ISSN 1007-9327 (print)
ISSN 2219-2840 (online)

World Journal of *Gastroenterology*

World J Gastroenterol 2021 September 7; 27(33): 5460-5624



Published by Baishideng Publishing Group Inc

World Journal of Gastroenterology

Contents

Weekly Volume 27 Number 33 September 7, 2021

THERAPEUTIC AND DIAGNOSTIC GUIDELINES

5460 Guidelines on postoperative magnetic resonance imaging in patients operated for cryptoglandular anal fistula: Experience from 2404 scans

Garg P, Kaur B, Yagnik VD, Dawka S, Menon GR

REVIEW

5474 Neutrophil extracellular traps in gastrointestinal cancer

Chu ZQ, Zhang KC, Chen L

5488 Microbiota and viral hepatitis: State of the art of a complex matter

Milosevic I, Russo E, Vujovic A, Barac A, Stevanovic O, Gitto S, Amedei A

5502 Clinical perspectives, assessment, and mechanisms of metabolic-associated fatty liver disease in patients with COVID-19

Campos-Murguía A, Román-Calleja BM, González-Regueiro JA, Hurtado-Díaz-de-León I, Solís-Ortega AA, Flores-García NC, García-Juárez I, Ruiz-Margáin A, Macías-Rodríguez RU

MINIREVIEWS

5520 Impact of COVID-19 on inflammatory bowel disease practice and perspectives for the future

Viganò C, Mulinacci G, Palermo A, Barisani D, Pirola L, Fichera M, Invernizzi P, Massironi S

5536 Surveillance for hepatocellular carcinoma in chronic viral hepatitis: Is it time to personalize it?

Demirtas CO, Brunetto MR

5555 Gut microbiota-derived metabolites as key mucosal barrier modulators in obesity

Wei YX, Zheng KY, Wang YG

ORIGINAL ARTICLE

Basic Study

5566 Adiponectin and the regulation of gastric content volume in the newborn rat

Wang H, Esemu-Ezewu P, Pan J, Ivanovska J, Gauda EB, Belik J

5575 Characterization of gut microbiome and metabolome in *Helicobacter pylori* patients in an underprivileged community in the United States

White B, Sterrett JD, Grigoryan Z, Lally L, Heinze JD, Alikhan H, Lowry CA, Perez LJ, DeSipio J, Phadtare S

Retrospective Study

5595 Gastric cancer mortality related to direct radiographic and endoscopic screening: A retrospective study

Hagiwara H, Moki F, Yamashita Y, Saji K, Iesaki K, Suda H

5610 Radiomics for predicting perineural invasion status in rectal cancer

Li M, Jin YM, Zhang YC, Zhao YL, Huang CC, Liu SM, Song B

LETTER TO THE EDITOR

5622 Comment on "Diagnostic approach to faecal incontinence: What test and when to perform?"

Wang JT, Miao YD, Guan QL

ABOUT COVER

Editorial Board Member of *World Journal of Gastroenterology*, Güray Can, MD, Associate Professor, Chief, Department of Gastroenterology, Bolu İzzet Baysal Education and Research Hospital, Bolu Abant İzzet Baysal University, Gölköy Campus, Bolu 14030, Turkey. guraycan@ibu.edu.tr

AIMS AND SCOPE

The primary aim of *World Journal of Gastroenterology* (*WJG*, *World J Gastroenterol*) is to provide scholars and readers from various fields of gastroenterology and hepatology with a platform to publish high-quality basic and clinical research articles and communicate their research findings online. *WJG* mainly publishes articles reporting research results and findings obtained in the field of gastroenterology and hepatology and covering a wide range of topics including gastroenterology, hepatology, gastrointestinal endoscopy, gastrointestinal surgery, gastrointestinal oncology, and pediatric gastroenterology.

INDEXING/ABSTRACTING

The *WJG* is now indexed in Current Contents®/Clinical Medicine, Science Citation Index Expanded (also known as SciSearch®), Journal Citation Reports®, Index Medicus, MEDLINE, PubMed, PubMed Central, and Scopus. The 2021 edition of Journal Citation Report® cites the 2020 impact factor (IF) for *WJG* as 5.742; Journal Citation Indicator: 0.79; IF without journal self cites: 5.590; 5-year IF: 5.044; Ranking: 28 among 92 journals in gastroenterology and hepatology; and Quartile category: Q2. The *WJG*'s CiteScore for 2020 is 6.9 and Scopus CiteScore rank 2020: Gastroenterology is 19/136.

RESPONSIBLE EDITORS FOR THIS ISSUE

Production Editor: *Ying-Yi Yuan*; **Production Department Director:** *Xiang Li*; **Editorial Office Director:** *Ze-Mao Gong*.

NAME OF JOURNAL
World Journal of Gastroenterology

ISSN
ISSN 1007-9327 (print) ISSN 2219-2840 (online)

LAUNCH DATE
October 1, 1995

FREQUENCY
Weekly

EDITORS-IN-CHIEF
Andrzej S Tarnawski, Subrata Ghosh

EDITORIAL BOARD MEMBERS
http://www.wjgnet.com/1007-9327/editorialboard.htm

PUBLICATION DATE
September 7, 2021

COPYRIGHT
© 2021 Baishideng Publishing Group Inc

INSTRUCTIONS TO AUTHORS
https://www.wjgnet.com/bpg/gerinfo/204

GUIDELINES FOR ETHICS DOCUMENTS
https://www.wjgnet.com/bpg/GerInfo/287

GUIDELINES FOR NON-NATIVE SPEAKERS OF ENGLISH
https://www.wjgnet.com/bpg/gerinfo/240

PUBLICATION ETHICS
https://www.wjgnet.com/bpg/GerInfo/288

PUBLICATION MISCONDUCT
https://www.wjgnet.com/bpg/gerinfo/208

ARTICLE PROCESSING CHARGE
https://www.wjgnet.com/bpg/gerinfo/242

STEPS FOR SUBMITTING MANUSCRIPTS
https://www.wjgnet.com/bpg/GerInfo/239

ONLINE SUBMISSION
https://www.f6publishing.com

© 2021 Baishideng Publishing Group Inc. All rights reserved. 7041 Koll Center Parkway, Suite 160, Pleasanton, CA 94566, USA

E-mail: bpgoffice@wjgnet.com https://www.wjgnet.com

World Journal of Gastroenterology

Submit a Manuscript: https://www.f6publishing.com

World J Gastroenterol 2021 September 7; 27(33): 5460-5473

DOI: 10.3748/wjg.v27.i33.5460

ISSN 1007-9327 (print) ISSN 2219-2840 (online)

THERAPEUTIC AND DIAGNOSTIC GUIDELINES

Guidelines on postoperative magnetic resonance imaging in patients operated for cryptoglandular anal fistula: Experience from 2404 scans

Pankaj Garg, Baljit Kaur, Vipul D Yagnik, Sushil Dawka, Geetha R Menon

ORCID number: Pankaj Garg 0000-0002-0800-3578; Baljit Kaur 0000-0002-3882-7578; Vipul D Yagnik 0000-0003-4008-6040; Sushil Dawka 0000-0002-9372-3683; Geetha R Menon 0000-0003-2491-0650.

Author contributions: Garg P conceived and designed the study, collected, and analyzed the data, revised the data, finally approved and submitted the manuscript (guarantor of the review); Kaur B and Yagnik VD collected, and analyzed the data, revised the data, finally approved and submitted the manuscript; Dawka S critically analyzed the data, reviewed and edited the manuscript, finally approved and submitted the manuscript; Menon GR analyzed the data, revised the data, finally approved and submitted the manuscript.

Conflict-of-interest statement: None of the authors, Garg P, Kaur B, Yagnik VD, Dawka S and Menon GR, have any conflict of interest.

Open-Access: This article is an open-access article that was selected by an in-house editor and fully peer-reviewed by external reviewers. It is distributed in accordance with the Creative

Pankaj Garg, Department of Colorectal Surgery, Garg Fistula Research Institute, Panchkula 134113, Haryana, India

Pankaj Garg, Department of Colorectal Surgery, Indus International Hospital, Mohali 140201, Punjab, India

Baljit Kaur, Department of Radiology, SSRD Magnetic Resonance Imaging Institute, Chandigarh 160011, Chandigarh, India

Vipul D Yagnik, Department of Surgical Gastroenterology, Nishtha Surgical Hospital and Research Center, Patan 384265, Gujarat, India

Sushil Dawka, Department of Surgery, SSR Medical College, Belle Rive, Mauritius

Geetha R Menon, Department of Statistics, Indian Council of Medical Research, New Delhi 110029, New Delhi, India

Corresponding author: Pankaj Garg, MBBS, MS, Associate Professor, Surgeon, Department of Colorectal Surgery, Garg Fistula Research Institute, House No 1042, Sector-15, Panchkula 134113, Haryana, India. drgargpankaj@yahoo.com

Abstract

Magnetic resonance imaging (MRI) is considered the gold standard for the evaluation of anal fistulas. There is sufficient literature available outlining the interpretation of fistula MRI before performing surgery. However, the interpretation of MRI becomes quite challenging in the postoperative period after the surgery of fistula has been undertaken. Incidentally, there are scarce data and no set guidelines regarding analysis of fistula MRI in the postoperative period. In this article, we discuss the challenges faced while interpreting the postoperative MRI, the timing of the postoperative MRI, the utility of MRI in the postoperative period for the management of anal fistulas, the importance of the active involvement and experience of the treating clinician in interpreting MRI scans, and the latest advancements in the field.

Key Words: Anal fistula; Magnetic resonance imaging; Postoperative; Hyperintensity; Internal opening

Commons Attribution NonCommercial (CC BY-NC 4.0) license, which permits others to distribute, remix, adapt, build upon this work non-commercially, and license their derivative works on different terms, provided the original work is properly cited and the use is non-commercial. See: http://creativecommons.org/Licenses/by-nc/4.0/

Manuscript source: Invited manuscript

Specialty type: Gastroenterology and hepatology

Country/Territory of origin: India

Peer-review report's scientific quality classification

Grade A (Excellent): 0
Grade B (Very good): B
Grade C (Good): 0
Grade D (Fair): 0
Grade E (Poor): 0

Received: May 8, 2021
Peer-review started: May 8, 2021
First decision: June 12, 2021
Revised: June 12, 2021
Accepted: August 5, 2021
Article in press: August 5, 2021
Published online: September 7, 2021

P-Reviewer: Dulskas A
S-Editor: Gao CC
L-Editor: Filipodia
P-Editor: Li JH

©The Author(s) 2021. Published by Baishideng Publishing Group Inc. All rights reserved.

Core Tip: Magnetic resonance imaging (MRI) plays a pivotal role in the preoperative management of anal fistulas, but there are little data on postoperative MRI. There are no existing guidelines available to the operating surgeon and the radiologist regarding the challenges faced, utility, timing, and other aspects of MRI interpretation of anal fistulas in the postoperative period. This is the first paper on this theme and presents the first guidelines to be formulated for postoperative MRI in anal fistula management. These guidelines are based on an extensive experience of interpreting 2404 MRI scans in 1719 patients, including 685 postoperative MRIs in 411 patients.

Citation: Garg P, Kaur B, Yagnik VD, Dawka S, Menon GR. Guidelines on postoperative magnetic resonance imaging in patients operated for cryptoglandular anal fistula: Experience from 2404 scans. *World J Gastroenterol* 2021; 27(33): 5460-5473
URL: https://www.wjgnet.com/1007-9327/full/v27/i33/5460.htm
DOI: https://dx.doi.org/10.3748/wjg.v27.i33.5460

INTRODUCTION

Anal fistulas are known and feared for their high rate of recurrence and risk to the continence mechanism if the anal sphincters are damaged during surgery[1-5]. Newer diagnostic modalities, especially magnetic resonance imaging (MRI) and transrectal ultrasound (TRUS)[6,7], have helped in better understanding the pathophysiology and management of the disease[8-11]. MRI is slightly better than TRUS and is considered the gold standard to assess anal fistulas[12]. Most colorectal surgeons prefer MRI over TRUS for managing anal fistulas[13]. A recent study showed that 97% of surgeons preferred MRI and only 12% opted for TRUS[13]. There is plenty of literature available on the role and interpretation of MRI in anal fistulas before surgery, but the same is not true about the postoperative period[12]. There are hardly any data on the role and interpretation of MRI in the postoperative period after fistula surgery[12]. This is the first paper in which the guidelines for postoperative MRI in anal fistulas are discussed, and they are presented under five headings (Table 1).

It is important to understand that fistula healing can be clinical or radiological[14,15]. The most common definition of clinical healing is cessation of pus discharge from all the external openings and the anus for at least 3 mo[14,15]. On the other hand, radiological healing is defined as complete healing of the internal opening, the intersphincteric portion of the fistula tract, and tracts in the ischiorectal fossa on MRI or TRUS[14,15].

CHALLENGES IN INTERPRETING THE MRI IN THE POSTOPERATIVE PERIOD

Interpretation of the MRI in the postoperative period is not straightforward and poses a few challenges[15]. The active (infected) fistula tracts and abscesses appear hyperintense on T2 and short tau inversion recovery (STIR) sequences. The main conundrum in the postoperative period is that inflammation of tissue due to surgical trauma also appears hyperintense (white) on T2 and STIR[15]. Another confusing feature is that the granulation tissue that leads to healing of the fistula appears hyperintense (white) on T2 and STIR[15,16] as well. Therefore, the overall picture can be quite confusing as all three (infected fistula, post-surgery inflammation and healing granulation tissue in the fistula tract) appear similar and therefore require careful assessment (Figure 1). This problem or confusion can be resolved if the check MRI is delayed for a few weeks[15,16].

After a few weeks, the postoperative inflammation of tissues subsides and the healing granulation tissue is converted to scar tissue when the fistula heals completely [16]. The scar tissue appears hypointense (black) on T2 and STIR (Figure 2). Therefore, after this time, any hyperintensity (white) on T2 and STIR would most likely indicate fistula persistence or fistula/abscess recurrence[16] (Figures 3 and 4).

Table 1 Guidelines for postoperative magnetic resonance imaging in management of anal fistulas

Guidelines for postoperative MRI in management of anal fistulas
(1) Challenges in interpreting the MRI in postoperative period
(2) Timing of postoperative MRI
(3) Utility of MRI in postoperative period for anal fistula management: Checking for missed tract and confirm adequate drainage of all abscesses; Checking for new abscess/tract development; Confirming healing of internal opening
(4) Active involvement and experience of clinician in interpreting MRI scans
(5) Other advancements

MRI: Magnetic resonance imaging.

Recommendation

An active fistula tract, post-surgery inflammation and healing granulation tissue in the fistula tract look similar on postoperative MRI and cause confusion. Waiting for a few weeks can resolve this confusion.

TIMING OF POSTOPERATIVE MRI

As discussed above, the timing of postoperative MRI assumes great significance if meaningful information is to be gained from it. The appropriate cut-off time period for performing MRI to confirm fistula healing should be 12 wk after the date of surgery [16]. However, MRI to check for a missed tract, inadequate drainage of an abscess or to identify a newly developed tract or abscess may be done at any time in the postoperative period as necessitated by the clinical picture.

By 12 wk after surgery, the postoperative inflammation of tissues subsides almost completely and fistula healing occurs completely in cases where fistula closure eventually occurs. In such cases with complete fistula healing, the hyperintense (white) active infected fistula tract or healing granulation tissue, both become hypointense (black) on T2 and STIR[12,16] (Figures 2 and 4-6).

Though a fistula may heal even before 12 wk (Figure 5) or the healing granulation tissue may persist beyond 12 wk after surgery, a minimum wait of 12 wk seems prudent[16]. Any wait greater than 12 wk is better; rather, the longer the delay in scheduling MRI, the clearer the picture (Figure 6). This is because, with greater delay in performing MRI (*e.g.*, 5-6 mo), all tissue inflammation and healing granulation tissue is expected to disappear, and any hyperintensity (white) on T2 and STIR would mean fistula persistence or fistula/abscess recurrence. However, most patients do not like to wait for such a long time (5-6 mo)[16].

Recommendation

The postoperative MRI to confirm fistula healing after surgery should be optimally done at least after 12 wk. However, the postoperative MRI to check for adequacy of abscess drainage or development of a new fistula tract may be scheduled as per clinical requirement.

UTILITY OF MRI IN THE POSTOPERATIVE PERIOD FOR ANAL FISTULA MANAGEMENT

MRI serves as an extremely useful tool in the armamentarium of surgeons managing complex anal fistulas. The main indications for performing MRI in the postoperative period after anal fistula surgery are as follow.

Checking for a missed tract or confirming adequate drainage of all abscesses: In complex fistulas with multiple tracts or abscesses, it is possible that a tract or an abscess may be missed during surgery or is inadequately drained[15]. This may lead to non-improvement or even deterioration of symptoms after surgery. An MRI in the postoperative period would lead to correct identification of the cause (missed fistula tract or inadequately drained abscess) (Figure 7) and timely intervention[16].

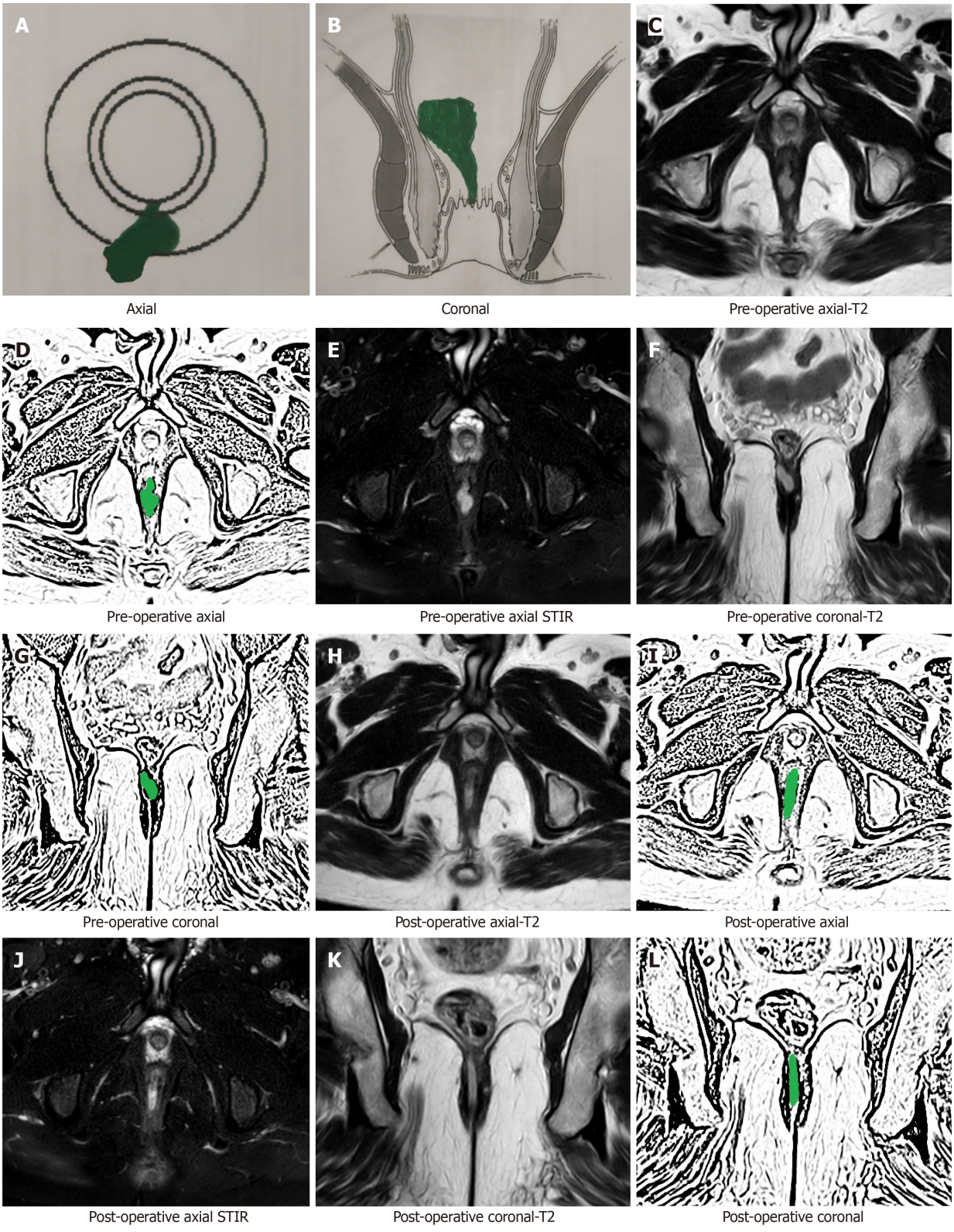


Figure 1 A 37-year-old male patient with a high posterior intersphincteric abscess was drained by transanal opening of the intersphincteric space procedure. Magnetic resonance imaging (MRI) done after 3 wk after surgery showed hyperintense signal (due to healing granulation tissue) at the same location similar to the hyperintense signal in the preoperative images (due to pus collection). A: Axial section (schematic diagram); B: Coronal section (schematic diagram); C: Pre-operative T2-weighted MRI; D: Sketch of pre-operative axial MRI image highlighting abscess (green color); E: Pre-operative short-T1 inversion recovery (STIR) axial MRI; F: Pre-operative T2-weighted coronal MRI; G: Sketch of pre-operative coronal MRI image highlighting abscess (green color); H: Postoperative T2-weighted axial MRI; I: Sketch of postoperative axial MRI image highlighting healing granulation tissue (green color); J: Postoperative STIR axial MRI; K: Postoperative T2-weighted coronal MRI; L: Sketch of postoperative coronal MRI image highlighting healing granulation tissue (green color). STIR: Short-T1 inversion recovery.

Checking for new abscess/tract development: There are instances when a patient

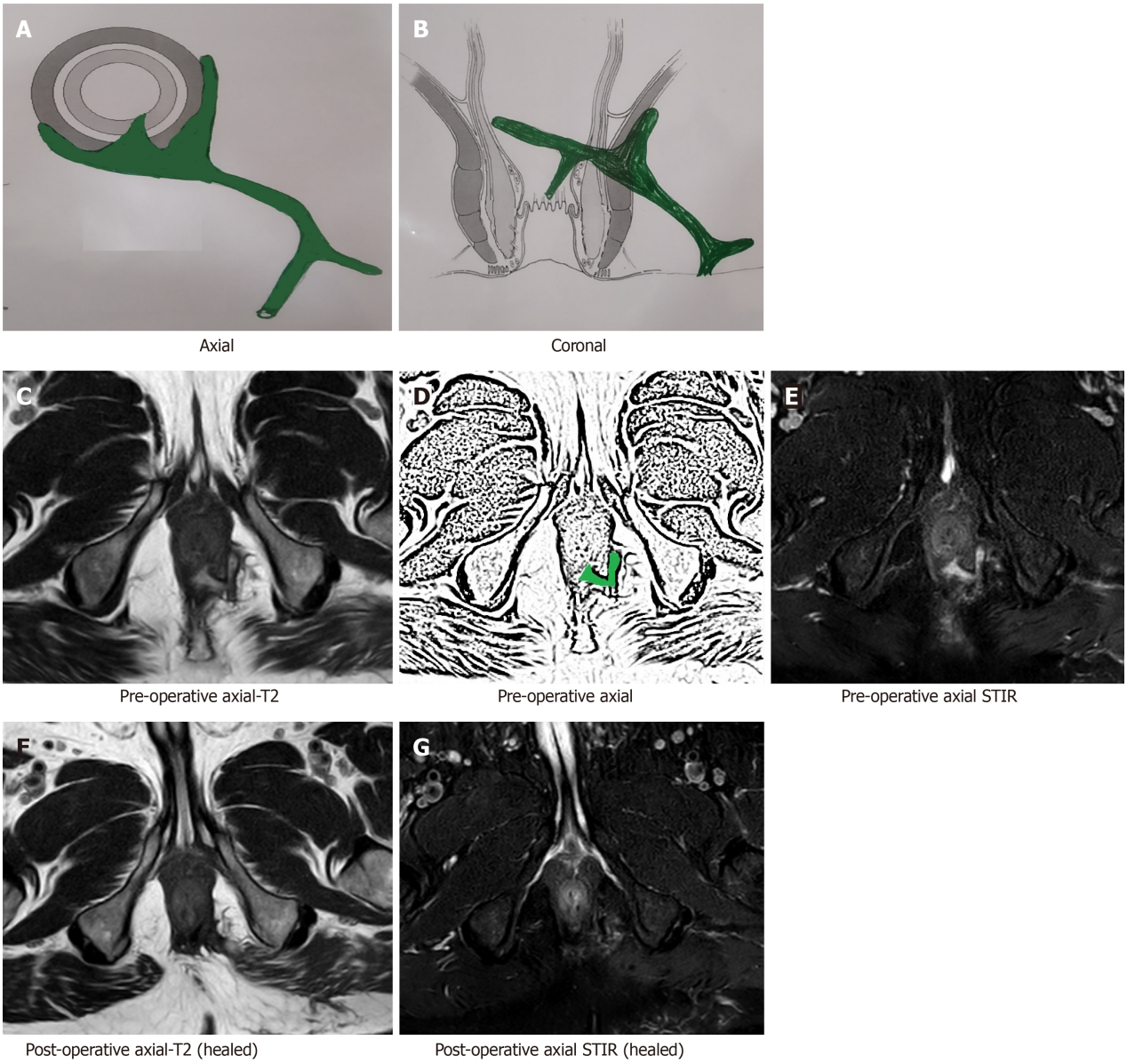


Figure 2 A 64-year-old male patient with a high transsphincteric fistula with multiple branches. Magnetic resonance imaging (MRI) done after 19 wk post-surgery showing fistula has healed completely. The hyperintense signal (white) in the preoperative images has turned hypointense (black). A: Axial section (schematic diagram); B: Coronal section (schematic diagram); C: Pre-operative T2-weighted axial MRI; D: Sketch of pre-operative axial MRI image highlighting internal opening and the intersphincteric portion of fistula tract (green color); E: Pre-operative short-T1 inversion recovery (STIR) axial MRI; F: Postoperative T2-weighted axial MRI (after 19 wk) showing completely healed fistula; G: Postoperative STIR axial MRI (after 19 wk) showing completely healed fistula. STIR: Short-T1 inversion recovery.

who was improving in the postoperative period starts to deteriorate due to development of fistula tracts or abscesses in new sites[15]. This could be due to undiagnosed tuberculosis (TB), Crohn's disease, or virulent microbes. An MRI would be of immense help in determining the presence as well as the location of the new tract or abscess and its subsequent management[16].

MRI is fairly accurate in assessing and confirming the healing of fistulas radiologically. Not uncommonly, the external opening of the fistula tract closes and the fistula appears healed clinically. However, the internal opening and intersphincteric component of the fistula tract have not healed and this leads to a recurrence weeks to months later[16] (Figures 3 and 4). This phenomenon of a fistula appearing healed followed by recurrence makes fistula management unpredictable and creates uncertainty in the minds of patients and surgeons alike. Therefore, many patients desire confirmation of whether the fistula which appears clinically healed has actually healed radiologically as well. This is especially true in patients who have suffered from multiple recurrences of the fistula[16].

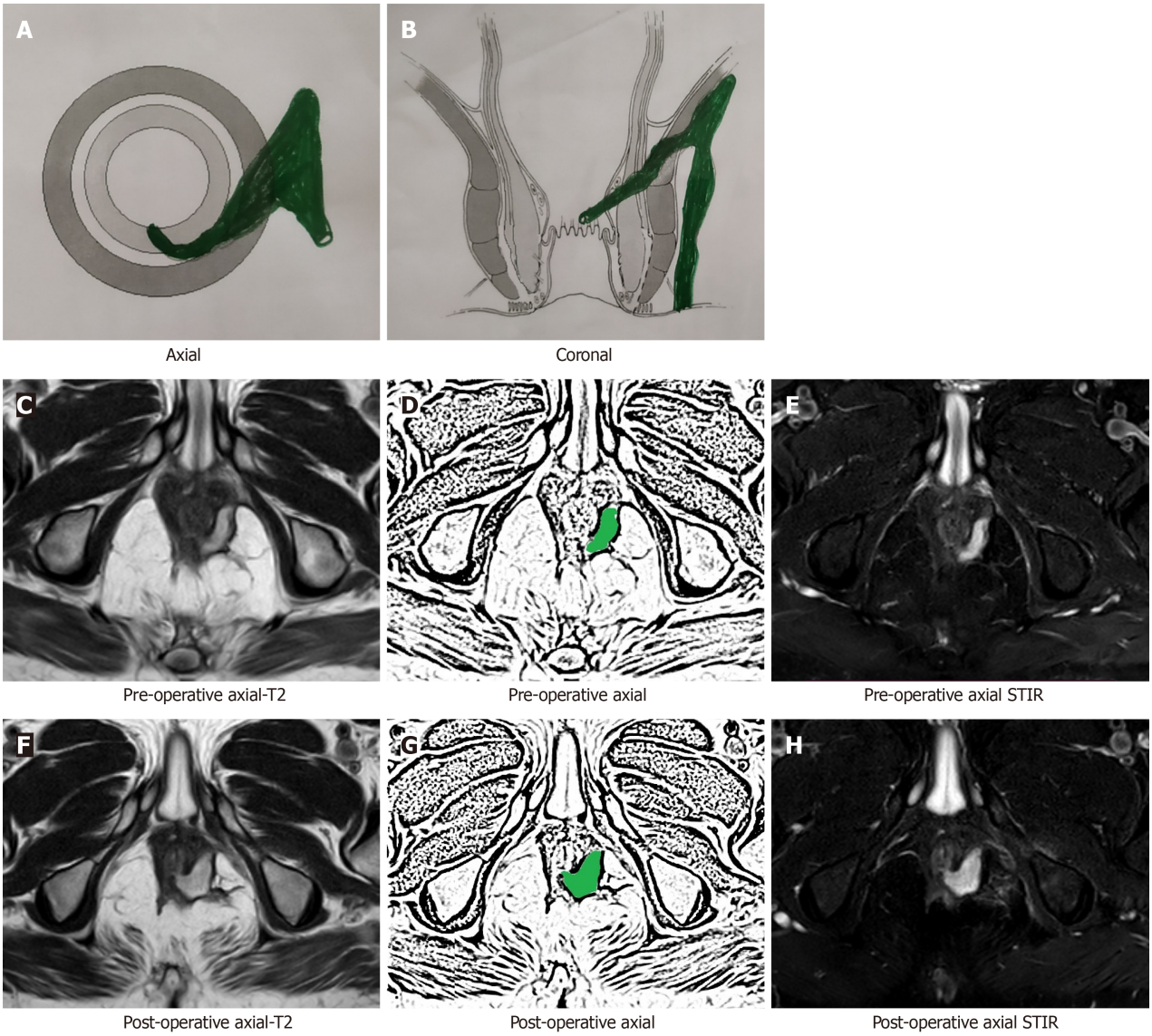


Figure 3 A 54-year-old male patient with a high transsphincteric fistula. The fistula appeared to have 'clinically' healed as the external opening had closed with cessation of all pus. However, magnetic resonance imaging (MRI) done after 28 wk post-surgery showed patent internal opening and widening of intersphincteric portion of fistula tract. A: Axial section (schematic diagram); B: Coronal section (schematic diagram); C: Pre-operative T2-weighted MRI; D: Sketch of pre-operative axial MRI image highlighting internal opening and the intersphincteric portion of fistula tract (green color); E: Pre-operative short-T1 inversion recovery (STIR) axial MRI; F: Postoperative T2-weighted axial MRI (after 28 wk) showing patent internal opening and persistent intersphincteric portion of fistula tract; G: Sketch of postoperative axial MRI image highlighting patent internal opening and persistent intersphincteric portion of fistula tract; H: Postoperative STIR axial MRI (after 28 wk) showing patent internal opening and persistent intersphincteric portion of fistula tract. STIR: Short-T1 inversion recovery.

Of all its benefits, this indication of MRI (to confirm fistula healing) is perhaps the most important of all motives for obtaining an MRI in the postoperative period[14]. It has been shown in a large study with long-term follow-up, that corroboration of clinical healing with radiological healing on MRI correlates quite well with actual long-term healing[14,15]. In a study of 125 patients of complex anal fistulas in whom the fistula had healed radiologically and who were followed-up for 38 mo, 99.2% (124/125) remained healed and only 1/125 patients had a recurrence on long-term [14]. This is important evidence that if clinical healing is corroborated by radiological healing on MRI, then the chances of long-term recurrence are minimal.

A fistula can be divided into three distinct parts for the purpose of MRI assessment: Internal opening; intersphincteric component of fistula tract; and component of fistula lateral to the external sphincter (external tracts).

The first two components, the internal opening and the intersphincteric component of the fistula tract, are deep and are difficult to assess on clinical examination, whereas the external tracts are relatively easy to assess clinically[14]. Second, any persistent infection in the external tracts leads to pus discharge from the external opening and will be clinically manifested. On the other hand, a fistula with healed external tract

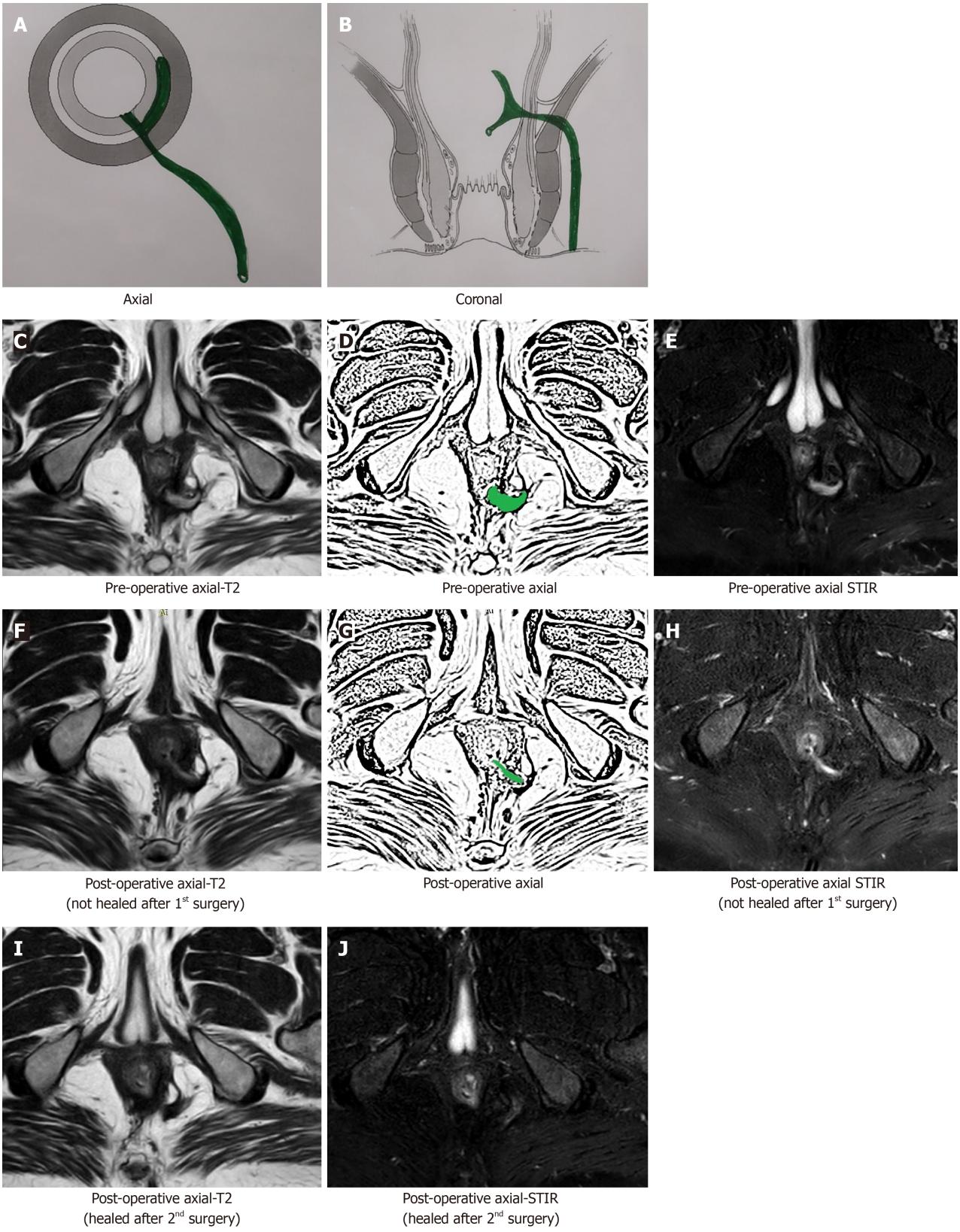


Figure 4 A 47-year-old male patient with a high transsphincteric fistula with supralevator extension. The fistula appeared to have 'clinically' healed as the external opening had closed with cessation of all pus. Magnetic resonance imaging (MRI) done after 26 wk post-surgery showed patent internal opening and active intersphincteric portion of the fistula tract [hyperintense on T2 and short-T1 inversion recovery (STIR)]. The patient was operated again. MRI done after 14 wk after 2nd surgery showed fistula has healed completely. The hyperintense signal (white) in the preoperative images has turned hypointense (black). A: Axial section (schematic diagram); B: Coronal section (schematic diagram); C: Pre-operative T2-weighted MRI; D: Sketch of pre-operative axial MRI image highlighting internal opening and the intersphincteric portion of fistula tract (green color); E: Pre-operative STIR axial MRI; F: Postoperative (26 wk after 1st surgery) T2-weighted axial MRI showing patent internal opening and persistent intersphincteric portion of fistula tract; G: Sketch highlighting patent internal opening and intersphincteric portion of fistula tract (green color); H: Postoperative (26 wk after 1st surgery) STIR axial MRI showing patent internal opening and persistent

intersphincteric portion of fistula tract; I: Postoperative (14 wk after 2nd surgery) T2-weighted axial MRI showing completely healed fistula; J: Postoperative (14 wk after 2nd surgery) STIR axial MRI showing completely healed fistula. STIR: Short-T1 inversion recovery.

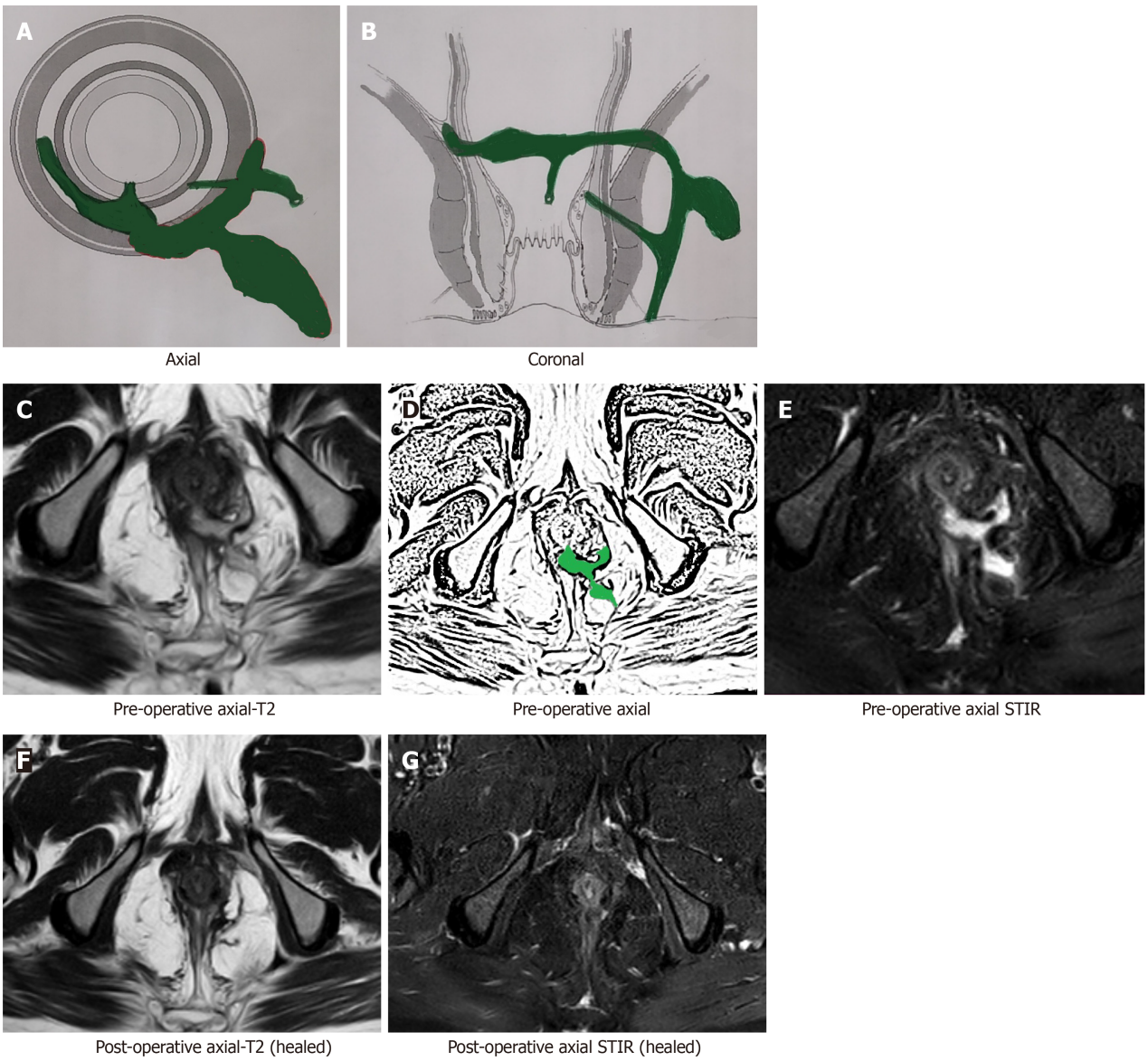


Figure 5 A 51-year-old male patient with a high transsphincteric fistula with multiple branches. Magnetic resonance imaging (MRI) done after 8 wk post-surgery showing fistula has healed completely. The hyperintense signal (white) in the preoperative images has turned hypointense (black). A: Axial section (schematic diagram); B: Coronal section (schematic diagram); C: Pre-operative T2-weighted axial MRI; D: Sketch of pre-operative axial MRI image highlighting internal opening, the intersphincteric portion of fistula tract and transsphincteric fistula tract (green color); E: Pre-operative short-T1 inversion recovery (STIR) axial MRI; F: Postoperative T2-weighted axial MRI (after 8 wk) showing completely healed fistula; G: Postoperative STIR axial MRI (after 8 wk) showing completely healed fistula. STIR: Short-T1 inversion recovery.

and closed external opening may have persistent infection/sepsis in the intersphincteric component of the fistula tract[14,15] (Figures 3 and 4). Such fistulas have no clinical manifestation for a few weeks and may appear healed even on clinical examination (Figures 3 and 4). Therefore, MRI is primarily useful in assessing the patency of the internal opening and assessing healing of the intersphincteric component of the fistula tract[14,15] (Figures 2 and 4-6). Moreover, once the internal opening and intersphincteric component of the fistula tract have healed completely, even the external tracts eventually heal in most cases. Therefore, a clinically healed fistula may be radiologically unhealed and such a fistula has a high likelihood of recurrence. On the other hand, a radiologically healed fistula with occasional serous discharge from the external opening for a few days (thus appearing clinically unhealed), has a high likelihood of healing and a low risk of recurrence.

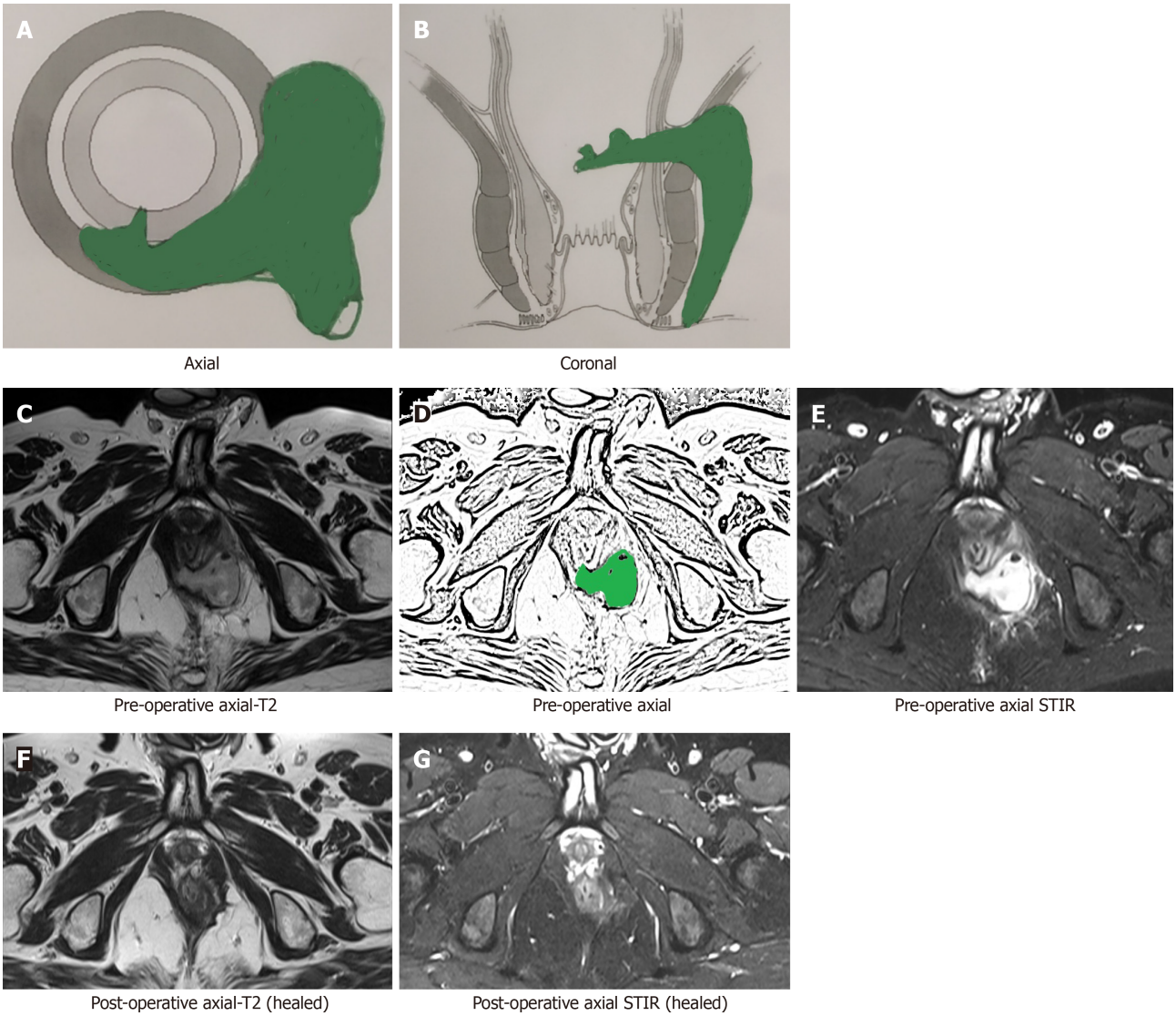


Figure 6 A 40-year-old male patient with a suprasphincteric fistula. Magnetic resonance imaging (MRI) done after 16 wk post-surgery showing fistula has healed completely. The hyperintense signal (white) in the preoperative images has turned hypointense (black). A: Axial section (schematic diagram); B: Coronal section (schematic diagram); C: Pre-operative T2-weighted axial MRI; D: Sketch of pre-operative axial MRI image highlighting internal opening and the intersphincteric portion of fistula tract (green color); E: Pre-operative short-T1 inversion recovery (STIR) axial MRI; F: Postoperative T2-weighted axial MRI (after 16 wk) showing completely healed fistula; G: Postoperative STIR axial MRI (after 16 wk) showing completely healed fistula. STIR: Short-T1 inversion recovery.

As mentioned above, the patent internal opening and actively infected intersphincteric component of the fistula tract appear hyperintense (white) on T2 and STIR (Figures 3 and 4) whereas the healed internal opening and intersphincteric component of fistula tract appear hypointense (black) on T2 and STIR (Figures 2 and 4-6).

Recommendation

The healing of the internal opening and the intersphincteric component of the fistula tract correlate very well with both immediate and long-term fistula healing.

ACTIVE INVOLVEMENT AND EXPERIENCE OF THE CLINICIAN IN INTERPRETING MRI SCANS

A pivotal point in the management of complex anal fistulas is the active involvement of the operating surgeon in the interpretation of MRI scans.

Apart from being slightly more sensitive than TRUS, the main advantage of MRI over TRUS is that MRI interpretation is not operator dependent[15]. MRI films can be meaningfully interpreted by anyone independent of who conducted the procedure.

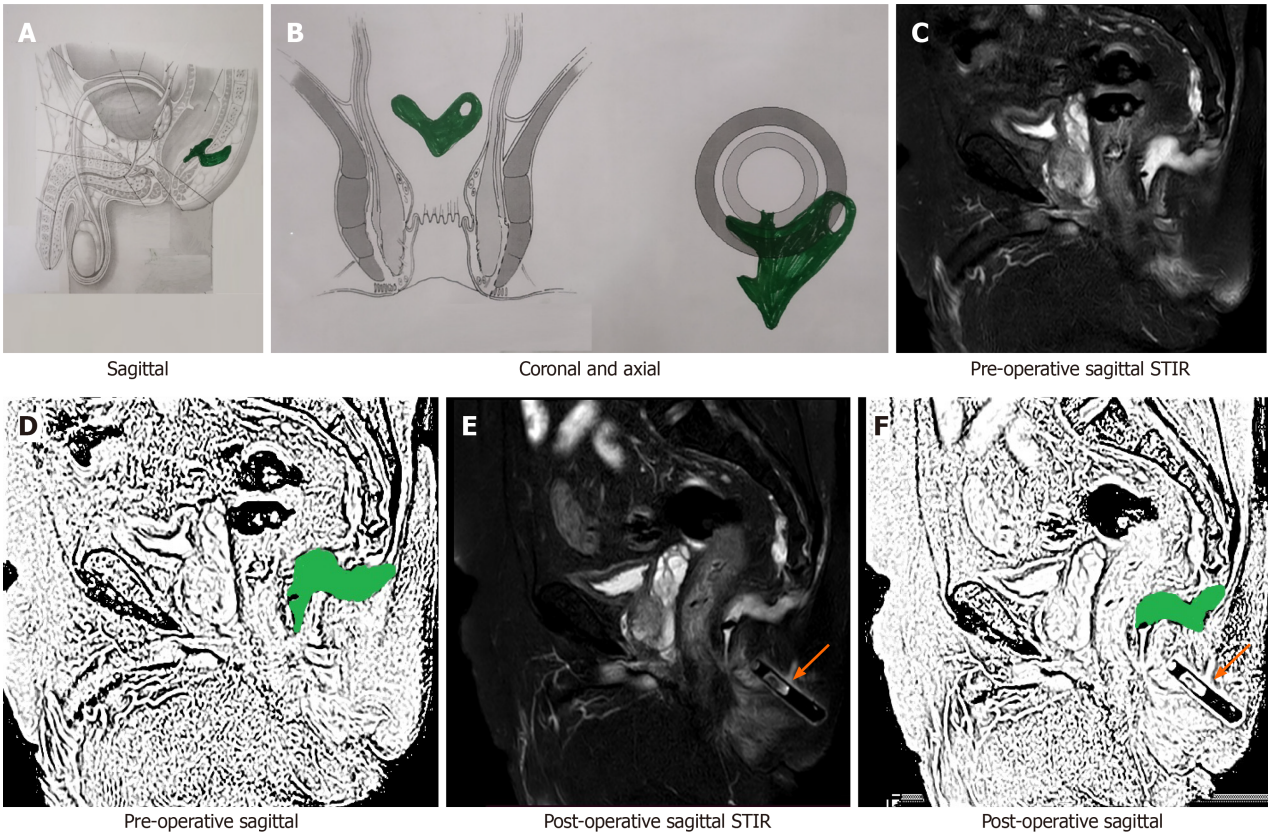


Figure 7 A 69-year-old male patient with a posterior fistula with a presacral abscess. A wide bore drainage tube was inserted into the cavity intraoperatively. However, the patient did not improve. Postoperative check magnetic resonance imaging (MRI) demonstrated that the tube was in the wrong plane and the presacral abscess was not properly drained. A: Axial section (schematic diagram); B: Coronal section (schematic diagram); C: Preoperative short-T1 inversion recovery (STIR) sagittal MRI; D: Sketch of pre-operative sagittal MRI image highlighting anal fistula and presacral abscess (green color); E: Postoperative STIR sagittal MRI showing drainage tube in the wrong plane and persistent presacral abscess; F: Sketch of postoperative sagittal MRI highlighting persisting anal fistula and presacral abscess (green color) (orange arrows show the drainage tube). STIR: Short-T1 inversion recovery.

This is a big advantage for the treating surgeon as the MRI scan can be analyzed in the office or operating room. We have realized that analyzing the MRI on computer *via* DVD/CD is more informative than interpreting it on films (hard copy). This is because each frame can be studied in high resolution on the monitor and can be enlarged as desired.

Active involvement of the surgeon in radiological analysis is important in preoperative management but holds even more significance in the postoperative management of complex anal fistulas. As the operating surgeon is well versed with the clinical picture, the operative procedure done and the postoperative course, he or she can correlate the radiological picture much better than the radiologist[5]. This holds true for other diseases as well but is far more applicable in managing complex anal fistulas. Needless to say, the full input of the radiologist needs to be considered in every case but the surgeon should be actively in the driver's seat alongside the radiologist while interpreting MRI scans. The surgeon should not passively make deductions from the radiologist's report.

Garg Fistula Research Institute is a specialized referral center for managing anal fistulas in North India. Over the last 8 years, 2404 MRI scans done in 1719 patients were analyzed at the institute[15]. Of the 1255/1719 patients who were operated for anal fistulas, 621/1255 patients had complex anal fistulas and 634/1255 had simple fistulas. Preoperative MRI (n = 1255) was done in all 1255 patients, whereas postoperative MRI (n = 685) was done in 411/1255 patients. Many patients required multiple postoperative MRI scans as their fistulas were more complex. The details are tabulated in Tables 2 and 3. The above data is mentioned in order to highlight a couple of points. First, the operating surgeon (Garg P) was actively involved in interpreting all the MRI scans along with the chief radiologist (Kaur B). The latter has the experience of reading more than 12000 anal fistula MRI scans over the last 30 years. Second, a reasonably high cure rate of 93.5% could be achieved over a long-term follow-up (median: 3 years) in this large cohort[15]. Active involvement of the operating surgeon in MRI interpretation was one of the key factors in achieving these

Table 2 Overview of magnetic resonance imaging scans done

Overview	
Total patients = 1719	Total MRI evaluated in 1719 patients = 2404
Total patients operated = 1255	Total MRI in 1255 operated patients = 1940
	Preoperative MRI in 1255 operated patients = 1255
Patients in whom postoperative	Number of MRI done in 411 patients = 685
MRI done = 411/1255	

MRI: Magnetic resonance imaging.

Table 3 Characteristics of operated anal fistula patients analyzed by magnetic resonance imaging

Parameter	Patients (*n* = 1255)
M/F	1078/177
Recurrent (%)	754 (60.1)
Associated abscess (%)	328 (25.7)
Multiple fistula tracts (%)	777 (61.9)
Horseshoe tract (%)	285 (22.7)
Supralevator or suprasphincteric tract (%)	162 (12.9)
Simple/complex fistulas	621/ 634
Fistula classification as per different classifications	
St James's University Hospital	I-193
	II-180
	III-150
	IV-570
	V- 162
Parks	I-375
	II-698
	III-162
	IV-0
Garg	I-265
	II-390
	III-83
	IV-355
	V- 162

Garg classification is a recently proposed classification (2017), which has been shown to correlate accurately with fistula complexity[15,16]. F: Female; M: Male.

results.

Approval for analyzing the data was obtained from the Indus International Hospital-Institute Ethics Committee. The patients were informed about the purpose of the study, and the study was conducted in accordance with the Declaration of Helsinki.

It is a standard recommendation to obtain pre-operative MRI in recurrent fistulas. However, there is no consensus on performing MRI in all patients including those with seemingly primary, simple fistulas on preoperative clinical examination. A recent large study highlighted that 34% of fistulas that appeared simple on clinical

examination turned out to be complex after an MRI was performed, leading to a change in surgical decision for these patients[16]. Considering the results of this study and since our institute is a referral center for anal fistulas, we perform MRI in all patients as a standard protocol. This might appear expensive, but it works out to be economical even if it prevents recurrence in half the patients. Additionally, as MRI is not very costly in our country (USD 75), it does not financially burden the patients. Therefore, the cost-effectiveness of performing MRI for all fistulas (including simple-looking fistulas) would depend on the prevailing cost and availability of MRI in the region, experience of the operating surgeon in clinical examination as well as his/her past experience, and correlation of the results of the clinical examination with actual fistula complexity.

Recommendation

The operating surgeon should be actively involved with the radiologist in interpreting preoperative as well as postoperative MRI scans for managing anal fistulas.

OTHER ADVANCEMENTS

Newer advancements like contrast-enhanced MRI and three-dimensional modelling are being evaluated for anal fistulas[9,17-22]. These have been utilized more in Crohn's disease rather than cryptoglandular fistulas. However, the data on their utility is limited, and the exact indications and advantages have not been outlined yet. Contrast-enhanced MRI might provide additional input in preoperative MRI scans, but its role in the postoperative period has not been studied in great detail[21]. Diffusion-weighted MRI (DW-MRI) is superior to fat-suppressed T2-weighted images in detecting fistula tracts and also helps avoid the need to administer contrast (gadolinium chelate) in many cases[9,20]. However, its role in postoperative management has not yet been evaluated[9,20].

Various MRI-based scoring systems have been developed based on disease severity. The first of these was the Van Assche scoring system[23] which has been modified and subsequently used[24-26]. However, these scores have been utilized only in fistulizing Crohn's disease and have not been evaluated in cryptoglandular fistulas. The major shortcoming of these scoring systems is that they are based on both fistula complexity and MRI features. A more complex fistula is assigned higher scores as per these scoring systems. These studies evaluated the correlation between postoperative fistula healing and the assigned scores. A fistula with lower scores was expected to heal more readily and *vice versa*. However, this correlation was not seen in many patients[26]. In summary, these scores did not correlate accurately with postoperative healing in Crohn's fistulizing disease. The point, perhaps overlooked by most of these studies, is that the scoring system primarily assessed fistula complexity. A complex fistula is expected to have a lower likelihood of healing, but this correlation may not always be accurate as, apart from complexity, fistula healing depends on additional factors. These include the surgeon's competence (a simple fistula treated by an inexperienced surgeon may recur), the procedure employed (an expert surgeon performing an inappropriate procedure in a simple fistula can cause a recurrence), associated comorbidities like diabetes, undetected fistulizing disease like TB, poor patient compliance *etc*. Therefore, it is not prudent to use a single scoring system to evaluate fistula complexity as well as to predict postoperative healing. Both these parameters should be assessed by separate scoring systems.

Recommendation

In future, DW-MRI, three-dimensional modelling scans and MRI-based scoring systems will play an important role in the interpretation of postoperative MRI after fistula surgery.

CONCLUSION

To conclude, this is the first paper in which the guidelines for postoperative MRI in anal fistulas have been discussed. Postoperative MRI is an extremely useful tool available to surgeons managing complex fistulas. Though its interpretation is somewhat more challenging than analyzing preoperative MRI, with diligence and adequate experience, the treating surgeon can acquire proficiency in interpreting

postoperative MRI as an active member of the clinician-radiologist team. This will go a long way in improving management of anal fistulas, especially complex ones.

REFERENCES

1 **Włodarczyk M**, Włodarczyk J, Sobolewska-Włodarczyk A, Trzciński R, Dziki Ł, Fichna J. Current concepts in the pathogenesis of cryptoglandular perianal fistula. *J Int Med Res* 2021; **49**: 300060520986669 [PMID: 33595349 DOI: 10.1177/0300060520986669]

2 **Mei Z**, Li Y, Zhang Z, Zhou H, Liu S, Han Y, Du P, Qin X, Shao Z, Ge M, Wang Q, Yang W. Development of screening tools to predict the risk of recurrence and related complications following anal fistula surgery: protocol for a prospective cohort study. *BMJ Open* 2020; **10**: e035134 [PMID: 32139494 DOI: 10.1136/bmjopen-2019-035134]

3 **Mei Z**, Wang Q, Zhang Y, Liu P, Ge M, Du P, Yang W, He Y. Risk Factors for Recurrence after anal fistula surgery: A meta-analysis. *Int J Surg* 2019; **69**: 153-164 [PMID: 31400504 DOI: 10.1016/j.ijsu.2019.08.003]

4 **Terra MP**, Beets-Tan RG, van der Hulst VP, Deutekom M, Dijkgraaf MG, Bossuyt PM, Dobben AC, Baeten CG, Stoker J. MRI in evaluating atrophy of the external anal sphincter in patients with fecal incontinence. *AJR Am J Roentgenol* 2006; **187**: 991-999 [PMID: 16985148 DOI: 10.2214/AJR.05.0386]

5 **Garcia-Aguilar J**, Belmonte C, Wong WD, Goldberg SM, Madoff RD. Anal fistula surgery. Factors associated with recurrence and incontinence. *Dis Colon Rectum* 1996; **39**: 723-729 [PMID: 8674361 DOI: 10.1007/BF02054434]

6 **Almeida IS**, Jayarajah U, Wickramasinghe DP, Samarasekera DN. Value of three-dimensional endoanal ultrasound scan (3D-EAUS) in preoperative assessment of fistula-in-ano. *BMC Res Notes* 2019; **12**: 66 [PMID: 30696490 DOI: 10.1186/s13104-019-4098-2]

7 **Youssef A**. The Ultrasound of Perianal External Opening. *Gastroenterol Hepatol Int J* 2017; **2**: 000128

8 **Waheed KB**, Shah WJ, Altaf B, Amjad M, Hameed F, Wasim S, UlHassan MZ, Abuabdullah ZM, Rajamonickam SN, Arulanatham ZJ. Magnetic resonance imaging findings in patients with initial manifestations of perianal fistulas. *Ann Saudi Med* 2020; **40**: 42-48 [PMID: 32026703 DOI: 10.5144/0256-4947.2020.42]

9 **Liu X**, Wang Z, Ren H, Ren A, Wang W, Yang X, Shi S. Evaluating postoperative anal fistula prognosis by diffusion-weighted MRI. *Eur J Radiol* 2020; **132**: 109294 [PMID: 33038577 DOI: 10.1016/j.ejrad.2020.109294]

10 **Rajkumar J**, Dharmendra K, Anirudh R, Akbar S, Nabeel N, Jayakrishna AR, Hema T, Shreya R. MRI Before Fistula Surgery: Will It Change the Operation? *Indian J Surg* 2019; **81**: 178-181 [DOI: 10.1007/s12262-018-1857-6]

11 **Balcı S**, Onur MR, Karaosmanoğlu AD, Karçaaltıncaba M, Akata D, Konan A, Özmen MN. MRI evaluation of anal and perianal diseases. *Diagn Interv Radiol* 2019; **25**: 21-27 [PMID: 30582572 DOI: 10.5152/dir.2018.17499]

12 **Halligan S**, Tolan D, Amitai MM, Hoeffel C, Kim SH, Maccioni F, Morrin MM, Mortele KJ, Rafaelsen SR, Rimola J, Schmidt S, Stoker J, Yang J. ESGAR consensus statement on the imaging of fistula-in-ano and other causes of anal sepsis. *Eur Radiol* 2020; **30**: 4734-4740 [PMID: 32307564 DOI: 10.1007/s00330-020-06826-5]

13 **Dekker L**, Zimmerman DDE, Smeenk RM, Schouten R, Han-Geurts IJM. Management of cryptoglandular fistula-in-ano among gastrointestinal surgeons in the Netherlands. *Tech Coloproctol* 2021; **25**: 709-719 [PMID: 33860363 DOI: 10.1007/s10151-021-02446-3]

14 **Garg P**, Yagnik VD, Kaur B, Menon GR, Dawka S. Role of MRI to confirm healing in complex high cryptoglandular anal fistulas: long-term follow-up of 151 cases. *Colorectal Dis* 2021 [PMID: 33900011 DOI: 10.1111/codi.15695]

15 **Garg P**, Kaur B, Goyal A, Yagnik VD, Dawka S, Menon GR. Lessons learned from an audit of 1250 anal fistula patients operated at a single center: A retrospective review. *World J Gastrointest Surg* 2021; **13**: 340-354 [PMID: 33968301 DOI: 10.4240/wjgs.v13.i4.340]

16 **Garg P**, Sodhi SS, Garg N. Management of Complex Cryptoglandular Anal Fistula: Challenges and Solutions. *Clin Exp Gastroenterol* 2020; **13**: 555-567 [PMID: 33204136 DOI: 10.2147/CEG.S198796]

17 **Lefrançois P**, Zummo-Soucy M, Olivié D, Billiard JS, Gilbert G, Garel J, Visée E, Manchec P, Tang A. Diagnostic performance of intravoxel incoherent motion diffusion-weighted imaging and dynamic contrast-enhanced MRI for assessment of anal fistula activity. *PLoS One* 2018; **13**: e0191822 [PMID: 29370278 DOI: 10.1371/journal.pone.0191822]

18 **Lam D**, Yong E, D'Souza B, Woods R. Three-Dimensional Modeling for Crohn's Fistula-in-Ano: A Novel, Interactive Approach. *Dis Colon Rectum* 2018; **61**: 567-572 [PMID: 29624551 DOI: 10.1097/DCR.0000000000001084]

19 **Baik J**, Kim SH, Lee Y, Yoon JH. Comparison of T2-weighted imaging, diffusion-weighted imaging and contrast-enhanced T1-weighted MR imaging for evaluating perianal fistulas. *Clin Imaging* 2017; **44**: 16-21 [PMID: 28395191 DOI: 10.1016/j.clinimag.2017.03.019]

20 **Dohan A**, Eveno C, Oprea R, Pautrat K, Placé V, Pocard M, Hoeffel C, Boudiaf M, Soyer P.

Diffusion-weighted MR imaging for the diagnosis of abscess complicating fistula-in-ano: preliminary experience. *Eur Radiol* 2014; **24**: 2906-2915 [PMID: 25038854 DOI: 10.1007/s00330-014-3302-y]

21 **Das GC**, Chakrabartty DK. Best non-contrast magnetic resonance imaging sequence and role of intravenous contrast administration in evaluation of perianal fistula with surgical correlation. *Abdom Radiol (NY)* 2021; **46**: 469-475 [PMID: 32734352 DOI: 10.1007/s00261-020-02616-1]

22 **Beckingham IJ**, Spencer JA, Ward J, Dyke GW, Adams C, Ambrose NS. Prospective evaluation of dynamic contrast enhanced magnetic resonance imaging in the evaluation of fistula in ano. *Br J Surg* 1996; **83**: 1396-1398 [PMID: 8944439 DOI: 10.1002/bjs.1800831022]

23 **Van Assche G**, Vanbeckevoort D, Bielen D, Coremans G, Aerden I, Noman M, D'Hoore A, Penninckx F, Marchal G, Cornillie F, Rutgeerts P. Magnetic resonance imaging of the effects of infliximab on perianal fistulizing Crohn's disease. *Am J Gastroenterol* 2003; **98**: 332-339 [PMID: 12591051 DOI: 10.1111/j.1572-0241.2003.07241.x]

24 **Wang WG**, Lu WZ, Yang CM, Yu KQ, He HB. Modified Van Assche magnetic resonance imaging-based score for assessing the clinical status of anal fistulas. *Medicine (Baltimore)* 2020; **99**: e20075 [PMID: 32384475 DOI: 10.1097/MD.0000000000020075]

25 **Hindryckx P**, Jairath V, Zou G, Feagan BG, Sandborn WJ, Stoker J, Khanna R, Stitt L, van Viegen T, Shackelton LM, Taylor SA, Santillan C, Mearadji B, D'Haens G, Richard MP, Panes J, Rimola J. Development and Validation of a Magnetic Resonance Index for Assessing Fistulas in Patients With Crohn's Disease. *Gastroenterology* 2019; **157**: 1233-1244.e5 [PMID: 31336124 DOI: 10.1053/j.gastro.2019.07.027]

26 **van Rijn KL**, Lansdorp CA, Tielbeek JAW, Nio CY, Buskens CJ, D'Haens GRAM, Löwenberg M, Stoker J. Evaluation of the modified Van Assche index for assessing response to anti-TNF therapy with MRI in perianal fistulizing Crohn's disease. *Clin Imaging* 2020; **59**: 179-187 [PMID: 31821976 DOI: 10.1016/j.clinimag.2019.10.007]

World Journal of Gastroenterology

Submit a Manuscript: https://www.f6publishing.com

World J Gastroenterol 2021 September 7; 27(33): 5474-5487

DOI: 10.3748/wjg.v27.i33.5474

ISSN 1007-9327 (print) ISSN 2219-2840 (online)

REVIEW

Neutrophil extracellular traps in gastrointestinal cancer

Zi-Qiang Chu, Ke-Cheng Zhang, Lin Chen

ORCID number: Zi-Qiang Chu 0000-0001-5993-149X; Ke-Cheng Zhang 0000-0002-9257-5607; Lin Chen 0000-0002-3507-673X.

Author contributions: Chu ZQ and Zhang KC contributed equally to this work; Chu ZQ designed and conceived the review; Chu ZQ and Zhang KC analysed the articles and wrote the manuscript; all authors have read and approved the final version.

Supported by Natural Science Foundation of Beijing for Youth, No. 7214252; and Program of Military Medicine for Youth, No. QNF19055.

Conflict-of-interest statement: The authors declare no potential conflicts of interest.

Open-Access: This article is an open-access article that was selected by an in-house editor and fully peer-reviewed by external reviewers. It is distributed in accordance with the Creative Commons Attribution NonCommercial (CC BY-NC 4.0) license, which permits others to distribute, remix, adapt, build upon this work non-commercially, and license their derivative works on different terms, provided the original work is properly cited and the use is non-commercial. See: http://creativecommons.org/Licenses/by-nc/4.0/

Zi-Qiang Chu, Graduate School, Chinese PLA General Hospital, Beijing 100853, China

Zi-Qiang Chu, Institute of Basic Medical Sciences, Chinese PLA General Hospital, Beijing 100853, China

Ke-Cheng Zhang, Lin Chen, Department of General Surgery, Chinese PLA General Hospital First Medical Center, Beijing 100853, China

Corresponding author: Lin Chen, MA, MD, Chief Doctor, Professor, Department of General Surgery, Chinese PLA General Hospital First Medical Center, No. 28 Fuxing Road, Beijing 100853, China. chenlin@301hospital.com.cn

Abstract

Gastrointestinal (GI) cancer is a high-risk malignancy and is characterized by high mortality and morbidity worldwide. Neutrophil extracellular traps (NETs), a weblike structure consisting of chromatin DNA with interspersed cytoplasmic and granule proteins, are extruded by activated neutrophils to entrap and kill bacteria and fungi. However, accumulating evidence shows that NETs are related to the progression and metastasis of cancer. In clinical studies, NETs infiltrate primary GI cancer tissues and are even more abundant in metastatic lesions. The quantity of NETs in peripheral blood is revealed to be associated with ascending clinical tumour stages, indicating the role of NETs as a prognostic markers in GI cancer. Moreover, several inhibitors of NETs or NET-related proteins have been discovered and used to exert anti-tumour effects *in vitro* or *in vivo*, suggesting that NETs can be regarded as targets in the treatment of GI cancer. In this review, we will focus on the role of NETs in gastric cancer and colorectal cancer, generalizing their effects on tumour-related thrombosis, invasion and metastasis. Recent reports are also listed to show the latest evidences of how NETs affect GI cancer. Additionally, notwithstanding the scarcity of systematic studies elucidating the underlying mechanisms of the interaction between NETs and cancer cells, we highlight the potential importance of NETs as biomarkers and anti-tumour therapeutic targets.

Key Words: Neutrophil extracellular traps; Gastric cancer; Colorectal cancer; Biomarkers; Therapeutic targets

©The Author(s) 2021. Published by Baishideng Publishing Group Inc. All rights reserved.

Manuscript source: Invited manuscript

Specialty type: Gastroenterology and hepatology

Country/Territory of origin: China

Peer-review report's scientific quality classification

Grade A (Excellent): A
Grade B (Very good): 0
Grade C (Good): 0
Grade D (Fair): 0
Grade E (Poor): 0

Received: January 26, 2021
Peer-review started: January 26, 2021
First decision: April 5, 2021
Revised: April 6, 2021
Accepted: August 11, 2021
Article in press: August 11, 2021
Published online: September 7, 2021

P-Reviewer: Caboclo JF
S-Editor: Liu M
L-Editor: A
P-Editor: Yuan YY



Core Tip: Neutrophil extracellular traps (NETs) have been reported to participate in progression and metastasis in gastrointestinal (GI) cancer. Recent reports demonstrate that NET formation is enhanced in GI cancer patients as well as some mouse models and that elevated levels of NETs indicate an adverse outcome in patients. Furthermore, NETs can trap disseminated cancer cells and assist the formation of metastatic lesions although the underlying mechanisms remain vague. More studies are needed before NETs can be used as reliable biomarkers and therapeutic targets in GI cancer.

Citation: Chu ZQ, Zhang KC, Chen L. Neutrophil extracellular traps in gastrointestinal cancer. *World J Gastroenterol* 2021; 27(33): 5474-5487
URL: https://www.wjgnet.com/1007-9327/full/v27/i33/5474.htm
DOI: https://dx.doi.org/10.3748/wjg.v27.i33.5474

INTRODUCTION

According to cancer statistics, gastric cancer (GC) ranks third globally in terms of mortality, while colorectal cancer (CRC) is the second leading cause of cancer-related death. Both constitute a major cause of cancer-related death worldwide[1,2]. Despite advances in the techniques applied for cancer treatment, surgical resection accompanied by adjuvant therapy (chemotherapy, radiotherapy and molecular targeted therapies) remains the primary approach[3]. However, the efficacy of aforementioned treatment is related to tumour heterogeneity in patients[4]. Once the tumour progresses and spreads to distant organs (*e.g.*, liver and lung), neither conventional surgery nor targeted therapies can reverse the dismal outcomes[5]. Therefore, it is of high importance in all future studies to understand the mechanisms of deterioration of GI cancer, by measuring not only the tumour itself, but also the surrounding cells that can be modified by the tumour to generate a supportive microenvironment; these cells include macrophages (tumour-associated macrophages), fibroblasts (cancer-associated fibroblasts) and neutrophils (tumour-associated neutrophils)[6,7].

Neutrophil extracellular traps (NETs) are extruded by activated neutrophils into the extracellular environment and have three-dimensional lattices, which are composed of decondensed chromatin with interspersed proteins such as neutrophil elastase (NE), cathepsin G, myeloperoxidase (MPO), histones and some other antimicrobial peptides [8,9]. NETs were originally discovered to ensnare and kill extracellular bacteria and fungi and may act as a physical barrier to impede the dissemination of microbes[10]. However, recent studies have revealed that NETs, if dysregulated, can contribute to the development or progression of some inflammatory or immune-related diseases[11,12], such as atherosclerosis[13], systemic lupus erythematosus (SLE)[14], diabetes[15], vasculitis[16], wound healing[17] and coronavirus disease 2019 (COVID-19)[18]. COVID-19 is still spreading worldwide, and clinical evidence shows that increased NET formation after the COVID-19 infection can be a potential biomarker for disease severity[19]; thus, targeting NETs may alleviate the condition of patients[20]. More work is needed before NETs can be used as reliable biomarkers in these diseases. In addition to the roles of NETs mentioned before, studies have expanded their biological scope and suggest that elevated numbers of neutrophils and levels of NETs in peripheral circulation are a hallmark of cancer[21]. Recently, NETs have been suggested to participate in the biological process of cancer[22-24]. Several studies have shown that NETs can cause hypercoagulability[25], accumulate in peripheral blood vessels and impair organ function[26], promote cancer development and metastasis[27-30], sequester circulating tumour cells[31,32], and even stimulate dormant cancer cells[33]. Therefore, more work needs to be done to elucidate the mechanism between NETs and cancer.

In this review, we will discuss the role of NETs in GC and CRC according to the latest findings and consider their potential of NETs as biomarkers and therapeutic targets.

NETS

The formation of NETs, known as NETosis, was first observed by Takei *et al*[34] *via* stimulation with phorbol-12-myristate-13-acetate (PMA) and is regarded as a novel form of neutrophil death that is different from apoptosis and necrosis. The antibacterial role of NETs was confirmed in 2004 and is dependent on the web-like structure [10]. The core scaffold of NETs is the nuclear DNA extruded from neutrophils and that forms a three-dimensional meshwork with a number of interspersed specific cytoplasmic and granular proteins[35]. Notwithstanding the lack of mechanistic or interventional studies investigating NET formation in peripheral circulation, initial studies suggest that NETs are released by dying neutrophils. This phenomenon of NET formation can be mainly described by at least two mechanisms. One mechanism requires the lytic suicide of neutrophils, while the other mechanism is independent of this process[36,37]. Neubert *et al*[38] demonstrated that entropic chromatin swelling is the major physical driving force of NETosis. In addition, other myeloid cells, such as human blood monocytes[39], mast cells[40] and eosinophils[41], have been discovered to release DNA networks. However, neutrophils seem to remain the main source of these networks because of their high efficiency of secretion.

The functions of NETs in defending against infection depend on the composition of the network, including the DNA itself, which is a chelator of divalent cations that possesses antibacterial ability. The citrullination of histones loosens their grip on DNA and provides a chance for interaction between DNA and bacteria[42]. Moreover, highly toxic modified histones, which constitute the major part of NET-associated proteins, are also mediators of bactericide[43]. Moreover, NE synergizes with MPO to assist the formation and antibacterial role of NETs[44]. More generally, NETs prevent dissemination of infection by entrapping microbes and facilitate their killing by bactericidal proteins which have been shown to be involved in both direct and indirect mechanisms. In addition, NETs are revealed to be vital factors in non-infectious diseases. Hakkim *et al*[45] suggested that the persistence of NETs exacerbates the autoimmune response and forms a vicious cycle in SLE. Similarly, studies on diabetes [15], vasculitis[16], wound healing[17] and COVID-19[18-20] have described the pathophysiological role of NETs.

Recently, an emerging role of NETs in promoting cancer progression has been described. Solid tumours are prone to generating a leukemoid reaction and pre-educate neutrophils to form extracellular DNA traps, and intratumoural NET formation is associated with thrombosis[46]. The accumulation of tumour-induced NETs in the peripheral circulation drives the systemic inflammation and vascular dysfunction in mice with cancer[26]. Leal *et al*[47] indicates that NETs serve as scaffolds and collaborate with tumour-derived procoagulant exosomes in the establishment of a prothrombotic phenotype in cancer. CXCL8 (interleukin-8, IL8) is a chemokine that can be produced by tumour cells and its role in promoting angiogenesis in cancer has been well discussed[48]. Furthermore, the presence of IL8 activates the extrusion of NETs with potential involvement in cancer progression and promotes cancer cell metastasis partially through AKT and STAT3 signalling pathways[49,50]. NETs produced by tumour-infiltrating neutrophils mediate the crosstalk between the tumour microenvironment and deterioration by regulating the HMGB1/RAGE/IL8 axis[51]. IL17 is a cytokine described as a protumourigenic factor involved in the initiation and development of cancer[52]. A recent study demonstrated that IL17 can induce NETosis through epithelial cell signalling to favour tumour growth[53]. Rocks *et al*[54] associated NETs with cancer cells and confirmed that the release of NETs favour tumour cell dissemination and colonization in organs.

Since the discovery of NETs, the role of neutrophils and NETs has attracted increasing attentions. Additional studies have reported on numerous stimuli that affect NET formation *in vitro* and *in vivo*. PMA, a potent artificial activator of the neutrophil respiratory burst, has been broadly applied to identify the mechanism of NETosis. Cytokines, such as the aforementioned IL8, IL17 and tumour necrosis factor alpha[55], have been investigated with respect to their role in expediting NET formation. Nicotine, a major addictive component of tobacco, is reported to induce NETosis in a dose-dependent manner, implying potential threats to human health[56]. Moreover, sulfasalazine, a drug used to treat inflammatory bowel disease and rheumatoid arthritis, has been found to significantly promote NETosis by accelerating lipid oxidation [57]. Most recently, Yasuda *et al*[58] established the relationship between NETosis and epigenetics and demonstrated that DNA demethylation enhances spontaneous NET formation by reinforcing PAD4 expression and histone citrullination.

NETS IN GC

GC is the fifth most common cancer and ranks third in terms of mortality worldwide. Several studies have tried to confirm the characteristics of NETs in GC and clarify the underlying mechanisms *in vitro* and *in vivo* (Table 1).

Notwithstanding advances in diagnosis and therapy, recurrence and metastasis are still common as a result of its high molecular and phenotypic heterogeneity[59], which contributes to a coagulable state that causes the proliferation and invasion of GC cells [60-63]. In GC patients, NET formation is significantly upregulated and its increased level is consistent with advanced TNM stage. Moreover, a procoagulant role of NETs in GC has been confirmed. When NETosis is inhibited by DNase I, the levels of TAT and D-dimers are downregulated. Furthermore, NETs obtained from GC patients can also stimulate control plasma to generate thrombin and fibrin[64].

A common target of metastatic gastrointestinal cancer is the peritoneal cavity[65]. The invention of heated intraperitoneal chemotherapy[66] and postoperative chemotherapy[67] has indeed reduced the rate of peritoneal recurrence and metastasis. However, limitations still exist with regard to the benefit of these treatments, and severe general toxicity has always been an unavoidable side effect. To elucidate the underlying mechanisms, Kanamaru *et al*[68,69] collected the peritoneal lavages from GC patients before and after radical surgery. Then NET formation emerged after short term culture of purified low-density neutrophils (LDNs) separated from the lavages fluids. Moreover, the majority of NET-like structures were discovered on the surface of omental tissue. In a *in vivo* study, GC cells lines such as MKN45, OCUM-1 and NUGC-4 were found attached to the NETs and remained healthy; this interaction was entirely prevented upon treatment with DNase I, which can degrade NETs.

Notwithstanding the advances of therapeutic strategies in GC, surgical resection remains the mainstay treatment. Therefore, the subsequent surgical stress, which suppresses immunity, constitutes one of the key factors that influence the prognosis of GC patients[70,71]. The percentage of LDNs in the peripheral circulation of GC patients who underwent abdominal surgery was elevated and *in vitro* studies observed the adhesion of cancer cells to NET structure, suggesting that partial adverse effects of surgical stress may be explained by the formation of NETs[72].

According to a pulmonary metastasis model of GC, accumulation of neutrophils in the adjacent vascular vessels has been found during the colonization of GC cells. Extracts from the root of *Salvia miltiorrhiza* (*Danshen*)[73], a medicinal plant used for cancer therapy, have been observed to prevent neutrophil trafficking to the metastatic sites and obstruct the formation of NETs *via* inhibitory activities on MPO and NADPH oxidase (NOX)[74]. A recent study has proposed that obstruction of NETosis by Cl-amidine or DNase I significantly suppresses the progression of GC cells by regulating the expression of apoptosis-associated genes, among which Bcl-2[75] levels were downregulated and the expression of Bax[76] and NF-κB p65[77] increased significantly[78].

NETS IN CRC

CRC is the third most frequent malignancy and second leading cause of cancer-related mortality worldwide. To date, metastasis and cancer-associated thrombosis are still the main causes of death in CRC patients. To address this issue, much work has been done or is currently in progress; recently, more attention has been drawn to the establishment of tumour microenvironment. Of note, recent accumulating evidence has shown that NETs may play a pivotal role in the progression of CRC (Table 2).

CRC patients are at high risk of venous thrombosis as a result of hypercoagulable state and the levels of NETs in the peripheral blood are positively related to cancer progression. A comparison between 60 newly diagnosed CRC patients and 20 healthy controls revealed that neutrophils in CRC patients can release more NETs, and this tendency parallels increased TAT levels and fibrin formation, which is indicative of a hypercoagulable state[79]. Thus, a vicious cycle can be established between activated platelets and neutrophils. Additionally, *in vitro* studies show that NETs can convert endothelial cells to a procoagulant phenotype[80]. Another study observed that NETs were concentrated in the centre of CRC tissues and reduced gradually towards adjacent normal tissues, and this characteristic could help surgeons determine a better surgical area through pathological examination of the tumour margins. Furthermore, tissue factor, a stimulus of coagulation and a pro-angiogenic factor, was discovered in NETs from the primary tumour and metastatic lymph nodes[81]. Altogether, the

Table 1 Role of neutrophil extracellular traps in gastric cancer

Ref.	Cell lines	Model (*in vitro*, *in vivo*, human)	Conclusion
Yang *et al*[64], 2015	-	Human	NETs contribute to the hypercoagulable state in GC patients with stage III/IV
Kanamaru *et al* [68], 2018	MKN45, NUGC-4, OCUM-1	*In vitro*, *in vivo*	NETs on peritoneal surface assist the clustering and growth of GC tumor cells disseminated in abdomen
Tao *et al*[74], 2018	BGC-823	*In vitro*, *in vivo*	NET formation is inhibited by Sal B and DHT I at the earlier stage
Kumagai *et al* [72], 2020	MKN45, NUGC-4, OCUM-1	*In vitro*, human	NETs formation is enhanced under surgical stress and can effectively trap circulating tumor cells
Li *et al*[78], 2020	BGC-823, SGC7901, MKN28	*In vitro*, human	NETs destruction promotes the apoptosis and inhibits the invasion of gastric cancer cells by regulating the expression of Bcl-2, Bax and NF-κB
Zhang *et al*[94], 2020	-	Human	NETs have novel diagnostic, therapeutic predictive, and prognostic value in GC patients

NETs: Neutrophil extracellular traps; GC: Gastric cancer.

Table 2 Role of neutrophil extracellular traps in colorectal cancer

Ref.	Cell lines	Model (*in vitro*, *in vivo*, human)	Conclusion
Arelaki *et al* [81], 2016	Caco-2	*In vitro*, human	NETs concentration is gradually reduced from the tumor mass to the distal margin
Tohme *et al* [83], 2016	MC38	*In vitro*, human	Surgical stress and intratumoral hypoxia induce NETs formation and NETs can trigger HMGB1 release and activate TLR9-dependent pathways to promote adhesion, proliferation, migration, and invasion in CRC
Richardson *et al* [84], 2017	-	Human	NET production in the later postoperative period appears to coincide with surgical recovery
Arelaki *et al* [88], 2018		Human	PolyP is present in human colon cancer and increase NETosis
Rayes *et al*[82], 2019	MC38, H59	*In vitro*, *in vivo*, human	Circulating NET levels are elevated in advanced CRC and blocking NETosis significantly inhibits spontaneous metastasis to the lung and liver
Yazdani *et al* [89], 2019	MC38, HCT116, Hepa 1-6, Huh7	*In vitro*, *in vivo*, human	NETs facilitate the growth of stressed cancer cells by altering their bioenergetics
Zhang *et al*[80], 2019	HUVECs	*In vitro*, human	NETs are involved in the progression of CRC and act as potential agonists in CRC-related hypercoagulability
Rayes *et al* [113], 2020	HT-29, MC38, A549	*In vitro*, *in vivo*, human	NET-associated CEACAM1 acts as a putative therapeutic target to prevent the metastatic progression of colon carcinoma
Shang *et al*[92], 2020	DKs-8, DKO-1, PMN	*In vitro*, *in vivo*, human	Exosomes may transfer mutant KRAS to recipient cells and trigger increases in IL-8 production, neutrophil recruitment and formation of NETs, eventually leading to the deterioration of CRC
Xia *et al*[105], 2020	MC38, HepG2	*In vitro*, *in vivo*	AAV-mediated DNase I liver gene transfer is a safe and effective modality to inhibit metastasis and represents a novel therapeutic strategy for CRC
Yang *et al*[91], 2020	HT29, MC38	*In vitro*, *in vivo*, human	A novel positive feedback between elevated tumorous IL-8 and NETs can promote CRC liver metastasis
Yang *et al*[93], 2020	HCT116, MDA-MB-231, MCF-7, 4T1, HEK293T, HeLa, E0771	*In vitro*, *in vivo*, human	CCDC25 mediates NET-dependent metastasis and is suggested to be a therapeutic target for the prevention of cancer metastasis

NETs: Neutrophil extracellular traps; CRC: Colorectal cancer; AAV: Adeno-associated virus.

presence of NETs contributes to thrombosis in CRC.

By analysing large-scale human data, Rayes *et al*[82] demonstrated that NETs can not only bind tumour cells but also promote metastasis. In addition, established preclinical models of gastrointestinal cancer revealed that tumours induce neutrophils to extrude NETs into the extracellular environment in the absence of surgical stress. Furthermore, NET formation could promote CRC metastasis after surgical stress[83,

84]. In a cohort study, increased postoperative NET formation was associated with disease-free survival in patients undergoing hepatic surgical resection, and the mouse model of surgical stress has obtained similar results. Further studies demonstrated that the hypoxic environment in solid tumours provides a favourable condition for NETosis and that NETs could in turn promote CRC progression by releasing HMGB1 [85], a DNA-binding protein that participates in the activation of TLR9[86]. Additionally, the protumourigenic effects of NETs are abolished by DNase and PAD4 inhibition[83]. Another clinical trial suggested that increased preoperative NETosis is related to an increased hospital stay and complications of CRC patients who undergo colorectal resection, suggesting a promising therapeutic benefit of surgery focused on the relationship between CRC and NETs[84].

In malignant and premalignant colon tissues, CD68+ polyP-expressing cells and NETosis were detected, suggesting a possible interaction between them in the tumour microenvironment. Further investigation indicates that polyP[87], which is secreted by activated platelets and could induce inflammation and thrombosis in CRC, may promote the formation of NETs[88]. A PAD4-KO mouse model, which is genetically incapable of NETosis, showed that inhibition of NETs halted CRC growth through its negative regulation of mitochondrial biogenesis-associated genes. Further studies show that CRC cells subjected to hypoxia have upregulated expression of HMGB1 [85], which acts as an inducer of NETosis, and NE released from NETs could assist tumour proliferation as a result of inducing mitochondrial biogenesis by activating the TLR4-p38-PGC1α pathway in CRC[89].

In CRC, IL8 has been reported to participate in growth, angiogenesis and metastasis [90]. High expression of IL8 also implicates adverse survival in patients. A recent study explains a promotional role of IL8 in the formation of NETs. *In vitro* adhesion system, CRC cells such as HT29 and MC38 cells are more prone to be entrapped into NETs than neutrophil monolayers, giving the chance for disseminated CRC cells to form micrometastases in the liver; this process can be enhanced by overexpression of IL8[91]. Another study focuses on exosomes secreted by CRC cells. The authors showed that exosomes derived from KRAS mutant cells could transfer mutant KRAS to receptors and upregulate IL8 Levels, eventually activating neutrophils to form NETs and leading to enhanced proliferation and invasion of cancer cells[92].

The aforementioned studies have highlighted an interaction between CRC cells and NETs, suggesting that NET formation is enhanced in tumours and that the increase in NETs can promote the progression and metastasis of CRC. Although several pathways have been described, the detailed mechanisms of how NETs interact with and boost the metastasis of CRC remain elusive. Most recently, a remarkable discovery not only precisely illustrates the underlying mechanism between CRC cells and NETs but also partially explains why CRC cells have a tendency to disseminate into the liver. Yang *et al*[93] investigated several metastatic lesions in the clinic and discovered the most abundant NET infiltration in liver metastases and the formation of NETs began before the appearance of the metastases. According to a pull-down assay, CCDC25, a potential cell-surface DNA receptor, was identified on the cytoplasmic membrane of cancer cells. Furthermore, amino acids 21-25 at the extracellular N-terminus of CCDC25 were found to be the binding site of NET-DNA. Further immunoprecipitation assays indicated that the intracellular C-terminus of CCDC25 binds integrin-linked kinase and that this interaction can be stimulated by NET-DNA, eventually inducing liver metastases of CRC cells *via* initiating the β-parvin-RACI-CDC42 cascade.

NETS AS POTENTIAL BIOMARKERS AND THERAPEUTIC TARGETS

An increasing number of investigations have suggested a protumourigenic role of NETs in providing a microenvironment favouring interactions and promoting cancer proliferation, thrombosis and metastasis in GI cancers. This has led to the question of whether NETs can act as potential biomarkers and therapeutic targets.

Zhang *et al*[94] compared the levels of NETs in different patient populations, suggesting that NETs, as a diagnostic biomarker, have better value than carcinoembryonic antigen (CEA) and carbohydrate antigen 19-9 in GC. Additionally, NET formation is associated with tumour stage, poor overall survival and poor recurrence-free survival. Moreover, tumour-infiltrating NETs has been demonstrated to be an independent prognostic biomarker according to the assessment of clinical outcomes of cancer patients[95-97]. Considering the potential diagnostic significance of NETs, conventional histological staining is ineffective for their detection in tissue. To solve

this problem, a protocol has been created to detect NETs in paraffin-embedded tissue [98]. Additionally, machine learning is described as a useful tool to quantitate NETosis [99]. Citrullinated histone H3, a central marker of NETs, is elevated in blood and regarded as a potential diagnostic and prognostic serum marker to predict the risk of venous thromboembolism and mortality in patients with advanced cancer[100-102]. A CitH3DNA binding assay has also been developed to quantify NET formation[103].

Taking into account the confirmed role of NETs in promoting the progression and metastasis of GI cancer cells, disruption of NETosis can be a possible new therapeutic strategy and the identification of NETosis inhibitors is of high interest. DNase I can degrade the DNA backbone of NETs and abrogate the protumourigenic ability of NETs in several aforementioned animal models. Moreover, DNase I has been safely used in cystic fibrosis and SLE patients[104], implying that DNase I can act as a promising candidate for the treatment of GI cancer patients. In a mouse model of CRC liver metastasis, an adeno-associated virus gene therapy vector was created to specifically express DNase I in the liver, inducing an inhibition of liver metastasis[105]. However, it is worth noting that everything is a double-edged sword. Inappropriate use of DNase I may lead to a systemic inflammatory response in patients[106]. Owing to the critical role of NE and PAD4 in the process of NETosis, NE inhibitors or PAD4-inhibitors are also commonly used to prevent the release of NETs. Nanoparticle-mediated delivery of NE inhibitors has been suggested as a feasible approach to decrease NETosis[107]. In addition, NOX inhibitors[108], MPO inhibitors[109] and RAF inhibitors[110] have been reported to arrest the inception of NETosis. Recently, a group of tetrahydroisoquinolines was found to be a novel class of NET formation inhibitors, but their underlying mechanism remains to be determined[111]. A drug screening of 126 compounds shows that appropriate use of anthracyclines (drugs used for cancer treatment) together with dexrazoxane could be a promising therapeutic candidate for suppressing NETosis without cytotoxicity against healthy neutrophils [112]. NET-associated CEA cell adhesion molecule 1 (CEACAM1) was identified by Rayes *et al*[113] Knockdown of CEACAM1 on NETs abrogates the adhesion between NETs and colon cancer cells, thus indicating a potential therapeutic therapy or preventing liver metastases. A novel study revealed that PKCα, a lamin kinase that mediates the phosphorylation of lamin B, contributes to the formation of NETs; hence, blocking PKCα provides a new perspective towards treating NET-associated cancer progression[114]. Since the application of 5-fluorouracil (5FU) has been shown to trigger the formation of NETs in the blood of cancer patients, Amph-PVP self-assembled nanoparticles are proposed as an efficient delivery system for 5FU to avoid the generation of NETs, partially improving the anticancer effect and reducing the risk of long-term metastasis[115]. The previously mentioned studies mainly focus on the inhibition of NETosis or the proteins assembled in NETs. Unusually, Cao and King [116] proposed that NETs per se can be utilized as an anti-tumour drug delivery vehicle. By re-engineering neutrophils, supercharged eGFP-TRAIL, an apoptosis-inducing chimeric protein, is expressed on NETs to entrap and kill tumour cells.

CONCLUSION

NETs, initially identified as a host defense system designed to trap and kill bacteria, have now been suggested to play an important tumorigenic role in many cancers. Accumulating evidence has shown that NETs are involved in GI cancers, including GC and CRC. As mentioned above, NET infiltration in primary tumour tissues implies a poor outcome in GI cancer patients, indicating that a rapid intraoperative histopathological examination of NETs in the resected tissue margins may help determine the range of surgical resection. Moreover, several cytokines and genetic mutations trigger the formation of NETs and NETs per se can promote the progression of cancer partially by initiating downstream signalling pathways. On the other hand, the fact that NETs can entrap disseminated cancer cells, combined with the situation that an abundance of NET infiltration in the liver is formed before metastases can be detected, increases the likelihood of liver metastasis and explains the high incidence of liver metastasis in patients with GI cancer.

Further studies are needed to elucidate the detailed underlying mechanism of the interaction between NETs and GI cancer. Clarifying the roles of NETs in cancer could open a new door in the design and development of therapeutic approaches. Transforming inhibitors of NETs into drugs that can be safely used in GI cancer patients or utilizing NETosis as a drug delivery system may evolve into promising anti-tumour therapies.

REFERENCES

1 **Siegel RL**, Miller KD, Jemal A. Cancer statistics, 2019. *CA Cancer J Clin* 2019; **69**: 7-34 [PMID: 30620402 DOI: 10.3322/caac.21551]

2 **Bray F**, Ferlay J, Soerjomataram I, Siegel RL, Torre LA, Jemal A. Global cancer statistics 2018: GLOBOCAN estimates of incidence and mortality worldwide for 36 cancers in 185 countries. *CA Cancer J Clin* 2018; **68**: 394-424 [PMID: 30207593 DOI: 10.3322/caac.21492]

3 **Saad ED**, Buyse M. Statistical aspects in adjuvant and neoadjuvant trials for gastrointestinal cancer in 2020: focus on time-to-event endpoints. *Curr Opin Oncol* 2020; **32**: 384-390 [PMID: 32541329 DOI: 10.1097/CCO.0000000000000636]

4 **Parikh AR**, Leshchiner I, Elagina L, Goyal L, Levovitz C, Siravegna G, Livitz D, Rhrissorrakrai K, Martin EE, Van Seventer EE, Hanna M, Slowik K, Utro F, Pinto CJ, Wong A, Danysh BP, de la Cruz FF, Fetter IJ, Nadres B, Shahzade HA, Allen JN, Blaszkowsky LS, Clark JW, Giantonio B, Murphy JE, Nipp RD, Roeland E, Ryan DP, Weekes CD, Kwak EL, Faris JE, Wo JY, Aguet F, Dey-Guha I, Hazar-Rethinam M, Dias-Santagata D, Ting DT, Zhu AX, Hong TS, Golub TR, Iafrate AJ, Adalsteinsson VA, Bardelli A, Parida L, Juric D, Getz G, Corcoran RB. Liquid *vs* tissue biopsy for detecting acquired resistance and tumour heterogeneity in gastrointestinal cancers. *Nat Med* 2019; **25**: 1415-1421 [PMID: 31501609 DOI: 10.1038/s41591-019-0561-9]

5 **Zhao Y**, Li J, Li D, Wang Z, Zhao J, Wu X, Sun Q, Lin PP, Plum P, Damanakis A, Gebauer F, Zhou M, Zhang Z, Schlösser H, Jauch KW, Nelson PJ, Bruns CJ. Tumour biology and multidisciplinary strategies of oligometastasis in gastrointestinal cancers. *Semin Cancer Biol* 2020; **60**: 334-343 [PMID: 31445220 DOI: 10.1016/j.semcancer.2019.08.026]

6 **Quail DF**, Joyce JA. Microenvironmental regulation of tumour progression and metastasis. *Nat Med* 2013; **19**: 1423-1437 [PMID: 24202395 DOI: 10.1038/nm.3394]

7 **Galdiero MR**, Bianchi P, Grizzi F, Di Caro G, Basso G, Ponzetta A, Bonavita E, Barbagallo M, Tartari S, Polentarutti N, Malesci A, Marone G, Roncalli M, Laghi L, Garlanda C, Mantovani A, Jaillon S. Occurrence and significance of tumour-associated neutrophils in patients with colorectal cancer. *Int J Cancer* 2016; **139**: 446-456 [PMID: 26939802 DOI: 10.1002/ijc.30076]

8 **Ravindran M**, Khan MA, Palaniyar N. Neutrophil Extracellular Trap Formation: Physiology, Pathology, and Pharmacology. *Biomolecules* 2019; **9**: 365 [PMID: 31416173 DOI: 10.3390/biom9080365]

9 **Dąbrowska D**, Jabłońska E, Garley M, Ratajczak-Wrona W, Iwaniuk A. New Aspects of the Biology of Neutrophil Extracellular Traps. *Scand J Immunol* 2016; **84**: 317-322 [PMID: 27667737 DOI: 10.1111/sji.12494]

10 **Brinkmann V**, Reichard U, Goosmann C, Fauler B, Uhlemann Y, Weiss DS, Weinrauch Y, Zychlinsky A. Neutrophil extracellular traps kill bacteria. *Science* 2004; **303**: 1532-1535 [PMID: 15001782 DOI: 10.1126/science.1092385]

11 **Papayannopoulos V**. Neutrophil extracellular traps in immunity and disease. *Nat Rev Immunol* 2018; **18**: 134-147 [PMID: 28990587 DOI: 10.1038/nri.2017.105]

12 **Bonaventura A**, Liberale L, Carbone F, Vecchié A, Diaz-Cañestro C, Camici GG, Montecucco F, Dallegri F. The Pathophysiological Role of Neutrophil Extracellular Traps in Inflammatory Diseases. *Thromb Haemost* 2018; **118**: 6-27 [PMID: 29304522 DOI: 10.1160/TH17-09-0630]

13 **Döring Y**, Soehnlein O, Weber C. Neutrophil Extracellular Traps in Atherosclerosis and Atherothrombosis. *Circ Res* 2017; **120**: 736-743 [PMID: 28209798 DOI: 10.1161/CIRCRESAHA.116.309692]

14 **O'Neil LJ**, Kaplan MJ, Carmona-Rivera C. The Role of Neutrophils and Neutrophil Extracellular Traps in Vascular Damage in Systemic Lupus Erythematosus. *J Clin Med* 2019; **8**: 1325 [PMID: 31466329 DOI: 10.3390/jcm8091325]

15 **Bryk AH**, Prior SM, Plens K, Konieczynska M, Hohendorff J, Malecki MT, Butenas S, Undas A. Predictors of neutrophil extracellular traps markers in type 2 diabetes mellitus: associations with a prothrombotic state and hypofibrinolysis. *Cardiovasc Diabetol* 2019; **18**: 49 [PMID: 30992036 DOI: 10.1186/s12933-019-0850-0]

16 **Söderberg D**, Segelmark M. Neutrophil extracellular traps in vasculitis, friend or foe? *Curr Opin Rheumatol* 2018; **30**: 16-23 [PMID: 28957962 DOI: 10.1097/BOR.0000000000000450]

17 **Kaur T**, Dumoga S, Koul V, Singh N. Modulating neutrophil extracellular traps for wound healing. *Biomater Sci* 2020; **8**: 3212-3223 [PMID: 32374321 DOI: 10.1039/d0bm00355g]

18 **Blasco A**, Coronado MJ, Hernández-Terciado F, Martín P, Royuela A, Ramil E, García D, Goicolea J, Del Trigo M, Ortega J, Escudier JM, Silva L, Bellas C. Assessment of Neutrophil Extracellular Traps in Coronary Thrombus of a Case Series of Patients With COVID-19 and Myocardial Infarction. *JAMA Cardiol* 2020; **6**: 1-6 [PMID: 33372956 DOI: 10.1001/jamacardio.2020.7308]

19 **Middleton EA**, He XY, Denorme F, Campbell RA, Ng D, Salvatore SP, Mostyka M, Baxter-Stoltzfus A, Borczuk AC, Loda M, Cody MJ, Manne BK, Portier I, Harris ES, Petrey AC, Beswick EJ, Caulin AF, Iovino A, Abegglen LM, Weyrich AS, Rondina MT, Egeblad M, Schiffman JD, Yost CC. Neutrophil extracellular traps contribute to immunothrombosis in COVID-19 acute respiratory distress syndrome. *Blood* 2020; **136**: 1169-1179 [PMID: 32597954 DOI: 10.1182/blood.2020007008]

20 **Barnes BJ**, Adrover JM, Baxter-Stoltzfus A, Borczuk A, Cools-Lartigue J, Crawford JM, Daßler-Plenker J, Guerci P, Huynh C, Knight JS, Loda M, Looney MR, McAllister F, Rayes R, Renaud S, Rousseau S, Salvatore S, Schwartz RE, Spicer JD, Yost CC, Weber A, Zuo Y, Egeblad M. Targeting

potential drivers of COVID-19: Neutrophil extracellular traps. *J Exp Med* 2020; **217**: e20200652 [PMID: 32302401 DOI: 10.1084/jem.20200652]

21 **Teramukai S**, Kitano T, Kishida Y, Kawahara M, Kubota K, Komuta K, Minato K, Mio T, Fujita Y, Yonei T, Nakano K, Tsuboi M, Shibata K, Furuse K, Fukushima M. Pretreatment neutrophil count as an independent prognostic factor in advanced non-small-cell lung cancer: an analysis of Japan Multinational Trial Organisation LC00-03. *Eur J Cancer* 2009; **45**: 1950-1958 [PMID: 19231158 DOI: 10.1016/j.ejca.2009.01.023]

22 **Jung HS**, Gu J, Kim JE, Nam Y, Song JW, Kim HK. Cancer cell-induced neutrophil extracellular traps promote both hypercoagulability and cancer progression. *PLoS One* 2019; **14**: e0216055 [PMID: 31034495 DOI: 10.1371/journal.pone.0216055]

23 **Park J**, Wysocki RW, Amoozgar Z, Maiorino L, Fein MR, Jorns J, Schott AF, Kinugasa-Katayama Y, Lee Y, Won NH, Nakasone ES, Hearn SA, Küttner V, Qiu J, Almeida AS, Perurena N, Kessenbrock K, Goldberg MS, Egeblad M. Cancer cells induce metastasis-supporting neutrophil extracellular DNA traps. *Sci Transl Med* 2016; **8**: 361ra138 [PMID: 27798263 DOI: 10.1126/scitranslmed.aag1711]

24 **Lerman I**, Hammes SR. Neutrophil elastase in the tumour microenvironment. *Steroids* 2018; **133**: 96-101 [PMID: 29155217 DOI: 10.1016/j.steroids.2017.11.006]

25 **Boone BA**, Murthy P, Miller-Ocuin J, Doerfler WR, Ellis JT, Liang X, Ross MA, Wallace CT, Sperry JL, Lotze MT, Neal MD, Zeh HJ 3rd. Chloroquine reduces hypercoagulability in pancreatic cancer through inhibition of neutrophil extracellular traps. *BMC Cancer* 2018; **18**: 678 [PMID: 29929491 DOI: 10.1186/s12885-018-4584-2]

26 **Cedervall J**, Zhang Y, Huang H, Zhang L, Femel J, Dimberg A, Olsson AK. Neutrophil Extracellular Traps Accumulate in Peripheral Blood Vessels and Compromise Organ Function in Tumour-Bearing Animals. *Cancer Res* 2015; **75**: 2653-2662 [PMID: 26071254 DOI: 10.1158/0008-5472.CAN-14-3299]

27 **Takesue S**, Ohuchida K, Shinkawa T, Otsubo Y, Matsumoto S, Sagara A, Yonenaga A, Ando Y, Kibe S, Nakayama H, Iwamoto C, Shindo K, Moriyama T, Nakata K, Miyasaka Y, Ohtsuka T, Toma H, Tominaga Y, Mizumoto K, Hashizume M, Nakamura M. Neutrophil extracellular traps promote liver micrometastasis in pancreatic ductal adenocarcinoma *via* the activation of cancerassociated fibroblasts. *Int J Oncol* 2020; **56**: 596-605 [PMID: 31894273 DOI: 10.3892/ijo.2019.4951]

28 **van der Windt DJ**, Sud V, Zhang H, Varley PR, Goswami J, Yazdani HO, Tohme S, Loughran P, O'Doherty RM, Minervini MI, Huang H, Simmons RL, Tsung A. Neutrophil extracellular traps promote inflammation and development of hepatocellular carcinoma in nonalcoholic steatohepatitis. *Hepatology* 2018; **68**: 1347-1360 [PMID: 29631332 DOI: 10.1002/hep.29914]

29 **Demers M**, Wong SL, Martinod K, Gallant M, Cabral JE, Wang Y, Wagner DD. Priming of neutrophils toward NETosis promotes tumour growth. *Oncoimmunology* 2016; **5**: e1134073 [PMID: 27467952 DOI: 10.1080/2162402X.2015.1134073]

30 **Kajioka H**, Kagawa S, Ito A, Yoshimoto M, Sakamoto S, Kikuchi S, Kuroda S, Yoshida R, Umeda Y, Noma K, Tazawa H, Fujiwara T. Targeting neutrophil extracellular traps with thrombomodulin prevents pancreatic cancer metastasis. *Cancer Lett* 2021; **497**: 1-13 [PMID: 33065249 DOI: 10.1016/j.canlet.2020.10.015]

31 **Cools-Lartigue J**, Spicer J, McDonald B, Gowing S, Chow S, Giannias B, Bourdeau F, Kubes P, Ferri L. Neutrophil extracellular traps sequester circulating tumour cells and promote metastasis. *J Clin Invest* 2013; **13**: 3446-3458 [PMID: 23863628 DOI: 10.1172/JCI67484]

32 **Najmeh S**, Cools-Lartigue J, Rayes RF, Gowing S, Vourtzoumis P, Bourdeau F, Giannias B, Berube J, Rousseau S, Ferri LE, Spicer JD. Neutrophil extracellular traps sequester circulating tumour cells *via* β1-integrin mediated interactions. *Int J Cancer* 2017; **140**: 2321-2330 [PMID: 28177522 DOI: 10.1002/ijc.30635]

33 **Albrengues J**, Shields MA, Ng D, Park CG, Ambrico A, Poindexter ME, Upadhyay P, Uyeminami DL, Pommier A, Küttner V, Bružas E, Maiorino L, Bautista C, Carmona EM, Gimotty PA, Fearon DT, Chang K, Lyons SK, Pinkerton KE, Trotman LC, Goldberg MS, Yeh JT, Egeblad M. Neutrophil extracellular traps produced during inflammation awaken dormant cancer cells in mice. *Science* 2018; **361** [PMID: 30262472 DOI: 10.1126/science.aao4227]

34 **Takei H**, Araki A, Watanabe H, Ichinose A, Sendo F. Rapid killing of human neutrophils by the potent activator phorbol 12-myristate 13-acetate (PMA) accompanied by changes different from typical apoptosis or necrosis. *J Leukoc Biol* 1996; **59**: 229-240 [PMID: 8603995 DOI: 10.1002/jlb.59.2.229]

35 **Sollberger G**, Tilley DO, Zychlinsky A. Neutrophil Extracellular Traps: The Biology of Chromatin Externalization. *Dev Cell* 2018; **44**: 542-553 [PMID: 29533770 DOI: 10.1016/j.devcel.2018.01.019]

36 **Yipp BG**, Kubes P. NETosis: how vital is it? *Blood* 2013; **122**: 2784-2794 [PMID: 24009232 DOI: 10.1182/blood-2013-04-457671]

37 **Pilsczek FH**, Salina D, Poon KK, Fahey C, Yipp BG, Sibley CD, Robbins SM, Green FH, Surette MG, Sugai M, Bowden MG, Hussain M, Zhang K, Kubes P. A novel mechanism of rapid nuclear neutrophil extracellular trap formation in response to Staphylococcus aureus. *J Immunol* 2010; **185**: 7413-7425 [PMID: 21098229 DOI: 10.4049/jimmunol.1000675]

38 **Neubert E**, Meyer D, Rocca F, Günay G, Kwaczala-Tessmann A, Grandke J, Senger-Sander S, Geisler C, Egner A, Schön MP, Erpenbeck L, Kruss S. Chromatin swelling drives neutrophil extracellular trap release. *Nat Commun* 2018; **9**: 3767 [PMID: 30218080 DOI: 10.1038/s41467-018-06263-5]

39 **Granger V**, Faille D, Marani V, Noël B, Gallais Y, Szely N, Flament H, Pallardy M, Chollet-Martin S, de Chaisemartin L. Human blood monocytes are able to form extracellular traps. *J Leukoc Biol* 2017; **102**: 775-781 [PMID: 28465447 DOI: 10.1189/jlb.3MA0916-411R]

40 **von Köckritz-Blickwede M**, Goldmann O, Thulin P, Heinemann K, Norrby-Teglund A, Rohde M, Medina E. Phagocytosis-independent antimicrobial activity of mast cells by means of extracellular trap formation. *Blood* 2008; **111**: 3070-3080 [PMID: 18182576 DOI: 10.1182/blood-2007-07-104018]

41 **Yousefi S**, Gold JA, Andina N, Lee JJ, Kelly AM, Kozlowski E, Schmid I, Straumann A, Reichenbach J, Gleich GJ, Simon HU. Catapult-like release of mitochondrial DNA by eosinophils contributes to antibacterial defense. *Nat Med* 2008; **14**: 949-953 [PMID: 18690244 DOI: 10.1038/nm.1855]

42 **Halverson TW**, Wilton M, Poon KK, Petri B, Lewenza S. DNA is an antimicrobial component of neutrophil extracellular traps. *PLoS Pathog* 2015; **11**: e1004593 [PMID: 25590621 DOI: 10.1371/journal.ppat.1004593]

43 **McDonald B**, Urrutia R, Yipp BG, Jenne CN, Kubes P. Intravascular neutrophil extracellular traps capture bacteria from the bloodstream during sepsis. *Cell Host Microbe* 2012; **12**: 324-333 [PMID: 22980329 DOI: 10.1016/j.chom.2012.06.011]

44 **Papayannopoulos V**, Metzler KD, Hakkim A, Zychlinsky A. Neutrophil elastase and myeloperoxidase regulate the formation of neutrophil extracellular traps. *J Cell Biol* 2010; **191**: 677-691 [PMID: 20974816 DOI: 10.1083/jcb.201006052]

45 **Hakkim A**, Fürnrohr BG, Amann K, Laube B, Abed UA, Brinkmann V, Herrmann M, Voll RE, Zychlinsky A. Impairment of neutrophil extracellular trap degradation is associated with lupus nephritis. *Proc Natl Acad Sci USA* 2010; **107**: 9813-9818 [PMID: 20439745 DOI: 10.1073/pnas.0909927107]

46 **Demers M**, Krause DS, Schatzberg D, Martinod K, Voorhees JR, Fuchs TA, Scadden DT, Wagner DD. Cancers predispose neutrophils to release extracellular DNA traps that contribute to cancer-associated thrombosis. *Proc Natl Acad Sci USA* 2012; **109**: 13076-13081 [PMID: 22826226 DOI: 10.1073/pnas.1200419109]

47 **Leal AC**, Mizurini DM, Gomes T, Rochael NC, Saraiva EM, Dias MS, Werneck CC, Sielski MS, Vicente CP, Monteiro RQ. Tumour-Derived Exosomes Induce the Formation of Neutrophil Extracellular Traps: Implications For The Establishment of Cancer-Associated Thrombosis. *Sci Rep* 2017; **7**: 6438 [PMID: 28743887 DOI: 10.1038/s41598-017-06893-7]

48 **Sanmamed MF**, Carranza-Rua O, Alfaro C, Oñate C, Martín-Algarra S, Perez G, Landazuri SF, Gonzalez A, Gross S, Rodriguez I, Muñoz-Calleja C, Rodríguez-Ruiz M, Sangro B, López-Picazo JM, Rizzo M, Mazzolini G, Pascual JI, Andueza MP, Perez-Gracia JL, Melero I. Serum interleukin-8 reflects tumour burden and treatment response across malignancies of multiple tissue origins. *Clin Cancer Res* 2014; **20**: 5697-5707 [PMID: 25224278 DOI: 10.1158/1078-0432.CCR-13-3203]

49 **Alfaro C**, Teijeira A, Oñate C, Pérez G, Sanmamed MF, Andueza MP, Alignani D, Labiano S, Azpilikueta A, Rodriguez-Paulete A, Garasa S, Fusco JP, Aznar A, Inogés S, De Pizzol M, Allegretti M, Medina-Echeverz J, Berraondo P, Perez-Gracia JL, Melero I. Tumour-Produced Interleukin-8 Attracts Human Myeloid-Derived Suppressor Cells and Elicits Extrusion of Neutrophil Extracellular Traps (NETs). *Clin Cancer Res* 2016; **22**: 3924-3936 [PMID: 26957562 DOI: 10.1158/1078-0432.CCR-15-2463]

50 **Cai Z**, Zhang M, Boafo Kwantwi L, Bi X, Zhang C, Cheng Z, Ding X, Su T, Wang H, Wu Q. Breast cancer cells promote self-migration by secreting interleukin 8 to induce NET formation. *Gene* 2020; **754**: 144902 [PMID: 32544496 DOI: 10.1016/j.gene.2020.144902]

51 **Zha C**, Meng X, Li L, Mi S, Qian D, Li Z, Wu P, Hu S, Zhao S, Cai J, Liu Y. Neutrophil extracellular traps mediate the crosstalk between glioma progression and the tumour microenvironment **via** the HMGB1/RAGE/IL-8 axis. *Cancer Biol Med* 2020; **17**: 154-168 [PMID: 32296583 DOI: 10.20892/j.issn.2095-3941.2019.0353]

52 **Zhang Q**, Liu S, Parajuli KR, Zhang W, Zhang K, Mo Z, Liu J, Chen Z, Yang S, Wang AR, Myers L, You Z. Interleukin-17 promotes prostate cancer *via* MMP7-induced epithelial-to-mesenchymal transition. *Oncogene* 2017; **36**: 687-699 [PMID: 27375020 DOI: 10.1038/onc.2016.240]

53 **Zhang Y**, Chandra V, Riquelme Sanchez E, Dutta P, Quesada PR, Rakoski A, Zoltan M, Arora N, Baydogan S, Horne W, Burks J, Xu H, Hussain P, Wang H, Gupta S, Maitra A, Bailey JM, Moghaddam SJ, Banerjee S, Sahin I, Bhattacharya P, McAllister F. Interleukin-17-induced neutrophil extracellular traps mediate resistance to checkpoint blockade in pancreatic cancer. *J Exp Med* 2020; **217**: e20190354 [PMID: 32860704 DOI: 10.1084/jem.20190354]

54 **Rocks N**, Vanwinge C, Radermecker C, Blacher S, Gilles C, Marée R, Gillard A, Evrard B, Pequeux C, Marichal T, Noel A, Cataldo D. Ozone-primed neutrophils promote early steps of tumour cell metastasis to lungs by enhancing their NET production. *Thorax* 2019; **74**: 768-779 [PMID: 31142617 DOI: 10.1136/thoraxjnl-2018-211990]

55 **Hudock KM**, Collins MS, Imbrogno M, Snowball J, Kramer EL, Brewington JJ, Gollomp K, McCarthy C, Ostmann AJ, Kopras EJ, Davidson CR, Srdiharan A, Arumugam P, Sengupta S, Xu Y, Worthen GS, Trapnell BC, Clancy JP. Neutrophil extracellular traps activate IL-8 and IL-1 expression in human bronchial epithelia. *Am J Physiol Lung Cell Mol Physiol* 2020; **319**: L137-L147 [PMID: 32159969 DOI: 10.1152/ajplung.00144.2019]

56 **Hosseinzadeh A**, Thompson PR, Segal BH, Urban CF. Nicotine induces neutrophil extracellular traps. *J Leukoc Biol* 2016; **100**: 1105-1112 [PMID: 27312847 DOI: 10.1189/jlb.3AB0815-379RR]

57 **Yotsumoto S**, Muroi Y, Chiba T, Ohmura R, Yoneyama M, Magarisawa M, Dodo K, Terayama N, Sodeoka M, Aoyagi R, Arita M, Arakawa S, Shimizu S, Tanaka M. Hyperoxidation of ether-linked phospholipids accelerates neutrophil extracellular trap formation. *Sci Rep* 2017; **7**: 16026 [PMID: 29167447 DOI: 10.1038/s41598-017-15668-z]

58 **Yasuda H**, Takishita Y, Morita A, Tsutsumi T, Tsuchiya M, Sato EF. DNA demethylation increases NETosis. *Arch Biochem Biophys* 2020; **689**: 108465 [PMID: 32561201 DOI: 10.1016/j.abb.2020.108465]

59 **Smyth EC**, Nilsson M, Grabsch HI, van Grieken NC, Lordick F. Gastric cancer. *Lancet* 2020; **396**: 635-648 [PMID: 32861308 DOI: 10.1016/S0140-6736(20)31288-5]

60 **Agnelli G**, Becattini C, Meyer G, Muñoz A, Huisman MV, Connors JM, Cohen A, Bauersachs R, Brenner B, Torbicki A, Sueiro MR, Lambert C, Gussoni G, Campanini M, Fontanella A, Vescovo G, Verso M; Caravaggio Investigators. Apixaban for the Treatment of Venous Thromboembolism Associated with Cancer. *N Engl J Med* 2020; **382**: 1599-1607 [PMID: 32223112 DOI: 10.1056/NEJMoa1915103]

61 **Kwon HC**, Oh SY, Lee S, Kim SH, Han JY, Koh RY, Kim MC, Kim HJ. Plasma levels of prothrombin fragment F1+2, D-dimer and prothrombin time correlate with clinical stage and lymph node metastasis in operable gastric cancer patients. *Jpn J Clin Oncol* 2008; **38**: 2-7 [PMID: 18258711 DOI: 10.1093/jjco/hym157]

62 **Lee KW**, Bang SM, Kim S, Lee HJ, Shin DY, Koh Y, Lee YG, Cha Y, Kim YJ, Kim JH, Park DJ, Kim HH, Oh D, Lee JS. The incidence, risk factors and prognostic implications of venous thromboembolism in patients with gastric cancer. *J Thromb Haemost* 2010; **8**: 540-547 [PMID: 20040044 DOI: 10.1111/j.1538-7836.2009.03731.x]

63 **Ay C**, Pabinger I, Cohen AT. Cancer-associated venous thromboembolism: Burden, mechanisms, and management. *Thromb Haemost* 2017; **117**: 219-230 [PMID: 27882374 DOI: 10.1160/TH16-08-0615]

64 **Yang C**, Sun W, Cui W, Li X, Yao J, Jia X, Li C, Wu H, Hu Z, Zou X. Procoagulant role of neutrophil extracellular traps in patients with gastric cancer. *Int J Clin Exp Pathol* 2015; **8**: 14075-14086 [PMID: 26823721]

65 **Kanda M**, Shimizu D, Tanaka H, Tanaka C, Kobayashi D, Hayashi M, Iwata N, Niwa Y, Yamada S, Fujii T, Sugimoto H, Murotani K, Fujiwara M, Kodera Y. Significance of SYT8 For the Detection, Prediction, and Treatment of Peritoneal Metastasis From Gastric Cancer. *Ann Surg* 2018; **267**: 495-503 [PMID: 28026832 DOI: 10.1097/SLA.0000000000002096]

66 **Gamboa AC**, Winer JH. Cytoreductive Surgery and Hyperthermic Intraperitoneal Chemotherapy for Gastric Cancer. *Cancers (Basel)* 2019; **11**: 1662 [PMID: 31717799 DOI: 10.3390/cancers11111662]

67 **Ilson DH**. Advances in the treatment of gastric cancer: 2019. *Curr Opin Gastroenterol* 2019; **35**: 551-554 [PMID: 31436556 DOI: 10.1097/MOG.0000000000000577]

68 **Kanamaru R**, Ohzawa H, Miyato H, Matsumoto S, Haruta H, Kurashina K, Saito S, Hosoya Y, Yamaguchi H, Yamashita H, Seto Y, Lefor AK, Sata N, Kitayama J. Low density neutrophils (LDN) in postoperative abdominal cavity assist the peritoneal recurrence through the production of neutrophil extracellular traps (NETs). *Sci Rep* 2018; **8**: 632 [PMID: 29330531 DOI: 10.1038/s41598-017-19091-2]

69 **Kanamaru R**, Ohzawa H, Miyato H, Yamaguchi H, Hosoya Y, Lefor AK, Sata N, Kitayama J. Neutrophil Extracellular Traps Generated by Low Density Neutrophils Obtained from Peritoneal Lavage Fluid Mediate Tumour Cell Growth and Attachment. *J Vis Exp* 2018; **(138)**: 58201 [PMID: 30124642 DOI: 10.3791/58201]

70 **Goldfarb Y**, Sorski L, Benish M, Levi B, Melamed R, Ben-Eliyahu S. Improving postoperative immune status and resistance to cancer metastasis: a combined perioperative approach of immunostimulation and prevention of excessive surgical stress responses. *Ann Surg* 2011; **253**: 798-810 [PMID: 21475023 DOI: 10.1097/SLA.0b013e318211d7b5]

71 **Angele MK**, Faist E. Clinical review: immunodepression in the surgical patient and increased susceptibility to infection. *Crit Care* 2002; **6**: 298-305 [PMID: 12225603 DOI: 10.1186/cc1514]

72 **Kumagai Y**, Ohzawa H, Miyato H, Horie H, Hosoya Y, Lefor AK, Sata N, Kitayama J. Surgical Stress Increases Circulating Low-Density Neutrophils Which May Promote Tumour Recurrence. *J Surg Res* 2020; **246**: 52-61 [PMID: 31561178 DOI: 10.1016/j.jss.2019.08.022]

73 **Chen X**, Guo J, Bao J, Lu J, Wang Y. The anticancer properties of Salvia miltiorrhiza Bunge (Danshen): a systematic review. *Med Res Rev* 2014; **34**: 768-794 [PMID: 24123144 DOI: 10.1002/med.21304]

74 **Tao L**, Xu M, Dai X, Ni T, Li D, Jin F, Wang H, Tao L, Pan B, Woodgett JR, Qian Y, Liu Y. Polypharmacological Profiles Underlying the Antitumour Property of *Salvia miltiorrhiza* Root (Danshen) Interfering with NOX-Dependent Neutrophil Extracellular Traps. *Oxid Med Cell Longev* 2018; **2018**: 4908328 [PMID: 30210653 DOI: 10.1155/2018/4908328]

75 **Du XY**, Liu X, Wang ZJ, Wang YY. SLPI promotes the gastric cancer growth and metastasis by regulating the expression of P53, Bcl-2 and Caspase-8. *Eur Rev Med Pharmacol Sci* 2017; **21**: 1495-1501 [PMID: 28429358]

76 **Lu C**, Cai D, Ma J. Pachymic Acid Sensitizes Gastric Cancer Cells to Radiation Therapy by Upregulating Bax through Hypoxia. *Am J Chin Med* 2018; **46**: 875-890 [PMID: 29737213 DOI: 10.1142/S0192415X18500465]

77 **Sokolova O**, Naumann M. NF-κB Signaling in Gastric Cancer. *Toxins (Basel)* 2017; **9**: 119 [PMID: 28350359 DOI: 10.3390/toxins9040119]

78 **Li R**, Zou X, Zhu T, Xu H, Li X, Zhu L. Destruction of Neutrophil Extracellular Traps Promotes the Apoptosis and Inhibits the Invasion of Gastric Cancer Cells by Regulating the Expression of Bcl-2, Bax and NF-κB. *Onco Targets Ther* 2020; **13**: 5271-5281 [PMID: 32606746 DOI: 10.2147/OTT.S227331]

79 **Ünlü B**, van Es N, Arindrarto W, Kiełbasa SM, Mei H, Westerga J, Middeldorp S, Kuppen PJK, Otten JMMB, Cannegieter S, Versteeg HH. Genes associated with venous thromboembolism in colorectal cancer patients. *J Thromb Haemost* 2018; **16**: 293-302 [PMID: 29247594 DOI: 10.1111/jth.13926]

80 **Zhang Y**, Wang C, Yu M, Zhao X, Du J, Li Y, Jing H, Dong Z, Kou J, Bi Y, Novakovic VA, Zhou J, Shi J. Neutrophil extracellular traps induced by activated platelets contribute to procoagulant activity in patients with colorectal cancer. *Thromb Res* 2019; **180**: 87-97 [PMID: 31271975 DOI: 10.1016/j.thromres.2019.06.005]

81 **Arelaki S**, Arampatzioglou A, Kambas K, Papagoras C, Miltiades P, Angelidou I, Mitsios A, Kotsianidis I, Skendros P, Sivridis E, Maroulakou I, Giatromanolaki A, Ritis K. Gradient Infiltration of Neutrophil Extracellular Traps in Colon Cancer and Evidence for Their Involvement in Tumour Growth. *PLoS One* 2016; **11**: e0154484 [PMID: 27136460 DOI: 10.1371/journal.pone.0154484]

82 **Rayes RF**, Mouhanna JG, Nicolau I, Bourdeau F, Giannias B, Rousseau S, Quail D, Walsh L, Sangwan V, Bertos N, Cools-Lartigue J, Ferri LE, Spicer JD. Primary tumours induce neutrophil extracellular traps with targetable metastasis promoting effects. *JCI Insight* 2019; **5**: e128008 [PMID: 31343990 DOI: 10.1172/jci.insight.128008]

83 **Tohme S**, Yazdani HO, Al-Khafaji AB, Chidi AP, Loughran P, Mowen K, Wang Y, Simmons RL, Huang H, Tsung A. Neutrophil Extracellular Traps Promote the Development and Progression of Liver Metastases after Surgical Stress. *Cancer Res* 2016; **76**: 1367-1380 [PMID: 26759232 DOI: 10.1158/0008-5472.CAN-15-1591]

84 **Richardson JJR**, Hendrickse C, Gao-Smith F, Thickett DR. Characterization of systemic neutrophil function in patients undergoing colorectal cancer resection. *J Surg Res* 2017; **220**: 410-418 [PMID: 28890131 DOI: 10.1016/j.jss.2017.07.036]

85 **Cheng KJ**, Alshawsh MA, Mejia Mohamed EH, Thavagnanam S, Sinniah A, Ibrahim ZA. HMGB1: an overview of its versatile roles in the pathogenesis of colorectal cancer. *Cell Oncol (Dordr)* 2020; **43**: 177-193 [PMID: 31677065 DOI: 10.1007/s13402-019-00477-5]

86 **Ni Q**, Zhang F, Liu Y, Wang Z, Yu G, Liang B, Niu G, Su T, Zhu G, Lu G, Zhang L, Chen X. A bi-adjuvant nanovaccine that potentiates immunogenicity of neoantigen for combination immunotherapy of colorectal cancer. *Sci Adv* 2020; **6**: eaaw6071 [PMID: 32206706 DOI: 10.1126/sciadv.aaw6071]

87 **Chrysanthopoulou A**, Kambas K, Stakos D, Mitroulis I, Mitsios A, Vidali V, Angelidou I, Bochenek M, Arelaki S, Arampatzioglou A, Galani IE, Skendros P, Couladouros EA, Konstantinides S, Andreakos E, Schäfer K, Ritis K. Interferon lambda1/IL-29 and inorganic polyphosphate are novel regulators of neutrophil-driven thromboinflammation. *J Pathol* 2017; **243**: 111-122 [PMID: 28678391 DOI: 10.1002/path.4935]

88 **Arelaki S**, Arampatzioglou A, Kambas K, Sivridis E, Giatromanolaki A, Ritis K. Mast cells co-expressing CD68 and inorganic polyphosphate are linked with colorectal cancer. *PLoS One* 2018; **13**: e0193089 [PMID: 29543850 DOI: 10.1371/journal.pone.0193089]

89 **Yazdani HO**, Roy E, Comerci AJ, van der Windt DJ, Zhang H, Huang H, Loughran P, Shiva S, Geller DA, Bartlett DL, Tsung A, Sheng T, Simmons RL, Tohme S. Neutrophil Extracellular Traps Drive Mitochondrial Homeostasis in Tumours to Augment Growth. *Cancer Res* 2019; **79**: 5626-5639 [PMID: 31519688 DOI: 10.1158/0008-5472.CAN-19-0800]

90 **Li J**, Huang L, Zhao H, Yan Y, Lu J. The Role of Interleukins in Colorectal Cancer. *Int J Biol Sci* 2020; **16**: 2323-2339 [PMID: 32760201 DOI: 10.7150/ijbs.46651]

91 **Yang L**, Liu L, Zhang R, Hong J, Wang Y, Wang J, Zuo J, Zhang J, Chen J, Hao H. IL-8 mediates a positive loop connecting increased neutrophil extracellular traps (NETs) and colorectal cancer liver metastasis. *J Cancer* 2020; **11**: 4384-4396 [PMID: 32489457 DOI: 10.7150/jca.44215]

92 **Shang A**, Gu C, Zhou C, Yang Y, Chen C, Zeng B, Wu J, Lu W, Wang W, Sun Z, Li D. Exosomal KRAS mutation promotes the formation of tumour-associated neutrophil extracellular traps and causes deterioration of colorectal cancer by inducing IL-8 expression. *Cell Commun Signal* 2020; **18**: 52 [PMID: 32228650 DOI: 10.1186/s12964-020-0517-1]

93 **Yang L**, Liu Q, Zhang X, Liu X, Zhou B, Chen J, Huang D, Li J, Li H, Chen F, Liu J, Xing Y, Chen X, Su S, Song E. DNA of neutrophil extracellular traps promotes cancer metastasis *via* CCDC25. *Nature* 2020; **583**: 133-138 [PMID: 32528174 DOI: 10.1038/s41586-020-2394-6]

94 **Zhang Y**, Hu Y, Ma C, Sun H, Wei X, Li M, Wei W, Zhang F, Yang F, Wang H, Gu K. Diagnostic, Therapeutic Predictive, and Prognostic Value of Neutrophil Extracellular Traps in Patients With Gastric Adenocarcinoma. *Front Oncol* 2020; **10**: 1036 [PMID: 32714865 DOI: 10.3389/fonc.2020.01036]

95 **Decker AS**, Pylaeva E, Brenzel A, Spyra I, Droege F, Hussain T, Lang S, Jablonska J. Prognostic Role of Blood NETosis in the Progression of Head and Neck Cancer. *Cells* 2019; **8**: 946 [PMID: 31438586 DOI: 10.3390/cells8090946]

96 **Jin W**, Xu HX, Zhang SR, Li H, Wang WQ, Gao HL, Wu CT, Xu JZ, Qi ZH, Li S, Ni QX, Liu L, Yu XJ. Tumour-Infiltrating NETs Predict Postsurgical Survival in Patients with Pancreatic Ductal Adenocarcinoma. *Ann Surg Oncol* 2019; **26**: 635-643 [PMID: 30374923 DOI: 10.1245/s10434-018-6941-4]

97 **Zhang H**, Lv H, Weng M, Wang H, Cata JP, Chen W, Miao C. Preoperative leukocytosis is associated with increased tumour-infiltrating neutrophil extracellular traps and worse outcomes in esophageal cancer. *Ann Transl Med* 2020; **8**: 441 [PMID: 32395485 DOI: 10.21037/atm.2020.03.190]

98 **Abu Abed U**, Brinkmann V. Immunofluorescence Labelling of Human and Murine Neutrophil Extracellular Traps in Paraffin-Embedded Tissue. *J Vis Exp* 2019 [PMID: 31566594 DOI: 10.3791/60115]

99 **Elsherif L**, Sciaky N, Metts CA, Modasshir M, Rekleitis I, Burris CA, Walker JA, Ramadan N, Leisner TM, Holly SP, Cowles MW, Ataga KI, Cooper JN, Parise LV. Machine Learning to Quantitate Neutrophil NETosis. *Sci Rep* 2019; **9**: 16891 [PMID: 31729453 DOI: 10.1038/s41598-019-53202-5]

100 **Thålin C**, Lundström S, Seignez C, Daleskog M, Lundström A, Henriksson P, Helleday T, Phillipson M, Wallén H, Demers M. Citrullinated histone H3 as a novel prognostic blood marker in patients with advanced cancer. *PLoS One* 2018; **13**: e0191231 [PMID: 29324871 DOI: 10.1371/journal.pone.0191231]

101 **Grilz E**, Mauracher LM, Posch F, Königsbrügge O, Zöchbauer-Müller S, Marosi C, Lang I, Pabinger I, Ay C. Citrullinated histone H3, a biomarker for neutrophil extracellular trap formation, predicts the risk of mortality in patients with cancer. *Br J Haematol* 2019; **186**: 311-320 [PMID: 30968400 DOI: 10.1111/bjh.15906]

102 **Mauracher LM**, Posch F, Martinod K, Grilz E, Däullary T, Hell L, Brostjan C, Zielinski C, Ay C, Wagner DD, Pabinger I, Thaler J. Citrullinated histone H3, a biomarker of neutrophil extracellular trap formation, predicts the risk of venous thromboembolism in cancer patients. *J Thromb Haemost* 2018; **16**: 508-518 [PMID: 29325226 DOI: 10.1111/jth.13951]

103 **Li M**, Lin C, Leso A, Nefedova Y. Quantification of Citrullinated Histone H3 Bound DNA for Detection of Neutrophil Extracellular Traps. *Cancers (Basel)* 2020; **12**: 3424 [PMID: 33218159 DOI: 10.3390/cancers12113424]

104 **Davis JC Jr**, Manzi S, Yarboro C, Rairie J, Mcinnes I, Averthelyi D, Sinicropi D, Hale VG, Balow J, Austin H, Boumpas DT, Klippel JH. Recombinant human Dnase I (rhDNase) in patients with lupus nephritis. *Lupus* 1999; **8**: 68-76 [PMID: 10025601 DOI: 10.1191/096120399678847380]

105 **Xia Y**, He J, Zhang H, Wang H, Tetz G, Maguire CA, Wang Y, Onuma A, Genkin D, Tetz V, Stepanov A, Terekhov S, Ukrainskaya V, Huang H, Tsung A. AAV-mediated gene transfer of DNase I in the liver of mice with colorectal cancer reduces liver metastasis and restores local innate and adaptive immune response. *Mol Oncol* 2020; **14**: 2920-2935 [PMID: 32813937 DOI: 10.1002/1878-0261.12787]

106 **Schauer C**, Janko C, Munoz LE, Zhao Y, Kienhöfer D, Frey B, Lell M, Manger B, Rech J, Naschberger E, Holmdahl R, Krenn V, Harrer T, Jeremic I, Bilyy R, Schett G, Hoffmann M, Herrmann M. Aggregated neutrophil extracellular traps limit inflammation by degrading cytokines and chemokines. *Nat Med* 2014; **20**: 511-517 [PMID: 24784231 DOI: 10.1038/nm.3547]

107 **Okeke EB**, Louttit C, Fry C, Najafabadi AH, Han K, Nemzek J, Moon JJ. Inhibition of neutrophil elastase prevents neutrophil extracellular trap formation and rescues mice from endotoxic shock. *Biomaterials* 2020; **238**: 119836 [PMID: 32045782 DOI: 10.1016/j.biomaterials.2020.119836]

108 **Fuchs TA**, Abed U, Goosmann C, Hurwitz R, Schulze I, Wahn V, Weinrauch Y, Brinkmann V, Zychlinsky A. Novel cell death program leads to neutrophil extracellular traps. *J Cell Biol* 2007; **176**: 231-241 [PMID: 17210947 DOI: 10.1083/jcb.200606027]

109 **Metzler KD**, Fuchs TA, Nauseef WM, Reumaux D, Roesler J, Schulze I, Wahn V, Papayannopoulos V, Zychlinsky A. Myeloperoxidase is required for neutrophil extracellular trap formation: implications for innate immunity. *Blood* 2011; **117**: 953-959 [PMID: 20974672 DOI: 10.1182/blood-2010-06-290171]

110 **Hakkim A**, Fuchs TA, Martinez NE, Hess S, Prinz H, Zychlinsky A, Waldmann H. Activation of the Raf-MEK-ERK pathway is required for neutrophil extracellular trap formation. *Nat Chem Biol* 2011; **7**: 75-77 [PMID: 21170021 DOI: 10.1038/nchembio.496]

111 **Martinez NE**, Zimmermann TJ, Goosmann C, Alexander T, Hedberg C, Ziegler S, Zychlinsky A, Waldmann H. Tetrahydroisoquinolines: New Inhibitors of Neutrophil Extracellular Trap (NET) Formation. *Chembiochem* 2017; **18**: 888-893 [PMID: 28240414 DOI: 10.1002/cbic.201600650]

112 **Khan MA**, D'Ovidio A, Tran H, Palaniyar N. Anthracyclines Suppress Both NADPH Oxidase-Dependent and -Independent NETosis in Human Neutrophils. *Cancers (Basel)* 2019; **11**: 1328 [PMID: 31500300 DOI: 10.3390/cancers11091328]

113 **Rayes RF**, Vourtzoumis P, Bou Rjeily M, Seth R, Bourdeau F, Giannias B, Berube J, Huang YH, Rousseau S, Camilleri-Broet S, Blumberg RS, Beauchemin N, Najmeh S, Cools-Lartigue J, Spicer JD, Ferri LE. Neutrophil Extracellular Trap-Associated CEACAM1 as a Putative Therapeutic Target to Prevent Metastatic Progression of Colon Carcinoma. *J Immunol* 2020; **204**: 2285-2294 [PMID: 32169849 DOI: 10.4049/jimmunol.1900240]

114 **Li Y**, Li M, Weigel B, Mall M, Werth VP, Liu ML. Nuclear envelope rupture and NET formation is driven by PKCα-mediated lamin B disassembly. *EMBO Rep* 2020; **21**: e48779 [PMID: 32537912 DOI: 10.15252/embr.201948779]

115 **Basyreva LY**, Voinova EV, Gusev AA, Mikhalchik EV, Kuskov AN, Goryachaya AV, Gusev SA, Shtilman MI, Velonia K, Tsatsakis AM. Fluorouracil neutrophil extracellular traps formation inhibited by polymer nanoparticle shielding. *Mater Sci Eng C Mater Biol Appl* 2020; **108**: 110382 [PMID: 31924010 DOI: 10.1016/j.msec.2019.110382]

116 **Cao TM**, King MR. Supercharged eGFP-TRAIL Decorated NETs to Ensnare and Kill Disseminated Tumour Cells. *Cell Mol Bioeng* 2020; **13**: 359-367 [PMID: 32952735 DOI: 10.1007/s12195-020-00639-8]

World Journal of Gastroenterology

Submit a Manuscript: https://www.f6publishing.com

World J Gastroenterol 2021 September 7; 27(33): 5488-5501

DOI: 10.3748/wjg.v27.i33.5488

ISSN 1007-9327 (print) ISSN 2219-2840 (online)

REVIEW

Microbiota and viral hepatitis: State of the art of a complex matter

Ivana Milosevic, Edda Russo, Ankica Vujovic, Aleksandra Barac, Olja Stevanovic, Stefano Gitto, Amedeo Amedei

ORCID number: Ivana Milosevic 0000-0002-5014-8949; Edda Russo 0000-0003-3141-1091; Ankica Vujovic 0000-0001-9570-215X; Aleksandra Barac 0000-0002-0132-2277; Olja Stevanovic 0000-0001-9306-2128; Stefano Gitto 0000-0002-8042-6508; Amedeo Amedei 0000-0002-6797-9343.

Author contributions: Russo E and Milosevic I contributed equally; Russo E, Milosevic I and Amedei A conceptualized the review; Milosevic I, Barak A, Vujovic A and Russo E wrote the paper; Milosevic I, Barak A, Vujovic A, Stevanovic O, and Russo E collected the data; Milosevic A, Barak A and Vujovic A, prepared the figures; Gitto S and Amedei A corrected the final version; Barak A, Russo E, and Amedei A acquired the funding; All authors critically revised the manuscript.

Supported by The Italian Ministry of University and Research (MIUR), the Foundation 'Ente Cassa di Risparmio di Firenze', No. FCR 2017.

Conflict-of-interest statement: Authors declare no any conflict of interest.

Open-Access: This article is an open-access article that was selected by an in-house editor and fully peer-reviewed by external reviewers. It is distributed in

Ivana Milosevic, Ankica Vujovic, Aleksandra Barac, Olja Stevanovic, Clinic for Infectious and Tropical Diseases, Clinical Centre of Serbia Faculty of Medicine, University of Belgrade, Belgrade 101801, Serbia

Edda Russo, Stefano Gitto, Amedeo Amedei, Department of Experimental and Clinical Medicine, University of Florence, Firenze 50100, Italy

Corresponding author: Ivana Milosevic, MD, Associate Professor, Clinic for Infectious and Tropical Diseases, Clinical Centre of Serbia Faculty of Medicine, University of Belgrade, Bul. Oslobodjenja 16, Belgrade 101801, Serbia. ivana.milosevic@med.bg.ac.rs

Abstract

Changes in gut microbiota influence both the gut and liver, which are strictly connected by the so-called "gut–liver axis". The gut microbiota acts as a major determinant of this relationship in the onset and clinical course of liver diseases. According to the results of several studies, gut dysbiosis is linked to viral hepatitis, mainly hepatitis C virus and hepatitis B virus infection. Gut bacteria-derived metabolites and cellular components are key molecules that affect liver function and modulate the pathology of viral hepatitis. Recent studies showed that the gut microbiota produces various molecules, such as peptidoglycans, lipopolysaccharides, DNA, lipoteichoic acid, indole-derivatives, bile acids, and trimethylamine, which are translocated to the liver and interact with liver immune cells causing pathological effects. Therefore, the existence of crosstalk between the gut microbiota and the liver and its implications on host health and pathologic status are essential factors impacting the etiology and therapeutic approach. Concrete mechanisms behind the pathogenic role of gut-derived components on the pathogenesis of viral hepatitis remain unclear and not understood. In this review, we discuss the current findings of research on the bidirectional relationship of the components of gut microbiota and the progression of liver diseases and viral hepatitis and *vice versa*. Moreover, this paper highlights the current therapeutic and preventive strategies, such as fecal transplantation, used to restore the gut microbiota composition and so improve host health.

Key Words: Gut microbiota; Hepatitis B virus; Hepatitis C virus; Liver diseases, Fecal transplantation

©The Author(s) 2021. Published by Baishideng Publishing Group Inc. All rights reserved.

accordance with the Creative Commons Attribution NonCommercial (CC BY-NC 4.0) license, which permits others to distribute, remix, adapt, build upon this work non-commercially, and license their derivative works on different terms, provided the original work is properly cited and the use is non-commercial. See: http://creativecommons.org/licenses/by-nc/4.0/

Manuscript source: Invited manuscript

Specialty type: Gastroenterology and hepatology

Country/Territory of origin: Serbia

Peer-review report's scientific quality classification

Grade A (Excellent): 0
Grade B (Very good): 0
Grade C (Good): C
Grade D (Fair): 0
Grade E (Poor): 0

Received: February 2, 2021
Peer-review started: February 2, 2021
First decision: March 14, 2021
Revised: March 26, 2021
Accepted: July 21, 2021
Article in press: July 21, 2021
Published online: September 7, 2021

P-Reviewer: Zheng H
S-Editor: Liu M
L-Editor: Webster JR
P-Editor: Yuan YY



Core Tip: Changes within the gut microbiota have an impact on the mutual crosstalk between intestinal microbiota and the liver. Gut dysbiosis is linked to viral hepatitis, mainly hepatitis C virus and hepatitis B virus infection. However, concrete mechanisms behind the pathogenic role of gut-derived components on the pathogenesis of viral hepatitis remain unclear. We discuss recent studies to understand the role of gut microbiota.

Citation: Milosevic I, Russo E, Vujovic A, Barac A, Stevanovic O, Gitto S, Amedei A. Microbiota and viral hepatitis: State of the art of a complex matter. *World J Gastroenterol* 2021; 27(33): 5488-5501
URL: https://www.wjgnet.com/1007-9327/full/v27/i33/5488.htm
DOI: https://dx.doi.org/10.3748/wjg.v27.i33.5488

INTRODUCTION

The gut contains a large, complex microbial community that has much more genetic material than the total human genome[1]. Gut microbiota (GM) acts as a major determinant of complex bidirectional communication between the gut and brain to maintain intestinal homeostasis and host health[2,3]. However, gastrointestinal tract bacteria produce several enzymes, metabolites, and cellular components that can contribute to many disorders such as liver disease[3], diabetes mellitus[4], inflammatory bowel disease[5], irritable bowel syndrome[6], obesity[7], colorectal cancer[8], and mental illness[9].

The term gut-liver axis refers to the anatomical and physiological connection between the gut and the liver[3]. The gut-liver axis is based on the very close anatomical relationship of these organs and consequently, enzymes, metabolites, and immune signals are transferred to the liver through the portal vein circulation[10-12]. These gut-derived metabolic products modulate immune functions and moderate liver disease formation, pathogenesis and treatment responses, by acting as signaling molecules[10-13].

The GM represents one of the main factors influencing the gut-liver axis and its role in the alteration of liver function has recently received considerable attention[3].

Gut dysbiosis may specifically lead to an inflammatory response due to increased production of pro-inflammatory cytokines, which are recognized by receptors in the portal circulation[10,12,14]. Production of these pro-inflammatory cytokines largely depends on the response of the innate immune system to the presence of microbial products[12]. It was documented that the GM profile in patients with chronic hepatitis differs considerably from that observed in healthy patients[15,16]. Moreover, the degree of liver insufficiency is closely related to the severity of gut dysbiosis[10]. Recent studies support the fact that GM dysbiosis helps the advancement of viral hepatitis infection[17]. During chronic viral hepatitis, the intestinal microbiota has a marked impact on viral host cell interaction as well as on viral replication[18]. *Escherichia coli* (*E. coli*), *Enterobacteriaceae*, *Enterococcus faecalis*, and *Faecalibacterium prausnitzii* represent the most harmful bacteria that can alter the good profile of GM in viral hepatitis and consequently lead to a decreased number of lactic acid species[19,20]. In addition, an increased number of *Candida sp*. in the stool is usually detected in patients with progression of hepatitis B virus (HBV), while *Neisseria, E. coli*, *Enterobacteriaceae*, *E. faecalis, F. prausnitzii*, and *Gemella* are the most common bacterial species present in the GM of patients with HBV and hepatitis C virus (HCV) infection and are correlated with the progression of liver disease[20-22].

This paper provides an overview of the state of the art of this complex matter. We discuss recent updates on the interactions of GM, liver diseases and viral hepatitis and potential therapeutic interventions that target the gut–liver axis.

GM in pathologic liver

As previously mentioned, the liver and intestine extensively interact *via* the biliary tract, the portal vein and systemic mediators. The liver is a crucial immunological organ, mainly enriched with innate immune cells and persistently exposed to numerous circulating nutrients, microbial components and metabolites in close contact with the intestinal tract. Liver compounds, on the other hand, mainly affect the GM

structure and integrity of the gut barrier, while intestinal conditions control the synthesis of bile acids, glucose and lipid metabolism in the liver. Currently, many lines of research have established a relationship between the GM and liver disease. Indeed, a concurrent surge in liver diseases and gastrointestinal and immune disorders confirms the crosstalk between the gut and the liver[23]. Among the liver diseases, the pathogenesis and progression of non-alcoholic fatty liver disease (NAFLD) and the most severe form non-alcoholic steatohepatitis (NASH), alcohol-related liver disease (ALD), primary biliary cholangitis (PBC), primary sclerosing cholangitis (PSC), cirrhosis and hepatocellular carcinoma (HCC) have been associated with changes in the gut-liver axis[24]. In light of this evidence, the latest advancements in the understanding of the gut-liver axis support studies to enhance liver disease treatment in microbiome-based, diagnostic, prognostic, and therapeutic modalities.

NAFLD

A large number of preclinical and clinical studies from the last decade have investigated the role of the GM in NAFLD and NASH, showing different results. In general, NAFLD patients display a decreased GM diversity[25,26], with a decrease of Bacteroidetes and Firmicutes, along with an increase of *Lactobacillus*[27]. Moreover, steatosis was related to an abundance of *Ruminococcus gnavus* and *Coprococcus* and lower bacterial diversity in NAFLD[28], while NAFLD severity was related to shifts in both GM composition and metabolic functions[29,30]. Recently, a correlation between specific immune cells and GM fecal signatures was observed in NAFLD. In detail, *F. prausnitzii* was negatively correlated with CD163+ and CD45+ cells, while *Prevotella* was negatively correlated with CD20+ cells[31]. In addition, a GM signature was also demonstrated in fibrotic NASH[32], where advanced liver fibrosis was related to augmented *Proteobacteria* levels, whereas Firmicutes were significantly decreased[32]. Patients with NASH also showed decreased *F. prausnitzii*, *Ruminococcus*, and *Coprococcus* abundance in comparison with healthy controls[27], while pediatric patients exhibited an increased abundance of *E. coli*[25]. In NASH patients, bacterial overgrowth can inhibit intestinal tight junction function and encourage epithelial barrier dysfunction[33]. Although several reports have evaluated the GM, much less has been reported regarding the virome, defined as the total collection of viruses in and on the human body. More advanced NAFLD was associated with reduced viral (and relative bacteriophages) diversity[34]. Additionally, a recent panel including microbiota features was able to detect NAFLD-cirrhosis[35], providing evidence for a fecal-microbiome derived profile to detect NAFLD. A choline-based diet has been shown to be compatible with NAFLD by GM structure changes that benefit bacteria that break down choline[36]. However, very recent animal model research, revealed sex variations in GM abundance changes, behaviors, and hepatic steatosis in response to dietary copper-fructose interaction in rats[37]. Finally, a particular symbiotic used for therapy changed the fecal microbiota in a placebo-controlled trial, but failed to change hepatic steatosis in subjects with NAFLD[38].

ALD

Several studies have been conducted in mouse and human models based on how alcohol can induce dysbiosis associated with microbiota, which in turn can lead to ALD pathogenesis and development[39]. Regarding the GM composition, ALD patients show lower levels of *Bifidobacterium*, *Enterobacterium* and *Lactobacillus spp.*[40-43], while cirrhotic patients with ALD showed an important reduction in Firmicutes and Bacteroidetes phyla[23,44]. In fecal samples, a reduction in *Lactobacillus spp.*, has been observed in alcoholic patients, whereas cirrhotic patients showed lower amounts of *Bifidobacterium spp.*[45,46]. In addition, the GM of alcoholics with liver cirrhosis contained increased levels of *Enterobactericeae*[41]. In general, an increase in the number of microorganisms was found in the small bowel of alcoholic patients[47-49], with higher levels of microbial metabolites in the blood compared to healthy controls [19,50]. During ALD progression, a shift in the GM profile from steatohepatitis to pre-cirrhosis to cirrhosis has been reported[51]. In addition, research on chronic alcoholics has demonstrated that bacterial overgrowth is central to disease progression[52]. These findings are also supported by mouse studies[53]. Alcohol-associated dysbiosis can decrease biosynthesis of long chain fatty acids (LCFA) in mice and LCFA supplementation can restore eubiosis. In fact, a significant correlation between *Lactobacillus*

spp. and bacterial LCFA has been observed in ALD patients[54,55]. Alcohol can also reduce the development of butyrate and the administration of butyrate modulates alcohol-induced liver damage in mice[56].

PBC

Patients with PBC show a significant general decrease in bacterial diversity[57]. Indeed, *Bacteroidetes spp*. were significantly decreased and *Haemophilus*, *Fusobacteria*, *Clostridium*, *Veillonella*, *Lactobacillus*, *Pseudomonas*, *Streptococcus*, *Klebsiella*, *Proteobacteria spp*. and *Enterobacteriaceae* were over-represented in PBC patients compared to healthy controls[57]. Cross-sectional research has shown that GM, metabolism and immune alterations are associated in PBC patients[58]. In detail, beneficial intestinal microbes, including *Lachnobacterium spp*., *Acidobacteria*, *Ruminococcus bromii* and *Bacteroides eggerthii*, were found to be depleted and higher levels of opportunistic pathogens, such as *Enterobacteriaceae*, y-*Proteobacteria*, *Neisseriaceae*, *etc*., were reported[58]. In the same study, PBC-related GM modulation was associated with increased markers of liver damage and serum inflammatory cytokinesis[58]. Moreover, a recent study[59] demonstrated that the concentration of particular secondary bile acids was inversely correlated with upregulated microbes in PBC patients, but was positively correlated with upregulated bacteria in healthy controls[59]. The relationships between clinical profiles, reaction to treatment with ursodeoxycholic acid and GM composition in patients with PBC have recently been studied[60], suggesting the decrease in *Faecalibacterium* as an innovative prognostic element in PBC.

PSC

Several reports investigating the role of GM in PSC show an overall reduction in GM diversity[61]. Alterations in biliary and fecal microbiome in PSC patients are characterized by higher abundance of *Lactobacillus*, *Fusobacterium*, and *Enterococcus* and low diversity[62,63]. In addition, PSC patients showed an overrepresentation of *Enterococcus*, *Rothia*, *Clostridium*, *Streptococcus*, *Haemophilus*, *Veillonella*, *Fusobacterium* and *Lactobacillus* genera[64,65]. In particular, *Veillonella* abundance was clearly increased in PSC patients matched with healthy controls[63]. Furthermore, the GM profile of PSC intestinal biopsies was distinguished by *Barnesiellaceae* abundance and a decline in *Clostridiales*[66,67]. The pathogenesis of PSC was linked with GM dysbiosis by causing *bacterobilia*, which in turn stimulates a pro-inflammatory mechanism contributing to fibrosis and inflammation in cholangiocytes[68,69].

HBV infection

Liver failure and disease progression in patients with chronic HBV infection was found to be connected to GM dysbiosis in a large proportion[18,70]. There are differences in the composition of the intestinal flora between patients with HBV and HCV infection (Figures 1 and 2). Compared to healthy controls, patients with chronic HBV infection showed an abundant *Anaerostipes* taxon[71,72]. Liu *et al*[70] aimed to find the differences in the GM composition of HBV and non-HBV non-HCV related HCC compared with healthy controls. HCC patients with HBV were found to harbor higher species richness, more potential anti-inflammatory bacteria (such as *Prevotella*, *Faecalibacterium*, *Pseudobutyrivibrio*, *Lachnoclostridium*, *Ruminoclostridium*), and fewer pro-inflammatory bacteria (such as *Escherichia-Shigella*, *Enterococcus*) while *Proteobacteria* abundance was decreased. The role of anti-inflammatory bacteria such as *Faecalibacterium* and *Prevotella* is in their anti-inflammatory and anti-carcinogenic potential[73], but HBV infection leads to their progressive decline compared to healthy subjects[70]. In addition, Ren *et al*[74] documented that butyrate-producing bacteria declined in early HCC HBV positive patients. This further indicated that HBV indeed plays a role in GM changes. In HBV infection, a beneficial bacterium, *Lachnospiraceae*, plays a role *via* a reduction in lipopolysaccharide (LPS) secretion and bacterial translocation[74,75]. The study by Lu *et al*[16] suggested that cirrhotic patients with HBV infection exhibit a decrease in *F. prausnitzii*, *E. faecalis*, *Enterobacteriaceae*, *Bifidobacteria* and lactic acid bacteria, while *Enterococcus* and *Enterobacteriaceae* levels are significantly increased compared to healthy individuals.

On the contrary, HBV and HCV negative patients with HCC harbored fewer potential anti-inflammatory bacteria and more pro-inflammatory bacteria. Taken together, these data indicated that GM plays an important role in the progression of

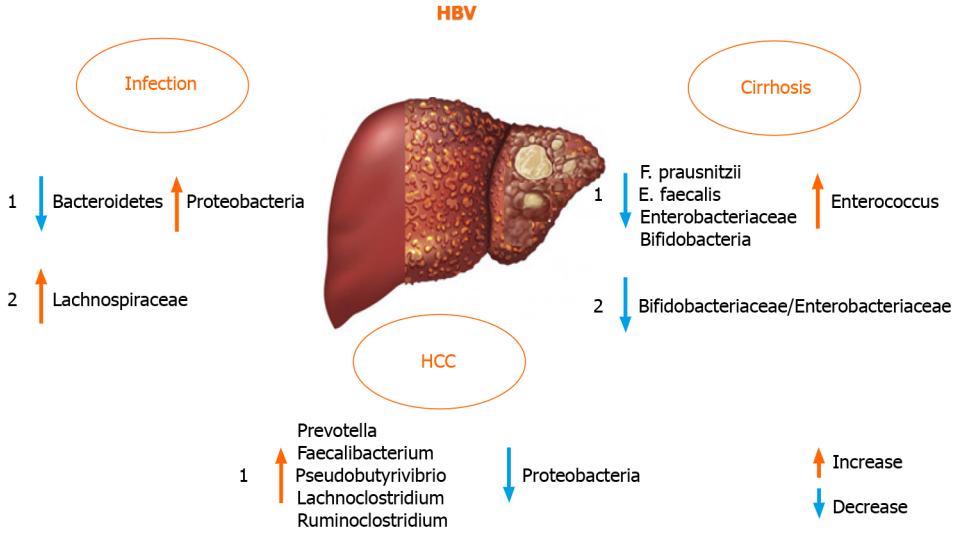


Figure 1 Differences in altered microbiota in patients with HBV during infection and cirrhosis. HBV: Hepatitis B virus; HCC: Hepatocellular carcinoma.

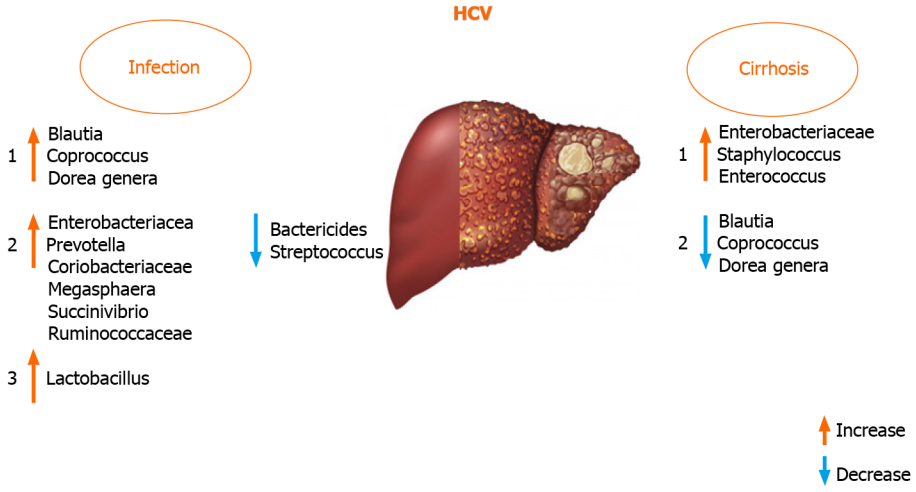


Figure 2 Differences in altered microbiota in patients with HCV during infection and cirrhosis. HCV: Hepatitis C virus.

HBV or non-HBV non-HCV related HCC. These findings were different from previous reports on HBV-induced liver diseases[16,70,76]. The discrepancy in these findings was probably due to the progression of liver diseases and the group of patients in evaluated studies. To analyze the GM role in HBV positive patients, it is appropriate to use a defined cohort of patients suffering from HBV infection[77], excluding patients with different etiologies of liver cirrhosis (including alcohol abuse) that itself may change the composition of the intestinal microbial community and the same might be true for other liver diseases[70,78]. Therefore, the discrepancy of fecal microbiota between HBV positive and HBV negative patients in the study by Liu *et al*[70] is perhaps due to the HBV infection[70,77].

Not only gut dysbiosis, but also dysbiosis of the oral microbiota was observed in HBV patients, and yellow tongue coating is suggestive of a reduction in *Bacteroidetes*, but an increase in *Proteobacteria*. Zhao *et al*[79] also suggested a positive correlation between serum HBV-DNA and the number of *Neisseriaceae* in oral microbiota.

Furthermore, the GM composition differed according to the level of alanine aminotransferase (ALT) in HBV patients[80,81]. *Desulfovibrio* had a positive correlation, while *Acidaminococcus* showed a negative correlation with high ALT level[81]. Lu *et al*[16] found a significantly decreased ratio of *Bifidobacteriaceae/Enterobacteriaceae* (B/E) in cirrhotic HBV positive patients, while Yun *et al*[72] observed no difference in the B/E ratio in non-cirrhotic HBV patients with positive HBsAg and normal or high ALT. These findings lead to the conclusion that the B/E ratio is disturbed only in the GM of patients with cirrhosis. However, another study observed that the *Megasphaera* genus

of the Firmicutes phylum was abundant in the HBsAg positive high ALT group compared to the normal ALT group. In HBsAg positive patients with normal ALT, butyrate-producing bacteria (*e.g.*, *Anaerostipes*) are more often present in GM compared to HBsAg negative patients[72]. These bacteria produce short-chain fatty acid as a by-product of lactate fermentation and butyrate. In Figure 1 we show the main microbiota alterations in HBV.

Recently, Wang *et al*[82] defined serum zonulin as an intestinal permeability marker and showed its association with AFP levels in HBV-associated liver cirrhosis and HCC, especially helpful in correlating it with advanced stages of these diseases[83]. It has been reported that the diagnostic model of one location may be not used in other locations, as the diagnostic efficiency declined when the geographic scale was increased[79]. The characteristic GM changes had the strongest relationship with the host location; thus, the diagnostic potential of microbial markers should consider these geographic differences[79].

HCV infection

The liver-gut interaction controls GM homeostasis during HCV infection, which might be an ideal model to study the interaction between the GM and liver[18,80]. A review of previous reports provides the rationale for the hypothesis that GM dysbiosis could also be employed as a biomarker and a therapeutic target to mitigate disease progression. Interestingly, HCV-RNA and HCVcoreAg were frequently found in the stool of patients with chronic HCV[84]. Therefore, direct interactions between virus particles and intestinal bacteria might facilitate or inhibit growth as in rotavirus infection[85]. Heidrich *et al*[86] found that progression of HCV infection is related to a reduced alpha diversity revealing that the relative abundance of phylotypes is associated with the stage of the disease. Additionally, Sultan *et al*[2] characterized the GM from a cohort of adult patients with HCV before starting any treatment and confirmed the presence of GM dysbiosis. Microbial taxa in HCV positive patients identified during this study were characterized by increased microbiota diversity, the enrichment of *Enterobacteriacea*, *Prevotella*, *Coriobacteriaceae*, *Megasphaera*, *Succinivibrio*, and *Ruminococcaceae*, and the depletion of *Bacteroides* and *Streptococcus*. In addition, the GM of HCV-infected subjects was characterized by the depletion of carbohydrates and lipid metabolism, specifically galactose, fructose, mannose, and sphingolipid metabolism. In the presence of HCV infection, microbiota-associated histidine metabolism was decreased, while the metabolism of cysteine and methionine and translation proteins was enriched compared to healthy controls[2]. The findings of Sultan *et al*[2] contradict previous literature that showed a decrease in GM diversity and changes within the abundance of some taxa such as *Prevotella*, *Ruminococcaceae*, *Enterobacteriacea*, and *Faecalibacterium* in patients with chronic HCV infection[2,15,86-88]. This could be due to many aspects such as different stages of the disease, treatment or other medication-related factors, different genotypes, demographics, diet, alcohol consumption or smoking. Specifically, treatment regimens were not controlled in most of these reports, which may obscure a possible key microbe, a protective role, or a diagnostic-related signal. The impact of specific treatment has also received significant attention in GM research in other health disorders[5,89,90].

It was documented that antiviral HCV treatment with ribavirin + pegylated interferon has no direct impact on gut dysbiosis, and in fact, it increases bile acids, which is very important in GM metabolism[91]. Some pathogenic bacteria such as *Enterobacteriaceae*, *Staphylococcus*, and *Enterococcus* decreased the steroid in HCV-infected cirrhotic patients, which normalized after direct-acting antivirals (DAAs). In addition, DAAs are helpful in improving GM, especially from the *Lachnospira* and *Dorea* genera, and in restoring TNF-α levels[92]. However, following DAA treatment, the expression of calprotectin, ZO1, and LPS was more intensive in HCV patients with cirrhosis[92]. Pérez-Matute *et al*[92] showed that the administration of DAAs in HCV patients was not able to improve GM bacterial richness. However, partial restoration of inflammation, alpha diversity and a few bacterial genera (except *Actinobacteria*) were observed after 3 mo in patients with a lower fibrosis degree, stressing the concept that gut dysbiosis and liver damage are gradual[92]. Liver fibrosis degree might be a key factor contributing to a definite GM profile. A lower abundance of *Akkermansia muciniphila* was also found in HCV infected patients with higher fibrosis degrees and it is proposed that these bacteria could have a major role in the evolution of HCV infection and liver damage. *Akkermansia muciniphila* is proposed as a new candidate for developing novel supplements with beneficial effects for GM recovery[93] and to intensify the action of DAAs at this level. These results confirm those previously observed with prior treatments in cirrhotic patients[94]. Thus, with severe liver damage, a greater impact on GM is observed, and, therefore, there are more difficulties to

counteract such changes with antivirals. These data highlight the need to treat patients as soon as possible in order to reverse the negative actions caused by HCV infection on GM diversity and future clinical correlated consequences.

It was found that *Blautia*, *Coprococcus*, and *Dorea* genera were increased in HCV positive patients, which is opposite to the lower presence of these bacteria observed in disease stage 4[95]. Such conflicting findings could be explained by the various fibrosis degrees of the study groups. Several studies have demonstrated an over-representation of *Veillonella* in cirrhotic patients (both, HBV and/or HCV infected) and its positive correlation with ALT or AST levels in serum[20,75,92]. In conclusion, the role of this genus in the GM of healthy people has not been completely revealed.

An increased presence of *Lactobacillus* in HCV-infected patients was found in very few studies, although the study cohorts were not uniform (treatment-naïve and patients under a treatment regimen)[86,92]. However, the impact on the progression of HCV infection of this genus and a few bacterial species belonging to that genus (such as *L. ruminis*) has to be specifically addressed, as some probiotics are supported by bacterial strains belonging to this genus[96]. The main microbiota alterations in HCV infection are reported in Figure 2.

The GM varies in patients with different HCV genotypes[86]. Statistically significant differences in GM composition between patients with and without liver cirrhosis are only found in genotype non-1. In genotype 1, differences in the microbial composition are associated with the persistent HCV infection rather than with the fibrosis stage. Therefore, studies investigating patients with liver diseases compared to healthy controls might overlook the influence of the underlying disease on the intestinal microbial communities, and so other diseases and stages of diseases need to be investigated for potential associations[15,75].

Cirrhosis

A recent study has shown that the GM has a lower abundance of *Bacteroidetes* and higher levels of *Prevotella*, *Enterococcus*, *Veillonella*, *Proteobacteria*, *Megasphaera*, *Burkholderia*, and *Fusobacteria* in patients with cirrhosis[20,43]. In the duodenal mucosa of cirrhotic patients, an overrepresentation of *Veillonella*, *Megasphaera*, *Dialister*, *Atopobium*, and *Prevotella* was reported, compared to controls. A reduction in diversity, a rise in immunostimulatory pathogens (*e.g.*, *Staphylococcaceae* and *Enterococcaceae*) and a decline in potentially beneficial *Firmicutes* (*e.g.*, *Ruminococcaceae* and *Lachnospiraceae*) have been identified with respect to the fecal microbiota in patients with cirrhosis[15]. Moreover, similar changes were detected in the colon mucosa[97], serum[98], and saliva[99] of patients with cirrhosis. Interestingly, the improvement in GM composition was correlated with the outcomes of patients with (*i.e.*, compensated *vs* uncompensated[100], inpatient *vs* outpatient, and noninfected and infected patients [19]), indicating microbiota alterations as potential new biomarkers. Intriguingly, a higher abundance of buccal-derived microflora was recorded in fecal specimens from cirrhosis patients, as well as dramatically altered salivary microbiome levels[15]. In a very recent and innovative study, an analogous microbiome profile was observed independently of the etiology of cirrhosis using a machine-learning-based methodology and matching their outcomes with other cohorts containing different etiologies of liver cirrhosis. These outcomes suggest that the etiology of liver disease tends to be less relevant regarding the GM alterations[101]. Such an approach may allow the non-invasive diagnosis of liver cirrhosis[101].

HCC

Alterations in the composition of the microbial profiles are suspected of having a role in carcinogenesis[1]. Indeed, recent studies suggested a correlation between particular bacterial profiles in HCC patients[74]. However, the contribution of GM to HCC pathogenesis is intricate: (1) A disturbed intestinal barrier brings a series of TLR ligands to the liver and activates the inflammatory response; (2) *via* downregulation of hepatocyte apoptosis and upregulation of hepatic stellar cell proliferation, the TLR signaling pathways mediate hepatocarcinogenesis[102]; and (3) Finally, impaired immunosurveillance is associated with abnormal GM in HCC. Moreover, microbiota dysbiosis can be related to HCC pathogenesis by increasing oxidative stress, steatosis, and the inflammatory response[103]. Additionally, the GM of HCC patients undergoing liver transplantation was compared to the GM of patients who did not have HCC, but had an analogous etiology of cirrhosis and MELD stage. An increased number of fecal *E. coli* was associated with HCC[104]. Moreover, the presence of *Helicobacter spp*. in HCC tissue samples indicated intestinal translocation as a possible trigger of tumorigenesis[105]. Finally, the GM structure could theoretically predict reaction rates in liver cancer patients treated with particular immune checkpoint

inhibitors[106], indicating the potential to harness the microbial flora for HCC immunotherapy[107].

Role of fecal microbiota transplantation in viral hepatitis - future directions

Different therapeutic approaches have been proposed to improve the health of patients with chronic viral hepatitis through the manipulation of GM composition, the modulation of immune signaling, and the production of metabolites[88,108]. It was found that some bacteria of the intestinal microbiota disappeared in patients who received antibiotics within 3 mo[109]. It is speculated that region and eating habits might affect the flora of HBV positive patients[109]. Fecal microbiota transplantation (FMT) is considered a promising new treatment option for HBV and HCV infection, due to its ability to restore GM dysbiosis[108].

Ren *et al*[110] reported a clinical trial of FMT for the treatment of HBeAg positive patients with chronic HBV with ongoing entecavir and tenofovir therapy. The results demonstrated that FMT induced HBeAg clearance in a significant number of patients that had persistent positive HBeAg even after long-term antiviral treatment. This result was especially encouraging for HBeAg positive patients who otherwise could not stop oral antiviral treatment[110]. In addition, this trial provided evidence that FMT could be a beneficial treatment option for modulating GM in patients with chronic HBV. HBV carriers might be suitable donors for FMT as their GM composition seems to be more appropriate compared to the healthy population. The results of Yang *et al*[108] confirmed that HBV carriers have altered GM although they are asymptomatic. The high treatment FMT potential from HBV carriers comes from the evidence that they are able to keep a long-life balance with the virus without developing clinical symptoms. These data confirm the previous allegations that the change in flora composition of HBV carriers may play an active role in the struggle between the human body and the virus[94,110]. Of course, more detailed studies are needed to verify these claims.

The use of probiotics in HBV positive patients was shown to be beneficial and suggested that probiotic VSL#3 plays an important role in the management of HBV infection[111]. In addition, the use of probiotics in HCV-infected patients with cirrhosis has been shown to be significantly beneficial[88]. It was suggested that during HCV infection, *L. acidophilus* and *Bifidobacterium spp.* can act as a supportive supplement with antiviral and antibacterial activities[112]. The results of Doskali *et al*[113] suggested that a healthy GM increases the cytotoxic effects of NK cells against viral infected cells; thus, inhibiting HCV replication. Finally, Yang *et al*[108] confirmed that some probiotics, such as lactic acid bacteria, may have a negative impact on disease progression. The results of Yang *et al*[108] indicated that the intake of *Lactobacillus* should be cautious as these bacteria are negatively associated with environmental adaptation, energy metabolism, and the immune system and may have an influence on the progression of HBV infection[70,108].

CONCLUSION

This literature review provides evidence on the association between gut dysbiosis and the clinical course of both chronic HBV and HCV infection. The evidence in humans seems to confirm the potential role of intestinal overgrowth of pathogenic bacteria and the development of chronic viral hepatitis observed in animal-based studies. In addition, current clinical trials with different therapeutic strategies have improved the present knowledge on the gut–liver axis, showing positive and encouraging results on how to overcome the battle with viral hepatitis. More studies on the liver-gut mechanistic interaction during HCV and HBV infection are still needed to unravel the cause-effect relationship between gut homeostasis and disease complications and to evaluate the efficacy of modulation of the GM as a preventive strategy against chronic viral hepatitis progression and especially the development of hepatocarcinoma.

ACKNOWLEDGEMENTS

The authors thank Dr. Elisangela Miceli, PhD and Dr. Savannah Devente for English revisions.

REFERENCES

1 **Russo E**, Amedei A. The Role of the Microbiota in the Genesis of Gastrointestinal Cancers. In: Frontiers in Anti-Infective Drug Discovery. Bentham e Books: 1-44 [DOI: 10.2174/9781681085623118070003]

2 **Sultan S**, El-Mowafy M, Elgaml A, El-Mesery M, El Shabrawi A, Elegezy M, Hammami R, Mottawea W. Alterations of the Treatment-Naive Gut Microbiome in Newly Diagnosed Hepatitis C Virus Infection. *ACS Infect Dis* 2021; **7**: 1059-1068 [PMID: 33119247 DOI: 10.1021/acsinfecdis.0c00432]

3 **Milosevic I**, Vujovic A, Barac A, Djelic M, Korac M, Radovanovic Spurnic A, Gmizic I, Stevanovic O, Djordjevic V, Lekic N, Russo E, Amedei A. Gut-Liver Axis, Gut Microbiota, and Its Modulation in the Management of Liver Diseases: A Review of the Literature. *Int J Mol Sci* 2019; **20**: 395 [PMID: 30658519 DOI: 10.3390/ijms20020395]

4 **Qin J**, Li Y, Cai Z, Li S, Zhu J, Zhang F, Liang S, Zhang W, Guan Y, Shen D, Peng Y, Zhang D, Jie Z, Wu W, Qin Y, Xue W, Li J, Han L, Lu D, Wu P, Dai Y, Sun X, Li Z, Tang A, Zhong S, Li X, Chen W, Xu R, Wang M, Feng Q, Gong M, Yu J, Zhang Y, Zhang M, Hansen T, Sanchez G, Raes J, Falony G, Okuda S, Almeida M, LeChatelier E, Renault P, Pons N, Batto JM, Zhang Z, Chen H, Yang R, Zheng W, Yang H, Wang J, Ehrlich SD, Nielsen R, Pedersen O, Kristiansen K. A metagenome-wide association study of gut microbiota in type 2 diabetes. *Nature* 2012; **490**: 55-60 [PMID: 23023125 DOI: 10.1038/nature11450]

5 **Mottawea W**, Chiang CK, Mühlbauer M, Starr AE, Butcher J, Abujamel T, Deeke SA, Brandel A, Zhou H, Shokralla S, Hajibabaei M, Singleton R, Benchimol EI, Jobin C, Mack DR, Figeys D, Stintzi A. Altered intestinal microbiota-host mitochondria crosstalk in new onset Crohn's disease. *Nat Commun* 2016; **7**: 13419 [PMID: 27876802 DOI: 10.1038/ncomms13419]

6 **Distrutti E**, Monaldi L, Ricci P, Fiorucci S. Gut microbiota role in irritable bowel syndrome: New therapeutic strategies. *World J Gastroenterol* 2016; **22**: 2219-2241 [PMID: 26900286 DOI: 10.3748/wjg.v22.i7.2219]

7 **Ray K**. Gut microbiota: Adding weight to the microbiota's role in obesity--exposure to antibiotics early in life can lead to increased adiposity. *Nat Rev Gastroenterol Hepatol* 2012; **9**: 615 [PMID: 22965425 DOI: 10.1038/nrgastro.2012.175]

8 **Arthur JC**, Perez-Chanona E, Mühlbauer M, Tomkovich S, Uronis JM, Fan TJ, Campbell BJ, Abujamel T, Dogan B, Rogers AB, Rhodes JM, Stintzi A, Simpson KW, Hansen JJ, Keku TO, Fodor AA, Jobin C. Intestinal inflammation targets cancer-inducing activity of the microbiota. *Science* 2012; **338**: 120-123 [PMID: 22903521 DOI: 10.1126/science.1224820]

9 **Valles-Colomer M**, Falony G, Darzi Y, Tigchelaar EF, Wang J, Tito RY, Schiweck C, Kurilshikov A, Joossens M, Wijmenga C, Claes S, Van Oudenhove L, Zhernakova A, Vieira-Silva S, Raes J. The neuroactive potential of the human gut microbiota in quality of life and depression. *Nat Microbiol* 2019; **4**: 623-632 [PMID: 30718848 DOI: 10.1038/s41564-018-0337-x]

10 **Grąt M**, Wronka KM, Krasnodębski M, Masior Ł, Lewandowski Z, Kosińska I, Grąt K, Stypułkowski J, Rejowski S, Wasilewicz M, Gałęcka M, Szachta P, Krawczyk M. Profile of Gut Microbiota Associated With the Presence of Hepatocellular Cancer in Patients With Liver Cirrhosis. *Transplant Proc* 2016; **48**: 1687-1691 [PMID: 27496472 DOI: 10.1016/j.transproceed.2016.01.077]

11 **Brenner DA**, Paik YH, Schnabl B. Role of Gut Microbiota in Liver Disease. *J Clin Gastroenterol* 2015; **49** Suppl 1: S25-S27 [PMID: 26447960 DOI: 10.1097/MCG.0000000000000391]

12 **Giannelli V**, Di Gregorio V, Iebba V, Giusto M, Schippa S, Merli M, Thalheimer U. Microbiota and the gut-liver axis: bacterial translocation, inflammation and infection in cirrhosis. *World J Gastroenterol* 2014; **20**: 16795-16810 [PMID: 25492994 DOI: 10.3748/wjg.v20.i45.16795]

13 **Vassallo G**, Mirijello A, Ferrulli A, Antonelli M, Landolfi R, Gasbarrini A, Addolorato G. Review article: Alcohol and gut microbiota - the possible role of gut microbiota modulation in the treatment of alcoholic liver disease. *Aliment Pharmacol Ther* 2015; **41**: 917-927 [PMID: 25809237 DOI: 10.1111/apt.13164]

14 **Chassaing B**, Etienne-Mesmin L, Gewirtz AT. Microbiota-liver axis in hepatic disease. *Hepatology* 2014; **59**: 328-339 [PMID: 23703735 DOI: 10.1002/hep.26494]

15 **Qin N**, Yang F, Li A, Prifti E, Chen Y, Shao L, Guo J, Le Chatelier E, Yao J, Wu L, Zhou J, Ni S, Liu L, Pons N, Batto JM, Kennedy SP, Leonard P, Yuan C, Ding W, Hu X, Zheng B, Qian G, Xu W, Ehrlich SD, Zheng S, Li L. Alterations of the human gut microbiome in liver cirrhosis. *Nature* 2014; **513**: 59-64 [PMID: 25079328 DOI: 10.1038/nature13568]

16 **Lu H**, Wu Z, Xu W, Yang J, Chen Y, Li L. Intestinal microbiota was assessed in cirrhotic patients with hepatitis B virus infection. Intestinal microbiota of HBV cirrhotic patients. *Microb Ecol* 2011; **61**: 693-703 [PMID: 21286703 DOI: 10.1007/s00248-010-9801-8]

17 **Xu D**, Huang Y, Wang J. Gut microbiota modulate the immune effect against hepatitis B virus infection. *Eur J Clin Microbiol Infect Dis* 2015; **34**: 2139-2147 [PMID: 26272175 DOI: 10.1007/s10096-015-2464-0]

18 **Sehgal R**, Bedi O, Trehanpati N. Role of Microbiota in Pathogenesis and Management of Viral Hepatitis. *Front Cell Infect Microbiol* 2020; **10**: 341 [PMID: 32850467 DOI: 10.3389/fcimb.2020.00341]

19 **Bajaj JS**, Heuman DM, Hylemon PB, Sanyal AJ, White MB, Monteith P, Noble NA, Unser AB, Daita K, Fisher AR, Sikaroodi M, Gillevet PM. Altered profile of human gut microbiome is associated with cirrhosis and its complications. *J Hepatol* 2014; **60**: 940-947 [PMID: 24374295

DOI: 10.1016/j.jhep.2013.12.019]
20 **Chen Y**, Ji F, Guo J, Shi D, Fang D, Li L. Dysbiosis of small intestinal microbiota in liver cirrhosis and its association with etiology. *Sci Rep* 2016; **6**: 34055 [PMID: 27687977 DOI: 10.1038/srep34055]
21 **Mohamadkhani A**. On the potential role of intestinal microbial community in hepatocarcinogenesis in chronic hepatitis B. *Cancer Med* 2018; **7**: 3095-3100 [PMID: 29761927 DOI: 10.1002/cam4.1550]
22 **Cui L**, Morris A, Ghedin E. The human mycobiome in health and disease. *Genome Med* 2013; **5**: 63 [PMID: 23899327 DOI: 10.1186/gm467]
23 **Hartmann P**, Seebauer CT, Schnabl B. Alcoholic liver disease: the gut microbiome and liver cross talk. *Alcohol Clin Exp Res* 2015; **39**: 763-775 [PMID: 25872593 DOI: 10.1111/acer.12704]
24 **Wang R**, Tang R, Li B, Ma X, Schnabl B, Tilg H. Gut microbiome, liver immunology, and liver diseases. *Cell Mol Immunol* 2021; **18**: 4-17 [PMID: 33318628 DOI: 10.1038/s41423-020-00592-6]
25 **Zhu L**, Baker SS, Gill C, Liu W, Alkhouri R, Baker RD, Gill SR. Characterization of gut microbiomes in nonalcoholic steatohepatitis (NASH) patients: a connection between endogenous alcohol and NASH. *Hepatology* 2013; **57**: 601-609 [PMID: 23055155 DOI: 10.1002/hep.26093]
26 **Jiang W**, Wu N, Wang X, Chi Y, Zhang Y, Qiu X, Hu Y, Li J, Liu Y. Dysbiosis gut microbiota associated with inflammation and impaired mucosal immune function in intestine of humans with non-alcoholic fatty liver disease. *Sci Rep* 2015; **5**: 8096 [PMID: 25644696 DOI: 10.1038/srep08096]
27 **Da Silva HE**, Teterina A, Comelli EM, Taibi A, Arendt BM, Fischer SE, Lou W, Allard JP. Nonalcoholic fatty liver disease is associated with dysbiosis independent of body mass index and insulin resistance. *Sci Rep* 2018; **8**: 1466 [PMID: 29362454 DOI: 10.1038/s41598-018-19753-9]
28 **Alferink LJM**, Radjabzadeh D, Erler NS, Vojinovic D, Medina-Gomez C, Uitterlinden AG, de Knegt RJ, Amin N, Ikram MA, Janssen HLA, Kiefte-de Jong JC, Metselaar HJ, van Duijn CM, Kraaij R, Darwish Murad S. Microbiomics, Metabolomics, Predicted Metagenomics, and Hepatic Steatosis in a Population-Based Study of 1,355 Adults. *Hepatology* 2021; **73**: 968-982 [PMID: 32530501 DOI: 10.1002/hep.31417]
29 **Boursier J**, Mueller O, Barret M, Machado M, Fizanne L, Araujo-Perez F, Guy CD, Seed PC, Rawls JF, David LA, Hunault G, Oberti F, Calès P, Diehl AM. The severity of nonalcoholic fatty liver disease is associated with gut dysbiosis and shift in the metabolic function of the gut microbiota. *Hepatology* 2016; **63**: 764-775 [PMID: 26600078 DOI: 10.1002/hep.28356]
30 **Raman M**, Ahmed I, Gillevet PM, Probert CS, Ratcliffe NM, Smith S, Greenwood R, Sikaroodi M, Lam V, Crotty P, Bailey J, Myers RP, Rioux KP. Fecal microbiome and volatile organic compound metabolome in obese humans with nonalcoholic fatty liver disease. *Clin Gastroenterol Hepatol* 2013; **11**: 868-75.e1 [PMID: 23454028 DOI: 10.1016/j.cgh.2013.02.015]
31 **Schwenger KJP**, Chen L, Chelliah A, Da Silva HE, Teterina A, Comelli EM, Taibi A, Arendt BM, Fischer S, Allard JP. Markers of activated inflammatory cells are associated with disease severity and intestinal microbiota in adults with nonalcoholic fatty liver disease. *Int J Mol Med* 2018; **42**: 2229-2237 [PMID: 30085339 DOI: 10.3892/ijmm.2018.3800]
32 **Loomba R**, Seguritan V, Li W, Long T, Klitgord N, Bhatt A, Dulai PS, Caussy C, Bettencourt R, Highlander SK, Jones MB, Sirlin CB, Schnabl B, Brinkac L, Schork N, Chen CH, Brenner DA, Biggs W, Yooseph S, Venter JC, Nelson KE. Gut Microbiome-Based Metagenomic Signature for Non-invasive Detection of Advanced Fibrosis in Human Nonalcoholic Fatty Liver Disease. *Cell Metab* 2019; **30**: 607 [PMID: 31484056 DOI: 10.1016/j.cmet.2019.08.002]
33 **Cani PD**, Amar J, Iglesias MA, Poggi M, Knauf C, Bastelica D, Neyrinck AM, Fava F, Tuohy KM, Chabo C, Waget A, Delmée E, Cousin B, Sulpice T, Chamontin B, Ferrières J, Tanti JF, Gibson GR, Casteilla L, Delzenne NM, Alessi MC, Burcelin R. Metabolic endotoxemia initiates obesity and insulin resistance. *Diabetes* 2007; **56**: 1761-1772 [PMID: 17456850 DOI: 10.2337/db06-1491]
34 **Lang S**, Demir M, Martin A, Jiang L, Zhang X, Duan Y, Gao B, Wisplinghoff H, Kasper P, Roderburg C, Tacke F, Steffen HM, Goeser T, Abraldes JG, Tu XM, Loomba R, Stärkel P, Pride D, Fouts DE, Schnabl B. Intestinal Virome Signature Associated With Severity of Nonalcoholic Fatty Liver Disease. *Gastroenterology* 2020; **159**: 1839-1852 [PMID: 32652145 DOI: 10.1053/j.gastro.2020.07.005]
35 **Caussy C**, Tripathi A, Humphrey G, Bassirian S, Singh S, Faulkner C, Bettencourt R, Rizo E, Richards L, Xu ZZ, Downes MR, Evans RM, Brenner DA, Sirlin CB, Knight R, Loomba R. A gut microbiome signature for cirrhosis due to nonalcoholic fatty liver disease. *Nat Commun* 2019; **10**: 1406 [PMID: 30926798 DOI: 10.1038/s41467-019-09455-9]
36 **Corbin KD**, Zeisel SH. Choline metabolism provides novel insights into nonalcoholic fatty liver disease and its progression. *Curr Opin Gastroenterol* 2012; **28**: 159-165 [PMID: 22134222 DOI: 10.1097/MOG.0b013e32834e7b4b]
37 **Song M**, Yuan F, Li X, Ma X, Yin X, Rouchka EC, Zhang X, Deng Z, Prough RA, McClain CJ. Analysis of sex differences in dietary copper-fructose interaction-induced alterations of gut microbial activity in relation to hepatic steatosis. *Biol Sex Differ* 2021; **12**: 3 [PMID: 33407877 DOI: 10.1186/s13293-020-00346-z]
38 **Scorletti E**, Afolabi PR, Miles EA, Smith DE, Almehmadi A, Alshathry A, Childs CE, Del Fabbro S, Bilson J, Moyses HE, Clough GF, Sethi JK, Patel J, Wright M, Breen DJ, Peebles C, Darekar A, Aspinall R, Fowell AJ, Dowman JK, Nobili V, Targher G, Delzenne NM, Bindels LB, Calder PC, Byrne CD. Synbiotics Alter Fecal Microbiomes, But Not Liver Fat or Fibrosis, in a Randomized Trial of Patients With Nonalcoholic Fatty Liver Disease. *Gastroenterology* 2020; **158**: 1597-1610

[PMID: 31987796 DOI: 10.1053/j.gastro.2020.01.031]
39 **Li F**, Duan K, Wang C, McClain C, Feng W. Probiotics and Alcoholic Liver Disease: Treatment and Potential Mechanisms. *Gastroenterol Res Pract* 2016; **2016**: 5491465 [PMID: 26839540 DOI: 10.1155/2016/5491465]
40 **Bull-Otterson L**, Feng W, Kirpich I, Wang Y, Qin X, Liu Y, Gobejishvili L, Joshi-Barve S, Ayvaz T, Petrosino J, Kong M, Barker D, McClain C, Barve S. Metagenomic analyses of alcohol induced pathogenic alterations in the intestinal microbiome and the effect of Lactobacillus rhamnosus GG treatment. *PLoS One* 2013; **8**: e53028 [PMID: 23326376 DOI: 10.1371/journal.pone.0053028]
41 **Tuomisto S**, Pessi T, Collin P, Vuento R, Aittoniemi J, Karhunen PJ. Changes in gut bacterial populations and their translocation into liver and ascites in alcoholic liver cirrhotics. *BMC Gastroenterol* 2014; **14**: 40 [PMID: 24564202 DOI: 10.1186/1471-230X-14-40]
42 **Bluemel S**, Williams B, Knight R, Schnabl B. Precision medicine in alcoholic and nonalcoholic fatty liver disease *via* modulating the gut microbiota. *Am J Physiol Gastrointest Liver Physiol* 2016; **311**: G1018-G1036 [PMID: 27686615 DOI: 10.1152/ajpgi.00245.2016]
43 **Davis BC**, Bajaj JS. The Human Gut Microbiome in Liver Diseases. *Semin Liver Dis* 2017; **37**: 128-140 [PMID: 28564721 DOI: 10.1055/s-0037-1602763]
44 **Kakiyama G**, Hylemon PB, Zhou H, Pandak WM, Heuman DM, Kang DJ, Takei H, Nittono H, Ridlon JM, Fuchs M, Gurley EC, Wang Y, Liu R, Sanyal AJ, Gillevet PM, Bajaj JS. Colonic inflammation and secondary bile acids in alcoholic cirrhosis. *Am J Physiol Gastrointest Liver Physiol* 2014; **306**: G929-G937 [PMID: 24699327 DOI: 10.1152/ajpgi.00315.2013]
45 **Kirpich IA**, Solovieva NV, Leikhter SN, Shidakova NA, Lebedeva OV, Sidorov PI, Bazhukova TA, Soloviev AG, Barve SS, McClain CJ, Cave M. Probiotics restore bowel flora and improve liver enzymes in human alcohol-induced liver injury: a pilot study. *Alcohol* 2008; **42**: 675-682 [PMID: 19038698 DOI: 10.1016/j.alcohol.2008.08.006]
46 **Leclercq S**, Matamoros S, Cani PD, Neyrinck AM, Jamar F, Stärkel P, Windey K, Tremaroli V, Bäckhed F, Verbeke K, de Timary P, Delzenne NM. Intestinal permeability, gut-bacterial dysbiosis, and behavioral markers of alcohol-dependence severity. *Proc Natl Acad Sci USA* 2014; **111**: E4485-E4493 [PMID: 25288760 DOI: 10.1073/pnas.1415174111]
47 **Bode C**, Kolepke R, Schäfer K, Bode JC. Breath hydrogen excretion in patients with alcoholic liver disease--evidence of small intestinal bacterial overgrowth. *Z Gastroenterol* 1993; **31**: 3-7 [PMID: 8447153]
48 **Hauge T**, Persson J, Danielsson D. Mucosal bacterial growth in the upper gastrointestinal tract in alcoholics (heavy drinkers). *Digestion* 1997; **58**: 591-595 [PMID: 9438608 DOI: 10.1159/000201507]
49 **Morencos FC**, de las Heras Castaño G, Martín Ramos L, López Arias MJ, Ledesma F, Pons Romero F. Small bowel bacterial overgrowth in patients with alcoholic cirrhosis. *Dig Dis Sci* 1995; **40**: 1252-1256 [PMID: 7781442 DOI: 10.1007/BF02065533]
50 **Parlesak A**, Schäfer C, Schütz T, Bode JC, Bode C. Increased intestinal permeability to macromolecules and endotoxemia in patients with chronic alcohol abuse in different stages of alcohol-induced liver disease. *J Hepatol* 2000; **32**: 742-747 [PMID: 10845660 DOI: 10.1016/s0168-8278(00)80242-1]
51 **Szabo G**. Gut-liver axis in alcoholic liver disease. *Gastroenterology* 2015; **148**: 30-36 [PMID: 25447847 DOI: 10.1053/j.gastro.2014.10.042]
52 **Mutlu EA**, Gillevet PM, Rangwala H, Sikaroodi M, Naqvi A, Engen PA, Kwasny M, Lau CK, Keshavarzian A. Colonic microbiome is altered in alcoholism. *Am J Physiol Gastrointest Liver Physiol* 2012; **302**: G966-G978 [PMID: 22241860 DOI: 10.1152/ajpgi.00380.2011]
53 **Yan AW**, Fouts DE, Brandl J, Stärkel P, Torralba M, Schott E, Tsukamoto H, Nelson KE, Brenner DA, Schnabl B. Enteric dysbiosis associated with a mouse model of alcoholic liver disease. *Hepatology* 2011; **53**: 96-105 [PMID: 21254165 DOI: 10.1002/hep.24018]
54 **Llopis M**, Cassard AM, Wrzosek L, Boschat L, Bruneau A, Ferrere G, Puchois V, Martin JC, Lepage P, Le Roy T, Lefèvre L, Langelier B, Cailleux F, González-Castro AM, Rabot S, Gaudin F, Agostini H, Prévot S, Berrebi D, Ciocan D, Jousse C, Naveau S, Gérard P, Perlemuter G. Intestinal microbiota contributes to individual susceptibility to alcoholic liver disease. *Gut* 2016; **65**: 830-839 [PMID: 26642859 DOI: 10.1136/gutjnl-2015-310585]
55 **Chen P**, Torralba M, Tan J, Embree M, Zengler K, Stärkel P, van Pijkeren JP, DePew J, Loomba R, Ho SB, Bajaj JS, Mutlu EA, Keshavarzian A, Tsukamoto H, Nelson KE, Fouts DE, Schnabl B. Supplementation of saturated long-chain fatty acids maintains intestinal eubiosis and reduces ethanol-induced liver injury in mice. *Gastroenterology* 2015; **148**: 203-214.e16 [PMID: 25239591 DOI: 10.1053/j.gastro.2014.09.014]
56 **Cresci GA**, Glueck B, McMullen MR, Xin W, Allende D, Nagy LE. Prophylactic tributyrin treatment mitigates chronic-binge ethanol-induced intestinal barrier and liver injury. *J Gastroenterol Hepatol* 2017; **32**: 1587-1597 [PMID: 28087985 DOI: 10.1111/jgh.13731]
57 **Tang R**, Wei Y, Li Y, Chen W, Chen H, Wang Q, Yang F, Miao Q, Xiao X, Zhang H, Lian M, Jiang X, Zhang J, Cao Q, Fan Z, Wu M, Qiu D, Fang JY, Ansari A, Gershwin ME, Ma X. Gut microbial profile is altered in primary biliary cholangitis and partially restored after UDCA therapy. *Gut* 2018; **67**: 534-541 [PMID: 28213609 DOI: 10.1136/gutjnl-2016-313332]
58 **Lv LX**, Fang DQ, Shi D, Chen DY, Yan R, Zhu YX, Chen YF, Shao L, Guo FF, Wu WR, Li A, Shi HY, Jiang XW, Jiang HY, Xiao YH, Zheng SS, Li LJ. Alterations and correlations of the gut microbiome, metabolism and immunity in patients with primary biliary cirrhosis. *Environ Microbiol*

2016; **18**: 2272-2286 [PMID: 27243236 DOI: 10.1111/1462-2920.13401]

59 **Chen W**, Wei Y, Xiong A, Li Y, Guan H, Wang Q, Miao Q, Bian Z, Xiao X, Lian M, Zhang J, Li B, Cao Q, Fan Z, Zhang W, Qiu D, Fang J, Gershwin ME, Yang L, Tang R, Ma X. Comprehensive Analysis of Serum and Fecal Bile Acid Profiles and Interaction with Gut Microbiota in Primary Biliary Cholangitis. *Clin Rev Allergy Immunol* 2020; **58**: 25-38 [PMID: 30900136 DOI: 10.1007/s12016-019-08731-2]

60 **Furukawa M**, Moriya K, Nakayama J, Inoue T, Momoda R, Kawaratani H, Namisaki T, Sato S, Douhara A, Kaji K, Kitade M, Shimozato N, Sawada Y, Saikawa S, Takaya H, Kitagawa K, Akahane T, Mitoro A, Yamao J, Tanaka Y, Yoshiji H. Gut dysbiosis associated with clinical prognosis of patients with primary biliary cholangitis. *Hepatol Res* 2020; **50**: 840-852 [PMID: 32346970 DOI: 10.1111/hepr.13509]

61 **Karlsen TH**. Primary sclerosing cholangitis: 50 years of a gut-liver relationship and still no love? *Gut* 2016; **65**: 1579-1581 [PMID: 27402486 DOI: 10.1136/gutjnl-2016-312137]

62 **Lemoinne S**, Kemgang A, Ben Belkacem K, Straube M, Jegou S, Corpechot C; Saint-Antoine IBD Network, Chazouillères O, Housset C, Sokol H. Fungi participate in the dysbiosis of gut microbiota in patients with primary sclerosing cholangitis. *Gut* 2020; **69**: 92-102 [PMID: 31003979 DOI: 10.1136/gutjnl-2018-317791]

63 **Kummen M**, Holm K, Anmarkrud JA, Nygård S, Vesterhus M, Høivik ML, Trøseid M, Marschall HU, Schrumpf E, Moum B, Røsjø H, Aukrust P, Karlsen TH, Hov JR. The gut microbial profile in patients with primary sclerosing cholangitis is distinct from patients with ulcerative colitis without biliary disease and healthy controls. *Gut* 2017; **66**: 611-619 [PMID: 26887816 DOI: 10.1136/gutjnl-2015-310500]

64 **Bajer L**, Kverka M, Kostovcik M, Macinga P, Dvorak J, Stehlikova Z, Brezina J, Wohl P, Spicak J, Drastich P. Distinct gut microbiota profiles in patients with primary sclerosing cholangitis and ulcerative colitis. *World J Gastroenterol* 2017; **23**: 4548-4558 [PMID: 28740343 DOI: 10.3748/wjg.v23.i25.4548]

65 **Sabino J**, Vieira-Silva S, Machiels K, Joossens M, Falony G, Ballet V, Ferrante M, Van Assche G, Van der Merwe S, Vermeire S, Raes J. Primary sclerosing cholangitis is characterised by intestinal dysbiosis independent from IBD. *Gut* 2016; **65**: 1681-1689 [PMID: 27207975 DOI: 10.1136/gutjnl-2015-311004]

66 **Torres J**, Bao X, Goel A, Colombel JF, Pekow J, Jabri B, Williams KM, Castillo A, Odin JA, Meckel K, Fasihuddin F, Peter I, Itzkowitz S, Hu J. The features of mucosa-associated microbiota in primary sclerosing cholangitis. *Aliment Pharmacol Ther* 2016; **43**: 790-801 [PMID: 26857969 DOI: 10.1111/apt.13552]

67 **Rossen NG**, Fuentes S, Boonstra K, D'Haens GR, Heilig HG, Zoetendal EG, de Vos WM, Ponsioen CY. The mucosa-associated microbiota of PSC patients is characterized by low diversity and low abundance of uncultured Clostridiales II. *J Crohns Colitis* 2015; **9**: 342-348 [PMID: 25547975 DOI: 10.1093/ecco-jcc/jju023]

68 **Tabibian JH**, Talwalkar JA, Lindor KD. Role of the microbiota and antibiotics in primary sclerosing cholangitis. *Biomed Res Int* 2013; **2013**: 389537 [PMID: 24232746 DOI: 10.1155/2013/389537]

69 **Mattner J**. Impact of Microbes on the Pathogenesis of Primary Biliary Cirrhosis (PBC) and Primary Sclerosing Cholangitis (PSC). *Int J Mol Sci* 2016; **17**: 1864 [PMID: 27834858 DOI: 10.3390/ijms17111864]

70 **Liu Q**, Li F, Zhuang Y, Xu J, Wang J, Mao X, Zhang Y, Liu X. Alteration in gut microbiota associated with hepatitis B and non-hepatitis virus related hepatocellular carcinoma. *Gut Pathog* 2019; **11**: 1 [PMID: 30675188 DOI: 10.1186/s13099-018-0281-6]

71 **Deng YD**, Peng XB, Zhao RR, Ma CQ, Li JN, Yao LQ. The intestinal microbial community dissimilarity in hepatitis B virus-related liver cirrhosis patients with and without at alcohol consumption. *Gut Pathog* 2019; **11**: 58 [PMID: 31788031 DOI: 10.1186/s13099-019-0337-2]

72 **Yun Y**, Chang Y, Kim HN, Ryu S, Kwon MJ, Cho YK, Kim HL, Cheong HS, Joo EJ. Alterations of the Gut Microbiome in Chronic Hepatitis B Virus Infection Associated with Alanine Aminotransferase Level. *J Clin Med* 2019; **8**: 173 [PMID: 30717396 DOI: 10.3390/jcm8020173]

73 **Hamer HM**, Jonkers D, Venema K, Vanhoutvin S, Troost FJ, Brummer RJ. Review article: the role of butyrate on colonic function. *Aliment Pharmacol Ther* 2008; **27**: 104-119 [PMID: 17973645 DOI: 10.1111/j.1365-2036.2007.03562.x]

74 **Ren Z**, Li A, Jiang J, Zhou L, Yu Z, Lu H, Xie H, Chen X, Shao L, Zhang R, Xu S, Zhang H, Cui G, Sun R, Wen H, Lerut JP, Kan Q, Li L, Zheng S. Gut microbiome analysis as a tool towards targeted non-invasive biomarkers for early hepatocellular carcinoma. *Gut* 2019; **68**: 1014-1023 [PMID: 30045880 DOI: 10.1136/gutjnl-2017-315084]

75 **Chen Y**, Yang F, Lu H, Wang B, Chen Y, Lei D, Wang Y, Zhu B, Li L. Characterization of fecal microbial communities in patients with liver cirrhosis. *Hepatology* 2011; **54**: 562-572 [PMID: 21574172 DOI: 10.1002/hep.24423]

76 **Wei X**, Yan X, Zou D, Yang Z, Wang X, Liu W, Wang S, Li X, Han J, Huang L, Yuan J. Abnormal fecal microbiota community and functions in patients with hepatitis B liver cirrhosis as revealed by a metagenomic approach. *BMC Gastroenterol* 2013; **13**: 175 [PMID: 24369878 DOI: 10.1186/1471-230X-13-175]

77 **Tsai KN**, Kuo CF, Ou JJ. Mechanisms of Hepatitis B Virus Persistence. *Trends Microbiol* 2018; **26**: 33-42 [PMID: 28823759 DOI: 10.1016/j.tim.2017.07.006]

78 **Betrapally NS**, Gillevet PM, Bajaj JS. Gut microbiome and liver disease. *Transl Res* 2017; **179**: 49-59 [PMID: 27477080 DOI: 10.1016/j.trsl.2016.07.005]

79 **Zhao Y**, Mao YF, Tang YS, Ni MZ, Liu QH, Wang Y, Feng Q, Peng JH, Hu YY. Altered oral microbiota in chronic hepatitis B patients with different tongue coatings. *World J Gastroenterol* 2018; **24**: 3448-3461 [PMID: 30122883 DOI: 10.3748/wjg.v24.i30.3448]

80 **Kanmani P**, Suganya K, Kim H. The Gut Microbiota: How Does It Influence the Development and Progression of Liver Diseases. *Biomedicines* 2020; **8**: 501 [PMID: 33207562 DOI: 10.3390/biomedicines8110501]

81 **Voukelatou P**, Vrettos I, Kalliakmanis A. Neurologic symptoms as the only manifestation of B_{12} deficiency in a young patient with normal hematocrit, MCV, peripheral blood smear and homocysteine levels. *Oxf Med Case Reports* 2016; **2016**: omw091 [PMID: 28031855 DOI: 10.1093/omcr/omw091]

82 **Wang WW**, Zhang Y, Huang XB, You N, Zheng L, Li J. Fecal microbiota transplantation prevents hepatic encephalopathy in rats with carbon tetrachloride-induced acute hepatic dysfunction. *World J Gastroenterol* 2017; **23**: 6983-6994 [PMID: 29097871 DOI: 10.3748/wjg.v23.i38.6983]

83 **Fasano A**. Intestinal permeability and its regulation by zonulin: diagnostic and therapeutic implications. *Clin Gastroenterol Hepatol* 2012; **10**: 1096-1100 [PMID: 22902773 DOI: 10.1016/j.cgh.2012.08.012]

84 **Heidrich B**, Steinmann E, Plumeier I, Kirschner J, Sollik L, Ziegert S, Engelmann M, Lehmann P, Manns MP, Pieper DH, Wedemeyer H. Frequent detection of HCV RNA and HCVcoreAg in stool of patients with chronic hepatitis C. *J Clin Virol* 2016; **80**: 1-7 [PMID: 27128354 DOI: 10.1016/j.jcv.2016.04.006]

85 **Kandasamy S**, Vlasova AN, Fischer D, Kumar A, Chattha KS, Rauf A, Shao L, Langel SN, Rajashekara G, Saif LJ. Differential Effects of Escherichia coli Nissle and Lactobacillus rhamnosus Strain GG on Human Rotavirus Binding, Infection, and B Cell Immunity. *J Immunol* 2016; **196**: 1780-1789 [PMID: 26800875 DOI: 10.4049/jimmunol.1501705]

86 **Heidrich B**, Vital M, Plumeier I, Döscher N, Kahl S, Kirschner J, Ziegert S, Solbach P, Lenzen H, Potthoff A, Manns MP, Wedemeyer H, Pieper DH. Intestinal microbiota in patients with chronic hepatitis C with and without cirrhosis compared with healthy controls. *Liver Int* 2018; **38**: 50-58 [PMID: 28561276 DOI: 10.1111/liv.13485]

87 **Inoue T**, Nakayama J, Moriya K, Kawaratani H, Momoda R, Ito K, Iio E, Nojiri S, Fujiwara K, Yoneda M, Yoshiji H, Tanaka Y. Gut Dysbiosis Associated With Hepatitis C Virus Infection. *Clin Infect Dis* 2018; **67**: 869-877 [PMID: 29718124 DOI: 10.1093/cid/ciy205]

88 **Preveden T**, Scarpellini E, Milić N, Luzza F, Abenavoli L. Gut microbiota changes and chronic hepatitis C virus infection. *Expert Rev Gastroenterol Hepatol* 2017; **11**: 813-819 [PMID: 28621554 DOI: 10.1080/17474124.2017.1343663]

89 **Gevers D**, Kugathasan S, Denson LA, Vázquez-Baeza Y, Van Treuren W, Ren B, Schwager E, Knights D, Song SJ, Yassour M, Morgan XC, Kostic AD, Luo C, González A, McDonald D, Haberman Y, Walters T, Baker S, Rosh J, Stephens M, Heyman M, Markowitz J, Baldassano R, Griffiths A, Sylvester F, Mack D, Kim S, Crandall W, Hyams J, Huttenhower C, Knight R, Xavier RJ. The treatment-naive microbiome in new-onset Crohn's disease. *Cell Host Microbe* 2014; **15**: 382-392 [PMID: 24629344 DOI: 10.1016/j.chom.2014.02.005]

90 **Forslund K**, Hildebrand F, Nielsen T, Falony G, Le Chatelier E, Sunagawa S, Prifti E, Vieira-Silva S, Gudmundsdottir V, Pedersen HK, Arumugam M, Kristiansen K, Voigt AY, Vestergaard H, Hercog R, Costea PI, Kultima JR, Li J, Jørgensen T, Levenez F, Dore J; MetaHIT consortium, Nielsen HB, Brunak S, Raes J, Hansen T, Wang J, Ehrlich SD, Bork P, Pedersen O. Disentangling type 2 diabetes and metformin treatment signatures in the human gut microbiota. *Nature* 2015; **528**: 262-266 [PMID: 26633628 DOI: 10.1038/nature15766]

91 **Ponziani FR**, Putignani L, Paroni Sterbini F, Petito V, Picca A, Del Chierico F, Reddel S, Calvani R, Marzetti E, Sanguinetti M, Gasbarrini A, Pompili M. Influence of hepatitis C virus eradication with direct-acting antivirals on the gut microbiota in patients with cirrhosis. *Aliment Pharmacol Ther* 2018; **48**: 1301-1311 [PMID: 30345704 DOI: 10.1111/apt.15004]

92 **Pérez-Matute P**, Íñiguez M, Villanueva-Millán MJ, Recio-Fernández E, Vázquez AM, Sánchez SC, Morano LE, Oteo JA. Short-term effects of direct-acting antiviral agents on inflammation and gut microbiota in hepatitis C-infected patients. *Eur J Intern Med* 2019; **67**: 47-58 [PMID: 31221551 DOI: 10.1016/j.ejim.2019.06.005]

93 **Cani PD**, de Vos WM. Next-Generation Beneficial Microbes: The Case of *Akkermansia muciniphila* . *Front Microbiol* 2017; **8**: 1765 [PMID: 29018410 DOI: 10.3389/fmicb.2017.01765]

94 **Bajaj JS**, Kassam Z, Fagan A, Gavis EA, Liu E, Cox IJ, Kheradman R, Heuman D, Wang J, Gurry T, Williams R, Sikaroodi M, Fuchs M, Alm E, John B, Thacker LR, Riva A, Smith M, Taylor-Robinson SD, Gillevet PM. Fecal microbiota transplant from a rational stool donor improves hepatic encephalopathy: A randomized clinical trial. *Hepatology* 2017; **66**: 1727-1738 [PMID: 28586116 DOI: 10.1002/hep.29306]

95 **Aly AM**, Adel A, El-Gendy AO, Essam TM, Aziz RK. Gut microbiome alterations in patients with stage 4 hepatitis C. *Gut Pathog* 2016; **8**: 42 [PMID: 27625705 DOI: 10.1186/s13099-016-0124-2]

96 **Kwak DS**, Jun DW, Seo JG, Chung WS, Park SE, Lee KN, Khalid-Saeed W, Lee HL, Lee OY, Yoon BC, Choi HS. Short-term probiotic therapy alleviates small intestinal bacterial overgrowth, but does not improve intestinal permeability in chronic liver disease. *Eur J Gastroenterol Hepatol* 2014; **26**: 1353-1359 [PMID: 25244414 DOI: 10.1097/MEG.0000000000000214]

97 **Bajaj JS**, Hylemon PB, Ridlon JM, Heuman DM, Daita K, White MB, Monteith P, Noble NA, Sikaroodi M, Gillevet PM. Colonic mucosal microbiome differs from stool microbiome in cirrhosis and hepatic encephalopathy and is linked to cognition and inflammation. *Am J Physiol Gastrointest Liver Physiol* 2012; **303**: G675-G685 [PMID: 22821944 DOI: 10.1152/ajpgi.00152.2012]

98 **Santiago A**, Pozuelo M, Poca M, Gely C, Nieto JC, Torras X, Román E, Campos D, Sarrabayrouse G, Vidal S, Alvarado-Tapias E, Guarner F, Soriano G, Manichanh C, Guarner C. Alteration of the serum microbiome composition in cirrhotic patients with ascites. *Sci Rep* 2016; **6**: 25001 [PMID: 27112233 DOI: 10.1038/srep25001]

99 **Bajaj JS**, Betrapally NS, Hylemon PB, Heuman DM, Daita K, White MB, Unser A, Thacker LR, Sanyal AJ, Kang DJ, Sikaroodi M, Gillevet PM. Salivary microbiota reflects changes in gut microbiota in cirrhosis with hepatic encephalopathy. *Hepatology* 2015; **62**: 1260-1271 [PMID: 25820757 DOI: 10.1002/hep.27819]

100 **Bajaj JS**, Vargas HE, Reddy KR, Lai JC, O'Leary JG, Tandon P, Wong F, Mitrani R, White MB, Kelly M, Fagan A, Patil R, Sait S, Sikaroodi M, Thacker LR, Gillevet PM. Association Between Intestinal Microbiota Collected at Hospital Admission and Outcomes of Patients With Cirrhosis. *Clin Gastroenterol Hepatol* 2019; **17**: 756-765 [PMID: 30036646 DOI: 10.1016/j.cgh.2018.07.022]

101 **Oh TG**, Kim SM, Caussy C, Fu T, Guo J, Bassirian S, Singh S, Madamba EV, Bettencourt R, Richards L, Yu RT, Atkins AR, Huan T, Brenner DA, Sirlin CB, Downes M, Evans RM, Loomba R. A Universal Gut-Microbiome-Derived Signature Predicts Cirrhosis. *Cell Metab* 2020; **32**: 901 [PMID: 33147487 DOI: 10.1016/j.cmet.2020.10.015]

102 **Dapito DH**, Mencin A, Gwak GY, Pradere JP, Jang MK, Mederacke I, Caviglia JM, Khiabanian H, Adeyemi A, Bataller R, Lefkowitch JH, Bower M, Friedman R, Sartor RB, Rabadan R, Schwabe RF. Promotion of hepatocellular carcinoma by the intestinal microbiota and TLR4. *Cancer Cell* 2012; **21**: 504-516 [PMID: 22516259 DOI: 10.1016/j.ccr.2012.02.007]

103 **Tripathi A**, Debelius J, Brenner DA, Karin M, Loomba R, Schnabl B, Knight R. The gut-liver axis and the intersection with the microbiome. *Nat Rev Gastroenterol Hepatol* 2018; **15**: 397-411 [PMID: 29748586 DOI: 10.1038/s41575-018-0011-z]

104 **Sheng L**, Jena PK, Hu Y, Liu HX, Nagar N, Kalanetra KM, French SW, Mills DA, Wan YY. Hepatic inflammation caused by dysregulated bile acid synthesis is reversible by butyrate supplementation. *J Pathol* 2017; **243**: 431-441 [PMID: 28892150 DOI: 10.1002/path.4983]

105 **Krüttgen A**, Horz HP, Weber-Heynemann J, Vucur M, Trautwein C, Haase G, Luedde T, Roderburg C. Study on the association of Helicobacter species with viral hepatitis-induced hepatocellular carcinoma. *Gut Microbes* 2012; **3**: 228-233 [PMID: 22572832 DOI: 10.4161/gmic.19922]

106 **Routy B**, Le Chatelier E, Derosa L, Duong CPM, Alou MT, Daillère R, Fluckiger A, Messaoudene M, Rauber C, Roberti MP, Fidelle M, Flament C, Poirier-Colame V, Opolon P, Klein C, Iribarren K, Mondragón L, Jacquelot N, Qu B, Ferrere G, Clémenson C, Mezquita L, Masip JR, Naltet C, Brosseau S, Kaderbhai C, Richard C, Rizvi H, Levenez F, Galleron N, Quinquis B, Pons N, Ryffel B, Minard-Colin V, Gonin P, Soria JC, Deutsch E, Loriot Y, Ghiringhelli F, Zalcman G, Goldwasser F, Escudier B, Hellmann MD, Eggermont A, Raoult D, Albiges L, Kroemer G, Zitvogel L. Gut microbiome influences efficacy of PD-1-based immunotherapy against epithelial tumors. *Science* 2018; **359**: 91-97 [PMID: 29097494 DOI: 10.1126/science.aan3706]

107 **Russo E**, Nannini G, Dinu M, Pagliai G, Sofi F, Amedei A. Exploring the food-gut axis in immunotherapy response of cancer patients. *World J Gastroenterol* 2020; **26**: 4919-4932 [PMID: 32952339 DOI: 10.3748/wjg.v26.i33.4919]

108 **Yang XA**, Lv F, Wang R, Chang Y, Zhao Y, Cui X, Li H, Yang S, Li S, Zhao X, Mo Z, Yang F. Potential role of intestinal microflora in disease progression among patients with different stages of Hepatitis B. *Gut Pathog* 2020; **12**: 50 [PMID: 33117435 DOI: 10.1186/s13099-020-00391-4]

109 **David LA**, Maurice CF, Carmody RN, Gootenberg DB, Button JE, Wolfe BE, Ling AV, Devlin AS, Varma Y, Fischbach MA, Biddinger SB, Dutton RJ, Turnbaugh PJ. Diet rapidly and reproducibly alters the human gut microbiome. *Nature* 2014; **505**: 559-563 [PMID: 24336217 DOI: 10.1038/nature12820]

110 **Ren YD**, Ye ZS, Yang LZ, Jin LX, Wei WJ, Deng YY, Chen XX, Xiao CX, Yu XF, Xu HZ, Xu LZ, Tang YN, Zhou F, Wang XL, Chen MY, Chen LG, Hong MZ, Ren JL, Pan JS. Fecal microbiota transplantation induces hepatitis B virus e-antigen (HBeAg) clearance in patients with positive HBeAg after long-term antiviral therapy. *Hepatology* 2017; **65**: 1765-1768 [PMID: 28027582 DOI: 10.1002/hep.29008]

111 **Dhiman RK**, Rana B, Agrawal S, Garg A, Chopra M, Thumburu KK, Khattri A, Malhotra S, Duseja A, Chawla YK. Probiotic VSL#3 reduces liver disease severity and hospitalization in patients with cirrhosis: a randomized, controlled trial. *Gastroenterology* 2014; **147**: 1327-1337 [PMID: 25450083 DOI: 10.1053/j.gastro.2014.08.031]

112 **Dore GJ**, Ward J, Thursz M. Hepatitis C disease burden and strategies to manage the burden (Guest Editors Mark Thursz, Gregory Dore and John Ward). *J Viral Hepat* 2014; **21** Suppl 1: 1-4 [PMID: 24713003 DOI: 10.1111/jvh.12253]

113 **Doskali M**, Tanaka Y, Ohira M, Ishiyama K, Tashiro H, Chayama K, Ohdan H. Possibility of adoptive immunotherapy with peripheral blood-derived $CD3^{-}CD56+$ and CD3+CD56+ cells for inducing antihepatocellular carcinoma and antihepatitis C virus activity. *J Immunother* 2011; **34**: 129-138 [PMID: 21304407 DOI: 10.1097/CJI.0b013e3182048c4e]

World Journal of Gastroenterology

Submit a Manuscript: https://www.f6publishing.com

World J Gastroenterol 2021 September 7; 27(33): 5502-5519

DOI: 10.3748/wjg.v27.i33.5502

ISSN 1007-9327 (print) ISSN 2219-2840 (online)

REVIEW

Clinical perspectives, assessment, and mechanisms of metabolic-associated fatty liver disease in patients with COVID-19

Alejandro Campos-Murguía, Berenice M Román-Calleja, José A González-Regueiro, Ivonne Hurtado-Díaz-de-León, Alberto Adrián Solís-Ortega, Nayelli C Flores-García, Ignacio García-Juárez, Astrid Ruiz-Margáin, Ricardo Ulises Macías-Rodríguez

ORCID number: Alejandro Campos-Murguía 0000-0002-2178-302X; Berenice M Román-Calleja 0000-0001-7624-9679; José A González-Regueiro 0000-0001-5211-4710; Ivonne Hurtado-Díaz-de-León 0000-0001-7300-2072; Alberto Adrián Solís-Ortega 0000-0003-2715-503X; Nayelli C Flores-García 0000-0003-3930-2682; Ignacio García-Juárez 0000-0003-2400-1887; Astrid Ruiz-Margáin 0000-0003-2779-8641; Ricardo Ulises Macías-Rodríguez 0000-0002-7637-4477.

Author contributions: Campos-Murguía A and Román-Calleja BM contributed equally to this article; Ruiz-Margáin A and Macías-Rodríguez RU contributed equally to the study conception and design; All authors contributed to acquisition of data, analysis of data, interpretation of data, drafting the article, making critical revisions for the content of the manuscript, writing and approving the final version of the article to be published.

Conflict-of-interest statement: The authors declare that they have no conflicting interests.

Open-Access: This article is an open-access article that was selected by an in-house editor and fully peer-reviewed by external

Alejandro Campos-Murguía, Berenice M Román-Calleja, José A González-Regueiro, Ivonne Hurtado-Díaz-de-León, Alberto Adrián Solís-Ortega, Nayelli C Flores-García, Ignacio García-Juárez, Astrid Ruiz-Margáin, Ricardo Ulises Macías-Rodríguez, Department of Gastroenterology, Instituto Nacional de Ciencias Médicas y Nutrición Salvador Zubirán, Mexico City 14080, Mexico

Astrid Ruiz-Margáin, Ricardo Ulises Macías-Rodríguez, Liver Fibrosis and Nutrition Lab (LFN-Lab), MICTLÁN-Network (Mechanisms of Liver Injury, Cell Death and Translational Nutrition in Liver Diseases- Research Network), Mexico City 14080, Mexico

Corresponding author: Ricardo Ulises Macías-Rodríguez, MD, MSc, PhD, Assistant Professor, Department of Gastroenterology, Instituto Nacional de Ciencias Médicas y Nutrición Salvador Zubirán, Vasco de Quiroga 15, Col. Belisario Domínguez Sección XVI, Mexico City 14080, Mexico. ricardomacro@yahoo.com.mx

Abstract

Metabolic diseases are highly prevalent worldwide and have been associated with adverse clinical outcomes, including mortality, in patients developing coronavirus disease (COVID-19). Because of the close relationship between metabolic diseases such as type 2 diabetes mellitus and obesity and the presence of metabolic-associated fatty liver disease (MAFLD), a high number of cases of patients affected by both MAFLD and COVID-19 would be expected, especially in high-risk populations. Some studies have shown an increased risk of adverse clinical outcomes, viral shedding, and deep vein thrombosis, especially in patients with MAFLD- related liver fibrosis. The predisposition to poor outcomes and severe acute respiratory syndrome coronavirus 2 infection in patients with MAFLD could be secondary to mechanisms common to both, including preexisting systemic chronic inflammation, endothelial dysfunction, and involvement of the renin-angiotensin system. Because of the increased risk of adverse outcomes, MAFLD should be screened in all patients admitted for COVID-19. Available computed tomography scans could be of help, assessment of liver fibrosis is also recommended, favoring noninvasive methods to limit the exposure of healthcare workers. Liver involvement in this population ranges from abnormalities in liver chemistry to hepatic steatosis in postmortem biopsies. Finally, preventive measures should be strongly advocated in patients already known to have MAFLD, including the use of telemedicine and vaccination in addition to general

reviewers. It is distributed in accordance with the Creative Commons Attribution NonCommercial (CC BY-NC 4.0) license, which permits others to distribute, remix, adapt, build upon this work non-commercially, and license their derivative works on different terms, provided the original work is properly cited and the use is non-commercial. See: http://creativecommons.org/Licenses/by-nc/4.0/

Manuscript source: Invited manuscript

Specialty type: Gastroenterology and hepatology

Country/Territory of origin: Mexico

Peer-review report's scientific quality classification

Grade A (Excellent): 0
Grade B (Very good): B
Grade C (Good): C
Grade D (Fair): 0
Grade E (Poor): 0

Received: January 28, 2021
Peer-review started: January 28, 2021
First decision: May 2, 2021
Revised: May 17, 2021
Accepted: August 5, 2021
Article in press: August 5, 2021
Published online: September 7, 2021

P-Reviewer: Du Y, Tuo BG
S-Editor: Ma YJ
L-Editor: Filipodia
P-Editor: Xing YX

measures.

Key Words: Metabolic-associated fatty liver disease; COVID-19; Mortality; Fibrosis; Histology; Epidemiology

©The Author(s) 2021. Published by Baishideng Publishing Group Inc. All rights reserved.

Core Tip: The coronavirus disease 2019 (COVID-19) pandemic arrived amid a population increasingly affected by metabolic diseases such as type 2 diabetes mellitus and metabolic-associated fatty liver disease (MAFLD). Patients with MAFLD can have chronic inflammation, endothelial dysfunction, and increased expression of angiotensin-converting enzyme 2 receptor, which could synergize with severe acute respiratory syndrome coronavirus 2 pathophysiology, predisposing to a greater risk of adverse outcomes. Interestingly a high prevalence of liver steatosis in postmortem samples of patients who had COVID-19 has been found. Moreover, the presence of liver fibrosis has been shown to worsen prognosis in those patients. As a result, all patients with COVID-19 should be assessed for the presence of these comorbidities and closely follow-up.

Citation: Campos-Murguía A, Román-Calleja BM, González-Regueiro JA, Hurtado-Díaz-de-León I, Solís-Ortega AA, Flores-García NC, García-Juárez I, Ruiz-Margáin A, Macías-Rodríguez RU. Clinical perspectives, assessment, and mechanisms of metabolic-associated fatty liver disease in patients with COVID-19. *World J Gastroenterol* 2021; 27(33): 5502-5519
URL: https://www.wjgnet.com/1007-9327/full/v27/i33/5502.htm
DOI: https://dx.doi.org/10.3748/wjg.v27.i33.5502

INTRODUCTION

In late 2019, a new coronavirus disease 2019 (COVID-19) caused by severe acute respiratory syndrome coronavirus 2 (SARS-CoV-2) was first described in Wuhan, China[1], and has since spread to the rest of the world[2]. The dimension of this pandemic can be partly explained by the higher level of transmissibility of SARS-CoV-2 and a higher number of asymptomatic carriers, compared with other viruses such as Middle East Respiratory Syndrome (MERS) and SARS-CoV[3]. SARS-CoV-2 belongs to the beta-coronavirus family, and together with MERS and SARS-CoV virus, has been responsible for a high fatality rate during outbreaks[4].

The clinical manifestations of SARS-CoV-2 infection are extensive, ranging from asymptomatic disease, mild respiratory symptoms, to severe disease that may require mechanical ventilation because of severe acute respiratory syndrome, with a high risk of death. Most patients dying from COVID-19 are clustered by the presence of risk factors including older age, obesity, and chronic and metabolic diseases[5-8]. Among the risk factors, highly prevalent metabolic diseases such as type 2 diabetes mellitus (T2DM), hypertension, and obesity, are of utmost importance, being associated with a more severe clinical course that includes the need for intubation, and death[9]. Nonalcoholic fatty liver disease (NAFLD), recently renamed as metabolic-associated fatty liver disease (MAFLD), is strongly related to metabolic comorbidities and insulin resistance. It is regarded as the hepatic manifestation of metabolic syndrome[10,11]. The most important predictor of liver and non-liver-related outcomes in patients with MAFLD is the presence of liver fibrosis[12]. The association between metabolic risk factors such as obesity and diabetes, and MAFLD, means that the probability of facing patients with MAFLD and COVID-19 is high. Therefore, understanding the possible mechanisms of synergism between these entities, epidemiology, risk factors, clinical assessment, and prevention is of great clinical relevance. This review addresses these topics, focusing on proposing ways to identify and manage MAFLD in patients with COVID-19.

EPIDEMIOLOGY OF MAFLD

MAFLD is the most prevalent chronic liver disease worldwide, found in 10%-30% of the general population. The prevalence varies across countries and at the same time it varies among different regions from the same country[13]. Several factors can explain the variability in the prevalence of MAFLD, including age, sex, genetic factors such as the PNPL3 allele, environmental factors such as the typical western diet and sedentary lifestyle, access to health care, and the diagnostic methods used in epidemiological studies, especially with its recent re-classification[13-15].

EPIDEMIOLOGY OF SARS-COV-2 INFECTION

As of July 29, 2021 the World Health Organization reported more than 195 million confirmed cases of COVID-19 infection worldwide, with a death toll of more than 4 million[16]. United States is the country with the most confirmed cases, followed by India, Brazil, Russia, and France, and the United Kingdom. The countries with the highest mortality are the United States, Brazil, India, Mexico, and Italy. Interestingly the fatality rate is considerably higher in countries like Mexico, Iran, and Peru. The disparity in mortality could have several explanations including population characteristics (*e.g.*, sex, age, presence of comorbidities, and genetic factors), time since the initial outbreak, outbreak management, quality of the healthcare system, and the number of testing and treatment options, including the availability of mechanical ventilation[17].

Figure 1 shows the ten countries with the most COVID-19 cases and the prevalence of NAFLD reported by each country[13,18-21]. It its noteworthy that of the ten countries five have a prevalence of NAFLD > 30%, four between 20% and 29.9%, and only one country has a prevalence < 10%. Figure 2 shows the countries with the highest case fatality rate, which refers to the proportion of deaths in the population diagnosed with the disease. The rate is disproportionally higher in Mexico, and once more, five of the countries have a prevalence of NAFLD > 30% and three have a prevalence between 20% and 29.9%. Although this is not a causal explanation, it is certainly an interesting association. Finally, Figure 3 shows the number of deaths adjusted for every 100,000 habitants in order to standardize the comparison. Two countries have rates > 30% and four have rates between 20% and 29.9% while the rest have rates between 10% and 19.9%.

PROPOSED MECHANISMS OF LIVER INJURY IN PATIENTS WITH MAFLD AND SARS-COV-2 INFECTION

Multiple factors in MAFLD contribute to liver damage and progression of the disease, beyond insulin resistance and oxidative stress alone, as was previously thought[22]. In general, three mechanisms are associated with a higher risk of adverse outcomes in patients with MAFLD who develop COVID-19. The relationship stems from the fact that MAFLD is a part of the metabolic syndrome, and shares the following characteristics: (1) A preexisting systemic inflammatory milieu (*i.e.* systemic chronic inflammation and insulin resistance); (2) Endothelial dysfunction; and (3) Differential regulation of the renin-angiotensin-aldosterone system (RAAS)[23-29].

Long-term inflammation is a common denominator in chronic metabolic diseases, including MAFLD[30]. Obese patients express 2.5-fold more tumor necrosis factor (TNF)-α in fat tissue compared with lean controls, and weight loss is accompanied by a decrease in TNF-α mRNA expression[31]. Contrary to the belief that patients with simple steatosis do not have inflammation, some studies have shown otherwise. In murine models, it has been shown that liver steatosis leads to inflammation through NF-kB activation and downstream cytokine production[32]. Patients with both NAFLD and nonalcoholic steatohepatitis (NASH) have significantly higher serum levels of IL-6 and CRP compared with healthy controls, where inflammation levels are similar in both stages[33,34]. Also CCL2/MCP-1, which regulates migration and infiltration of monocytes/macrophages was found to be increased in both NAFLD and NASH patients[33]. The studies reported that patients with NAFLD were characterized by low-grade systemic inflammation; furthermore, compared with healthy individuals, the presence of advanced liver fibrosis was accompanied by significantly higher markers of systemic circulatory dysfunction and higher levels of proinflam-

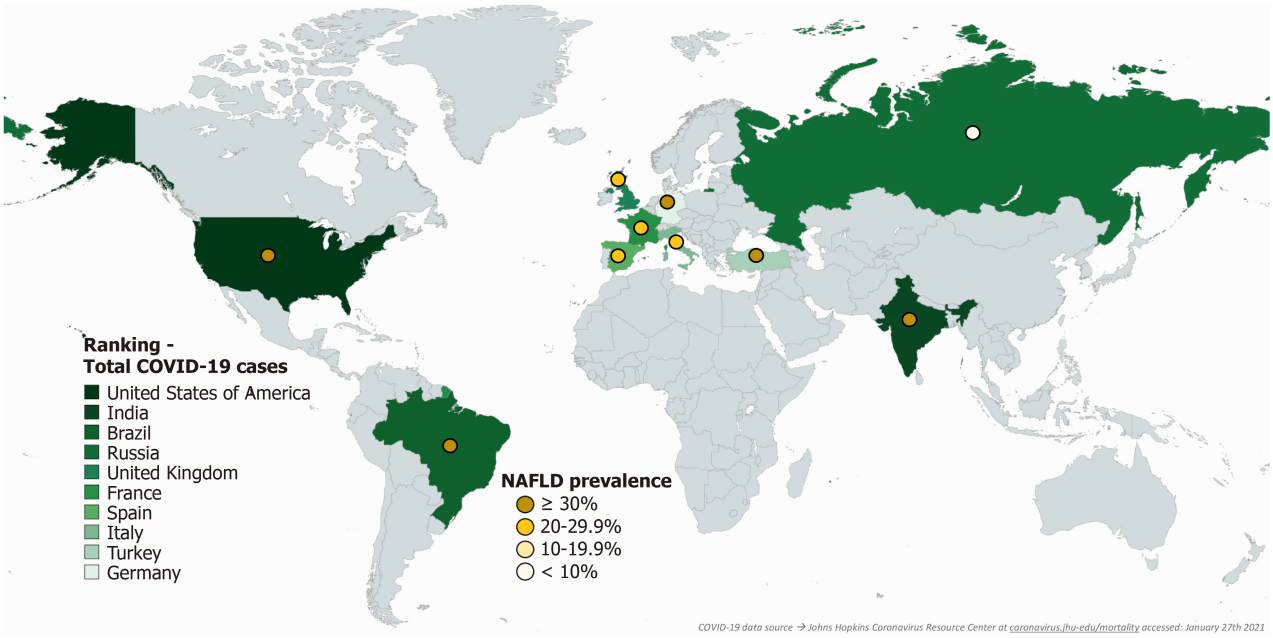


Figure 1 Total coronavirus disease 2019 cases and nonalcoholic fatty liver disease prevalence. United States of America 25439570, India 10689527, Brazil 8933356, Russia 3716228, United Kingdom 3700268, France 3138498, Spain 2629817, Italy 2485956, Turkey 2442350, Germany 2164043.

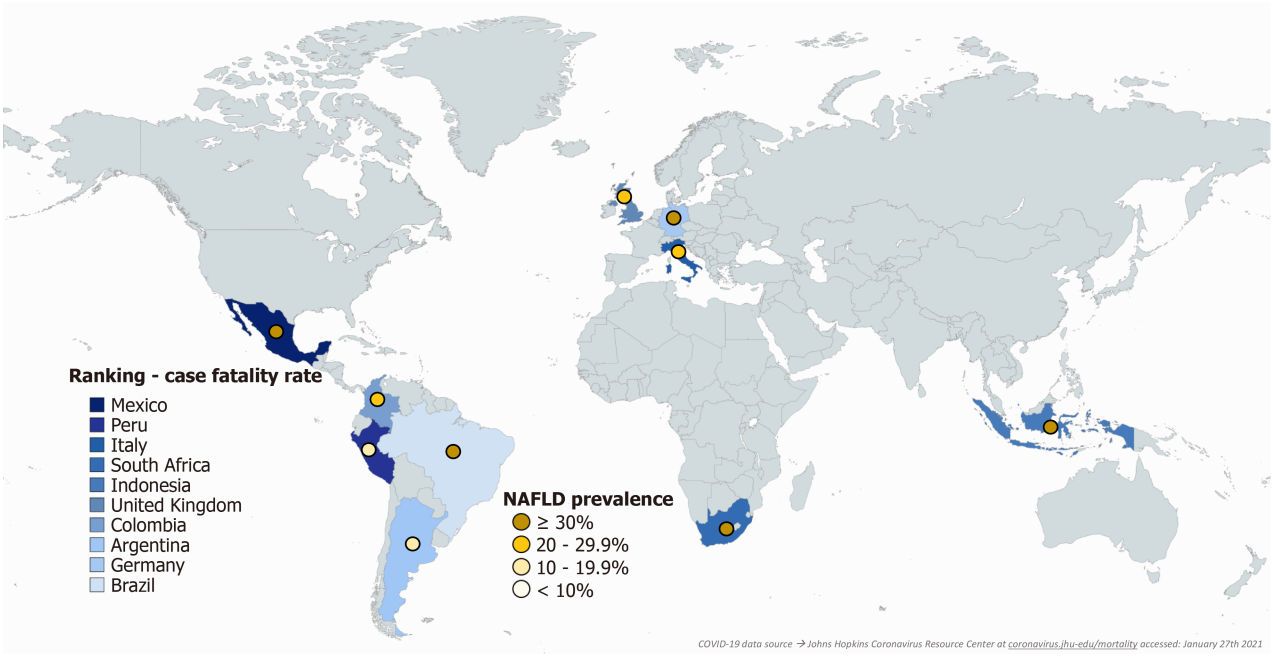


Figure 2 Coronavirus disease 2019 case fatality rate and nonalcoholic fatty liver disease prevalence. Mexico 8.5%, Peru 3.6%, Italy 3.5%, South Africa 2.9%, Indonesia 2.8%, United Kingdom 2.7%, Colombia 2.6%, Argentina 2.5%, Germany 2.5% and Brazil 2.5%. The prevalence of nonalcoholic fatty liver disease in those countries is indicated by the colored circles.

matory cytokines such as tumor necrosis factor (TNF)-α, interleukin (IL)-6, IL-8, monocyte chemoattractant protein (MCP)-1, interferon-γ–inducible protein (IP)-10, and macrophage inflammatory protein (MIP)-1b[35]. On the other hand, in patients with COVID-19, the presence of hyperinflammation, described as hypercytokinemia or "cytokine storm", immune hyperactivation, and even in some cases secondary hemophagocytic lymphohistiocytosis have been reported[1,36-38]. One of the cytokines reported to be elevated in patients with COVID-19 is IL-1B, which is the final effector of pyroptosis, a known mechanism of liver cell death[39,40]. Apart from IL-1B, other cytokines have been found to increase in COVID-19, including IL-6, IP-10, TNF, interferon-γ, vascular endothelial growth factor, and MIP 1α and 1β[36]. Obese patients with COVID-19 present a more prominent inflammatory profile than

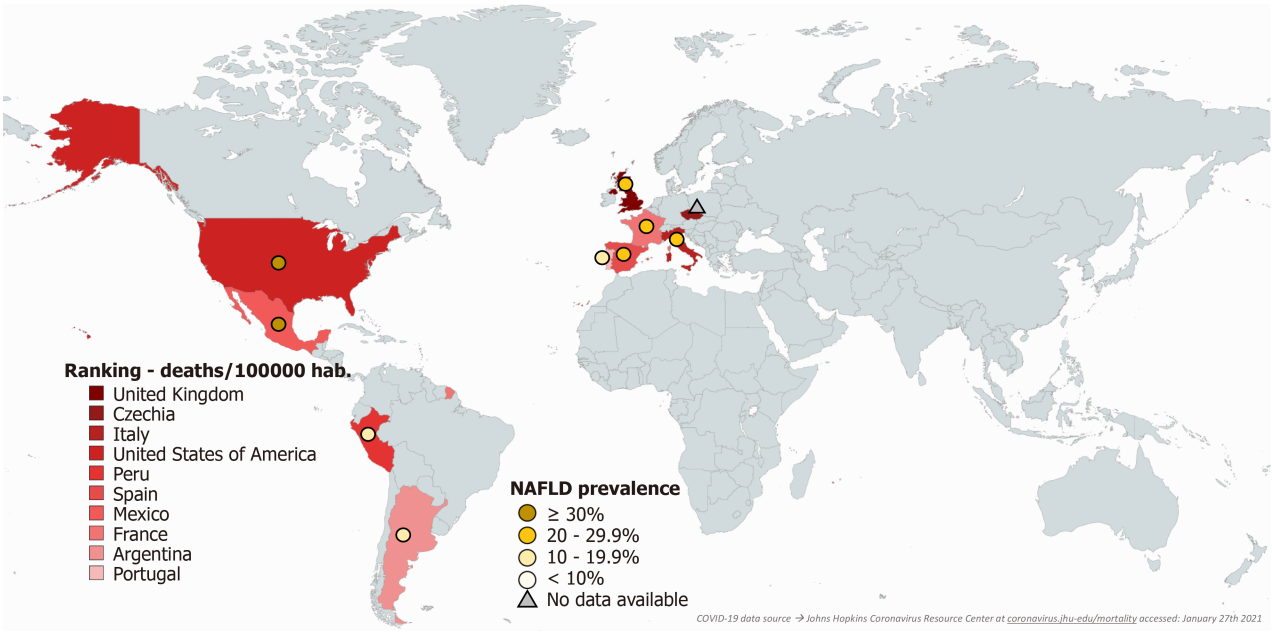


Figure 3 Number of deaths from coronavirus disease 2019 per 100000 habitants and nonalcoholic fatty liver disease prevalence. United Kingdom 150.94, Czechia 146.98, Italy 143.01, United States of America 129.94, Peru 125.38, Spain 121.55, Mexico 120.47, France 110.84, Portugal 107.10, Argentina 106.20.

nonobese COVID patients[41]. Dexamethasone has shown a mortality benefit in patients with severe COVID-19 because of its ability to inhibit the generation of cytokines and their deleterious effects[42]. The possible effect of an "acute-on-chronic inflammation" process in patients with MAFLD, including those with or without liver fibrosis, and COVID-19, deserves further research, including the possibility of different anti-inflammatory responses to corticosteroids such as dexamethasone.

Another point of convergence between COVID-19 and metabolic diseases such as MAFLD is endothelial dysfunction. Endothelial dysfunction has been described in patients with liver steatosis. Healthy individuals have better endothelial function than biopsy-proven NAFLD patients[27], which partially explains the increased risk of cardiovascular disease in that population[43]. Endothelial dysfunction results in a prothrombotic state leading to occlusion and micro thrombi formation in patients with COVID-19[44]. Moreover, endothelial dysfunction can result in insufficient nitric oxide and consequent vessel constriction[45]. Taken together, the studies show that preexisting endothelial dysfunction could explain the high prevalence of thrombosis in patients with COVID-19 and MAFLD[46].

Finally, some of the pathways involved in liver fibrosis, which is the key event determining the outcome in patients with NAFLD[12], are specially relevant and could have an important role in patients with COVID-19. One of them, the RAAS, is involved in liver fibrosis development, where angiotensin II induces a profibrogenic phenotype in stellate cells and has an important role in the pathophysiology of cirrhosis[47,48]. Similarly, RAAS has a role in the pathogenesis of NAFLD, where the hepatic local RAAS is overactivated, and more importantly, patients with NASH have significantly higher expression of angiotensin-converting enzyme 2 (*ACE2*) gene, suggesting that those patients have a greater risk of liver affection by SARS-CoV-2[49] given the fact that SARS-CoV-2 entry into the cell is accomplished through the binding and interaction of the spike glycoprotein (S-glycoprotein) andACE2[50]. This could partially explain the relationship between adverse outcomes and liver fibrosis in patients with MAFLD and COVID-19.

In conclusion, various mechanisms explain the association observed in different studies between MAFLD and/or fibrosis and adverse outcomes in patients with COVID-19, where its directionality is important to explain what happens in the liver. One is that a previous chronic state (*e.g.*, inflammation, endothelial dysfunction, differential regulation of the RAAS, *etc.*) "primes" the body to develop a stronger response upon SARS-CoV-2 infection, thereby increasing its lethality. Another possible scenario is that acute systemic inflammation induces a prosteatotic and profibrogenic response in patients with COVID-19. These mechanisms need further study in order to shed light on the main pathways explaining the relevance of MAFLD in patients with

COVID-19.

METABOLIC RISK FACTORS ASSOCIATED WITH SEVERE COVID-19

The risk of severe COVID-19 is higher in older individuals and in those with underlying medical comorbidities. The established risk factors for severe COVID-19, according to the Centers for Disease Control and Prevention (CDC), are T2DM, serious cardiovascular disease, obesity, chronic kidney disease, cancer, chronic obstructive pulmonary disease, immunocompromised state from solid organ transplant, smoking and sickle cell disease[51]. Given the association between MAFLD, obesity, and diabetes mellitus, it could be proposed as a high-risk metabolic condition[52,53].

Obesity

Obesity is a fast-growing public health problem. In 2016, 39% of the adult population worldwide were overweight and 13% were obese. There is a direct relationship between obesity and adverse clinical outcomes[54]. The association has also been observed in patients with SARS CoV2 infection, where observational data links obesity with an increased risk of severe disease and death[55-61]. In addition to the body mass index (BMI), visceral adiposity probably favors the development of severe COVID-19. This was addressed in a single-center cohort study in Italy, where the investigators found that abdominal adipose tissue distribution positively correlated with the risk of intensive care unit (ICU) admission in patients with COVID-19[62].

Diabetes mellitus

Diabetes is among the ten leading causes of death worldwide[63]. There is a relation between diabetes mellitus and the development of severe COVID-19[64-69]. In an observational cohort study, COVID-19-related mortality in people with diabetes mellitus was associated with the preceding level of hyperglycemia (HbA1c). In T2DM patients, the risk was significantly higher in those with an HbA1c > 7.5% and the risk increased as HbA1c levels did[70]. Another study found lower mortality in hospitalized patients with COVID-19 and T2DM with better glycemic control[65]. Conversely, Agarwal *et al*[71] did not find a clear association between HbA1c level and mortality in patients with diabetes and COVID-19, but the risk of mortality was greater in patients on previous insulin therapy.

The pathophysiological mechanisms that increase the risk of mortality in people with COVID 19 and obesity/diabetes mellitus are complex and not completely clear. The two factors have immune dysfunction characterized by a state of chronic low-grade inflammation in common[72,73]. There is evidence that patients with obesity and SARS CoV2 infection have a higher expression of inflammatory markers including IL6, IL-4, erythrocyte sedimentation rate, and high-sensitivity C-reactive protein (hsCRP) than nonobese patients[74].

SPECTRUM OF LIVER DAMAGE IN PATIENTS WITH MAFLD AND COVID-19

Several studies have been conducted to elucidate whether MAFLD is a risk factor for adverse clinical outcomes in patients with COVID-19. A summary of all of the studies, published until December 7, 2020 evaluating the association between MAFLD and clinical outcomes in patients with COVID-19 is presented in Table 1. It is important to acknowledge that comparison of the studies is limited by differences such as the number of available cases, the clinical outcomes evaluated, definitions of severity, demographic characteristics and comorbidities, and the methods of assessing both MAFLD and liver fibrosis. Despite this limitation, there are consistent results among the published data. All studies compared patients with or without MAFLD and all found different risk factors for the development of various poor clinical outcomes. Most studies concluded that MAFLD patients have an increased risk of developing abnormal liver function tests, liver injury, and severe disease in the acute setting of COVID-19. In addition, some studies found no differences in disease severity, disease progression, complications, or mortality among patients with or without MAFLD. Others emphasized that MAFLD only conferred an increased risk of severe disease in younger patients < 60 years of age, in those with advanced fibrosis detected by noninvasive methods such as the FIB-4 score or NAFLD fibrosis score (NFS) or with an

Table 1 Studies evaluating metabolic-associated fatty liver disease in coronavirus disease 2019 patients

Ref.	Type of study and population	MAFLD/non-MAFLD patients (*n*)	MAFLD diagnosis	Liver fibrosis criteria	Clinical outcomes	Results
Gao *et al* [61]	Cohort, *n* = 130 pts, China	65/65	Hepatic steatosis by CT and MAFLD consensus criteria	N/A	COVID-19 severity	MAFLD: Increased risk of severe COVID-19 (OR 4.07, 95%CI: 1.1-15.09, *P* = 0.003)
Ji *et al*[52]	Cohort, *n* = 202 pts, China	76/126	HSI > 36 points and/or abdominal US	N/A	Liver injury and COVID-19 severity	MAFLD: Increased risk of severe COVID-19 (44.7% *vs* 6.6%, *P* < 0.0001), abnormal liver function tests from admission to discharge (70% *vs* 11.1%, *P* < 0.0001) and longer viral shedding time (17.5 *vs* 12.1 d, *P* < 0.0001)
Targher *et al*[53]	Cohort, *n* = 310 pts, China	94/216	Hepatic steatosis by CT and MAFLD consensus criteria	FIB-4, NFS	COVID-19 severity	MAFLD: Intermediate/high FIB-4 increased risk of severe COVID-19 (OR 2.95, 95%CI: 1.37-6.34, *P* < 0.005), intermediate/high NFS increased risk of severe COVID-19 (OR 2.91, 95%CI: 1.20-7.06)
Huang *et al*[83]	Cohort, *n* = 280 pts, China	86/194	HSI >36 points	N/A	Laboratory abnormalities, liver injury, COVID-19 severity, clinical outcomes	MAFLD: Increased levels of white blood cells (5.5 *vs* 4.7, *P* < 0.001), lymphocytes (1.4 *vs* 1.2, p 0.041), ALT (34.5 *vs* 23, *P* < 0.0001) and GGT (34 *vs* 21, *P* < 0.001). No difference in severity, complications and clinical outcomes
Mahamid *et al*[84]	Case control, *n* = 71 pts, Israel	22/49	Hepatic steatosis by CT and MAFLD consensus criteria	N/A	COVID-19 severity	MAFLD: Increased risk of severe COVID-19 (men: OR 3.29, 95%CI 3.28-3.58, *P* = 0.001; women: 3.25, 95%CI: 3.09-3.47, *P* = 0.002)
Zhou *et al* [85]	Cohort, *n* = 327 pts, China	59/268	Hepatic steatosis by CT and MAFLD consensus criteria	N/A	COVID-19 severity in younger (< 60 yr of age) and elderly (< 60 yr of age) patients	MAFLD: Younger patients increased risk of severe COVID-19 (OR 2.67, 95%CI: 1.13-6.34, *P* = 0.03). Elderly patients no difference in COVID-19 severity
Chen *et al* [86]	Cohort, *n* = 342 pts, United States	178/164	HSI > 36 points for Asians and HSI > 39 points for non-Asians or imaging evidence of hepatic steatosis	N/A	Liver injury and COVID-19 severity	MAFLD: Increased risk of transaminitis (ALT > 5 × ULN) (OR 2.12, 95%CI: 1.03-4.37, *P* = 0.04), ICU admission (OR 1.60, 95%CI: 1.00-2.57, *P* = 0.05), intubation (OR 2.51, 95%CI: 1.52-4.16, *P* ≤ 0.001), and vasopressor use (OR 1.22, 95%CI: 1.11-1.34, *P* ≤ 0.001)
Zhou *et al* [87]	Cohort, *n* = 110 pts (all patients < 60 yr of age), China	55/55	Hepatic steatosis by CT and MAFLD consensus criteria	N/A	COVID-19 severity	MAFLD: Increased risk of severe COVID-19 (OR 4.07, 95%CI: 1.20-13.79, *P* = 0.02)
Pan *et al* [88]	Meta-analysis, *n* = 110 pts (all patients < 60 yr of age), China	401/892	Hepatic steatosis plus one of the following: overweight, type 2 diabetes mellitus or metabolic dysregulation	N/A	Pooled prevalence of MAFLD and COVID-19 severity	MAFLD: Prevalence of MAFLD in COVID-19 patients (OR 0.31, 95%CI: 0.28-0.35, I^2 = 38.8%, *P* = 0.1799). Increased risk of severe COVID-19 (OR 2.93, 95%CI: 1.87-4.60, I^2 = 34.3%, *P* = 0.166)
Bramante *et al*[75]	Cohort, *n* = 6700 pts, United States	373	ICD codes for NAFLD or NASH or BMI 30 kg/m^2 and elevated ALT	N/A	Admission or hospitalization for COVID-19	MAFLD: Increased risk of hospitalization (OR 1.43, 95%CI: 1.09-1.88, *P* < 0.01). Patients who had undergone bariatric surgery decreased risk of hospitalization (OR 0.22, 95%CI: 0.05-0.98, *P* < 0.05)
Lopez-Mendez *et al*[76]	Cross sectional, *n* = 155 pts, Mexico	66/89	HSI > 36 points	APRI, NFS and/or FIB-4	Prevalence of liver steatosis and fibrosis in COVID-19 patients, COVID-19 severity	MAFLD: Prevalence of steatosis 42.6% (66/155) and of advanced fibrosis 44.5% (69/155). Advanced liver fibrosis by FIB-4 increased risk of ICU admission (OR 1.74, 95%CI: 1.74-2.68, *P* = 0.023) and mortality (OR 6.45, 95%CI: 2.01-20.83, *P* = 0.002). No difference in disease severity
Forlano *et al*[77]	Cohort, *n* = 193 pts, United Kingdom	61/132	Imaging evidence of hepatic steatosis or previous diagnosis of MAFLD	FIB-4	ICU admission and in-hospital mortality	MAFLD: No difference in rates of ICU admission (OR 1.14, 95%CI: 0.53-2.5, *P* = 0.69) and in-hospital mortality (OR 0.86, 95%CI: 0.44-1.69, *P* = 0.67), regardless of the FIB-4 values (low <1.45, intermediate 1.45-3.25 or high > 3.25 risk of advanced

						fibrosis)
Mushtaq *et al*[78]	Cross sectional	320/269	HSI > 36 points	N/A	Mortality, COVID-19 severity, COVID-19 progression and liver injury	MAFLD: Increased risk of mild (OR 2.99, 95%CI: 1.62-4.37, P = 0.000) and moderate (OR 5.104, 95%CI: 3.21-6.99, P = 0.000) liver injury. No difference in disease severity, progression or mortality
Targher *et al*[79]	Cohort, n = 589 pts, Qatar	94/216	Hepatic steatosis by CT and MAFLD consensus criteria	N/A	COVID-19 severity according to NLR	MAFLD: MAFLD+NLR 2.8 (OR 5.32, 95%CI: 0.98-29.9, P = 0.053), non-MAFLD+NLR > 2.8 (OR 17.7, 95%CI: 3.89-80.6, P < 0.001), MAFLD+NLR>2.8 (OR 25.9, 95%CI: 5.32-127, P < 0.001) compared to those with non-MAFLD+NLR2.8. Patients with MAFLD and high NLR values have increased risk of severe COVID-19
Ji *et al*[46]	Cohort, n = 200 pts, China	125/75	HSI > 36 points and/or abdominal US	N/A	D-dimer levels	MAFLD: Increased D-dimer values at admission (0.72 *vs* 0.38 g/mL, P = 0.003) and peak levels (1.81 *vs* 0.63 g/mL, P = 0.003)
Ji *et al*[46]	Cohort, n = 81 pts (DVT 21 pts and non-DVT 60 pts), China	43/38	HSI > 36 points and/or abdominal US + Doppler US	N/A	Prevalence of MAFLD in DVT and non-DVT patients	MAFLD: Increased prevalence in patients with DVT compared to those without DVT (76% *vs* 45%, P = 0.01)
Sachdeva *et al*[80]	Systematic review and meta-analysis, n = 8142 pts, 8 studies (7 studies from China and 1 study from Israel)	833/7309	Imaging evidence of hepatic steatosis and MAFLD consensus criteria	N/A	COVID-19 severity	MAFLD: Increased risk of severe COVID-19 (OR 2.358, 95%CI: 1.902-2.923, P < 0.001)
Hashemi *et al*[81]	Cohort, n = 363 pts, United States	55/308 (69 w/CLD)	Imaging evidence or biopsy evidence of hepatic steatosis	N/A	Clinical outcomes	MAFLD: Increased risk of ICU admission (OR 2.30, 95%CI: 1.27-4.17, P = 0.03) and need of mechanical ventilation (OR 2.15, 95%CI: 1.18-3.91, P = 0.02). No difference in mortality rates

ALT: Alanine aminotransferase; BMI: Body mass index; CLD: Chronic liver disease; COVID-19: Coronavirus disease; 2019; CT: Computed tomography; DVT: Deep vein thrombosis; HSI: Hepatic steatosis index; MAFLD: Metabolic-associated fatty liver disease; N/A: Not available; NAFLD: Nonalcoholic fatty liver disease; NASH: Nonalcoholic steatohepatitis; NLR: Neutrophil/lymphocyte ratio; US; Ultrasound.

elevated neutrophil/lymphocyte ratio (NLR) of > 2.8. One study found that MAFLD patients had increased viral shedding time and another identified an increased risk of deep vein thrombosis[46,52,53,75-88].

HISTOLOGICAL FINDINGS

Information regarding liver histopathological findings in COVID-19 is scarce. Some case series have reported a high prevalence of liver steatosis in postmortem biopsies and autopsies, ranging between 48% and 75%. Sonzogni *et al*[89] reported liver biopsies from 48 patients who died from COVID-19 in northern Italy, none of whom had signs or symptoms of liver disease before and during hospitalization. Obesity was present in 16% of the patients, hypertension in 53%, and diabetes in 29%. Macrovesicular steatosis was observed in 48% of the samples; all patients with obesity had liver steatosis. The use of steroids was not reported in this paper. Lagana *et al*[90] reported the liver histology of 40 patients who died of COVID-19 in New York, 50% had diabetes and 75% had hypertension. The most common finding was macrovesicular steatosis, present in 75% of the patients. Interestingly, the distribution of liver steatosis was not typical of MAFLD and did not correlate with BMI or T2DM. Twenty-two patients (55%) received steroids during their hospital stay. Bradley *et al*[91] reported postmortem examinations performed on 14 patients who died of COVID-19 in Washington state. Liver steatosis was reported in 64% of the patients. Ten of the 14 patients had at least one metabolic disease (*i.e.* hypertension TD2M, dyslipidemia, or obesity), steroid use was not reported. A report of autopsy findings of 22 COVID-19 patients in Italy revealed microvacuolar and microvacuolar steatosis in 54% of the patients[92]. Table 2 further describes the studies.

Table 2 Histological findings from liver biopsies of coronavirus disease 2019 patients

Ref.	Inclusion criteria	Population characteristics *n* (%)	Histopathological results	
Sonzogni *et al*[89]	Postmortem SARS-CoV-2-positive patients. (*n* = 48)[1]; Male/Female (*n*): 35/13[1]; Age (yr): 71 (32-86)	No comorbidities: 6 (13.3); Hypertension 24 (53.3); Cardiovascular Disease (different than hypertension) 17 (37.8); Diabetes 13 (28.9); Obesity 7 (15.6); Kidney disease 10 (22.2); Pulmonary disease 5 (11.1)	Portal vein parietal fibrosis	Absent 39%; Focal 29%; Multifocal 22%; Diffuse 8%
			Herniated portal vein in periportal parenchyma	Absent 25%; Focal 37%; Multifocal 27%; Diffuse 10%
			Periportal abnormal vessels	Focal 56%; Multifocal 37%; Diffuse 6%
			Fibrosis	Absent 24%; Portal fibrosis 60%; Incomplete fibrous septa 16%
			Lobular inflammation	Absent 50%; Mild 48%; Moderate 2%; Severe 0%
			Portal inflammation	Absent 33%; Mild 66%; Moderate 0%; Severe 0%
			Vascular thrombosis	Partial portal 50%; Complete portal 23%; Incomplete sinusoidal 14%; Complete sinusoidal 12%
			Parenchymal confluent necrosis	Absent 65%; Mild 11%; Moderate 15%; Severe 12%
			Steatosis	Absent 46%; Small droplets 6%; Large droplets 2%; Mixed small and large 46%
Lagana *et al*[90]	Patients who died from illness related to COVID-19. (*n* = 40)[1]; Male/Female (*n*): 28/12[1]; Age (yr): 70 (66-80)	BMI, *N* = 32 mean (range) 26.5 (23.9-32.0); Chronic liver disease: 2 (13); Diabetes: 18 (50); Hypertension: 29 (76); Chronic kidney disease: 7 (22); Cardiac disease: 10 (36)	Lobular necroinflammation	20 (50%)
			Portal inflammation	20 (50%)
			Lobular apoptosis (individual hepatocytes)	10 (25%)
			Fat 0%–5%; 6%–33%; 34%–66%; 67%–100%	10 (25%); 19 (48%); 6 (15%); 5 (12%)
			Cholestasis	15 (38%)
Bradley *et al*[91]	Patients with a positive antemortem or post- mortem SARS-CoV-2. (*n* = 14)[1]; Male/Female: 6/8[1]; Age (yr): 73.5 (42-84)	-	Periportal lymphocytic inflammation	2 (14%)
			Centrilobular necrosis	4 (28%)
			Steatosis	9 (64%)
			Congestion	11 (78%)
Falasca *et al*[92]	Postmortem SARS-CoV-2-positive patients. (*n* = 22)[1]; Male/Female: 15/7[1]; Age (yr): 67.9 (27-92)	Chronic obstructive pulmonary disease: 6 (27.2); Cardiac disease: 8 (36.3); Malignancy: 5 (22.7); Hypertension: 4 (18.2); Diabetes: 4 (18.2); Kidney disease: 2 (9.1)	Inflammatory infiltrate	11 (50%)
			Congestion	10 (45.5%)
			Steatosis	12 (54.5%)

[1]Age was reported as median (interquartile range). SARS-CoV-2: Severe acute respiratory syndrome coronavirus 2; BMI: Body mass index.

Two explanations can be made of the high-frequency of macrovesicular steatosis in patients who died with severe COVID-19. The first is that the patients had liver steatosis before they acquired COVID-19, which represents a risk factor for mortality as the prevalence was higher than that reported in the general population[93]. MAFLD might contribute to the COVID-19-induced inflammatory "storm" through the hepatic release of proinflammatory cytokines, thereby contributing to the severity of the disease[79]. The second explanation is that liver steatosis developed in some patients during the course of the infection, with the etiology being multifactorial[90]. Hypoxia is associated with lipid homeostasis maintained by hypoxia-inducible factors (HIFs). HIFs regulate hepatic lipid metabolism to increase the liver lipid storage capacity[94,

95]. The corticosteroid therapy that is frequently given to patients with severe COVID-19 can cause hepatic steatosis. The effect can occur rapidly and is not usually clinically relevant[96]. Liver steatosis has been associated with viral infections, specifically hepatitis C virus infection, through impaired secretion, increased neosynthesis, and impaired degradation[97]. In summary, there is no pathophysiological evidence supporting SARS-CoV-2 as a direct cause of liver steatosis. However, as seen above, liver steatosis is a common histopathological finding in patients who died from severe COVID-19. The explanation of the findings is undoubtedly multifactorial, including a history of metabolic risk factors, use of corticosteroid therapy, and the universal presence of hypoxia in these patients.

FUTURE PERSPECTIVES IN PATIENTS WITH MAFLD AND COVID-19

MAFLD patients can be vulnerable to SARS-CoV-2 infection and COVID-19 complications because of the deleterious interaction of complex inflammatory pathways[98]. As we show in this review, based on currently available clinical evidence, patients with MAFLD have an increased risk of developing abnormal liver function tests and are more likely to progress to severe COVID-19[52,53,80-82,84,86-88]. Therefore, MAFLD should be considered a prognostic indicator for COVID-19.

We recommend taking these observations into account when assessing such patients. It is important to identify and closely monitor patients with preexisting liver diseases, including those with MAFLD. An Asia-Pacific position statement also recommends proper monitoring and management of blood pressure and glycemic control in MAFLD patients who have COVID-19, as it is associated with poor clinical outcomes[99]. As we do not yet know the long-term effects that COVID-19 can have on patients with MAFLD with respect to fibrosis, we also encourage long-term monitoring. Below, we discuss the available options for clinical assessment and prevention.

Clinical assessment

Given the high prevalence of MAFLD and the implications of liver fibrosis for the risk of adverse outcomes in patients with COVID-19[100], all patients admitted to hospital should be evaluated for the presence of MAFLD and assessed for the risk of liver fibrosis. Most patients with MAFLD are asymptomatic, and therefore, are not aware of their disease. Establishing the diagnosis of MAFLD requires the presence of metabolic risk factors such as overweight/obesity, T2DM, or evidence of metabolic dysregulation in addition to evidence of fat accumulation in the liver[101]. The first step in the evaluation of MAFLD and fibrosis in patients with COVID-19 should be to determine the presence of metabolic risk factors such as insulin resistance, T2DM, hypertension, obesity, and dyslipidemia. In those patients, the presence of liver steatosis should be determined either by imaging or by risk scores. The ideal imaging methods to assess liver fat content are ultrasound, transient elastography, or magnetic resonance imaging, however in the context of COVID-19 patients, the use of available images such as those derived from chest computed tomography (CT) scans can be useful, shorten the evaluation time, and limit the exposure of healthcare workers. Chest CT has high sensitivity and specificity for detecting lung lesions in patients with COVID-19 and is performed frequently in patients with severe disease[102]. Images of the liver and the upper pole of the spleen can be seen in chest CT scans. In those cases, the CT scan can be used to diagnose moderate and severe steatosis[101]. CT diagnostic criteria for steatosis are liver attenuation of at least ten Hounsfield Units (HU) less than that of the spleen or an absolute liver attenuation of less than 40 HU. These criteria have variable specificity (43%-95%) and high sensitivity (90%–100%)[103]. When a chest CT is not available or the image is not ideal, risk scores are a useful alternative. Several scores have been developed for that purpose, including the NAFLD liver fat score, the Framingham steatosis index (FSI), and the Dallas Steatosis Index. The NAFLD liver fat score is calculated using the presence of metabolic syndrome, T2DM, fasting serum insulin, fasting serum aspartate transaminase (AST)/alanine transaminase (ALT) ratio. A cutoff of 0.640 predicts increased liver fat content with a sensitivity of 86% and specificity of 71%[104]. The need of a serum insulin assay makes this score impractical in some hospitals. The FSI includes the patient age, sex, BMI, triglyceride level, hypertension, T2DM, and the ALT/AST ratio. At a cutoff point of 23, the FSI has a sensitivity of 79%, a specificity of 71%, a positive predictive value (PPV) of 50%, and a negative predictive value (NPV) of 90% for hepatic steatosis[105]. The disease severity index is a novel, recently developed score based on ALT level, DMI, age, sex, trigly-

ceride and glucose levels, T2DM, hypertension, and ethnicity. At a threshold of < 20% risk, MAFLD can be excluded with 86% sensitivity and 90% NPV[106]. A major drawback of these scores is that all of them require transaminase values, which may be elevated in patients with COVID-19[107], increasing the risk of overestimating the risk of liver steatosis.

For patients who meet the criteria for MAFLD, evaluation of fibrosis is essential. The gold standard for the evaluation of liver fibrosis is liver biopsy, however, as it is an invasive procedure, is not suitable for this clinical scenario. Elastography is another useful method, and it has become the noninvasive method of choice to quantify liver stiffness. However, liver inflammation caused by SARS-CoV-2 can by itself increase liver stiffness[108]. Furthermore, elastography is not widely available in all hospitals, and biosecurity measures could make it difficult to perform this evaluation of patients with COVID-19 and MAFLD. Noninvasive tools for the assessment of liver fibrosis include serologic tests, risk scores, and imaging studies[12]. None of the currently available biomarkers by itself has sufficient accuracy for diagnosing fibrosis, therefore, predictive scores have an important role in evaluating the risk of advanced fibrosis in patients with MAFLD. Among the prediction scores, FIB-4 index, NFS, the BARD score, FibroTest, HepatoScore, Hepamet fibrosis score (HFS), and AST/platelet ratio index (APRI) score, are the most widely used. Overall, predictive scores for fibrosis have high NPVs for excluding advanced fibrosis with low PPVs. Therefore, these scores may be confidently used for baseline risk stratification to exclude advanced fibrosis. A Fagan's nomogram analysis of post-test probability for detecting advanced fibrosis found that the HFS, HepatoScore and FibroMeter test to be the best noninvasive measures[12]. As mentioned before, a major disadvantage of these scores is the use of liver transaminases as a variable, and as previously known, patients with COVID-19 frequently have hypertransaminasemia, which would increase the risk of overestimating the presence of liver fibrosis. A confirmatory test should be made after the patient has been discharged and close follow-up should be continued.

Preventive measures

The general preventive recommendations for patients with MAFLD and liver fibrosis are those given for the general population, and include, wearing a mask when out in public or in areas without ventilation, practicing social distancing, and performing frequent hand hygiene. If possible, healthcare visits should be avoided in favor of telemedicine consultations[109]. It is important to mention that vaccination against SARS-CoV-2 has started worldwide and there are many doubts to be clarified regarding patients with liver diseases. We must keep in mind that several thousand people have participated in clinical trials of the different vaccines against SARS-CoV-2. However, there are few data on patients with liver diseases, and some trials have excluded such patients[110].

Three SARS-CoV-2 vaccines have been approved recently. The BNT162b2 vaccine (Pfizer-BioNTech) was evaluated in 43,448 participants of whom 0.6% (n = 214) had mild liver disease, only three had moderate or severe liver disease, 31% (n = 13218) of the participants had obesity, and 8.4% (n = 3163) had diabetes. In both conditions associated with MAFLD the vaccine safety and efficacy were high[111]. The ChAdOx1 nCoV-19 vaccine (AstraZeneca/University of Oxford), excluded individuals with chronic liver diseases, and only 135 (0.5%) patients with diabetes were included[112]. The mRNA-1273 vaccine (ModernaTX) was evaluated in 30,420 volunteers of whom 0.6% (n = 96) had unspecified liver disease, 9.5% (n = 2874) had diabetes, and 6.7% (n = 2046) had severe obesity[113]. Considering the high risk of severe COVID-19 in patients with chronic liver and metabolic diseases, the potential benefit of the newly developed vaccines outweigh the possible risks, therefore all patients should have the recommendation to get vaccinated and in those with with chronic liver diseases they should be counseled about the potential reduction in the immune response to the vaccine and the importance of continuing with the general preventive measures even after vaccination.

CONCLUSION

MAFLD is the most common liver disease worldwide and conveys an increased risk of adverse clinical outcomes in patients with COVID-19, especially in those patients with a high-risk of liver fibrosis. All patients with COVID-19, and principally those admitted to the hospital, should be screened for the presence of steatosis and fibrosis, and efforts should be made to promptly detect patients at risk for the provision of

early treatment. Close follow-up is encouraged after discharge. New studies of the pathophysiology, diagnostic approach, and the effectiveness of the available therapy and prevention are needed, aiming to improve the overall outcome in patients with MAFLD and COVID-19.

REFERENCES

1 **Huang C**, Wang Y, Li X, Ren L, Zhao J, Hu Y, Zhang L, Fan G, Xu J, Gu X, Cheng Z, Yu T, Xia J, Wei Y, Wu W, Xie X, Yin W, Li H, Liu M, Xiao Y, Gao H, Guo L, Xie J, Wang G, Jiang R, Gao Z, Jin Q, Wang J, Cao B. Clinical features of patients infected with 2019 novel coronavirus in Wuhan, China. *Lancet* 2020; **395**: 497-506 [PMID: 31986264 DOI: 10.1016/S0140-6736(20)30183-5]

2 **Johns Hopkins Coronavirus Resource Center**. COVID-19 Map. Johns Hopkins Coronavirus Resour. Cent. 2020 [cited 15 July 2020]. Available from: https://coronavirus.jhu.edu/map.html

3 **Romagnoli S**, Peris A, De Gaudio AR, Geppetti P. SARS-CoV-2 and COVID-19: From the Bench to the Bedside. *Physiol Rev* 2020; **100**: 1455-1466 [PMID: 32496872 DOI: 10.1152/physrev.00020.2020]

4 **Lu R**, Zhao X, Li J, Niu P, Yang B, Wu H, Wang W, Song H, Huang B, Zhu N, Bi Y, Ma X, Zhan F, Wang L, Hu T, Zhou H, Hu Z, Zhou W, Zhao L, Chen J, Meng Y, Wang J, Lin Y, Yuan J, Xie Z, Ma J, Liu WJ, Wang D, Xu W, Holmes EC, Gao GF, Wu G, Chen W, Shi W, Tan W. Genomic characterisation and epidemiology of 2019 novel coronavirus: implications for virus origins and receptor binding. *Lancet* 2020; **395**: 565-574 [PMID: 32007145 DOI: 10.1016/S0140-6736(20)30251-8]

5 **Fan VS**, Dominitz JA, Eastment MC, Locke E, Green P, Berry K, O'Hare AM, Shah JA, Crothers K, Ioannou GN. Risk Factors for testing positive for SARS-CoV-2 in a national US healthcare system. *Clin Infect Dis* 2020 [PMID: 33105485 DOI: 10.1093/cid/ciaa1624]

6 **Drefahl S**, Wallace M, Mussino E, Aradhya S, Kolk M, Brandén M, Malmberg B, Andersson G. A population-based cohort study of socio-demographic risk factors for COVID-19 deaths in Sweden. *Nat Commun* 2020; **11**: 5097 [PMID: 33037218 DOI: 10.1038/s41467-020-18926-3]

7 **Garibaldi BT**, Fiksel J, Muschelli J, Robinson ML, Rouhizadeh M, Perin J, Schumock G, Nagy P, Gray JH, Malapati H, Ghobadi-Krueger M, Niessen TM, Kim BS, Hill PM, Ahmed MS, Dobkin ED, Blanding R, Abele J, Woods B, Harkness K, Thiemann DR, Bowring MG, Shah AB, Wang MC, Bandeen-Roche K, Rosen A, Zeger SL, Gupta A. Patient Trajectories Among Persons Hospitalized for COVID-19 : A Cohort Study. *Ann Intern Med* 2021; **174**: 33-41 [PMID: 32960645 DOI: 10.7326/M20-3905]

8 **Munblit D**, Nekliudov NA, Bugaeva P, Blyuss O, Kislova M, Listovskaya E, Gamirova A, Shikhaleva A, Belyaev V, Timashev P, Warner JO, Comberiati P, Apfelbacher C, Bezrukov E, Politov ME, Yavorovskiy A, Bulanova E, Tsareva N, Avdeev S, Kapustina VA, Pigolkin YI, Dankwa EA, Kartsonaki C, Pritchard MG, Fomin V, Svistunov AA, Butnaru D, Glybochko P; Sechenov StopCOVID Research Team. Stop COVID Cohort: An Observational Study of 3480 Patients Admitted to the Sechenov University Hospital Network in Moscow City for Suspected Coronavirus Disease 2019 (COVID-19) Infection. *Clin Infect Dis* 2021; **73**: 1-11 [PMID: 33035307 DOI: 10.1093/cid/ciaa1535]

9 **Ayres JS**. A metabolic handbook for the COVID-19 pandemic. *Nat Metab* 2020; **2**: 572-585 [PMID: 32694793 DOI: 10.1038/s42255-020-0237-2]

10 **Sheka AC**, Adeyi O, Thompson J, Hameed B, Crawford PA, Ikramuddin S. Nonalcoholic Steatohepatitis: A Review. *JAMA* 2020; **323**: 1175-1183 [PMID: 32207804 DOI: 10.1001/jama.2020.2298]

11 **Watt MJ**, Miotto PM, De Nardo W, Montgomery MK. The Liver as an Endocrine Organ-Linking NAFLD and Insulin Resistance. *Endocr Rev* 2019; **40**: 1367-1393 [PMID: 31098621 DOI: 10.1210/er.2019-00034]

12 **Campos-Murguía A**, Ruiz-Margáin A, González-Regueiro JA, Macías-Rodríguez RU. Clinical assessment and management of liver fibrosis in non-alcoholic fatty liver disease. *World J Gastroenterol* 2020; **26**: 5919-5943 [PMID: 33132645 DOI: 10.3748/wjg.v26.i39.5919]

13 **Younossi Z**, Anstee QM, Marietti M, Hardy T, Henry L, Eslam M, George J, Bugianesi E. Global burden of NAFLD and NASH: trends, predictions, risk factors and prevention. *Nat Rev Gastroenterol Hepatol* 2018; **15**: 11-20 [PMID: 28930295 DOI: 10.1038/nrgastro.2017.109]

14 **Sharma P**, Kumar A. Metabolic dysfunction associated fatty liver disease increases risk of severe Covid-19. *Diabetes Metab Syndr* 2020; **14**: 825-827 [PMID: 32540736 DOI: 10.1016/j.dsx.2020.06.013]

15 **Eslam M**, Sanyal AJ, George J; International Consensus Panel. MAFLD: A Consensus-Driven Proposed Nomenclature for Metabolic Associated Fatty Liver Disease. *Gastroenterology* 2020; **158**: 1999-2014.e1 [PMID: 32044314 DOI: 10.1053/j.gastro.2019.11.312]

16 **World Health Organization**. WHO Coronavirus Disease (COVID-19) Dashboard. [cited 16 January 2021]. Available from: https://covid19.who.int/?gclid=EAIaIQobChMIq56a95Gi7gIVfTizAB3n3gdHEAAYASAAEgLx3fD_BwE

17 **Roser M**, Ritchie H, Ortiz-Ospina E. Coronavirus Disease (COVID-19)-Statistics and Research. [cited 17 January 2021]. Available from: https://www.sipotra.it/wp-

content/uploads/2020/03/Coronavirus-Disease-COVID-19-—Statistics-and-Research.pdf

18 **Leitão J**, Carvalhana S, Cochicho J, Silva AP, Velasco F, Medeiros I, Alves AC, Bourbon M, Oliveiros B, Rodrigues V, Sousa R, Sampaio F, Carvalho A, Cortez-Pinto H. Prevalence and risk factors of fatty liver in Portuguese adults. *Eur J Clin Invest* 2020; **50**: e13235 [PMID: 32289180 DOI: 10.1111/eci.13235]

19 **López-Velázquez JA**, Silva-Vidal KV, Ponciano-Rodríguez G, Chávez-Tapia NC, Arrese M, Uribe M, Méndez-Sánchez N. The prevalence of nonalcoholic fatty liver disease in the Americas. *Ann Hepatol* 2014; **13**: 166-178 [PMID: 24552858 DOI: 10.1186/1471-230X-14-42]

20 **Ye Q**, Zou B, Yeo YH, Li J, Huang DQ, Wu Y, Yang H, Liu C, Kam LY, Tan XXE, Chien N, Trinh S, Henry L, Stave CD, Hosaka T, Cheung RC, Nguyen MH. Global prevalence, incidence, and outcomes of non-obese or lean non-alcoholic fatty liver disease: a systematic review and meta-analysis. *Lancet Gastroenterol Hepatol* 2020; **5**: 739-752 [PMID: 32413340 DOI: 10.1016/S2468-1253(20)30077-7]

21 **Bernal-Reyes R**, Castro-Narro G, Malé-Velázquez R, Carmona-Sánchez R, González-Huezo MS, García-Juárez I, Chávez-Tapia N, Aguilar-Salinas C, Aiza-Haddad I, Ballesteros-Amozurrutia MA, Bosques-Padilla F, Castillo-Barradas M, Chávez-Barrera JA, Cisneros-Garza L, Flores-Calderón J, García-Compeán D, Gutiérrez-Grobe Y, Higuera de la Tijera MF, Kershenobich-Stalnikowitz D, Ladrón de Guevara-Cetina L, Lizardi-Cervera J, López-Cossio JA, Martínez-Vázquez S, Márquez-Guillén E, Méndez-Sánchez N, Moreno-Alcantar R, Poo-Ramírez JL, Ramos-Martínez P, Rodríguez-Hernández H, Sánchez-Ávila JF, Stoopen-Rometti M, Torre-Delgadillo A, Torres-Villalobos G, Trejo-Estrada R, Uribe-Esquivel M, Velarde-Ruiz Velasco JA. The Mexican consensus on nonalcoholic fatty liver disease. *Rev Gastroenterol Mex (Engl Ed)* 2019; **84**: 69-99 [PMID: 30711302 DOI: 10.1016/j.rgmx.2018.11.007]

22 **Friedman SL**, Neuschwander-Tetri BA, Rinella M, Sanyal AJ. Mechanisms of NAFLD development and therapeutic strategies. *Nat Med* 2018; **24**: 908-922 [PMID: 29967350 DOI: 10.1038/s41591-018-0104-9]

23 **Gao B**, Tsukamoto H. Inflammation in Alcoholic and Nonalcoholic Fatty Liver Disease: Friend or Foe? *Gastroenterology* 2016; **150**: 1704-1709 [PMID: 26826669 DOI: 10.1053/j.gastro.2016.01.025]

24 **Furman D**, Campisi J, Verdin E, Carrera-Bastos P, Targ S, Franceschi C, Ferrucci L, Gilroy DW, Fasano A, Miller GW, Miller AH, Mantovani A, Weyand CM, Barzilai N, Goronzy JJ, Rando TA, Effros RB, Lucia A, Kleinstreuer N, Slavich GM. Chronic inflammation in the etiology of disease across the life span. *Nat Med* 2019; **25**: 1822-1832 [PMID: 31806905 DOI: 10.1038/s41591-019-0675-0]

25 **Shoelson SE**, Lee J, Goldfine AB. Inflammation and insulin resistance. *J Clin Invest* 2006; **116**: 1793-1801 [PMID: 16823477 DOI: 10.1172/JCI29069]

26 **Dandona P**, Aljada A, Bandyopadhyay A. Inflammation: the link between insulin resistance, obesity and diabetes. *Trends Immunol* 2004; **25**: 4-7 [PMID: 14698276 DOI: 10.1016/j.it.2003.10.013]

27 **Al-Hamoudi W**, Alsadoon A, Hassanian M, Alkhalidi H, Abdo A, Nour M, Halwani R, Sanai F, Alsharaabi A, Alswat K, Hersi A, Albenmousa A, Alsaif F. Endothelial dysfunction in nonalcoholic steatohepatitis with low cardiac disease risk. *Sci Rep* 2020; **10**: 8825 [PMID: 32483260 DOI: 10.1038/s41598-020-65835-y]

28 **Villanova N**, Moscatiello S, Ramilli S, Bugianesi E, Magalotti D, Vanni E, Zoli M, Marchesini G. Endothelial dysfunction and cardiovascular risk profile in nonalcoholic fatty liver disease. *Hepatology* 2005; **42**: 473-480 [PMID: 15981216 DOI: 10.1002/hep.20781]

29 **Francque SM**, van der Graaff D, Kwanten WJ. Non-alcoholic fatty liver disease and cardiovascular risk: Pathophysiological mechanisms and implications. *J Hepatol* 2016; **65**: 425-443 [PMID: 27091791 DOI: 10.1016/j.jhep.2016.04.005]

30 **Monteiro R**, Azevedo I. Chronic inflammation in obesity and the metabolic syndrome. *Mediators Inflamm* 2010; **2010** [PMID: 20706689 DOI: 10.1155/2010/289645]

31 **Hotamisligil GS**, Arner P, Caro JF, Atkinson RL, Spiegelman BM. Increased adipose tissue expression of tumor necrosis factor-alpha in human obesity and insulin resistance. *J Clin Invest* 1995; **95**: 2409-2415 [PMID: 7738205 DOI: 10.1172/JCI117936]

32 **Cai D**, Yuan M, Frantz DF, Melendez PA, Hansen L, Lee J, Shoelson SE. Local and systemic insulin resistance resulting from hepatic activation of IKK-beta and NF-kappaB. *Nat Med* 2005; **11**: 183-190 [PMID: 15685173 DOI: 10.1038/nm1166]

33 **Haukeland JW**, Damås JK, Konopski Z, Løberg EM, Haaland T, Goverud I, Torjesen PA, Birkeland K, Bjøro K, Aukrust P. Systemic inflammation in nonalcoholic fatty liver disease is characterized by elevated levels of CCL2. *J Hepatol* 2006; **44**: 1167-1174 [PMID: 16618517 DOI: 10.1016/j.jhep.2006.02.011]

34 **Tarantino G**, Colicchio P, Conca P, Finelli C, Di Minno MN, Tarantino M, Capone D, Pasanisi F. Young adult obese subjects with and without insulin resistance: what is the role of chronic inflammation and how to weigh it non-invasively? *J Inflamm (Lond)* 2009; **6**: 6 [PMID: 19291292 DOI: 10.1186/1476-9255-6-6]

35 **Clària J**, Stauber RE, Coenraad MJ, Moreau R, Jalan R, Pavesi M, Amorós À, Titos E, Alcaraz-Quiles J, Oettl K, Morales-Ruiz M, Angeli P, Domenicali M, Alessandria C, Gerbes A, Wendon J, Nevens F, Trebicka J, Laleman W, Saliba F, Welzel TM, Albillos A, Gustot T, Benten D, Durand F, Ginès P, Bernardi M, Arroyo V; CANONIC Study Investigators of the EASL-CLIF Consortium and the European Foundation for the Study of Chronic Liver Failure (EF-CLIF). Systemic inflammation

in decompensated cirrhosis: Characterization and role in acute-on-chronic liver failure. *Hepatology* 2016; **64**: 1249-1264 [PMID: 27483394 DOI: 10.1002/hep.28740]

36 **Fajgenbaum DC**, June CH. Cytokine Storm. *N Engl J Med* 2020; **383**: 2255-2273 [PMID: 33264547 DOI: 10.1056/NEJMra2026131]

37 **Kalfaoglu B**, Almeida-Santos J, Tye CA, Satou Y, Ono M. T-cell dysregulation in COVID-19. *Biochem Biophys Res Commun* 2021; **538**: 204-210 [PMID: 33220925 DOI: 10.1016/j.bbrc.2020.10.079]

38 **Mehta P**, McAuley DF, Brown M, Sanchez E, Tattersall RS, Manson JJ; HLH Across Speciality Collaboration, UK. COVID-19: consider cytokine storm syndromes and immunosuppression. *Lancet* 2020; **395**: 1033-1034 [PMID: 32192578 DOI: 10.1016/S0140-6736(20)30628-0]

39 **Tay MZ**, Poh CM, Rénia L, MacAry PA, Ng LFP. The trinity of COVID-19: immunity, inflammation and intervention. *Nat Rev Immunol* 2020; **20**: 363-374 [PMID: 32346093 DOI: 10.1038/s41577-020-0311-8]

40 **Macías-Rodríguez RU**, Inzaugarat ME, Ruiz-Margáin A, Nelson LJ, Trautwein C, Cubero FJ. Reclassifying Hepatic Cell Death during Liver Damage: Ferroptosis-A Novel Form of Non-Apoptotic Cell Death? *Int J Mol Sci* 2020; **21** [PMID: 32121273 DOI: 10.3390/ijms21051651]

41 **McNeill JN**, Lau ES, Paniagua SM, Liu EE, Wang JK, Bassett IV, Selvaggi CA, Lubitz SA, Foulkes AS, Ho JE. The role of obesity in inflammatory markers in COVID-19 patients. *Obes Res Clin Pract* 2021; **15**: 96-99 [PMID: 33390322 DOI: 10.1016/j.orcp.2020.12.004]

42 **Sharun K**, Tiwari R, Dhama J, Dhama K. Dexamethasone to combat cytokine storm in COVID-19: Clinical trials and preliminary evidence. *Int J Surg* 2020; **82**: 179-181 [PMID: 32896649 DOI: 10.1016/j.ijsu.2020.08.038]

43 **Forlano R**, Mullish BH, Nathwani R, Dhar A, Thursz MR, Manousou P. Non-Alcoholic Fatty Liver Disease and Vascular Disease. *Curr Vascul Pharmacol* 2021; **19**: 269 [PMID: 32188385 DOI: 10.2174/1570161118666200318103001]

44 **Pons S**, Fodil S, Azoulay E, Zafrani L. The vascular endothelium: the cornerstone of organ dysfunction in severe SARS-CoV-2 infection. *Crit Care* 2020; **24**: 353 [PMID: 32546188 DOI: 10.1186/s13054-020-03062-7]

45 **Jin Y**, Ji W, Yang H, Chen S, Zhang W, Duan G. Endothelial activation and dysfunction in COVID-19: from basic mechanisms to potential therapeutic approaches. *Signal Transduct Target Ther* 2020; **5**: 293 [PMID: 33361764 DOI: 10.1038/s41392-020-00454-7]

46 **Ji D**, Zhang M, Qin E, Zhang L, Xu J, Wang Y, Cheng G, Wang F, Lau G. Letter to the Editor: Obesity, diabetes, non-alcoholic fatty liver disease and metabolic dysfunction associated fatty liver disease are proinflammatory hypercoagulable states associated with severe disease and thrombosis in Covid-19. *Metabolism* 2021; **115**: 154437 [PMID: 33220249 DOI: 10.1016/j.metabol.2020.154437]

47 **Bataller R**, Sancho-Bru P, Ginès P, Lora JM, Al-Garawi A, Solé M, Colmenero J, Nicolás JM, Jiménez W, Weich N, Gutiérrez-Ramos JC, Arroyo V, Rodés J. Activated human hepatic stellate cells express the renin-angiotensin system and synthesize angiotensin II. *Gastroenterology* 2003; **125**: 117-125 [PMID: 12851877 DOI: 10.1016/S0016-5085(03)00695-4]

48 **Di Pascoli M**, La Mura V. Renin-angiotensin-aldosterone system in cirrhosis: There's room to try! *Dig Liver Dis* 2019; **51**: 297-298 [PMID: 30220630 DOI: 10.1016/j.dld.2018.07.038]

49 **Fondevila MF**, Mercado-Gómez M, Rodríguez A, Gonzalez-Rellan MJ, Iruzubieta P, Valentí V, Escalada J, Schwaninger M, Prevot V, Dieguez C, Crespo J, Frühbeck G, Martinez-Chantar ML, Nogueiras R. Obese patients with NASH have increased hepatic expression of SARS-CoV-2 critical entry points. *J Hepatol* 2021; **74**: 469-471 [PMID: 33096086 DOI: 10.1016/j.jhep.2020.09.027]

50 **Yang J**, Petitjean SJL, Koehler M, Zhang Q, Dumitru AC, Chen W, Derclaye S, Vincent SP, Soumillion P, Alsteens D. Molecular interaction and inhibition of SARS-CoV-2 binding to the ACE2 receptor. *Nat Commun* 2020; **11**: 4541 [PMID: 32917884 DOI: 10.1038/s41467-020-18319-6]

51 **Centers for Disease Control and Prevention**. Science Brief: Evidence used to update the list of underlying medical conditions that increase a person's risk of severe illness from COVID-19. [cited 17 January 2021]. Available from: https://www.cdc.gov/coronavirus/2019-ncov/need-extra-precautions/evidence-table.html

52 **Ji D**, Qin E, Xu J, Zhang D, Cheng G, Wang Y, Lau G. Non-alcoholic fatty liver diseases in patients with COVID-19: A retrospective study. *J Hepatol* 2020; **73**: 451-453 [PMID: 32278005 DOI: 10.1016/j.jhep.2020.03.044]

53 **Targher G**, Mantovani A, Byrne CD, Wang XB, Yan HD, Sun QF, Pan KH, Zheng KI, Chen YP, Eslam M, George J, Zheng MH. Risk of severe illness from COVID-19 in patients with metabolic dysfunction-associated fatty liver disease and increased fibrosis scores. *Gut* 2020; **69**: 1545-1547 [PMID: 32414813 DOI: 10.1136/gutjnl-2020-321611]

54 **Flegal KM**, Kit BK, Orpana H, Graubard BI. Association of all-cause mortality with overweight and obesity using standard body mass index categories: a systematic review and meta-analysis. *JAMA* 2013; **309**: 71-82 [PMID: 23280227 DOI: 10.1001/jama.2012.113905]

55 **Lighter J**, Phillips M, Hochman S, Sterling S, Johnson D, Francois F, Stachel A. Obesity in Patients Younger Than 60 Years Is a Risk Factor for COVID-19 Hospital Admission. *Clin Infect Dis* 2020; **71**: 896-897 [PMID: 32271368 DOI: 10.1093/cid/ciaa415]

56 **Frank RC**, Mendez SR, Stevenson EK, Guseh JS, Chung M, Silverman MG. Obesity and the Risk of Intubation or Death in Patients With Coronavirus Disease 2019. *Crit Care Med* 2020; **48**: e1097-e1101 [PMID: 33045152 DOI: 10.1097/CCM.0000000000004553]

57 **Hur K**, Price CPE, Gray EL, Gulati RK, Maksimoski M, Racette SD, Schneider AL, Khanwalkar AR. Factors Associated With Intubation and Prolonged Intubation in Hospitalized Patients With COVID-19. *Otolaryngol Head Neck Surg* 2020; **163**: 170-178 [PMID: 32423368 DOI: 10.1177/0194599820929640]

58 **Simonnet A**, Chetboun M, Poissy J, Raverdy V, Noulette J, Duhamel A, Labreuche J, Mathieu D, Pattou F, Jourdain M; LICORN and the Lille COVID-19 and Obesity study group. High Prevalence of Obesity in Severe Acute Respiratory Syndrome Coronavirus-2 (SARS-CoV-2) Requiring Invasive Mechanical Ventilation. *Obesity (Silver Spring)* 2020; **28**: 1195-1199 [PMID: 32271993 DOI: 10.1002/oby.22831]

59 **Kalligeros M**, Shehadeh F, Mylona EK, Benitez G, Beckwith CG, Chan PA, Mylonakis E. Association of Obesity with Disease Severity Among Patients with Coronavirus Disease 2019. *Obesity (Silver Spring)* 2020; **28**: 1200-1204 [PMID: 32352637 DOI: 10.1002/oby.22859]

60 **Palaiodimos L**, Kokkinidis DG, Li W, Karamanis D, Ognibene J, Arora S, Southern WN, Mantzoros CS. Severe obesity, increasing age and male sex are independently associated with worse in-hospital outcomes, and higher in-hospital mortality, in a cohort of patients with COVID-19 in the Bronx, New York. *Metabolism* 2020; **108**: 154262 [PMID: 32422233 DOI: 10.1016/j.metabol.2020.154262]

61 **Gao F**, Zheng KI, Wang XB, Sun QF, Pan KH, Wang TY, Chen YP, Targher G, Byrne CD, George J, Zheng MH. Obesity Is a Risk Factor for Greater COVID-19 Severity. *Diabetes Care* 2020; **43**: e72-e74 [PMID: 32409499 DOI: 10.2337/dc20-0682]

62 **Battisti S**, Pedone C, Napoli N, Russo E, Agnoletti V, Nigra SG, Dengo C, Mughetti M, Conte C, Pozzilli P, Giampalma E, Strollo R. Computed Tomography Highlights Increased Visceral Adiposity Associated With Critical Illness in COVID-19. *Diabetes Care* 2020; **43**: e129-e130 [PMID: 32753457 DOI: 10.2337/dc20-1333]

63 **GBD 2017 Causes of Death Collaborators**. Global, regional, and national age-sex-specific mortality for 282 causes of death in 195 countries and territories, 1980-2017: a systematic analysis for the Global Burden of Disease Study 2017. *Lancet* 2018; **392**: 1736-1788 [PMID: 30496103 DOI: 10.1016/S0140-6736(18)32203-7]

64 **Richardson S**, Hirsch JS, Narasimhan M, Crawford JM, McGinn T, Davidson KW; the Northwell COVID-19 Research Consortium, Barnaby DP, Becker LB, Chelico JD, Cohen SL, Cookingham J, Coppa K, Diefenbach MA, Dominello AJ, Duer-Hefele J, Falzon L, Gitlin J, Hajizadeh N, Harvin TG, Hirschwerk DA, Kim EJ, Kozel ZM, Marrast LM, Mogavero JN, Osorio GA, Qiu M, Zanos TP. Presenting Characteristics, Comorbidities, and Outcomes Among 5700 Patients Hospitalized With COVID-19 in the New York City Area. *JAMA* 2020; **323**: 2052-2059 [PMID: 32320003 DOI: 10.1001/jama.2020.6775]

65 **Zhu L**, She ZG, Cheng X, Qin JJ, Zhang XJ, Cai J, Lei F, Wang H, Xie J, Wang W, Li H, Zhang P, Song X, Chen X, Xiang M, Zhang C, Bai L, Xiang D, Chen MM, Liu Y, Yan Y, Liu M, Mao W, Zou J, Liu L, Chen G, Luo P, Xiao B, Zhang Z, Lu Z, Wang J, Lu H, Xia X, Wang D, Liao X, Peng G, Ye P, Yang J, Yuan Y, Huang X, Guo J, Zhang BH. Association of Blood Glucose Control and Outcomes in Patients with COVID-19 and Pre-existing Type 2 Diabetes. *Cell Metab* 2020; **31**: 1068-1077.e3 [PMID: 32369736 DOI: 10.1016/j.cmet.2020.04.021]

66 **Bode B**, Garrett V, Messler J, McFarland R, Crowe J, Booth R, Klonoff DC. Glycemic Characteristics and Clinical Outcomes of COVID-19 Patients Hospitalized in the United States. *J Diabetes Sci Technol* 2020; **14**: 813-821 [PMID: 32389027 DOI: 10.1177/1932296820924469]

67 **Chen Y**, Yang D, Cheng B, Chen J, Peng A, Yang C, Liu C, Xiong M, Deng A, Zhang Y, Zheng L, Huang K. Clinical Characteristics and Outcomes of Patients With Diabetes and COVID-19 in Association With Glucose-Lowering Medication. *Diabetes Care* 2020; **43**: 1399-1407 [PMID: 32409498 DOI: 10.2337/dc20-0660]

68 **Fadini GP**, Morieri ML, Longato E, Avogaro A. Prevalence and impact of diabetes among people infected with SARS-CoV-2. *J Endocrinol Invest* 2020; **43**: 867-869 [PMID: 32222956 DOI: 10.1007/s40618-020-01236-2]

69 **Barron E**, Bakhai C, Kar P, Weaver A, Bradley D, Ismail H, Knighton P, Holman N, Khunti K, Sattar N, Wareham NJ, Young B, Valabhji J. Associations of type 1 and type 2 diabetes with COVID-19-related mortality in England: a whole-population study. *Lancet Diabetes Endocrinol* 2020; **8**: 813-822 [PMID: 32798472 DOI: 10.1016/S2213-8587(20)30272-2]

70 **Holman N**, Knighton P, Kar P, O'Keefe J, Curley M, Weaver A, Barron E, Bakhai C, Khunti K, Wareham NJ, Sattar N, Young B, Valabhji J. Risk factors for COVID-19-related mortality in people with type 1 and type 2 diabetes in England: a population-based cohort study. *Lancet Diabetes Endocrinol* 2020; **8**: 823-833 [PMID: 32798471 DOI: 10.1016/S2213-8587(20)30271-0]

71 **Agarwal S**, Schechter C, Southern W, Crandall JP, Tomer Y. Preadmission Diabetes-Specific Risk Factors for Mortality in Hospitalized Patients With Diabetes and Coronavirus Disease 2019. *Diabetes Care* 2020; **43**: 2339-2344 [PMID: 32769128 DOI: 10.2337/dc20-1543]

72 **Andersen CJ**, Murphy KE, Fernandez ML. Impact of Obesity and Metabolic Syndrome on Immunity. *Adv Nutr* 2016; **7**: 66-75 [PMID: 26773015 DOI: 10.3945/an.115.010207]

73 **Dhurandhar NV**, Bailey D, Thomas D. Interaction of obesity and infections. *Obes Rev* 2015; **16**: 1017-1029 [PMID: 26354800 DOI: 10.1111/obr.12320]

74 **Kang Z**, Luo S, Gui Y, Zhou H, Zhang Z, Tian C, Zhou Q, Wang Q, Hu Y, Fan H, Hu D. Obesity is a potential risk factor contributing to clinical manifestations of COVID-19. *Int J Obes (Lond)* 2020; **44**: 2479-2485 [PMID: 32921796 DOI: 10.1038/s41366-020-00677-2]

75 **Bramante C**, Tignanelli CJ, Dutta N, Jones E, Tamariz L, Clark JM, Usher M, Metlon-Meaux G, Ikramuddin S. Non-alcoholic fatty liver disease (NAFLD) and risk of hospitalization for Covid-19. *medRxiv* 2020 [PMID: 32909011 DOI: 10.1101/2020.09.01.20185850]

76 **Lopez-Mendez I**, Aquino-Matus J, Gall SM, Prieto-Nava JD, Juarez-Hernandez E, Uribe M, Castro-Narro G. Association of liver steatosis and fibrosis with clinical outcomes in patients with SARS-CoV-2 infection (COVID-19). *Ann Hepatol* 2021; **20**: 100271 [PMID: 33099028 DOI: 10.1016/j.aohep.2020.09.015]

77 **Forlano R**, Mullish BH, Mukherjee SK, Nathwani R, Harlow C, Crook P, Judge R, Soubieres A, Middleton P, Daunt A, Perez-Guzman P, Selvapatt N, Lemoine M, Dhar A, Thursz MR, Nayagam S, Manousou P. In-hospital mortality is associated with inflammatory response in NAFLD patients admitted for COVID-19. *PLoS One* 2020; **15**: e0240400 [PMID: 33031439 DOI: 10.1371/journal.pone.0240400]

78 **Mushtaq K**, Khan MU, Iqbal F, Alsoub DH, Chaudhry HS, Ata F, Iqbal P, Elfert K, Balaraju G, Almaslamani M, Al-Ejji K, AlKaabi S, Kamel YM. NAFLD is a predictor of liver injury in COVID-19 hospitalized patients but not of mortality, disease severity on the presentation or progression - The debate continues. *J Hepatol* 2021; **74**: 482-484 [PMID: 33223215 DOI: 10.1016/j.jhep.2020.09.006]

79 **Targher G**, Mantovani A, Byrne CD, Wang XB, Yan HD, Sun QF, Pan KH, Zheng KI, Chen YP, Eslam M, George J, Zheng MH. Detrimental effects of metabolic dysfunction-associated fatty liver disease and increased neutrophil-to-lymphocyte ratio on severity of COVID-19. *Diabetes Metab* 2020; **46**: 505-507 [PMID: 32505652 DOI: 10.1016/j.diabet.2020.06.001]

80 **Sachdeva S**, Khandait H, Kopel J, Aloysius MM, Desai R, Goyal H. NAFLD and COVID-19: a Pooled Analysis. *SN Compr Clin Med* 2020; 1-4 [PMID: 33173850 DOI: 10.1007/s42399-020-00631-3]

81 **Hashemi N**, Viveiros K, Redd WD, Zhou JC, McCarty TR, Bazarbashi AN, Hathorn KE, Wong D, Njie C, Shen L, Chan WW. Impact of chronic liver disease on outcomes of hospitalized patients with COVID-19: A multicentre United States experience. *Liver Int* 2020; **40**: 2515-2521 [PMID: 32585065 DOI: 10.1111/liv.14583]

82 **Gao F**, Zheng KI, Wang XB, Yan HD, Sun QF, Pan KH, Wang TY, Chen YP, George J, Zheng MH. Metabolic associated fatty liver disease increases coronavirus disease 2019 disease severity in nondiabetic patients. *J Gastroenterol Hepatol* 2021; **36**: 204-207 [PMID: 32436622 DOI: 10.1111/jgh.15112]

83 **Huang R**, Zhu L, Wang J, Xue L, Liu L, Yan X, Huang S, Li Y, Zhang B, Xu T, Li C, Ji F, Ming F, Zhao Y, Cheng J, Wang Y, Zhao H, Hong S, Chen K, Zhao XA, Zou L, Sang D, Shao H, Guan X, Chen X, Chen Y, Wei J, Zhu C, Wu C. Clinical features of COVID-19 patients with non-alcoholic fatty liver disease. *Hepatol Commun* 2020 [PMID: 32838108 DOI: 10.1002/hep4.1592]

84 **Mahamid M**, Nseir W, Khoury T, Mahamid B, Nubania A, Sub-Laban K, Schifter J, Mari A, Sbeit W, Goldin E. Nonalcoholic fatty liver disease is associated with COVID-19 severity independently of metabolic syndrome: a retrospective case-control study. *Eur J Gastroenterol Hepatol* 2020 [PMID: 32868652 DOI: 10.1097/MEG.0000000000001902]

85 **Zhou YJ**, Zheng KI, Wang XB, Yan HD, Sun QF, Pan KH, Wang TY, Ma HL, Chen YP, George J, Zheng MH. Younger patients with MAFLD are at increased risk of severe COVID-19 illness: A multicenter preliminary analysis. *J Hepatol* 2020; **73**: 719-721 [PMID: 32348790 DOI: 10.1016/j.jhep.2020.04.027]

86 **Chen VL**, Hawa F, Berinstein JA, Reddy CA, Kassab I, Platt KD, Hsu CY, Steiner CA, Louissaint J, Gunaratnam NT, Sharma P. Hepatic Steatosis Is Associated with Increased Disease Severity and Liver Injury in Coronavirus Disease-19. *Dig Dis Sci* 2020 [PMID: 32980956 DOI: 10.1007/s10620-020-06618-3]

87 **Zhou YJ**, Zheng KI, Wang XB, Sun QF, Pan KH, Wang TY, Ma HL, Chen YP, George J, Zheng MH. Metabolic-associated fatty liver disease is associated with severity of COVID-19. *Liver Int* 2020; **40**: 2160-2163 [PMID: 32573883 DOI: 10.1111/liv.14575]

88 **Pan L**, Huang P, Xie X, Xu J, Guo D, Jiang Y. Metabolic associated fatty liver disease increases the severity of COVID-19: A meta-analysis. *Dig Liver Dis* 2021; **53**: 153-157 [PMID: 33011088 DOI: 10.1016/j.dld.2020.09.007]

89 **Sonzogni A**, Previtali G, Seghezzi M, Grazia Alessio M, Gianatti A, Licini L, Morotti D, Zerbi P, Carsana L, Rossi R, Lauri E, Pellegrinelli A, Nebuloni M. Liver histopathology in severe COVID 19 respiratory failure is suggestive of vascular alterations. *Liver Int* 2020; **40**: 2110-2116 [PMID: 32654359 DOI: 10.1111/liv.14601]

90 **Lagana SM**, Kudose S, Iuga AC, Lee MJ, Fazlollahi L, Remotti HE, Del Portillo A, De Michele S, de Gonzalez AK, Saqi A, Khairallah P, Chong AM, Park H, Uhlemann AC, Lefkowitch JH, Verna EC. Hepatic pathology in patients dying of COVID-19: a series of 40 cases including clinical, histologic, and virologic data. *Mod Pathol* 2020; **33**: 2147-2155 [PMID: 32792598 DOI: 10.1038/s41379-020-00649-x]

91 **Bradley BT**, Maioli H, Johnston R, Chaudhry I, Fink SL, Xu H, Najafian B, Deutsch G, Lacy JM, Williams T, Yarid N, Marshall DA. Histopathology and ultrastructural findings of fatal COVID-19 infections in Washington State: a case series. *Lancet* 2020; **396**: 320-332 [PMID: 32682491 DOI: 10.1016/S0140-6736(20)31305-2]

92 **Falasca L**, Nardacci R, Colombo D, Lalle E, Di Caro A, Nicastri E, Antinori A, Petrosillo N, Marchioni L, Biava G, D'Offizi G, Palmieri F, Goletti D, Zumla A, Ippolito G, Piacentini M, Del Nonno F. Postmortem Findings in Italian Patients With COVID-19: A Descriptive Full Autopsy

Study of Cases With and Without Comorbidities. *J Infect Dis* 2020; **222**: 1807-1815 [PMID: 32914853 DOI: 10.1093/infdis/jiaa578]

93 **Browning JD**, Szczepaniak LS, Dobbins R, Nuremberg P, Horton JD, Cohen JC, Grundy SM, Hobbs HH. Prevalence of hepatic steatosis in an urban population in the United States: impact of ethnicity. *Hepatology* 2004; **40**: 1387-1395 [PMID: 15565570 DOI: 10.1002/hep.20466]

94 **Suzuki T**, Shinjo S, Arai T, Kanai M, Goda N. Hypoxia and fatty liver. *World J Gastroenterol* 2014; **20**: 15087-15097 [PMID: 25386057 DOI: 10.3748/wjg.v20.i41.15087]

95 **Rankin EB**, Rha J, Selak MA, Unger TL, Keith B, Liu Q, Haase VH. Hypoxia-inducible factor 2 regulates hepatic lipid metabolism. *Mol Cell Biol* 2009; **29**: 4527-4538 [PMID: 19528226 DOI: 10.1128/MCB.00200-09]

96 **National Institute of Diabetes and Digestive and Kidney Diseases**. Corticosteroids. 2012. Available from: https://www.niddk.nih.gov/

97 **Negro F**. Mechanisms and significance of liver steatosis in hepatitis C virus infection. *World J Gastroenterol* 2006; **12**: 6756-6765 [PMID: 17106922 DOI: 10.3748/wjg.v12.i42.6756]

98 **Portincasa P**, Krawczyk M, Smyk W, Lammert F, Di Ciaula A. COVID-19 and non-alcoholic fatty liver disease: Two intersecting pandemics. *Eur J Clin Invest* 2020; **50**: e13338 [PMID: 32589264 DOI: 10.1111/eci.13338]

99 **Wong GL**, Wong VW, Thompson A, Jia J, Hou J, Lesmana CRA, Susilo A, Tanaka Y, Chan WK, Gane E, Ong-Go AK, Lim SG, Ahn SH, Yu ML, Piratvisuth T, Chan HL; Asia-Pacific Working Group for Liver Derangement during the COVID-19 Pandemic. Management of patients with liver derangement during the COVID-19 pandemic: an Asia-Pacific position statement. *Lancet Gastroenterol Hepatol* 2020; **5**: 776-787 [PMID: 32585136 DOI: 10.1016/S2468-1253(20)30190-4]

100 **Ibáñez-Samaniego L**, Bighelli F, Usón C, Caravaca C, Fernández Carrillo C, Romero M, Barreales M, Perelló C, Madejón A, Marcos AC, Albillos A, Fernández I, García-Samaniego J, Calleja JL, Bañares R. Elevation of Liver Fibrosis Index FIB-4 Is Associated With Poor Clinical Outcomes in Patients With COVID-19. *J Infect Dis* 2020; **222**: 726-733 [PMID: 32563190 DOI: 10.1093/infdis/jiaa355]

101 **Eslam M**, Newsome PN, Sarin SK, Anstee QM, Targher G, Romero-Gomez M, Zelber-Sagi S, Wai-Sun Wong V, Dufour JF, Schattenberg JM, Kawaguchi T, Arrese M, Valenti L, Shiha G, Tiribelli C, Yki-Järvinen H, Fan JG, Grønbæk H, Yilmaz Y, Cortez-Pinto H, Oliveira CP, Bedossa P, Adams LA, Zheng MH, Fouad Y, Chan WK, Mendez-Sanchez N, Ahn SH, Castera L, Bugianesi E, Ratziu V, George J. A new definition for metabolic dysfunction-associated fatty liver disease: An international expert consensus statement. *J Hepatol* 2020; **73**: 202-209 [PMID: 32278004 DOI: 10.1016/j.jhep.2020.03.039]

102 **Xu B**, Xing Y, Peng J, Zheng Z, Tang W, Sun Y, Xu C, Peng F. Chest CT for detecting COVID-19: a systematic review and meta-analysis of diagnostic accuracy. *Eur Radiol* 2020; **30**: 5720-5727 [PMID: 32415585 DOI: 10.1007/s00330-020-06934-2]

103 **Wells MM**, Li Z, Addeman B, McKenzie CA, Mujoomdar A, Beaton M, Bird J. Computed Tomography Measurement of Hepatic Steatosis: Prevalence of Hepatic Steatosis in a Canadian Population. *Can J Gastroenterol Hepatol* 2016; **2016**: 4930987 [PMID: 27446844 DOI: 10.1155/2016/4930987]

104 **Kotronen A**, Peltonen M, Hakkarainen A, Sevastianova K, Bergholm R, Johansson LM, Lundbom N, Rissanen A, Ridderstråle M, Groop L, Orho-Melander M, Yki-Järvinen H. Prediction of non-alcoholic fatty liver disease and liver fat using metabolic and genetic factors. *Gastroenterology* 2009; **137**: 865-872 [PMID: 19524579 DOI: 10.1053/j.gastro.2009.06.005]

105 **Long MT**, Pedley A, Colantonio LD, Massaro JM, Hoffmann U, Muntner P, Fox CS. Development and Validation of the Framingham Steatosis Index to Identify Persons With Hepatic Steatosis. *Clin Gastroenterol Hepatol* 2016; **14**: 1172-1180.e2 [PMID: 27046482 DOI: 10.1016/j.cgh.2016.03.034]

106 **McHenry S**, Park Y, Browning JD, Sayuk G, Davidson NO. Dallas Steatosis Index Identifies Patients With Nonalcoholic Fatty Liver Disease. *Clin Gastroenterol Hepatol* 2020; **18**: 2073-2080.e7 [PMID: 31982611 DOI: 10.1016/j.cgh.2020.01.020]

107 **Kulkarni AV**, Kumar P, Tevethia HV, Premkumar M, Arab JP, Candia R, Talukdar R, Sharma M, Qi X, Rao PN, Reddy DN. Systematic review with meta-analysis: liver manifestations and outcomes in COVID-19. *Aliment Pharmacol Ther* 2020; **52**: 584-599 [PMID: 32638436 DOI: 10.1111/apt.15916]

108 **Effenberger M**, Grander C, Fritsche G, Bellmann-Weiler R, Hartig F, Wildner S, Seiwald S, Adolph TE, Zoller H, Weiss G, Tilg H. Liver stiffness by transient elastography accompanies illness severity in COVID-19. *BMJ Open Gastroenterol* 2020; **7** [PMID: 32665398 DOI: 10.1136/bmjgast-2020-000445]

109 **Centers for Disease Control and Prevention**. Certain Medical Conditions and Risk for Severe COVID-19 Illness. Available from: https://www.cdc.gov/coronavirus/2019-ncov/need-extra-precautions/people-with-medical-conditions.html

110 **Marjot T**, Webb GJ, Barritt AS, Ginès P, Lohse AW, Moon AM, Pose E, Trivedi P, Barnes E. SARS-CoV-2 vaccination in patients with liver disease: responding to the next big question. *Lancet Gastroenterol Hepatol* 2021; **6**: 156-158 [PMID: 33444545 DOI: 10.1016/S2468-1253(21)00008-X]

111 **Polack FP**, Thomas SJ, Kitchin N, Absalon J, Gurtman A, Lockhart S, Perez JL, Pérez Marc G, Moreira ED, Zerbini C, Bailey R, Swanson KA, Roychoudhury S, Koury K, Li P, Kalina WV, Cooper D, Frenck RW Jr, Hammitt LL, Türeci Ö, Nell H, Schaefer A, Ünal S, Tresnan DB, Mather S, Dormitzer PR, Şahin U, Jansen KU, Gruber WC; C4591001 Clinical Trial Group. Safety and

Efficacy of the BNT162b2 mRNA Covid-19 Vaccine. *N Engl J Med* 2020; **383**: 2603-2615 [PMID: 33301246 DOI: 10.1056/NEJMoa2034577]

112 **Voysey M**, Clemens SAC, Madhi SA, Weckx LY, Folegatti PM, Aley PK, Angus B, Baillie VL, Barnabas SL, Bhorat QE, Bibi S, Briner C, Cicconi P, Collins AM, Colin-Jones R, Cutland CL, Darton TC, Dheda K, Duncan CJA, Emary KRW, Ewer KJ, Fairlie L, Faust SN, Feng S, Ferreira DM, Finn A, Goodman AL, Green CM, Green CA, Heath PT, Hill C, Hill H, Hirsch I, Hodgson SHC, Izu A, Jackson S, Jenkin D, Joe CCD, Kerridge S, Koen A, Kwatra G, Lazarus R, Lawrie AM, Lelliott A, Libri V, Lillie PJ, Mallory R, Mendes AVA, Milan EP, Minassian AM, McGregor A, Morrison H, Mujadidi YF, Nana A, O'Reilly PJ, Padayachee SD, Pittella A, Plested E, Pollock KM, Ramasamy MN, Rhead S, Schwarzbold AV, Singh N, Smith A, Song R, Snape MD, Sprinz E, Sutherland RK, Tarrant R, Thomson EC, Török ME, Toshner M, Turner DPJ, Vekemans J, Villafana TL, Watson MEE, Williams CJ, Douglas AD, Hill AVS, Lambe T, Gilbert SC, Pollard AJ; Oxford COVID Vaccine Trial Group. Safety and efficacy of the ChAdOx1 nCoV-19 vaccine (AZD1222) against SARS-CoV-2: an interim analysis of four randomised controlled trials in Brazil, South Africa, and the UK. *Lancet* 2021; **397**: 99-111 [PMID: 33306989 DOI: 10.1016/S0140-6736(20)32661-1]

113 **Baden LR**, El Sahly HM, Essink B, Kotloff K, Frey S, Novak R, Diemert D, Spector SA, Rouphael N, Creech CB, McGettigan J, Khetan S, Segall N, Solis J, Brosz A, Fierro C, Schwartz H, Neuzil K, Corey L, Gilbert P, Janes H, Follmann D, Marovich M, Mascola J, Polakowski L, Ledgerwood J, Graham BS, Bennett H, Pajon R, Knightly C, Leav B, Deng W, Zhou H, Han S, Ivarsson M, Miller J, Zaks T; COVE Study Group. Efficacy and Safety of the mRNA-1273 SARS-CoV-2 Vaccine. *N Engl J Med* 2021; **384**: 403-416 [PMID: 33378609 DOI: 10.1056/NEJMoa2035389]

World Journal of Gastroenterology

Submit a Manuscript: https://www.f6publishing.com

World J Gastroenterol 2021 September 7; 27(33): 5520-5535

DOI: 10.3748/wjg.v27.i33.5520

ISSN 1007-9327 (print) ISSN 2219-2840 (online)

MINIREVIEWS

Impact of COVID-19 on inflammatory bowel disease practice and perspectives for the future

Chiara Viganò, Giacomo Mulinacci, Andrea Palermo, Donatella Barisani, Lorena Pirola, Maria Fichera, Pietro Invernizzi, Sara Massironi

ORCID number: Chiara Viganò 0000-0003-3401-1421; Giacomo Mulinacci 0000-0002-9398-893X; Andrea Palermo 0000-0001-8057-9398; Donatella Barisani 0000-0003-4592-6221; Lorena Pirola 0000-0002-2964-0664; Maria Fichera 0000-0002-5787-1371; Pietro Invernizzi 0000-0003-3262-1998; Sara Massironi 0000-0003-3214-8192.

Author contributions: Viganò C and Massironi S planned the work; Viganò C, Mulinacci G and Massironi S contributed to the design and conceptualization of the study; Mulinacci G and Palermo A wrote the first draft of the manuscript and edited figures and tables; Viganò C, Barisani D, Pirola L and Fichera M edited the subsequent versions of the manuscript; Viganò C and Massironi S revised the manuscript for relevant intellectual content; Invernizzi P corrected the final version; All the authors read and approved the final version of the manuscript.

Conflict-of-interest statement: All authors declare no conflict of interest.

Open-Access: This article is an open-access article that was selected by an in-house editor and fully peer-reviewed by external reviewers. It is distributed in

Chiara Viganò, Giacomo Mulinacci, Andrea Palermo, Lorena Pirola, Maria Fichera, Pietro Invernizzi, Sara Massironi, Division of Gastroenterology and Center for Autoimmune Liver Diseases, Department of Medicine and Surgery, University of Milano-Bicocca, Monza 20900, Italy

Chiara Viganò, Giacomo Mulinacci, Andrea Palermo, Lorena Pirola, Maria Fichera, Pietro Invernizzi, Sara Massironi, European Reference Network on Hepatological Diseases, San Gerardo Hospital, Monza 20900, Italy

Donatella Barisani, School of Medicine and Surgery, University of Milano-Bicocca, Monza 20900, Italy

Corresponding author: Chiara Viganò, MD, Doctor, Division of Gastroenterology and Center for Autoimmune Liver Diseases, Department of Medicine and Surgery, University of Milano-Bicocca, Via G. B. Pergolesi 33, Monza 20900, Italy. c.vigano@asst-monza.it

Abstract

Coronavirus disease 2019 (COVID-19) is an infectious disease caused by the novel coronavirus severe acute respiratory syndrome coronavirus 2 (SARS-CoV-2); since its first description in December 2019, it has rapidly spread to a global pandemic. Specific concerns have been raised concerning patients with inflammatory bowel diseases (IBD), which are chronic autoimmune inflammatory disorders of the gut that frequently require immunosuppressive and biological therapies to control their activity. Accumulating evidence has so far demonstrated that patients with IBD are not at increased risk of contracting severe acute respiratory syndrome coronavirus 2 infection. As for the general population, the identified risk factors for severe COVID-19 course among IBD patients have been established to be advanced age and the presence of comorbidities. Treatment with high-dose corticosteroids has also been associated with an increased risk of death in IBD patients with COVID-19. Information on COVID-19 is constantly evolving, with data growing at a rapid pace. This will guarantee better knowledge and stronger evidence to help physicians in the choice of the best therapeutic approach for each patient, concurrently controlling for the risk of IBD disease under treatment and the risk of COVID-19 adverse outcomes and balancing the two. Moreover, the impact of the enormous number of severe respiratory patients on healthcare systems and facilities has led to an unprecedented redeployment of healthcare resources, significantly impacting the care of patients with chronic diseases. In

accordance with the Creative Commons Attribution NonCommercial (CC BY-NC 4.0) license, which permits others to distribute, remix, adapt, build upon this work non-commercially, and license their derivative works on different terms, provided the original work is properly cited and the use is non-commercial. See: http://creativecommons.org/Licenses/by-nc/4.0/

Manuscript source: Invited manuscript

Specialty type: Gastroenterology and hepatology

Country/Territory of origin: Italy

Peer-review report's scientific quality classification

Grade A (Excellent): 0
Grade B (Very good): B
Grade C (Good): C
Grade D (Fair): 0
Grade E (Poor): 0

Received: January 28, 2021
Peer-review started: January 29, 2021
First decision: May 2, 2021
Revised: May 13, 2021
Accepted: August 2, 2021
Article in press: August 2, 2021
Published online: September 7, 2021

P-Reviewer: Bozkurt HS, Dahiya DS
S-Editor: Ma YJ
L-Editor: Filipodia
P-Editor: Xing YX

this newly changed environment, the primary aim is to avoid harm whilst still providing adequate management. Telemedicine has been applied and is strongly encouraged for patients without the necessity of infusion therapy and whose conditions are stable. The severe acute respiratory syndrome coronavirus 2 pandemic has already revolutionized the management of patients with chronic immune-mediated diseases such as IBD. Direct and indirect effects of the COVID-19 pandemic will be present for some time. This is the reason why continuous research, rapid solutions and constantly updated guidelines are of utmost importance. The aim of the present review is, therefore, to point out what has been learned so far as well as to pinpoint the unanswered questions and perspectives for the future.

Key Words: Inflammatory bowel disease; Ulcerative colitis; Crohn disease; COVID-19; SARS-CoV-2; Autoimmunity

©The Author(s) 2021. Published by Baishideng Publishing Group Inc. All rights reserved.

Core Tip: The Severe acute respiratory syndrome coronavirus 2 pandemic has abruptly impacted the management of patients with chronic immune-mediated diseases such as inflammatory bowel diseases. In a setting of general uncertainty, gastroenterologists have faced the need to rapidly reorganize facilities and redefine priorities in inflammatory bowel disease clinical management. With an enormous research effort, accumulating evidence is deepening our understanding of the multifaceted interaction of inflammatory bowel disease care and coronavirus disease 2019. Direct and indirect effects of the pandemic will be present for some time; it is, therefore, necessary to keep recommendations constantly updated.

Citation: Viganò C, Mulinacci G, Palermo A, Barisani D, Pirola L, Fichera M, Invernizzi P, Massironi S. Impact of COVID-19 on inflammatory bowel disease practice and perspectives for the future. *World J Gastroenterol* 2021; 27(33): 5520-5535
URL: https://www.wjgnet.com/1007-9327/full/v27/i33/5520.htm
DOI: https://dx.doi.org/10.3748/wjg.v27.i33.5520

INTRODUCTION

Until the beginning of this century, coronaviruses were known to cause common colds in humans. However, in 2002 and 2013, respectively, the severe acute respiratory syndrome coronavirus (SARS-CoV) and the Middle East Respiratory Syndrome-CoV emerged. Both viruses caused severe respiratory syndromes and were highly pathogenic for humans, with more than 8000 people infected and 919 death caused by SARS-CoV and 2494 cases and 858 death by Middle East Respiratory Syndrome-CoV [1,2]. The third coronavirus epidemic was first reported in December 2019 in Wuhan, China. A new coronavirus, firstly named 2019-nCov and then severe acute respiratory syndrome coronavirus 2 (SARS-CoV-2), was isolated[3]. The World Health Organization then proceeded to name the disease produced by SARS-CoV-2 as coronavirus disease 2019 (COVID-19). COVID-19 has rapidly spread to become a global pandemic, affecting populations in nearly all areas of the world, with high morbidity and mortality rates especially in elderly patients and those affected by chronic illnesses[4]. So far, COVID-19 has infected more than one hundred million people worldwide, causing more than two million deaths[5].

Inflammatory bowel diseases (IBD) encompass ulcerative colitis and Crohn's disease. They are chronic, relapsing, autoimmune inflammatory disorders of the gut, frequently requiring immunosuppressive and biological therapies to control disease activity. Patients with IBD, treated with immune suppressants, are at an increased risk of opportunistic and serious infections[6], including viral infection[7,8]. Hence, particular concerns have been raised for patients suffering from IBD throughout the SARS-CoV-2 pandemic[8], leading the medical community to rapidly generate research in this field and international organizations to release timely recommendations under constant and frequent review.

The gastroenterological community has faced an unprecedented challenge, requiring not only to adapt the therapeutic management of IBD patients and redefine medical priorities but also to reorganize health care facilities.

COVID-19 IN IBD PATIENTS

Accumulating evidence has demonstrated that angiotensin-converting enzyme 2 (ACE2) can mediate SARS-CoV-2 entry into cells[9]. Briefly, the spike protein of SARS-CoV-2 binds to the extracellular portion of ACE2, resulting in the internalization of the complex receptor-virus. This internalization process is favored by the presence of another protein, *i.e.* TMPRSS2, a protease that cleaves the intracellular portion of ACE2. Conversely, another transmembrane protein, called ADAM17, can cleave ACE2 generating its soluble form that could in turn act as a decoy receptor for the virus[10].

ACE2 and TMPRSS2 are physiologically expressed by different cells within the human body, including in the gastrointestinal tract, with peaking concentrations in the terminal ileum and colon. Various single nucleotide polymorphisms have been detected in both genes, but the data so far obtained studying different populations are controversial, not demonstrating a clear genetic predisposition to SARS-CoV-2 infection[11,12]. Nonetheless, in IBD-affected patients, levels of ACE2 are higher than in the general population[13], being the latter independently and differently regulated in the large and small intestines upon inflammation[14,15]. This feature could represent a significantly increased risk of contracting SARS-CoV-2 for IBD patients, even though inflammation also triggers the expression of ADAM17[16], which could have an opposite effect.

Another protein with an increased expression in both IBD and COVID-19 is interleukin 17 (IL-17)[17,18]. It is a cytokine produced and released by T helper 17 lymphocytes, displaying complex and variegate immune functions, and involved in the immune pathogenesis of IBD. In acute respiratory distress syndrome induced both by SARS-CoV-2 infection and other betacoronaviruses, IL-17 levels have been reported to be significantly elevated, and preliminary evidence supports its contribution to immunopathology[19]. Furthermore, it seems that synergism between IL-17 and other cytokines, *i.e.* IL-6, can promote viral replication[20]. The exact role of IL-17 expression and the risk of SARS-CoV-2 infection or COVID-19 disease course is still to be determined; however, agents endowed with anti-IL-17 function, among which probiotic strains of *Bifidobacteria*, have already been proposed as an adjunct therapeutic approach[21,22].

Based on these findings, it was initially hypothesized that patients with IBD could have an increased risk to become infected with SARS-CoV-2. However, the evidence collected so far suggests that the cumulative incidence of the infection [assessed through nasopharyngeal swab (NPS) tests] in IBD patients is similar or even lower to that observed in the general background population during the same pandemic period [23-26]. In a recent Danish nationwide population-based study on IBD-affected patients, the latter displayed a significantly lower prevalence than the general population (2.55% *vs* 3.7%; $P < 0.01$). Whether this occurred secondarily to a more stringent self-isolation and shielding of IBD patients as compared to healthy subjects is yet to be understood.

Furthermore, it seems that immunosuppressive treatments do not increase the risk of contracting SARS-CoV-2[27,28]. This aspect was also confirmed by seroprevalence studies, which showed similar seroprevalence in IBD patients treated with biological agents to the one determined in the general population from the same geographical region[29,30].

Regarding the clinical presentation of COVID-19 in IBD patients, the most frequent symptoms were fever and cough[31]. Yet, diarrhea was more commonly reported in IBD patients with SARS-CoV-2 compared to non-IBD patients, with a prevalence ranging from 8% to 49% in different studies[25,31-36] and a pooled estimate of 20%, which was twice as high as the cumulative prevalence of diarrhea in the general population of COVID-19 patients[31]. This could be attributed to the inflammatory disease itself, but it could also occur as a consequence of exacerbation of intestinal inflammation through a direct viral action on the intestinal epithelium, as suggested by the higher concentration of fecal calprotectin in infected patients with diarrhea[33]. Indeed, a recent cohort study reported a higher prevalence of diarrhea among IBD patients with COVID-19 as compared to non-infected patients, independently from baseline disease activity at multiple regression analyses[32].

Moreover, gastrointestinal (GI) symptoms, including diarrhea, have been described as the sole manifestations of COVID-19 in about 10% of patients[25,37], which is of particular relevance in patients with IBD since the infection could be misinterpreted as disease reactivation. It is therefore of paramount importance to raise awareness among clinicians on these specific clinical features of COVID-19 in patients with IBD and on the need for testing patients accordingly.

GI manifestations may actually help to spot SARS-CoV-2 infection in patients with negative NPS tests, through the assessment of stool samples. PCR testing for SARS-CoV-2 infection with NPS is the currently recommended diagnostic approach, yet false-negative results have occurred[38-43]. Explanations for this have included, besides poor specimen collection, absent or intermittent viral shedding from the upper airways and viral recovery in the oropharyngeal mucosa, whilst the virus may still be present in other tissues. Solid data demonstrated that fecal viral shedding may persist for up to nearly 5 wk following the negativity of NPS[44-48], being more prevalent in patients with GI symptoms in comparison to those with respiratory symptoms alone (73.3% *vs* 14.3%; P = 0.033)[49]. This may indicate that the virus can continue to replicate in the gut after being cleared from the respiratory tract, thus implying the possibility of fecal-oral transmission[45]. Although no clear evidence on the diagnostic performances of PCR testing on stools is available to date, patients with negative NPS and PCR positive stool samples were reported[46,50], and research in this field is rapidly evolving. The current knowledge allows us to speculate that testing for fecal SARS-CoV-2 RNA may be helpful as a complementary tool to the NPS, at least in patients presenting GI alterations and particularly in patients with IBD to distinguish infection from disease reactivation.

On the other hand, it is currently unknown if SARS-CoV-2 infection can interfere with IBD natural history, possibly inducing a disease reactivation. Very preliminary data from a Danish population study demonstrated no risk of relapse in a very small number of patients at 35 d of follow-up[51]; ongoing studies will help to clarify this point.

It has been very recently reported that patients with COVID-19 exhibit significant alterations in fecal microbiota composition, including an increase in opportunistic pathogens and the depletion of commensals. These alterations correlated both with fecal levels of SARS-CoV-2 and COVID-19 severity, irrespective of the medications received, and persisted up to 30 d after disease resolution[52,53]. Whether this persistent dysbiosis could have a role in the development of de novo IBD or in the progression of a pre-existing disease remains to be investigated.

When compared to non-IBD patients, the clinical course and severity of COVID-19 might be somewhat more severe, although definitive evidence is lacking. Data from the SECURE-IBD registry demonstrated, at the earlier stages of the pandemic, a trend toward increased age and sex-standardized mortality ratios compared to the general population in China, the United States and Italy, indicating up to 50% higher mortality in patients with IBD[54]. Though the data were originally not statistically significant, a more recent analysis, based on a total of 3493 reported cases, confirmed earlier findings and reached statistical significance[55]. However, this finding must be interpreted with caution due to the voluntary nature of reporting in the registry, which is therefore affected by several biases. Indeed, a recent population-based retrospective cohort study with propensity score matching for demographic and comorbidities found no difference in hospitalization and mortality for COVID-19 in IBD patients[36].

As in the case of the general population, identified risk factors for severe SARS-CoV-2 infection among IBD patients are advanced age and the presence of comorbidities[26,36,51,54,56].

When considering the risk connected with IBD medications at the time of viral infection, in the SECURE-IBD registry data analysis, systemic corticosteroid administration was positively associated with an increased risk of death (adjusted odds ratio (OR) = 11.62, 95% confidence interval (CI): 2.1-64.7); conversely, the use of anti-tumor necrosis factor (TNF) was associated with a lower rate of hospitalization or death (adjusted OR = 0.60, 95%CI: 0.38-0.96)[57]. A recently published retrospective multicenter study has also confirmed the negative impact of corticosteroids in IBD patients with COVID-19[36]. Similar data emerged from an analysis of 600 patients with rheumatic diseases in which glucocorticoid exposure correlated with a higher odds of hospitalization (OR = 2.05, 95%CI: 1.06-3.96), while the opposite occurred for anti-TNF agents (OR = 0.40, 95%CI: 0.19-0.81)[58].

This might be explained by a selective action of targeted therapies in contrasting some key mediators of the cytokine storm, a major factor in the occurrence of acute respiratory distress syndrome[59], which could counterpart the hypothetic risk of reduced viral clearance.

Conversely, the results from the RECOVERY Trial, the largest randomized controlled trial examining corticosteroids in the treatment of COVID-19 to date, demonstrated that treatment with dexamethasone in dose equivalents similar to those used for IBD treatment are indeed protective against adverse outcomes and mortality for patients hospitalized with COVID-19[60]. These data were confirmed by a recent meta-analysis considering a large number of SARS-CoV-2 infected patients included in seven clinical trials[61].

A possible explanation for such contrasting results may be related to the differential timing of steroid treatment, perhaps leading to diverse clinical scenarios. Indeed, we can speculate that the use of systemic steroids before contraction of a viral infection hampers the immune-system response, thus fostering viral replication. Conversely, treatment at later stages may quench the cytokine storm responsible for the onset of acute respiratory distress syndrome, positively impacting overall survival.

In the most recent analysis of the SECURE-IBD registry collecting 1439 cases and specifically analyzing the effect of IBD medications on COVID-19 course, thiopurine therapy, both alone and in combination with anti-TNF, has emerged as an independent risk factor for severe COVID-19 (aOR of 4.08 and 4.01, respectively) when compared with TNFα antagonist monotherapy[62]. Thiopurines have indeed previously been associated with increased risk of viral infection compared to anti-TNF agents [6]. However, data from the SECURE-IBD, though extremely helpful, need to be interpreted with caution since they are subject to reporting bias, and considering the high proportion of patients treated with anti-TNF agents, they might have overestimated the effect of thiopurines. Recently collected data from a nationwide population-based study of IBD patients with COVID-19, for instance, revealed no impact of immune modulators or biological therapies on the risk of hospitalization or death[51].

For what concerns anti-interleukin-12/23 and anti-integrins, limited data are available on their impact on the course of COVID-19, though general safety data suggests that they are not associated with a significant increased infectious risk. To date, the SECURE-IBD analysis demonstrated no differences compared to anti-TNF drugs[54].

Some concerns have been raised for tofacitinib since it may blunt the innate immune response to viral infection, including inhibition of interferon-gamma activity. Tofacitinib has so far been associated, both in clinical trials and in post-marketing monitoring, with an increased risk of infection, particularly of herpes zoster reactivation [63]. However preliminary data from the SECURE-IBD registry, though focused on a very small number of patients, showed no significant differences between tofacitinib-treated patients and other IBD patients in the occurrence of hospitalization, intensive care unit admission and severe COVID-19[64]. Moreover, recent preclinical evidence is emerging that tofacitinib treatment might in fact reduce ACE2 upregulation and ACE2-mediated intestinal viral uptake[65], and randomized clinical trials for the treatment of COVID-19 pneumonia are ongoing.

Last but not least, it should be kept in mind that the treatment-related risk of infection should be balanced against the disease activity related risk of infection. It has been previously demonstrated that the risk for systemic viral infections (cytomegalovirus and Epstein-Barr virus primary infections and reactivations) in IBD is significantly higher in patients with a clinically active disease[7]. Moreover, active disease is a known risk factor for malnutrition and may lead to hospitalization, thus again raising the infectious risk.

As for SARS-CoV-2 infection, preliminary data coming from two Italian studies identified a correlation between IBD activity and COVID-19 negative outcome[32,56], including a higher risk for pneumonia (OR = 10.25, P = 0.003) and death (OR = 8.45, P = 0.02)[56].

CONCEPT OF FRAILTY FOR IBD PATIENTS

Intensive efforts have been made by the scientific community to identify frail patients requiring more stringent social distancing and further precautions taken to limit the risk for SARS-CoV-2 infection. Since the presence of comorbidities correlates with a higher risk of severe COVID-19, most patients with chronic disorders are considered frail. Specifically regarding IBD patients, while initial data seem reassuring, they should also be regarded as frail. This has been recently supported by the data emerging from the SECURE-IBD registry, pointing towards increased sex-standardized mortality ratios in patients with IBD infected with COVID-19[55].

With these regards, early in the pandemic, the British Society of Gastroenterology categorized IBD patients into three risk groups, each associated with different necessities of social isolation (Table 1)[66]. This risk profiling remains substantially valid, also bearing in mind the newly accumulated evidence. Yet, since the pandemic diffusion varies greatly between countries and constantly fluctuates in severity across time, it is necessary to adapt preventive measures applied to each category accordingly. This would allow tailored preventive measures, according to individual fragility, risk of viral exposure and subsequent negative outcomes upon infection, avoiding on the other hand unnecessary limitations that can negatively impact patient quality of life.

GENERAL RECOMMENDATIONS AND CLINIC REORGANIZATION

Strict social distancing, regular use of face masks and meticulous sanitization of hands and frequently used surfaces, such as phones, tablets, desks, *etc*., with alcohol-based solutions remain the most important recommendations for the general population and should therefore apply to IBD patients as well.

Patients with IBD, still require regular medical follow-up and to some degree hospital access. In this setting, among the adopted general measures to reduce the risk of viral exposure, there has been the postponing of non-urgent outpatient visits and elective endoscopic procedures. As for the latter, the reduced distance between patients and hospital workers, and the air insufflation required by the procedure may increase the risk of SARS-CoV-2 transmission. Specific recommendations on endoscopy in IBD during the COVID-19 pandemic have been released[67].

The use of noninvasive inflammatory markers, such as C-reactive protein and fecal calprotectin for monitoring disease activity, should be encouraged during the pandemic[68]. Fecal calprotectin has been proven to correlate with endoscopic disease extension, mucosal healing and histological activity[69,70]. Home-test measurements of fecal calprotectin could be a valuable alternative, as evidence has demonstrated a good correlation with laboratory determinations[71].

Virtual clinics or online consultants are encouraged for patients without the necessity of infusion therapy and with stable disease, maintaining as much as possible the same timing as the originally scheduled visit. Several accessible and widely available digital technologies have been explored with exciting results[72]. Whenever hospital visits cannot be avoided, symptoms and fever checks at hospital entry, the social distancing of at least 2 m, the use of face masks and strict handwashing policies are highly recommended, even whenever not imposed by state laws.

Patients should ideally be provided with an emergency helpline, given the paramount importance of promptly controlling a disease flare.

Infusion units are dedicated spaces, often located within hospitals, which provide high-quality care during the administration of intravenous drugs for the treatment of several chronic disorders, including IBD. The infusion unit should be regarded as an essential service. A proper organization of the infusion unit is essential to guarantee the safety of both patients and healthcare workers, again through symptoms and fever checks at hospital entry, distancing of beds/chairs of at least 2 m, the use of face masks and strict hand and surface sanitization policies. Furthermore, the turnover of healthcare workers should be limited as much as possible to reduce the risk of viral spread[73]. A telephone screening for symptoms before the scheduled appointment time and rapid SARS-CoV-2 testing can also be considered, based on local epidemiology and resource availability.

Finally, home delivery of subcutaneous drugs should be implemented.

The stress on the healthcare system, with an extremely increased number of severe respiratory patients, has turned the spotlights on the importance to vaccinate people for common influenza virus and *Streptococcus pneumoniae*[74]. It is recommended that all patients with IBD are offered both vaccinations.

It is too early to bring conclusions; however, this pandemic might have sped up the process of a technological revolution in medicine, which will likely change the landscape for the management of patients with chronic diseases, including IBD, also with long-term benefit.

Table 1 British Society of Gastroenterology stratification of inflammatory bowel disease patients according to the risk of severe acute respiratory syndrome coronavirus 2 infection

Highest risk patients"shielding indicated"	Moderate risk patients"stringent social distancing"	Lowest risk patients"social distancing"
Patients who either have a comorbidity (respiratory, cardiac, hypertension or diabetes mellitus) and/or age ≥ 70 yr old and are on any "moderate risk" therapy for IBD (per middle column) and/or have moderate to severely active disease. Patients of any age regardless of comorbidities and who meet one or more of the following: (1) intravenous or oral steroids ≥ 20 mg prednisolone or equivalent per day (only while on this dose); (2) began biologic plus immunomodulator or systemic steroids within previous 6 wk; (3) moderate-to-severe active disease not controlled by "moderate risk" treatments; (4) short bowel syndrome requiring nutritional support; and (5) requirement for parenteral nutrition	Patients with moderate to severely active disease who are not on any of the medications in this column. Patients on the following medications: (1) anti-TNF (infliximab, adalimumab, golimumab) monotherapy; (2) biologic plus immunomodulatory in stable patients; (3) ustekinumab; (4) vedolizumab; (5) Thiopurines (azathioprine, mercaptopurine, tioguanine); (6) methotrexate; (7) calcineurin inhibitors (tacrolimus or ciclosporin); (8) JAK inhibitors (tofacitinib); (9) immunosuppressive trial medication; (10) mycophenolate mofetil; (11) thalidomide; and (12) prednisolone > 20 mg or equivalent per day	Patients on the following medications: (1) 5ASA; (2) rectal therapies; (3) orally administered topically acting steroids (budesonide or beclometasone); (4) therapies for bile acid diarrhea (colestyramine, colesevelam, colestipol); (5) anti-diarrheals (*e.g.*, loperamide); and (6) antibiotics for bacterial overgrowth or perianal disease

5ASA: 5-aminosalicylic acid; IBD: Inflammatory bowel diseases; JAK: Janus kinase; TNF: Tumor necrosis factor.

THERAPEUTIC MANAGEMENT OF IBD DURING SARS-COV-2 PANDEMIC

During this turbulent historical period, the care of chronic patients, including patients with IBD, has necessarily changed and is constantly evolving, reacting and adapting to the evolution of the pandemic.

As a general principle, we must not depart from solid evidence for the therapeutic management of IBD based solely on emergent data that, though extremely valuable, are certainly subject to many biases. Therefore, the principles of IBD management should remain largely unchanged during the pandemic, yet we certainly need to tailor patient care considering whether the patient is infected with SARS-CoV-2, has symptomatic manifestations of COVID-19 and shows underlying activity of the IBD.

Stable IBD course

Published guidelines, position statements and expert opinions agree in affirming that IBD patients with stable disease course and without SARS-CoV-2 infection should maintain the ongoing immunomodulatory treatment since the risk of disease reactivation outweighs the risk of SARS-CoV-2 infection (Table 2)[55,74-78]. As the pandemic ensued, the impossibility to reach hospitals has led to treatment discontinuation in some areas. Among 386 Chinese IBD patients on maintenance therapy during the epidemic[79], 107 (27.7%) have suspended medications, mostly biologics, with resulting disease relapses and hospitalization rates of approximately 25% and 50%, respectively.

Based on the available data, patients on high-dose corticosteroids (prednisolone dose ≥ 20 mg daily) should be informed about the higher risks they are exposed to and therefore encouraged to observe extra protective measures. It is more important than ever to minimize corticosteroid exposure and consider corticosteroid-sparing therapies where appropriate[57,62].

In patients with stable disease, a de-escalation of combination therapy with thiopurine and anti-TNF should be considered[62].

If necessary, it could also be considered to extend dose intervals of intravenous drug injection to reduce hospital visits; for instance, infliximab and vedolizumab infusions can be postponed up to every 8 wk and 10 wk, respectively[80,81]. The switch from infliximab to subcutaneous adalimumab treatment is not recommended, unless intravenous infusions cannot be performed safely; in fact, this elective shift is associated with loss of tolerance and efficacy within 1 year[82].

Patients with stable IBD and positivity for SARS-CoV-2 infection should be considered individually, simultaneously balancing the risk of inflammatory disease reactivation with the risk of severe COVID-19 course (Table 3).

Treatment with non-immunosuppressive medications (5-aminosalicylates) should be continued irrespectively of viral symptoms[74,78] , despite data from the SECURE-IBD registry indicating their association with severe COVID-19 disease course[57,62]. The unexpected nature of this finding from a biological perspective and the presence

Table 2 Summary of treatment in severe acute respiratory syndrome coronavirus-2 negative patients with stable inflammatory bowel disease disease course

Drug	Suggestions	Additional comments
	Continue therapy	
Salicylates	Yes	Data from the SECURE-IBD of possible harm need to be confirmed.
Locally acting steroids	Yes	No specific data available
Systemic steroids	Yes	Limit use to strictly necessary and taper rapidly
Azathioprine	Yes	Data from the SECURE-IBD of possible harm need to be confirmed, the risk of reactivation seems to outweigh the risk of continued treatment
Methotrexate	Yes	Limited data available
Anti-TNF	Yes	Data from the SECURE-IBD indicate better outcomes compared to other treatments; there are ongoing trials for the treatment of COVID-19
Vedolizumab, anti-IL-12/23	Yes	Limited data available
Tofacitinib	Yes	Limited data available

COVID-19: Coronavirus disease 2019; IBD: Inflammatory bowel diseases; IL: Interleukin; TNF: Tumor necrosis factors.

Table 3 Summary of treatment in severe acute respiratory syndrome coronavirus-2 positive patients with stable inflammatory bowel disease disease course

Drug	Suggestions	Additional comments
	Continue therapy	
Salicylates	Yes	A pause can be considered since data suggest a possible association of their use and poor COVID-19 outcome
Locally acting steroids	Yes	No data available
Systemic steroids	Rapid tapering	Dosage below 40 mg/d is suggested along with rapid tapering, particularly in patients without pneumonia and need for oxygen supplementation
Azathioprine	No	Delay treatment for 2 wk and/or until COVID-19 symptoms resolve
Methotrexate	No	Delay treatment for 2 wk and/or until COVID-19 symptoms resolve
Anti-TNF	No	Delay treatment for 2 wk and/or until COVID-19 symptoms resolve. Continued therapy may be considered in selected patients since no data demonstrated adverse outcome to date.
Vedolizumab, anti-IL-12/23	No	Delay treatment for 2 wk and/or until COVID-19 symptoms resolve
Janus kinase inhibitors	No	Delay treatment for 2 wk and/or until COVID-19 symptoms resolve

COVID-19: Coronavirus disease 2019; IL: Interleukin; TNF: Tumor necrosis factors.

of potential unmeasured confounders linked to data collection make further investigations necessary to confirm this association.

Corticosteroids should ideally be rapidly tapered off to the lowest possible dose in patients without symptoms or with mild symptoms. IBD patients presenting COVID-19 symptoms and requiring oxygen supplementation should probably maintain the dose equivalent to prednisone 40 mg/d since data from the RECOVERY trial has demonstrated the beneficial role of 6 mg of dexamethasone (equal to 40 mg prednisone) for up to 10 d in reducing 28 d mortality in patients receiving either invasive mechanical ventilation or oxygen supplementation[60].

The major guidelines state that patients positive for SARS-CoV-2 should interrupt the treatment with azathioprine, 6-mercaptopurine, biologics and Janus kinase inhibitors irrespective of the presence of COVID-19 symptoms[74,76].

However, uncertainty remains on the possibility of continuation of maintenance therapy with biologics in asymptomatic patients, with data from the SECURE-IBD registry and recent evidence suggesting no harm[54,83]. Even if these findings are insufficient to drive any solid conclusion, we might consider maintaining biologic agents in those patients with a high risk of IBD reactivation.

IBD disease reactivation

Telemedicine visits are encouraged as a first approach to gain insights into type and severity of symptoms reported by a patient. The cause underlying the symptoms should be deeply addressed in order to exclude an alternative diagnosis. In particular, all patients with IBD reactivation should undergo SARS-CoV-2 testing through NPS irrespective of respiratory symptoms[84]. Standard stool testing for bacterial and parasitic infections, including test for *Clostridioides difficile* toxins, should always be performed in patients presenting with diarrhea. Functional symptoms should also be considered during this stressful period.

A rapid assessment of the severity of disease activity is advisable, coupling clinical evaluation with noninvasive tests, including blood tests and fecal calprotectin. The reason for a disease flare should be quickly addressed (*i.e.* coinfection, drug immunogenicity or drug resistance) in order to be able to rapidly adjust medical therapy.

The need for face-to-face evaluation should be considered on a case-by-case basis, evaluating both clinical and biochemical parameters. Endoscopic procedures should be limited to what is strictly necessary for treatment decision; whenever possible, it should be replaced with ultrasound examinations or cross-sectional imaging[68].

SARS-CoV-2 negative patients. The management of IBD reactivation in SARS-CoV-2 negative patients should follow the current local and international guidelines, as it occurred in the pre-COVID era[74].

As stated, it appears to be even more important to minimize steroid exposure and consider steroid-sparing maintenance treatments if appropriate. There is currently no conclusive evidence to prefer one agent over another.

Patients must follow general and specific recommendations to reduce the risk of being infected with SARS-CoV-2, considering that active disease may represent an additional risk factor (Table 1).

SARS-CoV-2 positive patients. In mildly active disease a course of locally acting steroids can be instituted, despite the lack of specific evidence on the course of COVID-19. Alternatively, a reasonable approach would be to postpone treatment for 2 wk in order to observe the clinical course of COVID-19 and/or allow resolution of infection[85].

In a moderate to severe flare, there remain doubts about the use of systemic steroids, especially in patients without symptoms of COVID-19 or without need for oxygen supplementation. Indeed, besides the increased risk for adverse outcomes that emerged from the analysis of the SECURE-IBD registry data[54], in the RECOVERY trial patients receiving no respiratory support did not experience any benefit, but rather a trend toward harm was observed[60]. However, the role of high-dose systemic steroids in controlling the underlying IBD disease activity remains often pivotal.

Whenever necessary, a reasonable approach might be to limit the dose of prednisone to 40 mg daily, with rapid dose tapering and switch to maintenance biologic therapy[85].

When needed, biologic agents should be preferred as the first-choice treatment for the induction and maintenance of remission in IBD patients with SARS-CoV-2 since data available indicate their higher safety profile as compared to other drugs[6,54].

A strong emphasis needs to be put on the role of thromboprophylaxis for patients with both active IBD and SARS-CoV-2 infection, given the high rate of thrombotic complications observed in COVID-19 patients[85].

PSYCHOLOGICAL IMPLICATIONS OF SARS-COV-2 IN IBD PATIENTS

Since its first description in December 2019, COVID-19 has created a worldwide sense of fear, termed "coronaphobia," steeply increasing the incidence of various psychiatric manifestations[86]. Even before the pandemic onset, IBD patients were at an increased risk for mental health impairment and psychological comorbidities[87], with a reported incidence of depression and anxiety of up to four times higher than that of the general population[88,89]. During this pandemic, self-isolation, future uncertainty and lack of regular face-to-face contact with the referred physician will likely lead to

the amplification of latent psychopathological conditions or the development of new ones.

In the early phase of the pandemic, an online survey supported by the European Federation of Crohn's and Ulcerative Colitis Associations clearly demonstrated a communication gap between patients and physicians, as only 11% of patients had found relief from their worries from medical consultations[90].

Bearing all this in mind, the role of telemedicine, and perhaps of telepsychology, seems pivotal alongside a close-knit collaboration with patients' associations.

SARS-COV-2 VACCINATION

In December 2020 two mRNA vaccines and one replication-incompetent viral vector vaccine against SARS-CoV-2 have been approved, while many other candidates are currently in phase 3 testing. Vaccination campaigns have started in most countries with prioritization criteria mainly based on the risk of SARS-CoV-2 exposure and the risk of COVID-19 adverse outcomes.

Patients with IBD and other immune-mediated diseases were not included in the registration trials. Data on the safety and efficacy of SARS-CoV-2 vaccinations in these populations are therefore lacking.

The International Organization for the Study of Inflammatory Bowel Disease has recently released recommendations[91], mainly based on the extrapolation of safety and efficacy data from other vaccines.

Non-live vaccines are considered to be safe in patients with IBD, irrespective of immune-modifying treatments, though in the latter case it is acknowledged that the response may be to some degree blunted. In particular, previous studies have shown reduced response to influenza and pneumococcal vaccinations in IBD patients treated with immunosuppressant and anti-TNF agents[92-94]. Treatment with ustekinumab and vedolizumab, on the contrary, does not seem to impair response to influenza and pneumococcal vaccines[95,96].

Therefore, it is recommended that all IBD patients should be vaccinated against SARS-CoV-2, as soon as possible based on local policies, and irrespective of medications. According to the International Organization for the Study of Inflammatory Bowel Disease expert panel, the available SARS-CoV-2 vaccines are safe for patients with IBD, but patients should be informed that vaccine efficacy could be decreased when the latter are administered during corticosteroid therapy[91].

Further studies are definitively needed to assess the safety and efficacy of SARS-CoV-2 vaccines in IBD patients. Whether IBD patients on immune-modifying treatments may benefit from intensified vaccine administration regimen should also be evaluated.

CONCLUSION

Existing evidence shows that IBD patients are not at an increased risk for SARS-CoV-2 infection. As in the case of the general population, older age and presence of comorbidities are the primary risk factors for more severe COVID-19 course. Moreover, systemic steroids exposure has been consistently associated with COVID-19 negative outcomes. For what concerns the other class of IBD medications, no definite evidence of harm has emerged. In the clinical management of patients with IBD the risk of under treatment should be balanced against that of potential adverse outcomes of COVID-19, particularly in the setting of SARS-CoV-2 positive patients. Despite the lack of data, SARS-CoV-2 vaccination is recommended in IBD patients since the risk of the disease outweighs the uncertainty of potential adverse effects.

REFERENCES

1 **Peiris JS**, Guan Y, Yuen KY. Severe acute respiratory syndrome. *Nat Med* 2004; **10**: S88-S97 [PMID: 15577937 DOI: 10.1038/nm1143]

2 **Zaki AM**, van Boheemen S, Bestebroer TM, Osterhaus AD, Fouchier RA. Isolation of a novel coronavirus from a man with pneumonia in Saudi Arabia. *N Engl J Med* 2012; **367**: 1814-1820 [PMID: 23075143 DOI: 10.1056/NEJMoa1211721]

3 **Wu F**, Zhao S, Yu B, Chen YM, Wang W, Song ZG, Hu Y, Tao ZW, Tian JH, Pei YY, Yuan ML,

Zhang YL, Dai FH, Liu Y, Wang QM, Zheng JJ, Xu L, Holmes EC, Zhang YZ. A new coronavirus associated with human respiratory disease in China. *Nature* 2020; **579**: 265-269 [PMID: 32015508 DOI: 10.1038/s41586-020-2008-3]

4 **Yang X**, Yu Y, Xu J, Shu H, Xia J, Liu H, Wu Y, Zhang L, Yu Z, Fang M, Yu T, Wang Y, Pan S, Zou X, Yuan S, Shang Y. Clinical course and outcomes of critically ill patients with SARS-CoV-2 pneumonia in Wuhan, China: a single-centered, retrospective, observational study. Lancet Respir Med 2020; 8: 475-481 [PMID: 32105632 DOI: 10.1016/S2213-2600(20)30079-5]

5 **World Health Organization**. WHO Coronavirus (COVID-19) Dashboard. 2020. Available from: https://covid19.who.int/

6 **Kirchgesner J**, Lemaitre M, Carrat F, Zureik M, Carbonnel F, Dray-Spira R. Risk of Serious and Opportunistic Infections Associated With Treatment of Inflammatory Bowel Diseases. *Gastroenterology* 2018; **155**: 337-346.e10 [PMID: 29655835 DOI: 10.1053/j.gastro.2018.04.012]

7 **Wisniewski A**, Kirchgesner J, Seksik P, Landman C, Bourrier A, Nion-Larmurier I, Marteau P, Cosnes J, Sokol H, Beaugerie L; the Saint-Antoine IBD network. Increased incidence of systemic serious viral infections in patients with inflammatory bowel disease associates with active disease and use of thiopurines. *United European Gastroenterol J* 2020; **8**: 303-313 [PMID: 32529821 DOI: 10.1177/2050640619889763]

8 **Tinsley A**, Navabi S, Williams ED, Liu G, Kong L, Coates MD, Clarke K. Increased Risk of Influenza and Influenza-Related Complications Among 140,480 Patients With Inflammatory Bowel Disease. *Inflamm Bowel Dis* 2019; **25**: 369-376 [PMID: 30020478 DOI: 10.1093/ibd/izy243]

9 **Shang J**, Ye G, Shi K, Wan Y, Luo C, Aihara H, Geng Q, Auerbach A, Li F. Structural basis of receptor recognition by SARS-CoV-2. *Nature* 2020; **581**: 221-224 [PMID: 32225175 DOI: 10.1038/s41586-020-2179-y]

10 **Zipeto D**, Palmeira JDF, Argañaraz GA, Argañaraz ER. ACE2/ADAM17/TMPRSS2 Interplay May Be the Main Risk Factor for COVID-19. *Front Immunol* 2020; **11**: 576745 [PMID: 33117379 DOI: 10.3389/fimmu.2020.576745]

11 **Gómez J**, Albaiceta GM, García-Clemente M, López-Larrea C, Amado-Rodríguez L, Lopez-Alonso I, Hermida T, Enriquez AI, Herrero P, Melón S, Alvarez-Argüelles ME, Boga JA, Rojo-Alba S, Cuesta-Llavona E, Alvarez V, Lorca R, Coto E. Angiotensin-converting enzymes (ACE, ACE2) gene variants and COVID-19 outcome. *Gene* 2020; **762**: 145102 [PMID: 32882331 DOI: 10.1016/j.gene.2020.145102]

12 **Srivastava A**, Bandopadhyay A, Das D, Pandey RK, Singh V, Khanam N, Srivastava N, Singh PP, Dubey PK, Pathak A, Gupta P, Rai N, Sultana GNN, Chaubey G. Genetic Association of *ACE2* rs2285666 Polymorphism With COVID-19 Spatial Distribution in India. *Front Genet* 2020; **11**: 564741 [PMID: 33101387 DOI: 10.3389/fgene.2020.564741]

13 **Garg M**, Royce SG, Tikellis C, Shallue C, Batu D, Velkoska E, Burrell LM, Patel SK, Beswick L, Jackson A, Britto K, Lukies M, Sluka P, Wardan H, Hirokawa Y, Tan CW, Faux M, Burgess AW, Hosking P, Monagle S, Thomas M, Gibson PR, Lubel J. Imbalance of the renin-angiotensin system may contribute to inflammation and fibrosis in IBD: a novel therapeutic target? *Gut* 2020; **69**: 841-851 [PMID: 31409604 DOI: 10.1136/gutjnl-2019-318512]

14 **Nowak JK**, Lindstrøm JC, Kalla R, Ricanek P, Halfvarson J, Satsangi J. Age, Inflammation, and Disease Location Are Critical Determinants of Intestinal Expression of SARS-CoV-2 Receptor *ACE2* and *TMPRSS2* in Inflammatory Bowel Disease. *Gastroenterology* 2020; **159**: 1151-1154.e2 [PMID: 32413354 DOI: 10.1053/j.gastro.2020.05.030]

15 **Suárez-Fariñas M**, Tokuyama M, Wei G, Huang R, Livanos A, Jha D, Levescot A, Irizar H, Kosoy R, Cording S, Wang W, Losic B, Ungaro RC, Di'Narzo A, Martinez-Delgado G, Suprun M, Corley MJ, Stojmirovic A, Houten SM, Peters L, Curran M, Brodmerkel C, Perrigoue J, Friedman JR, Hao K, Schadt EE, Zhu J, Ko HM, Cho J, Dubinsky MC, Sands BE, Ndhlovu L, Cerf-Bensusan N, Kasarskis A, Colombel JF, Harpaz N, Argmann C, Mehandru S. Intestinal Inflammation Modulates the Expression of ACE2 and TMPRSS2 and Potentially Overlaps With the Pathogenesis of SARS-CoV-2-related Disease. *Gastroenterology* 2021; **160**: 287-301.e20 [PMID: 32980345 DOI: 10.1053/j.gastro.2020.09.029]

16 **Perrier C**, Arijs I, Staelens D, Breynaert C, Cleynen I, Covens K, Ferrante M, Van Assche G, Vermeire S, de Hertogh G, Schuit F, Rutgeerts P, Ceuppens JL. Interleukin-15 receptor α expression in inflammatory bowel disease patients before and after normalization of inflammation with infliximab. *Immunology* 2013; **138**: 47-56 [PMID: 23039249 DOI: 10.1111/imm.12014]

17 **Gálvez J**. Role of Th17 Cells in the Pathogenesis of Human IBD. *ISRN Inflamm* 2014; **2014**: 928461 [PMID: 25101191 DOI: 10.1155/2014/928461]

18 **Huang C**, Wang Y, Li X, Ren L, Zhao J, Hu Y, Zhang L, Fan G, Xu J, Gu X, Cheng Z, Yu T, Xia J, Wei Y, Wu W, Xie X, Yin W, Li H, Liu M, Xiao Y, Gao H, Guo L, Xie J, Wang G, Jiang R, Gao Z, Jin Q, Wang J, Cao B. Clinical features of patients infected with 2019 novel coronavirus in Wuhan, China. *Lancet* 2020; **395**: 497-506 [PMID: 31986264 DOI: 10.1016/S0140-6736(20)30183-5]

19 **Pacha O**, Sallman MA, Evans SE. COVID-19: a case for inhibiting IL-17? *Nat Rev Immunol* 2020; **20**: 345-346 [PMID: 32358580 DOI: 10.1038/s41577-020-0328-z]

20 **Hou W**, Jin YH, Kang HS, Kim BS. Interleukin-6 (IL-6) and IL-17 synergistically promote viral persistence by inhibiting cellular apoptosis and cytotoxic T cell function. *J Virol* 2014; **88**: 8479-8489 [PMID: 24829345 DOI: 10.1128/JVI.00724-14]

21 **Bozkurt HS**, Quigley EM. The probiotic *Bifidobacterium* in the management of Coronavirus: A theoretical basis. *Int J Immunopathol Pharmacol* 2020; **34**: 2058738420961304 [PMID: 33103512

DOI: 10.1177/2058738420961304]
22 **Bozkurt HS**, Kara B. A new treatment for ulcerative colitis: Intracolonic Bifidobacterium and xyloglucan application. *Eur J Inflamm* 2020; **18**: 205873922094262 [DOI: 10.1177/2058739220942626]
23 **Allocca M**, Fiorino G, Zallot C, Furfaro F, Gilardi D, Radice S, Danese S, Peyrin-Biroulet L. Incidence and Patterns of COVID-19 Among Inflammatory Bowel Disease Patients From the Nancy and Milan Cohorts. *Clin Gastroenterol Hepatol* 2020; **18**: 2134-2135 [PMID: 32360811 DOI: 10.1016/j.cgh.2020.04.071]
24 **Allocca M**, Chaparro M, Gonzalez HA, Bosca-Watts MM, Palmela C, D'Amico F, Zacharopoulou E, Kopylov U, Ellul P, Bamias G, Ntelis V, Lahat A, Mantzaris GJ, Papaconstantinou I, Katsanos K, Uspenskaya Y, Christodoulou D, Ben Horin S, Peyrin-Biroulet L, Torres J, Sebastian S, Gisbert JP, Danese S, Fiorino G. Patients with Inflammatory Bowel Disease Are Not at Increased Risk of COVID-19: A Large Multinational Cohort Study. *J Clin Med* 2020; **9** [PMID: 33142843 DOI: 10.3390/jcm9113533]
25 **Taxonera C**, Sagastagoitia I, Alba C, Mañas N, Olivares D, Rey E. 2019 novel coronavirus disease (COVID-19) in patients with inflammatory bowel diseases. *Aliment Pharmacol Ther* 2020; **52**: 276-283 [PMID: 32359205 DOI: 10.1111/apt.15804]
26 **Attauabi M**, Poulsen A, Theede K, Pedersen N, Larsen L, Jess T, Rosager Hansen M, Verner-Andersen MK, V Haderslev K, Berg Lødrup A, Molazahi A, Neumann A, Wase A, Seidelin JB, Burisch J. Prevalence and Outcomes of COVID-19 Among Patients With Inflammatory Bowel Disease-A Danish Prospective Population-based Cohort Study. *J Crohns Colitis* 2021; **15**: 540-550 [PMID: 33035299 DOI: 10.1093/ecco-jcc/jjaa205]
27 **Burke KE**, Kochar B, Allegretti JR, Winter RW, Lochhead P, Khalili H, Colizzo FP, Hamilton MJ, Chan WW, Ananthakrishnan AN. Immunosuppressive Therapy and Risk of COVID-19 Infection in Patients With Inflammatory Bowel Diseases. *Inflamm Bowel Dis* 2021; **27**: 155-161 [PMID: 33089863 DOI: 10.1093/ibd/izaa278]
28 **Khan N**, Patel D, Xie D, Lewis J, Trivedi C, Yang YX. Impact of Anti-Tumor Necrosis Factor and Thiopurine Medications on the Development of COVID-19 in Patients With Inflammatory Bowel Disease: A Nationwide Veterans Administration Cohort Study. *Gastroenterology* 2020; **159**: 1545-1546.e1 [PMID: 32479823 DOI: 10.1053/j.gastro.2020.05.065]
29 **Berte' R**, Mazza S, Stefanucci MR, Noviello D, Costa S, Ciafardini C, Mileti E, Mapelli M, Pasqualato S, Pinto S, Favale A, Vecchi M, Neurath MF, Atreya R, Fantini MC, Facciotti F, Caprioli F. Seroprevalence of SARS-CoV2 in IBD Patients Treated with Biologic Therapy. *J Crohns Colitis* 2021; **15**: 864-868 [PMID: 33211810 DOI: 10.1093/ecco-jcc/jjaa237]
30 **Armstrong GL**, Alter MJ, McQuillan GM, Margolis HS. The past incidence of hepatitis C virus infection: implications for the future burden of chronic liver disease in the United States. *Hepatology* 2000; **31**: 777-782 [PMID: 10706572 DOI: 10.1002/hep.510310332]
31 **D'Amico F**, Danese S, Peyrin-Biroulet L. Systematic Review on Inflammatory Bowel Disease Patients With Coronavirus Disease 2019: It Is Time to Take Stock. *Clin Gastroenterol Hepatol* 2020; **18**: 2689-2700 [PMID: 32777550 DOI: 10.1016/j.cgh.2020.08.003]
32 **Viganò C**, Massironi S, Pirola L, Cristoferi L, Fichera M, Bravo M, Mauri M, Redaelli AE, Dinelli ME, Invernizzi P. COVID-19 in Patients With Inflammatory Bowel Disease: A Single-center Observational Study in Northern Italy. *Inflamm Bowel Dis* 2020; **26**: e138-e139 [PMID: 32949238 DOI: 10.1093/ibd/izaa244]
33 **Lukin DJ**, Kumar A, Hajifathalian K, Sharaiha RZ, Scherl EJ, Longman RS; Jill Roberts Center Study Group Study Group; Weill Cornell Medicine-Gastrointestinal Study Group. Baseline Disease Activity and Steroid Therapy Stratify Risk of COVID-19 in Patients With Inflammatory Bowel Disease. *Gastroenterology* 2020; **159**: 1541-1544.e2 [PMID: 32479824 DOI: 10.1053/j.gastro.2020.05.066]
34 **Rodríguez-Lago I**, Ramírez de la Piscina P, Elorza A, Merino O, Ortiz de Zárate J, Cabriada JL. Characteristics and Prognosis of Patients With Inflammatory Bowel Disease During the SARS-CoV-2 Pandemic in the Basque Country (Spain). *Gastroenterology* 2020; **159**: 781-783 [PMID: 32330477 DOI: 10.1053/j.gastro.2020.04.043]
35 **Gubatan J**, Levitte S, Balabanis T, Patel A, Sharma A, Habtezion A. SARS-CoV-2 Testing, Prevalence, and Predictors of COVID-19 in Patients with Inflammatory Bowel Disease in Northern California. *Gastroenterology* 2020; **159**: 1141-1144.e2 [PMID: 32387541 DOI: 10.1053/j.gastro.2020.05.009]
36 **Singh S**, Khan A, Chowdhry M, Bilal M, Kochhar GS, Clarke K. Risk of Severe Coronavirus Disease 2019 in Patients With Inflammatory Bowel Disease in the United States: A Multicenter Research Network Study. *Gastroenterology* 2020; **159**: 1575-1578.e4 [PMID: 32522507 DOI: 10.1053/j.gastro.2020.06.003]
37 **Mao R**, Qiu Y, He JS, Tan JY, Li XH, Liang J, Shen J, Zhu LR, Chen Y, Iacucci M, Ng SC, Ghosh S, Chen MH. Manifestations and prognosis of gastrointestinal and liver involvement in patients with COVID-19: a systematic review and meta-analysis. *Lancet Gastroenterol Hepatol* 2020; **5**: 667-678 [PMID: 32405603 DOI: 10.1016/S2468-1253(20)30126-6]
38 **Xie X**, Zhong Z, Zhao W, Zheng C, Wang F, Liu J. Chest CT for Typical Coronavirus Disease 2019 (COVID-19) Pneumonia: Relationship to Negative RT-PCR Testing. *Radiology* 2020; **296**: E41-E45 [PMID: 32049601 DOI: 10.1148/radiol.2020200343]
39 **Ai T**, Yang Z, Hou H, Zhan C, Chen C, Lv W, Tao Q, Sun Z, Xia L. Correlation of Chest CT and RT-

PCR Testing for Coronavirus Disease 2019 (COVID-19) in China: A Report of 1014 Cases. *Radiology* 2020; **296**: E32-E40 [PMID: 32101510 DOI: 10.1148/radiol.2020200642]

40 **Fang Y**, Zhang H, Xie J, Lin M, Ying L, Pang P, Ji W. Sensitivity of Chest CT for COVID-19: Comparison to RT-PCR. *Radiology* 2020; **296**: E115-E117 [PMID: 32073353 DOI: 10.1148/radiol.2020200432]

41 **Yang Y**, Yang MH, Shen CG, Wang FX, Yuan J, Li JX, Zhang MX, Wang ZQ, Xing L, Wei JL, Peng L, Wong G, Zheng HX, Wu WB, Liao MF, Feng K, Li JM, Yang QT, Zhao JJ, Zhang Z, Liu L, Liu YX. Evaluating the accuracy of different respiratory specimens in the laboratory. 2020 Preprint. Available from: MedRxiv [DOI: 10.1101/2020.02.11.20021493]

42 **Zou L**, Ruan F, Huang M, Liang L, Huang H, Hong Z, Yu J, Kang M, Song Y, Xia J, Guo Q, Song T, He J, Yen HL, Peiris M, Wu J. SARS-CoV-2 Viral Load in Upper Respiratory Specimens of Infected Patients. *N Engl J Med* 2020; **382**: 1177-1179 [PMID: 32074444 DOI: 10.1056/NEJMc2001737]

43 **Wölfel R**, Corman VM, Guggemos W, Seilmaier M, Zange S, Müller MA, Niemeyer D, Jones TC, Vollmar P, Rothe C, Hoelscher M, Bleicker T, Brünink S, Schneider J, Ehmann R, Zwirglmaier K, Drosten C, Wendtner C. Virological assessment of hospitalized patients with COVID-2019. *Nature* 2020; **581**: 465-469 [PMID: 32235945 DOI: 10.1038/s41586-020-2196-x]

44 **Szymczak WA**, Goldstein DY, Orner EP, Fecher RA, Yokoda RT, Skalina KA, Narlieva M, Gendlina I, Fox AS. Utility of Stool PCR for the Diagnosis of COVID-19: Comparison of Two Commercial Platforms. *J Clin Microbiol* 2020; **58** [PMID: 32611796 DOI: 10.1128/JCM.01369-20]

45 **Wu Y**, Guo C, Tang L, Hong Z, Zhou J, Dong X, Yin H, Xiao Q, Tang Y, Qu X, Kuang L, Fang X, Mishra N, Lu J, Shan H, Jiang G, Huang X. Prolonged presence of SARS-CoV-2 viral RNA in faecal samples. *Lancet Gastroenterol Hepatol* 2020; **5**: 434-435 [PMID: 32199469 DOI: 10.1016/S2468-1253(20)30083-2]

46 **Zheng S**, Fan J, Yu F, Feng B, Lou B, Zou Q, Xie G, Lin S, Wang R, Yang X, Chen W, Wang Q, Zhang D, Liu Y, Gong R, Ma Z, Lu S, Xiao Y, Gu Y, Zhang J, Yao H, Xu K, Lu X, Wei G, Zhou J, Fang Q, Cai H, Qiu Y, Sheng J, Chen Y, Liang T. Viral load dynamics and disease severity in patients infected with SARS-CoV-2 in Zhejiang province, China, January-March 2020: retrospective cohort study. *BMJ* 2020; **369**: m1443 [PMID: 32317267 DOI: 10.1136/bmj.m1443]

47 **Wang W**, Xu Y, Gao R, Lu R, Han K, Wu G, Tan W. Detection of SARS-CoV-2 in Different Types of Clinical Specimens. *JAMA* 2020; **323**: 1843-1844 [PMID: 32159775 DOI: 10.1001/jama.2020.3786]

48 **Cheung KS**, Hung IFN, Chan PPY, Lung KC, Tso E, Liu R, Ng YY, Chu MY, Chung TWH, Tam AR, Yip CCY, Leung KH, Fung AY, Zhang RR, Lin Y, Cheng HM, Zhang AJX, To KKW, Chan KH, Yuen KY, Leung WK. Gastrointestinal Manifestations of SARS-CoV-2 Infection and Virus Load in Fecal Samples From a Hong Kong Cohort: Systematic Review and Meta-analysis. *Gastroenterology* 2020; **159**: 81-95 [PMID: 32251668 DOI: 10.1053/j.gastro.2020.03.065]

49 **Han C**, Duan C, Zhang S, Spiegel B, Shi H, Wang W, Zhang L, Lin R, Liu J, Ding Z, Hou X. Digestive Symptoms in COVID-19 Patients With Mild Disease Severity: Clinical Presentation, Stool Viral RNA Testing, and Outcomes. *Am J Gastroenterol* 2020; **115**: 916-923 [PMID: 32301761 DOI: 10.14309/ajg.0000000000000664]

50 **Chen L**, Lou J, Bai Y, Wang M. COVID-19 Disease With Positive Fecal and Negative Pharyngeal and Sputum Viral Tests. *Am J Gastroenterol* 2020; **115**: 790 [PMID: 32205644 DOI: 10.14309/ajg.0000000000000610]

51 **Derikx LAAP**, Lantinga MA, de Jong DJ, van Dop WA, Creemers RH, Römkens TEH, Jansen JM, Mahmmod N, West RL, Tan ACITL, Bodelier AGL, Gorter MHP, Boekema PJ, Halet ERC, Horjus CS, van Dijk MA, Hirdes MMC, Epping Stippel LSM, Jharap B, Lutgens MWMD, Russel MG, Gilissen LPL, Nauta S, van Bodegraven AA, Hoentjen F. Clinical Outcomes of Covid-19 in Patients With Inflammatory Bowel Disease: A Nationwide Cohort Study. *J Crohns Colitis* 2021; **15**: 529-539 [PMID: 33079178 DOI: 10.1093/ecco-jcc/jjaa215]

52 **Zuo T**, Zhang F, Lui GCY, Yeoh YK, Li AYL, Zhan H, Wan Y, Chung ACK, Cheung CP, Chen N, Lai CKC, Chen Z, Tso EYK, Fung KSC, Chan V, Ling L, Joynt G, Hui DSC, Chan FKL, Chan PKS, Ng SC. Alterations in Gut Microbiota of Patients With COVID-19 During Time of Hospitalization. *Gastroenterology* 2020; **159**: 944-955.e8 [PMID: 32442562 DOI: 10.1053/j.gastro.2020.05.048]

53 **Yeoh YK**, Zuo T, Lui GC, Zhang F, Liu Q, Li AY, Chung AC, Cheung CP, Tso EY, Fung KS, Chan V, Ling L, Joynt G, Hui DS, Chow KM, Ng SSS, Li TC, Ng RW, Yip TC, Wong GL, Chan FK, Wong CK, Chan PK, Ng SC. Gut microbiota composition reflects disease severity and dysfunctional immune responses in patients with COVID-19. *Gut* 2021; **70**: 698-706 [PMID: 33431578 DOI: 10.1136/gutjnl-2020-323020]

54 **SECURE-IBD Database**. Coronavirus and IBD Reporting Database. Available from: https://covidibd.org/

55 **Ungaro RC**, Kappelman MD, Rubin DT, Colombel JF. COVID-19 and Inflammatory Bowel Disease: Lessons Learned, Practical Recommendations, and Unanswered Questions. *Gastroenterology* 2021; **160**: 1447-1451 [PMID: 33387525 DOI: 10.1053/j.gastro.2020.12.042]

56 **Bezzio C**, Saibeni S, Variola A, Allocca M, Massari A, Gerardi V, Casini V, Ricci C, Zingone F, Amato A, Caprioli F, Lenti MV, Viganò C, Ascolani M, Bossa F, Castiglione F, Cortelezzi C, Grossi L, Milla M, Morganti D, Pastorelli L, Ribaldone DG, Sartini A, Soriano A, Manes G, Danese S, Fantini MC, Armuzzi A, Daperno M, Fiorino G; Italian Group for the Study of Inflammatory Bowel Disease (IG-IBD). Outcomes of COVID-19 in 79 patients with IBD in Italy: an IG-IBD study. *Gut* 2020; **69**: 1213-1217 [PMID: 32354990 DOI: 10.1136/gutjnl-2020-321411]

57 **Brenner EJ**, Ungaro RC, Gearry RB, Kaplan GG, Kissous-Hunt M, Lewis JD, Ng SC, Rahier JF, Reinisch W, Ruemmele FM, Steinwurz F, Underwood FE, Zhang X, Colombel JF, Kappelman MD. Corticosteroids, But Not TNF Antagonists, Are Associated With Adverse COVID-19 Outcomes in Patients With Inflammatory Bowel Diseases: Results From an International Registry. *Gastroenterology* 2020; **159**: 481-491.e3 [PMID: 32425234 DOI: 10.1053/j.gastro.2020.05.032]

58 **Gianfrancesco M**, Hyrich KL, Al-Adely S, Carmona L, Danila MI, Gossec L, Izadi Z, Jacobsohn L, Katz P, Lawson-Tovey S, Mateus EF, Rush S, Schmajuk G, Simard J, Strangfeld A, Trupin L, Wysham KD, Bhana S, Costello W, Grainger R, Hausmann JS, Liew JW, Sirotich E, Sufka P, Wallace ZS, Yazdany J, Machado PM, Robinson PC; COVID-19 Global Rheumatology Alliance. Characteristics associated with hospitalisation for COVID-19 in people with rheumatic disease: data from the COVID-19 Global Rheumatology Alliance physician-reported registry. *Ann Rheum Dis* 2020; **79**: 859-866 [PMID: 32471903 DOI: 10.1136/annrheumdis-2020-217871]

59 **Coperchini F**, Chiovato L, Croce L, Magri F, Rotondi M. The cytokine storm in COVID-19: An overview of the involvement of the chemokine/chemokine-receptor system. *Cytokine Growth Factor Rev* 2020; **53**: 25-32 [PMID: 32446778 DOI: 10.1016/j.cytogfr.2020.05.003]

60 **RECOVERY Collaborative Group**, Horby P, Lim WS, Emberson JR, Mafham M, Bell JL, Linsell L, Staplin N, Brightling C, Ustianowski A, Elmahi E, Prudon B, Green C, Felton T, Chadwick D, Rege K, Fegan C, Chappell LC, Faust SN, Jaki T, Jeffery K, Montgomery A, Rowan K, Juszczak E, Baillie JK, Haynes R, Landray MJ. Dexamethasone in Hospitalized Patients with Covid-19. *N Engl J Med* 2021; **384**: 693-704 [PMID: 32678530 DOI: 10.1056/NEJMoa2021436]

61 **WHO Rapid Evidence Appraisal for COVID-19 Therapies (REACT) Working Group**, Sterne JAC, Murthy S, Diaz JV, Slutsky AS, Villar J, Angus DC, Annane D, Azevedo LCP, Berwanger O, Cavalcanti AB, Dequin PF, Du B, Emberson J, Fisher D, Giraudeau B, Gordon AC, Granholm A, Green C, Haynes R, Heming N, Higgins JPT, Horby P, Jüni P, Landray MJ, Le Gouge A, Leclerc M, Lim WS, Machado FR, McArthur C, Meziani F, Møller MH, Perner A, Petersen MW, Savovic J, Tomazini B, Veiga VC, Webb S, Marshall JC. Association Between Administration of Systemic Corticosteroids and Mortality Among Critically Ill Patients With COVID-19: A Meta-analysis. *JAMA* 2020; **324**: 1330-1341 [PMID: 32876694 DOI: 10.1001/jama.2020.17023]

62 **Ungaro RC**, Brenner EJ, Gearry RB, Kaplan GG, Kissous-Hunt M, Lewis JD, Ng SC, Rahier JF, Reinisch W, Steinwurz F, Underwood FE, Zhang X, Colombel JF, Kappelman MD. Effect of IBD medications on COVID-19 outcomes: results from an international registry. *Gut* 2021; **70**: 725-732 [PMID: 33082265 DOI: 10.1136/gutjnl-2020-322539]

63 **Antonelli E**, Torti G, Bassotti G. Inhibitors of the Janus Kinases: A New Oral Treatment Option for Ulcerative Colitis. *J Clin Gastroenterol* 2019; **53**: 635-640 [PMID: 31373941 DOI: 10.1097/MCG.0000000000001250]

64 **Agrawal M**, Corn G, Shrestha S, Nielsen NM, Frisch M, Colombel JF, Jess T. Inflammatory bowel diseases among first-generation and second-generation immigrants in Denmark: a population-based cohort study. *Gut* 2021; **70**: 1037-1043 [PMID: 32895335 DOI: 10.1136/gutjnl-2020-321798]

65 **Spalinger MR**, Hai R, Li J, Santos AN, Nordgren TM, Tremblay ML, Eckmann L, Hanson E, Scharl M, Wu X, Boland BS, McCole DF. Identification of a Novel Susceptibility Marker for SARS-CoV-2 Infection in Human Subjects and Risk Mitigation with a Clinically Approved JAK Inhibitor in Human/Mouse Cells. *bioRxiv* 2020 [PMID: 33330862 DOI: 10.1101/2020.12.09.416586]

66 **BSG**. BSG expanded consensus advice for the management of IBD during the COVID-19 pandemic. Available from: https://www.bsg.org.uk/covid-19-advice/bsg-advice-for-management-of-inflammatory-bowel-diseases-during-the-covid-19-pandemic

67 **Iacucci M**, Cannatelli R, Labarile N, Mao R, Panaccione R, Danese S, Kochhar GS, Ghosh S, Shen B. Endoscopy in inflammatory bowel diseases during the COVID-19 pandemic and post-pandemic period. *Lancet Gastroenterol Hepatol* 2020; **5**: 598-606 [PMID: 32305075 DOI: 10.1016/S2468-1253(20)30119-9]

68 **Ng SC**, Mak JWY, Hitz L, Chowers Y, Bernstein CN, Silverberg MS. COVID-19 Pandemic: Which IBD Patients Need to Be Scoped-Who Gets Scoped Now, Who Can Wait, and how to Resume to Normal. *J Crohns Colitis* 2020; **14**: S791-S797 [PMID: 33085973 DOI: 10.1093/ecco-jcc/jjaa128]

69 **D'Amico F**, Bonovas S, Danese S, Peyrin-Biroulet L. Review article: faecal calprotectin and histologic remission in ulcerative colitis. *Aliment Pharmacol Ther* 2020; **51**: 689-698 [PMID: 32048751 DOI: 10.1111/apt.15662]

70 **Lin JF**, Chen JM, Zuo JH, Yu A, Xiao ZJ, Deng FH, Nie B, Jiang B. Meta-analysis: fecal calprotectin for assessment of inflammatory bowel disease activity. *Inflamm Bowel Dis* 2014; **20**: 1407-1415 [PMID: 24983982 DOI: 10.1097/MIB.0000000000000057]

71 **Heida A**, Knol M, Kobold AM, Bootsman J, Dijkstra G, van Rheenen PF. Agreement Between Home-Based Measurement of Stool Calprotectin and ELISA Results for Monitoring Inflammatory Bowel Disease Activity. *Clin Gastroenterol Hepatol* 2017; **15**: 1742-1749.e2 [PMID: 28606846 DOI: 10.1016/j.cgh.2017.06.007]

72 **Lees CW**, Regueiro M, Mahadevan U; International Organization for the Study of Inflammatory Bowel Disease. Innovation in Inflammatory Bowel Disease Care During the COVID-19 Pandemic: Results of a Global Telemedicine Survey by the International Organization for the Study of Inflammatory Bowel Disease. *Gastroenterology* 2020; **159**: 805-808.e1 [PMID: 32474119 DOI: 10.1053/j.gastro.2020.05.063]

73 **Scaldaferri F**, Pugliese D, Privitera G, Onali S, Lopetuso LR, Rizzatti G, Settanni CR, Pizzoferrato M, Schiavoni E, Turchini L, Amatucci V, Napolitano D, Bernabei T, Mora V, Laterza L, Papa A,

Guidi L, Rapaccini GL, Gasbarrini A, Armuzzi A. Impact of COVID-19 pandemic on the daily management of biotechnological therapy in inflammatory bowel disease patients: Reorganisational response in a high-volume Italian inflammatory bowel disease centre. *United European Gastroenterol J* 2020; **8**: 775-781 [PMID: 32438878 DOI: 10.1177/2050640620929133]

74 **Magro F**, Rahier JF, Abreu C, MacMahon E, Hart A, van der Woude CJ, Gordon H, Adamina M, Viget N, Vavricka S, Kucharzik T, Leone S, Siegmund B, Danese S, Peyrin-Biroulet L. Inflammatory Bowel Disease Management During the COVID-19 Outbreak: The Ten Do's and Don'ts from the ECCO-COVID Taskforce. *J Crohns Colitis* 2020; **14**: S798-S806 [PMID: 32722754 DOI: 10.1093/ecco-jcc/jjaa160]

75 **Mao R**, Liang J, Shen J, Ghosh S, Zhu LR, Yang H, Wu KC, Chen MH; Chinese Society of IBD, Chinese Elite IBD Union; Chinese IBD Quality Care Evaluation Center Committee. Implications of COVID-19 for patients with pre-existing digestive diseases. *Lancet Gastroenterol Hepatol* 2020; **5**: 425-427 [PMID: 32171057 DOI: 10.1016/S2468-1253(20)30076-5]

76 **Rubin DT**, Abreu MT, Rai V, Siegel CA; International Organization for the Study of Inflammatory Bowel Disease. Management of Patients With Crohn's Disease and Ulcerative Colitis During the Coronavirus Disease-2019 Pandemic: Results of an International Meeting. *Gastroenterology* 2020; **159**: 6-13.e6 [PMID: 32272113 DOI: 10.1053/j.gastro.2020.04.002]

77 **Kennedy NA**, Jones GR, Lamb CA, Appleby R, Arnott I, Beattie RM, Bloom S, Brooks AJ, Cooney R, Dart RJ, Edwards C, Fraser A, Gaya DR, Ghosh S, Greveson K, Hansen R, Hart A, Hawthorne AB, Hayee B, Limdi JK, Murray CD, Parkes GC, Parkes M, Patel K, Pollok RC, Powell N, Probert CS, Raine T, Sebastian S, Selinger C, Smith PJ, Stansfield C, Younge L, Lindsay JO, Irving PM, Lees CW. British Society of Gastroenterology guidance for management of inflammatory bowel disease during the COVID-19 pandemic. *Gut* 2020; **69**: 984-990 [PMID: 32303607 DOI: 10.1136/gutjnl-2020-321244]

78 **Rubin DT**, Feuerstein JD, Wang AY, Cohen RD. AGA Clinical Practice Update on Management of Inflammatory Bowel Disease During the COVID-19 Pandemic: Expert Commentary. *Gastroenterology* 2020; **159**: 350-357 [PMID: 32283100 DOI: 10.1053/j.gastro.2020.04.012]

79 **Chen J**, Peng X, Zhang M, Zhi M. Impact of Medication Discontinuation on Patients With Inflammatory Bowel Disease During the COVID-19 Outbreak. *Gastroenterology* 2021; **160**: 2223 [PMID: 32553758 DOI: 10.1053/j.gastro.2020.05.087]

80 **Sandborn WJ**, Feagan BG, Rutgeerts P, Hanauer S, Colombel JF, Sands BE, Lukas M, Fedorak RN, Lee S, Bressler B, Fox I, Rosario M, Sankoh S, Xu J, Stephens K, Milch C, Parikh A; GEMINI 2 Study Group. Vedolizumab as induction and maintenance therapy for Crohn's disease. *N Engl J Med* 2013; **369**: 711-721 [PMID: 23964933 DOI: 10.1056/NEJMoa1215739]

81 **Papamichael K**, Karatzas P, Mantzaris GJ. De-escalation of Infliximab Maintenance Therapy from 8- to 10-week Dosing Interval Based on Faecal Calprotectin in Patients with Crohn's Disease. *J Crohns Colitis* 2016; **10**: 371-372 [PMID: 26546496 DOI: 10.1093/ecco-jcc/jjv206]

82 **Van Assche G**, Vermeire S, Ballet V, Gabriels F, Noman M, D'Haens G, Claessens C, Humblet E, Vande Casteele N, Gils A, Rutgeerts P. Switch to adalimumab in patients with Crohn's disease controlled by maintenance infliximab: prospective randomised SWITCH trial. *Gut* 2012; **61**: 229-234 [PMID: 21948942 DOI: 10.1136/gutjnl-2011-300755]

83 **Mcgregor CG**, Adams A, Sadler R, Arancibia-Cárcamo CV, Satsangi J. Maintenance therapy with infliximab or vedolizumab in inflammatory bowel disease is not associated with increased SARS-CoV-2 seroprevalence: UK experience in the 2020 pandemic. 2020 Preprint. Available from: medRxiv [DOI: 10.1101/2020.12.12.20247841]

84 **Zingone F**, Savarino EV. Viral screening before initiation of biologics in patients with inflammatory bowel disease during the COVID-19 outbreak. *Lancet Gastroenterol Hepatol* 2020; **5**: 525 [PMID: 32220656 DOI: 10.1016/S2468-1253(20)30085-6]

85 **Allez M**, Fleshner P, Gearry R, Lakatos PL, Rubin DT. Care of the Patient With IBD Requiring Hospitalisation During the COVID-19 Pandemic. *J Crohns Colitis* 2020; **14**: S774-S779 [PMID: 32722757 DOI: 10.1093/ecco-jcc/jjaa150]

86 **Dubey S**, Biswas P, Ghosh R, Chatterjee S, Dubey MJ, Lahiri D, Lavie CJ. Psychosocial impact of COVID-19. *Diabetes Metab Syndr* 2020; **14**: 779-788 [PMID: 32526627 DOI: 10.1016/j.dsx.2020.05.035]

87 **Sajadinejad MS**, Asgari K, Molavi H, Kalantari M, Adibi P. Psychological issues in inflammatory bowel disease: an overview. *Gastroenterol Res Pract* 2012; **2012**: 106502 [PMID: 22778720 DOI: 10.1155/2012/106502]

88 **Graff LA**, Walker JR, Bernstein CN. Depression and anxiety in inflammatory bowel disease: a review of comorbidity and management. *Inflamm Bowel Dis* 2009; **15**: 1105-1118 [PMID: 19161177 DOI: 10.1002/ibd.20873]

89 **Neuendorf R**, Harding A, Stello N, Hanes D, Wahbeh H. Depression and anxiety in patients with Inflammatory Bowel Disease: A systematic review. *J Psychosom Res* 2016; **87**: 70-80 [PMID: 27411754 DOI: 10.1016/j.jpsychores.2016.06.001]

90 **D'Amico F**, Rahier JF, Leone S, Peyrin-Biroulet L, Danese S. Views of patients with inflammatory bowel disease on the COVID-19 pandemic: a global survey. *Lancet Gastroenterol Hepatol* 2020; **5**: 631-632 [PMID: 32411920 DOI: 10.1016/S2468-1253(20)30151-5]

91 **Siegel CA**, Melmed GY, McGovern DP, Rai V, Krammer F, Rubin DT, Abreu MT, Dubinsky MC; International Organization for the Study of Inflammatory Bowel Disease (IOIBD); International Organization for the Study of Inflammatory Bowel Diseases (IOIBD). SARS-CoV-2 vaccination for

patients with inflammatory bowel diseases: recommendations from an international consensus meeting. *Gut* 2021; **70**: 635-640 [PMID: 33472895 DOI: 10.1136/gutjnl-2020-324000]

92 **Fiorino G**, Lytras T, Younge L, Fidalgo C, Coenen S, Chaparro M, Allocca M, Arnott I, Bossuyt P, Burisch J, Campmans-Kuijpers M, de Ridder L, Dignass A, Drohan C, Feakins R, Gilardi D, Grosek J, Groß E, Hart A, Jäghult S, Katsanos K, Lönnfors S, Panis Y, Perovic M, Pierik M, Rimola J, Tulchinsky H, Gisbert JP. Quality of Care Standards in Inflammatory Bowel Diseases: a European Crohn's and Colitis Organisation [ECCO] Position Paper. *J Crohns Colitis* 2020; **14**: 1037-1048 [PMID: 32032423 DOI: 10.1093/ecco-jcc/jjaa023]

93 **Melmed GY**, Agarwal N, Frenck RW, Ippoliti AF, Ibanez P, Papadakis KA, Simpson P, Barolet-Garcia C, Ward J, Targan SR, Vasiliauskas EA. Immunosuppression impairs response to pneumococcal polysaccharide vaccination in patients with inflammatory bowel disease. *Am J Gastroenterol* 2010; **105**: 148-154 [PMID: 19755964 DOI: 10.1038/ajg.2009.523]

94 **Mamula P**, Markowitz JE, Piccoli DA, Klimov A, Cohen L, Baldassano RN. Immune response to influenza vaccine in pediatric patients with inflammatory bowel disease. *Clin Gastroenterol Hepatol* 2007; **5**: 851-856 [PMID: 17544875 DOI: 10.1016/j.cgh.2007.02.035]

95 **Caldera F**, Hillman L, Saha S, Wald A, Grimes I, Zhang Y, Sharpe AR, Reichelderfer M, Hayney MS. Immunogenicity of High Dose Influenza Vaccine for Patients with Inflammatory Bowel Disease on Anti-TNF Monotherapy: A Randomized Clinical Trial. *Inflamm Bowel Dis* 2020; **26**: 593-602 [PMID: 31504526 DOI: 10.1093/ibd/izz164]

96 **Brodmerkel C**, Wadman E, Langley RG, Papp KA, Bourcier M, Poulin Y, Ho V, Guenther L, Kunynetz R, Nigen S, Vender R, Wasel N, Hsu MC, Szapary P. Immune response to pneumococcus and tetanus toxoid in patients with moderate-to-severe psoriasis following long-term ustekinumab use. *J Drugs Dermatol* 2013; **12**: 1122-1129 [PMID: 24085047]

World Journal of Gastroenterology

Submit a Manuscript: https://www.f6publishing.com

World J Gastroenterol 2021 September 7; 27(33): 5536-5554

DOI: 10.3748/wjg.v27.i33.5536

ISSN 1007-9327 (print) ISSN 2219-2840 (online)

MINIREVIEWS

Surveillance for hepatocellular carcinoma in chronic viral hepatitis: Is it time to personalize it?

Coskun Ozer Demirtas, Maurizia Rossana Brunetto

ORCID number: Coskun Ozer Demirtas 0000-0002-0004-2740; Maurizia Rossana Brunetto 0000-0001-8364-9152.

Author contributions: Demirtas CO performed the literature search and wrote the paper; Brunetto MR critically revised the manuscript; All authors approved the final version of the manuscript.

Conflict-of-interest statement: The authors declare no conflict of interests for this article.

Open-Access: This article is an open-access article that was selected by an in-house editor and fully peer-reviewed by external reviewers. It is distributed in accordance with the Creative Commons Attribution NonCommercial (CC BY-NC 4.0) license, which permits others to distribute, remix, adapt, build upon this work non-commercially, and license their derivative works on different terms, provided the original work is properly cited and the use is non-commercial. See: http://creativecommons.org/Licenses/by-nc/4.0/

Manuscript source: Invited manuscript

Specialty type: Gastroenterology and hepatology

Coskun Ozer Demirtas, Department of Gastroenterology and Hepatology, Marmara University, School of Medicine, Istanbul 34854, Turkey

Maurizia Rossana Brunetto, Department of Clinical and Experimental Medicine, University Hospital of Pisa, Pisa 56125, Italy

Maurizia Rossana Brunetto, Hepatology Unit, University Hospital of Pisa, Pisa 56125, Italy

Maurizia Rossana Brunetto, Biostructure and Bio-imaging Institute, National Research Council of Italy, Naples 56125, Italy

Corresponding author: Coskun Ozer Demirtas, MD, Postdoctoral Fellow, Department of Gastroenterology and Hepatology, Marmara University, School of Medicine, Marmara Üniversitesi Göztepe Yerleşkesi, Istanbul 34854, Turkey. coskun_demirtas10@hotmail.com

Abstract

Surveillance with abdominal ultrasound with or without alpha-fetoprotein is recommended by clinical practice guidelines for patients who are considered to be at risk of developing hepatocellular carcinoma (HCC), including those with cirrhosis, advanced fibrosis and special subgroups of chronic hepatitis B (CHB). Application of the standard surveillance strategy to all patients with chronic liver disease (CLD) with or without cirrhosis imposes major sustainability and economic burdens on healthcare systems. Thus, a number of HCC risk scores were constructed, mainly from Asian cohorts, to stratify the HCC prediction in patients with CHB. Similarly, even if less than for CHB, a few scoring systems were developed for chronic hepatitis C patients or cirrhotic patients with CLD of different etiologies. Recently, a few newsworthy HCC-risk algorithms were developed for patients with cirrhosis using the combination of serologic HCC markers and clinical parameters. Overall, the HCC risk stratification appears at hand by several validated multiple score systems, but their optimal performance is obtained only in populations who show highly homogenous clinic-pathologic, epidemiologic, etiologic and therapeutic characteristics and this limitation poses a major drawback to their sustainable use in clinical practice. A better understanding of the dynamic process driving the progression from CLD to HCC derived from studies based on molecular approaches and genetics, epigenetics and liquid biopsy will enable the identification of new biomarkers to define the individual risk of HCC in the near future, with the possibility to achieve a real and cost/effective personalization of surveillance.

Country/Territory of origin: Turkey

Peer-review report's scientific quality classification
Grade A (Excellent): 0
Grade B (Very good): B
Grade C (Good): 0
Grade D (Fair): 0
Grade E (Poor): 0

Received: February 11, 2021
Peer-review started: February 11, 2021
First decision: April 18, 2021
Revised: April 28, 2021
Accepted: August 2, 2021
Article in press: August 2, 2021
Published online: September 7, 2021

P-Reviewer: Filipec Kanizaj T
S-Editor: Zhang H
L-Editor: Filipodia
P-Editor: Li JH

Key Words: Hepatocellular carcinoma; Surveillance; Chronic viral hepatitis; Risk score; Risk-stratification; Hepatitis B virus; Hepatitis C virus

©The Author(s) 2021. Published by Baishideng Publishing Group Inc. All rights reserved.

Core Tip: The risk of hepatocellular carcinoma (HCC) is not uniform and may increase due to underlying parameters in chronic viral hepatitis. Several clinical HCC risk scores and biomarker integrated algorithms have been proposed to stratify patients according to their HCC risk level. In the present review, we summarize the efforts for personalized HCC surveillance in the literature and discuss their applicability to clinical practice.

Citation: Demirtas CO, Brunetto MR. Surveillance for hepatocellular carcinoma in chronic viral hepatitis: Is it time to personalize it? *World J Gastroenterol* 2021; 27(33): 5536-5554
URL: https://www.wjgnet.com/1007-9327/full/v27/i33/5536.htm
DOI: https://dx.doi.org/10.3748/wjg.v27.i33.5536

INTRODUCTION

Hepatocellular carcinoma (HCC) is the fifth most common cancer and the second leading cause of cancer-related deaths globally[1]. The majority of HCC cases (> 90%), at least in the Western countries, occur in the setting of cirrhosis, as approximately one-third of patients with cirrhosis eventually develop HCC in the long term, with an annual risk of 1%-8%, varying upon several risk factors[2,3]. Globally, approximately 80% of HCC are associated with hepatitis B virus (HBV) or hepatitis C virus (HCV) infection and their geographical distribution depends on the epidemiology of the two viral infections. Most HCCs are associated with chronic hepatitis B (CHB) virus infection (> 60%) in Asian countries, whereas chronic hepatitis C (CHC) appears to be the most commonly established etiology for HCC in western countries[4]. However, in recent years, a progressive increase of HCC in patients with non-viral (mainly metabolic) liver disease has been reported[5].

CHB has carcinogenetic potential itself by several insertional mutagenetic routes, and up to 30% of CHB-related HCCs arise in non-cirrhotic liver, mainly in Asian patients[6]. Current management of CHB with long-term nucleotide analogues treatment by inhibiting HBV replication had been shown to decrease HCC incidence. Nevertheless, despite on-therapy virological remission, the annual incidence of HCC ranges from 0.01% to 5.4% in CHB[7]. In the last decade, wondrous new achievements occurred in the treatment of CHC, and sustained virological response (SVR) rates exceeded 95% with direct-acting antiviral (DAA) therapies[8]. Successful DAA treatment has resulted in a 71% reduction in HCC risk[9]. The HCC incidence fell from 3.6% to 1.8% per year with the DAA therapies[10]. However, many patients, after the clearance of HCV infection, maintain additional co-factors of liver disease (*i.e.* metabolic or alcohol-induced liver damage) that may contribute to the persistence of a significant HCC risk. Accordingly, a recent long-term study conducted in the Veterans cohort showed that HCC incidence remained stable at 1.5 to 2.3/100 person years, even up to 3.6 years, after DAA-induced SVR[11]. Cirrhosis is the primary risk factor for HCC regardless of liver disease etiology, with an annual HCC incidence greater than 1%[12]. CHC patients with cirrhosis and advanced fibrosis (F3) continue to have a significantly elevated risk of HCC despite achieving SVR and have stayed the target of surveillance programs. According to the general principles of surveillance, the definition of the target population must consider the incidence of HCC in a specific set of patients and the probability that effective therapies, particularly the curative ones, can be applied to these patients. Decision analysis and cost-effectiveness models suggest that an intervention is considered cost-effective if it provides life expectancy increases of at least 3 mo with a cost below the threshold of ultrasonography (US) of $50000 per year of lives saved[13]. Based on these premises, there is currently a general consensus on using abdominal US with or without alpha-fetoprotein (AFP) as a diagnostic tool to perform HCC surveillance.

Beyond the fact that several host-related (cirrhosis, chronic hepatic necroinflammation, older age, male sex, African origin, alcohol abuse, chronic co-infections with other hepatitis viruses or human immunodeficiency virus, diabetes or metabolic syndrome, active smoking, positive family history) and virus-related (high HBV-DNA and/or hepatitis B surface antigen [HBsAg] levels, HBV genotype C > B, specific mutations) factors influence the risk of HCC development[14], in the setting of CHB, HCC surveillance is recommended by American Association for the Study of Liver Diseases (AASLD), Asia-Pacific Association for the Study of Liver Diseases and European Association for the Study of Liver Diseases (EASL) for all patients with cirrhosis, hepatitis B carriers with a family history of HCC, Asian males older than 40 years, Asian females older than 50 years, and African males older than 20 years[15-18]. Additionally, all patients with chronic liver disease (CLD) and advanced fibrosis (F3) are also recommended to undergo HCC surveillance by EASL[18] (Table 1). In general, a cut-off for HCC incidence of 0.2%/year for hepatitis B, 1.5%/year for hepatitis C and all cirrhotics regardless of etiology is considered cost-effective for HCC surveillance, since it was first described in AASLD guidelines in 2005[19]. However, an area of uncertainty exists for CHC patients with viral clearance but F3 fibrosis. On one hand, the AASLD HCV guidance statement recommends HCC surveillance for this group, but on the other, the AASLD HCC guidance statement recommends surveillance only in presence of cirrhosis[16,20]. A recent study, using the Markov model, found out that HCC surveillance is cost-effective among CHC patients with cirrhosis but not for those with F3 fibrosis[21]. However, in clinical practice, the differentiation between advanced fibrosis (F3) and cirrhosis is not always straightforward. For this reason, EASL recommends HCC surveillance to patients with F3 fibrosis regardless of etiology, with a more clinically oriented approach. Given the limitations of the current surveillance protocols, several HCC risk scores have been developed mainly from Asian cohorts for patients with CHB. Even if in limited number, a few risk scores are also available for CHC or all-cirrhotic patients.

In this review, we summarize the characteristics and discuss the applicability of HCC-risk scores in clinical practice, with a special focus on chronic viral hepatitis. Several reviews investigated the impact of HCC risk scores on clinical practice in recent years, but newer scores and comparison studies have emerged since then[22-25]. Furthermore, new serologic biomarkers have been introduced for early detection of HCC with promising results, and some of them got involved in algorithms in combination with clinical and laboratory parameters.

HCC RISK SCORES FOR CHB PATIENTS

Risk scores for untreated CHB patients

The guide with age, gender, HBV-DNA, core promoter mutations, and cirrhosis (GAG-HCC) risk score was the first attempt to stratify HCC risk among CHB patients, which was published in 2009[26]. The study was conducted with 820 untreated CHB subjects (15% with cirrhosis) from Hong-Kong, and all patients were followed up for a median period of 77 mo. They showed that cirrhosis, age, gender, viral load, and precore mutation were independent predictors of HCC and used them all in the risk score. However, due to the unavailability of pre-core mutation assays in the routine clinical practice, they repeated the analysis without this variable and showed no loss of performance in the risk score. The area under the receiver-operating characteristics curve (AUROC) for GAG-HCC to predict HCC in 5 and 10 years was 0.87 and 0.88, respectively. The determined optimal cut-off value of 101 showed high sensitivity (88%) and specificity (78.7%) for the prediction of HCC at 10 years. Chinese University-HCC risk score (CU-HCC) was the second attempt for HCC risk stratification in CHB patients, which was published in 2010[27]. Using the same methodology, the investigators confirmed age, viral load, and cirrhosis as independent predictors of HCC during a median follow-up period of 10 years, with the addition of two markers of liver function (bilirubin and albumin). They proposed a three category risk score to distinguish low (< 5), intermediate (5-20), and high risk (> 20) CHB patients for HCC development. The model showed a good general performance in predicting 5- and 10-year HCC risk by showing AUROC values of 0.76 and 0.78, respectively. The 5-year HCC-free survival rates were 98.3%, 90.5%, and 78.9% in the low-, medium-, and high-risk groups, respectively. The determined cut-off value of 5 ruled out the risk of HCC development with high accuracy (negative predictive value [NPV] of 97.8% and 97.3 in training and validation cohorts, respectively), suggesting that HCC surveillance in low-risk group may not be cost-effective. Interestingly, the

Table 1 Patients for whom surveillance of hepatocellular carcinoma is recommended according to society guidelines

Cirrhotic patients regardless of etiology, Child-Pugh stage A-B[12-14]
Cirrhotic patients regardless of etiology, Child-Pugh stage C awaiting liver transplantation[12-14]
Asian male hepatitis B carriers over the age of 40 yr[12-14]
Asian female hepatitis B carriers over the age of 50 yr[12-14]
Hepatitis B carriers with a family history of HCC[12-14]
Non-cirrhotic F3 patients, regardless of etiology, may be considered for surveillance based on an individual risk assessment[14]

HCC: Hepatocellular carcinoma.

authors of GAG-HCC and CU-HCC, despite proposing their risk scores as tools to identify CHB patients at high risk for HCC development, never suggested their applicability in selecting candidates for HCC surveillance.

After two relatively small-sized studies, another HCC-risk score for untreated CHB patients without cirrhosis was proposed from Taiwan in 2010[28]. The risk estimation for hepatocellular carcinoma in chronic hepatitis B (REACH-B) score was developed in 3584 CHB Taiwanese patients without cirrhosis and validated in 1505 patients (18% of whom with cirrhosis) from Hong Kong and Korea[29]. The REACH-B score included male sex, age, alanine aminotransferase (ALT), hepatitis B e antigen (HBeAg), and HBV-DNA as parameters, but not cirrhosis, as the training cohort only consisted of patients without cirrhosis. Instead of using cut-off values, the score was proposed as a range from 0 to 17 points, with a progressively increasing risk of HCC development. The REACH-B score had a 5 and 10-year AUROC of 0.796 and 0.769 in the validation cohort. The 5 and 10-year AUROC values decreased to 0.698 and 0.647 in the analysis of the cirrhotic group only. This finding confirms that the presence of cirrhosis per se is a major determinant for HCC development. These findings suggest that the training cohort should reflect the overall population at HCC risk more balanced to produce a reliable score for use in clinical practice.

In the upcoming years, the score was revised (REACH-BII) with the inclusion of quantitative HBsAg, which proved to be an additional independent predictor for the development of HCC[30]. In 2014, REACH-B risk score went through a final modification in a South Korean cohort where liver stiffness measurement (LSM) by transient elastography substituted HBV-DNA level: The better performance of the modified score (AUROC values; mREACH-B: 0.814 *vs* REACH-B: 0.629) was consistent with the fact that the CHB patients included in the Korean study were under entecavir treatment[31]. Similar findings were reported by the investigators of the original REACH-B risk score study when they applied the old and modified score to CHB patients treated with nucleotide analogue[32].

Liver stiffness values, in addition to age, albumin and HBV-DNA were used by the group of investigators of the CU-HCC score in 2014, to develop a new score for untreated CHB patients, namely LSM-HCC[33]. The new scoring system ranged from 0 to 30, with an optimal cut-off value of 11 to identify patients at HCC risk. Patients with a LSM-HCC score lower than 11 had a very low 5-year risk for HCC, with 92% sensitivity, 71% specificity, and 100% NPV. In 2016, another HCC risk score was developed based on real-world data of 538 untreated CHB patients from Singapore, namely the real-world score-HCC (RWS-HCC)[34]. The RWS-HCC score included gender, age, cirrhosis, and AFP as independent predictors. Upon validation in 3353 patients from REACH-B, GAG-HCC and CU-HCC cohorts, RWS-HCC score had AUROC values of 0.767, 0.830, and 0.902 and NPV of 97.0%, 97.9%, and 93.0% respectively. In 2018, a novel score (HCC-ESC) was developed for 723 CHB patients who achieved HBeAg seroclearance; age, gender, cirrhosis, albumin, HBV-DNA, and ALT serum levels were the parameters of the risk score to identify the long-term risk. The HCC-ESC score showed an AUROC value of 0.92 in the validation cohort[35]. Finally, in 2019, another HCC risk score (AGED score) was proposed from a longer term (21-year follow-up period) cohort study[36]. The AGED score included age, gender, HBeAg status, and HBV-DNA as independent parameters. The AGED score categorized patients into three groups according to their HCC risk as low (0-4), intermediate (5-9), and high (10-12) risk using a 12-point score. A total of 1663 HBsAg-positive participants were recruited as the validation cohort, and the AGED score had AUROC values of 0.73 and 0.74.

Risk scores for treated CHB patients

At present, most CHB patients are under antiviral treatment, as it has a significant positive impact on the course of liver disease, reducing the progression to cirrhosis and its complications, including HCC[37,38]. Therefore, scores developed in cohorts of untreated CHB patients could not be adequate for treated patients because they include parameters that are not any more relevant in patients with sustained suppression of viral replication. PAGE-B is the first risk score developed in 1815 Caucasian CHB patients including those under nucleos(t)ide analogue (entecavir/tenofovir) treatment for at least 1 year[39]. This was a multicenter study where 1325 patients were set in derivation and 490 enrolled as validation cohort. The regression analysis identified age, gender, and platelet count as independent predictors of HCC. Cirrhosis was not included in the model, but the platelet count can be considered the surrogate marker for the cirrhotic (portal hypertension) stage. The c-statistic of PAGE-B score was found 0.82 in both the derivation and validation cohorts. Having a PAGE-B score < 9 (low risk), 10-17 (intermediate risk), > 18 (high risk) resulted in 5-year cumulative HCC incidences of 0%, 3%-4% and 16%-17%, respectively. The PAGE-B score shows a higher discriminatory ability in the identification of high-risk HBV patients from those with low-risk (100% NPV), contributing to define different surveillance strategies according to the individual risk. By contrast, the intermediate-risk group has to be considered as a borderline group, where the definition of individualized surveillance algorithm is more difficult. The original findings of the PAGE-B score were confirmed and validated in Spanish and South Korean cohorts[40,41]. In 2018, Kim *et al*[42] revised the PAGE-B risk score in 3001 Asian CHB patients receiving entecavir/tenofovir therapy by adding albumin to the PAGE-B risk score. They showed a significant improvement of prediction as compared to previous models, including CU-HCC, GAG-HCC, REACH-B, and PAGE-B, with an AUROC value of 0.82 at 5-year in HCC prediction and 100% NPV. Low- and intermediate-risk patients had an annual HCC development risk of approximately 0.2%-1%, which turned to be higher than 3% in the high-risk group. In an independent Asian HBV cohort, the mPAGE-B score showed similar accuracy with PAGE-B and GAG-HCC scores, but its discrimination ability was better than the REACH-B and CU-HCC scores[43]. PAGE-B and mPAGE-B risk scores showed promising results for adoption to HCC surveillance algorithm, particularly because of the very high NPV.

In 2017, the HCC-Risk Estimating Score in CHB patients under Entecavir (HCC-RESCUE) score based on age, gender, and cirrhosis was proposed for South Korean treated CHB patients[44]. The AUROC at 1, 3, and 5-year was 0.82, 0.81, and 0.81, respectively, in the validation cohort. In the same year, the age, platelet, AFP (APA)-B score was proposed from Taiwan[45]. It ranged from 0 to 15, with the optimal cut-off for low risk set at 6. The AUROCs for 2-, 3-, and 5-year HCC prediction was 0.939, 0.892, and 0.862, and the NPV for the low-risk group was 99.1% in the validation cohort.

In 2018, the cirrhosis, age, male gender, diabetes (CAMD) score, which aimed to predict HCC during antiviral treatment, was proposed by the analysis of population-wide data from the healthcare systems in Taiwan (training cohort of 23851 CHB patients) and Hong Kong (validation cohort of 19321 patients)[46]. The CAMD score was the first to integrate diabetes mellitus as a risk factor for HCC, extracted from the multivariable Cox proportional hazards model. These four parameters were weighed to develop the CAMD score ranging from 0 to 19 points, with the categorization of CHB patients in three groups as low (< 8), intermediate (9-12), and high (> 13) risk. Low-risk patients had an annual HCC incidence of 0.3%. The c-indices were higher than 0.75 within the first 5 years in the training and validation cohorts. The CAMD score can be easily computed with simple information at the baseline of treatment initiation.

In 2019, a multicenter study from Korea proposed the Age-Albumin-Sex-Liver cirrhosis (AASL-HCC) score[47]. Age, albumin, male gender, and cirrhosis were extracted as independent predictors of HCC development while under entecavir or tenofovir treatment in a cohort of 1242 consecutive treatment-naive HBV patients, who were followed from 2007 to 2017. Low (< 5), intermediate (6-19), and high (> 20) risk groups showed HCC incidence rates of 0%, 3.7%-7.4%, and 17.6%-30.9%, respectively. The AUROC value for HCC prediction in 3-year, 5-year and total follow-up period was 0.850, 0.805, and 0.797, respectively, in the validation cohort.

In 2020, a multicenter study, enrolling 8048 Asian CHB patients under antiviral treatment from 25 centers in the United States and Asian-Pacific region, developed the REAL-B score[48]. It includes seven variables (male gender, age, alcohol use, diabetes, baseline cirrhosis, platelet count, and AFP) to categorize patients into the following three groups: Those at low (0-3), moderate (7), and high (8-13) risk. All AUROCs for

HCC prediction were higher than 0.8 at 3, 5, and 10 years, with a better predictive performance than PAGE-B in the same cohort (AUROC values at same time points; 0.73-0.74). The previously described HCC-ESC score was revised in 2020 in a Korean cohort of CHB patients under antiviral treatment and called HCC-ESC$_{AVT}$[49]. The risk score targeted CHB patients with HBeAg seroclearance like the original version and used the following three parameters: Male gender, cirrhosis, and fibrosis-4 index. The AUROC values for 5-year HCC prediction were 0.770 and 0.774 in the training and validation cohorts, respectively.

Interpretation and comparison of CHB-specific HCC risk scores

CHB specific HCC risk scores are summarized in Table 2. Most of them had been developed in Asian CHB patients, resulting from the urgency to have an accurate, precise, simple-to-use HCC risk score to be used in routine clinical activity, particularly in geographical areas where the burden of HBV infection is higher. The majority were developed in Asian patients and were also validated in Caucasians with acceptable performance. Nevertheless, most validation performances were lower than in the training cohort. Accordingly, the validation studies with Caucasian CHB patients showed AUROC values ranging from 0.74 to 0.86 for GAG-HCC, 0.62 to 0.91 for CU-HCC, 0.54 to 0.77 for REACH-B, and 0.85 for RWS-HCC risk scores[41,50-54]. These findings indicate that specific features of the population significantly influence the risk of HCC development. On the other hand, it is well known that the duration of HBV infection and florid viral replication, HBV genotype, exposure to other oncogenic factors (such as aflatoxins), and co-morbidities play a relevant role in HCC development[14]. As a consequence, a universal and highly accurate HCC score is unrealistic. Conversely, a predictive model based on data reflecting the virologic and clinical features of a given geographical area will provide a reliable tool for the same specific population. Nevertheless, such a model will require continuous adjustments reflecting the dynamic variations of the population based on the changing patterns of both HBV epidemiology and cirrhosis prevalence, HBV population aging, the variable impact of antiviral treatment according to its timing during the CHB course, and the variations of all the other co-factors of liver disease. Accordingly, the GAG-HCC, CU-HCC, REACH-B, LSM-HCC, and RWS-HCC scores, all derived from untreated CHB cohorts, as they were developed from patients followed in the 1990s or early 2000s, are not any more of interest because at present most of HBsAg carriers with evidence of CHB are under antiviral therapy. Another vital issue is the prevalence of cirrhosis in the studied cohorts, which may modify and alter the power of other parameters significantly involved in the scoring systems. The best example for this issue is that the REACH-B score, derived from a cohort of purely non-cirrhotic patients, has degraded performance in validation studies involving cirrhotic patients. In general, all the validated risk scores showed high NPV (95% to 100%) in both the original and external validation cohorts, suggesting redundancy of standard surveillance strategy to low-risk groups. The high-risk groups showed a wide range of annual HCC incidence, ranging from 2.3% to 9.2%, in CHB specific risk scores. By contrast, it indicates that we require additional studies to stratify the individual risk and define new surveillance strategies with more sensitive imaging or serologic tools.

In conclusion, risk stratification is attainable by validated HCC risk scores, but the optimal performance is obtained only in populations with similar characteristics to those where the score was developed. Besides, continuous validation of the predictive models is required to adjust them according to the dynamic variation of all factors influencing the individual HCC risk.

HCC RISK SCORES FOR CHC PATIENTS

As compared to CHB, there are a few proposed modeling studies in CHC patients to predict their HCC risk (Table 3), and their major limitation is the lack of external validation cohorts for most. The latter drawback for their use in clinical practice is the heterogeneity of CHC patients. It may be due to different co-factors affecting the disease progression of HCV and different prevalence across the world. Furthermore, the availability of DAAs in clinical practice acted as a watershed in the clinical needs to optimize the management of CHC patients with advanced fibrosis or cirrhosis; the current unmet need is an algorithm to guide the clinician to personalize the surveillance according to the residual HCC risk. The antiviral treatment proved useful to improve the outcome of CHC and reduce the HCC incidence since the introduction of interferon and ribavirin[55]. However, patients with advanced liver disease had a

Table 2 Hepatocellular carcinoma prediction risk scores for chronic hepatitis B patients

Risk scores	Cohort: Patients/ratio of cirrhosis	Study population	Antiviral treatment	Variables	External validation
GAG-HCC (Yuen *et al* [26], 2009)	Training: 820/15%; Validation: -	Asian (Hong Kong)	No	Age; Gender; HBV-DNA; Cirrhosis	Asian, Caucasian
CU-HCC (Wong *et al*[27], 2010)	Training: 1055/38%; Validation: 428/16%	Asian (Hong Kong)	No	Age; Albumin; Bilirubin; HBV-DNA; Radiologic cirrhosis	Asian, Caucasian
REACH-B (Yang *et al* [29], 2011)	Training: 3584/0; Validation: 1505/18%	Asian (Taiwan)	No	Age; Gender; ALT; HBeAg status; HBV-DNA concentration	Asian, Caucasian
REACH-BII(Lee *et al*[30], 2013)	Training: 2227/0; Validation: 1113/0	Asian (Taiwan)	No	Age; Gender; ALT; HBeAg/HBV-DNA/HBsAg/Genotype status	- (Internal only)
mREACH-B (Lee *et al* [31], 2014)	Training: 192/46.9%; Validation: -	Asian (South Korea)	ETV	Gender; ALT; HBeAg status; LSM value	Asian
LSM-HCC (Wong *et al* [33], 2014)	Training: 1035/32%; Validation: 520/31%	Asian (Hong Kong)	No	Age; Albumin; HBV-DNA concentration; LSM value	Asian
RWS-HCC (Poh *et al*[34], 2016)	Training: 583/13.7%; Validation: 3353/NA	Asian (Singapore)	No	Age; Sex; Cirrhosis; AFP	Asian, Caucasian
PAGE-B (Papatheodoridis *et al* [39], 2016)	Training: 1325/20%; Validation: 490/48%	Caucasians (Europe)	ETV/TDF	Age; Gender; Platelet count	Asian, Caucasian
mPAGE-B (Kim *et al*[42], 2018)	Training: 2001/19%; Validation: 1000/20%	Asian (South Korea)	ETV/TDF	Age; Gender; Platelet count; Albumin	Asian
HCC-RESCUE (Sohn *et al* [44], 2017)	Training: 990/39%; Validation: 1071/35%	Asian (South Korea)	ETV	Age; Gender; Cirrhosis	Asian
APA-B (Chen *et al*[45], 2017)	Training: 883/36%; Validation: 442/236%	Asian (Taiwan)	ETV	Age; Platelet; AFP	Asian
HCC-ESC (Fung *et al*[35], 2018)	Training: 723/NA; Validation: -	Asian (Hong Kong)	No	Age; Gender; Cirrhosis; Hypoalbuminemia; HBV-DNA; ALT	-
CAMD (Hsu *et al*[46], 2018)	Training: 23851/26.4%; Validation: 19321/7.1%	Asian (Taiwan)	ETV/TDF	Age; Gender; Diabetes; Cirrhosis	Asian
AGED (Fan *et al*[36], 2019)	Training: 628/0%; Validation: 1663/0%	Asian (China)	No	Age; Gender; HBeAg status; HBV-DNA	- (Internal only)
AASL-HCC (Yu *et al*[47], 2019)	Training: 944/39%; Validation: 298/39%	Asian (South Korea)	ETV/TDF	Age; Gender; Albumin; Cirrhosis	Asian
REAL-B (Yang *et al*[48], 2020)	Training: 5365/20.2%; Validation: 2683/22.1%	Asian (Multiethnicity)	Yes (not specified)	Age; Gender; Alcohol use; Diabetes; Platelet count; Cirrhosis; AFP	- (Internal only)
HCC-ESC$_{AVT}$ (Lim *et al* [49], 2020)	Training: 769/41.5%; Validation: 1061/26.1%	Asian (South Korea)	ETV/TDF	Gender; Cirrhosis; Fibrosis-4 index	- (Internal only)

GAG-HCC: The guide with age, gender, hepatitis B virus DNA, core promoter mutations, and cirrhosis risk score; CU-HCC: Chinese University-hepatocellular carcinoma risk score; REACH-B: The risk estimation for hepatocellular carcinoma in chronic hepatitis B score; RWS: Real-world score; APA-B: Age, platelet, alpha-fetoprotein-B score; CAMD: Cirrhosis, age, male gender, diabetes score; AFP: Alpha-fetoprotein, ALT: Alanine aminotransferase, HBeAg: Hepatitis B e Antigen, HBV: Hepatitis B virus, LSM: Liver stiffness measurement.

significantly lower SVR rate and reduced compliance to treatment. Thus, the availability of scoring systems to identify individuals at higher risk of HCC development among those with advanced liver disease was perceived as a major clinical interest.

The first HCC risk score attempt was derived from the Hepatitis C Antiviral Long-Term Treatment Against Cirrhosis cohort in 2009[56]. During a median follow-up of 4.6 years, 48 of 1005 (4.8%) patients developed HCC, with a 5-year HCC incidence comparable in peginterferon-treated or untreated patients (5.4% *vs* 5.0%). The presence of cirrhosis together with older age, Black race, lower platelet count, higher alkaline phosphatase, esophageal varices, and smoking status identified patients at higher risk. A few years later, another study conducted on 11721 HCV-related cirrhotic patients from the Veterans Administration Hepatitis C Virus Clinical Case Registry in the United States investigated the possibility to develop an AFP-based algorithm where biomarkers of disease activity (ALT) and disease stage (platelet count) were used to

Table 3 Hepatocellular carcinoma prediction risk scores for chronic hepatitis C patients

Ref.	Cohort: Patients/ratio of cirrhosis	Study population	Variables	External validation
Lok *et al*[56], 2009	Training: 1050/41%; Validation: -	North America (United States HALT-C cohort)	Age; Race (Black); ALP; Esophageal varices; Ever smoked; Platelet count	-
Masuzaki *et al*[58], 2009	Training: 866/22.6%; Validation: -	Asian (Japan)	LSM	-
Chang *et al*[59], 2012	Training: 871/27.9%; Validation: -	Asian (Taiwan)	Age; Platelet count; AFP; Fibrosis stage	-
El-Serag HB *et al*[57], 2014	Training: 11721/100%; Validation: 52135/0	North America (United States Veterans Administration)	Age; ALT; Platelet; AFP	-
Ganne-Carrié *et al*[60],2016	Training: 720/100%; Validation: 360/100%	Caucasian (France)	Age; Past excessive alcohol intake; Platelet count; GGT; SVR status	-
Shiha *et al*[63], 2020 (GES)	Training: 2372/73.1%; Validation 1: 687/61.5%; Validation 2: 1314/70.6%	Egypt	Age; Gender; Fibrosis stage; Albumin; Alpha-feto protein	Egypt

AFP: Alpha-fetoprotein, ALP: Alkaline phosphatase, ALT: Alanine aminotransferase, GGT: Gamma-glutamyl transferase, LSM: Liver stiffness measurement, SVR: Sustained virologic response.

adjust the predictive accuracy of AFP[57]. At any given AFP value, low numbers of platelets and ALT and older age were associated with increased risk of HCC, and high levels of ALT and normal/high numbers of platelets were associated with low risk for HCC. The advantage of the model was its inclusion of routine laboratory tests and easy to manage parameters.

Two studies from Asia tackled the same issue with different approaches. Masuzaki *et al*[58] investigated the possibility to use LSM determined by FibroScan as a predictor of HCC in 866 HCV-infected patients. The cohort was prospectively followed for a mean period of 3 years after initial LSM determination. The odds ratio of HCC development was correlated with increasing LSM, and a LSM cut-off value of > 15 kPa had a greater association with HCC development. The other study from Taiwan enrolled 871 biopsy-proven CHC patients who achieved sustained response after peginterferon and ribavirin. They integrated the histologic fibrosis status with other parameters (age, AFP, low platelet counts) to define a HCC risk score[59]. Accordingly, low (< 10), intermediate (11-15), and high (> 16) risk groups had 1.37%, 9.14%, and 30.7% chances of HCC development, respectively. The authors proposed their novel risk score for HCC screening in CHC patients achieving SVR.

In 2016, a multicenter French cohort (ANRS CO12 CirVir) study with 1323 CHC-related cirrhosis patients was conducted to develop an individualized score for HCC prediction[60]. An 11-point risk score was established using the five variables independently associated with HCC (age > 50 years, past excessive alcohol intake, low platelet count, gamma-glutamyltransferase (GGT) > upper limit of normal, and absence of SVR). This new risk score was able to stratify the CHC-cirrhosis population into three groups according to HCC risk as low (< 3), intermediate (4-7), and high (> 8) risk. However, this score also lacked external validation.

In 2020, a different approach was used to refine HCC risk among patients with CHC-related cirrhosis from the same French cohort, by applying predictive machine learning approaches (Fine-Gray regression model) rather than traditional multivariate linear regression analysis[61]. The study was interesting in terms of bringing a new breath to risk-stratification models and personalized HCC-surveillance efforts. As expected, the authors showed that factors influencing the HCC risk varied after SVR. Only elevated AST, low platelet count, and shorter prothrombin time was independently associated with HCC risk after SVR, whereas there were six independent predictors (past excessive alcohol intake, genotype 1, elevated AFP, GGT, low platelet count, and albumin levels) before SVR. However, the interactions between the different parameters were quite complex, and eight different groups were identified with varying cancer risks and predictors depending on SVR achievement. The findings were interesting but not yet directly applicable in clinical practice. Nevertheless, the study showed that machine learning algorithms can refine the HCC risk assessment by revealing complex interactions between cancer predictors and eventually prompting more cost-effective tailored surveillance programs development.

An absolute simplified model was derived and proposed from 1088 Japanese CHC patients who achieved SVR after DAA in the same year[62]. They revealed age and AFP as independent predictors of HCC after achieving SVR with DAAs. Using AFP and age only, they developed a scoring system (0-2 points) where the incidence of HCC at 2-years was 0.3% in the 0 points group, 6.27% in the 1-point group, and 18.37% in the 2-points group. This oversimplified approach is captivating; however, external validation in different populations is required, as specific features, such as HCV epidemiology in the geographical area, could significantly influence the findings. The General Evaluation Score (GES) was recently proposed by a study performed in Egypt on 4400 patients, with cirrhosis or advanced fibrosis who achieved a SVR[63]. Age, sex, serum albumin, AFP and, pretreatment fibrosis stage was identified as risk factors for HCC and used to construct the risk score, and categorized CHC patients into three groups. The 2-year cumulative HCC incidence was 1.2%, 3.3%, 7.1% for low-, medium-, and high-risk groups, respectively. The GES score had high predictive ability in internal and external validation cohorts from Egypt with c-statistics values of 0.80 and 0.81. Unfortunately, the findings of this interesting and promising study cannot be generalized because it included only HCV genotype 4-infected patients.

Overall, it appears that in the setting of CHC patients from one side, the proposed scoring systems are lacking adequate external validation, which is mandatory to warrant their use in clinical practice. Furthermore, the high variability of the epidemiology of HCV infection (different genotype distribution worldwide, distinct modalities of HCV spreading in the various geographical area and overtime) is even more complicated than in HBV, necessitating the implementation of a model in a different context. Nevertheless, the evidence that the risk of HCC significantly declines over time in patients who achieved SVR underlines the urgent need for new algorithms to personalize the HCC surveillance and optimize its cost/benefit.

PREDICTION OF HCC RISK FOR PATIENTS WITH CLD OR OTHER RISK FACTORS

HCC prediction risk scores, regardless of underlying liver disease etiology, are summarized in Table 4. Flemming *et al*[64] developed an HCC risk prediction model to estimate the 1-year probability of HCC to assist clinicians with patient counseling by studying a large cohort of patients (n = 34932) with cirrhosis from the United States liver transplantation waiting list database. Thus, the authors did not mean to create a score to modify the surveillance of cirrhotic patients but to provide an individualized approach to HCC counseling based on specific patient characteristics. They identified six baseline variables (age, diabetes, race, etiology of cirrhosis, sex, and severity [ADRESS] of liver dysfunction) independently associated with HCC and the c-indices of the ADRESS-HCC risk model were 0.704 and 0.691 in the derivation and internal validation cohorts, respectively. The major limitation of the study was the selection of patients with advanced liver disease, as they were cirrhotic already on the transplant waitlist. In 2017, the Toronto Hepatocellular carcinoma Risk Index (THRI) was developed to predict 10-year HCC risk, using simple clinical and laboratory parameters (age, gender, etiology, platelet)[65]. The THRI weighed etiologies, including the SVR status of HCV-related cirrhosis, and its performance had been studied in three external validation cohorts from different regions (Netherlands, China, Turkey) with similar accuracy in predicting HCC development[65-67]. All AUROC values ranged from 0.75 to 0.80, using the same cut-off value of 240 to identify the high-risk HCC group.

Diabetes is a risk factor for HCC in patients with CLD. Li *et al*[68] in 2018 approached the issue in the other way round, developing a risk score system to predict the HCC risk in patients with diabetes. They studied a cohort of 31723 Taiwanese patients with type 2 diabetes mellitus, followed-up for 8.3 years, and the final model (scores ranging from -6 to 40 points) included age, gender, smoking status, hemoglobin A1c, glutamic-pyruvic transaminase, cirrhosis, hepatitis B, hepatitis C, anti-diabetic and anti-hyperlipidemic medications, and total/high-density lipoprotein cholesterol ratio. The 3-, 5-, and 10-year AUROC values to predict HCC risk were 0.81, 0.80, and 0.77.

More recently, an ambitious study aimed to develop a global universal HCC risk score to predict the HCC development for patients with chronic hepatitis, published by an international study group. A total of 17374 patients (10578 Asian and 2510 Caucasian treated CHB patients, 3566 CHC; 2489 of whom with cirrhosis and SVR, and 720 patients with non-viral hepatitis) from 11 international prospective observational

Table 4 Hepatocellular carcinoma prediction risk scores regardless of etiology

Risk scores	Cohort: Patients	Study population	Variables	External validation
ADRESS-HCC, (Flemming *et al* [64], 2014)	Training: 17124/100%; Validation:17808/100%	North America (United States)	Age; Diabetes; Race; Etiology of liver disease; Gender; Child-Pugh Score	- (Internal only)
THRI, (Sharma *et al*[65], 2017)	Training: 2079/100%; Validation: 1144/100%	Caucasian (Canada)	Age; Gender; Etiology of liver disease; Platelet count	Asian, Caucasian
TDS, (Li *et al*[68], 2018)	Training: 21149/NA; Validation:10574/NA	Asian (Taiwan)	Age; Gender; Smoking status; HbA1c; Glutamic-pyruvic transaminase; Cirrhosis; Hepatitis B virus; Hepatitis C virus; Anti-diabetic medication; Anti-hyperlipidemic medicaiton; Total/HDL cholesterol ratio	- (Internal only)
aMAP, (Fan *et al* [69], 2020)	Training: 3688/19.3%; Validation cohorts: 13686/11.4%-100%	Multicenter (Asian + Caucasian)	Age; Gender; Albumin-bilirubin score; Platelet count	Asian, Caucasian

THRI: Toronto hepatocellular carcinoma risk index; ADRESS: Age, diabetes, race, etiology of cirrhosis, sex, and severity; HbA1c: Hemoglobin A1c; HDL: High-density lipoprotein.

cohorts or randomized controlled trials were analyzed[69]. This study is unique in terms of having a large validation cohort from several ethnicities and etiologies; however, the majority were still CHB patients. The aMAP score was obtained from a training cohort of 3688 Asian patients and validated in nine cohorts with different etiologies and ethnicities. The score ranges from 0 to 100 and involves age, male, albumin-bilirubin score, and platelet count; the value of 50 was identified as the optimal cut-off to predict HCC, with a sensitivity of 85.7%-100% and 99.3%-100% NPV. The authors proposed their risk score, based on five common parameters, showing high performance regardless of etiology and ethnicity, as a potential new tool to establish a risk score-guided HCC surveillance strategy worldwide.

TUMOR MARKERS AND HCC RISK SCORES

Several serologic biomarkers, other than AFP that have already been discussed and included in some scoring systems, such as osteopontin, alpha-fetoprotein-L3 (AFP-L3), des-gamma-carboxy prothrombin (DCP), also known as the protein induced by vitamin K absence or antagonist II (PIVKAII), glypican-3, alpha-1-fucosidase, midikine, dikkopf-1, Golgi protein-73, squamose cell carcinoma antigen, and fucosylated glycoprotein, have been investigated for their potential role in HCC screening. Ideally, blood-based biomarkers with adequate sensitivity or specificity could enable early detection of HCC, avoiding cumbersome ultrasound-based surveillance. However, at present, none of the biomarkers has been validated in phase III clinical trials and are used in clinical practice, with the exclusion of AFP and PIVKAII, recommended by Japanese HCC guidelines, particularly in Japan[70]. This can be explained by the high heterogeneity of HCC biology, where several pathway alterations are involved in the tumorigenesis process[71]. Therefore, the combination of different biomarkers and the available clinical and laboratory variables has been evaluated to develop predictive scores (Table 5).

The GALAD algorithm combining three biomarkers (AFP, AFP-L3, and DCP) with sex and age showed a remarkable overall performance (AUROC values of 0.95, 92% sensitivity, and 85% specificity) that remained high (AUROC: 0.92, sensitivity 92%, specificity 79%) for early HCC detection[72]. The model was validated in independent cohorts from Japan, Germany, and Hong Kong, with overall sensitivity ranging from 80%-91%, specificity from 81%-90%, and AUROC values from 0.85 to 0.95[73]. Both in the original and validation studies, the etiologies were mixed and dominantly consisted of alcohol-related liver disease and CHC patients. The homogeneity of the studied cohorts as far as the etiology of CLD is concerned is critical as the diagnostic performance of the most widely used standardized HCC biomarkers, namely AFP and PIVKAII is significantly influenced by the etiology and activity of CLD, and their combination provides a better diagnostic accuracy[74]. Interestingly, the GALAD score showed an AUC of 0.96 in the identification of HCC in a German cohort of patients with nonalcoholic steatohepatitis (NASH), with comparable performance in patients

Table 5 Algorithmic approaches using the combination of serologic and clinical parameters for hepatocellular carcinoma risk prediction

Risk scores	Cohort: Patients/ratio of cirrhosis	Study population	Variables	External validation
GALAD score (Johnson *et al*[72], 2014)	HCC case: 670/90%; CLD control: 339/97%	Caucasian (England)	AFP; AFP-L3; DCP	Asian, Caucasian
Doylestown algorithm (Wang *et al*[76], 2016)	Training HCC case: 165/100%; CLD control: 195/100%; Validation 1 HCC case: 432/100%; CLD control: 438/100%; Validation 2 HCC case: 113/100%; CLD control: 586/100%; Validation 3 HCC case: 425/100%; CLD control: 804/100%	North America (United States)	Age; Gender; ALT; ALP; AFP; Fucosylated kininogen	North America (United States)
GALADUS score (Yang *et al*[75], 2019)	Training HCC case: 111/98%; CLD control: 180/85%; Validation HCC case: 233/100%; CLD control: 412/100%	North America (United States)	AFP; AFP-L3; DCP; Ultrasonography	North America (United States)
HES algorithm (Tayob *et al*[78, 79], 2019)	HCC case: 4804/100%; CLD control: 33627/100%	North American (United States Veterans Administration)	Age; Rate of AFP change; ALT; Platelet count; Etiology of cirrhosis	-

AFP: Alpha-fetoprotein; AFP-L3: Alpha-fetoprotein-L3; ALP: Alkaline phosphatase; ALT: Alanine aminotransferase; DCP: Des-gamma-carboxy-prothrombin, HCC: Hepatocellular carcinoma; CLD: Chronic liver disease.

with or without cirrhosis. A cut-off value of -0.63 GALAD score identified patients with HCC within Milan Criteria with an AUC of 0.91 (68% sensitivity and 93% specificity). The same threshold had been proposed to identify NASH patients who will have imaging diagnosis 200 d later. The GALAD score performance for HCC detection was also compared with liver US and showed to be superior. The combination of GALAD and US score further improved the performance score in a single-center cohort, achieving an area under the curve of 0.98[75]. Overall, these findings indicate that the GALAD score can detect patients with early-stage HCC and might facilitate surveillance of patients, particularly those with NASH, who are often obese, which limits the sensitivity of detection of liver cancer by US. However, the optimal cut-off value has to be defined to develop a shared and standardized surveillance algorithm. Another risk score, namely the Doylestown algorithm, incorporates two biomarkers (AFP and fucosylated kininogen) with two clinical (age, gender) and two laboratory (ALT and alkaline phosphatase) variables[76]. The Doylestown algorithm had an 89% detection rate for early HCCs with an AUROC value of 0.97 in low-AFP patients. The promising results of the Doylestown algorithm require adequate validation in larger and adequate cohort series.

In 2015, White *et al*[77] published an adjusted AFP-based algorithm for HCC detection in patients with HCV-related cirrhosis. It was the implementation of a previously reported score where age, platelets, ALT values, and interaction terms (AFP and ALT, and AFP and platelets) were used. In the new model, serial AFP measurements were included, showing an improvement in the overall performance. More recently, the Hospital Episode Statistics (HES) algorithm was validated in a cohort, which included 33627 patients with cirrhosis of any etiology who did not develop HCC during follow-up (controls) and 4804 patients with incident HCC (cases)[78]. At 90% specificity, the HES algorithm identified HCC cases with 52.56% sensitivity, compared to 48.13% sensitivity for the AFP assay alone, within 6 mo before diagnosis, which was an absolute improvement of 4.43% ($P < 0.0005$). Overall, the algorithm offers a modest advantage over AFP alone in HCC surveillance. The findings were substantially confirmed in a subsequent study, where the etiology of cirrhosis was added to the model[79].

POTENTIAL MOLECULAR CANDIDATES FOR INTEGRATION TO HCC RISK SCORES

Several lines of research are aiming to identify new biomarkers for detection of HCC at a very early stage. CancerSEEK is a recently proposed platform assessing eight circulating proteins (CA125, CEA, CA19-9, prolactin, hepatocyte growth factor, osteopontin, myeloperoxidase, and tissue inhibitor of metalloproteinases 1) and mutations in cell-free DNA[80]. By a machine-learning approach, an algorithm was

developed with an overall sensitivity of 70% and a specificity of 99% in detecting eight cancers, including HCC. A major limitation is that the study enrolled known cancers, whereas the aim would be to identify HCC in asymptomatic patients. Furthermore, using cancer gene panels in cell-free DNA could give rise to a high number of false-positive in healthy individuals[81]. A large number of other biomarkers, such as circulating tumor cells, microRNAs, tumor cell-free DNAs, tumor-derived/associated extracellular vesicles, metabolites, and proteins, are under investigation to obtain a liquid biopsy for HCC[82]. Another interesting approach has been proposed recently by Liu *et al*[83], who showed that a viral exposure signature (VES) obtained by a synthetic viral scan technology of viral antibodies could discriminate HCC with high confidence from at-risk individuals (area under the curve of 0.91 at baseline and 0.98 at diagnosis) or healthy volunteers. The VES was validated in at-risk patients in a prospective HCC cohort; however, larger prospective studies are needed to evaluate its utility in HCC surveillance.

Finally, germ-line single gene polymorphisms have also been analyzed in genome-wide association studies as specific host factors that determine HCC susceptibility for chronic viral hepatitis patients. *EGF, IFNL3, MICA, TLL1, MERTK, K27 of histone H3-H3K27ac* for CHC[84-90], and *KIF1B, STAT4,* and *HLA-DQB1/HLA-DBA2* for CHB patients were the most promising ones[91,92]. It is not very likely that a single germ-line genetic variant may affect HCC development in chronic viral hepatitis, but future attempts may include integrating them into HCC-risk scales. The future efforts will be incorporating molecular profiling into HCC-surveillance algorithms that could also identify targets for potential chemo-preventive interventions.

CONCLUSION

The epidemiology of CLD is rapidly changing, with a progressive reduction of viral hepatitis burden and an increase of non-alcoholic fatty liver diseases (NAFLD). Considering the significant rise in NAFLD-related HCC cases globally, the ability to stratify the risk of HCC is becoming another urgent need. HCC does also occur in patients with non-cirrhotic NAFLD but surveillance is not recommended to this group as incidence rates are lower than 1% a year[93]. The HCC risk stratification tools in patients with NAFLD is not discussed here, as the aim of the present article is to focus on HCC surveillance of patients with chronic viral hepatitis. The incidence of HCC has become highly heterogeneous within patients with chronic viral hepatitis since it differs significantly according to the period of both viral infection, the beginning of treatment, and the rate of cirrhosis. As a consequence, the incidence of HCC differs according to the geographical distribution of risk factors. Thus, the identification of appropriate tools for tailoring the HCC screening decisions according to the different subgroups of patients based on the CLD etiology, relevant clinicopathologic and epidemiologic factors is a growing need in clinical practice. The individually tailored HCC surveillance would imply a cost-effective application of personalized protocols using highly sensitive imaging techniques[94]. However, such an important medical need remains currently unmet and it appears unlikely that it will be fulfilled by a universal generalized score. The HCC-risk stratification models appear helpful to generate reliable and personalized HCC predictive scores only if the scoring system is applied to cohorts whose clinic-pathologic characteristics are highly similar to those of the original discovery cohort for the particular model.

On the other hand, the more widespread use of current HCC biomarkers to increase the specificity for identifying patients with a more significant risk is controversial. All HCC markers so far identified have a highly dis-homogeneous prevalence in patients with different etiology of CLD that imposes their use in multiple markers panels. Furthermore, the serum levels of HCC biomarkers change over time, and the detection of this velocity might improve their specificity. Their analytical cut-off needs to be better standardized in this regard. For instance, the levels of AFP are influenced by liver regeneration prompted by flares of intrahepatic necroinflammation; thus, the range of AFP normality values vary consistently from patients with chronic viral hepatitis and sustained antiviral response to those with metabolic-associated fatty liver disease and ongoing steatohepatitis. Future studies should address these issues using, for instance, algorithms of the combined dynamics of ALT and AFP levels.

In conclusion, according to existing knowledge, there is a strong recommendation to perform surveillance in patients with cirrhosis regardless of their liver disease etiology, origin, age, and sex. The question remains as to whether the time intervals of US screening can be safely reduced in lower risk cirrhotic patients who recovered from

chronic viral hepatitis and maintain normal liver function tests after sustained response to antiviral therapy. The issue of HCC surveillance is much more complicated in patients without cirrhosis. An ideal risk score system should define optimal cut-off values to discriminate high-risk HCCs with high annual HCC incidence (> 3%-5%) and high PPV and low-risk HCCs with high NPV (> 99%). Most of the existing risk scores for CHB reached or were close to this performance, but they did not target the non-cirrhotic patients specifically and were highly dis-homogeneous for the cirrhosis rate. For HCC-risk scores specific for CHC patients without cirrhosis, there is a lack of validation in independent cohorts and proposed scores are not yet representative of CHC patients with complete SVR in the current era of DAAs. Currently proposed HCC-risk scores are not yet standardized to be incorporated into sustainable HCC-surveillance decision algorithms, and more efforts should be made to personalize HCC surveillance in CHB patients without cirrhosis and CHC patients with F3 fibrosis, at least in the near future. Patients with cirrhosis have to undergo HCC-surveillance regardless of liver disease etiology and prospective, large-scale multinational study with stratification on the basis of underlying CLD etiology, fibrosis status, ethnicity (including Africans and other parts of the world) are required. The potential of such a study must include a dynamic calculation of HCC-risk scores every 6 mo. Individual molecular profiling will provide a crucial integration of HCC-surveillance decision algorithms and help identify high-risk target populations in the future, but they are currently not widely available.

REFERENCES

1 **Ferlay J**, Colombet M, Soerjomataram I, Mathers C, Parkin DM, Piñeros M, Znaor A, Bray F. Estimating the global cancer incidence and mortality in 2018: GLOBOCAN sources and methods. *Int J Cancer* 2019; **144**: 1941-1953 [PMID: 30350310 DOI: 10.1002/ijc.31937]

2 **Ioannou GN**, Splan MF, Weiss NS, McDonald GB, Beretta L, Lee SP. Incidence and predictors of hepatocellular carcinoma in patients with cirrhosis. *Clin Gastroenterol Hepatol* 2007; **5**: 938-945, 945.e1-945.e4 [PMID: 17509946 DOI: 10.1016/j.cgh.2007.02.039]

3 **Sangiovanni A**, Prati GM, Fasani P, Ronchi G, Romeo R, Manini M, Del Ninno E, Morabito A, Colombo M. The natural history of compensated cirrhosis due to hepatitis C virus: A 17-year cohort study of 214 patients. *Hepatology* 2006; **43**: 1303-1310 [PMID: 16729298 DOI: 10.1002/hep.21176]

4 **Global Burden of Disease Liver Cancer Collaboration**, Akinyemiju T, Abera S, Ahmed M, Alam N, Alemayohu MA, Allen C, Al-Raddadi R, Alvis-Guzman N, Amoako Y, Artaman A, Ayele TA, Barac A, Bensenor I, Berhane A, Bhutta Z, Castillo-Rivas J, Chitheer A, Choi JY, Cowie B, Dandona L, Dandona R, Dey S, Dicker D, Phuc H, Ekwueme DU, Zaki MS, Fischer F, Fürst T, Hancock J, Hay SI, Hotez P, Jee SH, Kasaeian A, Khader Y, Khang YH, Kumar A, Kutz M, Larson H, Lopez A, Lunevicius R, Malekzadeh R, McAlinden C, Meier T, Mendoza W, Mokdad A, Moradi-Lakeh M, Nagel G, Nguyen Q, Nguyen G, Ogbo F, Patton G, Pereira DM, Pourmalek F, Qorbani M, Radfar A, Roshandel G, Salomon JA, Sanabria J, Sartorius B, Satpathy M, Sawhney M, Sepanlou S, Shackelford K, Shore H, Sun J, Mengistu DT, Topór-Mądry R, Tran B, Ukwaja KN, Vlassov V, Vollset SE, Vos T, Wakayo T, Weiderpass E, Werdecker A, Yonemoto N, Younis M, Yu C, Zaidi Z, Zhu L, Murray CJL, Naghavi M, Fitzmaurice C. The Burden of Primary Liver Cancer and Underlying Etiologies From 1990 to 2015 at the Global, Regional, and National Level: Results From the Global Burden of Disease Study 2015. *JAMA Oncol* 2017; **3**: 1683-1691 [PMID: 28983565 DOI: 10.1001/jamaoncol.2017.3055]

5 **Garuti F**, Neri A, Avanzato F, Gramenzi A, Rampoldi D, Rucci P, Farinati F, Giannini EG, Piscaglia F, Rapaccini GL, Di Marco M, Caturelli E, Zoli M, Sacco R, Cabibbo G, Marra F, Mega A, Morisco F, Gasbarrini A, Svegliati-Baroni G, Foschi FG, Missale G, Masotto A, Nardone G, Raimondo G, Azzaroli F, Vidili G, Brunetto MR, Trevisani F; ITA. LI.CA study group. The changing scenario of hepatocellular carcinoma in Italy: an update. *Liver Int* 2021; **41**: 585-597 [PMID: 33219585 DOI: 10.1111/liv.14735]

6 **Desai A**, Sandhu S, Lai JP, Sandhu DS. Hepatocellular carcinoma in non-cirrhotic liver: A comprehensive review. *World J Hepatol* 2019; **11**: 1-18 [PMID: 30705715 DOI: 10.4254/wjh.v11.i1.1]

7 **Papatheodoridis GV**, Chan HL, Hansen BE, Janssen HL, Lampertico P. Risk of hepatocellular carcinoma in chronic hepatitis B: assessment and modification with current antiviral therapy. *J Hepatol* 2015; **62**: 956-967 [PMID: 25595883 DOI: 10.1016/j.jhep.2015.01.002]

8 **Falade-Nwulia O**, Suarez-Cuervo C, Nelson DR, Fried MW, Segal JB, Sulkowski MS. Oral Direct-Acting Agent Therapy for Hepatitis C Virus Infection: A Systematic Review. *Ann Intern Med* 2017; **166**: 637-648 [PMID: 28319996 DOI: 10.7326/M16-2575]

9 **Ioannou GN**, Green PK, Berry K. HCV eradication induced by direct-acting antiviral agents reduces the risk of hepatocellular carcinoma. *J Hepatol* 2017 [PMID: 28887168 DOI: 10.1016/j.jhep.2017.08.030]

10 **Kanwal F**, Kramer J, Asch SM, Chayanupatkul M, Cao Y, El-Serag HB. Risk of Hepatocellular

Cancer in HCV Patients Treated With Direct-Acting Antiviral Agents. *Gastroenterology* 2017; **153**: 996-1005.e1 [PMID: 28642197 DOI: 10.1053/j.gastro.2017.06.012]

11 **Kanwal F**, Kramer JR, Asch SM, Cao Y, Li L, El-Serag HB. Long-Term Risk of Hepatocellular Carcinoma in HCV Patients Treated With Direct Acting Antiviral Agents. *Hepatology* 2020; **71**: 44-55 [PMID: 31222774 DOI: 10.1002/hep.30823]

12 **Singal AG**, Lampertico P, Nahon P. Epidemiology and surveillance for hepatocellular carcinoma: New trends. *J Hepatol* 2020; **72**: 250-261 [PMID: 31954490 DOI: 10.1016/j.jhep.2019.08.025]

13 **McCabe C**, Claxton K, Culyer AJ. The NICE cost-effectiveness threshold: what it is and what that means. *Pharmacoeconomics* 2008; **26**: 733-744 [PMID: 18767894 DOI: 10.2165/00019053-200826090-00004]

14 **Fattovich G**, Bortolotti F, Donato F. Natural history of chronic hepatitis B: special emphasis on disease progression and prognostic factors. *J Hepatol* 2008; **48**: 335-352 [PMID: 18096267 DOI: 10.1016/j.jhep.2007.11.011]

15 **Omata M**, Cheng AL, Kokudo N, Kudo M, Lee JM, Jia J, Tateishi R, Han KH, Chawla YK, Shiina S, Jafri W, Payawal DA, Ohki T, Ogasawara S, Chen PJ, Lesmana CRA, Lesmana LA, Gani RA, Obi S, Dokmeci AK, Sarin SK. Asia-Pacific clinical practice guidelines on the management of hepatocellular carcinoma: a 2017 update. *Hepatol Int* 2017; **11**: 317-370 [PMID: 28620797 DOI: 10.1007/s12072-017-9799-9]

16 **Marrero JA**, Kulik LM, Sirlin CB, Zhu AX, Finn RS, Abecassis MM, Roberts LR, Heimbach JK. Diagnosis, Staging, and Management of Hepatocellular Carcinoma: 2018 Practice Guidance by the American Association for the Study of Liver Diseases. *Hepatology* 2018; **68**: 723-750 [PMID: 29624699 DOI: 10.1002/hep.29913]

17 **Terrault NA**, Lok ASF, McMahon BJ, Chang KM, Hwang JP, Jonas MM, Brown RS Jr, Bzowej NH, Wong JB. Update on prevention, diagnosis, and treatment of chronic hepatitis B: AASLD 2018 hepatitis B guidance. *Hepatology* 2018; **67**: 1560-1599 [PMID: 29405329 DOI: 10.1002/hep.29800]

18 **European Association for the Study of the Liver**. EASL Clinical Practice Guidelines: Management of hepatocellular carcinoma. *J Hepatol* 2018; **69**: 182-236 [PMID: 29628281 DOI: 10.1016/j.jhep.2018.03.019]

19 **Bruix J**, Sherman M; Practice Guidelines Committee; American Association for the Study of Liver Diseases. Management of hepatocellular carcinoma. *Hepatology* 2005; **42**: 1208-1236 [PMID: 16250051 DOI: 10.1002/hep.20933]

20 **AASLD-IDSA HCV Guidance Panel**. Hepatitis C Guidance 2018 Update: AASLD-IDSA Recommendations for Testing, Managing, and Treating Hepatitis C Virus Infection. *Clin Infect Dis* 2018; **67**: 1477-1492 [PMID: 30215672 DOI: 10.1093/cid/ciy585]

21 **Farhang Zangneh H**, Wong WWL, Sander B, Bell CM, Mumtaz K, Kowgier M, van der Meer AJ, Cleary SP, Janssen HLA, Chan KKW, Feld JJ. Cost Effectiveness of Hepatocellular Carcinoma Surveillance After a Sustained Virologic Response to Therapy in Patients With Hepatitis C Virus Infection and Advanced Fibrosis. *Clin Gastroenterol Hepatol* 2019; **17**: 1840-1849.e16 [PMID: 30580095 DOI: 10.1016/j.cgh.2018.12.018]

22 **Sherman M**. HCC Risk Scores: Useful or Not? *Semin Liver Dis* 2017; **37**: 287-295 [PMID: 29272891 DOI: 10.1055/s-0037-1607452]

23 **Wong VW**, Janssen HL. Can we use HCC risk scores to individualize surveillance in chronic hepatitis B infection? *J Hepatol* 2015; **63**: 722-732 [PMID: 26026875 DOI: 10.1016/j.jhep.2015.05.019]

24 **Lee HW**, Ahn SH. Prediction models of hepatocellular carcinoma development in chronic hepatitis B patients. *World J Gastroenterol* 2016; **22**: 8314-8321 [PMID: 27729738 DOI: 10.3748/wjg.v22.i37.8314]

25 **Voulgaris T**, Papatheodoridi M, Lampertico P, Papatheodoridis GV. Clinical utility of hepatocellular carcinoma risk scores in chronic hepatitis B. *Liver Int* 2020; **40**: 484-495 [PMID: 31884726 DOI: 10.1111/liv.14334]

26 **Yuen MF**, Tanaka Y, Fong DY, Fung J, Wong DK, Yuen JC, But DY, Chan AO, Wong BC, Mizokami M, Lai CL. Independent risk factors and predictive score for the development of hepatocellular carcinoma in chronic hepatitis B. *J Hepatol* 2009; **50**: 80-88 [PMID: 18977053 DOI: 10.1016/j.jhep.2008.07.023]

27 **Wong VW**, Chan SL, Mo F, Chan TC, Loong HH, Wong GL, Lui YY, Chan AT, Sung JJ, Yeo W, Chan HL, Mok TS. Clinical scoring system to predict hepatocellular carcinoma in chronic hepatitis B carriers. *J Clin Oncol* 2010; **28**: 1660-1665 [PMID: 20194845 DOI: 10.1200/JCO.2009.26.2675]

28 **Yang HI**, Sherman M, Su J, Chen PJ, Liaw YF, Iloeje UH, Chen CJ. Nomograms for risk of hepatocellular carcinoma in patients with chronic hepatitis B virus infection. *J Clin Oncol* 2010; **28**: 2437-2444 [PMID: 20368541 DOI: 10.1200/JCO.2009.27.4456]

29 **Yang HI**, Yuen MF, Chan HL, Han KH, Chen PJ, Kim DY, Ahn SH, Chen CJ, Wong VW, Seto WK; REACH-B Working Group. Risk estimation for hepatocellular carcinoma in chronic hepatitis B (REACH-B): development and validation of a predictive score. *Lancet Oncol* 2011; **12**: 568-574 [PMID: 21497551 DOI: 10.1016/S1470-2045(11)70077-8]

30 **Lee MH**, Yang HI, Liu J, Batrla-Utermann R, Jen CL, Iloeje UH, Lu SN, You SL, Wang LY, Chen CJ; R. E.V.E.A.L.-HBV Study Group. Prediction models of long-term cirrhosis and hepatocellular carcinoma risk in chronic hepatitis B patients: risk scores integrating host and virus profiles. *Hepatology* 2013; **58**: 546-554 [PMID: 23504622 DOI: 10.1002/hep.26385]

31 **Lee HW**, Yoo EJ, Kim BK, Kim SU, Park JY, Kim DY, Ahn SH, Han KH. Prediction of

development of liver-related events by transient elastography in hepatitis B patients with complete virological response on antiviral therapy. *Am J Gastroenterol* 2014; **109**: 1241-1249 [PMID: 24957159 DOI: 10.1038/ajg.2014.157]

32 **Yang HI**, Tseng TC, Liu J, Lee MH, Liu CJ, Su TH, Batrla-Utermann R, Chan HL, Kao JH, Chen CJ. Incorporating Serum Level of Hepatitis B Surface Antigen or Omitting Level of Hepatitis B Virus DNA Does not Affect Calculation of Risk for Hepatocellular Carcinoma in Patients Without Cirrhosis. *Clin Gastroenterol Hepatol* 2016; **14**: 461-468.e2 [PMID: 26598229 DOI: 10.1016/j.cgh.2015.10.033]

33 **Wong GL**, Chan HL, Wong CK, Leung C, Chan CY, Ho PP, Chung VC, Chan ZC, Tse YK, Chim AM, Lau TK, Wong VW. Liver stiffness-based optimization of hepatocellular carcinoma risk score in patients with chronic hepatitis B. *J Hepatol* 2014; **60**: 339-345 [PMID: 24128413 DOI: 10.1016/j.jhep.2013.09.029]

34 **Poh Z**, Shen L, Yang HI, Seto WK, Wong VW, Lin CY, Goh BB, Chang PE, Chan HL, Yuen MF, Chen CJ, Tan CK. Real-world risk score for hepatocellular carcinoma (RWS-HCC): a clinically practical risk predictor for HCC in chronic hepatitis B. *Gut* 2016; **65**: 887-888 [PMID: 26786688 DOI: 10.1136/gutjnl-2015-310818]

35 **Fung J**, Cheung KS, Wong DK, Mak LY, To WP, Seto WK, Lai CL, Yuen MF. Long-term outcomes and predictive scores for hepatocellular carcinoma and hepatitis B surface antigen seroclearance after hepatitis B e-antigen seroclearance. *Hepatology* 2018; **68**: 462-472 [PMID: 29534307 DOI: 10.1002/hep.29874]

36 **Fan C**, Li M, Gan Y, Chen T, Sun Y, Lu J, Wang J, Jin Y, Qian G, Gu J, Chen J, Tu H. A simple AGED score for risk classification of primary liver cancer: development and validation with long-term prospective HBsAg-positive cohorts in Qidong, China. *Gut* 2019; **68**: 948-949 [PMID: 29720409 DOI: 10.1136/gutjnl-2018-316525]

37 **Marcellin P**, Gane E, Buti M, Afdhal N, Sievert W, Jacobson IM, Washington MK, Germanidis G, Flaherty JF, Aguilar Schall R, Bornstein JD, Kitrinos KM, Subramanian GM, McHutchison JG, Heathcote EJ. Regression of cirrhosis during treatment with tenofovir disoproxil fumarate for chronic hepatitis B: a 5-year open-label follow-up study. *Lancet* 2013; **381**: 468-475 [PMID: 23234725 DOI: 10.1016/S0140-6736(12)61425-1]

38 **Yip TC**, Wong VW, Chan HL, Tse YK, Lui GC, Wong GL. Tenofovir Is Associated With Lower Risk of Hepatocellular Carcinoma Than Entecavir in Patients With Chronic HBV Infection in China. *Gastroenterology* 2020; **158**: 215-225.e6 [PMID: 31574268 DOI: 10.1053/j.gastro.2019.09.025]

39 **Papatheodoridis G**, Dalekos G, Sypsa V, Yurdaydin C, Buti M, Goulis J, Calleja JL, Chi H, Manolakopoulos S, Mangia G, Gatselis N, Keskin O, Savvidou S, de la Revilla J, Hansen BE, Vlachogiannakos I, Galanis K, Idilman R, Colombo M, Esteban R, Janssen HL, Lampertico P. PAGE-B predicts the risk of developing hepatocellular carcinoma in Caucasians with chronic hepatitis B on 5-year antiviral therapy. *J Hepatol* 2016; **64**: 800-806 [PMID: 26678008 DOI: 10.1016/j.jhep.2015.11.035]

40 **Kim MN**, Hwang SG, Rim KS, Kim BK, Park JY, Kim DY, Ahn SH, Han KH, Kim SU. Validation of PAGE-B model in Asian chronic hepatitis B patients receiving entecavir or tenofovir. *Liver Int* 2017; **37**: 1788-1795 [PMID: 28418595 DOI: 10.1111/liv.13450]

41 **Riveiro-Barciela M**, Tabernero D, Calleja JL, Lens S, Manzano ML, Rodríguez FG, Crespo J, Piqueras B, Pascasio JM, Comas C, Gutierrez ML, Aguirre A, Suárez E, García-Samaniego J, Rivero M, Acero D, Fernandez-Bermejo M, Moreno D, Sánchez-Pobre P, de Cuenca B, Moreno-Palomares JJ, Esteban R, Buti M. Effectiveness and Safety of Entecavir or Tenofovir in a Spanish Cohort of Chronic Hepatitis B Patients: Validation of the Page-B Score to Predict Hepatocellular Carcinoma. *Dig Dis Sci* 2017; **62**: 784-793 [PMID: 28078526 DOI: 10.1007/s10620-017-4448-7]

42 **Kim JH**, Kim YD, Lee M, Jun BG, Kim TS, Suk KT, Kang SH, Kim MY, Cheon GJ, Kim DJ, Baik SK, Choi DH. Modified PAGE-B score predicts the risk of hepatocellular carcinoma in Asians with chronic hepatitis B on antiviral therapy. *J Hepatol* 2018; **69**: 1066-1073 [PMID: 30075230 DOI: 10.1016/j.jhep.2018.07.018]

43 **Lee HW**, Kim SU, Park JY, Kim DY, Ahn SH, Han KH, Kim BK. External validation of the modified PAGE-B score in Asian chronic hepatitis B patients receiving antiviral therapy. *Liver Int* 2019; **39**: 1624-1630 [PMID: 31050379 DOI: 10.1111/liv.14129]

44 **Sohn W**, Cho JY, Kim JH, Lee JI, Kim HJ, Woo MA, Jung SH, Paik YH. Risk score model for the development of hepatocellular carcinoma in treatment-naïve patients receiving oral antiviral treatment for chronic hepatitis B. *Clin Mol Hepatol* 2017; **23**: 170-178 [PMID: 28506056 DOI: 10.3350/cmh.2016.0086]

45 **Chen CH**, Lee CM, Lai HC, Hu TH, Su WP, Lu SN, Lin CH, Hung CH, Wang JH, Lee MH, Peng CY. Prediction model of hepatocellular carcinoma risk in Asian patients with chronic hepatitis B treated with entecavir. *Oncotarget* 2017; **8**: 92431-92441 [PMID: 29190928 DOI: 10.18632/oncotarget.21369]

46 **Hsu YC**, Yip TC, Ho HJ, Wong VW, Huang YT, El-Serag HB, Lee TY, Wu MS, Lin JT, Wong GL, Wu CY. Development of a scoring system to predict hepatocellular carcinoma in Asians on antivirals for chronic hepatitis B. *J Hepatol* 2018; **69**: 278-285 [PMID: 29551708 DOI: 10.1016/j.jhep.2018.02.032]

47 **Yu JH**, Suh YJ, Jin YJ, Heo NY, Jang JW, You CR, An HY, Lee JW. Prediction model for hepatocellular carcinoma risk in treatment-naive chronic hepatitis B patients receiving entecavir/tenofovir. *Eur J Gastroenterol Hepatol* 2019; **31**: 865-872 [PMID: 30694912 DOI: 10.1097/MEG.0000000000001357]

48 **Yang HI**, Yeh ML, Wong GL, Peng CY, Chen CH, Trinh HN, Cheung KS, Xie Q, Su TH, Kozuka R, Lee DH, Ogawa E, Zhao C, Ning HB, Huang R, Li J, Zhang JQ, Ide T, Xing H, Iwane S, Takahashi H, Wong C, Lin CH, Hoang J, Le A, Henry L, Toyoda H, Ueno Y, Gane EJ, Eguchi Y, Kurosaki M, Wu C, Liu C, Shang J, Furusyo N, Enomoto M, Kao JH, Yuen MF, Yu ML, Nguyen MH. Real-World Effectiveness From the Asia Pacific Rim Liver Consortium for HBV Risk Score for the Prediction of Hepatocellular Carcinoma in Chronic Hepatitis B Patients Treated With Oral Antiviral Therapy. *J Infect Dis* 2020; **221**: 389-399 [PMID: 31550363 DOI: 10.1093/infdis/jiz477]

49 **Lim TS**, Lee HW, Lee JI, Kim IH, Lee CH, Jang BK, Chung WJ, Yim HJ, Suh SJ, Seo YS, Lee HA, Yu JH, Lee JW, Kim SG, Kim YS, Park SY, Tak WY, Kim SS, Cheong JY, Jeong SW, Jang JY, Rou WS, Lee BS, Kim SU; Korean Transient Elastography Study Group. Predictive score for hepatocellular carcinoma after hepatitis B e antigen loss in patients treated with entecavir or tenofovir. *J Viral Hepat* 2020; **27**: 1052-1060 [PMID: 32383246 DOI: 10.1111/jvh.13316]

50 **Papatheodoridis GV**, Dalekos GN, Yurdaydin C, Buti M, Goulis J, Arends P, Sypsa V, Manolakopoulos S, Mangia G, Gatselis N, Keskın O, Savvidou S, Hansen BE, Papaioannou C, Galanis K, Idilman R, Colombo M, Esteban R, Janssen HL, Lampertico P. Incidence and predictors of hepatocellular carcinoma in Caucasian chronic hepatitis B patients receiving entecavir or tenofovir. *J Hepatol* 2015; **62**: 363-370 [PMID: 25195548 DOI: 10.1016/j.jhep.2014.08.045]

51 **Arends P**, Sonneveld MJ, Zoutendijk R, Carey I, Brown A, Fasano M, Mutimer D, Deterding K, Reijnders JG, Oo Y, Petersen J, van Bömmel F, de Knegt RJ, Santantonio T, Berg T, Welzel TM, Wedemeyer H, Buti M, Pradat P, Zoulim F, Hansen B, Janssen HL; VIRGIL Surveillance Study Group. Entecavir treatment does not eliminate the risk of hepatocellular carcinoma in chronic hepatitis B: limited role for risk scores in Caucasians. *Gut* 2015; **64**: 1289-1295 [PMID: 25011935 DOI: 10.1136/gutjnl-2014-307023]

52 **Abu-Amara M**, Cerocchi O, Malhi G, Sharma S, Yim C, Shah H, Wong DK, Janssen HL, Feld JJ. The applicability of hepatocellular carcinoma risk prediction scores in a North American patient population with chronic hepatitis B infection. *Gut* 2016; **65**: 1347-1358 [PMID: 25934760 DOI: 10.1136/gutjnl-2014-309099]

53 **Brouwer WP**, van der Meer AJP, Boonstra A, Plompen EPC, Pas SD, de Knegt RJ, de Man RA, Ten Kate FJW, Janssen HLA, Hansen BE. Prediction of long-term clinical outcome in a diverse chronic hepatitis B population: Role of the PAGE-B score. *J Viral Hepat* 2017; **24**: 1023-1031 [PMID: 28544398 DOI: 10.1111/jvh.12727]

54 **Daheim M**, Lang S, Goeser T, Steffen HM, Demir M. Real-world risk score for hepatocellular carcinoma risk prediction in CHBV: a validation outside of Asia. *Gut* 2017; **66**: 1346-1347 [PMID: 27670373 DOI: 10.1136/gutjnl-2016-312993]

55 **Yu ML**, Lin SM, Chuang WL, Dai CY, Wang JH, Lu SN, Sheen IS, Chang WY, Lee CM, Liaw YF. A sustained virological response to interferon or interferon/ribavirin reduces hepatocellular carcinoma and improves survival in chronic hepatitis C: a nationwide, multicentre study in Taiwan. *Antivir Ther* 2006; **11**: 985-994 [PMID: 17302368]

56 **Lok AS**, Seeff LB, Morgan TR, di Bisceglie AM, Sterling RK, Curto TM, Everson GT, Lindsay KL, Lee WM, Bonkovsky HL, Dienstag JL, Ghany MG, Morishima C, Goodman ZD; HALT-C Trial Group. Incidence of hepatocellular carcinoma and associated risk factors in hepatitis C-related advanced liver disease. *Gastroenterology* 2009; **136**: 138-148 [PMID: 18848939 DOI: 10.1053/j.gastro.2008.09.014]

57 **El-Serag HB**, Kanwal F, Davila JA, Kramer J, Richardson P. A new laboratory-based algorithm to predict development of hepatocellular carcinoma in patients with hepatitis C and cirrhosis. *Gastroenterology* 2014; **146**: 1249-55.e1 [PMID: 24462733 DOI: 10.1053/j.gastro.2014.01.045]

58 **Masuzaki R**, Tateishi R, Yoshida H, Goto E, Sato T, Ohki T, Imamura J, Goto T, Kanai F, Kato N, Ikeda H, Shiina S, Kawabe T, Omata M. Prospective risk assessment for hepatocellular carcinoma development in patients with chronic hepatitis C by transient elastography. *Hepatology* 2009; **49**: 1954-1961 [PMID: 19434742 DOI: 10.1002/hep.22870]

59 **Chang KC**, Hung CH, Lu SN, Wang JH, Lee CM, Chen CH, Yen MF, Lin SC, Yen YH, Tsai MC, Tseng PL, Hu TH. A novel predictive score for hepatocellular carcinoma development in patients with chronic hepatitis C after sustained response to pegylated interferon and ribavirin combination therapy. *J Antimicrob Chemother* 2012; **67**: 2766-2772 [PMID: 22899800 DOI: 10.1093/jac/dks269]

60 **Ganne-Carrié N**, Layese R, Bourcier V, Cagnot C, Marcellin P, Guyader D, Pol S, Larrey D, de Lédinghen V, Ouzan D, Zoulim F, Roulot D, Tran A, Bronowicki JP, Zarski JP, Riachi G, Calès P, Péron JM, Alric L, Bourlière M, Mathurin P, Blanc JF, Abergel A, Serfaty L, Mallat A, Grangé JD, Attali P, Bacq Y, Wartelle C, Dao T, Benhamou Y, Pilette C, Silvain C, Christidis C, Capron D, Bernard-Chabert B, Zucman D, Di Martino V, Trinchet JC, Nahon P, Roudot-Thoraval F; ANRS CO12 CirVir Study Group. Nomogram for individualized prediction of hepatocellular carcinoma occurrence in hepatitis C virus cirrhosis (ANRS CO12 CirVir). *Hepatology* 2016; **64**: 1136-1147 [PMID: 27348075 DOI: 10.1002/hep.28702]

61 **Audureau E**, Carrat F, Layese R, Cagnot C, Asselah T, Guyader D, Larrey D, De Lédinghen V, Ouzan D, Zoulim F, Roulot D, Tran A, Bronowicki JP, Zarski JP, Riachi G, Calès P, Péron JM, Alric L, Bourlière M, Mathurin P, Blanc JF, Abergel A, Chazouillères O, Mallat A, Grangé JD, Attali P, d'Alteroche L, Wartelle C, Dao T, Thabut D, Pilette C, Silvain C, Christidis C, Nguyen-Khac E, Bernard-Chabert B, Zucman D, Di Martino V, Sutton A, Pol S, Nahon P; ANRS CO12 CirVir group. Personalized surveillance for hepatocellular carcinoma in cirrhosis - using machine learning adapted to HCV status. *J Hepatol* 2020; **73**: 1434-1445 [PMID: 32615276 DOI: 10.1016/j.jhep.2020.05.052]

62 **Tani J**, Morishita A, Sakamoto T, Takuma K, Nakahara M, Fujita K, Oura K, Tadokoro T, Mimura S, Nomura T, Yoneyama H, Kobara H, Himoto T, Tsutsui A, Senoh T, Nagano T, Ogawa C, Moriya A, Deguchi A, Takaguchi K, Masaki T. Simple scoring system for prediction of hepatocellular carcinoma occurrence after hepatitis C virus eradication by direct-acting antiviral treatment: All Kagawa Liver Disease Group Study. *Oncol Lett* 2020; **19**: 2205-2212 [PMID: 32194718 DOI: 10.3892/ol.2020.11341]

63 **Shiha G**, Waked I, Soliman R, Elbasiony M, Gomaa A, Mikhail NNH, Eslam M. GES: A validated simple score to predict the risk of HCC in patients with HCV-GT4-associated advanced liver fibrosis after oral antivirals. *Liver Int* 2020; **40**: 2828-2833 [PMID: 32946647 DOI: 10.1111/liv.14666]

64 **Flemming JA**, Yang JD, Vittinghoff E, Kim WR, Terrault NA. Risk prediction of hepatocellular carcinoma in patients with cirrhosis: the ADRESS-HCC risk model. *Cancer* 2014; **120**: 3485-3493 [PMID: 25042049 DOI: 10.1002/cncr.28832]

65 **Sharma SA**, Kowgier M, Hansen BE, Brouwer WP, Maan R, Wong D, Shah H, Khalili K, Yim C, Heathcote EJ, Janssen HLA, Sherman M, Hirschfield GM, Feld JJ. Toronto HCC risk index: A validated scoring system to predict 10-year risk of HCC in patients with cirrhosis. *J Hepatol* 2017 [PMID: 28844936 DOI: 10.1016/j.jhep.2017.07.033]

66 **Zhang H**, Zhu J, Xi L, Xu C, Wu A. Validation of the Toronto hepatocellular carcinoma risk index for patients with cirrhosis in China: a retrospective cohort study. *World J Surg Oncol* 2019; **17**: 75 [PMID: 31039803 DOI: 10.1186/s12957-019-1619-3]

67 **Demirtas CO**, Gunduz F, Kani HT, Keklikkiran C, Alahdab YO, Yilmaz Y, Duman DG, Atug O, Giral A, Aslan R, Cagatay NS, Ozkan B, Ozdogan OC. External validation of the Toronto hepatocellular carcinoma risk index in Turkish cirrhotic patients. *Eur J Gastroenterol Hepatol* 2020; **32**: 882-888 [PMID: 32395972 DOI: 10.1097/MEG.0000000000001685]

68 **Li TC**, Li CI, Liu CS, Lin WY, Lin CH, Yang SY, Lin CC. Risk score system for the prediction of hepatocellular carcinoma in patients with type 2 diabetes: Taiwan Diabetes Study. *Semin Oncol* 2018; **45**: 264-274 [PMID: 30342872 DOI: 10.1053/j.seminoncol.2018.07.006]

69 **Fan R**, Papatheodoridis G, Sun J, Innes H, Toyoda H, Xie Q, Mo S, Sypsa V, Guha IN, Kumada T, Niu J, Dalekos G, Yasuda S, Barnes E, Lian J, Suri V, Idilman R, Barclay ST, Dou X, Berg T, Hayes PC, Flaherty JF, Zhou Y, Zhang Z, Buti M, Hutchinson SJ, Guo Y, Calleja JL, Lin L, Zhao L, Chen Y, Janssen HLA, Zhu C, Shi L, Tang X, Gaggar A, Wei L, Jia J, Irving WL, Johnson PJ, Lampertico P, Hou J. aMAP risk score predicts hepatocellular carcinoma development in patients with chronic hepatitis. *J Hepatol* 2020; **73**: 1368-1378 [PMID: 32707225 DOI: 10.1016/j.jhep.2020.07.025]

70 **Kokudo N**, Takemura N, Hasegawa K, Takayama T, Kubo S, Shimada M, Nagano H, Hatano E, Izumi N, Kaneko S, Kudo M, Iijima H, Genda T, Tateishi R, Torimura T, Igaki H, Kobayashi S, Sakurai H, Murakami T, Watadani T, Matsuyama Y. Clinical practice guidelines for hepatocellular carcinoma: The Japan Society of Hepatology 2017 (4th JSH-HCC guidelines) 2019 update. *Hepatol Res* 2019; **49**: 1109-1113 [PMID: 31336394 DOI: 10.1111/hepr.13411]

71 **Craig AJ**, von Felden J, Garcia-Lezana T, Sarcognato S, Villanueva A. Tumour evolution in hepatocellular carcinoma. *Nat Rev Gastroenterol Hepatol* 2020; **17**: 139-152 [PMID: 31792430 DOI: 10.1038/s41575-019-0229-4]

72 **Johnson PJ**, Pirrie SJ, Cox TF, Berhane S, Teng M, Palmer D, Morse J, Hull D, Patman G, Kagebayashi C, Hussain S, Graham J, Reeves H, Satomura S. The detection of hepatocellular carcinoma using a prospectively developed and validated model based on serological biomarkers. *Cancer Epidemiol Biomarkers Prev* 2014; **23**: 144-153 [PMID: 24220911 DOI: 10.1158/1055-9965.EPI-13-0870]

73 **Berhane S**, Toyoda H, Tada T, Kumada T, Kagebayashi C, Satomura S, Schweitzer N, Vogel A, Manns MP, Benckert J, Berg T, Ebker M, Best J, Dechêne A, Gerken G, Schlaak JF, Weinmann A, Wörns MA, Galle P, Yeo W, Mo F, Chan SL, Reeves H, Cox T, Johnson P. Role of the GALAD and BALAD-2 Serologic Models in Diagnosis of Hepatocellular Carcinoma and Prediction of Survival in Patients. *Clin Gastroenterol Hepatol* 2016; **14**: 875-886.e6 [PMID: 26775025 DOI: 10.1016/j.cgh.2015.12.042]

74 **Ricco G**, Cavallone D, Cosma C, Caviglia GP, Oliveri F, Biasiolo A, Abate ML, Plebani M, Smedile A, Bonino F, Pontisso P, Brunetto MR. Impact of etiology of chronic liver disease on hepatocellular carcinoma biomarkers. *Cancer Biomark* 2018; **21**: 603-612 [PMID: 29278878 DOI: 10.3233/CBM-170551]

75 **Yang JD**, Addissie BD, Mara KC, Harmsen WS, Dai J, Zhang N, Wongjarupong N, Ali HM, Ali HA, Hassan FA, Lavu S, Cvinar JL, Giama NH, Moser CD, Miyabe K, Allotey LK, Algeciras-Schimnich A, Theobald JP, Ward MM, Nguyen MH, Befeler AS, Reddy KR, Schwartz M, Harnois DM, Yamada H, Srivastava S, Rinaudo JA, Gores GJ, Feng Z, Marrero JA, Roberts LR. GALAD Score for Hepatocellular Carcinoma Detection in Comparison with Liver Ultrasound and Proposal of GALADUS Score. *Cancer Epidemiol Biomarkers Prev* 2019; **28**: 531-538 [PMID: 30464023 DOI: 10.1158/1055-9965.EPI-18-0281]

76 **Wang M**, Devarajan K, Singal AG, Marrero JA, Dai J, Feng Z, Rinaudo JA, Srivastava S, Evans A, Hann HW, Lai Y, Yang H, Block TM, Mehta A. The Doylestown Algorithm: A Test to Improve the Performance of AFP in the Detection of Hepatocellular Carcinoma. *Cancer Prev Res (Phila)* 2016; **9**: 172-179 [PMID: 26712941 DOI: 10.1158/1940-6207.CAPR-15-0186]

77 **White DL**, Richardson P, Tayoub N, Davila JA, Kanwal F, El-Serag HB. The Updated Model: An Adjusted Serum Alpha-Fetoprotein-Based Algorithm for Hepatocellular Carcinoma Detection With Hepatitis C Virus-Related Cirrhosis. *Gastroenterology* 2015; **149**: 1986-1987 [PMID: 26519622 DOI:

10.1053/j.gastro.2015.10.004]

78 **Tayob N**, Christie I, Richardson P, Feng Z, White DL, Davila J, Corley DA, Kanwal F, El-Serag HB. Validation of the Hepatocellular Carcinoma Early Detection Screening (HES) Algorithm in a Cohort of Veterans With Cirrhosis. *Clin Gastroenterol Hepatol* 2019; **17**: 1886-1893.e5 [PMID: 30557738 DOI: 10.1016/j.cgh.2018.12.005]

79 **Tayob N**, Corley DA, Christie I, Almers L, Rahal AK, Richardson P, White DL, Davila J, Kanwal F, El-Serag HB. Validation of the Updated Hepatocellular Carcinoma Early Detection Screening Algorithm in a Community-Based Cohort of Patients With Cirrhosis of Multiple Etiologies. *Clin Gastroenterol Hepatol* 2021; **19**: 1443-1450.e6 [PMID: 32768590 DOI: 10.1016/j.cgh.2020.07.065]

80 **Cohen JD**, Li L, Wang Y, Thoburn C, Afsari B, Danilova L, Douville C, Javed AA, Wong F, Mattox A, Hruban RH, Wolfgang CL, Goggins MG, Dal Molin M, Wang TL, Roden R, Klein AP, Ptak J, Dobbyn L, Schaefer J, Silliman N, Popoli M, Vogelstein JT, Browne JD, Schoen RE, Brand RE, Tie J, Gibbs P, Wong HL, Mansfield AS, Jen J, Hanash SM, Falconi M, Allen PJ, Zhou S, Bettegowda C, Diaz LA Jr, Tomasetti C, Kinzler KW, Vogelstein B, Lennon AM, Papadopoulos N. Detection and localization of surgically resectable cancers with a multi-analyte blood test. *Science* 2018; **359**: 926-930 [PMID: 29348365 DOI: 10.1126/science.aar3247]

81 **Liu J**, Chen X, Wang J, Zhou S, Wang CL, Ye MZ, Wang XY, Song Y, Wang YQ, Zhang LT, Wu RH, Yang HM, Zhu SD, Zhou MZ, Zhang XC, Zhu HM, Qian ZY. Biological background of the genomic variations of cf-DNA in healthy individuals. *Ann Oncol* 2019; **30**: 464-470 [PMID: 30475948 DOI: 10.1093/annonc/mdy513]

82 **King LY**, Canasto-Chibuque C, Johnson KB, Yip S, Chen X, Kojima K, Deshmukh M, Venkatesh A, Tan PS, Sun X, Villanueva A, Sangiovanni A, Nair V, Mahajan M, Kobayashi M, Kumada H, Iavarone M, Colombo M, Fiel MI, Friedman SL, Llovet JM, Chung RT, Hoshida Y. A genomic and clinical prognostic index for hepatitis C-related early-stage cirrhosis that predicts clinical deterioration. *Gut* 2015; **64**: 1296-1302 [PMID: 25143343 DOI: 10.1136/gutjnl-2014-307862]

83 **Liu J**, Tang W, Budhu A, Forgues M, Hernandez MO, Candia J, Kim Y, Bowman ED, Ambs S, Zhao Y, Tran B, Wu X, Koh C, Surana P, Liang TJ, Guarnera M, Mann D, Rajaure M, Greten TF, Wang Z, Yu H, Wang XW. A Viral Exposure Signature Defines Early Onset of Hepatocellular Carcinoma. *Cell* 2020; **182**: 317-328.e10 [PMID: 32526205 DOI: 10.1016/j.cell.2020.05.038]

84 **Tanabe KK**, Lemoine A, Finkelstein DM, Kawasaki H, Fujii T, Chung RT, Lauwers GY, Kulu Y, Muzikansky A, Kuruppu D, Lanuti M, Goodwin JM, Azoulay D, Fuchs BC. Epidermal growth factor gene functional polymorphism and the risk of hepatocellular carcinoma in patients with cirrhosis. *JAMA* 2008; **299**: 53-60 [PMID: 18167406 DOI: 10.1001/jama.2007.65]

85 **Abu Dayyeh BK**, Yang M, Fuchs BC, Karl DL, Yamada S, Sninsky JJ, O'Brien TR, Dienstag JL, Tanabe KK, Chung RT; HALT-C Trial Group. A functional polymorphism in the epidermal growth factor gene is associated with risk for hepatocellular carcinoma. *Gastroenterology* 2011; **141**: 141-149 [PMID: 21440548 DOI: 10.1053/j.gastro.2011.03.045]

86 **Jiang G**, Yu K, Shao L, Yu X, Hu C, Qian P, Xie H, Li J, Zheng J, Zheng S. Association between epidermal growth factor gene +61A/G polymorphism and the risk of hepatocellular carcinoma: a meta-analysis based on 16 studies. *BMC Cancer* 2015; **15**: 314 [PMID: 25927412 DOI: 10.1186/s12885-015-1318-6]

87 **Kumar V**, Kato N, Urabe Y, Takahashi A, Muroyama R, Hosono N, Otsuka M, Tateishi R, Omata M, Nakagawa H, Koike K, Kamatani N, Kubo M, Nakamura Y, Matsuda K. Genome-wide association study identifies a susceptibility locus for HCV-induced hepatocellular carcinoma. *Nat Genet* 2011; **43**: 455-458 [PMID: 21499248 DOI: 10.1038/ng.809]

88 **Matsuura K**, Sawai H, Ikeo K, Ogawa S, Iio E, Isogawa M, Shimada N, Komori A, Toyoda H, Kumada T, Namisaki T, Yoshiji H, Sakamoto N, Nakagawa M, Asahina Y, Kurosaki M, Izumi N, Enomoto N, Kusakabe A, Kajiwara E, Itoh Y, Ide T, Tamori A, Matsubara M, Kawada N, Shirabe K, Tomita E, Honda M, Kaneko S, Nishina S, Suetsugu A, Hiasa Y, Watanabe H, Genda T, Sakaida I, Nishiguchi S, Takaguchi K, Tanaka E, Sugihara J, Shimada M, Kondo Y, Kawai Y, Kojima K, Nagasaki M, Tokunaga K, Tanaka Y; Japanese Genome-Wide Association Study Group for Viral Hepatitis. Genome-Wide Association Study Identifies TLL1 Variant Associated With Development of Hepatocellular Carcinoma After Eradication of Hepatitis C Virus Infection. *Gastroenterology* 2017; **152**: 1383-1394 [PMID: 28163062 DOI: 10.1053/j.gastro.2017.01.041]

89 **Hamdane N**, Jühling F, Crouchet E, El Saghire H, Thumann C, Oudot MA, Bandiera S, Saviano A, Ponsolles C, Roca Suarez AA, Li S, Fujiwara N, Ono A, Davidson I, Bardeesy N, Schmidl C, Bock C, Schuster C, Lupberger J, Habersetzer F, Doffoël M, Piardi T, Sommacale D, Imamura M, Uchida T, Ohdan H, Aikata H, Chayama K, Boldanova T, Pessaux P, Fuchs BC, Hoshida Y, Zeisel MB, Duong FHT, Baumert TF. HCV-Induced Epigenetic Changes Associated With Liver Cancer Risk Persist After Sustained Virologic Response. *Gastroenterology* 2019; **156**: 2313-2329.e7 [PMID: 30836093 DOI: 10.1053/j.gastro.2019.02.038]

90 **Calvaruso V**, Bruix J. Towards personalized screening for hepatocellular carcinoma: Still not there. *J Hepatol* 2020; **73**: 1319-1321 [PMID: 32771323 DOI: 10.1016/j.jhep.2020.06.032]

91 **Zhang H**, Zhai Y, Hu Z, Wu C, Qian J, Jia W, Ma F, Huang W, Yu L, Yue W, Wang Z, Li P, Zhang Y, Liang R, Wei Z, Cui Y, Xie W, Cai M, Yu X, Yuan Y, Xia X, Zhang X, Yang H, Qiu W, Yang J, Gong F, Chen M, Shen H, Lin D, Zeng YX, He F, Zhou G. Genome-wide association study identifies 1p36.22 as a new susceptibility locus for hepatocellular carcinoma in chronic hepatitis B virus carriers. *Nat Genet* 2010; **42**: 755-758 [PMID: 20676096 DOI: 10.1038/ng.638]

92 **Jiang DK**, Sun J, Cao G, Liu Y, Lin D, Gao YZ, Ren WH, Long XD, Zhang H, Ma XP, Wang Z,

Jiang W, Chen TY, Gao Y, Sun LD, Long JR, Huang HX, Wang D, Yu H, Zhang P, Tang LS, Peng B, Cai H, Liu TT, Zhou P, Liu F, Lin X, Tao S, Wan B, Sai-Yin HX, Qin LX, Yin J, Liu L, Wu C, Pei Y, Zhou YF, Zhai Y, Lu PX, Tan A, Zuo XB, Fan J, Chang J, Gu X, Wang NJ, Li Y, Liu YK, Zhai K, Hu Z, Liu J, Yi Q, Xiang Y, Shi R, Ding Q, Zheng W, Shu XO, Mo Z, Shugart YY, Zhang XJ, Zhou G, Shen H, Zheng SL, Xu J, Yu L. Genetic variants in STAT4 and HLA-DQ genes confer risk of hepatitis B virus-related hepatocellular carcinoma. *Nat Genet* 2013; **45**: 72-75 [PMID: 23242368 DOI: 10.1038/ng.2483]

93 **Perumpail RB**, Wong RJ, Ahmed A, Harrison SA. Hepatocellular Carcinoma in the Setting of Non-cirrhotic Nonalcoholic Fatty Liver Disease and the Metabolic Syndrome: US Experience. *Dig Dis Sci* 2015; **60**: 3142-3148 [PMID: 26250831 DOI: 10.1007/s10620-015-3821-7]

94 **Demirtas CO**, Gunduz F, Tuney D, Baltacioglu F, Kani HT, Bugdayci O, Alahdab YO, Ozdogan OC. Annual contrast-enhanced magnetic resonance imaging is highly effective in the surveillance of hepatocellular carcinoma among cirrhotic patients. *Eur J Gastroenterol Hepatol* 2020; **32**: 517-523 [PMID: 31524775 DOI: 10.1097/MEG.0000000000001528]

World Journal of Gastroenterology

Submit a Manuscript: https://www.f6publishing.com

World J Gastroenterol 2021 September 7; 27(33): 5555-5565

DOI: 10.3748/wjg.v27.i33.5555

ISSN 1007-9327 (print) ISSN 2219-2840 (online)

MINIREVIEWS

Gut microbiota-derived metabolites as key mucosal barrier modulators in obesity

Yan-Xia Wei, Kui-Yang Zheng, Yu-Gang Wang

ORCID number: Yan-Xia Wei 0000-0003-2706-957X; Kui-Yang Zheng 0000-0002-1896-7485; Yu-Gang Wang 0000-0002-0709-1924.

Author contributions: Wei Y performed the majority of the writing; Zheng K provided input in writing the paper; Wang Y provided input in writing the paper, designed the outline and coordinated the writing of the paper and prepared the figures.

Supported by The National Natural Science Foundation of China, No. 81770853 and No. 81970730.

Conflict-of-interest statement: There are no conflicts of interest associated with any of the senior authors or other coauthors who contributed to this manuscript.

Open-Access: This article is an open-access article that was selected by an in-house editor and fully peer-reviewed by external reviewers. It is distributed in accordance with the Creative Commons Attribution NonCommercial (CC BY-NC 4.0) license, which permits others to distribute, remix, adapt, build upon this work non-commercially, and license their derivative works on different terms, provided the original work is properly cited and the use is non-commercial. See: http://creativecommons.org/License

Yan-Xia Wei, Kui-Yang Zheng, Yu-Gang Wang, Laboratory of Infection and Immunity, Jiangsu Key Laboratory of Immunity and Metabolism, Department of Pathogenic Biology and Immunology, Xuzhou Medical University, Xuzhou 221004, Jiangsu Province, China

Corresponding author: Yu-Gang Wang, PhD, Professor, Laboratory of Infection and Immunity, Jiangsu Key Laboratory of Immunity and Metabolism, Department of Pathogenic Biology and Immunology, Xuzhou Medical University, No. 209 Tongshan Road, Xuzhou 221004, Jiangsu Province, China. wangyg@xzhmu.edu.cn

Abstract

A significant breakthrough in the field of obesity research was the demonstration that an obese phenotype could be manipulated by modulating the gut microbiota. An important next step is to elucidate a human-relevant "map" of microbiota-host interactions that regulate the metabolic health of the host. An improved understanding of this crosstalk is a prerequisite for optimizing therapeutic strategies to combat obesity. Intestinal mucosal barrier dysfunction is an important contributor to metabolic diseases and has also been found to be involved in a variety of other chronic inflammatory conditions, including cancer, neurodegeneration, and aging. The mechanistic basis for intestinal barrier dysfunction accompanying metabolic disorders remains poorly understood. Understanding the molecular and cellular modulators of intestinal barrier function will help devise improved strategies to counteract the detrimental systemic consequences of gut barrier breakage. Changes in the composition and function of the gut microbiota, *i.e.*, dysbiosis, are thought to drive obesity-related pathogenesis and may be one of the most important drivers of mucosal barrier dysfunction. Many effects of the microbiota on the host are mediated by microbiota-derived metabolites. In this review, we focus on several relatively well-studied microbial metabolites that can influence intestinal mucosal homeostasis and discuss how they might affect metabolic diseases. The design and use of microbes and their metabolites that are locally active in the gut without systemic side effects are promising novel and safe therapeutic modalities for metabolic diseases.

Key Words: Obesity; Metabolic diseases; Microbiota; Mucosal homeostasis; Gut; Microbial metabolites

©The Author(s) 2021. Published by Baishideng Publishing Group Inc. All rights reserved.

s/by-nc/4.0/

Manuscript source: Invited manuscript

Specialty type: Gastroenterology and hepatology

Country/Territory of origin: China

Peer-review report's scientific quality classification
Grade A (Excellent): 0
Grade B (Very good): B, B
Grade C (Good): C
Grade D (Fair): 0
Grade E (Poor): 0

Received: March 1, 2021
Peer-review started: March 1, 2021
First decision: April 17, 2021
Revised: April 24, 2021
Accepted: July 23, 2021
Article in press: July 23, 2021
Published online: September 7, 2021

P-Reviewer: Codoñer-Franch P, Durazzo M
S-Editor: Zhang H
L-Editor: Webster JR
P-Editor: Liu JH

Core Tip: The manner in which the gut microbiota influences obesity development remains incompletely understood. Recent studies have indicated that the changes in the gut barrier functions act as an important driver of metabolic disorders. There is currently an urgent need to define molecular and cellular modulators of intestinal mucosal barrier homeostasis. Here, we discuss the current understanding of microbiota-derived metabolites in regulating mucosal homeostasis and how they contribute to the metabolic health of the host.

Citation: Wei YX, Zheng KY, Wang YG. Gut microbiota-derived metabolites as key mucosal barrier modulators in obesity. *World J Gastroenterol* 2021; 27(33): 5555-5565
URL: https://www.wjgnet.com/1007-9327/full/v27/i33/5555.htm
DOI: https://dx.doi.org/10.3748/wjg.v27.i33.5555

INTRODUCTION

The gut microbiota is thought to function as an organ that can markedly influence human health and disease[1]. It plays an essential role in the progression of obesity and related metabolic syndromes[2-4]. Many effects of the microbiota on the host are mediated by microbiota-derived metabolites[5-8]. A complex interplay between the host immune system and the gut microbiota under normal physiological conditions maintains the mucosal barrier in a homeostatic state. This symbiotic relationship is often broken during the progression of obesity. Increased levels of circulating bacterial flagellin, lipopolysaccharides (LPS), and peptidoglycans are frequently observed in obesity and its complications due to mucosal barrier dysfunction[9-12]. The objective of this review is to provide an overview of the emerging field related to the role of gut microbiota-derived metabolites in regulating gut barrier function and metabolic health.

MUCOSAL HOMEOSTASIS IN OBESITY

Intestinal barrier dysfunction leads to the translocation of microbial molecules into the systemic circulation, resulting in a state of so-called "metabolic endotoxemia" that is considered to be one of the most important initiators of metabolic disease in obesity [13-16]. However, the mechanisms underlying barrier dysfunction accompanying metabolic syndrome remain poorly understood. Thus, there is an urgent need to elucidate the molecular and cellular modulators of intestinal mucosal barrier homeostasis to devise improved strategies to counteract metabolic disease progression. Hyperglycemia has been suggested as a contributor to obesity-associated dysfunctions of the intestinal barrier[17]; however, this condition may not be the initial trigger for barrier dysfunction, as hyperglycemia often occurs after metabolic syndrome manifestation. The gut microbiota is involved in the regulation of multiple host metabolic pathways *via* interactive host–microbiota interactions. Early phase alteration of the composition and function of the gut microbiota may induce intestinal barrier dysfunction and lead to the development of metabolic disorders. Here, we briefly review several microbial metabolites that regulate mucosal homeostasis.

Microbiota-derived short-chain fatty acids as regulators of mucosal homeostasis

Short-chain fatty acids (SCFAs) are derived predominantly from gut microbial fermentation of otherwise indigestible dietary fiber[18]. According to a clinical study, the major SCFA-producing bacteria promoted by dietary fibers in humans were found to be *Faecalibacterium prausnitzii* and *Eubacterium*, *Lactobacillus*, and *Bifidobacterium* species[19]. The roles of SCFAs in mucosal homeostasis and metabolic health are summarized in Figure 1.

SCFAs regulate gut epithelial cell metabolic programming: Gut epithelial cells express peroxisome proliferator-activated receptor gamma (PPAR-γ)[20], which can sense microbial-derived SCFAs (*e.g.*, butyrate). The activation of PPAR-γ by butyrate drives the energy metabolism of colonic epithelial cells toward beta-oxidation and limits the luminal bioavailability of oxygen[21-24]. This is important for maintaining

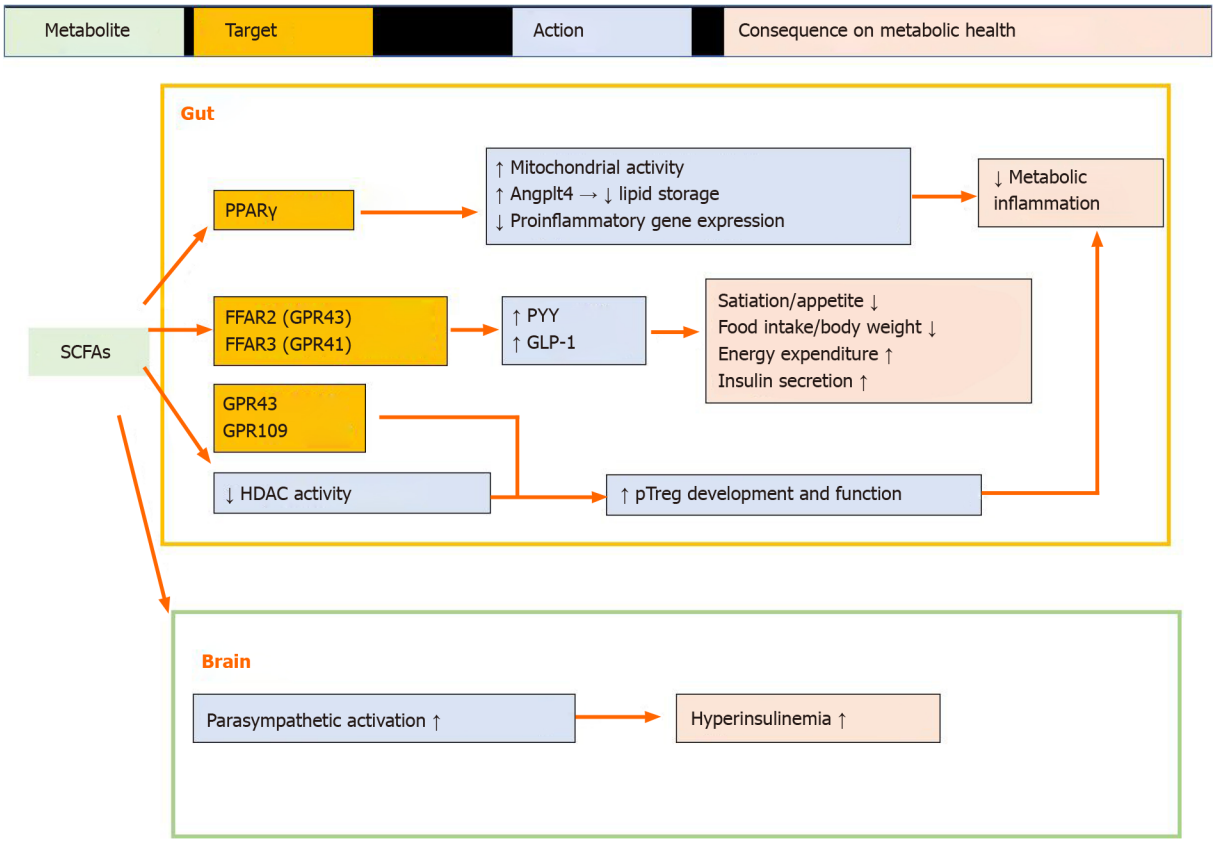


Figure 1 The roles of short-chain fatty acids in mucosal homeostasis and metabolic health. Short-chain fatty acids (SCFAs) can engage various molecular targets in the gut, and play positive roles in maintaining mucosal barrier integrity and systemic metabolic health *via* regulating gut epithelial cell metabolic programming by activating peroxisome proliferator-activated receptor gamma signals, maintaining immune homeostasis by promoting peripheral regulatory T helper cell development and functions, and stimulating energy expenditure and insulin secretion by releasing the gut hormones peptide tyrosine and glucagon-like peptide-1. SCFAs also exert some negative influences on host metabolic health *via* the gut–brain axis. Angplt4: Angiopoietin-like protein 4; FFAR: Free fatty acid receptor; GLP-1: Glucagon-like peptide-1; GPR: G-coupled receptor; HDAC: Histone deacetylase; PPAR: Peroxisome proliferator-activated receptor; pTreg: Peripheral regulatory T helper cell; PYY: Peptide tyrosine.

the colonic surface in a physiological hypoxic state, thereby limiting the aerobic outgrowth of facultative anaerobic bacteria[25]. Short-term high-fat diet (HFD) consumption can perturb epithelial PPAR-γ signals and disrupt the microbial and physiological ecosystems within the gut[26].

PPAR-γ activation by SCFAs can also increase angiopoietin-like protein 4 (ANGPTL4/FIAF) secretion from the gut epithelium[27]. ANGPTL4 is a circulating lipoprotein lipase inhibitor, and its expression levels can affect the process of dietary energy harvesting and storage in the host[28]. Additionally, PPAR-γ activation inhibits the transcription of proinflammatory genes induced by interferon (IFN) gamma and/or LPS[29].

Effects of SCFAs on gut hormones: The gut is the largest endocrine organ within the body and can release more than 20 different peptide hormones that are sensitive to gut nutrient content stimulation and function to regulate a variety of physiological processes[30]. As a gut nutrient, free fatty acids (FFAs) can serve as not only cellular energy sources but also natural ligands for a group of orphan G protein-coupled receptors (GPCRs), which are known as FFA receptors (FFARs) and are expressed in the gut epithelial cells to regulate gut peptide hormone production[31-34]. In particular, FFAR3 (GPR41) and FFAR2 (GPR43) are activated by SCFAs, primarily acetate, butyrate, and propionate[32]. SCFAs can stimulate the release of the anorexigenic hormone peptide tyrosine (PYY) and glucagon-like peptide-1 (GLP-1) from colonic L cells[30] *via* their cognate FFARs. The release of PYY into circulation after food intake can reduce energy intake[35]. GLP-1 can act directly on pancreatic beta cells to activate insulin secretion in a glucose-dependent manner[36]. Thus, SCFA-induced release of PYY and GLP-1 from colonic L-cells may play a role in preventing the development of obesity and its related complications[37].

Role of SCFAs in maintaining mucosal immune homeostasis: The gut microbiota has co-evolved with the intestinal immune system to facilitate the maintenance of mucosal homeostasis[38]. Regulatory T cells (Tregs) are critical for limiting intestinal inflammation[39]. SCFAs play an important role in the generation of peripheral Tregs and control Treg homeostasis and function within the gut[40,41]. Butyrate, acetate, and propionate are the major bacteria-derived SCFAs that control mucosal Treg differentiation and function[40]. Several mechanisms are involved in the promotion of mucosal Treg differentiation and function by SCFAs. First, SCFAs can regulate the size and function of the colonic Treg pool through the activation of GPCRs (GPR43 and/or GPR109)[40,42]. Second, SCFAs can regulate Treg differentiation by inhibiting histone deacetylase (HDAC)[43]. HDAC activity in T cells can be suppressed by acetate, propionate, and butyrate[43]. Butyrate enhances the acetylation of histone H3 Lysine 27 at the promoter and conserved non-coding sequence regions of the Foxp3 locus, which is critical for peripheral Treg generation to promote Foxp3 gene expression[41,44]. Furthermore, the HDAC inhibitory activity of butyrate and propionate promotes the ability of dendritic cells to support Treg differentiation by repressing the expression of LPS-responsive genes and by rendering lamina propria macrophages hyporesponsive[41,45]. Additionally, the binding of SCFAs with GPR43 expressed on neutrophils and eosinophils has been reported to dampen gut inflammatory responses [46]. Collectively, these data indicate that SCFAs can maintain mucosal immune homeostasis, particularly by inducing Treg generation and function, which may be beneficial for alleviating obesity and its related metabolic syndrome[37]. Consistent with this idea, fat-resident Tregs have been reported to be significantly reduced in obese hosts and Tregs protect against obesity-associated inflammation, insulin resistance, and other related metabolic disorders[47-49].

It should be noted that although SCFAs are generally thought to play positive roles in maintaining mucosal homeostasis, they exert negative impacts on host metabolism. In experimental studies involving mice, treatment with acetate promoted metabolic syndrome through the action of the gut–nervous system axis[50]. In a clinical trial, consumption of a propionate-containing meal resulted in the activation of catecholamine-related insulin counter-regulatory signals, thus leading to insulin resistance[51]. Approaches to avoid such negative impacts of SCFAs on host metabolism are warranted.

Role of microbiota-derived amino acid metabolites in mucosal homeostasis

Microbiota-derived tryptophan metabolites protect the gut barrier: Recent discoveries indicate that the gut microbiota modulates immune homeostasis and mucosal barrier physiology by modulating amino acid metabolism. Among the amino acids, the effects of aromatic amino acid tryptophan (Trp) derivatives produced by bacterial fermentation are relatively well studied. Gut microbiota can directly utilize Trp as a biosynthetic precursor for a large number of microbial metabolites, and approximately 4%–6% of Trp can also be further metabolized to indole, indican, tryptamine, skatole, and indole acid derivatives[52,53]. Trp can be converted into indole by tryptophanase, which is expressed in *Escherichia coli* and *Lactobacilli*[54], or into tryptamine by a Trp decarboxylase found in *Clostridium sporogenes*[55]. It can also be transformed into indoleacetic acid *via* an uncharacterized oxidative pathway or into indolepropionic acid (IPA) *via* a reductive pathway that requires a phenyllactate dehydratase that is found in *C. sporogenes*, *Peptostreptococcus anaerobius* CC14N, and three strains of *Clostridium cadaveris*[56].

Many indole derivatives, including IPA and indoleacrylic acid (IA) are ligands for the aryl hydrocarbon receptor (AhR)[54,57,58]. AhR signaling is crucial for intestinal homeostasis because it influences epithelial renewal, barrier integrity, and immune cell activity[59]. AhR mediates the activation of type 3 innate lymphoid cells to produce IL-22[60]. IL-22 plays an important role in maintaining the mucosal barrier and regulating host metabolic functions[61,62]. IPA induces IL-10R1 by activating AhR, thus exerting anti-inflammatory effects in the intestinal mucosa[58]. IA-AhR signaling promotes barrier function and mitigates LPS-stimulated inflammatory responses[63]. Indole-3-aldehyde (IAld) promotes AhR-dependent IL22 production to provide mucosal protection against inflammation induced by the fungus *Candida albicans*[57]. Trp-derived AhR ligands are reduced in both HFD-induced metabolic impairments in animals and in individuals with metabolic syndrome, and supplementation with an AhR agonist or an AhR ligand-producing *Lactobacillus* strain leads to the improvement of metabolic disorders[64,65].

Additionally, IPA has been reported to act as a ligand for the pregnane X receptor (PXR), and *in vivo*, PXR signals regulate mucosal integrity through toll-like receptor 4

[66]. Indole and IAld can also activate enteroendocrine cells through transient receptor potential ankyrin A1 to increase gut motility[67]. Gut microbiota-produced tryptamine activates intestinal epithelial GPCR serotonin receptor-4 (5-HT4R) to increase cAMP levels and drive colonic fluid secretion[68]. Collectively, Trp metabolites produced by the microbiota can protect gut barrier functions.

Microbiota-derived tyrosine metabolites regulate mucosal homeostasis: The aromatic amino acids phenylalanine, tyrosine (Tyr), and Trp share a decarboxylation pathway to generate trace amines, including phenylethylamine, tyramine, and tryptamine, respectively. Tyramine and tryptamine are high-affinity ligands for trace amine-associated receptor 1, which is expressed in the stomach, intestinal neuroendocrine cells, and pancreatic β cells, and regulates energy metabolism and modulates immune homeostasis[69,70].

Another common pathway involves aminotransaminase-mediated transamination, which subsequently undergoes oxidation and reduction, ultimately leading to the production of the corresponding acetic acid or propionic acid derivatives[56]. Desaminotyrosine (DAT, also known as 4-hydroxyphenylpropionic acid or p-hydroxyhydrocinnamic acid) is a degradation product derived from microbial Tyr metabolism. DAT can also be produced from microbial degradation of dietary flavonoids[71,72]. A recent study revealed that DAT protects the host from influenza virus infection by enhancing type I IFN signals[73]. Our recent data demonstrated that DAT supplementation alleviated HFD-induced fat mass accumulation and body weight increment, both of which are correlated with the anti-inflammatory effect of DAT with regard to maintaining mucosal immune homeostasis[7] (Summarized in Figure 2).

Bile acid modification by gut microbiota impacts mucosal homeostasis

Primary bile acids (BAs) are cholesterol metabolites that are produced in the liver and converted to secondary BAs by the gut microbiota[74]. The two key microbiota-dependent processes are BA deconjugation and 7α-hydroxylation. The enzyme bile salt hydrolase, which is produced by many commensal genera such as *Bacteroides*, *Clostridium*, and *Enterococcus*, deconjugates primary BAs. However, only a small number of known bacteria from the *Lachnospiraceae* and *Ruminococcaceae* families perform subsequent 7α-dehydroxylation to generate secondary BAs[75]. BAs are lipid solubilizers that are crucial for dietary lipid absorption and function as signaling molecules that coordinately regulate host metabolism and inflammation by interacting with their cognate cellular receptors, including the nuclear receptors farnesoid X receptor (FXR), PXR, vitamin D receptor, membrane G protein-coupled BA receptor 1 (also known as GPCR19 or TGR5), and sphingosine-1-phosphate receptor[76,77]. Different BA profiles can produce both agonists and antagonists of their cognate receptors, thus creating a great deal of complexity regarding the beneficial or deleterious influence of BAs and their derivatives on health and disease. In the gut, BA-TGR5 signaling leads to GLP-1 expression and secretion, whereas BA-FXR signaling inhibits GLP-1 production[78]. BAs influence gut-associated inflammation by regulating gut mucosal immune cells, including T helper cells expressing IL-17a and Tregs[79-81]. The BA-TGR5–cAMP–PKA axis inhibits NLRP3 inflammasome activation in macrophages[82]. Certain BAs can exert protective effects on the gut epithelium[83] or inhibit intestinal pathogens such as *Clostridium difficile*[84]. In an experimental model, tauroursodeoxycholic acid inhibited intestinal inflammation and barrier disruption in mice with nonalcoholic fatty liver disease[85]. *Parabacteroides distasonis*, one of the core members of the gut microbiota of humans, alleviates obesity and obesity-related dysfunction in mice, at least partially, based on its ability to produce secondary BAs[86] (Summarized in Figure 3).

Other dietary-derived microbial metabolites in regulating mucosal homeostasis

Polyphenols are a class of plant-derived macromolecules[87]. Approximately 90%–95% of dietary polyphenols are poorly absorbed and are partially processed by the gut microbiota[88]. Fermentation of polyphenols by the gut microbiota results in the production of bioactive metabolites that can affect host physiology. Urolithins are gut microbial metabolites derived from the polyphenol compounds, ellagitannins that are present in some fruits, nuts, and seeds (*e.g.*, pomegranates, black raspberries, raspberries, strawberries, walnuts, and almonds)[89]. Ellagitannins are hydrolyzed to ellagic acid under physiological conditions *in vivo*, and ellagic acid is then gradually metabolized by the gut microbiota to produce different types of urolithins. Urolithins have been demonstrated to protect against obesity and related metabolic diseases in animal studies[90]. These effects are related to their protective role in mucosal epithelial integrity and anti-inflammatory functions[91,92].

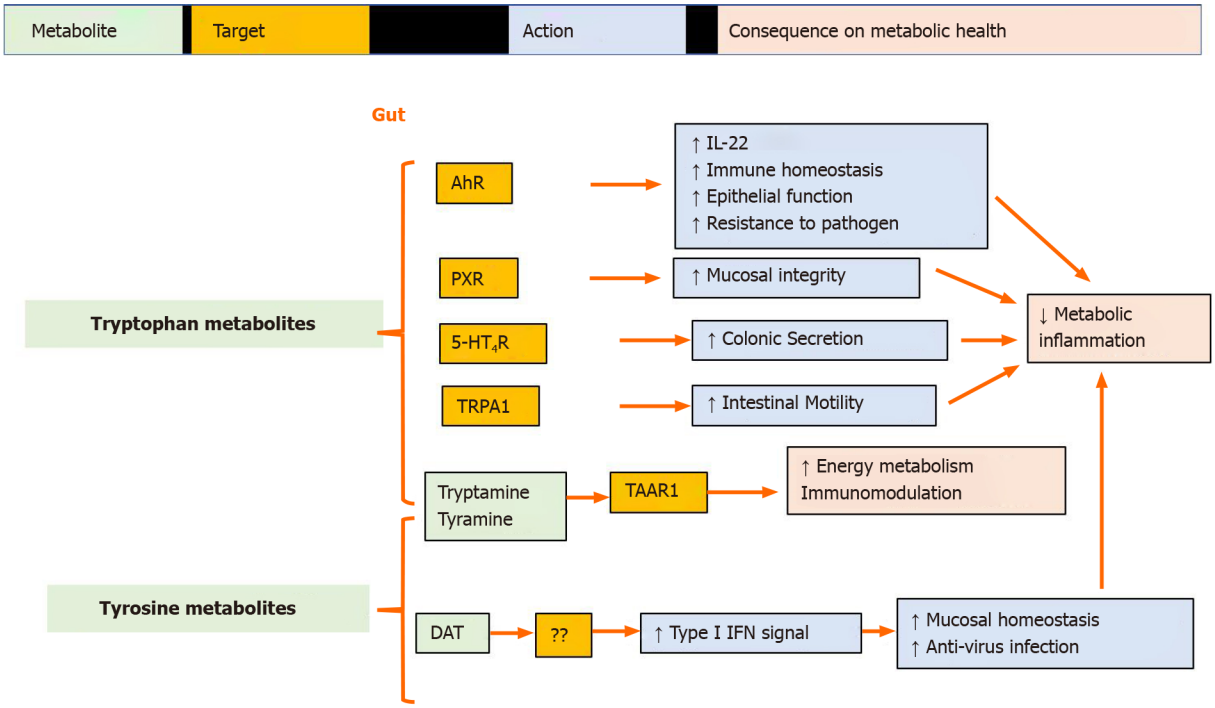


Figure 2 The roles of the indicated amino acid metabolites in mucosal homeostasis and metabolic health. Tryptophan and tyrosine metabolites can engage various molecular targets in the gut, and play positive roles in maintaining mucosal barrier integrity and regulating systemic metabolic health at least in part by modulating mucosal immune and epithelial cell functions *via* cytokine IL-22 or type I interferon, *etc.*, or by promoting host energy metabolism *via* trace amine-associated receptor 1. The question mark indicates that the molecular target of desaminotyrosine is currently unknown. 5-HT4R: Serotonin receptor-4; AhR: Aryl hydrocarbon receptor; DAT: Desaminotyrosine; PXR: Pregnane X receptor; TAAR1: Trace amine-associated receptor 1; TRPA1: Transient receptor potential ankyrin A1.

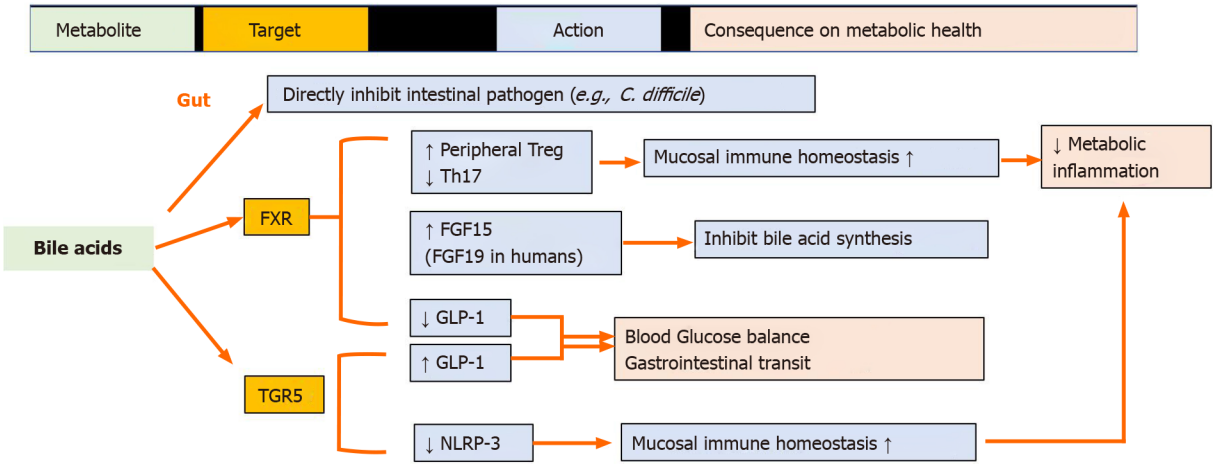


Figure 3 The roles of bile acids in mucosal homeostasis and metabolic health. Bile acids (BAs) have complicated roles in regulating mucosal immune cell activation and gut epithelial cell functions. Different BA profiles can produce both agonists and antagonists of their cognate receptors. Only the well-characterized intestinal targets of BAs and their actions are indicated here. FGF15: Fibroblast growth factor 15; FXR: Farnesoid X receptor; NLRP3: NLR family pyrin domain containing 3; TGR5: Membrane G protein-coupled bile acid receptor 1; Th17: T helper cells expressing IL-17a; Treg: Regulatory T helper cells.

Omega-6 polyunsaturated fatty acids (PUFAs) are abundant in the Western diet and can contribute to obesity and metabolic syndrome[93,94]. The increased ratio of omega-6/omega-3 fatty acids correlates with the incidence and prevalence of overweight individuals and obesity[94,95]. The gut microbiota confers host resistance to HFD-induced obesity by modulating dietary PUFA metabolism[96]. One of the metabolites is 10-hydroxy-cis-12-octadecenoic acid (HYA). HYA promotes GLP-1 secretion in colonic L cells and improves glucose homeostasis *via* the activation of GPR40 and GPR120. Additionally, HYA promotes intestinal peristalsis by acting as a low-affinity prostaglandin EP3 receptor agonist[96].

CONCLUSION

The gut microbiota plays a key role in obesity. Our current understanding of host–microbiota interactions remains in its early phase. Several challenges must be resolved before the field can be advanced. The design and use of microbes and their metabolites that are locally active in the gut without systemic side effects are promising novel and safe therapeutic modalities for metabolic diseases.

REFERENCES

1 **O'Hara AM**, Shanahan F. The gut flora as a forgotten organ. *EMBO Rep* 2006; **7**: 688-693 [PMID: 16819463 DOI: 10.1038/sj.embor.7400731]

2 **Lee CJ**, Sears CL, Maruthur N. Gut microbiome and its role in obesity and insulin resistance. *Ann N Y Acad Sci* 2020; **1461**: 37-52 [PMID: 31087391 DOI: 10.1111/nyas.14107]

3 **Amar J**, Chabo C, Waget A, Klopp P, Vachoux C, Bermúdez-Humarán LG, Smirnova N, Bergé M, Sulpice T, Lahtinen S, Ouwehand A, Langella P, Rautonen N, Sansonetti PJ, Burcelin R. Intestinal mucosal adherence and translocation of commensal bacteria at the early onset of type 2 diabetes: molecular mechanisms and probiotic treatment. *EMBO Mol Med* 2011; **3**: 559-572 [PMID: 21735552 DOI: 10.1002/emmm.201100159]

4 **Chassaing B**, Koren O, Goodrich JK, Poole AC, Srinivasan S, Ley RE, Gewirtz AT. Dietary emulsifiers impact the mouse gut microbiota promoting colitis and metabolic syndrome. *Nature* 2015; **519**: 92-96 [PMID: 25731162 DOI: 10.1038/nature14232]

5 **Taleb S**. Tryptophan Dietary Impacts Gut Barrier and Metabolic Diseases. *Front Immunol* 2019; **10**: 2113 [PMID: 31552046 DOI: 10.3389/fimmu.2019.02113]

6 **Ejtahed HS**, Angoorani P, Soroush AR, Hasani-Ranjbar S, Siadat SD, Larijani B. Gut microbiota-derived metabolites in obesity: a systematic review. *Biosci Microbiota Food Health* 2020; **39**: 65-76 [PMID: 32775123 DOI: 10.12938/bmfh.2019-026]

7 **Wei Y**, Gao J, Kou Y, Liu M, Meng L, Zheng X, Xu S, Liang M, Sun H, Liu Z, Wang Y. The intestinal microbial metabolite desaminotyrosine is an anti-inflammatory molecule that modulates local and systemic immune homeostasis. *FASEB J* 2020; **34**: 16117-16128 [PMID: 33047367 DOI: 10.1096/fj.201902900RR]

8 **Vallianou N**, Stratigou T, Christodoulatos GS, Dalamaga M. Understanding the Role of the Gut Microbiome and Microbial Metabolites in Obesity and Obesity-Associated Metabolic Disorders: Current Evidence and Perspectives. *Curr Obes Rep* 2019; **8**: 317-332 [PMID: 31175629 DOI: 10.1007/s13679-019-00352-2]

9 **Tuomi K**, Logomarsino JV. Bacterial Lipopolysaccharide, Lipopolysaccharide-Binding Protein, and Other Inflammatory Markers in Obesity and After Bariatric Surgery. *Metab Syndr Relat Disord* 2016; **14**: 279-288 [PMID: 27228236 DOI: 10.1089/met.2015.0170]

10 **Pekkala S**, Munukka E, Kong L, Pöllänen E, Autio R, Roos C, Wiklund P, Fischer-Posovszky P, Wabitsch M, Alen M, Huovinen P, Cheng S. Toll-like receptor 5 in obesity: the role of gut microbiota and adipose tissue inflammation. *Obesity (Silver Spring)* 2015; **23**: 581-590 [PMID: 25611816 DOI: 10.1002/oby.20993]

11 **Chan KL**, Tam TH, Boroumand P, Prescott D, Costford SR, Escalante NK, Fine N, Tu Y, Robertson SJ, Prabaharan D, Liu Z, Bilan PJ, Salter MW, Glogauer M, Girardin SE, Philpott DJ, Klip A. Circulating NOD1 Activators and Hematopoietic NOD1 Contribute to Metabolic Inflammation and Insulin Resistance. *Cell Rep* 2017; **18**: 2415-2426 [PMID: 28273456 DOI: 10.1016/j.celrep.2017.02.027]

12 **Hersoug LG**, Møller P, Loft S. Role of microbiota-derived lipopolysaccharide in adipose tissue inflammation, adipocyte size and pyroptosis during obesity. *Nutr Res Rev* 2018; **31**: 153-163 [PMID: 29362018 DOI: 10.1017/S0954422417000269]

13 **Winer DA**, Luck H, Tsai S, Winer S. The Intestinal Immune System in Obesity and Insulin Resistance. *Cell Metab* 2016; **23**: 413-426 [PMID: 26853748 DOI: 10.1016/j.cmet.2016.01.003]

14 **Wollam J**, Riopel M, Xu YJ, Johnson AMF, Ofrecio JM, Ying W, El Ouarrat D, Chan LS, Han AW, Mahmood NA, Ryan CN, Lee YS, Watrous JD, Chordia MD, Pan D, Jain M, Olefsky JM. Microbiota-Produced *N*-Formyl Peptide fMLF Promotes Obesity-Induced Glucose Intolerance. *Diabetes* 2019; **68**: 1415-1426 [PMID: 31010956 DOI: 10.2337/db18-1307]

15 **Zhao L**. The gut microbiota and obesity: from correlation to causality. *Nat Rev Microbiol* 2013; **11**: 639-647 [PMID: 23912213 DOI: 10.1038/nrmicro3089]

16 **Cani PD**, Amar J, Iglesias MA, Poggi M, Knauf C, Bastelica D, Neyrinck AM, Fava F, Tuohy KM, Chabo C, Waget A, Delmée E, Cousin B, Sulpice T, Chamontin B, Ferrières J, Tanti JF, Gibson GR, Casteilla L, Delzenne NM, Alessi MC, Burcelin R. Metabolic endotoxemia initiates obesity and insulin resistance. *Diabetes* 2007; **56**: 1761-1772 [PMID: 17456850 DOI: 10.2337/db06-1491]

17 **Thaiss CA**, Levy M, Grosheva I, Zheng D, Soffer E, Blacher E, Braverman S, Tengeler AC, Barak O, Elazar M, Ben-Zeev R, Lehavi-Regev D, Katz MN, Pevsner-Fischer M, Gertler A, Halpern Z, Harmelin A, Aamar S, Serradas P, Grosfeld A, Shapiro H, Geiger B, Elinav E. Hyperglycemia drives intestinal barrier dysfunction and risk for enteric infection. *Science* 2018; **359**: 1376-1383 [PMID: 29519916 DOI: 10.1126/science.aar3318]

18 **Makki K**, Deehan EC, Walter J, Bäckhed F. The Impact of Dietary Fiber on Gut Microbiota in Host Health and Disease. *Cell Host Microbe* 2018; **23**: 705-715 [PMID: 29902436 DOI: 10.1016/j.chom.2018.05.012]

19 **Zhao L**, Zhang F, Ding X, Wu G, Lam YY, Wang X, Fu H, Xue X, Lu C, Ma J, Yu L, Xu C, Ren Z, Xu Y, Xu S, Shen H, Zhu X, Shi Y, Shen Q, Dong W, Liu R, Ling Y, Zeng Y, Zhang Q, Wang J, Wang L, Wu Y, Zeng B, Wei H, Zhang M, Peng Y, Zhang C. Gut bacteria selectively promoted by dietary fibers alleviate type 2 diabetes. *Science* 2018; **359**: 1151-1156 [PMID: 29590046 DOI: 10.1126/science.aao5774]

20 **Su CG**, Wen X, Bailey ST, Jiang W, Rangwala SM, Keilbaugh SA, Flanigan A, Murthy S, Lazar MA, Wu GD. A novel therapy for colitis utilizing PPAR-gamma ligands to inhibit the epithelial inflammatory response. *J Clin Invest* 1999; **104**: 383-389 [PMID: 10449430 DOI: 10.1172/JCI7145]

21 **Lefebvre M**, Paulweber B, Fajas L, Woods J, McCrary C, Colombel JF, Najib J, Fruchart JC, Datz C, Vidal H, Desreumaux P, Auwerx J. Peroxisome proliferator-activated receptor gamma is induced during differentiation of colon epithelium cells. *J Endocrinol* 1999; **162**: 331-340 [PMID: 10467224 DOI: 10.1677/joe.0.1620331]

22 **Duszka K**, Oresic M, Le May C, König J, Wahli W. PPARγ Modulates Long Chain Fatty Acid Processing in the Intestinal Epithelium. *Int J Mol Sci* 2017; **18** [PMID: 29182565 DOI: 10.3390/ijms18122559]

23 **Dowdell AS**, Cartwright IM, Goldberg MS, Kostelecky R, Ross T, Welch N, Glover LE, Colgan SP. The HIF target ATG9A is essential for epithelial barrier function and tight junction biogenesis. *Mol Biol Cell* 2020; **31**: 2249-2258 [PMID: 32726170 DOI: 10.1091/mbc.E20-05-0291]

24 **Donohoe DR**, Garge N, Zhang X, Sun W, O'Connell TM, Bunger MK, Bultman SJ. The microbiome and butyrate regulate energy metabolism and autophagy in the mammalian colon. *Cell Metab* 2011; **13**: 517-526 [PMID: 21531334 DOI: 10.1016/j.cmet.2011.02.018]

25 **Byndloss MX**, Olsan EE, Rivera-Chávez F, Tiffany CR, Cevallos SA, Lokken KL, Torres TP, Byndloss AJ, Faber F, Gao Y, Litvak Y, Lopez CA, Xu G, Napoli E, Giulivi C, Tsolis RM, Revzin A, Lebrilla CB, Bäumler AJ. Microbiota-activated PPAR-γ signaling inhibits dysbiotic Enterobacteriaceae expansion. *Science* 2017; **357**: 570-575 [PMID: 28798125 DOI: 10.1126/science.aam9949]

26 **Tomas J**, Mulet C, Saffarian A, Cavin JB, Ducroc R, Regnault B, Kun Tan C, Duszka K, Burcelin R, Wahli W, Sansonetti PJ, Pédron T. High-fat diet modifies the PPAR-γ pathway leading to disruption of microbial and physiological ecosystem in murine small intestine. *Proc Natl Acad Sci USA* 2016; **113**: E5934-E5943 [PMID: 27638207 DOI: 10.1073/pnas.1612559113]

27 **Alex S**, Lange K, Amolo T, Grinstead JS, Haakonsson AK, Szalowska E, Koppen A, Mudde K, Haenen D, Al-Lahham S, Roelofsen H, Houtman R, van der Burg B, Mandrup S, Bonvin AM, Kalkhoven E, Müller M, Hooiveld GJ, Kersten S. Short-chain fatty acids stimulate angiopoietin-like 4 synthesis in human colon adenocarcinoma cells by activating peroxisome proliferator-activated receptor γ. *Mol Cell Biol* 2013; **33**: 1303-1316 [PMID: 23339868 DOI: 10.1128/MCB.00858-12]

28 **Bäckhed F**, Ding H, Wang T, Hooper LV, Koh GY, Nagy A, Semenkovich CF, Gordon JI. The gut microbiota as an environmental factor that regulates fat storage. *Proc Natl Acad Sci U S A* 2004; **101**: 15718-15723 [PMID: 15505215 DOI: 10.1073/pnas.0407076101]

29 **Li M**, Pascual G, Glass CK. Peroxisome proliferator-activated receptor gamma-dependent repression of the inducible nitric oxide synthase gene. *Mol Cell Biol* 2000; **20**: 4699-4707 [PMID: 10848596 DOI: 10.1128/mcb.20.13.4699-4707.2000]

30 **Murphy KG**, Bloom SR. Gut hormones and the regulation of energy homeostasis. *Nature* 2006; **444**: 854-859 [PMID: 17167473 DOI: 10.1038/nature05484]

31 **Kimura I**, Ichimura A, Ohue-Kitano R, Igarashi M. Free Fatty Acid Receptors in Health and Disease. *Physiol Rev* 2020; **100**: 171-210 [PMID: 31487233 DOI: 10.1152/physrev.00041.2018]

32 **Brown AJ**, Goldsworthy SM, Barnes AA, Eilert MM, Tcheang L, Daniels D, Muir AI, Wigglesworth MJ, Kinghorn I, Fraser NJ, Pike NB, Strum JC, Steplewski KM, Murdock PR, Holder JC, Marshall FH, Szekeres PG, Wilson S, Ignar DM, Foord SM, Wise A, Dowell SJ. The Orphan G protein-coupled receptors GPR41 and GPR43 are activated by propionate and other short chain carboxylic acids. *J Biol Chem* 2003; **278**: 11312-11319 [PMID: 12496283 DOI: 10.1074/jbc.M211609200]

33 **Tazoe H**, Otomo Y, Karaki S, Kato I, Fukami Y, Terasaki M, Kuwahara A. Expression of short-chain fatty acid receptor GPR41 in the human colon. *Biomed Res* 2009; **30**: 149-156 [PMID: 19574715 DOI: 10.2220/biomedres.30.149]

34 **Karaki S**, Tazoe H, Hayashi H, Kashiwabara H, Tooyama K, Suzuki Y, Kuwahara A. Expression of the short-chain fatty acid receptor, GPR43, in the human colon. *J Mol Histol* 2008; **39**: 135-142 [PMID: 17899402 DOI: 10.1007/s10735-007-9145-y]

35 **Batterham RL**, Cowley MA, Small CJ, Herzog H, Cohen MA, Dakin CL, Wren AM, Brynes AE, Low MJ, Ghatei MA, Cone RD, Bloom SR. Gut hormone PYY(3-36) physiologically inhibits food intake. *Nature* 2002; **418**: 650-654 [PMID: 12167864 DOI: 10.1038/nature00887]

36 **Drucker DJ**, Habener JF, Holst JJ. Discovery, characterization, and clinical development of the glucagon-like peptides. *J Clin Invest* 2017; **127**: 4217-4227 [PMID: 29202475 DOI: 10.1172/JCI97233]

37 **Chambers ES**, Viardot A, Psichas A, Morrison DJ, Murphy KG, Zac-Varghese SE, MacDougall K, Preston T, Tedford C, Finlayson GS, Blundell JE, Bell JD, Thomas EL, Mt-Isa S, Ashby D, Gibson GR, Kolida S, Dhillo WS, Bloom SR, Morley W, Clegg S, Frost G. Effects of targeted delivery of propionate to the human colon on appetite regulation, body weight maintenance and adiposity in

overweight adults. *Gut* 2015; **64**: 1744-1754 [PMID: 25500202 DOI: 10.1136/gutjnl-2014-307913]
38 **Lee YK**, Mazmanian SK. Has the microbiota played a critical role in the evolution of the adaptive immune system? *Science* 2010; **330**: 1768-1773 [PMID: 21205662 DOI: 10.1126/science.1195568]
39 **Whibley N**, Tucci A, Powrie F. Regulatory T cell adaptation in the intestine and skin. *Nat Immunol* 2019; **20**: 386-396 [PMID: 30890797 DOI: 10.1038/s41590-019-0351-z]
40 **Smith PM**, Howitt MR, Panikov N, Michaud M, Gallini CA, Bohlooly-Y M, Glickman JN, Garrett WS. The microbial metabolites, short-chain fatty acids, regulate colonic Treg cell homeostasis. *Science* 2013; **341**: 569-573 [PMID: 23828891 DOI: 10.1126/science.1241165]
41 **Arpaia N**, Campbell C, Fan X, Dikiy S, van der Veeken J, deRoos P, Liu H, Cross JR, Pfeffer K, Coffer PJ, Rudensky AY. Metabolites produced by commensal bacteria promote peripheral regulatory T-cell generation. *Nature* 2013; **504**: 451-455 [PMID: 24226773 DOI: 10.1038/nature12726]
42 **Singh N**, Gurav A, Sivaprakasam S, Brady E, Padia R, Shi H, Thangaraju M, Prasad PD, Manicassamy S, Munn DH, Lee JR, Offermanns S, Ganapathy V. Activation of Gpr109a, receptor for niacin and the commensal metabolite butyrate, suppresses colonic inflammation and carcinogenesis. *Immunity* 2014; **40**: 128-139 [PMID: 24412617 DOI: 10.1016/j.immuni.2013.12.007]
43 **Park J**, Kim M, Kang SG, Jannasch AH, Cooper B, Patterson J, Kim CH. Short-chain fatty acids induce both effector and regulatory T cells by suppression of histone deacetylases and regulation of the mTOR-S6K pathway. *Mucosal Immunol* 2015; **8**: 80-93 [PMID: 24917457 DOI: 10.1038/mi.2014.44]
44 **Furusawa Y**, Obata Y, Fukuda S, Endo TA, Nakato G, Takahashi D, Nakanishi Y, Uetake C, Kato K, Kato T, Takahashi M, Fukuda NN, Murakami S, Miyauchi E, Hino S, Atarashi K, Onawa S, Fujimura Y, Lockett T, Clarke JM, Topping DL, Tomita M, Hori S, Ohara O, Morita T, Koseki H, Kikuchi J, Honda K, Hase K, Ohno H. Commensal microbe-derived butyrate induces the differentiation of colonic regulatory T cells. *Nature* 2013; **504**: 446-450 [PMID: 24226770 DOI: 10.1038/nature12721]
45 **Chang PV**, Hao L, Offermanns S, Medzhitov R. The microbial metabolite butyrate regulates intestinal macrophage function *via* histone deacetylase inhibition. *Proc Natl Acad Sci U S A* 2014; **111**: 2247-2252 [PMID: 24390544 DOI: 10.1073/pnas.1322269111]
46 **Maslowski KM**, Vieira AT, Ng A, Kranich J, Sierro F, Yu D, Schilter HC, Rolph MS, Mackay F, Artis D, Xavier RJ, Teixeira MM, Mackay CR. Regulation of inflammatory responses by gut microbiota and chemoattractant receptor GPR43. *Nature* 2009; **461**: 1282-1286 [PMID: 19865172 DOI: 10.1038/nature08530]
47 **Li C**, Spallanzani RG, Mathis D. Visceral adipose tissue Tregs and the cells that nurture them. *Immunol Rev* 2020; **295**: 114-125 [PMID: 32162339 DOI: 10.1111/imr.12850]
48 **Zhao XY**, Zhou L, Chen Z, Ji Y, Peng X, Qi L, Li S, Lin JD. The obesity-induced adipokine sST2 exacerbates adipose T_{reg} and ILC2 depletion and promotes insulin resistance. *Sci Adv* 2020; **6**: eaay6191 [PMID: 32426492 DOI: 10.1126/sciadv.aay6191]
49 **Chen X**, Wu Y, Wang L. Fat-resident Tregs: an emerging guard protecting from obesity-associated metabolic disorders. *Obes Rev* 2013; **14**: 568-578 [PMID: 23534927 DOI: 10.1111/obr.12033]
50 **Perry RJ**, Peng L, Barry NA, Cline GW, Zhang D, Cardone RL, Petersen KF, Kibbey RG, Goodman AL, Shulman GI. Acetate mediates a microbiome-brain-β-cell axis to promote metabolic syndrome. *Nature* 2016; **534**: 213-217 [PMID: 27279214 DOI: 10.1038/nature18309]
51 **Tirosh A**, Calay ES, Tuncman G, Claiborn KC, Inouye KE, Eguchi K, Alcala M, Rathaus M, Hollander KS, Ron I, Livne R, Heianza Y, Qi L, Shai I, Garg R, Hotamisligil GS. The short-chain fatty acid propionate increases glucagon and FABP4 production, impairing insulin action in mice and humans. *Sci Transl Med* 2019; **11** [PMID: 31019023 DOI: 10.1126/scitranslmed.aav0120]
52 **Yokoyama MT**, Carlson JR. Microbial metabolites of tryptophan in the intestinal tract with special reference to skatole. *Am J Clin Nutr* 1979; **32**: 173-178 [PMID: 367144 DOI: 10.1093/ajcn/32.1.173]
53 **Alkhalaf LM**, Ryan KS. Biosynthetic manipulation of tryptophan in bacteria: pathways and mechanisms. *Chem Biol* 2015; **22**: 317-328 [PMID: 25794436 DOI: 10.1016/j.chembiol.2015.02.005]
54 **Hubbard TD**, Murray IA, Perdew GH. Indole and Tryptophan Metabolism: Endogenous and Dietary Routes to Ah Receptor Activation. *Drug Metab Dispos* 2015; **43**: 1522-1535 [PMID: 26041783 DOI: 10.1124/dmd.115.064246]
55 **Williams BB**, Van Benschoten AH, Cimermancic P, Donia MS, Zimmermann M, Taketani M, Ishihara A, Kashyap PC, Fraser JS, Fischbach MA. Discovery and characterization of gut microbiota decarboxylases that can produce the neurotransmitter tryptamine. *Cell Host Microbe* 2014; **16**: 495-503 [PMID: 25263219 DOI: 10.1016/j.chom.2014.09.001]
56 **Dodd D**, Spitzer MH, Van Treuren W, Merrill BD, Hryckowian AJ, Higginbottom SK, Le A, Cowan TM, Nolan GP, Fischbach MA, Sonnenburg JL. A gut bacterial pathway metabolizes aromatic amino acids into nine circulating metabolites. *Nature* 2017; **551**: 648-652 [PMID: 29168502 DOI: 10.1038/nature24661]
57 **Zelante T**, Iannitti RG, Cunha C, De Luca A, Giovannini G, Pieraccini G, Zecchi R, D'Angelo C, Massi-Benedetti C, Fallarino F, Carvalho A, Puccetti P, Romani L. Tryptophan catabolites from microbiota engage aryl hydrocarbon receptor and balance mucosal reactivity *via* interleukin-22. *Immunity* 2013; **39**: 372-385 [PMID: 23973224 DOI: 10.1016/j.immuni.2013.08.003]
58 **Alexeev EE**, Lanis JM, Kao DJ, Campbell EL, Kelly CJ, Battista KD, Gerich ME, Jenkins BR, Walk ST, Kominsky DJ, Colgan SP. Microbiota-Derived Indole Metabolites Promote Human and Murine Intestinal Homeostasis through Regulation of Interleukin-10 Receptor. *Am J Pathol* 2018; **188**: 1183-1194 [PMID: 29454749 DOI: 10.1016/j.ajpath.2018.01.011]
59 **Lamas B**, Natividad JM, Sokol H. Aryl hydrocarbon receptor and intestinal immunity. *Mucosal*

Immunol 2018; **11**: 1024-1038 [PMID: 29626198 DOI: 10.1038/s41385-018-0019-2]
60 **Qiu J**, Heller JJ, Guo X, Chen ZM, Fish K, Fu YX, Zhou L. The aryl hydrocarbon receptor regulates gut immunity through modulation of innate lymphoid cells. *Immunity* 2012; **36**: 92-104 [PMID: 22177117 DOI: 10.1016/j.immuni.2011.11.011]
61 **Wang X**, Ota N, Manzanillo P, Kates L, Zavala-Solorio J, Eidenschenk C, Zhang J, Lesch J, Lee WP, Ross J, Diehl L, van Bruggen N, Kolumam G, Ouyang W. Interleukin-22 alleviates metabolic disorders and restores mucosal immunity in diabetes. *Nature* 2014; **514**: 237-241 [PMID: 25119041 DOI: 10.1038/nature13564]
62 **Zou J**, Chassaing B, Singh V, Pellizzon M, Ricci M, Fythe MD, Kumar MV, Gewirtz AT. Fiber-Mediated Nourishment of Gut Microbiota Protects against Diet-Induced Obesity by Restoring IL-22-Mediated Colonic Health. *Cell Host Microbe* 2018; **23**: 41-53.e4 [PMID: 29276170 DOI: 10.1016/j.chom.2017.11.003]
63 **Wlodarska M**, Luo C, Kolde R, d'Hennezel E, Annand JW, Heim CE, Krastel P, Schmitt EK, Omar AS, Creasey EA, Garner AL, Mohammadi S, O'Connell DJ, Abubucker S, Arthur TD, Franzosa EA, Huttenhower C, Murphy LO, Haiser HJ, Vlamakis H, Porter JA, Xavier RJ. Indoleacrylic Acid Produced by Commensal Peptostreptococcus Species Suppresses Inflammation. *Cell Host Microbe* 2017; **22**: 25-37.e6 [PMID: 28704649 DOI: 10.1016/j.chom.2017.06.007]
64 **Natividad JM**, Agus A, Planchais J, Lamas B, Jarry AC, Martin R, Michel ML, Chong-Nguyen C, Roussel R, Straube M, Jegou S, McQuitty C, Le Gall M, da Costa G, Lecornet E, Michaudel C, Modoux M, Glodt J, Bridonneau C, Sovran B, Dupraz L, Bado A, Richard ML, Langella P, Hansel B, Launay JM, Xavier RJ, Duboc H, Sokol H. Impaired Aryl Hydrocarbon Receptor Ligand Production by the Gut Microbiota Is a Key Factor in Metabolic Syndrome. *Cell Metab* 2018; **28**: 737-749.e4 [PMID: 30057068 DOI: 10.1016/j.cmet.2018.07.001]
65 **Krishnan S**, Ding Y, Saedi N, Choi M, Sridharan GV, Sherr DH, Yarmush ML, Alaniz RC, Jayaraman A, Lee K. Gut Microbiota-Derived Tryptophan Metabolites Modulate Inflammatory Response in Hepatocytes and Macrophages. *Cell Rep* 2018; **23**: 1099-1111 [PMID: 29694888 DOI: 10.1016/j.celrep.2018.03.109]
66 **Venkatesh M**, Mukherjee S, Wang H, Li H, Sun K, Benechet AP, Qiu Z, Maher L, Redinbo MR, Phillips RS, Fleet JC, Kortagere S, Mukherjee P, Fasano A, Le Ven J, Nicholson JK, Dumas ME, Khanna KM, Mani S. Symbiotic bacterial metabolites regulate gastrointestinal barrier function *via* the xenobiotic sensor PXR and Toll-like receptor 4. *Immunity* 2014; **41**: 296-310 [PMID: 25065623 DOI: 10.1016/j.immuni.2014.06.014]
67 **Ye L**, Bae M, Cassilly CD, Jabba SV, Thorpe DW, Martin AM, Lu HY, Wang J, Thompson JD, Lickwar CR, Poss KD, Keating DJ, Jordt SE, Clardy J, Liddle RA, Rawls JF. Enteroendocrine cells sense bacterial tryptophan catabolites to activate enteric and vagal neuronal pathways. *Cell Host Microbe* 2021; **29**: 179-196.e9 [PMID: 33352109 DOI: 10.1016/j.chom.2020.11.011]
68 **Bhattarai Y**, Williams BB, Battaglioli EJ, Whitaker WR, Till L, Grover M, Linden DR, Akiba Y, Kandimalla KK, Zachos NC, Kaunitz JD, Sonnenburg JL, Fischbach MA, Farrugia G, Kashyap PC. Gut Microbiota-Produced Tryptamine Activates an Epithelial G-Protein-Coupled Receptor to Increase Colonic Secretion. *Cell Host Microbe* 2018; **23**: 775-785.e5 [PMID: 29902441 DOI: 10.1016/j.chom.2018.05.004]
69 **Liu Y**, Hou Y, Wang G, Zheng X, Hao H. Gut Microbial Metabolites of Aromatic Amino Acids as Signals in Host-Microbe Interplay. *Trends Endocrinol Metab* 2020; **31**: 818-834 [PMID: 32284282 DOI: 10.1016/j.tem.2020.02.012]
70 **Gainetdinov RR**, Hoener MC, Berry MD. Trace Amines and Their Receptors. *Pharmacol Rev* 2018; **70**: 549-620 [PMID: 29941461 DOI: 10.1124/pr.117.015305]
71 **Schoefer L**, Mohan R, Schwiertz A, Braune A, Blaut M. Anaerobic degradation of flavonoids by Clostridium orbiscindens. *Appl Environ Microbiol* 2003; **69**: 5849-5854 [PMID: 14532034 DOI: 10.1128/aem.69.10.5849-5854.2003]
72 **Saura-Calixto F**, Pérez-Jiménez J, Touriño S, Serrano J, Fuguet E, Torres JL, Goñi I. Proanthocyanidin metabolites associated with dietary fibre from in vitro colonic fermentation and proanthocyanidin metabolites in human plasma. *Mol Nutr Food Res* 2010; **54**: 939-946 [PMID: 20087856 DOI: 10.1002/mnfr.200900276]
73 **Steed AL**, Christophi GP, Kaiko GE, Sun L, Goodwin VM, Jain U, Esaulova E, Artyomov MN, Morales DJ, Holtzman MJ, Boon ACM, Lenschow DJ, Stappenbeck TS. The microbial metabolite desaminotyrosine protects from influenza through type I interferon. *Science* 2017; **357**: 498-502 [PMID: 28774928 DOI: 10.1126/science.aam5336]
74 **Ticho AL**, Malhotra P, Dudeja PK, Gill RK, Alrefai WA. Intestinal Absorption of Bile Acids in Health and Disease. *Compr Physiol* 2019; **10**: 21-56 [PMID: 31853951 DOI: 10.1002/cphy.c190007]
75 **Ridlon JM**, Harris SC, Bhowmik S, Kang DJ, Hylemon PB. Consequences of bile salt biotransformations by intestinal bacteria. *Gut Microbes* 2016; **7**: 22-39 [PMID: 26939849 DOI: 10.1080/19490976.2015.1127483]
76 **Parséus A**, Sommer N, Sommer F, Caesar R, Molinaro A, Ståhlman M, Greiner TU, Perkins R, Bäckhed F. Microbiota-induced obesity requires farnesoid X receptor. *Gut* 2017; **66**: 429-437 [PMID: 26740296 DOI: 10.1136/gutjnl-2015-310283]
77 **Ticho AL**, Malhotra P, Dudeja PK, Gill RK, Alrefai WA. Bile Acid Receptors and Gastrointestinal Functions. *Liver Res* 2019; **3**: 31-39 [PMID: 32368358 DOI: 10.1016/j.livres.2019.01.001]
78 **Shapiro H**, Kolodziejczyk AA, Halstuch D, Elinav E. Bile acids in glucose metabolism in health and disease. *J Exp Med* 2018; **215**: 383-396 [PMID: 29339445 DOI: 10.1084/jem.20171965]

79 **Hang S**, Paik D, Yao L, Kim E, Trinath J, Lu J, Ha S, Nelson BN, Kelly SP, Wu L, Zheng Y, Longman RS, Rastinejad F, Devlin AS, Krout MR, Fischbach MA, Littman DR, Huh JR. Bile acid metabolites control T_H17 and T_{reg} cell differentiation. *Nature* 2019; **576**: 143-148 [PMID: 31776512 DOI: 10.1038/s41586-019-1785-z]

80 **Song X**, Sun X, Oh SF, Wu M, Zhang Y, Zheng W, Geva-Zatorsky N, Jupp R, Mathis D, Benoist C, Kasper DL. Microbial bile acid metabolites modulate gut $ROR\gamma^+$ regulatory T cell homeostasis. *Nature* 2020; **577**: 410-415 [PMID: 31875848 DOI: 10.1038/s41586-019-1865-0]

81 **Campbell C**, McKenney PT, Konstantinovsky D, Isaeva OI, Schizas M, Verter J, Mai C, Jin WB, Guo CJ, Violante S, Ramos RJ, Cross JR, Kadaveru K, Hambor J, Rudensky AY. Bacterial metabolism of bile acids promotes generation of peripheral regulatory T cells. *Nature* 2020; **581**: 475-479 [PMID: 32461639 DOI: 10.1038/s41586-020-2193-0]

82 **Guo C**, Xie S, Chi Z, Zhang J, Liu Y, Zhang L, Zheng M, Zhang X, Xia D, Ke Y, Lu L, Wang D. Bile Acids Control Inflammation and Metabolic Disorder through Inhibition of NLRP3 Inflammasome. *Immunity* 2016; **45**: 802-816 [PMID: 27692610 DOI: 10.1016/j.immuni.2016.09.008]

83 **Barrasa JI**, Olmo N, Lizarbe MA, Turnay J. Bile acids in the colon, from healthy to cytotoxic molecules. *Toxicol In Vitro* 2013; **27**: 964-977 [PMID: 23274766 DOI: 10.1016/j.tiv.2012.12.020]

84 **Buffie CG**, Bucci V, Stein RR, McKenney PT, Ling L, Gobourne A, No D, Liu H, Kinnebrew M, Viale A, Littmann E, van den Brink MR, Jenq RR, Taur Y, Sander C, Cross JR, Toussaint NC, Xavier JB, Pamer EG. Precision microbiome reconstitution restores bile acid mediated resistance to Clostridium difficile. *Nature* 2015; **517**: 205-208 [PMID: 25337874 DOI: 10.1038/nature13828]

85 **Wang W**, Zhao J, Gui W, Sun D, Dai H, Xiao L, Chu H, Du F, Zhu Q, Schnabl B, Huang K, Yang L, Hou X. Tauroursodeoxycholic acid inhibits intestinal inflammation and barrier disruption in mice with non-alcoholic fatty liver disease. *Br J Pharmacol* 2018; **175**: 469-484 [PMID: 29139555 DOI: 10.1111/bph.14095]

86 **Wang K**, Liao M, Zhou N, Bao L, Ma K, Zheng Z, Wang Y, Liu C, Wang W, Wang J, Liu SJ, Liu H. Parabacteroides distasonis Alleviates Obesity and Metabolic Dysfunctions *via* Production of Succinate and Secondary Bile Acids. *Cell Rep* 2019; **26**: 222-235.e5 [PMID: 30605678 DOI: 10.1016/j.celrep.2018.12.028]

87 **Efenberger-Szmechtyk M**, Nowak A, Czyzowska A. Plant extracts rich in polyphenols: antibacterial agents and natural preservatives for meat and meat products. *Crit Rev Food Sci Nutr* 2021; **61**: 149-178 [PMID: 32043360 DOI: 10.1080/10408398.2020.1722060]

88 **Diotallevi C**, Fava F, Gobbetti M, Tuohy K. Healthy dietary patterns to reduce obesity-related metabolic disease: polyphenol-microbiome interactions unifying health effects across geography. *Curr Opin Clin Nutr Metab Care* 2020; **23**: 437-444 [PMID: 32941185 DOI: 10.1097/MCO.0000000000000697]

89 **Espín JC**, Larrosa M, García-Conesa MT, Tomás-Barberán F. Biological significance of urolithins, the gut microbial ellagic Acid-derived metabolites: the evidence so far. *Evid Based Complement Alternat Med* 2013; **2013**: 270418 [PMID: 23781257 DOI: 10.1155/2013/270418]

90 **Abdulrahman AO**, Kuerban A, Alshehri ZA, Abdulaal WH, Khan JA, Khan MI. Urolithins Attenuate Multiple Symptoms of Obesity in Rats Fed on a High-Fat Diet. *Diabetes Metab Syndr Obes* 2020; **13**: 3337-3348 [PMID: 33061495 DOI: 10.2147/DMSO.S268146]

91 **Zhao R**, Long X, Yang J, Du L, Zhang X, Li J, Hou C. Pomegranate peel polyphenols reduce chronic low-grade inflammatory responses by modulating gut microbiota and decreasing colonic tissue damage in rats fed a high-fat diet. *Food Funct* 2019; **10**: 8273-8285 [PMID: 31720661 DOI: 10.1039/c9fo02077b]

92 **Kujawska M**, Jodynis-Liebert J. Potential of the ellagic acid-derived gut microbiota metabolite - Urolithin A in gastrointestinal protection. *World J Gastroenterol* 2020; **26**: 3170-3181 [PMID: 32684733 DOI: 10.3748/wjg.v26.i23.3170]

93 **Galgani JE**, Uauy RD, Aguirre CA, Díaz EO. Effect of the dietary fat quality on insulin sensitivity. *Br J Nutr* 2008; **100**: 471-479 [PMID: 18394213 DOI: 10.1017/S0007114508894408]

94 **German JB**, Dillard CJ. Saturated fats: what dietary intake? *Am J Clin Nutr* 2004; **80**: 550-559 [PMID: 15321792 DOI: 10.1093/ajcn/80.3.550]

95 **Simopoulos AP**. An Increase in the Omega-6/Omega-3 Fatty Acid Ratio Increases the Risk for Obesity. *Nutrients* 2016; **8**: 128 [PMID: 26950145 DOI: 10.3390/nu8030128]

96 **Miyamoto J**, Igarashi M, Watanabe K, Karaki SI, Mukouyama H, Kishino S, Li X, Ichimura A, Irie J, Sugimoto Y, Mizutani T, Sugawara T, Miki T, Ogawa J, Drucker DJ, Arita M, Itoh H, Kimura I. Gut microbiota confers host resistance to obesity by metabolizing dietary polyunsaturated fatty acids. *Nat Commun* 2019; **10**: 4007 [PMID: 31488836 DOI: 10.1038/s41467-019-11978-0]

World Journal of Gastroenterology

Submit a Manuscript: https://www.f6publishing.com

World J Gastroenterol 2021 September 7; 27(33): 5566-5574

DOI: 10.3748/wjg.v27.i33.5566

ISSN 1007-9327 (print) ISSN 2219-2840 (online)

ORIGINAL ARTICLE

Basic Study

Adiponectin and the regulation of gastric content volume in the newborn rat

Huanhuan Wang, Paul Esemu-Ezewu, Jingyi Pan, Julijana Ivanovska, Estelle B Gauda, Jaques Belik

ORCID number: Huanhuan Wang 0000-0002-5006-629X; Paul Esemu-Ezewu 0000-0003-0561-1102; Jingyi Pan 0000-0002-5031-2710; Julijana Ivanovska 0000-0001-9045-1689; Estelle B Gauda 0000-0002-3245-3421; Jaques Belik 0000-0003-1470-7827.

Author contributions: Wang H, Esemu-Ezewu P, Pan J and Ivanovska J performed the experiments, acquired and analyzed the data and contributed to drafting the manuscript; Gauda EB and Belik J designed, coordinated the study and finalized the manuscript.

Supported by Canadian Institutes of Health Research, No. CIA310955.

Institutional animal care and use committee statement: All procedures were conducted in accordance with the Canadian Animals for Research Act and Canadian Council on Animal Care regulations, and the Hospital for Sick Children Research Institute Animal Care Committee approved the study, No. 1000046424.

Conflict-of-interest statement: The authors have no conflict of interest to declare.

Data sharing statement: Technical

Huanhuan Wang, Paul Esemu-Ezewu, Jingyi Pan, Julijana Ivanovska, Estelle B Gauda, Department of Paediatrics, The Hospital for Sick Children, Toronto M5G 1X8, Ontario, Canada

Jaques Belik, Department of Paediatrics and Physiology, The Hospital for Sick Children, Toronto M5G 1X8, Ontario, Canada

Corresponding author: Jaques Belik, FRCP (C), MD, Professor, Department of Paediatrics and Physiology, The Hospital for Sick Children, 555 University Ave, Toronto M5G 1X8, Ontario, Canada. jaques.belik@sickkids.ca

Abstract

BACKGROUND

Oral intake is dependent on the gastric ability to accommodate the food bolus. Comparatively, neonates have a smaller gastric capacity than adults and this may limit the volume of their milk intake. Yet, we previously reported that the newborn rat gastric milk volume is greatest after birth and, when normalized to body weight, decreases with postnatal age. Such age-dependent changes are not the result of intake differences, but greater gastric accommodation and reduced emptying rate.

AIM

Hypothesizing that breastmilk-derived adiponectin is the factor regulating gastric accommodation in neonates, we comparatively evaluated its effects on the rat fundic muscle tone at different postnatal ages.

METHODS

In freshly dispersed smooth muscle cells (SMC), we measured the adiponectin effect on the carbachol-induced length changes.

RESULTS

Adiponectin significantly reduced the carbachol-stimulated SMC shortening independently of age. In the presence of the inhibitor iberiotoxin, the adiponectin effect on SMC shortening was suppressed, suggesting that it is mediated *via* large-conductance Ca^{2+} sensitive K^+ channel activation. Lastly, we comparatively measured the newborn rat gastric milk curd adiponectin content in one- and two-week-old rats and found a 50% lower value in the latter.

CONCLUSION

appendix, statistical code, and dataset available from the corresponding author at jaques.belik@sickkids.ca.

ARRIVE guidelines statement: The authors have read the ARRIVE guidelines, and the manuscript was prepared and revised according to the ARRIVE guidelines.

Open-Access: This article is an open-access article that was selected by an in-house editor and fully peer-reviewed by external reviewers. It is distributed in accordance with the Creative Commons Attribution NonCommercial (CC BY-NC 4.0) license, which permits others to distribute, remix, adapt, build upon this work non-commercially, and license their derivative works on different terms, provided the original work is properly cited and the use is non-commercial. See: http://creativecommons.org/Licenses/by-nc/4.0/

Manuscript source: Invited manuscript

Specialty type: Gastroenterology and hepatology

Country/Territory of origin: Canada

Peer-review report's scientific quality classification

Grade A (Excellent): 0
Grade B (Very good): B
Grade C (Good): 0
Grade D (Fair): 0
Grade E (Poor): 0

Received: March 9, 2021
Peer-review started: March 9, 2021
First decision: May 1, 2021
Revised: May 12, 2021
Accepted: August 12, 2021
Article in press: August 12, 2021
Published online: September 7, 2021

P-Reviewer: Exbrayat JM
S-Editor: Wu YXJ
L-Editor: A
P-Editor: Liu JH

Adiponectin, a major component of breastmilk, downregulates fundic smooth muscle contraction potential, thus facilitating gastric volume accommodation. This rodent's adaptive response maximizes breastmilk intake volume after birth.

Key Words: Gastric emptying; Fundus; Smooth muscle; Breastmilk; Potassium channel; Development

©The Author(s) 2021. Published by Baishideng Publishing Group Inc. All rights reserved.

Core Tip: Gastric accommodation regulates the stomach content volume. Lactating rats continuously breastfeed to keep a full gastric milk volume and their gastric emptying time is directly related to the gastric content volume. Little is known about the gastric fundic accommodation regulatory factors early in life. In this study, breastmilk-derived adiponectin is shown to promote gastric fundic relaxation, thus playing an important regulatory role during the lactating period.

Citation: Wang H, Esemu-Ezewu P, Pan J, Ivanovska J, Gauda EB, Belik J. Adiponectin and the regulation of gastric content volume in the newborn rat. *World J Gastroenterol* 2021; 27(33): 5566-5574
URL: https://www.wjgnet.com/1007-9327/full/v27/i33/5566.htm
DOI: https://dx.doi.org/10.3748/wjg.v27.i33.5566

INTRODUCTION

Among other factors, oral intake depends on the gastric muscle accommodation to its content. The estimated receptive gastric milk volume is 20 mL for a full-term infant[1]. For an average full-term infant weighing 3.5 kg, this amounts to 5.7 mL/kg receptive gastric volume. The comparative adult gastric receptive volume has not been adequately assessed, but often referred to as 600 mL, or 8.5 mL/kg for a 70 kg body weight person. The implications of a lower gastric receptive capacity in the immediate neonatal period, specially, for preterm infants, requires further evaluation.

Comparative studies addressing the nutritional benefit and risks associated with lower (150-180 mL/kg/d) and higher (> 200 mL/kg/d) total enteral feed intake for preterm infants have been conducted. A recent metanalysis of such studies reported limited data and concluded that insufficient evidence is available[2]. Yet, at least one recent review on nutritional support strategies for preterm infants advised that more gestationally mature neonates can tolerate and benefit from a daily milk intake as high as 240 mL/kg/d or 20 mL/kg/feed[3].

Since the recommended maximum daily intake of milk exceeds the estimated stomach receptive volume, adaptive mechanisms must be present to overcome the reduced gastric functional capacity early in life. In adult life, the gastric accommodation response to the food bolus increases the stomach receptive volume by relaxes the fundic muscle thus enabling the stomach to accommodate a larger volume. The factors regulating this response are incompletely understood, but involve activation of the oropharynx, stomach and duodenum[4].

Aside from increasing total enteral intake, gastric accommodation may also have an important role in maximizing its content emptying potential. We have previously reported that the rat gastric functional capacity is increased during the immediate neonatal period and this facilitates its content emptying rate[5]. Figure 1 shows our previously reported data on the rat gastric content volume and emptying rates early in life[5]. The younger the rat, the higher is the gastric milk content, such that in the one-week pup the volume after breastfeeding, is two-fold greater, when compared with measurements obtained in the second week of life[5]. The mechanism accounting for the age-related gastric accommodation changes, early in life, is poorly understood and the main goal of the present study.

Adiponectin is an adipose tissue-derived adipokine that plays a major role in appetite regulation and other important physiological mechanisms[6]. The adiponectin concentration in human and rodent breastmilk, is more than 40 folds greater, when compared with the other major adipokines present[7,8]. The available evidence

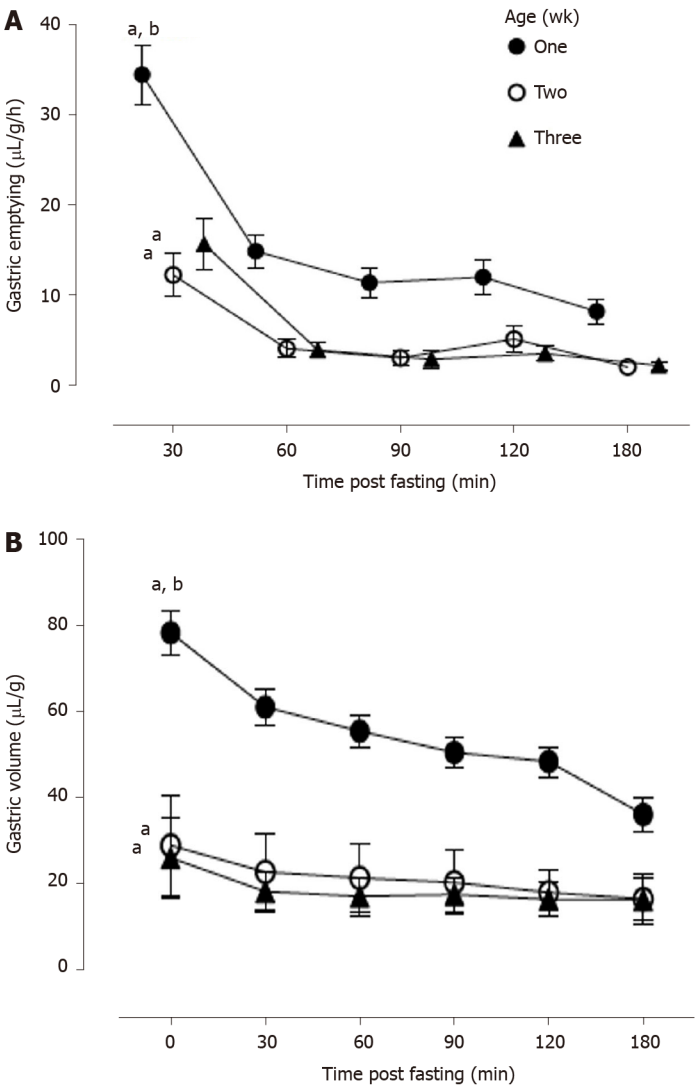


Figure 1 Gastric emptying rate (panel A) and related postprandial content volume (panel B) for one- (*n* = 30), two- (*n* = 10) and three-weeks old (*n* = 16) fasting rats[5]. Data are mean ± SE; [a]*P* < 0.01 *vs* other postprandial times; [b]*P* < 0.01 *vs* other ages by two-way ANOVA with multiple comparisons evaluated by the Tukey-Kramer test. Citation: Ferreira CHF, Shifrin Y, Pan J, Ivanovska J, McNamara PJ, Belik J. The newborn rat gastric emptying rate is volume and not developmentally dependent. Neurogastroenterology and motility: 2018; 30: e13233. Copyright© The Authors 2018. Published by Neurogastroenterol Motil. The authors have obtained the permission for figure using from the Publishing Group (Supplementary material).

suggest that breast-derived adiponectin may play a functional role in the regulation of gastric milk volume accommodation. Adiponectin receptors are present in fetal rodents' gastrointestinal tract[9] and in the adult rat, adiponectin modulates gastric tone[10].

A study comparatively evaluating the maternal breastmilk adiponectin content and their infants' gastric emptying time showed an inverse relationship between these parameters[11]. That is to say that the higher the maternal adiponectin breastmilk content, the slower is their infant's gastric emptying time. This suggest that adiponectin plays a facilitating role in the stomach receptive potential for milk volume by increasing gastric accommodation. Such regulatory role has not been previously evaluated in the newborn.

Therefore, the main goal of this study was to evaluate the adiponectin effect on the newborn rat gastric fundic muscle response to an agonist-induced contraction. We hypothesized that adiponectin downregulates the newborn fundic muscle tone thus allowing for greater accommodation to a larger milk volume, early in life.

MATERIALS AND METHODS

Design

Studies were conducted in a laboratory setting utilizing newborn and adult rat gastric tissue.

Animals

Sprague-Dawley (Charles River, Montreal, QC, Canada) newborn (3-7 d old; n = 9; female n = 5, male n = 4), juvenile (8-14 d old; n = 4 female n = 2, male n = 2) and adult (> 60 d old; n = 7 female n = 2, male n = 5) rats were studied. The adult rats were fed a regular rodent diet composed of animal and vegetable protein (Certified Rodent Diet 5002, LabDiet, St. Louis, MO, United States) and housed under standard lighting and temperature conditions.

The animals were sacrificed with pentobarbital sodium injection (60 mg/kg i.p). Immediately after death, the gastric tissue was removed fresh for functional studies. The gastric milk curd was completely removed intact, snap-frozen in liquid nitrogen and stored at -80°C for less than one month, for later processing. The rationale for studying this stomach anatomical segment relates to the fact that accommodation of the food bolus occurs in the gastric fundus.

Freshly dispersed smooth muscle cells

To evaluate the adiponectin effect on the gastric muscle contraction independently of its innervation, and other tissue factors, as well as under the more physiologic isotonic conditions, we measured the individual smooth muscle cells (SMC) shortening response to this metabolite. In summary, the gastric tissue was digested in 1 mL/mg collagenase and 0.01% Soybean Trypsin Inhibitor (ThermoFisher, Burlington, Ontario, Canada) and the SMCs were dispersed in DMEM cell culture media (Wisent, St. Bruno, Quebec, Canada). One hour after dispersion the SMCs were exposed to carbachol-at a final media concentration of 10^{-4} for 15 min, while maintained at 37°C and 5% CO_2 in a conventional incubator in the absence or presence of adiponectin (4 μl/mL). To study the mechanism by which adiponectin downregulates smooth muscle contraction, we evaluated the iberiotoxin (10^{-7} M) pre-incubation effect on the carbachol-induced response.

Following this, the cells were immediately fixed with 1% acrolein. Cells maintained for a similar duration in Calcium-free PBS media served as control. Light microscopy images at 20 × magnification was obtained using Leica DM IRE2 microscope (Wetzlar, Germany) and the cells' length were measured using ImageJ (NIH, Bethesda, MA, United States). H_2O_2-induced cells length changes (shortening) were expressed as percentage of average control SMC length. The cells were obtained from seven newborns and five adult animals. A minimum of 50 H_2O_2-exposed and control cells from age group were evaluated.

Milk curd adiponectin content

Milk curds were obtained from newborn (3-7 d) and juvenile (8-14 d) rats. The curd proteins were extracted, and their adiponectin content quantified by utilizing a commercially available ELISA kit (RRP300, R&D systems) according to the manufacturer's recommendations. Briefly, the pup's milk curd was carefully extracted from the gastric cavity at once, after they were euthanized. The curd was weighed and sonicated in RIPA buffer for 5-10 s three times. The mixture was centrifuged at 17949 g. The separated middle layer (skim milk) was used for adiponectin measurement and protein quantification.

Statistical analysis

Data were first evaluated to determine Gaussian distribution by Skewness, Kurtosis and Omnibus testing. Normally distributed data were analyzed by parametric tests. Group differences were statistically evaluated by unpaired Student's t-test or two-way ANOVA with multiple comparisons obtained by the Tukey-Kramer test. Statistical significance was determined at $P < 0.05$. All statistical analyses were performed with the Number Cruncher Statistical System software (NCSS, Kaysville, Utah). Data are presented as mean ± SE.

The sample size utilized for each experiment is listed in the Figure legends and refers to SMC number. Given their high yield, we utilized large sample sizes for freshly dispersed SMCs, to minimize the possibility of a type I error.

RESULTS

SMCs derived from rat's gastric fundus significantly shortened in response to carbachol stimulation. One-, two-weeks and adult SMC showed a similar response. Pre-incubation with adiponectin suppressed the carbachol-induced SMC shortening at all ages (Figure 2).

To investigate the mechanism accounting for the adiponectin-dependent effect on the agonist-induced newborn fundic SMC shortening, we tested the effect of iberiotoxin on the response (Figure 3). This large-conductance Ca^{2+} sensitive K^+ channel inhibitor was shown, by others, to be involved in the adiponectin-induced vascular smooth muscle relaxation[12]. Following pre-incubation with iberiotoxin the carbachol-induced SMC shortening was not altered by the presence of adiponectin. This observation suggests that the adiponectin downregulation of agonist induced fundic SMC shortening is mediated *via* modulation of large-conductance Ca^{2+} sensitive K^+ channels.

Lastly, as a surrogate measurement of the maternal breastmilk concentration, we evaluated the newborn rat milk curd adiponectin content at one- and two-weeks of age. Adiponectin was present at both ages, but the one-week milk curd adiponectin content was two-fold higher, when compared with values obtained from two-week old rats (Figure 4).

DISCUSSION

The findings of the present study suggest that breastmilk-derived adiponectin is the key regulator of gastric milk volume and clearance rate in the neonatal rat. Activation of large-conductance Ca^{2+} sensitive K^+ channels in fundic smooth muscle cells by adiponectin mediates this response.

Whereas in humans, the newborn enteral intake is dependent on milk offer, rodent pups can independently breastfeed on demand. This leads to the well-known observation of a consistently milk-filled stomach in suckling newborn rats. Experiments conducted decades ago showed that the regulation of gastric content in the newborn rat is not based on satiety, but stomach distention[13]. In a recently published study, we took advantage of this unique neonatal behavior to evaluate *in vivo,* the developmental pattern of gastric content volume and emptying time.

We showed that the rat gastric content volume, normalized to body weight, is highest at one-week, when compared with the later breastfeeding period[5]. In addition, the newborn rat's gastric milk emptying rate is directly proportional to the stomach's curd volume[5]. We further documented that a similar positive correlation between gastric milk volume and its emptying rate is present in preterm neonates[14].

Such observations imply that, in the immediate neonatal period, an operative physiological mechanism is present and geared at maximizing enteral intake to enhance gastric accommodation to the milk volume. The present study findings suggest that breastmilk-derived adiponectin is the factor responsible for this gastric accommodation response in newborn rats.

By downregulating the fundic smooth muscle agonist-induced contraction potential, adiponectin increases gastric accommodation thus maximizing the stomach's milk volume retention. As shown in this study, the developmental pattern of this response is mediated not by age differences in the gastric SMC properties, but by the post-partum changes in breastmilk adiponectin content.

Adiponectin is an adipokine primarily secreted by adipose tissue that has important physiological modulatory roles[15]. These include anti-inflammatory, antioxidant, antiatherosclerosis, appetite regulation and insulin-sensitizing effects. Yet, its presence in breastmilk raises provocative questions about its function in neonates.

Adiponectin is secreted by the breast adipose tissue and is the most abundant adipokine in human breast milk[7]. In humans, the breastmilk adiponectin content is highest in the early postpartum period and decreases overtime[16]. Similar pattern of breastmilk adiponectin content and postpartum changes were previously reported in rats[17], and the finding confirmed in the present study. Most importantly, adiponectin is rapidly taken-up by the gastrointestinal tract resulting in peak serum concentrations two hours after enteral administration in newborn mice[8]. This suggest that breastmilk-derived adiponectin plays a functional role early in life.

AdipoR1 and AdipoR2, the two adiponectin receptors are expressed during embryogenesis in mice, with the former being the predominant one in most tissues[9]. These receptors are also present in adult rodents' gastric tissue and the electrical field

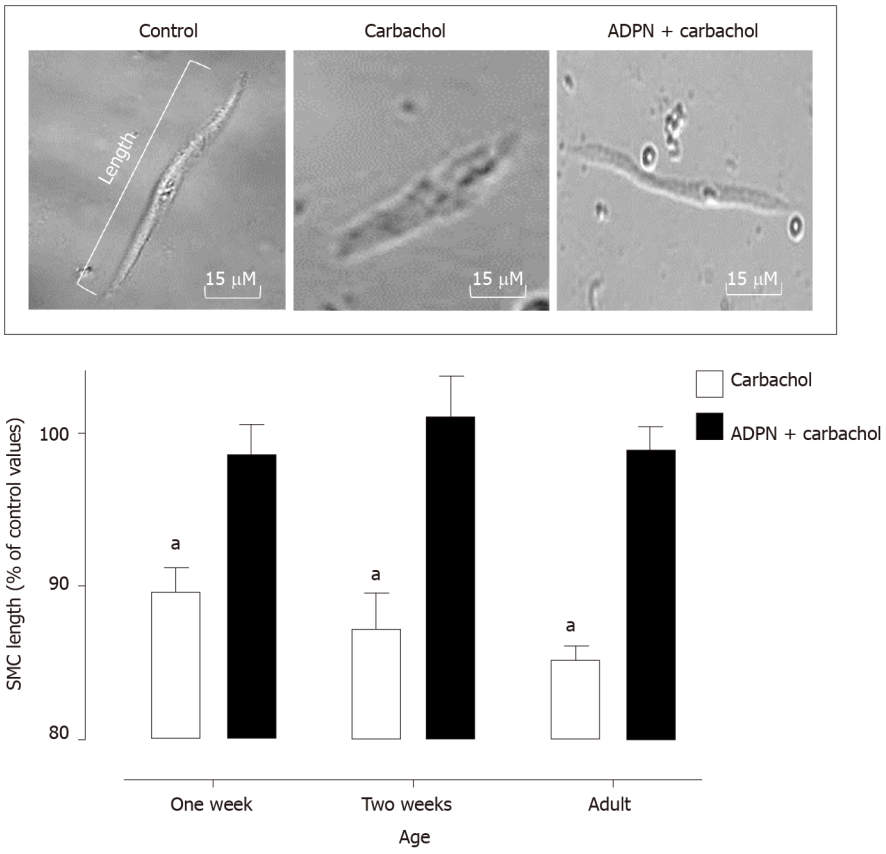


Figure 2 Smooth muscle cells shortening in response to carbachol stimulation (carbachol) in the absence and presence of adiponectin (ADPN + carbachol). Rat fundic smooth muscle cells (SMC) were freshly obtained from one- (*n* = 178: carbachol; *n* = 198: ADPN + carbachol), two-weeks (*n* = 109: carbachol; *n* = 93: ADPN + carbachol) old pups and adult rats (*n* = 924: carbachol; *n* = 564: ADPN + carbachol). Data are expressed as mean ± SE percentage of basal length measurements prior to contraction. $^{a}P < 0.01$ *vs* respective ADPN + carbachol. Insert shows representative SMC length measurements (magnification: 20 ×) under the different conditions. SMC: Smooth muscle cells.

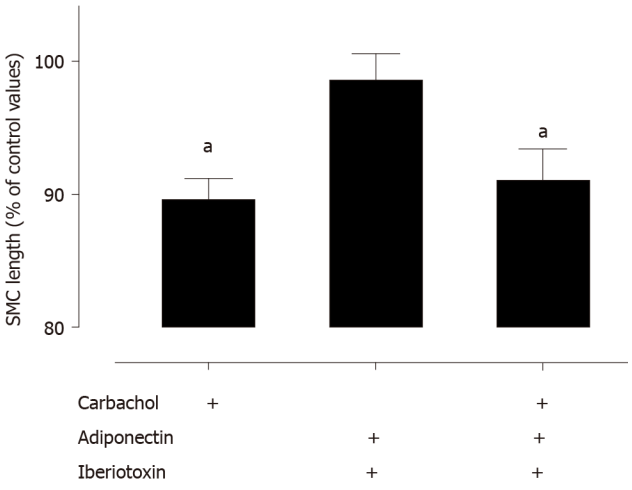


Figure 3 Newborn rat smooth muscle cell length expressed as a percentage of basal (non-stimulated; *n* = 178) length following pre-incubation with adiponectin and carbachol stimulation in the absence (*n* = 198) and pre-incubation presence of Iberiotoxin, a large-conductance Ca^{2+} sensitive K^{+} channel inhibitor (*n* = 96). Data are mean ± SE $^{a}P < 0.01$ *vs* basal smooth muscle cell length values. SMC: Smooth muscle cells.

stimulation contractile potential of its muscle is reduced in the presence of exogenous adiponectin[10,18]. Whether adiponectin modulates the nerve stimulus conduction, or the gastric smooth muscle itself if unclear since one study in adult mice showed an effect on the vagal nerve [18]. In adult mice, adiponectin downregulates gastric muscle cell excitability[19], but this report is the first to study fundic SMCs from a newborn

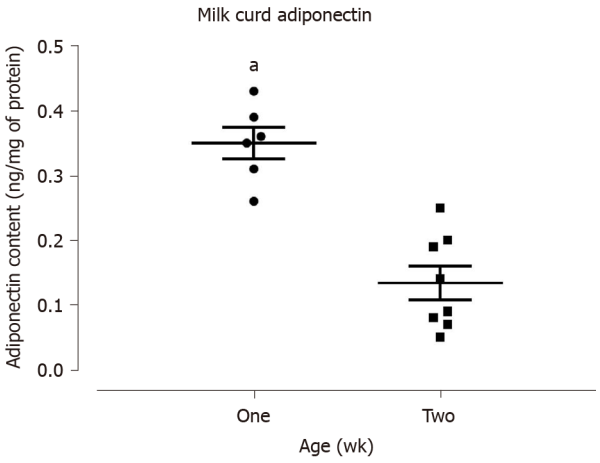


Figure 4 Freshly obtained, one-week old (*n* = 6) and two-weeks old (*n* = 8) rat milk curd adiponectin content. Data are shown as individual values and mean ± SE $^{a}P < 0.01$ *vs* two-weeks old values.

rodent.

Adiponectin not only reduces gastric muscle tone but has a similar effect on other smooth muscle dependent organs. In vascular tissue, adiponectin induces vasodilation [20] and reduces uterine contractions[21]. In the present study we evaluated the adiponectin effect on freshly dispersed rat SMCs from newborn, juvenile and adult animals. At all ages we documented a similar reduction in agonist-stimulated SMC shortening showing that adiponectin acts directly on the fundic muscle.

The signal-transduction pathway responsible for the adiponectin modulation of smooth muscle contraction remains unclear. In vascular tissue, adiponectin promotes endothelial-derived nitric oxide generation and it enhances its biological activity, both of which mediate the adiponectin vasodilatory response[22-24]. In addition, adiponectin has a direct effect on vascular smooth muscle large-conductance Ca^{2+} sensitive K^{+} channels that also result in reduced vasomotor tone[12,25].

The present data show that large-conductance Ca^{2+} sensitive K^{+} channels modulate the newborn rat gastric SMC contraction potential. Iberiotoxin, a large-conductance Ca^{2+} sensitive K^{+} channels inhibitor of rodent fundic muscle relaxation[26], suppressed the adiponectin-mediated reduction in the carbachol-induced shortening. Our findings are in keeping with the adult mice gastric fundus, where adiponectin hyperpolarized the SMC resting membrane potential resulting in reduced voltage-dependent Ca^{2+} currents[19].

In support of breastmilk being a major source of adiponectin to the newborn, we confirmed its presence in newborn and juvenile rats' milk curds. As previously shown to be the case for human breastmilk[16], we documented that the rat milk curds' adiponectin content was inversely proportional to postpartum age and two-fold lower in the second, when compared with first postnatal week.

Together our findings suggest that breastmilk-derived adiponectin plays an important role in the newborn rat milk volume intake. Human derived data support the current findings. An evaluation of mothers' breastmilk adiponectin content and their infants' gastric emptying time showed an inverse relationship between these parameters. The higher the breastmilk adiponectin the longer was the infant's gastric milk clearance[11].

This study has obvious limitations. Rat fundic SMCs agonist-induced shortening was used as a surrogate marker of gastric milk accommodation and the breastmilk adiponectin content was obtained from the newborn milk curds. Yet, it is well known that gastric accommodation to the food bolus depends on the fundic muscle relaxation [27] and thus the fundic SMC shortening response allows for the study of the adiponectin direct effect its muscle tone. Although the adiponectin content of the newborn gastric curd is probably not similar to the one from fresh breastmilk, if anything the former value is likely lower, when compared with breastmilk.

CONCLUSION

In conclusion, adiponectin reduces the gastric fundus motor tone allowing for greater

accommodation of the food bolus. This response is present in newborn-derived smooth muscle cells and mediated *via* large conductance Ca^{2+} sensitive K^+ channels. Breastmilk has a high adiponectin content and this adipokine likely enhances volume intake by increasing the gastric functional volume capacity (accommodation). These observations have translational importance since preterm infants are often fed either processed breastmilk or formula, both of which may not contain sufficient adiponectin to promote gastric fundic relaxation.

ARTICLE HIGHLIGHTS

Research background

Oral intake depends on the gastric ability to accommodate the food bolus. The preterm infant has a lower gastric capacity, normalized to body weight, when compared with adults, thus potentially limiting their milk intake. Yet, we previously shown that one-week rat pups milk intake is greater than observed, as they mature.

Research motivation

The main rationale for the study experiments was to understand the mechanism accounting for greater food accommodation early in life.

Research objectives

The main objective was to evaluate the hypothesis that the adiponectin in breast milk increases the newborn rat ability to accommodate the food bolus by reducing the fundic muscle tone.

Research methods

Rat freshly dispersed smooth muscle cells were used to measure the adiponectin effect on carbachol-induced fundic muscle shortening.

Research results

Adiponectin significantly reduced the carbachol-stimulated smooth muscle cells shortening independently of age, *via* large-conductance Ca^{2+} sensitive K^+ channel activation.

Research conclusions

Breast milk containing adiponectin regulates the newborn rat milk intake by increasing the gastric fundic accommodation potential.

Research perspectives

Maternal-neonatal interaction *via* breast milk components content provides a novel and likely important regulatory role on intake volume early in life.

REFERENCES

1 **Bergman NJ**. Neonatal stomach volume and physiology suggest feeding at 1-h intervals. *Acta Paediatr* 2013; **102**: 773-777 [PMID: 23662739 DOI: 10.1111/apa.12291]

2 **Abiramalatha T**, Thomas N, Gupta V, Viswanathan A, McGuire W. High *vs* standard volume enteral feeds to promote growth in preterm or low birth weight infants. *Cochrane Database Syst Rev* 2017; **9**: CD012413 [PMID: 28898404 DOI: 10.1002/14651858.CD012413.pub2]

3 **Hay WW Jr**. Nutritional Support Strategies for the Preterm Infant in the Neonatal Intensive Care Unit. *Pediatr Gastroenterol Hepatol Nutr* 2018; **21**: 234-247 [PMID: 30345236 DOI: 10.5223/pghn.2018.21.4.234]

4 **Vanden Berghe P**, Janssen P, Kindt S, Vos R, Tack J. Contribution of different triggers to the gastric accommodation reflex in humans. *Am J Physiol Gastrointest Liver Physiol* 2009; **297**: G902-G906 [PMID: 19846891 DOI: 10.1152/ajpgi.00046.2009]

5 **Ferreira CHF**, Shifrin Y, Pan J, Ivanovska J, McNamara PJ, Belik J. The newborn rat gastric emptying rate is volume and not developmentally dependent. *Neurogastroenterol Motil* 2018; **30**: e13233 [PMID: 29024213 DOI: 10.1111/nmo.13233]

6 **Gauda EB**, Master Z. Contribution of relative leptin and adiponectin deficiencies in premature infants to chronic intermittent hypoxia: Exploring a new hypothesis. *Respir Physiol Neurobiol* 2018; **256**: 119-127 [PMID: 29246449 DOI: 10.1016/j.resp.2017.12.003]

7 **Kratzsch J**, Bae YJ, Kiess W. Adipokines in human breast milk. *Best Pract Res Clin Endocrinol*

Metab 2018; **32**: 27-38 [PMID: 29549957 DOI: 10.1016/j.beem.2018.02.001]
8 **Newburg DS**, Woo JG, Morrow AL. Characteristics and potential functions of human milk adiponectin. *J Pediatr* 2010; **156**: S41-S46 [PMID: 20105665 DOI: 10.1016/j.jpeds.2009.11.020]
9 **Zhou Y**, Sun X, Jin L, Stringfield T, Lin L, Chen Y. Expression profiles of adiponectin receptors in mouse embryos. *Gene Expr Patterns* 2005; **5**: 711-715 [PMID: 15939384 DOI: 10.1016/j.modgep.2005.02.002]
10 **Idrizaj E**, Garella R, Castellini G, Mohr H, Pellegata NS, Francini F, Ricca V, Squecco R, Baccari MC. Adiponectin affects the mechanical responses in strips from the mouse gastric fundus. *World J Gastroenterol* 2018; **24**: 4028-4035 [PMID: 30254407 DOI: 10.3748/wjg.v24.i35.4028]
11 **Gridneva Z**, Kugananthan S, Hepworth AR, Tie WJ, Lai CT, Ward LC, Hartmann PE, Geddes DT. Effect of Human Milk Appetite Hormones, Macronutrients, and Infant Characteristics on Gastric Emptying and Breastfeeding Patterns of Term Fully Breastfed Infants. *Nutrients* 2016; **9** [PMID: 28036041 DOI: 10.3390/nu9010015]
12 **Weston AH**, Egner I, Dong Y, Porter EL, Heagerty AM, Edwards G. Stimulated release of a hyperpolarizing factor (ADHF) from mesenteric artery perivascular adipose tissue: involvement of myocyte BKCa channels and adiponectin. *Br J Pharmacol* 2013; **169**: 1500-1509 [PMID: 23488724 DOI: 10.1111/bph.12157]
13 **Lorenz DN**. Gastric emptying of milk in rat pups. *Am J Physiol* 1985; **248**: R732-R738 [PMID: 4003584 DOI: 10.1152/ajpregu.1985.248.6.R732]
14 **Ferreira CHF**, Martinez FE, Crott GC, Belik J. Gavage Feed Volume Determines the Gastric Emptying Rate in Preterm Infants. *J Pediatr Gastroenterol Nutr* 2018; **67**: e43-e46 [PMID: 29601436 DOI: 10.1097/MPG.0000000000001985]
15 **Cuerq C**, Morineau G, Dufour-Rainfray D, Vatier C, Fellahi S, Vigouroux C, Genoux A, Lacorte JM, Charchour R, Fève B, Capeau J, Collet C, Bastard JP; groupe de travail RIHN Adipokines. [Mutltifaceted biological roles of adiponectin]. *Ann Biol Clin (Paris)* 2020; **78**: 243-252 [PMID: 32540813 DOI: 10.1684/abc.2020.1562]
16 **Ley SH**, Hanley AJ, Sermer M, Zinman B, O'Connor DL. Associations of prenatal metabolic abnormalities with insulin and adiponectin concentrations in human milk. *Am J Clin Nutr* 2012; **95**: 867-874 [PMID: 22378730 DOI: 10.3945/ajcn.111.028431]
17 **Nozhenko Y**, Asnani-Kishnani M, Rodríguez AM, Palou A. Milk Leptin Surge and Biological Rhythms of Leptin and Other Regulatory Proteins in Breastmilk. *PLoS One* 2015; **10**: e0145376 [PMID: 26680765 DOI: 10.1371/journal.pone.0145376]
18 **Kentish SJ**, Ratcliff K, Li H, Wittert GA, Page AJ. High fat diet induced changes in gastric vagal afferent response to adiponectin. *Physiol Behav* 2015; **152**: 354-362 [PMID: 26074203 DOI: 10.1016/j.physbeh.2015.06.016]
19 **Idrizaj E**, Garella R, Castellini G, Francini F, Ricca V, Baccari MC, Squecco R. Adiponectin Decreases Gastric Smooth Muscle Cell Excitability in Mice. *Front Physiol* 2019; **10**: 1000 [PMID: 31447692 DOI: 10.3389/fphys.2019.01000]
20 **Fésüs G**, Dubrovska G, Gorzelniak K, Kluge R, Huang Y, Luft FC, Gollasch M. Adiponectin is a novel humoral vasodilator. *Cardiovasc Res* 2007; **75**: 719-727 [PMID: 17617391 DOI: 10.1016/j.cardiores.2007.05.025]
21 **Vyas V**, Guerra DD, Bok R, Powell T, Jansson T, Hurt KJ. Adiponectin links maternal metabolism to uterine contractility. *FASEB J* 2019; **33**: 14588-14601 [PMID: 31665924 DOI: 10.1096/fj.201901646R]
22 **Sena CM**, Pereira A, Fernandes R, Letra L, Seiça RM. Adiponectin improves endothelial function in mesenteric arteries of rats fed a high-fat diet: role of perivascular adipose tissue. *Br J Pharmacol* 2017; **174**: 3514-3526 [PMID: 28236429 DOI: 10.1111/bph.13756]
23 **Vanhoutte PM**, Zhao Y, Xu A, Leung SW. Thirty Years of Saying NO: Sources, Fate, Actions, and Misfortunes of the Endothelium-Derived Vasodilator Mediator. *Circ Res* 2016; **119**: 375-396 [PMID: 27390338 DOI: 10.1161/CIRCRESAHA.116.306531]
24 **Margaritis M**, Antonopoulos AS, Digby J, Lee R, Reilly S, Coutinho P, Shirodaria C, Sayeed R, Petrou M, De Silva R, Jalilzadeh S, Demosthenous M, Bakogiannis C, Tousoulis D, Stefanadis C, Choudhury RP, Casadei B, Channon KM, Antoniades C. Interactions between vascular wall and perivascular adipose tissue reveal novel roles for adiponectin in the regulation of endothelial nitric oxide synthase function in human vessels. *Circulation* 2013; **127**: 2209-2221 [PMID: 23625959 DOI: 10.1161/CIRCULATIONAHA.112.001133]
25 **Löhn M**, Dubrovska G, Lauterbach B, Luft FC, Gollasch M, Sharma AM. Periadventitial fat releases a vascular relaxing factor. *FASEB J* 2002; **16**: 1057-1063 [PMID: 12087067 DOI: 10.1096/fj.02-0024com]
26 **Kim M**, Han IS, Koh SD, Perrino BA. Roles of CaM kinase II and phospholamban in SNP-induced relaxation of murine gastric fundus smooth muscles. *Am J Physiol Cell Physiol* 2006; **291**: C337-C347 [PMID: 16510846 DOI: 10.1152/ajpcell.00397.2005]
27 **Currò D**, Ipavec V, Preziosi P. Neurotransmitters of the non-adrenergic non-cholinergic relaxation of proximal stomach. *Eur Rev Med Pharmacol Sci* 2008; **12**: 53-62 [PMID: 18924444]

World Journal of Gastroenterology

Submit a Manuscript: https://www.f6publishing.com

World J Gastroenterol 2021 September 7; 27(33): 5575-5594

DOI: 10.3748/wjg.v27.i33.5575

ISSN 1007-9327 (print) ISSN 2219-2840 (online)

ORIGINAL ARTICLE

Basic Study

Characterization of gut microbiome and metabolome in *Helicobacter pylori* patients in an underprivileged community in the United States

Brian White, John D Sterrett, Zoya Grigoryan, Lauren Lally, Jared D Heinze, Hyder Alikhan, Christopher A Lowry, Lark J Perez, Joshua DeSipio, Sangita Phadtare

ORCID number: Brian White 0000-0003-2288-6044; John D Sterrett 0000-0002-0931-7181; Zoya Grigoryan 0000-0003-2726-5247; Lauren Lally 0000-0001-6285-3533; Jared D Heinze 0000-0002-6747-8119; Hyder Alikhan 0000-0003-3979-4488; Christopher A Lowry 0000-0003-3920-5575; Lark J Perez 0000-0002-6920-7996; Joshua DeSipio 0000-0002-0949-1681; Sangita Phadtare 0000-0002-4388-6150.

Author contributions: White B, Sterrett JD and Grigoryan Z contributed equally to the work; DeSipio J, and Phadtare S designed and coordinated the study; Grigoryan Z and Lally L collected patient samples and data; Phadtare S performed the sample processing for 16S rRNA gene sequencing; Heinze JD provided guidance for sample processing methodology; Grigoryan Z and Phadtare S performed the 16S rRNA sequencing data analysis; Sterrett JD and Lowry CA created the analysis codes essential for analysis and provided guidance for data analysis; Alikhan H and Perez LJ performed the fatty acid analysis; Lally L and White B carried out literature search; White B, Sterrett JD, Lowry CA, Perez LJ, DeSipio J and Phadtare S interpreted the analyzed data and wrote the final

Brian White, Sangita Phadtare, Department of Biomedical Sciences, Cooper Medical School of Rowan University, Camden, NJ 08103, United States

John D Sterrett, Jared D Heinze, Christopher A Lowry, Department of Integrative Physiology, University of Colorado Boulder, Boulder, CO 80309, United States

Zoya Grigoryan, Department of Internal Medicine, Lenox Hill Hospital, NYC, NY 10075, United States

Lauren Lally, Department of Internal Medicine, Thomas Jefferson University Hospital, Philadelphia, PA 19107, United States

Hyder Alikhan, Department of Biological Sciences, Rowan University, Glassboro, NJ 08028, United States

Lark J Perez, Department of Chemistry and Biochemistry, Rowan University, Glassboro, NJ 08028, United States

Joshua DeSipio, Department of Gastroenterology, Cooper University Hospital, Camden, NJ 08103, United States

Corresponding author: Sangita Phadtare, BSc, MSc, PhD, Professor, Department of Biomedical Sciences, Cooper Medical School of Rowan University, 401 S Broadway, Camden, NJ 08103, United States. phadtare@rowan.edu

Abstract

BACKGROUND

Helicobacter pylori (*H. pylori*), a bacterium that infects approximately half of the world's population, is associated with various gastrointestinal diseases, including peptic ulcers, non-ulcer dyspepsia, gastric adenocarcinoma, and gastric lymphoma. As the burden of antibiotic resistance increases, the need for new adjunct therapies designed to facilitate *H. pylori* eradication and reduce negative distal outcomes associated with infection has become more pressing. Characterization of the interactions between *H. pylori*, the fecal microbiome, and fecal fatty acid metabolism, as well as the mechanisms underlying these interactions, may offer new therapeutic approaches.

draft of the manuscript; all authors approved the final version of the article.

Supported by The Camden Health Research Initiative grant to Sangita Phadtare.

Institutional review board statement: This study received approval by the Cooper Health System Institutional Review Board (IRB) (17-077EX) and all the steps were carried out as *per* the standards set by the IRB.

Institutional animal care and use committee statement: There are no animals used in the study.

Conflict-of-interest statement: The authors report no conflicts of interest.

Data sharing statement: The code is available at https://github.com/sterrettJD/H-pylori-microbiome-analysis. Volcano plot data are included as Supplementary Tables 1-3 (Supplementary Table 1: Volcano plot data with all Helicobacter data set; Supplementary Table 2: Volcano plot data with High Bacteroidetes; Supplementary Table 3: Volcano plot data with High Firmicutes).

Open-Access: This article is an open-access article that was selected by an in-house editor and fully peer-reviewed by external reviewers. It is distributed in accordance with the Creative Commons Attribution NonCommercial (CC BY-NC 4.0) license, which permits others to distribute, remix, adapt, build upon this work non-commercially, and license their derivative works on different terms, provided the original work is properly cited and the use is non-commercial. See: http://creativecommons.org/Licenses/by-nc/4.0/

Manuscript source: Invited manuscript

Specialty type: Gastroenterology and hepatology

Country/Territory of origin: United

AIM

To characterize the gut microbiome and metabolome in *H. pylori* patients in a socioeconomically challenged and underprivileged inner-city community.

METHODS

Stool samples from 19 *H. pylori* patients and 16 control subjects were analyzed. *16S rRNA* gene sequencing was performed on normalized pooled amplicons using the Illumina MiSeq System using a MiSeq reagent kit v2. Alpha and beta diversity analyses were performed in QIIME 2. Non-targeted fatty acid analysis of the samples was carried out using gas chromatography-mass spectrometry, which measures the total content of 30 fatty acids in stool after conversion into their corresponding fatty acid methyl esters. Multi-dimensional scaling (MDS) was performed on Bray-Curtis distance matrices created from both the metabolomics and microbiome datasets and a Procrustes test was performed on the metabolomics and microbiome MDS coordinates.

RESULTS

Fecal microbiome analysis showed that alpha diversity was lowest in *H. pylori* patients over 40 years of age compared to control subjects of similar age group. Beta diversity analysis of the samples revealed significant differences in microbial community structure between *H. pylori* patients and control subjects across all ages. Thirty-eight and six taxa had lower and higher relative abundance in *H. pylori* patients, respectively. Taxa that were enriched in *H. pylori* patients included *Atopobium*, Gemellaceae, Micrococcaceae, Gemellales and *Rothia* (*R. mucilaginosa*). Notably, relative abundance of the phylum Verrucomicrobia was decreased in *H. pylori* patients compared to control subjects. Procrustes analysis showed a significant relationship between the microbiome and metabolome datasets. Stool samples from *H. pylori* patients showed increases in several fatty acids including the polyunsaturated fatty acids (PUFAs) 22:4n6, 22:5n3, 20:3n6 and 22:2n6, while decreases were noted in other fatty acids including the PUFA 18:3n6. The pattern of changes in fatty acid concentration correlated to the Bacteroidetes:Firmicutes ratio determined by *16S rRNA* gene analysis.

CONCLUSION

This exploratory study demonstrates *H. pylori*-associated changes to the fecal microbiome and fecal fatty acid metabolism. Such changes may have implications for improving eradication rates and minimizing associated negative distal outcomes.

Key Words: Gut microbiome; Metabolome; *Helicobacter pylori*; Antibiotic resistance; Dysbiosis; Eradication

©The Author(s) 2021. Published by Baishideng Publishing Group Inc. All rights reserved.

Core Tip: *Helicobacter pylori* (*H. pylori*) infects half of the world's population and is associated with various diseases, including malignancy. Research of microbiome and metabolomic changes associated with *H. pylori* may hold therapeutic potential. We sought to characterize the fecal microbiome and fatty acid metabolism among *H. pylori* patients in our community. We observed differences in alpha and beta diversity among *H. pylori* patients compared to controls, particularly for those over 40 years old. Changes in several fecal fatty acids, including those associated with anti-inflammatory activity, were observed. Our findings may have implications for improving *H. pylori* eradication and minimizing associated negative distal outcomes.

Citation: White B, Sterrett JD, Grigoryan Z, Lally L, Heinze JD, Alikhan H, Lowry CA, Perez LJ, DeSipio J, Phadtare S. Characterization of gut microbiome and metabolome in *Helicobacter pylori* patients in an underprivileged community in the United States. *World J Gastroenterol* 2021; 27(33): 5575-5594

URL: https://www.wjgnet.com/1007-9327/full/v27/i33/5575.htm

DOI: https://dx.doi.org/10.3748/wjg.v27.i33.5575

States

Peer-review report's scientific quality classification
Grade A (Excellent): A
Grade B (Very good): 0
Grade C (Good): C
Grade D (Fair): D, D
Grade E (Poor): 0

Received: March 31, 2021
Peer-review started: March 31, 2021
First decision: June 23, 2021
Revised: July 2, 2021
Accepted: August 13, 2021
Article in press: August 13, 2021
Published online: September 7, 2021

P-Reviewer: Krzyżek P, Neri M, Werawatganon D, Zhang J
S-Editor: Fan JR
L-Editor: A
P-Editor: Yuan YY

INTRODUCTION

Helicobacter pylori (*H. pylori*), a bacterium found in the stomach of roughly half of the world's population, is associated with various gastrointestinal diseases, including peptic ulcers, non-ulcer dyspepsia, gastric adenocarcinoma, and gastric lymphoma. Although many infections are asymptomatic, eradication of *H. pylori* has been shown to reduce the incidence of gastric cancer and is thus universally recommended[1]. For decades, clarithromycin-based triple therapy was considered the first-line therapy for *H. pylori* eradication and associated gastric cancer prevention. Following the global trend in emerging antibiotic resistance, rates of clarithromycin, metronidazole, and levofloxacin resistance among *H. pylori* strains have increased markedly, causing an alarmingly high rate of eradication failure[2]. In the absence of universally available antibiotic susceptibility testing, current guidelines advocate for the use of empiric quadruple therapy strategies; however, the efficacy of these regimens may be limited by dual resistance, local availability, and patient adherence[3].

As the burden of antibiotic resistance increases, the need for new adjunct therapies designed to facilitate *H. pylori* eradication and reduce negative distal outcomes associated with infection has become more pressing. The relationship between *H. pylori* and the microbiome has garnered particular attention of late[4]. With the advent of high throughput *16S rRNA* gene sequencing methods and open-source software for subsequent analysis and visualization, researchers have been able to characterize changes in microbial diversity and community structure, as well as specific taxa that are differentially abundant in association with particular phenotypes[5]. Many studies have focused on *H. pylori*-mediated changes to the gastric microbiome, in which data have demonstrated variable effects on multiple metrics of microbial diversity and community structure[4]. *H. pylori*-associated gastric dysbiosis is particularly significant in the context of studies which suggest increased relative abundance of particular taxa, including *Lactobacillus* and *Lachnospiraceae*, among patients who develop premalignant lesions and gastric cancer[6,7]. *H. pylori*-associated gastric dysbiosis has also prompted researchers to evaluate the adjunct therapeutic role of probiotics, which may increase the rate of *H. pylori* eradication and limit negative side effects of antibiotic treatment[8-11].

More recently, researchers have also focused on the impact of *H. pylori* infection on distal gut, *i.e.*, fecal microbiota. Despite *H. pylori's* role as an almost exclusively gastric pathogen, animal and clinical studies have demonstrated alterations in distal gut microbiota associated with *H. pylori* infection[12-15]. The mechanisms by which gastric *H. pylori* infection may influence the distal gut microbiome are unclear, although authors have speculated that multiple factors, including alterations in hydrochloric acid secretion, gastrointestinal hormones, and immune regulation, may be involved [12-14]. As stated above, microbiome modulation with probiotics may have a role in improving eradication rates and minimizing adverse effects of antibiotics. Additionally, *H. pylori*-mediated changes to the distal gut microbiome may be significant in the context of research that implicates gut dysbiosis in the development of colorectal cancer (CRC)[16]. Indeed, authors of a large case-control study found that seropositivity for the *H. pylori* virulence factor VacA was associated with increased odds of CRC[17]. The well-documented associations between gut dysbiosis, type 2 diabetes, and metabolic syndrome has also prompted speculation about the role of *H. pylori*-associated gut dysbiosis in diabetes, which has been associated with *H. pylori* infection [18-21]. Further characterization of the interactions between *H. pylori* and the gut microbiome, as well as the mechanisms underlying these interactions, may lead to a better understanding of the role of microbiome modulation in *H. pylori* therapy, as well as the development of novel therapies and screening tools aimed at the negative distal outcomes associated with *H. pylori* infection, including CRC and metabolic diseases.

Given the association between *H. pylori* infection and gastrointestinal inflammation, attention has also been paid to compounds with anti-inflammatory activity, including fatty acids. Polyunsaturated fatty acid (PUFA) supplementation in particular may have therapeutic potential for *H. pylori* treatment *via* multiple mechanisms, including suppression of inflammatory cytokines and enzymes and direct bacteriocidal effects *via* disruption of cell membranes[22-24]. 10-hydroxy-cis-12-octadecenoic acid (10-HOE; a linoleic acid derivative) and docosahexaenoic acid (DHA) have both been shown to inhibit *in vitro* growth of *H. pylori* and gastric infection in mouse models[25,26]. Nevertheless, the effects of *H. pylori* infection on fatty acid metabolism in the gastrointestinal tract are not completely understood. Furthermore, the extent to which such metabolomic changes may relate to alterations in the gastrointestinal microbiota are unknown. Notably, short-chain fatty acids (SCFAs) produced by gut microbiota

are thought to play a role in intestinal homeostasis, regulation of immune function, and dysbiosis in the setting of inflammatory bowel disease, which is associated with decreased levels of these important molecules[27,28]. Exploration of changes in fatty acid production and metabolism associated with *H. pylori*-mediated alterations of the fecal microbiome is warranted, as it may reveal strategies to inhibit the cascade of events leading to neoplasia.

Previously, we studied the pattern of *H. pylori* prevalence and antibiotic resistance in our socioeconomically challenged and underprivileged inner-city community[29]. As a next step, we then sought to characterize the gut microbiome associated with *H. pylori* infection in our patients. We further explored interactions among *H. pylori* infection, the gut microbiota, and the gut metabolome by comparing stool fatty acid profiles between subjects with and without *H. pylori* infection. Our overarching goal is to identify potential targets for intervention that could improve *H. pylori* eradication rates and limit associated negative distal outcomes.

MATERIALS AND METHODS

Patients and sample collection

Patients presenting to the Cooper Digestive Health Institute in Camden, New Jersey were recruited for our study. *H. pylori* patients at least 18 years of age and diagnosed *via* biopsy between June 1, 2017 and December 31, 2019, were eligible for inclusion. Patients less than 18 years old, pregnant women, patients taking antibiotics at the time of recruitment or sampling, and non-English speaking patients were excluded from participation. *H. pylori*-positive patients are identified in our electronic medical record system (EPIC) by ICD-9 codes of 041.86, 531.90, 535.60, 795.79, 008.47, 531.00, V12.08. Histological examination of the biopsied samples showed positive outcome indicating *H. pylori* infection. Control participants were recruited from a healthy population, also seen at Cooper Health Institute for well visits. The control subjects were screened for lack of previous history and current documentation for *H. pylori* infection as well as lack of any GI-related symptoms before recruitment. Their stools were tested by reverse transcription-polymerase chain reaction (PCR) based biprobe assay for presence of *H. pylori* DNA[30]. None of the stool samples from the control subjects showed presence of *H. pylori* DNA. Informed consent was obtained by one of several Institutional Review Board (IRB)-approved team members. Surveys about demographic information and relevant medical history were collected. Information on diagnosis, disease features, medication, history of antibiotic use, and treatment regimen were collected from the electronic medical record. Patients were asked to provide a stool sample before initiating eradication therapy, and samples were collected and stored in Stool Nucleic Acid Collection and Preservation Tubes (Cat. No. 45630, 45660, Norgen Biotek Corp., Thorold, Ontario, Canada) prior to freezing at –80 ℃ as described previously[29].

Processing of samples and 16S rRNA gene sequencing

Total genomic bacterial DNA extraction was performed from frozen fecal samples using the Qiagen DNeasy PowerSoil HTP Kit (Cat. No. 12955-4, Qiagen, Valencia, CA, United States). Adequate DNA yield was confirmed using NanoDrop spectrophotometry. For high throughput sequencing, 515F–806R Golay barcodes were used to target the hypervariable V4 region of the *16S rRNA* gene, which is highly conserved and ideal for gut microbiome analysis. Marker genes in isolated DNA were PCR-amplified using GoTaq Master Mix (Cat. No. M5133, Promega, Madison, WI, United States) as described in Caporaso *et al*[31]. PCR products were cleaned and normalized using the SequalPrep™ Normalization Plate Kit (Cat. No. A1051001, ThermoFisher, Waltham, MA, United States) following the manufacturer's instructions. Purification of PCR product amplicons was performed with the QIAquick PCR Purification Kit (Cat. No. 28104, Qiagen). Quantification of the PCR amplified library was performed with the Invitrogen™ Quant-iT™ PicoGreen™ dsDNA Assay Kit (Cat. No. P7589, ThermoFisher). *16S rRNA* gene sequencing was performed on normalized pooled amplicons using the Illumina MiSeq System using a MiSeq reagent kit v2 (300 cycles; Cat. No. MS-102-2002, Illumina Inc.). FASTQ files for reads 1 (forward), 2 (reverse), and the index (barcode) read were generated using the BCL-to-FASTQ file converter bcl2fastq (ver. 2.17.1.14, Illumina, Inc.). Sequencing of the samples was conducted at the University of Colorado Boulder BioFrontiers Next-Gen Sequencing core facility.

Sequencing data analysis

Analysis was performed using Python-based packages (Python 3.6.12), QIIME 2 2019.4 (denoising and taxonomy assignment), Quantitative Insights Into Microbial Ecology (QIIME) 2 2020.11 (statistical testing), and Linear Discriminant Analysis (LDA) using LDA Effect Size (LEfSe)[32,33]. Sequences were de-multiplexed, then filtered and clustered into sub-operational taxonomic units (sOTUs) using QIIME 2 DADA2[34]. A masked phylogenetic tree was created using MAFFT *via* QIIME2[35,36]. Taxonomy was assigned using a naïve-Bayes classifier based on the latest Greengenes *16S rRNA* gene database available as of August 2019 *via* the QIIME 2 interface (gg_13_8). Additional Python packages (SciPy.stats, Scikit-bio) were used for statistical tests on QIIME 2-generated data. Inter-class comparisons were made based on attributes of our population including: *H. pylori* status, gender, age group, race, education, and alcohol use. Alpha and beta diversity analyses were performed in QIIME 2, rarefied to an even sampling depth of 22400[37]. Alpha diversity was assessed by Faith's phylogenetic diversity, chao1 index, and observed OTUs. Differences in alpha diversity between groups were determined by Kruskal-Wallis non-parametric rank test for categorical variables or by Fisher Z transformation on Spearman rho values for differences between alpha diversity correlations with numeric data across groups. Bacterial composition (beta diversity) was analyzed by principal coordinate analyses (PCoA) of both unweighted and weighted unique fraction metric (UniFrac) phylogenetic distance matrices[38-41]. Beta diversity was assessed for statistical significance between groups using Monte Carlo permutations [Adonis and permutational multivariate analysis of variance (PERMANOVA)], and dispersion of group samples was assessed using permutational analysis of multivariate dispersions (PERMDISP)[42,43]. Comparisons of relative abundances of microbial taxa between groups were performed using LEfSe with the Segata *et al*[44] online interface. Taxa with an LDA value of 2.0 or greater and a two-tailed P value ≤ 0.05 with Kruskal-Wallis and pairwise Wilcoxon analyses were considered significantly enriched. The code is available at https://github.com/sterrettJD/H-pylori-microbiome-analysis.

Non-targeted fatty acid analysis

Collected fecal samples were stored at –80 ℃ until analysis. Sample preparation and analysis were performed using gas chromatography-mass spectrometry (GC-MS) by Metabolon, Inc. (Durham, NC, United States). This method (Metabolon TAM112-002) measures the total content of 30 fatty acids in stool samples after conversion into their corresponding fatty acid methyl esters (FAMEs). The measured concentrations are provided in weight corrected μg/g of sample. NQ (not quantified-below the lower limit of quantification) values were treated as a concentration of 0.001 mg/mL.

Briefly, stool samples were homogenized and the suspension was weighed out in a 100 mg aliquot in a test tube. Liquid/Liquid extraction was performed to extract fatty acids and remove the nucleic acid preservative. A 250 μL aliquot of each extract was transferred to a clean analysis tube. The solvent was removed by evaporation under a stream of nitrogen. Internal standard solution was added to the dried sample extracts, quality controls (QCs), and calibration standards. The solvent was again removed by evaporation under a stream of nitrogen. The dried samples and QCs were subjected to methylation/transmethylation with methanol/sulfuric acid, resulting in the formation of the corresponding methyl esters (FAME) of free fatty acids and conjugated fatty acids. The reaction mixture was neutralized and extracted with hexanes. An aliquot of the hexanes layer was injected onto a 7890A/5975C GC-MS system (Agilent Technologies, Santa Clara, CA, United States). Mass spectrometric analysis was performed in the single ion monitoring positive mode with electron ionization. Quantitation was performed using both linear and quadratic regression analysis generated from fortified calibration standards prepared immediately prior to each run. Raw data were collected and processed using Agilent MassHunter GC-MS Acquisition B.07.04.2260 and Agilent MassHunter Workstation Software Quantitative Analysis for GC-MS B.09.00/ Build 9.0.647.0. Data reduction was performed using Microsoft Office 365 ProPlus Excel. Volcano plot data are included as Supplementary Tables 1-3 (Supplementary Table 1: Volcano plot data with all *Helicobacter* data set; Supplementary Table 2: Volcano plot data with High Bacteroidetes; Supplementary Table 3: Volcano plot data with High Firmicutes).

Procrustes analysis

Multi-dimensional scaling (MDS, using the Python package Scikit-learn) was performed on Bray-Curtis distance matrices created from both the fecal metabolome and fecal microbiome datasets (using the Python package SciPy.distance), and a Procrustes

test was performed on the metabolomics and microbiome MDS coordinates. As described by Peres-Neto and Jackson, a Procrustes randomization test (PROTEST) was performed by randomly sampling the MDS coordinates and performing a Procrustes test on the reordered coordinates 10000 times, and the *P* value was calculated based on the portion of randomized Procrustes tests with resulting m^2 (Gower's statistic) scores lower than the Procrustes m^2 score of the observed datasets[45].

Ethics approval

This study received approval by the Cooper Health System IRB (17-077EX) and all the steps were carried out as *per* the standards set by the IRB.

RESULTS

Fecal microbiome analysis

Selected demographic attributes of our participants are presented in Table 1. Fecal microbiome analysis of 35 stool samples collected from 19 *H. pylori* patients and 16 healthy control subjects was carried out. The mean number of reads *per* sample was 269462 with a minimum of 22483 reads/sample. Rarefaction was set to 22400 for even sampling based on this minimum. We analyzed the association of each of the factors included in Table 1 with alpha and beta diversity (*via* Kruskal-Wallis and PERMANOVA for nominal variables or *via* Spearman correlation and Mantel test for numerical variables, respectively). Age was the only factor that showed statically significant differences (*P* value of $\leq$ 0.05) in alpha diversity in the *H. pylori* patients compared to the control participants, with *H. pylori* patients over 40 years of age having lower richness than control participants over 40 years of age. Significant differences in community composition and group dispersion were seen between *H. pylori* patients and control participants.

Information was collected about each participant regarding (1) If they had been treated for *H. pylori* infection in the past; (2) If so, the date infection was diagnosed; (3) Treatments given; and (4) Outcomes: Eradication testing with dates. Only one patient had *H. pylori* infection 10 years ago and had successfully completed treatment at that time. History about antibiotic treatments for any infection and proton pump inhibitors (PPIs) use for both *H. pylori* patients and control subjects in the past five years was also documented and these data values were included in the statistical analyses. Our statistical analyses showed that the differences seen in *H. pylori* patients were not due to the previous treatments.

Analysis of alpha diversity

Chao1 index alpha diversity between *H. pylori* patients and control subjects and regression analysis of observed OTUs by age are shown in Figure 1. Alpha diversity, which estimates the diversity of a microbial community within a sample, incorporates the number of different OTUs and their respective abundance in each sample. Alpha diversity was lowest in *H. pylori* patients over 40 years of age, who had significantly lower Chao1 scores compared to control subjects over 40 years of age (Kruskal-Wallis $H = 6.036$, $P = 0.014$). *H. pylori* patients over 40 years old also had lower Chao1 scores approaching statistical significance when compared to *H. pylori* patients under 40 (Kruskal-Wallis $H = 2.813$, $P = 0.094$). Additionally, the correlation of age with observed OTUs (Figure 1B), Faith's phylogenetic diversity, and Chao1 was consistently different between *H. pylori* patients *vs* control subjects, as evidenced by a Fisher *Z* transformation on Spearman rank correlation *rho* values (observed OTUs: *H. pylori rho* = –0.21 *vs* control *rho* = 0.50, Fisher $P = 0.041$; Faith: *H. pylori rho* = –0.04 *vs* control *rho* = 0.57, Fisher $P = 0.067$; Chao1: *H. pylori rho* = –0.15 *vs* control *rho* = 0.44, Fisher $P = 0.097$).

Analysis of beta diversity

Next we analyzed beta diversity of our samples, which estimates how samples differ from each other. An unweighted UniFrac PCoA plot of *H. pylori* patients *vs* control subjects is shown in Figure 2. Adonis testing revealed that current *H. pylori* infection represented 7% of the variation in unweighted UniFrac beta diversity ($F = 2.523$, $R^2 = 0.071$, $P = 0.002$). Additionally, unweighted UniFrac PERMANOVAs identified significant differences between *H. pylori* patients and control subjects ($F = 2.523$, $P = 0.001$). Furthermore, unweighted UniFrac PERMDISP did not reveal differences in dispersion among *H. pylori* patients *vs* control subjects ($F = 0.0506$, $P = 0.809$), but

Table 1 Patient demographics and clinical characteristics

	Total (*n* = 35)	*H. pylori* patients (*n* = 19)	Control (*n* = 16)
Sex, *n* (%)			
Male	19 (54)	13 (68)	6 (38)
Female	16 (46)	6 (32)	10 (62)
Age, *n* (%)			
18-40	15 (43)	3 (16)	12 (75)
> 40	20 (57)	16 (84)	4 (25)
Highest education, *n* (%)			
Less than high school	2 (6)	2 (11)	0 (0)
High school	12 (34)	11 (58)	1 (6)
Undergraduate	4 (11)	2 (11)	2 (13)
Graduate	15 (43)	3 (16)	12 (75)
Post-graduate	1 (3)	0 (0)	1 (6)
Race, *n* (%)			
African American	8 (23)	6 (32)	2 (12)
Asian American	2 (6)	0 (0)	2 (12)
Caucasian	13 (37)	1 (5)	12 (75)
Non-White Hispanic	8 (23)	8 (42)	0 (0)
Other	3 (9)	3 (16)	0 (0)
Smoker	5 (14)	4 (21)	1 (6)
Past *H. pylori* treatment	1 (3)	1 (5)	0 (0)
Duodenal ulcer	1 (3)	1 (5)	0 (0)
Non-ulcer dyspepsia	14 (40)	10 (53)	4 (25)

H. pylori: *Helicobacter pylori*.

weighted UniFrac PERMDISP did (F = 6.82955, P = 0.017). We also explored the effect of the use of PPIs *via* beta diversity analysis as PPIs are the medications commonly given to *H. pylori* patients and we had previously noted their influence on the antibiotic resistance of *H. pylori*[29]. Unweighted UniFrac PERMANOVA identified differences between PPI users and non-users across all participants (F = 1.939, P = 0.012), though the magnitude of the effect was smaller than that seen for *H. pylori* infection as described above. It should also be noted that only four *H. pylori* patients and one control subject were on PPI at the time of study and sample collection, so its contribution to the results described here may not be significant.

LDA effect size

LEfSe scores for taxa that were differentially distributed across *H. pylori* patients *vs* control subjects are shown in Figure 3. Thirty-eight taxa had lower relative abundance in *H. pylori* patients relative to healthy control subjects, and six taxa had higher relative abundance in *H. pylori* patients relative to healthy control subjects. Taxa that were enriched in *H. pylori* patients include *Atopobium,* Gemellaceae, Micrococcaceae, Gemellales and *Rothia* (*R. mucilaginosa*). Figure 4 shows the arcsin square root transformed relative abundances of each phylum, grouped by *H. pylori* status. Notably, relative abundance of the phylum Verrucomicrobia, and its main constituent, *Akkermansia muciniphila*, was decreased in *H. pylori* patients compared to control subjects.

Procrustes analysis

The Procrustes randomization test was carried out to investigate the relationship between the fecal microbiome and fecal metabolome. Procrustes analysis identified a significant relationship between the two datasets, as the resulting P value of 0.017

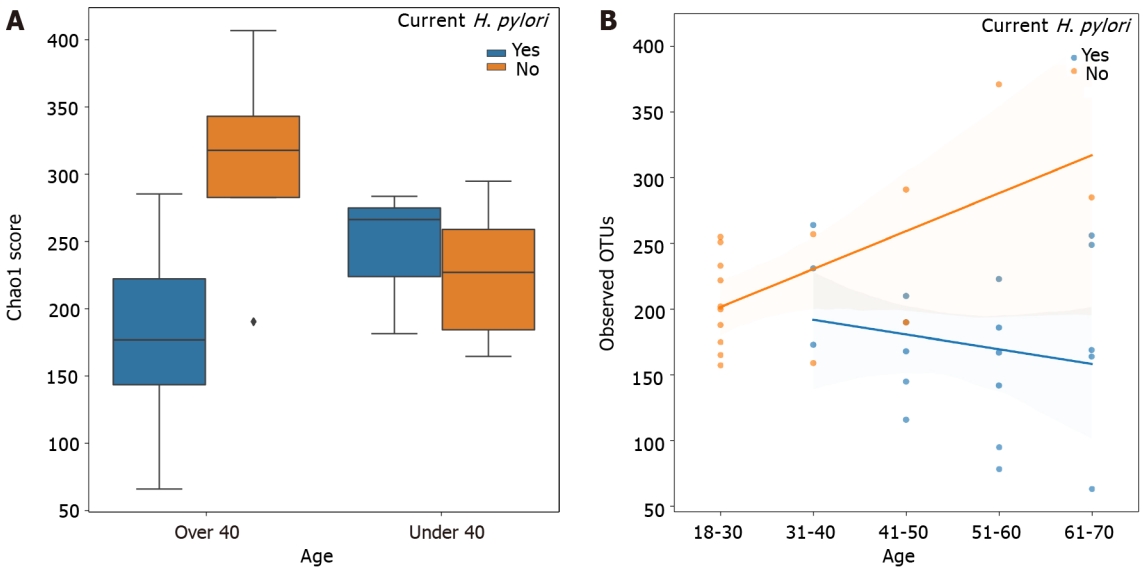


Figure 1 Chao1 index alpha diversity and observed operational taxonomic units by *Helicobacter pylori* status stratified by age. A: Chao1 index alpha diversity is compared between *Helicobacter pylori* (*H. pylori*) patients (blue) and control subjects (orange), subgrouped by age. *H. pylori* patients over 40 years old (n = 16) had significantly lower Chao1 scores compared to control subjects over 40 (n = 4) (Kruskal-Wallis H = 6.036, P = 0.014). Boxes represent 1st and 3rd quartiles, and central lines represent median values. Whiskers represent non-outlier high and low values. Points show outliers, which were determined by having a distance from the 1st or 3rd quartile greater than 1.5 times the interquartile range; B: Observed operational taxonomic units (operational taxonomic units) are compared between *H. pylori* patients (blue, n = 19) and control subjects (orange, n = 16), as a function of age. Shading around the regression lines indicates 95% confidence intervals. OTU: Operational taxonomic units; *H. pylori*: *Helicobacter pylori*.

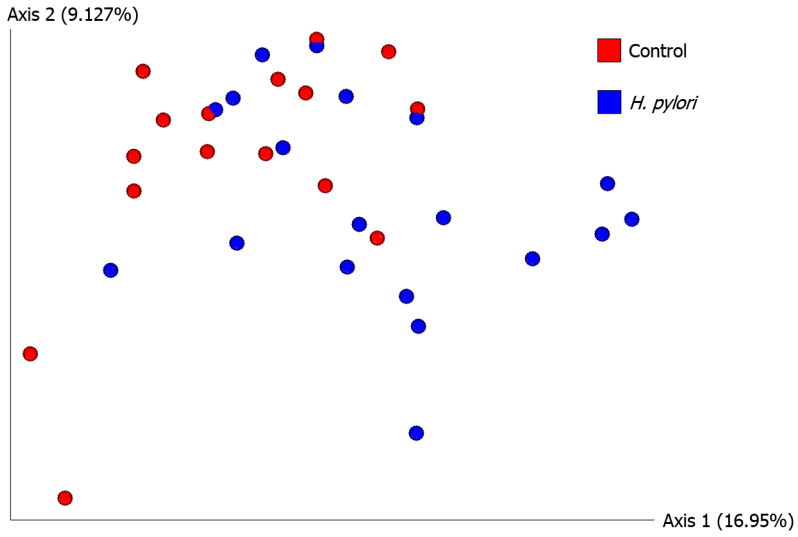


Figure 2 Beta diversity analysis by unweighted UniFrac principal coordinate analysis. Unweighted principal coordinate analysis (PCoA) plot is shown comparing *Helicobacter pylori* (*H. pylori*) patients (blue, n = 19) to control subjects (red, n = 16). Significant differences between *H. pylori* patients and control subjects were identified by unweighted UniFrac PERMANOVA (F = 2.523, P = 0.001). The proportion of variance explained by each principal coordinate axis is denoted in the corresponding axis label; PCo1 explains 16.95% of the variability and PCo2 explains 9.13% of the variability. *H. pylori*: *Helicobacter pylori*.

indicates that the correspondence of each participant's fecal microbiome to their fecal metabolome was better than 98% of randomly sampled simulations (Figure 5).

Fecal fatty acid analysis

To evaluate the impact of *H. pylori* infection on fatty acid composition, we performed non-targeted metabolomics analysis of a panel of 30 fatty acids including long chain fatty acids (LCFAs), monounsaturated fatty acids (MUFAs) and PUFAs. We prepared a volcano plot evaluating changes in fatty acid profile for the entire population of *H. pylori* patient samples relative to healthy control subjects (Figure 6A). In addition, we prepared separate volcano plots for subgroups of the *H. pylori* patients with high Bacteroidetes and high Firmicutes based on *16S rRNA* gene analysis (Figure 6B and C).

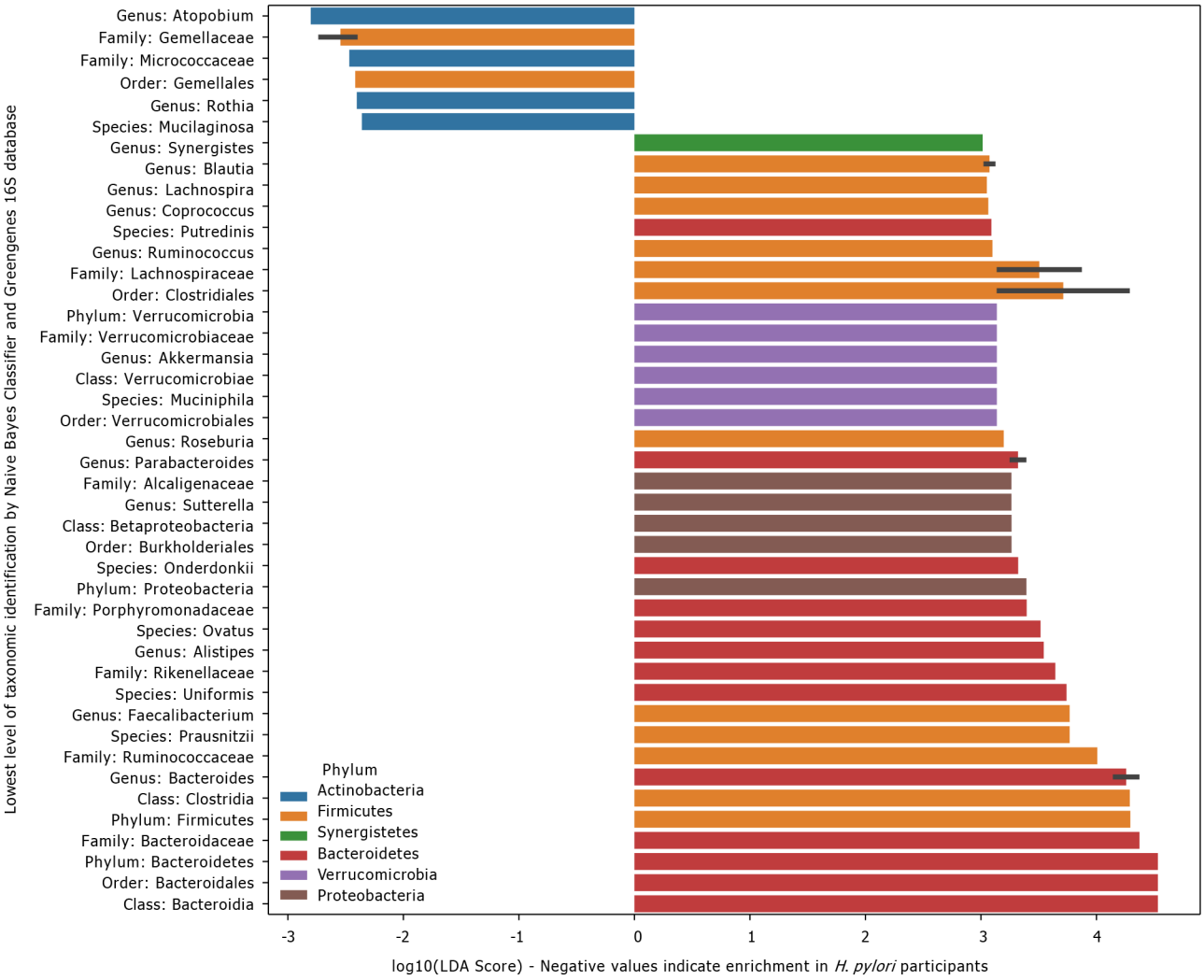


Figure 3 Linear discriminant analysis effect size scores for taxa enriched in *Helicobacter pylori* or control participants. Linear discriminant analysis effect size (LEfSe) scores for taxa that were differentially distributed across *Helicobacter pylori* (*H. pylori*) patients (n = 19) *vs* control subjects (n = 16) *via* Kruskal-Wallis and Wilcoxon tests with two-tailed α = 0.05. Negative values represent taxa that were enriched in *H. pylori* patients, whereas positive values represent taxa that were enriched in control subjects. Error bars represent a 95% confidence interval and are only present if the listed taxonomic identity was the lowest level classified for multiple operational taxonomic units highlighted by LEfSe. Color represents the phylum. *H. pylori*: *Helicobacter pylori*.

See Supplementary Tables 1-3 for the full volcano plot data. Volcano plots allow for the plotting of *P* values *vs* fatty acid fold change from control samples for all evaluated fatty acids.

Stool samples from *H. pylori* patients showed increases in several fatty acids including the PUFAs 22:4n6, 22:5n3, 20:3n6 and 22:2n6 while decreases were noted in fatty acids including the PUFA 18:3n6, relative to healthy control subjects. The pattern of changes in fatty acid concentration was correlated to the Bacteroidetes:Firmicutes ratio (determined by *16S rRNA* gene analysis). Among the sub-population of *H. pylori* patients identified to have high Bacteroidetes (Bacteroidetes:Firmicutes ratio ≥ 1 standard deviation above the ratio in control participants, n = 7) we found several fatty acids that were diminished relative to control participants including the LCFAs 24:0, 22:0 and 15:0 along with MUFAs 20:1n9 and 18:1n9. By contrast, in the sub-population of *H. pylori* patients identified to have high Firmicutes (Firmicutes:Bacteroidetes ratio ≥ 1 standard deviation above ratios in control participants; n = 4) a distinct set of fatty acids were found to be significantly increased and decreased relative to control participants. In this subpopulation of *H. pylori* patients we observed increases in the PUFA 22:2n6 and decreases in PUFAs 18:3n6 and 20:4n3 relative to control participants.

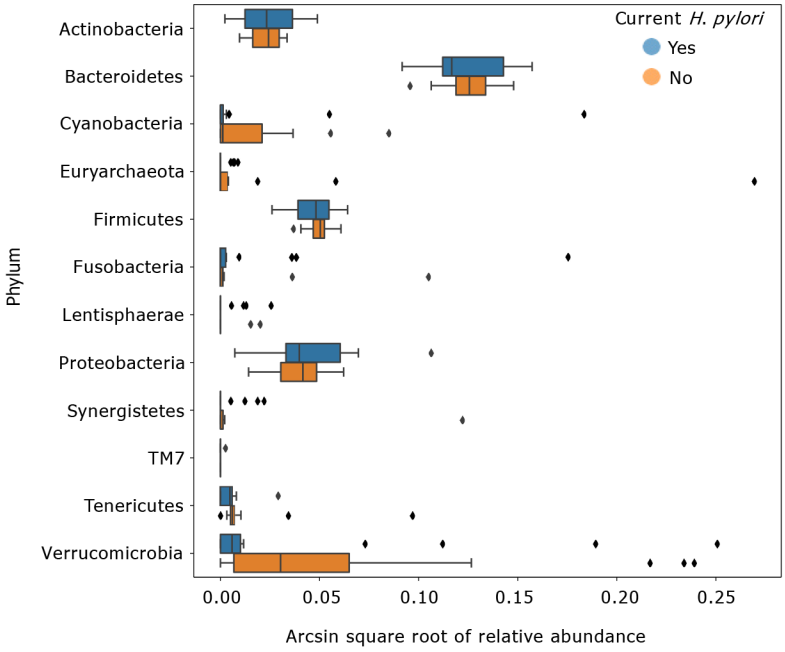


Figure 4 Transformed relative abundances of phyla grouped by *Helicobacter pylori* infection. Arcsin square root transformed relative abundances of each phylum, grouped by *Helicobacter pylori* (*H. pylori*) status. Bacterial relative abundances of *H. pylori* patients (n = 19) are shown in blue, whereas healthy controls (n = 16) are shown in orange. Boxes represent the 1st and 3rd quartiles, and vertical lines in the middle of the boxes represent median values. Whiskers represent the lowest and highest non-outlier values. Points show outliers, which were determined by having a distance from the 1st or 3rd quartile greater than 1.5 times the interquartile range. Of note, relative abundances of Verrucomicrobia were significantly lower in *H. pylori* patients compared to healthy controls (Kruskal-Wallis H = 4.455, P = 0.034). *H. pylori*: *Helicobacter pylori*.

DISCUSSION

As little is known about the microbiome of *H. pylori* patients in an underprivileged community, this study is useful due to its exploratory nature. A sample size calculation for microbiome analysis was not thus performed prior to collecting samples. Casals-Pascual *et al*[46] outline that in human microbiome studies knowledge of the baseline microbiome diversity and composition, along with knowledge of the magnitude of changes that confer clinically relevant outcomes are important for determining sample size. However, this could not easily be predicted in our sample demographic due to lack of previous research. Though the effects of *H. pylori* and low socioeconomic status (SES) on the gut microbiome have been investigated separately in previous studies, the two states (*H. pylori* infection and low SES) could potentially have conflicting relationships with diversity and composition, making it difficult to determine the baseline microbiome diversity and composition without large assumptions. Thus, much of this study provides the baseline to characterize the microbiome of *H. pylori* patients in an underserved population, which was previously understudied to a degree by which sample size calculations would have required a large number of assumptions. Though the power is likely weak in this study, especially for post-hoc analyses such as alpha diversity in *H. pylori* patients over 40 years of age *vs* control participants over 40 years of age, multiple lines of evidence, including both the Kruskal-Wallis test with age group and the Spearman correlation with actual age support the relationship in our sample. These results can provide a basis for future study design and power calculations.

Our sample size is modest in part due to the limitations posed by the socioeconomic and cultural attributes of our patient population and logistic challenges associated with sample collection. Camden County has the lowest median income and highest poverty and unemployment rates in southern New Jersey. It also has the lowest educational attainment and the greatest socioeconomic disparities among ethnic minority groups. More than one third of the population in Camden City, where our hospital is located, lives below the national poverty line, and the median household income is USD $26105[47]. Our local community is thus considered one of the poorest and most economically distressed communities in the United States. A significant fraction of adults over 25 years old (almost one quarter) have not completed high school. It is possible that this influences patients' appreciation of the relevance of the study and willingness to participate. A significant portion of potential participants

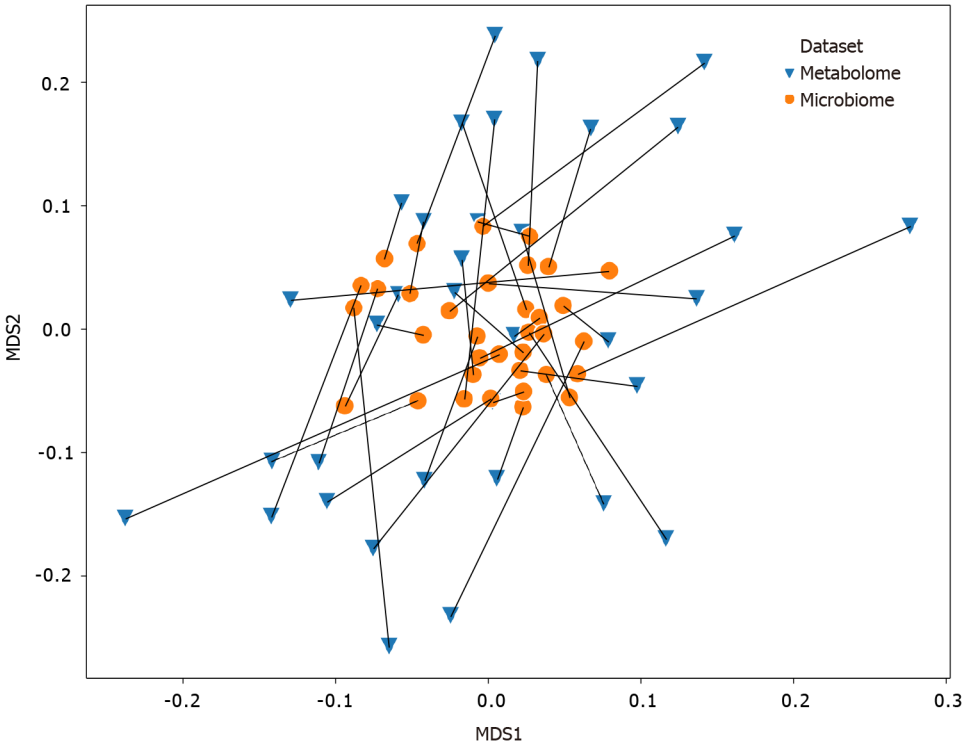


Figure 5 Procrustes-transformed Bray-Curtis multi-dimensional scaling of microbiome and metabolome. Connections between the fecal microbiome and fecal metabolome Bray-Curtis multi-dimensional scaling plots. The microbiome data shown here have been transformed by the Procrustes analysis to minimize disparity between the two datasets, and lines have been drawn to indicate microbiome and metabolome from the same participants. Orange dots represent the microbiomes, whereas blue triangles represent the metabolomes. The Procrustes randomization test showed a significant relationship between the datasets (m^2 = 0.86, P = 0.017). MDS: Multi-dimensional scaling.

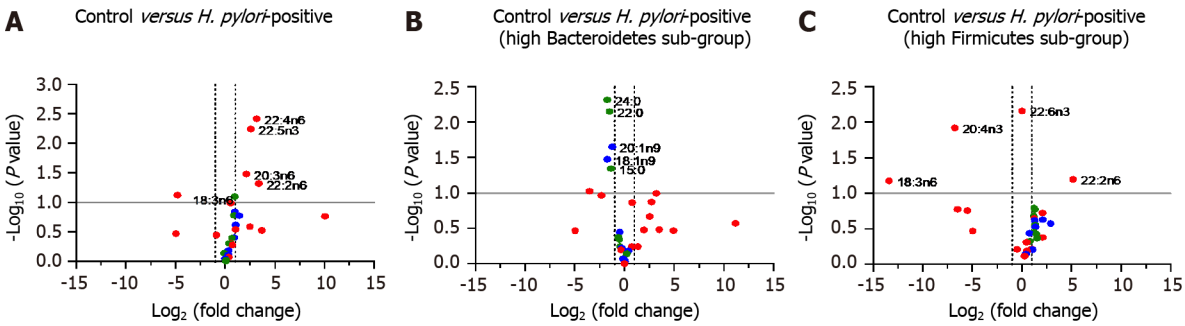


Figure 6 Volcano plots of composition of evaluated fatty acids. A: Control *vs* entire *Helicobacter pylori* (*H. pylori*) patient group; B: Control *vs* sub-group of *H. pylori* patients identified as having high ratio of Bacteroidetes to Firmicutes (n = 7 of 19 patients); C: Control *vs* sub-group of *H. pylori* patients identified as having high ratio of Firmicutes to Bacteroidetes (n = 4 of 19 patients). Selected long-chain fatty acids (green), monounsaturated fatty acids (blue) and polyunsaturated fatty acids (red) are highlighted. *H. pylori*: *Helicobacter pylori*.

were excluded due to non-English-speaking status, thus being unable to partake in the informed consent process. Logistic challenges imposed by the process of stool sample collection also limited the number of subjects. A large number of potential participants were unable to return to the clinic for stool sample delivery due to poor transportation access or inability to leave employment or domestic responsibilities during the window for sample collection (after diagnosis but prior to initiation of antibiotics). Nonetheless, the present study yielded meaningful results.

H. pylori infection was associated with significantly decreased fecal microbial diversity relative to over the age of 40 years. Among all participants, correlations between age and multiple metrics of microbial alpha diversity were consistently different between *H. pylori* patients and control subjects. *H. pylori* was also shown to account for a significant portion of the variation in beta diversity between infected patients and control subjects. Collectively, these results may suggest an *H. pylori*-mediated alteration of the fecal microbiome that progresses with age. While other

authors have attributed decreased diversity of gastric microbiota to the ability of *H. pylori* to outcompete other species, secretion of antibacterial peptides, and local pH alterations, the mechanisms by which *H. pylori* affect distal gut microbiota remain unclear[4,48-50]. Although our study was not designed to uncover these mechanisms, multiple factors hypothesized by other authors, including alterations in hydrochloric acid secretion, gastrointestinal hormones, and immune regulation, may be involved in the mediation of distal gut dysbiosis[12-14]. The impact of *H. pylori* on fecal microbial diversity observed in our study may be reversible, as a recent study showed that *H. pylori* eradication could restore gastric microbial diversity to levels seen in uninfected controls[51].

Less likely is the possibility that the data reflect a preceding decrease in gut microbial diversity that facilitates *H. pylori* infection, potentially mediated by other factors or exposures that accumulate with age. In other words, patients who experience decreased gut microbial diversity as they age, potentially mediated by diet or chronic inflammation, may be more prone to *H. pylori* infection, particularly by mid-adulthood. In our previous study of 2014 *H. pylori* patients, we observed that 80% of our patients were above the age of 40 years, consistent with studies showing increased prevalence of *H. pylori* infection with age in both developing and developed countries [29,52]. Antibiotic exposure is known to alter the gut microbiome, and increased rates of antibiotic-resistant *H. pylori* among older adults have been attributed to increased antibiotic use compared to younger patients[53,54]. Conceivably, decreased gut microbial diversity induced by cumulative antibiotic exposure could create an intragastric niche for *H. pylori*, and antibiotic-resistant *H. pylori* strains in particular, to thrive. However, *H. pylori* infection is thought to be acquired in infancy and carried through to adulthood, and this observation would not be consistent with preceding microbiome alteration facilitating *de novo H. pylori* infection in adulthood[55].

LEfSe showed that multiple taxa were differentially enriched or depleted in stool from *H. pylori* patients compared to controls. The significance of differential expression of these taxa is unknown; however, certain taxa stand out. The enrichment of *Atopobium* in *H. pylori* patients is notable in the context of a metagenomic analysis that revealed increased *Atopobium parvulum* abundance among patients with colorectal intramucosal carcinomas[56]. Although *H. pylori* is predominantly associated with gastric cancers, a recent meta-analysis suggested a significantly increased risk of CRC as well, and our data suggest that *H. pylori*-associated increases in *Atopobium* abundance may have a role in the distal gut carcinogenesis[57].

Over-representation of *Rothia mucilaginosa*, a commensal oral microbe, has previously been observed in fecal samples from patients with primary sclerosing cholangitis (PSC)[58]. Because of the sensitivity of *R. mucilaginosa* to gastric fluid, Bajer *et al*[58] hypothesized that its presence in PSC patients represented contamination of the intestine *via* previous endoscopic retrograde cholangiopancreatography. The enrichment of *Rothia* sp. in fecal samples from our *H. pylori* patients may reflect the potent gastric acid suppression by *H. pylori*, allowing translocation of swallowed oral flora to the distal gut. The clinical consequences of the colonization of the distal gut by *Rothia* sp. are unknown, although the bacteria has been implicated as a cause of myriad syndromes, including dental caries, pneumonia, and bacteremia, particularly in immunocompromised patients[59]. The increased abundance of Gemellaceae in *H. pylori* patients is consistent with the observation of increased organisms from the *Gemella* genus in patients with current *H. pylori* infection reported by Gao *et al*[60]. Increased relative abundance of Gemellaceae in the Crohn's ileum has been reported by other groups[61,62].

Interestingly, the phylum Verrucomicrobia was significantly depleted in *H. pylori* patients. Verrucomicrobia includes *Akkermansia muciniphila*, a mucus-residing commensal bacterium of the large intestine. *A. muciniphila* is an obligate chemoorganotroph, utilizing mucus as a sole carbon, nitrogen, and energy source that produces SCFAs including acetate, propionate, and, to a smaller extent, 1,2-propanediol[63,64]. Our study was not designed to study this aspect in detail, but the decreased relative abundance of Verrucomicrobia may suggest disruption of the gut mucosal environment by *H. pylori*. In a mouse stress model, exposure to chronic psychosocial stress resulted in expansion of *Helicobacter* spp., which has been demonstrated to proliferate in response to glucocorticoid administration as well as psychosocial stress exposure [65]. Specifically, stress-induced increases in *Helicobacter* spp. were associated with increases in other *Proteobacteria* spp., including unidentified genera belonging to the Enterobacteraceae and Desulfovibrionaceae families. Concurrently, relative abundance of *Mucispirillum*, an obligate mucus-residing bacterium, decreased; a decline of *Mucispirillum* in rodents is associated with early disruption of the gastrointestinal surface mucus layer and a prolonged delay to recovery after the period of pathogen clearance

[66]. Potential disruption of the gut mucosa by *H. pylori* infection is also consistent with decreased relative abundance of *Faecalibacterium prausnitzii*. *F. prausnitzii* is an important gram-positive human commensal that produces butyrate and other SCFA through the fermentation of dietary fiber. Reduced relative abundance of *F. prausnitzii* has been associated with inflammatory conditions including Crohn's disease, obesity, asthma, and stress-related psychiatric disorders in which inflammation is a risk factor, such as major depressive disorder[67-70].

Strategies to promote increased gastric microbial diversity among patients with *H. pylori* infection, particularly those over 40 years of age, may hold therapeutic potential in eradicating infection, and some clinical trials with adjunctive probiotic formulas have shown promising results in this regard[71]. Likewise, treatment of gut dysbiosis in patients with *H. pylori* infection may limit its associated pathologies. Reduced fecal microbiome diversity is associated with multiple disease markers including increased adiposity, insulin resistance, dyslipidemia, and a pro-inflammatory state[72]. *H. pylori* infection is associated with higher rates of diabetes, specifically, and addressing gut dysbiosis in such patients could conceivably aid primary dietary and pharmacologic strategies to achieve glycemic control and insulin sensitivity[20]. Rehabilitation of the gut microbiota in patients with *H. pylori* may also have a role in minimizing the risk of malignancy. Mouse studies suggest that the carcinogenic effects of *H. pylori* partly depend on interactions with the gut microbiome, and persistent infection with *H. pylori* may create a niche favorable for taxa that are found in increased abundance in gastric cancer, including *Lactobacillus* and *Lachnospiraceae*[73,74]. It has been suggested that lactic acid bacteria can influence gastric cancer by a number of mechanisms such as (1) Supply of exogenous lactate, that acts as a fuel source for cancer cells; (2) Production of reactive oxygen species and N-nitroso compounds; and (3) By allowing colonization of carcinogenic non-*H. pylori* bacteria[75]. Accordingly, reversal of abnormalities in gut microbiota associated with *H. pylori* may also limit its carcinogenic potential. Finally, consideration must be given to the effects of *H. pylori* treatment on the gut microbiome, as data suggest that current therapies may be associated with dysbiosis and subsequent adverse effects[76]. Several factors including lifestyle and diet can act as confounders in analysis of the diversity and composition of the gut microbiome. However, given the challenges associated with controlling for such variables, their presence should not prohibit drawing meaningful conclusions from significant observations of gut dysbiosis in association with *H. pylori*.

While evaluating changes in the LCFAs palmitic (16:0) and stearic (18:0) concentrations, we found that palmitic acid concentrations were increased in our test samples compared to control samples [625.23 ± 598.82 mg/g (n = 18) *vs* 334.10 ± 284.58 mg/g (n = 12)], whereas concentrations of stearic acid were comparable between populations. Interestingly, when we evaluated the high Firmicutes (> 1.4:1 Firmicutes:Bacteroidetes, n = 4) sub-group compared to the high Bacteroidetes (> 2.7:1 Bacteroidetes:Firmicutes, n = 7) sub-group of our test population, we found the concentrations of both these LCFAs to be diminished in the high Bacteroidetes population while the concentrations of both were enhanced in the high Firmicutes sub-population. This is consistent with previous studies in mice where administration of LCFA-rich diets resulted in an observed increase in Firmicutes to Bacteroidetes ratio[77]. Ktsoyan *et al*[78] implicated a characteristic profile of serum LCFA concentrations in association with *H. pylori* infection compared to healthy controls. It is plausible that diet can modulate the impact of *H. pylori* on the gut microbiome, which in turn may relate to different disease phenotypes, *i.e.*, asymptomatic infection, peptic ulcer disease, and gastric cancer.

The accumulation of the saturated LCFAs is regulated under normal physiological conditions by desaturation of 16:0 to 16:1n7, elongation of 16:0 to 18:0 and/or desaturation of 18:0 to 18:1n9 which can be further elongated to 20:1n9 (Figure 7). While only small changes in concentrations of these MUFAs were noted between our *H. pylori* patients and control subjects, the changes in MUFA concentrations in our high Firmicutes and high Bacteroidetes sub-populations showed more significant and consistent changes across the series of MUFAs. The concentration of 16:1n7, 18:1n9 and 20:1n9 were decreased in the high Bacteroidetes sub-group, whereas these MUFAs were slightly increased in the high Firmicutes sub-group. Interestingly, this contrasts published data on the benefits of high MUFA diets in animal models and humans. In previous studies, high MUFA diets have been reported to lead to increased ratios of Bacteroidetes to Firmicutes and were correlated with reductions in several disease indicators[77]. Together, these observations may suggest that either the patients in our high Bacteroidetes sub-population have severely limited MUFA production/intake, contrasting previous work on MUFA rich diets or that the endogenous biosynthetic pathways for MUFA production are dysregulated in this patient population.

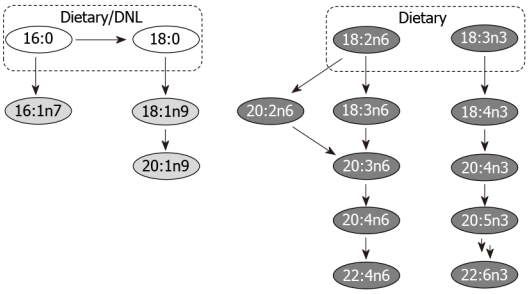


Figure 7 Major metabolic pathways. Selected long-chain fatty acids (no fill), monounsaturated fatty acids (light grey fill) and polyunsaturated fatty acids (dark grey fill) are highlighted. Although many of the fatty acids shown may be supplemented by diet, key parent members of these pathways acquired from *de novo* lipogenesis and/or diet are indicated. DNL: *De novo* lipogenesis.

The range of PUFAs observed endogenously have essential physiological roles and are produced from dietary alpha-linolenic acid (18:3n3) and linoleic acid (18:2n6). We observed that both of these dietary PUFAs were increased in our test samples compared to the control samples. In humans, C18:3n3 is converted through multiple steps to eicosapentaenoic acid (20:5n3) and DHA (22:6n3), whereas 18:2n6 proceeds to produce arachidonic acid (AA, 20:4n6) (Figure 7). As these two biosynthetic pathways share enzymes for their respective dehydration and elongation steps, they are antagonistic to each other. In general, a high 18:3n3 (n-3 fatty acid) diet is correlated with positive physiological effects whereas a high 18:2n6 (n-6 fatty acid) diet is correlated with metabolic dysbiosis and negative physiological effects[79,80]. Accordingly a balanced dietary intake of n-6/n-3 fatty acids is recommended to be 1:1-2:1, although the average ratio in a typical Western diet has been reported to be > 15:1[81]. In accordance with published ratios for n-6/n-3 fatty acid intake in Western diets, we find the ratio of 18:2n6/18:3n3 to be 22:1 in our control samples and 15:1 in our *H. pylori* patient test samples.

Endogenously, the essential dietary fatty acid 18:3n3 undergoes multiple dehydration and elongation steps to produce docosapentaenoic acid (DPA, 22:5n3) and DHA (22:6n3). For all intermediates along this biosynthetic pathway, with exception to 18:3n3 and 22:5n3, we observe concentrations at or below the limit of quantification for the majority of samples making an evaluation of the individual steps of this biosynthesis pathway difficult.

Contrasting the low concentrations observed for 18:3n3 and fatty acids produced along this biosynthetic pathway, higher overall concentrations were observed for fatty acids derived from 18:2n6, perhaps reflecting the higher concentration of dietary n-6 fatty acids as described earlier. In humans, the dietary fatty acid, 18:2n6 undergoes dehydration to produce 18:3n6. This intermediate undergoes a subsequent elongation to produce 20:3n6, which is dehydrated to 20:4n6 (AA). Alternatively, 18:2n6 can undergo elongation first to produce 20:2n6, which is dehydrated to produce 20:3n6 (Figure 7).

We found that the early steps in the metabolism of 18:2n6 were significantly impacted in all of our *H. pylori* samples by comparison of downstream fatty acid metabolites to controls. Most notably, in all *H. pylori* test samples the concentration of 18:3n6 was significantly diminished. Concentration of 18:3n6 was 10.7 ± 18.2 mg/g (n = 12) in the control samples and 0.36 ± 1.50 mg/g (n = 18) in the test samples. While we would anticipate that this deficiency in dehydration of 18:2n6 would lead to lower levels of fatty acid metabolites downstream of 18:3n6, this is not the case. In fact, by the following biosynthetic step, *i.e.*, elongation to produce 20:3n6, the fatty acid concentration of 20:3n6 in test samples was found to be higher than in controls. These higher concentrations were also reflected in arachidonic acid (20:4n6) and adrenic acid (22:4n6). It is plausible that the alternative *d-8-desaturase* mediated route *via* 20:2n6 may be prominent in these *H. pylori* patient samples, which are marked by a deficiency in *d-6-desaturase* mediated pathway *via* 18:3n6[82]. We observed a striking decrease in the concentration of the PUFA C18:3n6 in *H. pylori* infected patients. Interestingly, among the multiple liposomal fatty acids evaluated by Thamphiwatana *et al*[83], only the linolenic acid formulation (C18:3) showed bactericidal activity by impacting the *H. pylori* membrane structure and stability.

As the burden of antibiotic resistance grows, populations like ours are impacted greatly by the high prevalence of *H. pylori* colonization. As eradication by a one-size-fits-all approach becomes more and more difficult, it becomes even more important to look towards strategies that can provide insight into community attributes that can

help guide targeted therapies, predict likelihood of treatment outcomes, and possibly create strategies towards mitigating the impact of increased antibiotic usage. A greater, more individualized understanding of gut microbiome features among patients experiencing *H. pylori* colonization, especially in our underserved population, will pave the way for better community impact and reduce healthcare burdens of repeated treatment and mounting antibiotic resistance. As gut dysbiosis is inextricably tied not only to *H. pylori* infection but also to the use of antibiotics itself, the cycle of treatment and re-treatment may very well only further exacerbate vulnerability to enteric pathogens. Our results add to the growing evidence suggesting that *H. pylori* is associated with alterations in distal gut microbiota, particularly in those over 40 years of age. Strategies to better understand gut dysbiosis features among affected groups may create opportunities for improving eradication rates and reducing negative associated distal outcomes.

CONCLUSION

This exploratory study demonstrates *H. pylori*-associated changes to the fecal microbiome and fecal fatty acid metabolism. Such changes may have implications for improving eradication rates and minimizing associated negative distal outcomes.

ARTICLE HIGHLIGHTS

Research background

Helicobacter pylori (*H. pylori*), a bacterium that infects approximately half of the world's population, is associated with various gastrointestinal diseases, including peptic ulcers, non-ulcer dyspepsia, gastric adenocarcinoma, and gastric lymphoma. Following the global trend in emerging antibiotic resistance, rates of clarithromycin, metronidazole, and levofloxacin resistance among *H. pylori* strains have increased markedly, causing high rates of eradication failure.

Research motivation

As the burden of antibiotic resistance increases, the need for new adjunct therapies designed to facilitate *H. pylori* eradication and reduce negative distal outcomes associated with infection has become more pressing. Characterization of the interactions between *H. pylori*, the fecal microbiome, and fecal fatty acid metabolism, as well as the mechanisms underlying these interactions, may offer new therapeutic approaches.

Research objectives

The aim of this study is to characterize the fecal microbiome and metabolome in *H. pylori* patients in a socioeconomically challenged and underprivileged inner-city community.

Research methods

Stool samples from 19 *H. pylori* patients and 16 control subjects were analyzed. *16S rRNA* gene sequencing was performed on normalized pooled amplicons using the Illumina MiSeq System using a MiSeq reagent kit v2. Alpha and beta diversity analyses were performed in QIIME 2. Non-targeted fatty acid analysis of the samples was carried out using gas chromatography-mass spectrometry, which measures the total content of 30 fatty acids in stool after conversion into their corresponding fatty acid methyl esters. Multi-dimensional scaling (MDS) was performed on Bray-Curtis distance matrices created from both the metabolomics and microbiome datasets and a Procrustes test was performed on the metabolomics and microbiome MDS coordinates.

Research results

Fecal microbiome analysis showed that alpha diversity was lowest in *H. pylori* patients over 40 years of age compared to control subjects of similar age group. Beta diversity analysis of the samples revealed significant differences in microbial community structure between *H. pylori* patients and control subjects across all ages. Thirty-eight and six taxa were identified by Linear Discriminant Analysis (LDA) using LDA Effect Size to be enriched in *H. pylori* patients *vs* control individuals, respectively. Taxa that

were enriched in *H. pylori* patients included *Atopobium,* Gemellaceae, Micrococcaceae, Gemellales and *Rothia* (*R. mucilaginosa)*. Notably, relative abundance of the phylum Verrucomicrobia was decreased in *H. pylori* patients compared to control subjects. Procrustes analysis showed a significant relationship between the microbiome and metabolome datasets. Stool samples from *H. pylori* patients showed increases in several fatty acids including the polyunsaturated fatty acids (PUFAs) 22:4n6, 22:5n3, 20:3n6 and 22:2n6, while decreases were noted in other fatty acids including the PUFA 18:3n6. The pattern of changes in fatty acid concentration correlated to the Bacteroidetes:Firmicutes ratio determined by *16S rRNA* gene analysis.

Research conclusions

The study suggests *H. pylori*-associated changes to the fecal microbiome and fecal fatty acid metabolism. Such changes may have implications for improving eradication rates and minimizing associated negative distal outcomes.

Research perspectives

Future study with greater power should be directed to confirming the distal gut dysbiosis and changes to fecal fatty acid metabolism seen in our exploratory analysis of patients with *H. pylori* infection, as well as towards exploring the relationships between such phenomena and eradication success, colorectal cancer, and metabolic disease.

ACKNOWLEDGEMENTS

We thank Drs. Robert Cooper, Anjali Mone and Sanket Patel for their help in the collection of some of the samples for the study; these were also approved in the IRB protocol.

REFERENCES

1 **Lee YC**, Chiang TH, Chou CK, Tu YK, Liao WC, Wu MS, Graham DY. Association Between Helicobacter pylori Eradication and Gastric Cancer Incidence: A Systematic Review and Meta-analysis. *Gastroenterology* 2016; **150**: 1113-1124.e5 [PMID: 26836587 DOI: 10.1053/j.gastro.2016.01.028]

2 **Savoldi A**, Carrara E, Graham DY, Conti M, Tacconelli E. Prevalence of Antibiotic Resistance in Helicobacter pylori: A Systematic Review and Meta-analysis in World Health Organization Regions. *Gastroenterology* 2018; **155**: 1372-1382.e17 [PMID: 29990487 DOI: 10.1053/j.gastro.2018.07.007]

3 **Fallone CA**, Moss SF, Malfertheiner P. Reconciliation of Recent Helicobacter pylori Treatment Guidelines in a Time of Increasing Resistance to Antibiotics. *Gastroenterology* 2019; **157**: 44-53 [PMID: 30998990 DOI: 10.1053/j.gastro.2019.04.011]

4 **Sheh A**, Fox JG. The role of the gastrointestinal microbiome in Helicobacter pylori pathogenesis. *Gut Microbes* 2013; **4**: 505-531 [PMID: 23962822 DOI: 10.4161/gmic.26205]

5 **Caporaso JG**, Kuczynski J, Stombaugh J, Bittinger K, Bushman FD, Costello EK, Fierer N, Peña AG, Goodrich JK, Gordon JI, Huttley GA, Kelley ST, Knights D, Koenig JE, Ley RE, Lozupone CA, McDonald D, Muegge BD, Pirrung M, Reeder J, Sevinsky JR, Turnbaugh PJ, Walters WA, Widmann J, Yatsunenko T, Zaneveld J, Knight R. QIIME allows analysis of high-throughput community sequencing data. *Nat Methods* 2010; **7**: 335-336 [PMID: 20383131 DOI: 10.1038/nmeth.f.303]

6 **Eun CS**, Kim BK, Han DS, Kim SY, Kim KM, Choi BY, Song KS, Kim YS, Kim JF. Differences in gastric mucosal microbiota profiling in patients with chronic gastritis, intestinal metaplasia, and gastric cancer using pyrosequencing methods. *Helicobacter* 2014; **19**: 407-416 [PMID: 25052961 DOI: 10.1111/hel.12145]

7 **Aviles-Jimenez F**, Vazquez-Jimenez F, Medrano-Guzman R, Mantilla A, Torres J. Stomach microbiota composition varies between patients with non-atrophic gastritis and patients with intestinal type of gastric cancer. *Sci Rep* 2014; **4**: 4202 [PMID: 24569566 DOI: 10.1038/srep04202]

8 **Tang B**, Tang L, Huang C, Tian C, Chen L, He Z, Yang G, Zuo L, Zhao G, Liu E, Wang S, Lin H, He J, Yang S. The Effect of Probiotics Supplementation on Gut Microbiota After Helicobacter pylori Eradication: A Multicenter Randomized Controlled Trial. *Infect Dis Ther* 2021; **10**: 317-333 [PMID: 33270205 DOI: 10.1007/s40121-020-00372-9]

9 **Ojetti V**, Bruno G, Ainora ME, Gigante G, Rizzo G, Roccarina D, Gasbarrini A. Impact of Lactobacillus reuteri Supplementation on Anti-Helicobacter pylori Levofloxacin-Based Second-Line Therapy. *Gastroenterol Res Pract* 2012; **2012**: 740381 [PMID: 22690211 DOI: 10.1155/2012/740381]

10 **Du YQ**, Su T, Fan JG, Lu YX, Zheng P, Li XH, Guo CY, Xu P, Gong YF, Li ZS. Adjuvant probiotics improve the eradication effect of triple therapy for Helicobacter pylori infection. *World J Gastroenterol* 2012; **18**: 6302-6307 [PMID: 23180952 DOI: 10.3748/wjg.v18.i43.6302]

11 **Shi X**, Zhang J, Mo L, Shi J, Qin M, Huang X. Efficacy and safety of probiotics in eradicating Helicobacter pylori: A network meta-analysis. *Medicine (Baltimore)* 2019; **98**: e15180 [PMID: 30985706 DOI: 10.1097/MD.0000000000015180]

12 **Heimesaat MM**, Fischer A, Plickert R, Wiedemann T, Loddenkemper C, Göbel UB, Bereswill S, Rieder G. Helicobacter pylori induced gastric immunopathology is associated with distinct microbiota changes in the large intestines of long-term infected Mongolian gerbils. *PLoS One* 2014; **9**: e100362 [PMID: 24941045 DOI: 10.1371/journal.pone.0100362]

13 **Kienesberger S**, Cox LM, Livanos A, Zhang XS, Chung J, Perez-Perez GI, Gorkiewicz G, Zechner EL, Blaser MJ. Gastric Helicobacter pylori Infection Affects Local and Distant Microbial Populations and Host Responses. *Cell Rep* 2016; **14**: 1395-1407 [PMID: 26854236 DOI: 10.1016/j.celrep.2016.01.017]

14 **Frost F**, Kacprowski T, Rühlemann M, Bang C, Franke A, Zimmermann K, Nauck M, Völker U, Völzke H, Biffar R, Schulz C, Mayerle J, Weiss FU, Homuth G, Lerch MM. Helicobacter pylori infection associates with fecal microbiota composition and diversity. *Sci Rep* 2019; **9**: 20100 [PMID: 31882864 DOI: 10.1038/s41598-019-56631-4]

15 **Dash NR**, Khoder G, Nada AM, Al Bataineh MT. Exploring the impact of Helicobacter pylori on gut microbiome composition. *PLoS One* 2019; **14**: e0218274 [PMID: 31211818 DOI: 10.1371/journal.pone.0218274]

16 **Song M**, Chan AT, Sun J. Influence of the Gut Microbiome, Diet, and Environment on Risk of Colorectal Cancer. *Gastroenterology* 2020; **158**: 322-340 [PMID: 31586566 DOI: 10.1053/j.gastro.2019.06.048]

17 **Butt J**, Varga MG, Blot WJ, Teras L, Visvanathan K, Le Marchand L, Haiman C, Chen Y, Bao Y, Sesso HD, Wassertheil-Smoller S, Ho GYF, Tinker LE, Peek RM, Potter JD, Cover TL, Hendrix LH, Huang LC, Hyslop T, Um C, Grodstein F, Song M, Zeleniuch-Jacquotte A, Berndt S, Hildesheim A, Waterboer T, Pawlita M, Epplein M. Serologic Response to Helicobacter pylori Proteins Associated With Risk of Colorectal Cancer Among Diverse Populations in the United States. *Gastroenterology* 2019; **156**: 175-186.e2 [PMID: 30296434 DOI: 10.1053/j.gastro.2018.09.054]

18 **Qin J**, Li Y, Cai Z, Li S, Zhu J, Zhang F, Liang S, Zhang W, Guan Y, Shen D, Peng Y, Zhang D, Jie Z, Wu W, Qin Y, Xue W, Li J, Han L, Lu D, Wu P, Dai Y, Sun X, Li Z, Tang A, Zhong S, Li X, Chen W, Xu R, Wang M, Feng Q, Gong M, Yu J, Zhang Y, Zhang M, Hansen T, Sanchez G, Raes J, Falony G, Okuda S, Almeida M, LeChatelier E, Renault P, Pons N, Batto JM, Zhang Z, Chen H, Yang R, Zheng W, Yang H, Wang J, Ehrlich SD, Nielsen R, Pedersen O, Kristiansen K. A metagenome-wide association study of gut microbiota in type 2 diabetes. *Nature* 2012; **490**: 55-60 [PMID: 23023125 DOI: 10.1038/nature11450]

19 **Vrieze A**, Van Nood E, Holleman F, Salojärvi J, Kootte RS, Bartelsman JF, Dallinga-Thie GM, Ackermans MT, Serlie MJ, Oozeer R, Derrien M, Druesne A, Van Hylckama Vlieg JE, Bloks VW, Groen AK, Heilig HG, Zoetendal EG, Stroes ES, de Vos WM, Hoekstra JB, Nieuwdorp M. Transfer of intestinal microbiota from lean donors increases insulin sensitivity in individuals with metabolic syndrome. *Gastroenterology* 2012; **143**: 913-6.e7 [PMID: 22728514 DOI: 10.1053/j.gastro.2012.06.031]

20 **Jeon CY**, Haan MN, Cheng C, Clayton ER, Mayeda ER, Miller JW, Aiello AE. Helicobacter pylori infection is associated with an increased rate of diabetes. *Diabetes Care* 2012; **35**: 520-525 [PMID: 22279028 DOI: 10.2337/dc11-1043]

21 **Yang YJ**, Sheu BS. Metabolic Interaction of Helicobacter pylori Infection and Gut Microbiota. *Microorganisms* 2016; **4** [PMID: 27681909 DOI: 10.3390/microorganisms4010015]

22 **Thompson L**, Cockayne A, Spiller RC. Inhibitory effect of polyunsaturated fatty acids on the growth of Helicobacter pylori: a possible explanation of the effect of diet on peptic ulceration. *Gut* 1994; **35**: 1557-1561 [PMID: 7828972 DOI: 10.1136/gut.35.11.1557]

23 **Correia M**, Michel V, Osório H, El Ghachi M, Bonis M, Boneca IG, De Reuse H, Matos AA, Lenormand P, Seruca R, Figueiredo C, Machado JC, Touati E. Crosstalk between Helicobacter pylori and gastric epithelial cells is impaired by docosahexaenoic acid. *PLoS One* 2013; **8**: e60657 [PMID: 23577140 DOI: 10.1371/journal.pone.0060657]

24 **Bergsson G**, Steingrímsson O, Thormar H. Bactericidal effects of fatty acids and monoglycerides on Helicobacter pylori. *Int J Antimicrob Agents* 2002; **20**: 258-262 [PMID: 12385681 DOI: 10.1016/s0924-8579(02)00205-4]

25 **Correia M**, Michel V, Matos AA, Carvalho P, Oliveira MJ, Ferreira RM, Dillies MA, Huerre M, Seruca R, Figueiredo C, Machado JC, Touati E. Docosahexaenoic acid inhibits Helicobacter pylori growth in vitro and mice gastric mucosa colonization. *PLoS One* 2012; **7**: e35072 [PMID: 22529974 DOI: 10.1371/journal.pone.0035072]

26 **Matsui H**, Takahashi T, Murayama SY, Kawaguchi M, Matsuo K, Nakamura M. Protective efficacy of a hydroxy fatty acid against gastric Helicobacter infections. *Helicobacter* 2017; **22** [PMID: 28834011 DOI: 10.1111/hel.12430]

27 **Parada Venegas D**, De la Fuente MK, Landskron G, González MJ, Quera R, Dijkstra G, Harmsen HJM, Faber KN, Hermoso MA. Short Chain Fatty Acids (SCFAs)-Mediated Gut Epithelial and Immune Regulation and Its Relevance for Inflammatory Bowel Diseases. *Front Immunol* 2019; **10**: 277 [PMID: 30915065 DOI: 10.3389/fimmu.2019.00277]

28 **Corrêa-Oliveira R**, Fachi JL, Vieira A, Sato FT, Vinolo MA. Regulation of immune cell function by short-chain fatty acids. *Clin Transl Immunology* 2016; **5**: e73 [PMID: 27195116 DOI: 10.1038/cti.2016.17]

29 **Singh H**, Chung H, Awan I, Mone A, Cooper R, Patel S, Grigoryan Z, Ishida Y, Papachristou C, Judge T, DeSipio J, Phadtare S. Designing strategies for eradication of Helicobacter pylori based on prevalence patterns of infection and antibiotic resistance in a low-income, medically underserved community in the United States. *Helicobacter* 2021; **26**: e12769 [PMID: 33167084 DOI: 10.1111/hel.12769]

30 **Redondo JJ**, Keller PM, Zbinden R, Wagner K. A novel RT-PCR for the detection of Helicobacter pylori and identification of clarithromycin resistance mediated by mutations in the 23S rRNA gene. *Diagn Microbiol Infect Dis* 2018; **90**: 1-6 [PMID: 29111147 DOI: 10.1016/j.diagmicrobio.2017.09.014]

31 **Caporaso JG**, Lauber CL, Walters WA, Berg-Lyons D, Huntley J, Fierer N, Owens SM, Betley J, Fraser L, Bauer M, Gormley N, Gilbert JA, Smith G, Knight R. Ultra-high-throughput microbial community analysis on the Illumina HiSeq and MiSeq platforms. *ISME J* 2012; **6**: 1621-1624 [PMID: 22402401 DOI: 10.1038/ismej.2012.8]

32 **Bolyen E**, Rideout JR, Dillon MR, Bokulich NA, Abnet CC, Al-Ghalith GA, Alexander H, Alm EJ, Arumugam M, Asnicar F, Bai Y, Bisanz JE, Bittinger K, Brejnrod A, Brislawn CJ, Brown CT, Callahan BJ, Caraballo-Rodríguez AM, Chase J, Cope EK, Da Silva R, Diener C, Dorrestein PC, Douglas GM, Durall DM, Duvallet C, Edwardson CF, Ernst M, Estaki M, Fouquier J, Gauglitz JM, Gibbons SM, Gibson DL, Gonzalez A, Gorlick K, Guo J, Hillmann B, Holmes S, Holste H, Huttenhower C, Huttley GA, Janssen S, Jarmusch AK, Jiang L, Kaehler BD, Kang KB, Keefe CR, Keim P, Kelley ST, Knights D, Koester I, Kosciolek T, Kreps J, Langille MGI, Lee J, Ley R, Liu YX, Loftfield E, Lozupone C, Maher M, Marotz C, Martin BD, McDonald D, McIver LJ, Melnik AV, Metcalf JL, Morgan SC, Morton JT, Naimey AT, Navas-Molina JA, Nothias LF, Orchanian SB, Pearson T, Peoples SL, Petras D, Preuss ML, Pruesse E, Rasmussen LB, Rivers A, Robeson MS 2nd, Rosenthal P, Segata N, Shaffer M, Shiffer A, Sinha R, Song SJ, Spear JR, Swafford AD, Thompson LR, Torres PJ, Trinh P, Tripathi A, Turnbaugh PJ, Ul-Hasan S, van der Hooft JJJ, Vargas F, Vázquez-Baeza Y, Vogtmann E, von Hippel M, Walters W, Wan Y, Wang M, Warren J, Weber KC, Williamson CHD, Willis AD, Xu ZZ, Zaneveld JR, Zhang Y, Zhu Q, Knight R, Caporaso JG. Reproducible, interactive, scalable and extensible microbiome data science using QIIME 2. *Nat Biotechnol* 2019; **37**: 852-857 [PMID: 31341288 DOI: 10.1038/s41587-019-0209-9]

33 **McDonald D**, Clemente JC, Kuczynski J, Rideout JR, Stombaugh J, Wendel D, Wilke A, Huse S, Hufnagle J, Meyer F, Knight R, Caporaso JG. The Biological Observation Matrix (BIOM) format or: how I learned to stop worrying and love the ome-ome. *Gigascience* 2012; **1**: 7 [PMID: 23587224 DOI: 10.1186/2047-217X-1-7]

34 **Callahan BJ**, McMurdie PJ, Rosen MJ, Han AW, Johnson AJ, Holmes SP. DADA2: High-resolution sample inference from Illumina amplicon data. *Nat Methods* 2016; **13**: 581-583 [PMID: 27214047 DOI: 10.1038/nmeth.3869]

35 **Katoh K**, Standley DM. MAFFT multiple sequence alignment software version 7: improvements in performance and usability. *Mol Biol Evol* 2013; **30**: 772-780 [PMID: 23329690 DOI: 10.1093/molbev/mst010]

36 **Price MN**, Dehal PS, Arkin AP. FastTree 2--approximately maximum-likelihood trees for large alignments. *PLoS One* 2010; **5**: e9490 [PMID: 20224823 DOI: 10.1371/journal.pone.0009490]

37 **Weiss S**, Xu ZZ, Peddada S, Amir A, Bittinger K, Gonzalez A, Lozupone C, Zaneveld JR, Vázquez-Baeza Y, Birmingham A, Hyde ER, Knight R. Normalization and microbial differential abundance strategies depend upon data characteristics. *Microbiome* 2017; **5**: 27 [PMID: 28253908 DOI: 10.1186/s40168-017-0237-y]

38 **Lozupone C**, Knight R. UniFrac: a new phylogenetic method for comparing microbial communities. *Appl Environ Microbiol* 2005; **71**: 8228-8235 [PMID: 16332807 DOI: 10.1128/AEM.71.12.8228-8235.2005]

39 **Lozupone C**, Lladser ME, Knights D, Stombaugh J, Knight R. UniFrac: an effective distance metric for microbial community comparison. *ISME J* 2011; **5**: 169-172 [PMID: 20827291 DOI: 10.1038/ismej.2010.133]

40 **Vázquez-Baeza Y**, Pirrung M, Gonzalez A, Knight R. EMPeror: a tool for visualizing high-throughput microbial community data. *Gigascience* 2013; **2**: 16 [PMID: 24280061 DOI: 10.1186/2047-217X-2-16]

41 **Legendre P**, Legendre L. Numerical Ecology. 3rd ed. Elsevier, 2012 [DOI: 10.1016/s0304-3800(00)00291-x]

42 **Anderson MJ**. A new method for non-parametric multivariate analysis of variance. *Austral Ecology* 2001; **26**: 32-46 [DOI: 10.1046/j.1442-9993.2001.01070.x]

43 **Oksanen J**, Blanchet FG, Friendly M, Kindt R, Legendre P, McGlinn D, Minchin PR, O'Hara RB, Simpson GL, Solymos P, Stevens MHH, Szoecs E, Wagner H. vegan: Community Ecology Package, 2018. [cited 10 March 2021]. Available from: https://CRAN.R-project.org/package=vegan

44 **Segata N**, Izard J, Waldron L, Gevers D, Miropolsky L, Garrett WS, Huttenhower C. Metagenomic biomarker discovery and explanation. *Genome Biol* 2011; **12**: R60 [PMID: 21702898 DOI: 10.1186/gb-2011-12-6-r60]

45 **Peres-Neto PR**, Jackson DA. How well do multivariate data sets match? *Oecologia* 2001; **129**: 169-178 [PMID: 28547594 DOI: 10.1007/s004420100720]

46 **Casals-Pascual C**, González A, Vázquez-Baeza Y, Song SJ, Jiang L, Knight R. Microbial Diversity in Clinical Microbiome Studies: Sample Size and Statistical Power Considerations. *Gastroenterology* 2020; **158**: 1524-1528 [PMID: 31930986 DOI: 10.1053/j.gastro.2019.11.305]

47 **Data USA: Camden City, New Jersey**. QuickFacts: United States Census Bureau, 2019. [cited 10 March 2021]. Available from: https://gistbok.ucgis.org/bok-topics/united-states-census-data

48 **Noto JM**, Peek RM Jr. The gastric microbiome, its interaction with Helicobacter pylori, and its potential role in the progression to stomach cancer. *PLoS Pathog* 2017; **13**: e1006573 [PMID: 28982167 DOI: 10.1371/journal.ppat.1006573]

49 **Zhao Y**, Gao X, Guo J, Yu D, Xiao Y, Wang H, Li Y. Helicobacter pylori infection alters gastric and tongue coating microbial communities. *Helicobacter* 2019; **24**: e12567 [PMID: 30734438 DOI: 10.1111/hel.12567]

50 **Das A**, Pereira V, Saxena S, Ghosh TS, Anbumani D, Bag S, Das B, Nair GB, Abraham P, Mande SS. Gastric microbiome of Indian patients with Helicobacter pylori infection, and their interaction networks. *Sci Rep* 2017; **7**: 15438 [PMID: 29133866 DOI: 10.1038/s41598-017-15510-6]

51 **Guo Y**, Zhang Y, Gerhard M, Gao JJ, Mejias-Luque R, Zhang L, Vieth M, Ma JL, Bajbouj M, Suchanek S, Liu WD, Ulm K, Quante M, Li ZX, Zhou T, Schmid R, Classen M, Li WQ, You WC, Pan KF. Effect of *Helicobacter pylori* on gastrointestinal microbiota: a population-based study in Linqu, a high-risk area of gastric cancer. *Gut* 2020; **69**: 1598-1607 [PMID: 31857433 DOI: 10.1136/gutjnl-2019-319696]

52 **Pounder RE**, Ng D. The prevalence of Helicobacter pylori infection in different countries. *Aliment Pharmacol Ther* 1995; **9** Suppl 2: 33-39 [PMID: 8547526]

53 **Ji Z**, Han F, Meng F, Tu M, Yang N, Zhang J. The Association of Age and Antibiotic Resistance of Helicobacter Pylori: A Study in Jiaxing City, Zhejiang Province, China. *Medicine (Baltimore)* 2016; **95**: e2831 [PMID: 26937912 DOI: 10.1097/MD.0000000000002831]

54 **Zullo A**, Perna F, Hassan C, Ricci C, Saracino I, Morini S, Vaira D. Primary antibiotic resistance in Helicobacter pylori strains isolated in northern and central Italy. *Aliment Pharmacol Ther* 2007; **25**: 1429-1434 [PMID: 17539982 DOI: 10.1111/j.1365-2036.2007.03331.x]

55 **Jones NL**, Sherman PM. Helicobacter pylori infection in children. *Curr Opin Pediatr* 1998; **10**: 19-23 [PMID: 9529633 DOI: 10.1097/00008480-199802000-00005]

56 **Yachida S**, Mizutani S, Shiroma H, Shiba S, Nakajima T, Sakamoto T, Watanabe H, Masuda K, Nishimoto Y, Kubo M, Hosoda F, Rokutan H, Matsumoto M, Takamaru H, Yamada M, Matsuda T, Iwasaki M, Yamaji T, Yachida T, Soga T, Kurokawa K, Toyoda A, Ogura Y, Hayashi T, Hatakeyama M, Nakagama H, Saito Y, Fukuda S, Shibata T, Yamada T. Metagenomic and metabolomic analyses reveal distinct stage-specific phenotypes of the gut microbiota in colorectal cancer. *Nat Med* 2019; **25**: 968-976 [PMID: 31171880 DOI: 10.1038/s41591-019-0458-7]

57 **Yang F**, Xu YL, Zhu RF. Helicobacter pylori infection and the risk of colorectal carcinoma: a systematic review and meta-analysis. *Minerva Med* 2019; **110**: 464-470 [PMID: 31368293 DOI: 10.23736/S0026-4806.19.05942-1]

58 **Bajer L**, Kverka M, Kostovcik M, Macinga P, Dvorak J, Stehlikova Z, Brezina J, Wohl P, Spicak J, Drastich P. Distinct gut microbiota profiles in patients with primary sclerosing cholangitis and ulcerative colitis. *World J Gastroenterol* 2017; **23**: 4548-4558 [PMID: 28740343 DOI: 10.3748/wjg.v23.i25.4548]

59 **Ramanan P**, Barreto JN, Osmon DR, Tosh PK. Rothia bacteremia: a 10-year experience at Mayo Clinic, Rochester, Minnesota. *J Clin Microbiol* 2014; **52**: 3184-3189 [PMID: 24951810 DOI: 10.1128/JCM.01270-14]

60 **Gao JJ**, Zhang Y, Gerhard M, Mejias-Luque R, Zhang L, Vieth M, Ma JL, Bajbouj M, Suchanek S, Liu WD, Ulm K, Quante M, Li ZX, Zhou T, Schmid R, Classen M, Li WQ, You WC, Pan KF. Association Between Gut Microbiota and *Helicobacter pylori*-Related Gastric Lesions in a High-Risk Population of Gastric Cancer. *Front Cell Infect Microbiol* 2018; **8**: 202 [PMID: 29971220 DOI: 10.3389/fcimb.2018.00202]

61 **Gevers D**, Kugathasan S, Denson LA, Vázquez-Baeza Y, Van Treuren W, Ren B, Schwager E, Knights D, Song SJ, Yassour M, Morgan XC, Kostic AD, Luo C, González A, McDonald D, Haberman Y, Walters T, Baker S, Rosh J, Stephens M, Heyman M, Markowitz J, Baldassano R, Griffiths A, Sylvester F, Mack D, Kim S, Crandall W, Hyams J, Huttenhower C, Knight R, Xavier RJ. The treatment-naive microbiome in new-onset Crohn's disease. *Cell Host Microbe* 2014; **15**: 382-392 [PMID: 24629344 DOI: 10.1016/j.chom.2014.02.005]

62 **Haberman Y**, Tickle TL, Dexheimer PJ, Kim MO, Tang D, Karns R, Baldassano RN, Noe JD, Rosh J, Markowitz J, Heyman MB, Griffiths AM, Crandall WV, Mack DR, Baker SS, Huttenhower C, Keljo DJ, Hyams JS, Kugathasan S, Walters TD, Aronow B, Xavier RJ, Gevers D, Denson LA. Pediatric Crohn disease patients exhibit specific ileal transcriptome and microbiome signature. *J Clin Invest* 2014; **124**: 3617-3633 [PMID: 25003194 DOI: 10.1172/JCI75436]

63 **Derrien M**, Vaughan EE, Plugge CM, de Vos WM. Akkermansia muciniphila gen. nov., sp. nov., a human intestinal mucin-degrading bacterium. *Int J Syst Evol Microbiol* 2004; **54**: 1469-1476 [PMID: 15388697 DOI: 10.1099/ijs.0.02873-0]

64 **Ottman N**, Davids M, Suarez-Diez M, Boeren S, Schaap PJ, Martins Dos Santos VAP, Smidt H, Belzer C, de Vos WM. Genome-Scale Model and Omics Analysis of Metabolic Capacities of *Akkermansia muciniphila* Reveal a Preferential Mucin-Degrading Lifestyle. *Appl Environ Microbiol* 2017; **83** [PMID: 28687644 DOI: 10.1128/AEM.01014-17]

65 **Hemmings SMJ**, Malan-Müller S, van den Heuvel LL, Demmitt BA, Stanislawski MA, Smith DG, Bohr AD, Stamper CE, Hyde ER, Morton JT, Marotz CA, Siebler PH, Braspenning M, Van Criekinge W, Hoisington AJ, Brenner LA, Postolache TT, McQueen MB, Krauter KS, Knight R, Seedat S, Lowry CA. The Microbiome in Posttraumatic Stress Disorder and Trauma-Exposed Controls: An

Exploratory Study. *Psychosom Med* 2017; **79**: 936-946 [PMID: 28700459 DOI: 10.1097/PSY.0000000000000512]

66 **Belzer C**, Gerber GK, Roeselers G, Delaney M, DuBois A, Liu Q, Belavusava V, Yeliseyev V, Houseman A, Onderdonk A, Cavanaugh C, Bry L. Dynamics of the microbiota in response to host infection. *PLoS One* 2014; **9**: e95534 [PMID: 25014551 DOI: 10.1371/journal.pone.0095534]

67 **Sokol H**, Pigneur B, Watterlot L, Lakhdari O, Bermúdez-Humarán LG, Gratadoux JJ, Blugeon S, Bridonneau C, Furet JP, Corthier G, Grangette C, Vasquez N, Pochart P, Trugnan G, Thomas G, Blottière HM, Doré J, Marteau P, Seksik P, Langella P. Faecalibacterium prausnitzii is an anti-inflammatory commensal bacterium identified by gut microbiota analysis of Crohn disease patients. *Proc Natl Acad Sci USA* 2008; **105**: 16731-16736 [PMID: 18936492 DOI: 10.1073/pnas.0804812105]

68 **Newton RJ**, McLellan SL, Dila DK, Vineis JH, Morrison HG, Eren AM, Sogin ML. Sewage reflects the microbiomes of human populations. *mBio* 2015; **6**: e02574 [PMID: 25714718 DOI: 10.1128/mBio.02574-14]

69 **Jiang H**, Ling Z, Zhang Y, Mao H, Ma Z, Yin Y, Wang W, Tang W, Tan Z, Shi J, Li L, Ruan B. Altered fecal microbiota composition in patients with major depressive disorder. *Brain Behav Immun* 2015; **48**: 186-194 [PMID: 25882912 DOI: 10.1016/j.bbi.2015.03.016]

70 **Martín R**, Miquel S, Benevides L, Bridonneau C, Robert V, Hudault S, Chain F, Berteau O, Azevedo V, Chatel JM, Sokol H, Bermúdez-Humarán LG, Thomas M, Langella P. Functional Characterization of Novel *Faecalibacterium prausnitzii* Strains Isolated from Healthy Volunteers: A Step Forward in the Use of *F. prausnitzii* as a Next-Generation Probiotic. *Front Microbiol* 2017; **8**: 1226 [PMID: 28713353 DOI: 10.3389/fmicb.2017.01226]

71 **Ji J**, Yang H. Using Probiotics as Supplementation for *Helicobacter pylori* Antibiotic Therapy. *Int J Mol Sci* 2020; **21** [PMID: 32046317 DOI: 10.3390/ijms21031136]

72 **Le Chatelier E**, Nielsen T, Qin J, Prifti E, Hildebrand F, Falony G, Almeida M, Arumugam M, Batto JM, Kennedy S, Leonard P, Li J, Burgdorf K, Grarup N, Jørgensen T, Brandslund I, Nielsen HB, Juncker AS, Bertalan M, Levenez F, Pons N, Rasmussen S, Sunagawa S, Tap J, Tims S, Zoetendal EG, Brunak S, Clément K, Doré J, Kleerebezem M, Kristiansen K, Renault P, Sicheritz-Ponten T, de Vos WM, Zucker JD, Raes J, Hansen T; MetaHIT consortium, Bork P, Wang J, Ehrlich SD, Pedersen O. Richness of human gut microbiome correlates with metabolic markers. *Nature* 2013; **500**: 541-546 [PMID: 23985870 DOI: 10.1038/nature12506]

73 **Lofgren JL**, Whary MT, Ge Z, Muthupalani S, Taylor NS, Mobley M, Potter A, Varro A, Eibach D, Suerbaum S, Wang TC, Fox JG. Lack of commensal flora in Helicobacter pylori-infected INS-GAS mice reduces gastritis and delays intraepithelial neoplasia. *Gastroenterology* 2011; **140**: 210-220 [PMID: 20950613 DOI: 10.1053/j.gastro.2010.09.048]

74 **Lertpiriyapong K**, Whary MT, Muthupalani S, Lofgren JL, Gamazon ER, Feng Y, Ge Z, Wang TC, Fox JG. Gastric colonisation with a restricted commensal microbiota replicates the promotion of neoplastic lesions by diverse intestinal microbiota in the Helicobacter pylori INS-GAS mouse model of gastric carcinogenesis. *Gut* 2014; **63**: 54-63 [PMID: 23812323 DOI: 10.1136/gutjnl-2013-305178]

75 **Vinasco K**, Mitchell HM, Kaakoush NO, Castaño-Rodríguez N. Microbial carcinogenesis: Lactic acid bacteria in gastric cancer. *Biochim Biophys Acta Rev Cancer* 2019; **1872**: 188309 [PMID: 31394110 DOI: 10.1016/j.bbcan.2019.07.004]

76 **Hsu PI**, Pan CY, Kao JY, Tsay FW, Peng NJ, Kao SS, Wang HM, Tsai TJ, Wu DC, Chen CL, Tsai KW; Taiwan Acid-related Disease (TARD) Study Group. Helicobacter pylori eradication with bismuth quadruple therapy leads to dysbiosis of gut microbiota with an increased relative abundance of Proteobacteria and decreased relative abundances of Bacteroidetes and Actinobacteria. *Helicobacter* 2018; **23**: e12498 [PMID: 29897654 DOI: 10.1111/hel.12498]

77 **Machate DJ**, Figueiredo PS, Marcelino G, Guimarães RCA, Hiane PA, Bogo D, Pinheiro VAZ, Oliveira LCS, Pott A. Fatty Acid Diets: Regulation of Gut Microbiota Composition and Obesity and Its Related Metabolic Dysbiosis. *Int J Mol Sci* 2020; **21** [PMID: 32521778 DOI: 10.3390/ijms21114093]

78 **Ktsoyan ZA**, Beloborodova NV, Sedrakyan AM, Osipov GA, Khachatryan ZA, Kelly D, Manukyan GP, Arakelova KA, Hovhannisyan AI, Olenin AY, Arakelyan AA, Ghazaryan KA, Aminov RI. Profiles of Microbial Fatty Acids in the Human Metabolome are Disease-Specific. *Front Microbiol* 2010; **1**: 148 [PMID: 21687748 DOI: 10.3389/fmicb.2010.00148]

79 **Fu Y**, Wang Y, Gao H, Li D, Jiang R, Ge L, Tong C, Xu K. Associations among Dietary Omega-3 Polyunsaturated Fatty Acids, the Gut Microbiota, and Intestinal Immunity. *Mediators Inflamm* 2021; **2021**: 8879227 [PMID: 33488295 DOI: 10.1155/2021/8879227]

80 **Kaliannan K**, Wang B, Li XY, Kim KJ, Kang JX. A host-microbiome interaction mediates the opposing effects of omega-6 and omega-3 fatty acids on metabolic endotoxemia. *Sci Rep* 2015; **5**: 11276 [PMID: 26062993 DOI: 10.1038/srep11276]

81 **Simopoulos AP**. The importance of the ratio of omega-6/omega-3 essential fatty acids. *Biomed Pharmacother* 2002; **56**: 365-379 [PMID: 12442909 DOI: 10.1016/s0753-3322(02)00253-6]

82 **Zárate R**, El Jaber-Vazdekis N, Tejera N, Pérez JA, Rodríguez C. Significance of long chain polyunsaturated fatty acids in human health. *Clin Transl Med* 2017; **6**: 25 [PMID: 28752333 DOI: 10.1186/s40169-017-0153-6]

83 **Thamphiwatana S**, Gao W, Obonyo M, Zhang L. In vivo treatment of Helicobacter pylori infection with liposomal linolenic acid reduces colonization and ameliorates inflammation. *Proc Natl Acad Sci USA* 2014; **111**: 17600-17605 [PMID: 25422427 DOI: 10.1073/pnas.1418230111]

World Journal of Gastroenterology

Submit a Manuscript: https://www.f6publishing.com

World J Gastroenterol 2021 September 7; 27(33): 5595-5609

DOI: 10.3748/wjg.v27.i33.5595

ISSN 1007-9327 (print) ISSN 2219-2840 (online)

ORIGINAL ARTICLE

Retrospective Study

Gastric cancer mortality related to direct radiographic and endoscopic screening: A retrospective study

Hiroaki Hagiwara, Fumitaka Moki, Yukiko Yamashita, Kazuki Saji, Keigo Iesaki, Hiromitsu Suda

ORCID number: Hiroaki Hagiwara 0000-0001-7081-3574; Fumitaka Moki 0000-0002-7280-6666; Yukiko Yamashita 0000-0001-9719-6107; Kazuki Saji 0000-0002-7815-9084; Keigo Iesaki 0000-0003-3567-2838; Hiromitsu Suda 0000-0003-2991-8125.

Author contributions: Hagiwara H designed the study, collected data, and wrote the paper; Moki F performed the follow-up survey and conducted the statistical analysis; Yamashita Y, Saji K, Iesaki K, and Suda H provided clinical advice.

Institutional review board statement: This study was reviewed and approved by the Gunma Prefecture Health and Welfare Department and Maebashi Medical Association.

Informed consent statement: Written informed consent to use screening results for research purposes was obtained from all participants of gastric cancer screening in Maebashi City, Japan.

Conflict-of-interest statement: The authors declare that they have no conflict of interest.

Data sharing statement: No additional data are available.

Open-Access: This article is an

Hiroaki Hagiwara, Department of Internal Medicine, Hagiwara Clinic, Maebashi 379-2106, Gunma, Japan

Hiroaki Hagiwara, Fumitaka Moki, Yukiko Yamashita, Kazuki Saji, Keigo Iesaki, Hiromitsu Suda, Maebashi Medical Association, Maebashi 371-0035, Gunma, Japan

Fumitaka Moki, Gunma Health Foundation, Maebashi 371-0005, Gunma, Japan

Yukiko Yamashita, Department of Internal Medicine and Surgery, Yamashita Clinic, Maebashi 371-0016, Gunma, Japan

Kazuki Saji, Department of Internal Medicine, Saji Clinic, Maebashi 371-0133, Gunma, Japan

Keigo Iesaki, Department of Internal Medicine, Iesaki Clinic, Maebashi 371-0805, Gunma, Japan

Hiromitsu Suda, Department of Pediatrics, Suda Kids Clinic, Maebashi 371-0813, Gunma, Japan

Corresponding author: Hiroaki Hagiwara, MD, Director, Department of Internal Medicine, Hagiwara Clinic, 1585-2 Arakomachi, Maebashi 379-2106, Gunma, Japan. hagiwaras@dab.hi-ho.ne.jp

Abstract

BACKGROUND

Despite its decreased incidence in Japan, gastric cancer continues among the leading causes of cancer-related deaths in both men and women. Accordingly, efforts are still required to lower the mortality rate of gastric cancer in Japan. Maebashi City introduced endoscopic gastric cancer screening in 2004, and participants are able to choose between direct radiography and endoscopy. Hence, we expected to see a decrease in mortality rate from gastric cancer after introducing endoscopic screening and a difference in mortality rate reduction between screening methods.

AIM

To evaluate the impact on gastric cancer mortality rate of two types of gastric cancer screening in Maebashi City, Japan.

METHODS

open-access article that was selected by an in-house editor and fully peer-reviewed by external reviewers. It is distributed in accordance with the Creative Commons Attribution NonCommercial (CC BY-NC 4.0) license, which permits others to distribute, remix, adapt, build upon this work non-commercially, and license their derivative works on different terms, provided the original work is properly cited and the use is non-commercial. See: http://creativecommons.org/Licenses/by-nc/4.0/

Manuscript source: Unsolicited manuscript

Specialty type: Gastroenterology and hepatology

Country/Territory of origin: Japan

Peer-review report's scientific quality classification

Grade A (Excellent): 0
Grade B (Very good): B
Grade C (Good): C, C
Grade D (Fair): D
Grade E (Poor): 0

Received: April 6, 2021
Peer-review started: April 6, 2021
First decision: June 24, 2021
Revised: July 9, 2021
Accepted: August 12, 2021
Article in press: August 12, 2021
Published online: September 7, 2021

P-Reviewer: Li BF, Li K, Sun QL, Yang Y
S-Editor: Fan JR
L-Editor: A
P-Editor: Yuan YY

Participants aged 40 to 79 years of the Maebashi City gastric cancer screening program in 2006 who were screened by direct radiography (n = 11155) or endoscopy (n = 10747) were included. Participants were followed until March 31, 2012, by cross-referencing their data against the Gunma Prefecture cancer registry data. We compared the detection rate of gastric cancers. Then, we compared the mortality rate between the two groups. The Cox proportional hazards model was used to estimate the hazard ratio (HR) of gastric cancer death. Finally, the reduction in gastric cancer mortality rate associated with each screening method was evaluated.

RESULTS

Gastric cancer was detected in 22 participants undergoing direct radiography (detection rate, 0.20%) and in 52 participants undergoing endoscopy (detection rate, 0.48%). However, most gastric cancers detected by endoscopic screening were early cancers that may not have resulted in death. We found no significant difference in gastric cancer mortality rate between participants receiving annual screening and those who do not. When the number of gastric cancer deaths in the direct radiography group was set as 1 in the Cox proportional hazard analysis, the HR of gastric cancer death was 1.368 (95%CI: 0.7308–2.562) in the overall group of participants. The results showed no significant difference between the two screening methods in any of the analysis groups.

CONCLUSION

Although endoscopic screening detected more gastric cancer than direct radiographic screening, no significant difference in the reduction of gastric cancer mortality rate between the two screening methods was found.

Key Words: Gastric cancer; Radiography; Endoscopy; Population-based cancer screening; Mortality reduction

©The Author(s) 2021. Published by Baishideng Publishing Group Inc. All rights reserved.

Core Tip: Although the incidence rate has declined in Japan, gastric cancer is still the leading cause of cancer-related deaths in men and women. Therefore, Japan still needs to work hard to reduce the death rate of gastric cancer. Maebashi City introduced endoscopic gastric cancer screening in 2004. Endoscopic screening detects more gastric cancer than direct radiographic screening does, but both screening methods have similar effects on reducing the mortality rate from gastric cancer.

Citation: Hagiwara H, Moki F, Yamashita Y, Saji K, Iesaki K, Suda H. Gastric cancer mortality related to direct radiographic and endoscopic screening: A retrospective study. *World J Gastroenterol* 2021; 27(33): 5595-5609
URL: https://www.wjgnet.com/1007-9327/full/v27/i33/5595.htm
DOI: https://dx.doi.org/10.3748/wjg.v27.i33.5595

INTRODUCTION

In 2017, 24.5 million patients globally had a cancer diagnosis, and 9.6 million patients died of cancer. Of these deaths, 861000 were due to gastric cancer (men, n = 542000; women, n = 319000). Furthermore, gastric cancer was the third-highest cause of death among men dying from cancer and the fourth-highest in women dying from cancer[1].

In Japan, the prevalence of *Helicobacter pylori* (*Hp*) infection—a known cause of gastric cancer—has decreased, and the incidence of gastric cancer and the age-adjusted mortality rate from gastric cancer have also been decreasing. Nonetheless, in 2018 gastric cancer was the second-highest cause of death among Japanese men dying from any cancer and the fourth-highest among Japanese women dying from any cancer[2]. Accordingly, further efforts are still required to lower the mortality rate of gastric cancer in Japan.

In Japan, for many years, gastric cancer mass screening programs conducted by municipal governments were performed by using indirect radiography to examine large numbers of people, and direct radiography was used to examine individual patients at medical institutions. However, in 2015 the Gastric Cancer Screening Guidelines were revised to recommend endoscopy for organized gastric cancer screening[3]. Accordingly, many municipal governments subsequently started using endoscopy rather than indirect radiography for gastric cancer screening.

In Maebashi City, endoscopic gastric cancer screening was introduced in 2004, and subsequently, participants were able to choose between direct radiography and endoscopy[4]. Therefore, we examined clinical data from participants in the Maebashi City gastric cancer screening program in 2006 to assess whether the mortality rate from gastric cancer decreased after the introduction of endoscopic screening.

MATERIALS AND METHODS

Study design and participants

Citizens aged 40 years and older are eligible to participate in the Maebashi City gastric cancer screening as part of their personal health check, and participants can choose between direct radiography and endoscopy every year. Gastric cancer screening is conducted at practitioner clinics or at hospitals in Maebashi City that have elected to participate in the screening program, and institutions do not have to fulfill any eligibility criteria to participate. In 2006, 23963 citizens participated in gastric cancer screening, accounting for 20.5% of the overall eligible population. A total of 12014 participants underwent direct radiographic screening and 11949 endoscopic screening.

The present study included participants aged 40 to 79 years; 79 years was chosen as the upper age limit because, in Japan, the average lifespan is 79.00 years in men and 85.81 years in women[5]. A total of 21802 participants were included, comprising 11155 individuals who underwent direct radiography and 10747 who underwent endoscopy.

First, we investigated the number of gastric cancers detected and the cancer stage at detection. Next, we compared the detection rate between the two participant groups undergoing direct radiography or endoscopy. Then, we compared the mortality rate between the two groups. The clinical data of the present study cohort, including the name, sex, date of birth, and history of participation in gastric cancer screening, were extracted from the Maebashi Medical Association cancer screening database. The participants were followed up until March 31, 2012, using the Gunma Prefectural Cancer Registry data. The 2006 Maebashi City gastric cancer screening was conducted from May 2006 until the end of February 2007, and participants could choose to be screened by either of the two imaging methods. The follow-up period ranged from 5 years, 1 mo, to 5 years, 11 mo.

The two screening methods are offered by at least 80 institutions each year. Direct radiographic examination is performed by the standard imaging method (8-image method). For endoscopic gastric cancer screening, 30 to 40 images are taken that cover the esophagus and duodenum. Screening physicians are required to submit the images to the Maebashi Medical Association, where they are reviewed by two other physicians commissioned by the Maebashi Medical Association; these physicians check the quality and look for missed lesions (secondary review). Generally, endoscopic images are reviewed by physicians who are board-certified by the Japan Gastroenterological Endoscopy Society.

All procedures followed were in accordance with the ethical standards of the responsible committee on human experimentation (institutional and national) and with the Helsinki Declaration of 1964 and later versions.

Outcomes

The primary outcome was death from gastric cancer. We compared the incidence rate of the primary outcome between the two screening methods in the whole group of participants and between those participants who had also participated in the gastric cancer screening in the previous year and those who had not.

The secondary outcome was the incidence rate of death from any cancer except gastric cancer, and the same comparisons were performed for the secondary outcome as for the primary outcome.

To obtain additional information on causes of death, we compared the data in the Gunma Prefectural Cancer Registry with the death certificates.

The accuracy of the 2006 Gunma Prefectural Cancer Registry was low with 40.5% of incidence cancer rate registered as death certified only; however, the data of death was perfectly obtained.

Statistical analysis

We compared the participants' background factors between the two groups using Fisher's exact test and Student's *t*-test. The Cox proportional hazards model was used to estimate the hazard ratio (HR) of gastric cancer death, and death from any cancer other than gastric cancer, in the overall group of participants and the subsets of participants who had or had not participated in gastric cancer screening in the previous year. HRs were adjusted for sex and age group. Finally, the average covariate method was used to estimate and plot the survival curve adjusted for sex and age groups[6,7]. All test statistics were 2-tailed, and a *P* value less than 0.05 was considered to indicate a statistically significant difference. Analyses were performed with EZR (easy-R)[8]. The use of Gunma Cancer Registry data was approved by Gunma Prefecture. The statistical review of the study was performed by Moki F from Gunma Health Foundation.

RESULTS

Participants and gastric cancer detection rates

The percentages of male participants and participants aged 60 years or older were slightly higher in the endoscopic screening group (Table 1). Similar results were found in the subsets of participants who had also participated in the screening in the previous year (Table 2) and those who had not (Table 3).

Among all screening program participants, gastric cancer was detected in 25 participants undergoing direct radiography (detection rate, 0.21%) and in 72 participants undergoing endoscopy (detection rate, 0.60%). Thus, the gastric cancer detection rate with endoscopy was triple that of direct radiography. In the participants aged from 40 to 79 years, gastric cancer was detected in 22 individuals undergoing direct radiography (detection rate, 0.20%) and in 52 individuals undergoing endoscopy (detection rate, 0.48%). Thus, endoscopic screening detected gastric cancer in participants aged 80 years or over more frequently than direct radiographic screening.

In the participants aged from 40 to 79 years, the categories of gastric cancer lesions detected by direct radiographic screening and respective numbers and percentages of participants were as follows: Stage IA, n = 6 (27.2%); stage IB, n = 2 (9.1%); stage II, n = 3 (13.6%); stage IIIA, n = 1 (4.5%); stage IIIB, n = 4 (18.2%); stage IV, n = 5 (22.7%); and unspecified stage, n = 1 (4.5%). The respective data for gastric cancer detected by endoscopic screening were as follows: Stage IA, n = 30 (57.7%); stage IB, n = 3 individuals (5.8%); stage II, n = 6 (11.5%); stage IIIA, n = 1 (1.9%); stage IIIB, n = 2 (3.8%); stage IV, n = 7 (13.5%); and unspecified stage, n = 3 (5.8%)[9]. The stage IA gastric cancer lesions detected by endoscopic screening were treated by endoscopic submucosal dissection (ESD) in 21 of the 30 individuals, and all 6 of the stage IA lesions detected by direct radiographic screening were treated by gastrectomy.

Gastric cancer mortality rates

Gastric cancer deaths were detected in 17 of the 11 155 individuals who underwent direct radiography and in 23 of the 10 747 individuals who underwent endoscopy. The five-year survival by the Kaplan-Meier method was 0.998 (95%CI: 0.998–0.999) in individuals who underwent direct radiography and 0.998 (95%CI: 0.997–0.999) in individuals who underwent endoscopy. Overall, no significant difference was observed between the two screening methods (P = 0.285) (Figure 1). Among participants who had not participated in screening in the previous year, gastric cancer deaths were detected in 10 of 4 382 individuals who underwent direct radiography and in 16 of 6 915 individuals who underwent endoscopy. The five-year survival rate was 0.998 (95%CI: 0.996–0.999) in individuals who underwent direct radiography and 0.998 (95%CI: 0.996–0.999) in individuals who underwent endoscopy. No significant difference was observed between the two screening methods (P = 0.971) (Figure 2). Among participants who had also undergone screening in the previous year, gastric cancer deaths were detected in 7 of 6 773 individuals who underwent direct radiography and 7 of 3832 individuals who underwent endoscopy. The five-year survival rate was 0.999 (95%CI: 0.998–1.000) in individuals who underwent direct radiography and 0.998 (95%CI: 0.996–0.999) in individuals who underwent endoscopy. Again, no significant difference was observed between the two methods (P = 0.280) (Figure 3).

Table 1 Characteristics of individuals aged 40 to 79 years who participated in gastric cancer screening in Maebashi City, Japan, in 2006

		Screening method		
		Endoscopy	Radiography	*P* value
Participants, *n*		10747	11155	
Sex, *n* (%)	Male	4323 (40.2)	4103 (36.8)	< 0.001
	Female	6424 (59.8)	7052 (63.2)	
Age group, *n* (%)	40–49 yr	952 (8.9)	1005 (9.0)	NA
	50–59 yr	2043 (19.0)	2264 (20.3)	
	60–69 yr	3667 (34.1)	3986 (35.7)	
	70–79 yr	4085 (38.0)	3900 (35.0)	
Age group, *n* (%)	40–59 yr	2995 (27.9)	3269 (29.3)	0.019
	60–79 yr	7752 (72.1)	7886 (70.7)	
Age, mean (SD), yr		64.75 (9.69)	64.30 (9.57)	< 0.001

NA: No significant.

Table 2 Characteristics of individuals aged 40 to 79 years who participated in gastric cancer screening in Maebashi City, Japan, in 2006 and did not subsequently receive annual screening

		Screening method		
		Endoscopy	Radiography	*P* value
Participants, *n*		6915	4382	
Sex, *n* (%)	Male	2680 (38.8)	1570 (35.8)	0.002
	Female	4235 (61.2)	2812 (64.2)	
Age group, *n* (%)	40–49 yr	764 (11.0)	552 (12.6)	NA
	50–59 yr	1483 (21.4)	1032 (23.6)	
	60–69 yr	2372 (34.3)	1528 (34.9)	
	70–79 yr	2296 (33.2)	1270 (29.0)	
Age group, *n* (%)	40–59 yr	2247 (32.5)	1584 (36.1)	< 0.001
	60–79 yr	4668 (67.5)	2798 (63.9)	
Age, mean (SD), yr		63.54 (9.99)	62.51 (10.08)	< 0.001

NA: No significant.

A Cox hazard analysis was conducted. Because the proportional hazard was not maintained for participants who had not participated in the previous year, the HR was estimated for participants who had also participated in the screening in the previous year and those who did not. When the number of gastric cancer deaths in the direct radiography group was set as 1 in the Cox proportional hazard analysis, the adjusted HR of gastric cancer death was 1.368 (95%CI: 0.7308–2.562) in the overall group of participants and 1.600 (95%CI: 0.5604–4.569) in the subset of participants who had also participated in gastric cancer screening in the previous year. These results showed no significant difference between the two screening methods in any of the analysis groups (Table 4).

Mortality rates for any cancer

Deaths from any cancer other than gastric cancer occurred in 163 of 11 155 individuals who underwent direct radiography and 178 of 10 747 individuals who underwent endoscopy. The five-year survival rate was 0.987 (95%CI: 0.985–0.989) in individuals who underwent direct radiography and 0.986 (95%CI: 0.984–0.988) in individuals who

Table 3 Characteristics of individuals aged 40 to 79 years who participated in gastric cancer screening in Maebashi City, Japan, in 2006 and subsequently received annual screening

		Screening method		
		Endoscopy	Radiography	*P* value
Participants, *n*		3832	6773	
Sex, *n* (%)	Male	1643 (42.9)	2533 (37.4)	< 0.001
	Female	2189 (57.1)	4240 (62.6)	
Age group, *n* (%)	40–49 yr	188 (4.9)	453 (6.7)	NA
	50–59 yr	560 (14.6)	1232 (18.2)	
	60–69 yr	1295 (33.8)	2458 (36.3)	
	70–79 yr	1789 (46.7)	2630 (38.8)	
Age group, *n* (%)	40–59 yr	748 (19.5)	1685 (24.9)	< 0.001
	60–79 yr	3084 (80.5)	5088 (75.1)	
Age, mean (SD), b		66.95 (8.71)	65.46 (9.03)	< 0.001

NA: No significant.

Table 4 Cox proportional hazards analyses of gastric cancer deaths in individuals aged 40 to 79 years who participated in gastric cancer screening in Maebashi City, Japan, in 2006

	Screening method	Participants, *n* (%)	Gastric cancer deaths, *n* (%)	Adjusted reduction rate[1]	95%CI
All participants	Radiography	11155	17	1.000	
	Endoscopy	10747	23	1.368	0.7308–2.562
Participants receiving annual screening after 2006	Radiography	6773	7	1.000	
	Endoscopy	3832	7	1.600	0.5604–4.569

[1]Adjusted for sex and age group (40–59 years and 60–79 years).

underwent endoscopy. No significant difference between the two screening methods was observed in the overall population (P = 0.249) (Figure 4A).

Among participants who had not participated in screening in the previous year, gastric cancer deaths were detected in 77 of 4 382 individuals who underwent direct radiography and 110 of 6 915 individuals who underwent endoscopy. The five-year survival rate was 0.985 (95%CI: 0.981–0.988) in individuals who underwent direct radiography and 0.986 (95%CI: 0.983–0.989) in individuals who underwent endoscopy. No significant difference was observed between the two screening methods (P = 0.509) (Figure 4B).

Among participants who had also participated in screening in the previous year, gastric cancer deaths were detected in 86 of 6 773 individuals who underwent direct radiography and 68 of 3 832 individuals who underwent endoscopy. The five-year survival rate was 0.988 (95%CI: 0.985–0.990) in individuals who underwent direct radiography and 0.985 (95%CI: 0.981–0.989) in individuals who underwent endoscopy. A significant difference was observed between the two screening methods (P = 0.038) (Figure 4C). The Cox proportional hazard test was conducted. For participants who had not participated in the previous year, the Cox hazard was not maintained. Accordingly, the HR was estimated for the overall population and participants who had also participated in the screening in the previous year.

When the number of deaths from any cancer other than gastric cancer in the participants who received direct radiographic screening was set as 1 in the Cox proportional hazard analysis, the adjusted HR of deaths from any cancer other than gastric cancer was 1.090 (95%CI: 0.8813-1.3480) in the overall group, 1.284 (95%CI: 0.9334–1.7650) in the participants who had also participated in the screening in the previous year. Again, no significant difference was found between the two screening

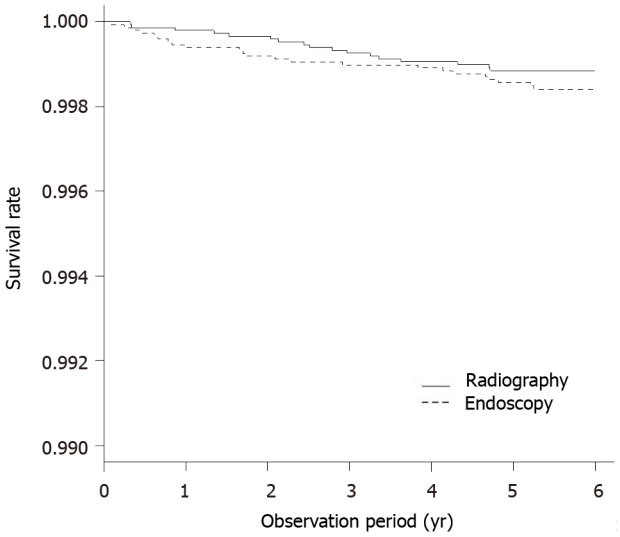


Figure 1 Survival curves of gastric cancer deaths in all individuals aged 40 to 79 years old who participated in gastric cancer screening in Maebashi City, Japan, in 2006. Survival curves are adjusted for sex and age group (40–59 years and 60–79 years). No significant difference was observed in the 5-year survival rate between the direct radiography and the endoscopy groups (P = 0.285).

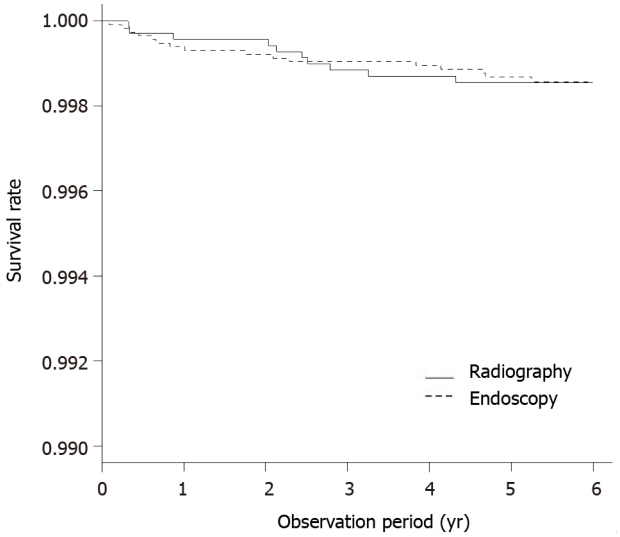


Figure 2 Survival curves of gastric cancer deaths in individuals aged 40 to 79 years old who participated in gastric cancer screening in Maebashi City, Japan, in 2006 and did not subsequently receive annual screening. Survival curves are adjusted for sex and age group (40–59 years and 60–79 years). No significant difference was observed in the 5-year survival rate between the direct radiography and the endoscopy groups (P = 0.971).

methods in terms of death from any cancer except gastric cancer (Table 5).

DISCUSSION

In this study, we examined clinical data from participants in the Maebashi City gastric cancer screening program in 2006 to assess whether the mortality rate from gastric cancer decreased after endoscopy was introduced as an additional screening method in addition to direct radiography. We found that although endoscopy detected more gastric cancers than direct radiography, the mortality rate from gastric cancer showed no difference between the two screening methods. Hence, endoscopy likely detected relatively slowly progressing gastric cancer (mainly differentiated gastric cancer common in older adults), whereas failed to detect gastric cancer that rapidly progresses in the early stage.

Hamashima *et al*[10] performed a study, the Tottori Cohort Study, on data from gastric cancer screening by radiography and endoscopy conducted in Yonago City and

Table 5 Cox proportional hazards analyses of all cancer deaths, without gastric cancer, in individuals aged 40 to 79 years who participated in gastric cancer screening in Maebashi City, Japan, in 2006

	Screening method	Participants, *n* (%)	Cancer deaths[1], *n* (%)	Adjusted reduction rate[2]	95%CI
All participants	Radiography	11155	163	1.000	
	Endoscopy	10747	178	1.090	0.8813–1.3480
Participants receiving annual screening after 2006	Radiography	6773	86	1.000	
	Endoscopy	3832	68	1.284	0.9334–1.7650

[1]Gastric cancer deaths are not included.
[2]Adjusted for sex and age group (40–59 years and 60–79 years).

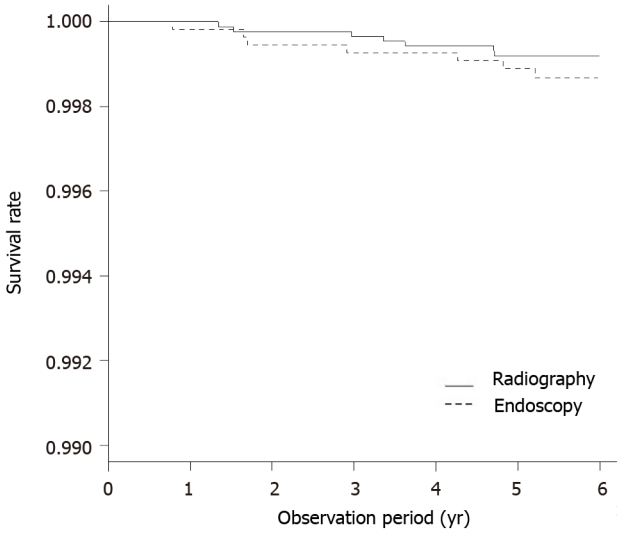


Figure 3 Survival curves of gastric cancer deaths in individuals aged 40 to 79 years old who participated in gastric cancer screening in Maebashi City, Japan, in 2006 and subsequently received annual screening. Survival curves are adjusted for sex and age group (40–59 years and 60–79 years). No significant difference was observed in the 5-year survival rate between the direct radiography and the endoscopy groups (P = 0.280).

Tottori City in 2007 and 2008[10]. This study included people aged 40 to 79 years who had not participated in gastric cancer screening in the previous year and followed them until the end of 2013 by using data from the Tottori Prefectural cancer registry. The authors reported that endoscopic screening reduced the gastric cancer mortality rate by 67% compared with radiographic screening[10]. In contrast, our study results found that the introduction of endoscopy in an organized gastric cancer screening program did not significantly reduce the gastric cancer mortality rate compared with direct radiographic screening. In Tottori Prefecture, institutions are allowed to conduct endoscopic screening if they perform at least 50 endoscopies annually, submit arbitrary endoscopic films, and attend seminars specified by the Tottori Prefecture Health Promoting Council[11]. In Maebashi City, institutions do not have to fulfill any particular eligibility criteria, and all of the institutions wishing to conduct endoscopic screening are allowed to participate in the gastric cancer screening program. Accordingly, the institutions conducting endoscopic screening in Yonago City and Tottori City may have achieved higher accuracy than those in Maebashi City, which may explain the inconsistent findings between the Tottori Cohort Study and our study.

Endoscopy of the upper gastrointestinal tract has become the more common evaluation method in routine clinical care in Japan. In 2014, endoscopies were performed in 527086 patients *per* month at hospitals and in 378195 patients *per* month at general clinics; and in 2017, in 572409 and 500447 patients *per* month, respectively. Thus, the use of endoscopy has increased markedly in recent years, especially at general clinics[12].

In Japan, endoscopies are not always performed by endoscopists with specialized training in the procedure, particularly at general clinics, and most of the general clinics in Maebashi City that routinely perform endoscopies participated in the 2006 gastric

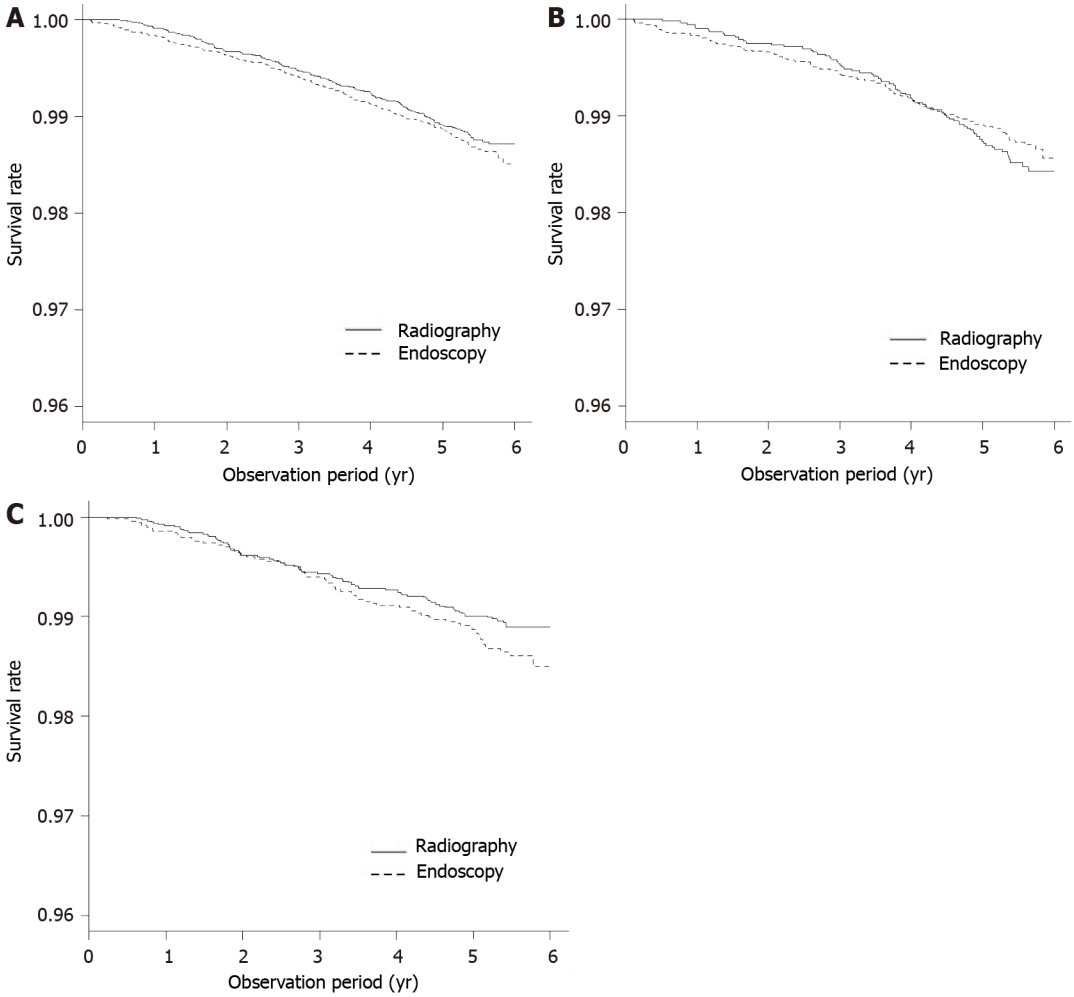


Figure 4 Survival curves of all cancer deaths, other than gastric cancer, in individuals aged 40 to 79 years old who participated in gastric cancer screening in Maebashi City, Japan, in 2006. Survival curves are adjusted for sex and age group (40–59 years and 60–79 years). A: All participants; B: Participants not receiving annual screening; C: Participants receiving annual screening. No significant differences were observed in the 5-year survival rate between the direct radiography and the endoscopy groups in both A and B (A: $P = 0.249$, B: $P = 0.509$). A significant difference was observed between the direct radiography and the endoscopy groups in C ($P = 0.038$).

cancer screening. In this study, endoscopies were performed by endoscopy experts only at 22 of the 82 participating clinics. Shimodate *et al*[13] reported that expert physicians certified by the Japan Gastroenterological Endoscopy Society detected gastric cancer in 1462 patients and that the gastric cancer lesions had been missed in the previous endoscopies in 157 of these patients; in 13 of the 157 patients, the lesion had progressed to advanced gastric cancer at the time of detection. Hosokawa *et al*[14] evaluated the precision of endoscopy for cancer detection and found a false-negative rate during the three years after endoscopy of 22.2%. They also reported that the false-negative rate was higher when the screening doctors had less experience. However, false-negative results were observed in 19.6% of patients even when the endoscopy was performed by trained doctors certified by the Japan Gastroenterological Endoscopy Society. In recent years, the quality of endoscopy devices and their images has increased substantially, but to our knowledge, no study has clarified whether the false-negative rate of diagnosing cancer has decreased.

Physicians of varying skill levels participate in endoscopic gastric cancer screening. Therefore, secondary review of endoscopic images by physicians who are board-certified by the Japan Gastroenterological Endoscopy Society is considered mandatory to compensate for any skill gaps among physicians and to standardize image interpretation[11]. Secondary review of endoscopic images was reported to decrease failures in identifying cancer and reduce the number of unnecessary biopsies[15,16]. Nevertheless, double-checking of images cannot achieve its mission if the inside of the stomach has not been thoroughly and systematically investigated and photographed and if a lesion site is missed during photography or the lesion image is unclear. A study that examined previously taken images to find reasons for false-negative cases

found that the physician had failed to take an image of the lesion site in 16.4% of the cases, even at institutions where a trained doctor certified by the Japan Gastroenterological Endoscopy Society was available[14]. An earlier study we performed also found that no endoscopic image was taken of the lesion site in 39.5% of the false-negative cases among participants in the 2006 to 2007 gastric cancer screening[17].

The "Manual for Organized Gastric Endoscopic Screening" published by the Japanese Society of Gastrointestinal Cancer Screening specifies that physicians who are qualified to perform endoscopic gastric cancer screening include expert physicians certified by Japanese endoscopy-related medical societies, physicians who have been performing endoscopies in at least 100 individuals annually, and physicians who have at least the equivalent ability to investigate the stomach and take endoscopic images [11]. This level of experience and skill in performing endoscopies is necessary to completely monitor and photograph the inside of the stomach so that the number of false-negative results of gastric cancer screening can be reduced as far as possible.

The efficacy of radiographic screening in reducing mortality has been well verified. A recent study found that the efficacy of radiographic screening in reducing gastric cancer mortality rate is equivalent to that of endoscopic screening[18]. In contrast, another study found that radiographic screening did not show efficacy in reducing the gastric cancer mortality rate[19]. The Japan Gastroenterological Endoscopy Society has recommended "a new radiography method" based on a double-contrast examination that uses high-density, low-viscosity barium sulfate[20]. Radiographic screening by this new method was reported to increase the detection rate of early cancer and reduce the requirement rate for detailed examinations when compared with the conventional screening method that uses medium-density barium sulfate[21,22].

The maximum follow-up period in our study was 5 years and 11 mo (*i.e.*, 71 mo). Early cancer was reported to become advanced cancer over 44 mo and to lead to death over 75 mo[23]. The Tottori Cohort Study showed a significant difference in gastric cancer mortality rate from 3 years after the screening. Therefore, the present study may have had a different result if the follow-up period were longer.

In the present study, we were unable to evaluate the difference between the two screening methods based on the number of times participants had previously undergone gastric cancer screening because we did not know how many participants newly received endoscopic screening after receiving direct radiographic screening in the previous year. Participants in the screening program were allowed to choose the screening method freely and could change the screening method from year to year, so we also had difficulties acquiring the history of participation in each screening method. Therefore, in the present study, we divided the participants into three analysis groups: The whole group of participants, participants who had also participated in the screening in the previous year, and participants who had not participated in the previous year. We conducted survival curve analyses for each of these three analysis sets and calculated gastric cancer mortality and the proportional HR for the mortality rate for any cancer other than gastric cancer. For the mortality rate from any cancer other than gastric cancer, among participants who had also participated in the screening in the previous year, survival analysis detected a difference between individuals undergoing direct radiography and individuals undergoing endoscopy. However, no difference was found with the Cox proportional hazard model. This may be due to slight differences in demographic characteristics between the two screening groups for participants who had also participated in screening the year prior. The reason for this may be as follows. When comparing the screening database *vs* the cancer registration, patients diagnosed with cancer prior to the study period were excluded in both groups. However, the quality of the cancer registration was low, and, therefore, cancer patients may have been included in the analysis set, resulting in a bias. Hence, for participants who had also participated in screening the previous year, differences in demographic characteristics between screening groups may exist for those with gastric cancer mortality. However, this effect is considered less significant when restricted to gastric cancer.

The analyses revealed no significant difference between the screening methods in any of the analysis sets, suggesting no noteworthy difference in the history of undergoing either of the two screening methods.

Stage IA gastric cancer detected by endoscopy was treated by ESD in 70% of the participants who were found to have a lesion. Intramucosal gastric cancer was more commonly detected by endoscopic screening. On the other hand, all cases of stage IA cancer detected by direct radiographic screening were treated by gastrectomy. Therefore, introducing direct radiographic screening and endoscopic screening has made it possible to detect gastric cancer in earlier stages. The Maebashi City gastric cancer screening detected higher percentages of stage III and IV gastric cancers than those

reported by other authors. Six of the seven participants who were found by endoscopic screening to have a stage IV lesion, and both of the participants who were found by endoscopic screening to have a stage IIIB lesion, had initially undergone endoscopic screening, and five participants who were found by direct radiography to have stage IV cancer and one of the four participants who were found by direct radiography to have stage IIIB cancer had initially undergone direct radiographic screening. We previously reported that stage III and stage IV cancers were more often detected among participants who reported the presence of stomach pain or appetite loss or both on the medical questionnaire for gastric cancer screening[24]. The Maebashi City gastric cancer screening may have included a larger number of participants with such symptoms, even though people with these symptoms are normally supposed to undergo examination at a clinical practice rather than gastric cancer screening.

Endoscopy is able to detect early gastric cancers more frequently than direct radiography, and endoscopic detection of early cancer may be related to overdiagnosis of gastric cancer. In fact, the number of gastric cancers detected by endoscopic screening has previously been reported to be twice the predicted number[25]. Moreover, endoscopic screening detected gastric cancer in a very large number of participants aged 80 years or over. Therefore, the gastric cancer screening system in Japan should be amended to provide an upper age limit.

Infection with *Hp*, current smoking, and salt and alcohol intake are known risk factors of gastric cancer. A previous study reported odds ratios of 2.56 for *Hp* infection, 1.61 for current smoking, 1.34 for salt intake, and 1.19 for alcohol intake[26]. We did not investigate the presence of *Hp* infection in participants in the 2006 Maebashi City gastric cancer screening because testing for *Hp* infection only began to be covered by health insurance in 2013. We also did not investigate smoking, salt intake, or drinking habits. Smoking and alcohol drinking are also risk factors for other cancers, but the present study found no significant difference between the two screening methods in terms of mortality rate from any cancer, which indicates that our comparison of the two screening methods had no risk factor-related bias.

The number of participants undergoing direct radiographic gastric cancer screening has decreased since its peak of 6.9 million or more in 2012[27]. Therefore, the introduction of endoscopic screening was needed to attain the government's target participation rate of 50%. In Maebashi City, in 2003, a total of 18494 citizens (equivalent to a participation rate of 15.8%) participated in gastric cancer screening by direct radiography alone. In 2015, when endoscopic screening was introduced, the number of participants increased to 33607 (participation rate, 28.8%). Nevertheless, it will be challenging to increase the participation rate further if the current screening system remains as it is now, partly because of the lack of qualified staff to perform the screening procedures. We need to establish a screening system that corresponds to the risk of developing gastric cancer and conduct gastric cancer screening efficiently, taking into account a possible reduction in the incidence rate of gastric cancer associated with a reduction in the incidence rate of *Hp* infection.

The present study had some limitations. First, because of the low reporting rate to the Gunma Prefecture cancer registry in 2006, we were unable to determine whether the gastric cancer incidence rate in screening participants was similar across the two screening methods, even though we were able to collect information on cancer deaths from death certificates. Therefore, the incidences of gastric cancer may not be completely accurate. Second, the group of participants undergoing endoscopic screening was highly likely to include a large number of people who had been instructed to undergo endoscopy because of the result of their previous direct radiographic screening; however, we were not able to collect such data. Third, compliance with the screening operation manual and precision control, including secondary review, were insufficient because the present screening was conducted at an early stage after the introduction of endoscopic screening. Because of these limitations, the usefulness of endoscopic screening should be further evaluated in a larger number of participants. In addition, we expect that future studies will examine this topic in regions where endoscopic screening has been newly introduced.

CONCLUSION

We used the data from the Maebashi City gastric cancer screening program in 2006 to compare the efficacy of direct radiography and endoscopy in reducing the gastric cancer mortality rate. In Maebashi City, a larger number of older adults participated in endoscopic gastric cancer screening than in direct radiographic screening. As a result,

endoscopic screening detected more early gastric cancers than direct radiographic screening; however, the mortality rate showed no significant difference between the two screening methods. For future gastric cancer screening, physicians' technical level gap across screening institutions should be corrected, and physicians' interpretation accuracy in secondary review should also be further supported.

ARTICLE HIGHLIGHTS

Research background

Gastric cancer is among the leading causes of cancer mortality worldwide, including in Japan. Initiatives have been implemented to lower the mortality rate of gastric cancer in Japan, including mass screening programs. In 2015, guidelines were revised to recommend endoscopy.

Research motivation

In Maebashi City, endoscopic gastric cancer screening was introduced in 2004, allowing eligible participants to choose between direct radiography and endoscopy. Comparing outcomes is essential to reduce gastric cancer mortality and ensure an effective and efficient screening program.

Research objectives

This study aimed to assess whether the mortality rate from gastric cancer decreased after the introduction of endoscopic screening in Maebashi City and compare gastric cancer mortality rates between screening methods.

Research methods

A retrospective analysis of the Maebashi City Gastric Cancer Screening Program in 2006 was conducted. Participants aged 40 to 79 were screened by direct radiography (n = 11155) or endoscopy (n = 10747) and followed until March 31, 2012. Data was cross-referenced against the Gunma Prefecture cancer registry data. The detection rate of gastric cancer and gastric cancer mortality rate were compared between the two screening groups.

Research results

Gastric cancer detection rate for direct radiography was 0.20% and 0.48% for endoscopy; however, endoscopic screening detected a higher number of early-stage cancers that may not have resulted in death. No significant difference in gastric cancer mortality rate was found between participants who underwent annual screening and those who did not. In addition, no significant difference was found in gastric cancer mortality rate between direct radiographic screening and endoscopic screening (P = 0.285). The five-year survival by the Kaplan-Meier method was 0.998 (95%CI: 0.998–0.999) in individuals who underwent direct radiography and 0.998 (95%CI: 0.997–0.999) in individuals who underwent endoscopy.

Research conclusions

No significant difference in gastric cancer mortality rate was found between direct radiographic screening and endoscopic screening. Screening programs should address gaps in endoscopists' skill levels across screening institutions to ensure the quality of endoscopic examination. Finally, an efficient gastric cancer screening system should consider gastric cancer risk by combining endoscopic and radiographic screening.

Research perspectives

Further research with a larger number of participants and high-quality cancer incidence data is needed to better clarify the usefulness of population-based endoscopic screening.

ACKNOWLEDGEMENTS

The authors are deeply grateful to the doctors at medical institutions in Maebashi City for performing gastric cancer screening and secondary reading, as well as the staff members of the Maebashi Medical Association office for collecting data on gastric

cancer screening.

REFERENCES

1 **Global Burden of Disease Cancer Collaboration**, Fitzmaurice C, Abate D, Abbasi N, Abbastabar H, Abd-Allah F, Abdel-Rahman O, Abdelalim A, Abdoli A, Abdollahpour I, Abdulle ASM, Abebe ND, Abraha HN, Abu-Raddad LJ, Abualhasan A, Adedeji IA, Advani SM, Afarideh M, Afshari M, Aghaali M, Agius D, Agrawal S, Ahmadi A, Ahmadian E, Ahmadpour E, Ahmed MB, Akbari ME, Akinyemiju T, Al-Aly Z, AlAbdulKader AM, Alahdab F, Alam T, Alamene GM, Alemnew BTT, Alene KA, Alinia C, Alipour V, Aljunid SM, Bakeshei FA, Almadi MAH, Almasi-Hashiani A, Alsharif U, Alsowaidi S, Alvis-Guzman N, Amini E, Amini S, Amoako YA, Anbari Z, Anber NH, Andrei CL, Anjomshoa M, Ansari F, Ansariadi A, Appiah SCY, Arab-Zozani M, Arabloo J, Arefi Z, Aremu O, Areri HA, Artaman A, Asayesh H, Asfaw ET, Ashagre AF, Assadi R, Ataeinia B, Atalay HT, Ataro Z, Atique S, Ausloos M, Avila-Burgos L, Avokpaho EFGA, Awasthi A, Awoke N, Ayala Quintanilla BP, Ayanore MA, Ayele HT, Babaee E, Bacha U, Badawi A, Bagherzadeh M, Bagli E, Balakrishnan S, Balouchi A, Bärnighausen TW, Battista RJ, Behzadifar M, Bekele BB, Belay YB, Belayneh YM, Berfield KKS, Berhane A, Bernabe E, Beuran M, Bhakta N, Bhattacharyya K, Biadgo B, Bijani A, Bin Sayeed MS, Birungi C, Bisignano C, Bitew H, Bjørge T, Bleyer A, Bogale KA, Bojia HA, Borzì AM, Bosetti C, Bou-Orm IR, Brenner H, Brewer JD, Briko AN, Briko NI, Bustamante-Teixeira MT, Butt ZA, Carreras G, Carrero JJ, Carvalho F, Castro C, Castro F, Catalá-López F, Cerin E, Chaiah Y, Chanie WF, Chattu VK, Chaturvedi P, Chauhan NS, Chehrazi M, Chiang PP, Chichiabellu TY, Chido-Amajuoyi OG, Chimed-Ochir O, Choi JJ, Christopher DJ, Chu DT, Constantin MM, Costa VM, Crocetti E, Crowe CS, Curado MP, Dahlawi SMA, Damiani G, Darwish AH, Daryani A, das Neves J, Demeke FM, Demis AB, Demissie BW, Demoz GT, Denova-Gutiérrez E, Derakhshani A, Deribe KS, Desai R, Desalegn BB, Desta M, Dey S, Dharmaratne SD, Dhimal M, Diaz D, Dinberu MTT, Djalalinia S, Doku DT, Drake TM, Dubey M, Dubljanin E, Duken EE, Ebrahimi H, Effiong A, Eftekhari A, El Sayed I, Zaki MES, El-Jaafary SI, El-Khatib Z, Elemineh DA, Elkout H, Ellenbogen RG, Elsharkawy A, Emamian MH, Endalew DA, Endries AY, Eshrati B, Fadhil I, Fallah Omrani V, Faramarzi M, Farhangi MA, Farioli A, Farzadfar F, Fentahun N, Fernandes E, Feyissa GT, Filip I, Fischer F, Fisher JL, Force LM, Foroutan M, Freitas M, Fukumoto T, Futran ND, Gallus S, Gankpe FG, Gayesa RT, Gebrehiwot TT, Gebremeskel GG, Gedefaw GA, Gelaw BK, Geta B, Getachew S, Gezae KE, Ghafourifard M, Ghajar A, Ghashghaee A, Gholamian A, Gill PS, Ginindza TTG, Girmay A, Gizaw M, Gomez RS, Gopalani SV, Gorini G, Goulart BNG, Grada A, Ribeiro Guerra M, Guimaraes ALS, Gupta PC, Gupta R, Hadkhale K, Haj-Mirzaian A, Hamadeh RR, Hamidi S, Hanfore LK, Haro JM, Hasankhani M, Hasanzadeh A, Hassen HY, Hay RJ, Hay SI, Henok A, Henry NJ, Herteliu C, Hidru HD, Hoang CL, Hole MK, Hoogar P, Horita N, Hosgood HD, Hosseini M, Hosseinzadeh M, Hostiuc M, Hostiuc S, Househ M, Hussen MM, Ileanu B, Ilic MD, Innos K, Irvani SSN, Iseh KR, Islam SMS, Islami F, Jafari Balalami N, Jafarinia M, Jahangiry L, Jahani MA, Jahanmehr N, Jakovljevic M, James SL, Javanbakht M, Jayaraman S, Jee SH, Jenabi E, Jha RP, Jonas JB, Jonnagaddala J, Joo T, Jungari SB, Jürisson M, Kabir A, Kamangar F, Karch A, Karimi N, Karimian A, Kasaeian A, Kasahun GG, Kassa B, Kassa TD, Kassaw MW, Kaul A, Keiyoro PN, Kelbore AG, Kerbo AA, Khader YS, Khalilarjmandi M, Khan EA, Khan G, Khang YH, Khatab K, Khater A, Khayamzadeh M, Khazaee-Pool M, Khazaei S, Khoja AT, Khosravi MH, Khubchandani J, Kianipour N, Kim D, Kim YJ, Kisa A, Kisa S, Kissimova-Skarbek K, Komaki H, Koyanagi A, Krohn KJ, Bicer BK, Kugbey N, Kumar V, Kuupiel D, La Vecchia C, Lad DP, Lake EA, Lakew AM, Lal DK, Lami FH, Lan Q, Lasrado S, Lauriola P, Lazarus JV, Leigh J, Leshargie CT, Liao Y, Limenih MA, Listl S, Lopez AD, Lopukhov PD, Lunevicius R, Madadin M, Magdeldin S, El Razek HMA, Majeed A, Maleki A, Malekzadeh R, Manafi A, Manafi N, Manamo WA, Mansourian M, Mansournia MA, Mantovani LG, Maroufizadeh S, Martini SMS, Mashamba-Thompson TP, Massenburg BB, Maswabi MT, Mathur MR, McAlinden C, McKee M, Meheretu HAA, Mehrotra R, Mehta V, Meier T, Melaku YA, Meles GG, Meles HG, Melese A, Melku M, Memiah PTN, Mendoza W, Menezes RG, Merat S, Meretoja TJ, Mestrovic T, Miazgowski B, Miazgowski T, Mihretie KMM, Miller TR, Mills EJ, Mir SM, Mirzaei H, Mirzaei HR, Mishra R, Moazen B, Mohammad DK, Mohammad KA, Mohammad Y, Darwesh AM, Mohammadbeigi A, Mohammadi H, Mohammadi M, Mohammadian M, Mohammadian-Hafshejani A, Mohammadoo-Khorasani M, Mohammadpourhodki R, Mohammed AS, Mohammed JA, Mohammed S, Mohebi F, Mokdad AH, Monasta L, Moodley Y, Moosazadeh M, Moossavi M, Moradi G, Moradi-Joo M, Moradi-Lakeh M, Moradpour F, Morawska L, Morgado-da-Costa J, Morisaki N, Morrison SD, Mosapour A, Mousavi SM, Muche AA, Muhammed OSS, Musa J, Nabhan AF, Naderi M, Nagarajan AJ, Nagel G, Nahvijou A, Naik G, Najafi F, Naldi L, Nam HS, Nasiri N, Nazari J, Negoi I, Neupane S, Newcomb PA, Nggada HA, Ngunjiri JW, Nguyen CT, Nikniaz L, Ningrum DNA, Nirayo YL, Nixon MR, Nnaji CA, Nojomi M, Nosratnejad S, Shiadeh MN, Obsa MS, Ofori-Asenso R, Ogbo FA, Oh IH, Olagunju AT, Olagunju TO, Oluwasanu MM, Omonisi AE, Onwujekwe OE, Oommen AM, Oren E, Ortega-Altamirano DDV, Ota E, Otstavnov SS, Owolabi MO, P A M, Padubidri JR, Pakhale S, Pakpour AH, Pana A, Park EK, Parsian H, Pashaei T, Patel S, Patil ST, Pennini A, Pereira DM, Piccinelli C, Pillay JD, Pirestani M, Pishgar F, Postma MJ, Pourjafar H, Pourmalek F, Pourshams A, Prakash S, Prasad N, Qorbani M, Rabiee M, Rabiee N, Radfar A, Rafiei A, Rahim F, Rahimi M,

Rahman MA, Rajati F, Rana SM, Raoofi S, Rath GK, Rawaf DL, Rawaf S, Reiner RC, Renzaho AMN, Rezaei N, Rezapour A, Ribeiro AI, Ribeiro D, Ronfani L, Roro EM, Roshandel G, Rostami A, Saad RS, Sabbagh P, Sabour S, Saddik B, Safiri S, Sahebkar A, Salahshoor MR, Salehi F, Salem H, Salem MR, Salimzadeh H, Salomon JA, Samy AM, Sanabria J, Santric Milicevic MM, Sartorius B, Sarveazad A, Sathian B, Satpathy M, Savic M, Sawhney M, Sayyah M, Schneider IJC, Schöttker B, Sekerija M, Sepanlou SG, Sepehrimanesh M, Seyedmousavi S, Shaahmadi F, Shabaninejad H, Shahbaz M, Shaikh MA, Shamshirian A, Shamsizadeh M, Sharafi H, Sharafi Z, Sharif M, Sharifi A, Sharifi H, Sharma R, Sheikh A, Shirkoohi R, Shukla SR, Si S, Siabani S, Silva DAS, Silveira DGA, Singh A, Singh JA, Sisay S, Sitas F, Sobngwi E, Soofi M, Soriano JB, Stathopoulou V, Sufiyan MB, Tabarés-Seisdedos R, Tabuchi T, Takahashi K, Tamtaji OR, Tarawneh MR, Tassew SG, Taymoori P, Tehrani-Banihashemi A, Temsah MH, Temsah O, Tesfay BE, Tesfay FH, Teshale MY, Tessema GA, Thapa S, Tlaye KG, Topor-Madry R, Tovani-Palone MR, Traini E, Tran BX, Tran KB, Tsadik AG, Ullah I, Uthman OA, Vacante M, Vaezi M, Varona Pérez P, Veisani Y, Vidale S, Violante FS, Vlassov V, Vollset SE, Vos T, Vosoughi K, Vu GT, Vujcic IS, Wabinga H, Wachamo TM, Wagnew FS, Waheed Y, Weldegebreal F, Weldesamuel GT, Wijeratne T, Wondafrash DZ, Wonde TE, Wondmieneh AB, Workie HM, Yadav R, Yadegar A, Yadollahpour A, Yaseri M, Yazdi-Feyzabadi V, Yeshaneh A, Yimam MA, Yimer EM, Yisma E, Yonemoto N, Younis MZ, Yousefi B, Yousefifard M, Yu C, Zabeh E, Zadnik V, Moghadam TZ, Zaidi Z, Zamani M, Zandian H, Zangeneh A, Zaki L, Zendehdel K, Zenebe ZM, Zewale TA, Ziapour A, Zodpey S, Murray CJL. Global, Regional, and National Cancer Incidence, Mortality, Years of Life Lost, Years Lived With Disability, and Disability-Adjusted Life-Years for 29 Cancer Groups, 1990 to 2017: A Systematic Analysis for the Global Burden of Disease Study. *JAMA Oncol* 2019; **5**: 1749-1768 [PMID: 31560378 DOI: 10.1001/jamaoncol.2019.2996]

2 **National Cancer Center**. Cancer Information Services. [cited 4 December 2020]. Available from: https://ganjoho.jp/reg_stat/statistics/stat/summary.html

3 **Hamashima C**; Systematic Review Group and Guideline Development Group for Gastric Cancer Screening Guidelines. Update version of the Japanese Guidelines for Gastric Cancer Screening. *Jpn J Clin Oncol* 2018; **48**: 673-683 [PMID: 29889263 DOI: 10.1093/jjco/hyy077]

4 **Hagiwara H**, Yamashita Y, Yagi T, Koitabashi T, Ishida M, Sekiguchi T, Imai T. Present situation and problems in individual gastric cancer screening conducted by endoscopy at multiple facilities. *J Gastrointestinal Cancer Screen* 2008; **46**: 472-481

5 **Ministry of Health**, Labour and Welfare. [cited 14 December 2020]. Available from: https://www.mhlw.go.jp/toukei/saikin/hw/Life/Life06/01.html

6 **Neuberger J**, Altman DG, Christensen E, Tygstrup N, Williams R. Use of a prognostic index in evaluation of liver transplantation for primary biliary cirrhosis. *Transplantation* 1986; **41**: 713-716 [PMID: 3520987 DOI: 10.1097/00007890-198606000-00009]

7 **Nieto FJ**, Coresh J. Adjusting survival curves for confounders: a review and a new method. *Am J Epidemiol* 1996; **143**: 1059-1068 [PMID: 8629613 DOI: 10.1093/oxfordjournals.aje.a008670]

8 **Kanda Y**. Investigation of the freely available easy-to-use software 'EZR' for medical statistics. *Bone Marrow Transplant* 2013; **48**: 452-458 [PMID: 23208313 DOI: 10.1038/bmt.2012.244]

9 **Japanese Gastric Cancer Association**. Japanese Classification of Gastric Carcinoma. 13th edition. Tokyo: KANEHARA&Co., Ltd, 1999: 39

10 **Hamashima C**, Shabana M, Okada K, Okamoto M, Osaki Y. Mortality reduction from gastric cancer by endoscopic and radiographic screening. *Cancer Sci* 2015; **106**: 1744-1749 [PMID: 26432528 DOI: 10.1111/cas.12829]

11 **The Japanese Society of Gastrointestinal Cancer Screening**. Quality Assurance of Endoscopic Screening for Gastric Cancer in Japanese Communities. 2017. [cited 14 December 2020]. Available from: https://www.jsgcs.or.jp

12 **e-Stat**. Official Statistics of Japan. [Cited 14 December 2020]. Available from: https://www.e-stat.go.jp/dbview?sid=0003026748,003026801,0003289757,0003289801

13 **Shimodate Y**, Mizuno M, Doi A, Nishimura N, Mouri H, Matsueda K, Yamamoto H. Gastric superficial neoplasia: high miss rate but slow progression. *Endosc Int Open* 2017; **5**: E722-E726 [PMID: 28791319 DOI: 10.1055/s-0043-110076]

14 **Hosokawa O**, Hattori M, Takeda T, Watanabe K, Fujita M. Accuracy of endoscopy in detecting gastric cancer. *J Gastroenterol Mass Sur* 2004; **42**: 33-39

15 **Ogoshi K**, Narisawa R, Kato T, Saito Y, Funakoshi K, Kinameri K. Evaluation of endoscopic screening for gastric cancer in Niigata City: the reduction of the mortality rate. *J Gastrointestinal Cancer Screen* 2009; **47**: 531-541

16 **Ohno K**, Takabatake I, Nishimura G, Ueno T, Kaji K, Hashiba A, Takeda Y. Examination of the Kanazawa-shi method (the third reading shadow) in multicenter endoscopic for gastric cancer. *Gastric Cancer* 2014; **52**: 715-722

17 **Hagiwara H**, Yamashita Y, Yagi T, Koitabashi T, Moki F. Current status of use of transnasal endoscopy in personal health checkup and its accuracy in screening gastric cancers at multiple institutions. *J Gastrointestinal Cancer Screen* 2009; **47**: 683-692 [DOI: 10.11404/jsgcs.47.683]

18 **Matsumoto S**, Ishikawa S, Yoshida Y. Reduction of gastric cancer mortality by endoscopic and radiographic screening in an isolated island: A retrospective cohort study. *Aust J Rural Health* 2013; **21**: 319-324 [PMID: 24299436 DOI: 10.1111/ajr.12064]

19 **Hamashima C**, Ogoshi K, Okamoto M, Shabana M, Kishimoto T, Fukao A. A community-based, case-control study evaluating mortality reduction from gastric cancer by endoscopic screening in

Japan. *PLoS One* 2013; **8**: e79088 [PMID: 24236091 DOI: 10.1371/journal.pone.0079088]

20 **The Japanese Society of Gastrointestinal Cancer Screening**. New Guidelines of Radiography for Gastric Cancer Screening. 2011. [cited 14 December 2020]. Available from: https://www.jsgcs.or.jp

21 **Shimizu K**, Kunihiro K, Onoda H, Tanabe M, Matsukuma M, Matsunaga N. Evaluation of gastric mass screening during the shift to a new standard method focused on the detection of early gastric cancers. *Nihon Shoukaki Gan Kenshin Gakkai zasshi* 2009; **47**: 35-42

22 **Murakami H**, Tuchigame T, Murata Y, Awazu Y, Maeda M, Ogata I, Nishi J. Evaluation of mass screening for stomach cancers. *Nihon Shoukaki Gan Kenshin Gakkai zasshi* 2007; **45**: 399-404

23 **Tsukuma H**, Oshima A, Narahara H, Morii T. Natural history of early gastric cancer: a non-concurrent, long term, follow up study. *Gut* 2000; **47**: 618-621 [PMID: 11034575 DOI: 10.1136/gut.47.5.618]

24 **Hagiwara H**, Moki F, Sekiguchi T, Yamashita Y, Yagi T, Koitabashi T. Effectiveness of gastroendoscopic examination in individual screening for stomach cancer. *Nihon Shoukaki Gan Kenshin Gakkai zasshi* 2015; **53**: 376-382

25 **Hamashima C**, Sobue T, Muramatsu Y, Saito H, Moriyama N, Kakizoe T. Comparison of observed and expected numbers of detected cancers in the research center for cancer prevention and screening program. *Jpn J Clin Oncol* 2006; **36**: 301-308 [PMID: 16735372 DOI: 10.1093/jjco/hyl022]

26 **Poorolajal J**, Moradi L, Mohammadi Y, Cheraghi Z, Gohari-Ensaf F. Risk factors for stomach cancer: a systematic review and meta-analysis. *Epidemiol Health* 2020; **42**: e2020004 [PMID: 32023777 DOI: 10.4178/epih.e2020004]

27 **The Japanese Society of Gastrointestinal Cancer Screening**. Annual Report of Gastrointestinal Cancer Screening 2014. [cited 14 December 2020]. Available from: https://www.jsgcs.or.jp

World Journal of Gastroenterology

Submit a Manuscript: https://www.f6publishing.com

World J Gastroenterol 2021 September 7; 27(33): 5610-5621

DOI: 10.3748/wjg.v27.i33.5610

ISSN 1007-9327 (print) ISSN 2219-2840 (online)

ORIGINAL ARTICLE

Retrospective Study

Radiomics for predicting perineural invasion status in rectal cancer

Mou Li, Yu-Mei Jin, Yong-Chang Zhang, Ya-Li Zhao, Chen-Cui Huang, Sheng-Mei Liu, Bin Song

ORCID number: Mou Li 0000-0002-7101-5942; Yu-Mei Jin 0000-0001-6606-8049; Yong-Chang Zhang 0000-0003-0402-2525; Ya-Li Zhao 0000-0002-8895-1972; Chen-Cui Huang 0000-0003-3307-6872; Sheng-Mei Liu 0000-0003-4575-0799; Bin Song 0000-0002-7269-2101.

Author contributions: Song B and Li M designed the research; Jin YM and Liu SM collected the data; Li M, Zhang YC, Zhao YL, and Huang CC analyzed the data; Li M and Song B wrote the paper; all authors have read and approved the final manuscript.

Institutional review board statement: This study was reviewed and approved by the Ethics Committee of West China Hospital of Sichuan University (Approved No.1159).

Informed consent statement: Patients were not required to give informed consent to the study because the analysis used anonymous clinical data that were obtained after each patient agreed to treatment by written consent.

Conflict-of-interest statement: Zhao YL and Huang CC are employed by the company Beijing Deepwise & League of PHD Technology Co., Ltd. The remaining authors declare no conflicts-of-interest related to this article.

Mou Li, Yu-Mei Jin, Sheng-Mei Liu, Bin Song, Department of Radiology, West China Hospital of Sichuan University, Chengdu 610041, Sichuan Province, China

Yong-Chang Zhang, Department of Radiology, Chengdu Seventh People's Hospital, Chengdu 610213, Sichuan Province, China

Ya-Li Zhao, Chen-Cui Huang, Department of Research Collaboration, R&D Center, Beijing Deepwise & League of PHD Technology Co., Ltd, Beijing 100080, China

Corresponding author: Bin Song, MD, Chief Doctor, Professor, Department of Radiology, West China Hospital of Sichuan University, No. 37 Guoxue Alley, Chengdu 610041, Sichuan Province, China. songlab_radiology@163.com

Abstract

BACKGROUND

Perineural invasion (PNI), as a key pathological feature of tumor spread, has emerged as an independent prognostic factor in patients with rectal cancer (RC). The preoperative stratification of RC patients according to PNI status is beneficial for individualized treatment and improved prognosis. However, the preoperative evaluation of PNI status is still challenging.

AIM

To establish a radiomics model for evaluating PNI status preoperatively in RC patients.

METHODS

This retrospective study enrolled 303 RC patients in a single institution from March 2018 to October 2019. These patients were classified as the training cohort (n = 242) and validation cohort (n = 61) at a ratio of 8:2. A large number of intra- and peritumoral radiomics features were extracted from portal venous phase images of computed tomography (CT). After deleting redundant features, we tested different feature selection (n = 6) and machine-learning (n = 14) methods to form 84 classifiers. The best performing classifier was then selected to establish Rad-score. Finally, the clinicoradiological model (combined model) was developed by combining Rad-score with clinical factors. These models for predicting PNI were compared using receiver operating characteristic curve (ROC) analysis and area under the ROC curve (AUC).

RESULTS

One hundred and forty-four of the 303 patients were eventually found to be PNI-

Data sharing statement: No additional data are available.

Open-Access: This article is an open-access article that was selected by an in-house editor and fully peer-reviewed by external reviewers. It is distributed in accordance with the Creative Commons Attribution NonCommercial (CC BY-NC 4.0) license, which permits others to distribute, remix, adapt, build upon this work non-commercially, and license their derivative works on different terms, provided the original work is properly cited and the use is non-commercial. See: http://creativecommons.org/Licenses/by-nc/4.0/

Manuscript source: Unsolicited manuscript

Specialty type: Gastroenterology and hepatology

Country/Territory of origin: China

Peer-review report's scientific quality classification
Grade A (Excellent): 0
Grade B (Very good): B
Grade C (Good): C
Grade D (Fair): 0
Grade E (Poor): 0

Received: June 2, 2021
Peer-review started: June 2, 2021
First decision: June 25, 2021
Revised: July 3, 2021
Accepted: August 11, 2021
Article in press: August 11, 2021
Published online: September 7, 2021

P-Reviewer: Dulskas A, Peltrini R
S-Editor: Liu M
L-Editor: A
P-Editor: Guo X

positive. Clinical factors including CT-reported T stage (cT), N stage (cN), and carcinoembryonic antigen (CEA) level were independent risk factors for predicting PNI preoperatively. We established Rad-score by logistic regression analysis after selecting features with the L1-based method. The combined model was developed by combining Rad-score with cT, cN, and CEA. The combined model showed good performance to predict PNI status, with an AUC of 0.828 [95% confidence interval (CI): 0.774-0.873] in the training cohort and 0.801 (95%CI: 0.679-0.892) in the validation cohort. For comparison of the models, the combined model achieved a higher AUC than the clinical model (cT + cN + CEA) achieved ($P < 0.001$ in the training cohort, and $P = 0.045$ in the validation cohort).

CONCLUSION
The combined model incorporating Rad-score and clinical factors can provide an individualized evaluation of PNI status and help clinicians guide individualized treatment of RC patients.

Key Words: Radiomics; Perineural invasion; Rectal cancer; Computed tomography; Preoperative prediction; Model building

©The Author(s) 2021. Published by Baishideng Publishing Group Inc. All rights reserved.

Core Tip: In this study, a radiomics model integrating Rad-score and clinical factors was developed and validated for predicting perineural invasion status in patients with rectal cancer. Radiomics features were extracted from intra- and peritumoral regions. This radiomics model showed good performance and outperformed the clinical factors. Therefore, the combined model might assist in predicting perineural invasion status and improving prognosis of patients with rectal cancer.

Citation: Li M, Jin YM, Zhang YC, Zhao YL, Huang CC, Liu SM, Song B. Radiomics for predicting perineural invasion status in rectal cancer. *World J Gastroenterol* 2021; 27(33): 5610-5621
URL: https://www.wjgnet.com/1007-9327/full/v27/i33/5610.htm
DOI: https://dx.doi.org/10.3748/wjg.v27.i33.5610

INTRODUCTION

Rectal cancer (RC) is one of the most common cancers of the digestive tract worldwide, with a growing morbidity[1]. In the last decade, the combination of neoadjuvant chemoradiotherapy (nCRT) and surgery has improved local control of locally advanced RC, but it does not significantly affect prognosis[2]. Different biological characteristics of RC may cause different treatment responses, risks of distant metastasis, and outcomes[3].

Recently, there is an increasing interest in perineural invasion (PNI) as a potential route of tumor spread, in addition to the well-known routes of direct extension, lymphatic metastasis, and hematogenous metastasis[4]. PNI refers to the biological process characterized by cancer cells invading the nerves and spreading along the nerve sheaths[5,6]. This process can be found in the main tumor and peritumoral area [7,8]. Previous studies have demonstrated the prognostic value of PNI in RC in terms of both recurrence and survival[9-11]. Other studies have shown that PNI can be an indicator for identifying patients who can benefit from nCRT and postoperative adjuvant chemotherapy[12,13]. Therefore, understanding PNI status in advance is helpful for clinicians to make individualized treatment plans for RC patients.

However, PNI status can only be confirmed by assessing the pathology of surgical specimens. In other words, neither biopsy nor imaging examinations [computed tomography (CT)/magnetic resonance imaging (MRI)] can accurately determine PNI status of RC[6]. Recent advances in radiomics have enabled researchers to extract numerous quantitative features from medical images and provide a comprehensive overview of heterogeneity in tumors[14]. Latterly, radiomics analysis has been used to predict PNI status in colorectal cancer[14,15]. Considering the higher incidence of PNI

in RC (compared with colon cancer)[16], several researchers evaluated the performance of MRI-based radiomics for PNI prediction in RC[6,17,18]. However, the sample sizes in the previous studies were really small (PNI^+: 26-32). At present, there is still a lack of CT-based radiomics research in this field. Therefore, we aimed to evaluate the predictive value of CT-based radiomics for PNI prediction in a bigger cohort of RC patients.

MATERIALS AND METHODS

Patients

The local ethics committee approved this study (document number: 1159), and the requirement of informed consent was waived because of the retrospective nature of this study.

The RC patients were reviewed by browsing the radiological and pathological databases from March 2018 to October 2019. A total of 303 patients (170 men and 133 women, mean age 58.9 ± 11.7 years, age range 23-86 years) were enrolled, according to the following inclusion criteria: (1) Adults with histologically confirmed rectal adenocarcinoma; (2) Clinical materials such as enhanced CT images and tumor markers were complete; and (3) No prior therapy before CT examination. The exclusion criteria were as follows: (1) Quality of CT images was poor; (2) Patients treated without surgery; and (3) Patients with other malignant tumors besides RC. The patient recruitment pathway is shown in Figure 1. The workflow of the radiomics analysis is shown in Figure 2.

The clinical and pathological data of each patient were derived from medical records. The baseline data including age, sex, tumor volume, location, tumor markers [carcinoembryonic antigen (CEA), carbohydrate antigen (CA) 19-9, and CA125], pathological TNM stage, and histological grade are shown in Table 1.

Reference standard for pathology

All patients with RC were diagnosed by pathology based on resected specimens. The pathological confirmatory reports were acquired from electronic medical records. PNI status was defined as positive, if (1) At least 33% of the nerve circumference was surrounded by cancer cells (without invasion of nerve sheath); or (2) Cancer cells were within any layer of the nerve sheath[6,19].

CT examination and evaluation

In our hospital, the chest-abdomen-pelvis enhanced CT is used to detect both primary and metastatic lesions for patients with clinically suspected RC. The CT scanners were restricted to Somatom Definition AS+ and Somatom Definition Flash in this study. The parameters of CT examinations are shown in the Supplementary material.

Two experienced radiologists (10 years' and 5 years' experience in abdominal imaging) were assigned to review CT images. The identification of patients was removed from CT images, and the readers were blinded to all clinical and pathological information. The CT-reported T stage (cT) and N stage (cN) were determined by summarizing the results of the two readers (Table 1). The inter-observer variability of cT/cN was evaluated by a weighted kappa statistics test. Because CT is limited to distinguish T1 from T2 in RC, lesions of cT1 were classified as cT2 in this study. When reviewing the CT images, the radiologists solved disagreements by discussion.

Feature extraction and model building

The stability of radiomics features was tested on 20 patients. One radiologist drew volumes of interest (VOIs) twice for evaluating intra-class correlation coefficient (intra-ICC), and the other drew VOIs once for evaluating inter- ICC. The features with ICC < 0.75 were deleted according to the commonly admitted knowledge: ICC < 0.5, poor reliability; 0.5-0.75, moderate reliability; ICC > 0.75, good reliability[20]. The main tumor and peritumoral area were separately drawn slice by slice to obtain intra- and peritumoral features (Figure 2).

The CT images were resampled to a pixel spacing of 1.0 mm in three anatomical directions. Then high- and low-pass wavelet filters, Laplacian-of-Gaussian filters, and other transformation methods such as square, square root, logarithm, exponential, gradient, lbp2d, and lbp3 were used to pre-process the original images. Radiomics features were extracted by using PyRadiomics[21]. A total of 4214 features (three types: First-order statistics, shape features, and texture features) were extracted from

Table 1 Baseline characteristics of the study population

Characteristics	PNI$^+$ (*n* = 144)	PNI$^-$ (*n* = 159)	*P* value	The training set(*n* = 242)	The validation set(*n* = 61)	*P* value
Age (mean ± SD, yr)	58.9 ± 11.8	58.9 ± 11.7	0.952	58.4 ± 11.9	60.8 ± 10.2	0.162
Sex (male/female)	77/67	93/66	0.379	140/102	30/31	0.223
Volume (cm^3)	19.7	20.8	0.132	20.1	20.8	0.847
Location[1]			0.075			0.045
Middle-low	101	96		164	33	
High	43	63		78	28	
cT stage (T1-2/T3/T4)	25/98/21	57/90/12	< 0.001	61/156/25	21/32/8	0.222
cN stage (N0/N1/N2)	31/52/61	75/59/25	< 0.001	89/84/69	17/27/17	0.313
Neoadjuvant therapy (+/-)	25/119	37/122	0.203	51/191	11/50	0.599
CEA (+/-) (positive ≥ 5 ng/mL)	77/67	56/103	0.001	107/135	26/35	0.823
CA19-9 (+/-) (positive ≥ 30 U/mL)	43/101	35/124	0.119	64/178	14/47	0.577
CA125 (+/-) (positive ≥ 24 U/mL)	20/124	15/144	0.226	20/222	3/58	0.378
pT stage (T1/T2/T3/T4)	0/15/117/12	8/44/95/12	< 0.001	6/48/171/17	2/11/41/7	0.584
pN stage (0/N1/N2)	29/74/41	81/56/22	< 0.001	88/101/53	22/29/10	0.579
Stage (I/II/III)	10/28/115	38/43/78	< 0.001	40/48/154	8/14/39	0.731
Histologic grade (G1/G2/G3)	1/105/38	2/133/24	0.014	2/189/51	1/49/11	0.523
Rad-score	0.60 ± 0.19	0.40 ± 0.20	< 0.001	0.50±0.21	0.49 ± 0.23	0.805

[1]Location: Low (0-5 cm from the anal verge), middle (5.1-10 cm from the anal verge), and high (10.1-15 cm from the anal verge). This table summarized the results of cT-stage and cN-stage for the two readers. CT: Computed tomography; PNI: Perineural invasion; CEA: Carcinoembryonic antigen; CA19-9: Carbohydrate antigen 19-9; CA125: Carbohydrate antigen 125; cT stage: Computed tomography-reported T stage; cN stage: Computed tomography-reported N stage; pT stage: Pathological T stage; pN stage: Pathological N stage.

intra- and peritumoral regions. Z-score was used to normalize the features for eliminating the differences in the value scales. Redundant features were randomly removed by correlation analysis with a threshold of 0.48. Then the features were selected using six different methods (analysis of variance, Pearson, mutual information, L1-based, tree-based, and recursive). Subsequently, 14 different machine-learning methods were used to build 84 classifiers. The optimal parameters were adjusted to improve the area under the receiver operating characteristic (ROC) curve (AUC) of the test set and output the best classifier (Rad-score).

Statistically significant risk variables (Rad-score and clinical factors) from the univariate logistic regression analysis were then entered into a multivariate analysis for developing the clinical and combined models. A nomogram was generated for the combined model visualization, graphical evaluation of variable importance, and the calculation of predictive accuracy. ROC curve analyses were performed to assess the diagnostic performance of the models.

Statistical analysis

All statistical analyses were performed using R software (version 3.6.1), SPSS (version 21), Stata (version 15.0), and Medcalc (version 15.2.2). Differences of the factors in Table 1 were assessed by chi-square test or Fisher's exact test, Mann-Whitney test, and *t*-test. AUCs of the models were compared by DeLong's test.

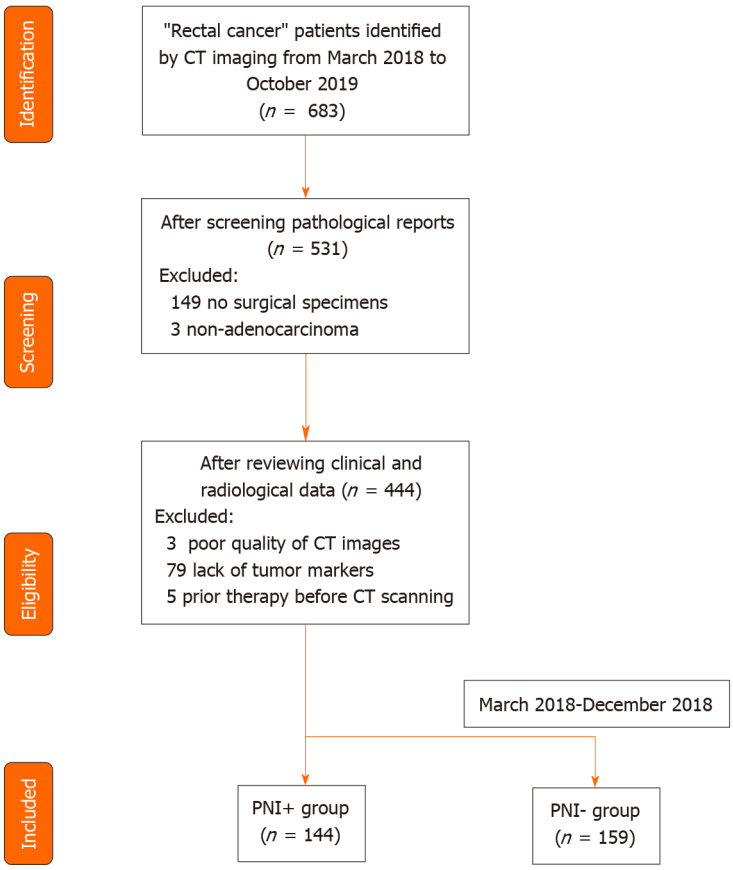


Figure 1 Flowchart of patients' recruitment pathway. CT: Computed tomography; PNI: Perineural invasion.

RESULTS

Patient characteristics

A total of 303 RC patients (144 PNI^+ and 159 PNI^-) were enrolled in this study. Clinical factors such as cT/cN stage, CEA (+/-), pathological T/N stage, and grade had significant differences between PNI^+ and PNI^- groups (Table 1). The weighted kappa coefficients of cT and cN between two readers were 0.709 [95% confidence interval (CI): 0.630-0.789] and 0.849 (95%CI: 0.801-0.897), which showed substantial consistency for cT and almost perfect consistency for cN (0.41-0.60, moderate, 0.61-0.80, substantial and 0.81-1.00, almost perfect)[22]. There were no significant differences in sex, age, volume, location, CA19-9, and CA125 between PNI^+ and PNI^- groups (Table 1). The patients were randomly divided into the training cohort (n = 242) and the validation cohort (n = 61). Except for location (P = 0.045), there were no significant differences in other factors between the training and validation groups (Table 1).

Feature selection and model building

A total of 3095 features (1490 intratumoral and 1605 peritumoral) had good reliability with ICC > 0.75. After deleting redundant features, we selected only seven intratumoral and 13 peritumoral features using the L1-based method. Rad-score was established by logistic regression, as shown in Supplementary material. Rad-score was an independent risk factor for predicting PNI [odds ratio (OR) = 3.148, P < 0.001]. As for clinical factors, CEA, cT, and cN were independent risk factors for predicting PNI preoperatively (OR = 2.528, 1.636, and 1.458; P = 0.003, 0.087, and 0.001, respectively), as shown in Table 2. The factor location had a significant difference in the univariate logistic regression analysis; however, it was excluded by multivariate analysis (Table 2). Thus, the combined model (Rad-score + CEA + cT + cN) was built by multivariate logistic regression analysis. The formula of the combined model is shown in Supplementary material.

A nomogram was generated for the visualization of the combined model (Figure 3). Higher total score obtained from the nomogram is associated with greater predicted risk of PNI. The combined model had good fit according to the Hosmer-Lemeshow test (P = 0.122). In the calibration curve of the nomogram (Figure 4), the y axis

Table 2 Risk factors selected by logistic regression analysis

Variables	Univariate		Multivariate	
	OR	*P* value	OR	*P* value
Age	1.001	0.961	-	-
Sex	0.787	0.358	-	-
Volume	1.000	1.000	-	-
Location	1.779	0.050	1.470	0.265
cT stage	2.328	< 0.001	1.636	0.087
cN stage	1.550	< 0.001	1.458	0.001
CEA	2.631	< 0.001	2.528	0.003
CA19-9	1.478	0.182	-	-
CA125	0.717	0.484	-	-
Rad-score	3.012	< 0.001	3.148	< 0.001

If *P* value < 0.1, variables were included in the model. CEA: Carcinoembryonic antigen; CA19-9: Carbohydrate antigen 19-9; CA125: Carbohydrate antigen 125; OR: Odds ratio.

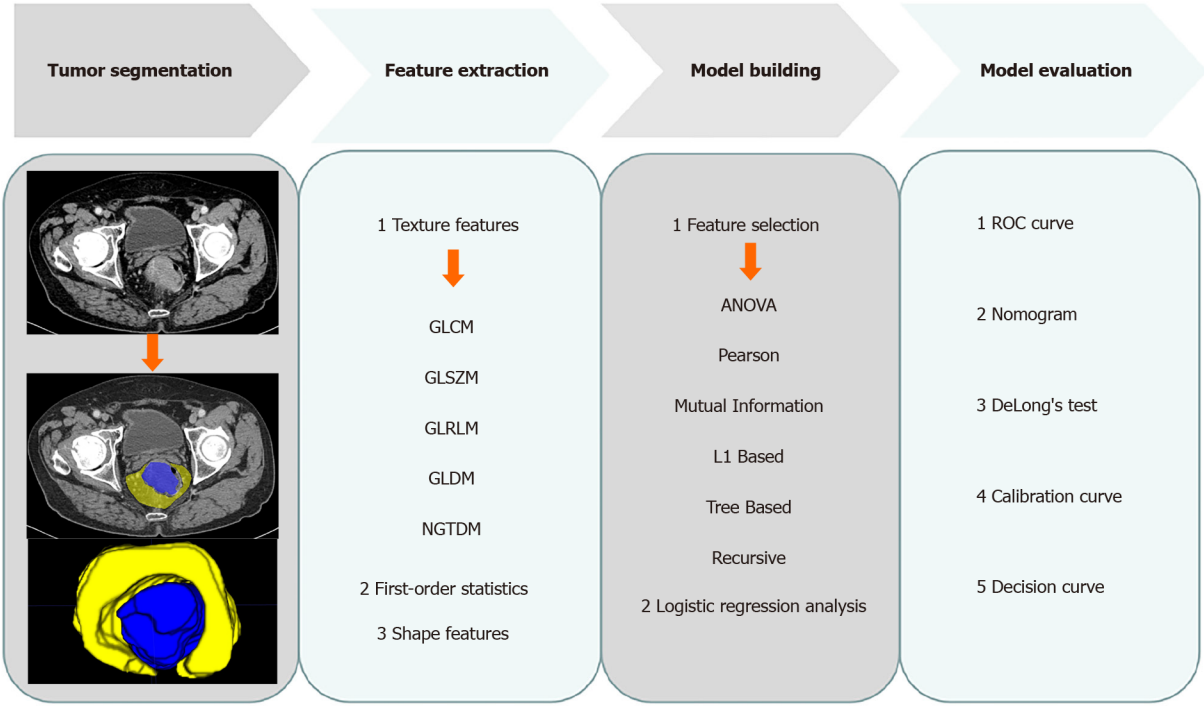


Figure 2 Radiomics workflow. GLCM: Gray level co-occurrence matrix; GLSZM: Gray level size zone matrix; GLRLM: Gray level run length matrix; GLDM: Gray level dependence matrix; NGTDM: Neighbouring gray tone difference matrix; ANOVA: Analysis of variance; ROC: Receiver operating characteristic curve.

represents the actual observed probability of PNI, and the x axis represents the predicted probability of PNI. A locally weighted regression line (solid line) of calibration plots is used to demonstrate the general trend of predicted risk. The model had a good agreement between the predicted and observed probability, because the solid line was close to the reference line (dotted line) in this study. This conclusion was consistent with the result of the Hosmer-Lemeshow test. However, among patients with predicted probability > 83%, the model overestimated actual risk of PNI$^+$ (about 15% at most). The decision curve was performed to assess the clinical usefulness of the combined model in predicting PNI. The net benefit is measured on the y axis. Figure 4 shows that the combined model (nomogram) obtained more benefit than "treat all", "treat none", Rad-score, and the clinical model, when the threshold probability was

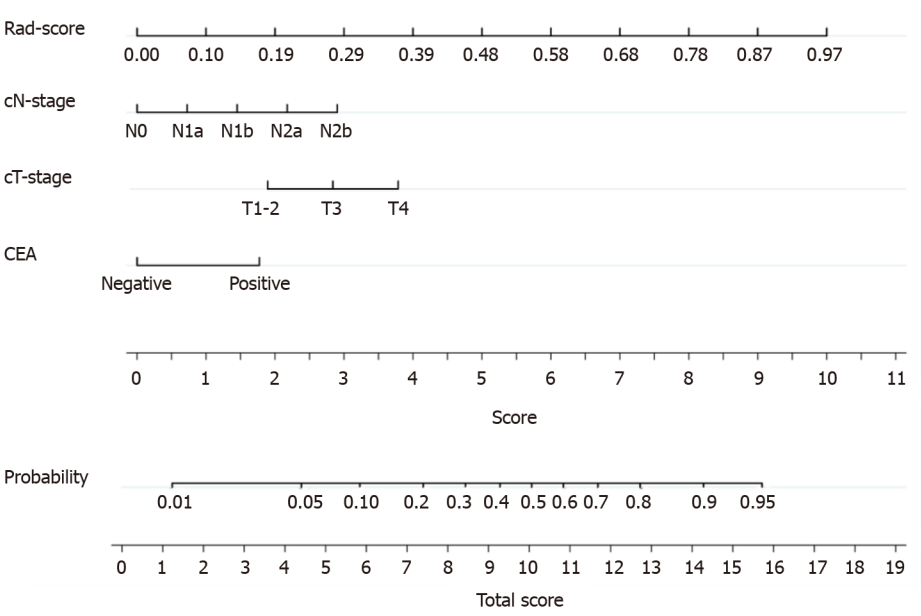


Figure 3 The nomogram was developed in the training cohort. Sum the points of variables in the "score" axis to get the total points. The risk of perineural invasion is the corresponding value on the "probability" axis. CEA: Carcinoembryonic antigen; cT: Computed tomography-reported T stage; cN: Computed tomography-reported N stage.

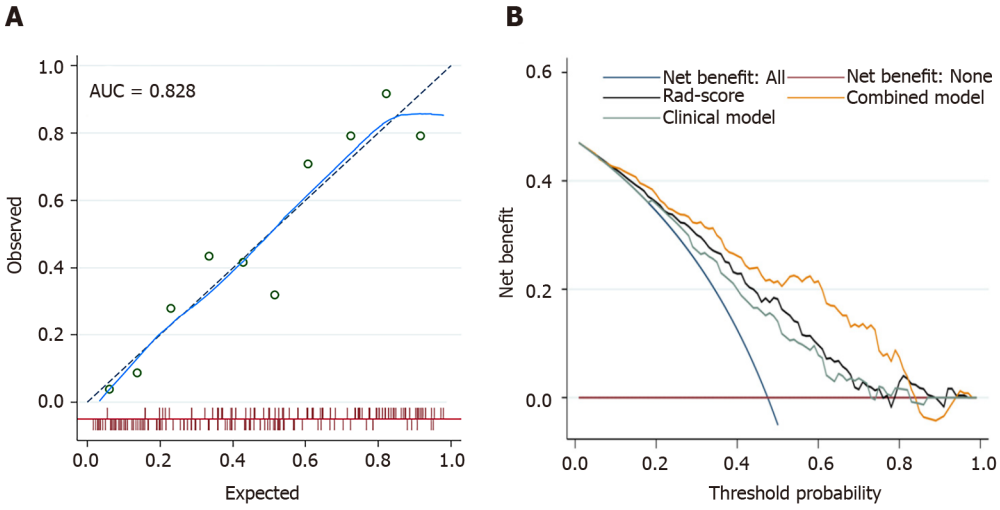


Figure 4 The fit and usefulness evaluation of the nomogram. A: The calibration curve of the nomogram shows a good agreement between the predicted and observed risks in the training cohort; B: The decision curve demonstrates that the nomogram (combined model) obtains more benefit than "treat all", "treat none", Rad-score, and the clinical model, when the threshold probability is in the range of 10% to 83%. AUC: Area under the receiver operating characteristic curve.

found to be in the range of 10% to 83%.

Classification results

In the case of the clinical model (cT + cN + CEA), the resulting AUCs were 0.718 (95%CI: 0.657-0.774) in the training cohort and 0.674 (95%CI: 0.542-0.789) in the validation cohort. Improved performance was achieved by adding Rad-score to the clinical factors. The AUCs of the combined model (0.828; 95%CI: 0.774-0.873 in the training cohort and 0.801; 95%CI: 0.679-0.892 in the validation cohort) were higher than those of the clinical model ($P < 0.001$ and $P = 0.045$, respectively), as shown in Table 3 and Figure 5. The combined model had a higher AUC than Rad-score (AUC = 0.828 *vs* 0.760, $P = 0.020$) in the training cohort. However, there was no significant difference between the combined model and Rad-score in the validation cohort (AUC = 0.801 *vs* 0.782, $P = 0.640$).

Table 3 Comparisons of variables and models in the training and validation cohorts

	The training set				The validation set			
	AUC	SEN (%)	SPE (%)	*P* value	AUC	SEN (%)	SPE (%)	*P* value
CEA	0.597 (0.533-0.660)	50.00	76.38	< 0.001	0.635 (0.502-0.754)	96.55	40.63	0.042
cT stage	0.613 (0.549-0.675)	84.35	33.86	< 0.001	0.589 (0.456-0.714)	75.86	43.75	0.004
cN stage	0.670 (0.607-0.729)	42.61	84.25	< 0.001	0.684 (0.553-0.797)	86.21	40.63	0.045
Rad-score	0.760 (0.701-0.812)	72.17	69.29	0.020	0.782 (0.658-0.878)	68.97	78.12	0.640
Clinical model	0.718 (0.657-0.774)	63.48	70.08	< 0.001	0.674 (0.542-0.789)	65.52	71.87	0.045
Combined model	0.828 (0.774-0.873)	66.09	88.19		0.801 (0.679-0.892)	62.07	93.75	

P value: Compared with the combined model by DeLong's test. AUC: Area under the receiver operating characteristic curve; SEN: Sensitivity; SPE: Specificity; CEA: Carcinoembryonic antigen.

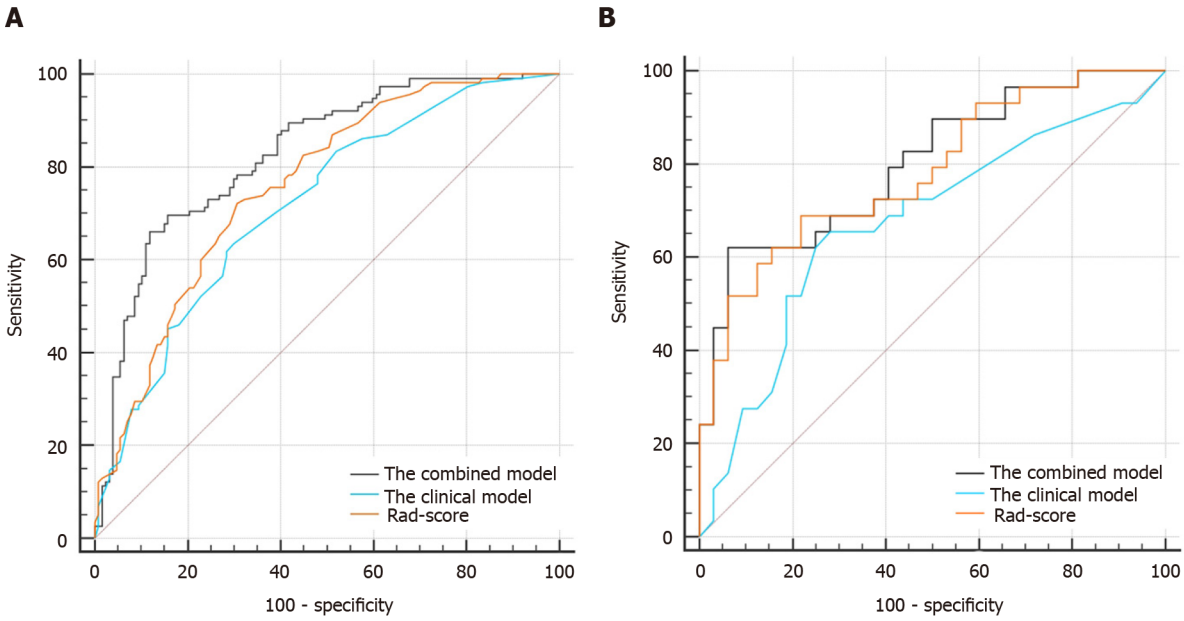


Figure 5 The comparisons of receiver operating characteristic curves in this study. A: In the training cohort: Area under the receiver operating characteristic curve (AUC) = 0.828 for the combined model, 0.718 for the clinical model, and 0.760 for Rad-score; B: In the validation cohort: AUC = 0.801 for the combined model, 0.674 for the clinical model, and 0.782 for Rad-score.

Subgroup analysis

In the cohort of patients treated with nCRT, the AUC of the combined model was higher than that of the clinical model (AUC = 0.853 *vs* 0.710, *P* = 0.011) (Table 4). Among stage III patients, the combined model still had a higher AUC than the clinical model (AUC = 0.796 *vs* 0.630, *P* < 0.001). As for the performance among stage II patients, the combined model failed to outperform the clinical model (AUC = 0.670 *vs* 0.553, *P* = 0.098). Considering the difference between the upper third RC and middle-lower RC in prognosis[23], we performed a subgroup analysis showing that the AUC of the combined model in upper RC group (0.817; 95%CI: 0.730-0.885) was similar with that of the middle-lower RC group (0.824; 95%CI: 0.764-0.875).

DISCUSSION

In this study, a combined model showing potential for predicting PNI of RC outperformed the clinical model (AUC = 0.828 *vs* 0.718, *P* < 0.001 in the training cohort; 0.801 *vs* 0.674, *P* = 0.045 in the validation cohort), indicating that adding Rad-score to the clinical factors improved the predictive value. However, model calibration was not perfect due to the modest overestimation of PNI risk for high-risk patients.

Table 4 Subgroup analyses of the models in the whole cohort

	The clinical model			The combined model			*P* value
Subgroups	**AUC**	**SEN (%)**	**SPE (%)**	**AUC**	**SEN (%)**	**SPE (%)**	
nCRT							
With (*n* = 62)	0.710 (0.581-0.818)	68.00	75.68	0.853 (0.740-0.930)	68.00	89.19	0.011
Without (*n* = 241)	0.712 (0.650-0.768)	48.74	83.61	0.814 (0.759-0.861)	65.55	87.70	< 0.001
Stage							
II (*n* = 62)	0.553 (0.422-0.680)	21.05	93.02	0.670 (0.538-0.784)	36.84	100.00	0.098
III (*n* = 193)	0.630 (0.558-0.698)	56.52	69.23	0.796 (0.732-0.851)	73.04	79.49	< 0.001

P value: Comparisons between the clinical model and combined model. AUC: Area under the receiver operating characteristic curve; SEN: Sensitivity; SPE: Specificity; nCRT: Neoadjuvant chemoradiotherapy.

It has been shown in recent studies that PNI is not only the simple diffusion of cancer cells along connective tissues covering the nerve sheath, but also the interaction of a variety of neurotrophic factors and chemokines between cancer cells and the surrounding microenvironment[5,6]. This process may induce cancer invasion, local recurrence, and metastasis, resulting in poor prognosis. Accurate prediction of PNI helps to evaluate prognosis of RC patients. Currently, the sole approach to determine PNI status is the pathological examination of surgical specimens. Preoperative prediction of PNI helps the formulation of individualized treatment[16,24]. For example, PNI$^+$ patients should accept more aggressive treatment; for instance, nCRT.

In contrast to CT and MRI, radiomics may achieve desirable outcomes for predicting PNI by extracting high-throughput features that can quantify differences between tissues invisible to the naked eyes. Different MRI-based radiomics models have been reported in RC[6,17,18]. However, the sample sizes in the previous studies were small (PNI$^+$: 26-32). In our study, a total of 144 PNI$^+$ patients were enrolled, which increased the reliability of the conclusion.

As for the methodology of radiomics, the machine-learning methods used in our study and previous studies were similar. However, the previous studies only included the intratumoral region, ignoring the peritumoral region in which PNI can also appear [7]. There is evidence that radiomics features of peritumoral regions can offer information about biological characteristics of other tumors, such as gastric[25], breast [26], and lung[27] cancer. Different from the previous studies[6,17,18], we built the model by using both peri- and intratumoral regions, and the model had comparable AUCs with the previous MRI-based models[6,18]. The specificities of our model were 88.19% in the training cohort and 93.75% in the validation cohort, as shown in Table 3, indicating low false-positive rate (misdiagnosis rate) for detecting PNI. However, the sensitivities were low (66.09% in the training cohort and 62.07% in the validation cohort).

In terms of clinical factors, cT and cN included in our model revealed a higher risk of PNI in patients with more advanced RC, which was consistent with the conclusion of a meta-analysis[28]. As for Rad-score, it was more important than clinical factors in the prediction of PNI, due to its longer axis in the nomogram. For example, a PNI$^+$ lesion in Figure 2 was incorrectly identified as PNI$^-$ by the clinical model (CEA = negative, cT = T3, cN = N1a) and correctly determined after adding Rad-score (0.805) to the clinical model with a total score of 12 points in the nomogram, showing a probability of 73% to be PNI$^+$.

Referring to the 62 patients receiving nCRT, we found that AUC of the combined model was improved (0.853; 95%CI: 0.740-0.930), suggesting that this model was also suitable for patients treated with nCRT. With the consideration of individualized evaluation of RC patients with different stages, the combined model obtained a higher AUC than the clinical model for stage III patients (AUC = 0.796 *vs* 0.630, $P < 0.001$). However, the combined model failed to outperform the clinical model among stage II patients (AUC = 0.670 *vs* 0.553, $P = 0.098$), which might be caused by the small sample size of stage II patients. As for the subgroup analysis of location, the combined model had similar predictive values in upper RC group (AUC = 0.817) and in middle-lower RC group (AUC = 0.824), indicating good applicability of the model for both upper and middle-lower RC patients.

There were several limitations to this study. Firstly, bias may have existed due to the retrospective design of this study. Secondly, PNI^- patients from January 2019 to October 2019 were not included, because the current PNI^- patients were sufficient to complete this radiomics analysis. Thirdly, all patients were enrolled from a single institution. In the future, it is necessary to conduct a multicenter validation to extend the versatility of the radiomics model.

CONCLUSION

A combined model incorporating a radiomics signature and clinical factors was described in this study. This model can provide assistance in the individualized prediction of PNI status in patients with RC.

ARTICLE HIGHLIGHTS

Research background

Perineural invasion (PNI) has emerged as an independent prognostic factor in patients with rectal cancer (RC). The preoperative prediction of PNI status is beneficial for individualized treatment and improved prognosis.

Research motivation

Nowadays, preoperative assessment of PNI status is still challenging.

Research objectives

To build a radiomics prediction model for evaluating PNI status preoperatively in RC patients.

Research methods

We enrolled 303 RC patients in a single institution from March 2018 to October 2019. These patients were classified as the training cohort (n = 242) and validation cohort (n = 61). A large number of intra- and peritumoral radiomics features were extracted to build the Rad-score and combined model.

Research results

Our study enrolled more patients (144 PNI^+ and 159 PNI^-) than previous studies[6,17,18]. Rad-score was built by logistic regression analysis. The combined model was developed by combining Rad-score with computed tomography (CT)-reported T stage and N stage, and carcinoembryonic antigen. The combined model showed good performance to predict PNI status, with an area under the receiver operating characteristic curve of 0.828 [95% confidence interval (CI): 0.774-0.873] in the training cohort and 0.801 (95%CI: 0.679-0.892) in the validation cohort.

Research conclusions

The combined model incorporating Rad-score and clinical factors helps to provide an individualized PNI status evaluation.

Research perspectives

Other biological characteristics besides PNI are also related to the prognosis of RC patients; for instance, intramural lymphovascular invasion (LVI). Intramural LVI cannot be determined by magnetic resonance imaging and CT. Therefore, using radiomics or deep learning to predict intramural LVI of RC is valuable in the future.

REFERENCES

1 **Siegel RL**, Miller KD, Goding Sauer A, Fedewa SA, Butterly LF, Anderson JC, Cercek A, Smith RA, Jemal A. Colorectal cancer statistics, 2020. *CA Cancer J Clin* 2020; **70**: 145-164 [PMID: 32133645 DOI: 10.3322/caac.21601]

2 **Lombardi R**, Cuicchi D, Pinto C, Di Fabio F, Iacopino B, Neri S, Tardio ML, Ceccarelli C, Lecce F, Ugolini G, Pini S, Di Tullio P, Taffurelli M, Minni F, Martoni A, Cola B. Clinically-staged T3N0 rectal cancer: is preoperative chemoradiotherapy the optimal treatment? *Ann Surg Oncol* 2010; **17**:

838-845 [PMID: 20012700 DOI: 10.1245/s10434-009-0796-7]
3 **Meng X**, Xia W, Xie P, Zhang R, Li W, Wang M, Xiong F, Liu Y, Fan X, Xie Y, Wan X, Zhu K, Shan H, Wang L, Gao X. Preoperative radiomic signature based on multiparametric magnetic resonance imaging for noninvasive evaluation of biological characteristics in rectal cancer. *Eur Radiol* 2019; **29**: 3200-3209 [PMID: 30413959 DOI: 10.1007/s00330-018-5763-x]
4 **Kim CH**, Yeom SS, Lee SY, Kim HR, Kim YJ, Lee KH, Lee JH. Prognostic Impact of Perineural Invasion in Rectal Cancer After Neoadjuvant Chemoradiotherapy. *World J Surg* 2019; **43**: 260-272 [PMID: 30151676 DOI: 10.1007/s00268-018-4774-8]
5 **Liebig C**, Ayala G, Wilks JA, Berger DH, Albo D. Perineural invasion in cancer: a review of the literature. *Cancer* 2009; **115**: 3379-3391 [PMID: 19484787 DOI: 10.1002/cncr.24396]
6 **Chen J**, Chen Y, Zheng D, Pang P, Zhang H, Zheng X, Liao J. Pretreatment MR-based radiomics nomogram as potential imaging biomarker for individualized assessment of perineural invasion status in rectal cancer. *Abdom Radiol (NY)* 2021; **46**: 847-857 [PMID: 32870349 DOI: 10.1007/s00261-020-02710-4]
7 **Ueno H**, Hase K, Mochizuki H. Criteria for extramural perineural invasion as a prognostic factor in rectal cancer. *Br J Surg* 2001; **88**: 994-1000 [PMID: 11442534 DOI: 10.1046/j.0007-1323.2001.01810.x]
8 **Ceyhan GO**, Liebl F, Maak M, Schuster T, Becker K, Langer R, Demir IE, Hartel M, Friess H, Rosenberg R. The severity of neural invasion is a crucial prognostic factor in rectal cancer independent of neoadjuvant radiochemotherapy. *Ann Surg* 2010; **252**: 797-804 [PMID: 21037435 DOI: 10.1097/SLA.0b013e3181fcab8d]
9 **Sun Q**, Liu T, Liu P, Luo J, Zhang N, Lu K, Ju H, Zhu Y, Wu W, Zhang L, Fan Y, Liu Y, Li D, Liu L. Perineural and lymphovascular invasion predicts for poor prognosis in locally advanced rectal cancer after neoadjuvant chemoradiotherapy and surgery. *J Cancer* 2019; **10**: 2243-2249 [PMID: 31258728 DOI: 10.7150/jca.31473]
10 **Peng J**, Sheng W, Huang D, Venook AP, Xu Y, Guan Z, Cai S. Perineural invasion in pT3N0 rectal cancer: the incidence and its prognostic effect. *Cancer* 2011; **117**: 1415-1421 [PMID: 21425141 DOI: 10.1002/cncr.25620]
11 **Huang CM**, Huang CW, Huang MY, Lin CH, Chen CF, Yeh YS, Ma CJ, Huang CJ, Wang JY. Coexistence of perineural invasion and lymph node metastases is a poor prognostic factor in patients with locally advanced rectal cancer after preoperative chemoradiotherapy followed by radical resection and adjuvant chemotherapy. *Med Princ Pract* 2014; **23**: 465-470 [PMID: 25012611 DOI: 10.1159/000363604]
12 **Nikberg M**, Chabok A, Letocha H, Kindler C, Glimelius B, Smedh K. Lymphovascular and perineural invasion in stage II rectal cancer: a report from the Swedish colorectal cancer registry. *Acta Oncol* 2016; **55**: 1418-1424 [PMID: 27732105 DOI: 10.1080/0284186X.2016.1230274]
13 **Song JH**, Yu M, Kang KM, Lee JH, Kim SH, Nam TK, Jeong JU, Jang HS, Lee JW, Jung JH. Significance of perineural and lymphovascular invasion in locally advanced rectal cancer treated by preoperative chemoradiotherapy and radical surgery: Can perineural invasion be an indication of adjuvant chemotherapy? *Radiother Oncol* 2019; **133**: 125-131 [PMID: 30935568 DOI: 10.1016/j.radonc.2019.01.002]
14 **Huang Y**, He L, Dong D, Yang C, Liang C, Chen X, Ma Z, Huang X, Yao S, Tian J, Liu Z. Individualized prediction of perineural invasion in colorectal cancer: development and validation of a radiomics prediction model. *Chin J Cancer Res* 2018; **30**: 40-50 [PMID: 29545718 DOI: 10.21147/j.issn.1000-9604.2018.01.05]
15 **Huang X**, Liu J, Wu G, Chen S, Pc FJ, Xie W, Tang W. Development and Validation of a Nomogram for Preoperative Prediction of Perineural Invasion in Colorectal Cancer. *Med Sci Monit* 2019; **25**: 1709-1717 [PMID: 30837449 DOI: 10.12659/MSM.914900]
16 **Yang Y**, Huang X, Sun J, Gao P, Song Y, Chen X, Zhao J, Wang Z. Prognostic value of perineural invasion in colorectal cancer: a meta-analysis. *J Gastrointest Surg* 2015; **19**: 1113-1122 [PMID: 25663635 DOI: 10.1007/s11605-015-2761-z]
17 **Guo Y**, Wang Q, Guo Y, Zhang Y, Fu Y, Zhang H. Preoperative prediction of perineural invasion with multi-modality radiomics in rectal cancer. *Sci Rep* 2021; **11**: 9429 [PMID: 33941817 DOI: 10.1038/s41598-021-88831-2]
18 **Yang YS**, Qiu YJ, Zheng GH, Gong HP, Ge YQ, Zhang YF, Feng F, Wang YT. High resolution MRI-based radiomic nomogram in predicting perineural invasion in rectal cancer. *Cancer Imaging* 2021; **21**: 40 [PMID: 34039436 DOI: 10.1186/s40644-021-00408-4]
19 **Bakst RL**, Wong RJ. Mechanisms of Perineural Invasion. *J Neurol Surg B Skull Base* 2016; **77**: 96-106 [PMID: 27123385 DOI: 10.1055/s-0036-1571835]
20 **Benchoufi M**, Matzner-Lober E, Molinari N, Jannot AS, Soyer P. Interobserver agreement issues in radiology. *Diagn Interv Imaging* 2020; **101**: 639-641 [PMID: 32958434 DOI: 10.1016/j.diii.2020.09.001]
21 **van Griethuysen JJM**, Fedorov A, Parmar C, Hosny A, Aucoin N, Narayan V, Beets-Tan RGH, Fillion-Robin JC, Pieper S, Aerts HJWL. Computational Radiomics System to Decode the Radiographic Phenotype. *Cancer Res* 2017; **77**: e104-e107 [PMID: 29092951 DOI: 10.1158/0008-5472.CAN-17-0339]
22 **Roldán-Nofuentes JA**, Amro RM. Combination of the weighted kappa coefficients of two binary diagnostic tests. *J Biopharm Stat* 2018; **28**: 909-926 [PMID: 29172996 DOI: 10.1080/10543406.2017.1402781]

23 **Clancy C**, Flanagan M, Marinello F, O'Neill BD, McNamara D, Burke JP. Comparative Oncologic Outcomes of Upper Third Rectal Cancers: A Meta-analysis. *Clin Colorectal Cancer* 2019; **18**: e361-e367 [PMID: 31445919 DOI: 10.1016/j.clcc.2019.07.004]

24 **Cienfuegos JA**, Rotellar F, Baixauli J, Beorlegui C, Sola JJ, Arbea L, Pastor C, Arredondo J, Hernández-Lizoáin JL. Impact of perineural and lymphovascular invasion on oncological outcomes in rectal cancer treated with neoadjuvant chemoradiotherapy and surgery. *Ann Surg Oncol* 2015; **22**: 916-923 [PMID: 25190129 DOI: 10.1245/s10434-014-4051-5]

25 **Jiang Y**, Wang H, Wu J, Chen C, Yuan Q, Huang W, Li T, Xi S, Hu Y, Zhou Z, Xu Y, Li G, Li R. Noninvasive imaging evaluation of tumor immune microenvironment to predict outcomes in gastric cancer. *Ann Oncol* 2020; **31**: 760-768 [PMID: 32240794 DOI: 10.1016/j.annonc.2020.03.295]

26 **Braman N**, Prasanna P, Whitney J, Singh S, Beig N, Etesami M, Bates DDB, Gallagher K, Bloch BN, Vulchi M, Turk P, Bera K, Abraham J, Sikov WM, Somlo G, Harris LN, Gilmore H, Plecha D, Varadan V, Madabhushi A. Association of Peritumoral Radiomics With Tumor Biology and Pathologic Response to Preoperative Targeted Therapy for HER2 (ERBB2)-Positive Breast Cancer. *JAMA Netw Open* 2019; **2**: e192561 [PMID: 31002322 DOI: 10.1001/jamanetworkopen.2019.2561]

27 **Pérez-Morales J**, Tunali I, Stringfield O, Eschrich SA, Balagurunathan Y, Gillies RJ, Schabath MB. Peritumoral and intratumoral radiomic features predict survival outcomes among patients diagnosed in lung cancer screening. *Sci Rep* 2020; **10**: 10528 [PMID: 32601340 DOI: 10.1038/s41598-020-67378-8]

28 **Knijn N**, Mogk SC, Teerenstra S, Simmer F, Nagtegaal ID. Perineural Invasion is a Strong Prognostic Factor in Colorectal Cancer: A Systematic Review. *Am J Surg Pathol* 2016; **40**: 103-112 [PMID: 26426380 DOI: 10.1097/PAS.0000000000000518]

World Journal of Gastroenterology

Submit a Manuscript: https://www.f6publishing.com

World J Gastroenterol 2021 September 7; 27(33): 5622-5624

DOI: 10.3748/wjg.v27.i33.5622

ISSN 1007-9327 (print) ISSN 2219-2840 (online)

LETTER TO THE EDITOR

Comment on "Diagnostic approach to faecal incontinence: What test and when to perform?"

Jiang-Tao Wang, Yan-Dong Miao, Quan-Lin Guan

ORCID number: Jiang-Tao Wang 0000-0002-1222-164X; Yan-Dong Miao 0000-0002-1429-8915; Quan-Lin Guan 0000-0003-4947-8016.

Author contributions: Wang JT and Miao YD designed and performed the research; Wang JT wrote this comment; Guan QL revised the manuscript.

Conflict-of-interest statement: All authors declare having no conflict of interests.

Open-Access: This article is an open-access article that was selected by an in-house editor and fully peer-reviewed by external reviewers. It is distributed in accordance with the Creative Commons Attribution NonCommercial (CC BY-NC 4.0) license, which permits others to distribute, remix, adapt, build upon this work non-commercially, and license their derivative works on different terms, provided the original work is properly cited and the use is non-commercial. See: http://creativecommons.org/Licenses/by-nc/4.0/

Manuscript source: Invited manuscript

Specialty type: Gastroenterology and hepatology

Country/Territory of origin: China

Jiang-Tao Wang, Yan-Dong Miao, The First Clinical Medical College of Lanzhou University, Lanzhou University, Lanzhou 730000, Gansu Province, China

Quan-Lin Guan, Department of Oncology, The First Hospital of Lanzhou University, Lanzhou University, Lanzhou 730000, Gansu Province, China

Corresponding author: Quan-Lin Guan, MD, PhD, Chief Doctor, Full Professor, Department of Oncology, The First Hospital of Lanzhou University, Lanzhou University, No. 1 Donggang West Road, Chengguan District, Lanzhou 730000, Gansu Province, China.
guanquanlin@yeah.net

Abstract

We recently read with interest the article "Diagnostic approach to faecal incontinence: What test and when to perform?". This is a comprehensive and practical review, which has particular significance for guiding clinicians to improve the examination strategy. Although we appreciate their work very much, based on the in-depth analysis of this research, we found some detailed problems in the article and will give our comments in this letter. If the author can further improve the relevant research, it will be valuable.

Key Words: Faecal; Incontinence; Manometry; Diagnostic; Pathophysiology; Tools

©The Author(s) 2021. Published by Baishideng Publishing Group Inc. All rights reserved.

Core Tip: Faecal incontinence (FI) has caused social, psychological, and economic pressure on an increasing number of people. It is essential to explore the diagnostic strategies and treatment techniques for FI. We read with great interest the article "Diagnostic approach to faecal incontinence: What test and when to perform?". This article had substantial clinical reference value and minor problems. We want to share our views and opinions on this valuable work.

Citation: Wang JT, Miao YD, Guan QL. Comment on "Diagnostic approach to faecal incontinence: What test and when to perform?". *World J Gastroenterol* 2021; 27(33): 5622-5624

URL: https://www.wjgnet.com/1007-9327/full/v27/i33/5622.htm

Peer-review report's scientific quality classification
Grade A (Excellent): 0
Grade B (Very good): 0
Grade C (Good): C, C
Grade D (Fair): 0
Grade E (Poor): 0

Received: May 9, 2021
Peer-review started: May 9, 2021
First decision: June 12, 2021
Revised: June 21, 2021
Accepted: August 20, 2021
Article in press: August 20, 2021
Published online: September 7, 2021

P-Reviewer: Acharyya BC, Tadros M
S-Editor: Fan JR
L-Editor: A
P-Editor: Guo X

DOI: https://dx.doi.org/10.3748/wjg.v27.i33.5622

TO THE EDITOR

We read with pleasure the article "Diagnostic approach to faecal incontinence: What test and when to perform?"[1]. Within this article, the authors analyzed and summarized systematically the assessment and examination of patients with faecal incontinence (FI), thereby providing a valuable reference for clinicians. The salient highlight of this review was that it not only systematically expounded the etiology and pathogenesis of FI but also combined clinical evaluation and inspection strategies and provided unique insights into the structured and step-by-step method of evaluating and diagnosing FI. This research has a strong reference and practical value for sorting out the management strategies for FI and overcoming limitations. We found some details through further research and analysis and anticipate a discussion with the authors.

First, the authors analyzed the etiology and clinicopathologic features of patients with FI and described the diagnostic strategies including high-resolution anorectal manometry, perineal ultrasound, transrectal ultrasound, endopelvic magnetic resonance imaging, and electromyography of the anal sphincter. The use of a standardized quality-of-life assessment tool to define the extent and impact of FI is the first step in assessing patients with FI[2,3]. For instance, the PERFECT system in the modified OXFORD scale is available for evaluating vaginal and rectal resections. However, the most critical step was not detailed in this review.

From this paper, the authors concluded that the incidence of FI had no differences in both males and females, but the pathogenesis is different. To this end, we have reviewed a great deal of relevant literature and obtained different conclusions. For example, a study from the United States reported that the prevalence of FI is 2.2%, with 63% in females and 37% in males, and approximately 30% of patients are over 65 years of age[4]. Consequently, we conclude that females are more likely to develop FI owing to their physiology and childbearing experiences[5]. In addition, the factors that cause FI are different in women and men, with women being more susceptible to anal sphincter disorders due to obstetric trauma and reduced pelvic floor muscle training (PFMT), whereas men are more likely to suffer from anorectal sensory disturbances [6]. Based on a careful analysis of the authors' list of etiologies and risk factors for FI, we found that some factors overlooked are becoming increasingly important with the increasing incidence of rectal tumors and gynecology in women. For example, undergoing rectal surgery, pelvic radiotherapy, or the presence of the tumor or inflammatory stricture (IBM) is usually accompanied by impaired rectal storage function and decreased compliance[3]. Therefore, we consider that the abovementioned factors should be supplemented.

Finally, the authors provided a review of common tools and strategies for diagnosing FI, which in turn provides guidance and reference for clinical application. Unfortunately, after extensive reading of the associated papers, we found that such strategies were insufficiently comprehensive. For example, an increasing number of studies recommend the usage of NS neurostimulation electrodes for diagnosis and treatment as a preliminary step in the absence of contraindications[7,8]. In 2012, Cochrane *et al*. conducted a meta-analysis of 21 studies and found that there is a lack of sufficient trials to support the effectiveness of pure anal sphincter exercise and biologic therapy. Consequently, a combination of biofeedback and PFMT with other methods is recommended (*e.g.*, neuroelectrical stimulation combined with techniques) may improve the overall outcome[9].

In summary, this review can be a valuable basis and reference for the diagnosis of patients with FI and is of particular practical value for guiding clinicians in the development of screening strategies. Of course, we only offer our comments based on the existing literature or data on the shortcomings of this review, and more comprehensive and clinically verified examination strategies and treatments are expected to be served for patients with FI.

REFERENCES

1 **Sbeit W**, Khoury T, Mari A. Diagnostic approach to faecal incontinence: What test and when to perform? *World J Gastroenterol* 2021; **27**: 1553-1562 [PMID: 33958842 DOI:

10.3748/wjg.v27.i15.1553]
2 **Vaizey CJ**, Carapeti E, Cahill JA, Kamm MA. Prospective comparison of faecal incontinence grading systems. *Gut* 1999; **44**: 77-80 [PMID: 9862829 DOI: 10.1136/gut.44.1.77]
3 **Saldana Ruiz N**, Kaiser AM. Fecal incontinence - Challenges and solutions. *World J Gastroenterol* 2017; **23**: 11-24 [PMID: 28104977 DOI: 10.3748/wjg.v23.i1.11]
4 **Nelson R**, Norton N, Cautley E, Furner S. Community-based prevalence of anal incontinence. *JAMA* 1995; **274**: 559-561 [PMID: 7629985]
5 **Kumar N**, Kumar D. Fecal incontinence and rectal prolapse. *Indian J Gastroenterol* 2019; **38**: 465-469 [PMID: 32002830 DOI: 10.1007/s12664-020-01014-1]
6 **Mazur-Bialy AI**, Kołomańska-Bogucka D, Opławski M, Tim S. Physiotherapy for Prevention and Treatment of Fecal Incontinence in Women-Systematic Review of Methods. *J Clin Med* 2020; **9** [PMID: 33053702 DOI: 10.3390/jcm9103255]
7 **Kenefick NJ**, Vaizey CJ, Nicholls RJ, Cohen R, Kamm MA. Sacral nerve stimulation for faecal incontinence due to systemic sclerosis. *Gut* 2002; **51**: 881-883 [PMID: 12427794 DOI: 10.1136/gut.51.6.881]
8 **Maeda Y**, O'Connell PR, Lehur PA, Matzel KE, Laurberg S; European SNS Bowel Study Group. Sacral nerve stimulation for faecal incontinence and constipation: a European consensus statement. *Colorectal Dis* 2015; **17**: O74-O87 [PMID: 25603960 DOI: 10.1111/codi.12905]
9 **Norton C**, Chelvanayagam S, Wilson-Barnett J, Redfern S, Kamm MA. Randomized controlled trial of biofeedback for fecal incontinence. *Gastroenterology* 2003; **125**: 1320-1329 [PMID: 14598248 DOI: 10.1016/j.gastro.2003.09.039]

Published by **Baishideng Publishing Group Inc**
7041 Koll Center Parkway, Suite 160, Pleasanton, CA 94566, USA
Telephone: +1-925-3991568
E-mail: bpgoffice@wjgnet.com
Help Desk: https://www.f6publishing.com/helpdesk
https://www.wjgnet.com

© 2021 Baishideng Publishing Group Inc. All rights reserved.

ISSN 1007-9327 (print)
ISSN 2219-2840 (online)

World Journal of *Gastroenterology*

World J Gastroenterol 2021 September 14; 27(34): 5625-5795



Published by Baishideng Publishing Group Inc

World Journal of Gastroenterology

Contents

Weekly Volume 27 Number 34 September 14, 2021

EDITORIAL

5625 Serrated lesions: A challenging enemy

Trovato A, Turshudzhyan A, Tadros M

REVIEW

5630 Liver disorders in COVID-19, nutritional approaches and the use of phytochemicals

Vargas-Mendoza N, García-Machorro J, Angeles-Valencia M, Martínez-Archundia M, Madrigal-Santillán EO, Morales-González Á, Anguiano-Robledo L, Morales-González JA

5666 Recent advances in blood-based and artificial intelligence-enhanced approaches for gastrointestinal cancer diagnosis

Li LS, Guo XY, Sun K

5682 Liver disease and COVID-19: The link with oxidative stress, antioxidants and nutrition

Ristic-Medic D, Petrovic S, Arsic A, Vucic V

MINIREVIEWS

5700 Updates in diagnosis and management of pancreatic cysts

Lee LS

5715 Artificial intelligence for hepatitis evaluation

Liu W, Liu X, Peng M, Chen GQ, Liu PH, Cui XW, Jiang F, Dietrich CF

5727 Machine perfusion of the liver: Putting the puzzle pieces together

Boteon YL, Martins PN, Muiesan P, Schlegel A

ORIGINAL ARTICLE

Retrospective Cohort Study

5737 *MTNR1B* polymorphisms with *CDKN2A* and *MGMT* methylation status are associated with poor prognosis of colorectal cancer in Taiwan

Lee CC, Kuo YC, Hu JM, Chang PK, Sun CA, Yang T, Li CW, Chen CY, Lin FH, Hsu CH, Chou YC

Retrospective Study

5753 Validation of conventional non-invasive fibrosis scoring systems in patients with metabolic associated fatty liver disease

Wu YL, Kumar R, Wang MF, Singh M, Huang JF, Zhu YY, Lin S

Observational Study

5764 Secular decreasing trends in gastric cancer incidence in Taiwan: A population-based cancer registry study

Lin YT, Chiang CJ, Yang YW, Huang SP, You SL

World Journal of Gastroenterology

Weekly Volume 27 Number 34 September 14, 2021

Contents

META-ANALYSIS

5775 Dietary intake in patients with chronic pancreatitis: A systematic review and meta-analysis

Ul Ain Q, Bashir Y, Kelleher L, Bourne DM, Egan SM, McMahon J, Keaskin L, Griffin OM, Conlon KC, Duggan SN

LETTER TO THE EDITOR

5793 Relationship between nonalcoholic fatty liver disease and chronic kidney disease could start in childhood

Di Sessa A, Guarino S, Melone R, De Simone RF, Marzuillo P, Miraglia del Giudice E

Contents

ABOUT COVER

Editorial Board Member of *World Journal of Gastroenterology*, Konstantinos Triantafyllou, MD, PhD, FEBGH, Professor, Hepatogastroenterology Unit, 2nd Department of Propaedeutic Internal Medicine, Medical School, National and Kapodistian University of Athens, Attikon University General Hospital, 1, Rimini Street, Athens 12462, Greece. ktriant@med.uoa.gr

AIMS AND SCOPE

The primary aim of *World Journal of Gastroenterology* (*WJG*, *World J Gastroenterol*) is to provide scholars and readers from various fields of gastroenterology and hepatology with a platform to publish high-quality basic and clinical research articles and communicate their research findings online. *WJG* mainly publishes articles reporting research results and findings obtained in the field of gastroenterology and hepatology and covering a wide range of topics including gastroenterology, hepatology, gastrointestinal endoscopy, gastrointestinal surgery, gastrointestinal oncology, and pediatric gastroenterology.

INDEXING/ABSTRACTING

The *WJG* is now indexed in Current Contents®/Clinical Medicine, Science Citation Index Expanded (also known as SciSearch®), Journal Citation Reports®, Index Medicus, MEDLINE, PubMed, PubMed Central, and Scopus. The 2021 edition of Journal Citation Report® cites the 2020 impact factor (IF) for *WJG* as 5.742; Journal Citation Indicator: 0.79; IF without journal self cites: 5.590; 5-year IF: 5.044; Ranking: 28 among 92 journals in gastroenterology and hepatology; and Quartile category: Q2. The *WJG*'s CiteScore for 2020 is 6.9 and Scopus CiteScore rank 2020: Gastroenterology is 19/136.

RESPONSIBLE EDITORS FOR THIS ISSUE

Production Editor: *Ji-Hong Liu*; **Production Department Director:** *Yu-Jie Ma*; **Editorial Office Director:** *Ze-Mao Gong*.

NAME OF JOURNAL
World Journal of Gastroenterology

ISSN
ISSN 1007-9327 (print) ISSN 2219-2840 (online)

LAUNCH DATE
October 1, 1995

FREQUENCY
Weekly

EDITORS-IN-CHIEF
Andrzej S Tarnawski, Subrata Ghosh

EDITORIAL BOARD MEMBERS
http://www.wjgnet.com/1007-9327/editorialboard.htm

PUBLICATION DATE
September 14, 2021

COPYRIGHT
© 2021 Baishideng Publishing Group Inc

INSTRUCTIONS TO AUTHORS
https://www.wjgnet.com/bpg/gerinfo/204

GUIDELINES FOR ETHICS DOCUMENTS
https://www.wjgnet.com/bpg/GerInfo/287

GUIDELINES FOR NON-NATIVE SPEAKERS OF ENGLISH
https://www.wjgnet.com/bpg/gerinfo/240

PUBLICATION ETHICS
https://www.wjgnet.com/bpg/GerInfo/288

PUBLICATION MISCONDUCT
https://www.wjgnet.com/bpg/gerinfo/208

ARTICLE PROCESSING CHARGE
https://www.wjgnet.com/bpg/gerinfo/242

STEPS FOR SUBMITTING MANUSCRIPTS
https://www.wjgnet.com/bpg/GerInfo/239

ONLINE SUBMISSION
https://www.f6publishing.com

© 2021 Baishideng Publishing Group Inc. All rights reserved. 7041 Koll Center Parkway, Suite 160, Pleasanton, CA 94566, USA
E-mail: bpgoffice@wjgnet.com https://www.wjgnet.com

World Journal of Gastroenterology

Submit a Manuscript: https://www.f6publishing.com

World J Gastroenterol 2021 September 14; 27(34): 5625-5629

DOI: 10.3748/wjg.v27.i34.5625

ISSN 1007-9327 (print) ISSN 2219-2840 (online)

EDITORIAL

Serrated lesions: A challenging enemy

Alexa Trovato, Alla Turshudzhyan, Micheal Tadros

ORCID number: Alexa Trovato 0000-0003-2411-9834; Alla Turshudzhyan 0000-0001-6867-7569; Micheal Tadros 0000-0003-3118-3893.

Author contributions: Trovato A, Turshudzhyan A, and Tadros M all wrote the manuscript and contributed equally to this work; all authors have read and approve the final manuscript.

Conflict-of-interest statement: There are no financial arrangements to disclose in the development of this editorial from any of the authors. All appropriate consent was obtained. There is no conflict of interest to disclose from any of the authors.

Open-Access: This article is an open-access article that was selected by an in-house editor and fully peer-reviewed by external reviewers. It is distributed in accordance with the Creative Commons Attribution NonCommercial (CC BY-NC 4.0) license, which permits others to distribute, remix, adapt, build upon this work non-commercially, and license their derivative works on different terms, provided the original work is properly cited and the use is non-commercial. See: http://creativecommons.org/Licenses/by-nc/4.0/

Manuscript source: Invited manuscript

Alexa Trovato, Albany Medical College, Albany, NY 12208, United States

Alla Turshudzhyan, Department of Medicine, University of Connecticut, School of Medicine, Farmingdale, CT 06032, United States

Micheal Tadros, Department of Gastroenterology, Albany Medical Center, Albany, NY 12208, United States

Corresponding author: Micheal Tadros, FACG, MD, Associate Professor, Doctor, Department of Gastroenterology, Albany Medical Center, 43 New Scotland Ave, Albany, NY 12208, United States. tadrosm1@amc.edu

Abstract

The serrated pathway accounts for 30%-35% of colorectal cancer (CRC). Unlike hyperplastic polyps, both sessile serrated lesions (SSLs) and traditional serrated adenomas are premalignant lesions, yet SSLs are considered to be the principal serrated precursor of CRCs. Serrated lesions represent a challenge in detection, classification, and removal–contributing to post-colonoscopy cancer. Therefore, it is of the utmost importance to characterize these lesions properly to ensure complete removal. A retrospective cohort study developed a diagnostic scoring system for SSLs to facilitate their detection endoscopically and subsequent removal. From the study, it can be ascertained that both indistinct border and mucus cap are essential in both recognizing and diagnosing serrated lesions. The proximal colon poses technical challenges for some endoscopists, which is why high-quality colonoscopy plays such an important role. The indistinct border of some SSLs poses another challenge due to difficult complete resection. Overall, it is imperative that gastroenterologists use the key features of mucus cap, indistinct borders, and size of at least five millimeters along with a high-quality colonoscopy and a good bowel preparation to improve the SSL detection rate.

Key Words: Sessile serrated lesions; Colonoscopy; Polyps; Colorectal cancer screening; Hyperplastic polyps; Traditional serrated adenomas

©The Author(s) 2021. Published by Baishideng Publishing Group Inc. All rights reserved.

Core Tip: Serrated lesions represent a challenge in detection, classification, and removal. The mucus cap, flat nature, and indistinct borders make these lesions difficult

Specialty type: Gastroenterology and hepatology

Country/Territory of origin: United States

Peer-review report's scientific quality classification
Grade A (Excellent): A
Grade B (Very good): 0
Grade C (Good): 0
Grade D (Fair): 0
Grade E (Poor): 0

Received: May 3, 2021
Peer-review started: May 3, 2021
First decision: June 2, 2021
Revised: June 11, 2021
Accepted: August 17, 2021
Article in press: August 17, 2021
Published online: September 14, 2021

P-Reviewer: Teramoto-Matsubara OT
S-Editor: Fan JR
L-Editor: A
P-Editor: Xing YX

to localize endoscopically. Therefore, it is important to characterize these lesions properly to ensure complete removal and a reduction in post-colonoscopy cancer. A study recently developed a diagnostic scoring system for sessile serrated lesions to facilitate their detection endoscopically and removal. The study shows that both indistinct border and mucus cap are essential in both recognizing and diagnosing serrated lesions, further emphasizing the importance of a good colon preparation and a high-quality colonoscopy.

Citation: Trovato A, Turshudzhyan A, Tadros M. Serrated lesions: A challenging enemy. *World J Gastroenterol* 2021; 27(34): 5625-5629
URL: https://www.wjgnet.com/1007-9327/full/v27/i34/5625.htm
DOI: https://dx.doi.org/10.3748/wjg.v27.i34.5625

INTRODUCTION

The serrated pathway accounts for 30%-35% of colorectal cancer (CRC)[1]. Serrated lesions are characterized histologically by a saw-tooth or serrated glandular pattern, likely secondary to a lack of apoptosis of dividing cells in the colonic crypts, resulting in the cells folding onto each other and giving it a serrated appearance. While a variety of molecular mechanisms contribute to neoplastic progression, hypermethylation of DNA promoter regions resulting in a CpG island methylator phenotype is believed to be the major mechanism driving the serrated pathway to CRC[2] . According to the 2019 World Health Organization 5th edition classification, serrated colorectal lesions can be further defined into four main categories: Hyperplastic polyps (HPs), with microvesicular (MVHP) and goblet cell-rich subtypes; sessile serrated lesion (SSL) and SSL with dysplasia, both previously known as SSA/Ps with or without cytological dysplasia; traditional serrated adenoma (TSA); and serrated adenoma, unclassified[3]. HPs are the most common non-neoplastic polyps in the colon, typically located in the rectosigmoid region and are often less than five millimeters in size. These polyps are polypoid in appearance and do not exhibit dysplasia and therefore do not increase the risk of CRC[4]. SSLs are usually more prevalent in the proximal colon and have a smooth surface with a "cloud-like" appearance[2]. They can be flat or sessile, and may be covered in mucus. TSAs can be pedunculated or sessile in appearance and are typically found in the rectosigmoid colon. Unlike HPs, both SSLs and TSAs are premalignant lesions, yet SSLs are considered to be the principal serrated precursor of CRCs[5]. Therefore, SSLs must be distinguished from HPs to ensure an accurate diagnosis.

THE CHALLENGES OF SERRATED LESIONS

Serrated lesions represent a challenge in detection, classification, and removal. As portrayed in Figure 1, the mucus cap, flat nature, and indistinct borders makes these lesions difficult to localize endoscopically, resulting in them being incompletely removed or easily missed[6]. In terms of classification, SSLs may initially be misclassified as HPs due to similarities in histological appearance. Serrated lesions may exhibit MVHP pathology in some areas, but display SSL morphology, blurring the lines between SSLs and HPs and resulting in a misclassification and misdiagnosis[5]. In fact, certain factors such as location in the proximal colon as well as size greater than five millimeters have been shown to change the pathological diagnosis of HP to SSL[7]. For all of these reasons combined with the fact that they tend to exhibit a more rapid progression to cancer, SSLs play a role in post-colonoscopy cancer[6]. Therefore, it is of utmost importance to characterize these lesions properly to ensure complete removal and a reduction in post-colonoscopy cancer. Nishizawa *et al*[8] 2021 performed a retrospective cohort study to develop a diagnostic scoring system for SSLs to facilitate their detection endoscopically and subsequent removal.

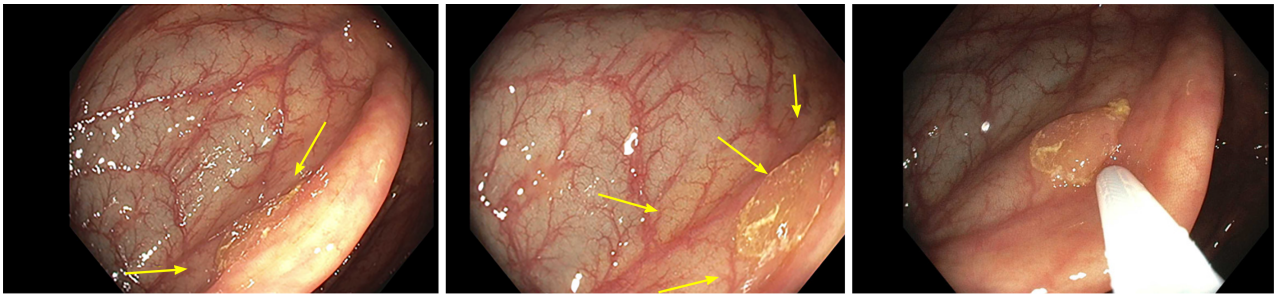


Figure 1 Flat polyp with visible mucus cap and indistinct border identified on colonoscopy at hepatic flexure. This polyp was only able to be visualized with an excellent bowel prep.

DIAGNOSTIC SCORING SYSTEM FOR SERRATED LESIONS

Nishizawa *et al*[8] 2021 collected data on serrated lesions diagnosed either by endoscopic or pathologic means. They analyzed 232 polyps that were diagnosed as serrated polyps, and univariate analysis determined that the proximal colon location ($P = 0.003$), size greater than five millimeters ($P < 0.001$), presence of mucus cap ($P < 0.001$), presence of cloud-like surface ($P < 0.001$), and presence of microvascular vessels ($P = 0.024$) were significantly associated with the presence of SSLs. Through multivariate analysis, mucus cap ($P = 0.005$), size greater than five millimeters ($P = 0.033$), and indistinct borders ($P = 0.033$) were deemed as characteristics independently associated with the diagnosis of SSLs. Each of these characteristics were assigned one point, the sum of them defining the endoscopic SSL diagnosis score. Through receiver-operating characteristic curve analysis, a cut-off score of three was determined to be most optimal, resulting in prediction of pathological SSLs with a 75% sensitivity, 80% specificity, and 78.4% accuracy. Overall, the authors determined that serrated polyps with a size greater than five millimeters, presence of a mucus cap, and indistinct borders should be removed during colonoscopy[8].

THE IMPORTANCE OF AN EXCELLENT BOWEL PREP AND HIGH-QUALITY COLONOSCOPY

From the study, it can be ascertained that both indistinct border and mucus cap are essential in recognizing and diagnosing serrated lesions. The mucus cap can mimic the appearance of a benign mucus collection and thus be missed by the untrained eye easily on colonoscopy. A practical word of advice would be to wash the mucus gently starting at the edge to observe if there is polyp tissue hiding underneath. This further emphasizes the importance of a good colon preparation and a high-quality colonoscopy. Bowel preparation should be adequate to consistently allow for detection of polyps greater than five millimeters after leftover stool suctioning[9]. It is important to note that chyme from the small intestine can coat the proximal colon when bowel preparation agents are given the day prior to the procedure, resulting in impaired detection of flat lesions[10]. Furthermore, as the time interval between the end of bowel preparation and the start of colonoscopy increases by the hour, the likelihood of having a good or excellent bowel preparation of the cecum is decreased by ten percent [11]. Splitting of bowel cleansing to half of the preparation given on the day of the procedure has shown to have overwhelmingly superior efficacy when compared to traditional regimen[12]. Split dose leads to higher adenoma detection rate and several guidelines have endorsed its use[13,14].

The proximal colon poses technical challenges for some endoscopists, which is why high-quality colonoscopy plays such an important role. Both retroflexion and second-look techniques have been shown to improve adenoma detection rate in the right colon[15,16]. Retroflexion in the right colon is a maneuver in which the colonoscope makes a U-turn, allowing better visualization of the proximal sides of the haustral folds[17]. A 2017 meta-analysis found that retroflexion detected 17% of adenomas of the right colon that would have otherwise been missed on conventional colonoscopy [15]. Superiority of retroflexion to the second examination has not been confirmed. Second examination of the right colon has been shown to improve adenoma detection rate by a very similar amount and may be preferred over retroflexion as it is an easier

maneuver to perform[16].

The indistinct border of some SSLs poses another challenge due to difficulty of complete resection. For instance, studies have suggested that residual tissue determined to be complete after polypectomy ranges from 6.5%-22.7%[18]. A pooled analysis from eight surveillance studies that followed patients with adenoma post-colonoscopy suggested that roughly 20% of malignancies were due to incomplete resection while nearly 50% of post-colonoscopy malignancies were acquired from missed lesions[19]. It is recommended that the type of resection method (*e.g.*, cold snare, hot snare, EMR) is thoroughly documented. It is also recommended that, if resected en block, non-pedunculated lesions are to be pinned to a flat surface prior to being submitted to pathology and be measured for the depth of the submucosal invasion[10].

CONCLUSION

The key constituents of the diagnostic score proposed by Nishizawa *et al*[8] 2021 provide essential information about the nature of the serrated lesions. It is imperative that gastroenterologists use those key features along with a high-quality colonoscopy and a good bowel preparation to improve the SSL detection rate. The article also stresses the importance of complete resection of the SSL and training of endoscopists to recognize and fully resect such challenging lesions.

REFERENCES

1 **Singh R**, Zorrón Cheng Tao Pu L, Koay D, Burt A. Sessile serrated adenoma/polyps: Where are we at in 2016? *World J Gastroenterol* 2016; **22**: 7754-7759 [PMID: 27678358 DOI: 10.3748/wjg.v22.i34.7754]

2 **Higuchi T**, Sugihara K, Jass JR. Demographic and pathological characteristics of serrated polyps of colorectum. *Histopathology* 2005; **47**: 32-40 [PMID: 15982321 DOI: 10.1111/j.1365-2559.2005.02180.x]

3 **Nagtegaal ID**, Odze RD, Klimstra D, Paradis V, Rugge M, Schirmacher P, Washington KM, Carneiro F, Cree IA; WHO Classification of Tumours Editorial Board. The 2019 WHO classification of tumours of the digestive system. *Histopathology* 2020; **76**: 182-188 [PMID: 31433515 DOI: 10.1111/his.13975]

4 **Laiyemo AO**, Murphy G, Sansbury LB, Wang Z, Albert PS, Marcus PM, Schoen RE, Cross AJ, Schatzkin A, Lanza E. Hyperplastic polyps and the risk of adenoma recurrence in the polyp prevention trial. *Clin Gastroenterol Hepatol* 2009; **7**: 192-197 [PMID: 18849014 DOI: 10.1016/j.cgh.2008.08.031]

5 **Rex DK**, Ahnen DJ, Baron JA, Batts KP, Burke CA, Burt RW, Goldblum JR, Guillem JG, Kahi CJ, Kalady MF, O'Brien MJ, Odze RD, Ogino S, Parry S, Snover DC, Torlakovic EE, Wise PE, Young J, Church J. Serrated lesions of the colorectum: review and recommendations from an expert panel. *Am J Gastroenterol* 2012; **107**: 1315-29; quiz 1314, 1330 [PMID: 22710576 DOI: 10.1038/ajg.2012.161]

6 **Iwatate M**, Kitagawa T, Katayama Y, Tokutomi N, Ban S, Hattori S, Hasuike N, Sano W, Sano Y, Tamano M. Post-colonoscopy colorectal cancer rate in the era of high-definition colonoscopy. *World J Gastroenterol* 2017; **23**: 7609-7617 [PMID: 29204060 DOI: 10.3748/wjg.v23.i42.7609]

7 **Niv Y**. Changing pathological diagnosis from hyperplastic polyp to sessile serrated adenoma: systematic review and meta-analysis. *Eur J Gastroenterol Hepatol* 2017; **29**: 1327-1331 [PMID: 29049128 DOI: 10.1097/MEG.0000000000000994]

8 **Nishizawa T**, Yoshida S, Toyoshima A, Yamada T, Sakaguchi Y, Irako T, Ebinuma H, Kanai T, Koike K, Toyoshima O. Endoscopic diagnosis for colorectal sessile serrated lesions. *World J Gastroenterol* 2021; **27**: 1321-1329 [PMID: 33833485 DOI: 10.3748/wjg.v27.i13.1321]

9 **Gupta S**, Lieberman D, Anderson JC, Burke CA, Dominitz JA, Kaltenbach T, Robertson DJ, Shaukat A, Syngal S, Rex DK. Recommendations for Follow-Up After Colonoscopy and Polypectomy: A Consensus Update by the US Multi-Society Task Force on Colorectal Cancer. *Gastrointest Endosc* 2020; **91**: 463-485.e5 [PMID: 32044106 DOI: 10.1016/j.gie.2020.01.014]

10 **Johnson DA**, Barkun AN, Cohen LB, Dominitz JA, Kaltenbach T, Martel M, Robertson DJ, Boland CR, Giardello FM, Lieberman DA, Levin TR, Rex DK; US Multi-Society Task Force on Colorectal Cancer. Optimizing adequacy of bowel cleansing for colonoscopy: recommendations from the US multi-society task force on colorectal cancer. *Gastroenterology* 2014; **147**: 903-924 [PMID: 25239068 DOI: 10.1053/j.gastro.2014.07.002]

11 **Siddiqui AA**, Yang K, Spechler SJ, Cryer B, Davila R, Cipher D, Harford WV. Duration of the interval between the completion of bowel preparation and the start of colonoscopy predicts bowel-preparation quality. *Gastrointest Endosc* 2009; **69**: 700-706 [PMID: 19251013 DOI: 10.1016/j.gie.2008.09.047]

12 **Cohen LB**. Split dosing of bowel preparations for colonoscopy: an analysis of its efficacy, safety, and

tolerability. *Gastrointest Endosc* 2010; **72**: 406-412 [PMID: 20579994 DOI: 10.1016/j.gie.2010.04.001]

13 **Jover R**, Zapater P, Polanía E, Bujanda L, Lanas A, Hermo JA, Cubiella J, Ono A, González-Méndez Y, Peris A, Pellisé M, Seoane A, Herreros-de-Tejada A, Ponce M, Marín-Gabriel JC, Chaparro M, Cacho G, Fernández-Díez S, Arenas J, Sopeña F, de-Castro L, Vega-Villaamil P, Rodríguez-Soler M, Carballo F, Salas D, Morillas JD, Andreu M, Quintero E, Castells A; COLONPREV study investigators. Modifiable endoscopic factors that influence the adenoma detection rate in colorectal cancer screening colonoscopies. *Gastrointest Endosc* 2013; **77**: 381-389.e1 [PMID: 23218945 DOI: 10.1016/j.gie.2012.09.027]

14 **Wexner SD**, Beck DE, Baron TH, Fanelli RD, Hyman N, Shen B, Wasco KE; American Society of Colon and Rectal Surgeons; American Society for Gastrointestinal Endoscopy; Society of American Gastrointestinal and Endoscopic Surgeons. A consensus document on bowel preparation before colonoscopy: prepared by a task force from the American Society of Colon and Rectal Surgeons (ASCRS), the American Society for Gastrointestinal Endoscopy (ASGE), and the Society of American Gastrointestinal and Endoscopic Surgeons (SAGES). *Gastrointest Endosc* 2006; **63**: 894-909 [PMID: 16733101 DOI: 10.1016/j.gie.2006.03.918]

15 **Cohen J**, Grunwald D, Grossberg LB, Sawhney MS. The Effect of Right Colon Retroflexion on Adenoma Detection: A Systematic Review and Meta-analysis. *J Clin Gastroenterol* 2017; **51**: 818-824 [PMID: 27683963 DOI: 10.1097/MCG.0000000000000695]

16 **Núñez Rodríguez MH**, Díez Redondo P, Riu Pons F, Cimavilla M, Hernández L, Loza A, Pérez-Miranda M. Proximal retroflexion *vs* second forward view of the right colon during screening colonoscopy: A multicentre randomized controlled trial. *United European Gastroenterol J* 2020; **8**: 725-735 [PMID: 32379535 DOI: 10.1177/2050640620924210]

17 **Rex DK**, Vemulapalli KC. Retroflexion in colonoscopy: why? *Gastroenterology* 2013; **144**: 882-883 [PMID: 23499952 DOI: 10.1053/j.gastro.2013.01.077]

18 **Pohl H**, Srivastava A, Bensen SP, Anderson P, Rothstein RI, Gordon SR, Levy LC, Toor A, Mackenzie TA, Rosch T, Robertson DJ. Incomplete polyp resection during colonoscopy-results of the complete adenoma resection (CARE) study. *Gastroenterology* 2013; **144**: 74-80.e1 [PMID: 23022496 DOI: 10.1053/j.gastro.2012.09.043]

19 **Robertson DJ**, Lieberman DA, Winawer SJ, Ahnen DJ, Baron JA, Schatzkin A, Cross AJ, Zauber AG, Church TR, Lance P, Greenberg ER, Martínez ME. Colorectal cancers soon after colonoscopy: a pooled multicohort analysis. *Gut* 2014; **63**: 949-956 [PMID: 23793224 DOI: 10.1136/gutjnl-2012-303796]

World Journal of Gastroenterology

Submit a Manuscript: https://www.f6publishing.com

World J Gastroenterol 2021 September 14; 27(34): 5630-5665

DOI: 10.3748/wjg.v27.i34.5630

ISSN 1007-9327 (print) ISSN 2219-2840 (online)

REVIEW

Liver disorders in COVID-19, nutritional approaches and the use of phytochemicals

Nancy Vargas-Mendoza, Jazmín García-Machorro, Marcelo Angeles-Valencia, Marlet Martínez-Archundia, Eduardo Osiris Madrigal-Santillán, Ángel Morales-González, Liliana Anguiano-Robledo, José A Morales-González

ORCID number: Nancy Vargas-Mendoza 0000-0002-2528-5538; Jazmín García-Machorro 0000-0002-3630-5979; Marcelo Angeles-Valencia 0000-0003-1016-9769; Marlet Martínez-Archundia 0000-0002-6140-8953; Eduardo Osiris Madrigal-Santillán 0000-0001-7254-6350; Ángel Morales-González 0000-0003-2920-8078; Liliana Anguiano-Robledo 0000-0001-7435-0087; José A Morales-González 0000-0002-5980-0980.

Author contributions: The authors contributed equally to the development of the manuscript; All authors read and approved the final version.

Supported by SIP Project, No. SIP-20200341 and No. SIP-20200453; and Consejo Nacional de Ciencia y Tecnología (CONACyT) Grants, No. PAACTI 312807.

Conflict-of-interest statement: The authors declare that they have no conflicting interests.

Open-Access: This article is an open-access article that was selected by an in-house editor and fully peer-reviewed by external reviewers. It is distributed in accordance with the Creative Commons Attribution NonCommercial (CC BY-NC 4.0)

Nancy Vargas-Mendoza, Jazmín García-Machorro, Marcelo Angeles-Valencia, Laboratorio de Medicina de Conservacion, Instituto Politécnico Nacional, México 11340, Mexico

Marlet Martínez-Archundia, Laboratorio de Diseño y Desarrollo de Nuevos Fármacos e Innovación Biotécnológica, Instituto Politécnico Nacional, México 11340, Mexico

Eduardo Osiris Madrigal-Santillán, Escuela Superior de Medicina, Instituto Politécnico Nacional, México 11340, Mexico

Ángel Morales-González, Escuela Superior de Cómputo, Instituto Politécnico Nacional, México 07738, Mexico

Liliana Anguiano-Robledo, Laboratorio de Farmacología Molecular, Instituto Politécnico Nacional, México 11340, Mexico

José A Morales-González, Laboratorio Medicina de Conservación, Escuela Superior de Medicina, Instituto Politécnico Nacional, México 11340, Mexico

Corresponding author: José A Morales-González, MD, PhD, Academic Research, Professor, Laboratorio Medicina de Conservación, Escuela Superior de Medicina, Instituto Politécnico Nacional, Plan de San Luis y Díaz Mirón, Col. Casco de Santo Tomás, Del. Miguel Hidalgo, Mexico 11340, Mexico. jmorales101@yahoo.com.mx

Abstract

Coronavirus disease 2019 (COVID-19), which is caused by severe acute respiratory syndrome-coronavirus-2 (SARS-CoV-2), has affected millions of people globally. It was declared a pandemic by the World Health Organization in March 2020. The hyperinflammatory response to the entry of SARS-CoV-2 into the host through angiotensin-converting enzyme 2 is the result of a "cytokine storm" and the high oxidative stress responsible for the associated symptomatology. Not only respiratory symptoms are reported, but gastrointestinal symptoms (diarrhea, vomiting, and nausea) and liver abnormalities (high levels of aspartate aminotransferase, alanine aminotransferase transaminases, and bilirubin) are observed in at least 30% of patients. Reduced food intake and a delay in medical services may lead to malnutrition, which increases mortality and poor outcomes. This review provides some strategies to identify malnutrition and establishes nutritional approaches for the management of COVID-19 and liver injury, taking

license, which permits others to distribute, remix, adapt, build upon this work non-commercially, and license their derivative works on different terms, provided the original work is properly cited and the use is non-commercial. See: http://creativecommons.org/Licenses/by-nc/4.0/

Manuscript source: Invited manuscript

Specialty type: Gastroenterology and hepatology

Country/Territory of origin: Mexico

Peer-review report's scientific quality classification
Grade A (Excellent): A
Grade B (Very good): 0
Grade C (Good): 0
Grade D (Fair): 0
Grade E (Poor): 0

Received: January 27, 2021
Peer-review started: January 27, 2021
First decision: May 13, 2021
Revised: May 19, 2021
Accepted: July 19, 2021
Article in press: July 19, 2021
Published online: September 14, 2021

P-Reviewer: Tumminello G
S-Editor: Ma YJ
L-Editor: Filipodia
P-Editor: Yuan YY

energy and nutrient requirements and their impact on the immune response into account. The roles of certain phytochemicals in the prevention of the disease or as promising target drugs in the treatment of this disease are also considered.

Key Words: COVID-19; Infection; Liver; Nutrition therapy; Phytochemicals

©The Author(s) 2021. Published by Baishideng Publishing Group Inc. All rights reserved.

Core Tip: The Coronavirus disease 2019 (COVID-19) outbreak caused by severe acute respiratory syndrome-coronavirus-2 (SARS-CoV-2), was declared a pandemic by the World Health Organization in 2020. It has since affected millions of persons worldwide. In some cases, entry of the virus into the cell leads to a hyperinflammatory response, giving rise to all of the associated symptomatology. Liver abnormalities have been detected frequently during the course of COVID-19, with or without related symptoms. Herein we discuss the infectious process, the response to the immune system and to the oxidative stress induced, and provide a brief guideline for nutritional therapy in patients affected by SARS-CoV-2 and liver injury.

Citation: Vargas-Mendoza N, García-Machorro J, Angeles-Valencia M, Martínez-Archundia M, Madrigal-Santillán EO, Morales-González Á, Anguiano-Robledo L, Morales-González JA. Liver disorders in COVID-19, nutritional approaches and the use of phytochemicals. *World J Gastroenterol* 2021; 27(34): 5630-5665
URL: https://www.wjgnet.com/1007-9327/full/v27/i34/5630.htm
DOI: https://dx.doi.org/10.3748/wjg.v27.i34.5630

INTRODUCTION

Severe acute respiratory syndrome-coronavirus-2 (SARS-CoV-2) belongs to the family of coronaviruses; the genome is +ssRNA, which is nonsegmented and has a size of 30 kb[1,2]. In the cytoplasm of the host cell, it can be translated immediately into protein, as occurs with messenger (m)RNA. The genome encodes 16 nonstructural proteins (nsps) that are not part of the virion and have various functions in genome replication, protein processing, viral assembly, the exit of viral progeny, and others[3]. It also codes for four structural proteins, including spike (S), nucleocapsid (N), membrane (M), and envelope (E) that are required to constitute the complete virus particle (Figure 1)[2,4]. The origin of the disease may be from BatCov RaTG13 (GenBank: MN996532), a relatively close virus and one that was isolated from horseshoe bats[5]. SARS-CoV-2 causes the disease known as coronavirus disease 2019 (COVID-19). Since March 2020, a pandemic has been declared, and up to December 31, 2020, 81475053 cases were confirmed and 1798050 deaths had been reported. The global lethality rate is 2.22%[6].

SARS-CoV-2 can affect various organs that express the entry receptor. The main receptor described is angiotensin-converting enzyme 2 (ACE2)[1]. Distribution of the ACE2 protein was investigated by immunohistochemistry, and the protein was found present in endothelial cells from small and large arteries and veins, arterial smooth muscle cells, myofibroblasts, the membrane of fat cells in various organs, and in the basal layer of nonkeratinizing squamous epithelium. Importantly, ACE2 is expressed in nasal and oral mucosae and the nasopharynx in type I and type II alveolar epithelial cells in normal lungs, which explains the respiratory tract infection. Gastrointestinal manifestations can be explained by the presence of the receptor in smooth muscle cells and in the endothelium of vessels in the stomach, small intestine, and colon. In addition, the receptor can be found in the brush border of enterocytes in the small intestine, including the duodenum, jejunum, and ileum, but not in enterocytes of the colon. In the kidney, weak glomerular visceral ACE2 staining was observed, whereas parietal epithelial cells were moderately positive. In the skin, ACE2 was present in the basal cell layer of the epidermis extending to the basal cell layer of hair follicles. Smooth muscle cells surrounding the sebaceous glands were also positive for ACE2. In the brain, ACE2 receptors were found in only endothelial and smooth muscle cells[7]. Some of the extra respiratory manifestations can be explained by the previous fin-

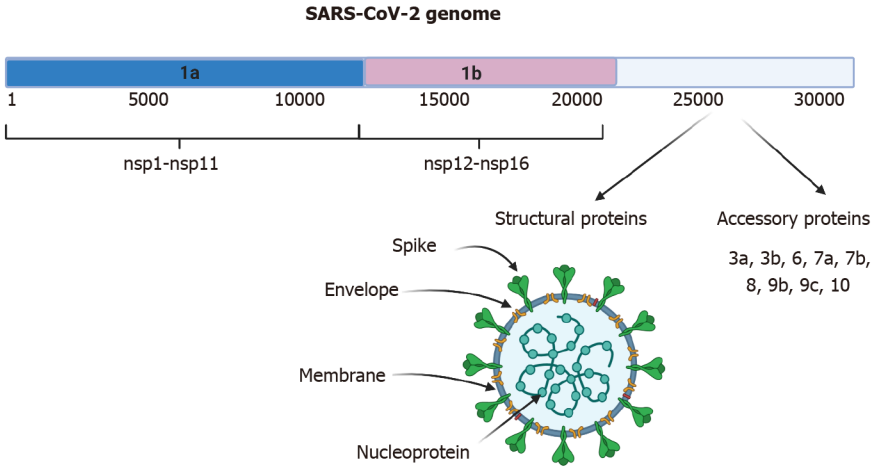


Figure 1 Genome and structure of severe acute respiratory syndrome-coronavirus-2. The 30-kb severe acute respiratory syndrome-coronavirus-2 virus genome is shown. It possesses different open reading frames (ORFs). ORF 1a generates the nonstructural proteins (nsp) from nsp1-nsp11, ORF 1b generates proteins nsp12-nsp16. The spike, envelope, membrane, and nucleoprotein structural proteins and accessory proteins are generated from the 3' region. Created with BioRender.com. SARS-CoV-2: Severe acute respiratory syndrome-coronavirus-2.

dings. However, several alterations, such as those related to the liver, require explanation. The underlying mechanisms of acute liver injury associated with COVID-19 have yet to be determined. The possible mechanisms of damage are described below.

PATHOPHISIOLOGY IN COVID-19 INFECTION

Viral receptor

The ACE2 receptor has been described as the main entry receptor for the SARS-CoV and SARS-CoV-2 viruses, and it is abundantly expressed in the cells of the biliary system (*i.e.* cholangiocytes)[7]. Thus, it has been implicated in elevated levels of alkaline phosphatase and gamma-glutamyl transferase (GGT). However, those changes have been found in a small number of patients[8], compared with elevated levels of aminotransferases directly related to functions of hepatocytes that do not express the ACE2 receptor (Figure 2)[9].

Direct damage of liver cells by SARS-CoV-2 has been reported, based on ultrastructural changes and SARS-CoV-2 viral particles observed in the cytoplasm of hepatocytes by transmission electron microscopy of liver biopsies of two COVID-19 who subsequently died, one of acute respiratory distress syndrome (ARDS) and the other of septic shock distress syndrome[10]. In a subsequent letter to the editor[11], multiple observations were made indicating that the elevation of alanine aminotransferase (ALT) and aspartate aminotransferase (AST) were not sufficient for the condition to be called acute liver injury, the number of biopsies performed were those of two patients, the characteristics of liver cell renewal could be mistaken for hepatic injury, "corona-like" particles could have been intrahepatic cholesterol crystals, and lamellations, or "crown-like" structures are observed in patients with nonalcoholic fatty liver disease.

In addition to the above observations, we would ask how the virus enters cells that do not have the receptor? In the case of cells with high phagocytic capacity that could swallow the virus, viral replication capacity would have to be investigated by the detection of nonstructural proteins. In the case of suspected viral reservoir cells, detecting at least some of the viral structural proteins would require staining, as has been reported for other viruses[12].

On the other hand, SARS-CoV-2 can use transmembrane protease serine 2 (TMPRSS2), which has not been detected in the liver, to enter cells. However, other transmembrane serine proteases have been detected, in particular furin and hepsin (in Huh7-25-CD81 cells)[13]. In three-dimensional (3D) culture systems, liver bile duct-derived progenitor cells form "liver ductal organoids" that retain their tissue-of-origin commitment and genetic stability. In a SARS-CoV-2 infection model with human liver ductal organoids, cholangiocytes expressing ACE2 and TMPRSS2 were preserved *ex vivo* in long-term culture. In addition, the expression of TMPRSS2 mRNA was found in

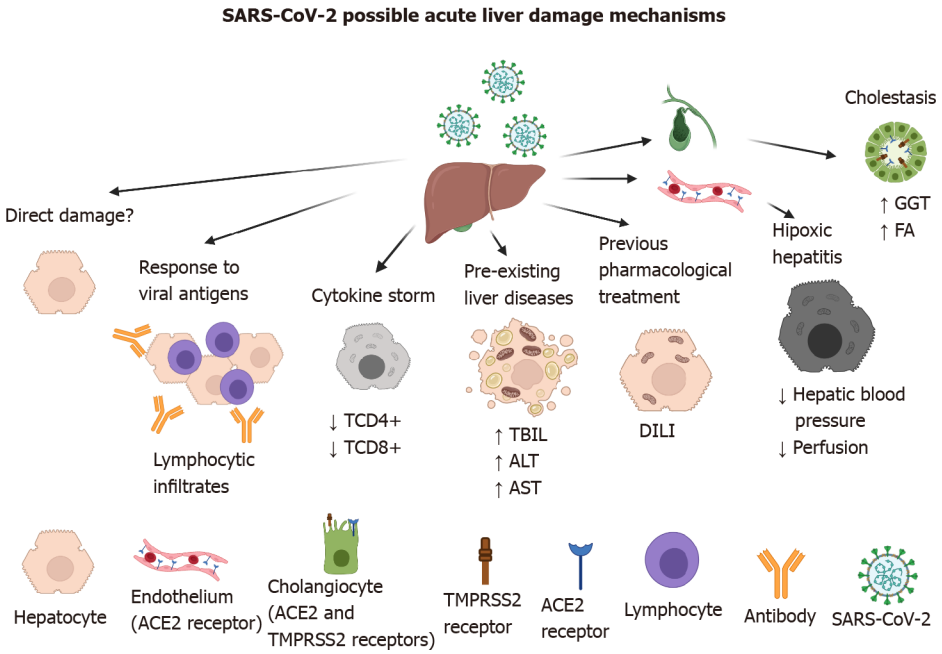


Figure 2 Possible mechanisms of acute liver damage by severe acute respiratory syndrome-coronavirus-2 infection. Direct damage to the hepatocyte is does not occur because it does not possess the viral entry receptor. However, indirect damage-associated with the immune response against viral antigens, cytokine storm, pre-existing liver diseases such as hepatitis A, B, and C viruses infection, and treatment with hepatotoxic drugs like acetaminophen, remdesivir, lopinavir, *etc.* has been characterized. In severely affected patients, oxygen deficiency can give rise to hypoxic hepatitis. Severe acute respiratory syndrome-coronavirus-2 damage to cholangiocytes has been documented, because they both possess the angiotensin-converting enzyme 2 and transmembrane protease serine 2 receptors. Created with BioRender.com. ACE2: Angiotensin-converting enzyme 2; ALT: Alanine aminotransferase; AST: Aspartate aminotransferase; DILI: Drug-induced liver injury; FA: Alkaline phosphatase; GGT: Gamma-glutamyl transferase;SARS-CoV-2: Severe acute respiratory syndrome-coronavirus-2; TBIL: Total bilirubin; TMPRSS2: Transmembrane protease serine 2.

a subset of hepatocytes and cholangiocytes[14]. In other experiments, human liver ductal organoids showed increased expression of viral mRNA 24 h after being infected with SARS-CoV-2[15]. The experimental evidence suggests that viral receptors are not static and that they can be regulated by mechanisms that involve the presence of the virus and have not yet been described.

Response against viral antigens

Damage to the liver is known to be caused by hepatotropic viruses that replicate in the liver (*e.g.*, hepatitis A, B, C, and E viruses). However, some viruses that attack the respiratory tract can cause liver damage, from small alterations in transaminases to fulminant liver failure, for example, the influenza virus[16,17], parvovirus[18], and respiratory syncytial virus bronchiolitis[19]. In general, hepatitis is thought to be a consequence of an immune response to viral antigens and to the loss of regulation of the inflammatory response. SARS-CoV-2 infection has been associated with hepatitis characterized by focal lobular lymphocytic infiltrates[20]. SARS-CoV-2 viral antigens were recently detected in liver as nucleocapsids and spike proteins[21].

Cytokine storm

The first line of antiviral defense is the innate immune response, initiated by the production of interferon (IFN) type 1 or IFN-α/β[22,23]. IFN-α/β binds to its cellular receptor and initiates autocrine and paracrine signaling to stimulate the expression of genes involved in the antiviral response (interferon-stimulated genes, *ISG*), in order to build resistance to infection and limit the spread of the virus. However, poor interferon response and high viral replication have been characterized in severe cases of COVID-19[24]. High viral replication stimulates an exaggerated systemic inflammatory response that is related to a sustained elevation of interleukin (IL)-1β, IL-2, IL-7, IL-8, IL-9, IL-10, IL-17, granulocyte colony-stimulating factor (G-CSF), granulocyte-macrophage colony-stimulating factor (GM)-CSF, IFN-γ, TNF-α, interferon γ-induced protein 10 kDa (IP-10), monocyte chemoattractant protein (MCP)-1, macrophage inflammatory protein (MIP)1α, and MIP-1β, and decreases in CD4+ T cell (TCD4+) and TCD8+ cell counts[25-27]. The latter could contribute to altered liver function[28] and to activation of the coagulation cascade[29,30], and an alteration of iron homeostasis

with elevated ferritin levels[31].

Pre-existing liver diseases

Correlations between the severity of COVID-19 and chronic diseases such as diabetes mellitus, arterial hypertension, obesity, renal alterations, and cardiovascular disease have been clearly described[32-34]. Regarding the impact of liver diseases on the progression of COVID-19, ALT and AST activity, and the concentration of C-reactive protein (CRP) have been related to the prediction of disease severity. The prediction of mortality was correlated with liver failure, total bilirubin, platelet count, and serum albumin concentration. Chronic hepatitis B and chronic liver disease were not related to disease severity, the requirement for treatment in the intensive care unit (ICU), or mortality[35]. In another study, 17 inactive hepatitis B virus carriers with SARS-CoV-2 co-infection were found to have abnormal liver function tests (total bilirubin, ALT, and AST)[36]. Thus, it is not clear whether pre-existing liver diseases, such as viral hepatitis, are associated with the severity of COVID-19 infection[37].

Previous pharmacological treatment

The liver contributes mainly to the elimination of lipophilic drugs by increasing their solubility, therefore facilitating their elimination through the cytochrome P450 isoenzyme complex. Therefore, it is important to inquire whether patients diagnosed with COVID-19 are using medications for the treatment of chronic diseases or even anti-influenza or antipyretic drugs[38]. Drugs that are especially potentially hepatotoxic, such as acetaminophen, lopinavir/ritonavir, remdesivir, corticosteroids, and immune modulators, should be taken into account[39] because they can predispose to drug-induced liver injury.

Hypoxic hepatitis

Ischemic hepatitis, also known as hypoxic hepatitis or liver shock, is defined as extensive and potentially severe predominantly centrilobular hepatocellular necrosis resulting from a significant decrease in hepatic perfusion. In patients with severe COVID-19, mechanical ventilation, or hemodynamic disturbance and the occurrence of a sudden drop in systemic blood pressure, can lead to a reduction in hepatic blood pressure, decreased perfusion, and hepatocellular hypoxia. The pathogenesis involves hepatic ischemia and hepatic venous congestion because of elevated central venous pressure, which can predispose the hepatocytes to irreversible hypoxic injury[39,40]. Additionally, the hypoxia can directly affect the tissue–oxygen demand[41].

LIVER MANIFESTATIONS IN COVID-19

Various hepatic manifestations associated with COVID-19 have been documented, ranging from mild enzyme disruption to acute hepatic injury (Figure 3). The manifestations can be grouped into enzymatic (ALT and AST), metabolic (hypoglycemia and hyperammonemia), secretory (hyperbilirubinemia), synthetic (hypoalbuminemia and prothrombin time), and degradation (D-dimer) dysfunctions. Cholestasis with impaired GGT and alkaline phosphatase (FA) is rare, but it is suggested that it may be caused by the dysfunction of the bile duct cells rather than by liver cell damage[8].

Enzymatic liver dysfunction

Liver enzyme abnormalities in patients with COVID-19 are usually transient and are associated with disease severity. Alanine and aspartate aminotransferases (ALT and AST) are generally found to be elevated in the serum and are more often observed in hospitalized patients[33,42-44] than in patients with subclinical disease. Acute hepatic injury can be diagnosed by an ALT at 10 times the upper reference limit and by AST at three times the appropriate upper reference limit[45].

Metabolic liver dysfunction

Hypoglycemia and hyperammonemia suggest liver failure and have not been found in COVID-19 patients, but there is a hypothesis that coronaviruses can cause a transient dysfunction of pancreatic beta cells[46], leading to acute hyperglycemia and relative insulin deficiency. The hypothesis is supported by a previous study including 39 patients with SARS and without a history of diabetes. Twenty of the patients developed diabetes, all but two temporarily. In addition, ACE2 has been identified in the pancreas of patients with SARS[47].

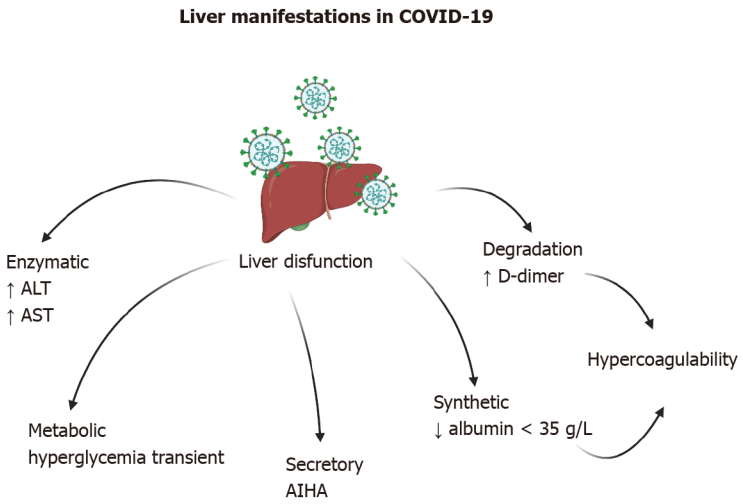


Figure 3 Liver manifestations in coronavirus disease 2019 are quite varied. Increased transaminases and hypercoagulability have been observed in the majority of patients. In rare cases, autoimmune hemolytic anemia has been observed. Created with BioRender.com. AIHA: autoimmune hemolytic anemia; ALT: Alanine aminotransferase; AST: Aspartate aminotransferase; COVID-19: Coronavirus disease 2019.

Secretory liver dysfunction (hyperbilirubinemia)

Regarding bilirubin, no relationship has been directly associated with SARS-CoV-2. However, there are reports of autoimmune hemolytic anemia (AIHA) in patients with symptomatic COVID-19[48,49]. Additionally, there is a report of a patient without clear evidence of SARS-CoV-2 infection for 2 wk and a subsequent positive PCR test. The final diagnosis was AIHA secondary to COVID-19)[50].

Synthetic liver dysfunction (hypoalbuminemia) elevated prothrombin time

Albumin is a protein synthesized in the liver and has a serum half-life of approximately 21 d[51]. In the majority of cases, a decrease in serum albumin can be explained by two factors, either a decrease in its synthesis in the liver) or an increase in renal permeability. However, the prevalence of hypoalbuminemia (< 35 g/L) in COVID-19 patients was increased in critically ill patients in an ICU, but liver damage or albuminuria were not detected. hypoalbuminemia was associated with high-sensitivity C-Reactive protein (hs-CRP) and elevated D-dimer, which is considered to be a marker of thrombin. Therefore, an attempt was made to establish a cause–effect relationship between hypoalbuminemia and hypercoagulability, in that albumin possesses anticoagulant and antiplatelet activity[52]. In a separate study, it was determined that hypoalbuminemia (< 35 g/L) on hospital admission increased the risk of death in COVID-19 patients by at least six-fold. Lower albumin levels on hospital admission can predict the outcome of COVID-19 independently of other known indicators, such as lymphocyte count or comorbidities[32,53].

D-dimer levels

D-dimer is the end-product of fibrin degradation, and it serves as a serological indicator of the activation of coagulation and of the fibrinolytic system. D-dimer levels have been reported as elevated in patients with COVID-19 and have been used as a tool for the prediction of disease severity in 178 studies[54]. In one study, it was determined that elevated D-dimer levels predicted in-hospital mortality in patients with COVID-19[55]. However, the usefulness of D-dimer is diminished by poor reporting of the values. The majority of publications did not identify either the assay manufacturer or the D-dimer product used for the determination. The majority of the authors did not identify whether D-dimer values were reported as D-dimer units or fibrinogen equivalent units (FEU), which differ by approximately ×2. The studies did not report normal cutoff values, and the units of comparison were not the same[56].

IMMUNE SYSTEM AND OXIDATIVE STRESS

Response of the immune system in infection by SARS-CoV-2

The innate immunological system functions as the first line of defense of the host

against infection by SARS-CoV-2; it is crucial for identifying and eliminating the infected cells, and at the same time, for coordinating an adaptive immunity response [57]. The immune response of the host in cases of COVID-19 can be described as an early local immune response (antiviral defense) and a later local/systemic response phase, followed by uncontrolled inflammatory responses and cytokine storm syndromes (Figure 4)[58]. Because SARS-CoV-2 initially affects the upper respiratory tract, its first interactions with the immunological system during the inductive and effector phases, should take place predominantly on the surfaces of the respiratory and oral mucosae[57,59]. Exposure to the virus antigens causes immunoglobulin (Ig)A-mediated responses in the mucosa[60,61] that can be accompanied by the systemic production of IgA, but the systemic production can be absent, transitory, or delayed [61]. The response involving IgA antibodies of the mucosa that maintains an essentially noninflammatory medium[59] and can be particularly prevalent in young people with a mild infection by SARS-CoV-2 without evidence of pneumonia[61].

If the immunological system of the individual does not counteract the virus during the initial phase of exposure through a rapid early response, the virus advances to the lower respiratory tract (LRT)[62,63]. Once the virus reaches terminal respiratory pathways and the alveoli, B and T cells are activated, which results in the production of specific anti-SARS-CoV-2 antibodies[61], with the predominance of an inflammatory environment dominated by IgG[59]. The S and N proteins are the two principal antigens of the coronavirus that induce the production of Ig[64,65]. The IgA, IgM, and IgG antibodies against the N and S proteins, and the IgM and IgG antibodies against the protein receptor-binding domain, as well as the presence of neutralizing antibodies (nAbs) against SARS-CoV-2 are positive from day 1 after the appearance of symptoms [64]. The antibody levels, especially IgG, increase during the disease course, while a limited increase of IgA and IgM is observed[64]. The antibodies against the S1 and N antigens persist for at least 3 mo after the infection[60,65]. In addition, higher levels of nAbs as well as IgG and IgM antibodies and anti-S1 and -N antibodies have been observed in patients with very severe symptoms[9]. In addition, depletion of memory B cells of IgM was associated with worse outcomes, including a higher mortality rate and a greater risk of developing superimposed infections[66].

In response to viral invasion, the innate immunological system recognizes viral nucleic acids by host recognition-pattern (HRP) receptors, which are expressed in innate immune cells (*e.g.*, neutrophils, dendritic cells, epithelial cells, and macrophages)[67], and by toll-like receptors (TLRs) and retinoic acid-inducible gene I-like (NOD-like) receptors (NLRs) (Figure 4C). For the production of cytokines and the induction of an antiviral state[57,58], as a response to specific pathogen-associated molecular patterns and damage-associated molecular patterns (DAMPs)[57,68]. HRP receptors can activate antiviral responses in neighboring cells and recruit innate and adaptive immune cells and the participation of phagocytes such as macrophages and neutrophils, as well as natural killer (NK) cells[59,68].

Once the virus was detected by an HRP receptor, intracellular signaling pathways are triggered that activate interferon regulatory factor 3 (IRF3) and the nuclear factor kappa beta (NF-κB) signaling cascade[58]. The initial phase of the production of interferon (IFN) mediated by IRF3 performs the initial phase of the innate immune response to detect and brake viral replication[69]. Viral detection stimulates the production of type-1 and type-3 IFN, which results in the expression of interferon-simulated genes ISG (*IRF1*, *IFI44L*, and *IFIT3*) and antiviral genes (*OAS3* and *ADAR*) [70], and the release of large amounts of inflammatory procytokines like interferon gamma (IFN-γ), interleukin (IL)-1RA, IL-6, IL-8, IL-10, and IL-19, monocyte chemoattractant protein 1 (MCP-1), MCP-2, and MCP-3, bonding with C-X-C motif chemokines, including CXCL9, CXCL10, and CXCL5, and tumor necrosis factor alpha (TNF-α)[71]. Stimulation of TLRs activates NF-κB, giving rise to the production of inflammatory markers deriving from monocytes (IL-1, TNF-α, and IL-6) to control the infection by means of direct antiviral pathways and the recruitment of other leukocytes[67]. Signaling is elevated 24 h after infection by SARS-CoV-2, leading to the progressive loss of the pulmonary alveolar epithelial function[62]. The activation of complement, and especially of the C5a/C5aR1 axis, was also implicated in the pulmonary pathology of COVID-19[71].

HRP receptors, particularly the nucleotide-binding oligomerization domain-like (NOD)-like receptor (NLR) family, subsequent to the SARS-CoV-2 infection, assemble a multiprotein complex called inflammasome NLRP3, which results in the activation of caspase-1. Activated caspase-1 splits from the pro-interleukin IL-1β, pro-IL-18, and gasdermin D (GSDMD) and releases the GSDMD N-terminal fragment that can be oligomerized within membranes to form membrane pores and "pyroptosis"[57]. The excision of caspase-1-dependent GSDMD leads to the release of IL-1β and IL-18[72],

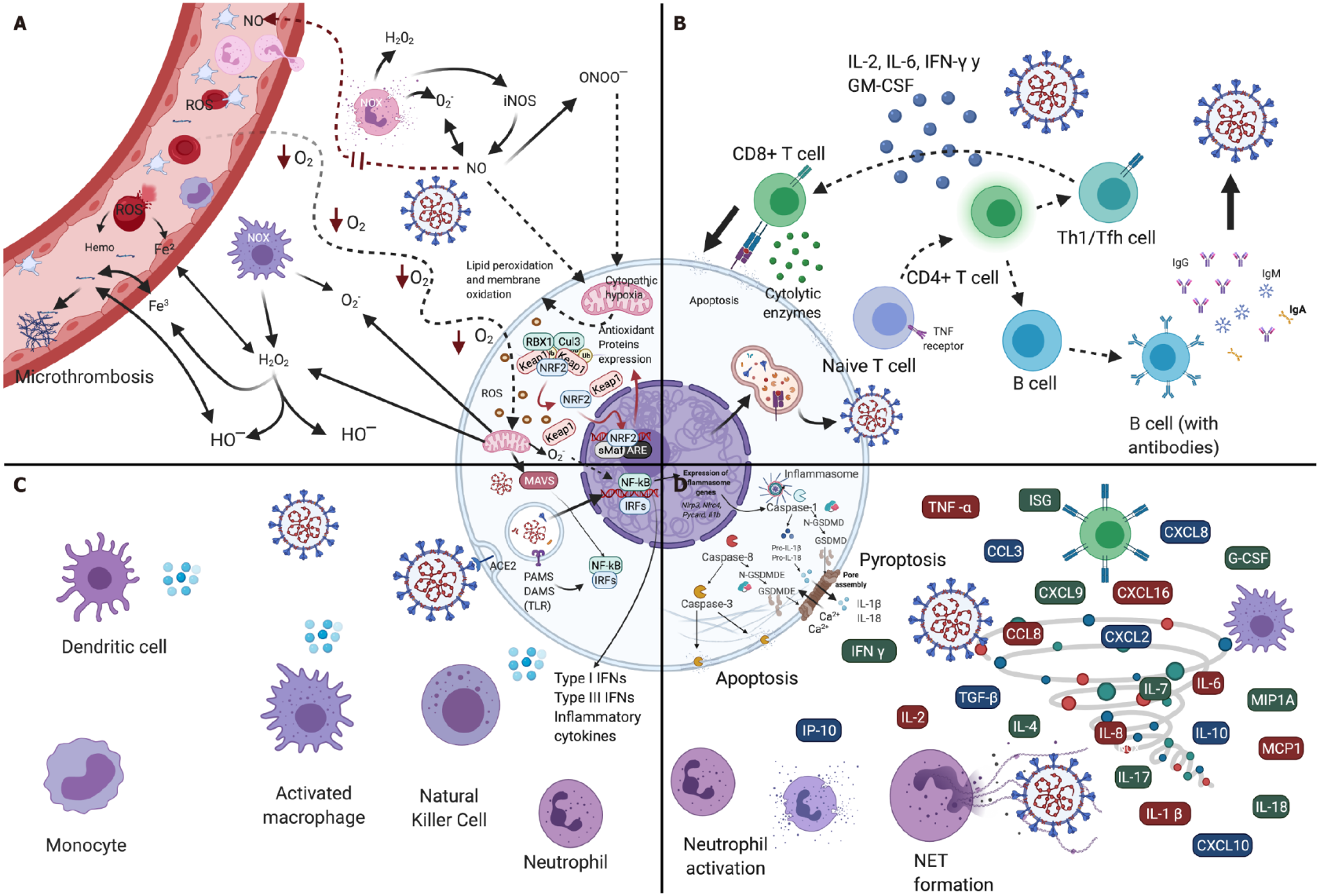


Figure 4 Immune response and oxidative stress in severe acute respiratory syndrome-coronavirus-2 infection. A: Oxidative stress; B: Adaptive immune response; C: Innate immune response; D: Cytokine storm. Created with BioRender.com.

which are key mediators of the inflammatory response, and their increase in the plasma have been correlated with COVID-19 mortality or severity[73]. Apoptosis, another type of cell death, also occurs during SARS-CoV-2 infection and is driven by the excision of the caspase-8, -9, -10 initiators of the executioner caspase-3 and -7. Apoptotic caspase-3 activates gasdermin E (GSDME) to induce the lytic form of cell death; the protein ORF3a of the SARS-CoV-2 virus also induces the excision of caspase-8 and -9 and causes apoptosis[57]. The activation associated with the death pathways of the inflammatory cells can give rise to critical tissue damage, severe inflammation, and lactate dehydrogenase (LDH), which is a marker of cell death that has high concentrations in COVID-19 patients. The LDH concentration is considered a predictive factor for the early recognition of pulmonary lesions in severe cases[74].

Macrophages are a key respiratory system. They produce chemokines and IFN-β. Infected dendritic cells (DCs) produce antiviral cytokines, like IFN-α and IFN-β; the proinflammatory cytokine TNF, IL-6, and high levels of the inflammatory chemokines CCL3, CCL5, CCL2, and CXCL10. The cytokines/chemokines are key factors for the chemotaxis of neutrophils, monocytes, and activated T cells[75]. Activated neutrophils, whose main function is the elimination of pathogens and dendrites by means of phagocytosis[67], release leukotrienes and reactive oxygen species (ROS) that induce local damage to pneumocytes and the endothelium, which in turn leads directly to acute lung lesions[68].

Neutrophils can also develop DNA networks called neutrophilic extracellular traps (NETs)[68] through the process of NETosis, or the release of nucleic acids enveloped in histones, which retain viral particles and promote the inactivation of the viral infection and cytokine production to restrict replication of the virus[67]. NETosis is conditioned to the production of ROS by means of nicotinamide adenine dinucleotide phosphate (NADPH) oxidase. In addition to the physical containment promoted by NETosis, NETs contain proteases and cytotoxic enzymes that permit the neutrophils to centralize lethal proteins at the sites of infection. A variety of stimuli, including toxic factors, viruses, and proinflammatory cytokines such as TNF-α and IL-8, can drive neutrophils to release NETs (Figure 4D)[67]. The uncontrolled production of NETs is correlated with the severity of the disease and the extension of the pulmonary lesion, with acute respiratory insufficiency and multiple organic dysfunction syndromes[76]. NETs also contribute to the formation of thrombi, or immunothrombosis, which can amplify the production of cytokines[68]. The inflammatory process comprises a triggering of thrombotic complications that are usually observed in patients with COVID-19, and immunothrombotic dysregulation appears to be an important marker of the severity of the disease[77,78]. In SARS-CoV-2, elevation of the neutrophil/lymphocyte ratio (NLR), a marker of infection and systemic inflammation, suggests a poor disease prognosis. In addition, patients with COVID-19 have the lowest lymphocyte count and the highest neutrophil count and NLR during severe disease[67,79,80].

The inflammatory responses in the respiratory system intended to eliminate SARS-CoV-2 result in the generation of metabolic-acid waste material that, together with an increase in respiratory muscular work, lead to the development of metabolic acidosis. Metabolic acidosis compromises adaptive cellular immunity and the efficient eradication of SARS-CoV-2[81]. Activated neutrophils and the T lymphocytes depend mainly on glycolytic metabolism for their proliferation, differentiation, and function, which results in the accumulation of lactic acid[81]. A low pH induces anergy in CD8+ T cells, suppresses NK cells, and inhibits the function of CD4+ T cells. Acidosis also increases the levels of circulating glucocorticoids; thus, their anti-inflammatory and immunosuppressor properties compromise immunity against viruses to an even greater degree[81].

Infection by SARS-CoV-2 promotes mechanisms that antagonize proinflammatory signals, particularly the signaling of IFN-I and IFN-III, but increases the expression of chemokines and proinflammatory cytokines in order to counteract the host's innate immune response[57,58,63]. Thus, the expansion and early differentiation of T cells depend on the direct action of IFN-I[82]. The descending production of interferons promotes intracellular antiviral defenses in neighboring epithelial cells that can limit viral dissemination, while the release of IL-6 and IL-1β from other immune cells promotes neutrophil recruitment and immune cell activation[68].

The three most critical components of the adaptive immune responses are viral protein-specific CD4+ T cells, CD8+ T cells, and nAbs. The nAbs produced by B cells can bind to and neutralize the extracellular SARS-CoV-2 proteins. If the Abs cannot prevent the virus from entering cells, cytotoxic CD8+ T cells are called upon to destroy the cells directly infected with their granules[83,84]. Pulmonary cytotoxic CD8+ T cells recognize and induce apoptosis in cells infected through direct mechanisms (*i.e.*

cell–cell contact) and indirect mechanisms with the participation of the perforin and granzyme-secreted cytolytic enzymes, as well as with the cytokines IFN-γ and TNF-α [85]. However, cytotoxic cells by nature do not prevent the infection, they destroy already infected cells, thus reducing propagation of the infection (Figure 4B)[59]. Transitory increases of the CD8 effector T and memory T cells constitute an effective and efficient response during early viral infection[81]. High counts of CD8+ T cells in the lungs are correlated with better control of SARS-CoV-2[80,85].

CD4+ T cells, the third arm, are auxiliaries and coordinators of the production of Abs and of the activation of the cytotoxic CD8+ T cells[83,84]. After being infected with SARS-CoV-2, CD4+ T cells are activated and differentiate to Th1 cells or circulating T follicular helper T cells (Tfh)[68,80] that secrete proinflammatory cytokines, such as IL-2, IL-6, IFN-γ, and granulocyte-macrophage colony-stimulating factor (GM-CSF)[68] that participate in the activation, proliferation, and differentiation of cytotoxic T lymphocytes. In addition, elevated levels of cytokines secreted by Th2 cells, such as IL-4 and IL-10), which inhibit Th1 inflammatory responses have been reported[86]. The severity of SARS-CoV-2 infection has been related to diminished adaptive immunity responses, mainly because of depletion of T cells and lymphopenia[80], alteration of the differentiation of T follicular helper (Tfh) cells[63,87], low levels of CD8+ NK cells[83], CD4+ auxiliary T cells[87], and memory T cells[84]. However, Abs by themselves do not correlate with the severity of the disease[64,83]. It is probable that the level of inflammation and the amount of proinflammatory cytokines are associated with the activation and depletion of T cells, but it has not yet been determined whether the early response reaches a state of depletion in individuals with severe hyperinflammation[63,70].

Lymphocytes gradually decrease as the disease advances, which results in immunosuppression manifested as atrophy of the organs of the immune system, secondary infection, and multiple organ dysfunction syndrome[75]. Lymphopenia is consistent with overrepresentation of nonfunctional T lymphocytes, with increased percentages of virgin Th lymphocytes (*i.e.* CD45RA+, CXCR3−, CCR4−, CCR6−, and CCR10−) and a persistent low frequency of markers associated with effector memory T cells, TFH cells, and regulatory T cells (Tregs)[80]. Lymphocytopenia is negatively correlated with inflammatory biochemical parameters (ferritin, fibrinogen, PCR, D-dimer, LDH) and the percentage of lymphocytes and positively correlated with the neutrophil count [80]. From an immunological point of view, lymphopenia could depend on the possibly dysfunctional deactivation of dendritic cells and on the increased concentration of cytokines such as TNF-α, IL-6, and IL-10, which act as negative regulators of the proliferation and survival of the T lymphocytes[88]. The production of acute-phase proteins such as ferritin and CRP, in addition to affecting the equilibrium of pro- and anticoagulant pathways (*i.e.* increasing D-dimer), can induce lymphocyte apoptosis [82].

The host capacity to generate efficient T cell responses after infection by SARS-CoV-2 probably depends on the directed epitopes, the presence or absence of pre-existing cross-reactive T cells, and genetic factors such as the human lymphocyte antigen (HLA) type, and the repertory of T cell receptors (TCRs)[85]. Given that activated T cells in elderly persons and in those with chronic disease present reduced responses to IFN-I, a longer time is needed to generate effective adaptive immune responses because of the deterioration of the immune functions such as the production of virgin T cells and memory T cells, which diminish with aging[84], and present asynchronous immune responses with high Ab levels and weak T cell responses[83]. Delayed activation of SARS-CoV-2-specific T cells and a reduction of the clarification of the virus increase the risk of cytokine storm, the earlier appearance of severe disease, and increased mortality[68].

In contrast with innate immune responses, which are produced before the infection and participate fully in the elimination of the virus, the adaptive immune responses begin 4-7 d after infection. If the body does not generate effective adaptive antiviral responses in time to eliminate the virus, the innate immune responses will be maintained, but without eliminating the virus in an effective manner and even leading to systemic inflammatory responses and the uncontrolled release of inflammatory cytokines[68].

The inflammatory cytokine storm, also known as the cytokine release syndrome, is a severe excessive immune response caused by positive biofeedback circuit damage of immune cells by the cytokines[67,75,87]. The formation of a cytokine storm leads to a "suicide attack" that not only limits additional propagation of the virus, but also induces secondary tissue damage[68]. The marked release of proinflammatory cytokines causes lymphopenia, lymphocyte dysfunction, granulocyte and monocyte anomalies[58], coagulation disorders such as capillary extravasation syndrome, formation

of thrombi, and even the combined immunodeficiency syndrome[76,81]. A series of destructive effects on tissues, including destabilization of the interactions among endothelial cells, damage to the vascular barrier, diffuse alveolar damage characterized by the formation of hyaline membranes[13], ARDS[57,68], tissue toxicities that affect the respiratory, hematological, gastrointestinal, cardiovascular, renal, hepatic, and neurological systems[89], multiorgan failure[80] and, ultimately death may occur [58,68,75,76]. Despite the large number of studies much of the physiology of the immune response in COVID-19 has yet to be described.

Oxidative stress and infection by SARS-CoV-2

Oxidative stress is the result of disequilibrium between the oxidant system, which consists principally of free radicals, ROS), and reactive nitrogen species (RNS), and the antioxidant systems that neutralize the free radicals[90]. Reactive oxygen and nitrogen species (RONS) are characterized by unpaired valance electrons, obliging them to react with diverse biological molecules[90,91]. ROS comprise the hydroxyl (OH) radicals, superoxide anion (O_2^-), singlet oxygen ($^1O_2$), hydrogen peroxide (H_2O_2), and ozone (O_3). RNS include nitric oxide (NO), peroxynitrite ($ONOO^-$), nitrosyl cation (NO^+), the nitrosyl anion (NO^-), and nitrose acid (NH_2O_2)[90]. Under physiological conditions, the reactive species play an important role in cellular signaling (redox signaling) and the regulation of cytokines, and growth factors such as immunomodulators, cellular differentiation, and others. However, when the equilibrium of oxidant agents and antioxidant systems is disturbed, harmful effects are generated[90,91]. The damage caused by free radicals affects cellular membranes by lipid peroxidation, oxidation, protein denaturalization, DNA damage that can induce inflammatory immune responses and increase the risk of mutations and tumorigenesis, and apoptosis[90]. In general, hydroxyl radicals are highly reactive and are responsible for the greatest cellular damage modification of biomolecules induced by ROS. H_2O_2 is considered the least harmful and can travel to and penetrate cell membranes, and the superoxide is intermediately harmful[92].

In the pathology of COVID-19, the cytokine storm is an important source of endogenous oxidative stress, and excessive production of ROS that in turn stimulates the increased release of cytokines, causing an exaggeration of the already initiated inflammatory responses (Figure 4A)[93-97]. The interaction of ROS and cytokines generates a self-sustaining cycle involving the cytokine storm and the production of oxidative stress that eventually leads to a high pulmonary protein exudate with a low hemoglobin carrier, the generation of free radicals and proteases, and an increase in the permeability and entry of edematous fluid into the alveoli. The results in deficient gas exchange in the lungs, pulmonary hypoxia, cytopathic hypoxia, damage to the epithelium, acute pulmonary lesions, disseminated coagulation, multiorgan failure and death in patients with COVID-19[95-98].

The cytokine storm with hyperinflammation accompanied by cytopenia and hyperferritinemia is known to generate ROS, by means of the Fenton reaction ($Fe^{2+} + H_2O_2 \rightarrow Fe^{3+} + HO^- + HO^-$). Additionally, the cytokines and endotoxins stimulate an isoform of nitric oxide synthase (iNOS), the inducible isoform NO, which stimulates the production of NO that in turn reacts with the superoxide to yield peroxynitrite ($ONOO^-$)[90,96]. Both peroxynitrite and NO are toxic to mitochondria, producing dysfunctional mitochondria that, in turn, result in cytopathic hypoxia[96,99]. In addition, they cause a possible oxidative storm with all of the harmful effects of RONS, in particular the peroxidation of lipids and oxidation of membrane proteins that contribute to the transformation and hyalinization of the pulmonary alveolar membranes, with lethal respiratory difficulty[90].

SARS-CoV-2 activates oxidant-sensitive pathways through inflammatory responses following activation of the NF-κB pathway[93]. The reduction of oxygen saturation leads to the generation of superoxide radicals and H_2O_2 by the mitochondria. Hydrogen peroxide triggers the expression of genes that positively regulate proinflammatory cytokines, such as IL-1, IL-6, and TNF-α, and inducible nitric oxide synthase (iNOS) by means of the activation of the (iNOS) NF-κB pathway[94,96,98,100]. That, together with the ROS, activates NLRP3 inflammasomes[101]. IFN-γ, IL-1β, IL-2, IL-6, and TNF-α stimulate the generation of NO[96]. IL-6 and TNF-α give rise to superoxide generation in neutrophils, and hydrogen peroxide stimulates the generation of IL-6[98, 102]. In cyclical fashion, the proinflammatory cytokines activate macrophages, neutrophils, and endothelial cells through NADPH oxidase (NOx) to produce more superoxide and H_2O_2. Patients with COVID-19 exhibit an overactivation of NOx2, a mechanism that favors ischemic events related to thrombotic events and associated with severe disease[103].

At the same time, the IFN-γ pathways are activated by oxidative stress induced by the inflammation intended to combat the infection by the virus[33]. Circulation of the inflammatory cytokines and ROS damage erythrocytes, leading to the generation of heme and free iron and diminish the circulating nitric oxide (NO), which worsens the existing ischemia of the organs. Deterioration of the mitochondria leads to cytopathic hypoxia, which results in a partial reduction of oxygen with the generation of ROS and the reduced energy production[98]. In addition, macrophages and activated neutrophils produce respiratory bursts that generate superoxide radicals and H_2O_2[94,98] that maintain the oxidative stress[98].

Poorly coordinated iron, especially in the presence of high concentrations of oxygen and reducers have the potential to generate hydrogen peroxide, superoxide, and hydroxyl radicals in the lung[92]. The radical superoxide anion reduces Fe (III) to Fe (II) that, in the presence of H_2O_2, produces hydroxyl radicals ($^{\bullet}OH$), which are extremely toxic and promote the formation of lipid peroxidases in the cell membrane and the oxidation of proteins, causing cell death by apoptosis[94]. Hydroxyl radicals plus free iron convert soluble plasma fibrinogen into abnormal fibrin clots in the form of enzymatic degradation-resistant dense and entangled deposits, leading to microthrombosis in the vascular system and in the microcirculation[95,96].

Oxidative damage resulting from SARS-CoV-2 infection can produce viral mutations that affect the immunological response. In addition, overproduction of ROS suppresses T-lymphocyte responses and results in weakened adaptive immunity[94], altering the structure and function of the circulating lymphocytes, principally $TCD4^{+}$, with selective depletion reduced antiviral activity of CD8+[94] T cells. In general, the host response to stress and to combat an inflammatory condition is marked by a strong increase of the cortisol level. Cortisol supports the mechanisms of the host immunological defense in a permissive manner, and high levels of cortisol suppress inflammation and prevent tissue damage[93]. However, in the case of severe COVID-19, patients can develop a corticosteroid insufficiency related to a critical disease[93]. It is known that overproduction of ROS and the weakening of antioxidants are needed for viral replication and the subsequent disease associated with the virus[97]. Viral infections alter antioxidant mechanisms leading to an unbalanced oxidative-antioxidant state and consequent oxidative cellular damage. Exposure to various pro-oxidants generally leads to activation of nuclear factor erythroid 2-related factor 2 (Nrf2) and to an increase of the expression of components of the antioxidant response. However, respiratory virus infections have also been associated with inhibition of the Nrf2 pathways that leads to inflammation and oxidative damage[97]. Nrf2 is a transcription factor responsible for the adaptation of cells and tissues including alveolar epithelium, endothelium, and macrophages to electrophilic or oxidative stress. Under normal conditions, Nrf2 is found in the cytoplasm bound to its inhibitor Keap1, which is directed to Nrf2 for ubiquination and later degradation. In the presence of electrophiles or ROS, the Keap1–Nrf2 complex dissociates and Nrf2 migrates to the nucleus where it stimulates the transcription of target genes with sequences of antioxidant response elements in their promoters[104]. Nrf2 controls the expression of the genes that participate in the antioxidant response, redox homeostasis, and the biogenesis of the mitochondria, *etc.* In addition, Nrf2 functions as a transcription repressor that inhibits the expression of inflammatory cytokines in the macrophages (*e.g.*, IL-1β, IL-6, and TNF-α)[95]. SARS-CoV-2 can interfere with the equilibrium between the transcription factor NF-κB involved in the expression of cytokines and in the activation of Nrf2, responsible for the expression of antioxidant enzymes[96], including hemoxygenase 1 (HO-1), superoxide dismutase 1 (SOD1), superoxide dismutase 3 (SOD3), glutathione S-transferase (GST), catalase (CAT), and glutathione peroxidase (GPx)[96]. Nrf2 also regulates the increase in the production of the antioxidant enzymes NAD(P)H and quinone oxidoreductase (NQO1), and enzymes needed for the biosynthesis of glutathione, which functions as the main cellular antioxidant[95]. In patients with SARS-CoV-2 infection, deficiencies in systems protection against free radicals, as well as deficits in superoxide dismutases (SODs), CAT, and reduced glutathione (GSH) have been described[94].

Oxidative stress is already increased in the elderly and people with diabetes and chronic cardiovascular diseases[90,91]. Increase in the stress level in response to viral infection affords a possible explanation of the severity of COVID-19 in such patients. In addition, elderly individuals may particularly vulnerable to infection by SARS-CoV-2 because the level and the activity of Nrf2 diminish with age[98]. Therefore, aging is not only associated with alterations in the response to adaptive immunity, but also to a proinflammatory state in the host[97].

NUTRITIONAL MANAGEMENT AND APPROACHES

Malnutrition in patients with COVID-19 infection

SARS-COV-2 infection and the resulting COVID-19 may cause multiorgan failure in addition to respiratory symptoms, including gastrointestinal (GI) and liver dysfunction, which can be complicated in the elderly or in the presence of comorbidities. There are complications associated with prolonged ICU stays; thus, the longer the ICU stay, the greater the risk of malnutrition. Malnutrition, mostly undernutrition, is the result of inadequate food intake or altered nutrient assimilation, and when it is caused by disease, different degrees of acute or chronic inflammation contribute to the state. Inflammation induces the elevation of resting expenditure, anorexia, and reduced intake. Such catabolic conditions modify body composition, with waste of muscle mass that alters functionality along and clinical outcomes[105]. Indeed, malnutrition may develop as a result of the physiological effects of SARS-COV-2, management procedures such as ventilation. Limited access of patients to direct consultations with healthcare professionals because of confinement impairs the identification of risk factors for malnutrition as well detection of the reduced food intake. Unplanned weight loss and the diminution of muscle mass induce a catabolic state in the patient, with an impact on mobility and, in turn, a poor quality of life and an increased risk of mortality, in addition to the complication of polymorbidities. As a consequence of malnutrition, immune function can be reduced, respiratory and muscle strength may be impaired, which delay recovery and result in longer hospital stays with poor outcomes. Thus, the additional use of healthcare services increases costs.

Based on the previous statement, malnutrition should be identified as an early step in the assessment of patients with SARS-CoV-2 infection, especially in patients with a high risk of mortality or of poor outcomes, such as older adults and polymorbid individuals. The identification of malnutrition is crucial for establishing effective nutritional support in order to improve food consumption, nutritional status, the patient's health prognosis, and even to prevent the occurrence of COVID-19 in the future. Particularly in the COVID-19 crisis, food and nutrient absorption is often impaired by nausea, vomiting, and diarrhea, the main GI symptoms, which lead to enhanced malnutrition. The international meta-analysis of McClave *et al*[106] of 47 studies in 10890 patients who were analyzed to determine the prevalence of liver and GI manifestations resulting from COVID-19 established consultative management of patients. Nausea/vomiting was a very frequent GI manifestation with a pooled prevalence of 7.8% (95%CI, 7.1%-8-5%) followed by diarrhea in 7.7% (95%CI, 7.2%-8.2%) and abdominal pain in 2.7% (95%CI, 2.0-3.4%). Moreover, ALT had a pooled prevalence of 15% (95%CI, 13.6%-16.5%) and AST had a prevalence of 15% (95%CI, 13.6%-15.4%) as manifestations of liver disorders. A cohort study of patients with COVID-19 in Hong Kong revealed that GI symptoms were present in 17.6% of patients and that diarrhea appeared to be the most common symptom. In the meta-analysis, the RNA virus was detected in 48.1% (95%CI, 38.3%-57-9%) of stool samples, and 70.3% (95%CI, 49.6%-85.1%) of the samples were collected after respiratory samples were found to be negative. Therefore, good management must be considered as a low risk of infection through endoscopic procedures or saving stool samples[107]. Thus, it is suggested that, prior to the administration of any treatment, it is necessary to evaluate the nutritional status of every infected patient.

In clinical practice, malnutrition is assessed with various tools (Table 1). The European Society for Clinical Nutrition and Metabolism (ESPEN) recommends using the Malnutrition Universal Screening Tool (MUST) for the identification of malnutrition in patients diagnosed with COVID-19[100]. The MUST instrument was designed for persons at risk of malnutrition, not only in those who are underweight but also in obese individuals. In patients with SARS-COV-2, loss of appetite is very frequent because of symptoms such as shortness of breath, loss of taste and smell, muscle pain, fatigue, and general discomfort. Related symptoms may contribute to insufficient achievement of energy and nutrient demands, thus promoting unplanned weight loss. To perform the MUST assessment, simple objective measurements of weight and height are needed to estimate the body mass index (BMI) in addition to weight at 3-6 mo previously. The acute disease effect denoted no nutritional intake for more than 5 d. However, even if conditions do not allow for obtaining objective measurements, screening can be carried out utilizing other measurement options, such as ulna length to estimate height and mid-upper-arm circumference. The latter are very useful for subjective BMI estimation in that healthcare personal and professionals, the patients' family members, or the patients themselves are able to obtain them. Nevertheless, if the patients are in the ICU or at home, and if it is not possible to obtain the measurements in any manner, the second step comprises the subjective

Table 1 Tools for malnutrition detection in patients with coronavirus disease 2019 and liver injury

Tool	Target patients	Criteria
MUST	Low weight	Objective criteria:
		Objective measures: weight and height to obtain BMI
		Other measures (optional): ulna length and mid upper arm circumference
		Weight loss in las 3-6 mo
	Obese patients	Subjective criteria:
		Reduced food intake in last 5 d: clinical management, psychological factors
		Weight loss appearance (clothes, jewelry)
NRS-2002	Hospitalized individuals	BMI
		Weight loss within 3 mo
		Reduced dietary intake in last week
NUTRIC score	Hospitalized patients at ICU	Age
		Days hospitalized or in the ICU
		Number of comorbidities
		IL-6 levels (optional)
		APACHE II score
		SOFA score
APACHE II score	Patients at ICU (predicting mortality)	Age
		Temperature
		Mean arterial pressure
		pH
		Heart rate/pulse
		Respiratory rate
		Sodium, potassium levels
		Creatinine
		Acute renal failure
SOFA score	Patients at ICU (estimation of mortality)	PaO_2
		FiO_2
		Medical ventilation
		Platelets level
		Glasgow Coma Scale
		Bilirubin levels
		Mean arterial pressure or administration of vasoactive agents required
		Creatinine levels
		Is a COVID-19 patient?
GLIM	Individuals at risk in general	Phenotypic criteria:
		Weight loss
		Low BMI
		Loss of muscle mass
		Etiologic criteria:

NRF-NPT	Detection of malnutrition in liver patients disease	Reduced food intake or assimilation
		Presence of disease or inflammation
		Unplanned weight loss in las 3-6 mo
		BMI
		Reduced dietary intake and uncompleted meals

BMI: Body mass index; GLIM: Global Leadership Initiative of Malnutrition; ICU: Intensive care unit; MUST: Malnutrition Universal Screening Tool; NRF-NPT: Royal Free Hospital-Nutritional Prioritizing Tool. NRS-2002: Nutrition Risk Screening-2002; NUTRIC: Nutrition risk in the critically ill; SOFA: Sequential Organ Failure Assessment.

criteria. The patient is asked to seek information related to reduced food consumption during the last 5 d or more, apparent weight loss visible in clothes and jewelry, changes in smell and taste perception if the cause of the reduced food intake is due to related symptoms in COVID-19 described previously, clinical management (ventilation, medication, and sedation), or because of the influence of physiological factors (social restriction, anxiety, and depression). The subjective criteria are useful to estimate a low, medium, or high risk of malnutrition under different circumstances, considering the limitations of infection-control restrictions instituted by local policies. It is highly recommended that patients remaining at home also perform a complete MUST assessment following progress after the implementation of nutritional strategies.

Several tools developed for assessment of hospitalized patients have been applied in COVID-19. Nutrition Risk Screening-2002 (NRS-2002) criteria, also recommended by ESPEN, predict malnutrition in hospitalized individuals and are recommended by the American College of Gastroenterology (ACG) guidelines for nutrition therapy[106]. NRS-2002 takes into account BMI; weight loss within the past 3 mo; reduced dietary intake in the previous week, and an ICU stay. In addition, the Nutrition Risk in the Critically ill (NUTRIC) score[108-111] is designed for patients, particularly for those in the ICU, and for those who can benefit from nutritional therapy considering their age, days hospitalized or time in the ICU, number of comorbidities, IL-6 Levels (optional). The Acute Physiology And Health Evaluation II (APACHE II) score[112,113], which is the most widely used tool for predicting mortality in the ICU, and the Sequential Organ Failure Assessment (SOFA) score[114,115], which estimates ICU mortality based on clinical data and laboratory results have both been used in COVID-19 clinical trials[116].

Recently, the Global Leadership Initiative on Malnutrition (GLIM), which includes the leading clinical nutrition societies worldwide, achieved a consensus with the purpose of establishing global criteria for the diagnosis of malnutrition in clinical practice. Such a consensus is a two-step approach. The first consists of the identification of "at risk" status by validated screening tools, and the second is the assessment for the diagnosis and categorization of the severity of the malnutrition[117]. According to this, three phenotypic criteria were highlighted: weight loss; reduced muscle mass, and low BMI, along with two etiological criteria, reduced food intake or assimilation and the presence of disease or inflammation. Therefore, the diagnosis of malnutrition requires at least one phenotypic and one etiologic criterion. The stratification of the phenotypic metric considers stage 1 (moderate) and stage 2 (severe) [117].

In patients with liver damage caused by COVID-19, the risk of malnutrition may be increased by the presence of GI-associated abnormalities. In severe cases of COVID-19 infection, liver injury has most commonly been observed. At the same time, patients with previous liver damage represent more critical cases of COVID-19[118]. The incidence of liver injury ranges from 14%-53%[8]. Approximately one-third of the infected population reported altered aminotransferase levels. Liver damage may affect glucose, amino acid, and lipid metabolism, and result in poor clearance of lactate and protein catabolism as a consequence of hyperaminoacidemia, and hyperammonemia, which contributes to malnutrition. On the other hand, it is crucial to determine whether the liver injury is a consequence of pre-existing liver injury (cirrhosis, viral hepatitis, NASH, and ASH) or the result of COVID-19 infection and/or the reported drug-induced liver injury. In conjunction with the MUST and NRS-2002 tools for malnutrition assessment, ESPEN recommends the Royal Free Hospital-Nutritional Prioritizing tool (RFH-NPT), which has been developed for the detection of malnutrition in patients with liver disease[119]. RFH-NPT is a validated tool very similar

to NRS-2002, but it has demonstrated greater sensitivity for the identification of malnutrition in liver diseases. The screening tool considers nearly the same indicators, namely unplanned weight loss in the previous 3-6 mo, BMI, reduced dietary intake, and uncompleted meals. The stratification scale is based scores of 1 (low risk), 2 (moderate risk), and 2-7 (high risk)[120]. Thus, in patients with COVID-19 and liver damage, the use of at least two of these options for the detection of malnutrition could be reasonable.

Nutrition strategies for liver injury in COVID-19

In COVID-19, disease complications are basically the result of a hyperinflammatory response mediated by cytokine storm and several immune-related stimuli mentioned above. Thus, nutrition treatment should be designed to strengthen the immune system during the COVID-19 crisis, providing nutrients that relieve inflammation and oxidative stress. Whether liver injury emerges as a consequence of COVID-19 or pre-existing before infection, nutrition strategies should also correct liver and GI manifestations as related symptoms to prevent or treat the associated malnutrition.

Energy and nutrient recommendations

Liver injury associated with COVID-19, as in any disease, could enhance inflammation, which alters the metabolic rate. In critically ill patients, it is recommended to estimate energy needs by means of indirect calorimetry considering all of the conditions for sterility during the measurement procedure. Significant increases in resting energy expenditure (REE) in patients with acute liver failure (ALF, 18%-30%)[121], alcoholic hepatitis (55%)[122] and alcoholic cirrhosis (26%)[123] have been reported. Hypermetabolism reported in patients with liver cirrhosis (> 30%)[124] could be related to effect of delay in the improvement of body composition on clinical outcomes. Hence, because of the individual variability in liver damage, REE should be measured by indirect calorimetry. Recently, the estimation of REE with a less-expensive handheld calorimeter method based on a respiratory quotient of 0.85, and which is very accurate for REE has been proposed[125]. However, when accessibility to calorimetric equipment is limited, prediction equations for the estimation of energy expenditure could be employed. A summary of caloric and nutrient recommendations is shown in Table 2. Caloric intake should be 1500-2000 kcal/d for normal maintenance by oral diets, with an increase of 400-500 kcals under conditions of stress or in an infection crisis[126]. ESPEN guidelines[100] suggest 27 kcal/kg body weight (Bw)/day in polymorbid patients and in patients > 65 years of age. For low-weight or older patients, it is suggested to achieve 30 kcal/kg Bw/day. In malnourished cirrhotic patients with muscle depletion, the energy supply must provide 30-35 kcal/kg Bw/day. Contrariwise, in overweight or obese patients with liver disease, the prognosis may be worse. In such cases, obesity has been associated with portal hypertension[127]. For that reason, an increased energy intake is not recommended. Nonetheless, all energy recommendations must be adjusted individually, taking into account disease severity, mobility, physical activity, and tolerance. In severely underweight patients, the energy supply must be carefully administered in order to prevent the refeeding syndrome, which is very common in such patients. Whenever possible, oral feeding should be the first energy and nutrient-supply option. When oral feeding is not feasible, support nutrition therapy by nasogastric tube through enteral nutrition (EN) or parenteral nutrition (PN) should be available as the next step.

Proteins in the diet are known to be crucial nutrients for gut-associated lymphoid tissue, as are active immunoglobulins, which act against infection in the gut mucosa[128]. The consumption of high-value proteins that contain essential amino acids is associated with immune responses, for example, adequate production of antibodies; activation of T and B lymphocytes, macrophages, and NK cells; and the production of cytokines and other immune elements that prevent infectious diseases[129]. In addition, in order to prevent body weight loss and muscle mass, > 1 g/kg Bw/day of protein intake is recommended for patients with anorexia or reduced food intake. In general, 1 g/kg Bw/day is sufficient to meet the requirement, but protein intake should be adapted to individual needs according to disease status, physical activity, and tolerance. Overall, 70-100 g/d of protein are acceptable in the oral diet, preferably consumed from animal (milk, yogurt, meat, fish, chicken, and cheese) and vegetable sources (beans, soy, nuts, and peas)[126]. Oral nutrition supplements (ONS) are a fairly good option when the goals of oral feeding are not fully achieved. In the latter cases, ONS are suggested to supply 150-400 kcals and 15-30 g of protein and should be consumed for at least 1 mo[100,126].

Table 2 Energy and nutrient recommendations for patients with coronavirus disease 2019 with or without liver injury

Energy/Nutrient	Criteria	Recommendation
Estimation of REE	All individuals with COVID-19	Estimation by indirect calorimetry
		Prediction equations
Calories	Normal oral diets	1500-2000 kcals/d
		Increase 400-500 kcals in stress or infection crisis
	Polymorbid, old patients > 65 yr	27 kcals/kg Bw/day
	Low weight, older patients	30 kcals/kg Bw/day
	Malnourish chronic patients and muscle depletion	30-35 kcals/kg Bw/day
	-Patients with COVID-19 outside ICU	ONS with low oral intolerance:
		150-400 kcals/service
		70-100 g protein/service
		Carbohydrates, fiber, PUFAs, vitamins, minerals, probiotics
		Consuming for a month
Protein	Normal individuals (prevent loss and muscle mass)	1 g/kg Bw/day
		70-100 g/d
		Form animal (milk, yogurt, meat, fish, chicken, cheese) and vegetable sources (beans, soy, nuts, peas)
	Patients with liver cirrhosis sarcopenic	1.2-1.5 g/kg Bw/day
	Obese sarcopenic	Oral supplementation of BCAA 0.20-0.25 g/kg Bw/day or 30 g/d
		Glutamine and arginine supplementation
Carbohydrates/fat	Patients with COVID-19 without respiratory impairment	Ratio 70:30 carbohydrates/fat
		Medium and low glycemic
		Fiber 25-30 g/d
		PUFAs: DHA, EPA, ALA
	Patients with ventilator support	Ratio 50:50 carbohydrates/fat
Vitamins	All individuals with COVID-19	A, C, D, E, folate, B_6 and B_{12} (monitoring in patients with liver abnormalities)
Minerals	All individuals with COVID-19	Zinc, copper, selenium (monitoring in patients with liver abnormalities)
	Critically ill patients	EN after 24-36 h. after ICU admission
		Initiate with trophic low-dose (10-20 mL/h.)
		Polymeric formula: 15-20 kcals/kg Bw and 1.2-2.0 g/kg Bw/day of protein vitamins, minerals, fiber, probiotics
		Provide 70%-80% needs in over 1 wk
	Sever obese patients BMI > 50	Energy 22-25 kcals/kg IBW
		Protein 2 g/kg per day (Class I, II) or 2.5 g/kg IBW/day of (Class III)
		Vitamins, minerals, fiber, probiotics
	Gastric intolerance individuals	Use prokinetics
		Post-pyloric feeding in persistence intolerance or at high risk of aspiration
	Patients with no GI feasible	PN recommended
	Poor nutrition status	Limit the use of omega-6 soy-based ILE during first week
	Prolonged stay at ICU	Mixture of lipids such as olive oil based ILE or SMOF (soy,

	medium chain triglycerides, olive oil, fish oil)

ALA: Alpha linoleic acid; BCAA: Branch chain amino acids; DHA: Docosahexaenoic acid; EN: Enteral nutrition; EPA: Eicosanoid acid; GI: Gastrointestinal; IBW: Ideal body weight; ICU: Intensive care unit; ILE: Intravenous lipid emulsion. ONS: Oral nutritional supplements; PN: Parenteral nutrition; PUFAs: Polyunsaturated fatty acids; REE: Resting energy expenditure.

In liver injury, nutritional approaches must be attended to according to the type and grade of the lesion(s). In patients with acute liver failure, nutrition therapy must be centered on providing sufficient energy in the form of glucose and fatty acids along with vitamins and mineral elements, preventing hypoglycemia and hypertriglyceridemia, and protein and amino acid sources adequate to avoid catabolism and to promote protein synthesis. Patients with liver cirrhosis are very likely to experience malnutrition and muscle wasting because of a decrease in protein synthesis and increased total protein breakdown. The recommendation is 1.2-1.5 g/kg Bw/day of protein to ameliorate protein synthesis in patients with sarcopenia, including those with obese sarcopenia, preferably with high-quality proteins from animal and vegetable sources in oral diets. In those with poor tolerance of protein, vegetable sources are acceptable[119]. It is preferable to distribute the intake in 3-5 meals a day, avoiding long starvation periods. A late evening snack of protein and carbohydrates has been shown to be very effective in improving nitrogen balance in cirrhotic patients[130, 131]. Oral supplementation with isoleucine, leucine, valine, and branched chain amino acids (BCAA) has been useful for patients with intolerance to protein with liver encephalopathy. In liver dysfunction, low BCAA levels are regularly observed in addition to high levels of tryptophan, aromatic amino acids, and sulfur-containing amino acids. The imbalance of amino acids may induce liver encephalopathy. Hence, the administration of 0.20-0.25 g/kg Bw/day or 30 g/d of BCAA has beneficial effects on the patient's mental state after episodes of encephalopathy and on improvement of protein metabolism[132,133]. In addition, BCAA supplementation in protein-restricted diets has been associated with improvement of the intestinal immune defense by increasing the levels of jejunal and ileal immunoglobulins and protecting duodenal villous morphology[134]. Some amino acids are responsible for modulating the immune response; for instance, glutamine activates protein participation with extracellular signal-regulated kinases (ERKs) and c-Jun N-terminal (JNKS) kinases in signal transduction, triggering transcription factor activation, and the expression of genes regulating the proliferation of lymphocytes, macrophages, and neutrophils. Moreover, glutamine induces the expression of some cytokines, including IL-6, TNF-α, and IFN-γ, and certain surface markers of lymphocytes[135]. Under catabolic and hypercatabolic conditions, glutamine has an essential role in metabolism; therefore, it is widely utilized in clinical nutrition under conditions of immunosuppression[135, 136]. On the other hand, arginine and its downstream metabolites citrulline and ornithine are involved in T cell activation, and promoting and modulating innate and adaptive immune responses[137].

During liver injury, the metabolism of glucose is altered, the glucose oxidation rate is reduced, and the glucose production rate in the liver is low because of the depletion of glycogen stores despite increased gluconeogenesis. Glucose deposition in skeletal muscle and liver as glycogen is impaired. At the same time, glucose uptake in tissues is reduced because of insulin resistance in response to high secretion and reduced degradation[138,139]. Lipid metabolism reflects an augmented rate of lipid oxidation parallel to insulin resistance. Additionally, the plasma levels of essential and polyunsaturated fatty acids are reduced in relation to the nutritional status and to the severity of the injury[140]. In patients with COVID-19, the ratio of carbohydrates to fat should fall within the range of 70:30 for patients without respiratory impairment and within 50:50 in patients on ventilatory support[141]. Nonetheless, it is noteworthy to take into consideration the previously mentioned changes in glucose and lipid metabolism in patients with liver disorders. In oral diets, low glycemic index foods, such as vegetables, whole grains, and legumes, are preferable rather than those with high glycemic/glycemic loads, which have been associated with the immediate increase of the inflammatory cytokines IL-6 and TNF-α[89] and CRP[142]. In parallel, fatty acids (FAs) have also been associated with the immune response, impacting on macrophages, epithelial cells, lymphocytes, neutrophils, dendritic cells, and lymphoid cells [143]. The consumption of saturated and trans-FAs from processed and fried foods has been correlated with the elevation of hs-CRP, IL-6, and TNF-α[144]. In influenza A virus infection, a diet rich in saturated FAs has been associated with impaired immune viral response, resulting in higher viral loads in the lung and heart, inducing inflam-

mation and tissue damage[145]. Contrariwise, polyunsaturated FAs, particularly omega-3 FAs, have a potent anti-inflammatory effect. Omega-3 FA eicosapentaenoic acid (EPA) and docosahexaenoic acid (DHA), consumed mainly from fish and seafoods, including α-linolenic acid (ALA) consumed from plant sources, have been reported to initiate anti-inflammatory signaling[143]. In epithelial cells in the lungs, gut, and skin, omega-3 FAs are capable of activating nuclear and transmembrane receptors and can restore a compromised barrier defense and reducing the production of anti-inflammatory mediators such as IL-1β, TNF-α, interferon gamma (IFN-γ), and lipopolysaccharides (LPSs)[69]. Also, they reduce the expression of ERK1/2 MAPK, NF-κB, and COX-2, the main signaling pathways of the inflammatory response[69]. In viral infections, supplementation with omega-3 FAs appears to inhibit the production of TNF-α, IL-1β, IL-6, and IL-8 and reduce the production of ROS. In critically ill patients in the ICU, the addition of fish oil rich in omega-3/antioxidants in the enteral formula appears to enhance the response to oxygen therapy, improve clinical outcomes, and shorten ICU stays[146,147].

For patients outside the ICU, nutrition treatment should begin early, within 24-48 h of hospitalization, orally and mainly in older and polymorbid patients, whose nutritional situation may be compromised. The use of ONS could be fully applicable in patients with COVID-19 and liver injury in order to prevent or treat malnutrition and reestablish liver function. ONS are recommended to meet energy, macronutrient (carbohydrate, protein, and lipids) and micronutrient (vitamins and mineral elements) needs. Fiber and probiotics are suggested to promote optimal intestinal function. The increase of dietary fiber from whole grains benefits gut microbiome composition and is also correlated with reducing both systemic and gut inflammation by reducing IL-6, TNF-α, and hs-CRP, and by increasing short chain fatty acids (SCFAs)[74]. SCFA are produced by gut microbiota as a result of dietary fermentation. They are potential activators of anti-inflammatory signaling cascades and inhibitors of proinflammatory cytokines, as well as the reduced expression of NF-kB[72]. Furthermore, dietary fiber has been reported to promote healthy gut microbiota, which is related to inhibition of systemic inflammation and enhanced mucosal thickness, protecting the gut barrier from the infiltration of pathogens[77]. Dietary fiber is also thought to influence the gut microbiome and respiratory function, and it is noteworthy that, in some cases, the macrophage response to respiratory viruses is linked to the composition of the gut microbiome[148].

Vitamins and minerals in nutrition therapy

Some vitamins and mineral elements have attracted special attention because of the potential benefit that they may have during the COVID-19 crisis. In general, treatment with vitamins A, C, D, and E, folate, vitamin B_6 and B_{12}, and minerals including zinc, selenium, copper, iron, and calcium is recommended as ONS as well as by consumption of natural food sources in the diet. To date, there is no consistent evidence to support the idea that the previously mentioned vitamins and minerals possess a potential effect in preventing or treating the COVID-19. Nonetheless, in agreement with previous data regarding their effect on reducing flu symptoms and possessing antioxidant benefits, the consumption of vitamin C is suggested for consumption within a range of 1-2 g in persons at risk of respiratory infections[149]. Vitamin C exerts an influence on the immune system and on the production, development, and maturation of lymphocytes, and in the promotion of phagocytosis and chemotaxis of leukocytes during infection[82,150]. In pneumonia, vitamin C has been found to reduce ROS and inflammation by inhibiting the activation of NF-κB that, in turn, decreases IL-1, IL-8, IL-6, and TNF-α production, and reduces DNA damage and LPS-induced ROS[82]. In various trials that investigated the treatment of sepsis and ARDS vitamin C was found to reduce TNF-α and IL-1β and increase CAT, SOD, and glutathione levels[151]; in that regard, vitamin C supplementation could be beneficial in COVID-19.

Regarding vitamin D, recent investigations have pointed out its role in preventing infections, including COVID-19. Vitamin D has been described as possessing anti-inflammatory and immunomodulatory effects and may interfere with viral replication, probably by its effects on innate and adaptive responses by the modulation of defensins and cathelicidins and reduction of the Th1 helper cell response[152]. Furthermore, vitamin D participates in the activation of regulatory T cells and Th2 cells along with a decrease of proinflammatory cytokines, such as TNFα and IFNγ, which are involved in the pathogenesis of ARDS, by Th1 cells[153]. Vitamin D deficiency is correlated with an increase of susceptibility to infections and increased autoimmunity; its benefits are thus highlighted in persons with low levels of vitamin D[154]. One of the possible mechanisms by which vitamin D could impair the entry of COVID-19 into

host cells is by suppressing the adhesion molecule CD26/DDP4, a key element for viral entry[155]. Another possible mechanism of lung protection is through regulation of the renin–angiotensin system to inhibit viral entry and replication[156].

It appears that the role of vitamin A in preventing the effects of COVID-19 is not fully understood, but it is known that retinoic acid, the most active retinoid form of vitamin A, has an impact on the production of IL-1β and IL-1 receptor antagonists by means of alveolar macrophages and the consequent infiltration of neutrophils into the lungs during the course of ARDS. Retinoic acid contributes to surfactant production, which may be another way to protect against ARDS. Meanwhile, carotenes attenuate ROS production, diminishing the level of oxidative stress in the lungs. Under conditions of vitamin A deficiency, epithelial damage is often observed during viral infections, as is the increase of susceptibility of the host to respiratory viruses like influenza and SARS-CoV[156].

The most relevant activity of vitamin E is it antioxidant activity, which protects against free radicals like superoxides. In addition, the vitamin E effect is associated with the immune response of lymphocytes, NK cells, and neutrophils, which decline in the elderly[157]. Vitamin E supplementation in older adults was shown to enhance immune cell functions including neutrophil chemotaxis and phagocytosis, NK cell activity, and mitogen-induced lymphocyte proliferation[158].

With regard to the vitamin B group, vitamins B_6, B_9 (folate), and B_{12} are considered relevant to immune function in the context of the COVID-19 pandemic framework [159]. Low concentrations of B_6 influence on lymphocyte maturation, antibody responses, and the cytotoxic activity of NK cells. Folate intervenes in the response of Th1 and NK cells and in optimal antibody production[160]. Two mechanisms have been proposed by which folate may blunt the COVID-19 infection. The first is the significance of the homocysteine-mediated trans-sulfuration pathway and of ferroptotic stress that leads to cell death[88]. The second is the probable disruption of furin protease activity involved in SARS-CoV-2 spike protein cleavage, as mentioned previously[161]. Vitamin B_{12} also participates in antibody responses and circulating lymphocyte levels. In DNA synthesis, which is important for cell replication, B_{12} restores an abnormal ratio of CD4+/CD8+ T cells, and its deficiency may be associated with the impairment of the immune response to viruses and bacteria in conjunction with suppressed NK cells[86]. Hence, the consumption of folate, B_6, and B_{12}, is recommended, and they should be integrated within nutrition therapy.

The trace minerals zinc, copper, and selenium are intricately involved in immune function. Zinc is highlighted because of its immunomodulatory effects on NK cell activity and macrophage and neutrophil function, complementary activity, and T cell-mediated function. Antioxidant activity has been attributed to trace minerals because they are cofactors of antioxidant metalloenzymes such as SOD. Zinc deficiency is implicated in the systemic activation of NF-κB[162]. Zinc might reduce viral replication and attenuate GI and respiratory symptoms related to COVID-19. Additionally, zinc at low doses (2 μmol/L) can prevent SARS-CoV replication by inhibiting SARS RNA polymerase[163]. Increased intracellular levels of zinc enhance the therapeutic effect of some drugs employed in the treatment of COVID-19, such as chloroquine, disulfiram, and tetracycline[164]. Recent evidence supports the idea that maintaining optimal levels of zinc is fundamental for resistance in the host response in COVID-19 and for preventing other viral infections[165]. A clinical study of four patients treated with oral administration of a high dose of a zinc salt, based on previous data that zinc shortens the duration of a cold, reported rapid improvement of the symptomatology [166]. Therefore, alone or in combination with other drugs, zinc is being investigated in several trials to determine its effectiveness in the prevention or treatment of COVID-19.

Selenium is considered another important trace element with antioxidant and anti-inflammatory effects. Selenium, together with vitamin D deficiency, probably impairs immune responses to COVID-19 and increases the severity of the disease[167]. In contrast, other clinical studies reveal that the recovery rate in surviving patients was related to increased selenium levels in patients with COVID-19[168,169]. Selenium is intricately involved in a wide range of immune activities, such as T cell activation, maturation, differentiation, and proliferation. It exerts antiviral activity by regulating the TCD4+ response, modulating TCD8+ and NK cells with cytotoxic activity, and it has a crucial role in the production of antibodies[170]. It is thought that a selenium deficiency has an influence on the high incidence of thromboembolism in patients critically ill with COVID-19 in the ICU[171]. A possible explanation is that low selenium levels are correlated with an abnormal thromboxane A_2-to-prostacyclin I_2 ratio, which is implicated in vasoconstriction and coagulation[172]. However, further studies are needed for clarification[170].

Copper protects DNA integrity by reducing oxidative damage, and its deficiency alters the immune response and promotes infectious diseases. Copper appears to participate in immune cell differentiation and to inhibit viral replication. It exerts an influence on the optimal functioning of NK cells, lymphocytes, neutrophils, macrophages, and monocytes. Supplementation with high doses of copper (7.8 mg/d) was shown to improve the activity of antioxidant enzymes and to activate SOD, ceruloplasmin, and benzylamine oxidase. However, the high dose affected neutrophils, serum IL-2R, and the levels of anti-influenza virus antibodies[173]. In this framework, copper has been proposed as a target element, together with others, such as zinc, in the treatment of COVID-19[174]. The antiviral properties attributed to copper would act directly with the virus by blocking structural proteins or by improving immune cell functioning[159]. Following this line of reasoning, optimal plasma levels of copper can elevate innate and adaptive immune responses to promote best action against SARS-CoV-2. Therefore, it must be part of regimens for COVID-19 prevention and therapy[175].

Nutritional support in critically ill patients with COVID-19 and liver injury

The hyperinflammatory response is one of the main characteristics of patients critically ill with COVID-19. Accordingly, the GI tract could play a central role in modulation of the inflammatory response, as it is the largest immune organ in the body, with the greatest microbiome. Nutritional therapy through EN strengthens gut barrier defenses and the microbial burden by providing luminal nutrients that impair dysbiosis and stimulate the anti-inflammatory response[176]. EN nutrition should start early, within 24-36 h after admission to the ICU or within 12 h of mechanical ventilation. To avoid refeeding syndrome, EN should be initiated with low trophic doses (10-20 mL/h) of a standard isosmotic polymeric formula that supplies 15-20 kcal/kg Bw and 1.2-2.0 g/kg Bw/day of protein, considering the actual body weight. The goal is to provide 70-80% of energy needs during 1 wk. In obese individuals with a BMI of 30-50, EN provides 11-14 kcals/kg Bw/day; for patients with severe obesity with a BMI >50 energy 22-25 kcal/kg Bw and 2 g/kg/d (classes I and II) or 2.5 g/kg/d (class III), taking into account the ideal body weight (IBW)[102]. Various complications may occur in patients with EN, such as GI disorders (*e.g.*, diarrhea, vomiting, and nausea) and mechanical disorders related to intubation and metabolic disorders (*e.g.*, hyperglycemia and an electrolyte imbalance). Thereafter, close monitoring is required to prevent difficulties[177]. In patients with gastric intolerance, prokinetics may alleviate symptoms and promote motility, but post-pyloric feeding should be performed in the persistence of intolerance or in patients with a high risk of aspiration[118].

For patients in whom GI feeding is not feasible, PN should be considered. Patients with a poor nutrition status, significant intolerance to EN, or those with a prolonged length-of-stay in the ICU, are potential candidates for PN. To avoid proinflammatory infusion, it is suggested to limit the use of omega-6 soy-based intravenous lipid emulsion (ILE) in week 1 or to change to a mixture of lipids, such as olive oil-based ILE or to soy, medium chain triglycerides, olive oil, and fish oil (SMOF)[102]. PN complications include catheter-related bloodstream infections and PN liver-associated damage[99]. At present, there are no reported cases associated with these complications. Nevertheless, the background must be taken into account for patients with sustained PN[126].

Certain other aspects must be taken into consideration when determining nutritional support in the patient. For instance, in liver injury, the primary treatment goal is against the COVID-19 infection, using antivirals, antibiotics, symptomatic support, oxygen therapy, and anti-inflammatory drugs, *etc.* It has been reported that some of the antivirals and drugs employed to treat this infection did cause liver damage[55, 178], and clinicians should consider reducing the dose or discontinuing the drug(s). In patients with severe COVID-19, AST, ALT, total bilirubin, albumin, and certain other liver function indicators are significantly increased. However, the indices gradually returned to normal levels during recovery. With moderate liver damage, the organ function was restored without special treatment[179]. Consequently, moderate-to-severe cases require the regular monitoring of liver indicators, including AST, ALT, alkaline phosphatase, bilirubin, GGT, albumin, and prothrombin time. In severe cases, hepatoprotective drugs should be administered with caution[8] and the patient should probably be referred to the hepatology service for further specialized management. Mildly elevated indicators may not require specific liver treatment or hepatoprotective drugs[118].

ROLE OF PHYTOCHEMICALS IN COVID-19 THERAPY

The outbreak of COVID-19 has revolutionized medical science, and has been accompanied by the absence of a definitive treatment in addition to the unknown long-term effectiveness of recently approved vaccines. That has encouraged researchers to design target drugs in the fight against COVID-19 and also to seek further therapeutic options. Phytochemicals are molecules that are biologically active and that generally derive from plants or vegetable sources. Phytochemicals provide benefits when they are consumed in foods, supplements, or as medicinal ingredients. For several years, these compounds have been extensively studied from different perspectives. To date, 5000 bioactive compounds have been identified and classified into different groups depending their chemical features or biological activities. The groups include polyphenolic compounds, carotenoids, alkaloids, and sulfur/nitrogen compounds. Each group comprises a wide variety of molecules with high biological potential. The most predominant biological activities are the result of antioxidant, antitumor, anticancer, anti-inflammatory, antimutagenic, detoxifying, and immunomodulatory properties [180,181]. Moreover, various phytochemicals have antiviral activity that is shown to be more effective than that of antivirals, in addition to being generally better tolerated and having fewer adverse effects[182]. Two modalities have been proposed by which phytochemicals may induce protection against the virus, including (1) direct interaction with the structure of the virus and (2), enhancement of endogenous cytoprotective systems. In both cases, some of the compounds have proven to be effective. For the purpose of this review, some of these will be discussed briefly within the framework of COVID-19 and liver injury.

Direct interaction with the virus

From structural studies of SARS-CoV-2, it has been possible to determine the major drug targets, which include 3-chymotrypsin-like protease ($3CL^{pro}$), papain-like protease (PL^{pro}), RNA-dependent RNA polymerase, and spike (S) proteins. The S proteins are considered potential therapeutic targets because the virus attaches itself to the ACE2 receptor through these proteins, leading to fusion with the host cell. Subsequently, the virus releases its genetic material for RNA replication, building new viruses. As the proteins participate in the process, are attractive targets of antiviral drugs and phytochemicals[183].

Previous studies of SARS-CoV and Middle East Respiratory Syndrome provided relevant information for understanding the behavior of SARS-CoV-2 and the effectiveness of natural compounds that inhibit viral activity. Among the compounds that appear to possess effective antiviral activity against coronaviruses silvestrol, tryptanthrin, scutellarein, saikosaponin B2, quercetin, myricetin, caffeic acid, isobavachalcone, psoralidin, and lectins. The majority are extracted from natural herbs that are very commonly used in traditional medicines. Many of the bioactive compounds depend on enzyme inhibition for their antiviral effects[184]. It appears that polyphenols are the most effective antiviral compounds. For example, quercetin inhibits the protease $3CL^{pro}$, which has a crucial role in viral transcription. The inhibitory concentration (IC_{50}) of quercetin was reported to be 8.6 ± 3.2 μmol/L against SARS-CoV PL^{pro} [185]. Quercetin has shown to be effective in inhibiting the influenza virus, poliovirus, adenovirus, Epstein-Barr virus, and hepatitis C virus, among others[182].

A few computer modeling studies have been performed to screen the targeted biding sites of phytochemicals with SARS-CoV-2. Recently, Kurman *et al*[76] used molecular docking or molecular dynamics (MD) software to predict phytochemical interactions with Nps15, a nidoviral RNA uridylate-specific endoribonuclease (NendoU) protein commonly present in coronaviruses, and responsible for interfering with the innate immune response. It was found that 50 phytochemicals had the potential to bond with Nsp15 and obstruct viral replication. The phytochemicals with the effective bonding potential were sarsasapogenin, ursonic acid, curcumin, ajmalicine, novobiocin, silymarin and aranotin, piperine, gingerol, rosmarinic acid, and alpha terpinyl acetate, suggestive of potential use as inhibitors of SARS-CoV-2 replication. In another MD simulation study, phytochemicals from the Aryurvedic medicinal plants *Withania somnifera* (Ashwagandha), *Tinospora cordifolia* (Giloy), and *Ocimuvingm sanctum* (Tulsi), identified as anolide V, somniferine, tinocordiside, vicenin, ursolic acid, and isoorientin 4′-*O*-glucoside 2′′-*O*-*p*-hydroxybenzoagte, potentially inhibited the main protease M^{pro} or the $3Cl^{pro}$ of SARS-CoV-2. The authors suggested that such active compounds were safe, and that the drug-likeness test and their absorption, distribution, metabolism, excretion, and toxicity (ADMET) profile predicted their potential effectiveness[186]. In an in-silico MD study of 32 phytocompounds, Swargiary *et al*[187] found that amentoflavone and gallocatechin gallate were

potential inhibitors of $3CL^{pro}$ and PL^{pro} and might be promising drug candidates for the treatment of SARS-CoV-2. However, the findings of in-silico studies require support by in vivo research to determine their mechanism of action.

Activation of cytoprotective systems

In addition, phytochemicals can also induce protection against SARS-CoV-2 by activating cytoprotective systems. A variety of these compounds have been shown to trigger signaling pathways related to endogenous defenses such as Nrf2/Keap1/ARE. Nuclear factor erythroid 2-related factor 1 (Nrf2) is a nuclear transcription factor coded by the *NFE2L2* gene. It is known as the master regulator of cytoprotection and antioxidant responses[188]. Nrf2 impacts approximately 250 genes involved in antioxidant responses, detoxification, cell growth, proliferation, differentiation, energy metabolism, and apoptosis. Under homeostatic conditions, Nrf2 binds to its negative regulator Keap1 in the cytosol, but the electrophilic molecules that result, such as ROS, encourage Nrf2 dissociation from Keap1 and further translocation into the nucleus to bind the specific DNA sequence. The antioxidant response elements (ARE) elicit the expression of several genes involved in cell protection, including antioxidant enzymes, phase-II detoxifying enzymes, NAD(P)H quinone oxidoreductase 1 (NQO1), and the enzymes involved in glutathione synthesis and metabolism *via* musculo-aponeurotic fibrosarcoma proteins (s-Maf)[189]. The redox-sensitive Nrf2/Keap1/ARE signaling pathway has a fundamental role in preserving homeostasis caused by oxidative stress, inflammation, diabetes, cardiovascular diseases, cancer, neurodegeneration, liver-kidney injury, and aging[190]. According to the evidence, some phytochemicals possess the ability to activate the Nrf2/Keap1/ARE pathway. They are called "Nrf2 bioactivators", but few have been broadly studied. Sulphoraphane (SFN), an isothiocyanate found in *Brassica* species like broccoli, is the most potent Nrf2 bioactivator. Taking into account the "CD value", which refers to the amount of a certain compound necessary to double NQO1 activity in murine hepatoma cells (hepg2)[191], SFN requires 0.2 μmol/L, and other phytochemicals, such as quercetin, require, 2.5 μmol/L, with curcumin requiring 2.7 μmol/L, and silymarin, 3.5 μmol/L. It is important to bear in mind that the lower the amount required, the more potent the phytochemical is considered to be. Other phytochemicals have been found to activate Nrf2, including andrographolides, quercetin, β-carotene, genistein, lutein, resveratrol, and zeaxanthin [192]. SFN activates nuclear respiratory factor (NRF) by means of a direct reaction with the electrophilic isothiocyanate group, changing the covalent linking of the Keap1 cysteine residues. SFN has thus been extensively employed in several protocols for the treatment of inflammation, cancer, diabetes; and cardiovascular, neurodegenerative, lung, hepatic, and kidney damage. SFN is considered to be an anticancer, antiproliferative, antioxidant, and anti-inflammatory agent[193,194]. The Nrf2/Keap1/ARE pathway is ubiquitously active, which may be the reason why certain phytochemicals could be promising protectors under different clinical situations.

To our knowledge, silymarin (SM) could be one of the most remarkable phytochemicals from the COVID-19 and liver injury perspective. SM is a blend of seven flavonolignans (65%-80%) obtained from the extract of *Silybum marianum*. The main flavonolignan is silybin (50%-70%) and its isoforms silybin A and silybin B. Isosilybin, silychristin, isosilychristin, and silydianin and their isoforms are the remaining flavonolignan constituents. SM has been used as a traditional medicine since ancient times by physicians and herbalists to treat acute and chronic liver abnormalities because of its antioxidant, anti-inflammatory, and antibiotic activities[101]. The mechanisms of action of SM are not yet fully elucidated, but involve triggering the Nrf2/Keap1/ARE signaling pathway. Various in vitro and in vivo trials have demonstrated the efficacy of SM in Nrf2 activation. Likewise, in SFN, the reported benefits are not only found in liver injury models[195,196] but have also been described in lung[197], neurodegenerative[198], cardio–renal[199], gastric ulcer[200], and neurotoxicity[201] models, among others. Furthermore, an in-silico MD study revealed the affinity of six SM flavonolignans (silybin A, silybin B, isosilybin A, isosilychristin, taxifolin, and silydianin) for bonding Keap1 by electrostatic and van der Waals interactions, as well as hydrogen bonds. That could partially explain the ability of SM to induce the activation of the Nrf2/Keap1/ARE signaling pathway[202].

Moreover, recent investigations have identified SM antiviral activity against hepatitis C and B, dengue, influenza, Chikungunya, and HIV[203]. SM even proved to inhibit the entry and attachment of enterovirus 71 (EV-A71), which is responsible for causing hand, food, and mouth disease in childhood, more effectively than the positive control, balcalein[204]. Together with previously mentioned results of MD studies with regard to potential SM and COVID-19 inhibition, it is suggested that SM or its flavonolignans should be considered as very promising drugs for the treatment of

COVID-19 and liver injury.

Curcumin is another phytochemical with potential for treating SARS-CoV-2 and liver damage. Curcumin is the main polyphenol in turmeric, present the rhizome of *Curcuma longa* and other species. In traditional medicine, it is used as an anti-inflammatory, antiseptic, analgesic, antimalarial, and as an insect repellent[205]. Current evidence supports the ability of curcumin to attenuate oxidative stress produced by ROS and RNS. Curcumin induces the antioxidant enzymes GST and γ-Glutamyl cysteine ligase (γ-GCL) and, at the same time, inhibits ROS-producing enzymes (oxidases, lipooxygenase, xanthine hydrogenase, and cyclooxygenase) and removes peroxide radicals, hydrogen peroxide, hydroxyl radicals, oxygen, and nitric oxide. The activities are associated with regulation of the Nrf2/Keap1/ARE pathway in addition to the modulation of other transcription factors, such as NF-kB and AP1[206]. In rat hepatic stellate-T6 (HSC-T6) cells, curcumin reduced the levels of malonaldehyde (MDA), and ROS treated with glucose oxidase, upregulated the nuclear translocation of Nrf2, augmenting glutathione levels, and reduced the expression of smooth muscle α-actin and extracellular matrix molecules[207]. In a rat model of arthritis, curcumin reduced inflammation by increasing methionine sulfoxide reductase A and the antioxidant enzymes CAT, SOD, and GPx[208]. In macrophages and RAW264.7 cells, curcumin protected cells from stress by inducing H_2O_2, triggering the Nrf2/Keap1/ARE pathway and the expression of antioxidant enzymes, thus promoting cell survival [209]. Additional evidence that supports the effect of curcumin on Nrf2 activation, curcumin is also described as an antiviral. Curcumin interacts with viral proteins on the cell surface, impairing entry of the virus. It also interacts with RNA polymerase and other proteins to hamper replication and may also interact with protease M^{pro}[210, 211]. In the previously mentioned MD study, curcumin was an effective inhibitor of the SARS-CoV-2 Nps15 protein. The hyperinflammatory response initiated in the "cytokine storm" is also weakened by curcumin, which interferes in the NF-κB and MAPK inflammatory pathways to reduce the expression of the proinflammatory cytokines IFN-γ, monocyte chemoattractant protein 1 (MCP)-1, IL-6, IL-10, and TNF-α [212]. Curcumin appears to prevent apoptosis and lung fibrosis by inhibiting the TGF-β pathway[213]. The envelope protein of SARS-CoV-2 is the smallest of the four structural proteins of the virus and it is known to participate in the viral entry process. We have performed some in-silico studies to investigate that protein.

Molecular modeling of the SARS-CoV-2 envelope protein

The three-dimensional model of the SARS-CoV-2 envelope protein of was built using Modeller 9.23 Software and considering the crystal structure of the transmembrane region of the envelope protein of SARS-CoV (PDB: 5X29). The resulting model represents a homo-pentamer of the E protein of SARS-CoV-2.

Docking analysis of the compounds of interest

Docking studies were used to predict the binding affinity of the compounds of interest and the SARS-CoV-2 envelope protein. Results of the analysis of silibylin, curcumina, and sulfuraphane were performed with Autodock 4.2 (Table 3 and Figure 5). The input files were prepared with the AutoDock Tools 1.5.2 graphic interface[214]. A grid box of 120 Å × 120 Å × 120 Å and a grid spacing of 0.375 Å was used for the docking studies. The Lamarckian genetic algorithm was selected for the sampling score, considering a randomized initial population of 100 and a maximum number of energy evaluations of 10^7.

CONCLUSION

The current pandemic situation caused by COVID-19 infection has generated global changes in not only human health, but in all economic, political, and social levels. The lack of an effective vaccine that prevents COVID-19 infections and the absence of an effective treatment that reduces multiorgan consequences, only allows us to establish guidelines and recommendations based on direct experience with patients and observing what works and what does not and to make decisions supported by science. In this review, we attempted to provide an outline of how hyperinflammatory and oxidative stress responses to COVID-19 infection may cause liver injury or worsen a pre-existing one. GI-related symptoms, such as diarrhea, vomiting, nausea, and reduced food intake, along with a delay in medical attention, promote weight loss. Malnutrition increases mortality, hospital stay, and poor outcomes, in addition to high economic costs. The detection of malnutrition is thus crucial for establishing optimal

Table 3 Curcumina, silibylin, sulfuraphane evaluation by Autodock 4.2

Ligand	Binding energy (kcal/mol)	kI μmol/L	Residue interactions
Curcumine	-4.6	428.13	Phe 23, Val 25, Leu 28, Phe 26, Thr 30, Val 26
Silybin	-5.73	62.57	Phe 23, Phe 26, Val 29
Sulforaphane	-3.75	1.79	Val 29, Phe 26, Val 25, Ala 22, Phe 23, Leu 27

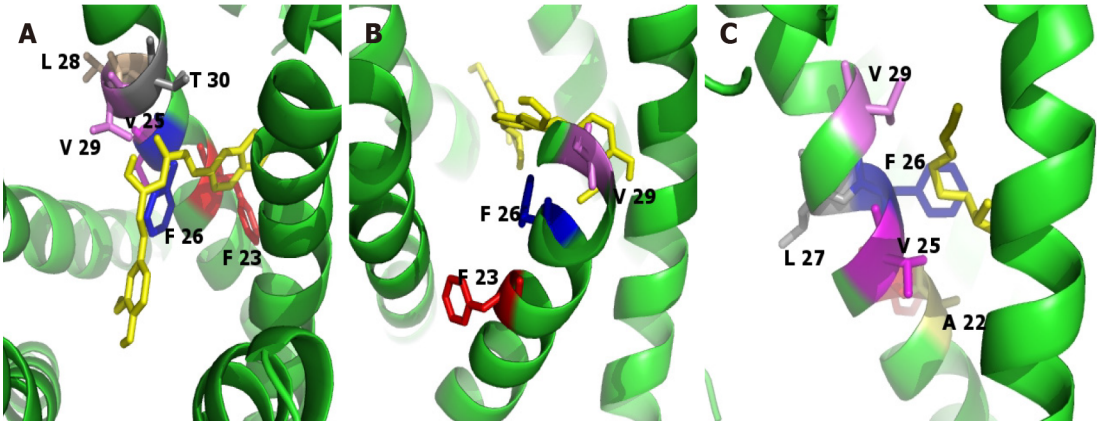


Figure 5 Graphic representation of the binding poses of the ligands on the envelope protein of severe acute respiratory syndrome-coronavirus-2. Images were carried out using Pymol. Homo-pentamer of the E protein of severe acute respiratory syndrome-coronavirus-2 is shown in green, and the ligand is shown in yellow. Surrounded residues are shown in different colors and labeled as indicated. A: Curcumine; B: Silybin; C: Sulforaphane.

nutritional therapy. the nutritional guidelines for patients with SARS-CoV-2 infection and liver injury are based on the statements of international clinical nutrition associations and the currently available evidence. Maintaining an optimal nutritional state is fundamental for preventing infection or overcoming SARS-CoV-2. Herein, the key role of providing sufficient energy, protein, lipids, and carbohydrates is clarified. Furthermore, the function of vitamins and trace minerals impacting the immune response is explained. To complete the nutritional approaches, we considered the use of phytochemicals as potential components of the therapy because of the possible benefits that they might offer during the COVID-19 crisis. The interactions (*i.e.* possible antiviral effects) of phytochemicals such curcumine, sulphoraphane, and silybin with the viral envelope protein have been demonstrated in-silico. The latter is an open door to researchers in the race to find tools to help overcome this pandemic in the best possible manner.

ACKNOWLEDGEMENTS

Nancy Vargas-Mendoza and Marcelo Angeles-Valencia are scholarship holders for their postgraduate studies by the Consejo Nacional de Ciencia y Tecnología (CONACyT) and the BEIFI program, Instituto Politécnico Nacional, Mexico.

REFERENCES

1 **Mittal A**, Manjunath K, Ranjan RK, Kaushik S, Kumar S, Verma V. COVID-19 pandemic: Insights into structure, function, and hACE2 receptor recognition by SARS-CoV-2. *PLoS Pathog* 2020; **16**: e1008762 [PMID: 32822426 DOI: 10.1371/journal.ppat.1008762]
2 **Palacios Cruz M**, Santos E, Velázquez Cervantes MA, León Juárez M. COVID-19, a worldwide public health emergency. *Rev Clin Esp* 2020 [PMID: 32204922 DOI: 10.1016/j.rceng.2020.03.001]
3 **Yoshimoto FK**. The Proteins of Severe Acute Respiratory Syndrome Coronavirus-2 (SARS CoV-2 or n-COV19), the Cause of COVID-19. *Protein J* 2020; **39**: 198-216 [PMID: 32447571 DOI: 10.1007/s10930-020-09901-4]
4 **Fehr AR**, Perlman S. Coronaviruses: an overview of their replication and pathogenesis. *Methods Mol Biol* 2015; **1282**: 1-23 [PMID: 25720466 DOI: 10.1007/978-1-4939-2438-7_1]
5 **Zhou P**, Yang XL, Wang XG, Hu B, Zhang L, Zhang W, Si HR, Zhu Y, Li B, Huang CL, Chen HD,

Chen J, Luo Y, Guo H, Jiang RD, Liu MQ, Chen Y, Shen XR, Wang X, Zheng XS, Zhao K, Chen QJ, Deng F, Liu LL, Yan B, Zhan FX, Wang YY, Xiao GF, Shi ZL. A pneumonia outbreak associated with a new coronavirus of probable bat origin. *Nature* 2020; **579**: 270-273 [PMID: 32015507 DOI: 10.1038/s41586-020-2012-7]

6 **WHO**. Coronavirus disease (COVID-19) pandemic. 2020. [cited 31 December 2020]. Available from: https://www.who.int/es/emergencies/diseases/novel-coronavirus-2019

7 **Hamming I**, Timens W, Bulthuis ML, Lely AT, Navis G, van Goor H. Tissue distribution of ACE2 protein, the functional receptor for SARS coronavirus. A first step in understanding SARS pathogenesis. *J Pathol* 2004; **203**: 631-637 [PMID: 15141377 DOI: 10.1002/path.1570]

8 **Zhang C**, Shi L, Wang FS. Liver injury in COVID-19: management and challenges. *Lancet Gastroenterol Hepatol* 2020; **5**: 428-430 [PMID: 32145190 DOI: 10.1016/S2468-1253(20)30057-1]

9 **Gu J**, Han B, Wang J. COVID-19: Gastrointestinal Manifestations and Potential Fecal-Oral Transmission. *Gastroenterology* 2020; **158**: 1518-1519 [PMID: 32142785 DOI: 10.1053/j.gastro.2020.02.054]

10 **Wang Y**, Liu S, Liu H, Li W, Lin F, Jiang L, Li X, Xu P, Zhang L, Zhao L, Cao Y, Kang J, Yang J, Li L, Liu X, Li Y, Nie R, Mu J, Lu F, Zhao S, Lu J, Zhao J. SARS-CoV-2 infection of the liver directly contributes to hepatic impairment in patients with COVID-19. *J Hepatol* 2020; **73**: 807-816 [PMID: 32437830 DOI: 10.1016/j.jhep.2020.05.002]

11 **Philips CA**, Ahamed R, Augustine P. SARS-CoV-2 related liver impairment - perception may not be the reality. *J Hepatol* 2020; **73**: 991-992 [PMID: 32454042 DOI: 10.1016/j.jhep.2020.05.025]

12 **Pedro KD**, Henderson AJ, Agosto LM. Mechanisms of HIV-1 cell-to-cell transmission and the establishment of the latent reservoir. *Virus Res* 2019; **265**: 115-121 [PMID: 30905686 DOI: 10.1016/j.virusres.2019.03.014]

13 **Esumi M**, Ishibashi M, Yamaguchi H, Nakajima S, Tai Y, Kikuta S, Sugitani M, Takayama T, Tahara M, Takeda M, Wakita T. Transmembrane serine protease TMPRSS2 activates hepatitis C virus infection. *Hepatology* 2015; **61**: 437-446 [PMID: 25203900 DOI: 10.1002/hep.27426]

14 **Pirola CJ**, Sookoian S. SARS-CoV-2 virus and liver expression of host receptors: Putative mechanisms of liver involvement in COVID-19. *Liver Int* 2020; **40**: 2038-2040 [PMID: 32352224 DOI: 10.1111/liv.14500]

15 **Zhao B**, Ni C, Gao R, Wang Y, Yang L, Wei J, Lv T, Liang J, Zhang Q, Xu W, Xie Y, Wang X, Yuan Z, Zhang R, Lin X. Recapitulation of SARS-CoV-2 infection and cholangiocyte damage with human liver ductal organoids. *Protein Cell* 2020; **11**: 771-775 [PMID: 32303993 DOI: 10.1007/s13238-020-00718-6]

16 **Polakos NK**, Cornejo JC, Murray DA, Wright KO, Treanor JJ, Crispe IN, Topham DJ, Pierce RH. Kupffer cell-dependent hepatitis occurs during influenza infection. *Am J Pathol* 2006; **168**: 1169-1178; quiz 1404-1405 [PMID: 16565492 DOI: 10.2353/ajpath.2006.050875]

17 **Morton A**. Presumed acute fatty liver of pregnancy following influenza A hepatitis. *Obstet Med* 2017; **10**: 186-188 [PMID: 29225680 DOI: 10.1177/1753495X17695173]

18 **Pardi DS**, Romero Y, Mertz LE, Douglas DD. Hepatitis-associated aplastic anemia and acute parvovirus B19 infection: a report of two cases and a review of the literature. *Am J Gastroenterol* 1998; **93**: 468-470 [PMID: 9517662 DOI: 10.1111/j.1572-0241.1998.468_1.x]

19 **Eisenhut M**, Thorburn K, Ahmed T. Transaminase levels in ventilated children with respiratory syncytial virus bronchiolitis. *Intensive Care Med* 2004; **30**: 931-934 [PMID: 15024569 DOI: 10.1007/s00134-004-2236-2]

20 **Chau TN**, Lee KC, Yao H, Tsang TY, Chow TC, Yeung YC, Choi KW, Tso YK, Lau T, Lai ST, Lai CL. SARS-associated viral hepatitis caused by a novel coronavirus: report of three cases. *Hepatology* 2004; **39**: 302-310 [PMID: 14767982 DOI: 10.1002/hep.20111]

21 **Cheung CCL**, Goh D, Lim X, Tien TZ, Lim JCT, Nerurkar SN, Shihleone L, Cheow PC, Chan CY, Koh YX, Tan TT, Kalimuddin S, David Tai WM, Ng JL, Hong Low JG, Yeong J, Hon Lim TK. Residual SARS-CoV-2 viral antigens detected in gastrointestinal and hepatic tissues from two recovered COVID-19 patients. 2020 Preprint. Available from: medRxiv:2020.10.28.20219014 [DOI: 10.1101/2020.10.28.20219014]

22 **Channappanavar R**, Fehr AR, Vijay R, Mack M, Zhao J, Meyerholz DK, Perlman S. Dysregulated Type I Interferon and Inflammatory Monocyte-Macrophage Responses Cause Lethal Pneumonia in SARS-CoV-Infected Mice. *Cell Host Microbe* 2016; **19**: 181-193 [PMID: 26867177 DOI: 10.1016/j.chom.2016.01.007]

23 **Ye Q**, Wang B, Mao J. The pathogenesis and treatment of the `Cytokine Storm' in COVID-19. *J Infect* 2020; **80**: 607-613 [PMID: 32283152 DOI: 10.1016/j.jinf.2020.03.037]

24 **Bouayad A**. Innate immune evasion by SARS-CoV-2: Comparison with SARS-CoV. *Rev Med Virol* 2020; **30**: 1-9 [PMID: 32734714 DOI: 10.1002/rmv.2135]

25 **Pedersen SF**, Ho YC. SARS-CoV-2: a storm is raging. *J Clin Invest* 2020; **130**: 2202-2205 [PMID: 32217834 DOI: 10.1172/JCI137647]

26 **Gubernatorova EO**, Gorshkova EA, Polinova AI, Drutskaya MS. IL-6: Relevance for immunopathology of SARS-CoV-2. *Cytokine Growth Factor Rev* 2020; **53**: 13-24 [PMID: 32475759 DOI: 10.1016/j.cytogfr.2020.05.009]

27 **McGonagle D**, Sharif K, O'Regan A, Bridgewood C. The Role of Cytokines including Interleukin-6 in COVID-19 induced Pneumonia and Macrophage Activation Syndrome-Like Disease. *Autoimmun Rev* 2020; **19**: 102537 [PMID: 32251717 DOI: 10.1016/j.autrev.2020.102537]

28 **Li Y**, Xiao SY. Hepatic involvement in COVID-19 patients: Pathology, pathogenesis, and clinical

implications. *J Med Virol* 2020; **92**: 1491-1494 [PMID: 32369204 DOI: 10.1002/jmv.25973]
29 **de Lucena TMC**, da Silva Santos AF, de Lima BR, de Albuquerque Borborema ME, de Azevêdo Silva J. Mechanism of inflammatory response in associated comorbidities in COVID-19. *Diabetes Metab Syndr* 2020; **14**: 597-600 [PMID: 32417709 DOI: 10.1016/j.dsx.2020.05.025]
30 **Wu D**, Yang XO. TH17 responses in cytokine storm of COVID-19: An emerging target of JAK2 inhibitor Fedratinib. *J Microbiol Immunol Infect* 2020; **53**: 368-370 [PMID: 32205092 DOI: 10.1016/j.jmii.2020.03.005]
31 **Edeas M**, Saleh J, Peyssonnaux C. Iron: Innocent bystander or vicious culprit in COVID-19 pathogenesis? *Int J Infect Dis* 2020; **97**: 303-305 [PMID: 32497811 DOI: 10.1016/j.ijid.2020.05.110]
32 **Chen R**, Liang W, Jiang M, Guan W, Zhan C, Wang T, Tang C, Sang L, Liu J, Ni Z, Hu Y, Liu L, Shan H, Lei C, Peng Y, Wei L, Liu Y, Peng P, Wang J, Chen Z, Li G, Zheng Z, Qiu S, Luo J, Ye C, Zhu S, Liu X, Cheng L, Ye F, Zheng J, Zhang N, Li Y, He J, Li S, Zhong N; Medical Treatment Expert Group for COVID-19. Risk Factors of Fatal Outcome in Hospitalized Subjects With Coronavirus Disease 2019 From a Nationwide Analysis in China. *Chest* 2020; **158**: 97-105 [PMID: 32304772 DOI: 10.1016/j.chest.2020.04.010]
33 **Guan WJ**, Ni ZY, Hu Y, Liang WH, Ou CQ, He JX, Liu L, Shan H, Lei CL, Hui DSC, Du B, Li LJ, Zeng G, Yuen KY, Chen RC, Tang CL, Wang T, Chen PY, Xiang J, Li SY, Wang JL, Liang ZJ, Peng YX, Wei L, Liu Y, Hu YH, Peng P, Wang JM, Liu JY, Chen Z, Li G, Zheng ZJ, Qiu SQ, Luo J, Ye CJ, Zhu SY, Zhong NS; China Medical Treatment Expert Group for Covid-19. Clinical Characteristics of Coronavirus Disease 2019 in China. *N Engl J Med* 2020; **382**: 1708-1720 [PMID: 32109013 DOI: 10.1056/NEJMoa2002032]
34 **Zádori N**, Váncsa S, Farkas N, Hegyi P, Erőss B; KETLAK Study Group. The negative impact of comorbidities on the disease course of COVID-19. *Intensive Care Med* 2020; **46**: 1784-1786 [PMID: 32601834 DOI: 10.1007/s00134-020-06161-9]
35 **Váncsa S**, Hegyi PJ, Zádori N, Szakó L, Vörhendi N, Ocskay K, Földi M, Dembrovszky F, Dömötör ZR, Jánosi K, Rakonczay Z Jr, Hartmann P, Horváth T, Erőss B, Kiss S, Szakács Z, Németh D, Hegyi P, Pár G. Pre-existing Liver Diseases and On-Admission Liver-Related Laboratory Tests in COVID-19: A Prognostic Accuracy Meta-Analysis With Systematic Review. *Front Med (Lausanne)* 2020; **7**: 572115 [PMID: 33282888 DOI: 10.3389/fmed.2020.572115]
36 **Lin Y**, Yuan J, Long Q, Hu J, Deng H, Zhao Z, Chen J, Lu M, Huang A. Patients with SARS-CoV-2 and HBV co-infection are at risk of greater liver injury. *Genes Dis* 2021; **8**: 484-492 [PMID: 33225036 DOI: 10.1016/j.gendis.2020.11.005]
37 **Boettler T**, Newsome PN, Mondelli MU, Maticic M, Cordero E, Cornberg M, Berg T. Care of patients with liver disease during the COVID-19 pandemic: EASL-ESCMID position paper. *JHEP Rep* 2020; **2**: 100113 [PMID: 32289115 DOI: 10.1016/j.jhepr.2020.100113]
38 **Ferron PJ**, Gicquel T, Mégarbane B, Clément B, Fromenty B. Treatments in Covid-19 patients with pre-existing metabolic dysfunction-associated fatty liver disease: A potential threat for drug-induced liver injury? *Biochimie* 2020; **179**: 266-274 [PMID: 32891697 DOI: 10.1016/j.biochi.2020.08.018]
39 **Bertolini A**, van de Peppel IP, Bodewes FAJA, Moshage H, Fantin A, Farinati F, Fiorotto R, Jonker JW, Strazzabosco M, Verkade HJ, Peserico G. Abnormal Liver Function Tests in Patients With COVID-19: Relevance and Potential Pathogenesis. *Hepatology* 2020; **72**: 1864-1872 [PMID: 32702162 DOI: 10.1002/hep.31480]
40 **Kavoliuniene A**, Vaitiekiene A, Cesnaite G. Congestive hepatopathy and hypoxic hepatitis in heart failure: a cardiologist's point of view. *Int J Cardiol* 2013; **166**: 554-558 [PMID: 22656043 DOI: 10.1016/j.ijcard.2012.05.003]
41 **Salehi B**, Calina D, Docea AO, Koirala N, Aryal S, Lombardo D, Pasqua L, Taheri Y, Marina Salgado Castillo C, Martorell M, Martins N, Iriti M, Suleria HAR, Sharifi-Rad J. Curcumin's Nanomedicine Formulations for Therapeutic Application in Neurological Diseases. *J Clin Med* 2020; **9** [PMID: 32033365 DOI: 10.3390/jcm9020430]
42 **Huang C**, Wang Y, Li X, Ren L, Zhao J, Hu Y, Zhang L, Fan G, Xu J, Gu X, Cheng Z, Yu T, Xia J, Wei Y, Wu W, Xie X, Yin W, Li H, Liu M, Xiao Y, Gao H, Guo L, Xie J, Wang G, Jiang R, Gao Z, Jin Q, Wang J, Cao B. Clinical features of patients infected with 2019 novel coronavirus in Wuhan, China. *Lancet* 2020; **395**: 497-506 [PMID: 31986264 DOI: 10.1016/S0140-6736(20)30183-5]
43 **Alqahtani SA**, Schattenberg JM. Liver injury in COVID-19: The current evidence. *United European Gastroenterol J* 2020; **8**: 509-519 [PMID: 32450787 DOI: 10.1177/2050640620924157]
44 **Li J**, Fan JG. Characteristics and Mechanism of Liver Injury in 2019 Coronavirus Disease. *J Clin Transl Hepatol* 2020; **8**: 13-17 [PMID: 32274341 DOI: 10.14218/JCTH.2020.00019]
45 **Dufour DR**, Lott JA, Nolte FS, Gretch DR, Koff RS, Seeff LB. Diagnosis and monitoring of hepatic injury. II. Recommendations for use of laboratory tests in screening, diagnosis, and monitoring. *Clin Chem* 2000; **46**: 2050-2068 [PMID: 11106350 DOI: 10.1093/clinchem/46.12.2050]
46 **Ilias I**, Zabuliene L. Hyperglycemia and the novel Covid-19 infection: Possible pathophysiologic mechanisms. *Med Hypotheses* 2020; **139**: 109699 [PMID: 32240876 DOI: 10.1016/j.mehy.2020.109699]
47 **Yang JK**, Lin SS, Ji XJ, Guo LM. Binding of SARS coronavirus to its receptor damages islets and causes acute diabetes. *Acta Diabetol* 2010; **47**: 193-199 [PMID: 19333547 DOI: 10.1007/s00592-009-0109-4]
48 **Lopez C**, Kim J, Pandey A, Huang T, DeLoughery TG. Simultaneous onset of COVID-19 and autoimmune haemolytic anaemia. *Br J Haematol* 2020; **190**: 31-32 [PMID: 32369626 DOI:

10.1111/bjh.16786]
49 **Lazarian G**, Quinquenel A, Bellal M, Siavellis J, Jacquy C, Re D, Merabet F, Mekinian A, Braun T, Damaj G, Delmer A, Cymbalista F. Autoimmune haemolytic anaemia associated with COVID-19 infection. *Br J Haematol* 2020; **190**: 29-31 [PMID: 32374906 DOI: 10.1111/bjh.16794]
50 **Jawed M**, Hart E, Saeed M. Haemolytic anaemia: a consequence of COVID-19. *BMJ Case Rep* 2020; **13** [PMID: 33303503 DOI: 10.1136/bcr-2020-238118]
51 **Rothschild MA**, Oratz M, Schreiber SS. Serum albumin. *Hepatology* 1988; **8**: 385-401 [PMID: 3281888 DOI: 10.1002/hep.1840080234]
52 **Violi F**, Ceccarelli G, Cangemi R, Alessandri F, D'Ettorre G, Oliva A, Pastori D, Loffredo L, Pignatelli P, Ruberto F, Venditti M, Pugliese F, Mastroianni CM. Hypoalbuminemia, Coagulopathy, and Vascular Disease in COVID-19. *Circ Res* 2020; **127**: 400-401 [PMID: 32508261 DOI: 10.1161/CIRCRESAHA.120.317173]
53 **Huang J**, Cheng A, Kumar R, Fang Y, Chen G, Zhu Y, Lin S. Hypoalbuminemia predicts the outcome of COVID-19 independent of age and co-morbidity. *J Med Virol* 2020; **92**: 2152-2158 [PMID: 32406952 DOI: 10.1002/jmv.26003]
54 **U.S. NIH National Library of Medicine**. COVID-19 Information. 2020. [cited 31 December 2020]. Available from: https://www.clinicaltrials.gov/
55 **Wang Y**, Zhang D, Du G, Du R, Zhao J, Jin Y, Fu S, Gao L, Cheng Z, Lu Q, Hu Y, Luo G, Wang K, Lu Y, Li H, Wang S, Ruan S, Yang C, Mei C, Wang Y, Ding D, Wu F, Tang X, Ye X, Ye Y, Liu B, Yang J, Yin W, Wang A, Fan G, Zhou F, Liu Z, Gu X, Xu J, Shang L, Zhang Y, Cao L, Guo T, Wan Y, Qin H, Jiang Y, Jaki T, Hayden FG, Horby PW, Cao B, Wang C. Remdesivir in adults with severe COVID-19: a randomised, double-blind, placebo-controlled, multicentre trial. *Lancet* 2020; **395**: 1569-1578 [PMID: 32423584 DOI: 10.1016/S0140-6736(20)31022-9]
56 **Favaloro EJ**, Thachil J. Reporting of D-dimer data in COVID-19: some confusion and potential for misinformation. *Clin Chem Lab Med* 2020; **58**: 1191-1199 [PMID: 32432563 DOI: 10.1515/cclm-2020-0573]
57 **Lee S**, Channappanavar R, Kanneganti TD. Coronaviruses: Innate Immunity, Inflammasome Activation, Inflammatory Cell Death, and Cytokines. *Trends Immunol* 2020; **41**: 1083-1099 [PMID: 33153908 DOI: 10.1016/j.it.2020.10.005]
58 **Liu BM**, Hill HR. Role of Host Immune and Inflammatory Responses in COVID-19 Cases with Underlying Primary Immunodeficiency: A Review. *J Interferon Cytokine Res* 2020; **40**: 549-554 [PMID: 33337932 DOI: 10.1089/jir.2020.0210]
59 **Russell MW**, Moldoveanu Z, Ogra PL, Mestecky J. Mucosal Immunity in COVID-19: A Neglected but Critical Aspect of SARS-CoV-2 Infection. *Front Immunol* 2020; **11**: 611337 [PMID: 33329607 DOI: 10.3389/fimmu.2020.611337]
60 **Isho B**, Abe KT, Zuo M, Jamal AJ, Rathod B, Wang JH, Li Z, Chao G, Rojas OL, Bang YM, Pu A, Christie-Holmes N, Gervais C, Ceccarelli D, Samavarchi-Tehrani P, Guvenc F, Budylowski P, Li A, Paterson A, Yue FY, Marin LM, Caldwell L, Wrana JL, Colwill K, Sicheri F, Mubareka S, Gray-Owen SD, Drews SJ, Siqueira WL, Barrios-Rodiles M, Ostrowski M, Rini JM, Durocher Y, McGeer AJ, Gommerman JL, Gingras AC. Persistence of serum and saliva antibody responses to SARS-CoV-2 spike antigens in COVID-19 patients. *Sci Immunol* 2020; **5** [PMID: 33033173 DOI: 10.1101/2020.08.01.20166553]
61 **Cervia C**, Nilsson J, Zurbuchen Y, Valaperti A, Schreiner J, Wolfensberger A, Raeber ME, Adamo S, Weigang S, Emmenegger M, Hasler S, Bosshard PP, De Cecco E, Bächli E, Rudiger A, Stüssi-Helbling M, Huber LC, Zinkernagel AS, Schaer DJ, Aguzzi A, Kochs G, Held U, Probst-Müller E, Rampini SK, Boyman O. Systemic and mucosal antibody responses specific to SARS-CoV-2 during mild *vs* severe COVID-19. *J Allergy Clin Immunol* 2021; **147**: 545-557.e9 [PMID: 33221383 DOI: 10.1016/j.jaci.2020.10.040]
62 **Chakraborty J**, Banerjee I, Vaishya R, Ghosh S. Bioengineered in Vitro Tissue Models to Study SARS-CoV-2 Pathogenesis and Therapeutic Validation. *ACS Biomater Sci Eng* 2020; **6**: 6540 [PMID: 33320635 DOI: 10.1021/acsbiomaterials.0c01226]
63 **Karlsson AC**, Humbert M, Buggert M. The known unknowns of T cell immunity to COVID-19. *Sci Immunol* 2020; **5** [PMID: 33208380 DOI: 10.1126/sciimmunol.abe8063]
64 **Ren L**, Zhang L, Chang, Wang J, Hu Y, Chen H, Guo L, Wu C, Wang C, Wang Y, Wang G, Yang S, Dela Cruz CS, Sharma L, Wang L, Zhang D. The kinetics of humoral response and its relationship with the disease severity in COVID-19. *Commun Biol* 2020; **3**: 780 [PMID: 33311543 DOI: 10.1038/s42003-020-01526-8]
65 **Hashem AM**, Algaissi A, Almahboub SA, Alfaleh MA, Abujamel TS, Alamri SS, Alluhaybi KA, Hobani HI, AlHarbi RH, Alsulaiman RM, ElAssouli MZ, Hala S, Alharbi NK, Alhabbab RY, AlSaieedi AA, Abdulaal WH, Bukhari A, Al-Somali AA, Alofi FS, Khogeer AA, Pain A, Alkayyal AA, Almontashiri NAM, Ahmad BM, Li X. Early Humoral Response Correlates with Disease Severity and Outcomes in COVID-19 Patients. *Viruses* 2020; **12** [PMID: 33291713 DOI: 10.1101/2020.09.21.20198309]
66 **Lenti MV**, Aronico N, Pellegrino I, Boveri E, Giuffrida P, Borrelli de Andreis F, Morbini P, Vanelli L, Pasini A, Ubezio C, Melazzini F, Rascaroli A, Antoci V, Merli S, Di Terlizzi F, Sabatini U, Cambiè G, Tenore A, Picone C, Vanoli A, Arcaini L, Baldanti F, Paulli M, Corazza GR, Di Sabatino A. Depletion of circulating IgM memory B cells predicts unfavourable outcome in COVID-19. *Sci Rep* 2020; **10**: 20836 [PMID: 33257775 DOI: 10.1038/s41598-020-77945-8]
67 **Borges L**, Pithon-Curi TC, Curi R, Hatanaka E. COVID-19 and Neutrophils: The Relationship

between Hyperinflammation and Neutrophil Extracellular Traps. *Mediators Inflamm* 2020; **2020**: 8829674 [PMID: 33343232 DOI: 10.1155/2020/8829674]

68 **Tang L**, Yin Z, Hu Y, Mei H. Controlling Cytokine Storm Is Vital in COVID-19. *Front Immunol* 2020; **11**: 570993 [PMID: 33329533 DOI: 10.3389/fimmu.2020.570993]

69 **Calder PC**. Omega-3 polyunsaturated fatty acids and inflammatory processes: nutrition or pharmacology? *Br J Clin Pharmacol* 2013; **75**: 645-662 [PMID: 22765297 DOI: 10.1111/j.1365-2125.2012.04374.x]

70 **Desai N**, Neyaz A, Szabolcs A, Shih AR, Chen JH, Thapar V, Nieman LT, Solovyov A, Mehta A, Lieb DJ, Kulkarni AS, Jaicks C, Xu KH, Raabe MJ, Pinto CJ, Juric D, Chebib I, Colvin RB, Kim AY, Monroe R, Warren SE, Danaher P, Reeves JW, Gong J, Rueckert EH, Greenbaum BD, Hacohen N, Lagana SM, Rivera MN, Sholl LM, Stone JR, Ting DT, Deshpande V. Temporal and spatial heterogeneity of host response to SARS-CoV-2 pulmonary infection. *Nat Commun* 2020; **11**: 6319 [PMID: 33298930 DOI: 10.1038/s41467-020-20139-7]

71 **Blot M**, Bour JB, Quenot JP, Bourredjem A, Nguyen M, Guy J, Monier S, Georges M, Large A, Dargent A, Guilhem A, Mouries-Martin S, Barben J, Bouhemad B, Charles PE, Chavanet P, Binquet C, Piroth L; LYMPHONIE study group. The dysregulated innate immune response in severe COVID-19 pneumonia that could drive poorer outcome. *J Transl Med* 2020; **18**: 457 [PMID: 33272291 DOI: 10.1186/s12967-020-02646-9]

72 **Tan J**, McKenzie C, Potamitis M, Thorburn AN, Mackay CR, Macia L. The role of short-chain fatty acids in health and disease. *Adv Immunol* 2014; **121**: 91-119 [PMID: 24388214 DOI: 10.1016/B978-0-12-800100-4.00003-9]

73 **Rodrigues TS**, Sa KS, Ishimoto AY, Becerra A, Oliveira S, Almeida L, Goncalves AV, Perucello DB, Andrade WA, Castro R, Veras FP, Toller-Kawahisa JE, Nascimento DC, de Lima MH, Silva CM, Caetite DB, Martins RB, Castro IA, Pontelli MC, de Barros FC, do Amaral NB, Giannini MC, Bonjorno LP, Lopes MIF, Benatti MN, Santana RC, Vilar FC, Auxiliadora-Martins M, Luppino-Assad R, de Almeida SC, de Oliveira FR, Batah SS, Siyuan L, Cunha TM, Alves-Filho JC, Cunha FQ, Cunha LD, Frantz FG, Kohlsdorf T, Fabro AT, Arruda E, de Oliveira RD, Louzada-Junior P, Zamboni DS. Inflammasome activation in COVID-19 patients. 2020 Preprint [DOI: 10.1101/2020.08.05.20168872]

74 **Pol K**, Christensen R, Bartels EM, Raben A, Tetens I, Kristensen M. Whole grain and body weight changes in apparently healthy adults: a systematic review and meta-analysis of randomized controlled studies. *Am J Clin Nutr* 2013; **98**: 872-884 [PMID: 23945718 DOI: 10.3945/ajcn.113.064659]

75 **Zhang Y**, Chen Y, Meng Z. Immunomodulation for Severe COVID-19 Pneumonia: The State of the Art. *Front Immunol* 2020; **11**: 577442 [PMID: 33240265 DOI: 10.3389/fimmu.2020.577442]

76 **Kumar S**, Kashyap P, Chowdhury S, Kumar S, Panwar A, Kumar A. Identification of phytochemicals as potential therapeutic agents that binds to Nsp15 protein target of coronavirus (SARS-CoV-2) that are capable of inhibiting virus replication. *Phytomedicine* 2021; **85**: 153317 [PMID: 32943302 DOI: 10.1016/j.phymed.2020.153317]

77 **Myhrstad MCW**, Tunsjø H, Charnock C, Telle-Hansen VH. Dietary Fiber, Gut Microbiota, and Metabolic Regulation-Current Status in Human Randomized Trials. *Nutrients* 2020; **12** [PMID: 32210176 DOI: 10.3390/nu12030859]

78 **Nicolai L**, Leunig A, Brambs S, Kaiser R, Weinberger T, Weigand M, Muenchhoff M, Hellmuth JC, Ledderose S, Schulz H, Scherer C, Rudelius M, Zoller M, Höchter D, Keppler O, Teupser D, Zwißler B, von Bergwelt-Baildon M, Kääb S, Massberg S, Pekayvaz K, Stark K. Immunothrombotic Dysregulation in COVID-19 Pneumonia Is Associated With Respiratory Failure and Coagulopathy. *Circulation* 2020; **142**: 1176-1189 [PMID: 32755393 DOI: 10.1161/CIRCULATIONAHA.120.048488]

79 **Sun S**, Cai X, Wang H, He G, Lin Y, Lu B, Chen C, Pan Y, Hu X. Abnormalities of peripheral blood system in patients with COVID-19 in Wenzhou, China. *Clin Chim Acta* 2020; **507**: 174-180 [PMID: 32339487 DOI: 10.1016/j.cca.2020.04.024]

80 **Gutiérrez-Bautista JF**, Rodriguez-Nicolas A, Rosales-Castillo A, Jiménez P, Garrido F, Anderson P, Ruiz-Cabello F, López-Ruz MÁ. Negative Clinical Evolution in COVID-19 Patients Is Frequently Accompanied With an Increased Proportion of Undifferentiated Th Cells and a Strong Underrepresentation of the Th1 Subset. *Front Immunol* 2020; **11**: 596553 [PMID: 33324414 DOI: 10.3389/fimmu.2020.596553]

81 **Liao WH**, Yang GG, Henneberg M. The renin-angiotensin-aldosterone system inhibitors in COVID-19: from acidosis to ventilation and immunity. *Swiss Med Wkly* 2020; **150**: w20444 [PMID: 33306813 DOI: 10.4414/smw.2020.20444]

82 **Chen Y**, Luo G, Yuan J, Wang Y, Yang X, Wang X, Li G, Liu Z, Zhong N. Vitamin C mitigates oxidative stress and tumor necrosis factor-alpha in severe community-acquired pneumonia and LPS-induced macrophages. *Mediators Inflamm* 2014; **2014**: 426740 [PMID: 25253919 DOI: 10.1155/2014/426740]

83 **Shi Y**, Zhou G, Li Q. Asynchronous actions of immune responses in COVID-19 patients. *Signal Transduct Target Ther* 2020; **5**: 284 [PMID: 33277465 DOI: 10.1038/s41392-020-00424-z]

84 **Kalpakci Y**, Hacibekiroglu T, Trak G, Karacaer C, Demirci T, Kocayigit H, Sunu C, Varim C, Falay M. Comparative evaluation of memory T cells in COVID-19 patients and the predictive role of CD4+CD8+ double positive T lymphocytes as a new marker. *Rev Assoc Med Bras (1992)* 2020; **66**: 1666-1672 [PMID: 33331574 DOI: 10.1590/1806-9282.66.12.1666]

85 **Shomuradova AS**, Vagida MS, Sheetikov SA, Zornikova KV, Kiryukhin D, Titov A, Peshkova IO, Khmelevskaya A, Dianov DV, Malasheva M, Shmelev A, Serdyuk Y, Bagaev DV, Pivnyuk A, Shcherbinin DS, Maleeva AV, Shakirova NT, Pilunov A, Malko DB, Khamaganova EG, Biderman B, Ivanov A, Shugay M, Efimov GA. SARS-CoV-2 Epitopes Are Recognized by a Public and Diverse Repertoire of Human T Cell Receptors. *Immunity* 2020; **53**: 1245-1257.e5 [PMID: 33326767 DOI: 10.1016/j.immuni.2020.11.004]

86 **Saeed F**, Nadeem M, Ahmed RS, Tahir Nadeem M, Arshad MS, Ullah A. Studying the impact of nutritional immunology underlying the modulation of immune responses by nutritional compounds – a review. *Food Agric Immunol* 2016; **27**: 205 [DOI: 10.1080/09540105.2015.1079600]

87 **Bacher P**, Rosati E, Esser D, Martini GR, Saggau C, Schiminsky E, Dargvainiene J, Schröder I, Wieters I, Khodamoradi Y, Eberhardt F, Vehreschild MJGT, Neb H, Sonntagbauer M, Conrad C, Tran F, Rosenstiel P, Markewitz R, Wandinger KP, Augustin M, Rybniker J, Kochanek M, Leypoldt F, Cornely OA, Koehler P, Franke A, Scheffold A. Low-Avidity CD4^{+} T Cell Responses to SARS-CoV-2 in Unexposed Individuals and Humans with Severe COVID-19. *Immunity* 2020; **53**: 1258-1271.e5 [PMID: 33296686 DOI: 10.1016/j.immuni.2020.11.016]

88 **Singh Y**, Gupta G, Kazmi I, Al-Abbasi FA, Negi P, Chellappan DK, Dua K. SARS CoV-2 aggravates cellular metabolism mediated complications in COVID-19 infection. *Dermatol Ther* 2020; **33**: e13871 [PMID: 32558055 DOI: 10.1111/dth.13871]

89 **Bulló M**, Casas R, Portillo MP, Basora J, Estruch R, García-Arellano A, Lasa A, Juanola-Falgarona M, Arós F, Salas-Salvadó J. Dietary glycemic index/load and peripheral adipokines and inflammatory markers in elderly subjects at high cardiovascular risk. *Nutr Metab Cardiovasc Dis* 2013; **23**: 443-450 [PMID: 22209741 DOI: 10.1016/j.numecd.2011.09.009]

90 **Ntyonga-Pono MP**. COVID-19 infection and oxidative stress: an under-explored approach for prevention and treatment? *Pan Afr Med J* 2020; **35**: 12 [PMID: 32528623 DOI: 10.11604/pamj.2020.35.2.22877]

91 **Suhail S**, Zajac J, Fossum C, Lowater H, McCracken C, Severson N, Laatsch B, Narkiewicz-Jodko A, Johnson B, Liebau J, Bhattacharyya S, Hati S. Role of Oxidative Stress on SARS-CoV (SARS) and SARS-CoV-2 (COVID-19) Infection: A Review. *Protein J* 2020; **39**: 644-656 [PMID: 33106987 DOI: 10.1007/s10930-020-09935-8]

92 **Muhoberac BB**. What Can Cellular Redox, Iron, and Reactive Oxygen Species Suggest About the Mechanisms and Potential Therapy of COVID-19? *Front Cell Infect Microbiol* 2020; **10**: 569709 [PMID: 33381464 DOI: 10.3389/fcimb.2020.569709]

93 **Dutta S**, Sengupta P. SARS-CoV-2 infection, oxidative stress and male reproductive hormones: can testicular-adrenal crosstalk be ruled-out? *J Basic Clin Physiol Pharmacol* 2020; **31** [PMID: 32889794 DOI: 10.1515/jbcpp-2020-0205]

94 **Bakadia BM**, Boni BOO, Ahmed AAQ, Yang G. The impact of oxidative stress damage induced by the environmental stressors on COVID-19. *Life Sci* 2021; **264**: 118653 [PMID: 33115606 DOI: 10.1016/j.lfs.2020.118653]

95 **Zinovkin RA**, Grebenchikov OA. Transcription Factor Nrf2 as a Potential Therapeutic Target for Prevention of Cytokine Storm in COVID-19 Patients. *Biochemistry (Mosc)* 2020; **85**: 833-837 [PMID: 33040727 DOI: 10.1134/S0006297920070111]

96 **Cecchini R**, Cecchini AL. SARS-CoV-2 infection pathogenesis is related to oxidative stress as a response to aggression. *Med Hypotheses* 2020; **143**: 110102 [PMID: 32721799 DOI: 10.1016/j.mehy.2020.110102]

97 **Delgado-Roche L**, Mesta F. Oxidative Stress as Key Player in Severe Acute Respiratory Syndrome Coronavirus (SARS-CoV) Infection. *Arch Med Res* 2020; **51**: 384-387 [PMID: 32402576 DOI: 10.1016/j.arcmed.2020.04.019]

98 **Wu J**. Tackle the free radicals damage in COVID-19. *Nitric Oxide* 2020; **102**: 39-41 [PMID: 32562746 DOI: 10.1016/j.niox.2020.06.002]

99 **Xu ZW**, Li YS. Pathogenesis and treatment of parenteral nutrition-associated liver disease. *Hepatobiliary Pancreat Dis Int* 2012; **11**: 586-593 [PMID: 23232629 DOI: 10.1016/s1499-3872(12)60229-x]

100 **Barazzoni R**, Bischoff SC, Breda J, Wickramasinghe K, Krznaric Z, Nitzan D, Pirlich M, Singer P; endorsed by the ESPEN Council. ESPEN expert statements and practical guidance for nutritional management of individuals with SARS-CoV-2 infection. *Clin Nutr* 2020; **39**: 1631-1638 [PMID: 32305181 DOI: 10.1016/j.clnu.2020.03.022]

101 **Federico A**, Dallio M, Loguercio C. Silymarin/Silybin and Chronic Liver Disease: A Marriage of Many Years. *Molecules* 2017; **22** [PMID: 28125040 DOI: 10.3390/molecules22020191]

102 **Patel JJ**, Martindale RG, McClave SA. Relevant Nutrition Therapy in COVID-19 and the Constraints on Its Delivery by a Unique Disease Process. *Nutr Clin Pract* 2020; **35**: 792-799 [PMID: 32786117 DOI: 10.1002/ncp.10566]

103 **Violi F**, Oliva A, Cangemi R, Ceccarelli G, Pignatelli P, Carnevale R, Cammisotto V, Lichtner M, Alessandri F, De Angelis M, Miele MC, D'Ettorre G, Ruberto F, Venditti M, Pugliese F, Mastroianni CM. Nox2 activation in Covid-19. *Redox Biol* 2020; **36**: 101655 [PMID: 32738789 DOI: 10.1016/j.redox.2020.101655]

104 **Motohashi H**, Yamamoto M. Nrf2-Keap1 defines a physiologically important stress response mechanism. *Trends Mol Med* 2004; **10**: 549-557 [PMID: 15519281 DOI: 10.1016/j.molmed.2004.09.003]

105 **Cederholm T**, Barazzoni R, Austin P, Ballmer P, Biolo G, Bischoff SC, Compher C, Correia I,

Higashiguchi T, Holst M, Jensen GL, Malone A, Muscaritoli M, Nyulasi I, Pirlich M, Rothenberg E, Schindler K, Schneider SM, de van der Schueren MA, Sieber C, Valentini L, Yu JC, Van Gossum A, Singer P. ESPEN guidelines on definitions and terminology of clinical nutrition. *Clin Nutr* 2017; **36**: 49-64 [PMID: 27642056 DOI: 10.1016/j.clnu.2016.09.004]

106 **McClave SA**, DiBaise JK, Mullin GE, Martindale RG. ACG Clinical Guideline: Nutrition Therapy in the Adult Hospitalized Patient. *Am J Gastroenterol* 2016; **111**: 315-334; quiz 335 [PMID: 26952578 DOI: 10.1038/ajg.2016.28]

107 **Cheung KS**, Hung IFN, Chan PPY, Lung KC, Tso E, Liu R, Ng YY, Chu MY, Chung TWH, Tam AR, Yip CCY, Leung KH, Fung AY, Zhang RR, Lin Y, Cheng HM, Zhang AJX, To KKW, Chan KH, Yuen KY, Leung WK. Gastrointestinal Manifestations of SARS-CoV-2 Infection and Virus Load in Fecal Samples From a Hong Kong Cohort: Systematic Review and Meta-analysis. *Gastroenterology* 2020; **159**: 81-95 [PMID: 32251668 DOI: 10.1053/j.gastro.2020.03.065]

108 **Heyland DK**, Dhaliwal R, Jiang X, Day AG. Identifying critically ill patients who benefit the most from nutrition therapy: the development and initial validation of a novel risk assessment tool. *Crit Care* 2011; **15**: R268 [PMID: 22085763 DOI: 10.1186/cc10546]

109 **Kalaiselvan MS**, Renuka MK, Arunkumar AS. Use of Nutrition Risk in Critically ill (NUTRIC) Score to Assess Nutritional Risk in Mechanically Ventilated Patients: A Prospective Observational Study. *Indian J Crit Care Med* 2017; **21**: 253-256 [PMID: 28584426 DOI: 10.4103/ijccm.IJCCM_24_17]

110 **Rosa M**, Heyland DK, Fernandes D, Rabito EI, Oliveira ML, Marcadenti A. Translation and adaptation of the NUTRIC Score to identify critically ill patients who benefit the most from nutrition therapy. *Clin Nutr ESPEN* 2016; **14**: 31-36 [PMID: 28531396 DOI: 10.1016/j.clnesp.2016.04.030]

111 **Compher C**, Chittams J, Sammarco T, Nicolo M, Heyland DK. Greater Protein and Energy Intake May Be Associated With Improved Mortality in Higher Risk Critically Ill Patients: A Multicenter, Multinational Observational Study. *Crit Care Med* 2017; **45**: 156-163 [PMID: 28098623 DOI: 10.1097/CCM.0000000000002083]

112 **Knaus WA**, Draper EA, Wagner DP, Zimmerman JE. APACHE II: a severity of disease classification system. *Crit Care Med* 1985; **13**: 818-829 [PMID: 3928249 DOI: 10.1097/00003246-198510000-00009]

113 **Capuzzo M**, Valpondi V, Sgarbi A, Bortolazzi S, Pavoni V, Gilli G, Candini G, Gritti G, Alvisi R. Validation of severity scoring systems SAPS II and APACHE II in a single-center population. *Intensive Care Med* 2000; **26**: 1779-1785 [PMID: 11271085 DOI: 10.1007/s001340000715]

114 **Vincent JL**, Moreno R, Takala J, Willatts S, De Mendonça A, Bruining H, Reinhart CK, Suter PM, Thijs LG. The SOFA (Sepsis-related Organ Failure Assessment) score to describe organ dysfunction/failure. On behalf of the Working Group on Sepsis-Related Problems of the European Society of Intensive Care Medicine. *Intensive Care Med* 1996; **22**: 707-710 [PMID: 8844239 DOI: 10.1007/BF01709751]

115 **Cárdenas-Turanzas M**, Ensor J, Wakefield C, Zhang K, Wallace SK, Price KJ, Nates JL. Cross-validation of a Sequential Organ Failure Assessment score-based model to predict mortality in patients with cancer admitted to the intensive care unit. *J Crit Care* 2012; **27**: 673-680 [PMID: 22762932 DOI: 10.1016/j.jcrc.2012.04.018]

116 **Zhou F**, Yu T, Du R, Fan G, Liu Y, Liu Z, Xiang J, Wang Y, Song B, Gu X, Guan L, Wei Y, Li H, Wu X, Xu J, Tu S, Zhang Y, Chen H, Cao B. Clinical course and risk factors for mortality of adult inpatients with COVID-19 in Wuhan, China: a retrospective cohort study. *Lancet* 2020; **395**: 1054-1062 [PMID: 32171076 DOI: 10.1016/S0140-6736(20)30566-3]

117 **Cederholm T**, Jensen GL, Correia MITD, Gonzalez MC, Fukushima R, Higashiguchi T, Baptista G, Barazzoni R, Blaauw R, Coats AJS, Crivelli AN, Evans DC, Gramlich L, Fuchs-Tarlovsky V, Keller H, Llido L, Malone A, Mogensen KM, Morley JE, Muscaritoli M, Nyulasi I, Pirlich M, Pisprasert V, de van der Schueren MAE, Siltharm S, Singer P, Tappenden K, Velasco N, Waitzberg D, Yamwong P, Yu J, Van Gossum A, Compher C; GLIM Core Leadership Committee, GLIM Working Group. GLIM criteria for the diagnosis of malnutrition - A consensus report from the global clinical nutrition community. *J Cachexia Sarcopenia Muscle* 2019; **10**: 207-217 [PMID: 30920778 DOI: 10.1002/jcsm.12383]

118 **Aguila EJT**, Cua IHY, Dumagpi JEL, Francisco CPD, Raymundo NTV, Sy-Janairo MLL, Cabral-Prodigalidad PAI, Lontok MAD. COVID-19 and its effects on the digestive system and endoscopy practice. *JGH Open* 2020; **4**: 324-331 [PMID: 32514432 DOI: 10.1002/jgh3.12358]

119 **Plauth M**, Bernal W, Dasarathy S, Merli M, Plank LD, Schütz T, Bischoff SC. ESPEN guideline on clinical nutrition in liver disease. *Clin Nutr* 2019; **38**: 485-521 [PMID: 30712783 DOI: 10.1016/j.clnu.2018.12.022]

120 **Arora S**, Mattina C, McAnenny C, O'Sullivan N, McGeeney L, Calder N, Gatiss G, Davidson B, Morgan MY. The development and validation of a nutritional prioritising tool for use in patients with chronic liver disease. *J Hepatol* 2012; **56**: S241 [DOI: 10.1016/S0168-8278(12)60621-7]

121 **Schneeweiss B**, Pammer J, Ratheiser K, Schneider B, Madl C, Kramer L, Kranz A, Ferenci P, Druml W, Grimm G. Energy metabolism in acute hepatic failure. *Gastroenterology* 1993; **105**: 1515-1521 [PMID: 8224656 DOI: 10.1016/0016-5085(93)90159-a]

122 **John WJ**, Phillips R, Ott L, Adams LJ, McClain CJ. Resting energy expenditure in patients with alcoholic hepatitis. *JPEN J Parenter Enteral Nutr* 1989; **13**: 124-127 [PMID: 2709599 DOI: 10.1177/0148607189013002124]

123 **Levine JA**, Harris MM, Morgan MY. Energy expenditure in chronic alcohol abuse. *Eur J Clin*

Invest 2000; **30**: 779-786 [PMID: 10998077 DOI: 10.1046/j.1365-2362.2000.00708.x]

124 **Müller MJ**, Böttcher J, Selberg O, Weselmann S, Böker KH, Schwarze M, von zur Mühlen A, Manns MP. Hypermetabolism in clinically stable patients with liver cirrhosis. *Am J Clin Nutr* 1999; **69**: 1194-1201 [PMID: 10357739 DOI: 10.1093/ajcn/69.6.1194]

125 **Glass C**, Hipskind P, Cole D, Lopez R, Dasarathy S. Handheld calorimeter is a valid instrument to quantify resting energy expenditure in hospitalized cirrhotic patients: a prospective study. *Nutr Clin Pract* 2012; **27**: 677-688 [PMID: 22668853 DOI: 10.1177/0884533612446195]

126 **Aguila EJT**, Cua IHY, Fontanilla JAC, Yabut VLM, Causing MFP. Gastrointestinal Manifestations of COVID-19: Impact on Nutrition Practices. *Nutr Clin Pract* 2020; **35**: 800-805 [PMID: 32668037 DOI: 10.1002/ncp.10554]

127 **Berzigotti A**, Albillos A, Villanueva C, Genescá J, Ardevol A, Augustín S, Calleja JL, Bañares R, García-Pagán JC, Mesonero F, Bosch J; Ciberehd SportDiet Collaborative Group. Effects of an intensive lifestyle intervention program on portal hypertension in patients with cirrhosis and obesity: The SportDiet study. *Hepatology* 2017; **65**: 1293-1305 [PMID: 27997989 DOI: 10.1002/hep.28992]

128 **Amaral JF**, Foschetti DA, Assis FA, Menezes JS, Vaz NM, Faria AM. Immunoglobulin production is impaired in protein-deprived mice and can be restored by dietary protein supplementation. *Braz J Med Biol Res* 2006; **39**: 1581-1586 [PMID: 17160267 DOI: 10.1590/s0100-879x2006001200009]

129 **Li P**, Yin YL, Li D, Kim SW, Wu G. Amino acids and immune function. *Br J Nutr* 2007; **98**: 237-252 [PMID: 17403271 DOI: 10.1017/S000711450769936X]

130 **Swart GR**, Zillikens MC, van Vuure JK, van den Berg JW. Effect of a late evening meal on nitrogen balance in patients with cirrhosis of the liver. *BMJ* 1989; **299**: 1202-1203 [PMID: 2513050 DOI: 10.1136/bmj.299.6709.1202]

131 **Zillikens MC**, van den Berg JW, Wattimena JL, Rietveld T, Swart GR. Nocturnal oral glucose supplementation. The effects on protein metabolism in cirrhotic patients and in healthy controls. *J Hepatol* 1993; **17**: 377-383 [PMID: 8315266 DOI: 10.1016/s0168-8278(05)80221-1]

132 **Les I**, Doval E, García-Martínez R, Planas M, Cárdenas G, Gómez P, Flavià M, Jacas C, Mínguez B, Vergara M, Soriano G, Vila C, Esteban R, Córdoba J. Effects of branched-chain amino acids supplementation in patients with cirrhosis and a previous episode of hepatic encephalopathy: a randomized study. *Am J Gastroenterol* 2011; **106**: 1081-1088 [PMID: 21326220 DOI: 10.1038/ajg.2011.9]

133 **Gluud LL**, Dam G, Les I, Marchesini G, Borre M, Aagaard NK, Vilstrup H. Branched-chain amino acids for people with hepatic encephalopathy. *Cochrane Database Syst Rev* 2017; **5**: CD001939 [PMID: 28518283 DOI: 10.1002/14651858.CD001939.pub4]

134 **Ren M**, Zhang SH, Zeng XF, Liu H, Qiao SY. Branched-chain Amino Acids are Beneficial to Maintain Growth Performance and Intestinal Immune-related Function in Weaned Piglets Fed Protein Restricted Diet. *Asian-Australas J Anim Sci* 2015; **28**: 1742-1750 [PMID: 26580442 DOI: 10.5713/ajas.14.0131]

135 **Cruzat V**, Macedo Rogero M, Noel Keane K, Curi R, Newsholme P. Glutamine: Metabolism and Immune Function, Supplementation and Clinical Translation. *Nutrients* 2018; **10** [PMID: 30360490 DOI: 10.20944/preprints201809.0459.v1]

136 **Shah AM**, Wang Z, Ma J. Glutamine Metabolism and Its Role in Immunity, a Comprehensive Review. *Animals (Basel)* 2020; **10** [PMID: 32092847 DOI: 10.3390/ani10020326]

137 **Kim SH**, Roszik J, Grimm EA, Ekmekcioglu S. Impact of l-Arginine Metabolism on Immune Response and Anticancer Immunotherapy. *Front Oncol* 2018; **8**: 67 [PMID: 29616189 DOI: 10.3389/fonc.2018.00067]

138 **Selberg O**, Burchert W, vd Hoff J, Meyer GJ, Hundeshagen H, Radoch E, Balks HJ, Müller MJ. Insulin resistance in liver cirrhosis. Positron-emission tomography scan analysis of skeletal muscle glucose metabolism. *J Clin Invest* 1993; **91**: 1897-1902 [PMID: 8486761 DOI: 10.1172/JCI116407]

139 **Müller MJ**, Willmann O, Rieger A, Fenk A, Selberg O, Lautz HU, Bürger M, Balks HJ, von zur Mühlen A, Schmidt FW. Mechanism of insulin resistance associated with liver cirrhosis. *Gastroenterology* 1992; **102**: 2033-2041 [PMID: 1587421 DOI: 10.1016/0016-5085(92)90329-w]

140 **Croci I**, Byrne NM, Choquette S, Hills AP, Chachay VS, Clouston AD, O'Moore-Sullivan TM, Macdonald GA, Prins JB, Hickman IJ. Whole-body substrate metabolism is associated with disease severity in patients with non-alcoholic fatty liver disease. *Gut* 2013; **62**: 1625-1633 [PMID: 23077135 DOI: 10.1136/gutjnl-2012-302789]

141 **Gomes F**, Schuetz P, Bounoure L, Austin P, Ballesteros-Pomar M, Cederholm T, Fletcher J, Laviano A, Norman K, Poulia KA, Ravasco P, Schneider SM, Stanga Z, Weekes CE, Bischoff SC. ESPEN guidelines on nutritional support for polymorbid internal medicine patients. *Clin Nutr* 2018; **37**: 336-353 [PMID: 28802519 DOI: 10.1016/j.clnu.2017.06.025]

142 **Neuhouser ML**, Schwarz Y, Wang C, Breymeyer K, Coronado G, Wang CY, Noar K, Song X, Lampe JW. A low-glycemic load diet reduces serum C-reactive protein and modestly increases adiponectin in overweight and obese adults. *J Nutr* 2012; **142**: 369-374 [PMID: 22190020 DOI: 10.3945/jn.111.149807]

143 **Radzikowska U**, Rinaldi AO, Çelebi Sözener Z, Karaguzel D, Wojcik M, Cypryk K, Akdis M, Akdis CA, Sokolowska M. The Influence of Dietary Fatty Acids on Immune Responses. *Nutrients* 2019; **11** [PMID: 31817726 DOI: 10.3390/nu11122990]

144 **Innis SM**. Dietary lipids in early development: relevance to obesity, immune and inflammatory disorders. *Curr Opin Endocrinol Diabetes Obes* 2007; **14**: 359-364 [PMID: 17940463 DOI: 10.1097/MED.0b013e3282be90b9]

145 **Siegers JY**, Novakovic B, Hulme KD, Marshall RJ, Bloxham CJ, Thomas WG, Reichelt ME, Leijten L, van Run P, Knox K, Sokolowski KA, Tse BWC, Chew KY, Christ AN, Howe G, Bruxner TJC, Karolyi M, Pawelka E, Koch RM, Bellmann-Weiler R, Burkert F, Weiss G, Samanta RJ, Openshaw PJM, Bielefeldt-Ohmann H, van Riel D, Short KR. A High-Fat Diet Increases Influenza A Virus-Associated Cardiovascular Damage. *J Infect Dis* 2020; **222**: 820-831 [PMID: 32246148 DOI: 10.1093/infdis/jiaa159]

146 **Singer P**, Shapiro H. Enteral omega-3 in acute respiratory distress syndrome. *Curr Opin Clin Nutr Metab Care* 2009; **12**: 123-128 [PMID: 19202383 DOI: 10.1097/MCO.0b013e328322e70f]

147 **Dushianthan A**, Cusack R, Burgess VA, Grocott MP, Calder PC. Immunonutrition for acute respiratory distress syndrome (ARDS) in adults. *Cochrane Database Syst Rev* 2019; **1**: CD012041 [PMID: 30677127 DOI: 10.1002/14651858.CD012041.pub2]

148 **Schenck LP**, Surette MG, Bowdish DM. Composition and immunological significance of the upper respiratory tract microbiota. *FEBS Lett* 2016; **590**: 3705-3720 [PMID: 27730630 DOI: 10.1002/1873-3468.12455]

149 **Zabetakis I**, Lordan R, Norton C, Tsoupras A. COVID-19: The Inflammation Link and the Role of Nutrition in Potential Mitigation. *Nutrients* 2020; **12** [PMID: 32438620 DOI: 10.3390/nu12051466]

150 **Hemilä H**. Vitamin C and Infections. *Nutrients* 2017; **9** [PMID: 28353648 DOI: 10.3390/nu9040339]

151 **Erol N**, Saglam L, Saglam YS, Erol HS, Altun S, Aktas MS, Halici MB. The Protection Potential of Antioxidant Vitamins Against Acute Respiratory Distress Syndrome: a Rat Trial. *Inflammation* 2019; **42**: 1585-1594 [PMID: 31081527 DOI: 10.1007/s10753-019-01020-2]

152 **Grant WB**, Lahore H, McDonnell SL, Baggerly CA, French CB, Aliano JL, Bhattoa HP. Evidence that Vitamin D Supplementation Could Reduce Risk of Influenza and COVID-19 Infections and Deaths. *Nutrients* 2020; **12** [PMID: 32252338 DOI: 10.20944/preprints202003.0235.v2]

153 **Jeffery LE**, Burke F, Mura M, Zheng Y, Qureshi OS, Hewison M, Walker LS, Lammas DA, Raza K, Sansom DM. 1,25-Dihydroxyvitamin D3 and IL-2 combine to inhibit T cell production of inflammatory cytokines and promote development of regulatory T cells expressing CTLA-4 and FoxP3. *J Immunol* 2009; **183**: 5458-5467 [PMID: 19843932 DOI: 10.4049/jimmunol.0803217]

154 **Aranow C**. Vitamin D and the immune system. *J Investig Med* 2011; **59**: 881-886 [PMID: 21527855 DOI: 10.2310/JIM.0b013e31821b8755]

155 **Vankadari N**, Wilce JA. Emerging WuHan (COVID-19) coronavirus: glycan shield and structure prediction of spike glycoprotein and its interaction with human CD26. *Emerg Microbes Infect* 2020; **9**: 601-604 [PMID: 32178593 DOI: 10.1080/22221751.2020.1739565]

156 **Jovic TH**, Ali SR, Ibrahim N, Jessop ZM, Tarassoli SP, Dobbs TD, Holford P, Thornton CA, Whitaker IS. Could Vitamins Help in the Fight Against COVID-19? *Nutrients* 2020; **12** [PMID: 32842513 DOI: 10.3390/nu12092550]

157 **Wu D**, Meydani SN. Age-associated changes in immune function: impact of vitamin E intervention and the underlying mechanisms. *Endocr Metab Immune Disord Drug Targets* 2014; **14**: 283-289 [PMID: 25244230 DOI: 10.2174/1871530314666140922143950]

158 **Calder PC**, Carr AC, Gombart AF, Eggersdorfer M. Optimal Nutritional Status for a Well-Functioning Immune System Is an Important Factor to Protect against Viral Infections. *Nutrients* 2020; **12** [PMID: 32340216 DOI: 10.3390/nu12041181]

159 **Galmés S**, Serra F, Palou A. Current State of Evidence: Influence of Nutritional and Nutrigenetic Factors on Immunity in the COVID-19 Pandemic Framework. *Nutrients* 2020; **12** [PMID: 32911778 DOI: 10.3390/nu12092738]

160 **Troen AM**, Mitchell B, Sorensen B, Wener MH, Johnston A, Wood B, Selhub J, McTiernan A, Yasui Y, Oral E, Potter JD, Ulrich CM. Unmetabolized folic acid in plasma is associated with reduced natural killer cell cytotoxicity among postmenopausal women. *J Nutr* 2006; **136**: 189-194 [PMID: 16365081 DOI: 10.1093/jn/136.1.189]

161 **Sheybani Z**, Dokoohaki MH, Negahdaripour M, Dehdashti M, Zolghadr AR. The Role of Folic Acid in the Management of Respiratory Disease Caused by COVID-19. *ChemRexiv* 2020 [DOI: 10.26434/chemrxiv.12034980]

162 **Jarosz M**, Olbert M, Wyszogrodzka G, Młyniec K, Librowski T. Antioxidant and anti-inflammatory effects of zinc. Zinc-dependent NF-κB signaling. *Inflammopharmacology* 2017; **25**: 11-24 [PMID: 28083748 DOI: 10.1007/s10787-017-0309-4]

163 **te Velthuis AJ**, van den Worm SH, Sims AC, Baric RS, Snijder EJ, van Hemert MJ. Zn(2+) inhibits coronavirus and arterivirus RNA polymerase activity *in vitro* and zinc ionophores block the replication of these viruses in cell culture. *PLoS Pathog* 2010; **6**: e1001176 [PMID: 21079686 DOI: 10.1371/journal.ppat.1001176]

164 **Doboszewska U**, Wlaź P, Nowak G, Młyniec K. Targeting zinc metalloenzymes in coronavirus disease 2019. *Br J Pharmacol* 2020; **177**: 4887-4898 [PMID: 32671829 DOI: 10.1111/bph.15199]

165 **Razzaque MS**. COVID-19 Pandemic: Can Maintaining Optimal Zinc Balance Enhance Host Resistance? *Tohoku J Exp Med* 2020; **251**: 175-181 [PMID: 32641644 DOI: 10.1620/tjem.251.175]

166 **Finzi E**. Treatment of SARS-CoV-2 with high dose oral zinc salts: A report on four patients. *Int J Infect Dis* 2020; **99**: 307-309 [PMID: 32522597 DOI: 10.1016/j.ijid.2020.06.006]

167 **Im JH**, Je YS, Baek J, Chung MH, Kwon HY, Lee JS. Nutritional status of patients with COVID-19. *Int J Infect Dis* 2020; **100**: 390-393 [PMID: 32795605 DOI: 10.1016/j.ijid.2020.08.018]

168 **Zhang J**, Taylor EW, Bennett K, Saad R, Rayman MP. Association between regional selenium status and reported outcome of COVID-19 cases in China. *Am J Clin Nutr* 2020; **111**: 1297-1299

[PMID: 32342979 DOI: 10.1093/ajcn/nqaa095]

169 **Moghaddam A**, Heller RA, Sun Q, Seelig J, Cherkezov A, Seibert L, Hackler J, Seemann P, Diegmann J, Pilz M, Bachmann M, Minich WB, Schomburg L. Selenium Deficiency Is Associated with Mortality Risk from COVID-19. *Nutrients* 2020; **12** [PMID: 32708526 DOI: 10.20944/preprints202007.0113.v1]

170 **Bae M**, Kim H. Mini-Review on the Roles of Vitamin C, Vitamin D, and Selenium in the Immune System against COVID-19. *Molecules* 2020; **25** [PMID: 33207753 DOI: 10.3390/molecules25225346]

171 **Klok FA**, Kruip MJHA, van der Meer NJM, Arbous MS, Gommers DAMPJ, Kant KM, Kaptein FHJ, van Paassen J, Stals MAM, Huisman MV, Endeman H. Incidence of thrombotic complications in critically ill ICU patients with COVID-19. *Thromb Res* 2020; **191**: 145-147 [PMID: 32291094 DOI: 10.1016/j.thromres.2020.04.013]

172 **Haberland A**, Neubert K, Kruse I, Behne D, Schimk I. Consequences of long-term selenium-deficient diet on the prostacyclin and thromboxane release from rat aorta. *Biol Trace Elem Res* 2001; **81**: 71-78 [PMID: 11508333 DOI: 10.1385/bter:81:1:71]

173 **Turnlund JR**, Jacob RA, Keen CL, Strain JJ, Kelley DS, Domek JM, Keyes WR, Ensunsa JL, Lykkesfeldt J, Coulter J. Long-term high copper intake: effects on indexes of copper status, antioxidant status, and immune function in young men. *Am J Clin Nutr* 2004; **79**: 1037-1044 [PMID: 15159234 DOI: 10.1093/ajcn/79.6.1037]

174 **Andreou A**, Trantza S, Filippou D, Sipsas N, Tsiodras S. COVID-19: The Potential Role of Copper and N-acetylcysteine (NAC) in a Combination of Candidate Antiviral Treatments Against SARS-CoV-2. *In Vivo* 2020; **34**: 1567-1588 [PMID: 32503814 DOI: 10.21873/invivo.11946]

175 **Raha S**, Mallick R, Basak S, Duttaroy AK. Is copper beneficial for COVID-19 patients? *Med Hypotheses* 2020; **142**: 109814 [PMID: 32388476 DOI: 10.1016/j.mehy.2020.109814]

176 **Martindale R**, Patel JJ, Taylor B, Arabi YM, Warren M, McClave SA. Nutrition Therapy in Critically Ill Patients With Coronavirus Disease 2019. *JPEN J Parenter Enteral Nutr* 2020; **44**: 1174-1184 [PMID: 32462719 DOI: 10.1002/jpen.1930]

177 **Bodoky G**, Kent-Smith L. Basics in clinical nutrition: Complications of enteral nutrition. *E Spen Eur E J Clin Nutr Metab* 2009; **4** [DOI: 10.1016/j.eclnm.2009.05.003]

178 **Fan Z**, Chen L, Li J, Cheng X, Yang J, Tian C, Zhang Y, Huang S, Liu Z, Cheng J. Clinical Features of COVID-19-Related Liver Functional Abnormality. *Clin Gastroenterol Hepatol* 2020; **18**: 1561-1566 [PMID: 32283325 DOI: 10.1016/j.cgh.2020.04.002]

179 **Wu J**, Song S, Cao HC, Li LJ. Liver diseases in COVID-19: Etiology, treatment and prognosis. *World J Gastroenterol* 2020; **26**: 2286-2293 [PMID: 32476793 DOI: 10.3748/wjg.v26.i19.2286]

180 **López-Romero D**, Izquierdo-Vega JA, Morales-González JA, Madrigal-Bujaidar E, Chamorro-Cevallos G, Sánchez-Gutiérrez M, Betanzos-Cabrera G, Alvarez-Gonzalez I, Morales-González Á, Madrigal-Santillán E. Evidence of Some Natural Products with Antigenotoxic Effects. Part 2: Plants, Vegetables, and Natural Resin. *Nutrients* 2018; **10** [PMID: 30544726 DOI: 10.3390/nu10121954]

181 **Izquierdo-Vega JA**, Morales-González JA, SánchezGutiérrez M, Betanzos-Cabrera G, Sosa-Delgado SM, Sumaya-Martínez MT, Morales-González Á, Paniagua-Pérez R, Madrigal-Bujaidar E, Madrigal-Santillán E.
Evidence of Some Natural Products with Antigenotoxic Effects. Part 1: Fruits and Polysaccharides. *Nutrients* 2017; **9** [PMID: 28157162 DOI: 10.3390/nu9020102]

182 **Ben-Shabat S**, Yarmolinsky L, Porat D, Dahan A. Antiviral effect of phytochemicals from medicinal plants: Applications and drug delivery strategies. *Drug Deliv Transl Res* 2020; **10**: 354-367 [PMID: 31788762 DOI: 10.1007/s13346-019-00691-6]

183 **Wu C**, Liu Y, Yang Y, Zhang P, Zhong W, Wang Y, Wang Q, Xu Y, Li M, Li X, Zheng M, Chen L, Li H. Analysis of therapeutic targets for SARS-CoV-2 and discovery of potential drugs by computational methods. *Acta Pharm Sin B* 2020; **10**: 766-788 [PMID: 32292689 DOI: 10.1016/j.apsb.2020.02.008]

184 **Mani JS**, Johnson JB, Steel JC, Broszczak DA, Neilsen PM, Walsh KB, Naiker M. Natural product-derived phytochemicals as potential agents against coronaviruses: A review. *Virus Res* 2020; **284**: 197989 [PMID: 32360300 DOI: 10.1016/j.virusres.2020.197989]

185 **Park JY**, Yuk HJ, Ryu HW, Lim SH, Kim KS, Park KH, Ryu YB, Lee WS. Evaluation of polyphenols from Broussonetia papyrifera as coronavirus protease inhibitors. *J Enzyme Inhib Med Chem* 2017; **32**: 504-515 [PMID: 28112000 DOI: 10.1080/14756366.2016.1265519]

186 **Shree P**, Mishra P, Selvaraj C, Singh SK, Chaube R, Garg N, Tripathi YB. Targeting COVID-19 (SARS-CoV-2) main protease through active phytochemicals of ayurvedic medicinal plants - *Withania somnifera* (Ashwagandha), *Tinospora cordifolia* (Giloy) and *Ocimum sanctum* (Tulsi) - a molecular docking study. *J Biomol Struct Dyn* 2020; 1-14 [PMID: 32851919 DOI: 10.1080/07391102.2020.1810778]

187 **Swargiary A**, Mahmud S, Saleh MA. Screening of phytochemicals as potent inhibitor of 3-chymotrypsin and papain-like proteases of SARS-CoV2: an in silico approach to combat COVID-19. *J Biomol Struct Dyn* 2020; 1-15 [PMID: 33089730 DOI: 10.1080/07391102.2020.1835729]

188 **Moi P**, Chan K, Asunis I, Cao A, Kan YW. Isolation of NF-E2-related factor 2 (Nrf2), a NF-E2-like basic leucine zipper transcriptional activator that binds to the tandem NF-E2/AP1 repeat of the beta-globin locus control region. *Proc Natl Acad Sci USA* 1994; **91**: 9926-9930 [PMID: 7937919 DOI: 10.1073/pnas.91.21.9926]

189 **Bryan HK**, Olayanju A, Goldring CE, Park BK. The Nrf2 cell defence pathway: Keap1-dependent

and -independent mechanisms of regulation. *Biochem Pharmacol* 2013; **85**: 705-717 [PMID: 23219527 DOI: 10.1016/j.bcp.2012.11.016]

190 **Tu W**, Wang H, Li S, Liu Q, Sha H. The Anti-Inflammatory and Anti-Oxidant Mechanisms of the Keap1/Nrf2/ARE Signaling Pathway in Chronic Diseases. *Aging Dis* 2019; **10**: 637-651 [PMID: 31165007 DOI: 10.14336/AD.2018.0513]

191 **Houghton CA**, Fassett RG, Coombes JS. Sulforaphane: translational research from laboratory bench to clinic. *Nutr Rev* 2013; **71**: 709-726 [PMID: 24147970 DOI: 10.1111/nure.12060]

192 **Houghton CA**, Fassett RG, Coombes JS. Sulforaphane and Other Nutrigenomic Nrf2 Activators: Can the Clinician's Expectation Be Matched by the Reality? *Oxid Med Cell Longev* 2016; **2016**: 7857186 [PMID: 26881038 DOI: 10.1155/2016/7857186]

193 **de Figueiredo SM**, Binda NS, Nogueira-Machado JA, Vieira-Filho SA, Caligiorne RB. The antioxidant properties of organosulfur compounds (sulforaphane). *Recent Pat Endocr Metab Immune Drug Discov* 2015; **9**: 24-39 [PMID: 25944116 DOI: 10.2174/1872214809666150505164138]

194 **Kamal MM**, Akter S, Lin CN, Nazzal S. Sulforaphane as an anticancer molecule: mechanisms of action, synergistic effects, enhancement of drug safety, and delivery systems. *Arch Pharm Res* 2020; **43**: 371-384 [PMID: 32152852 DOI: 10.1007/s12272-020-01225-2]

195 **Liu Y**, Yu Q, Chen Y. Effect of silibinin on CFLAR-JNK pathway in oleic acid-treated HepG2 cells. *Biomed Pharmacother* 2018; **108**: 716-723 [PMID: 30248539 DOI: 10.1016/j.biopha.2018.09.089]

196 **Ou Q**, Weng Y, Wang S, Zhao Y, Zhang F, Zhou J, Wu X. Silybin Alleviates Hepatic Steatosis and Fibrosis in NASH Mice by Inhibiting Oxidative Stress and Involvement with the Nf-κB Pathway. *Dig Dis Sci* 2018; **63**: 3398-3408 [PMID: 30191499 DOI: 10.1007/s10620-018-5268-0]

197 **Zhao F**, Shi D, Li T, Li L, Zhao M. Silymarin attenuates paraquat-induced lung injury *via* Nrf2-mediated pathway in vivo and in vitro. *Clin Exp Pharmacol Physiol* 2015; **42**: 988-998 [PMID: 26173462 DOI: 10.1111/1440-1681.12448]

198 **Zhou J**, Chao G, Li Y, Wu M, Zhong S, Feng Z. Activation of NRF2/ARE by isosilybin alleviates A β25-35-induced oxidative stress injury in HT-22 cells. *Neurosci Lett* 2016; **632**: 92-97 [PMID: 27567700 DOI: 10.1016/j.neulet.2016.08.043]

199 **Abdelsalam HM**, Samak MA, Alsemeh AE. Synergistic therapeutic effects of Vitis vinifera extract and Silymarin on experimentally induced cardiorenal injury: The pertinent role of Nrf2. *Biomed Pharmacother* 2019; **110**: 37-46 [PMID: 30458346 DOI: 10.1016/j.biopha.2018.11.053]

200 **Arafa Keshk W**, Zahran SM, Katary MA, Abd-Elaziz Ali D. Modulatory effect of silymarin on nuclear factor-erythroid-2-related factor 2 regulated redox status, nuclear factor-κB mediated inflammation and apoptosis in experimental gastric ulcer. *Chem Biol Interact* 2017; **273**: 266-272 [PMID: 28648817 DOI: 10.1016/j.cbi.2017.06.022]

201 **Li L**, Sun HY, Liu W, Zhao HY, Shao ML. Silymarin protects against acrylamide-induced neurotoxicity *via* Nrf2 signalling in PC12 cells. *Food Chem Toxicol* 2017; **102**: 93-101 [PMID: 28137608 DOI: 10.1016/j.fct.2017.01.021]

202 **Vargas-Mendoza N**, Morales-González Á, Morales-Martínez M, Soriano-Ursúa MA, Delgado-Olivares L, Sandoval-Gallegos EM, Madrigal-Bujaidar E, Álvarez-González I, Madrigal-Santillán E, Morales-Gonzalez JA. Flavolignans from Silymarin as Nrf2 Bioactivators and Their Therapeutic Applications. *Biomedicines* 2020; **8** [PMID: 32423098 DOI: 10.3390/biomedicines8050122]

203 **Liu CH**, Jassey A, Hsu HY, Lin LT. Antiviral Activities of Silymarin and Derivatives. *Molecules* 2019; **24** [PMID: 31010179 DOI: 10.3390/molecules24081552]

204 **Lalani SS**, Anasir MI, Poh CL. Antiviral activity of silymarin in comparison with baicalein against EV-A71. *BMC Complement Med Ther* 2020; **20**: 97 [PMID: 32293397 DOI: 10.1186/s12906-020-2880-2]

205 **Lestari ML**, Indrayanto G. Curcumin. *Profiles Drug Subst Excip Relat Methodol* 2014; **39**: 113-204 [PMID: 24794906 DOI: 10.1016/B978-0-12-800173-8.00003-9]

206 **Asouri M**, Ataee R, Ahmadi AA, Amini A, Moshaei MR. Antioxidant and free radical scavenging activities of curcumin. *Asian J Chem* 2013; **25**: 7593 [DOI: 10.14233/ajchem.2013.15308]

207 **Liu Z**, Dou W, Zheng Y, Wen Q, Qin M, Wang X, Tang H, Zhang R, Lv D, Wang J, Zhao S. Curcumin upregulates Nrf2 nuclear translocation and protects rat hepatic stellate cells against oxidative stress. *Mol Med Rep* 2016; **13**: 1717-1724 [PMID: 26676408 DOI: 10.3892/mmr.2015.4690]

208 **Meshkibaf MH**, Maleknia M, Noroozi S. Effect of curcumin on gene expression and protein level of methionine sulfoxide reductase A (MSRA), SOD, CAT and GPx in Freund's adjuvant inflammation-induced male rats. *J Inflamm Res* 2019; **12**: 241-249 [PMID: 31564949 DOI: 10.2147/JIR.S212577]

209 **Lin X**, Bai D, Wei Z, Zhang Y, Huang Y, Deng H, Huang X. Curcumin attenuates oxidative stress in RAW264.7 cells by increasing the activity of antioxidant enzymes and activating the Nrf2-Keap1 pathway. *PLoS One* 2019; **14**: e0216711 [PMID: 31112588 DOI: 10.1371/journal.pone.0216711]

210 **Zahedipour F**, Hosseini SA, Sathyapalan T, Majeed M, Jamialahmadi T, Al-Rasadi K, Banach M, Sahebkar A. Potential effects of curcumin in the treatment of COVID-19 infection. *Phytother Res* 2020; **34**: 2911-2920 [PMID: 32430996 DOI: 10.1002/ptr.6738]

211 **Mathew D**, Hsu WL. Antiviral potential of curcumin. *J Functional Foods* 2018; **40**: 692 [DOI: 10.1016/j.jff.2017.12.017]

212 **Mollazadeh H**, Cicero AFG, Blesso CN, Pirro M, Majeed M, Sahebkar A. Immune modulation by curcumin: The role of interleukin-10. *Crit Rev Food Sci Nutr* 2019; **59**: 89-101 [PMID: 28799796 DOI: 10.1080/10408398.2017.1358139]

213 **Avasarala S**, Zhang F, Liu G, Wang R, London SD, London L. Curcumin modulates the inflammatory response and inhibits subsequent fibrosis in a mouse model of viral-induced acute respiratory distress syndrome. *PLoS One* 2013; **8**: e57285 [PMID: 23437361 DOI: 10.1371/journal.pone.0057285]

214 **Morris GM**, Huey R, Lindstrom W, Sanner MF, Belew RK, Goodsell DS, Olson AJ. AutoDock4 and AutoDockTools4: Automated docking with selective receptor flexibility. *J Comput Chem* 2009; **30**: 2785-2791 [PMID: 19399780 DOI: 10.1002/jcc.21256]

World Journal of Gastroenterology

Submit a Manuscript: https://www.f6publishing.com

World J Gastroenterol 2021 September 14; 27(34): 5666-5681

DOI: 10.3748/wjg.v27.i34.5666

ISSN 1007-9327 (print) ISSN 2219-2840 (online)

REVIEW

Recent advances in blood-based and artificial intelligence-enhanced approaches for gastrointestinal cancer diagnosis

Li-Shi Li, Xiang-Yu Guo, Kun Sun

ORCID number: Li-Shi Li 0000-0003-2117-7529; Xiang-Yu Guo 0000-0001-5835-490X; Kun Sun 0000-0002-9883-1616.

Author contributions: Sun K outlined the article; Li LS and Guo XY performed the literature review and wrote the paper; Sun K revised the manuscript critically for important intellectual content and approved the final version for submission.

Supported by Guangdong Basic and Applied Basic Research Foundation, No. 2019A1515110173; BGI-research, No. BGIRSZ2020007; and Shenzhen Bay Laboratory.

Conflict-of-interest statement: There is no conflict of interest associated with any of the senior author or other coauthors who contributed their efforts in this manuscript.

Open-Access: This article is an open-access article that was selected by an in-house editor and fully peer-reviewed by external reviewers. It is distributed in accordance with the Creative Commons Attribution NonCommercial (CC BY-NC 4.0) license, which permits others to distribute, remix, adapt, build upon this work non-commercially, and license their derivative works on different terms, provided the

Li-Shi Li, School of Chemical Biology and Biotechnology, Shenzhen Graduate School, Peking University, Shenzhen 518055, Guangdong Province, China

Li-Shi Li, Xiang-Yu Guo, Kun Sun, Institute of Cancer Research, Shenzhen Bay Laboratory, Shenzhen 518132, Guangdong Province, China

Kun Sun, BGI-Shenzhen, Shenzhen 518083, Guangdong Province, China

Corresponding author: Kun Sun, PhD, Assistant Professor, Institute of Cancer Research, Shenzhen Bay Laboratory, Rm B302, Guangming International Innovation Center, Guangming District, Shenzhen 518132, Guangdong Province, China. sunkun@szbl.ac.cn

Abstract

Gastrointestinal (GI) cancers are among the most common cancer types and leading causes of cancer-related deaths worldwide. There is a tremendous clinical need for effective early diagnosis for better healthcare of GI cancer patients. In this article, we provide a short overview of the recent advances in GI cancer diagnosis. In the first part, we discuss the applications of blood-based biomarkers, such as plasma circulating cell-free DNA, circulating tumor cells, extracellular vesicles, and circulating cell-free RNA, for cancer liquid biopsies. In the second part, we review the current trends of artificial intelligence (AI) for pathology image and tissue biopsy analysis for GI cancer, as well as deep learning-based approaches for purity assessment of tissue biopsies. We further provide our opinions on the future directions in blood-based and AI-enhanced approaches for GI cancer diagnosis, and we think that these fields will have more intensive integrations with clinical needs in the near future.

Key Words: Liquid biopsy; Plasma cell-free DNA; Circulating tumor cell; Extracellular vesicle; Exosome; Artificial intelligence

©The Author(s) 2021. Published by Baishideng Publishing Group Inc. All rights reserved.

Core Tip: Recent studies have discovered a variety of blood-based biomarkers with great potential in improving the diagnosis and surveillance of gastrointestinal (GI) cancers. In this article, we review the latest advances in the diagnosis of various GI

original work is properly cited and the use is non-commercial. See: http://creativecommons.org/Licenses/by-nc/4.0/

Manuscript source: Invited manuscript

Specialty type: Gastroenterology and hepatology

Country/Territory of origin: China

Peer-review report's scientific quality classification

Grade A (Excellent): 0
Grade B (Very good): B, B
Grade C (Good): C
Grade D (Fair): 0
Grade E (Poor): 0

Received: January 27, 2021
Peer-review started: January 27, 2021
First decision: May 2, 2021
Revised: May 14, 2021
Accepted: August 3, 2021
Article in press: August 3, 2021
Published online: September 14, 2021

P-Reviewer: Park WS, Vymetalkova V
S-Editor: Ma YJ
L-Editor: Wang TQ
P-Editor: Liu JH

cancers, focusing on emerging blood-based liquid biopsy assays and artificial intelligence-enhanced approaches. We also discuss purity assessment approaches for tissue biopsies, which is an important issue in cancer studies, especially those applicable in metastatic GI cancers.

Citation: Li LS, Guo XY, Sun K. Recent advances in blood-based and artificial intelligence-enhanced approaches for gastrointestinal cancer diagnosis. *World J Gastroenterol* 2021; 27(34): 5666-5681
URL: https://www.wjgnet.com/1007-9327/full/v27/i34/5666.htm
DOI: https://dx.doi.org/10.3748/wjg.v27.i34.5666

INTRODUCTION

Gastrointestinal (GI) cancers, which include tumors from the colon, rectum, stomach, pancreas, esophagus, anus, gallbladder, liver, and bile duct, are among the most common cancer types and leading causes of cancer-related deaths worldwide[1]. Colorectal cancer (CRC), in particular, is the third most common cancer in men (9%) and women (8%) in the United States[1-3]. Most patients with GI cancers are in the advanced stage upon diagnosis and have relatively poor prognosis outcome. For example, the overall 5-year survival rate for patients with hepatocellular carcinoma (HCC) is around 20%[3], while the survival rate for early stage patients is as high as 70%[1,3]. This is because various efficient treatment strategies, such as surgical resection and organ transplantation, are feasible for early-stage patients only. Hence, early diagnosis is of high clinical significance for better healthcare of cancer patients.

Pathological analysis of the tumor tissue is currently the "gold standard" for clinical diagnosis of cancers[4,5]. In particular, image-based computed tomography (CT) colonography, optical colonoscopy, and endoscopic biopsy are mostly widely used in the diagnosis of GI cancers. Recent studies have demonstrated that blood-based approaches, also known as liquid biopsy, offer substantial advantages over conventional tissue biopsy-based diagnostic methods, including minimally invasive nature, cost-efficiency, clinical convenience for real-time monitoring, and the potential to promote higher patient compliance. Major analytes in current liquid biopsy studies include circulating cell-free DNA (cfDNA), circulating tumor cells (CTCs), as well as extracellular vesicles (EVs) that transport the biomolecules from tumor cells, such as lipids, proteins, DNA fragment, and RNAs[6-9]. Moreover, advances and integration of artificial intelligence (AI) have brought revolutionary changes to the clinical and translational cancer studies[10-12], especially in cancer diagnosis. The identification and utilization of disease-specific biomarkers, and development of exquisite diagnostic algorithms are both highly valuable for early diagnosis of cancers.

In this article, we provide an overview of current approaches for GI cancer diagnosis, especially in CRC and HCC. We focus on blood-based biomarkers, as well as AI algorithms for image-based tissue biopsies. We review the identification of biomarkers and development of diagnostic methods, and provide our opinions on future directions in early diagnosis of GI cancers.

BLOOD-BASED LIQUID BIOPSY APPROACHES

With the advantages of being highly efficient, minimally invasive, and cost-effective, liquid biopsy has become an emerging technique for early diagnosis of cancers. Tumor-derived cell-free DNA in peripheral blood provide a surrogate for researchers/clinicians to investigate the genomic and epigenomic landscape as well as dynamics during treatment of malignant tumors[13,14]. Conventionally, liquid biopsy approaches cover the analysis of various circulating components, including cfDNA, cfRNA, CTCs, and tumor-associated EVs (Figure 1)[15], and significant progress has been made in these areas in the past few years (Table 1).

Circulating cell-free DNA

cfDNA molecules in plasma originate from various tissues in human body. In cancer

Table 1 Biomarkers for blood-based liquid biopsy in gastrointestinal cancers

Cancer type	Biomarker type	Biomarkers	No. of patients /controls	Accuracy	Ref.
GC	cfDNA copy number	*HER2* gene	60/30	Sn = 73.3%, Sp = 93.3%	[19]
GC	cfDNA methylation	BARHL2	128/30	Sn = 90%, Sp = 100%	[104]
GC	CTC	CTC level	116/31	Sn = 85.3%, Sp = 90.3%	[49]
GC	Exosomal lncRNA	lncRNA-UEGC1	10/5	AUC = 0.876	[105]
GC	Exosomal lncRNA	lncRNA-pcsk2-2:1	63/29	Sn = 84%, Sp = 86.5%	[77]
GC	Exosomal lncRNA	lncRNA-GNAQ6:1	43/27	AUC = 0.732	[71]
GC	Exosomal lncRNA	lncRNA-HOTTIP	126/120	AUC = 0.827	[106]
GC	Exosomal miRNA	miR-1246	117/82	AUC = 0.843	[107]
GC	Serum cfRNA	miR-10b-5p, miR-195-5p, miR-185-5p, miR-296-5p, miR-132-3p, and miR-20a-3p	441/233	AUC = 0.702	[68]
GC	Serum cfRNA	miR-21	50/50	Sn = 88.4%, Sp = 79.6%	[81]
GC	Serum cfRNA	miR-30a-5p, miR-659-3p and miR-3917	354	AUC = 0.82	[82]
GC	Serum cfRNA	B3GALT5-AS1	107/87	AUC = 0.816	[108]
CRC	CTC mRNA	ECT2 gene	90/151	AUC = 0.821	[61]
CRC	Serum cfRNA	miR-21, miR-29a, miR-125b	160/77	AUC = 0.827	[86]
CRC	Serum cfRNA	miR-30a-5p	138/60	Sn = 77.5%, Sp = 78.3%	[109]
CRC	cfDNA methylation	SFRP2	62/55	Sn = 69.4%, Sp = 87.3%	[21]
CRC	CTC protein	CD133+CD54+CD44+ Protein	10/10	Sn = 88.2%, Sp = 92.4%	[62]
CRC	Exosomal miRNA	miR-27a, miR-130a	40/40	AUC = 0.773	[110]
CRC	Exosomal miRNA	miR-125a-3p	50/50	AUC = 0.685	[111]
CRC	Exosomal protein	CPNE3	92/32	Sn = 67.5%, Sp = 84.4%	[112]
PC	CTC protein	Vimentin	100/30	AUC = 0.968	[58]
PC	cfDNA methylation	BNC1, ADAMTS1	39/95	Sn = 94.8%, Sp = 91.6%	[23]
PC	cfDNA methylation	CDO1	160	Sn = 95%	[24]
PC	CTC	CTC level	126	Sn = 100%, Sp = 88.6%	[113]
PC	Exosomal lncRNA	CLDN1, TIMP1, MAL2, MARCH2, ITIH2, HIST1H2BK, KRT19 and FGA	284/117	AUC = 0.931	[79]
PC	Exosomal miRNA	miR-21	27	AUC = 0.9	[76]
PC	Exosomal miRNA	miR-155	27	AUC = 0.89	[76]
PC	Exosomal miRNA	miR-451a	56	Sn = 69.2%, Sp = 70.8%	[114]
PC	Exosomal miRNA	miR-133a	110/64	Sn = 90.6%, Sp = 87.2%, AUC = 0.893	[115]
HCC	cfDNA methylation	cfDNA 5hmC	1204/958	AUC = 0.846	[30]
HCC	Exosomal miRNA	miR-10b-5p	90/28	AUC = 0.934	[75]
HCC	Exosomal mRNA	hnRNPH1	88/68	Sn = 85.2%, Sp = 76.5%	[80]
HCC	Plasma cfRNA	hsa_circ_0000976, hsa_circ_0007750 and hsa_circ_0139897	158/53	AUC = 0.863	[85]
HCC	Serum cfRNA	miR-143	131/122	Sn = 80.3%, Sp = 82.4%	[87]
HCC	Serum cfRNA	miR-132, miR-212`	80/42	Sn = 93.75%, Sp = 63.44%	[116]

GC: Gastric cancer; CRC: Colorectal cancer; PC: Pancreatic cancer; HCC: Hepatocellular carcinoma; Sn: Sensitivity; Sp: Specificity; AUC: Area under the

curve.

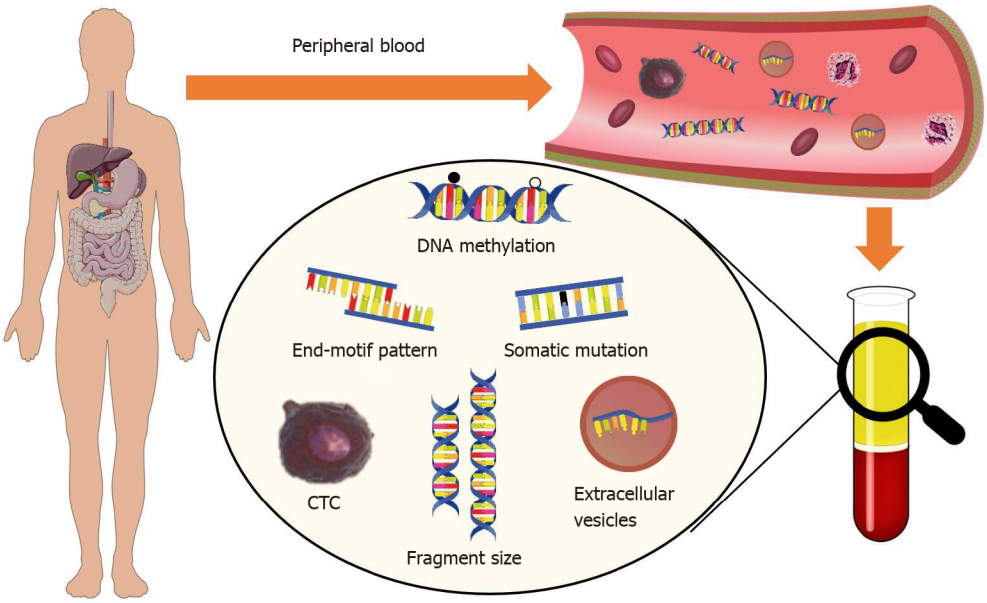


Figure 1 Blood-based liquid biopsy in cancer diagnosis. In the peripheral blood of cancer patients, circulating cell-free nucleic acids, circulating tumor cells, and extracellular vesicles carry the tumor-associated information, which allow noninvasive diagnosis of cancer patients.

patients, the dying tumor cells release their DNA, which contains the tumor-specific signatures, including somatic mutations, copy number aberrations (CNAs), and altered DNA methylation profiles, into the circulation (which is known as ctDNA). However, tumor-derived cfDNA usually account for a small fraction of the total cfDNA, and the concentration is even lower in early-stage cancer patients, which largely limits the accuracy of most cfDNA-based liquid biopsy assays. To this end, in recent studies, researcher have explored the application of extra-deep sequencing and discovered a broad range of tumor-related signals in cfDNA to further improve their performance in bother diagnosis and prognosis monitoring.

Conventional genomic and epigenomic alterations: Somatic mutations are one of the most widely studied tumor-associated genomic alterations. In a proof-of-concept study, through extra-high sequencing of cfDNA in HCC patients, researchers are able to non-invasively resolve the mutation landscape of the tumor with high accuracy[16], which would be informative in guiding the therapeutic strategies for cancer patients. The somatic mutations in cfDNA are widely utilized used as biomarkers for early diagnosis and prognosis monitoring. For example, in pancreatic cancer (PC), the overall survival of patients with detectable KRAS mutation in cfDNA was significantly shorter than that of patients without such mutations[17]. Notably, the somatic mutations detected in cfDNA may not solely come from the tumors. In fact, recent studies have proven that clonal hematopoiesis also introduces somatic mutations which are detectable in cfDNA. Hence, it is highly recommended to analyze the blood cells in parallel to cfDNA in somatic mutation-oriented studies.

CNA is another widely used biomarker in cancer diagnosis and prognosis monitoring. For example, Shoda *et al*[18] found that the copy number status of *HER2* gene in cfDNA is a potential biomarker for predicting the risk of recurrence and monitoring the effects of treatment for patients with gastric cancer (GC); Chen *et al*[19] showed that in GC, patients with stable chromosomes were sensitive to drug treatment while patients with detectable chromosomal instability in cfDNA were resistant to treatment, demonstrating the potential of cfDNA in predicting treatment responses.

DNA modifications, mostly 5-methylcytosine (5mC) and 5-hydroxymethylcytosine (5hmC), are abundant epigenetic regulators in the human genome. These modifications are known to affect gene expression, and suffer from gross abnormalities in almost all kinds of tumors. In cancer patients, such modifications are detectable in cfDNA and could be used to point to the tissue origin of the tumor. For example, Chan *et al*[20] analyzed the CNA and 5mC profiles of cfDNA simultaneously using whole-

genome bisulfite sequencing technology, demonstrating that flexible combination of these two biomarkers would benefit in cancer diagnosis in various clinical scenarios; Li *et al*[21] showed that methylated *SFRP2* in cfDNA has the potential to serve as a non-invasive biomarker for CRC screening; Gai *et al*[22] reported the application of DNA methylation biomarkers in differentiating CRC patients with and without liver metastases. Eissa *et al*[23] reported that the methylation of *BNC1* and *ADAMTS1* gene promoters could be used for PC diagnosis and screening with an area under the curve (AUC) of 0.95. The hypermethylation of cysteine dioxygenase 1 gene (*CDO1*) could distinguish pancreatic ductal adenocarcinoma (PDAC) patients from healthy controls with a sensitivity of 95%[24]. Besides diagnosis, Kim *et al*[25] showed that low methylation of ST-alpha and L1 of cfDNA are associated with a shorter overall survival in GC patients; Harada *et al*[26] suggested that GC patients with a high methylation level in the promoter of *CDO1* gene in cfDNA had a significantly worse prognosis. Similarly, Zhang *et al*[27] found that, in PDAC patients, the methylation of *PCDH10* gene was associated with a shorter disease-free survival. On the other hand, recent studies have suggested that 5hmC-based biomarkers in cfDNA are highly predictive of colorectal, gastric, and liver cancers with superior performance over conventional protein-based biomarkers[28-30]. Through genome-wide profiling of 5hmC in cfDNA as well as genomic DNA (gDNA) of paired tumor and adjacent normal tissues from patients with colorectal, gastric, liver, and other cancers, Li *et al*[21] discovered robust cancer-associated 5hmC signatures in cfDNA for cancer diagnosis. In another study, Cai *et al*[29] utilized the highly sensitive 5hmC-Seal assay to profile the genome-wide 5hmC landscape in cfDNA samples from 2554 HCC patients and found that liver-related 5hmC biomarkers show a remarkable capacity for distinguishing early HCC from high-risk non-cancerous subjects with chronic hepatitis B virus infection or liver cirrhosis. These studies demonstrated that DNA methylation-based biomarkers have favorable clinical value in cancer diagnosis, molecular characterization of the tumor, and prognosis monitoring of the patients, especially in GI cancers.

Emerging cfDNA fragmentomic features: Plasma cell-free DNA is known as naturally fragmented, small molecules. Recent studies have revealed that the tumor-derived DNA possess a remarkable difference in fragmentation characteristics compared to the background DNA (which mostly comes from the hematopoietic system)[31], and demonstrated the clinical significance of these features in the diagnosis of various GI cancers.

CfDNA molecules show a dominant size peak at 166 bp and most of them are shorter than 200 bp, and this phenomenon is believed to correlate with the nucleosome structure[32]. In cancer patients, tumor-derived cfDNA is even shorter than the background DNA[33]. Hence, it is doable to enrich the tumor-derived cfDNA through selection of shorter cfDNA molecules in principle. Indeed, Mouliere *et al*[34] demonstrated the enrichment of tumor-derived cfDNA in fragment sizes between 90 and 150 bp in a cohort of 344 plasma samples from various cancer patients. They also showed that using an integrated analysis of cfDNA at different size ranges, they could classify CRC patients from healthy individuals with a high specificity of 94%[34].

Besides size pattern, recent studies further showed that the relationship between the fragmentation pattern and nucleosome structure could point to the tissue origin of cfDNA[35,36]. In particular, cfDNA of different origins tends to have different preferences on fragment ends. Jiang *et al*[16] compared the genome-wide fragment end patterns of cfDNA in one HCC patient and one non-cancerous control; they reported that many genomic loci show significantly higher chances to serve as fragment ends (which they called "preferred-ends") in the HCC patient, and the usage of such genomic loci could differentiate HCC patients from non-cancerous controls with a favorable accuracy. Moreover, the same team further showed that the nucleotide frequencies (or motifs) at the cfDNA end, which are believed to correlate with nuclease cutting preference, also change in various cancers[37,38]. In fact, they found a nuclease, DNAS1L3, which plays key roles in the apoptotic fragmentation process and shows strong sequence preferences when cutting the DNA[39]. Interestingly, this gene is significantly down-regulated in many cancers and thus affects the end motif pattern of the tumor-derived DNA[37]. The discovery of these novel biomarkers largely extends our knowledgebase on both the biology of cfDNA and cancer biomarkers; these novel biomarkers also promise the development of less complex and cheaper assays than those based on the conventional genomic/epigenomic biomarkers. However, most current studies are still in proof-of-principle stage, thus large-scale validation studies are essential to assure the performances before clinical investigations.

Circulating tumor cells

CTCs are released into the bloodstream of patients through the blood vessels and lymphatic vessels. When the primary cancer cells acquire an increased propensity for migration, invasiveness, and resistance, these tumor cells will invade through the tissue surrounding their site of origin and keep invading until they enter the blood or the lymphatic system, and become the CTCs[40,41]. Although most of CTCs will die within hours, only a small part of them can potentially form a new cancerous lesion at a distant site and grow into a new metastasis[42,43].

There are many commercial kits for CTC isolation and enrichments. CTC isolation and enrichment are mostly based on their physical and immunological properties. The physical features of CTCs, such as the size, density, and electric charge, are utilized to enrich CTCs from blood. For example, ISET (isolation by size of epithelial tumor cells) system and a microfluidic chip developed by Haber' lab filter CTCs from blood by the size of CTCs[44-46], CAP (centrifugal affinity plate) system isolates CTCs by the density gradient centrifugation[47], and ApoStream system enriches CTCs by dielectrophoretic field-flow fractionation[48,49]. Enriching CTCs based on the immunological properties of CTCs depends on the antigens expressed on the surface of epithelial cells, including epithelial cell adhesion molecule (EpCAM) and cytokeratin (CK). CellSearch is the first and only FDA-approved test for capturing CTCs that express EpCAM by using immunomagnetic beads[50,51]. There also are some methods that combine epithelial marker immunofluorescence staining with automated microscopy, such as NYONE[52]. At the protein level, fluorescence *in situ* hybridization (FISH) has been utilized for identifying chromosomal rearrangements in CTCs [53]. Immunocytochemistry (ICC) is the major technique that is used by several commercial kits for isolating CTCs, including ApoStream and OcoQuick. Flow cytometry is another protein analysis method employed for CTC isolation. The analysis of genetic information of CTCs is mainly based on PCR and next-generation sequencing (NGS), such as RNA-based digital PCR and single-cell sequencing[54,55]. Due to the low concentration and fragile property of CTCs and limitations of current methods, combination and further optimization may achieve better enrichment and detection for CTCs.

The clinical application of CTCs depends on the number of CTCs and the information about protein expression and gene mutation in CTCs. Kang *et al*[56] showed that for individuals with two or more CTCs per 7.5 mL of blood, 97.1% of them were GC patients in their cohort. The increased number of CTCs after treatment was also correlated with early recurrence[27]. Zhang *et al*[27] showed that in GC patients, the patients with five or more CTCs per 7.5 mL in postoperative blood had a significantly shorter overall survival and disease-free survival compared to those with less CTCs. The protein expression patterns in CTCs are also an important biomarker for cancer diagnosis. Around 50% GC patients with CK^+CD44^+ CTCs were diagnosed with distant metastases[57]. Wei *et al*[58] found that, in 76% of PDAC patients, vimentin was upregulated in CTCs, and a high level of vimentin in CTCs was associated with a shorter recurrence-free survival. Similarly, PDAC patients with CTCs that expressed high levels of mucin 1 (MUC-1) and cancer stem cell markers, such as ALDH, CD133, and CD44, were associated with a worse overall survival and tumor recurrence[59,60]. Chen *et al*[61] found up-regulated expression of ECT2 in CTCs from patients with CRC. Fang *et al*[62] found that CRC patients with liver metastasis showed a higher percentage of $^+CD133^+CD54^+$ $CD44^+$ cell subpopulations. Moreover, the upregulated genes in CTCs, such as *SHH*, *SMO*, *POU5F1B*, and *ALCAM*, were demonstrated as potential markers for therapeutic response and prognosis prediction in PC patients[63]. In HCC patients, Zhou *et al*[64] discovered that the presence of EpCAM $mRNA^+$ CTCs was associated with early recurrence when combined with Treg/$CD4^+$ T cell ratio.

Exosomes

Exosomes are membrane-bound extracellular nanovesicles (EVs) released by many types of cells, having a size ranging from 30 to 150 nm. Exosomes have been found in various bodily fluids, including plasma, urine, and malignant ascites[65]. Exosomes are involved in mechanisms of cell-cell communication in physiological and pathological tissues through transporting biomolecules, such as lipids, proteins, mRNA, microRNAs, and DNA fragments, and the intercellular transfer of signal components[66,67]. Tumor-associated exosomes are larger than those derived from healthy cells and are enriched with different types of mediators of tumorigenesis, including proteins, growth factors, immunomodulatory molecules, and nucleic acids that arise from the cytoplasm of donor cancer cells[68].

In the last decade, a significant number of studies have focused their attention on the exosome-mediated cross-talk which can promote the activation of signaling pathways and reprogram the functions of recipient cells through their cargo transfer that occurs between cancer and normal cells, especially in the tumor microenvironment[65,69-71].

Several examples of exosome biomarkers, such as proteins, microRNAs, and long non-coding RNAs (lncRNAs), have been shown to have the potential for the diagnosis and prognosis of specific types of cancer. For example, GPC-1 was identified as a diagnostic exosome marker for PC and CRC. CD9 and CD147 were found to be upregulated in exosomes derived from serum of CRC patients[72]. Previously, seven miRNAs including let-7a, miR-21, miR-23a, miR-155, miR-223, miR-1246, and miR-1229 were reported to be highly expressed in the serum exosomes of CRC patients and were significantly decreased after surgical resection[73]. MiR-103 was reported to be delivered from hepatoma cell-derived exosomes into endothelial cells, and induced metastasis[74]. In HCC patients, serum exosomal miR-10b-5p was fond to upregulated and could be used to distinguish HCC patients from healthy controls with an AUC of 0.934[75]. Nakamura *et al*[76] found that exosomal miR-21 and miR-155 were significantly upregulated in PDAC patients compared to chronic pancreatitis patients. In GC patients, exosomal lncRNA pcsk2-2:1 and lncRNA GNAQ-6:1 were significantly downregulated and could be served as biomarkers for early diagnosis for GC[77,78]. Yu *et al*[79] developed a panel of eight exosomal RNAs, which could distinguish PDAC patients from chronic pancreatitis patients with an AUC of 0.931. The exosomal mRNA *hnRNPH1* was found to have a high expression level in HCC patients and could be used to distinguish HCC patients from chronic hepatitis B patients with an AUC of 0.865[80]. Furthermore, lncRNAs, such as *LncRNA-ARSR*, *Lnc-sox2ot*, and *LncRNA-h19*, were showed to be associated with tumor progression[72,81].

Circulating cell-free tumor RNAs

Circulating cell-free RNAs (cfRNAs) are also present in the blood circulation and have the potential to serve as cancer biomarkers for cancer diagnosis. CfRNAs may be released into the blood through mechanisms of cell death or exosome-mediated signaling by living cells.

Historically, the study of cfRNA has focused on a small group of known cancer-related mRNA, miRNAs, and lncRNAs[76-78,82]. For instance, miR-21 showed an increased expression level in GC patients, which could serve as a classification biomarker with an 88.4% sensitivity and 79.6% specificity[83]. Huang *et al*[84] designed a panel of six miRNAs that were upregulated in the serum of GC patients, which showed an AUC of 0.702 in distinguishing GC patients from healthy controls. Shimura *et al*[85] found that three miRNAs (miR-30a-5p, miR-659-3p, and miR-3917) were overexpressed in GC patients who had peritoneal metastasis and could be used to distinguish patients with or without peritoneal metastasis with an AUC of 0.82. Yamada *et al*[86] showed that the expression of three serum miRNAs, including miR-21, miR-29a, and miR-125b, could discriminate CRC patients from healthy ones with an AUC of 0.827. In HCC patients, serum miR-143 was downregulated and could distinguish HCC patients from healthy controls with an AUC of 0.831[87]. Another study showed that a panel of three plasma circRNAs were found to distinguish HCC patients from healthy ones with an AUC of 0.863[88].

AI-ENHANCED ALGORITHMS FOR IMAGE-BASED AND TISSUE-BASED PATHOLOGY ANALYSIS

The early diagnosis and prognosis of a cancer type have become a necessity in cancer research. Image-based and tissue biopsy-based pathology analyses are considered to be the "gold standard" for their accuracy and effectiveness for cancer screening.

In recent years, AI has become an emerging field with the advances of computational power and massive amounts of learning data. Over the last two decades, different machine learning (ML) algorithms, such as support vector machines (SVM), random forest (RF), and artificial neural networks (ANNs), have been widely used in the field of medicine[89-91]. More recently, convolutional neural networks (CNN), a novel algorithm, show its great potential in processing and interpreting radiological and pathological images (Figure 2)[92,93]. Previous studies demonstrated that a multilayer CNN with pre-trained GoogleNet Inception v3 architecture on skin cancer level prediction could achieve comparable results to dermatologists[94]. Similarly, another image-based deep learning model proposed by Kermany *et al*[10] in analyzing optical

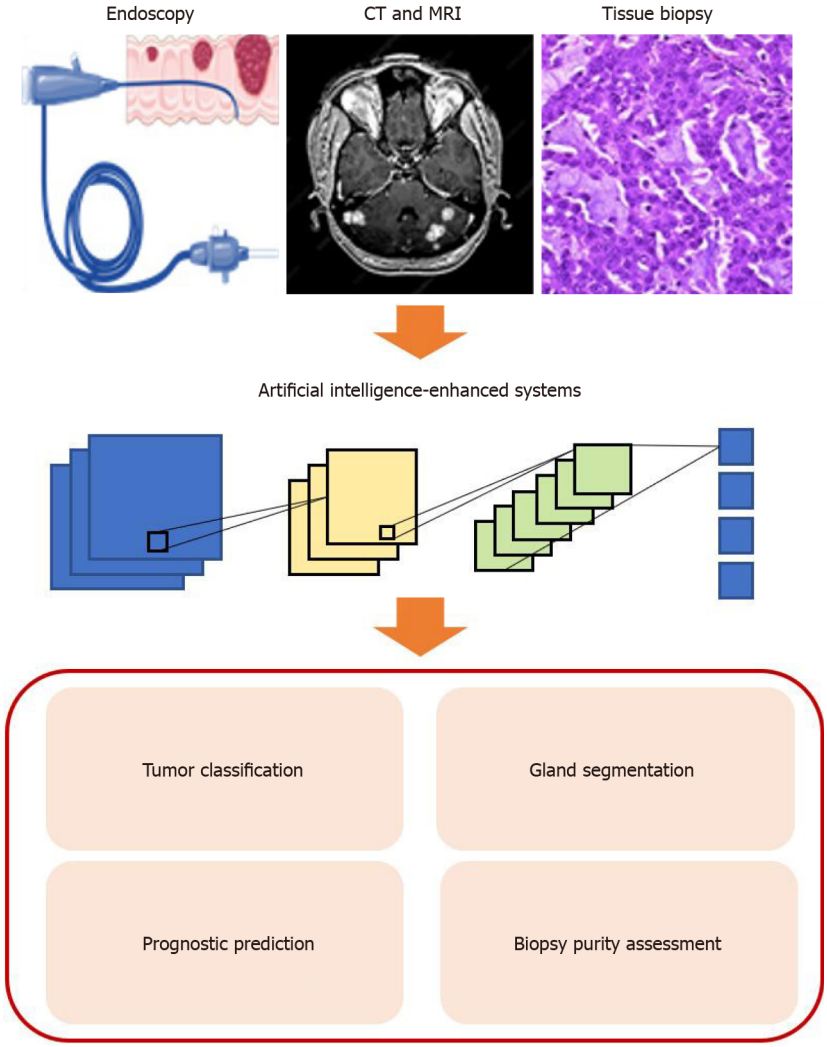


Figure 2 Applications of artificial intelligence in medical area. The effective combination of artificial intelligence and big data can provide efficient and accurate clinical-decision support for physicians. CT: Computed tomography; MRI: Magnetic resonance imaging.

coherence tomography (OCT) images of the retina is on par with the ophthalmologist, with an accuracy of 96.6%, sensitivity of 97.8%, and specificity of 97.4% on the four-class classification problem. Most importantly, both studies utilized transfer learning when training the model to save the training time, which is also a widely used technique in training an ML model in medical images due to the lack of training data in most cases[95].

Traditionally, the most effective and direct method of screening colorectal carcinoma is endoscopy, particularly colonoscopy[96]. Abdominal computerized tomography (CT) or abdominal magnetic resonance imaging (MRI) are employed when more precise and additional information is needed about the lesion to help assess cancer and look for any signs of spread. However, these methods are usually labor-intensive and time-consuming and require professional knowledge. In the era of big data, the number of colonoscopy examinations and radiology screening is enormously increasing[96]. To this end, the deep learning-based radiology and digital pathology workflow could assist the radiologists and pathologists to diagnose diseases in various aspects, such as tumor classification, gland segment, tumor microenvironment analysis, and prognostic survival prediction, to ease their ever-growing workload and improve their efficiency[92]. More recently, Luo *et al*[97] built a real-time Gastrointestinal Artificial Intelligence Diagnostic System (GRAIDS) for the diagnosis of upper GI cancer through analysis of imaging data from clinical endoscopies. The GRAIDS achieved a high diagnostic accuracy in detecting upper GI cancers and had a similar predicted sensitivity as expert endoscopies and outperformed the non-expert endoscopies. Besides, they performed a multi-center study and further validated the system from the other five primary care hospitals, thus indicating the general applicability of GRAIDS.

Apart from AI application in colonoscopy, CT, and MRI images, the digital pathology also drew much attention from researchers, in particular adopting deep learning on the whole slide images (WSIs)[92,98-100]. However, the WSIs are multi-gigabyte images, present high morphological variance, and contain various types of artifacts. Such circumstances prevent CNN directly from applying to the high-resolution images. On the other hand, typically small labeled datasets in pathological images impede the generality of the deep learning model[101]. Kermany *et al*[102] developed a multiple-instance learning-based deep learning system that only used the reported annotated datasets to tackle the limited number of labeled images and the AUCs were all above 0.98 when testing on multiple cancer types. Joseph *et al*[96] introduced a novel machine learning-based system on prediction of CRC outcome for whole digitized haematoxylin and eosin (HE) stained histopathology slides in learning heterogeneous and discriminant contents. They demonstrated the effectiveness of the method and presented a detailed analysis of its different elements which corroborate its ability to extract and learn salient, discriminative, and clinically meaningful content.

At present, pathological analysis of tissue biopsies is still the most widely approach in cancer diagnosis. Recent studies have shown that combination of molecular data and deep learning approach could predict the cancerous status and tissue origin of pan-cancer biopsies with high accuracy. For instance, Sun *et al*[103] developed GeneCT, which showed an overall accuracy of 98.2% in differentiating tumor samples from adjacent normal samples, and an overall accuracy of 98.6% in predicting the tissue origins of the biopsies. In addition, as tissue biopsy is one of the most widely materials in cancer studies, and the purity of the biopsies is crucial for appropriate project design and correct interpretation of the data. To this end, Fan *et al*[12] showed that the low prediction accuracy of GeneCT in some datasets suggested impurity of the samples. The performance of GeneCT was further evaluated using metastatic tumor samples, which is a common scenario in GI cancers. As a result, GeneCT shows potential as an accurate classification tool for tissue biopsy-based diagnosis, as well as an easy-to-use quality-control tool for cancer studies.

CONCLUSION

GI malignancies, especially CRC and HCC, are common cancers that lead to death of patients with cancers worldwide. Liquid biopsy plays an important role in early-stage GI cancer diagnosis as a noninvasive tumor detection strategy. Biomarkers including cfDNA, CTCs, and exosomes of liquid biopsy are widely used for the detection of tumor-associated molecules. The advantages of cfDNA, such as high amount, being relatively stable and easy for extraction and preservation, mostly representing the information from the major tumor clone, and the significant features including fragment sizes, the proportion of fragment, the end-motif, and genomic alterations, make it the preferential and accurate biomarker for the cancer diagnosis. CTCs are also important liquid biomarkers because they not only contain direct molecular information from the tumor clone but also can be cultured *in vitro*. However, CTCs are very rare and require fresh blood for isolation.

The potential of liquid biopsy in clinical practice is enormous in the future. However, there are several challenges that need to be resolved for the utility of liquid biopsy in clinical diagnosis. First, standardization should be established for the sample collection and storage conditions, and biomarker molecules and the suitable detection and analysis strategy depend on sample type. Second, tumor-associated molecule detection techniques require high sensitivity for early tumor detection and high specificity for early-stage tumor screening. At the same time, the low content of tumor biomarkers and the varied interference factors in the circulation make the high requirements for the high sensitivity and specificity of detection strategies. Reducing purification steps could shorten the time of sample treatment and reduce the cost, and optimization of the throughput platform could help to increase both the sensitivity and specificity of the biomarkers.

AI based on machine learning and deep learning is widely used in all walks of life. Recently, rapid developments have been made in the utility of AI in medicine areas and showed promising results in terms of accuracy for cancer diagnosis. However, the scale and quality of the training and validation datasets of most of the studies were relatively limited to apply this technique in clinical practice. Moreover, it also requires the external cross-validation, especially in tumor classification. Therefore, future studies with a larger number of datasets with high-quality annotations and external

cross-validation are required for routine practice-level validation.

ACKNOWLEDGEMENTS

We would like to thank Ms. Qi Wang from Shenzhen Bay Laboratory for her technical assistance.

REFERENCES

1 **Siegel RL**, Miller KD, Jemal A. Cancer statistics, 2020. *CA Cancer J Clin* 2020; **70**: 7-30 [PMID: 31912902 DOI: 10.3322/caac.21590]
2 **Siegel RL**, Miller KD, Goding Sauer A, Fedewa SA, Butterly LF, Anderson JC, Cercek A, Smith RA, Jemal A. Colorectal cancer statistics, 2020. *CA Cancer J Clin* 2020; **70**: 145-164 [PMID: 32133645 DOI: 10.3322/caac.21601]
3 **Society AC**. Cancer Facts & Figures 2021: Atlanta: American Cancer Society, 2021
4 **Moore H**, Dodd N. Computed tomographic colonography (CTC); colorectal cancer diagnosis with CTC in an Auckland population. *J Med Imaging Radiat Oncol* 2013; **57**: 572-575 [PMID: 24119271 DOI: 10.1111/1754-9485.12062]
5 **Greenhill C**. Colorectal cancer: CTC for diagnosing symptomatic colorectal cancer. *Nat Rev Gastroenterol Hepatol* 2013; **10**: 198 [PMID: 23458893 DOI: 10.1038/nrgastro.2013.37]
6 **Fici P**. Cell-Free DNA in the Liquid Biopsy Context: Role and Differences Between ctDNA and CTC Marker in Cancer Management. *Methods Mol Biol* 2019; **1909**: 47-73 [PMID: 30580422 DOI: 10.1007/978-1-4939-8973-7_4]
7 **Keup C**, Storbeck M, Hauch S, Hahn P, Sprenger-Haussels M, Tewes M, Mach P, Hoffmann O, Kimmig R, Kasimir-Bauer S. Cell-Free DNA Variant Sequencing Using CTC-Depleted Blood for Comprehensive Liquid Biopsy Testing in Metastatic Breast Cancer. *Cancers (Basel)* 2019; **11** [PMID: 30781720 DOI: 10.3390/cancers11020238]
8 **Nanduri LK**, Hissa B, Weitz J, Schölch S, Bork U. The prognostic role of circulating tumor cells in colorectal cancer. *Expert Rev Anticancer Ther* 2019; **19**: 1077-1088 [PMID: 31778322 DOI: 10.1080/14737140.2019.1699065]
9 **Maltoni R**, Palleschi M, Ravaioli S, Tumedei MM, Rocca A, Melegari E, Altini M, Puccetti M, Manunta S, Bravaccini S. Cell-Free DNA Variant Sequencing Using CTC-Depleted Blood for Comprehensive Liquid Biopsy Testing in Metastatic Breast Cancer. *Cell Transplant* 2020; **29**: 963689720925057 [PMID: 32584148 DOI: 10.1177/0963689720925057]
10 **Kermany DS**, Goldbaum M, Cai W, Valentim CCS, Liang H, Baxter SL, McKeown A, Yang G, Wu X, Yan F, Dong J, Prasadha MK, Pei J, Ting MYL, Zhu J, Li C, Hewett S, Ziyar I, Shi A, Zhang R, Zheng L, Hou R, Shi W, Fu X, Duan Y, Huu VAN, Wen C, Zhang ED, Zhang CL, Li O, Wang X, Singer MA, Sun X, Xu J, Tafreshi A, Lewis MA, Xia H, Zhang K. Identifying Medical Diagnoses and Treatable Diseases by Image-Based Deep Learning. *Cell* 2018; **172**: 1122-1131.e9 [PMID: 29474911 DOI: 10.1016/j.cell.2018.02.010]
11 **He B**, Lu Q, Lang J, Yu H, Peng C, Bing P, Li S, Zhou Q, Liang Y, Tian G. A New Method for CTC Images Recognition Based on Machine Learning. *Front Bioeng Biotechnol* 2020; **8**: 897 [PMID: 32850745 DOI: 10.3389/fbioe.2020.00897]
12 **Fan F**, Chen D, Zhao Y, Wang H, Sun H, Sun K. Rapid preliminary purity evaluation of tumor biopsies using deep learning approach. *Comput Struct Biotechnol J* 2020; **18**: 1746-1753 [PMID: 32695267 DOI: 10.1016/j.csbj.2020.06.007]
13 **Yeh P**, Hunter T, Sinha D, Ftouni S, Wallach E, Jiang D, Chan YC, Wong SQ, Silva MJ, Vedururu R, Doig K, Lam E, Arnau GM, Semple T, Wall M, Zivanovic A, Agarwal R, Petrone P, Jones K, Westerman D, Blombery P, Seymour JF, Papenfuss AT, Dawson MA, Tam CS, Dawson SJ. Circulating tumour DNA reflects treatment response and clonal evolution in chronic lymphocytic leukaemia. *Nat Commun* 2017; **8**: 14756 [PMID: 28303898 DOI: 10.1038/ncomms14756]
14 **Hao X**, Luo H, Krawczyk M, Wei W, Wang W, Wang J, Flagg K, Hou J, Zhang H, Yi S, Jafari M, Lin D, Chung C, Caughey BA, Li G, Dhar D, Shi W, Zheng L, Hou R, Zhu J, Zhao L, Fu X, Zhang E, Zhang C, Zhu JK, Karin M, Xu RH, Zhang K. DNA methylation markers for diagnosis and prognosis of common cancers. *Proc Natl Acad Sci USA* 2017; **114**: 7414-7419 [PMID: 28652331 DOI: 10.1073/pnas.1703577114]
15 **Buechler C**, Aslanidis C. Role of lipids in pathophysiology, diagnosis and therapy of hepatocellular carcinoma. *Biochim Biophys Acta Mol Cell Biol Lipids* 2020; **1865**: 158658 [PMID: 32058031 DOI: 10.1016/j.bbalip.2020.158658]
16 **Jiang P**, Sun K, Tong YK, Cheng SH, Cheng THT, Heung MMS, Wong J, Wong VWS, Chan HLY, Chan KCA, Lo YMD, Chiu RWK. Preferred end coordinates and somatic variants as signatures of circulating tumor DNA associated with hepatocellular carcinoma. *Proc Natl Acad Sci USA* 2018; **115**: E10925-E10933 [PMID: 30373822 DOI: 10.1073/pnas.1814616115]
17 **Zhang Q**, Peng J, Ye M, Weng W, Tan C, Ni S, Huang D, Sheng W, Wang L. KRAS Mutation Predicted More Mirometastases and Closer Resection Margins in Patients with Colorectal Cancer

Liver Metastases. *Ann Surg Oncol* 2020; **27**: 1164-1173 [PMID: 31720935 DOI: 10.1245/s10434-019-08065-5]

18 **Shoda K**, Ichikawa D, Fujita Y, Masuda K, Hiramoto H, Hamada J, Arita T, Konishi H, Komatsu S, Shiozaki A, Kakihara N, Okamoto K, Taniguchi H, Imoto I, Otsuji E. Monitoring the HER2 copy number status in circulating tumor DNA by droplet digital PCR in patients with gastric cancer. *Gastric Cancer* 2017; **20**: 126-135 [PMID: 26874951 DOI: 10.1007/s10120-016-0599-z]

19 **Chen Z**, Zhang C, Zhang M, Li B, Niu Y, Chen L, Yang J, Lu S, Gao J, Shen L. Chromosomal instability of circulating tumor DNA reflect therapeutic responses in advanced gastric cancer. *Cell Death Dis* 2019; **10**: 697 [PMID: 31541076 DOI: 10.1038/s41419-019-1907-4]

20 **Chan KC**, Jiang P, Chan CW, Sun K, Wong J, Hui EP, Chan SL, Chan WC, Hui DS, Ng SS, Chan HL, Wong CS, Ma BB, Chan AT, Lai PB, Sun H, Chiu RW, Lo YM. Noninvasive detection of cancer-associated genome-wide hypomethylation and copy number aberrations by plasma DNA bisulfite sequencing. *Proc Natl Acad Sci USA* 2013; **110**: 18761-18768 [PMID: 24191000 DOI: 10.1073/pnas.1313995110]

21 **Li H**, Wang Z, Zhao G, Ma Y, Chen Y, Xue Q, Zheng M, Fei S. Performance of a MethyLight assay for methylated SFRP2 DNA detection in colorectal cancer tissue and serum. *Int J Biol Markers* 2019; **34**: 54-59 [PMID: 30852954 DOI: 10.1177/1724600818820536]

22 **Gai W**, Ji L, Lam WKJ, Sun K, Jiang P, Chan AWH, Wong J, Lai PBS, Ng SSM, Ma BBY, Wong GLH, Wong VWS, Chan HLY, Chiu RWK, Lo YMD, Chan KCA. Liver- and Colon-Specific DNA Methylation Markers in Plasma for Investigation of Colorectal Cancers with or without Liver Metastases. *Clin Chem* 2018; **64**: 1239-1249 [PMID: 29903871 DOI: 10.1373/clinchem.2018.290304]

23 **Eissa MAL**, Lerner L, Abdelfatah E, Shankar N, Canner JK, Hasan NM, Yaghoobi V, Huang B, Kerner Z, Takaesu F, Wolfgang C, Kwak R, Ruiz M, Tam M, Pisanic TR 2nd, Iacobuzio-Donahue CA, Hruban RH, He J, Wang TH, Wood LD, Sharma A, Ahuja N. Promoter methylation of ADAMTS1 and BNC1 as potential biomarkers for early detection of pancreatic cancer in blood. *Clin Epigenetics* 2019; **11**: 59 [PMID: 30953539 DOI: 10.1186/s13148-019-0650-0]

24 **Nishizawa N**, Harada H, Kumamoto Y, Kaizu T, Katoh H, Tajima H, Ushiku H, Yokoi K, Igarashi K, Fujiyama Y, Okuwaki K, Iwai T, Watanabe M, Yamashita K. Diagnostic potential of hypermethylation of the cysteine dioxygenase 1 gene (CDO1) promoter DNA in pancreatic cancer. *Cancer Sci* 2019; **110**: 2846-2855 [PMID: 31325200 DOI: 10.1111/cas.14134]

25 **Kim Y**, Wen X, Jeong S, Cho NY, Kim WH, Kang GH. Combinatory low methylation statuses of SAT-α and L1 are associated with shortened survival time in patients with advanced gastric cancer. *Gastric Cancer* 2019; **22**: 37-47 [PMID: 29926315 DOI: 10.1007/s10120-018-0852-8]

26 **Harada H**, Hosoda K, Moriya H, Mieno H, Ema A, Ushiku H, Washio M, Nishizawa N, Ishii S, Yokota K, Tanaka Y, Kaida T, Soeno T, Kosaka Y, Watanabe M, Yamashita K. Cancer-specific promoter DNA methylation of Cysteine dioxygenase type 1 (CDO1) gene as an important prognostic biomarker of gastric cancer. *PLoS One* 2019; **14**: e0214872 [PMID: 30934021 DOI: 10.1371/journal.pone.0214872]

27 **Zhang Q**, Shan F, Li Z, Gao J, Li Y, Shen L, Ji J, Lu M. A prospective study on the changes and clinical significance of pre-operative and post-operative circulating tumor cells in resectable gastric cancer. *J Transl Med* 2018; **16**: 171 [PMID: 29925382 DOI: 10.1186/s12967-018-1544-1]

28 **Li W**, Zhang X, Lu X, You L, Song Y, Luo Z, Zhang J, Nie J, Zheng W, Xu D, Wang Y, Dong Y, Yu S, Hong J, Shi J, Hao H, Luo F, Hua L, Wang P, Qian X, Yuan F, Wei L, Cui M, Zhang T, Liao Q, Dai M, Liu Z, Chen G, Meckel K, Adhikari S, Jia G, Bissonnette MB, Zhao Y, Zhang W, He C, Liu J. 5-Hydroxymethylcytosine signatures in circulating cell-free DNA as diagnostic biomarkers for human cancers. *Cell Res* 2017; **27**: 1243-1257 [PMID: 28925386 DOI: 10.1038/cr.2017.121]

29 **Cai J**, Chen L, Zhang Z, Zhang X, Lu X, Liu W, Shi G, Ge Y, Gao P, Yang Y, Ke A, Xiao L, Dong R, Zhu Y, Yang X, Wang J, Zhu T, Yang D, Huang X, Sui C, Qiu S, Shen F, Sun H, Zhou W, Zhou J, Nie J, Zeng C, Stroup EK, Chiu BC, Lau WY, He C, Wang H, Zhang W, Fan J. Genome-wide mapping of 5-hydroxymethylcytosines in circulating cell-free DNA as a non-invasive approach for early detection of hepatocellular carcinoma. *Gut* 2019; **68**: 2195-2205 [PMID: 31358576 DOI: 10.1136/gutjnl-2019-318882]

30 **Xiao Z**, Wu W, Wu C, Li M, Sun F, Zheng L, Liu G, Li X, Yun Z, Tang J, Yu Y, Luo S, Sun W, Feng X, Cheng Q, Tao X, Wu S, Tao J. 5-Hydroxymethylcytosine signature in circulating cell-free DNA as a potential diagnostic factor for early-stage colorectal cancer and precancerous adenoma. *Mol Oncol* 2021; **15**: 138-150 [PMID: 33107199 DOI: 10.1002/1878-0261.12833]

31 **Sun K**, Jiang P, Chan KC, Wong J, Cheng YK, Liang RH, Chan WK, Ma ES, Chan SL, Cheng SH, Chan RW, Tong YK, Ng SS, Wong RS, Hui DS, Leung TN, Leung TY, Lai PB, Chiu RW, Lo YM. Plasma DNA tissue mapping by genome-wide methylation sequencing for noninvasive prenatal, cancer, and transplantation assessments. *Proc Natl Acad Sci USA* 2015; **112**: E5503-E5512 [PMID: 26392541 DOI: 10.1073/pnas.1508736112]

32 **Sun K**, Jiang P, Wong AIC, Cheng YKY, Cheng SH, Zhang H, Chan KCA, Leung TY, Chiu RWK, Lo YMD. Size-tagged preferred ends in maternal plasma DNA shed light on the production mechanism and show utility in noninvasive prenatal testing. *Proc Natl Acad Sci USA* 2018; **115**: E5106-E5114 [PMID: 29760053 DOI: 10.1073/pnas.1804134115]

33 **Underhill HR**, Kitzman JO, Hellwig S, Welker NC, Daza R, Baker DN, Gligorich KM, Rostomily RC, Bronner MP, Shendure J. Fragment Length of Circulating Tumor DNA. *PLoS Genet* 2016; **12**: e1006162 [PMID: 27428049 DOI: 10.1371/journal.pgen.1006162]

34 **Mouliere F**, Chandrananda D, Piskorz AM, Moore EK, Morris J, Ahlborn LB, Mair R, Goranova T, Marass F, Heider K, Wan JCM, Supernat A, Hudecova I, Gounaris I, Ros S, Jimenez-Linan M, Garcia-Corbacho J, Patel K, Østrup O, Murphy S, Eldridge MD, Gale D, Stewart GD, Burge J, Cooper WN, van der Heijden MS, Massie CE, Watts C, Corrie P, Pacey S, Brindle KM, Baird RD, Mau-Sørensen M, Parkinson CA, Smith CG, Brenton JD, Rosenfeld N. Enhanced detection of circulating tumor DNA by fragment size analysis. *Sci Transl Med* 2018; **10** [PMID: 30404863 DOI: 10.1126/scitranslmed.aat4921]

35 **Snyder MW**, Kircher M, Hill AJ, Daza RM, Shendure J. Cell-free DNA Comprises an In Vivo Nucleosome Footprint that Informs Its Tissues-Of-Origin. *Cell* 2016; **164**: 57-68 [PMID: 26771485 DOI: 10.1016/j.cell.2015.11.050]

36 **Ulz P**, Thallinger GG, Auer M, Graf R, Kashofer K, Jahn SW, Abete L, Pristauz G, Petru E, Geigl JB, Heitzer E, Speicher MR. Inferring expressed genes by whole-genome sequencing of plasma DNA. *Nat Genet* 2016; **48**: 1273-1278 [PMID: 27571261 DOI: 10.1038/ng.3648]

37 **Jiang P**, Sun K, Peng W, Cheng SH, Ni M, Yeung PC, Heung MMS, Xie T, Shang H, Zhou Z, Chan RWY, Wong J, Wong VWS, Poon LC, Leung TY, Lam WKJ, Chan JYK, Chan HLY, Chan KCA, Chiu RWK, Lo YMD. Plasma DNA End-Motif Profiling as a Fragmentomic Marker in Cancer, Pregnancy, and Transplantation. *Cancer Discov* 2020; **10**: 664-673 [PMID: 32111602 DOI: 10.1158/2159-8290.CD-19-0622]

38 **Sun K**, Jiang P, Cheng SH, Cheng THT, Wong J, Wong VWS, Ng SSM, Ma BBY, Leung TY, Chan SL, Mok TSK, Lai PBS, Chan HLY, Sun H, Chan KCA, Chiu RWK, Lo YMD. Orientation-aware plasma cell-free DNA fragmentation analysis in open chromatin regions informs tissue of origin. *Genome Res* 2019; **29**: 418-427 [PMID: 30808726 DOI: 10.1101/gr.242719.118]

39 **Serpas L**, Chan RWY, Jiang P, Ni M, Sun K, Rashidfarrokhi A, Soni C, Sisirak V, Lee WS, Cheng SH, Peng W, Chan KCA, Chiu RWK, Reizis B, Lo YMD. *Dnase1 L3* deletion causes aberrations in length and end-motif frequencies in plasma DNA. *Proc Natl Acad Sci USA* 2019; **116**: 641-649 [PMID: 30593563 DOI: 10.1073/pnas.1815031116]

40 **Hanahan D**, Weinberg RA. Hallmarks of cancer: the next generation. *Cell* 2011; **144**: 646-674 [PMID: 21376230 DOI: 10.1016/j.cell.2011.02.013]

41 **Plaks V**, Koopman CD, Werb Z. Cancer. Circulating tumor cells. *Science* 2013; **341**: 1186-1188 [PMID: 24031008 DOI: 10.1126/science.1235226]

42 **Heitzer E**, Auer M, Gasch C, Pichler M, Ulz P, Hoffmann EM, Lax S, Waldispuehl-Geigl J, Mauermann O, Lackner C, Höfler G, Eisner F, Sill H, Samonigg H, Pantel K, Riethdorf S, Bauernhofer T, Geigl JB, Speicher MR. Complex tumor genomes inferred from single circulating tumor cells by array-CGH and next-generation sequencing. *Cancer Res* 2013; **73**: 2965-2975 [PMID: 23471846 DOI: 10.1158/0008-5472.CAN-12-4140]

43 **Vignot S**, Frampton GM, Soria JC, Yelensky R, Commo F, Brambilla C, Palmer G, Moro-Sibilot D, Ross JS, Cronin MT, André F, Stephens PJ, Lazar V, Miller VA, Brambilla E. Next-generation sequencing reveals high concordance of recurrent somatic alterations between primary tumor and metastases from patients with non-small-cell lung cancer. *J Clin Oncol* 2013; **31**: 2167-2172 [PMID: 23630207 DOI: 10.1200/JCO.2012.47.7737]

44 **Hofman V**, Ilie MI, Long E, Selva E, Bonnetaud C, Molina T, Vénissac N, Mouroux J, Vielh P, Hofman P. Detection of circulating tumor cells as a prognostic factor in patients undergoing radical surgery for non-small-cell lung carcinoma: comparison of the efficacy of the CellSearch Assay™ and the isolation by size of epithelial tumor cell method. *Int J Cancer* 2011; **129**: 1651-1660 [PMID: 21128227 DOI: 10.1002/ijc.25819]

45 **Pailler E**, Oulhen M, Billiot F, Galland A, Auger N, Faugeroux V, Laplace-Builhé C, Besse B, Loriot Y, Ngo-Camus M, Hemanda M, Lindsay CR, Soria JC, Vielh P, Farace F. Method for semi-automated microscopy of filtration-enriched circulating tumor cells. *BMC Cancer* 2016; **16**: 477 [PMID: 27417942 DOI: 10.1186/s12885-016-2461-4]

46 **Edd JF**, Mishra A, Dubash TD, Herrera S, Mohammad R, Williams EK, Hong X, Mutlu BR, Walsh JR, Machado de Carvalho F, Aldikacti B, Nieman LT, Stott SL, Kapur R, Maheswaran S, Haber DA, Toner M. Microfluidic concentration and separation of circulating tumor cell clusters from large blood volumes. *Lab Chip* 2020; **20**: 558-567 [PMID: 31934715 DOI: 10.1039/c9lc01122f]

47 **Lee SW**, Hyun KA, Kim SI, Kang JY, Jung HI. Enrichment of circulating tumor cells using a centrifugal affinity plate system. *J Chromatogr A* 2014; **1373**: 25-30 [PMID: 25435456 DOI: 10.1016/j.chroma.2014.11.027]

48 **Balasubramanian P**, Kinders RJ, Kummar S, Gupta V, Hasegawa D, Menachery A, Lawrence SM, Wang L, Ferry-Galow K, Davis D, Parchment RE, Tomaszewski JE, Doroshow JH. Antibody-independent capture of circulating tumor cells of non-epithelial origin with the ApoStream® system. *PLoS One* 2017; **12**: e0175414 [PMID: 28403214 DOI: 10.1371/journal.pone.0175414]

49 **Le Du F**, Fujii T, Kida K, Davis DW, Park M, Liu DD, Wu W, Chavez-MacGregor M, Barcenas CH, Valero V, Tripathy D, Reuben JM, Ueno NT. EpCAM-independent isolation of circulating tumor cells with epithelial-to-mesenchymal transition and cancer stem cell phenotypes using ApoStream® in patients with breast cancer treated with primary systemic therapy. *PLoS One* 2020; **15**: e0229903 [PMID: 32214335 DOI: 10.1371/journal.pone.0229903]

50 **Swennenhuis JF**, Reumers J, Thys K, Aerssens J, Terstappen LW. Efficiency of whole genome amplification of single circulating tumor cells enriched by CellSearch and sorted by FACS. *Genome Med* 2013; **5**: 106 [PMID: 24286536 DOI: 10.1186/gm510]

51 **Huebner H**, Fasching PA, Gumbrecht W, Jud S, Rauh C, Matzas M, Paulicka P, Friedrich K, Lux

MP, Volz B, Gass P, Häberle L, Meier-Stiegen F, Hartkopf A, Neubauer H, Almstedt K, Beckmann MW, Fehm TN, Ruebner M. Filtration based assessment of CTCs and CellSearch® based assessment are both powerful predictors of prognosis for metastatic breast cancer patients. *BMC Cancer* 2018; **18**: 204 [PMID: 29463222 DOI: 10.1186/s12885-018-4115-1]

52 **Hendricks A**, Brandt B, Geisen R, Dall K, Röder C, Schafmayer C, Becker T, Hinz S, Sebens S. Isolation and Enumeration of CTC in Colorectal Cancer Patients: Introduction of a Novel Cell Imaging Approach and Comparison to Cellular and Molecular Detection Techniques. *Cancers (Basel)* 2020; **12** [PMID: 32947903 DOI: 10.3390/cancers12092643]

53 **Wang A**, Li Z, Wang Q, Bai Y, Ji X, Fu T, Ji K, Xue Y, Han T, Wu X, Zhang J, Yang Y, Xu G, Bu Z, Ji J. Diagnostic value of negative enrichment and immune fluorescence *in situ* hybridization for intraperitoneal free cancer cells of gastric cancer. *Chin J Cancer Res* 2019; **31**: 945-954 [PMID: 31949396 DOI: 10.21147/j.issn.1000-9604.2019.06.10]

54 **Miyamoto DT**, Lee RJ, Kalinich M, LiCausi JA, Zheng Y, Chen T, Milner JD, Emmons E, Ho U, Broderick K, Silva E, Javaid S, Kwan TT, Hong X, Dahl DM, McGovern FJ, Efstathiou JA, Smith MR, Sequist LV, Kapur R, Wu CL, Stott SL, Ting DT, Giobbie-Hurder A, Toner M, Maheswaran S, Haber DA. An RNA-Based Digital Circulating Tumor Cell Signature Is Predictive of Drug Response and Early Dissemination in Prostate Cancer. *Cancer Discov* 2018; **8**: 288-303 [PMID: 29301747 DOI: 10.1158/2159-8290.CD-16-1406]

55 **Winter M**, Cai Z, Winkler K, Georgiou K, Inglis D, Lavranos T, Rezaei M, Warkiani M, Thierry B. Circulating tumour cell RNA characterisation from colorectal cancer patient blood after inertial microfluidic enrichment. *MethodsX* 2019; **6**: 1512-1520 [PMID: 31304099 DOI: 10.1016/j.mex.2019.06.012]

56 **Kang HM**, Kim GH, Jeon HK, Kim DH, Jeon TY, Park DY, Jeong H, Chun WJ, Kim MH, Park J, Lim M, Kim TH, Cho YK. Circulating tumor cells detected by lab-on-a-disc: Role in early diagnosis of gastric cancer. *PLoS One* 2017; **12**: e0180251 [PMID: 28662130 DOI: 10.1371/journal.pone.0180251]

57 **Szczepanik A**, Sierzega M, Drabik G, Pituch-Noworolska A, Kołodziejczyk P, Zembala M. CD44^{+} cytokeratin-positive tumor cells in blood and bone marrow are associated with poor prognosis of patients with gastric cancer. *Gastric Cancer* 2019; **22**: 264-272 [PMID: 30056567 DOI: 10.1007/s10120-018-0858-2]

58 **Wei T**, Zhang X, Zhang Q, Yang J, Chen Q, Wang J, Li X, Chen J, Ma T, Li G, Gao S, Lou J, Que R, Wang Y, Dang X, Zheng L, Liang T, Bai X. Vimentin-positive circulating tumor cells as a biomarker for diagnosis and treatment monitoring in patients with pancreatic cancer. *Cancer Lett* 2019; **452**: 237-243 [PMID: 30905814 DOI: 10.1016/j.canlet.2019.03.009]

59 **Dotan E**, Alpaugh RK, Ruth K, Negin BP, Denlinger CS, Hall MJ, Astsaturov I, McAleer C, Fittipaldi P, Thrash-Bingham C, Meropol NJ, Cohen SJ. Prognostic Significance of MUC-1 in Circulating Tumor Cells in Patients With Metastatic Pancreatic Adenocarcinoma. *Pancreas* 2016; **45**: 1131-1135 [PMID: 26967453 DOI: 10.1097/MPA.0000000000000619]

60 **Poruk KE**, Blackford AL, Weiss MJ, Cameron JL, He J, Goggins M, Rasheed ZA, Wolfgang CL, Wood LD. Circulating Tumor Cells Expressing Markers of Tumor-Initiating Cells Predict Poor Survival and Cancer Recurrence in Patients with Pancreatic Ductal Adenocarcinoma. *Clin Cancer Res* 2017; **23**: 2681-2690 [PMID: 27789528 DOI: 10.1158/1078-0432.CCR-16-1467]

61 **Chen CJ**, Sung WW, Chen HC, Chern YJ, Hsu HT, Lin YM, Lin SH, Peck K, Yeh KT. Early Assessment of Colorectal Cancer by Quantifying Circulating Tumor Cells in Peripheral Blood: ECT2 in Diagnosis of Colorectal Cancer. *Int J Mol Sci* 2017; **18** [PMID: 28362321 DOI: 10.3390/ijms18040743]

62 **Fang C**, Fan C, Wang C, Huang Q, Meng W, Yu Y, Yang L, Peng Z, Hu J, Li Y, Mo X, Zhou Z. CD133+CD54+CD44+ circulating tumor cells as a biomarker of treatment selection and liver metastasis in patients with colorectal cancer. *Oncotarget* 2016; **7**: 77389-77403 [PMID: 27764803 DOI: 10.18632/oncotarget.12675]

63 **Amantini C**, Morelli MB, Nabissi M, Piva F, Marinelli O, Maggi F, Bianchi F, Bittoni A, Berardi R, Giampieri R, Santoni G. Expression Profiling of Circulating Tumor Cells in Pancreatic Ductal Adenocarcinoma Patients: Biomarkers Predicting Overall Survival. *Front Oncol* 2019; **9**: 874 [PMID: 31552188 DOI: 10.3389/fonc.2019.00874]

64 **Zhou Y**, Wang B, Wu J, Zhang C, Zhou Y, Yang X, Zhou J, Guo W, Fan J. Association of preoperative EpCAM Circulating Tumor Cells and peripheral Treg cell levels with early recurrence of hepatocellular carcinoma following radical hepatic resection. *BMC Cancer* 2016; **16**: 506 [PMID: 27439521 DOI: 10.1186/s12885-016-2526-4]

65 **Mittelbrunn M**, Sánchez-Madrid F. Intercellular communication: diverse structures for exchange of genetic information. *Nat Rev Mol Cell Biol* 2012; **13**: 328-335 [PMID: 22510790 DOI: 10.1038/nrm3335]

66 **Théry C**, Zitvogel L, Amigorena S. Exosomes: composition, biogenesis and function. *Nat Rev Immunol* 2002; **2**: 569-579 [PMID: 12154376 DOI: 10.1038/nri855]

67 **Scavo MP**, Depalo N, Tutino V, De Nunzio V, Ingrosso C, Rizzi F, Notarnicola M, Curri ML, Giannelli G. Exosomes for Diagnosis and Therapy in Gastrointestinal Cancers. *Int J Mol Sci* 2020; **21** [PMID: 31935918 DOI: 10.3390/ijms21010367]

68 **Bebelman MP**, Smit MJ, Pegtel DM, Baglio SR. Biogenesis and function of extracellular vesicles in cancer. *Pharmacol Ther* 2018; **188**: 1-11 [PMID: 29476772 DOI: 10.1016/j.pharmthera.2018.02.013]

69 **Carpelan-Holmström MA**, Haglund CH, Roberts PJ. Differences in serum tumor markers between colon and rectal cancer. Comparison of CA 242 and carcinoembryonic antigen. *Dis Colon Rectum* 1996; **39**: 799-805 [PMID: 8674374 DOI: 10.1007/BF02054447]

70 **Brzozowski JS**, Jankowski H, Bond DR, McCague SB, Munro BR, Predebon MJ, Scarlett CJ, Skelding KA, Weidenhofer J. Lipidomic profiling of extracellular vesicles derived from prostate and prostate cancer cell lines. *Lipids Health Dis* 2018; **17**: 211 [PMID: 30193584 DOI: 10.1186/s12944-018-0854-x]

71 **Alzahrani FA**, El-Magd MA, Abdelfattah-Hassan A, Saleh AA, Saadeldin IM, El-Shetry ES, Badawy AA, Alkarim S. Potential Effect of Exosomes Derived from Cancer Stem Cells and MSCs on Progression of DEN-Induced HCC in Rats. *Stem Cells Int* 2018; **2018**: 8058979 [PMID: 30224923 DOI: 10.1155/2018/8058979]

72 **Xiao Y**, Zhong J, Zhong B, Huang J, Jiang L, Jiang Y, Yuan J, Sun J, Dai L, Yang C, Li Z, Wang J, Zhong T. Exosomes as potential sources of biomarkers in colorectal cancer. *Cancer Lett* 2020; **476**: 13-22 [PMID: 32044357 DOI: 10.1016/j.canlet.2020.01.033]

73 **Lane RE**, Korbie D, Hill MM, Trau M. Extracellular vesicles as circulating cancer biomarkers: opportunities and challenges. *Clin Transl Med* 2018; **7**: 14 [PMID: 29855735 DOI: 10.1186/s40169-018-0192-7]

74 **Nedaeinia R**, Manian M, Jazayeri MH, Ranjbar M, Salehi R, Sharifi M, Mohaghegh F, Goli M, Jahednia SH, Avan A, Ghayour-Mobarhan M. Circulating exosomes and exosomal microRNAs as biomarkers in gastrointestinal cancer. *Cancer Gene Ther* 2017; **24**: 48-56 [PMID: 27982021 DOI: 10.1038/cgt.2016.77]

75 **Cho HJ**, Eun JW, Baek GO, Seo CW, Ahn HR, Kim SS, Cho SW, Cheong JY. Serum Exosomal MicroRNA, miR-10b-5p, as a Potential Diagnostic Biomarker for Early-Stage Hepatocellular Carcinoma. *J Clin Med* 2020; **9** [PMID: 31968558 DOI: 10.3390/jcm9010281]

76 **Nakamura S**, Sadakari Y, Ohtsuka T, Okayama T, Nakashima Y, Gotoh Y, Saeki K, Mori Y, Nakata K, Miyasaka Y, Onishi H, Oda Y, Goggins M, Nakamura M. Pancreatic Juice Exosomal MicroRNAs as Biomarkers for Detection of Pancreatic Ductal Adenocarcinoma. *Ann Surg Oncol* 2019; **26**: 2104-2111 [PMID: 30820789 DOI: 10.1245/s10434-019-07269-z]

77 **Cai C**, Zhang H, Zhu Y, Zheng P, Xu Y, Sun J, Zhang M, Lan T, Gu B, Li S, Ma P. Serum Exosomal Long Noncoding RNA pcsk2-2:1 As A Potential Novel Diagnostic Biomarker For Gastric Cancer. *Onco Targets Ther* 2019; **12**: 10035-10041 [PMID: 31819499 DOI: 10.2147/OTT.S229033]

78 **Li S**, Zhang M, Zhang H, Hu K, Cai C, Wang J, Shi L, Ma P, Xu Y, Zheng P. Exosomal long noncoding RNA lnc-GNAQ-6:1 may serve as a diagnostic marker for gastric cancer. *Clin Chim Acta* 2020; **501**: 252-257 [PMID: 31730812 DOI: 10.1016/j.cca.2019.10.047]

79 **Yu S**, Li Y, Liao Z, Wang Z, Qian L, Zhao J, Zong H, Kang B, Zou WB, Chen K, He X, Meng Z, Chen Z, Huang S, Wang P. Plasma extracellular vesicle long RNA profiling identifies a diagnostic signature for the detection of pancreatic ductal adenocarcinoma. *Gut* 2020; **69**: 540-550 [PMID: 31562239 DOI: 10.1136/gutjnl-2019-318860]

80 **Xu H**, Dong X, Chen Y, Wang X. Serum exosomal hnRNPH1 mRNA as a novel marker for hepatocellular carcinoma. *Clin Chem Lab Med* 2018; **56**: 479-484 [PMID: 29252188 DOI: 10.1515/cclm-2017-0327]

81 **Baassiri A**, Nassar F, Mukherji D, Shamseddine A, Nasr R, Temraz S. Exosomal Non Coding RNA in LIQUID Biopsies as a Promising Biomarker for Colorectal Cancer. *Int J Mol Sci* 2020; **21** [PMID: 32092975 DOI: 10.3390/ijms21041398]

82 **Redis RS**, Calin S, Yang Y, You MJ, Calin GA. Cell-to-cell miRNA transfer: from body homeostasis to therapy. *Pharmacol Ther* 2012; **136**: 169-174 [PMID: 22903157 DOI: 10.1016/j.pharmthera.2012.08.003]

83 **Wu J**, Li G, Wang Z, Yao Y, Chen R, Pu X, Wang J. Circulating MicroRNA-21 Is a Potential Diagnostic Biomarker in Gastric Cancer. *Dis Markers* 2015; **2015**: 435656 [PMID: 26063956 DOI: 10.1155/2015/435656]

84 **Huang Z**, Zhu D, Wu L, He M, Zhou X, Zhang L, Zhang H, Wang W, Zhu J, Cheng W, Chen Y, Fan Y, Qi L, Yin Y, Zhu W, Shu Y, Liu P. Six Serum-Based miRNAs as Potential Diagnostic Biomarkers for Gastric Cancer. *Cancer Epidemiol Biomarkers Prev* 2017; **26**: 188-196 [PMID: 27756776 DOI: 10.1158/1055-9965.EPI-16-0607]

85 **Shimura T**, Toden S, Kandimalla R, Toiyama Y, Okugawa Y, Kanda M, Baba H, Kodera Y, Kusunoki M, Goel A. Genomewide Expression Profiling Identifies a Novel miRNA-Based Signature for the Detection of Peritoneal Metastasis in Patients With Gastric Cancer. *Ann Surg* 2019 [PMID: 31663973 DOI: 10.1097/SLA.0000000000003647]

86 **Yamada A**, Horimatsu T, Okugawa Y, Nishida N, Honjo H, Ida H, Kou T, Kusaka T, Sasaki Y, Yagi M, Higurashi T, Yukawa N, Amanuma Y, Kikuchi O, Muto M, Ueno Y, Nakajima A, Chiba T, Boland CR, Goel A. Serum miR-21, miR-29a, and miR-125b Are Promising Biomarkers for the Early Detection of Colorectal Neoplasia. *Clin Cancer Res* 2015; **21**: 4234-4242 [PMID: 26038573 DOI: 10.1158/1078-0432.CCR-14-2793]

87 **Zhang J**, Lin H, Wang XY, Zhang DQ, Chen JX, Zhuang Y, Zheng XL. Predictive value of microRNA-143 in evaluating the prognosis of patients with hepatocellular carcinoma. *Cancer Biomark* 2017; **19**: 257-262 [PMID: 28436387 DOI: 10.3233/CBM-160357]

88 **Yu J**, Ding WB, Wang MC, Guo XG, Xu J, Xu QG, Yang Y, Sun SH, Liu JF, Qin LX, Liu H, Yang F, Zhou WP. Plasma circular RNA panel to diagnose hepatitis B virus-related hepatocellular carcinoma: A large-scale, multicenter study. *Int J Cancer* 2020; **146**: 1754-1763 [PMID: 31456215

DOI: 10.1002/ijc.32647]
89 **Kourou K**, Exarchos TP, Exarchos KP, Karamouzis MV, Fotiadis DI. Machine learning applications in cancer prognosis and prediction. *Comput Struct Biotechnol J* 2015; **13**: 8-17 [PMID: 25750696 DOI: 10.1016/j.csbj.2014.11.005]
90 **Jiménez Pérez M**, Grande RG. Application of artificial intelligence in the diagnosis and treatment of hepatocellular carcinoma: A review. *World J Gastroenterol* 2020; **26**: 5617-5628 [PMID: 33088156 DOI: 10.3748/wjg.v26.i37.5617]
91 **Jin P**, Ji X, Kang W, Li Y, Liu H, Ma F, Ma S, Hu H, Li W, Tian Y. Artificial intelligence in gastric cancer: a systematic review. *J Cancer Res Clin Oncol* 2020; **146**: 2339-2350 [PMID: 32613386 DOI: 10.1007/s00432-020-03304-9]
92 **Thakur N**, Yoon H, Chong Y. Current Trends of Artificial Intelligence for Colorectal Cancer Pathology Image Analysis: A Systematic Review. *Cancers (Basel)* 2020; **12** [PMID: 32668721 DOI: 10.3390/cancers12071884]
93 **Wang Y**, He X, Nie H, Zhou J, Cao P, Ou C. Application of artificial intelligence to the diagnosis and therapy of colorectal cancer. *Am J Cancer Res* 2020; **10**: 3575-3598 [PMID: 33294256]
94 **Esteva A**, Kuprel B, Novoa RA, Ko J, Swetter SM, Blau HM, Thrun S. Dermatologist-level classification of skin cancer with deep neural networks. *Nature* 2017; **542**: 115-118 [PMID: 28117445 DOI: 10.1038/nature21056]
95 **Cheplygina V**, de Bruijne M, Pluim JPW. Not-so-supervised: A survey of semi-supervised, multi-instance, and transfer learning in medical image analysis. *Med Image Anal* 2019; **54**: 280-296 [PMID: 30959445 DOI: 10.1016/j.media.2019.03.009]
96 **Joseph DA**, Meester RG, Zauber AG, Manninen DL, Winges L, Dong FB, Peaker B, van Ballegooijen M. Colorectal cancer screening: Estimated future colonoscopy need and current volume and capacity. *Cancer* 2016; **122**: 2479-2486 [PMID: 27200481 DOI: 10.1002/cncr.30070]
97 **Luo H**, Xu G, Li C, He L, Luo L, Wang Z, Jing B, Deng Y, Jin Y, Li Y, Li B, Tan W, He C, Seeruttun SR, Wu Q, Huang J, Huang DW, Chen B, Lin SB, Chen QM, Yuan CM, Chen HX, Pu HY, Zhou F, He Y, Xu RH. Real-time artificial intelligence for detection of upper gastrointestinal cancer by endoscopy: a multicentre, case-control, diagnostic study. *Lancet Oncol* 2019; **20**: 1645-1654 [PMID: 31591062 DOI: 10.1016/S1470-2045(19)30637-0]
98 **Zhen SH**, Cheng M, Tao YB, Wang YF, Juengpanich S, Jiang ZY, Jiang YK, Yan YY, Lu W, Lue JM, Qian JH, Wu ZY, Sun JH, Lin H, Cai XJ. Deep Learning for Accurate Diagnosis of Liver Tumor Based on Magnetic Resonance Imaging and Clinical Data. *Front Oncol* 2020; **10**: 680 [PMID: 32547939 DOI: 10.3389/fonc.2020.00680]
99 **Kiani A**, Uyumazturk B, Rajpurkar P, Wang A, Gao R, Jones E, Yu Y, Langlotz CP, Ball RL, Montine TJ, Martin BA, Berry GJ, Ozawa MG, Hazard FK, Brown RA, Chen SB, Wood M, Allard LS, Ylagan L, Ng AY, Shen J. Impact of a deep learning assistant on the histopathologic classification of liver cancer. *NPJ Digit Med* 2020; **3**: 23 [PMID: 32140566 DOI: 10.1038/s41746-020-0232-8]
100 **Chen M**, Zhang B, Topatana W, Cao J, Zhu H, Juengpanich S, Mao Q, Yu H, Cai X. Classification and mutation prediction based on histopathology H&E images in liver cancer using deep learning. *NPJ Precis Oncol* 2020; **4**: 14 [PMID: 32550270 DOI: 10.1038/s41698-020-0120-3]
101 **Dimitriou N**, Arandjelović O, Caie PD. Deep Learning for Whole Slide Image Analysis: An Overview. *Front Med (Lausanne)* 2019; **6**: 264 [PMID: 31824952 DOI: 10.3389/fmed.2019.00264]
102 **Campanella G**, Hanna MG, Geneslaw L, Miraflor A, Werneck Krauss Silva V, Busam KJ, Brogi E, Reuter VE, Klimstra DS, Fuchs TJ. Clinical-grade computational pathology using weakly supervised deep learning on whole slide images. *Nat Med* 2019; **25**: 1301-1309 [PMID: 31308507 DOI: 10.1038/s41591-019-0508-1]
103 **Sun K**, Wang J, Wang H, Sun H. GeneCT: a generalizable cancerous status and tissue origin classifier for pan-cancer biopsies. *Bioinformatics* 2018; **34**: 4129-4130 [PMID: 29947737 DOI: 10.1093/bioinformatics/bty524]
104 **Yamamoto H**, Watanabe Y, Oikawa R, Morita R, Yoshida Y, Maehata T, Yasuda H, Itoh F. BARHL2 Methylation Using Gastric Wash DNA or Gastric Juice Exosomal DNA is a Useful Marker For Early Detection of Gastric Cancer in an H. pylori-Independent Manner. *Clin Transl Gastroenterol* 2016; **7**: e184 [PMID: 27441821 DOI: 10.1038/ctg.2016.40]
105 **Lin LY**, Yang L, Zeng Q, Wang L, Chen ML, Zhao ZH, Ye GD, Luo QC, Lv PY, Guo QW, Li BA, Cai JC, Cai WY. Tumor-originated exosomal lncUEGC1 as a circulating biomarker for early-stage gastric cancer. *Mol Cancer* 2018; **17**: 84 [PMID: 29690888 DOI: 10.1186/s12943-018-0834-9]
106 **Oehme F**, Krahl S, Gyorffy B, Muessle B, Rao V, Greif H, Ziegler N, Lin K, Thepkaysone ML, Polster H, Tonn T, Schneider M, Weitz J, Baenke F, Kahlert C. Low level of exosomal long non-coding RNA *HOTTIP* is a prognostic biomarker in colorectal cancer. *RNA Biol* 2019; **16**: 1339-1345 [PMID: 31251124 DOI: 10.1080/15476286.2019.1637697]
107 **Shi Y**, Wang Z, Zhu X, Chen L, Ma Y, Wang J, Yang X, Liu Z. Exosomal miR-1246 in serum as a potential biomarker for early diagnosis of gastric cancer. *Int J Clin Oncol* 2020; **25**: 89-99 [PMID: 31506750 DOI: 10.1007/s10147-019-01532-9]
108 **Feng W**, Zong W, Li Y, Shen X, Cui X, Ju S. Abnormally expressed long noncoding RNA B3GALT5-AS1 may serve as a biomarker for the diagnostic and prognostic of gastric cancer. *J Cell Biochem* 2020; **121**: 557-565 [PMID: 31338903 DOI: 10.1002/jcb.29296]
109 **Sun Y**, Yang B, Lin M, Yu H, Chen H, Zhang Z. Identification of serum miR-30a-5p as a diagnostic and prognostic biomarker in colorectal cancer. *Cancer Biomark* 2019; **24**: 299-305 [PMID:

30829615 DOI: 10.3233/CBM-182129]
110 **Liu X**, Pan B, Sun L, Chen X, Zeng K, Hu X, Xu T, Xu M, Wang S. Circulating Exosomal miR-27a and miR-130a Act as Novel Diagnostic and Prognostic Biomarkers of Colorectal Cancer. *Cancer Epidemiol Biomarkers Prev* 2018; **27**: 746-754 [PMID: 29739748 DOI: 10.1158/1055-9965.EPI-18-0067]
111 **Wang J**, Yan F, Zhao Q, Zhan F, Wang R, Wang L, Zhang Y, Huang X. Circulating exosomal miR-125a-3p as a novel biomarker for early-stage colon cancer. *Sci Rep* 2017; **7**: 4150 [PMID: 28646161 DOI: 10.1038/s41598-017-04386-1]
112 **Sun B**, Li Y, Zhou Y, Ng TK, Zhao C, Gan Q, Gu X, Xiang J. Circulating exosomal CPNE3 as a diagnostic and prognostic biomarker for colorectal cancer. *J Cell Physiol* 2019; **234**: 1416-1425 [PMID: 30078189 DOI: 10.1002/jcp.26936]
113 **Court CM**, Ankeny JS, Sho S, Winograd P, Hou S, Song M, Wainberg ZA, Girgis MD, Graeber TG, Agopian VG, Tseng HR, Tomlinson JS. Circulating Tumor Cells Predict Occult Metastatic Disease and Prognosis in Pancreatic Cancer. *Ann Surg Oncol* 2018; **25**: 1000-1008 [PMID: 29442211 DOI: 10.1245/s10434-017-6290-8]
114 **Takahasi K**, Iinuma H, Wada K, Minezaki S, Kawamura S, Kainuma M, Ikeda Y, Shibuya M, Miura F, Sano K. Usefulness of exosome-encapsulated microRNA-451a as a minimally invasive biomarker for prediction of recurrence and prognosis in pancreatic ductal adenocarcinoma. *J Hepatobiliary Pancreat Sci* 2018; **25**: 155-161 [PMID: 29130611 DOI: 10.1002/jhbp.524]
115 **Wang Z**. Diagnostic performance for declined microRNA-133a in pancreatic cancer. *J Cell Biochem* 2019 [PMID: 31773791 DOI: 10.1002/jcb.29547]
116 **Wang F**, Wang J, Ju L, Chen L, Cai W, Yang J. Diagnostic and prognostic potential of serum miR-132/212 cluster in patients with hepatocellular carcinoma. *Ann Clin Biochem* 2018; **55**: 576-582 [PMID: 29357677 DOI: 10.1177/0004563218755815]

World Journal of Gastroenterology

Submit a Manuscript: https://www.f6publishing.com

World J Gastroenterol 2021 September 14; 27(34): 5682-5699

DOI: 10.3748/wjg.v27.i34.5682

ISSN 1007-9327 (print) ISSN 2219-2840 (online)

REVIEW

Liver disease and COVID-19: The link with oxidative stress, antioxidants and nutrition

Danijela Ristic-Medic, Snjezana Petrovic, Aleksandra Arsic, Vesna Vucic

ORCID number: Danijela Ristic-Medic 0000-0002-7041-4220; Snjezana Petrovic 0000-0002-1387-9777; Aleksandra Arsic 0000-0001-8498-9415; Vesna Vucic 0000-0002-8563-594X.

Author contributions: Ristic-Medic D designed the review; Ristic-Medic D, Petrovic S and Arsic A analyzed and interpreted the data and drafted the manuscript; Vucic V critically revised the paper.

Supported by the Ministry of Education, Science and Technological Development of the Republic of Serbia, No. 451-03-9/2021-14/200015.

Conflict-of-interest statement: The authors declare that they have no competing interests.

Open-Access: This article is an open-access article that was selected by an in-house editor and fully peer-reviewed by external reviewers. It is distributed in accordance with the Creative Commons Attribution NonCommercial (CC BY-NC 4.0) license, which permits others to distribute, remix, adapt, build upon this work non-commercially, and license their derivative works on different terms, provided the original work is properly cited and the use is non-commercial. See: http://creativecommons.org/License

Danijela Ristic-Medic, Snjezana Petrovic, Aleksandra Arsic, Vesna Vucic, Group for Nutritional Biochemistry and Dietology, Centre of Research Excellence in Nutrition and Metabolism, National Institute for Medical Research, University of Belgrade, Belgrade 11129, Serbia

Corresponding author: Danijela Ristic-Medic, MD, Professor, Group for Nutritional Biochemistry and Dietology, Centre of Research Excellence in Nutrition and Metabolism, National Institute for Medical Research, University of Belgrade, Tadeusa Koscuska 1, PO Box 102, Belgrade 11129, Serbia. dristicmedic@gmail.com

Abstract

Varying degrees of liver injuries have been reported in patients infected with the severe acute respiratory syndrome-coronavirus-2 (SARS-CoV-2). In general, oxidative stress is actively involved in initiation and progression of liver damage. The liver metabolizes various compounds that produce free radicals. Maintaining the oxidative/antioxidative balance is important in coronavirus disease 2019 (COVID-19) patients. Antioxidant vitamins, essential trace elements and food compounds, such as polyphenols, appear to be promising agents, with effects in oxidative burst. Deficiency of these nutrients suppresses immune function and increases susceptibility to COVID-19. Daily micronutrient intake is necessary to support anti-inflammatory and antioxidative effects but for immune function may be higher than current recommended dietary intake. Antioxidant supplements (β-carotene, vitamin A, vitamin C, vitamin E, and selenium) could have a potential role in patients with liver damage. Available evidence suggests that supplementing the diet with a combination of micronutrients may help to optimize immune function and reduce the risk of infection. Clinical trials based on the associations of diet and SARS-CoV-2 infection are lacking. Unfortunately, it is not possible to definitively determine the dose, route of administration and best timing to intervene with antioxidants in COVID-19 patients because clinical trials are still ongoing. Until then, hopefully, this review will enable clinicians to understand the impact of micronutrient dietary intake and liver status assessment in COVID-19 patients.

Key Words: SARS-CoV-2; COVID-19; Liver injury; Antioxidants; Nutrients; Treatment

©The Author(s) 2021. Published by Baishideng Publishing Group Inc. All rights reserved.

s/by-nc/4.0/

Manuscript source: Invited manuscript

Specialty type: Nutrition and dietetics

Country/Territory of origin: Serbia

Peer-review report's scientific quality classification
Grade A (Excellent): 0
Grade B (Very good): 0
Grade C (Good): C
Grade D (Fair): 0
Grade E (Poor): 0

Received: January 28, 2021
Peer-review started: January 29, 2021
First decision: March 29, 2021
Revised: April 11, 2021
Accepted: August 17, 2021
Article in press: August 17, 2021
Published online: September 14, 2021

P-Reviewer: Sakina NL
S-Editor: Liu M
L-Editor: A
P-Editor: Li JH

Core Tip: In this review, we highlight the importance of an optimal micronutrient intake and status to boost the immune system, providing special emphasis on liver injury during the coronavirus disease 2019 (commonly known as COVID-19) crisis and focusing on the most relevant nutrients that reduce oxidative stress.

Citation: Ristic-Medic D, Petrovic S, Arsic A, Vucic V. Liver disease and COVID-19: The link with oxidative stress, antioxidants and nutrition. *World J Gastroenterol* 2021; 27(34): 5682-5699
URL: https://www.wjgnet.com/1007-9327/full/v27/i34/5682.htm
DOI: https://dx.doi.org/10.3748/wjg.v27.i34.5682

INTRODUCTION

Since its first appearance in December 2019 in Wuhan, China, coronavirus disease 2019 (COVID-19), caused by the severe acute respiratory syndrome-coronavirus-2 (SARS-CoV-2), has spread swiftly around the world. The angiotensin converting enzyme 2 (ACE2) receptor has been identified as the target vehicle for the virus entrance into the host cell[1]. After binding of SARS-CoV-2, the bioavailability of ACE2 is reduced and angiotensin 2 becomes extremely available to promote oxidative stress cascades and inflammatory responses, which in turn contribute to the pathological host responses and the severity of disease[2,3]. The multiple organ involvement is mainly attributed to the wide distribution of ACE2 receptors[4]. Incidence of liver injury in SARS-CoV-2–infected patients is about 36% (range: 21%–52%)[1].

Any liver damage occurring during the COVID-19 course or treatment, in patients with or without previous liver diseases, could be considered as COVID-19-associated liver injury[4]. The presence of ACE2 receptors in hepatic cholangiocytes has pointed out the possibility of direct infection and active SARS-CoV-2 replication in the liver[5]. Many studies have also shown that COVID-19-associated liver injuries can be induced and/or exacerbated by the inflammatory response, endothelial changes, hypoxia and coagulopathy characteristic of severe disease course[4]. Accordingly, higher rates of liver dysfunction have been detected in critically ill COVID-19 patients[6]. In addition, compatibility between histological alternations and impaired blood flow has been found through the post-mortem analysis of COVID-19 patients' liver samples. Marked derangement of intrahepatic blood vessels, including portal vein fibrosis and wall inflammation, herniated portal vein with activated Kupffer cells containing large necrotic debris, and vascular thrombosis accompanied with high D-dimer (≥ 500 ng/dL) and high platelet count, have been observed[7].

In addition to impaired blood flow, more than a 50% of post-mortem liver samples of COVID-19 patients have shown the presence of large, small or mixed fatty droplets in hepatic parenchyma, a condition known as hepatic steatosis[7]. More recently, the hepatic steatosis, which is commonly associated with comorbidities such as metabolic syndrome, diabetes, obesity and hypertension, has also been recognized as an independent risk factor for severe disease in patients with COVID-19, significantly contributing to greater incidence of critical illness and lethality[8].

POSSIBLE MECHANISMS OF LIVER INJURY IN COVID-19

The main biochemical findings in COVID-19-affected liver are elevated transaminase aspartate aminotransferase (commonly referred to as AST) and alanine transaminase (ALT), which are above referent range in 20.0%-22.5% and 14.6%-20.1% COVID-19 cases, respectively. The increase of AST and ALT is followed by slightly increased total bilirubin in 35% of cases, as well as elevated alkaline phosphatase and gamma-glutamyl transferase in 6.1% and 21.1% of COVID-19 patients, respectively[4]. A meta-analysis of 25 relevant studies showed that COVID-19 survivors accounted for a lower percent of patients and lower increase of these parameters, compared with non-survivors. Moreover, cured patients had lower levels of total bilirubin and lactate dehydrogenase, higher level of albumin and lower proportion of markedly decreased albumin than patients who succumbed to the disease[9].

Until now, proposed mechanisms of COVID-19-associated liver injuries are: (1) Systemic inflammatory response; (2) Hypoxia–reperfusion injury; (3) Drug-induced liver injury; (4) Direct viral infection; and (5) Coexisting chronic liver disease [non-alcoholic fatty liver disease (NAFLD), alcoholic liver disease (commonly referred to as ALD), hepatitis B virus and/or hepatitis C virus infection, hepatocellular carcinoma, *etc.*] (Figure 1).

Systemic inflammatory response is an extensive body inflammatory activity. It begins when SARS-CoV-2 lung infection activates alveolar macrophages and lung epithelial cells to promote massive release of proinflammatory cytokines, particularly interleukin (IL)-6, tumor necrosis factor (TNF), and IL-1β[10]. Acting locally, these cytokines increase permeability of the lung endothelium and support further dissemination of the pathogen, but after reaching the circulation they spread through the body and induce excessive immune response, with deleterious impact on many organs (Figure 1). Proinflammatory cytokines further hyperactivate monocytes, macrophages and T lymphocytes, generating a self-producing loop which results in cytokines overwhelming the system [*i.e.* cytokine storm syndrome (also known as CSS)]. Thus, the cytokine storm can result in multiorgan damage, including to the liver[2].

In addition to CSS, hypoxia, as a consequence of pulmonary failure, is one of the most important factors causing secondary liver injury in COVID-19 patients[11]. Low or no circulation, reduced oxygen supply and lipid accumulation in hepatocytes during shock, and the hypoxic state lead to marked increases in reactive oxygen species (ROS) and their peroxidation products[12]. These hypoxia-induced products are directly involved in hepatic cell damage and death (Figure 1); while, on the other hand, they can act as second messengers to activate redox-sensitive transcription factors. They exaggerate the release of multiple proinflammatory factors and cause hepatocyte apoptosis, followed by further infiltration of inflammatory cells into hepatic tissue and consequent liver damage/failure[13]. However, the main part of liver injury caused by disturbed blood flow occurs during reperfusion, rather than at the time of the hypoxic state[14].

During the course of the COVID-19 epidemic, infected patients have been treated with different antipyretics (*e.g.*, paracetamol, ibuprofen), analgetics (*e.g.*, caffeine), anti-inflammatory agents (*e.g.*, aminosalicylates, corticosteroids), antirheumatics (*e.g.*, chloroquine, hydroxychloroquine) and antiviral agents (*e.g.*, baricitinib, abidol, lopinavir, ritonavir, remdesivir), and many of these drugs are hepatotoxic[15]. However, despite reports on more frequent liver injuries in critically ill COVID-19 patients[11,16,17], there is no evidence on liver dysfunction induced exclusively by drugs in severe SARS-CoV-2 infection.

Abundant expression of ACE2 receptors makes the liver susceptible to direct infection by SARS-CoV-2[1,11]. Up-regulated expression of ACE2 receptors in hepatocytes of COVID-19 patients that suffer from severe hypoxia has also been found. Yet, there is no evidence of viral replication inside hepatocytes. On the other side, the liver harbors the body's largest macrophage pool, indicating that the liver damage may be caused by lymphocytes recognizing infected hepatocytes and consequently inducing a cell death process[1].

OXIDATIVE STRESS, LIVER DISEASES AND COVID-19

Oxidative stress plays an important role in liver diseases. Although both ROS and reactive nitrogen species (RNS) are involved in normal physiological processes, excessive amounts of either can destroy the major cellular components, proteins, lipids, and DNA. Chronic liver diseases are one of the biggest risk factors for liver complications in COVID-19, and commonly these diseases are marked by increased oxidative stress[18]. In chronic liver diseases, function in all types of cells is altered including hepatocyte, stellate, endothelial and Kupffer cells and their impaired gene expression led to increased liver damage[19]. Oxidative stress and mitochondrial dysfunction have a key role in the development of NAFLD. Mitochondrial dysfunction implies not only the formation of ROS and RNS, glutathione (GSH) depletion, and protein oxidation but also inhibition of the β-oxidation of lipids, increased steatosis, and lipid accumulation in hepatocytes[18]. ROS are generated in a lipid-rich environment, leading to lipid peroxidation (LPO) and further production and release of very reactive products of LPO. These LPO products impair the respiratory chain in hepatocytes, leading to impaired oxidative phosphorylation, reduced ATP synthesis, and further increase ROS production[20]. Moreover, ROS, along with products of LPO, induce activation of several cytokines, including TNF-α, IL-6 and IL-8, as well as cell

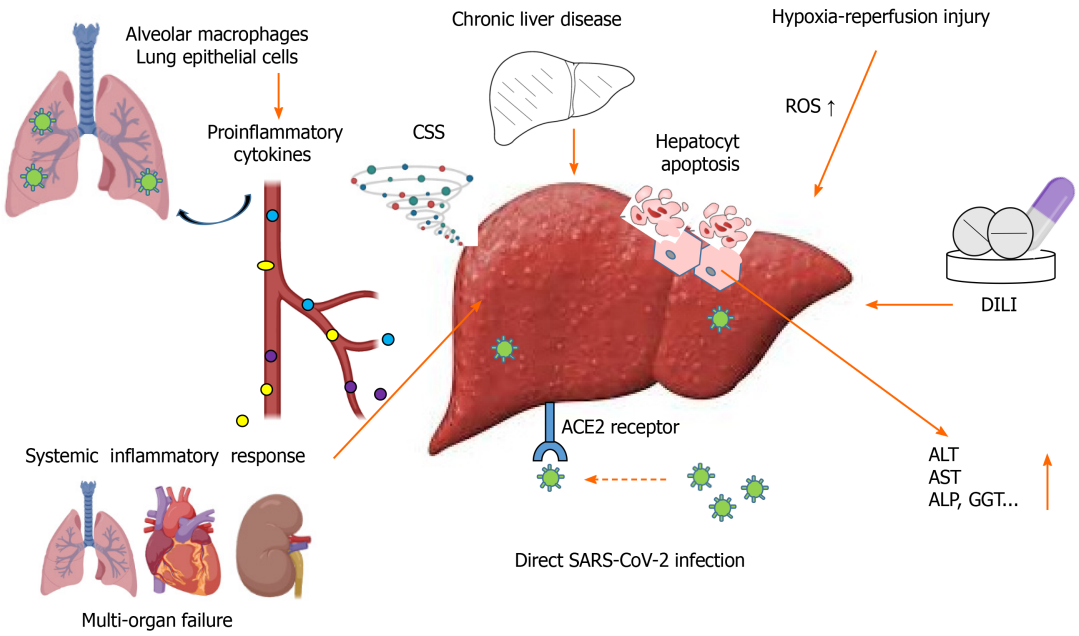


Figure 1 Pathophysiological mechanisms of coronavirus disease 2019-associated liver injuries. Created with BioRender.com. ACE2: Angiotensin converting enzyme 2; ALP: Alkaline phosphatase; ALT: Alanine transaminase; AST: Aspartate aminotransferase; CSS: Cytokine storm syndrome; DILI: Drug-induced liver injury; GGT: Gamma-glutamyl transferase; ROS: Reactive oxygen species.

death and fibrosis[21]. Furthermore, decreased activity of antioxidative enzymes, particularly superoxide dismutase and catalase, and lower level of coenzyme Q10 had been noticed in patients with liver diseases[22].

Most mechanisms of tissue damage due to SARS-CoV-2 infection are directly associated with oxidative stress[23]. Nevertheless, according to our knowledge, there are no studies about the parameters of oxidative stress in patients with SARS-CoV-2 infection. However, Polonikov *et al*[24] recently showed that people who had lower GSH levels before infection developed a more severe form of the disease than those with optimal GSH levels and suggested the crucial role of GSH in determining individual responsiveness to SARS-CoV-2 infection and disease pathogenesis.

In addition to producing $O_2$and H_2O_2, the cell infected by SARS-CoV-2 also produces IL-18 and IL-1β[2]. Besides, T lymphocytes and natural killer (NK) cells produce TNF-α, interferon (IFN)-γ, and IL-1β and stimulate the production of other proinflammatory cytokines, including IL-6 which contributes to the cytokine storm [25]. Additionally, IL-6 acts on liver cells, which in turn increase the synthesis of fibrinogen, plasminogen activator inhibitor-1, and C-reactive protein (CRP). The levels of these molecules rise consistently in COVID-19 patients[26]. Since liver diseases are associated with disturbed redox balance and inflammation, SARS-CoV-2 infection can lead to serious manifestations and lethality in COVID-19 patients.

Considering that the more recent studies recognize oxidative stress as a key player in COVID-19 severity, the free radical scavenging by specific natural and/or synthetic antioxidants would be beneficial in preventing the progression of COVID-19[23]. Among others, some natural plant compounds, such as polyphenols, are known to have anti-inflammatory, antioxidative and antiapoptotic properties[27,28] that make them potentially beneficial in the effort to improve therapies for the most vulnerable SARS-CoV-2-infected patients.

ANTIOXIDANT NUTRIENTS, DIET AND COVID-19

Vitamins and minerals are actively involved in neutralizing the harmful effects of oxidative species that induce liver damages. Their deficiency suppresses immune function and increases to the risk of infection. Patients with liver steatosis have increased LPO markers and proinflammatory cytokines as well as reduced total plasma antioxidant capacity (TAC)[29]. Literature data presented that vitamins (A, C, D, E, B6, B12, and folate), omega-3 fatty acids and minerals such as zinc, selenium, iron, magnesium and copper have important and common roles in maintaining the

immune system[30]. Inadequate dietary intake and/ or status of these micronutrients contribute to a decrease in resistance to infections, and consequently increased disease burden[31] Zhang and Liu[32] pointed out that in the assessment of micronutrients besides vitamins A, D, B, C and omega-3 fatty acids in COVID-19 patients, trace elements (selenium, zinc, and iron) should also be considered. Anti-inflammatory dietary index and dietary TAC are emphasized as a concept of the association between nutrients, dietary sources, eating habits, inflammation, and oxidative stress[33,34]. Omega-3 fatty acids, vitamin A and vitamin C, as well as polyphenols (widely present in plant-based foods) are known nutritional ingredients with anti-inflammatory and antioxidant properties[35]. There is evidence that supplementation with higher daily doses of nutrients (vitamins D, C, E, zinc and omega-3 fatty acids) than recommended might have a beneficial effect in patients with COVID-19, potentially reducing the viral load and the duration of hospitalization[31,36-38]. Oxidative stress contributes to the onset and progression of liver damage through related pathological mechanism[35]. According to a recent study by de Oliveira *et al*[39] NAFLD patients with lower hepatic injury have higher dietary TAC. It suggests a that increased consumption of foods with naturally high TAC leads to reduced production of LPO[39].

Vitamin A

Liver injury is associated with impaired vitamin A homeostasis. Vitamin A plays a role in regulating the production of IL-2 (promoting T cell growth) and proinflammatory TNF-α, which activates the microbial action of macrophages[31]. Also, vitamin A is involved in the phagocytic and oxidative explosive activities of macrophages activated during inflammation[40]. Vitamin A and some other retinoids show important immunomodulatory properties, by increasing the efficiency of actions of type 1 IFNs (*e.g.*, IFN-I), which are important antiviral cytokines[41]. Thus, retinoids promoted increase antiviral responses mediated by IFN-I. There is evidence that activation of retinoid signaling can strongly inhibit coronaviruses[42]. Thus, retinoids could possibly suppress viral replication in COVID-19 patients and may interfere with the cellular uptake of SARS-CoV-2 by inhibiting ACE2[43].

Dietary plant sources of vitamin A are carotenoids, such as β-carotene, while animal sources are rich in retinyl esters. Major food sources of vitamin A are presented in Table 1. β-carotene is known as a scavenger of ROS[44]. It also enhances T lymphocyte response, NK cell activity, and IL-2 production[45]. Liver represents the largest pool of retinyl esters in hepatic stellate cells. In hepatitis C-infected patients, vitamin A deficiency is associated with a lack of response to IFN as antiviral therapy[46]. Further, NAFLD is associated with declining circulating and hepatic retinol levels[30], and patients with NAFLD have higher risk for SARS-CoV-2 infections[47]. Adequate daily intake (about 650 μg/d for women and 750 μg/d for men) and liver storage below 80% in a healthy person are required to keep retinol levels in plasma around 2 μmol/L[45]. Data from 10 western European countries, demonstrated that low levels of vitamin A are associated with the incidence and mortality of COVID-19[41]. Vitamin A deficiency can occur during SARS-CoV-2 infection due to effects on the lung and liver body stores caused by inflammation process[48], suggesting importance of supplementation during this disease[49].

Vitamin D

Vitamin D is involved in several functions in the body, including increasing the oxidative burst potential of macrophages, and biosynthesis of superoxide dismutase. Furthermore, it suppresses the expression of proinflammatory cytokines, while promotes the expression of anti-inflammatory cytokines. In patients with chronic liver diseases, vitamin D deficiency is often reported[50], due to impaired synthesis of vitamin D–binding protein and hydroxylation of vitamin D. In spite of available *in vitro* and *in vivo* evidence, the therapeutic effect of vitamin D in liver disease still remain controversial[51]. Further studies will be required to clarify whether vitamin D have beneficial effects on liver diseases.

Vitamin D is actively involved in antioxidant, immunomodulatory, and antiviral responses. It induces the expression of enzymes involved in the antioxidant defense system. Also, it increases the levels of GSH, and suppresses the expression of NADPH oxidase. This way, vitamin D affects the reduction of oxidative stress and cellular oxidation[2]. Since deficiency of vitamin D is a global health challenge, the need for vitamin D supplementation has been a notable topic of research and discussion during the COVID-19 pandemic. Further, vitamin D deficiency elevates the vulnerability to acute viral respiratory infections[52]. Thus, supplementation with vitamin D enhances the innate immune responses to influenza and viral hepatitis C[53,54]. Vitamin D receptor is also expressed in pulmonary tissue.

Table 1 Ongoing clinical trials of antioxidant supplementation in coronavirus disease 2019 patients

Antioxidants and nutrients	Plant and/or animal sources	Potential target pathways	Recommended dietary intake; Effective dose for respiratory infection)	Registered clinical trials of COVID-19, rial number	Intervention dose	Primary outcome
Vitamin A	Carrots (raw); Cantaloupe; Mango; Salmon; Eggs	Role in immune competence; Immunomodulatory action	900/700 μg M/F	IRCT20200319046819N1[49]	25000 IU vitamin A and 600000 IU vitamin D per day, 300 IU vitamin E twice a week, 2000 mg vitamin C 4 times in a day, amp vitamin B; Soluvit in a day, for 1 wk	Weight, height, BMI; Severity of pulmonary involvement (CT scan); Respiratory support (invasive or non-invasive); WBC, CRP, IL6, TNF-α, IFN-γ, ESR; Body temperature; Organ involvement; Hospital duration; Mortality
Vitamin D	Portabella mushrooms; Dairy products; Eggs; Fish	Maintenance of cell physical barrier integrity; Increased antimicrobial protein production; Anti-inflammatory state; ACE2 and other members of the RAS expression	5- 15 μg; 20-50 μg[60]	NCT04334005[61]	25000 IU vitamin D	Mortality, all-cause mortality within 14 d
				NCT04344041[62]	400000 IU/or 50000 IU	Serum 25(OH)D3 changes during treatment
				NCT04636086[63]	50000 IU vitamin D ; 25000 IU vitamin D ; Days 1-4, 8,15, 22, 29 and 36	Vitamin D serum concentration, clinical improvement, biological markers
				NCT04621058[64]	D deficiency (< 30 ng/mL) 0.532 mg vitamin D (< 40 ng/mL): 0.266 mg vitamin D	Mortality reduction, lent of hospital reduction
				NCT04483635[65]	100000 IU vitamin D tab. baseline + 10000 IU/wk; 16 wk	Change in incidence laboratory-confirmed COVID-19 infection
				NCT04386850[66]	25 μg 25(OH)D3; 2 mo	Hospitalization, disease duration, death, mortality, ventilation
Vitamin C	Oranges; Lemon; Green and red peppers; Tomato; Broccoli; Brussel sprouts; Cabbage; Cauliflower; Spinach; Sweet potato; Winter squash	Antioxidant capacity; Immunomodulatory effects on interferon production; Cytokine production down-regulation	40-80 mg; 6–8 g[77]	NCT04323514[74]	10 g vitamin C infusion	Hospital mortality
				NCT04530539[75]	1000 mg vitamin C	Severity of symptoms
				NCT04682574[76]	30 g/d 2 d with standard treatment	Partial pressure of oxygen in arterial blood to fraction of inspired oxygen
Vitamin E	Sunflower seeds; Nuts; Almonds; Blueberries; Kivi; Broccoli	Antioxidant action; Immunomodulatory effects	7–10 mg; 30–200 mg[82]			
Zinc	Pumpkin and squash seeds nuts; Soybean; Beef; Mollusks; Lamb	Reduces ROS in viral infections; Replication inhibition; Immunomodulatory effects; Antibody production; NK cell activity; Cytokine production by mononuclear cells; Chemotaxis response reduction; Neutrophil respiratory burst reduction	8–14 mg; 30–50 mg[43]	NCT04335084[90]	Zinc, vitamin D, vitamin C 12 wk and hydroxychloroquine for 1 d	Prevention of COVID-19 symptoms recorded in a daily diary
Selenium	Sunflower seeds; Coconut meat; Mollusks; Salmon;	Antioxidant balanceROS balance in inflammatory processes	60–70 mg			

	Turkey; Ham					
Copper	Cashew nuts; Tofu; Mushrooms; Beef; Oyster; Cereals; Roots, tubers: Sweet potato; Quinoa	Role in immunity antimicrobial action due to copper toxicity; Enhance macrophage activity in lung infection	900 μg			
Curcumin	Rhizome of turmeric (*Curcuma longa*)	Antioxidant capacity; Virus-ACE2 interaction reduction; ACE2 level increase; Antiviral activities SARS-CoV-2 protease, spike glycoprotein-RBD and PD-ACE2 binding		IRCT20200611047735N1[114]	160 mg curcumin; 2 wk	Immune responses (IFN-γ, IL-17, IL-4 and TGF-β)
				IRCT20121216011763N46 [115]	1000 mg curcumin + 10 mg piperine twice/day, 2 wk	Clinical symptoms, duration, severity, inflammatory mediators
Silymarin	Milk thistle *(Silybum marianum)*	Antioxidant capacity; Anti-inflammatory; p38 MAPK pathway antiviral		NCT04394208[116]	420 mg/d; 3 divided doses	Clinical outcome duration of mechanical ventilation hospitalization

ACE2: Angiotensin converting enzyme 2; COVID-19: Coronavirus disease 2019; CRP: C-reactive protein; CT: Computed tomography; ESR: Erythrocyte sedimentation rate; IFN-γ: Interferon-gamma; IL: Interleukin; NK: Natural killer; PD: Protease domain; RAS: Renin-angiotensin system; RBD: Receptor binding domain; ROS: Reactive oxygen species; SARS-CoV-2: Severe acute respiratory syndrome-coronavirus-2; tab.: Tablet; TGF-β: Transforming growth factor-beta; TNF-α: Tumor necrosis factor-alpha; WBC: White blood cell.

The immunomodulatory effect of this vitamin are well established, and the supplements seems to be useful in the prevention or treatment of COVID-19. Vitamin D supplementation stimulates the binding of angiotensin-II to the ACE2 receptor, thereby diminishing the number of SARS-CoV-2 particles that can bind to ACE2 receptors and enter the cells[55,56]. Two meta-analysis reported that COVID-19 patients with a low blood vitamin D levels have worse prognoses[57] and that the risk of SARS-CoV-2 infection was significantly increased in patients with low levels of vitamin D[58]. CRP, as marker of inflammation and the cytokine storm, was highly expressed in COVID-19 patients with severe symptoms and correlate with vitamin deficiency[59]. Therefore, vitamin D could act as an adjuvant therapeutic for the treatment of this novel virus[60]. Ongoing clinical trials of vitamin D supplementation [61-66] in patients with COVID-19 are presented in Table 1.

Vitamin C

Vitamin C has a key antioxidant role, maintains cellular redox balance and protects against free radicals (ROS and RNS) during oxidative fight[67]. Also, vitamin C regenerates oxidized vitamin E, GSH and carotenoids, modifies pro-inflammatory cytokine production, and lower blood histamine. The meta-analysis reported that administration of high doses of vitamin C was associated with a reduction in-hospital mortality among patients with severe sepsis[68]. The hepatoprotective property of water soluble vitamin C is attributed to its antioxidant action, Animal models have lent strong evidence that vitamin C supplementation significantly decreases hepatic markers of oxidative stress, hepatocellular ballooning, and inflammation[69]. The prooxidant potential of vitamin C is enhanced with the presence of iron and copper catalysts *in vitro*. Through the Fenton reaction, the antiviral activity of vitamin C

increases, resulting in the formation of hydroxyl radicals from hydrogen peroxide. High intake of vitamin C may be an effective choice in the early treatment of COVID-19[70,71]. Several clinical studies evaluating vitamin C infusion in patients with COVID-19 are in progress (Table 1)[72-76]. It is indisputable that consumption of citrus fruits and vegetables that contain vitamin C is important in supporting the immune system during the COVID-19 pandemic[77].

Vitamin E

Vitamin E is a well-known fat-soluble vitamin, with a high antioxidant potential, which combats free radicals by a chain-breaking effect and protects cells from oxidative damage. Also, vitamin E enhances production of IL-2 and reduces production of prostaglandin E. Thus, vitamin E indirectly saves T cell function[32]. In addition, blood level of vitamin E inversely correlates with the number of products of oxidative stress, which is in line with the degree of liver injury. The potential mechanisms of action of vitamin E against COVID-19 involve the antioxidant properties of vitamin E derivatives that increase the integrity of the cell membrane and improve the adaptive response of the immune system to viral infections of the respiratory tract[78]. Natural isomers of vitamin E, α and γ tocopherols also have ROS scavenging potential. Taking vitamin E with vitamin C or alone, facilitates the removal of free radicals formed in the liver tissue[50]. The results of a meta-analysis[79] revealed that vitamin E supplementation significantly reduced AST, ALT, steatosis, inflammation, and hepatocellular ballooning. Vitamin E is also shown to be effective for normalizing ALT levels in patients with chronic liver injury in doses of 600 mg, while 800 IU is recommended for nondiabetic patients with nonalcoholic steatohepatitis (commonly known as NASH)[80,81]. As reviewed by Sahin *et al*[43], 200 IU vitamin E has no effect on lower respiratory infection but treatment with 800 IJ increases resistance to respiratory infections. Vitamins E and C in combination have been suggested as a useful antioxidant therapy in treating critically ill COVID-19 patients with gastric cardia complications. Major food sources of vitamin E and recommended dietary intake[82] are presented in Table 1.

Vitamins B6 and B12

Vitamin B6 is essential cofactor for metabolism of amino acids, which are structural components of cytokines. It has been shown that higher levels of the active form of vitamin B6, pyridoxal 5'-phosphate (PLP) in plasma with parallel reduction in liver PLP is linked to the lower inflammation rate[32]. Adequate vitamin B_6 (and B_{12}) supplementation in COVID-19 patients has been included in current protocols for the treatment[83], in order to regulate the altered homocysteine metabolism caused by the corona virus. Vitamin B6 administration at higher doses can decrease levels of inflammatory markers such as the TNF-α and IL-6, as well as D-dimer values, preventing coagulopathy in COVID-19 patients[84]. Methylcobalamin supplements may improve clinical deterioration during SARS-CoV-2 infection and decrease COVID-19-related symptoms and organ damage[85]. Combination of vitamin B_{12} (500 μg), vitamin D (1000 IU) and magnesium supplements was also shown to reduce COVID-19 severity symptoms and reduce the need for oxygen and intensive care support[86].

Zinc

Zinc enhances the function of antioxidant proteins and it is well known on its antioxidant activity, including protection against ROS and RNS[43]. It also has a strong anti-inflammatory action, reduces proliferation of proinflammatory Th17 and Th9 cells, and thus decreases release of proinflammatory cytokines such as TNF-α, IL-2 and IL-6. Zinc is potentially considered a major mineral during SARS-CoV-2 infection due to its dual immunomodulatory and antiviral effects. Indirect data suggest that zinc may decrease the activity of ACE2[43]. In NAFLD patients, with comorbidities such as old age, overweight, immune disturbance, diabetes and atherosclerosis, zinc deficiency and low body status may increase the risk of severe COVID-19 illness[34]. However, in the latest meta-analyses of 12 randomized control studies, the decrease of IL-6, increase of IL-2 and no ameliorative effects on TNF-α level due to zinc supplementation has been found[87].

Recent studies have shown that zinc supplementation is able to decrease SARS-CoV-2 infections, due to inhibition of viral uncoating, binding, and replication. It is reported by Finzi *et al*[88] that the clinical respiratory symptoms were improved in COVID-19 patients supplemented with high dose of zinc citrate, zinc gluconate or zinc acetate. Roy *et al*[89] suggested the combined use of curcumin and zinc treatment. The authors speculated that zinc in synergy with curcumin might promote the synthesis of

ionophore complexes, leading to the synchronized and improved antiviral activity. Curcumas exert an antiviral effect by inhibiting entry of the virus into the cell, while zinc inhibits the RNA polymerase. Major food sources of zinc, recommended dietary intake[43], and ongoing study that examines the effect of zinc supplementation in preventing COVID-19 symptoms[90] are presented in Table 1.

Selenium

As a part of selenoproteins, selenium has essential role in regulation of redox reactions, particularly in suppression of ROS produced during oxidative stress. Deficiency of selenium in the diet, concomitant with elevated oxidative stress in the host tissue, may lead to alteration of viral genome. The activity of selenoproteins in antioxidant defense, affects function of host leukocytes and NK cells[43], while selenium deficiency alters immune response by reducing proliferation of T cells, the lymphocyte-mediated toxicity, and NK cell activity[91]. Besides being pointed out as a promising treatment for COVID-19[92], crucial role of selenium in the SARS-CoV-2 emergence and spread has been suggested. Low selenium status in the host affects the viral genome[93], leading to the virus becoming more virulent[92]. Dietary supplementation of selenium can stimulate the activity of cytotoxic effector cells in COVID-19 [94].

The meta-analysis of antioxidants effects in COVID-19 patients revealed decreased mortality and the requirement of mechanical ventilation, but no shorter time in intensive care unit (ICU) due to antioxidant therapies (predominantly based in supplementation of selenium)[95,96]. However, in meta-analysis performed by Allingstrup and Afshari[97], no clear results supporting beneficial effect of selenium supplementation in critically ill patients, including less days on a ventilation and shorter ICU and hospital stay, was shown. The elevated ratio of thromboxane A2 to prostacyclin I2 followed by vasoconstriction and blood coagulation, has been found in animal models deficient in selenium[93]. The same mechanism possible explains the venous thromboembolism in COVID-19 patients with selenium deficiency.

Iron

Among many other physiological roles, iron is known to regulate production and action of cytokines. It is also involved in the generation of ROS in neutrophils, which presents pathogen-killing activity during oxidative burst[31]. In hepatitis C, enhanced hepcidin production favors viral persistence, while the inflammation during SARS-CoV-2 infection might be associated with promotion of hepcidin production. Elevated hepcidin reduces iron uptake in the gut, thus diminishing the effect of iron supplementation. Even more, the sequestration of iron in macrophages, hepatocytes and enterocytes, can be reduced by hepcidin[98]. When SARS-CoV-2 colonizes these cells, the accumulated iron is used for viral replication. Evidence in the context of SARS-CoV, based on the previous studies, indicates that iron is important for viral replication, which is why iron is a promising adjuvant therapeutic agent in treating the SARS-CoV-2 infection[99].

Copper

Being a part of copper/zinc-superoxide dismutase, an enzyme essential for anti-ROS defense, copper accumulates at sites of inflammation and acts as a free-radical scavenger[100]. Due to its activity in maintaining intracellular antioxidant balance, an important role for copper in the inflammatory response has been suggested. In general, it is important for IL-2 production and response, as well as for antibody production. Between 80% and 95% of copper is transported by ceruloplasmin, the levels of which are increased in response to inflammation and infection. Changes in copper homeostasis are a crucial component of respiratory burst. Copper has distinctive antimicrobial properties and helps to destroy a broad range of microorganisms[101]. It competes with zinc for the same absorption site, and the copper deficiency is likely to occur when zinc orally supplemented at high doses. Copper deficiency has been identified in liver disease, in NAFLD associated with insulin resistance, steatosis, and an accelerated progression of NASH[102,103]. Copper has proven to be capable of inactivating different types of viruses, such as influenza A/WSN/33 and recently SARS-CoV-2[104]. SARS-CoV-2 is very sensitive to the copper surface[105], thus copper may be proposed for supplementation during COVID-19 treatment[106].

Magnesium

Magnesium is involved in several functions in the body, including antioxidant

defense. It assists in DNA protection against oxidative damage and diminishes the production of superoxide anion radical[31]. It is hypothesized that a low magnesium status may encourage transition from mild to critical clinical manifestations of the SARS-CoV-2 infection[107]. Magnesium also maintains proper lung function and reduces the risk of airway hyper-reactivity. It has been noticed that magnesium deficiency is related to reduced activity of immune cells and increased levels of IL-6, which is recognized as a key player in the COVID-19 associated cytokine storm[108]. According to a recent study by Tan *et al*[86] , the concomitant oral supplementation of vitamin D, magnesium, and vitamin B12 decreases clinical deterioration in patients with COVID-19. It should be noted that magnesium has a relationship to vitamin D physiology. This suggests that magnesium could contribute to the beneficial effects of vitamin D on COVID-19 outcomes.

Polyphenols

Polyphenols are a large class of bioactive compounds from plants, which exert protective effects against oxidative stress, ultraviolet radiations, and different pathogens. Although there are more than 8000 polyphenolic compounds, all of them contain one or more phenolic rings with hydroxyl groups. The most common polyphenols are flavonoids (including, flavonols, isoflavones, flavones, flavanones, flavan-3-ols and anthocyanins), while nonflavonoids are phenolic acids (gallic, ellagic, chlorogenic or hydoxycinnamic), stilbenes (resveratrol), and lignans[109]. The antiviral activities of some polyphenolic compounds are well documented in the literature. Among the targeted viruses are hepatitis B and C viruses, herpes simplex virus-1, influenza A virus, and Epstein-Barr virus[110]. However, data on their effects on coronaviruses are still sparse.

Polyphenols could exert their anti-SARS-CoV-2 potential in several ways. The first one is inhibition of virus entry into the host cells. Since the spike (S) protein is the sole protein of coronaviruses responsible for its fusion with host cells, it is a meaningful target for antiviral therapies. Several polyphenols have demonstrated the interference with the S protein *in vitro*. In particular, luteolin and quercetin prevented SARS-CoV-2 infection of Vero E6 cells[111], while emodin interfered with the interaction between S protein and its receptor ACE2 in the same cells[112]. Hesperidin has shown a similar effect on the S protein-ACE2 interaction as emodin, and curcumin and several polyphenols from Citrus species also possess a high affinity to S protein[110].

The fusion of S protein and ACE2 could also be prevented by targeting ACE2. Some polyphenols, such as curcumin and resveratrol, down-regulate expression and function of ACE2, thereby affecting severity of COVID-19. Further, Jena *et al*[113] recently published a computational study that showed flavonoids such as catechin and curcumin could bind the ACE2, impeding its interaction with the virus, but these implications have not been confirmed *in vivo* so far. Ongoing studies that examine the effect of curcumin and silymarin supplementation on clinical outcomes in COVID-19 patients[114-116] are presented in Table 1.

Considering that ACE2 is abundantly expressed in the liver, this organ represents a potential target for direct infection and cytotoxicity caused by an active viral replication in hepatic cells[117]. Accordingly, persons with chronic liver disease can have serious consequences on health after SARS-CoV-2 infection, and polyphenols dietary intake could diminish these complications.

Aloe vera is one of the nutraceuticals with the strongest antiviral potential, with quercetin and kaempferol as the most active components against viruses. They both effectively reduce the viral replication of the influenza virus *in vitro*, and also reduce oxidative damage in the lungs and liver of infected mice[118]. Therefore, quercetin and kaempferol are good candidates for preclinical and clinical studies on the liver protection in SARS-CoV-2 infection.

Green tea and coffee are commonly consumed beverages worldwide and important sources of polyphenols. The polyphenols from green tea: Gallocatechin-3-gallate, epigallocatechin gallate, and epicatechingallate are recognized as potential weapon to battle SARS-CoV-2[119]. Moreover, both coffee and green tea have been shown to lower prevalence of metabolic syndrome, type 2 diabetes, and NAFLD[120].

Another mechanism for the beneficial effects of polyphenols in COVID-19 is the suppression of inflammatory response of the host. The above-mentioned cytokine storm, that has been responsible for lethal outcome in many patients worldwide, may be reduced by several polyphenols, including curcumin, resveratrol, emodin, epigallocatechin, gallate, naringenin, apigenin, and kaempferol[121]. All these polyphenols have shown potential to reduce level of proinflammatory cytokines *in vitro* and *in vivo*; although, their beneficial effects against SARS-CoV-2 need to be confirmed in clinical studies.

The severe inflammatory response could also lead to immune-mediated damage of the liver[118]. In line with this, polyphenol mediates the body's fight against the cytokine storm, which would protect the liver as well. Nevertheless, clinical studies on the hepatoprotective potential of different polyphenols in patients with COVID-19 are urgently needed to confirm this hypothesis.

Omega-3 fatty acids

Fatty acids are important players in hepatic lipid metabolism. Omega-3 fatty acids promote fat oxidation and decrease endogenous lipid synthesis by altering gene expression[122]. Patients with liver ALD have low levels of omega-3 fatty acids[123]. Despite genetic and anthropometric factors that could influence their benefits, eicosapentaenoic acid (EPA) and docosahexaenoic acid (DHA) possess a strong anti-inflammatory potential. Thus, a dietary intake of 250 mg/d is recommended for maintaining optimal health[36]. A study by Zheng *et al*[124] showed a statistically significant association between NAFLD and the severity of COVID-19 in obese patients and those with metabolic syndrome and fatty liver, while a study by Mahamid *et al*[47] showed that NAFLD is a significant risk factor for severe COVID-19 independently of both sex or metabolic syndrome. Also, NAFLD patients, in particular those with associated obesity, commonly have an impaired omega-3 fatty acid level and an increased omega-6/omega-3 ratio that can be ameliorated by a nutritional intervention[125,126].

The European Society for Parenteral and Enteral Nutrition has recently declared that omega-3 fatty acids can increase oxygenation in COVID-19 patients[127,128]. Bistrian[129] proposed parenteral supplementation with high doses of EPA and DHA (4–6 g/d), for treatment of patients with severe COVID-19, to inhibit cytokine storm and reduce the inflammation. The possible benefits and risk of omega-3 fatty acid intervention for patients with COVID-19 have been reviewed[130]. The authors concluded that although EPA and DHA may positively affect resolution of inflammation and recovery in patients with COVID-19, excess of EPA and/or DHA can induce LPO of cell membranes, resulting in cell damage due to elevated oxidative stress. This could be prevented by a concomitant supplementation with antioxidants, such as vitamin C and E[30,36]. However, based on the clinical trials that have been completed to date, it is still difficult to determine the optimal dose, route and timing of omega-3 fatty acids administration in COVID-19 patients. Until randomized clinical test data are validated, omega-3 fatty acid supplementation, especially at high doses, must be performed carefully in patients with COVID-19.

Dietary patterns

The COVID-19 pandemic provides nutrition researchers with new opportunities to keep the public, especially those in high-risk groups, constantly informed about the potential benefits of good nutrition and healthy eating habits for prevention and therapy in COVID-19[40,131]. The most vulnerable are the elderly, due to a declined gastrointestinal uptake of micronutrients and macronutrients[132]. Many studies have shown association between a high intake of plant foods, fruit and vegetables and low levels of inflammatory parameters.

There is strong evidence of a favorable impact of the Mediterranean diet on IL-6 and CRP values[133]. Traditionally, the Mediterranean diet is characterized by low intake of simple carbohydrates, high consumption of olive oil, fiber, fresh fruit and vegetables, legumes, whole grains, olives, nuts and fish, moderate consumption of dairy products and poultry, low intake of red meat, many condiments and spices, and regular but moderate wine intake. Oleic acid consumption, which is abundant in olive oil, is also a feature. These components directly affect the synthesis of various antioxidant enzymes and may reduce liver tissue damage generated by oxidative stress[134].

Numerous studies have also shown the anti-inflammatory effect of the dietary approach stop hypertension (referred to as DASH) diet[135]. The ability of nutrients rich in antioxidants (bayberry juice, chocolate, onion, lettuce, and tomato products) to increase TAC in plasma and thereby reduce NAFLD through modifications of oxidative stress is well documented[34]. However, proper nutrition and nutrition support can help battle against COVID-19 by improving immune responses and aiding inflammatory processes[40,136].

CONCLUSION

Foods rich in vitamins, minerals, polyphenols and other bioactive compounds may decrease inflammatory pathway activity and prevent liver damage in COVID-19 patients. An important additional aspect is their ability to control oxidative stress. Antioxidants supplementation during the COVID-19 pandemic crisis should respect nutritional status and serum levels of relevant nutrients in patients. It is essential to recognize nutritional deficiencies in COVID-19 patients, and to intervene to improve their status. Constant public informing about balanced diet and healthy eating habits is important in the prevention of SARS-CoV-2 infection.

REFERENCES

1 **Lizardo-Thiebaud MJ**, Cervantes-Alvarez E, Limon-de la Rosa N, Tejeda-Dominguez F, Palacios-Jimenez M, Méndez-Guerrero O, Delaye-Martinez M, Rodriguez-Alvarez F, Romero-Morales B, Liu WH, Huang CA, Kershenobich D, Navarro-Alvarez N. Direct or Collateral Liver Damage in SARS-CoV-2-Infected Patients. *Semin Liver Dis* 2020; **40**: 321-330 [PMID: 32886936 DOI: 10.1055/s-0040-1715108]

2 **Beltrán-García J**, Osca-Verdegal R, Pallardó FV, Ferreres J, Rodríguez M, Mulet S, Sanchis-Gomar F, Carbonell N, García-Giménez JL. Oxidative Stress and Inflammation in COVID-19-Associated Sepsis: The Potential Role of Anti-Oxidant Therapy in Avoiding Disease Progression. *Antioxidants (Basel)* 2020; **9**: 936 [PMID: 33003552 DOI: 10.3390/antiox9100936]

3 **Laforge M**, Elbim C, Frère C, Hémadi M, Massaad C, Nuss P, Benoliel JJ, Becker C. Tissue damage from neutrophil-induced oxidative stress in COVID-19. *Nat Rev Immunol* 2020; **20**: 515-516 [PMID: 32728221 DOI: 10.1038/s41577-020-0407-1]

4 **Soldo J**, Heni M, Königsrainer A, Häring HU, Birkenfeld AL, Peter A. Increased Hepatic ACE2 Expression in NAFL and Diabetes-A Risk for COVID-19 Patients? *Diabetes Care* 2020; **43**: e134-e136 [PMID: 32753456 DOI: 10.2337/dc20-1458]

5 **Nardo AD**, Schneeweiss-Gleixner M, Bakail M, Dixon ED, Lax SF, Trauner M. Pathophysiological mechanisms of liver injury in COVID-19. *Liver Int* 2021; **41**: 20-32 [PMID: 33190346 DOI: 10.1111/liv.14730]

6 **Morgan K**, Samuel K, Vandeputte M, Hayes PC, Plevris JN. SARS-CoV-2 Infection and the Liver. *Pathogens* 2020; **9**: 430 [PMID: 32486188 DOI: 10.3390/pathogens9060430]

7 **Zhang C**, Shi L, Wang FS. Liver injury in COVID-19: management and challenges. *Lancet Gastroenterol Hepatol* 2020; **5**: 428-430 [PMID: 32145190 DOI: 10.1016/S2468-1253(20)30057-1]

8 **Sonzogni A**, Previtali G, Seghezzi M, Grazia Alessio M, Gianatti A, Licini L, Morotti D, Zerbi P, Carsana L, Rossi R, Lauri E, Pellegrinelli A, Nebuloni M. Liver histopathology in severe COVID 19 respiratory failure is suggestive of vascular alterations. *Liver Int* 2020; **40**: 2110-2116 [PMID: 32654359 DOI: 10.1111/liv.14601]

9 **Palomar-Lever A**, Barraza G, Galicia-Alba J, Echeverri-Bolaños M, Escarria-Panesso R, Padua-Barrios J, Halabe-Cherem J, Hernandez-Molina G, Chargoy-Loustaunau TN, Kimura-Hayama E. Hepatic steatosis as an independent risk factor for severe disease in patients with COVID-19: A computed tomography study. *JGH Open* 2020; **4**: 1102-1107 [PMID: 32838045 DOI: 10.1002/jgh3.12395]

10 **Ye L**, Chen B, Wang Y, Yang Y, Zeng J, Deng G, Deng Y, Zeng F. Prognostic value of liver biochemical parameters for COVID-19 mortality. *Ann Hepatol* 2021; **21**: 100279 [PMID: 33157267 DOI: 10.1016/j.aohep.2020.10.007]

11 **Zhong P**, Xu J, Yang D, Shen Y, Wang L, Feng Y, Du C, Song Y, Wu C, Hu X, Sun Y. COVID-19-associated gastrointestinal and liver injury: clinical features and potential mechanisms. *Signal Transduct Target Ther* 2020; **5**: 256 [PMID: 33139693 DOI: 10.1038/s41392-020-00373-7]

12 **Feng G**, Zheng KI, Yan QQ, Rios RS, Targher G, Byrne CD, Poucke SV, Liu WY, Zheng MH. COVID-19 and Liver Dysfunction: Current Insights and Emergent Therapeutic Strategies. *J Clin Transl Hepatol* 2020; **8**: 18-24 [PMID: 32274342 DOI: 10.14218/JCTH.2020.00018]

13 **Huang C**, Li Q, Xu W, Chen L. Molecular and cellular mechanisms of liver dysfunction in COVID-19. *Discov Med* 2020; **30**: 107-112 [PMID: 33382966]

14 **Henrion J**. Ischemia/reperfusion injury of the liver: pathophysiologic hypotheses and potential relevance to human hypoxic hepatitis. *Acta Gastroenterol Belg* 2000; **63**: 336-347 [PMID: 11233516]

15 **Olry A**, Meunier L, Délire B, Larrey D, Horsmans Y, Le Louët H. Drug-Induced Liver Injury and COVID-19 Infection: The Rules Remain the Same. *Drug Saf* 2020; **43**: 615-617 [PMID: 32514859 DOI: 10.1007/s40264-020-00954-z]

16 **Boeckmans J**, Rodrigues RM, Demuyser T, Piérard D, Vanhaecke T, Rogiers V. COVID-19 and drug-induced liver injury: a problem of plenty or a petty point? *Arch Toxicol* 2020; **94**: 1367-1369 [PMID: 32266419 DOI: 10.1007/s00204-020-02734-1]

17 **Fan Z**, Chen L, Li J, Cheng X, Yang J, Tian C, Zhang Y, Huang S, Liu Z, Cheng J. Clinical Features of COVID-19-Related Liver Functional Abnormality. *Clin Gastroenterol Hepatol* 2020; **18**: 1561-1566 [PMID: 32283325 DOI: 10.1016/j.cgh.2020.04.002]

18 **Grattagliano I**, de Bari O, Bernardo TC, Oliveira PJ, Wang DQ, Portincasa P. Role of mitochondria in nonalcoholic fatty liver disease--from origin to propagation. *Clin Biochem* 2012; **45**: 610-618 [PMID: 22484459 DOI: 10.1016/j.clinbiochem.2012.03.024]

19 **Zhu R**, Wang Y, Zhang L, Guo Q. Oxidative stress and liver disease. *Hepatol Res* 2012; **42**: 741-749 [PMID: 22489668 DOI: 10.1111/j.1872-034X.2012.00996.x]

20 **Ucar F**, Sezer S, Erdogan S, Akyol S, Armutcu F, Akyol O. The relationship between oxidative stress and nonalcoholic fatty liver disease: Its effects on the development of nonalcoholic steatohepatitis. *Redox Rep* 2013; **18**: 127-133 [PMID: 23743495 DOI: 10.1179/1351000213Y.0000000050]

21 **Rolo AP**, Teodoro JS, Palmeira CM. Role of oxidative stress in the pathogenesis of nonalcoholic steatohepatitis. *Free Radic Biol Med* 2012; **52**: 59-69 [PMID: 22064361 DOI: 10.1016/j.freeradbiomed.2011.10.003]

22 **Yesilova Z**, Yaman H, Oktenli C, Ozcan A, Uygun A, Cakir E, Sanisoglu SY, Erdil A, Ates Y, Aslan M, Musabak U, Erbil MK, Karaeren N, Dagalp K. Systemic markers of lipid peroxidation and antioxidants in patients with nonalcoholic Fatty liver disease. *Am J Gastroenterol* 2005; **100**: 850-855 [PMID: 15784031 DOI: 10.1111/j.1572-0241.2005.41500.x]

23 **Schönrich G**, Raftery MJ, Samstag Y. Devilishly radical NETwork in COVID-19: Oxidative stress, neutrophil extracellular traps (NETs), and T cell suppression. *Adv Biol Regul* 2020; **77**: 100741 [PMID: 32773102 DOI: 10.1016/j.jbior.2020.100741]

24 **Polonikov A**. Endogenous Deficiency of Glutathione as the Most Likely Cause of Serious Manifestations and Death in COVID-19 Patients. *ACS Infect Dis* 2020; **6**: 1558-1562 [PMID: 32463221 DOI: 10.1021/acsinfecdis.0c00288]

25 **Libby P**, Lüscher T. COVID-19 is, in the end, an endothelial disease. *Eur Heart J* 2020; **41**: 3038-3044 [PMID: 32882706 DOI: 10.1093/eurheartj/ehaa623]

26 **Wright FL**, Vogler TO, Moore EE, Moore HB, Wohlauer MV, Urban S, Nydam TL, Moore PK, McIntyre RC Jr. Fibrinolysis Shutdown Correlation with Thromboembolic Events in Severe COVID-19 Infection. *J Am Coll Surg* 2020; **231**: 193-203.el [PMID: 32422349 DOI: 10.1016/j.jamcollsurg.2020.05.007]

27 **Vučić V**, Grabež M, Trchounian A, Arsić A. Composition and Potential Health Benefits of Pomegranate: A Review. *Curr Pharm Des* 2019; **25**: 1817-1827 [PMID: 31298147 DOI: 10.2174/1381612825666190708183941]

28 **Petrovic S**, Arsic A, Ristic-Medic D, Cvetkovic Z, Vucic V. Lipid Peroxidation and Antioxidant Supplementation in Neurodegenerative Diseases: A Review of Human Studies. *Antioxidants (Basel)* 2020; **9**: 1128 [PMID: 33202952 DOI: 10.3390/antiox9111128]

29 **Coelho JM**, Cansanção K, Perez RM, Leite NC, Padilha P, Ramalho A, Peres W. Association between serum and dietary antioxidant micronutrients and advanced liver fibrosis in non-alcoholic fatty liver disease: an observational study. *PeerJ* 2020; **8**: e9838 [PMID: 32995080 DOI: 10.7717/peerj.9838]

30 **Calder PC**, Carr AC, Gombart AF, Eggersdorfer M. Optimal Nutritional Status for a Well-Functioning Immune System Is an Important Factor to Protect against Viral Infections. *Nutrients* 2020; **12**: 1181 [PMID: 32340216 DOI: 10.3390/nu12041181]

31 **Gombart AF**, Pierre A, Maggini S. A Review of Micronutrients and the Immune System-Working in Harmony to Reduce the Risk of Infection. *Nutrients* 2020; **12**: 236 [PMID: 31963293 DOI: 10.3390/nu12010236]

32 **Zhang L**, Liu Y. Potential interventions for novel coronavirus in China: A systematic review. *J Med Virol* 2020; **92**: 479-490 [PMID: 32052466 DOI: 10.1002/jmv.25707]

33 **Shivappa N**, Steck SE, Hurley TG, Hussey JR, Hébert JR. Designing and developing a literature-derived, population-based dietary inflammatory index. *Public Health Nutr* 2014; **17**: 1689-1696 [PMID: 23941862 DOI: 10.1017/S1368980013002115]

34 **Sohouli MH**, Fatahi S, Sayyari A, Olang B, Shidfar F. Associations between dietary total antioxidant capacity and odds of non-alcoholic fatty liver disease (NAFLD) in adults: a case-control study. *J Nutr Sci* 2020; **9**: e48 [PMID: 33244400 DOI: 10.1017/jns.2020.39]

35 **Iddir M**, Brito A, Dingeo G, Fernandez Del Campo SS, Samouda H, La Frano MR, Bohn T. Strengthening the Immune System and Reducing Inflammation and Oxidative Stress through Diet and Nutrition: Considerations during the COVID-19 Crisis. *Nutrients* 2020; **12**: 1562 [PMID: 32471251 DOI: 10.3390/nu12061562]

36 **Calder PC**. Nutrition, immunity and COVID-19. *BMJ Nutr Prev Health* 2020; **3**: 74-92 [PMID: 33230497 DOI: 10.1136/bmjnph-2020-000085]

37 **Hemilä H**, Chalker E. Vitamin C Can Shorten the Length of Stay in the ICU: A Meta-Analysis. *Nutrients* 2019; **11**: 708 [PMID: 30934660 DOI: 10.3390/nu11040708]

38 **Grant WB**, Lahore H, McDonnell SL, Baggerly CA, French CB, Aliano JL, Bhattoa HP. Evidence that Vitamin D Supplementation Could Reduce Risk of Influenza and COVID-19 Infections and Deaths. *Nutrients* 2020; **12**: 988 [PMID: 32252338 DOI: 10.3390/nu12040988]

39 **de Oliveira DG**, de Faria Ghetti F, Moreira APB, Hermsdorff HHM, de Oliveira JM, de Castro Ferreira LEVV. Association between dietary total antioxidant capacity and hepatocellular ballooning in nonalcoholic steatohepatitis: a cross-sectional study. *Eur J Nutr* 2019; **58**: 2263-2270 [PMID: 30019089 DOI: 10.1007/s00394-018-1776-0]

40 **Budhwar S**, Sethi K, Chakraborty M. A Rapid Advice Guideline for the Prevention of Novel Coronavirus Through Nutritional Intervention. *Curr Nutr Rep* 2020; **9**: 119-128 [PMID: 32578027

DOI: 10.1007/s13668-020-00325-1]
41 **Galmés S**, Serra F, Palou A. Current State of Evidence: Influence of Nutritional and Nutrigenetic Factors on Immunity in the COVID-19 Pandemic Framework. *Nutrients* 2020; **12**: 2738 [PMID: 32911778 DOI: 10.3390/nu12092738]
42 **Trasino SE**. A role for retinoids in the treatment of COVID-19? *Clin Exp Pharmacol Physiol* 2020; **47**: 1765-1767 [PMID: 32459003 DOI: 10.1111/1440-1681.13354]
43 **Sahin E**, Orhan C, Uckun FM, Sahin K. Clinical Impact Potential of Supplemental Nutrients as Adjuncts of Therapy in High-Risk COVID-19 for Obese Patients. *Front Nutr* 2020; **7**: 580504 [PMID: 33195370 DOI: 10.3389/fnut.2020.580504]
44 **Stipp M**. SARS-CoV-2: Micronutrient Optimization in Supporting Host Immunocompetence. *Int J Clin Case Rep Rev IJCCR* 2020; **2** [DOI: 10.31579/2690-4861/024]
45 **Saeed A**, Dull aart RPF, Schreuder TCMA, Blokzijl H, Faber KN. Disturbed Vitamin A Metabolism in Non-Alcoholic Fatty Liver Disease (NAFLD). *Nutrients* 2017; **10** [PMID: 29286303 DOI: 10.3390/nu10010029]
46 **Bitetto D**, Bortolotti N, Falleti E, Vescovo S, Fabris C, Fattovich G, Cussigh A, Cmet S, Fornasiere E, Ceriani E, Pirisi M, Toniutto P. Vitamin A deficiency is associated with hepatitis C virus chronic infection and with unresponsiveness to interferon-based antiviral therapy. *Hepatology* 2013; **57**: 925-933 [PMID: 23213086 DOI: 10.1002/hep.26186]
47 **Mahamid M**, Nseir W, Khoury T, Mahamid B, Nubania A, Sub-Laban K, Schifter J, Mari A, Sbeit W, Goldin E. Nonalcoholic fatty liver disease is associated with COVID-19 severity independently of metabolic syndrome: a retrospective case-control study. *Eur J Gastroenterol Hepatol* 2020; epub ahead of print [PMID: 32868652 DOI: 10.1097/MEG.0000000000001902]
48 **Stephensen CB**, Lietz G. Vitamin A in resistance to and recovery from infection: relevance to SARS-CoV2. *Br J Nutr* 2021; 1-10 [PMID: 33468263 DOI: 10.1017/S0007114521000246]
49 **Bitarafan S**. Impact of vitamin B, A, D, E, C supplementation on improvement and mortality rate in patients with COVID-19 admitted in intensive care unit. [accessed 2020 Dec 15]. In: IRCT.ir/trial/ [Internet]. Teheran: Iranian Registry of Clinical Trails. Available from: https://www.irct.ir/trial/46838 IRCT registration number: IRCT20200319046819N1
50 **Kozeniecki M**, Ludke R, Kerner J, Patterson B. Micronutrients in Liver Disease: Roles, Risk Factors for Deficiency, and Recommendations for Supplementation. *Nutr Clin Pract* 2020; **35**: 50-62 [PMID: 31840874 DOI: 10.1002/ncp.10451]
51 **Elangovan H**, Chahal S, Gunton JE. Vitamin D in liver disease: Current evidence and potential directions. *Biochim Biophys Acta Mol Basis Dis* 2017; **1863**: 907-916 [PMID: 28064017 DOI: 10.1016/j.bbadis.2017.01.001]
52 **Alexander J**, Tinkov A, Strand TA, Alehagen U, Skalny A, Aaseth J. Early Nutritional Interventions with Zinc, Selenium and Vitamin D for Raising Anti-Viral Resistance Against Progressive COVID-19. *Nutrients* 2020; **12**: 2358 [PMID: 32784601 DOI: 10.3390/nu12082358]
53 **Zdrenghea MT**, Makrinioti H, Bagacean C, Bush A, Johnston SL, Stanciu LA. Vitamin D modulation of innate immune responses to respiratory viral infections. *Rev Med Virol* 2017; **27** [PMID: 27714929 DOI: 10.1002/rmv.1909]
54 **Abu-Mouch S**, Fireman Z, Jarchovsky J, Zeina AR, Assy N. Vitamin D supplementation improves sustained virologic response in chronic hepatitis C (genotype 1)-naïve patients. *World J Gastroenterol* 2011; **17**: 5184-5190 [PMID: 22215943 DOI: 10.3748/wjg.v17.i47.5184]
55 **Rafiullah M**. Can a Combination of AT1R Antagonist and Vitamin D Treat the Lung Complication of COVID-19? *Am J Med Sci* 2020; **360**: 338-341 [PMID: 32736832 DOI: 10.1016/j.amjms.2020.07.018]
56 **Lanham-New SA**, Webb AR, Cashman KD, Buttriss JL, Fallowfield JL, Masud T, Hewison M, Mathers JC, Kiely M, Welch AA, Ward KA, Magee P, Darling AL, Hill TR, Greig C, Smith CP, Murphy R, Leyland S, Bouillon R, Ray S, Kohlmeier M. Vitamin D and SARS-CoV-2 virus/COVID-19 disease. *BMJ Nutr Prev Health* 2020; **3**: 106-110 [PMID: 33230499 DOI: 10.1136/bmjnph-2020-000089]
57 **Ghasemian R**, Shamshiria A, Heydari, K; Malekan M; Alizadeh-Navaei R; Ebrahimzadeh MA; Jafarpour H; Shahmirzadi AR; Khodabandeh M; Seyfari B; Motamedzadeh A, Dadgostar E, Aalinezhad M, Sedaghat M, Behnamfar N, Asadi A, Zarandi B, Razzaghi N, Vahid Yaghoubi Naei V, Hessami A, Azizi A, Mohseni R, Skamsirian D. The Role of Vitamin D in The Age of COVID-19: A Systematic Review and Meta-Analysis Along with an Ecological Approach. 2020 Preprint. Available from: medRxiv: 20123554 [DOI: 10.1101/2020.06.05.20123554]
58 **Munshi R**, Hussein MH, Toraih EA, Elshazli RM, Jardak C, Sultana N, Youssef MR, Omar M, Attia AS, Fawzy MS, Killackey M, Kandil E, Duchesne J. Vitamin D insufficiency as a potential culprit in critical COVID-19 patients. *J Med Virol* 2021; **93**: 733-740 [PMID: 32716073 DOI: 10.1002/jmv.26360]
59 **Daneshkhah A**, Eshein A, Subramanian H, Roy HK, Backman V. The role of vitamin d in suppressing cytokine storm in COVID-19 patients and associated mortality. 2020 Preprint. Available from: medRxiv: 20058578 [DOI: 10.1101/2020.04.08.20058578]
60 **McCartney DM**, Byrne DG. Optimisation of Vitamin D Status for Enhanced Immuno-protection Against Covid-19. *Ir Med J* 2020; **113**: 58 [PMID: 32268051]
61 **Garzón MC**. Vitamin D on Prevention and Treatment of COVID-19 (COVITD-19). [accessed 2020 Dec 15]. In: ClinicalTrials.gov [Internet]. Bethesda (MD): U.S. National Library of Medicine. Available from: https://clinicaltrials.gov/ct2/show/NCT04334005 ClinicalTrials.gov Identifier:

NCT04334005
62 **Annweiler C**. COVID-19 and Vitamin D Supplementation: a Multicenter Randomized Controlled Trial of High Dose Versus Standard Dose Vitamin D3 in High-risk COVID-19 Patients (CoVitTrial). [accessed 2020 Dec 15]. In: ClinicalTrials.gov [Internet]. Bethesda (MD) U.S.National Library of Medicine. Available from: https://clinicaltrials.gov/ct2/show/NCT04344041 ClinicalTrials.gov Identifier: NCT04344041
63 **Rousseau AF**. Effect of Vitamin D on Hospitalized Adults With COVID-19 Infection. [accessed 2020 Dec 15]. In: ClinicalTrials.gov [Internet]. Bethesda (MD): U.S. National Library of Medicine. Available from: https://clinicaltrials.gov/ct2/show/NCT04636086 ClinicalTrials.gov Identifier: NCT04636086
64 **Duran-Cantolla C**. Efficacy of Vitamin D Treatment in Mortality Reduction Due to COVID-19. [accessed 2020 Dec 15]. In: ClinicalTrials.gov [Internet]. Bethesda (MD): U.S. National Library of Medicine. Available from: https://clinicaltrials.gov/ct2/show/NCT04621058 ClinicalTrials.gov Identifier: NCT04621058
65 **Ducharme FM**. PRevention of COVID-19 With Oral Vitamin D Supplemental Therapy in Essential health Care Teams (PROTECT). [accessed 2020 Dec 15]. In: ClinicalTrials.gov [Internet]. Bethesda (MD): U.S. National Library of Medicine. Available from: https://clinicaltrials.gov/ct2/show/NCT04483635 ClinicalTrials.gov Identifier: NCT04483635
66 **Sahraian M**. Oral 25-hydroxyvitamin D3 and COVID-19. [accessed 2020 Dec 15]. In: ClinicalTrials.gov [Internet]. Bethesda (MD): U.S. National Library of Medicine. Available from: https://clinicaltrials.gov/ct2/show/NCT04386850 ClinicalTrials.gov Identifier: NCT04386850
67 **Shakoor H**, Feehan J, Al Dhaheri AS, Ali HI, Platat C, Ismail LC, Apostolopoulos V, Stojanovska L. Immune-boosting role of vitamins D, C, E, zinc, selenium and omega-3 fatty acids: Could they help against COVID-19? *Maturitas* 2021; **143**: 1-9 [PMID: 33308613 DOI: 10.1016/j.maturitas.2020.08.003]
68 **Carr AC**. Vitamin C administration in the critically ill: a summary of recent meta-analyses. *Crit Care* 2019; **23**: 265 [PMID: 31362775 DOI: 10.1186/s13054-019-2538-y]
69 **Rezazadeh A**, Yazdanparast R, Molaei M. Amelioration of diet-induced nonalcoholic steatohepatitis in rats by Mn-salen complexes *via* reduction of oxidative stress. *J Biomed Sci* 2012; **19**: 26 [PMID: 22375551 DOI: 10.1186/1423-0127-19-26]
70 **Erol A**. High-dose intravenous vitamin C treatment for COVID-19. 2020 Preprint. Available from: OSF Preprints [DOI: 10.31219/osf.io/p7ex8]
71 **Holford P**, Carr AC, Jovic TH, Ali SR, Whitaker IS, Marik PE, Smith AD. Vitamin C-An Adjunctive Therapy for Respiratory Infection, Sepsis and COVID-19. *Nutrients* 2020; **12**: 3760 [PMID: 33297491 DOI: 10.3390/nu12123760]
72 **Liu F**, Zhu Y, Zhang J, Li Y, Peng Z. Intravenous high-dose vitamin C for the treatment of severe COVID-19: study protocol for a multicentre randomised controlled trial. *BMJ Open* 2020; **10**: e039519 [PMID: 32641343 DOI: 10.1136/bmjopen-2020-039519]
73 **Waqas Khan HM**, Parikh N, Megala SM, Predeteanu GS. Unusual Early Recovery of a Critical COVID-19 Patient After Administration of Intravenous Vitamin C. *Am J Case Rep* 2020; **21**: e925521 [PMID: 32709838 DOI: 10.12659/AJCR.925521]
74 **Corrao S**. Use of Ascorbic Acid in Patients with COVID 19. [accessed 2020 Dec 15]. In: ClinicalTrials.gov [Internet]. Bethesda (MD): U.S. National Library of Medicine. Available from: https://clinicaltrials.gov/ct2/show/NCT04323514 ClinicalTrials.gov Identifier: NCT04323514
75 **Fogleman C**. The Effect of Melatonin and Vitamin C on COVID-19. [accessed 2020 Dec 15]. In: ClinicalTrials.gov [Internet]. Bethesda (MD): U.S. National Library of Medicine. Available from: https://clinicaltrials.gov/ct2/show/NCT04530539 ClinicalTrials.gov Identifier: NCT04530539
76 **Hafeez MM**. Role of Mega Dose of Vitamin C in Critical COVID-19 Patients. [accessed 2020 Dec 15]. In: ClinicalTrials.gov [Internet]. Bethesda (MD): U.S. National Library of Medicine. Available from: https://clinicaltrials.gov/ct2/show/NCT04682574 ClinicalTrials.gov Identifier: NCT04682574
77 **Hemilä H**. Vitamin C and Infections. *Nutrients* 2017; **9**: 339 [PMID: 28353648 DOI: 10.3390/nu9040339]
78 **Jovic TH**, Ali SR, Ibrahim N, Jessop ZM, Tarassoli SP, Dobbs TD, Holford P, Thornton CA, Whitaker IS. Could Vitamins Help in the Fight Against COVID-19? *Nutrients* 2020; **12**: 2550 [PMID: 32842513 DOI: 10.3390/nu12092550]
79 **Sato K**, Gosho M, Yamamoto T, Kobayashi Y, Ishii N, Ohashi T, Nakade Y, Ito K, Fukuzawa Y, Yoneda M. Vitamin E has a beneficial effect on nonalcoholic fatty liver disease: a meta-analysis of randomized controlled trials. *Nutrition* 2015; **31**: 923-930 [PMID: 26059365 DOI: 10.1016/j.nut.2014.11.018]
80 **Ji HF**, Sun Y, Shen L. Effect of vitamin E supplementation on aminotransferase levels in patients with NAFLD, NASH, and CHC: results from a meta-analysis. *Nutrition* 2014; **30**: 986-991 [PMID: 24976430 DOI: 10.1016/j.nut.2014.01.016]
81 **Kawanaka M**, Mahmood S, Niiyama G, Izumi A, Kamei A, Ikeda H, Suehiro M, Togawa K, Sasagawa T, Okita M, Nakamura H, Yodoi J, Yamada G. Control of oxidative stress and reduction in biochemical markers by Vitamin E treatment in patients with nonalcoholic steatohepatitis: a pilot study. *Hepatol Res* 2004; **29**: 39-41 [PMID: 15135345 DOI: 10.1016/j.hepres.2004.02.002]
82 **Hemilä H**. Vitamin E administration may decrease the incidence of pneumonia in elderly males. *Clin Interv Aging* 2016; **11**: 1379-1385 [PMID: 27757026 DOI: 10.2147/CIA.S114515]
83 **Shakoor H**, Feehan J, Mikkelsen K, Al Dhaheri AS, Ali HI, Platat C, Ismail LC, Stojanovska L,

Apostolopoulos V. Be well: A potential role for vitamin B in COVID-19. *Maturitas* 2021; **144**: 108-111 [PMID: 32829981 DOI: 10.1016/j.maturitas.2020.08.007]

84 **Desbarats J**. Pyridoxal 5'-phosphate to mitigate immune dysregulation and coagulopathy in COVID-19. 2020 Preprint. Available from: Preprints: 202005.0144 [DOI: 10.20944/preprints202005.0144.v1]

85 **dos Santos LMJ**. Can vitamin B12 be an adjuvant to COVID-19 treatment? *GSC Bio Pharm Sci* 2020; **11**: 01-05 [DOI: 10.30574/gscbps.2020.11.3.0155]

86 **Tan CW**, Ho LP, Kalimuddin S, Cherng BPZ, Teh YE, Thien SY, Wong HM, Tern PJW, Chandran M, Chay JWM, Nagarajan C, Sultana R, Low JGH, Ng HJ. Cohort study to evaluate the effect of vitamin D, magnesium, and vitamin B_{12} in combination on progression to severe outcomes in older patients with coronavirus (COVID-19). *Nutrition* 2020; **79-80**: 111017 [PMID: 33039952 DOI: 10.1016/j.nut.2020.111017]

87 **Faghfouri AH**, Baradaran B, Khabbazi A, Khaje Bishak Y, Zarezadeh M, Tavakoli-Rouzbehani OM, Faghfuri E, Payahoo L, Alipour M, Alipour B. Invited Letter to Editor in response to Profiling Inflammatory Cytokines Following Zinc Supplementation: A Systematic Review and Meta-analysis of Randomized Controlled Trials. *Br J Nutr* 2021; 1-5 [PMID: 33762049 DOI: 10.1017/S0007114521001070]

88 **Finzi E**. Treatment of SARS-CoV-2 with high dose oral zinc salts: A report on four patients. *Int J Infect Dis* 2020; **99**: 307-309 [PMID: 32522597 DOI: 10.1016/j.ijid.2020.06.006]

89 **Roy A**, Sarkar B, Celik C, Ghosh A, Basu U, Jana M, Jana A, Gencay A, Can Sezgin G, Ildiz N, Dam P, Mandal AK, Ocsoy I. Can concomitant use of zinc and curcumin with other immunity-boosting nutraceuticals be the arsenal against COVID-19? *Phytother Res* 2020; **34**: 2425-2428 [PMID: 32488956 DOI: 10.1002/ptr.6766]

90 **Hazan S**. A Study of Hydroxychloroquine, Vitamin C, Vitamin D, and Zinc for the Prevention of COVID-19 Infection (HELPCOVID-19). [accessed 2020 Dec 15]. In: ClinicalTrials.gov [Internet]. Bethesda (MD): U.S. National Library of Medicine. Available from: https://clinicaltrials.gov/ct2/show/NCT04335084 ClinicalTrials.gov Identifier: NCT04335084

91 **Ivory K**, Prieto E, Spinks C, Armah CN, Goldson AJ, Dainty JR, Nicoletti C. Selenium supplementation has beneficial and detrimental effects on immunity to influenza vaccine in older adults. *Clin Nutr* 2017; **36**: 407-415 [PMID: 26803169 DOI: 10.1016/j.clnu.2015.12.003]

92 **Zhang J**, Taylor EW, Bennett K, Saad R, Rayman MP. Association between regional selenium status and reported outcome of COVID-19 cases in China. *Am J Clin Nutr* 2020; **111**: 1297-1299 [PMID: 32342979 DOI: 10.1093/ajcn/nqaa095]

93 **Bae M**, Kim H. Mini-Review on the Roles of Vitamin C, Vitamin D, and Selenium in the Immune System against COVID-19. *Molecules* 2020; **25**: 5346 [PMID: 33207753 DOI: 10.3390/molecules25225346]

94 **Kieliszek M**, Lipinski B. Selenium supplementation in the prevention of coronavirus infections (COVID-19). *Med Hypotheses* 2020; **143**: 109878 [PMID: 32464491 DOI: 10.1016/j.mehy.2020.109878]

95 **Park SJ**, Yim GW, Paik H, Lee N, Lee S, Lee M, Kim HS. Efficacy and safety of intravenous administration of high-dose selenium for preventing chemotherapy-induced peripheral neuropathy in platinum-sensitive recurrent ovarian, fallopian or primary peritoneal cancer: study protocol for a phase III, double-blind, randomized study. *J Gynecol Oncol* 2021; epub ahead of print [PMID: 34132071 DOI: 10.3802/jgo.2021.32.e73]

96 **Zhao Y**, Yang M, Mao Z, Yuan R, Wang L, Hu X, Zhou F, Kang H. The clinical outcomes of selenium supplementation on critically ill patients: A meta-analysis of randomized controlled trials. *Medicine (Baltimore)* 2019; **98**: e15473 [PMID: 31096444 DOI: 10.1097/MD.0000000000015473]

97 **Allingstrup M**, Afshari A. Selenium supplementation for critically ill adults. *Cochrane Database Syst Rev* 2015; CD003703 [PMID: 26214143 DOI: 10.1002/14651858.CD003703.pub3]

98 **Camaschella C**, Nai A, Silvestri L. Iron metabolism and iron disorders revisited in the hepcidin era. *Haematologica* 2020; **105**: 260-272 [PMID: 31949017 DOI: 10.3324/haematol.2019.232124]

99 **Liu W**, Zhang S, Nekhai S, Liu S. Depriving Iron Supply to the Virus Represents a Promising Adjuvant Therapeutic Against Viral Survival. *Curr Clin Microbiol Rep* 2020; 1-7 [PMID: 32318324 DOI: 10.1007/s40588-020-00140-w]

100 **Fedele D**, De Francesco A, Riso S, Collo A. Obesity, malnutrition, and trace element deficiency in the coronavirus disease (COVID-19) pandemic: An overview. *Nutrition* 2021; **81**: 111016 [PMID: 33059127 DOI: 10.1016/j.nut.2020.111016]

101 **Hutasoit N**, Kennedy B, Hamilton S, Luttick A, Rahman Rashid RA, Palanisamy S. Sars-CoV-2 (COVID-19) inactivation capability of copper-coated touch surface fabricated by cold-spray technology. *Manuf Lett* 2020; **25**: 93-97 [PMID: 32904558 DOI: 10.1016/j.mfglet.2020.08.007]

102 **Chakravarthy MV**, Waddell T, Banerjee R, Guess N. Nutrition and Nonalcoholic Fatty Liver Disease: Current Perspectives. *Gastroenterol Clin North Am* 2020; **49**: 63-94 [PMID: 32033765 DOI: 10.1016/j.gtc.2019.09.003]

103 **van Doremalen N**, Bushmaker T, Morris DH, Holbrook MG, Gamble A, Williamson BN, Tamin A, Harcourt JL, Thornburg NJ, Gerber SI, Lloyd-Smith JO, de Wit E, Munster VJ. Aerosol and Surface Stability of SARS-CoV-2 as Compared with SARS-CoV-1. *N Engl J Med* 2020; **382**: 1564-1567 [PMID: 32182409 DOI: 10.1056/NEJMc2004973]

104 **Yu L**, Liou IW, Biggins SW, Yeh M, Jalikis F, Chan LN, Burkhead J. Copper Deficiency in Liver Diseases: A Case Series and Pathophysiological Considerations. *Hepatol Commun* 2019; **3**: 1159-

1165 [PMID: 31388635 DOI: 10.1002/hep4.1393]
105 **Altarelli M**, Ben-Hamouda N, Schneider A, Berger MM. Copper Deficiency: Causes, Manifestations, and Treatment. *Nutr Clin Pract* 2019; **34**: 504-513 [PMID: 31209935 DOI: 10.1002/ncp.10328]
106 **Raha S**, Mallick R, Basak S, Duttaroy AK. Is copper beneficial for COVID-19 patients? *Med Hypotheses* 2020; **142**: 109814 [PMID: 32388476 DOI: 10.1016/j.mehy.2020.109814]
107 **Wallace TC**. Combating COVID-19 and Building Immune Resilience: A Potential Role for Magnesium Nutrition? *J Am Coll Nutr* 2020; **39**: 685-693 [PMID: 32649272 DOI: 10.1080/07315724.2020.1785971]
108 **Iotti S**, Wolf F, Mazur A, Maier JA. The COVID-19 pandemic: is there a role for magnesium? *Magnes Res* 2020; **33**: 21-27 [PMID: 32554340 DOI: 10.1684/mrh.2020.0465]
109 **Annunziata G**, Jiménez-García M, Capó X, Moranta D, Arnone A, Tenore GC, Sureda A, Tejada S. Microencapsulation as a tool to counteract the typical low bioavailability of polyphenols in the management of diabetes. *Food Chem Toxicol* 2020; **139**: 111248 [PMID: 32156568 DOI: 10.1016/j.fct.2020.111248]
110 **Utomo RY**, Ikawati M, Meiyanto E. Revealing the Potency of Citrus and Galangal Constituents to Halt SARS-CoV-2 Infection. 2020 Preprint. Available from: Preprints: 2020030214 [DOI: 10.20944/preprints202003.0214.v1]
111 **Yi L**, Li Z, Yuan K, Qu X, Chen J, Wang G, Zhang H, Luo H, Zhu L, Jiang P, Chen L, Shen Y, Luo M, Zuo G, Hu J, Duan D, Nie Y, Shi X, Wang W, Han Y, Li T, Liu Y, Ding M, Deng H, Xu X. Small molecules blocking the entry of severe acute respiratory syndrome coronavirus into host cells. *J Virol* 2004; **78**: 11334-11339 [PMID: 15452254 DOI: 10.1128/JVI.78.20.11334-11339.2004]
112 **Ho TY**, Wu SL, Chen JC, Li CC, Hsiang CY. Emodin blocks the SARS coronavirus spike protein and angiotensin-converting enzyme 2 interaction. *Antiviral Res* 2007; **74**: 92-101 [PMID: 16730806 DOI: 10.1016/j.antiviral.2006.04.014]
113 **Jena AB**, Kanungo N, Nayak V, Chainy GBN, Dandapat J. Catechin and curcumin interact with S protein of SARS-CoV2 and ACE2 of human cell membrane: insights from computational studies. *Sci Rep* 2021; **11**: 2043 [PMID: 33479401 DOI: 10.1038/s41598-021-81462-7]
114 **Nikpoor AR**. Evaluation of the effect of nano micelles containing curcumin (Sina Ccurcumin) as a therapeutic supplement in patients with COVID-19 and investigating of immune responses balance changes following treatment: A randomized double blind clinical trial. [accessed 2020 Dec 15] In: IRCT.ir/trial/ [Internet]. Teheran: Iranian Registry of Clinical Trails. Available from: https://www.irct.ir/trial/48843 IRCT registration number: IRCT20200611047735N1
115 **Askari G**. Effect of curcumin-piperine supplementation on disease duration, severity and clinical signs, and inflammatory factors in patients with coronavirus (COVID-19): A randomized, double-blind, placebo-controlled clinical trial study. [accessed 2020 Dec 15] In: IRCT.ir/trial/ [Internet]. Teheran: Iranian Registry of Clinical Trails. Available from: https://www.irct.ir/trial/47529 IRCT registration number: IRCT20121216011763N46
116 **Salem K**. Silymarin in COVID-19 Pneumonia (SCOPE). [accessed 2020 Dec 15]. In: ClinicalTrials.gov [Internet]. Bethesda (MD): U.S. National Library of Medicine. Available from: https://clinicaltrials.gov/ct2/show/NCT04394208 ClinicalTrials.gov Identifier: NCT04394208
117 **Sun J**, Aghemo A, Forner A, Valenti L. COVID-19 and liver disease. *Liver Int* 2020; **40**: 1278-1281 [PMID: 32251539 DOI: 10.1111/liv.14470]
118 **Limanaqi F**, Busceti CL, Biagioni F, Lazzeri G, Forte M, Schiavon S, Sciarretta S, Frati G, Fornai F. Cell Clearing Systems as Targets of Polyphenols in Viral Infections: Potential Implications for COVID-19 Pathogenesis. *Antioxidants (Basel)* 2020; **9**: 1105 [PMID: 33182802 DOI: 10.3390/antiox9111105]
119 **Semiz S**, Serdarevic F. Prevention and Management of Type 2 Diabetes and Metabolic Syndrome in the Time of COVID-19: Should We Add a Cup of Coffee? *Front Nutr* 2020; **7**: 581680 [PMID: 33123550 DOI: 10.3389/fnut.2020.581680]
120 **Paraiso IL**, Revel JS, Stevens JF. Potential use of polyphenols in the battle against COVID-19. *Curr Opin Food Sci* 2020; **32**: 149-155 [PMID: 32923374 DOI: 10.1016/j.cofs.2020.08.004]
121 **Zahedipour F**, Hosseini SA, Sathyapalan T, Majeed M, Jamialahmadi T, Al-Rasadi K, Banach M, Sahebkar A. Potential effects of curcumin in the treatment of COVID-19 infection. *Phytother Res* 2020; **34**: 2911-2920 [PMID: 32430996 DOI: 10.1002/ptr.6738]
122 **Abenavoli L**, Greco M, Milic N, Accattato F, Foti D, Gulletta E, Luzza F. Effect of Mediterranean Diet and Antioxidant Formulation in Non-Alcoholic Fatty Liver Disease: A Randomized Study. *Nutrients* 2017; **9**: 870 [PMID: 28805669 DOI: 10.3390/nu9080870]
123 **Ristić-Medić D**, Takić M, Vučić V, Kandić D, Kostić N, Glibetić M. Abnormalities in the serum phospholipids fatty acid profile in patients with alcoholic liver cirrhosis - a pilot study. *J Clin Biochem Nutr* 2013; **53**: 49-54 [PMID: 23874070 DOI: 10.3164/jcbn.12-79]
124 **Zheng KI**, Gao F, Wang XB, Sun QF, Pan KH, Wang TY, Ma HL, Chen YP, Liu WY, George J, Zheng MH. Letter to the Editor: Obesity as a risk factor for greater severity of COVID-19 in patients with metabolic associated fatty liver disease. *Metabolism* 2020; **108**: 154244 [PMID: 32320741 DOI: 10.1016/j.metabol.2020.154244]
125 **López-Bautista F**, Barbero-Becerra VJ, Ríos MY, Ramírez-Cisneros MÁ, Sánchez-Pérez CA, Ramos-Ostos MH, Uribe M, Chávez-Tapia NC, Juárez-Hernández E. Dietary consumption and serum pattern of bioactive fatty acids in NAFLD patients. *Ann Hepatol* 2020; **19**: 482-488 [PMID: 32717363 DOI: 10.1016/j.aohep.2020.06.008]

126 **Ristic-Medic D**, Kovacic M, Takic M, Arsic A, Petrovic S, Paunovic M, Jovicic M, Vucic V. Calorie-Restricted Mediterranean and Low-Fat Diets Affect Fatty Acid Status in Individuals with Nonalcoholic Fatty Liver Disease. *Nutrients* 2020; **13**: 15 [PMID: 33374554 DOI: 10.3390/nu13010015]

127 **Darwesh AM**, Bassiouni W, Sosnowski DK, Seubert JM. Can N-3 polyunsaturated fatty acids be considered a potential adjuvant therapy for COVID-19-associated cardiovascular complications? *Pharmacol Ther* 2021; **219**: 107703 [PMID: 33031856 DOI: 10.1016/j.pharmthera.2020.107703]

128 **Barazzoni R**, Bischoff SC, Breda J, Wickramasinghe K, Krznaric Z, Nitzan D, Pirlich M, Singer P; endorsed by the ESPEN Council. ESPEN expert statements and practical guidance for nutritional management of individuals with SARS-CoV-2 infection. *Clin Nutr* 2020; **39**: 1631-1638 [PMID: 32305181 DOI: 10.1016/j.clnu.2020.03.022]

129 **Bistrian BR**. Parenteral Fish-Oil Emulsions in Critically Ill COVID-19 Emulsions. *JPEN J Parenter Enteral Nutr* 2020; **44**: 1168 [PMID: 32384188 DOI: 10.1002/jpen.1871]

130 **Rogero MM**, Leão MC, Santana TM, Pimentel MVMB, Carlini GCG, da Silveira TFF, Gonçalves RC, Castro IA. Potential benefits and risks of omega-3 fatty acids supplementation to patients with COVID-19. *Free Radic Biol Med* 2020; **156**: 190-199 [PMID: 32653511 DOI: 10.1016/j.freeradbiomed.2020.07.005]

131 **Fernández-Quintela A**, Milton-Laskibar I, Trepiana J, Gómez-Zorita S, Kajarabille N, Léniz A, González M, Portillo MP. Key Aspects in Nutritional Management of COVID-19 Patients. *J Clin Med* 2020; **9**: 2589 [PMID: 32785121 DOI: 10.3390/jcm9082589]

132 **Jaggers GK**, Watkins BA, Rodriguez RL. COVID-19: repositioning nutrition research for the next pandemic. *Nutr Res* 2020; **81**: 1-6 [PMID: 32795724 DOI: 10.1016/j.nutres.2020.07.005]

133 **Billingsley HE**, Carbone S. The antioxidant potential of the Mediterranean diet in patients at high cardiovascular risk: an in-depth review of the PREDIMED. *Nutr Diabetes* 2018; **8**: 13 [PMID: 29549354 DOI: 10.1038/s41387-018-0025-1]

134 **Bhattacharjee B**, Pal PK, Chattopadhyay A, Bandyopadhyay D. Oleic acid protects against cadmium induced cardiac and hepatic tissue injury in male Wistar rats: A mechanistic study. *Life Sci* 2020; **244**: 117324 [PMID: 31958420 DOI: 10.1016/j.lfs.2020.117324]

135 **Ardestani ME**, Onvani S, Esmailzadeh A, Feizi A, Azadbakht L. Adherence to Dietary Approaches to Stop Hypertension (DASH) Dietary Pattern in Relation to Chronic Obstructive Pulmonary Disease (COPD): A Case-Control Study. *J Am Coll Nutr* 2017; **36**: 549-555 [PMID: 28862922 DOI: 10.1080/07315724.2017.1326858]

136 **Morais AHA**, Aquino JS, da Silva-Maia JK, Vale SHL, Maciel BLL, Passos TS. Nutritional status, diet and viral respiratory infections: perspectives for severe acute respiratory syndrome coronavirus 2. *Br J Nutr* 2021; **125**: 851-862 [PMID: 32843118 DOI: 10.1017/S0007114520003311]

World Journal of Gastroenterology

Submit a Manuscript: https://www.f6publishing.com

World J Gastroenterol 2021 September 14; 27(34): 5700-5714

DOI: 10.3748/wjg.v27.i34.5700

ISSN 1007-9327 (print) ISSN 2219-2840 (online)

MINIREVIEWS

Updates in diagnosis and management of pancreatic cysts

Linda S Lee

ORCID number: Linda S Lee 0000-0001-9921-8920.

Author contributions: Lee LS is sole author of this review.

Conflict-of-interest statement: No conflict of interest.

Open-Access: This article is an open-access article that was selected by an in-house editor and fully peer-reviewed by external reviewers. It is distributed in accordance with the Creative Commons Attribution NonCommercial (CC BY-NC 4.0) license, which permits others to distribute, remix, adapt, build upon this work non-commercially, and license their derivative works on different terms, provided the original work is properly cited and the use is non-commercial. See: http://creativecommons.org/Licenses/by-nc/4.0/

Manuscript source: Invited manuscript

Specialty type: Gastroenterology and hepatology

Country/Territory of origin: United States

Peer-review report's scientific quality classification

Grade A (Excellent): 0
Grade B (Very good): B
Grade C (Good): C
Grade D (Fair): 0

Linda S Lee, Division of Gastroenterology, Hepatology and Endoscopy, Brigham and Women's Hospital, Boston, MA 02115, United States

Corresponding author: Linda S Lee, MD, Associate Professor, Director, Division of Gastroenterology, Hepatology and Endoscopy, Brigham and Women's Hospital, 75 Francis St, Boston, MA 02115, United States. llee@bwh.harvard.edu

Abstract

Incidental pancreatic cysts are commonly encountered with some cysts having malignant potential. The most common pancreatic cystic neoplasms include serous cystadenoma, mucinous cystic neoplasm and intraductal papillary mucinous neoplasm. Risk stratifying pancreatic cysts is important in deciding whether patients may benefit from endoscopic ultrasound (EUS) or surgical resection. Surgery should be reserved for patients with malignant cysts or cysts at high risk for developing malignancy as suggested by various risk features including solid mass, nodule and dilated main pancreatic duct. EUS may supplement magnetic resonance imaging findings for cysts that remain indeterminate or have concerning features on imaging. Various cyst fluid markers including carcinoembryonic antigen, glucose, amylase, cytology, and DNA markers help distinguish mucinous from nonmucinous cysts. This review will guide the practicing gastroenterologist in how to evaluate incidental pancreatic cysts and when to consider referral for EUS or surgery. For presumed low risk cysts, surveillance strategies will be discussed. Managing pancreatic cysts requires an individualized approach that is directed by the various guidelines.

Key Words: Pancreatic cyst; Intraductal papillary mucinous neoplasm; Endoscopic ultrasound-guided fine needle aspiration; Serous cystadenoma; Surveillance; Carcinoembryonic antigen

©The Author(s) 2021. Published by Baishideng Publishing Group Inc. All rights reserved.

Core Tip: Incidental pancreatic cysts are common, and some have malignant potential. magnetic resonance imaging of the pancreas should be used to risk stratify pancreatic cysts and decide whether patients may benefit from endoscopic ultrasound or surgical resection. Presumed low risk cysts should undergo surveillance unless the patient is not a surgical candidate or has a pseudocyst or serous cystadenoma. We discuss the approach to diagnosis and management of incidental pancreatic cysts.

Grade E (Poor): 0

Received: February 28, 2021
Peer-review started: February 28, 2021
First decision: April 18, 2021
Revised: May 14, 2021
Accepted: August 20, 2021
Article in press: August 20, 2021
Published online: September 14, 2021

P-Reviewer: Corrales FJ, Fiori E
S-Editor: Wang JL
L-Editor: A
P-Editor: Xing YX

Citation: Lee LS. Updates in diagnosis and management of pancreatic cysts. *World J Gastroenterol* 2021; 27(34): 5700-5714
URL: https://www.wjgnet.com/1007-9327/full/v27/i34/5700.htm
DOI: https://dx.doi.org/10.3748/wjg.v27.i34.5700

INTRODUCTION

Pancreatic cysts are typically discovered incidentally with the increased use and quality of abdominal imaging. They are identified in up to 20% of magnetic resonance imaging (MRI) and 3% of computed tomography (CT) scans with older patients more likely to have pancreatic cysts[1-3]. The malignant potential of some pancreatic cysts creates consternation for patients and providers alike. A retrospective study of Veterans Administration patients with pancreatic cysts noted a hazard ratio of 19.64 for pancreatic cancer[4]. However, other studies of incidental pancreatic cysts demonstrated lower risk of malignancy with a hazard ratio of 3.0 for pancreatic adenocarcinoma[5]. The American Gastroenterological Association (AGA) technical review of incidental pancreatic cysts estimated incident risk of malignancy at 0.24% per year with a prevalent malignant risk of 0.25% at the time the cyst is identified[6].

The most commonly encountered benign pancreatic cysts include serous cystadenoma (SCA), mucinous cystic neoplasm (MCN), and intraductal papillary mucinous neoplasm (IPMN). MCN and IPMN have varying malignant potential. SCAs classically appear lobular with multiple septations and microcysts (Figure 1). If densely septated, the cyst can appear mass-like on imaging and endoscopic ultrasound (EUS). A central scar which may be calcified is pathognomonic for SCA but occurs in only 15-20% of all SCA. A surgical series reported 51% preoperative diagnostic accuracy mainly based on radiologic imaging studies for SCA[7]. On pathology, SCA are defined by glycogen-containing cuboidal epithelial cells. The natural history of SCAs may involve slow gradual growth, which occurs in less than half of all SCAs with cysts larger than 4 cm potentially growing faster[8,9].

MCNs are defined by the presence of ovarian-like stroma, which explains why they occur almost exclusively in women. On imaging, MCNs are usually characterized by unilocular cysts in the body and/or tail (Figure 2). Peripheral calcifications of the wall or septa can occur in about 25% of MCNs. Approximately 15% of resected MCNs contain invasive cancer, and risk factors for malignancy include size > 6 cm, enhancing nodule, thick irregular wall, and peripheral calcifications[6,10]. While MCNs have malignant potential, less than 0.4% of MCNs smaller than 3 cm without a nodule harbor high-grade dysplasia or invasive cancer[11]. This has led to the suggestion by some that not all MCNs must be resected.

IPMNs are more common with radiologic and histologic subtypes that confer different risks of malignancy. Main duct IPMNs (MD-IPMN) have the highest malignant potential (approximately 60%-80%) and are characterized by diffuse or segmental dilatation of the main pancreatic duct to > 5 mm from a cystic tumor producing mucus within the duct (Figure 3)[12]. Branch duct IPMNs (BD-IPMN) arise within the branches of a nondilated main pancreatic duct (Figure 4) with malignant risk ranging from 3% to 26%[6,12]. Mixed type IPMNs have features of both MD-IPMN and BD-IPMN with approximately 20% to 30% of BD-IPMN ultimately proven to be mixed type IPMN following surgical resection[13]. The malignant potential of mixed type IPMN is comparable to MD-IPMN although mixed type IPMN with only microscopic involvement of the main pancreatic duct may carry less malignant risk [14]. High risk features for malignant IPMNs include solid component, enhancing nodule, main pancreatic duct dilation > 1 cm, jaundice and cytology with high-grade dysplasia or cancer, which were associated with lower 5-year survival compared with size > 3 cm, main pancreatic duct 5-9 mm, pancreatitis and non-enhancing nodules[15]. Other findings potentially associated with development of risk features include rapid rate of growth > 2.5 mm per year, body mass index > 26.4, smoking, and history of extrapancreatic malignancy[15-17]. Gastric histology is associated with a more benign course and more commonly found with BD-IPMN and microscopic mixed type IPMN while intestinal histology tends to occur with MD-IPMNs[18]. The less common pancreatobiliary and oncocytic histologic subtypes are mainly associated with high-grade dysplasia[19].

Solid pseudopapillary neoplasms (SPEN) also have malignant potential with characteristic pseudopapillae and cystic spaces containing hemorrhage and cholesterol clefts in myxoid stroma alternating with solid tissue. Therefore, these lesions appear solid

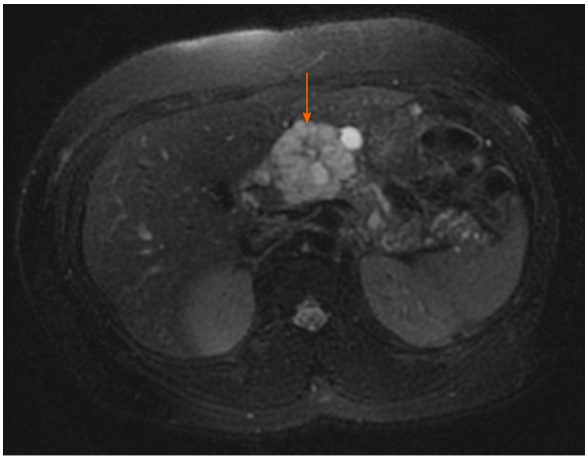


Figure 1 Magnetic resonance imaging of microcystic serous cystadenoma in body of pancreas (arrow)[23].

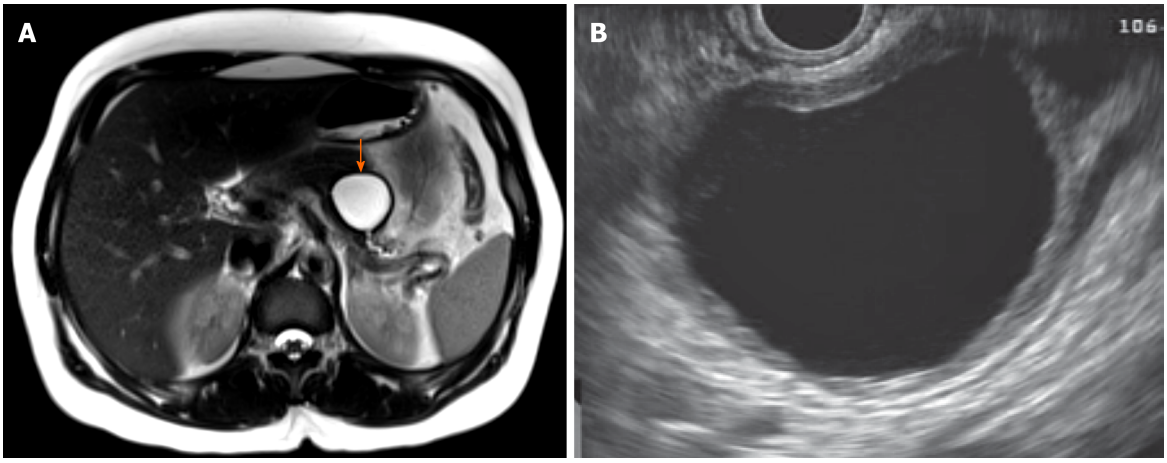


Figure 2 Magnetic resonance imaging and endoscopic ultrasound of mucinous cystic neoplasm appearing unilocular with a thick wall (arrow)[23]. A: Magnetic resonance imaging; B: Endoscopic ultrasound.

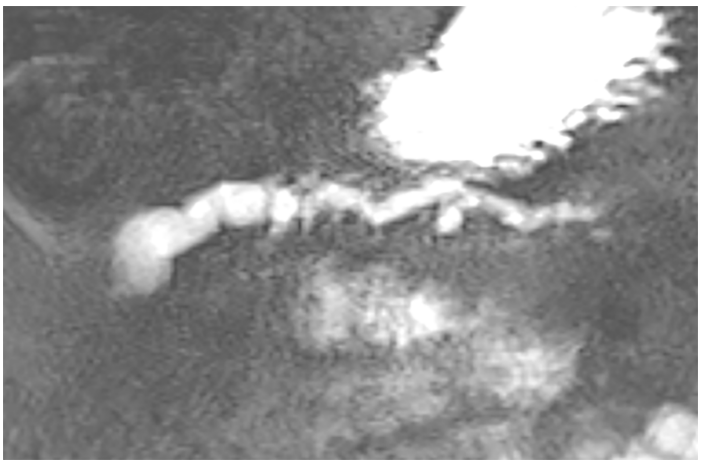


Figure 3 Magnetic resonance cholangiopancreatography of main duct intraductal papillary mucinous neoplasm[23].

and cystic, and typically occur in young women (Figure 5).

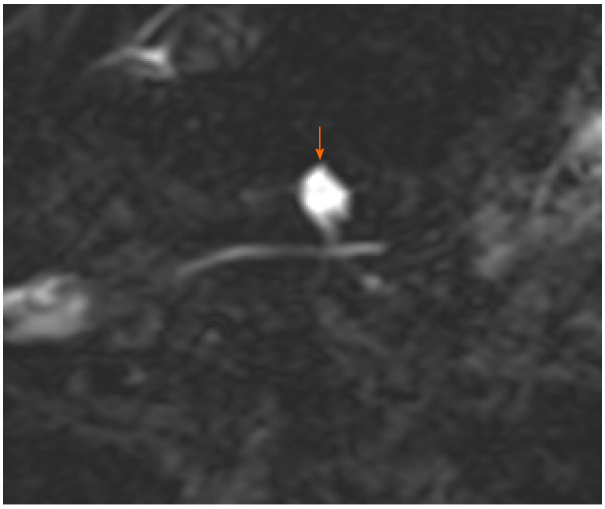


Figure 4 Magnetic resonance cholangiopancreatography of branch duct intraductal papillary mucinous neoplasm communicating with nondilated main pancreatic duct (arrow)[23].

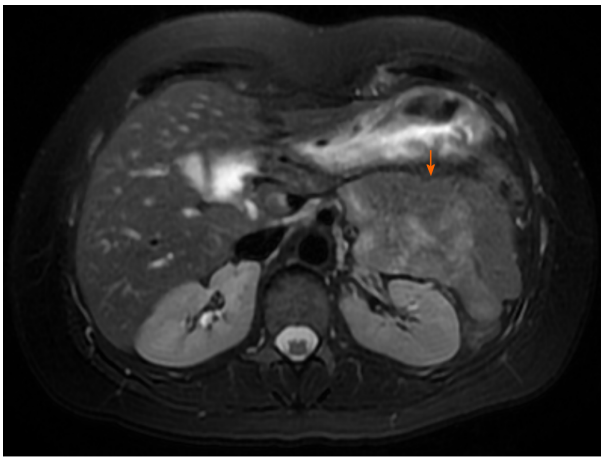


Figure 5 Magnetic resonance imaging of solid pseudopapillary neoplasm (arrow)[23].

APPROACH TO DIAGNOSIS OF THE INCIDENTAL PANCREATIC CYST

Evaluating a patient with an incidental pancreatic cyst should begin with a targeted history focused on acute or chronic pancreatitis and family history of pancreatic cancer or hereditary cancer syndromes associated with increased risk of pancreatic cancer. Patients at increased risk of pancreatic cancer due to family history should be managed differently and these patients are not the focus of this review. For those with incidental cysts, MRI pancreas with magnetic resonance cholangiopancreatography in 1.5 or 3 tesla should be performed. MRI has 55% to 76% accuracy for differentiating benign from malignant cysts while it is only 40% to 50% accurate for diagnosing the specific type of cyst[20]. MRI is superior for identifying communication between the main pancreatic duct and cyst, and thus better at diagnosing BD-IPMNs. If MRI cannot be performed, pancreatic protocol CT with contrast-enhanced images during the pancreatic and portal venous phases should be obtained. The imaging findings will help determine whether EUS is needed for further diagnostic evaluation, the patient should undergo surgical resection, or begin a surveillance program. The overarching questions when reviewing imaging are: (1) Is the cyst malignant; (2) If not, is it a mucinous cyst; and (3) If it is a mucinous cyst, what is the malignant potential[21-23]?

Before embarking on further evaluation for incidental pancreatic cysts, discussion should occur with select patients about whether ongoing management fits with the patients' overall clinical status. All pancreatic cyst guidelines agree that patients who are not surgically fit do not need ongoing surveillance. A study of 725 patients with IPMNs noted that patients with higher Charlson comorbidity index ≥ 7 were 11 times

more likely to die from non-IPMN related causes within 3 years of cyst diagnosis and had significantly shorter median survival (43 mo *vs* 180 mo)[24]. Another study used the Adult Comorbidity Evaluation 27 scoring system in 793 patients with IPMNs followed for over a year with similar conclusions that patients with higher scores were more likely to die from non-IPMN related causes[25]. These may help risk stratify patients with multiple comorbidities who likely will not need ongoing attention to their cysts. The other group of patients who do not need ongoing evaluation include those with pseudocysts or SCAs although the European cyst guideline suggests a one-time surveillance MRI one year after identification of SCAs[26].

The multiple guidelines that have been proposed to assist clinicians with managing pancreatic cystic lesions share many commonalities although the AGA guideline is the significant outlier (Table 1)[12,20,26-28]. The controversial AGA guideline increased the threshold for sending a patient to EUS-FNA as well as surgery from one to at least two risk features. While this may be expected to decrease the unnecessary resection of benign cysts, the impact on the negative predictive value has not been proven[29,30]. In our experience, we found similar rates of missing malignant cysts when comparing the International Association of Pancreatology Fukuoka and AGA guidelines (19% by Fukuoka, 25% by AGA) and preventing unnecessary surgeries (69% by Fukuoka, 74% by AGA)[29]. Therefore, the guidelines all serve as guides but cannot dictate management of patients with pancreatic cysts.

EUS

Following radiologic imaging, the role of EUS in the diagnostic work-up of pancreatic cysts includes evaluating cysts that are indeterminate or have risk features, or if EUS may change management. EUS-FNA is helpful in differentiating mucinous from nonmucinous cysts when imaging is indeterminate and in diagnosing suspected cystic neuroendocrine tumors and solid pseudopapillary neoplasms[31]. The Fukuoka and AGA guidelines offer guidance on whom to select for EUS-FNA based on presence of specific risk features. The Fukuoka guideline for suspected MCN and IPMN recommends EUS for patients with any one of these clinical or radiologic worrisome features (pancreatitis, size ≥ 3 cm, enhancing nodule < 5 mm, main pancreatic duct 5-9 mm, thick cyst wall, abrupt change in main pancreatic duct diameter with upstream parenchymal atrophy, lymphadenopathy, elevated serum CA 19-9, cyst growth ≥ 5 mm/2 years)[12]. On the other hand, the AGA guideline suggests EUS-FNA only for cysts with two high-risk imaging features (size ≥ 3 cm, solid component, or dilated main pancreatic duct) or if significant changes develop in the cyst during surveillance [27]. However, it is certainly reasonable to perform EUS-FNA in certain situations even with a single risk feature such as a solid component or significantly dilated main pancreatic duct given the relatively high risk of malignancy associated with these features.

EUS imaging is limited in diagnostic accuracy for identifying mucinous cysts with only 51% accuracy[32]. Moreover, among expert endosonographers there remains wide variation in interobserver agreement of neoplastic features[33,34]. Agreement is reportedly best for nodules, moderate for solid component and cystic communication with pancreatic duct, and fair for suspicion of malignancy[34].

Endosonographers can distinguish nodules from mucus by comparing the echogenicity relative to adjacent tissue and assessing the mobility of the structure with patient repositioning and probing with the needle. Nodules appear iso- or hypoechoic without a smooth edge or hyperechoic rim compared with mucus which have a smooth-edged hyperechoic rim surrounding a hypoechoic center[35]. Contrast-enhanced harmonic EUS, which involves intravenous injection of special contrast agents that highlight microvasculature differences between normal and abnormal tissue, appears helpful in not only diagnosing nodules, but also differentiating high-grade dysplasia and cancerous nodules from nodules with low-grade dysplasia[36]. Nodules taller than 5 mm have greater association with malignancy.

Cyst fluid analysis

Because of the inadequate diagnostic capabilities of EUS imaging alone, intense interest has focused on searching for the ideal cyst fluid marker whether protein, DNA, RNA, metabolite that would diagnose the cyst, distinguish a mucinous from nonmucinous cyst, and predict malignant progression of the cyst. Cyst fluid for cytology typically has low diagnostic yield with less than 50% sensitivity for mucinous lesions, however, it is helpful when positive for a specific diagnosis. Similarly, cytology is highly specific for malignancy with at best 60% sensitivity for malignancy [27,37]. Fluid cytology appears more useful for SPEN with 70-81% accuracy and cystic neuroendocrine tumors with 70%-89% diagnostic yield[38-41]. Cyst fluid from

Table 1 Key Features of pancreatic cyst guidelines

Specifics of Guidelines	2015 AGA	2017 Fukuoka	2017 ACG	2017 ACR	2018 European Study Group
Patient population	Incidental pancreatic cysts	Suspected MCN and IPMN	All pancreatic cysts	Incidental pancreatic cysts	All pancreatic cysts
Threshold for EUS and/or surgery	At least 2 risk factors	1 risk factor	1 risk factor	1 risk factor	1 risk factor
Surveillance recommendations in unresected cysts	MRI in 1 year, then every 2 yr	Surveillance based on cyst size	Surveillance based on cyst size	Surveillance based on cyst size and age	Surveillance based on cyst size and diagnosis
Stopping surveillance	(1) After 5 yr of stability without development of high-risk features; (2) Surgically unfit; and (3) Select resected cysts including BD-IPMN with no, low or moderate-grade dysplasia	(1) Surgically unfit; and (2) Following resection of serous cystadenoma and MCN without invasive cancer	(1) Surgically unfit; (2) Following resection of serous cystadenoma and MCN without invasive cancer; and (3) Individualize approach to patients > 75	(1) 9-10 yr and stop at age 80; and (2) For cysts discovered > age 80, limited surveillance for 4 yr only if stable	Surgically unfit

AGA: American Gastroenterological Association; ACG: American College of Gastroenterology; EUS: Endoscopic ultrasound; MRI: Magnetic resonance imaging; MCN: Mucinous cystic neoplasm; IPMN: Intraductal papillary mucinous neoplasm; BD-IPMN: Branch duct-intraductal papillary mucinous neoplasm.

pancreatic lymphangioma has a characteristic chylous appearance, elevated triglyceride levels, and numerous benign lymphocytes[42]. Improved diagnostic yield for mucinous or malignant cysts by 29% has been reported with cyst wall cytology, obtained by repeatedly passing the needle back and forth through the collapsed cyst wall[43]. Therefore, cyst wall cytology may be preferred over fluid alone, unless copious fluid is available for cytology. A small study suggests greater diagnostic yield with EUS-fine needle biopsy using a core biopsy needle[44].

If there is enough fluid, before sending it for analysis it should be evaluated for string sign, which is highly specific (95%) for a mucinous cyst[45]. This is defined as cyst fluid extending for at least 1 cm and 1 s from the tip of the EUS needle or between two fingers that are separated after placing a drop of fluid on them. The remaining fluid should be sent for carcinoembryonic antigen (CEA), amylase, glucose and potentially DNA analyses (Table 2).

While CEA is not predictive of malignancy, it remains the most widely used and accurate tumor marker for differentiating mucinous from non-mucinous pancreatic cysts[46]. However, it does not distinguish IPMN from MCN. Other limitations with CEA assays are they were validated for serum but not for cyst fluid, and significant CEA variation exists among different assays[47]. The appropriate CEA threshold is debated with CEA greater than 192 ng/mL having 73% sensitivity and 84% specificity for mucinous cysts[32]. Cyst fluid glucose may be more accurate than CEA for mucinous cysts with a recent meta-analysis reporting 91% sensitivity and 75% specificity for glucose compared with 67% sensitivity and 80% specificity for CEA[48]. A common cutoff used for cyst fluid glucose in diagnosing mucinous cysts is < 50 mg/dL. Very low CEA levels < 5 ng/mL are specific for SCA, pseudocyst, or cystic neuroendocrine tumor[49]. Amylase is helpful in excluding pseudocysts if less than 250 U/L[49].

DNA analysis of cyst aspirates may be helpful especially when less than 0.5cc of fluid is available as this precludes many chemistry and tumor marker analyses. A recent meta-analysis noted that KRAS and GNAS mutations were more accurate for diagnosing mucinous cysts and IPMNs than CEA alone[50]. Other studies have noted high specificity > 90% for mucinous cysts and IPMNs but lower sensitivity (65%) with KRAS and GNAS[51]. Using both CEA and KRAS may be increase sensitivity to 83% for mucinous cysts but at the expense of specificity (85%)[52]. How useful DNA mutations are for identifying cysts with high-grade dysplasia or cancer remains to be determined with some preliminary studies of various DNA mutation panels suggesting high sensitivity and specificity[53,54]. Our study found the addition of DNA analysis consisting of KRAS, loss of heterozygosity, DNA quantity and quality did not improve upon the Sendai guideline in detecting malignant cysts[55].

Table 2 Cyst fluid studies

Cyst fluid test	Test characteristics	Diagnosis
String sign ≥ 1 cm, ≥ 1 s	95% specificity, 94% positive predictive value	Mucinous
Cyst fluid cytology	63% sensitivity	-
Cyst wall cytology	29% increased diagnostic yield	-
CEA > 192 ng/mL	75% sensitivity, 84% specificity	Mucinous
CEA < 5 ng/mL	50% sensitivity, 95% specificity	Serous cystadenoma, pseudocyst, cystic neuroendocrine tumor
Amylase < 250 U/L	44% sensitivity, 98% specificity	Excludes pseudocyst
Glucose < 50 mg/dL	89% sensitivity, 78% specificity	Mucinous
KRAS/*GNAS* mutation	89% sensitivity, 100% specificity	Mucinous

CEA: Carcinoembryonic antigen.

Needle-based confocal laser endomicroscopy and microbiopsy forceps

Newer tools during EUS that may improve diagnosis of pancreatic cysts include needle-based confocal laser endomicroscopy (nCLE) (Mauna Kea Technologies, Paris, France) and microbiopsy forceps (Steris, Mentor, OH, Figure 6). Both require passing the nCLE probe or microbiopsy forceps through a 19-gauge needle, which limits the size and location of cysts eligible for these techniques. EUS-nCLE allows real-time microscopic imaging of the cyst wall. Visualizing a superficial vascular network pattern is consistent with SCA with 56% to over 90% sensitivity and 100% specificity (Figure 7)[56,57]. Sensitivity for mucinous cysts ranges from 66% to over 90% with finger-like papilla consistent with IPMN (Figure 8) and epithelial bands seen in MCN [56,58]. The most common complication with nCLE is pancreatitis which ranges from 1.2% to 12%. Recommended techniques to minimize pancreatitis include preloading the nCLE probe in the FNA needle, nCLE duration less than 10 minutes and avoiding brushing the tip of the nCLE probe along the cyst wall.

A systematic review of 9 studies with 463 patients undergoing EUS with microbiopsy forceps reported 68.6% diagnostic accuracy with near 10% complications [59]. A death has been reported in Europe following this procedure as well as up to 4% severe complications[60]. Therefore, while nCLE and microbiopsy forceps are exciting tools that may improve diagnosis of pancreatic cysts, further studies are necessary to understand their safety profile as well as the optimal place these tools have amidst the currently available cyst fluid markers.

SURGICAL RESECTION

Surgery should be considered for patients with cysts that are symptomatic, malignant, or at high-risk for malignancy. Stratifying the malignant risk of a pancreatic cyst is simplest when the diagnosis of the cyst is known, but also possible for indeterminate cysts by assessing for risk features. Surgical resection is recommended for symptomatic SCAs only[20,26]. On the other hand, resection of MCNs should be considered for all patients or select higher risk patients with symptoms, nodule or size ≥ 4 cm[12,26]. Similarly, due to higher malignant risk of MD-IPMN and mixed type IPMNs, surgical resection is suggested for these lesions[12,26]. Resection is recommended for select BD-IPMN with a risk feature. Absolute indications for resection include main pancreatic duct ≥ 1 cm, enhancing nodule ≥ 5 mm, solid mass, jaundice, or cytology suspicious or positive for malignancy. Relative indications for resection of BD-IPMN include main pancreatic duct 5-9 mm, cyst ≥ 4 cm, enhancing nodule < 5 mm, growth rate ≥ 5 mm/year, serum CA 19-9 ≥ 37 U/mL, acute pancreatitis, or new onset diabetes. SPENs are considered premalignant with up to 15% incidence of local invasion or metastatic disease[39]. Given their malignant potential, favorable post-resection outcomes, and occurrence in mainly young women, referral for surgical resection is most appropriate[20,26].

The AGA guideline is the outlier by requiring the presence of at least 2 risk features before sending a patient to surgery. In the AGA technical review, 15% of all resected pancreatic cyst specimens had invasive malignancy while the rate of high-grade



Figure 6 Microbiopsy forceps through endoscopic ultrasound needle.

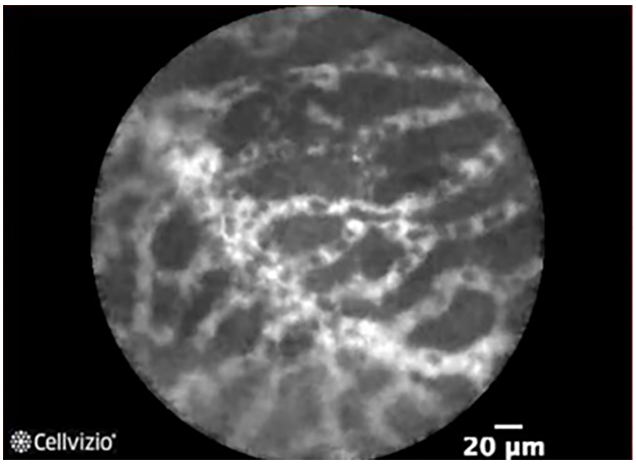


Figure 7 Superficial vascular network in serous cystadenoma. Courtesy of Mauna Kea Technologies.

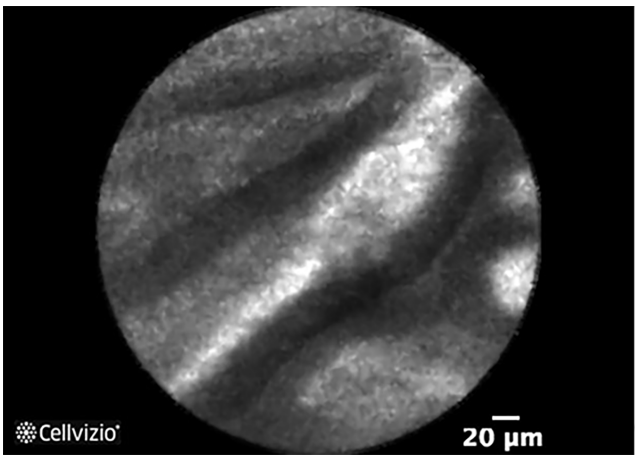


Figure 8 Papillary projections in intraductal papillary mucinous neoplasm. Courtesy of Mauna Kea Technologies.

dysplasia was not assessed[6]. Of surgically resected IPMNs, 25% had invasive malignancy and 42% had either high-grade dysplasia and/or invasive malignancy[6]. Whether resecting IPMN with low-grade dysplasia in 58% of cases is acceptable can be debated, but as a result, the AGA guideline increased the threshold for surgery to requiring 2 risk features (solid component, dilated main pancreatic duct, and/or concerning features on EUS-FNA) in the hopes of improving the positive predictive value for resecting pancreatic cysts[27]. However, this has not proven true from multiple studies including our experience[29]. A recent meta-analysis comparing the

Fukuoka and AGA guidelines reported they both had similarly modest sensitivity (67% and 59%, respectively) and specificity (64% and 77%, respectively) for detecting high-grade dysplasia and invasive cancer[61].

The AGA technical review identified the following as the greatest risk factors for malignancy in incidental pancreatic cysts: solid component [odds ratio (OR) 7.7], cyst size > 3 cm (OR 3), and dilated main pancreatic duct (MPD) (OR 2.4)[6]. One caveat is that the included studies used varying definitions for dilated main pancreatic duct ranging from ≥ 3mm to > 6 mm. Studies have suggested that the degree of main pancreatic duct dilation correlates with varying malignant potential with higher risk associated with duct > 7-8 mm[62,63]. Regarding cyst size, a study of 563 resected and radiologically diagnosed BD-IPMN noted that 18% of cysts > 3 cm had high-grade dysplasia or invasive cancer, while no malignancy was detected in cysts < 2 cm and no high-grade dysplasia was noted in lesions < 1 cm[64]. Larger cysts seem associated with development of high-risk features including nodule and main pancreatic duct dilation[16]. Assessment of cyst size and nodules may vary depending on the imaging modality. EUS may be more accurate than CT or MRI for cyst size measurements and for detecting nodules[35,65].

Careful surgical planning is important with MD-IPMN, and partial pancreatectomy is reasonable in cases with segmental dilation or diffuse dilation with focal lesions[12]. Resection should continue until the margins are negative for high-grade dysplasia and cancer. However, determining how much pancreas to resect in MD-IPMN with diffuse dilation without focal lesions can be challenging. ERCP with pancreatoscopy and/or intraductal ultrasound (IDUS) and EUS may help with surgical planning. Case series have suggested the utility of pancreatoscopy with or without IDUS in mapping IPMNs preoperatively leading to more or less extensive surgeries than previously planned in about 60% of patients[26,66,67]. Therefore, these tools may be used selectively to guide surgical planning. Regarding total pancreatectomy, some suggest this should be reserved for younger healthy patients who will tolerate brittle diabetes or exocrine insufficiency postoperatively while others advocate for this in all patients with diffuse main pancreatic duct dilation or those with family history of pancreatic cancer[12,26].

SURVEILLANCE

Patients with cysts at low risk for malignancy and following resection of certain cysts should undergo surveillance. MRI is preferred over CT for surveillance due to reduced radiation exposure and potentially improved ability to detect communication with the main pancreatic duct and nodules[20,26,28]. Recent reports of gadolinium deposition in the brain has raised concern over repeated injections of gadolinium during surveillance MRIs[68]. A few studies have suggested that MRI performed with *vs* without gadolinium did not change management decisions[69,70]. Non-contrast MRI scans have demonstrated similar efficacy to contrast-enhanced MRI in discerning benign from malignant disease[69]. Therefore, surveillance MRIs may be performed without gadolinium unless concerning findings are noted on the non-contrast MRI.

Surveillance is recommended at various intervals for unresected pancreatic cystic neoplasms depending on size and other criteria for different guidelines (Table 3)[12,20,26-28]. The surveillance interval may be lengthened if there are no concerning features or changes found on repeated testing[26,27]. If a cyst had been followed with imaging every 6 mo, this may be extended to every year while annual surveillance may be lengthened to biennial follow-up. Similarly, if new onset or worsening diabetes or concerning changes (risk features) develop on imaging, surveillance interval should be shortened and/or EUS performed and patient referred to a multidisciplinary pancreas center.

While the other gastroenterology guidelines suggest surveillance intervals based on cyst size and other factors without an explicit recommendation to stop surveillance except in surgically unfit patients, the AGA guideline endorses a simplified surveillance protocol of MRI in 1 year and then every 2 years for 5 years followed by stopping if the cyst remains stable without developing high risk features[27]. This is perhaps the most controversial aspect of the AGA guideline. Numerous long-term surveillance studies have been published following the release of the AGA guidelines, most of which noted low risk of malignancies developing after 5 years of surveillance. A Japanese study of 1404 patients with BD-IPMN excluding cysts with nodules or main pancreatic duct dilation > 1 cm noted gradually increasing incidence rates of cancer over time (3.3% at 5 years, 6.6% at 10 years and 15% at 15 years)[71]. Long-term surveillance of 1036 BD-IPMNs without worrisome or high-risk features in Italy found

Table 3 Surveillance recommendations from pancreatic cyst guidelines

2015 AGA	2017 Fukuoka	2017 ACG	2017 ACR	2018 European Study Group
Repeat 1 yr then q2 years until 5 yr	< 1 cm: q2-3 years	< 1 cm: q2 years x4 years	< 1.5 cm + < 65-year-old: q1 year x5, q2 years x2	< 1.5 cm: q1 year x3 years then q2 years
	1-2 cm: q1 year x2 years	1-2 cm: q1 year x3 years then q2 years x4 years	< 1.5 cm + ≥ 65-year-old: q2 years x5	≥ 1.5 cm: q6 mo x2 then q1 year
	2-3 cm: EUS in 3-6 mo then increase interval and alternate with MRI	2-3 cm: MRI/EUS q6-12 mo x3 years then q1 year x4 years	1.5-1.9 cm connected to MPD: q1 year x5 then q2 years x2	IPMN or MCN: q6 mo x2 then q1 year
	> 3 cm: MRI alternate with EUS q3-6 mo	> 3 cm: Consider referral to multidisciplinary pancreas group; MRI/EUS q6 mo x3 years, then MRI/EUS q1 year x4 years	2-2.5 cm connected to MPD or 1.5-2.5 cm without MPD connection or > 2.5 cm: q6 mo x4 then q1 year x2 then q2 years x3	

AGA: American Gastroenterological Association; ACG: American College of Gastroenterology; EUS: Endoscopic ultrasound; MRI: Magnetic resonance imaging; MCN: Mucinous cystic neoplasm; IPMN: Intraductal papillary mucinous neoplasm; MPD: Main pancreatic duct.

1.1% developed cancer after median 62 mo follow-up[72]. Development of worrisome features or cyst size growth > 2.5 mm/year were associated with risk for cancer. Another study of 363 patients with BD-IPMN followed for over 5 years noted that cyst size > 1.5 cm was associated with higher risk of developing cancer (7.5% *vs* 0.9%)[73]. Therefore, surveillance should not be stopped for all patients after 5 years, and in fact, should continue for most patients except those who are no longer surgical candidates. As discussed earlier, various comorbidity scoring systems including the Charlson comorbidity index and Adult Comorbidity Evaluation 27 scoring system may serve as aides to identify patients at higher risk from their comorbidities than their pancreatic cyst[24,25]. These patients likely would not benefit from ongoing surveillance. The American College of Gastroenterology guideline also suggests individualizing surveillance in patients over 75 years old analogous to the United States Preventive Services Taskforce recommendations for colon cancer screening.

Following surgical resection of SCA or MCN without invasive features, surveillance is not necessary as resection is considered curative. This is because no recurrence of MCN without invasive cancer was noted in patients after nearly 5 years[74]. For higher risk IPMNs including high-grade dysplasia at the surgical margins, non-intestinal subtype, or family history of pancreatic cancer, the Fukuoka guideline recommends repeat imaging at least every 6 mo[12]. For other IPMNs, surveillance every 6-12 mo is suggested. Those with resected invasive cancer should continue surveillance as per patients with pancreatic ductal adenocarcinoma. The AGA guideline supports postoperative surveillance only following resection of high-grade dysplasia or invasive cancer with MRI every 2 years[27]. A concern with this recommendation is that early recurrences, especially in patients with invasive cancer, may be missed.

Unresolved questions remain regarding surveillance including the optimal surveillance interval and duration in unresected cysts.

CONCLUSION

While the various guidelines provide a foundation for managing pancreatic cysts, the approach to each patient with a pancreatic cyst should be individualized based on clinical status and comorbidities, risk of malignancy, and personal preferences. A good quality MRI of the pancreas may help identify malignant and mucinous cysts. If the diagnosis of the cyst remains uncertain or there are concerning features on imaging, EUS should be pursued although the ideal diagnostic markers and tools remain elusive. Surgical resection should be reserved for patients with high risk features including solid mass, nodule or dilated main pancreatic duct. The ongoing challenge with surgical referral remains accurately identifying signs predictive of malignancy that allow early surgery to improve long-term survival while sparing patients with low-risk cysts the morbidity and mortality of pancreatic surgery. High quality studies are necessary to discover better diagnostic markers and tools, to improve risk stratification of patients, and to understand the optimal interval and duration of

surveillance.

REFERENCES

1 **de Oliveira PB**, Puchnick A, Szejnfeld J, Goldman SM. Prevalence of incidental pancreatic cysts on 3 tesla magnetic resonance. *PLoS One* 2015; **10**: e0121317 [PMID: 25798910 DOI: 10.1371/journal.pone.0121317]

2 **Megibow AJ**, Baker ME, Gore RM, Taylor A. The incidental pancreatic cyst. *Radiol Clin North Am* 2011; **49**: 349-359 [PMID: 21333781 DOI: 10.1016/j.rcl.2010.10.008]

3 **Chu LC**, Singhi AD, Haroun RR, Hruban RH, Fishman EK. The many faces of pancreatic serous cystadenoma: Radiologic and pathologic correlation. *Diagn Interv Imaging* 2017; **98**: 191-202 [PMID: 27614585 DOI: 10.1016/j.diii.2016.08.005]

4 **Munigala S**, Gelrud A, Agarwal B. Risk of pancreatic cancer in patients with pancreatic cyst. *Gastrointest Endosc* 2016; **84**: 81-86 [PMID: 26524643 DOI: 10.1016/j.gie.2015.10.030]

5 **Chernyak V**, Flusberg M, Haramati LB, Rozenblit AM, Bellin E. Incidental pancreatic cystic lesions: is there a relationship with the development of pancreatic adenocarcinoma and all-cause mortality? *Radiology* 2015; **274**: 161-169 [PMID: 25117591 DOI: 10.1148/radiol.14140796]

6 **Scheiman JM**, Hwang JH, Moayyedi P. American gastroenterological association technical review on the diagnosis and management of asymptomatic neoplastic pancreatic cysts. *Gastroenterology* 2015; **148**: 824-48.e22 [PMID: 25805376 DOI: 10.1053/j.gastro.2015.01.014]

7 **Kang JS**, Kim HJ, Choi YJ, Byun Y, Lee JM, Han Y, Kim H, Kwon W, Jang JY. Clinicoradiological features of resected serous cystic neoplasms according to morphological subtype and preoperative tentative diagnosis: can radiological characteristics distinguish serous cystic neoplasms from other lesions? *Ann Surg Treat Res* 2020; **98**: 247-253 [PMID: 32411629 DOI: 10.4174/astr.2020.98.5.247]

8 **Jais B**, Rebours V, Malleo G, Salvia R, Fontana M, Maggino L, Bassi C, Manfredi R, Moran R, Lennon AM, Zaheer A, Wolfgang C, Hruban R, Marchegiani G, Fernández Del Castillo C, Brugge W, Ha Y, Kim MH, Oh D, Hirai I, Kimura W, Jang JY, Kim SW, Jung W, Kang H, Song SY, Kang CM, Lee WJ, Crippa S, Falconi M, Gomatos I, Neoptolemos J, Milanetto AC, Sperti C, Ricci C, Casadei R, Bissolati M, Balzano G, Frigerio I, Girelli R, Delhaye M, Bernier B, Wang H, Jang KT, Song DH, Huggett MT, Oppong KW, Pererva L, Kopchak KV, Del Chiaro M, Segersvard R, Lee LS, Conwell D, Osvaldt A, Campos V, Aguero Garcete G, Napoleon B, Matsumoto I, Shinzeki M, Bolado F, Fernandez JM, Keane MG, Pereira SP, Acuna IA, Vaquero EC, Angiolini MR, Zerbi A, Tang J, Leong RW, Faccinetto A, Morana G, Petrone MC, Arcidiacono PG, Moon JH, Choi HJ, Gill RS, Pavey D, Ouaïssi M, Sastre B, Spandre M, De Angelis CG, Rios-Vives MA, Concepcion-Martin M, Ikeura T, Okazaki K, Frulloni L, Messina O, Lévy P. Serous cystic neoplasm of the pancreas: a multinational study of 2622 patients under the auspices of the International Association of Pancreatology and European Pancreatic Club (European Study Group on Cystic Tumors of the Pancreas). *Gut* 2016; **65**: 305-312 [PMID: 26045140 DOI: 10.1136/gutjnl-2015-309638]

9 **Tseng JF**, Warshaw AL, Sahani DV, Lauwers GY, Rattner DW, Fernandez-del Castillo C. Serous cystadenoma of the pancreas: tumor growth rates and recommendations for treatment. *Ann Surg* 2005; **242**: 413-9; discussion 419 [PMID: 16135927 DOI: 10.1097/01.sla.0000179651.21193.2c]

10 **Sakorafas GH**, Smyrniotis V, Reid-Lombardo KM, Sarr MG. Primary pancreatic cystic neoplasms revisited: part II. Mucinous cystic neoplasms. *Surg Oncol* 2011; **20**: e93-101 [PMID: 21251815 DOI: 10.1016/j.suronc.2010.12.003]

11 **Nguyen D**, Dawson DW, Hines OJ, Reber HA, Donahue TR. Mucinous cystic neoplasms of the pancreas: are we overestimating malignant potential? *Am Surg* 2014; **80**: 915-919 [PMID: 25264629]

12 **Tanaka M**, Fernández-Del Castillo C, Kamisawa T, Jang JY, Levy P, Ohtsuka T, Salvia R, Shimizu Y, Tada M, Wolfgang CL. Revisions of international consensus Fukuoka guidelines for the management of IPMN of the pancreas. *Pancreatology* 2017; **17**: 738-753 [PMID: 28735806 DOI: 10.1016/j.pan.2017.07.007]

13 **Fritz S**, Werner J, Büchler MW. Reply to Letter: "Sendai Consensus Guidelines for Branch-duct IPMN: Guidelines Are Just Guidelines". *Ann Surg* 2015; **262**: e66 [PMID: 24646531 DOI: 10.1097/SLA.0000000000000545]

14 **Sahora K**, Fernández-del Castillo C, Dong F, Marchegiani G, Thayer SP, Ferrone CR, Sahani DV, Brugge WR, Warshaw AL, Lillemoe KD, Mino-Kenudson M. Not all mixed-type intraductal papillary mucinous neoplasms behave like main-duct lesions: implications of minimal involvement of the main pancreatic duct. *Surgery* 2014; **156**: 611-621 [PMID: 25081232 DOI: 10.1016/j.surg.2014.04.023]

15 **Capurso G**, Crippa S, Vanella G, Traini M, Zerboni G, Zaccari P, Belfiori G, Gentiluomo M, Pessarelli T, Petrone MC, Campa D, Falconi M, Arcidiacono PG. Factors Associated With the Risk of Progression of Low-Risk Branch-Duct Intraductal Papillary Mucinous Neoplasms. *JAMA Netw Open* 2020; **3**: e2022933 [PMID: 33252689 DOI: 10.1001/jamanetworkopen.2020.22933]

16 **Han Y**, Lee H, Kang JS, Kim JR, Kim HS, Lee JM, Lee KB, Kwon W, Kim SW, Jang JY. Progression of Pancreatic Branch Duct Intraductal Papillary Mucinous Neoplasm Associates With Cyst Size. *Gastroenterology* 2018; **154**: 576-584 [PMID: 29074452 DOI: 10.1053/j.gastro.2017.10.013]

17 **Overbeek KA**, Alblas M, Gausman V, Kandel P, Schweber AB, Brooks C, Van Riet PA, Wallace

MB, Gonda TA, Cahen DL, Bruno MJ. Development of a stratification tool to identify pancreatic intraductal papillary mucinous neoplasms at lowest risk of progression. *Aliment Pharmacol Ther* 2019; **50**: 789-799 [PMID: 31429105 DOI: 10.1111/apt.15440]

18 **Yamada S**, Fujii T, Shimoyama Y, Kanda M, Nakayama G, Sugimoto H, Koike M, Nomoto S, Fujiwara M, Nakao A, Kodera Y. Clinical implication of morphological subtypes in management of intraductal papillary mucinous neoplasm. *Ann Surg Oncol* 2014; **21**: 2444-2452 [PMID: 24562937 DOI: 10.1245/s10434-014-3565-1]

19 **Patra KC**, Bardeesy N, Mizukami Y. Diversity of Precursor Lesions For Pancreatic Cancer: The Genetics and Biology of Intraductal Papillary Mucinous Neoplasm. *Clin Transl Gastroenterol* 2017; **8**: e86 [PMID: 28383565 DOI: 10.1038/ctg.2017.3]

20 **Elta GH**, Enestvedt BK, Sauer BG, Lennon AM. ACG Clinical Guideline: Diagnosis and Management of Pancreatic Cysts. *Am J Gastroenterol* 2018; **113**: 464-479 [PMID: 29485131 DOI: 10.1038/ajg.2018.14]

21 **Lee LS**. Diagnostic approach to pancreatic cysts. *Curr Opin Gastroenterol* 2014; **30**: 511-517 [PMID: 25003604 DOI: 10.1097/MOG.0000000000000098]

22 **Lee LS**. Incidental Cystic Lesions in the Pancreas: Resect? *Curr Treat Options Gastroenterol* 2014; **12**: 333-349 [PMID: 24903582 DOI: 10.1007/s11938-014-0019-6]

23 **Chiang AL**, Lee LS. Clinical approach to incidental pancreatic cysts. *World J Gastroenterol* 2016; **22**: 1236-1245 [PMID: 26811661 DOI: 10.3748/wjg.v22.i3.1236]

24 **Sahora K**, Ferrone CR, Brugge WR, Morales-Oyarvide V, Warshaw AL, Lillemoe KD, Fernández-del Castillo C. Effects of Comorbidities on Outcomes of Patients With Intraductal Papillary Mucinous Neoplasms. *Clin Gastroenterol Hepatol* 2015; **13**: 1816-1823 [PMID: 25956837 DOI: 10.1016/j.cgh.2015.04.177]

25 **Kawakubo K**, Tada M, Isayama H, Sasahira N, Nakai Y, Takahara N, Miyabayashi K, Yamamoto K, Mizuno S, Mohri D, Kogure H, Sasaki T, Yamamoto N, Tateishi R, Hirano K, Ijichi H, Tateishi K, Koike K. Risk for mortality from causes other than pancreatic cancer in patients with intraductal papillary mucinous neoplasm of the pancreas. *Pancreas* 2013; **42**: 687-691 [PMID: 23211374 DOI: 10.1097/MPA.0b013e318270ea97]

26 **European Study Group on Cystic Tumours of the Pancreas**. European evidence-based guidelines on pancreatic cystic neoplasms. *Gut* 2018; **67**: 789-804 [PMID: 29574408 DOI: 10.1136/gutjnl-2018-316027]

27 **Vege SS**, Ziring B, Jain R, Moayyedi P; Clinical Guidelines Committee; American Gastroenterology Association. American gastroenterological association institute guideline on the diagnosis and management of asymptomatic neoplastic pancreatic cysts. *Gastroenterology* 2015; **148**: 819-22; quize12 [PMID: 25805375 DOI: 10.1053/j.gastro.2015.01.015]

28 **Megibow AJ**, Baker ME, Morgan DE, Kamel IR, Sahani DV, Newman E, Brugge WR, Berland LL, Pandharipande PV. Management of Incidental Pancreatic Cysts: A White Paper of the ACR Incidental Findings Committee. *J Am Coll Radiol* 2017; **14**: 911-923 [PMID: 28533111 DOI: 10.1016/j.jacr.2017.03.010]

29 **Lee A**, Kadiyala V, Lee LS. Evaluation of AGA and Fukuoka Guidelines for EUS and surgical resection of incidental pancreatic cysts. *Endosc Int Open* 2017; **5**: E116-E122 [PMID: 28210708 DOI: 10.1055/s-0042-118703]

30 **Singhi AD**, Zeh HJ, Brand RE, Nikiforova MN, Chennat JS, Fasanella KE, Khalid A, Papachristou GI, Slivka A, Hogg M, Lee KK, Tsung A, Zureikat AH, McGrath K. American Gastroenterological Association guidelines are inaccurate in detecting pancreatic cysts with advanced neoplasia: a clinicopathologic study of 225 patients with supporting molecular data. *Gastrointest Endosc* 2016; **83**: 1107-1117.e2 [PMID: 26709110 DOI: 10.1016/j.gie.2015.12.009]

31 **Kadiyala V**, Lee LS. Endosonography in the diagnosis and management of pancreatic cysts. *World J Gastrointest Endosc* 2015; **7**: 213-223 [PMID: 25789091 DOI: 10.4253/wjge.v7.i3.213]

32 **Brugge WR**, Lewandrowski K, Lee-Lewandrowski E, Centeno BA, Szydlo T, Regan S, del Castillo CF, Warshaw AL. Diagnosis of pancreatic cystic neoplasms: a report of the cooperative pancreatic cyst study. *Gastroenterology* 2004; **126**: 1330-1336 [PMID: 15131794 DOI: 10.1053/j.gastro.2004.02.013]

33 **de Jong K**, Verlaan T, Dijkgraaf MG, Poley JW, van Dullemen H, Bruno MJ, Fockens P. Interobserver agreement for endosonography in the diagnosis of pancreatic cysts. *Endoscopy* 2011; **43**: 579-584 [PMID: 21717378 DOI: 10.1055/s-0030-1256434]

34 **Ahmad NA**, Kochman ML, Brensinger C, Brugge WR, Faigel DO, Gress FG, Kimmey MB, Nickl NJ, Savides TJ, Wallace MB, Wiersema MJ, Ginsberg GG. Interobserver agreement among endosonographers for the diagnosis of neoplastic versus non-neoplastic pancreatic cystic lesions. *Gastrointest Endosc* 2003; **58**: 59-64 [PMID: 12838222 DOI: 10.1067/mge.2003.298]

35 **Zhong N**, Zhang L, Takahashi N, Shalmiyev V, Canto MI, Clain JE, Deutsch JC, DeWitt J, Eloubeidi MA, Gleeson FC, Levy MJ, Mallery S, Raimondo M, Rajan E, Stevens T, Topazian M. Histologic and imaging features of mural nodules in mucinous pancreatic cysts. *Clin Gastroenterol Hepatol* 2012; **10**: 192-198, 198.e1 [PMID: 21982970 DOI: 10.1016/j.cgh.2011.09.029]

36 **Kamata K**, Kitano M, Omoto S, Kadosaka K, Miyata T, Yamao K, Imai H, Sakamoto H, Harwani Y, Chikugo T, Chiba Y, Matsumoto I, Takeyama Y, Kudo M. Contrast-enhanced harmonic endoscopic ultrasonography for differential diagnosis of pancreatic cysts. *Endoscopy* 2016; **48**: 35-41 [PMID: 26605974 DOI: 10.1055/s-0034-1393564]

37 **Maker AV**, Lee LS, Raut CP, Clancy TE, Swanson RS. Cytology from pancreatic cysts has marginal

utility in surgical decision-making. *Ann Surg Oncol* 2008; **15**: 3187-3192 [PMID: 18766406 DOI: 10.1245/s10434-008-0110-0]

38 **Karsenti D**, Caillol F, Chaput U, Perrot B, Koch S, Vuitton L, Jacques J, Valats JC, Poincloux L, Subtil C, Chabrun E, Williet N, Vanbiervliet G, Belkhodja H, Charachon A, Wangermez M, Coron E, Cholet F, Privat J, Le Baleur Y, Bichard P, Ah Soune P, Lecleire S, Palazzo M; from the GRAPHE. Safety of Endoscopic Ultrasound-Guided Fine-Needle Aspiration for Pancreatic Solid Pseudopapillary Neoplasm Before Surgical Resection: A European Multicenter Registry-Based Study on 149 Patients. *Pancreas* 2020; **49**: 34-38 [PMID: 31856077 DOI: 10.1097/MPA.0000000000001460]

39 **Law JK**, Ahmed A, Singh VK, Akshintala VS, Olson MT, Raman SP, Ali SZ, Fishman EK, Kamel I, Canto MI, Dal Molin M, Moran RA, Khashab MA, Ahuja N, Goggins M, Hruban RH, Wolfgang CL, Lennon AM. A systematic review of solid-pseudopapillary neoplasms: are these rare lesions? *Pancreas* 2014; **43**: 331-337 [PMID: 24622060 DOI: 10.1097/MPA.0000000000000061]

40 **Ridtitid W**, Halawi H, DeWitt JM, Sherman S, LeBlanc J, McHenry L, Coté GA, Al-Haddad MA. Cystic pancreatic neuroendocrine tumors: outcomes of preoperative endosonography-guided fine needle aspiration, and recurrence during long-term follow-up. *Endoscopy* 2015; **47**: 617-625 [PMID: 25763832 DOI: 10.1055/s-0034-1391712]

41 **Lee LS**. Diagnosis of pancreatic neuroendocrine tumors and the role of endoscopic ultrasound. *Gastroenterol Hepatol (N Y)* 2010; **6**: 520-522 [PMID: 20978556]

42 **Barnes EL**, Lee LS. Got milk? *Gastroenterology* 2015; **148**: e1-e2 [PMID: 25637836 DOI: 10.1053/j.gastro.2014.09.035]

43 **Hong SK**, Loren DE, Rogart JN, Siddiqui AA, Sendecki JA, Bibbo M, Coben RM, Meckes DP, Kowalski TE. Targeted cyst wall puncture and aspiration during EUS-FNA increases the diagnostic yield of premalignant and malignant pancreatic cysts. *Gastrointest Endosc* 2012; **75**: 775-782 [PMID: 22317883 DOI: 10.1016/j.gie.2011.12.015]

44 **Phan J**, Dawson D, Sedarat A, Fejleh MP, Marya N, Thaker AM, Rogers M, Kim S, Muthusamy VR. Clinical Utility of Obtaining Endoscopic Ultrasound-Guided Fine-Needle Biopsies for Histologic Analyses of Pancreatic Cystic Lesions. *Gastroenterology* 2020; **158**: 475-477.e1 [PMID: 31738913 DOI: 10.1053/j.gastro.2019.10.048]

45 **Bick BL**, Enders FT, Levy MJ, Zhang L, Henry MR, Abu Dayyeh BK, Chari ST, Clain JE, Farnell MB, Gleeson FC, Kendrick ML, Pearson RK, Petersen BT, Rajan E, Vege SS, Topazian M. The string sign for diagnosis of mucinous pancreatic cysts. *Endoscopy* 2015; **47**: 626-631 [PMID: 25730281 DOI: 10.1055/s-0034-1391484]

46 **Ngamruengphong S**, Bartel MJ, Raimondo M. Cyst carcinoembryonic antigen in differentiating pancreatic cysts: a meta-analysis. *Dig Liver Dis* 2013; **45**: 920-926 [PMID: 23790480 DOI: 10.1016/j.dld.2013.05.002]

47 **Boot C**. A review of pancreatic cyst fluid analysis in the differential diagnosis of pancreatic cyst lesions. *Ann Clin Biochem* 2014; **51**: 151-166 [PMID: 24097809 DOI: 10.1177/0004563213503819]

48 **Faias S**, Cravo M M, Chaves P, Pereira L. A comparative analysis of glucose and carcinoembryonic antigen in diagnosis of pancreatic mucinous cysts: a systematic review and meta-analysis. *Gastrointest Endosc* 2021 [PMID: 33508302 DOI: 10.1016/j.gie.2021.01.021]

49 **van der Waaij LA**, van Dullemen HM, Porte RJ. Cyst fluid analysis in the differential diagnosis of pancreatic cystic lesions: a pooled analysis. *Gastrointest Endosc* 2005; **62**: 383-389 [PMID: 16111956 DOI: 10.1016/s0016-5107(05)01581-6]

50 **McCarty TR**, Paleti S, Rustagi T. Molecular analysis of EUS-acquired pancreatic cyst fluid for KRAS and GNAS mutations for diagnosis of intraductal papillary mucinous neoplasia and mucinous cystic lesions: a systematic review and meta-analysis. *Gastrointest Endosc* 2021; **93**: 1019-1033.e5 [PMID: 33359054 DOI: 10.1016/j.gie.2020.12.014]

51 **Singhi AD**, Nikiforova MN, Fasanella KE, McGrath KM, Pai RK, Ohori NP, Bartholow TL, Brand RE, Chennat JS, Lu X, Papachristou GI, Slivka A, Zeh HJ, Zureikat AH, Lee KK, Tsung A, Mantha GS, Khalid A. Preoperative GNAS and KRAS testing in the diagnosis of pancreatic mucinous cysts. *Clin Cancer Res* 2014; **20**: 4381-4389 [PMID: 24938521 DOI: 10.1158/1078-0432.CCR-14-0513]

52 **Al-Haddad M**, DeWitt J, Sherman S, Schmidt CM, LeBlanc JK, McHenry L, Coté G, El Chafic AH, Luz L, Stuart JS, Johnson CS, Klochan C, Imperiale TF. Performance characteristics of molecular (DNA) analysis for the diagnosis of mucinous pancreatic cysts. *Gastrointest Endosc* 2014; **79**: 79-87 [PMID: 23845445 DOI: 10.1016/j.gie.2013.05.026]

53 **Singhi AD**, McGrath K, Brand RE, Khalid A, Zeh HJ, Chennat JS, Fasanella KE, Papachristou GI, Slivka A, Bartlett DL, Dasyam AK, Hogg M, Lee KK, Marsh JW, Monaco SE, Ohori NP, Pingpank JF, Tsung A, Zureikat AH, Wald AI, Nikiforova MN. Preoperative next-generation sequencing of pancreatic cyst fluid is highly accurate in cyst classification and detection of advanced neoplasia. *Gut* 2018; **67**: 2131-2141 [PMID: 28970292 DOI: 10.1136/gutjnl-2016-313586]

54 **Springer S**, Wang Y, Dal Molin M, Masica DL, Jiao Y, Kinde I, Blackford A, Raman SP, Wolfgang CL, Tomita T, Niknafs N, Douville C, Ptak J, Dobbyn L, Allen PJ, Klimstra DS, Schattner MA, Schmidt CM, Yip-Schneider M, Cummings OW, Brand RE, Zeh HJ, Singhi AD, Scarpa A, Salvia R, Malleo G, Zamboni G, Falconi M, Jang JY, Kim SW, Kwon W, Hong SM, Song KB, Kim SC, Swan N, Murphy J, Geoghegan J, Brugge W, Fernandez-Del Castillo C, Mino-Kenudson M, Schulick R, Edil BH, Adsay V, Paulino J, van Hooft J, Yachida S, Nara S, Hiraoka N, Yamao K, Hijioka S, van der Merwe S, Goggins M, Canto MI, Ahuja N, Hirose K, Makary M, Weiss MJ, Cameron J, Pittman M, Eshleman JR, Diaz LA Jr, Papadopoulos N, Kinzler KW, Karchin R, Hruban RH, Vogelstein B,

Lennon AM. A combination of molecular markers and clinical features improve the classification of pancreatic cysts. *Gastroenterology* 2015; **149**: 1501-1510 [PMID: 26253305 DOI: 10.1053/j.gastro.2015.07.041]

55 **Li ZH**, Zhong LQ, Mu WN, Wu YH. Toxicity of Tributyltin in Juvenile Common Carp (Cyprinus Carpio): Physiological Responses, Hepatic Gene Expression, and Stress Protein Profiling. *J Biochem Mol Toxicol* 2016; **30**: 91-96 [PMID: 26418422 DOI: 10.1002/jbt.21767]

56 **Napoleon B**, Palazzo M, Lemaistre AI, Caillol F, Palazzo L, Aubert A, Buscail L, Maire F, Morellon BM, Pujol B, Giovannini M. Needle-based confocal laser endomicroscopy of pancreatic cystic lesions: a prospective multicenter validation study in patients with definite diagnosis. *Endoscopy* 2019; **51**: 825-835 [PMID: 30347425 DOI: 10.1055/a-0732-5356]

57 **Keane MG**, Wehnert N, Perez-Machado M, Fusai GK, Thorburn D, Oppong KW, Carroll N, Metz AJ, Pereira SP. A prospective trial of CONfocal endomicroscopy in CYSTic lesions of the pancreas: CONCYST-01. *Endosc Int Open* 2019; **7**: E1117-E1122 [PMID: 31475228 DOI: 10.1055/a-0957-2976]

58 **Kadayifci A**, Atar M, Basar O, Forcione DG, Brugge WR. Needle-Based Confocal Laser Endomicroscopy for Evaluation of Cystic Neoplasms of the Pancreas. *Dig Dis Sci* 2017; **62**: 1346-1353 [PMID: 28281172 DOI: 10.1007/s10620-017-4521-2]

59 **Balaban VD**, Cazacu IM, Pinte L, Jinga M, Bhutani MS, Saftoiu A. EUS-through-the-needle microbiopsy forceps in pancreatic cystic lesions: A systematic review. *Endosc Ultrasound* 2021; **10**: 19-24 [PMID: 32611848 DOI: 10.4103/eus.eus_23_20]

60 **Kovacevic B**, Klausen P, Rift CV, Toxværd A, Grossjohann H, Karstensen JG, Brink L, Hassan H, Kalaitzakis E, Storkholm J, Hansen CP, Hasselby JP, Vilmann P. Clinical impact of endoscopic ultrasound-guided through-the-needle microbiopsy in patients with pancreatic cysts. *Endoscopy* 2021; **53**: 44-52 [PMID: 32693411 DOI: 10.1055/a-1214-6043]

61 **Wu J**, Wang Y, Li Z, Miao H. Accuracy of Fukuoka and American Gastroenterological Association Guidelines for Predicting Advanced Neoplasia in Pancreatic Cyst Neoplasm: A Meta-Analysis. *Ann Surg Oncol* 2019; **26**: 4522-4536 [PMID: 31617119 DOI: 10.1245/s10434-019-07921-8]

62 **Abdeljawad K**, Vemulapalli KC, Schmidt CM, Dewitt J, Sherman S, Imperiale TF, Al-Haddad M. Prevalence of malignancy in patients with pure main duct intraductal papillary mucinous neoplasms. *Gastrointest Endosc* 2014; **79**: 623-629 [PMID: 24094923 DOI: 10.1016/j.gie.2013.08.024]

63 **Sugimoto M**, Elliott IA, Nguyen AH, Kim S, Muthusamy VR, Watson R, Hines OJ, Dawson DW, Reber HA, Donahue TR. Assessment of a Revised Management Strategy for Patients With Intraductal Papillary Mucinous Neoplasms Involving the Main Pancreatic Duct. *JAMA Surg* 2017; **152**: e163349 [PMID: 27829085 DOI: 10.1001/jamasurg.2016.3349]

64 **Sahora K**, Mino-Kenudson M, Brugge W, Thayer SP, Ferrone CR, Sahani D, Pitman MB, Warshaw AL, Lillemoe KD, Fernandez-del Castillo CF. Branch duct intraductal papillary mucinous neoplasms: does cyst size change the tip of the scale? *Ann Surg* 2013; **258**: 466-475 [PMID: 24022439 DOI: 10.1097/SLA.0b013e3182a18f48]

65 **Du C**, Chai NL, Linghu EQ, Li HK, Sun LH, Jiang L, Wang XD, Tang P, Yang J. Comparison of endoscopic ultrasound, computed tomography and magnetic resonance imaging in assessment of detailed structures of pancreatic cystic neoplasms. *World J Gastroenterol* 2017; **23**: 3184-3192 [PMID: 28533675 DOI: 10.3748/wjg.v23.i17.3184]

66 **Cheon YK**, Cho YD, Jeon SR, Moon JH, Jeong SW, Hur KY, Jin SY, Lee JS. Pancreatic resection guided by preoperative intraductal ultrasonography for intraductal papillary mucinous neoplasm. *Am J Gastroenterol* 2010; **105**: 1963-1969 [PMID: 20407429 DOI: 10.1038/ajg.2010.169]

67 **Tyberg A**, Raijman I, Siddiqui A, Arnelo U, Adler DG, Xu MM, Nassani N, Sejpal DV, Kedia P, Nah Lee Y, Gress FG, Ho S, Gaidhane M, Kahaleh M. Digital Pancreaticocholangioscopy for Mapping of Pancreaticobiliary Neoplasia: Can We Alter the Surgical Resection Margin? *J Clin Gastroenterol* 2019; **53**: 71-75 [PMID: 29517713 DOI: 10.1097/MCG.0000000000001008]

68 **Choi JW**, Moon WJ. Gadolinium Deposition in the Brain: Current Updates. *Korean J Radiol* 2019; **20**: 134-147 [PMID: 30627029 DOI: 10.3348/kjr.2018.0356]

69 **Nougaret S**, Reinhold C, Chong J, Escal L, Mercier G, Fabre JM, Guiu B, Molinari N. Incidental pancreatic cysts: natural history and diagnostic accuracy of a limited serial pancreatic cyst MRI protocol. *Eur Radiol* 2014; **24**: 1020-1029 [PMID: 24569848 DOI: 10.1007/s00330-014-3112-2]

70 **Macari M**, Lee T, Kim S, Jacobs S, Megibow AJ, Hajdu C, Babb J. Is gadolinium necessary for MRI follow-up evaluation of cystic lesions in the pancreas? *AJR Am J Roentgenol* 2009; **192**: 159-164 [PMID: 19098196 DOI: 10.2214/AJR.08.1068]

71 **Oyama H**, Tada M, Takagi K, Tateishi K, Hamada T, Nakai Y, Hakuta R, Ijichi H, Ishigaki K, Kanai S, Kogure H, Mizuno S, Saito K, Saito T, Sato T, Suzuki T, Takahara N, Morishita Y, Arita J, Hasegawa K, Tanaka M, Fukayama M, Koike K. Long-term Risk of Malignancy in Branch-Duct Intraductal Papillary Mucinous Neoplasms. *Gastroenterology* 2020; **158**: 226-237.e5 [PMID: 31473224 DOI: 10.1053/j.gastro.2019.08.032]

72 **Marchegiani G**, Andrianello S, Pollini T, Caravati A, Biancotto M, Secchettin E, Bonamini D, Malleo G, Bassi C, Salvia R. "Trivial" Cysts Redefine the Risk of Cancer in Presumed Branch-Duct Intraductal Papillary Mucinous Neoplasms of the Pancreas: A Potential Target for Follow-Up Discontinuation? *Am J Gastroenterol* 2019; **114**: 1678-1684 [PMID: 31449158 DOI: 10.14309/ajg.0000000000000378]

73 **Pergolini I**, Sahora K, Ferrone CR, Morales-Oyarvide V, Wolpin BM, Mucci LA, Brugge WR, Mino-Kenudson M, Patino M, Sahani DV, Warshaw AL, Lillemoe KD, Fernández-Del Castillo C. Long-

term Risk of Pancreatic Malignancy in Patients With Branch Duct Intraductal Papillary Mucinous Neoplasm in a Referral Center. *Gastroenterology* 2017; **153**: 1284-1294.e1 [PMID: 28739282 DOI: 10.1053/j.gastro.2017.07.019]

74 **Gil E**, Choi SH, Choi DW, Heo JS, Kim MJ. Mucinous cystic neoplasms of the pancreas with ovarian stroma. *ANZ J Surg* 2013; **83**: 985-990 [PMID: 23072713 DOI: 10.1111/j.1445-2197.2012.06295.x]

World Journal of Gastroenterology

Submit a Manuscript: https://www.f6publishing.com

World J Gastroenterol 2021 September 14; 27(34): 5715-5726

DOI: 10.3748/wjg.v27.i34.5715

ISSN 1007-9327 (print) ISSN 2219-2840 (online)

MINIREVIEWS

Artificial intelligence for hepatitis evaluation

Wei Liu, Xue Liu, Mei Peng, Gong-Quan Chen, Peng-Hua Liu, Xin-Wu Cui, Fan Jiang, Christoph F Dietrich

ORCID number: Wei Liu 0000-0001-7777-5507; Xue Liu 0000-0003-4148-6812; Mei Peng 0000-0001-7809-9440; Gong-Quan Chen 0000-0002-4204-6133; Peng-Hua Liu 0000-0003-1981-7451; Xin-Wu Cui 0000-0003-3890-6660; Fan Jiang 0000-0001-8896-2009; Christoph F Dietrich 0000-0001-6015-6347.

Author contributions: Cui XW, Jiang F, and Dietrich CF established the design and conception of the paper; Liu W, Liu X, Peng M, Chen GQ, Liu PH, Jiang F, Cui XW, and Dietrich CF explored the literature data; Liu W provided the first draft of the manuscript, which was discussed and revised critically for intellectual content by Liu X, Peng M, Chen GQ, Liu PH, Jiang F, Cui XW, and Dietrich CF; all authors discussed the statement and conclusions and approved the final version to be published.

Supported by the National Natural Science Foundation of China, No. 82071953; and Department of Science and Technology of Hunan Province, No. 2020SK52103.

Conflict-of-interest statement: There is no conflict of interest associated with any of the senior author or other coauthors who contributed their efforts in this manuscript.

Open-Access: This article is an open-access article that was

Wei Liu, Xue Liu, Mei Peng, Fan Jiang, Department of Medical Ultrasound, The Second Hospital of Anhui Medical University, Hefei 230601, Anhui Province, China

Gong-Quan Chen, Department of Medical Ultrasound, Minda Hospital of Hubei Minzu University, Enshi 445000, Hubei Province, China

Peng-Hua Liu, Department of Medical Ultrasound, The First Affiliated Hospital of Shaoyang University, Shaoyang 422000, Hunan Province, China

Xin-Wu Cui, Sino-German Tongji-Caritas Research Center of Ultrasound in Medicine, Department of Medical Ultrasound, Tongji Hospital, Tongji Medical College, Huazhong University of Science and Technology, Wuhan 430030, Hubei Province, China

Christoph F Dietrich, Department Allgemeine Innere Medizin, Kliniken Hirslanden Beau Site, Salem und Permanence, Bern 3626, Switzerland

Corresponding author: Xin-Wu Cui, MD, PhD, Professor, Sino-German Tongji-Caritas Research Center of Ultrasound in Medicine, Department of Medical Ultrasound, Tongji Hospital, Tongji Medical College, Huazhong University of Science and Technology, No. 1095 Jiefang Avenue, Wuhan 430030, Hubei Province, China. cuixinwu@live.cn

Abstract

Recently, increasing attention has been paid to the application of artificial intelligence (AI) to the diagnosis of diverse hepatic diseases, which comprises traditional machine learning and deep learning. Recent studies have shown the possible value of AI based data mining in predicting the incidence of hepatitis, classifying the different stages of hepatitis, diagnosing or screening for hepatitis, forecasting the progression of hepatitis, and predicting response to antiviral drugs in chronic hepatitis C patients. More importantly, AI based on radiology has been proven to be useful in predicting hepatitis and liver fibrosis as well as grading hepatocellular carcinoma (HCC) and differentiating it from benign liver tumors. It can predict the risk of vascular invasion of HCC, the risk of hepatic encephalopathy secondary to hepatitis B related cirrhosis, and the risk of liver failure after hepatectomy in HCC patients. In this review, we summarize the application of AI in hepatitis, and identify the challenges and future perspectives.

Key Words: Machine learning; Deep learning; Radiomics; Hepatitis; Fibrosis; Hepatocellular carcinoma

©The Author(s) 2021. Published by Baishideng Publishing Group Inc. All rights reserved.

selected by an in-house editor and fully peer-reviewed by external reviewers. It is distributed in accordance with the Creative Commons Attribution NonCommercial (CC BY-NC 4.0) license, which permits others to distribute, remix, adapt, build upon this work non-commercially, and license their derivative works on different terms, provided the original work is properly cited and the use is non-commercial. See: http://creativecommons.org/Licenses/by-nc/4.0/

Manuscript source: Invited manuscript

Specialty type: Gastroenterology and hepatology

Country/Territory of origin: China

Peer-review report's scientific quality classification

Grade A (Excellent): 0
Grade B (Very good): 0
Grade C (Good): C, C
Grade D (Fair): 0
Grade E (Poor): 0

Received: March 1, 2021
Peer-review started: March 1, 2021
First decision: April 18, 2021
Revised: April 28, 2021
Accepted: August 2, 2021
Article in press: August 2, 2021
Published online: September 14, 2021

P-Reviewer: Borzi L
S-Editor: Zhang H
L-Editor: Wang TQ
P-Editor: Liu JH



Core Tip: Currently, there is a need of a comprehensive review to introduce the applications of artificial intelligence (AI) in hepatitis. We first discuss the possible value of AI based data mining in predicting the incidence of hepatitis, classifying the different stages of hepatitis, diagnosing or screening for hepatitis, forecasting the progression of hepatitis, and predicting response to antiviral drugs in chronic hepatitis C patients. In addition, we introduce the applications of AI based on radiology in predicting hepatitis and liver fibrosis, grading hepatocellular carcinoma (HCC) and differentiating it from benign liver tumors, and predicting the risk of vascular invasion of HCC as well as the risk of hepatic encephalopathy secondary to hepatitis B related cirrhosis.

Citation: Liu W, Liu X, Peng M, Chen GQ, Liu PH, Cui XW, Jiang F, Dietrich CF. Artificial intelligence for hepatitis evaluation. *World J Gastroenterol* 2021; 27(34): 5715-5726
URL: https://www.wjgnet.com/1007-9327/full/v27/i34/5715.htm
DOI: https://dx.doi.org/10.3748/wjg.v27.i34.5715

INTRODUCTION

Artificial intelligence (AI) is a new discipline that aims to simulate, extend, and expand human intelligence and integrates theory, method, and application research and development[1]. According to the different algorithms of AI, AI is usually divided into traditional AI (*e.g.*, traditional machine learning) and deep learning (based on neural network structure) in the medical field[2]. Compared with traditional AI, deep learning can directly apply the image to the learning process without manual feature extraction, while traditional machine learning needs manual recognition and extraction of different features. Therefore, deep learning has the advantage of no manual extraction of various features, which makes its learning process faster, intelligent, and accurate. In addition, deep learning can iterate and improve from past mistakes, but it needs more big data and more result analysis to fully show its robust and precise efficiency[3].

Lately, AI technology has been at the forefront of scientific research. The benefits of the AI model in various fields have triggered an upsurge in the use of this technology for data mining and analysis in more areas, and it has also attracted attention in the field of medicine and biological cognition[4]. For instance, AI has been widely used in the examination of superficial glands such as the thyroid and breast to assist radiologists to evaluate whether nodules are benign or malignant, with a high level of accuracy. The accuracy is lower than that of senior radiologists but higher than that of junior radiologists[5-7]. Some literature has reported the application of AI technology based on data mining or radiology in predicting hepatitis, evaluating fibrosis, and diagnosing benign and malignant liver masses[8-10].

This systematic review is intended to ascertain the clinical utility in routine practice of AI based on data mining, predict the incidence of hepatitis A, B, C, or E, categorize the different stages of hepatitis B, predict the progression of hepatitis C in veterans, and diagnose or screen for hepatitis B. Particularly, this review focuses on the application of deep learning or radiomics based on radiology to stage hepatic fibrosis, predict the occurrence of HCC, identify microvascular invasion, and predict the risk of liver failure after hepatectomy in HCC patients.

HEPATITIS DETECTION BASED ON DATA MINING

Predicting incidence of hepatitis

Newborn babies are required to be vaccinated with hepatitis B vaccine in numerous countries, which has reduced the incidence of hepatitis worldwide. However, viral hepatitis is still a serious health problem[11]. Hence, Guan *et al*[12] designed the AI model of artificial neural network (ANN) and autoregressive integrated moving average (ARIMA) with hepatitis data mined from Liaoning Disease Control and Prevention Center, which aimed to forecast the incidence of hepatitis A. They extracted data concerning the incidence of hepatitis A from 1987 to 2001 in the above-mentioned Disease Control and Prevention Center. The incidence of hepatitis A from

1981 to 1997 was taken as the training group and from 1998 to 2001 as the validation group. The forecasting statistical effect value and the correlation coefficient are summarized in Table 1. Intelligently mining hepatitis B-related medical record data from local health websites authorized by the local Health Commission, the AI model of ARIMA (0, 1, 1) and ElmanNN (Elman neural network) with eight neurons were established by Zheng *et al*[13]. From January 2012 to August 2019, the local health bureau reported 486983 cases of hepatitis B. Hepatitis B incidence from January 2012 to December 2018 was used to build and train ARIMA (0, 1, 1) model and ElmanNN model with eight neurons, and hepatitis B incidence from January 2019 to August 2019 was used to validate ARIMA (0, 1, 1) model and ElmanNN with eight neurons, with root-mean-square error (RMSE) and mean absolute error (MAE) applied to evaluate the prediction effect of the model. The RMSE and MAE of the above-mentioned ARIMA (0, 1, 1) model and ElmanNN with eight neurons are shown in Table 1. Gan *et al*[14] also tried to forecast the incidence of hepatitis B using a hybrid model combing Grey system and BP-ANN (back propagation artificial neural networks), with trained and validated data collected from National Health Commission. From 2003 to 2012, 10486959 cases of hepatitis B were reported by National Health Commission. Compared with the above data, the prediction effect of a hybrid model, Grey model (1, 1) and Grey model (2, 1), was calculated. The predictive results are summarized in Table 1. The results showed that the hybrid algorithm was superior to the Grey model algorithm in all assessment norms, and a better prediction effect was achieved. Intending to predict the incidence of hepatitis E, Guo *et al*[15] mined monthly incidence and cases of hepatitis E from the local Center for Disease Control and Prevention as samples. All above-mentioned data were collected from January 2005 to December 2017 in the local Centers for Disease Control. The monthly incidence and cases from January 2005 to June 2015 were used as the input variable to establish an AI model of the ARIMA, supporter vector machine (SVM), and long-short time memory neural network (LSTM), and those from July 2015 to December 2017 as the validating group. The assessment indexes of the ARIMA, SVM, and LSTM models were RMSE and MAE, whose corresponding values are given in Table 1.

Classifying different stages of hepatitis

According to the serological level of transaminase and serological titer of hepatitis B antigen or antibody, hepatitis B can be categorized into five stages: I, HBeAg (+) chronic infection; II, HBeAg (+) chronic hepatitis; III, HBeAg (-) chronic infection; IV, HBeAg (-) chronic hepatitis; V, HBsAg (-) stage. For young doctors, it can be difficult to accurately classify the clinical types of hepatitis. Therefore, with 52 patients included, an automated diagnosis of hepatitis B using multilayer mamdani fuzzy inference system expert system (ADHB-ML-MFIS) was established by Ahmad *et al*[16] to categorize the different stages of hepatitis B. In the ADHB-ML-MFIS expert system, there were two levels of input variables. The input variables of the first layer were transaminase, and the input variables of the second layer were serological markers of hepatitis B. The diagnostic accuracy of the ADHB-ML-MFIS expert system for differentiating stages of hepatitis B was 92.2% with the detailed results shown in Table 1.

Diagnosing or screening for hepatitis

Raman spectroscopy has been used to diagnose hepatitis B, showing a superior performance compared to traditional serological tests. Obtaining 119 confirmed hepatitis B virus (HBV) infected samples from histopathology department, Khan *et al*[8] combined Raman spectroscopy with pattern recognition technology, and established an AI model based on the SVM algorithm and radial basis function to diagnose hepatitis B. In the study, the AI model achieved high diagnostic performance for hepatitis B, with the data presented in Table 1. Collecting data from 1134 blood samples, Wang *et al*[17] proposed a method for promptly screening hepatitis B patients and non-hepatitis B patients using serum Raman spectroscopy combined with LSTM. Then, LSTM was used to train the spectral data. Several models can distinguish hepatitis B from non-hepatitis B, with the highest diagnostic efficacy acquired by serum Raman spectroscopy combined with LSTM. The accuracy of serum Raman spectroscopy combined with LSTM for screening hepatitis B from non-hepatitis B was 0.9732. About 50% of hepatitis C virus (HCV) infected persons worldwide have not been diagnosed or treated, and it remains a significant risk factor for human health [18]. Thus, it is vital that clinicians could find these undiagnosed patients with hepatitis C infection, a nowadays-treatable disease. With 120023 HCV patients and 9601900 non-HCV patients used as modeling data, Doyle *et al*[19]developed five kinds of AI models attempting to find undiagnosed hepatitis C infection: Logistic regression, gradient boosting trees, gradient boosting trees with temporal variables, stacked

Table 1 Hepatitis detection based on data mining

No.	Task	Algorithms	Sample size (type)	Evaluation index	Ref.
1	Predicting incidence of hepatitis A	ANN; ARIMA	N/A (CDC data)	ANN: Correlation coefficient 0.71; ARIMA: Correlation coefficient 0.66	[12]
2	Predicting incidence of hepatitis B	ARIMA; ElmanNN	486983 cases (data from health commission)	ARIMA: RMSE 0.94, MAE 0.81; ElmanNN: RMSE 0.89, MAE 0.70	[13]
3	Forecasting incidence of hepatitis B	Hybrid method (combing GM and BP-ANN)	10486959 cases (data from health ministry)	R 0.9495, RMSE 4.863 × 10^3, MAE 3.9704 × 10^4	[14]
4	Prediction of incidence of hepatitis E	ARIMA; SVM; LSTM	N/A (CDC data)	ARIMA: RMSE 0.022, MAE 0.018; SVM: RMSE 0.0204, MAE 0.0167; LSTM: RMSE 0.01, MAE 0.011	[15]
5	Automated classification of the different stages of hepatitis B	ADHB-ML-MFIS expert system	52 patients (serological data)	Overall accuracy: 0.922; No hepatitis accuracy: 1; Due to infection accuracy: 0.75; Acute HBV accuracy: 0.95; Chronic HBV accuracy: 0.91	[16]
6	Analyzing HBV infection from normal blood samples	Polynomial function; RBF	119 serum samples from HBV infected patients (Raman spectroscopy data)	Polynomial kernel (order-2): Quadratic programming/least squares: Accuracy 98%, precision 97%, sensitivity 100%, specificity 95%; RBF kernel (RBF sigma-2): Quadratic programming: accuracy 94%, precision 90%, sensitivity 100%, specificity 87%; RBF kernel (RBF sigma-2): Least squares: Accuracy 95%, precision 92%, sensitivity 100%, specificity 90%	[8]
7	Rapidly screening hepatitis B from non-hepatitis B	LSTM	1134 blood samples (Raman spectroscopy data)	Accuracy 97.32%, sensitivity 97.87%, specificity 96.77%, precision 96.84%	[17]
8	Finding undiagnosed patients with hepatitis C infection	Logistic regression; Gradient boosting trees; Gradient boosting trees with temporal variables; Stacked ensemble; Random forest	9721923 patients (data from the patient's medical history)	The stacked ensemble had a specificity of 0.99 and precision of 0.97 at a recall level of 0.50	[19]
9	Predicting hepatitis C virus progression among veterans	CS Cox modellongitudinal Cox model; CS boosting modelLongitudinal-boosting model	72683 CHC individuals (VHA data)	CS Cox model: Concordance 0.746; Longitudinal Cox model: Concordance 0.764; CS boosting model: Concordance 0.758; Longitudinal-boosting model: Concordance 0.774	[20]
10	Forecasting response to IFN plus RIB treatment in HCV patients	ANN	300 patients (serological data)	The diagnostic accuracy rose from 52% (ANN 2) to 70% (ANN 6)	[21]

ANN: Artificial neural network; ARIMA: Autoregressive integrated moving average; CDC: Centers for Disease Control; RMSE: Root-mean-square error; MAE: Mean absolute error; GM: Grey model, BP-ANN: Back propagation artificial neural networks; SVM: Supporter vector machine; LSTM: Long-short time memory neural network; ADHB-ML-MFIS: Automated diagnosis of hepatitis B using multilayer Mamdani fuzzy inference; HBV: Hepatitis B virus; RBF: Gaussian radial basic function; CHC: Chronic hepatitis C virus; VHA: National Veterans Health Administration; IFN: Interferon; RIB: Ribavirin, HCV: Hepatitis C virus.

ensemble, and random forest. All these models mined data from demographics, risk factors, symptoms, treatments, and procedures relevant to HCV from the patient's medical history. At different recall levels, the models had different diagnostic performances. For example, the stacked ensemble had a specificity of 0.99 and precision of 0.97 at a recall level of 0.50.

Forecasting progression of hepatitis

Liver biopsy is the gold standard for the evaluation of liver fibrosis and cirrhosis. However, liver biopsy is an invasive examination and carries the risk of causing liver bleeding. In clinical practice, aspartate aminotransferase-to-platelet ratio index (APRI) and radiology are often used to forecast hepatic fibrosis and cirrhosis. In Konerman *et al*[20]'s study, aiming to predict HCV progression among veterans, they developed the cross-sectional (CS) Cox model, longitudinal Cox model, CS boosting model, and longitudinal-boosting model with 72683 chronic hepatitis C (CHC) individuals and matched control data searched from National Veterans Health Administration between 2000 and 2016. The calculated value of APRI > 2 after time zero for two consecutive times indicated the progression of liver cirrhosis. The predictive

concordance of the above-mentioned four models is given in Table 1.

Predicting response to antiviral drugs in CHC patients

The combined administration of interferon-alpha (IFN) and ribavirin (RIB) is the first-line recommended treatment regimen for patients with CHC. However, the cure rate is still low and the incidence of side effects is high. Therefore, there is an urgent need for doctors in the hepatology or infection departments to evaluate the response of patients with CHC to the combinative administration of IFN and RIB. Hence, Maiellaro *et al*[21] retrospectively analyzed 300 patients treated with IFN plus RIB through an ANN, intending to predict the response to the treatment. The range of positive predictive value and negative predictive value of the ANN model for predicting the treatment response of patients with CHC to the combined administration of IFN and RIB was 57%-75% and 52%-71%, respectively.

HEPATITIS EVALUATION BASED ON RADIOLOGY

Radiology plays an important role in evaluating a range of hepatic diseases, such as hepatitis, hepatic fibrosis, HCC, vascular invasion of liver cancer, and even HE. With the rapid development of computer technology and AI, radiomics and deep learning have become hot topics in the field of medical imaging. Compared with traditional AI, deep learning is a more advanced and intelligent learning algorithm, which was based on a neural network structure inspired by the human brain[22,23]. Radiomics has also been developed recently. It can adopt a variety of methods to extract numerous quantitative features from ultrasound, computed tomography (CT), and magnetic resonance imaging (MRI) images, then select the quantitative features related to the task, finally providing clinicians with a model based on radiomics to evaluate diagnostic and prognostic information[24,25].

Predicting clinical severity in alcohol-associated hepatitis patients

Tana *et al*[26] included 34 patients with alcohol-associated hepatitis (AAH) and 35 control subjects in their study to extract texture features from computed tomography images based on random forest and deep learning convolutional neural network algorithms, which evaluated the diagnostic value of CT texture analysis for clinical severity (most notably aspartate aminotransferase) in AAH patients. Recursive feature elimination using random forest identified 23 top features for AAH categorizing, and the accuracy of deep learning for diagnosing AAH was 70% in the validation set.

Diagnosing or grading liver fibrosis

According to the METAVIR scoring system[27], hepatic fibrosis can be divided into five categories: F0, no fibrosis; F1, portal fibrosis without septa; F2, portal fibrosis and few septa; F3, numerous septa without cirrhosis; F4, cirrhosis. Significant fibrosis is defined as ≥ F2. Based on radiomics or deep learning algorithms, multifarious imaging modalities have been applied to diagnose or stage liver fibrosis, such as ultrasound, contrast or non-contrast CT, CT texture, MRI, or gadoxetic acid–enhanced hepato-biliary phase MR.

A study including 144 HBV infected patients, evaluated the performance of multiparametric ultrasomics for the diagnosis of significant hepatic fibrosis[9]. Conventional ultrasomics, original radiofrequency, and contrast-enhanced micro-flow features comprise the multiparametric ultrasomics for clinicians to diagnose diseases and monitor treatment regimens. Multiparametric ultrasomics used Adaboost, random forest, and SVM algorithms for predicting significant liver fibrosis, with results summarized in Table 2. With 466 patients (401 with chronic hepatitis B, 65 without fibrosis) undergoing partial hepatectomy used as the data of the training group and test group of transfer learning (TL) radiomics, Xue *et al*[28] discussed the diagnostic value of transfer learning radiomics based on multimodal ultrasound in the grading of liver fibrosis. As the name suggests, TL moves a network trained on a large data set on to other related tasks, thus avoiding the over fitting problem caused by insufficient training data in conventional deep learning. Results showed that the area under the curve (AUC) of TL was statistically higher than that of non-TL, and the AUC of multimodal ultrasound imaging was larger than that of single modality ultrasound imaging. Hence, multimodal ultrasound imaging based on TL could usefully be applied to the staging of liver fibrosis.

Table 2 Hepatitis or hepatitis associated lesion detection based on radiology

No.	Task	Algorithms (model)	Sample size (type)	Evaluation index	Ref.
1	Predicting clinical severity in AAH patients	Random forest; Convolutional neural network	69 cases (CT texture features)	Accuracy: 82.4% of RFE-RF in the test set; Accuracy: 70% of CNN in the test set	[26]
2	Assessing significant liver fibrosis by multiparametric ultrasomics data	Adaboost; Random forest; SVM (multiparametric ultrasomics)	144 HBV infected patients (multiparametric ultrasomics)	AUROC: 0.85 ± 0.01 of Adaboost, random forest, SVM in multiparametric ultrasomics including conventional ultrasomics, ORF and CEMF	[9]
3	Grading liver fibrosis	Inception-V3 network (transfer learning)	466 patients (multimodal ultrasound)	AUCs of TL in GM + EM reached 0.950, 0.932, and 0.930, respectively, for grading S4, ≥ S3, and ≥ S2an	[28]
4	Predicting cirrhosis	LASSO (radiomics nomogram)	144 cases of HBV patients (CT features and clinical factors)	AUROC: 0.915 in the training cohort, 0.872 in the validation cohort, overall correctly classified rate of 82.0%	[29]
5	Differentiating hepatic fibrosis' grade	RFC (CTTA-based models); SVM (CTTA-based models)	30 fibrosis patients (CT texture features)	Train AUC 0.95 in RFC (model 1); Test AUC 0.90 in RFC (model 1); Train AUC 0.88 in SVM (model 2); Test AUC 0.76 in SVM (model 2)	[30]
6	Assessing liver fibrosis severity	A prototype convolutional neural network	558 cases (CT images)	AUCs were 0.82, 0.85, and 0.88 of Vol_L/Vol_S in diagnosing advanced fibrosis, cirrhosis, and decompensated cirrhosis in the whole study population	[31]
7	Staging liver fibrosis	Convolutional neural network	634 fibrosis patients (MR images and MR/virus)	AUCs were 0.84, 0.84, and 0.85 of the model full for diagnosing F4, ≥ F3, and ≥ F2 in the test set, respectively	[34]
8	Assessing liver fibrosis in chronic hepatitis B	Convolution neural network (DLRE)	398 HBV patients (shear wave elastography)	AUCs of DLRE 1.00, 0.99, and 0.99 for classifying F4, ≥ F3, and ≥ F2 in the training set and 0.97, 0.98, and 0.85 in the validation set	[35]
9	Diagnosing FNH from HCC in the non-cirrhotic liver	LASSO (radiomics nomogram)	156 patients (CT images and clinical factors)	Accuracy: 92.4% in the training set, 89.2% in the validation set	[38]
10	Diagnosing HCC	LASSO (radiomics signature)	211 patients (MR images)	AUROC: 0.861 in the training set, 0.810 in the validation set	[39]
11	Preoperative prediction of HCC grade	LASSO (combined model with clinical factors and radiomics signature)	170 HCC patients (MR images and clinical factors)	AUROC: 0.742, 0.786, and 0.800 based on T1WI images, T2WI images, and combined T1WI and T2WI images in the combined model	[41]
12	Predicting MVI risk in HBV-related HCC preoperatively	LASSO (radiomics nomogram)	304 HCC patients (CT images and AFP)	AUROC: 0.846 in the training set, 0.844 in the validation set	[43]
13	Preoperative prediction of MVI in HCC patients	LASSO (combined model)	157 HCC patients (CT images and clinical factors)	AUROC: 0.835 in the training dataset, 0.801 in the validation dataset	[44]
14	Predicting risk of HE complicated by hepatitis B related cirrhosis	LASSO (integrated model of radiomics and clinical features)	304 cirrhosis patients (CT images and clinical factors)	Accuracy: 0.93 in the training cohort, 0.83 in the testing cohort	[45]
15	Predicting liver failure in cirrhotic patients with HCC after major hepatectomy	LASSO (integrated radiomics-based mode)	101 HCC patients (MR images and clinical factors)	Accuracy: 0.802 in radiomics-based model	[47]

AAH: Alcohol-associated hepatitis; CT: Computed tomography; RFE-RF: Recursive feature elimination using random forest; CNN: Convolutional neural network; SVM: Supporter vector machine; HBV: Hepatitis B virus; AUROC: Area under the receiver operating curve; ORF: Original radiofrequency; CEMF: Contrast-enhanced micro-flow; AUC: Area under curve; TL: Transfer learning; GM: Gray scale modality; EM: Elastogram modality; LASSO: Least absolute shrinkage and selection operator; RFC: Random forest classifier; CTTA: Computed tomography texture analysis; VolL: Liver volume; VolS: Spleen volume; MR: Magnetic resonance; DLRE: Deep learning radiomics of shear wave elastography; FNH: Focal nodular hyperplasia; HCC: Hepatocellular carcinoma; MVI: Microvascular invasion; AFP: Alpha-fetoprotein; HE: Hepatic encephalopathy.

In another study, Wang *et al*[29] included 144 HBV patients with hepatic fibrosis

confirmed by liver biopsy who underwent unenhanced CT examinations in their study and successfully extracted 25 cirrhosis-related CT features to construct a radiomics signature using the SVM algorithm. In addition to the CT features that were closely related to liver cirrhosis, the specific clinical factors (alanine transaminase, aspartate aminotransferase, globulin, and international normalized ratio) were also closely related to liver cirrhosis. Combining the radiomics signature and clinical factors, a radiomics-based nomogram was established, and the results demonstrated that the area under the receiver operating curve (AUROC) of the radiomics nomogram was 0.915 and 0.872 in the training and validation cohorts, respectively. CT texture analysis (CTTA) revealed the biological and pathological features of diverse liver diseases by analyzing the characteristics and distribution of pixels in medical images, and extracted texture features that were difficult to recognize by the naked eye. To explore the diagnostic value of CTTA in low- and high-grade hepatic fibrosis, Budai *et al*[30] included 30 patients with liver fibrosis in the study. They extracted 354 CT texture features and constructed a CTTA-based model using a random forest classifier (RFC) algorithm and SVM algorithm, respectively. The AUROC of the CTTA-based model based on the RFC algorithm in predicting fibrosis grade was 0.90 in both the first and second analyses. The AUC of the CTTA-based model using the SVM algorithm in predicting liver fibrosis in analysis I was 0.76, and 0.91 in analysis II that was the highest prediction rate. Son *et al*[31] also evaluated liver fibrosis severity using splenic volume (measured on portal venous phase CT images). They proposed a convolution neural network (CNN) based on a three-dimensional U-net, with 513 chronic liver disease patients and 45 healthy liver subjects taken as modeled data, dividing the liver and spleen into many segments. By using the calculus method, the volume of hepatic and splenic segments in each thin slice was first calculated, then the volume of the liver and spleen in each thin slice was calculated, and finally, the volume of the liver and spleen amounted to the volume of the liver and spleen in each thin slice multiplied by the thickness of each thin slice. Then, they evaluated the correlation between liver and spleen volume indexes [Vol_S (spleen volume), Vol_L (liver volume), and Vol_S/Vol_L] and liver fibrosis severity and their diagnostic value in liver fibrosis severity. The results demonstrated that the AUCs were 0.82, 0.85, and 0.88 of Vol_L/Vol_S for the diagnosis of advanced fibrosis, cirrhosis, and decompensated cirrhosis in the entire study population, which outperformed the Vol_L.

A variety of methods have been used to detect the stage of liver fibrosis, such as serological markers and elasticity scores based on ultrasound[32,33]. Yasaka *et al*[34] specifically included 534 patients with hepatic fibrosis into training datasets and 100 fibrosis patients into test sets, analyzing the diagnostic value of deep CNN using gadoxetic acid-enhanced hepatobiliary phase MR images and MR/virus model for liver fibrosis. The results showed that AUCs were 0.84, 0.84, and 0.85 of the model full (combined MR images and MR/virus model) for diagnosing F4, ≥ F3, and ≥ F2 in test sets, respectively, while 0.81, 0.84, and 0.83 of MR/virus model for diagnosing F4, ≥ F3, and ≥ F2 in test sets.

Previous studies have been limited to single-center studies to explore the diagnostic value of ultrasound, CT, or MRI images-based radiomics or deep learning model for liver fibrosis. Wang *et al*[35] subsequently carried out a prospective multicenter study based on deep learning radiomics of shear wave elastography (DLRE) to assess the diagnostic performance for evaluating liver fibrosis in chronic hepatitis B, and compare it with 2D-SWE (shear wave elastography) and serological biomarkers [APRI and fibrosis index based on four factors (FIB-4)]. A total of 398 patients from 12 hospitals in China with 1990 2D-SWE images were included in the study, and a DLRE model was established using the CNN algorithm. The results showed that the AUCs of DLRE were 0.97, 0.98, 0.85 for classifying F4, ≥ F3, and ≥ F2 in the validation set, which statistically outperformed 2D-SWE and serological biomarkers (APRI and FIB-4) except 2D-SWE in ≥ F2. Simplified structural flowchart of convolutional neural network architecture for staging liver fibrosis can be seen in Figure 1.

Diagnosing HCC

Typical focal nodular hyperplasia (FNH) has central cicatricial foci, which is enhanced in the arterial phase (AP), and the enhancement degree gradually decreases to low density in the portal venous phase (PVP). Atypical FNH has no central cicatricial foci and shows low perfusion, even hemorrhage, necrosis, and calcification on enhanced CT, which makes it difficult to differentiate atypical FNH from HCC[36,37]. Hence, Nie *et al*[38] aimed to establish a radiomics nomogram model based on CT for differentiating FNH from HCC. A total of 156 patients with FNH and HCC were divided into a training group and test group of the above-mentioned radiomics nomogram model. Initially, 4227 radiomics features were extracted from the regions of interest (ROIs) on

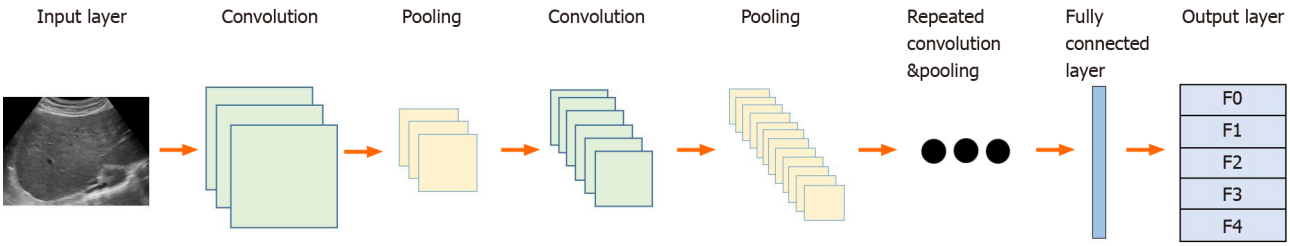


Figure 1 Simplified structural flowchart of convolutional neural network architecture for staging liver fibrosis. After repeatedly convoluting and pooling the input layer images, the extracted high-dimensional manageable features are fed into the fully connected layer and the classification task is performed by expressing the class probabilities through the output layer.

hepatic CT scan. After selection for inter- and intra-class correlation coefficients (ICCs) > 0.75 and statistical difference between the two groups, 764 radiomics features were entered into least absolute shrinkage and selection operator (LASSO) regression, and finally, ten features were used for the construction of a radiomics signature. After multivariate logistic regression calculation, old age, HBV infection, and early enhancement (with a washout pattern) were used to establish the clinical factors model. Three models were then established: Radiomics signature model, clinical factors model, and radiomics nomogram model (clinical factors and radiomics signature combined). The predictive performance of the radiomics nomogram model was superior to those of the other constructed models. The accuracy of the radiomics nomogram model for diagnosing HCC was 92.4% and 89.2% in the training and validation datasets, respectively.

To confirm the value of the AI model for predicting HCC, Jiang *et al*[39] implemented a prospective study to compare the diagnostic differences of the 2018 European Association for the Study of the Liver (EASL) criteria, Liver Imaging Reporting and Data System (LI-RADS) criteria, and a radiomics signature model for diagnosing HCC. They included 211 patients with surgically confirmed focal liver lesions (165 HCC patients, 30 non-HCC malignancies patients, and 16 non-HCC benign lesions patients) who were randomly divided into a training cohort (n = 133) and a validation cohort (n = 78). The results demonstrated that the AUROCs of HCC risk in all nodules calculated by EASL v2018 criteria, LR5/LR5V in LI-RADS v2018 criteria, and radiomics signature model were 0.811, 0.841, and 0.810, respectively. The benignity and malignancy of liver tumors are usually based on Edmondson grade. Generally speaking, low-grade liver tumors conform to Edmondson I/II, while high-grade liver tumors conform to Edmondson III/IV[40]. Wu *et al*[41] included 125 HCC patients in the training group and 45 HCC patients in the validation group to predict the grade of HCC patients based on unenhanced MRI radiomics. The MRI image was uploaded to ITK-SNAP software, and the ROI was depicted along the edge of the tumor on each TIWI and T2WI segment with radiomics features extracted from ROI. A total of 656 radiomics features were extracted. After LASSO regression selection, 14, 18, and 20 features were selected based on T1WI, T2WI, and combined T1WI and T2WI, respectively. Finally, the combined model was established with results summarized in Table 2.

Predicting microvascular invasion of HCC

The occurrence of microvascular invasion (MVI) often reduces the 5-year survival rate of HCC patients, which is closely related to the poor prognosis of HCC patients[42]. Peng *et al*[43] randomly assigned 304 cases of eligible HCC patients to the training group and validation group. IBEX software was used to extract radiomics features from the ROI of enhanced CT images in each of the HCC patients. In this study, 980 candidate radiomics features were generated from each patient, and after screening by LASSO with λ chosen smallest cross-validation error, eight radiomics features were selected to establish the radiomics signature. Radiomics signature, together with radiologic features (non-smooth tumor margin, internal arteries, and hypoattenuating halos) and alpha-fetoprotein > 20 ng/mL, was used to construct the radiomics nomogram, whose AUROC values for predicting MVI status were 0.846 and 0.844 in the training and validation sets, respectively. Ma *et al*[44] also discussed the value of preoperative radiomics nomogram for diagnosing MVI in HCC patients based on enhanced CT; 110 HCC patients were randomly assigned to the training cohort (MVI+ group 37 cases, MVI-group 73 cases), and 47 HCC patients to the validation cohort (MVI+ group 18 cases, MVI-group 29 cases). The ROI was drawn by an experienced

radiologist using ITK-SNAP software in AP, PVP, and delayed phase (DP) images on CT along the visible borders of the lesion. Initially, in the AP, PVP, and DP images, 647 radiomics features were extracted. After screening by ICC and concordance correlation coefficient ≥ 0.75 and LASSO method, finally, five AP features, seven PVP features, and nine DP features were selected. In predicting HCC invasion of MVI, PVP and radiomics signature outperformed AP and DP, hence, the PVP radiomics signature with the effective clinical factors constituted the combined model, whose AUCs were 0.835 and 0.801 in the training and validation groups, respectively for diagnosing MVI status in HCC.

Predicting HE secondary to hepatitis B related cirrhosis

Decompensated liver cirrhosis is often accompanied by multiple complications, of which HE is the most serious complication. Therefore, it is worthwhile to try to predict hepatic fibrosis patients who are susceptible to HE to provide early prevention and treatment[45]. A total of 304 cases of first-diagnosed hepatitis B-related cirrhosis were included in their study, 212 cases in the training group (HE = 38, non-HE = 174) and 92 cases in the validation group (HE = 21, non-HE = 71). Initially, 356 radiomics features were picked from the ROI of a patient's liver enhanced CT. After three times selection, 19 radiomics features were applied to construct a radiomics model. Three clinical factors related to HE, including serum albumin, ascites, and collateral circulation, were used to establish a clinical factor model. The results showed that, in the training and validation cohorts, the model combining radiomics and clinical features had an accuracy rate of 0.93 and 0.83 in predicting the risk of HE complicated by hepatitis B cirrhosis, respectively, while the corresponding values were 0.89 and 0.84 for radiomics model, and 0.83 and 0.77 for the clinical model.

Predicting liver failure in cirrhotic patients with HCC after major hepatectomy

Postoperative hepatic failure is the most serious complication in HCC patients after hepatectomy, which not only prolongs the hospitalization time of patients but also increases the mortality of patients[46]. Zhu *et al*[47] included 101 eligible HCC patients who had a major liver resection, to use preoperative gadoxetic acid-enhanced MRI for predicting liver failure based on the radiomics model. Removing the necessary structures, on the hepatobiliary phase image of the above-mentioned patient, experienced radiologists drew ROIs of the liver along the edge of the whole hepatic parenchyma. Through screening for ICC > 0.75 and LASSO regression, five features were employed to establish a radiomics signature. Then, the radiomics signature and ICG-R15 (a variable in the clinical factors model) were incorporated to establish a radiomics-based model. The results showed that the accuracy of the radiomics-based model in predicting postoperative liver failure was 0.802.

CONCLUSION

AI can mine data from patients' medical records, the Centers for Disease Control and Prevention in countries or regions, and serological markers. Raman spectroscopy can predict the incidence of hepatitis, classify the different stages of hepatitis, diagnose or screen hepatitis, forecast the progression of hepatitis, and predict response to antiviral drugs in CHC patients with a high level of diagnostic performance. AI, especially deep learning or radiomics, can predict hepatitis, predict liver fibrosis and its grade, differentiate HCC from the benign liver tumor, predict the risk of vascular invasion of HCC, predict the risk of HE complicated by hepatitis B related cirrhosis, and predict the risk of liver failure after hepatectomy in HCC patients, with good levels of accuracy.

Limitations and future perspectives

At present, all reviewed studies using AI are mostly single-center research, and the amount of data in the training sets may be insufficient. In the future, people should build an internet database or hospital, and disease-related information from various countries or regions could be uploaded to the internet database or hospital so that AI researchers can obtain more disease-related information with different demographics, geographic areas, *etc*., to carry out multicenter research, and establish a more robust and inclusive AI model for clinical use.

REFERENCES

1 **Angermueller C**, Pärnamaa T, Parts L, Stegle O. Deep learning for computational biology. *Mol Syst Biol* 2016; **12**: 878 [PMID: 27474269 DOI: 10.15252/msb.20156651]
2 **Zhou LQ**, Wang JY, Yu SY, Wu GG, Wei Q, Deng YB, Wu XL, Cui XW, Dietrich CF. Artificial intelligence in medical imaging of the liver. *World J Gastroenterol* 2019; **25**: 672-682 [PMID: 30783371 DOI: 10.3748/wjg.v25.i6.672]
3 **Chan HP**, Samala RK, Hadjiiski LM, Zhou C. Deep Learning in Medical Image Analysis. *Adv Exp Med Biol* 2020; **1213**: 3-21 [PMID: 32030660 DOI: 10.1007/978-3-030-33128-3_1]
4 **Gore JC**. Artificial intelligence in medical imaging. *Magn Reson Imaging* 2020; **68**: A1-A4 [PMID: 31857130 DOI: 10.1016/j.mri.2019.12.006]
5 **Liang X**, Yu J, Liao J, Chen Z. Convolutional Neural Network for Breast and Thyroid Nodules Diagnosis in Ultrasound Imaging. *Biomed Res Int* 2020; **2020**: 1763803 [PMID: 32420322 DOI: 10.1155/2020/1763803]
6 **Wang F**, Liu X, Yuan N, Qian B, Ruan L, Yin C, Jin C. Study on automatic detection and classification of breast nodule using deep convolutional neural network system. *J Thorac Dis* 2020; **12**: 4690-4701 [PMID: 33145042 DOI: 10.21037/jtd-19-3013]
7 **Dong F**, She R, Cui C, Shi S, Hu X, Zeng J, Wu H, Xu J, Zhang Y. One step further into the blackbox: a pilot study of how to build more confidence around an AI-based decision system of breast nodule assessment in 2D ultrasound. *Eur Radiol* 2021; **31**: 4991-5000 [PMID: 33404698 DOI: 10.1007/s00330-020-07561-7]
8 **Khan S**, Ullah R, Khan A, Ashraf R, Ali H, Bilal M, Saleem M. Analysis of hepatitis B virus infection in blood sera using Raman spectroscopy and machine learning. *Photodiagnosis Photodyn Ther* 2018; **23**: 89-93 [PMID: 29787817 DOI: 10.1016/j.pdpdt.2018.05.010]
9 **Li W**, Huang Y, Zhuang BW, Liu GJ, Hu HT, Li X, Liang JY, Wang Z, Huang XW, Zhang CQ, Ruan SM, Xie XY, Kuang M, Lu MD, Chen LD, Wang W. Multiparametric ultrasomics of significant liver fibrosis: A machine learning-based analysis. *Eur Radiol* 2019; **29**: 1496-1506 [PMID: 30178143 DOI: 10.1007/s00330-018-5680-z]
10 **Zhen S**, Cai X. Letter to the Editor: Predicting Survival After Hepatocellular Carcinoma Resection Using Deep-Learning on Histological Slides. *Hepatology* 2021; **73**: 2077-2078 [PMID: 32894573 DOI: 10.1002/hep.31543]
11 **Lavanchy D**. Hepatitis B virus epidemiology, disease burden, treatment, and current and emerging prevention and control measures. *J Viral Hepat* 2004; **11**: 97-107 [PMID: 14996343 DOI: 10.1046/j.1365-2893.2003.00487.x]
12 **Guan P**, Huang DS, Zhou BS. Forecasting model for the incidence of hepatitis A based on artificial neural network. *World J Gastroenterol* 2004; **10**: 3579-3582 [PMID: 15534910 DOI: 10.3748/wjg.v10.i24.3579]
13 **Zheng Y**, Zhang L, Zhu X, Guo G. A comparative study of two methods to predict the incidence of hepatitis B in Guangxi, China. *PLoS One* 2020; **15**: e0234660 [PMID: 32579598 DOI: 10.1371/journal.pone.0234660]
14 **Gan R**, Chen X, Yan Y, Huang D. Application of a hybrid method combining grey model and back propagation artificial neural networks to forecast hepatitis B in china. *Comput Math Methods Med* 2015; **2015**: 328273 [PMID: 25815044 DOI: 10.1155/2015/328273]
15 **Guo Y**, Feng Y, Qu F, Zhang L, Yan B, Lv J. Prediction of hepatitis E using machine learning models. *PLoS One* 2020; **15**: e0237750 [PMID: 32941452 DOI: 10.1371/journal.pone.0237750]
16 **Ahmad G**, Khan MA, Abbas S, Athar A, Khan BS, Aslam MS. Automated Diagnosis of Hepatitis B Using Multilayer Mamdani Fuzzy Inference System. *J Healthc Eng* 2019; **2019**: 6361318 [PMID: 30867895 DOI: 10.1155/2019/6361318]
17 **Wang X**, Tian S, Yu L, Lv X, Zhang Z. Rapid screening of hepatitis B using Raman spectroscopy and long short-term memory neural network. *Lasers Med Sci* 2020; **35**: 1791-1799 [PMID: 32285292 DOI: 10.1007/s10103-020-03003-4]
18 **Yehia BR**, Schranz AJ, Umscheid CA, Lo Re V 3rd. The treatment cascade for chronic hepatitis C virus infection in the United States: a systematic review and meta-analysis. *PLoS One* 2014; **9**: e101554 [PMID: 24988388 DOI: 10.1371/journal.pone.0101554]
19 **Doyle OM**, Leavitt N, Rigg JA. Finding undiagnosed patients with hepatitis C infection: an application of artificial intelligence to patient claims data. *Sci Rep* 2020; **10**: 10521 [PMID: 32601354 DOI: 10.1038/s41598-020-67013-6]
20 **Konerman MA**, Beste LA, Van T, Liu B, Zhang X, Zhu J, Saini SD, Su GL, Nallamothu BK, Ioannou GN, Waljee AK. Machine learning models to predict disease progression among veterans with hepatitis C virus. *PLoS One* 2019; **14**: e0208141 [PMID: 30608929 DOI: 10.1371/journal.pone.0208141]
21 **Maiellaro PA**, Cozzolongo R, Marino P. Artificial neural networks for the prediction of response to interferon plus ribavirin treatment in patients with chronic hepatitis C. *Curr Pharm Des* 2004; **10**: 2101-2109 [PMID: 15279549 DOI: 10.2174/1381612043384240]
22 **Chartrand G**, Cheng PM, Vorontsov E, Drozdzal M, Turcotte S, Pal CJ, Kadoury S, Tang A. Deep Learning: A Primer for Radiologists. *Radiographics* 2017; **37**: 2113-2131 [PMID: 29131760 DOI: 10.1148/rg.2017170077]
23 **Lee JG**, Jun S, Cho YW, Lee H, Kim GB, Seo JB, Kim N. Deep Learning in Medical Imaging: General Overview. *Korean J Radiol* 2017; **18**: 570-584 [PMID: 28670152 DOI:

10.3348/kjr.2017.18.4.570]
24 **Gillies RJ**, Kinahan PE, Hricak H. Radiomics: Images Are More than Pictures, They Are Data. *Radiology* 2016; **278**: 563-577 [PMID: 26579733 DOI: 10.1148/radiol.2015151169]
25 **Lee G**, Lee HY, Park H, Schiebler ML, van Beek EJR, Ohno Y, Seo JB, Leung A. Radiomics and its emerging role in lung cancer research, imaging biomarkers and clinical management: State of the art. *Eur J Radiol* 2017; **86**: 297-307 [PMID: 27638103 DOI: 10.1016/j.ejrad.2016.09.005]
26 **Tana MM**, McCoy D, Lee B, Patel R, Lin J, Ohliger MA. Texture features from computed tomography correlate with markers of severity in acute alcohol-associated hepatitis. *Sci Rep* 2020; **10**: 17980 [PMID: 33087739 DOI: 10.1038/s41598-020-74599-4]
27 **Husain A**, Chiwhane A, Kirnake V. Non-invasive assessment of liver fibrosis in alcoholic liver disease. *Clin Exp Hepatol* 2020; **6**: 125-130 [PMID: 32728629 DOI: 10.5114/ceh.2020.95739]
28 **Xue LY**, Jiang ZY, Fu TT, Wang QM, Zhu YL, Dai M, Wang WP, Yu JH, Ding H. Transfer learning radiomics based on multimodal ultrasound imaging for staging liver fibrosis. *Eur Radiol* 2020; **30**: 2973-2983 [PMID: 31965257 DOI: 10.1007/s00330-019-06595-w]
29 **Wang JC**, Fu R, Tao XW, Mao YF, Wang F, Zhang ZC, Yu WW, Chen J, He J, Sun BC. A radiomics-based model on non-contrast CT for predicting cirrhosis: make the most of image data. *Biomark Res* 2020; **8**: 47 [PMID: 32963787 DOI: 10.1186/s40364-020-00219-y]
30 **Budai BK**, Tóth A, Borsos P, Frank VG, Shariati S, Fejér B, Folhoffer A, Szalay F, Bérczi V, Kaposi PN. Three-dimensional CT texture analysis of anatomic liver segments can differentiate between low-grade and high-grade fibrosis. *BMC Med Imaging* 2020; **20**: 108 [PMID: 32957949 DOI: 10.1186/s12880-020-00508-w]
31 **Son JH**, Lee SS, Lee Y, Kang BK, Sung YS, Jo S, Yu E. Assessment of liver fibrosis severity using computed tomography-based liver and spleen volumetric indices in patients with chronic liver disease. *Eur Radiol* 2020; **30**: 3486-3496 [PMID: 32055946 DOI: 10.1007/s00330-020-06665-4]
32 **Talwalkar JA**, Kurtz DM, Schoenleber SJ, West CP, Montori VM. Ultrasound-based transient elastography for the detection of hepatic fibrosis: systematic review and meta-analysis. *Clin Gastroenterol Hepatol* 2007; **5**: 1214-1220 [PMID: 17916549 DOI: 10.1016/j.cgh.2007.07.020]
33 **Friedrich-Rust M**, Ong MF, Martens S, Sarrazin C, Bojunga J, Zeuzem S, Herrmann E. Performance of transient elastography for the staging of liver fibrosis: a meta-analysis. *Gastroenterology* 2008; **134**: 960-974 [PMID: 18395077 DOI: 10.1053/j.gastro.2008.01.034]
34 **Yasaka K**, Akai H, Kunimatsu A, Abe O, Kiryu S. Liver Fibrosis: Deep Convolutional Neural Network for Staging by Using Gadoxetic Acid-enhanced Hepatobiliary Phase MR Images. *Radiology* 2018; **287**: 146-155 [PMID: 29239710 DOI: 10.1148/radiol.2017171928]
35 **Wang K**, Lu X, Zhou H, Gao Y, Zheng J, Tong M, Wu C, Liu C, Huang L, Jiang T, Meng F, Lu Y, Ai H, Xie XY, Yin LP, Liang P, Tian J, Zheng R. Deep learning Radiomics of shear wave elastography significantly improved diagnostic performance for assessing liver fibrosis in chronic hepatitis B: a prospective multicentre study. *Gut* 2019; **68**: 729-741 [PMID: 29730602 DOI: 10.1136/gutjnl-2018-316204]
36 **Yu Y**, Lin X, Chen K, Chai W, Hu S, Tang R, Zhang J, Cao L, Yan F. Hepatocellular carcinoma and focal nodular hyperplasia of the liver: differentiation with CT spectral imaging. *Eur Radiol* 2013; **23**: 1660-1668 [PMID: 23306709 DOI: 10.1007/s00330-012-2747-0]
37 **Grazioli L**, Bondioni MP, Faccioli N, Gambarini S, Tinti R, Schneider G, Kirchin M. Solid focal liver lesions: dynamic and late enhancement patterns with the dual phase contrast agent gadobenate dimeglumine. *J Gastrointest Cancer* 2010; **41**: 221-232 [PMID: 20405242 DOI: 10.1007/s12029-010-9145-0]
38 **Nie P**, Yang G, Guo J, Chen J, Li X, Ji Q, Wu J, Cui J, Xu W. A CT-based radiomics nomogram for differentiation of focal nodular hyperplasia from hepatocellular carcinoma in the non-cirrhotic liver. *Cancer Imaging* 2020; **20**: 20 [PMID: 32093786 DOI: 10.1186/s40644-020-00297-z]
39 **Jiang H**, Liu X, Chen J, Wei Y, Lee JM, Cao L, Wu Y, Duan T, Li X, Ma L, Song B. Man or machine? *Cancer Imaging* 2019; **19**: 84 [PMID: 31806050 DOI: 10.1186/s40644-019-0266-9]
40 **Edmondson HA**, Steiner PE. Primary carcinoma of the liver: a study of 100 cases among 48,900 necropsies. *Cancer* 1954; **7**: 462-503 [PMID: 13160935 DOI: 10.1002/1097-0142(195405)7:3<462::aid-cncr2820070308>3.0.co;2-e]
41 **Wu M**, Tan H, Gao F, Hai J, Ning P, Chen J, Zhu S, Wang M, Dou S, Shi D. Predicting the grade of hepatocellular carcinoma based on non-contrast-enhanced MRI radiomics signature. *Eur Radiol* 2019; **29**: 2802-2811 [PMID: 30406313 DOI: 10.1007/s00330-018-5787-2]
42 **Bruix J**, Llovet JM. Hepatitis B virus and hepatocellular carcinoma. *J Hepatol* 2003; **39** Suppl 1: S59-S63 [PMID: 14708679 DOI: 10.1016/s0168-8278(03)00140-5]
43 **Peng J**, Zhang J, Zhang Q, Xu Y, Zhou J, Liu L. A radiomics nomogram for preoperative prediction of microvascular invasion risk in hepatitis B virus-related hepatocellular carcinoma. *Diagn Interv Radiol* 2018; **24**: 121-127 [PMID: 29770763 DOI: 10.5152/dir.2018.17467]
44 **Ma X**, Wei J, Gu D, Zhu Y, Feng B, Liang M, Wang S, Zhao X, Tian J. Preoperative radiomics nomogram for microvascular invasion prediction in hepatocellular carcinoma using contrast-enhanced CT. *Eur Radiol* 2019; **29**: 3595-3605 [PMID: 30770969 DOI: 10.1007/s00330-018-5985-y]
45 **Cao JM**, Yang JQ, Ming ZQ, Wu JL, Yang LQ, Chen TW, Li R, Ou J, Zhang XM, Mu QW, Li HJ, Hu J. A radiomics model of liver CT to predict risk of hepatic encephalopathy secondary to hepatitis B related cirrhosis. *Eur J Radiol* 2020; **130**: 109201 [PMID: 32738462 DOI: 10.1016/j.ejrad.2020.109201]
46 **Lock JF**, Reinhold T, Malinowski M, Pratschke J, Neuhaus P, Stockmann M. The costs of

postoperative liver failure and the economic impact of liver function capacity after extended liver resection--a single-center experience. *Langenbecks Arch Surg* 2009; **394**: 1047-1056 [PMID: 19533168 DOI: 10.1007/s00423-009-0518-4]

47 **Zhu WS**, Shi SY, Yang ZH, Song C, Shen J. Radiomics model based on preoperative gadoxetic acid-enhanced MRI for predicting liver failure. *World J Gastroenterol* 2020; **26**: 1208-1220 [PMID: 32231424 DOI: 10.3748/wjg.v26.i11.1208]

World Journal of Gastroenterology

Submit a Manuscript: https://www.f6publishing.com

World J Gastroenterol 2021 September 14; 27(34): 5727-5736

DOI: 10.3748/wjg.v27.i34.5727

ISSN 1007-9327 (print) ISSN 2219-2840 (online)

MINIREVIEWS

Machine perfusion of the liver: Putting the puzzle pieces together

Yuri L Boteon, Paulo N Martins, Paolo Muiesan, Andrea Schlegel

ORCID number: Yuri L Boteon 0000-0002-1709-9284; Paulo N Martins 0000-0001-9333-0233; Paolo Muiesan 0000-0002-7389-6691; Andrea Schlegel 0000-0002-9385-9847.

Author contributions: Boteon YL designed this study; Boteon YL, Martins PN, Muiesan P and Schlegel A performed the literature review and analysis; Boteon YL drafted the manuscript; Boteon YL, Martins PN, Muiesan P, and Schlegel A reviewed the manuscript critically; All authors contributed to editing and approved the final manuscript version.

Conflict-of-interest statement: The authors have no conflicts of interest to disclose.

Open-Access: This article is an open-access article that was selected by an in-house editor and fully peer-reviewed by external reviewers. It is distributed in accordance with the Creative Commons Attribution NonCommercial (CC BY-NC 4.0) license, which permits others to distribute, remix, adapt, build upon this work non-commercially, and license their derivative works on different terms, provided the original work is properly cited and the use is non-commercial. See: http://creativecommons.org/Licenses/by-nc/4.0/

Manuscript source: Invited

Yuri L Boteon, Liver Unit, Hospital Israelita Albert Einstein, São Paulo 05652-900, Brazil

Yuri L Boteon, Instituto Israelita de Ensino e Pesquisa Albert Einstein, Faculdade Israelita de Ci ências da Saúde Albert Einstein, São Paulo 05652-900, Brazil

Paulo N Martins, Department of Surgery, Transplant Division, University of Massachusetts Medical School, Worcester, MA 01655, United States

Paolo Muiesan, Andrea Schlegel, Hepatobiliary Unit, Careggi University Hospital, University of Florence, Florence 50134, Italy

Andrea Schlegel, Department of Visceral Surgery and Transplantation, University Hospital Zurich, Swiss HPB and Transplant Center, Zurich 8091, Switzerland

Corresponding author: Yuri L Boteon, MD, PhD, Doctor, Professor, Surgeon, Liver Unit, Hospital Israelita Albert Einstein, Jardim Leonor, São Paulo 05652-900, São Paulo, Brazil. yuri.boteon@einstein.br

Abstract

The realm of extended criteria liver transplantation created the 'adjacent possible' for dynamic organ preservation. Machine perfusion of the liver greatly expanded donor organ preservation possibilities, reaching before unattainable goals, including the mitigation of ischemia-reperfusion injury, viability assessment, and organ reconditioning prior to transplantation. However, current scientific evidence lacks uniformity between studies, perfusion protocols, and acceptance criteria. Construction of collaborative research networks for sharing knowledge should, therefore, enable the development of high-level evidence and guidelines for machine perfusion utilization, including donor acceptance criteria. Finally, this approach shall guarantee conditions for further progress to occur.

Key Words: Machine perfusion of the liver; Liver transplantation; Organ donation; Extended criteria donors; Liver preservation; Clinical trials

©The Author(s) 2021. Published by Baishideng Publishing Group Inc. All rights reserved.

Core Tip: The frequent use of extended criteria donor organs unveiled the limits of static cold storage and created the conditions for the renewed interest in dynamic organ preservation. Indeed, several studies have suggested the superiority of this method over

manuscript

Specialty type: Transplantation

Country/Territory of origin: Brazil

Peer-review report's scientific quality classification

Grade A (Excellent): 0
Grade B (Very good): B
Grade C (Good): C
Grade D (Fair): 0
Grade E (Poor): 0

Received: March 2, 2021
Peer-review started: March 2, 2021
First decision: April 17, 2021
Revised: May 3, 2021
Accepted: July 21, 2021
Article in press: July 21, 2021
Published online: September 14, 2021

P-Reviewer: Baiocchi L, Zhou S
S-Editor: Liu M
L-Editor: Filipodia
P-Editor: Liu JH

static cold storage for these high-risk donors. However, controversy still exists between different machine perfusion modalities and even amongst studies employing the same method, compromising the strength of the available evidence. With the currently fragmented efforts, the development of collaborative networks will produce collective outcomes that will expand the boundaries of current knowledge.

Citation: Boteon YL, Martins PN, Muiesan P, Schlegel A. Machine perfusion of the liver: Putting the puzzle pieces together. *World J Gastroenterol* 2021; 27(34): 5727-5736
URL: https://www.wjgnet.com/1007-9327/full/v27/i34/5727.htm
DOI: https://dx.doi.org/10.3748/wjg.v27.i34.5727

INTRODUCTION

Previously disregarded and surpassed by the simplicity of static cold storage (SCS), dynamic organ preservation found the 'adjacent possible' in the realm of extended criteria donors (ECD) liver transplantation. Over the last few years, the liver transplantation community has experienced a surge in studies investigating the safety and efficacy of dynamic preservation[1-5]. This event is mainly a consequence of the increased use of ECD organs in order to attend to the growing demand for donor livers. The use of these high-risk organs exposed the limitations of SCS and posed a threat to recipients due to the risk of early allograft dysfunction and even primary non-function; thus, they are often discarded[6,7]. Therefore, at present, ECD liver transplantation has given the possibility to revisit and develop further machine perfusion techniques, previously hindered by the lack of appropriate conditions (*e.g.*, complexity, specific perfusates, and devices, costs). Figure 1 illustrates the evolution of conditions favouring the renewed interest in machine perfusion of the liver (MPL).

DYNAMIC ORGAN PRESERVATION AND ISCHAEMIA-REPERFUSION INJURY MITIGATION

The keystone of dynamic organ preservation is the mitigation of ischemia-reperfusion injury (IRI). IRI is responsible for the inflammatory-mediated tissue injury involved in transplantation and is ultimately associated with adverse results, such as early allograft dysfunction and primary non-function[8]. Dynamic preservation is characterized by a continuous flow of an oxygenated solution, preventing ischemic damage to the cells. In addition, the continuous flow of the perfusate provides nutrients and removes toxic metabolic waste products[7].

Diverse techniques of MPL are currently under research, while a few are currently clinically implemented. These include the *ex-situ* (normothermic, hypothermic, subnormothermic, controlled oxygenated rewarming), the *in-situ* modalities (normothermic regional perfusion, NRP), and the ischemia-free organ transplantation [2-4,6,9-12]. Furthermore, combinations of techniques have more recently gained the attention of the transplant community (*e.g.*, cold-to-warm, hypothermic plus normothermic, NRP plus hypothermic or normothermic *ex-situ* perfusion)[13-18]. Also, *ex-situ* normothermic machine perfusion (NMP) can be performed in a preservation approach during organ transportation or in an end-ischemic method, whereby the organ will be perfused after arrival at the transplant centre[7]. Hypothermic machine perfusion (HMP) can be done using an oxygen pre-charged perfusate or an actively oxygenated perfusate — with perfusion *via* portal vein exclusively (hypothermic oxygenated perfusion, HOPE) or in association with the hepatic artery (dual HOPE, D-HOPE)[3,5]. Although HMP is currently used in an end-ischemic approach, a device for hypothermic perfusion during organ transportation is under clinical investigation in the United States (clinical trials.gov, NCT number 03484455).

Albeit all these techniques hold the potential to benefit ECD livers, clearly controversy exists about the best strategy. Currently, the two most studied modalities are NMP and HMP. Both can be performed *ex-situ* in an end-ischemic approach for organs from donors after brain death (DBD) and donors after circulatory death (DCD). Furthermore, due to the need to increase DCD organ utilization avoiding its associated

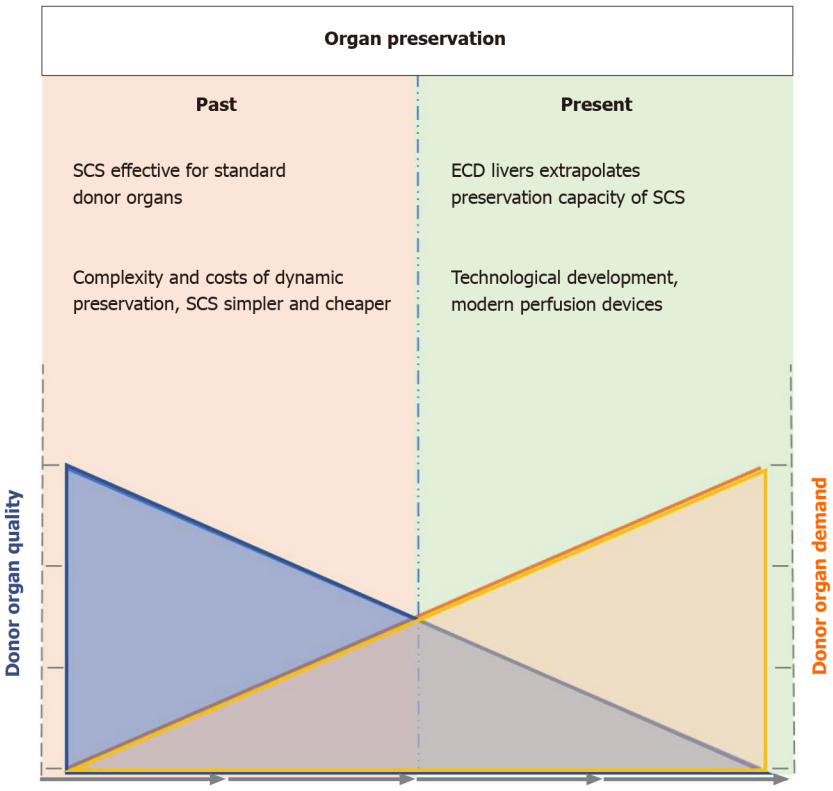


Figure 1 Conditions favouring the development of machine perfusion of the liver. At the start of transplantation, the utilization of good quality donor organs and the low price and simplicity of static cold storage (SCS) favoured its general use. However, the rise in demand for liver transplantation and the donor organ demographic change imposed a frequent utilization of extended criteria donor (ECD) organs. ECD liver transplantation presented inferior results, exposing the limitations of SCS. This scenario, allied to the technological development, created a favourable environment and renewed interest in dynamic organ preservation.

post-transplant complications, NRP is routinely applied in a few countries, including Spain, France, and Italy. NRP alleviates the warm ischemic injury to the organ and induces initial normothermic reperfusion in the donor. Thereby, it allows assessment of viability markers (most lactate and transaminases) which help to decide whether the organ must be declined or not. Several studies currently evidenced the benefits of this technique for DCD liver transplantation[11,19].

Despite consistently attending the primary aim to mitigate IRI, questions are still emerging about the mechanistic pathways involved in this process within each method[8,20]. In fact, benefits vary slightly between techniques mainly as a consequence of the physical properties employed by the methods and the moment of application. Table 1 describes the potential advantages of different MPL techniques in clinical studies. Notably, only three of the mentioned studies were randomized and the study of Ghinolfi *et al*[21] included only 10 patients[2,21,22].

ORGAN VIABILITY ASSESSMENT IN LIVER TRANSPLANTATION: CONTINUOUS FLOW FOR REAL-TIME ANALYSIS

Once inducing reperfusion, whilst NMP abbreviates the cold ischemia time, it results in full activation of the aerobic mitochondrial respiration with reactive oxygen species production and release. Further downstream processes are triggered with subsequent oxidative tissue damage and initiation of the inflammatory cascade[8,23]. The fully physiologically active organ allows real-time assessment of its metabolic functioning, which is currently mostly based on lactate clearance and bile production[6,24]. However, definitive viability criteria are not yet characterized and validated[25].

We are currently transitioning from a combination of hepatocyte function-based criteria to a more comprehensive assessment that incorporates cholangiocyte function. The Birmingham group developed pioneer clinical viability criteria, which included: Lactate clearance, evidence of bile production, perfusate pH stability, hepatic artery flow and portal vein flow, and homogeneous graft perfusion with soft consistency of parenchyma[6]. Later, Watson *et al*[24] advocated using changes in lactate, in glucose

Table 1 Potential benefits of the different modalities of machine perfusion of the liver on clinical studies

	Safety and feasibility	Prevention of early allograft dysfunction	Prevention of biliary complications	Prolonged preservation time	Viability assessment	Therapeutic interventions
Normothermic regional perfusion[1]	Yes[11,19,46]	Yes[11,19,46]	Yes[11,19,46]	No data available yet	Yes[11,46]	No data available yet
Normothermic machine perfusion	Yes[2,6,21,42,50,51]	Yes[2,6,42]	No data available yet	Yes[2,6]	Yes[6,24,26,50,51]	Yes[43][2]
Subnormothermic machine perfusion	No data available yet	No data available yet	No data available yet	No data available yet	No data available yet	No data available yet
Hypothermic machine perfusion	Yes[3,37]	Yes[3,37]	Yes[3,22,37]	Yes[39][2]	Yes[34]	No data available yet
Controlled oxygenated rewarming	Yes[9,47]	Yes[9,47]	No data available yet	No data available yet	No data available yet	No data available yet
Combined modalities (HMP + NMP)	Yes[14,15]	No data available yet	No data available yet	Yes[39][2]	Yes[14,15]	No data available yet
Ischaemia-free liver transplantation[3]	Yes[12,48]	Yes[48,49]	No data available yet	No data available yet	No data available yet	No data available yet

[1]Only suitable for donors after circulatory death.
[2]Only pre-clinical studies available so far.
[3]Only suitable for donors after brain death. HMP: Hypothermic machine perfusion; NMP: Normothermic machine perfusion.

and transaminases, and the ability to maintain a stable perfusate pH without bicarbonate supplementation to consider an organ viable. Most recently, the Groningen group highlighted the importance of bile composition analysis during viability assessment (biliary bicarbonate, pH, glucose, lactate dehydrogenase); and their viability criteria already included bile flow and its properties on the analysis[26]. Another study, evaluating discarded donor livers, demonstrated a low hepatocellular injury during NMP; with, however, an elevated bile duct injury on histology[27]. Notably, the impact of MPL on the peribiliary glands and peribiliary vascular plexus, rather than solely bile duct injury, deserves attention. This is because if damage to the bile duct cannot be avoided, establishing a healthy environment to the peribiliary glands contributes to the regenerative capacity of this structure, possibly preventing the development of nonanastomotic strictures[28-30]. The relevance of biliary biomarkers to assess cholangiocyte function and bile duct viability is currently a research topic in liver transplantation[31].

The importance of biliary analysis was indirectly reinforced by another study investigating discarded donor livers, the VITTAL (Viability testing and transplantation of marginal livers) trial[6]. Despite excellent synthetic function with isolated bile flow assessment, a significant proportion of organs developed biliary complications, even requiring retransplantation[6]. In accordance, recently, Eshmuminov *et al*[32] questioned the value of bile formation as a marker of a deteriorating liver function. These findings were paralleled by previous studies, concluding that continuous bile production alone appears not sufficient enough to evaluate liver viability during *ex-situ* machine perfusion[27]. In this study, porcine and human livers were perfused for up to 1 wk and the authors demonstrated good bile production once appropriate drug-induced stimuli were offered[27]. Finally, they suggest the response to vasoconstrictors and hormones as viability markers for liver function. Interestingly, part of the viable livers included in the study from Eshmuminov *et al*[27,33] was initially declined for transplantation based on elevated flavin mononucleotide (FMN) levels during HOPE[34].

Conversely, HMP —usually performed at temperatures between 4 °C and 12 °C — keeps the organ at a low metabolic rate, making the assessment of most of its function more challenging. Despite that, actively oxygenated HMP techniques act seemingly on the mitochondria, restoring the electron transport chain and enhancing the mitochondrial oxidative phosphorylation and adenosine triphosphate production[8,23]. Despite the different metabolic status during HMP, more than 2000 molecules can be quantified from perfusates[34]. Recent viability assessment during HOPE focused on mitochondria function and injury. Muller *et al*[34] identified the first biomarker of organ viability during HMP, the FMN. FMN is a molecule in mitochondria complex I, which is released during organ reperfusion concomitantly and from the same pocket

as reactive oxygen species[35,36]. The number of released FMN molecules was also assessed during different perfusion modalities and authors found a higher FMN release during normothermic liver perfusion[36]. Therefore, ultimately, it reflects the severity of IRI, the mitochondrial injury and dysfunction[36]. The authors from Zurich found a strong correlation between perfusate FMN levels' — fluorometric readings after 30 min of HMP — and post-transplant outcome parameters (hospital stay, cumulative complications, and 90-d graft loss)[34]. Importantly, based on the autofluorescence properties, FMN can be measured in real-time using a spectrometer [34]. This mitochondrial parameter was further validated during NRP and NMP in kidneys and livers. Data presented by Wang *et al*[36] supported the entire concept of mitochondrial injury quantification through FMN release and concluded that this marker appears useful during various preservation approaches.

Table 2 summarizes parameters tested in clinical studies to assess the viability of donor organs during MPL prior to transplantation. Importantly, current studies included different parameters within their viability criteria. In addition, even when the same parameters were investigated, thresholds and the timepoints analysed varied.

A WAY BEYOND PRESERVATION: ORGAN RECONDITIONING

Moving organ preservation forward, MPL extrapolates the simple concept of mitigation of donor organ damage before transplantation; in the interim, the dynamic preservation aims to improve the quality of the donated organs or, in other words, recondition them. This step further is fundamental to increase ECD organ utilization once they were exposed to more severe damage and carry a high risk to receptors if SCS is applied.

Non-randomized single-centre clinical studies have confirmed the ability of HMP to enhance the results of ECD liver transplantation[3,10,37]. Dutkowski *et al*[37] suggested that high-risk DCD organs — associated with most severe IRI, poor clinical outcomes, and a high rate of post-operative complications — submitted to the HOPE technique for 1-2 h prior to transplantation have similar outcomes to standard DBD organs, including the length of hospital stay and biliary complications. Later, the same group compared HOPE-treated DCD livers to a matched cohort of DCD organs without further intervention. The perfused livers presented lower post-transplant alanine aminotransferase levels, decreased biliary complication rate, and increased 1-year graft survival[3]. More recently, Schlegel *et al*[38] reported a 5-year graft survival of 94% for transplanted HOPE-treated DCD livers against 78% for untreated DCD organs. Similar benefits were also found in D-HOPE studies led by the Groningen group[30]. van Rijn *et al*[22] recently published a randomized clinical trial on HMP with 160 patients transplanted with DCD organs. The study reached its primary endpoint, D-HOPE-perfused DCD livers had a lower incidence of symptomatic non-anastomotic biliary stricture (6%) compared to 18% in the control group (P = 0.03). This study also demonstrated that D-HOPE reduced the occurrence of early allograft dysfunction post-transplantation[22].

Importantly, evolving evidence supports the safety of performing D-HOPE for up to 24 h, which may improve transplant logistics[39]. A recent study suggested that HOPE plays a protective role in preventing hepatocellular carcinoma recurrence after liver transplantation, which is possible due to protection from IRI, downstream inflammation, and subsequent pro-tumour-recurrence environment[40,41].

A large multicentre trial recently evidenced preservation NMP was able to reduce in 50% the hepatocellular enzyme releases post-operatively, increasing organ utilization rate and preservation time[2]. Nevertheless, NMP did not reduce biliary complications rate post-transplant and, also, did not impact on graft or patient survival[2]. Similar results were found in another study wherein end-ischemic NMP was used[42]. The Birmingham group applied NMP to discarded donor livers, 71% of the perfused organs were transplanted. Although this study reported 100% 90-d patient and graft survival, perfusion did not prevent non-anastomotic biliary stricture (incidence of 18%), and four recipients required retransplantation within 542 d[6]. Albeit the near-physiological conditions of donor organs during NMP favours the assessment of their metabolic functions, the ability of NMP per se to recondition ECD organs is still controversial. Whether a severely damaged organ would recover after activation of the damaging IRI machinery during NMP without any further intervention is not clear. Seemingly, additional support must be required[8,13,43,44].

The uncertainty about NMP reconditioning properties is counterbalanced by evident advantages. The organ's full metabolism facilitates its viability assessment,

Table 2 Parameters employed in clinical studies to assess the viability of donor organs before transplantation

Ref.	Method	Perfusate parameters	Bile parameters	Perfusion parameters
Watson *et al*[11]	NRP	Within 2 h of NRP: Alanine transaminase up to 500 IU/L, providing no continued rise between the first and second hours		
Muller *et al* [34]	HMP	At least 1 h of HMP: Threshold at 10000 A.U. (100 ng FMN/mL perfusate) to refuse livers regardless of the use of a DCD or DBD liver		
Watson *et al*[32]	NMP	No timepoint defined: Changes in lactate, glucose, and transaminase concentrations and the ability of the liver to maintain perfusate pH without supplemental bicarbonate		
Matton *et al*[26]	NMP		Within 2.5 h of NMP: Bicarbonate concentration > 18 mmol/L, pH > 7.48, glucose concentration < 16 mmol/L, bile/perfusate glucose concentration ratio < 0.67, and LDH concentration < 3689 U/L	
de Vries *et al*[14]	NMP	Within 150 min of NMP: Lactate concentration within "normal" values (0.5-1.7 mmol/L); pH within normal values (7.35-7.45), without continuing sodium bicarbonate supplementation	Within 150 min of NMP: Cumulative bile production of ≥ 10 mL and ≥ 4 mL in the preceding hour. pH > 7.45	
Mergental *et al*[6]	NMP	Within 4 h of NMP: Lactate ≤ 2.5 mmol/L; and two or more parameters: pH ≥ 7.30; Evidence of glucose metabolism	Within 4 h of NMP: Evidence of bile production	Within 4 h of NMP: HA flow ≥ 150 mL/min and PV flow ≥ 500 mL/min; and homogenous perfusion of the parenchyma
Cardini *et al*[50]	NMP	Within 2 h of NMP: Rapid decrease and maintenance of lactate to physiological levels, maintenance of physiological pH values without sodium bicarbonate supplementation, and glucose consumption. Remarkably high transaminases and LDH levels and a severe rise of these parameters are deemed warning signals	Within 2 h of NMP: Bile production and bile pH are indicators for bile duct viability and function	
Reiling *et al*[51]	NMP	Within 2 h of NMP: Lactate clearance to < 2 mmol/L. Within 4 h of NMP: Evidence of glucose metabolism. Maintenance of physiological pH without continuing administration of sodium bicarbonate	Within 4 h of NMP: Bile production (no lower limit)	Within 4 h of NMP: Stable hepatic arterial and portal venous flows. Homogeneous graft perfusion with soft consistency of parenchyma

DCD: Donation after circulatory death; DBD: Donation after brain death; HA: Hepatic artery; HMP: Hypothermic machine perfusion; LDH: Lactate dehydrogenase; NMP: Normothermic machine perfusion; NRP: Normothermic regional perfusion; PV: Portal vein.

increases the surgeon's confidence, and allows safe prolonged organ preservation[2,6]. This ambiguity opened up an opportunity for further additions to the technique, for example, combinations of perfusion modalities and pharmacological interventions[15,43]. Combinations of perfusion modalities may merge both techniques' benefits; experimental and clinical studies have already suggested the possibility to enhance the reconditioning of the most severely damaged organs with the realization of HMP before NMP[13-15,17]. Similarly, pharmacological interventions may mitigate IRI and improve donor organ metabolic recovery, which has been suggested in pre-clinical studies investigating discarded steatotic donor livers[43]. For a comprehensive review on pharmacological agents used in MPL, please refer to Resch *et al*[45].

FINAL CONSIDERATIONS

Although several studies currently have demonstrated the benefits of dynamic organ preservation, limitations of this evidence exist. This is because significant variability of technicalities occurs even between studies employing the same method. For example, for NMP, parameters such as the rewarming period, arterial and portal vein perfusion pressure, and perfusate constitution vary between studies. Similarly, studies diverge on the perfusion duration, either replacing SCS during organ transportation or performed as an end-ischemic approach at the recipient transplant centre. For HMP, similar challenges also occur. So far, most studies focused on organs with a short period of cold ischemia time and, also, the level of perfusate oxygenation differs

between them. Adopting standardized protocols might enable the construction of large perfusion databases, which may unveil further advantages of MPL.

In addition, the foundation of large networks to develop studies collaboratively must benefit even further the era of machine perfusion in liver transplantation. The development of large collaborative perfusion groups working collectively may allow reliable comparison between perfusion modalities and, even, identify which technology is most beneficial to each specific organ.

CONCLUSION

Over the last few years, machine perfusion in liver transplantation gathered momentum, though it seems the construction of definitive evidence is still needed. This is mainly because of current disjointed individual efforts with non-standardization of methods and publication of single-centre non-randomized small studies. Dynamic organ preservation must thrive on collaborative networks wherein collective outcomes must consolidate its actual benefits (viability assessment, prolonged organ preservation, and organ reconditioning) and create the conditions for further progress to occur. Pharmacological *ex-situ* treatments and investigation of the impact of this technology on specific donor organs are some possibilities within reach, lying in the realm of the possible.

ACKNOWLEDGEMENTS

This paper presents independent research supported by the Brazilian Ministry of Health *via* the Support Program for Organizational Development of the SUS (PROADI-SUS) at the Hospital Israelita Albert Einstein. The views expressed are those of the author(s) and not necessarily those of the Ministry of Health, the PROADI-SUS, or the Hospital Israelita Albert Einstein. We are extremely grateful to the staff from the Hospital Israelita Albert Einstein and Hospital Municipal Vila Santa Catarina, whose continued support provides resources and intellectual input that is shaping the thoughts and future strategies for the continuing development of our research.

REFERENCES

1 **Serifis N**, Matheson R, Cloonan D, Rickert CG, Markmann JF, Coe TM. Machine Perfusion of the Liver: A Review of Clinical Trials. *Front Surg* 2021; **8**: 625394 [PMID: 33842530 DOI: 10.3389/fsurg.2021.625394]

2 **Nasralla D**, Coussios CC, Mergental H, Akhtar MZ, Butler AJ, Ceresa CDL, Chiocchia V, Dutton SJ, García-Valdecasas JC, Heaton N, Imber C, Jassem W, Jochmans I, Karani J, Knight SR, Kocabayoglu P, Malagò M, Mirza D, Morris PJ, Pallan A, Paul A, Pavel M, Perera MTPR, Pirenne J, Ravikumar R, Russell L, Upponi S, Watson CJE, Weissenbacher A, Ploeg RJ, Friend PJ; Consortium for Organ Preservation in Europe. A randomized trial of normothermic preservation in liver transplantation. *Nature* 2018; **557**: 50-56 [PMID: 29670285 DOI: 10.1038/s41586-018-0047-9]

3 **Dutkowski P**, Polak WG, Muiesan P, Schlegel A, Verhoeven CJ, Scalera I, DeOliveira ML, Kron P, Clavien PA. First Comparison of Hypothermic Oxygenated PErfusion Versus Static Cold Storage of Human Donation After Cardiac Death Liver Transplants: An International-matched Case Analysis. *Ann Surg* 2015; **262**: 764-770; discussion 770 [PMID: 26583664 DOI: 10.1097/SLA.0000000000001473]

4 **op den Dries S**, Karimian N, Sutton ME, Westerkamp AC, Nijsten MW, Gouw AS, Wiersema-Buist J, Lisman T, Leuvenink HG, Porte RJ. Ex vivo normothermic machine perfusion and viability testing of discarded human donor livers. *Am J Transplant* 2013; **13**: 1327-1335 [PMID: 23463950 DOI: 10.1111/ajt.12187]

5 **Graham JA**, Guarrera JV. "Resuscitation" of marginal liver allografts for transplantation with machine perfusion technology. *J Hepatol* 2014; **61**: 418-431 [PMID: 24768755 DOI: 10.1016/j.jhep.2014.04.019]

6 **Mergental H**, Laing RW, Kirkham AJ, Perera MTPR, Boteon YL, Attard J, Barton D, Curbishley S, Wilkhu M, Neil DAH, Hübscher SG, Muiesan P, Isaac JR, Roberts KJ, Abradelo M, Schlegel A, Ferguson J, Cilliers H, Bion J, Adams DH, Morris C, Friend PJ, Yap C, Afford SC, Mirza DF. Transplantation of discarded livers following viability testing with normothermic machine perfusion. *Nat Commun* 2020; **11**: 2939 [PMID: 32546694 DOI: 10.1038/s41467-020-16251-3]

7 **Ceresa CDL**, Nasralla D, Jassem W. Normothermic Machine Preservation of the Liver: State of the Art. *Curr Transplant Rep* 2018; **5**: 104-110 [PMID: 29564207 DOI: 10.1007/s40472-018-0186-9]

8 **Gilbo N**, Catalano G, Salizzoni M, Romagnoli R. Liver graft preconditioning, preservation and

reconditioning. *Dig Liver Dis* 2016; **48**: 1265-1274 [PMID: 27448845 DOI: 10.1016/j.dld.2016.06.031]

9 **Hoyer DP**, Mathé Z, Gallinat A, Canbay AC, Treckmann JW, Rauen U, Paul A, Minor T. Controlled Oxygenated Rewarming of Cold Stored Livers Prior to Transplantation: First Clinical Application of a New Concept. *Transplantation* 2016; **100**: 147-152 [PMID: 26479280 DOI: 10.1097/TP.0000000000000915]

10 **Guarrera JV**, Henry SD, Samstein B, Reznik E, Musat C, Lukose TI, Ratner LE, Brown RS Jr, Kato T, Emond JC. Hypothermic machine preservation facilitates successful transplantation of "orphan" extended criteria donor livers. *Am J Transplant* 2015; **15**: 161-169 [PMID: 25521639 DOI: 10.1111/ajt.12958]

11 **Watson CJE**, Hunt F, Messer S, Currie I, Large S, Sutherland A, Crick K, Wigmore SJ, Fear C, Cornateanu S, Randle LV, Terrace JD, Upponi S, Taylor R, Allen E, Butler AJ, Oniscu GC. In situ normothermic perfusion of livers in controlled circulatory death donation may prevent ischemic cholangiopathy and improve graft survival. *Am J Transplant* 2019; **19**: 1745-1758 [PMID: 30589499 DOI: 10.1111/ajt.15241]

12 **He X**, Guo Z, Zhao Q, Ju W, Wang D, Wu L, Yang L, Ji F, Tang Y, Zhang Z, Huang S, Wang L, Zhu Z, Liu K, Zhu Y, Gao Y, Xiong W, Han M, Liao B, Chen M, Ma Y, Zhu X, Huang W, Cai C, Guan X, Li XC, Huang J. The first case of ischemia-free organ transplantation in humans: A proof of concept. *Am J Transplant* 2018; **18**: 737-744 [PMID: 29127685 DOI: 10.1111/ajt.14583]

13 **Westerkamp AC**, Karimian N, Matton AP, Mahboub P, van Rijn R, Wiersema-Buist J, de Boer MT, Leuvenink HG, Gouw AS, Lisman T, Porte RJ. Oxygenated Hypothermic Machine Perfusion After Static Cold Storage Improves Hepatobiliary Function of Extended Criteria Donor Livers. *Transplantation* 2016; **100**: 825-835 [PMID: 26863473 DOI: 10.1097/TP.0000000000001081]

14 **de Vries Y**, Matton APM, Nijsten MWN, Werner MJM, van den Berg AP, de Boer MT, Buis CI, Fujiyoshi M, de Kleine RHJ, van Leeuwen OB, Meyer P, van den Heuvel MC, de Meijer VE, Porte RJ. Pretransplant sequential hypo- and normothermic machine perfusion of suboptimal livers donated after circulatory death using a hemoglobin-based oxygen carrier perfusion solution. *Am J Transplant* 2019; **19**: 1202-1211 [PMID: 30588774 DOI: 10.1111/ajt.15228]

15 **van Leeuwen OB**, de Vries Y, Fujiyoshi M, Nijsten MWN, Ubbink R, Pelgrim GJ, Werner MJM, Reyntjens KMEM, van den Berg AP, de Boer MT, de Kleine RHJ, Lisman T, de Meijer VE, Porte RJ. Transplantation of High-risk Donor Livers After Ex Situ Resuscitation and Assessment Using Combined Hypo- and Normothermic Machine Perfusion: A Prospective Clinical Trial. *Ann Surg* 2019; **270**: 906-914 [PMID: 31633615 DOI: 10.1097/SLA.0000000000003540]

16 **Friend PJ**, Dengu F. Expanding the Scope of Donation After Circulatory Death Liver Transplantation. *Liver Transpl* 2021; **27**: 325-326 [PMID: 33098747 DOI: 10.1002/lt.25924]

17 **De Carlis L**, De Carlis R, Lauterio A, Di Sandro S, Ferla F, Zanierato M. Sequential Use of Normothermic Regional Perfusion and Hypothermic Machine Perfusion in Donation After Cardiac Death Liver Transplantation With Extended Warm Ischemia Time. *Transplantation* 2016; **100**: e101-e102 [PMID: 27495774 DOI: 10.1097/TP.0000000000001419]

18 **Ghinolfi D**, Dondossola D, Rreka E, Lonati C, Pezzati D, Cacciatoinsilla A, Kersik A, Lazzeri C, Zanella A, Peris A, Maggioni M, Biancofiore G, Reggiani P, Morganti R, De Simone P, Rossi G. Sequential Use of Normothermic Regional and Ex Situ Machine Perfusion in Donation After Circulatory Death Liver Transplant. *Liver Transpl* 2021; **27**: 385-402 [PMID: 32949117 DOI: 10.1002/lt.25899]

19 **Savier E**, Lim C, Rayar M, Orlando F, Boudjema K, Mohkam K, Lesurtel M, Mabrut JY, Pittau G, Begdadi N, Cherqui D, Adam R, Dondero F, Sepulveda A, Soubrane O, Bucur P, Barbier L, Salame E, Jasseron C, Antoine C, Riou B, Scatton O. Favorable Outcomes of Liver Transplantation from Controlled Circulatory Death Donors Using Normothermic Regional Perfusion Compared to Brain Death Donors. *Transplantation* 2020; **104**: 1943-1951 [PMID: 32639402 DOI: 10.1097/TP.0000000000003372]

20 **Weissenbacher A**, Vrakas G, Nasralla D, Ceresa CDL. The future of organ perfusion and re-conditioning. *Transpl Int* 2019; **32**: 586-597 [PMID: 30980772 DOI: 10.1111/tri.13441]

21 **Ghinolfi D**, Rreka E, De Tata V, Franzini M, Pezzati D, Fierabracci V, Masini M, Cacciatoinsilla A, Bindi ML, Marselli L, Mazzotti V, Morganti R, Marchetti P, Biancofiore G, Campani D, Paolicchi A, De Simone P. Pilot, Open, Randomized, Prospective Trial for Normothermic Machine Perfusion Evaluation in Liver Transplantation From Older Donors. *Liver Transpl* 2019; **25**: 436-449 [PMID: 30362649 DOI: 10.1002/lt.25362]

22 **van Rijn R**, Schurink IJ, de Vries Y, van den Berg AP, Cortes Cerisuelo M, Darwish Murad S, Erdmann JI, Gilbo N, de Haas RJ, Heaton N, van Hoek B, Huurman VAL, Jochmans I, van Leeuwen OB, de Meijer VE, Monbaliu D, Polak WG, Slangen JJG, Troisi RI, Vanlander A, de Jonge J, Porte RJ; DHOPE-DCD Trial Investigators. Hypothermic Machine Perfusion in Liver Transplantation - A Randomized Trial. *N Engl J Med* 2021; **384**: 1391-1401 [PMID: 33626248 DOI: 10.1056/NEJMoa2031532]

23 **Hofmann J**, Otarashvili G, Meszaros A, Ebner S, Weissenbacher A, Cardini B, Oberhuber R, Resch T, Öfner D, Schneeberger S, Troppmair J, Hautz T. Restoring Mitochondrial Function While Avoiding Redox Stress: The Key to Preventing Ischemia/Reperfusion Injury in Machine Perfused Liver Grafts? *Int J Mol Sci* 2020; **21**: 3132 [PMID: 32365506 DOI: 10.3390/ijms21093132]

24 **Watson CJE**, Kosmoliaptsis V, Pley C, Randle L, Fear C, Crick K, Gimson AE, Allison M, Upponi S, Brais R, Jochmans I, Butler AJ. Observations on the ex situ perfusion of livers for transplantation.

Am J Transplant 2018; **18**: 2005-2020 [PMID: 29419931 DOI: 10.1111/ajt.14687]
25 **Watson CJE**, Jochmans I. From "Gut Feeling" to Objectivity: Machine Preservation of the Liver as a Tool to Assess Organ Viability. *Curr Transplant Rep* 2018; **5**: 72-81 [PMID: 29564205 DOI: 10.1007/s40472-018-0178-9]
26 **Matton APM**, de Vries Y, Burlage LC, van Rijn R, Fujiyoshi M, de Meijer VE, de Boer MT, de Kleine RHJ, Verkade HJ, Gouw ASH, Lisman T, Porte RJ. Biliary Bicarbonate, pH, and Glucose Are Suitable Biomarkers of Biliary Viability During Ex Situ Normothermic Machine Perfusion of Human Donor Livers. *Transplantation* 2019; **103**: 1405-1413 [PMID: 30395120 DOI: 10.1097/TP.0000000000002500]
27 **Eshmuminov D**, Schuler MJ, Becker D, Bautista Borrego L, Mueller M, Hagedorn C, Häusler S, Steiger J, Tibbitt MW, Dutkowski P, Rudolf von Rohr P, Stieger B, Hefti M, Clavien PA. Bile formation in long-term ex situ perfused livers. *Surgery* 2021; **169**: 894-902 [PMID: 33422346 DOI: 10.1016/j.surg.2020.11.042]
28 **de Jong IEM**, Matton APM, van Praagh JB, van Haaften WT, Wiersema-Buist J, van Wijk LA, Oosterhuis D, Iswandana R, Suriguga S, Overi D, Lisman T, Carpino G, Gouw ASH, Olinga P, Gaudio E, Porte RJ. Peribiliary Glands Are Key in Regeneration of the Human Biliary Epithelium After Severe Bile Duct Injury. *Hepatology* 2019; **69**: 1719-1734 [PMID: 30506902 DOI: 10.1002/hep.30365]
29 **Weeder PD**, van Rijn R, Porte RJ. Machine perfusion in liver transplantation as a tool to prevent non-anastomotic biliary strictures: Rationale, current evidence and future directions. *J Hepatol* 2015; **63**: 265-275 [PMID: 25770660 DOI: 10.1016/j.jhep.2015.03.008]
30 **van Rijn R**, van Leeuwen OB, Matton APM, Burlage LC, Wiersema-Buist J, van den Heuvel MC, de Kleine RHJ, de Boer MT, Gouw ASH, Porte RJ. Hypothermic oxygenated machine perfusion reduces bile duct reperfusion injury after transplantation of donation after circulatory death livers. *Liver Transpl* 2018; **24**: 655-664 [PMID: 29369470 DOI: 10.1002/lt.25023]
31 **Gaurav R**, Atulugama N, Swift L, Butler AJ, Upponi S, Brais R, Allison M, Watson CJE. Bile Biochemistry Following Liver Reperfusion in the Recipient and Its Association With Cholangiopathy. *Liver Transpl* 2020; **26**: 1000-1009 [PMID: 32108995 DOI: 10.1002/lt.25738]
32 **Watson CJE**, Kosmoliaptsis V, Randle LV, Gimson AE, Brais R, Klinck JR, Hamed M, Tsyben A, Butler AJ. Normothermic Perfusion in the Assessment and Preservation of Declined Livers Before Transplantation: Hyperoxia and Vasoplegia-Important Lessons From the First 12 Cases. *Transplantation* 2017; **101**: 1084-1098 [PMID: 28437389 DOI: 10.1097/TP.0000000000001661]
33 **Eshmuminov D**, Becker D, Bautista Borrego L, Hefti M, Schuler MJ, Hagedorn C, Muller X, Mueller M, Onder C, Graf R, Weber A, Dutkowski P, Rudolf von Rohr P, Clavien PA. An integrated perfusion machine preserves injured human livers for 1 week. *Nat Biotechnol* 2020; **38**: 189-198 [PMID: 31932726 DOI: 10.1038/s41587-019-0374-x]
34 **Muller X**, Schlegel A, Kron P, Eshmuminov D, Würdinger M, Meierhofer D, Clavien PA, Dutkowski P. Novel Real-time Prediction of Liver Graft Function During Hypothermic Oxygenated Machine Perfusion Before Liver Transplantation. *Ann Surg* 2019; **270**: 783-790 [PMID: 31592808 DOI: 10.1097/SLA.0000000000003513]
35 **Chouchani ET**, Pell VR, Gaude E, Aksentijević D, Sundier SY, Robb EL, Logan A, Nadtochiy SM, Ord ENJ, Smith AC, Eyassu F, Shirley R, Hu CH, Dare AJ, James AM, Rogatti S, Hartley RC, Eaton S, Costa ASH, Brookes PS, Davidson SM, Duchen MR, Saeb-Parsy K, Shattock MJ, Robinson AJ, Work LM, Frezza C, Krieg T, Murphy MP. Ischaemic accumulation of succinate controls reperfusion injury through mitochondrial ROS. *Nature* 2014; **515**: 431-435 [PMID: 25383517 DOI: 10.1038/nature13909]
36 **Wang L**, Thompson E, Bates L, Pither TL, Hosgood SA, Nicholson ML, Watson CJE, Wilson C, Fisher AJ, Ali S, Dark JH. Flavin Mononucleotide as a Biomarker of Organ Quality-A Pilot Study. *Transplant Direct* 2020; **6**: e600 [PMID: 32904032 DOI: 10.1097/TXD.0000000000001046]
37 **Dutkowski P**, Schlegel A, de Oliveira M, Müllhaupt B, Neff F, Clavien PA. HOPE for human liver grafts obtained from donors after cardiac death. *J Hepatol* 2014; **60**: 765-772 [PMID: 24295869 DOI: 10.1016/j.jhep.2013.11.023]
38 **Schlegel A**, Muller X, Kalisvaart M, Muellhaupt B, Perera MTPR, Isaac JR, Clavien PA, Muiesan P, Dutkowski P. Outcomes of DCD liver transplantation using organs treated by hypothermic oxygenated perfusion before implantation. *J Hepatol* 2019; **70**: 50-57 [PMID: 30342115 DOI: 10.1016/j.jhep.2018.10.005]
39 **Brüggenwirth IMA**, van Leeuwen OB, de Vries Y, Bodewes SB, Adelmeijer J, Wiersema-Buist J, Lisman T, Martins PN, de Meijer VE, Porte RJ. Extended hypothermic oxygenated machine perfusion enables *ex situ* preservation of porcine livers for up to 24 hours. *JHEP Rep* 2020; **2**: 100092 [PMID: 32195456 DOI: 10.1016/j.jhepr.2020.100092]
40 **Mueller M**, Kalisvaart M, O'Rourke J, Shetty S, Parente A, Muller X, Isaac J, Muellhaupt B, Muiesan P, Shah T, Clavien PA, Schlegel A, Dutkowski P. Hypothermic Oxygenated Liver Perfusion (HOPE) Prevents Tumor Recurrence in Liver Transplantation From Donation After Circulatory Death. *Ann Surg* 2020; **272**: 759-765 [PMID: 32889870 DOI: 10.1097/SLA.0000000000004258]
41 **Li CX**, Man K, Lo CM. The Impact of Liver Graft Injury on Cancer Recurrence Posttransplantation. *Transplantation* 2017; **101**: 2665-2670 [PMID: 28665890 DOI: 10.1097/TP.0000000000001844]
42 **Ceresa CDL**, Nasralla D, Watson CJE, Butler AJ, Coussios CC, Crick K, Hodson L, Imber C, Jassem W, Knight SR, Mergental H, Ploeg RJ, Pollok JM, Quaglia A, Shapiro AMJ, Weissenbacher A, Friend PJ. Transient Cold Storage Prior to Normothermic Liver Perfusion May Facilitate Adoption of

a Novel Technology. *Liver Transpl* 2019; **25**: 1503-1513 [PMID: 31206217 DOI: 10.1002/lt.25584]

43 **Goumard C**, Turco C, Sakka M, Aoudjehane L, Lesnik P, Savier E, Conti F, Scatton O. Ex-Vivo Pharmacological Defatting of the Liver: A Review. *J Clin Med* 2021; **10**: 1253 [PMID: 33803539 DOI: 10.3390/jcm10061253]

44 **Harada N**, Yoshizumi T, Mori M. Current review of machine perfusion in liver transplantation from the Japanese perspective. *Surg Today*2021 epub ahead of print [PMID: 33754175 DOI: 10.1007/s00595-021-02265-x]

45 **Resch T**, Cardini B, Oberhuber R, Weissenbacher A, Dumfarth J, Krapf C, Boesmueller C, Oefner D, Grimm M, Schneeberger S. Transplanting Marginal Organs in the Era of Modern Machine Perfusion and Advanced Organ Monitoring. *Front Immunol* 2020; **11**: 631 [PMID: 32477321 DOI: 10.3389/fimmu.2020.00631]

46 **Oniscu GC**, Randle LV, Muiesan P, Butler AJ, Currie IS, Perera MT, Forsythe JL, Watson CJ. In situ normothermic regional perfusion for controlled donation after circulatory death--the United Kingdom experience. *Am J Transplant* 2014; **14**: 2846-2854 [PMID: 25283987 DOI: 10.1111/ajt.12927]

47 **Hoyer DP**, Benkö T, Manka P, von Horn C, Treckmann JW, Paul A, Minor T. Long-term Outcomes After Controlled Oxygenated Rewarming of Human Livers Before Transplantation. *Transplant Direct* 2020; **6**: e542 [PMID: 32309628 DOI: 10.1097/TXD.0000000000000987]

48 **Zhang Z**, Tang Y, Zhao Q, Wang L, Zhu C, Ju W, Wang D, Yang L, Wu L, Chen M, Huang S, Gao N, Zhu Z, Zhang Y, Sun C, Xiong W, Shen Y, Ma Y, Hu A, Zhu X, Rong J, Cai C, Guo Z, He X. Association of Perfusion Characteristics and Posttransplant Liver Function in Ischemia-Free Liver Transplantation. *Liver Transpl* 2020; **26**: 1441-1454 [PMID: 32542994 DOI: 10.1002/lt.25825]

49 **Chen M**, Chen Z, Lin X, Hong X, Ma Y, Huang C, He X, Ju W. Application of ischaemia-free liver transplantation improves prognosis of patients with steatotic donor livers - a retrospective study. *Transpl Int* 2021; **34**: 1261-1270 [PMID: 33484201 DOI: 10.1111/tri.13828]

50 **Cardini B**, Oberhuber R, Fodor M, Hautz T, Margreiter C, Resch T, Scheidl S, Maglione M, Bösmüller C, Mair H, Frank M, Augustin F, Griesmacher A, Schennach H, Martini J, Breitkopf R, Eschertzhuber S, Pajk W, Obwegeser A, Tilg H, Watson C, Öfner D, Weissenbacher A, Schneeberger S. Clinical Implementation of Prolonged Liver Preservation and Monitoring Through Normothermic Machine Perfusion in Liver Transplantation. *Transplantation* 2020; **104**: 1917-1928 [PMID: 32371845 DOI: 10.1097/TP.0000000000003296]

51 **Reiling J**, Butler N, Simpson A, Hodgkinson P, Campbell C, Lockwood D, Bridle K, Santrampurwala N, Britton L, Crawford D, Dejong CHC, Fawcett J. Assessment and Transplantation of Orphan Donor Livers: A Back-to-Base Approach to Normothermic Machine Perfusion. *Liver Transpl* 2020; **26**: 1618-1628 [PMID: 32682340 DOI: 10.1002/lt.25850]

World Journal of Gastroenterology

Submit a Manuscript: https://www.f6publishing.com

World J Gastroenterol 2021 September 14; 27(34): 5737-5752

DOI: 10.3748/wjg.v27.i34.5737

ISSN 1007-9327 (print) ISSN 2219-2840 (online)

ORIGINAL ARTICLE

Retrospective Cohort Study

MTNR1B polymorphisms with *CDKN2A* and *MGMT* methylation status are associated with poor prognosis of colorectal cancer in Taiwan

Chia-Cheng Lee, Yu-Cheng Kuo, Je-Ming Hu, Pi-Kai Chang, Chien-An Sun, Tsan Yang, Chuan-Wang Li, Chao-Yang Chen, Fu-Huang Lin, Chih-Hsiung Hsu, Yu-Ching Chou

ORCID number: Chia-Cheng Lee 0000-0002-7450-504X; Yu-Cheng Kuo 0000-0002-7673-5164; Je-Ming Hu 0000-0002-7377-0984; Pi-Kai Chang 0000-0002-8641-3230; Chien-An Sun 0000-0001-9041-0537; Tsan Yang 0000-0002-8265-6438; Chuan-Wang Li 0000-0001-8108-8988; Chao-Yang Chen 0000-0002-2246-7635; Fu-Huang Lin 0000-0001-9878-9625; Chih-Hsiung Hsu 0000-0003-4423-4231; Yu-Ching Chou 0000-0003-4823-6541.

Author contributions: Hsu CH and Chou YC contributed equally to this work; Lee CC, Hsu CH and Chou YC designed the research; Sun CA, Yang T and Li CW performed the research; Hu JM, Chang PK and Chen CY collected the data; Lee CC, Kuo YC, Hsu CH, Lin FH and Chou YC analyzed the data; Lee CC, Hsu CH and Chou YC wrote the paper.

Supported by the grant from the Ministry of National Defense-Medical Affairs Bureau, Taiwan, No. MND-MAB-110-109 and No. MND-MAB-D-111059.

Institutional review board statement: This study was approved by the TSGH Institutional Review Board

Chia-Cheng Lee, Je-Ming Hu, Pi-Kai Chang, Chao-Yang Chen, Division of Colorectal Surgery, Department of Surgery, Tri-Service General Hospital, National Defense Medical Center, Taipei 114, Taiwan

Chia-Cheng Lee, Medical Informatics Office, Tri-Service General Hospital, National Defense Medical Center, Taipei 114, Taiwan

Yu-Cheng Kuo, Fu-Huang Lin, Chih-Hsiung Hsu, Yu-Ching Chou, School of Public Health, National Defense Medical Center, Taipei 114, Taiwan

Chien-An Sun, Department of Public Health, College of Medicine, Fu-Jen Catholic University, New Taipei City 24205, Taiwan

Chien-An Sun, Big Data Research Center, College of Medicine, Fu-Jen Catholic University, New Taipei City 24205, Taiwan

Tsan Yang, Department of Health Business Administration, Meiho University, Pingtung 91202, Taiwan

Chuan-Wang Li, Department and Graduate Institute of Microbiology and Immunology, National Defense Medical Center, Taipei 114, Taiwan

Chuan-Wang Li, Institute of Preventive Medicine, National Defense Medical Center, New Taipei City 237, Taiwan

Corresponding author: Yu-Ching Chou, PhD, Professor, School of Public Health, National Defense Medical Center, No. 161 Sec. 6, Minquan E. Road, Neihu District, Taipei 114, Taiwan. trishow@mail.ndmctsgh.edu.tw

Abstract

BACKGROUND

Identifying novel colorectal cancer (CRC) prognostic biomarkers is crucial to helping clinicians make appropriate therapy decisions. Melatonin plays a major role in managing the circadian rhythm and exerts oncostatic effects on different kinds of tumours.

(TSGHIRB approval number: 098-05-292 and 2-105-05-129).

Informed consent statement: Written informed consent was obtained from all patients before enrollment into the study to evaluate their prognosis.

Conflict-of-interest statement: We have no financial relationships to disclose.

Data sharing statement: No additional data are available.

Open-Access: This article is an open-access article that was selected by an in-house editor and fully peer-reviewed by external reviewers. It is distributed in accordance with the Creative Commons Attribution NonCommercial (CC BY-NC 4.0) license, which permits others to distribute, remix, adapt, build upon this work non-commercially, and license their derivative works on different terms, provided the original work is properly cited and the use is non-commercial. See: http://creativecommons.org/Licenses/by-nc/4.0/

Manuscript source: Invited manuscript

Specialty type: Oncology

Country/Territory of origin: Taiwan

Peer-review report's scientific quality classification

Grade A (Excellent): 0
Grade B (Very good): B
Grade C (Good): C, C
Grade D (Fair): 0
Grade E (Poor): 0

Received: April 15, 2021
Peer-review started: April 15, 2021
First decision: June 23, 2021
Revised: June 30, 2021
Accepted: August 23, 2021
Article in press: August 23, 2021
Published online: September 14, 2021

P-Reviewer: Ji G, Mogulkoc R, Xie M
S-Editor: Zhang H
L-Editor: A

AIM

To explore the relationship between *MTNR1B* single-nucleotide polymorphism (SNPs) combined with gene hypermethylation and CRC prognosis.

METHODS

A total of 94 CRC tumour tissues were investigated. Genotyping for the four *MTNR1B* SNPs (rs1387153, rs2166706, rs10830963, and rs1447352) was performed using multiplex polymerase chain reaction. The relationships between the *MTNR1B* SNPs and CRC 5-year overall survival (OS) was assessed by calculating hazard ratios with 95%CIs.

RESULTS

All SNPs (rs1387153, rs2166706, rs10830963, and rs1447352) were correlated with decreased 5-year OS. In stratified analysis, rs1387153, rs10830963, and rs1447352 risk genotype combined with CDKN2A and MGMT methylation status were associated with 5-year OS. A strong cumulative effect of the four polymorphisms on CRC prognosis was observed. Four haplotypes of *MTNR1B* SNPs were also associated with the 5-year OS. *MTNR1B* SNPs combined with *CDKN2A* and *MGMT* gene methylation status could be used to predict shorter CRC survival.

CONCLUSION

The novel genetic biomarkers combined with epigenetic biomarkers may be predictive tool for CRC prognosis and thus could be used to individualise treatment for patients with CRC.

Key Words: Colorectal cancer; Melatonin; Hypermethylation; Polymorphism; Prognosis; Biomarker

©The Author(s) 2021. Published by Baishideng Publishing Group Inc. All rights reserved.

Core Tip: In this retrospective cohort study, we found that *MTNR1B* single-nucleotide polymorphism were associated with a significantly increased risk of colorectal cancer (CRC) 5-year overall survival. A strong cumulative effect of the four polymorphisms on CRC prognosis was observed. This study indicated the novel genetic biomarkers, *MTNR1B*, combined with *CDKN2A* and *MGMT* gene methylation statuses, maybe a predictive tool for CRC prognosis.

Citation: Lee CC, Kuo YC, Hu JM, Chang PK, Sun CA, Yang T, Li CW, Chen CY, Lin FH, Hsu CH, Chou YC. *MTNR1B* polymorphisms with *CDKN2A* and *MGMT* methylation status are associated with poor prognosis of colorectal cancer in Taiwan. *World J Gastroenterol* 2021; 27(34): 5737-5752
URL: https://www.wjgnet.com/1007-9327/full/v27/i34/5737.htm
DOI: https://dx.doi.org/10.3748/wjg.v27.i34.5737

INTRODUCTION

Colorectal cancer (CRC) is the third most newly diagnosed cancer and second most frequent cause of cancer-related deaths worldwide[1]. The sudden increase in the incidence of CRC in Taiwan may be associated with obesity, a sedentary lifestyle, and unhealthy dietary habits resulting from improvement of the economy[2]. However, these well-known risk factors cannot wholly account for the increased incidence of CRC. Extensive studies have demonstrated that genetic and epigenetic variations influence personal CRC susceptibility and prognosis[3-6]. Finding novel CRC prognostic biomarkers is crucial because it would help clinicians in making appropriate decisions. Melatonin, which plays a central role in the management of circadian rhythm, has been identified in the pineal retina, lymphocytes, bone marrow, and gastrointestinal tract[7]. Several epidemiological studies have indicated that melatonin exerts oncostatic effects, including antioxidant activity, stimulation of apoptosis, regulation of prosurvival signalling and tumour metabolism, inhibition of

P-Editor: Liu JH

angiogenesis, metastasis, and induction of epigenetic alteration[8] on different types of tumours[9-11]. Melatonin prevents metastases, increases the 1-year longevity of patients with resected CRC, and enhances myelotoxicity, lymphocytopenia, and other undesirous haematological and immunological side effects. Furthermore, melatonin reduces neurotoxicity, weakness, insomnia, and psychological stress. These effects have been reported when melatonin is administered as a single pharmaceutical agent or coadministered with the usual first-line and second-line schedules for radiotherapy and chemotherapy[12]. The growing interest in understanding the association between melatonin and colorectal carcinogenesis has led to thorough studies regarding the presence of unique melatonin binding sites in the human colon's intestinal mucosa and submucosa. The melatonin receptor MT2, one of the largest superfamilies of G-protein linked receptors and encoded by *MTNR1B*, is generally responsible for mediating the downstream effects of melatonin[13]. In 2006, Ekmekcioglu *et al*[14] reported that MT2 was involved in the antiproliferative action of melatonin. Some research demonstrated that the levels of melatonin are regulated through its biosynthesis from the amino acid tryptophan, which is mediated by MT2[15]. Research analyses have demonstrated reduced expression of MT2 in tumour mucosa compared with the normal mucosa in patients with CRC[16,17]. This may be caused by MT2 downregulation, which reduces protection against CRC and facilitates the development of CRC tumours. In vitro findings indicate that melatonin triggers p53 phosphorylation through the activation of MT2[18].

Studies have reported an association between *MTNR1B* gene polymorphisms and impaired insulin secretion, higher fasting glucose level, increased risk of type 2 diabetes, and gestational diabetes[19,20]. However, the effect of *MTNR1B* gene polymorphisms on CRC sensitivity is little understood. Many studies have demonstrated that *CDKN2A* is more frequently methylated in poorly differentiated, lymphatic metastasis of CRC[21]. In addition, the hypermethylation state of DNA repair genes, *MGMT* and *MLH1*, which are silenced, and have been shown to be correlated with specific mutations in tumor DNA, such as *KRAS* mutations or microsatellite instability, respectively[22]. Furthermore, aberrant promoter methylation of the *CDKN2A, MGMT*, and *MLH1* genes has been reported to be related to adenoma-carcinoma sequence and could serve as a diagnostic prognostic marker of CRC[23,24].

In the present study, a hospital-based retrospective cohort study was conducted to evaluate the effects of *MTNR1B* gene polymorphisms rs1387153, rs2166706, rs10830963, and rs1447352 and their haplotypes on the 5-year overall survival (OS) of patients with CRC and to analyse interactions based on the methylation status of the *CDKN2A* and *MGMT* genes. We hypothesised that the influence of *MTNR1B* gene variation combined with the hypermethylation of *CDKN2A* and *MGMT* genes would predict the prognosis and provide clinical recommendations for optimal treatment of CRC.

MATERIALS AND METHODS

Samples and DNA extraction

A retrospective cohort study, described in detail elsewhere[24-27], was conducted to predict the OS of patients with CRC in Taiwan. Among this cohort, 94 tumour tissues were collected from patients with CRC, which was diagnosed in the Tri-Service General Hospital (TSGH), Taiwan, from 2006 to 2010. The 5-year prognosis was assessed using the tumour tissues. The TSGH Colon and Rectum Division's clinical practice guideline requires enrolees to return once every 3 mo in the first year after surgical resection and once every 3–6 mo thereafter. Written informed consent was obtained from all patients before participation in the study. The TSGH Institutional Review Board approved this study (TSGHIRB approval number: 098-05-292 and 2-105-05-129). Data regarding registered patients—including sex, surgical age (permanent variable), adjuvant chemotherapy, histologic grade and location of the tumour, and survival—were collected from the TSGH's cancer registry database and analyzed to investigate the association with *MTNR1B* genotyping. All methods were performed in accordance with the relevant guidelines and regulations. OS was defined as the time from the date of surgery to the date of death from any cause or the last follow-up date before December 31, 2010. Cellulose-coated magnetic beads were employed to extract genomic DNA from the tumour tissues stored at −80 °C in a liquid nitrogen tank by using the MagCore Compact Automated Nucleic Acid Extractor (catalogue no. MCA0801; RBC Bioscience, Taipei, Taiwan) and Genomic DNA Tissue Kit (catalogue

no. 69504; Qiagen, Taipei, Taiwan).

MTNR1B genotyping

The *MTNR1B* gene polymorphisms rs1387153, rs2166706, rs10830963, and rs1447352 were screened using the Agena MassARRAY platform with iPLEX gold chemistry (Agena, San Diego, CA, United States). The detailed genotyping protocols have been reported elsewhere[28,29]. Following the manufacturer guide, the specific polymerase chain reaction (PCR) primer and extension primer sequences were designed using the Assay Designer software package (v.4.0). A 1-μL genomic DNA sample (10 ng/μL) was employed in multiplex PCR in 5-μL volumes containing 1 unit of Taq polymerase, 500 nmol of each PCR primer mix, and 2.5 mmol/L of each dNTP (Agena, PCR accessory and Enzyme kit). Thermocycling was performed at 94 °C for 4 min, which was followed by 45 cycles at 94 °C for 20 s, 56 °C for 30 s, 72 °C for 1 min, and then 72 °C for 3 min. Unincorporated dNTPs were deactivated using 0.3 U of shrimp alkaline phosphatase. Single-base extension reaction was performed using iPLEX enzyme, terminator mix, and extension primer mix; this was followed by 94 °C for 30 s, 40 cycles at 94 °C for 5 s, 5 inner-cycles at 56 °C for 5 s, 80 °C for 5 s, and finally 72 °C for 3 min (Agena, iPLEX gold kit). After cation exchange resin was added to remove residual salt from the reaction, 7 nL of the purified primer extension reaction was loaded onto the matrix pad of a SpectroCHIP (Agena). The SpectroCHIPs were analysed using a MassARRAY Analyzer 4, and clustering analysis was performed using TYPER 4.0 software.

Methylation-specific-PCR

We analyzed *CDKN2A*, *hMLH1*, and *MGMT* DNA methylation in the promoter regions through methylation-specific polymerase chain reaction (MS-PCR), as described in our earlier study[25]. Perform MS-PCR with 1.2-μL aliquots of forward and reverse primers, with 12.5 μL HotStart Taq Premix (RBC Bioscience) and bisulfite-converted DNA according to the manufacturer's protocol. The sequences, annealing temperature of individual primer used for amplification, and MS-PCR product sizes are illustrated in Table 1. The MS-PCR procedures were in accordance with the previous study[25]: first, 10 min at 95 °C; then, 35 cycles of 30-s denaturation at 95 °C, 30-s annealing, and 48-s extension at 72 °C; finally, 4-min extension at 72 °C. After the amplification, MS-PCR products were mixed with a loading buffer, electrophoresed on 2% agarose gel by using 0.2-μL gel-stained dye for 25 min, and visualized using an ultraviolet transilluminator.

Statistical analysis

Student's *t*-tests were performed to analyse continuous variables, and χ^2 tests were performed for statistical analyses of categorical variables (IBM SPSS Statistics 22). The existence of a Hardy–Weinberg equilibrium per single-nucleotide polymorphism (SNP) was assessed using two goodness-of-fit tests. Linkage disequilibrium (LD) among genotyped SNPs was obtained using the Haploview 4.2 programme. The minor allele frequencies of four *MTNR1B* gene polymorphisms (rs1387153, rs2166706, rs10830963, and rs1447352) are higher than 5% in an ethnic Chinese population according to data in the dbSNP database.

The relationships between the *MTNR1B* SNPs and 5-year OS of patients with CRC and between the cumulative effect of *MTNR1B* SNPs and 5-year OS of CRC were assessed using adjusted hazard ratios (aHRs) with 95%CIs, calculated using Cox proportional-hazards analyses and adjusted for all the aforementioned patient-level and hospital-level characteristics.

Haplotype frequencies for these SNPs combinations were first estimated using haplo.stats (version 12.1) for the R statistical package and then verified using Haploview 4.2. These software programmes employ expectation–maximisation algorithms when constructing the haplotypes. All statistical tests were two-sided, and $P < 0.05$ was considered statistically significant.

RESULTS

In this study, 94 CRC tumor samples from the TSGH tumor bank were analyzed. LD was evaluated for all *MTNR1B* SNP pairs. The Lewontin's D' values of the pairs were 1.00 (rs1387153: rs2166706), 0.90 (rs1387153: rs10830963), and 0.88 (rs1387153: rs1447352); and the R2 values were 0.98, 1.00, and 1.00, respectively. Four haplotypes with frequencies of 0.034 (T-C-G-A), 0.011 (C-T-C-A), 0.011 (C-T-C-G), and 0.472 (C-T-

Table 1 Primer sequences, annealing temperature and product size for methylation-specific polymerase of target genes

Genes		Forward primer (5'→3')	Annealing temperature (oC)	Product size (bp)
CDKN2A	M	F: TTATTAGAGGGTGGGGCGGATCGC	62	150
		R: GACCCCGAACCGCGACCGTAA		
	U	F: TTATTAGAGGGTGGGGTGGATTGT	62	151
		R: CAACCCCAAACCACAACCATAA		
MLH1	M	F: ACGTAGACGTTTTATTAGGGTCGC	60	118
		R: CCTCATCGTAACTACCCGCG		
	U	F: TTTTGATGTAGATGTTTTATTAGGGTTGT	60	124
		R: ACCACCTCATCATAACTACCCACA		
MGMT	M	F: TTTCGACGTTCGTAGGTTTTCGC	53	81
		R: GCACTCTTCCGAAAACGAAACG		
	U	F: TTTGTGTTTTGATGTTTGTAGGTTTTTGT	53	93
		R: AACTCCACACTCTTCCAAAAACAAAACA		

MSP: Methylation-specific polymerase chain reaction; M: Methylation; U: Unmethylation.

G-A) were selected for the haplotype association analysis. The relationship between the *MTNR1B* genotype and the demographic and clinicopathological features of patients with CRC was evaluated. Among the patients with CRC, 41.5% were men; the mean age at surgery was 64.2 ± 13.8 years; 51.0% were at stage III–IV; and 19.1% of the patients died during the study period. Table 2 and Table 3 show that certain possible CRC risk factors, such as age, sex, tumor-node-metastasis stage, and *CDKN2A*, *MLH1* and *MGMT* genes methylation status, were not significantly associated with the *MTNR1B* genotype. However, tumor location and survival were associated with a *MTNR1B* polymorphism. The relationships between each *MTNR1B* genotype were analyzed to determine their association with 5-year OS in patients with CRC using Cox proportional-hazards models adjusted for age, sex, stage, adjuvant chemotherapy, tumor location, and the methylation status of the *CDKN2A, MLH1* and *MGMT* genes (Table 4). All SNPs were associated with lower 5-year OS. The variant types of rs1387153 (TT *vs* CC + CT: aHR = 6.23, 95%CI = 2.01–19.3), rs2166706 (CC *vs* TT + TC: aHR = 6.40, 95%CI = 2.21–18.6), rs10830963 (GG *vs* CC + CG: aHR = 7.43, 95%CI = 2.63–21.1), and rs1447352 (AA *vs* GG + GA: aHR = 4.28, 95%CI = 1.32–13.9) decreased the 5-year OS in patients with CRC.

We further examined the relationship between each SNP and the 5-year OS, with data stratified by the methylation status of the *CDKN2A* and *MGMT* genes (Table 5). Particularly, 5-year OS was significantly reduced in the rs1387153 and rs1447352 polymorphism subgroups of unmethylation of the *MGMT* gene (aHR = 8.57, 95%CI = 1.67–44.1; aHR = 19.4, 95%CI = 2.94–128, respectively) compared with the opposite subgroups. In contrast, we determined that the rs1447352 polymorphism was related to a higher risk of mortality in the subjects with methylation of the *CDKN2A* gene (aHR = 9.40, 95%CI = 1.02 –86.8). Besides, rs10830963 exhibited a significant association with 5-year OS in the subgroups with hypermethylation of the *CDKN2A* gene (aHR = 27.2, 95%CI = 3.12–233). According to the small number of hypermethylation *MLH1* gene, we could not perform the *MLH1* gene methylation-stratified analysis.

The cumulative effects of four SNPs were then evaluated. We selected polymorphism to classify the risk based on genotypes, in accordance with the findings summarised in Table 4: TT *vs* CC + CT for rs1387153, CC *vs* TT + TC for rs2166706, GG *vs* CC + CG for rs10830963, and AA *vs* GG + GA for rs1447352. The subjects were classified into five groups on the basis of their genotypical risk score (0, 1, 2, 3, and 4), and the significance of the linear trend was then evaluated. The risk of poor CRC prognosis significantly increased with an increase in the SNP risk genotypes (P_{trend} < 0.001, Table 6). Furthermore, patients were divided into two groups on the basis of the number of risk genotypes, forming the < 2 and ≥ 2 SNP risk genotypes groups. The 5-year OS was significantly different between the group with two or more SNP risk genotypes and the comparison group (aHR = 5.81, 95%CI = 2.03-16.6).

Table 2 Clinical characteristics of colorectal cancer patients and *MTNR1B* genotypes (rs1387153 and rs2166706)

No of subjects	Total	rs1387153 (C>T)						rs2166706 (T>C)					
		CC (%)	CT (%)	TT (%)	*P* value	CC + CT (%)	*P* value	TT (%)	TC (%)	CC (%)	*P* value	TT + TC (%)	*P* value
Sex													
Male	39 (41.5)	8 (34.8)	20 (41.7)	10 (47.6)	0.69	28 (39.4)	0.62	8 (36.4)	20 (40.8)	11 (47.8)	0.73	28 (39.4)	0.63
Female	55 (58.5)	15 (65.2)	28 (58.3)	11 (52.4)		43 (60.6)		14 (63.6)	29 (59.2)	12 (52.2)		43 (60.6)	
Age at surgery													
mean ± SD (yr)	64.2 ± 13.8	66.8 ± 13.8	61.7 ± 13.8	67.0 ± 13.3	0.20	63.3 ± 13.9	0.29	67.4 ± 13.8	61.8 ± 13.8	65.6 ± 13.5	0.24	63.6 ± 13.9	0.54
< 65	50 (53.2)	12 (52.2)	27 (56.2)	10 (47.6)	0.80	39 (54.9)	0.62	11 (50.0)	27 (55.1)	12 (52.2)	0.92	38 (53.5)	1.00
≥ 65	44 (46.8)	11 (47.8)	21 (43.8)	11 (52.4)		32 (45.1)		11 (50.0)	22 (44.9)	11 (47.8)		33 (46.5)	
Stage													
I	12 (12.8)	2 (8.7)	6 (12.5)	4 (19.0)	0.31	8 (11.3)	0.12	2 (9.1)	6.1 (2.2)	4 (17.4)	0.24	8 (11.3)	0.08
II	34 (36.2)	9 (39.1)	18 (37.5)	6 (28.6)		27 (38.0)		8 (36.4)	19 (38.8)	7 (30.4)		27 (38.0)	
III	30 (31.9)	10 (43.5)	16 (33.3)	4 (19.0)		26 (36.6)		10 (45.5)	16 (32.7)	4 (17.4)		26 (36.6)	
IV	18 (19.1)	2 (8.7)	8 (16.7)	7 (33.3)		10 (14.1)		2 (9.1)	8 (16.3)	8 (34.8)		10 (14.1)	
Adjuvant chemotherapy[a]													
No	23 (24.5)	5 (22.7)	12 (25.5)	6 (33.3)	0.74	17 (24.6)	0.55	5 (23.8)	12 (25.5)	6 (30.0)	0.90	17 (25.0)	0.77
Yes	65 (69.1)	17 (77.3)	35 (74.5)	12 (66.7)		52 (75.4)		16 (76.2)	35 (74.5)	4 (70.0)		51 (75.0)	
Tumor location[a]													
Colon	74 (78.7)	21 (95.5)	41 (87.2)	11 (61.1)	< 0.001	62 (89.9)	< 0.001	20 (95.2)	41 (87.2)	13 (65.0)	0.02	61 (89.7)	0.01
Rectum	14 (14.9)	1 (4.5)	6 (12.5)	7 (38.9)		7 (10.1)		1 (4.8)	6 (12.8)	7 (35.0)		7 (10.3)	
CDKN2A gene													
Unmethylation	43 (45.7)	13 (56.5)	19 (39.6)	10 (47.6)	0.40	32 (45.1)	1.00	12 (54.5)	21 (42.9)	10 (43.5)	0.64	33 (46.5)	0.99
Methylation	51 (54.3)	10 (43.5)	29 (60.4)	11 (52.4)		39 (54.9)		10 (45.5)	28 (57.1)	13 (56.5)		38 (53.5)	
MLH1 gene													
Unmethylation	77 (81.9)	20 (87.0)	38 (79.2)	17 (81.0)	0.73	58 (81.7)	1.00	19 (86.4)	39 (79.6)	19 (82.6)	0.79	58 (81.7)	1.00
Methylation	17 (18.1)	3 (13.0)	10 (20.8)	4 (19.0)		13 (18.3)		3 (13.6)	10 (20.4)	4 (17.4)		13 (18.3)	
MGMT gene													

Unmethylation	46 (48.9)	8 (34.8)	26 (54.2)	12 (57.1)	0.24	34 (47.9)	0.62	8 (36.4)	25 (51.0)	13 (56.5)	0.37	33 (46.5)	0.55
Methylation	48 (51.1)	15 (65.2)	22 (45.8)	9 (42.9)		37 (52.1)		14 (63.6)	24 (49.0)	10 (43.5)		38 (53.5)	
Death in 5 yr													
No	76 (80.9)	21 (91.3)	41 (85.4)	13 (61.9)	0.03	62 (87.3)	0.02	20 (90.9)	42 (85.7)	14 (60.9)	0.02	62 (87.3)	0.01
Yes	18 (19.1)	2 (8.7)	7 (14.6)	8 (38.1)		9 (12.7)		2 (9.1)	7 (14.3)	9 (39.1)		9 (12.7)	

[a]The total number of patients with colorectal cancer does not correspond because of missing data. CRC: Colorectal cancer.

Haplotype analysis was performed to determine the relationship between haplotypes of the studied SNPs (rs1387153, rs2166706, rs10830963, and rs1447352) and the 5-year OS. Four haplotypes were screened and two demonstrated significance. The T-C-G-A haplotype contributed to reduced 5-year OS (aHR = 2.75, 95%CI = 1.82–11.2), whereas the C-T-C-G haplotype reduced the risk of mortality (aHR = 0.21, 95%CI = 0.06–0.71, Table 7). No significant relationship with the 5-year OS was evident for the C-T-G-A haplotype (aHR = 1.96, 95%CI = 0.44–8.66) or the C-T-C-A haplotype (aHR = 0.70, 95%CI = 0.28–1.72).

DISCUSSION

In this retrospective cohort study, we examined the associations between four *MTNR1B* gene polymorphisms (rs1387153, rs2166706, rs10830963, and rs1447352) and CRC outcomes in terms of OS. Correlations between all SNPs and the 5-year OS were identified. In stratified analysis, the rs1387153 and rs1447352 risk genotypes were determined to be associated with 5-year OS in the unmethylation *MGMT* gene subgroup. In contrast, the rs10830963 and rs1447352 risk genotypes with hypermethylation *CDKN2A* gene had a higher risk of death in five years. Four haplotypes of *MTNR1B* SNPs were also determined to be associated with increased risk of mortality. This study is one of a few that has reported an association between *MTNR1B* SNPs and the 5-year OS in patients with CRC. The *MTNR1B* gene location of both rs1387153 and rs2166706 is > 11 kb upstream. The variant rs10830963 is located in an intronic region, whereas the variant rs1447352 is located at approximately 4.5 kb from the *MTNR1B* gene[30]. Qiu *et al*[31] indicated that these SNPs may influence the *MTNR1B* expression, causing a functional deficiency of melatonin. De Luis *et al*[32] demonstrated that rs10830963 was associated with an increased *MTNR1B* mRNA expression and the expression of other genes that may affect the energy balance role of melatonin[33]. However, the potential role and regulation of the other three SNPs in the *MTNR1B* expression are poorly understood[34].

Table 3 Clinical characteristics of colorectal cancer patients and *MTNR1B* genotypes (rs10830963 and rs1447352)

Variables	Total	rs10830963 (C>G)						rs1447352 (A>G)					
		CC (%)	CG (%)	GG (%)	*P* value	CC + CG (%)	*P* value	GG (%)	GA (%)	AA (%)	*P* value	GG + GA (%)	*P* value
Sex													
Male	39 (41.5)	7 (33.3)	22 (44.9)	10 (43.5)	0.66	29 (41.4)	1.00	4 (66.7)	16 (43.2)	19 (38.0)	0.40	20 (46.5)	0.53
Female	55 (58.5)	14 (66.7)	27 (55.1)	13 (56.5)		41 (58.6)		2 (33.3)	21 (56.8)	31 (62.0)		23 (53.5)	
Age at surgery													
mean ± SD (yr)	64.2 ± 13.8	67.0 ± 14.0	61.4 ± 13.9	66.8 ± 13.1	0.16	63.1 ± 14.0	0.26	69.7 ± 14.1	64.4 ± 14.0	63.0 ± 13.8	0.53	65.1 ± 14.0	0.47
< 65	50 (53.2)	11 (52.4)	28 (57.1)	11 (47.8)	0.75	39 (55.7)	0.63	3 (50.0)	18 (48.6)	29 (58.0)	0.68	21 (48.8)	0.41
≥ 65	44 (46.8)	10 (47.6)	21 (42.9)	12 (52.2)		31 (44.3)		3 (50.0)	19 (51.4)	21 (42.0)		22 (51.2)	
Stage													
I	12 (12.8)	2 (9.5)	6 (12.2)	4 (17.4)	0.56	8 (11.4)	0.30	0 (0)	4 (10.8)	8 (16.0)	0.54	4 (9.3)	0.60
II	34 (36.2)	8 (38.1)	18 (36.7)	7 (30.4)		26 (37.1)		1 (16.7)	15 (40.5)	17 (34.0)		16 (37.2)	
III	30 (31.9)	9 (42.9)	16 (32.7)	5 (21.7)		25 (35.7)		4 (66.7)	12 (32.4)	14 (28.0)		16 (37.2)	
IV	18 (19.1)	2 (9.5)	9 (18.4)	7 (30.4)		11 (15.7)		1 (16.7)	6 (16.2)	11 (22.0)		7 (16.3)	
Adjuvant chemotherapy[a]													
No	23 (24.5)	5 (23.8)	12 (25.5)	6 (30.0)	0.90	17 (25.0)	0.77	1 (16.7)	8 (22.2)	14 (30.4)	0.61	9 (21.4)	0.47
Yes	65 (69.1)	16 (76.2)	35 (74.5)	14 (70.0)		51 (75.0)		5 (83.3)	28 (77.8)	32 (69.6)		33 (78.6)	
Tumor location[a]													
Colon	74 (78.7)	20 (95.2)	41 (87.2)	13 (65.0)	0.02	61 (89.7)	0.01	6 (100)	34 (94.4)	34 (73.9)	0.02	40 (95.2)	< 0.001
Rectum	14 (14.9)	1 (4.85)	6 (12.8)	7 (35.0)		7 (10.3)		0 (0)	2 (5.6)	12 (26.1)		2 (4.8)	
CDKN2A gene													
Unmethylation	43 (45.7)	12 (57.1)	17 (34.7)	13 (56.5)	0.10	29 (41.4)	0.31	4 (66.7)	16 (43.2)	22 (44.0)	0.55	20 (46.5)	0.97
Methylation	51 (54.3)	9 (42.9)	32 (65.3)	10 (43.5)		41 (58.6)		2 (33.3)	21 (56.8)	28 (56.0)		23 (53.5)	
MLH1 gene													
Unmethylation	77 (81.9)	18 (85.7)	39 (79.6)	19 (82.6)	0.83	57 (81.4)	1.00	5 (83.3)	31 (83.8)	40 (80.0)	0.90	36 (83.7)	0.79
Methylation	17 (18.1)	3 (14.3)	10 (20.4)	4 (17.4)		13 (18.6)		1 (16.7)	6 (16.2)	10 (20.0)		7 (16.3)	
MGMT gene													

Unmethylation	46 (48.9)	8 (38.1)	26 (53.1)	12 (52.2)	0.50	34 (48.6)	0.95	4 (66.7)	18 (48.6)	24 (48.0)	0.68	22 (51.2)	0.92
Methylation	48 (51.1)	13 (61.9)	23 (46.9)	11 (47.8)		36 (51.4)		2 (33.3)	19 (51.4)	26 (52.0)		21 (48.8)	
Death in 5 yr													
No	76 (80.9)	19 (90.5)	43 (87.8)	13 (56.5)	< 0.001	62 (88.6)	< 0.001	6 (100)	33 (89.2)	36 (72.0)	0.06	39 (90.7)	0.03
Yes	18 (19.1)	2 (9.5)	6 (12.2)	10 (43.5)		8 (11.4)		0 (0)	4 (10.8)	14 (28.0)		4 (9.3)	

[a]The total number of patients with colorectal cancer does not correspond because of missing data. CRC: Colorectal cancer.

Mechanisms involving the oncostatic effect of melatonin binding to MT1 and MT2 receptors in CRC have been reported in numerous studies. An *in vitro* study conducted by Karasek *et al*[35] determined that both MT1 and MT2 were part of the oncostatic action of melatonin on Colon 38 adenocarcinoma cells. Furthermore, activation of the tumour suppressor *p53* gene by melatonin is reportedly directly controlled by MT1 and MT2. Melatonin's suppression of cell proliferation and clonogenic activity is impaired because of the lack of either receptor[18]. León *et al*[16] demonstrated an association between reduced MT1 and MT2 expression and increased malignancy in CRC in 54 Spanish patients with CRC. Moreover, expression of the tumour markers CD44 and CD133 was negatively correlated with MT1 and MT2 expression in patients with CRC[17]. Furthermore, the role of the MT1 receptor in gastric adenocarcinoma was demonstrated in patients over the age of 50 years[36]. In the present study, we determined that four *MTNR1B* gene polymorphisms were significantly associated with the 5-year OS of patients with CRC, with a cumulative effect on prediction for poorer prognosis. Few studies have assessed the relationship between *MTNR1B* gene polymorphisms and CRC prognosis. However, some type 2 diabetes susceptibility genes are correlated with metastasis development[37]. Nasrabadi *et al*[38] indicated that high expression of MT2 was associated with gastric adenocarcinoma, because MT2 receptors enhance the secretion of bicarbonate by stimulating calcium release into the mucosa of enterochromaffin cells. Numerous reports have indicated that *MTNR1B* SNPs are associated with fasting glucose level, obesity, carbohydrate disorders, and type 2 diabetes, which are crucial metabolic risk factors for CRC[39,40]. Indeed, Johnson *et al*[41] reviewed the association between colorectal cancer and type 2 diabetes and indicated that there is a positive and observational correlation. Besides, the GG genotype of the variant rs10830963 was discovered to significantly increase the risk of breast cancer than the CC genotype[39,42]. Moreover, the AA genotype of the variant rs10765576 was correlated with lower risk of breast cancer compared with the GG or GA major allele among Chinese women[13].

Data concerning the effect of gene methylation modification on the association between *MTNR1B* gene polymorphisms and CRC prognosis are scarce. The case-only analysis performed by Das *et al*[43] assessed the potential interactions and associations between epigenetics, genetics, and the risk of oesophageal cancer. Das *et al*[43]

Table 4 Relationship between *MTNR1B* single-nucleotide polymorphism and 5-year overall survival of colorectal cancer patients

	No. of subjects	No. of cases (%)	Crude		Adjusted[a]	
			HR	95%CI	HR	95%CI
rs1387153 (C>T)						
CC	23	2 (11.8)	1.00	Referent	1.00	Referent
CT	48	7 (41.2)	1.65	(0.34 to 7.95)	1.98	(0.40 to 9.82)
TT	21	8 (47.1)	6.03	(1.28 to 28.4)	10.6	(1.87 to 59.5)
TT *vs* CC + CT			4.18	(1.61 to 10.9)	6.23	(2.01 to 19.3)
rs2166706 (T>C)						
TT	22	2 (11.1)	1.00	Referent	1.00	Referent
TC	49	7 (38.9)	1.55	(0.32 to 7.47)	1.91	(0.39 to 9.45)
CC	23	9 (50.0)	5.74	(1.24 to 26.6)	10.5	(1.96 to 56.4)
CC *vs* TT + TC			4.15	(1.65 to 10.5)	6.40	(2.21 to 18.6)
rs10830963 (C>G)						
CC	21	2 (11.1)	1.00	Referent	1.00	Referent
CG	49	6 (33.3)	1.19	(0.24 to 5.91)	1.40	(0.27 to 7.22)
GG	23	10 (55.6)	5.79	(1.27 to 26.5)	9.46	(1.90 to 47.1)
GG *vs* CC + CG			5.09	(2.01 to 12.9)	7.43	(2.63 to 21.1)
rs1447352 (A>G)						
AA	50	14 (77.8)	1.00	Referent	1.00	Referent
GA	37	4 (22.2)	0.36	(0.12 to 1.08)	0.31	(0.10 to 0.99)
GG	6	0 (0)	N/A	N/A	N/A	N/A
AA *vs* GG + GA			3.37	(1.11 to 10.2)	4.28	(1.32 to 13.9)

[a]Adjusted for age, sex, stage, adjuvant chemotherapy, tumor location and the methylation status of *CDKN2A, MLH1* and *MGMT* gene. HR: Hazard ratio; N/A: Not applicable.

determined that *CDKN2A* methylation and the *p53* polymorphism were significantly associated with oesophageal cancer risk. DNA methylation can regulate gene expression by modifying chromatin complexes and recruiting methyl-CpG domain-binding proteins around CpG islands, and this is the most common epigenetic alteration. There was a clinical study had revealed the feasibility of using specific gene methylation statuses as biomarkers for CRC prognosis[44]. For instance, the hypermethylation of *CDKN2A* and *MGMT* promoters has been suggested to be independently correlated with poorer prognosis (including metastasis, recurrence, and mortality) in patients with CRC[45,46]. Our findings demonstrated that the risk of mortality in *CDKN2A* hypermethylation patients with rs10830963 or rs1447352 risk genotype was higher than that in the opposing subgroups. However, SNPs−rs1387153 and rs1447352 with unmethylation of the *MGMT* gene were associated with poorer CRC prognosis. All these findings regarding the correlation with gene promoter methylation status and polymorphisms suggest an overlap and crosstalk between the involved pathways, adversely affecting cancer prognosis, and indicate a strong correlation between genetic and epigenetic factors in the Taiwanese population. Therefore, *CDKN2A* and *MGMT* methylation status and *MTNR1B* SNPs may be used as molecular targets for predicting CRC prognosis. The efficiency of any single polymorphic site for risk detection is usually limited because of the multistep model of colorectal carcinogenesis. The benefits of using a combination of several SNPs are well-documented[47]. Our analysis revealed a significant cumulative effect, which was observed as *MTNR1B* SNPs correlating with the 5-year OS, which indicates that using more risk genotypes may improve the accuracy of CRC prognoses. Furthermore, the risk of mortality in individuals with the TT genotype rs1387153, CC genotype rs2166706, and GG genotype rs10830963 may be 2.75-fold higher than that in other haplotypes.

Table 5 Stratified effect between gene promoter region methylation and *MTNR1B* genotypes for 5-year overall survival of colorectal cancer patients

		No. of subjects	No. of cases (%)	Crude		Adjusted[a]	
				HR	95%CI	HR	95%CI
rs1387153 (C>T)							
TT *vs* CC + CT	CDKN2A						
	U	10	4 (40.0)	5.01	(1.33 to 18.9)	10.4	(1.17 to 92.4)
	M	11	4 (36.4)	3.83	(0.96 to 15.3)	8.86	(1.08 to 72.8)
	MGMT						
	U	12	5 (41.7)	3.63	(1.05 to 12.6)	8.57	(1.67 to 44.1)
	M	9	3 (33.3)	4.93	(1.10 to 22.1)	3.05	(0.33 to 28.0)
rs2166706 (T>C)							
CC *vs* TT + TC	CDKN2A						
	U	10	4 (40.0)	5.02	(1.33 to 19.0)	10.4	(1.17 to 92.4)
	M	13	5 (38.5)	3.96	(1.06 to 14.7)	10.1	(1.49 to 68.0)
	MGMT						
	U	13	5 (38.5)	3.07	(0.89 to 10.7)	6.28	(1.54 to 25.7)
	M	23	9 (39.1)	6.25	(1.56 to 25.1)	8.28	(0.95 to 72.3)
rs10830963 (C>G)							
GG *vs* CC + CG	CDKN2A						
	U	13	5 (38.5)	4.63	(1.24 to 17.3)	8.47	(1.57 to 45.6)
	M	10	5 (50.0)	5.61	(1.51 to 20.9)	27.2	(3.12 to 233)
	MGMT						
	U	12	5 (41.7)	3.47	(1.00 to 12.0)	8.50	(1.98 to 36.5)
	M	11	5 (45.5)	7.91	(1.89 to 33.2)	9.80	(1.42 to 67.5)
rs1447352 (A>G)							
AA *vs* GG + GA	CDKN2A						
	U	22	6 (27.3)	2.05	(0.51 to 8.22)	2.28	(0.51 to 10.2)
	M	28	8 (28.6)	7.34	(0.92 to 58.7)	9.40	(1.02 to 86.8)
	MGMT						
	U	24	8 (33.3)	3.94	(0.84 to 18.6)	19.4	(2.94 to 128)
	M	26	6 (23.1)	2.77	(0.56 to 13.7)	2.04	(0.35 to 12.0)

[a]Adjusted for age, sex, stage, adjuvant chemotherapy, tumor location and the methylation status of *CDKN2A* and *MLH1* or *MGMT* and *MLH1* gene. U: Unmethylation; M: Methylation; HR: Hazard ratio.

Certain limitations to the present study should be considered. First, limitations are inherent in any retrospective cohort study. Second, our sample size was not sufficiently large enough to provide a more precise estimate of the association between *MTNR1B* SNPs and CRC prognosis. Third, our preliminary retrospective cohort study was not designed to clarify the pathophysiology of how the risk genotype of the *MTNR1B* gene reduces postoperative survival. In addition, data regarding registered patients were collected from the TSGH's cancer registry database. Other potential risk factors, such as dietary habits, obesity, and combined primary diseases were unavailable from the database. Furthermore, this study did not include normal colorectal tissues, *i.e.* we could not describe *MTNR1B* polymorphic variants in normal colorectal tissues. The results of the present study should be verified using a large-scale study that controls for confounding variables, such as lifestyle, carcinogen exposure, and diet, among others.

Table 6 Cumulative effect of *MTNR1B* single-nucleotide polymorphism associated with 5-year overall survival of colorectal cancer patients

	No. of subjects	No. of cases (%)	Crude		Adjusted[a]	
			HR	95%CI	HR	95%CI
No. of SNP risk genotypes						
0	41	3 (7.3)	1.00	Referent	1.00	Referent
1	25	4 (16.0)	2.27	(0.51 to 10.1)	2.60	(0.55 to 12.2)
2	7	3 (42.9)	6.40	(1.29 to 317)	6.89	(1.16 to 41.0)
3	1	0 (0)	N/A	N/A	N/A	N/A
4	18	7 (38.9)	7.60	(1.96 to 29.5)	14.0	(2.94 to 66.3)
P for trend				< 0.001		< 0.001
≥ 2 of SNP risk genotypes	26	10 (38.5)	4.00	(1.58 to 10.1)	5.81	(2.03 to 16.6)

[a]Adjusted for age, sex, stage, adjuvant chemotherapy, tumor location and the methylation status of *CDKN2A*, *MLH1* and *MGMT* gene. SNP: Single-nucleotide polymorphism; U: Unmethylation; M: Methylation; HR: Hazard ratio; N/A: Not applicable.

Table 7 Relationship between haplotypes of *MTNR1B* single-nucleotide polymorphism and 5-year overall survival of colorectal cancer patients

Haplotypes	Survival group (%)	Death group (%)	Crude		Adjusted[a]	
			HR	95%CI	HR	95%CI
T-C-G-A	42.0	68.4	2.58	(1.27 to 5.28)	2.75	(1.82 to 11.2)
C-T-G-A	2.7	5.3	1.74	(0.42 to 7.26)	1.96	(0.44 to 8.66)
C-T-C-G	30.0	7.9	0.23	(0.07 to 0.76)	0.21	(0.06 to 0.71)
C-T-C-A	22.0	15.8	0.73	(0.30 to 1.76)	0.70	(0.28 to 1.72)

[a]Adjusted for age, sex, stage, adjuvant chemotherapy, tumor location. The reference is the set of all the other haplotypes when one haplotype is regarded as an analyzed item. HR: Hazard ratio.

CONCLUSION

In summary, we conducted a retrospective cohort study to investigate the association between *MTNR1B* SNPs and CRC prognosis in those with different gene methylation statuses. All polymorphisms were correlated with 5-year OS. Three SNPs (rs1387153, rs10830963, and rs1447352) were associated with enhanced mortality risk when combined with different *CDKN2A* or *MGMT* gene methylation status. Furthermore, we observed a strong cumulative effect of *MTNR1B* SNPs on the 5-year OS of patients with CRC. Our findings indicate that *MTNR1B* SNPs combined with *CDKN2A* and *MGMT* gene methylation statuses may be predictive biomarkers for CRC prognosis. This study offers insights into novel genetic and epigenetic biomarkers for the prediction of CRC prognosis, and the findings could be used to individualise the treatment of patients with CRC.

ARTICLE HIGHLIGHTS

Research background

Melatonin plays a central role in the management of circadian rhythm and was identified in the gastrointestinal tract. Epidemiological studies demonstrated that melatonin has oncostatic effects including induction of epigenetic alteration on different types of tumours. The melatonin receptor MT2 encoded by *MTNR1B* is generally responsible for mediating the downstream effects of melatonin. The expression of MT2 in tumour mucosa is lower than the normal mucosa in patients with

colorectal cancer (CRC).

Research motivation

Growing studies have investigated the association between melatonin and CRC carcinogenesis. However, the relationship between *MTNR1B* gene polymorphisms and CRC sensitivity is not clear. To analyze the effects of *MTNR1B* gene polymorphisms on CRC prognosis and evaluate the interactions with aberrant promoter methylation of the *CDKN2A* and *MGMT* genes will be of great significance.

Research objectives

In our study, we aimed to explore the association between *MTNR1B* single-nucleotide polymorphism (SNPs) and the 5-year overall survival (OS) of CRC patients. To further assess the interaction between *MTNR1B* SNPs and *CDKN2A* and *MGMT* gene methylation, we examined the relationship between each SNP and the 5-year OS, with data stratified by the methylation status of the *CDKN2A* and *MGMT* gene.

Research methods

Ninety four CRC patients from Taiwan were enrolled to evaluate the association between *MTNR1B* SNPs, *CDKN2A*, *MGMT* gene hypermethylation and 5-year OS. The *MTNR1B* gene polymorphisms were screened using the Agena MassARRAY platform with iPLEX gold chemistry. The promoter methylation status of *CDKN2A* and *MGMT* was assessed using methylation-specific polymerase chain reaction. Associations of the genetic and epigenetic effect and 5-year OS were assessed using the Cox proportional hazards regression model.

Research results

In this retrospective cohort study, we found that *MTNR1B* SNPs was associated with a significantly increased risk of CRC 5-year OS. A strong cumulative effect of the four polymorphisms on CRC prognosis was observed. In stratified analysis, rs1387153, and rs1447352 risk genotype were determined to be associated with 5-year OS in the unmethylation *MGMT* gene subgroup. In contrast, rs10830963 and rs1447352 risk genotype with hypermethylation *CDKN2A* gene had a higher risk of death in five years. Four haplotypes of MTNR1B SNPs were also determined to be associated with increased risk of mortality.

Research conclusions

This study is one of few reports which demonstrated the association between MTNR1B SNPs and the 5-year OS in patients with CRC. Our data identified these novel genetic biomarkers combined with *CDKN2A* and *MGMT* methylation status for the prediction of CRC prognosis, and the findings could be used to individualise the treatment of patients with CRC.

Research perspectives

Based on our findings, the novel genetic biomarkers, *MTNR1B*, combined with *CDKN2A* and *MGMT* gene methylation statuses could be a predictive tool for CRC prognosis. The new set of markers may help physicians make treatment decisions based on the prognostic information and would improve the OS of patients with CRC. This study warrant further investigation of the underlying mechanisms related to oncostatic effects of *MTNR1B* on CRC.

REFERENCES

1 **Bray F**, Ferlay J, Soerjomataram I, Siegel RL, Torre LA, Jemal A. Global cancer statistics 2018: GLOBOCAN estimates of incidence and mortality worldwide for 36 cancers in 185 countries. *CA Cancer J Clin* 2018; **68**: 394-424 [PMID: 30207593 DOI: 10.3322/caac.21492]

2 **Tseng CH**. Diabetes, metformin use, and colon cancer: a population-based cohort study in Taiwan. *Eur J Endocrinol* 2012; **167**: 409-416 [PMID: 22778198 DOI: 10.1530/EJE-12-0369]

3 **Lv Z**, Xu Q, Sun L, Wen J, Fang X, Xing C, Yuan Y. Four novel polymorphisms in long non-coding RNA HOTTIP are associated with the risk and prognosis of colorectal cancer. *Biosci Rep* 2019; **39** [PMID: 30940774 DOI: 10.1042/BSR20180573]

4 **Lam K**, Pan K, Linnekamp JF, Medema JP, Kandimalla R. DNA methylation based biomarkers in colorectal cancer: A systematic review. *Biochim Biophys Acta* 2016; **1866**: 106-120 [PMID: 27385266 DOI: 10.1016/j.bbcan.2016.07.001]

5 **Kim TO**, Park J, Kang MJ, Lee SH, Jee SR, Ryu DY, Yang K, Yi JM. DNA hypermethylation of a

selective gene panel as a risk marker for colon cancer in patients with ulcerative colitis. *Int J Mol Med* 2013; **31**: 1255-1261 [PMID: 23546389 DOI: 10.3892/ijmm.2013.1317]
6 **Lech G**, Słotwiński R, Słodkowski M, Krasnodębski IW. Colorectal cancer tumour markers and biomarkers: Recent therapeutic advances. *World J Gastroenterol* 2016; **22**: 1745-1755 [PMID: 26855534 DOI: 10.3748/wjg.v22.i5.1745]
7 **Acuña-Castroviejo D**, Escames G, Venegas C, Díaz-Casado ME, Lima-Cabello E, López LC, Rosales-Corral S, Tan DX, Reiter RJ. Extrapineal melatonin: sources, regulation, and potential functions. *Cell Mol Life Sci* 2014; **71**: 2997-3025 [PMID: 24554058 DOI: 10.1007/s00018-014-1579-2]
8 **Li Y**, Li S, Zhou Y, Meng X, Zhang JJ, Xu DP, Li HB. Melatonin for the prevention and treatment of cancer. *Oncotarget* 2017; **8**: 39896-39921 [PMID: 28415828 DOI: 10.18632/oncotarget.16379]
9 **Seely D**, Wu P, Fritz H, Kennedy DA, Tsui T, Seely AJ, Mills E. Melatonin as adjuvant cancer care with and without chemotherapy: a systematic review and meta-analysis of randomized trials. *Integr Cancer Ther* 2012; **11**: 293-303 [PMID: 22019490 DOI: 10.1177/1534735411425484]
10 **Zhao M**, Wan J, Zeng K, Tong M, Lee AC, Ding J, Chen Q. The Reduction in Circulating Melatonin Level May Contribute to the Pathogenesis of Ovarian Cancer: A Retrospective Study. *J Cancer* 2016; **7**: 831-836 [PMID: 27162542 DOI: 10.7150/jca.14573]
11 **Brown SB**, Hankinson SE, Eliassen AH, Reeves KW, Qian J, Arcaro KF, Wegrzyn LR, Willett WC, Schernhammer ES. Urinary melatonin concentration and the risk of breast cancer in Nurses' Health Study II. *Am J Epidemiol* 2015; **181**: 155-162 [PMID: 25587174 DOI: 10.1093/aje/kwu261]
12 **Gil-Martín E**, Egea J, Reiter RJ, Romero A. The emergence of melatonin in oncology: Focus on colorectal cancer. *Med Res Rev* 2019; **39**: 2239-2285 [PMID: 30950095 DOI: 10.1002/med.21582]
13 **Deming SL**, Lu W, Beeghly-Fadiel A, Zheng Y, Cai Q, Long J, Shu XO, Gao YT, Zheng W. Melatonin pathway genes and breast cancer risk among Chinese women. *Breast Cancer Res Treat* 2012; **132**: 693-699 [PMID: 22138747 DOI: 10.1007/s10549-011-1884-5]
14 **Ekmekcioglu C**. Melatonin receptors in humans: biological role and clinical relevance. *Biomed Pharmacother* 2006; **60**: 97-108 [PMID: 16527442 DOI: 10.1016/j.biopha.2006.01.002]
15 **Slominski RM**, Reiter RJ, Schlabritz-Loutsevitch N, Ostrom RS, Slominski AT. Melatonin membrane receptors in peripheral tissues: distribution and functions. *Mol Cell Endocrinol* 2012; **351**: 152-166 [PMID: 22245784 DOI: 10.1016/j.mce.2012.01.004]
16 **León J**, Casado J, Carazo A, Sanjuán L, Maté A, Muñoz de Rueda P, de la Cueva P, Quiles R, Ruíz S, Ruíz-Extremera A, Salmerón J. Gender-related invasion differences associated with mRNA expression levels of melatonin membrane receptors in colorectal cancer. *Mol Carcinog* 2012; **51**: 608-618 [PMID: 21809392 DOI: 10.1002/mc.20832]
17 **Casado J**, Iñigo-Chaves A, Jiménez-Ruiz SM, Ríos-Arrabal S, Carazo-Gallego Á, González-Puga C, Núñez MI, Ruíz-Extremera Á, Salmerón J, León J. AA-NAT, MT1 and MT2 Correlates with Cancer Stem-Like Cell Markers in Colorectal Cancer: Study of the Influence of Stage and p53 Status of Tumors. *Int J Mol Sci* 2017; **18** [PMID: 28604612 DOI: 10.3390/ijms18061251]
18 **Santoro R**, Mori F, Marani M, Grasso G, Cambria MA, Blandino G, Muti P, Strano S. Blockage of melatonin receptors impairs p53-mediated prevention of DNA damage accumulation. *Carcinogenesis* 2013; **34**: 1051-1061 [PMID: 23354312 DOI: 10.1093/carcin/bgt025]
19 **Tarnowski M**, Malinowski D, Safranow K, Dziedziejko V, Pawlik A. MTNR1A and MTNR1B gene polymorphisms in women with gestational diabetes. *Gynecol Endocrinol* 2017; **33**: 395-398 [PMID: 28084098 DOI: 10.1080/09513590.2016.1276556]
20 **Patel R**, Rathwa N, Palit SP, Ramachandran AV, Begum R. Association of melatonin &MTNR1B variants with type 2 diabetes in Gujarat population. *Biomed Pharmacother* 2018; **103**: 429-434 [PMID: 29674279 DOI: 10.1016/j.biopha.2018.04.058]
21 **Kim MS**, Lee J, Sidransky D. DNA methylation markers in colorectal cancer. *Cancer Metastasis Rev* 2010; **29**: 181-206 [PMID: 20135198 DOI: 10.1007/s10555-010-9207-6]
22 **Hiraoka S**, Kato J, Horii J, Saito S, Harada K, Fujita H, Kuriyama M, Takemoto K, Uraoka T, Yamamoto K. Methylation status of normal background mucosa is correlated with occurrence and development of neoplasia in the distal colon. *Hum Pathol* 2010; **41**: 38-47 [PMID: 19733896 DOI: 10.1016/j.humpath.2009.06.002]
23 **Imperiale TF**, Ransohoff DF, Itzkowitz SH, Levin TR, Lavin P, Lidgard GP, Ahlquist DA, Berger BM. Multitarget stool DNA testing for colorectal-cancer screening. *N Engl J Med* 2014; **370**: 1287-1297 [PMID: 24645800 DOI: 10.1056/NEJMoa1311194]
24 **Chang HF**, Wu CC, Sun CA, Chu CM, Lin FG, Hsieh JF, Hsu CH, Huang CH, Yang T, Tsai YM, Kuan JC, Chou YC. Clinical stage and risk of recurrence and mortality: interaction of DNA methylation factors in patients with colorectal cancer. *J Investig Med* 2016; **64**: 1200-1207 [PMID: 27296458 DOI: 10.1136/jim-2016-000086]
25 **Kuan JC**, Wu CC, Sun CA, Chu CM, Lin FG, Hsu CH, Kan PC, Lin SC, Yang T, Chou YC. DNA methylation combinations in adjacent normal colon tissue predict cancer recurrence: evidence from a clinical cohort study. *PLoS One* 2015; **10**: e0123396 [PMID: 25815725 DOI: 10.1371/journal.pone.0123396]
26 **Hsu CH**, Hsiao CW, Sun CA, Wu WC, Yang T, Hu JM, Huang CH, Liao YC, Chen CY, Lin FH, Chou YC. Novel methylation gene panel in adjacent normal tissues predicts poor prognosis of colorectal cancer in Taiwan. *World J Gastroenterol* 2020; **26**: 154-167 [PMID: 31988582 DOI: 10.3748/wjg.v26.i2.154]
27 **Hsu CH**, Hsiao CW, Sun CA, Wu WC, Yang T, Hu JM, Liao YC, Huang CH, Chen CY, Lin FH,

Chou YC. Multiple gene promoter methylation and clinical stage in adjacent normal tissues: Effect on prognosis of colorectal cancer in Taiwan. *Sci Rep* 2020; **10**: 145 [PMID: 31924802 DOI: 10.1038/s41598-019-56691-6]

28 **Zou M**, Li R, Wang JY, Wang K, Wang YN, Li Y, Ji FX, Sun SN, Huang SS, Fan HH, Huang CP, Zhang X, Zhu JH. Association analyses of variants of SIPA1L2, MIR4697, GCH1, VPS13C, and DDRGK1 with Parkinson's disease in East Asians. *Neurobiol Aging* 2018; **68**: 159.e7-159.e14 [PMID: 29622492 DOI: 10.1016/j.neurobiolaging.2018.03.005]

29 **Huang CY**, Lin YC, Shiue HS, Chen WJ, Su CT, Pu YS, Ao PL, Hsueh YM. Comparison of arsenic methylation capacity and polymorphisms of arsenic methylation genes between bladder cancer and upper tract urothelial carcinoma. *Toxicol Lett* 2018; **295**: 64-73 [PMID: 29859237 DOI: 10.1016/j.toxlet.2018.05.035]

30 **Liao S**, Liu Y, Tan Y, Gan L, Mei J, Song W, Chi S, Dong X, Chen X, Deng S. Association of genetic variants of melatonin receptor 1B with gestational plasma glucose level and risk of glucose intolerance in pregnant Chinese women. *PLoS One* 2012; **7**: e40113 [PMID: 22768333 DOI: 10.1371/journal.pone.0040113]

31 **Qiu XS**, Tang NL, Yeung HY, Lee KM, Hung VW, Ng BK, Ma SL, Kwok RH, Qin L, Qiu Y, Cheng JC. Melatonin receptor 1B (MTNR1B) gene polymorphism is associated with the occurrence of adolescent idiopathic scoliosis. *Spine (Phila Pa 1976)* 2007; **32**: 1748-1753 [PMID: 17632395 DOI: 10.1097/BRS.0b013e3180b9f0ff]

32 **Lyssenko V**, Nagorny CL, Erdos MR, Wierup N, Jonsson A, Spégel P, Bugliani M, Saxena R, Fex M, Pulizzi N, Isomaa B, Tuomi T, Nilsson P, Kuusisto J, Tuomilehto J, Boehnke M, Altshuler D, Sundler F, Eriksson JG, Jackson AU, Laakso M, Marchetti P, Watanabe RM, Mulder H, Groop L. Common variant in MTNR1B associated with increased risk of type 2 diabetes and impaired early insulin secretion. *Nat Genet* 2009; **41**: 82-88 [PMID: 19060908 DOI: 10.1038/ng.288]

33 **de Luis DA**, Izaola O, Primo D, Aller R. Association of the rs10830963 polymorphism in melatonin receptor type 1B (MTNR1B) with metabolic response after weight loss secondary to a hypocaloric diet based in Mediterranean style. *Clin Nutr* 2018; **37**: 1563-1568 [PMID: 28869073 DOI: 10.1016/j.clnu.2017.08.015]

34 **Wang T**, Wang XT, Lai R, Ling HW, Zhang F, Lu Q, Lv DM, Yin XX. *MTNR1B* Gene Polymorphisms Are Associated With the Therapeutic Responses to Repaglinide in Chinese Patients With Type 2 Diabetes Mellitus. *Front Pharmacol* 2019; **10**: 1318 [PMID: 31787898 DOI: 10.3389/fphar.2019.01318]

35 **Karasek M**, Carrillo-Vico A, Guerrero JM, Winczyk K, Pawlikowski M. Expression of melatonin MT(1) and MT(2) receptors, and ROR alpha(1) receptor in transplantable murine Colon 38 cancer. *Neuro Endocrinol Lett* 2002; **23** Suppl 1: 55-60 [PMID: 12019353]

36 **Nasrabadi NN**, Sargazi F, Shokrzadeh M, Abediankenari S, Hoseini SV, Najafi M, Haghi-Aminjan H, Mirmajidi SH, Ataee R. Expression of MT1 receptor in patients with gastric adenocarcinoma and its relationship with clinicopathological features. *Neuro Endocrinol Lett* 2018; **39**: 111-118 [PMID: 30183205]

37 **Vincent EE**, Yaghootkar H. Using genetics to decipher the link between type 2 diabetes and cancer: shared aetiology or downstream consequence? *Diabetologia* 2020; **63**: 1706-1717 [PMID: 32705315 DOI: 10.1007/s00125-020-05228-y]

38 **Nasrabadi NN**, Ataee R, Abediankenari S, Shokrzadeh M, Najafi M, Hoseini SV, Jan HH. Expression of MT2 receptor in patients with gastric adenocarcinoma and its relationship with clinicopathological features. *J Gastrointest Cancer* 2014; **45**: 54-60 [PMID: 24142542 DOI: 10.1007/s12029-013-9552-0]

39 **Ziółko E**, Kokot T, Skubis A, Sikora B, Szota-Czyż J, Kruszniewska-Rajs C, Wierzgoń J, Mazurek U, Grochowska-Niedworok E, Muc-Wierzgoń M. The profile of melatonin receptors gene expression and genes associated with their activity in colorectal cancer: a preliminary report. *J Biol Regul Homeost Agents* 2015; **29**: 823-828 [PMID: 26753642]

40 **Lopez-Minguez J**, Saxena R, Bandín C, Scheer FA, Garaulet M. Late dinner impairs glucose tolerance in MTNR1B risk allele carriers: A randomized, cross-over study. *Clin Nutr* 2018; **37**: 1133-1140 [PMID: 28455106 DOI: 10.1016/j.clnu.2017.04.003]

41 **Johnson JA**, Carstensen B, Witte D, Bowker SL, Lipscombe L, Renehan AG; Diabetes and Cancer Research Consortium. Diabetes and cancer (1): evaluating the temporal relationship between type 2 diabetes and cancer incidence. *Diabetologia* 2012; **55**: 1607-1618 [PMID: 22476947 DOI: 10.1007/s00125-012-2525-1]

42 **Zienolddiny S**, Haugen A, Lie JA, Kjuus H, Anmarkrud KH, Kjærheim K. Analysis of polymorphisms in the circadian-related genes and breast cancer risk in Norwegian nurses working night shifts. *Breast Cancer Res* 2013; **15**: R53 [PMID: 23822714 DOI: 10.1186/bcr3445]

43 **Das M**, Sharma SK, Sekhon GS, Mahanta J, Phukan RK, Jalan BK. p16 gene silencing along with p53 single-nucleotide polymorphism and risk of esophageal cancer in Northeast India. *Tumour Biol* 2017; **39**: 1010428317698384 [PMID: 28459370 DOI: 10.1177/1010428317698384]

44 **Okugawa Y**, Grady WM, Goel A. Epigenetic Alterations in Colorectal Cancer: Emerging Biomarkers. *Gastroenterology* 2015; **149**: 1204-1225.e12 [PMID: 26216839 DOI: 10.1053/j.gastro.2015.07.011]

45 **Bihl MP**, Foerster A, Lugli A, Zlobec I. Characterization of CDKN2A(p16) methylation and impact in colorectal cancer: systematic analysis using pyrosequencing. *J Transl Med* 2012; **10**: 173 [PMID: 22925370 DOI: 10.1186/1479-5876-10-173]

46 **Konishi K**, Watanabe Y, Shen L, Guo Y, Castoro RJ, Kondo K, Chung W, Ahmed S, Jelinek J, Boumber YA, Estecio MR, Maegawa S, Kondo Y, Itoh F, Imawari M, Hamilton SR, Issa JP. DNA methylation profiles of primary colorectal carcinoma and matched liver metastasis. *PLoS One* 2011; **6**: e27889 [PMID: 22132162 DOI: 10.1371/journal.pone.0027889]

47 **Li X**, Liu W, Feng F, Hu X, Yuan P, Yan J, Yang Y. [Association between adiponectin rs2241766, rs1501299 polymorphisms and the risk of colorectal cancer]. *Zhonghua Liu Xing Bing Xue Za Zhi* 2014; **35**: 195-199 [PMID: 24739564]

World Journal of Gastroenterology

Submit a Manuscript: https://www.f6publishing.com

World J Gastroenterol 2021 September 14; 27(34): 5753-5763

DOI: 10.3748/wjg.v27.i34.5753

ISSN 1007-9327 (print) ISSN 2219-2840 (online)

ORIGINAL ARTICLE

Retrospective Study

Validation of conventional non-invasive fibrosis scoring systems in patients with metabolic associated fatty liver disease

Yin-Lian Wu, Rahul Kumar, Ming-Fang Wang, Medha Singh, Jiao-Feng Huang, Yue-Yong Zhu, Su Lin

ORCID number: Yin-Lian Wu 0000-0001-9298-8367; Rahul Kumar 0000-0002-5092-4821; Ming-Fang Wang 0000-0001-7306-955X; Medha Singh 0000-0002-3258-0658; Jiao-Feng Huang 0000-0003-1383-6897; Yue-Yong Zhu 0000-0002-0746-4911; Su Lin 0000-0001-7517-9859.

Author contributions: Wu YL, Kumar R and Lin S designed the study; Wang MF and Singh M analyzed the data; Huang JF collected the data; Wu YL and Kumar R wrote the paper; Zhu YY and Lin S supervised the study; Wu YL and Kumar R contributed equally to this work; All authors contributed to the manuscript for important intellectual content and approved the submission.

Supported by Chinese National 13th Five-Year Plan's Science and Technology Projects, No. 2017ZX10202201.

Institutional review board statement: The study protocol was approved by the Institutional Review Board of the First Affiliated Hospital of Fujian Medical University and was in accordance with the Declaration of Helsinki.

Informed consent statement: All study participants, or their legal guardian, provided informed written consent prior to study

Yin-Lian Wu, Ming-Fang Wang, Jiao-Feng Huang, Yue-Yong Zhu, Su Lin, Department of Hepatology, Hepatology Research Institute, The First Affiliated Hospital, Fujian Medical University, Fuzhou 350005, Fujian Province, China

Rahul Kumar, Department of Gastroenterology and Hepatology, Duke-NUS academic Medical Centre, Changi General Hospital, Singapore 529889, Singapore

Medha Singh, Department of General Medicine, Tan Tock Seng Hospital, Singapore 308433, Singapore

Corresponding author: Su Lin, MD, PhD, Associate Chief Physician, Professor, Department of Hepatology, Hepatology Research Institute, The First Affiliated Hospital, Fujian Medical University, No. 20 Chazhong Road, Taijiang District, Fuzhou 350005, Fujian Province, China. sumer5129@fjmu.edu.cn

Abstract

BACKGROUND

Non-invasive fibrosis scores are not yet validated in the newly defined metabolic associated fatty liver disease (MAFLD).

AIM

To evaluate the diagnostic performance of four non-invasive scores including aspartate aminotransferase to platelet ratio index (APRI), fibrosis-4 index (FIB-4), body mass index, aspartate aminotransferase/alanine aminotransferase ratio, diabetes score (BARD), and nonalcoholic fatty liver disease fibrosis score (NFS) in patients with MAFLD.

METHODS

Consecutive patients with histologically confirmed MAFLD were included. The discrimination ability of different non-invasive scores was compared.

RESULTS

A total of 417 patients were included; 156 (37.4%) of them had advanced fibrosis (Metavir ≥ F3). The area under receiver operating characteristic curve of FIB-4, NFS, APRI, and BARD for predicting advanced fibrosis was 0.736, 0.724, 0.671, and 0.609, respectively. The area under receiver operating characteristic curve of FIB-4 and NFS was similar (P = 0.523), while the difference between FIB-4 and APRI (P = 0.001) and FIB-4 and BARD (P < 0.001) was statistically significant. The

enrollment.

Conflict-of-interest statement: The authors have no conflict of interest to declare.

Data sharing statement: Data are available on request.

Open-Access: This article is an open-access article that was selected by an in-house editor and fully peer-reviewed by external reviewers. It is distributed in accordance with the Creative Commons Attribution NonCommercial (CC BY-NC 4.0) license, which permits others to distribute, remix, adapt, build upon this work non-commercially, and license their derivative works on different terms, provided the original work is properly cited and the use is non-commercial. See: http://creativecommons.org/licenses/by-nc/4.0/

Manuscript source: Unsolicited manuscript

Specialty type: Gastroenterology and hepatology

Country/Territory of origin: China

Peer-review report's scientific quality classification

Grade A (Excellent): A
Grade B (Very good): B
Grade C (Good): 0
Grade D (Fair): 0
Grade E (Poor): 0

Received: January 6, 2021
Peer-review started: January 6, 2021
First decision: May 5, 2021
Revised: May 15, 2021
Accepted: July 29, 2021
Article in press: July 29, 2021
Published online: September 14, 2021

P-Reviewer: Sawada K
S-Editor: Gao CC
L-Editor: Filipodia
P-Editor: Liu JH

best thresholds of FIB-4, NFS, APRI, and BARD for diagnosis of advanced fibrosis in MAFLD were 1.05, -2.1, 0.42, and 2. A subgroup analysis showed that FIB-4, APRI, and NFS performed worse in the pure MAFLD group than in the hepatitis B virus-MAFLD group.

CONCLUSION

APRI and BARD scores do not perform well in MAFLD. The FIB-4 and NFS could be more useful, but a new threshold is needed. Novel non-invasive scoring systems for fibrosis are required for MAFLD.

Key Words: Metabolic associated fatty liver disease; Non-invasive fibrosis scores; Fibrosis-4 index; Non-alcoholic fatty liver disease fibrosis score; Aspartate aminotransferase to platelet ratio index; BARD

©The Author(s) 2021. Published by Baishideng Publishing Group Inc. All rights reserved.

Core Tip: Metabolic associated fatty liver disease (MAFLD) is a new concept proposed in 2020 to redefine fatty liver disease. The utility of non-invasive fibrosis scores as well as their optimal thresholds for MAFLD remains unknown. We validated the conventional non-invasive scores including aspartate aminotransferase to platelet ratio index, fibrosis-4 index, body mass index, aspartate aminotransferase/alanine aminotransferase ratio, diabetes score, and nonalcoholic fatty liver disease fibrosis score in patients with MAFLD. The results indicate that the conventional scores may lead to a high rate of misdiagnosis in MAFLD. A novel scoring system for fibrosis is urgently needed.

Citation: Wu YL, Kumar R, Wang MF, Singh M, Huang JF, Zhu YY, Lin S. Validation of conventional non-invasive fibrosis scoring systems in patients with metabolic associated fatty liver disease. *World J Gastroenterol* 2021; 27(34): 5753-5763
URL: https://www.wjgnet.com/1007-9327/full/v27/i34/5753.htm
DOI: https://dx.doi.org/10.3748/wjg.v27.i34.5753

INTRODUCTION

Nonalcoholic fatty liver disease (NAFLD), defined as excessive fat accumulation in liver cells in the absence of other liver diseases, has become a new epidemic due to its growing prevalence[1,2]. To date, NAFLD is believed to affect more than a quarter of the global population[2,3]. The natural history of NAFLD is highly variable; however, it is believed to progress through various fibrosis stages to end up in liver cirrhosis in a significant number of patients. The development and grade of liver fibrosis are strongly related with the adverse outcomes of NAFLD[4-6]. Thus, it is critical to identify patients with advanced fibrosis to optimize the management of NAFLD.

Liver biopsy is currently regarded as the "gold standard" for the diagnosis of liver fibrosis. However, due to the high prevalence of NAFLD, it is impossible to perform a biopsy for each patient. Moreover, the inherent issues including safety, sampling errors, and the inter- and intraobserver variation limit its application[7,8]. These limitations warrant the need for non-invasive scores for assessing liver fibrosis.

Numerous non-invasive assessment tools have been developed for diagnosis of advanced fibrosis[9]. The most widely used non-invasive scores include aspartate aminotransferase (AST) to platelet ratio index (APRI), fibrosis-4 index (FIB-4), body mass index (BMI), AST/alanine aminotransferase (ALT) ratio, diabetes score (BARD), and NAFLD fibrosis score (NFS). Most of them have been tested in subjects with NAFLD, showing great diagnostic accuracy in predicting fibrosis[10-13].

Metabolic associated fatty liver disease (MAFLD) is a recently proposed concept to replace NAFLD[14]. Significantly different from NAFLD, the MAFLD definition does not require the exclusion of any chronic liver diseases; however, the presence of metabolic associated disease or dysfunction is required[15,16]. It is known that metabolic profiles are associated with a risk for severe fibrosis in patients with NAFLD [17]. The MAFLD population has been found to have higher non-fibrosis scores than

NAFLD individuals[18]. Thus, in the light of the new concept of MAFLD, which incorporates metabolic disorder, the performance of these non-invasive models requires re-evaluation and further validation. This study aimed to evaluate the utility of conventional non-invasive scoring systems in MAFLD.

MATERIALS AND METHODS

Ethics

The study protocol was approved by the Institutional Review Board of the First Affiliated Hospital of Fujian Medical University and was in accordance with the Declaration of Helsinki. Written consent forms were obtained from all patients. The data was anonymized prior to the analysis.

Patients

Consecutive patients with histologically confirmed MAFLD admitted to the First Affiliated Hospital of Fujian Medical University from 2005 to 2015 were retrospectively analyzed in this study.

Histologic evaluation

All patients enrolled in this study underwent percutaneous liver biopsy under ultrasonic guidance. The liver specimens were fixed in formalin, embedded in paraffin, and stained with hematoxylin and eosin and Masson's trichrome. The minimum biopsy length was 15 mm, and at least six portal areas were required[19]. Histopathological slides were reviewed independently by two pathologists experienced in reading liver histopathology slides and were blinded to the patient's clinical data.

Fatty liver was defined as the presence of steatosis in at least 5% of hepatocytes. The liver fibrosis was graded as 0 to 4 points according to the Metavir fibrosis stage[20], where 0 = absence of fibrosis; 1 = perisinusoidal or periportal; 2 = perisinusoidal and portal/periportal; 3 = bridging fibrosis; 4 = cirrhosis. Advanced fibrosis was defined as stage 3 or 4 fibrosis (bridging fibrosis or cirrhosis).

Diagnosis of MAFLD

The diagnosis of MAFLD was based on the following criteria[15]: A histological evidence of hepatic steatosis and the presence of one of the following three conditions: BMI ≥ 23 kg/m^2, presence of type 2 diabetes mellitus, or evidence of metabolic dysregulation. The metabolic dysregulation was defined by the presence of at least two of the following conditions: (1) Waist circumference ≥ 90 cm in men and 80 cm in women; (2) Blood pressure ≥ 130/85 mmHg or specific drug treatment; (3) Plasma triglycerides ≥ 1.70 mmol/L or specific drug treatment; (4) Plasma high-density lipoprotein cholesterol < 1.0 mmol/L for men and < 1.3 mmol/L for women or specific drug treatment; (5) Prediabetes (*i.e.* fasting glucose levels 5.6-6.9 mmol/L or 2 h post-load glucose levels 7.8-11.0 mmol/L or glycated hemoglobin 5.7%-6.4%; (6) Homeostasis model assessment-insulin resistance score ≥ 2.5; and (7) Plasma high-sensitivity C-reactive protein level > 2 mg/L.

According to the result of hepatitis B surface antigen (HBsAg) seropositivity, patients were divided into pure MAFLD group (HBsAg negative) and hepatitis B virus (HBV)-MAFLD group (HBsAg positive for > 6 mo) for the purpose of subgroup analysis.

Demographic and laboratory evaluation

The following data were collected at the time of biopsy from all patients: age, gender, BMI, waist circumference, history of diabetes, and hypertension. Laboratory parameters were as follows: Blood cell count, AST, ALT, γ-glutamyl transpeptidase, albumin, globulin, bilirubin, fasting plasma glucose, total cholesterol, high-density lipoprotein cholesterol, low-density lipoprotein cholesterol, triglyceride, urea, creatinine, uric acid, fasting insulin, glycated hemoglobin, high-sensitivity C-reactive protein, and HBsAg.

All biochemical assessments were performed by standard laboratory methods. Non-invasive liver fibrosis assessment scores included APRI, FIB-4, BARD, and NFS, which were calculated based on previously published formulas as shown in Table 1[10,12,21,22].

Table 1 An overview of formulas and cutoffs for determining non-invasive marker panels for detection of liver fibrosis[10-12,21,22]

Formula	Equation	Lower cutoff	Higher cutoff
FIB-4	[Age (yr) × AST (IU/L)]/{platelet count (10^9/L) × [ALT(IU/L)]$^{1/2}$}	1.3	2.67[11]
		1.45	3.25[22]
APRI	[(AST/ULN)/platelet count (10^9/L)] × 100	0.5	1.5[21]
NFS	-1.675 + 0.037 × age (yr) + 0.094 × BMI (kg/m^2) + 1.13 × IFG/diabetes (yes = 1, no = 0) + 0.99 × AST/ALT-0.013 × platelet count (× 10^9/L) - 0.66 × albumin (g/dL)	-0.676	1.455[10]
BARD	Scale 0-4; BMI ≥ 28 kg/m^2 = 1 point; AST/ALT ≥ 0.8 = 2 points; Diabetes = 1 point	2[12]	

ALT: Alanine aminotransferase; APRI: Aspartate aminotransferase to platelet ratio index; AST: Aspartate aminotransferase; BARD: Body mass index, aspartate aminotransferase/alanine aminotransferase ratio, diabetes score; BMI: Body mass index; FIB-4: Fibrosis-4 index; IFG: Impaired fasting glucose; NFS: Nonalcoholic fatty liver disease fibrosis score; ULN: Upper limit of normal.

Statistical analysis

Continuous variables are expressed as mean ± SD or median (interquartile range) and were compared using Student's *t* test in the case of normally distributed data or Mann-Whitney test in the remaining cases. Categorical variables are expressed as counts (percentages) and evaluated by χ^2 test or the Fisher's exact test. The diagnostic accuracy of conventional non-invasive scoring systems was evaluated by the receiver operating characteristic (ROC) curve. The best cut-off values to determine the presence of advanced fibrosis were chosen based on Youden's index. The discrimination ability of the different models was compared using area under ROC curve (AUROC), positive predictive value (PPV), negative predictive value (NPV), sensitivity, specificity, and accuracy. Statistical analyses were performed using the SPSS software, version 18.0 (SPSS, Chicago, IL, United States) and MedCalc software version 15.2.2 (MedCalc Software, Mariakerke, Belgium). A P value < 0.05 was considered statistically significant.

RESULTS

Baseline characteristics of the patients

A total of 417 patients with biopsy-proven MAFLD were included in this study (Figure 1). All patients were treatment-naïve and did not receive nucleosides analogue treatment before biopsy. The mean age was 40.54 ± 10.95 years, and the BMI was 25.48 ± 2.66 kg/m^2. Of them, 354 (84.9%) were male, 82 (19.7%) had type 2 diabetes mellitus, 42 (10.1%) had hypertension, and 156 (37.4%) had advanced fibrosis (Table 2). Liver histological examination showed that 272 (76.0%) HBV-MAFLD patients had significant inflammation (grade ≥ 2). Antiviral therapy was initiated when chronic hepatitis B was diagnosed with the presence of significant inflammation (grade ≥ 2) or significant liver fibrosis (stage ≥ 2). Patients with advanced fibrosis were significantly older and had higher AST and lower albumin, triglyceride, and platelet counts. In addition, the FIB-4 (P < 0.001), NFS (P < 0.001), APRI (P = 0.003) and BARD (P < 0.001) scores were all significantly higher in patients with advanced fibrosis compared with patients with no/mild fibrosis.

Performance of FIB-4, NFS, APRI, and BARD for advanced fibrosis in MAFLD

The ROC curves were used to evaluate the utility of non-invasive scoring systems to identify advanced fibrosis (Figure 2). The AUROC was greatest for FIB-4 [0.736; 95% confidence interval (CI): 0.691-0.778] followed by NFS (0.724; 95%CI: 0.679-0.767), APRI (0.671; 95%CI: 0.623-0.715), and BARD (0.609; 95%CI: 0.560-0.656). The comparison between AUROCs showed that the discrimination abilities of FIB-4 and NFS were similar (P = 0.523). Similar results were also noted in NFS and APRI (P = 0.080). The differences between FIB-4 and APRI (P = 0.001), FIB-4 and BARD (P < 0.001), as well as NFS and BARD (P < 0.001) were statistically significant.

Table 3 summarizes the best cutoff values developed for prediction of advanced fibrosis by the four non-invasive models and the validation of previously reported cutoffs (for NAFLD) in this MAFLD cohort[10-12,21,22]. The best cutoff scores of FIB-4,

Table 2 Baseline characteristics of the patients

	Overall, *n* = 417	No/mild fibrosis, *n* = 261	Advanced fibrosis, *n* = 156	*P* value
Age (yr)	40.54 ± 10.95	39.42 ± 11.39	42.41 ± 9.94	0.007
Male, *n* (%)	354 (84.9)	219 (83.9)	135 (86.5)	0.468
BMI (kg/m^2)	25.48 ± 2.66	25.51 ± 2.56	25.42 ± 2.83	0.757
Diabetes mellitus, *n* (%)	82 (19.7)	46 (17.6)	36 (23.1)	0.175
Hypertension, *n* (%)	42 (10.1)	30 (11.5)	12 (7.7)	0.212
ALB (g/L)	42.53 ± 4.96	43.65 ± 5.14	40.65 ± 3.98	< 0.001
GLO (g/L)	29.88 ± 14.11	29.11 ± 6.00	31.13 ± 21.53	0.160
ALT (U/L)	133.07 ± 199.05	126.93 ± 151.37	143.33 ± 260.27	0.416
AST (U/L)	70.69 ± 85.14	63.24 ± 62.19	83.17 ± 112.77	0.021
GGT (U/L)	89.64 ± 109.58	88.75 ± 117.46	91.11 ± 95.28	0.832
FPG (mmol/L)	5.34 ± 1.42	5.28 ± 1.20	5.45 ± 1.73	0.251
Cr (μmol/L)	73.41 ± 13.71	74.00 ± 13.50	72.41 ± 14.07	0.273
UA (μmol/L)	368.49 ± 82.08	377.02 ± 83.87	353.77 ± 76.98	0.007
TG (mmol/L)	1.67 ± 1.12	1.78 ± 1.45	1.48 ± 0.71	0.016
HDL-C (mmol/L)	1.12 ± 0.30	1.12 ± 0.29	1.12 ± 0.33	0.959
PLT (× 10^9/L)	204.00 ± 64.22	221.00 ± 62.76	175.52 ± 56.22	< 0.001
FIB-4	1.48 ± 1.64	1.19 ± 1.65	1.97 ± 1.49	< 0.001
APRI	1.03 ± 1.72	0.84 ± 1.33	1.34 ± 2.19	0.003
NFS	-2.16 ± 1.38	-2.56 ± 1.24	-1.50 ± 1.33	< 0.001
BARD (%)				< 0.001
0	209 (50.1)	145 (55.6)	64 (41.0)	
1	86 (20.6)	59 (22.6)	27 (17.3)	
2	92 (22.1)	48 (18.4)	44 (28.2)	
3	25 (6.0)	8 (3.1)	17 (10.9)	
4	5 (1.2)	1 (0.4)	4 (2.6)	

ALB: Albumin; ALT: Alanine aminotransferase; APRI: Aspartate aminotransferase to platelet ratio index; AST: Aspartate aminotransferase; BARD: Body mass index, aspartate aminotransferase/alanine aminotransferase ratio, diabetes score; BMI: Body mass index; Cr: Creatinine; FIB-4: Fibrosis-4 index; FPG: Fasting plasma glucose; GGT: γ-Glutamyl transpeptidase; GLO: Globulin; HDL-C: High-density lipoprotein cholesterol; NFS: Non-alcoholic fatty liver disease fibrosis score; PLT: Platelet; TG: Triglyceride; UA: Uric acid.

APRI, NFS, and BARD for the diagnosis of advanced fibrosis in MAFLD were 1.05, 0.42, -2.1, and 2, respectively. Most cutoff scores were lower than the prior reported thresholds for each model. Using the newly developed thresholds, the sensitivity, specificity, PPV, and NPV of the above four models ranged from 41.7%-81.4%, 44.4%-78.2%, 46.7%-55.8%, and 69.2%-80.0%, respectively (Table 3).

With the previously reported cutoff value of 1.30 (lower) and 2.67 (higher) of FIB-4 for advanced fibrosis, the PPV was only 57.3% and 69.2%, and the NPV was 74.6% and 65.9%, respectively. Similar results were found for the NFS score; the PPV and NPV of the well-accepted threshold (-1.455) were only 56.0% and 70.6% (Table 3).

The accuracy of the FIB-4 and NFS scores, irrespective of the numerical value of cutoff used, was only 63.8%-68.8%. The accuracy was even lower for APRI and BARD (58.3%-64.5%). On the other hand, 20%-35% patients with biopsy-proven advanced fibrosis were misdiagnosed as no advanced fibrosis by these four scores (Table 3).

Performance of the non-invasive scores in HBV-MAFLD and pure MAFLD subgroups

According to the result of HBsAg, patients were divided into HBV-MAFLD (359, 86.1%) and pure MAFLD (58, 13.9%) subgroups. The difference in the baseline characteristics between HBV-MAFLD and pure MAFLD had been presented in our previous

Table 3 Comparison of the diagnostic value among fibrosis-4 index, nonalcoholic fatty liver disease fibrosis score, aspartate aminotransferase to platelet ratio index, and body mass index, aspartate aminotransferase/alanine aminotransferase ratio, diabetes score in metabolic associated fatty liver disease

	Cutoffs	AUROC	Accuracy, %	Advanced fibrosis being missed, %[1]	Sensitivity, %	Specificity, %	PPV, %	NPV, %	Youden index
FIB-4	**1.05**	**0.736**	**66.2**	**20.3**	**73.7**	**61.7**	**53.5**	**79.7**	**0.354**
	1.30		68.1	25.4	57.7	74.3	57.3	74.6	0.320
	1.45		68.8	26.5	52.6	78.5	59.4	73.5	0.311
	2.67		66.2	34.1	17.3	95.4	69.2	65.9	0.127
	3.25		66.7	34.4	14.1	98.1	81.5	65.6	0.122
NFS	**-2.100**	**0.724**	**68.1**	**20.9**	**70.5**	**66.7**	**55.8**	**79.1**	**0.372**
	-1.455		66.2	29.5	44.9	78.9	56.0	70.6	0.238
	0.676		63.8	36.5	4.5	99.2	77.8	63.5	0.037
APRI	**0.42**	**0.671**	**58.3**	**20.0**	**81.4**	**44.4**	**46.7**	**80.0**	**0.258**
	0.50		59.2	24.7	71.2	52.5	47.2	75.3	0.237
	1.50		63.3	34.6	22.4	87.7	52.2	65.4	0.101
BARD	**2**	**0.609**	**64.5**	**30.8**	**41.7**	**78.2**	**53.3**	**69.2**	**0.199**

Best cutoff value in bold.

[1]The percentage was calculated as the number of advanced fibrosis being missed diagnosed/the number of patients who were diagnosed as no advanced fibrosis by the non-invasive score × 100%. APRI: Aspartate aminotransferase to platelet ratio index; AUROC: Area under the receiver operating characteristic curve; BARD: Body mass index, aspartate aminotransferase/alanine aminotransferase ratio, diabetes score; FIB-4: Fibrosis-4 index; NFS: Nonalcoholic fatty liver disease fibrosis score; NPV: Negative predictive value; PPV: Positive predictive value.

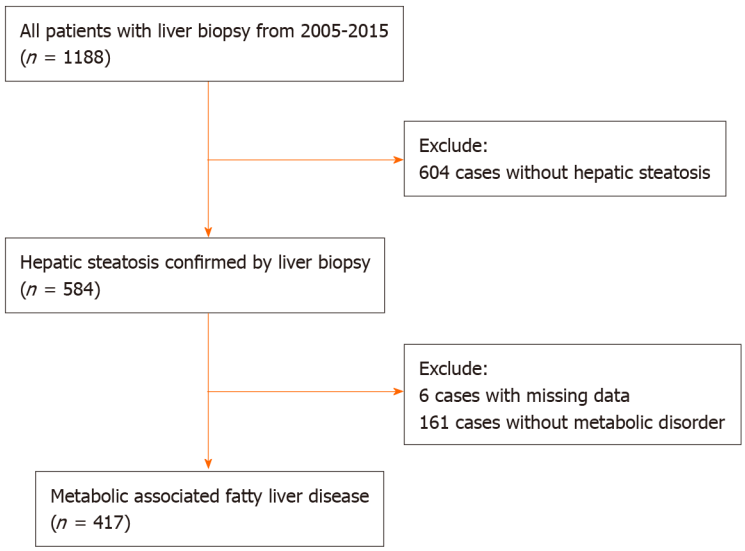


Figure 1 Flow chart of case selection.

work[23] and is shown in Supplementary Table 1. Briefly, the HBV-MAFLD group had higher ALT (135.82 ± 210.31 U/L *vs* 119.76 ± 118.19 U/L) and AST (71.70 ± 88.63 U/L *vs* 65.55 ± 63.28 U/L) levels and lower platelet (198.59 ± 60.33) × 10^9/L *vs* (237.47 ± 76.97) × 10^9/L levels than the pure MAFLD group. The AUROCs of FIB-4, NFS, and APRI in the HBV-MAFLD group was 0.738, 0.725, and 0.671, respectively, which were all higher than in the pure MAFLD group (FIB-4 0.658, NFS 0.692, and APRI 0.633). The AUROC of BARD was lower in the HBV-MAFLD group than in the pure MAFLD group (0.609 *vs* 0.644). Using different thresholds mentioned above, the overall performance of the FIB-4, APRI, and NFS, including sensitivity, specificity, PPV and

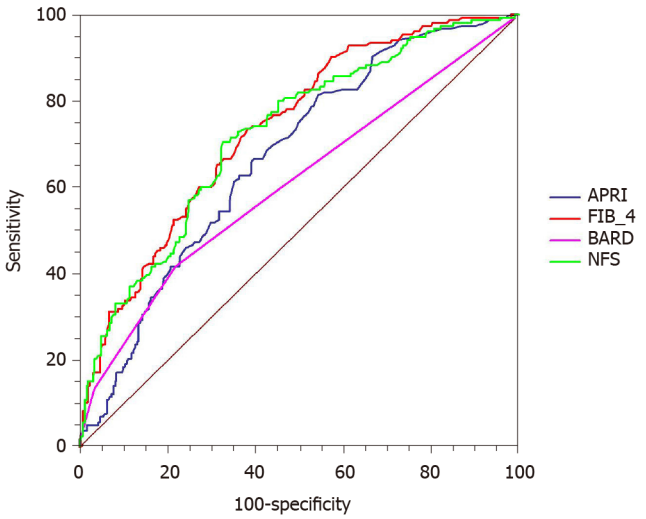


Figure 2 Receiver operating characteristic curves of different scores for advanced fibrosis. APRI: Aspartate aminotransferase to platelet ratio index; FIB-4: Fibrosis-4 index; NFS: Nonalcoholic fatty liver disease fibrosis score.

NPV, was better in the HBV-MAFLD group. The BARD score performed better in the pure MAFLD population (Table 4).

DISCUSSION

Non-invasive scoring systems are widely used to identify or exclude advanced fibrosis in patients with chronic liver disease. The main finding of our study is that FIB-4 and NFS performed better than APRI and BARD in MAFLD patients. These scores are more useful in HBV-MAFLD than in pure MAFLD population. However, the performance of all above models was not as good as previously reported in NAFLD.

The non-invasive fibrosis scoring systems are derived from widely available clinical, laboratory, and anthropometric parameters. Although the APRI and BARD scores are more user-friendly, their discrimination ability in prediction of advanced fibrosis is not satisfactory in this group of MAFLD patients. The AUROC of BARD was 0.609, and the accuracy was less than 65%. It is not a surprising result as the two variables for calculating BARD score (BMI and diabetes) were also variables for the diagnosis of MAFLD. This led to lower sensitivity and higher false positivity for detecting advanced fibrosis in MAFLD patients, thus the BARD score should not be recommended for MAFLD patients in clinical practice. Although APRI score was easy to calculate, it did not perform well in MAFLD as well. The NPV did not exceed 80%, and the PPV was only around 50% at any cutoff value tested. Thus, APRI should not be used for assessment of advanced fibrosis in the MAFLD population either.

The calculations of FIB-4 and NFS require the use of more complex formulas and may not be easy to use. Even though the results of our study indicate that both FIB-4 and NFS significantly outperform APRI and BARD for the prediction of advanced fibrosis in MAFLD, the NPV and PPV of these two models did not reach the similar values reported by previous studies using the cohort of NAFLD patients[10,11,24]. According to the previously reported studies on patients with NAFLD[10,11,24], when the cutoff of the FIB-4 and NFS was set at 1.3 and -1.455, respectively, the NPV increased from 90% to 93%. When the cutoff of the FIB-4 was set at 2.67, the PPV could reach 80%. However, in our cohort of MAFLD patients, by using the aforementioned cutoffs, or the new threshold found in the present study, the NPV did not exceed 75%, and PPV did not exceed 70%. This finding is of utmost clinical importance and indicates that in the light of the new concept of MAFLD, newer non-invasive fibrosis scores need to be developed and validated to assess the presence of advanced fibrosis in patients with MAFLD. Another worrying yet important finding of our study is that the use of these non-invasive fibrosis scores, even with the new cutoffs, led to a misdiagnosis of no advanced fibrosis in 20%-35% of the patients in this cohort (Table 3) when the histology actually showed the presence of advanced fibrosis.

The occurrence of HBV infection and fatty liver disease is frequently seen in Asian countries[25]. As our cohort consisted of 359 (86.1%) patients with chronic HBV

Table 4 Comparison of the diagnostic value among fibrosis-4 index, non-alcoholic fatty liver disease fibrosis score, aspartate aminotransferase to platelet ratio index, and body mass index, aspartate aminotransferase/alanine aminotransferase ratio, diabetes score in hepatitis B virus-metabolic associated fatty liver disease (group A) and pure metabolic associated fatty liver disease (group B) subgroups

	Cutoffs	AUROC		Accuracy, %		Sensitivity, %		Specificity, %		PPV, %		NPV, %	
		A	B	A	B	A	B	A	B	A	B	A	B
FIB-4	1.05	0.738	0.658	67.7	56.9	74.8	55.6	62.7	57.1	58.2	19.2	78.2	87.5
	1.30			68.2	67.2	58.5	44.4	75.0	71.4	61.9	22.2	72.3	87.5
	1.45			68.5	70.7	54.4	22.2	78.3	79.6	63.5	16.7	71.2	84.8
	2.67			63.2	84.5	17.0	22.2	95.3	95.9	71.4	50.0	62.3	87.0
	3.25			63.5	86.2	13.6	22.2	98.1	98.0	83.3	66.7	62.1	87.3
NFS	-2.100	0.725	0.692	68.2	67.2	70.1	77.8	67.0	65.3	59.5	29.2	76.3	94.1
	-1.455			64.9	74.1	44.2	55.6	79.2	77.6	59.6	31.3	67.2	90.5
	0.676			60.4	84.5	4.1	11.1	99.5	98.0	85.7	50.0	59.9	85.7
APRI	0.42	0.671	0.633	59.3	51.7	81.6	77.8	43.9	46.9	50.2	21.2	77.5	92.0
	0.50			60.2	55.2	70.7	77.8	52.8	51.0	51.0	22.6	72.3	92.6
	1.50			61.0	77.6	23.1	11.1	87.3	89.8	55.7	16.7	62.1	84.6
BARD	2	0.609	0.644	63.0	74.1	42.2	33.3	77.4	81.6	56.4	25.0	65.9	87.0

APRI: Aspartate aminotransferase to platelet ratio index; AUROC: Area under the receiver operating characteristic curve; BARD: Body mass index, aspartate aminotransferase/alanine aminotransferase ratio, diabetes score; FIB-4: Fibrosis-4 index; NFS: Non-alcoholic fatty liver disease fibrosis score; NPV: Negative predictive value; PPV: Positive predictive value.

infection, we performed a subgroup analysis to test the performance of the non-invasive scores in a pure MAFLD group, which is very close to previous NAFLD and HBV-MAFLD group. Three of the four non-invasive models (FIB-4, NFS, and APRI) performed even worse in the pure MAFLD group than in the HBV-MAFLD group. We speculate that the higher levels of ALT and AST and lower platelets in HBV-MAFLD might result in higher scores of the non-invasive models and make them easier to discriminate the advanced fibrosis. As MAFLD is a new entity, this result further reinforces the need to develop and validate novel scoring systems for fibrosis in the MAFLD population.

The strength of our study is that, to our knowledge, this is the first validation of conventional non-invasive fibrosis scoring systems in a large sample of histology-proven MAFLD. However, this study has some limitations. Firstly, a large proportion of included patients (86%) had concomitant chronic HBV infection, which could be a potential limitation as the western MAFLD population differs substantially from Asia's population in the HBsAg seropositivity rates, the results may only be applicable to a subset of the entire MAFLD pool namely HBV-MAFLD, which is the most important subtype of MAFLD in clinical practice in Asia. Secondly, as our study is a single-center study with only an Asian population, the findings will need further validation in other Asian and western cohorts.

CONCLUSION

APRI and BARD scores do not perform well and are not suitable for the diagnosis of advanced fibrosis in MAFLD. The FIB-4 and NFS could be more useful, and we propose a new threshold of 1.05 and -2.1, respectively, which had the best diagnostic performance for advanced fibrosis. There is an urgent need of a novel non-invasive scoring system for predicting advanced fibrosis in patients with MAFLD including its subtypes.

ARTICLE HIGHLIGHTS

Research background

Metabolic associated fatty liver disease (MAFLD) is a new concept proposed in 2020. The clinical features of MAFLD would be different from nonalcoholic fatty liver disease.

Research motivation

Non-invasive fibrosis scores have been tested in subjects with nonalcoholic fatty liver disease showing great diagnostic accuracy in predicting fibrosis. But the utility of non-invasive fibrosis scores, as well as their optimal thresholds, needs re-evaluation in MAFLD.

Research objectives

This study aimed to evaluate the diagnostic performance of four non-invasive scores including aspartate aminotransferase to platelet ratio index (APRI), fibrosis-4 index (FIB-4), body mass index, aspartate aminotransferase/alanine aminotransferase ratio, and diabetes score (BARD), and nonalcoholic fatty liver disease fibrosis score (NFS) in patients with MAFLD.

Research methods

Consecutive patients with histologically-confirmed MAFLD admitted to a single medical center were included. The discrimination ability of different non-invasive scores was compared.

Research results

A total of 417 patients were included; 156 (37.4%) of them had advanced fibrosis. The area under receiver operating characteristic curve of FIB-4, NFS, APRI, and BARD for predicting advanced fibrosis were 0.736, 0.724, 0.671, and 0.609, respectively. The area under receiver operating characteristic curve of FIB-4 and NFS was similar (P = 0.523), while the difference between FIB-4 and APRI (P = 0.001) and FIB-4 and BARD (P < 0.001) was statistically significant. The best thresholds of FIB-4, NFS, APRI, and BARD for diagnosis of advanced fibrosis in MAFLD were 1.05, -2.1, 0.42, and 2, respectively. A subgroup analysis showed that FIB-4, APRI, and NFS performed worse in the pure MAFLD group than the HBV-MAFLD group.

Research conclusions

APRI and BARD scores do not perform well in MAFLD. The FIB-4 and NFS could be more useful, but a new threshold is needed.

Research perspectives

MAFLD is a new entity. The results of this study indicate the conventional scores may lead to misdiagnosis, and the development of novel scoring systems to assess fibrosis in the MAFLD population is urgently needed.

REFERENCES

1 **Chalasani N**, Younossi Z, Lavine JE, Charlton M, Cusi K, Rinella M, Harrison SA, Brunt EM, Sanyal AJ. The diagnosis and management of nonalcoholic fatty liver disease: Practice guidance from the American Association for the Study of Liver Diseases. *Hepatology* 2018; **67**: 328-357 [PMID: 28714183 DOI: 10.1002/hep.29367]

2 **Younossi Z**, Anstee QM, Marietti M, Hardy T, Henry L, Eslam M, George J, Bugianesi E. Global burden of NAFLD and NASH: trends, predictions, risk factors and prevention. *Nat Rev Gastroenterol Hepatol* 2018; **15**: 11-20 [PMID: 28930295 DOI: 10.1038/nrgastro.2017.109]

3 **Sarin SK**, Kumar M, Eslam M, George J, Al Mahtab M, Akbar SMF, Jia J, Tian Q, Aggarwal R, Muljono DH, Omata M, Ooka Y, Han KH, Lee HW, Jafri W, Butt AS, Chong CH, Lim SG, Pwu RF, Chen DS. Liver diseases in the Asia-Pacific region: a Lancet Gastroenterology & Hepatology Commission. *Lancet Gastroenterol Hepatol* 2020; **5**: 167-228 [PMID: 31852635 DOI: 10.1016/S2468-1253(19)30342-5]

4 **Angulo P**, Kleiner DE, Dam-Larsen S, Adams LA, Bjornsson ES, Charatcharoenwitthaya P, Mills PR, Keach JC, Lafferty HD, Stahler A, Haflidadottir S, Bendtsen F. Liver Fibrosis, but No Other Histologic Features, Is Associated With Long-term Outcomes of Patients With Nonalcoholic Fatty Liver Disease. *Gastroenterology* 2015; **149**: 389-97.e10 [PMID: 25935633 DOI:

10.1053/j.gastro.2015.04.043]
5 **Hagström H**, Nasr P, Ekstedt M, Hammar U, Stål P, Hultcrantz R, Kechagias S. Fibrosis stage but not NASH predicts mortality and time to development of severe liver disease in biopsy-proven NAFLD. *J Hepatol* 2017; **67**: 1265-1273 [PMID: 28803953 DOI: 10.1016/j.jhep.2017.07.027]
6 **Vilar-Gomez E**, Calzadilla-Bertot L, Wai-Sun Wong V, Castellanos M, Aller-de la Fuente R, Metwally M, Eslam M, Gonzalez-Fabian L, Alvarez-Quiñones Sanz M, Conde-Martin AF, De Boer B, McLeod D, Hung Chan AW, Chalasani N, George J, Adams LA, Romero-Gomez M. Fibrosis Severity as a Determinant of Cause-Specific Mortality in Patients With Advanced Nonalcoholic Fatty Liver Disease: A Multi-National Cohort Study. *Gastroenterology* 2018; **155**: 443-457.e17 [PMID: 29733831 DOI: 10.1053/j.gastro.2018.04.034]
7 **Ratziu V**, Charlotte F, Heurtier A, Gombert S, Giral P, Bruckert E, Grimaldi A, Capron F, Poynard T; LIDO Study Group. Sampling variability of liver biopsy in nonalcoholic fatty liver disease. *Gastroenterology* 2005; **128**: 1898-1906 [PMID: 15940625 DOI: 10.1053/j.gastro.2005.03.084]
8 **European Association for Study of Liver**. Asociacion Latinoamericana para el Estudio del Higado. EASL-ALEH Clinical Practice Guidelines: Non-invasive tests for evaluation of liver disease severity and prognosis. *J Hepatol* 2015; **63**: 237-264 [PMID: 25911335 DOI: 10.1016/j.jhep.2015.04.006]
9 **Castera L**, Friedrich-Rust M, Loomba R. Noninvasive Assessment of Liver Disease in Patients With Nonalcoholic Fatty Liver Disease. *Gastroenterology* 2019; **156**: 1264-1281.e4 [PMID: 30660725 DOI: 10.1053/j.gastro.2018.12.036]
10 **Angulo P**, Hui JM, Marchesini G, Bugianesi E, George J, Farrell GC, Enders F, Saksena S, Burt AD, Bida JP, Lindor K, Sanderson SO, Lenzi M, Adams LA, Kench J, Therneau TM, Day CP. The NAFLD fibrosis score: a noninvasive system that identifies liver fibrosis in patients with NAFLD. *Hepatology* 2007; **45**: 846-854 [PMID: 17393509 DOI: 10.1002/hep.21496]
11 **Shah AG**, Lydecker A, Murray K, Tetri BN, Contos MJ, Sanyal AJ; Nash Clinical Research Network. Comparison of noninvasive markers of fibrosis in patients with nonalcoholic fatty liver disease. *Clin Gastroenterol Hepatol* 2009; **7**: 1104-1112 [PMID: 19523535 DOI: 10.1016/j.cgh.2009.05.033]
12 **Harrison SA**, Oliver D, Arnold HL, Gogia S, Neuschwander-Tetri BA. Development and validation of a simple NAFLD clinical scoring system for identifying patients without advanced disease. *Gut* 2008; **57**: 1441-1447 [PMID: 18390575 DOI: 10.1136/gut.2007.146019]
13 **Kolhe KM**, Amarapurkar A, Parikh P, Chaubal A, Chauhan S, Khairnar H, Walke S, Ingle M, Pandey V, Shukla A. Aspartate transaminase to platelet ratio index (APRI) but not FIB-5 or FIB-4 is accurate in ruling out significant fibrosis in patients with non-alcoholic fatty liver disease (NAFLD) in an urban slum-dwelling population. *BMJ Open Gastroenterol* 2019; **6**: e000288 [PMID: 31275584 DOI: 10.1136/bmjgast-2019-000288]
14 **Eslam M**, Sanyal AJ, George J; International Consensus Panel. MAFLD: A Consensus-Driven Proposed Nomenclature for Metabolic Associated Fatty Liver Disease. *Gastroenterology* 2020; **158**: 1999-2014.e1 [PMID: 32044314 DOI: 10.1053/j.gastro.2019.11.312]
15 **Eslam M**, Newsome PN, Sarin SK, Anstee QM, Targher G, Romero-Gomez M, Zelber-Sagi S, Wai-Sun Wong V, Dufour JF, Schattenberg JM, Kawaguchi T, Arrese M, Valenti L, Shiha G, Tiribelli C, Yki-Järvinen H, Fan JG, Grønbæk H, Yilmaz Y, Cortez-Pinto H, Oliveira CP, Bedossa P, Adams LA, Zheng MH, Fouad Y, Chan WK, Mendez-Sanchez N, Ahn SH, Castera L, Bugianesi E, Ratziu V, George J. A new definition for metabolic dysfunction-associated fatty liver disease: An international expert consensus statement. *J Hepatol* 2020; **73**: 202-209 [PMID: 32278004 DOI: 10.1016/j.jhep.2020.03.039]
16 **Fouad Y**, Waked I, Bollipo S, Gomaa A, Ajlouni Y, Attia D. What's in a name? *Liver Int* 2020; **40**: 1254-1261 [PMID: 32301554 DOI: 10.1111/liv.14478]
17 **Petta S**, Eslam M, Valenti L, Bugianesi E, Barbara M, Cammà C, Porzio M, Rosso C, Fargion S, George J, Craxì A. Metabolic syndrome and severity of fibrosis in nonalcoholic fatty liver disease: An age-dependent risk profiling study. *Liver Int* 2017; **37**: 1389-1396 [PMID: 28235154 DOI: 10.1111/liv.13397]
18 **Lin S**, Huang J, Wang M, Kumar R, Liu Y, Liu S, Wu Y, Wang X, Zhu Y. Comparison of MAFLD and NAFLD diagnostic criteria in real world. *Liver Int* 2020; **40**: 2082-2089 [PMID: 32478487 DOI: 10.1111/liv.14548]
19 **Bravo AA**, Sheth SG, Chopra S. Liver biopsy. *N Engl J Med* 2001; **344**: 495-500 [PMID: 11172192 DOI: 10.1056/nejm200102153440706]
20 **Bedossa P**, Poynard T. An algorithm for the grading of activity in chronic hepatitis C. The METAVIR Cooperative Study Group. *Hepatology* 1996; **24**: 289-293 [PMID: 8690394 DOI: 10.1002/hep.510240201]
21 **Wai CT**, Greenson JK, Fontana RJ, Kalbfleisch JD, Marrero JA, Conjeevaram HS, Lok AS. A simple noninvasive index can predict both significant fibrosis and cirrhosis in patients with chronic hepatitis C. *Hepatology* 2003; **38**: 518-526 [PMID: 12883497 DOI: 10.1053/jhep.2003.50346]
22 **Sterling RK**, Lissen E, Clumeck N, Sola R, Correa MC, Montaner J, S Sulkowski M, Torriani FJ, Dieterich DT, Thomas DL, Messinger D, Nelson M; APRICOT Clinical Investigators. Development of a simple noninvasive index to predict significant fibrosis in patients with HIV/HCV coinfection. *Hepatology* 2006; **43**: 1317-1325 [PMID: 16729309 DOI: 10.1002/hep.21178]
23 **Wang MF**, Wan B, Wu YL, Huang JF, Zhu YY, Li YB. Clinic-pathological features of metabolic associated fatty liver disease with hepatitis B virus infection. *World J Gastroenterol* 2021; **27**: 336-344 [PMID: 33584066 DOI: 10.3748/wjg.v27.i4.336]

24 **McPherson S**, Stewart SF, Henderson E, Burt AD, Day CP. Simple non-invasive fibrosis scoring systems can reliably exclude advanced fibrosis in patients with non-alcoholic fatty liver disease. *Gut* 2010; **59**: 1265-1269 [PMID: 20801772 DOI: 10.1136/gut.2010.216077]

25 **Polaris Observatory Collaborators**. Global prevalence, treatment, and prevention of hepatitis B virus infection in 2016: a modelling study. *Lancet Gastroenterol Hepatol* 2018; **3**: 383-403 [PMID: 29599078 DOI: 10.1016/S2468-1253(18)30056-6]

World Journal of Gastroenterology

Submit a Manuscript: https://www.f6publishing.com

World J Gastroenterol 2021 September 14; 27(34): 5764-5774

DOI: 10.3748/wjg.v27.i34.5764

ISSN 1007-9327 (print) ISSN 2219-2840 (online)

ORIGINAL ARTICLE

Observational Study

Secular decreasing trends in gastric cancer incidence in Taiwan: A population-based cancer registry study

Yen-Tzeng Lin, Chun-Ju Chiang, Ya-Wen Yang, Shih-Pei Huang, San-Lin You

ORCID number: Yen-Tzeng Lin 0000-0003-0596-1583; Chun-Ju Chiang 0000-0002-1330-5319; Ya-Wen Yang 0000-0001-6330-6830; Shih-Pei Huang 0000-0003-3075-5853; San-Lin You 0000-0002-3192-3356.

Author contributions: Lin YT, Huang SP, and You SL conceived and designed the study; Chiang CJ and You SL acquired the data; Lin YT and Yang YW performed the data analyses; Lin YT, Huang SP, and You SL drafted the manuscript; Lin YT, Huang SP, and You SL assisted in interpretation of the data; Lin YT, Chiang CJ, Yang YW, Huang SP, and You SL critically revised the manuscript for intellectual content.

Institutional review board statement: The study was reviewed and approved by the Fu Jen Catholic University Institutional Review Board.

Informed consent statement: This research protocol was approved by the Institutional Review Board of Fu-Jen Catholic University (C107034).

Conflict-of-interest statement: There are no conflicts of interest to report.

Data sharing statement: No

Yen-Tzeng Lin, School of Medicine, College of Medicine, Fu Jen Catholic University, New Taipei City 242008, Taiwan

Chun-Ju Chiang, Ya-Wen Yang, Institute of Epidemiology and Preventive Medicine, College of Public Health, National Taiwan University, Taipei 10617, Taiwan

Shih-Pei Huang, Department of Medical Education & Bioethics, Graduate Institute of Medical Education & Bioethics, National Taiwan University College of Medicine, Taipei 10051, Taiwan

San-Lin You, School of Medicine & Big Data Research Center, Fu Jen Catholic University, New Taipei City 242008, Taiwan

Corresponding author: Shih-Pei Huang, MD, PhD, Adjunct Assistant Professor, Doctor, Department of Medical Education & Bioethics, Graduate Institute of Medical Education & Bioethics, National Taiwan University College of Medicine, No. 1 Jen Ai Road, Section 1, Taipei 10051, Taiwan. esphuang.imbd@gmail.com

Abstract

BACKGROUND

Gastric cancer remains a leading cause of cancer death worldwide. In Taiwan, gastric cancer is the sixth leading cause of cancer mortality in both males and females.

AIM

To evaluate secular trends in gastric cancer incidence according to age, sex, and *Helicobacter pylori* (*H. pylori*) treatment in Taiwan.

METHODS

In this population-based study, we used the national Taiwan Cancer Registry database. Annual percent changes in incidence rates were used to describe secular trends in incidence rates and sex ratios of gastric cancer in Taiwan. Pearson's product-moment correlation coefficients were used to analyze the correlation between annual age-adjusted incidence rates and the annual number of patients treated with antibiotic therapy for *H. pylori* infection.

RESULTS

The annual percent changes showed continuously decreasing rates of gastric

cancer among both males and females. However, the decreasing trends differed by sex, with an annual percent change of -2.58% in males and -2.14% in females. The age-specific incidence rates increased with age. Within the same age group, more recent time periods showed lower incidence rates than greater time periods. Similarly, the sex ratio was lower in later birth cohorts than in earlier birth cohorts. Age-adjusted incidence rates substantially decreased with increasing numbers of patients being treated with antibiotic therapy for *H. pylori* infection during 2005 to 2016 (r = 0.72).

CONCLUSION

We observed steadily decreasing trends with differential sex ratios in the incidence of gastric cancer in Taiwan. These results support *H. pylori* eradication programs in Taiwan.

Key Words: Gastric cancer; Population-based study; Taiwan Cancer Registry; Sex difference; *Helicobacter pylori*; *Helicobacter pylori* eradication

©The Author(s) 2021. Published by Baishideng Publishing Group Inc. All rights reserved.

Core Tip: Gastric cancer remains a leading cause of cancer death worldwide. In this population-based study, we used the national Taiwan Cancer Registry database to evaluate secular trends in gastric cancer incidence in Taiwan. Annual percent changes showed continuously decreasing rates of gastric cancer among both males and females, with an annual percent change of -2.58% in males and -2.14% in females. Age-specific incidence rates increased with age. Within the same age group, the sex ratio was lower in later birth cohorts than in earlier birth cohorts. Age-adjusted incidence rates substantially decreased with the increase in patients newly treated with anti-*Helicobacter pylori* treatment.

Citation: Lin YT, Chiang CJ, Yang YW, Huang SP, You SL. Secular decreasing trends in gastric cancer incidence in Taiwan: A population-based cancer registry study. *World J Gastroenterol* 2021; 27(34): 5764-5774
URL: https://www.wjgnet.com/1007-9327/full/v27/i34/5764.htm
DOI: https://dx.doi.org/10.3748/wjg.v27.i34.5764

INTRODUCTION

Gastric cancer is one of the leading causes of cancer death worldwide. Data from GLOBOCAN 2020 shows an age-standardized incidence rate of gastric cancer of 15.8 per 100000 persons for males and 7.0 per 100000 persons for females, with a mortality rate of 11.0 per 100000 persons in males and 4.9 per 100000 persons in females[1]. In Taiwan, gastric cancer was the sixth leading cause of cancer death for both males and females in 2018[2].

Gastric cancer is a multifactorial disease; its risk factors include alcohol drinking, tobacco smoking, gastric ulcer, and atrophic gastritis, whereas the intake of fresh fruits and vegetables is probably protective[3]. A previous study demonstrated that anti-*Helicobacter pylori* (*H. pylori*) treatment has the potential to decrease the risk of gastric cancer[4]. Moreover, a study by Chiang *et al*[5] showed that the effectiveness of *H. pylori* eradication in reducing gastric cancer incidence and mortality was 53% [95% confidence interval (CI): 30% to 69%, P < 0.001] and 25% (95%CI: -14% to 51%, P = 0.18), respectively. This study aimed to investigate secular trends in the incidence of gastric cancer and its association with *H. pylori* eradication programs in Taiwan.

MATERIALS AND METHODS

Data sources

We obtained data on gastric cancer incidence from 1979 to 2016 from the national

additional data are available.

STROBE statement: The authors have read the STROBE statement, and the manuscript was prepared and revised according to the STROBE statement.

Open-Access: This article is an open-access article that was selected by an in-house editor and fully peer-reviewed by external reviewers. It is distributed in accordance with the Creative Commons Attribution NonCommercial (CC BY-NC 4.0) license, which permits others to distribute, remix, adapt, build upon this work non-commercially, and license their derivative works on different terms, provided the original work is properly cited and the use is non-commercial. See: http://creativecommons.org/Licenses/by-nc/4.0/

Manuscript source: Unsolicited manuscript

Specialty type: Gastroenterology and hepatology

Country/Territory of origin: Taiwan

Peer-review report's scientific quality classification
Grade A (Excellent): A
Grade B (Very good): B
Grade C (Good): C, C
Grade D (Fair): 0
Grade E (Poor): 0

Received: March 23, 2021
Peer-review started: March 23, 2021
First decision: April 29, 2021
Revised: May 11, 2021
Accepted: August 6, 2021
Article in press: August 6, 2021
Published online: September 14, 2021

P-Reviewer: Cai ZL, Dong QJ, Keikha M
S-Editor: Liu M
L-Editor: Wang TQ
P-Editor: Yuan YY

population-based Taiwan Cancer Registry (TCR) database. The TCR database has been collecting data on newly diagnosed cancer cases since 1979. The TCR's accuracy was such that the percentage of death certificate only cases was 0.91%, and the proportion of morphologically verified cases reached 92.23%[6]. In addition, the completeness of the TCR database was reported to be 98.44% in 2016[6]. All cases of primary gastric cancer in this analysis were classified based on the International Classification of Diseases for Oncology, third edition (codes C16.0–C16.9)[7]. We identified subjects who received anti-*H. pylori* treatment from 2005 to 2016, based on Anatomical Therapeutic Chemical Classification codes from Taiwan's National Health Insurance Research Database, which included treatment with clarithromycin, amoxicillin, metronidazole, and tetracycline[8].

Statistical analysis

Age-specific and age-adjusted incidence rates per 100000 person-years were calculated according to the 2000 World Health Organization standard population[9]. The incidence data were divided into ten 5-year age groups (25-29, 30-34, 35-39, 40-44, 45-49, 50-54, 55-59, 60-64, 65-69, and 70-74) and seven 5-year time periods. Birth cohorts were divided into five 10-year age groups (25-34, 35-44, 45-54, 55-64, and 65-74). We calculated age-adjusted incidence rates for the period from 1979 to 2016 and age-specific incidence rates for the period from 1981 to 2015, for birth cohorts representing the years 1906 to 2005.

To describe linear trends by time period, we computed the annual percent change (APC) in incidence rate and tested whether the corresponding changes in rates were significant. We also used the Pearson's product-moment correlation coefficient to analyze the correlation between the annual age-adjusted incidence rate and the annual number of patients treated with antibiotic therapy for *H. pylori* infection. The research protocol was approved by the Institutional Review Board of Fu-Jen Catholic University (C107034).

RESULTS

Age-adjusted incidence rates

The age-adjusted incidence rates of gastric cancer show that rates for males were volatile between the years of 1981 to 2002 but steadily decreased from 2002 to 2016, with an average APC (AAPC) of -2.58% (Figure 1). However, the incidence rates for females slightly increased between the years of 1979 to 1997 and then gradually decreased from 1997 to 2016, with an AAPC of -2.14% (Figure 1).

Age-specific incidence rates

Looking at age-specific incidence rates by sex for the years of 1981 to 2015, we found that age-specific incidence rates of gastric cancer increased with age, with the highest incidence rate occurring among the oldest age group across all time periods (Figure 2). Among the same age group, more recent time periods showed lower incidence rates than earlier time periods. For example, among males aged 60-64 years, the incidence rate per 100000 persons during 2011-2015 was 44.42, which was lower than the incidence rate for 1996-2000, which had an incidence rate of 62.41. Moreover, among the same age group, the decreasing trend in age-specific incidence was more evident in males than in females (Figure 2).

The age-specific incidence rates by birth cohort for both males and females are shown in Figure 3. In both males and females, older birth cohorts had higher incidence rates than younger birth cohorts within the same age group. Moreover, among the same birth cohort, incidence rates increased more significantly by age in males than in females (Figure 3).

Sex ratios of age-adjusted incidence rates

We also found that the sex ratios of age-adjusted incidence rates decreased from 1981 to 2016 (Figure 4A). Males had higher age-adjusted incidence rates than females, with sex ratios ranging from 2.5 in 1979 to 1.9 in 2016, with an AAPC of -0.67% during the study period. During time periods prior to 1990, age-specific sex ratios were higher in older age groups, whereas the sex ratios were more consistent during time periods after 1996 (Figure 4B). Sex ratios of age-specific incidence rates by birth cohort showed that among the same age group, sex ratios were higher in earlier birth cohorts than in later birth cohorts. Whereas the sex ratios were close to 1 in the 35-44 age group, the

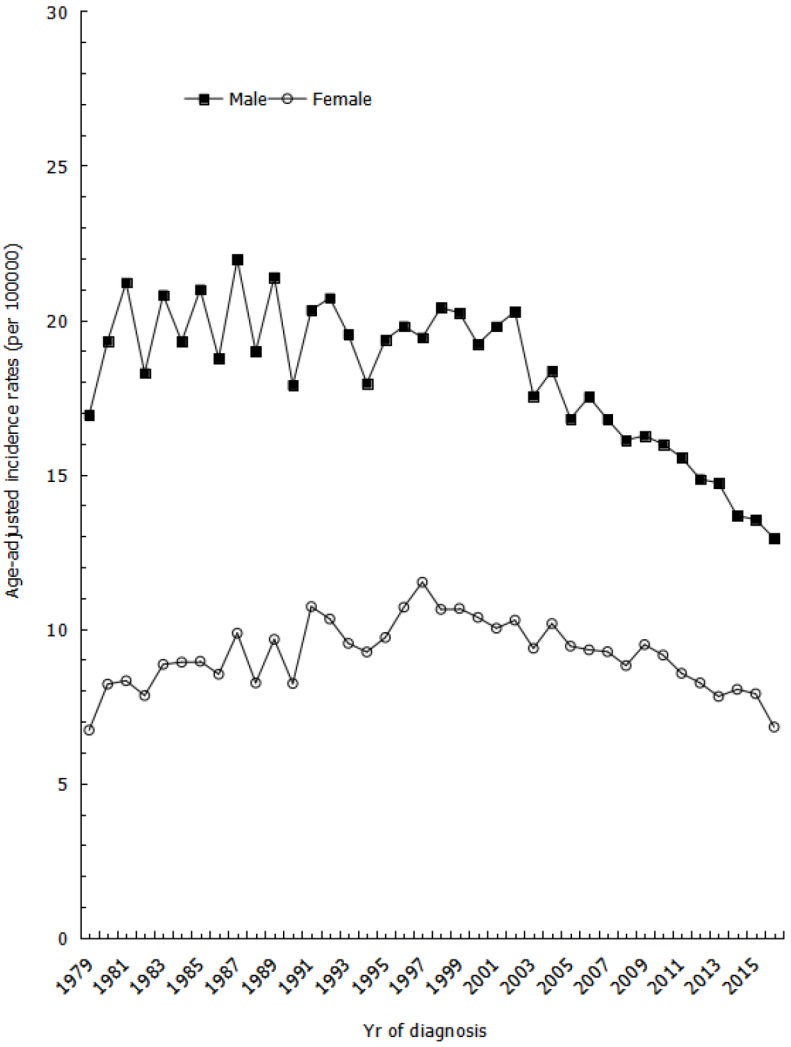


Figure 1 Secular trends in age-adjusted incidence rates of gastric cancer in Taiwan. 1979-2016, showing steadily decreasing rates in males from 2002 to 2016, with an Average Annual Percent Change (AAPC) of -2.58%, and gradually decreasing rates in females from 1997 to 2016, with an AAPC of -2.14%.

sex ratios were all less than 1 in the 25-34 age group (Figure 4C).

Association with H. pylori treatment

Furthermore, we also investigated the association between gastric cancer incidence and *H. pylori* treatment (Figure 5). During 2005 to 2016, the age-adjusted incidence rates decreased substantially along with increasing numbers of patients newly treated with antibiotic therapy for *H. pylori* infection (r = 0.72).

DISCUSSION

This population-based study found an overall secular trend of declining gastric cancer incidence in Taiwan from 1979 to 2016. Age-adjusted incidence rates decreased after 2002, with a statistically significant trend in both males and females; although, our results were slightly lower than estimates from other East Asian countries in terms of proportion changes. For example, one study from Japan found a decreasing trend with an AAPC of -1.4%, while another study from China found an AAPC of -3.7%[10]. Meanwhile, Taiwan showed an AAPC in incidence rate of -1.62% from 1996 to 2013 [11]. The downward trend in incidence was greater in males during earlier years, but this difference has since diminished in recent years. Furthermore, the downward trend observed from 2002 to 2016 was higher in males than in females, with an AAPC of -2.59% in males and -2.40% in females. Our proportion changes were slightly lower than estimates from other Asian countries, as shown in a study by Bertuccio *et al*[12]. One possible reason for the discrepancy may be that our study period began in the 1980s, after the incidence of gastric cancer had already been steadily declining for

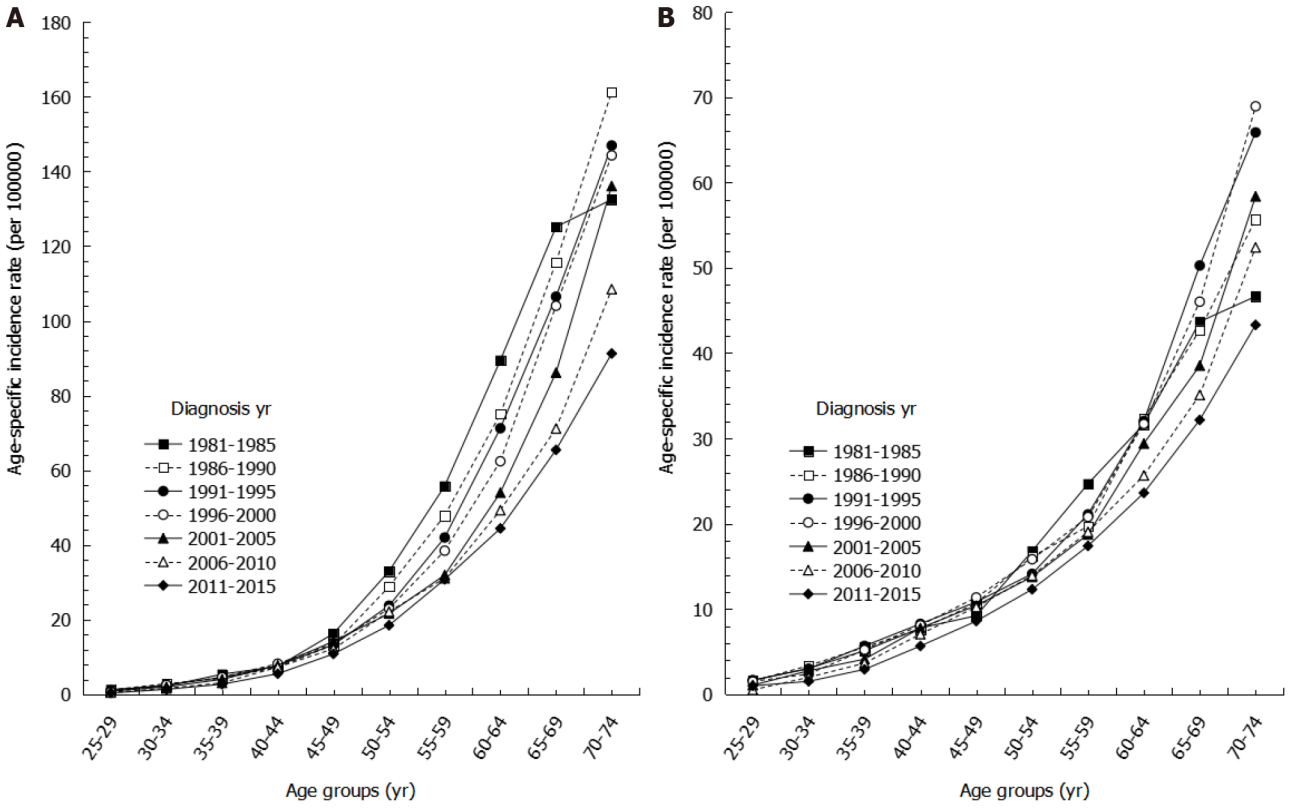


Figure 2 Age-specific incidence rates of gastric cancer in Taiwan by time period during 1981-2015. A: Among males; B: Females, showing lower incidence rates in more recent time periods than in earlier time periods. The decreasing trend was more evident in males than in females.

several decades.

As the development of gastric cancer is a multistage process arising from different risk factors, the decline in incidence rates in Taiwan may be attributable to the following reasons. First, the Taiwanese government launched an *H. pylori* eradication program in 1997[13]. Although anti-*H. pylori* treatments started in 1997, the number of patients treated with antibiotic therapy was unstable during the first decade. Therefore, we show results ranging from 2005 to 2016, which show a strong association between the number of patients treated with *H. pylori* treatment and age-adjusted incidence rates (r = 0.72) (Figure 5).

Several clinical studies have demonstrated the prophylactic role of *H. pylori*-eradication in the prevention of gastric cancer. For instance, in a Swedish study[14] of 39154 patients undergoing hip replacement, prophylactic antibiotic treatment conferred a reduction in gastric cancer risk after 5 years (odds ratio: 0.6; 95%CI: 0.3 to 1.2). In addition, another Japanese study reported that *H. pylori* eradication inhibited the development of gastric cancer after endoscopic resection during a follow-up period of 3 years[15]. Ever since the government approved *H. pylori* eradication, there has been a decreasing trend in peptic ulcers in Taiwan[13,16]. The mass eradication of *H. pylori* infection was launched in 2004 among a high-risk Taiwanese population with prevalent *H. pylori* infection that were living on the Matsu Islands, and continued until 2018. As a result of this effort, the prevalence rates of *H. pylori* decreased from 64.2% to 15.0%, with reinfection rates of less than 1% per person-year[5]. In one Taiwanese study of 80255 peptic ulcer patients, early *H. pylori* eradication conferred a reduction in early gastric cancer risk (hazard ratio: 0.77)[17]. In addition, this study also showed that early *H. pylori* eradication reduced the standardized incidence ratio of gastric cancer from 1.60 to 1.05 (95%CI: 0.96 to 1.14). Together with results from these studies, our findings provide supportive evidence that the eradication of *H. pylori* infection may be associated with a substantial reduction in gastric cancer incidence.

Second, dietary and lifestyle habits in Taiwan have improved in the past few decades. Earlier studies showed that the consumption of foods containing nitrosamine [18] and cigarette smoking[19] were risk factors for gastric cancer. However, the increased use of refrigerators as a method of food preservation led to a decreased consumption of preserved foods containing nitrosamine and provided the constant availability of fresh food[20]. In Taiwan, a national public survey claimed that the

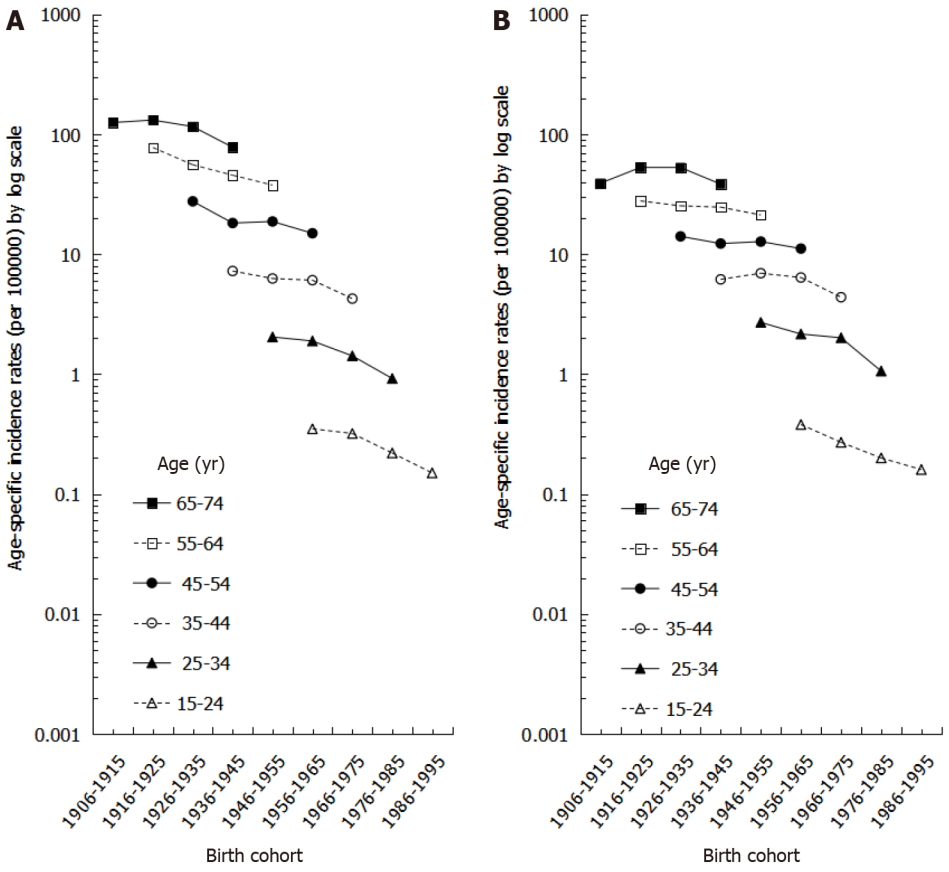


Figure 3 Age-specific incidence rates of gastric cancer in Taiwan by birth cohort during 1906-2005. A: Among males; B: Females, showing higher incidence rates in older birth cohorts than in younger birth cohorts within the same age group. Within the same birth cohort, incidence rates increased by age more evidently in males than in females.

popularization rate of refrigerators was approximately 99.14% in 1991 compared to a popularization rate of only 74.19% in 1976, with 3.6% of families even owning two refrigerators[21]. In regard to cigarette smoking, the Tobacco Hazards Prevention Act was implemented in January 2009, and the prevalence of smoking in adults over 40 years of age dropped from 12.25% in 2001 to 8.18% in 2013[22].

Our age-adjusted incidence rates were slightly lower than estimates from other East Asian countries in terms of proportion change. The reason may be that there has been no evident decline in alcohol consumption, another known risk factor for gastric cancer[23]. Surveys in Taiwan showed that the prevalence of alcohol drinking among males was 38.2% in 2001 and 24.2% in 2013, while the prevalence among females was 9.2% in 2001 and 9.3% in 2013[24]. Furthermore, obesity is also associated with an increased risk of gastric cancer[25-27]. The body mass index of the Taiwanese population has increased over time. The prevalence of having a body mass index ≥ 24 kg/m^2 among males rose from 33.4% during 1993-1996 to 52.1% during 2013-2016 and among females, rose from 33.0% during 1993-1996 to 37.4% during 2013-2016[28].

We also showed a steady decrease in sex ratios. In our results examining sex ratios by birth cohort, younger age groups had lower sex ratios, especially in the 25-34 age group, which had a ratio lower than 1, indicating that males accounted for a lower incidence of gastric cancer. The trends in sex ratios by birth cohort are similar to the intestinal type of gastric cancer based on histopathology and non-cardia site based on anatomic site[29]. We speculate that the decreasing trend in gastric cancer may be mainly attributed to declines in the intestinal type histology because the intestinal type of gastric cancer affects males and older age groups more frequently[30], leading to a greater decrease in incidence among males than among females. Furthermore, the dominant risk factors for gastric cancer, especially for non-cardia cancer, are diet, cigarette smoking, and *H. pylori* infection, whereas the risk factors for cardia cancer are obesity, gastroesophageal reflux, and Barrett's esophagus[31]. This may explain why the corresponding decrease in Taiwan is mainly in non-cardia gastric cancer, as the prevalence of risk factors such as poor diet, smoking, and *H. Pylori* infection are decreasing in Taiwan.

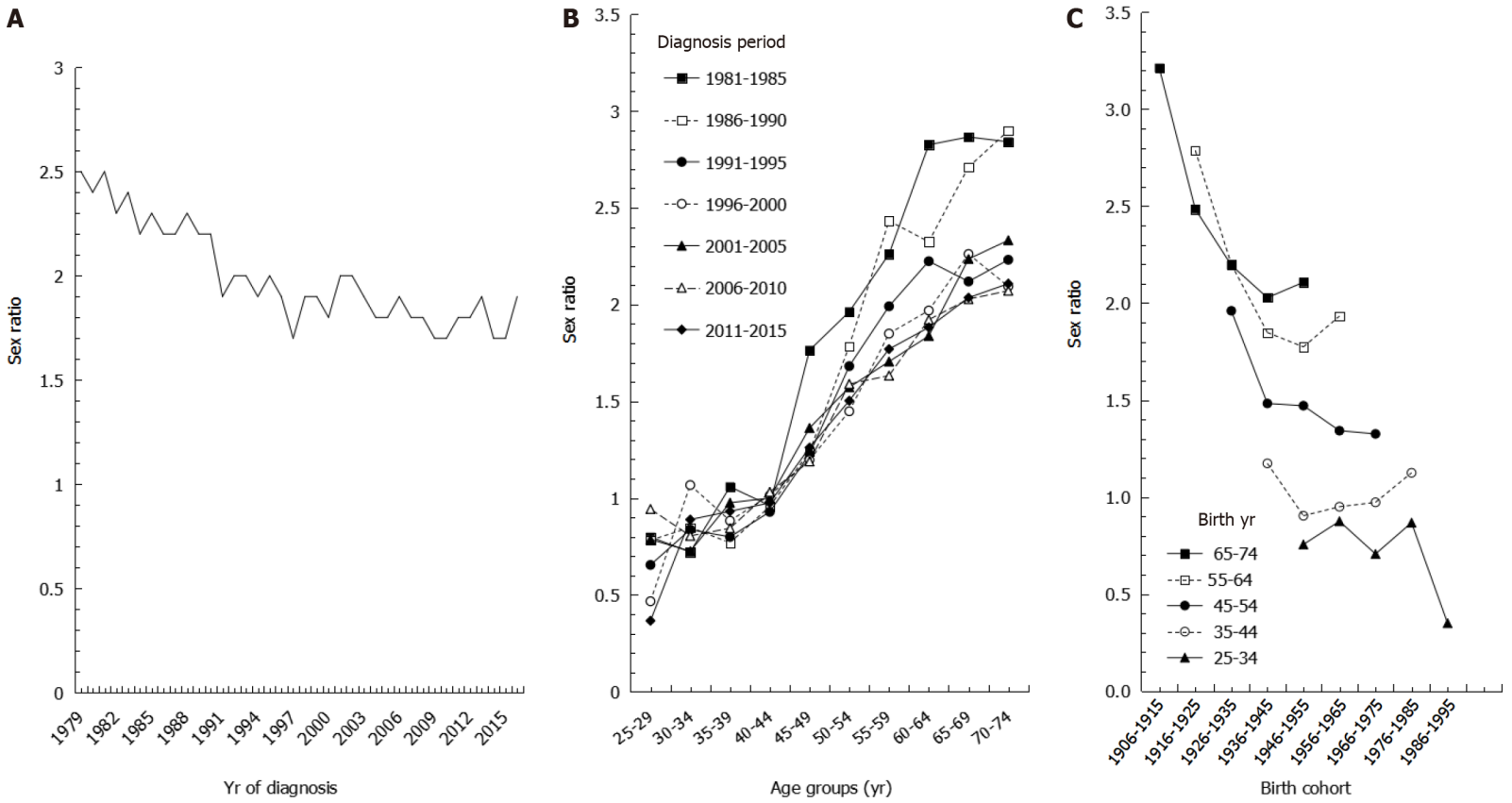


Figure 4 Sex ratios of gastric cancer in Taiwan during 1979-2016. A: Decreasing trends in age-adjusted incidence rates; B: Sex ratios by time period, showing a more consistent trend after 1996; C: Sex ratios in earlier birth cohorts were higher than later birth cohorts.

Regarding the sex ratios in age-specific incidence, we found a large curve in sex ratios around 45-59 years of age. Lindblad *et al*[32] indicated that estrogen may prevent gastric cancer, and our results are in accordance with females in this age group being exposed to some protective factors against gastric cancer, such as estrogen and reproductive factors. The growth of gastric cancer cells may be stimulated during low concentrations of estrogen, such as in young females and postmenopausal women, while the growth of cancer cells may be inhibited in females with high concentrations of estrogen[33,34].

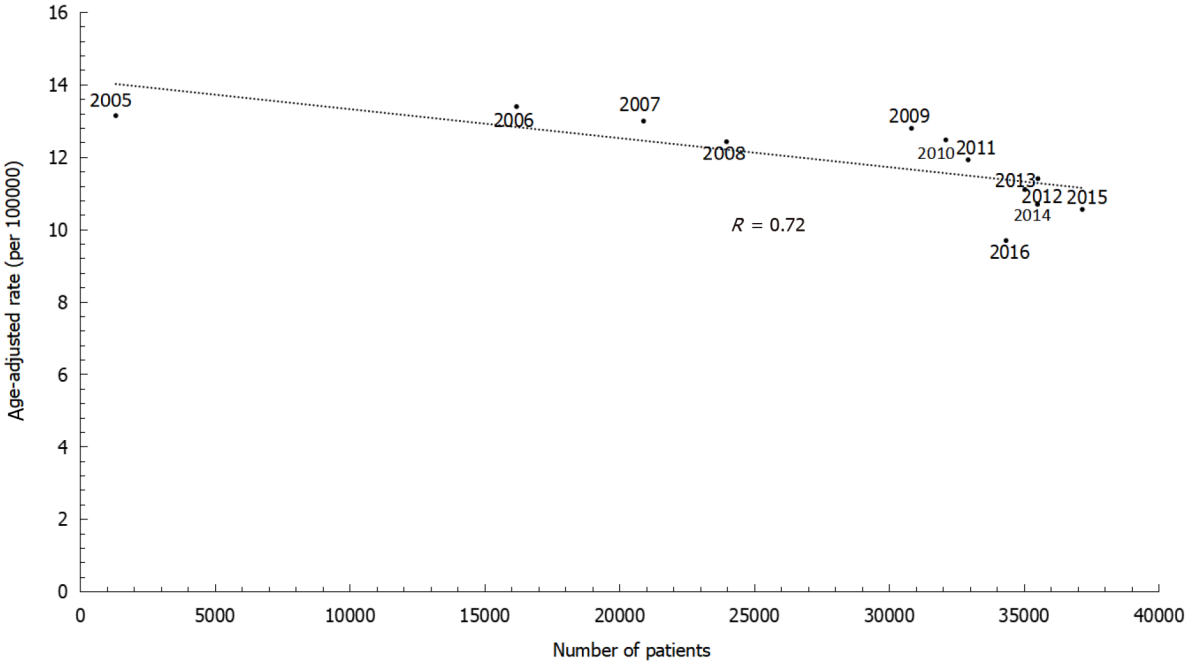


Figure 5 Correlation between numbers of patients with *Helicobacter pylori* infection newly treated with antibiotic therapy and age-adjusted incidence rates showed a substantial decrease with an *r* coefficient of 0.72 in Taiwan, 2005-2016.

In this study, we summarize the descriptive epidemiology of gastric cancer incidence in Taiwan during a period of almost 40 years and show that gastric cancer incidence has steadily declined during this period. However, there are several limitations to our study. First, due to limitations of the database, we were unable to confirm whether the declines in gastric cancer incidence are attributable to differential histologic types and anatomic sites. An earlier study showed a decreased standardized incidence ratio of non-cardia gastric cancer after *H. pylori* eradication, but this eradication did not influence the overall risk for cardia gastric cancer[35]. Also, as for pathological patterns, another study in Taiwan showed significantly decreasing trends in the incidence of adenocarcinoma. However, there was no evident decrease in the incidences of mucosa-associated lymphoid tissue lymphoma and diffuse large B-cell lymphoma[11]. Therefore, further studies are needed to investigate the relationship between *H. pylori* and the histologic type and anatomic site of gastric cancer. Second, this study did not investigate ecological correlations since there was no adjustment for other confounders, such as dietary and lifestyle habits, due to the limitations of the databases.

CONCLUSION

In conclusion, we show continuously decreasing rates of gastric cancer in both sexes, increasing age-specific incidence rates with age, lower sex ratios in later birth cohorts, and decreasing age-adjusted incidence rates with increasing anti-*H. pylori* treatment. The results support the need to further address the issue of mass anti-*H. pylori* treatment in areas with a high prevalence rate of *H. pylori* infection in order to eliminate the threat of *H. pylori*-associated gastric cancer.

ARTICLE HIGHLIGHTS

Research background

Gastric cancer is a multifactorial cancer and is a leading cause of cancer death worldwide. In Taiwan, gastric cancer is the sixth leading cause of cancer mortality.

Research motivation

We desired to discover the association between gastric cancer incidence and potential

factors, including anti-*Helicobacter pylori* (*H. pylori*) treatment.

Research objectives

The objective of this study was to observe secular trends in gastric cancer incidence according to age, sex, and the implementation of a nationwide *H. pylori* treatment program in Taiwan.

Research methods

We used the national Taiwan Cancer Registry database in this population-based study. Annual percent changes in incidence rates were used to describe secular trends in incidence rates and sex ratios of gastric cancer in Taiwan and to study the relationship between its incidence and potential risk factors, including anti-*H. pylori* treatment. Pearson's product-moment correlation coefficients were used to analyze the correlation between annual age adjusted incidence rates and the annual number of patients treated with antibiotic therapy for *H. pylori* infection.

Research results

The annual percent changes showed steadily decreasing rates of gastric cancer in both sexes. However, the decreasing trends differed by sex, with an annual percent change of -2.58% in males and -2.14% in females. The age-specific incidence rates increased with age. Among the same age group, more recent time periods showed lower incidence rates than earlier time periods. Within the same age group, the sex ratio was lower in later birth cohorts than in earlier birth cohorts. In addition, age-adjusted incidence rates decreased substantially with increasing numbers of patients newly treated with antibiotic therapy during 2005 to 2016 for *H. pylori* infection (r = 0.72).

Research conclusions

We observed steadily decreasing trends with differential sex ratios in the incidence of gastric cancer in Taiwan. The results also support the association between trends in gastric cancer incidence and the implementation of *H. pylori* eradication programs in Taiwan.

Research perspectives

Further long-term cohort studies are needed to investigate the relationship between *H. pylori* treatment and gastric cancer histologic type and anatomic site and should include adjusting for other confounders, such as dietary and lifestyle habits and genetic susceptibility.

REFERENCES

1 **Ferlay J**, Ervik M, Lam F, Colombet M, Mery L, Pineros M, Znoar A, Soerjomataram I, Bray F. Global Cancer Observatory: Cancer Today. Lyon, France: International Agency for Research on Cancer, 2020

2 **Ministry of Health and Welfare**. Cancer Registry Annual Report. Department of Health, editor. Taiwan, Republic of China, 2021

3 **Guggenheim DE**, Shah MA. Gastric cancer epidemiology and risk factors. *J Surg Oncol* 2013; **107**: 230-236 [PMID: 23129495 DOI: 10.1002/jso.23262]

4 **IARC Helicobacter pylori Working Group**. Helicobater pylori Eradication as a Strategy for Gastric Cancer Prevention. In: IARC Working Group Reports, No 8. International Agency for Research on Cancer, editor. Lyon, France, 2014

5 **Chiang TH**, Chang WJ, Chen SL, Yen AM, Fann JC, Chiu SY, Chen YR, Chuang SL, Shieh CF, Liu CY, Chiu HM, Chiang H, Shun CT, Lin MW, Wu MS, Lin JT, Chan CC, Graham DY, Chen HH, Lee YC. Mass eradication of *Helicobacter pylori* to reduce gastric cancer incidence and mortality: a long-term cohort study on Matsu Islands. *Gut* 2021; **70**: 243-250 [PMID: 32792335 DOI: 10.1136/gutjnl-2020-322200]

6 **Ministry of Health and Welfare**. Cancer Registry Annual Report, 2016. In: Health Promotion Administration. Taiwan, Republic of China, 2016

7 **Clarke CA**, Undurraga DM, Harasty PJ, Glaser SL, Morton LM, Holly EA. Changes in cancer registry coding for lymphoma subtypes: reliability over time and relevance for surveillance and study. *Cancer Epidemiol Biomarkers Prev* 2006; **15**: 630-638 [PMID: 16614102 DOI: 10.1158/1055-9965.EPI-05-0549]

8 **Liou JM**, Chang CY, Chen MJ, Chen CC, Fang YJ, Lee JY, Wu JY, Luo JC, Liou TC, Chang WH, Tseng CH, Wu CY, Yang TH, Chang CC, Wang HP, Sheu BS, Lin JT, Bair MJ, Wu MS; Taiwan Gastrointestinal Disease and Helicobacter Consortium. The Primary Resistance of Helicobacter pylori

in Taiwan after the National Policy to Restrict Antibiotic Consumption and Its Relation to Virulence Factors-A Nationwide Study. *PLoS One* 2015; **10**: e0124199 [PMID: 25942450 DOI: 10.1371/journal.pone.0124199]

9 **Ahmad OB**, Boschi-Pinto C, Lopez AD. Age standardization of rates: A new WHO standard. 2001. [cited 10 March 2021]. Available from: https://www.who.int/healthinfo/paper31.pdf

10 **Luo G**, Zhang Y, Guo P, Wang L, Huang Y, Li K. Global patterns and trends in stomach cancer incidence: Age, period and birth cohort analysis. *Int J Cancer* 2017; **141**: 1333-1344 [PMID: 28614909 DOI: 10.1002/ijc.30835]

11 **Chang JS**, Kuo SH, Chu PY, Shan YS, Tsai CR, Tsai HJ, Chen LT. The Epidemiology of Gastric Cancers in the Era of *Helicobacter pylori* Eradication: A Nationwide Cancer Registry-Based Study in Taiwan. *Cancer Epidemiol Biomarkers Prev* 2019; **28**: 1694-1703 [PMID: 31350264 DOI: 10.1158/1055-9965.EPI-19-0355]

12 **Bertuccio P**, Chatenoud L, Levi F, Praud D, Ferlay J, Negri E, Malvezzi M, La Vecchia C. Recent patterns in gastric cancer: a global overview. *Int J Cancer* 2009; **125**: 666-673 [PMID: 19382179 DOI: 10.1002/ijc.24290]

13 **Wu CY**, Wu CH, Wu MS, Wang CB, Cheng JS, Kuo KN, Lin JT. A nationwide population-based cohort study shows reduced hospitalization for peptic ulcer disease associated with H pylori eradication and proton pump inhibitor use. *Clin Gastroenterol Hepatol* 2009; **7**: 427-431 [PMID: 19264578 DOI: 10.1016/j.cgh.2008.12.029]

14 **Akre K**, Signorello LB, Engstrand L, Bergström R, Larsson S, Eriksson BI, Nyrén O. Risk for gastric cancer after antibiotic prophylaxis in patients undergoing hip replacement. *Cancer Res* 2000; **60**: 6376-6380 [PMID: 11103800]

15 **Uemura N**, Mukai T, Okamoto S, Yamaguchi S, Mashiba H, Taniyama K, Sasaki N, Haruma K, Sumii K, Kajiyama G. Effect of Helicobacter pylori eradication on subsequent development of cancer after endoscopic resection of early gastric cancer. *Cancer Epidemiol Biomarkers Prev* 1997; **6**: 639-642 [PMID: 9264278]

16 **Lee YC**, Lin JT. Screening and treating Helicobacter pylori infection for gastric cancer prevention on the population level. *J Gastroenterol Hepatol* 2017; **32**: 1160-1169 [PMID: 28087975 DOI: 10.1111/jgh.13726]

17 **Wu CY**, Kuo KN, Wu MS, Chen YJ, Wang CB, Lin JT. Early Helicobacter pylori eradication decreases risk of gastric cancer in patients with peptic ulcer disease. *Gastroenterology* 2009; **137**: 1641-1648 [PMID: 19664631 DOI: 10.1053/j.gastro.2009.07.060]

18 **Hsiung HY**, Fann JC, Yen AM, Chen SL, Chiu SY, Ku TH, Liu TY, Chen HH, Lin MW. Stage-specific Dietary Factors Associated with the Correa Multistep and Multifactorial Process of Human Gastric Carcinogenesis. *Nutr Cancer* 2016; **68**: 598-610 [PMID: 27042805 DOI: 10.1080/01635581.2016.1156712]

19 **Kneller RW**, You WC, Chang YS, Liu WD, Zhang L, Zhao L, Xu GW, Fraumeni JF Jr, Blot WJ. Cigarette smoking and other risk factors for progression of precancerous stomach lesions. *J Natl Cancer Inst* 1992; **84**: 1261-1266 [PMID: 1640486 DOI: 10.1093/jnci/84.16.1261]

20 **Kelley JR**, Duggan JM. Gastric cancer epidemiology and risk factors. *J Clin Epidemiol* 2003; **56**: 1-9 [PMID: 12589864 DOI: 10.1016/s0895-4356(02)00534-6]

21 **Directorate-General of Budget**. Report on the survey of personal income & distribution in Taiwan area of the republic of China. [cited 4 August 2021]. In: Taiwan, Republic of China: Executive Yuan, 1994 [Internet]. Available from: https://win.dgbas.gov.tw/fies/doc/result/83.pdf

22 **Shih YH**, Chang HY, Lu MI, Hurng BS. Time trend of prevalence of self-reported cataract and its association with prolonged sitting in Taiwan from 2001 and 2013. *BMC Ophthalmol* 2014; **14**: 128 [PMID: 25370503 DOI: 10.1186/1471-2415-14-128]

23 **Scherübl H**. Alcohol Use and Gastrointestinal Cancer Risk. *Visc Med* 2020; **36**: 175-181 [PMID: 32775347 DOI: 10.1159/000507232]

24 **Lai YJ**, Hu HY, Lee YL, Ko MC, Ku PW, Yen YF, Chu D. Frequency of alcohol consumption and risk of type 2 diabetes mellitus: A nationwide cohort study. *Clin Nutr* 2019; **38**: 1368-1372 [PMID: 30448092 DOI: 10.1016/j.clnu.2018.06.930]

25 **Wang FW**, Tu MS, Mar GY, Chuang HY, Yu HC, Cheng LC, Hsu PI. Prevalence and risk factors of asymptomatic peptic ulcer disease in Taiwan. *World J Gastroenterol* 2011; **17**: 1199-1203 [PMID: 21448426 DOI: 10.3748/wjg.v17.i9.1199]

26 **Lee HH**, Wu HY, Chuang YC, Chang AS, Chao HH, Chen KY, Chen HK, Lai GM, Huang HH, Chen CJ. Epidemiologic characteristics and multiple risk factors of stomach cancer in Taiwan. *Anticancer Res* 1990; **10**: 875-881 [PMID: 2382983]

27 **Song M**, Choi JY, Yang JJ, Sung H, Lee Y, Lee HW, Kong SH, Lee HJ, Kim HH, Kim SG, Yang HK, Kang D. Obesity at adolescence and gastric cancer risk. *Cancer Causes Control* 2015; **26**: 247-256 [PMID: 25471061 DOI: 10.1007/s10552-014-0506-z]

28 **Lai YJ**, Hu HY, Lee YL, Ku PW, Yen YF, Chu D. Association between obesity and risk of chronic kidney disease: A nationwide Cohort study in Taiwan. *Nutr Metab Cardiovasc Dis* 2017; **27**: 1008-1014 [PMID: 28986076 DOI: 10.1016/j.numecd.2017.08.006]

29 **Wu H**, Rusiecki JA, Zhu K, Potter J, Devesa SS. Stomach carcinoma incidence patterns in the United States by histologic type and anatomic site. *Cancer Epidemiol Biomarkers Prev* 2009; **18**: 1945-1952 [PMID: 19531677 DOI: 10.1158/1055-9965.EPI-09-0250]

30 **Vauhkonen M**, Vauhkonen H, Sipponen P. Pathology and molecular biology of gastric cancer. *Best Pract Res Clin Gastroenterol* 2006; **20**: 651-674 [PMID: 16997151 DOI: 10.1016/j.bpg.2006.03.016]

31 **Crew KD**, Neugut AI. Epidemiology of gastric cancer. *World J Gastroenterol* 2006; **12**: 354-362 [PMID: 16489633 DOI: 10.3748/wjg.v12.i3.354]

32 **Lindblad M**, Ye W, Rubio C, Lagergren J. Estrogen and risk of gastric cancer: a protective effect in a nationwide cohort study of patients with prostate cancer in Sweden. *Cancer Epidemiol Biomarkers Prev* 2004; **13**: 2203-2207 [PMID: 15598781]

33 **Ur Rahman MS**, Cao J. Estrogen receptors in gastric cancer: Advances and perspectives. *World J Gastroenterol* 2016; **22**: 2475-2482 [PMID: 26937135 DOI: 10.3748/wjg.v22.i8.2475]

34 **Sipponen P**, Correa P. Delayed rise in incidence of gastric cancer in females results in unique sex ratio (M/F) pattern: etiologic hypothesis. *Gastric Cancer* 2002; **5**: 213-219 [PMID: 12491079 DOI: 10.1007/s101200200037]

35 **Doorakkers E**, Lagergren J, Engstrand L, Brusselaers N. *Helicobacter pylori* eradication treatment and the risk of gastric adenocarcinoma in a Western population. *Gut* 2018; **67**: 2092-2096 [PMID: 29382776 DOI: 10.1136/gutjnl-2017-315363]

World Journal of Gastroenterology

Submit a Manuscript: https://www.f6publishing.com

World J Gastroenterol 2021 September 14; 27(34): 5775-5792

DOI: 10.3748/wjg.v27.i34.5775

ISSN 1007-9327 (print) ISSN 2219-2840 (online)

META-ANALYSIS

Dietary intake in patients with chronic pancreatitis: A systematic review and meta-analysis

Qurat Ul Ain, Yasir Bashir, Linda Kelleher, David M Bourne, Suzanne M Egan, Jean McMahon, Laura Keaskin, Oonagh M Griffin, Kevin C Conlon, Sinead N Duggan

ORCID number: Qurat Ul Ain 0000-0002-1904-0550; Yasir Bashir 0000-0001-8902-8883; Linda Kelleher 0000-0003-2484-514X; David M Bourne 0000-0002-1492-8710; Suzanne M Egan 0000-0003-1092-789X; Jean McMahon 0000-0001-7955-9146; Laura Keaskin 0000-0001-5039-2901; Oonagh M Griffin 0000-0003-2326-3009; Kevin C Conlon 0000-0002-3703-7080; Sinead N Duggan 0000-0002-4517-4384.

Author contributions: Ul Ain Q, Egan SM, McMahon J, Conlon KC and Duggan SN contributed to design of study; Ul Ain Q and Bashir Y contributed to acquisition of data, independent reviewer; Ul Ain Q, Bashir Y, and Duggan SN contributed to analysis and interpretation of data; Ul Ain Q and Duggan SN drafted and finally approved the article; Bashir Y, Kelleher L, Bourne DM, Egan SM, McMahon J, Griffin OM and Conlon KC critically revised and finally approved the article; Kelleher L, Bourne DM, Egan SM, McMahon J, Keaskin L, Griffin OM and Conlon KC contributed to interpretation of data; Duggan SN conceived the study, and is the overall guarantor of the study.

Supported by The Meath Foundation of Tallaght University Hospital, No. 117/2020.

Qurat Ul Ain, Yasir Bashir, Suzanne M Egan, Laura Keaskin, Oonagh M Griffin, Kevin C Conlon, Sinead N Duggan, Professorial Surgical Unit, Department of Surgery, Trinity College Dublin, Dublin 24 D24 NR0A, Ireland

Linda Kelleher, Department of Nutrition and Dietetics, Tallaght University Hospital, Dublin 24 D24 NR0A, Ireland

David M Bourne, Department of Newcastle Nutrition, Freeman Hospital, Newcastle Upon Tyne NE77DN, United Kingdom

Jean McMahon, Library and Information Services Tallaght, Tallaght University Hospital, Dublin 24 D24 NR0A, Ireland

Oonagh M Griffin, Department of Nutrition and Dietetics, St. Vincent's University Hospital, Dublin 4 D04 T6F4, Ireland

Corresponding author: Sinead N Duggan, RD, PhD, Senior Research Fellow, Professorial Surgical Unit, Department of Surgery, Trinity College Dublin, Dublin 24 D24 NR0A, Ireland. duggansi@tcd.ie

Abstract

BACKGROUND

A progressive reduction in the secretion of pancreatic enzymes in patients with chronic pancreatitis (CP) results in malabsorption and ultimate malnutrition. However, the pathogenesis of malnutrition is multifactorial and other factors such as chronic inflammation, alcohol excess and poor dietary intake all contribute. Patients may restrict their dietary intake due to poor appetite or to avoid gastrointestinal symptoms and abdominal pain. Whilst up to half of patients with chronic pancreatitis are reportedly malnourished, the dietary intake of patients with CP is relatively understudied and has not been systematically reviewed to date.

AIM

To perform a systematic review and meta-analysis of the dietary intakes of patients with CP compared to healthy controls, and to compare the dietary intake of patients with alcohol-related CP and non-alcohol-related CP.

METHODS

Conflict-of-interest statement: The authors declare no conflicts of interest.

PRISMA 2009 Checklist statement: The authors have read the PRISMA 2009 checklist and the manuscript was prepared and revised according to the PRISMA 2009 checklist.

Open-Access: This article is an open-access article that was selected by an in-house editor and fully peer-reviewed by external reviewers. It is distributed in accordance with the Creative Commons Attribution NonCommercial (CC BY-NC 4.0) license, which permits others to distribute, remix, adapt, build upon this work non-commercially, and license their derivative works on different terms, provided the original work is properly cited and the use is non-commercial. See: http://creativecommons.org/Licenses/by-nc/4.0/

Manuscript source: Invited manuscript

Specialty type: Surgery

Country/Territory of origin: Ireland

Peer-review report's scientific quality classification

Grade A (Excellent): 0
Grade B (Very good): B
Grade C (Good): 0
Grade D (Fair): 0
Grade E (Poor): 0

Received: February 26, 2021
Peer-review started: February 26, 2021
First decision: May 1, 2021
Revised: May 26, 2021
Accepted: August 18, 2021
Article in press: August 18, 2021
Published online: September 14, 2021

P-Reviewer: Lei C
S-Editor: Ma YJ
L-Editor: A
P-Editor: Liu JH

A systematic literature search was performed using EMBASE, MEDLINE, and Cochrane review on studies published between 1946 and August 30th, 2019. Adult subjects with a diagnosis of CP who had undergone dietary assessment were included in the systematic review (qualitative analysis). Studies on patients with other pancreatic diseases or who had undergone pancreatic surgery were not included. Studies comparing the dietary intake of patients with CP to that of healthy controls were included in the meta-analysis (quantitative analysis). Meta-analysis was performed using Review Manager 5.3. Newcastle Ottawa Scale (NOS) was used to assess quality of studies.

RESULTS

Of 6715 studies retrieved in the search, 23 were eligible for qualitative analysis while 12 were eligible for quantitative analysis. In the meta-analysis, the total energy (calorie) intake of patients with CP was similar to that of healthy controls [mean difference (MD): 171.3; 95% confidence interval (CI): -226.01, 568.5; P = 0.4], however patients with CP consumed significantly fewer non-alcohol calories than controls [MD: -694.1; 95%CI: -1256.1, (-132.1); P = 0.02]. CP patients consumed more protein, but carbohydrate and fat intakes did not differ significantly. Those with alcohol-related CP consumed more mean (standard deviation) calories than CP patients with a non-alcohol aetiology [2642 (1090) kcal and 1372 (394) kcal, respectively, P = 0.046], as well as more protein, fat, but not carbohydrate.

CONCLUSION

Although patients with CP had similar calorie intake to controls, studies that analysed the contribution of alcohol to energy intake showed that patients with CP consumed fewer non-alcohol calories than healthy controls. A high calorie intake, made up to a large degree by alcohol, may in part contribute to poor nutritional status in CP.

Key Words: Systematic review; Meta-analysis; Chronic pancreatitis; Dietary intake; Undernutrition; Alcohol-related chronic pancreatitis

©The Author(s) 2021. Published by Baishideng Publishing Group Inc. All rights reserved.

Core Tip: Patients with chronic pancreatitis appear to have a similar dietary intake to heathy controls, however, this diet may be made up of alcohol-derived calories to a considerable degree. This may account for the poor nutritional status frequently observed in this population.

Citation: Ul Ain Q, Bashir Y, Kelleher L, Bourne DM, Egan SM, McMahon J, Keaskin L, Griffin OM, Conlon KC, Duggan SN. Dietary intake in patients with chronic pancreatitis: A systematic review and meta-analysis. *World J Gastroenterol* 2021; 27(34): 5775-5792
URL: https://www.wjgnet.com/1007-9327/full/v27/i34/5775.htm
DOI: https://dx.doi.org/10.3748/wjg.v27.i34.5775

INTRODUCTION

Chronic pancreatitis (CP) is a progressive, inflammatory disease of the pancreas, causing progressive fibrosis and eventual destruction of the gland[1]. Along with a gradual loss of pancreatic endocrine and exocrine function, a chronic hyper-inflammatory state increases the risk of undernutrition[2,3]. Almost 50% of CP patients are known to be undernourished[4], the reasons for which are multifactorial.

Maldigestion and malabsorption commonly co-exist with suboptimal dietary intake. Patients may self-restrict to ease symptoms of malabsorption, nausea, early satiety, and abdominal pain. Misleading dietary instructions or selective over-restriction of diet, for instance a fat-free diet to manage steatorrhea, may further cause suboptimal intake[5,6]. For some, chronic excess alcohol consumption may displace food resulting in reduced intake of dietary nutrients[7], while heavy smoking may further reduce appetite[8]. Further complications, including type 3c diabetes and chronic pain, and

maldigestive symptoms including nausea, steatorrhoea, abdominal bloating and or discomfort may worsen already poor dietary intake in the latter stages of the disease [9].

In patients with CP, the prevalence of nutrient deficiencies and their consequences have been widely reported[10-14] however little is known regarding the dietary intake of patients with CP. One study on dietary intake in CP reported that 52% of the patients lost weight following diagnosis of CP, with those who lost weight consuming significantly fewer calories than those who did not[15]. Conversely in another study, patients with calcifying CP consumed higher amount of fats and proteins[16]. Therefore, despite being a digestive disease, no study has systematically reviewed dietary intake in CP.

To address this gap, we undertook a systematic review of published observational studies reporting dietary intake in patients with CP. Specifically, the primary objective was to compare energy (calorie) and macronutrient intake in CP patients with that of healthy controls. The secondary objectives were to determine if dietary intake in CP differed according to aetiology, and to determine and compare the micronutrient intakes of patients with CP with that of controls.

MATERIALS AND METHODS

This study adhered to the Preferred Reporting Items for Systematic Reviews (PRISMA) guidelines[17]. No ethical approval was required due to the nature of the study.

Under the guidance of medical librarian (J.M), Ovid Medline (1946 to August 30th, 2019), Embase (1980 to September 30th, 2019) and Cochrane Review were searched. The search strategy was developed for MEDLINE and translated for use in EMBASE. Finally, we searched the Cochrane central register of control trials to assess for any available trials on our search. We searched for articles with a combination of exploded versions of Medical Subject Headings (MeSH) and keywords as follows: ("Pancreatitis, Chronic", chronic pancreatitis) AND "diet", "dietary intake", "food intake", "food quality", "nutrient intake", "nutritional assessment", "nutrition intake", "nutrition survey", "nutritional survey", "nutritional surveys", "food", "diet history", "dietary history", "food frequency questionnaire", "food diary", "food diaries", "calorie intake", energy intake", "carbohydrates", "dietary protein", "dietary fats", "vitamins", "minerals", "macronutrient intake", "micronutrient intake", "eating", "diet pattern", "dietary pattern", "diet records", "dietary records", "diet quality", "dietary quality", "diet assessment", "dietary assessment".

Boolean operator "OR" was used to assess between each Mesh term and "AND" was used to combine the searches for chronic pancreatitis and dietary intake. Additionally, bibliographies of included studies, and abstracts of pertinent scientific conferences were also manually reviewed for other relevant articles. The search was not limited by language.

Criteria for inclusion/exclusion

To be included, studies had to have quantified the dietary intake of patients with chronic pancreatitis. The PICO[18] model was used to determine the inclusion criteria as follows: patient population (adults of both sexes with a confirmed diagnosis of CP) with the data of interest (studies that measured dietary intake by any recognised means, including food-frequency questionnaires (FFQs), diet histories, food diaries, electronic ('app') measurement, or any other validated technique. Data on controls (healthy or non-pancreatitis) were recorded, if available. Publications had to be available in full text. Studies on patients with active acute pancreatitis, pancreatic carcinoma, cystic fibrosis, and total pancreatectomy were excluded. Data from children under the age of 18, those on enteral/parenteral nutrition, elemental diet or additional supplementation *via* parenteral routes were excluded. Duplicates, case-reports, reviews, editorial/comments, abstracts only, and animal studies were also excluded. Intervention studies where the diet was modified before assessment were excluded, unless baseline unmodified dietary assessment was available. However, data from patients that may have received dietary advice as part of routine clinical care were not excluded.

Study selection

Two reviewers (QS and YB) independently reviewed abstracts and titles of the citations to determine suitability for final inclusion. Disagreement was resolved with discussion or if required, consultation with the third reviewer (SND). Once potentially

relevant studies were identified, full publications were sought, and the selection criteria were applied.

Quality assessment

Quality and risk of bias was assessed using the Newcastle-Ottawa scale (NOS)[19]. A total score of 9 stars can be awarded to each study based on: Up to four stars for the patient selection criteria, two stars for comparability of participants on the basis of design or analysis, and three stars for ascertainment of exposure. The study was deemed to be low quality (0-3 stars), moderate quality (4-6 stars), or high quality (7-9 stars) according to this scoring system.

Data extraction

For each eligible study, the following data were extracted: study details, patient characteristics (age, ethnicity, gender, smoking status, alcohol consumption, BMI), clinical details (disease status, diagnostic criteria, complications, duration of disease, controls if included), dietary intake (energy intake (calories), macronutrient intake (carbohydrate, fat, protein), vitamin intake (vitamins A, B, C, D, E and K), and mineral intake (iron and calcium). We attempted to contact study authors to clarify data where required.

Statistical analysis

Data were analysed using Review Manager (RevMan, version 5.3.5, The Copenhagen Nordic Cochrane Center, The Cochrane Collaboration, 2014). Data were presented as mean (g/d for macronutrients and kcal/d for caloric intake) and corresponding standard deviation (SD). Data were pooled using a random-effects model to give the most conservative estimates. Statistical heterogeneity was calculated as I^2 (presented as 0%-100%). Values < 40% were considered as relatively unimportant, 40%-60% moderate heterogeneity and > 60% indicated substantial heterogeneity. P values < 0.05 were considered statistically significant. Publication bias was assessed using Egger's test. Subgroup analysis for statistical associations were done using SPSS (version 20, IBM, United States).

RESULTS

Study identification and characteristics

The PRISMA flow diagram is shown in Figure 1. Table 1 summarises the 23 articles retrieved in the search, representing 1,577 patients with confirmed CP (based on clinical symptoms and/or radiology). Of these, 12 studies comparing dietary intake of CP patients to that of controls were eligible for meta-analysis, representing 1048 patients with CP and 1,965 control subjects. Most case-controlled studies[6,7,15,20-29] recruited healthy controls, while five studies compared CP patients to patients with alcoholic cirrhosis[6,7,23,25,30], and one study[31] compared patients with pancreatic steatorrhea to those with intestinal steatorrhea. Nine studies originated from Asia (predominantly India), seven from Europe (predominantly France), five from the United States, two from South/Central America, and one each from Africa and Australasia. Most studies were done in the out-patient setting (22 studies)[6,7,15,20-30,32-34] while two studies[31,35] assessed hospitalised patients, and one study[36] assessed dietary intake by means of an international survey. All but three studies[26,29,36] were single centre.

Dietary assessment methods

Regarding dietary assessment, a variety of methods were used (some studies used combined methods to estimate intake). Four studies used food diaries (between 3 and 7 d diaries), 9 studies used food frequency questionnaires (FFQ, of which one used a software technology VioScreen), six studies used a 24-h recall method, one study used a 7-d recall method, three studies employed a diet history method, four studies (all conducted in the 1970s or 1980s) referenced a particular dietary assessment technique, and attempts to obtain the original references were not successful, and five studies did not report the exact dietary assessment method employed. Twenty-two out of the 23 included studies used an a posteriori or data- driven approach to assess diet quality, while one study used a priori measure of diet quality (diet indices)[24], specifically the healthy eating index (HEI) and Mediterranean diet score (MED). Dietary assessment was performed by a dietitian (n = 15) or nutritionist (n = 2) in most cases, and 6 studies

Table 1 Demographic description of studies included in systematic review

Ref.	Setting (subgroup)	Groups (*n*)		GenderM/F		Age (mean ± SD, yr)		BMI (mean ± SD, kg/m²)		Dietary assessment method (by whom)	NOS
		CP, *n* (type)	Control, *n* (type)	CP	Control	CP	Control	CP	Control		
Durbec *et al* [40]	Clinic (Marseille)	193 (142 alcohol-related)	490 (no PC, diabetes, liver disease)	193/0	490/0	44.5 ± 10.5	46.6 ± 13.3	20.2	24.2	Standardised questionnaire [39](dietitian)	6
	Clinic (9 countries)	247	521 (healthy)	247/0	521/0	44.8 ± 13.4	46.7 ± 9.9	20.5	24.1	As above (dietitian)	6
Pitchumoni *et al*[30]	Clinic	36 (36 alcohol-related)	26 (cirrhosis)	NR	NR	NR	NR	NR	NR	NR ("detailed survey", method not specified) (nutritionist)	4
Uscanga *et al* [35]	Hospital	23 (23 alcohol-related)	20 (healthy)	21/2	-	41.2 ± 12.2	-	-	-	NR (nutritionist)	6
Guarnier *et al* [27]	Clinic	14 (8 alcohol-related)	-	14/0	-	50 ± 11	-	21.8 (X)	-	Diet history and FFQ (dietitian)	5
Mezey *et al*[7]	Hospital	42 (42 alcohol related)	28 (healthy)	25/17	19/9	40.7 ± 1.6	39.5 ± 1.8	NR	NR	NR (dietitian)	6
Balakrishnan *et al*[36]	Clinic(India)	28	23 (free of diabetes and digestive disease)	-	-	32.4	24.7	16.2	18.4	Questionnaire [40] (dietitian)	7
Balakrishnan *et al*[36]	Clinic(France)	25	17 (free from diabetes and digestive disease)	-	-	45.7	39.9	21.6	21.7	FFQ (dietitian)	7
Dani *et al*[29]	Clinic(Belo Horizonte)	28 (28 alcohol-related)	28 (healthy)	-	-	-	-	-	-	NR (NR)	5
Dani *et al*[29]	Clinic(Sao Paulo)	40 (40 alcohol-related)	40 (healthy)	-	-	-	-	-	-	NR (NR)	5
Noel-Jorand *et al*[20]	Clinic	31 (31 alcohol-related)	34 (non-alcoholic, 'normal' controls)	25/6	28/6	39.6 ± 6.0	44.8 ± 9.0	22 ± 2.7	22.9 ± 2.8	Standardised questionnaire [41] (NR, 'highly trained person')	6
Laugier *et al* [26]	Clinic(African)	34 (34 alcohol-related)	40 (healthy)	33/1	39/1	39.1 ± 1.3	35.2 ± 1.7	NR	NR	Questionnaire [40] (NR) (dietitian)	5
Laugier *et al* [26]	Clinic (French)	87	430 (healthy)	-	41/6	40.6 ± 1.3	46.6 ± 0.8	NR	NR	As above (NR)	5
Nakamura *et al*[6]	Clinic	38 (29 alcohol-related; 8 idiopathic)	35 (healthy)	36/2	-	52.3 ± 11.3	51.6 ± 11.1	20.1 ± 2.1	23.6 ± 3.2	3-7-d food diary (dietitian)	5
Lévy *et al*[23]	Hospital or attending clinic	56 (56 alcohol-related)	50 (healthy)	n/a	-	44.8 ± 8.4	43.1 ± 8.9	NR	NR	NR "Detailed survey" (NR)	5
Nakamura *et al*[31]	Hospital	15 (15 pancreatic steatorrhoea)	7 (7 intestinal steatorrhoea)	15/0	5/2	54.3 ± 7.5	52.4 ± 22.2	18.4 ± 2.6	19.4 ± 1.0	3-7 d food diary (NR)	4
Vaona *et al* [21]	Clinic	40	75 (healthy)	40/0	75/0	50 ± 10.0	50 ± 10.0	21.9 ± 3.1	26.1 ± 3.1	7-d food diary and 24-h recall (dietitian)	6
Singh *et al* [33][1]	Clinic	76 (60% tropical PC; 40% alcohol-related)	-	63/13	-	32 (NR)	-	NR	-	FFQFor *n* = 20 subgroup, 24-h dietary recall (dietitian)	5
Hamberg *et al*[38]	Clinic	6 (6 alcohol-related)	-	4/2	-	50.3 ± 8.6	-	NR	-	3-d food diary and diet history (dietitian)	5
Midha *et al* [22]	Clinic	120 (idiopathic CP)	120 (healthy subjects attending	74/46	NR (sex-matched)	29.6 ±	NR (age-matched)	19.4 ± 3.4	21.3 ± 3.7	24 dietary recall and FFQ	5

			gastroenterology OPD)			10.5				(dietitian)	
Singh *et al* [39]	Clinic (Group 1 in RCT)	29	-	24/5	-	32 ± 10.0	-	17.2 ± 1.2	-	FFQ and 24-h recall (dietitian)	5
Singh *et al* [39]	Clinic (Group 2 in RCT)	31	-	26/5	-	28 ± 10.0	-	16.7 ± 1.6	-		
Tinju *et al*[37] [1]	Clinic	94 (23% alcohol-related, 44% tropical, 28% idiopathic)	-	61/3[1]	n/a	40.2 ± 13[1]	-	NR	NR	FFQ and 24-h recall (dietitian)	5
Sathiaraj *et al* [15]	Clinic	89 (89 tropical PC diagnosed within 1 yr)	101	60/29	-	32.1 ± 14	NR	NR	NR	FFQ (dietitian)	6
Quilliot *et al* [28]	Clinic	80 (80 alcohol-related)	20 (healthy)	75/5	NR	57.6 ± 9.1	44 ± 11	25.7 ± 4.5	25 ± 2	7-d dietary recall and FFQ (NR)	5
Sobral-Oliveira *et al* [25]	Clinic	20 (20 alcohol-related, current non-drinkers)	16 (healthy never drinkers)	20/0	16/0	54.1 ± 11.4	54.1 ± 18.1	23.7 ± 4.6	26 ± 3.7	7-d diet history (dietitian)	6
Turner *et al* [32]	Clinic	83	-	61/22	-	43.4 (NR)	-	23.8 (NR)	-	24-h dietary recall (NR)	6
Roberts *et al* [24]	Clinic	52 (40% alcohol-related, 23% idiopathic, 12 autoimmune)	48(healthy)	35/17	19/29	50 ± 15.0	54 ± 13.0	24 ± 6.0	31 ± 8.0	FFQ (Vioscreen software) (NR)	6

[1]No demographic or additional clinical details were provided for the n = 20 subgroup of patient with additional dietary assessment.
CP: Chronic pancreatitis; NOS: Newcastle Ottawa scale; FFQ: Food frequency questionnaire; BMI: Body mass index; M: Male; F: Female; NR: Not reported; RCT: Randomised controlled trial; PC: Pancreatitis cancer.

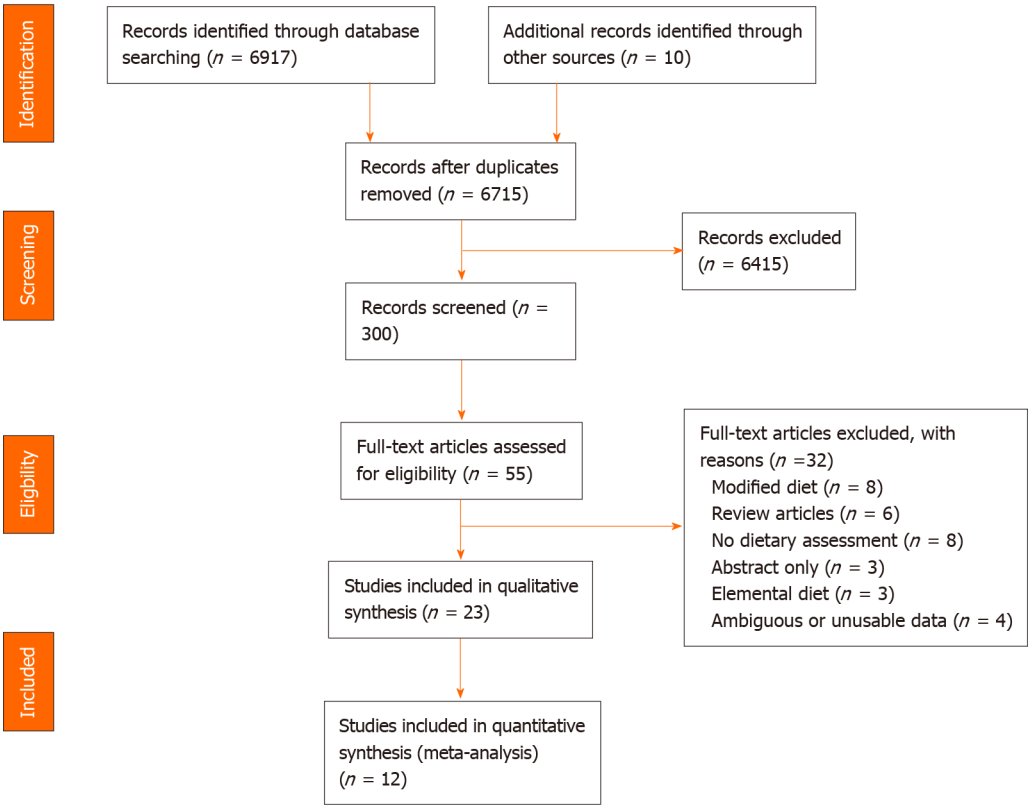


Figure 1 PRISMA flowchart: Preferred reporting items for systematic review and meta-analysis.

did not characterise the individual conducting the assessment. Only six of the 23 studies were published in the last 10 years (2010 or later). Seven studies had been published more than 30 years ago (earlier than 1990).

Participants

Patients with CP had a pooled average age of 43 years (range 29-57.6 years), while healthy controls had a pooled average age of 45 years (range 24.7-54 years). 19 studies reported gender distribution, 1152 (86.8%) of CP patients were male while 175 (13.2%) were female. Thirteen studies reported the BMI of CP patients (pooled mean BMI 21.5 kg/m^2, range 16.2-25.7 kg/m^2), while the reported mean BMI of controls was 24.8 kg/m^2 (range 18.4-27.3 kg/m^2). The average BMI of CP patients from studies conducted on subjects from Eastern/African countries was lower than those conducted on subjects from Western countries (US, Europe) (BMI 18.2 and 22.5 kg/m^2 respectively, P = 0.042). When comparing control subjects from studies from Eastern and Western countries the BMIs did not differ (20.5 and 25 kg/m^2 respectively, P = 0.066).

Study quality

According to the NOS for quality assessment, one study[36] was deemed to be "high-quality" while no studies were deemed to be "low-quality", with the remainder being medium-quality.

Quantitative analysis

Meta-analysis was used to combine study results. Ten studies reported energy (calorie) intakes for both patients with CP and healthy controls, and two studies reported data for geographic groups separately, which were reported independently in the forest plot. There was no difference between the energy intakes of patients with CP and healthy controls (MD: 171.3; 95%CI: -226.01, 568.5; P = 0.4) (Figure 2A), however when analysing data from four studies reporting the intake of non-alcohol calories (five separate study groups), patients with CP consumed significantly fewer non-alcohol calories than healthy controls [MD: -694.1; 95%CI: -1256.1, (-132.1); P = 0.02] (Figure 2B). From 13 studies (16 separate study groups), patients with CP had a higher intake of protein than healthy controls (MD: 14.2; 95%CI: 7.99, 20.49; P < 0.001, Figure 2C). From 11 studies (15 separate study groups), the consumption of carbohydrate (MD: 14.05; 95%CI: -34.03, 62.12; P = 0.57, Figure 2D) did not differ between groups. Similarly, from 12 studies (16 separate study groups) the intake of dietary fat (MD: 8.69; 95%CI: -0.21, 17.59; P = 0.06, Figure 2E) did not differ between the groups. Heterogeneity was considerably high for all outcome measures.

Qualitative analysis

Energy intake and macronutrient composition: Macro- and micronutrient intakes of patients and controls in all studies included in the systematic review are summarised in Table 2. For patients with CP, energy (calorie) intake ranged from 842 to 4178 kcal/d, while the energy intake of controls ranged from 810 to 4178 kcal/d. Where there was higher energy intake among patients with CP, the reasons varied between studies. High calorie consumption was due to higher fat and protein intake in one study[23], higher carbohydrate intake in one study[21], and due to a high intake of all macronutrients in another[35]. In one study[7], the calorie intake was high due to excessive alcohol consumption, with alcohol comprising 50% of total caloric intake. The percentage of energy intake consumed as carbohydrate ranged from 22.1% to 73%, the percentage of energy consumed as protein ranged from 9.1% to 21.3%, and the percentage of energy consumed as fat ranged from 16 to 35%. For controls, the corresponding percentages were 27.5% to 61% (carbohydrate), 10.5% to 16.8% (protein) and 19.8% to 36.6% (fat). In the majority of studies reporting lower energy intake among patients with CP, those with poor energy intake showed some form of malnutrition (defined by lower BMI/loss of weight) after onset of disease when compared to controls. In one study that compared subtypes of CP[37], patients with tropical CP had the lowest intake of energy, attributable to a low intake of dietary fat.

Protein intake: Twenty studies[6,7,15,20-27,29,30,32,33,35-40] determined the protein intake of patients with CP, 15 of which were controlled[6,7,20-26,29,30,32,35-37,40]. Of those, 13 studies[6,7,20-26,29,35-37,40] compared the protein intake of CP patients to that of healthy controls, while one study compared to patients with alcoholic cirrhosis [30] and another to patients with acute pancreatitis[32]. The protein intake of patients with CP ranged from 35 to 145 g/d, compared to 45 to 117g/d among healthy controls. Five studies[20,26,29,35,40] reported that patients with CP consumed a higher intake of protein than healthy controls. In one of these studies[40], the relative risk of developing CP increased as a function of the quantity of protein (and alcohol) consumed. Another study on African patients[26] reported that high protein intake

Table 2 Dietary intake of patients with chronic pancreatitis and controls from studies included in systematic review

Ref.	Number of subjects		Energy intake kcal/d (SD)		Carbohydrate intake g/d (SD)		Protein intake g/d (SD)		Fats intake g/d (SD)		Alcohol intake g/d (SD)	
	CP	Control	CP	Control	CP	Control	CP	Control	CP	Control	CP	Control
Durbec *et al* [40]	193 (Marseille)	490	NR	NR	452.5 (178.1)	300.4 (104.4)	123.8 (56.4)	94.8 (29.5)	122.6 (50.4)	96.97 (28.8)	144 (78.7)	43.6 (56.6)
	247 (International)	521	NR	NR	389 (174.3)	305 (111.8)	119.2 (61)	96.1 (33.9)	115.7 (54.1)	97.8 (32.9)	149.9 (89.1)	37.2 (55.1)
Pitchumoni *et al*[30]	36	26	1050[1] (523)	810[1] (330)	NR	NR	67 (22)	56 (23)	59 (33)	40 (22)	> 200	> 200
Uscanga *et al* [35]	23	20	3367 (748.6)	2332 (548.9)	532.6 (157.7)	357.3 (109.3)	117.6 (26.2)	84.4 (19.9)	83.7 (29.4)	64.4 (17.7)	203.9 (100.2)	NR
Guarnier *et al* [27]	14	UC	1893 (296)	UC	258.5 (44.3)	UC	66.5 (10.3)	UC	66.5 (14.8)	UC	NR	UC
Mezey *et al*[7][2]	42	28	2,514 (142)	2298 (115)	139.2 (10.0)	221 (13.7)	57.1 (4.8)	76.2 (4.8)	53.8 (4.2)	85.6 (3.7)	177.8 (14.5)	47.7 (11.6)
Balakrishnan *et al*[36][2]	28 (India)	23	1966 (154.8)	2012 (173.6)	354 (22.4)	385.7 (37.2)	55.7 (5.8)	51.3 (4.9)	23.4 (2.8)	25.5 (3.4)	NR	NR
	105 (France)	476	3411 (NR)	2453 (NR)	452.5 (178)	300.3 (104.4)	123.8 (56.4)	94.8 (29.5)	122.6 (50.4)	96.9 (28.8)	NR	NR
Dani *et al*[29]	28 (Belo Horizonte)	28	NR	NR	282(21.9)	220(12.2)	64(3.9)	45(3.8)	40(4.3)	34(3.4)	396.6(286.0)	NR
	40 (Sao Paulo)	40	NR	NR	270 (21.6)	319 (19.3)	100 (5.9)	80 (4.8)	97 (4.8)	85 (4.7)	295.3 (171.3)	NR
Noel-Jorand *et al*[20]	31	34	NR	1919 (NR)	NR	133 (NR)	119 (NR)	86 (NR)	120 (NR)	70 (NR)	232 (NR)	< 20 (NR)
Laugier *et al* [26][2]	34 (Africa)	40	2339 (56.8)	2366 (55.3)	301 (15.2)	395 (10.1)	145 (5.9)	117 (3.4)	66 (3.8)	35 (2.6)	130 (12.7)	34 (5.5)
	87 (France)	430	3409 (45.4)	2454 (55.3)	452 (21.8)	300 (6.5)	124 (7.1)	95 (1.8)	123 (6.3)	97 (1.7)	150 (11.4)	43 (3.8)
Nakamura *et al*[6]	38	35	1650 (366)	2564 (477)	237 (63.9)	382 (82.5)	73 (15)	96 (17.5)	38 (12.3)	56 (13.6)	58 (130.6)	78 (110.4)
Lévy *et al*[23]	56	50	4178 (1906-13345)	4178 (1433-6418)	295 (108.8-541)	290 (797-772)	117 (34.6-162.7)	109 (22.6-181.6)	171 (59.7-447.7)	145 (42.2-332.7)	17.5[3] (0.9-64.5)	17.8[3] (2.3-50.4)
Nakamura *et al*[31]	15	7	1674 (188.2)	1985 (226.8)	NR	NR	NR	NR	45(8)	54(7.9)	NR	NR
Vaona *et al*[21]	40	75	2584[4] (850.2)	2103[4] (528.5)	362 (168)	250 (120)	95 (33)	88 (33)	76 (25)	83 (38)	37 (44)	32 (26)
Singh *et al*[33]	20	UC	1760 (375)	UC	274 (55)	UC	48 (13)	UC	53 (23)	UC	NR	UC
Hamberg *et al* [38][2]	7	UC	NR	UC	NR	UC	36.8 (8.46)	UC	NR	UC	NR	UC
Midha *et al* [22]	120	120	1650 (699)	1663 (499)	262 (125)	257 (108)	56 (24)	54 (16)	38 (20)	47 (17)	NR	NR
Singh *et al*[39]	29 (Group 1)[5]	UC	2188 (672)	UC	346 (140)	UC	73 (24)	UC	52 (24)	UC	NR	UC
	31 (Group 2)[5]	UC	2053 (689)	UC	324 (126)	UC	69 (22)	UC	48 (18)	UC	NR	UC
Tinju *et al*[37][6]	100	UC	1398 (515.9)	UC	231 (98.8)	UC	47 (18.8)	UC	37 (18.7)	UC	NR	UC
Sathiaraj *et al* [15]	89	101	1093 (257)	NR	195 (56)	UC	31 (10)	NR	19 (7)	NR	NR	NR
Quilliot *et al* [28]	80	20	2512 (644)	NR	NR	NR	NR	NR	NR	NR	NR	NR

Sobral-Oliveira *et al* [25]	20	16	1637 (546)	1622 (542)	224 (87)	225 (79)	71 (24)	70 (21)	51 (17)	49 (23)	253 (229)	NR
Turner *et al* [32]	83	54	842 (NR)	1143 (NR)	89 (NR)	116 (NR)	46 (NR)	60 (NR)	25 (NR)	48 (NR)	80 (NR)	30 (NR)
Roberts *et al* [24]	52	48	1549 (NR)	1664 (NR)	208 (NR)	181 (NR)	66 (NR)	60 (NR)	52 (NR)	62 (NR)	NR	NR

[1]Results presented non-alcoholic calories only.
[2]Results expressed as mean ± SE.
[3]Expressed as kg of pure alcohol/kg body weight.
[4]Results presented as kJ/d- converted to kcal/d.
[5]Results from two groups of an interventional presented, both groups represent baseline nutrient intake.
[6]Results compared to population survey, no controls recruited. CP: Chronic pancreatitis; SD: Standard deviation; UC: Uncontrolled; NR: Not reported.

was mostly derived from high bean consumption. Eight studies[6,7,15,27,32,33,36,37] reported the opposite: that patients with CP consumed less protein than controls, with protein intake being 20% lower than the recommended daily allowance in two studies [33,37]. Five of these eight studies were conducted in Eastern countries, specifically India and Japan. One study[36] compared protein intake in patients with India with that of patients in France, finding that intake was lower in the former. Three studies considered the source of dietary protein[6,20,23]. Of these, two studies[6,23] reported that patients with CP consumed more animal-based protein than controls.

Carbohydrate intake: Eighteen studies[6,7,15,21-27,29,32,33,35-37,39,40] analysed the carbohydrate intake of patients with CP, of which 13 studies[6,7,21-26,29,32,35,36,40] were controlled. In the 13 controlled studies, there were 17 separate groups studied. Among controlled studies, carbohydrate intake ranged from 89 to 533 g for patients with CP, and 116 to 386 g for controls. Of the controlled studies, three[21,26,35] reported that patients with CP had a higher intake of carbohydrates than controls (in one of those studies[26], only one of the study arms reported that patients with CP consumed significantly more carbohydrate than controls). Four studies reported the opposite[6,7,26,32], stating that patients with CP consumed lower amounts of carbohydrates than controls (in one of those studies[26], only the African group reported that patients with CP consumed significantly less carbohydrate than controls). The other controlled studies reported no significant difference in carbohydrate intake between patients with CP and controls.

Fat intake: Seven studies[18,21,23,24,33,34,38] reported a higher intake of dietary fat in patients with CP than in controls. In several studies, a higher intake of fat was associated with the development of CP[18,21,24,33,38] and earlier onset of disease[18,38]. Three studies provided details on the source of dietary fat[6,20,23]. In one study[6] conducted in Japan, CP patients had statistically lower fat intake from both animal and plant sources, but significantly higher intake of marine fat (fish oil). Two studies analysed patients' intake of saturated fat, monounsaturated and polyunsaturated fat [20,23], reporting that patients with alcohol-associated CP consumed significantly more dietary fat than both control patients with cirrhosis[20,23] and healthy controls [20].

Alcohol intake: Noel-Jorand and colleagues[20] noted that patients with CP had reached the same threshold of alcohol consumption as patients with alcoholic liver cirrhosis prior to diagnosis of their respective diseases (204-232 g/d per subject), however those who developed CP consumed alcohol over a shorter time-frame than those who developed cirrhosis. Lévy *et al*[23] similarly reported that patients with CP had a lower mean duration than those with alcoholic cirrhosis. Durbec *et al*[40] reported that the total quantity of alcohol consumed, as well as the duration of consumption, prior to diagnosis was lower in women than in men. This was mirrored in a study from the United States in which women with CP had a lower duration of alcohol consumption than men with CP[7]. Three studies compared patients with alcohol-related CP to those with CP of other causes. Patients with alcohol-related CP consumed more calories[35,37], carbohydrate[35] and protein[29]. Table 3 compares intake between those with alcohol-related CP and CP of other causes. Those with alcohol-related CP had a higher overall energy intake than those with non-alcohol-related CP, along with a higher protein and fat intake, but not carbohydrate intake.

Table 3 Energy (calorie), protein, carbohydrate, and fat intake of patients with alcohol-related chronic pancreatitis[7,18,21,23,24,28,33] compared to those with non-alcohol-related chronic pancreatitis[14,20]

	Alcohol-related chronic pancreatitis (*n* = 208)	Non- alcohol-related chronic pancreatitis (*n* = 209)	*P* value
Energy, kcal/d (SD)	2642 (1090)	1372 (394)	0.046[1]
Carbohydrate, g/d (SD)	243 (194)	229 (47)	0.85
Protein, g/d (SD)	102 (32)	46(15)	0.02[1]
Fat, g/d (SD)	91 (43)	29 (13)	0.01[1]

[1]Statistically different.
SD: Standard deviation.

Geographical differences: Studies reporting a higher consumption of energy were mostly conducted in Western countries (United States, Europe, Mexico), and the majority were published over 20 years ago. Studies reporting a lower consumption of energy tended to arise from Eastern countries (mainly India and Japan), and the majority had been published more recently. The consumption of carbohydrate and protein appeared to be similar in Western and Eastern countries, while the average intake of fat was lower in eastern/African countries (mean 35.8 g/d) compared to Western countries (mean 75 g/d).

Micronutrient intake: Only four studies measured micronutrient intake (Table 4), of which two studies were controlled (both recruited healthy controls). Vitamin A was expressed in various forms and it was not clear which specific form was presented in some cases. In a controlled study from Japan[6], controls consumed more vitamin A, vitamin B1, vitamin B2, calcium and iron, but not vitamin C.

DISCUSSION

This is the first systematic review to quantify the nutritional intake of patients with CP. While total calorie consumption was not different between patients with CP and healthy controls, patients with CP consumed significantly fewer non-alcohol calories than controls. Those with CP also consumed significantly more protein than healthy controls, however the intake of carbohydrate and fat did not differ. When comparing patients with alcohol-related CP to those with a non-alcohol aetiology, patients with alcohol-related CP consumed more calories, protein and fat than controls, but consumed a similar amount of carbohydrates. This review has highlighted the dearth of research on this topic in general. Only five of the studies retrieved in the search were published in the ten years preceding this paper.

The contribution of alcohol to overall energy intake is an important finding. Five studies were meta-analysed to compare non-alcohol caloric intake to that of healthy controls. In one study from the US on alcohol-related CP, as much as half of all calories consumed were derived from alcohol[7]. In another study conducted both in France and Africa, percentage calories from alcohol were as high as 31% and 39% respectively [24]. The contribution of alcohol to weight is not straightforward. Each gram of alcohol provides 7.1 (29.7 kJ) kcal whereas each gram of carbohydrate approximately provides 4 kcal/g[41], therefore, those consuming large amounts of alcohol should eventually gain excess weight. However, in a Brazilian study comparing asymptomatic alcohol-aetiology CP patients to non-pancreatitis patients with excessive alcohol consumption and healthy controls, patients with CP had lower BMI, body fat and lean body mass, despite a higher alcohol-derived caloric consumption. They also had magnesium and vitamin deficiencies, as well dyslipidaemia and increased risk of cardiovascular disease[25]. Calories derived from alcohol have no nutritive value. Where the same amount of calories was consumed by two groups of non-pancreatic healthy subjects (one receiving calories from carbohydrates and the other receiving the same calories from alcohol), those obtaining energy from alcohol did not gain weight, even when alcohol-derived calorie consumption was increased[42]. Malnutrition secondary to alcohol consumption is multi-factorial and not just due to non-nutritive calorie provision. One study reported that patients consuming high levels of alcohol (23% of

Table 4 Studies analysing micronutrient intake in patients with chronic pancreatitis and controls

Ref.		Vitamin A (SD), IU	Vitamin B1 (SD) mg	Vitamin B2 (SD) mg	Vitamin C (mg)	Vitamin D (mcg)	Vitamin E (IU/mg)	Vitamin K (mg)	Calcium (SD), mg	Iron (SD), mg
Nakamura *et al*[6]	CP	2337.9 (3018.9)	0.9 (0.3)	1.28 (0.4)	98.5 (38.5)	NM	NM	NM	501.5 (145.4)	9.9 (2.7)
	Control[1]	4016.3 (4902.7)	1.21 (0.3)	1.61 (0.5)	85.0 (48.2)	NM	NM	NM	624.3 (227.2)	12.1 (2.8)
Tinju *et al* [37]	CP	M: 3659.7 (6546.8); F: 3888.4 (3936.1)	NM	NM	M: 54.0 (70.5); F: 50.0 (68.7)	NM	NM	NM	M: 496.3 (307.9); F: 485.8 (272)	M: 11.4 (6.7); F: 7.1 (2.8)
	Control	UC	UC	UC	UC	UC	UC	UC	UC	UC
Turner *et al* [32][2]	CP	278 (μg/d)	NM	NM	25.3	NM	NM	NM	NM	NM
	Control	UC	UC	UC	UC	UC	UC	UC	UC	UC
Roberts *et al* [24][3]	CP	744.4 (RAE)	NM	NM	NM	5.88	11.77	64	NM	NM
	Control[2]	651.3 (RAE)	NM	NM	NM	4.03	11.54	99.5	NM	NM

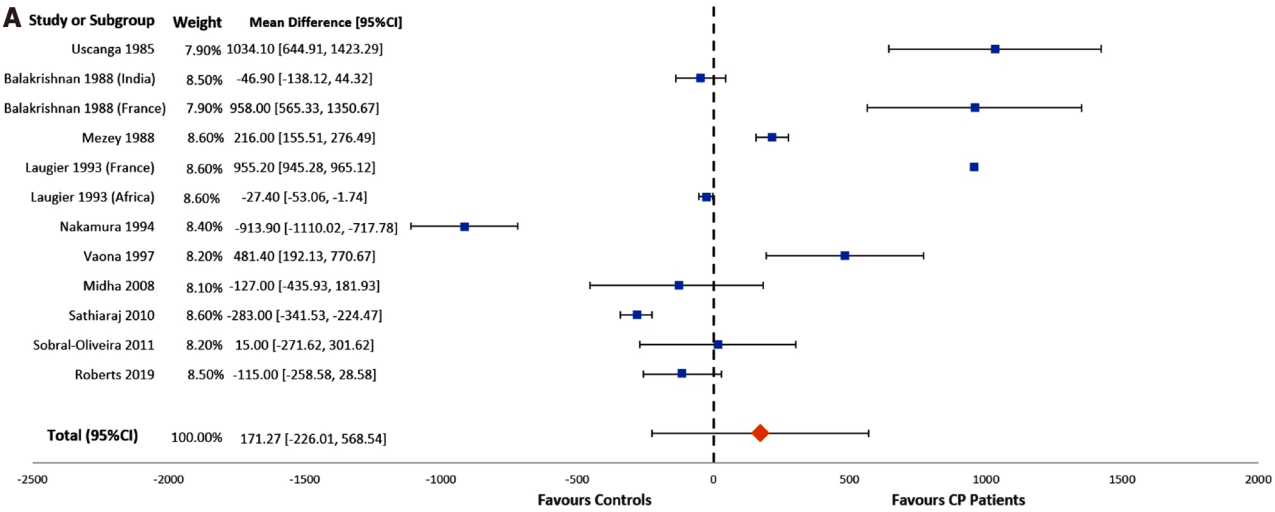
[1]Healthy controls.
[2]Study presented data for "CP present" *vs* "CP absent", however both groups were pancreatitis patients, there were no controls. No standard deviation provided.
[3]Data are expressed as median, no inter-quartile range provided. NM: Not measured; UC: Uncontrolled; M: Male; F: Female; RAE: Retinol activity equivalent.

total calories) tended to displace carbohydrate intake. However, where alcohol intake was higher than 30% of total calories, the intake of proteins, fat and vitamins declined considerably[43].

As well as being responsible for the development of CP and the progression of disease, and aside from the effects of nutrient displacement, a high intake of alcohol is known to directly contribute to malnutrition. Alcohol has direct toxic effects on the gastrointestinal tract and liver, leading to impaired digestion, reduced absorption of nutrients into the blood, and impaired utilisation or increased degradation of those nutrients. As well as causing malabsorption, alcohol also increases systemic inflammation increasing energy requirement, and leading to weight loss[44]. All these effects occur independently and parallel to the decreased secretion of pancreatic enzymes and chronic inflammation that occur as a consequence of CP, hence, cumulative damage occurs in CP patients with excessive alcohol consumption. Patients with CP may reduce their intake of alcohol following diagnosis[24], however most studies show that they continue to consume high quantities of alcohol[45].

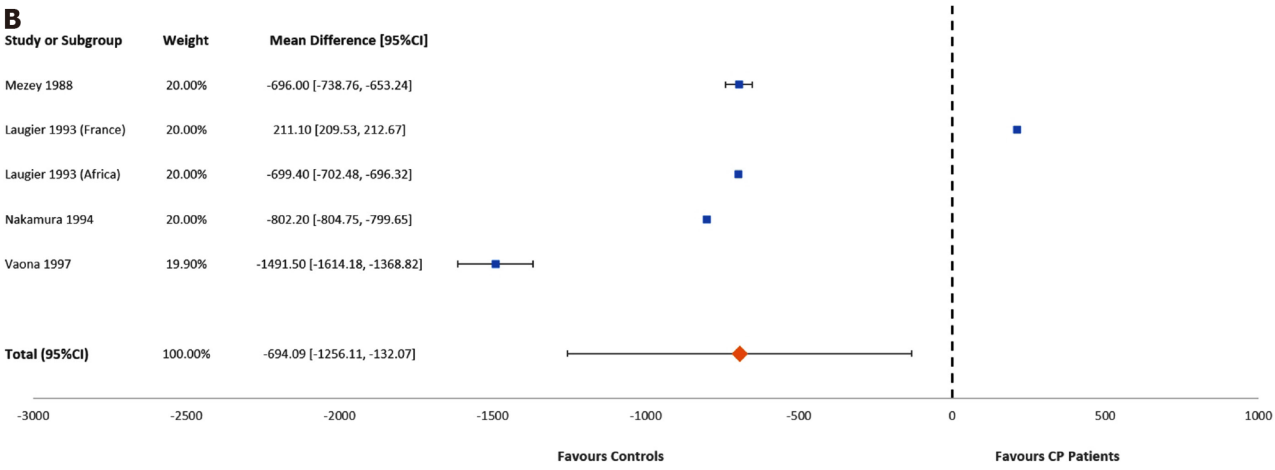
Patients with CP may not be classically underweight, however they may be sarcopenic, defined as low skeletal muscle mass, low muscle strength, and low muscle function leading to impaired physical performance[46,47]. A systematic review[47] reported that sarcopenia is prevalent in 17%-64% of patients with CP, and negatively affects outcomes such as quality of life, hospitalisation, mortality and may be associated with a lower islet yield following total pancreatectomy with islet autotransplantation. Sarcopenic obesity describes the state where excess body weight and reduced muscle mass or strength occur simultaneously. In the 12 studies meta-analysed for total calorie intake, only seven reported BMI. Of those, all reported a mean BMI in the underweight or normal BMI range for patients with CP. Only two of the five studies meta-analysed for non-alcohol calorie intake reported BMI, with both reporting BMI to be in the normal range. Crucially, BMI alone is a poor indicator of individual nutritional status and body composition, with sarcopenia being present independent of BMI[47-49]. In addition, impaired measures of functional capacity (such as hand-grip strength) have been reported in patients with CP, independent of weight or BMI[12,50]. Contrary to the 'textbook' description of an underweight patient, those with CP are frequently overweight or obese[12]. In the present review, whilst none of the studies measured sarcopenia or sarcopenic obesity, patients with CP appeared to have an adequate or high caloric consumption. However, a high percentage of calories as alcohol might explain the nutritional deficits reported in some.

The issue of the macronutrient composition of the diet is more complex. In our meta-analysis of 12 studies (investigating 16 different study populations), we showed that patients with CP consumed significantly more dietary protein compared to



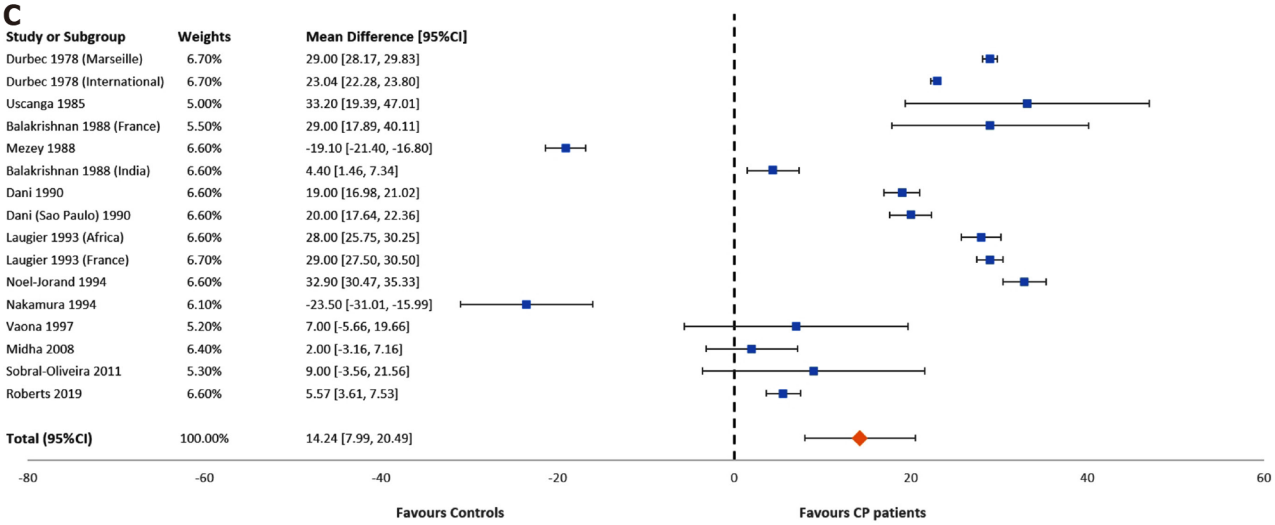
Heterogeneity: Tau² = 479500.12; Chi² = 7417.17, df = 11 (P < 0.00001); I^2 = 100%

Test for overall effect: Z = 0.84 (P = 0.40)



Heterogeneity: Tau² = 410254.49; Chi² = 575839.15, df = 4 (P < 0.00001); I^2 = 100%

Test for overall effect: Z = 2.42 (P = 0.02)



Heterogeneity: Tau² = 151.86; Chi² = 2328.30, df = 15 (P < 0.00001); I^2 = 99%

Test for overall effect: Z = 4.47 (P < 0.00001)

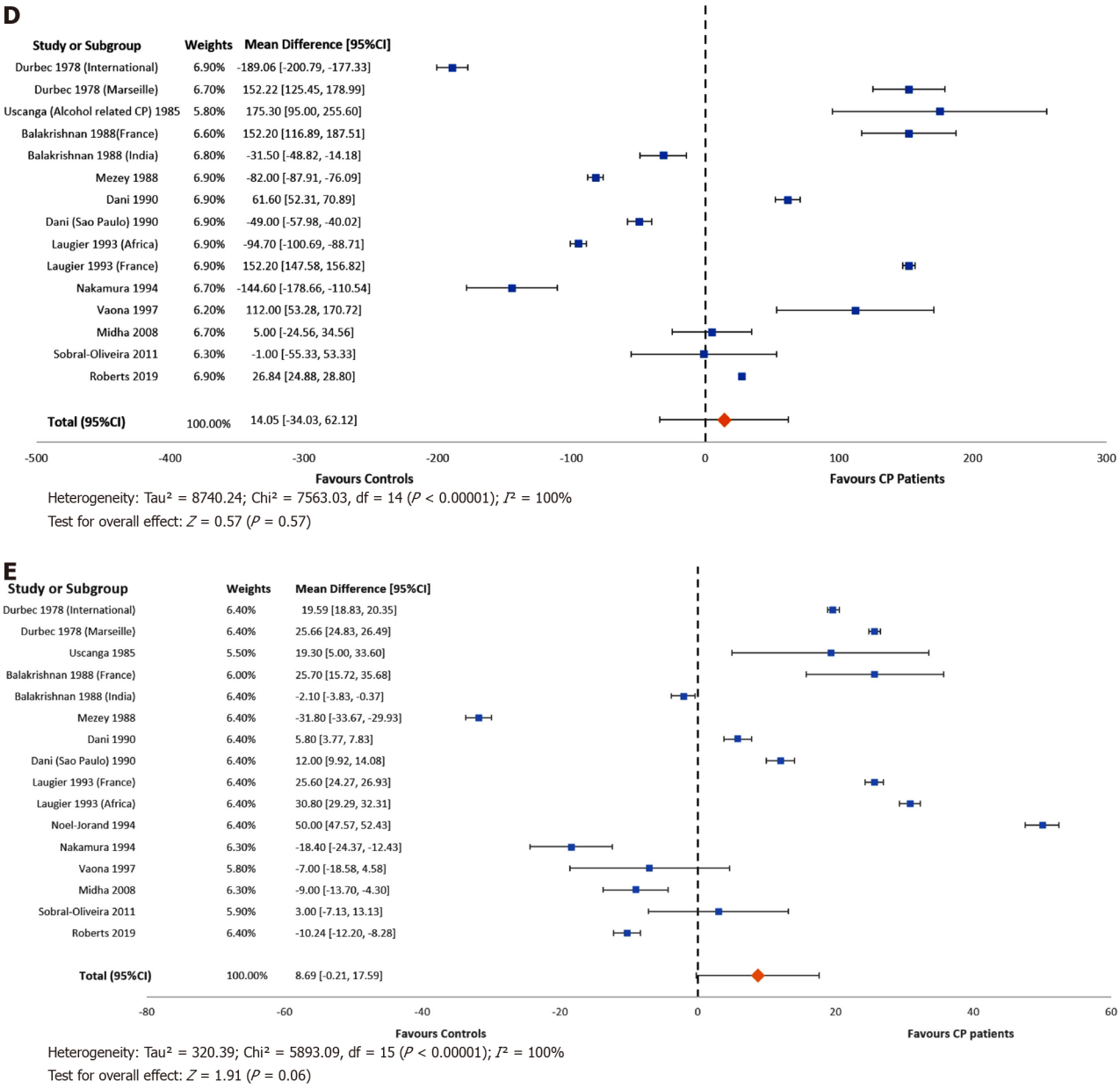


Figure 2 Forest plots of (A) energy intake in calories per day, (B) non-alcohol energy intake in calories per day, (C) protein intake in grams per day, (D) carbohydrate intake in grams per day, and (E) fat intake in grams per day of patients with chronic pancreatitis compared to healthy controls. CP: Chronic pancreatitis.

healthy controls. Recently-published consensus guidelines state that patients with CP do not need to follow specific restrictions on protein, fat or carbohydrate intake, but instead should follow a "well-balanced" diet, except for those who are malnourished, where a high protein, high calorie dietary pattern is warranted[9,51]. It is not known if patients included in the meta-analysis had received dietary counselling at any time preceding their inclusion in the studies. Several studies have examined the role of protein intake in the development of CP. In a paper published in 1973, Sarles *et al*[16] reported the results of an international study of dietary intake in CP in 16 countries across 4 continents. The study, which did not meet the criteria for inclusion into the systematic review, reported that subjects with alcoholism who developed chronic calcific pancreatitis had higher protein and fat intakes than controls. Conversely in a subgroup from India, chronic calcific pancreatitis was found in 'occasional alcoholics' who were deficient in protein. In a study published in the same decade by the same author[40], two study groups were assessed, including a group from France, and a second group of Caucasian patients from 9 international centres. This study also recruited controls and was eligible for inclusion in the systematic review and meta-analysis. It found that there was a small increase in the relative risk of developing chronic pancreatitis with increased protein intake, although the study counselled

against a "protein-poor" diet due to the risk of malabsorption and protein deficiency. Most studies reporting a high protein intake for patients with CP had recruited patients with an alcohol aetiology[7,21,23,24,28]. Studies on patients with non-alcohol aetiology appeared to report a lower protein intake[20].

Regarding fat intake, the study by Durbec and Sarles[40] reported that both a low-fat and high-fat diet increased the relative risk of developing chronic pancreatitis, suggesting consumption of an "average fat" diet (85-110 g fat per day). Perhaps unexpectedly, our meta-analysis showed that there was no difference in fat intake between patients with CP and healthy controls. The forest plot (Figure 2E) shows that most studies reported that patients had a higher intake than controls, and the p-value was just above the arbitrary 0.05. Patients were traditionally advised to follow a low-fat (or even fat-free) diet in an effort to reduce the symptom burden associated with pancreatic exocrine insufficiency. The most recent guidelines[9,51] recommend against restricting fat intake for all but the most severe cases of intractable malabsorption. This is in part because protein and carbohydrate are similarly malabsorbed, resulting in adverse symptoms, and simple fat restriction does not address this fact. Furthermore, achieving protein requirement is also more difficult with a restrictive diet. Treatment with optimal dosage of PERT treats malabsorption of all macronutrients and allows for a more "normal" dietary intake. The studies described above, suggesting that higher dietary intakes of protein and fat might be related to the development of CP, were published during the 1970s, before the importance of adequate treatment with PERT was appreciated. The relationship between the development of CP, the macronutrient composition of the diet, along with the interplay between nutritional status and alcohol intake are therefore not well understood.

There is a clear gap in the literature on the dietary intake of micronutrients in CP. Only four studies[6,24,32,37] have investigated this, one of which was uncontrolled [32]. Only one study measured the dietary intake of fat-soluble vitamins D, E and K [24]. However, this is a critical issue for patients with CP, who are known to have micronutrient deficiency. Again, a high intake of calories with little nutritive value is certain to exacerbate nutritional deficiencies[12,52-58].

This study was also the first to systematically review the methodology of dietary assessment techniques for this patient group, finding considerable heterogeneity, which presented a clear challenge for the interpretation of data, and thereby limits the generalisability of results. A notable number of studies did not report the methods used, while others utilised retrospective techniques and some used prospective methods such as food diaries. Each method carries its own risk of bias. For example, retrospective techniques such as FFQs and dietary recall may be affected by recall bias, as well with problems with subject memory, cognition and motivation. The reported nutrient intake in some studies appeared to be considerably high compared to contemporaneous national surveys. For example, Lévy *et al*[23] reported the dietary intake of newly diagnosed alcoholic CP patients from 1995 and reported an intake for both groups in excess of 4,000 kcal and 100 g protein per day. This is considerably higher than values reported by other national surveys around that time, including the French national dietary study from 1993-94 [mean energy intake in males of 2,390 kcal of which 16.6% came from protein (approximately 99g)[59]]. Similarly, the Irish North-South Food Consumption Survey 1997-99 found that men aged 18-64 years had a mean energy intake of 2,632kcal and 100g protein[60]. FFQs, used in the French study, have been shown to overestimate energy intake[59]. However, this study was not eligible for inclusion in the meta-analysis due to incompatible data.

Limitations and strengths

This systematic review was limited by the heterogenous nature of the included studies. More importantly, the method of dietary assessment differed considerably between studies, which may account for the wide range of intakes reported and may have resulted in both under- and over-estimation of actual intake. However, the meta-analysis was designed to report the differences in intake between patients with CP and controls rather than absolute values (and the methodology for patients and controls was the same within each individual study), which should minimise this error. In addition, the meta-analysis compared patients with CP to healthy controls only, and excluded studies with other types of controls. Hence, despite inter-group heterogeneity, intra-group diversity was minimal. Furthermore, as heterogeneity is high in large scale studies, this may have further added to the heterogeneity observed, as most of our included studies recruited large patient numbers. Only 12 of the 23 studies retrieved were deemed eligible for meta-analysis, and fewer were suitable for some of the analyses, such as non-alcohol calories. This was in part due to the inclusion of studies that recruited healthy controls only.

Only six studies were published within the last ten years. Nonetheless, we believe that the results are applicable to present-day patients. A potential variable was the inclusion of a wide range of ethnic groups. The differences in nutrient intake reported may have been a consequence of geographic location rather than the effect of CP. However, the inclusion of healthy controls from the same geographic region as the patients with CP would have minimised this limitation. In addition, most patients with CP recruited to the various studies were male, but the same restriction wasn't applied for controls. Therefore, the gender differences might explain higher caloric intake by CP patients in some studies. No study had compared dietary intake by gender. As with all systematic reviews, this study was inherently limited by the quality of the studies included, although only one study was deemed to be of low quality. In some cases, different units and methods of reporting were used, necessitating extrapolation or recalculation.

CONCLUSION

This systematic review and meta-analysis supports the notion that while patients consume apparently adequate energy, the quality of the dietary intake is poor, in part due to the contribution of alcohol to overall energy intake. This review has also highlighted the critical lack of recent studies on this topic. Further studies should aim to characterise the dietary intake of patients with CP, with robust study designs and adequate sample size. Longitudinal research would help to determine the effects of various dietary patterns and alcohol abuse on diet. Intervention studies of therapeutic dietary strategies as well as early dietetic consultation in patients with CP are sorely needed.

ARTICLE HIGHLIGHTS

Research background

Patients with chronic pancreatitis (CP) are a high risk of developing malnutrition due to progressive exocrine insufficiency, malabsorption, and adverse gastro-intestinal symptoms. Poor dietary intake and excess alcohol consumption may exacerbate malnutrition.

Research motivation

Although CP is a digestive disease, little is known regarding the dietary intake of patients with this condition, and no systematic reviews or meta-analyses have been undertaken to date.

Research objectives

The purpose of this systematic review and meta-analysis was to compare the macronutrient and micronutrient intake of patients with CP to that of healthy subjects, and to determine if there was a difference in dietary intake according to aetiology.

Research methods

With the guidance of a medical librarian, we conducted a search of multiple databases including Ovid Medline, EMBASE and Cochrane Review.

Research results

Twenty-three studies were retrieved in the search and included in the systematic review (representing 1577 patients with CP), of which 12 were eligible for meta-analysis (representing 1048 patients with CP and 1965 healthy controls). There was no statistical difference in the energy (calorie) intakes of patients with CP and controls. However, when analysing studies reporting non-alcohol calorie consumption, patients with CP consumed significantly fewer calories than health control subjects. Those with CP consumed more protein than healthy controls, but there was no difference in the consumption of carbohydrate and fat. Heterogeneity was considerably high for all outcome measures. A broad variety of methods was used in the various studies to estimate dietary intake, and most had been published more than ten years prior to this review.

Research conclusions

This was the first meta-analysis to evaluate the dietary intake of patients with CP. Although the calorie intake of patients with CP did not differ from that of healthy controls, studies that analysed the contribution of alcohol to energy intake showed that those with CP consumed fewer non-alcohol calories than controls. This may contribute to the poor nutritional status of patients with CP.

Research perspectives

The considerable heterogeneity made it difficult to make general conclusions, and the broad range of dietary assessment methods used means that under-or over-estimation of intake may have occurred. There were few data for micronutrient intake, a considerable research gap considering the common occurrence of biochemical deficiency in this patient group. There were few recently-published studies. Future studies should aim to characterise the dietary macronutrient and micronutrient intakes of patients with CP with robust methodology and study design.

REFERENCES

1 **Sarles H**. Etiopathogenesis and definition of chronic pancreatitis. *Dig Dis Sci* 1986; **31**: 91S-107S [PMID: 3525051 DOI: 10.1007/BF01295992]
2 **Rasch S**, Valantiene I, Mickevicius A, Beer S, Rosendahl J, Charnley RM, Robinson SM. Chronic pancreatitis: Do serum biomarkers provide an association with an inflammageing phenotype? *Pancreatology* 2016; **16**: 708-714 [PMID: 27554641 DOI: 10.1016/j.pan.2016.08.004]
3 **Hébuterne X**, Hastier P, Péroux JL, Zeboudj N, Delmont JP, Rampal P. Resting energy expenditure in patients with alcoholic chronic pancreatitis. *Dig Dis Sci* 1996; **41**: 533-539 [PMID: 8617130 DOI: 10.1007/BF02282334]
4 **Armbrecht U**. [Chronic pancreatitis: weight loss and poor physical performance - experience from a specialized rehabilitation centre]. *Rehabilitation (Stuttg)* 2001; **40**: 332-336 [PMID: 11742423 DOI: 10.1055/s-2001-18966]
5 **Goebell H**, Hotz J, Hoffmeister H. Hypercaloric nutrition as aetiological factor in chronic pancreatitis. *Z Gastroenterol* 1980; **18**: 94-97 [PMID: 7385939]
6 **Nakamura T**, Arai Y, Terada A, Kudoh K, Imamura K, Machida K, Kikuchi H, Takebe K. Dietary analysis of Japanese patients with chronic pancreatitis in stable conditions. *J Gastroenterol* 1994; **29**: 756-762 [PMID: 7874272 DOI: 10.1007/BF02349283]
7 **Mezey E**, Kolman CJ, Diehl AM, Mitchell MC, Herlong HF. Alcohol and dietary intake in the development of chronic pancreatitis and liver disease in alcoholism. *Am J Clin Nutr* 1988; **48**: 148-151 [PMID: 3389321 DOI: 10.1093/ajcn/48.1.148]
8 **Audrain-McGovern J**, Benowitz NL. Cigarette smoking, nicotine, and body weight. *Clin Pharmacol Ther* 2011; **90**: 164-168 [PMID: 21633341 DOI: 10.1038/clpt.2011.105]
9 **Arvanitakis M**, Ockenga J, Bezmarevic M, Gianotti L, Krznarić Ž, Lobo DN, Löser C, Madl C, Meier R, Phillips M, Rasmussen HH, Van Hooft JE, Bischoff SC. ESPEN guideline on clinical nutrition in acute and chronic pancreatitis. *Clin Nutr* 2020; **39**: 612-631 [PMID: 32008871 DOI: 10.1016/j.clnu.2020.01.004]
10 **Duggan SN**, O'Sullivan M, Hamilton S, Feehan SM, Ridgway PF, Conlon KC. Patients with chronic pancreatitis are at increased risk for osteoporosis. *Pancreas* 2012; **41**: 1119-1124 [PMID: 22836855 DOI: 10.1097/MPA.0b013e31824abb4d]
11 **Duggan SN**, Smyth ND, Murphy A, Macnaughton D, O'Keefe SJ, Conlon KC. High prevalence of osteoporosis in patients with chronic pancreatitis: a systematic review and meta-analysis. *Clin Gastroenterol Hepatol* 2014; **12**: 219-228 [PMID: 23856359 DOI: 10.1016/j.cgh.2013.06.016]
12 **Duggan SN**, Smyth ND, O'Sullivan M, Feehan S, Ridgway PF, Conlon KC. The prevalence of malnutrition and fat-soluble vitamin deficiencies in chronic pancreatitis. *Nutr Clin Pract* 2014; **29**: 348-354 [PMID: 24727205 DOI: 10.1177/0884533614528361]
13 **Martínez-Moneo E**, Stigliano S, Hedström A, Kaczka A, Malvik M, Waldthaler A, Maisonneuve P, Simon P, Capurso G. Deficiency of fat-soluble vitamins in chronic pancreatitis: A systematic review and meta-analysis. *Pancreatology* 2016; **16**: 988-994 [PMID: 27681502 DOI: 10.1016/j.pan.2016.09.008]
14 **Hoogenboom SA**, Lekkerkerker SJ, Fockens P, Boermeester MA, van Hooft JE. Systematic review and meta-analysis on the prevalence of vitamin D deficiency in patients with chronic pancreatitis. *Pancreatology* 2016; **16**: 800-806 [PMID: 27453461 DOI: 10.1016/j.pan.2016.07.010]
15 **Sathiaraj E**, Gupta S, Chutke M, Mahurkar S, Mansard MJ, Rao GV, Reddy DN. Malnutrition is not an etiological factor in the development of tropical pancreatitis--a case-control study of southern Indian patients. *Trop Gastroenterol* 2010; **31**: 169-174 [PMID: 21560520]
16 **Sarles H**. An international survey on nutrition and pancreatitis. *Digestion* 1973; **9**: 389-403 [PMID: 4206286 DOI: 10.1159/000197468]
17 **Moher D**, Liberati A, Tetzlaff J, Altman DG; PRISMA Group. Preferred reporting items for systematic reviews and meta-analyses: the PRISMA statement. *Int J Surg* 2010; **8**: 336-341 [PMID:

20171303 DOI: 10.1016/j.ijsu.2010.02.007]
18 **Eriksen MB**, Frandsen TF. The impact of patient, intervention, comparison, outcome (PICO) as a search strategy tool on literature search quality: a systematic review. *J Med Libr Assoc* 2018; **106**: 420-431 [PMID: 30271283 DOI: 10.5195/jmla.2018.345]
19 **Wells GA**, Shea B, O'Connell D, Peterson J, Welch V, Losos M, P Tugwell. The Newcastle-Ottawa Scale (NOS) for assessing the quality of nonrandomised studies in meta-analyses. Oxford; 2000
20 **Noel-Jorand MC**, Bras J. A comparison of nutritional profiles of patients with alcohol-related pancreatitis and cirrhosis. *Alcohol Alcohol* 1994; **29**: 65-74 [PMID: 8003119]
21 **Vaona B**, Armellini F, Bovo P, Rigo L, Zamboni M, Brunori MP, Dall'O E, Filippini M, Talamini G, Di Francesco V, Frulloni L, Micciolo R, Cavallini G. Food intake of patients with chronic pancreatitis after onset of the disease. *Am J Clin Nutr* 1997; **65**: 851-854 [PMID: 9062539 DOI: 10.1093/ajcn/65.3.851]
22 **Midha S**, Singh N, Sachdev V, Tandon RK, Joshi YK, Garg PK. Cause and effect relationship of malnutrition with idiopathic chronic pancreatitis: prospective case-control study. *J Gastroenterol Hepatol* 2008; **23**: 1378-1383 [PMID: 18554234 DOI: 10.1111/j.1440-1746.2008.05459.x]
23 **Lévy P**, Mathurin P, Roqueplo A, Rueff B, Bernades P. A multidimensional case-control study of dietary, alcohol, and tobacco habits in alcoholic men with chronic pancreatitis. *Pancreas* 1995; **10**: 231-238 [PMID: 7624300 DOI: 10.1097/00006676-199504000-00003]
24 **Roberts KM**, Golian P, Nahikian-Nelms M, Hinton A, Madril P, Basch K, Conwell D, Hart PA. Does the Healthy Eating Index and Mediterranean Diet Score Identify the Nutritional Adequacy of Dietary Patterns in Chronic Pancreatitis? *Dig Dis Sci* 2019; **64**: 2318-2326 [PMID: 30798461 DOI: 10.1007/s10620-019-05536-3]
25 **Sobral-Oliveira MB**, Faintuch J, Guarita DR, Oliveira CP, Carrilho FJ. Nutritional profile of asymptomatic alcoholic patients. *Arq Gastroenterol* 2011; **48**: 112-118 [PMID: 21709952 DOI: 10.1590/S0004-28032011000200006]
26 **Laugier R**, Bernard JP, Laroche R, Kadende P, N'Dabaneze E, Saunière JF, Dupuy P. Exocrine pancreatic secretion in normal controls and chronic calcifying pancreatitis patients from Burundi: possible dietary influences. *Digestion* 1993; **54**: 54-60 [PMID: 8513989 DOI: 10.1159/000201012]
27 **Guarnieri G**, Toigo G, Situlin R, Crapesi L, Del Bianco MA, Zanettovich A, Mandero E, Resetta G. Muscle biopsy studies on protein-energy malnutrition in patients with chronic relapsing pancreatitis. *Infusionsther Klin Ernahr* 1986; **13**: 166, 168-171 [PMID: 2428750 DOI: 10.1159/000222135]
28 **Quilliot D**, Forbes A, Dubois F, Gueant JL, Ziegler O. Carotenoid deficiency in chronic pancreatitis: the effect of an increase in tomato consumption. *Eur J Clin Nutr* 2011; **65**: 262-268 [PMID: 21119697 DOI: 10.1038/ejcn.2010.232]
29 **Dani R**, Mott CB, Guarita DR, Nogueira CE. Epidemiology and etiology of chronic pancreatitis in Brazil: a tale of two cities. *Pancreas* 1990; **5**: 474-478 [PMID: 2381901]
30 **Pitchumoni CS**, Sonnenshein M, Candido FM, Panchacharam P, Cooperman JM. Nutrition in the pathogenesis of alcoholic pancreatitis. *Am J Clin Nutr* 1980; **33**: 631-636 [PMID: 7355847 DOI: 10.1093/ajcn/33.3.631]
31 **Nakamura T**, Takebe K, Tando Y, Arai Y, Yamada N, Ishii M, Kikuchi H, Imamura K. Faecal triglycerides and fatty acids in the differential diagnosis of pancreatic insufficiency and intestinal malabsorption in patients with low fat intakes. *J Int Med Res* 1995; **23**: 48-55 [PMID: 7774758 DOI: 10.1177/030006059502300106]
32 **Turner RC**, Brazionis LB, McDermott R. Intake patterns of food nutrients and other substances associated with chronic pancreatitis. *Pancreatology* 2013; **13**: 33-37 [PMID: 23395567 DOI: 10.1016/j.pan.2012.12.004]
33 **Singh N**, Joshi YK, Saraya A, Tandon RK. Nutritional profile of patients with chronic pancreatitis. *Asia Pac J Clin Nutr* 1999; **8**: 19-23 [PMID: 24393731 DOI: 10.1046/j.1440-6047.1999.00041.x]
34 **Lin Y**, Tamakoshi A, Hayakawa T, Ogawa M, Ohno Y; Research Committee on Intractable Pancreatic Diseases. Associations of alcohol drinking and nutrient intake with chronic pancreatitis: findings from a case-control study in Japan. *Am J Gastroenterol* 2001; **96**: 2622-2627 [PMID: 11569685 DOI: 10.1111/j.1572-0241.2001.04121.x]
35 **Uscanga L**, Robles-Díaz G, Sarles H. Nutritional data and etiology of chronic pancreatitis in Mexico. *Dig Dis Sci* 1985; **30**: 110-113 [PMID: 3967558 DOI: 10.1007/BF01308194]
36 **Balakrishnan V**, Sauniere JF, Hariharan M, Sarles H. Diet, pancreatic function, and chronic pancreatitis in south India and France. *Pancreas* 1988; **3**: 30-35 [PMID: 3362842 DOI: 10.1097/00006676-198802000-00006]
37 **Tinju J**, Reshmi S, Rajesh G, Balakrishnan V. Anthropometric, biochemical, clinical and dietary assessment for malnutrition in south Indian patients with chronic pancreatitis. *Trop Gastroenterol* 2010; **31**: 285-290 [PMID: 21568144]
38 **Hamberg O**, Andersen V, Sonne J, Larsen S, Vilstrup H. Urea synthesis in patients with chronic pancreatitis: relation to glucagon secretion and dietary protein intake. *Clin Nutr* 2001; **20**: 493-501 [PMID: 11883997 DOI: 10.1054/clnu.2001.0476]
39 **Singh S**, Midha S, Singh N, Joshi YK, Garg PK. Dietary counseling versus dietary supplements for malnutrition in chronic pancreatitis: a randomized controlled trial. *Clin Gastroenterol Hepatol* 2008; **6**: 353-359 [PMID: 18328440 DOI: 10.1016/j.cgh.2007.12.040]
40 **Durbec JP**, Sarles H. Multicenter survey of the etiology of pancreatic diseases. Relationship between the relative risk of developing chronic pancreaitis and alcohol, protein and lipid consumption. *Digestion* 1978; **18**: 337-350 [PMID: 750261 DOI: 10.1159/000198221]

41 **Westerfeld WW**, Schulman MP. Metabolism and caloric value of alcohol. *J Am Med Assoc* 1959; **170**: 197-203 [PMID: 13641007 DOI: 10.1001/jama.1959.63010020007016]

42 **Pirola RC**, Lieber CS. The energy cost of the metabolism of drugs, including ethanol. *Pharmacology* 1972; **7**: 185-196 [PMID: 5054589 DOI: 10.1159/000136288]

43 **Gruchow HW**, Sobocinski KA, Barboriak JJ. Alcohol, nutrient intake, and hypertension in US adults. *JAMA* 1985; **253**: 1567-1570 [PMID: 3974035 DOI: 10.1001/jama.253.11.1567]

44 **Wang HJ**, Zakhari S, Jung MK. Alcohol, inflammation, and gut-liver-brain interactions in tissue damage and disease development. *World J Gastroenterol* 2010; **16**: 1304-1313 [PMID: 20238396 DOI: 10.3748/wjg.v16.i11.1304]

45 **Coté GA**, Yadav D, Slivka A, Hawes RH, Anderson MA, Burton FR, Brand RE, Banks PA, Lewis MD, Disario JA, Gardner TB, Gelrud A, Amann ST, Baillie J, Money ME, O'Connell M, Whitcomb DC, Sherman S; North American Pancreatitis Study Group. Alcohol and smoking as risk factors in an epidemiology study of patients with chronic pancreatitis. *Clin Gastroenterol Hepatol* 2011; **9**: 266-73; quiz e27 [PMID: 21029787 DOI: 10.1016/j.cgh.2010.10.015]

46 **Cruz-Jentoft AJ**, Bahat G, Bauer J, Boirie Y, Bruyère O, Cederholm T, Cooper C, Landi F, Rolland Y, Sayer AA, Schneider SM, Sieber CC, Topinkova E, Vandewoude M, Visser M, Zamboni M; Writing Group for the European Working Group on Sarcopenia in Older People 2 (EWGSOP2), and the Extended Group for EWGSOP2. Sarcopenia: revised European consensus on definition and diagnosis. *Age Ageing* 2019; **48**: 16-31 [PMID: 30312372 DOI: 10.1093/ageing/afy169]

47 **Kuan LL**, Dennison AR, Garcea G. Prevalence and Impact of Sarcopenia in Chronic Pancreatitis: A Review of the Literature. *World J Surg* 2021; **45**: 590-597 [PMID: 33165641 DOI: 10.1007/s00268-020-05828-0]

48 **OConnor D**, Kok T, Purcell C, Duggan S, Conlon K. Investigating the prevalence of sarcopenia in chronic pancreatitis in an irish cohort: A CT-scan based pilot study. *Pancreatology* 2014; **3**: S74 [DOI: 10.1016/j.pan.2014.05.628]

49 **Olesen SS**, Büyükuslu A, Køhler M, Rasmussen HH, Drewes AM. Sarcopenia associates with increased hospitalization rates and reduced survival in patients with chronic pancreatitis. *Pancreatology* 2019; **19**: 245-251 [PMID: 30665702 DOI: 10.1016/j.pan.2019.01.006]

50 **Verhaegh BP**, Reijven PL, Prins MH, Brouns JH, Masclee AA, Keulemans YC. Nutritional status in patients with chronic pancreatitis. *Eur J Clin Nutr* 2013; **67**: 1271-1276 [PMID: 24129361 DOI: 10.1038/ejcn.2013.199]

51 **Löhr JM**, Dominguez-Munoz E, Rosendahl J, Besselink M, Mayerle J, Lerch MM, Haas S, Akisik F, Kartalis N, Iglesias-Garcia J, Keller J, Boermeester M, Werner J, Dumonceau JM, Fockens P, Drewes A, Ceyhan G, Lindkvist B, Drenth J, Ewald N, Hardt P, de Madaria E, Witt H, Schneider A, Manfredi R, Brøndum FJ, Rudolf S, Bollen T, Bruno M; HaPanEU/UEG Working Group. United European Gastroenterology evidence-based guidelines for the diagnosis and therapy of chronic pancreatitis (HaPanEU). *United European Gastroenterol J* 2017; **5**: 153-199 [PMID: 28344786 DOI: 10.1177/2050640616684695]

52 **de Rijk FE**, Kempeneers MA, Bruno MJ, Besselink MG, van Goor H, Boermeester MA, van Geenen EJ, van Hooft JE, van Santvoort HC, Verdonk RC; Dutch Pancreatitis Study Group. Suboptimal care for chronic pancreatitis patients revealed by moderate to low adherence to the United European Gastroenterology evidence-based guidelines (HaPanEU): A Netherlands nationwide analysis. *United European Gastroenterol J* 2020; **8**: 764-774 [PMID: 32588790 DOI: 10.1177/2050640620937610]

53 **Sikkens EC**, Cahen DL, Koch AD, Braat H, Poley JW, Kuipers EJ, Bruno MJ. The prevalence of fat-soluble vitamin deficiencies and a decreased bone mass in patients with chronic pancreatitis. *Pancreatology* 2013; **13**: 238-242 [PMID: 23719594 DOI: 10.1016/j.pan.2013.02.008]

54 **Duggan SN**, Purcell C, Kilbane M, O'Keane M, McKenna M, Gaffney P, Ridgway PF, Boran G, Conlon KC. An association between abnormal bone turnover, systemic inflammation, and osteoporosis in patients with chronic pancreatitis: a case-matched study. *Am J Gastroenterol* 2015; **110**: 336-345 [PMID: 25623657 DOI: 10.1038/ajg.2014.430]

55 **Lindkvist B**, Phillips ME, Domínguez-Muñoz JE. Clinical, anthropometric and laboratory nutritional markers of pancreatic exocrine insufficiency: Prevalence and diagnostic use. *Pancreatology* 2015; **15**: 589-597 [PMID: 26243045 DOI: 10.1016/j.pan.2015.07.001]

56 **Quilliot D**, Dousset B, Guerci B, Dubois F, Drouin P, Ziegler O. Evidence that diabetes mellitus favors impaired metabolism of zinc, copper, and selenium in chronic pancreatitis. *Pancreas* 2001; **22**: 299-306 [PMID: 11291933 DOI: 10.1097/00006676-200104000-00012]

57 **Papazachariou IM**, Martinez-Isla A, Efthimiou E, Williamson RC, Girgis SI. Magnesium deficiency in patients with chronic pancreatitis identified by an intravenous loading test. *Clin Chim Acta* 2000; **302**: 145-154 [PMID: 11074071 DOI: 10.1016/S0009-8981(00)00363-6]

58 **Vujasinovic M**, Hedström A, Maisonneuve P, Valente R, von Horn H, Löhr JM, Haas SL. Zinc deficiency in patients with chronic pancreatitis. *World J Gastroenterol* 2019; **25**: 600-607 [PMID: 30774274 DOI: 10.3748/wjg.v25.i5.600]

59 **Volatier JL**, Verger P. Recent national French food and nutrient intake data. *Br J Nutr* 1999; **81** Suppl 2: S57-S59 [PMID: 10999027 DOI: 10.1017/s0007114599000902]

60 **Harrington KE**, McGowan MJ, Kiely M, Robson PJ, Livingstone MB, Morrissey PA, Gibney MJ. Macronutrient intakes and food sources in Irish adults: findings of the North/South Ireland Food Consumption Survey. *Public Health Nutr* 2001; **4**: 1051-1060 [PMID: 11820918 DOI: 10.1079/phn2001186]

World Journal of Gastroenterology

Submit a Manuscript: https://www.f6publishing.com

World J Gastroenterol 2021 September 14; 27(34): 5793-5795

DOI: 10.3748/wjg.v27.i34.5793

ISSN 1007-9327 (print) ISSN 2219-2840 (online)

LETTER TO THE EDITOR

Relationship between nonalcoholic fatty liver disease and chronic kidney disease could start in childhood

Anna Di Sessa, Stefano Guarino, Rosa Melone, Rossella Francesca De Simone, Pierluigi Marzuillo, Emanuele Miraglia del Giudice

ORCID number: Anna Di Sessa 0000-0002-5877-3757; Stefano Guarino 0000-0002-0551-5236; Rosa Melone 0000-0001-6897-5742; Rossella Francesca De Simone 0000-0001-5807-7121; Pierluigi Marzuillo 0000-0003-4682-0170; Emanuele Miraglia del Giudice 0000-0002-1492-076X.

Author contributions: Di Sessa A wrote the letter; Di Sessa A, Miraglia del Giudice E and Marzuillo P conceived the manuscript; Miraglia del Giudice E supervised the manuscript drafting; Guarino S, Melone R and De Simone RF reviewed the literature data; each author contributed important intellectual content during manuscript drafting or revision.

Conflict-of-interest statement: Nothing to declare.

Open-Access: This article is an open-access article that was selected by an in-house editor and fully peer-reviewed by external reviewers. It is distributed in accordance with the Creative Commons Attribution NonCommercial (CC BY-NC 4.0) license, which permits others to distribute, remix, adapt, build upon this work non-commercially, and license their derivative works on different terms, provided the original work is properly cited and

Anna Di Sessa, Stefano Guarino, Rosa Melone, Rossella Francesca De Simone, Pierluigi Marzuillo, Emanuele Miraglia del Giudice, Department of Woman, Child, and General and Specialized Surgery, University of Campania Luigi Vanvitelli, Naples 80138, Italy

Corresponding author: Pierluigi Marzuillo, MD, PhD, Assistant Professor, Department of Woman, Child, and General and Specialized Surgery, University of Campania Luigi Vanvitelli, Via de Crecchio, Naples 80138, Italy. pierluigi.marzuillo@gmail.com

Abstract

The relationship between nonalcoholic fatty liver disease (NAFLD) and chronic kidney disease (CKD) has gained considerable scientific interest in adults over the past few years. However, this association has recently emerged in children. Several published studies have suggested a role for NAFLD as a risk factor for CKD from the earliest age, with a potential influence of the major NAFLD risk polymorphisms, resulting in an increased risk of both cardiovascular and metabolic diseases. In view of the progressive course and increased cardio-metabolic risk closely related to NAFLD and CKD, we focused on the link between these diseases in childhood.

Key Words: Nonalcoholic fatty liver disease; Chronic kidney disease; Children; Liver

©The Author(s) 2021. Published by Baishideng Publishing Group Inc. All rights reserved.

Core Tip: Nonalcoholic fatty liver disease has been linked to chronic kidney disease in childhood. Due to the intrinsic cardiometabolic burden related to both diseases, we highlighted the importance of knowledge of this relationship in pediatric patients.

Citation: Di Sessa A, Guarino S, Melone R, De Simone RF, Marzuillo P, Miraglia del Giudice E. Relationship between nonalcoholic fatty liver disease and chronic kidney disease could start in childhood. *World J Gastroenterol* 2021; 27(34): 5793-5795

URL: https://www.wjgnet.com/1007-9327/full/v27/i34/5793.htm

DOI: https://dx.doi.org/10.3748/wjg.v27.i34.5793

the use is non-commercial. See: http://creativecommons.org/Licenses/by-nc/4.0/

Manuscript source: Unsolicited manuscript

Specialty type: Gastroenterology and hepatology

Country/Territory of origin: Italy

Peer-review report's scientific quality classification

Grade A (Excellent): 0
Grade B (Very good): B, B
Grade C (Good): 0
Grade D (Fair): 0
Grade E (Poor): 0

Received: May 4, 2021
Peer-review started: May 4, 2021
First decision: June 12, 2021
Revised: June 21, 2021
Accepted: August 6, 2021
Article in press: August 6, 2021
Published online: September 14, 2021

P-Reviewer: Ali H, Du Y
S-Editor: Fan JR
L-Editor: Kerr C
P-Editor: Liu JH

TO THE EDITOR

We read with interest the review by Mantovani *et al*[1] on the challenging association of nonalcoholic fatty liver disease (NAFLD) with chronic kidney disease (CKD)[1]. The authors provided a comprehensive overview on this association, linking two chronic diseases with a serious cardiometabolic burden and potentially leading to end-stage organ injury, by discussing both pathophysiological and therapeutic aspects.

In our opinion, it is important to underline that the relationship between NAFLD and CKD already occurs in childhood. Parallel to the increasing prevalence of childhood obesity, NAFLD has become the most common chronic liver disease in pediatric patients[2-4]. As demonstrated in adults, there is convincing evidence in children indicating NAFLD as a risk factor for CKD later in life[5-9]. Owing to the shared metabolic pathogenesis (including ectopic lipid accumulation and insulin resistance)[10], NAFLD has been found to be closely inter-related with renal dysfunction in childhood[9,11-14]. There is compelling evidence of a significant reduction in estimated glomerular filtration rate (eGFR) in obese children with NAFLD[8,12,14], as well as possible modulation of the main NAFLD genes (including the I148M *PNPLA3* variant[5,15-17], the E167K allele of *TM6SF2,* and *HSD17B13*)[5, 15]. Early impairments in renal function (such as reduced eGFR and/or abnormal albuminuria) have been observed in children with obesity and NAFLD and linked to the severity of liver disease[8,12-14].

We wish to draw readers' attention to the early subclinical renal involvement in children with obesity and NAFLD. In view of the greater cardiometabolic risk (including type 2 diabetes, cardiovascular disease, and metabolic syndrome)[18-21] of these patients and the potential genetic influence of NAFLD polymorphisms, findings from these studies might have important clinical and prognostic implications at an early age. In our opinion, all children with obesity should undergo abdominal ultrasound to detect fatty liver[22], and careful monitoring with intensive lifestyle-dietary intervention programs. In the future, NAFLD management may also include genetic characterization, which could represent a crucial step to counteract the development of cardiovascular and metabolic disorders already occurring in childhood.

REFERENCES

1 **Mantovani A**, Petracca G, Beatrice G, Tilg H, Byrne CD, Targher G. Non-alcoholic fatty liver disease and risk of incident diabetes mellitus: an updated meta-analysis of 501 022 adult individuals. *Gut* 2021; **70**: 962-969 [PMID: 32938692 DOI: 10.1136/gutjnl-2020-322572]
2 **Sahota AK**, Shapiro WL, Newton KP, Kim ST, Chung J, Schwimmer JB. Incidence of Nonalcoholic Fatty Liver Disease in Children: 2009-2018. *Pediatrics* 2020; **146** [PMID: 33214329 DOI: 10.1542/peds.2020-0771]
3 **Shaunak M**, Byrne CD, Davis N, Afolabi P, Faust SN, Davies JH. Non-alcoholic fatty liver disease and childhood obesity. *Arch Dis Child* 2021; **106**: 3-8 [PMID: 32409495 DOI: 10.1136/archdischild-2019-318063]
4 **Dunn W**, Schwimmer JB. The obesity epidemic and nonalcoholic fatty liver disease in children. *Curr Gastroenterol Rep* 2008; **10**: 67-72 [PMID: 18417045 DOI: 10.1007/s11894-008-0011-1]
5 **Di Sessa A**, Guarino S, Passaro AP, Liguori L, Umano GR, Cirillo G, Miraglia Del Giudice E, Marzuillo P. NAFLD and renal function in children: is there a genetic link? *Expert Rev Gastroenterol Hepatol* 2021; 1-10 [PMID: 33851883 DOI: 10.1080/17474124.2021.1906649]
6 **Musso G**, Gambino R, Tabibian JH, Ekstedt M, Kechagias S, Hamaguchi M, Hultcrantz R, Hagström H, Yoon SK, Charatcharoenwitthaya P, George J, Barrera F, Hafliðadóttir S, Björnsson ES, Armstrong MJ, Hopkins LJ, Gao X, Francque S, Verrijken A, Yilmaz Y, Lindor KD, Charlton M, Haring R, Lerch MM, Rettig R, Völzke H, Ryu S, Li G, Wong LL, Machado M, Cortez-Pinto H, Yasui K, Cassader M. Association of non-alcoholic fatty liver disease with chronic kidney disease: a systematic review and meta-analysis. *PLoS Med* 2014; **11**: e1001680 [PMID: 25050550 DOI: 10.1371/journal.pmed.1001680]
7 **Targher G**, Chonchol M, Zoppini G, Abaterusso C, Bonora E. Risk of chronic kidney disease in patients with non-alcoholic fatty liver disease: is there a link? *J Hepatol* 2011; **54**: 1020-1029 [PMID: 21145850 DOI: 10.1016/j.jhep.2010.11.007]
8 **Yodoshi T**, Arce-Clachar AC, Sun Q, Fei L, Bramlage K, Xanthakos SA, Flores F, Mouzaki M. Glomerular Hyperfiltration Is Associated with Liver Disease Severity in Children with Nonalcoholic Fatty Liver Disease. *J Pediatr* 2020; **222**: 127-133 [PMID: 32381466 DOI: 10.1016/j.jpeds.2020.03.038]
9 **Pacifico L**, Perla FM, Roggini M, Andreoli G, D'Avanzo M, Chiesa C. A Systematic Review of NAFLD-Associated Extrahepatic Disorders in Youths. *J Clin Med* 2019; **8** [PMID: 31213030 DOI: 10.3390/jcm8060868]

10 **Byrne CD**, Targher G. NAFLD as a driver of chronic kidney disease. *J Hepatol* 2020; **72**: 785-801 [PMID: 32059982 DOI: 10.1016/j.jhep.2020.01.013]

11 **Manco M**, Ciampalini P, DeVito R, Vania A, Cappa M, Nobili V. Albuminuria and insulin resistance in children with biopsy proven non-alcoholic fatty liver disease. *Pediatr Nephrol* 2009; **24**: 1211-1217 [PMID: 19242728 DOI: 10.1007/s00467-009-1134-9]

12 **Lin H**, Fu J, Chen X, Huang K, Wu W, Liang L. [Early identification of impaired renal function in obese children with non-alcoholic fatty liver disease]. *Zhejiang Da Xue Xue Bao Yi Xue Ban* 2013; **42**: 381-387 [PMID: 24022925]

13 **Machado MV**, Gonçalves S, Carepa F, Coutinho J, Costa A, Cortez-Pinto H. Impaired renal function in morbid obese patients with nonalcoholic fatty liver disease. *Liver Int* 2012; **32**: 241-248 [PMID: 22098270 DOI: 10.1111/j.1478-3231.2011.02623.x]

14 **Pacifico L**, Bonci E, Andreoli GM, Di Martino M, Gallozzi A, De Luca E, Chiesa C. The Impact of Nonalcoholic Fatty Liver Disease on Renal Function in Children with Overweight/Obesity. *Int J Mol Sci* 2016; **17** [PMID: 27472326 DOI: 10.3390/ijms17081218]

15 **Targher G**, Mantovani A, Alisi A, Mosca A, Panera N, Byrne CD, Nobili V. Relationship Between PNPLA3 rs738409 Polymorphism and Decreased Kidney Function in Children With NAFLD. *Hepatology* 2019; **70**: 142-153 [PMID: 30912854 DOI: 10.1002/hep.30625]

16 **Mantovani A**, Zusi C, Sani E, Colecchia A, Lippi G, Zaza GL, Valenti L, Byrne CD, Maffeis C, Bonora E, Targher G. Association between PNPLA3rs738409 polymorphism decreased kidney function in postmenopausal type 2 diabetic women with or without non-alcoholic fatty liver disease. *Diabetes Metab* 2019; **45**: 480-487 [PMID: 30763699 DOI: 10.1016/j.diabet.2019.01.011]

17 **Musso G**, Cassader M, Gambino R. PNPLA3 rs738409 and TM6SF2 rs58542926 gene variants affect renal disease and function in nonalcoholic fatty liver disease. *Hepatology* 2015; **62**: 658-659 [PMID: 25482317 DOI: 10.1002/hep.27643]

18 **Goldner D**, Lavine JE. Nonalcoholic Fatty Liver Disease in Children: Unique Considerations and Challenges. *Gastroenterology* 2020; **158**: 1967-1983.e1 [PMID: 32201176 DOI: 10.1053/j.gastro.2020.01.048]

19 **Bendor CD**, Bardugo A, Pinhas-Hamiel O, Afek A, Twig G. Cardiovascular morbidity, diabetes and cancer risk among children and adolescents with severe obesity. *Cardiovasc Diabetol* 2020; **19**: 79 [PMID: 32534575 DOI: 10.1186/s12933-020-01052-1]

20 **Peng L**, Wu S, Zhou N, Zhu S, Liu Q, Li X. Clinical characteristics and risk factors of nonalcoholic fatty liver disease in children with obesity. *BMC Pediatr* 2021; **21**: 122 [PMID: 33711964 DOI: 10.1186/s12887-021-02595-2]

21 **Scapaticci S**, D'Adamo E, Mohn A, Chiarelli F, Giannini C. Non-Alcoholic Fatty Liver Disease in Obese Youth With Insulin Resistance and Type 2 Diabetes. *Front Endocrinol (Lausanne)* 2021; **12**: 639548 [PMID: 33889132 DOI: 10.3389/fendo.2021.639548]

22 **Marzuillo P**, Grandone A, Perrone L, Miraglia Del Giudice E. Controversy in the diagnosis of pediatric non-alcoholic fatty liver disease. *World J Gastroenterol* 2015; **21**: 6444-6450 [PMID: 26074683 DOI: 10.3748/wjg.v21.i21.6444]

Published by **Baishideng Publishing Group Inc**
7041 Koll Center Parkway, Suite 160, Pleasanton, CA 94566, USA
Telephone: +1-925-3991568
E-mail: bpgoffice@wjgnet.com
Help Desk: https://www.f6publishing.com/helpdesk
https://www.wjgnet.com

© 2021 Baishideng Publishing Group Inc. All rights reserved.

ISSN 1007-9327 (print)
ISSN 2219-2840 (online)

World Journal of *Gastroenterology*

World J Gastroenterol 2021 September 21; 27(35): 5796-5988



Published by Baishideng Publishing Group Inc

World Journal of Gastroenterology

Contents

Weekly Volume 27 Number 35 September 21, 2021

EDITORIAL

5796 Induced pluripotent stem cells as an innovative model to study drug induced pancreatitis

Genova E, Stocco G, Decorti G

OPINION REVIEW

5803 Screening for nonalcoholic fatty liver disease-when, who and how?

Dietrich CG, Rau M, Geier A

REVIEW

5822 Environmental perspectives of COVID-19 outbreaks: A review

Samanta P, Ghosh AR

5851 Pancreatic cancer in 2021: What you need to know to win

Tonini V, Zanni M

5890 Gastrinoma and Zollinger Ellison syndrome: A roadmap for the management between new and old therapies

Rossi RE, Elvevi A, Citterio D, Coppa J, Invernizzi P, Mazzaferro V, Massironi S

MINIREVIEWS

5908 Optical diagnosis of colorectal polyps using convolutional neural networks

Kader R, Hadjinicolaou AV, Georgiades F, Stoyanov D, Lovat LB

5919 Liver-spleen axis dysfunction in COVID-19

Cococcia S, Lenti MV, Santacroce G, Achilli G, Borrelli de Andreis F, Di Sabatino A

5932 Primary gastric non-Hodgkin lymphomas: Recent advances regarding disease pathogenesis and treatment

Diamantidis MD, Papaioannou M, Hatjiharissi E

ORIGINAL ARTICLE

Basic Study

5946 Proteomics identifies a novel role of fibrinogen-like protein 1 in Crohn's disease

Sun XL, Qiao LC, Gong J, Wen K, Xu ZZ, Yang BL

Retrospective Study

5958 Effectiveness and safety of over-the-scope clip in closing perforations after duodenal surgery

Wang ZZ, Zhou XB, Wang Y, Mao XL, Ye LP, Yan LL, Chen YH, Song YQ, Cai Y, Xu SW, Li SW

5967 Hepatic perivascular epithelioid cell tumor: Clinicopathological analysis of 26 cases with emphasis on disease management and prognosis

Zhang S, Yang PP, Huang YC, Chen HC, Chen DL, Yan WT, Yang NN, Li Y, Li N, Feng ZZ

5978 Diagnosis of focal liver lesions with deep learning-based multi-channel analysis of hepatocyte-specific contrast-enhanced magnetic resonance imaging

Stollmayer R, Budai BK, Tóth A, Kalina I, Hartmann E, Szoldán P, Bérczi V, Maurovich-Horvat P, Kaposi PN

Contents

ABOUT COVER

Editorial Board Member of *World Journal of Gastroenterology*, Haruhiko Sugimura, PhD, MD, Vice President, Hamamatsu University School of Medicine; Professor and Chairman of the Department of Tumor Pathology, Hamamatsu University School of Medicine, 1-20-1 Handayama, Higashi-ku, Hamamatsu 431-3192, Japan. hsugimur@hama-med.ac.jp

AIMS AND SCOPE

The primary aim of *World Journal of Gastroenterology* (*WJG*, *World J Gastroenterol*) is to provide scholars and readers from various fields of gastroenterology and hepatology with a platform to publish high-quality basic and clinical research articles and communicate their research findings online. *WJG* mainly publishes articles reporting research results and findings obtained in the field of gastroenterology and hepatology and covering a wide range of topics including gastroenterology, hepatology, gastrointestinal endoscopy, gastrointestinal surgery, gastrointestinal oncology, and pediatric gastroenterology.

INDEXING/ABSTRACTING

The *WJG* is now indexed in Current Contents®/Clinical Medicine, Science Citation Index Expanded (also known as SciSearch®), Journal Citation Reports®, Index Medicus, MEDLINE, PubMed, PubMed Central, and Scopus. The 2021 edition of Journal Citation Report® cites the 2020 impact factor (IF) for *WJG* as 5.742; Journal Citation Indicator: 0.79; IF without journal self cites: 5.590; 5-year IF: 5.044; Ranking: 28 among 92 journals in gastroenterology and hepatology; and Quartile category: Q2. The *WJG*'s CiteScore for 2020 is 6.9 and Scopus CiteScore rank 2020: Gastroenterology is 19/136.

RESPONSIBLE EDITORS FOR THIS ISSUE

Production Editor: *Yan-Xia Xing*; **Production Department Director:** *Xiang Li*; **Editorial Office Director:** *Ze-Mao Gong*.

NAME OF JOURNAL
World Journal of Gastroenterology

ISSN
ISSN 1007-9327 (print) ISSN 2219-2840 (online)

LAUNCH DATE
October 1, 1995

FREQUENCY
Weekly

EDITORS-IN-CHIEF
Andrzej S Tarnawski, Subrata Ghosh

EDITORIAL BOARD MEMBERS
http://www.wjgnet.com/1007-9327/editorialboard.htm

PUBLICATION DATE
September 21, 2021

COPYRIGHT
© 2021 Baishideng Publishing Group Inc

INSTRUCTIONS TO AUTHORS
https://www.wjgnet.com/bpg/gerinfo/204

GUIDELINES FOR ETHICS DOCUMENTS
https://www.wjgnet.com/bpg/GerInfo/287

GUIDELINES FOR NON-NATIVE SPEAKERS OF ENGLISH
https://www.wjgnet.com/bpg/gerinfo/240

PUBLICATION ETHICS
https://www.wjgnet.com/bpg/GerInfo/288

PUBLICATION MISCONDUCT
https://www.wjgnet.com/bpg/gerinfo/208

ARTICLE PROCESSING CHARGE
https://www.wjgnet.com/bpg/gerinfo/242

STEPS FOR SUBMITTING MANUSCRIPTS
https://www.wjgnet.com/bpg/GerInfo/239

ONLINE SUBMISSION
https://www.f6publishing.com

© 2021 Baishideng Publishing Group Inc. All rights reserved. 7041 Koll Center Parkway, Suite 160, Pleasanton, CA 94566, USA
E-mail: bpgoffice@wjgnet.com https://www.wjgnet.com

World Journal of Gastroenterology

Submit a Manuscript: https://www.f6publishing.com

World J Gastroenterol 2021 September 21; 27(35): 5796-5802

DOI: 10.3748/wjg.v27.i35.5796

ISSN 1007-9327 (print) ISSN 2219-2840 (online)

EDITORIAL

Induced pluripotent stem cells as an innovative model to study drug induced pancreatitis

Elena Genova, Gabriele Stocco, Giuliana Decorti

ORCID number: Elena Genova 0000-0002-6692-6573; Gabriele Stocco 0000-0003-0964-5879; Giuliana Decorti 0000-0002-9714-6246.

Author contributions: Genova E, Stocco G and Decorti G designed the research study, reviewed and edited the manuscript; Genova E performed the research and wrote the manuscript; all authors have read and approved the final manuscript.

Supported by Italian Ministry of Health (IRCCS Burlo Garofolo), No. RC 7_2014.

Conflict-of-interest statement: Authors have nothing to disclose.

Open-Access: This article is an open-access article that was selected by an in-house editor and fully peer-reviewed by external reviewers. It is distributed in accordance with the Creative Commons Attribution NonCommercial (CC BY-NC 4.0) license, which permits others to distribute, remix, adapt, build upon this work non-commercially, and license their derivative works on different terms, provided the original work is properly cited and the use is non-commercial. See: http://creativecommons.org/Licenses/by-nc/4.0/

Manuscript source: Invited

Elena Genova, Giuliana Decorti, Institute for Maternal and Child Health, IRCCS Burlo Garofolo, Trieste 34137, Italy

Gabriele Stocco, Department of Life Sciences, University of Trieste, Trieste 34127, Italy

Giuliana Decorti, Department of Medical, Surgical and Health Sciences, University of Trieste, Trieste 34127, Italy

Corresponding author: Giuliana Decorti, MD, Full Professor, Institute for Maternal and Child Health, IRCCS Burlo Garofolo, Via dell'Istria 65, Trieste 34137, Italy. decorti@units.it

Abstract

Drug-induced pancreatitis is a gastrointestinal adverse effect concerning about 2% of drugs. The majority of cases are mild to moderate but severe episodes can also occur, leading to hospitalization or even death. Unfortunately, the mechanisms of this adverse reaction are still not clear, hindering its prevention, and the majority of data available of this potentially life-threatening adverse effect are limited to case reports leading to a probable underestimation of this event. In particular, in this editorial, special attention is given to thiopurine-induced pancreatitis (TIP), an idiosyncratic adverse reaction affecting around 5% of inflammatory bowel disease (IBD) patients taking thiopurines as immunosuppressants, with a higher incidence in the pediatric population. Validated biomarkers are not available to assist clinicians in the prevention of TIP, also because of the inaccessibility of the pancreatic tissue, which limits the possibility to perform dedicated cellular and molecular studies. In this regard, induced pluripotent stem cells (iPSCs) and the exocrine pancreatic differentiated counterpart could be a great tool to investigate the cellular and molecular mechanisms underlying the development of this undesirable event. This particular type of stem cells is obtained by reprogramming adult cells, including fibroblasts and leukocytes, with a set of transcription factors known as the Yamanaka's factors. Maintaining unaltered the donors' genetic heritage, iPSCs represent an innovative model to study the mechanisms of adverse drug reactions in individual patients' tissues not easily obtainable from human probands. Indeed, iPSCs can differentiate under adequate stimuli into almost any somatic lineage, opening a new world of opportunities for researchers. Several works are already available in the literature studying liver, central nervous system and cardiac cells derived from iPSCs and adverse drug effects. However, to our knowledge no studies have been performed on exocrine pancreas differentiated from iPSCs and drug-induced pancreatitis, so far. Hence, in

manuscript

Specialty type: Gastroenterology and hepatology

Country/Territory of origin: Italy

Peer-review report's scientific quality classification

Grade A (Excellent): A
Grade B (Very good): B
Grade C (Good): C
Grade D (Fair): 0
Grade E (Poor): 0

Received: March 17, 2021
Peer-review started: March 17, 2021
First decision: April 16, 2021
Revised: April 27, 2021
Accepted: August 30, 2021
Article in press: August 30, 2021
Published online: September 21, 2021

P-Reviewer: Maharshi S, Nayudu SK, Soliman YY
S-Editor: Fan JR
L-Editor: A
P-Editor: Yuan YY

this editorial we focus specifically on the description of the study of the mechanisms of TIP by using IBD patient-specific iPSCs and exocrine pancreatic differentiated cells as innovative *in vitro* models.

Key Words: Induced pluripotent stem cells; Therapy personalization; Patient-specific cells; Drug-induced pancreatitis; Thiopurines; Inflammatory bowel disease

©The Author(s) 2021. Published by Baishideng Publishing Group Inc. All rights reserved.

Core Tip: About 5% of inflammatory bowel disease patients develop pancreatitis after thiopurine administration. The mechanism of this adverse effect is still not clear making it difficult to prevent. By differentiating induced pluripotent stem cells into their pancreatic exocrine counterpart, it is possible to set up innovative personalized *in vitro* models to study this adverse effect in a more effective way.

Citation: Genova E, Stocco G, Decorti G. Induced pluripotent stem cells as an innovative model to study drug induced pancreatitis. *World J Gastroenterol* 2021; 27(35): 5796-5802
URL: https://www.wjgnet.com/1007-9327/full/v27/i35/5796.htm
DOI: https://dx.doi.org/10.3748/wjg.v27.i35.5796

INTRODUCTION

Gastrointestinal adverse effects are common especially with orally absorbed drugs and may result in undesirable consequences leading to the reduction of treatment efficacy and, in the most serious cases, to therapy interruption with associated healthcare costs. To better study and prevent these adverse events there is the need for dedicated clinical investigation[1]. Over the past years, adverse drug reactions (ADRs) have been widely studied also for their negative effect on the development of new drugs[2,3].

Among the different ADRs, drug-induced pancreatitis has become increasingly recognized as an important cause of acute pancreatitis with a wide range of drug classes involved in its development[4]. Unfortunately, the majority of data available of this potentially life-threatening ADR are principally limited to case reports, leading to a probably underestimated incidence, reported to be around 2%[4]. Furthermore, the mechanisms of drug-induced pancreatitis of many drugs are still not clear, making it difficult to determine a definitive association of causality between specific medications and acute pancreatitis, and in only less than 10% of cases the real cause has been determined. Drugs known to induce pancreatitis have been classified considering the number of case reports, the recurrence of pancreatitis with a re-challenge with the drug, consistent latency between the drug assumption and the onset of acute pancreatitis and the exclusion of alternative causes such as alcohol assumption or gallstones [4,5] (Table 1).

Interestingly, certain types of ADRs are reported to be more frequent in patients affected by specific diseases. An important example is thiopurine-induced pancreatitis (TIP), an idiosyncratic ADR affecting more frequently inflammatory bowel disease (IBD) patients taking thiopurines, such as azathioprine and mercaptopurine[6]. In the vast majority of cases, TIP is manageable, however patients have to stop the treatment and to be sometimes hospitalized until the symptoms are resolved[7]. The higher incidence of this adverse event in IBD patients, especially in the pediatric population, suggests that molecular mechanisms involved in the disease may contribute to TIP predisposition[6]. However, mechanisms determining TIP predisposition are still unknown and only hypotheses have been postulated. In particular, the mechanisms proposed can be divided into three different groups: genetic predisposition[8,9], alteration in thiopurine biotransformation[7] and abnormalities in innate or adaptative immunity[10].

The thiopurines azathioprine, mercaptopurine and thioguanine undergo an extensive biotransformation catalyzed by several enzymes[11]. Regarding genetic predisposition, TIP seems unrelated to candidate variants on important genes of the thiopurine biotransformation pathway, such as *TPMT, ITPA* and *NUDT15*, well-known to induce severe ADRs, including myelosuppression and hematologic toxicity[12,13].

Table 1 Classification system of drugs related to pancreatitis development[4,5]

Class	
Class Ia	At least one case report with positive rechallenge, excluding other possible causes such as alcohol, gallstones and other drugs
Class Ib	At least one case report with positive rechallenge but not excluding other possible causes
Class II	At least four cases in the literature without rechallenge but with consistent latency in greater than 75% of cases
Class III	At least two cases in the literature without rechallenge and consistent latency
Class IV	Single case reported in the literature not fitting the previous described classed without rechallenge

Recently, two different research groups have found a strong association between the Class II *HLA* gene region polymorphism rs2647087 and TIP[8,9], but more efforts are needed to translate these variants into clinical practice. TIP development may be also related to direct damage to the exocrine pancreatic cells or to an accumulation of toxic metabolites (biotransformation hypothesis). However, pancreatitis frequently occurs early after thiopurine administration, making the accumulation of toxic metabolites unlikely, while more probably immunological reactions are involved. However, direct toxicity of thiopurines or their metabolites on patients' pancreatic cells cannot be completely excluded[7,10].

To study and discover TIP mechanisms and predisposition, innovative patient-specific *in vitro* models could be helpful and decisive. In this regard, induced pluripotent stem cells (iPSCs) and their differentiated counterpart are widely used to set up groundbreaking personalized *in vitro* models representative of patients' genetic background. The peculiar characteristics of these cells allow to set up *in vitro* models to study disease mechanisms and ADRs with the purpose to personalize patients' therapy, improving the disease outcome. The iPSC model can be a great tool to better understand, and thus prevent, ADRs in particular in comparison to animal models and immortalized cells. Indeed, the predisposition to a specific ADR may be related to the individual genetic patients' background, leading to a wide range of toxicities of different severity[14]. Therefore, the iPSC technology, matching the donor's genetic background, can be extremely helpful for developing patient-specific assays. Indeed, by using iPSCs, it seems reasonable to precisely mimic the patients' susceptibility to an abnormal response to a specific drug, setting up powerful assays useful to identify predictive biomarkers. In the last years, many different models[15] have been developed using the iPSC technology, including the differentiation into pancreatic exocrine cells[16].

PATIENT-SPECIFIC IPSCS AS AN IN VITRO MODEL TO STUDY DRUG-INDUCED PANCREATITIS

Patient-specific iPSCs can be obtained by reprogramming patients' fibroblasts or peripheral blood mononuclear cells using the four Yamanaka's factors OCT4, SOX2, KLF4 and MYC, forcing somatic cells to an embryonic-like state[17,18]. Differentiation of iPSCs allows to generate almost any kind of somatic cells using appropriate protocols. In the literature it is possible to find a wide range of differentiation possibilities including neural-like cells, hepatocytes, enterocytes, pancreatic endocrine cells and many others as recently reviewed by our group[15]. These cells, being patient-specific, have been frequently used to model and study individual susceptibility to develop ADRs. For example, regarding gastrointestinal toxicity, some groups have already tried to model hepatocytes[19-21] and enterocytes[22,23] to study drug-induced liver injury and intestinal toxicity, respectively. However, in comparison to other ADRs, drug-induced pancreatitis has not been deeply studied yet. A limited number of protocols[16,24-26] are available in the literature to generate pancreatic exocrine cells starting from iPSCs in comparison to the endocrine counterpart[15]. To the best of our knowledge, our group recently evaluated for the first time the mechanisms behind TIP predisposition using iPSCs and pancreatic differentiated cells of pediatric patients affected by IBD that developed or not TIP. Differentiation of iPSCs in pancreatic exocrine cells was performed using the protocol developed by Takizawa-Shirasawa *et al*[16]. Briefly, different stimuli were added to the culture medium in 4 different steps (Figure 1). To characterize cells obtained during each differentiation step, genetic expression of specific genetic markers was analyzed and confirmed:

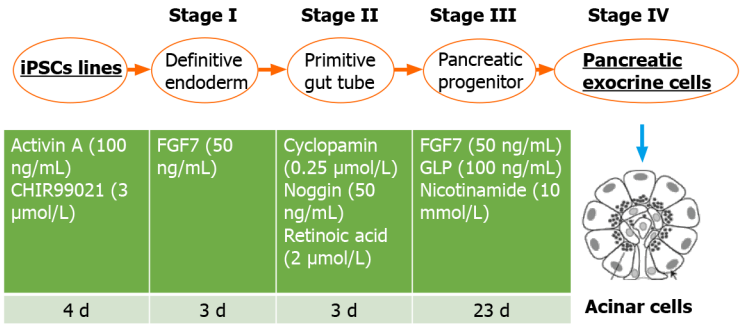


Figure 1 Differentiation of induced pluripotent stem cells into pancreatic cells towards a 4 steps protocol. iPSCs: Induced pluripotent stem cells; d: Days of culture.

OCT4 for undifferentiated cells (iPSCs), *FOXA2* and *SOX17* for definitive endoderm (stage I), *PDX1* for pancreatic progenitors (stage III) and amylase, in particular its pancreatic isoforms *AMY2A* and *AMY2B* for pancreatic exocrine cells (stage IV).

The gold standard of cytotoxicity assay showed an almost double *in vitro* sensitivity of TIP cases cells to thiopurines, more marked in iPSCs rather than in the differentiated counterpart, after mercaptopurine and thioguanine exposure. *TPMT* variants (rs1142345, rs1800460 and rs1800462) were excluded as a possible cause of this different sensitivity because all patients resulted wild-type.

The results obtained are encouraging, however some limitations have to be overcome in the next future. For instance, the differentiation protocol to obtain exocrine pancreatic cells could be further improved in terms of efficiency based on the more recent studies performed by Hohwieler *et al*[24] and Ito *et al*[25] which used 3D culture methods and the distinction between acinar and ductal cell type, by analyzing the expression of different genetic and protein markers such as amylase and chymotrypsin C for acinar cells, and SOX9 and cytokeratin 19 for ductal cells[24,25]. An important point to consider is if the amylase markers are sufficient to reflect terminal differentiation. Beside studies considering the mRNA levels of these markers[24,25], more functional studies, evaluating the amylase protein concentrations and enzyme activity, should be implemented. These comparisons would allow to ensure that terminal differentiation is as representative as possible of the *in vivo* models. Another important point to focus, linked to pancreatic cell generation, is the time necessary that is too long for a clinical application of this *in vitro* model for TIP predisposition screening. Studies are now ongoing to partially resolve this limitation trying to develop more efficient and faster ready-to-use patient-specific pancreatic exocrine differentiated cells. The cost of hospitalization after a pancreatitis event has been recently calculated, resulting in around 8000 € *per* patient[27]. Considering an incidence of pancreatitis of 5%, we can estimate that every 20 patients treated with azathioprine one will be at risk of pancreatitis. Therefore, to be cost-effective, the analysis should amount to 400 €, considering only the cost of the analysis, without evaluating the health benefit[28]. Current costs are still higher but there is a trend toward reduction; indeed, the iPSC technology is still expensive and costs have to be reduced before they can be introduced into clinical practice. In particular, characterization costs are high, but several suggestions to address this limitation have been already proposed such as SNP microarray technology for the routine karyotyping and cost-effective methods such as innovative flow cytometry analyses to assess cell surface expression of pluripotent markers[29].

Beyond technical limitations, it is conceivable that thiopurines do not directly reach the pancreatic tissue unmodified, but rather as metabolites. Therefore, to improve the clinical relevance of the *in vitro* model, patient-specific pancreatic cells would need to be exposed to a representative mixture of thiopurine metabolites or to conditioned media of other thiopurine metabolizing cells such as hepatocytes[30]. Moreover, it is important to keep in mind that TIP predisposition could be influenced by the contribution of the immune system that, in predisposed patients, could be activated for unknown reasons after thiopurine administration attacking the pancreatic tissue. This aspect has to be considered, modeled and studied as well[7,31]. Finally, data obtained have to be confirmed in a larger cohort of patients that now includes 3 cases and 3 controls already analyzed while 2 cases and 2 controls still have to be analyzed.

CLINICAL IMPLICATIONS

Drug-induced pancreatitis represents an important clinical issue for different reasons including therapy interruption, reduction of treatment efficacy, the need for unnecessary diagnostic procedures and treatment for the adverse effect resolution[1] with associated healthcare costs. Moreover, in recent years an increasing number of drugs have been associated with pancreatitis development although its recognition by clinicians is still limited because of the lack of biomarkers useful to prevent this ADR.

CONCLUSION

Drug-induced pancreatitis is a growing problem related to several drugs and TIP recapitulates well all complications related to the development of this ADR. The possibility of studying TIP by an iPSC-based model seems a great opportunity to investigate TIP mechanisms that still remain not clear. The *in vitro* model established in our laboratory has proven to be suitable for studying and investigating TIP predisposition in a personalized way in pediatric IBD patients. Alongside thiopurines, several other drugs such as asparaginase, nilotinib and pazopanib can cause pancreatitis. Therefore, the *in vitro* model developed in this study could be applied also to study the sensitivity of other drugs with the purpose of pancreatitis prevention.

REFERENCES

1 **Philpott HL**, Nandurkar S, Lubel J, Gibson PR. Drug-induced gastrointestinal disorders. *Frontline Gastroenterol* 2014; **5**: 49-57 [PMID: 28839751 DOI: 10.1136/flgastro-2013-100316]

2 **Guengerich FP**. Mechanisms of drug toxicity and relevance to pharmaceutical development. *Drug Metab Pharmacokinet* 2011; **26**: 3-14 [PMID: 20978361 DOI: 10.2133/dmpk.dmpk-10-rv-062]

3 **Timilsina M**, Tandan M, d'Aquin M, Yang H. Discovering Links Between Side Effects and Drugs Using a Diffusion Based Method. *Sci Rep* 2019; **9**: 10436 [PMID: 31320740 DOI: 10.1038/s41598-019-46939-6]

4 **Weissman S**, Aziz M, Perumpail RB, Mehta TI, Patel R, Tabibian JH. Ever-increasing diversity of drug-induced pancreatitis. *World J Gastroenterol* 2020; **26**: 2902-2915 [PMID: 32587438 DOI: 10.3748/wjg.v26.i22.2902]

5 **Badalov N**, Baradarian R, Iswara K, Li J, Steinberg W, Tenner S. Drug-induced acute pancreatitis: an evidence-based review. *Clin Gastroenterol Hepatol* 2007; **5**: 648-61; quiz 644 [PMID: 17395548 DOI: 10.1016/j.cgh.2006.11.023]

6 **Ramos LR**, Sachar DB, DiMaio CJ, Colombel JF, Torres J. Inflammatory Bowel Disease and Pancreatitis: A Review. *J Crohns Colitis* 2016; **10**: 95-104 [PMID: 26351384 DOI: 10.1093/ecco-jcc/jjv153]

7 **Stocco G**, Lanzi G, Yue F, Giliani S, Sasaki K, Tommasini A, Pelin M, Martelossi S, Ventura A, Decorti G. Patients' Induced Pluripotent Stem Cells to Model Drug Induced Adverse Events: A Role in Predicting Thiopurine Induced Pancreatitis? *Curr Drug Metab* 2015; **17**: 91-98 [PMID: 26526832 DOI: 10.2174/1389200216666151103120220]

8 **Heap GA**, Weedon MN, Bewshea CM, Singh A, Chen M, Satchwell JB, Vivian JP, So K, Dubois PC, Andrews JM, Annese V, Bampton P, Barnardo M, Bell S, Cole A, Connor SJ, Creed T, Cummings FR, D'Amato M, Daneshmend TK, Fedorak RN, Florin TH, Gaya DR, Greig E, Halfvarson J, Hart A, Irving PM, Jones G, Karban A, Lawrance IC, Lee JC, Lees C, Lev-Tzion R, Lindsay JO, Mansfield J, Mawdsley J, Mazhar Z, Parkes M, Parnell K, Orchard TR, Radford-Smith G, Russell RK, Reffitt D, Satsangi J, Silverberg MS, Sturniolo GC, Tremelling M, Tsianos EV, van Heel DA, Walsh A, Watermeyer G, Weersma RK, Zeissig S, Rossjohn J, Holden AL; International Serious Adverse Events Consortium; IBD Pharmacogenetics Study Group, Ahmad T. HLA-DQA1-HLA-DRB1 variants confer susceptibility to pancreatitis induced by thiopurine immunosuppressants. *Nat Genet* 2014; **46**: 1131-1134 [PMID: 25217962 DOI: 10.1038/ng.3093]

9 **Wilson A**, Jansen LE, Rose RV, Gregor JC, Ponich T, Chande N, Khanna R, Yan B, Jairath V, Khanna N, Sey M, Beaton M, McIntosh K, Teft WA, Kim RB. HLA-DQA1-HLA-DRB1 polymorphism is a major predictor of azathioprine-induced pancreatitis in patients with inflammatory bowel disease. *Aliment Pharmacol Ther* 2018; **47**: 615-620 [PMID: 29270995 DOI: 10.1111/apt.14483]

10 **Weersma RK**, Batstra MR, Kleibeuker JH, van Dullemen HM. Are pancreatic autoantibodies associated with azathioprine-induced pancreatitis in Crohn's disease? *JOP* 2008; **9**: 283-289 [PMID: 18469440]

11 **Zaza G**, Cheok M, Krynetskaia N, Thorn C, Stocco G, Hebert JM, McLeod H, Weinshilboum RM, Relling MV, Evans WE, Klein TE, Altman RB. Thiopurine pathway. *Pharmacogenet Genomics* 2010; **20**: 573-574 [PMID: 19952870 DOI: 10.1097/FPC.0b013e328334338f]

12 **Zabala-Fernández W**, Barreiro-de Acosta M, Echarri A, Carpio D, Lorenzo A, Castro J, Martínez-

Ares D, Pereira S, Martin-Granizo I, Corton M, Carracedo A, Barros F. A pharmacogenetics study of TPMT and ITPA genes detects a relationship with side effects and clinical response in patients with inflammatory bowel disease receiving Azathioprine. *J Gastrointestin Liver Dis* 2011; **20**: 247-253 [PMID: 21961091]

13 **Moriyama T**, Nishii R, Perez-Andreu V, Yang W, Klussmann FA, Zhao X, Lin TN, Hoshitsuki K, Nersting J, Kihira K, Hofmann U, Komada Y, Kato M, McCorkle R, Li L, Koh K, Najera CR, Kham SK, Isobe T, Chen Z, Chiew EK, Bhojwani D, Jeffries C, Lu Y, Schwab M, Inaba H, Pui CH, Relling MV, Manabe A, Hori H, Schmiegelow K, Yeoh AE, Evans WE, Yang JJ. NUDT15 polymorphisms alter thiopurine metabolism and hematopoietic toxicity. *Nat Genet* 2016; **48**: 367-373 [PMID: 26878724 DOI: 10.1038/ng.3508]

14 **Wilke RA**, Lin DW, Roden DM, Watkins PB, Flockhart D, Zineh I, Giacomini KM, Krauss RM. Identifying genetic risk factors for serious adverse drug reactions: current progress and challenges. *Nat Rev Drug Discov* 2007; **6**: 904-916 [PMID: 17971785 DOI: 10.1038/nrd2423]

15 **Genova E**, Cavion F, Lucafò M, Leo L, Pelin M, Stocco G, Decorti G. Induced pluripotent stem cells for therapy personalization in pediatric patients: Focus on drug-induced adverse events. *World J Stem Cells* 2019; **11**: 1020-1044 [PMID: 31875867 DOI: 10.4252/wjsc.v11.i12.1020]

16 **Takizawa-Shirasawa S**, Yoshie S, Yue F, Mogi A, Yokoyama T, Tomotsune D, Sasaki K. FGF7 and cell density are required for final differentiation of pancreatic amylase-positive cells from human ES cells. *Cell Tissue Res* 2013; **354**: 751-759 [PMID: 23996199 DOI: 10.1007/s00441-013-1695-6]

17 **Fusaki N**, Ban H, Nishiyama A, Saeki K, Hasegawa M. Efficient induction of transgene-free human pluripotent stem cells using a vector based on Sendai virus, an RNA virus that does not integrate into the host genome. *Proc Jpn Acad Ser B Phys Biol Sci* 2009; **85**: 348-362 [PMID: 19838014 DOI: 10.2183/pjab.85.348]

18 **Takahashi K**, Yamanaka S. Induction of pluripotent stem cells from mouse embryonic and adult fibroblast cultures by defined factors. *Cell* 2006; **126**: 663-676 [PMID: 16904174 DOI: 10.1016/j.cell.2006.07.024]

19 **Kondo Y**, Iwao T, Nakamura K, Sasaki T, Takahashi S, Kamada N, Matsubara T, Gonzalez FJ, Akutsu H, Miyagawa Y, Okita H, Kiyokawa N, Toyoda M, Umezawa A, Nagata K, Matsunaga T, Ohmori S. An efficient method for differentiation of human induced pluripotent stem cells into hepatocyte-like cells retaining drug metabolizing activity. *Drug Metab Pharmacokinet* 2014; **29**: 237-243 [PMID: 24334537 DOI: 10.2133/dmpk.dmpk-13-rg-104]

20 **Kang SJ**, Lee HM, Park YI, Yi H, Lee H, So B, Song JY, Kang HG. Chemically induced hepatotoxicity in human stem cell-induced hepatocytes compared with primary hepatocytes and HepG2. *Cell Biol Toxicol* 2016; **32**: 403-417 [PMID: 27287938 DOI: 10.1007/s10565-016-9342-0]

21 **Liu J**, Brzeszczynska J, Samuel K, Black J, Palakkan A, Anderson RA, Gallagher R, Ross JA. Efficient episomal reprogramming of blood mononuclear cells and differentiation to hepatocytes with functional drug metabolism. *Exp Cell Res* 2015; **338**: 203-213 [PMID: 26256888 DOI: 10.1016/j.yexcr.2015.08.004]

22 **Kondo S**, Mizuno S, Hashita T, Iwao T, Matsunaga T. Using human iPS cell-derived enterocytes as novel *in vitro* model for the evaluation of human intestinal mucosal damage. *Inflamm Res* 2018; **67**: 975-984 [PMID: 30317465 DOI: 10.1007/s00011-018-1193-0]

23 **Ozawa T**, Takayama K, Okamoto R, Negoro R, Sakurai F, Tachibana M, Kawabata K, Mizuguchi H. Generation of enterocyte-like cells from human induced pluripotent stem cells for drug absorption and metabolism studies in human small intestine. *Sci Rep* 2015; **5**: 16479 [PMID: 26559489 DOI: 10.1038/srep16479]

24 **Hohwieler M**, Illing A, Hermann PC, Mayer T, Stockmann M, Perkhofer L, Eiseler T, Antony JS, Müller M, Renz S, Kuo CC, Lin Q, Sendler M, Breunig M, Kleiderman SM, Lechel A, Zenker M, Leichsenring M, Rosendahl J, Zenke M, Sainz B Jr, Mayerle J, Costa IG, Seufferlein T, Kormann M, Wagner M, Liebau S, Kleger A. Human pluripotent stem cell-derived acinar/ductal organoids generate human pancreas upon orthotopic transplantation and allow disease modelling. *Gut* 2017; **66**: 473-486 [PMID: 27633923 DOI: 10.1136/gutjnl-2016-312423]

25 **Ito K**, Matsuura K, Mihara Y, Sakamoto Y, Hasegawa K, Kokudo N, Shimizu T. Delivery of pancreatic digestive enzymes into the gastrointestinal tract by pancreatic exocrine tissue transplant. *Sci Rep* 2019; **9**: 5922 [PMID: 30976035 DOI: 10.1038/s41598-019-42362-z]

26 **Huang L**, Holtzinger A, Jagan I, BeGora M, Lohse I, Ngai N, Nostro C, Wang R, Muthuswamy LB, Crawford HC, Arrowsmith C, Kalloger SE, Renouf DJ, Connor AA, Cleary S, Schaeffer DF, Roehrl M, Tsao MS, Gallinger S, Keller G, Muthuswamy SK. Ductal pancreatic cancer modeling and drug screening using human pluripotent stem cell- and patient-derived tumor organoids. *Nat Med* 2015; **21**: 1364-1371 [PMID: 26501191 DOI: 10.1038/nm.3973]

27 **Wilson A**, Wang Q, Choi YH, Ponich T, Gregor JC, Chande N, Yan B, Sey M, Beaton M, Kim RB. Pretreatment HLADQA1-HLADRB1 Testing for the Prevention of Azathioprine-Induced Pancreatitis in Inflammatory Bowel Disease: A Prospective Cohort Study. *Clin Transl Gastroenterol* 2021; **12**: e00332 [PMID: 33821842 DOI: 10.14309/ctg.0000000000000332]

28 **Owens DK**. Interpretation of cost-effectiveness analyses. *J Gen Intern Med* 1998; **13**: 716-717 [PMID: 9798822 DOI: 10.1046/j.1525-1497.1998.00211.x]

29 **Malihi G**, Nikoui V, Elson EL. A review on qualifications and cost effectiveness of induced pluripotent stem cells (IPSCs)-induced cardiomyocytes in drug screening tests. *Arch Physiol Biochem* 2020; 1-12 [PMID: 32783745 DOI: 10.1080/13813455.2020.1802600]

30 **Vikingsson S**, Carlsson B, Almer SH, Peterson C. Monitoring of thiopurine metabolites in patients

with inflammatory bowel disease-what is actually measured? *Ther Drug Monit* 2009; **31**: 345-350 [PMID: 19363461 DOI: 10.1097/FTD.0b013e3181a1ea58]

31 **Hung WY**, Abreu Lanfranco O. Contemporary review of drug-induced pancreatitis: A different perspective. *World J Gastrointest Pathophysiol* 2014; **5**: 405-415 [PMID: 25400984 DOI: 10.4291/wjgp.v5.i4.405]

World Journal of Gastroenterology

Submit a Manuscript: https://www.f6publishing.com

World J Gastroenterol 2021 September 21; 27(35): 5803-5821

DOI: 10.3748/wjg.v27.i35.5803

ISSN 1007-9327 (print) ISSN 2219-2840 (online)

OPINION REVIEW

Screening for nonalcoholic fatty liver disease-when, who and how?

Christoph G Dietrich, Monika Rau, Andreas Geier

ORCID number: Christoph G Dietrich 0000-0001-6927-7970; Monika Rau 0000-0003-1219-4044; Andreas Geier 0000-0002-9626-5083.

Author contributions: Dietrich CG and Geier A developed the concept of this review; all authors contributed to the manuscript.

Conflict-of-interest statement: CGD reports personal speaker fees from Falk Foundation. MR declares no conflict of interest. AG serves as advisor and steering committee member for AbbVie, Alexion, Bayer, BMS, CSL Behring, Eisai, Gilead, Intercept, Ipsen, Merz, MSD, Novartis, Pfizer, Roche, Sanofi-Aventis, Sequana and as speaker for AbbVie, Alexion, BMS, CSL Behring, Falk, Gilead, Intercept, Merz, MSD, Novartis, Roche, Sequana. AG also received research support from Intercept and Falk (NAFLD CSG), Novartis.

Open-Access: This article is an open-access article that was selected by an in-house editor and fully peer-reviewed by external reviewers. It is distributed in accordance with the Creative Commons Attribution NonCommercial (CC BY-NC 4.0) license, which permits others to distribute, remix, adapt, build upon this work non-commercially, and license their derivative works on different terms, provided the original work is properly cited and

Christoph G Dietrich, Department of Internal Medicine, Bethlehem Health Center, Stolberg 52222, Germany

Monika Rau, Department of Internal Medicine II, University Hospital Würzburg, Würzburg 97080, Germany

Andreas Geier, Department of Medicine II, University Hospital Würzburg, Würzburg 97080, Germany

Corresponding author: Christoph G Dietrich, MD, PhD, Chief Doctor, Department of Internal Medicine, Bethlehem Health Center, Steinfeldstr. 5, Stolberg 52222, Germany. christoph.g.dietrich@googlemail.com

Abstract

Nonalcoholic fatty liver disease (NAFLD) is becoming a frequent liver disease, especially in patients with metabolic syndrome and especially in Western countries. Complications of NAFLD comprise progressive fibrosis, cirrhosis and hepatocellular carcinoma. NAFLD also represents an independent risk factor for cardiovascular disease, extrahepatic neoplasia and other organ damage, such as renal insufficiency. Given the epidemiological importance of the disease, new developments in specific treatment of the disease and the wide availability of noninvasive techniques in estimating steatosis and fibrosis, NAFLD should be subject to screening programs, at least in countries with a high prevalence of the disease. The review discusses prerequisites for screening, cost-effectiveness, current guideline recommendations, suitability of techniques for screening and propositions for the following questions: Who should be screened? Who should perform screening? How should screening be performed? It is time for a screening program in patients at risk for NAFLD.

Key Words: Screening; Nonalcoholic fatty liver disease; Diabetes; Liver fibrosis; Cirrhosis

©The Author(s) 2021. Published by Baishideng Publishing Group Inc. All rights reserved.

Core Tip: Nonalcoholic fatty liver disease (NAFLD) is becoming more important in Western countries and leads to serious complications in patients with progressive disease. The epidemiological, clinical and technical requirements for screening for this disease are fulfilled and are outlaid in this review. It is time to consider a screening program for NAFLD.

the use is non-commercial. See: http://creativecommons.org/Licenses/by-nc/4.0/

Manuscript source: Invited manuscript

Specialty type: Gastroenterology and hepatology

Country/Territory of origin: Germany

Peer-review report's scientific quality classification

Grade A (Excellent): 0
Grade B (Very good): B
Grade C (Good): 0
Grade D (Fair): 0
Grade E (Poor): 0

Received: March 16, 2021
Peer-review started: March 16, 2021
First decision: May 1, 2021
Revised: May 13, 2021
Accepted: August 30, 2021
Article in press: August 30, 2021
Published online: September 21, 2021

P-Reviewer: Maevskaya M
S-Editor: Fan JR
L-Editor: Y
P-Editor: Yuan YY



Citation: Dietrich CG, Rau M, Geier A. Screening for nonalcoholic fatty liver disease-when, who and how? *World J Gastroenterol* 2021; 27(35): 5803-5821
URL: https://www.wjgnet.com/1007-9327/full/v27/i35/5803.htm
DOI: https://dx.doi.org/10.3748/wjg.v27.i35.5803

INTRODUCTION

Nonalcoholic fatty liver disease (NAFLD) is the most common liver disease worldwide, with rising prevalence to an estimate of 25% in Western populations[1]. NAFLD is regarded as one component of metabolic syndrome, including obesity, insulin resistance or type 2 diabetes mellitus (T2DM), hypertension, and dyslipidemia. Recently, the new term metabolic dysfunction-associated fatty liver disease has been proposed to emphasize this association[2]. Over the next decade, the number of patients with advanced fibrosis stages is expected to rise further together with an increasing incidence of complications [nonalcoholic steato hepatitis (NASH)-related end stage liver disease, *e.g.* hepatic decompensation, liver cancer and mortality][3]. In this recent modeling, the number of NAFLD patients in the United States, the EU5 (France, Germany, Italy, Spain, United Kingdom) and China was estimated to be 85.3 million, 72.2 million and 211 million, respectively, whereby in the same countries, more than 17.3 million, 12.6 million and 32.6 million patients were predicted to have NASH[3]. The number of NASH patients with advanced fibrosis is expected to more than double until 2030. Similar but slightly more conservative calculations have been obtained with different modeling methodologies but confirm the extent of the clinical problem[4]. In addition to liver-related morbidity and mortality, it is important to emphasize that NAFLD patients have increased cardiovascular mortality, which together cause an enormous socioeconomic impact in industrialized countries[4]. The fact that NAFLD has become the most frequent disease entity on the liver transplant waiting list in the UNOS network documents the need for early detection and intervention in the future[5]. Given the sheer frequency of patients with obesity, metabolic syndrome and NAFLD worldwide, it is remarkable that this disease entity has been overlooked by clinicians and the pharmaceutical industry for a considerable period of time, and no widely established algorithms for screening exist. The global burden of disease documents the burning need to establish clinical care structures and diagnostic algorithms to cope with the increasing number of patients at risk.

A multistep diagnostic screening algorithm is recommended in current guidelines in Western countries and combines an initial ultrasound (US) examination with subsequent risk prediction tools such as the Fibrosis-4 (FIB-4) or NAFLD fibrosis score (NFS) followed by transient elastography (TE) stratification for liver biopsy[6,7]. Increasing public and professional awareness as well as the implementation of screening algorithms in primary and secondary care will lead to a more frequent diagnosis of NAFLD patients at different stages of the disease (NAFL, noncirrhotic NASH, NASH with cirrhosis) in the near future. For the histological assessment of NAFLD, different systems are used for scoring in clinical practice [*e.g.*, NAFLD activity score (NAS)][8]. The definite histopathological diagnosis of NAFL *vs* NASH is based on the simultaneous presence of steatosis, ballooning and inflammation, which are required for the diagnosis of "NASH" in the European SAF/FLIP algorithm[9].

Of the different histologic features of NASH, fibrosis has been identified as the strongest predictor of adverse clinical outcomes, including decompensation and liver-related death[10-14]. The latest meta-analysis showed that the stage of biopsy-confirmed liver fibrosis is a strong predictor of future all-cause mortality and morbidity in NAFLD with and without adjustment for key potential confounding variables[15]. It became clear that evaluation of the fibrosis stage is even more fundamental than scoring necroinflammation or diagnosing NASH. Several options for the noninvasive evaluation of liver fibrosis in NASH, such as elastography devices and blood tests, are available[16]. Despite recent progress in noninvasive tests (NITs) for the evaluation of liver fibrosis in NAFLD, the diagnosis of NASH is still often based on liver biopsy, an invasive procedure not suitable for the large proportion of the general population affected by NAFLD. To identify patients with an increased risk, the NFS was introduced in 2007 as a simple scoring system to distinguish NAFLD with and without advanced fibrosis (fibrosis stages 3 and 4)[17]. Subsequently, further fibrosis tests, including the FIB-4 index, Fibrotest/Fibrosure, enhanced liver fibrosis (ELF) test, and liver stiffness measurement (LSM) by vibration-controlled TE, have entered clinical practice[18-21]. Of relevance for fibrosis screening, these NITs show excellent

AUROCs for the diagnosis of advanced fibrosis and cirrhosis[22]. Furthermore, repeated testing of FIB-4 within 5 years improved the identification of individuals at an increased risk of severe liver disease in the general population[23]. In light of a multistep screening algorithm, the performance has been further improved by the sequential combination of different NITs for advanced fibrosis, thereby refining the patient referral pathway between primary care or diabetologists and liver specialists [24]. Sequential combinations of FIB-4 (or NFS) and TE with a lower cut-off to rule-out advanced fibrosis and a higher cut-off to rule-in cirrhosis can increase the specificity and thereby reduce the need for liver biopsies from 33% to 19%[25]. The ultimate goal of screening measures is to identify patients at high risk for liver-related events and unfavorable overall outcomes. Longitudinal retrospective studies have demonstrated that NITs calibrated on liver fibrosis are prognostic markers to stratify the risk of liver-related outcomes and mortality in NAFLD patients[26].

Comparative diagnostic accuracy studies for established and novel biomarkers and combinations thereof are ongoing in the European LITMUS and United States NIBLE consortia[27]. It will be interesting to learn whether and which of the novel biomarkers outperforms the established freely available routine scores NFS and FIB-4. At the same time, biomarker screening strategies are currently being tested to establish validated numbers of patients to test to identify NASH patients with advanced fibrosis suitable for specific treatment.

The following review gives an overview of current guideline recommendations and answers the question of when, whom and how to screen in the different clinical settings.

RECOMMENDATIONS FOR NAFLD SCREENING IN RECENT GUIDELINES

Several guidelines worldwide have already taken a position on screening for NAFLD. The consensus is that screening in the general population is not recommended[6,7,28,29]. AASLD also discourages screening in high-risk groups because of the current lack of treatment options, unclear value of screening tests, and unclear cost-effectiveness. However, "a high index of suspicion" for the presence of NAFLD in diabetes mellitus type 2 patients is advised[7]. The Asian guideline takes a similarly noncommittal view, which also does not explicitly recommend screening in risk groups (here T2DM and obesity) but merely describes it as worth considering[29].

In contrast, specific screening recommendations can be found in the Latin American and European guidelines. Here, NAFLD screening is recommended for patients with repeatedly altered liver enzymes, features of metabolic syndrome, or obesity [body mass index (BMI) > 30] according to Latin American guidelines[28]. In the same direction, patients with insulin resistance and metabolic syndrome, especially manifest type 2 diabetes, should also be screened for the presence of NAFLD according to the European recommendation, regardless of the level of liver enzymes[6]. Both guidelines primarily recommend abdominal US as the initial examination to determine the presence of steatosis. Serum fibrosis tests are considered appropriate for further risk stratification[6,28], with the Latin American guideline decidedly recommending determination of FIB-4 and NFS. Elastography, as a more reliable method, is also mentioned[28] but is considered secondary due to its lack of availability in many places.

The guidelines differ in their treatment of patients in whom serum fibrosis scores indicate intermediate fibrosis risk. While the European algorithm recommends both high-risk and intermediate-risk patients for referral to the hepatologist[6], the Latin American guidelines suggest that this should only be the case for patients > 50 years of age with diabetes or obesity[28].

The basis of the differing recommendations is an ultimate lack of data on the efficacy and efficiency of structured screening and on the effectiveness of the therapeutic efforts that begin after NAFLD has been diagnosed in the context of screening. There are also discrepancies between the lack of widespread availability of specific examination procedures and the desire for screening results that are as sensitive and specific as possible and avoid overloading specialists by referring numerous false-positive screened patients.

SCREENING–WHEN? IS IT TIME FOR A NAFLD SCREENING PROGRAM?

Prerequisites for a disease to justify screening

In 1968, Wilson and Jungner formulated basic criteria for the usefulness of screening procedures for a particular disease in a paper by the WHO[30,31]. These criteria include peculiarities of the disease (significant burden of disease in the population and knowledge of etiology and stages of disease) and of reaching a diagnosis (simple test acceptable to patients) as well as organizational requirements (available facilities for diagnosis and therapy). In general, these criteria already apply for NAFLD for some time.

However, the authors also point out that efficient therapy as well as cost-effectiveness of screening must be present[30]. Here, important new developments have occurred in recent years that make screening for NAFLD much more justified than in the past.

The general progress in diagnosing and treating liver disease led an expert group 2016 to the proposal that screening for liver fibrosis (independent from the underlying disease) may now be feasible even for the general population[32].

For a long time, missing therapeutic options were a major argument against NAFLD screening, since lifestyle changes could only be maintained in a minority of patients and NASH-specific drugs were not even developed. In the meantime, several new drugs acting on various pathophysiological processes in NASH have entered clinical development. Current drug classes being investigated for NASH treatment are agonists of nuclear receptors such as FXR agonists (including FGF19), peroxisome proliferator-activated receptors agonists, chemokine receptor inhibitors, thyroid hormone receptor-β agonists and analogs of enterohepatic hormones such as GLP-1 and FGF21 or SGLT2 inhibitors[33]. Despite disappointment by negative interim results from three out of four recent phase 3 trials, the process of approval is ongoing for obeticholic acid as the only drug with a significant benefit in the phase 3 interim analysis. Obeticholic acid is an obvious candidate for the first conditional approval as a NASH therapeutic in the near future. However, even before approval of new drugs, NAFLD patients "at risk" should be offered to participate in ongoing clinical trials, particularly those with drug combinations, since the future will putatively be a more efficient combination therapy of two different drug classes with complementary effects[33].

Cost-effectiveness of NAFLD screening

Decisions on the target population for screening are mostly driven by cost-effectiveness and depend on the prevalence of the disease in the target population and health outcomes measured as quality-adjusted life-years (QALYs). Unfortunately, the cost-effectiveness of noninvasive liver tests in NAFLD is scarcely available in the literature.

However, the cost-effectiveness of noninvasive screening for alcohol-related liver fibrosis has been investigated in more detail[34]. For low prevalence populations, a screening strategy involving a blood-based noninvasive fibrosis test (ELF) in the first-line follow-up with LSM in intermediate- or high-risk individuals in the second-line follow-up was most cost-effective, both short- and long-term, depending on whether diagnostic testing had lasting or temporary effects on abstinence rates. The study documents that the effect of screening measures strongly depends on the therapeutic options and the size of the treatment effect. Moreover, for high-prevalence populations, direct referral to LSM was highly cost-effective.

In contrast to the growing burden of disease, a cross-sectional study of the public health response to NAFLD among experts in 29 European countries in 2018 and 2019 revealed a general lack of national policies, awareness campaigns and civil society involvement and only a few epidemiological registries[35]. Only one-third of the countries reported having national recommendations for NAFLD screening in all patients with diabetes, obesity and/or metabolic syndrome.

Data on cost-effectiveness need to be interpreted in the context of the national health system, economy and availability of treatment. Nevertheless, available data for certain diagnostic measures allow at least some general insight and can be used as part of evidence-informed decision making. As the most basic diagnostic method, ultrasonography screening for NAFLD has been found to be cost-effective in Thailand for patients with metabolic syndrome participating in an intensive weight reduction program when compared with no screening[36]. Differences in the age of the target population have been observed, since screening before 45 years was cost saving, while screening at 45 to 64 years was cost-effective.

The cost-effectiveness of LSM by TE has only been assessed in comparison to liver biopsy as the invasive reference method. In a systematic analysis covering four cost-effectiveness and four cost-utility studies[37], high-quality cost-effectiveness studies suggested that TE is less costly but also less accurate than liver biopsy (which is not surprising since histology is still regarded as the diagnostic gold standard). The incremental cost-effectiveness ratio (ICER) of TE improves with a greater level of diagnostic accuracy and a higher degree of liver fibrosis. Similar data have been obtained in a Canadian systematic review of existing TE cost-effectiveness studies from the perspective of the Ontario Ministry of Health and Long-Term Care[38]. For a primary economic evaluation, decision analytic models were used to compare short-term costs and outcomes of TE compared to liver biopsy. Again, data suggested that TE leads to cost savings but is less effective than liver biopsy in the diagnosis of liver fibrosis. Of note, TE became more economically attractive in a high-risk population with a higher degree of liver fibrosis. No studies have assessed the cost-effectiveness of TE with controlled attenuation parameter (CAP)-based fat quantification for the diagnosis of liver steatosis.

It remains open whether NAFLD screening can become cost-effective in the near future with a further increasing number of at-risk NAFLD patients in Western countries. Investigators from six prospective cohorts in Europe and Asia used patients with mostly alcohol-related liver disease to explore the cost-effectiveness of TE as a screening method to detect liver fibrosis against standard of care in a primary care pathway[39]. In 6295 participants, TE with the proposed cutoffs for the diagnosis of significant fibrosis (≥ F2) of 9.1 kPa in general population settings and 9.5 kPa in at-risk populations outperformed fibrosis scores in terms of accuracy. Screening with TE was cost-effective, with mean ICER ranging from 2570 €/QALY for a population at risk of alcohol-related liver disease (age ≥ 45 years) to 6217 €/QALY in the general population [39]. Overall, there was a 12% chance of TE screening, even though it was cost saving across countries and populations. This study clearly documents that screening for liver fibrosis with TE can be a cost-effective intervention for European and Asian populations, even in primary care, and may even be cost saving.

For various other screening tools, a comparative cost-utility model analysis of different annual noninvasive screening strategies has been conducted in Canada using a third-party payer perspective in a general population compared to screening in a high-risk obese or diabetic population[40]. The investigated screening algorithms involved the NFS, cytokeratin-18, TE and acoustic radiation force impulse (ARFI) imaging for detecting advanced fibrosis (≥ F3). Liver biopsy and magnetic resonance elastography were compared as confirmation methods. Compared with no screening, screening in high-risk obese or diabetic populations was more cost-effective than in the unselected general population. Interestingly, liver biopsy confirmation was not found to be cost-effective. These data suggest that annual NASH screening can be cost-effective in high-risk obese or diabetic populations in a Western country.

Using a different simulation model in the United States, the effectiveness and cost-effectiveness of US screening for NAFLD followed by liver biopsy has been assessed for type 2 diabetic patients[41]. In this more basic NASH screening strategy, all patients received a one-time screening US, individuals with hyperechogenicity on US underwent subsequent liver biopsy, and those found to have NASH received medical therapy to decrease disease progression. Screening for NASH decreased the number of individuals who developed cirrhosis by 12.9% and resulted in an 11.9% reduction in liver-related deaths. However, the screening strategy resulted in only 0.02 fewer QALYs due to the disutility associated with treatment and was dominated by the "no screening" strategy[41]. The impact of treatment efficacy and treatment-related side effects became clear in this study because when the model excluded the treatment-related quality-of-life decrement, screening became cost-effective. This study documents that treatment-associated side effects are relevant for quality of life and impact QALYs and the suitability of screening.

Referral strategies between primary care and secondary care by specialists have also been investigated. Given the high prevalence of NAFLD in Western countries, the optimal evaluation of NAFLD likely involves triage by a primary care physician (PCP) with advanced disease managed by gastroenterologists or hepatologists. Screening in a cohort of 10000 simulated United States-American patients with NAFLD performed in either PCP or referral clinics was simulated[42]. Risk stratification by the PCP using the NFS alone costs approximately 20% more *per* QALY than usual care costs. In the microsimulation, at a willingness-to-pay threshold of $100000, the NFS alone in the PCP setting was the most cost-effective strategy in 94.2% of samples, followed by the combination NFS/vibration-controlled transient elastography in the PCP setting (5.6%) and usual care in 0.2%[42]. This study indicates that risk stratification of pa-

tients with NAFLD in primary care is a cost-effective strategy that should be further explored in clinical practice.

Finally, the outcome of the entire diagnostic chain is relevant for decision making upon screening. This certainly includes the likelihood of referral to the specialist after obtaining a risk surrogate (which is often moderate at best), the availability of effective drugs for the target disease (in case of NASH to be established) and relevant side effects of the treatment impacting quality of life. Taking into account the emerging awareness campaigns among the public and PCPs and ongoing phase 3 treatment studies for NASH patients, it is likely that the impact of screening on the overall outcome could improve over the near future.

WHO TO SCREEN?

NAFLD is an asymptomatic disease in the early phase, often leading to a late diagnosis [43]. In a large population-based, cross-sectional study from Barcelona, the authors found elevated liver stiffness (as defined with TE > 6.8 kPa) in 9% of the participants, and NAFLD was the leading etiology (followed by alcohol risk consumption)[44]. Risk factors for elevated liver stiffness included obesity, type 2 diabetes and the presence of metabolic syndrome (each with a prevalence of elevated liver stiffness in 20%–30%). This study convincingly underlines the importance of NAFLD in the general population but especially in the known risk groups. While the prevalence of NAFLD in the general population is quite high (20%-30%), only approximately 7%-10% of NAFLD patients develop relevant complications of this disease, such as advanced fibrosis, cirrhosis or hepatocellular carcinoma (HCC)[45,46] (Figure 1). Thus, screening the entire population cannot (yet) be justified because too many patients would suffer overdiagnosis and possibly overtherapy. For advanced testing or invasive diagnostic measures such as liver biopsy, which applies to a selected patient population of still 3%-5%, primary testing to rule out low-risk individuals appears mandatory.

These numbers from the general population, however, do not apply to patient groups with increased NAFLD prevalence and increased risk for advanced disease. In the presence of the risk factors diabetes and obesity, the prevalence of NAFLD increases to 75%[47,48]. Diabetes and obesity are clear independent risk factors for the development of NASH-related fibrosis[46,47] and other factors of the metabolic syndrome are closely associated[49]. In addition, patients with these underlying diseases are more likely to develop complications of NAFLD[48]. Consequently, screening in the group of patients with these risk factors for complications is particularly important[50]. Elevated liver enzymes alone are sufficient as a reason for screening but are not sufficient as a sole decision criterion, as relevant NAFLD with fibrosis or cirrhosis may be present even with normal transaminases[51-53].

These facts warrant screening of this risk population[54], especially at higher HbA1c levels[54]. In some cohorts, patients with NAFLD also had an older age > 50 years in addition to the above risk factors[55-57], and an increased prevalence of NAFLD and advanced fibrosis has been shown in men[57]. These risk factors reflect quite well the collective for which screening for NAFLD is repeatedly discussed in the current literature or even concrete recommendations exist[6,7,28,29].

NAFLD is linked to several other diseases and is connected to metabolic disturbances. It is straightforward to consider the presence of NAFLD in patients with such concomitant diseases, one of the most important being coronary heart disease. Additionally, NAFLD should also be considered, depending on the advancement of the respective disease, in diseases such as polycystic ovary syndrome, sleep apnea, hypothyroidism, depression, renal insufficiency or psoriasis[7,58-60]. Making a specific screening recommendation for these patients is probably not warranted at this time; further risk profiles are needed here to justify such screening in selected patient groups with these diseases.

General screening of close relatives is also not reasonable despite some familial clustering and genetic factors (*e.g.*, *PNPLA3*[61]) that may influence the course of NAFLD. The penetrance of these genetic risk factors is too low to justify screening in the presence alone (RR 3.26 for the histological presence of NAFLD *per* effect allele [62]). However, relatives with the presence of the abovementioned risk factors should definitely be screened for the presence of NAFLD[6]. Screening with diabetes type 2 as a central risk factor again has very recently been shown to be cost effective in the United States by avoiding advanced liver-specific disease and endpoints (all calculated screening models based on US and AST, with an ICER between $17000 and $35000/QALY[63], see also ***Cost-effectiveness of NAFLD screening***).

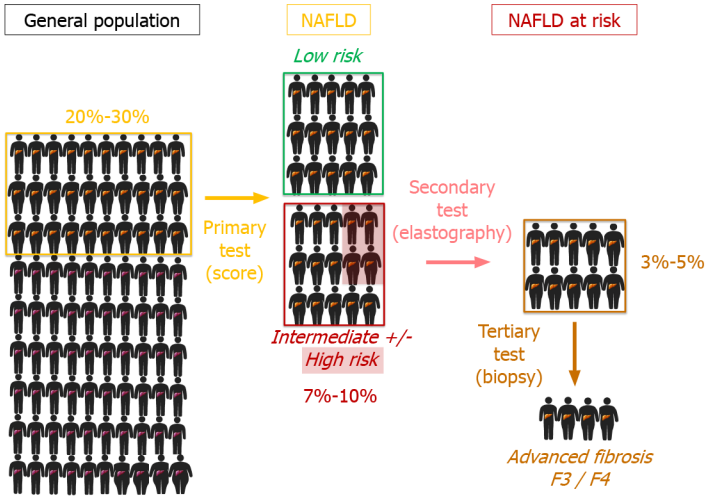


Figure 1 Nonalcoholic fatty liver disease patient proportions according to risk assessment. Stepwise enrichment of nonalcoholic fatty liver disease (NAFLD) patients at risk for advanced fibrosis using a three-step strategy with score-based primary testing in a subgroup of the general population at risk for NAFLD and elastometric secondary testing to identify candidate patients for liver biopsy represents the third and final step in most algorithms. Patients with a diagnosis of NAFLD by either surrogate scores or ultrasound (20%-30% of the general population) are divided into low-risk *vs* intermediate-to-high-risk subgroups (the latter 7%-10% of the general population). After elastometry testing, half of these subjects can be assigned to a high likelihood of advanced fibrosis F3/F4 and should be subjected to liver biopsy. NAFLD: Nonalcoholic fatty liver disease.

WHO SCREENS?

A decision about who carries out screening is determined by the care structures of a particular health care system rather than by the efficacy of particular screening procedures. Even if certain diagnostic procedures proved to be cost-efficient for screening (*e.g.*, LSM as shown above in section 3), the lack of a broad availability of LSM-determining procedures may preclude its application. Consequently, more broadly available blood-based tests are needed, and the design of a screening algorithm must then be aligned with the capabilities of those performing the screening[64-66].

In many countries, almost all patients are primarily cared for by PCPs. A certain proportion of patients defined in the at-risk population (see above) are assigned to specialists (diabetologists/endocrinologists, cardiologists), but numerous patients with diabetes mellitus, obesity, and arterial hypertension are also treated exclusively by PCPs (*e.g.*, in the context of so-called disease management programs). In Europe, screening algorithms are implemented in a total of only 5 countries and are located in the primary health care sector in all of these countries (Belgium, Denmark, Czech Republic, Slovakia, and United Kingdom[35]). However, there are sometimes considerable structural differences in the health care systems of these countries.

Due to access to patients, comprehensive risk population screening in many countries can only be in the hands of PCPs, possibly supported by diabetologists and cardiologists. This group of physicians is particularly suited to broadly identify the major risk diseases for NAFLD and thus to determine the individual NAFLD risk in these patients[67]. This assessment is also in line with existing EASL recommendations [6] and a recently developed algorithm for general practitioners and diabetologists [68]. Direct referral of all patients at risk to hepatologists is not feasible. The need for a screening filter at the primary care level to prevent unnecessary referrals to specialists is shown by data from England ("Camden and Islington NAFLD pathway"[69]) and the United States[70]. In both studies, almost 90% of unnecessary referrals could be avoided by structured screening at the primary care provider level. On the other hand, in an American study, more than 25% of NAFLD patients referred to a hepatologist without screening already had advanced fibrosis (characterized as at least F3 with TE measurement[54]).

Data on awareness of NAFLD at GP level are rare. In the United States, data from the United States Veteran Affairs Database showed that NAFLD is significantly underdiagnosed in primary care patients[71]. Patients with abnormal alanine aminotransferase (ALT)/glutamate pyruvate transaminase (GPT) without other known liver disease (viral hepatitis and alcohol use were largely excluded by data analysis) were detected in only 40% of cases in this study, received a suspected diagnosis of NAFLD in only 21%, received therapeutic counseling in only 15% and were referred to a specialist in only 3% of cases. Initially, there is no reason to assume that the situation

in other countries differs significantly from these results. A study by the professional association of gastroenterologists in private practice in Germany (bng) showed for a cohort of NAFLD patients in secondary care that approximately 10% of these patients already had advanced fibrosis according to FIB-4 screening, but even these patients were not consistently counseled or guided regarding therapy[55]. Only 27% of patients with presumed advanced fibrosis in this study received nutritional counseling. In this respect, education and training activities for PCPs are definitely necessary to increase awareness of the presence and risks of NAFLD and to create acceptance for screening. Diabetologists and cardiologists should also be included by these measures, as they should also be involved in screening due to their spectrum of patients they treat.

Integration of primary care identification of patients at risk for the presence of NAFLD, particularly with advanced fibrosis, into secondary testing facilities at a specialist setting is a crucial issue for the overall efficacy of a screening algorithm (Figure 2). Dedicated elastography platforms have been established at several places, such as in our own center[72]. The likelihood of referral of "intermediate or high risk" individuals to secondary care, the proportion of subjects with "indeterminate" test results (the so-called "gray zone" of respective score-based tests) and the availability of advanced testing platforms for referral are relevant factors at this interface. As pointed out, existing or emerging networks between PCPs and specialists are key to optimizing a bidirectional transition into secondary testing and, in case of "low risk", back to long-term observation and basic treatment in a primary setting.

HOW TO SCREEN?

Value of transabdominal ultrasonography of the liver in NAFLD

US is a widely available, cost-effective, radiation-free method that allows assessment of hepatic fatty degeneration[73]. Hepatic fatty degeneration results in an increase in the echogenicity of the liver parenchyma (*e.g.*, compared with the renal parenchyma). US is thus suitable as a screening method for NAFLD. However, steatosis below 10% of hepatocytes is not detected, and up to 20% is unreliably detected[74] (especially with microvesicular fatty degeneration). In moderate and severe hepatic steatosis, good sensitivity (85%-96%) is achieved with specificity up to 98%[75]. The best results are seen above a liver fat content of 12.5%, where AUROC values under consideration of different echographic parameters reached comparable results to H-magnetic resonance spectroscopy (MRS)[76]. With the above referenced threshold, exclusion of steatosis by US is not completely possible. With regard to possible fibrosis of the liver, US diagnostics do not allow reliable determination and staging[73].

Noninvasive measurement of hepatic steatosis and fibrosis by elastography

US-based shear wave elastography techniques are well suited as a method for measuring liver stiffness to detect or exclude advanced liver fibrosis and cirrhosis in NASH. In addition, FibroScan, for example, now also offers the possibility of quantifying the fat content of the liver *via* the measurement of additional parameters.

The CAP measurement integrated in the FibroScan achieved AUROC values between 0.7[77] and 0.84[78] in studies with more than 400 patients each for (histologically confirmed) steatosis of > 33% and > 66%.

Different elastography techniques are now available on the market, and a differentiated overview cannot be given here but is available elsewhere[79]. While TE using FibroScan requires the purchase of a dedicated device, other techniques, such as ARFI imaging (Siemens), Elast-PQ (Philipps), and supersonic shear-wave elastography (SWE, Aixplorer), offer the advantage of being integrated into routine US equipment [73].

In large cohorts from Europe and Asia, the reliability of TE, its superiority over fibrosis scores, and even its cost-effectiveness have been demonstrated, at least for certain at-risk populations, in determining liver fibrosis of different origins[39]. TE is also well suited for quantifying fibrosis in NAFLD. Here, sensitivity, specificity, and AUROC values improve as fibrosis progresses, reaching values of approximately 92% and 0.89 for cirrhosis (F4), respectively[77,80]. Difficulties in estimating fibrosis in obese patients with the normal (M) probe[81] were countered by the company's introduction of an XL probe for particularly obese patients, which provides reliable values and is automatically chosen if the patient has appropriate physical conditions [82,83].

Apart from slight differences in patients with different body types, the diagnostic value of the different elastography methods in determining liver fibrosis in NAFLD

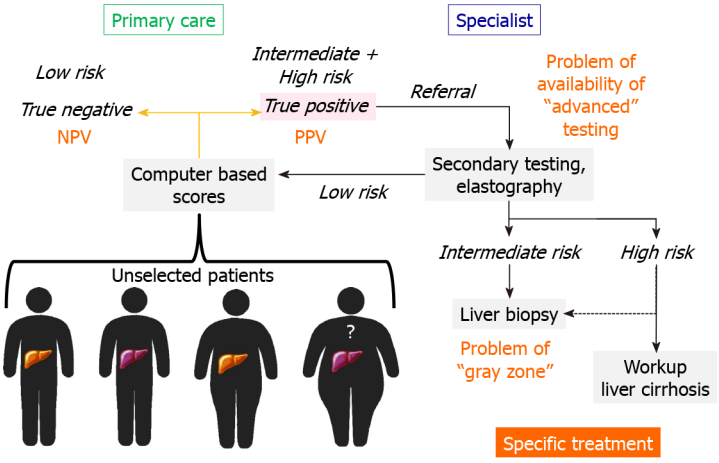


Figure 2 Linking primary care to hepatology. Unselected patients from the general population are most likely in contact with primary care. In primary care, patients at risk for the presence of nonalcoholic fatty liver disease and according to computer-based scores at risk for advanced fibrosis should be transferred into secondary testing facilities at a specialist setting. Critical for the overall efficacy of a screening algorithm are the likelihood of referral of "intermediate or high risk" individuals to secondary care, the proportion of subjects with "indeterminate" test results ("gray zone" of score-based tests) and the availability of advanced testing platforms for referral. NPV: Negative predictive value; PPV: Positive predictive value.

patients appears to be similar. Several studies with different populations and study designs yielded similar AUROC values for TE, SSI, ARFI, and 2D-SWE[84-86]. However, problems with a tendency to overestimate fibrosis occurred in bariatric, extremely obese (median BMI 47 kg/sqm) patients for both TE and ARFI, where the ELF score was actually superior to these two elastography methods[87]. Nevertheless, the procedures should also be well suited for screening most patients. The availability of the methods is very heterogeneous, so broad screening with elastography is currently not possible.

Value of magnetic resonance imaging and computed tomography in the diagnosis and screening of NAFLD

The availability of computed tomography (CT) is bound to institutions with large medical devices but is well reproducible and reliably determines the fat content of the liver by measuring organ density[73]. In a meta-analysis comparing different radiological methods, CT performed rather modestly with a sensitivity of 46%-72%[88]. At least moderate hepatic fatty degeneration can be diagnosed if the density ratio of the liver and spleen on native CT has a cutoff value > 1.1[89]. Dual-energy CT has been able to show promising results for quantifying fat content in the liver in smaller cohorts, even in comparison with magnetic resonance imaging[90]. However, such techniques are poorly validated and not widely available. Overall, CT should not be used as a primary screening method for detecting NAFLD because of its cost, lack of broad availability, and substantial radiation exposure.

Magnetic resonance imaging (MRI), though also a large medical device, is a radiologic imaging modality without any radiation exposure. Certain modalities of MRI can be used to determine both the fat content of the liver and the fibrosis stage quite reliably[73]. MR-based quantification of liver fat content using proton density fat fraction (PDFF) has high linearity and precision with simple postprocessing[91], but it is also not suitable for screening large risk groups because of cost and effort[92]. Compared with histology as a reference standard and in comparison to CAP, PDFF-based determinations have a higher diagnostic accuracy for detecting steatosis (histological grade 1-3) with an AUROC of 0.96 up to 0.99, a sensitivity of 96%, and a specificity of 100%[93,94]. MRS has the highest accuracy for fat assessment in the literature[88,92,95] but is currently limited to research centers due to a lack of standardization of methodology and high costs for hardware and software requirements [73].

MR elastography measures liver stiffness significantly more reliably than US-based elastography techniques[85,96]. In a biopsy-controlled study of 100 patients, an AUROC of 0.98 was achieved at 40 Hz[97]. A joint analysis from 12 studies with over 900 patients still showed summary AUROC values of 0.93-0.95[98]. MR elastography also correlated better to clinical fibrosis parameters and scores than TE[99] but remains restricted to specialized centers[92].

Multiparametric MRI with determination of fat content (by PDFF or spectroscopy) and fibrosis (by MR elastography) was superior to the respective FibroScan-based non-MR methods (CAP for steatosis and TE for fibrosis) in a comprehensive new study [100] and cost-effective for risk stratification of NAFLD in a United Kingdom study [101]. Nevertheless, these methods are not (yet) suitable for broad screening due to lack of availability and high costs.

Laboratory chemistry scores

Because screening must be performed primarily by PCPs, screening tools must be widely available, inexpensive, and noninvasive[58,66,67]. This allows screening to be performed on a day-to-day basis and, more importantly, increases the acceptance of screening by the physicians performing it. The two-step design with the verification of steatosis and fibrosis risk improves the specificity (and in some cases even the sensitivity) of screening[65,102]. Positively screened patients must be transferred to a hepatologist for further evaluation. In this context, the proportion of positively screened patients should not be too large to avoid overloading hepatologists[65,103]. The extent of the diagnostic "gray zone" is of particular importance in this regard and can vary substantially from test to test. In any case, however, patients with prolonged or repeated elevations of GPT/ALT should be referred for further evaluation (as is usually the case), as they are generally at increased risk for liver disease or injury[51, 104,105].

There are significant differences between different countries and health care systems in the availability and cost-effectiveness of different screening tools. However, despite the limited sensitivity of US, this procedure is an attractive screening option for PCPs because of its ease of performance. More technically sophisticated and sensitive procedures such as CAP or elastography are generally not available at this level of care.

Steatosis scores correlate with insulin resistance. Their diagnostic performance for steatosis depends on the degree of fatty degeneration, fibrosis, and inflammation[106]. Assuming at least moderate steatosis is relevant, the performance of the fatty liver index (FLI) and NAFLD liver fat score is best, with the highest AUROC values with a positive predictive value of 99%, but without safe exclusion of steatosis below the cutoff[106-108]. Only the FLI can easily be obtained from routine values in family practice (see Table 1) and should therefore be used when US is not feasible[109].

Fibrosis scores also vary in both availability and quality of information. In this regard, the sensitivity and specificity of each score for significant fibrosis, advanced fibrosis, and cirrhosis are quite different and additionally vary depending on the population screened (population screening *vs* high-risk screening *vs* screening of confirmed NAFLD)[110]. Scores that require the determination of expensive specialty laboratory parameters are not suitable for primary care screening, nor are scores that include, at least in part, unavailable laboratory parameters or instrumental procedures. Although these special scores are superior to routine scores, as expected[111], and would also improve specificity in combination with them[112], the lack of availability and the lack of acceptance of these special scores by general practitioners, based in part on complicated determination, hinder their widespread use. This applies, for example, to the ELF test[113] (hyaluronic acid, TIMP-1, and procollagen peptide), which is of similar prognostic value to liver biopsy[114], and the fibrometer VCTE test (with elastography), which is also superior to purely laboratory chemistry-clinical indices [24].

Scores with readily available routine parameters for fibrosis risk include NFS, FIB-4 score, APRI score, Forns score, and BARD score. The first two (NFS, FIB-4) are superior to the last three (APRI, Forns, BARD) in screening fibrosis in the NAFLD cohort[115,116]. In a recent systematic review, this could be confirmed, especially for the hardest endpoint (mortality)[117]. These two scores (FIB-4 and NFS) are also suitable for screening patients with normal ALT[118] and can be easily determined *via* internet-based calculators.

In population screening, all scores have significant weaknesses and are therefore of limited use for this question[110]. However, the discriminatory performance of all tests is significantly better in high-risk collectives[110]. Although the FIB-4 score was initially developed for the detection of hepatitis C virus fibrosis[119], it has since been validated[120] and compared[121] in NAFLD collectives and may be considered suitable in principle for liver fibrosis of other etiologies. The FIB-4 score has an additional advantage over the NFS in that no albumin value is needed and that the proportion of intermediate tested patients is somewhat smaller[65,116]. However, both scores have lower specificity in patients > 65 years of age[122], which may increase the referral rate to the specialist due to a higher proportion of false-positive screened

Table 1 Scores for diagnosing steatosis and fibrosis with parameters used

	Routine parameters											Special parameters		
Scores for Steatosis	**AST**	**ALT**	**yGT**	**Platelets**	**TG**	**Bilirubin**	**BMI**	**Waist**	**Age**	**Sex**	**Diab.**	**A2M**	**HA**	**Other**
FLI			X		X		X	X						
HSI	X	X					X			X	X			
Steato-Test		X	X		X	X			X	X	Gluc	X		Apo-A1, Haptoglobin, Cholesterol
NAFLD-LFS	X	X									X			Insulin
VAI					X		X	X						
TyG					X						Gluc			
Scores for fibrosis														
NFS	X	X		X			X		X		X			Albumin
FIB-4	X	X		X					X					
APRI	X			X										
ELF													X	PIIINP, TIMP-1
Fibrotest		X	X			X						X		Haptoglobin,Apo-A1
Fibrometer (V2G) ((V3G))	X		((X)), for HA	X					X	(X)		X	X	Prothrombin, Urea
NIKEI	X	X				X			X					

New fibrometer versions (V2G, V3G) and their respective parameters labeled with brackets: (V2G) and ((V3G)). AST: Aspartate-aminotransferase; ALT: Alanine-aminotransferase; yGT: gamma-glutamyltransferase; TG: triglycerides; BMI: Body mass index; Diab.: Diabetes; A2M: Alpha-2-microglobulin; HA: Hyaluronic acid; Gluc: Glucose; PIIINP: Procollagen-III-peptide; TIMP-1: Tissue inhibitor of metalloproteinases I; Apo-A1: Apo-A1-lipoprotein; FLI: Fatty liver index; HIS: Hepatic steatosis index; NAFLD-LFS: Nonalcoholic fatty liver-liver fat score; VAI: Visceral adiposity index; TyG: Triglyceride and glucose index; NFS: NAFLD fibrosis score; FIB-4: Fibrosis-4; APRI: AST-platelet-ratio index; ELF: Enhanced liver fibrosis; NIKEI: Noninvasive Koeln-Essen-index.

patients. Data from a screening study of type 2 diabetes patients show that the use of age-adjusted cutoffs on FIB-4 (in delineating negative *vs* intermediate) reduces the number of patients tested intermediate (from 38.3% to 15.4%[65]). Repeated measurements of laboratory scores could also help to identify patients at risk of severe liver disease in the general population, as was recently shown for repeated measurements of FIB-4 within 5 years[23].

The screening strategy proposed in Figure 3 relies on recent proposals and takes into account the aforementioned prerequisites of high-risk screening by PCPs but may not currently be evidence-based in several areas. In particular, this concerns the handling of the intermediate-risk group, the screening interval in low-risk patients, and the cost-effectiveness of the entire algorithm. In addition, the screening recommendation given requires further education and possibly training of PCPs about the prevalence and prognosis of NAFLD.

CONCLUSION

It is time for NAFLD screening. NAFLD is hard to diagnose in the early phase of the disease. The prevalence of this disease is increasing in countries with Western lifestyles, and the complication rate (inflammation, fibrosis, cirrhosis and HCC) is high in patients with metabolic dysfunction. Additionally, there are inexpensive noninvasive tools for the diagnosis of steatosis and fibrosis, leading to a reliable identification of persons at risk who can be referred to hepatologists. Apart from lifestyle modification, there are evolving drug treatments shortly before approval or in the late phases of clinical trials.

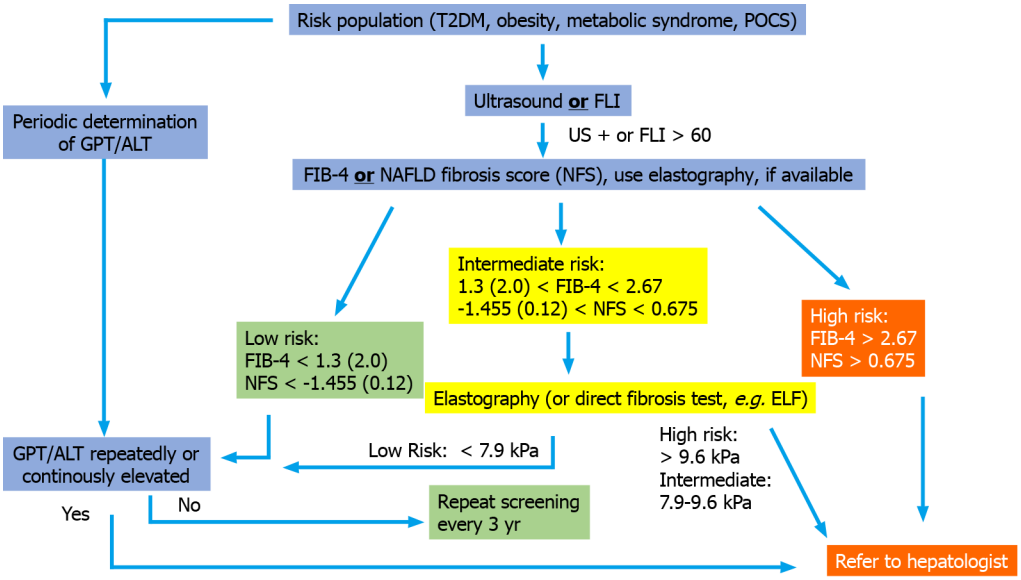


Figure 3 Possible screening algorithm that can be modified according to availability but contains the two main elements (detection of steatosis and fibrosis risk) and can be performed in the primary care physician's office. The algorithm corresponds well to the so-called European algorithm of the EASL-EASD-EASO Clinical Practice Guidelines[6] and to a recently proposed approach for family physicians and diabetologists[68] but is simpler to use. The sequences of fatty liver index and Fibrosis-4 (FIB-4) have been decisively studied for screening in a high-risk population of type 2 diabetes patients[65]. The use of age-adjusted cutoff values (in parentheses) is reasonable to reduce the high proportion of intermediate tested individuals. The sequential use of FIB-4, nonalcoholic fatty liver disease fibrosis score or enhanced liver fibrosis in the intermediate group has not been investigated in studies so far, but there are first studies on the basic sequential use of noninvasive fibrosis scores[123]. FLI: Fatty liver index; FIB-4: Fibrosis-4; T2DM: Type 2 diabetes mellitu; NFS: Nonalcoholic fatty liver disease fibrosis score; GPT: Glutamate pyruvate transaminase; ALT: Alanine aminotransferase.

Studies show that screening for NAFLD, at least for a risk population, is cost effective and will help to prevent serious hepatic consequences of pandemic metabolic dysfunction. However, it will not be easy to implement comprehensive screening programs in all countries since there are large structural differences between national health systems. For example, the extent of availability of elastography will decide in each country, whether this promising technique can be used in broad screening approaches or whether US and lab scores will be necessary for PCPs to conduct screening for NAFLD. Therefore, each screening algorithm (as the one depicted in Figure 3) should be adapted locally depending on the broad availability of methods for detecting steatosis and fibrosis. Additionally, the screening population (*i.e.* the patients with an amount of risk factors high enough for qualifying for the screening program) has to be determined in each country individually depending on the epidemiology of NAFLD in this country.

So what is to be done? We have to increase awareness for NAFLD and its consequences in the population and in primary care. National professional gastroenterology and hepatology societies have to develop guidelines for screening programs depending on the structure of the population and health care system of their respective country. National health systems must implement reimbursement for the tools needed for reliable screening. Hepatologists should prepare for rising numbers of patients referred for risk stratification and specific counseling.

REFERENCES

1 **Younossi ZM**, Koenig AB, Abdelatif D, Fazel Y, Henry L, Wymer M. Global epidemiology of nonalcoholic fatty liver disease-Meta-analytic assessment of prevalence, incidence, and outcomes. *Hepatology* 2016; **64**: 73-84 [PMID: 26707365 DOI: 10.1002/hep.28431]

2 **Eslam M**, Newsome PN, Sarin SK, Anstee QM, Targher G, Romero-Gomez M, Zelber-Sagi S, Wai-Sun Wong V, Dufour JF, Schattenberg JM, Kawaguchi T, Arrese M, Valenti L, Shiha G, Tiribelli C, Yki-Järvinen H, Fan JG, Grønbæk H, Yilmaz Y, Cortez-Pinto H, Oliveira CP, Bedossa P, Adams LA, Zheng MH, Fouad Y, Chan WK, Mendez-Sanchez N, Ahn SH, Castera L, Bugianesi E, Ratziu V, George J. A new definition for metabolic dysfunction-associated fatty liver disease: An international expert consensus statement. *J Hepatol* 2020; **73**: 202-209 [PMID: 32278004 DOI: 10.1016/j.jhep.2020.03.039]

3 **Estes C**, Anstee QM, Arias-Loste MT, Bantel H, Bellentani S, Caballeria J, Colombo M, Craxi A,

Crespo J, Day CP, Eguchi Y, Geier A, Kondili LA, Kroy DC, Lazarus JV, Loomba R, Manns MP, Marchesini G, Nakajima A, Negro F, Petta S, Ratziu V, Romero-Gomez M, Sanyal A, Schattenberg JM, Tacke F, Tanaka J, Trautwein C, Wei L, Zeuzem S, Razavi H. Modeling NAFLD disease burden in China, France, Germany, Italy, Japan, Spain, United Kingdom, and United States for the period 2016-2030. *J Hepatol* 2018; **69**: 896-904 [PMID: 29886156 DOI: 10.1016/j.jhep.2018.05.036]

4 **Younossi ZM**, Blissett D, Blissett R, Henry L, Stepanova M, Younossi Y, Racila A, Hunt S, Beckerman R. The economic and clinical burden of nonalcoholic fatty liver disease in the United States and Europe. *Hepatology* 2016; **64**: 1577-1586 [PMID: 27543837 DOI: 10.1002/hep.28785]

5 **Wong RJ**, Aguilar M, Cheung R, Perumpail RB, Harrison SA, Younossi ZM, Ahmed A. Nonalcoholic steatohepatitis is the second leading etiology of liver disease among adults awaiting liver transplantation in the United States. *Gastroenterology* 2015; **148**: 547-555 [PMID: 25461851 DOI: 10.1053/j.gastro.2014.11.039]

6 **European Association for the Study of the Liver (EASL)**; European Association for the Study of Diabetes (EASD); European Association for the Study of Obesity (EASO). EASL-EASD-EASO Clinical Practice Guidelines for the management of non-alcoholic fatty liver disease. *Diabetologia* 2016; **59**: 1121-1140 [PMID: 27053230 DOI: 10.1007/s00125-016-3902-y]

7 **Chalasani N**, Younossi Z, Lavine JE, Charlton M, Cusi K, Rinella M, Harrison SA, Brunt EM, Sanyal AJ. The diagnosis and management of nonalcoholic fatty liver disease: Practice guidance from the American Association for the Study of Liver Diseases. *Hepatology* 2018; **67**: 328-357 [PMID: 28714183 DOI: 10.1002/hep.29367]

8 **Kleiner DE**, Brunt EM, Van Natta M, Behling C, Contos MJ, Cummings OW, Ferrell LD, Liu YC, Torbenson MS, Unalp-Arida A, Yeh M, McCullough AJ, Sanyal AJ; Nonalcoholic Steatohepatitis Clinical Research Network. Design and validation of a histological scoring system for nonalcoholic fatty liver disease. *Hepatology* 2005; **41**: 1313-1321 [PMID: 15915461 DOI: 10.1002/hep.20701]

9 **Bedossa P**, Poitou C, Veyrie N, Bouillot JL, Basdevant A, Paradis V, Tordjman J, Clement K. Histopathological algorithm and scoring system for evaluation of liver lesions in morbidly obese patients. *Hepatology* 2012; **56**: 1751-1759 [PMID: 22707395 DOI: 10.1002/hep.25889]

10 **Angulo P**, Kleiner DE, Dam-Larsen S, Adams LA, Bjornsson ES, Charatcharoenwitthaya P, Mills PR, Keach JC, Lafferty HD, Stahler A, Haflidadottir S, Bendtsen F. Liver Fibrosis, but No Other Histologic Features, Is Associated With Long-term Outcomes of Patients With Nonalcoholic Fatty Liver Disease. *Gastroenterology* 2015; **149**: 389-97.e10 [PMID: 25935633 DOI: 10.1053/j.gastro.2015.04.043]

11 **Dulai PS**, Singh S, Patel J, Soni M, Prokop LJ, Younossi Z, Sebastiani G, Ekstedt M, Hagstrom H, Nasr P, Stal P, Wong VW, Kechagias S, Hultcrantz R, Loomba R. Increased risk of mortality by fibrosis stage in nonalcoholic fatty liver disease: Systematic review and meta-analysis. *Hepatology* 2017; **65**: 1557-1565 [PMID: 28130788 DOI: 10.1002/hep.29085]

12 **Ekstedt M**, Hagström H, Nasr P, Fredrikson M, Stål P, Kechagias S, Hultcrantz R. Fibrosis stage is the strongest predictor for disease-specific mortality in NAFLD after up to 33 years of follow-up. *Hepatology* 2015; **61**: 1547-1554 [PMID: 25125077 DOI: 10.1002/hep.27368]

13 **Hagström H**, Nasr P, Ekstedt M, Hammar U, Stål P, Hultcrantz R, Kechagias S. Fibrosis stage but not NASH predicts mortality and time to development of severe liver disease in biopsy-proven NAFLD. *J Hepatol* 2017; **67**: 1265-1273 [PMID: 28803953 DOI: 10.1016/j.jhep.2017.07.027]

14 **Hagström H**, Nasr P, Ekstedt M, Kechagias S, Stål P, Bedossa P, Hultcrantz R. SAF score and mortality in NAFLD after up to 41 years of follow-up. *Scand J Gastroenterol* 2017; **52**: 87-91 [PMID: 27616339 DOI: 10.1080/00365521.2016.1230779]

15 **Taylor RS**, Taylor RJ, Bayliss S, Hagström H, Nasr P, Schattenberg JM, Ishigami M, Toyoda H, Wai-Sun Wong V, Peleg N, Shlomai A, Sebastiani G, Seko Y, Bhala N, Younossi ZM, Anstee QM, McPherson S, Newsome PN. Association Between Fibrosis Stage and Outcomes of Patients With Nonalcoholic Fatty Liver Disease: A Systematic Review and Meta-Analysis. *Gastroenterology* 2020; **158**: 1611-1625.e12 [PMID: 32027911 DOI: 10.1053/j.gastro.2020.01.043]

16 **Geier A**, Boursier J. Non-invasive diagnosis of patients with 'at-risk' NAFLD : only fibrosis counts? *Gut* 2020; **69**: 1164-1165 [PMID: 32220903 DOI: 10.1136/gutjnl-2020-320785]

17 **Angulo P**, Hui JM, Marchesini G, Bugianesi E, George J, Farrell GC, Enders F, Saksena S, Burt AD, Bida JP, Lindor K, Sanderson SO, Lenzi M, Adams LA, Kench J, Therneau TM, Day CP. The NAFLD fibrosis score: a noninvasive system that identifies liver fibrosis in patients with NAFLD. *Hepatology* 2007; **45**: 846-854 [PMID: 17393509 DOI: 10.1002/hep.21496]

18 **Ratziu V**, Massard J, Charlotte F, Messous D, Imbert-Bismut F, Bonyhay L, Tahiri M, Munteanu M, Thabut D, Cadranel JF, Le Bail B, de Ledinghen V, Poynard T; LIDO Study Group; CYTOL study group. Diagnostic value of biochemical markers (FibroTest-FibroSURE) for the prediction of liver fibrosis in patients with non-alcoholic fatty liver disease. *BMC Gastroenterol* 2006; **6**: 6 [PMID: 16503961 DOI: 10.1186/1471-230X-6-6]

19 **Guha IN**, Parkes J, Roderick P, Chattopadhyay D, Cross R, Harris S, Kaye P, Burt AD, Ryder SD, Aithal GP, Day CP, Rosenberg WM. Noninvasive markers of fibrosis in nonalcoholic fatty liver disease: Validating the European Liver Fibrosis Panel and exploring simple markers. *Hepatology* 2008; **47**: 455-460 [PMID: 18038452 DOI: 10.1002/hep.21984]

20 **McPherson S**, Stewart SF, Henderson E, Burt AD, Day CP. Simple non-invasive fibrosis scoring systems can reliably exclude advanced fibrosis in patients with non-alcoholic fatty liver disease. *Gut* 2010; **59**: 1265-1269 [PMID: 20801772 DOI: 10.1136/gut.2010.216077]

21 **Yoneda M**, Yoneda M, Fujita K, Inamori M, Tamano M, Hiriishi H, Nakajima A. Transient elastography in patients with non-alcoholic fatty liver disease (NAFLD). *Gut* 2007; **56**: 1330-1331 [PMID: 17470477 DOI: 10.1136/gut.2007.126417]

22 **Anstee QM**, Lawitz EJ, Alkhouri N, Wong VW, Romero-Gomez M, Okanoue T, Trauner M, Kersey K, Li G, Han L, Jia C, Wang L, Chen G, Subramanian GM, Myers RP, Djedjos CS, Kohli A, Bzowej N, Younes Z, Sarin S, Shiffman ML, Harrison SA, Afdhal NH, Goodman Z, Younossi ZM. Noninvasive Tests Accurately Identify Advanced Fibrosis due to NASH: Baseline Data From the STELLAR Trials. *Hepatology* 2019; **70**: 1521-1530 [PMID: 31271665 DOI: 10.1002/hep.30842]

23 **Hagström H**, Talbäck M, Andreasson A, Walldius G, Hammar N. Repeated FIB-4 measurements can help identify individuals at risk of severe liver disease. *J Hepatol* 2020; **73**: 1023-1029 [PMID: 32621944 DOI: 10.1016/j.jhep.2020.06.007]

24 **Boursier J**, Guillaume M, Leroy V, Irlès M, Roux M, Lannes A, Foucher J, Zuberbuhler F, Delabaudière C, Barthelon J, Michalak S, Hiriart JB, Peron JM, Gerster T, Le Bail B, Riou J, Hunault G, Merrouche W, Oberti F, Pelade L, Fouchard I, Bureau C, Calès P, de Ledinghen V. New sequential combinations of non-invasive fibrosis tests provide an accurate diagnosis of advanced fibrosis in NAFLD. *J Hepatol* 2019; **71**: 389-396 [PMID: 31102719 DOI: 10.1016/j.jhep.2019.04.020]

25 **Mózes FE**, Lee JA, Selvaraj EA, Jayaswal ANA, Trauner M, Boursier J, Fournier C, Staufer K, Stauber RE, Bugianesi E, Younes R, Gaia S, Lupșor-Platon M, Petta S, Shima T, Okanoue T, Mahadeva S, Chan WK, Eddowes PJ, Hirschfield GM, Newsome PN, Wong VW, de Ledinghen V, Fan J, Shen F, Cobbold JF, Sumida Y, Okajima A, Schattenberg JM, Labenz C, Kim W, Lee MS, Wiegand J, Karlas T, Yılmaz Y, Aithal GP, Palaniyappan N, Cassinotto C, Aggarwal S, Garg H, Ooi GJ, Nakajima A, Yoneda M, Ziol M, Barget N, Geier A, Tuthill T, Brosnan MJ, Anstee QM, Neubauer S, Harrison SA, Bossuyt PM, Pavlides M; LITMUS Investigators. Diagnostic accuracy of non-invasive tests for advanced fibrosis in patients with NAFLD: an individual patient data meta-analysis. *Gut* 2021 [PMID: 34001645 DOI: 10.1136/gutjnl-2021-324243]

26 **Angulo P**, Bugianesi E, Bjornsson ES, Charatcharoenwitthaya P, Mills PR, Barrera F, Haflidadottir S, Day CP, George J. Simple noninvasive systems predict long-term outcomes of patients with nonalcoholic fatty liver disease. *Gastroenterology* 2013; **145**: 782-9.e4 [PMID: 23860502 DOI: 10.1053/j.gastro.2013.06.057]

27 **Hardy T**, Wonders K, Younes R, Aithal GP, Aller R, Allison M, Bedossa P, Betsou F, Boursier J, Brosnan MJ, Burt A, Cobbold J, Cortez-Pinto H, Day CP, Dufour JF, Ekstedt M, Francque S, Harrison S, Miele L, Nasr P, Papatheodoridis G, Petta S, Tiniakos D, Torstenson R, Valenti L, Holleboom AG, Yki-Jarvinen H, Geier A, Romero-Gomez M, Ratziu V, Bugianesi E, Schattenberg JM, Anstee QM; LITMUS Consortium. The European NAFLD Registry: A real-world longitudinal cohort study of nonalcoholic fatty liver disease. *Contemp Clin Trials* 2020; **98**: 106175 [PMID: 33045403 DOI: 10.1016/j.cct.2020.106175]

28 **Arab JP**, Dirchwolf M, Álvares-da-Silva MR, Barrera F, Benítez C, Castellanos-Fernandez M, Castro-Narro G, Chavez-Tapia N, Chiodi D, Cotrim H, Cusi K, de Oliveira CPMS, Díaz J, Fassio E, Gerona S, Girala M, Hernandez N, Marciano S, Masson W, Méndez-Sánchez N, Leite N, Lozano A, Padilla M, Panduro A, Paraná R, Parise E, Perez M, Poniachik J, Restrepo JC, Ruf A, Silva M, Tagle M, Tapias M, Torres K, Vilar-Gomez E, Costa Gil JE, Gadano A, Arrese M. Latin American Association for the study of the liver (ALEH) practice guidance for the diagnosis and treatment of non-alcoholic fatty liver disease. *Ann Hepatol* 2020; **19**: 674-690 [PMID: 33031970 DOI: 10.1016/j.aohep.2020.09.006]

29 **Wong VW**, Chan WK, Chitturi S, Chawla Y, Dan YY, Duseja A, Fan J, Goh KL, Hamaguchi M, Hashimoto E, Kim SU, Lesmana LA, Lin YC, Liu CJ, Ni YH, Sollano J, Wong SK, Wong GL, Chan HL, Farrell G. Asia-Pacific Working Party on Non-alcoholic Fatty Liver Disease guidelines 2017-Part 1: Definition, risk factors and assessment. *J Gastroenterol Hepatol* 2018; **33**: 70-85 [PMID: 28670712 DOI: 10.1111/jgh.13857]

30 **Andermann A**, Blancquaert I, Beauchamp S, Déry V. Revisiting Wilson and Jungner in the genomic age: a review of screening criteria over the past 40 years. *Bull World Health Organ* 2008; **86**: 317-319 [PMID: 18438522 DOI: 10.2471/blt.07.050112]

31 **Sturdy S**, Miller F, Hogarth S, Armstrong N, Chakraborty P, Cressman C, Dobrow M, Flitcroft K, Grossman D, Harris R, Hoebee B, Holloway K, Kinsinger L, Krag M, Löblová O, Löwy I, Mackie A, Marshall J, O'Hallahan J, Rabeneck L, Raffle A, Reid L, Shortland G, Steele R, Tarini B, Taylor-Phillips S, Towler B, van der Veen N, Zappa M. Half a Century of Wilson & Jungner: Reflections on the Governance of Population Screening. *Wellcome Open Res* 2020; **5**: 158 [PMID: 32923689 DOI: 10.12688/wellcomeopenres.16057.2]

32 **Ginès P**, Graupera I, Lammert F, Angeli P, Caballeria L, Krag A, Guha IN, Murad SD, Castera L. Screening for liver fibrosis in the general population: a call for action. *Lancet Gastroenterol Hepatol* 2016; **1**: 256-260 [PMID: 28404098 DOI: 10.1016/S2468-1253(16)30081-4]

33 **Rau M**, Geier A. An update on drug development for the treatment of nonalcoholic fatty liver disease - from ongoing clinical trials to future therapy. *Expert Rev Clin Pharmacol* 2021; **14**: 333-340 [PMID: 33535836 DOI: 10.1080/17512433.2021.1884068]

34 **Asphaug L**, Thiele M, Krag A, Melberg HO. Cost-Effectiveness of Noninvasive Screening for Alcohol-Related Liver Fibrosis. *Hepatology* 2020; **71**: 2093-2104 [PMID: 31595545 DOI: 10.1002/hep.30979]

35 **Lazarus JV**, Ekstedt M, Marchesini G, Mullen J, Novak K, Pericàs JM, Roel E, Romero-Gómez M,

Ratziu V, Tacke F, Cortez-Pinto H, Anstee QM; EASL International Liver Foundation NAFLD Policy Review Collaborators. A cross-sectional study of the public health response to non-alcoholic fatty liver disease in Europe. *J Hepatol* 2020; **72**: 14-24 [PMID: 31518646 DOI: 10.1016/j.jhep.2019.08.027]

36 **Phisalprapa P**, Supakankunti S, Charatcharoenwitthaya P, Apisarnthanarak P, Charoensak A, Washirasaksiri C, Srivanichakorn W, Chaiyakunapruk N. Cost-effectiveness analysis of ultrasonography screening for nonalcoholic fatty liver disease in metabolic syndrome patients. *Medicine (Baltimore)* 2017; **96**: e6585 [PMID: 28445256 DOI: 10.1097/MD.0000000000006585]

37 **van Katwyk S**, Coyle D, Cooper C, Pussegoda K, Cameron C, Skidmore B, Brener S, Moher D, Thavorn K. Transient elastography for the diagnosis of liver fibrosis: a systematic review of economic evaluations. *Liver Int* 2017; **37**: 851-861 [PMID: 27699993 DOI: 10.1111/liv.13260]

38 **Thavorn K**, Coyle D. Transient Elastography and Controlled Attenuation Parameter for Diagnosing Liver Fibrosis and Steatosis in Ontario: An Economic Analysis. *Ont Health Technol Assess Ser* 2015; **15**: 1-58 [PMID: 26664666]

39 **Serra-Burriel M**, Graupera I, Torán P, Thiele M, Roulot D, Wai-Sun Wong V, Neil Guha I, Fabrellas N, Arslanow A, Expósito C, Hernández R, Lai-Hung Wong G, Harman D, Darwish Murad S, Krag A, Pera G, Angeli P, Galle P, Aithal GP, Caballeria L, Castera L, Ginès P, Lammert F; investigators of the LiverScreen Consortium. Transient elastography for screening of liver fibrosis: Cost-effectiveness analysis from six prospective cohorts in Europe and Asia. *J Hepatol* 2019; **71**: 1141-1151 [PMID: 31470067 DOI: 10.1016/j.jhep.2019.08.019]

40 **Zhang E**, Wartelle-Bladou C, Lepanto L, Lachaine J, Cloutier G, Tang A. Cost-utility analysis of nonalcoholic steatohepatitis screening. *Eur Radiol* 2015; **25**: 3282-3294 [PMID: 25994191 DOI: 10.1007/s00330-015-3731-2]

41 **Corey KE**, Klebanoff MJ, Tramontano AC, Chung RT, Hur C. Screening for Nonalcoholic Steatohepatitis in Individuals with Type 2 Diabetes: A Cost-Effectiveness Analysis. *Dig Dis Sci* 2016; **61**: 2108-2117 [PMID: 26825843 DOI: 10.1007/s10620-016-4044-2]

42 **Tapper EB**, Hunink MG, Afdhal NH, Lai M, Sengupta N. Cost-Effectiveness Analysis: Risk Stratification of Nonalcoholic Fatty Liver Disease (NAFLD) by the Primary Care Physician Using the NAFLD Fibrosis Score. *PLoS One* 2016; **11**: e0147237 [PMID: 26905872 DOI: 10.1371/journal.pone.0147237]

43 **Bertot LC**, Jeffrey GP, Wallace M, MacQuillan G, Garas G, Ching HL, Adams LA. Nonalcoholic fatty liver disease-related cirrhosis is commonly unrecognized and associated with hepatocellular carcinoma. *Hepatol Commun* 2017; **1**: 53-60 [PMID: 29404433 DOI: 10.1002/hep4.1018]

44 **Caballería L**, Pera G, Arteaga I, Rodríguez L, Alumà A, Morillas RM, de la Ossa N, Díaz A, Expósito C, Miranda D, Sánchez C, Prats RM, Urquizu M, Salgado A, Alemany M, Martinez A, Majeed I, Fabrellas N, Graupera I, Planas R, Ojanguren I, Serra M, Torán P, Caballería J, Ginès P. High Prevalence of Liver Fibrosis Among European Adults With Unknown Liver Disease: A Population-Based Study. *Clin Gastroenterol Hepatol* 2018; **16**: 1138-1145.e5 [PMID: 29452268 DOI: 10.1016/j.cgh.2017.12.048]

45 **Younossi Z**, Anstee QM, Marietti M, Hardy T, Henry L, Eslam M, George J, Bugianesi E. Global burden of NAFLD and NASH: trends, predictions, risk factors and prevention. *Nat Rev Gastroenterol Hepatol* 2018; **15**: 11-20 [PMID: 28930295 DOI: 10.1038/nrgastro.2017.109]

46 **Cohen JC**, Horton JD, Hobbs HH. Human fatty liver disease: old questions and new insights. *Science* 2011; **332**: 1519-1523 [PMID: 21700865 DOI: 10.1126/science.1204265]

47 **Jarvis H**, Craig D, Barker R, Spiers G, Stow D, Anstee QM, Hanratty B. Metabolic risk factors and incident advanced liver disease in non-alcoholic fatty liver disease (NAFLD): A systematic review and meta-analysis of population-based observational studies. *PLoS Med* 2020; **17**: e1003100 [PMID: 32353039 DOI: 10.1371/journal.pmed.1003100]

48 **Chen K**, Sng WK, Quah JH, Liu J, Chong BY, Lee HK, Wang XF, Tan NC, Chang PE, Tan HC, Bee YM, Goh GBB. Clinical spectrum of non-alcoholic fatty liver disease in patients with diabetes mellitus. *PLoS One* 2020; **15**: e0236977 [PMID: 32822391 DOI: 10.1371/journal.pone.0236977]

49 **Sookoian S**, Pirola CJ. Systematic review with meta-analysis: risk factors for non-alcoholic fatty liver disease suggest a shared altered metabolic and cardiovascular profile between lean and obese patients. *Aliment Pharmacol Ther* 2017; **46**: 85-95 [PMID: 28464369 DOI: 10.1111/apt.14112]

50 **Caussy C**. Should We Screen High-Risk Populations for NAFLD? *Curr Hepatology Rep* 2019; **18**: 433-443 [DOI: 10.1007/s11901-019-00497-7]

51 **Mofrad P**, Contos MJ, Haque M, Sargeant C, Fisher RA, Luketic VA, Sterling RK, Shiffman ML, Stravitz RT, Sanyal AJ. Clinical and histologic spectrum of nonalcoholic fatty liver disease associated with normal ALT values. *Hepatology* 2003; **37**: 1286-1292 [PMID: 12774006 DOI: 10.1053/jhep.2003.50229]

52 **Browning JD**, Szczepaniak LS, Dobbins R, Nuremberg P, Horton JD, Cohen JC, Grundy SM, Hobbs HH. Prevalence of hepatic steatosis in an urban population in the United States: impact of ethnicity. *Hepatology* 2004; **40**: 1387-1395 [PMID: 15565570 DOI: 10.1002/hep.20466]

53 **Fracanzani AL**, Valenti L, Bugianesi E, Andreoletti M, Colli A, Vanni E, Bertelli C, Fatta E, Bignamini D, Marchesini G, Fargion S. Risk of severe liver disease in nonalcoholic fatty liver disease with normal aminotransferase levels: a role for insulin resistance and diabetes. *Hepatology* 2008; **48**: 792-798 [PMID: 18752331 DOI: 10.1002/hep.22429]

54 **Shieh C**, Halegoua-De Marzio DL, Hung ML, Fenkel JM, Herrine SK. Timely diagnosis and staging of non-alcoholic fatty liver disease using transient elastography and clinical parameters. *JGH Open*

2020; **4**: 1002-1006 [PMID: 33102776 DOI: 10.1002/jgh3.12385]

55 **Hofmann WP**, Buggisch P, Schubert L, Dikopoulos N, Schwenzer J, Muche M, Felten G, Heyne R, Ingiliz P, Schmidt A, Stein K, Wedemeyer H, Berg T, Wiegand J, Lammert F, Zeuzem S, Schattenberg JM. The Fatty Liver Assessment in Germany (FLAG) cohort study identifies large heterogeneity in NAFLD care. *JHEP Rep* 2020; **2**: 100168 [PMID: 32964201 DOI: 10.1016/j.jhepr.2020.100168]

56 **Labenz C**, Huber Y, Kalliga E, Nagel M, Ruckes C, Straub BK, Galle PR, Wörns MA, Anstee QM, Schuppan D, Schattenberg JM. Predictors of advanced fibrosis in non-cirrhotic non-alcoholic fatty liver disease in Germany. *Aliment Pharmacol Ther* 2018; **48**: 1109-1116 [PMID: 30288767 DOI: 10.1111/apt.14976]

57 **Teeratorn N**, Piyachaturawat P, Thanapirom K, Chaiteerakij R, Sonsiri K, Komolmit P, Tangkijvanich P, Rerknimitr R, Adams L, Treeprasertsuk S. Screening for non-alcoholic fatty liver disease in community setting: A cohort study using controlled attenuation parameter-transient elastography. *JGH Open* 2020; **4**: 245-250 [PMID: 32280772 DOI: 10.1002/jgh3.12252]

58 **Rinella ME**. Screening for nonalcoholic fatty liver disease in patients with atherosclerotic coronary disease? *Hepatology* 2016; **63**: 688-690 [PMID: 26566595 DOI: 10.1002/hep.28341]

59 **Mantovani A**, Gisondi P, Lonardo A, Targher G. Relationship between Non-Alcoholic Fatty Liver Disease and Psoriasis: A Novel Hepato-Dermal Axis? *Int J Mol Sci* 2016; **17**: 217 [PMID: 26861300 DOI: 10.3390/ijms17020217]

60 **Heitmann J**, Frings VG, Geier A, Goebeler M, Kerstan A. Non-alcoholic fatty liver disease and psoriasis - is there a shared proinflammatory network? *J Dtsch Dermatol Ges* 2021; **19**: 517-528 [PMID: 33768700 DOI: 10.1111/ddg.14425]

61 **Romeo S**, Kozlitina J, Xing C, Pertsemlidis A, Cox D, Pennacchio LA, Boerwinkle E, Cohen JC, Hobbs HH. Genetic variation in PNPLA3 confers susceptibility to nonalcoholic fatty liver disease. *Nat Genet* 2008; **40**: 1461-1465 [PMID: 18820647 DOI: 10.1038/ng.257]

62 **Speliotes EK**, Yerges-Armstrong LM, Wu J, Hernaez R, Kim LJ, Palmer CD, Gudnason V, Eiriksdottir G, Garcia ME, Launer LJ, Nalls MA, Clark JM, Mitchell BD, Shuldiner AR, Butler JL, Tomas M, Hoffmann U, Hwang SJ, Massaro JM, O'Donnell CJ, Sahani DV, Salomaa V, Schadt EE, Schwartz SM, Siscovick DS; NASH CRN; GIANT Consortium; MAGIC Investigators, Voight BF, Carr JJ, Feitosa MF, Harris TB, Fox CS, Smith AV, Kao WH, Hirschhorn JN, Borecki IB; GOLD Consortium. Genome-wide association analysis identifies variants associated with nonalcoholic fatty liver disease that have distinct effects on metabolic traits. *PLoS Genet* 2011; **7**: e1001324 [PMID: 21423719 DOI: 10.1371/journal.pgen.1001324]

63 **Noureddin M**, Jones C, Alkhouri N, Gomez EV, Dieterich DT, Rinella ME; NASHNET. Screening for Nonalcoholic Fatty Liver Disease in Persons with Type 2 Diabetes in the United States Is Cost-effective: A Comprehensive Cost-Utility Analysis. *Gastroenterology* 2020; **159**: 1985-1987.e4 [PMID: 32763241 DOI: 10.1053/j.gastro.2020.07.050]

64 **Nones RB**, Ivantes CP, Pedroso MLA. Can FIB4 and NAFLD fibrosis scores help endocrinologists refer patients with non-alcoholic fat liver disease to a hepatologist? *Arch Endocrinol Metab* 2017; **61**: 276-281 [PMID: 28225987 DOI: 10.1590/2359-3997000000233]

65 **Ciardullo S**, Muraca E, Perra S, Bianconi E, Zerbini F, Oltolini A, Cannistraci R, Parmeggiani P, Manzoni G, Gastaldelli A, Lattuada G, Perseghin G. Screening for non-alcoholic fatty liver disease in type 2 diabetes using non-invasive scores and association with diabetic complications. *BMJ Open Diabetes Res Care* 2020; **8** [PMID: 32049637 DOI: 10.1136/bmjdrc-2019-000904]

66 **Castera L**. Non-invasive tests for liver fibrosis in NAFLD: Creating pathways between primary healthcare and liver clinics. *Liver Int* 2020; **40** Suppl 1: 77-81 [PMID: 32077617 DOI: 10.1111/liv.14347]

67 **Pandyarajan V**, Gish RG, Alkhouri N, Noureddin M. Screening for Nonalcoholic Fatty Liver Disease in the Primary Care Clinic. *Gastroenterol Hepatol (N Y)* 2019; **15**: 357-365 [PMID: 31391806]

68 **Younossi ZM**, Corey KE, Alkhouri N, Noureddin M, Jacobson I, Lam B, Clement S, Basu R, Gordon SC, Ravendhra N, Puri P, Rinella M, Scudera P, Singal AK, Henry L; US Members of the Global Nash Council. Clinical assessment for high-risk patients with non-alcoholic fatty liver disease in primary care and diabetology practices. *Aliment Pharmacol Ther* 2020; **52**: 513-526 [PMID: 32598051 DOI: 10.1111/apt.15830]

69 **Srivastava A**, Gailer R, Tanwar S, Trembling P, Parkes J, Rodger A, Suri D, Thorburn D, Sennett K, Morgan S, Tsochatzis EA, Rosenberg W. Prospective evaluation of a primary care referral pathway for patients with non-alcoholic fatty liver disease. *J Hepatol* 2019; **71**: 371-378 [PMID: 30965069 DOI: 10.1016/j.jhep.2019.03.033]

70 **Leung M**, Piao C, Sarkar S. NAFLD referral patterns in a large US academic center. *J Hepatol* 2020; **73**: 218-219 [PMID: 32273138 DOI: 10.1016/j.jhep.2019.12.026]

71 **Blais P**, Husain N, Kramer JR, Kowalkowski M, El-Serag H, Kanwal F. Nonalcoholic fatty liver disease is underrecognized in the primary care setting. *Am J Gastroenterol* 2015; **110**: 10-14 [PMID: 24890441 DOI: 10.1038/ajg.2014.134]

72 **Alsenbesy M**, Rau M, Weiss J, Götze O, Geier A. A 2-step fast-track elastometry service for advanced workup of nonalcoholic fatty liver disease (NAFLD) patients - single-center real-world experience of outpatient clinical practice. *Z Gastroenterol* 2019; **57**: 1209-1217 [PMID: 31610584 DOI: 10.1055/a-0981-6484]

73 **Roeb E**, Steffen HM, Bantel H, Baumann U, Canbay A, Demir M, Drebber U, Geier A, Hampe J,

Hellerbrand C, Pathil-Warth A, Schattenberg JM, Schramm C, Seitz HK, Stefan N, Tacke F, Tannapfel A, Lynen Jansen P, Bojunga J. [S2k Guideline non-alcoholic fatty liver disease]. *Z Gastroenterol* 2015; **53**: 668-723 [PMID: 26167698 DOI: 10.1055/s-0035-1553193]

74 **Ryan CK**, Johnson LA, Germin BI, Marcos A. One hundred consecutive hepatic biopsies in the workup of living donors for right lobe liver transplantation. *Liver Transpl* 2002; **8**: 1114-1122 [PMID: 12474149 DOI: 10.1053/jlts.2002.36740]

75 **Dasarathy S**, Dasarathy J, Khiyami A, Joseph R, Lopez R, McCullough AJ. Validity of real time ultrasound in the diagnosis of hepatic steatosis: a prospective study. *J Hepatol* 2009; **51**: 1061-1067 [PMID: 19846234 DOI: 10.1016/j.jhep.2009.09.001]

76 **Bril F**, Ortiz-Lopez C, Lomonaco R, Orsak B, Freckleton M, Chintapalli K, Hardies J, Lai S, Solano F, Tio F, Cusi K. Clinical value of liver ultrasound for the diagnosis of nonalcoholic fatty liver disease in overweight and obese patients. *Liver Int* 2015; **35**: 2139-2146 [PMID: 25847730 DOI: 10.1111/liv.12840]

77 **Eddowes PJ**, Sasso M, Allison M, Tsochatzis E, Anstee QM, Sheridan D, Guha IN, Cobbold JF, Deeks JJ, Paradis V, Bedossa P, Newsome PN. Accuracy of FibroScan Controlled Attenuation Parameter and Liver Stiffness Measurement in Assessing Steatosis and Fibrosis in Patients With Nonalcoholic Fatty Liver Disease. *Gastroenterology* 2019; **156**: 1717-1730 [PMID: 30689971 DOI: 10.1053/j.gastro.2019.01.042]

78 **de Lédinghen V**, Vergniol J, Capdepont M, Chermak F, Hiriart JB, Cassinotto C, Merrouche W, Foucher J, Brigitte le B. Controlled attenuation parameter (CAP) for the diagnosis of steatosis: a prospective study of 5323 examinations. *J Hepatol* 2014; **60**: 1026-1031 [PMID: 24378529 DOI: 10.1016/j.jhep.2013.12.018]

79 **Honda Y**, Yoneda M, Imajo K, Nakajima A. Elastography Techniques for the Assessment of Liver Fibrosis in Non-Alcoholic Fatty Liver Disease. *Int J Mol Sci* 2020; **21** [PMID: 32516937 DOI: 10.3390/ijms21114039]

80 **Kwok R**, Tse YK, Wong GL, Ha Y, Lee AU, Ngu MC, Chan HL, Wong VW. Systematic review with meta-analysis: non-invasive assessment of non-alcoholic fatty liver disease--the role of transient elastography and plasma cytokeratin-18 fragments. *Aliment Pharmacol Ther* 2014; **39**: 254-269 [PMID: 24308774 DOI: 10.1111/apt.12569]

81 **Castéra L**, Foucher J, Bernard PH, Carvalho F, Allaix D, Merrouche W, Couzigou P, de Lédinghen V. Pitfalls of liver stiffness measurement: a 5-year prospective study of 13,369 examinations. *Hepatology* 2010; **51**: 828-835 [PMID: 20063276 DOI: 10.1002/hep.23425]

82 **Myers RP**, Pomier-Layrargues G, Kirsch R, Pollett A, Duarte-Rojo A, Wong D, Beaton M, Levstik M, Crotty P, Elkashab M. Feasibility and diagnostic performance of the FibroScan XL probe for liver stiffness measurement in overweight and obese patients. *Hepatology* 2012; **55**: 199-208 [PMID: 21898479 DOI: 10.1002/hep.24624]

83 **Wong VW**, Irles M, Wong GL, Shili S, Chan AW, Merrouche W, Shu SS, Foucher J, Le Bail B, Chan WK, Chan HL, de Ledinghen V. Unified interpretation of liver stiffness measurement by M and XL probes in non-alcoholic fatty liver disease. *Gut* 2019; **68**: 2057-2064 [PMID: 30658997 DOI: 10.1136/gutjnl-2018-317334]

84 **Lee MS**, Bae JM, Joo SK, Woo H, Lee DH, Jung YJ, Kim BG, Lee KL, Kim W. Prospective comparison among transient elastography, supersonic shear imaging, and ARFI imaging for predicting fibrosis in nonalcoholic fatty liver disease. *PLoS One* 2017; **12**: e0188321 [PMID: 29176844 DOI: 10.1371/journal.pone.0188321]

85 **Furlan A**, Tublin ME, Yu L, Chopra KB, Lippello A, Behari J. Comparison of 2D Shear Wave Elastography, Transient Elastography, and MR Elastography for the Diagnosis of Fibrosis in Patients With Nonalcoholic Fatty Liver Disease. *AJR Am J Roentgenol* 2020; **214**: W20-W26 [PMID: 31714842 DOI: 10.2214/AJR.19.21267]

86 **Jiang W**, Huang S, Teng H, Wang P, Wu M, Zhou X, Ran H. Diagnostic accuracy of point shear wave elastography and transient elastography for staging hepatic fibrosis in patients with non-alcoholic fatty liver disease: a meta-analysis. *BMJ Open* 2018; **8**: e021787 [PMID: 30139901 DOI: 10.1136/bmjopen-2018-021787]

87 **Karlas T**, Dietrich A, Peter V, Wittekind C, Lichtinghagen R, Garnov N, Linder N, Schaudinn A, Busse H, Prettin C, Keim V, Tröltzsch M, Schütz T, Wiegand J. Evaluation of Transient Elastography, Acoustic Radiation Force Impulse Imaging (ARFI), and Enhanced Liver Function (ELF) Score for Detection of Fibrosis in Morbidly Obese Patients. *PLoS One* 2015; **10**: e0141649 [PMID: 26528818 DOI: 10.1371/journal.pone.0141649]

88 **Bohte AE**, van Werven JR, Bipat S, Stoker J. The diagnostic accuracy of US, CT, MRI and 1H-MRS for the evaluation of hepatic steatosis compared with liver biopsy: a meta-analysis. *Eur Radiol* 2011; **21**: 87-97 [PMID: 20680289 DOI: 10.1007/s00330-010-1905-5]

89 **Iwasaki M**, Takada Y, Hayashi M, Minamiguchi S, Haga H, Maetani Y, Fujii K, Kiuchi T, Tanaka K. Noninvasive evaluation of graft steatosis in living donor liver transplantation. *Transplantation* 2004; **78**: 1501-1505 [PMID: 15599315 DOI: 10.1097/01.tp.0000140499.23683.0d]

90 **Hyodo T**, Yada N, Hori M, Maenishi O, Lamb P, Sasaki K, Onoda M, Kudo M, Mochizuki T, Murakami T. Multimaterial Decomposition Algorithm for the Quantification of Liver Fat Content by Using Fast-Kilovolt-Peak Switching Dual-Energy CT: Clinical Evaluation. *Radiology* 2017; **283**: 108-118 [PMID: 28212047 DOI: 10.1148/radiol.2017160130]

91 **Yokoo T**, Serai SD, Pirasteh A, Bashir MR, Hamilton G, Hernando D, Hu HH, Hetterich H, Kühn JP, Kukuk GM, Loomba R, Middleton MS, Obuchowski NA, Song JS, Tang A, Wu X, Reeder SB,

Sirlin CB; RSNA-QIBA PDFF Biomarker Committee. Linearity, Bias, and Precision of Hepatic Proton Density Fat Fraction Measurements by Using MR Imaging: A Meta-Analysis. *Radiology* 2018; **286**: 486-498 [PMID: 28892458 DOI: 10.1148/radiol.2017170550]

92 **Caussy C**, Johansson L. Magnetic resonance-based biomarkers in nonalcoholic fatty liver disease and nonalcoholic steatohepatitis. *Endocrinol Diabetes Metab* 2020; **3**: e00134 [PMID: 33102797 DOI: 10.1002/edm2.134]

93 **Imajo K**, Kessoku T, Honda Y, Tomeno W, Ogawa Y, Mawatari H, Fujita K, Yoneda M, Taguri M, Hyogo H, Sumida Y, Ono M, Eguchi Y, Inoue T, Yamanaka T, Wada K, Saito S, Nakajima A. Magnetic Resonance Imaging More Accurately Classifies Steatosis and Fibrosis in Patients With Nonalcoholic Fatty Liver Disease Than Transient Elastography. *Gastroenterology* 2016; **150**: 626-637.e7 [PMID: 26677985 DOI: 10.1053/j.gastro.2015.11.048]

94 **Park CC**, Nguyen P, Hernandez C, Bettencourt R, Ramirez K, Fortney L, Hooker J, Sy E, Savides MT, Alquiraish MH, Valasek MA, Rizo E, Richards L, Brenner D, Sirlin CB, Loomba R. Magnetic Resonance Elastography vs Transient Elastography in Detection of Fibrosis and Noninvasive Measurement of Steatosis in Patients With Biopsy-Proven Nonalcoholic Fatty Liver Disease. *Gastroenterology* 2017; **152**: 598-607.e2 [PMID: 27911262 DOI: 10.1053/j.gastro.2016.10.026]

95 **Cowin GJ**, Jonsson JR, Bauer JD, Ash S, Ali A, Osland EJ, Purdie DM, Clouston AD, Powell EE, Galloway GJ. Magnetic resonance imaging and spectroscopy for monitoring liver steatosis. *J Magn Reson Imaging* 2008; **28**: 937-945 [PMID: 18821619 DOI: 10.1002/jmri.21542]

96 **Hsu C**, Caussy C, Imajo K, Chen J, Singh S, Kaulback K, Le MD, Hooker J, Tu X, Bettencourt R, Yin M, Sirlin CB, Ehman RL, Nakajima A, Loomba R. Magnetic Resonance vs Transient Elastography Analysis of Patients With Nonalcoholic Fatty Liver Disease: A Systematic Review and Pooled Analysis of Individual Participants. *Clin Gastroenterol Hepatol* 2019; **17**: 630-637.e8 [PMID: 29908362 DOI: 10.1016/j.cgh.2018.05.059]

97 **Loomba R**, Cui J, Wolfson T, Haufe W, Hooker J, Szeverenyi N, Ang B, Bhatt A, Wang K, Aryafar H, Behling C, Valasek MA, Lin GY, Gamst A, Brenner DA, Yin M, Glaser KJ, Ehman RL, Sirlin CB. Novel 3D Magnetic Resonance Elastography for the Noninvasive Diagnosis of Advanced Fibrosis in NAFLD: A Prospective Study. *Am J Gastroenterol* 2016; **111**: 986-994 [PMID: 27002798 DOI: 10.1038/ajg.2016.65]

98 **Liang Y**, Li D. Magnetic resonance elastography in staging liver fibrosis in non-alcoholic fatty liver disease: a pooled analysis of the diagnostic accuracy. *BMC Gastroenterol* 2020; **20**: 89 [PMID: 32252641 DOI: 10.1186/s12876-020-01234-x]

99 **Choi SJ**, Kim SM, Kim YS, Kwon OS, Shin SK, Kim KK, Lee K, Park IB, Choi CS, Chung DH, Jung J, Paek M, Lee DH. Magnetic Resonance-Based Assessments Better Capture Pathophysiologic Profiles and Progression in Nonalcoholic Fatty Liver Disease. *Diabetes Metab J* 2020 [PMID: 33108854 DOI: 10.4093/dmj.2020.0137]

100 **Lee YS**, Yoo YJ, Jung YK, Kim JH, Seo YS, Yim HJ, Kim IH, Lee SY, Kim BH, Kim JW, Lee CH, Yeon JE, Kwon SY, Um SH, Byun KS. Multiparametric MR Is a Valuable Modality for Evaluating Disease Severity of Nonalcoholic Fatty Liver Disease. *Clin Transl Gastroenterol* 2020; **11**: e00157 [PMID: 32251018 DOI: 10.14309/ctg.0000000000000157]

101 **Eddowes PJ**, McDonald N, Davies N, Semple SIK, Kendall TJ, Hodson J, Newsome PN, Flintham RB, Wesolowski R, Blake L, Duarte RV, Kelly CJ, Herlihy AH, Kelly MD, Olliff SP, Hübscher SG, Fallowfield JA, Hirschfield GM. Utility and cost evaluation of multiparametric magnetic resonance imaging for the assessment of non-alcoholic fatty liver disease. *Aliment Pharmacol Ther* 2018; **47**: 631-644 [PMID: 29271504 DOI: 10.1111/apt.14469]

102 **Grecian SM**, McLachlan S, Fallowfield JA, Kearns PKA, Hayes PC, Guha NI, Morling JR, Glancy S, Williamson RM, Reynolds RM, Frier BM, Zammitt NN, Price JF, Strachan MWJ. Non-invasive risk scores do not reliably identify future cirrhosis or hepatocellular carcinoma in Type 2 diabetes: The Edinburgh type 2 diabetes study. *Liver Int* 2020; **40**: 2252-2262 [PMID: 32638496 DOI: 10.1111/liv.14590]

103 **Blond E**, Disse E, Cuerq C, Drai J, Valette PJ, Laville M, Thivolet C, Simon C, Caussy C. EASL-EASD-EASO clinical practice guidelines for the management of non-alcoholic fatty liver disease in severely obese people: do they lead to over-referral? *Diabetologia* 2017; **60**: 1218-1222 [PMID: 28352941 DOI: 10.1007/s00125-017-4264-9]

104 **Verma S**, Jensen D, Hart J, Mohanty SR. Predictive value of ALT levels for non-alcoholic steatohepatitis (NASH) and advanced fibrosis in non-alcoholic fatty liver disease (NAFLD). *Liver Int* 2013; **33**: 1398-1405 [PMID: 23763360 DOI: 10.1111/liv.12226]

105 **Lee TY**, Wu JC, Yu SH, Lin JT, Wu MS, Wu CY. The occurrence of hepatocellular carcinoma in different risk stratifications of clinically noncirrhotic nonalcoholic fatty liver disease. *Int J Cancer* 2017; **141**: 1307-1314 [PMID: 28509327 DOI: 10.1002/ijc.30784]

106 **Fedchuk L**, Nascimbeni F, Pais R, Charlotte F, Housset C, Ratziu V; LIDO Study Group. Performance and limitations of steatosis biomarkers in patients with nonalcoholic fatty liver disease. *Aliment Pharmacol Ther* 2014; **40**: 1209-1222 [PMID: 25267215 DOI: 10.1111/apt.12963]

107 **Cheung CL**, Lam KS, Wong IC, Cheung BM. Non-invasive score identifies ultrasonography-diagnosed non-alcoholic fatty liver disease and predicts mortality in the USA. *BMC Med* 2014; **12**: 154 [PMID: 25204761 DOI: 10.1186/s12916-014-0154-x]

108 **Lind L**, Johansson L, Ahlström H, Eriksson JW, Larsson A, Risérus U, Kullberg J, Oscarsson J. Comparison of four non-alcoholic fatty liver disease detection scores in a Caucasian population. *World J Hepatol* 2020; **12**: 149-159 [PMID: 32685107 DOI: 10.4254/wjh.v12.i4.149]

109 **Byrne CD**, Targher G. EASL-EASD-EASO Clinical Practice Guidelines for the management of non-alcoholic fatty liver disease: is universal screening appropriate? *Diabetologia* 2016; **59**: 1141-1144 [PMID: 27053232 DOI: 10.1007/s00125-016-3910-y]

110 **Hagström H**, Talbäck M, Andreasson A, Walldius G, Hammar N. Ability of Noninvasive Scoring Systems to Identify Individuals in the Population at Risk for Severe Liver Disease. *Gastroenterology* 2020; **158**: 200-214 [PMID: 31563624 DOI: 10.1053/j.gastro.2019.09.008]

111 **Staufer K**, Halilbasic E, Spindelboeck W, Eilenberg M, Prager G, Stadlbauer V, Posch A, Munda P, Marculescu R, Obermayer-Pietsch B, Stift J, Lackner C, Trauner M, Stauber RE. Evaluation and comparison of six noninvasive tests for prediction of significant or advanced fibrosis in nonalcoholic fatty liver disease. *United European Gastroenterol J* 2019; **7**: 1113-1123 [PMID: 31662868 DOI: 10.1177/2050640619865133]

112 **Inadomi C**, Takahashi H, Ogawa Y, Oeda S, Imajo K, Kubotsu Y, Tanaka K, Kessoku T, Okada M, Isoda H, Akiyama T, Fukushima H, Yoneda M, Anzai K, Aishima S, Nakajima A, Eguchi Y. Accuracy of the Enhanced Liver Fibrosis test, and combination of the Enhanced Liver Fibrosis and non-invasive tests for the diagnosis of advanced liver fibrosis in patients with non-alcoholic fatty liver disease. *Hepatol Res* 2020; **50**: 682-692 [PMID: 32090397 DOI: 10.1111/hepr.13495]

113 **Vali Y**, Lee J, Boursier J, Spijker R, Löffler J, Verheij J, Brosnan MJ, Böcskei Z, Anstee QM, Bossuyt PM, Zafarmand MH; LITMUS systematic review team(†). Enhanced liver fibrosis test for the non-invasive diagnosis of fibrosis in patients with NAFLD: A systematic review and meta-analysis. *J Hepatol* 2020; **73**: 252-262 [PMID: 32275982 DOI: 10.1016/j.jhep.2020.03.036]

114 **Parkes J**, Roderick P, Harris S, Day C, Mutimer D, Collier J, Lombard M, Alexander G, Ramage J, Dusheiko G, Wheatley M, Gough C, Burt A, Rosenberg W. Enhanced liver fibrosis test can predict clinical outcomes in patients with chronic liver disease. *Gut* 2010; **59**: 1245-1251 [PMID: 20675693 DOI: 10.1136/gut.2009.203166]

115 **Xiao G**, Zhu S, Xiao X, Yan L, Yang J, Wu G. Comparison of laboratory tests, ultrasound, or magnetic resonance elastography to detect fibrosis in patients with nonalcoholic fatty liver disease: A meta-analysis. *Hepatology* 2017; **66**: 1486-1501 [PMID: 28586172 DOI: 10.1002/hep.29302]

116 **Boursier J**, Vergniol J, Guillet A, Hiriart JB, Lannes A, Le Bail B, Michalak S, Chermak F, Bertrais S, Foucher J, Oberti F, Charbonnier M, Fouchard-Hubert I, Rousselet MC, Calès P, de Lédinghen V. Diagnostic accuracy and prognostic significance of blood fibrosis tests and liver stiffness measurement by FibroScan in non-alcoholic fatty liver disease. *J Hepatol* 2016; **65**: 570-578 [PMID: 27151181 DOI: 10.1016/j.jhep.2016.04.023]

117 **Lee J**, Vali Y, Boursier J, Spijker R, Anstee QM, Bossuyt PM, Zafarmand MH. Prognostic accuracy of FIB-4, NAFLD fibrosis score and APRI for NAFLD-related events: A systematic review. *Liver Int* 2021; **41**: 261-270 [PMID: 32946642 DOI: 10.1111/liv.14669]

118 **Yoneda M**, Imajo K, Eguchi Y, Fujii H, Sumida Y, Hyogo H, Ono M, Suzuki Y, Kawaguchi T, Aoki N, Sata M, Kanemasa K, Kohgo Y, Saibara T, Chayama K, Itoh Y, Yoshikawa T, Anzai K, Fujimoto K, Okanoue T, Nakajima A; Japan Study Group of Nonalcoholic Fatty Liver Disease (JSG-NAFLD). Noninvasive scoring systems in patients with nonalcoholic fatty liver disease with normal alanine aminotransferase levels. *J Gastroenterol* 2013; **48**: 1051-1060 [PMID: 23184095 DOI: 10.1007/s00535-012-0704-y]

119 **Sterling RK**, Lissen E, Clumeck N, Sola R, Correa MC, Montaner J, S Sulkowski M, Torriani FJ, Dieterich DT, Thomas DL, Messinger D, Nelson M; APRICOT Clinical Investigators. Development of a simple noninvasive index to predict significant fibrosis in patients with HIV/HCV coinfection. *Hepatology* 2006; **43**: 1317-1325 [PMID: 16729309 DOI: 10.1002/hep.21178]

120 **Sumida Y**, Yoneda M, Hyogo H, Itoh Y, Ono M, Fujii H, Eguchi Y, Suzuki Y, Aoki N, Kanemasa K, Fujita K, Chayama K, Saibara T, Kawada N, Fujimoto K, Kohgo Y, Yoshikawa T, Okanoue T; Japan Study Group of Nonalcoholic Fatty Liver Disease (JSG-NAFLD). Validation of the FIB4 index in a Japanese nonalcoholic fatty liver disease population. *BMC Gastroenterol* 2012; **12**: 2 [PMID: 22221544 DOI: 10.1186/1471-230X-12-2]

121 **Sun W**, Cui H, Li N, Wei Y, Lai S, Yang Y, Yin X, Chen DF. Comparison of FIB-4 index, NAFLD fibrosis score and BARD score for prediction of advanced fibrosis in adult patients with non-alcoholic fatty liver disease: A meta-analysis study. *Hepatol Res* 2016; **46**: 862-870 [PMID: 26763834 DOI: 10.1111/hepr.12647]

122 **McPherson S**, Hardy T, Dufour JF, Petta S, Romero-Gomez M, Allison M, Oliveira CP, Francque S, Van Gaal L, Schattenberg JM, Tiniakos D, Burt A, Bugianesi E, Ratziu V, Day CP, Anstee QM. Age as a Confounding Factor for the Accurate Non-Invasive Diagnosis of Advanced NAFLD Fibrosis. *Am J Gastroenterol* 2017; **112**: 740-751 [PMID: 27725647 DOI: 10.1038/ajg.2016.453]

123 **Yang M**, Jiang L, Wang Y, Li X, Zou Z, Han T, Nan Y, Lu F, Zhao J. Step layered combination of noninvasive fibrosis models improves diagnostic accuracy of advanced fibrosis in nonalcoholic fatty liver disease. *J Gastrointestin Liver Dis* 2019; **28**: 289-296 [PMID: 31517325 DOI: 10.15403/jgld-420]

World Journal of Gastroenterology

Submit a Manuscript: https://www.f6publishing.com

World J Gastroenterol 2021 September 21; 27(35): 5822-5850

DOI: 10.3748/wjg.v27.i35.5822

ISSN 1007-9327 (print) ISSN 2219-2840 (online)

REVIEW

Environmental perspectives of COVID-19 outbreaks: A review

Palas Samanta, Apurba Ratan Ghosh

ORCID number: Palas Samanta 0000-0001-9369-7502; Apurba Ratan Ghosh 0000-0003-1454-7720.

Author contributions: Samanta P contributed to the conceptualization, writing- original draft preparation, software running; Ghosh AR contributed to the conceptualization, supervision, writing- reviewing and editing.

Conflict-of-interest statement: The authors have no conflicts of interest to declare.

Open-Access: This article is an open-access article that was selected by an in-house editor and fully peer-reviewed by external reviewers. It is distributed in accordance with the Creative Commons Attribution NonCommercial (CC BY-NC 4.0) license, which permits others to distribute, remix, adapt, build upon this work non-commercially, and license their derivative works on different terms, provided the original work is properly cited and the use is non-commercial. See: http://creativecommons.org/Licenses/by-nc/4.0/

Manuscript source: Invited manuscript

Specialty type: Public, environmental and occupational health

Country/Territory of origin: India

Palas Samanta, Department of Environmental Science, Sukanta Mahavidyalaya, University of North Bengal, Dhupguri 735210, West Bengal, India

Apurba Ratan Ghosh, Department of Environmental Science, The University of Burdwan, Burdwan 713104, West Bengal, India

Corresponding author: Palas Samanta, PhD, Assistant Professor, Department of Environmental Science, Sukanta Mahavidyalaya, University of North Bengal, Dhupguri, Jalpaiguri, Dhupguri 735210, West Bengal, India. samanta.palas2010@gmail.com

Abstract

The coronavirus disease 2019 (COVID-19) pandemic, caused by the novel virus severe acute respiratory syndrome coronavirus 2 (SARS-CoV-2), began in December 2019 in China and has led to a global public health emergency. Previously, it was known as 2019-nCoV and caused disease mainly through respiratory pathways. The COVID-19 outbreak is ranked third globally as the most highly pathogenic disease of the twenty-first century, after the outbreak of SARS-CoV and Middle East respiratory syndrome in 2002 and 2012, respectively. Clinical, laboratory, and diagnostic methodology have been demonstrated in some observational studies. No systematic reviews on COVID-19 have been published regarding the integration of COVID-19 outbreaks (monitoring, fate and treatment) with environmental and human health perspectives. Accordingly, this review systematically addresses environmental aspects of COVID-19 outbreak such as the origin of SARS-CoV-2, epidemiological characteristics, diagnostic methodology, treatment options and technological advancement for the prevention of COVID-19 outbreaks. Finally, we integrate COVID-19 outbreaks (monitoring, fate and treatment) with environmental and human health perspectives. We believe that this review will help to understand the SARS-CoV-2 outbreak as a multipurpose document, not only for the scientific community but also for global citizens. Countries should adopt emergency preparedness such as prepare human resources, infrastructure and facilities to treat severe COVID-19 as the virus spreads rapidly globally.

Key Words: COVID-19; SARS-CoV-2 virus; Environmental perspectives; Epidemiological characteristics; Public health; Emergency preparedness

©The Author(s) 2021. Published by Baishideng Publishing Group Inc. All rights reserved.

Peer-review report's scientific quality classification
Grade A (Excellent): 0
Grade B (Very good): B, B
Grade C (Good): 0
Grade D (Fair): 0
Grade E (Poor): 0

Received: December 14, 2020
Peer-review started: December 14, 2020
First decision: January 7, 2021
Revised: January 10, 2021
Accepted: August 12, 2021
Article in press: August 12, 2021
Published online: September 21, 2021

P-Reviewer: Jiang T, Pan H
S-Editor: Gong ZM
L-Editor: Webster JR
P-Editor: Ma YJ

Core Tip: This review is the first attempt to integrate coronavirus disease 2019 (COVID-19) outbreaks (monitoring, fate and treatment) with respect to environmental and human health perspectives. Briefly, the paper systematically addresses the environmental aspects of the COVID-19 outbreak such as the origin of severe acute respiratory syndrome coronavirus 2, epidemiological characteristics, diagnostic methodology, treatment options and technological advancement for the prevention of COVID-19 outbreaks.

Citation: Samanta P, Ghosh AR. Environmental perspectives of COVID-19 outbreaks: A review. *World J Gastroenterol* 2021; 27(35): 5822-5850
URL: https://www.wjgnet.com/1007-9327/full/v27/i35/5822.htm
DOI: https://dx.doi.org/10.3748/wjg.v27.i35.5822

INTRODUCTION

A series of patients with unidentified pneumonia, caused by β-coronavirus, was reported in late December 2019 in Wuhan (Hubei Province), China. Coronavirus disease 2019 (COVID-19) outbreaks are clinically very similar to viral pneumonia. A number of experts from the PRC Centers for Disease Control declared that this respiratory disorder (alternatively known as novel coronavirus pneumonia, NCP) was caused by a novel coronavirus[1]. The World Health Organization (WHO) initially named the disease as 2019-nCoV (2019-novel coronavirus) on January 12, 2020. It was officially later named COVID-19 on February 11, 2020 by the WHO. On the same date, the International Committee on Taxonomy of Viruses named the virus as severe acute respiratory syndrome coronavirus 2 (SARS-CoV-2) after developing the genome sequence from a COVID-19 patient in Wuhan on January 7, 2020. The virus belongs to the β-coronavirus family, which is very prevalent in nature among other families. Similar to other viruses, the SARS-CoV-2 also has many natural hosts including different intermediate and final hosts, which makes it challenging for scientific communities to treat and prevent COVID-19 outbreaks. It has higher transmission and infection potential but causes a lower mortality rate compared with SARS-CoV and Middle East respiratory syndrome (MERS-CoV)[2]. The genomic sequence of SARS-CoV-2 revealed that it has 79.5% and 96% similarity with SARS-CoV and bat coronavirus, respectively[1], which implies that bats might be the source of SARS-CoV-2. Although the COVID-19 outbreak started in China, the virus has spread to over 213 countries with the highest rate of infection in the United States, Italy, France, and Spain among others as per data published by the WHO on December 13, 2020 (Figure 1). There are approximately 202608306 confirmed SARS-CoV-2 cases and 4293591 deaths worldwide. Consequently, COVID-19 has emerged as a global threat to public health and is steadily growing due to human-to-human transmission. Moreover, this transmission also spreads in different environmental sectors such as water, air, soil, sewage and fecal matter[3]. Additionally, this process is accelerated by a number of meteorological factors namely temperature, weather, humidity and air quality parameters including particulate matter, SOx, NOx and carbon, *etc*. Therefore, a better understanding of the global consequences of COVID-19 is required with regard to environmental perspectives. Accordingly, this review will address the origin of SARS-CoV-2, route of transmission, pathogenesis, epidemiological characteristics, diagnostic methodology, treatment options and technological advancement for the prevention of COVID-19 outbreaks with regard to environmental perspectives in order to acquire the latest understanding of this new infectious disease of which certain immediate as well as long-term remedial measures can be explored.

EPIDEMIOLOGY OF THE COVID-19 OUTBREAK

Origin of the COVID-19 outbreak

SARS-CoV-2 is a β-coronavirus and is enveloped with non-segmented Orthocoronavirinae subfamily RNA[4]. Among the four genera, γ- and δ-CoV infect birds while α- and β-CoV infect mammals including humans (Table 1). The α- and β-CoV have six

Table 1 Details of coronavirus (genus, species and receptor)

Genus	Species	Targets	Receptor
α-CoV	Alphacoronavirus 1:	Mammals	
	Feline coronavirus serotype 2		Aminopeptidase N
	Canine coronavirus serotype 2		Aminopeptidase N
	Transmissible gastroenteritis virus		Aminopeptidase N
	Human coronavirus 229E		Aminopeptidase N
	Human coronavirus NL63		ACE2
	Porcine epidemic diarrhea coronavirus		Aminopeptidase N
	Rhinolophus bat coronavirus HKU2		
	Scotophilus bat coronavirus 512/05		
	Miniopterus bat coronavirus 1		
	Miniopterus bat coronavirus HKU8		
β-CoV	Betacoronavirus 1:	Mammals	
	Bovine coronavirus		Neu 5,9 Ac2
	Human coronavirus OC43		Neu 5,9 Ac2
	Equine coronavirus		
	Human enteric coronavirus		
	Porcine haemagglutinating encephalomyelitis virus		
	Canine respiratory coronavirus		
	Murine coronavirus:		
	Mouse hepatitis virus		CEACAM1
	Rat coronavirus		
	Puffinosis virus		
	Hedgehog coronavirus 1		
	Human coronavirus HKU1		
	Middle East respiratory syndrome-related coronavirus		
	Pipistrellus bat coronavirus HKU5		
	Rousettus bat coronavirus HKU9		
	Severe acute respiratory syndrome-related coronavirus		
	SARS-CoV		
	SARS-CoV-2		ACE2
	Rhinolophus bat viruses		
	Tylonycteris bat coronavirus HKU4		
γ-CoV	Avian coronavirus:	Birds	
	IBV (turkey, pheasant, duck, goose and pigeon)		
	Beluga Whale coronavirus SW1		
δ-CoV	Bulbul coronavirus HKU11	Birds	
	Thrush coronavirus HKU12		
	Munia coronavirus HKU13		
	Porcine coronavirus HKU15		

ACE2: Angiotensin-converting enzyme 2; SARS-CoV-2: Severe acute respiratory syndrome coronavirus 2.

variants. Among them α-CoVs variants (HCoV-229E and HCoV-NL63), and β

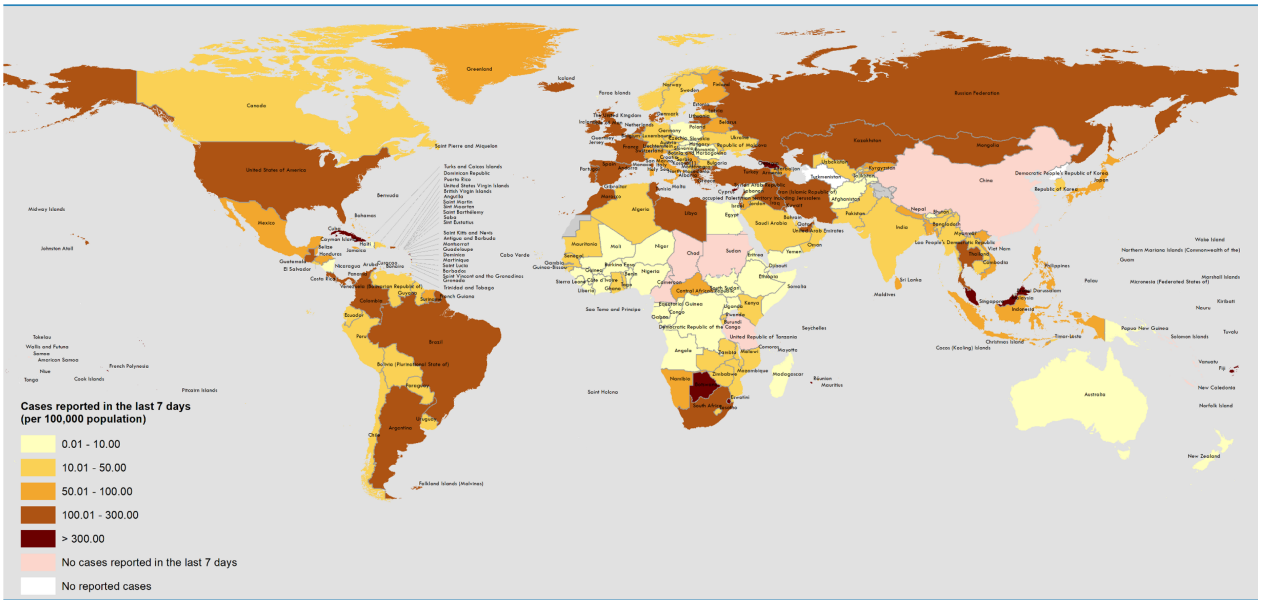


Figure 1 Geographical distribution of coronavirus disease 2019 outbreaks. Source: https://www.who.int/publications/m/item/weekly-epidemiological-update-on-covid-19---10-august-2021 (data as reported at 4:58 pm CET on August 10, 2021).

-CoVs variants (HCoV-HKU1 and HCoV-OC43) have lower pathogenic capability in humans and cause mild respiratory symptoms similar to the common cold. Only β-CoVs variants (SARS-CoV and MERS-CoV) have severe pathogenic capability in humans. This pandemic started in Wuhan specifically in a seafood wet market, on December 12, 2019. Several studies have demonstrated that bats are natural hosts of SARS-CoV-2 and animals such as snakes, turtles and pangolins are intermediate hosts of SARS-CoV-2.

Previously, snakes were thought to be involved in COVID-19 outbreaks by Ji *et al*[5] but this hypothesis was rejected by Zhang *et al*[6] who did not find any similarity in genome sequence between snakes and COVID-19 patients. In another study, researchers found an approximately 96.2% genome sequence similarity between SARS-CoV-2 and bat coronavirus (CoV RaTG13)[7]. In addition, the genomic sequence of SARS-CoV-2 matched with 79.5% of the genome sequence of SARS-CoV[8]. These findings implied that bats were the suspected source of COVID-19 outbreaks as well as the natural host of this virus. The virus was finally transmitted to humans *via* unknown intermediate hosts from bats. However, few bats are sold in the Wuhan seafood market[9]. Accordingly, scientists are trying to determine the intermediate sources such as snakes, turtles and pangolins. Xu *et al*[10] found approximately 99% genomic similarity between SARS-CoV-2 and pangolins. Furthermore, they revealed that pangolins are the potential intermediate host of SARS-CoV-2. Apart from these studies, to date there is no adequate evidence on the virus origin regarding potential intermediate hosts and the natural host of SARS-CoV-2. Therefore, SARS-CoV-2 could use angiotensin-converting enzyme 2 (ACE2), similar to SARS-CoV receptor for human infection[7]. However, there is controversy regarding the infectious potential of COVID-19 patients to transmit the disease during the incubation period. Recently, the WHO reported that cats may be the carrier of this virus, whereas other domestic animals like ducks, hens and dogs may not be carriers of this deadly virus.

Transmission of COVID-19

The animal-human interface is not a new concept. Zoonotic diseases with a wildlife reservoir have long been recognized as significant public health problems. Indeed, up to three-quarters of infectious diseases that cause human infections are known to be zoonotic[11]. Apart from this, the complexity of animal, human, and environmental factors is thought to play a critical role in its emergence[12]. On the other hand, contact with infected patients and droplets are considered to be major transmission routes of COVID-19. Aerosol transmission is another important route of SARS-CoV-2 infection. By contrast, SARS-CoV and MERS-CoV transmission are mainly reported through nosocomial transmission. However, human-to-human SARS-CoV-2 transmission occurs mainly through close contact between COVID-19 patients or friends or carriers and between family members including relatives. It can be spread rapidly in

healthcare workers (up to 50%) and patients (62–79%) similar to SARS-CoV and MERS-CoV and is considered the most common route of infection[13]. It is also assumed that consumption of wild animals who are the hosts of SARS-CoV-2 and humans in close contact with these animals are suspected to be the route of entry of SARS-CoV-2 and its mode of transmission. However, this route of SARS-CoV-2 transmission remains controversial and requires further study.

To date, 1 million people around the world have tested positive for this virus, but only 4 cases have so far been reported in which pets showed positive for SARS-CoV-2. These involved 2 dogs and 2 cats, the owners had COVID-19 and are believed to be the most likely source of transmission to their pets. The dogs showed clinical signs, but one of the cats did not have signs of illness. In late March 2020, health officials in Belgium reported that a cat from Liège province had also tested positive for SARS-CoV-2. Nevertheless, the US Centers for Disease Control and Prevention (CDC), WHO, and key animal health organizations have all issued statements aiming to calm people's fears about their pets being a source of the novel virus[14-16]. In this regard, the World Organization for Animal Health has emphasized that "there is no justification in taking measures against companion animals which may compromise their welfare". Furthermore, given the speculation that wild live animal species may be linked to this pandemic, this collaborative approach will also require the expertise of wildlife forensic specialists.

SARS-CoV-2 has also been detected in saliva, the gastrointestinal tract, urine and stool. In particular, the gastrointestinal tract or digestive tract has been recognized as another route of SARS-CoV-2 infection based on a bioinformatics study[17]. SARS-CoV-2 has been detected in gastrointestinal mucosal tissue of COVID-19 patients[18]. In addition, it has also been detected in tears and conjunctival secretions of COVID-19 patients[19]. Intrauterine vertical transmission from pregnant women to the newborn is temporarily excluded due to a lack of adequate data on pregnant women infected with SARS-CoV-2[20].

Prevalence of COVID-19

A number of researchers estimated the basic reproduction number (R_0) to calculate the number of people affected by secondary infections. Generally, it represents the number of people with COVID-19 but in a completely susceptible population without intervention[21]. Using the SEIR model, Wu *et al*[22] recorded an R_0 value for SARS-CoV-2 in the range of 2.47-2.86, while Majumder and Kenneth[23] estimated the R_0 value to be 2.0–3.3 based on the IDEA model. By contrast, other β-CoV viruses namely SARS-CoV and MERS-CoV showed an R_0 value in the range of 2.2–3.6 and 2.0–6.7, respectively[24,25], which indicated that SARS-CoV-2 has higher transmissibility than SARS-CoV and MERS-CoV. In China, 87% of cases were in the age group 30 to 79 years and 3% cases were noted to be aged ≥ 80 years, while female cases were only 41.9%[26,27]. Additionally, 81% of cases were classified as mild, 14% cases were severe and 5% cases were very critical. In another study, it was reported that the overall case-fatality rate (CFR) was 2.3%; however, in the age groups 70-79 and ≥80 years, the CFRs were 8.0% and 14.8%, respectively[22]. These findings clearly indicated that elderly males are more susceptible to SARS-CoV-2 compared with other groups. In addition, the virus affected those elderly males with chronic diseases such as diabetes, hypertension, heart disease, *etc*.[20]. In summary, the prevalence of COVID-19 is very high, and it can spread very rapidly within countries and outside countries.

Virus susceptibility and incubation period

Generally, elderly people aged between 55 and 75 years are more susceptible to SARS-CoV-2 infection. Currently, it has been found that the virus is also infecting middle-aged people aged between 25 and 50 years. The average age of patients across 18 studies was 51.97 years (95%CI: 46.06%-57.89%), 55.9% were male (95%CI: 51.6%–60.1%). Additionally, 36.8% cases showed comorbidities (95%CI: 24.7%-48.9%), the most significant being hypertension (18.6%; 95%CI, 8.1–29.0%), cardiovascular disease (14.4%; 95%CI: 5.7%–23.1%), and diabetes (11.9%; 95%CI: 9.1%-14.6%), among others[28]. Children account for 1% to 3% of COVID-19 cases across countries and likely experience an asymptomatic infection (mild or no symptoms on infection) compared with adults. Zhong *et al*[29] demonstrated that the virus has an average median incubation period of about 3 d but it can range between 0 and 24 d, and the average median time from symptomatic onset to death is 14 d. They also found that mortality rises in patients with comorbidities or a surgical history before virus infection. Generally, the average median latency period for SARS-CoV-2 infection was 4 d, the average interval to hospital admission after onset of symptoms was 3.8 d, and the average time to death after admission to hospital was 17.4 d[30]. Another study

reported that the time to appearance of COVID-19 symptoms to death ranged between 6 and 41 d with a median period 14 d[22]. They also showed that this period was age-dependent and related to the patient's immune system status. The prevalence was greater in patients aged over 70 years compared with those less than 70 years. According to the WHO, the incubation period for COVID-19 ranged from 2 to 10 d. By contrast, for MERS-CoV infection the average median latency was 7 d[31]. However, in COVID-19, the maximum latency was observed to be 24 d, which was high compared with SARS and MERS. This indicated that SARS-CoV-2 has a higher risk of transmission. Accordingly, in comparison with SARS and MERS, SARS-CoV-2 has a shorter median incubation period. Recent data showed that elderly people (aged above 75 years) have a shorter median interval, *i.e.*, 11.5 d from symptom onset to death in comparison to COVID-19 patients (20 d). This finding indicated that disease progression is more rapid in elderly people compared to younger people[1].

GENOMIC STRUCTURE AND PATHOPHYSIOLOGY

Genomic structure

SARS-CoV-2, a β-coronavirus, is a single-stranded RNA virus with a diameter ranging between 80 nm and 120 nm. Currently, four types of coronavirus are present in nature: α-, β-, δ- and γ- coronavirus. The γ- and δ-CoV infect birds, while α- and β-CoV infect mammals. Details of these coronaviruses are presented in Table 1. There are six coronaviruses causing human infection including SARS-CoV and MERS-CoV. The complete genome sequence of SARS-CoV-2 is closest to SARS-like bat CoV (MG772933). There is approximately 79% homology in genome sequence between SARS-CoV-2 and SARS[9]. In addition, the complete genomic sequence of SARS-CoV-2 is approximately 29.9 kb, while SARS-CoV and MERS-CoV have a genome length of 27.9 kb and 30.1 kb, respectively[8,32]. The SARS-CoV-2 genome contains a variable number of open reading frames (ORFs) ranging between 6 and 11[33]. Two-thirds are located mainly in the first ORF (ORF1a/b) which encodes 16 non-structural proteins (NSP) and translates polyproteins (pp1a and pp1ab), while the remaining ORFs encode accessory and structural proteins. The remainder of the RNA virus encodes four essential structural proteins, including the spike (S) glycoprotein, small envelope (E) protein, matrix (M) protein, and nucleocapsid (N) protein, and several accessory proteins, that interfere with the host innate immune response[34]. Frameshift mutation between ORF1a and ORF1b is mainly responsible for the production of pp1a and pp1ab polypeptides that are regulated by chymotrypsin-like protease (3CLpro) or main protease (Mpro), and this process produces 16 non-structural proteins (NSPs) with the help of papain-like proteases[35]. Therefore, SARS-CoV-2 pathophysiology and virulence are thought to be linked with NSPs and structural protein functions.

Pathophysiology

The pathophysiology of COVID-19 produces pneumonia which seems to be very complex. The pathological mechanism is presented in Figure 2. A group of researchers claimed that viral infection is caused by an immune reaction through the "cytokine storm"[36,37]. The main protagonist of this "cytokine storm" is interleukin 6 (IL-6). Generally, activated leukocytes are primarily responsible for IL-6 production and IL-6 acts on a number of cells and tissues. It stimulates acute phase protein production and regulates thermoregulation, bone structure and central nervous system functions[36,37]. However, its main role is pro-inflammatory actions. COVID-19 enhances IL-6 level, which is implicated in the pathogenesis of the cytokine release syndrome (CRS), which is an acute systemic inflammatory syndrome characterized by fever and multiple organ dysfunction[36,37].

Another group of researchers demonstrated that SARS-CoV-2 uses angiotensin converting enzyme 2 (ACE2) receptor for both cross-species and human-to-human transmission[1,38]. The virion S-glycoprotein present on the virus surface interacts with ACE2 receptors on human cells to spread the infection[39]. S-glycoprotein contains two subunits, S1 and S2. The S1 determines the virus-host range and cellular tropism in the key function domain – RBD (receptor-binding domain), while S2 is responsible for cell membrane-virus fusion by two tandem domains, heptad repeats 1 (HR1) and HR2[40,41]. Following membrane fusion, viral RNA is released into the cytoplasm, and the uncoated RNA is induced to produce pp1a and pp1ab polypeptides with the help of either chymotrypsin-like protease (3CLpro) or main protease (Mpro), which encode 16 non-structural proteins (NSPs) in the presence of papain-like proteases, and finally form a replication-transcription complex (RTC) in double-

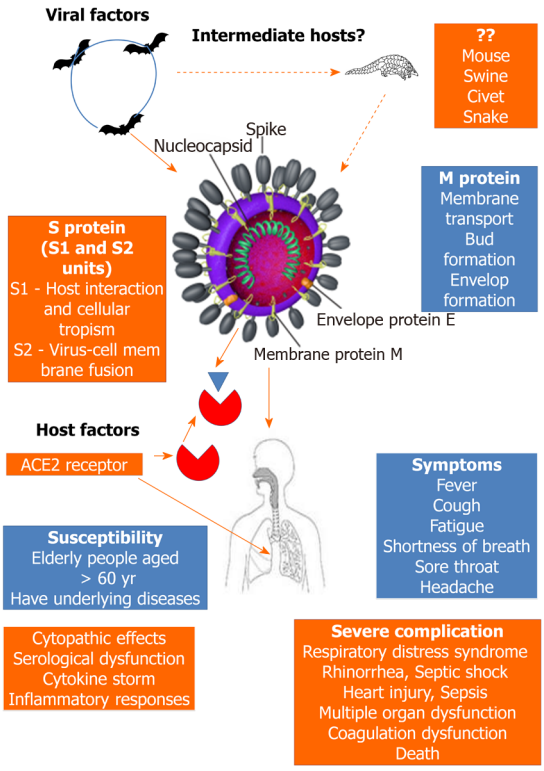


Figure 2 Pathogenesis of severe acute respiratory syndrome coronavirus 2 (viral and host factors). ACE2: Angiotensin-converting enzyme 2.

membrane vesicles[8]. Subsequently, the RTC replicates continuously and synthesizes sub-genomic RNAs[42] to encode accessory proteins and structural proteins. This newly formed genomic RNA, envelopes glycoproteins and nucleocapsid proteins mediated through the endoplasmic reticulum (ER) and Golgi[43] are assembled together to form viral buds. Finally, these newly formed virion-containing vesicles are fused with plasma membrane to release the virus and cause infection through mucous membranes, especially nasal and larynx mucosa, and then enter the lungs through the respiratory tract.

These ACE2 receptors are very important in the spread of COVID-19. They are mainly found in the lower respiratory tract of humans. After entry through mucous membranes, especially nasal and larynx mucosa, the virus enters directly into the lungs through the respiratory tract. In the next step, the virus attacks other target organs which contain ACE2 receptors, such as the lungs, heart, renal system and gastrointestinal tract[36,37]. Accordingly, the binding affinity of this virus-receptor has been intensively studied using different approaches. Systematic detection analysis showed that SARS-CoV-2 S-glycoprotein binding capacity with ACE2 was 10-fold higher than SARS-CoV as shown under cryo-electron microscopy of the SARS-CoV-2 S protein in pre-fusion conformation[39]. Recently, Wu *et al*[9] demonstrated moderate genomic and phylogenetic similarity with SARS-CoV but higher similarity with bat CoV genome sequence, particularly in the S-glycoprotein and RBD. They also found that there were no amino acid substitutions occurring in the NSP7, NSP13, envelope, matrix, or accessory proteins p6 and 8b at the protein level, except in NSP2, NSP3, spike protein, underpinning the subdomain, *i.e.*, RBD. Another recent study demonstrated that mutation of NSP2 and NSP3 plays an important role in infection and SARS-CoV-2 differentiation. However, this mechanism of SARS-CoV-2 infection in humans *via* S-protein binding with ACE2 is unclear, as is the interaction strength for risk transmission. Accordingly, the WHO was also unable to clarify the mechanism of COVID-19. This has led to further investigations regarding potential human-to-human transmission and the pathophysiological mechanisms of COVID-19 outbreaks.

CLINICAL CHARACTERISTICS OF COVID-19 INFECTION

Being an acute respiratory infection, COVID-19 is initiated in the respiratory tract, primarily by droplets, respiratory secretions, and direct contact. After entry, the virus

affects a number of organs or systems (Figure 3). The clinical symptoms of COVID-19 vary from asymptomatic or paucisymptomatic forms to clinical conditions. In particular, all patients are divided into general, severe, and critical patient groups. The most common clinical symptoms of COVID-19 are fever (87.9%), cough (67.7%), fatigue (38.1%), sputum production (33.4%), shortness of breath (18.6%), sore throat (13.9%), and headache (13.6%)[27,44]. The development of these symptoms may occur within 3 d of viral infection. On the other hand, other symptoms may occur 9 d after virus infection. Of these, fever and cough are the dominant COVID-19 symptoms. The incidence of diarrhea (3.7%) and vomiting (5.0%) is very rare[27,44]. However, it is very difficult to accurately distinguish COVID-19 from other viral respiratory infections. The CDC included loss of taste or smell, pink eye, muscle pain, intense chills, headache and sore throat as COVID symptoms. In severe cases, symptoms such as acute respiratory distress syndrome, rhinorrhea, dyspnea, gastrointestinal disorders, septic shock, mental stress, acute heart injury, sepsis, multiple organ dysfunction syndrome (MODS), secondary infection and even death may occur[8,34]. Critical COVID-19 patients with severe respiratory failure require an intensive care unit (ICU) or ventilation support. However, the occurrence of upper respiratory symptoms and gastrointestinal symptoms are very rare compared with other symptoms. In addition to this, the elderly and those who have underlying diseases (*i.e.*, chronic obstructive pulmonary disease, hypertension, diabetes, cardiovascular disease) are very prone to COVID-19 and develop symptoms such as metabolic acidosis, acute respiratory distress syndrome, coagulation dysfunction and even death [8,45]. Sometimes, COVID-19 patients experience acute heart injury, arrhythmia, impaired renal function and abnormal liver function such as the formation of microvesicular steatosis (50.7%) at the time of admission[1,45,46].

Hematological assays revealed that most patients had decreased white blood cell counts, and lymphocytopenia[27]. In the case of critical patients, neutrophil count, D-dimer, blood urea, creatinine and lymphocyte levels decreased markedly. In another study, a reduction in albumin level (75.8%; 95%CI, 30.5%-100.0%), higher C-reactive protein (58.3%; 95%CI: 21.8%-94.7%) and lactate dehydrogenase (LDH) levels (57.0%; 95%CI: 38.0%-76.0%), higher lymphopenia level (43.1%; 95%CI, 18.9%-67.3%), and higher erythrocyte sedimentation rate (ESR) (41.8%; 95%CI: 0.0-92.8%) and other clinical manifestations were recorded[28]. Additionally, inflammatory factors, which indicated the immune status of patients, namely IL-6, IL-10, and tumor necrosis factor-α (TNF-α) are also markedly increased. In critical patients (admitted to the ICU), higher IL-2, IL-7, IL-10, granulocyte colony-stimulating factor (GCSF), 10 kD interferon gamma-induced protein (IP-10), monocyte chemoattractant protein-1 (MCP-1), macrophage inflammatory protein 1-α (MIP-1α), and TNF-α levels in plasma were observed[8,45]. In patients with severe COVID-19 [admitted to the ICU; 20.3% cases (95%CI, 10.0–30.6%)], 32.8% of patients experienced ARDS (95%CI: 13.7%–51.8%), 13.0% patients had acute cardiac injury (95%CI: 4.1%-21.9%), 7.9% patients experienced acute kidney injury (95%CI: 1.8-14.0%), 6.2% cases (95%CI: 3.1%-9.3%) developed shock and 13.9% cases (95%CI 6.2%-21.5%) experienced fatal outcomes[28]. Furthermore, 96.8% of all patients (95%CI: 94.9%-98.7%) had RNAemia in blood and nasopharyngeal aspirates (NPA)[28].

IMMUNOPATHOLOGICAL RESPONSES

Immunological symptoms are generally caused due to binding of virus S proteins with ACE2 at the receptor, usually in the endosome Toll-like receptor (TLR) 3, TLR7, TLR8, and TLR9[8,47]. Retinoic-acid inducible gene I (RIG-I) of the virus, melanoma differentiation-associated gene 5 (MDA5) of the cytosol and nucleotidyltransferase cyclic GMP-AMP synthase (cGAS) are generally responsible for the spread of COVID-19[8, 48,49]. Viral infection activates nuclear factor-κB (NF-κB) and interferon regulatory factor 3 (IRF3) to produce type I interferons (IFN-α/β) and pro-inflammatory cytokines as immune mediators (*i.e.*, innate immunity) to prevent infection[8,50]. As a result, the plasma levels of some cytokines and chemokines are elevated in COVID-19 patients such as IL-1, IL-2, IL-4, IL-7, IL-10, IL-12, IL-13, IL-17, GCSF, macrophage colony-stimulating factor (MCSF), IP-10, MCP-1, MIP-1α, hepatocyte growth factor (HGF), IFN-γ and TNF-α[20,45,51]. Generally, these inflammatory responses were noted in the lower airway and lung[52]. Consequently, these trigger immune signaling and produce the "cytokine storm' within the body leading to a very critical condition in COVID-19 patients.

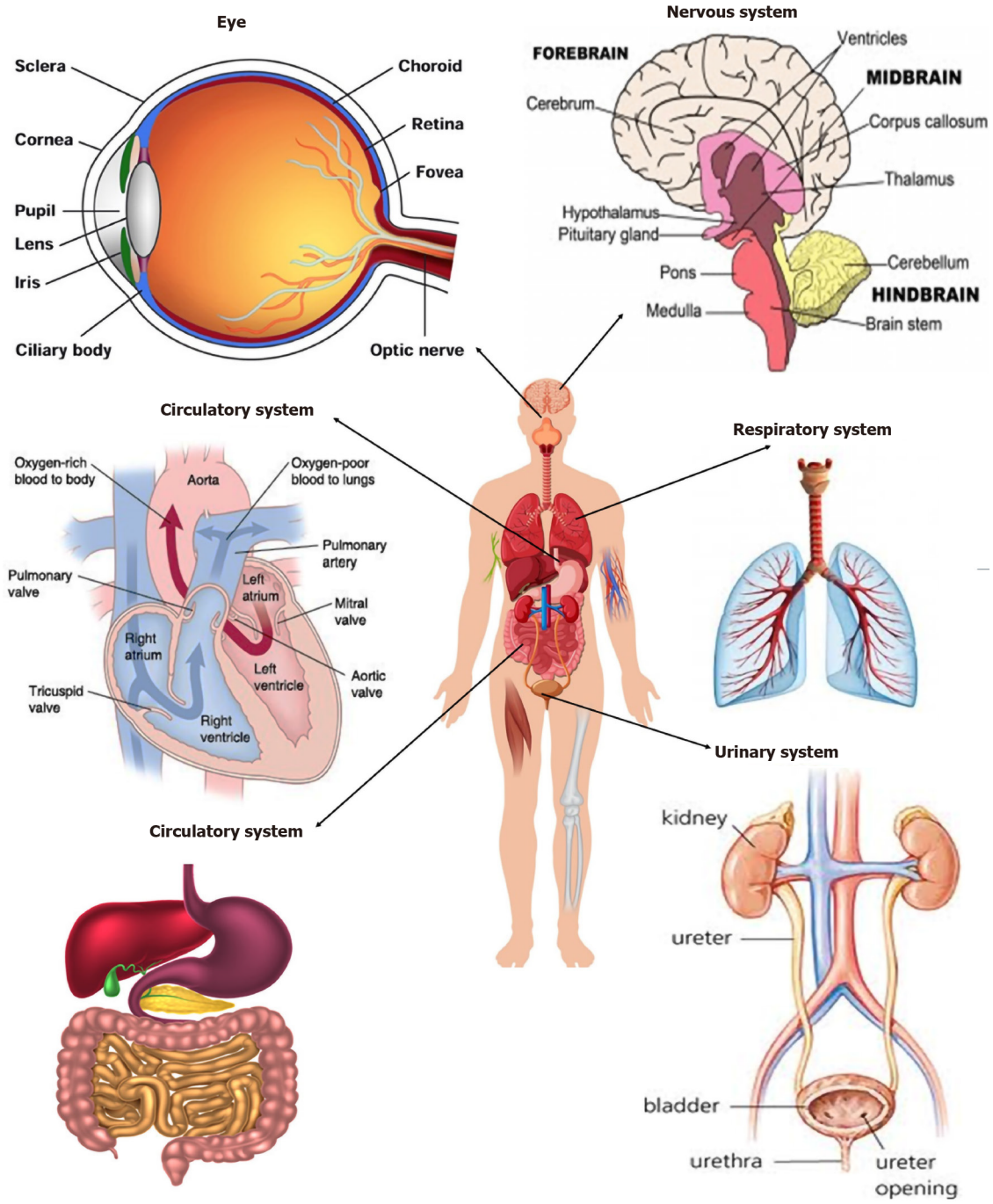


Figure 3 Coronavirus disease 2019 in organs or systems (Images were taken www.google.com).

DIAGNOSIS OF COVID-19

Since the outbreak of COVID-19, a number of diagnostic tools have been used to detect the infection. The classical Koch's postulates method was used to detect the infection in Wuhan[22]. This method is very expensive and time-consuming as it uses electron microscopy. In some countries, radiography was used to detect the viral infection such as a chest computed tomography (CT) scan. CT scan is an important tool in diagnosing COVID-19 pneumonia. Typical COVID-19 pneumonia features were observed by CT. and CT imaging showed ground-glass opacities (56.4%-65%), an air bronchogram (47%), bilateral patchy shadowing (51.8%), consolidations (50%), smooth or irregular interlobular septal thickening (35%), thickening of adjacent pleura (32%), sometimes rounded morphology, peripheral and lower lobe involvement and a peripheral lung distribution in COVID patients[27,53,54]. A very recent study recorded bilateral chest CT findings in 90% patients, and proved its sensitivity (97%) in detecting COVID-19 [55]. However, in another study clinical scientists found that some patients with

confirmed COVID-19 had normal CT scans[53]. Therefore, the diagnosis of COVID-19 is very confusing. Moreover, this technique mainly determines pneumonia. Accordingly, scientists are looking for an alternative method which is more reliable and confirmative. The detection of viral nucleic acid from nasal and throat swab samples, cough, sputum or other respiratory tract samples is the golden diagnostic method for COVID-19 detection. This method uses RT-PCR technology to detect viral infection. Although, this method has high specificity, false-negative results may occur due to low sensitivity and the testing time is too long. In the case of false-positive tests, the WHO recommends resampling and further testing. In this regard, serologic testing is an important diagnostic tool to detect patients who have either current or previous infection but have a negative PCR test[56,57]. In this technique, basic parameters are tested to detect the COVID-19, namely white blood cell count, neutrophil and lymphocyte count, D-dimer, blood urea, and creatinine estimation to identify the appearance of leukopenia, leukocytosis, and lymphopenia as COVID-19 symptoms[58, 59]. In another study, it was demonstrated that 82.1% of COVID patients are lymphopenic, 33.7% patients are leukopenic and 36.2% patients are thrombocytopenic [1]. In addition, another group of researchers recommended elevated plasma levels of C-reactive protein, lactate dehydrogenase, creatinine kinase, transaminase, abnormal myocardial enzyme spectrum or creatinine as COVID-19 indicators[27,45]. They also showed that cytokine release syndrome is an important vital indicator of disease progression. On the other hand, Wan *et al*[60] demonstrated higher IL-6 and IL-10 levels, and lower CD4+T and CD8+T levels as indicators of COVID-19.

Currently, a number of technological inventions are ongoing to detect COVID-19 in a simplistic pathway. Different technological inventions such as the more organized sequencing library (SHERRY) in China, SHERLOCK technology in China, FELUDA in India *etc.*, have been developed as testing tools for rapid detection of COVID-19[6,61]. However, clinical verification of these technological inventions has not been undertaken to date, and once approved, they will be a major breakthrough in technology to diagnose COVID-19 rapidly and economically.

GLOBAL SCENARIOS OF COVID-19 OUTBREAKS

Since its outbreak in Wuhan, China in late December 2019, SARS-CoV-2 infection is spreading very rapidly across the globe. COVID-19 has affected 202608306 people and caused around 4293591 deaths (Table 2). The inter-continental spread is described in Table 2. Figure 4 shows COVID-19 outbreaks in different countries. In the beginning, the Asian countries namely China and South Korea were the epicenter of COVID-19 until the first week of February. Up to August 10, 2021, there have been 93826 confirmed cases and 4636 deaths in China (WHO). In Korea the first COVID case was recorded on January 20, 2020. Since then, about 212448 cases have been confirmed and 2125 deaths recorded in Korea. The epicenter then moved from Asian countries to European countries mainly Italy and Spain. COVID-19 was recorded in Italy on January 30, 2020, and was found in France and Spain on January 24, 2020 and January 31, 2020, respectively. In particular, in Italy, the United Kingdom, France, Germany and Spain it affected people more seriously; approximately 4400617, 6094243, 6310933, 3800048, and 4627770 confirmed cases and 128242, 130357, 112288, 92291, and 82125 deaths were recorded in these countries, respectively, up to August 10, 2021. Among the European countries, mortality rate was highest in Italy due to its travel connection with China. In the middle of March, the virus epicenter moved to the United States and other American countries. The United States and Canada were the most affected countries during this phase. Although the first COVID-19 patient was recorded in late January, 2020 the first death was confirmed in February. In the USA, the first COVID-19 patient died in the middle of March. On August 10, 2021, the USA had recorded the greatest number of confirmed cases and deaths worldwide. The death rate is 206 per million people, which is the tenth highest rate globally. The first COVID-19 patient in Canada was reported on January 27, 2020. On August 10, 2021 there have been 36780480 and 1442087 confirmed cases in the USA and Canada, respectively, and 633799 and 26678 deaths, respectively. In the middle of April, the virus epicenter moved to Russia and India. As of August 10, 2021, there have been 6469910 and 31997017 confirmed cases in Russia and India, respectively, and the number of deaths is 165650 and 428715, respectively. However, the first confirmed COVID-19 case was recorded on January 30, 2020 in Kerala state and January 31, 2020 in Russia. The virus infection in these countries took a very long time to spread due to the implementation of different control measures. The details of COVID-19 cases in India are presented in

Table 2 Coronavirus disease 2019 outbreaks based on the World Health Organization (data as reported at 7.07 PM CEST on August 10, 2021)

Items	Confirmed cases	Deaths
Globally	202608306	4293591
Africa	5156790	122537
Americas	78718104	2032256
Eastern Mediterranean	13169171	243217
Europe	61333662	1231439
South-East Asia	39271048	593565
Western Pacific	4958767	70564



Figure 4 Coronavirus disease 2019 routes of transmission across countries. Figure modified after Ali and Alharbi (2020)[68], an Elsevier journal.

Table 3. However, according to fatality rate data, Belgium (15% fatality) is highest, followed by the United Kingdom (15%), France (14.7%), Italy (13.6%) and the Netherlands (12.3%) (John Hopkins Bulletin).

TREATMENT OF COVID-19

Antiviral drug treatment

Presently, COVID-19 treatment is based on symptomatic findings. To date, there is no precise treatment method, but currently the WHO, CDC and Food and Drug Administration have recommended certain drugs for COVID-19 treatment. The effectiveness

Table 3 Coronavirus disease 2019 state-wise status in India (as on August 10, 2021; Ministry of Home Affairs, GoI)

No.	Name of State / UT	Total confirmed cases*	Cured/discharged/migrated	Deaths**
1	Andaman and Nicobar Islands	7546	7412	129
2	Andhra Pradesh		1950623	13549
3	Arunachal Pradesh	50372	47520	246
4	Assam		558720	5404
5	Bihar		715303	9646
6	Chandigarh	61984	61146	811
7	Chhattisgarh		988004	13540
8	Dadar Nagar Haveli	10656	10612	4
9	Delhi		1411235	25067
10	Goa		167884	3164
11	Gujarat		814778	10077
12	Haryana		759769	9650
13	Himachal Pradesh		202569	3519
14	Jammu and Kashmir		316957	4390
15	Jharkhand		342074	5130
16	Karnataka		2859552	36817
17	Kerala		3377691	17852
18	Ladakh	20393	20117	207
19	Madhya Pradesh		781307	10514
20	Maharashtra		6151956	134064
21	Manipur		96128	1657
22	Meghalaya	69358	63450	1174
23	Mizoram	44520	32854	168
24	Odisha		971391	6554
25	Puducherry		119031	1800
26	Punjab		582753	16320
27	Rajasthan		944670	8954
28	Tamil Nadu		2522470	34340
29	Telengana		637789	3828
30	Tripura	80208	77230	767
31	Uttarakhand		328569	7368
32	Uttar Pradesh		1685449	22774
33	West Bengal		1505808	18240
34	Nagaland	28709	25906	585
35	Sikkim	27908	24544	355
36	Lakshadweep	10257	10112	51

and limitations of each drug are summarized in Table 4[62]. The existing drugs for treating COVID-19 patients are remdesivir, chloroquine, hydroxychloroquine, tocilizumab, lopinavir-ritonavir, azithromycin, baloxavir, favipiravir, *etc.*[63]. Remdesivir, is most prominent for treating COVID-19 patients[64]. The efficacy of remdesivir in treating patients has been reported globally[63-65]. Recently, the ChAdOx1 vaccine developed by the University of Oxford's Jenner Institute and the Oxford Vaccine Group has proved effective in combatting COVID-19. More recently,

Table 4 Recommended drugs for coronavirus disease 2019 treatments (Food and Drug Administration and World Health Organization)

Common drugs	Dose	Mechanism
Chloroquine; Antimalarial	50% for GFR < 10 mL/min	*In vitro* activity and has immunomodulating properties Inhibits viral enzymes or processes such as viral DNA and RNA polymerase, viral protein glycosylation, virus assembly, new virus particle transport, and virus release ACE2 inhibition due to acidification at cell membrane surface, inhibits fusion of virus, and cytokine release
Hydroxychloroquine; Antimalarial	800 mg orally on day one, followed by 400 mg/d orally for four to seven days	Same as chloroquine
Chloroquine phosphate; Antimalarial	1 g orally on day one, followed by 500 mg/d orally for four to seven days	Same as chloroquine
Remdesivir; Nucleoside Analogue	200 mg IV on day 1 followed by 100 mg IV daily on days two to five or 200 mg IV on day 1 followed by 100 mg IV daily on days two to ten	*In vitro* activity; Inhibitor of RNA-dependent RNA polymerases (RdRps) Remdesivir-TP competes with adenosine-triphosphate for incorporation into nascent viral RNA chains Once incorporated into the viral RNA at position i, RDV-TP terminates RNA synthesis at position i+3 Because RDV-TP does not cause immediate chain termination (i.e., 3 additional nucleotides are incorporated after RDV-TP), the drug appears to evade proofreading by viral exoribonuclease (an enzyme thought to excise nucleotide analogue inhibitors)
Azithromycin; Macrolide Antibacterial	500 mg on day one, followed by 250 mg daily for four days	Prevents bacterial superinfection, has immunomodulatory action on pulmonary inflammatory disorders Downregulates inflammatory responses and reduces excessive cytokine production associated with respiratory viral infections; however, its direct effects on viral clearance are uncertain Immunomodulatory mechanisms include reducing chemotaxis of neutrophils (PMNs) to lungs by inhibiting cytokines (*i.e.*, IL-8), inhibition of mucus hypersecretion, decreased production of ROS, accelerating neutrophil apoptosis, blocking activation of nuclear transcription factors
Lopinavir; Ritonavir; HIV protease inhibitor	400 mg/ritonavir 100 mg orally twice daily for up to 21 d	*In vitro* animal model studies show potential activity for other coronaviruses (SARS-CoV and MERS-CoV) Lopinavir and ritonavir may bind to Mpro, a key enzyme for virus replication and suppress virus activity
Tocilizumab; Interleukin-6 (IL-6) Receptor-InhibitingMonoclonal Antibody	4-8 mg/kg infused over more than 60 min (additional dose after 12 h)	Cytokine release syndrome; Inhibits IL-6-mediated signaling by competitively binding to both soluble and membrane-bound IL-6 receptors. IL-6 involved in T-cell activation, immunoglobulin secretion induction, hepatic acute-phase protein synthesis initiation, and hematopoietic precursor cell proliferation and differentiation stimulation
Baloxavir; Antiviral	80 mg orally on day 1 and on day 4, and another dose of 80 mg on day 7 (as needed); not to exceed 3 total doses	Active against influenza viruses; *In vitro* antiviral activity against SARS-CoV-2 demonstrated in one trial
Favipiravir; Antiviral	1600 mg twice daily on day 1, then 600 mg twice daily for 7-10 d; Severe: 1600 mg every 12 h on day 1, then 600 mg every 12 h days 2-10	*In vitro* activity against Vero E6 cells

SARS-CoV-2: Severe acute respiratory syndrome coronavirus 2.

Russia has reportedly developed a coronavirus vaccine named Sputnik V.

Chinese medicine treatment

A number of Chinese medicines have been used to treat COVID-19 patients. According to the Academy of Sciences, Shuanghuanglian oral liquid is most prominent and inhibits SARS-CoV-2. Several studies reported that baicalin, chlorogenic acid and forsythin present in Shuanghuanglian oral liquid have certain inhibitory effects on various viruses and bacteria including SARS-CoV-2[66]; however, the detailed mechanism is not yet known. Lianhuaqingwen capsules have also been used to treat

SARS-CoV-2 infected people as well as other diseases such as influenza viruses, including H7N9 by reducing inflammatory factors[1,17].

Unani medicine treatment

These are plant-based treatments, called Ayurvedic treatments, and these treatments are nontoxic and have no side effects. Different plant parts are used to treat anti-viral activities[67]. The most important plants are *Glycyrrhiza glabra, Allium cepa, Allium sativum, Ocimum sanctum, Ocimum tenuiflorum, Piper nigrum, Cinnamomum verum, Daucus maritimus, Curcuma longa, etc.* Administration of the aqueous extracts of these plants along with lemon juice and honey is very effective for flu and the common cold [68]. According to Fiore *et al*[69] *Glycyrrhiza glabra* plant extract is effective in treating viruses such as SARS related coronavirus, HIV-1, respiratory syncytial virus, varicella zoster, hepatitis A, B, C, and cytomegalovirus herpes. Similarly, Wang *et al*[70] indicated that *Glycyrrhiza glabra* also has antiviral and antimicrobial activities. Therefore, *Glycyrrhiza glabra* plant extract along with other plants may be useful in controlling COVID-19. Accordingly, the Government of India has recommended Ayurveda treatment methods to improve immunity (Table 5).

Homeopathic treatment

Arsenic album-30 is considered beneficial for viral infections. Recently, the Directorate of AYUSH, New Delhi, India has issued an order on January 30, 2020 to take prophylactic medicine to avoid coronavirus infection. Dr Rajan Sankaran has recommended Camphor 1M as a potential medicine for COVID-19 (https://www.boomlive.in/coronavirus-outbreak/homoeopathy-can-be-used-as-adjuvant-to-covid-19-treatment-dr-anil-khurana-7997). They recommended 4 pills of Arsenic album-30 medicine once daily on an empty stomach for 3 d. It is highly diluted arsenic trioxide and works as a homeopathic prophylaxis. Accordingly, the Homeopathy Department of Kerala Government is administering *Arsenicum Album* 30C as a preventive medicine to boost immunity in COVID-19 patients and it was approved by the Department of AYUSH, GoI (https://gulfnews.com/world/asia/india/covid-19-kerala-government-distributes-homeopathy-medicine-to-boost-immunity-1.1588091249686). However, to date, there is no clinical evidence that Arsenic album-30 is an effective medicine. As a result, the use of these medicines to manage COVID-19 has been criticized globally. Mathie *et al*[71] reported that *Arsenicum album* medicine is effective in reducing fever, runny nose, headache, and sore throat in patients with swine flu. Therefore, the use of homeopathy in COVID-19 management is debatable and requires further scientific study.

Immuno-booster treatment

Boosting the body's immunity is a potential individual protocol as COVID-19 pathogenesis is caused by a disproportionate immune response. Therefore, it is important to take supplements to boost both innate and adaptive immune response. Interferon is reported to inhibit viral infection and in particular, recombinant interferon α is effective for SARS-like viruses. Additionally, interferon was reported to be an effective inhibitor of MERS-CoV replication[72]. These findings indicated that interferon could be used to treat COVID-19 infection. Intravenous immunoglobulin might be the safest immune modulator for all age groups, and could help to inhibit pro-inflammatory cytokine production and to increase anti-inflammatory mediators[1,73]. Moreover, thymosin alpha-1 (Ta1) is used as an immune booster for SARS patients to effective control the disease[74]. Accordingly, intravenous immunoglobulin and Ta1 may also be used for the treatment of COVID-19. Recently, different immune-booster drugs have been used to treat COVID-19 such as neuraminidase inhibitors (*e.g.*, oseltamivir used to treat influenza). Apart from these, citrus fruits, dry fruits (almonds, walnuts, and dates) are very effective in improving the immune system. Vitamin A, C, D and E, and zinc supplements are effective in older patients. Additionally, adequate sleep, regular exercise and stress avoidance is essential to boost the immune system[68].

Plasma therapy

Due to lack of appropriate vaccines and specific drugs, plasma therapy could be an effective way to treat COVID-19. Previously, convalescent plasma therapy was proved to be an effective treatment option for SARS patients and those with H1N1 influenza [75,76]. From an immunological perspective, it was observed that recovered COVID-19 patients produced specific antibodies against SARS-CoV-2, and therefore their serum could be used to prevent re-infection. Additionally, these antibodies can limit the

Table 5 Unani drugs for coronavirus disease 2019 treatment (Source: Department of AYUSH, Government of India)

Unani drugs	Doses
Symptomatic treatments	
SharbatUnnab	10-20 mL twice a day
TiryaqArba	3-5 g twice a day
TiryaqNazla	5 g twice a day
KhamiraMarwareed	3-5 g once a day
ArqAjeeb	4-8 drops in fresh water and four times a day
Habb e IkseerBukhar (fever)	2 pills with lukewarm water twice daily
SharbatNazla	10 mL mixed in 100 mL of lukewarm water twice daily
Qurs e Suaal	2 tablets to be chewed twice daily
Decoction	
Behidana	3 g
Unnab	7 nos
Sapistan	7 nos
Darchini	3 g
Banafsha	5 g
Berg-e-Gaozabaan	7 g
Sore throat	
Khashkhash; Bazrulbanj; Post Khashkhash; Barg e Moard (Habbulaas); Tukhm e kahuMukashar; GuleSurkh	Any of them @12 g (each)

production of virus in the acute phase and help to clear the virus if injected during the first week of the viremia peak. Therefore, plasma globulin specific to SARS-CoV-2 has to be prepared from recovered COVID-19 patients. Recently, the Delhi Government successfully applied plasma therapy to treat COVID-19 patients.

In summary, in addition to the abovementioned treatments for COVID-19, auxiliary blood purification treatment (mainly used for severe NCP patients) could be used as an alternative therapy. According to Zarbock *et al*[77] the ACE2 receptor, the key receptor of SARS-CoV-2, is highly expressed in human kidney (100 times higher than in the lung). Kidney is one of the target organs for SARS-CoV-2; therefore, continuous blood purification could reduce renal recovery during COVID-19. Additionally, the kidney suffers from cytokine storms under severe COVID-19 infection. Therefore, blood purification technology could be an alternative method for removing inflammatory factors, eliminating cytokine storms, correcting electrolyte imbalances and maintaining acid–base status[1]. In addition, randomized double-blind clinical trials should be used as standard methodology for large sample sizes to determine antiviral drug efficacy in clinical practice. Currently, in India the discharge policy for COVID-19 recovered patients is based on 3 tier COVID-19 facilities and the categorization of patients is based on clinical severity. The revised discharge policy is indicated in Figure 5.

PREVENTION OF COVID-19 OUTBREAKS

COVID-19 has affected all sectors of society. Therefore, prevention is the best practice to reduce the impact of COVID-19 considering the lack of effective treatments. This can be achieved through a variety of means as follows:

Individual measures

Individual measures are essential in reducing the spread of COVID-19 at the community level. Community level spread is mainly caused when an infected person is in close contact with other healthy individuals. According to the WHO, the following individual measures should be taken to reduce the contamination level such

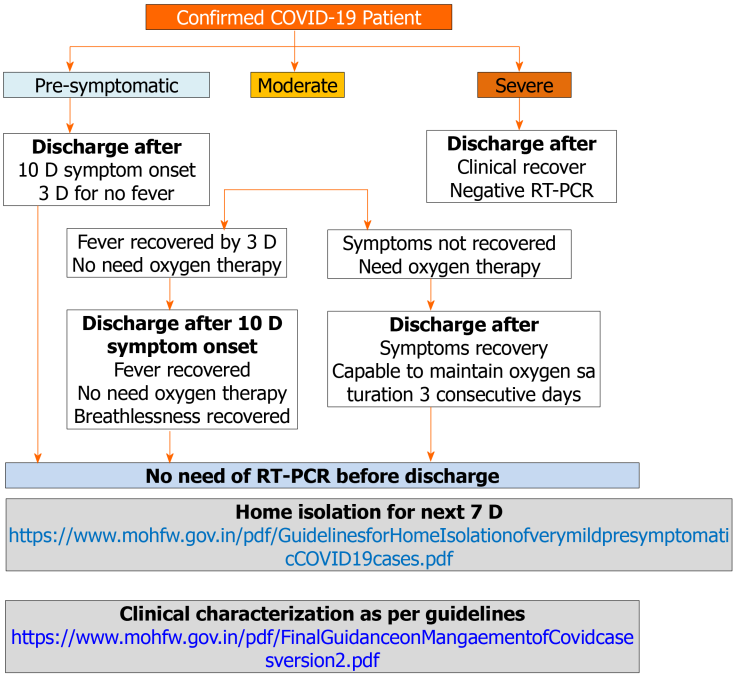


Figure 5 Discharge policies adopted by the Indian government. COVID-19: Coronavirus disease 2019.

as the use of face masks; respiratory hygiene by covering the mouth and nose with a bent elbow or tissue during coughing or sneezing; washing hands regularly with soap or disinfectant (containing at least 60% alcohol); avoiding contact with infected people, maintaining an appropriate distance (at least 2 m) from coughing or sneezing people; refraining from touching eyes, nose, and mouth with unwashed hands and finally, following advice from the healthcare provider.

Community level measures, social lockdown

Social lockdown is the restriction of inter-individual physical contact. Generally, it is a community level measure. The prime objective of social lockdown is to avoid two people from different families or nearby inhabitants coming in close contact with each other[78]. However, minimal and emergency movement of the general public is allowed under this condition. The emergency services (medical care, food security, general security and medicine supply) vary in different countries. However, in severe situations, emergency services such as the food and medical supply chain can also be closed as external or internal body fluid discharges such as coughs, sneezes, saliva *etc.* from COVID-19 patients infect healthy persons due to its easy transmissibility. Another objective of social lockdown is to allow the community to develop mild or full resistance to a mutated virus[78]. Moreover, it provides researchers more time to work on medicine or vaccines production. Considering the advantages of social lockdown, many nations across the globe have started different degrees of social lockdown to prevent SARS-CoV-2 infection.

International social lockdown progress

Some of the international social lockdown campaigns have been addressed here to understand COVID-19 preventive measures. Since the outbreak of COVID-19, China was the first country to implement social lockdown, which occurred in the last week of January 2020 in Wuhan city, the epicenter of the COVID-19 outbreak. During lockdown, buses and cars were allowed to run but domestic flights and trains were cancelled in various cities, and around 760 million people were under lockdown[29]. Accordingly, the WHO praised China as they had taken "perhaps the most ambitious, agile and aggressive disease containment effort in history"[79-81]. After China, Italy was the second country to adopt social lockdown. In Italy, social lockdown was declared on February 21, 2020 in northern Italy covering only 50000 people. Considering the disease incidence, the Federal government of Italy declared whole country lockdown on March 9, 2020. Only public transport was partially allowed, and a public pass system was initiated to ride buses or board flights on an emergency basis [82].

COVID-19 in the USA was spreading very rapidly with a high death rate since its first official COVID-19 case. Higher infection was mainly due to either higher migrant movement or a higher rate of clinical diagnosis[83]. Hence, following the high death and infection rate in the USA, the Trump government implemented the first lockdown on March 19, 2020 but to achieve total control of COVID-19, the American government extended the lockdown period to April 30, 2020 on March 30, 2020. The Trump government explained the second lockdown as follows "The better you do, the faster this whole nightmare will end. Therefore, we will be extending our guidelines to April 30th to slow the spread." Accordingly, the Director of NIH recommended the people of the USA to adapt to the lockdown voluntarily and stringently[84]. Most of the African countries had started to implement social distancing in the middle of March and ended it between May 10 and May 20, 2020. The same window was also used by most European countries. Social distancing in Bangladesh was implemented by Prime Minister Sheikh Hasina very late on March 25, 2020 and ended on May 16, 2020. Other countries such as Pakistan and Sri Lanka started to implement social distancing on March 24, 2020 which ended on May 9, 2020. Additionally, Sri Lanka declared a curfew to maintain strict social distancing.

Social lockdown status in India

Being a populous country, a large portion of the population lives in places of high density and their unhygienic lifestyle results in frequent infectious and epidemic diseases[85]. Therefore, as World Bank data have indicated India is still struggling to improve its health care system and is unable to provide sufficient hospital beds for its citizens. India can only afford 0.7 hospital beds per 1000 people, the doctor: population ratio is 1:1800 (standard is 1:1000), and the total number of ventilators available is 48000[86]. Considering this, the Government of India under Prime Minister Narendra Modi declared a Janata Curfew for 14-h (from 7 a.m. to 9 p.m.) on March 22, 2020 prior to total lockdown. Except for 'essential services' (police, medical services, media and home delivery) everyone took part in the curfew. According to Swiss firm IQAir, at least 75 Indian districts took part and helped to control the spread of SARS-CoV-2, which had an immediate positive effect, especially in Delhi, which is known as one of the world's most polluted capital cities. This resulted in a massive change in New Delhi's Air Quality Index (AQI). This was mainly due to a huge reduction in vehicular traffic; during lockdown there was a 70% reduction in the demand for petroleum oil. India is the third largest user of oil, after the USA and China. After that a nationwide lockdown for 21 days (except emergency services) was declared on March 24, 2020. The government implemented the following restrictions: (1) ban on people from stepping out of their homes; (2) closed all services and shops except pharmacies, hospitals, banks, grocery shops and other essential services; (3) closed all commercial and private establishments (only work-from-home allowed); (4) suspended all educational, training, and research institutions; (5) closed all places of worship; (6) suspended all non-essential public and private transport; (7) prohibited all social, political, sports, entertainment, academic, cultural, and religious activities; and (8) suspended entry of all international commercial flights from March 22. During the first phase of lockdown, the infection rate was not as high as that in the USA, Spain and Italy. It was previously reported that temperature may adversely affect virus infection [87]. Considering the influence of the upcoming Indian hot and humid summer, the health experts urged the Government to extend the lockdown. Many international news agencies described this strict lockdown by the Indian government as harsh, intensive and mismanaged[88,89]. However, the WHO declared that "the measures taken by India to break the community spread of COVID-19 by the lockdown was a very early, scientific and timely decision"[90]. In the words of Dr. David Nabarro, special envoy on the disease, WHO "*The lockdown in India was quite early on, when there was relatively a small number of cases detected. This was really a far-sighted decision because it gave the whole country the opportunity to come to terms with the reality of this enemy. People understood that there is a virus in our midst. It gave time to develop capacities at the local level for interrupting transmission and sorting out hospitals. Of course, there is a lot of debate and criticism, and inevitably with a lot of frustration and anger that life is being disturbed in this way. It is very, very upsetting. I think it is courageous of the government, honestly, to take this step and provoke this enormous public debate and let the frustration come out, to accept that there will be hundreds of millions of people whose lives are being disrupted. For poor people on daily wages, this is a massive sacrifice they are making. And to do it now at an early stage as opposed to waiting three or four weeks later when the virus is much more widespread was very courageous*[91]."

In the second phase, PM Modi extended the nationwide lockdown on April 14, 2002 until May 3, with a conditional relaxation after April 20. On April 16, lockdown areas

were classified as "red, orange and green zones", indicating the presence of infection hotspots, some infection, no infections, respectively. On April 20, the government announced relaxations in different sectors such as agriculture including dairy, aquaculture and plantations, selling of farming products, cargo transportation including trucks, trains and planes following social distancing norms[92]. On April 25, the government allowed the opening of small retail shops with half-staff following social distancing norms. On April 29, the Ministry of Home Affairs allowed inter-state movement of migrant people following the guidelines laid down by the government. An additional extension (May 4 – May 17) was granted by Government of India on May 1, 2020 with additional relaxation to curb the infection.

In this phase, the whole country was categorized into three zones namely red zones (130 districts), orange zones (284 districts) and green zones (319 districts). Red zones were areas with high infection and a high doubling rate, orange zones had comparatively fewer cases and green zones had no cases in the past 21 days. Normal movement was allowed in green zones with buses (50% capacity). In orange zones, only private and hired vehicles but no public transportation was allowed, while red zones were under complete lockdown. The government then implemented a fourth phase of lockdown to prevent COVID-19 between May 18 and May 31, 2020. On May 30, the government extended the ongoing lockdown until June 30 for only containment zones with services resumed in a phased-manner from 8 June. This was termed "Unlock 1.0". The second phase of unlock, called Unlock 2.0, was announced for the period of 1 to 31 July, followed by the easing of restrictions. Currently, Unlock 3.0 has been announced for August.

ENVIRONMENTAL PERSPECTIVES: INFLUENCE AND IMPACTS

The lockdown period has greatly helped the environment to rejuvenate, simply due to a reduction in pollution level to a large extent.

Longevity of SARS-CoV-2 in the environment

SARS-CoV-2 can remain suspended for approximately 30 min as an aerosol (< 5 μm). SARS-CoV-2 remained viable in aerosols for up to 3 h, with a reduction in infectious titer from $10^{3.5}$ to $10^{2.7}$ $TCID_{50}$ per L of air. SARS-CoV-2 is more stable on plastic and stainless steel than on copper and cardboard[78]. The virus has the longest life on plastic and steel, surviving up to 72 h but the total number of virus particles decreases sharply over this time ($10^{3.7}$ to $10^{0.6}$ $TCID_{50}$ per mL of medium after 72 h on plastic and $10^{3.7}$ to $10^{0.6}$ $TCID_{50}$ per mL after 48 h on stainless steel). On copper, it survives up to 4 h [78]. On cardboard, it survives up to 24 h, which suggests packages that arrived in the mail should have only low levels of the virus. On copper and cardboard, the virus is undetectable by 8 and 48 h, respectively[78]. The half-life of SARS-CoV-2 is similar to SARS-CoV-1 in aerosols, with a median of approximately 1.1 to 1.2 h and 95% credible intervals of 0.64 to 2.64 for SARS-CoV-2 and 0.78 to 2.43 for SARS-CoV-1[78]. The half-life of these two viruses is also similar on copper. On cardboard, the half-life of SARS-CoV-2 is longer than SARS-CoV-1. The longest viability was detected on stainless steel and plastic; the estimated median half-life of SARS-CoV-2 is 5.6 h on stainless steel and 6.8 h on plastic[78].

Meteorological influence

The COVID-19 pandemic is spreading globally irrespective of meteorological influence. Meteorological factors such as temperature, weather conditions and humidity are thought to play a vital role in COVID-19 transmission. At the beginning of the outbreak, it was speculated that COVID-19 may decrease with increasing air temperature as the outbreak occurred in the winter months[93]. Additionally, air temperature was relatively low in those months in comparison with Spring and/or Summer months. Accordingly, Zhou and Xie[94] demonstrated there is no concrete evidence of a decrease in COVID-19 when ambient temperature increases. Recently, Ma *et al*[95] indicated the positive influence of temperature and humidity on COVID-19 *i.e.*, increase in temperature and humidity decreases the number of COVID-19 deaths. This study was also conducted in same time period (January-February) as the study by Zhou and Xie[94]. A similar positive influence of meteorological factors on COVID-19 in various countries[96,97] was demonstrated. In addition to meteorological factors, Ramadhan[96] highlighted very high mobility and high density of people resulted in fast transmission of COVID-19 in Jakarta.

Influence on air quality

COVID-19 transmission has a direct impact on air quality namely particulate matter, SOx, NOx and carbon, *etc*. Standard air quality is essential in maintaining human health. However, almost 91% of the world's population lives in very poor air quality that exceeds the permissible limits[98], resulting in approximately 8% of deaths globally mainly in Asia, Africa and parts of Europe[98]. Coccia[99] demonstrated that cities (North Italy) with poor air quality (PM_{10} or ozone) increased the probability of COVID-19, mainly due to air pollution-to-human rather than human-to-human transmission. Another study from the same city indicated that prolonged exposure to poor air quality (PM_{10}, $PM_{2.5}$, O_3, SOx and NO_2) boosts COVID-19 incidence and even death in elderly people who have severe respiratory and cardiovascular disorders[97].

On the other hand, COVID-19 has significantly improved the air quality globally, particularly during lockdown periods due to the cessation of social activity, industrial activity, institutional activity, *etc*. Columbia University reported that the amount of carbon monoxide and carbon dioxide in New York City was reduced by 5% and 10%, respectively. During February 2020, carbon emission was decreased by 25% in China, which was last recorded during the economic crisis of 2008-2009. NASA's OMI instrument measured a 36% reduction in NO_2 concentration in China as well as in Italy, Spain, and France during February 2020 (these countries declared lockdown before other European nations). The level of particulate matter ($PM_{2.5}$) in London, Cardiff, and Bristol was less following the implementation of lockdown. PM induces inflammation in lung cells and exposure to PM increases the susceptibility and severity of COVID-19 symptoms.

In China, there was a profound decline in air pollution (greenhouse gases) during January and February as recorded by NASA using satellite images due to the decrease in industrial, business and transportation activity. Accordingly, the China's Ministry of Ecology and Environment declared that it is 'good quality, air days'.

An approximately 43%, 31%, 10%, and 18% decrease in $PM_{2.5}$, PM_{10}, CO, and NO_2 levels, respectively, were observed in India during COVID-19 lockdown compared to previous years[100]. The AQI was reduced by 44%, 33%, 29%, 15% and 32% in north, south, east, central and western India, respectively. In New Delhi, the AQI was reduced to as low as 93, and in Mumbai it decreased to 90 from 161 and 153, respectively.

Due to quarantine, NO_2 level was reduced by 22.8 μg/m^3 and 12.9 μg/m^3 in Wuhan and China, respectively. $PM_{2.5}$ level dropped by 1.4 μg/m^3 in Wuhan but in another 367 cities it was decreased by 18.9 μg/m^3[103]. After two weeks of lockdown in Spain, the black carbon and NO_2 level decreased markedly (-45 to -51%)[102]. However, O_3 level increased (+33 to +57%, 8 h daily), probably due to lower titration of O_3 by NO due to lower NOx level[102]. Additionally, the Copernicus Atmosphere Monitoring Service (CAMS) of the European Union observed a drop in $PM_{2.5}$ level during February 2020 in comparison with the previous three years. In China, according to CAMS[103], an approximately 20%–30% decrease in $PM_{2.5}$ was recorded in different parts of China during February 2020 compared with monthly averages in February 2017, 2018 and 2019. It is likely that the improvement in air quality around the globe was recorded due to COVID-19 control measures mainly by lockdown and quarantine[104-108]. During this period the demand for petroleum oil was reduced by 20% worldwide.

Furthermore, different national and international media on 10th February reported increased SO_2 concentration of approximately 1,350 μg/m^3 in Wuhan and Chongqing cities due to mass cremation of COVID-19 victims based on a screenshot image from *windy.com*. These were the results of the GEOS-5 Model. On the other hand, The Sun showed that this was not certain but mainly due to the cremation of virus-infected victims. Accordingly, The Sun (https://archive.is/ShAfz), *WION* (https://archive.is/Cdz4d) and IndiaTimes (https://timesofindia.indiatimes.com/times-fact-check/news/fact-check-satellite-images-showing-high-levels-of-sulphur-dioxide-indicate-mass-cremations-in-china/articleshow/74130633.cms) demonstrated that the mass cremations in Wuhan and Chongqing cities could be the prime reason for increased SO_2 concentration. Dr Arlindo M da Silva, from the Global Modeling and Assimilation Office, stated that GEOS-5 sulfur dioxide models do not "assimilate real satellite data" to confirm the image of *windy.com*. The China National Environmental Monitoring Center and the Center for Satellite Application on Environment and Ecology and the Chinese Academy of Sciences explained that the SO_2 data fluctuated between 4 and 8 μg/m^3, which was over 200 times less than the data shown on the website.

Influence on noise level and water quality

Environmental noise produced mainly by industrial or commercial operations, transit

vehicles, and many other sources cause serious health problems in the population [109]. The implementation of quarantine and lockdown due to COVID-19 preventive measures by most governments around the globe has compelled people to stay at home. The use of private and public transportation including trains and planes decreased significantly. Additionally, all commercial activities, shopping complexes and industrial operations stopped almost entirely. Accordingly, it is thought that noise level should have reduced; however, there are currently no studies on this issue. Most studies are confined to air quality assessment. Therefore, more attention should be focused on this environmental aspect.

Water quality in freshwater and marine ecosystems is also expected to improve globally. The lack of tourists, as a result of social distancing, has caused a significant change in beaches around the world. Coastal areas are important natural assets, which provide recreation and tourism, and fishing activities. These services are crucial for the nutrition and survival of coastal animals and human communities, and impart intrinsic values[110]. The lack of tourists has resulted in less pollution, especially plastics and wastes as well as reduced drainage volume into water bodies. A lower pollution level in aquatic ecosystems improves the health of the ecosystem by improving the health of aquatic organisms. In undisturbed habitats, olive ridley turtles were able to lay their eggs in Odisha's Gahirmatha beach and Rushikulya roockery. A number of dolphins were observed jumping in the water at the Marine Drive of Mumbai in the Arabian Sea, and the Canals of Venice are now full of fish and dolphins, as the water has sufficient time for sediments to settle to the bottom. According to Sunita Narain, the environmental activist, also the Director General of the Centre for Science and Environment (CSE), explained that, "*Right after this health crisis subsides, it is imperative to get the economy back in shape. People need to get back to work and continue leading their lives. This is just a phase. People can learn from it. However, we require long-term solutions like that of the utilization of clean energy, conservation of forests, and efficient waste management systems in order to see real impact.*" According to R. Ramamurthy, COVID-19 is an eye-opener. For example, beaches such as those of Acapulco (Mexico), Barcelona (Spain), or Salinas (Ecuador) are now cleaner with crystal clear waters[101]. This aspect also needs further study to understand the impact of COVID-19.

Influence on waste generation and waste recycling

A number of environmental issues such as air and water pollution, soil erosion, and deforestation are responsible for direct or indirect generation of organic and inorganic waste[111]. Home quarantine measures, established across most countries as COVID-19 measures, have expanded online shopping dramatically. Accordingly, online procurement systems enhanced the generation of inorganic waste due to packaging, in addition to enhanced organic waste generation by households. Furthermore, medical waste generation is also high. In Wuhan, around 240 metric tons of medical waste is generated per day since the COVID-19 outbreak, which is too high compared with previous years (average 50 tons)[45]. Calma[112] reported that in countries like the USA garbage generation due to personal protective equipment such as masks and gloves have increased significantly compared with previous years.

Waste recycling is a common and effective way to prevent pollution, save energy, and conserve natural resources; simultaneously, it is a major environmental problem across the globe[113,114]. Although wastes are generated in high volume globally, at present it is impossible for all countries to recycle these wastes due to the further spread of SARS-CoV-2 infection. Accordingly, the USA has closed waste recycling totally due to COVID-19. Affected European countries have also restricted waste management during this outbreak[101]. For example, Italy totally prohibited infected residents from sorting their waste. Industry also seized the use of reusable bags, as single-use plastic can harbor viruses[115]. China has implemented the use of additional disinfectant in wastewater treatment plants to strengthen their disinfection process to prevent the new coronavirus spreading *via* wastewater. However, to date, there is no evidence of the survival of SARS-CoV-2 in drinking water or wastewater [116].

Other indirect influences on the environment

Wildlife is also affected by SARS-CoV-2. In a USA sanctuary, one tiger was reported to be coronavirus positive. In a Chinese sanctuary, two pangolins died due to the virus infection. It also affected the movement of migratory birds. Different migratory birds are now visiting places where they never visited before due to high pollution levels. It has also forced the UN organization to postpone the Annual Climate Change Conference, *i.e.*, COP-26, which was scheduled to be held at Glasgow in the UK in

November 2020.

SOCIAL IMPACTS

COVID-19 outbreaks have adversely affected different sectors of society with big losses globally in terms of both monetary and personal loss, which cannot be accurately estimated. However, some aspects can be addressed here. Globalization is a chain process; therefore, it will collapse if a single chain stops working. In particular, the economy of countries is adversely affected. Functions, especially business meetings, sports events, scientific conferences, running educational institutes, fashion shows, and wedding parties are to be avoided, which has a big social impact on society. In the educational sector, many countries banned the running of schools, colleges and universities as well as students attending classes, which has deprived the students of a good quality education. This loss poses a large problem not only in monetary matters but also a big disadvantage to the students and their families mainly due to psychological stress. Apart from this, the tourism sector and industrial sectors are facing a major problem due to lack of labor. Prices of commodities are increasing, which has had a negative impact on poor people worldwide. Implementation of lockdown has had an enormous negative impact on poor people especially their daily wage as they are unable to earn. According to the ILO, half of permanent employees will be deprived of work, particularly in the Asia and Pacific regions. In India, 90% of workers from unorganized sectors were highly affected. In addition, production in eight major sectors was reduced by 6.5%, which obviously affected the industrial production index. According to an estimate by the IATA there was a loss of about $113 billion during the lockdown period so far. However, the positive effect of social lockdown is spending more time with family members as well as friends but without physical meetings. It has positive effects on health and accordingly improves immunity.

This pandemic has had a serious impact on major festivals around the world, which may lead to secondary epidemic burnout and stress-related absenteeism. The Public Health Department of England has mentioned 14 ways to protect mental health during the pandemic. The WHO has recommended two most effective protocols, the R-TEP (Recent Traumatic Episode Protocol) and G-TEP (Group Traumatic Episode Protocol) to treat the invisible and psychological wounds of trauma in these situations. *'The Lancet'* documented the psychological impact of quarantine in people which included low mood, insomnia, stress, anxiety, anger, irritability, emotional exhaustion, depression and post-traumatic stress symptoms. Some people have a higher risk because of long-term absenteeism from work due to illness and burnout, which has led to a loss of productivity of approximately 35% in these workers (America's State of Mind Report). In the case of patients who are in quarantine with their children they are facing major mental disorders such as trauma-related health disorder.

It is obvious that this pandemic has both long- and short-term implications on public mental health. Poor mental health may be the result of social isolation and loneliness. It is reported that 47% cases showed negative mental health effects due to worry or stress related to coronavirus, in particular, the situation is very pronounced among older adults and households with adolescents. Research has shown that older adults are at higher risk of poor mental health due to loneliness and bereavement. It also showed that job loss enhances depression, anxiety, distress, and low self-esteem and a higher rate of disorders. In the USA, 30 million students and subsequently their families face physical, social, and mental health impairment. During this pandemic, mental health illness among adolescents has been exacerbated, and over 12% of adolescents aged between 12 and 17 years have depression and/or anxiety. Closures of non-essential businesses and disruption to livelihood have a negative impact on mental health. It has been observed that people with low incomes (about 26%) experience major negative mental health impacts (worry, 17% and stress, 14%) compared with high income groups. Presently, the Coronavirus Aid, Relief, and Economic Security Act (CARES Act) endorsed the need for emergency services to improve the mental health conditions of remote people. According to the CDC, people who suffer from chronic illness such as chronic lung disease, asthma, chronic cardiovascular disease, and diabetes are at high risk of severe illness due to COVID-19.

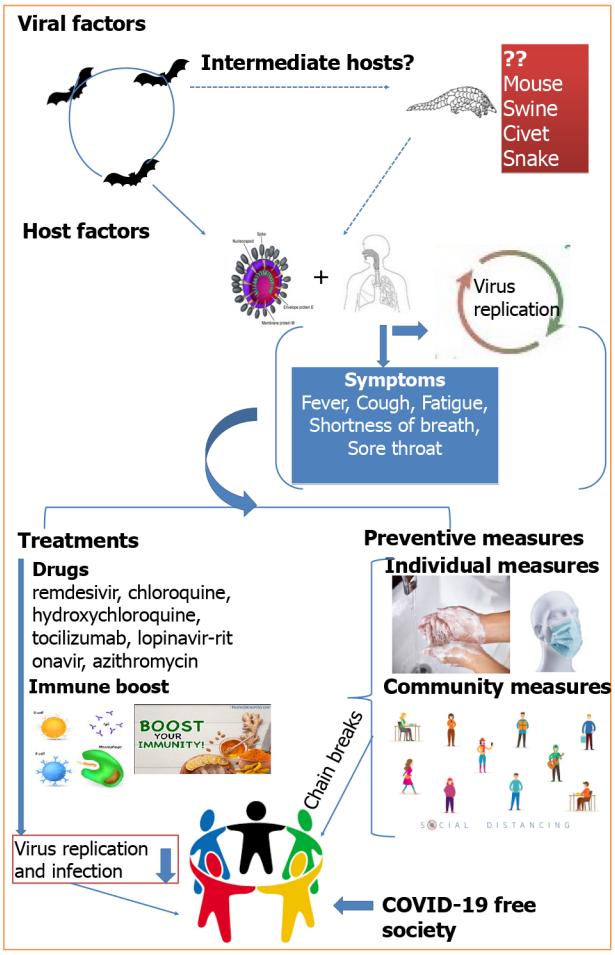


Figure 6 Schematic presentation of the management of coronavirus disease 2019 outbreaks. COVID-19: Coronavirus disease 2019.

RECURRENCE OF COVID19

Although a large number of individuals recover from COVID-19, the incidence of SARS-CoV-2 RNA recurrence has been recorded in various countries. To date, the incidence of recurrent SARS-CoV-2 in recovered individuals ranges from 7.35 to 21.4% [117]. Bonifácio *et al*[118] reported the recurrence of COVID-19 in a female nurse from Brazil. Following her recovery, two family members developed flu-like symptoms and tested positive for COVID-19 by RT-PCR. The next day, the nurse experienced malaise, myalgia, severe headache, fatigue, weakness, feverish sensation, sore throat, anosmia and dysgeusia. Hoang[119] estimated that 15% (95%CI, 12% to 19%) of patients (among 3,644 patients, recovering from COVID-19) tested positive for SARS-CoV-2. In addition, Hoang[119] documented that the proportion was 14% (95%CI, 11% to 17%) in China and 31% (95%CI: 26%-37%) in Korea. Furthermore, he demonstrated that among recurrent cases, 39% (95%CI: 31%-48%) experienced at least one comorbidity. The estimates for times from disease onset to admission, from admission to discharge, and from discharge to RNA positive conversion were 4.8, 16.4, and 10.4 d, respectively [119]. Loconsole *et al*[120] reported the recurrence of COVID-19 in a 48-year-old man from Italy who developed dyspnea and chest pain. The recurrence of COVID-19 has been reported around the world, and raises questions about the durability and quality of immune protection from SARS-CoV-2 as well as the quality of treatment options.

FUTURE PERSPECTIVES

COVID-19 has been an unprecedented disaster around the globe in every aspect, especially environmental health, social and economic aspects. This pandemic originated from bats. People worldwide are consuming different animals including bats, cats, snakes, mice, rats, pigs, dogs, *etc*., as food stuff. Accordingly, our future generation must be provided with substantial knowledge before consuming these

animals as food. Furthermore, people should be informed about the negative impact of these foods as they may harbor dangerous microbes. Emphasis should be given to providing adequate health care facilities to all people across countries including a greater number of health care systems, health insurance *etc.* This pandemic has highlighted the lack of health care facilities across the globe. Therefore, investment is needed in science and technology to establish specialized research centers to fight against such disasters in the future. In addition, more scientific studies are needed especially on viral diseases, mosquito-and insect-based diseases, bacterial infections, cancer, *etc.*, to combat any future pandemics. Currently, no medicine or vaccines have been identified to treat or eradicate COVID-19. Therefore, efforts should be focused on developing effective medicine or vaccines to treat COVID-19 through technological advancements.

CONCLUSION

This review provides an insight into the current status of COVID-19 (to date) from an environmental perspective. COVID-19 is a zoonotic disease, which originated from bats in Wuhan, China and was declared a pandemic by the WHO. The main symptoms are high fever, cough, shortness of breath and fatigue, which are similar to those of SARS. COVID-19 is highly infectious and transmissible through either aerosol droplets or close contact. The virus has spread to 213 countries/territories with approximately 202608306 confirmed cases and 4293591 deaths up to August 10, 2021. SARS-CoV-2 binds to human ACE2 and infects humans. Elderly people are more prone to SARS-CoV-2 compared to other age groups. To date, there is no specific medicine or vaccines for COVID-19. Currently, drugs such as remdesivir, chloroquine, hydroxychloroquine, tocilizumab, lopinavir-ritonavir, azithromycin, *etc.*, are used to treat SARS-CoV-2 infection. However, no drug is able to induce full recovery in COVID-19 patients. Remdesivir is effective in treating the virus. Recently, the ChAdOx1 vaccine was developed by the University of Oxford's Jenner Institute and the Oxford Vaccine Group. More recently, Russia has developed a coronavirus vaccine, named Sputnik V but these are still in the testing phase. Therefore, boosting the immune response could be an effective way to improve viral resistance. Accordingly, prevention and management are currently the best solution to control COVID-19. Therefore, it is essential that we follow the preventive measures, management and quarantine strictly laid down by the concerned government (Figure 6). Source reduction as an individual protective measure is the best way to control the infection. Lockdown as a social strategy is considered an indirect, but effective alternative tool to control spread of the virus. Additionally, the pandemic has had a direct impact on the environment, society and economy. Therefore, we should promote science and technology to develop vaccines or specific drugs to combat COVID-19.

ACKNOWLEDGEMENTS

The authors would like to thank the Department of Environmental Science of Sukanta Mahavidyalaya and The University of Burdwan for allowing working from home during the lockdown period.

REFERENCES

1 **Wang L**, Wang Y, Ye D, Liu Q. Review of the 2019 novel coronavirus (SARS-CoV-2) based on current evidence. *Int J Antimicrob Agents* 2020; **55**: 105948 [PMID: 32201353 DOI: 10.1016/j.ijantimicag.2020.105948]

2 **Liu Y**, Gayle AA, Wilder-Smith A, Rocklöv J. The reproductive number of COVID-19 is higher compared to SARS coronavirus. *J Travel Med* 2020; **27** [PMID: 32052846 DOI: 10.1093/jtm/taaa021]

3 **Núñez-Delgado A**. What do we know about the SARS-CoV-2 coronavirus in the environment? *Sci Total Environ* 2020; **727**: 138647 [PMID: 32315907 DOI: 10.1016/j.scitotenv.2020.138647]

4 **Zhu N**, Zhang D, Wang W, Li X, Yang B, Song J, Zhao X, Huang B, Shi W, Lu R, Niu P, Zhan F, Ma X, Wang D, Xu W, Wu G, Gao GF, Tan W; China Novel Coronavirus Investigating and Research Team. A Novel Coronavirus from Patients with Pneumonia in China, 2019. *N Engl J Med* 2020; **382**: 727-733 [PMID: 31978945 DOI: 10.1056/NEJMoa2001017]

5 **Ji W**, Wang W, Zhao X, Zai J, Li X. Cross-species transmission of the newly identified coronavirus

2019-nCoV. *J Med Virol* 2020; **92**: 433-440 [PMID: 31967321 DOI: 10.1002/jmv.25682]

6 **Zhang C**, Zheng W, Huang X, Bell EW, Zhou X, Zhang Y. Protein Structure and Sequence Reanalysis of 2019-nCoV Genome Refutes Snakes as Its Intermediate Host and the Unique Similarity between Its Spike Protein Insertions and HIV-1. *J Proteome Res* 2020; **19**: 1351-1360 [PMID: 32200634 DOI: 10.1021/acs.jproteome.0c00129]

7 **Zhou P**, Yang XL, Wang XG, Hu B, Zhang L, Zhang W, Si HR, Zhu Y, Li B, Huang CL, Chen HD, Chen J, Luo Y, Guo H, Jiang RD, Liu MQ, Chen Y, Shen XR, Wang X, Zheng XS, Zhao K, Chen QJ, Deng F, Liu LL, Yan B, Zhan FX, Wang YY, Xiao GF, Shi ZL. A pneumonia outbreak associated with a new coronavirus of probable bat origin. *Nature* 2020; **579**: 270-273 [PMID: 32015507 DOI: 10.1038/s41586-020-2012-7]

8 **Guo YR**, Cao QD, Hong ZS, Tan YY, Chen SD, Jin HJ, Tan KS, Wang DY, Yan Y. The origin, transmission and clinical therapies on coronavirus disease 2019 (COVID-19) outbreak - an update on the status. *Mil Med Res* 2020; **7**: 11 [PMID: 32169119 DOI: 10.1186/s40779-020-00240-0]

9 **Wu A**, Peng Y, Huang B, Ding X, Wang X, Niu P, Meng J, Zhu Z, Zhang Z, Wang J, Sheng J, Quan L, Xia Z, Tan W, Cheng G, Jiang T. Genome Composition and Divergence of the Novel Coronavirus (2019-nCoV) Originating in China. *Cell Host Microbe* 2020; **27**: 325-328 [PMID: 32035028 DOI: 10.1016/j.chom.2020.02.001]

10 **Xu X**, Chen P, Wang J, Feng J, Zhou H, Li X, Zhong W, Hao P. Evolution of the novel coronavirus from the ongoing Wuhan outbreak and modeling of its spike protein for risk of human transmission. *Sci China Life Sci* 2020; **63**: 457-460 [PMID: 32009228 DOI: 10.1007/s11427-020-1637-5]

11 **Kruse H**, kirkemo AM, Handeland K. Wildlife as source of zoonotic infections. *Emerg Infect Dis* 2004; **10**: 2067-2072 [PMID: 15663840 DOI: 10.3201/eid1012.040707]

12 NMA. COVID-19 and pets: When pandemic meets panic. *Forensic Sci Int Rep* 2020; **2**: 100090 [DOI: 10.1016/j.fsir.2020.100090]

13 **Chowell G**, Abdirizak F, Lee S, Lee J, Jung E, Nishiura H, Viboud C. Transmission characteristics of MERS and SARS in the healthcare setting: a comparative study. *BMC Med* 2015; **13**: 210 [PMID: 26336062 DOI: 10.1186/s12916-015-0450-0]

14 **British Veterinary Association**. Coronavirus and animals. [cited 3 April 2020]. Available from: https://www.bva.co.uk/news-and-blog/news-article/coronavirus-disease-covid-19-updates-for-the-veterinary-profession/

15 **Centers for Disease Control and Prevention**. Coronavirus Disease 2019 (COVID-19). If You Have Animals, (2020). [cited 6 April 2020]. Available from: https://www.cdc.gov/coronavirus/2019-ncov/daily-life-coping/animals.html

16 **World Organisation for Animal Health (OIE)**. Questions and Answers on the 2019 Coronavirus Disease (COVID-19), (2020). [cited 3 April 2020]. Available from: https://www.oie.int/en/scientific-expertise/specific-information-and-recommendations/questions-andanswers-on-2019novel-coronavirus/

17 **Wang W**, Tang J, Wei F. Updated understanding of the outbreak of 2019 novel coronavirus (2019-nCoV) in Wuhan, China. *J Med Virol* 2020; **92**: 441-447 [PMID: 31994742 DOI: 10.1002/jmv.25689]

18 **Xiao F**, Tang M, Zheng X, Liu Y, Li X, Shan H. Evidence for Gastrointestinal Infection of SARS-CoV-2. *Gastroenterology* 2020; **158**: 1831-1833.e3 [PMID: 32142773 DOI: 10.1053/j.gastro.2020.02.055]

19 **Xia J**, Tong J, Liu M, Shen Y, Guo D. Evaluation of coronavirus in tears and conjunctival secretions of patients with SARS-CoV-2 infection. *J Med Virol* 2020; **92**: 589-594 [PMID: 32100876 DOI: 10.1002/jmv.25725]

20 **Chen N**, Zhou M, Dong X, Qu J, Gong F, Han Y, Qiu Y, Wang J, Liu Y, Wei Y, Xia J, Yu T, Zhang X, Zhang L. Epidemiological and clinical characteristics of 99 cases of 2019 novel coronavirus pneumonia in Wuhan, China: a descriptive study. *Lancet* 2020; **395**: 507-513 [PMID: 32007143 DOI: 10.1016/S0140-6736(20)30211-7]

21 **Remais J**. Modelling environmentally-mediated infectious diseases of humans: transmission dynamics of schistosomiasis in China. *Adv Exp Med Biol* 2010; **673**: 79-98 [PMID: 20632531 DOI: 10.1007/978-1-4419-6064-1_6]

22 **Wu JT**, Leung K, Leung GM. Nowcasting and forecasting the potential domestic and international spread of the 2019-nCoV outbreak originating in Wuhan, China: a modelling study. *Lancet* 2020; **395**: 689-697 [PMID: 32014114 DOI: 10.1016/S0140-6736(20)30260-9]

23 **Majumder MS**, Mandl KD. Early Transmissibility Assessment of a Novel Coronavirus in Wuhan, China. *SSRN* 2020; 3524675 [PMID: 32714102 DOI: 10.2139/ssrn.3524675]

24 **Lipsitch M**, Cohen T, Cooper B, Robins JM, Ma S, James L, Gopalakrishna G, Chew SK, Tan CC, Samore MH, Fisman D, Murray M. Transmission dynamics and control of severe acute respiratory syndrome. *Science* 2003; **300**: 1966-1970 [PMID: 12766207 DOI: 10.1126/science.1086616]

25 **Majumder MS**, Rivers C, Lofgren E, Fisman D. Estimation of MERS-Coronavirus Reproductive Number and Case Fatality Rate for the Spring 2014 Saudi Arabia Outbreak: Insights from Publicly Available Data. *PLoS Curr* 2014; **6** [PMID: 25685622 DOI: 10.1371/currents.outbreaks.98d2f8f3382d84f390736cd5f5fe133c]

26 **Wu Z**, McGoogan JM. Characteristics of and Important Lessons From the Coronavirus Disease 2019 (COVID-19) Outbreak in China: Summary of a Report of 72 314 Cases From the Chinese Center for Disease Control and Prevention. *JAMA* 2020; **323**: 1239-1242 [PMID: 32091533 DOI: 10.1001/jama.2020.2648]

27 **Guan WJ**, Ni ZY, Hu Y, Liang WH, Ou CQ, He JX, Liu L, Shan H, Lei CL, Hui DSC, Du B, Li LJ, Zeng G, Yuen KY, Chen RC, Tang CL, Wang T, Chen PY, Xiang J, Li SY, Wang JL, Liang ZJ, Peng YX, Wei L, Liu Y, Hu YH, Peng P, Wang JM, Liu JY, Chen Z, Li G, Zheng ZJ, Qiu SQ, Luo J, Ye CJ, Zhu SY, Zhong NS; China Medical Treatment Expert Group for Covid-19. Clinical Characteristics of Coronavirus Disease 2019 in China. *N Engl J Med* 2020; **382**: 1708-1720 [PMID: 32109013 DOI: 10.1056/NEJMoa2002032]

28 **Rodriguez-Morales AJ**, Cardona-Ospina JA, Gutiérrez-Ocampo E, Villamizar-Peña R, Holguin-Rivera Y, Escalera-Antezana JP, Alvarado-Arnez LE, Bonilla-Aldana DK, Franco-Paredes C, Henao-Martinez AF, Paniz-Mondolfi A, Lagos-Grisales GJ, Ramírez-Vallejo E, Suárez JA, Zambrano LI, Villamil-Gómez WE, Balbin-Ramon GJ, Rabaan AA, Harapan H, Dhama K, Nishiura H, Kataoka H, Ahmad T, Sah R; Latin American Network of Coronavirus Disease 2019-COVID-19 Research (LANCOVID-19). Electronic address: https://www.lancovid.org. Clinical, laboratory and imaging features of COVID-19: A systematic review and meta-analysis. *Travel Med Infect Dis* 2020; **34**: 101623 [PMID: 32179124 DOI: 10.1016/j.tmaid.2020.101623]

29 **Zhong R**, Mozur P, Tame TYT. Coronavirus, mao-style social control blankets china. The New Yorks Times. [cited 10 April 2020]. Available from: https://www.nytimes.com/2020/02/15/business/china-coronavirus-lockdown.html

30 **Lessler J**, Reich NG, Brookmeyer R, Perl TM, Nelson KE, Cummings DA. Incubation periods of acute respiratory viral infections: a systematic review. *Lancet Infect Dis* 2009; **9**: 291-300 [PMID: 19393959 DOI: 10.1016/S1473-3099(09)70069-6]

31 **Cho SY**, Kang JM, Ha YE, Park GE, Lee JY, Ko JH, Kim JM, Kang CI, Jo IJ, Ryu JG, Choi JR, Kim S, Huh HJ, Ki CS, Kang ES, Peck KR, Dhong HJ, Song JH, Chung DR, Kim YJ. MERS-CoV outbreak following a single patient exposure in an emergency room in South Korea: an epidemiological outbreak study. *Lancet* 2016; **388**: 994-1001 [PMID: 27402381 DOI: 10.1016/S0140-6736(16)30623-7]

32 **de Wit E**, van Doremalen N, Falzarano D, Munster VJ. SARS and MERS: recent insights into emerging coronaviruses. *Nat Rev Microbiol* 2016; **14**: 523-534 [PMID: 27344959 DOI: 10.1038/nrmicro.2016.81]

33 **Belouzard S**, Millet JK, Licitra BN, Whittaker GR. Mechanisms of coronavirus cell entry mediated by the viral spike protein. *Viruses* 2012; **4**: 1011-1033 [PMID: 22816037 DOI: 10.3390/v4061011]

34 **Lupia T**, Scabini S, Mornese Pinna S, Di Perri G, De Rosa FG, Corcione S. 2019 novel coronavirus (2019-nCoV) outbreak: A new challenge. *J Glob Antimicrob Resist* 2020; **21**: 22-27 [PMID: 32156648 DOI: 10.1016/j.jgar.2020.02.021]

35 **Letko M**, Marzi A, Munster V. Functional assessment of cell entry and receptor usage for SARS-CoV-2 and other lineage B betacoronaviruses. *Nat Microbiol* 2020; **5**: 562-569 [PMID: 32094589 DOI: 10.1038/s41564-020-0688-y]

36 **Bennardo F**, Buffone C, Giudice A. New therapeutic opportunities for COVID-19 patients with Tocilizumab: Possible correlation of interleukin-6 receptor inhibitors with osteonecrosis of the jaws. *Oral Oncol* 2020; **106**: 104659 [PMID: 32209313 DOI: 10.1016/j.oraloncology.2020.104659]

37 **Chen C**, Zhang XR, Ju ZY, He WF. [Advances in the research of mechanism and related immunotherapy on the cytokine storm induced by coronavirus disease 2019]. *Zhonghua Shao Shang Za Zhi* 2020; **36**: 471-475 [PMID: 32114747 DOI: 10.3760/cma.j.cn501120-20200224-00088]

38 **Hoffmann M**, Kleine-Weber H, Krüger N, Müller M, Drosten C, Pöhlmann S. The novel coronavirus 2019 (2019-nCoV) uses the SARS-coronavirus receptor ACE2 and the cellular protease TMPRSS2 for entry into target cells. 2020 Preprint. Available from: bioRxiv [DOI: 10.1101/2020.01.31.929042]

39 **Wrapp D**, Wang N, Corbett KS, Goldsmith JA, Hsieh CL, Abiona O, Graham BS, McLellan JS. Cryo-EM structure of the 2019-nCoV spike in the prefusion conformation. *Science* 2020; **367**: 1260-1263 [PMID: 32075877 DOI: 10.1126/science.abb2507]

40 **Xia S**, Zhu Y, Liu M, Lan Q, Xu W, Wu Y, Ying T, Liu S, Shi Z, Jiang S, Lu L. Fusion mechanism of 2019-nCoV and fusion inhibitors targeting HR1 domain in spike protein. *Cell Mol Immunol* 2020; **17**: 765-767 [PMID: 32047258 DOI: 10.1038/s41423-020-0374-2]

41 **Yu F**, Du L, Ojcius DM, Pan C, Jiang S. Measures for diagnosing and treating infections by a novel coronavirus responsible for a pneumonia outbreak originating in Wuhan, China. *Microbes Infect* 2020; **22**: 74-79 [PMID: 32017984 DOI: 10.1016/j.micinf.2020.01.003]

42 **de Wilde AH**, Snijder EJ, Kikkert M, van Hemert MJ. Host Factors in Coronavirus Replication. *Curr Top Microbiol Immunol* 2018; **419**: 1-42 [PMID: 28643204 DOI: 10.1007/82_2017_25]

43 **Perrier A**, Bonnin A, Desmarets L, Danneels A, Goffard A, Rouillé Y, Dubuisson J, Belouzard S. The C-terminal domain of the MERS coronavirus M protein contains a *trans*-Golgi network localization signal. *J Biol Chem* 2019; **294**: 14406-14421 [PMID: 31399512 DOI: 10.1074/jbc.RA119.008964]

44 **Yang Y**, Lu Q, Liu M, Wang Y, Zhang A, Jalali N, Dean NE, Longini I, Halloran ME, Xu B, Zhang XA, Wang LP, Liu W, Fang LQ. Epidemiological and clinical features of the 2019 novel coronavirus outbreak in China. 2020 Preprint. Available from: medRxiv [DOI: 10.1101/2020.02.10.20021675]

45 **Huang C**, Wang Y, Li X, Ren L, Zhao J, Hu Y, Zhang L, Fan G, Xu J, Gu X, Cheng Z, Yu T, Xia J, Wei Y, Wu W, Xie X, Yin W, Li H, Liu M, Xiao Y, Gao H, Guo L, Xie J, Wang G, Jiang R, Gao Z, Jin Q, Wang J, Cao B. Clinical features of patients infected with 2019 novel coronavirus in Wuhan, China. *Lancet* 2020; **395**: 497-506 [PMID: 31986264 DOI: 10.1016/S0140-6736(20)30183-5]

46 **Li Z**, Wu M, Guo J, Yao J, Liao X, Song S, et al Caution on kidney dysfunctions of 2019-nCoV patients. 2020 Preprint. Available from: medRxiv [DOI: 10.1101/2020.02.08.20021212]

47 **Wu J**, Chen ZJ. Innate immune sensing and signaling of cytosolic nucleic acids. *Annu Rev Immunol* 2014; **32**: 461-488 [PMID: 24655297 DOI: 10.1146/annurev-immunol-032713-120156]

48 **Wu J**, Sun L, Chen X, Du F, Shi H, Chen C, Chen ZJ. Cyclic GMP-AMP is an endogenous second messenger in innate immune signaling by cytosolic DNA. *Science* 2013; **339**: 826-830 [PMID: 23258412 DOI: 10.1126/science.1229963]

49 **Yoo JS**, Kato H, Fujita T. Sensing viral invasion by RIG-I like receptors. *Curr Opin Microbiol* 2014; **20**: 131-138 [PMID: 24968321 DOI: 10.1016/j.mib.2014.05.011]

50 **Kawai T**, Akira S. The role of pattern-recognition receptors in innate immunity: update on Toll-like receptors. *Nat Immunol* 2010; **11**: 373-384 [PMID: 20404851 DOI: 10.1038/ni.1863]

51 **Liu Y**, Zhang C, Huang F, Yang Y, Wang F, Yuan J, Zhang Z, Qin Y, Li X, Zhao D, Li S, Tan S, Wang Z, Li J, Shen C, Peng L, Wu W, Cao M, Xing L, Xu Z, Chen L, Zhou C, Liu WJ, Liu L, Jiang C. 2019-novel coronavirus (2019-nCoV) infections trigger an exaggerated cytokine response aggravating lung injury. 2020 Preprint. Available from: ChinaXiv

52 **Liu Q**, Wang R, Qu G, Wang Y, Liu P, Zhu Y. General anatomy report of novel coronavirus pneumonia death corpse. *J Forensic Med* 2020; **36**: 19-21

53 **Chung M**, Bernheim A, Mei X, Zhang N, Huang M, Zeng X, Cui J, Xu W, Yang Y, Fayad ZA, Jacobi A, Li K, Li S, Shan H. CT Imaging Features of 2019 Novel Coronavirus (2019-nCoV). *Radiology* 2020; **295**: 202-207 [PMID: 32017661 DOI: 10.1148/radiol.2020200230]

54 **Shi H**, Han X, Jiang N, Cao Y, Alwalid O, Gu J, Fan Y, Zheng C. Radiological findings from 81 patients with COVID-19 pneumonia in Wuhan, China: a descriptive study. *Lancet Infect Dis* 2020; **20**: 425-434 [PMID: 32105637 DOI: 10.1016/S1473-3099(20)30086-4]

55 **Ai T**, Yang Z, Hou H, Zhan C, Chen C, Lv W, Tao Q, Sun Z, Xia L. Correlation of Chest CT and RT-PCR Testing for Coronavirus Disease 2019 (COVID-19) in China: A Report of 1014 Cases. *Radiology* 2020; **296**: E32-E40 [PMID: 32101510 DOI: 10.1148/radiol.2020200642]

56 **Lim CC**, Tan CS, Kaushik M, Tan HK. Initiating acute dialysis at earlier Acute Kidney Injury Network stage in critically ill patients without traditional indications does not improve outcome: a prospective cohort study. *Nephrology (Carlton)* 2015; **20**: 148-154 [PMID: 25395245 DOI: 10.1111/nep.12364]

57 **Liang W**, Guan W, Chen R, Wang W, Li J, Xu K, Li C, Ai Q, Lu W, Liang H, Li S, He J. Cancer patients in SARS-CoV-2 infection: a nationwide analysis in China. *Lancet Oncol* 2020; **21**: 335-337 [PMID: 32066541 DOI: 10.1016/S1470-2045(20)30096-6]

58 **Lagier JC**, Colson P, Tissot Dupont H, Salomon J, Doudier B, Aubry C, Gouriet F, Baron S, Dudouet P, Flores R, Ailhaud L, Gautret P, Parola P, La Scola B, Raoult D, Brouqui P. Testing the repatriated for SARS-Cov2: Should laboratory-based quarantine replace traditional quarantine? *Travel Med Infect Dis* 2020; **34**: 101624 [PMID: 32179125 DOI: 10.1016/j.tmaid.2020.101624]

59 **Lippi G**, Simundic AM, Plebani M. Potential preanalytical and analytical vulnerabilities in the laboratory diagnosis of coronavirus disease 2019 (COVID-19). *Clin Chem Lab Med* 2020; **58**: 1070-1076 [PMID: 32172228 DOI: 10.1515/cclm-2020-0285]

60 **Wan S**, Yi Q, Fan S, Lv J, Zhang X, Guo L, Lang C, Xiao Q, Xiao K, Yi Z, Qiang M, Xiang J, Zhang B, Chen Y. Characteristics of lymphocyte subsets and cytokines in peripheral blood of 123 hospitalized patients with 2019 novel coronavirus pneumonia (NCP). 2020 Preprint. Available from: medRxiv [DOI: 10.1101/2020.02.10.20021832]

61 **Di L**, Fu Y, Sun Y, Li J, Liu L, Yao J, Wang G, Wu Y, Lao K, Lee RW, Zheng G, Xu J, Oh J, Wang D, Xie XS, Huang Y, Wang J. RNA sequencing by direct tagmentation of RNA/DNA hybrids. *Proc Natl Acad Sci USA* 2020; **117**: 2886-2893 [PMID: 31988135 DOI: 10.1073/pnas.1919800117]

62 **Smith T**, Bushek J, LeClaire A, Prosser T. COVID-19 Drug Therapy. Available from: https://www.elsevier.com/__data/assets/pdf_file/0007/988648/COVID-19-Drug-Therapy_2020-8-28.pdf

63 **Di Gennaro F**, Pizzol D, Marotta C, Antunes M, Racalbuto V, Veronese N, Smith L. Coronavirus Diseases (COVID-19) Current Status and Future Perspectives: A Narrative Review. *Int J Environ Res Public Health* 2020; **17** [PMID: 32295188 DOI: 10.3390/ijerph17082690]

64 **Wang M**, Cao R, Zhang L, Yang X, Liu J, Xu M, Shi Z, Hu Z, Zhong W, Xiao G. Remdesivir and chloroquine effectively inhibit the recently emerged novel coronavirus (2019-nCoV) in vitro. *Cell Res* 2020; **30**: 269-271 [PMID: 32020029 DOI: 10.1038/s41422-020-0282-0]

65 **Holshue ML**, DeBolt C, Lindquist S, Lofy KH, Wiesman J, Bruce H, Spitters C, Ericson K, Wilkerson S, Tural A, Diaz G, Cohn A, Fox L, Patel A, Gerber SI, Kim L, Tong S, Lu X, Lindstrom S, Pallansch MA, Weldon WC, Biggs HM, Uyeki TM, Pillai SK; Washington State 2019-nCoV Case Investigation Team. First Case of 2019 Novel Coronavirus in the United States. *N Engl J Med* 2020; **382**: 929-936 [PMID: 32004427 DOI: 10.1056/NEJMoa2001191]

66 **Lu HT**, Yang JC, Yuan ZC, Sheng WH, Yan WH. [Effect of combined treatment of Shuanghuanglian and recombinant interferon alpha 2a on coxsackievirus B3 replication in vitro]. *Zhongguo Zhong Yao Za Zhi* 2000; **25**: 682-684 [PMID: 12525074]

67 **Kim HY**, Eo EY, Park H, Kim YC, Park S, Shin HJ, Kim K. Medicinal herbal extracts of Sophorae radix, Acanthopanacis cortex, Sanguisorbae radix and Torilis fructus inhibit coronavirus replication in vitro. *Antivir Ther* 2010; **15**: 697-709 [PMID: 20710051 DOI: 10.3851/IMP1615]

68 **Ali I**, Alharbi OML. COVID-19: Disease, management, treatment, and social impact. *Sci Total*

Environ 2020; **728**: 138861 [PMID: 32344226 DOI: 10.1016/j.scitotenv.2020.138861]
69 **Fiore C**, Eisenhut M, Krausse R, Ragazzi E, Pellati D, Armanini D, Bielenberg J. Antiviral effects of Glycyrrhiza species. *Phytother Res* 2008; **22**: 141-148 [PMID: 17886224 DOI: 10.1002/ptr.2295]
70 **Wang L**, Yang R, Yuan B, Liu Y, Liu C. The antiviral and antimicrobial activities of licorice, a widely-used Chinese herb. *Acta Pharm Sin B* 2015; **5**: 310-315 [PMID: 26579460 DOI: 10.1016/j.apsb.2015.05.005]
71 **Mathie RT**, Baitson ES, Frye J, Nayak C, Manchanda RK, Fisher P. Homeopathic treatment of patients with influenza-like illness during the 2009 A/H1N1 influenza pandemic in India. *Homeopathy* 2013; **102**: 187-192 [PMID: 23870378 DOI: 10.1016/j.homp.2013.04.001]
72 **Mustafa S**, Balkhy H, Gabere MN. Current treatment options and the role of peptides as potential therapeutic components for Middle East Respiratory Syndrome (MERS): A review. *J Infect Public Health* 2018; **11**: 9-17 [PMID: 28864360 DOI: 10.1016/j.jiph.2017.08.009]
73 **Gilardin L**, Bayry J, Kaveri SV. Intravenous immunoglobulin as clinical immune-modulating therapy. *CMAJ* 2015; **187**: 257-264 [PMID: 25667260 DOI: 10.1503/cmaj.130375]
74 **Kumar V**, Jung YS, Liang PH. Anti-SARS coronavirus agents: a patent review (2008 - present). *Expert Opin Ther Pat* 2013; **23**: 1337-1348 [PMID: 23905913 DOI: 10.1517/13543776.2013.823159]
75 **Soo YO**, Cheng Y, Wong R, Hui DS, Lee CK, Tsang KK, Ng MH, Chan P, Cheng G, Sung JJ. Retrospective comparison of convalescent plasma with continuing high-dose methylprednisolone treatment in SARS patients. *Clin Microbiol Infect* 2004; **10**: 676-678 [PMID: 15214887 DOI: 10.1111/j.1469-0691.2004.00956.x]
76 **Hung IF**, To KK, Lee CK, Lee KL, Chan K, Yan WW, Liu R, Watt CL, Chan WM, Lai KY, Koo CK, Buckley T, Chow FL, Wong KK, Chan HS, Ching CK, Tang BS, Lau CC, Li IW, Liu SH, Chan KH, Lin CK, Yuen KY. Convalescent plasma treatment reduced mortality in patients with severe pandemic influenza A (H1N1) 2009 virus infection. *Clin Infect Dis* 2011; **52**: 447-456 [PMID: 21248066 DOI: 10.1093/cid/ciq106]
77 **Zarbock A**, Kellum JA, Schmidt C, Van Aken H, Wempe C, Pavenstädt H, Boanta A, Gerß J, Meersch M. Effect of Early vs Delayed Initiation of Renal Replacement Therapy on Mortality in Critically Ill Patients With Acute Kidney Injury: The ELAIN Randomized Clinical Trial. *JAMA* 2016; **315**: 2190-2199 [PMID: 27209269 DOI: 10.1001/jama.2016.5828]
78 **van Doremalen N**, Bushmaker T, Morris DH, Holbrook MG, Gamble A, Williamson BN, Tamin A, Harcourt JL, Thornburg NJ, Gerber SI, Lloyd-Smith JO, de Wit E, Munster VJ. Aerosol and Surface Stability of SARS-CoV-2 as Compared with SARS-CoV-1. *N Engl J Med* 2020; **382**: 1564-1567 [PMID: 32182409 DOI: 10.1056/NEJMc2004973]
79 **World Health Organization**. Clinical Management of Severe Acute Respiratory Infection (SARI) When COVID-19 Disease Is Suspected. Interim Guidance. 2020 [DOI: 10.15557/PiMR.2020.0003]
80 **WHO**. Report of the WHO-China joint mission on coronavirus disease 2019 (COVID-19). Available from: https://www.who.int/docs/default-source/coronaviruse/who-chinajoint-mission-on-COVID-19-final-report.pdf. 2020b
81 **WHO**. Rolling updates on coronavirus disease (COVID-19). [Accessed April 10, 2020] Available from: https://www.who.int/emergencies/diseases/novel-coronavirus-2019/events-as-they-happen
82 **BBC**. Coronavirus: Venice carnival closes as Italy imposes lockdown. Available from: https://www.bbc.com/news/world-europe-51602007,2020a
83 **Rasheed Z**, Allahoum R, Siddiqui U. Trump extends US social distancing until April 30: live updates. 2020. Available from: https://www.aljazeera.com/news/2020/03/trump-weighs-coronavirus-lockdown-york-live-updates-200328234401911.html
84 **Collins F**. To beat COVID-19, social distancing is a must. 2020. Available from: https://directorsblog.nih.gov/2020/03/19/to-beat-COVID-19-social-distancing-is-a-must/
85 **Naidoo D**, Schembri A, Cohen M. The health impact of residential retreats: a systematic review. *BMC Complement Altern Med* 2018; **18**: 8 [PMID: 29316909 DOI: 10.1186/s12906-017-2078-4]
86 **World Bank**. Hospital beds (per 1,000 people). [cited 10 April 2020]. Available from: https://data.worldbank.org/indicator/sh.med.beds.zs
87 **Chin AWH**, Chu JTS, Perera MRA, Hui KPY, Yen HL, Chan MCW, Peiris M, Poon LLM. Stability of SARS-CoV-2 in different environmental conditions. *Lancet Microbe* 2020; **1**: e10 [PMID: 32835322 DOI: 10.1016/S2666-5247(20)30003-3]
88 **Daniyal S**. India is enforcing the harshest and most extensive COVID-19 Lockdown in the world. [cited 11 April 2020]. Available from: https://qz.com/india/1828915/indias-coronavirus-lockdown-harsherthan-china-italy pakistan/
89 **Abidi A**, Jacinto L. Lack of compassion, more than resources, marks india's deadly lockdown mismanagement. [cited 11 April 2020]. Available from: https://www.france24.com/en/20200401-lack-of-compassion-more-than-resources-marks-india-s-deadly-lockdown-mismanagement
90 **Kumar A**. Coronavirus: WHO lauds Modi government's social outreach during lockdown. [cited 11 April 2020]. Available from: https://www.indiatoday.in/india/story/who-coronavirus-lockdownindia-economic-stimulus-package-1662392-2020-04-02
91 **Sharma S**. Lockdown in India was early, far-sighted and courageous': WHO envoy. [cited 25 October 2020]. Available from: https://www.hindustantimes.com/india-news/Lockdown-in-india-was-early-thiswas-far-sighted courageous-move-who-special-envoy-on-COVID-19/storywNdCkNVOqV5gCN8Du9jJ3N.html
92 **BBC**. Coronavirus deaths exceed SARS fatalities in 2003. [cited 11 April 2020]. Available from:

https://www.bbc.com/news/world-asia-china-51431087

93 **Barcelo D**. An environmental and health perspective for COVID-19 outbreak: Meteorology and air quality influence, sewage epidemiology indicator, hospitals disinfection, drug therapies and recommendations. *J Environ Chem Eng* 2020; **8**: 104006 [PMID: 32373461 DOI: 10.1016/j.jece.2020.104006]

94 **Xie J**, Zhu Y. Association between ambient temperature and COVID-19 infection in 122 cities from China. *Sci Total Environ* 2020; **724**: 138201 [PMID: 32408450 DOI: 10.1016/j.scitotenv.2020.138201]

95 **Ma Y**, Zhao Y, Liu J, He X, Wang B, Fu S, Yan J, Niu J, Zhou J, Luo B. Effects of temperature variation and humidity on the death of COVID-19 in Wuhan, China. *Sci Total Environ* 2020; **724**: 138226 [PMID: 32408453 DOI: 10.1016/j.scitotenv.2020.138226]

96 **Tosepu R**, Gunawan J, Effendy DS, Ahmad OAI, Lestari H, Bahar H, Asfian P. Correlation between weather and Covid-19 pandemic in Jakarta, Indonesia. *Sci Total Environ* 2020; **725**: 138436 [PMID: 32298883 DOI: 10.1016/j.scitotenv.2020.138436]

97 **Conticini E**, Frediani B, Caro D. Can atmospheric pollution be considered a co-factor in extremely high level of SARS-CoV-2 lethality in Northern Italy? *Environ Pollut* 2020; **261**: 114465 [PMID: 32268945 DOI: 10.1016/j.envpol.2020.114465]

98 **WHO**. Air pollution. [cited 5 April 2020]. Available from: https://www.who.int/health-topics/air-pollution#tab=tab_1

99 **Coccia M**. Factors determining the diffusion of COVID-19 and suggested strategy to prevent future accelerated viral infectivity similar to COVID. *Sci Total Environ* 2020; **729**: 138474 [PMID: 32498152 DOI: 10.1016/j.scitotenv.2020.138474]

100 **Sharma S**, Zhang M, Anshika, Gao J, Zhang H, Kota SH. Effect of restricted emissions during COVID-19 on air quality in India. *Sci Total Environ* 2020; **728**: 138878 [PMID: 32335409 DOI: 10.1016/j.scitotenv.2020.138878]

101 **Zambrano-Monserrate MA**, Ruano MA, Sanchez-Alcalde L. Indirect effects of COVID-19 on the environment. *Sci Total Environ* 2020; **728**: 138813 [PMID: 32334159 DOI: 10.1016/j.scitotenv.2020.138813]

102 **Tobías A**, Carnerero C, Reche C, Massagué J, Via M, Minguillón MC, Alastuey A, Querol X. Changes in air quality during the lockdown in Barcelona (Spain) one month into the SARS-CoV-2 epidemic. *Sci Total Environ* 2020; **726**: 138540 [PMID: 32302810 DOI: 10.1016/j.scitotenv.2020.138540]

103 **CAMS**. [cited 5 April 2020]. Available from: https://atmosphere.copernicus.eu/amid-coronavirus-outbreak-copernicusmonitors-reduction-particulate-matter-pm25-over-china

104 **Ceylan Z**. Estimation of COVID-19 prevalence in Italy, Spain, and France. *Sci Total Environ* 2020; **729**: 138817 [PMID: 32360907 DOI: 10.1016/j.scitotenv.2020.138817]

105 **Ibarra-Vega D**. Lockdown, one, two, none, or smart. Modeling containing covid-19 infection. A conceptual model. *Sci Total Environ* 2020; **730**: 138917 [PMID: 32387821 DOI: 10.1016/j.scitotenv.2020.138917]

106 **Mahato S**, Pal S, Ghosh KG. Effect of lockdown amid COVID-19 pandemic on air quality of the megacity Delhi, India. *Sci Total Environ* 2020; **730**: 139086 [PMID: 32375105 DOI: 10.1016/j.scitotenv.2020.139086]

107 **Ogen Y**. Assessing nitrogen dioxide (NO_2) levels as a contributing factor to coronavirus (COVID-19) fatality. *Sci Total Environ* 2020; **726**: 138605 [PMID: 32302812 DOI: 10.1016/j.scitotenv.2020.138605]

108 **Prata DN**, Rodrigues W, Bermejo PH. Temperature significantly changes COVID-19 transmission in (sub)tropical cities of Brazil. *Sci Total Environ* 2020; **729**: 138862 [PMID: 32361443 DOI: 10.1016/j.scitotenv.2020.138862]

109 **Zambrano-Monserrate MA**, Ruano MA. Does environmental noise affect housing rental prices in developing countries? *Land Use Policy* 2019; **87**: 104059 [DOI: 10.1016/j.landusepol.2019.104059]

110 **Zambrano-Monserrate MA**, Silva-Zambrano CA, Ruano MA. The economic value of natural protected areas in Ecuador: a case of Villamil Beach National Recreation Area. *Ocean Coast Manage* 2018; **157**: 193-202 [DOI: 10.1016/j.ocecoaman.2018.02.020]

111 **Schanes K**, Dobernig K, Gözet B. Food waste matters-a systematic review of household food waste practices and their policy implications. *J Clean Prod* 2018; **182**: 978-991 [DOI: 10.1016/j.jclepro.2018.02.030]

112 **Calma J**. The COVID-19 pandemic is generating tons of medical waste. [cited 5 April 2020]. Available from: https://www.theverge.com/2020/3/26/21194647/the-covid-19-pandemic-is-generating-tons-of-medical-waste

113 **Liu M**, Tan S, Zhang M, He G, Chen Z, Fu Z, Luan C. Waste paper recycling decision system based on material flow analysis and life cycle assessment: A case study of waste paper recycling from China. *J Environ Manage* 2020; **255**: 109859 [PMID: 32063319 DOI: 10.1016/j.jenvman.2019.109859]

114 **Ma B**, Li X, Jiang Z, Jiang J. Recycle more, waste more? *J Clean Prod* 2019; **206**: 870-877 [DOI: 10.1016/j.jclepro.2018.09.063]

115 **Bir B**. Single-use items not safest option amid COVID-19. [cited 5 April 2020]. Available from: https://www.aa.com.tr/en/health/single-use-items-not-safest-option-amidcovid-19/1787067

116 **WHO**. Water, sanitation, hygiene, and waste management for COVID-19. [cited 5 April 2020]. Available from: https://www.who.int/publications-detail/water-sanitation-hygiene-andwaste

management-for-covid-19

117 **Xiao AT**, Tong YX, Zhang S. False negative of RT-PCR and prolonged nucleic acid conversion in COVID-19: Rather than recurrence. *J Med Virol* 2020; **92**: 1755-1756 [PMID: 32270882 DOI: 10.1002/jmv.25855]

118 **Bonifácio LP**, Pereira APS, Araújo DCAE, Balbão VDMP, Fonseca BALD, Passos ADC, Bellissimo-Rodrigues F. Are SARS-CoV-2 reinfection and Covid-19 recurrence possible? *Rev Soc Bras Med Trop* 2020; **53**: e20200619 [PMID: 32965458 DOI: 10.1590/0037-8682-0619-2020]

119 **Hoang T**. Characteristics of COVID-19 recurrence: a systematic review and meta-analysis. 2020 Preprint. Available from: medRxiv [DOI: 10.1101/2020.09.05.20189134]

120 **Loconsole D**, Passerini F, Palmieri VO, Centrone F, Sallustio A, Pugliese S, Grimaldi LD, Portincasa P, Chironna M. Recurrence of COVID-19 after recovery: a case report from Italy. *Infection* 2020; **48**: 965-967 [PMID: 32415334 DOI: 10.1007/s15010-020-01444-1]

World Journal of Gastroenterology

Submit a Manuscript: https://www.f6publishing.com

World J Gastroenterol 2021 September 21; 27(35): 5851-5889

DOI: 10.3748/wjg.v27.i35.5851

ISSN 1007-9327 (print) ISSN 2219-2840 (online)

REVIEW

Pancreatic cancer in 2021: What you need to know to win

Valeria Tonini, Manuel Zanni

ORCID number: Valeria Tonini 0000-0003-3130-2928; Manuel Zanni 0000-0001-7732-7739.

Author contributions: Tonini V and Zanni M wrote the manuscript; both authors reviewed and approved the final version.

Conflict-of-interest statement: No conflict of interest.

Open-Access: This article is an open-access article that was selected by an in-house editor and fully peer-reviewed by external reviewers. It is distributed in accordance with the Creative Commons Attribution NonCommercial (CC BY-NC 4.0) license, which permits others to distribute, remix, adapt, build upon this work non-commercially, and license their derivative works on different terms, provided the original work is properly cited and the use is non-commercial. See: http://creativecommons.org/Licenses/by-nc/4.0/

Manuscript source: Invited manuscript

Specialty type: Gastroenterology and hepatology

Country/Territory of origin: Italy

Peer-review report's scientific quality classification

Grade A (Excellent): 0

Grade B (Very good): B, B

Valeria Tonini, Department of Medical Sciences and Surgery, University of Bologna-Emergency Surgery Unit, IRCCS Sant'Orsola Hospital, Bologna 40121, Italy

Manuel Zanni, University of Bologna, Emergency Surgery Unit, IRCCS Sant'Orsola Hospital, Bologna 40121, Italy

Corresponding author: Valeria Tonini, MD, PhD, Professor, Surgeon, Surgical Oncologist, Department of Medical Sciences and Surgery, University of Bologna- Emergency Surgery Unit, IRCCS Sant'Orsola Hospital, Via Massarenti 9, Bologna 40121, Italy. valeria.tonini@unibo.it

Abstract

Pancreatic cancer is one of the solid tumors with the worst prognosis. Five-year survival rate is less than 10%. Surgical resection is the only potentially curative treatment, but the tumor is often diagnosed at an advanced stage of the disease and surgery could be performed in a very limited number of patients. Moreover, surgery is still associated with high post-operative morbidity, while other therapies still offer very disappointing results. This article reviews every aspect of pancreatic cancer, focusing on the elements that can improve prognosis. It was written with the aim of describing everything you need to know in 2021 in order to face this difficult challenge.

Key Words: Pancreatic cancer treatment; Advanced pancreatic cancer; Metastatic pancreatic cancer; Pancreatic cancer surgery; Pancreatic cancer chemotherapy; Pancreatic cancer screening

©The Author(s) 2021. Published by Baishideng Publishing Group Inc. All rights reserved.

Core Tip: Pancreatic cancer is a very dangerous enemy and the results are still very unsatisfactory. But we have not given up. Research is running fast on many paths, without losing its enthusiasm.The number of articles published on this subject in the last two years is impressive. I have tried to summarize all the most significant data from the different lines of research, ranging from screening and early diagnosis to new developments in surgery and associated therapies. I hope I have succeeded in the task of describing as comprehensively as possible the most promising fields of research available to us today, in order to achieve the improved results we desire.

Citation: Tonini V, Zanni M. Pancreatic cancer in 2021: What you need to know to win. *World*

Grade C (Good): 0
Grade D (Fair): 0
Grade E (Poor): 0

Received: January 28, 2021
Peer-review started: January 28, 2021
First decision: June 14, 2021
Revised: July 14, 2021
Accepted: August 23, 2021
Article in press: August 23, 2021
Published online: September 21, 2021

P-Reviewer: Sato H
S-Editor: Gao CC
L-Editor: A
P-Editor: Li JH



J Gastroenterol 2021; 27(35): 5851-5889
URL: https://www.wjgnet.com/1007-9327/full/v27/i35/5851.htm
DOI: https://dx.doi.org/10.3748/wjg.v27.i35.5851

INTRODUCTION

Pancreatic cancer is currently the seventh leading cause of cancer death worldwide and the fourth following lung, colorectal and breast cancers in the United States and Europe. It will become the third by 2030. It is an age-related neoplasm and this trend is similar between males and females. In particular the number of both deaths and incident cases peaked at the ages of 65-69 years in males, whereas the peak in females was observed at the ages of 75-79 years[1-4]. The commonly used term "pancreatic cancer" usually refers to ductal adenocarcinoma (PDAC), which represents 85% of all pancreatic tumor[4]. Complete surgical resection significantly prolongs survival, but the tumor is often diagnosed at an advanced stage and only a small percentage of patients are therefore candidates for surgery. Moreover, surgery is still associated with high post-operative morbidity. Despite ongoing developments, PDAC remains one of the most difficult tumors to treat, and the five-year survival rate is less than 10%[5]. There are four fundamental challenges that underlie the high mortality. First, the retroperitoneal location of the pancreas, deep in the abdomen, protects growing tumors from detection. The symptoms are late and therefore the diagnosis is made when the tumor is already in an advanced stage. Second, PDAC has an aggressive biology characterized by early metastasis and 50% of patients has metastatic disease at presentation. In addition, a large number of patients undergoing surgery develop metastases within 4 years. This suggests the presence of micrometastasis in apparently localized cases[6]. Third, pancreatic cancer dramatically weakens patients, limiting their ability to withstand aggressive treatments. Finally, it shows resistance to many antineoplastic therapies[7,8]. Advances in prevention, screening, early detection, and therapy, particularly on new frontiers, are essential to improve outcomes. This article has been written with the aim of describing everything you need to know in 2021 in order to face this difficult challenge.

NON-FAMILIAL RISK FACTORS AND PREVENTION

Identification of risk factors, high-risk populations and early detection markers is the first and crucial step to change the pancreatic cancer horizon[9]. PDAC incidence rates are nearly four times higher in high-income countries such as the United States and Western European countries than in middle- and low-income countries[3]. The different incidence seems to be related with different lifestyles.

Obesity, smoking, alcohol consumption and type 2 diabetes are considered non-familial risk factors for pancreatic cancer. Chronic pancreatitis, cystic fibrosis and intraductal papillary mucinous neoplasm (IPMN) should also be considered. An increased risk of pancreatic cancer has been observed following gastrectomy[10-17].

One-third of all cancers could have been prevented through lifestyle correction[18]. A 2020 European prospective study (EPIC) evaluated the association between the healthy lifestyle index score and PDAC[19-22]. Healthy lifestyle habits were inversely related to the risk of PDAC. Adherence to healthy behaviors, corresponding to a three-point increase in the score, was associated with a 16%-23% lower risk. The result summarizes many previous studies[23-29] and support the adoption of healthy lifestyles in PDAC prevention.

A recent nutrigenomic study has highlighted nutrients capable of preventing cancer through epigenetic modifications. An optimal diet should include omega 3 fatty acids, polyphenols, folic acid, selenium and zinc. Particularly important for PDAC prevention could be the epigallocatechin, a polyphenol from tea and green tea[30,31].

Data linking type 2 diabetes with pancreatic cancer suggest that the new onset of diabetes in a lean older adult should prompt consideration of PDAC. This is even more valid if new-onset diabetes is associated with unintentional weight loss[32-34]. A Mayo Clinic study evaluated the use of computed tomography (CT) at the time of diabetes diagnosis in otherwise asymptomatic patients. A higher likelihood of showing potentially resectable tumors was observed compared with scans performed six months later[32]. However, CT screening of all elderly subjects with new-onset

diabetes is not feasible[33]. With the identification of these characteristics that differentiate pancreatic cancer-associated diabetes from other cases of new-onset diabetes, perhaps the guidelines will updacate[35].

HEREDITARY RISKS FACTORS

PDAC can be hereditary. There are two categories of inherited risk for PDAC: Genetic syndromes (20% of cases) and familial pancreatic cancer (80%). Familial pancreatic cancer is defined as a predisposition that is based on familial clustering in families in which there is at least one pair of first-degree relative (FDR) relatives with PDAC in the absence of a known genetic syndrome. Genetic syndromes that predispose to pancreatic cancer are listed in Table 1. Table 1 also shows in parentheses the frequencies of mutated genes in PDAC patients[36-42].

Knowledge of inherited risk factors is important because it allows us an effective stratification and management of patients. According to American Society of Clinical Oncology and National Comprehensive Cancer Network guidelines, all patients diagnosed with PDAC should be evaluated to understand if there is a risk of familial predisposition to cancer. All patients should undergo risk assessment for syndromes associated with an increased risk of PDAC. Germline genetic testing is recommended for patients with PDAC and an unremarkable family history[43,44].

SCREENING

Screening aims to detect preinvasive lesions (IPMNs and pancreatic intraepithelial neoplasias) with high-grade neoplastic changes and early invasive tumors that are more amenable to potentially curative resection[45-49].

Candidates for screening

(1) Patients with Peutz-Jeghers syndrome or CDKN2A mutation, regardless of family history; (2) BRCA2 mutation with at least one affected FDR or at least two affected relatives of any degree; (3) BRCA1, partner and localizer of BRCA2 (PALB2), ataxia-telangiectasia mutated (ATM), and Lynch syndrome mutation carriers with one or more affected FDRs; (4) Hereditary pancreatitis with a PRSS1 mutation; and (5) Regardless of gene mutation status: (a) At least three affected relatives on the same side of the family, of whom at least one is an FDR of the individual being considered for surveillance; (b) At least two affected relatives who are FDRs of each other, of whom at least one is an FDR of the individual being considered for surveillance; and (c) At least two affected relatives on the same side of the family, of whom at least one is an FDR of the individual being considered for surveillance.

General population-based screening for average-risk patients is not recommended [33] because the average lifetime risk for developing PDAC is too low[49].

Screening modality

The current recommendation provides for the execution of endoscopic ultrasonography (EUS) or magnetic resonance imaging (MRI)/magnetic resonance cholangiopancreatography (MRCP). It has been demonstrated that they detect more lesion as compared with CT scan[50]. Screening is recommended at age 50 years or 10 years younger than the youngest relative with PDAC in familial pancreatic cancer relatives. In other cases, screening is carried out between 35 and 45 years. For patients with a normal pancreas on imaging, repeat the procedure every year alternating EUS and MRCP. The age for stopping screening should be individualized based on each patient's medical status, life expectancy, and preferences.

SURGICAL RESECTION FOR IPMNS AND OTHER CYSTIC LESIONS

Surgical resection is indicated in patients with any of the following[45]: (1) Solid pancreatic lesion ≥ 5 mm of indeterminate pathology or if additional evaluation does not yield a definitive preoperative diagnosis; (2) Any positive fine-needle aspiration (FNA) result, except for a pancreatic neuroendocrine tumor; (3) Main-duct IPMNs with any one of the following: (a) Main pancreatic duct dilation of ≥ 10 mm; (b) Main pancreatic duct stricture; or (c) Mural nodules; (4) Branch duct IPMNs (BD-IPMNs)

Table 1 Genetic syndromes predisposing to pancreatic cancer (the frequency of mutated genes among patients with pancreatic ductal adenocarcinoma is indicated in brackets)

Genetic syndrome	Mutated genes
Hereditary breast/ovarian cancer syndrome[36,37]	*BRCA1* (0.7%), *BRCA2* (1.4%), *PALB2* (1%)
Familial atypical multiple mole melanoma syndrome[38]	*CDKN2A* (0.7%)
Peutz-Jeghers syndrome[39]	*STK11*
Familial adenomatous polyposis	*APC* (0.4%)
Lynch syndrome[40]	*MLH1*, *MSH2* (0.4%), *PMS2* (0.3%)
Hereditary pancreatitis[41]	*PRSS1*, *SPINK1*
Ataxia telangectasia[42]	*ATM* (1.4%)
Li-Fraumeni syndrome[42]	*P53* (0.4%)

with any one of the following: (a) Rapid growth (> 5 mm over six months); (b) Mural nodules or an enhancing solid component; (c) Abrupt main pancreatic duct caliber change with distal atrophy (even if no mass is visible); (d) Main pancreatic duct dilation of ≥ 10 mm; (e) Positive cytology; or (f) Associated symptoms of pancreatitis, jaundice, or pancreatic-type pain; or (5) Asymptomatic main pancreatic duct stricture with an associated suspicious mass.

For patients who do not meet these criteria for surgery, repeat imaging in three months if worrisome features are present[47,51]. Worrisome features include the following: (1) Solid lesion with main pancreatic duct size of 5 mm to 9 mm in diameter; (2) Main pancreatic duct stricture and/or dilation ≥ 6 mm of unknown etiology without an associated mass; and (3) Solid lesion < 5 mm of uncertain significance.

Repeat imaging in six months is recommended for patients who have the following imaging abnormalities: (1) Cystic lesion (presumed BD-IPMN) ≥ 3 cm in size; (2) Cystic lesion with associated main pancreatic duct 5 mm to 9 mm; (3) Cystic lesion associated with lymphadenopathy; (4) Cyst growth rate of ≥ 5 mm in two years; and (5) Increased serum carbohydrate antigen 19-9 (CA 19-9).

Individuals without worrisome features of malignancy should undergo repeat imaging in 12 mo[47,51].

Screening/surveillance should be continued until the patient is no longer a surgical candidate.

A 2020 paper analyzed the benefits of screening. Nine out of 10 screen-detected PDAC were resectable, with a three-year survival of 85%, compared with 25% in PDAC detected outside surveillance. With continued follow-up of patients with resectable PDAC, the five-year overall survival (OS) rate was 60%[49].

BIOMARKERS AND EARLY DETECTION

Different biomarkers are being evaluated to improve early diagnosis of tumor not detectable by imaging and to differentiate cancer and high-grade dysplasia from benign disease[52].

Blood tests

The most useful serum tumor marker for PDAC is CA 19-9. It is recommended adding this test when there are worrisome features on abdominal imaging. The sensitivity and the specificity of elevated CA 19-9 to detect PDAC are 79% and 82%, respectively[53-55]. It becomes more precise when used in combination with CA 125[56,57]. Other carbohydrate markers, such as CA 50, CA 72.4 and CA 242, were extensively analyzed in PDAC patients. Although they exhibited less sensitivity than CA 19-9 for the diagnosis, they improved specificity[58-61]. Satake and Takeuchi[62] also studied SPan-1 and DUPAN-2. SPan-1 has a high sensitivity for PDAC (81.4%), but the specificity (67.5%) and diagnostic accuracy (71%) are lower than those of CA19-9. SPan-1 may be considered as an additional useful serum marker, but it does not significantly improve the diagnostic accuracy obtained with CA 19-9. In contrast, DUPAN-2 has a high specificity (85.3%) and low sensitivity (47.7%). Furthermore, it seems that serum levels of DUPAN-2 are influenced by liver function. SPan-1 and DUPAN-2 unfortunately have not yet shown the sensitivity and specificity needed to

be used for early detection[62,63].

A huge step forward in the early detection of pancreatic cancer could come from studying cell-free DNA (cfDNA), which consists of circulating double-stranded DNA molecules that can be found in plasma or blood serum. From the analysis of these molecules, it is possible to understand if we are in the presence of a tumor DNA and to go back to the tissue of origin. By analyzing the methylation status of two genes in cfDNA, ADAMTS1 and BNC1, early stage cancer can be identified with a sensitivity of 94.8% and a specificity of 91.6%[64].

Innovative discoveries have also been made in the field of RNA. Abnormal microRNA expressions are potential diagnostic markers for several cancers, including PDAC. Multiple microRNA tests performed in combination with CA 19-9 can improve diagnostic accuracy, particularly miR-216[65-69]. Permuth *et al*[70] demonstrated that a combination of eight lncRNAs helps in the differential diagnosis between malignant and non-malignant IPMNs. Furthermore, three lncRNAs (HAND2-AS1, CTD-2033D15.2, and lncRNA-TGF) could be exploited as early diagnostic biomarkers of IPMN[71,72].

Pancreatic juice and pancreatic cyst fluid

Pancreatic juice collected at the time of ERCP and cyst fluid obtained by EUS-guided FNA can be analyzed for molecular markers. These procedures also have broad potential in terms of early diagnosis of PDAC. Next-generation sequencing can be performed at low cost to detect low-frequency mutations. Potential markers include mutant GNAS (specific for IPMNs) and mutant KRAS. TP53, SMAD4, PIK3CA, PTEN, and AKT1 mutants are also useful as they correlate with IPMN-associated tumors[73-75]. According to Suenaga *et al*[76], a pancreatic juice collection, to ensure optimal yield of mutations for pancreatic screening assays, should be performed 10 min after secretin administration. The authors detected 40 patients with KRAS mutations in pancreatic juice out of 45 undergoing surveillance with EUS, reconfirming the usefulness of these analysis[76].

There are many other biomarkers that are currently being validated for clinical use, such as mucins (MUC). Normal pancreatic ductal epithelium expresses low levels of MUC, while an upregulation of MUC occurs in BD-IPMNs and more pronounced changes in expression in PDAC. Normal pancreatic ductal epithelium expresses low levels of MUC, while upregulation of MUC occurs in BD-IPMN and PDAC[77-83]. The analysis of mucin changes in the fluid of pancreatic cysts allows us to differentiate mucinous from non-mucinous pancreatic cysts with high sensitivity and specificity and to diagnose PDACs associated with IPMN at an early stage[84]. MUC4 and MUC16 have been reported to be 100% specific for PDAC, while associated with sensitivities of 63% and 67%, respectively[85].

Interesting data were reported about interleukins (IL). Higher concentrations of IL-1b, IL-5, and IL-8 have been identified in cystic lesions with high grade dysplasia or malignancy[86]. IL-1b is a potentially useful factor in differentiating high-risk from low-risk pancreatic cysts.

The Das-1 monoclonal antibody is also capable of detecting pancreatic cysts at risk of malignancy with high levels of sensitivity (88%) and specificity (98%)[87,88]. Das-1, IL and MUC could be used in conjunction with clinical guidelines to identify patients at risk for malignancy.

Saliva

Saliva is a suitable substance for screening because it is obtained in a simple and noninvasive manner. In addition, salivary mRNA is relatively stable and informative for disease diagnosis, including cancer. Zhang *et al*[89] identified 7 up-regulated genes (MBD3L2, KRAS, STIM2, DMXL2, ACRV1, DMD, and CABLES1) and 5 down-regulated genes (TK2, GLTSCR2, CDKL3, TPT1, and DPM1) in subjects with PDAC compared with healthy controls or those with chronic pancreatitis. A combination of 4 mRNAs (MBD3L2, KRAS, ACRV1, and DPM1) can discriminate diseased patients from healthy ones with sensitivity and specificity over 90%[89]. Xie *et al*[90] worked on miR-3679-5p and miR-940. The former is down-regulated, while the latter is up-regulated in PDAC patients compared to controls. The combination of the two miRNAs identifies diseased subjects with sensitivity and specificity of 70%. The same group evaluated the expression of salivary long non-coding RNAs (lincRNAs). They identified HOTAIR and PV1T as significantly up-regulated lincRNAs in the PDAC group compared with controls and benign pancreatic tumors. The combination of salivary HOTAIR and PVT1 differentiated PDAC from healthy controls with a sensitivity of 78.2% and specificity of 90.9% and PDAC from benign tumors with a sensitivity of 81.8% and specificity of 95%[90,91]. Another important mRNA studied in

serum, urine, and saliva is MIR1246. Salivary expression of miR-1246 is related to serum CA19-9 levels[92]. Significantly higher expression of MIR1246 in serum and urine was observed in patients with cancer compared with healthy controls. Ishige *et al* [93] observed an AUC for MIR1246 in serum of 0.87 (sensitivity, 92.3%; specificity, 73.3%), for MIR1246 in urine of 0.90 (sensitivity, 90.2%; specificity, 83.3%). Combining the expression of MIR1246 in serum and urine resulted in a sensitivity of 85%. These results indicate that MIR246 may be a useful diagnostic biomarker for pancreatic cancer. The accuracy further increases if we consider miR-1246 and miR-4644 simultaneously[92].

Urine

Several biomarkers have also been evaluated in urine. Radon *et al*[94] used three protein biomarkers (REG1A, TFF1 and LYVE1) to form a powerful urinary panel that can detect patients with stages I-II PDAC, with over 90% accuracy. Brezgyte *et al*[95] found four miRNAs (miR-143, miR-204 and miR-223) in significantly higher amounts and one miRNA (miR-30e) in lower amounts in the urine of PDAC Stage I patients compared to the healthy population. These miRNAs (except for miR-204) also showed a decreased expression in Stage II-IV compared to Stage I[95]. However, more studies are needed to validate the clinical utility of these biomarkers.

CLINICAL FEATURES

The presenting symptoms in patients with PDAC varies according to location. Tumors in the body and tail present with pain and weight loss, while tumor of the head cause jaundice and steatorrhea[96]. Pain associated with PDAC is usually insidious, visceral, generally epigastric, radiating to the sides or straight through to the back. It is worse by eating or lying supine at night. Rarely, it develops acutely on account of acute pancreatitis due to tumoral occlusion of the main pancreatic duct[97]. Pancreatic cancer may result in an onset of diabetes mellitus[98,99]. The hypercoagulable state that accompanies PDAC can result in Trousseau syndrome, which consists of superficial, sometimes migratory thrombophlebitis[100]. Thromboembolic complications occur more commonly in patients with tumors arising in the tail or body of the pancreas[101]. Skin manifestations could occur as paraneoplastic phenomena[102]. Rarely, erythematous subcutaneous areas of nodular fat necrosis (pancreatic panniculitis), typically located on the legs, may be evident. It is more frequent in patients with the acinar cell variant of PDAC. It is not pathognomonic for an PDAC, because it has also been described in associated with pancreatic neuroendocrine tumors, IPMNs and chronic pancreatitis[103].

When assessing symptoms, it should be borne in mind that PDAC tends to infiltrate nearby organs and structures and to give distant metastases very early. Local extension typically involves adjacent structures, such as the duodenum, the portal vein (PV), or the superior mesenteric vessels. PDAC also show a striking tendency toward perineural invasion, both within and beyond the pancreas. The difficulty in achieving a wide resection margin due to the proximity to the vessels accounts for the fact that the retroperitoneal tissue behind the head of the pancreas represents the most common site of disease recurrence. Sometimes the tumor extends to the spleen, adrenal glands, vertebral column, transverse colon, and/or stomach. In these cases, tumors are not resectable. Tumor may metastasize to regional peripancreatic lymph nodes or less often to distant lymph node, peri-gastric, mesenteric, omental or porta-hepatic nodes. Distant metastasis may affect the liver, peritoneum, lungs, and less frequently, bone. Signs of advanced, incurable disease include an abdominal mass, ascites, Virchow's node, Sister Mary Joseph's node or a palpable rectal shelf. Pancreatic cancer is the origin of a cutaneous metastasis to the umbilicus in 7% to 9% of cases[104].

DIAGNOSIS

CT

CT is considered the gold standard for pancreatic cancer's diagnosis. Protocol pancreatic CT is performed for evaluation of suspected PDAC or if a routine CT scan was not sufficient for initial staging[105,106]. This protocol consists of evaluating the patient at different stages of contrast injection. The arterial phase provides excellent opacification of the celiac axis, superior mesenteric artery (SMA), and peripancreatic

arteries. An attenuation difference between tumor and normal pancreas is best achieved after peak enhancement of the aorta in the arterial phase but before the one of the liver, in the portal venous phase. This is sometimes termed the "pancreatic phase". The portal venous phase provides better enhancement of the superior mesenteric vein (SMV), splenic and PVs. In addition, peak hepatic enhancement, which optimizes the detection of hepatic metastases, also occurs in the portal venous phase[107,108].

The typical CT appearance of a PDAC is an ill-defined hypoattenuating mass within the pancreas. Smaller lesions may be iso-attenuating, making difficult their identification[109]. Secondary signs of PDAC include a dilatation of the pancreatic duct or common bile duct, parenchymal atrophy, and contour abnormalities. Dilation of both the pancreatic duct and the common bile duct, commonly referred to as the "double duct sign" is not diagnostic for a pancreatic head malignancy[110]. Routine preoperative CT helps to identify hepatic vascular anatomy and prepares the surgeon for any potential vascular anomalies. It can detect hemodynamically significant arterial stenosis[111]. The contrast-enhanced CT scan is the best technique for PDAC staging [112] and it is essential to detect vascular invasion. CT criteria for vascular invasion include arterial embedment in the tumor mass or venous obliteration, tumor involvement exceeding one-half the circumference of the vessel, vessel wall irregularity, vessel caliber stenosis, or a "teardrop" sign of the SMV[113]. Classic CT criteria for vascular involvement are not reliable in patients who have undergone neoadjuvant therapy with a highly active chemotherapy combination such as mFOLFIRINOX (mFFX). In such cases, surgical exploration may be the only method to assess resectability[114].

MRI

Contrast-enhanced MRI of the pancreas may be useful in staging patients at initial presentation. MRI is the best technique for detection of small liver metastases[115]. The importance of MRI also lies in the ability to diagnose pancreatic cancer by identifying changes in the body that indicate systemic effects of PDAC. It has been well recognized that anorexia, sarcopenia, and weight loss are hallmarks of PDAC. Consequently, it can be used to measure adipose and muscle mass in high-risk populations to identify early disease[116-118].

EUS

EUS is considered the most sensitive method to detect early neoplasia in the pancreas. PDAC on EUS appears as a hypoechoic mass, typically with dilation of the proximal pancreatic duct and the border of the lesion may have an irregular contour. This is the best accurate technique for local T and N staging, and for predicting vascular invasion. However, EUS is inferior to CT for evaluation of distant metastases. In addition, the specificity of EUS for excluding vascular invasion in small tumors is limited, particularly when inflammatory changes are present[119].

EUS is mainly used as part of the workup to obtain fine needle aspiration or biopsy material in patients suspected of having a PDAC[120]. EUS is not readily accessible and as a result is considered a complementary modality to the pancreatic protocol CT. Emerging area for endoscopic ultrasound includes the incorporation of elastography. Elastography shows significantly lower elasticity values for PDAC than for normal pancreatic tissue[121]. Incorporation of elastography in the evaluation of solid pancreatic lesions improves diagnostic accuracy[122,123].

Endoscopic retrograde cholangiopancreatography

A meta-analysis demonstrated a 92% sensitivity and 96% specificity of endoscopic retrograde cholangiopancreatography (ERCP) in the diagnosis of PDAC[124]. Findings suggestive of a malignant tumor of the pancreatic head include stenosis or obstruction of the common and pancreatic bile ducts (the "double duct" sign), a pancreatic duct stenosis greater than 1 cm in length, and pancreatic duct obstruction. In addition, ERCP provides an opportunity to collect tissue samples for cytohistologic analysis [124].

Some early-stage pancreatic tumors are not detected by CT, MRI, or EUS. Especially for carcinoma in situ, localized stenosis of the main pancreatic duct is often the only imaging finding. Pancreatic duct imaging evaluation by ERCP and subsequent pancreatic juice cytology are critical for diagnosis.

On the other hand, ERCP is an invasive procedure that can cause acute pancreatitis, bleeding, and cholangitis. Consequently, it has purely therapeutic value for patients with cholestasis due to tumor obstruction of the biliary system and require placement of a biliary stent[125].

Positron emission tomography

The role of positron emission tomography (PET) is limited for PDAC due to the high number of false positives and false negatives[126]. However, the degree of fluorodeoxyglucose (FDG) uptake correlates with histopathology, aggressiveness, and metastatic potential[127,128]. According to a meta-analysis, PET/CT is more accurate than CT in detecting distant metastases. Preoperatively, it may therefore be useful in avoiding unnecessary resection if unexpected metastases are found[129,130]. After treatment, FDG-PET is instead used to detect residual or recurrent cancer. It can also be applied to assess and monitor response to therapy in unresectable or metastatic disease[127,131].

Other molecular imaging agents including overexpressed proteins, signaling pathways, and tumor stroma may also be used[132]. Among these, promising results appear to involve 68Ga-cicratide, an integrin αvβ6-specific radiotracer, which has favorable pharmacokinetics and is capable of detecting pancreatic cancer lesions and monitoring response to therapy[133]. Another molecular imaging method that is of interest for early detection is hyperpolarized MRI. It can identify metabolic aberrations in the pancreas that indicate preneoplasia[134].

Staging laparoscopy

Sub-centimeter metastases of the liver or peritoneum that are rarely visible by CT, MRI or PET may be visualized laparoscopically. Up to one-third of patients thought to be resectable by imaging will be found to be unresectable based upon laparoscopic findings[135,136].

Some experts suggest a selective approach to staging laparoscopy, limiting the procedure to those with the highest likelihood of occult metastatic disease[137,138]. First, this includes tumors of the body or tail of the pancreas that appear potentially resectable by CT scan. Second, it includes large (> 3 cm) primary tumors and patients with a high initial CA 19-9 level (> 100 units/mL)[139].

Biopsy

Biopsy of a pancreatic mass can be performed either percutaneously or *via* EUS. EUS-guided FNA is the best modality for obtaining a tissue diagnosis. EUS-FNA is a safe method with a 0.98% morbidity and a 0.02% mortality. Although the most common adverse events of EUS-FNA include pancreatitis and postprocedural pain, there is also some concern regarding tumor cell seeding[140]. According to a study by Yane *et al* [141] the cumulative needle tract seeding rate at five years was 3.8%. However the preoperative EUS-FNA has no negative effect on recurrence-free survival and OS.

In many cases, the diagnosis will not yet be histologically confirmed. Once PDAC is suspected on imaging studies, the next step is generally a staging evaluation rather than biopsy. Patients who are fit for major surgery and who appear to have potentially resectable PDAC, they do not necessarily need a biopsy before surgery. Biopsy could be indicated if there is evidence of systemic spread or local evidence of unresectability on staging studies. It is also indicated if the patient is unfit for major surgery or if other diagnoses need to be excluded[142,143].

Pancreatic incidentaloma

A 2014 systematic review[144] evaluated 5 studies enrolling patients with incidentalomas and concluded that most solid lesions are malignant. Histologic definition of a solid lesion of the pancreas should be the first option, as opposed to radiologic monitoring alone. It is important to avoid operating on benign solid lesions such as chronic focal pancreatitis or autoimmune pancreatitis.

In case of cystic lesion, surgery is the first option for cystadenomamucinous and IPMN with high-risk stigmata. A recent review defined high-risk stigmata as the presence of obstructive jaundice, vascularized mural nodules ≥ 5 mm, main duct diameter ≥ 10 mm[145].

STAGING

The goal of the staging workup is to delineate the extent of disease spread and to identify patients who are eligible for resection with curative intent. Patients with PDAC can be staged according to the eighth edition of TNM system of American Joint Committee on Cancer (AJCC). However, most clinicians use a four-tiered staging system including resectable, borderline resectable, locally advanced (LA), and

metastatic cancer[146,147] (Table 2). In 2017, a classification was published, by the International Association of Pancreatology, which redefines the concept of resectability in relation to biological risk and patient conditions[148]. Table 3 summarizes the different resectability criteria assumed by the different scientific societies.

SURGERY

Surgical resection is the only potentially curative treatment. Unfortunately, PDAC is often diagnosed at an advanced stage and radical surgery could be performed in a very limited number of patients. The surgical interventions that can be performed are different depending on the tumour location and extension. In all cases the operation involves the removal of the tumour with free margins and at least twelve lymph nodes, which are necessary for staging. Tumors of the head require more complex operations, which still have a high operative morbidity. In high-frequency surgical centres mortality after pancreatoduodenectomy (PD) is now less than 2%, but post-operative morbidity remains high, 30%-50%. Anastomotic dehiscences, are the most serious post-operative complication. They are difficult to manage and are unfortunately associated with a still high mortality rate. Tumors of the tail and body require easier operations than head tumors, with a low operative morbidity and mortality. Unfortunately, because of their late symptomatology, they are more frequently unresectable.

Pancreaticoduodenectomy

PD is the classic operation performed for pancreatic tumors of the head or uncinate process. Conventional pancreaticoduodenectomy involves removal of the pancreatic head, duodenum, first 15 cm of the jejunum, common bile duct, gallbladder, and a partial gastrectomy. It is a complex procedure and patients may experience several complications. These complications could be intra-operative or post-operative[149,150].

The most important intraoperative complication of PD is bleeding. Most patients undergoing PD for PDAC have an obstructive jaundice with associated coagulopathy. Bleeding can occur from multiple sites during the various phases of mobilization and resection, so hemostasis must be monitored and assured before reconstruction begins.

Postoperative complications can be further divided into short-term and long-term complications. The short-term ones are pancreatic fistula, delayed gastric emptying, and postoperative bleeding. The long-term ones are biliary stenosis and cholangitis, pancreatitis, peptic ulcer disease, small bowel obstruction, and incisional hernia[149,150].

Modifications of the conventional PD procedure have been developed in an attempt to improve outcomes or minimize the morbidity associated with this operation. The pylorus-preserving pancreaticoduodenectomy preserves the gastric antrum, pylorus, and proximal 3 cm to 6 cm of the duodenum. It can decrease the incidence of post-operative dumping, marginal ulceration, and bile reflux gastritis, without negative effect on the morbidity, mortality and long-term survival[151]. Instead, the subtotal stomach-preserving pancreaticoduodenectomy is performed with the aims to preserve as much stomach as possible, minimizing the delayed gastric emptying that are associated with preserving the pyloric ring in the face of vagal denervation. In this procedure, the duodenum, pylorus, and 1 cm to 2 cm of stomach are resected with the pancreatic specimen. Although described, this modification has yet to be validated, and it is uncommonly performed[152].

The "Artery-first" approach is a surgical technique or set of techniques that have in common the dissection of the main arterial vasculature involved in pancreatic cancer, prior to performing any irreversible surgical step (transection of the pancreatic neck or bile duct division). The "Artery-first" approach has the potential to reduce blood loss and increase R0 resection rates and OS, as demonstrated in a recent meta-analysis[153].

Modified child reconstruction aims to reduce the incidence of cholangitis due to digestive reflux through hepatic-digiunal anastomosis. In case of pancreatic-digiunal anastomosis, the hepatic-digiunal anastomosis is made downstream of the previous one. In case of pancreatico-gastric anastomosis, the hepatico-digiunal anastomosis is made near the previously closed loop. Whatever the type of pancreatico-digestive anastomosis, the digestive anastomosis (gastro-digiunal or duodeno-digiunal) is made 60 cm downstream of the hepatico-digiunal anastomosis, to reduce digestive reflux into the biliary tract.

Table 2 Resectability criteria

Resectability status		Resectable	Borderline resectable	Locally advanced
Arterial involvement	Celiac artery	None	≤ 180°; > 180°, without involvement of aorta o GDA (body/tail)	>180° (head/uncinate); Solid tumor contact with CA and aorta
	SMA common hepatic artery	None	≤ 180°; Solit tumor contact without extension into CA or hepatic artery biforcation	> 180°
Venous involvement (portal vein/smv)		None; ≤ 180° contact without contour irregularity	> 180°; ≤ 180° with contour irregularity or thrombosis, with reconstructible PV/SMV; Solid tumor contact with IVC	Unreconstractible PV/SMV due to tumor involvement or occlusion

CA: Celiac artery; GDA: Gastroduodenal artery; IVC: Inferior vena cava; PV: Portal vein; SMA: Superior mesenteric artery; SMV: Superior mesenteric vein.

Table 3 Resectability criteria and societies

Vessel involvement	NCCN 2019	MDACC	ACTO	AHPBA/SSAT/SSO
CA abutment (≤ 180°)	Borderline	Borderline	Borderline	Unresectable
CA encasement (> 180°)	Borderline (body/tail); locally advanced (head/uncinate)	Unresectable	Unresectable	Unresectable
SMA abutment (< 180°); SMA encasement (> 180°); CHA abutment or encasement	Borderline; Locally advanced; Borderline	Borderline; Unresectable; Borderline	Borderline; Unresectable; Borderline	Borderline; Unresectable; Borderline
PV/SMV encasement (> 180°) or abutment (≤ 180°) with contour abnormality	Borderline	Borderline	Borderline	Borderline

ACTO: Alliance for Clinical Trials in Oncology; AHPBA: American Hepato-Pancreato-Biliary Association; CA: Celiac artery; CHA: Common hepatic artery; MDACC: The University of Texas MD Anderson Cancer Center; NCCN: National Comprehensive Cancer Network; PV: Portal vein; SMA: Superior mesenteric artery; SMV: Superior mesenteric vein; SSAT: Society for Surgery of the Alimentary Tract; SSO: Society for Surgical Oncology.

Post-operative pancreatic fistula (POPF) is the main and most frequent complication after pancreatic resection surgery. It is caused by leakage of pancreatic juice into the abdominal cavity, which is collected and conveyed to the outside by the drains normally placed at the end of surgery or during postoperative care if necessary. The diagnosis is made on the basis of the quality of the drainage fluid (varying from transparent to coffee-colored to brown) and the value of amylase in the fluid itself, greater than three times the normal limit of serum amylase[149,150].

POPFs are classified into three grades based on clinical impact. Grade A fistulas do not involve any special intervention and do not significantly modify the postoperative hospital stay. Grade B fistulas require a longer postoperative stay, the retention of surgical drains, the possible placement of additional drains under radiological guidance, antibiotic therapy and the use of artificial nutrition (enteral or parenteral). In grade C fistulas, reoperation is required to resolve the complication.

Several methods have been used to reduce the risk of pancreatic fistula, including the use of octreotide, pancreatic duct occlusion, pancreatic duct stenting, pancreaticojejunostomy, anastomosis modification, and pancreaticogastrostomy. The efficacy of octreotide in preventing POPF is still a hotly debated topic. According to a 2020 meta-analysis[154], somatostatin analogs did not affect POPF after PD, but rather appeared to be associated with a lower rate of POPF after distal pancratectomy. Therefore, reconstruction technique is the most important factor in reducing the risk of this complication. Recently, interesting results concern the blumgart anastomosis (BA), which combines the duct-mucosal principle with the transpancreatic U-suture technique. Unlike other duct-mucosal anastomoses such as Cattell-Warren anastomosis and Kakita anastomosis, U-shaped sutures and horizontal mattress suture technique are used in BA. The difference is that Blumgart's technique involves the placement of 3 to 6 transpancreatic and digestive seromuscular U-sutures to bring the pancreatic stump and jejunum closer together. A meta-analysis conducted by Ricci *et al* [155] demonstrated the ability of BA to reduce the risk of pancreatic fistula compared with non-blumgart duct-to-mucosal anastomoses (non-BA DtoM). The reduction seems clinically significant, with a number needed to treat of 9 which means that one pancreatic fistula can be avoided every ten patients treated with BA instead of non-BA

DtoM[155,156].

Indications for the preoperative treatment of jaundice in patients who are candidates for surgery are still under debate. It increases post-operative complications and should be reserved to patients with cholangitis or with bilirubin levels greater than 15 mg/dL[157].

Distal pancreasectomy

Distal pancreasectomy with splenectomy is the conventional operation for PDAC located in the body or tail of the pancreas. It can provide a margin-negative resection and ensure a sampling of at least 12 regional lymph nodes. A systematic review, that included 29 observational studies, found less blood loss and reduced length of hospital stay in patients operated with laparoscopic approach. However, the laparoscopic technique has some disadvantages that may lead to inadequate resection margins: Technical difficulties, inability to palpate the gland, difficulty in closing the pancreatic stump. Generally, surgeons advocate an open approach when the concern for malignancy is high, reserving laparoscopic resection for benign or premalignant indications[158-160].

Petrucciani *et al*[161] evaluated the prognosis of patients with positive surgical margin (R1). A better OS was observed in patients with R0 margin *vs* R1. However, an extension of the surgical resection following R1 pancreasectomy did not improve long term survival.

Total pancreasectomy

Sometimes, because of the extent or location of the tumor, a total pancreasectomy is required to achieve microscopically negative resection margins[162,163]. However, the metabolic consequences of this procedure, which include permanent exocrine insufficiency and brittle diabetes, have a detrimental impact on the quality of life and long-term survival[164]. A recent study showed a moderately reduced summary score of 76%, compared with a general population score of 86% using the EORTC QLQ-C30 questionnaire to evaluate the overall quality of life. Diarrhea is the most important symptom[165].

Lymphadenectomy

Tomlinson *et al*[166] evaluated the minimum number of lymph nodes removed during pancreasectomy that are essential for proper staging. They consider a number of 15 Lymph nodes as the optimal cut-off. Therefore, the cut-off of 12 lymph nodes reported by Schwarz, represents a more easily threshold value, but sufficient for correct staging.

Standard lymphadenectomy should strive to resect lymph node stations 5, 6, 8a, 12b1, 12b2, 12c, 13a, 13b, 14a, 14b, 17a, and 17b[167].

In some centres, mainly in Japan, surgeons routinely perform extensive lymph node dissection, including all 8, 9, all 12, all 14, 16a2, and 16b1 lymph nodes. A systematic review comparing standard *vs* extended lymphadenectomy demonstrated that there are no differences in OS between the two groups at one, three, or five years. However, the risk of complications was significantly increased after extended lymphadenectomy [168].

Vascular resection

If the pancreatic tumor involves the PV or SMV, pancreatic resection with PV or SMV resection may be considered: (1) When the vascular resection allows for adequate vascular flow; (2) When the tumor does not involve the SMA or hepatic artery; and (3) When an R0 resection can be accomplished. Nevertheless, many surgeons prefer to treat patients with PV or SMV involvement with neoadjuvant systemic chemotherapy before surgery.

A systematic review of 12 single-center reports concluded that pancreasectomy with PV/SMV resection is a safe and feasible procedure. It increases the number of patients who can undergo curative surgery and improves long term prognosis in a selected group of patients[169]. However, post-operative morbidity and mortality increase markedly when arterial resections are performed and few data are available to support these procedures[170-172].

Open vs minimally invasive approach

A systematic review identified 27 retrospective studies, including close to 7000 patients who underwent pancreasectomy (1306 minimally invasive, 5603 open)[173]. The laparoscopic approach was associated with longer operative times [mean difference (MD) 71 min], but lower intraoperative blood loss (MD -300 mL). The rate of

lymph node retrieval was significantly higher in the minimally invasive group (MD 1.34 nodes), and the likelihood of an R0 resection was also higher (odds ratio 1.45). Hospital stay, postoperative hemorrhage and wound infection were significantly lower in the laparoscopic group, while the rate of overall mortality, reoperations, vascular resection, pancreatic fistula, delayed gastric emptying and bile leak were similar between the two groups[174-176].

In some high-volume surgical centres, robotic-assisted pancreatic resection has been adopted. Experienced surgeon reported the same morbidity and mortality of open surgery. Decreased blood loss, higher number of adequate lymphadenectomy and improved gastric emptying are reported in some studies. These results may improve OS, but, because robotic-assisted pancreasectomy is still in its infancy, available long-term oncologic outcomes are limited[177-181].

CHEMOTHERAPY FOR RESECTABLE AND BORDERLINE RESECTABLE PANCREATIC CANCER

The only treatment with curative potential for pancreatic cancer is surgery. Five-year survival ranges from 10% to 25%.

For patients with PDAC resectable or borderline resectable, surgical resection is followed by adjuvant chemotherapy. Some high-volume centers also use neoadjuvant therapy in these categories of patients[182,183].

Adjuvant chemotherapy

Several adjuvant chemotherapy regimens have been evaluated in randomized controlled trials[184-190]. Currently, mFFX is the recommended therapy for patients with a good performance status. Gemcitabine (+/- capecitabine) remains a treatment option for patients not sufficiently fit or with contraindications to mFFX[182,191]. Because mFFX has a high toxicity, Brown University Oncology Research Group suggests FOLFOX + nab-paclitaxel (FOLFOX-A) as an alternative[192].

According to a meta-analysis[193], S1 was ranked best for overall and disease-free survival followed by mFFX. Whilst there was no significant difference between S1 and mFFX for OS, S1 had significantly longer disease-free survival (MD 2.8 mo) and was ranked best for lowest overall and haematological grade 3/4 toxicities[194]. However, the results should be interpreted with care, as S-1 has shown good results in the Asian population, but its performance in Caucasians remains unclear due to the different expression of cytochrome P-450.

Adjuvant chemotherapy should be administered between 28 and 59 d after surgery. This timing appears to provide better survival than administering before 28 or after 59 d[182,194].

A 2020 study compared the efficacy between adjuvant chemotherapy and chemoradiation therapy in relation to AJCC stage. Monochemotherapy and combination chemotherapy + chemoradiotherapy (CRT) showed better OS and disease free survival than CRT alone in patients with AJCC stage III, whereas there was no significant difference in OS in patients with AJCC stage I/II[195].

Neoadjuvant chemotherapy

The main purpose of neoadjuvant chemotherapy (NACT) differs according to the stage. For patients with BR-PDAC the objective of the therapy is to decrease tumor size and to control the micro metastases. For patients with primary resectable PDAC the purpose is to increase the proportion of patients receiving chemotherapy, because half of patients undergoing surgery, do not receive adjuvant chemotherapy due to postoperative morbidity or poor general condition[196].

In 2020, important advances were made in this field. For patients with BR-PDAC several studies confirmed the benefits on R0 resection rates and survival of NACT with mFFX[197-200] or multi-agent gemcitabine[201]. Moreover, in the PREOPANC-1 trial, patients receiving neoadjuvant CRT with gemcitabine obtained the same benefits of mFFX[202]. A study of the University of Texas showed that patients who received neoadjuvant CRT had significantly improved R0 resection rates, lymph node resection rates, and locoregional recurrence rates, compared with those who received NACT [203]. Although early data suggest the importance of integrating both NACT and CRT into the treatment, large prospective trial data are lacking[204]. New evidence for a standard regimen for BR-PDAC will be established by the result of the ESPAC-5F trial (ISRCTN89500674)[205].

For primary resectable cancer, the potential benefit of NACT has been validated, particularly when initiated within 6 wk of diagnosis[206]. The SWOG S1505 study observed that patients who received gemcitabine and nab-paclitaxel had a greater pathologic response and median survival comparable to those who received mFFX [207]. Several chemotherapeutic agents for resectable pancreatic cancer are currently being studied in several RCTs[208]. The NorPACT-1 study[209] and the Panache-01 study[210] are evaluating the effect of NACT with mFFX, and the NEONAX study [211] of NACT with 2 cycles of nab-paclitaxel/ gemcitabine.

In the Asian population, treatment regimens differ. The Prep-02/JSAP-05 study study demonstrated, in patients with resectable PDAC, that NACT with gemcitabine plus S-1 (GS therapy) improves median OS compared with initial surgery (37 mo vs 27 mo). The resection rate and morbidity of surgery remain the same[212].

Based on these results, the latest Japanese guidelines recommend GS therapy as standard neoadjuvant therapy for patients with resectable PDAC. In this regimen, patients receive intravenous gemcitabine at a dose of 1000 mg/m2 on days 1 and 8, plus oral S-1, twice daily, at a dose based on body surface area (80, 100, 120 mg/d) on days 1-14 every 3 wk for 2 cycles. For patients with BR-PDAC, they recommend NACT, but have refrained from recommending any specific regimens[212-214]. Among several ongoing RCTs on treatments for borderline resectable pancreatic cancer, a Japanese trial is comparing neoadjuvant therapy with gemcitabine plus nab-paclitaxel and CRT therapy with S-1[215].

A subset of patients does not respond to NACT. There is therefore a need to find markers that can predict response to NACT. At the moment the best ones seem to be GRP78, CADM1, PGES2 and RUXF[216] (Table 4).

CHEMOTHERAPY FOR LA PANCREATIC CANCER

Thirty to forty percent of patients with PDAC are initially diagnosed LA PDAC[182, 215]. LA PDAC is still nonmetastatic, but due to the local growth, curative resection is not possible at the time of diagnosis. Treatment involves chemotherapy with regimens that are also used in the metastatic setting, such as mFFX or gemcitabine plus nab-paclitaxel[217-219]. A small percentage of patients, with excellent response to chemotherapy, may become eligible for surgical resection. The majority have incurable disease. A systematic review of studies investigating mFFX in LA-PDAC revealed a median OS ranging from 10.0 mo to 32.7 mo[220], while in the LAPACT study, about the Nab-Paclitaxel + Gemcitabine regimen, OS 18.8 mo[221]. Recently, Kunzmann *et al* [222] compared two different NACT regimens, mFFX and gemcitabine plus nab-paclitaxel. The mFFX was superior in both the conversion rate to surgery (45.0% *vs* 30.6%) and the rate of R0 resections achieved (74% *vs* 68%). A subsequent study confirmed that mFFX patients had greater tumor size reduction, fewer positive lymph nodes, longer OS and distant metastasis-free survival compared to the nab-P/G patients[223].

The role of CRT for LA disease is still unclear. According to the LAP07 study, CRT improves the rate of local control but does not prolong survival in patients with LA PDAC after treatment with chemotherapy (gemcitabine with or without erlotinib) [224]. It is unclear whether these conclusions still hold true in the setting of newer combination chemotherapy regimens and improved radiation therapy techniques, such as stereotactic radiation therapy and proton therapy. The PAULA-1 study compared two cohorts of LAPDAC patients treated with stereotactic body radiotherapy (SBRT) ± chemotherapy *vs* CRT ± chemotherapy in terms of local control, distant metastases-free survival (DMFS), progression-free survival (PFS), OS, and toxicity. Patients treated with SBRT showed higher local control rate and similar OS, DMFS, PFS and toxicity compared to CRT[225].

CHEMOTHERAPY FOR METASTATIC PDAC

Half of patients have metastatic disease at the time of diagnosis. The primary treatment is systemic chemotherapy, with the goal of increasing survival and palliating cancer-related symptoms. Both mFFX and gemcitabine plus nab-paclitaxel improve median OS compared to gemcitabine monotherapy[226,227]. In clinical practice, for patients who are fitter, mFFX is generally preferred, reserving gemcitabine plus nab-paclitaxel as a second-line option if they have adequate performance status[228,229]. For patients who have received first-line gemcitabine and

Table 4 Phase of trial and level of evidence of trial about chemotherapy for resectable and borderline resectable pancreatic ductal adenocarcinoma

Ref.	Phase of trial	Level of evidence
Neoptolemos *et al*[185]	III	II
Oettle *et al*[186]	III	I
Neoptolemos *et al*[187]	III	I
Neoptolemos *et al*[188]	III	I
Conroy *et al*[189]	III	I
You *et al*[195]	III	II
van Roessel *et al*[198]	IV	II
Versteijne *et al*[202]	III	II
Ghaneh *et al*[205]	II	II
Sohal *et al*[207]	IV	II
Labori *et al*[209]	III	II
Schwarz *et al*[210]	II	I
Ettrich *et al*[211]	II	II
Motoi *et al*[212]	III	II
UMIN-CTR Clinical Trial[215] (UMIN000026858)	III	II

have progressed, a good option might be the combination of fluorouracil plus leucovorin with nanoliposomal irinotecan[230]. Golan *et al*[231] evaluated patients with metastatic PDAC and BRCA1-2 germline mutation. In these patients, disease progression had not occurred during at least 4 mo of first-line platinum derivative-based chemotherapy. Patients were randomized to receive olaparib or placebo. Olaparib showed a benefit in terms of PFS and a relatively safe toxicity profile. Although AIFA has not yet approved the indication, this study suggests a role for olaparib as maintenance therapy[231].

Finally, we look forward to the results of the AVENGER 500 trial (NCT03504423) to evaluate the efficacy of mFFX with or without CPI-613. CPI613 (devimistat) is an inhibitor of pyruvate dehydrogenase and a-ketoglutarate, key enzymes of the Krebs cycle. It has already shown good results in a phase I study[232].

STROMA-TARGETING THERAPY

Although chemotherapy is the recommended treatment for patients with advanced PDAC, its efficacy is not satisfactory. The major hurdle is considered the dense dysplastic stroma. The stroma components occupy more than 70% of the total tumor volume. The dense desmoplastic stroma of PDAC leads to vascular compression and a hypoxic microenvironment, which in turn influences drug pharmacokinetics/pharmacodynamics. It also prevents proper action of immune system cells, which are unable to reach the target site. The result is a chemoresistant and immunoresistant tumor[233,234].

One of the major components of the PDAC stroma is hyaluronic acid (HA). HA promotes the survival, proliferation, and migration of tumor cells[235]. HA is a potential therapeutic target using pegylated hyaluronidase (PEGPH20). The HALO-109-202 study demonstrated that PEGPH20, combined with Abraxane (nab-paclitaxel) and gemcitabine, improves progression-free and OS in patients with high HA levels [236]. However, poor results were obtained from the subsequent HALO-109-301 study (NCT02715804). Another element to be acted upon is the Hedgehog signaling pathway, which is generally overactivated in pancreatic cancer. Vismodegib, in combination with gemcitabine or erlotinib, was studied for this purpose. It did not significantly affect survival compared with these two drugs administered as monotherapy[237,238].

In tumors, Angiotensin II activates transforming growth factor-β through the AT1R and stimulates proliferation, so several angiotensin system inhibitors have been used to target PDAC stroma[233]. One study evaluated the efficacy of mFFX combined with losartan in a neoadjuvant regimen in patients with LA PDAC. The therapy was associated with an increased R0 resection rate[239].

A clinical trial evaluated the efficacy of focused ultrasound combined with gemcitabine microbubble delivery in PDAC patients. Patients treated with the combination tolerated multiple chemotherapy cycles of gemcitabine. A prolongation of median survival by almost 9 mo and, in 50% of cases, a reduction in tumor size were observed[240].

Poor results were obtained from stroma depletion in clinical settings. They are due to the fact that, although stroma-targeting therapy enhances the delivery of chemotherapeutic agents, it might also promote tumor chemoresistance and metastasis (a double-edged sword)[241]. According to several experts, future research should focus on the tumor ECM biology, biomarkers correlated with treatment benefit (as ADAM12)[242] and pharmacological agents able to alter the tumor microenvironment (TME). One of the most interesting discoveries in this regard involves clodronate liposomes. They prevent metastasis formation by inhibiting the activity of PDAC-associated macrophages and altering the microenvironment of key organs that are sites of metastatic invasion. They are therefore valuable candidates to be evaluated in combination with target therapy against stroma[243].

IMMUNOTHERAPY

Immune checkpoint inhibitors

Checkpoint inhibitors activates the function "kill the tumor" of the immune system, targeting immune checkpoint molecules (PD-1, PD-L1, CTLA-4) that negatively regulate T-cell function. Although they resulted in remarkable successes in other cancers, ipilimumab, BMS-936559 and tremelimumab showed little efficacy in PDAC [244-247]. The reasons of failure of immune checkpoint inhibitors are the low baseline PD-1+ T-cell infiltration into the tumor and a paucity of neoepitopes[248,249]. Indeed, in a very small subset of PDAC patients with a high burden of microsatellite instability (MSI-high) PD-1 inhibitor is effective and was recently FDA approved[250,251].

Currently, the development of immune checkpoint inhibitors for PDAC is focused on combination therapy with chemotherapeutic agents[252-255].

Therapeutic cancer vaccines

Therapeutic cancer vaccines present of immunogenic tumor antigens to the immune system, resulting in activation of the anti-cancer response. GVAX is an allogeneic vaccine irradiated with tumor cells engineered to express GM-CSF. It was studied alone and in combination with CRS-207 and cyclophoshamide, however it didn't correlate with improved survival[256,257].

More promising results were instead obtained with KIF20A-66[258-260].

K-RAS vaccines have been tested in the past, but data remain unclear and with no prominent advantages in metastatic patients[261-264].

We are currently awaiting the results of some studies: (1) TLP0-001, a phase III study of a dendritic cell (DC) vaccine loaded with WT1 peptides in patients with advanced PDAC refractory to standard chemotherapy[265,266]; (2) A clinical trial using GV1001 with GM-CSF in patients with LA-PDAC in combination with gemcitabine chemotherapy, tadalafil and radiation therapy (NCT01342224); and (3) NCT01836432, NCT02405585 and NCT01072981 evaluating algenpantucel-L in combination with chemotherapy and CRT therapy. They involve patients with borderline resectable and LA unresectable PDAC.

CAR-T cell

CAR-T cell therapy is a type of adoptive cell therapy. CAR-T cells are T lymphocytes that are extracted from a patient's blood sample or from a donor by apheresis, genetically modified to express the receptor for chimeric antigen (CAR), and cultured in the laboratory. They are then re-infused into the patient. The resulting T cells are able to recognize tumor cells and activate the immune system response against the disease[267]. The target antigens of CAR-T cells include mesothelin, prostate stem cell antigen (PSCA), CEA, HER2, MUC-1, and CD133[268,269]. In a study of metastatic PDAC, autologous mesothelin-specific T lymphocytes improved PFS in two patients of the six examined. An additional patient had complete remission of all liver metastases

[270].

Combination of immunotherapy drugs was experienced and showed good results over time. Le *et al*[271] compared the efficacy of Ipilimumab as monotherapy (arm 1) and Ipilimumab in combination with GVAX (arm 2) in patients with already treated PDAC. Combination therapy showed an increase in median OS (5.7 mo *vs* 3.6 mo) and 1-year OS (27% *vs* 7%). Chung *et al*[272] evaluated the combination of Pembrolizumab with modified p53-expressing Ankara vaccinia virus (p53MVA). Three of eleven patients experienced disease stabilization by 30, 32, and 49 wk. Good OS and PFS results were also obtained using DC and cytokine-induced killer cell immunotherapy in combination with S-1 chemotherapy, compared with chemotherapy or supportive care alone[256].

Several trials of immunotherapy-based treatment combinations with targeted agents are ongoing for patients with pancreatic cancer[273-275].

Oncolytic viruses

Oncolytic viruses are modified therapeutic drugs that selectively infect and self-replicate in tumor cells with tumor-dissolving effect. They also activate the anti-tumor immunity and change the TME from an immunosuppressed state to an immune-activated state. Futhermore, oncolytic viruses have the advantages of specificity, low toxicity, and low drug resistance[276]. Adenovirus, Herpes Simplex Virus, Protoparvovirus, Reovirus and Vaccinia Virus have been tested. However most of the studies have shown unsatisfactory results. The only positive results derive from ParvOryx02 (NCT02653313). A single-arm study published in 2020 showed an encouraging efficacy of pembrolizumab in combination with Pelareorep and chemotherapy in patients progressed after first-line treatment[277-281] (Table 5).

GENETIC MUTATION AND TARGET THERAPY

Some genetic alterations produce cellular changes in neoplastic cells that are potentially therapeutically targetable. BRAF mutations occur in 1%-3% of PDAC. They showed to be targetable in metastatic colon cancer where the combination of Encorafenib and Cetuximab has recently been approved[282,283]. Encorafenib and Cetuximab should also be evaluated in PDAC. Furthermore, pancreatic tumors with NTRK gene fusions can be treated with tropomyosin receptor kinase inhibitors[284, 285]. Similarly, some wild-type Kras pancreatic tumors hosting somatic NRG1 gene fusions respond to treatment with a kinase inhibitor of the HER family[286,287].

However, the results of the targeted therapies have been unsatisfactory, mainly due to the low life expectancy. There is no time to sequence the tumors and develop a treatment based on mutations[288].

The exceptions were the germline alterations. Patients with mutations of BRCA1, BRCA2 or PALB1 are remarkably sensitive to treatment with DNA cross-linking agents, such as platinum-based drugs, and poly(ADP-ribose) polymerase (PARP) inhibitors[289-291]. Patients with Lynch syndrome (MSI-high) respond well to treatment with immune checkpoint inhibitors[292-294] and those with ATM mutations could respond to the drugs, targeting the ATR-checkpoint kinase 1 (Chk1) pathway [295,296].

The elephant in the targeted therapy room remains Kras[297]. It has been considered "undrinkable"[297-299] because the protein lacks an efficient small-molecule binding pocket and has a high affinity for cellular guanosine triphosphate (GTP), which is highly concentrated in the cytoplasm. Furthermore, other than the GTP/GDP binding pocket, KRAS has no other pockets for small-molecule inhibitor binding. A druggable variant of Kras appears to be G12C. Enormous progress has been made in this regard and several drugs (AMG 510, MRTX849, JNJ-74699157 and LY3499446) are currently in clinical trials[299]. The importance of these can be deduced from the fact that 95% of pancreatic cancers harbor mutations in the Kras gene (the four Kras mountains, TP53, CDKN2A and SMAD4 present in > 50% of tumors)[300,301]. Although Kras G12C mutations are only a small fraction of Kras mutations in PDAC, these drugs represent a chance to take down a previously thought invincible adversary.

PANCREATIC CANCER AND GUT MICROBIOTA

Recent studies have shown the gut microbiota (GM) may play a role in the

Table 5 Phase and level of evidence of trials about immunotherapy for pancreatic ductal adenocarcinoma

Ref.	Phase of trial	Level of evidence
Royal *et al*[245]	II	II
Brahmer *et al*[246]	I	I
O'Reilly *et al*[247]	II	II
Tumeh *et al*[248]	II	III
Le *et al*[250]	II	II
Le *et al*[251]	II	II
Wainberg *et al*[252]	I	II
Weiss *et al*[253]	Ib/II	II
National Institute of Public Health[254] (JapicCTI-184230,ONO-4538)	II	II
Wang-Gillam *et al*[255]	II	II
Le *et al*[257]	IIb	I
Asahara *et al*[258]	I/II	II
Suzuki *et al*[259]	II	III
Miyazawa *et al*[260]	II	II
Wedén *et al*[261]	IV	III
Toubaji *et al*[262]	I	III
Abou-Alfa *et al*[263]	I/II	III
Cohn *et al*[264]	I	III
Katsuda *et al*[265]	III	I
Katsuda *et al*[266]	I/II	II
Beatty *et al*[270]	I	III
Le *et al*[271]	Ib	II
Chung *et al*[272]	I	III
Wang-Gillam *et al*[273]	I	III
Reiss *et al*[274]	II	III
Desai *et al*[275]	Ib/II	Ongoing trial
Chang *et al*[278]	I	III
Noonan *et al*[279]	II	II
Mahalingam *et al*[280]	Ib	III

development of PDAC and its response to therapy. GM alterations result in reduced mucus thickness, leading to decreased antimicrobial defenses and increased exposure to bacterial components such as LPS, flagellin, single or doubled DNA and CpG DNA. These agents activate Toll-like-receptors and trigger chronic inflammation that are related to carcinogenesis. Moreover, inflammation and dysbiosis lead to mutation of Kras, that accelerates carcinogenesis, activating nuclear factor-κB pathway[302-304].

Several bacterial products are considered potential carcinogens. Cyclomodulins promote tumorigenesis through active interference with host cell cycles. Colibactin and Bacteroides fragilis toxin act synergistically with Escherichia coli to create double-stranded DNA damage[305]. E. coli cytotoxic necrotizing factor and CagA lead to uncontrolled cell proliferation, while cytolytic distending toxin and cycle inhibitory factor participate in genetic alterations and induce hyperploidy even in the absence of cell division[306]. The presence of an *Helicobacter pylori* infection and high concentrations of Fusobacterium spp and Porphyromonas gingivalis (bacteria generally present in the oral cavity) are associated with an increased risk of pancreatic cancer [307-310].

Moreover, other studies correlated a large number of microbes with immune suppression, downregulation of tumor suppressive pathways and the upregulation of oncogenic pathways[311].

Dysbiosis is also related to obesity, chronic pancreatitis and diabetes, well-established risk factors of PDAC[312,313].

Because it participates in drug metabolism and biotransformation and immune regulation, the GM is implicated in the efficacy of chemotherapeutic agents[314]. The innate immune response activated by the GM potentiates the action of oxaliplatin [315]. Gentamicin activity may be reduced by the enzymes pyrimidine nucleoside phosphorylase and cytidine deaminase, which are produced by Gamma-proteobacteria and mycoplasmas within PDAC. Thus, these data suggest the possibility of modulating GM to counteract the chemoresistance characteristic of pancreatic cancer [316].

Intratumoral microorganisms can play a key role in anticancer therapy[317]. Indeed, they can stimulate host immune responses with positive or negative impacts on therapy. *Gammaproteobacteria*, *Escherichia Coli* and *Fusobacteria* are most commonly present in PDAC. Gamma proteobacteria contain the enzyme CDD which could be responsible for the ineffectiveness of gemcitabine[318]. Escheria Coli is capable of inducing chemical changes in the structure of gemcitabine, fludarabine, cladribine, and CB1954[319]. The desmoplastic response induced by tumor cells is dependent on MyD88. It is activated by Fusobacterium species.

The intratumoral microbiota thus emerges as a major proponent of the chemo-immunoresistant phenotype of pancreatic cancer and is related to long-term survival in PDAC patients.

PROGNOSIS

The most important prognostic factor is tumor stage. The median survival time after resection for patients with stage IA, IB, IIA, IIB, and III was 38, 24, 18, 17, and 14 mo, respectively[320]. Other factors may influence the prognosis of PDAC after surgery: Surgical margin status, tumor grading, presence of lymphatic invasion, preoperative and postoperative serum levels of CA 19-9, and cigarette smoking[321-329]. Squamous subtypes have a poor prognosis. They are enriched with TP53 and KDM6A mutations, upregulation of TP63ΔN transcriptional network, hypermethylation of pancreatic endoderm cell fate determining genes[330].

Several studies have investigated novel factors influencing prognosis: (1) Increased expression of CDK1 and CCNA2 is associated with poor prognosis, although they may be potential therapeutic targets[331]; (2) The autophagy regulatory genes MET and RIPK2 play a prognostic role in PDAC[332]; (3) High expression of GPDAC2, GPDAC3 and GPDAC5 has been significantly associated with favorable survival[333]; (4) High expression of Hic-5 is negatively correlated with postoperative survival time, as Hic-5 stimulates tumor proliferation, migration, and invasion[334]; (5) PRMT1 promotes pancreatic cancer growth by increasing cellular β-catenin levels and predicts poor prognosis[335]; (6) Patients with first recurrence in the lung have a better prognosis than patients with first recurrence in the liver[336]; (7) Increased levels of ZIP4 correlate with poorer survival. ZIP4 inhibits the expression of the gemcitabine transporter ENT1, so that cells take up smaller amounts of the drug. Activation of this pathway participates in the chemoresistance of pancreatic cancers[337]; (8) The highly upregulated in liver cancer (HULC) lncRNA distinguishes patients with pancreatic cancer, patients with benign pancreatic disease, and healthy subjects and correlates with TNM stage. Subjects with low HULC expression have significantly higher 3- and 5-year OS than those with high expression. Therefore, HULC lncRNA could be considered an effective marker for the diagnosis and prognosis of PDAC[338]; (9) Upregulation of TYMS leads to unfavorable OS and RFS[339]; and (10) The GINS complex has four subunits, encoded by the GINS1, GINS2, GINS3, and GINS4 genes, all of which are overexpressed in PDAC. The expression of each member is associated with the histological grade of PDAC and is a negative prognostic marker[340].

CONCLUSION

Pancreatic cancer is a very treacherous, dangerous enemy and the results are still very unsatisfactory. But we have not given up. Research is running fast on many paths, without losing its enthusiasm. It is proof that we are encircling it, and at the end, we

will win. The success of a fight is linked to the ability to move from one failure to another without losing one's enthusiasm.

REFERENCES

1 **GBD 2017 Pancreatic Cancer Collaborators**. The global, regional, and national burden of pancreatic cancer and its attributable risk factors in 195 countries and territories, 1990-2017: a systematic analysis for the Global Burden of Disease Study 2017. *Lancet Gastroenterol Hepatol* 2019; **4**: 934-947 [PMID: 31648972 DOI: 10.1016/S2468-1253(19)30347-4]

2 **GBD 2015 Mortality and Causes of Death Collaborators**. Global, regional, and national life expectancy, all-cause mortality, and cause-specific mortality for 249 causes of death, 1980-2015: a systematic analysis for the Global Burden of Disease Study 2015. *Lancet* 2016; **388**: 1459-1544 [PMID: 27733281 DOI: 10.1016/S0140-6736(16)31012-1]

3 **Bray F**, Ferlay J, Soerjomataram I, Siegel RL, Torre LA, Jemal A. Global cancer statistics 2018: GLOBOCAN estimates of incidence and mortality worldwide for 36 cancers in 185 countries. *CA Cancer J Clin* 2018; **68**: 394-424 [PMID: 30207593 DOI: 10.3322/caac.21492]

4 **Ilic M**, Ilic I. Epidemiology of pancreatic cancer. *World J Gastroenterol* 2016; **22**: 9694-9705 [PMID: 27956793 DOI: 10.3748/wjg.v22.i44.9694]

5 **Oldfield LE**, Connor AA, Gallinger S. Molecular Events in the Natural History of Pancreatic Cancer. *Trends Cancer* 2017; **3**: 336-346 [PMID: 28718411 DOI: 10.1016/j.trecan.2017.04.005]

6 **Siegel RL**, Miller KD, Jemal A. Cancer statistics, 2020. *CA Cancer J Clin* 2020; **70**: 7-30 [PMID: 31912902 DOI: 10.3322/caac.21590]

7 **Grasso C**, Jansen G, Giovannetti E. Drug resistance in pancreatic cancer: Impact of altered energy metabolism. *Crit Rev Oncol Hematol* 2017; **114**: 139-152 [PMID: 28477742 DOI: 10.1016/j.critrevonc.2017.03.026]

8 **He J**, Blair AB, Groot VP, Javed AA, Burkhart RA, Gemenetzis G, Hruban RH, Waters KM, Poling J, Zheng L, Laheru D, Herman JM, Makary MA, Weiss MJ, Cameron JL, Wolfgang CL. Is a Pathological Complete Response Following Neoadjuvant Chemoradiation Associated With Prolonged Survival in Patients With Pancreatic Cancer? *Ann Surg* 2018; **268**: 1-8 [PMID: 29334562 DOI: 10.1097/SLA.0000000000002672]

9 **Singhi AD**, Koay EJ, Chari ST, Maitra A. Early Detection of Pancreatic Cancer: Opportunities and Challenges. *Gastroenterology* 2019; **156**: 2024-2040 [PMID: 30721664 DOI: 10.1053/j.gastro.2019.01.259]

10 **Bosetti C**, Lucenteforte E, Silverman DT, Petersen G, Bracci PM, Ji BT, Negri E, Li D, Risch HA, Olson SH, Gallinger S, Miller AB, Bueno-de-Mesquita HB, Talamini R, Polesel J, Ghadirian P, Baghurst PA, Zatonski W, Fontham E, Bamlet WR, Holly EA, Bertuccio P, Gao YT, Hassan M, Yu H, Kurtz RC, Cotterchio M, Su J, Maisonneuve P, Duell EJ, Boffetta P, La Vecchia C. Cigarette smoking and pancreatic cancer: an analysis from the International Pancreatic Cancer Case-Control Consortium (Panc4). *Ann Oncol* 2012; **23**: 1880-1888 [PMID: 22104574 DOI: 10.1093/annonc/mdr541]

11 **Carreras-Torres R**, Johansson M, Gaborieau V, Haycock PC, Wade KH, Relton CL, Martin RM, Davey Smith G, Brennan P. The Role of Obesity, Type 2 Diabetes, and Metabolic Factors in Pancreatic Cancer: A Mendelian Randomization Study. *J Natl Cancer Inst* 2017; **109** [PMID: 28954281 DOI: 10.1093/jnci/djx012]

12 **Li D**, Morris JS, Liu J, Hassan MM, Day RS, Bondy ML, Abbruzzese JL. Body mass index and risk, age of onset, and survival in patients with pancreatic cancer. *JAMA* 2009; **301**: 2553-2562 [PMID: 19549972 DOI: 10.1001/jama.2009.886]

13 **O'Rorke MA**, Cantwell MM, Cardwell CR, Mulholland HG, Murray LJ. Can physical activity modulate pancreatic cancer risk? *Int J Cancer* 2010; **126**: 2957-2968 [PMID: 19856317 DOI: 10.1002/ijc.24997]

14 **Huang J**, Magnusson M, Törner A, Ye W, Duberg AS. Risk of pancreatic cancer among individuals with hepatitis C or hepatitis B virus infection: a nationwide study in Sweden. *Br J Cancer* 2013; **109**: 2917-2923 [PMID: 24178755 DOI: 10.1038/bjc.2013.689]

15 **Amundadottir L**, Kraft P, Stolzenberg-Solomon RZ, Fuchs CS, Petersen GM, Arslan AA, Bueno-de-Mesquita HB, Gross M, Helzlsouer K, Jacobs EJ, LaCroix A, Zheng W, Albanes D, Bamlet W, Berg CD, Berrino F, Bingham S, Buring JE, Bracci PM, Canzian F, Clavel-Chapelon F, Clipp S, Cotterchio M, de Andrade M, Duell EJ, Fox JW Jr, Gallinger S, Gaziano JM, Giovannucci EL, Goggins M, González CA, Hallmans G, Hankinson SE, Hassan M, Holly EA, Hunter DJ, Hutchinson A, Jackson R, Jacobs KB, Jenab M, Kaaks R, Klein AP, Kooperberg C, Kurtz RC, Li D, Lynch SM, Mandelson M, McWilliams RR, Mendelsohn JB, Michaud DS, Olson SH, Overvad K, Patel AV, Peeters PH, Rajkovic A, Riboli E, Risch HA, Shu XO, Thomas G, Tobias GS, Trichopoulos D, Van Den Eeden SK, Virtamo J, Wactawski-Wende J, Wolpin BM, Yu H, Yu K, Zeleniuch-Jacquotte A, Chanock SJ, Hartge P, Hoover RN. Genome-wide association study identifies variants in the ABO locus associated with susceptibility to pancreatic cancer. *Nat Genet* 2009; **41**: 986-990 [PMID: 19648918 DOI: 10.1038/ng.429]

16 **Yamada A**, Komaki Y, Komaki F, Micic D, Zullow S, Sakuraba A. Risk of gastrointestinal cancers in patients with cystic fibrosis: a systematic review and meta-analysis. *Lancet Oncol* 2018; **19**: 758-

767 [PMID: 29706374 DOI: 10.1016/S1470-2045(18)30188-8]
17 **Pergolini I**, Sahora K, Ferrone CR, Morales-Oyarvide V, Wolpin BM, Mucci LA, Brugge WR, Mino-Kenudson M, Patino M, Sahani DV, Warshaw AL, Lillemoe KD, Fernández-Del Castillo C. Long-term Risk of Pancreatic Malignancy in Patients With Branch Duct Intraductal Papillary Mucinous Neoplasm in a Referral Center. *Gastroenterology* 2017; **153**: 1284-1294.e1 [PMID: 28739282 DOI: 10.1053/j.gastro.2017.07.019]
18 **IARC Working Group on the Evaluation of Carcinogenic Risks to Humans**. Personal habits and indoor combustions. Volume 100 E. A review of human carcinogens. *IARC Monogr Eval Carcinog Risks Hum* 2012; **100**: 1-538 [PMID: 23193840]
19 **Riboli E**, Hunt KJ, Slimani N, Ferrari P, Norat T, Fahey M, Charrondière UR, Hémon B, Casagrande C, Vignat J, Overvad K, Tjønneland A, Clavel-Chapelon F, Thiébaut A, Wahrendorf J, Boeing H, Trichopoulos D, Trichopoulou A, Vineis P, Palli D, Bueno-De-Mesquita HB, Peeters PH, Lund E, Engeset D, González CA, Barricarte A, Berglund G, Hallmans G, Day NE, Key TJ, Kaaks R, Saracci R. European Prospective Investigation into Cancer and Nutrition (EPIC): study populations and data collection. *Public Health Nutr* 2002; **5**: 1113-1124 [PMID: 12639222 DOI: 10.1079/PHN2002394]
20 **McKenzie F**, Biessy C, Ferrari P, Freisling H, Rinaldi S, Chajès V, Dahm CC, Overvad K, Dossus L, Lagiou P, Trichopoulos D, Trichopoulou A, Bueno-de-Mesquita HB, May A, Peeters PH, Weiderpass E, Sanchez MJ, Navarro C, Ardanaz E, Ericson U, Wirfält E, Travis RC, Romieu I. Healthy Lifestyle and Risk of Cancer in the European Prospective Investigation Into Cancer and Nutrition Cohort Study. *Medicine (Baltimore)* 2016; **95**: e2850 [PMID: 27100409 DOI: 10.1097/MD.0000000000002850]
21 **Chajès V**, Biessy C, Byrnes G, Deharveng G, Saadatian-Elahi M, Jenab M, Peeters PH, Ocké M, Bueno-de-Mesquita HB, Johansson I, Hallmans G, Manjer J, Wirfält E, Jakszyn P, González CA, Huerta JM, Martinez C, Amiano P, Suárez LR, Ardanaz E, Tjønneland A, Halkjaer J, Overvad K, Jakobsen MU, Berrino F, Pala V, Palli D, Tumino R, Vineis P, de Magistris MS, Spencer EA, Crowe FL, Bingham S, Khaw KT, Linseisen J, Rohrmann S, Boeing H, Nöethlings U, Olsen KS, Skeie G, Lund E, Trichopoulou A, Zilis D, Oustoglou E, Clavel-Chapelon F, Riboli E, Slimani N. Ecological-level associations between highly processed food intakes and plasma phospholipid elaidic acid concentrations: results from a cross-sectional study within the European prospective investigation into cancer and nutrition (EPIC). *Nutr Cancer* 2011; **63**: 1235-1250 [PMID: 22043987 DOI: 10.1080/01635581.2011.617530]
22 **Saadatian-Elahi M**, Slimani N, Chajès V, Jenab M, Goudable J, Biessy C, Ferrari P, Byrnes G, Autier P, Peeters PH, Ocké M, Bueno de Mesquita B, Johansson I, Hallmans G, Manjer J, Wirfält E, González CA, Navarro C, Martinez C, Amiano P, Suárez LR, Ardanaz E, Tjønneland A, Halkjaer J, Overvad K, Jakobsen MU, Berrino F, Pala V, Palli D, Tumino R, Vineis P, Santucci de Magistris M, Spencer EA, Crowe FL, Bingham S, Khaw KT, Linseisen J, Rohrmann S, Boeing H, Noethlings U, Olsen KS, Skeie G, Lund E, Trichopoulou A, Oustoglou E, Clavel-Chapelon F, Riboli E. Plasma phospholipid fatty acid profiles and their association with food intakes: results from a cross-sectional study within the European Prospective Investigation into Cancer and Nutrition. *Am J Clin Nutr* 2009; **89**: 331-346 [PMID: 19056549 DOI: 10.3945/ajcn.2008.26834]
23 **Jiao L**, Mitrou PN, Reedy J, Graubard BI, Hollenbeck AR, Schatzkin A, Stolzenberg-Solomon R. A combined healthy lifestyle score and risk of pancreatic cancer in a large cohort study. *Arch Intern Med* 2009; **169**: 764-770 [PMID: 19398688 DOI: 10.1001/archinternmed.2009.46]
24 **Ferrari P**, Licaj I, Muller DC, Kragh Andersen P, Johansson M, Boeing H, Weiderpass E, Dossus L, Dartois L, Fagherazzi G, Bradbury KE, Khaw KT, Wareham N, Duell EJ, Barricarte A, Molina-Montes E, Sanchez CN, Arriola L, Wallström P, Tjønneland A, Olsen A, Trichopoulou A, Benetou V, Trichopoulos D, Tumino R, Agnoli C, Sacerdote C, Palli D, Li K, Kaaks R, Peeters P, Beulens JW, Nunes L, Gunter M, Norat T, Overvad K, Brennan P, Riboli E, Romieu I. Lifetime alcohol use and overall and cause-specific mortality in the European Prospective Investigation into Cancer and nutrition (EPIC) study. *BMJ Open* 2014; **4**: e005245 [PMID: 24993766 DOI: 10.1136/bmjopen-2014-005245]
25 **Naudin S**, Li K, Jaouen T, Assi N, Kyrø C, Tjønneland A, Overvad K, Boutron-Ruault MC, Rebours V, Védié AL, Boeing H, Kaaks R, Katzke V, Bamia C, Naska A, Trichopoulou A, Berrino F, Tagliabue G, Palli D, Panico S, Tumino R, Sacerdote C, Peeters PH, Bueno-de-Mesquita HBA, Weiderpass E, Gram IT, Skeie G, Chirlaque MD, Rodríguez-Barranco M, Barricarte A, Quirós JR, Dorronsoro M, Johansson I, Sund M, Sternby H, Bradbury KE, Wareham N, Riboli E, Gunter M, Brennan P, Duell EJ, Ferrari P. Lifetime and baseline alcohol intakes and risk of pancreatic cancer in the European Prospective Investigation into Cancer and Nutrition study. *Int J Cancer* 2018; **143**: 801-812 [PMID: 29524225 DOI: 10.1002/ijc.31367]
26 **Molina-Montes E**, Sánchez MJ, Buckland G, Bueno-de-Mesquita HB, Weiderpass E, Amiano P, Wark PA, Kühn T, Katzke V, Huerta JM, Ardanaz E, Quirós JR, Affret A, His M, Boutron-Ruault MC, Peeters PH, Ye W, Sund M, Boeing H, Iqbal K, Ohlsson B, Sonestedt E, Tjønneland A, Petersen KE, Travis RC, Skeie G, Agnoli C, Panico S, Palli D, Tumino R, Sacerdote C, Freisling H, Huybrechts I, Overvad K, Trichopoulou A, Bamia C, Vasilopoulou E, Wareham N, Khaw KT, Cross AJ, Ward HA, Riboli E, Duell EJ. Mediterranean diet and risk of pancreatic cancer in the European Prospective Investigation into Cancer and Nutrition cohort. *Br J Cancer* 2017; **116**: 811-820 [PMID: 28170373 DOI: 10.1038/bjc.2017.14]
27 **Rawla P**, Thandra KC, Sunkara T. Pancreatic cancer and obesity: epidemiology, mechanism, and

preventive strategies. *Clin J Gastroenterol* 2019; **12**: 285-291 [PMID: 30788774 DOI: 10.1007/s12328-019-00953-3]

28 **Genkinger JM**, Kitahara CM, Bernstein L, Berrington de Gonzalez A, Brotzman M, Elena JW, Giles GG, Hartge P, Singh PN, Stolzenberg-Solomon RZ, Weiderpass E, Adami HO, Anderson KE, Beane-Freeman LE, Buring JE, Fraser GE, Fuchs CS, Gapstur SM, Gaziano JM, Helzlsouer KJ, Lacey JV Jr, Linet MS, Liu JJ, Park Y, Peters U, Purdue MP, Robien K, Schairer C, Sesso HD, Visvanathan K, White E, Wolk A, Wolpin BM, Zeleniuch-Jacquotte A, Jacobs EJ. Central adiposity, obesity during early adulthood, and pancreatic cancer mortality in a pooled analysis of cohort studies. *Ann Oncol* 2015; **26**: 2257-2266 [PMID: 26347100 DOI: 10.1093/annonc/mdv355]

29 **Song S**, Wang B, Zhang X, Hao L, Hu X, Li Z, Sun S. Long-Term Diabetes Mellitus Is Associated with an Increased Risk of Pancreatic Cancer: A Meta-Analysis. *PLoS One* 2015; **10**: e0134321 [PMID: 26222906 DOI: 10.1371/journal.pone.0134321]

30 **Bimonte S**, Cascella M, Leongito M, Palaia R, Caliendo D, Izzo F, Cuomo A. An overview of pre-clinical studies on the effects of (-)-epigallocatechin-3-gallate, a catechin found in green tea, in treatment of pancreatic cancer. *Recenti Prog Med* 2017; **108**: 282-287 [PMID: 28631776 DOI: 10.1701/2715.27715]

31 **Nasir A**, Bullo MMH, Ahmed Z, Imtiaz A, Yaqoob E, Jadoon M, Ahmed H, Afreen A, Yaqoob S. Nutrigenomics: Epigenetics and cancer prevention: A comprehensive review. *Crit Rev Food Sci Nutr* 2020; **60**: 1375-1387 [PMID: 30729798 DOI: 10.1080/10408398.2019.1571480]

32 **Pelaez-Luna M**, Takahashi N, Fletcher JG, Chari ST. Resectability of presymptomatic pancreatic cancer and its relationship to onset of diabetes: a retrospective review of CT scans and fasting glucose values prior to diagnosis. *Am J Gastroenterol* 2007; **102**: 2157-2163 [PMID: 17897335 DOI: 10.1111/j.1572-0241.2007.01480.x]

33 **US Preventive Services Task Force**, Owens DK, Davidson KW, Krist AH, Barry MJ, Cabana M, Caughey AB, Curry SJ, Doubeni CA, Epling JW Jr, Kubik M, Landefeld CS, Mangione CM, Pbert L, Silverstein M, Simon MA, Tseng CW, Wong JB. Screening for Pancreatic Cancer: US Preventive Services Task Force Reaffirmation Recommendation Statement. *JAMA* 2019; **322**: 438-444 [PMID: 31386141 DOI: 10.1001/jama.2019.10232]

34 **Yuan C**, Babic A, Khalaf N, Nowak JA, Brais LK, Rubinson DA, Ng K, Aguirre AJ, Pandharipande PV, Fuchs CS, Giovannucci EL, Stampfer MJ, Rosenthal MH, Sander C, Kraft P, Wolpin BM. Diabetes, Weight Change, and Pancreatic Cancer Risk. *JAMA Oncol* 2020; **6**: e202948 [PMID: 32789511 DOI: 10.1001/jamaoncol.2020.2948]

35 **Naudin S**, Viallon V, Hashim D, Freisling H, Jenab M, Weiderpass E, Perrier F, McKenzie F, Bueno-de-Mesquita HB, Olsen A, Tjønneland A, Dahm CC, Overvad K, Mancini FR, Rebours V, Boutron-Ruault MC, Katzke V, Kaaks R, Bergmann M, Boeing H, Peppa E, Karakatsani A, Trichopoulou A, Pala V, Masala G, Panico S, Tumino R, Sacerdote C, May AM, van Gils CH, Rylander C, Borch KB, Chirlaque López MD, Sánchez MJ, Ardanaz E, Quirós JR, Amiano Exezarreta P, Sund M, Drake I, Regnér S, Travis RC, Wareham N, Aune D, Riboli E, Gunter MJ, Duell EJ, Brennan P, Ferrari P. Healthy lifestyle and the risk of pancreatic cancer in the EPIC study. *Eur J Epidemiol* 2020; **35**: 975-986 [PMID: 31564045 DOI: 10.1007/s10654-019-00559-6]

36 **Lal G**, Liu G, Schmocker B, Kaurah P, Ozcelik H, Narod SA, Redston M, Gallinger S. Inherited predisposition to pancreatic adenocarcinoma: role of family history and germ-line p16, BRCA1, and BRCA2 mutations. *Cancer Res* 2000; **60**: 409-416 [PMID: 10667595]

37 **Holter S**, Borgida A, Dodd A, Grant R, Semotiuk K, Hedley D, Dhani N, Narod S, Akbari M, Moore M, Gallinger S. Germline BRCA Mutations in a Large Clinic-Based Cohort of Patients With Pancreatic Adenocarcinoma. *J Clin Oncol* 2015; **33**: 3124-3129 [PMID: 25940717 DOI: 10.1200/JCO.2014.59.7401]

38 **Goldstein AM**, Fraser MC, Struewing JP, Hussussian CJ, Ranade K, Zametkin DP, Fontaine LS, Organic SM, Dracopoli NC, Clark WH Jr. Increased risk of pancreatic cancer in melanoma-prone kindreds with p16INK4 mutations. *N Engl J Med* 1995; **333**: 970-974 [PMID: 7666916 DOI: 10.1056/NEJM199510123331504]

39 **van Lier MG**, Wagner A, Mathus-Vliegen EM, Kuipers EJ, Steyerberg EW, van Leerdam ME. High cancer risk in Peutz-Jeghers syndrome: a systematic review and surveillance recommendations. *Am J Gastroenterol* 2010; **105**: 1258-64; author reply 1265 [PMID: 20051941 DOI: 10.1038/ajg.2009.725]

40 **Park JG**, Park YJ, Wijnen JT, Vasen HF. Gene-environment interaction in hereditary nonpolyposis colorectal cancer with implications for diagnosis and genetic testing. *Int J Cancer* 1999; **82**: 516-519 [PMID: 10404064 DOI: 10.1002/(sici)1097-0215(19990812)82:4<516::aid-ijc8>3.0.co;2-u]

41 **Whitcomb DC**. Inflammation and Cancer V. Chronic pancreatitis and pancreatic cancer. *Am J Physiol Gastrointest Liver Physiol* 2004; **287**: G315-G319 [PMID: 15246966 DOI: 10.1152/ajpgi.00115.2004]

42 **Yurgelun MB**, Chittenden AB, Morales-Oyarvide V, Rubinson DA, Dunne RF, Kozak MM, Qian ZR, Welch MW, Brais LK, Da Silva A, Bui JL, Yuan C, Li T, Li W, Masuda A, Gu M, Bullock AJ, Chang DT, Clancy TE, Linehan DC, Findeis-Hosey JJ, Doyle LA, Thorner AR, Ducar MD, Wollison BM, Khalaf N, Perez K, Syngal S, Aguirre AJ, Hahn WC, Meyerson ML, Fuchs CS, Ogino S, Hornick JL, Hezel AF, Koong AC, Nowak JA, Wolpin BM. Germline cancer susceptibility gene variants, somatic second hits, and survival outcomes in patients with resected pancreatic cancer. *Genet Med* 2019; **21**: 213-223 [PMID: 29961768 DOI: 10.1038/s41436-018-0009-5]

43 **Stoffel EM**, McKernin SE, Brand R, Canto M, Goggins M, Moravek C, Nagarajan A, Petersen GM,

Simeone DM, Yurgelun M, Khorana AA. Evaluating Susceptibility to Pancreatic Cancer: ASCO Provisional Clinical Opinion. *J Clin Oncol* 2019; **37**: 153-164 [PMID: 30457921 DOI: 10.1200/JCO.18.01489]

44 **Ohmoto A**, Yachida S, Morizane C. Genomic Features and Clinical Management of Patients with Hereditary Pancreatic Cancer Syndromes and Familial Pancreatic Cancer. *Int J Mol Sci* 2019; **20** [PMID: 30699894 DOI: 10.3390/ijms20030561]

45 **Goggins M**, Overbeek KA, Brand R, Syngal S, Del Chiaro M, Bartsch DK, Bassi C, Carrato A, Farrell J, Fishman EK, Fockens P, Gress TM, van Hooft JE, Hruban RH, Kastrinos F, Klein A, Lennon AM, Lucas A, Park W, Rustgi A, Simeone D, Stoffel E, Vasen HFA, Cahen DL, Canto MI, Bruno M; International Cancer of the Pancreas Screening (CAPS) consortium. Management of patients with increased risk for familial pancreatic cancer: updated recommendations from the International Cancer of the Pancreas Screening (CAPS) Consortium. *Gut* 2020; **69**: 7-17 [PMID: 31672839 DOI: 10.1136/gutjnl-2019-319352]

46 **Syngal S**, Brand RE, Church JM, Giardiello FM, Hampel HL, Burt RW; American College of Gastroenterology. ACG clinical guideline: Genetic testing and management of hereditary gastrointestinal cancer syndromes. *Am J Gastroenterol* 2015; **110**: 223-62; quiz 263 [PMID: 25645574 DOI: 10.1038/ajg.2014.435]

47 **Brand RE**, Lerch MM, Rubinstein WS, Neoptolemos JP, Whitcomb DC, Hruban RH, Brentnall TA, Lynch HT, Canto MI; Participants of the Fourth International Symposium of Inherited Diseases of the Pancreas. Advances in counselling and surveillance of patients at risk for pancreatic cancer. *Gut* 2007; **56**: 1460-1469 [PMID: 17872573 DOI: 10.1136/gut.2006.108456]

48 **Aslanian HR**, Lee JH, Canto MI. AGA Clinical Practice Update on Pancreas Cancer Screening in High-Risk Individuals: Expert Review. *Gastroenterology* 2020; **159**: 358-362 [PMID: 32416142 DOI: 10.1053/j.gastro.2020.03.088]

49 **Hirono S**, Yamaue H. Surgical strategy for intraductal papillary mucinous neoplasms of the pancreas. *Surg Today* 2020; **50**: 50-55 [PMID: 31807871 DOI: 10.1007/s00595-019-01931-5]

50 **Canto MI**, Hruban RH, Fishman EK, Kamel IR, Schulick R, Zhang Z, Topazian M, Takahashi N, Fletcher J, Petersen G, Klein AP, Axilbund J, Griffin C, Syngal S, Saltzman JR, Mortele KJ, Lee J, Tamm E, Vikram R, Bhosale P, Margolis D, Farrell J, Goggins M; American Cancer of the Pancreas Screening (CAPS) Consortium. Frequent detection of pancreatic lesions in asymptomatic high-risk individuals. *Gastroenterology* 2012; **142**: 796-804; quiz e14 [PMID: 22245846 DOI: 10.1053/j.gastro.2012.01.005]

51 **Grover S**, Syngal S. Hereditary pancreatic cancer. *Gastroenterology* 2010; **139**: 1076-1080, 1080.e1 [PMID: 20727885 DOI: 10.1053/j.gastro.2010.08.012]

52 **Matthaei H**, Schulick RD, Hruban RH, Maitra A. Cystic precursors to invasive pancreatic cancer. *Nat Rev Gastroenterol Hepatol* 2011; **8**: 141-150 [PMID: 21383670 DOI: 10.1038/nrgastro.2011.2]

53 **Del Chiaro M**, Verbeke CS, Kartalis N, Pozzi Mucelli R, Gustafsson P, Hansson J, Haas SL, Segersvärd R, Andren-Sandberg Å, Löhr JM. Short-term Results of a Magnetic Resonance Imaging-Based Swedish Screening Program for Individuals at Risk for Pancreatic Cancer. *JAMA Surg* 2015; **150**: 512-518 [PMID: 25853369 DOI: 10.1001/jamasurg.2014.3852]

54 **Tanaka M**, Fernández-del Castillo C, Adsay V, Chari S, Falconi M, Jang JY, Kimura W, Levy P, Pitman MB, Schmidt CM, Shimizu M, Wolfgang CL, Yamaguchi K, Yamao K; International Association of Pancreatology. International consensus guidelines 2012 for the management of IPMN and MCN of the pancreas. *Pancreatology* 2012; **12**: 183-197 [PMID: 22687371 DOI: 10.1016/j.pan.2012.04.004]

55 **Canto MI**, Kerdsirichairat T, Yeo CJ, Hruban RH, Shin EJ, Almario JA, Blackford A, Ford M, Klein AP, Javed AA, Lennon AM, Zaheer A, Kamel IR, Fishman EK, Burkhart R, He J, Makary M, Weiss MJ, Schulick RD, Goggins MG, Wolfgang CL. Surgical Outcomes After Pancreatic Resection of Screening-Detected Lesions in Individuals at High Risk for Developing Pancreatic Cancer. *J Gastrointest Surg* 2020; **24**: 1101-1110 [PMID: 31197699 DOI: 10.1007/s11605-019-04230-z]

56 **Lennon AM**, Wolfgang CL, Canto MI, Klein AP, Herman JM, Goggins M, Fishman EK, Kamel I, Weiss MJ, Diaz LA, Papadopoulos N, Kinzler KW, Vogelstein B, Hruban RH. The early detection of pancreatic cancer: what will it take to diagnose and treat curable pancreatic neoplasia? *Cancer Res* 2014; **74**: 3381-3389 [PMID: 24924775 DOI: 10.1158/0008-5472.CAN-14-0734]

57 **Goonetilleke KS**, Siriwardena AK. Systematic review of carbohydrate antigen (CA 19-9) as a biochemical marker in the diagnosis of pancreatic cancer. *Eur J Surg Oncol* 2007; **33**: 266-270 [PMID: 17097848 DOI: 10.1016/j.ejso.2006.10.004]

58 **Rawla P**, Sunkara T, Gaduputi V. Epidemiology of Pancreatic Cancer: Global Trends, Etiology and Risk Factors. *World J Oncol* 2019; **10**: 10-27 [PMID: 30834048 DOI: 10.14740/wjon1166]

59 **Meng Q**, Shi S, Liang C, Liang D, Xu W, Ji S, Zhang B, Ni Q, Xu J, Yu X. Diagnostic and prognostic value of carcinoembryonic antigen in pancreatic cancer: a systematic review and meta-analysis. *Onco Targets Ther* 2017; **10**: 4591-4598 [PMID: 28979147 DOI: 10.2147/OTT.S145708]

60 **Ni XG**, Bai XF, Mao YL, Shao YF, Wu JX, Shan Y, Wang CF, Wang J, Tian YT, Liu Q, Xu DK, Zhao P. The clinical value of serum CEA, CA19-9, and CA242 in the diagnosis and prognosis of pancreatic cancer. *Eur J Surg Oncol* 2005; **31**: 164-169 [PMID: 15698733 DOI: 10.1016/j.ejso.2004.09.007]

61 **Khomiak A**, Brunner M, Kordes M, Lindblad S, Miksch RC, Öhlund D, Regel I. Recent Discoveries of Diagnostic, Prognostic and Predictive Biomarkers for Pancreatic Cancer. *Cancers (Basel)* 2020; **12** [PMID: 33147766 DOI: 10.3390/cancers12113234]

62 **Satake K**, Takeuchi T. Comparison of CA19-9 with other tumor markers in the diagnosis of cancer of the pancreas. *Pancreas* 1994; **9**: 720-724 [PMID: 7846015 DOI: 10.1097/00006676-199411000-00008]

63 **Bussom S**, Saif MW. Methods and rationale for the early detection of pancreatic cancer. Highlights from the "2010 ASCO Gastrointestinal Cancers Symposium". Orlando, FL, USA. January 22-24, 2010. *JOP* 2010; **11**: 128-130 [PMID: 20208319]

64 **Eissa MAL**, Lerner L, Abdelfatah E, Shankar N, Canner JK, Hasan NM, Yaghoobi V, Huang B, Kerner Z, Takaesu F, Wolfgang C, Kwak R, Ruiz M, Tam M, Pisanic TR 2nd, Iacobuzio-Donahue CA, Hruban RH, He J, Wang TH, Wood LD, Sharma A, Ahuja N. Promoter methylation of ADAMTS1 and BNC1 as potential biomarkers for early detection of pancreatic cancer in blood. *Clin Epigenetics* 2019; **11**: 59 [PMID: 30953539 DOI: 10.1186/s13148-019-0650-0]

65 **Shen SY**, Singhania R, Fehringer G, Chakravarthy A, Roehrl MHA, Chadwick D, Zuzarte PC, Borgida A, Wang TT, Li T, Kis O, Zhao Z, Spreafico A, Medina TDS, Wang Y, Roulois D, Ettayebi I, Chen Z, Chow S, Murphy T, Arruda A, O'Kane GM, Liu J, Mansour M, McPherson JD, O'Brien C, Leighl N, Bedard PL, Fleshner N, Liu G, Minden MD, Gallinger S, Goldenberg A, Pugh TJ, Hoffman MM, Bratman SV, Hung RJ, De Carvalho DD. Sensitive tumour detection and classification using plasma cell-free DNA methylomes. *Nature* 2018; **563**: 579-583 [PMID: 30429608 DOI: 10.1038/s41586-018-0703-0]

66 **Cirmena G**, Dameri M, Ravera F, Fregatti P, Ballestrero A, Zoppoli G. Assessment of Circulating Nucleic Acids in Cancer: From Current Status to Future Perspectives and Potential Clinical Applications. *Cancers (Basel)* 2021; **13** [PMID: 34298675 DOI: 10.3390/cancers13143460]

67 **Bloomston M**, Frankel WL, Petrocca F, Volinia S, Alder H, Hagan JP, Liu CG, Bhatt D, Taccioli C, Croce CM. MicroRNA expression patterns to differentiate pancreatic adenocarcinoma from normal pancreas and chronic pancreatitis. *JAMA* 2007; **297**: 1901-1908 [PMID: 17473300 DOI: 10.1001/jama.297.17.1901]

68 **Duell EJ**, Lujan-Barroso L, Sala N, Deitz McElyea S, Overvad K, Tjonneland A, Olsen A, Weiderpass E, Busund LT, Moi L, Muller D, Vineis P, Aune D, Matullo G, Naccarati A, Panico S, Tagliabue G, Tumino R, Palli D, Kaaks R, Katzke VA, Boeing H, Bueno-de-Mesquita HBA, Peeters PH, Trichopoulou A, Lagiou P, Kotanidou A, Travis RC, Wareham N, Khaw KT, Ramon Quiros J, Rodríguez-Barranco M, Dorronsoro M, Chirlaque MD, Ardanaz E, Severi G, Boutron-Ruault MC, Rebours V, Brennan P, Gunter M, Scelo G, Cote G, Sherman S, Korc M. Plasma microRNAs as biomarkers of pancreatic cancer risk in a prospective cohort study. *Int J Cancer* 2017; **141**: 905-915 [PMID: 28542740 DOI: 10.1002/ijc.30790]

69 **Liu J**, Gao J, Du Y, Li Z, Ren Y, Gu J, Wang X, Gong Y, Wang W, Kong X. Combination of plasma microRNAs with serum CA19-9 for early detection of pancreatic cancer. *Int J Cancer* 2012; **131**: 683-691 [PMID: 21913185 DOI: 10.1002/ijc.26422]

70 **Permuth JB**, Chen DT, Yoder SJ, Li J, Smith AT, Choi JW, Kim J, Balagurunathan Y, Jiang K, Coppola D, Centeno BA, Klapman J, Hodul P, Karreth FA, Trevino JG, Merchant N, Magliocco A, Malafa MP, Gillies R. Linc-ing Circulating Long Non-coding RNAs to the Diagnosis and Malignant Prediction of Intraductal Papillary Mucinous Neoplasms of the Pancreas. *Sci Rep* 2017; **7**: 10484 [PMID: 28874676 DOI: 10.1038/s41598-017-09754-5]

71 **Ding J**, Li Y, Zhang Y, Fan B, Li Q, Zhang J. Identification of key lncRNAs in the tumorigenesis of intraductal pancreatic mucinous neoplasm by coexpression network analysis. *Cancer Med* 2020; **9**: 3840-3851 [PMID: 32239802 DOI: 10.1002/cam4.2927]

72 **Nasca V**, Chiaravalli M, Piro G, Esposito A, Salvatore L, Tortora G, Corbo V, Carbone C. Intraductal Pancreatic Mucinous Neoplasms: A Tumor-Biology Based Approach for Risk Stratification. *Int J Mol Sci* 2020; **21** [PMID: 32887490 DOI: 10.3390/ijms21176386]

73 **Kanda M**, Knight S, Topazian M, Syngal S, Farrell J, Lee J, Kamel I, Lennon AM, Borges M, Young A, Fujiwara S, Seike J, Eshleman J, Hruban RH, Canto MI, Goggins M. Mutant GNAS detected in duodenal collections of secretin-stimulated pancreatic juice indicates the presence or emergence of pancreatic cysts. *Gut* 2013; **62**: 1024-1033 [PMID: 22859495 DOI: 10.1136/gutjnl-2012-302823]

74 **Kanda M**, Sadakari Y, Borges M, Topazian M, Farrell J, Syngal S, Lee J, Kamel I, Lennon AM, Knight S, Fujiwara S, Hruban RH, Canto MI, Goggins M. Mutant TP53 in duodenal samples of pancreatic juice from patients with pancreatic cancer or high-grade dysplasia. *Clin Gastroenterol Hepatol* 2013; **11**: 719-30.e5 [PMID: 23200980 DOI: 10.1016/j.cgh.2012.11.016]

75 **Singhi AD**, McGrath K, Brand RE, Khalid A, Zeh HJ, Chennat JS, Fasanella KE, Papachristou GI, Slivka A, Bartlett DL, Dasyam AK, Hogg M, Lee KK, Marsh JW, Monaco SE, Ohori NP, Pingpank JF, Tsung A, Zureikat AH, Wald AI, Nikiforova MN. Preoperative next-generation sequencing of pancreatic cyst fluid is highly accurate in cyst classification and detection of advanced neoplasia. *Gut* 2018; **67**: 2131-2141 [PMID: 28970292 DOI: 10.1136/gutjnl-2016-313586]

76 **Suenaga M**, Dudley B, Karloski E, Borges M, Irene Canto M, Brand RE, Goggins M. The Effect of Pancreatic Juice Collection Time on the Detection of KRAS Mutations. *Pancreas* 2018; **47**: 35-39 [PMID: 29200129 DOI: 10.1097/MPA.0000000000000956]

77 **Garcia-Carracedo D**, Chen ZM, Qiu W, Huang AS, Tang SM, Hruban RH, Su GH. PIK3CA mutations in mucinous cystic neoplasms of the pancreas. *Pancreas* 2014; **43**: 245-249 [PMID: 24518503 DOI: 10.1097/MPA.0000000000000034]

78 **Garcia-Carracedo D**, Turk AT, Fine SA, Akhavan N, Tweel BC, Parsons R, Chabot JA, Allendorf JD, Genkinger JM, Remotti HE, Su GH. Loss of PTEN expression is associated with poor prognosis

in patients with intraductal papillary mucinous neoplasms of the pancreas. *Clin Cancer Res* 2013; **19**: 6830-6841 [PMID: 24132918 DOI: 10.1158/1078-0432.CCR-13-0624]

79 **Kaur S**, Kumar S, Momi N, Sasson AR, Batra SK. Mucins in pancreatic cancer and its microenvironment. *Nat Rev Gastroenterol Hepatol* 2013; **10**: 607-620 [PMID: 23856888 DOI: 10.1038/nrgastro.2013.120]

80 **Nagata K**, Horinouchi M, Saitou M, Higashi M, Nomoto M, Goto M, Yonezawa S. Mucin expression profile in pancreatic cancer and the precursor lesions. *J Hepatobiliary Pancreat Surg* 2007; **14**: 243-254 [PMID: 17520199 DOI: 10.1007/s00534-006-1169-2]

81 **Moniaux N**, Chaturvedi P, Varshney GC, Meza JL, Rodriguez-Sierra JF, Aubert JP, Batra SK. Human MUC4 mucin induces ultra-structural changes and tumorigenicity in pancreatic cancer cells. *Br J Cancer* 2007; **97**: 345-357 [PMID: 17595659 DOI: 10.1038/sj.bjc.6603868]

82 **Gold DV**, Modrak DE, Ying Z, Cardillo TM, Sharkey RM, Goldenberg DM. New MUC1 serum immunoassay differentiates pancreatic cancer from pancreatitis. *J Clin Oncol* 2006; **24**: 252-258 [PMID: 16344318 DOI: 10.1200/JCO.2005.02.8282]

83 **Haab BB**, Porter A, Yue T, Li L, Scheiman J, Anderson MA, Barnes D, Schmidt CM, Feng Z, Simeone DM. Glycosylation variants of mucins and CEACAMs as candidate biomarkers for the diagnosis of pancreatic cystic neoplasms. *Ann Surg* 2010; **251**: 937-945 [PMID: 20395854 DOI: 10.1097/SLA.0b013e3181d7738d]

84 **Sinha J**, Cao Z, Dai J, Tang H, Partyka K, Hostetter G, Simeone DM, Feng Z, Allen PJ, Brand RE, Haab BB. A Gastric Glycoform of MUC5AC Is a Biomarker of Mucinous Cysts of the Pancreas. *PLoS One* 2016; **11**: e0167070 [PMID: 27992432 DOI: 10.1371/journal.pone.0167070]

85 **Horn A**, Chakraborty S, Dey P, Haridas D, Souchek J, Batra SK, Lele SM. Immunocytochemistry for MUC4 and MUC16 is a useful adjunct in the diagnosis of pancreatic adenocarcinoma on fine-needle aspiration cytology. *Arch Pathol Lab Med* 2013; **137**: 546-551 [PMID: 23544943 DOI: 10.5858/arpa.2011-0229-OA]

86 **Maker AV**, Katabi N, Qin LX, Klimstra DS, Schattner M, Brennan MF, Jarnagin WR, Allen PJ. Cyst fluid interleukin-1beta (IL1beta) levels predict the risk of carcinoma in intraductal papillary mucinous neoplasms of the pancreas. *Clin Cancer Res* 2011; **17**: 1502-1508 [PMID: 21266527 DOI: 10.1158/1078-0432.CCR-10-1561]

87 **Hao S**, Takahashi C, Snyder RA, Parikh AA. Stratifying Intraductal Papillary Mucinous Neoplasms by Cyst Fluid Analysis: Present and Future. *Int J Mol Sci* 2020; **21** [PMID: 32050465 DOI: 10.3390/ijms21031147]

88 **Das KK**, Geng X, Brown JW, Morales-Oyarvide V, Huynh T, Pergolini I, Pitman MB, Ferrone C, Al Efishat M, Haviland D, Thompson E, Wolfgang C, Lennon AM, Allen P, Lillemoe KD, Fields RC, Hawkins WG, Liu J, Castillo CF, Das KM, Mino-Kenudson M. Cross Validation of the Monoclonal Antibody Das-1 in Identification of High-Risk Mucinous Pancreatic Cystic Lesions. *Gastroenterology* 2019; **157**: 720-730.e2 [PMID: 31175863 DOI: 10.1053/j.gastro.2019.05.014]

89 **Zhang L**, Farrell JJ, Zhou H, Elashoff D, Akin D, Park NH, Chia D, Wong DT. Salivary transcriptomic biomarkers for detection of resectable pancreatic cancer. *Gastroenterology* 2010; **138**: 949-57.e1 [PMID: 19931263 DOI: 10.1053/j.gastro.2009.11.010]

90 **Xie Z**, Yin X, Gong B, Nie W, Wu B, Zhang X, Huang J, Zhang P, Zhou Z, Li Z. Salivary microRNAs show potential as a noninvasive biomarker for detecting resectable pancreatic cancer. *Cancer Prev Res (Phila)* 2015; **8**: 165-173 [PMID: 25538087 DOI: 10.1158/1940-6207.CAPR-14-0192]

91 **Satoh K**. Molecular Approaches Using Body Fluid for the Early Detection of Pancreatic Cancer. *Diagnostics (Basel)* 2021; **11** [PMID: 33671729 DOI: 10.3390/diagnostics11020375]

92 **Setti G**, Pezzi ME, Viani MV, Pertinhez TA, Cassi D, Magnoni C, Bellini P, Musolino A, Vescovi P, Meleti M. Salivary MicroRNA for Diagnosis of Cancer and Systemic Diseases: A Systematic Review. *Int J Mol Sci* 2020; **21** [PMID: 32019170 DOI: 10.3390/ijms21030907]

93 **Ishige F**, Hoshino I, Iwatate Y, Chiba S, Arimitsu H, Yanagibashi H, Nagase H, Takayama W. MIR1246 in body fluids as a biomarker for pancreatic cancer. *Sci Rep* 2020; **10**: 8723 [PMID: 32457495 DOI: 10.1038/s41598-020-65695-6]

94 **Radon TP**, Massat NJ, Jones R, Alrawashdeh W, Dumartin L, Ennis D, Duffy SW, Kocher HM, Pereira SP, Guarner posthumous L, Murta-Nascimento C, Real FX, Malats N, Neoptolemos J, Costello E, Greenhalf W, Lemoine NR, Crnogorac-Jurcevic T. Identification of a Three-Biomarker Panel in Urine for Early Detection of Pancreatic Adenocarcinoma. *Clin Cancer Res* 2015; **21**: 3512-3521 [PMID: 26240291 DOI: 10.1158/1078-0432.CCR-14-2467]

95 **Brezgyte G**, Shah V, Jach D, Crnogorac-Jurcevic T. Non-Invasive Biomarkers for Earlier Detection of Pancreatic Cancer-A Comprehensive Review. *Cancers (Basel)* 2021; **13** [PMID: 34072842 DOI: 10.3390/cancers13112722]

96 **Porta M**, Fabregat X, Malats N, Guarner L, Carrato A, de Miguel A, Ruiz L, Jariod M, Costafreda S, Coll S, Alguacil J, Corominas JM, Solà R, Salas A, Real FX. Exocrine pancreatic cancer: symptoms at presentation and their relation to tumour site and stage. *Clin Transl Oncol* 2005; **7**: 189-197 [PMID: 15960930 DOI: 10.1007/BF02712816]

97 **Mujica VR**, Barkin JS, Go VL. Acute pancreatitis secondary to pancreatic carcinoma. Study Group Participants. *Pancreas* 2000; **21**: 329-332 [PMID: 11075985 DOI: 10.1097/00006676-200011000-00001]

98 **Chari ST**, Leibson CL, Rabe KG, Ransom J, de Andrade M, Petersen GM. Probability of pancreatic cancer following diabetes: a population-based study. *Gastroenterology* 2005; **129**: 504-511 [PMID:

16083707 DOI: 10.1016/j.gastro.2005.05.007]
99 **Aggarwal G**, Kamada P, Chari ST. Prevalence of diabetes mellitus in pancreatic cancer compared to common cancers. *Pancreas* 2013; **42**: 198-201 [PMID: 23000893 DOI: 10.1097/MPA.0b013e3182592c96]
100 **Khorana AA**, Fine RL. Pancreatic cancer and thromboembolic disease. *Lancet Oncol* 2004; **5**: 655-663 [PMID: 15522652 DOI: 10.1016/S1470-2045(04)01606-7]
101 **Pinzon R**, Drewinko B, Trujillo JM, Guinee V, Giacco G. Pancreatic carcinoma and Trousseau's syndrome: experience at a large cancer center. *J Clin Oncol* 1986; **4**: 509-514 [PMID: 3958764 DOI: 10.1200/JCO.1986.4.4.509]
102 **Bravo-Piris J**, Villaron LG, Martinez C, Garcia-Perez A. Pipillon-Lefèvre syndrome: report of two familial cases. *Dermatologica* 1976; **152**: 168-176 [PMID: 133038 DOI: 10.1111/j.1365-2230.1992.tb02541.x]
103 **Marcos P**, Kieselova K, Cunha M. Pancreatic Panniculitis. *Am J Gastroenterol* 2017; **112**: 1218 [PMID: 28766564 DOI: 10.1038/ajg.2017.161]
104 **Galvañ VG**. Sister Mary Joseph's nodule. *Ann Intern Med* 1998; **128**: 410 [PMID: 9490607 DOI: 10.7326/0003-4819-128-5-199803010-00017]
105 **Lee ES**, Lee JM. Imaging diagnosis of pancreatic cancer: a state-of-the-art review. *World J Gastroenterol* 2014; **20**: 7864-7877 [PMID: 24976723 DOI: 10.3748/wjg.v20.i24.7864]
106 **Garces-Descovich A**, Beker K, Jaramillo-Cardoso A, James Moser A, Mortele KJ. Applicability of current NCCN Guidelines for pancreatic adenocarcinoma resectability: analysis and pitfalls. *Abdom Radiol (NY)* 2018; **43**: 314-322 [PMID: 29392370 DOI: 10.1007/s00261-018-1459-6]
107 **Wong JC**, Raman S. Surgical resectability of pancreatic adenocarcinoma: CTA. *Abdom Imaging* 2010; **35**: 471-480 [PMID: 19468791 DOI: 10.1007/s00261-009-9539-2]
108 **Fletcher JG**, Wiersema MJ, Farrell MA, Fidler JL, Burgart LJ, Koyama T, Johnson CD, Stephens DH, Ward EM, Harmsen WS. Pancreatic malignancy: value of arterial, pancreatic, and hepatic phase imaging with multi-detector row CT. *Radiology* 2003; **229**: 81-90 [PMID: 14519871 DOI: 10.1148/radiol.2291020582]
109 **Yoon SH**, Lee JM, Cho JY, Lee KB, Kim JE, Moon SK, Kim SJ, Baek JH, Kim SH, Lee JY, Han JK, Choi BI. Small (≤ 20 mm) pancreatic adenocarcinomas: analysis of enhancement patterns and secondary signs with multiphasic multidetector CT. *Radiology* 2011; **259**: 442-452 [PMID: 21406627 DOI: 10.1148/radiol.11101133]
110 **Shukla PJ**, Barreto SG, Kulkarni A, Nagarajan G, Fingerhut A. Vascular anomalies encountered during pancreatoduodenectomy: do they influence outcomes? *Ann Surg Oncol* 2010; **17**: 186-193 [PMID: 19838756 DOI: 10.1245/s10434-009-0757-1]
111 **Chu LC**, Goggins MG, Fishman EK. Diagnosis and Detection of Pancreatic Cancer. *Cancer J* 2017; **23**: 333-342 [PMID: 29189329 DOI: 10.1097/PPO.0000000000000290]
112 **Li H**, Zeng MS, Zhou KR, Jin DY, Lou WH. Pancreatic adenocarcinoma: the different CT criteria for peripancreatic major arterial and venous invasion. *J Comput Assist Tomogr* 2005; **29**: 170-175 [PMID: 15772532 DOI: 10.1097/01.rct.0000155060.73107.83]
113 **Xia BT**, Fu B, Wang J, Kim Y, Ahmad SA, Dhar VK, Levinsky NC, Hanseman DJ, Habib DA, Wilson GC, Smith M, Olowokure OO, Kharofa J, Al Humaidi AH, Choe KA, Abbott DE. Does radiologic response correlate to pathologic response in patients undergoing neoadjuvant therapy for borderline resectable pancreatic malignancy? *J Surg Oncol* 2017; **115**: 376-383 [PMID: 28105634 DOI: 10.1002/jso.24538]
114 **Holzapfel K**, Reiser-Erkan C, Fingerle AA, Erkan M, Eiber MJ, Rummeny EJ, Friess H, Kleeff J, Gaa J. Comparison of diffusion-weighted MR imaging and multidetector-row CT in the detection of liver metastases in patients operated for pancreatic cancer. *Abdom Imaging* 2011; **36**: 179-184 [PMID: 20563868 DOI: 10.1007/s00261-010-9633-5]
115 **Motosugi U**, Ichikawa T, Morisaka H, Sou H, Muhi A, Kimura K, Sano K, Araki T. Detection of pancreatic carcinoma and liver metastases with gadoxetic acid-enhanced MR imaging: comparison with contrast-enhanced multi-detector row CT. *Radiology* 2011; **260**: 446-453 [PMID: 21693662 DOI: 10.1148/radiol.11103548]
116 **Carrara G**, Pecorelli N, De Cobelli F, Cristel G, Damascelli A, Beretta L, Braga M. Preoperative sarcopenia determinants in pancreatic cancer patients. *Clin Nutr* 2017; **36**: 1649-1653 [PMID: 27789123 DOI: 10.1016/j.clnu.2016.10.014]
117 **Ozola Zalite I**, Zykus R, Francisco Gonzalez M, Saygili F, Pukitis A, Gaujoux S, Charnley RM, Lyadov V. Influence of cachexia and sarcopenia on survival in pancreatic ductal adenocarcinoma: a systematic review. *Pancreatology* 2015; **15**: 19-24 [PMID: 25524484 DOI: 10.1016/j.pan.2014.11.006]
118 **Prado CM**, Lieffers JR, McCargar LJ, Reiman T, Sawyer MB, Martin L, Baracos VE. Prevalence and clinical implications of sarcopenic obesity in patients with solid tumours of the respiratory and gastrointestinal tracts: a population-based study. *Lancet Oncol* 2008; **9**: 629-635 [PMID: 18539529 DOI: 10.1016/S1470-2045(08)70153-0]
119 **Schmocker RK**, Vanness DJ, Greenberg CC, Havlena JA, LoConte NK, Weiss JM, Neuman HB, Leverson G, Smith MA, Winslow ER. Utilization of preoperative endoscopic ultrasound for pancreatic adenocarcinoma. *HPB (Oxford)* 2017; **19**: 465-472 [PMID: 28237627 DOI: 10.1016/j.hpb.2017.01.017]
120 **Hartwig W**, Schneider L, Diener MK, Bergmann F, Büchler MW, Werner J. Preoperative tissue diagnosis for tumours of the pancreas. *Br J Surg* 2009; **96**: 5-20 [PMID: 19016272 DOI:

10.1002/bjs.6407]
121 **Lee TH**, Cho YD, Cha SW, Cho JY, Jang JY, Jeong SW, Choi HJ, Moon JH. Endoscopic ultrasound elastography for the pancreas in Korea: a preliminary single center study. *Clin Endosc* 2013; **46**: 172-177 [PMID: 23614128 DOI: 10.5946/ce.2013.46.2.172]
122 **Chantarojanasiri T**, Kongkam P. Endoscopic ultrasound elastography for solid pancreatic lesions. *World J Gastrointest Endosc* 2017; **9**: 506-513 [PMID: 29085561 DOI: 10.4253/wjge.v9.i10.506]
123 **Okasha H**, Elkholy S, El-Sayed R, Wifi MN, El-Nady M, El-Nabawi W, El-Dayem WA, Radwan MI, Farag A, El-Sherif Y, Al-Gemeie E, Salman A, El-Sherbiny M, El-Mazny A, Mahdy RE. Real time endoscopic ultrasound elastography and strain ratio in the diagnosis of solid pancreatic lesions. *World J Gastroenterol* 2017; **23**: 5962-5968 [PMID: 28932088 DOI: 10.3748/wjg.v23.i32.5962]
124 **Niederau C**, Grendell JH. Diagnosis of pancreatic carcinoma. Imaging techniques and tumor markers. *Pancreas* 1992; **7**: 66-86 [PMID: 1557348 DOI: 10.1097/00006676-199201000-00011]
125 **Vozzo CF**, Sanaka MR. Endoscopic Management of Pancreaticobiliary Disease. *Surg Clin North Am* 2020; **100**: 1151-1168 [PMID: 33128885 DOI: 10.1016/j.suc.2020.08.006]
126 **Alauddin MM**, De Palatis L. Current and Future Trends in Early Detection of Pancreatic Cancer: Molecular Targets and PET Probes. *Curr Med Chem* 2015; **22**: 3370-3389 [PMID: 26295468 DOI: 10.2174/0929867322666150821094015]
127 **Moradi F**, Iagaru A. The Role of Positron Emission Tomography in Pancreatic Cancer and Gallbladder Cancer. *Semin Nucl Med* 2020; **50**: 434-446 [PMID: 32768007 DOI: 10.1053/j.semnuclmed.2020.04.002]
128 **Li XX**, Liu NB, Zhu L, Yuan XK, Yang CW, Ren P, Gong LL, Zhao LJ, Xu WG, Wang P. Consequences of additional use of contrast-enhanced (18)F-FDG PET/CT in target volume delineation and dose distribution for pancreatic cancer. *Br J Radiol* 2015; **88**: 20140590 [PMID: 25939819 DOI: 10.1259/bjr.20140590]
129 **Wang L**, Dong P, Wang WG, Tian BL. Positron emission tomography modalities prevent futile radical resection of pancreatic cancer: A meta-analysis. *Int J Surg* 2017; **46**: 119-125 [PMID: 28890410 DOI: 10.1016/j.ijsu.2017.09.003]
130 **Santhosh S**, Mittal BR, Bhasin DK, Rana SS, Gupta R, Das A, Nada R. Fluorodeoxyglucose-positron emission tomography/computed tomography performs better than contrast-enhanced computed tomography for metastasis evaluation in the initial staging of pancreatic adenocarcinoma. *Ann Nucl Med* 2017; **31**: 575-581 [PMID: 28689356 DOI: 10.1007/s12149-017-1193-0]
131 **Daamen LA**, Groot VP, Goense L, Wessels FJ, Borel Rinkes IH, Intven MPW, van Santvoort HC, Molenaar IQ. The diagnostic performance of CT *vs* FDG PET-CT for the detection of recurrent pancreatic cancer: a systematic review and meta-analysis. *Eur J Radiol* 2018; **106**: 128-136 [PMID: 30150034 DOI: 10.1016/j.ejrad.2018.07.010]
132 **England CG**, Hernandez R, Eddine SB, Cai W. Molecular Imaging of Pancreatic Cancer with Antibodies. *Mol Pharm* 2016; **13**: 8-24 [PMID: 26620581 DOI: 10.1021/acs.molpharmaceut.5b00626]
133 **Feng X**, Wang Y, Lu D, Xu X, Zhou X, Zhang H, Zhang T, Zhu H, Yang Z, Wang F, Li N, Liu Z. Clinical Translation of a ^{68}Ga-Labeled Integrin $\alpha_v\beta_6$-Targeting Cyclic Radiotracer for PET Imaging of Pancreatic Cancer. *J Nucl Med* 2020; **61**: 1461-1467 [PMID: 32086242 DOI: 10.2967/jnumed.119.237347]
134 **Serrao EM**, Kettunen MI, Rodrigues TB, Dzien P, Wright AJ, Gopinathan A, Gallagher FA, Lewis DY, Frese KK, Almeida J, Howat WJ, Tuveson DA, Brindle KM. MRI with hyperpolarised [1-13C]pyruvate detects advanced pancreatic preneoplasia prior to invasive disease in a mouse model. *Gut* 2016; **65**: 465-475 [PMID: 26347531 DOI: 10.1136/gutjnl-2015-310114]
135 **Mayo SC**, Austin DF, Sheppard BC, Mori M, Shipley DK, Billingsley KG. Evolving preoperative evaluation of patients with pancreatic cancer: does laparoscopy have a role in the current era? *J Am Coll Surg* 2009; **208**: 87-95 [PMID: 19228509 DOI: 10.1016/j.jamcollsurg.2008.10.014]
136 **Allen VB**, Gurusamy KS, Takwoingi Y, Kalia A, Davidson BR. Diagnostic accuracy of laparoscopy following computed tomography (CT) scanning for assessing the resectability with curative intent in pancreatic and periampullary cancer. *Cochrane Database Syst Rev* 2016; **7**: CD009323 [PMID: 27383694 DOI: 10.1002/14651858.CD009323.pub3]
137 **Pisters PW**, Lee JE, Vauthey JN, Charnsangavej C, Evans DB. Laparoscopy in the staging of pancreatic cancer. *Br J Surg* 2001; **88**: 325-337 [PMID: 11260096 DOI: 10.1046/j.1365-2168.2001.01695.x]
138 **Fong ZV**, Alvino DML, Fernández-Del Castillo C, Mehtsun WT, Pergolini I, Warshaw AL, Chang DC, Lillemoe KD, Ferrone CR. Reappraisal of Staging Laparoscopy for Patients with Pancreatic Adenocarcinoma: A Contemporary Analysis of 1001 Patients. *Ann Surg Oncol* 2017; **24**: 3203-3211 [PMID: 28718038 DOI: 10.1245/s10434-017-5973-5]
139 **Karachristos A**, Scarmeas N, Hoffman JP. CA 19-9 Levels predict results of staging laparoscopy in pancreatic cancer. *J Gastrointest Surg* 2005; **9**: 1286-1292 [PMID: 16332484 DOI: 10.1016/j.gassur.2005.06.008]
140 **Wang KX**, Ben QW, Jin ZD, Du YQ, Zou DW, Liao Z, Li ZS. Assessment of morbidity and mortality associated with EUS-guided FNA: a systematic review. *Gastrointest Endosc* 2011; **73**: 283-290 [PMID: 21295642 DOI: 10.1016/j.gie.2010.10.045]
141 **Yane K**, Kuwatani M, Yoshida M, Goto T, Matsumoto R, Ihara H, Okuda T, Taya Y, Ehira N, Kudo T, Adachi T, Eto K, Onodera M, Sano I, Nojima M, Katanuma A. Non-negligible rate of needle tract seeding after endoscopic ultrasound-guided fine-needle aspiration for patients undergoing distal

pancreatectomy for pancreatic cancer. *Dig Endosc* 2020; **32**: 801-811 [PMID: 31876309 DOI: 10.1111/den.13615]

142 **Zhang L**, Sanagapalli S, Stoita A. Challenges in diagnosis of pancreatic cancer. *World J Gastroenterol* 2018; **24**: 2047-2060 [PMID: 29785074 DOI: 10.3748/wjg.v24.i19.2047]

143 **Clarke DL**, Clarke BA, Thomson SR, Garden OJ, Lazarus NG. The role of preoperative biopsy in pancreatic cancer. *HPB (Oxford)* 2004; **6**: 144-153 [PMID: 18333068 DOI: 10.1080/13651820410030862]

144 **Pezzilli R**. Asymptomatic lesions of the pancreas: an overview. *J Gastroenterol Hepatol Res* 2014; **3**: 1216-1219

145 **Tanaka M**, Fernández-Del Castillo C, Kamisawa T, Jang JY, Levy P, Ohtsuka T, Salvia R, Shimizu Y, Tada M, Wolfgang CL. Revisions of international consensus Fukuoka guidelines for the management of IPMN of the pancreas. *Pancreatology* 2017; **17**: 738-753 [PMID: 28735806 DOI: 10.1016/j.pan.2017.07.007]

146 **van Roessel S**, Kasumova GG, Verheij J, Najarian RM, Maggino L, de Pastena M, Malleo G, Marchegiani G, Salvia R, Ng SC, de Geus SW, Lof S, Giovinazzo F, van Dam JL, Kent TS, Busch OR, van Eijck CH, Koerkamp BG, Abu Hilal M, Bassi C, Tseng JF, Besselink MG. International Validation of the Eighth Edition of the American Joint Committee on Cancer (AJCC) TNM Staging System in Patients With Resected Pancreatic Cancer. *JAMA Surg* 2018; **153**: e183617 [PMID: 30285076 DOI: 10.1001/jamasurg.2018.3617]

147 **Bockhorn M**, Uzunoglu FG, Adham M, Imrie C, Milicevic M, Sandberg AA, Asbun HJ, Bassi C, Büchler M, Charnley RM, Conlon K, Cruz LF, Dervenis C, Fingerhutt A, Friess H, Gouma DJ, Hartwig W, Lillemoe KD, Montorsi M, Neoptolemos JP, Shrikhande SV, Takaori K, Traverso W, Vashist YK, Vollmer C, Yeo CJ, Izbicki JR; International Study Group of Pancreatic Surgery. Borderline resectable pancreatic cancer: a consensus statement by the International Study Group of Pancreatic Surgery (ISGPS). *Surgery* 2014; **155**: 977-988 [PMID: 24856119 DOI: 10.1016/j.surg.2014.02.001]

148 **Isaji S**, Mizuno S, Windsor JA, Bassi C, Fernández-Del Castillo C, Hackert T, Hayasaki A, Katz MHG, Kim SW, Kishiwada M, Kitagawa H, Michalski CW, Wolfgang CL. International consensus on definition and criteria of borderline resectable pancreatic ductal adenocarcinoma 2017. *Pancreatology* 2018; **18**: 2-11 [PMID: 29191513 DOI: 10.1016/j.pan.2017.11.011]

149 **Brown JA**, Zenati MS, Simmons RL, Al Abbas AI, Chopra A, Smith K, Lee KKW, Hogg ME, Zeh HJ, Paniccia A, Zureikat AH. Long-Term Surgical Complications After Pancreatoduodenectomy: Incidence, Outcomes, and Risk Factors. *J Gastrointest Surg* 2020; **24**: 1581-1589 [PMID: 32410174 DOI: 10.1007/s11605-020-04641-3]

150 **Seiler CA**, Wagner M, Bachmann T, Redaelli CA, Schmied B, Uhl W, Friess H, Büchler MW. Randomized clinical trial of pylorus-preserving duodenopancreatectomy *vs* classical Whipple resection-long term results. *Br J Surg* 2005; **92**: 547-556 [PMID: 15800958 DOI: 10.1002/bjs.4881]

151 **Hüttner FJ**, Fitzmaurice C, Schwarzer G, Seiler CM, Antes G, Büchler MW, Diener MK. Pylorus-preserving pancreaticoduodenectomy (pp Whipple) *vs* pancreaticoduodenectomy (classic Whipple) for surgical treatment of periampullary and pancreatic carcinoma. *Cochrane Database Syst Rev* 2016; **2**: CD006053 [PMID: 26905229 DOI: 10.1002/14651858.CD006053.pub6]

152 **Karim SAM**, Abdulla KS, Abdulkarim QH, Rahim FH. The outcomes and complications of pancreaticoduodenectomy (Whipple procedure): Cross sectional study. *Int J Surg* 2018; **52**: 383-387 [PMID: 29438817 DOI: 10.1016/j.ijsu.2018.01.041]

153 **Mora-Oliver I**, Garcés-Albir M, Dorcaratto D, Muñoz-Forner E, Izquierdo Moreno A, Carbonell-Aliaga MP, Sabater L. Pancreatoduodenectomy with artery-first approach. *Minerva Chir* 2019; **74**: 226-236 [PMID: 30600965 DOI: 10.23736/S0026-4733.18.07944-0]

154 **Li Z**, Wei A, Xia N, Zheng L, Yang D, Ye J, Xiong J, Hu W. Blumgart anastomosis reduces the incidence of pancreatic fistula after pancreaticoduodenectomy: a systematic review and meta-analysis. *Sci Rep* 2020; **10**: 17896 [PMID: 33087777 DOI: 10.1038/s41598-020-74812-4]

155 **Ricci C**, Ingaldi C, Alberici L, Pagano N, Mosconi C, Marasco G, Minni F, Casadei R. Blumgart Anastomosis After Pancreaticoduodenectomy. A Comprehensive Systematic Review, Meta-Analysis, and Meta-Regression. *World J Surg* 2021; **45**: 1929-1939 [PMID: 33721074 DOI: 10.1007/s00268-021-06039-x]

156 **Fang Y**, Gurusamy KS, Wang Q, Davidson BR, Lin H, Xie X, Wang C. Meta-analysis of randomized clinical trials on safety and efficacy of biliary drainage before surgery for obstructive jaundice. *Br J Surg* 2013; **100**: 1589-1596 [PMID: 24264780 DOI: 10.1002/bjs.9260]

157 **Schorn S**, Vogel T, Demir IE, Demir E, Safak O, Friess H, Ceyhan GO. Do somatostatin-analogues have the same impact on postoperative morbidity and pancreatic fistula in patients after pancreaticoduodenectomy and distal pancreatectomy? *Pancreatology* 2020; **20**: 1770-1778 [PMID: 33121847 DOI: 10.1016/j.pan.2020.10.043]

158 **Ammori BJ**, Ayiomamitis GD. Laparoscopic pancreaticoduodenectomy and distal pancreatectomy: a UK experience and a systematic review of the literature. *Surg Endosc* 2011; **25**: 2084-2099 [PMID: 21298539 DOI: 10.1007/s00464-010-1538-4]

159 **Mehrabi A**, Hafezi M, Arvin J, Esmaeilzadeh M, Garoussi C, Emami G, Kössler-Ebs J, Müller-Stich BP, Büchler MW, Hackert T, Diener MK. A systematic review and meta-analysis of laparoscopic *vs* open distal pancreatectomy for benign and malignant lesions of the pancreas: it's time to randomize. *Surgery* 2015; **157**: 45-55 [PMID: 25482464 DOI: 10.1016/j.surg.2014.06.081]

160 **Pierce RA**, Spitler JA, Hawkins WG, Strasberg SM, Linehan DC, Halpin VJ, Eagon JC, Brunt LM,

Frisella MM, Matthews BD. Outcomes analysis of laparoscopic resection of pancreatic neoplasms. *Surg Endosc* 2007; **21**: 579-586 [PMID: 17180287 DOI: 10.1007/s00464-006-9022-x]

161 **Petrucciani N**, Nigri G, Debs T, Giannini G, Sborlini E, Antolino L, Aurello P, D'Angelo F, Gugenheim J, Ramacciato G. Frozen section analysis of the pancreatic margin during pancreaticoduodenectomy for cancer: Does extending the resection to obtain a secondary R0 provide a survival benefit? *Pancreatology* 2016; **16**: 1037-1043 [PMID: 27697467 DOI: 10.1016/j.pan.2016.09.004]

162 **Winter JM**, Cameron JL, Campbell KA, Arnold MA, Chang DC, Coleman J, Hodgin MB, Sauter PK, Hruban RH, Riall TS, Schulick RD, Choti MA, Lillemoe KD, Yeo CJ. 1423 pancreaticoduodenectomies for pancreatic cancer: A single-institution experience. *J Gastrointest Surg* 2006; **10**: 1199-210; discussion 1210 [PMID: 17114007 DOI: 10.1016/j.gassur.2006.08.018]

163 **Schmidt CM**, Glant J, Winter JM, Kennard J, Dixon J, Zhao Q, Howard TJ, Madura JA, Nakeeb A, Pitt HA, Cameron JL, Yeo CJ, Lillemoe KD. Total pancreatectomy (R0 resection) improves survival over subtotal pancreatectomy in isolated neck margin positive pancreatic adenocarcinoma. *Surgery* 2007; **142**: 572-8; discussion 578 [PMID: 17950350 DOI: 10.1016/j.surg.2007.07.016]

164 **Karpoff HM**, Klimstra DS, Brennan MF, Conlon KC. Results of total pancreatectomy for adenocarcinoma of the pancreas. *Arch Surg* 2001; **136**: 44-7; discussion 48 [PMID: 11146775 DOI: 10.1001/archsurg.136.1.44]

165 **Scholten L**, Stoop TF, Del Chiaro M, Busch OR, van Eijck C, Molenaar IQ, de Vries JH, Besselink MG; Dutch Pancreatic Cancer Group. Systematic review of functional outcome and quality of life after total pancreatectomy. *Br J Surg* 2019; **106**: 1735-1746 [PMID: 31502658 DOI: 10.1002/bjs.11296]

166 **Tomlinson JS**, Jain S, Bentrem DJ, Sekeris EG, Maggard MA, Hines OJ, Reber HA, Ko CY. Accuracy of staging node-negative pancreas cancer: a potential quality measure. *Arch Surg* 2007; **142**: 767-723; discussion 773 [PMID: 17709731 DOI: 10.1001/archsurg.142.8.767]

167 **Tol JA**, Gouma DJ, Bassi C, Dervenis C, Montorsi M, Adham M, Andrén-Sandberg A, Asbun HJ, Bockhorn M, Büchler MW, Conlon KC, Fernández-Cruz L, Fingerhut A, Friess H, Hartwig W, Izbicki JR, Lillemoe KD, Milicevic MN, Neoptolemos JP, Shrikhande SV, Vollmer CM, Yeo CJ, Charnley RM; International Study Group on Pancreatic Surgery. Definition of a standard lymphadenectomy in surgery for pancreatic ductal adenocarcinoma: a consensus statement by the International Study Group on Pancreatic Surgery (ISGPS). *Surgery* 2014; **156**: 591-600 [PMID: 25061003 DOI: 10.1016/j.surg.2014.06.016]

168 **Sun J**, Yang Y, Wang X, Yu Z, Zhang T, Song J, Zhao H, Wen J, Du Y, Lau WY, Zhang Y. Meta-analysis of the efficacies of extended and standard pancreatoduodenectomy for ductal adenocarcinoma of the head of the pancreas. *World J Surg* 2014; **38**: 2708-2715 [PMID: 24912627 DOI: 10.1007/s00268-014-2633-9]

169 **Zgliczynski S**, Gietka-Czernel M, Gorowski T, Bednarski A, Chomicki O, Jastrzebska W, Makowska A, Niegowska E, Pucilowska J, Soszynski P. Results of 131I theory for 2,000 thyrotoxic patients: do the effects depend on the dose? *Exp Clin Endocrinol* 1991; **97**: 286-291 [PMID: 1915646 DOI: 10.1245/s10434-008-0281-8]

170 **Gurusamy KS**, Kumar S, Davidson BR, Fusai G. Resection *vs* other treatments for locally advanced pancreatic cancer. *Cochrane Database Syst Rev* 2014; CD010244 [PMID: 24578248 DOI: 10.1002/14651858.CD010244.pub2]

171 **Yamada S**, Fujii T, Sugimoto H, Nomoto S, Takeda S, Kodera Y, Nakao A. Aggressive surgery for borderline resectable pancreatic cancer: evaluation of National Comprehensive Cancer Network guidelines. *Pancreas* 2013; **42**: 1004-1010 [PMID: 23532000 DOI: 10.1097/MPA.0b013e31827b2d7c]

172 **Mollberg N**, Rahbari NN, Koch M, Hartwig W, Hoeger Y, Büchler MW, Weitz J. Arterial resection during pancreatectomy for pancreatic cancer: a systematic review and meta-analysis. *Ann Surg* 2011; **254**: 882-893 [PMID: 22064622 DOI: 10.1097/SLA.0b013e31823ac299]

173 **Wang S**, Shi N, You L, Dai M, Zhao Y. Minimally invasive surgical approach *vs* open procedure for pancreaticoduodenectomy: A systematic review and meta-analysis. *Medicine (Baltimore)* 2017; **96**: e8619 [PMID: 29390259 DOI: 10.1097/MD.0000000000008619]

174 **Palanivelu C**, Senthilnathan P, Sabnis SC, Babu NS, Srivatsan Gurumurthy S, Anand Vijai N, Nalankilli VP, Praveen Raj P, Parthasarathy R, Rajapandian S. Randomized clinical trial of laparoscopic *vs* open pancreatoduodenectomy for periampullary tumours. *Br J Surg* 2017; **104**: 1443-1450 [PMID: 28895142 DOI: 10.1002/bjs.10662]

175 **Poves I**, Burdío F, Morató O, Iglesias M, Radosevic A, Ilzarbe L, Visa L, Grande L. Comparison of Perioperative Outcomes Between Laparoscopic and Open Approach for Pancreatoduodenectomy: The PADULAP Randomized Controlled Trial. *Ann Surg* 2018; **268**: 731-739 [PMID: 30138162 DOI: 10.1097/SLA.0000000000002893]

176 **Croome KP**, Farnell MB, Que FG, Reid-Lombardo KM, Truty MJ, Nagorney DM, Kendrick ML. Total laparoscopic pancreaticoduodenectomy for pancreatic ductal adenocarcinoma: oncologic advantages over open approaches? *Ann Surg* 2014; **260**: 633-8; discussion 638 [PMID: 25203880 DOI: 10.1097/SLA.0000000000000937]

177 **Boone BA**, Zenati M, Hogg ME, Steve J, Moser AJ, Bartlett DL, Zeh HJ, Zureikat AH. Assessment of quality outcomes for robotic pancreaticoduodenectomy: identification of the learning curve. *JAMA Surg* 2015; **150**: 416-422 [PMID: 25761143 DOI: 10.1001/jamasurg.2015.17]

178 **Wang SE**, Shyr BU, Chen SC, Shyr YM. Comparison between robotic and open

pancreaticoduodenectomy with modified Blumgart pancreaticojejunostomy: A propensity score-matched study. *Surgery* 2018; **164**: 1162-1167 [PMID: 30093277 DOI: 10.1016/j.surg.2018.06.031]

179 **Zureikat AH**, Postlewait LM, Liu Y, Gillespie TW, Weber SM, Abbott DE, Ahmad SA, Maithel SK, Hogg ME, Zenati M, Cho CS, Salem A, Xia B, Steve J, Nguyen TK, Keshava HB, Chalikonda S, Walsh RM, Talamonti MS, Stocker SJ, Bentrem DJ, Lumpkin S, Kim HJ, Zeh HJ 3rd, Kooby DA. A Multi-institutional Comparison of Perioperative Outcomes of Robotic and Open Pancreaticoduodenectomy. *Ann Surg* 2016; **264**: 640-649 [PMID: 27433907 DOI: 10.1097/SLA.0000000000001869]

180 **Nassour I**, Tohme S, Hoehn R, Adam MA, Zureikat AH, Alessandro P. Safety and oncologic efficacy of robotic compared to open pancreaticoduodenectomy after neoadjuvant chemotherapy for pancreatic cancer. *Surg Endosc* 2021; **35**: 2248-2254 [PMID: 32440928 DOI: 10.1007/s00464-020-07638-w]

181 **Baimas-George M**, Watson M, Murphy KJ, Iannitti D, Baker E, Ocuin L, Vrochides D, Martinie JB. Robotic pancreaticoduodenectomy may offer improved oncologic outcomes over open surgery: a propensity-matched single-institution study. *Surg Endosc* 2020; **34**: 3644-3649 [PMID: 32328825 DOI: 10.1007/s00464-020-07564-x]

182 **Mizrahi JD**, Surana R, Valle JW, Shroff RT. Pancreatic cancer. *Lancet* 2020; **395**: 2008-2020 [PMID: 32593337 DOI: 10.1016/S0140-6736(20)30974-0]

183 **Perri G**, Prakash L, Qiao W, Varadhachary GR, Wolff R, Fogelman D, Overman M, Pant S, Javle M, Koay EJ, Herman J, Kim M, Ikoma N, Tzeng CW, Lee JE, Katz MHG. Postoperative Chemotherapy Benefits Patients Who Received Preoperative Therapy and Pancreatectomy for Pancreatic Adenocarcinoma. *Ann Surg* 2020; **271**: 996-1002 [PMID: 31895709 DOI: 10.1097/SLA.0000000000003763]

184 **Müller PC**, Frey MC, Ruzza CM, Nickel F, Jost C, Gwerder C, Hackert T, Z'graggen K, Kessler U. Neoadjuvant Chemotherapy in Pancreatic Cancer: An Appraisal of the Current High-Level Evidence. *Pharmacology* 2021; **106**: 143-153 [PMID: 32966993 DOI: 10.1159/000510343]

185 **Neoptolemos JP**, Stocken DD, Friess H, Bassi C, Dunn JA, Hickey H, Beger H, Fernandez-Cruz L, Dervenis C, Lacaine F, Falconi M, Pederzoli P, Pap A, Spooner D, Kerr DJ, Büchler MW; European Study Group for Pancreatic Cancer. A randomized trial of chemoradiotherapy and chemotherapy after resection of pancreatic cancer. *N Engl J Med* 2004; **350**: 1200-1210 [PMID: 15028824 DOI: 10.1056/NEJMoa032295]

186 **Oettle H**, Neuhaus P, Hochhaus A, Hartmann JT, Gellert K, Ridwelski K, Niedergethmann M, Zülke C, Fahlke J, Arning MB, Sinn M, Hinke A, Riess H. Adjuvant chemotherapy with gemcitabine and long-term outcomes among patients with resected pancreatic cancer: the CONKO-001 randomized trial. *JAMA* 2013; **310**: 1473-1481 [PMID: 24104372 DOI: 10.1001/jama.2013.279201]

187 **Neoptolemos JP**, Stocken DD, Bassi C, Ghaneh P, Cunningham D, Goldstein D, Padbury R, Moore MJ, Gallinger S, Mariette C, Wente MN, Izbicki JR, Friess H, Lerch MM, Dervenis C, Oláh A, Butturini G, Doi R, Lind PA, Smith D, Valle JW, Palmer DH, Buckels JA, Thompson J, McKay CJ, Rawcliffe CL, Büchler MW; European Study Group for Pancreatic Cancer. Adjuvant chemotherapy with fluorouracil plus folinic acid *vs* gemcitabine following pancreatic cancer resection: a randomized controlled trial. *JAMA* 2010; **304**: 1073-1081 [PMID: 20823433 DOI: 10.1001/jama.2010.1275]

188 **Neoptolemos JP**, Palmer DH, Ghaneh P, Psarelli EE, Valle JW, Halloran CM, Faluyi O, O'Reilly DA, Cunningham D, Wadsley J, Darby S, Meyer T, Gillmore R, Anthoney A, Lind P, Glimelius B, Falk S, Izbicki JR, Middleton GW, Cummins S, Ross PJ, Wasan H, McDonald A, Crosby T, Ma YT, Patel K, Sherriff D, Soomal R, Borg D, Sothi S, Hammel P, Hackert T, Jackson R, Büchler MW; European Study Group for Pancreatic Cancer. Comparison of adjuvant gemcitabine and capecitabine with gemcitabine monotherapy in patients with resected pancreatic cancer (ESPAC-4): a multicentre, open-label, randomised, phase 3 trial. *Lancet* 2017; **389**: 1011-1024 [PMID: 28129987 DOI: 10.1016/S0140-6736(16)32409-6]

189 **Conroy T**, Hammel P, Hebbar M, Ben Abdelghani M, Wei AC, Raoul JL, Choné L, Francois E, Artru P, Biagi JJ, Lecomte T, Assenat E, Faroux R, Ychou M, Volet J, Sauvanet A, Breysacher G, Di Fiore F, Cripps C, Kavan P, Texereau P, Bouhier-Leporrier K, Khemissa-Akouz F, Legoux JL, Juzyna B, Gourgou S, O'Callaghan CJ, Jouffroy-Zeller C, Rat P, Malka D, Castan F, Bachet JB; Canadian Cancer Trials Group and the Unicancer-GI–PRODIGE Group. FOLFIRINOX or Gemcitabine as Adjuvant Therapy for Pancreatic Cancer. *N Engl J Med* 2018; **379**: 2395-2406 [PMID: 30575490 DOI: 10.1056/NEJMoa1809775]

190 **Parmar A**, Chaves-Porras J, Saluja R, Perry K, Rahmadian AP, Santos SD, Ko YJ, Berry S, Doherty M, Chan KKW. Adjuvant treatment for resected pancreatic adenocarcinoma: A systematic review and network meta-analysis. *Crit Rev Oncol Hematol* 2020; **145**: 102817 [PMID: 31955005 DOI: 10.1016/j.critrevonc.2019.102817]

191 **Galvano A**, Castiglia M, Rizzo S, Silvestris N, Brunetti O, Vaccaro G, Gristina V, Barraco N, Bono M, Guercio G, Graceffa G, Fulfaro F, Gori S, Bazan V, Russo A. Moving the Target on the Optimal Adjuvant Strategy for Resected Pancreatic Cancers: A Systematic Review with Meta-Analysis. *Cancers (Basel)* 2020; **12** [PMID: 32110977 DOI: 10.3390/cancers12030534]

192 **Raufi AG**, Breakstone R, Leonard K, Charpentier K, Beard R, Renaud J, Cavanaugh L, Sturtevant A, MacKinnon K, Almhanna K, Olszewski A, Safran HP. Adjuvant FOLFOX+Nab-Paclitaxel (FOLFOX-A) for Pancreatic Cancer: A Brown University Oncology Research Group Phase II Study

(BrUOG295). *Am J Clin Oncol* 2020; **43**: 857-860 [PMID: 32976178 DOI: 10.1097/COC.0000000000000762]

193 **Kamarajah SK**, Bundred JR, Alrawashdeh W, Manas D, White SA. A systematic review and network meta-analysis of phase III randomised controlled trials for adjuvant therapy following resection of pancreatic ductal adenocarcinoma (PDAC). *HPB (Oxford)* 2020; **22**: 649-659 [PMID: 31894014 DOI: 10.1016/j.hpb.2019.12.001]

194 **Ma SJ**, Oladeru OT, Miccio JA, Iovoli AJ, Hermann GM, Singh AK. Association of Timing of Adjuvant Therapy With Survival in Patients With Resected Stage I to II Pancreatic Cancer. *JAMA Netw Open* 2019; **2**: e199126 [PMID: 31411712 DOI: 10.1001/jamanetworkopen.2019.9126]

195 **You MS**, Ryu JK, Huh G, Chun JW, Paik WH, Lee SH, Kim YT. Comparison of efficacy between adjuvant chemotherapy and chemoradiation therapy for pancreatic cancer: AJCC stage-based approach. *World J Clin Oncol* 2020; **11**: 747-760 [PMID: 33033696 DOI: 10.5306/wjco.v11.i9.747]

196 **Janssen QP**, O'Reilly EM, van Eijck CHJ, Groot Koerkamp B. Neoadjuvant Treatment in Patients With Resectable and Borderline Resectable Pancreatic Cancer. *Front Oncol* 2020; **10**: 41 [PMID: 32083002 DOI: 10.3389/fonc.2020.00041]

197 **Murphy JE**, Wo JY, Ryan DP, Jiang W, Yeap BY, Drapek LC, Blaszkowsky LS, Kwak EL, Allen JN, Clark JW, Faris JE, Zhu AX, Goyal L, Lillemoe KD, DeLaney TF, Fernández-Del Castillo C, Ferrone CR, Hong TS. Total Neoadjuvant Therapy With FOLFIRINOX Followed by Individualized Chemoradiotherapy for Borderline Resectable Pancreatic Adenocarcinoma: A Phase 2 Clinical Trial. *JAMA Oncol* 2018; **4**: 963-969 [PMID: 29800971 DOI: 10.1001/jamaoncol.2018.0329]

198 **van Roessel S**, van Veldhuisen E, Klompmaker S, Janssen QP, Abu Hilal M, Alseidi A, Balduzzi A, Balzano G, Bassi C, Berrevoet F, Bonds M, Busch OR, Butturini G, Del Chiaro M, Conlon KC, Falconi M, Frigerio I, Fusai GK, Gagnière J, Griffin O, Hackert T, Halimi A, Klaiber U, Labori KJ, Malleo G, Marino MV, Mortensen MB, Nikov A, Lesurtel M, Keck T, Kleeff J, Pandé R, Pfeiffer P, Pietrasz D, Roberts KJ, Sa Cunha A, Salvia R, Strobel O, Tarvainen T, Bossuyt PM, van Laarhoven HWM, Wilmink JW, Groot Koerkamp B, Besselink MG; European-African Hepato-Pancreato-Biliary Association. Evaluation of Adjuvant Chemotherapy in Patients With Resected Pancreatic Cancer After Neoadjuvant FOLFIRINOX Treatment. *JAMA Oncol* 2020; **6**: 1733-1740 [PMID: 32910170 DOI: 10.1001/jamaoncol.2020.3537]

199 **Yoo C**, Hwang I, Song TJ, Lee SS, Jeong JH, Park DH, Seo DW, Lee SK, Kim MH, Byun JH, Park JH, Hwang DW, Song KB, Lee JH, Lee W, Chang HM, Kim KP, Kim SC, Ryoo BY. FOLFIRINOX in borderline resectable and locally advanced unresectable pancreatic adenocarcinoma. *Ther Adv Med Oncol* 2020; **12**: 1758835920953294 [PMID: 32983266 DOI: 10.1177/1758835920953294]

200 **Oba A**, Ho F, Bao QR, Al-Musawi MH, Schulick RD, Del Chiaro M. Neoadjuvant Treatment in Pancreatic Cancer. *Front Oncol* 2020; **10**: 245 [PMID: 32185128 DOI: 10.3389/fonc.2020.00245]

201 **Giovinazzo F**, Soggiu F, Jang JY, Versteijne E, van Tienhoven G, van Eijck CH, Han Y, Choi SH, Kang CM, Zalupski M, Ahmad H, Yentz S, Helton S, Rose JB, Takishita C, Nagakawa Y, Abu Hilal M. Gemcitabine-Based Neoadjuvant Treatment in Borderline Resectable Pancreatic Ductal Adenocarcinoma: A Meta-Analysis of Individual Patient Data. *Front Oncol* 2020; **10**: 1112 [PMID: 32850319 DOI: 10.3389/fonc.2020.01112]

202 **Versteijne E**, Suker M, Groothuis K, Akkermans-Vogelaar JM, Besselink MG, Bonsing BA, Buijsen J, Busch OR, Creemers GM, van Dam RM, Eskens FALM, Festen S, de Groot JWB, Groot Koerkamp B, de Hingh IH, Homs MYV, van Hooft JE, Kerver ED, Luelmo SAC, Neelis KJ, Nuyttens J, Paardekooper GMRM, Patijn GA, van der Sangen MJC, de Vos-Geelen J, Wilmink JW, Zwinderman AH, Punt CJ, van Eijck CH, van Tienhoven G; Dutch Pancreatic Cancer Group. Preoperative Chemoradiotherapy Versus Immediate Surgery for Resectable and Borderline Resectable Pancreatic Cancer: Results of the Dutch Randomized Phase III PREOPANC Trial. *J Clin Oncol* 2020; **38**: 1763-1773 [PMID: 32105518 DOI: 10.1200/JCO.19.02274]

203 **Cloyd JM**, Chen HC, Wang X, Tzeng CD, Kim MP, Aloia TA, Vauthey JN, Lee JE, Katz MHG. Chemotherapy Versus Chemoradiation as Preoperative Therapy for Resectable Pancreatic Ductal Adenocarcinoma: A Propensity Score Adjusted Analysis. *Pancreas* 2019; **48**: 216-222 [PMID: 30629022 DOI: 10.1097/MPA.0000000000001231]

204 **Grossberg AJ**, Chu LC, Deig CR, Fishman EK, Hwang WL, Maitra A, Marks DL, Mehta A, Nabavizadeh N, Simeone DM, Weekes CD, Thomas CR Jr. Multidisciplinary standards of care and recent progress in pancreatic ductal adenocarcinoma. *CA Cancer J Clin* 2020; **70**: 375-403 [PMID: 32683683 DOI: 10.3322/caac.21626]

205 **Ghaneh P**, Palmer DH, Cicconi S, Halloran C, Psarelli EE, Rawcliffe CL, Sripadam R, Mukherjee S, Wadsley J, Al-Mukhtar A, Jiao LR, Wasan HS, Carter R, Graham JS, Ammad F, Evans J, Tjaden C, Hackert T, Buchler MW, Neoptolemos JP; European Study Group for Pancreatic Cancer (ESPAC). ESPAC-5F: four-arm, prospective, multicenter, international randomized phase II trial of immediate surgery compared with neoadjuvant gemcitabine plus capecitabine (GEMCAP) or MFFX or chemoradiotherapy (CRT) in patients with borderline resectable pancreatic cancer. *J Clin Oncol* 2020; **38** (15_Suppl): 4505 [DOI: 10.1200/JCO.2020.38.15_suppl.4505]

206 **Gamboa AC**, Rupji M, Switchenko JM, Lee RM, Turgeon MK, Meyer BI, Russell MC, Cardona K, Kooby DA, Maithel SK, Shah MM. Optimal timing and treatment strategy for pancreatic cancer. *J Surg Oncol* 2020; **122**: 457-468 [PMID: 32470166 DOI: 10.1002/jso.25976]

207 **Sohal D**, Duong MT, Ahmad SA, Gandhi N, Beg MS. SWOG S1505: Results of perioperative chemotherapy (peri-op CTx) with mFFX *vs* gemcitabine/nab-paclitaxel (Gem/nabP) for resectable pancreatic ductal adenocarcinoma (PRA). *J Clin Oncol* 2020; **38** (15_Suppl): 4504

208 **Motoi F**, Unno M. Adjuvant and neoadjuvant treatment for pancreatic adenocarcinoma. *Jpn J Clin Oncol* 2020; **50**: 483-489 [PMID: 32083290 DOI: 10.1093/jjco/hyaa018]

209 **Labori KJ**, Lassen K, Hoem D, Grønbech JE, Søreide JA, Mortensen K, Smaaland R, Sorbye H, Verbeke C, Dueland S. Neoadjuvant chemotherapy *vs* surgery first for resectable pancreatic cancer (Norwegian Pancreatic Cancer Trial - 1 (NorPACT-1)) - study protocol for a national multicentre randomized controlled trial. *BMC Surg* 2017; **17**: 94 [PMID: 28841916 DOI: 10.1186/s12893-017-0291-1]

210 **Schwarz L**, Vernerey D, Bachet JB, Tuech JJ, Portales F, Michel P, Cunha AS. Resectable pancreatic adenocarcinoma neo-adjuvant FOLF(IRIN)OX-based chemotherapy - a multicenter, non-comparative, randomized, phase II trial (PANACHE01-PRODIGE48 study). *BMC Cancer* 2018; **18**: 762 [PMID: 30041614 DOI: 10.1186/s12885-018-4663-4]

211 **Ettrich TJ**, Berger AW, Perkhofer L, Daum S, König A, Dickhut A, Wittel U, Wille K, Geissler M, Algül H, Gallmeier E, Atzpodien J, Kornmann M, Muche R, Prasnikar N, Tannapfel A, Reinacher-Schick A, Uhl W, Seufferlein T. Neoadjuvant plus adjuvant or only adjuvant nab-paclitaxel plus gemcitabine for resectable pancreatic cancer - the NEONAX trial (AIO-PAK-0313), a prospective, randomized, controlled, phase II study of the AIO pancreatic cancer group. *BMC Cancer* 2018; **18**: 1298 [PMID: 30594153 DOI: 10.1186/s12885-018-5183-y]

212 **Motoi F**, Kosuge T, Ueno H, Yamaue H, Satoi S, Sho M, Honda G, Matsumoto I, Wada K, Furuse J, Matsuyama Y, Unno M; Study Group of Preoperative Therapy for Pancreatic Cancer (Prep) and Japanese Study Group of Adjuvant Therapy for Pancreatic cancer (JSAP). Randomized phase II/III trial of neoadjuvant chemotherapy with gemcitabine and S-1 *vs* upfront surgery for resectable pancreatic cancer (Prep-02/JSAP05). *Jpn J Clin Oncol* 2019; **49**: 190-194 [PMID: 30608598 DOI: 10.1093/jjco/hyy190]

213 **Okusaka T**, Nakamura M, Yoshida M, Kitano M, Uesaka K, Ito Y, Furuse J, Hanada K, Okazaki K; Committee for Revision of Clinical Guidelines for Pancreatic Cancer of the Japan Pancreas Society. Clinical Practice Guidelines for Pancreatic Cancer 2019 From the Japan Pancreas Society: A Synopsis. *Pancreas* 2020; **49**: 326-335 [PMID: 32132516 DOI: 10.1097/MPA.0000000000001513]

214 **Okusaka T**, Furuse J. Recent advances in chemotherapy for pancreatic cancer: evidence from Japan and recommendations in guidelines. *J Gastroenterol* 2020; **55**: 369-382 [PMID: 31997007 DOI: 10.1007/s00535-020-01666-y]

215 **UMIN-CTR Clinical Trial**. Randomized phase II/III study of gemcitabine and nab-paclitaxel therapy vs S-1 and concurrent radiotherapy as neoadjuvant treatment for Borderline resectable pancreatic cancer. [cited 21 Dec 2019]. In: UMIN-CTR Clinical Trial [Internet]. Available from: https://upload.umin.ac.jp/cgi-open-bin/ctr_e/ctr_view.cgi?recptno=R000030821

216 **Sahni S**, Nahm C, Krisp C, Molloy MP, Mehta S, Maloney S, Itchins M, Pavlakis N, Clarke S, Chan D, Gill AJ, Howell VM, Samra J, Mittal A. Identification of Novel Biomarkers in Pancreatic Tumor Tissue to Predict Response to Neoadjuvant Chemotherapy. *Front Oncol* 2020; **10**: 237 [PMID: 32195182 DOI: 10.3389/fonc.2020.00237]

217 **Hammel P**, Lacy J, Portales F, Sobrero AF, Pazo Cid RA, Mozo JLM, Terrebonne E, Dowden SD, Li JS, Ong TJ, Nydam T, Philip PA. Phase II LAPACT trial of nab-paclitaxel (nab-P) plus gemcitabine (G) for patients with locally advanced pancreatic cancer (LAPDAC). *J Clin Oncol* 2018; **36** (suppl 4): 204

218 **Marthey L**, Sa-Cunha A, Blanc JF, Gauthier M, Cueff A, Francois E, Trouilloud I, Malka D, Bachet JB, Coriat R, Terrebonne E, De La Fouchardière C, Manfredi S, Solub D, Lécaille C, Thirot Bidault A, Carbonnel F, Taieb J. FOLFIRINOX for locally advanced pancreatic adenocarcinoma: results of an AGEO multicenter prospective observational cohort. *Ann Surg Oncol* 2015; **22**: 295-301 [PMID: 25037971 DOI: 10.1245/s10434-014-3898-9]

219 **Weniger M**, Moir J, Damm M, Maggino L, Kordes M, Rosendahl J, Ceyhan GO, Schorn S; RESPECT-study group. Respect - A multicenter retrospective study on preoperative chemotherapy in locally advanced and borderline resectable pancreatic cancer. *Pancreatology* 2020; **20**: 1131-1138 [PMID: 32739267 DOI: 10.1016/j.pan.2020.06.012]

220 **Suker M**, Beumer BR, Sadot E, Marthey L, Faris JE, Mellon EA, El-Rayes BF, Wang-Gillam A, Lacy J, Hosein PJ, Moorcraft SY, Conroy T, Hohla F, Allen P, Taieb J, Hong TS, Shridhar R, Chau I, van Eijck CH, Koerkamp BG. FOLFIRINOX for locally advanced pancreatic cancer: a systematic review and patient-level meta-analysis. *Lancet Oncol* 2016; **17**: 801-810 [PMID: 27160474 DOI: 10.1016/S1470-2045(16)00172-8]

221 **Philip PA**, Lacy J, Portales F, Sobrero A, Pazo-Cid R, Manzano Mozo JL, Kim EJ, Dowden S, Zakari A, Borg C, Terrebonne E, Rivera F, Sastre J, Bathini V, López-Trabada D, Asselah J, Saif MW, Shiansong Li J, Ong TJ, Nydam T, Hammel P. Nab-paclitaxel plus gemcitabine in patients with locally advanced pancreatic cancer (LAPACT): a multicentre, open-label phase 2 study. *Lancet Gastroenterol Hepatol* 2020; **5**: 285-294 [PMID: 31953079 DOI: 10.1016/S2468-1253(19)30327-9]

222 **Kunzmann V**, Algül H, Goekkurt E, Siegler GM, Martens UM, Waldschmidt D, Pelzer U, Hennes E, Fuchs M, Siveke J, Kullmann F, Boeck S, Ettrich TJ, Ferenczy P, Keller R, Germer C, Stein H, Hartlapp I, Klein I, Heinemann V. Conversion rate in locally advanced pancreatic cancer (LAPDAC) after nab-paclitaxel/gemcitabine- or MFFX-based induction chemotherapy (NEOLAP): final results of a multicenter randomised phase II AIO trial. *Ann Oncol* 2019; **30**: v253

223 **Wolfe AR**, Prabhakar D, Yildiz VO, Cloyd JM, Dillhoff M, Abushahin L, Alexandra Diaz D, Miller ED, Chen W, Frankel WL, Noonan A, Williams TM. Neoadjuvant-modified FOLFIRINOX *vs* nab-paclitaxel plus gemcitabine for borderline resectable or locally advanced pancreatic cancer patients

who achieved surgical resection. *Cancer Med* 2020; **9**: 4711-4723 [PMID: 32415696 DOI: 10.1002/cam4.3075]

224 **Hammel P**, Huguet F, van Laethem JL, Goldstein D, Glimelius B, Artru P, Borbath I, Bouché O, Shannon J, André T, Mineur L, Chibaudel B, Bonnetain F, Louvet C; LAP07 Trial Group. Effect of Chemoradiotherapy *vs* Chemotherapy on Survival in Patients With Locally Advanced Pancreatic Cancer Controlled After 4 Months of Gemcitabine With or Without Erlotinib: The LAP07 Randomized Clinical Trial. *JAMA* 2016; **315**: 1844-1853 [PMID: 27139057 DOI: 10.1001/jama.2016.4324]

225 **Arcelli A**, Buwenge M, Macchia G, Bertini F, Guido A, Deodato F, Cilla S, Scotti V, Rosetto ME, Djan I, Parisi S, Mattiucci GC, Cellini F, Fiore M, Bonomo P, Belgioia L, Niespolo RM, Gabriele P, Di Marco M, Simoni N, Mazzarotto R, Morganti AG; AIRO (Italian Association of Radiation Oncology and Clinical Oncology) Gastrointestinal Study Group. Stereotactic body radiotherapy *vs* conventionally fractionated chemoradiation in locally advanced pancreatic cancer: A multicenter case-control study (PAULA-1). *Cancer Med* 2020; **9**: 7879-7887 [PMID: 32910549 DOI: 10.1002/cam4.3330]

226 **Conroy T**, Desseigne F, Ychou M, Bouché O, Guimbaud R, Bécouarn Y, Adenis A, Raoul JL, Gourgou-Bourgade S, de la Fouchardière C, Bennouna J, Bachet JB, Khemissa-Akouz F, Péré-Vergé D, Delbaldo C, Assenat E, Chauffert B, Michel P, Montoto-Grillot C, Ducreux M; Groupe Tumeurs Digestives of Unicancer; PRODIGE Intergroup. FOLFIRINOX *vs* gemcitabine for metastatic pancreatic cancer. *N Engl J Med* 2011; **364**: 1817-1825 [PMID: 21561347 DOI: 10.1056/NEJMoa1011923]

227 **Von Hoff DD**, Ervin T, Arena FP, Chiorean EG, Infante J, Moore M, Seay T, Tjulandin SA, Ma WW, Saleh MN, Harris M, Reni M, Dowden S, Laheru D, Bahary N, Ramanathan RK, Tabernero J, Hidalgo M, Goldstein D, Van Cutsem E, Wei X, Iglesias J, Renschler MF. Increased survival in pancreatic cancer with nab-paclitaxel plus gemcitabine. *N Engl J Med* 2013; **369**: 1691-1703 [PMID: 24131140 DOI: 10.1056/NEJMoa1304369]

228 **Chan KKW**, Guo H, Cheng S, Beca JM, Redmond-Misner R, Isaranuwatchai W, Qiao L, Earle C, Berry SR, Biagi JJ, Welch S, Meyers BM, Mittmann N, Coburn N, Arias J, Schwartz D, Dai WF, Gavura S, McLeod R, Kennedy ED. Real-world outcomes of FOLFIRINOX *vs* gemcitabine and nab-paclitaxel in advanced pancreatic cancer: A population-based propensity score-weighted analysis. *Cancer Med* 2020; **9**: 160-169 [PMID: 31724340 DOI: 10.1002/cam4.2705]

229 **Wang Y**, Camateros P, Cheung WY. A Real-World Comparison of FOLFIRINOX, Gemcitabine Plus nab-Paclitaxel, and Gemcitabine in Advanced Pancreatic Cancers. *J Gastrointest Cancer* 2019; **50**: 62-68 [PMID: 29143916 DOI: 10.1007/s12029-017-0028-5]

230 **Wang-Gillam A**, Li CP, Bodoky G, Dean A, Shan YS, Jameson G, Macarulla T, Lee KH, Cunningham D, Blanc JF, Hubner RA, Chiu CF, Schwartsmann G, Siveke JT, Braiteh F, Moyo V, Belanger B, Dhindsa N, Bayever E, Von Hoff DD, Chen LT; NAPOLI-1 Study Group. Nanoliposomal irinotecan with fluorouracil and folinic acid in metastatic pancreatic cancer after previous gemcitabine-based therapy (NAPOLI-1): a global, randomised, open-label, phase 3 trial. *Lancet* 2016; **387**: 545-557 [PMID: 26615328 DOI: 10.1016/S0140-6736(15)00986-1]

231 **Golan T**, Hammel P, Reni M, Van Cutsem E, Macarulla T, Hall MJ, Park JO, Hochhauser D, Arnold D, Oh DY, Reinacher-Schick A, Tortora G, Algül H, O'Reilly EM, McGuinness D, Cui KY, Schlienger K, Locker GY, Kindler HL. Maintenance Olaparib for Germline *BRCA*-Mutated Metastatic Pancreatic Cancer. *N Engl J Med* 2019; **381**: 317-327 [PMID: 31157963 DOI: 10.1056/NEJMoa1903387]

232 **Alistar A**, Morris BB, Desnoyer R, Klepin HD, Hosseinzadeh K, Clark C, Cameron A, Leyendecker J, D'Agostino R Jr, Topaloglu U, Boteju LW, Boteju AR, Shorr R, Zachar Z, Bingham PM, Ahmed T, Crane S, Shah R, Migliano JJ, Pardee TS, Miller L, Hawkins G, Jin G, Zhang W, Pasche B. Safety and tolerability of the first-in-class agent CPI-613 in combination with modified FOLFIRINOX in patients with metastatic pancreatic cancer: a single-centre, open-label, dose-escalation, phase 1 trial. *Lancet Oncol* 2017; **18**: 770-778 [PMID: 28495639 DOI: 10.1016/S1470-2045(17)30314-5]

233 **Jiang B**, Zhou L, Lu J, Wang Y, Liu C, You L, Guo J. Stroma-Targeting Therapy in Pancreatic Cancer: One Coin With Two Sides? *Front Oncol* 2020; **10**: 576399 [PMID: 33178608 DOI: 10.3389/fonc.2020.576399]

234 **von Ahrens D**, Bhagat TD, Nagrath D, Maitra A, Verma A. The role of stromal cancer-associated fibroblasts in pancreatic cancer. *J Hematol Oncol* 2017; **10**: 76 [PMID: 28351381 DOI: 10.1186/s13045-017-0448-5]

235 **Provenzano PP**, Hingorani SR. Hyaluronan, fluid pressure, and stromal resistance in pancreas cancer. *Br J Cancer* 2013; **108**: 1-8 [PMID: 23299539 DOI: 10.1038/bjc.2012.569]

236 **Hingorani SR**, Zheng L, Bullock AJ, Seery TE, Harris WP, Sigal DS, Braiteh F, Ritch PS, Zalupski MM, Bahary N, Oberstein PE, Wang-Gillam A, Wu W, Chondros D, Jiang P, Khelifa S, Pu J, Aldrich C, Hendifar AE. HALO 202: Randomized Phase II Study of PEGPH20 Plus Nab-Paclitaxel/Gemcitabine Versus Nab-Paclitaxel/Gemcitabine in Patients With Untreated, Metastatic Pancreatic Ductal Adenocarcinoma. *J Clin Oncol* 2018; **36**: 359-366 [PMID: 29232172 DOI: 10.1200/JCO.2017.74.9564]

237 **Catenacci DV**, Junttila MR, Karrison T, Bahary N, Horiba MN, Nattam SR, Marsh R, Wallace J, Kozloff M, Rajdev L, Cohen D, Wade J, Sleckman B, Lenz HJ, Stiff P, Kumar P, Xu P, Henderson L, Takebe N, Salgia R, Wang X, Stadler WM, de Sauvage FJ, Kindler HL. Randomized Phase Ib/II Study of Gemcitabine Plus Placebo or Vismodegib, a Hedgehog Pathway Inhibitor, in Patients With

Metastatic Pancreatic Cancer. *J Clin Oncol* 2015; **33**: 4284-4292 [PMID: 26527777 DOI: 10.1200/JCO.2015.62.8719]

238 **McCleary-Wheeler AL**, Carr RM, Palmer SR, Smyrk TC, Allred JB, Almada LL, Tolosa EJ, Lamberti MJ, Marks DL, Borad MJ, Molina JR, Qi Y, Lingle WL, Grothey A, Pitot HC, Jatoi A, Northfelt DW, Bryce AH, McWilliams RR, Okuno SH, Haluska P, Kim GP, Colon-Otero G, Lowe VJ, Callstrom MR, Ma WW, Bekaii-Saab T, Hung MC, Erlichman C, Fernandez-Zapico ME. Phase 1 trial of Vismodegib and Erlotinib combination in metastatic pancreatic cancer. *Pancreatology* 2020; **20**: 101-109 [PMID: 31787526 DOI: 10.1016/j.pan.2019.11.011]

239 **Murphy JE**, Wo JY, Ryan DP, Clark JW, Jiang W, Yeap BY, Drapek LC, Ly L, Baglini CV, Blaszkowsky LS, Ferrone CR, Parikh AR, Weekes CD, Nipp RD, Kwak EL, Allen JN, Corcoran RB, Ting DT, Faris JE, Zhu AX, Goyal L, Berger DL, Qadan M, Lillemoe KD, Talele N, Jain RK, DeLaney TF, Duda DG, Boucher Y, Fernández-Del Castillo C, Hong TS. Total Neoadjuvant Therapy With FOLFIRINOX in Combination With Losartan Followed by Chemoradiotherapy for Locally Advanced Pancreatic Cancer: A Phase 2 Clinical Trial. *JAMA Oncol* 2019; **5**: 1020-1027 [PMID: 31145418 DOI: 10.1001/jamaoncol.2019.0892]

240 **Dimcevski G**, Kotopoulis S, Bjånes T, Hoem D, Schjøtt J, Gjertsen BT, Biermann M, Molven A, Sorbye H, McCormack E, Postema M, Gilja OH. A human clinical trial using ultrasound and microbubbles to enhance gemcitabine treatment of inoperable pancreatic cancer. *J Control Release* 2016; **243**: 172-181 [PMID: 27744037 DOI: 10.1016/j.jconrel.2016.10.007]

241 **Cooke VG**, LeBleu VS, Keskin D, Khan Z, O'Connell JT, Teng Y, Duncan MB, Xie L, Maeda G, Vong S, Sugimoto H, Rocha RM, Damascena A, Brentani RR, Kalluri R. Pericyte depletion results in hypoxia-associated epithelial-to-mesenchymal transition and metastasis mediated by met signaling pathway. *Cancer Cell* 2012; **21**: 66-81 [PMID: 22264789 DOI: 10.1016/j.ccr.2011.11.024]

242 **Veenstra VL**, Damhofer H, Waasdorp C, van Rijssen LB, van de Vijver MJ, Dijk F, Wilmink HW, Besselink MG, Busch OR, Chang DK, Bailey PJ, Biankin AV, Kocher HM, Medema JP, Li JS, Jiang R, Pierce DW, van Laarhoven HWM, Bijlsma MF. ADAM12 is a circulating marker for stromal activation in pancreatic cancer and predicts response to chemotherapy. *Oncogenesis* 2018; **7**: 87 [PMID: 30442938 DOI: 10.1038/s41389-018-0096-9]

243 **Griesmann H**, Drexel C, Milosevic N, Sipos B, Rosendahl J, Gress TM, Michl P. Pharmacological macrophage inhibition decreases metastasis formation in a genetic model of pancreatic cancer. *Gut* 2017; **66**: 1278-1285 [PMID: 27013602 DOI: 10.1136/gutjnl-2015-310049]

244 **Morrison AH**, Byrne KT, Vonderheide RH. Immunotherapy and Prevention of Pancreatic Cancer. *Trends Cancer* 2018; **4**: 418-428 [PMID: 29860986 DOI: 10.1016/j.trecan.2018.04.001]

245 **Royal RE**, Levy C, Turner K, Mathur A, Hughes M, Kammula US, Sherry RM, Topalian SL, Yang JC, Lowy I, Rosenberg SA. Phase 2 trial of single agent Ipilimumab (anti-CTLA-4) for locally advanced or metastatic pancreatic adenocarcinoma. *J Immunother* 2010; **33**: 828-833 [PMID: 20842054 DOI: 10.1097/CJI.0b013e3181eec14c]

246 **Brahmer JR**, Tykodi SS, Chow LQ, Hwu WJ, Topalian SL, Hwu P, Drake CG, Camacho LH, Kauh J, Odunsi K, Pitot HC, Hamid O, Bhatia S, Martins R, Eaton K, Chen S, Salay TM, Alaparthy S, Grosso JF, Korman AJ, Parker SM, Agrawal S, Goldberg SM, Pardoll DM, Gupta A, Wigginton JM. Safety and activity of anti-PD-L1 antibody in patients with advanced cancer. *N Engl J Med* 2012; **366**: 2455-2465 [PMID: 22658128 DOI: 10.1056/NEJMoa1200694]

247 **O'Reilly EM**, Oh DY, Dhani N, Renouf DJ, Lee MA, Sun W, Fisher G, Hezel A, Chang SC, Vlahovic G, Takahashi O, Yang Y, Fitts D, Philip PA. Durvalumab With or Without Tremelimumab for Patients With Metastatic Pancreatic Ductal Adenocarcinoma: A Phase 2 Randomized Clinical Trial. *JAMA Oncol* 2019; **5**: 1431-1438 [PMID: 31318392 DOI: 10.1001/jamaoncol.2019.1588]

248 **Tumeh PC**, Harview CL, Yearley JH, Shintaku IP, Taylor EJ, Robert L, Chmielowski B, Spasic M, Henry G, Ciobanu V, West AN, Carmona M, Kivork C, Seja E, Cherry G, Gutierrez AJ, Grogan TR, Mateus C, Tomasic G, Glaspy JA, Emerson RO, Robins H, Pierce RH, Elashoff DA, Robert C, Ribas A. PD-1 blockade induces responses by inhibiting adaptive immune resistance. *Nature* 2014; **515**: 568-571 [PMID: 25428505 DOI: 10.1038/nature13954]

249 **Humphris JL**, Patch AM, Nones K, Bailey PJ, Johns AL, McKay S, Chang DK, Miller DK, Pajic M, Kassahn KS, Quinn MC, Bruxner TJ, Christ AN, Harliwong I, Idrisoglu S, Manning S, Nourse C, Nourbakhsh E, Stone A, Wilson PJ, Anderson M, Fink JL, Holmes O, Kazakoff S, Leonard C, Newell F, Waddell N, Wood S, Mead RS, Xu Q, Wu J, Pinese M, Cowley MJ, Jones MD, Nagrial AM, Chin VT, Chantrill LA, Mawson A, Chou A, Scarlett CJ, Pinho AV, Rooman I, Giry-Laterriere M, Samra JS, Kench JG, Merrett ND, Toon CW, Epari K, Nguyen NQ, Barbour A, Zeps N, Jamieson NB, McKay CJ, Carter CR, Dickson EJ, Graham JS, Duthie F, Oien K, Hair J, Morton JP, Sansom OJ, Grützmann R, Hruban RH, Maitra A, Iacobuzio-Donahue CA, Schulick RD, Wolfgang CL, Morgan RA, Lawlor RT, Rusev B, Corbo V, Salvia R, Cataldo I, Tortora G, Tempero MA; Australian Pancreatic Cancer Genome Initiative, Hofmann O, Eshleman JR, Pilarsky C, Scarpa A, Musgrove EA, Gill AJ, Pearson JV, Grimmond SM, Waddell N, Biankin AV. Hypermutation In Pancreatic Cancer. *Gastroenterology* 2017; **152**: 68-74.e2 [PMID: 27856273 DOI: 10.1053/j.gastro.2016.09.060]

250 **Le DT**, Uram JN, Wang H, Bartlett BR, Kemberling H, Eyring AD, Skora AD, Luber BS, Azad NS, Laheru D, Biedrzycki B, Donehower RC, Zaheer A, Fisher GA, Crocenzi TS, Lee JJ, Duffy SM, Goldberg RM, de la Chapelle A, Koshiji M, Bhaijee F, Huebner T, Hruban RH, Wood LD, Cuka N, Pardoll DM, Papadopoulos N, Kinzler KW, Zhou S, Cornish TC, Taube JM, Anders RA, Eshleman JR, Vogelstein B, Diaz LA Jr. PD-1 Blockade in Tumors with Mismatch-Repair Deficiency. *N Engl*

J Med 2015; **372**: 2509-2520 [PMID: 26028255 DOI: 10.1056/NEJMoa1500596]

251 **Le DT**, Durham JN, Smith KN, Wang H, Bartlett BR, Aulakh LK, Lu S, Kemberling H, Wilt C, Luber BS, Wong F, Azad NS, Rucki AA, Laheru D, Donehower R, Zaheer A, Fisher GA, Crocenzi TS, Lee JJ, Greten TF, Duffy AG, Ciombor KK, Eyring AD, Lam BH, Joe A, Kang SP, Holdhoff M, Danilova L, Cope L, Meyer C, Zhou S, Goldberg RM, Armstrong DK, Bever KM, Fader AN, Taube J, Housseau F, Spetzler D, Xiao N, Pardoll DM, Papadopoulos N, Kinzler KW, Eshleman JR, Vogelstein B, Anders RA, Diaz LA Jr. Mismatch repair deficiency predicts response of solid tumors to PD-1 blockade. *Science* 2017; **357**: 409-413 [PMID: 28596308 DOI: 10.1126/science.aan6733]

252 **Wainberg ZA**, Hochster HS, Kim EJH, George B, Kalyan A, Chiorean EG, Waterhouse DM, Gutierrez M, Parikh AR, Jain R, Carrizosa DR, Soliman HH, Bhore R, Banerjee S, Lyons L, Louis CU, Ong TJ, O'Dwyer PJ. Phase I study of nivolumab (Nivo) + nab-paclitaxel (nab-P) + gemcitabine (Gem) in advanced pancreatic cancer (APDAC). *J Clin Oncol* 2019; **37**: 298

253 **Weiss GJ**, Blaydorn L, Beck J, Bornemann-Kolatzki K, Urnovitz H, Schütz E, Khemka V. Phase Ib/II study of gemcitabine, nab-paclitaxel, and pembrolizumab in metastatic pancreatic adenocarcinoma. *Invest New Drugs* 2018; **36**: 96-102 [PMID: 29119276 DOI: 10.1007/s10637-017-0525-1]

254 **National Institute of Public Health**. ONO-4538 Phase II Study (ONO-4538–83/TASUKI-83). [cited 21 Dec 2019]. In: National Institute of Public Health [Internet]. Available from: https://rctportal.niph.go.jp/en/detail?trial_id=JapicCTI-184230

255 **Wang-Gillam A**, O'Reilly EM, Bendell JC, Wainberg ZA, Borazanci EH, Bahary N, O'Hara MH, Beatty GL, Pant S, Cohen DJ, Leong S, Beg MS, Yu KH, Evans TRJ, Seufferlein T, Okusaka T, Phillips P, Liu X, Perna SK, Le DT. A randomized phase II study of cabiralizumab (cabira) + nivolumab (nivo) ± chemotherapy (chemo) in advanced pancreatic ductal adenocarcinoma (PDAC). *J Clin Oncol* 2019; **37**: TPS465

256 **Schizas D**, Charalampakis N, Kole C, Economopoulou P, Koustas E, Gkotsis E, Ziogas D, Psyrri A, Karamouzis MV. Immunotherapy for pancreatic cancer: A 2020 update. *Cancer Treat Rev* 2020; **86**: 102016 [PMID: 32247999 DOI: 10.1016/j.ctrv.2020.102016]

257 **Le DT**, Picozzi VJ, Ko AH, Wainberg ZA, Kindler H, Wang-Gillam A, Oberstein P, Morse MA, Zeh HJ 3rd, Weekes C, Reid T, Borazanci E, Crocenzi T, LoConte NK, Musher B, Laheru D, Murphy A, Whiting C, Nair N, Enstrom A, Ferber S, Brockstedt DG, Jaffee EM. Results from a Phase IIb, Randomized, Multicenter Study of GVAX Pancreas and CRS-207 Compared with Chemotherapy in Adults with Previously Treated Metastatic Pancreatic Adenocarcinoma (ECLIPSE Study). *Clin Cancer Res* 2019; **25**: 5493-5502 [PMID: 31126960 DOI: 10.1158/1078-0432.CCR-18-2992]

258 **Asahara S**, Takeda K, Yamao K, Maguchi H, Yamaue H. Phase I/II clinical trial using HLA-A24-restricted peptide vaccine derived from KIF20A for patients with advanced pancreatic cancer. *J Transl Med* 2013; **11**: 291 [PMID: 24237633 DOI: 10.1186/1479-5876-11-291]

259 **Suzuki N**, Hazama S, Iguchi H, Uesugi K, Tanaka H, Hirakawa K, Aruga A, Hatori T, Ishizaki H, Umeda Y, Fujiwara T, Ikemoto T, Shimada M, Yoshimatsu K, Shimizu R, Hayashi H, Sakata K, Takenouchi H, Matsui H, Shindo Y, Iida M, Koki Y, Arima H, Furukawa H, Ueno T, Yoshino S, Nakamura Y, Oka M, Nagano H. Phase II clinical trial of peptide cocktail therapy for patients with advanced pancreatic cancer: VENUS-PC study. *Cancer Sci* 2017; **108**: 73-80 [PMID: 27783849 DOI: 10.1111/cas.13113]

260 **Miyazawa M**, Katsuda M, Maguchi H, Katanuma A, Ishii H, Ozaka M, Yamao K, Imaoka H, Kawai M, Hirono S, Okada KI, Yamaue H. Phase II clinical trial using novel peptide cocktail vaccine as a postoperative adjuvant treatment for surgically resected pancreatic cancer patients. *Int J Cancer* 2017; **140**: 973-982 [PMID: 27861852 DOI: 10.1002/ijc.30510]

261 **Wedén S**, Klemp M, Gladhaug IP, Møller M, Eriksen JA, Gaudernack G, Buanes T. Long-term follow-up of patients with resected pancreatic cancer following vaccination against mutant K-ras. *Int J Cancer* 2011; **128**: 1120-1128 [PMID: 20473937 DOI: 10.1002/ijc.25449]

262 **Toubaji A**, Achtar M, Provenzano M, Herrin VE, Behrens R, Hamilton M, Bernstein S, Venzon D, Gause B, Marincola F, Khleif SN. Pilot study of mutant ras peptide-based vaccine as an adjuvant treatment in pancreatic and colorectal cancers. *Cancer Immunol Immunother* 2008; **57**: 1413-1420 [PMID: 18297281 DOI: 10.1007/s00262-008-0477-6]

263 **Abou-Alfa GK**, Chapman PB, Feilchenfeldt J, Brennan MF, Capanu M, Gansukh B, Jacobs G, Levin A, Neville D, Kelsen DP, O'Reilly EM. Targeting mutated K-ras in pancreatic adenocarcinoma using an adjuvant vaccine. *Am J Clin Oncol* 2011; **34**: 321-325 [PMID: 20686403 DOI: 10.1097/COC.0b013e3181e84b1f]

264 **Cohn A**, Morse MA, O'Neil B, Whiting S, Coeshott C, Ferraro J, Bellgrau D, Apelian D, Rodell TC. Whole Recombinant Saccharomyces cerevisiae Yeast Expressing Ras Mutations as Treatment for Patients With Solid Tumors Bearing Ras Mutations: Results From a Phase 1 Trial. *J Immunother* 2018; **41**: 141-150 [PMID: 29528991 DOI: 10.1097/CJI.0000000000000219]

265 **Katsuda M**, Miyazawa M, Kawai M, Hirono S, Okada KI, Shimizu A, Kitahata Y, Yamaue H. A phase III, double-blind, randomized clinical trial comparing S-1 in combination with DC vaccine loaded with WT1 peptides (TLP0-001) or placebo for the patients with advanced pancreatic cancer refractory to standard chemotherapy. *J Clin Oncol* 2017; **35**: TPS4153

266 **Katsuda M**, Miyazawa M, Ojima T, Katanuma A, Hakamada K, Sudo K, Asahara S, Endo I, Ueno M, Hara K, Yamada S, Fujii T, Satoi S, Ioka T, Ohira M, Akahori T, Kitano M, Nagano H, Furukawa M, Adachi T, Yamaue H. A double-blind randomized comparative clinical trial to

evaluate the safety and efficacy of dendritic cell vaccine loaded with WT1 peptides (TLP0-001) in combination with S-1 in patients with advanced pancreatic cancer refractory to standard chemotherapy. *Trials* 2019; **20**: 242 [PMID: 31029154 DOI: 10.1186/s13063-019-3332-5]

267 **Liu J**, Zhong JF, Zhang X, Zhang C. Allogeneic CD19-CAR-T cell infusion after allogeneic hematopoietic stem cell transplantation in B cell malignancies. *J Hematol Oncol* 2017; **10**: 35 [PMID: 28143567 DOI: 10.1186/s13045-017-0405-3]

268 **June CH**, O'Connor RS, Kawalekar OU, Ghassemi S, Milone MC. CAR T cell immunotherapy for human cancer. *Science* 2018; **359**: 1361-1365 [PMID: 29567707 DOI: 10.1126/science.aar6711]

269 **Wu J**, Cai J. Dilemma and Challenge of Immunotherapy for Pancreatic Cancer. *Dig Dis Sci* 2021; **66**: 359-368 [PMID: 32140943 DOI: 10.1007/s10620-020-06183-9]

270 **Beatty GL**, O'Hara MH, Lacey SF, Torigian DA, Nazimuddin F, Chen F, Kulikovskaya IM, Soulen MC, McGarvey M, Nelson AM, Gladney WL, Levine BL, Melenhorst JJ, Plesa G, June CH. Activity of Mesothelin-Specific Chimeric Antigen Receptor T Cells Against Pancreatic Carcinoma Metastases in a Phase 1 Trial. *Gastroenterology* 2018; **155**: 29-32 [PMID: 29567081 DOI: 10.1053/j.gastro.2018.03.029]

271 **Le DT**, Lutz E, Uram JN, Sugar EA, Onners B, Solt S, Zheng L, Diaz LA Jr, Donehower RC, Jaffee EM, Laheru DA. Evaluation of ipilimumab in combination with allogeneic pancreatic tumor cells transfected with a GM-CSF gene in previously treated pancreatic cancer. *J Immunother* 2013; **36**: 382-389 [PMID: 23924790 DOI: 10.1097/CJI.0b013e31829fb7a2]

272 **Chung V**, Kos FJ, Hardwick N, Yuan Y, Chao J, Li D, Waisman J, Li M, Zurcher K, Frankel P, Diamond DJ. Evaluation of safety and efficacy of p53MVA vaccine combined with pembrolizumab in patients with advanced solid cancers. *Clin Transl Oncol* 2019; **21**: 363-372 [PMID: 30094792 DOI: 10.1007/s12094-018-1932-2]

273 **Wang-Gillam A**, Lockhart AC, Tan BR, Suresh R, Lim KH, Ratner L, Morton A, Huffman J, Marquez S, Boice N, DeNardo DG. Phase I study of defactinib combined with pembrolizumab and gemcitabine in patients with advanced cancer. *J Clin Oncol* 2018; **36**: 2561

274 **Reiss KA**, Mick R, O'Hara MH, Teitelbaum UR, Karasic TB, Schneider CJ, O'Dwyer PJ, Karlson D, Cowden S, Fuhrer MJ, Carpenter EL, Pantel AA, Makvandi M, Mankoff DA, Nathanson K, Maxwell KN, Beatty GL, Domchek SM. A randomized phase II trial of niraparib plus either nivolumab or ipilimumab in patients with advanced pancreatic cancer whose cancer has not progressed on platinum-based therapy. *J Clin Oncol* 2019; **37**: TPS4161

275 **Desai J**, Kortmansky JS, Segal NH, Fakih M, Oh DY, Kim KP, Rahma OE, Ko AH, Chung HC, Alsina M, Yeh KH, Li S, Al-Sakaff NJA, Patel J, Barak H, Wang J, Zhang X, Bleul C, Cha E, Lee J. MORPHEUS: A phase Ib/II study platform evaluating the safety and clinical efficacy of cancer immunotherapy (CIT)—based combinations in gastrointestinal (GI) cancers. *J Clin Oncol* 2019; **37**: TPS467

276 **Rahal A**, Musher B. Oncolytic viral therapy for pancreatic cancer. *J Surg Oncol* 2017; **116**: 94-103 [PMID: 28407327 DOI: 10.1002/jso.24626]

277 **Eissa IR**, Bustos-Villalobos I, Ichinose T, Matsumura S, Naoe Y, Miyajima N, Morimoto D, Mukoyama N, Zhiwen W, Tanaka M, Hasegawa H, Sumigama S, Aleksic B, Kodera Y, Kasuya H. The Current Status and Future Prospects of Oncolytic Viruses in Clinical Trials against Melanoma, Glioma, Pancreatic, and Breast Cancers. *Cancers (Basel)* 2018; **10** [PMID: 30261620 DOI: 10.3390/cancers10100356]

278 **Chang KJ**, Senzer NN, Binmoeller K, Goldsweig H, Coffin R. Phase I dose-escalation study of talimogene laherparepvec (T-VEC) for advanced pancreatic cancer (ca). *J Clin Oncol* 2012; **30**: e14546

279 **Noonan AM**, Farren MR, Geyer SM, Huang Y, Tahiri S, Ahn D, Mikhail S, Ciombor KK, Pant S, Aparo S, Sexton J, Marshall JL, Mace TA, Wu CS, El-Rayes B, Timmers CD, Zwiebel J, Lesinski GB, Villalona-Calero MA, Bekaii-Saab TS. Randomized Phase 2 Trial of the Oncolytic Virus Pelareorep (Reolysin) in Upfront Treatment of Metastatic Pancreatic Adenocarcinoma. *Mol Ther* 2016; **24**: 1150-1158 [PMID: 27039845 DOI: 10.1038/mt.2016.66]

280 **Mahalingam D**, Wilkinson GA, Eng KH, Fields P, Raber P, Moseley JL, Cheetham K, Coffey M, Nuovo G, Kalinski P, Zhang B, Arora SP, Fountzilas C. Pembrolizumab in Combination with the Oncolytic Virus Pelareorep and Chemotherapy in Patients with Advanced Pancreatic Adenocarcinoma: A Phase Ib Study. *Clin Cancer Res* 2020; **26**: 71-81 [PMID: 31694832 DOI: 10.1158/1078-0432.CCR-19-2078]

281 **Haller SD**, Monaco ML, Essani K. The Present Status of Immuno-Oncolytic Viruses in the Treatment of Pancreatic Cancer. *Viruses* 2020; **12** [PMID: 33213031 DOI: 10.3390/v12111318]

282 **Aguirre AJ**, Nowak JA, Camarda ND, Moffitt RA, Ghazani AA, Hazar-Rethinam M, Raghavan S, Kim J, Brais LK, Ragon D, Welch MW, Reilly E, McCabe D, Marini L, Anderka K, Helvie K, Oliver N, Babic A, Da Silva A, Nadres B, Van Seventer EE, Shahzade HA, St Pierre JP, Burke KP, Clancy T, Cleary JM, Doyle LA, Jajoo K, McCleary NJ, Meyerhardt JA, Murphy JE, Ng K, Patel AK, Perez K, Rosenthal MH, Rubinson DA, Ryou M, Shapiro GI, Sicinska E, Silverman SG, Nagy RJ, Lanman RB, Knoerzer D, Welsch DJ, Yurgelun MB, Fuchs CS, Garraway LA, Getz G, Hornick JL, Johnson BE, Kulke MH, Mayer RJ, Miller JW, Shyn PB, Tuveson DA, Wagle N, Yeh JJ, Hahn WC, Corcoran RB, Carter SL, Wolpin BM. Real-time Genomic Characterization of Advanced Pancreatic Cancer to Enable Precision Medicine. *Cancer Discov* 2018; **8**: 1096-1111 [PMID: 29903880 DOI: 10.1158/2159-8290.CD-18-0275]

283 **Bernabe-Ramirez C**, Patel R, Chahal J, Saif MW. Treatment options in BRAF-mutant metastatic

colorectal cancer. *Anticancer Drugs* 2020; **31**: 545-557 [PMID: 32304411 DOI: 10.1097/CAD.0000000000000940]

284 **O'Reilly EM**, Hechtman JF. Tumour response to TRK inhibition in a patient with pancreatic adenocarcinoma harbouring an NTRK gene fusion. *Ann Oncol* 2019; **30**: viii36-viii40 [PMID: 31605106 DOI: 10.1093/annonc/mdz385]

285 **Solomon JP**, Linkov I, Rosado A, Mullaney K, Rosen EY, Frosina D, Jungbluth AA, Zehir A, Benayed R, Drilon A, Hyman DM, Ladanyi M, Sireci AN, Hechtman JF. NTRK fusion detection across multiple assays and 33,997 cases: diagnostic implications and pitfalls. *Mod Pathol* 2020; **33**: 38-46 [PMID: 31375766 DOI: 10.1038/s41379-019-0324-7]

286 **Aguirre AJ**. Oncogenic NRG1 Fusions: A New Hope for Targeted Therapy in Pancreatic Cancer. *Clin Cancer Res* 2019; **25**: 4589-4591 [PMID: 31164372 DOI: 10.1158/1078-0432.CCR-19-1280]

287 **Jones MR**, Williamson LM, Topham JT, Lee MKC, Goytain A, Ho J, Denroche RE, Jang G, Pleasance E, Shen Y, Karasinska JM, McGhie JP, Gill S, Lim HJ, Moore MJ, Wong HL, Ng T, Yip S, Zhang W, Sadeghi S, Reisle C, Mungall AJ, Mungall KL, Moore RA, Ma Y, Knox JJ, Gallinger S, Laskin J, Marra MA, Schaeffer DF, Jones SJM, Renouf DJ. *NRG1* Gene Fusions Are Recurrent, Clinically Actionable Gene Rearrangements in *KRAS* Wild-Type Pancreatic Ductal Adenocarcinoma. *Clin Cancer Res* 2019; **25**: 4674-4681 [PMID: 31068372 DOI: 10.1158/1078-0432.CCR-19-0191]

288 **Thompson ED**, Roberts NJ, Wood LD, Eshleman JR, Goggins MG, Kern SE, Klein AP, Hruban RH. The genetics of ductal adenocarcinoma of the pancreas in the year 2020: dramatic progress, but far to go. *Mod Pathol* 2020; **33**: 2544-2563 [PMID: 32704031 DOI: 10.1038/s41379-020-0629-6]

289 **Chantrill LA**, Nagrial AM, Watson C, Johns AL, Martyn-Smith M, Simpson S, Mead S, Jones MD, Samra JS, Gill AJ, Watson N, Chin VT, Humphris JL, Chou A, Brown B, Morey A, Pajic M, Grimmond SM, Chang DK, Thomas D, Sebastian L, Sjoquist K, Yip S, Pavlakis N, Asghari R, Harvey S, Grimison P, Simes J, Biankin AV; Australian Pancreatic Cancer Genome Initiative (APGI); Individualized Molecular Pancreatic Cancer Therapy (IMPaCT) Trial Management Committee of the Australasian Gastrointestinal Trials Group (AGITG). Precision Medicine for Advanced Pancreas Cancer: The Individualized Molecular Pancreatic Cancer Therapy (IMPaCT) Trial. *Clin Cancer Res* 2015; **21**: 2029-2037 [PMID: 25896973 DOI: 10.1158/1078-0432.CCR-15-0426]

290 **Kuo KK**, Hsiao PJ, Chang WT, Chuang SC, Yang YH, Wuputra K, Ku CC, Pan JB, Li CP, Kato K, Liu CJ, Wu DC, Yokoyama KK. Therapeutic Strategies Targeting Tumor Suppressor Genes in Pancreatic Cancer. *Cancers (Basel)* 2021; **13** [PMID: 34359820 DOI: 10.3390/cancers13153920]

291 **Yarchoan M**, Myzak MC, Johnson BA 3rd, De Jesus-Acosta A, Le DT, Jaffee EM, Azad NS, Donehower RC, Zheng L, Oberstein PE, Fine RL, Laheru DA, Goggins M. Olaparib in combination with irinotecan, cisplatin, and mitomycin C in patients with advanced pancreatic cancer. *Oncotarget* 2017; **8**: 44073-44081 [PMID: 28454122 DOI: 10.18632/oncotarget.17237]

292 **Aung KL**, Fischer SE, Denroche RE, Jang GH, Dodd A, Creighton S, Southwood B, Liang SB, Chadwick D, Zhang A, O'Kane GM, Albaba H, Moura S, Grant RC, Miller JK, Mbabaali F, Pasternack D, Lungu IM, Bartlett JMS, Ghai S, Lemire M, Holter S, Connor AA, Moffitt RA, Yeh JJ, Timms L, Krzyzanowski PM, Dhani N, Hedley D, Notta F, Wilson JM, Moore MJ, Gallinger S, Knox JJ. Genomics-Driven Precision Medicine for Advanced Pancreatic Cancer: Early Results from the COMPASS Trial. *Clin Cancer Res* 2018; **24**: 1344-1354 [PMID: 29288237 DOI: 10.1158/1078-0432.CCR-17-2994]

293 **Singhi AD**, George B, Greenbowe JR, Chung J, Suh J, Maitra A, Klempner SJ, Hendifar A, Milind JM, Golan T, Brand RE, Zureikat AH, Roy S, Schrock AB, Miller VA, Ross JS, Ali SM, Bahary N. Real-Time Targeted Genome Profile Analysis of Pancreatic Ductal Adenocarcinomas Identifies Genetic Alterations That Might Be Targeted With Existing Drugs or Used as Biomarkers. *Gastroenterology* 2019; **156**: 2242-2253.e4 [PMID: 30836094 DOI: 10.1053/j.gastro.2019.02.037]

294 **Luchini C**, Brosens LAA, Wood LD, Chatterjee D, Shin JI, Sciammarella C, Fiadone G, Malleo G, Salvia R, Kryklyva V, Piredda ML, Cheng L, Lawlor RT, Adsay V, Scarpa A. Comprehensive characterisation of pancreatic ductal adenocarcinoma with microsatellite instability: histology, molecular pathology and clinical implications. *Gut* 2021; **70**: 148-156 [PMID: 32350089 DOI: 10.1136/gutjnl-2020-320726]

295 **Choi M**, Kipps T, Kurzrock R. ATM Mutations in Cancer: Therapeutic Implications. *Mol Cancer Ther* 2016; **15**: 1781-1791 [PMID: 27413114 DOI: 10.1158/1535-7163.MCT-15-0945]

296 **Nanda N**, Roberts NJ. *ATM* Serine/Threonine Kinase and its Role in Pancreatic Risk. *Genes (Basel)* 2020; **11** [PMID: 31963441 DOI: 10.3390/genes11010108]

297 **Mukhopadhyay S**, Goswami D, Adiseshaiah PP, Burgan W, Yi M, Guerin TM, Kozlov SV, Nissley DV, McCormick F. Undermining Glutaminolysis Bolsters Chemotherapy While NRF2 Promotes Chemoresistance in KRAS-Driven Pancreatic Cancers. *Cancer Res* 2020; **80**: 1630-1643 [PMID: 31911550 DOI: 10.1158/0008-5472.CAN-19-1363]

298 **Janes MR**, Zhang J, Li LS, Hansen R, Peters U, Guo X, Chen Y, Babbar A, Firdaus SJ, Darjania L, Feng J, Chen JH, Li S, Long YO, Thach C, Liu Y, Zarieh A, Ely T, Kucharski JM, Kessler LV, Wu T, Yu K, Wang Y, Yao Y, Deng X, Zarrinkar PP, Brehmer D, Dhanak D, Lorenzi MV, Hu-Lowe D, Patricelli MP, Ren P. Targeting KRAS Mutant Cancers with a Covalent G12C-Specific Inhibitor. *Cell* 2018; **172**: 578-589.e17 [PMID: 29373830 DOI: 10.1016/j.cell.2018.01.006]

299 **Nagasaka M**, Li Y, Sukari A, Ou SI, Al-Hallak MN, Azmi AS. KRAS G12C Game of Thrones, which direct KRAS inhibitor will claim the iron throne? *Cancer Treat Rev* 2020; **84**: 101974 [PMID:

32014824 DOI: 10.1016/j.ctrv.2020.101974]

300 **Jones S**, Zhang X, Parsons DW, Lin JC, Leary RJ, Angenendt P, Mankoo P, Carter H, Kamiyama H, Jimeno A, Hong SM, Fu B, Lin MT, Calhoun ES, Kamiyama M, Walter K, Nikolskaya T, Nikolsky Y, Hartigan J, Smith DR, Hidalgo M, Leach SD, Klein AP, Jaffee EM, Goggins M, Maitra A, Iacobuzio-Donahue C, Eshleman JR, Kern SE, Hruban RH, Karchin R, Papadopoulos N, Parmigiani G, Vogelstein B, Velculescu VE, Kinzler KW. Core signaling pathways in human pancreatic cancers revealed by global genomic analyses. *Science* 2008; **321**: 1801-1806 [PMID: 18772397 DOI: 10.1126/science.1164368]

301 **Waddell N**, Pajic M, Patch AM, Chang DK, Kassahn KS, Bailey P, Johns AL, Miller D, Nones K, Quek K, Quinn MC, Robertson AJ, Fadlullah MZ, Bruxner TJ, Christ AN, Harliwong I, Idrisoglu S, Manning S, Nourse C, Nourbakhsh E, Wani S, Wilson PJ, Markham E, Cloonan N, Anderson MJ, Fink JL, Holmes O, Kazakoff SH, Leonard C, Newell F, Poudel B, Song S, Taylor D, Waddell N, Wood S, Xu Q, Wu J, Pinese M, Cowley MJ, Lee HC, Jones MD, Nagrial AM, Humphris J, Chantrill LA, Chin V, Steinmann AM, Mawson A, Humphrey ES, Colvin EK, Chou A, Scarlett CJ, Pinho AV, Giry-Laterriere M, Rooman I, Samra JS, Kench JG, Pettitt JA, Merrett ND, Toon C, Epari K, Nguyen NQ, Barbour A, Zeps N, Jamieson NB, Graham JS, Niclou SP, Bjerkvig R, Grützmann R, Aust D, Hruban RH, Maitra A, Iacobuzio-Donahue CA, Wolfgang CL, Morgan RA, Lawlor RT, Corbo V, Bassi C, Falconi M, Zamboni G, Tortora G, Tempero MA; Australian Pancreatic Cancer Genome Initiative, Gill AJ, Eshleman JR, Pilarsky C, Scarpa A, Musgrove EA, Pearson JV, Biankin AV, Grimmond SM. Whole genomes redefine the mutational landscape of pancreatic cancer. *Nature* 2015; **518**: 495-501 [PMID: 25719666 DOI: 10.1038/nature14169]

302 **Cani PD**. Human gut microbiome: hopes, threats and promises. *Gut* 2018; **67**: 1716-1725 [PMID: 29934437 DOI: 10.1136/gutjnl-2018-316723]

303 **Maekawa T**, Fukaya R, Takamatsu S, Itoyama S, Fukuoka T, Yamada M, Hata T, Nagaoka S, Kawamoto K, Eguchi H, Murata K, Kumada T, Ito T, Tanemura M, Fujimoto K, Tomita Y, Tobe T, Kamada Y, Miyoshi E. Possible involvement of Enterococcus infection in the pathogenesis of chronic pancreatitis and cancer. *Biochem Biophys Res Commun* 2018; **506**: 962-969 [PMID: 30401562 DOI: 10.1016/j.bbrc.2018.10.169]

304 **Wang S**, Dong W, Liu L, Xu M, Wang Y, Liu T, Zhang Y, Wang B, Cao H. Interplay between bile acids and the gut microbiota promotes intestinal carcinogenesis. *Mol Carcinog* 2019; **58**: 1155-1167 [PMID: 30828892 DOI: 10.1002/mc.22999]

305 **Cougnoux A**, Dalmasso G, Martinez R, Buc E, Delmas J, Gibold L, Sauvanet P, Darcha C, Déchelotte P, Bonnet M, Pezet D, Wodrich H, Darfeuille-Michaud A, Bonnet R. Bacterial genotoxin colibactin promotes colon tumour growth by inducing a senescence-associated secretory phenotype. *Gut* 2014; **63**: 1932-1942 [PMID: 24658599 DOI: 10.1136/gutjnl-2013-305257]

306 **Nougayrède JP**, Taieb F, De Rycke J, Oswald E. Cyclomodulins: bacterial effectors that modulate the eukaryotic cell cycle. *Trends Microbiol* 2005; **13**: 103-110 [PMID: 15737728 DOI: 10.1016/j.tim.2005.01.002]

307 **Bao Y**, Spiegelman D, Li R, Giovannucci E, Fuchs CS, Michaud DS. History of peptic ulcer disease and pancreatic cancer risk in men. *Gastroenterology* 2010; **138**: 541-549 [PMID: 19818786 DOI: 10.1053/j.gastro.2009.09.059]

308 **Mitsuhashi K**, Nosho K, Sukawa Y, Matsunaga Y, Ito M, Kurihara H, Kanno S, Igarashi H, Naito T, Adachi Y, Tachibana M, Tanuma T, Maguchi H, Shinohara T, Hasegawa T, Imamura M, Kimura Y, Hirata K, Maruyama R, Suzuki H, Imai K, Yamamoto H, Shinomura Y. Association of Fusobacterium species in pancreatic cancer tissues with molecular features and prognosis. *Oncotarget* 2015; **6**: 7209-7220 [PMID: 25797243 DOI: 10.18632/oncotarget.3109]

309 **Fan X**, Alekseyenko AV, Wu J, Peters BA, Jacobs EJ, Gapstur SM, Purdue MP, Abnet CC, Stolzenberg-Solomon R, Miller G, Ravel J, Hayes RB, Ahn J. Human oral microbiome and prospective risk for pancreatic cancer: a population-based nested case-control study. *Gut* 2018; **67**: 120-127 [PMID: 27742762 DOI: 10.1136/gutjnl-2016-312580]

310 **Li Q**, Jin M, Liu Y, Jin L. Gut Microbiota: Its Potential Roles in Pancreatic Cancer. *Front Cell Infect Microbiol* 2020; **10**: 572492 [PMID: 33117731 DOI: 10.3389/fcimb.2020.572492]

311 **Chakladar J**, Kuo SZ, Castaneda G, Li WT, Gnanasekar A, Yu MA, Chang EY, Wang XQ, Ongkeko WM. The Pancreatic Microbiome is Associated with Carcinogenesis and Worse Prognosis in Males and Smokers. *Cancers (Basel)* 2020; **12** [PMID: 32962112 DOI: 10.3390/cancers12092672]

312 **Rogers CJ**, Prabhu KS, Vijay-Kumar M. The microbiome and obesity-an established risk for certain types of cancer. *Cancer J* 2014; **20**: 176-180 [PMID: 24855004 DOI: 10.1097/PPO.0000000000000049]

313 **Qin J**, Li Y, Cai Z, Li S, Zhu J, Zhang F, Liang S, Zhang W, Guan Y, Shen D, Peng Y, Zhang D, Jie Z, Wu W, Qin Y, Xue W, Li J, Han L, Lu D, Wu P, Dai Y, Sun X, Li Z, Tang A, Zhong S, Li X, Chen W, Xu R, Wang M, Feng Q, Gong M, Yu J, Zhang Y, Zhang M, Hansen T, Sanchez G, Raes J, Falony G, Okuda S, Almeida M, LeChatelier E, Renault P, Pons N, Batto JM, Zhang Z, Chen H, Yang R, Zheng W, Yang H, Wang J, Ehrlich SD, Nielsen R, Pedersen O, Kristiansen K. A metagenome-wide association study of gut microbiota in type 2 diabetes. *Nature* 2012; **490**: 55-60 [PMID: 23023125 DOI: 10.1038/nature11450]

314 **Sousa T**, Paterson R, Moore V, Carlsson A, Abrahamsson B, Basit AW. The gastrointestinal microbiota as a site for the biotransformation of drugs. *Int J Pharm* 2008; **363**: 1-25 [PMID: 18682282 DOI: 10.1016/j.ijpharm.2008.07.009]

315 **Iida N**, Dzutsev A, Stewart CA, Smith L, Bouladoux N, Weingarten RA, Molina DA, Salcedo R, Back T, Cramer S, Dai RM, Kiu H, Cardone M, Naik S, Patri AK, Wang E, Marincola FM, Frank KM, Belkaid Y, Trinchieri G, Goldszmid RS. Commensal bacteria control cancer response to therapy by modulating the tumor microenvironment. *Science* 2013; **342**: 967-970 [PMID: 24264989 DOI: 10.1126/science.1240527]

316 **Vande Voorde J**, Sabuncuoğlu S, Noppen S, Hofer A, Ranjbarian F, Fieuws S, Balzarini J, Liekens S. Nucleoside-catabolizing enzymes in mycoplasma-infected tumor cell cultures compromise the cytostatic activity of the anticancer drug gemcitabine. *J Biol Chem* 2014; **289**: 13054-13065 [PMID: 24668817 DOI: 10.1074/jbc.M114.558924]

317 **Pushalkar S**, Hundeyin M, Daley D, Zambirinis CP, Kurz E, Mishra A, Mohan N, Aykut B, Usyk M, Torres LE, Werba G, Zhang K, Guo Y, Li Q, Akkad N, Lall S, Wadowski B, Gutierrez J, Kochen Rossi JA, Herzog JW, Diskin B, Torres-Hernandez A, Leinwand J, Wang W, Taunk PS, Savadkar S, Janal M, Saxena A, Li X, Cohen D, Sartor RB, Saxena D, Miller G. The Pancreatic Cancer Microbiome Promotes Oncogenesis by Induction of Innate and Adaptive Immune Suppression. *Cancer Discov* 2018; **8**: 403-416 [PMID: 29567829 DOI: 10.1158/2159-8290.CD-17-1134]

318 **Geller LT**, Barzily-Rokni M, Danino T, Jonas OH, Shental N, Nejman D, Gavert N, Zwang Y, Cooper ZA, Shee K, Thaiss CA, Reuben A, Livny J, Avraham R, Frederick DT, Ligorio M, Chatman K, Johnston SE, Mosher CM, Brandis A, Fuks G, Gurbatri C, Gopalakrishnan V, Kim M, Hurd MW, Katz M, Fleming J, Maitra A, Smith DA, Skalak M, Bu J, Michaud M, Trauger SA, Barshack I, Golan T, Sandbank J, Flaherty KT, Mandinova A, Garrett WS, Thayer SP, Ferrone CR, Huttenhower C, Bhatia SN, Gevers D, Wargo JA, Golub TR, Straussman R. Potential role of intratumor bacteria in mediating tumor resistance to the chemotherapeutic drug gemcitabine. *Science* 2017; **357**: 1156-1160 [PMID: 28912244 DOI: 10.1126/science.aah5043]

319 **Lehouritis P**, Cummins J, Stanton M, Murphy CT, McCarthy FO, Reid G, Urbaniak C, Byrne WL, Tangney M. Local bacteria affect the efficacy of chemotherapeutic drugs. *Sci Rep* 2015; **5**: 14554 [PMID: 26416623 DOI: 10.1038/srep14554]

320 **Kamarajah SK**, Burns WR, Frankel TL, Cho CS, Nathan H. Validation of the American Joint Commission on Cancer (AJCC) 8th Edition Staging System for Patients with Pancreatic Adenocarcinoma: A Surveillance, Epidemiology and End Results (SEER) Analysis. *Ann Surg Oncol* 2017; **24**: 2023-2030 [PMID: 28213792 DOI: 10.1245/s10434-017-5810-x]

321 **Raut CP**, Tseng JF, Sun CC, Wang H, Wolff RA, Crane CH, Hwang R, Vauthey JN, Abdalla EK, Lee JE, Pisters PW, Evans DB. Impact of resection status on pattern of failure and survival after pancreaticoduodenectomy for pancreatic adenocarcinoma. *Ann Surg* 2007; **246**: 52-60 [PMID: 17592291 DOI: 10.1097/01.sla.0000259391.84304.2b]

322 **Crippa S**, Guarneri G, Belfiori G, Partelli S, Pagnanelli M, Gasparini G, Balzano G, Lena MS, Rubini C, Doglioni C, Zamboni G, Falconi M. Positive neck margin at frozen section analysis is a significant predictor of tumour recurrence and poor survival after pancreatodudenectomy for pancreatic cancer. *Eur J Surg Oncol* 2020; **46**: 1524-1531 [PMID: 32098733 DOI: 10.1016/j.ejso.2020.02.013]

323 **Meyer W**, Jurowich C, Reichel M, Steinhäuser B, Wünsch PH, Gebhardt C. Pathomorphological and histological prognostic factors in curatively resected ductal adenocarcinoma of the pancreas. *Surg Today* 2000; **30**: 582-587 [PMID: 10930222 DOI: 10.1007/s005950070096]

324 **Sohn TA**, Yeo CJ, Cameron JL, Koniaris L, Kaushal S, Abrams RA, Sauter PK, Coleman J, Hruban RH, Lillemoe KD. Resected adenocarcinoma of the pancreas-616 patients: results, outcomes, and prognostic indicators. *J Gastrointest Surg* 2000; **4**: 567-579 [PMID: 11307091 DOI: 10.1016/s1091-255x(00)80105-5]

325 **Chang DK**, Johns AL, Merrett ND, Gill AJ, Colvin EK, Scarlett CJ, Nguyen NQ, Leong RW, Cosman PH, Kelly MI, Sutherland RL, Henshall SM, Kench JG, Biankin AV. Margin clearance and outcome in resected pancreatic cancer. *J Clin Oncol* 2009; **27**: 2855-2862 [PMID: 19398572 DOI: 10.1200/JCO.2008.20.5104]

326 **Helm J**, Centeno BA, Coppola D, Melis M, Lloyd M, Park JY, Chen DT, Malafa MP. Histologic characteristics enhance predictive value of American Joint Committee on Cancer staging in resectable pancreas cancer. *Cancer* 2009; **115**: 4080-4089 [PMID: 19626671 DOI: 10.1002/cncr.24503]

327 **Kinsella TJ**, Seo Y, Willis J, Stellato TA, Siegel CT, Harpp D, Willson JK, Gibbons J, Sanabria JR, Hardacre JM, Schulak JP. The impact of resection margin status and postoperative CA19-9 Levels on survival and patterns of recurrence after postoperative high-dose radiotherapy with 5-FU-based concurrent chemotherapy for resectable pancreatic cancer. *Am J Clin Oncol* 2008; **31**: 446-453 [PMID: 18838880 DOI: 10.1097/COC.0b013e318168f6c4]

328 **Pelucchi C**, Galeone C, Polesel J, Manzari M, Zucchetto A, Talamini R, Franceschi S, Negri E, La Vecchia C. Smoking and body mass index and survival in pancreatic cancer patients. *Pancreas* 2014; **43**: 47-52 [PMID: 24177141 DOI: 10.1097/MPA.0b013e3182a7c74b]

329 **Yuan C**, Morales-Oyarvide V, Babic A, Clish CB, Kraft P, Bao Y, Qian ZR, Rubinson DA, Ng K, Giovannucci EL, Ogino S, Stampfer MJ, Gaziano JM, Sesso HD, Cochrane BB, Manson JE, Fuchs CS, Wolpin BM. Cigarette Smoking and Pancreatic Cancer Survival. *J Clin Oncol* 2017; **35**: 1822-1828 [PMID: 28358654 DOI: 10.1200/JCO.2016.71.2026]

330 **Jiang P**, Zhang M, Gui L, Zhang K. Expression patterns and prognostic values of the *cyclin-dependent kinase 1* and *cyclin A2* gene cluster in pancreatic adenocarcinoma. *J Int Med Res* 2020; **48**: 300060520930113 [PMID: 33290118 DOI: 10.1177/0300060520930113]

331 **Bailey P**, Chang DK, Nones K, Johns AL, Patch AM, Gingras MC, Miller DK, Christ AN, Bruxner TJ, Quinn MC, Nourse C, Murtaugh LC, Harliwong I, Idrisoglu S, Manning S, Nourbakhsh E, Wani S, Fink L, Holmes O, Chin V, Anderson MJ, Kazakoff S, Leonard C, Newell F, Waddell N, Wood S, Xu Q, Wilson PJ, Cloonan N, Kassahn KS, Taylor D, Quek K, Robertson A, Pantano L, Mincarelli L, Sanchez LN, Evers L, Wu J, Pinese M, Cowley MJ, Jones MD, Colvin EK, Nagrial AM, Humphrey ES, Chantrill LA, Mawson A, Humphris J, Chou A, Pajic M, Scarlett CJ, Pinho AV, Giry-Laterriere M, Rooman I, Samra JS, Kench JG, Lovell JA, Merrett ND, Toon CW, Epari K, Nguyen NQ, Barbour A, Zeps N, Moran-Jones K, Jamieson NB, Graham JS, Duthie F, Oien K, Hair J, Grützmann R, Maitra A, Iacobuzio-Donahue CA, Wolfgang CL, Morgan RA, Lawlor RT, Corbo V, Bassi C, Rusev B, Capelli P, Salvia R, Tortora G, Mukhopadhyay D, Petersen GM; Australian Pancreatic Cancer Genome Initiative, Munzy DM, Fisher WE, Karim SA, Eshleman JR, Hruban RH, Pilarsky C, Morton JP, Sansom OJ, Scarpa A, Musgrove EA, Bailey UM, Hofmann O, Sutherland RL, Wheeler DA, Gill AJ, Gibbs RA, Pearson JV, Waddell N, Biankin AV, Grimmond SM. Genomic analyses identify molecular subtypes of pancreatic cancer. *Nature* 2016; **531**: 47-52 [PMID: 26909576 DOI: 10.1038/nature16965]

332 **Li X**, Li Z, Zhu H, Yu X. Autophagy Regulatory Genes MET and RIPK2 Play a Prognostic Role in Pancreatic Ductal Adenocarcinoma: A Bioinformatic Analysis Based on GEO and TCGA. *Biomed Res Int* 2020; **2020**: 8537381 [PMID: 33204717 DOI: 10.1155/2020/8537381]

333 **Liu JQ**, Liao XW, Wang XK, Yang CK, Zhou X, Liu ZQ, Han QF, Fu TH, Zhu GZ, Han CY, Su H, Huang JL, Ruan GT, Yan L, Ye XP, Peng T. Prognostic value of Glypican family genes in early-stage pancreatic ductal adenocarcinoma after pancreaticoduodenectomy and possible mechanisms. *BMC Gastroenterol* 2020; **20**: 415 [PMID: 33302876 DOI: 10.1186/s12876-020-01560-0]

334 **Qian B**, Wei L, Yang Z, He Q, Chen H, Wang A, Yang D, Li Q, Li J, Zheng S, Fu W. Hic-5 in pancreatic stellate cells affects proliferation, apoptosis, migration, invasion of pancreatic cancer cells and postoperative survival time of pancreatic cancer. *Biomed Pharmacother* 2020; **121**: 109355 [PMID: 31683179 DOI: 10.1016/j.biopha.2019.109355]

335 **Song C**, Chen T, He L, Ma N, Li JA, Rong YF, Fang Y, Liu M, Xie D, Lou W. PRMT1 promotes pancreatic cancer growth and predicts poor prognosis. *Cell Oncol (Dordr)* 2020; **43**: 51-62 [PMID: 31520395 DOI: 10.1007/s13402-019-00435-1]

336 **Kurahara H**, Maemura K, Mataki Y, Tanoue K, Iino S, Kawasaki Y, Idichi T, Arigami T, Mori S, Shinden Y, Higashi M, Ueno S, Shinchi H, Natsugoe S. Lung recurrence and its therapeutic strategy in patients with pancreatic cancer. *Pancreatology* 2020; **20**: 89-94 [PMID: 31787525 DOI: 10.1016/j.pan.2019.11.015]

337 **Liu M**, Zhang Y, Yang J, Cui X, Zhou Z, Zhan H, Ding K, Tian X, Yang Z, Fung KA, Edil BH, Postier RG, Bronze MS, Fernandez-Zapico ME, Stemmler MP, Brabletz T, Li YP, Houchen CW, Li M. ZIP4 Increases Expression of Transcription Factor ZEB1 to Promote Integrin α3β1 Signaling and Inhibit Expression of the Gemcitabine Transporter ENT1 in Pancreatic Cancer Cells. *Gastroenterology* 2020; **158**: 679-692.e1 [PMID: 31711924 DOI: 10.1053/j.gastro.2019.10.038]

338 **Ou ZL**, Luo Z, Lu YB. Long non-coding RNA HULC as a diagnostic and prognostic marker of pancreatic cancer. *World J Gastroenterol* 2019; **25**: 6728-6742 [PMID: 31857775 DOI: 10.3748/wjg.v25.i46.6728]

339 **Fu Z**, Jiao Y, Li Y, Ji B, Jia B, Liu B. TYMS presents a novel biomarker for diagnosis and prognosis in patients with pancreatic cancer. *Medicine (Baltimore)* 2019; **98**: e18487 [PMID: 31861032 DOI: 10.1097/MD.0000000000018487]

340 **Bu F**, Zhu X, Yi X, Luo C, Lin K, Zhu J, Hu C, Liu Z, Zhao J, Huang C, Zhang W, Huang J. Expression Profile of GINS Complex Predicts the Prognosis of Pancreatic Cancer Patients. *Onco Targets Ther* 2020; **13**: 11433-11444 [PMID: 33192076 DOI: 10.2147/OTT.S275649]

World Journal of Gastroenterology

Submit a Manuscript: https://www.f6publishing.com

World J Gastroenterol 2021 September 21; 27(35): 5890-5907

DOI: 10.3748/wjg.v27.i35.5890

ISSN 1007-9327 (print) ISSN 2219-2840 (online)

REVIEW

Gastrinoma and Zollinger Ellison syndrome: A roadmap for the management between new and old therapies

Roberta Elisa Rossi, Alessandra Elvevi, Davide Citterio, Jorgelina Coppa, Pietro Invernizzi, Vincenzo Mazzaferro, Sara Massironi

ORCID number: Roberta Elisa Rossi 0000-0003-4208-4372; Alessandra Elvevi 0000-0001-9841-2051; Davide Citterio 0000-0002-0708-8733; Jorgelina Coppa 0000-0003-2466-0524; Pietro Invernizzi 0000-0003-3262-1998; Vincenzo Mazzaferro 0000-0002-4013-8085; Sara Massironi 0000-0003-3214-8192.

Author contributions: Rossi RE designed the research; Rossi RE, Elvevi A, Citterio D, and Massironi S performed the literature search and wrote the first draft of the paper; Rossi RE, Massironi S, Coppa J, Invernizzi P, and Mazzaferro V revised the manuscript for important intellectual content; Rossi RE and Massironi S wrote the final version of the paper; All of the authors approved the final version for publication.

Conflict-of-interest statement: The authors declare no conflict of interest for this article.

Open-Access: This article is an open-access article that was selected by an in-house editor and fully peer-reviewed by external reviewers. It is distributed in accordance with the Creative Commons Attribution NonCommercial (CC BY-NC 4.0) license, which permits others to distribute, remix, adapt, build

Roberta Elisa Rossi, Davide Citterio, Jorgelina Coppa, Vincenzo Mazzaferro, HPB Surgery, Hepatology and Liver Transplantation, ENETS Center of Excellence, Fondazione IRCCS Istituto Nazionale Tumori (INT, National Cancer Institute), Milan 20133, Italy

Roberta Elisa Rossi, Department of Pathophysiology and Transplantation, University of Milan, Milan 20122, Italy

Alessandra Elvevi, Pietro Invernizzi, Sara Massironi, Division of Gastroenterology and Center for Autoimmune Liver Diseases, Department of Medicine and Surgery, University of Milano-Bicocca, Monza 20900, Italy

Alessandra Elvevi, Pietro Invernizzi, Sara Massironi, European Reference Network on Hepatological Diseases (ERN RARE-LIVER), San Gerardo Hospital, Monza 20033, Italy

Vincenzo Mazzaferro, Department of Oncology and Hemato-Oncology, University of Milan, Milan 20122, Italy

Corresponding author: Roberta Elisa Rossi, MD, PhD, HPB Surgery, Hepatology and Liver Transplantation, ENETS Center of Excellence, Fondazione IRCCS Istituto Nazionale Tumori (INT, National Cancer Institute), *via* Giacomo Venezian, Milan 20133, Italy.
robertaelisa.rossi@gmail.com

Abstract

Zollinger-Ellison syndrome (ZES) associated with pancreatic or duodenal gastrinoma is characterized by gastric acid hypersecretion, which typically leads to gastroesophageal reflux disease, recurrent peptic ulcers, and chronic diarrhea. As symptoms of ZES are nonspecific and overlap with other gastrointestinal disorders, the diagnosis is often delayed with an average time between the onset of symptoms and final diagnosis longer than 5 years. The critical step for the diagnosis of ZES is represented by the initial clinical suspicion. Hypergastrinemia is the hallmark of ZES; however, hypergastrinemia might recognize several causes, which should be ruled out in order to make a final diagnosis. Gastrin levels > 1000 pg/mL and a gastric pH below 2 are considered to be diagnostic for gastrinoma; some specific tests, including esophageal pH-recording and secretin test, might be useful in selected cases, although they are not widely available. Endoscopic ultrasound is very useful for the diagnosis and the local staging of the primary tumor in patients with ZES, particularly in the setting of multiple endocrine neoplasia type 1. Some controversies about the management of these

upon this work non-commercially, and license their derivative works on different terms, provided the original work is properly cited and the use is non-commercial. See: http://creativecommons.org/licenses/by-nc/4.0/

Manuscript source: Invited manuscript

Specialty type: Gastroenterology and hepatology

Country/Territory of origin: Italy

Peer-review report's scientific quality classification

Grade A (Excellent): 0
Grade B (Very good): 0
Grade C (Good): C
Grade D (Fair): 0
Grade E (Poor): 0

Received: March 15, 2021
Peer-review started: March 15, 2021
First decision: April 17, 2021
Revised: April 29, 2021
Accepted: August 10, 2021
Article in press: August 10, 2021
Published online: September 21, 2021

P-Reviewer: Prisciandaro M
S-Editor: Gao CC
L-Editor: Filipodia
P-Editor: Xing YX

tumors also exist. For the localized stage, the combination of proton pump inhibitory therapy, which usually resolves symptoms, and surgery, whenever feasible, with curative intent represents the hallmark of gastrinoma treatment. The high expression of somatostatin receptors in gastrinomas makes them highly responsive to somatostatin analogs, supporting their use as anti-proliferative agents in patients not amenable to surgical cure. Other medical options for advanced disease are super-imposable to other neuroendocrine neoplasms, and studies specifically focused on gastrinomas only are scant and often limited to case reports or small retrospective series. The multidisciplinary approach remains the cornerstone for the proper management of this composite disease. Herein, we reviewed available literature about gastrinoma-associated ZES with a specific focus on differential diagnosis, providing potential diagnostic and therapeutic algorithms.

Key Words: Gastrinoma; Zollinger-Ellison syndrome; Neuroendocrine neoplasms; Pancreatic neuroendocrine neoplasm; Duodenal neuroendocrine neoplasm; Diagnosis; Therapy

©The Author(s) 2021. Published by Baishideng Publishing Group Inc. All rights reserved.

Core Tip: As symptoms of Zollinger-Ellison syndrome are nonspecific and overlap with other gastrointestinal disorders, most of these patients are usually referred to general gastroenterologists, leading to a diagnostic delay. A better disease awareness together with the maintenance of a high index of suspicion are necessary to make the final diagnosis. The proper management of Zollinger-Ellison syndrome due to a gastrinoma include both the medical treatment for symptom's relief and surgery whenever feasible with curative intent; the multidisciplinary approach, with close cooperation between gastroenterologists and surgeons, and the referral to tertiary centers with great expertise in the neuroendocrine field are mandatory.

Citation: Rossi RE, Elvevi A, Citterio D, Coppa J, Invernizzi P, Mazzaferro V, Massironi S. Gastrinoma and Zollinger Ellison syndrome: A roadmap for the management between new and old therapies. *World J Gastroenterol* 2021; 27(35): 5890-5907
URL: https://www.wjgnet.com/1007-9327/full/v27/i35/5890.htm
DOI: https://dx.doi.org/10.3748/wjg.v27.i35.5890

INTRODUCTION

Zollinger-Ellison syndrome (ZES) was firstly described in 1955 as associated with a neuroendocrine neoplasm (NEN) capable of ectopic gastrin secretion (namely gastrinoma)[1], resulting in gastric acid hypersecretion, which typically leads to gastroesophageal reflux disease (GERD), recurrent peptic ulcers, and chronic diarrhea. The terms gastrinoma and ZES have been frequently used as synonymous, although gastrinoma refers to the NEN secreting gastrin, whereas ZES refers to the clinical manifestations of the disease. ZES has an incidence of 1-1.5 cases/million per year[2]. Gastrinomas are NENs located in the duodenum (70%), pancreas (25%), and rarely (5%), in other sites, including stomach, liver, ovary, and lung. Gastrinoma is the most frequent functioning duodenal NEN and the second most frequently occurring functional pancreatic NEN (pNEN), following insulinoma; in turn, 15% of functioning pNENs is represented by gastrinoma. It may be sporadic, which is generally diagnosed between the ages of 50 and 70 years with a male to female ratio of 1.5-2:1 [3], whilst 20%-30% of the patients develop ZES in the context of a genetic syndrome known as multiple endocrine neoplasia type 1 (MEN-1)[4].

The diagnosis of ZES is not always straightforward due to both non-specific symptoms and confounding factors including proton pump inhibitor (PPI) therapy, which might temporarily relieve symptoms. Furthermore, as these patients tend to be referred to gastroenterologists because of diarrhea and/or reflux disease disorder, despite a better awareness of the disease, the diagnosis might be challenging for those

gastroenterologists with low experience in the neuroendocrine setting as well as for many oncologists who are less used to dealing with diarrhea and reflux disease. As a consequence, the average time between the onset of symptoms and the final diagnosis is often longer than 5 years[5,6], and nearly 25% of patients are metastatic at the first diagnosis and show a worse prognosis when compared to non-metastatic patients in whom the surgical management is associated with a promising 15-year survival rate of > 80%[7].

Furthermore, some controversies about the management of these tumors still exist, particularly regarding the exact role of surgery or medical treatment and the possible role of somatostatin analogs (SSAs)[3]. Given that gastrinoma and ZES need both a proper medical treatment for symptom relief and a surgical procedure whenever feasible, the multidisciplinary approach, with close cooperation between clinicians and surgeons, remains the cornerstone for proper management of this composite disease, which should be always referred to tertiary centers.

Herein, we review from a critical point of view current knowledge about gastrinoma-associated ZES, also providing potential diagnostic and therapeutic algorithms based on both evidence from literature and own personal experience.

METHODOLOGY

Bibliographical searches were performed in PubMed using the following keywords: Gastrinoma; Zollinger Ellison syndrome; neuroendocrine neoplasms; pancreatic neuroendocrine neoplasm; duodenal neuroendocrine neoplasm; diagnosis; therapy; guidelines. We searched for all relevant articles published over the last 10 years. The reference lists from the studies returned by the electronic search were manually searched to identify further relevant reports. The reference lists from all available review articles, primary studies, and proceedings of major meetings were also considered. Articles published as abstracts were included, whereas non-English language papers were excluded.

CLINICAL PRESENTATION

ZES is characterized by gastric acid hypersecretion and consequent hyperchlorhydria resulting in severe acid-related peptic disease and diarrhea. The symptoms usually resolve when gastric acid secretion is controlled pharmacologically with PPIs[8,9]; of note, the disappearance of diarrhea following PPI treatment is typical of ZES and represents one of the factors contributing to the diagnostic delay. According to data from the literature, common symptoms include abdominal pain (75%), diarrhea (73%), heartburn (44%), and weight loss (17%)[6,8,10]. As these symptoms are both not specific and often less severe due to concomitant PPI treatment, the final diagnosis is often delayed and patients are diagnosed with irritable bowel syndrome or reflux disease by gastroenterologists with low or no knowledge of the disease[8,11].

The endoscopic features are also not specific and might include erosions and ulcers [12], however, ZES patients often present with multiple ulcers located at unusual sites, *e.g.*, beyond the first or second portion of the duodenum[8,13]. Furthermore, enlarged gastric folds can be present in more than 90% of patients with ZES[11].

One should keep in mind that approximately 25% of gastrinomas occur in the context of MEN-1, which is characterized by the presence of parathyroid, pancreatic-duodenal, and pituitary tumors[14]; thus the occurrence of unexplained hypercalcemia might be a sign for possible MEN-1 syndrome-associated ZES[15,16], also taken into account that primary hyperparathyroidism is generally the presenting feature in the majority of cases of MEN-1 syndrome[8,16,17]. Of note, parathyroidectomy usually improves gastrin levels and basal acid output[16]. Finally, in ZES/MEN-1 patients, type 2 gastric NENs might occur[3].

DIFFERENTIAL DIAGNOSIS

Symptoms of ZES are nonspecific and overlap with other gastrointestinal (GI) disorders, which explains the frequent diagnostic delay.

As concerns chronic diarrhea in ZES, this is sustained by hyperchlorhydria and sodium and water malabsorption due to hypergastrinemia[18]. As afore-mentioned,

diarrhea is one of the most frequent symptoms in ZES; up to 75% of patients manifest diarrhea[19], and this could be the sole presenting symptom in 3%-10% of the patients [20]. Moreover, chronic diarrhea is one of the most frequent symptoms requiring gastroenterologist referral; its diagnostic workup could be challenging because many different causes could cooperate to diarrhea development and recurrence (*e.g.*, dietary habits, drugs). Recent British Society of Gastroenterology (BSG) guidelines for chronic diarrhea[21] tried to classify different causes of chronic diarrhea (Table 1) and to standardize a diagnostic work-up in these patients. Since hormone-secreting tumors are considered rare causes of chronic diarrhea, BSG guidelines suggest testing patients for these tumors only when other causes of diarrhea have been excluded. From a clinical point of view, the association between chronic diarrhea with both other ZES suggestive symptoms (*e.g.*, chronic peptic ulcer disease) and clinical response to PPIs may be helpful in diagnosing this challenging syndrome, taking into account that the delay in diagnosis of ZES remains between 6 to 9 years from the first clinical presentation[9,19].

Abdominal pain and heartburn are frequently reported as symptoms of ZES[9]. As well as diarrhea, they are sustained by hyperchlorhydria, which directly damages GI mucosa, causing ulcers and erosions. Abdominal pain could be associated with peptic ulcers, which, differently from *Helicobacter pylo*ri or non-steroidal anti-inflammatory drug-related ulcers, are multiple, located at unusual locations (*e.g.*, the third part of the duodenum, small bowel) and complicated by bleeding, penetration, perforation, or strictures[8,13,19].

Similar to peptic ulcer disease, chronic GERD is one of the most frequent manifestations of ZES[13]. Heartburn and regurgitation are the most typical symptoms, which are super-imposable to symptoms associated with typical GERD; differently from the typical syndrome, patients with ZES often present esophageal strictures due to over-exposition to acid reflux.

Again, the association between these symptoms and chronic diarrhea, after exclusion of other common GI etiologies, might raise the suspicion of ZES, which requires specific tests in order to get the final diagnosis.

DIAGNOSIS

The diagnosis of ZES is quite challenging, also considered that the critical point is the initial suspicion of ZES. A suggested diagnostic algorithm is represented in Figure 1.

ZES is a clinical syndrome characterized by the following triad: (1) gastric acid hypersecretion, sustained by (2) fasting serum hypergastrinemia causing (3) peptic ulcer disease and diarrhea[1]. Hypergastrinemia is sustained by a gastrinoma, a rare NEN (located primarily in the duodenum or pancreas) that secretes gastrin.

Since ZES symptoms can be explained almost entirely by acid hypersecretion, PPIs, which significantly decrease acid secretion, can mitigate or resolve ZES symptoms, making ZES diagnosis even more challenging than in the past[9,22], but avoiding severe ZES complications.

Hypergastrinemia is the hallmark of ZES; however, hypergastrinemia might recognize several causes, which should be ruled out in order to make a final diagnosis of ZES[23]. In detail, it can be distinguished between (1) appropriate hypergastrinemia, due to atrophic gastritis (with or without pernicious anemia), anti-secretory therapy (PPIs or high-dose histamine H2-receptor antagonist, namely famotidine), chronic renal failure, *Helicobacter pylori*-related pan-gastritis, vagotomy, and (2) inappropriate hypergastrinemia that can be observed in ZES (sporadic or associated with MEN-1), antral-predominant *Helicobacter pylori* infection, retained-antrum syndrome, gastric-outlet obstruction, extensive small-bowel resection.

The diagnosis of ZES requires the demonstration of inappropriate gastrin secretion associated with gastric hyperchlorhydria, which corresponds to a gastric pH < 2[5]. Normal fasting gastrin levels are < 100 pg/mL; levels > 300 pg/mL are highly suspicious, and levels > 1000 pg/mL together with a gastric pH below 2 are considered to be diagnostic for gastrinoma[2,9,24]. Naso-gastric tube aspiration has classically been used to estimate gastric pH, but it can be uncomfortable for patients and can underestimate gastric acid output; alternatively, gastric pH can be measured during upper GI endoscopy, by aspiration of gastric juice for pH determination using either pH paper or a pH meter; while endoscopic sampling was shown to overestimate total acid volume, it provided more reproducible results and offered greater patient tolerance than nasogastric tube placement[5,23,25,26]. To avoid false-negative results, fasting serum gastrin levels and gastric pH should be measured after PPI withdrawal

Table 1 Differential diagnosis of chronic diarrhea[21]

Common	Infrequent	Rare
IBS-diarrhea	Small bowel bacterial overgrowth	Small bowel enteropathies (*i.e.* Whipple's disease, tropical sprue, amyloid, *etc.*)
Bile acid diarrhea	Mesenteric ischemia	Hypoparathyroidism
Diet (artificial sweeteners, caffeine, FODMAP malabsorption, *etc.*)	Lymphoma	Addison's disease
Colonic neoplasia	Surgical causes (small bowel resection, incontinence, *etc.*)	**Hormone secreting tumors** (*i.e.* VIPoma, gastrinoma, carcinoid)
IBD	Chronic pancreatitis	Autonomic neuropathy
Celiac disease	Radiation enteropathy	Factitious diarrhea
Drugs (antibiotics, NSAID, *etc.*)	Pancreatic carcinoma	Brainerd diarrhea
Overflow diarrhea	Hyperthyroidism	
	Diabetes	
	Chronic infections (*i.e.* giardiasis)	
	Cystic fibrosis	

FODMAP: Fermentable Oligosaccharides, Disaccharides, Monosaccharides, and Polyols; IBS: Irritable bowel syndrome; NSAID: Nonsteroidal anti-inflammatory drugs.

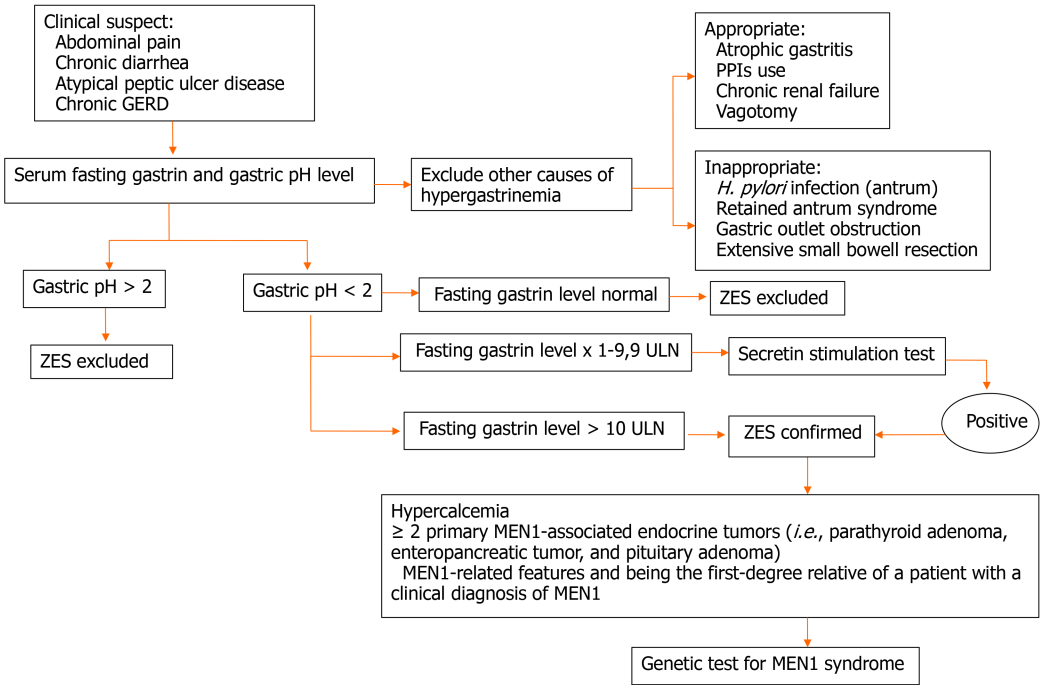


Figure 1 A suggested diagnostic algorithm is depicted. GERD: Gastroesophageal reflux disease; *H. pylori*: *Helicobacter pylori*; MEN-1: Multiple endocrine neoplasia type 1; PPIs: Proton pump inhibitors; ULN: Upper limit of normal; ZES: Zollinger Ellison syndrome.

[2,6,27]. However, PPI withdrawal could be dangerous for ZES patients, because it could bring a dramatic increase in gastric acid secretion, hence causing severe peptic ulcer disease and its complications[23], thus the decision to stop the treatment should be tailored to every single patient. Then, it is usually suggested to start histamine H2-receptor antagonists (*i.e.* famotidine) as soon as PPIs are stopped in order to prevent complications due to gastric acid hypersecretion. Having a shorter duration of action compared to PPIs, H2-antagonists could be used until the evening before serum gastrin and gastric pH tests[23].

Imaging and ultrasound endoscopy (endoscopic ultrasound)

Localization of the primary tumor and its metastases is the first diagnostic step when ZES associated with gastrinoma is suspected.

Contrast-enhanced computed tomography (CT) scan is useful to identify primary tumor > 1 cm, pancreatic head tumors, and liver metastases, with a sensitivity between 59% and 78% and a specificity between 95% and 98%, respectively. Conversely, sensitivity decreases for tumor size < 1 cm and extra-pancreatic locations[28,29].

Contrast-enhanced magnetic resonance imaging (MRI) showed high specificity (namely 100%) in detecting small pancreatic tumors and liver metastases, whereas sensibility is sub-optimal varying from 25% to 85%. Of note, MRI showed a higher sensibility for liver metastases detection when compared to CT scan[28,30].

Somatostatin receptor scintigraphy (Octreoscan®) has been used to localize gastrinomas[8,31]. This test involves the administration of indium radio-labeled octreotide, which binds selectively to somatostatin receptors found on gastrinoma cells. It showed quite good sensitivity (between 77% and 78%) and a good specificity (93%-94%) for primary tumor detection and its metastases, although sensitivity decreases for small tumors (< 1 cm)[32]. Diagnostic accuracy of somatostatin receptor scintigraphy (Octreoscan®) can be improved by performing it in combination with single-photon emission CT (SRS-SPECT)[28]. Different studies showed higher sensitivity and specificity in primary tumor detection, 78%-88% and 97%, respectively, when compared to Octreoscan® alone[33-35].

In more recent years, somatostatin receptor positron emission tomography (PET) techniques have shown great promise for improving the localization of gastrinomas as well as other NENs[36-39] and for the detection of distant metastases, including bone lesions. The radioisotope ^{68}Ga can be ligated to peptides that bind to somatostatin receptors found in abundance on the NEN surface[36]. This technique showed a higher sensibility and specificity (72%-100% and 83%-100%, respectively) when compared to the aforementioned diagnostic techniques in localizing the primary tumor, especially small size tumors[36,37,40]. Combining ^{68}Ga-radiotracers with traditional CT scans (PET/CT) further enhances diagnostic accuracy compared to PET alone, showing a sensitivity of 93% and a specificity of 96% in primary tumor detection [41]. Gallium-^{68}PET-scan should be always included in the diagnostic pathway of all NENs, including gastrinoma, in order to both identify the primary tumor and stage the disease.

Endoscopic ultrasound (EUS) has become an important diagnostic tool to localize gastrinomas, particularly small (*i.e.* < 2 cm) pancreatic lesions; its sensitivity and specificity are 75%-100% and 95%, respectively, for pancreatic tumors. Unfortunately, its sensitivity dramatically decreases in cases of duodenal localization, ranging from 38% to 63%[28,42]. A further advantage of this technique is the possibility of taking cytologic/histologic samples through a fine needle aspiration/biopsy (FNA/B) to confirm the diagnosis of NEN, even if false-negative results are possible mainly due to poor sampling adequacy. EUS-FNA/B is now considered the primary sampling technique for pancreatic tumors, with a sensitivity ranging between 80% and 90%, specificity at 96%[43], and a sampling adequacy rate of 83%-93%[44].

When used as a screening modality in asymptomatic patients with MEN-1, EUS has been reported to be more accurate than CT scan to detect smaller tumors[45]. Therefore, its diagnostic ability has led experts to recommend it as an annual screening modality for all patients with MEN-1, although recent evidence suggests that the growth rate of small pNENs (*i.e.* < 2 cm) is low and that EUS screening frequency can likely be extended[14,46].

Esophageal pH-recording

Since one of the most common symptoms of ZES is GERD, it could be argued that esophageal pH-monitoring could be a useful tool to diagnose ZES. Recent BSG guidelines for esophageal manometry and esophageal pH monitoring[47] stated indications to perform esophageal pH-monitoring, also including as an indication GERD symptoms that did not respond to double dose of PPIs. This technique allows to diagnose an increased acid exposure, to evaluate the association between symptoms and acid or non-acid reflux, and to identify different phenotypes of upper symptoms (*i.e.* non-erosive reflux disease, hypersensitive esophagus, and functional heartburn).

ZES is not usually included in diagnosis performed by esophageal pH-monitoring, and, consequently, ZES reference standard for esophageal pH-monitoring is lacking. However, evidence of a high number of acidic reflux episodes (*i.e.* esophageal pH < 4), a high number of long (*i.e.* > 5 min) reflux episodes, a high percentage of time with esophageal pH < 4, both on a double dose of PPIs and off PPIs, could raise the

suspicion of abnormal gastric acid secretion. This hypothesis should be confirmed by prospective studies; however, considering the rarity of this syndrome, it would be very difficult to obtain standard values to use in clinical practice; therefore, despite its potential utility, this test is not currently included in the standard diagnostic workup of gastrinoma.

Secretin provocative test

Secretin provocative test in ZES diagnosis founds its application in controversial cases, that is patients with suspected ZES, gastric pH < 2 but fasting serum gastrin < × 10 upper limit of normal[9]. To perform a secretin stimulation test, fasting gastrin levels are obtained before intravenous (IV) administration of secretin and then 2, 5, and 10 min after infusion[25]. Patients with gastrinomas exhibit an inappropriate increase in gastrin production in response to secretin infusion[9]. This mechanism can be explained in part by the fact that secretin receptors are expressed directly on the gastrinoma cell surface[48]. Different cut-offs for positive tests have been proposed, including an absolute increase in gastrin concentration ≥ 110 pg/mL or ≥ 200 pg/mL or a 50% increase in gastrin concentration[49]. However, previous data suggested that a positive secretin-provocative test (≥ 120 pg/mL increase) has a sensitivity of 94% and specificity of 100%, respectively[50]. According to data from the literature, a false-negative response can occur in 6% to 20% of patients[51,52], whereas false-positive responses, ranging from 15% to 39% in different studies[52,53], are found in patients with pernicious anemia or chronic PPI use.

In order to reduce the risk of false-positive results, PPI treatment should be withdrawn, but, again, the decision should be discussed in a case-by-case manner to limit the risk of severe complications (*e.g.*, perforation or bleeding). This might partially explain the reason why the secretin test can be difficult to be performed and should be reserved for strictly selected cases when the diagnosis is not straightforward.

MEN-1

MEN-1 is an autosomal dominant disorder, whose incidence has been estimated from random postmortem studies to be 0.25%, and to be 1%-18% in patients with primary hyperparathyroidism, 16%-38% in patients with gastrinomas, and less than 3% in patients with pituitary tumors[14]. From a clinical point of view, MEN-1 syndrome includes the occurrence of parathyroid adenoma (90%), entero-pancreatic tumor (30%-70%), being gastrinoma the most frequent (40%), and pituitary adenoma (30%-40%). Other tumors that might occur in MEN-1 patients are adrenal cortical tumor (40%), pheochromocytoma (< 1%), bronchopulmonary NEN (2%), thymic NEN (2%), gastric NEN (10%), lipomas, (30%), angiofibromas (85%), collagenomas (70%), and meningiomas (8%)[14].

In patients with an established diagnosis of gastrinoma-related ZES, MEN-1 syndrome might be present in approximately 25% of the cases. The presence of hypercalcemia due to hyperparathyroidism is one of the first signs. However, the diagnosis might be challenging in this specific setting as ZES does not usually develop in the absence of primary hyperparathyroidism, and hypergastrinemia has also been reported to be associated with hypercalcemia as a confounding factor[15]. Furthermore, parathyroidectomy leads to restoration of normocalcemia and improvement in clinical symptoms and biochemical abnormalities in as many as 20% of MEN-1 patients with ZES[14]. Moreover, staging and localization with CT or MRI is even more challenging in the setting of MEN-1 due to the presence of numerous small tumors < 1 cm in size[27,28]. A high index of suspicion must be maintained if a patient with chronic diarrhea and unexplained peptic ulcer disease presents with primary hyperparathyroidism. The genetic test for MEN-1 syndrome should be performed in a selected subgroup of patients, namely (1) in patients with two or more primary MEN-1-associated endocrine tumors (*e.g.*, parathyroid adenoma, entero-pancreatic tumor, and pituitary adenoma) or hypercalcemia associated with an endocrine tumor; and (2) patients showing MEN-1-related features and being the first-degree relative of a patient with a clinical diagnosis of MEN-1[14].

THERAPY

The management of gastrinoma and ZES includes both a proper medical treatment for symptom's relief and surgery with curative intent whenever feasible. A proposed therapeutic algorithm is represented in Figure 2.

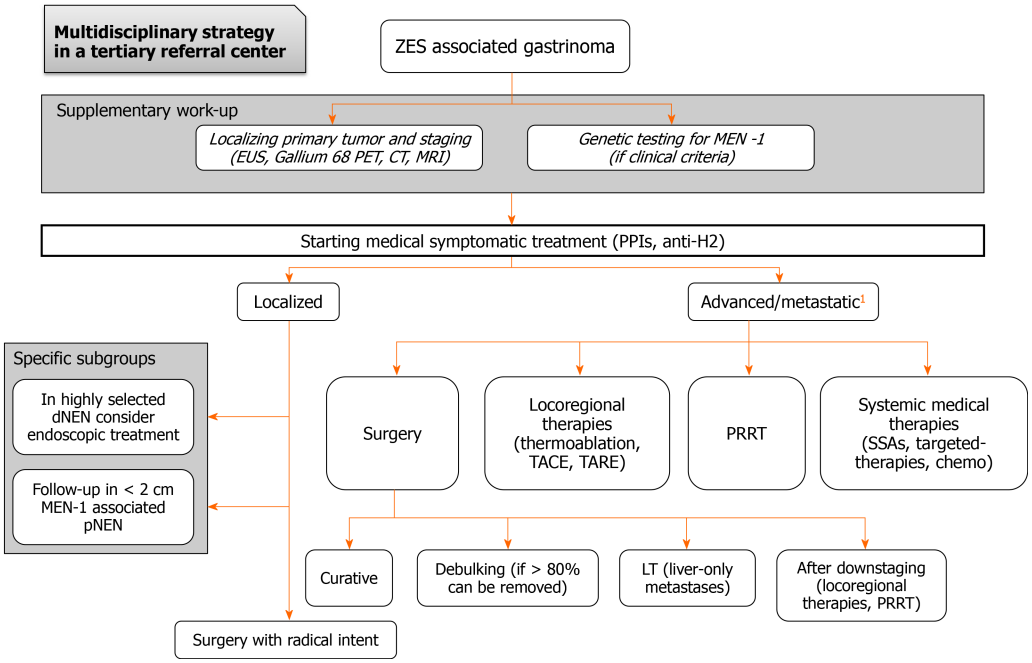


Figure 2 A proposed therapeutic algorithm is represented based on both evidence from literature and personal own experience. [1]Allocation driving prognostic factors are performance status, age, metastatic disease burden and pattern, comorbidities. CT: Computed tomography; dNEN: Duodenal neuroendocrine neoplasm; EUS: Endoscopic ultrasound; H2: Histamine receptor 2: LT: Orthotopic liver transplantation; MEN-1: Multiple endocrine neoplasia type 1; MRI: Magnetic resonance imaging; PET: Positron emission tomography; pNEN: Pancreatic NEN; PPIs: Proton pump inhibitors; PRRT: Peptide-radioreceptor therapy; SSAs: Somatostatin analogs; TACE: Transarterial chemoembolization; TARE: Transarterial radioembolization; ZES: Zollinger Ellison syndrome.

Surgery

The role of surgery in the treatment of gastrinoma has changed completely from the introduction of PPIs in the 1980s. In fact, before the advent of an effective anti-secretory therapy, surgery was performed to control acid hypersecretion, mainly removing the target cells of gastrin through total gastrectomy. These operations were, by the way, affected by a high mortality rate due to acid-related complications in the postoperative course. With the use of PPIs, gastric hypersecretion was no longer a problem, and the main determinant of prognosis became the gastrinoma itself because of its malignant potential and surgical excision started to be proposed as a potentially curative therapy. From 1981, the National Institute of Health began a prospective study recruiting patients with ZES for surgical therapy, with a well-designed surgical protocol in order to capture the long-term results of the best available surgical approach. The study reported a 10-year overall survival (OS) and disease-free survival (DFS) of 94% and 34%, respectively[54]. Therefore, surgery has gradually changed its role and gastrinoma resection has started to be increasingly proposed to patients eligible for resection. Currently, across the most important guidelines, surgical excision is generally recommended either for sporadic gastrinoma or for MEN-1 associated gastrinoma if complete tumor removal is possible[2,55-58]. Subsequent studies reported a 20 year OS of 58%-71%, a 20-year disease-related survival of 73%-88%[59], and a 10-year DFS of 25%-50%[60]. Surgery of the primary tumor also demonstrated to reduce the occurrence of liver metastases[61-63], which are one of the main determinants of prognosis, and to improve DFS in comparison with non-surgical management[62].

The majority of gastrinomas (from 60% to 90% depending on the series)[42,60] occur in the duodenum, and, since these are often very small lesions (less than 1 cm) and located at the submucosal layer, tumor detection is not so straightforward. Therefore, the surgical technique should follow a stepwise approach to search for the tumor even in case of negative preoperative imaging. In this context, surgery has firstly a diagnostic purpose, which is quite uncommon in modern surgery and, given the peculiarity of this technique and the rarity of the disease, it should be performed by experienced surgeons in tertiary referral centers. After a complete abdominal exploration, the duodenum and the pancreatic head are mobilized (Kocher maneuver) and carefully palpated. Intra-operative ultrasound with a linear probe is then performed on the duodenum and pancreas looking for the primary tumor and on the liver in search for liver metastases. Intra-operative endoscopy is performed thereafter

advancing the scope into the duodenum; duodenal gastrinomas may be found through trans-illumination of the bowel wall as non-trans-illuminated spots. If a lesion is identified, it should be marked with a suture and the duodenum opened around it for a full-thickness excision. If the described steps fail to reveal any lesion, a 3 cm longitudinal incision is made on the anterior aspect of the second portion of the duodenum, and the entire duodenal wall is palpated. Suspicious lesions are excised with a full-thickness rim of normal tissue and sent for pathology. The duodenum is then closed transversally, if possible, to minimize the risk of strictures[64,65]. In the hands of an experienced surgeon, lesions could be found in 98% of imaging-negative ZES patients, with a 50% curative rate[59], similar to that of imaging-positive patients. These findings suggest that surgery should be performed as soon as possible in sporadic ZES, despite negative imaging findings. Pancreatic gastrinomas should be enucleated if located 3 mm or farther from the main pancreatic duct. Conversely, lesions that are closer to the pancreatic duct require distal pancreatectomy with or without splenectomy if located in the body or tail of the gland and pancreaticoduodenectomy if located in the head/neck. Pancreaticoduodenectomy or distal pancreatectomy may be necessary also for local recurrence after enucleation[66].

Regional lymph nodes should always be removed because nodal metastases are present in almost half of the patients[54,67] and lymphadenectomy has been associated with increased DFS[68], as reported also for other pNENs[69-71]. The presence of primary gastrinoma located in a lymph node is controversial, however, several studies reported long disease-free survivors after resection of only a positive lymph node[72, 73], and this supports the role of routine lymphadenectomy.

Since pancreaticoduodenectomy provides complete removal of the regional lymph nodes of the pancreatic head, the results in terms of DFS are better with respect to enucleation because of the higher chance of radicality[54,67]. However, given the high postoperative morbidity and the good prognosis also of patients with small residual disease, pancreaticoduodenectomy is not recommended as the standard operation for these patients[2,55-58]. Generally, the indication for surgery should always follow a thorough risk/benefit assessment within a multidisciplinary tumor board aiming at maximum radicality and minimum morbidity. This is particularly the case for MEN-1 patients; in these patients, who have generally an earlier age of onset, pNENs should be resected in low-risk patients, and surgery is generally recommended for tumors larger than 2 cm[14,58]. However, according to most authorities, as well as all guidelines, surgical resection for an attempted cure should be performed in ZES patients whenever possible[2,27,58]. This is particularly true for functioning duodenal NENs, including gastrinomas, which have been reported to express a high metastatic potential[74], thus a radical surgical approach should be the first choice in this specific setting. However, in highly selected cases (*i.e.* duodenal lesions ≤ 1 cm, limited to the submucosal layer and without lymph nodal involvement), endoscopic resection might also be considered, although the risk of undetected micro-metastases might represent an issue.

Another controversial issue is laparoscopic surgery; while it is widely adopted for pNENs, its role for gastrinomas is limited to patients in whom preoperative imaging gives an accurate definition of tumor location. Unfortunately, as already mentioned, extensive exploration is often needed for diagnostic purposes. In these cases, laparoscopy is inadequate, and laparotomy is mandatory.

The role of surgical resection in ZES patients with advanced metastatic disease or even with extensive invasive localized disease is not well-defined. In this setting, the possibility of surgical removal of all resectable tumors (cytoreductive surgery, debulking surgery) should be considered, and surgery is generally recommended if ≥ 80% of all disease can be removed (generally feasible in 5%-15% of all metastatic gastrinomas), although only a few reports containing primarily gastrinomas treated with this approach are currently available[10,72].

Finally, in highly selected metastatic gastrinomas, with liver-only metastases and fulfilling strict inclusion criteria, liver transplantation might be considered, even if its use remains controversial and the risk of tumor recurrence represents an issue[58].

Liver-directed therapies

Studies specifically focused on liver-directed therapies in the context of gastrinomas are scant; however, as for other NENs, the embolization approaches in the setting of gastrinoma are generally reserved for patients with metastatic unresectable hepatic metastases either limited to the liver or with a liver-predominant disease, particularly if locally symptomatic[10,58]. Of note, liver-directed therapies are used less frequently in ZES than in other metastatic NENs, because in ZES, the hormone excess-state can be well-controlled medically.

Medical treatment

Among functioning NENs, gastrinoma is the most frequent type. There are two therapeutic goals in the management of patients with gastrinoma: The control of gastric acid hypersecretion and the treatment of the tumor itself.

Antisecretory medications

The therapy for syndrome control is based on PPI (*e.g.*, omeprazole, esomeprazole, lansoprazole, pantoprazole, *etc.*), which are highly effective drugs and considered the drugs of choice for suppressing acid secretion. PPIs effectively block gastric acid secretion by irreversibly binding to and inhibiting the hydrogen-potassium ATPase pump on the luminal surface of the parietal cell membrane. Theoretically, the choice and titration of anti-secretory therapy should be guided by the parameters of gastric acid secretions such as basal acid output (to reduce it below 10 mEq/h)[75], since using symptoms alone as a signal of efficacy might be misleading, even if in many centers these methods are not available. Therefore, in most cases, PPI therapy is started at an empirical maximized dosage. The recommended initial dose of omeprazole is 60 mg/daily or esomeprazole 120 mg/daily, lansoprazole 45 mg/daily, rabeprazole 60 mg/daily, pantoprazole 120 mg/daily, divided, twice-a-day[75-78]. The type of PPI used seems not to be of relevance and a systematic review of 12 randomized trials examining the relative effectiveness of different PPI doses and dosing regimens found no consistent differences in symptom resolution and esophagitis healing rates[79]. IV PPIs are indicated in patients with clinically significant upper GI bleeding from a suspected peptic ulcer. Omeprazole, pantoprazole, and esomeprazole are the only PPIs available as an IV formulation. The other patients can be treated with oral preparation.

As concerns efficacy, PPIs have significantly decreased the morbidity and mortality resulting from severe ulcer disease[80]. In 60% of patients, ulcer healing occurs within 2 wk; in 90%-100% of patients, healing occurs within 4 wk. PPIs are generally safe, even when used in high doses.

Once an effective clinical control of the peptic disease has been achieved, a gradual dose reduction is generally suggested[81,82]. In a study by Metz *et al*[83], 37 patients received high-dose omeprazole for almost 2 years, and nearly 50% were able to lower the dose down to 20 mg once daily, with 95% of patients experiencing safe long-term reductions in their medication dose. PPIs are generally well tolerated and can control hypergastrinemia in ZES for > 10 years (although some patients experience low vitamin B12 levels)[84].

No tachyphylaxis has been described. Therefore, the long duration of action, the fewer adverse effects, and the high potency make them superior to H2 blockers.

Regarding the use of H2-receptor antagonists in ZES, the dose usually is 4-8 times higher than the dose administered to patients with peptic ulcer disease. Although a good success rate exists, this treatment has been reported to fail in 50% of patients. Therefore, these drugs are never the first choice.

Only when PPIs are unable to control gastric acid secretion, SSAs can be considered, as they reduce gastrin secretion, even if they do not represent a first-line treatment at least for symptom control.

Even if this is not a treatment currently approved in localized gastrinoma, it is worth mentioning that in animals, the cholecystokinin-2 receptor antagonist YF476 has been shown to inhibit the development of enterochromaffin-like cell-tumors in susceptible animals with induced hypergastrinemia. Therefore, this drug could represent a potential option in ZES, not only to inhibit hypergastrinemia but also to prevent gastric NEN type 2 (*e.g.*, associated with ZES/MEN-1). Furthermore, there continues to be interest in the development of cholecystokinin-2 receptor antagonists as anti-secretory agents[85]. However, strong evidence supporting the role of these molecules in this specific setting is lacking.

Anti-proliferative treatment

Approximately one-third of ZES patients present with metastatic disease to the liver [10,86]. There are several systemic therapeutic options for advanced gastrinoma, not substantially different from the ones for other NENs, however, studies evaluating specific response rates in gastrinomas alone are limited.

SSAs like octreotide and lanreotide are highly effective in controlling the symptoms associated with hormone hypersecretion in all functioning tumors[87,88]; furthermore, they can reduce gastrin levels and their anti-proliferative effect has been demonstrated in PROMID and CLARINET studies[89,90]. However, in these studies only a few cases of gastrinoma were included, and, even if different case reports and case series suggested the role of SSAs in controlling gastrin secretion and symptoms in ZES

patients[91-94], to date only a few studies with a very low number of patients investigated specifically the role of SSAs in ZES[3].

The multitargeted tyrosine kinase inhibitor, sunitinib, has demonstrated an improved progression-free survival from 5.5 mo to 11.4 mo in metastatic pNENs[95]. Moreover, based on the results of two randomized, double-blind, prospective, placebo-controlled studies, the mammalian target of rapamycin-inhibitor everolimus has been approved in advanced both pancreatic[96] and extra-pNENs[96]. However, there are no specific studies on the effects of sunitinib/everolimus in the specific setting of gastrinomas.

Streptozocin, 5-fluorouracil, and doxorubicin have been used, with the response rate reported to be as high as 69%[97]. Despite these reported response rates, the true radiologic response rate is more probably between 10% and 40%[98,99]. More recently, anti-proliferative activity has also been shown for temozolomide. Data came from retrospective studies[100] as well as from a prospective randomized study comparing capecitabine plus temozolomide to temozolomide alone in pNENs that revealed a median progression-free survival longer in the combination arm (22.7 mo *vs* 14.4 mo, hazard ratio 0.58, $P = 0.023$), but satisfactory in both[101]. Moreover, a recent real-world analysis confirmed the combination of capecitabine and temozolomide as an active treatment for metastatic NENs[102]. Because of these studies, the use of capecitabine plus temozolomide has become routine for advanced pNENs, including gastrinomas.

Lastly, peptide receptor radionuclide therapy (PRRT) may be the most promising systemic therapy, and it has been repeatedly reported as particularly useful for symptom relief in functioning forms, even if this aspect might be less important in the setting of gastrinomas due to concomitant PPI treatment which is considered to be the first-line approach for symptoms' control[10]. Two different isotopes have been used in most studies: ^{90}Yttrium (^{90}Y)- or ^{177}Lutetium (^{177}Lu)-labeled SSAs[103]. The approval of PRRT treatment comes from the promising results of a double-blinded, control phase 3 trial (NETTER-1)[104] in patients with advanced unresectable, midgut carcinoids and the results of treatment of 510 patients with advanced pNENs and other NENs[105,106]. According to data from the literature, gastrinomas are one of the malignant pNENs that were most responsive to PRRT; however, they also had one of the highest recurrence rates leading to a poorer prognosis[103,105]. In detail, in one study including 11 patients with metastatic ZES[107] treated with either ^{90}Y-and/or ^{177}Lu-labeled SSAs, the mean serum gastrin decreased by 81%, complete response occurred in 9%, partial tumor response in 45%, tumor stabilization in 45%, with a persistence of the antitumor effect for a median period of 14 mo in 64% of the cases. Another study[108] involving 30 gastrinoma patients treated with ^{90}Y-labeled SSAs reported a partial response rate of 33% with a mean OS time of 40 mo.

CONCLUSION

As the diagnosis of ZES is challenging; the maintenance of a high index of suspicion is necessary to get the final diagnosis. Better disease awareness is useful to reduce the diagnostic delay, particularly due to the improper referral of patients to physicians with low or no expertise in the neuroendocrine field. The association between typical symptoms including chronic diarrhea, reflux disorder, and recurrent peptic disease particularly at unusual sites should raise the suspicion of ZES after exclusion of alternative and more common GI etiologies. The possibility of an underlying MEN-1 syndrome should be always considered, particularly in young patients with concomitant hypercalcemia suggestive of hyperparathyroidism and/or familiar history of MEN-1. A fasting gastrin level is generally the first step and confounding factors such as PPI use need to be considered. Gastric pH, esophageal pH-recording, and possibly a secretin stimulation test might be necessary as well, although the decision to perform them should be tailored to every single patient, considered both the need to withdraw PPI treatment and the limited availability of these tests in routine clinical practice. Tumor localization must be performed and EUS with the possibility of getting a sampling through FNA is considered to be a more accurate technique than conventional imaging for small lesions. Given the high expression of STTRs in gastrinomas, gallium-68PET-scan should be always included in the diagnostic pathway of all NENs, including gastrinoma, in order to both identify the primary tumor and to stage the disease.

Regarding the treatment of the localized disease, the two milestones are represented by PPIs for symptoms' control and surgery with curative intent. The role of surgery in

the treatment of gastrinoma has changed completely from the introduction of PPIs. In the past, total gastrectomy represented the sole effective treatment to treat ZES by removing the end-organ target of gastrin. With the use of PPIs, gastric hypersecretion was no longer considered a problem and surgical excision started to be proposed as a potentially curative therapy. Surgical removal of the primary tumor (and possibly its metastases) with curative intent should be, indeed, always performed. Unfortunately, the diagnosis is often made when the disease is too advanced for a surgical approach. The first step, again, is represented by syndrome control, based on PPIs, which are considered to be the drugs of choice for suppressing acid secretion. In order to achieve tumor growth control, SSAs constitute a viable option; studies specifically focused on advanced gastrinomas are scanty and often retrospective, however, according to data from the literature, treatments for the advanced disease are super-imposable to other NENs and include targeted therapies, chemotherapy, and PRRT. As there is a need for both a proper medical treatment for symptom's relief and a surgical procedure whenever feasible with curative intent, the multidisciplinary approach, with close cooperation between clinicians and surgeons, remains the cornerstone for proper management of this composite disease. Due to the risk of overlapping ZES with other GI common disorders, referral to tertiary centers with great expertise in the neuroendocrine field is mandatory.

ACKNOWLEDGEMENTS

Pietro Invernizzi and Sara Massironi are members of the European Reference Network on Hepatological Diseases (ERN RARE LIVER), and they thank AMAF Monza ONLUS and AIRCS for their support.

REFERENCES

1 **Zollinger RM**, Ellison EH. Primary peptic ulcerations of the jejunum associated with islet cell tumors of the pancreas. *Ann Surg* 1955; **142**: 709-23; discussion, 724 [PMID: 13259432 DOI: 10.1097/00000658-195510000-00015]

2 **Falconi M**, Eriksson B, Kaltsas G, Bartsch DK, Capdevila J, Caplin M, Kos-Kudla B, Kwekkeboom D, Rindi G, Klöppel G, Reed N, Kianmanesh R, Jensen RT; Vienna Consensus Conference participants. ENETS Consensus Guidelines Update for the Management of Patients with Functional Pancreatic Neuroendocrine Tumors and Non-Functional Pancreatic Neuroendocrine Tumors. *Neuroendocrinology* 2016; **103**: 153-171 [PMID: 26742109 DOI: 10.1159/000443171]

3 **Guarnotta V**, Martini C, Davì MV, Pizza G, Colao A, Faggiano A; NIKE group. The Zollinger-Ellison syndrome: is there a role for somatostatin analogues in the treatment of the gastrinoma? *Endocrine* 2018; **60**: 15-27 [PMID: 29019150 DOI: 10.1007/s12020-017-1420-4]

4 **Ito T**, Igarashi H, Jensen RT. Zollinger-Ellison syndrome: recent advances and controversies. *Curr Opin Gastroenterol* 2013; **29**: 650-661 [PMID: 24100728 DOI: 10.1097/MOG.0b013e328365efb1]

5 **Ito T**, Cadiot G, Jensen RT. Diagnosis of Zollinger-Ellison syndrome: increasingly difficult. *World J Gastroenterol* 2012; **18**: 5495-5503 [PMID: 23112541 DOI: 10.3748/wjg.v18.i39.5495]

6 **Jensen RT**, Niederle B, Mitry E, Ramage JK, Steinmuller T, Lewington V, Scarpa A, Sundin A, Perren A, Gross D, O'Connor JM, Pauwels S, Kloppel G; Frascati Consensus Conference; European Neuroendocrine Tumor Society. Gastrinoma (duodenal and pancreatic). *Neuroendocrinology* 2006; **84**: 173-182 [PMID: 17312377 DOI: 10.1159/000098009]

7 **Keutgen XM**, Nilubol N, Kebebew E. Malignant-functioning neuroendocrine tumors of the pancreas: A survival analysis. *Surgery* 2016; **159**: 1382-1389 [PMID: 26704781 DOI: 10.1016/j.surg.2015.11.010]

8 **Gibril F**, Jensen RT. Zollinger-Ellison syndrome revisited: diagnosis, biologic markers, associated inherited disorders, and acid hypersecretion. *Curr Gastroenterol Rep* 2004; **6**: 454-463 [PMID: 15527675 DOI: 10.1007/s11894-004-0067-5]

9 **Mendelson AH**, Donowitz M. Catching the Zebra: Clinical Pearls and Pitfalls for the Successful Diagnosis of Zollinger-Ellison Syndrome. *Dig Dis Sci* 2017; **62**: 2258-2265 [PMID: 28776139 DOI: 10.1007/s10620-017-4695-7]

10 **Jensen RT**, Ito T. Gastrinoma. 2020 Nov 21. In: Feingold KR, Anawalt B, Boyce A, Chrousos G, de Herder WW, Dhatariya K, Dungan K, Grossman A, Hershman JM, Hofland J, Kalra S, Kaltsas G, Koch C, Kopp P, Korbonits M, Kovacs CS, Kuohung W, Laferrère B, McGee EA, McLachlan R, Morley JE, New M, Purnell J, Sahay R, Singer F, Stratakis CA, Trence DL, Wilson DP, editors. Endotext [Internet]. South Dartmouth (MA): MDText.com, Inc.; 2000 [PMID: 25905301]

11 **Wilcox CM**, Seay T, Arcury JT, Mohnen J, Hirschowitz BI. Zollinger-Ellison syndrome: presentation, response to therapy, and outcome. *Dig Liver Dis* 2011; **43**: 439-443 [PMID: 21193359 DOI: 10.1016/j.dld.2010.11.007]

12 **Hatta W**, Iijima K, Koike T, Kondo Y, Ara N, Asanuma K, Uno K, Asano N, Imatani A, Shimosegawa T. Endoscopic findings for predicting gastric acid secretion status. *Dig Endosc* 2015; **27**: 582-589 [PMID: 25556402 DOI: 10.1111/den.12427]

13 **Roy PK**, Venzon DJ, Shojamanesh H, Abou-Saif A, Peghini P, Doppman JL, Gibril F, Jensen RT. Zollinger-Ellison syndrome. Clinical presentation in 261 patients. *Medicine (Baltimore)* 2000; **79**: 379-411 [PMID: 11144036 DOI: 10.1097/00005792-200011000-00004]

14 **Thakker RV**, Newey PJ, Walls GV, Bilezikian J, Dralle H, Ebeling PR, Melmed S, Sakurai A, Tonelli F, Brandi ML; Endocrine Society. Clinical practice guidelines for multiple endocrine neoplasia type 1 (MEN1). *J Clin Endocrinol Metab* 2012; **97**: 2990-3011 [PMID: 22723327 DOI: 10.1210/jc.2012-1230]

15 **Gibril F**, Schumann M, Pace A, Jensen RT. Multiple endocrine neoplasia type 1 and Zollinger-Ellison syndrome: a prospective study of 107 cases and comparison with 1009 cases from the literature. *Medicine (Baltimore)* 2004; **83**: 43-83 [PMID: 14747767 DOI: 10.1097/01.md.0000112297.72510.32]

16 **Norton JA**, Venzon DJ, Berna MJ, Alexander HR, Fraker DL, Libutti SK, Marx SJ, Gibril F, Jensen RT. Prospective study of surgery for primary hyperparathyroidism (HPT) in multiple endocrine neoplasia-type 1 and Zollinger-Ellison syndrome: long-term outcome of a more virulent form of HPT. *Ann Surg* 2008; **247**: 501-510 [PMID: 18376196 DOI: 10.1097/SLA.0b013e31815efda5]

17 **Davì MV**, Boninsegna L, Dalle Carbonare L, Toaiari M, Capelli P, Scarpa A, Francia G, Falconi M. Presentation and outcome of pancreaticoduodenal endocrine tumors in multiple endocrine neoplasia type 1 syndrome. *Neuroendocrinology* 2011; **94**: 58-65 [PMID: 21464564 DOI: 10.1159/000326164]

18 **Aamar A**, Madhani K, Virk H, Butt Z. Zollinger-Ellison Syndrome: A Rare Case of Chronic Diarrhea. *Gastroenterology Res* 2016; **9**: 103-104 [PMID: 28058079 DOI: 10.14740/gr734w]

19 **Campana D**, Piscitelli L, Mazzotta E, Bonora M, Serra C, Salomone L, Corinaldesi R, Tomassetti P. Zollinger-Ellison syndrome. Diagnosis and therapy. *Minerva Med* 2005; **96**: 187-206 [PMID: 16175161]

20 **Simmons LH**, Guimaraes AR, Zukerberg LR. Case records of the Massachusetts General Hospital. Case 6-2013. A 54-year-old man with recurrent diarrhea. *N Engl J Med* 2013; **368**: 757-765 [PMID: 23425169 DOI: 10.1056/NEJMcpc1208149]

21 **Arasaradnam RP**, Brown S, Forbes A, Fox MR, Hungin P, Kelman L, Major G, O'Connor M, Sanders DS, Sinha R, Smith SC, Thomas P, Walters JRF. Guidelines for the investigation of chronic diarrhoea in adults: British Society of Gastroenterology, 3rd edition. *Gut* 2018; **67**: 1380-1399 [PMID: 29653941 DOI: 10.1136/gutjnl-2017-315909]

22 **Corleto VD**, Annibale B, Gibril F, Angeletti S, Serrano J, Venzon DJ, Delle Fave G, Jensen RT. Does the widespread use of proton pump inhibitors mask, complicate and/or delay the diagnosis of Zollinger-Ellison syndrome? *Aliment Pharmacol Ther* 2001; **15**: 1555-1561 [PMID: 11563994 DOI: 10.1046/j.1365-2036.2001.01085.x]

23 **Metz DC**. Diagnosis of the Zollinger–Ellison syndrome. *Clin Gastroenterol Hepatol* 2012; **10**: 126-130 [PMID: 21806955 DOI: 10.1016/j.cgh.2011.07.012]

24 **Epelboym I**, Mazeh H. Zollinger-Ellison syndrome: classical considerations and current controversies. *Oncologist* 2014; **19**: 44-50 [PMID: 24319020 DOI: 10.1634/theoncologist.2013-0369]

25 **Phan J**, Benhammou JN, Pisegna JR. Gastric Hypersecretory States: Investigation and Management. *Curr Treat Options Gastroenterol* 2015; **13**: 386-397 [PMID: 26342486 DOI: 10.1007/s11938-015-0065-8]

26 **Oh DS**, Wang HS, Ohning GV, Pisegna JR. Validation of a new endoscopic technique to assess acid output in Zollinger-Ellison syndrome. *Clin Gastroenterol Hepatol* 2006; **4**: 1467-1473 [PMID: 17101299 DOI: 10.1016/j.cgh.2006.08.015]

27 **Kulke MH**, Anthony LB, Bushnell DL, de Herder WW, Goldsmith SJ, Klimstra DS, Marx SJ, Pasieka JL, Pommier RF, Yao JC, Jensen RT; North American Neuroendocrine Tumor Society (NANETS). NANETS treatment guidelines: well-differentiated neuroendocrine tumors of the stomach and pancreas. *Pancreas* 2010; **39**: 735-752 [PMID: 20664472 DOI: 10.1097/MPA.0b013e3181ebb168]

28 **Krampitz GW**, Norton JA. Current management of the Zollinger-Ellison syndrome. *Adv Surg* 2013; **47**: 59-79 [PMID: 24298844 DOI: 10.1016/j.yasu.2013.02.004]

29 **Reznek RH**. CT/MRI of neuroendocrine tumours. *Cancer Imaging* 2006; **6**: S163-S177 [PMID: 17114072 DOI: 10.1102/1470-7330.2006.9037]

30 **Thoeni RF**, Mueller-Lisse UG, Chan R, Do NK, Shyn PB. Detection of small, functional islet cell tumors in the pancreas: selection of MR imaging sequences for optimal sensitivity. *Radiology* 2000; **214**: 483-490 [PMID: 10671597 DOI: 10.1148/radiology.214.2.r00fe32483]

31 **Metz DC**, Jensen RT. Gastrointestinal neuroendocrine tumors: pancreatic endocrine tumors. *Gastroenterology* 2008; **135**: 1469-1492 [PMID: 18703061 DOI: 10.1053/j.gastro.2008.05.047]

32 **Stokkel MP**, Rietbergen DD, Korse CM, Taal BG. Somatostatin receptor scintigraphy and chromogranin A assay in staging and follow-up of patients with well-differentiated neuroendocrine tumors. *Nucl Med Commun* 2011; **32**: 731-737 [PMID: 21633314 DOI: 10.1097/MNM.0b013e328347a895]

33 **Ruf J**, von Wedel F, Furth C, Denecke T, Stelter L, Steffen IG, Schütte K, Arend J, Ulrich G, Klose S, Bornschein J, Apostolova I, Amthauer H. Significance of a Single-Time-Point Somatostatin

Receptor SPECT/Multiphase CT Protocol in the Diagnostic Work-up of Gastroenteropancreatic Neuroendocrine Neoplasms. *J Nucl Med* 2016; **57**: 180-185 [PMID: 26609177 DOI: 10.2967/jnumed.115.161117]

34 **Wong KK**, Gandhi A, Viglianti BL, Fig LM, Rubello D, Gross MD. Endocrine radionuclide scintigraphy with fusion single photon emission computed tomography/computed tomography. *World J Radiol* 2016; **8**: 635-655 [PMID: 27358692 DOI: 10.4329/wjr.v8.i6.635]

35 **Sainz-Esteban A**, Olmos R, González-Sagrado M, González ML, Ruiz MÁ, García-Talavera P, Gamazo C, Villanueva JG, Cobo A, de Luis D. Contribution of ^{111}In-pentetreotide SPECT/CT imaging to conventional somatostatin receptor scintigraphy in the detection of neuroendocrine tumours. *Nucl Med Commun* 2015; **36**: 251-259 [PMID: 25369750 DOI: 10.1097/MNM.0000000000000239]

36 **Johnbeck CB**, Knigge U, Kjær A. PET tracers for somatostatin receptor imaging of neuroendocrine tumors: current status and review of the literature. *Future Oncol* 2014; **10**: 2259-2277 [PMID: 25471038 DOI: 10.2217/fon.14.139]

37 **Gabriel M**, Decristoforo C, Kendler D, Dobrozemsky G, Heute D, Uprimny C, Kovacs P, Von Guggenberg E, Bale R, Virgolini IJ. 68Ga-DOTA-Tyr3-octreotide PET in neuroendocrine tumors: comparison with somatostatin receptor scintigraphy and CT. *J Nucl Med* 2007; **48**: 508-518 [PMID: 17401086 DOI: 10.2967/jnumed.106.035667]

38 **Skoura E**, Michopoulou S, Mohmaduvesh M, Panagiotidis E, Al Harbi M, Toumpanakis C, Almukhailed O, Kayani I, Syed R, Navalkissoor S, Ell PJ, Caplin ME, Bomanji J. The Impact of 68Ga-DOTATATE PET/CT Imaging on Management of Patients with Neuroendocrine Tumors: Experience from a National Referral Center in the United Kingdom. *J Nucl Med* 2016; **57**: 34-40 [PMID: 26471695 DOI: 10.2967/jnumed.115.166017]

39 **Sharma P**, Arora S, Mukherjee A, Pal S, Sahni P, Garg P, Khadgawat R, Thulkar S, Bal C, Kumar R. Predictive value of 68Ga-DOTANOC PET/CT in patients with suspicion of neuroendocrine tumors: is its routine use justified? *Clin Nucl Med* 2014; **39**: 37-43 [PMID: 24152621 DOI: 10.1097/RLU.0000000000000257]

40 **Wild D**, Bomanji JB, Benkert P, Maecke H, Ell PJ, Reubi JC, Caplin ME. Comparison of 68Ga-DOTANOC and 68Ga-DOTATATE PET/CT within patients with gastroenteropancreatic neuroendocrine tumors. *J Nucl Med* 2013; **54**: 364-372 [PMID: 23297077 DOI: 10.2967/jnumed.112.111724]

41 **Geijer H**, Breimer LH. Somatostatin receptor PET/CT in neuroendocrine tumours: update on systematic review and meta-analysis. *Eur J Nucl Med Mol Imaging* 2013; **40**: 1770-1780 [PMID: 23873003 DOI: 10.1007/s00259-013-2482-z]

42 **Norton JA**, Jensen RT. Resolved and unresolved controversies in the surgical management of patients with Zollinger-Ellison syndrome. *Ann Surg* 2004; **240**: 757-773 [PMID: 15492556 DOI: 10.1097/01.sla.0000143252.02142.3e]

43 **Zilli A**, Arcidiacono PG, Conte D, Massironi S. Clinical impact of endoscopic ultrasonography on the management of neuroendocrine tumors: lights and shadows. *Dig Liver Dis* 2018; **50**: 6-14 [PMID: 29102525 DOI: 10.1016/j.dld.2017.10.007]

44 **Atiq M**, Bhutani MS, Bektas M, Lee JE, Gong Y, Tamm EP, Shah CP, Ross WA, Yao J, Raju GS, Wang X, Lee JH. EUS-FNA for pancreatic neuroendocrine tumors: a tertiary cancer center experience. *Dig Dis Sci* 2012; **57**: 791-800 [PMID: 21964743 DOI: 10.1007/s10620-011-1912-7]

45 **Thomas-Marques L**, Murat A, Delemer B, Penfornis A, Cardot-Bauters C, Baudin E, Niccoli-Sire P, Levoir D, Choplin Hdu B, Chabre O, Jovenin N, Cadiot G; Groupe des Tumeurs Endocrines (GTE). Prospective endoscopic ultrasonographic evaluation of the frequency of nonfunctioning pancreaticoduodenal endocrine tumors in patients with multiple endocrine neoplasia type 1. *Am J Gastroenterol* 2006; **101**: 266-273 [PMID: 16454829 DOI: 10.1111/j.1572-0241.2006.00367.x]

46 **Kappelle WF**, Valk GD, Leenders M, Moons LM, Bogte A, Siersema PD, Vleggaar FP. Growth rate of small pancreatic neuroendocrine tumors in multiple endocrine neoplasia type 1: results from an endoscopic ultrasound based cohort study. *Endoscopy* 2017; **49**: 27-34 [PMID: 27975336 DOI: 10.1055/s-0042-119402]

47 **Trudgill NJ**, Sifrim D, Sweis R, Fullard M, Basu K, McCord M, Booth M, Hayman J, Boeckxstaens G, Johnston BT, Ager N, De Caestecker J. British Society of Gastroenterology guidelines for oesophageal manometry and oesophageal reflux monitoring. *Gut* 2019; **68**: 1731-1750 [PMID: 31366456 DOI: 10.1136/gutjnl-2018-318115]

48 **Long SH**, Berna MJ, Thill M, Pace A, Pradhan TK, Hoffmann KM, Serrano J, Jensen RT. Secretin-receptor and secretin-receptor-variant expression in gastrinomas: correlation with clinical and tumoral features and secretin and calcium provocative test results. *J Clin Endocrinol Metab* 2007; **92**: 4394-4402 [PMID: 17711922 DOI: 10.1210/jc.2007-0986]

49 **Metz DC**, Buchanan M, Purich E, Fein S. A randomized controlled crossover study comparing synthetic porcine and human secretins with biologically derived porcine secretin to diagnose Zollinger-Ellison Syndrome. *Aliment Pharmacol Ther* 2001; **15**: 669-676 [PMID: 11328261 DOI: 10.1046/j.1365-2036.2001.00976.x]

50 **Berna MJ**, Hoffmann KM, Long SH, Serrano J, Gibril F, Jensen RT. Serum gastrin in Zollinger-Ellison syndrome: II. Prospective study of gastrin provocative testing in 293 patients from the National Institutes of Health and comparison with 537 cases from the literature. evaluation of diagnostic criteria, proposal of new criteria, and correlations with clinical and tumoral features. *Medicine (Baltimore)* 2006; **85**: 331-364 [PMID: 17108779 DOI: 10.1097/MD.0b013e31802b518c]

51 **Poitras P**, Gingras MH, Rehfeld JF. Secretin stimulation test for gastrin release in Zollinger-Ellison syndrome: to do or not to do? *Pancreas* 2013; **42**: 903-904 [PMID: 23851427 DOI: 10.1097/MPA.0b013e318298df75]

52 **Kuiper P**, Biemond I, Masclee AA, Jansen JB, Verspaget HW, Lamers CB. Diagnostic efficacy of the secretin stimulation test for the Zollinger-Ellison syndrome: an intra-individual comparison using different dosages in patients and controls. *Pancreatology* 2010; **10**: 14-18 [PMID: 20299818 DOI: 10.1159/000265936]

53 **Shah P**, Singh MH, Yang YX, Metz DC. Hypochlorhydria and achlorhydria are associated with false-positive secretin stimulation testing for Zollinger-Ellison syndrome. *Pancreas* 2013; **42**: 932-936 [PMID: 23851430 DOI: 10.1097/MPA.0b013e3182847b2e]

54 **Norton JA**, Fraker DL, Alexander HR, Venzon DJ, Doppman JL, Serrano J, Goebel SU, Peghini PL, Roy PK, Gibril F, Jensen RT. Surgery to cure the Zollinger-Ellison syndrome. *N Engl J Med* 1999; **341**: 635-644 [PMID: 10460814 DOI: 10.1056/nejm199908263410902]

55 **Jensen RT**, Cadiot G, Brandi ML, de Herder WW, Kaltsas G, Komminoth P, Scoazec JY, Salazar R, Sauvanet A, Kianmanesh R; Barcelona Consensus Conference participants. ENETS Consensus Guidelines for the management of patients with digestive neuroendocrine neoplasms: functional pancreatic endocrine tumor syndromes. *Neuroendocrinology* 2012; **95**: 98-119 [PMID: 22261919 DOI: 10.1159/000335591]

56 **Kunz PL**, Reidy-Lagunes D, Anthony LB, Bertino EM, Brendtro K, Chan JA, Chen H, Jensen RT, Kim MK, Klimstra DS, Kulke MH, Liu EH, Metz DC, Phan AT, Sippel RS, Strosberg JR, Yao JC; North American Neuroendocrine Tumor Society. Consensus guidelines for the management and treatment of neuroendocrine tumors. *Pancreas* 2013; **42**: 557-577 [PMID: 23591432 DOI: 10.1097/MPA.0b013e31828e34a4]

57 **Howe JR**, Merchant NB, Conrad C, Keutgen XM, Hallet J, Drebin JA, Minter RM, Lairmore TC, Tseng JF, Zeh HJ, Libutti SK, Singh G, Lee JE, Hope TA, Kim MK, Menda Y, Halfdanarson TR, Chan JA, Pommier RF. The North American Neuroendocrine Tumor Society Consensus Paper on the Surgical Management of Pancreatic Neuroendocrine Tumors. *Pancreas* 2020; **49**: 1-33 [PMID: 31856076 DOI: 10.1097/MPA.0000000000001454]

58 **Pavel M**, Öberg K, Falconi M, Krenning EP, Sundin A, Perren A, Berruti A; ESMO Guidelines Committee. Gastroenteropancreatic neuroendocrine neoplasms: ESMO Clinical Practice Guidelines for diagnosis, treatment and follow-up. *Ann Oncol* 2020; **31**: 844-860 [PMID: 32272208 DOI: 10.1016/j.annonc.2020.03.304]

59 **Norton JA**, Fraker DL, Alexander HR, Jensen RT. Value of surgery in patients with negative imaging and sporadic Zollinger-Ellison syndrome. *Ann Surg* 2012; **256**: 509-517 [PMID: 22868363 DOI: 10.1097/SLA.0b013e318265f08d]

60 **Norton JA**, Alexander HR, Fraker DL, Venzon DJ, Gibril F, Jensen RT. Does the use of routine duodenotomy (DUODX) affect rate of cure, development of liver metastases, or survival in patients with Zollinger-Ellison syndrome? *Ann Surg* 2004; **239**: 617-25; discussion 626 [PMID: 15082965 DOI: 10.1097/01.sla.0000124290.05524.5e]

61 **Weber HC**, Venzon DJ, Lin JT, Fishbein VA, Orbuch M, Strader DB, Gibril F, Metz DC, Fraker DL, Norton JA. Determinants of metastatic rate and survival in patients with Zollinger-Ellison syndrome: a prospective long-term study. *Gastroenterology* 1995; **108**: 1637-1649 [PMID: 7768367 DOI: 10.1016/0016-5085(95)90124-8]

62 **Norton JA**, Fraker DL, Alexander HR, Gibril F, Liewehr DJ, Venzon DJ, Jensen RT. Surgery increases survival in patients with gastrinoma. *Ann Surg* 2006; **244**: 410-419 [PMID: 16926567 DOI: 10.1097/01.sla.0000234802.44320.a5]

63 **Fraker DL**, Norton JA, Alexander HR, Venzon DJ, Jensen RT. Surgery in Zollinger-Ellison syndrome alters the natural history of gastrinoma. *Ann Surg* 1994; **220**: 320-8; discussion 328 [PMID: 7916560 DOI: 10.1097/00000658-199409000-00008]

64 **Sugg SL**, Norton JA, Fraker DL, Metz DC, Pisegna JR, Fishbeyn V, Benya RV, Shawker TH, Doppman JL, Jensen RT. A prospective study of intraoperative methods to diagnose and resect duodenal gastrinomas. *Ann Surg* 1993; **218**: 138-144 [PMID: 8342993 DOI: 10.1097/00000658-199308000-00004]

65 **Norton JA**, Doppman JL, Jensen RT. Curative resection in Zollinger-Ellison syndrome. Results of a 10-year prospective study. *Ann Surg* 1992; **215**: 8-18 [PMID: 1531004 DOI: 10.1097/00000658-199201000-00012]

66 **Norton JA**, Krampitz GW, Poultsides GA, Visser BC, Fraker DL, Alexander HR, Jensen RT. Prospective Evaluation of Results of Reoperation in Zollinger-Ellison Syndrome. *Ann Surg* 2018; **267**: 782-788 [PMID: 29517561 DOI: 10.1097/SLA.0000000000002122]

67 **Giovinazzo F**, Butturini G, Monsellato D, Malleo G, Marchegiani G, Bassi C. Lymph nodes metastasis and recurrences justify an aggressive treatment of gastrinoma. *Updates Surg* 2013; **65**: 19-24 [PMID: 23417896 DOI: 10.1007/s13304-013-0201-8]

68 **Bartsch DK**, Waldmann J, Fendrich V, Boninsegna L, Lopez CL, Partelli S, Falconi M. Impact of lymphadenectomy on survival after surgery for sporadic gastrinoma. *Br J Surg* 2012; **99**: 1234-1240 [PMID: 22864882 DOI: 10.1002/bjs.8843]

69 **Liu P**, Zhang X, Shang Y, Lu L, Cao F, Sun M, Tang Z, Vollmar B, Gong P. Lymph node ratio, but not the total number of examined lymph nodes or lymph node metastasis, is a predictor of overall survival for pancreatic neuroendocrine neoplasms after surgical resection. *Oncotarget* 2017; **8**: 89245-89255 [PMID: 29179516 DOI: 10.18632/oncotarget.19184]

70 **Conrad C**, Kutlu OC, Dasari A, Chan JA, Vauthey JN, Adams DB, Kim M, Fleming JB, Katz MH, Lee JE. Prognostic Value of Lymph Node Status and Extent of Lymphadenectomy in Pancreatic Neuroendocrine Tumors Confined To and Extending Beyond the Pancreas. *J Gastrointest Surg* 2016; **20**: 1966-1974 [PMID: 27714644 DOI: 10.1007/s11605-016-3243-7]

71 **Curran T**, Pockaj BA, Gray RJ, Halfdanarson TR, Wasif N. Importance of lymph node involvement in pancreatic neuroendocrine tumors: impact on survival and implications for surgical resection. *J Gastrointest Surg* 2015; **19**: 152-60; discussion 160 [PMID: 25118642 DOI: 10.1007/s11605-014-2624-z]

72 **Norton JA**, Alexander HR, Fraker DL, Venzon DJ, Gibril F, Jensen RT. Possible primary lymph node gastrinoma: occurrence, natural history, and predictive factors: a prospective study. *Ann Surg* 2003; **237**: 650-7; discussion 657 [PMID: 12724631 DOI: 10.1097/01.SLA.0000064375.51939.48]

73 **Chen Y**, Deshpande V, Ferrone C, Blaszkowsky LS, Parangi S, Warshaw AL, Lillemoe KD, Fernandez-Del Castillo C. Primary lymph node gastrinoma: A single institution experience. *Surgery* 2017; **162**: 1088-1094 [PMID: 28705492 DOI: 10.1016/j.surg.2017.05.017]

74 **Massironi S**, Campana D, Partelli S, Panzuto F, Rossi RE, Faggiano A, Brighi N, Falconi M, Rinzivillo M, Delle Fave G, Colao AM, Conte D. Heterogeneity of Duodenal Neuroendocrine Tumors: An Italian Multi-center Experience. *Ann Surg Oncol* 2018; **25**: 3200-3206 [PMID: 30054824 DOI: 10.1245/s10434-018-6673-5]

75 **Jensen RT**, Fraker DL. Zollinger-Ellison syndrome. Advances in treatment of gastric hypersecretion and the gastrinoma. *JAMA* 1994; **271**: 1429-1435 [PMID: 7513768 DOI: 10.1001/jama.271.18.1429]

76 **Metz DC**, Pisegna JR, Fishbeyn VA, Benya RV, Jensen RT. Control of gastric acid hypersecretion in the management of patients with Zollinger-Ellison syndrome. *World J Surg* 1993; **17**: 468-480 [PMID: 8362529 DOI: 10.1007/BF01655106]

77 **Hirschowitz BI**, Simmons J, Mohnen J. Clinical outcome using lansoprazole in acid hypersecretors with and without Zollinger-Ellison syndrome: a 13-year prospective study. *Clin Gastroenterol Hepatol* 2005; **3**: 39-48 [PMID: 15645403 DOI: 10.1016/S1542-3565(04)00606-8]

78 **Metz DC**, Comer GM, Soffer E, Forsmark CE, Cryer B, Chey W, Pisegna JR. Three-year oral pantoprazole administration is effective for patients with Zollinger-Ellison syndrome and other hypersecretory conditions. *Aliment Pharmacol Ther* 2006; **23**: 437-444 [PMID: 16423003 DOI: 10.1111/j.1365-2036.2006.02762.x]

79 **Ip S**, Bonis P, Tatsioni A, Raman G, Chew P, Kupelnick B, Fu L, DeVine D, Lau J. Comparative Effectiveness of Management Strategies For Gastroesophageal Reflux Disease [Internet]. Rockville (MD): Agency for Healthcare Research and Quality (US); 2005 Dec. Report No.: 06-EHC003-EF [PMID: 21348043]

80 **Quatrini M**, Castoldi L, Rossi G, Cesana BM, Peracchi M, Bardella MT. A follow-up study of patients with Zollinger-Ellison syndrome in the period 1966-2002: effects of surgical and medical treatments on long-term survival. *J Clin Gastroenterol* 2005; **39**: 376-380 [PMID: 15815204 DOI: 10.1097/01.mcg.0000159221.77913.ac]

81 **Maton PN**, Vinayek R, Frucht H, McArthur KA, Miller LS, Saeed ZA, Gardner JD, Jensen RT. Long-term efficacy and safety of omeprazole in patients with Zollinger-Ellison syndrome: a prospective study. *Gastroenterology* 1989; **97**: 827-836 [PMID: 2777040 DOI: 10.1016/0016-5085(89)91485-6]

82 **Poitras P**, Gingras MH, Rehfeld JF. The Zollinger-Ellison syndrome: dangers and consequences of interrupting antisecretory treatment. *Clin Gastroenterol Hepatol* 2012; **10**: 199-202 [PMID: 21871248 DOI: 10.1016/j.cgh.2011.08.012]

83 **Metz DC**, Pisegna JR, Fishbeyn VA, Benya RV, Feigenbaum KM, Koviack PD, Jensen RT. Currently used doses of omeprazole in Zollinger-Ellison syndrome are too high. *Gastroenterology* 1992; **103**: 1498-1508 [PMID: 1426868 DOI: 10.1016/0016-5085(92)91170-9]

84 **Norton JA**, Foster DS, Ito T, Jensen RT. Gastrinomas: Medical or Surgical Treatment. *Endocrinol Metab Clin North Am* 2018; **47**: 577-601 [PMID: 30098717 DOI: 10.1016/j.ecl.2018.04.009]

85 **Dockray GJ**, Moore A, Varro A, Pritchard DM. Gastrin receptor pharmacology. *Curr Gastroenterol Rep* 2012; **14**: 453-459 [PMID: 22983899 DOI: 10.1007/s11894-012-0293-1]

86 **Ellison EC**, Johnson JA. The Zollinger-Ellison syndrome: a comprehensive review of historical, scientific, and clinical considerations. *Curr Probl Surg* 2009; **46**: 13-106 [PMID: 19059523 DOI: 10.1067/j.cpsurg.2008.09.001]

87 **Tomassetti P**, Migliori M, Gullo L. Slow-release lanreotide treatment in endocrine gastrointestinal tumors. *Am J Gastroenterol* 1998; **93**: 1468-1471 [PMID: 9732927 DOI: 10.1111/j.1572-0241.1998.465_q.x]

88 **Eriksson B**, Renstrup J, Imam H, Oberg K. High-dose treatment with lanreotide of patients with advanced neuroendocrine gastrointestinal tumors: clinical and biological effects. *Ann Oncol* 1997; **8**: 1041-1044 [PMID: 9402179 DOI: 10.1023/A:1008205415035]

89 **Rinke A**, Müller HH, Schade-Brittinger C, Klose KJ, Barth P, Wied M, Mayer C, Aminossadati B, Pape UF, Bläker M, Harder J, Arnold C, Gress T, Arnold R; PROMID Study Group. Placebo-controlled, double-blind, prospective, randomized study on the effect of octreotide LAR in the control of tumor growth in patients with metastatic neuroendocrine midgut tumors: a report from the PROMID Study Group. *J Clin Oncol* 2009; **27**: 4656-4663 [PMID: 19704057 DOI: 10.1200/JCO.2009.22.8510]

90 **Caplin ME**, Pavel M, Ćwikła JB, Phan AT, Raderer M, Sedláčková E, Cadiot G, Wolin EM, Capdevila J, Wall L, Rindi G, Langley A, Martinez S, Blumberg J, Ruszniewski P; CLARINET

Investigators. Lanreotide in metastatic enteropancreatic neuroendocrine tumors. *N Engl J Med* 2014; **371**: 224-233 [PMID: 25014687 DOI: 10.1056/NEJMoa1316158]

91 **Saijo F**, Naito H, Funayama Y, Fukushima K, Shibata C, Hashimoto A, Kitayama T, Nagao M, Matsuno S, Sasaki I. Octreotide in control of multiple liver metastases from gastrinoma. *J Gastroenterol* 2003; **38**: 905-908 [PMID: 14564638 DOI: 10.1007/s00535-002-1170-8]

92 **Granberg D**, Jacobsson H, Oberg K, Gustavsson J, Lehtihet M. Regression of a large malignant gastrinoma on treatment with Sandostatin LAR: a case report. *Digestion* 2008; **77**: 92-95 [PMID: 18376130 DOI: 10.1159/000122229]

93 **Yamaguchi M**, Yamada Y, Hosokawa Y, Iwamoto R, Tamba S, Ihara A, Yamamoto K, Hoshida Y, Matsuzawa Y. Long-term suppressive effect of octreotide on progression of metastatic gastrinoma with multiple endocrine neoplasia type 1: seven-year follow up. *Intern Med* 2010; **49**: 1557-1563 [PMID: 20686291 DOI: 10.2169/internalmedicine.49.3607]

94 **Ruszniewski P**, Laucournet H, Elouaer-Blanc L, Mignon M, Bonfils S. Long-acting somatostatin (SMS 201-995) in the management of Zollinger-Ellison syndrome: evidence for sustained efficacy. *Pancreas* 1988; **3**: 145-152 [PMID: 2897687 DOI: 10.1097/00006676-198804000-00006]

95 **Raymond E**, Dahan L, Raoul JL, Bang YJ, Borbath I, Lombard-Bohas C, Valle J, Metrakos P, Smith D, Vinik A, Chen JS, Hörsch D, Hammel P, Wiedenmann B, Van Cutsem E, Patyna S, Lu DR, Blanckmeister C, Chao R, Ruszniewski P. Sunitinib malate for the treatment of pancreatic neuroendocrine tumors. *N Engl J Med* 2011; **364**: 501-513 [PMID: 21306237 DOI: 10.1056/NEJMoa1003825]

96 **Yao JC**, Shah MH, Ito T, Bohas CL, Wolin EM, Van Cutsem E, Hobday TJ, Okusaka T, Capdevila J, de Vries EG, Tomassetti P, Pavel ME, Hoosen S, Haas T, Lincy J, Lebwohl D, Öberg K; RAD001 in Advanced Neuroendocrine Tumors, Third Trial (RADIANT-3) Study Group. Everolimus for advanced pancreatic neuroendocrine tumors. *N Engl J Med* 2011; **364**: 514-523 [PMID: 21306238 DOI: 10.1056/NEJMoa1009290]

97 **Moertel CG**, Hanley JA, Johnson LA. Streptozocin alone compared with streptozocin plus fluorouracil in the treatment of advanced islet-cell carcinoma. *N Engl J Med* 1980; **303**: 1189-1194 [PMID: 6252466 DOI: 10.1056/nejm198011203032101]

98 **Prakash L**, Bhosale P, Cloyd J, Kim M, Parker N, Yao J, Dasari A, Halperin D, Aloia T, Lee JE, Vauthey JN, Fleming JB, Katz MH. Role of Fluorouracil, Doxorubicin, and Streptozocin Therapy in the Preoperative Treatment of Localized Pancreatic Neuroendocrine Tumors. *J Gastrointest Surg* 2017; **21**: 155-163 [PMID: 27634306 DOI: 10.1007/s11605-016-3270-4]

99 **Kouvaraki MA**, Ajani JA, Hoff P, Wolff R, Evans DB, Lozano R, Yao JC. Fluorouracil, doxorubicin, and streptozocin in the treatment of patients with locally advanced and metastatic pancreatic endocrine carcinomas. *J Clin Oncol* 2004; **22**: 4762-4771 [PMID: 15570077 DOI: 10.1200/JCO.2004.04.024]

100 **Cives M**, Ghayouri M, Morse B, Brelsford M, Black M, Rizzo A, Meeker A, Strosberg J. Analysis of potential response predictors to capecitabine/temozolomide in metastatic pancreatic neuroendocrine tumors. *Endocr Relat Cancer* 2016; **23**: 759-767 [PMID: 27552969 DOI: 10.1530/ERC-16-0147]

101 **Kunz PL**, Catalano PJ, Nimeiri H, Fisher GA, Longacre TA, Suarez CJ, Yao JC, Kulke MH, Hendifar AE, Shanks JC, Shah MH, Zalupski M, Schmulbach EL, Reidy DL, Strosberg JR, O'Dwyer PJ, Benson AB. A randomized study of temozolomide or temozolomide and capecitabine in patients with advanced pancreatic neuroendocrine tumors: A trial of the ECOG-ACRIN Cancer Research Group (E2211). *J Clin Oncol* 2018; **36**: 4004-4004 [DOI: 10.1200/jco.2018.36.15_suppl.4004]

102 **Bongiovanni A**, Liverani C, Foca F, Fausti V, Di Menna G, Mercatali L, De Vita A, Riva N, Calpona S, Miserocchi G, Spadazzi C, Cocchi C, Ibrahim T. Temozolomide Alone or Combined with Capecitabine for the Treatment of Metastatic Neuroendocrine Neoplasia: a "Real World" data analysis. *Neuroendocrinology* 2020 [PMID: 33221806 DOI: 10.1159/000513218]

103 **Ito T**, Igarashi H, Jensen RT. Therapy of metastatic pancreatic neuroendocrine tumors (pNETs): recent insights and advances. *J Gastroenterol* 2012; **47**: 941-960 [PMID: 22886480 DOI: 10.1007/s00535-012-0642-8]

104 **Strosberg J**, El-Haddad G, Wolin E, Hendifar A, Yao J, Chasen B, Mittra E, Kunz PL, Kulke MH, Jacene H, Bushnell D, O'Dorisio TM, Baum RP, Kulkarni HR, Caplin M, Lebtahi R, Hobday T, Delpassand E, Van Cutsem E, Benson A, Srirajaskanthan R, Pavel M, Mora J, Berlin J, Grande E, Reed N, Seregni E, Öberg K, Lopera Sierra M, Santoro P, Thevenet T, Erion JL, Ruszniewski P, Kwekkeboom D, Krenning E; NETTER-1 Trial Investigators. Phase 3 Trial of ^{177}Lu-Dotatate for Midgut Neuroendocrine Tumors. *N Engl J Med* 2017; **376**: 125-135 [PMID: 28076709 DOI: 10.1056/NEJMoa1607427]

105 **Kwekkeboom DJ**, de Herder WW, Kam BL, van Eijck CH, van Essen M, Kooij PP, Feelders RA, van Aken MO, Krenning EP. Treatment with the radiolabeled somatostatin analog [177 Lu-DOTA 0,Tyr3]octreotate: toxicity, efficacy, and survival. *J Clin Oncol* 2008; **26**: 2124-2130 [PMID: 18445841 DOI: 10.1200/JCO.2007.15.2553]

106 **Kwekkeboom DJ**, Teunissen JJ, Bakker WH, Kooij PP, de Herder WW, Feelders RA, van Eijck CH, Esser JP, Kam BL, Krenning EP. Radiolabeled somatostatin analog [177Lu-DOTA0,Tyr3]octreotate in patients with endocrine gastroenteropancreatic tumors. *J Clin Oncol* 2005; **23**: 2754-2762 [PMID: 15837990 DOI: 10.1200/JCO.2005.08.066]

107 **Grozinsky-Glasberg S**, Barak D, Fraenkel M, Walter MA, Müeller-Brand J, Eckstein J, Applebaum

L, Shimon I, Gross DJ. Peptide receptor radioligand therapy is an effective treatment for the long-term stabilization of malignant gastrinomas. *Cancer* 2011; **117**: 1377-1385 [PMID: 21425137 DOI: 10.1002/cncr.25646]

108 **Dumont RA**, Seiler D, Marincek N, Brunner P, Radojewski P, Rochlitz C, Müller-Brand J, Maecke HR, Briel M, Walter MA. Survival after somatostatin based radiopeptide therapy with (90)Y-DOTATOC vs. (90)Y-DOTATOC plus (177)Lu-DOTATOC in metastasized gastrinoma. *Am J Nucl Med Mol Imaging* 2015; **5**: 46-55 [PMID: 25625026 DOI: 10.7892/boris.67183]

World Journal of Gastroenterology

Submit a Manuscript: https://www.f6publishing.com

World J Gastroenterol 2021 September 21; 27(35): 5908-5918

DOI: 10.3748/wjg.v27.i35.5908

ISSN 1007-9327 (print) ISSN 2219-2840 (online)

MINIREVIEWS

Optical diagnosis of colorectal polyps using convolutional neural networks

Rawen Kader, Andreas V Hadjinicolaou, Fanourios Georgiades, Danail Stoyanov, Laurence B Lovat

ORCID number: Rawen Kader 0000-0001-9133-0838; Andreas V Hadjinicolaou 0000-0002-6520-443X; Fanourios Georgiades 0000-0003-0440-2720; Danail Stoyanov 0000-0002-0980-3227; Laurence B Lovat 0000-0003-4542-3915.

Author contributions: Kader R, Hadjinicolaou AV and Georgiades F performed the literature review and wrote the manuscript; Stoyanov D and Lovat LB revised the manuscript; All authors have read and approved the final manuscript.

Conflict-of-interest statement: Rawen Kader is supported by the Wellcome/EPSRC Centre for Interventional and Surgical Sciences (WEISS) at UCL; [203145Z/16/Z]. Danail Stoyanov owns shares in Odin Vision and Digital Surgery Ltd. Laurence B Lovat owns shares in Odin Vision. The remaining authors declare no conflict of interest.

Open-Access: This article is an open-access article that was selected by an in-house editor and fully peer-reviewed by external reviewers. It is distributed in accordance with the Creative Commons Attribution NonCommercial (CC BY-NC 4.0) license, which permits others to distribute, remix, adapt, build upon this work non-commercially,

Rawen Kader, Danail Stoyanov, Laurence B Lovat, Wellcome/EPSRC Centre for Interventional and Surgical Sciences, University College London, London W1W 7TY, United Kingdom

Rawen Kader, Laurence B Lovat, Division of Surgery and Interventional Sciences, University College London, London W1W 7TY, United Kingdom

Andreas V Hadjinicolaou, MRC Cancer Unit, Department of Gastroenterology, University of Cambridge, Cambridge CB2 0QQ, United Kingdom

Fanourios Georgiades, Department of Surgery, University of Cambridge, Cambridge CB2 0QQ, United Kingdom

Danail Stoyanov, Department of Computer Science, University College London, London W1W 7TY, United Kingdom

Corresponding author: Rawen Kader, BMed, MBBS, MRCP, Research Fellow, Wellcome/EPSRC Centre for Interventional and Surgical Sciences, University College London, Charles Bell House, 43-45 Foley Street, Fitzrovia, London W1W 7TY, United Kingdom.
r.kader@nhs.net

Abstract

Colonoscopy remains the gold standard investigation for colorectal cancer screening as it offers the opportunity to both detect and resect pre-malignant and neoplastic polyps. Although technologies for image-enhanced endoscopy are widely available, optical diagnosis has not been incorporated into routine clinical practice, mainly due to significant inter-operator variability. In recent years, there has been a growing number of studies demonstrating the potential of convolutional neural networks (CNN) to enhance optical diagnosis of polyps. Data suggest that the use of CNNs might mitigate the inter-operator variability amongst endoscopists, potentially enabling a "resect and discard" or "leave in" strategy to be adopted in real-time. This would have significant financial benefits for healthcare systems, avoid unnecessary polypectomies of non-neoplastic polyps and improve the efficiency of colonoscopy. Here, we review advances in CNN for the optical diagnosis of colorectal polyps, current limitations and future directions.

Key Words: Artificial intelligence; Deep learning; Convolutional neural networks; Computer aided diagnosis; Optical diagnosis; Colorectal polyps

and license their derivative works on different terms, provided the original work is properly cited and the use is non-commercial. See: http://creativecommons.org/Licenses/by-nc/4.0/

Manuscript source: Invited manuscript

Specialty type: Gastroenterology and hepatology

Country/Territory of origin: United Kingdom

Peer-review report's scientific quality classification

Grade A (Excellent): A
Grade B (Very good): 0
Grade C (Good): 0
Grade D (Fair): 0
Grade E (Poor): 0

Received: February 27, 2021
Peer-review started: February 27, 2021
First decision: April 18, 2021
Revised: April 29, 2021
Accepted: August 24, 2021
Article in press: August 24, 2021
Published online: September 21, 2021

P-Reviewer: Cavdar SC
S-Editor: Ma YJ
L-Editor: A
P-Editor: Li JH

©The Author(s) 2021. Published by Baishideng Publishing Group Inc. All rights reserved.

Core Tip: A convolutional neural network (CNN) is a specific type of artificial intelligence deep learning. These networks may play an important role in the coming years in assisting endoscopists to optically diagnose colorectal polyps. CNNs can mitigate the inter-operator variability amongst endoscopists, potentially enabling a "resect and discard" or "leave in" strategy to be adopted. This would improve the efficiency of colonoscopy, reduce healthcare costs and reduce adverse events for patients by avoiding unnecessary resections of non-neoplastic polyps. In this article, we expand on the most relevant studies in this field and discuss limitations and future directions that will determine fulfilment of the potential of CNN in the optical diagnosis of colorectal polyps.

Citation: Kader R, Hadjinicolaou AV, Georgiades F, Stoyanov D, Lovat LB. Optical diagnosis of colorectal polyps using convolutional neural networks. *World J Gastroenterol* 2021; 27(35): 5908-5918
URL: https://www.wjgnet.com/1007-9327/full/v27/i35/5908.htm
DOI: https://dx.doi.org/10.3748/wjg.v27.i35.5908

INTRODUCTION

Colorectal cancer (CRC) is the third most commonly diagnosed cancer worldwide[1] and thus, a significant burden on global healthcare systems. Most CRCs develop in a relatively predictable, stepwise sequence from mutation-accumulating neoplastic polyps, such as adenomas and sessile serrated lesions (SSL)[2]. Current evidence-based societal guidelines unequivocally accept colonoscopy to be the gold standard tool for screening of CRC[3]. Colonoscopy offers the opportunity to both detect and resect neoplastic polyps[4] and its implementation, especially as part of bowel cancer screening programs, has been linked to a significant reduction in the incidence of the CRC and CRC-related mortality[5].

Over 90% of polyps detected at colonoscopy are either small (6-9 mm) or diminutive (≤ 5 mm), entities that are thought to harbour a very low risk for developing into CRC [6]. Furthermore, almost half of these polyps are non-neoplastic in nature; and frequently hyperplastic[7]. Accurate differentiation of neoplastic from non-neoplastic polyps can prevent the unnecessary resection of the latter, avoiding an intervention which is not cost-effective and which carries risks of significant morbidity[8].

Recent years have seen significant research activity in the use of artificial intelligence (AI), particularly convolutional neural networks (CNN), to optically diagnose colorectal polyps. The field is gaining increasing momentum. The aim of this review article is to summarise and critically appraise the available medical literature related to advances in CNN for optical diagnosis of colorectal polyps and highlight the field's current limitations and future directions.

OPTICAL DIAGNOSIS

The term "optical diagnosis" refers to the use of advanced imaging techniques for real-time, *in-vivo* polyp characterisation and evaluation to guide therapeutic decisions[9]. Accurate optical diagnosis of diminutive polyps would enable identification of hyperplastic polyps in the rectosigmoid region, where they are commonly found, and allow the endoscopist to confidently take a "diagnose and leave" approach instead of resecting the lesion. Equally, for diminutive adenomas, accurate optical diagnosis would prompt the endoscopist to remove the lesion on the spot and discard the specimen without the need for histological assessment ("resect and discard"strategy) [9].

The American Society of Gastrointestinal Endoscopy established the Preservation and Incorporation of Valuable endoscopic Innovations (PIVI) to provide thresholds that are required of endoscopic technology in order to implement a "resect and discard"(PIVI 1) and "diagnose and leave" (PIVI 2) strategy[9]. PIVI 1 requires ≥ 90%

concordance in post-polypectomy surveillance intervals when comparing the combination of optical diagnosis for diminutive adenomas with histopathology assessment of all other polyps against decisions based solely on histopathology evaluation of all identified polyps[10]. PIVI 2 requires a technology to achieve a negative predictive value (NPV) of ≥ 90% for diminutive adenomatous polyps in the rectosigmoid region[9].

There has been extensive research in image enhanced endoscopy (IEE), such as narrow band imaging (NBI), to assist endoscopists in optical diagnosis to characterise diminutive polyps[11-13]. Using IEE, expert endoscopists in academic centres have consistently demonstrated an optical diagnosis accuracy that exceeds PIVI thresholds [14-16], however, studies have often found community and non-expert endoscopists to fall short of these minimal thresholds[17]. An example is the multi-centre DISCARD-2 study which evaluated the optical diagnosis accuracy of 28 community endoscopists using NBI. Disappointingly, the endoscopists' optical diagnosis derived colonoscopy surveillance intervals only matched 68% of the histopathology derived intervals[18]. Although widely available, technologies for optical diagnosis has not been incorporated into routine clinical practice with one of the main barriers being the inter-operator variability amongst endoscopists[19].

WHAT IS A CONVOLUTIONAL NEURAL NETWORK?

AI is the ability of computers to perform tasks that traditionally require human intelligence (Figure 1)[20]. Machine learning (ML) is a subset of AI, whereby computers continuously learn from data without explicit human programming[21]. This can be used to predicate a polyp's histology. ML models can be trained using unsupervised or supervised techniques. Unsupervised learning is when the input and output data are not paired. Supervised ML is more labour intensive as it requires paired input and output data for training. An example of a supervised ML model for optical diagnosis is to annotate a bounding box around a polyp (input data), commonly referred to as a region of interest, and label it with the histology of the polyp (output data). The model automatically learns to extract features that allow it to differentiate polyp subtypes and output a diagnosis based on the histology classification system it was trained with but the annotation process is time consuming for the clinician.

Deep learning is a subset of ML, whereby algorithms use multiple layers within a neural network[22], mimicking the human brain, to extract high level features from input data. CNNs are the most commonly used network in the application of deep learning to optically diagnose polyps. They provide an objective output, bypassing the human inter and intra-operator variability, and can develop classification algorithms without exhaustive effort as they do not require human-crafted feature extraction or extensive pre-processing of data[23].

Building a CNN model typically involves three separate datasets; a training set, a validation set and a test set[24]. The training set is used to develop the model so that it predicts a label (*e.g.*, adenomatous or hyperplastic polyp for polyp characterisation) based on features extracted from the endoscopic image by the algorithm itself. The validation set is used to avoid over-fitting into the training dataset through fine tuning of the hyperparameters of the model. Finally, the testing set is used as an independent dataset to evaluate the generalisability of the CNN. With smaller datasets, cross-validation can be used to assess the model's robustness. In cross-validation, the data is split into equal parts (*e.g.*, 4 parts), with one part held out as a validation dataset. This process is repeated multiple times, with the results of each split eventually pooled together to decide how robust the model is[24]. CNNs evaluated using cross-validation should still be assessed against an independent test set to examine their generalisability[24].

CONVOLUTIONAL NEURAL NETWORKS AND OPTICAL DIAGNOSIS

It is only in the last few years that the use of CNNs in optical diagnosis of colorectal polyps has been extensively investigated, with various studies emerging (Table 1). Many of these studies have in fact demonstrated the capability of CNNs to surpass the PIVI 2 threshold in order to support a "leave in" strategy for rectosigmoid hyperplastic polyps (Table 2). This was first demonstrated by Chen *et al*[25], who used a single centre, retrospective, still image dataset of 2157 polyps to train a CNN and reported a

Table 1 Summary of the studies on convolutional neural network algorithms for the optical diagnosis of colorectal polyps

Ref.	Study design (training/testing)	Multi-centre study	Dataset	Image quality	Classification system	Lesion number (training/testing)	SSL excluded	Endoscopic processor	Image modality (training)	Real-time capability
Komeda *et al* [37]	Retrospective	Single	Video	Not specified	Adenoma/non-adenoma	Not specified/10	No	Not specified	WLI, NBI, chromoendoscopy	Not specified
Chen *et al*[25]	Retrospective/prospective	Single	Still	HQ	Hyperplastic/neoplastic	2157/284	Yes	Olympus 260 + 290	Magnified NBI	Real-time (approximately 450 ms)
Byrne *et al* [23]	Retrospective/prospective	Single	Video	All images	NICE Type 1/NICE Type 2	220/125	Yes	Olympus 190	NBI-NF	Real-time (approximately 50 ms)
Zachariah *et al*[26]	Prospective	Two	Still	Adequate and HQ	Adenomatous/serrated polyp	5278/634	No	Olympus 190 (90%), 180 (7%), Pentax i10(3%)	WLI, NBI, i-SCAN	Real-time (approximately 13 ms)
Ozawa *et al* [38]	Retrospective/prospective	Single	Still	HQ	Hyperplastic/adenomatous/SSL/CRC/other	WLI: 17566/783 NBI: 2865/290	No	Olympus 260 + 290	WLI, NBI	Real-time (approximately 20 ms)
Jin *et al*[31]	Retrospective/prospective	Single	Still	HQ	Hyperplastic/adenomatous	2150/300	Yes	Olympus 290	NBI-NF	Real-time (approximately 10 ms)
Song *et al*[39]	Retrospective/prospective	Single	Still	HQ	Serrated polyp/benign adenoma/MSM/DSMC	624/545	No	Olympus 290	NBI-NF	Real-time (approximately 20-40 ms)
Rodriguez-Diaz *et al*[28]	Retrospective/prospective	Two	Still	Not specified	Neoplastic (adenomas, CRC)/non-neoplastic (hyperplastic, normal)	607/280	Training: Yes Testing: No	Olympus 190	NBI-NF, NBI (digital magnification)	Real-time (approximately 100 ms)
van der Zander *et al* [27]	Retrospective/prospective	Not specified	Still	HQ	Benign (hyperplastic)/pre-malignant (adenomatous, SSL, T1 CRC)	398/60	No	Fujifilm, Pentax	WLI, BLI, i-SCAN	Real-time (approximately 14.8 ms)

SSL: Sessile serrated lesion; WLI: White light imaging; BLI: Blue light imaging; NBI: Narrow band imaging; NBI-NF: Narrow band imaging–near focus; NICE: NBI International Colorectal Endoscopic; HQ: High-quality; CRC: Colorectal cancer; MSMC: Mucosal or superficial submucosal cancer; DSMC: Deep submucosal cancer.

sensitivity for identifying adenomas of 96.3% , specificity 78.1%, and NPV of 91.5% when evaluating a test set of 284 colonic and rectal diminutive adenomatous and hyperplastic polyps. Using colonic diminutive polyps is a common strategy to assess against PIVI 2 due to difficulties in obtaining large datasets of diminutive rectosigmoid polyps. An important limitation of this study is that it used magnified narrow-band

Table 2 Summary of the per-polyp results of studies on convolutional neural network algorithms for the optical diagnosis of colorectal polyps (cross-validation results not included)

Ref.	Image Modality (testing)	Sensitivity (%)	Specificity (%)	PPV (%)	NPV (%)	Accuracy for neoplasia (%)	PIVI 1 achieved (%)	PIVI 2 achieved (%)
Komeda *et al*[37]	Not specified	-	-	-	-	70	-	-
Chen *et al*[25]	Magnified NBI	96.3	78.1	89.6	91.5	90.1	-	Yes (91.5)
Byrne *et al*[23]	NBI-NF	98	83	90	97	94	-	Yes (97)
Zachariah *et al*[26]	NBI	-	-	-	96.5	93.1	Yes (98.3)	Yes (96.5)
	WLI	-	-	-	88.9	92.8	Yes (90.8)	No (88.9)
Ozawa *et al*[38][1]	NBI	97	-	84	88	-	-	-
	WLI	98	-	85	88	-	-	-
Jin *et al*	NBI-NF	83.3	91.7	93.3	78.6	86.7	-	-
Song *et al*[39]	NBI-NF (test set 1)	84.1	74	88.3	67.7	-	-	-
	NBI-NF (test set 2)	88.5	72.1	88.6	84.7	-	-	-
Rodriguez-Diaz *et al*[28]	NBI-NF (90%) + NBI (10%)	95	88	-	93	-	Yes (94 (20/90 LC))	Yes (98 (6/68 LC))
van der Zander *et al*[27]	WLI + BLI	95.6	93.3	97.7	87.5	95.0	-	No (87.5)

[1]Per frame analysis reported only.

WLI: White light imaging; BLI: Blue light imaging; NBI: Narrow band imaging; NBI-NF: Narrow band imaging–near focus; PIVI: Preservation and Incorporation of Valuable endoscopic Innovations; PPV: Positive predictor value; NPV: Negative predictor value; LC: Low-confidence.

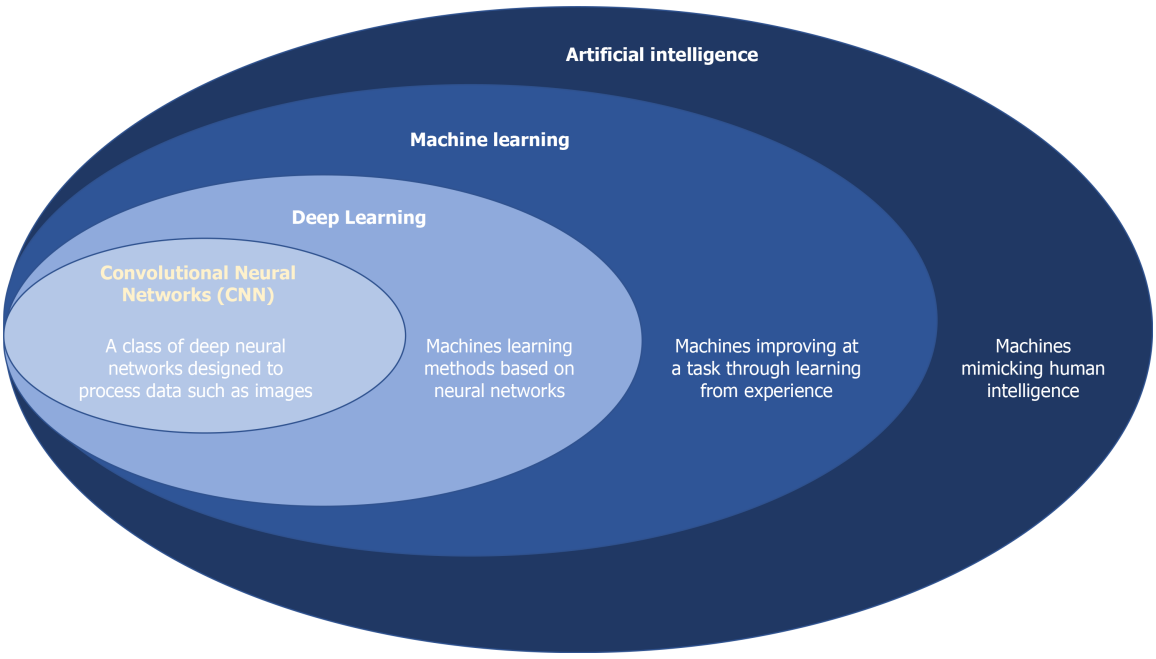


Figure 1 The relationship between convolutional neural networks, deep learning, machine learning and artificial intelligence.

imaging (NBI) data. This recently developed modality is not yet readily available in most endoscopy departments, although it will become more widely used with time.

Byrne *et al*[23] further advanced the field by training a CNN with NBI-near focus (NBI-NF) which is more commonly used in Europe and North America. It was trained with 220 polyp positive videos and when tested against 125 diminutive polyps which were collected prospectively, the model diagnosed 106 polyps with high confidence, achieving a sensitivity for identifying NBI International Colorectal Endoscopic (NICE)

type 1 polyps of 98%, specificity 83% and NPV of 97%. A novelty worth highlighting in this study was the use of images derived from videos, an approach that reduces selection bias compared to retrospective still images as endoscopists usually capture high quality polyp views that are free from motion blur and surface artifact. An additional advantage of this CNN is that it simplified the clinical workflow as it automatically diagnoses polyps without requiring a still image of the polyp to be captured. Limitations of the study are that SSLs, normal tissue and lymphoid aggregates were excluded from the final analysis and the videos used to train and test the CNN were captured from colonoscopies performed by a single expert endoscopist and hence, potentially less generalisable to novice users.

The most commonly used imaging modalities amongst community endoscopists are white light imaging (WLI) and NBI without magnification. Using a large retrospective still image training set of 5278 polyps and tested against 634 polyps, Zachariah *et al*[26]'s CNN fell short of ***PIVI*** 2 in WLI (NPV of 88.9% and accuracy 92.8%) but achieved the threshold in NBI without magnification (NPV of 90.8% and accuracy 93.1%). This study advanced the field as it demonstrated the capabilities of CNNs to optically diagnose polyps in standard NBI modality and also to differentiate adenomas from serrated polyps through the inclusion of SSLs in its dataset.

Whilst the majority of CNNs have been trained and tested using Olympus data, studies are emerging using data from other manufacturers. van der Zander *et al*[27] recently developed a CNN using Fujifilm data in high definition white light (HDWL) and blue light imaging (BLI). The CNN was more efficacious when it used a unique multimodal imaging approach where it combined both HDWL and BLI images of the same polyp in its decision process compared to a single imaging modality. When evaluated against 60 prospectively collected diminutive polyps, it did not reach the ***PIVI*** 2 threshold with a NPV of 87.5% but did achieve an optical diagnosis accuracy of 95% (sensitivity for identifying pre-malignant polyps 95.6% and specificity 93.3%) and demonstrated superiority to both expert and novice endoscopists in human benchmark testing.

In comparison to PIVI 2, there are fewer studies evaluating the performance of CNNs against PIVI 1. The CNN presented in Zachariah *et al*[26] reached PIVI 1 thresholds in both WLI and NBI with normal magnification, achieving concordance with histology-based colonoscopy surveillance intervals in 90.9% and 98.3% of patients, for each respective modality. Rodrigues-Diaz *et al*[28] used a single centre retrospective still image dataset to train a CNN with 607 polyps and tested against 90 diminutive polyps where it achieved a high confidence diagnosis in 78% of cases, with a 94% agreement with histology-based colonoscopy surveillance intervals. Tested against 68 rectosigmoid polyps, the model diagnosed 88% of polyps with high confidence, achieving PIVI 2 thresholds with a NPV of 97%.

There is also potential to expand the use of optical diagnosis CNNs outside of the "resect and discard" and "leave in strategy". A dilemma that can complicate issuing post-polypectomy surveillance intervals is discrepancies between endoscopic and histological diagnosis and classification of polyps with tissue fragmentation in the specimen retrieval process playing an important role. Shahidi *et al*[29]'s proof of concept study used a CNN to resolve discrepancies in polyps ≤ 3 mm in size. Tested against 900 polyps that were ≤ 3 mm and optically diagnosed as adenomatous by an expert endoscopist, the CNN diagnosed the adenomas with high confidence in 644 polyps, with 256 polyps deemed to be of sub-optimal imaging quality. However, of these high confidence diagnoses, the pathologists diagnosed 15.4% as normal mucosa, 13.2% as hyperplastic polyp and 0.3% as SSL. In this context, a CNN could help to mitigate against the risk of under-surveillance.

Whilst CNN's diagnostic accuracy excels in many studies, without real-time capabilities, they would have no clinical utility. Prior to the era of deep learning, computer aided diagnosis algorithms lacked real-time capability, but most CNNs do not share this problem and often process data at a rate that exceeds the 25 frames per second that is generated in a video recording of a colonoscopy procedure. Given the excellent performance in ex-vivo studies and the real-time capabilities displayed by CNNs, the future appears promising for their integration in colonoscopy.

TRANSPARENCY OF CONVOLUTIONAL NEURAL NETWORKS

The complexity of CNN models' decision process is often referred to as a "black box" and represents an important barrier to its acceptance by both clinicians and patients [30]. Opening the ''black box'' to display the raw features which informed the CNN's

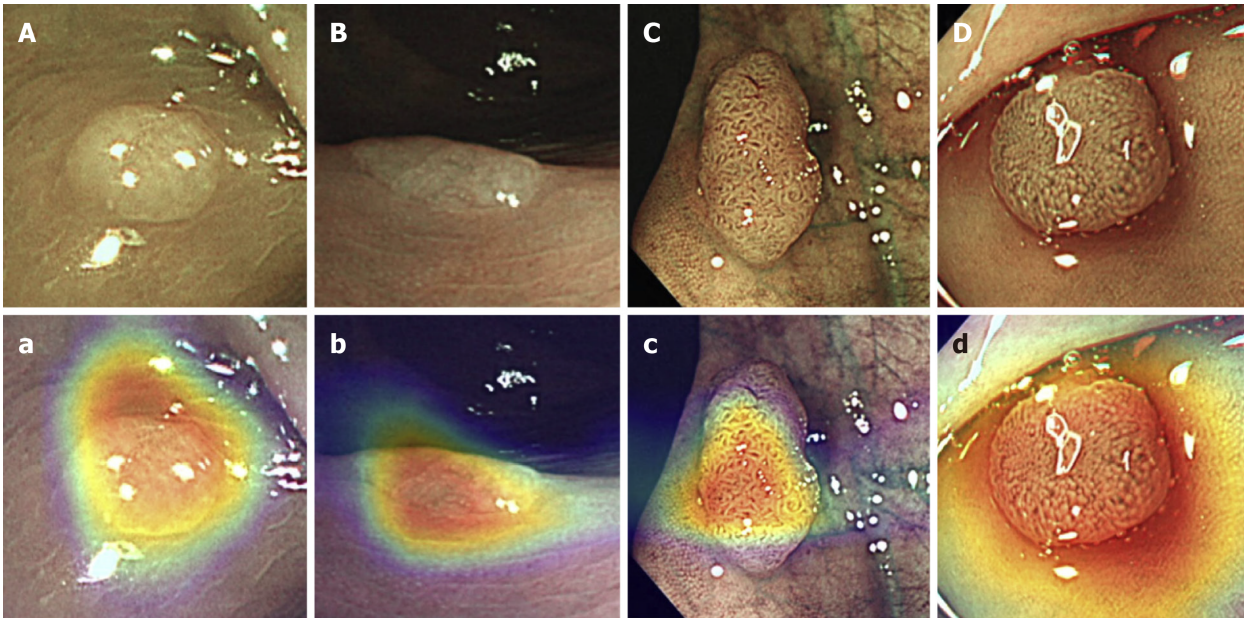


Figure 2 Illustration of coloured heatmaps, overlaid to the polyp, which demonstrates the regions that most likely contributed to the convolutional neural networks's diagnosis. A, B, C, D: Original narrow band imaging (NBI) of polyps; a, b, c, d: Coloured heatmap overlaid on the NBI image; Red: Higher probability that this region informed the convolutional neural networks (CNN)'s diagnosis; Blue: Lower probability that this region informed the CNN's diagnosis. Images adapted and modified with permission from the publisher[31]. Citation: Jin EH, Lee D, Bae JH, Kang HY, Kwak MS, Seo JY, Yang JI, Yang SY, Lim SH, Yim JY, Lim JH, Chung GE, Chung SJ, Choi JM, Han YM, Kang SJ, Lee J, Chan Kim H, Kim JS. Improved Accuracy in Optical Diagnosis of Colorectal Polyps Using Convolutional Neural Networks. *Gastroenterology* 2020; 158(8): 2169-2179. Copyright© The Authors 2020. Published by Elsevier.

decision is important for transparency especially from a safety standpoint[28]. Transparency can help identify biases within the neural network and aid root-cause analyses in cases of patient harm, for example, if a neoplastic polyp that subsequently develops into a CRC is originally misdiagnosed as non-neoplastic by the CNN model.

For polyp characterisation, important steps have been taken to open the black box. Jin *et al*[31] developed a CNN that generated a coloured heat map, overlaid to the polyp, to help the endoscopist comprehend the specific aspects of the image that contributed to the CNN's prediction (Figure 2). This could help the endoscopist to decide which information is relevant and which decisions are truly based on appropriate image analysis. If, for example, the heatmap is overlaid to normal mucosa, then the endoscopist would quickly be able to appreciate this and disregard the CNN's diagnosis.

More recently, in order to further enhance CNN transparency, Rodriguez-Diaz *et al*[28] developed a colour coded segmentation model (Figure 3). In this model, the CNN divides the polyp into distinct segments to allow the endoscopist to identify the specific regions within the image that is informing the CNN's decision. The CNN predicts the histology of each subregion of the segmented polyp, with high confidence neoplastic diagnoses coloured in red, high confidence non-neoplastic in green, and low confidence/indeterminate diagnoses in yellow, with the final predication resulting from an aggregate of all the analysed regions. The end result is a detailed spatial colour coded histology map of the polyp surface, which the endoscopist can visualise and incorporate into their decision process[28], enhancing the interpretability of this CNN model in comparison to others. However, an important limitation to this advanced CNN is that it currently lacks the ability to operate at a video rate.

Further research in the interpretability of CNN models is required to improve its acceptance[32] and accelerate its translation to clinical practise.

LIMITATIONS AND FUTURE DIRECTIONS

Despite the promise shown by CNNs this far, it is crucial to recognise that there are various limitations that need to be overcome before they can become part of the endoscopic clinical workflow. The most significant limitations are the reliance on retrospective datasets[33], which are inherently subject to selection bias, and the lack of prospective studies and randomised controlled trials[34]. Most studies train and test

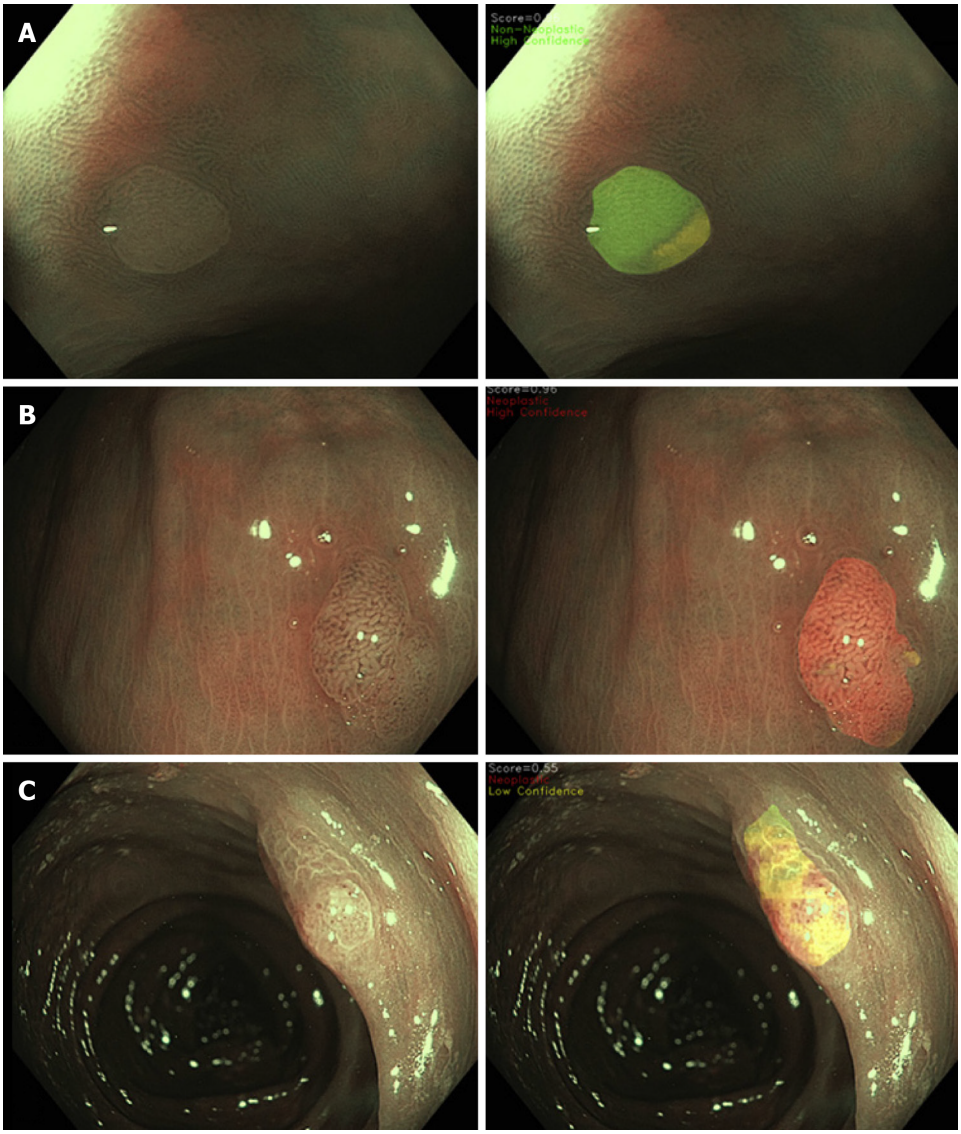


Figure 3 Spatial colour coded histology map which allows the user to visualise the sub-regions of the polyp surface that contributed to the convolutional neural networks's decision process. A: Hyperplastic polyps; B: Adenomatous polyps; C: Sessile serrated lesions; Red: High-confidence neoplastic diagnosis; Green: High-confidence non-neoplastic diagnosis; Yellow: Indeterminate or low-confidence diagnosis. Adapted from Ref. [28]. Citation: Rodriguez-Diaz E, Baffy G, Lo WK, Mashimo H, Vidyarthi G, Mohapatra SS, Singh SK. Real-time artificial intelligence-based histologic classification of colorectal polyps with augmented visualization. *Gastrointest Endosc* 2021; 93: 662-670. Copyright© The Authors 2021. Published by Elsevier.

CNNs using high quality images of polyps, free from "noise" such as motion blur and polyp surface artifact (*e.g.*, mucus, stool or blood). The extent to which CNNs pre-clinical results are reproducible in the real-world setting, where 'noise' is frequently encountered, remains to be seen.

To the best of our knowledge, there have been no prospective randomised controlled clinical trials evaluating optical diagnosis CNN *in-vivo*. This is partly due to clinical trials being time consuming and expensive, and an alternative pragmatic approach could be the use of a benchmark test in the form a publicly available external dataset to compare different CNN models[35]. No such datasets currently exist for polyp characterisation and therefore the generalisability of CNN models remains poorly understood. Generalisability refers to the CNN performance with different endoscope models and clinical settings from the site that the data was generated to train the CNN. To date, only one study[36] has evaluated generalisability, and this was limited to a small testing set of 69 polyp images from two population cohorts (Australian and Japanese) using two separate endoscope manufactures (Olympus and Fujifilm). Despite the small test-set, this study highlighted the concerns of generalisability as the operator area under the curve fell from 94.3% for the internal set, to 84.5% and 90.3% for the external testing sets (NBI and BLI respectively).

Another important limitation is that studies often exclude polyps that are not adenomas or hyperplastic polyps, restricting the possible classification outputs of CNNs. This, in turn, limits their clinical utility as polyps such as SSL and inflammatory polyps would be misclassified due to limitations in the initial training phase of the CNNs when the categorisation system is established.

Research in this field is likely to continue to expand and future directions to consider include: (1) Guidelines to identify the role of CNNs in the clinical workflow, specifically, whether it is a second reader, a concurrent reader or a provider of an independent diagnosis[30]; (2) Prospective multi-centre randomised clinical trials; (3) Publicly available external datasets for benchmark testing and evaluation of the generalisability of CNN models in different clinical settings and population cohorts; and (4) Acquiring datasets inclusive of all polyp sub-types to advance CNN classification systems.

CONCLUSION

In summary, this is an exciting time for the endoscopy community. CNNs diagnostic performance has excelled in ex-vivo studies and in human benchmarking testing. CNNs are likely to be a key adjunct in optically diagnosing polyps and have renewed optimism that implementation of a "resect and discard" and "leave in" strategy is feasible due to the potential to alleviate the inter-operator variability amongst endoscopists. This would bring significant financial benefits to healthcare systems, avoid unnecessary polypectomies of non-neoplastic polyps and improve the efficiency of colonoscopy. However, prospective multi-centre randomised controlled trials and publicly available datasets for benchmark testing are required to further evaluate the efficacy and generalisability of CNNs. Furthermore, with these models now emerging in endoscopy units, it's imperative that guidelines are developed to establish their role in the clinical workflow.

REFERENCES

1 **Bray F**, Ferlay J, Soerjomataram I, Siegel RL, Torre LA, Jemal A. Global cancer statistics 2018: GLOBOCAN estimates of incidence and mortality worldwide for 36 cancers in 185 countries. *CA Cancer J Clin* 2018; **68**: 394-424 [PMID: 30207593 DOI: 10.3322/caac.21492]

2 **Song M**, Emilsson L, Bozorg SR, Nguyen LH, Joshi AD, Staller K, Nayor J, Chan AT, Ludvigsson JF. Risk of colorectal cancer incidence and mortality after polypectomy: a Swedish record-linkage study. *Lancet Gastroenterol Hepatol* 2020; **5**: 537-547 [PMID: 32192628 DOI: 10.1016/S2468-1253(20)30009-1]

3 **US Preventive Services Task Force**. Bibbins-Domingo K, Grossman DC, Curry SJ, Davidson KW, Epling JW Jr, García FAR, Gillman MW, Harper DM, Kemper AR, Krist AH, Kurth AE, Landefeld CS, Mangione CM, Owens DK, Phillips WR, Phipps MG, Pignone MP, Siu AL. Screening for Colorectal Cancer: US Preventive Services Task Force Recommendation Statement. *JAMA* 2016; **315**: 2564-2575 [PMID: 27304597 DOI: 10.1001/jama.2016.5989]

4 **Rutter MD**, East J, Rees CJ, Cripps N, Docherty J, Dolwani S, Kaye PV, Monahan KJ, Novelli MR, Plumb A, Saunders BP, Thomas-Gibson S, Tolan DJM, Whyte S, Bonnington S, Scope A, Wong R, Hibbert B, Marsh J, Moores B, Cross A, Sharp L. British Society of Gastroenterology/Association of Coloproctology of Great Britain and Ireland/Public Health England post-polypectomy and post-colorectal cancer resection surveillance guidelines. *Gut* 2020; **69**: 201-223 [PMID: 31776230 DOI: 10.1136/gutjnl-2019-319858]

5 **Zauber AG**, Winawer SJ, O'Brien MJ, Lansdorp-Vogelaar I, van Ballegooijen M, Hankey BF, Shi W, Bond JH, Schapiro M, Panish JF, Stewart ET, Waye JD. Colonoscopic polypectomy and long-term prevention of colorectal-cancer deaths. *N Engl J Med* 2012; **366**: 687-696 [PMID: 22356322 DOI: 10.1056/NEJMoa1100370]

6 **Lieberman D**, Moravec M, Holub J, Michaels L, Eisen G. Polyp size and advanced histology in patients undergoing colonoscopy screening: implications for CT colonography. *Gastroenterology* 2008; **135**: 1100-1105 [PMID: 18691580 DOI: 10.1053/j.gastro.2008.06.083]

7 **Rex DK**, Overhiser AJ, Chen SC, Cummings OW, Ulbright TM. Estimation of impact of American College of Radiology recommendations on CT colonography reporting for resection of high-risk adenoma findings. *Am J Gastroenterol* 2009; **104**: 149-153 [PMID: 19098863 DOI: 10.1038/ajg.2008.35]

8 **El Hajjar A**, Rey JF. Artificial intelligence in gastrointestinal endoscopy: general overview. *Chin Med J (Engl)* 2020; **133**: 326-334 [PMID: 31929362 DOI: 10.1097/CM9.0000000000000623]

9 **ASGE Technology Committee**. Abu Dayyeh BK, Thosani N, Konda V, Wallace MB, Rex DK, Chauhan SS, Hwang JH, Komanduri S, Manfredi M, Maple JT, Murad FM, Siddiqui UD, Banerjee S.

ASGE Technology Committee systematic review and meta-analysis assessing the ASGE PIVI thresholds for adopting real-time endoscopic assessment of the histology of diminutive colorectal polyps. *Gastrointest Endosc* 2015; **81**: 502.e1-502.e16 [PMID: 25597420 DOI: 10.1016/j.gie.2014.12.022]

10 **Rex DK**. Can we do resect and discard with AI-assisted colon polyp 'optical biopsy'? *Tech Gastrointest Endosc* 2019; 150638 [DOI: 10.1016/j.tgie.2019.150638]

11 **Ignjatovic A**, East JE, Suzuki N, Vance M, Guenther T, Saunders BP. Optical diagnosis of small colorectal polyps at routine colonoscopy (Detect InSpect ChAracterise Resect and Discard; DISCARD trial): a prospective cohort study. *Lancet Oncol* 2009; **10**: 1171-1178 [PMID: 19910250 DOI: 10.1016/S1470-2045(09)70329-8]

12 **Ignjatovic A**, Thomas-Gibson S, East JE, Haycock A, Bassett P, Bhandari P, Man R, Suzuki N, Saunders BP. Development and validation of a training module on the use of narrow-band imaging in differentiation of small adenomas from hyperplastic colorectal polyps. *Gastrointest Endosc* 2011; **73**: 128-133 [PMID: 21184878 DOI: 10.1016/j.gie.2010.09.021]

13 **Rastogi A**, Keighley J, Singh V, Callahan P, Bansal A, Wani S, Sharma P. High accuracy of narrow band imaging without magnification for the real-time characterization of polyp histology and its comparison with high-definition white light colonoscopy: a prospective study. *Am J Gastroenterol* 2009; **104**: 2422-2430 [PMID: 19584829 DOI: 10.1038/ajg.2009.403]

14 **Repici A**, Hassan C, Radaelli F, Occhipinti P, De Angelis C, Romeo F, Paggi S, Saettone S, Cisarò F, Spaander M, Sharma P, Kuipers EJ. Accuracy of narrow-band imaging in predicting colonoscopy surveillance intervals and histology of distal diminutive polyps: results from a multicenter, prospective trial. *Gastrointest Endosc* 2013; **78**: 106-114 [PMID: 23582472 DOI: 10.1016/j.gie.2013.01.035]

15 **Wallace MB**, Crook JE, Coe S, Ussui V, Staggs E, Almansa C, Patel MK, Bouras E, Cangemi J, Keaveny A, Picco M, Riegert-Johnson D. Accuracy of *in vivo* colorectal polyp discrimination by using dual-focus high-definition narrow-band imaging colonoscopy. *Gastrointest Endosc* 2014; **80**: 1072-1087 [PMID: 24973171 DOI: 10.1016/j.gie.2014.05.305]

16 **Singh R**, Jayanna M, Navadgi S, Ruszkiewicz A, Saito Y, Uedo N. Narrow-band imaging with dual focus magnification in differentiating colorectal neoplasia. *Dig Endosc* 2013; **25** Suppl 2: 16-20 [PMID: 23617643 DOI: 10.1111/den.12075]

17 **Rees CJ**, Rajasekhar PT, Wilson A, Close H, Rutter MD, Saunders BP, East JE, Maier R, Moorghen M, Muhammad U, Hancock H, Jayaprakash A, MacDonald C, Ramadas A, Dhar A, Mason JM. Narrow band imaging optical diagnosis of small colorectal polyps in routine clinical practice: the Detect Inspect Characterise Resect and Discard 2 (DISCARD 2) study. *Gut* 2017; **66**: 887-895 [PMID: 27196576 DOI: 10.1136/gutjnl-2015-310584]

18 **Kuiper T**, Marsman WA, Jansen JM, van Soest EJ, Haan YC, Bakker GJ, Fockens P, Dekker E. Accuracy for optical diagnosis of small colorectal polyps in nonacademic settings. *Clin Gastroenterol Hepatol* 2012; **10**: 1016-20; quiz e79 [PMID: 22609999 DOI: 10.1016/j.cgh.2012.05.004]

19 **Ladabaum U**, Fioritto A, Mitani A, Desai M, Kim JP, Rex DK, Imperiale T, Gunaratnam N. Real-time optical biopsy of colon polyps with narrow band imaging in community practice does not yet meet key thresholds for clinical decisions. *Gastroenterology* 2013; **144**: 81-91 [PMID: 23041328 DOI: 10.1053/j.gastro.2012.09.054]

20 **Sharma P**, Pante A, Gross SA. Artificial intelligence in endoscopy. *Gastrointest Endosc* 2020; **91**: 925-931 [PMID: 31874161 DOI: 10.1016/j.gie.2019.12.018]

21 **Alagappan M**, Brown JRG, Mori Y, Berzin TM. Artificial intelligence in gastrointestinal endoscopy: The future is almost here. *World J Gastrointest Endosc* 2018; **10**: 239-249 [PMID: 30364792 DOI: 10.4253/wjge.v10.i10.239]

22 **Vakli P**, Deák-Meszlényi RJ, Hermann P, Vidnyánszky Z. Transfer learning improves resting-state functional connectivity pattern analysis using convolutional neural networks. *Gigascience* 2018; **7** [PMID: 30395218 DOI: 10.1093/gigascience/giy130]

23 **Byrne MF**, Chapados N, Soudan F, Oertel C, Linares Pérez M, Kelly R, Iqbal N, Chandelier F, Rex DK. Real-time differentiation of adenomatous and hyperplastic diminutive colorectal polyps during analysis of unaltered videos of standard colonoscopy using a deep learning model. *Gut* 2019; **68**: 94-100 [PMID: 29066576 DOI: 10.1136/gutjnl-2017-314547]

24 **van der Sommen F**, de Groof J, Struyvenberg M, van der Putten J, Boers T, Fockens K, Schoon EJ, Curvers W, de With P, Mori Y, Byrne M, Bergman JJGHM. Machine learning in GI endoscopy: practical guidance in how to interpret a novel field. *Gut* 2020; **69**: 2035-2045 [PMID: 32393540 DOI: 10.1136/gutjnl-2019-320466]

25 **Chen PJ**, Lin MC, Lai MJ, Lin JC, Lu HH, Tseng VS. Accurate Classification of Diminutive Colorectal Polyps Using Computer-Aided Analysis. *Gastroenterology* 2018; **154**: 568-575 [PMID: 29042219 DOI: 10.1053/j.gastro.2017.10.010]

26 **Zachariah R**, Samarasena J, Luba D, Duh E, Dao T, Requa J, Ninh A, Karnes W. Prediction of Polyp Pathology Using Convolutional Neural Networks Achieves "Resect and Discard" Thresholds. *Am J Gastroenterol* 2020; **115**: 138-144 [PMID: 31651444 DOI: 10.14309/ajg.0000000000000429]

27 **van der Zander QEW**, Schreuder RM, Fonollà R, Scheeve T, van der Sommen F, Winkens B, Aepli P, Hayee B, Pischel AB, Stefanovic M, Subramaniam S, Bhandari P, de With PHN, Masclee AAM, Schoon EJ. Optical diagnosis of colorectal polyp images using a newly developed computer-aided diagnosis system (CADx) compared with intuitive optical diagnosis. *Endoscopy* 2020 [PMID: 33368056 DOI: 10.1055/a-1343-1597]

28 **Rodriguez-Diaz E**, Baffy G, Lo WK, Mashimo H, Vidyarthi G, Mohapatra SS, Singh SK. Real-time artificial intelligence-based histologic classification of colorectal polyps with augmented visualization. *Gastrointest Endosc* 2021; **93**: 662-670 [PMID: 32949567 DOI: 10.1016/j.gie.2020.09.018]

29 **Shahidi N**, Rex DK, Kaltenbach T, Rastogi A, Ghalehjegh SH, Byrne MF. Use of Endoscopic Impression, Artificial Intelligence, and Pathologist Interpretation to Resolve Discrepancies Between Endoscopy and Pathology Analyses of Diminutive Colorectal Polyps. *Gastroenterology* 2020; **158**: 783-785.e1 [PMID: 31863741 DOI: 10.1053/j.gastro.2019.10.024]

30 **Ahmad OF**, Mori Y, Misawa M, Kudo SE, Anderson JT, Bernal J, Berzin TM, Bisschops R, Byrne MF, Chen PJ, East JE, Eelbode T, Elson DS, Gurudu SR, Histace A, Karnes WE, Repici A, Singh R, Valdastri P, Wallace MB, Wang P, Stoyanov D, Lovat LB. Establishing key research questions for the implementation of artificial intelligence in colonoscopy: a modified Delphi method. *Endoscopy* 2021; **53**: 893-901 [PMID: 33167043 DOI: 10.1055/a-1306-7590]

31 **Jin EH**, Lee D, Bae JH, Kang HY, Kwak MS, Seo JY, Yang JI, Yang SY, Lim SH, Yim JY, Lim JH, Chung GE, Chung SJ, Choi JM, Han YM, Kang SJ, Lee J, Chan Kim H, Kim JS. Improved Accuracy in Optical Diagnosis of Colorectal Polyps Using Convolutional Neural Networks with Visual Explanations. *Gastroenterology* 2020; **158**: 2169-2179.e8 [PMID: 32119927 DOI: 10.1053/j.gastro.2020.02.036]

32 **Yang YJ**, Bang CS. Application of artificial intelligence in gastroenterology. *World J Gastroenterol* 2019; **25**: 1666-1683 [PMID: 31011253 DOI: 10.3748/wjg.v25.i14.1666]

33 **Namikawa K**, Hirasawa T, Yoshio T, Fujisaki J, Ozawa T, Ishihara S, Aoki T, Yamada A, Koike K, Suzuki H, Tada T. Utilizing artificial intelligence in endoscopy: a clinician's guide. *Expert Rev Gastroenterol Hepatol* 2020; **14**: 689-706 [PMID: 32500760 DOI: 10.1080/17474124.2020.1779058]

34 **Pannala R**, Krishnan K, Melson J, Parsi MA, Schulman AR, Sullivan S, Trikudanathan G, Trindade AJ, Watson RR, Maple JT, Lichtenstein DR. Artificial intelligence in gastrointestinal endoscopy. *VideoGIE* 2020; **5**: 598-613 [PMID: 33319126 DOI: 10.1016/j.vgie.2020.08.013]

35 **Misawa M**, Kudo SE, Mori Y, Hotta K, Ohtsuka K, Matsuda T, Saito S, Kudo T, Baba T, Ishida F, Itoh H, Oda M, Mori K. Development of a computer-aided detection system for colonoscopy and a publicly accessible large colonoscopy video database (with video). *Gastrointest Endosc* 2021; **93**: 960-967.e3 [PMID: 32745531 DOI: 10.1016/j.gie.2020.07.060]

36 **Zorron Cheng Tao Pu L**, Maicas G, Tian Y, Yamamura T, Nakamura M, Suzuki H, Singh G, Rana K, Hirooka Y, Burt AD, Fujishiro M, Carneiro G, Singh R. Computer-aided diagnosis for characterization of colorectal lesions: comprehensive software that includes differentiation of serrated lesions. *Gastrointest Endosc* 2020; **92**: 891-899 [PMID: 32145289 DOI: 10.1016/j.gie.2020.02.042]

37 **Komeda Y**, Handa H, Watanabe T, Nomura T, Kitahashi M, Sakurai T, Okamoto A, Minami T, Kono M, Arizumi T, Takenaka M, Hagiwara S, Matsui S, Nishida N, Kashida H, Kudo M. Computer-Aided Diagnosis Based on Convolutional Neural Network System for Colorectal Polyp Classification: Preliminary Experience. *Oncology* 2017; **93** Suppl 1: 30-34 [PMID: 29258081 DOI: 10.1159/000481227]

38 **Ozawa T**, Ishihara S, Fujishiro M, Kumagai Y, Shichijo S, Tada T. Automated endoscopic detection and classification of colorectal polyps using convolutional neural networks. *Therap Adv Gastroenterol* 2020; **13**: 1756284820910659 [PMID: 32231710 DOI: 10.1177/1756284820910659]

39 **Song EM**, Park B, Ha CA, Hwang SW, Park SH, Yang DH, Ye BD, Myung SJ, Yang SK, Kim N, Byeon JS. Endoscopic diagnosis and treatment planning for colorectal polyps using a deep-learning model. *Sci Rep* 2020; **10**: 30 [PMID: 31913337 DOI: 10.1038/s41598-019-56697-0]

World Journal of Gastroenterology

Submit a Manuscript: https://www.f6publishing.com

World J Gastroenterol 2021 September 21; 27(35): 5919-5931

DOI: 10.3748/wjg.v27.i35.5919

ISSN 1007-9327 (print) ISSN 2219-2840 (online)

MINIREVIEWS

Liver-spleen axis dysfunction in COVID-19

Sara Cococcia, Marco Vincenzo Lenti, Giovanni Santacroce, Giovanna Achilli, Federica Borrelli de Andreis, Antonio Di Sabatino

ORCID number: Sara Cococcia 0000-0002-1507-6513; Marco Vincenzo Lenti 0000-0002-6654-4911; Giovanni Santacroce 0000-0002-0544-0414; Giovanna Achilli 0000-0002-4763-0945; Federica Borrelli de Andreis 0000-0003-2933-8825; Antonio Di Sabatino 0000-0002-0302-8645.

Author contributions: All authors significantly participated in the drafting of the manuscript or in its critical revision for important intellectual content and the approval of the final submitted version; Cococcia S, Borrelli de Andreis F, Santacroce G, and Achilli G wrote the manuscript; Di Sabatino A and Lenti MV supervised the other authors, reviewed the paper, and carried out the final critical revision for important intellectual content.

Conflict-of-interest statement: The authors declare that there are no conflicts of interest.

Open-Access: This article is an open-access article that was selected by an in-house editor and fully peer-reviewed by external reviewers. It is distributed in accordance with the Creative Commons Attribution NonCommercial (CC BY-NC 4.0) license, which permits others to distribute, remix, adapt, build upon this work non-commercially, and license their derivative works on different terms, provided the

Sara Cococcia, Marco Vincenzo Lenti, Giovanni Santacroce, Giovanna Achilli, Federica Borrelli de Andreis, Antonio Di Sabatino, First Department of Internal Medicine, San Matteo Hospital Foundation, University of Pavia, Pavia 27100, Italy

Sara Cococcia, Department of Gastroenterology, Royal Free Hospital, London NW3 2QG, United Kingdom

Corresponding author: Marco Vincenzo Lenti, MD, Academic Research, Research Assistant Professor, First Department of Internal Medicine, San Matteo Hospital Foundation, University of Pavia, Viale Golgi 19, Pavia 27100, Italy. marco.lenti@unipv.it

Abstract

Coronavirus disease 2019 (COVID-19), caused by the novel severe acute respiratory syndrome coronavirus 2 (SARS-CoV-2), is an acute infectious disease that spreads mainly through the respiratory route. Besides interstitial pneumonia, a number of other clinical manifestations were noticed in COVID-19 patients. In particular, liver and spleen dysfunctions have been described both as complications of COVID-19 and as potential predisposing factors for severe COVID-19. Liver damage is rather common in COVID-19 patients, and it is most likely multifactorial, caused by the direct insult of SARS-CoV-2 to the liver by the cytokine storm triggered by the virus, by the use of hepatotoxic drugs, and as a consequence of hypoxia. Although generally mild, liver impairment has been found to be associated with a higher rate of intensive care unit admission. A higher mortality rate was reported among chronic liver disease patients. Instead, spleen impairment in patients with COVID-19 has been poorly described. The main anatomical changes are the architectural derangement of the B cell compartment, white pulp atrophy, and reduction or absence of lymphoid follicles, while, from a functional point of view, the IgM memory B cell pool is markedly depleted. The outcome of COVID-19 in asplenic or hyposplenic patients is yet to be defined. In this review, we will summarise the current knowledge regarding the impact of SARS-CoV-2 on the liver and spleen function, as well as the outcome of patients with a pre-existent liver disease or defective spleen function.

Key Words: Asplenia; Chronic liver disease; IgM memory B cell; Liver transplantation; Transaminase

©The Author(s) 2021. Published by Baishideng Publishing Group Inc. All rights reserved.

original work is properly cited and the use is non-commercial. See: http://creativecommons.org/Licenses/by-nc/4.0/

Manuscript source: Invited manuscript

Specialty type: Gastroenterology and hepatology

Country/Territory of origin: Italy

Peer-review report's scientific quality classification

Grade A (Excellent): A
Grade B (Very good): B
Grade C (Good): 0
Grade D (Fair): 0
Grade E (Poor): 0

Received: March 21, 2021
Peer-review started: March 21, 2021
First decision: April 29, 2021
Revised: May 1, 2021
Accepted: August 17, 2021
Article in press: August 17, 2021
Published online: September 21, 2021

P-Reviewer: Guo WZ, Montasser IF
S-Editor: Ma YJ
L-Editor: Filipodia
P-Editor: Wu RR

Core Tip: The severe acute respiratory syndrome coronavirus 2 has rapidly spread worldwide, primarily causing interstitial pneumonia, although many other organs can be involved. Here, we will discuss the current knowledge regarding the liver and spleen involvement caused by this infection.

Citation: Cococcia S, Lenti MV, Santacroce G, Achilli G, Borrelli de Andreis F, Di Sabatino A. Liver-spleen axis dysfunction in COVID-19. *World J Gastroenterol* 2021; 27(35): 5919-5931
URL: https://www.wjgnet.com/1007-9327/full/v27/i35/5919.htm
DOI: https://dx.doi.org/10.3748/wjg.v27.i35.5919

INTRODUCTION

In December 2019, a novel coronavirus-related pneumonia was detected in a Chinese group of patients[1]. The pathogen was later named severe acute respiratory syndrome coronavirus 2 (SARS-CoV-2)[2], and on 30th January 2020 the World Health Organization publicly declared the outbreak of the new virus-related disease, the so-called coronavirus disease 19 (COVID-19)[3].

The most common clinical manifestations of SARS-CoV-2 infection include fever, dry cough, dyspnoea, fatigue, and myalgia[4,5], but the increasing information in published literature reported a wide spectrum of extrapulmonary symptoms and signs, especially arising from the gastrointestinal tract[6]. Hepatic involvement in COVID-19 patients has been largely documented in several observational studies, highlighting a significant prevalence of liver impairment in hospitalized individuals and a correlation with the severity of the disease[7,8]. COVID-19 implications for individuals with a pre-existent chronic liver disease (CLD) have also been evaluated, and a few studies have focused on the management and prognosis of post-transplant patients[9,10].

Little is known about the splenic involvement in COVID-19 patients. The spleen plays a fundamental role in the immune system modulation, regulating the T and B cell responses to the antigenic targets in the blood, and the tropism of the coronaviruses for the spleen has been documented[11]. Although splenic alterations in autoptic specimens have already been shown, and these anatomical changes might contribute to the abnormal immune reaction occurring in COVID-19[12], data on prognosis of COVID-19 individuals with splenic function impairment have been poorly investigated so far.

In this review, we aim at elucidating the pathological role of SARS-CoV-2 in patients with hepatic and splenic involvement, ranging from specific biochemical alterations to any histopathological modifications. Secondly, our purpose is to evaluate the impact of COVID-19 in individuals with a pre-existent diagnosis of hepatic disease or defective spleen function or asplenia.

MATERIALS AND METHODS

From January to March 2021 we searched on MEDLINE (PubMed) by using the medical subject heading terms "liver", "hepatic", "spleen", "splenectomy", "hyposplenic" matched with "coronavirus", "COVID-19", "SARS-CoV-2" for all articles published since database inception. More than 3000 papers were found with this search strategy, most of which were not strictly related to the subject of this review. Hence, we selected human studies exploring relationships between COVID-19 and liver or spleen function, as well as the outcomes of COVID-19 patients with CLD or spleen hypofunction/asplenia. Given the high number of papers and senior authors (SC, MVL, ADS), after a careful review, we selected the most important or representative ones, summarising current evidence. We also searched for additional papers in the reference lists of review articles, and they were included if deemed appropriate.

LIVER IMPAIRMENT IN COVID-19

Pathogenesis

Since the most recent studies reporting clinical manifestation of COVID-19 were carried out, the alteration of liver function tests (LFTs) has been reported[4,13-15]. These abnormalities, which still have an unclear clinical significance, have been repeatedly reported in patients suffering from a more severe disease[4,16-18]. The exact cause of liver damage during SARS-CoV-2 infection is partly unknown and most likely multifactorial (Figure 1)[18]. One of the possible explanations has been found in the direct insult of SARS-CoV-2 to the liver through the binding of the virus to the angiotensin-converting enzyme 2 (ACE2) receptor, which represents the main cell entry receptor for the virus[19-21]. ACE2 receptors, which are key players in regulating arterial blood pressure, are expressed in almost any tissue of the human body, especially in the lungs, kidneys, gut, liver and brain. Their polymorphisms may lead to a cardiovascular disease and a stroke[22]. However, the ACE2 receptor is highly expressed by cholangiocytes rather than hepatocytes; therefore, the hepatic damage would be channelled through the bile duct dysfunction, which might alter the immune responses and liver regeneration[20]. Nonetheless, it should be noted that alkaline phosphatase (ALP) is not constantly raised in these patients[23].

In addition to the aforementioned mechanisms, the cytokine storm resulting from the excessive immune response triggered by the virus could be another factor leading to liver damage[23,24]. An excessive increase in pro-inflammatory cytokines has been found in a high percentage of critically-ill COVID-19 patients, alongside with a reduction in T cells and an increase in the neutrophilic count. The hypothesis that the lymphocytopenia and C-reactive protein (CRP) levels are independently correlated to the presence of liver damage has been proposed, suggesting a role of the cytokine storm in causing liver dysfunction[25]. This hypothesis has also been proved with regard to organs other than the liver, including heart and kidneys[26], supporting the idea that the cytokine storm may cause shock and tissue damage. Another contributing factor is the use of potentially hepatotoxic drugs, including antibiotics (*e.g.*, macrolides), antiviral agents especially used during the first wave of the pandemic, corticosteroids, and paracetamol[23,24]. Lastly, liver damage can be caused by hypoxia, as a result of severe respiratory failure[23,24,27].

Clinical findings

Liver abnormalities are rather common in COVID-19 patients. The proportion of COVID-19 inpatients with an elevated alanine aminotransferase (ALT) has been found to be as high as 36%, and a higher proportion (46%) also had raised aspartate aminotransferase (AST)[18,28]. On the contrary, ALP or gamma-glutamyl transpeptidase (GGT) alterations were reported more rarely[18,29]. Although rather common, in most cases liver injury is mild and it usually manifests in more critically-ill patients[18,30,31]. A mild-to-moderate increase of ALT was reported in 43/87 patients (49.4%), and a higher mortality rate was observed among those with deranged LFT who had developed acute respiratory distress syndrome (ARDS)[29]. Similarly, Richardson *et al*[7], who enrolled more than 5000 patients with liver involvement, showed that acute hepatic injury, although rare, was associated with higher mortality. Liver involvement was reported in 2700 patients (39%), and 1% of the whole cohort developed acute liver injury. Another study enrolling more than 2000 patients confirmed these findings, reporting acute liver injury in a quarter of the included patients and severe liver injury in only 6.4% of the patients. However, this small proportion had a more complex clinical course, including intensive care admission and intubation need in more than 60% of the cases, renal replacement therapy in a third, and mortality as high as 42%[31]. A low incidence of severe liver injury (9%) was also reported by a German study enrolling 44 patients of which 6 had deranged ALT. Also, the German cohort reported AST to be more commonly deranged than ALT[28].

Although generally mild, liver impairment has been found to be associated to a higher rate of intensive care unit admission[30,32], as well as to a longer hospital stay [33]. Ponziani *et al*[30] reported liver involvement in 161 out of 515 patients enrolled (31.3%) and no cases of severe acute liver injury. Moreover, although liver involvement led to a higher need for intensive care, no increase in mortality was recorded among those patients. However, conflicting data have been published on the role of liver impairment in increasing mortality in patients without pre-existing liver disease. Medetalibeyoglu *et al*[32] reported that AST/ALT ratio was a good predictor of mortality (area under the curve [AUC]: 0.713; P = 0.0001) in a cohort of 554 individuals enrolled in Turkey, and that AST and ALT levels were independently

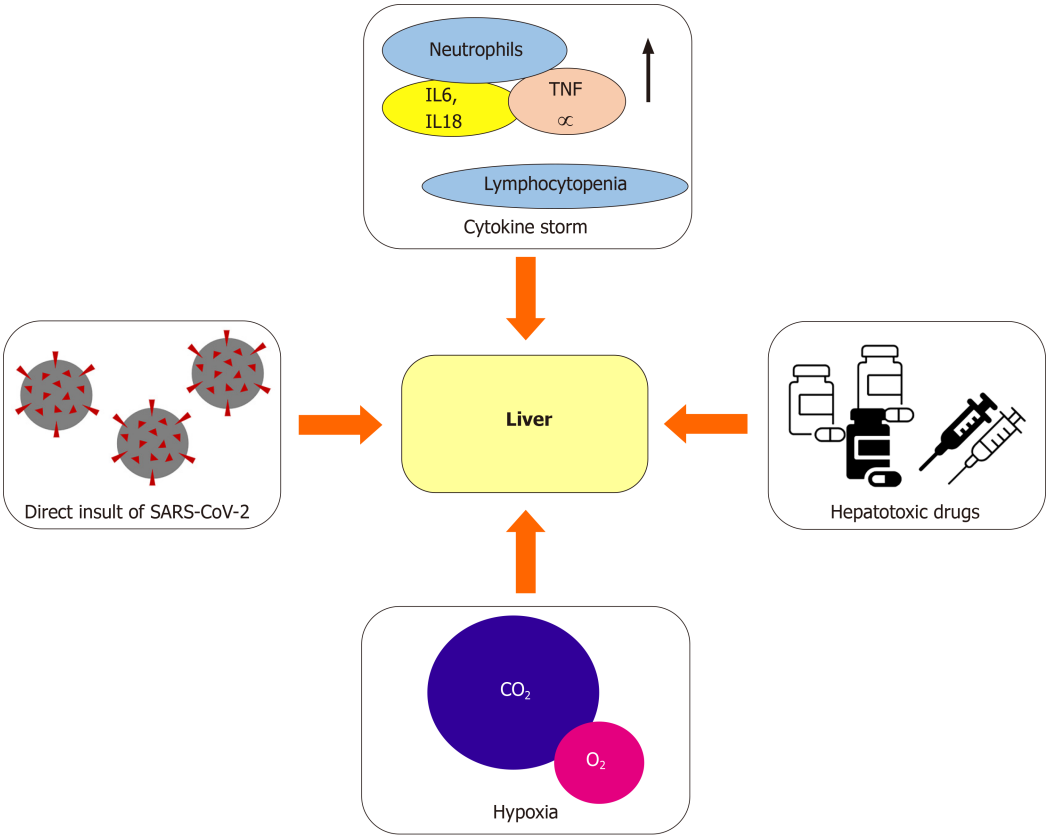


Figure 1 Putative mechanisms of liver damage in coronavirus disease 2019. IL: Interleukin; SARS-CoV-2: Severe acute respiratory syndrome coronavirus 2; TNF: Tumour necrosis factor.

associated with an increased need for intensive care and with mortality (P = 0.001). Table 1 reports the main studies focusing on liver abnormalities in COVID-19 patients.

Histological features

Limited data are available about histological liver findings in COVID-19 patients. Lagana *et al*[34] reported the histological features of 40 patients who died of COVID-19-related complications and who had liver biochemical abnormalities. Two-thirds of the included patients presented macrovesicular steatosis, which was most commonly panlobular, while 2 patients (7%) showed active steatohepatitis. Half of the included patients had mild lobular necroinflammation and, therefore, active hepatitis, which was mild in 80% of the cases and moderate in the remaining 20%. Similarly, portal inflammation was reported in 20 patients, 3 of which had interface hepatitis. Lobular mild and focal cholestasis changes were observed in 15 (38%) cases. Although the ACE2 receptor is mainly expressed by cholangiocytes in the liver, ductopenia was not reported. Vascular alterations (*i.e.* phlebosclerosis, portal arteriolar muscular hyperplasia, focal fibrinoid necrosis, and sinusoidal thrombus) were less common (15%). Interestingly, no significant correlation was found between laboratory and histological findings. Wang *et al*[35] demonstrated, in 2 deceased COVID-19 patients, that SARS-CoV-2 can infect the liver causing direct cytopathy. They also reported massive hepatic apoptosis as well as binuclear hepatocytes. However, due to the small sample size, further studies are needed to confirm these preliminary findings.

COVID-19 IN PATIENTS WITH A PRE-EXISTING CLD

Immune dysregulation is known to affect people with CLD or cirrhosis, leading to the concern that these patients are at higher risk of having a more severe form of COVID-19[36]. A limited number of studies have investigated the role of COVID-19 in patients with a pre-existing CLD and most of them only included a limited number of patients from a restricted geographical area. It is to be noted that all these studies reported a higher mortality rate among CLD patients[37-43]. Marjot *et al*[43] conducted one of the largest studies of CLD cases (745 patients) from 29 different countries. They showed

Table 1 Main studies reporting liver involvement in patients without pre-existing liver disease

Ref.	Country	Patients	Liver involvement criteria	Patients with liver involvement, *n* (%)	Main findings
Fan *et al*[33]	China	148	ALT > 40 U/L or AST > 35 U/L	55 (37.2)	Abnormal liver function is common in COVID-19 inpatients, leading to a longer hospital stay
Goyal *et al*[17]	United States	375	ALT > 40 U/L	120 (32)	Mechanically ventilated patients more likely to have liver involvement.
Lenti *et al*[29]	Italy	100	ALT or GGT > 50 U/L	58/93 (62.4)	Liver involvement correlate to higher mortality and ICU need in those who develop ARDS
Medetalibeyoglu *et al*[32]	Turkey	554	ALT or AST > 40 U/L	153 (27.6)	Higher rate of moderate-to-severe pneumonia and ICU admission need in patients with liver involvement
Phipps *et al*[31]	United States	2273	ALT > 50 U/L	537 (24)	Severe liver involvement was rare (6.4%) and led to worse outcomes (ICU admission, higher mortality)
Ponziani *et al*[30]	Italy	515	AST > 45 U/I orALT > 45 U/I orGGT > 61	161 (31.3)	No cases of severe liver injury in this cohort. Liver involvement was generally mild and, although correlated to a higher need of ICU care, not associated to higher mortality
Richardson *et al*[7]	United States	5700	ALT > 60	2176 (39)	Acute liver injury occurred in 1% of the included patients and was associated with higher mortality
Schattenberg *et al*[28]	Germany	44	ALT >50 U/L	6/38 (15.8)	Severe liver involvement was rare (9%), with AST more commonly deranged than ALT

ALT: Alanine aminotransferase; ARDS: Acute severe respiratory distress syndrome; AST: Aspartate aminotransferase; COVID-19: Coronavirus disease 2019; GGT; Gamma-glutamyl transpeptidase; ICU: Intensive care unit.

that CLD was associated with increased mortality according to the Child-Pugh class. They reported an increase in mortality, ranging from 19% in Child-Pugh-A patients to 51% in Child-Pugh-C patients. Although mortality has consistently reported to be increased in CLD patients, respiratory failure was found to be the main cause of death in these patients. Interestingly, alcohol-related liver disease was found to be independently associated to higher mortality. Liver decompensation was also reported to be common in cirrhotic patients (46%) with half of them having acute-on-chronic liver failure[44].

Among patients with CLD, liver transplant recipients were thought to represent a high risk category due to their frailty, comorbidities, and immunosuppressant therapy. Only few studies evaluated their clinical outcomes, showing conflicting results. Additionally, the majority of these studies are small case series in which patients did not always have the confirmation of SARS-CoV-2 infection[45-49]. Complying with preventive measures (*i.e.* frequent hand washing/sanitisation, use of surgical mask in public places and avoidance of public or crowded places) has been found effective to reduce the infection rate in this population[49]. A large multinational registry-based study[50], including 151 transplanted patients with laboratory-confirmed infection, showed that liver transplantation was not independently associated with higher mortality, hospitalisation rate or intensive care unit admission, whereas age and comorbidities were[47,50]. Tables 2 and 3 report the main studies focusing respectively on the outcome of COVID-19 in patients with CLD and in those with a transplanted liver.

SPLEEN IMPAIRMENT IN COVID-19

Spleen impairment in patients with COVID-19 has been poorly described. It is assumed that it may be driven by several mechanisms, including direct organ attack by the virus, cytokine-mediated immune pathogenesis, microvascular dysfunction, and lymphocyte apoptosis (Figure 2)[51].

Coronavirus detection in biopsies and autopsies has shown a tropism of this virus family for the spleen. The first available evidence is related to studies carried out on patients infected with SARS-CoV[11,52] and in experimental models of the Middle East respiratory syndrome[53]. In 2020, through immunohistochemistry techniques and the real-time reverse-transcript polymerase chain reaction assay, the SARS-CoV-2 nucleocapsid protein and the RNA were detected in the spleen tissue[54-56].

Table 2 Main studies reporting outcomes in patients with pre-existing chronic liver disease

Ref.	Country	Patients	Patients with CLD, *n* (%)	Main findings
Bajaj *et al*[40]	United States	272	37 (13.6)	Higher mortality in cirrhotic COVID-19 positive patients
Hashemi *et al*[41]	United States	363	69 (19)	CLD patients had higher ICU admission and mechanical ventilation rate. CLD was a predictor of mortality
Iavarone *et al*[42]	Italy	50	50 (100)	COVID-19 infection led to liver function deterioration. CLD patients had increased mortality
Marjot *et al*[43]	International	1365	745 (54.6)	CLD correlate to higher mortality rate according to the CPT class. ALD was an independent risk factor for mortality
Qi *et al*[39]	China	21	21 (100)	Respiratory failure was the cause of death in most patients
Singh *et al*[37]	United States	250	60 (46.1)	Pre-existing CLD patients had higher hospitalisation and mortality rates
Sarin *et al*[38]	International	228	228 (100)	Decompensation of pre-existing CLD occurred in one fifth of cirrhotic patients

CLD: Chronic liver disease; COVID-19: Coronavirus disease 2019.

Table 3 Main studies reporting outcomes in liver transplant patients

Ref.	Country	Patients	Patients with LT	Main findings
Bhoori *et al*[45]	Italy	151 (COVID status unknown)	151 (100)	3 deaths recorded in long-term LT recipient on low immunosuppressant dose
Belli *et al*[47]	International	103	103 (100)	Mortality might correlate with age and longer time since LT
Donato *et al*[49]	Italy	640 (8 COVID positive)	640 (100)	Low prevalence of infection in LT patients who adhere to preventive measures
Lee *et al*[48]	United States	38	38 (100)	High mortality in LT patients regardless of time since transplant
Pereira *et al*[46]	United States	90	14 (15)	Solid organ transplant recipient had more severe outcomes
Webb *et al*[50]	International	778	151 (19.4)	LT patients did not have a higher mortality, ICU admission or hospitalisation rate; age and comorbidities correlated with outcomes

COVID: Coronavirus disease; ICU: Intensive care unit; LT: Liver transplant.

This tropism of coronaviruses for the spleen, as for other organs, seems to be mediated by the presence of the ACE2 receptor. In fact, a study published in 2004 already described ACE2 receptors in the red pulp sinus endothelium[57]. More recent studies have confirmed the expression of ACE2 receptor in the splenic tissue, although at lower levels compared to others (*i.e.* small intestine, testis, kidneys, heart, thyroid, and adipose tissue)[58,59]. These studies also highlighted no difference, according to sex and age, in ACE2 receptor expression. Further immunohistochemical studies detected this receptor in tissue-resident CD169+ macrophages[54].

Autopsy studies have revealed interesting anatomical changes in the spleen during SARS-CoV-2 infection[60-63], including a reduction in the splenic cellular composition, with a specific depletion of T and B lymphocyte pools. Some authors assumed that this lymphocytopenia was linked to SARS-CoV-2-induced apoptosis, *via* Fas/Fas-ligand signalling, as well as increased interleukin (IL)-6 secretion by macrophages[54]. Furthermore, other frequent histopathological features were the white pulp atrophy and the reduction or absence of lymphoid follicles, with increased red pulp to white pulp proportion. In addition, spleen autopsies frequently showed a congested and haemorrhagic appearance. Microscopic studies of splenic vessels revealed, in many cases, a splenic infarction due to arterial thrombosis and proliferation of fibrous tissue in the sinuses.

Table 4 Summary of the main studies reporting coronavirus disease 2019 related spleen dysfunction

Ref.	Country	Patients	Patients with spleen involvement, *n* (%)	Main findings
Feng *et al*[54]	China	6	6 (100)	ACE2 expression on tissue-resident CD169+ macrophages in spleen; viral NP antigen found in ACE2+ cells in spleen; direct damage of spleen tissue (lymph follicle depletion, splenic nodule atrophy, lymphocyte reduction, *etc*.)
Remmelink *et al*[55]	Belgium	17	11 (65)	SARS-CoV-2 RNA detected in spleen autopsy samples by RT-PCR assay
Sekulic *et al* [56]	United States	2	2 (100)	SARS-CoV-2 RNA detected at high level in spleen FFPE samples by RT-PCR assay
Han *et al*[58]	China	7356	NA	Expression of ACE2 in spleen tissue (lower than in other tissues), without difference according to sex
Li *et al*[59]	China	31	NA	Expression of ACE2 in spleen tissue (lower than in other tissues), without difference according to sex and age
Xu *et al*[60]	China	10	10 (100)	Decrease in spleen cell composition with decrease in lymphocyte components, white pulp atrophied, lymphoid follicles decreased or absent, increase in red pulp to white pulp ratio
Menter *et al* [61]	Switzerland	21	6 (29)	Acute splenitis and/or septic neutrophilic leucocytosis of the red pulp, suggesting vascular disfunction in patients with COVID-19
Lax *et al*[62]	Austria	11	10 (90)	White pulp atrophy due to lymphocyte depletion, areas of haemorrhage with acute or chronic congestion
Duarte-Neto *et al*[63]	Brazil	5	5 (100)	Lymphoid hypoplasia in 100%, red pulp haemorrhages in 60%, splenitis in 40%, extramedullary haematopoiesis in 50%, endothelial changes in 80%, vasculitis and arterial thrombus in 20%
Lenti *et al*[29]	Italy	63	55 (87.3)	IgM memory B cell depletion that correlates with increased mortality and superimposed infections
Kaneko *et al* [65]	United States	11	11 (100)	Loss of spleen germinal centres due to depletion of Bcl-6+ germinal centre B cells and Bcl-6+ germinal centre T follicular helper cells, resulting in a dysregulated humoral immune response

COVID-19: Coronavirus disease 2019; FFPE: Formalin-fixed paraffin-embedded; NA: Not available; NP: Nucleocapsid protein; RT-PCR: Real-time reverse-transcript polymerase chain reaction; SARS-CoV-2: Severe acute respiratory syndrome coronavirus 2.

The functional impact of these anatomical damages has been poorly investigated. A recent study[12] assessed the splenic immunological function through the detection of circulating IgM+ IgD+ CD27+ B lymphocytes, also known as IgM memory B cells, a unique B cell population in the marginal zone of the spleen which plays a major role in early inflammatory responses, including those caused by viral and bacterial infections [64]. A high prevalence of persistent IgM memory B cell depletion was demonstrated in patients with COVID-19, resulting in a higher mortality rate and an increased risk of developing superimposed bacterial infections. Other molecular studies have suggested that the loss of germinal centres may be due to the depletion of Bcl-6+ germinal centre B cells and Bcl-6+ germinal centre T follicular helper cells, resulting in a dysregulated immune response during the SARS-CoV-2 infection[65]. Although further studies are needed, it can be assumed that splenic involvement could be one of the causes of immune perturbations associated with severe COVID-19[66]. It still has to be ascertained whether the spleen immunological defect is reversible or not. Conversely, the haemocateretic function, assessed by counting pitted red cells (PRCs; red cells with membrane abnormalities [pits] visible under interference phase microscopy[67]) was preserved in patients with acute COVID-19, contrary to what happens in asplenia and spleen hypofunction[12]. The long average life span of circulating erythrocytes (approximately 120 d) might explain the lack of PRC increase in the acute phase of COVID-19.

COVID-19 IN ASPLENIC OR HYPOSPLENIC PATIENTS

It is well known that asplenic or hyposplenic patients are predisposed to a greater risk of developing serious infections or overwhelming post-splenectomy infections, due to the defect in mounting the immune response against encapsulated bacteria[67,68].

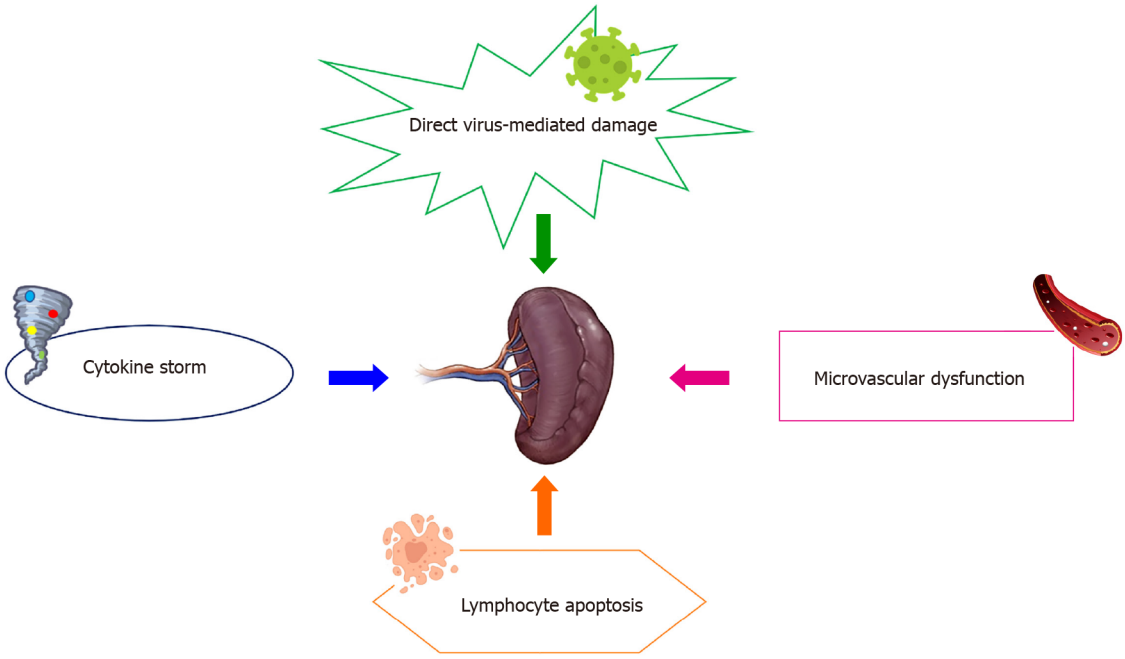


Figure 2 Putative mechanisms of spleen damage in coronavirus disease 2019.

Starting from these premises, it would be interesting to know whether patients with asplenia or spleen dysfunction could be more susceptible to Sars-CoV-2, both in terms of severity and incidence of the disease. Indeed, apart from a document drafted by the British Society of Haematology, stating that asplenic and hyposplenic patients are not exposed to a major risk of COVID-19, data regarding this population are completely missing[69]. Moreover, it is unknown whether patients who might develop spleen hypofunction as a consequence of COVID-19 could be more exposed to infections sustained by encapsulated bacteria and less responsive to vaccine immune-prophylaxis.

According to a single-centre, longitudinal, prospective, study conducted in an academic, tertiary referral hospital from Northern Italy, asplenic/hyposplenic patients did not seem to have an increased risk of developing COVID-19. The study had the purpose of characterising the spleen function, through circulating IgM memory B cell and PRC detection, in patients with COVID-19, in relation to their clinical outcome. Overall, 66 COVID-19 patients (mean age: 74 ± 16.6 years; 29 females) were enrolled; three patients had been splenectomised for trauma, all of them having IgM memory B cell depletion, and one of them died. Most COVID-19 patients had marked IgM memory B cell depletion, and this was associated to a higher mortality rate and a higher risk of developing superimposed infections[12]. Another important study conducted to identify, quantify, and analyse factors associated with COVID-19-related death in one of the largest cohort studies on this topic conducted so far (primary care records of 17278392 adults were linked to 10926 COVID-19-related deaths), considered asplenia as a comorbidity of interest. The results showed that 0.2% of the study population were affected by asplenia, and that the proportion of COVID-19-related death was 0.14%. In addition, asplenic COVID-19 patients had a 1.62 higher risk of death than individuals with a normal spleen function[70].

Indeed, further studies are needed to clarify the impact of SARS-CoV-2 in patients without a spleen or with spleen dysfunction. Table 4 reports the main studies reporting COVID-19 related spleen dysfunction.

CONCLUSION

While the involvement of the respiratory system in SARS-CoV-2 infection is well established, the impact on the liver and spleen has not been explored much. Some studies have shown a direct tropism of the virus for these organs, and this may be one of the mechanisms underlying their damage, in association with the systemic inflammatory response. Regarding the liver, its involvement seems to be quite common, especially in more severe cases of infection, resulting in a worse prognosis for these

patients. The spleen involvement, on the other hand, has been poorly investigated. The splenic immune function appears to be defective in COVID-19 patients, resulting in a higher mortality rate and superimposed infections. Further studies may lead to a better diagnostic and therapeutic approach in SARS-CoV-2-infected patients, especially those with pre-existing liver and spleen diseases, who seem to be at higher risk of a worse outcome.

ACKNOWLEDGEMENTS

Dr. Marco Vincenzo Lenti is grateful to the University of Pavia for supporting his research projects. We thank Intermediate SRL for having proofread the paper.

REFERENCES

1 **Wang C**, Horby PW, Hayden FG, Gao GF. A novel coronavirus outbreak of global health concern. *Lancet* 2020; **395**: 470-473 [PMID: 31986257 DOI: 10.1016/S0140-6736(20)30185-9]
2 **Coronaviridae Study Group of the International Committee on Taxonomy of Viruses**. The species Severe acute respiratory syndrome-related coronavirus: classifying 2019-nCoV and naming it SARS-CoV-2. *Nat Microbiol* 2020; **5**: 536-544 [PMID: 32123347 DOI: 10.1038/s41564-020-0695-z]
3 **Eurosurveillance Editorial Team**. Note from the editors: World Health Organization declares novel coronavirus (2019-nCoV) sixth public health emergency of international concern. *Euro Surveill* 2020; **25** [PMID: 32019636 DOI: 10.2807/1560-7917.ES.2020.25.5.200131e]
4 **Huang C**, Wang Y, Li X, Ren L, Zhao J, Hu Y, Zhang L, Fan G, Xu J, Gu X, Cheng Z, Yu T, Xia J, Wei Y, Wu W, Xie X, Yin W, Li H, Liu M, Xiao Y, Gao H, Guo L, Xie J, Wang G, Jiang R, Gao Z, Jin Q, Wang J, Cao B. Clinical features of patients infected with 2019 novel coronavirus in Wuhan, China. *Lancet* 2020; **395**: 497-506 [PMID: 31986264 DOI: 10.1016/S0140-6736(20)30183-5]
5 **Wang D**, Hu B, Hu C, Zhu F, Liu X, Zhang J, Wang B, Xiang H, Cheng Z, Xiong Y, Zhao Y, Li Y, Wang X, Peng Z. Clinical Characteristics of 138 Hospitalized Patients With 2019 Novel Coronavirus-Infected Pneumonia in Wuhan, China. *JAMA* 2020; **323**: 1061-1069 [PMID: 32031570 DOI: 10.1001/jama.2020.1585]
6 **Marasco G**, Lenti MV, Cremon C, Barbaro MR, Stanghellini V, Di Sabatino A, Barbara G. Implications of SARS-CoV-2 infection for neurogastroenterology. *Neurogastroenterol Motil* 2021; **33**: e14104 [PMID: 33591607 DOI: 10.1111/nmo.14104]
7 **Richardson S**, Hirsch JS, Narasimhan M, Crawford JM, McGinn T, Davidson KW; the Northwell COVID-19 Research Consortium, Barnaby DP, Becker LB, Chelico JD, Cohen SL, Cookingham J, Coppa K, Diefenbach MA, Dominello AJ, Duer-Hefele J, Falzon L, Gitlin J, Hajizadeh N, Harvin TG, Hirschwerk DA, Kim EJ, Kozel ZM, Marrast LM, Mogavero JN, Osorio GA, Qiu M, Zanos TP. Presenting Characteristics, Comorbidities, and Outcomes Among 5700 Patients Hospitalized With COVID-19 in the New York City Area. *JAMA* 2020; **323**: 2052-2059 [PMID: 32320003 DOI: 10.1001/jama.2020.6775]
8 **Guan WJ**, Ni ZY, Hu Y, Liang WH, Ou CQ, He JX, Liu L, Shan H, Lei CL, Hui DSC, Du B, Li LJ, Zeng G, Yuen KY, Chen RC, Tang CL, Wang T, Chen PY, Xiang J, Li SY, Wang JL, Liang ZJ, Peng YX, Wei L, Liu Y, Hu YH, Peng P, Wang JM, Liu JY, Chen Z, Li G, Zheng ZJ, Qiu SQ, Luo J, Ye CJ, Zhu SY, Zhong NS; China Medical Treatment Expert Group for Covid-19. Clinical Characteristics of Coronavirus Disease 2019 in China. *N Engl J Med* 2020; **382**: 1708-1720 [PMID: 32109013 DOI: 10.1056/NEJMoa2002032]
9 **Becchetti C**, Zambelli MF, Pasulo L, Donato MF, Invernizzi F, Detry O, Dahlqvist G, Ciccarelli O, Morelli MC, Fraga M, Svegliati-Baroni G, van Vlierberghe H, Coenraad MJ, Romero MC, de Gottardi A, Toniutto P, Del Prete L, Abbati C, Samuel D, Pirenne J, Nevens F, Dufour JF; COVID-LT group. COVID-19 in an international European liver transplant recipient cohort. *Gut* 2020; **69**: 1832-1840 [PMID: 32571972 DOI: 10.1136/gutjnl-2020-321923]
10 **Fernández-Ruiz M**, Andrés A, Loinaz C, Delgado JF, López-Medrano F, San Juan R, González E, Polanco N, Folgueira MD, Lalueza A, Lumbreras C, Aguado JM. COVID-19 in solid organ transplant recipients: A single-center case series from Spain. *Am J Transplant* 2020; **20**: 1849-1858 [PMID: 32301155 DOI: 10.1111/ajt.15929]
11 **Zhan J**, Deng R, Tang J, Zhang B, Tang Y, Wang JK, Li F, Anderson VM, McNutt MA, Gu J. The spleen as a target in severe acute respiratory syndrome. *FASEB J* 2006; **20**: 2321-2328 [PMID: 17077309 DOI: 10.1096/fj.06-6324com]
12 **Lenti MV**, Aronico N, Pellegrino I, Boveri E, Giuffrida P, Borrelli de Andreis F, Morbini P, Vanelli L, Pasini A, Ubezio C, Melazzini F, Rascaroli A, Antoci V, Merli S, Di Terlizzi F, Sabatini U, Cambiè G, Tenore A, Picone C, Vanoli A, Arcaini L, Baldanti F, Paulli M, Corazza GR, Di Sabatino A. Depletion of circulating IgM memory B cells predicts unfavourable outcome in COVID-19. *Sci Rep* 2020; **10**: 20836 [PMID: 33257775 DOI: 10.1038/s41598-020-77945-8]
13 **Yang J**, Zheng Y, Gou X, Pu K, Chen Z, Guo Q, Ji R, Wang H, Wang Y, Zhou Y. Prevalence of comorbidities and its effects in patients infected with SARS-CoV-2: a systematic review and meta-

analysis. *Int J Infect Dis* 2020; **94**: 91-95 [PMID: 32173574 DOI: 10.1016/j.ijid.2020.03.017]
14 **Grasselli G**, Zangrillo A, Zanella A, Antonelli M, Cabrini L, Castelli A, Cereda D, Coluccello A, Foti G, Fumagalli R, Iotti G, Latronico N, Lorini L, Merler S, Natalini G, Piatti A, Ranieri MV, Scandroglio AM, Storti E, Cecconi M, Pesenti A; COVID-19 Lombardy ICU Network. Baseline Characteristics and Outcomes of 1591 Patients Infected With SARS-CoV-2 Admitted to ICUs of the Lombardy Region, Italy. *JAMA* 2020; **323**: 1574-1581 [PMID: 32250385 DOI: 10.1001/jama.2020.5394]
15 **Borges do Nascimento IJ**, Cacic N, Abdulazeem HM, von Groote TC, Jayarajah U, Weerasekara I, Esfahani MA, Civile VT, Marusic A, Jeroncic A, Carvas Junior N, Pericic TP, Zakarija-Grkovic I, Meirelles Guimarães SM, Luigi Bragazzi N, Bjorklund M, Sofi-Mahmudi A, Altujjar M, Tian M, Arcani DMC, O'Mathúna DP, Marcolino MS. Novel Coronavirus Infection (COVID-19) in Humans: A Scoping Review and Meta-Analysis. *J Clin Med* 2020; **9** [PMID: 32235486 DOI: 10.3390/jcm9040941]
16 **Shi H**, Han X, Jiang N, Cao Y, Alwalid O, Gu J, Fan Y, Zheng C. Radiological findings from 81 patients with COVID-19 pneumonia in Wuhan, China: a descriptive study. *Lancet Infect Dis* 2020; **20**: 425-434 [PMID: 32105637 DOI: 10.1016/S1473-3099(20)30086-4]
17 **Goyal P**, Choi JJ, Pinheiro LC, Schenck EJ, Chen R, Jabri A, Satlin MJ, Campion TR Jr, Nahid M, Ringel JB, Hoffman KL, Alshak MN, Li HA, Wehmeyer GT, Rajan M, Reshetnyak E, Hupert N, Horn EM, Martinez FJ, Gulick RM, Safford MM. Clinical Characteristics of Covid-19 in New York City. *N Engl J Med* 2020; **382**: 2372-2374 [PMID: 32302078 DOI: 10.1056/NEJMc2010419]
18 **Bertolini A**, van de Peppel IP, Bodewes FAJA, Moshage H, Fantin A, Farinati F, Fiorotto R, Jonker JW, Strazzabosco M, Verkade HJ, Peserico G. Abnormal Liver Function Tests in Patients With COVID-19: Relevance and Potential Pathogenesis. *Hepatology* 2020; **72**: 1864-1872 [PMID: 32702162 DOI: 10.1002/hep.31480]
19 **Du M**, Cai G, Chen F, Christiani DC, Zhang Z, Wang M. Multiomics Evaluation of Gastrointestinal and Other Clinical Characteristics of COVID-19. *Gastroenterology* 2020; **158**: 2298-2301.e7 [PMID: 32234303 DOI: 10.1053/j.gastro.2020.03.045]
20 **Chai X**, Hu L, Zhang Y, Han W, Lu Z, Ke A, Zhou J, Shi G, Fang N, Fan J, Cai J, Lan F. Specific ACE2 Expression in Cholangiocytes May Cause Liver Damage After 2019-nCoV Infection. *bioRxiv* 2020 [DOI: 10.1101/2020.02.03.931766]
21 **Wu J**, Song S, Cao HC, Li LJ. Liver diseases in COVID-19: Etiology, treatment and prognosis. *World J Gastroenterol* 2020; **26**: 2286-2293 [PMID: 32476793 DOI: 10.3748/wjg.v26.i19.2286]
22 **Samavati L**, Uhal BD. ACE2, Much More Than Just a Receptor for SARS-COV-2. *Front Cell Infect Microbiol* 2020; **10**: 317 [PMID: 32582574 DOI: 10.3389/fcimb.2020.00317]
23 **Cha MH**, Regueiro M, Sandhu DS. Gastrointestinal and hepatic manifestations of COVID-19: A comprehensive review. *World J Gastroenterol* 2020; **26**: 2323-2332 [PMID: 32476796 DOI: 10.3748/wjg.v26.i19.2323]
24 **Yang RX**, Zheng RD, Fan JG. Etiology and management of liver injury in patients with COVID-19. *World J Gastroenterol* 2020; **26**: 4753-4762 [PMID: 32921955 DOI: 10.3748/wjg.v26.i32.4753]
25 **Lu L**, Shuang L, Manman X, Yu P, Zheng S, Duan Z, Liu J, Chen Y, Li J. Risk factors related to hepatic injury in patients with corona virus disease 2019. *medRxiv* 2020
26 **Cao X**. COVID-19: immunopathology and its implications for therapy. *Nat Rev Immunol* 2020; **20**: 269-270 [PMID: 32273594 DOI: 10.1038/s41577-020-0308-3]
27 **Zhang C**, Shi L, Wang FS. Liver injury in COVID-19: management and challenges. *Lancet Gastroenterol Hepatol* 2020; **5**: 428-430 [PMID: 32145190 DOI: 10.1016/S2468-1253(20)30057-1]
28 **Schattenberg JM**, Labenz C, Wörns MA, Menge P, Weinmann A, Galle PR, Sprinzl MF. Patterns of liver injury in COVID-19 - a German case series. *United European Gastroenterol J* 2020; **8**: 814-819 [PMID: 32588791 DOI: 10.1177/2050640620931657]
29 **Lenti MV**, Borrelli de Andreis F, Pellegrino I, Klersy C, Merli S, Miceli E, Aronico N, Mengoli C, Di Stefano M, Cococcia S, Santacroce G, Soriano S, Melazzini F, Delliponti M, Baldanti F, Triarico A, Corazza GR, Pinzani M, Di Sabatino A; Internal Medicine Covid-19 Team. Impact of COVID-19 on liver function: results from an internal medicine unit in Northern Italy. *Intern Emerg Med* 2020; **15**: 1399-1407 [PMID: 32651938 DOI: 10.1007/s11739-020-02425-w]
30 **Ponziani FR**, Del Zompo F, Nesci A, Santopaolo F, Ianiro G, Pompili M, Gasbarrini A; "Gemelli against COVID-19" group. Liver involvement is not associated with mortality: results from a large cohort of SARS-CoV-2-positive patients. *Aliment Pharmacol Ther* 2020; **52**: 1060-1068 [PMID: 32628793 DOI: 10.1111/apt.15996]
31 **Phipps MM**, Barraza LH, LaSota ED, Sobieszczyk ME, Pereira MR, Zheng EX, Fox AN, Zucker J, Verna EC. Acute Liver Injury in COVID-19: Prevalence and Association with Clinical Outcomes in a Large U.S. Cohort. *Hepatology* 2020; **72**: 807-817 [PMID: 32473607 DOI: 10.1002/hep.31404]
32 **Medetalibeyoglu A**, Catma Y, Senkal N, Ormeci A, Cavus B, Kose M, Bayramlar OF, Yildiz G, Akyuz F, Kaymakoglu S, Tukek T. The effect of liver test abnormalities on the prognosis of COVID-19. *Ann Hepatol* 2020; **19**: 614-621 [PMID: 32920162 DOI: 10.1016/j.aohep.2020.08.068]
33 **Fan Z**, Chen L, Li J, Cheng X, Yang J, Tian C, Zhang Y, Huang S, Liu Z, Cheng J. Clinical Features of COVID-19-Related Liver Functional Abnormality. *Clin Gastroenterol Hepatol* 2020; **18**: 1561-1566 [PMID: 32283325 DOI: 10.1016/j.cgh.2020.04.002]
34 **Lagana SM**, Kudose S, Iuga AC, Lee MJ, Fazlollahi L, Remotti HE, Del Portillo A, De Michele S, de Gonzalez AK, Saqi A, Khairallah P, Chong AM, Park H, Uhlemann AC, Lefkowitch JH, Verna EC. Hepatic pathology in patients dying of COVID-19: a series of 40 cases including clinical,

histologic, and virologic data. *Mod Pathol* 2020; **33**: 2147-2155 [PMID: 32792598 DOI: 10.1038/s41379-020-00649-x]

35 **Wang Y**, Liu S, Liu H, Li W, Lin F, Jiang L, Li X, Xu P, Zhang L, Zhao L, Cao Y, Kang J, Yang J, Li L, Liu X, Li Y, Nie R, Mu J, Lu F, Zhao S, Lu J, Zhao J. SARS-CoV-2 infection of the liver directly contributes to hepatic impairment in patients with COVID-19. *J Hepatol* 2020; **73**: 807-816 [PMID: 32437830 DOI: 10.1016/j.jhep.2020.05.002]

36 **Albillos A**, Lario M, Álvarez-Mon M. Cirrhosis-associated immune dysfunction: distinctive features and clinical relevance. *J Hepatol* 2014; **61**: 1385-1396 [PMID: 25135860 DOI: 10.1016/j.jhep.2014.08.010]

37 **Singh S**, Khan A. Clinical Characteristics and Outcomes of Coronavirus Disease 2019 Among Patients With Preexisting Liver Disease in the United States: A Multicenter Research Network Study. *Gastroenterology* 2020; **159**: 768-771.e3 [PMID: 32376408 DOI: 10.1053/j.gastro.2020.04.064]

38 **Sarin SK**, Choudhury A, Lau GK, Zheng MH, Ji D, Abd-Elsalam S, Hwang J, Qi X, Cua IH, Suh JI, Park JG, Putcharoen O, Kaewdech A, Piratvisuth T, Treeprasertsuk S, Park S, Wejnaruemarn S, Payawal DA, Baatarkhuu O, Ahn SH, Yeo CD, Alonzo UR, Chinbayar T, Loho IM, Yokosuka O, Jafri W, Tan S, Soo LI, Tanwandee T, Gani R, Anand L, Esmail ES, Khalaf M, Alam S, Lin CY, Chuang WL, Soin AS, Garg HK, Kalista K, Batsukh B, Purnomo HD, Dara VP, Rathi P, Al Mahtab M, Shukla A, Sharma MK, Omata M; APASL COVID Task Force, APASL COVID Liver Injury Spectrum Study (APCOLIS Study-NCT 04345640). Pre-existing liver disease is associated with poor outcome in patients with SARS CoV2 infection; The APCOLIS Study (APASL COVID-19 Liver Injury Spectrum Study). *Hepatol Int* 2020; **14**: 690-700 [PMID: 32623632 DOI: 10.1007/s12072-020-10072-8]

39 **Qi X**, Liu Y, Wang J, Fallowfield JA, Li X, Shi J, Pan H, Zou S, Zhang H, Chen Z, Li F, Luo Y, Mei M, Liu H, Wang Z, Li J, Yang H, Xiang H, Liu T, Zheng MH, Liu C, Huang Y, Xu D, Kang N, He Q, Gu Y, Zhang G, Shao C, Liu D, Zhang L, Kawada N, Jiang Z, Wang F, Xiong B, Takehara T, Rockey DC; COVID-Cirrhosis-CHESS Group. Clinical course and risk factors for mortality of COVID-19 patients with pre-existing cirrhosis: a multicentre cohort study. *Gut* 2021; **70**: 433-436 [PMID: 32434831 DOI: 10.1136/gutjnl-2020-321666]

40 **Bajaj JS**, Garcia-Tsao G, Biggins SW, Kamath PS, Wong F, McGeorge S, Shaw J, Pearson M, Chew M, Fagan A, de la Rosa Rodriguez R, Worthington J, Olofson A, Weir V, Trisolini C, Dwyer S, Reddy KR. Comparison of mortality risk in patients with cirrhosis and COVID-19 compared with patients with cirrhosis alone and COVID-19 alone: multicentre matched cohort. *Gut* 2021; **70**: 531-536 [PMID: 32660964 DOI: 10.1136/gutjnl-2020-322118]

41 **Hashemi N**, Viveiros K, Redd WD, Zhou JC, McCarty TR, Bazarbashi AN, Hathorn KE, Wong D, Njie C, Shen L, Chan WW. Impact of chronic liver disease on outcomes of hospitalized patients with COVID-19: A multicentre United States experience. *Liver Int* 2020; **40**: 2515-2521 [PMID: 32585065 DOI: 10.1111/liv.14583]

42 **Iavarone M**, D'Ambrosio R, Soria A, Triolo M, Pugliese N, Del Poggio P, Perricone G, Massironi S, Spinetti A, Buscarini E, Viganò M, Carriero C, Fagiuoli S, Aghemo A, Belli LS, Lucà M, Pedaci M, Rimondi A, Rumi MG, Invernizzi P, Bonfanti P, Lampertico P. High rates of 30-day mortality in patients with cirrhosis and COVID-19. *J Hepatol* 2020; **73**: 1063-1071 [PMID: 32526252 DOI: 10.1016/j.jhep.2020.06.001]

43 **Marjot T**, Moon AM, Cook JA, Abd-Elsalam S, Aloman C, Armstrong MJ, Pose E, Brenner EJ, Cargill T, Catana MA, Dhanasekaran R, Eshraghian A, García-Juárez I, Gill US, Jones PD, Kennedy J, Marshall A, Matthews C, Mells G, Mercer C, Perumalswami PV, Avitabile E, Qi X, Su F, Ufere NN, Wong YJ, Zheng MH, Barnes E, Barritt AS 4th, Webb GJ. Outcomes following SARS-CoV-2 infection in patients with chronic liver disease: An international registry study. *J Hepatol* 2021; **74**: 567-577 [PMID: 33035628 DOI: 10.1016/j.jhep.2020.09.024]

44 **Patrono D**, Lupo F, Canta F, Mazza E, Mirabella S, Corcione S, Tandoi F, De Rosa FG, Romagnoli R. Outcome of COVID-19 in liver transplant recipients: A preliminary report from Northwestern Italy. *Transpl Infect Dis* 2020; **22**: e13353 [PMID: 32500942 DOI: 10.1111/tid.13353]

45 **Bhoori S**, Rossi RE, Citterio D, Mazzaferro V. COVID-19 in long-term liver transplant patients: preliminary experience from an Italian transplant centre in Lombardy. *Lancet Gastroenterol Hepatol* 2020; **5**: 532-533 [PMID: 32278366 DOI: 10.1016/S2468-1253(20)30116-3]

46 **Pereira MR**, Mohan S, Cohen DJ, Husain SA, Dube GK, Ratner LE, Arcasoy S, Aversa MM, Benvenuto LJ, Dadhania DM, Kapur S, Dove LM, Brown RS Jr, Rosenblatt RE, Samstein B, Uriel N, Farr MA, Satlin M, Small CB, Walsh TJ, Kodiyanplakkal RP, Miko BA, Aaron JG, Tsapepas DS, Emond JC, Verna EC. COVID-19 in solid organ transplant recipients: Initial report from the US epicenter. *Am J Transplant* 2020; **20**: 1800-1808 [PMID: 32330343 DOI: 10.1111/ajt.15941]

47 **Belli LS**, Duvoux C, Karam V, Adam R, Cuervas-Mons V, Pasulo L, Loinaz C, Invernizzi F, Patrono D, Bhoori S, Ciccarelli O, Morelli MC, Castells L, Lopez-Lopez V, Conti S, Fondevila C, Polak W. COVID-19 in liver transplant recipients: preliminary data from the ELITA/ELTR registry. *Lancet Gastroenterol Hepatol* 2020; **5**: 724-725 [PMID: 32505228 DOI: 10.1016/S2468-1253(20)30183-7]

48 **Lee BT**, Perumalswami PV, Im GY, Florman S, Schiano TD; COBE Study Group. COVID-19 in Liver Transplant Recipients: An Initial Experience From the US Epicenter. *Gastroenterology* 2020; **159**: 1176-1178.e2 [PMID: 32442561 DOI: 10.1053/j.gastro.2020.05.050]

49 **Donato MF**, Invernizzi F, Lampertico P, Rossi G. Health Status of Patients Who Underwent Liver Transplantation During the Coronavirus Outbreak at a Large Center in Milan, Italy. *Clin Gastroenterol Hepatol* 2020; **18**: 2131-2133.e1 [PMID: 32334081 DOI: 10.1016/j.cgh.2020.04.041]

50 **Webb GJ**, Marjot T, Cook JA, Aloman C, Armstrong MJ, Brenner EJ, Catana MA, Cargill T, Dhanasekaran R, García-Juárez I, Hagström H, Kennedy JM, Marshall A, Masson S, Mercer CJ, Perumalswami PV, Ruiz I, Thaker S, Ufere NN, Barnes E, Barritt AS 4th, Moon AM. Outcomes following SARS-CoV-2 infection in liver transplant recipients: an international registry study. *Lancet Gastroenterol Hepatol* 2020; **5**: 1008-1016 [PMID: 32866433 DOI: 10.1016/S2468-1253(20)30271-5]

51 **Li H**, Liu L, Zhang D, Xu J, Dai H, Tang N, Su X, Cao B. SARS-CoV-2 and viral sepsis: observations and hypotheses. *Lancet* 2020; **395**: 1517-1520 [PMID: 32311318 DOI: 10.1016/S0140-6736(20)30920-X]

52 **Tang JW**, To KF, Lo AW, Sung JJ, Ng HK, Chan PK. Quantitative temporal-spatial distribution of severe acute respiratory syndrome-associated coronavirus (SARS-CoV) in post-mortem tissues. *J Med Virol* 2007; **79**: 1245-1253 [PMID: 17607787 DOI: 10.1002/jmv.20873]

53 **Chu H**, Zhou J, Wong BH, Li C, Chan JF, Cheng ZS, Yang D, Wang D, Lee AC, Yeung ML, Cai JP, Chan IH, Ho WK, To KK, Zheng BJ, Yao Y, Qin C, Yuen KY. Middle East Respiratory Syndrome Coronavirus Efficiently Infects Human Primary T Lymphocytes and Activates the Extrinsic and Intrinsic Apoptosis Pathways. *J Infect Dis* 2016; **213**: 904-914 [PMID: 26203058 DOI: 10.1093/infdis/jiv380]

54 **Feng Z**, Diao B, Wang R, Wang G, Wang C, Tan Y, Liu L, Liu Y, Yuan Z, Ren L, Wu Y, Chen Y. The Novel Severe Acute Respiratory Syndrome Coronavirus 2 (SARS-CoV-2) Directly Decimates Human Spleens and Lymph Nodes. medRxiv 2020

55 **Remmelink M**, De Mendonça R, D'Haene N, De Clercq S, Verocq C, Lebrun L, Lavis P, Racu ML, Trépant AL, Maris C, Rorive S, Goffard JC, De Witte O, Peluso L, Vincent JL, Decaestecker C, Taccone FS, Salmon I. Unspecific post-mortem findings despite multiorgan viral spread in COVID-19 patients. *Crit Care* 2020; **24**: 495 [PMID: 32787909 DOI: 10.1186/s13054-020-03218-5]

56 **Sekulic M**, Harper H, Nezami BG, Shen DL, Sekulic SP, Koeth AT, Harding CV, Gilmore H, Sadri N. Molecular Detection of SARS-CoV-2 Infection in FFPE Samples and Histopathologic Findings in Fatal SARS-CoV-2 Cases. *Am J Clin Pathol* 2020; **154**: 190-200 [PMID: 32451533 DOI: 10.1093/ajcp/aqaa091]

57 **Hamming I**, Timens W, Bulthuis ML, Lely AT, Navis G, van Goor H. Tissue distribution of ACE2 protein, the functional receptor for SARS coronavirus. A first step in understanding SARS pathogenesis. *J Pathol* 2004; **203**: 631-637 [PMID: 15141377 DOI: 10.1002/path.1570]

58 **Han T**, Kang J, Li G, Ge J, Gu J. Analysis of 2019-nCoV receptor ACE2 expression in different tissues and its significance study. *Ann Transl Med* 2020; **8**: 1077 [PMID: 33145296 DOI: 10.21037/atm-20-4281]

59 **Li MY**, Li L, Zhang Y, Wang XS. Expression of the SARS-CoV-2 cell receptor gene ACE2 in a wide variety of human tissues. *Infect Dis Poverty* 2020; **9**: 45 [PMID: 32345362 DOI: 10.1186/s40249-020-00662-x]

60 **Xu X**, Chang XN, Pan HX, Su H, Huang B, Yang M, Luo DJ, Weng MX, Ma L, Nie X. [Pathological changes of the spleen in ten patients with coronavirus disease 2019(COVID-19) by postmortem needle autopsy]. *Zhonghua Bing Li Xue Za Zhi* 2020; **49**: 576-582 [PMID: 32340089 DOI: 10.3760/cma.j.cn112151-20200401-00278]

61 **Menter T**, Haslbauer JD, Nienhold R, Savic S, Hopfer H, Deigendesch N, Frank S, Turek D, Willi N, Pargger H, Bassetti S, Leuppi JD, Cathomas G, Tolnay M, Mertz KD, Tzankov A. Postmortem examination of COVID-19 patients reveals diffuse alveolar damage with severe capillary congestion and variegated findings in lungs and other organs suggesting vascular dysfunction. *Histopathology* 2020; **77**: 198-209 [PMID: 32364264 DOI: 10.1111/his.14134]

62 **Lax SF**, Skok K, Zechner P, Kessler HH, Kaufmann N, Koelblinger C, Vander K, Bargfrieder U, Trauner M. Pulmonary Arterial Thrombosis in COVID-19 With Fatal Outcome : Results From a Prospective, Single-Center, Clinicopathologic Case Series. *Ann Intern Med* 2020; **173**: 350-361 [PMID: 32422076 DOI: 10.7326/M20-2566]

63 **Duarte-Neto AN**, Monteiro RAA, da Silva LFF, Malheiros DMAC, de Oliveira EP, Theodoro-Filho J, Pinho JRR, Gomes-Gouvêa MS, Salles APM, de Oliveira IRS, Mauad T, Saldiva PHN, Dolhnikoff M. Pulmonary and systemic involvement in COVID-19 patients assessed with ultrasound-guided minimally invasive autopsy. *Histopathology* 2020; **77**: 186-197 [PMID: 32443177 DOI: 10.1111/his.14160]

64 **Seifert M**, Przekopowitz M, Taudien S, Lollies A, Ronge V, Drees B, Lindemann M, Hillen U, Engler H, Singer BB, Küppers R. Functional capacities of human IgM memory B cells in early inflammatory responses and secondary germinal center reactions. *Proc Natl Acad Sci U S A* 2015; **112**: E546-E555 [PMID: 25624468 DOI: 10.1073/pnas.1416276112]

65 **Kaneko N**, Kuo HH, Boucau J, Farmer JR, Allard-Chamard H, Mahajan VS, Piechocka-Trocha A, Lefteri K, Osborn M, Bals J, Bartsch YC, Bonheur N, Caradonna TM, Chevalier J, Chowdhury F, Diefenbach TJ, Einkauf K, Fallon J, Feldman J, Finn KK, Garcia-Broncano P, Hartana CA, Hauser BM, Jiang C, Kaplonek P, Karpell M, Koscher EC, Lian X, Liu H, Liu J, Ly NL, Michell AR, Rassadkina Y, Seiger K, Sessa L, Shin S, Singh N, Sun W, Sun X, Ticheli HJ, Waring MT, Zhu AL, Alter G, Li JZ, Lingwood D, Schmidt AG, Lichterfeld M, Walker BD, Yu XG, Padera RF Jr, Pillai S; Massachusetts Consortium on Pathogen Readiness Specimen Working Group. Loss of Bcl-6-Expressing T Follicular Helper Cells and Germinal Centers in COVID-19. *Cell* 2020; **183**: 143-157.e13 [PMID: 32877699 DOI: 10.1016/j.cell.2020.08.025]

66 **Kuri-Cervantes L**, Pampena MB, Meng W, Rosenfeld AM, Ittner CAG, Weisman AR, Agyekum

RS, Mathew D, Baxter AE, Vella LA, Kuthuru O, Apostolidis SA, Bershaw L, Dougherty J, Greenplate AR, Pattekar A, Kim J, Han N, Gouma S, Weirick ME, Arevalo CP, Bolton MJ, Goodwin EC, Anderson EM, Hensley SE, Jones TK, Mangalmurti NS, Luning Prak ET, Wherry EJ, Meyer NJ, Betts MR. Comprehensive mapping of immune perturbations associated with severe COVID-19. *Sci Immunol* 2020; **5** [PMID: 32669287 DOI: 10.1126/sciimmunol.abd7114]

67 **Di Sabatino A**, Carsetti R, Corazza GR. Post-splenectomy and hyposplenic states. *Lancet* 2011; **378**: 86-97 [PMID: 21474172 DOI: 10.1016/S0140-6736(10)61493-6]

68 **Kruetzmann S**, Rosado MM, Weber H, Germing U, Tournilhac O, Peter HH, Berner R, Peters A, Boehm T, Plebani A, Quinti I, Carsetti R. Human immunoglobulin M memory B cells controlling Streptococcus pneumoniae infections are generated in the spleen. *J Exp Med* 2003; **197**: 939-945 [PMID: 12682112 DOI: 10.1084/jem.20022020]

69 **Ryan K**, Cooper N, Eleftheriou P, Garg M, Grainger J, Hill Q, Howard J, Kesse-Adu R, Lugthart S, Laffan M, McDonald V, Misbah S, Pavord S. Guidance on shielding for Children and Adults with splenectomy or splenic dysfunction during the COVID-19 pandemic. British Society of Haematology. [cited 4 July 2020]. Available from: https://b-s-h.org.uk/media/18292/covid19-bsh-guidance-on-splenectomy-v2-fnal-6-may2020_.pdf

70 **Williamson EJ**, Walker AJ, Bhaskaran K, Bacon S, Bates C, Morton CE, Curtis HJ, Mehrkar A, Evans D, Inglesby P, Cockburn J, McDonald HI, MacKenna B, Tomlinson L, Douglas IJ, Rentsch CT, Mathur R, Wong AYS, Grieve R, Harrison D, Forbes H, Schultze A, Croker R, Parry J, Hester F, Harper S, Perera R, Evans SJW, Smeeth L, Goldacre B. Factors associated with COVID-19-related death using OpenSAFELY. *Nature* 2020; **584**: 430-436 [PMID: 32640463 DOI: 10.1038/s41586-020-2521-4]

World Journal of Gastroenterology

Submit a Manuscript: https://www.f6publishing.com

World J Gastroenterol 2021 September 21; 27(35): 5932-5945

DOI: 10.3748/wjg.v27.i35.5932

ISSN 1007-9327 (print) ISSN 2219-2840 (online)

MINIREVIEWS

Primary gastric non-Hodgkin lymphomas: Recent advances regarding disease pathogenesis and treatment

Michael D Diamantidis, Maria Papaioannou, Evdoxia Hatjiharissi

ORCID number: Michael D Diamantidis 0000-0002-0041-5930; Maria Papaioannou 0000-0002-1999-9622; Evdoxia Hatjiharissi 0000-0002-8233-0542.

Author contributions: Diamantidis MD performed the literature review and wrote the manuscript; Hatjiharissi E wrote the manuscript, performed the literature review and corrected the manuscript; Papaioannou M wrote and corrected the manuscript.

Conflict-of-interest statement: All authors declare they have no conflicts of interest.

Open-Access: This article is an open-access article that was selected by an in-house editor and fully peer-reviewed by external reviewers. It is distributed in accordance with the Creative Commons Attribution NonCommercial (CC BY-NC 4.0) license, which permits others to distribute, remix, adapt, build upon this work non-commercially, and license their derivative works on different terms, provided the original work is properly cited and the use is non-commercial. See: http://creativecommons.org/Licenses/by-nc/4.0/

Manuscript source: Invited manuscript

Michael D Diamantidis, Department of Hematology, Thalassemia and Sickle Cell Disease Unit, General Hospital of Larissa, Larissa 41221, Thessaly, Greece

Maria Papaioannou, Evdoxia Hatjiharissi, Division of Hematology, First Department of Internal Medicine, AHEPA General Hospital, Aristotle University of Thessaloniki, Thessaloniki 54636, Greece

Corresponding author: Evdoxia Hatjiharissi, MD, PhD, Consultant Hematologist, Division of Hematology, First Department of Internal Medicine, AHEPA General Hospital, Aristotle University of Thessaloniki, St. Kiriakidis 1, Thessaloniki 54636, Greece.
ehatjiharissi@gmail.com

Abstract

Primary gastric lymphomas (PGLs) are distinct lymphoproliferative neoplasms described as heterogeneous entities clinically and molecularly. Their main histological types are diffuse large B-cell lymphoma (DLBCL) or mucosa-associated lymphoma tissue. PGL has been one of the main fields of clinical research of our group in recent years. Although gastric DLBCLs are frequent, sufficient data to guide optimal care are scarce. Until today, a multidisciplinary approach has been applied, including chemotherapy, surgery, radiotherapy or a combination of these treatments. In this minireview article, we provide an overview of the clinical manifestations, diagnosis and staging of these diseases, along with their molecular pathogenesis and the most important related clinical published series. We then discuss the scientific gaps, perils and pitfalls that exist regarding the aforementioned studies, in parallel with the unmet need for future research and comment on the proper methodology for such retrospective studies. Aiming to fill this gap, we retrospectively evaluated the trends in clinical presentation, management and outcome among 165 patients with DLBCL PGL who were seen in our institutions in 1980-2014. The study cohort was divided into two subgroups, comparing the main 2 therapeutic options [cyclophosphamide doxorubicin vincristine prednisone (CHOP) *vs* rituximab-CHOP (R-CHOP)]. A better outcome with immunochemotherapy (R-CHOP) was observed. In the next 2 mo, we will present the update of our study with the same basic conclusion.

Key Words: Primary gastric lymphoma; Extranodal non-Hodgkin's lymphoma; Diffuse large B-cell lymphoma; Mucosa-associated lymphoid tissue; Immunochemotherapy; Rituximab-cyclophosphamide doxorubicin vincristine prednisone

Specialty type: Gastroenterology and hepatology

Country/Territory of origin: Greece

Peer-review report's scientific quality classification

Grade A (Excellent): 0
Grade B (Very good): B, B
Grade C (Good): 0
Grade D (Fair): D
Grade E (Poor): 0

Received: March 22, 2021
Peer-review started: March 22, 2021
First decision: June 14, 2021
Revised: June 27, 2021
Accepted: August 30, 2021
Article in press: August 30, 2021
Published online: September 21, 2021

P-Reviewer: Ahmed M, Li G, Saito M
S-Editor: Gao CC
L-Editor: A
P-Editor: Liu JH

©The Author(s) 2021. Published by Baishideng Publishing Group Inc. All rights reserved.

Core Tip: A few small, heterogeneous, retrospective studies have attempted to determine the optimal treatment for gastric diffuse large B-cell lymphoma, investigating the role of chemotherapy +/- rituximab, surgery and radiation in patient outcomes. Our retrospective research suggests that a better outcome is observed for these patients after the introduction of immunochemotherapy (rituximab-cyclophosphamide doxorubicin vincristine prednisone). Because statistical analysis might differ among various studies, it is crucial to correctly define the terms freedom from progression and lymphoma-specific survival. The latter provides information on whether the patients died from lymphoma or from other causes.

Citation: Diamantidis MD, Papaioannou M, Hatjiharissi E. Primary gastric non-Hodgkin lymphomas: Recent advances regarding disease pathogenesis and treatment. *World J Gastroenterol* 2021; 27(35): 5932-5945
URL: https://www.wjgnet.com/1007-9327/full/v27/i35/5932.htm
DOI: https://dx.doi.org/10.3748/wjg.v27.i35.5932

INTRODUCTION

Primary gastric lymphomas (PGLs) are a diverse group of lymphoproliferative disorders that originate from the stomach and comprise many different histologic types. Either of diffuse large B-cell lymphoma (DLBCL) subtype or mucosa-associated lymphoma tissue (MALT) histology, PGL is the second most common gastric malignancy globally, following the adenocarcinoma of the stomach[1,2]. The latter is the most common form of gastric cancer and the fifth most common malignancy in the world[3]. Despite the fact that prevention and treatment of *Helicobacter pylori* infection (*H. pylori* I) has led to a decrease in its overall incidence, gastric cancer remains the 3rd most deadly cancer, with an estimated 783000 deaths in 2018 worldwide[4,5]. Therefore, accurately recognizing and diagnosing gastric cancer from gastric lymphomas is important, as these diseases are treated differently, and any confusion may result in inappropriate treatment management.

The gastrointestinal tract (GIT) is the most common site for the development of extranodal lymphomas. The incidence of these neoplasms has been increasing in recent years[2,6]. The stomach represents 30%-40% of all extranodal lymphomas and 55%-65% of all GI lymphomas. The incidence of PGL varies from 4% to 20% of extranodal non-Hodgkin lymphomas (NHLs) and reaches up to 5% of primary gastric neoplasms[2]. The incidence of PGL is estimated to be 1 per 100000 in Western countries[7]. B-cell lymphomas are more frequent in these countries than in Eastern countries[1].

To date, the term PGL was originally used to describe lymphomas that arise from the stomach. However, within the medical literature, controversy exists regarding the definition, staging and treatment of this entity. Most cases of PGLs are B-cell subtypes of NHLs. The majority of these subtypes have DLBCL histology and are classified as DLBCL of the stomach, not otherwise specified (NOS).

PGLs are histologically heterogeneous neoplasms. This contributes to a different biology, clinical presentation and prognosis and subsequently determines special therapeutic needs for each subtype[8,9]. For example, certain subtypes of PGLs, such as DLBCL, are more aggressive than others and require immediate therapy[8], whereas for patients with MALT histology, unique management is usually applied ranging from watch and wait to antibiotic-based treatment[9].

As stated above, PGLs are histologically, biologically and clinically heterogeneous neoplasms. Although gastric DLBCL is an extranodal high-grade lymphoma, it is considered less aggressive than its nodal counterpart and other extranodal DLBCL locations. Its appropriate treatment has not been satisfactorily determined, and treatment choices vary considerably. Human immunodeficiency virus, Epstein-Barr infection, hepatitis B virus, human T-cell lymphotropic virus 1, immunosuppression, celiac disease, inflammatory bowel disease, and *H. pylori* I have all been implicated in the factors predisposing patients to PGLs, increasing the risk of developing the disease [1,2,10]. PGL usually occurs in patients older than 50 years. There are many older

patients over 80 years of age. Males are more prone to be diagnosed with PGL with a 2-3-fold higher risk than females[2].

This review mainly focuses on DLBCL gastric lymphoma, which is one of the main fields of our clinical research and comments briefly on MALT lymphoma. The molecular etiology and pathophysiology of DLBCL gastric lymphomas and the available clinical data for their optimal management will be discussed. In parallel, a brief review of the MALT subtype that represents almost 50% of PGLs will also be provided. This review aims to meet the therapeutic needs of those who are involved and/or interested in the treatment of GI-DLBCL lymphomas and extensively focuses on the role of rituximab, the first in class anti-CD20 monoclonal antibody (mAb), in the outcome of patients with PGL of the DLBCL subtype.

CLINICAL MANIFESTATIONS AND DIAGNOSIS

The stomach is the most common site for the development of extranodal lymphomas in the GI tract, accounting for 60% of cases, followed by the small bowel, ileum, cecum, colon and rectum[7]. Distinguishing PGL from secondary dissemination of the stomach due to primary nodal lymphoma can be difficult. No peripheral and mediastinal lymphadenopathy at the time of diagnosis, no spleen or liver infiltration and normal blood counts are in contrast to the presence of a secondary gastric lymphoma[11].

The diagnosis of PGL can be delayed for many years due to the presence of nonspecific symptoms, mimicking peptic ulcer disease, gastritis, functional gastric or even pancreatic disorder. The main symptoms include nausea, vomiting, anorexia, abdominal distention, fullness or pain, indigestion, dyspepsia and weight loss, whereas weakness, night sweats, fever, jaundice, hematemesis or melena are less common[2,7]. An obvious epigastric mass or perforation is rare as an initial presentation[7,10,12].

An appropriate endoscopic evaluation with generously sized tissue samples is the hallmark of diagnosis. The diagnostic accuracy of endoscopic biopsy is very high, reaching 90%. Endoscopic ultrasonography can improve this diagnostic accuracy. The diagnosis becomes difficult when there is deep infiltration and preservation of the mucosa. Computed tomography (CT), magnetic resonance imaging (MRI) and 18F-fluorodeoxyglucose positron emission tomography (FDG-PET) assist in the diagnosis and staging of PGL[1,7]. Sporadically, PGL might present as multifocal, clonally identical foci surrounded by macroscopically unaffected tissue. Thus, gastric mapping of unaffected mucosa is strongly recommended[13]. Bone marrow infiltration, B symptoms and elevated lactate dehydrogenase (LDH) are more frequently encountered in nodal lymphomas than in gastric lymphomas[13].

Different staging systems have been proposed for PGLs. The Ann Arbor staging system, which is widely used for primary nodal lymphomas, is considered unsatisfactory as PGLs originate from the lining of the stomach instead of the lymph nodes[7,13]. In recent years, a more specific Lugano staging system for PGLs was proposed and applied based on the Lugano score[14,15], which includes the following stages: Stage IE — Lymphoma is confined to the GIT (single lesion or multiple noncontiguous lesions): IE1 = mucosa, submucosa; IE2 = muscularis propria, serosa; Stage II — Lymphoma extends into the abdomen from the primary site within the GI tract: II1 = local nodal involvement; II2 = distant nodal involvement; Stage IIE — Penetration of serosa to involve adjacent organs or tissues; Stage IV — Disseminated extranodal involvement or concomitant supra diaphragmatic nodal involvement. Note: Stage III does not exist because gastric lymphoma is always below the diaphragm.

A complete staging work-up includes the following: Biochemical examinations, chest, abdomen and pelvis CT scan, bone marrow biopsy, thorough endoscopy including biopsies from the stomach, duodenum and gastroesophageal junction, endoscopic ultrasound, evaluation of the Waldeyer ring, investigation for *H. pylori* I, routine histology and immunohistochemistry. Cytogenetic studies and even fluorescence in situ hybridization (FISH) can all be used in biopsies to provide the appropriate information needed for optimal treatment. PET/CT scans have documented diagnostic and prognostic value only for DLBCL lymphomas, in contrast to MALT gastric lymphomas, which can be reported as false-negative because of the small tumor burden of the disease and their indolent behavior[13]. However, there is an unmet need regarding the use of PET scans in the clinical setting to guide treatment. Usually, this examination is performed before and after the end of treatment to guide therapeutic decisions as a standard of care. Because the stomach is

an abdominal organ, it is unclear how PET scans can assist in the aforementioned necessary clinical decisions.

In general, the prognosis of extranodal lymphomas varies according to the affected organ; it is poor in the testis, central nervous system (CNS) and intestine, whereas it is quite good in the stomach, mediastinum and bone. Nevertheless, PGL is an aggressive malignancy characterized by rapid growth. However, the prognosis of DLBCL PGL is relatively good, with a 5-year overall survival (OS) higher than 80%[7].

COMPARISON AMONG CLINICAL STUDIES/TREATMENT

The optimal treatment for DLBCL PGLs is not clear, because prospective clinical studies are missing. In the past, a spectrum of treatment approaches was applied, ranging from gastrectomy or radiotherapy alone to chemotherapy (cyclophosphamide doxorubicin vincristine prednisone, CHOP) or the combination of chemotherapy plus radiotherapy and surgery. Wang *et al*[16] compared surgery over conservative treatment in a retrospective study. Conservative treatment in this study included chemotherapy (CHOP) or radiotherapy alone, chemotherapy plus radiotherapy or *H. pylori* I eradication (HPE). The authors found superiority of surgery alone compared with conservative treatment in the DLBCL type regarding prognosis, but not in the MALT type[16]. Currently, the role of surgical resection has been minimized, even in cases of extreme intestinal obstruction, as immunochemotherapy can induce rapid and complete resolution of large obstructing tumor masses. Gastrectomy is restricted to the management of major complications, including perforation or hemorrhage of DLBCL PGLs.

In contrast, other studies demonstrated that DLBCL PGL is a potentially curable disease with rituximab-CHOP (R-CHOP)-like treatment, leading to long-term survival [17]. Investigators found that surgical treatment did not offer survival benefits when compared with chemotherapy for 5-year progression-free survival (PFS) and OS estimates and that no significant differences were noted in these endpoints for patients treated with R-CHOP or conventional chemotherapy[18].

Sohn *et al*[19] directly compared CHOP *vs* R-CHOP as a front-line approach in 93 patients with DLBCL PGL. With a median follow-up of 48 mo, no differences were noted among the 2 groups regarding OS, EFS and CR. High serum levels of β2-microglobulin were associated with worse OS and EFS in patients who received R-CHOP[19]. In a retrospective analysis of 95 Japanese patients, the clinical outcomes of gastric DLBCL were extremely favorable for localized-stage patients in the rituximab era. Conversely, these treatments were poor for advanced-stage patients[20]. Interestingly, an effective approach in treating deeply infiltrated DLBCL PGL patients by switching fractioned R-CHOP (rituximab d0, 50% dose of CHOP d1 and d5) to standard R-CHOP cycles guided by endoscopic ultrasonography has been proposed [21].

The following factors were identified as having a negative impact on survival: age above 65, Eastern Cooperative Oncology Group 2-3, B symptoms, bulky disease, IPI 3-4, more than 3 treatment lines, and absence of response to first-line treatment[17].

Conversely, other factors were considered negative for prognosis in the subsequent study: elevated LDH levels, chemotherapy or radiotherapy alone or the combination of chemotherapy plus radiotherapy[16]. The non-germinal center B-cell-like lymphoma (GCB) subtype has also been associated with shorter OS[18]. *H. pylori* I negativity, advanced Lugano stage and elevated LDH levels have been reported as adverse prognostic factors in gastric DLBCL[22].

Low serum albumin at diagnosis was the only risk factor for developing gastric complications, such as bleeding and stenosis, in patients with gastric DLBCL who received R-CHOP[23]. Furthermore, a low CD4:CD8 ratio at diagnosis is an independent poor prognostic factor for subsequent OS and EFS24 (24 mo after diagnosis) in patients with gastric DLBCL[24]. Finally, the microRNA miR-150 is reportedly a negative independent prognostic biomarker for primary GI DLBCL[25].

Some patients with DLBCL PGL also have a MALT component. The 5-year PFS and OS estimates were similar when de novo DLBCL patients were compared with DLBCL/MALT patients, suggesting that patients with a MALT component, along with DLBCL, might have the same biological type of lymphoma as de novo DLBCL patients [18]. In such DLBCL/MALT cases, an important deregulation of Bcl-2 and an upregulation of p53 protein of uncertain clinical significance have been observed[26]. A synopsis of the studies comparing R-CHOP *vs* CHOP for DLBCL PGLs is shown in Table 1. Indeed, there is a lack of a head-to-head comparison between CHOP and R-

Table 1 Studies comparing rituximab-cyclophosphamide doxorubicin vincristine prednisone *vs* cyclophosphamide doxorubicin vincristine prednisone for diffuse large B-cell lymphoma primary gastric lymphomas

Ref.		Number of Pts	R-CHOP OS	CHOP OS	R-CHOP PFS	CHOP PFS	Comments
Sohn *et al* [19], 2012	Double-arm Retrospective Study (R-CHOP *vs* CHOP as 1st line treatment)	93 (55 R-CHOP, 38 CHOP)	3-yr 84.7% ($P > 0.05$)	3-yr 94.7% ($P > 0.05$)	3-yr 81.7% (EFS) ($P > 0.05$)	3-yr 86% (EFS) ($P > 0.05$)	CR: (CHOP: 93.9%), (R-CHOP: 92.5%)
Liu *et al* [62], 2018	Double-arm Retrospective Study (diagnosis: 1973-2000 era *vs* 2001-2014 era of immuno-CT)	SEER Database 7051 [(4186, 1973-2000), (2865, 2001-2014)	5-yr 53% ($P = 0.001$)	5-yr 47% ($P = 0.001$)			
Tanaka *et al*[20], 2012	Single-arm Retrospective Study (R-CHOP)	95	3-yr 91% (localized disease); 3-yr 95% (localized disease); 3-yr 64% (localized disease)		3-yr 91% (localized disease); 3-yr 92% (localized disease); 3-yr 43% (localized disease)		6c. R-CHOP; 3-4 c. R-CHOP plus radiotherapy; R-CHOP ± radiotherapy
Couto *et al*[17], 2021	Single-arm Retrospective Study (R-CHOP)	101	Not reached		Not reached		80% CR (after 1st line); 54% CR (3 yrs FU)

R-CHOP: Rituximab-cyclophosphamide doxorubicin vincristine prednisone; CHOP: Cyclophosphamide doxorubicin vincristine prednisone; OS: Overall survival; PFS: Progression-free survival; EFS: Event free survival; CR: Complete remission; CT: Computed tomography; FU: Follow-up.

CHOP in PGLs.

Regarding the role of radiotherapy, more data are available for patients with gastric MALT lymphoma or early-stage gastric lymphoma. When there is an unsatisfactory response to HPE, recurrence after HPE or in MALT cases negative for *H. pylori* I, gastric radiotherapy of the entire stomach plus irradiation of the pathological and perigastric lymph nodes (30-440 Gy, 15-20 fractions) has been proposed. However, it is less clear whether radiotherapy should be applied in cases of DLBCL PGLs. However, involved-field radiotherapy has a role, especially for patients with DLBCL PGL of advanced stage who achieve partial remission (PR) after immunochemotherapy (R-CHOP)[27]. R-CHOP plus additional local treatment for gastric lesions (*e.g.*, consolidative radiotherapy or surgical resection) has also been recommended[28]. Alternatively, several studies have found that in the era of immunochemotherapy (R-CHOP), radiotherapy does not improve OS[29-31]. The side effects of radiotherapy should always be taken into account in clinical decision making[27].

Despite the presence of several clinical series involving primary gastric DLBCL lymphomas mainly addressing the issue of selecting the optimal treatment, there are sporadic single cases in the literature[22,32-34]. Some very rare, more aggressive cases of DLBCL lymphoma originating from the stomach and infiltrating the adrenals bilaterally have been reported[32,34]. The first patient presented with nausea, vomiting, abdominal pain and hypotension, was treated with glucocorticoids and died after developing respiratory failure, severe hypotension refractory to vasopressors and severe metabolic acidosis[34]. The second case was a DLBCL, PGL of the non-germinal center (non-GC) type. This patient received 8 cycles of rituximab therapy, 6 cycles of CHOP and 3 cycles of prophylactic intrathecal chemotherapy. The patient maintained a CR for approximately 14 mo after the completion of the aforementioned treatment. The latter is in favor of the hypothesis that DLBCL lymphomas of the stomach have a better prognosis than other DLBCL nodal and extranodal lymphomas. In contrast to the very dismal prognosis of primary adrenal lymphomas (PALs)[35], this patient survived, likely because the primary neoplasm was gastric DLBCL, which has better biological and clinical behavior for unknown molecular reasons (even though it is considered an aggressive neoplasm, being DLBCL).

Regarding the role of HPE, Nakamura *et al*[36] studied 420 patients with gastric MALT lymphoma and found a significant responsiveness to HPE therapy (77%), with treatment failure (relapse or progressive disease) occurring in only 9% of the patients. However, this primary refractory disease was not associated with a dismal outcome, as the subsequent therapy still yielded a 90% OS rate after 10 years[36].

Nevertheless, even though HPE has already been established as an optimal strategy for the management of gastric MALT lymphoma, there are conflicting results, either in favor of or against HPE for patients with DLBCL PGLs. Thus, HPE has been reported to be a suitable strategy for patients with DLBCL PGLs[37,38]. The concept of a less

aggressive biological behavior for *H. pylori* I-dependent gastric DLBCL has been proposed with the suggestion to apply HPE in such cases[39]. However, it is not clear how accurately these lymphomas can be distinguished. Alternatively, high-grade gastric lymphomas can rapidly progress if they do not respond to HPE. The loss of *H. pylori* I dependency and the possible high-grade lymphomatic evolution/transformation are separate and distinct events in the natural history of PGL[38,40]. The description of defined molecular markers linked to *H. pylori* I dependency of PGLs is beyond the scope of this article.

Moreover, a substantial portion of early-stage *H. pylori* I-positive gastric de novo DLBCLs remain *H. pylori* I-dependent and respond to antibiotic treatment (HPE). Prospective studies to validate these findings are needed[41]. Our personal opinion is that HPE should not be applied as monotherapy, even in the early stage of *H. pylori* I-positive DLBCL PGLs.

MOLECULAR PATHOGENESIS

Extranodal lymphomas are distinct types of lymphomas that show a predilection for anatomical sites harboring extranodal lymphoid tissue, such as the CNS, testis, mediastinum, bone and GIT, in contrast to the typical pattern of the nodal counterpart in the lymph nodes for nodal lymphomas[42]. Extranodal lymphomas can even appear in immune-privileged (sanctuary) sites (CNS, testis) or arise in sites of chronic inflammation, effusions or other closed spaces within the body. The complex mechanisms of local immune evasion leading to extranodal lymphoproliferations have not been fully elucidated[43]. The capacity of mature lymphocytes to recirculate between blood and lymphoid tissue and to migrate to extranodal anatomical sites is crucial for the pathogenesis of the disease. During this process, lymphocytes interact with endothelial venules, mediated by receptor molecules (integrins and lymphocytes)[44].

The role of specific B-cell receptor (BCR) antigens has been proposed in the process of lymphomagenesis. Oncogenic translocations during BCR development and generation (VDJ rearrangement), the activation of mature B-cells and the germinal center reaction, the mechanisms of loss of immunological self-tolerance, and the role of infectious agents and autoantigens are all hallmarks and basic elements of lymphomagenesis, a complex multifactorial process, in both aggressive and indolent lymphomas[45]. Gastric DLBCL is a high-grade lymphoma compared to low-grade MALT lymphomas. Whether DLBCL transforms from low-grade MALT lymphoma or whether it arises de novo in the stomach is unknown. DLBCL gastric lymphoma has been associated with a lower CR and shorter survival than MALT lymphoma[2,46]. Nevertheless, transformed DLBCLs from MALTs are CD10- and Bcl-2-negative, while de novo DLBCLs are CD10- and Bcl-2-positive[31,46].

The oncogene Bcl-6 is located on chromosome 3q27 and is frequently present in the majority of extranodal high-grade lymphomas. Conversely, Bcl-2 oncogene expression was significantly lower in gastric lymphomas than in other primary extranodal high-grade B-cell lymphomas (HGBCLs). p53 protein expression did not differ significantly between these 2 groups[2].

Primary gastric DLBCL

DLBCL is described by diffuse proliferation of large, atypical cells, with vesicular nuclei, prominent nucleoli, and basophilic cytoplasm. These cells typically express CD19, CD20, CD22 and CD79a (pan-B-cell markers). Bcl-6 is expressed in 60% of cases. FISH can identify poor prognostic subtypes of DLBCL, such as double-hit (DH) or triple-hit (TH) lymphomas (high-grade, B-cells), characterized by translocations of MYC and Bcl-2 and/or Bcl-6[47,48]. DH or TH lymphomas are defined by their genetic aberrations, irrespective of their morphology. Genetic variability has been documented for DLBCL PGL[47]. Gene expression profiling distinguishes DLBCL into GCB and non-GCB or activated B-cell-like (ABC) subtypes based on the cell of origin profile. ABC lymphomas show a worse prognosis than GCB lymphomas[49]. In routine diagnostic practice, this screening is conducted by immunohistochemistry based on the assessment of three markers (CD10, bcl-6 and MUM1)[50] (Figure 1).

More analytically, ABC DLBCLs are characterized by nuclear factor kappa beta (NF-κB) activation, showing a higher frequency of Bcl-2 amplifications, Bcl-6 rearrangements and recurrent mutations of MYD88, PRDM1 and CD79B, whereas GCB-like DLBCLs are enriched for activating EZH2 and Bcl-2 mutations, defined by perturbations/molecular defects in the JAK/STAT and PI3K/AKT signaling pathways [48]. EZH2 overexpression has been associated with inferior outcomes in patients with

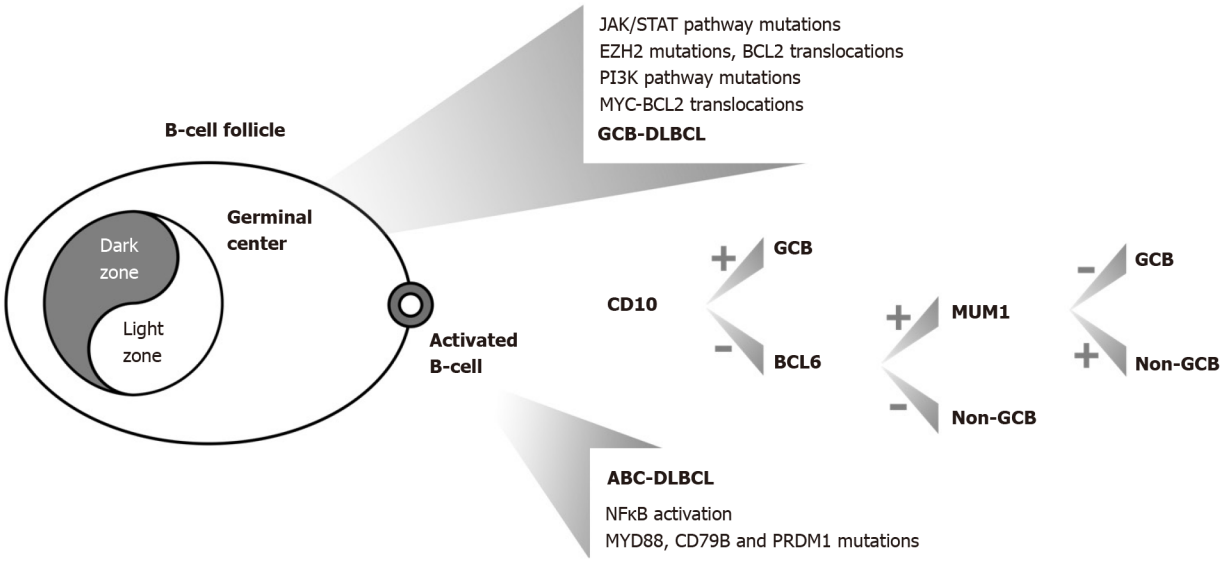


Figure 1 Primary gastric diffuse large B-cell lymphoma lymphomas and related molecular lesions. GCB: Germinal center B-cell lymphoma; ABC: Activated B-cell-like lymphoma; the combination of MYC plus BCL2 translocations corresponds to 'double hit lymphomas'; DLBCL: Diffuse large B-cell lymphoma; NF-κβ: Nuclear factor κappa beta.

DLBCL PGL[51] (Figure 1).

Interestingly, 2 HGBCLs were included in the recent revised WHO classification of lymphoid neoplasms. These entities are clinically and biologically distinct from DLBCL NOS and Burkitt lymphoma (BL). The HGBCL, NOS entity includes cases previously termed 'unclassifiable, with features intermediate between DLBCL and BL', or showing blastoid morphology but lacking DH/TH translocations[49].

High levels of Bcl-6 expression were found in GCB gastric lymphomas, whereas in the non-GCB cases, a high Bcl-6 expression level correlated importantly with mutations producing Bcl-6 deregulation, even if in the latter cases no correlation was found between survival rates[2].

Clinical studies addressing the role of programmed cell death 1 (PD-1) and its ligand (PD-L1) have shown promising results. PD-1 blockade in patients with PD-L1 expression on tumor cells has been linked with clinical responses. Investigators from Japan evaluated the role of PD-L1 expression on neoplastic and non neoplastic immune cells in the microenvironment (miPD-L1) in a retrospective study of patients with GI DLBCL lymphoma. They found that elevated miPD-L1 expression had a favorable impact on the outcome of these DLBCL patients, regardless of the anatomical site of the disease[52].

Gastric MALT lymphoma

MALT lymphoma is a low-grade B-cell NHL, and the majority of cases (approximately 90%) are directly related to *H. pylori* I. However, 10% of gastric MALT lymphomas are *H. pylori* I negative[53]. Chronic *H. pylori* I of the gastric mucosa and the accompanying inflammation have been strongly linked to MALT lymphomagenesis. Moreover, abnormalities in the expression of various miRNAs contribute to the neoplastic gastric phenotype[54,55].

H. pylori I expresses proteins related to the corresponding genes, contributing to the related lymphomagenesis from the bacterium. These are cytotoxin-associated gene A (CagA), vacuolization cytotoxin A (VacA) and heat shock proteins (Hsps). The Cag pathogenicity island (a common gene sequence considered responsible for the pathophysiology of the infection) contains over 40 genes, which mainly code for a complex type IV secretion system. This pathogenicity island is usually absent from *H. pylori* I strains isolated from asymptomatic human carriers. The CagA protein is frequently co-expressed with the vacuolating cytotoxin VacA[56].

Hamoudi *et al*[57] established the connection between abnormal NF-κB signaling due to the chromosomal translocations, t(11;18)(q21;q21)/*API2-MALT1*, t(1;14)(p22;q32)/BCL10-IGH, t(14;18) (q32;q21)/IGH-MALT1 and t(3;14) (p13;q32)/FOXP1-IGH,in gastric MALT lymphomas[57,58] (Figure 2).

MALT1 and BCL10 proteins are involved in surface immune receptor-mediated activation of the NF-κB transcription factor; chromosomal translocations involving

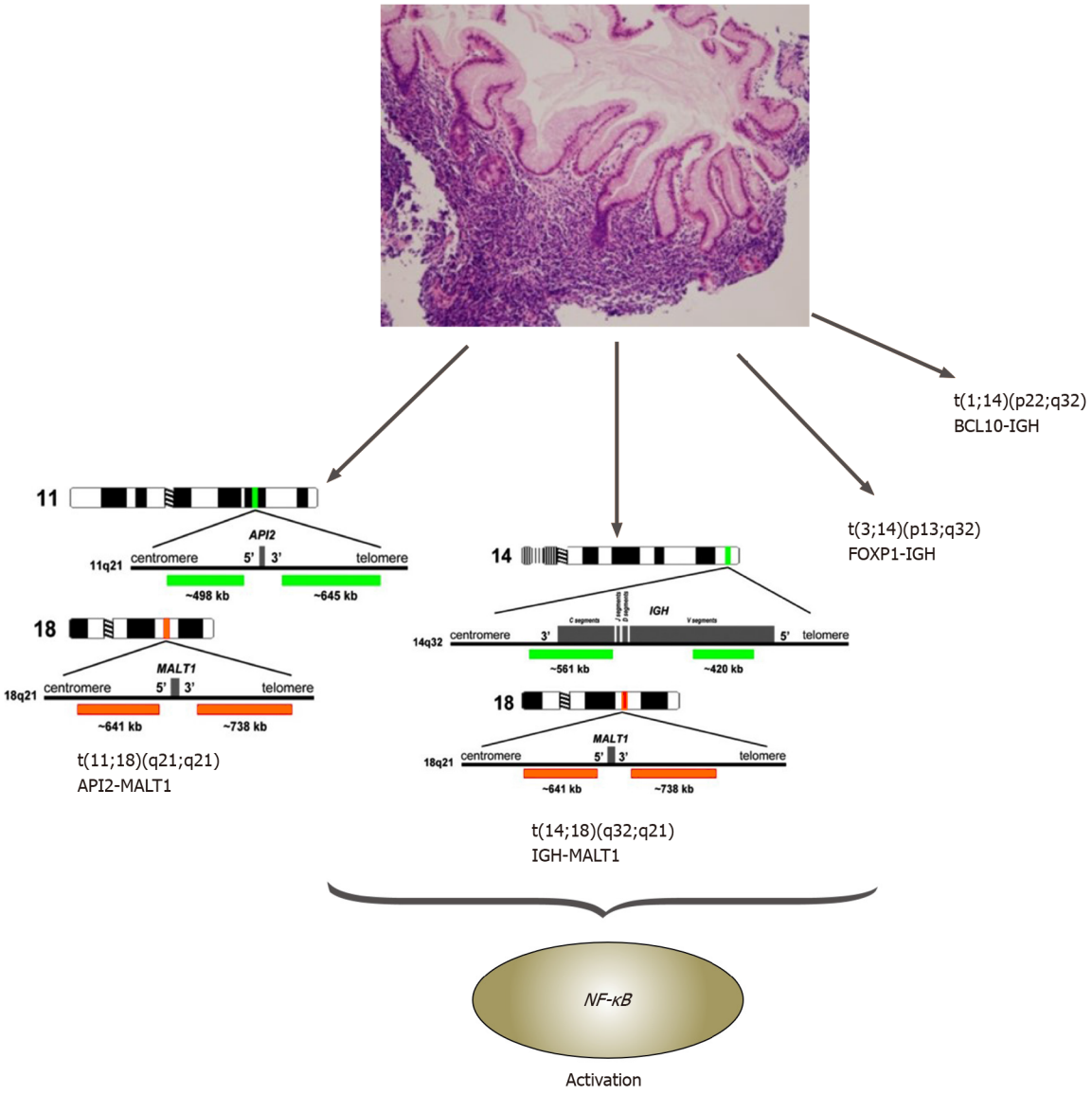


Figure 2 Gastric mucosa-associated lymphoid tissue lymphomas and related chromosomal translocations. BCL: B-cell lymphoma; FOXP: Forkhead box protein; IGH: Immunoglobulin heavy (chain); MALT: Mucosa-associated lymphoid tissue; NF-κB: Nuclear factor κappa beta.

these genes are believed to exert their oncogenic activities through constitutive activation of the NF-κB pathway, leading to the expression of numerous genes important for cell survival and proliferation[40,55,57,58] (Figure 2).

In gastric MALT lymphoma, t(11;18)/*API2-MALT1* is the most frequent translocation, detected in 20% of cases. This translocation fuses the N-terminal region of *API2* to the C-terminal region of *MALT1* and generates a functional chimeric fusion, which can activate the NF-κB pathway. Clinically, t(11;18) is more frequently associated with the absence of *H. pylori* I, and the majority of translocation-positive cases do not respond to HPE therapy. Interestingly, t(11;18)-positive cases rarely transform to DLBCL[55,58].

Gastric MALT lymphoma is indirectly influenced by *H. pylori* I through T-cell stimulation, and recent studies have shown that *H. pylori*-triggering chemokines and their receptors, *H. pylori*-associated epigenetic changes, *H. pylori*-regulated miRNA expression and tumor infiltration by $CD4^+$ $CD25^+$ regulatory T cells contribute to lymphomagenesis of gastric MALT lymphoma (Figure 3). Recent studies have also demonstrated that the translocation of CagA into B lymphocytes inhibits apoptosis through p53 accumulation, BAD phosphorylation and the upregulation of Bcl-2 and Bcl-XL expression (Figure 3). In gastric MALT lymphoma, CagA may stimulate lymphomagenesis directly through the regulation of signal transduction, and intracellular CagA is associated with *H. pylori* I dependence. These findings represent a substantial paradigm shift compared with the classical theory of *H. pylori*-reactive T cells contributing indirectly to the development of MALT lymphoma[40].

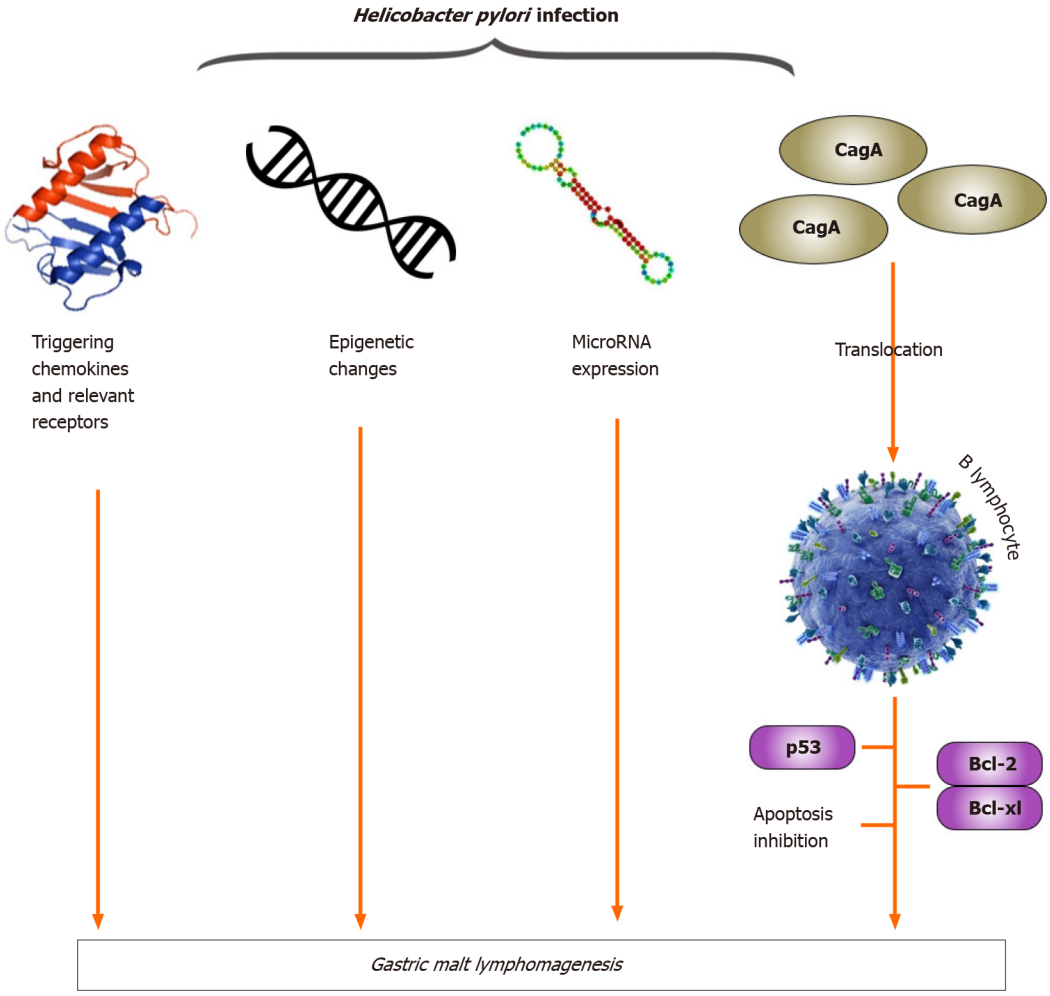


Figure 3 *Helicobacter pylori* infection, molecular mechanisms and gastric mucosa-associated lymphoid tissue lymphomagenesis. BCL: B-cell lymphoma; Bcl-XL: B-cell leukemia XL; CagA: Cytotoxin-associated gene A.

Other cytogenetic aberrations, often associated with one of the four main chromosomal translocations described above, include trisomies 3, 12 and/or 18, which can also present as a sole abnormality in one-fifth of the total cases. Somatic missense mutations in PIM1 and cMYC have been reported in 46% of MALT gastric lymphomas and in 30% of transformed MALT lymphomas. The majority of these genetic lesions are not MALT lymphoma specific. Aberrant somatic hypermutation can still be encountered in indolent lymphomas, such as MALT, but not at the extent noted in DLBCL lymphomas[40,55,58]. Interestingly, the loss of the chemokine receptor CXCR4 and the upregulation of CXCR7 have been associated with the progression of gastric MALT lymphoma to DLBCL lymphoma[59]. Furthermore, lower expression of the microRNA miR-34a has also been linked to the transition from MALT to DLBCL lymphoma[54]. Finally, among the proposed pathogenetic etiologies for *H. pylori*-negative MALT lymphoma cases, genetic alterations in NF-κB signaling are the main hypothesis[53].

SCIENTIFIC GAPS

While gastric DLBCLs are frequent, sufficient data to guide optimal care are still limited. In the past, gastrectomy was the treatment of choice for these patients. Nevertheless, due to the observed high morbidity rates linked with this procedure, novel therapeutic approaches have emerged, such as radiation and combination chemotherapy. Hence, until today, a multidisciplinary approach has been applied, including chemotherapy, surgery, radiotherapy or a combination of these modalities.

Today, immunochemotherapy with R-CHOP is the most acceptable option for treating gastric DLBCL, as for nodal DLBCL. R-CHOP was established as a standard approach for DLBCL patients; in the study of patients aged 60-80 years, the rate of

complete response (CR) was significantly higher in the group that received R-CHOP *vs* CHOP[60]. Since then, a few small, heterogeneous, retrospective studies have attempted to determine the optimal management of gastric DLBCL, investigating the role of immunochemotherapy, surgery and radiation in patient outcomes[16-21,23,61-63].

Significant advances in diagnosis, treatment and response assessment options over the last years have been made in the field of high-grade lymphomas. Molecular characterization of DLBCL has also described 3 major lymphoma subgroups that correlate with distinct biological and clinical behavior (ABCs, GCBs, double hit lymphomas), supporting the rationale for distinct therapeutic options[48]. However, these advances were extracted from nodal DLBCL, while the intrinsic pathogenesis of primary gastric DLBCL is unclear, and similar studies on this particular type of lymphoma are lacking.

The heterogeneity of the various clinical retrospective studies investigating the outcomes of patients with DLBCL PGLs is impressive. For example, these studies differ in the number of patients, in the time intervals when each therapeutic approach was applied, or in the type of therapeutic approaches compared. Other studies calculate surgery alone and other surgeries with chemotherapy and/or radiotherapy, without separating treatment subgroups of patients. Some researchers place all DLBCL patients together into the statistical analysis, regardless of the anatomical site (stomach, intestine). Hence, comparisons are difficult and not head-to-head. Thus, evidence-based conclusions cannot be drawn, and these results should be regarded with caution.

Finally, the use of various staging systems combined with the variability in the applied procedures for staging make the application of meaningful comparisons among the published series difficult.

CURRENT AND FUTURE RESEARCH — FRONTIER PERSPECTIVE

We retrospectively evaluated the clinical profile and the patterns of outcome among patients who were treated after the diagnosis of aggressive, B-cell, primary endocrine lymphoma (another type of extranodal lymphoma). The patients were diagnosed with either primary testicular lymphoma, primary thyroid lymphoma (PTHL), or PAL. Better outcomes were observed in patients with PTHL for whom the median OS had not been reached until the end date of the study, whereas the PAL group had the worst prognosis[35].

To better understand the nature and outcome of extranodal DLBCL PGL, we described patients' and disease characteristics and assessed trends in treatment options, management and outcome among 159 newly diagnosed patients with primary gastric DLBCL who were seen in our institutions in the years 1971-2017.

Previously, we retrospectively evaluated the trends in clinical presentation, management and outcome among 165 consecutive patients with biopsy-proven primary gastric DLBCL who were seen in 1980-2014. The study cohort was divided into two subgroups based on the era of treatment (CHOP *vs* R-CHOP, before and after the initiation of rituximab). A better outcome after immunochemotherapy (R-CHOP) was observed comparatively[64].

Our novel manuscript and update of the same cohort of patients will be sent for peer review within the next 2 mo (under preparation). We have been preparing and analyzing it for years, focusing on the proper methodology and aiming to correct the perils and pitfalls seen in other relevant studies in the past. We will still have the same conclusion that a better outcome has been noted for the R-CHOP patient cohort, as in the past[64]. However, there are individual variations of the results regarding the OS and freedom from progression (FFP) time intervals, which will be analyzed accordingly, now that a longer follow-up of the patients has been achieved.

The term FFP is based on the strict scientific definition for this type of lymphoma and is preferable to define the aforementioned important endpoint for retrospective clinical studies. PFS has disadvantages in nonrandomized studies because in such studies, there is a lack of specific or concrete criteria for the comparison between time intervals (fixed check points), necessary for the re-evaluation of the disease and the definition of relapse in a similar way (for example, with CT or MRI). However, the term PFS is more widely used in the literature in an equivalent meaning for these lymphomas without being absolutely accurate or to the point in a strict scientific sense. We especially focused on defining FFP accurately, as this is crucial for this novel study. FFP for our novel update will be measured from the initiation of the first treatment until relapse or until death or until the last day of the study for the non

relapsed patients or until the day of the last follow-up for the censored patients (lost to follow-up).

Per-protocol analysis will be used in our clinical research compared to intention-to-treat analysis. The latter is considered a better marker of treatment efficacy for prospective, randomized studies and not for retrospective studies.

Finally, lymphoma-specific survival, another important endpoint, will be measured from diagnosis until the time of death from lymphoma. The number of patients who died from causes other than lymphoma was not calculated at this endpoint. As the long-year follow-up continued, we noted a proportion of our patients dying from lymphoma but also other patients dying from causes other than lymphoma. This analysis is important because it attributes the specific hazard ratio to DLBCL gastric lymphoma (death risk) and separates causes of death other than lymphoma for patients who have survived longer. Importantly, when a patient died from another cause in addition to lymphoma, there was no relapse because the patient was in follow-up. Thus, the possible drug might have protected the patient from relapse, and these patients contributed to the studied time-to-event analysis.

CONCLUSION

In conclusion, retrospective studies, despite their limitations, if conducted with the correct methodology, can provide useful clinical information for treating patients. Our research in recent years has shown that immunochemotherapy (R-CHOP) is the optimal treatment for patients with DLBCL PGLs, as it is associated with a better outcome.

ACKNOWLEDGEMENTS

The authors would like to thank Tsangalas E for the preparation of the figures of this work.

REFERENCES

1 **Peng JC**, Zhong L, Ran ZH. Primary lymphomas in the gastrointestinal tract. *J Dig Dis* 2015; **16**: 169-176 [PMID: 25678011 DOI: 10.1111/1751-2980.12234]

2 **Juárez-Salcedo LM**, Sokol L, Chavez JC, Dalia S. Primary Gastric Lymphoma, Epidemiology, Clinical Diagnosis, and Treatment. *Cancer Control* 2018; **25**: 1073274818778256 [PMID: 29779412 DOI: 10.1177/1073274818778256]

3 **Milano AF**. 20-Year Comparative Survival and Mortality of Cancer of the Stomach by Age, Sex, Race, Stage, Grade, Cohort Entry Time-Period, Disease Duration & Selected ICD-O-3 Oncologic Phenotypes: *A Systematic Review of 157,258 Cases for Diagnosis Years 1973-2014: (SEER*Stat 8.3.4)*. *J Insur Med* 2019; **48**: 5-23 [PMID: 31609640 DOI: 10.17849/insm-48-1-1-19.1]

4 **Rawla P**, Barsouk A. Epidemiology of gastric cancer: global trends, risk factors and prevention. *Prz Gastroenterol* 2019; **14**: 26-38 [PMID: 30944675 DOI: 10.5114/pg.2018.80001]

5 **Zhang X**, Yang J, Huang Q, Lyu J. Prognostic factors in patients with gastric adenocarcinoma using competing-risk analysis: a study of cases in the SEER database. *Scand J Gastroenterol* 2019; **54**: 1015-1021 [PMID: 31382800 DOI: 10.1080/00365521.2019.1649456]

6 **Violeta Filip P**, Cuciureanu D, Sorina Diaconu L, Maria Vladareanu A, Silvia Pop C. MALT lymphoma: epidemiology, clinical diagnosis and treatment. *J Med Life* 2018; **11**: 187-193 [PMID: 30364585 DOI: 10.25122/jml-2018-0035]

7 **Ferreri AJ**, Montalbán C. Primary diffuse large B-cell lymphoma of the stomach. *Crit Rev Oncol Hematol* 2007; **63**: 65-71 [PMID: 17339119 DOI: 10.1016/j.critrevonc.2007.01.003]

8 **Ikoma N**, Badgwell BD, Mansfield PF. Multimodality Treatment of Gastric Lymphoma. *Surg Clin North Am* 2017; **97**: 405-420 [PMID: 28325194 DOI: 10.1016/j.suc.2016.11.012]

9 **Fischbach W**. Long-term follow-up of gastric lymphoma after stomach conserving treatment. *Best Pract Res Clin Gastroenterol* 2010; **24**: 71-77 [PMID: 20206110 DOI: 10.1016/j.bpg.2009.12.005]

10 **Shirwaikar Thomas A**, Schwartz M, Quigley E. Gastrointestinal lymphoma: the new mimic. *BMJ Open Gastroenterol* 2019; **6**: e000320 [PMID: 31645987 DOI: 10.1136/bmjgast-2019-000320]

11 **Dawson IM**, Cornes JS, Morson BC. Primary malignant lymphoid tumours of the intestinal tract. Report of 37 cases with a study of factors influencing prognosis. *Br J Surg* 1961; **49**: 80-89 [PMID: 13884035 DOI: 10.1002/bjs.18004921319]

12 **Malipatel R**, Patil M, Pritilata Rout P, Correa M, Devarbhavi H. Primary Gastric Lymphoma: Clinicopathological Profile. *Euroasian J Hepatogastroenterol* 2018; **8**: 6-10 [PMID: 29963454 DOI:

10.5005/jp-journals-10018-1250]
13 **Psyrri A**, Papageorgiou S, Economopoulos T. Primary extranodal lymphomas of stomach: clinical presentation, diagnostic pitfalls and management. *Ann Oncol* 2008; **19**: 1992-1999 [PMID: 18647965 DOI: 10.1093/annonc/mdn525]
14 **Cheson BD**, Fisher RI, Barrington SF, Cavalli F, Schwartz LH, Zucca E, Lister TA; Alliance, Australasian Leukaemia and Lymphoma Group; Eastern Cooperative Oncology Group; European Mantle Cell Lymphoma Consortium; Italian Lymphoma Foundation; European Organisation for Research; Treatment of Cancer/Dutch Hemato-Oncology Group; Grupo Español de Médula Ósea; German High-Grade Lymphoma Study Group; German Hodgkin's Study Group; Japanese Lymphorra Study Group; Lymphoma Study Association; NCIC Clinical Trials Group; Nordic Lymphoma Study Group; Southwest Oncology Group; United Kingdom National Cancer Research Institute. Recommendations for initial evaluation, staging, and response assessment of Hodgkin and non-Hodgkin lymphoma: the Lugano classification. *J Clin Oncol* 2014; **32**: 3059-3068 [PMID: 25113753 DOI: 10.1200/jco.2013.54.8800]
15 **Barrington SF**, Mikhaeel NG, Kostakoglu L, Meignan M, Hutchings M, Müeller SP, Schwartz LH, Zucca E, Fisher RI, Trotman J, Hoekstra OS, Hicks RJ, O'Doherty MJ, Hustinx R, Biggi A, Cheson BD. Role of imaging in the staging and response assessment of lymphoma: consensus of the International Conference on Malignant Lymphomas Imaging Working Group. *J Clin Oncol* 2014; **32**: 3048-3058 [PMID: 25113771 DOI: 10.1200/jco.2013.53.5229]
16 **Wang YG**, Zhao LY, Liu CQ, Pan SC, Chen XL, Liu K, Zhang WH, Yang K, Chen XZ, Zhang B, Chen ZX, Chen JP, Zhou ZG, Hu JK. Clinical characteristics and prognostic factors of primary gastric lymphoma: A retrospective study with 165 cases. *Medicine (Baltimore)* 2016; **95**: e4250 [PMID: 27495029 DOI: 10.1097/MD.0000000000004250]
17 **Couto ME**, Oliveira I, Domingues N, Viterbo L, Martins Â, Moreira I, Espírito-Santo A, Chacim S, Moreira C, Pereira D, Henrique R, Mariz J. Gastric Diffuse Large B-Cell Lymphoma: A Single-Center 9-Year Experience. *Indian J Hematol Blood Transfus* 2021; 1-5 [PMID: 33424149 DOI: 10.1007/s12288-020-01391-9]
18 **Li X**, Xia B, Guo S, Zhan Z, Zhang L, Zhao D, Wu X, Zhang Y. A retrospective analysis of primary gastric diffuse large B-cell lymphoma with or without concomitant mucosa-associated lymphoid tissue (MALT) lymphoma components. *Ann Hematol* 2013; **92**: 807-815 [PMID: 23417758 DOI: 10.1007/s00277-013-1701-9]
19 **Sohn BS**, Kim SM, Yoon DH, Kim S, Lee DH, Kim JH, Lee SW, Huh J, Suh C. The comparison between CHOP and R-CHOP in primary gastric diffuse large B cell lymphoma. *Ann Hematol* 2012; **91**: 1731-1739 [PMID: 22752193 DOI: 10.1007/s00277-012-1512-4]
20 **Tanaka T**, Shimada K, Yamamoto K, Hirooka Y, Niwa Y, Sugiura I, Kitamura K, Kosugi H, Kinoshita T, Goto H, Nakamura S. Retrospective analysis of primary gastric diffuse large B cell lymphoma in the rituximab era: a multicenter study of 95 patients in Japan. *Ann Hematol* 2012; **91**: 383-390 [PMID: 21822617 DOI: 10.1007/s00277-011-1306-0]
21 **Liu Y**, Liu Y, Zhao P, Zhang Q, Liu X, Lv F, Hong X, Cao J, Xue K. Switching Fractioned R-CHOP Cycles to Standard R-CHOP Cycles Guided by Endoscopic Ultrasonography in Treating Patients with Primary Gastric Diffuse Large B-Cell Lymphoma. *Cancer Manag Res* 2020; **12**: 5041-5048 [PMID: 32612391 DOI: 10.2147/CMAR.S260974]
22 **Goto A**, Nishikawa J, Ito S, Hideura E, Ogawa R, Hashimoto S, Okamoto T, Sakaida I. A Rapidly Developing Diffuse Large B cell Lymphoma of the Stomach. *J Gastrointest Cancer* 2019; **50**: 657-659 [PMID: 29623599 DOI: 10.1007/s12029-018-0098-z]
23 **Kadota T**, Seo S, Fuse H, Ishii G, Itoh K, Yano T, Kaneko K, Tsukasaki K. Complications and outcomes in diffuse large B-cell lymphoma with gastric lesions treated with R-CHOP. *Cancer Med* 2019; **8**: 982-989 [PMID: 30730104 DOI: 10.1002/cam4.1982]
24 **Bai Z**, Li Z, Guan T, Wang L, Wang J, Wu S, Su L. Primary Gastric Diffuse Large B-Cell Lymphoma: Prognostic Factors in the Immuno-Oncology Therapeutics Era. *Turk J Haematol* 2020; **37**: 193-202 [PMID: 32160735 DOI: 10.4274/tjh.galenos.2020.2019.0332]
25 **Wang X**, Kan Y, Chen L, Ge P, Ding T, Zhai Q, Yu Y, Wang X, Zhao Z, Yang H, Liu X, Li L, Qiu L, Qian Z, Zhang H, Wang Y, Zhao H. miR-150 is a negative independent prognostic biomarker for primary gastrointestinal diffuse large B-cell lymphoma. *Oncol Lett* 2020; **19**: 3487-3494 [PMID: 32269622 DOI: 10.3892/ol.2020.11452]
26 **Yonezumi M**, Suzuki R, Suzuki H, Yoshino T, Oshima K, Hosokawa Y, Asaka M, Morishima Y, Nakamura S, Seto M. Detection of AP12-MALT1 chimaeric gene in extranodal and nodal marginal zone B-cell lymphoma by reverse transcription polymerase chain reaction (PCR) and genomic long and accurate PCR analyses. *Br J Haematol* 2001; **115**: 588-594 [PMID: 11736940 DOI: 10.1046/j.1365-2141.2001.03158.x]
27 **Aleman BM**, Haas RL, van der Maazen RW. Role of radiotherapy in the treatment of lymphomas of the gastrointestinal tract. *Best Pract Res Clin Gastroenterol* 2010; **24**: 27-34 [PMID: 20206106 DOI: 10.1016/j.bpg.2009.12.002]
28 **Kang HJ**, Lee HH, Jung SE, Park KS, O JH, Jeon YW, Choi BO, Cho SG. Pattern of failure and optimal treatment strategy for primary gastric diffuse large B-cell lymphoma treated with R-CHOP chemotherapy. *PLoS One* 2020; **15**: e0238807 [PMID: 32960887 DOI: 10.1371/journal.pone.0238807]
29 **Avilés A**, Nambo MJ, Neri N, Huerta-Guzmán J, Cuadra I, Alvarado I, Castañeda C, Fernández R, González M. The role of surgery in primary gastric lymphoma: results of a controlled clinical trial.

Ann Surg 2004; **240**: 44-50 [PMID: 15213617 DOI: 10.1097/01.sla.0000129354.31318.f1]
30 **Cuccurullo R**, Govi S, Ferreri AJ. De-escalating therapy in gastric aggressive lymphoma. *World J Gastroenterol* 2014; **20**: 8993-8997 [PMID: 25083073]
31 **Olszewska-Szopa M**, Wróbel T. Gastrointestinal non-Hodgkin lymphomas. *Adv Clin Exp Med* 2019; **28**: 1119-1124 [PMID: 31414733 DOI: 10.17219/acem/94068]
32 **Wakabayashi M**, Sekiguchi Y, Shimada A, Ichikawa K, Sugimoto K, Tomita S, Izumi H, Nakamura N, Sawada T, Ohta Y, Komatsu N, Noguchi M. Diffuse large B-cell lymphoma solely involving bilateral adrenal glands and stomach: report of an extremely rare case with review of the literature. *Int J Clin Exp Pathol* 2014; **7**: 8190-8197 [PMID: 25550871]
33 **Ceniceros-Cabrales AP**, Sánchez-Fernández P. Perforated gastric diffuse large B-cell lymphoma: A case report and literature review. *Rev Gastroenterol Mex (Engl Ed)* 2019; **84**: 412-414 [PMID: 30245175 DOI: 10.1016/j.rgmx.2018.07.004]
34 **Hassan M**, Mandal AK, Sidhu JS, Cardenas LM. Gastric diffuse large B-cell lymphoma with bilateral adrenal metastasis. *BMJ Case Rep* 2019; **12** [PMID: 31272994 DOI: 10.1136/bcr-2019-229758]
35 **Hatjiharissi E**, Diamantidis MD, Papaioannou M, Dimou T, Chrisoulidou A, Patakiouta F, Constantinou N, Pazaitou-Panayiotou K. Long-term outcome of primary endocrine non-Hodgkin lymphomas: does the site make the difference? *QJM* 2013; **106**: 623-630 [PMID: 23426729 DOI: 10.1093/qjmed/hct048]
36 **Nakamura S**, Sugiyama T, Matsumoto T, Iijima K, Ono S, Tajika M, Tari A, Kitadai Y, Matsumoto H, Nagaya T, Kamoshida T, Watanabe N, Chiba T, Origasa H, Asaka M; JAPAN GAST Study Group. Long-term clinical outcome of gastric MALT lymphoma after eradication of Helicobacter pylori: a multicentre cohort follow-up study of 420 patients in Japan. *Gut* 2012; **61**: 507-513 [PMID: 21890816 DOI: 10.1136/gutjnl-2011-300495]
37 **Ferreri AJ**, Govi S, Ponzoni M. The role of Helicobacter pylori eradication in the treatment of diffuse large B-cell and marginal zone lymphomas of the stomach. *Curr Opin Oncol* 2013; **25**: 470-479 [PMID: 23942292 DOI: 10.1097/01.cco.0000432523.24358.15]
38 **Paydas S**. Helicobacter pylori eradication in gastric diffuse large B cell lymphoma. *World J Gastroenterol* 2015; **21**: 3773-3776 [PMID: 25852262 DOI: 10.3748/wjg.v21.i13.3773]
39 **Kuo SH**, Yeh KH, Chen LT, Lin CW, Hsu PN, Hsu C, Wu MS, Tzeng YS, Tsai HJ, Wang HP, Cheng AL. Helicobacter pylori-related diffuse large B-cell lymphoma of the stomach: a distinct entity with lower aggressiveness and higher chemosensitivity. *Blood Cancer J* 2014; **4**: e220 [PMID: 24949857 DOI: 10.1038/bcj.2014.40]
40 **Kuo SH**, Cheng AL. Helicobacter pylori and mucosa-associated lymphoid tissue: what's new. *Hematology Am Soc Hematol Educ Program* 2013; **2013**: 109-117 [PMID: 24319171 DOI: 10.1182/asheducation-2013.1.109]
41 **Kuo SH**, Yeh KH, Wu MS, Lin CW, Hsu PN, Wang HP, Chen LT, Cheng AL. Helicobacter pylori eradication therapy is effective in the treatment of early-stage H pylori-positive gastric diffuse large B-cell lymphomas. *Blood* 2012; **119**: 4838-44; quiz 5057 [PMID: 22403257 DOI: 10.1182/blood-2012-01-404194]
42 **Ollila TA**, Olszewski AJ. Extranodal Diffuse Large B Cell Lymphoma: Molecular Features, Prognosis, and Risk of Central Nervous System Recurrence. *Curr Treat Options Oncol* 2018; **19**: 38 [PMID: 29931605 DOI: 10.1007/s11864-018-0555-8]
43 **King RL**, Goodlad JR, Calaminici M, Dotlic S, Montes-Moreno S, Oschlies I, Ponzoni M, Traverse-Glehen A, Ott G, Ferry JA. Lymphomas arising in immune-privileged sites: insights into biology, diagnosis, and pathogenesis. *Virchows Arch* 2020; **476**: 647-665 [PMID: 31863183 DOI: 10.1007/s00428-019-02698-3]
44 **Taal BG**, Burgers JM. Primary non-Hodgkin's lymphoma of the stomach: endoscopic diagnosis and the role of surgery. *Scand J Gastroenterol Suppl* 1991; **188**: 33-37 [PMID: 1775939 DOI: 10.3109/00365529109111227]
45 **Thurner L**, Hartmann S, Neumann F, Hoth M, Stilgenbauer S, Küppers R, Preuss KD, Bewarder M. Role of Specific B-Cell Receptor Antigens in Lymphomagenesis. *Front Oncol* 2020; **10**: 604685 [PMID: 33363034 DOI: 10.3389/fonc.2020.604685]
46 **Bautista-Quach MA**, Ake CD, Chen M, Wang J. Gastrointestinal lymphomas: Morphology, immunophenotype and molecular features. *J Gastrointest Oncol* 2012; **3**: 209-225 [PMID: 22943012 DOI: 10.3978/j.issn.2078-6891.2012.024]
47 **Lin P**, Medeiros LJ. The impact of MYC rearrangements and "double hit" abnormalities in diffuse large B-cell lymphoma. *Curr Hematol Malig Rep* 2013; **8**: 243-252 [PMID: 23892979 DOI: 10.1007/s11899-013-0169-y]
48 **Abramson JS**. Hitting back at lymphoma: How do modern diagnostics identify high-risk diffuse large B-cell lymphoma subsets and alter treatment? *Cancer* 2019; **125**: 3111-3120 [PMID: 31287161 DOI: 10.1002/cncr.32145]
49 **Foukas PG**, Bisig B, de Leval L. Recent advances upper gastrointestinal lymphomas: molecular updates and diagnostic implications. *Histopathology* 2021; **78**: 187-214 [PMID: 33382495 DOI: 10.1111/his.14289]
50 **Hans CP**, Weisenburger DD, Greiner TC, Gascoyne RD, Delabie J, Ott G, Müller-Hermelink HK, Campo E, Braziel RM, Jaffe ES, Pan Z, Farinha P, Smith LM, Falini B, Banham AH, Rosenwald A, Staudt LM, Connors JM, Armitage JO, Chan WC. Confirmation of the molecular classification of diffuse large B-cell lymphoma by immunohistochemistry using a tissue microarray. *Blood* 2004; **103**: 275-282 [PMID: 14504078 DOI: 10.1182/blood-2003-05-1545]

51 **Liu Y**, Yu K, Li M, Zeng K, Wei J, Li X, Liu Y, Zhao D, Fan L, Yu Z, Wang Y, Li Z, Zhang W, Bai Q, Yan Q, Guo Y, Wang Z, Guo S. EZH2 overexpression in primary gastrointestinal diffuse large B-cell lymphoma and its association with the clinicopathological features. *Hum Pathol* 2017; **64**: 213-221 [PMID: 28438623 DOI: 10.1016/j.humpath.2017.04.011]

52 **Ishikawa E**, Nakamura M, Shimada K, Tanaka T, Satou A, Kohno K, Sakakibara A, Furukawa K, Yamamura T, Miyahara R, Nakamura S, Kato S, Fujishiro M. Prognostic impact of PD-L1 expression in primary gastric and intestinal diffuse large B-cell lymphoma. *J Gastroenterol* 2020; **55**: 39-50 [PMID: 31493237 DOI: 10.1007/s00535-019-01616-3]

53 **Asano N**, Iijima K, Koike T, Imatani A, Shimosegawa T. Helicobacter pylori-negative gastric mucosa-associated lymphoid tissue lymphomas: A review. *World J Gastroenterol* 2015; **21**: 8014-8020 [PMID: 26185372 DOI: 10.3748/wjg.v21.i26.8014]

54 **Vasilatou D**, Sioulas AD, Pappa V, Papanikolaou IS, Triantafyllou K, Dimitriadis GD, Papageorgiou SG. The role of miRNAs and epigenetic mechanisms in primary gastric mucosa-associated lymphoid tissue lymphoma. *Future Oncol* 2016; **12**: 1587-1593 [PMID: 27079806 DOI: 10.2217/fon-2016-0038]

55 **Troppan K**, Wenzl K, Neumeister P, Deutsch A. Molecular Pathogenesis of MALT Lymphoma. *Gastroenterol Res Pract* 2015; **2015**: 102656 [PMID: 25922601 DOI: 10.1155/2015/102656]

56 **Amedei A**, Cappon A, Codolo G, Cabrelle A, Polenghi A, Benagiano M, Tasca E, Azzurri A, D'Elios MM, Del Prete G, de Bernard M. The neutrophil-activating protein of Helicobacter pylori promotes Th1 immune responses. *J Clin Invest* 2006; **116**: 1092-1101 [PMID: 16543949 DOI: 10.1172/jci27177]

57 **Hamoudi RA**, Appert A, Ye H, Ruskone-Fourmestraux A, Streubel B, Chott A, Raderer M, Gong L, Wlodarska I, De Wolf-Peeters C, MacLennan KA, de Leval L, Isaacson PG, Du MQ. Differential expression of NF-kappaB target genes in MALT lymphoma with and without chromosome translocation: insights into molecular mechanism. *Leukemia* 2010; **24**: 1487-1497 [PMID: 20520640 DOI: 10.1038/leu.2010.118]

58 **Nakamura S**, Matsumoto T. Helicobacter pylori and gastric mucosa-associated lymphoid tissue lymphoma: recent progress in pathogenesis and management. *World J Gastroenterol* 2013; **19**: 8181-8187 [PMID: 24363507 DOI: 10.3748/wjg.v19.i45.8181]

59 **Deutsch AJ**, Steinbauer E, Hofmann NA, Strunk D, Gerlza T, Beham-Schmid C, Schaider H, Neumeister P. Chemokine receptors in gastric MALT lymphoma: loss of CXCR4 and upregulation of CXCR7 is associated with progression to diffuse large B-cell lymphoma. *Mod Pathol* 2013; **26**: 182-194 [PMID: 22936065 DOI: 10.1038/modpathol.2012.134]

60 **Coiffier B**, Lepage E, Briere J, Herbrecht R, Tilly H, Bouabdallah R, Morel P, Van Den Neste E, Salles G, Gaulard P, Reyes F, Lederlin P, Gisselbrecht C. CHOP chemotherapy plus rituximab compared with CHOP alone in elderly patients with diffuse large-B-cell lymphoma. *N Engl J Med* 2002; **346**: 235-242 [PMID: 11807147 DOI: 10.1056/NEJMoa011795]

61 **Ge Z**, Liu Z, Hu X. Anatomic distribution, clinical features, and survival data of 87 cases primary gastrointestinal lymphoma. *World J Surg Oncol* 2016; **14**: 85 [PMID: 26988370 DOI: 10.1186/s12957-016-0821-9]

62 **Liu PP**, Xia Y, Bi XW, Wang Y, Sun P, Yang H, Li ZM, Jiang WQ. Trends in Survival of Patients with Primary Gastric Diffuse Large B-Cell Lymphoma: An Analysis of 7051 Cases in the SEER Database. *Dis Markers* 2018; **2018**: 7473935 [PMID: 30410635 DOI: 10.1155/2018/7473935]

63 **Taal BG**, Burgers JM, van Heerde P, Hart AA, Somers R. The clinical spectrum and treatment of primary non-Hodgkin's lymphoma of the stomach. *Ann Oncol* 1993; **4**: 839-846 [PMID: 8117603 DOI: 10.1093/oxfordjournals.annonc.a058390]

64 **Hatjiharissi E**, Diamantidis M, Papadopoulou A, Chatzileontiadou S, Gerofotis A, Pouptsis A, Karabatzakis N, Pentidou K, Patakiouta F, Konstantinou N, Papaioannou M. Long-term follow-up of patients with non-Hodgkin primary diffuse large B-cell lymphoma of the stomach: Better outcome after immunochemotherapy. *Hematol Oncol* 2017; **35**: 377 [DOI: 10.1002/hon.2439_136]

World Journal of Gastroenterology

Submit a Manuscript: https://www.f6publishing.com

World J Gastroenterol 2021 September 21; 27(35): 5946-5957

DOI: 10.3748/wjg.v27.i35.5946

ISSN 1007-9327 (print) ISSN 2219-2840 (online)

ORIGINAL ARTICLE

Basic Study

Proteomics identifies a novel role of fibrinogen-like protein 1 in Crohn's disease

Xue-Liang Sun, Li-Chao Qiao, Jing Gong, Ke Wen, Zhi-Zhong Xu, Bo-Lin Yang

ORCID number: Xue-Liang Sun 0000-0001-8520-6937; Li-Chao Qiao 0000-0002-0292-2936; Jing Gong 0000-0001-8423-3706; Ke Wen 0000-0003-3925-6567; Zhi-Zhong Xu 0000-0002-1725-7190; Bo-Lin Yang 0000-0002-2474-4085.

Author contributions: Sun XL and Yang BL contributed to designing the study; Sun XL, Qiao LC and Gong J contributed to performing the experiments; Wen K and Xu ZZ contributed to sample collection and statistical analysis; Sun XL and Qiao LC contributed to manuscript drafting; all authors made critical revisions to the manuscript and approved the final version of the article to be published.

Supported by National Natural Science Foundation of China, No. 82074431; The Open Projects of the Discipline of Chinese Medicine of Nanjing University of Chinese Medicine Supported by the Subject of Academic Priority Discipline of Jiangsu Higher Education Institutions, No. ZYX03KF034; and Suzhou Municipal Science and Technology Bureau, No. SYSD2020253 and No. SS202085.

Institutional review board statement: The study was approved by the Ethics Committee of the Affiliated Hospital of Nanjing University of Chinese

Xue-Liang Sun, Li-Chao Qiao, Jing Gong, Bo-Lin Yang, First Clinical Medical College, The Affiliated Hospital of Nanjing University of Chinese Medicine, Nanjing 210029, Jiangsu Province, China

Xue-Liang Sun, Ke Wen, Zhi-Zhong Xu, Department of Colorectal Surgery, Suzhou TCM Hospital Affiliated to Nanjing University of Chinese Medicine, Suzhou 215000, Jiangsu Province, China

Bo-Lin Yang, Department of Colorectal Surgery, Jiangsu Province Hospital of Chinese Medicine, Nanjing 210029, Jiangsu Province, China

Corresponding author: Bo-Lin Yang, MD, Chief Doctor, First Clinical Medical College, The Affiliated Hospital of Nanjing University of Chinese Medicine, No. 155 Hanzhong Road, Nanjing 210029, Jiangsu Province, China. yfy0051@njucm.edu.cn

Abstract

BACKGROUND

Crohn's disease (CD) is an incurable intestinal disorder with unclear etiology and pathogenesis. Currently, there is a lack of specific biomarkers and drug targets for CD in clinical practice. It is essential to identify the precise pathophysiological mechanism of CD and investigate new therapeutic targets.

AIM

To explore a new biomarker and therapeutic target for CD and verify its role in the CD pathological mechanism.

METHODS

Proteomics was performed to quantify the protein profile in the plasma of 20 CD patients and 20 matched healthy controls. Hub genes among the selected differentially expressed proteins (DEPs) were detected *via* the MCODE plugin in Cytoscape software. The expression level of one hub gene with an immunoregulatory role that interested us was verified in the inflamed intestinal tissues of 20 CD patients by immunohistochemical analysis. After that, the effects of the selected hub gene on the intestinal inflammation of CD were identified in a CD cell model by examining the levels of proinflammatory cytokines by enzyme-linked immunosorbent assays and the expression of the NF-κB signalling pathway by quantitative real-time PCR analysis and Western blot assays.

Medicine (2018NL-171-02).

Conflict-of-interest statement: To the best of our knowledge, no conflict of interest exists.

Data sharing statement: No additional data are available.

Open-Access: This article is an open-access article that was selected by an in-house editor and fully peer-reviewed by external reviewers. It is distributed in accordance with the Creative Commons Attribution NonCommercial (CC BY-NC 4.0) license, which permits others to distribute, remix, adapt, build upon this work non-commercially, and license their derivative works on different terms, provided the original work is properly cited and the use is non-commercial. See: http://creativecommons.org/licenses/by-nc/4.0/

Manuscript source: Unsolicited manuscript

Specialty type: Gastroenterology and hepatology

Country/Territory of origin: China

Peer-review report's scientific quality classification

Grade A (Excellent): 0
Grade B (Very good): B
Grade C (Good): 0
Grade D (Fair): 0
Grade E (Poor): 0

Received: March 5, 2021
Peer-review started: March 5, 2021
First decision: April 5, 2021
Revised: April 7, 2021
Accepted: August 10, 2021
Article in press: August 10, 2021
Published online: September 21, 2021

P-Reviewer: Kumar S
S-Editor: Gong ZM
L-Editor: Wang TQ
P-Editor: Xing YX

RESULTS

Thirty-five DEPs were selected from 393 credible proteins identified by proteomic analysis. Among the DEPs, fibrinogen-like protein 1 (*FGL1*), which attracted our attention due to its function in the regulation of the immune response, had 1.722-fold higher expression in the plasma of CD patients and was identified as a hub gene by MCODE. Furthermore, the expression of *FGL1* in the intestinal mucosal and epithelial tissues of CD patients was also upregulated ($P < 0.05$). *In vitro*, the mRNA levels of *FGL1* and *NF-κB*; the protein expression levels of FGL1, IKKα, IKKβ, p-IKKα/β, p-IκBα, and p-p65; and the concentrations of the proinflammatory cytokines IL-1β, IL-6, IL-17, and TNF-α were increased ($P < 0.05$) after stimulation with lipopolysaccharide, which were reversed by knockdown of FGL1 with siRNA transfection ($P < 0.05$). Conversely, FGL1 overexpression enhanced the abovementioned results ($P < 0.05$).

CONCLUSION

FGL1 can induce intestinal inflammation by activating the canonical NF-κB signalling pathway, and it may be considered a potential biomarker and therapeutic target for CD.

Key Words: Crohn's disease; Fibrinogen-like protein 1; Proteomics; NF-κB pathway

©The Author(s) 2021. Published by Baishideng Publishing Group Inc. All rights reserved.

Core Tip: In this study, fibrinogen-like protein 1 (FGL1) was identified to be significantly upregulated in the plasma and intestinal mucosa of Crohn's disease (CD) patients. *In vitro*, silencing FGL1 downregulated the levels of the proinflammatory cytokines IL-1β, IL-6, IL-17, and TNF-α. Furthermore, FGL1 knockdown suppressed the mRNA expression of *NF-κB* and the protein levels of IKKα, IKKβ, p-IKKα/β, p-IκBα, and p-p65. These results could be reversed by the overexpression of FGL1. Taken together, these data suggest that FGL1 may induce intestinal inflammation by activating the canonical NF-κB signalling pathway and has the potential to be a therapeutic target for CD.

Citation: Sun XL, Qiao LC, Gong J, Wen K, Xu ZZ, Yang BL. Proteomics identifies a novel role of fibrinogen-like protein 1 in Crohn's disease. *World J Gastroenterol* 2021; 27(35): 5946-5957
URL: https://www.wjgnet.com/1007-9327/full/v27/i35/5946.htm
DOI: https://dx.doi.org/10.3748/wjg.v27.i35.5946

INTRODUCTION

Crohn's disease (CD) is a chronic, idiopathic intestinal inflammatory disease affecting any segment of the gastrointestinal tract. Although CD is believed to be a result of an imbalanced interaction among genetic susceptibility, environmental factors, the intestinal microflora, and the immune system, the precise pathogenesis is still not entirely clear[1]. Consequently, CD remains incurable even though great advancement has been achieved in medical therapy. Symptoms evolving in a relapsing and remitting manner indicate that CD has a progressive disease course that may induce complications, such as abscess, fistula, and stricture development. Eventually, up to 70% of CD patients require at least one intestinal surgery over their lifetime[2]. Targeted therapy is anticipated to change the natural course of CD, and even to cure it.

Currently, anti-tumor necrosis factor (TNF) agents (infliximab, adalimumab, and certolizumab pegol) are the most potent drugs for inducing and maintaining remission of CD. Unfortunately, anti-TNF treatment failure is common. Primary non-response occurs in 21.9% of infliximab-treated CD patients and 26.8% of adalimumab-treated patients[3]. More than 60% of patients treated with infliximab or adalimumab do not achieve deep remission[3]. These data indicate that increased TNF-α levels may be the result of an immunoinflammatory response instead of the cause. Vedolizumab blocking the α4β7 integrin can induce endoscopic remission in approximately one-

third of CD patients at week 52[4]. The decreased long-term efficacy of biologic medications makes it urgent to investigate new therapeutic targets for CD.

Omics techniques, including genomics, metabolomics, and proteomics, have been applied to explore potential biomarkers and targets for CD in recent years. It is widely known that cellular function and biological behaviour are primarily regulated by proteins. The protein domain is likely the most ubiquitously affected in disease development, treatment response, and physical recovery. Hence, it is promising to reveal the crucial changes in CD pathogenesis and discover novel drug targets by proteomics directly profiling protein expression. Proteomic techniques are classified into three major stages: Discovery, verification, and validation. Currently, the application of proteomics in CD remains in the initial discovery phase[5].

In the present study, we applied proteomics to identify differentially expressed proteins (DEPs) in the plasma of CD patients in an attempt to discover a potential biomarker and therapeutic target for CD. Our data showed that fibrinogen-like protein 1 (FGL1) was significantly upregulated in the plasma of CD patients. FGL1, also known as hepassocin or hepatocyte-derived fibrinogen-related protein 1 (HFREP1), is a hepatocyte-secreted protein that belongs to the fibrinogen family[6]. However, FGL1 lacks a platelet-binding site, a cross-linking region, and a thrombin-sensitive site, which are crucial for fibrin clot formation. Several studies have demonstrated that FGL1 can regulate immune systems to induce inflammatory response and tumor immune evasion[7,8]. To date, whether FGL1 is correlated with the development of CD remains unclear. Therefore, we further verified the expression of FGL1 in intestinal tissues of CD patients and validated its crucial role in the pathogenesis of CD *in vitro*.

MATERIALS AND METHODS

Clinical samples

Plasma samples were collected from 20 treatment-naive patients with CD and 20 age- and sex-matched healthy individuals between July 2017 and August 2018. The protein profiles in the plasma were analysed by tandem mass tag (TMT)-based quantitative proteomics. Paraffin-embedded mucosal biopsy specimens from an additional 20 treatment-naive patients with active CD and 20 matched healthy individuals undergoing colonoscopy screening were obtained for immunohistochemical examination. The protocols of this study were approved by the ethics committee of the Affiliated Hospital of Nanjing University of Chinese Medicine (2018NL-171-02). All patients provided informed consent.

TMT-based quantitative proteomics

Plasma samples were homogenized in sodium dodecyl sulfate (SDS) lysis buffer. Centrifugation was performed to collect the supernatant. Total protein concentrations were quantified using a bicinchoninic acid (BCA) assay (Thermo Scientific, United States). Protein extracts were reduced with reducing buffer (10 mmol/L dithiothreitol, 8 mol/L urea, and 100 mmol/L tetraethylammonium bromide (TEAB), pH 8.0) at 60 °C for 1 h. All samples were alkylated with iodoacetamide for 40 min at room temperature in the dark. After centrifugation, the protein pellets were digested with TEAB (100 mmol/L) and sequencing-grade trypsin (1 μg/μL) at 37 °C for 12 h.

For TMT labelling, 100 μL of protein sample was incubated with a mixed solution of 41 μL of TMT labelling reagent (Thermo Fisher Scientific, United States) and 41 μL of anhydrous acetonitrile for 1 h at room temperature. The reaction was terminated with 8 μL of 5% hydroxylamine. The samples from the CD patients were labelled with TMT-130 and TMT-131, while those from the healthy controls were labelled with TMT-126 and TMT-127.

The TMT-labelled peptides were eluted by using an Agilent Zorbax Extend-C18 column (2.1 mm × 150 mm, 5 μm) and fractionated with a high-performance liquid chromatography (HPLC) system at a flow rate of 300 μL/min. The elution gradient was set to 98%, 95%, 75%, 60%, and 10%. The collected peptides were loaded on a reverse-phase trap column (C18, 100 μm × 20 mm, Thermo Fisher Scientific, United States) and enriched on an analysis column (C18, 75 μm × 150 mm, Thermo Fisher Scientific, United States) following redissolution in nano-HPLC buffer (HPLC water containing 0.1% formic acid). The flow rate was 300 nL/min, and the linear elution gradient was set as 5%, 30%, 50%, and 100%.

For mass spectrometry (MS) survey scans, the ion spray voltage, interface heating temperature, MS resolution, and ion population were set to 1,800 V, 250 °C, 70000, and 1×10^6, respectively. The precursor ion was acquired at 300-1600 m/z. A maximum of

10 precursors were selected for higher-energy collisional dissociation with analysis in an LTQ Orbitrap Velos Pro (Thermo Fisher Scientific, United States), and the normal chemical energy was 32%. For MS/MS detection, the tandem MS resolution, ion population, ion maximum injection time, and dynamic exclusion time were set to 17500, 2×10^5, 80 ms, and 30 s, respectively.

Quantitative proteomic analysis

The raw proteomic data were analysed using Proteome Discoverer software (version 2.2, Thermo Fisher Scientific, United States) and searched against the UniProtKB database (Hunam, 2015-09, 88473 sequences). Andromeda was used as the search engine with the following parameters: (1) *Homo sapiens* taxonomy; (2) Q Exactive plus as instrument type; (3) Trypsin as the proteolytic enzyme, with two missed cleavages allowed; (4) TMT 6 plex and cysteine carbamidomethylations as fixed modifications; (5) Oxidation of methionine as a variable modification; (6) 20 ppm as the MS tolerance; and (7) Seven amino acids as minimum cut-off for peptide length. A false discovery rate (FDR) of less than 1% was set to refine the results.

For quantitative analysis, the TMT reporter ion intensity of each protein was analysed using Proteome Discoverer software. Proteins with empty values were discarded. Student's *t* test was performed to examine the difference in each protein between the two groups with Perseus software. Proteins with a fold change > 1.5 or < 0.67 and a *P* value < 0.05 were considered to be DEPs.

Bioinformatics analysis

Genes of DEPs were visualized in Cytoscape software (version 3.7.2), in which the MCODE plugin was used to select significant modules for identification of hub genes. Subsequently, the hub genes were input into the Search Tool for the Retrieval of Interacting Genes/Proteins (STRING) database (https://string-db.org/) to construct a protein-protein interaction (PPI) network. The Database for Annotation, Visualization and Integrated Discovery (DAVID) database (https://david.ncifcrf.gov/) was applied for gene ontology (GO) enrichment analysis. Reactome pathway analysis (https://www.reactome.org/) was performed for pathway enrichment analysis.

Immunohistochemical staining

Immunohistochemical staining was implemented to detect the expression of FGL1 in inflamed intestinal tissues of CD patients and normal intestinal biopsies. Mucosal biopsy specimens were fixed in 10% neutral formalin for 24 h. Afterwards, they were embedded in paraffin and cut into 5 μm sections. The sections were deparaffinized and rehydrated and then incubated in citrate buffer (pH 6.0) for antigen retrieval. After endogenous peroxidase activity was quenched with 3% hydrogen peroxide, the samples were incubated in 1% bovine serum albumin (BSA) to block non-specific immunoglobulin binding. Subsequently, the slides were incubated with an anti-FGL1 antibody (1:200 dilution, 16000-1-AP, Proteintech, United States) at 4 °C overnight. Following washing with phosphate buffered saline (PBS), the slides were incubated with a secondary IgG antibody (1:1000 dilution, ab6721, Abcam, United Kingdom) at room temperature for 1 h, counterstained with haematoxylin, and stained with a diaminobenzidine kit (DAB, Beyotime, China). All the sections were visualized under a light microscope (Nikon 80i, Japan). ImageJ software (version 1.52) was used to calculate the integrated optical density (IOD) values.

Cell culture and treatment

The human colonic adenoma cell line HT-29 (ATCC, United States) was cultured with Dulbecco's modified Eagle's medium, supplemented with 10% fetal bovine serum, 100 μg/mL penicillin, and 100 U/mL streptomycin at 37 °C with 5% CO_2. The HT-29 cells were stimulated with 100 ng/mL lipopolysaccharide (LPS, Sigma, United States) to establish a cell model of intestinal inflammation. To uncover the impact of FGL1 on intestinal inflammation, the HT-29 cells were transfected with *FGL1* siRNA and plasmid DNA (Nanjing KeyGen Biotech Co., Ltd., China) before stimulation with LPS. The transfection efficiency was determined by examining the mRNA expression of *FGL1*.

Quantitative real-time PCR analysis

Total RNA in HT-29 cells was extracted using a TRIzol reagent kit (Takara, Japan) according to the manufacturer's instructions. A PrimeScript RT reagent kit (Takara, Japan) was used for reverse transcription of the extracted RNA into cDNA. Quantitative real-time PCR (qRT-PCR) was conducted to detect the mRNA expression

of *FGL1* and *NF-κB* by using a SYBR green kit (Takara, Japan). The housekeeping gene β-actin was used for normalization to an endogenous reference. The relative gene expression was evaluated by using the $2^{-\Delta\Delta Ct}$ method. The sequences of the PCR primers are as follows: *FGL1*-forward: 5′-ATGGCAAAGGTGTTCAGTTTCA-3′, reverse: 5′-ACAATCTGCATACTGCCTCTTG-3′; *NF-κB*-forward: 5′-GAAGCACGAATGACAGAGGC-3′, reverse: 5′-GCTTGGCGGATTAGCTCTTTT-3′; and β-actin-forward: 5′-CATGTACGTTGCTATCCAGGC-3′, reverse: 5′-CTCCTTAATGTCACGCACGAT-3′.

Enzymelinked immunosorbent assay

The levels of the proinflammatory cytokines IL-1β, IL-6, IL-17, and TNF-α (Sigma, United States) in the culture medium collected after 48 h were examined by enzyme linked immunosorbent assay (ELISA) according to the manufacturer's protocol.

Western blot assay

Cells lysed with radioimmunoprecipitation assay (RIPA) lysis buffer were centrifuged at 12000 *g* for 20 min at 4 °C. Protein concentrations in the collected supernatant were quantified with a BCA assay kit. After equal amounts of protein (20 μg/well) were loaded and separated by sodium dodecyl sulfate-polyacrylamide gel electrophoresis (SDS-PAGE), they were transferred onto polyvinylidene difluoride (PVDF) membranes and incubated in 5% BSA for 1 h at room temperature. The membranes were washed with Tris-borate saline containing 0.1% Tween-20 (TBST) and were incubated with primary antibodies against FGL1 (1:1000 dilution, 16000-1-AP, Proteintech, United States), IKKα (1:1000 dilution, ab32041, Abcam, United Kingdom), IKKβ (1:1000 dilution, ab32135, Abcam), p-IKKα/β (1:1000 dilution, ab194528, Abcam), IκBα (1:1000 dilution, ab32518, Abcam), p-IκBα (1:1000 dilution, ab133462, Abcam), NF-κB (p65, 1:1000 dilution, ab32536, Abcam), p-p65 (1:1000 dilution, ab76302, Abcam) and β-actin (1:1000 dilution, 20536-1-AP, Proteintech) at 4 °C overnight. The membranes were washed with TBST again and incubated with a horseradish peroxidase (HRP)-conjugated secondary antibody for 1 h at room temperature. The blots were imaged using enhanced chemiluminescence (ECL). ImageJ software was used to calculate the protein signal grey values.

Statistical analysis

All data were statistically analysed with SPSS 22.0 (SPSS Inc., United States). Continuous variables with a normal distribution are summarized using the mean ± SD, which in a skewness distribution are expressed as the median with range. The Mann-Whitney *U* test, Student's *t* tests, and chi-square test were performed to compare numerical variables and categorical variables as appropriate. One-way analysis of variance was used for multi-group comparisons. A two-sided *P* value < 0.05 was considered statistically significant.

RESULTS

Patients' characteristics

Twenty treatment-naive CD patients and 20 healthy controls were recruited for plasma proteomic analysis. The diagnostic criteria for CD referred to the clinical guidelines of the American College of Gastroenterology (ACG)[9]. Thirteen males and seven females with a median age of 20.5 (14-43) years were included in the CD group, and eleven males and nine females with a median age of 24.5 (18-46) years were included in the normal control group. Baseline demographic characteristics were comparable between the two groups ($P > 0.05$).

Colonoscopic biopsy specimens from an additional 20 treatment-naive patients with active CD and 20 healthy controls were used for immunohistochemical staining. There was no significant difference in sex distribution, age, or biopsy site between the two groups ($P > 0.05$). The baseline clinical characteristics of patients for plasma proteomic detection and immunohistochemical analysis are presented in Tables 1 and 2, respectively.

FGL1 is significantly upregulated in plasma proteomic analysis

Plasma samples in each group were randomly divided into four subclusters. A total of 393 credible proteins were identified by proteomic analysis, among which 35 had differential expression between the two groups (Figure 1A). Among the DEPs, FGL1

Table 1 Clinical characteristics of patients for plasma proteomic analysis

Item	Crohn's disease (*n* = 20)	Normal control (*n* = 20)	*P* value
Sex			
Male	13	11	0.519
Female	7	9	
Median age (range), yr	20.5 (14-43)	24.5 (18-46)	0.069
Disease location in the endoscopy			
Ileum	6	N/A	
Colon	6	N/A	
Ileocolon	8	N/A	

N/A: Not applicable.

Table 2 Clinical characteristics of patients for immunohistochemical assay

Item	Crohn's disease (*n* = 20)	Normal control (*n* = 20)	*P* value
Sex			
Male	15	13	0.731
Female	5	7	
Age (mean ± SD), yr	27.1 ± 7.9	25.6 ± 4.5	0.465
Biopsy site			
Terminal ileum	8	5	0.832
Ascending colon	2	1	
Transverse colon	2	2	
Descending colon	2	4	
Sigmoid colon	4	6	
Rectum	2	2	

SD: Standard deviation.

attracted our attention because of its function in the regulation of the immune response. The expression level of FGL1 in the plasma of CD patients was 1.722-fold greater than that in healthy people (Figure 1B). Three MCODE modules were established to screen hub genes *via* Cytoscape software. As *FGL1* was contained in the 3rd module, the genes in this module were used for further bioinformatics analysis. Figure 1C shows the PPI network of the genes. GO enrichment analysis showed that the genes were involved in the biological processes of platelet degranulation, acute phase response, platelet activation, and negative regulation of endopeptidase activity, and the molecular functions of heparin binding and serine-type endopeptidase inhibitor activity. Reactome pathway analysis demonstrated that the genes were related to the common pathway of fibrin clot formation and the pathways of platelet degranulation, peptide ligand-binding receptors, haemostasis, G alpha (i) signalling events, and innate immune system.

FGL1 expression is increased in intestinal tissues of CD patients

Immunohistochemical analysis was performed to verify the expression of FGL1 in the intestinal tissues of CD patients. The results demonstrated that the FGL1 levels in the intestinal mucosal and epithelial tissues were higher than those in the normal intestinal tissues ($P < 0.01$, Figure 2).

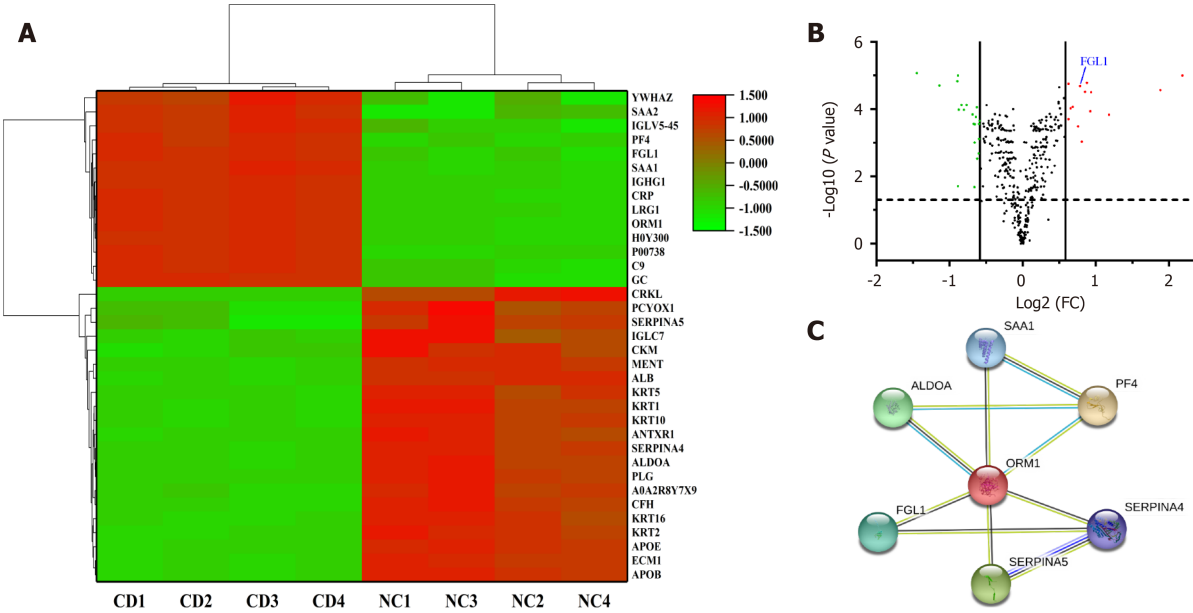


Figure 1 Fibrinogen-like protein 1 expression in the plasma of Crohn's disease patients. A: Heat map showing 35 differentially expressed proteins between Crohn's disease (CD) patients and healthy individuals, among which fibrinogen-like protein 1 (FGL1) expression was upregulated in the CD group; B: The FGL1 expression level in the plasma of CD patients was 1.722-fold greater than that in healthy people; C: Protein-protein interaction network of an MCODE module containing *FGL1* as a hub gene. CD: Crohn's disease; NC: Normal control; FGL1: Fibrinogen-like protein 1.

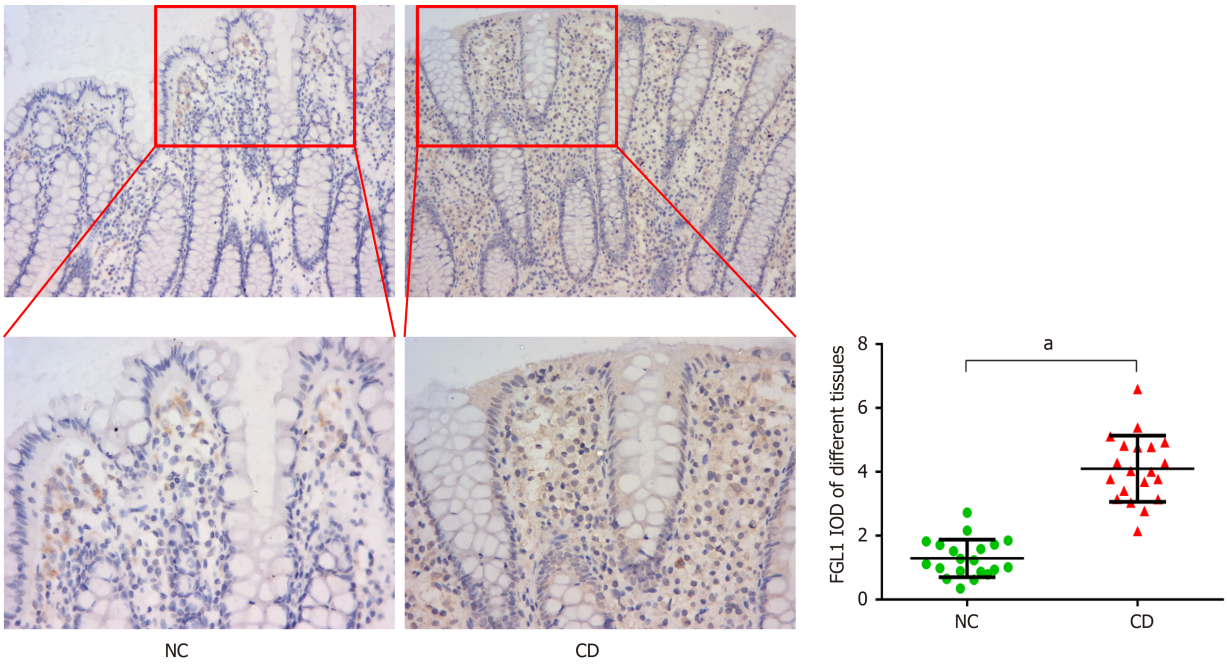


Figure 2 Fibrinogen-like protein 1 expression, as determined by immunohistochemical analysis (× 200, × 400), was increased in the intestinal mucosal and epithelial tissues of Crohn's disease patients. [a]*P* < 0.01 *vs* normal control group. NC: Normal control group; CD: Crohn's disease group; FGL1: Fibrinogen-like protein 1.

FGL1 mediates the expression of proinflammatory cytokines in intestinal epithelial cells

To investigate the regulation of intestinal inflammation by FGL1, proinflammatory cytokines were detected by ELISA after *FGL1* siRNA and plasmids were transfected into HT-29 cells. After LPS stimulation, the IL-1β, IL-6, IL-17, and TNF-α levels were significantly upregulated. FGL1 knockdown reversed the expression of IL-1β, IL-6, IL-17, and TNF-α, while overexpression of FGL1 elevated the levels of the four proinflammatory cytokines ($P < 0.05$, Figure 3).

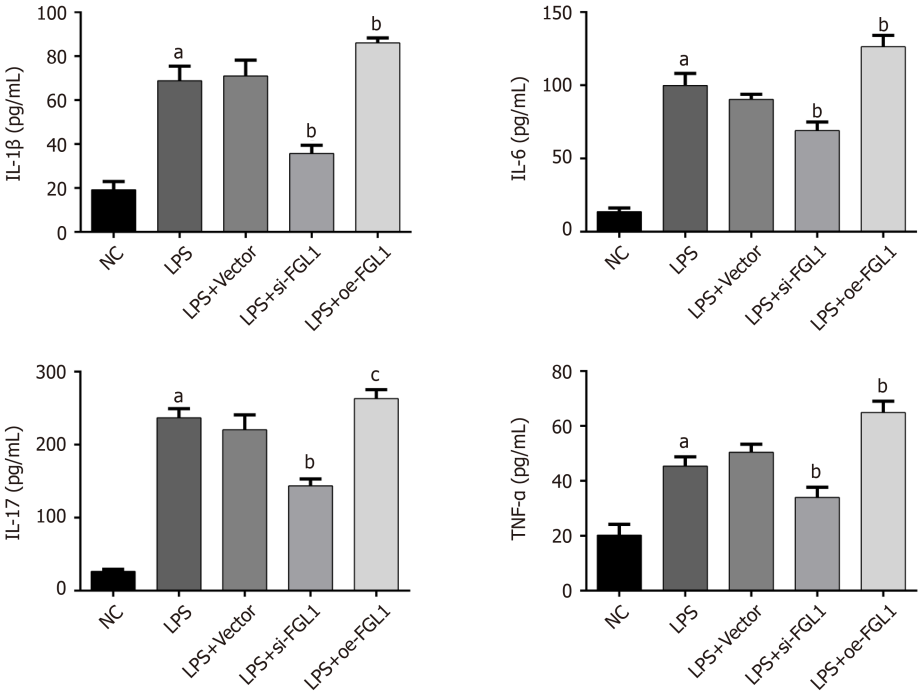


Figure 3 Expression of proinflammatory cytokines in different groups, as determined by enzyme linked immunosorbent assay. $^{a}P < 0.01$ *vs* normal control group; $^{b}P < 0.01$, $^{c}P < 0.05$ *vs* lipopolysaccharide. NC: Normal control group; LPS: Crohn's disease (CD) model induced by lipopolysaccharide (LPS); LPS+Vector: Transfected with an empty vector based on the CD model; LPS+si-FGL1: Transfected with FGL1 siRNA based on the CD model; LPS+oe-FGL1: Transfected with the FGL1 plasmid based on the CD model; FGL1: Fibrinogen-like protein 1.

FGL1 activates the NF-κB signalling pathway

Given that NF-κB plays a fundamental role in the intestinal inflammation of CD, the modulation of the NF-κB signalling pathway by FGL1 was investigated. The mRNA expression levels of *FGL1* and *NF-κB* were increased by LPS stimulation. After intervention with *FGL1* siRNA, the mRNA expression levels of *FGL1* and *NF-κB* were both downregulated, while the mRNA levels were enhanced following FGL1 overexpression with plasmid transfection ($P < 0.01$, Figure 4A and B).

The exact mechanism by which FGL1 regulates the NF-κB signalling pathway was revealed by Western blot assay. The protein levels of FGL1, IKKα, IKKβ, p-IKKα/β, p-IκBα, and p-p65 were upregulated in HT-29 cells stimulated with LPS ($P < 0.05$). *FGL1* gene knockdown inhibited the protein expression of FGL1 and downregulated the protein expression of IKKα, IKKβ, p-IKKα/β, p-IκBα, and p-p65 ($P < 0.05$). Conversely, the overexpression of the *FGL1* gene enhanced the protein expression of FGL1, IKKα, IKKβ, p-IKKα/β, p-IκBα, and p-p65 ($P < 0.05$, Figure 4C).

DISCUSSION

In the present study, we took advantage of proteomics for a large-scale screen of DEPs between the plasma of CD patients and healthy people. The expression of *FGL1*, a hub gene among the DEPs, was increased in the plasma of CD patients, which was verified in intestinal mucosal and epithelial tissues. Furthermore, FGL1 was validated to exacerbate the inflammatory response in intestinal epithelial cells by activating the NF-κB signalling pathway.

At present, knowledge about the etiology and pathogenesis of CD is limited, which makes it incurable. Hence, it is essential to detect potential drug targets for CD. As proteins are directly involved in nearly all pathophysiological processes, proteomics has become a hotspot tool for the discovery of novel biomarkers or therapeutic targets for CD, differential diagnosis between CD and ulcerative colitis, and disease stratification by examining and quantifying thousands of proteins encoded by the genome in a holistic manner[10-13]. To our knowledge, the present study revealed for the first time by proteomics that FGL1 may be a key contributor to CD onset and progression.

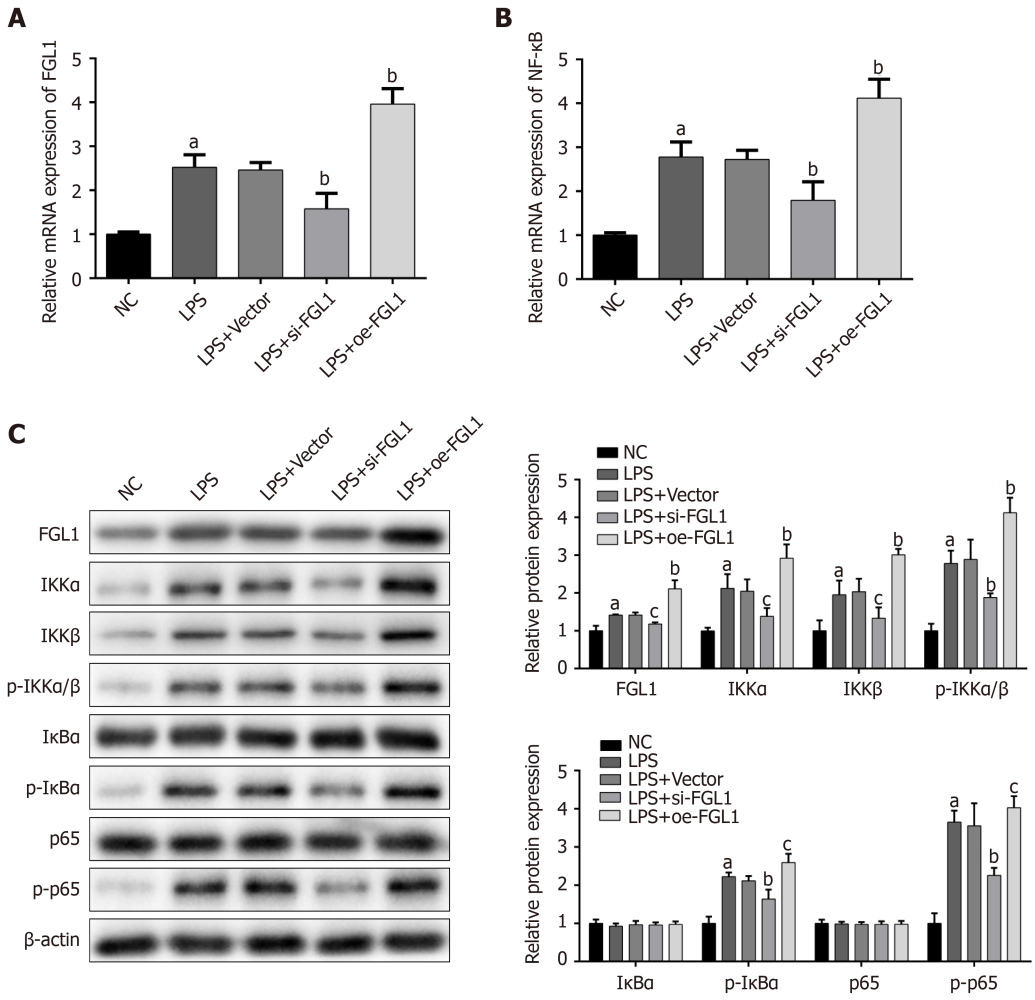


Figure 4 Impact of fibrinogen-like protein 1 on the NF-κB signalling pathway. A and B: Effect of knockdown or overexpression of fibrinogen-like protein 1 (FGL1) on the mRNA expression of *FGL1* and *NF-κB*, as determined by quantitative real-time PCR assay; C: Effect of FGL1 on the protein expression of related proteins in the canonical NF-κB signalling pathway, as determined by Western blot assay. $^{a}P < 0.01$ *vs* NC; $^{b}P < 0.01$, $^{c}P < 0.05$ *vs* LPS. NC: Normal control group; LPS: Crohn's disease (CD) model induced by LPS; LPS+Vector: Transfected with an empty vector based on the CD model; LPS+si-FGL1: Transfected with FGL1 siRNA based on the CD model; LPS+oe-FGL1: Transfected with the FGL1 plasmid based on the CD model; LPS: Lipopolysaccharide; FGL1: Fibrinogen-like protein 1.

Accumulating evidence has demonstrated that FGL1 plays a prominent role in the pathogenesis of various diseases, including hepatocellular carcinoma, gastric cancer, lung cancer, diabetes mellitus, and obesity[14-19]. Additionally, FGL1 is also considered a potential biomarker and drug target in certain inflammatory conditions. FGL1 may promote liver injury-induced inflammation *via* the IL-6/STAT3 signalling pathway[20]. Proteomics revealed that FGL1 is a specific biomarker for predicting the progression of rheumatoid arthritis[7]. This finding displays a fundamental role of FGL1 in regulating immune-mediated inflammation.

Pierre and colleagues have demonstrated that CD relapse is correlated with the innate immune response of the liver[21]. Given that FGL1 is a liver-derived protein and is involved in the innate immune system pathway, we hypothesize that FGL1 may influence the pathophysiology of CD based on the evidence of increased expression of FGL1 in the plasma and intestinal tissues of CD patients. Although FGL1 has been demonstrated to be a potent target for cancer immunotherapy, its precise role in CD therapy is unknown[8]. To unravel the mystery, a cell experiment was designed in the current study that focused on the FGL1-mediated regulation of signalling by NF-κB, an important proinflammatory transcription factor for inflammatory disorders.

Activation of NF-κB plays a central role in the induction and exacerbation of the intestinal inflammatory response of CD patients[22]. The NF-κB family consists of p65 (RELA), RELB, c-REL, p50/p105 (NF-κB1), and p52/p100 (NF-κB2). Activated p65 can translocate into the nucleus to upregulate the transcriptional expression of proinflammatory cytokines. In the present study, the mRNA and protein levels of FGL1 and NF-κB and the concentrations of IL-1β, IL-6, IL-17, and TNF-α were markedly upregulated

in HT-29 cells stimulated with LPS, and these effects were reversed by depleting FGL1 with specific siRNA. Correspondingly, the expression of NF-κB and the four proinflammatory cytokines was enhanced following overexpression of FGL1. These results indicate that FGL1 may promote the intestinal inflammatory response by activating NF-κB signalling. The canonical pathway of NF-κB activation involves the IKK complex, consisting of NEMO, IKKα, and IKKβ, and the IκB protein family, including IκBα, IκBβ, and IκBe. After stimulation, IKKα and IKKβ activation promotes phosphorylation of IκBα. Degradation of phosphorylated IκBα releases the p65-p50 dimer for nuclear translocation[23]. In this study, the protein expression levels of IKKα , IKKβ, p-IKKα/β, p-IκBα, and p-p65 were decreased after knockdown of FGL1 compared to those in the cell model, and the inverse effect was verified by overexpression of FGL1. Therefore, FGL1 may induce intestinal inflammation by activating the canonical NF-κB pathway.

CONCLUSION

In summary, we found for the first time that the expression of FGL1 is considerably upregulated in the plasma and intestinal mucosal and epithelial tissues of CD patients. FGL1 might induce intestinal inflammation by activating the canonical NF-κB signalling pathway to stimulate the secretion of proinflammatory cytokines, such as IL-1β, IL-6, IL-17, and TNF-α. Hence, FGL1 may be considered a potential biomarker and therapeutic target for CD. However, given the exploratory design of our study, the precise role of FGL1 in the pathogenesis of CD needs to be deeply investigated and further validated.

ACKNOWLEDGEMENT

The authors are deeply grateful to Fan Yang from the Faculty of Art and Science, St. George Campus, University of Toronto, for helping us analyze the data in the statistics of this study.

ARTICLE HIGHLIGHTS

Research background

Currently, the etiology and pathogenesis of Crohn's disease (CD) are not completely known, which makes it incurable. It is urgent to reveal the pathophysiological mechanism of CD and investigate new therapeutic targets.

Research motivation

To explore a potential therapeutic target for CD and verify its role in the CD pathological mechanism.

Research objectives

In this study, we attempted to find a potential therapeutic target for CD and verify its role in the CD pathological mechanism *in vitro*.

Research methods

Proteomics was implemented to quantify the protein profile in the plasma of CD patients. Among the differentially expressed proteins, a hub gene that could regulate the immune response was selected for further study. The expression of the selected hub gene in the inflamed intestinal mucosa was verified by immunohistochemical staining. *In vitro*, the effects of the hub gene on the expression of proinflammatory cytokines and the NF-κB signalling pathway were evaluated by ELISA, qRT-PCR, and Western blot analysis.

Research results

Fibrinogen-like protein 1 (*FGL1*), as a hub gene of the differentially expressed proteins, was confirmed to be markedly upregulated in the plasma and intestinal mucosa of CD patients. Silencing FGL1 downregulated the levels of the proinflammatory cytokines IL-1β, IL-6, IL-17, and TNF-α. Furthermore, FGL1 knockdown repressed the mRNA

expression of *NF-κB* and the protein levels of IKKα, IKKβ, p-IKKα/β, p-IκBα, and p-p65. Overexpression of FGL1 enhanced these results.

Research conclusions

FGL1 may promote intestinal inflammation modulated by the canonical NF-κB signalling pathway and has the potential to be a therapeutic target for CD.

Research perspectives

Our findings indicate a critical role of FGL1 in the onset and progression of CD, which may serve as a potential prognostic biomarker and therapeutic target for CD.

REFERENCES

1 **Torres J**, Mehandru S, Colombel JF, Peyrin-Biroulet L. Crohn's disease. *Lancet* 2017; **389**: 1741-1755 [PMID: 27914655 DOI: 10.1016/S0140-6736(16)31711-1]

2 **Patel KV**, Darakhshan AA, Griffin N, Williams AB, Sanderson JD, Irving PM. Patient optimization for surgery relating to Crohn's disease. *Nat Rev Gastroenterol Hepatol* 2016; **13**: 707-719 [PMID: 27780971 DOI: 10.1038/nrgastro.2016.158]

3 **Kennedy NA**, Heap GA, Green HD, Hamilton B, Bewshea C, Walker GJ, Thomas A, Nice R, Perry MH, Bouri S, Chanchlani N, Heerasing NM, Hendy P, Lin S, Gaya DR, Cummings JRF, Selinger CP, Lees CW, Hart AL, Parkes M, Sebastian S, Mansfield JC, Irving PM, Lindsay J, Russell RK, McDonald TJ, McGovern D, Goodhand JR, Ahmad T; UK Inflammatory Bowel Disease Pharmacogenetics Study Group. Predictors of anti-TNF treatment failure in anti-TNF-naive patients with active luminal Crohn's disease: a prospective, multicentre, cohort study. *Lancet Gastroenterol Hepatol* 2019; **4**: 341-353 [PMID: 30824404 DOI: 10.1016/S2468-1253(19)30012-3]

4 **Löwenberg M**, Vermeire S, Mostafavi N, Hoentjen F, Franchimont D, Bossuyt P, Hindryckx P, Rispens T, de Vries A, van der Woude CJ, Berends S, Ambarus CA, Mathot R, Clasquin E, Baert F, D'Haens G. Vedolizumab Induces Endoscopic and Histologic Remission in Patients With Crohn's Disease. *Gastroenterology* 2019; **157**: 997-1006.e6 [PMID: 31175865 DOI: 10.1053/j.gastro.2019.05.067]

5 **Gisbert JP**, Chaparro M. Clinical Usefulness of Proteomics in Inflammatory Bowel Disease: A Comprehensive Review. *J Crohns Colitis* 2019; **13**: 374-384 [PMID: 30307487 DOI: 10.1093/ecco-jcc/jjy158]

6 **Yamamoto T**, Gotoh M, Sasaki H, Terada M, Kitajima M, Hirohashi S. Molecular cloning and initial characterization of a novel fibrinogen-related gene, HFREP-1. *Biochem Biophys Res Commun* 1993; **193**: 681-687 [PMID: 8390249 DOI: 10.1006/bbrc.1993.1678]

7 **Liu S**, Guo Y, Lu L, Lu J, Ke M, Xu T, Lu Y, Chen W, Wang J, Kong D, Shen Q, Zhu Y, Tan W, Ji W, Zhou W. Fibrinogen-Like Protein 1 Is a Novel Biomarker for Predicting Disease Activity and Prognosis of Rheumatoid Arthritis. *Front Immunol* 2020; **11**: 579228 [PMID: 33123164 DOI: 10.3389/fimmu.2020.579228]

8 **Wang J**, Sanmamed MF, Datar I, Su TT, Ji L, Sun J, Chen L, Chen Y, Zhu G, Yin W, Zheng L, Zhou T, Badri T, Yao S, Zhu S, Boto A, Sznol M, Melero I, Vignali DAA, Schalper K. Fibrinogen-like Protein 1 Is a Major Immune Inhibitory Ligand of LAG-3. *Cell* 2019; **176**: 334-347.e12 [PMID: 30580966 DOI: 10.1016/j.cell.2018.11.010]

9 **Lichtenstein GR**, Loftus EV, Isaacs KL, Regueiro MD, Gerson LB, Sands BE. ACG Clinical Guideline: Management of Crohn's Disease in Adults. *Am J Gastroenterol* 2018; **113**: 481-517 [PMID: 29610508 DOI: 10.1038/ajg.2018.27]

10 **Tyers M**, Mann M. From genomics to proteomics. *Nature* 2003; **422**: 193-197 [PMID: 12634792 DOI: 10.1038/nature01510]

11 **Titz B**, Gadaleta RM, Lo Sasso G, Elamin A, Ekroos K, Ivanov NV, Peitsch MC, Hoeng J. Proteomics and Lipidomics in Inflammatory Bowel Disease Research: From Mechanistic Insights to Biomarker Identification. *Int J Mol Sci* 2018; **19** [PMID: 30223557 DOI: 10.3390/ijms19092775]

12 **Starr AE**, Deeke SA, Ning Z, Chiang CK, Zhang X, Mottawea W, Singleton R, Benchimol EI, Wen M, Mack DR, Stintzi A, Figeys D. Proteomic analysis of ascending colon biopsies from a paediatric inflammatory bowel disease inception cohort identifies protein biomarkers that differentiate Crohn's disease from UC. *Gut* 2017; **66**: 1573-1583 [PMID: 27216938 DOI: 10.1136/gutjnl-2015-310705]

13 **Townsend P**, Zhang Q, Shapiro J, Webb-Robertson BJ, Bramer L, Schepmoes AA, Weitz KK, Mallette M, Moniz H, Bright R, Merrick M, Shah SA, Sands BE, Leleiko N. Serum Proteome Profiles in Stricturing Crohn's Disease: A Pilot Study. *Inflamm Bowel Dis* 2015; **21**: 1935-1941 [PMID: 26199992 DOI: 10.1097/MIB.0000000000000445]

14 **Wang J**, Wei W, Tang Q, Lu L, Luo Z, Li W, Lu Y, Pu J. Oxysophocarpine suppresses hepatocellular carcinoma growth and sensitizes the therapeutic blockade of anti-Lag-3 *via* reducing FGL1 expression. *Cancer Med* 2020; **9**: 7125-7136 [PMID: 32810392 DOI: 10.1002/cam4.3151]

15 **Sun C**, Gao W, Liu J, Cheng H, Hao J. FGL1 regulates acquired resistance to Gefitinib by inhibiting apoptosis in non-small cell lung cancer. *Respir Res* 2020; **21**: 210 [PMID: 32778129 DOI: 10.1186/s12931-020-01477-y]

16 **Bie F**, Wang G, Qu X, Wang Y, Huang C, Du J. Loss of FGL1 induces epithelialmesenchymal transition and angiogenesis in LKB1 mutant lung adenocarcinoma. *Int J Oncol* 2019; **55**: 697-707 [PMID: 31322182 DOI: 10.3892/ijo.2019.4838]
17 **Wu HT**, Ou HY, Hung HC, Su YC, Lu FH, Wu JS, Yang YC, Wu CL, Chang CJ. A novel hepatokine, HFREP1, plays a crucial role in the development of insulin resistance and type 2 diabetes. *Diabetologia* 2016; **59**: 1732-1742 [PMID: 27221093 DOI: 10.1007/s00125-016-3991-7]
18 **Kang L**, Li HY, Ou HY, Wu P, Wang SH, Chang CJ, Lin SY, Wu CL, Wu HT. Role of placental fibrinogen-like protein 1 in gestational diabetes. *Transl Res* 2020; **218**: 73-80 [PMID: 32006524 DOI: 10.1016/j.trsl.2020.01.001]
19 **Wu HT**, Chen SC, Fan KC, Kuo CH, Lin SY, Wang SH, Chang CJ, Li HY. Targeting fibrinogen-like protein 1 is a novel therapeutic strategy to combat obesity. *FASEB J* 2020; **34**: 2958-2967 [PMID: 31908014 DOI: 10.1096/fj.201901925R]
20 **Liu Z**, Ukomadu C. Fibrinogen-like protein 1, a hepatocyte derived protein is an acute phase reactant. *Biochem Biophys Res Commun* 2008; **365**: 729-734 [PMID: 18039467 DOI: 10.1016/j.bbrc.2007.11.069]
21 **Pierre N**, Baiwir D, Huynh-Thu VA, Mazzucchelli G, Smargiasso N, De Pauw E, Bouhnik Y, Laharie D, Colombel JF, Meuwis MA, Louis E; GETAID (Groupe d'Etude Thérapeutique des Affections Inflammatoires du tube Digestif). Discovery of biomarker candidates associated with the risk of short-term and mid/long-term relapse after infliximab withdrawal in Crohn's patients: a proteomics-based study. *Gut* 2020 [PMID: 33106355 DOI: 10.1136/gutjnl-2020-322100]
22 **Atreya I**, Atreya R, Neurath MF. NF-kappaB in inflammatory bowel disease. *J Intern Med* 2008; **263**: 591-596 [PMID: 18479258 DOI: 10.1111/j.1365-2796.2008.01953.x]
23 **Rius-Pérez S**, Pérez S, Martí-Andrés P, Monsalve M, Sastre J. Nuclear Factor Kappa B Signaling Complexes in Acute Inflammation. *Antioxid Redox Signal* 2020; **33**: 145-165 [PMID: 31856585 DOI: 10.1089/ars.2019.7975]

World Journal of Gastroenterology

Submit a Manuscript: https://www.f6publishing.com

World J Gastroenterol 2021 September 21; 27(35): 5958-5966

DOI: 10.3748/wjg.v27.i35.5958

ISSN 1007-9327 (print) ISSN 2219-2840 (online)

ORIGINAL ARTICLE

Retrospective Study

Effectiveness and safety of over-the-scope clip in closing perforations after duodenal surgery

Zhen-Zhen Wang, Xian-Bin Zhou, Yi Wang, Xin-Li Mao, Li-Ping Ye, Ling-Ling Yan, Ya-Hong Chen, Ya-Qi Song, Yue Cai, Shi-Wen Xu, Shao-Wei Li

ORCID number: Zhen-Zhen Wang 0000-0002-6274-2646; Xian-Bin Zhou 0000-0003-0048-7456; Yi Wang 0000-0002-9817-1769; Xin-Li Mao 0000-0003-4548-1867; Li-Ping Ye 0000-0001-9839-2062; Ling-Ling Yan 0000-0001-5103-9886; Ya-Hong Chen 0000-0003-0004-0187; Ya-Qi Song 0000-0001-9648-8159; Yue Cai 0000-0002-7201-6525; Shi-Wen Xu 0000-0001-6774-1979; Shao-Wei Li 0000-0002-3276-1037.

Author contributions: Wang ZZ, Zhou XB, Wang Y, Mao XL, and Ye LP participated in the clinical treatment; Xu SW, Yan LL, and Li SW wrote the original draft; Song YQ, Cai Y, and Chen YH undertook validation, writing, review, and editing; all authors contributed to the article and approved the submitted version.

Supported by Program of Taizhou Science and Technology Grant, No. 20ywb29; Medical Health Science and Technology Project of Zhejiang Province, No. 2021PY083 and No. 2019KY239; Key Technology Research and Development Program of Zhejiang Province, No. 2019C03040; Major Research Program of Taizhou Enze Medical Center Grant, No. 19EZZDA2; and Open Fund of Key Laboratory of Key Laboratory of Minimally Invasive Techniques & Rapid

Zhen-Zhen Wang, Xian-Bin Zhou, Yi Wang, Xin-Li Mao, Li-Ping Ye, Ling-Ling Yan, Ya-Qi Song, Yue Cai, Shao-Wei Li, Key Laboratory of Minimally Invasive Techniques and Rapid Rehabilitation of Digestive System Tumor of Zhejiang Province, Taizhou Hospital of Zhejiang Province Affiliated to Wenzhou Medical University, Linhai 317000, Zhejiang Province, China

Zhen-Zhen Wang, Xian-Bin Zhou, Yi Wang, Xin-Li Mao, Li-Ping Ye, Ling-Ling Yan, Ya-Qi Song, Yue Cai, Shao-Wei Li, Department of Gastroenterology, Taizhou Hospital of Zhejiang Province Affiliated to Wenzhou Medical University, Linhai 317000, Zhejiang Province, China

Ya-Hong Chen, Health Management Center, Taizhou Hospital of Zhejiang Province Affiliated to Wenzhou Medical University, Linhai 317000, Zhejiang Province, China

Shi-Wen Xu, Taizhou Hospital of Zhejiang Province, Wenzhou Medical University, Linhai 317000, Zhejiang Province, China

Corresponding author: Shao-Wei Li, PhD, Academic Fellow, Assistant Professor, Associate Research Scientist, Instructor, Key Laboratory of Minimally Invasive Techniques and Rapid Rehabilitation of Digestive System Tumor of Zhejiang Province, Taizhou Hospital of Zhejiang Province Affiliated to Wenzhou Medical University, No. 150 Xinmen Street, Linhai 317000, Zhejiang Province, China. li_shaowei81@hotmail.com

Abstract

BACKGROUND

Endoscopic resection of duodenal subepithelial lesions (SELs) is a difficult procedure with a high risk of perforation. At present, dealing with perforation after endoscopic resection of duodenal SELs is still considered a great challenge.

AIM

To evaluate the effectiveness and safety of an over-the-scope clip (OTSC) in the treatment of perforation post-endoscopic resection of duodenal SELs.

METHODS

From May 2015 to November 2019, 18 patients with perforation following endoscopic resection of duodenal SELs were treated with OTSCs. Data comprising the rate of complete resection, closure of intraprocedural perforation, delayed bleeding, delayed perforation, and postoperative infection were extracted.

Rehabilitation of Digestive System Tumor of Zhejiang Province, No. 21SZDSYS01 and No. 21SZDSYS09.

Institutional review board statement: The study was reviewed and approved by the Ethics Committee of Taizhou Hospital of Zhejiang Province affiliated to Wenzhou Medical University Institutional Review Board (approval No. K20210412).

Informed consent statement: All study participants, or their legal guardian, provided informed written consent prior to study enrollment.

Conflict-of-interest statement: The authors declare that they have no conflict interests.

Data sharing statement: No additional data are available.

Open-Access: This article is an open-access article that was selected by an in-house editor and fully peer-reviewed by external reviewers. It is distributed in accordance with the Creative Commons Attribution NonCommercial (CC BY-NC 4.0) license, which permits others to distribute, remix, adapt, build upon this work non-commercially, and license their derivative works on different terms, provided the original work is properly cited and the use is non-commercial. See: http://creativecommons.org/Licenses/by-nc/4.0/

Manuscript source: Invited manuscript

Specialty type: Gastroenterology and hepatology

Country/Territory of origin: China

Peer-review report's scientific quality classification

Grade A (Excellent): 0
Grade B (Very good): B, B, B
Grade C (Good): 0
Grade D (Fair): 0
Grade E (Poor): 0

Received: May 10, 2021
Peer-review started: May 10, 2021
First decision: June 27, 2021

RESULTS

The rate of complete removal of duodenal SELs and successful closure of the perforation was 100%. The median perforation size was 1 cm in diameter. Seventeen patients had minor intraoperative bleeding, while the remaining 1 patient had considerable amount of bleeding during the procedure. Seven patients had postoperative abdominal infections, of which 1 patient developed an abscess in the right iliac fossa and another patient developed septic shock. All 18 patients recovered and were discharged. No delayed bleeding or perforation was reported. The mean time taken to resume normal diet after the procedure was 6.5 d. The mean postoperative hospital stay was 9.5 d. No residual or recurrent lesions were detected during the follow-up period (15-66 mo).

CONCLUSION

Closing a perforation after endoscopic resection of duodenal SELs with OTSCs seems to be an effective and reasonably safe therapeutic method.

Key Words: Over-the-scope clip; Duodenal subepithelial lesion; Endoscopic resection; Perforation; Effectiveness; Safety

©The Author(s) 2021. Published by Baishideng Publishing Group Inc. All rights reserved.

Core Tip: This study presents the use of over-the-scope clip in closing duodenal perforation of 18 patients. We believe that our study makes a significant contribution to the literature because dealing with perforation after endoscopic resection of duodenal subepithelial lesions is challenging. This study aimed to evaluate the effectiveness and safety of over-the-scope clip in closing perforation after endoscopic resection of duodenal subepithelial lesions. The rate of successful closure was 100%. No delayed perforation occurred in any of the patients. Seven patients had postoperative infection, of which 1 patient developed septic shock and underwent surgery. All 18 patients recovered.

Citation: Wang ZZ, Zhou XB, Wang Y, Mao XL, Ye LP, Yan LL, Chen YH, Song YQ, Cai Y, Xu SW, Li SW. Effectiveness and safety of over-the-scope clip in closing perforations after duodenal surgery. *World J Gastroenterol* 2021; 27(35): 5958-5966
URL: https://www.wjgnet.com/1007-9327/full/v27/i35/5958.htm
DOI: https://dx.doi.org/10.3748/wjg.v27.i35.5958

INTRODUCTION

Duodenal subepithelial lesions (SELs) include Brunner's adenomas, lipomas, heterotopic pancreas, leiomyomas, neuroendocrine tumors, and gastrointestinal stromal tumors (GISTs). Most of these are benign, while some lesions, such as neuroendocrine tumors and GISTs, are potentially malignant[1-3]. Resection of these lesions may contribute to improvement in diagnosis and treatment outcomes.

Surgery, including pancreatoduodenectomy and limited resection, is the most basic treatment for duodenal lesions. However, due to the complexity of the operation, risk of trauma, high incidence of postoperative complications, poor quality of life of patients after surgery, and other difficulties, these surgeries are not easily consented by patients, which also puts the medical staff in a difficult position. With the recent development of minimally invasive endoscopic treatment technologies, such as endoscopic submucosal dissection (ESD), endoscopic muscularis excavation, and endoscopic full-thickness resection, endoscopic treatment has become increasingly popular, which brings hope for the use of minimally invasive treatment of duodenal SELs in the future.

However, endoscopic resection of duodenal SELs is still regarded as a challenging procedure due to a high risk of perforation. The incidence of perforations in duodenal ESD has been reported to range from 6.7%-36.6% during the procedure and 0%-14.3% during the postoperative period[1,4-7]. Management of perforations after endoscopic removal of duodenal SELs is particularly challenging. However, this may be achieved

Revised: July 8, 2021
Accepted: August 18, 2021
Article in press: August 18, 2021
Published online: September 21, 2021

P-Reviewer: Masaki S, Seicean A
S-Editor: Gao CC
L-Editor: Filipodia
P-Editor: Liu JH

by using over-the-scope clips (OTSCs). An OTSC was developed as an endoscopic full-thickness gastrointestinal closure device and has become one of the treatment options for gastrointestinal perforation because it is less invasive compared to conventional surgical closure. At present, there are few reports on endoscopic resection of duodenal SELs and endoscopic methods for the management of perforations[1,2,8,9]. To explore further this area, this study aimed to assess the effectiveness and safety of OTSCs in the treatment of perforation after endoscopic resection of duodenal SELs.

MATERIALS AND METHODS

Patients

This was a retrospective study and was approved by the ethics committee of Taizhou Hospital of Zhejiang Province (Linhai, China). The study included 18 consecutive patients who were treated with OTSCs to close perforations that resulted after endoscopic resection of duodenal SELs, from May 2015 to November 2019. Patients were recruited if they met all of the following criteria: (1) Patients with duodenal SELs diagnosed by computed tomography and endoscopic ultrasound (EUS) with a high-frequency miniprobe (UM-2R, 12 MHz; UM-3R, 20 MHz, Olympus Optical, Tokyo, Japan); (2) Patients who underwent endoscopic resection of duodenal SELs and had intraoperative or postoperative perforations; (3) The duodenal perforation was closed using an OTSC; and (4) Patients who were able to tolerate general anesthesia and had no blood coagulation disorders prior to the procedure.

Before the endoscopic procedure, informed consent was obtained from all 18 patients. Patients were also informed that an OTSC might be used, and surgical intervention might be required in case of unsuccessful resection of the lesion or the occurrence of severe complications that cannot be successfully managed by endoscopic methods and conservative treatment.

The main outcome measurements were as follows: (1) The rate of complete closure of intraprocedural perforation; (2) Delayed perforation rate; and (3) Postoperative infection rate. All endoscopic resection procedures were performed by an experienced endoscopist in a sterile operating room while the patients were under general anesthesia with tracheal intubation.

Endoscopic procedures

The main equipment and accessories used were as follows: A single-accessory channel endoscope (Q260J; Olympus) with a transparent cap (ND-201-11802; Olympus) attached to its tip, an argon plasma coagulation unit (APC 300; ERBE, Tübingen, Germany), a high-frequency electronic cutting device (ICC 200; ERBE), a hook knife (KD-620LR; Olympus), an insulated-tip knife (KD-611L, IT2; Olympus), hot biopsy forceps (FD-410LR; Olympus), foreign body forceps (FG-B-24, Kangjin, Changzhou, China), a snare (SD-230U-20; Olympus), a carbon dioxide insufflator (Olympus), twin graspers (Ovesco Endoscopy AG, Tuebingen, Germany), an OTSC (12/6 t-type, Ovesco Endoscopy AG,), a titanium clip (HX-600-135; Olympus and M00522600), and endoloop (Leo Medical Co., Ltd, Changzhou, China).

Endoscopic resection was performed as follows (Figure 1): (1) Several marking dots were initially made around the lesion using a needle-knife to define the border; (2) A submucosal elevation was made by injection of solution (100 mL saline plus 1 mL epinephrine and 2 mL indigo carmine); (3) Subsequently, the mucosa was incised with a hook knife outside the border to reveal the lesion; (4) A circumferential excavation was made as deep as the submucosa or muscularis propria layer around the lesion using an insulated tip knife; (5) After the lesion was completely resected, it was removed using a snare or foreign body forceps; and (6) Duodenal tissues adjacent to the perforation were clamped with twin graspers and then drawn into the transparent cap of the OTSC device until they were fully inhaled into the transparent cap following which the OTSC closure system was released to close the wound. If defect closure was not complete, several clip and/or endoloops were used to close the remaining portions. The mucosa defect was closed with several clips in a 'side to center' manner, and an endoloop was placed to trap all the clips. Finally, the endoloop was slowly tightened, and all the clips were tied together with the endoloop[8].

Postoperative management and follow-up

After the operation, all patients were treated with postoperative fasting, gastrointestinal decompression, proton-pump inhibitors, and antibiotics for infection prevention. Oral intake was gradually resumed depending on the speed of recovery.

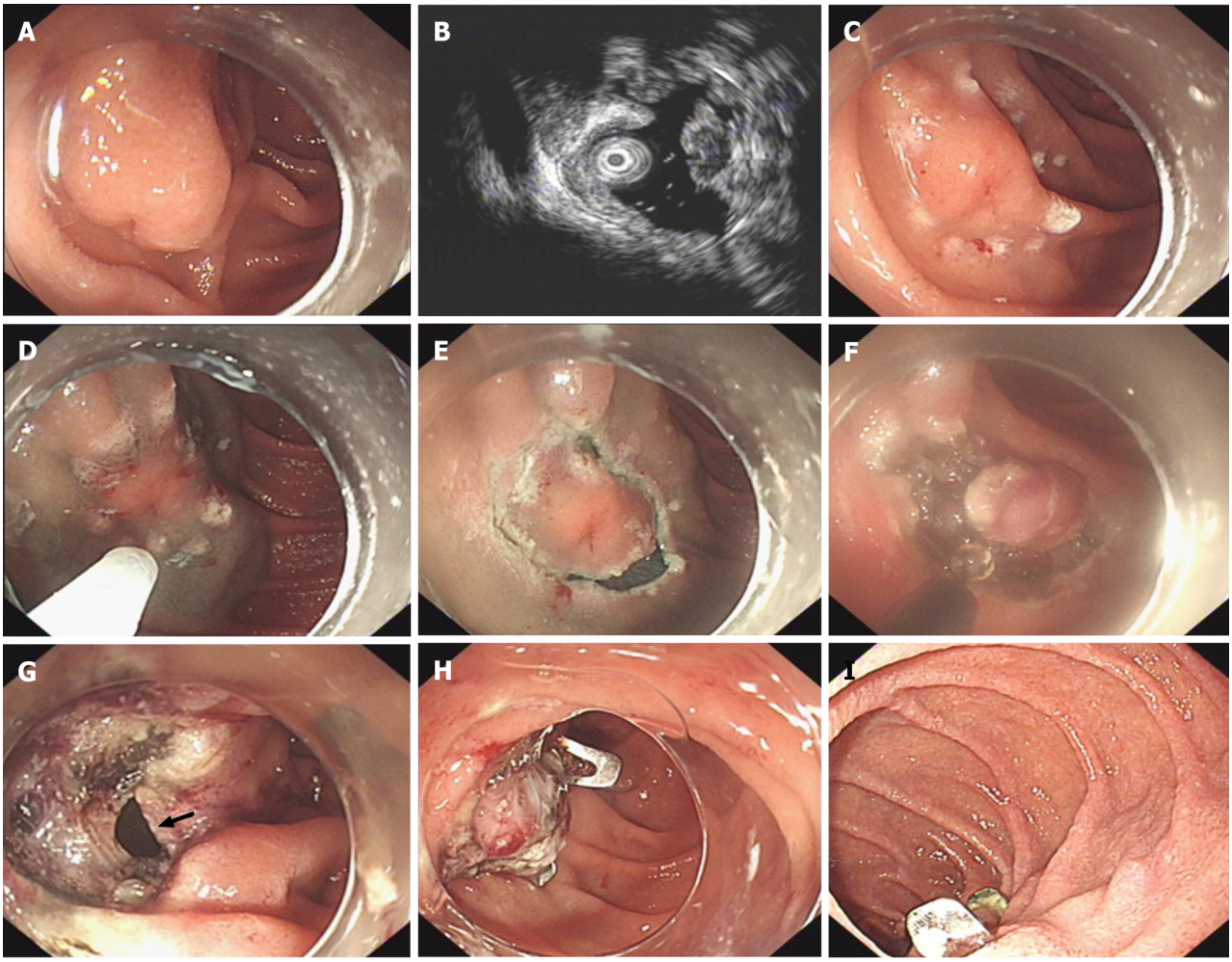


Figure 1 Endoscopic resection of a subepithelial lesion located in the descending duodenum with perforation closure using an over-the-scope clip. A: Endoscopic view of a subepithelial lesion located in the descending duodenum; B: Endoscopic ultrasound evaluation of the same lesion; C: Several marking dots are made around the lesion; D: Injection solution used to elevate the submucosa; E: The mucosa is incised outside the marking dots; F: A circumferential excavation is made as deep as the submucosa around the lesion; G: A duodenal perforation is observed (black arrow) after removal of the lesion; H: The perforation is closed with an over-the-scope clip; I: Healed wound 9 mo after the procedure.

Every patient underwent follow-up endoscopies to monitor wound healing at 3 mo and 6 mo after endoscopic resection. EUS was performed to check for residual lesions after 3 mo. Patients with potentially malignant lesions, such as neuroendocrine tumors and GISTs, were monitored by endoscopy and/or EUS to detect recurrent lesions, and abdominal US and/or computed tomography to detect distant metastasis every 12 mo.

Statistical analysis

Data were analyzed using SPSS software (version 20.0; SPSS Inc., Armonk, NY, United States). Descriptive statistics were used for this study. The median was used for variables with a skewed distribution, while the mean was used in the case of a normal distribution of variables. Enumeration data are expressed as case numbers and percentages (%).

RESULTS

Clinical characteristics and therapeutic outcome

Patient information is summarized in Table 1 and therapeutic outcomes, are described in Table 2. The rate of successful *en bloc* resection was 100%. The vertical and horizontal margins of all specimens were tumor-free. Thus, the complete resection rate was 100%.

Table 1 Clinical characteristics of the 18 patients with duodenal subepithelial lesions, *n* (%)

Patients	
Median age, yr (range)	53.5 (29-74)
Gender	
Male	8 (44.4)
Female	10 (55.6)
Symptom	
Upper abdominal pain	3 (16.7)
Abdominal distention	4 (22.2)
Melena	5 (27.8)
Asymptomatic	6 (33.3)
Lesions	
Median size, cm (range)	2.0 (1.3-5.0)
Location of lesion	
Duodenal bulb	11 (61.1)
Descending junction of duodenal bulb	4 (22.2)
Descending duodenum	3 (16.7)
Origination of lesion	
Submucosal layer	9 (50.0)
Muscularis propria layer	9 (50.0)

All 18 patients had intraoperative perforations. The median perforation size was 1 cm in diameter (range, 0.5-3.0 cm). The wound was closed with an OTSC in 6 cases, an OTSC + a titanium clip in 1 case, and an OTSC + a titanium clip + an endoloop in 5 cases. The rate of successful intraprocedural perforation closure was 100%.

Seventeen patients had minor intraoperative bleeding. The remaining 1 patient, who had a tumor originating from the lamina propria, growing mainly out of the lumen, with rich blood supply, had considerable amount of bleeding during the procedure. All patients were treated with hot biopsy forceps to achieve hemostasis during the procedure.

None of the patients developed delayed bleeding or perforation. Seven patients had postoperative abdominal infections and were administered intensive antibiotic therapy. Among the 7 patients, 1 patient developed an abscess in the right iliac fossa that improved after puncture and drainage, while another patient developed septic shock and received peritoneal lavage and underwent distal subtotal gastrectomy with duodenal bulb resection. All 18 patients recovered and were discharged. The mean time taken to resume normal diet after the procedure was 6.5 d. The mean postoperative hospital stay was 9.5 d.

Follow-up

The median follow-up period after the procedure was 27 mo (range, 15-66 mo). No residual or recurrent lesions, duodenal stenosis, or adhesions were detected during the follow-up period in any of the patients.

DISCUSSION

Currently, endoscopic resection of duodenal SELs is a challenging procedure with a high risk of perforation. Published studies about endoscopic resection of duodenal SELs and endoscopic methods for management of perforations are limited[1,2,8,9]. In this study, we used OTSCs to close perforations in 18 patients. The rate of complete removal of duodenal SELs and successful perforation closure was 100%. No delayed bleeding or perforation occurred in any of the patients. This suggests that the use of OTSCs can effectively close perforations following endoscopic resection of duodenal

Table 2 Therapeutic outcome and adverse events of endoscopic resection for duodenal subepithelial lesions, *n* (%)

Therapeutic outcome and adverse events	
Complete resection	18 (100)
Histology diagnosis	
Brunner's adenoma	1 (5.6)
Heterotopic pancreas	7 (38.9)
GIST	7 (38.9)
Very low risk	1 (5.6)
Low risk	6 (33.3)
Neuroendocrine tumors	3 (16.6)
Complication	
Delayed perforation	0 (0)
Delayed bleeding	0 (0)
Postoperative infection	7 (38.9)
Mean time of diet recovery after the procedure, d (range)	6.5 (2-14)
Mean hospital stay after the procedure, d (range)	9.5 (4-18)
Median follow-up period, mo (range)	27 (15-66)

GIST: Gastrointestinal stromal tumor.

SELs when performed by an experienced endoscopist.

The clinical manifestations of duodenal SELs are nonspecific and related to the location, size, growth pattern, presence of mucosal ulcers, and invasion or compression of adjacent organs. Most duodenal lesions have no symptoms and are usually found incidentally during endoscopic examinations. Clinical symptoms such as gastrointestinal bleeding, abdominal pain, and abdominal distention may occur when the lesion is very large or when an ulcer develops on the surface of the lesion.

Though most duodenal SELs, such as lipomas, Brunner's adenomas, heterotopic pancreas, and cysts, are benign, some including neuroendocrine tumors and GISTs are potentially malignant[1-3]. Endoscopy and EUS are of great value in the diagnosis of duodenal SELs; however, they may be difficult to diagnose on some occasions. Patients with duodenal SELs can be monitored by endoscopy, especially for asymptomatic tumors that lack high-risk features as identified by EUS[10]. However, surveillance using only endoscopy may increase the risk of delayed diagnosis of a malignancy[11]. Furthermore, the difficulty of the operation and risk of combined evisceration will increase if the lesion is large. In such cases, removal of the lesion is inevitable.

Traditional surgical approaches for duodenal lesions, including pancreatoduodenectomy and limited resection, are traumatic and may result in serious complications, such as bleeding, perforation, and infection. Considering these potential risks associated with surgical therapy, endoscopic treatment is used as an alternative choice, which may be safer, more effective, and is minimally invasive. However, endoscopic resection of duodenal SELs is still considered to be a challenging procedure because the duodenal lumen is narrow and the initial part (ball to lower part) is an anti-c loop, which renders the endoscope unstable. Moreover, the abundant blood vessels and Brunner glands in the submucosa of the duodenum make it difficult to lift the mucosa after injection. In addition, compared to other parts of the gastrointestinal tract, the muscularis propria layer of the duodenum is soft and thin, and the posterior wall lacks the serosal layer; therefore, perforation can occur easily during or after the endoscopic resection of duodenal lesions, especially duodenal SELs[8]. The incidence of intraprocedural perforations in duodenal ESD has been reported to range from 6.7%-36.6%, and is 0%-14.3% in delayed perforations[1,4-7]. Moreover, emergency operations have been performed in 3.3%-25.0% of patients due to intraprocedural uncontrollable perforation or delayed perforation[1,4-7]. Our previous study reported that the perforation rate of endoscopic resection of duodenal SELs in our hospital was 7.4%[8].

Perioperative perforation associated with endoscopic therapy was previously considered a serious complication that usually requires surgery. With the development of endoscopic suture instruments and techniques, patients with iatrogenic gastrointestinal perforation can be successfully managed using endoscopic methods and conservative treatment without surgical intervention[12,13]. Thus, most perforations related to endoscopic treatment are no longer life-threatening complications. However, endoscopic closure of perforations after endoscopic resection of duodenal SELs remains a great challenge.

In the past, titanium clips were used for endoscopic closure of gastrointestinal perforations, especially for small acute perforations (< 5 mm). However, a titanium clip has a narrow wingspan and lacks the ability to approximate adequately the margins of the defect. Consequently, the rate of leakage after repairing a large perforation of more than 1 cm is high as the seal is confined to the surface rather than the full-thickness of the mucosa[14-16]. An OTSC has a greater holding strength[16,17]; it can clamp the entire wall of the lumen and grasp more tissue. The design can manage full-thickness perforations with diameters of up to 3 cm[14]. Moreover, the gap between the teeth of an OTSC allows blood to pass through to avoid tissue necrosis. The advantage of an OTSC lies in its ease of use, ability to close defects between 1 and 3 cm with a single clip, and safety, which allows endoscopists to deal effectively with acute perforations immediately after identification[18]. Thus, OTSCs are easy to operate and can effectively shorten operation times. Moreover, The European Society of Gastrointestinal Endoscopy recommends OTSCs for endoscopic closure of iatrogenic perforations[18]. According to a systematic review, the success rate of using OTSCs to manage perforations was 85.3%, while 9.4% of patients still required surgical intervention after an OTSC placement to achieve complete closure [19]. Voermans *et al*[14] reported 12 cases of duodenal perforation that were treated with OTSCs, nine of which were effectively closed, with an overall success rate of 75%. In our study, the rate of successful closure of intraprocedural perforations was 100%. However, we have also used a titanium clip in 1 case and a titanium clip along with an endoloop in 5 cases. It seems that if the perforation is larger than 1.5 cm, using an OTSC alone may fail to achieve complete closure. We speculate that the combination of OTSC, titanium clip, and endoloops may be more effective. Given that the duodenal lumen is narrow, caution should be exercised to avoid grasping too much tissue to avoid further narrowing of the lumen while deploying the OTSC in the duodenum. In our study, no duodenal stenosis was detected in any patient during the follow-up period.

The duodenum is exposed to pancreatic juices and bile, causing delayed perforations more likely to occur after endoscopic resection of duodenal lesions. Complete closure of the wound facilitates prevention of delayed perforation[6,7,17]. Due to its the strong tightening force and the gap between its teeth, an OTSC can manage to close full-thickness duodenal perforations and avoid tissue necrosis, which effectively reduces the occurrence of delayed perforations. A carbon dioxide pump is also recommended to use with endoscopic treatment, especially when a perforation occurs. The use of gastrointestinal decompression after endoscopic closure of perforation is helpful for the absorption of gas and liquid in the intestinal cavity. It also reduces tension in the wound, and promotes wound healing, which can reduce the incidence of delayed perforations. In this study, we placed a jejunal nutrition tube next to the wound and a gastrointestinal decompression tube to extract gas and digestive juice. Thereafter, none of the patients developed delayed perforations.

The duodenum is an interperitoneal organ, most of which is located in the retroperitoneum. After perforation or full-thickness resection, digestive fluid from the duodenum (mainly bile and pancreatic juice) flows into the peritoneal cavity or retroperitoneal cavity, which may cause serious abdominal or retroperitoneal infection. In our study, 7 patients (38.9%) had postoperative abdominal infection, including 1 who developed an abscess in the right iliac fossa and another who developed septic shock. Severe infection in the 2 cases were considered to be caused by long operation times and large amounts of digestive juice entering the abdominal cavity. Timely conversion of the endoscopic procedure to surgery or combining with laparoscopy when the resection is found to be difficult may help avoid such complications.

Due to their strong holding strength, OTSCs are more difficult to detach spontaneously from the mucosa than normal titanium clips. The OTSC is made of nitinol, which has favorable biocompatibility. Thus, this device is considered a permanent implanted material. However, OTSCs should be removed in the following circumstances: (1) Poor healing; (2) OTSC misplacement; (3) Repeat biopsy/therapy or further treatment; (4) Adverse events after OTSC implantation, such as ulcers and

stenosis of the digestive tract; (5) Removal after recovery; and (6) Patient's wishes[20]. In our study, there were no such indications for removal. During the follow-up period, OTSCs detached spontaneously in most cases.

This study has a few limitations. First, this was a single-center retrospective study and the sample size was relatively small; therefore, selection bias may have been present. Second, since this was a retrospective study, it lacked randomized and control samples. Third, our institution is a tertiary endoscopic center in Zhejiang Province where the procedures were performed by an experienced operator; thus, the results of this study may not be applicable to all other endoscopic centers.

CONCLUSION

Closing of perforations after endoscopic resection of duodenal SELs with OTSCs is an effective and reasonably safe therapeutic method. However, this procedure should be performed by an experienced endoscopic team. If the endoscopic procedure fails or the postoperative complications are difficult to manage, the patient should be planned to undergo surgery immediately.

ARTICLE HIGHLIGHTS

Research background

Currently, endoscopic resection of duodenal subepithelial lesions (SELs) is a challenging procedure with a high risk of perforation.

Research motivation

It is importance to deal with perforation after endoscopic resection of duodenal SELs. However, so far, there were few reports on endoscopic methods for management of perforations.

Research objectives

We aim to evaluate the effectiveness and safety of over-the-scope clip (OTSC) in the closing the perforation after endoscopic resection of duodenal SELs.

Research methods

This was a retrospective study. We collected data of 18 consecutive patients who were treated with OTSCs to close the perforation after endoscopic resection of duodenal SELs and analyzed the rate of complete resection, closure of intraprocedural perforation, delayed bleeding, delayed perforation, and postoperative infection.

Research results

All the perforations after endoscopic resection of duodenal SELs were successfully closed. No delayed bleeding or perforation occurred in any of the patients.

Research conclusions

OTSC can effectively and safely close the perforations after endoscopic resection of duodenal SELs by an experienced endoscopist.

Research perspectives

We need to expand the sample size to confirm further the effectiveness and safety of OTSC in closing the perforation after endoscopic resection of duodenal SELs. In addition, the long-term outcome of OTSC should be observed by extending the follow-up time.

REFERENCES

1 **Matsumoto S**, Miyatani H, Yoshida Y. Endoscopic submucosal dissection for duodenal tumors: a single-center experience. *Endoscopy* 2013; **45**: 136-137 [PMID: 22930172 DOI: 10.1055/s-0032-1310123]

2 **Musumba C**, Sonson R, Tutticci N, Nanda K, Bourke MJ. Endoscopic submucosal dissection of a duodenal neuroendocrine tumor. *Gastrointest Endosc* 2014; **79**: 716 [PMID: 24368076 DOI:

10.1016/j.gie.2013.11.011]
3 **Xu GQ**, Wu YQ, Wang LJ, Chen HT. Values of endoscopic ultrasonography for diagnosis and treatment of duodenal protruding lesions. *J Zhejiang Univ Sci B* 2008; **9**: 329-334 [PMID: 18381809 DOI: 10.1631/jzus.B0710546]
4 **Hoteya S**, Yahagi N, Iizuka T, Kikuchi D, Mitani T, Matsui A, Ogawa O, Yamashita S, Furuhata T, Yamada A, Kimura R, Nomura K, Kuribayashi Y, Kaise M. Endoscopic submucosal dissection for nonampullary large superficial adenocarcinoma/adenoma of the duodenum: feasibility and long-term outcomes. *Endosc Int Open* 2013; **1**: 2-7 [PMID: 26135505 DOI: 10.1055/s-0033-1359232]
5 **Jung JH**, Choi KD, Ahn JY, Lee JH, Jung HY, Choi KS, Lee GH, Song HJ, Kim DH, Kim MY, Bae SE, Kim JH. Endoscopic submucosal dissection for sessile, nonampullary duodenal adenomas. *Endoscopy* 2013; **45**: 133-135 [PMID: 23364841 DOI: 10.1055/s-0032-1326178]
6 **Nonaka S**, Oda I, Tada K, Mori G, Sato Y, Abe S, Suzuki H, Yoshinaga S, Nakajima T, Matsuda T, Taniguchi H, Saito Y, Maetani I. Clinical outcome of endoscopic resection for nonampullary duodenal tumors. *Endoscopy* 2015; **47**: 129-135 [PMID: 25314330 DOI: 10.1055/s-0034-1390774]
7 **Yamamoto Y**, Yoshizawa N, Tomida H, Fujisaki J, Igarashi M. Therapeutic outcomes of endoscopic resection for superficial non-ampullary duodenal tumor. *Dig Endosc* 2014; **26** Suppl 2: 50-56 [PMID: 24750149 DOI: 10.1111/den.12273]
8 **Ye LP**, Mao XL, Zheng HH, Zhang Y, Shen LY, Zhou XB, Zhu LH. Safety of endoscopic resection for duodenal subepithelial lesions with wound closure using clips and an endoloop: an analysis of 68 cases. *Surg Endosc* 2017; **31**: 1070-1077 [PMID: 27387179 DOI: 10.1007/s00464-016-5065-9]
9 **Schmidt A**, Bauder M, Riecken B, von Renteln D, Muehleisen H, Caca K. Endoscopic full-thickness resection of gastric subepithelial tumors: a single-center series. *Endoscopy* 2015; **47**: 154-158 [PMID: 25380509 DOI: 10.1055/s-0034-1390786]
10 **Demetri GD**, von Mehren M, Antonescu CR, DeMatteo RP, Ganjoo KN, Maki RG, Pisters PW, Raut CP, Riedel RF, Schuetze S, Sundar HM, Trent JC, Wayne JD. NCCN Task Force report: update on the management of patients with gastrointestinal stromal tumors. *J Natl Compr Canc Netw* 2010; **8** Suppl 2: S1-41; quiz S42 [PMID: 20457867 DOI: 10.6004/jnccn.2010.0116]
11 **Białek A**, Wiechowska-Kozłowska A, Pertkiewicz J, Polkowski M, Milkiewicz P, Karpińska K, Ławniczak M, Starzyńska T. Endoscopic submucosal dissection for treatment of gastric subepithelial tumors (with video). *Gastrointest Endosc* 2012; **75**: 276-286 [PMID: 22032850 DOI: 10.1016/j.gie.2011.08.029]
12 **Yoshizumi F**, Yasuda K, Kawaguchi K, Suzuki K, Shiraishi N, Kitano S. Submucosal tunneling using endoscopic submucosal dissection for peritoneal access and closure in natural orifice transluminal endoscopic surgery: a porcine survival study. *Endoscopy* 2009; **41**: 707-711 [PMID: 19670139 DOI: 10.1055/s-0029-1214959]
13 **Guo J**, Liu Z, Sun S, Liu X, Wang S, Ge N, Wang G, Qi Y. Endoscopic full-thickness resection with defect closure using an over-the-scope clip for gastric subepithelial tumors originating from the muscularis propria. *Surg Endosc* 2015; **29**: 3356-3362 [PMID: 25701060 DOI: 10.1007/s00464-015-4076-2]
14 **Voermans RP**, Le Moine O, von Renteln D, Ponchon T, Giovannini M, Bruno M, Weusten B, Seewald S, Costamagna G, Deprez P, Fockens P; CLIPPER Study Group. Efficacy of endoscopic closure of acute perforations of the gastrointestinal tract. *Clin Gastroenterol Hepatol* 2012; **10**: 603-608 [PMID: 22361277 DOI: 10.1016/j.cgh.2012.02.005]
15 **Verlaan T**, Voermans RP, van Berge Henegouwen MI, Bemelman WA, Fockens P. Endoscopic closure of acute perforations of the GI tract: a systematic review of the literature. *Gastrointest Endosc* 2015; **82**: 618-28.e5 [PMID: 26005015 DOI: 10.1016/j.gie.2015.03.1977]
16 **Singhal S**, Changela K, Papafragkakis H, Anand S, Krishnaiah M, Duddempudi S. Over the scope clip: technique and expanding clinical applications. *J Clin Gastroenterol* 2013; **47**: 749-756 [PMID: 23751852 DOI: 10.1097/MCG.0b013e318296ecb9]
17 **Mori H**, Shintaro F, Kobara H, Nishiyama N, Rafiq K, Kobayashi M, Nakatsu T, Miichi N, Suzuki Y, Masaki T. Successful closing of duodenal ulcer after endoscopic submucosal dissection with over-the-scope clip to prevent delayed perforation. *Dig Endosc* 2013; **25**: 459-461 [PMID: 23368742 DOI: 10.1111/j.1443-1661.2012.01363.x]
18 **Paspatis GA**, Dumonceau JM, Barthet M, Meisner S, Repici A, Saunders BP, Vezakis A, Gonzalez JM, Turino SY, Tsiamoulos ZP, Fockens P, Hassan C. Diagnosis and management of iatrogenic endoscopic perforations: European Society of Gastrointestinal Endoscopy (ESGE) Position Statement. *Endoscopy* 2014; **46**: 693-711 [PMID: 25046348 DOI: 10.1055/s-0034-1377531]
19 **Bartell N**, Bittner K, Kaul V, Kothari TH, Kothari S. Clinical efficacy of the over-the-scope clip device: A systematic review. *World J Gastroenterol* 2020; **26**: 3495-3516 [PMID: 32655272 DOI: 10.3748/wjg.v26.i24.3495]
20 **Ou YH**, Kong WF, Li LF, Chen PS, Deng SH, He FJ, Peng QQ, Yue H. Methods for Endoscopic Removal of Over-the-Scope Clip: A Systematic Review. *Can J Gastroenterol Hepatol* 2020; **2020**: 5716981 [PMID: 32908852 DOI: 10.1155/2020/5716981]

World Journal of Gastroenterology

Submit a Manuscript: https://www.f6publishing.com

World J Gastroenterol 2021 September 21; 27(35): 5967-5977

DOI: 10.3748/wjg.v27.i35.5967

ISSN 1007-9327 (print) ISSN 2219-2840 (online)

ORIGINAL ARTICLE

Retrospective Study

Hepatic perivascular epithelioid cell tumor: Clinicopathological analysis of 26 cases with emphasis on disease management and prognosis

Shan Zhang, Pan-Pan Yang, Yu-Chen Huang, Hong-Chun Chen, De-Li Chen, Wen-Tian Yan, Ning-Ning Yang, Yuan Li, Nan Li, Zhen-Zhong Feng

ORCID number: Shan Zhang 0000-0001-7891-6906; Pan-Pan Yang 0000-0003-3633-6844; Yu-Chen Huang 0000-0002-7740-5634; Hong-Chun Chen 0000-0002-7751-5390; De-Li Chen 0000-0002-4593-9295; Wen-Tian Yan 0000-0001-5260-4701; Ning-Ning Yang 0000-0003-0691-7293; Yuan Li 0000-0002-8178-5131; Nan Li 0000-0002-5522-4252; Zhen-Zhong Feng 0000-0001-9385-3157.

Author contributions: Zhang S and Feng ZZ designed the study; Zhang S and Yang PP performed the experiments; Li Y prepared the slices; Zhang S, Huang YC, Chen HC, Yan WT, and Yang NN collected and analyzed the data; Feng ZZ and Li N reviewed the histopathology and IHC results; Chen DL provided critical comments on the manuscript; Zhang S, Yang PP, and Feng ZZ wrote the manuscript; all authors read and approved the final manuscript.

Supported by the Anhui Provincial Natural Science Foundation, No. 1908085MH275; Bengbu Medical College Key projects of Natural Science Foundation, No. BYKF1710; and Bengbu City-Bengbu Medical College Joint Science and Technology Project,

Shan Zhang, Department of Pathology, The Second People's Hospital of Hefei, Hefei 230011, Anhui Province, China

Pan-Pan Yang, Zhen-Zhong Feng, Department of Pathology, The Second Affiliated Hospital of Anhui Medical University, Hefei 230601, Anhui Province, China

Yu-Chen Huang, Hong-Chun Chen, Wen-Tian Yan, Ning-Ning Yang, Nan Li, Department of Pathology, The First Affiliated Hospital of Bengbu Medical College, Bengbu 233000, Anhui Province, China

De-Li Chen, Department of Gastrointestinal Surgery, The First Affiliated Hospital of Bengbu Medical College, Bengbu 233000, Anhui Province, China

Yuan Li, Department of Pathology, The First Affiliated Hospital of University of Science and Technology of China, Anhui Provincial Hospital, Hefei 230001, Anhui Province, China

Corresponding author: Zhen-Zhong Feng, PhD, Professor, Department of Pathology, The Second Affiliated Hospital of Anhui Medical University, No. 678 Furong Road, Hefei 230601, Anhui Province, China. fzz18297301626@163.com

Abstract

BACKGROUND

Perivascular epithelioid cell tumor (PEComa) is an uncommon tumor of mesenchymal origin. Cases of PEComa in the liver are extremely rare.

AIM

To analyze the clinicopathological features and treatment of hepatic PEComa and to evaluate the prognosis after different treatments.

METHODS

Clinical and pathological data of 26 patients with hepatic PEComa were collected. All cases were analyzed by immunohistochemistry and clinical follow-up.

RESULTS

This study included 17 females and 9 males, with a median age of 50 years.

No. BYLK201812.

Institutional review board statement: This study was approved by the Ethics and Research Committees of the First Affiliated Hospital of Bengbu Medical College (Anhui Province, China).

Informed consent statement: Informed written consent was obtained from all the patients.

Conflict-of-interest statement: The authors declare no conflicts of interest for this manuscript.

Data sharing statement: No additional data are available.

Open-Access: This article is an open-access article that was selected by an in-house editor and fully peer-reviewed by external reviewers. It is distributed in accordance with the Creative Commons Attribution NonCommercial (CC BY-NC 4.0) license, which permits others to distribute, remix, adapt, build upon this work non-commercially, and license their derivative works on different terms, provided the original work is properly cited and the use is non-commercial. See: http://creativecommons.org/Licenses/by-nc/4.0/

Manuscript source: Unsolicited manuscript

Specialty type: Gastroenterology and hepatology

Country/Territory of origin: China

Peer-review report's scientific quality classification

Grade A (Excellent): A
Grade B (Very good): B
Grade C (Good): 0
Grade D (Fair): 0
Grade E (Poor): 0

Received: March 29, 2021
Peer-review started: March 29, 2021
First decision: May 28, 2021
Revised: May 29, 2021
Accepted: August 13, 2021
Article in press: August 13, 2021
Published online: September 21, 2021

Lesions were located in the left hepatic lobe in 13 cases, in the right lobe in 11, and in the caudate lobe in 2. The median tumor diameter was 6.5 cm. Light microscopy revealed that the tumor cells were mainly composed of epithelioid cells. The cytoplasm contained heterogeneous eosinophilic granules. There were thick-walled blood vessels, around which tumor cells were radially arranged. Immunohistochemical analysis of pigment-derived and myogenic markers in PEComas revealed that 25 cases were HMB45 (+), 23 were Melan-A (+), and 22 SMA (+). TFE3 and Desmin were negative in all cases. All the fluorescence *in situ* hybridization samples were negative for *TFE3* gene break-apart probe. Tumor tissues were collected by extended hepatic lobe resection or simple hepatic tumor resection as the main treatments. Median follow-up was 62.5 mo. None of the patients had metastasis or recurrence, and there were no deaths due to the disease.

CONCLUSION

Hepatic PEComa highly expresses melanin and smooth muscle markers, and generally exhibits an inert biological behavior. The prognosis after extended hepatic lobe resection and simple hepatic tumor resection is semblable.

Key Words: Hepatic tumor; Perivascular epithelioid cells; PEComa; Immunohistochemistry; Treatment; Prognosis

©The Author(s) 2021. Published by Baishideng Publishing Group Inc. All rights reserved.

Core Tip: Hepatic perivascular epithelioid cell tumor (PEComa) exhibits an inert biological behavior, and its diagnosis, treatment, and follow-up are challenging. Our study revealed that there was no difference in the prognosis between simple resection of liver tumor and extended resection of liver lobe. Optimal surgical resection currently is the best treatment option, and radiotherapy, chemotherapy, and immunotherapy may become more effective in future. The number of cases in the current retrospective study was limited by the rarity of hepatic PEComa. Therefore, further multicenter, larger-cohort studies are warranted to investigate the clinicopathological features and biological behavior of hepatic PEComa.

Citation: Zhang S, Yang PP, Huang YC, Chen HC, Chen DL, Yan WT, Yang NN, Li Y, Li N, Feng ZZ. Hepatic perivascular epithelioid cell tumor: Clinicopathological analysis of 26 cases with emphasis on disease management and prognosis. *World J Gastroenterol* 2021; 27(35): 5967-5977
URL: https://www.wjgnet.com/1007-9327/full/v27/i35/5967.htm
DOI: https://dx.doi.org/10.3748/wjg.v27.i35.5967

INTRODUCTION

Perivascular epithelioid cells were first described in 1992 by Bonetti *et al*[1]. In 2013, the World Health Organization[2] defined perivascular epithelioid cell tumor (PEComa) as "a mesenchymal tumor, which shows a local association with the vessel wall and usually expresses melanocyte markers and smooth muscle markers." Bonetti *et al*[1] were the first to propose the concept of a PEComa family, which includes angiomyolipoma, clear cell sugar tumor of the lung, lymphangioleiomyomatosis, and a group of histologically and immunophenotypically similar tumors that include primary extrapulmonary sugar tumor, clear cell myomelanocytic tumor, and abdominopelvic sarcoma of perivascular epithelioid cells. PEComas are mainly composed of eosinophilic and clear epithelioid cells, which are usually arranged in nests of different sizes associated with blood vessels[3,4]. The diagnosis of PEComa relies on its pathological features, including epithelioid cellular shapes with ample clear to eosinophilic cytoplasm, and in some cases, arrangement around thick-walled blood vessels and immunohistochemical phenotypes, including melanocyte and smooth muscle markers[1,4,5]. Cases of PEComa in the liver are extremely rare[6], and surgical resection currently is the most effective therapeutic strategy to cure patients or prolong

P-Reviewer: Yasukawa K
S-Editor: Wu YXJ
L-Editor: Wang TQ
P-Editor: Xing YX

the survival period. In this study, the clinical and pathological features, immunohistochemical phenotypes, and information on treatment modalities of 26 cases of hepatic PEComa were collected, and the effects of different surgical methods on prognosis were evaluated to provide information for the guidance of clinical treatment.

MATERIALS AND METHODS

Patient selection

The study included 17 women and 9 men who were diagnosed with hepatic PEComa for the first time. Tumor tissue samples were collected at the time of diagnosis between January 2010 and December 2018 at the First Affiliated Hospital of Bengbu Medical College (Anhui Province, China). None of the patients received preoperative radio- or chemo-therapy. Sixteen patients underwent extended hepatic lobe resection, eight underwent simple hepatic tumor resection, and two received the oral mTOR inhibitor sirolimus. None of the 26 patients had metastasis or recurrence, and there were no deaths due to the disease. Only two patients with extended liver lobectomy had a poor prognosis (one had postoperative pain in the liver area, and the other was diagnosed with liver cancer 2 years after surgery). Informed consent was obtained from all patients. The study protocol was approved by the ethics committees of the hospitals partaking in this study.

Imageological examination

Imaging data of all patients were collected and reviewed by two experienced physicians who analyzed the imaging characteristics of the patients.

Histological observation and immunohistochemical analysis

Two experienced pathologists reviewed hematoxylin and eosin-stained sections of each tissue sample, marked the representative regions of tissue blocks, and assessed the following histological features: Tumor boundary (infiltration), tumor cell structure (trabecular and nested), tumor cell type (epithelial and fusiform), cytological features (cytoplasm and nucleus), nuclear features (atypical and pleomorphic), presence of pleomorphic tumor cells, and tumor necrosis.

Immunohistochemical staining was conducted on 4-μm-thick serial PEComa tissue sections using the standard ElivisionTM Plus/HRP detection system (Fuzhou Maixin Biotechnology, Fuzhou, China) and DAB substrate, generating a brown color. The antibodies, clones, dilutions, and pretreatment conditions used, as well as the positively stained sites, are listed in Table 1. Serial sections were incubated in parallel with rabbit IgG instead of the primary antibody as a negative control. Immunoreactivity was graded according to the percentage of positive tumor cells (0, negative; 1+, 1%-5%; 2+, 6%-25%; 3+, 26%-50%; 4+, 51%-100%), and tumor cell immunoreactivity was also semi-qualitatively graded: Weak, heterogeneous, or strong[7,8]. For calculation of IHC totals, a score of 1+ with weak, heterogeneous, or strong staining was considered positive for all antibodies except TFE3. A minimum of 3+ was required for TFE3 immunopositivity[8].

Fluorescence in situ hybridization

FISH was performed on paraffin-embedded tissue sections with a thickness of 4 μm and labeled with a *TFE3* gene break-apart probe (Guangzhou Anbiping Medical, Guangzhou, Guangdong Province, China). For probe preparation, *TFE3* gene was labeled with green fluorescence on the centromere side and red fluorescence on the telomere side. FISH interpretation criteria are as follows: The positive pattern for *TFE3* translocation should be 1 red, 1 green, and 1 fusion (yellow) signal in females, and 1 red, 1 green, and 1 negative signal in males; the pattern for intact *TFE3* alleles should be 2 fusion (yellow) signals in females and 1 fusion (yellow) signal in males. When the distance between the red and green signals exceeds 1 fusion signal size, it is interpreted as a red-green signal separation. A case was scored as positive if at least 10% of 100 scored nuclei showed a split signal pattern.

Table 1 Antibodies used in this study

Antigen	Clone	Dilution	Antigen retrieval	Localization
HMB-45	HMB-45	1:400	None	Cytoplasm
Melan-A	A103	1:200	Citrate buffer pressure cook	Cytoplasm
SMA	1A4	1:20000	None	Cytoplasm
Desmin	D33	1:500	None	Cytoplasm
S100 protein	Polyclonal	1:4000	Citrate buffer pressure cook	Cytoplasm/nucleus
Hepatocyte	OCH1E5	1:1000	Citrate buffer pressure cook	Cytoplasm
Vimentin	V9	1:200	Citrate buffer pressure cook	Cytoplasm
CD34	QBEnd/10	1:500	Citrate buffer pressure cook	Cell membrane
TFE-3	MRQ-0663	1:500	ETDA buffer pressure cook	Nucleus
Ki-67	MX006	1:200	Citrate buffer pressure cook	Nucleus

RESULTS

Clinical features

The clinical and pathological data for all 26 cases are summarized in Table 2. We enrolled 26 patients, including 17 females and 9 males. The median patient age was 50 years (range, 26–77 years). Of the 26 patients, 23 had liver-occupying lesions, 2 had hepatic hemangioma, and 1 had hepatic hamartoma. Six patients had a history of liver disease (cysts, hamartoma, or hemangioma). The most common site of tumors was the left hepatic lobe. Sixteen patients underwent extended hepatic lobe resection, eight underwent simple hepatic tumor resection, and two were treated only with the mTOR inhibitor sirolimus (both patients were treated for 8 mo). The clinical symptoms of hepatic PEComa were non-specific. Most patients were admitted to one of our hospitals because of space-occupying lesions in the liver during medical examination, nausea, vomiting, loss of appetite, or weight loss. During physical examination, the abdomen was soft, with no tenderness or rebound tenderness, occasional contact with the ribs at the liver margin, and no pain in the liver area. Some patients experienced compression pain under the ribs and xiphoid, or in the right abdomen when the tumor involved the caudate lobe, or in the right kidney.

Imaging findings

B-ultrasound usually revealed strong echoes in the liver, the boundary was clear, and the internal echo was uneven, suggesting that the liver had substantial space-occupying lesions (data not shown). Plain computed tomography (CT) scans commonly revealed an irregular soft tissue density (Figure 1A). Enhanced scanning in the arterial phase revealed obvious enhancement of the mass edge and of central heterogeneity (Figure 1B). Portal vein scanning revealed a low mass density (Figure 1C). Magnetic resonance imaging (MRI) revealed a solid cystic space in the liver, and tumors had clear boundaries and uneven internal signal (data not shown).

Macroscopic features

The median tumor diameter was 6.5 cm (range, 0.5-13.0 cm). PEComa tumors were located in the liver parenchyma and were round or oval. The surface was smooth and occasionally highlighted the surface of the liver. The boundary was clear and appeared to be enveloped. Tumors did not invade the surrounding tissue. The cut surface was solid and grayish yellow, had a slightly hard texture, and showed loose necrotic tissue in the center. The liver tissue surrounding the tumor was normal, and the lymph nodes in the hilar region were not swollen. Focal hemorrhage and necrosis were seen in two cases.

Microscopic features

Microscopically, the tumor cells were clearly distinct from normal liver cells, and were largely composed of proliferating epithelioid cells and spindle cells, nested in trabeculae or lamellae. In most cases, the tumor cell nest was surrounded by capillaries. Tumor cells were arranged radially around the thick-walled blood vessels (Figure 2A). Tumor cells were polygonal and cytoplasm was translucent, with hetero-

Table 2 Clinicopathological features of the 26 cases of hepatic PEComa

No.	Sex/age (yr)	Tumor location	Tumor size (cm)	First diagnosis	Treatment	Follow-up (mo) and prognosis
1	F/40	Left lobe	2.5	Left lobe occupying lesion	Left hepatic tumor simple resection	91, favorable prognosis
2	M/57	Left lobe	7.5	Left lobe occupying lesion	Left hepatic tumor simple resection	80, favorable prognosis
3	F/58	Left lobe	8.5	Left lobe occupying lesion	Left hepatic tumor simple resection	79, favorable prognosis
4	F/48	Right lobe	8.0	Right lobe occupying lesion	Right hepatic tumor simple resection	69, favorable prognosis
5	F/64	Right lobe	7.0	Right lobe occupying lesion	Right hepatic tumor simple resection	66, favorable prognosis
6	M/72	Right lobe	8.0	Right lobe occupying lesion	Right hepatic tumor simple resection	59, favorable prognosis
7	F/26	Right lobe	3.0	Right hepatic hamartoma	Extended hepatic lobe resection	55, favorable prognosis
8	M/47	Right lobe	6.5	Right lobe occupying lesion	mTOR inhibitor-sirolimus	51, favorable prognosis
9	F/47	Left lobe	5.5	Left lobe occupying lesion	Extended hepatic lobe resection	25, favorable prognosis
10	M/72	Right lobe	8.0	Right lobe occupying lesion	Extended right hepatic lobe resection	57, favorable prognosis
11	F/56	Right lobe	8.0	Right lobe occupying lesion	mTOR inhibitor-sirolimus	32, favorable prognosis
12	F/54	Right lobe	13.0	Left lobe occupying lesion	Extended left hepatic lobe resection	99, favorable prognosis
13	F/41	Caudate lobe	8.0	Caudate lobe occupying lesion	Caudate hepatic tumor simple resection	98, favorable prognosis
14	F/46	Left lobe	2.0	Left lobe occupying lesion	Extended left hepatic lobe resection	99, favorable prognosis
15	F/54	Right lobe	8.0	Right hepatic hemangioma	Extended Rright hepatic lobe resection	84, favorable prognosis
16	F/41	Caudate lobe	6.0	Caudate lobe occupying lesion	Extended caudate hepatic lobe resection	87, hepatic pain often occurs after discharge
17	M/45	Right lobe	0.5	Right hepatic hemangioma	Extended hepatic lobe resection	85, favorable prognosis
18	F/66	Right lobe	5.5	Right lobe occupying lesion	Extended hepatic lobe resection	59, favorable prognosis
19	F/43	Right lobe	2.8	Right lobe occupying lesion	Extended hepatic lobe resection	47, favorable prognosis
20	F/41	Left lobe	5.0	Left lobe occupying lesion	Extended hepatic lobe resection	49, reoperation for liver cancer in 2017
21	M/52	Left lobe	7.5	Left lobe occupying lesion	Left hepatic tumor simple resection	48, favorable prognosis
22	F/48	Right lobe	9.5	Right lobe occupying lesion	Extended right hepatic lobe resection	71, favorable prognosis
23	M/58	Left lobe	4.0	Left lobe occupying lesion	Left hepatic tumor simple resection	70, favorable prognosis
24	M/77	Left lobe	4.0	Left lobe occupying lesion	Extended left hepatic lobe resection	47, favorable prognosis
25	M/62	Left lobe	6.5	Left lobe occupying lesion	Extended left hepatic lobe resection	36, favorable prognosis
26	F/45	Left lobe	3.0	Left lobe occupying lesion	Extended left hepatic lobe resection	35, favorable prognosis

geneous eosinophilic particles; tumor nuclei were round or oval, nucleoli were

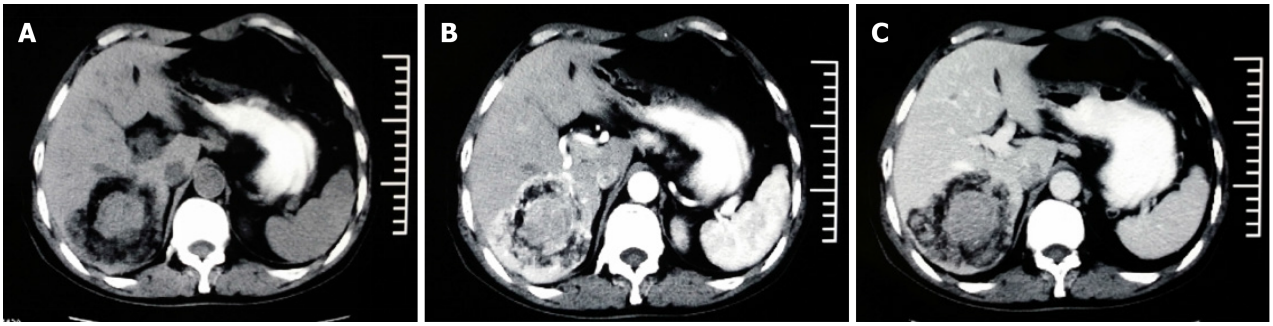


Figure 1 Computed tomography scans of the right hepatic lobe of a 72-year-old male patient with PEComa (patient 10). A: Plain computed tomography scan showing an irregular soft tissue density shadow; B: Enhanced scan showing obvious enhancement of the mass margin and of central heterogeneity in the arterial phase; C: Portal vein scan showing a low mass density.

obvious, chromatin was sparse, part of the cells were heteromorphic, and mitotic figures were not common. Collagen fibers were observed in the interstitium and were generally feathery, and a few fibers were accompanied by hemorrhage and necrosis (Figure 2B).

Immunohistochemistry findings are summarized in Table 3. Of the 26 cases, 25 were HMB45 (+), usually with multifocal or diffuse distribution and occasionally, with scattered distribution (Figure 2C), 23 were Melan-A (+) (Figure 2D), 22 were SMA (+) (Figure 2E), 20 were VIM (+), and 12 were S-100 (+). Only three cases showed focal staining (1%-5%) for TFE3. All tumors were desmin (–) (Figure 2F). The positive rate for Ki-67 was < 10%. All cases expressed at least one smooth muscle or melanocyte marker. FISH showed that no abnormal *TFE3* separation signal was found in 26 cases of hepatic PEComa (Figure 3).

Treatment and follow-up

Sixteen patients underwent extended hepatic lobe resection, eight underwent simple hepatic tumor resection, and two were treated with the mTOR inhibitor sirolimus. During a follow-up period of 25 mo to 99 mo, none of the 26 patients had metastasis or recurrence, and there were no deaths due to the disease. Only two patients with extended liver lobectomy had a poor prognosis (one had postoperative pain in the liver area, and the other was diagnosed with liver cancer 2 years after surgery). There was no difference in patient prognosis between the two surgical treatment methods, and long-term follow-up indicated that the patients went into remission.

DISCUSSION

Hepatic PEComa is a rare mesenchymal tumor derived from pericytes. Ultrasound, CT, and MRI are commonly used for preoperative diagnosis of PEComa. On contrast-enhanced CT, PEComa is characterized by vascular proliferation and arteriovenous connections[5,9,10]. MRI scans have revealed significant enhancement in PEComa in the arterial phase, but not in the portal venous and delayed phases[10]. Contrast-enhanced ultrasonography is another commonly used diagnostic method, in which the contrast agent characteristically reaches the tumor rapidly and drains the arterial blood rapidly to the vein[11]. However, due to the different proportions of smooth muscle cells, adipose tissue, blood vessels, and rare tumors, the accuracy of preoperative diagnosis is currently low. In our study, only one patient was diagnosed with hepatic PEComa before undergoing surgery.

Martignoni *et al*[12] defined PEComa as a tumor that is composed mainly of epithelioid cells and is closely associated with dilated blood vessels and contains eosinophils, but not fat cells or disordered blood vessels. The final diagnosis of PEComa currently depends on pathological features and immunohistochemical analysis. Hepatic PEComa is mainly composed of proliferating epithelioid cells and spindle cells. The tumor cells are polygonal, have translucent cytoplasm, and contain eosinophilic particles, and thick-walled blood vessels are visible in the tumors. Epithelioid cells are arranged radially around thick-walled blood vessels. Feather-like collagen fibers are visible. Nearly all PEComas have specific immunological characteristics, with melanocyte markers (*e.g.*, HMB-45 and/or melan-A) and smooth muscle markers (*e.g.*, SMA) being strongly expressed[11,13], whereas desmin, hepatocyte-

Table 3 Immunohistochemical features of the 26 cases of hepatic PEComa

Target protein	Positive cases (*n*)/total	% Positive
HMB45	25/26	96.2
Melan-A	23/26	88.5
SMA	22/26	83.6
Desmin	1/26*	3.8
S100	14/26	53.8
Hepatocyte	9/26	34.6
Vimentin	20/26	76.9
CD34	18/26	69.2
TFE3	0/26	0
Ki-67 (> 10%)	1/26	3.8

Weakly positive (1%-5%), only scattered cells.

specific antigen, and TFE3 are generally negative. In this study, 25 cases were HMB-45 (+), 17 were SMA (+), and only 3 showed focal staining (1%-5%) for TFE3.

TFE3 is a member of the MiTF family of transcription factors. A recent study[14] showed that *TFE3* gene rearrangements occur in approximately 14% of PEComas. Similar to other *TFE3* translocation-associated tumors, TFE3 (+) PEComa usually exhibits an acinar structure and epithelioid cell morphology, shows aggressive biological behavior, and has a poor prognosis. *PSF-TFE3* gene fusion has been detected in gastrointestinal tract PEComa, but fusion partners in other cases remain unknown [15]. In this study, TFE3 expression was weak and detected in only three patients with small tumors and typical morphological PEComa images, and was associated with a low malignancy and good prognosis. Moreover, no break-apart of the *TFE3* gene was detected by FISH method. Whether there is a *TFE3* fusion gene still needs to be confirmed by subsequent studies. This suggests that liver PEComa may be less malignant than PEComas in other organs.

PEComas are mainly benign tumors[16] that usually do not recur after surgical resection; however, some are malignant, and their biological behavior has not been fully elucidated. In 2005, Folpe *et al*[17] reviewed 26 cases of PEComa of soft tissue and gynecological origin, and suggested to classify PEComa into benign, uncertain malignant potential, and malignant. Further, the authors proposed seven evaluation criteria for PEComa malignancies: (1) Tumor size > 5 cm; (2) Infiltration and growth into surrounding normal tissue; (3) High nuclear grade; (4) Excessive cells; (5) Mitotic figures in > 1/50 high-power fields; (6) Coagulative necrosis of tumor; and (7) Vascular invasion. PEComas with two or more of these features are considered to be malignant, and tumors with only nuclear polymorphism, multinucleated giant cells, or tumors > 5 cm in size are considered to have malignant potential[18].

Because of the rare disease types and the scarcity of cases, treatment plans for hepatic PEComa can only be developed based on statistical analysis of a small number of cases. Surgical resection currently is the main means of treating hepatic PEComa. In clinical practice, surgical methods are usually selected based on the tumor size and on whether the tumor is benign or malignant. Larger and malignant tumors are removed by extended hepatic lobe resection, whereas simple hepatic tumor resection is used for smaller or benign tumors. In this study, the 26 cases showed clinical and biological manifestations of inertness, and no morphological criteria for malignant PEComa. Sixteen patients underwent extended hepatic lobe resection, eight underwent simple hepatic tumor resection, and two received sirolimus. The survival rate of the patients treated with the three different modalities was good, and there was no significant difference among the treatments. Hepatic pain complications were reported only in a few cases with extended lobe resection. It has been reported that when the tumor diameter is less 5 cm, resection can be suspended or regular follow-up suffices[18].

Current data do not support that chemo- or radio-therapy improves the survival time in patients with PEComa[12]; however, sirolimus is expected to improve outcomes either when used alone or in combination with other treatments[4,10,19,20]. A 31-year-old woman with hepatic PEComa showed a significant reduction in tumor

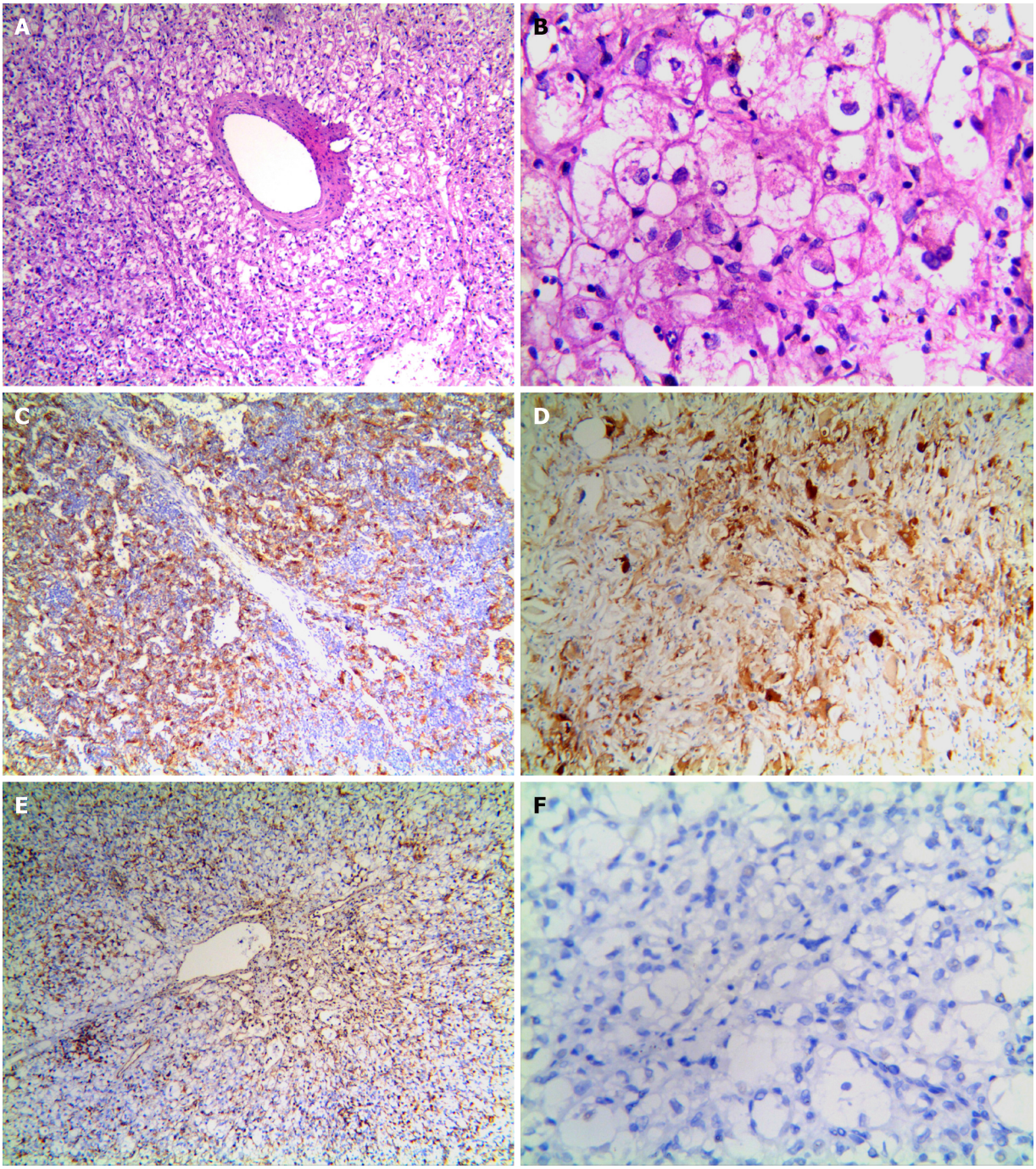


Figure 2 Morphologic appearance of hepatic PEComa. A: Tumor cells consists of proliferating epithelioid cells nested in trabeculae or lamellae and radially arranged around thick-walled vessels (HE, magnification: 100 ×); B: Tumor cells are polygonal, have translucent cytoplasm, and contain uneven eosinophilic granules. Nuclei are round or oval, with a clear nucleolus and sparse chromatin. Interstitial collagen fibers are feathery (HE, magnification, 400 ×); C: Immunoreactivity for HMB45 was detected in the cytoplasm of tumor cells in contrast to normal liver cells, which were negative for this marker (magnification, 100 ×); D: Increased expression of Melan-A was observed in both the cytoplasm and nuclei of carcinoma cells, whereas normal cells displayed lower expression of this marker (magnification, 100 ×); E: Vimentin was detected in the cytoplasm of tumor cells (magnification, 100 ×), whereas normal tissues were negative for this marker (magnification, 100 ×); F: Desmin immunoreactivity was not detected in tumor cells and normal tissues (magnification, 400 ×). Elivision™ Plus/HRP was used.

volume after 8 mo of treatment with sirolimus[19]. After subsequent surgical resection, there were no complications and the prognosis was favorable. This suggests that hepatic PEComa has a better prognosis when surgery is combined with chemotherapy [13,14]. In addition, Wagner *et al*[21] treated three patients with PEComa with sirolimus and found that the tumors responded to the drug, suggesting that sirolimus can be used alone or in combination to treat PEComa. Italiano *et al*[22] reported similar efficacy in a number of cases. However, large-scale clinical trials are needed. Numerous previous studies and this study showed that hepatic PEComa displays an inert biological behavior. However, due to the heterogeneous nature of PEComa, the

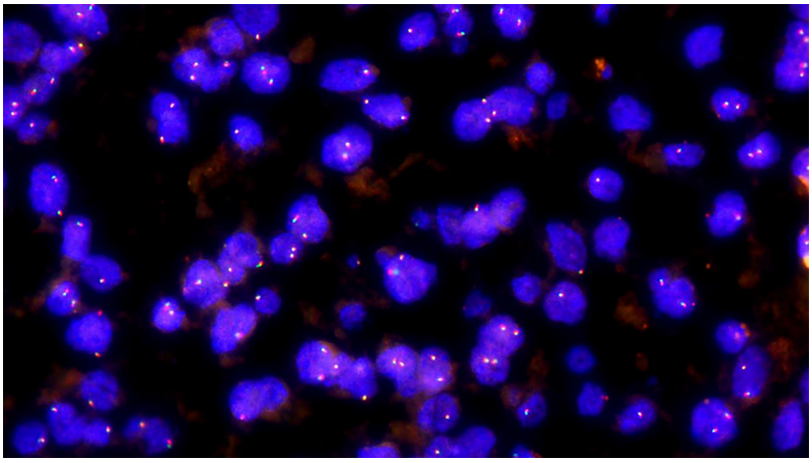


Figure 3 FISH detection of *TFE3* gene break-apart in hepatic PEComa. Most of the tumor cells show fused (yellow) signals, and the distance between the red and green signals is less than 1 fusion signal. For each sample, 100 cells were counted. Only less than 10% of tumor cells showed break-apart signals (magnification, 1000 ×).

existing diagnostic criteria cannot accurately determine the nature of this tumor, which has led to overtreatment in some cases. In addition, because the nature of hepatic PEComa is not entirely clear, there is no standard treatment, and it is difficult to develop an optimal treatment plan. Therefore, clinical observation and follow-up of more cases, and the establishment of a clinical online registration system for hepatic PEComa are needed to provide clinical data for future exploration of the differentiation and distribution of the disease and the development of more accurate diagnostic criteria.

CONCLUSION

Hepatic PEComa is a rare mesenchymal tumor that exhibits an inert biological behavior, and its diagnosis, treatment, and follow-up are challenging. Our study of 26 cases of hepatic PEComa revealed that there was no difference in the prognosis between simple resection of liver tumor and extended resection of liver lobe. Optimal surgical resection currently is the best treatment option, and radiotherapy, chemotherapy, and immunotherapy may become more effective in future[4,9]. The number of cases in the current retrospective study was limited by the rarity of hepatic PEComa. Therefore, further multicenter, larger-cohort studies are warranted to investigate the clinicopathological features and biological behavior of hepatic PEComa.

ARTICLE HIGHLIGHTS

Research background

Perivascular epithelioid cell tumor (PEComa) is an uncommon tumor of mesenchymal origin. Cases of PEComa in the liver are extremely rare.

Research motivation

Cases of PEComa in the liver are extremely rare, and surgical resection currently is the most effective therapeutic strategy to cure patients or prolong the survival period. In this study, the clinical and pathological features, immunohistochemical phenotypes, and information on treatment modalities of 26 cases of hepatic PEComa were collected, and the effects of different surgical methods on prognosis were evaluated to provide information for the guidance of clinical treatment.

Research objectives

We aimed to analyze the clinicopathological features and treatment of hepatic PEComa and to evaluate the prognosis after different treatments.

Research methods

Clinical and pathological data of 26 patients with hepatic PEComa were collected. All cases were analyzed by immunohistochemistry and clinical follow-up.

Research results

This study included 17 females and 9 males, with a median age of 50 years. Lesions were located in the left hepatic lobe in 13 cases, in the right lobe in 11, and in the caudate lobe in 2. The median tumor diameter was 6.5 cm. Light microscopy revealed that the tumor cells were mainly composed of epithelioid cells. The cytoplasm contained heterogeneous eosinophilic granules. There were thick-walled blood vessels, around which tumor cells were radially arranged. Immunohistochemical analysis of pigment-derived and myogenic markers in PEComa tumors revealed that 25 cases were HMB45 (+), 23 were Melan-A (+), and 22 SMA (+). TFE3 and Desmin were negative in all cases. All the FISH samples were negative for *TFE3* gene break-apart probe. Tumor tissues were collected by extended hepatic lobe resection or simple hepatic tumor resection as the main treatments. Median follow-up was 62.5 mo. None of the patients had metastasis or recurrence, and there were no deaths due to the disease.

Research conclusions

Hepatic PEComa is a rare mesenchymal tumor that exhibits an inert biological behavior, and its diagnosis, treatment, and follow-up are challenging. Our study of 26 cases of hepatic PEComa revealed that there was no difference in the prognosis between simple resection of liver tumor and extended resection of liver lobe. Optimal surgical resection currently is the best treatment option, and radiotherapy, chemotherapy, and immunotherapy may become more effective in future.

Research perspectives

The number of cases in the current retrospective study was limited by the rarity of hepatic PEComa. Therefore, further multicenter, larger-cohort studies are warranted to investigate the clinicopathological features and biological behavior of hepatic PEComa.

REFERENCES

1 **Bonetti F**, Pea M, Martignoni G, Zamboni G. PEC and sugar. *Am J Surg Pathol* 1992; **16**: 307-308 [PMID: 1599021 DOI: 10.1097/00000478-199203000-00013]

2 **Abhirup B**, Kaushal K, Sanket M, Ganesh N. Malignant hepatic perivascular epithelioid cell tumor (PEComa) - Case report and a brief review. *J Egypt Natl Canc Inst* 2015; **27**: 239-242 [PMID: 26071321 DOI: 10.1016/j.jnci.2015.05.004]

3 **Hornick JL**, Fletcher CD. PEComa: what do we know so far? *Histopathology* 2006; **48**: 75-82 [PMID: 16359539 DOI: 10.1111/j.1365-2559.2005.02316.x]

4 **Parfitt JR**, Bella AJ, Izawa JI, Wehrli BM. Malignant neoplasm of perivascular epithelioid cells of the liver. *Arch Pathol Lab Med* 2006; **130**: 1219-1222 [PMID: 16879028 DOI: 10.5858/2006-130-1219-MNOPEC]

5 **Fang SH**, Zhou LN, Jin M, Hu JB. Perivascular epithelioid cell tumor of the liver: a report of two cases and review of the literature. *World J Gastroenterol* 2007; **13**: 5537-5539 [PMID: 17907305 DOI: 10.3748/wjg.v13.i41.5537]

6 **Strzelczyk JM**, Durczynski A, Szymanski D, Jablkowski M, Dworniak D, Sporny S. Primary perivascular epithelioid cell tumor (PEComa) of the liver: report of a case. *Surg Today* 2009; **39**: 916-921 [PMID: 19784736 DOI: 10.1007/s00595-009-3945-5]

7 **Schoolmeester JK**, Dao LN, Sukov WR, Wang L, Park KJ, Murali R, Hameed MR, Soslow RA. TFE3 translocation-associated perivascular epithelioid cell neoplasm (PEComa) of the gynecologic tract: morphology, immunophenotype, differential diagnosis. *Am J Surg Pathol* 2015; **39**: 394-404 [PMID: 25517951 DOI: 10.1097/PAS.0000000000000349]

8 **Schoolmeester JK**, Howitt BE, Hirsch MS, Dal Cin P, Quade BJ, Nucci MR. Perivascular epithelioid cell neoplasm (PEComa) of the gynecologic tract: clinicopathologic and immunohistochemical characterization of 16 cases. *Am J Surg Pathol* 2014; **38**: 176-188 [PMID: 24418852 DOI: 10.1097/PAS.0000000000000133]

9 **Högemann D**, Flemming P, Kreipe H, Galanski M. Correlation of MRI and CT findings with histopathology in hepatic angiomyolipoma. *Eur Radiol* 2001; **11**: 1389-1395 [PMID: 11519547 DOI: 10.1007/s003300000750]

10 **Tan Y**, Xiao EH. Hepatic perivascular epithelioid cell tumor (PEComa): dynamic CT, MRI, ultrasonography, and pathologic features--analysis of 7 cases and review of the literature. *Abdom Imaging* 2012; **37**: 781-787 [PMID: 22278345 DOI: 10.1007/s00261-012-9850-1]

11 **Akitake R**, Kimura H, Sekoguchi S, Nakamura H, Seno H, Chiba T, Fujimoto S. Perivascular epithelioid cell tumor (PEComa) of the liver diagnosed by contrast-enhanced ultrasonography. *Intern Med* 2009; **48**: 2083-2086 [PMID: 20009396 DOI: 10.2169/internalmedicine.48.2133]

12 **Martignoni G**, Pea M, Reghellin D, Zamboni G, Bonetti F. PEComas: the past, the present and the future. *Virchows Arch* 2008; **452**: 119-132 [PMID: 18080139 DOI: 10.1007/s00428-007-0509-1]

13 **Bergamo F**, Maruzzo M, Basso U, Montesco MC, Zagonel V, Gringeri E, Cillo U. Neoadjuvant sirolimus for a large hepatic perivascular epithelioid cell tumor (PEComa). *World J Surg Oncol* 2014; **12**: 46 [PMID: 24575738 DOI: 10.1186/1477-7819-12-46]

14 **Argani P**, Aulmann S, Illei PB, Netto GJ, Ro J, Cho HY, Dogan S, Ladanyi M, Martignoni G, Goldblum JR, Weiss SW. A distinctive subset of PEComas harbors TFE3 gene fusions. *Am J Surg Pathol* 2010; **34**: 1395-1406 [PMID: 20871214 DOI: 10.1097/PAS.0b013e3181f17ac0]

15 **Tanaka M**, Kato K, Gomi K, Matsumoto M, Kudo H, Shinkai M, Ohama Y, Kigasawa H, Tanaka Y. Perivascular epithelioid cell tumor with SFPQ/PSF-TFE3 gene fusion in a patient with advanced neuroblastoma. *Am J Surg Pathol* 2009; **33**: 1416-1420 [PMID: 19606011 DOI: 10.1097/PAS.0b013e3181a9cd6c]

16 **Selvaggi F**, Risio D, Claudi R, Cianci R, Angelucci D, Pulcini D, D'Aulerio A, Legnini M, Cotellese R, Innocenti P. Malignant PEComa: a case report with emphasis on clinical and morphological criteria. *BMC Surg* 2011; **11**: 3 [PMID: 21272348 DOI: 10.1186/1471-2482-11-3]

17 **Folpe AL**, Mentzel T, Lehr HA, Fisher C, Balzer BL, Weiss SW. Perivascular epithelioid cell neoplasms of soft tissue and gynecologic origin: a clinicopathologic study of 26 cases and review of the literature. *Am J Surg Pathol* 2005; **29**: 1558-1575 [PMID: 16327428 DOI: 10.1097/01.pas.0000173232.22117.37]

18 **Tang D**, Wang J, Tian Y, Li Q, Yan H, Wang B, Xiong L. Hepatic perivascular epithelioid cell tumor: Case report and brief literature review. *Medicine (Baltimore)* 2016; **95**: e5572 [PMID: 28002331 DOI: 10.1097/MD.0000000000005572]

19 **Khaja F**, Carilli A, Baidas S, Sriharan A, Norford S. PEComa: A Perivascular Epithelioid Cell Tumor in the Liver-A Case Report and Review of the Literature. *Case Rep Med* 2013; **2013**: 904126 [PMID: 24489554 DOI: 10.1155/2013/904126]

20 **Bleeker JS**, Quevedo JF, Folpe AL. "Malignant" perivascular epithelioid cell neoplasm: risk stratification and treatment strategies. *Sarcoma* 2012; **2012**: 541626 [PMID: 22619565 DOI: 10.1155/2012/541626]

21 **Wagner AJ**, Malinowska-Kolodziej I, Morgan JA, Qin W, Fletcher CD, Vena N, Ligon AH, Antonescu CR, Ramaiya NH, Demetri GD, Kwiatkowski DJ, Maki RG. Clinical activity of mTOR inhibition with sirolimus in malignant perivascular epithelioid cell tumors: targeting the pathogenic activation of mTORC1 in tumors. *J Clin Oncol* 2010; **28**: 835-840 [PMID: 20048174 DOI: 10.1200/JCO.2009.25.2981]

22 **Italiano A**, Delcambre C, Hostein I, Cazeau AL, Marty M, Avril A, Coindre JM, Bui B. Treatment with the mTOR inhibitor temsirolimus in patients with malignant PEComa. *Ann Oncol* 2010; **21**: 1135-1137 [PMID: 20215136 DOI: 10.1093/annonc/mdq044]

World Journal of Gastroenterology

Submit a Manuscript: https://www.f6publishing.com

World J Gastroenterol 2021 September 21; 27(35): 5978-5988

DOI: 10.3748/wjg.v27.i35.5978

ISSN 1007-9327 (print) ISSN 2219-2840 (online)

ORIGINAL ARTICLE

Retrospective Study

Diagnosis of focal liver lesions with deep learning-based multi-channel analysis of hepatocyte-specific contrast-enhanced magnetic resonance imaging

Róbert Stollmayer, Bettina K Budai, Ambrus Tóth, Ildikó Kalina, Erika Hartmann, Péter Szoldán, Viktor Bérczi, Pál Maurovich-Horvat, Pál N Kaposi

ORCID number: Róbert Stollmayer 0000-0003-4673-7588; Bettina K Budai 0000-0002-3982-7887; Ambrus Tóth 0000-0002-1150-957X; Ildikó Kalina 0000-0002-2647-9123; Erika Hartmann 0000-0001-6073-9286; Péter Szoldán 0000-0002-3808-8541; Viktor Bérczi 0000-0003-4386-2527; Pál Maurovich-Horvat 0000-0003-0885-736X; Pál N Kaposi 0000-0002-7150-3495.

Author contributions: Stollmayer R designed and performed the research and wrote the paper; Budai BK and Tóth A contributed to data collection and analysis; Kalina I and Hartmann E provided clinical advice; Szoldán P contributed to the analysis; Bérczi V and Maurovich-Horvat P supervised the report; Kaposi PN designed the research, contributed to the analysis and supervised the report; all authors have read and approved the final manuscript.

Institutional review board statement: The present study has been approved by the institutional ethics committee of Semmelweis University (Semmelweis University Regional and Institutional Committee of Science and Research Ethics) according to

Róbert Stollmayer, Bettina K Budai, Ambrus Tóth, Ildikó Kalina, Viktor Bérczi, Pál Maurovich-Horvat, Pál N Kaposi, Department of Radiology, Medical Imaging Centre, Faculty of Medicine, Semmelweis University, Budapest 1083, Hungary

Erika Hartmann, Department of Transplantation and Surgery, Faculty of Medicine, Semmelweis University, Budapest 1082, Hungary

Péter Szoldán, MedInnoScan Research and Development Ltd., Budapest 1112, Hungary

Corresponding author: Bettina K Budai, MD, Department of Radiology, Medical Imaging Centre, Faculty of Medicine, Semmelweis University, Korányi Sándor st. 2., Budapest 1083, Hungary. budai.bettina@med.semmelweis-univ.hu

Abstract

BACKGROUND

The nature of input data is an essential factor when training neural networks. Research concerning magnetic resonance imaging (MRI)-based diagnosis of liver tumors using deep learning has been rapidly advancing. Still, evidence to support the utilization of multi-dimensional and multi-parametric image data is lacking. Due to higher information content, three-dimensional input should presumably result in higher classification precision. Also, the differentiation between focal liver lesions (FLLs) can only be plausible with simultaneous analysis of multi-sequence MRI images.

AIM

To compare diagnostic efficiency of two-dimensional (2D) and three-dimensional (3D)-densely connected convolutional neural networks (DenseNet) for FLLs on multi-sequence MRI.

METHODS

We retrospectively collected T2-weighted, gadoxetate disodium-enhanced arterial phase, portal venous phase, and hepatobiliary phase MRI scans from patients with focal nodular hyperplasia (FNH), hepatocellular carcinomas (HCC) or liver metastases (MET). Our search identified 71 FNH, 69 HCC and 76 MET. After volume registration, the same three most representative axial slices from all

sequences were combined into four-channel images to train the 2D-DenseNet264 network. Identical bounding boxes were selected on all scans and stacked into 4D volumes to train the 3D-DenseNet264 model. The test set consisted of 10-10-10 tumors. The performance of the models was compared using area under the receiver operating characteristic curve (AUROC), specificity, sensitivity, positive predictive values (PPV), negative predictive values (NPV), and f1 scores.

RESULTS

The average AUC value of the 2D model (0.98) was slightly higher than that of the 3D model (0.94). Mean PPV, sensitivity, NPV, specificity and f1 scores (0.94, 0.93, 0.97, 0.97, and 0.93) of the 2D model were also superior to metrics of the 3D model (0.84, 0.83, 0.92, 0.92, and 0.83). The classification metrics of FNH were 0.91, 1.00, 1.00, 0.95, and 0.95 using the 2D and 0.90, 0.90, 0.95, 0.95, and 0.90 using the 3D models. The 2D and 3D networks' performance in the diagnosis of HCC were 1.00, 0.80, 0.91, 1.00, and 0.89 and 0.88, 0.70, 0.86, 0.95, and 0.78, respectively; while the evaluation of MET lesions resulted in 0.91, 1.00, 1.00, 0.95, and 0.95 and 0.75, 0.90, 0.94, 0.85, and 0.82 using the 2D and 3D networks, respectively.

CONCLUSION

Both 2D and 3D-DenseNets can differentiate FNH, HCC and MET with good accuracy when trained on hepatocyte-specific contrast-enhanced multi-sequence MRI volumes.

Key Words: Artificial intelligence; Multi-parametric magnetic resonance imaging; Hepatocyte-specific contrast; Densely connected convolutional network; Hepatocellular carcinoma; Focal nodular hyperplasia

©The Author(s) 2021. Published by Baishideng Publishing Group Inc. All rights reserved.

Core Tip: Our study aimed to assess the performance of two-dimensional (2D) and three-dimensional (3D) densely connected convolutional neural networks (DenseNets) in the classification of focal liver lesions (FLLs) based on multi-parametric magnetic resonance imaging (MRI) with hepatocyte-specific contrast. We used multi-channel data input to train our networks and found that both 2D and 3D-DenseNets can differentiate between focal nodular hyperplasias, hepatocellular carcinomas or liver metastases with excellent accuracy. We conclude that DensNets can reliably classify FLLs based on multi-parametric and hepatocyte-specific post-contrast MRI. Meanwhile, multi-channel input is advantageous when the number of clinical cases available for model training is limited.

Citation: Stollmayer R, Budai BK, Tóth A, Kalina I, Hartmann E, Szoldán P, Bérczi V, Maurovich-Horvat P, Kaposi PN. Diagnosis of focal liver lesions with deep learning-based multi-channel analysis of hepatocyte-specific contrast-enhanced magnetic resonance imaging. *World J Gastroenterol* 2021; 27(35): 5978-5988
URL: https://www.wjgnet.com/1007-9327/full/v27/i35/5978.htm
DOI: https://dx.doi.org/10.3748/wjg.v27.i35.5978

INTRODUCTION

Artificial intelligence (AI)-based analysis is one of the fastest evolving fields in medical imaging, thanks to the rapid development of medical physics, electronic engineering, and computer science. The need for computer-aided diagnostics has been further amplified by the continuously increasing demand for imaging studies and the arrival of new modalities that put extra pressure on radiologists while also increasing the probability of diagnostic errors[1]. Meanwhile, deep learning (DL)-based algorithms have started to gain attention among medical researchers, since they provide excellent reproducibility and the ability to quantify aspects of imaging data unobservable to the human eye, resulting in automatically generated statistical reports and predictions, such as the potential of malignancy or metastatic spread and automated volume

the World Medical Association guidelines and Declaration of Helsinki, revised in 2000 in Edinburgh, No. SE-RKEB 136/2019.

Informed consent statement: As this is a retrospective study, in compliance with the Hungarian legal code, the need for written patient consent was waived by the ethics committee. Patients were not required to give informed consent to the study because the analysis used only anonymized clinical data that were obtained after each patient agreed to treatment and gave written informed consent to the MRI scan in compliance with our institutional protocol.

Conflict-of-interest statement: The authors have no financial relationships to disclose.

Data sharing statement: Additional anonymized data are available upon request from the corresponding author.

Open-Access: This article is an open-access article that was selected by an in-house editor and fully peer-reviewed by external reviewers. It is distributed in accordance with the Creative Commons Attribution-NonCommercial (CC BY-NC 4.0) license, which permits others to distribute, remix, adapt, build upon this work non-commercially, and license their derivative works on different terms, provided the original work is properly cited and the use is non-commercial. See: http://creativecommons.org/Licenses/by-nc/4.0/

Manuscript source: Invited manuscript

Specialty type: Gastroenterology and hepatology

Country/Territory of origin: Hungary

Peer-review report's scientific quality classification

Grade A (Excellent): 0
Grade B (Very good): B
Grade C (Good): 0
Grade D (Fair): 0

Grade E (Poor): 0

Received: April 30, 2021
Peer-review started: April 30, 2021
First decision: June 23, 2021
Revised: July 7, 2021
Accepted: August 25, 2021
Article in press: August 25, 2021
Published online: September 21, 2021

P-Reviewer: Bork U
S-Editor: Fan JR
L-Editor: A
P-Editor: Xing YX

assessment, among other uses. Nowadays, AI has become compatible with the full spectrum of imaging modalities and has evolved the capacity to diagnose lesions in various organ systems with greater accuracy than a human reader[2]. The processed data often include two-dimensional (2D) slices or three-dimensional (3D) image volumes; moreover, in the case of magnetic resonance imaging (MRI) studies, the different sequences are condensed into a multi-channel input. Due to their efficiency, convolutional neural networks (CNNs) have replaced other machine learning (ML) approaches in most image classification and segmentation tasks[3,4]. Recently, densely connected CNNs (DenseNets) have become more popular than plain CNN architectures. DenseNets use shortcut connections between the convolutional layers to facilitate gradient flow and optimize the number of trainable parameters. In return, these networks yield improved accuracy and efficiency in medical image classification tasks[5].

Focal liver lesions (FLLs) are common incidental findings during imaging studies, and the work-up often requires further diagnostic procedures, such as dynamic contrast-enhanced ultrasound, computed tomography and liver biopsy. Meanwhile, the excellent soft-tissue contrast, volumetric image acquisition and avoidance of ionizing radiation make multi-phase dynamic post-contrast MRI the primary tool for detection and characterization of liver lesions. The use of hepatocyte-specific contrast agents (HSAs), such as gadoxetic acid and gadobenate dimeglumine, further improves the sensitivity and specificity of the diagnosis of FLLs, as the enhancement characteristics of these lesions in the hepatobiliary phase (HBP) correlates with hepatocyte uptake[6,7]. Additionally, HSA-enhanced MRI is capable of detecting lesions smaller than 10 mm, making it an optimal modality for the early detection of liver metastases (METs)[8].

In the present study, we compared the performance of 2D and 3D-DenseNets in the classification of three types of FLLs, including focal nodular hyperplasia (FNH), hepatocellular carcinoma (HCC) and MET. To guarantee the highest possible prediction rate, we used HSA-enhanced multi-phase dynamic post-contrast MRI scans for the classification task. According to our knowledge, this is the first study to evaluate 2D and 3D-DenseNets for the diagnosis of FLLs and using multi-channel images combining four different MRI sequences. The reporting of this study follows the STROBE Statement checklist of items[9].

MATERIALS AND METHODS

Patient and MRI study selection

In our single-center study, we retrospectively collected multi-phasic MRI studies of patients with FNHs, HCCs or METs, that were acquired using Primovist (gadoxetate disodium), an HSA, from the picture archiving and communication system of the Medical Imaging Centre of our university. As this is a retrospective study, the need for written patient consent was waived by the Institutional Research Ethics Committee. The collected images were acquired between November 2017 and October 2020 using a Philips Ingenia 1.5 T scanner (Cambridge, MA, United States). T2-weighted (T2w) spectral-attenuated inversion recovery (commonly referred to as SPAIR), arterial phase (HAP), portal venous phase (PVP), and HBP scans were collected from each eligible patient for further analysis. Included lesions were either histologically confirmed or exhibited typical characteristics of the given lesion type with MRI. Patients younger than 18 years of age at the time of imaging were excluded from the study. Table 1 contains details of patient demographics, properties of each lesion class, and metastatic lesion origin.

Data preparation and dataset creation

MRI scans were exported as DICOM files, that were then anonymized to remove the patients' social security numbers, birth date, sex, age, body weight, and date of the imaging study. Anonymized PVP and HBP files were resampled and spatially aligned to the corresponding T2w volume using BSpline as a non-rigid registration method *via* an open-source visualization and medical image computing software, called 3D Slicer (www.slicer.org). 3D Slicer was also used for annotation cropping and file conversion [10,11]. Lesions were annotated by cubic regions of interest (referred to as ROIs). The lesions were then cropped from the aligned HAP, PVP, HBP, and T2w volumes using the same ROI. The cropped volumes were saved as NIfTI files, which were then combined into one four-dimensional (4D) file for each lesion (Figure 1). Cropped lesions were randomly sorted into datasets. After 10-10 lesions were added to the test

Table 1 Patient demographics, imaging properties of each lesion class, and details of metastatic lesion origin

Patent properties	FNH	HCC	MET	Total
Number of patients	42	13	14	69
Age in years at imaging, mean ± SD	45 ± 12	66 ± 5	57 ± 10	54 ± 14
Sex				
Male	11	8	8	27
Female	31	5	6	42
Lesion properties				
Number	71	69	76	216
Primary type				
CRC			21	
Leiomyosarcoma			18	
GI adenocc. or cholangiocc.			15	
Breast cc.			11	
Pancreas cc.			7	
Neuroendocrine ileum cc.			3	
Papillary thyroid cc.			1	

cc.: Carcinoma; CRC: Colorectal cancer; FNH: Focal nodular hyperplasia; GI: Gastrointestinal; HCC: Hepatocellular carcinoma; MET: Metastasis; SD: Standard deviation; T: Tesla.

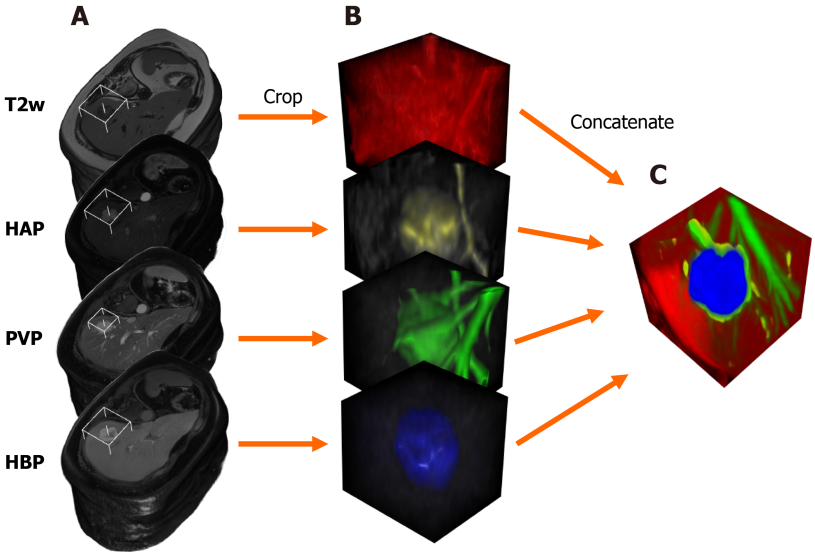


Figure 1 Steps of input data preparation for the three-dimensional densely connected convolutional neural network. A: Three-dimensionally rendered whole volumes at the level of the lesion (indicated by the white frame); B: Cropped cubic volumes containing the lesion; C: The four cubic volumes are concatenated into one four-dimensional file; each volume is represented by a different color. T2w: T2-weighted; HAP: Hepatic arterial phase; PVP: Portal venous phase; HBP: Hepatobiliary phase.

and validation dataset from each class, the remaining tumors were added to the training dataset. NIfTI files were sliced up into axial PNG images. The resulting T2w, HAP, PVP, and HBP PNG files were concatenated (Figure 2) using a custom-written computer program in Python. The training and validation datasets contained three axial slices of each lesion (*i.e.* three most representative axial slices of the NIfTI files), while the test set consisted of only one slice from each lesion.

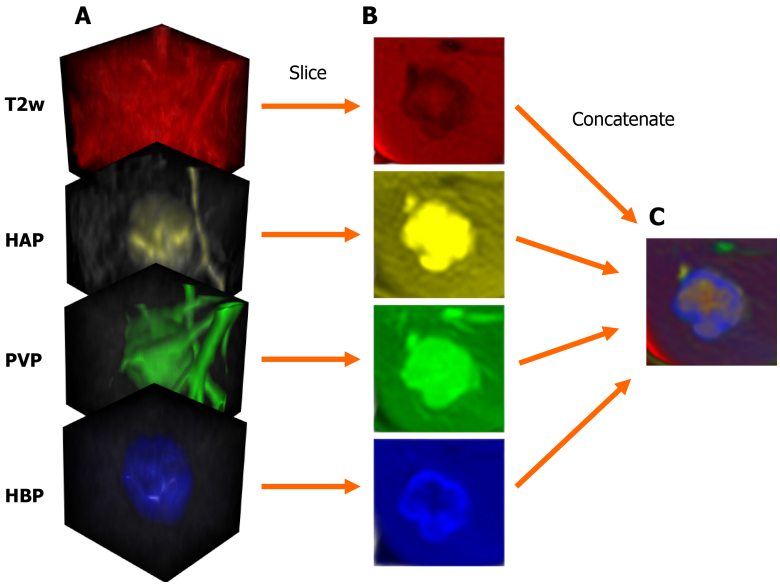


Figure 2 Steps of input data preparation for the two-dimensional densely connected convolutional neural network. A: Cubic magnetic resonance image volumes containing the lesion; B: Axial slices acquired from the cropped volumes; C: The four axial slices are concatenated into one three-dimensional image; each slice is represented by a different color. T2w: T2-weighted; HAP: Hepatic arterial phase; PVP: Portal venous phase; HBP: Hepatobiliary phase.

Data processing, training, and testing

Parameters of concatenated files were modified *via* transform functions. Image pixel intensity was scaled between -1.0 minimum and 1.0 maximum values. Data augmentation transforms were applied to the training samples, including random rotation (70° range along two axes) and zoom (0.7–1.4 scaling) to enrich training data. PNGs were resized to 64 × 64 resolution. Transformed images were converted to tensors (2D images were converted into 3D tensors, with the additional dimension equaling the number of network input channels), which were then fed to DenseNet264 that used 2D convolutional layers[5].

In the case of the 3D-DenseNet264 network, NIfTI voxels were resampled to isovolumetric shape, voxel intensities were rescaled between -1.0 minimum and 1.0 maximum value and NIfTI files were resized to 64 × 64 × 64 spatial resolution. The four NIfTI files were concatenated (T2w, HAP, PVP, HBP) to be used as multi-channel input for the 3D CNN. We used random 90° rotation (along two spatial axes), random 60° rotation (along x and y axes), random zoom (between 0.8 and 1.35), and random flipping on the training samples. MR volumes were converted to 4D tensors (number of channels, x-, y- and z-dimensions) that were used as network input. We used DenseNet264 models through the Pytorch-based open-source Medical Open Network For Artificial Intelligence (*i.e.* MONAI) framework[12]. We used categorical cross-entropy loss to measure the prediction error of the network during training and an Adam optimizer to update model parameters[13]. Networks were trained for 70 epochs. Using a Tesla T4 graphical processing unit, the 2D network was trained for 18 min, while the 3D CNN was trained for 41 min. Validation set area under the receiver operating characteristic curve (AUROC) values were calculated after each epoch, and the model with the highest average AUC value was saved as the final model.

The trained models were used to make predictions on an independent test dataset consisting of 10 lesions from each class. The tumor type with the highest probability, according to the last softmax layer of the convolutional networks, was chosen as the predicted lesion type *via* an argmax function, encoding the predicted diagnosis as 1, while the predicted incorrect classes as 0. Specificity, sensitivity, f1 score, positive predictive value (PPV), negative predictive value (NPV) were calculated for each class based on these outputs.

Classification performance was also measured using AUC values of each class, calculated from the softmax layer probability outputs. DeLong's test was used to determine the statistical significance between the test performance of the 2D and 3D classifiers[14].

RESULTS

The 2D model achieved the highest average validation set AUC after the 46th epoch, while the best average AUC value of the 3D network was reached after the 62nd epoch. These models were saved and then used to make test set predictions (Figure 3).

The finalized 2D and 3D networks were evaluated on the same independent test set, consisting of 10 lesions from each tumor type. On the independent test set, the finalized 2D model achieved 0.9900 [95% confidence interval (CI): 0.9664–1.0000], 0.9600 (95%CI: 0.8786–1.0000) and 0.9950 (95%CI: 0.9811–1.0000) AUC values for FNH, HCC and MET respectively, with an average AUC of 0.9783 (95%CI: 0.9492–1.0000). The finalized 3D model achieved 0.9700 (95%CI: 0.9077–1.0000), 0.9050 (95%CI: 0.7889–1.0000) and 0.9550 (95%CI: 0.8890–1.0000) AUC values for FNH, HCC and MET diagnosis, and an average AUC value of 0.9433 (95%CI: 0.8942–0.9924) on the test dataset (Figure 4). No statistically significant difference was found between the diagnostic performance of the 2D and 3D classifiers based on the ROC curve comparison for the three classes (Z = 0.7007, P = 0.4835 for FNH; Z = 0.7812, P = 0.4347 for HCC; Z = 1.3069, P = 0.1913 for MET). The 2D input data achieved excellent results in the distinction between all three lesion classes, similar to the 3D network (Table 2). Both networks achieved excellent PPV, sensitivity, f1 score, NPV, and specificity values for all three classes. The highest diagnostic accuracy was achieved by both networks for FNH and MET, while both networks demonstrated lower AUC values for HCC (Table 2). PPV, sensitivity, f1 score, specificity and an NPV of 0.9091, 1.0000, 0.9524, 0.9500, 1.000 values were achieved by the 2D model for FNH diagnosis. The 3D network performed FNH classification with similar PPV (0.9000), sensitivity (0.9000), f1 score (0.9000), specificity (0.9500) and NPV (0.9500) values as the 2D network. During HCC classification both the 2D and 3D models reached acceptable metrics with PPVs of 1.000 and 0.8750, sensitivities of 0.8000 and 0.7000, f1 scores of 0.8889 and 0.7778, specificities of 1.000 and 0.9500, lastly NPVs of 0.9091 and 0.8636. For the differentiation of METs from FNHs and HCCs the use of the 2D DenseNet resulted in a PPV of 0.9091, sensitivity of 1.000, f1 score of 0.9524, specificity of 0.9500 and NPV of 1.000, while the 3D DenseNet achieved values of 0.7500, 0.9000, 0.8182, 0.8500 and 0.9444 for PPV, sensitivity, f1 score, specificity and NPV respectively. On average, both the 2D and 3D trained models could distinguish FNHs, HCCs and METs reliably with PPVs of 0.9394 and 0.8417, sensitivities of 0.9333 and 0.8333, f1 scores of 0.9312 and 0.8320, specificities of 0.9667 and 0.9167, NPVs of 0.9697 and 0.9194.

In addition, these results are supported by the extraction of attention maps from the trained models using test set images. We implemented an open-source software (M3d-CAM) to visualize the most important regions for diagnosis-making[15]. The extracted attention maps may correlate with the certainty with which a model classifies FLLs. By marking the areas within images, based on which the model makes a decision, attention maps form optimal bases of training dataset tailoring for certain radiological or other medical computer vision tasks by focusing on image regions that are difficult to analyze for the trained neural network (Figure 5).

DISCUSSION

FLLs are common findings during liver imaging, and the differentiation of benign and malignant types of FLLs is a significant diagnostic challenge, as imaging signs may overlap between different pathologies which can substantially alter the therapeutic decision. Therefore, precise and reproducible differential diagnosis of FLLs is critical for optimal patient management.

Today, the most accurate imaging modality to diagnose FLLs is multi-phase dynamic contrast-enhanced MRI. Extracellular contrast agents (ECAs) are commonly used to perform multi-phase dynamic post-contrast MRI studies to differentiate between lesions based on their distinct contrast enhancement patterns, such as HAP hyper-enhancement or washout in the PVP[16]. In comparison to ECAs, HSAs are taken up by hepatocytes and (in part) excreted through the biliary tract; thus, they can better differentiate between those lesions that consist of functionally active and impaired hepatocytes or those that are extrahepatic in origin[7]. This behavior of HSAs is utilized for making a distinction between FNH and hepatocellular adenoma, or to detect small foci of HCC and MET within the surrounding liver parenchyma[17,18].

In the current study, we evaluated different AI models on liver MRI images for the prediction of 216 FLLs compiled from three different types of lesions, namely FNHs, HCCs and METs. To ensure that the models could achieve the highest possible

Table 2 Evaluation metrics of the two-dimensional and three-dimensional densely connected convolutional neural networks

Input data	PPV	Sensitivity	F1 score	Specificity	NPV
FNH 2D	0.9091	1.0000	0.9524	0.9500	1.0000
3D	0.9000	0.9000	0.9000	0.9500	0.9500
HCC 2D	1.0000	0.8000	0.8889	1.0000	0.9091
3D	0.8750	0.7000	0.7778	0.9500	0.8636
MET 2D	0.9091	1.0000	0.9524	0.9500	1.0000
3D	0.7500	0.9000	0.8182	0.8500	0.9444
Mean 2D	0.9394	0.9333	0.9312	0.9667	0.9697
3D	0.8417	0.8333	0.8320	0.9167	0.9194

2D: Two-dimensional; 3D: Three-dimensional; FNH: Focal nodular hyperplasia; HCC: Hepatocellular carcinoma; MET: Metastasis; NPV: Negative predictive value; PPV: Positive predictive value.

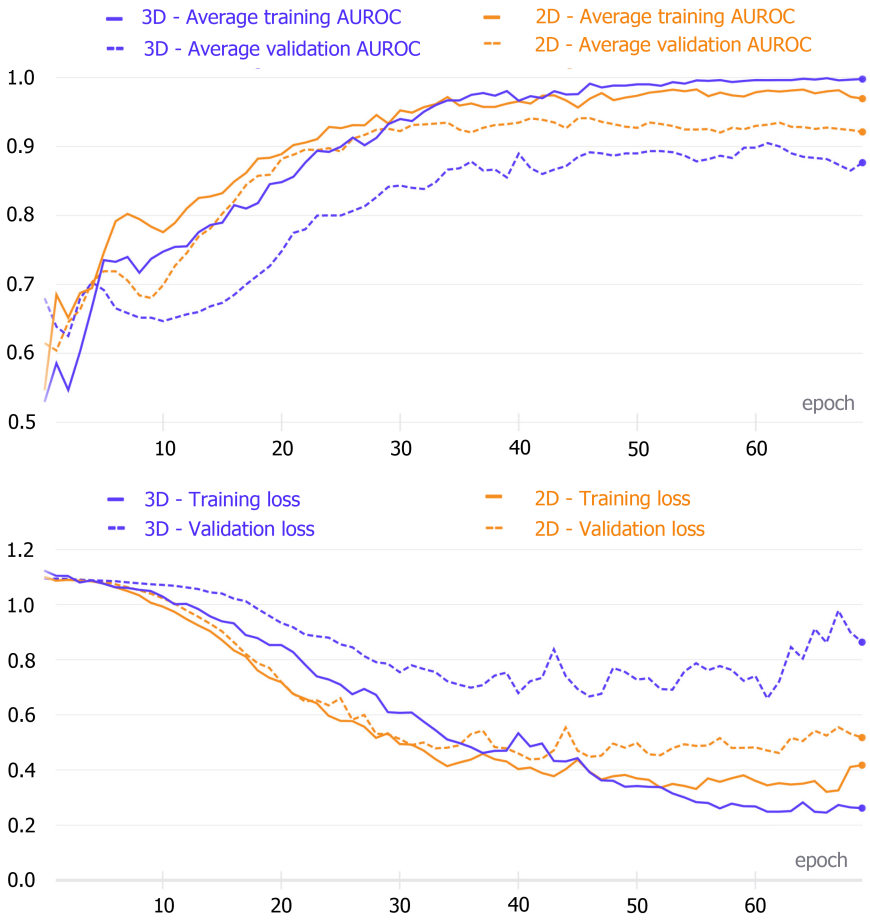


Figure 3 Comparison of the training evaluation metric curves and loss curves. The upper figure shows the area under the receiver operating characteristic curve (AUROC) values after each training epoch of the two-dimensional (2D) and three-dimensional (3D) densely connected convolutional neural networks (DenseNets). The best average AUC was obtained after the 46th (2D network) and 62nd (3D network) epochs. The lower figure indicates the loss values for each training epoch of the two networks. 2D: Two-dimensional; 3D: Three-dimensional; AUROC: Area under the receiver operating characteristic curve.

prediction rate, we narrowed down our data collection to only those four MRI sequences that provided the highest tissue contrast compared to the neighboring parenchyma or depicted distinctive imaging features of the lesion types. For the same reason, we used only HSA-enhanced scans for the analysis. We collected post-contrast images from HAP, PVP and HBP, and a T2w SPAIR image in the case of each lesion. A similar image analysis strategy was used by Hamm *et al*[19], who predicted 494 FLLs from six categories, including simple cyst, cavernous hemangioma, FNH, HCC,

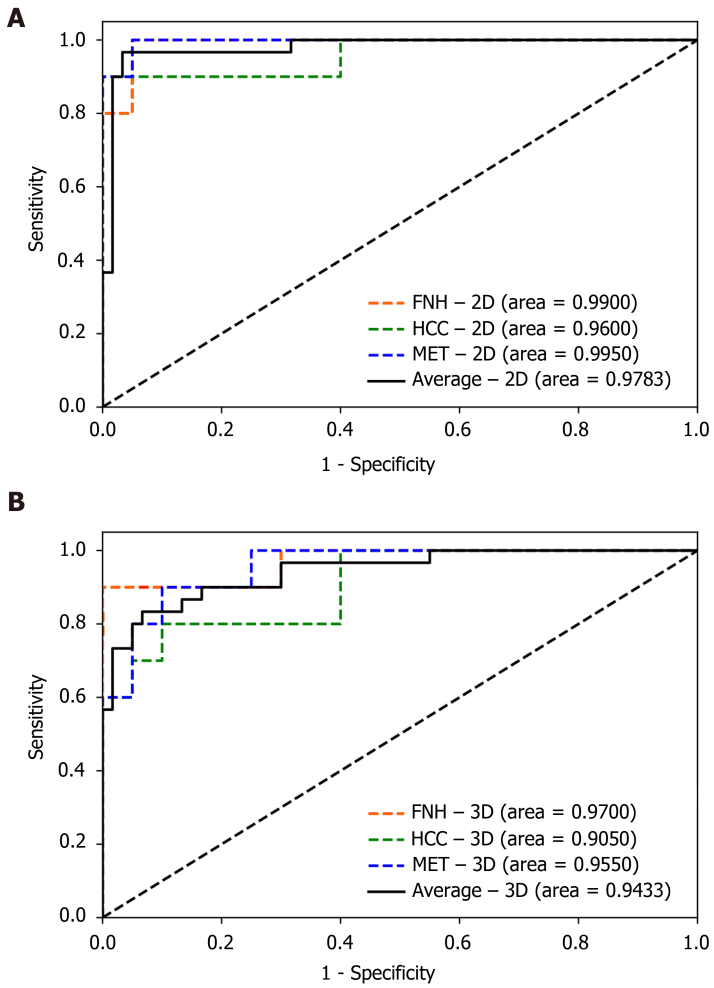


Figure 4 Receiver operating characteristic curves of the two-dimensional and three-dimensional densely connected convolutional neural network 264 models' performance on the test set. A: Two-dimensional; B: Three-dimensional. 2D: Two-dimensional; 3D: Three-dimensional; FNH: Focal nodular hyperplasia; HCC: Hepatocellular carcinoma; MET: Metastasis.

intrahepatic cholangiocarcinoma, and colorectal cancer METs using a 3D CNN model. The authors used HAP, PVP and delayed venous phase MRI images for the classification of the FLLs. They reported that the CNN model demonstrated 0.92 accuracy, 0.92 sensitivity and 0.98 specificity. The disadvantage of this study compared to ours was that it did not include HBP images, with only ECA images used for the MRI scans.

There are a handful of studies that included conventional ML methods and achieved reasonably good results. Wu *et al*[20], for example, extracted radiomics features from non-enhanced multi-parametric MRI images of FLLs and used them in ML models to differentiate between hepatic haemangioma and HCC. The final classifier achieved an AUC of 0.89, a sensitivity of 0.822 and a specificity of 0.714. Jansen *et al*[21], in their 2019 paper, used traditional ML methods for the same problem achieving an average accuracy of 0.77 for five major FLL types.

Our models' performance in the test set was comparable to or even surpassed those from previous publications, as the AUC, sensitivity and specificity were excellent for both the 2D (0.9783, 0.9333 and 0.9667 respectively) and 3D (0.9433, 0.8333 and 0.9167 respectively) architectures, which demonstrates the robustness of our data collection and analysis.

The quality and quantity of input data are pivotal when training neural networks. MRI liver tumor analysis using DL methods has steeply increased, but there is evidence lacking to support the use of 2D or 3D data. The additional dimension in 3D network inputs makes them computationally more demanding and the different data augmentation methods and hyperparameters must be well chosen to avoid artifacts. The 2D neural networks have the advantage of pretraining, which may improve classification accuracy[16,22,23]. Our study supports the results of Wang *et al*[24] and Hamm *et al*[19], emphasizing the need for multi-channel input volumes in order to achieve better accuracy. In contrast to these approaches, we have also utilized HBP

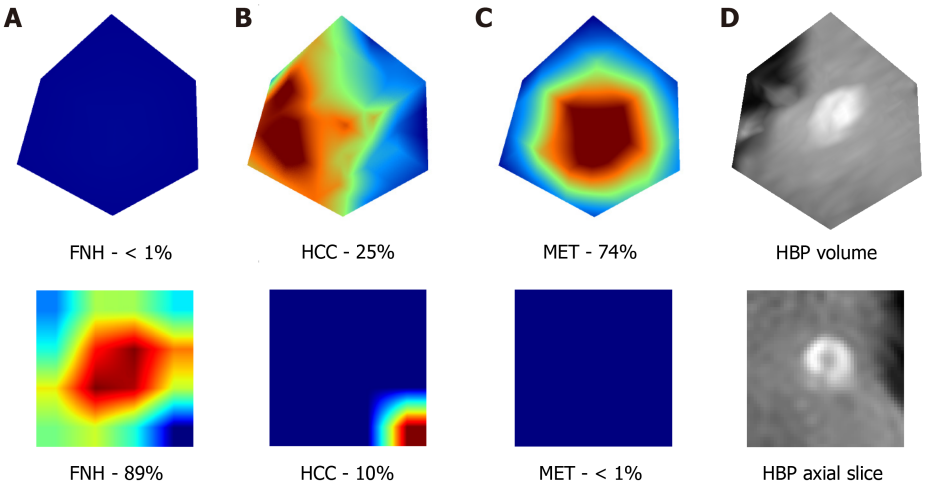


Figure 5 Visualization of the attention maps extracted from the two-dimensional and three-dimensional densely connected convolutional neural networks compared to the hepatobiliary phase input images. Two-dimensional (lower row) and three-dimensional (upper row) attention maps (column A-C) and hepatobiliary phase (column D) images were extracted from the 3rd dense block of the trained network. A-C: Two-dimensional (lower row) and three-dimensional (upper row) attention maps; D: Hepatobiliary phase images. Column A contains the attention maps for focal nodular hyperplasia (FNH), column B for hepatocellular carcinoma, and column C for metastasis diagnosis. The correct diagnosis is FNH in this case. Probabilities for different lesion classes are annotated below each attention map. The red areas are more important for the classification than other image regions. FNH: Focal nodular hyperplasia; HCC: Hepatocellular carcinoma; MET: Metastasis; HBP: Hepatobiliary phase.

images, thereby increasing the number of input channels to four in order to improve accuracy and additionally trained 2D CNNs, proving them to be just as effective classifiers as 3D models.

The selected architecture of the DL model can substantially alter classification accuracy. It is a novelty of our analysis that compared to previous examinations we utilized a DenseNet architecture. DenseNets contain multiple dense blocks, where each layer is connected with the residuals from previous layers. DenseNets require fewer trainable parameters at the same depth than conventional CNNs, as newly learned features are shared through all layers[5]. Our results are among the first to indicate that this highly efficient network design can enhance the performance of AI models for the classification of multi-parametric MRI images of FLLs.

Our study's limitations are the low number of patients involved, the retrospective nature of the study, and that it was conducted within a single institute. Further improvement may be achieved by additional data collection (including additional lesion classes) and the use of more MRI volumes and different data augmentation methods as well as the use of pre-trained networks.

CONCLUSION

Based on our study, we can say that routinely acquired radiological image materials can be used for analysis with AI methods, such as CNNs. According to our results, densely connected CNNs trained on multi-sequence MRI scans can be promising new alternatives to single-phase approaches; furthermore, the use of multi-dimensional input volumes can help the AI-based diagnosis of FLLs. According to our results, 3D and 2D DenseNets can reach similar performance in the differentiation of FLLs based on a small dataset of MRI images. The use of gadoxetate disodium-enhanced MRI scans can also enhance the diagnostic performance of MRI-based hepatic lesion classification.

ARTICLE HIGHLIGHTS

Research background

Interest in medical applications of artificial intelligence (AI) has steeply risen in the last few years. As one of the most obvious beneficiaries of the advances in computer vision, radiology research has also put AI in a prominent position. Convolutional

neural networks are the state-of-the-art methods used in computer vision. Focal liver lesions (FLLs) are common findings during imaging, which can best be evaluated *via* hepatocyte-specific contrast-enhanced magnetic resonance imaging (MRI).

Research motivation

Though convolutional neural networks are widely used for medical image research purposes, the effect of input, such as data dimensionality and the effect of multiple input channels, has not yet been widely examined in this area. MRI volumes presumably hold more complex information about each lesion; as such, three-dimensional inputs may be more difficult to process and properly use for classification tasks in comparison to two-dimensional axial slices. The combination of multiple MRI sequences in addition to the use of hepatocyte-specific contrast agents (HSAs) may also affect diagnostic accuracy.

Research objectives

Our research aimed to compare two- and three-dimensional DenseNets264 networks for the multi-phasic hepatocyte-specific contrast-enhanced MRI-based classification of FLLs.

Research methods

T2-weighted, arterial phase, portal venous phase, and hepatobiliary phase volumes of focal nodular hyperplasias, hepatocellular carcinomas and liver metastases were used to train the two models. Diagnostic performance was evaluated on an independent test set, based on area under the curve, positive and negative predictive values (NPVs), sensitivity, specificity and f1 score.

Research results

The study found that *via* the use of either two- or three-dimensional convolutional neural networks and the combination of multiple MRI sequences, the average area under the curve, sensitivity, specificity, NPV, positive predictive value and f1 scores of comparable level can be achieved.

Research conclusions

According to our findings, two- and three-dimensional networks can both be used for highly accurate differentiation of multiple classes of FLLs by combining multiple MRI phases and using HSAs.

Research perspectives

This study's findings can help to clarify the potential applicability of two- and three-dimensional multi-channel MRI images for the convolutional neural network-based classification of FLLs using HSAs.

ACKNOWLEDGEMENTS

The authors would like to express their gratitude to Dr. Endre Szabó, mathematician from the Alfréd Rényi Institute of Mathematics of The Hungarian Academy of Sciences, for expert review of the manuscript and discussion of the AI analysis and statistical methods. The authors also thank Tamás Wentzel and Lilla Petovsky, technicians of the MRI unit of the Medical Imaging Center, Semmelweis University, for their enthusiasm for the current research and professionalism during patient examinations.

REFERENCES

1 **Bhargavan M**, Kaye AH, Forman HP, Sunshine JH. Workload of radiologists in United States in 2006-2007 and trends since 1991-1992. *Radiology* 2009; **252**: 458-467 [PMID: 19508987 DOI: 10.1148/radiol.2522081895]

2 **Bi WL**, Hosny A, Schabath MB, Giger ML, Birkbak NJ, Mehrtash A, Allison T, Arnaout O, Abbosh C, Dunn IF, Mak RH, Tamimi RM, Tempany CM, Swanton C, Hoffmann U, Schwartz LH, Gillies RJ, Huang RY, Aerts HJWL. Artificial intelligence in cancer imaging: Clinical challenges and applications. *CA Cancer J Clin* 2019; **69**: 127-157 [PMID: 30720861 DOI: 10.3322/caac.21552]

3 **Kim J**, Min JH, Kim SK, Shin SY, Lee MW. Detection of Hepatocellular Carcinoma in Contrast-

Enhanced Magnetic Resonance Imaging Using Deep Learning Classifier: A Multi-Center Retrospective Study. *Sci Rep* 2020; **10**: 9458 [PMID: 32527998 DOI: 10.1038/s41598-020-65875-4]

4 **Singh SP**, Wang L, Gupta S, Goli H, Padmanabhan P, Gulyás B. 3D Deep Learning on Medical Images: A Review. *Sensors (Basel)* 2020; **20** [PMID: 32906819 DOI: 10.3390/s20185097]

5 **Huang G**, Liu Z, Pleiss G, Van Der Maaten L, Weinberger K. Convolutional Networks with Dense Connectivity. *IEEE Trans Pattern Anal Mach Intell* 2019 [PMID: 31135351 DOI: 10.1109/TPAMI.2019.2918284]

6 **Kim YY**, Park MS, Aljoqiman KS, Choi JY, Kim MJ. Gadoxetic acid-enhanced magnetic resonance imaging: Hepatocellular carcinoma and mimickers. *Clin Mol Hepatol* 2019; **25**: 223-233 [PMID: 30661336 DOI: 10.3350/cmh.2018.0107]

7 **Thian YL**, Riddell AM, Koh DM. Liver-specific agents for contrast-enhanced MRI: role in oncological imaging. *Cancer Imaging* 2013; **13**: 567-579 [PMID: 24434892 DOI: 10.1102/1470-7330.2013.0050]

8 **Coenegrachts K**. Magnetic resonance imaging of the liver: New imaging strategies for evaluating focal liver lesions. *World J Radiol* 2009; **1**: 72-85 [PMID: 21160723 DOI: 10.4329/wjr.v1.i1.72]

9 **von Elm E**, Altman DG, Egger M, Pocock SJ, Gøtzsche PC, Vandenbroucke JP; STROBE Initiative. The Strengthening the Reporting of Observational Studies in Epidemiology (STROBE) statement: guidelines for reporting observational studies. *J Clin Epidemiol* 2008; **61**: 344-349 [PMID: 18313558 DOI: 10.1016/j.jclinepi.2007.11.008]

10 **Fedorov A**, Beichel R, Kalpathy-Cramer J, Finet J, Fillion-Robin JC, Pujol S, Bauer C, Jennings D, Fennessy F, Sonka M, Buatti J, Aylward S, Miller JV, Pieper S, Kikinis R. 3D Slicer as an image computing platform for the Quantitative Imaging Network. *Magn Reson Imaging* 2012; **30**: 1323-1341 [PMID: 22770690 DOI: 10.1016/j.mri.2012.05.001]

11 **Klein S**, Staring M, Pluim JP. Evaluation of optimization methods for nonrigid medical image registration using mutual information and B-splines. *IEEE Trans Image Process* 2007; **16**: 2879-2890 [PMID: 18092588 DOI: 10.1109/tip.2007.909412]

12 **Zenodo**. The MONAI Consortium. Project MONAI. [cited 10 March 2021]. Available from: https://www.f6publishing.com/Forms/Manuscript/Editorial/ReviewAndEditProcess.aspx?id=WJG-27-5978

13 **Kingma DP**, Ba J. Adam: A method for stochastic optimization. 2014 Preprint. Available from: arXiv:1412.6980v9

14 **DeLong ER**, DeLong DM, Clarke-Pearson DL. Comparing the areas under two or more correlated receiver operating characteristic curves: a nonparametric approach. *Biometrics* 1988; **44**: 837-845 [PMID: 3203132]

15 **Gotkowski K**, Gonzalez C, Bucher A, Mukhopadhyay A. M3d-CAM: A PyTorch library to generate 3D data attention maps for medical deep learning. 2020 Preprint. Available from: arXiv:2007.00453v1

16 **Matos AP**, Velloni F, Ramalho M, AlObaidy M, Rajapaksha A, Semelka RC. Focal liver lesions: Practical magnetic resonance imaging approach. *World J Hepatol* 2015; **7**: 1987-2008 [PMID: 26261689 DOI: 10.4254/wjh.v7.i16.1987]

17 **Granata V**, Fusco R, de Lutio di Castelguidone E, Avallone A, Palaia R, Delrio P, Tatangelo F, Botti G, Grassi R, Izzo F, Petrillo A. Diagnostic performance of gadoxetic acid-enhanced liver MRI *vs* multidetector CT in the assessment of colorectal liver metastases compared to hepatic resection. *BMC Gastroenterol* 2019; **19**: 129 [PMID: 31340755 DOI: 10.1186/s12876-019-1036-7]

18 **Grieser C**, Steffen IG, Kramme IB, Bläker H, Kilic E, Perez Fernandez CM, Seehofer D, Schott E, Hamm B, Denecke T. Gadoxetic acid enhanced MRI for differentiation of FNH and HCA: a single centre experience. *Eur Radiol* 2014; **24**: 1339-1348 [PMID: 24658870 DOI: 10.1007/s00330-014-3144-7]

19 **Hamm CA**, Wang CJ, Savic LJ, Ferrante M, Schobert I, Schlachter T, Lin M, Duncan JS, Weinreb JC, Chapiro J, Letzen B. Deep learning for liver tumor diagnosis part I: development of a convolutional neural network classifier for multi-phasic MRI. *Eur Radiol* 2019; **29**: 3338-3347 [PMID: 31016442 DOI: 10.1007/s00330-019-06205-9]

20 **Wu J**, Liu A, Cui J, Chen A, Song Q, Xie L. Radiomics-based classification of hepatocellular carcinoma and hepatic haemangioma on precontrast magnetic resonance images. *BMC Med Imaging* 2019; **19**: 23 [PMID: 30866850 DOI: 10.1186/s12880-019-0321-9]

21 **Jansen MJA**, Kuijf HJ, Veldhuis WB, Wessels FJ, Viergever MA, Pluim JPW. Automatic classification of focal liver lesions based on MRI and risk factors. *PLoS One* 2019; **14**: e0217053 [PMID: 31095624 DOI: 10.1371/journal.pone.0217053]

22 **Liu Z**, Tang H, Lin Y, Han SJapa. Point-voxel cnn for efficient 3d deep learning. 2020 Preprint. Available from: arXiv:1907.03739v2

23 **Morid MA**, Borjali A, Del Fiol G. A scoping review of transfer learning research on medical image analysis using ImageNet. *Comput Biol Med* 2021; **128**: 104115 [PMID: 33227578 DOI: 10.1016/j.compbiomed.2020.104115]

24 **Wang C**, Hamm C, Letzen B, Duncan J. A probabilistic approach for interpretable deep learning in liver cancer diagnosis. SPIE Medical Imaging. United States, California, San Diego: SPIE, 2019

Published by **Baishideng Publishing Group Inc**
7041 Koll Center Parkway, Suite 160, Pleasanton, CA 94566, USA
Telephone: +1-925-3991568
E-mail: bpgoffice@wjgnet.com
Help Desk: https://www.f6publishing.com/helpdesk
https://www.wjgnet.com

© 2021 Baishideng Publishing Group Inc. All rights reserved.

ISSN 1007-9327 (print)
ISSN 2219-2840 (online)

World Journal of *Gastroenterology*

World J Gastroenterol 2021 September 28; 27(36): 5989-6160



Published by Baishideng Publishing Group Inc

World Journal of Gastroenterology

Contents

Weekly Volume 27 Number 36 September 28, 2021

FRONTIER

5989 Fluorescent cholangiography: An up-to-date overview twelve years after the first clinical application

Pesce A, Piccolo G, Lecchi F, Fabbri N, Diana M, Feo CV

REVIEW

6004 Histone methylation in pancreatic cancer and its clinical implications

Liu XY, Guo CH, Xi ZY, Xu XQ, Zhao QY, Li LS, Wang Y

6025 Hepatitis B virus infection and hepatocellular carcinoma in sub-Saharan Africa: Implications for elimination of viral hepatitis by 2030?

Amponsah-Dacosta E

MINIREVIEWS

6039 Liver disease in the era of COVID-19: Is the worst yet to come?

Mikolasevic I, Bozic D, Pavić T, Ruzic A, Hauser G, Radic M, Radic-Kristo D, Razov-Radas M, Puljiz Z, Milic S

6053 Treatment of hepatitis B virus infection in children and adolescents

Stinco M, Rubino C, Trapani S, Indolfi G

ORIGINAL ARTICLE

Basic Study

6064 CircRNA_0084927 promotes colorectal cancer progression by regulating miRNA-20b-3p/glutathione S-transferase mu 5 axis

Liu F, Xiao XL, Liu YJ, Xu RH, Zhou WJ, Xu HC, Zhao AG, Xu YX, Dang YQ, Ji G

6079 Exosomal microRNA-588 from M2 polarized macrophages contributes to cisplatin resistance of gastric cancer cells

Cui HY, Rong JS, Chen J, Guo J, Zhu JQ, Ruan M, Zuo RR, Zhang SS, Qi JM, Zhang BH

Case Control Study

6093 Evaluation of biomarkers, genetic mutations, and epigenetic modifications in early diagnosis of pancreatic cancer

Rah B, Banday MA, Bhat GR, Shah OJ, Jeelani H, Kawoosa F, Yousuf T, Afroze D

Retrospective Study

6110 Impact of radiogenomics in esophageal cancer on clinical outcomes: A pilot study

Brancato V, Garbino N, Mannelli L, Aiello M, Salvatore M, Franzese M, Cavaliere C

6128 Clinicopathological characteristics and longterm survival of patients with synchronous multiple primary gastrointestinal stromal tumors: A propensity score matching analysis

Wu H, Li C, Li H, Shang L, Jing HY, Liu J, Fang Z, Du FY, Liu Y, Fu MD, Jiang KW, Li LP

Observational Study

6142 Urotensin II levels in patients with inflammatory bowel disease

Alicic D, Martinovic D, Rusic D, Zivkovic PM, Tadin Hadjina I, Vilovic M, Kumric M, Tokic D, Supe-Domic D, Lupi-Ferandin S, Bozic J

CASE REPORT

6154 Inverted Meckel's diverticulum diagnosed using capsule endoscopy: A case report

El Hajra Martínez I, Calvo M, Martínez-Porras JL, Gomez-Pimpollo Garcia L, Rodriguez JL, Leon C, Calleja Panero JL

ABOUT COVER

Editorial Board Member of *World Journal of Gastroenterology*, Mark D Gorrell, BSc, PhD, Professor of Liver Science, Head, Liver Enzymes in Metabolism and Inflammation Program, Centenary Institute, Faculty of Medicine and Health, The University of Sydney, New South Wales 2006, Australia. m.gorrell@centenary.org.au

AIMS AND SCOPE

The primary aim of *World Journal of Gastroenterology* (*WJG*, *World J Gastroenterol*) is to provide scholars and readers from various fields of gastroenterology and hepatology with a platform to publish high-quality basic and clinical research articles and communicate their research findings online. *WJG* mainly publishes articles reporting research results and findings obtained in the field of gastroenterology and hepatology and covering a wide range of topics including gastroenterology, hepatology, gastrointestinal endoscopy, gastrointestinal surgery, gastrointestinal oncology, and pediatric gastroenterology.

INDEXING/ABSTRACTING

The *WJG* is now indexed in Current Contents®/Clinical Medicine, Science Citation Index Expanded (also known as SciSearch®), Journal Citation Reports®, Index Medicus, MEDLINE, PubMed, PubMed Central, and Scopus. The 2021 edition of Journal Citation Report® cites the 2020 impact factor (IF) for *WJG* as 5.742; Journal Citation Indicator: 0.79; IF without journal self cites: 5.590; 5-year IF: 5.044; Ranking: 28 among 92 journals in gastroenterology and hepatology; and Quartile category: Q2. The *WJG*'s CiteScore for 2020 is 6.9 and Scopus CiteScore rank 2020: Gastroenterology is 19/136.

RESPONSIBLE EDITORS FOR THIS ISSUE

Production Editor: *Jia-Hui Li*; **Production Department Director:** *Yu-Jie Ma*; **Editorial Office Director:** *Ze-Mao Gong*.

NAME OF JOURNAL
World Journal of Gastroenterology

ISSN
ISSN 1007-9327 (print) ISSN 2219-2840 (online)

LAUNCH DATE
October 1, 1995

FREQUENCY
Weekly

EDITORS-IN-CHIEF
Andrzej S Tarnawski, Subrata Ghosh

EDITORIAL BOARD MEMBERS
http://www.wjgnet.com/1007-9327/editorialboard.htm

PUBLICATION DATE
September 28, 2021

COPYRIGHT
© 2021 Baishideng Publishing Group Inc

INSTRUCTIONS TO AUTHORS
https://www.wjgnet.com/bpg/gerinfo/204

GUIDELINES FOR ETHICS DOCUMENTS
https://www.wjgnet.com/bpg/GerInfo/287

GUIDELINES FOR NON-NATIVE SPEAKERS OF ENGLISH
https://www.wjgnet.com/bpg/gerinfo/240

PUBLICATION ETHICS
https://www.wjgnet.com/bpg/GerInfo/288

PUBLICATION MISCONDUCT
https://www.wjgnet.com/bpg/gerinfo/208

ARTICLE PROCESSING CHARGE
https://www.wjgnet.com/bpg/gerinfo/242

STEPS FOR SUBMITTING MANUSCRIPTS
https://www.wjgnet.com/bpg/GerInfo/239

ONLINE SUBMISSION
https://www.f6publishing.com

© 2021 Baishideng Publishing Group Inc. All rights reserved. 7041 Koll Center Parkway, Suite 160, Pleasanton, CA 94566, USA

E-mail: bpgoffice@wjgnet.com https://www.wjgnet.com

World Journal of Gastroenterology

Submit a Manuscript: https://www.f6publishing.com

World J Gastroenterol 2021 September 28; 27(36): 5989-6003

DOI: 10.3748/wjg.v27.i36.5989

ISSN 1007-9327 (print) ISSN 2219-2840 (online)

FRONTIER

Fluorescent cholangiography: An up-to-date overview twelve years after the first clinical application

Antonio Pesce, Gaetano Piccolo, Francesca Lecchi, Nicolò Fabbri, Michele Diana, Carlo Vittorio Feo

ORCID number: Antonio Pesce 0000-0002-7560-551X; Gaetano Piccolo 0000-0002-4942-7705; Francesca Lecchi 0000-0002-7568-4967; Nicolò Fabbri 0000-0001-7039-3717; Michele Diana 0000-0002-1390-8486; Carlo Vittorio Feo 0000-0003-0699-5689.

Author contributions: Pesce A and Piccolo G designed the research; Pesce A, Piccolo G, Fabbri N, and Lecchi F researched and wrote the manuscript; Diana M and Feo CV supervised the paper; all authors have read and approved the final manuscript.

Conflict-of-interest statement: The corresponding author declares that the manuscript has been submitted on behalf of all authors. All authors declare that they have no competing interests.

Open-Access: This article is an open-access article that was selected by an in-house editor and fully peer-reviewed by external reviewers. It is distributed in accordance with the Creative Commons Attribution Non Commercial (CC BY-NC 4.0) license, which permits others to distribute, remix, adapt, build upon this work non-commercially, and license their derivative works on different terms, provided the original work is properly cited and the use is non-commercial. See: http://creativecommons.org/License

Antonio Pesce, Nicolò Fabbri, Carlo Vittorio Feo, Department of Surgery, Section of General Surgery, Ospedale del Delta, Azienda USL of Ferrara, University of Ferrara, Ferrara 44023, Italy

Gaetano Piccolo, Francesca Lecchi, Department of Health Sciences, University of Milan, Unit of Hepato-Bilio-Pancreatic and Digestive Surgery, San Paolo Hospital, Milano 20142, Italy

Michele Diana, Department of General, Digestive and Endocrine Surgery, University Hospital of Strasbourg, IRCAD, Research Institute Against Digestive Cancer, ICUBE lab, PHOTONICS for Health, University of Strasbourg, Strasbourg Cedex F-67091, France

Corresponding author: Antonio Pesce, MD, PhD, Research Fellow, Surgeon, Department of Surgery, Section of General Surgery, Ospedale del Delta, Azienda USL of Ferrara, University of Ferrara, Via Valle Oppio 2, Lagosanto (FE), Ferrara 44023, Italy. antonio.pesce@ausl.fe.it

Abstract

Laparoscopic cholecystectomy (LC) is one of the most frequently performed gastrointestinal surgeries worldwide. Bile duct injury (BDI) represents the most serious complication of LC, with an incidence of 0.3%-0.7%, resulting in significant perioperative morbidity and mortality, impaired quality of life, and high rates of subsequent medico-legal litigation. In most cases, the primary cause of BDI is the misinterpretation of biliary anatomy, leading to unexpected biliary lesions. Near-infrared fluorescent cholangiography is widely spreading in clinical practice to delineate biliary anatomy during LC in elective and emergency settings. The primary aim of this article was to perform an up-to-date overview of the evolution of this method 12 years after the first clinical application in 2009 and to highlight all advantages and current limitations according to the available scientific evidence.

Key Words: Laparoscopic cholecystectomy; Bile duct injury; Biliary anatomy; Fluorescent cholangiography; Indocyanine green

©The Author(s) 2021. Published by Baishideng Publishing Group Inc. All rights reserved.

Core Tip: Fluorescence image-guided surgery is one of the most recent innovations in

s/by-nc/4.0/

Manuscript source: Invited manuscript

Specialty type: Gastroenterology and hepatology

Country/Territory of origin: Italy

Peer-review report's scientific quality classification

Grade A (Excellent): 0
Grade B (Very good): B, B, B, B
Grade C (Good): 0
Grade D (Fair): 0
Grade E (Poor): 0

Received: April 15, 2021
Peer-review started: April 15, 2021
First decision: July 1, 2021
Revised: July 10, 2021
Accepted: August 30, 2021
Article in press: August 30, 2021
Published online: September 28, 2021

P-Reviewer: Ghannam WM, Grosek J, Komatsu S, Wang SY
S-Editor: Wang LL
L-Editor: A
P-Editor: Xing YX

laparoscopic and robotic surgery. The visualization of biliary anatomy using fluorescence during surgery is becoming one of the most promising frontier approaches in minimally invasive surgery. This novel method is a powerful tool to detect biliary variants that could guide surgeons during dissection to prevent major bile duct lesions, and it has enormous potential to be considered the gold standard during all cholecystectomies. The up-to-date overview of this method confirms the efficacy of indocyanine green fluorescence cholangiography in detecting biliary anatomy, its importance as a teaching tool for young surgeons, and the effects on the reduction of conversion rate and bile duct injury, even if further considerable research remains necessary to optimize its use.

Citation: Pesce A, Piccolo G, Lecchi F, Fabbri N, Diana M, Feo CV. Fluorescent cholangiography: An up-to-date overview twelve years after the first clinical application. *World J Gastroenterol* 2021; 27(36): 5989-6003
URL: https://www.wjgnet.com/1007-9327/full/v27/i36/5989.htm
DOI: https://dx.doi.org/10.3748/wjg.v27.i36.5989

INTRODUCTION

Laparoscopic cholecystectomy (LC) is one of the most frequently performed gastrointestinal surgeries worldwide. Bile duct injury (BDI) represents the most serious complication of LC, with an incidence of 0.3% to 0.7%, resulting in significant perioperative morbidity and mortality, impaired quality of life, and high rates of subsequent medico-legal litigation[1,2]. In most cases, the primary cause of BDI is the misinterpretation of biliary anatomy, leading surgeons to unexpected biliary lesions (71%-97% of all cases)[3,4]. Various methods have been proposed and used to prevent iatrogenic biliary tract lesions[4]. Among them, near-infrared fluorescent cholangiography (NIRF-C) is widely spreading in clinical practice to delineate biliary anatomy during LC in elective and emergency settings. It is becoming one of the most popular and promising clinical applications in minimally invasive surgery[5,6]. In 2006, Stiles BM *et al*[7] first proposed fluorescent cholangiography in a mouse model by exploiting the unique auto fluorescent properties of bile for the intraoperative identification of the biliary anatomy in mice. The first application in humans was performed and described by *Ishizawa et al*[8] a few years later (2009). This classical method involves the intravenous injection of indocyanine green (ICG) dye before surgery. ICG binds to plasma proteins, with albumin as the principal carrier (95%), and is eliminated exclusively by the liver. The excitation of ICG by means of near-infrared light causes fluorescence, thereby delineating the anatomy of the biliary elements in real time. This innovative method was introduced as a means to prevent bile duct injuries during LC due to a better visualization of biliary anatomy during dissection. In 2015, we performed a systematic review of available studies by analyzing the efficacy of the novel technique in detecting bile duct structures during surgery. Detection rates of the biliary anatomy in 590 pooled patients were as follows: Cystic duct (CD) 96.2% (94.7%-97.7%), common hepatic duct (CHD) 78.1% (74.8%-81.4%), CD-CHD junction 72.0% (69.0%-75.0%), and common bile duct (CBD) 86.0% (83.3%-88.8%)[9]. Overall, these preliminary studies indicated that ICG fluorescence cholangiography is highly sensitive for the detection of extrahepatic biliary anatomy and may facilitate the prevention of bile duct injuries. Over the years, several single-center experiences from different countries[10-12] have been published regarding the usefulness of ICG fluorescence cholangiography in detecting biliary anatomy and analyzing patient outcomes after LC. The level of scientific evidence on ICG fluorescence cholangiography remains low. However, recent studies have significantly propelled the literature forward.

The primary aim of this article was to perform an up-to-date overview of the evolution of this method 12 years after its first clinical application and to highlight all the advantages and current limitations according to the available scientific literature.

TECHNIQUES

ICG administration can be performed in two different ways. The classical method described by Ishizawa T *et al*[8] in 2009 consists of the intravenous injection of ICG 30 min before surgery. Biliary visualization should be obtained prior to any dissection, during the dissection of the hepatocystic triangle, and after complete dissection according to the critical view of safety (CVS) method[13,14].This approach enables surgeons to check the biliary anatomy intraoperatively at any time. Recently, Dip F *et al*[15] summarized 10 important steps for the correct performance of fluorescent cholangiography during LC. The first two steps involve ICG intravenous administration and complete exposure of the hepatoduodenal ligament prior to any dissection. The primary objective of step 3 is the localization of the main biliary structures after the partial dissection of the hepatocystic triangle. Steps 4-7 are characterized by the identification of the CD, gallbladder-CD junction, CD-CHD junction, and CBD; step 8 is the identification of the cystic artery, in some cases by repeating ICG injection for fluorescent angiography to detect any anatomical arterial variations; step 9 is called "time-out", and it consists of the re-evaluation of the CVS before clipping and cutting any structures (as shown in Figures 1-2). After completing gallbladder removal, near-infrared (NIR) light should be turned on to identify any potential biliary leaks from the liver bed (step 10). At the current stage, there are two unresolved issues regarding NIRF-C, *i.e.*, the dose and the time required to obtain an optimal bile duct-to-liver fluorescence ratio >1. An elevated background liver signal may hinder the correct visualization of biliary anatomy. The dose and the time of administration of ICG are quite variable, as reported in the literature[16]. A recent study with data from the European Fluorescence Image-Guided Surgery (FIGS) registry[17] has shown a wide disparity in ICG dose and timing in NIRF-C across different European countries. Boogerd L *et al*[18] demonstrated that the highest bile duct-to-liver ratio was achieved 3 to 7 h after administration of 5 mg of ICG and 5 to 25 h after administration of 10 mg of ICG. Another study by Zarrinpar A *et al*[19] confirmed that a single dose of 0.25 mg/kg administered at least 45 min prior to visualization of the hepatocystic triangle facilitates intra-operative anatomical identification. Recently, Chen Q *et al*[20] demonstrated that the optimal effect of fluorescent cholangiography can be achieved by injecting 10 mg of ICG 10 to 12 h prior to surgery. Matsumura M *et al*[21] recommended the administration of 0.25 mg/kg ICG on the evening before surgery, as it may increase bile duct detectability in fluorescence cholangiography during LC. Based on our experience, we think that the administration of ICG 45 to 60 min before surgery is—from a logistical point of view - more practical since most patients are usually hospitalized on the same day as the surgical procedure. Indeed, the debate remains open, and a consensus conference may help the surgical community.

The direct injection of ICG into the gallbladder is a technique that allows overcoming the strong background signal in the liver. Liu YY *et al*[22] were the first to describe intracholecystic ICG administration during LC in a porcine model, proving the feasibility and usefulness of this technique to achieve adequate CVS. Few clinical studies of NIR cholecystocholangiography with direct ICG injection into the gallbladder were conducted, namely, two case reports, one case-control study, and a few prospective cohort studies, for a total of 80 patients, of whom 49 underwent surgery for symptomatic cholelithiasis and 31 for acute cholecystitis[22-26], as summarized in Table 1.

Liu YY *et al*[22] and Škrabec C *et al*[23] conducted the two widest studies, namely, a prospective cohort study of 46 patients and a case-control study including 20 patients, respectively. The authors described two different routes for intracholecystic ICG injection, *i.e.*, percutaneous transhepatic gallbladder drainage (trans-PTGBD) and intra-operative direct gallbladder puncture. A 1 mL amount of an ICG bile solution was used (ICG concentration = 0.025 mg/mL) made from a combination of 9 mL of bile mixed with 1 mL of a preparation of ICG and sterile water at a concentration of 0.25 mg/mL. NIR cholecystocholangiography with direct gallbladder injection was more successful in acute cholecystitis patients who underwent early or interval LC after the preliminary positioning of a PTGBD. Among all cases reported in the literature, only one patient required conversion to open cholecystectomy due to acute necrotic cholecystitis, which precluded safe laparoscopic dissection.

Intracholecystic ICG injection provides relevant advantages compared to intravenous NIR cholecystocholangiography, such as the real-time visualization of the biliary anatomy, including the gallbladder neck and Hartmann's pouch, which are safe landmarks to start the dissection. Additionally, the timing of ICG injection is irrelevant, and small dosages can be used.

Table 1 Cholecysto-cholangiography with direct intra-gallbladder indocyanine green injection

Ref.	Type of publication	No. of patients	No. of patients with gallbladder lithiasis	No. of patients with acute cholecystitis	Technique	Complication	Conversion to open surgery
Jao *et al* [26], 2020	Case series	2	0	2	2 trans-PTGBD cases	Lymphatic spillage	0
Nitta *et al* [24], 2020	Case report	1	0	1	1 case through DGBP	-	0
Škrabecet al [23], 2020	Case-controlled study	20	19	1	20 cases through DGBP	ICG bile leakage in 1 case; No progression of dye into the CD in 3 cases	1
Liu *et al* [22], 2017	Cohort study	46	21	25	18 trans-PTGBD cases; 28 cases through DGBP	ICG leakage in 5 cases	0
Graves *et al* [25], 2017	Cohort study	11	9	2	11 cases through DGBP	No progression of dye into the CD in 1 case	0

PTGBD: Percutaneous transhepatic gallbladder drainage; DGBP: Direct gallbladder puncture; ICG: Indocyanine green; CD: Cystic duct.

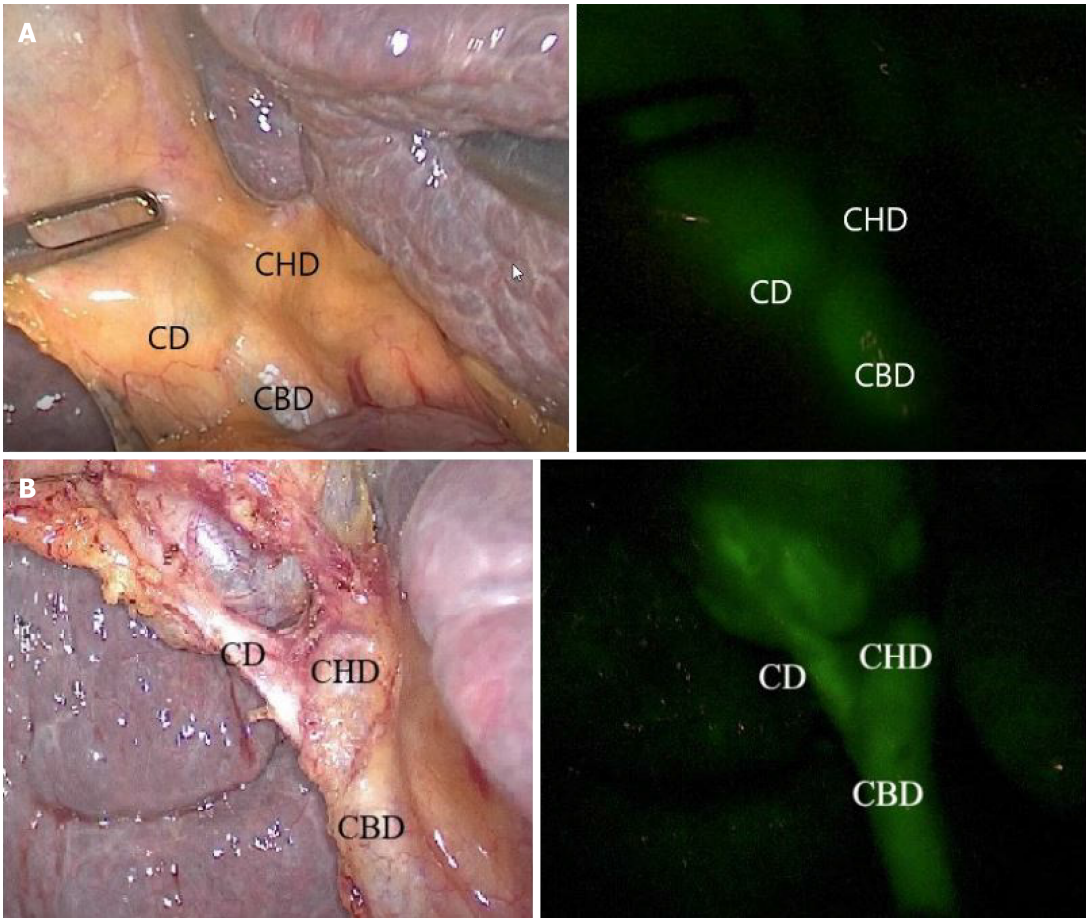


Figure 1 Intra-operative real-time identification of biliary structures in a cirrhotic patient, with visible light to the left and NIRF-C to the right. A: Pre-dissection visualization of biliary anatomy; B: After complete dissection. One can observe the posterior implantation of the cystic duct on the common hepatic duct. CD: Cystic duct; CHD: Common hepatic duct; CBD: Common bile duct.

The downside of direct ICG injection lies in the possibility of ICG bile leakage or lymph spillage during gallbladder dissection for acute cholecystitis, as ICG may enter through the necrotic gallbladder mucosa into the submucosal lymphatic drainage. In regard to the widest experiences reported in the literature[22,23], ICG bile leakage occurred in six patients in whom ICG was directly injected through a fine-needle puncture. Another limitation lies in the absence of progression of the dye into the CD

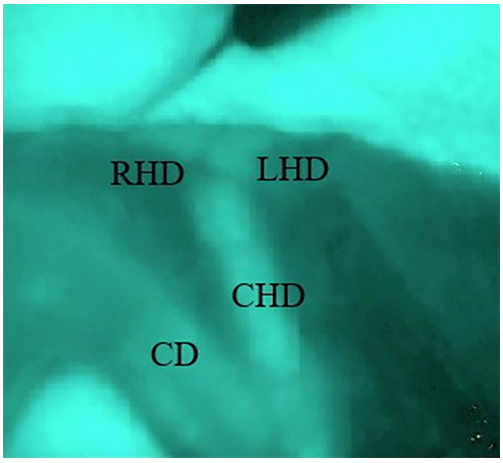


Figure 2 Classical extrahepatic biliary anatomy with identification of the right and left hepatic ducts using near-infrared fluorescent cholangiography. CD: Cystic duct; CHD: Common hepatic duct; RHD: Right hepatic duct; LHD: Left hepatic duct.

in cases of stone obstruction.

Based on the available data, we suggest that larger studies are necessary to validate the technique of intracholecystic ICG injection for NIR fluorescent cholangiography.

ICG FLUORESCENT CHOLANGIOGRAPHY IN PATIENTS WITH ACUTE CHOLECYSTITIS

Early LC is the gold standard treatment for patients with mild (grade I) and moderate (grade II) acute cholecystitis who have no response to initial (within 24 h) conservative treatment if performed within 72 h from the onset of symptoms according to 2018 Tokyo guidelines[27].

Fluorescent cholangiography may be very challenging in an emergency setting, when inflammation and adhesions at the hepatoduodenal ligament may impair the identification of biliary elements during dissection. Reaching the CVS may be particularly difficult in such situations[28].

In a recent meta-analysis, Dip F *et al*[29] suggested that using NIRF-C during elective cholecystectomy led to decreased BDI and conversion to open surgery compared to white light alone. However, there are limited data about its feasibility in an emergency setting. The identification of biliary structures may be challenging, especially in cases where there is an abundance of adhesions and severe inflammation of the gallbladder wall and surrounding tissues[9].

The literature contains four articles that provide data of patients who underwent LC for acute cholecystitis with NIR devices, *i.e.*, two cohort studies[30,31], one international European registry[17], and one randomized controlled trial (RCT)[32] are reported in Table 2.

In a large retrospective study involving 184 consecutive patients, Daskalaki E *et al*[31] reported the results of 24 patients who underwent robotic cholecystectomies (RCs) with ICG fluorescence for acute and gangrenous cholecystitis. The authors evaluated the detection rate of four biliary structures, *i.e.*, CD, CHD, CBD, and CD-CHD junction. In this subset of challenging surgical cases, the CD, CHD, CBD, and CD-CHD junction were successfully visualized in 91.6%, 79.1%, 79.1%, and 75% of cases, respectively.

Agnus V *et al*[17] reported data from the Euro-FIGS database, which enrolled 314 cases from 12 European surgical centers, including patients affected by symptomatic cholelithiasis (n = 248) and patients with acute cholecystitis (n = 58). A 5-point Likert scale was used to evaluate the quality of biliary anatomy visualization before and after the dissection of the hepatocystic triangle during LC with NIR devices. When the two groups (cholelithiasis *vs* acute cholecystitis) were compared, lower visualization quality scores were obtained in the CD group (2.76 ± 1.9 *vs* 3.54 ± 1.6, P = 0.001) and CD-CHD junction (2.43 ± 2 *vs* 3 ± 1.9, P = 0.04) before the preliminary dissection. The impact of variable inflammation on the visualization score of the biliary tree was also confirmed by means of multivariate linear regression analysis.

Table 2 Fluorescent cholangiography in patients with acute cholecystitis

Ref.	Type of publication	Procedure	No. of patients
Agnus *et al*[17], 2020	Euro-FIGS registry	LC	58
Dip *et al*[32], 2020	RCT	LC	44
Di Maggio *et al*[30], 2020	Prospective cohort study	LC	16
Daskalaki *et al*[31], 2014	Retrospective cohort study	RC	24
Yoshiya *et al*[33], 2019	Retrospective cohort study	LC after-PTGBD	130

FIGS: Fluorescence image-guided surgery; RCT: Randomized controlled trial; LC: Laparoscopic cholecystectomy; RC: Robotic cholecystectomy; PTGBD: Percutaneous transhepatic gallbladder drainage.

Similar data have been reported in a single-blinded randomized controlled trial[32] comparing the efficacy of NIR fluorescent cholangiography *vs* white light alone. The primary objective was the structure detection rate, defined as the total number of patients in whom a particular biliary structure was detected, both before and after dissection, in each study arm, divided by the total number of patients in each arm. The authors found that the degree of gallbladder inflammation was the most important variable, affecting the detection of CD and CBD before and after dissection, respectively, and of the CD-gallbladder junction only after dissection.

The usefulness of NIRF-C was also confirmed by Yoshiya S *et al*[33] during LC after PTGBD in patients with severe acute cholecystitis. The ICG fluorescence cholangiography group showed a significantly shorter operative time, a lower conversion rate, and a lower proportion of subtotal cholecystectomies[33].

NIR fluorescence cholangiography in emergency cholecystectomies is a safe and useful tool to prevent BDI during LC. However, the available data require further elaboration in randomized controlled studies in larger numbers of patients with acute cholecystitis undergoing LC with the aid of intra-operative fluorescent cholangiography.

DETECTION OF BILIARY VARIANTS USING ICG FLUORESCENCE

Various reports have underlined the importance of fluorescence image-guided cholecystectomy in detecting biliary variants. Fluorescent cholangiography allows the intraoperative identification of subvesical Luschka's ducts[34,35], aberrant bile ducts [36-38], anatomical CD variations[39], and gallbladder aberrations[40,41].

In specific studies, the diagnostic accuracy of NIRF-C in the evaluation of CD anatomy has been compared to that of magnetic resonance cholangiopancreatography (MRCP), which is the gold standard radiology diagnostic tool for the preoperative study of the biliary tree[42,43]. Pesce A *et al*[44] evaluated the ability of the two imaging methods to identify three selected features, namely, the insertion of CD, CD-CHD junction, and CD course. The level of insertion, course, and wall implantation of the CD were achieved by means of NIRF-C with diagnostic accuracy values of 65.2%, 78.3%, and 91.3%, respectively, in comparison with MRCP data.

In 2017, Diana M *et al*[45] prospectively evaluated the combination of three imaging modalities during robotic cholecystectomy, *i.e.*, virtual reality 3D modeling of MRCP, NIRF-C, and intraoperative cholangiogram (IOC). Surprisingly, expert hepatobiliary radiologists missed 5 out of 8 anatomical variants on preoperative MRCP, while surgeons were able to identify all variants through a virtual surgical exploration complemented with intraoperative fluorescent cholangiography.

In another observational study in 65 patients by Hiwatashi K *et al*[46], the authors found a statistically significant correlation between the delineation of CD using ICG cholangiography and preoperative MRCP.

Based on the current scientific literature (RCTs shown in Table 3), we strongly believe that NIRF-C is a useful tool to detect biliary variants that could guide surgeons during dissection to prevent any major bile duct lesions.

Table 3 Recruiting randomized controlled trials using indocyanine green fluorescence cholangiography

Study coordinator; NCT No.	Participating country	No. of patients	Period study	Published data	Main outcome	Controlled group	Dose indocyanine green	Dosing time	Conversion to open surgery	Bile duct injury
Dip *et al*[32]; NCT 02702843	United States	639	April 2016	*Ann Surg* 2020	Identification of biliary anatomy	White light	0.05 mg/kg	> 45 min prior to surgery	One patient for bleeding	No
Lehrskov *et al* [50]; NCT 02344654	Denmark	120	March 2015-August 2018	*Br J Surg* 2020	Visualization of the critical junction	Intraoperative cholangiogram	0.05 mg/kg	After intubation	No	No
van den Bos *et al*[61]; NCT 02558556	The Netherlands	308	January 2016	Ongoing	Time to achieve critical view of safety	White light	2.5 mg	After intubation	NA	NA
Koong *et al* [60] ; NCT04228835	Malaysia	63	March2017-July 2019	*Asian J Surg* 2021	Time to achieve critical view of safety	White light	2.5 mg	Before induction of anesthesia	No	No

NA: Not available.

FLUORESCENT CHOLANGIOGRAPHY *VS* STANDARD INTRAOPERATIVE CHOLANGIOGRAPHY

NIRF-C has been recognized as providing some advantages over conventional radiographic IOC, such as feasibility and safety, real-time visualization of biliary anatomy with safer dissection of the hepatocystic triangle, the lack of a learning curve, reduced X-ray exposure, and reduced costs and operative times[5,47-49]. In a Danish randomized controlled single-blind clinical trial[50], the authors compared NIRF-C *vs* IOC. They demonstrated that fluorescent cholangiography has the same capacity to identify the CVS, and is significantly faster and easier to perform than X-ray cholangiography[50]. In a recent meta-analysis by Lim SH *et al*[51], the authors concluded that there was no difference in the visualization of the CD, CBD, and CD-CBD junction using ICG fluorescence cholangiography compared to IOC. However, the ICG group reported increased rates of CHD visualization.

Dip F *et al*[52] analyzed medical costs and stated that the median cost of ICG fluorescence cholangiography was cheaper than that of IOC (13.97 ± 4.3 *vs* 778.43 ± 0.4 USD per patient, $P = 0.0001$).

Quaresima S *et al*[53] proposed that NIRF-C is a safe and effective procedure for the early recognition of anatomical biliary landmarks, with an important reduction in operative times compared to LC with intraoperative cholangiography.

In an article by Prevot F *et al*[54], the authors analyzed the ability to identify the CD, the CD-hepatic duct junction, and the CBD using fluorescence in comparison with standard IOC. The results of this study suggested that ICG fluorescence cholangiography is more effective than IOC in identifying the biliary tract after dissection.

In conclusion, we believe that there is considerable scientific evidence supporting the usefulness of NIRF-C with important advantages over conventional intraoperative cholangiography. NIRF-C represents a powerful real-time diagnostic tool for the detection of extrahepatic biliary anatomy during LC. Advantages and current limitations are summarized in Table 4.

FLUORESCENT CHOLANGIOGRAPHY IN OBESE PATIENTS

As reported in previous studies[9,31,55-57], the presence of dense adipose tissue surrounding the hepatocystic triangle may negatively affect the visualization of extrahepatic biliary tract using fluorescence. Obesity may represent a limitation of NIRF-C because NIR light has a penetration capability of only 5 to 10 mm[7-9]. In 2016, Dip F *et al*[58] conducted a prospective study to evaluate the accuracy of NIRF-C in obese *vs* non-obese patients. The results showed no difference in hepatic duct, CBD, or accessory duct detection rates between the two groups ($P = 0.09$, 0.16, and 0.66,

Table 4 Advantages and current limitations of fluorescent cholangiography in comparison to intraoperative cholangiogram and laparoscopic ultrasonography

Advantages	Limitations
Real-time visualization of biliary anatomy in elective and emergent settings	Limited in patients with specific conditions, such as overweight and obesity; it needs a preliminary dissection and exposure of the hepatocystic triangle
Safer dissection of the hepatocystic triangle	Limited scientific evidence in the setting of acute cholecystitis
Detection of biliary variants and biliary leaks	High variability about indocyanine green dose and dosing time
Implementing method in combination with adequate dissection and identification technique to achieve critical view of safety	Detection of bile duct stones
Feasibility and safety	Need for consensus conference and international guidelines
Reduced medical costs	
Time/faster	
Lack of X-ray exposure	
Simplicity and lack of learning curve	
Teaching tool for young surgeons	
Possibility to associate fluorescent angiography	
Strong potential to become a gold standard during all cholecystectomies	

respectively) before and after dissection of the hepatocystic triangle.

On the other hand, a German study[59] suggested that a BMI > 25 kg/m² and male sex significantly reduced the identification rate of CD before dissection of the hepatocystic triangle.

In a randomized controlled multicenter trial[32] comparing ICG *vs* white light alone, an increased BMI was associated with a reduced detection of most biliary structures in both groups, especially before dissection.

In general, our opinion is to use fluorescence to perform a complete dissection of the hepatocystic triangle in overweight and obese patients to obtain a good quality visualization of the biliary anatomy. In difficult cases where the surgeon is not able to clearly check the biliary anatomy, the surgeon should respect a sufficient thickness between the dissecting site and the main bile duct by working close to the gallbladder infundibulum to avoid unexpected biliary lesions. NIR imaging cannot be considered a substitute for good dissection and structure identification.

FLUORESCENT INCISIONLESS CHOLANGIOGRAPHY AS A TEACHING TOOL FOR YOUNG SURGEONS

It is well established that the risk of BDI correlates with the quality of the procedure performed, rather than the number of cases seen by the surgeon[1,2]. A clear identification of the biliary anatomy is crucial to perform a safe cholecystectomy and achieving CVS is now being taught as a key step of the operation to young surgeons[4,13]. In a recent randomized controlled trial[60], the time to achieve CVS from the gallbladder fundus retraction was measured by analyzing different levels of difficulty. The mean time, expressed in minutes, to achieve CVS was 22.3 ± 12.9 in the ICG-LC group (n = 30) and 22.8 ± 14.3 in the conventional LC group (P = 0.867). The authors concluded that fluorescent cholangiography may be a useful tool in difficult LC and in surgical training. A randomized controlled multicenter Dutch trial (FALCON trial) regarding the time to visualize CVS with NIRF-C compared to white light alone is still ongoing[61]. However, biliary structures are not always easily visualized laparoscopically. Fluorescence incisionless cholangiography may be a promising tool for training new surgeons in safe laparoscopic cholecystectomies by helping with biliary anatomy identification. To date, few studies have been conducted regarding the potential role of this technique in surgical training programs[62-64].

In 2016, Roy M *et al*[62] tested the ability of surgical students and residents to identify major biliary structures at NIR light. Participants were shown pictures taken at the same stage of hepatocystic triangle dissection in 10 cases of LC, first with NIR

light and then with Xenon white light. Both students and residents had a higher success rate of biliary tree identification with NIR fluorescence cholangiography. The authors also underlined the importance of NIRF-C to achieve appropriate intraoperative communication to guide residents, as it allows us to point out glowing structures in real time.

Similarly, in 2020, Rungsakulkij N *et al*[63] conducted a study to investigate the beneficial impact of fluorescence cholangiography on the ability of surgical residents to identify biliary structures. Participants were asked to identify the CD and artery, CBD and CHD in five LC videos, first without fluorescence, and then with NIRF-C. The results showed a higher misidentification rate among surgical residents in the without-FC modality than in the with-FC modality, proving the benefit of the technique among trainees.

In a study by Pesce A *et al*[47] on the usefulness of fluorescent cholangiography for biliary anatomy identification, surgical residents completed a survey on the perceived benefits of the technique. Responses were measured with a Likert scale. All participants agreed that NIRF-C facilitates the dissection of the hepatocystic triangle, hence being a useful adjuvant to training programs; 92% of respondents found the method easy to perform; 88% declared that it was effective in visualizing the biliary tree, and 84% found that the image quality was good. Consequently, residents consider the novel method a useful tool to visualize biliary anatomy and perform a safe dissection of the hepatocystic triangle, decreasing the risk of BDI.

From these experiences, it is safe to conclude that there is a large consensus regarding the beneficial role of NIRF-C in the training process of young surgeons. However, larger studies proving the benefits on the skills of surgical residents are required for the technique to be routinely performed in a teaching setting.

FLUORESCENT CHOLANGIOGRAPHY AND DETECTION OF BILIARY STONES

To date, there is no evidence that FC can effectively identify CBD stones by replacing IOC[64,65]. Intraoperative laparoscopic ultrasound (IOUS) could well represent a valid alternative to IOC in the detection of CBD stones[66,67]. Current limitations are related to the difficult learning curve and the lack of randomized controlled trials[66]. According to Daskalaki M *et al*[27], ICG fluorescence cholangiography can help to detect CD dilation and gallbladder stones (as shown in Figure 3), but it cannot rule out the presence of CBD stones. In a recent correspondence by Labil PL and Aroori S published in *Br J Surg*[65], the authors suggested performing an RCT comparing IOUS with X-ray and/or fluorescence cholangiography in LCto detect a difference in the rate of bile duct stone identification, as well as viewing the critical junction.

NIRF-C AND ROBOTIC CHOLECYSTECTOMY

Since the introduction of the robotic surgical platform in the 2000s, approximately 10% of all cholecystectomies are performed robotically[68] today. ICG technology was soon incorporated into the robotic platform, and the first case series involved patients who underwent single-incision or multiport robotic cholecystectomy (RC) with NIRF-C, as summarized in Table 5.

In a large retrospective cohort study including 184 patients, Daskalaki D *et al*[31] proved the feasibility of this technique. The four main biliary structures (CD, CHD, CD-CHD junction, CBD) were recognized using fluorescence imaging in 83% of cases. At least one structure was visualized in 99% of cases. Similar data have been reported by other authors[55,69-71].

Spinoglio G *et al*[70] showed that after dissection of the hepatocystic triangle, the visualization rates for each structure (CD, CHD, CD-CHD junction, CBD) increased to 97%. In addition, the rate of patients with two or three ducts visualized with NIR fluorescent cholangiography increased from 91% to 97% and from 86% to 95% before and after dissection, respectively.

In recent years, some authors compared data of patients who underwent robotic cholecystectomy with the use of ICG *vs* conventional LC[72,73]. In a retrospective cohort study, Sharma S *et al*[72] analyzed 287 consecutive cases, including 96 RCs and 191 LCs. The authors found a lower open conversion rate in the robotic cohort (2.1% *vs* 8.9% in LC), although this difference was not statistically significant.

Table 5 Studies reporting robotic cholecystectomy and near-infrared fluorescent cholangiography

Ref.	Type of publication	No. of patients	Technique	Incidence of conversion rate to open surgery (%)
Sharma *et al*[72], 2017	Retrospective cohort study	96	RC	2.1
Gangemi *et al*[73], 2017	Retrospective cohort study	676	RC	0.15
Maker *et al*[71], 2017	Cohort study	35	RC	NR
Daskalaki *et al*[31], 2014	Retrospective cohort study	184	RC	0.00
Spinoglio *et al*[70], 2013	Cohort study	45	SIRC	0.00
Buchs *et al*[55], 2013	Cohort study	23	SIRC	0.00
Buchs *et al*[69], 2012	Prospective cohort study	12	SIRC	0.00

RC: Robotic cholecystectomy; SIRC: Single-incision robotic cholecystectomy; NR: Not reported.

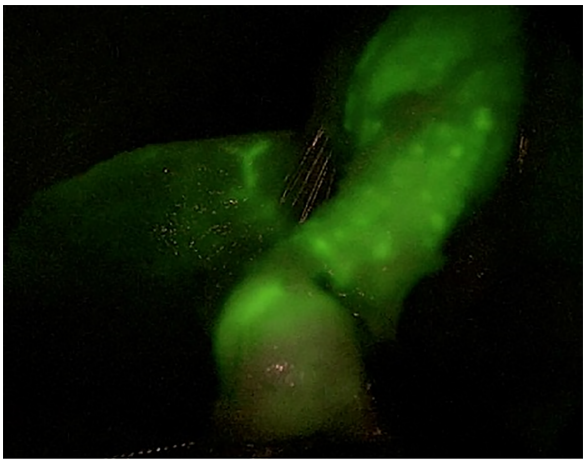


Figure 3 Identification of cystic duct stones by means of fluorescence.

Gangemi A *et al*[73] conducted a case-control study comparing the outcomes of ICG-aided RC *vs* LC at the University of Illinois (Chicago, United States). The authors reported a statistically significant difference between RC performed with the help of ICG and traditional LC in terms of the overall open conversion rate (0.15% *vs* 4.5%), open conversion rate in the acute setting (0.76% *vs* 9.57%), mean blood loss during surgery (14.37 mL *vs* 21.08 mL), and minor biliary injury rate (0.15% *vs* 1.04%). Additionally, a biliary tree anomaly was found in 2.07% of patients who underwent ICG-aided RC compared to 0.69% of patients who underwent LC with conventional intraoperative cholangiography.

Recently, Dip *et al*[29] conducted a meta-analysis evaluating whether NIFC with ICG could reduce conversion to open surgery and bile duct injuries during laparoscopic and robotic cholecystectomy. Patients who underwent ICG-aided RC showed a marked reduction in the rate of conversion to open surgery compared to RC without NIFC (weighted rate: 12/10.000 *vs* 322/10.000). Similar data were reported in the ICG-aided LC group (weighted rate: 23/10.000 *vs* 255/10.000). For BDI, a reduction was reported in the ICG-aided LC group compared to LC without NIFC (weighted rate: 23/10.000 *vs* 255/10.000), while no difference was noted regarding RC with and without NIFC. In conclusion, we believe that the use of NIRF-C may reduce the conversion rate in both minimally invasive procedures, laparoscopic and robotic cholecystectomy, while the reduction rate only exists in LC for BDI. However, further studies are required.

CONSENSUS CONFERENCES AND GUIDELINES

During the 4th International Congress of Fluorescence-Guided Surgery in Boca Raton, Florida in 2017, Dip F *et al*[74] conducted a pilot survey of 51 attending surgeons who

routinely performed laparoscopic cholecystectomies to identify their surgical practice and perceptions of intraoperative fluorescent cholangiography. Ten experts in ICG fluorescence-guided LC from North and South America, Europe, and Asia designed the survey for conference attendees. Seventy-eight percent of respondents underlined the importance for surgeons of having a noninvasive, simple, and reproducible diagnostic tool to identify the extrahepatic biliary anatomy in real time. In general, they recommended the routine use of NIRF-C during LC as a complimentary imaging technique, and 93.3% of them felt that the procedure would be useful in surgical training programs.

In a recent state-of-the-art consensus conference on the prevention of BDI during cholecystectomy published in *Annals of Surgery*[75], a pool of experts from five surgical societies (Society of Gastrointestinal and Endoscopic Surgeons, Americas Hepato-Pancreato-Biliary Association, International Hepato-Pancreato-Biliary Association, Society for Surgery of the Alimentary Tract, and European Association for Endoscopic Surgery) analyzed the scientific evidence among surgical practices to prevent bile duct injuries. At question 5B, *i.e.*, "Should intraoperative NIR biliary imaging with white light versus white light biliary imaging alone be used to limit the risk or severity of BDI during LC?", they answered the following question: We suggest that the use of NIR imaging may be considered an adjunct to white light alone to identify the biliary anatomy during cholecystectomy (conditional recommendation, very low certainty of evidence).

However, in a Delphi survey of 19 international experts in fluorescence-guided surgery attending a 1 d consensus meeting in Frankfurt, Germany in September 2019, fluorescence imaging was almost unanimously perceived to be both effective and safe across a broad range of clinical settings[76]. No specific recommendations were given for fluorescent cholangiography. Moreover, the safety of ICG dye has been underlined: the risk of adverse reactions to ICG injection, such as anaphylactic shock, is very small (approximately 0.003% at doses exceeding 0.5 mg/kg) according to the literature data [9,77].

CONCLUSION

The results of the current up-to-date overview confirmed the efficacy of ICG-fluorescence cholangiography in detecting biliary anatomy, its importance as a teaching tool for young surgeons, and the effects on the reduction of conversion rate and BDI, even if further considerable research remains necessary to optimize its use. This frontier method has enormous potential to become the gold standard during all cholecystectomies in elective and emergency settings due to its safety and limited costs. However, clear clinical guidelines are necessary for the surgical community.

REFERENCES

1 **Nuzzo G**, Giuliante F, Giovannini I, Ardito F, D'Acapito F, Vellone M, Murazio M, Capelli G. Bile duct injury during laparoscopic cholecystectomy: results of an Italian national survey on 56 591 cholecystectomies. *Arch Surg* 2005; **140**: 986-992 [PMID: 16230550 DOI: 10.1001/archsurg.140.10.986]

2 **Way LW**, Stewart L, Gantert W, Liu K, Lee CM, Whang K, Hunter JG. Causes and prevention of laparoscopic bile duct injuries: analysis of 252 cases from a human factors and cognitive psychology perspective. *Ann Surg* 2003; **237**: 460-469 [PMID: 12677139 DOI: 10.1097/01.SLA.0000060680.92690.E9]

3 **Pesce A**, Portale TR, Minutolo V, Scilletta R, Li Destri G, Puleo S. Bile duct injury during laparoscopic cholecystectomy without intraoperative cholangiography: a retrospective study on 1,100 selected patients. *Dig Surg* 2012; **29**: 310-314 [PMID: 22986956 DOI: 10.1159/000341660]

4 **Pesce A**, Palmucci S, La Greca G, Puleo S. Iatrogenic bile duct injury: impact and management challenges. *Clin Exp Gastroenterol* 2019; **12**: 121-128 [PMID: 30881079 DOI: 10.2147/CEG.S169492]

5 **Majlesara A**, Golriz M, Hafezi M, Saffari A, Stenau E, Maier-Hein L, Müller-Stich BP, Mehrabi A. Indocyanine green fluorescence imaging in hepatobiliary surgery. *Photodiagnosis Photodyn Ther* 2017; **17**: 208-215 [PMID: 28017834 DOI: 10.1016/j.pdpdt.2016.12.005]

6 **Baiocchi GL**, Diana M, Boni L. Indocyanine green-based fluorescence imaging in visceral and hepatobiliary and pancreatic surgery: State of the art and future directions. *World J Gastroenterol* 2018; **24**: 2921-2930 [PMID: 30038461 DOI: 10.3748/wjg.v24.i27.2921]

7 **Stiles BM**, Adusumilli PS, Bhargava A, Fong Y. Fluorescent cholangiography in a mouse model: an innovative method for improved laparoscopic identification of the biliary anatomy. *Surg Endosc*

2006; **20**: 1291-1295 [PMID: 16858526 DOI: 10.1007/s00464-005-0664-x]
8 **Ishizawa T**, Tamura S, Masuda K, Aoki T, Hasegawa K, Imamura H, Beck Y, Kokudo N. Intraoperative fluorescent cholangiography using indocyanine green: a biliary road map for safe surgery. *J Am Coll Surg* 2009; **208**: e1-e4 [PMID: 19228492 DOI: 10.1016/j.jamcollsurg.2008.09.024]
9 **Pesce A**, Piccolo G, La Greca G, Puleo S. Utility of fluorescent cholangiography during laparoscopic cholecystectomy: A systematic review. *World J Gastroenterol* 2015; **21**: 7877-7883 [PMID: 26167088 DOI: 10.3748/wjg.v21.i25.7877]
10 **Igami T**, Nojiri M, Shinohara K, Ebata T, Yokoyama Y, Sugawara G, Mizuno T, Yamaguchi J, Nagino M. Clinical value and pitfalls of fluorescent cholangiography during single-incision laparoscopic cholecystectomy. *Surg Today* 2016; **46**: 1443-1450 [PMID: 27002714 DOI: 10.1007/s00595-016-1330-8]
11 **Broderick RC**, Lee AM, Cheverie JN, Zhao B, Blitzer RR, Patel RJ, Soltero S, Sandler BJ, Jacobsen GR, Doucet JJ, Horgan S. Fluorescent cholangiography significantly improves patient outcomes for laparoscopic cholecystectomy. *Surg Endosc* 2020 [PMID: 33052527 DOI: 10.1007/s00464-020-08045-x]
12 **Bleszynski MS**, DeGirolamo KM, Meneghetti AT, Chiu CJ, Panton ON. Fluorescent Cholangiography in Laparoscopic Cholecystectomy: An Updated Canadian Experience. *Surg Innov* 2020; **27**: 38-43 [PMID: 31744398 DOI: 10.1177/1553350619885792]
13 **Strasberg SM**, Brunt LM. Rationale and use of the critical view of safety in laparoscopic cholecystectomy. *J Am Coll Surg* 2010; **211**: 132-138 [PMID: 20610259 DOI: 10.1016/j.jamcollsurg.2010.02.053]
14 **Ishizawa T**, Bandai Y, Ijichi M, Kaneko J, Hasegawa K, Kokudo N. Fluorescent cholangiography illuminating the biliary tree during laparoscopic cholecystectomy. *Br J Surg* 2010; **97**: 1369-1377 [PMID: 20623766 DOI: 10.1002/bjs.7125]
15 **Dip F**, Aleman R, Frieder JS, Gomez CO, Menzo EL, Szomstein S, Rosenthal RJ. Understanding intraoperative fluorescent cholangiography: ten steps for an effective and successful procedure. *Surg Endosc* 2021 [PMID: 33475844 DOI: 10.1007/s00464-020-08219-7]
16 **van den Bos J**, Wieringa FP, Bouvy ND, Stassen LPS. Optimizing the image of fluorescence cholangiography using ICG: a systematic review and ex vivo experiments. *Surg Endosc* 2018; **32**: 4820-4832 [PMID: 29777357 DOI: 10.1007/s00464-018-6233-x]
17 **Agnus V**, Pesce A, Boni L, Van Den Bos J, Morales-Conde S, Paganini AM, Quaresima S, Balla A, La Greca G, Plaudis H, Moretto G, Castagnola M, Santi C, Casali L, Tartamella L, Saadi A, Picchetto A, Arezzo A, Marescaux J, Diana M. Fluorescence-based cholangiography: preliminary results from the IHU-IRCAD-EAES EURO-FIGS registry. *Surg Endosc* 2020; **34**: 3888-3896 [PMID: 31591654 DOI: 10.1007/s00464-019-07157-3]
18 **Boogerd LSF**, Handgraaf HJM, Huurman VAL, Lam HD, Mieog JSD, van der Made WJ, van de Velde CJH, Vahrmeijer AL. The Best Approach for Laparoscopic Fluorescence Cholangiography: Overview of the Literature and Optimization of Dose and Dosing Time. *Surg Innov* 2017; **24**: 386-396 [PMID: 28457194 DOI: 10.1177/1553350617702311]
19 **Zarrinpar A**, Dutson EP, Mobley C, Busuttil RW, Lewis CE, Tillou A, Cheaito A, Hines OJ, Agopian VG, Hiyama DT. Intraoperative Laparoscopic Near-Infrared Fluorescence Cholangiography to Facilitate Anatomical Identification: When to Give Indocyanine Green and How Much. *Surg Innov* 2016; **23**: 360-365 [PMID: 26964557 DOI: 10.1177/1553350616637671]
20 **Chen Q**, Zhou R, Weng J, Lai Y, Liu H, Kuang J, Zhang S, Wu Z, Wang W, Gu W. Extrahepatic biliary tract visualization using near-infrared fluorescence imaging with indocyanine green: optimization of dose and dosing time. *Surg Endosc* 2020 [PMID: 33026517 DOI: 10.1007/s00464-020-08058-6]
21 **Matsumura M**, Kawaguchi Y, Kobayashi Y, Kobayashi K, Ishizawa T, Akamatsu N, Kaneko J, Arita J, Kokudo N, Hasegawa K. Indocyanine green administration a day before surgery may increase bile duct detectability on fluorescence cholangiography during laparoscopic cholecystectomy. *J Hepatobiliary Pancreat Sci* 2021; **28**: 202-210 [PMID: 33091224 DOI: 10.1002/jhbp.855]
22 **Liu YY**, Liao CH, Diana M, Wang SY, Kong SH, Yeh CN, Dallemagne B, Marescaux J, Yeh TS. Near-infrared cholecystocholangiography with direct intragallbladder indocyanine green injection: preliminary clinical results. *Surg Endosc* 2018; **32**: 1506-1514 [PMID: 28916859 DOI: 10.1007/s00464-017-5838-9]
23 **Gené Škrabec C**, Pardo Aranda F, Espín F, Cremades M, Navinés J, Zárate A, Cugat E. Fluorescent cholangiography with direct injection of indocyanine green (ICG) into the gallbladder: a safety method to outline biliary anatomy. *Langenbecks Arch Surg* 2020; **405**: 827-832 [PMID: 32827267 DOI: 10.1007/s00423-020-01967-z]
24 **Nitta T**, Kataoka J, Ohta M, Ueda Y, Senpuku S, Kurashima Y, Shimizu T, Ishibashi T. Laparoscopic cholecystectomy for cholecystitis using direct gallbladder indocyanine green injection fluorescence cholangiography: A case report. *Ann Med Surg (Lond)* 2020; **57**: 218-222 [PMID: 32793342 DOI: 10.1016/j.amsu.2020.07.057]
25 **Graves C**, Ely S, Idowu O, Newton C, Kim S. Direct Gallbladder Indocyanine Green Injection Fluorescence Cholangiography During Laparoscopic Cholecystectomy. *J Laparoendosc Adv Surg Tech A* 2017; **27**: 1069-1073 [PMID: 28574801 DOI: 10.1089/lap.2017.0070]
26 **Jao ML**, Wang YY, Wong HP, Bachhav S, Liu KC. Intracholecystic administration of indocyanine green for fluorescent cholangiography during laparoscopic cholecystectomy-A two-case report. *Int J*

Surg Case Rep 2020; **68**: 193-197 [PMID: 32172195 DOI: 10.1016/j.ijscr.2020.02.054]

27 **Okamoto K**, Suzuki K, Takada T, Strasberg SM, Asbun HJ, Endo I, Iwashita Y, Hibi T, Pitt HA, Umezawa A, Asai K, Han HS, Hwang TL, Mori Y, Yoon YS, Huang WS, Belli G, Dervenis C, Yokoe M, Kiriyama S, Itoi T, Jagannath P, Garden OJ, Miura F, Nakamura M, Horiguchi A, Wakabayashi G, Cherqui D, de Santibañes E, Shikata S, Noguchi Y, Ukai T, Higuchi R, Wada K, Honda G, Supe AN, Yoshida M, Mayumi T, Gouma DJ, Deziel DJ, Liau KH, Chen MF, Shibao K, Liu KH, Su CH, Chan ACW, Yoon DS, Choi IS, Jonas E, Chen XP, Fan ST, Ker CG, Giménez ME, Kitano S, Inomata M, Hirata K, Inui K, Sumiyama Y, Yamamoto M. Tokyo Guidelines 2018: flowchart for the management of acute cholecystitis. *J Hepatobiliary Pancreat Sci* 2018; **25**: 55-72 [PMID: 29045062 DOI: 10.1002/jhbp.516]

28 **Alander JT**, Kaartinen I, Laakso A, Pätilä T, Spillmann T, Tuchin VV, Venermo M, Välisuo P. A review of indocyanine green fluorescent imaging in surgery. *Int J Biomed Imaging* 2012; **2012**: 940585 [PMID: 22577366 DOI: 10.1155/2012/940585]

29 **Dip F**, Lo Menzo E, White KP, Rosenthal RJ. Does near-infrared fluorescent cholangiography with indocyanine green reduce bile duct injuries and conversions to open surgery during laparoscopic or robotic cholecystectomy? *Surgery* 2021; **169**: 859-867 [PMID: 33478756 DOI: 10.1016/j.surg.2020.12.008]

30 **Di Maggio F**, Hossain N, De Zanna A, Husain D, Bonomo L. Near-Infrared Fluorescence Cholangiography can be a Useful Adjunct during Emergency Cholecystectomies. *Surg Innov* 2020; 1553350620958562 [PMID: 32936054 DOI: 10.1177/1553350620958562]

31 **Daskalaki D**, Fernandes E, Wang X, Bianco FM, Elli EF, Ayloo S, Masrur M, Milone L, Giulianotti PC. Indocyanine green (ICG) fluorescent cholangiography during robotic cholecystectomy: results of 184 consecutive cases in a single institution. *Surg Innov* 2014; **21**: 615-621 [PMID: 24616013 DOI: 10.1177/1553350614524839]

32 **Dip F**, LoMenzo E, Sarotto L, Phillips E, Todeschini H, Nahmod M, Alle L, Schneider S, Kaja L, Boni L, Ferraina P, Carus T, Kokudo N, Ishizawa T, Walsh M, Simpfendorfer C, Mayank R, White K, Rosenthal RJ. Randomized Trial of Near-infrared Incisionless Fluorescent Cholangiography. *Ann Surg* 2019; **270**: 992-999 [PMID: 30614881 DOI: 10.1097/SLA.0000000000003178]

33 **Yoshiya S**, Minagawa R, Kamo K, Kasai M, Taketani K, Yukaya T, Kimura Y, Koga T, Kai M, Kajiyama K, Yoshizumi T. Usability of Intraoperative Fluorescence Imaging with Indocyanine Green During Laparoscopic Cholecystectomy After Percutaneous Transhepatic Gallbladder Drainage. *World J Surg* 2019; **43**: 127-133 [PMID: 30105635 DOI: 10.1007/s00268-018-4760-1]

34 **Kitamura H**, Tsuji T, Yamamoto D, Takahashi T, Kadoya S, Kurokawa M, Bando H. Efficiency of fluorescent cholangiography during laparoscopic cholecystectomy for subvesical bile ducts: A case report. *Int J Surg Case Rep* 2019; **57**: 194-196 [PMID: 30981075 DOI: 10.1016/j.ijscr.2019.03.042]

35 **Iwasaki T**, Takeyama Y, Yoshida Y, Kawaguchi K, Matsumoto M, Murase T, Kamei K, Takebe A, Matsumoto I, Nakai T. Identification of aberrant subvesical bile duct by using intraoperative fluorescent cholangiography: A case report. *Int J Surg Case Rep* 2019; **61**: 115-118 [PMID: 31357101 DOI: 10.1016/j.ijscr.2019.07.013]

36 **Tsuruda Y**, Okumura H, Setoyama T, Hiwatashi K, Minami K, Ando K, Wada M, Maenohara S, Natsugoe S. Laparoscopic cholecystectomy with aberrant bile duct detected by intraoperative fluorescent cholangiography concomitant with angiography: A case report. *Int J Surg Case Rep* 2018; **51**: 14-16 [PMID: 30130667 DOI: 10.1016/j.ijscr.2018.08.009]

37 **Bozzay J**, Vicente D, Jessie EM, Rodriguez CJ. Identification of Abnormal Biliary Anatomy Utilizing Real-Time Near-Infrared Cholangiography: A Report of Two Cases. *Case Rep Gastrointest Med* 2017; **2017**: 8628206 [PMID: 28536662 DOI: 10.1155/2017/8628206]

38 **Asai Y**, Igami T, Ebata T, Yokoyama Y, Mizuno T, Yamaguchi J, Onoe S, Watanabe N, Nagino M. Application of fluorescent cholangiography during single-incision laparoscopic cholecystectomy in the cystohepatic duct without preoperative diagnosis. *ANZ J Surg* 2021; **91**: 470-472 [PMID: 32681758 DOI: 10.1111/ans.16162]

39 **Kim NS**, Jin HY, Kim EY, Hong TH. Cystic duct variation detected by near-infrared fluorescent cholangiography during laparoscopic cholecystectomy. *Ann Surg Treat Res* 2017; **92**: 47-50 [PMID: 28090506 DOI: 10.4174/astr.2017.92.1.47]

40 **Naganuma S**, Ishida H, Konno K, Hamashima Y, Hoshino T, Naganuma H, Komatsuda T, Ohyama Y, Yamada N, Ishida J, Masamune O. Sonographic findings of anomalous position of the gallbladder. *Abdom Imaging* 1998; **23**: 67-72 [PMID: 9437066 DOI: 10.1007/s002619900287]

41 **Nojiri M**, Igami T, Toyoda Y, Ebata T, Yokoyama Y, Sugawara G, Mizuno T, Yamaguchi J, Nagino M. Application of fluorescent cholangiography during single-incision laparoscopic cholecystectomy for cholecystitis with a right-sided round ligament: Preliminary experience. *J Minim Access Surg* 2018; **14**: 244-246 [PMID: 29226884 DOI: 10.4103/jmas.JMAS_159_17]

42 **Shanmugam V**, Beattie GC, Yule SR, Reid W, Loudon MA. Is magnetic resonance cholangiopancreatography the new gold standard in biliary imaging? *Br J Radiol* 2005; **78**: 888-893 [PMID: 16177010 DOI: 10.1259/bjr/51075444]

43 **Griffin N**, Charles-Edwards G, Grant LA. Magnetic resonance cholangiopancreatography: the ABC of MRCP. *Insights Imaging* 2012; **3**: 11-21 [PMID: 22695995 DOI: 10.1007/s13244-011-0129-9]

44 **Pesce A**, La Greca G, Esposto Ultimo L, Basile A, Puleo S, Palmucci S. Effectiveness of near-infrared fluorescent cholangiography in the identification of cystic duct-common hepatic duct anatomy in comparison to magnetic resonance cholangio-pancreatography: a preliminary study. *Surg Endosc* 2020; **34**: 2715-2721 [PMID: 31598878 DOI: 10.1007/s00464-019-07158-2]

45 **Diana M**, Soler L, Agnus V, D'Urso A, Vix M, Dallemagne B, Faucher V, Roy C, Mutter D, Marescaux J, Pessaux P. Prospective Evaluation of Precision Multimodal Gallbladder Surgery Navigation: Virtual Reality, Near-infrared Fluorescence, and X-ray-based Intraoperative Cholangiography. *Ann Surg* 2017; **266**: 890-897 [PMID: 28742709 DOI: 10.1097/SLA.0000000000002400]

46 **Hiwatashi K**, Okumura H, Setoyama T, Ando K, Ogura Y, Aridome K, Maenohara S, Natsugoe S. Evaluation of laparoscopic cholecystectomy using indocyanine green cholangiography including cholecystitis: A retrospective study. *Medicine (Baltimore)* 2018; **97**: e11654 [PMID: 30045318 DOI: 10.1097/MD.0000000000011654]

47 **Pesce A**, Latteri S, Barchitta M, Portale TR, Di Stefano B, Agodi A, Russello D, Puleo S, La Greca G. Near-infrared fluorescent cholangiography - real-time visualization of the biliary tree during elective laparoscopic cholecystectomy. *HPB (Oxford)* 2018; **20**: 538-545 [PMID: 29292071 DOI: 10.1016/j.hpb.2017.11.013]

48 **Pesce A**, Diana M. Critical View of Safety During Laparoscopic Cholecystectomy: From the Surgeon's Eye to Fluorescent Vision. *Surg Innov* 2018; **25**: 197-198 [PMID: 29557253 DOI: 10.1177/1553350618763200]

49 **Dip FD**, Asbun D, Rosales-Velderrain A, Lo Menzo E, Simpfendorfer CH, Szomstein S, Rosenthal RJ. Cost analysis and effectiveness comparing the routine use of intraoperative fluorescent cholangiography with fluoroscopic cholangiogram in patients undergoing laparoscopic cholecystectomy. *Surg Endosc* 2014; **28**: 1838-1843 [PMID: 24414461 DOI: 10.1007/s00464-013-3394-5]

50 **Lehrskov LL**, Westen M, Larsen SS, Jensen AB, Kristensen BB, Bisgaard T. Fluorescence or X-ray cholangiography in elective laparoscopic cholecystectomy: a randomized clinical trial. *Br J Surg* 2020; **107**: 655-661 [PMID: 32057103 DOI: 10.1002/bjs.11510]

51 **Lim SH**, Tan HTA, Shelat VG. Comparison of indocyanine green dye fluorescent cholangiography with intra-operative cholangiography in laparoscopic cholecystectomy: a meta-analysis. *Surg Endosc* 2021; **35**: 1511-1520 [PMID: 33398590 DOI: 10.1007/s00464-020-08164-5]

52 **Dip F**, Roy M, Lo Menzo E, Simpfendorfer C, Szomstein S, Rosenthal RJ. Routine use of fluorescent incisionless cholangiography as a new imaging modality during laparoscopic cholecystectomy. *Surg Endosc* 2015; **29**: 1621-1626 [PMID: 25277476 DOI: 10.1007/s00464-014-3853-7]

53 **Quaresima S**, Balla A, Palmieri L, Seitaj A, Fingerhut A, Ursi P, Paganini AM. Routine near infra-red indocyanine green fluorescent cholangiography vs intraoperative cholangiography during laparoscopic cholecystectomy: a case-matched comparison. *Surg Endosc* 2020; **34**: 1959-1967 [PMID: 31309307 DOI: 10.1007/s00464-019-06970-0]

54 **Osayi SN**, Wendling MR, Drosdeck JM, Chaudhry UI, Perry KA, Noria SF, Mikami DJ, Needleman BJ, Muscarella P 2nd, Abdel-Rasoul M, Renton DB, Melvin WS, Hazey JW, Narula VK. Near-infrared fluorescent cholangiography facilitates identification of biliary anatomy during laparoscopic cholecystectomy. *Surg Endosc* 2015; **29**: 368-375 [PMID: 24986018 DOI: 10.1007/s00464-014-3677-5]

55 **Buchs NC**, Pugin F, Azagury DE, Jung M, Volonte F, Hagen ME, Morel P. Real-time near-infrared fluorescent cholangiography could shorten operative time during robotic single-site cholecystectomy. *Surg Endosc* 2013; **27**: 3897-3901 [PMID: 23670747 DOI: 10.1007/s00464-013-3005-5]

56 **Aoki T**, Murakami M, Yasuda D, Shimizu Y, Kusano T, Matsuda K, Niiya T, Kato H, Murai N, Otsuka K, Kusano M, Kato T. Intraoperative fluorescent imaging using indocyanine green for liver mapping and cholangiography. *J Hepatobiliary Pancreat Sci* 2010; **17**: 590-594 [PMID: 19844652 DOI: 10.1007/s00534-009-0197-0]

57 **Vlek SL**, van Dam DA, Rubinstein SM, de Lange-de Klerk ESM, Schoonmade LJ, Tuynman JB, Meijerink WJHJ, Ankersmit M. Biliary tract visualization using near-infrared imaging with indocyanine green during laparoscopic cholecystectomy: results of a systematic review. *Surg Endosc* 2017; **31**: 2731-2742 [PMID: 27844236 DOI: 10.1007/s00464-016-5318-7]

58 **Dip F**, Nguyen D, Montorfano L, Szretter Noste ME, Lo Menzo E, Simpfendorfer C, Szomstein S, Rosenthal R. Accuracy of Near Infrared-Guided Surgery in Morbidly Obese Subjects Undergoing Laparoscopic Cholecystectomy. *Obes Surg* 2016; **26**: 525-530 [PMID: 26224370 DOI: 10.1007/s11695-015-1781-9]

59 **Pax V**, Schneider-Koriath S, Scholz M, Wießner R, Ludwig K. [Fluorescence Cholangiography in Comparison to Radiographic Cholangiography During Laparoscopic Cholecystectomy]. *Zentralbl Chir* 2018; **143**: 35-41 [PMID: 29166696 DOI: 10.1055/s-0043-117495]

60 **Koong JK**, Ng GH, Ramayah K, Koh PS, Yoong BK. Early identification of the critical view of safety in laparoscopic cholecystectomy using indocyanine green fluorescence cholangiography: A randomised controlled study. *Asian J Surg* 2021; **44**: 537-543 [PMID: 33223453 DOI: 10.1016/j.asjsur.2020.11.002]

61 **van den Bos J**, Schols RM, Luyer MD, van Dam RM, Vahrmeijer AL, Meijerink WJ, Gobardhan PD, van Dam GM, Bouvy ND, Stassen LP. Near-infrared fluorescence cholangiography assisted laparoscopic cholecystectomy vs conventional laparoscopic cholecystectomy (FALCON trial): study protocol for a multicentre randomised controlled trial. *BMJ Open* 2016; **6**: e011668 [PMID: 27566635 DOI: 10.1136/bmjopen-2016-011668]

62 **Roy M**, Dip F, Nguyen D, Simpfendorfer CH, Menzo EL, Szomstein S, Rosenthal RJ. Fluorescent incisionless cholangiography as a teaching tool for identification of Calot's triangle. *Surg Endosc* 2017; **31**: 2483-2490 [PMID: 27778170 DOI: 10.1007/s00464-016-5250-x]

63 **Rungsakulkij N**, Thewmorakot S, Suragul W, Vassanasiri W, Tangtawee P, Muangkaew P, Mingphruedhi S, Aeesoa S. Fluorescence cholangiography enhances surgical residents' biliary delineation skill for laparoscopic cholecystectomies. *World J Gastrointest Surg* 2020; **12**: 93-103 [PMID: 32218892 DOI: 10.4240/wjgs.v12.i3.93]

64 **van de Graaf FW**, Zaïmi I, Stassen LPS, Lange JF. Safe laparoscopic cholecystectomy: A systematic review of bile duct injury prevention. *Int J Surg* 2018; **60**: 164-172 [PMID: 30439536 DOI: 10.1016/j.ijsu.2018.11.006]

65 **Labib PL**, Aroori S. Intraoperative ultrasound vs fluorescence and X-ray cholangiography for the identification of bile duct stones, biliary anatomy and bile duct injury during laparoscopic cholecystectomy: Time for a randomized controlled trial? *Br J Surg* 2020; **107**: e563 [PMID: 32841376 DOI: 10.1002/bjs.11862]

66 **Dili A**, Bertrand C. Laparoscopic ultrasonography as an alternative to intraoperative cholangiography during laparoscopic cholecystectomy. *World J Gastroenterol* 2017; **23**: 5438-5450 [PMID: 28839445 DOI: 10.3748/wjg.v23.i29.5438]

67 **Machi J**, Johnson JO, Deziel DJ, Soper NJ, Berber E, Siperstein A, Hata M, Patel A, Singh K, Arregui ME. The routine use of laparoscopic ultrasound decreases bile duct injury: a multicenter study. *Surg Endosc* 2009; **23**: 384-388 [PMID: 18528611 DOI: 10.1007/s00464-008-9985-x]

68 **Spinoglio G**, Lenti LM, Maglione V, Lucido FS, Priora F, Bianchi PP, Grosso F, Quarati R. Single-site robotic cholecystectomy (SSRC) versus single-incision laparoscopic cholecystectomy (SILC): comparison of learning curves. First European experience. *Surg Endosc* 2012; **26**: 1648-1655 [PMID: 22179472 DOI: 10.1007/s00464-011-2087-1]

69 **Buchs NC**, Hagen ME, Pugin F, Volonte F, Bucher P, Schiffer E, Morel P. Intra-operative fluorescent cholangiography using indocyanin green during robotic single site cholecystectomy. *Int J Med Robot* 2012; **8**: 436-440 [PMID: 22648637 DOI: 10.1002/rcs.1437]

70 **Spinoglio G**, Priora F, Bianchi PP, Lucido FS, Licciardello A, Maglione V, Grosso F, Quarati R, Ravazzoni F, Lenti LM. Real-time near-infrared (NIR) fluorescent cholangiography in single-site robotic cholecystectomy (SSRC): a single-institutional prospective study. *Surg Endosc* 2013; **27**: 2156-2162 [PMID: 23271272 DOI: 10.1007/s00464-012-2733-2]

71 **Maker AV**, Kunda N. A Technique to Define Extrahepatic Biliary Anatomy Using Robotic Near-Infrared Fluorescent Cholangiography. *J Gastrointest Surg* 2017; **21**: 1961-1962 [PMID: 28585107 DOI: 10.1007/s11605-017-3455-5]

72 **Sharma S**, Huang R, Hui S, Smith MC, Chung PJ, Schwartzman A, Sugiyama G. The utilization of fluorescent cholangiography during robotic cholecystectomy at an inner-city academic medical center. *J Robot Surg* 2018; **12**: 481-485 [PMID: 29181777 DOI: 10.1007/s11701-017-0769-y]

73 **Gangemi A**, Danilkowicz R, Elli FE, Bianco F, Masrur M, Giulianotti PC. Could ICG-aided robotic cholecystectomy reduce the rate of open conversion reported with laparoscopic approach? *J Robot Surg* 2017; **11**: 77-82 [PMID: 27435700 DOI: 10.1007/s11701-016-0624-6]

74 **Dip F**, Sarotto L, Roy M, Lee A, LoMenzo E, Walsh M, Carus T, Schneider S, Boni L, Ishizawa T, Kokudo N, White K, Rosenthal RJ. Incisionless fluorescent cholangiography (IFC): a pilot survey of surgeons on procedural familiarity, practices, and perceptions. *Surg Endosc* 2020; **34**: 675-685 [PMID: 31062156 DOI: 10.1007/s00464-019-06814-x]

75 **Brunt LM**, Deziel DJ, Telem DA, Strasberg SM, Aggarwal R, Asbun H, Bonjer J, McDonald M, Alseidi A, Ujiki M, Riall TS, Hammill C, Moulton CA, Pucher PH, Parks RW, Ansari MT, Connor S, Dirks RC, Anderson B, Altieri MS, Tsamalaidze L, Stefanidis D; and the Prevention of Bile Duct Injury Consensus Work Group. Safe Cholecystectomy Multi-society Practice Guideline and State of the Art Consensus Conference on Prevention of Bile Duct Injury During Cholecystectomy. *Ann Surg* 2020; **272**: 3-23 [PMID: 32404658 DOI: 10.1097/SLA.0000000000003791]

76 **Dip F**, Boni L, Bouvet M, Carus T, Diana M, Falco J, Gurtner GC, Ishizawa T, Kokudo N, Lo Menzo E, Low PS, Masia J, Muehrcke D, Papay FA, Pulitano C, Schneider-Koraith S, Sherwinter D, Spinoglio G, Stassen L, Urano Y, Vahrmeijer A, Vibert E, Warram J, Wexner SD, White K, Rosenthal RJ. Consensus Conference Statement on the General Use of Near-Infrared Fluorescence Imaging and Indocyanine Green Guided Surgery: Results of a Modified Delphi Study. *Ann Surg* 2020 [PMID: 33214476 DOI: 10.1097/SLA.0000000000004412]

77 **Benya R**, Quintana J, Brundage B. Adverse reactions to indocyanine green: a case report and a review of the literature. *Cathet Cardiovasc Diagn* 1989; **17**: 231-233 [PMID: 2670244 DOI: 10.1002/ccd.1810170410]

World Journal of Gastroenterology

Submit a Manuscript: https://www.f6publishing.com

World J Gastroenterol 2021 September 28; 27(36): 6004-6024

DOI: 10.3748/wjg.v27.i36.6004

ISSN 1007-9327 (print) ISSN 2219-2840 (online)

REVIEW

Histone methylation in pancreatic cancer and its clinical implications

Xing-Yu Liu, Chuan-Hao Guo, Zhi-Yuan Xi, Xin-Qi Xu, Qing-Yang Zhao, Li-Sha Li, Ying Wang

ORCID number: Xing-Yu Liu 0000-0001-5800-2787; Chuan-Hao Guo 0000-0001-5801-0453; Zhi-Yuan Xi 0000-0002-3747-3042; Xin-Qi Xu 0000-0002-7688-7619; Qing-Yang Zhao 0000-0002-0386-5507; Li-Sha Li 0000-0003-4048-5981; Ying Wang 0000-0003-1633-0007.

Author contributions: Liu XY, Guo CH, Xi ZY, Xu XQ, and Zhao QY drafted the manuscript and designed the tables; Li LS and Wang Y designed and revised the manuscript; All authors have read and approved the final manuscript.

Conflict-of-interest statement: The authors have no conflicts of interests or financial disclosures relevant to this manuscript.

Open-Access: This article is an open-access article that was selected by an in-house editor and fully peer-reviewed by external reviewers. It is distributed in accordance with the Creative Commons Attribution NonCommercial (CC BY-NC 4.0) license, which permits others to distribute, remix, adapt, build upon this work non-commercially, and license their derivative works on different terms, provided the original work is properly cited and the use is non-commercial. See: http://creativecommons.org/Licenses/by-nc/4.0/

Manuscript source: Invited manuscript

Xing-Yu Liu, Xin-Qi Xu, Qing-Yang Zhao, Ying Wang, The First Hospital of Jilin University, Jilin University, Changchun 130021, Jilin Province, China

Chuan-Hao Guo, Zhi-Yuan Xi, Li-Sha Li, The Key Laboratory of Pathobiology, Ministry of Education, College of Basic Medical Sciences, Jilin University, Changchun 130021, Jilin Province, China

Corresponding author: Ying Wang, MM, Technologist-In-Charge, The First Hospital of Jilin University, Jilin University, No. 126 Xinmin Street, Changchun 130021, Jilin Province, China. wangying_jy@jlu.edu.cn

Abstract

Pancreatic cancer (PC) is an aggressive human cancer. Appropriate methods for the diagnosis and treatment of PC have not been found at the genetic level, thus making epigenetics a promising research path in studies of PC. Histone methylation is one of the most complicated types of epigenetic modifications and has proved crucial in the development of PC. Histone methylation is a reversible process regulated by readers, writers, and erasers. Some writers and erasers can be recognized as potential biomarkers and candidate therapeutic targets in PC because of their unusual expression in PC cells compared with normal pancreatic cells. Based on the impact that writers have on the development of PC, some inhibitors of writers have been developed. However, few inhibitors of erasers have been developed and put to clinical use. Meanwhile, there is not enough research on the reader domains. Therefore, the study of erasers and readers is still a promising area. This review focuses on the regulatory mechanism of histone methylation, and the diagnosis and chemotherapy of PC based on it. The future of epigenetic modification in PC research is also discussed.

Key Words: Pancreatic cancer; Epigenetics; Histone modification; Methylation; Demethylation; Clinical application

©The Author(s) 2021. Published by Baishideng Publishing Group Inc. All rights reserved.

Core Tip: Pancreatic cancer is a highly lethal malignancy of the digestive tract that is difficult to diagnose and treat. Histone methylation/demethylation equilibrium is altered in carcinogenesis, resulting in changes in chromatin structure and gene expression. Not only are histone methylation writers related to histone methylation

Specialty type: Gastroenterology and hepatology

Country/Territory of origin: China

Peer-review report's scientific quality classification

Grade A (Excellent): 0
Grade B (Very good): 0
Grade C (Good): C, C
Grade D (Fair): 0
Grade E (Poor): 0

Received: January 27, 2021
Peer-review started: January 27, 2021
First decision: February 25, 2021
Revised: March 12, 2021
Accepted: April 22, 2021
Article in press: April 22, 2021
Published online: September 28, 2021

P-Reviewer: Kobayashi S, Tada M
S-Editor: Gao CC
L-Editor: Filipodia
P-Editor: Li JH



erasers but histone methylation is also related to other epigenetic modifications. Therefore, histone methylation is addressed as a potentially important chemotherapy drug target.

Citation: Liu XY, Guo CH, Xi ZY, Xu XQ, Zhao QY, Li LS, Wang Y. Histone methylation in pancreatic cancer and its clinical implications. *World J Gastroenterol* 2021; 27(36): 6004-6024
URL: https://www.wjgnet.com/1007-9327/full/v27/i36/6004.htm
DOI: https://dx.doi.org/10.3748/wjg.v27.i36.6004

INTRODUCTION

Pancreatic cancer (PC) is a malignant tumor. The lack of adequate diagnostics for PC limits the efficacy of the few currently available treatment options. Current diagnostic methods include clinical biomarkers, imaging, biopsy, *etc.* To date, carcinoembryonic antigen 19 (CA-19) is the only PC clinical biomarker approved by the U.S. Food and Drug Administration[1], but the use of CA-19 is limited by its inadequate sensitivity and specificity[2,3]. Percutaneous biopsy can result in micrometastases in younger patients who receive surgery, so it is only appropriate for inoperable patients[4]. Current diagnostic methods are either inaccurate or limited. Conventional treatment methods for PC mainly include surgery, adjuvant chemotherapy, drug therapy, and radiation therapy[5]. Surgery remains the most important treatment, followed by adjuvant chemotherapy[5]. At present, only 15% to 20% patients can be surgically treated after diagnosis, and only 20% of the patients survive 5 years after receiving surgery[6,7]. Regarding chemotherapy, gemcitabine and other drugs have proved effective for advanced and metastatic PC, but the development of drug resistance has limited the effectiveness[8]. The survival rate of PC patients has not changed much in the past 40 years[8]. The robust molecular biomarkers need to be developed for diagnosis and targeted therapies.

Cancer development is a complex process involving both genetic and epigenetic changes. Genome instability, regulated by both genetic mutations and epigenetic modifications, contributes to tumor progression[9]. The concept of epigenetics itself is evolving with the increase of our knowledge of the molecular mechanism and regulation of gene expression. It is currently widely acknowledged that epigenetics is the study of alternations in gene expression patterns without changes in DNA sequences[10]. Epigenetic modifications include DNA methylation, histone modification and non-coding RNAs. Epigenetic modifications present a new direction for cancer prevention, clinical diagnosis, and drug development.

Histone modification is one of the most important and complicated epigenetic regulatory mechanisms and is crucial in PC. Histone modification affects chromatin structure, transcription, and DNA repair process[11]. Histone modification takes part in the regulation of chromatin architecture and specific loci regulation by recruiting cell-specific transcription factors and interacting with initiation and elongation factors [12]. Histone modification also regulates the transcription process by influencing RNA processing[12]. In terms of regulating chromatin structure, histone modification affects the higher-order chromatin structure by changing the interactions of histones with DNA, and/or by recruiting chromatin remodeling complexes indirectly[13-15].

Histone modifications include histone acetylation, methylation, phosphorylation, and ubiquitination. Histone methylation plays crucial roles in the development of PC. Therefore, this review focuses on histone methylation and its clinical applications.

HISTONE METHYLATION

Post-translational methylation in histone tails is a reversible dynamic chromatin modification. Methyl is dynamically added by methyltransferases-writers, removed by demethylase-erasers, and interpreted by effector proteins-readers[16]. Readers recognize specific sites and promote the recruitment of transcription factors or chromatin-associated protein complexes and bind to histones to enable the localization of enzymes to specific targets[17].

Histone methylation takes place on the residues of arginine, lysine, and histidine. According to the amino acid residues modified, there are arginine residue methyltransferases and lysine residue methyltransferases[18]. Histone arginine methylation is a universal post-translational modification, and aberrant histone arginine methylation is strongly associated with carcinogenesis and metastasis[19]. Arginine residues may be differentially methylated by different types of protein arginine N-methyltransferases (PRMTs)[19].

The maintenance of the balance between histone methylation and demethylation is fundamental to normal cellular development and function[20,21]. The break of the balance between histone methylation and demethylation results in oncogenesis and progression[21,22]. Corresponding to writers, erasers can be divided into arginine residue demethylases and lysine residue demethylases. However, current research on histone arginine residue demethylases is limited, so we only discuss lysine residue demethylases. Based on their mechanism of action, lysine demethylases (KDMs) are classified into two families: Flavin adenine dinucleotide (FAD)-dependent and Fe(II) and 2-oxoglutarate (2OG)-dependent[23-25].

The appropriate localization of histone methyltransferase and histone demethylase is dependent on the readers that can recognize histone modifications[26]. The reader can either be an independent polypeptide or a part of methyltransferase/demethylase [27-31]. Some reader domains such as chromodomain[32,33], Tudor domain[34], tryptophan-aspartic acid 40 (WD40) domain[35,36] and plant homeodomain (PHD) finger[37,38] are well known. These reader domains all have their own specific structure[32-38].

HISTONE METHYLATION WRITERS IN PC

Among histone methylation, arginine and lysine methylation are the most widely studied in PC[39]. Histone methylation is performed mainly by two types of writers: PRMTs and lysine methyltransferases (KMTs) (Table 1), with S-adenosyl-L-methionine (SAM) as the methyl donor[40].

PRMTs

PRMTs catalyze the transfer of a methyl group from SAM to a guanidino-nitrogen atom[41]. Three types of methylated arginine residues are found in mammalian cells: Asymmetric dimethyl-arginine (ADMA), symmetric dimethyl-arginine (SDMA) and monomethyl-arginine (MMA)[41]. Depending on their catalytic activity, PRMTs can be classified in three types[42]. Type I PRMTs are responsible for producing ADMA, whose methyl groups are linked to the same guanidino nitrogen atom. Type II PRMTs add the methyl groups on each of the guanidino nitrogen atom of arginine symmetrically, producing SDMA[42]. PRMT7 is the sole member of type III, exclusively catalyzing the formation of MMA[43]. PRMT1 and PRMT5 function in PC[44,45]. PRMT1 belongs to type I and PRMT5 belongs to type II[42].

PRMT1: PRMT1 is the founding member of the PRMT family, and PRMT1 can methylate histone H4 at arginine 3. This modification is associated with transcriptional activation[44]. Upregulation of PRMT1 is found in various cancer types[46-49]. PRMT1 is highly expressed in pancreatic ductal adenocarcinoma (PDAC) cells, and elevated PRMT1 levels predict a poor clinical outcome[44]. PRMT1 promotes PC cell growth *in vitro* and *in vivo*[44]. PRMT1 increases the β-catenin protein level in PC cells[44]. Overactivation of β-catenin signaling promotes the growth, migration, and metastasis of PC cells[50-52]. PRMT1 downregulation inhibits PC cell proliferation and invasion [53]. GLI family zinc finger 1 (Gli1) is a substrate of PRMT1 in PDAC. Methylation of Gli1 at R597 by PRMT1 promotes its transcriptional activity by enhancing the binding of Gli1 to the promoters of its target gene[54]. Interruption of Gli1 methylation attenuates oncogenic functions of Gli1 and sensitizes PDAC cells to gemcitabine treatment[54].

PRMT5: PRMT5 is a type II writer, responsible for symmetric demethylation[19,55]. PRMT5 regulates the expression of a wide spectrum of target genes by modifying the chromatin structure or transcriptional machinery[56]. Specifically, PRMT5 can catalyze the methylation of arginine 8 on histone H3 and arginine 3 on histone H4 (H4R3)[57]. High expression of PRMT5 has been observed in various cancers. PRMT5 expression improves cancer cell survival, proliferation, migration and metabolism while inhibiting cancer cell apoptosis[55]. PRMT5 expression is significantly upregulated in PC tissues[56]. PRMT5 promotes tumorigenesis and PC cell proliferation[45]. PRMT5

Table 1 Histone methyltransferases play a major role in pancreatic cancer

Family	Subfamily	Alias	Site	Function in pancreatic cancer
PRMTs	PRMT1	HRMT1L2, HMT2, ANM1	H4R3me2a	Increase the β-catenin protein level; Methylate Gli1 at R597[44,54]
	PRMT5	HRMT1L5, SKB1, HSL7	H3R2me2s	Silence the expression of the tumor suppressor FBW7; Promote EMT *via* activating EGFR/ AKT/β-catenin signaling[45,56,188,189]
KMTs	SMYD3	ZNFN3A1, ZMYND1	H4K5me3	Affect the PC progression by regulating MMP-2; Potentiate Ras signaling through methylation of MAP3K2[62,64]
	EZH2	KMT6, WVS, ENX-1	H3K27me3	Suppress miR-139-5p expression by upregulating H3K27me3; Repress the E-cadherin by tri-methylation of H3K27[78,190]

All current research on reprogramming histone methyltransferases that play a role in pancreatic cancer. EMT: Epithelial-mesenchymal transition; FBW7: F-Box and WD repeat domain containing 7; KMTs: Histone lysine methyltransferases; PC: Pancreatic cancer; PRMTs: Protein arginine N-methyltransferases.

promotes cell migration, invasion, and the epithelial-mesenchymal transition (EMT) *via* activating EGFR/AKT/β-catenin signaling in PC cells[45]. PRMT5 knockdown reduces glucose intake and lactate levels in PC cells[56]. PRMT5 can inhibit the expression of F-Box and WD repeat domain containing 7 (FBW7)[58,59]. PRMT5 inhibits FBW7 *via* suppression of *FBW7* gene promoter activity and elevation of cMyc stability, leading to tumorigenicity and aerobic glycolysis in PC cells[56]. PRMT5 induces the phosphorylation of epidermal growth factor receptor (EGFR) at Y1068 and Y1172[45]. Then PRMT5 activates phosphorylation of AKT and its downstream GSK3β [45].

KMTs

KMTs transfer one, two, or three methyl-groups to histone lysine residues[60]. KMTs are categorized into two protein families based on catalytic domain sequence similarity and structural organization[61]. Two major writers, SMYD3 (KMT3E) and EZH2 (KMT6), are related to PC[62,63]. SMYD3 is a member of SET and MYND-domain family[64]. EZH2 belongs to the polycomb family[61].

SMYD3: SMYD3 belongs to the SET and MYND-domain family. SMYD3 can promote the proliferation, migration, and invasion of many types of cancer[64]. SMYD3 is a protooncogene in liver, colon and breast tissue based on its high level of endogenous expression and cancer-related promoter polymorphism[65-70]. SMYD3 is upregulated in PC. SMYD3 is positively associated with caspase-3 and MMP-2 expression in PC tissues[62]. Active Src phosphorylates p300 in the nucleus, and then the complex binds to HMGA2 and SMYD3 genes. Therefore, HMGA2 and SMYD3 are regulated to promote PC cell migration and invasion[71].

EZH2: EZH2 is the enzymatic subunit of polycomb repressive complex 2 (PRC2), a complex that methylates lysine 27 of histone H3(H3K27) to promote transcriptional silencing[72]. High expression of EZH2 protein has been associated with several cancers[73-75]. EZH2 is overexpressed in PC[76]. FBW7 interacts with EZH2 and downregulates EZH2 *via* ubiquitination and degradation in PC cells[76]. Downregulation of FBW7 induces high EZH2 protein expression and promotes tumor progression in PC[76]. Long non-coding RNA (lncRNA) *BLACAT1* facilitates proliferation, migration, and aerobic glycolysis of PC cells by repressing *CDKN1C via* EZH2-induced histone H3 lysine 27 trimethylation (H3K27me3)[77]. EZH2 regulates the expression of miR-139-5p *via* H3K27me3, and the EZH2/miR-139-5p axis participates in the progression of PC, whereby downregulation of EZH2 and upregulation of miR-139-5p repress the EMT and lymph node metastasis of PC[78]. EZH2 can bind to the promoters of P15 and KLF2 to induce H3K27me3[79]. LncRNA *SNHG15* knockdown inhibits PC cell proliferation and tumorigenesis while inducing cell apoptosis, and the *SNHG15*-mediated oncogenic effect is partly by repressing P15 and KLF2 expression *via* EZH2-induced H3K27me3[79].

HISTONE METHYLATION ERASERS IN PC

The demethylation of arginine and lysine in histone tails is the two main forms of histone demethylation. Due to the large gaps in research on arginine demethylation, the main situation of KDMs in PC will be mainly described. KDMs can catalyze monomethyl, dimethyl or trimethyl labeling of histone lysine residues[12]. There is some evidence that occurrence, development, and therapy of PC are all related to KDMs[80,81] (Table 2).

KDM1

Flavin-dependent KDMs are a subfamily of amine oxidases that catalyze the selective posttranslational oxidative demethylation of methyl lysine side chains within substrates[82]. Two subtypes of KDMs, KDM1A and KDM1B, are related to PC[83,84]. They are expressed at high levels in PC tissues. To date, the expression patterns and physiological functions of KDM1A/LSD1 in PC have not been fully elucidated. KDM1A and hypoxia inducible factor-1α (HIF1α) are the interaction partners of the homeobox protein PROX1[85,86]. KDM1A acts synergistically with HIF1α in maintaining glycolysis[87]. Compared with KDM1A, KDM1B/LSD2 lacks a "tower domain" and has a zinc finger domain in the N-terminal region, which makes KDM1B endowed with different biochemical properties[24,25,88]. KDM1B is related to many important biological functions, including transcriptional regulation, genome imprinting, somatic cell reprogramming, DNA methylation, and signal transduction [89-92]. The downregulation of KDM1B can inhibit PC cell proliferation and promote PC cell apoptosis *in vitro*[93,94].

JmjC domain-containing protein family

JmjC domain-containing (JMJD) protein family is a type of Fe (II) and α-ketoglutarate-dependent dioxygenases. The JMJD protein family now consists of 33 members. There are 18 members with the ability to demethylate H3K4, H3K9, H3K27, H3K36, and H4K20[23,95-108].

KDM2B: KDM2B acts on H3K36 demethylation. KDM2B enhances the bypass of primary cell senescence by directly binding to tumor suppressor gene *CDKN2A* sites and demethylating histones, thereby guiding the recruitment of PRC2; thus, it plays an important role in cell cycle progression and senescence[109,110]. KDM2B regulates cell proliferation, migration, and angiogenesis[111-113]. KDM2B plays a crucial role in poorly differentiated PDAC, and there is an interaction between EZH2 and KDM2B [114].

KDM3A: KDM3A/JMJD1A, one member of the JMJD1 family, participates in transcriptional regulation by demethylating monomethyl or dimethyl H3K9[115,116]. Since cells are heterogeneous in early PDAC tissues, new progress has been made in the study of PDAC morphology, which is specifically manifested by the upregulation of *DCLK1* expression[117]. KDM3A plays a key role in the upregulation of *DCLK1* expression, and KDM3A expression inhibitors can inhibit the malignant properties of PDAC[118].

KDM4: The KDM4 subfamily consists of 12 demethylases including KDM4A, B, C, and D, which can catalyze the removal of inhibitory trimethyl marker of H3K9 and H3K36 related to transcription[98,119]. KDM4A, B, and D play a role in PC mainly. The interaction between regulatory factor X-associated protein RFXAP and KDM4A can disrupt DNA damage repair[120]. RFAXP is a key transcription factor for MHC II molecules[121,122]. It can bind to the promoter of *KDM4A* and induce its expression [120]. In PC, Fisetin can interact with RFXAP/KDM4A to inhibit PC tumor growth *in vivo* and cell proliferation *in vitro*[120]. In PC, KDM4B shows the ability to downregulate E-cadherin[123]. The high nuclear expression of KDM4D in the samples of pancreatic resection margins significantly and independently predicts an earlier recurrence in PC patients[124].

KDM5: KDM5 subfamily consists of four members, KDM5A, KDM5B, KDM5C, and KDM5D[125]. The role of KDM5 family in PC is not completely clear. KDM5A is associated with the development of PC[126]. KDM5A inhibits the expression of mitochondrial pyruvate carrier-1 (MPC-1) and controls the metabolites of pyruvate in mitochondria in PDAC[126]. Upregulation of MPC-1 seems to inhibit the development of cancer. Therefore, it can be inferred that KDM5A promotes the development of PDAC.

Table 2 Histone demethylase that plays a major role in pancreatic cancer

Family	Subfamily		Alias	Site	Function in pancreatic cancer
KDM1	KDM1A		LSD1	H3K4me1	Promote the occurrence of cancer[83]
	KDM1B		LSD2, AOF1	H3K4me2	Related to tumor tissue apoptosis[84]
Jumonji C	KDM2B		Ndy1, FBXL10, JHDM1B	H3K4me3, H3K36me2	Promote senescence of primary cells[109,110]
	KDM3A		JMJD1A, JHDM2A	H3K9me2 (preferential), H3K9me1	Regulate biological and pathological processes, including embryonic development, stem cell self-renewal and differentiation, genome integrity and tumorigenesis[191,192]
	KDM4 family	KDM4A	JMJD2A	H3K36me3, H3K9me3	Destruction of homologous recombination[120,138]
		KDM4B	JMJD2B	H3K9me3	Promote epithelial-mesenchymal transition[123]
		KDM4D	JMJD2D	H3K9me2/me3	Stimulates *in vitro* proliferation and cell survival, and plays a vital role in DNA double-strand break repair[193,194]
	KDM5A		JARID1A, RBBP2	H3K4me2	Promote the inhibition of active transcription and repair of DNA double-strand breaks[139,195]
	KDM6 family	KDM6A	UTX	H3K27me2/me3	The effect of KDM6A on PC tissue is currently unclear[196]
		KDM6B	JMJD3	H3K27me2/me3	Enhance the aggressiveness of cancer cells[176]
	PHD finger and zinc finger protein family	KDM7A	JHDM1D	H3K9me2, H3K27me2	May be related to the upregulation of E-cadherin gene expression[93]

All current research on reprogramming histone demethylases that play a role in pancreatic cancer. The table is sorted by family. PC: Pancreatic cancer; PHD: Plant homeodomain.

KDM6: KDM6 subfamily is mainly composed of KDM6A/UTX, its paralogs UTY and KDM6B[127]. They can demethylate the dimethyl and trimethyl groups of H3K27. They play important roles in the occurrence and development of many cancers. KDM6A/UTX has been the most frequently mutated epigenetic regulator in cancers including PC[128-133]. In addition, KDM6A also antagonizes PRC2-mediated H3K27 trimethylation catalyzed by EZH2, thereby regulating development[99,104,134]. KDM6A has not been found to function in PC tissues. Downregulation of KDM6B is widespread in many cancer cells[135,136]. Almost all pancreatic epithelial tissues have been detected *KRAS* gene mutations before they become cancerous[137]. KDM6B, which is located downstream of the *KRAS* gene, is upregulated in the pre-tumor phase of pancreatic intraepithelial tumors[138]. It is worth noting that the expression of KDM6B decreases with cancer development.

KDM7 (PHF and ZF protein subfamily): At present, the effect of KDM7 subfamily on PC has been seldom developed. According to relevant data, KDM7A may be related to the occurrence and development of PC[139].

READER DOMAIN IN WRITERS AND ERASERS

PHD fingers are central "readers" of histone post-translational modifications. They recognize specific histone modifications and bind to histone to ensure the different enzymes to locate in special targets[140,141]. They are structurally conserved, represented by the canonical C4HC2C/H sequence coordinating two zinc ions. They present in many chromatin-modifying proteins, such as demethylases or methyltransferases, or act as scaffolding proteins that can connect multi-subunit enzymatic complexes with a particular genomic region[30,140,141]. In this part, we will discuss how PHD fingers regulate histone methylation/demethylation and their binding substrates (Table 3).

Regulation of writers by PHD finger

KMT2A-E all have PHD fingers, but the number of PHD fingers in these proteins is different. KMT2A and KMT2B have four PHD fingers, while KMT2C has eight PHD fingers and KMT2D has seven PHD fingers, but KMT2E only has one PHD finger.

Table 3 Different enzymes and plant homeodomain finger domain

Type of enzyme	Name of enzyme	PHD domain	Histone substrates	Function
Histone demethylation enzyme	KDM1B/LSD2	PHD	H3K4me2	Unknown[25]
	KDM2A	PHD	H3K36me2/me1	Unknown[150]
	KDM4A-C	Two PHD	Unknown	Unknown[155,197]
	KDM5A	PHD1	Unmethylated H3K4 histone tail	PHD1 finger by H3 N-terminal tail peptides stabilizes binding of the substrate to the catalytic finger and improves the catalytic efficiency of demethylation[198,199]
		PHD2	Unmodified H3K4	Unknown[158]
		PHD3	H3K4me3	PHD3 finger can recruit substrate and it relates to demethylation propagation along nucleosomes *via* a positive-feedback regulatory mechanism[151,199]
	KDM5B	PHD1	H3K4me0	PHD1 finger recognizes the N-terminus of histone H3, provides an anchoring mechanism for KDM5B and PHD1-H3K4me0 is interaction is important for inhibition of migration[17]
		PHD2	Couldn't bind to histone	Unknown[17]
		PHD3	H3K4me3/H3K4me0	PHD3 finger detects H3K4me3, anchors at chromatin and spreads the transcriptionally inactive state
	KDM5C	PHD1	H3K4	PHD1 finger stabilizes the substrate peptide and helps to position the H3K4 in the JmjC finger exactly[162]
	PHF8(KDM7subfamily)	PHD1	Suppressive marks on H3K9me2/me3 and H3K27me2/me3 and H4k20me2/me3	PHD1 finger plays a significant role in PHF8 substrate recognition and helps to improve substrate affinity and specificity[164]
Histone methylation enzyme	KMT2A, KMT2B	PHD1	Unknown	PHD1 finger is necessary for a context-dependent regulation of holocomplex formation and implicated in tumor suppression[143]
		PHD2	Unknown	PHD2 finger shows the E3 ubiquitin ligase activity and involve in homo-dimerization[144,200]. Mutation in PHD2 will enhance transactivation ability and help to recruit target gene promoters
		PHD3	H3K4me3/me2	Unclear, one possibility is binding of H3K4me3 by PHD3 is necessary for the transcription-promoting effects of KMT2A/2B, another is to set a broad, methylated chromatin finger[145]
		PHD4	Unknown	PHD4 finger mediates intramolecular interactions between the N-terminal and C-terminal fragments of KMT2A with PHD1, and improves its stability[143]
	KMT2C	Eight PHD fingers	Unknown	These fingers help KMT2C to recruit to its target genes correctly[30,146]
	KMT2D	Seven PHD fingers	Unmodified histone H4 and asymmetrical H4R3me2	These fingers are essential for methyltransferase activity of KMT2D and KMT2D-mediated differentiation[201]
	KMT2E	PHD	H3K4me3	PHD finger binds to H3K4me3 specially and facilitates the recruitment of KMT2E to active transcription chromatin regions[148,149,202]

All current research on the regulation of writers and erasers by plant homeodomain domain. "Unknown" means that the corresponding literature was not mentioned. This table is sorted by types and subfamilies of enzymes. JmjC: Jumonji C; KMT: Histone lysine methyltransferase; PHD: Plant homeodomain.

There are 24 PHD fingers in KMT2A-E[142].

Regulation of KMT2A and KMT2B by PHD finger: KMT2A and KMT2B have similar domain architecture and both contain three consecutive PHD fingers, PHD1-3. These consecutive PHD fingers are followed by a bromodomain and the fourth PHD4 finger [142]. The precise function of PHD1 finger in KMT2A and KMT2B is unclear, but it can regulate the intramolecular interactions between N-terminal and C-terminal segments [143]. PHD1 fingers are necessary for holocomplex formation and are implicated in

tumor suppression[143]. PHD2 finger has an E3 ubiquitin ligase in the presence of the E2-conjugating enzyme CDC34[144]. Mutation of the PHD2 finger will cause increased transactivation ability of KMT2A and its recruitment to target genes[142], because of increased protein stability[144]. PHD3 finger binds to H3K4me3/me2, but the affinity between PHD3 finger and H3K4me2 is eight times lower than the affinity between PHD3 finger and H3K4me3[145]. Although PHD3 finger can recognize H3K4me3, the special function of KMT2A in transcriptional maintenance is unclear[145]. One possibility is that binding of H3K4me3 by PHD3 finger is necessary for the transcription-promoting effects of KMT2A, and another possibility is that newly deposited H3K4me3 mark helps KMT2A slide along the gene to set a broad, methylated chromatin domain[145]. The stability of KMT2A is dependent on its intramolecular interaction which is mediated *via* its PHD1 finger with PHD4 finger and the phenylalanine/tyrosine-rich domain of KMT2A[143]. Therefore, PHD4 finger in KMT2A can improve the stability of KMT2A in case of hydrolysis.

Regulation of KMT2C by PHD finger: KMT2C contains eight PHD fingers while KMT2D contains seven PHD fingers[142]. Although the function of PHD fingers in KMT2C is unclear, the functional extended PHD finger is important for KMT2C to be recruited to its target genes[146]. PHD4, PHD5, and PHD6 in KMT2D are tandem and these tandem PHDs can bind to unmethylated or asymmetrically demethylated H4 arginine3[147]. This connection is important for nucleosomal methylation activity and mediates stem cell differentiation by KMT2D[147]. But this binding ability is repressed by symmetrical demethylation on arginine-3 of histone H4 (H4R3me2s), because H4R3me2s can hinder the histone binding ability and catalytic activity in PHD4-6[142,147].

Regulation of KMT2E by PHD finger: The binding of KMT2E and histone is based on its single PHD finger which can bind to H3K4me3, and this special spatial structure of KMT2E makes it possible to recognize H3K4me3[148]. Although KMT2E can also bind to H3K4me2 and H3K4me1, the stability of binding of H3K4me2 and KMT2E is five times weaker than H3K4me3, while the stability of binding of H3K4me1 and KMT2E is sixteen times weaker than H3K4me3[148]. This can facilitate the recruitment of KMT2E to active transcription chromatin regions[148,149].

Regulation of erasers by PHD finger

PHD fingers can be found in KDMs[150,151]. These PHD fingers bind to the tail of H3 to enable the localization of enzymes to specific targets[152], and promote the recruitment of transcription factors or chromatin-associated protein complexes[17].

Regulation of KDM4 subfamily by PHD finger: PHD fingers can be found in KDM4 subfamily. KDM4A, KDM4B, and KDM4C have a catalytic histone demethylase domain, double PHD and Tudor domains, whereas KDM4D contains only a catalytic domain and lacks PHD and Tudor domains[153,154]. Although KDM4A-C have PHD fingers, the function of PHD fingers is unclear[155].

Regulation of KDM5 subfamily by PHD finger: KDM5 subfamily, including KDM5A-D, catalyze demethylation of the transcriptionally activating trimethylated and demethylated lysine-4 mark on H3[100,103,156,157]. KDM5A contains three PHD fingers (PHD1, PHD2, PHD3). Qualitative pull-down assays with isolated PHD1 domain of KDM5A show that it binds to unmodified H3K4 peptide[158]. The PHD1 finger preferentially recognizes unmethylated H3K4 histone tail, which is a KDM5A-mediated trimethylation products of H3K4 (H3K4me3) demethylation[151]. The function of PHD2 finger is unknown. PHD3 finger has been studied in the context of its fusion with nucleoporin NUP98 and it specifically binds to the H3K4me3, with a decrease in affinity for lower methylation states[17,158]. Since these preferred binding substrates are the products of KDM5A-mediated demethylation, a model in which demethylation can propagate along nucleosomes *via* a positive-feedback regulatory mechanism, has been put forward[151].

The KDM5B PHD1 finger can recognize the N-terminus of H3, which is unmodified or methylated at Lys9[17]. The KDM5B PHD2 finger cannot bind to histone. The KDM5B PHD3 finger prefers to bind to H3K4me3[17]. The PHD1 finger specifically binds to H3K4me0, and the PHD3 finger is selective for H3K4me3. A combination of two 'readers' capable of recognizing distinctive epigenetic marks is likely to impact KDM5B activity. Binding of PHD1 to H3K4me0 may provide an anchoring mechanism for KDM5B to sense H3K4me3 through PHD3 and slide along the H3K4me3-enriched promoters, demethylating nearby methylated H3K4 and further spreading the

transcriptionally inactive state of chromatin[17]. In addition, abrogation of H3 tail recognition by point mutation in the PHD1 domain of KDM5B decreases H3K4 demethylation in cells, resulting in the repression of tumor suppressor genes[159]. Therefore, the importance of interaction between PHD1 and H3 tail is proved.

Similarly, the PHD1 finger domain in KDM5C is close to the JmjC domain, and the linker of JmjC domain is 13 amino acids long and is expected to recognize and bind to H3K9me3[157,160]. Although the PHD1 domain is not necessary for the demethylase activity, it helps to recognize the substrate peptide[157,161]. The interaction between PHD1 domain and JmjC domain stabilizes the substrate peptide and the PHD1 domain can help precisely position H3K4 in the JmjC domain[162].

Regulation of KDM7 by PHD finger: PHF8 belongs to KDM7 subfamily and transcriptionally removes suppressive demethylation and monomethylation of lysine 9 and 27 on H3 and lysine 20 on H4[163]. PHF8 has a PHD finger which is closed to the catalytic domain. PHD finger in PHF8 plays a significant role in PHF8 substrate recognition, because it helps to improve substrate affinity and specificity[164]. PHF8 can be recruited to the promoters through the combination of its PHD finger and H3K4me2/3 during the cell cycle transition from G1 to S[107]. Although the functions of PHD fingers can be found in gastric cancer[165], breast cancer[166], colorectal cancer[167], lung cancer[168], *etc*., the functions of PHD finger are still unclear in PC.

CLINICAL APPLICATION

Epigenetic genes play vital roles in maintaining structural stability and physiological functions of normal chromosomes and are deficient in some patients with PC, thereby serving as potential targets for correcting these deficiencies and precisely killing these aberrant PC cells[169]. The discovery of histone methyltransferases, demethylases and their active sites has provided new insights in the diagnosis and treatment of PC. The active sites and mechanism of the inhibitors in PC treatment are shown in Table 4.

Histone modifications define the previously unrecognized subsets of PC patients with different epigenetic states and therefore represent the prognostic and predictive biomarkers that can be used to guide clinical decisions, such as the use of fluorouracil chemotherapy[170]. H3K4me2, H3K9me2, or H3K18AC expressed at low levels are positively correlated with the poor prognosis of PC[170]. EZH2 expression is higher in PC cells than in normal cells; thus, EZH2 can be used as a potential biomarker for early diagnosis of PDAC[171]. High expression of KDM4D in benign cells near the edge of surgically resected PC tissues is predictive of early recurrence[124]. The discovery of epigenetic biomarkers can provide a great reference for early diagnosis, drug selection and surgery prognosis of PC.

SMYD3 is a candidate therapeutic target against PC, lung cancer and potentially other RAS-driven tumors[172]. In mice, complete loss of SMYD3 function with no apparent phenotype suggests that SMYD3 inhibitors, as chemotherapeutic agents, cause minimal collateral toxicity. The clinically used combination of Raf protein kinase or dual specificity threonine/tyrosine kinase inhibitors and SMYD3 inhibitors can reduce drug toxicity and suppress the development of drug resistance[172].

SMYD3 inhibitor piperidine-4-formamide-acetanilide compound, BCI-121, is a small molecule inhibitor that significantly inhibits proliferation in PC cell lines with high expression of SMYD3. BCI-121 and histone competitively bind to SMYD3; BCI-121 binds inside the lysine channel, which connects cofactor binding sites and histone peptide binding sites[173].

The PRMT5 inhibitor EZP015556 targets *MTAP* (a gene commonly lost in PC) negative tumors, which indicates that it is an effective treatment for a subpopulation of *MTAP* positive tumors. According to the individualized medication approach, the therapeutic response in different patient-derived organoids (PDOs), developed directly from patient tumor tissue is different. The PDO model is used to validate the effectiveness of PMRT5 inhibition as a potential treatment for PDAC[174]. EZH2 expression in PC cells is significantly higher than that in normal pancreatic duct cells and fibroblasts. 3-Deazaneplanocin A (DZNeP) regulates the expression of EZH2 and H3K27me3, synergically enhancing the anti-proliferative activity of gemcitabine and significantly increasing the apoptosis rate of cells[175]. DZNeP is an S-adenosine homocysteine hydrolase inhibitor. DZNeP also enhances the mRNA and protein expression of nucleoside transporter HENT1/HCNT1[175]. The combination of DZNeP and DZNeP/gemcitabine significantly reduces the growth volume of PDAC spheres in selective medium[175].

Table 4 Inhibitors for the treatment of pancreatic cancer

Drug type	Drug name	Active site	Mechanism	Effect	Targeting tumors
Relating to histone methyltransferase	SMYD3 inhibitor piperidine-4-formamide-acetylaniline compound (BCI-121)	It competes with histones to bind SMYD3, binding sites are formed within the SET and post-SET fingers and contained in a deep and narrow substrate binding cavity	BCI-121 is a competitive inhibitor significantly inhibits; SMYD3-substrate interaction and chromatin recruitment	It inhibits cancer cell growth and accumulates during the cell cycle S	High expression of SMYD3 protein in cancer cell lines (pancreatic cancer, lung, prostate and ovarian cancer)[173]
	PRMT5 inhibitor EZP015556	MTAP	-	It works for MTAP He and MTAP PDO	A negative tumor MTAP (a commonly lost gene in pancreatic cancer) [174]
	EZH2 inhibitor 3-Dazocycline A (DZNeP)	It regulates EZH2 and H3K27me3 protein expression	DZNeP inhibit the activity of S-adenosine-L-homocysteine (AdoHcy) hydrolase, which reversely hydrolyzes AdoHcy to adenosine and homocysteine, thereby inhibiting histone methylation	It synergistically enhanced antiproliferative activity of gemcitabine and significantly increased apoptosis rate	Pancreatic ductal carcinoma[175]
Relating to histone demethylase	BET inhibitor JQ1 related to KDM6A	Reducing activity and p63 levels of MYC pathways	GLI1 is the main target gene of the Hh pathway JQ1 reduces the mRNA and protein levels of primary human CAFs. TGF-β is an interstitial activator that JQ1 its induced response	Altered KMT2C (MLL3)-KDM6A (UTX)- PRC2 regulating axis	Pancreatic ductal carcinoma[169,176, 177]

All current research on inhibitors for the treatment of pancreatic cancer developed based on histone methylation modification. "-" means that the content does not exist here. This table is sorted according to the correlation with histone methyltransferases and demethylases. CAF: Cancer-associated fibroblast; KMT: Histone lysine methyltransferases; PDO: Patient-derived organoid; PRC2: Polycomb repressive complex 2; TGF-β: Transforming growth factor β.

Bromodomain and extra-terminal (BET) inhibitors and EZH2 inhibitors are designed to rescue the dysregulated KMT2C/MLL3-KDM6A/UTX-PRC2 regulatory axis and have achieved preliminary success in preclinical models. The regulatory axis regulates the expression of various downstream tumor suppressor genes[169]. Therefore, rebalancing this axis represents a new approach to PDAC therapy.

Defects in KDM6A make sex-specific squamous PC sensitive to bromouracil and BET inhibitors[169]. BET inhibitor JQ1 reverses squamous cell differentiation and inhibits tumor growth *in vivo* by decreasing MYC pathway activity and p63 levels [176]. JQ1 affects cancer-associated fibroblast (CAF) activation by acting on the Hedgehog and TGF-β pathways. JQ1 inhibitor converts α-SMA-positive CAFs to α-SMA-negative CAFs, but does not eliminate CAFs[177].

Small molecules containing 8-hydroxyquinoline structure are competitive inhibitors of KDM4 (also known as JMJD2) family, binding active iron to inhibit the activity of KDM4 and regulate demethylation of H3K9 sites[178]. KDM4C inhibitor SD70 can inhibit the growth of prostate cancer cells[179].

Many types of inhibitors of KDM1A have been reported, but the inhibitors of this enzyme are mainly targeted at acute myeloid leukemia or small cell lung cancer, *etc.* And there are few studies on PC. For example, SP2509 is a noncompetitive inhibitor, and is used in current clinical trials for the treatment of acute myeloid leukemia or small cell lung cancer[180]. Ory-1001 effectively inactivates LSD1 and is highly selective for FAD-dependent ammonia oxidase[181]. The application of histone demethylase inhibitors in the treatment of PC is still limited, so it is necessary to strengthen the exploration of the treatment of PC based on the existing research.

FUTURE DIRECTIONS

Histone writers and erasers do not work independently. In fact, the interactions between writers and erasers include the positive correlativity between EZH2 and KDM2B, and the synergistic effects of EZH2 and KDM6A[182,183]. In bladder cancer, the H3K27 demethylase KDM6A gene often has mutations[131,184]. This makes cancer tissues that have lost KDM6A more vulnerable to EZH2 attack[185]. This accelerates the onset of tumors. The expression of EZH2 and KDM2B in ovarian cancer is

positively correlated[183]. Therefore, knocking down the KDM2B gene is beneficial to inhibit the migration of ovarian cancer cells *in vitro*.

Many problems remain in the research of histone modifications. Research on histone methyltransferases is relatively adequate, but there are few articles about the mechanism of SMYD2, so SMYD2 is not mentioned in our review. Current research on histone arginine residue demethylases has not yet fully achieved results. Therefore, only histone lysine residue demethylases are discussed. However, the effect of KDM7 subfamily demethylases on PC has seldom been proved, so only some guesses about the effect of KDM7A are mentioned. Besides, the study of the interactions between writers and erasers in PC is still in a blank state. The role of the reader domain in PC remains unclear. This review only lists the roles of the PHD domain in the localization of histone modifications and the recruitment of related protein complexes. Reader domain is still a potential research direction in PC.

The study of histone methylation and demethylation has enlightening effects on the diagnosis, treatment, and prognosis of PC. Histone modifications can be used to predict in the prognosis of PC patients[171]. Histone methyltransferase and demethylase inhibitors are used clinically to treat PC. The corresponding inhibitors act on the signal regulatory pathway and change the signal expression of downstream target cells, thus regulating the growth and development of cancer cells. At present, the research of histone demethylase inhibitors is inadequate. Therefore, histone demethylase inhibitors need to be further explored.

The effect of histone modifications on PC is interdependent. The interactions between histone modifications and other epigenetic forms can influence the occurrence and progression of cancers such as cervical cancer and breast cancer. The effect of these interactions enlightens the research on PC. DNA methylation and the expression of miRNAs can be regulated by histone methyltransferases and demethylases, thereby causing alternations of developing process of cancer. Histone methyltransferase EZH2 epigenetically silences tumor-suppressor miRNAs, such as miR-139-5p, miR-125b, miR-101, let-7c and miR-200b, thereby promoting cancer cell metastasis[186]. Histone demethylase KDM5B targets H3K4 demethylation of miR-let-7e and promotes tumor cell proliferation through epigenetically inhibiting the tumor suppressor miR[187]. The combination of EZH2 and promoter region induces the expression of specific target protein H3K27me3, thereby reducing the expression of downstream gene, DNA (cytosine-5)-methyltransferase 3A (DNMT3A)[10]. EZH2-H3K27me3-DNMT3A is the key factor of regulating cervical total stimulus molecule Tim-3/galectin-9, which results in immune escape in the process of malignant transformation[10]. It is reasonable to speculate that the interaction between histone methylation and other epigenetic modifications may also play a role in PC. This opinion draws some inspiration and reference to future research of PC.

CONCLUSION

This review focuses on the mechanism of histone methylation in PC. Histone methylation is mainly regulated by writer, reader and eraser. Writer refers to histone methyltransferase, eraser refers to histone demethylase and reader refers to the modification domain of histone methyltransferase and demethylase. Reader can be an independent polypeptide or a component of methyltransferase and demethylase. On the one hand, histone methyltransferase can promote the proliferation and invasion of PC cells. On the other hand, histone methyltransferase can inhibit the proliferation of cancer cells. Histone demethylase promotes the occurrence of PC and is related to apoptosis. Reader domain plays a role in guiding related methyltransferases and demethylases to identify corresponding sites during the methylation and demethylation process.

REFERENCES

1 **Daoud AZ**, Mulholland EJ, Cole G, McCarthy HO. MicroRNAs in Pancreatic Cancer: biomarkers, prognostic, and therapeutic modulators. *BMC Cancer* 2019; **19**: 1130 [PMID: 31752758 DOI: 10.1186/s12885-019-6284-y]

2 **Duffy MJ**, Sturgeon C, Lamerz R, Haglund C, Holubec VL, Klapdor R, Nicolini A, Topolcan O, Heinemann V. Tumor markers in pancreatic cancer: a European Group on Tumor Markers (EGTM) status report. *Ann Oncol* 2010; **21**: 441-447 [PMID: 19690057 DOI: 10.1093/annonc/mdp332]

3 **Ansari D**, Torén W, Zhou Q, Hu D, Andersson R. Proteomic and genomic profiling of pancreatic

cancer. *Cell Biol Toxicol* 2019; **35**: 333-343 [PMID: 30771135 DOI: 10.1007/s10565-019-09465-9]
4 **Goral V**. Pancreatic Cancer: Pathogenesis and Diagnosis. *Asian Pac J Cancer Prev* 2015; **16**: 5619-5624 [PMID: 26320426 DOI: 10.7314/apjcp.2015.16.14.5619]
5 **Dumont R**, Puleo F, Collignon J, Meurisse N, Chavez M, Seidel L, Gast P, Polus M, Loly C, Delvenne P, Meunier P, Hustinx R, Deroover A, Detry O, Louis E, Martinive P, Van Daele D. A single center experience in resectable pancreatic ductal adenocarcinoma : the limitations of the surgery-first approach. Critical review of the literature and proposals for practice update. *Acta Gastroenterol Belg* 2017; **80**: 451-461 [PMID: 29560639]
6 **Puckett Y**, Garfield K. Pancreatic Cancer 2021 [PMID: 30085538]
7 **Labori KJ**, Katz MH, Tzeng CW, Bjørnbeth BA, Cvancarova M, Edwin B, Kure EH, Eide TJ, Dueland S, Buanes T, Gladhaug IP. Impact of early disease progression and surgical complications on adjuvant chemotherapy completion rates and survival in patients undergoing the surgery first approach for resectable pancreatic ductal adenocarcinoma - A population-based cohort study. *Acta Oncol* 2016; **55**: 265-277 [PMID: 26213211 DOI: 10.3109/0284186X.2015.1068445]
8 **Zeng S**, Pöttler M, Lan B, Grützmann R, Pilarsky C, Yang H. Chemoresistance in Pancreatic Cancer. *Int J Mol Sci* 2019; **20** [PMID: 31514451 DOI: 10.3390/ijms20184504]
9 **Hanahan D**, Weinberg RA. Hallmarks of cancer: the next generation. *Cell* 2011; **144**: 646-674 [PMID: 21376230 DOI: 10.1016/j.cell.2011.02.013]
10 **Zhang L**, Tian S, Pei M, Zhao M, Wang L, Jiang Y, Yang T, Zhao J, Song L, Yang X. Crosstalk between histone modification and DNA methylation orchestrates the epigenetic regulation of the costimulatory factors, Tim3 and galectin9, in cervical cancer. *Oncol Rep* 2019; **42**: 2655-2669 [PMID: 31661141 DOI: 10.3892/or.2019.7388]
11 **Ning B**, Li W, Zhao W, Wang R. Targeting epigenetic regulations in cancer. *Acta Biochim Biophys Sin (Shanghai)* 2016; **48**: 97-109 [PMID: 26508480 DOI: 10.1093/abbs/gmv116]
12 **Greer EL**, Shi Y. Histone methylation: a dynamic mark in health, disease and inheritance. *Nat Rev Genet* 2012; **13**: 343-357 [PMID: 22473383 DOI: 10.1038/nrg3173]
13 **Suganuma T**, Workman JL. Signals and combinatorial functions of histone modifications. *Annu Rev Biochem* 2011; **80**: 473-499 [PMID: 21529160 DOI: 10.1146/annurev-biochem-061809-175347]
14 **Bell O**, Tiwari VK, Thomä NH, Schübeler D. Determinants and dynamics of genome accessibility. *Nat Rev Genet* 2011; **12**: 554-564 [PMID: 21747402 DOI: 10.1038/nrg3017]
15 **de Almeida SF**, Grosso AR, Koch F, Fenouil R, Carvalho S, Andrade J, Levezinho H, Gut M, Eick D, Gut I, Andrau JC, Ferrier P, Carmo-Fonseca M. Splicing enhances recruitment of methyltransferase HYPB/Setd2 and methylation of histone H3 Lys36. *Nat Struct Mol Biol* 2011; **18**: 977-983 [PMID: 21792193 DOI: 10.1038/nsmb.2123]
16 **Hyun K**, Jeon J, Park K, Kim J. Writing, erasing and reading histone lysine methylations. *Exp Mol Med* 2017; **49**: e324 [PMID: 28450737 DOI: 10.1038/emm.2017.11]
17 **Klein BJ**, Piao L, Xi Y, Rincon-Arano H, Rothbart SB, Peng D, Wen H, Larson C, Zhang X, Zheng X, Cortazar MA, Peña PV, Mangan A, Bentley DL, Strahl BD, Groudine M, Li W, Shi X, Kutateladze TG. The histone-H3K4-specific demethylase KDM5B binds to its substrate and product through distinct PHD fingers. *Cell Rep* 2014; **6**: 325-335 [PMID: 24412361 DOI: 10.1016/j.celrep.2013.12.021]
18 **Varier RA**, Timmers HT. Histone lysine methylation and demethylation pathways in cancer. *Biochim Biophys Acta* 2011; **1815**: 75-89 [PMID: 20951770 DOI: 10.1016/j.bbcan.2010.10.002]
19 **Zhang J**, Jing L, Li M, He L, Guo Z. Regulation of histone arginine methylation/demethylation by methylase and demethylase (Review). *Mol Med Rep* 2019; **19**: 3963-3971 [PMID: 30942418 DOI: 10.3892/mmr.2019.10111]
20 **McCabe MT**, Mohammad HP, Barbash O, Kruger RG. Targeting Histone Methylation in Cancer. *Cancer J* 2017; **23**: 292-301 [PMID: 28926430 DOI: 10.1097/PPO.0000000000000283]
21 **Chi P**, Allis CD, Wang GG. Covalent histone modifications--miswritten, misinterpreted and mis-erased in human cancers. *Nat Rev Cancer* 2010; **10**: 457-469 [PMID: 20574448 DOI: 10.1038/nrc2876]
22 **Shi Y**, Lan F, Matson C, Mulligan P, Whetstine JR, Cole PA, Casero RA, Shi Y. Histone demethylation mediated by the nuclear amine oxidase homolog LSD1. *Cell* 2004; **119**: 941-953 [PMID: 15620353 DOI: 10.1016/j.cell.2004.12.012]
23 **Tsukada Y**, Fang J, Erdjument-Bromage H, Warren ME, Borchers CH, Tempst P, Zhang Y. Histone demethylation by a family of JmjC domain-containing proteins. *Nature* 2006; **439**: 811-816 [PMID: 16362057 DOI: 10.1038/nature04433]
24 **Karytinos A**, Forneris F, Profumo A, Ciossani G, Battaglioli E, Binda C, Mattevi A. A novel mammalian flavin-dependent histone demethylase. *J Biol Chem* 2009; **284**: 17775-17782 [PMID: 19407342 DOI: 10.1074/jbc.M109.003087]
25 **Fang R**, Barbera AJ, Xu Y, Rutenberg M, Leonor T, Bi Q, Lan F, Mei P, Yuan GC, Lian C, Peng J, Cheng D, Sui G, Kaiser UB, Shi Y, Shi YG. Human LSD2/KDM1b/AOF1 regulates gene transcription by modulating intragenic H3K4me2 methylation. *Mol Cell* 2010; **39**: 222-233 [PMID: 20670891 DOI: 10.1016/j.molcel.2010.07.008]
26 **Torres IO**, Fujimori DG. Functional coupling between writers, erasers and readers of histone and DNA methylation. *Curr Opin Struct Biol* 2015; **35**: 68-75 [PMID: 26496625 DOI: 10.1016/j.sbi.2015.09.007]
27 **Musselman CA**, Khorasanizadeh S, Kutateladze TG. Towards understanding methyllysine readout. *Biochim Biophys Acta* 2014; **1839**: 686-693 [PMID: 24727128 DOI: 10.1016/j.bbagrm.2014.04.001]

28 **Upadhyay AK**, Horton JR, Zhang X, Cheng X. Coordinated methyl-lysine erasure: structural and functional linkage of a Jumonji demethylase domain and a reader domain. *Curr Opin Struct Biol* 2011; **21**: 750-760 [PMID: 21872465 DOI: 10.1016/j.sbi.2011.08.003]

29 **Verrier L**, Vandromme M, Trouche D. Histone demethylases in chromatin cross-talks. *Biol Cell* 2011; **103**: 381-401 [PMID: 21736555 DOI: 10.1042/BC20110028]

30 **Musselman CA**, Kutateladze TG. Handpicking epigenetic marks with PHD fingers. *Nucleic Acids Res* 2011; **39**: 9061-9071 [PMID: 21813457 DOI: 10.1093/nar/gkr613]

31 **Lalonde ME**, Cheng X, Côté J. Histone target selection within chromatin: an exemplary case of teamwork. *Genes Dev* 2014; **28**: 1029-1041 [PMID: 24831698 DOI: 10.1101/gad.236331.113]

32 **Hard R**, Li N, He W, Ross B, Mo GCH, Peng Q, Stein RSL, Komives E, Wang Y, Zhang J, Wang W. Deciphering and engineering chromodomain-methyllysine peptide recognition. *Sci Adv* 2018; **4**: eaau1447 [PMID: 30417094 DOI: 10.1126/sciadv.aau1447]

33 **Yap KL**, Zhou MM. Structure and mechanisms of lysine methylation recognition by the chromodomain in gene transcription. *Biochemistry* 2011; **50**: 1966-1980 [PMID: 21288002 DOI: 10.1021/bi101885m]

34 **El Agha E**, Kramann R, Schneider RK, Li X, Seeger W, Humphreys BD, Bellusci S. Mesenchymal Stem Cells in Fibrotic Disease. *Cell Stem Cell* 2017; **21**: 166-177 [PMID: 28777943 DOI: 10.1016/j.stem.2017.07.011]

35 **Bergamin E**, Blais A, Couture JF. Keeping them all together: β-propeller domains in histone methyltransferase complexes. *J Mol Biol* 2014; **426**: 3363-3375 [PMID: 24853063 DOI: 10.1016/j.jmb.2014.05.010]

36 **Xu C**, Min J. Structure and function of WD40 domain proteins. *Protein Cell* 2011; **2**: 202-214 [PMID: 21468892 DOI: 10.1007/s13238-011-1018-1]

37 **Adams-Cioaba MA**, Min J. Structure and function of histone methylation binding proteins. *Biochem Cell Biol* 2009; **87**: 93-105 [PMID: 19234526 DOI: 10.1139/O08-129]

38 **Liu R**, Gao J, Yang Y, Qiu R, Zheng Y, Huang W, Zeng Y, Hou Y, Wang S, Leng S, Feng D, Yu W, Sun G, Shi H, Teng X, Wang Y. PHD finger protein 1 (PHF1) is a novel reader for histone H4R3 symmetric dimethylation and coordinates with PRMT5-WDR77/CRL4B complex to promote tumorigenesis. *Nucleic Acids Res* 2018; **46**: 6608-6626 [PMID: 29846670 DOI: 10.1093/nar/gky461]

39 **Ma F**, Zhang CY. Histone modifying enzymes: novel disease biomarkers and assay development. *Expert Rev Mol Diagn* 2016; **16**: 297-306 [PMID: 26750583 DOI: 10.1586/14737159.2016.1135057]

40 **Morera L**, Lübbert M, Jung M. Targeting histone methyltransferases and demethylases in clinical trials for cancer therapy. *Clin Epigenetics* 2016; **8**: 57 [PMID: 27222667 DOI: 10.1186/s13148-016-0223-4]

41 **Poulard C**, Corbo L, Le Romancer M. Protein arginine methylation/demethylation and cancer. *Oncotarget* 2016; **7**: 67532-67550 [PMID: 27556302 DOI: 10.18632/oncotarget.11376]

42 **Rakow S**, Pullamsetti SS, Bauer UM, Bouchard C. Assaying epigenome functions of PRMTs and their substrates. *Methods* 2020; **175**: 53-65 [PMID: 31542509 DOI: 10.1016/j.ymeth.2019.09.014]

43 **Zurita-Lopez CI**, Sandberg T, Kelly R, Clarke SG. Human protein arginine methyltransferase 7 (PRMT7) is a type III enzyme forming ω-NG-monomethylated arginine residues. *J Biol Chem* 2012; **287**: 7859-7870 [PMID: 22241471 DOI: 10.1074/jbc.M111.336271]

44 **Song C**, Chen T, He L, Ma N, Li JA, Rong YF, Fang Y, Liu M, Xie D, Lou W. PRMT1 promotes pancreatic cancer growth and predicts poor prognosis. *Cell Oncol (Dordr)* 2020; **43**: 51-62 [PMID: 31520395 DOI: 10.1007/s13402-019-00435-1]

45 **Ge L**, Wang H, Xu X, Zhou Z, He J, Peng W, Du F, Zhang Y, Gong A, Xu M. PRMT5 promotes epithelial-mesenchymal transition *via* EGFR-β-catenin axis in pancreatic cancer cells. *J Cell Mol Med* 2020; **24**: 1969-1979 [PMID: 31851779 DOI: 10.1111/jcmm.14894]

46 **Choucair A**, Pham TH, Omarjee S, Jacquemetton J, Kassem L, Trédan O, Rambaud J, Marangoni E, Corbo L, Treilleux I, Le Romancer M. The arginine methyltransferase PRMT1 regulates IGF-1 signaling in breast cancer. *Oncogene* 2019; **38**: 4015-4027 [PMID: 30692633 DOI: 10.1038/s41388-019-0694-9]

47 **Li Z**, Wang D, Lu J, Huang B, Wang Y, Dong M, Fan D, Li H, Gao Y, Hou P, Li M, Liu H, Pan ZQ, Zheng J, Bai J. Methylation of EZH2 by PRMT1 regulates its stability and promotes breast cancer metastasis. *Cell Death Differ* 2020; **27**: 3226-3242 [PMID: 32895488 DOI: 10.1038/s41418-020-00615-9]

48 **He L**, Hu Z, Sun Y, Zhang M, Zhu H, Jiang L, Zhang Q, Mu D, Zhang J, Gu L, Yang Y, Pan FY, Jia S, Guo Z. PRMT1 is critical to FEN1 expression and drug resistance in lung cancer cells. *DNA Repair (Amst)* 2020; **95**: 102953 [PMID: 32861926 DOI: 10.1016/j.dnarep.2020.102953]

49 **Li M**, An W, Xu L, Lin Y, Su L, Liu X. The arginine methyltransferase PRMT5 and PRMT1 distinctly regulate the degradation of anti-apoptotic protein $CFLAR_L$ in human lung cancer cells. *J Exp Clin Cancer Res* 2019; **38**: 64 [PMID: 30736843 DOI: 10.1186/s13046-019-1064-8]

50 **Yu L**, Li X, Li H, Chen H, Liu H. Rab11a sustains GSK3β/Wnt/β-catenin signaling to enhance cancer progression in pancreatic cancer. *Tumour Biol* 2016; **37**: 13821-13829 [PMID: 27481517 DOI: 10.1007/s13277-016-5172-1]

51 **Ji M**, Fan D, Yuan L, Zhang Y, Dong W, Peng X. EBP50 inhibits pancreatic cancer cell growth and invasion by targeting the β-catenin/E-cadherin pathway. *Exp Ther Med* 2015; **10**: 1311-1316 [PMID: 26622484 DOI: 10.3892/etm.2015.2684]

52 **Zhou W**, Li Y, Gou S, Xiong J, Wu H, Wang C, Yan H, Liu T. MiR-744 increases tumorigenicity of pancreatic cancer by activating Wnt/β-catenin pathway. *Oncotarget* 2015; **6**: 37557-37569 [PMID: 26485754 DOI: 10.18632/oncotarget.5317]

53 **Lin Z**, Chen Y, Lin Z, Chen C, Dong Y. Overexpressing PRMT1 Inhibits Proliferation and Invasion in Pancreatic Cancer by Inverse Correlation of ZEB1. *IUBMB Life* 2018; **70**: 1032-1039 [PMID: 30194893 DOI: 10.1002/iub.1917]

54 **Wang Y**, Hsu JM, Kang Y, Wei Y, Lee PC, Chang SJ, Hsu YH, Hsu JL, Wang HL, Chang WC, Li CW, Liao HW, Chang SS, Xia W, Ko HW, Chou CK, Fleming JB, Wang H, Hwang RF, Chen Y, Qin J, Hung MC. Oncogenic Functions of Gli1 in Pancreatic Adenocarcinoma Are Supported by Its PRMT1-Mediated Methylation. *Cancer Res* 2016; **76**: 7049-7058 [PMID: 27758883 DOI: 10.1158/0008-5472.Can-16-0715]

55 **Yuan Y**, Nie H. Protein arginine methyltransferase 5: a potential cancer therapeutic target. *Cell Oncol (Dordr)* 2021; **44**: 33-44 [PMID: 33469838 DOI: 10.1007/s13402-020-00577-7]

56 **Qin Y**, Hu Q, Xu J, Ji S, Dai W, Liu W, Xu W, Sun Q, Zhang Z, Ni Q, Zhang B, Yu X, Xu X. PRMT5 enhances tumorigenicity and glycolysis in pancreatic cancer *via* the FBW7/cMyc axis. *Cell Commun Signal* 2019; **17**: 30 [PMID: 30922330 DOI: 10.1186/s12964-019-0344-4]

57 **Kim H**, Ronai ZA. PRMT5 function and targeting in cancer. *Cell Stress* 2020; **4**: 199-215 [PMID: 32743345 DOI: 10.15698/cst2020.08.228]

58 **Davis RJ**, Welcker M, Clurman BE. Tumor suppression by the Fbw7 ubiquitin ligase: mechanisms and opportunities. *Cancer Cell* 2014; **26**: 455-464 [PMID: 25314076 DOI: 10.1016/j.ccell.2014.09.013]

59 **Shimizu K**, Nihira NT, Inuzuka H, Wei W. Physiological functions of FBW7 in cancer and metabolism. *Cell Signal* 2018; **46**: 15-22 [PMID: 29474981 DOI: 10.1016/j.cellsig.2018.02.009]

60 **Black JC**, Van Rechem C, Whetstine JR. Histone lysine methylation dynamics: establishment, regulation, and biological impact. *Mol Cell* 2012; **48**: 491-507 [PMID: 23200123 DOI: 10.1016/j.molcel.2012.11.006]

61 **McGrath J**, Trojer P. Targeting histone lysine methylation in cancer. *Pharmacol Ther* 2015; **150**: 1-22 [PMID: 25578037 DOI: 10.1016/j.pharmthera.2015.01.002]

62 **Zhu CL**, Huang Q. Overexpression of the SMYD3 Promotes Proliferation, Migration, and Invasion of Pancreatic Cancer. *Dig Dis Sci* 2020; **65**: 489-499 [PMID: 31441002 DOI: 10.1007/s10620-019-05797-y]

63 **Patil S**, Steuber B, Kopp W, Kari V, Urbach L, Wang X, Küffer S, Bohnenberger H, Spyropoulou D, Zhang Z, Versemann L, Bösherz MS, Brunner M, Gaedcke J, Ströbel P, Zhang JS, Neesse A, Ellenrieder V, Singh SK, Johnsen SA, Hessmann E. EZH2 Regulates Pancreatic Cancer Subtype Identity and Tumor Progression *via* Transcriptional Repression of *GATA6*. *Cancer Res* 2020; **80**: 4620-4632 [PMID: 32907838 DOI: 10.1158/0008-5472.CAN-20-0672]

64 **Giakountis A**, Moulos P, Sarris ME, Hatzis P, Talianidis I. Smyd3-associated regulatory pathways in cancer. *Semin Cancer Biol* 2017; **42**: 70-80 [PMID: 27554136 DOI: 10.1016/j.semcancer.2016.08.008]

65 **Foreman KW**, Brown M, Park F, Emtage S, Harriss J, Das C, Zhu L, Crew A, Arnold L, Shaaban S, Tucker P. Structural and functional profiling of the human histone methyltransferase SMYD3. *PLoS One* 2011; **6**: e22290 [PMID: 21779408 DOI: 10.1371/journal.pone.0022290]

66 **Hamamoto R**, Furukawa Y, Morita M, Iimura Y, Silva FP, Li M, Yagyu R, Nakamura Y. SMYD3 encodes a histone methyltransferase involved in the proliferation of cancer cells. *Nat Cell Biol* 2004; **6**: 731-740 [PMID: 15235609 DOI: 10.1038/ncb1151]

67 **Hamamoto R**, Silva FP, Tsuge M, Nishidate T, Katagiri T, Nakamura Y, Furukawa Y. Enhanced SMYD3 expression is essential for the growth of breast cancer cells. *Cancer Sci* 2006; **97**: 113-118 [PMID: 16441421 DOI: 10.1111/j.1349-7006.2006.00146.x]

68 **Silva FP**, Hamamoto R, Kunizaki M, Tsuge M, Nakamura Y, Furukawa Y. Enhanced methyltransferase activity of SMYD3 by the cleavage of its N-terminal region in human cancer cells. *Oncogene* 2008; **27**: 2686-2692 [PMID: 17998933 DOI: 10.1038/sj.onc.1210929]

69 **Tsuge M**, Hamamoto R, Silva FP, Ohnishi Y, Chayama K, Kamatani N, Furukawa Y, Nakamura Y. A variable number of tandem repeats polymorphism in an E2F-1 binding element in the 5' flanking region of SMYD3 is a risk factor for human cancers. *Nat Genet* 2005; **37**: 1104-1107 [PMID: 16155568 DOI: 10.1038/ng1638]

70 **Wang H**, Liu Y, Tan W, Zhang Y, Zhao N, Jiang Y, Lin C, Hao B, Zhao D, Qian J, Lu D, Jin L, Wei Q, Lin D, He F. Association of the variable number of tandem repeats polymorphism in the promoter region of the SMYD3 gene with risk of esophageal squamous cell carcinoma in relation to tobacco smoking. *Cancer Sci* 2008; **99**: 787-791 [PMID: 18294291 DOI: 10.1111/j.1349-7006.2008.00729.x]

71 **Paladino D**, Yue P, Furuya H, Acoba J, Rosser CJ, Turkson J. A novel nuclear Src and p300 signaling axis controls migratory and invasive behavior in pancreatic cancer. *Oncotarget* 2016; **7**: 7253-7267 [PMID: 26695438 DOI: 10.18632/oncotarget.6635]

72 **Kim KH**, Roberts CW. Targeting EZH2 in cancer. *Nat Med* 2016; **22**: 128-134 [PMID: 26845405 DOI: 10.1038/nm.4036]

73 **Bao Y**, Oguz G, Lee WC, Lee PL, Ghosh K, Li J, Wang P, Lobie PE, Ehmsen S, Ditzel HJ, Wong A, Tan EY, Lee SC, Yu Q. EZH2-mediated PP2A inactivation confers resistance to HER2-targeted breast cancer therapy. *Nat Commun* 2020; **11**: 5878 [PMID: 33208750 DOI: 10.1038/s41467-020-19704-x]

74 **Biswas A**, Mukherjee G, Kondaiah P, Desai KV. Both EZH2 and JMJD6 regulate cell cycle genes in breast cancer. *BMC Cancer* 2020; **20**: 1159 [PMID: 33246425 DOI: 10.1186/s12885-020-07531-8]

75 **Chen J**, Wang F, Xu H, Xu L, Chen D, Wang J, Huang S, Wen Y, Fang L. Long Non-Coding RNA SNHG1 Regulates the Wnt/β-Catenin and PI3K/AKT/mTOR Signaling Pathways *via* EZH2 to Affect the Proliferation, Apoptosis, and Autophagy of Prostate Cancer Cell. *Front Oncol* 2020; **10**: 552907 [PMID: 33194612 DOI: 10.3389/fonc.2020.552907]

76 **Jin X**, Yang C, Fan P, Xiao J, Zhang W, Zhan S, Liu T, Wang D, Wu H. CDK5/FBW7-dependent ubiquitination and degradation of EZH2 inhibits pancreatic cancer cell migration and invasion. *J Biol Chem* 2017; **292**: 6269-6280 [PMID: 28242758 DOI: 10.1074/jbc.M116.764407]

77 **Zhou X**, Gao W, Hua H, Ji Z. LncRNA-BLACAT1 Facilitates Proliferation, Migration and Aerobic Glycolysis of Pancreatic Cancer Cells by Repressing CDKN1C *via* EZH2-Induced H3K27me3. *Front Oncol* 2020; **10**: 539805 [PMID: 33072570 DOI: 10.3389/fonc.2020.539805]

78 **Ma J**, Zhang J, Weng YC, Wang JC. EZH2-Mediated microRNA-139-5p Regulates Epithelial-Mesenchymal Transition and Lymph Node Metastasis of Pancreatic Cancer. *Mol Cells* 2018; **41**: 868-880 [PMID: 30304920 DOI: 10.14348/molcells.2018.0109]

79 **Ma Z**, Huang H, Wang J, Zhou Y, Pu F, Zhao Q, Peng P, Hui B, Ji H, Wang K. Long non-coding RNA SNHG15 inhibits P15 and KLF2 expression to promote pancreatic cancer proliferation through EZH2-mediated H3K27me3. *Oncotarget* 2017; **8**: 84153-84167 [PMID: 29137412 DOI: 10.18632/oncotarget.20359]

80 **Rotili D**, Mai A. Targeting Histone Demethylases: A New Avenue for the Fight against Cancer. *Genes Cancer* 2011; **2**: 663-679 [PMID: 21941621 DOI: 10.1177/1947601911417976]

81 **Suzuki T**, Terashima M, Tange S, Ishimura A. Roles of histone methyl-modifying enzymes in development and progression of cancer. *Cancer Sci* 2013; **104**: 795-800 [PMID: 23560485 DOI: 10.1111/cas.12169]

82 **Burg JM**, Link JE, Morgan BS, Heller FJ, Hargrove AE, McCafferty DG. KDM1 class flavin-dependent protein lysine demethylases. *Biopolymers* 2015; **104**: 213-246 [PMID: 25787087 DOI: 10.1002/bip.22643]

83 **Scoumanne A**, Chen X. The lysine-specific demethylase 1 is required for cell proliferation in both p53-dependent and -independent manners. *J Biol Chem* 2007; **282**: 15471-15475 [PMID: 17409384 DOI: 10.1074/jbc.M701023200]

84 **Shi Y**, Whetstine JR. Dynamic regulation of histone lysine methylation by demethylases. *Mol Cell* 2007; **25**: 1-14 [PMID: 17218267 DOI: 10.1016/j.molcel.2006.12.010]

85 **Liu Y**, Zhang JB, Qin Y, Wang W, Wei L, Teng Y, Guo L, Zhang B, Lin Z, Liu J, Ren ZG, Ye QH, Xie Y. PROX1 promotes hepatocellular carcinoma metastasis by way of up-regulating hypoxia-inducible factor 1α expression and protein stability. *Hepatology* 2013; **58**: 692-705 [PMID: 23505027 DOI: 10.1002/hep.26398]

86 **Ouyang H**, Qin Y, Liu Y, Xie Y, Liu J. Prox1 directly interacts with LSD1 and recruits the LSD1/NuRD complex to epigenetically co-repress CYP7A1 transcription. *PLoS One* 2013; **8**: e62192 [PMID: 23626788 DOI: 10.1371/journal.pone.0062192]

87 **Qin Y**, Zhu W, Xu W, Zhang B, Shi S, Ji S, Liu J, Long J, Liu C, Liu L, Xu J, Yu X. LSD1 sustains pancreatic cancer growth *via* maintaining HIF1α-dependent glycolytic process. *Cancer Lett* 2014; **347**: 225-232 [PMID: 24561118 DOI: 10.1016/j.canlet.2014.02.013]

88 **Chen F**, Yang H, Dong Z, Fang J, Wang P, Zhu T, Gong W, Fang R, Shi YG, Li Z, Xu Y. Structural insight into substrate recognition by histone demethylase LSD2/KDM1b. *Cell Res* 2013; **23**: 306-309 [PMID: 23357850 DOI: 10.1038/cr.2013.17]

89 **Ciccone DN**, Su H, Hevi S, Gay F, Lei H, Bajko J, Xu G, Li E, Chen T. KDM1B is a histone H3K4 demethylase required to establish maternal genomic imprints. *Nature* 2009; **461**: 415-418 [PMID: 19727073 DOI: 10.1038/nature08315]

90 **van Essen D**, Zhu Y, Saccani S. A feed-forward circuit controlling inducible NF-κB target gene activation by promoter histone demethylation. *Mol Cell* 2010; **39**: 750-760 [PMID: 20832726 DOI: 10.1016/j.molcel.2010.08.010]

91 **Lin SL**, Chang DC, Lin CH, Ying SY, Leu D, Wu DT. Regulation of somatic cell reprogramming through inducible mir-302 expression. *Nucleic Acids Res* 2011; **39**: 1054-1065 [PMID: 20870751 DOI: 10.1093/nar/gkq850]

92 **Katz TA**, Huang Y, Davidson NE, Jankowitz RC. Epigenetic reprogramming in breast cancer: from new targets to new therapies. *Ann Med* 2014; **46**: 397-408 [PMID: 25058177 DOI: 10.3109/07853890.2014.923740]

93 **Wang Y**, Sun L, Luo Y, He S. Knockdown of KDM1B inhibits cell proliferation and induces apoptosis of pancreatic cancer cells. *Pathol Res Pract* 2019; **215**: 1054-1060 [PMID: 30846414 DOI: 10.1016/j.prp.2019.02.014]

94 **Noble P**, Vyas M, Al-Attar A, Durrant S, Scholefield J, Durrant L. High levels of cleaved caspase-3 in colorectal tumour stroma predict good survival. *Br J Cancer* 2013; **108**: 2097-2105 [PMID: 23591201 DOI: 10.1038/bjc.2013.166]

95 **Cloos PA**, Christensen J, Agger K, Maiolica A, Rappsilber J, Antal T, Hansen KH, Helin K. The putative oncogene GASC1 demethylates tri- and dimethylated lysine 9 on histone H3. *Nature* 2006; **442**: 307-311 [PMID: 16732293 DOI: 10.1038/nature04837]

96 **Fodor BD**, Kubicek S, Yonezawa M, O'Sullivan RJ, Sengupta R, Perez-Burgos L, Opravil S, Mechtler K, Schotta G, Jenuwein T. Jmjd2b antagonizes H3K9 trimethylation at pericentric heterochromatin in mammalian cells. *Genes Dev* 2006; **20**: 1557-1562 [PMID: 16738407 DOI:

10.1101/gad.388206]
97 **Klose RJ**, Yamane K, Bae Y, Zhang D, Erdjument-Bromage H, Tempst P, Wong J, Zhang Y. The transcriptional repressor JHDM3A demethylates trimethyl histone H3 Lysine 9 and lysine 36. *Nature* 2006; **442**: 312-316 [PMID: 16732292 DOI: 10.1038/nature04853]
98 **Whetstine JR**, Nottke A, Lan F, Huarte M, Smolikov S, Chen Z, Spooner E, Li E, Zhang G, Colaiacovo M, Shi Y. Reversal of histone lysine trimethylation by the JMJD2 family of histone demethylases. *Cell* 2006; **125**: 467-481 [PMID: 16603238 DOI: 10.1016/j.cell.2006.03.028]
99 **Agger K**, Cloos PA, Christensen J, Pasini D, Rose S, Rappsilber J, Issaeva I, Canaani E, Salcini AE, Helin K. UTX and JMJD3 are histone H3K27 demethylases involved in HOX gene regulation and development. *Nature* 2007; **449**: 731-734 [PMID: 17713478 DOI: 10.1038/nature06145]
100 **Christensen J**, Agger K, Cloos PA, Pasini D, Rose S, Sennels L, Rappsilber J, Hansen KH, Salcini AE, Helin K. RBP2 belongs to a family of demethylases, specific for tri-and dimethylated lysine 4 on histone 3. *Cell* 2007; **128**: 1063-1076 [PMID: 17320161 DOI: 10.1016/j.cell.2007.02.003]
101 **De Santa F**, Totaro MG, Prosperini E, Notarbartolo S, Testa G, Natoli G. The histone H3 Lysine-27 demethylase Jmjd3 Links inflammation to inhibition of polycomb-mediated gene silencing. *Cell* 2007; **130**: 1083-1094 [PMID: 17825402 DOI: 10.1016/j.cell.2007.08.019]
102 **Frescas D**, Guardavaccaro D, Bassermann F, Koyama-Nasu R, Pagano M. JHDM1B/FBXL10 is a nucleolar protein that represses transcription of ribosomal RNA genes. *Nature* 2007; **450**: 309-313 [PMID: 17994099 DOI: 10.1038/nature06255]
103 **Klose RJ**, Yan Q, Tothova Z, Yamane K, Erdjument-Bromage H, Tempst P, Gilliland DG, Zhang Y, Kaelin WG Jr. The retinoblastoma binding protein RBP2 is an H3K4 demethylase. *Cell* 2007; **128**: 889-900 [PMID: 17320163 DOI: 10.1016/j.cell.2007.02.013]
104 **Lan F**, Bayliss PE, Rinn JL, Whetstine JR, Wang JK, Chen S, Iwase S, Alpatov R, Issaeva I, Canaani E, Roberts TM, Chang HY, Shi Y. A histone H3 Lysine 27 demethylase regulates animal posterior development. *Nature* 2007; **449**: 689-694 [PMID: 17851529 DOI: 10.1038/nature06192]
105 **Tahiliani M**, Mei P, Fang R, Leonor T, Rutenberg M, Shimizu F, Li J, Rao A, Shi Y. The histone H3K4 demethylase SMCX links REST target genes to X-linked mental retardation. *Nature* 2007; **447**: 601-605 [PMID: 17468742 DOI: 10.1038/nature05823]
106 **Yamane K**, Tateishi K, Klose RJ, Fang J, Fabrizio LA, Erdjument-Bromage H, Taylor-Papadimitriou J, Tempst P, Zhang Y. PLU-1 is an H3K4 demethylase involved in transcriptional repression and breast cancer cell proliferation. *Mol Cell* 2007; **25**: 801-812 [PMID: 17363312 DOI: 10.1016/j.molcel.2007.03.001]
107 **Liu W**, Tanasa B, Tyurina OV, Zhou TY, Gassmann R, Liu WT, Ohgi KA, Benner C, Garcia-Bassets I, Aggarwal AK, Desai A, Dorrestein PC, Glass CK, Rosenfeld MG. PHF8 mediates histone H4 Lysine 20 demethylation events involved in cell cycle progression. *Nature* 2010; **466**: 508-512 [PMID: 20622854 DOI: 10.1038/nature09272]
108 **Kim TD**, Oh S, Shin S, Janknecht R. Regulation of tumor suppressor p53 and HCT116 cell physiology by histone demethylase JMJD2D/KDM4D. *PLoS One* 2012; **7**: e34618 [PMID: 22514644 DOI: 10.1371/journal.pone.0034618]
109 **Tzatsos A**, Pfau R, Kampranis SC, Tsichlis PN. Ndy1/KDM2B immortalizes mouse embryonic fibroblasts by repressing the Ink4a/Arf locus. *Proc Natl Acad Sci U S A* 2009; **106**: 2641-2646 [PMID: 19202064 DOI: 10.1073/pnas.0813139106]
110 **Tzatsos A**, Paskaleva P, Lymperi S, Contino G, Stoykova S, Chen Z, Wong KK, Bardeesy N. Lysine-specific demethylase 2B (KDM2B)-let-7-enhancer of zester homolog 2 (EZH2) pathway regulates cell cycle progression and senescence in primary cells. *J Biol Chem* 2011; **286**: 33061-33069 [PMID: 21757686 DOI: 10.1074/jbc.M111.257667]
111 **He J**, Kallin EM, Tsukada Y, Zhang Y. The H3K36 demethylase Jhdm1b/Kdm^{2}b regulates cell proliferation and senescence through p15(Ink4b). *Nat Struct Mol Biol* 2008; **15**: 1169-1175 [PMID: 18836456 DOI: 10.1038/nsmb.1499]
112 **Pfau R**, Tzatsos A, Kampranis SC, Serebrennikova OB, Bear SE, Tsichlis PN. Members of a family of JmjC domain-containing oncoproteins immortalize embryonic fibroblasts *via* a JmjC domain-dependent process. *Proc Natl Acad Sci U S A* 2008; **105**: 1907-1912 [PMID: 18250326 DOI: 10.1073/pnas.0711865105]
113 **Kottakis F**, Polytarchou C, Foltopoulou P, Sanidas I, Kampranis SC, Tsichlis PN. FGF-2 regulates cell proliferation, migration, and angiogenesis through an NDY1/KDM2B-miR-101-EZH2 pathway. *Mol Cell* 2011; **43**: 285-298 [PMID: 21777817 DOI: 10.1016/j.molcel.2011.06.020]
114 **Tzatsos A**, Paskaleva P, Ferrari F, Deshpande V, Stoykova S, Contino G, Wong KK, Lan F, Trojer P, Park PJ, Bardeesy N. KDM2B promotes pancreatic cancer *via* Polycomb-dependent and -independent transcriptional programs. *J Clin Invest* 2013; **123**: 727-739 [PMID: 23321669 DOI: 10.1172/JCI64535]
115 **Yamane K**, Toumazou C, Tsukada Y, Erdjument-Bromage H, Tempst P, Wong J, Zhang Y. JHDM2A, a JmjC-containing H3K9 demethylase, facilitates transcription activation by androgen receptor. *Cell* 2006; **125**: 483-495 [PMID: 16603237 DOI: 10.1016/j.cell.2006.03.027]
116 **Okada Y**, Scott G, Ray MK, Mishina Y, Zhang Y. Histone demethylase JHDM2A is critical for Tnp1 and Prm1 transcription and spermatogenesis. *Nature* 2007; **450**: 119-123 [PMID: 17943087 DOI: 10.1038/nature06236]
117 **Bailey JM**, Alsina J, Rasheed ZA, McAllister FM, Fu YY, Plentz R, Zhang H, Pasricha PJ, Bardeesy N, Matsui W, Maitra A, Leach SD. DCLK1 marks a morphologically distinct subpopulation of cells with stem cell properties in preinvasive pancreatic cancer. *Gastroenterology*

2014; **146**: 245-256 [PMID: 24096005 DOI: 10.1053/j.gastro.2013.09.050]

118 **Dandawate P**, Ghosh C, Palaniyandi K, Paul S, Rawal S, Pradhan R, Sayed AAA, Choudhury S, Standing D, Subramaniam D, Padhye SB, Gunewardena S, Thomas SM, Neil MO, Tawfik O, Welch DR, Jensen RA, Maliski S, Weir S, Iwakuma T, Anant S, Dhar A. The Histone Demethylase KDM3A, Increased in Human Pancreatic Tumors, Regulates Expression of DCLK1 and Promotes Tumorigenesis in Mice. *Gastroenterology* 2019; **157**: 1646-1659.e11 [PMID: 31442435 DOI: 10.1053/j.gastro.2019.08.018]

119 **Labbé RM**, Holowatyj A, Yang ZQ. Histone lysine demethylase (KDM) subfamily 4: structures, functions and therapeutic potential. *Am J Transl Res* 2013; **6**: 1-15 [PMID: 24349617]

120 **Ding G**, Xu X, Li D, Chen Y, Wang W, Ping D, Jia S, Cao L. Fisetin inhibits proliferation of pancreatic adenocarcinoma by inducing DNA damage *via* RFXAP/KDM4A-dependent histone H3K36 demethylation. *Cell Death Dis* 2020; **11**: 893 [PMID: 33093461 DOI: 10.1038/s41419-020-03019-2]

121 **Gokturk B**, Artac H, van Eggermond MJ, van den Elsen P, Reisli İ. Type III bare lymphocyte syndrome associated with a novel RFXAP mutation: a case report. *Int J Immunogenet* 2012; **39**: 362-364 [PMID: 22390233 DOI: 10.1111/j.1744-313X.2012.01105.x]

122 **Hanna S**, Etzioni A. MHC class I and II deficiencies. *J Allergy Clin Immunol* 2014; **134**: 269-275 [PMID: 25001848 DOI: 10.1016/j.jaci.2014.06.001]

123 **Li S**, Wu L, Wang Q, Li Y, Wang X. KDM4B promotes epithelial-mesenchymal transition through up-regulation of ZEB1 in pancreatic cancer. *Acta Biochim Biophys Sin (Shanghai)* 2015; **47**: 997-1004 [PMID: 26511091 DOI: 10.1093/abbs/gmv107]

124 **Isohookana J**, Haapasaari KM, Soini Y, Karihtala P. KDM4D Predicts Recurrence in Exocrine Pancreatic Cells of Resection Margins from Patients with Pancreatic Adenocarcinoma. *Anticancer Res* 2018; **38**: 2295-2302 [PMID: 29599352 DOI: 10.21873/anticanres.12474]

125 **Rasmussen PB**, Staller P. The KDM5 family of histone demethylases as targets in oncology drug discovery. *Epigenomics* 2014; **6**: 277-286 [PMID: 25111482 DOI: 10.2217/epi.14.14]

126 **Cui J**, Quan M, Xie D, Gao Y, Guha S, Fallon MB, Chen J, Xie K. A novel KDM5A/MPC-1 signaling pathway promotes pancreatic cancer progression *via* redirecting mitochondrial pyruvate metabolism. *Oncogene* 2020; **39**: 1140-1151 [PMID: 31641207 DOI: 10.1038/s41388-019-1051-8]

127 **Hong S**, Cho YW, Yu LR, Yu H, Veenstra TD, Ge K. Identification of JmjC domain-containing UTX and JMJD3 as histone H3 Lysine 27 demethylases. *Proc Natl Acad Sci U S A* 2007; **104**: 18439-18444 [PMID: 18003914 DOI: 10.1073/pnas.0707292104]

128 **Bailey P**, Chang DK, Nones K, Johns AL, Patch AM, Gingras MC, Miller DK, Christ AN, Bruxner TJ, Quinn MC, Nourse C, Murtaugh LC, Harliwong I, Idrisoglu S, Manning S, Nourbakhsh E, Wani S, Fink L, Holmes O, Chin V, Anderson MJ, Kazakoff S, Leonard C, Newell F, Waddell N, Wood S, Xu Q, Wilson PJ, Cloonan N, Kassahn KS, Taylor D, Quek K, Robertson A, Pantano L, Mincarelli L, Sanchez LN, Evers L, Wu J, Pinese M, Cowley MJ, Jones MD, Colvin EK, Nagrial AM, Humphrey ES, Chantrill LA, Mawson A, Humphris J, Chou A, Pajic M, Scarlett CJ, Pinho AV, Giry-Laterriere M, Rooman I, Samra JS, Kench JG, Lovell JA, Merrett ND, Toon CW, Epari K, Nguyen NQ, Barbour A, Zeps N, Moran-Jones K, Jamieson NB, Graham JS, Duthie F, Oien K, Hair J, Grützmann R, Maitra A, Iacobuzio-Donahue CA, Wolfgang CL, Morgan RA, Lawlor RT, Corbo V, Bassi C, Rusev B, Capelli P, Salvia R, Tortora G, Mukhopadhyay D, Petersen GM; Australian Pancreatic Cancer Genome Initiative, Munzy DM, Fisher WE, Karim SA, Eshleman JR, Hruban RH, Pilarsky C, Morton JP, Sansom OJ, Scarpa A, Musgrove EA, Bailey UM, Hofmann O, Sutherland RL, Wheeler DA, Gill AJ, Gibbs RA, Pearson JV, Waddell N, Biankin AV, Grimmond SM. Genomic analyses identify molecular subtypes of pancreatic cancer. *Nature* 2016; **531**: 47-52 [PMID: 26909576 DOI: 10.1038/nature16965]

129 **Biankin AV**, Waddell N, Kassahn KS, Gingras MC, Muthuswamy LB, Johns AL, Miller DK, Wilson PJ, Patch AM, Wu J, Chang DK, Cowley MJ, Gardiner BB, Song S, Harliwong I, Idrisoglu S, Nourse C, Nourbakhsh E, Manning S, Wani S, Gongora M, Pajic M, Scarlett CJ, Gill AJ, Pinho AV, Rooman I, Anderson M, Holmes O, Leonard C, Taylor D, Wood S, Xu Q, Nones K, Fink JL, Christ A, Bruxner T, Cloonan N, Kolle G, Newell F, Pinese M, Mead RS, Humphris JL, Kaplan W, Jones MD, Colvin EK, Nagrial AM, Humphrey ES, Chou A, Chin VT, Chantrill LA, Mawson A, Samra JS, Kench JG, Lovell JA, Daly RJ, Merrett ND, Toon C, Epari K, Nguyen NQ, Barbour A, Zeps N; Australian Pancreatic Cancer Genome Initiative, Kakkar N, Zhao F, Wu YQ, Wang M, Muzny DM, Fisher WE, Brunicardi FC, Hodges SE, Reid JG, Drummond J, Chang K, Han Y, Lewis LR, Dinh H, Buhay CJ, Beck T, Timms L, Sam M, Begley K, Brown A, Pai D, Panchal A, Buchner N, De Borja R, Denroche RE, Yung CK, Serra S, Onetto N, Mukhopadhyay D, Tsao MS, Shaw PA, Petersen GM, Gallinger S, Hruban RH, Maitra A, Iacobuzio-Donahue CA, Schulick RD, Wolfgang CL, Morgan RA, Lawlor RT, Capelli P, Corbo V, Scardoni M, Tortora G, Tempero MA, Mann KM, Jenkins NA, Perez-Mancera PA, Adams DJ, Largaespada DA, Wessels LF, Rust AG, Stein LD, Tuveson DA, Copeland NG, Musgrove EA, Scarpa A, Eshleman JR, Hudson TJ, Sutherland RL, Wheeler DA, Pearson JV, McPherson JD, Gibbs RA, Grimmond SM. Pancreatic cancer genomes reveal aberrations in axon guidance pathway genes. *Nature* 2012; **491**: 399-405 [PMID: 23103869 DOI: 10.1038/nature11547]

130 **Hoadley KA**, Yau C, Wolf DM, Cherniack AD, Tamborero D, Ng S, Leiserson MDM, Niu B, McLellan MD, Uzunangelov V, Zhang J, Kandoth C, Akbani R, Shen H, Omberg L, Chu A, Margolin AA, Van't Veer LJ, Lopez-Bigas N, Laird PW, Raphael BJ, Ding L, Robertson AG, Byers LA, Mills GB, Weinstein JN, Van Waes C, Chen Z, Collisson EA; Cancer Genome Atlas Research

Network, Benz CC, Perou CM, Stuart JM. Multiplatform analysis of 12 cancer types reveals molecular classification within and across tissues of origin. *Cell* 2014; **158**: 929-944 [PMID: 25109877 DOI: 10.1016/j.cell.2014.06.049]

131 **van Haaften G**, Dalgliesh GL, Davies H, Chen L, Bignell G, Greenman C, Edkins S, Hardy C, O'Meara S, Teague J, Butler A, Hinton J, Latimer C, Andrews J, Barthorpe S, Beare D, Buck G, Campbell PJ, Cole J, Forbes S, Jia M, Jones D, Kok CY, Leroy C, Lin ML, McBride DJ, Maddison M, Maquire S, McLay K, Menzies A, Mironenko T, Mulderrig L, Mudie L, Pleasance E, Shepherd R, Smith R, Stebbings L, Stephens P, Tang G, Tarpey PS, Turner R, Turrell K, Varian J, West S, Widaa S, Wray P, Collins VP, Ichimura K, Law S, Wong J, Yuen ST, Leung SY, Tonon G, DePinho RA, Tai YT, Anderson KC, Kahnoski RJ, Massie A, Khoo SK, Teh BT, Stratton MR, Futreal PA. Somatic mutations of the histone H3K27 demethylase gene UTX in human cancer. *Nat Genet* 2009; **41**: 521-523 [PMID: 19330029 DOI: 10.1038/ng.349]

132 **Waddell N**, Pajic M, Patch AM, Chang DK, Kassahn KS, Bailey P, Johns AL, Miller D, Nones K, Quek K, Quinn MC, Robertson AJ, Fadlullah MZ, Bruxner TJ, Christ AN, Harliwong I, Idrisoglu S, Manning S, Nourse C, Nourbakhsh E, Wani S, Wilson PJ, Markham E, Cloonan N, Anderson MJ, Fink JL, Holmes O, Kazakoff SH, Leonard C, Newell F, Poudel B, Song S, Taylor D, Waddell N, Wood S, Xu Q, Wu J, Pinese M, Cowley MJ, Lee HC, Jones MD, Nagrial AM, Humphris J, Chantrill LA, Chin V, Steinmann AM, Mawson A, Humphrey ES, Colvin EK, Chou A, Scarlett CJ, Pinho AV, Giry-Laterriere M, Rooman I, Samra JS, Kench JG, Pettitt JA, Merrett ND, Toon C, Epari K, Nguyen NQ, Barbour A, Zeps N, Jamieson NB, Graham JS, Niclou SP, Bjerkvig R, Grützmann R, Aust D, Hruban RH, Maitra A, Iacobuzio-Donahue CA, Wolfgang CL, Morgan RA, Lawlor RT, Corbo V, Bassi C, Falconi M, Zamboni G, Tortora G, Tempero MA; Australian Pancreatic Cancer Genome Initiative, Gill AJ, Eshleman JR, Pilarsky C, Scarpa A, Musgrove EA, Pearson JV, Biankin AV, Grimmond SM. Whole genomes redefine the mutational landscape of pancreatic cancer. *Nature* 2015; **518**: 495-501 [PMID: 25719666 DOI: 10.1038/nature14169]

133 **Witkiewicz AK**, McMillan EA, Balaji U, Baek G, Lin WC, Mansour J, Mollaee M, Wagner KU, Koduru P, Yopp A, Choti MA, Yeo CJ, McCue P, White MA, Knudsen ES. Whole-exome sequencing of pancreatic cancer defines genetic diversity and therapeutic targets. *Nat Commun* 2015; **6**: 6744 [PMID: 25855536 DOI: 10.1038/ncomms7744]

134 **Welstead GG**, Creyghton MP, Bilodeau S, Cheng AW, Markoulaki S, Young RA, Jaenisch R. X-linked H3K27me3 demethylase Utx is required for embryonic development in a sex-specific manner. *Proc Natl Acad Sci U S A* 2012; **109**: 13004-13009 [PMID: 22826230 DOI: 10.1073/pnas.1210787109]

135 **Agger K**, Cloos PA, Rudkjaer L, Williams K, Andersen G, Christensen J, Helin K. The H3K27me3 demethylase JMJD3 contributes to the activation of the INK4A-ARF locus in response to oncogene- and stress-induced senescence. *Genes Dev* 2009; **23**: 1171-1176 [PMID: 19451217 DOI: 10.1101/gad.510809]

136 **Barradas M**, Anderton E, Acosta JC, Li S, Banito A, Rodriguez-Niedenführ M, Maertens G, Banck M, Zhou MM, Walsh MJ, Peters G, Gil J. Histone demethylase JMJD3 contributes to epigenetic control of INK4a/ARF by oncogenic RAS. *Genes Dev* 2009; **23**: 1177-1182 [PMID: 19451218 DOI: 10.1101/gad.511109]

137 **Kanda M**, Matthaei H, Wu J, Hong SM, Yu J, Borges M, Hruban RH, Maitra A, Kinzler K, Vogelstein B, Goggins M. Presence of somatic mutations in most early-stage pancreatic intraepithelial neoplasia. *Gastroenterology* 2012; **142**: 730-733.e9 [PMID: 22226782 DOI: 10.1053/j.gastro.2011.12.042]

138 **Yamamoto K**, Tateishi K, Kudo Y, Sato T, Yamamoto S, Miyabayashi K, Matsusaka K, Asaoka Y, Ijichi H, Hirata Y, Otsuka M, Nakai Y, Isayama H, Ikenoue T, Kurokawa M, Fukayama M, Kokudo N, Omata M, Koike K. Loss of histone demethylase KDM6B enhances aggressiveness of pancreatic cancer through downregulation of C/EBPα. *Carcinogenesis* 2014; **35**: 2404-2414 [PMID: 24947179 DOI: 10.1093/carcin/bgu136]

139 **Pan MR**, Hsu MC, Chen LT, Hung WC. G9a orchestrates PCL3 and KDM7A to promote histone H3K27 methylation. *Sci Rep* 2015; **5**: 18709 [PMID: 26688070 DOI: 10.1038/srep18709]

140 **Aasland R**, Gibson TJ, Stewart AF. The PHD finger: implications for chromatin-mediated transcriptional regulation. *Trends Biochem Sci* 1995; **20**: 56-59 [PMID: 7701562 DOI: 10.1016/s0968-0004(00)88957-4]

141 **Sanchez R**, Zhou MM. The PHD finger: a versatile epigenome reader. *Trends Biochem Sci* 2011; **36**: 364-372 [PMID: 21514168 DOI: 10.1016/j.tibs.2011.03.005]

142 **Ali M**, Hom RA, Blakeslee W, Ikenouye L, Kutateladze TG. Diverse functions of PHD fingers of the MLL/KMT2 subfamily. *Biochim Biophys Acta* 2014; **1843**: 366-371 [PMID: 24291127 DOI: 10.1016/j.bbamcr.2013.11.016]

143 **Yokoyama A**, Ficara F, Murphy MJ, Meisel C, Naresh A, Kitabayashi I, Cleary ML. Proteolytically cleaved MLL subunits are susceptible to distinct degradation pathways. *J Cell Sci* 2011; **124**: 2208-2219 [PMID: 21670200 DOI: 10.1242/jcs.080523]

144 **Wang J**, Muntean AG, Wu L, Hess JL. A subset of mixed lineage leukemia proteins has plant homeodomain (PHD)-mediated E3 Ligase activity. *J Biol Chem* 2012; **287**: 43410-43416 [PMID: 23129768 DOI: 10.1074/jbc.M112.423855]

145 **Chang PY**, Hom RA, Musselman CA, Zhu L, Kuo A, Gozani O, Kutateladze TG, Cleary ML. Binding of the MLL PHD3 finger to histone H3K4me3 is required for MLL-dependent gene transcription. *J Mol Biol* 2010; **400**: 137-144 [PMID: 20452361 DOI: 10.1016/j.jmb.2010.05.005]

146 **Mathioudaki A**, Ljungström V, Melin M, Arendt ML, Nordin J, Karlsson Å, Murén E, Saksena P, Meadows JRS, Marinescu VD, Sjöblom T, Lindblad-Toh K. Targeted sequencing reveals the somatic mutation landscape in a Swedish breast cancer cohort. *Sci Rep* 2020; **10**: 19304 [PMID: 33168853 DOI: 10.1038/s41598-020-74580-1]

147 **Dhar SS**, Lee SH, Kan PY, Voigt P, Ma L, Shi X, Reinberg D, Lee MG. Trans-tail regulation of MLL4-catalyzed H3K4 methylation by H4R3 symmetric dimethylation is mediated by a tandem PHD of MLL4. *Genes Dev* 2012; **26**: 2749-2762 [PMID: 23249737 DOI: 10.1101/gad.203356.112]

148 **Ali M**, Rincón-Arano H, Zhao W, Rothbart SB, Tong Q, Parkhurst SM, Strahl BD, Deng LW, Groudine M, Kutateladze TG. Molecular basis for chromatin binding and regulation of MLL5. *Proc Natl Acad Sci U S A* 2013; **110**: 11296-11301 [PMID: 23798402 DOI: 10.1073/pnas.1310156110]

149 **Lemak A**, Yee A, Wu H, Yap D, Zeng H, Dombrovski L, Houliston S, Aparicio S, Arrowsmith CH. Solution NMR structure and histone binding of the PHD domain of human MLL5. *PLoS One* 2013; **8**: e77020 [PMID: 24130829 DOI: 10.1371/journal.pone.0077020]

150 **Klose RJ**, Kallin EM, Zhang Y. JmjC-domain-containing proteins and histone demethylation. *Nat Rev Genet* 2006; **7**: 715-727 [PMID: 16983801 DOI: 10.1038/nrg1945]

151 **Torres IO**, Kuchenbecker KM, Nnadi CI, Fletterick RJ, Kelly MJ, Fujimori DG. Histone demethylase KDM5A is regulated by its reader domain through a positive-feedback mechanism. *Nat Commun* 2015; **6**: 6204 [PMID: 25686748 DOI: 10.1038/ncomms7204]

152 **Tsai WW**, Wang Z, Yiu TT, Akdemir KC, Xia W, Winter S, Tsai CY, Shi X, Schwarzer D, Plunkett W, Aronow B, Gozani O, Fischle W, Hung MC, Patel DJ, Barton MC. TRIM24 Links a non-canonical histone signature to breast cancer. *Nature* 2010; **468**: 927-932 [PMID: 21164480 DOI: 10.1038/nature09542]

153 **Hillringhaus L**, Yue WW, Rose NR, Ng SS, Gileadi C, Loenarz C, Bello SH, Bray JE, Schofield CJ, Oppermann U. Structural and evolutionary basis for the dual substrate selectivity of human KDM4 histone demethylase family. *J Biol Chem* 2011; **286**: 41616-41625 [PMID: 21914792 DOI: 10.1074/jbc.M111.283689]

154 **Trojer P**, Zhang J, Yonezawa M, Schmidt A, Zheng H, Jenuwein T, Reinberg D. Dynamic Histone H1 Isotype 4 Methylation and Demethylation by Histone Lysine Methyltransferase G9a/KMT1C and the Jumonji Domain-containing JMJD2/KDM4 Proteins. *J Biol Chem* 2009; **284**: 8395-8405 [PMID: 19144645 DOI: 10.1074/jbc.M807818200]

155 **Berry WL**, Janknecht R. KDM4/JMJD2 histone demethylases: epigenetic regulators in cancer cells. *Cancer Res* 2013; **73**: 2936-2942 [PMID: 23644528 DOI: 10.1158/0008-5472.CAN-12-4300]

156 **Højfeldt JW**, Agger K, Helin K. Histone lysine demethylases as targets for anticancer therapy. *Nat Rev Drug Discov* 2013; **12**: 917-930 [PMID: 24232376 DOI: 10.1038/nrd4154]

157 **Iwase S**, Lan F, Bayliss P, de la Torre-Ubieta L, Huarte M, Qi HH, Whetstine JR, Bonni A, Roberts TM, Shi Y. The X-linked mental retardation gene SMCX/JARID1C defines a family of histone H3 Lysine 4 demethylases. *Cell* 2007; **128**: 1077-1088 [PMID: 17320160 DOI: 10.1016/j.cell.2007.02.017]

158 **Wang GG**, Song J, Wang Z, Dormann HL, Casadio F, Li H, Luo JL, Patel DJ, Allis CD. Haematopoietic malignancies caused by dysregulation of a chromatin-binding PHD finger. *Nature* 2009; **459**: 847-851 [PMID: 19430464 DOI: 10.1038/nature08036]

159 **Zhang Y**, Yang H, Guo X, Rong N, Song Y, Xu Y, Lan W, Zhang X, Liu M, Cao C. The PHD1 finger of KDM5B recognizes unmodified H3K4 during the demethylation of histone H3K4me2/3 by KDM5B. *Protein Cell* 2014; **5**: 837-850 [PMID: 24952722 DOI: 10.1007/s13238-014-0078-4]

160 **Shi X**, Hong T, Walter KL, Ewalt M, Michishita E, Hung T, Carney D, Peña P, Lan F, Kaadige MR, Lacoste N, Cayrou C, Davrazou F, Saha A, Cairns BR, Ayer DE, Kutateladze TG, Shi Y, Côté J, Chua KF, Gozani O. ING2 PHD domain links histone H3 Lysine 4 methylation to active gene repression. *Nature* 2006; **442**: 96-99 [PMID: 16728974 DOI: 10.1038/nature04835]

161 **Johansson C**, Velupillai S, Tumber A, Szykowska A, Hookway ES, Nowak RP, Strain-Damerell C, Gileadi C, Philpott M, Burgess-Brown N, Wu N, Kopec J, Nuzzi A, Steuber H, Egner U, Badock V, Munro S, LaThangue NB, Westaway S, Brown J, Athanasou N, Prinjha R, Brennan PE, Oppermann U. Structural analysis of human KDM5B guides histone demethylase inhibitor development. *Nat Chem Biol* 2016; **12**: 539-545 [PMID: 27214403 DOI: 10.1038/nchembio.2087]

162 **Peng Y**, Alexov E. Cofactors-loaded quaternary structure of lysine-specific demethylase 5C (KDM5C) protein: Computational model. *Proteins* 2016; **84**: 1797-1809 [PMID: 27696497 DOI: 10.1002/prot.25162]

163 **Zhu Z**, Wang Y, Li X, Xu L, Wang X, Sun T, Dong X, Chen L, Mao H, Yu Y, Li J, Chen PA, Chen CD. PHF8 is a histone H3K9me2 demethylase regulating rRNA synthesis. *Cell Res* 2010; **20**: 794-801 [PMID: 20531378 DOI: 10.1038/cr.2010.75]

164 **Horton JR**, Upadhyay AK, Qi HH, Zhang X, Shi Y, Cheng X. Enzymatic and structural insights for substrate specificity of a family of jumonji histone lysine demethylases. *Nat Struct Mol Biol* 2010; **17**: 38-43 [PMID: 20023638 DOI: 10.1038/nsmb.1753]

165 **Zhang H**, Song Y, Yang C, Wu X. UHRF1 mediates cell migration and invasion of gastric cancer. *Biosci Rep* 2018; **38** [PMID: 30352833 DOI: 10.1042/bsr20181065]

166 **Guo X**, Xu Y, Wang P, Li Z, Yang H. Crystallization and preliminary crystallographic analysis of a PHD domain of human JARID1B. *Acta Crystallogr Sect F Struct Biol Cryst Commun* 2011; **67**: 907-910 [PMID: 21821892 DOI: 10.1107/S1744309111021981]

167 **Thompson B**, Townsley F, Rosin-Arbesfeld R, Musisi H, Bienz M. A new nuclear component of the Wnt signalling pathway. *Nat Cell Biol* 2002; **4**: 367-373 [PMID: 11988739 DOI: 10.1038/ncb786]

168 **Wang J**, Zhong M, Liu B, Sha L, Lun Y, Zhang W, Li X, Wang X, Cao J, Ning A, Huang M. Expression and functional analysis of novel molecule - Latcripin-13 domain from Lentinula edodes C91-3 produced in prokaryotic expression system. *Gene* 2015; **555**: 469-475 [PMID: 25447899 DOI: 10.1016/j.gene.2014.11.014]

169 **Qian Y**, Gong Y, Fan Z, Luo G, Huang Q, Deng S, Cheng H, Jin K, Ni Q, Yu X, Liu C. Molecular alterations and targeted therapy in pancreatic ductal adenocarcinoma. *J Hematol Oncol* 2020; **13**: 130 [PMID: 33008426 DOI: 10.1186/s13045-020-00958-3]

170 **Manuyakorn A**, Paulus R, Farrell J, Dawson NA, Tze S, Cheung-Lau G, Hines OJ, Reber H, Seligson DB, Horvath S, Kurdistani SK, Guha C, Dawson DW. Cellular histone modification patterns predict prognosis and treatment response in resectable pancreatic adenocarcinoma: results from RTOG 9704. *J Clin Oncol* 2010; **28**: 1358-1365 [PMID: 20142597 DOI: 10.1200/JCO.2009.24.5639]

171 **Hinton J**, Callan R, Bodine C, Glasgow W, Brower S, Jiang SW, Li J. Potential epigenetic biomarkers for the diagnosis and prognosis of pancreatic ductal adenocarcinomas. *Expert Rev Mol Diagn* 2013; **13**: 431-443 [PMID: 23782251 DOI: 10.1586/erm.13.38]

172 **Mazur PK**, Reynoird N, Khatri P, Jansen PW, Wilkinson AW, Liu S, Barbash O, Van Aller GS, Huddleston M, Dhanak D, Tummino PJ, Kruger RG, Garcia BA, Butte AJ, Vermeulen M, Sage J, Gozani O. SMYD3 Links lysine methylation of MAP3K2 to Ras-driven cancer. *Nature* 2014; **510**: 283-287 [PMID: 24847881 DOI: 10.1038/nature13320]

173 **Peserico A**, Germani A, Sanese P, Barbosa AJ, Di Virgilio V, Fittipaldi R, Fabini E, Bertucci C, Varchi G, Moyer MP, Caretti G, Del Rio A, Simone C. A SMYD3 Small-Molecule Inhibitor Impairing Cancer Cell Growth. *J Cell Physiol* 2015; **230**: 2447-2460 [PMID: 25728514 DOI: 10.1002/jcp.24975]

174 **Driehuis E**, van Hoeck A, Moore K, Kolders S, Francies HE, Gulersonmez MC, Stigter ECA, Burgering B, Geurts V, Gracanin A, Bounova G, Morsink FH, Vries R, Boj S, van Es J, Offerhaus GJA, Kranenburg O, Garnett MJ, Wessels L, Cuppen E, Brosens LAA, Clevers H. Pancreatic cancer organoids recapitulate disease and allow personalized drug screening. *Proc Natl Acad Sci U S A* 2019 [PMID: 31818951 DOI: 10.1073/pnas.1911273116]

175 **Avan A**, Crea F, Paolicchi E, Funel N, Galvani E, Marquez VE, Honeywell RJ, Danesi R, Peters GJ, Giovannetti E. Molecular mechanisms involved in the synergistic interaction of the EZH2 inhibitor 3-deazaneplanocin A with gemcitabine in pancreatic cancer cells. *Mol Cancer Ther* 2012; **11**: 1735-1746 [PMID: 22622284 DOI: 10.1158/1535-7163.MCT-12-0037]

176 **Andricovich J**, Perkail S, Kai Y, Casasanta N, Peng W, Tzatsos A. Loss of KDM6A Activates Super-Enhancers to Induce Gender-Specific Squamous-like Pancreatic Cancer and Confers Sensitivity to BET Inhibitors. *Cancer Cell* 2018; **33**: 512-526.e8 [PMID: 29533787 DOI: 10.1016/j.ccell.2018.02.003]

177 **Yamamoto K**, Tateishi K, Kudo Y, Hoshikawa M, Tanaka M, Nakatsuka T, Fujiwara H, Miyabayashi K, Takahashi R, Tanaka Y, Ijichi H, Nakai Y, Isayama H, Morishita Y, Aoki T, Sakamoto Y, Hasegawa K, Kokudo N, Fukayama M, Koike K. Stromal remodeling by the BET bromodomain inhibitor JQ1 suppresses the progression of human pancreatic cancer. *Oncotarget* 2016; **7**: 61469-61484 [PMID: 27528027 DOI: 10.18632/oncotarget.11129]

178 **King ON**, Li XS, Sakurai M, Kawamura A, Rose NR, Ng SS, Quinn AM, Rai G, Mott BT, Beswick P, Klose RJ, Oppermann U, Jadhav A, Heightman TD, Maloney DJ, Schofield CJ, Simeonov A. Quantitative high-throughput screening identifies 8-hydroxyquinolines as cell-active histone demethylase inhibitors. *PLoS One* 2010; **5**: e15535 [PMID: 21124847 DOI: 10.1371/journal.pone.0015535]

179 **Jin C**, Yang L, Xie M, Lin C, Merkurjev D, Yang JC, Tanasa B, Oh S, Zhang J, Ohgi KA, Zhou H, Li W, Evans CP, Ding S, Rosenfeld MG. Chem-seq permits identification of genomic targets of drugs against androgen receptor regulation selected by functional phenotypic screens. *Proc Natl Acad Sci U S A* 2014; **111**: 9235-9240 [PMID: 24928520 DOI: 10.1073/pnas.1404303111]

180 **Sonnemann J**, Zimmermann M, Marx C, Ebert F, Becker S, Lauterjung ML, Beck JF. LSD1 (KDM1A)-independent effects of the LSD1 inhibitor SP2509 in cancer cells. *Br J Haematol* 2018; **183**: 494-497 [PMID: 29205263 DOI: 10.1111/bjh.14983]

181 **Fang Y**, Liao G, Yu B. LSD1/KDM1A inhibitors in clinical trials: advances and prospects. *J Hematol Oncol* 2019; **12**: 129 [PMID: 31801559 DOI: 10.1186/s13045-019-0811-9]

182 **Yamagishi M**, Uchimaru K. Targeting EZH2 in cancer therapy. *Curr Opin Oncol* 2017; **29**: 375-381 [PMID: 28665819 DOI: 10.1097/CCO.0000000000000390]

183 **Kuang Y**, Lu F, Guo J, Xu H, Wang Q, Xu C, Zeng L, Yi S. Histone demethylase KDM2B upregulates histone methyltransferase EZH2 expression and contributes to the progression of ovarian cancer *in vitro* and in vivo. *Onco Targets Ther* 2017; **10**: 3131-3144 [PMID: 28706445 DOI: 10.2147/OTT.S134784]

184 **Lawrence MS**, Stojanov P, Mermel CH, Robinson JT, Garraway LA, Golub TR, Meyerson M, Gabriel SB, Lander ES, Getz G. Discovery and saturation analysis of cancer genes across 21 tumour types. *Nature* 2014; **505**: 495-501 [PMID: 24390350 DOI: 10.1038/nature12912]

185 **Ler LD**, Ghosh S, Chai X, Thike AA, Heng HL, Siew EY, Dey S, Koh LK, Lim JQ, Lim WK, Myint SS, Loh JL, Ong P, Sam XX, Huang D, Lim T, Tan PH, Nagarajan S, Cheng CW, Ho H, Ng LG, Yuen J, Lin PH, Chuang CK, Chang YH, Weng WH, Rozen SG, Tan P, Creasy CL, Pang ST, McCabe MT, Poon SL, Teh BT. Loss of tumor suppressor KDM6A amplifies PRC2-regulated transcriptional repression in bladder cancer and can be targeted through inhibition of EZH2. *Sci*

Transl Med 2017; **9** [PMID: 28228601 DOI: 10.1126/scitranslmed.aai8312]

186 **Au SL**, Wong CC, Lee JM, Fan DN, Tsang FH, Ng IO, Wong CM. Enhancer of zeste homolog 2 epigenetically silences multiple tumor suppressor microRNAs to promote liver cancer metastasis. *Hepatology* 2012; **56**: 622-631 [PMID: 22370893 DOI: 10.1002/hep.25679]

187 **Mitra D**, Das PM, Huynh FC, Jones FE. Jumonji/ARID1 B (JARID1B) protein promotes breast tumor cell cycle progression through epigenetic repression of microRNA let-7e. *J Biol Chem* 2011; **286**: 40531-40535 [PMID: 21969366 DOI: 10.1074/jbc.M111.304865]

188 **Kwak YT**, Guo J, Prajapati S, Park KJ, Surabhi RM, Miller B, Gehrig P, Gaynor RB. Methylation of SPT5 regulates its interaction with RNA polymerase II and transcriptional elongation properties. *Mol Cell* 2003; **11**: 1055-1066 [PMID: 12718890 DOI: 10.1016/s1097-2765(03)00101-1]

189 **Jansson M**, Durant ST, Cho EC, Sheahan S, Edelmann M, Kessler B, La Thangue NB. Arginine methylation regulates the p53 response. *Nat Cell Biol* 2008; **10**: 1431-1439 [PMID: 19011621 DOI: 10.1038/ncb1802]

190 **Han T**, Jiao F, Hu H, Yuan C, Wang L, Jin ZL, Song WF, Wang LW. EZH2 promotes cell migration and invasion but not alters cell proliferation by suppressing E-cadherin, partly through association with MALAT-1 in pancreatic cancer. *Oncotarget* 2016; **7**: 11194-11207 [PMID: 26848980 DOI: 10.18632/oncotarget.7156]

191 **Kooistra SM**, Helin K. Molecular mechanisms and potential functions of histone demethylases. *Nat Rev Mol Cell Biol* 2012; **13**: 297-311 [PMID: 22473470 DOI: 10.1038/nrm3327]

192 **Pfister SX**, Ahrabi S, Zalmas LP, Sarkar S, Aymard F, Bachrati CZ, Helleday T, Legube G, La Thangue NB, Porter AC, Humphrey TC. SETD2-dependent histone H3K36 trimethylation is required for homologous recombination repair and genome stability. *Cell Rep* 2014; **7**: 2006-2018 [PMID: 24931610 DOI: 10.1016/j.celrep.2014.05.026]

193 **Lee GS**, Subramanian N, Kim AI, Aksentijevich I, Goldbach-Mansky R, Sacks DB, Germain RN, Kastner DL, Chae JJ. The calcium-sensing receptor regulates the NLRP3 inflammasome through Ca2+ and cAMP. *Nature* 2012; **492**: 123-127 [PMID: 23143333 DOI: 10.1038/nature11588]

194 **Khoury-Haddad H**, Nadar-Ponniah PT, Awwad S, Ayoub N. The emerging role of lysine demethylases in DNA damage response: dissecting the recruitment mode of KDM4D/JMJD2D to DNA damage sites. *Cell Cycle* 2015; **14**: 950-958 [PMID: 25714495 DOI: 10.1080/15384101.2015.1014147]

195 **Horton JR**, Liu X, Gale M, Wu L, Shanks JR, Zhang X, Webber PJ, Bell JSK, Kales SC, Mott BT, Rai G, Jansen DJ, Henderson MJ, Urban DJ, Hall MD, Simeonov A, Maloney DJ, Johns MA, Fu H, Jadhav A, Vertino PM, Yan Q, Cheng X. Structural Basis for KDM5A Histone Lysine Demethylase Inhibition by Diverse Compounds. *Cell Chem Biol* 2016; **23**: 769-781 [PMID: 27427228 DOI: 10.1016/j.chembiol.2016.06.006]

196 **Gong F**, Clouaire T, Aguirrebengoa M, Legube G, Miller KM. Histone demethylase KDM5A regulates the ZMYND8-NuRD chromatin remodeler to promote DNA repair. *J Cell Biol* 2017; **216**: 1959-1974 [PMID: 28572115 DOI: 10.1083/jcb.201611135]

197 **Liu H**, Liu L, Holowatyj A, Jiang Y, Yang ZQ. Integrated genomic and functional analyses of histone demethylases identify oncogenic KDM2A isoform in breast cancer. *Mol Carcinog* 2016; **55**: 977-990 [PMID: 26207617 DOI: 10.1002/mc.22341]

198 **Longbotham JE**, Chio CM, Dharmarajan V, Trnka MJ, Torres IO, Goswami D, Ruiz K, Burlingame AL, Griffin PR, Fujimori DG. Histone H3 binding to the PHD1 domain of histone demethylase KDM5A enables active site remodeling. *Nat Commun* 2019; **10**: 94 [PMID: 30626866 DOI: 10.1038/s41467-018-07829-z]

199 **Lan F**, Collins RE, De Cegli R, Alpatov R, Horton JR, Shi X, Gozani O, Cheng X, Shi Y. Recognition of unmethylated histone H3 Lysine 4 Links BHC80 to LSD1-mediated gene repression. *Nature* 2007; **448**: 718-722 [PMID: 17687328 DOI: 10.1038/nature06034]

200 **Fair K**, Anderson M, Bulanova E, Mi H, Tropschug M, Diaz MO. Protein interactions of the MLL PHD fingers modulate MLL target gene regulation in human cells. *Mol Cell Biol* 2001; **21**: 3589-3597 [PMID: 11313484 DOI: 10.1128/mcb.21.10.3589-3597.2001]

201 **Li SS**, Jiang WL, Xiao WQ, Li K, Zhang YF, Guo XY, Dai YQ, Zhao QY, Jiang MJ, Lu ZJ, Wan R. KMT2D deficiency enhances the anti-cancer activity of L48H37 in pancreatic ductal adenocarcinoma. *World J Gastrointest Oncol* 2019; **11**: 599-621 [PMID: 31435462 DOI: 10.4251/wjgo.v11.i8.599]

202 **Zhang X**, Novera W, Zhang Y, Deng LW. MLL5 (KMT2E): structure, function, and clinical relevance. *Cell Mol Life Sci* 2017; **74**: 2333-2344 [PMID: 28188343 DOI: 10.1007/s00018-017-2470-8]

World Journal of Gastroenterology

Submit a Manuscript: https://www.f6publishing.com

World J Gastroenterol 2021 September 28; 27(36): 6025-6038

DOI: 10.3748/wjg.v27.i36.6025

ISSN 1007-9327 (print) ISSN 2219-2840 (online)

REVIEW

Hepatitis B virus infection and hepatocellular carcinoma in sub-Saharan Africa: Implications for elimination of viral hepatitis by 2030?

Edina Amponsah-Dacosta

ORCID number: Edina Amponsah-Dacosta 0000-0002-3913-0457.

Author contributions: Amponsah-Dacosta E defined the topic, performed the literature search, screened, and reviewed the literature, and wrote the manuscript.

Supported by The Harry Crossley Postdoctoral Research Fellowship 2021.

Conflict-of-interest statement: The author has no conflict of interest to disclose.

Open-Access: This article is an open-access article that was selected by an in-house editor and fully peer-reviewed by external reviewers. It is distributed in accordance with the Creative Commons Attribution NonCommercial (CC BY-NC 4.0) license, which permits others to distribute, remix, adapt, build upon this work non-commercially, and license their derivative works on different terms, provided the original work is properly cited and the use is non-commercial. See: http://creativecommons.org/Licenses/by-nc/4.0/

Manuscript source: Invited manuscript

Edina Amponsah-Dacosta, Vaccines for Africa Initiative, School of Public Health and Family Medicine, University of Cape Town, Cape Town 7925, Western Cape, South Africa

Corresponding author: Edina Amponsah-Dacosta, PhD, Postdoctoral Fellow, Vaccines for Africa Initiative, School of Public Health and Family Medicine, University of Cape Town, Anzio Road, Observatory, Cape Town 7925, Western Cape, South Africa. edina.amponsah-dacosta@uct.ac.za

Abstract

Elimination of viral hepatitis in sub-Saharan Africa by 2030 is an ambitious feat. However, as stated by the World Health Organization, there are unprecedented opportunities to act and make significant contributions to the elimination target. With 60 million people chronically infected with hepatitis B virus (HBV) of whom 38800 are at risk of developing highly fatal hepatocellular carcinoma (HCC) every year, sub-Saharan Africa faces one of the greatest battles towards elimination of viral hepatitis. There is a need to examine progress in controlling the disproportionate burden of HBV-associated HCC in sub-Saharan Africa within the context of this elimination target. By scaling-up coverage of hepatitis B birth dose and early childhood vaccination, we can significantly reduce new cases of HCC by as much as 50% within the next three to five decades. Given the substantial reservoir of chronic HBV carriers however, projections show that HCC incidence and mortality rates in sub-Saharan Africa will double by 2040. This warrants urgent public health attention. The trends in the burden of HCC over the next two decades, will be determined to a large extent by progress in achieving early diagnosis and appropriate linkage to care for high-risk chronic HBV infected persons.

Key Words: Hepatitis B virus; Viral hepatitis, Hepatocellular Carcinoma; Elimination; Human Immunodeficiency Virus; Sub-Saharan Africa

©The Author(s) 2021. Published by Baishideng Publishing Group Inc. All rights reserved.

Core Tip: Chronic hepatitis B virus (HBV) infection is the primary risk factor for

Specialty type: Gastroenterology and hepatology

Country/Territory of origin: South Africa

Peer-review report's scientific quality classification
Grade A (Excellent): 0
Grade B (Very good): B
Grade C (Good): 0
Grade D (Fair): 0
Grade E (Poor): 0

Received: February 28, 2021
Peer-review started: February 28, 2021
First decision: May 1, 2021
Revised: May 10, 2021
Accepted: August 13, 2021
Article in press: August 13, 2021
Published online: September 28, 2021

P-Reviewer: Peng S
S-Editor: Wang JL
L-Editor: Webster JR
P-Editor: Li JH

hepatocellular carcinoma (HCC) in sub-Saharan Africa. In 2020, HBV-associated HCC accounted for approximately 36700 deaths. By 2040, it is projected that approximately 72200 people will die each year from this disease without an intensive public health response. The high mortality-to-incidence ratio associated with HCC in sub-Saharan Africa suggests significant inequities in access to appropriate health care. This review examines the evidence on the extent of the disease burden in sub-Saharan Africa and advocates for prioritizing HCC control as part of ongoing viral hepatitis elimination strategies within this region.

Citation: Amponsah-Dacosta E. Hepatitis B virus infection and hepatocellular carcinoma in sub-Saharan Africa: Implications for elimination of viral hepatitis by 2030? *World J Gastroenterol* 2021; 27(36): 6025-6038
URL: https://www.wjgnet.com/1007-9327/full/v27/i36/6025.htm
DOI: https://dx.doi.org/10.3748/wjg.v27.i36.6025

INTRODUCTION

Despite the availability of a safe and effective prophylactic vaccine since 1982, chronic hepatitis B which is a serious liver disease caused by hepatitis B virus (HBV), remains a major global public health threat. Estimates from the World Health Organization's (WHO) current Global Hepatitis Report suggest that in 2015, 3.5% (257 million persons) of the world's population were living with chronic hepatitis B, with the Western Pacific and sub-Saharan African regions bearing the brunt (68%) of the disease burden (WHO, 2017). In addition to this, 887000 deaths due to HBV-associated hepatic sequelae such as acute hepatitis, liver cirrhosis and liver cancer or hepatocellular carcinoma (HCC), were recorded worldwide[1].

With an estimated 830180 associated deaths recorded in 2020, liver cancer remains a leading cause of cancer-related death worldwide, third only to lung (1.8 million deaths) and colorectal (935153 deaths) cancers[2]. Globally, incidence rates of liver cancer have remained high, with 905677 newly diagnosed cases in 2020 [compared to 748000 (5.9% of all cancers) new cases in 2008, for example[3]], representing 4.7% of all cancer cases recorded in that year alone[2]. The most common type of malignant transformation in the liver is HCC (75%-85%), followed by intrahepatic cholangiocarcinoma (10%-15%), with other rare types accounting for the remainder of all primary liver cancers. The geographic distribution of the incidence of HCC tends to mirror that of its major risk factors, chronic hepatitis B and hepatitis C virus (HCV) infection, which account for approximately 56% and 20% of all HCC cases, respectively[2,4-6]. This implies that the highest incidence rates [age-standardized incidence rate (ASIR) > 20 cases per 100000 persons per year] of HCC are recorded in hepatitis B endemic countries including those in sub-Saharan Africa, while non-endemic regions like Europe and North America report relatively lower incidence rates (ASIR < 10 cases per 100000 persons per year)[2,7-9]. A further cause for concern in most resource limited countries within regions like sub-Saharan Africa where HCC screening and diagnostic services, and medical interventions are often inadequate, is the poor survival and extremely high mortality rates associated with HCC. Approximately 93% of patients die within a year of the onset of symptoms[7,9-11]. Evidently, elimination of viral hepatitis caused by HBV and HCV presents the best opportunity to reduce the incidence of HCC, especially in regions like sub-Saharan Africa, where the disease burden and need for intervention are oftentimes the greatest.

Recognizing the devastating impact of viral hepatitis on global health, the WHO in May 2016 adopted a Global Health Sector Strategy on Viral Hepatitis aimed at achieving a 90% reduction in new cases and a 65% reduction in mortality due to HBV and HCV infection, towards an ambitious target of eliminating viral hepatitis by 2030 [12]. To eliminate chronic hepatitis B, the health service targets to be attained by 2030 include; 90% coverage of routine childhood hepatitis B vaccination, a reduction in mother-to-child transmission (MTCT) of HBV such as through > 90% coverage of hepatitis B birth dose vaccination, 100% of all blood donations screened for HBV, 90% of all HBV infections diagnosed, and 80% of eligible persons with chronic hepatitis B linked to appropriate treatment and care[12]. While largely in the planning phase of executing this global strategy, a recent WHO report suggests that overall, member

states are making progress in developing national viral hepatitis management guidelines and strategic plans towards attaining the elimination targets, although availability of dedicated funding to support implementation appears to be an important challenge in some countries[13].

To contribute to the knowledgebase on the scope of the burden of chronic hepatitis B in sub-Saharan Africa, the status and public health response to HBV-associated HCC in sub-Saharan Africa are reviewed. Opportunities and challenges towards achieving the 2030 viral hepatitis elimination target – at least where chronic hepatitis B and HCC are concerned – are also identified, with the intent of arguing for continued financial and technical investments to support ongoing health sector strategies and interventions within sub-Saharan Africa.

GLOBAL BURDEN OF CHRONIC HEPATITIS B

The seroprevalence of chronic hepatitis B which is based on the detection of the hepatitis B surface antigen (HBsAg) within the general population, is highly variable worldwide. This variability is demonstrated by substantial regional and inter-country disparities in the burden of the disease. Available estimates[14] suggest that HBsAg prevalence rates in the Americas, for example, range from < 2% in countries like the United States of America, Mexico, and Guatemala, to 13.55% (95%CI: 9.00-19.89) in Haiti. In the South East Asian region, HBsAg prevalence rates range from 0.82% (95%CI: 0.80–0.84) in Nepal to as high as 6.42% (95%CI: 6.37–6.47) in Thailand. Overall, countries within the Eastern Mediterranean and European regions mostly have lower-intermediate endemicity levels (HBsAg prevalence ranging from 2% to 4.99%) while the Western Pacific can be classified as a high-intermediate endemic region with most countries recording HBsAg prevalence rates > 5%. Within the African region, the lowest HBsAg prevalence rates are reported in countries like Seychelles [0.48% (95%CI: 0.12-1.90)], Eritrea [2.49% (95%CI: 2.32-2.67)], and Algeria [2.89% (95%CI: 2.50-3.33)], while Mauritania [16.16% (95%CI: 14.92-17.49)], Liberia [17.55% (95%CI: 15.70-19.55)], Swaziland [19% (95%CI: 17.65-20.43)], and South Sudan [22.38% (95%CI: 20.10-24.83)] have recorded some of the highest prevalence estimates[14].

EPIDEMIOLOGICAL SHIFT IN THE BURDEN OF CHRONIC HEPATITIS B IN SUB-SAHARAN AFRICA

Historically, sub-Saharan Africa has been classified as hyper-endemic for chronic hepatitis B based on the detection of HBsAg among ≥ 8% of the general population. Table 1 shows the variable prevalence of HBsAg among populations in some sub-Saharan African countries prior to introduction of universal hepatitis B vaccination and how this has changed over time post-vaccine introduction[15-47]. At the peak of the hepatitis B epidemic in sub-Saharan Africa, the disease burden was characterized by a preponderance of horizontal transmission of HBV among young children (between 1-4 years of age), 30%-50% of whom would go on to develop chronic hepatitis B, and later progress to potentially fatal sequelae (mainly liver cirrhosis and HCC) within 30-50 years after infection[15,29,48]. This contrasts with HBV infection acquired during adulthood which carries a considerably lower risk (< 5%) of progression to chronic disease as observed in non-endemic regions of the world.

Currently, the prevalence of HBsAg in sub-Saharan Africa is reported to be 6.1%, equating to 60 million people living with chronic hepatitis B, of which approximately 4.8 million are children < 5 years of age[1]. The decline in the prevalence of HBsAg within the population can be largely attributed to the success of universal childhood hepatitis B vaccination programmes implemented in sub-Saharan Africa since the early 1990s[49]. In most sub-Saharan African countries, the first dose of the hepatitis B vaccine is administered at 6 weeks of age, with the remainder of the regimen completed within the 1st year of life in an effort to interrupt transmission and prevent incident HBV infection in early childhood. Coverage of the third dose of the hepatitis B vaccine in the region is currently estimated at 73%[50]. Countries like The Gambia and South Africa with longstanding hepatitis B vaccination programmes have achieved marked declines in incident infections over time, especially among children < 5 years of age (Table 1).

Despite this success, we are still decades away from realizing the full benefits of universal childhood hepatitis B vaccination programmes in sub-Saharan Africa, given

Table 1 Prevalence of hepatitis B surface antigen among pre- *vs* post-hepatitis B vaccine introduction populations in some sub-Saharan African countries

Country	Year of hepatitis B vaccine introduction[1]	Prevalence of HBsAg (%)		
		Pre-vaccine introduction	Post-vaccine introduction	
			< 15-yr-olds	≥ 15-yr-olds
Burundi	2004	11.0[15]	2.6[16]	1.0-4.6[17]
Democratic Republic of Congo	2007	> 20.7[18]	2.2[19]	3.7[19]
Ethiopia	2007	11.0[20]	4.4[21]	7.4[22]
Gambia	1990	20.0[23]	0.4[24]	10.0[25]
Kenya	2002	11.4[26]	0.9[16]	3.4[27]
Mali	2003	> 8.7[28]	4.9[16]	8.5[16]
Mozambique	2001	14.6[29]	3.7[16]	4.5[30]
Namibia	2009	14.0[31]	2.7[32]	1.8[33]
Nigeria	2004	13.3[34]	11.5[35]	8.2[36]
Rwanda	2002	Approximately 5.0[37]	1.7[16]	2.2[38]
Senegal	2004	11.8[39]	1.6[40]	> 11.0[41]
South Africa	1995	9.6[15]	0.4[42]	4.0[43]
Uganda	2002	10.3[44]	0.6[45]	4.1[45]
Zimbabwe	2000	15.4[46]	4.4[16]	3.3[47]

[1]The year the hepatitis B vaccine was introduced into national Expanded Programme on Immunization. HBsAg: Hepatitis B surface antigen.

the protracted natural history of chronic hepatitis B, and the long interval between early childhood infection and development of chronic sequelae[51,52]. As such, high prevalence rates of HBsAg persist among a reservoir of adult populations, including women of childbearing age, most of whom were born before the introduction of the hepatitis B vaccine or were not fully vaccinated in infancy (Table 1). This continues to feed the epidemic in sub-Saharan Africa, contributing to the 87890 HBV-associated deaths (approximately 10% of the global total) recorded each year[1]. What further compounds the situation in sub-Saharan Africa is the disproportionate burden of human immunodeficiency virus (HIV) co-infection (69% of all HBV-HIV co-infected persons reside in sub-Saharan Africa) which is associated with a more severe prognosis than that observed in HBV mono-infected individuals[53-55]. Emerging evidence also suggests that perinatal transmission or MTCT of HBV, which was previously presumed to be insignificant in the epidemiology of chronic hepatitis B in sub-Saharan Africa, actually contributes to 367250 incident HBV infections (twice the number of paediatric HIV infections) among neonates annually[56]. In fact, the risk of HBV MTCT increases by up to 2.5-fold among the substantial population of HBV-HIV co-infected pregnant women in sub-Saharan Africa, compared to their HBV mono-infected counterparts[57-60]. This is concerning, given that perinatally acquired HBV infections carry a 90% risk of progression to chronic hepatitis B. This implies that hepatitis B vaccination from 6 weeks of age may be inadequate in preventing incident HBV infections among neonates, especially where the burden of maternal HBV-HIV co-infection is high and prevention of HBV MTCT (PMTCT) strategies are sub-optimal, as is the case in most sub-Saharan African countries. This is a stark contrast to HIV MTCT in sub-Saharan Africa which is on course for elimination due to rapid expansion of antenatal screening and access to timely HIV antiretroviral therapy[61]. The marked decline in HIV MTCT has led to a growing population of HIV-exposed uninfected children in sub-Saharan Africa. Of the 14.8 million HIV-exposed uninfected children in the world, 90% live in sub-Saharan Africa[62]. Although inconclusive, there is some evidence to suggest that HIV-exposed uninfected children may have a modified immune response to hepatitis B vaccination and may also be at increased risk for HBV infection, presenting an additional complexity to elimination strategies in sub-Saharan Africa[58,63-66].

EPIDEMIOLOGICAL TRENDS IN HBV-ASSOCIATED HCC IN SUB-SAHARAN AFRICA

Of the 60 million people currently living with chronic hepatitis B in sub-Saharan Africa, 38800 are at risk of developing HCC every year, characterized by an aggressive clinical course[2,67,68]. In addition, approximately 93% (36700) of persons with HCC will die within a year of their diagnosis without appropriate and timely medical intervention[2,11,67]. Most of these HCC cases (and deaths) will occur among a predominantly male population (sex ratio of 2:1) with age at diagnosis ranging between 38-67 years (compared to 50-70 years in resource rich countries), who are in their prime reproductive and working years, draining productive capacity, and placing a further burden on already strained economic, societal, and health, systems in sub-Saharan Africa[9,11,69-71]. While cases of paediatric HCC are diagnosed more frequently in some sub-Saharan African countries than those in Europe and North America for example, they remain uncommon when compared to the HCC incidence among adult populations[72-75]. Within the next two decades, HCC incidence and mortality rates in sub-Saharan Africa are predicted to double (Figure 1[67,76,77]) unless addressed through reforms in regional and national health policy and practice, including intensifying prevention, diagnostic and treatment strategies, in a whole system approach.

A comparison of the 2020 estimates of age-standardized liver cancer (mainly HCC) incidence and mortality (ASMR) rates in sub-Saharan Africa *vs* other regions of the world is shown in Figure 2[2,67,78]. With ASIRs of 8.1 and 4.2, and ASMRs of 7.8 and 4.0 per 100000 persons per year among men and women, respectively, HCC is a common cause of cancer-related morbidity and mortality in sub-Saharan Africa. There are substantial regional variations in HCC incidence and mortality rates across sub-Saharan Africa. Among males for example, the highest HCC ASIRs (> 12.9 per 100000 persons per year) and ASMRs (> 12.6 per 100000 persons per year) are recorded in West African countries, while East African countries generally appear to experience a lower burden (ASIRs < 5.1 and ASMRs < 4.9 per 100000 persons per year) of the disease (Figures 3 and 4)[2,67,78]. It should be noted however, that the true burden of HCC in sub-Saharan Africa is grossly underestimated by as much as 40%, given that cases are often underreported due to challenges in effectively diagnosing the disease, while the quality and coverage of data in population-based cancer registries are suboptimal[9,11,79].

The overall HCC mortality-to-incidence ratio (MIR = 0.95) in sub-Saharan Africa is comparable to that in the Western Pacific and South-East Asian regions (MIR = 0.95) but higher than that in Northern America (MIR = 0.82)[80]. This high MIR reflects disparities in outcomes of HCC in sub-Saharan Africa compared to resource-rich regions, owing to limited availability and accessibility of diagnostic and treatment services[81,82]. These disparities go beyond the clinical context and are rooted in socio-economic inequities. A recent South African study[82] investigating trends in liver cancer-associated mortality found key socio-economic and sex disparities. The average MIR for black South African men and women was 4.0 and 3.3 respectively, compared to 2.2 and 1.8 among their white counterparts. This underscores the inequities in HCC prognosis experienced by socio-economically disadvantaged populations[82]. Evidently, addressing the disproportionate burden of HCC in sub-Saharan Africa will require careful consideration of socio-economic and demographic inequities prevalent within its population.

PREDOMINANCE OF HBV-ASSOCIATED HEPATOCARCINOGENESIS IN SUB-SAHARAN AFRICA

The association of chronic hepatitis B with the development of most cases of HCC [attributable fraction, AF = 50% (95%CI: 39-60)] occurring among sub-Saharan African populations is well established in the literature[5,6,83,84]. The remainder of HCC cases are typically associated with HCV infection [AF = 21% (95%CI: 13-32)] and exposure to the dietary carcinogen, aflatoxin B1, although metabolic syndrome is emerging as an important risk factor in sub-Saharan Africa[6,85-88]. In comparison, the major risk factors for HCC development in low incidence regions of the world (North America, and Western, Central, and Eastern Europe) include host and environmental factors such as genetic predisposition to primary liver cancer, chronic alcohol intake, obesity, hemochromatosis, and exposure to nitrosamines, followed by HCV infection[71,89-

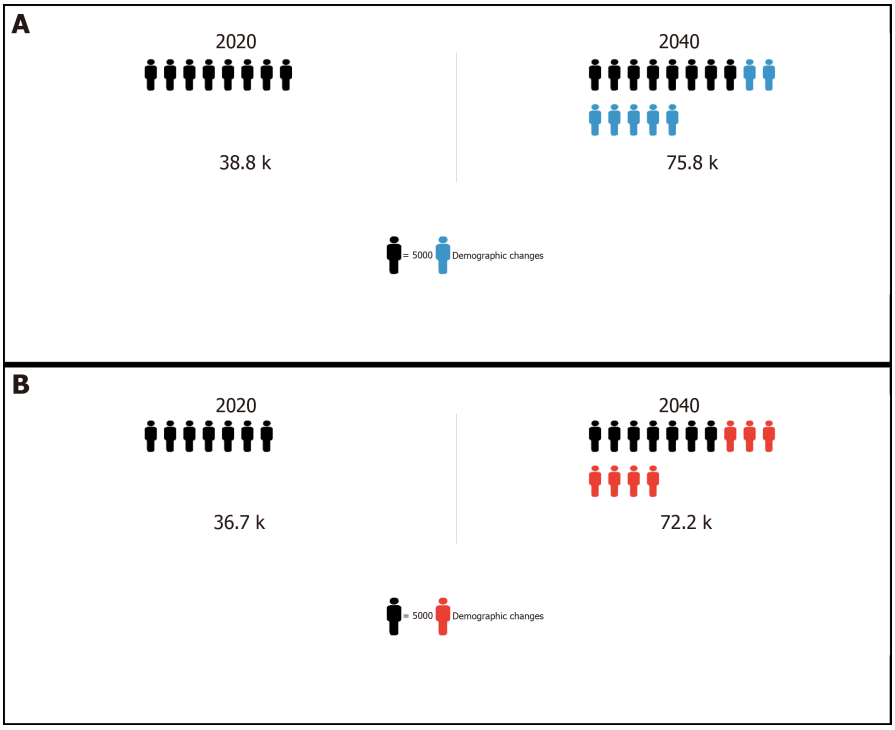


Figure 1 Projected increase in estimated number of cases and deaths due to cancers of the liver and intrahepatic bile ducts within sub-Saharan Africa from 2020 to 2040[67,76,77]. GLOBOCAN 2020 (https://gco.iarc.fr/). A: Estimated number of cases from 2020 to 2040, both sexes, age (0-85+); B: Estimated number of deaths from 2020 to 2040, both sexes, age (0-85+).

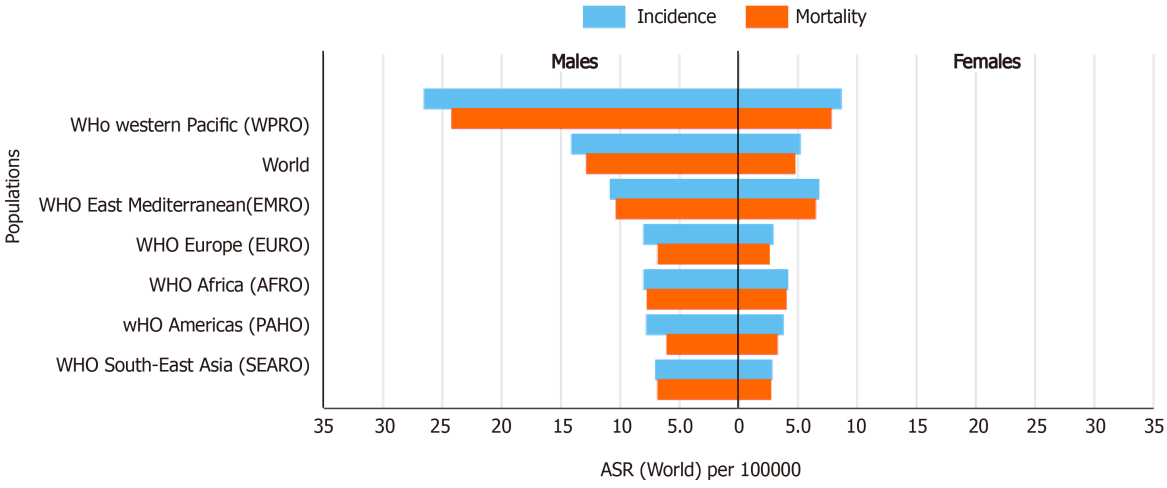
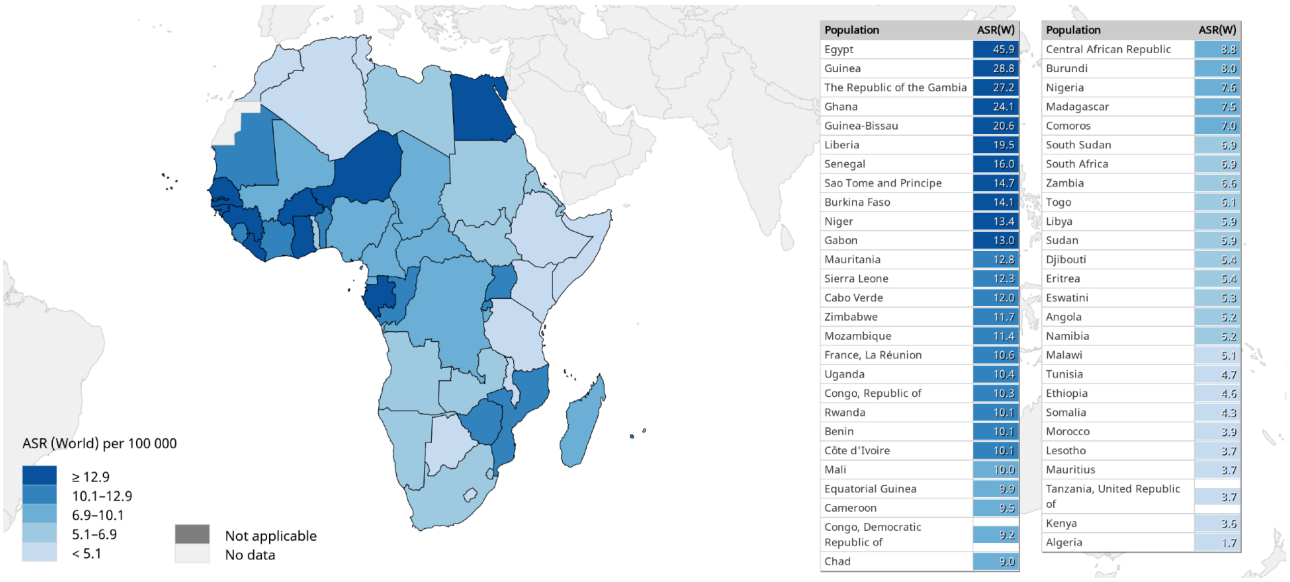


Figure 2 Estimated age-standardized liver cancer incidence and mortality rates per 100000 persons per year shown worldwide in 2020[2,67,78]. GLOBOCAN 2020 (https://gco.iarc.fr/). WHO: World Health Organization; ASR: Liver cancer age standardized incidence rate.

91]. It is worth noting however, that the potential for interaction among these different risk factors, leading to synergistic or additive effects in the development of HCC in both endemic and non-endemic regions of the world cannot be undervalued.

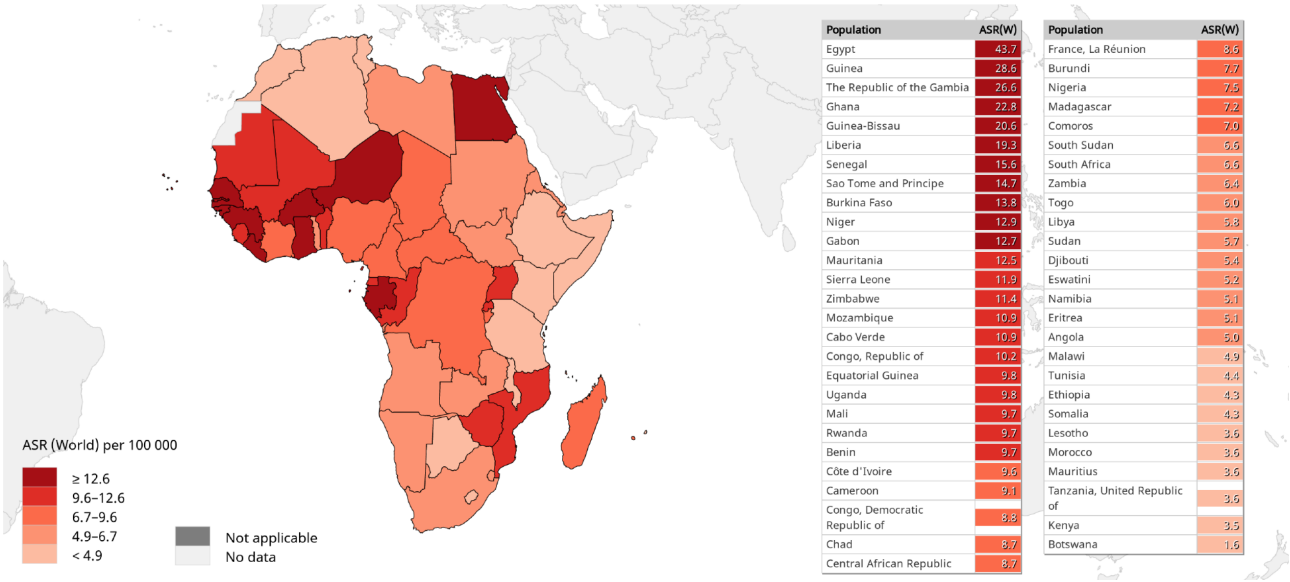
The mechanism underlying HBV-associated hepatocarcinogenesis is multifactorial, involving various direct and indirect viral mechanisms required to stimulate the host oncogenic pathway and achieve hepatocyte transformation[92,93]. These mechanisms, which may act synergistically, include integration of the viral DNA into host genome, persistent and enhanced HBV replication, as well as infection with specific HBV genotypes and HBV genetic variants. Important HBV-specific risk factors involved in the development of HCC have been identified in previous studies conducted in sub-Saharan Africa. In a recent case control study, Atsama Amougou *et al*[94] demonstrated the role of circulating quasi-genotypes and viral genetic variations in HBV-



Population	ASR(W)
Egypt	45.9
Guinea	28.8
The Republic of the Gambia	27.2
Ghana	24.1
Guinea-Bissau	20.6
Liberia	19.5
Senegal	16.0
Sao Tome and Principe	14.7
Burkina Faso	14.1
Niger	13.4
Gabon	13.0
Mauritania	12.8
Sierra Leone	12.3
Cabo Verde	12.0
Zimbabwe	11.7
Mozambique	11.4
France, La Réunion	10.6
Uganda	10.4
Congo, Republic of	10.3
Rwanda	10.1
Benin	10.1
Côte d'Ivoire	10.1
Mali	10.0
Equatorial Guinea	9.9
Cameroon	9.5
Congo, Democratic Republic of	9.2
Chad	9.0

Population	ASR(W)
Central African Republic	8.8
Burundi	8.0
Nigeria	7.6
Madagascar	7.5
Comoros	7.0
South Sudan	6.9
South Africa	6.9
Zambia	6.6
Togo	6.1
Libya	5.9
Sudan	5.9
Djibouti	5.4
Eritrea	5.4
Eswatini	5.3
Angola	5.2
Namibia	5.2
Malawi	5.1
Tunisia	4.7
Ethiopia	4.6
Somalia	4.3
Morocco	3.9
Lesotho	3.7
Mauritius	3.7
Tanzania, United Republic of	3.7
Kenya	3.6
Algeria	1.7

Figure 3 Estimated age-standardized liver cancer incidence rates per 100000 persons per year in males in Africa (2020)[2,67,78]. GLOBOCAN 2020 (https://gco.iarc.fr/). The designations employed and the presentation of the material in this publication do not imply the expression of any opinion whatsoever on the part of the World Health Organization/International Agency for Research on Cancer concerning the legal status of any country, territory, city, or area or of its authorities, or concerning the delimitation of its frontiers or boundaries. Dotted or dashed lines on maps represent approximate borderlines for which there may not yet be full agreement.



Population	ASR(W)
Egypt	43.7
Guinea	28.6
The Republic of the Gambia	26.6
Ghana	22.8
Guinea-Bissau	20.6
Liberia	19.3
Senegal	15.6
Sao Tome and Principe	14.7
Burkina Faso	13.8
Niger	12.9
Gabon	12.7
Mauritania	12.5
Sierra Leone	11.9
Zimbabwe	11.4
Mozambique	10.9
Cabo Verde	10.9
Congo, Republic of	10.2
Equatorial Guinea	9.8
Uganda	9.8
Mali	9.7
Rwanda	9.7
Benin	9.7
Côte d'Ivoire	9.6
Cameroon	9.1
Congo, Democratic Republic of	8.8
Chad	8.7
Central African Republic	8.7

Population	ASR(W)
France, La Réunion	8.6
Burundi	7.7
Nigeria	7.5
Madagascar	7.2
Comoros	7.0
South Sudan	6.6
South Africa	6.6
Zambia	6.4
Togo	6.0
Libya	5.8
Sudan	5.7
Djibouti	5.4
Eswatini	5.2
Namibia	5.1
Eritrea	5.1
Angola	5.0
Malawi	4.9
Tunisia	4.4
Ethiopia	4.3
Somalia	4.3
Lesotho	3.6
Morocco	3.6
Mauritius	3.6
Tanzania, United Republic of	3.5
Kenya	3.5
Botswana	1.6

Figure 4 Estimated age-standardized liver cancer mortality rates per 100000 persons per year in males in Africa (2020)[2,67,78]. GLOBOCAN 2020 (https://gco.iarc.fr/). The designations employed and the presentation of the material in this publication do not imply the expression of any opinion whatsoever on the part of the World Health Organization/International Agency for Research on Cancer concerning the legal status of any country, territory, city, or area or of its authorities, or concerning the delimitation of its frontiers or boundaries. Dotted or dashed lines on maps represent approximate borderlines for which there may not yet be full agreement.

associated hepatocarcinogenesis among Cameroonian HCC patients. A previous study [95] conducted in South Africa found an increasing risk of HCC with increasing HBV viremia, showing an increasing trend in odds ratio (OR) from ≥ 2000 IU/mL (OR = 8.55, 95%CI: 3.00 ± 24.54) to ≥ 200000 IU/mL (OR 16.93, 95%CI: 8.65 ± 33.13). While this finding is consistent with that from another study conducted in The Gambia, there is evidence to suggest that low-level viremia may also be a significant risk factor for HCC[96]. The South African study further demonstrated a 4-fold increase in the risk of developing HCC among participants with occult HBV infection (HBsAg negative but HBV DNA positive infections) compared to controls[95]. Interestingly, a previous longitudinal study conducted in The Gambia which followed chronic carriers of HBV

over a median duration of 28.4 years (interquartile rage = 17.7-32.7) found that maternal HBsAg positivity – as a proxy of MTCT of HBV – was statistically significantly ($P < 0.001$) associated with a higher incidence of HCC [crude incidence rates of 89.2 (95%CI: 22.3–356.8) *vs* 0 (unadjusted) per 100 000 persons per year, among those born to HBsAg positive *vs* HBsAg negative mothers][70]. Based on these findings, the authors recommend further investigation into the feasibility of scaling-up implementation of hepatitis B birth dose vaccination and other PMTCT strategies within sub-Saharan Africa in order to interrupt incident HBV infections among neonates[70]. Of the 111 countries which report having introduced a hepatitis B birth dose as part of national routine immunization programmes, only 11 (Algeria, Botswana, Cabo Verde, Côte d'Ivoire, The Gambia, Mauritania, Namibia, Nigeria, Sao Tome and Principe, Senegal, and Zambia) are in Africa[50]. While the global coverage of the birth dose is reported to be suboptimal (43%), that in the sub-Saharan African region is even more dismal at an estimated 6%[50]. When considered together with the reported low coverage of maternal screening for HBV infection and linkage to antiviral prophylaxis, current PMTCT strategies are inadequate to significantly reduce perinatal transmission and avert neonatal HBV infections within the region[97,98].

CHALLENGES AFFECTING MANAGEMENT OF HBV-ASSOCIATED HCC IN SUB-SAHARAN AFRICA

Management of chronic hepatitis B involves suppressing HBV viremia and minimizing the risk of progression to liver cirrhosis, chronic liver failure and HCC, using oral nucleotide/nucleoside analogues like tenofovir disoproxil fumarate (TDF) and entecavir. Treatment with nucleotide/nucleoside analogues is indicated in chronic carriers with elevated HBV viremia, elevated liver enzymes, and evidence of liver fibrosis and cirrhosis. Appropriate linkage to care requires the identification of chronically infected individuals who are eligible for treatment through HBV screening programmes[99]. It is estimated that < 1% of chronic HBV infected individuals in sub-Saharan Africa are currently being diagnosed[100]. In addition, there are major gaps in determining treatment eligibility. Significant limitations have been identified when applying internationally recommended treatment eligibility criteria in the sub-Saharan African context. Only 10%–15% of persons with liver cirrhosis are detected for linkage to appropriate treatment[99-102].

Low uptake of HBV screening and treatment services in sub-Saharan Africa has been attributed to the lack of publicly funded, national HBV screening and treatment programmes. This leaves the responsibility for seeking an HBV test to the patient, which is highly detrimental when considered in the context of limited public awareness of the virus, and the asymptomatic nature of the infection until onset of late-stage sequelae[103]. As currently available nucleotide/nucleoside analogues cannot eradicate intrahepatic HBV DNA, treatment is typically lifelong, and this amounts to a significant cost[100,102]. A recent WHO report indicates that by 2019, < 8 of the 47 member states within the WHO African region (WHO AFRO) had established subsidized HBV treatment programmes[16]. This suggests that a substantial proportion of chronic HBV carriers continue to incur undue financial burden as a consequence of paying out-of-pocket for the treatment they need, while others may be unable to afford it altogether. In Ghana, the annual cost of TDF is estimated at $670 which, when considered against an average annual income of $1778, is a major constraint to accessing lifesaving treatment[104]. It should not come as a surprise then that most patients in sub-Saharan Africa present to health care facilities with established liver cirrhosis or symptomatic advanced-stage HCC, at which point the prognosis is grim and therapeutic options are limited to palliative care.

TOWARDS ELIMINATION OF CHRONIC HEPATITIS B AND CONTROL OF HCC IN SUB-SAHARAN AFRICA

Future trends in the burden of HCC in sub-Saharan Africa will be determined by our progress in preventing new HBV infections, screening and treating existing chronic hepatitis B cases, as well as detecting and appropriately managing HCC. As part of a scorecard to monitor progress towards elimination of viral hepatitis within WHO AFRO in 2019, six core indicators were listed; (1) development of national hepatitis policies in the form of a national strategic plan for viral hepatitis; (2) implementation

of hepatitis B birth dose vaccination; (3) achieving > 90% national coverage of the third dose of the hepatitis B vaccine; (4) being on track for the HBV and HCV 2020 testing target; (5) implementation of a national hepatitis treatment programme; and (6) commemoration of World Hepatitis Day in 2018. Overall, most sub-Saharan African countries were found lagging in almost all indicators[16].

Within the next decade, there is a need to scale-up primary prevention of incident HBV infections in sub-Saharan Africa. Despite adopting resolutions to improve hepatitis B birth dose and routine childhood vaccination in WHO AFRO by 2020, implementation and coverage of the birth dose remains unacceptably low, while coverage of routine childhood vaccination remains well below the global average of 84%[49,105,106]. Recognizing the significant threat of HBV MTCT to public health in sub-Saharan Africa, there have been renewed calls to expand access to the hepatitis B birth dose and leverage HIV PMTCT infrastructure in screening pregnant women and providing timely prophylaxis[56,98,107]. The future research agenda in sub-Saharan Africa should include investigating the need for tailored hepatitis B vaccination strategies for unique populations like HIV-exposed uninfected children.

As national governments grapple with the feasibility of implementing subsidized hepatitis surveillance and treatment programmes, the success of the HIV test and treat model in sub-Saharan Africa has been recognized as an opportunity to expand screening and antiviral treatment for chronic hepatitis B in the interim. To ensure a comprehensive package of care, there is a need to prioritize integration of cost-effective point-of-care screening tests with good diagnostic accuracy, guided by appropriate treatment eligibility criteria[49,108].

Within the past decade, there have been significant advances in the development of new diagnostic and therapeutic approaches for HCC, with prospects for further innovation in the field[109,110]. These advances present unique opportunities to improve surveillance and management of HCC. Biannual surveillance among high-risk chronic carriers of HBV using both liver ultrasonography and serum α-fetoprotein concentrations, is commonly used for early detection of progression to HCC. Curative treatment approaches for early-stage HCC include surgical resection, tumour ablation, or liver transplantation. For advanced-stage HCC, combination treatment using atezolizumab and bevacizumab over sorafenib alone, have shown promising long-term outcomes in phase III clinical trials[110]. Other immunotherapeutic agents for the treatment of late-stage HCC have also been recently explored[109]. While all these advancements present much needed opportunities to improve the quality of life of patients with HCC, the cost and feasibility of implementation within the sub-Saharan African public health context are always important considerations.

CONCLUSION

Ultimately, sub-Saharan Africa faces one of the toughest battles against chronic hepatitis B and HCC. Despite this, there are opportunities to achieve significant reductions in incident HBV infections and alter future trends in the burden of HCC. This calls for strong political will, regional coordination, and effective partnerships with donor agencies and non-governmental organizations in order to mobilize financial investments and technical support. Finally, the role of advocacy and awareness campaigns like World Hepatitis Day in enabling public ownership and demand for accessible, equitable, and quality health services cannot be undervalued.

REFERENCES

1 **World Health Organization**. Global hepatitis report, 2017. Geneva: World Health Organization, 2017

2 **Sung H**, Ferlay J, Siegel RL, Laversanne M, Soerjomataram I, Jemal A, Bray F. Global Cancer Statistics 2020: GLOBOCAN Estimates of Incidence and Mortality Worldwide for 36 Cancers in 185 Countries. *CA Cancer J Clin* 2021; **71**: 209-249 [PMID: 33538338 DOI: 10.3322/caac.21660]

3 **Ferlay J**, Shin HR, Bray F, Forman D, Mathers C, Parkin DM. Estimates of worldwide burden of cancer in 2008: GLOBOCAN 2008. *Int J Cancer* 2010; **127**: 2893-2917 [PMID: 21351269 DOI: 10.1002/ijc.25516]

4 **Herbst DA**, Reddy KR. Risk factors for hepatocellular carcinoma. *Clin Liver Dis (Hoboken)* 2012; **1**: 180-182 [PMID: 31186882 DOI: 10.1002/cld.111]

5 **de Martel C**, Maucort-Boulch D, Plummer M, Franceschi S. World-wide relative contribution of hepatitis B and C viruses in hepatocellular carcinoma. *Hepatology* 2015; **62**: 1190-1200 [PMID:

26146815 DOI: 10.1002/hep.27969]
6 **Maucort-Boulch D**, de Martel C, Franceschi S, Plummer M. Fraction and incidence of liver cancer attributable to hepatitis B and C viruses worldwide. *Int J Cancer* 2018; **142**: 2471-2477 [PMID: 29388206 DOI: 10.1002/ijc.31280]
7 **Ozakyol A**. Global Epidemiology of Hepatocellular Carcinoma (HCC Epidemiology). *J Gastrointest Cancer* 2017; **48**: 238-240 [PMID: 28626852 DOI: 10.1007/s12029-017-9959-0]
8 **Tang A**, Hallouch O, Chernyak V, Kamaya A, Sirlin CB. Epidemiology of hepatocellular carcinoma: target population for surveillance and diagnosis. *Abdom Radiol (NY)* 2018; **43**: 13-25 [PMID: 28647765 DOI: 10.1007/s00261-017-1209-1]
9 **Zakharia K**, Luther CA, Alsabbak H, Roberts LR. Hepatocellular carcinoma: Epidemiology, pathogenesis and surveillance - implications for sub-Saharan Africa. *S Afr Med J* 2018; **108**: 35-40 [PMID: 30182911 DOI: 10.7196/SAMJ.2018.v108i8b.13499]
10 **Kew MC**. Hepatocellular carcinoma in developing countries: Prevention, diagnosis and treatment. *World J Hepatol* 2012; **4**: 99-104 [PMID: 22489262 DOI: 10.4254/wjh.v4.i3.99]
11 **Kew MC**. Epidemiology of hepatocellular carcinoma in sub-Saharan Africa. *Ann Hepatol* 2013; **12**: 173-182 [PMID: 23396727]
12 **World Health Organization**. Global health sector strategy on viral hepatitis 2016–2021: towards ending viral hepatitis. Geneva: World Health Organization, 2016
13 **Smith S**, Harmanci H, Hutin Y, Hess S, Bulterys M, Peck R, Rewari B, Mozalevskis A, Shibeshi M, Mumba M, Le LV, Ishikawa N, Nolna D, Sereno L, Gore C, Goldberg DJ, Hutchinson S. Global progress on the elimination of viral hepatitis as a major public health threat: An analysis of WHO Member State responses 2017. *JHEP Rep* 2019; **1**: 81-89 [PMID: 32039355 DOI: 10.1016/j.jhepr.2019.04.002]
14 **Schweitzer A**, Horn J, Mikolajczyk RT, Krause G, Ott JJ. Estimations of worldwide prevalence of chronic hepatitis B virus infection: a systematic review of data published between 1965 and 2013. *Lancet* 2015; **386**: 1546-1555 [PMID: 26231459 DOI: 10.1016/S0140-6736(15)61412-X]
15 **Kiire CF**. The epidemiology and prophylaxis of hepatitis B in sub-Saharan Africa: a view from tropical and subtropical Africa. *Gut* 1996; **38** Suppl 2: S5-12 [PMID: 8786055 DOI: 10.1136/gut.38.suppl_2.s5]
16 **World Health Organization Regional Office for Africa**. Hepatitis scorecard for the WHO Africa Region implementing the hepatitis elimination strategy. 2019. Available from: https://www.afro.who.int/publications/hepatitis-scorecard-who-africa-region-implementing-hepatitis-elimination-strategy
17 **Kwizera R**, Moibéni A, Shenawy F, Youssif M. The prevalence of hepatitis B and C among blood donors at the National Blood Transfusion Center (CNTS) in Burundi. *Pan Afr Med J* 2018; **31**: 119 [PMID: 31037179 DOI: 10.11604/pamj.2018.31.119.14571]
18 **Werner GT**, Frösner GG, Fresenius K. Prevalence of serological hepatitis A and B markers in a rural area of northern Zaire. *Am J Trop Med Hyg* 1985; **34**: 620-624 [PMID: 2988353 DOI: 10.4269/ajtmh.1985.34.620]
19 **Thompson P**, Parr JB, Holzmayer V, Carrel M, Tshefu A, Mwandagalirwa K, Muwonga J, Welo PO, Fwamba F, Kuhns M, Jhaveri R, Meshnick SR, Cloherty G. Seroepidemiology of Hepatitis B in the Democratic Republic of the Congo. *Am J Trop Med Hyg* 2019; **101**: 226-229 [PMID: 31074406 DOI: 10.4269/ajtmh.18-0883]
20 **Tsega E**, Mengesha B, Nordenfelt E, Hansson BG, Lindberg J. Prevalence of hepatitis B virus markers among Ethiopian blood donors: is HBsAg screening necessary? *Trop Geogr Med* 1987; **39**: 336-340 [PMID: 3451408]
21 **Argaw B**, Mihret A, Aseffa A, Tarekegne A, Hussen S, Wachamo D, Shimelis T, Howe R. Sero-prevalence of hepatitis B virus markers and associated factors among children in Hawassa City, southern Ethiopia. *BMC Infect Dis* 2020; **20**: 528 [PMID: 32698884 DOI: 10.1186/s12879-020-05229-7]
22 **Belyhun Y**, Maier M, Mulu A, Diro E, Liebert UG. Hepatitis viruses in Ethiopia: a systematic review and meta-analysis. *BMC Infect Dis* 2016; **16**: 761 [PMID: 27993129 DOI: 10.1186/s12879-016-2090-1]
23 **Fortuin M**, Chotard J, Jack AD, Maine NP, Mendy M, Hall AJ, Inskip HM, George MO, Whittle HC. Efficacy of hepatitis B vaccine in the Gambian expanded programme on immunisation. *Lancet* 1993; **341**: 1129-1131 [PMID: 8097813 DOI: 10.1016/0140-6736(93)93137-p]
24 **Peto TJ**, Mendy ME, Lowe Y, Webb EL, Whittle HC, Hall AJ. Efficacy and effectiveness of infant vaccination against chronic hepatitis B in the Gambia Hepatitis Intervention Study (1986-90) and in the nationwide immunisation program. *BMC Infect Dis* 2014; **14**: 7 [PMID: 24397793 DOI: 10.1186/1471-2334-14-7]
25 **Bittaye M**, Idoko P, Ekele BA, Obed SA, Nyan O. Hepatitis B virus sero-prevalence amongst pregnant women in the Gambia. *BMC Infect Dis* 2019; **19**: 259 [PMID: 30876397 DOI: 10.1186/s12879-019-3883-9]
26 **Hyams KC**, Okoth FA, Tukei PM, Mugambi M, Johnson B, Morrill JC, Gray GC, Woody JN. Epidemiology of hepatitis B in eastern Kenya. *J Med Virol* 1989; **28**: 106-109 [PMID: 2786919 DOI: 10.1002/jmv.1890280210]
27 **Awili HO**, Gitao GC, Muchemi GM. Seroprevalence and Risk Factors for Hepatitis B Virus Infection in Adolescent Blood Donors within Selected Counties of Western Kenya. *Biomed Res Int* 2020; **2020**: 8578172 [PMID: 32685533 DOI: 10.1155/2020/8578172]

28 **Maupas P**, Chiron JP, Goudeau A, Coursaget P, Perrin J, Barin F, Yvonnet B, Dubois F, Duflo B, Duflo-Moreau B, Sidibe S, Diallo AN. [Epidemiology and pathologic results of chronic carriers state of hepatitis B in Mali]. *Bull Soc Pathol Exot Filiales* 1981; **74**: 722-732 [PMID: 7343138]

29 **Kiire CF**. Hepatitis B infection in sub-Saharan Africa. The African Regional Study Group. *Vaccine* 1990; **8** Suppl: S107-12; discussion S134 [PMID: 2139278 DOI: 10.1016/0264-410x(90)90229-f]

30 **Mabunda N**, Zicai AF, Ismael N, Vubil A, Mello F, Blackard JT, Lago B, Duarte V, Moraes M, Lewis L, Jani I. Molecular and serological characterization of occult hepatitis B among blood donors in Maputo, Mozambique. *Mem Inst Oswaldo Cruz* 2020; **115**: e200006 [PMID: 32997000 DOI: 10.1590/0074-02760200006]

31 **Botha JF**, Ritchie MJ, Dusheiko GM, Mouton HW, Kew MC. Hepatitis B virus carrier state in black children in Ovamboland: role of perinatal and horizontal infection. *Lancet* 1984; **1**: 1210-1212 [PMID: 6144925 DOI: 10.1016/s0140-6736(84)91694-5]

32 **Mhata P**, Rennie TW, Small LF, Nyarang'o PM, Chagla Z, Hunter CJ. Distribution of hepatitis B virus infection in Namibia. *S Afr Med J* 2017; **107**: 882-886 [PMID: 29022533 DOI: 10.7196/SAMJ.2017.v107i10.12171]

33 **Mavenyengwa RT**, Mukesi M, Chipare I, Shoombe E. Prevalence of human immunodeficiency virus, syphilis, hepatitis B and C in blood donations in Namibia. *BMC Public Health* 2014; **14**: 424 [PMID: 24884633 DOI: 10.1186/1471-2458-14-424]

34 **Nasidi A**, Harry TO, Vyazov SO, Munube GM, Azzan BB, Ananiev VA. Prevalence of hepatitis B infection markers in representative areas of Nigeria. *Int J Epidemiol* 1986; **15**: 274-276 [PMID: 3721692 DOI: 10.1093/ije/15.2.274]

35 **Ezeilo MC**, Engwa GA, Iroha RI, Odimegwu DC. Seroprevalence and Associated Risk Factors of Hepatitis B Virus Infection Among Children in Enugu Metropolis. *Virology (Auckl)* 2018; **9**: 1178122X18792859 [PMID: 30150873 DOI: 10.1177/1178122X18792859]

36 **Federal Ministry of Health**, Nigeria. Nigeria HIV/AIDS Indicator and Impact Survey (NAIIS) 2018: Technical Report. Abuja, Nigeria; 2019. Available from: https://www.naiis.ng/resource/NAIIS-Report-2018.pdf

37 **Twagirumugabe T**, Swaibu G, Walker TD, Lindh M, Gahutu JB, Bergström T, Norder H. Hepatitis B virus strains from Rwandan blood donors are genetically similar and form one clade within subgenotype A1. *BMC Infect Dis* 2017; **17**: 32 [PMID: 28056881 DOI: 10.1186/s12879-016-2149-z]

38 **Makuza JD**, Nisingizwe MP, Rwema JOT, Dushimiyimana D, Habimana DS, Umuraza S, Serumondo J, Ngwije A, Semakula M, Gupta N, Nsanzimana S, Janjua NZ. Role of unsafe medical practices and sexual behaviours in the hepatitis B and C syndemic and HIV co-infection in Rwanda: a cross-sectional study. *BMJ Open* 2020; **10**: e036711 [PMID: 32660951 DOI: 10.1136/bmjopen-2019-036711]

39 **Barin F**, Perrin J, Chotard J, Denis F, N'Doye R, Diop Mar I, Chiron JP, Coursaget P, Goudeau A, Maupas P. Cross-sectional and longitudinal epidemiology of hepatitis B in Senegal. *Prog Med Virol* 1981; **27**: 148-162 [PMID: 6972051]

40 **Lô G**, Sow-Sall A, Diop-Ndiaye H, Babacar N, Diouf NN, Daffé SM, Ndao B, Thiam M, Mbow M, Soumboundou MB, Lemoine M, Sylla-Niang M, Ndiaye O, Boye CS, Mboup S, Touré-Kane NC. Hepatitis B virus (HBV) infection amongst children in Senegal: current prevalence and seroprotection level. *Pan Afr Med J* 2019; **32**: 140 [PMID: 31303913 DOI: 10.11604/pamj.2019.32.140.14485]

41 **Coste M**, De Sèze M, Diallo A, Carrieri MP, Marcellin F, Boyer S; ANRS 12356 AmBASS Study Group. Burden and impacts of chronic hepatitis B infection in rural Senegal: study protocol of a cross-sectional survey in the area of Niakhar (AmBASS ANRS 12356). *BMJ Open* 2019; **9**: e030211 [PMID: 31320358 DOI: 10.1136/bmjopen-2019-030211]

42 **Prabdial-Sing N**, Makhathini L, Smit SB, Manamela MJ, Motaze NV, Cohen C, Suchard MS. Hepatitis B sero-prevalence in children under 15 years of age in South Africa using residual samples from community-based febrile rash surveillance. *PLoS One* 2019; **14**: e0217415 [PMID: 31150445 DOI: 10.1371/journal.pone.0217415]

43 **Samsunder N**, Ngcapu S, Lewis L, Baxter C, Cawood C, Khanyile D, Kharsany ABM. Seroprevalence of hepatitis B virus: Findings from a population-based household survey in KwaZulu-Natal, South Africa. *Int J Infect Dis* 2019; **85**: 150-157 [PMID: 31202910 DOI: 10.1016/j.ijid.2019.06.005]

44 **Bwogi J**, Braka F, Makumbi I, Mishra V, Bakamutumaho B, Nanyunja M, Opio A, Downing R, Biryahwaho B, Lewis RF. Hepatitis B infection is highly endemic in Uganda: findings from a national serosurvey. *Afr Health Sci* 2009; **9**: 98-108 [PMID: 19652743]

45 **Ministry of Health**, Uganda. Uganda Population-based HIV Impact Assessment (UPHIA) 2016–2017: Final Report: Kampala, Ministry of Health; 2019. Available from: https://phia.icap.columbia.edu/wp-content/uploads/2019/07/UPHIA_Final_Report_Revise_07.11.2019_Final_for-web.pdf

46 **Tswana S**, Chetsanga C, Nyström L, Moyo S, Nzara M, Chieza L. A sero-epidemiological cross-sectional study of hepatitis B virus in Zimbabwe. *S Afr Med J* 1996; **86**: 72-75 [PMID: 8685787]

47 **Mavenyengwa RT**, Moyo SR, Nordbø SA. Streptococcus agalactiae colonization and correlation with HIV-1 and HBV seroprevalence in pregnant women from Zimbabwe. *Eur J Obstet Gynecol Reprod Biol* 2010; **150**: 34-38 [PMID: 20189288 DOI: 10.1016/j.ejogrb.2010.02.021]

48 **Kew MC**. Epidemiology of chronic hepatitis B virus infection, hepatocellular carcinoma, and hepatitis B virus-induced hepatocellular carcinoma. *Pathol Biol (Paris)* 2010; **58**: 273-277 [PMID:

20378277 DOI: 10.1016/j.patbio.2010.01.005]
49 **Spearman CW**, Afihene M, Ally R, Apica B, Awuku Y, Cunha L, Dusheiko G, Gogela N, Kassianides C, Kew M, Lam P, Lesi O, Lohouès-Kouacou MJ, Mbaye PS, Musabeyezu E, Musau B, Ojo O, Rwegasha J, Scholz B, Shewaye AB, Tzeuton C, Sonderup MW; Gastroenterology and Hepatology Association of sub-Saharan Africa (GHASSA). Hepatitis B in sub-Saharan Africa: strategies to achieve the 2030 elimination targets. *Lancet Gastroenterol Hepatol* 2017; **2**: 900-909 [PMID: 29132759 DOI: 10.1016/S2468-1253(17)30295-9]
50 **World Health Organization**. World Health Organization/UNICEF joint reporting process. Geneva: World Health Organization/UNICEF, 2020
51 **Hadziyannis SJ**. Natural history of chronic hepatitis B in Euro-Mediterranean and African countries. *J Hepatol* 2011; **55**: 183-191 [PMID: 21238520 DOI: 10.1016/j.jhep.2010.12.030]
52 **Croagh CM**, Lubel JS. Natural history of chronic hepatitis B: phases in a complex relationship. *World J Gastroenterol* 2014; **20**: 10395-10404 [PMID: 25132755 DOI: 10.3748/wjg.v20.i30.10395]
53 **Kew MC**. Hepatitis B virus / human immunodeficiency virus co-infection and its hepatocarcinogenic potential in sub-saharan black africans. *Hepat Mon* 2012; **12**: e7876 [PMID: 23166538 DOI: 10.5812/hepatmon.7876]
54 **Matthews PC**, Geretti AM, Goulder PJ, Klenerman P. Epidemiology and impact of HIV coinfection with hepatitis B and hepatitis C viruses in Sub-Saharan Africa. *J Clin Virol* 2014; **61**: 20-33 [PMID: 24973812 DOI: 10.1016/j.jcv.2014.05.018]
55 **Platt L**, French CE, McGowan CR, Sabin K, Gower E, Trickey A, McDonald B, Ong J, Stone J, Easterbrook P, Vickerman P. Prevalence and burden of HBV co-infection among people living with HIV: A global systematic review and meta-analysis. *J Viral Hepat* 2020; **27**: 294-315 [PMID: 31603999 DOI: 10.1111/jvh.13217]
56 **Keane E**, Funk AL, Shimakawa Y. Systematic review with meta-analysis: the risk of mother-to-child transmission of hepatitis B virus infection in sub-Saharan Africa. *Aliment Pharmacol Ther* 2016; **44**: 1005-1017 [PMID: 27630001 DOI: 10.1111/apt.13795]
57 **Andersson MI**, Maponga TG, Ijaz S, Barnes J, Theron GB, Meredith SA, Preiser W, Tedder RS. The epidemiology of hepatitis B virus infection in HIV-infected and HIV-uninfected pregnant women in the Western Cape, South Africa. *Vaccine* 2013; **31**: 5579-5584 [PMID: 23973500 DOI: 10.1016/j.vaccine.2013.08.028]
58 **Chasela CS**, Kourtis AP, Wall P, Drobeniuc J, King CC, Thai H, Teshale EH, Hosseinipour M, Ellington S, Codd MB, Jamieson DJ, Knight R, Fitzpatrick P, Kamili S, Hoffman I, Kayira D, Mumba N, Kamwendo DD, Martinson F, Powderly W, Teo CG, van der Horst C; BAN Study Team. Hepatitis B virus infection among HIV-infected pregnant women in Malawi and transmission to infants. *J Hepatol* 2014; **60**: 508-514 [PMID: 24211737 DOI: 10.1016/j.jhep.2013.10.029]
59 **Thumbiran NV**, Moodley D, Parboosing R, Moodley P. Hepatitis B and HIV co-infection in pregnant women: indication for routine antenatal hepatitis B virus screening in a high HIV prevalence setting. *S Afr Med J* 2014; **104**: 307-309 [PMID: 25118561 DOI: 10.7196/samj.7299]
60 **Kafeero HM**, Ndagire D, Ocama P, Walusansa A, Sendagire H. Sero-prevalence of human immunodeficiency virus-hepatitis B virus (HIV-HBV) co-infection among pregnant women attending antenatal care (ANC) in sub-Saharan Africa (SSA) and the associated risk factors: a systematic review and meta-analysis. *Virol J* 2020; **17**: 170 [PMID: 33160386 DOI: 10.1186/s12985-020-01443-6]
61 **UNAIDS**. UNAIDS data 2020. 2nd edition, February 2021. Available from: https://www.unaids.org/sites/default/files/media_asset/2020_aids-data-book_en.pdf
62 **Slogrove AL**, Powis KM, Johnson LF, Stover J, Mahy M. Estimates of the global population of children who are HIV-exposed and uninfected, 2000-18: a modelling study. *Lancet Glob Health* 2020; **8**: e67-e75 [PMID: 31791800 DOI: 10.1016/S2214-109X(19)30448-6]
63 **Jones CE**, Naidoo S, De Beer C, Esser M, Kampmann B, Hesseling AC. Maternal HIV infection and antibody responses against vaccine-preventable diseases in uninfected infants. *JAMA* 2011; **305**: 576-584 [PMID: 21304083 DOI: 10.1001/jama.2011.100]
64 **Njom Nlend AE**, Nguwoh PS, Ngounouh CT, Tchidjou HK, Pieme CA, Otélé JM, Penlap V, Colizzi V, Moyou RS, Fokam J. HIV-Infected or -Exposed Children Exhibit Lower Immunogenicity to Hepatitis B Vaccine in Yaoundé, Cameroon: An Appeal for Revised Policies in Tropical Settings? *PLoS One* 2016; **11**: e0161714 [PMID: 27656883 DOI: 10.1371/journal.pone.0161714]
65 **Baruti K**, Lentz K, Anderson M, Ajibola G, Phinius BB, Choga WT, Mbangiwa T, Powis KM, Sebunya T, Blackard JT, Lockman S, Moyo S, Shapiro R, Gaseitsiwe S. Hepatitis B virus prevalence and vaccine antibody titers in children HIV exposed but uninfected in Botswana. *PLoS One* 2020; **15**: e0237252 [PMID: 32764801 DOI: 10.1371/journal.pone.0237252]
66 **Tamandjou Tchuem C**, Cotton MF, Nel E, Tedder R, Preiser W, Violari A, Bobat R, Hovind L, Aaron L, Montepiedra G, Mitchell C, Andersson MI. Viral hepatitis B and C in HIV-exposed South African infants. *BMC Pediatr* 2020; **20**: 563 [PMID: 33357228 DOI: 10.1186/s12887-020-02479-x]
67 **Ferlay J**, Colombet M, Soerjomataram I, Mathers C, Parkin DM, Piñeros M, Znaor A, Bray F. Estimating the global cancer incidence and mortality in 2018: GLOBOCAN sources and methods. *Int J Cancer* 2019; **144**: 1941-1953 [PMID: 30350310 DOI: 10.1002/ijc.31937]
68 **Okeke E**, Davwar PM, Roberts L, Sartorius K, Spearman W, Malu A, Duguru M. Epidemiology of Liver Cancer in Africa: Current and Future Trends. *Semin Liver Dis* 2020; **40**: 111-123 [PMID: 31726474 DOI: 10.1055/s-0039-3399566]
69 **Howell J**, Ladepa NG, Lemoinea M, Thursza MR. , Taylor-Robinsona SD. Hepatitis B in sub-

Saharan Africa. *South Sudan Med J* 2014; **7**: 59-61

70 **Shimakawa Y**, Lemoine M, Njai HF, Bottomley C, Ndow G, Goldin RD, Jatta A, Jeng-Barry A, Wegmuller R, Moore SE, Baldeh I, Taal M, D'Alessandro U, Whittle H, Njie R, Thursz M, Mendy M. Natural history of chronic HBV infection in West Africa: a longitudinal population-based study from The Gambia. *Gut* 2016; **65**: 2007-2016 [PMID: 26185161 DOI: 10.1136/gutjnl-2015-309892]

71 **Yang JD**, Mohamed EA, Aziz AO, Shousha HI, Hashem MB, Nabeel MM, Abdelmaksoud AH, Elbaz TM, Afihene MY, Duduyemi BM, Ayawin JP, Gyedu A, Lohouès-Kouacou MJ, Ndam AW, Moustafa EF, Hassany SM, Moussa AM, Ugiagbe RA, Omuemu CE, Anthony R, Palmer D, Nyanga AF, Malu AO, Obekpa S, Abdo AE, Siddig AI, Mudawi HM, Okonkwo U, Kooffreh-Ada M, Awuku YA, Nartey YA, Abbew ET, Awuku NA, Otegbayo JA, Akande KO, Desalegn HM, Omonisi AE, Ajayi AO, Okeke EN, Duguru MJ, Davwar PM, Okorie MC, Mustapha S, Debes JD, Ocama P, Lesi OA, Odeghe E, Bello R, Onyekwere C, Ekere F, Igetei R, Mah'moud MA, Addissie B, Ali HM, Gores GJ, Topazian MD, Roberts LR; Africa Network for Gastrointestinal and Liver Diseases. Characteristics, management, and outcomes of patients with hepatocellular carcinoma in Africa: a multicountry observational study from the Africa Liver Cancer Consortium. *Lancet Gastroenterol Hepatol* 2017; **2**: 103-111 [PMID: 28403980 DOI: 10.1016/S2468-1253(16)30161-3]

72 **Moore SW**, Millar AJ, Hadley GP, Ionescu G, Kruger M, Poole J, Stones D, Wainwright L, Chitnis M, Wessels G. Hepatocellular carcinoma and liver tumors in South African children: a case for increased prevalence. *Cancer* 2004; **101**: 642-649 [PMID: 15274079 DOI: 10.1002/cncr.20398]

73 **Seleye-Fubara D**, Jebbin NJ. Hepatocellular carcinoma in Port Harcourt, Nigeria: clinicopathologic study of 75 cases. *Ann Afr Med* 2007; **6**: 54-57 [PMID: 18240703 DOI: 10.4103/1596-3519.55716]

74 **Carreira H**, Lorenzoni C, Carrilho C, Ferro J, Sultane T, Garcia C, Amod F, Augusto O, Silva-Matos C, La Vecchia C, Lunet N. Spectrum of pediatric cancers in Mozambique: an analysis of hospital and population-based data. *Pediatr Hematol Oncol* 2014; **31**: 498-508 [PMID: 24852201 DOI: 10.3109/08880018.2014.909547]

75 **Stefan C**, Bray F, Ferlay J, Liu B, Maxwell Parkin D. Cancer of childhood in sub-Saharan Africa. *Ecancermedicalscience* 2017; **11**: 755 [PMID: 28900468 DOI: 10.3332/ecancer.2017.755]

76 **Bray F**, Møller B. Predicting the future burden of cancer. *Nat Rev Cancer* 2006; **6**: 63-74 [PMID: 16372017 DOI: 10.1038/nrc1781]

77 **Ferlay J**, Laversanne M, Ervik M, Lam F, Colombet M, Mery L, Piñeros M, Znaor A, Soerjomataram I, Bray F. Global Cancer Observatory: Cancer Tomorrow. Lyon: International Agency for Research on Cancer, 2020

78 **Ferlay J**, Ervik M, Lam F, Colombet M, Mery L, Piñeros M, Znaor A, Soerjomataram I, Bray F. Global Cancer Observatory: Cancer Today. Lyon, France: International Agency for Research on Cancer, 2020

79 **Sartorius K**, Sartorius B, Aldous C, Govender PS, Madiba TE. Global and country underestimation of hepatocellular carcinoma (HCC) in 2012 and its implications. *Cancer Epidemiol* 2015; **39**: 284-290 [PMID: 25922178 DOI: 10.1016/j.canep.2015.04.006]

80 **Wang CC**, Tsai MC, Peng CM, Lee HL, Chen HY, Yang TW, Sung WW, Lin CC. Favorable liver cancer mortality-to-incidence ratios of countries with high health expenditure. *Eur J Gastroenterol Hepatol* 2017; **29**: 1397-1401 [PMID: 29023320 DOI: 10.1097/MEG.0000000000000969]

81 **Spearman CW**, Sonderup MW. Health disparities in liver disease in sub-Saharan Africa. *Liver Int* 2015; **35**: 2063-2071 [PMID: 26053588 DOI: 10.1111/liv.12884]

82 **Mak D**, Sengayi M, Chen WC, Babb de Villiers C, Singh E, Kramvis A. Liver cancer mortality trends in South Africa: 1999-2015. *BMC Cancer* 2018; **18**: 798 [PMID: 30086727 DOI: 10.1186/s12885-018-4695-9]

83 **Kirk GD**, Lesi OA, Mendy M, Akano AO, Sam O, Goedert JJ, Hainaut P, Hall AJ, Whittle H, Montesano R. The Gambia Liver Cancer Study: Infection with hepatitis B and C and the risk of hepatocellular carcinoma in West Africa. *Hepatology* 2004; **39**: 211-219 [PMID: 14752840 DOI: 10.1002/hep.20027]

84 **Otedo A**, Simbiri KO, Were V, Ongati O, Estambale BA. Risk factors for liver Cancer in HIV endemic areas of Western Kenya. *Infect Agent Cancer* 2018; **13**: 41 [PMID: 30607173 DOI: 10.1186/s13027-018-0214-5]

85 **Kirk GD**, Lesi OA, Mendy M, Szymañska K, Whittle H, Goedert JJ, Hainaut P, Montesano R. 249(ser) TP53 mutation in plasma DNA, hepatitis B viral infection, and risk of hepatocellular carcinoma. *Oncogene* 2005; **24**: 5858-5867 [PMID: 16007211 DOI: 10.1038/sj.onc.1208732]

86 **Kew MC**. Aflatoxins as a cause of hepatocellular carcinoma. *J Gastrointestin Liver Dis* 2013; **22**: 305-310 [PMID: 24078988]

87 **Kew MC**. Hepatitis C virus-induced hepatocellular carcinoma in sub-Saharan Africa. *J Afr Cancer* 2013; **5**: 169-174 [DOI: 10.1007/s12558-013-0275-8]

88 **Amponsah-Dacosta E**, Tamandjou Tchuem C, Anderson M. Chronic hepatitis B-associated liver disease in the context of human immunodeficiency virus co-infection and underlying metabolic syndrome. *World J Virol* 2020; **9**: 54-66 [PMID: 33362998 DOI: 10.5501/wjv.v9.i5.54]

89 **Yu MC**, Yuan JM. Environmental factors and risk for hepatocellular carcinoma. *Gastroenterology* 2004; **127**: S72-S78 [PMID: 15508106 DOI: 10.1016/j.gastro.2004.09.018]

90 **Baecker A**, Liu X, La Vecchia C, Zhang ZF. Worldwide incidence of hepatocellular carcinoma cases attributable to major risk factors. *Eur J Cancer Prev* 2018; **27**: 205-212 [PMID: 29489473 DOI: 10.1097/CEJ.0000000000000428]

91 **Petruzziello A**. Epidemiology of Hepatitis B Virus (HBV) and Hepatitis C Virus (HCV) Related

Hepatocellular Carcinoma. *Open Virol J* 2018; **12**: 26-32 [PMID: 29541276 DOI: 10.2174/1874357901812010026]

92 **Levrero M**, Zucman-Rossi J. Mechanisms of HBV-induced hepatocellular carcinoma. *J Hepatol* 2016; **64**: S84-S101 [PMID: 27084040 DOI: 10.1016/j.jhep.2016.02.021]

93 **Torresi J**, Tran BM, Christiansen D, Earnest-Silveira L, Schwab RHM, Vincan E. HBV-related hepatocarcinogenesis: the role of signalling pathways and innovative ex vivo research models. *BMC Cancer* 2019; **19**: 707 [PMID: 31319796 DOI: 10.1186/s12885-019-5916-6]

94 **Atsama Amougou M**, Marchio A, Bivigou-Mboumba B, Noah Noah D, Banai R, Atangana PJA, Fewou Moundipa P, Pineau P, Njouom R. Enrichment in selected genotypes, basal core and precore mutations of hepatitis B virus in patients with hepatocellular carcinoma in Cameroon. *J Viral Hepat* 2019; **26**: 1086-1093 [PMID: 31106515 DOI: 10.1111/jvh.13131]

95 **Mak D**, Babb de Villiers C, Chasela C, Urban MI, Kramvis A. Analysis of risk factors associated with hepatocellular carcinoma in black South Africans: 2000-2012. *PLoS One* 2018; **13**: e0196057 [PMID: 29718992 DOI: 10.1371/journal.pone.0196057]

96 **Mendy ME**, Welzel T, Lesi OA, Hainaut P, Hall AJ, Kuniholm MH, McConkey S, Goedert JJ, Kaye S, Rowland-Jones S, Whittle H, Kirk GD. Hepatitis B viral load and risk for liver cirrhosis and hepatocellular carcinoma in The Gambia, West Africa. *J Viral Hepat* 2010; **17**: 115-122 [PMID: 19874478 DOI: 10.1111/j.1365-2893.2009.01168.x]

97 **Polaris Observatory Collaborators**. Global prevalence, treatment, and prevention of hepatitis B virus infection in 2016: a modelling study. *Lancet Gastroenterol Hepatol* 2018; **3**: 383-403 [PMID: 29599078 DOI: 10.1016/S2468-1253(18)30056-6]

98 **Wilson P**, Parr JB, Jhaveri R, Meshnick SR. Call to Action: Prevention of Mother-to-Child Transmission of Hepatitis B in Africa. *J Infect Dis* 2018; **217**: 1180-1183 [PMID: 29351639 DOI: 10.1093/infdis/jiy028]

99 **Sonderup MW**, Dusheiko G, Desalegn H, Lemoine M, Tzeuton C, Taylor-Robinson SD, Spearman CW. Hepatitis B in sub-Saharan Africa-How many patients need therapy? *J Viral Hepat* 2020; **27**: 560-567 [PMID: 31800145 DOI: 10.1111/jvh.13247]

100 **Béguelin C**, Fall F, Seydi M, Wandeler G. The current situation and challenges of screening for and treating hepatitis B in sub-Saharan Africa. *Expert Rev Gastroenterol Hepatol* 2018; **12**: 537-546 [PMID: 29737218 DOI: 10.1080/17474124.2018.1474097]

101 **Desalegn H**, Aberra H, Berhe N, Gundersen SG, Johannessen A. Are non-invasive fibrosis markers for chronic hepatitis B reliable in sub-Saharan Africa? *Liver Int* 2017; **37**: 1461-1467 [PMID: 28222249 DOI: 10.1111/liv.13393]

102 **Lemoine M**, Thursz MR. Battlefield against hepatitis B infection and HCC in Africa. *J Hepatol* 2017; **66**: 645-654 [PMID: 27771453 DOI: 10.1016/j.jhep.2016.10.013]

103 **Boye S**, Shimakawa Y, Vray M, Giles-Vernick T. Limited Awareness of Hepatitis B but Widespread Recognition of Its Sequelae in Rural Senegal: A Qualitative Study. *Am J Trop Med Hyg* 2020; **102**: 637-643 [PMID: 31971148 DOI: 10.4269/ajtmh.19-0477]

104 **Adjei CA**, Stutterheim SE, Naab F, Ruiter RAC. Barriers to chronic Hepatitis B treatment and care in Ghana: A qualitative study with people with Hepatitis B and healthcare providers. *PLoS One* 2019; **14**: e0225830 [PMID: 31794577 DOI: 10.1371/journal.pone.0225830]

105 **World Health Organization Regional Office for Africa**. Sixty-fourth session of the WHO Regional Committee for Africa. 2014. Available from: https://www.afro.who.int/about-us/governance/sessions/sixty-fourth-session-who-regional-committee-africa

106 **World Health Organization Regional Office for Africa**. Regional strategic plan for immunization 2014 – 2020. 2015. Available from: https://www.afro.who.int/sites/default/files/2017-06/oms-ivb-rvap-afro-en-20150408_final_sent140317.pdf

107 **Andersson MI**, Rajbhandari R, Kew MC, Vento S, Preiser W, Hoepelman AI, Theron G, Cotton M, Cohn J, Glebe D, Lesi O, Thursz M, Peters M, Chung R, Wiysonge C. Mother-to-child transmission of hepatitis B virus in sub-Saharan Africa: time to act. *Lancet Glob Health* 2015; **3**: e358-e359 [PMID: 26087980 DOI: 10.1016/S2214-109X(15)00056-X]

108 **Stockdale AJ**, Geretti AM. Chronic hepatitis B infection in sub-Saharan Africa: a grave challenge and a great hope. *Trans R Soc Trop Med Hyg* 2015; **109**: 421-422 [PMID: 26065660 DOI: 10.1093/trstmh/trv044]

109 **Jia L**, Gao Y, He Y, Hooper JD, Yang P. HBV induced hepatocellular carcinoma and related potential immunotherapy. *Pharmacol Res* 2020; **159**: 104992 [PMID: 32505833 DOI: 10.1016/j.phrs.2020.104992]

110 **Yang JD**, Heimbach JK. New advances in the diagnosis and management of hepatocellular carcinoma. *BMJ* 2020; **371**: m3544 [PMID: 33106289 DOI: 10.1136/bmj.m3544]

World Journal of Gastroenterology

Submit a Manuscript: https://www.f6publishing.com

World J Gastroenterol 2021 September 28; 27(36): 6039-6052

DOI: 10.3748/wjg.v27.i36.6039

ISSN 1007-9327 (print) ISSN 2219-2840 (online)

MINIREVIEWS

Liver disease in the era of COVID-19: Is the worst yet to come?

Ivana Mikolasevic, Dorotea Bozic, Tajana Pavić, Alen Ruzic, Goran Hauser, Marija Radic, Delfa Radic-Kristo, Melanija Razov-Radas, Zeljko Puljiz, Sandra Milic

ORCID number: Ivana Mikolasevic 0000-0001-9676-0642; Dorotea Bozic 0000-0001-9234-4203; Tajana Pavić 0000-0002-0370-5001; Alen Ruzic 0000-0001-5031-2975; Goran Hauser 0000-0002-4758-1717; Marija Radic 0000-0002-7746-2065; Delfa Radic-Kristo 0000-0002-2827-7808; Melanija Razov-Radas 0000-0003-4530-4350; Zeljko Puljiz 0000-0002-3465-4227; Sandra Milic 0000-0002-6635-5360.

Author contributions: Mikolasevic I researched the database, wrote the manuscript and is the guarantor of this work; Bozic D, Pavić T, Ruzic A, Hauser G, Milic S, Radic M, Radic-Kristo D, Razov-Radas M and Puljiz Z contributed to the discussion and reviewed/edited the manuscript.

Conflict-of-interest statement: Authors declare no conflict of interest for this article.

Open-Access: This article is an open-access article that was selected by an in-house editor and fully peer-reviewed by external reviewers. It is distributed in accordance with the Creative Commons Attribution NonCommercial (CC BY-NC 4.0) license, which permits others to distribute, remix, adapt, build upon this work non-commercially, and license their derivative works on different terms, provided the original work is properly cited and

Ivana Mikolasevic, Goran Hauser, Sandra Milic, Department of Gastroenterology, Clinical Hospital Center Rijeka, Rijeka 51000, Croatia

Ivana Mikolasevic, Department of Gastroenterology, University Hospital Merkur, Zagreb 10000, Croatia

Ivana Mikolasevic, Alen Ruzic, Goran Hauser, Sandra Milic, Faculty of Medicine, University of Rijeka, Rijeka 51000, Croatia

Dorotea Bozic, Zeljko Puljiz, Department for Gastroenterology and Hepatology, University Hospital Center Split, Split 21000, Croatia

Tajana Pavić, Department of Gastroenterology and Hepatology, Faculty of Medicine, Sestre Milosrdnice University Hospital Center, Zagreb 10000, Croatia

Alen Ruzic, Clinic for Cardiology, University Hospital Center Rijeka, Rijeka 51000, Croatia

Goran Hauser, Faculty of Health Studies, University of Rijeka, Rijeka 51000, Croatia

Marija Radic, Delfa Radic-Kristo, Faculty of Medicine, Zagreb 10000, Croatia

Delfa Radic-Kristo, Department of Hematology, University Hospital Merkur, Zagreb 10000, Croatia

Melanija Razov-Radas, Division of Gastroenterology, General Hospital Zadar, Zadar 23000, Croatia

Zeljko Puljiz, University of Split, School of Medicine, Split 21000, Croatia

Corresponding author: Ivana Mikolasevic, PhD, Professor, Department of Gastroenterology, Clinical Hospital Center Rijeka, Kresimirova 42, Rijeka 51000, Croatia.
ivana.mikolasevic@gmail.com

Abstract

The global social, economic and political crises related to coronavirus disease 2019 (COVID-19) presumably had more indirect than direct negative impacts on health systems. Drastic lifestyle changes, social isolation and distancing, and individual and global financial crises resulted in robust populations forfeiting healthy habits and seeking comfort in alcoholic beverages, drugs and unhealthy diets. The inevitable consequences are increases in the incidence of nonalcoholic fatty liver disease, viral hepatitis, acute alcoholic hepatitis, liver cirrhosis decompensation

the use is non-commercial. See: http://creativecommons.org/Licenses/by-nc/4.0/

Manuscript source: Invited manuscript

Specialty type: Gastroenterology and hepatology

Country/Territory of origin: Croatia

Peer-review report's scientific quality classification

Grade A (Excellent): 0
Grade B (Very good): 0
Grade C (Good): C, C, C, C
Grade D (Fair): 0
Grade E (Poor): 0

Received: February 28, 2021
Peer-review started: February 28, 2021
First decision: July 3, 2021
Revised: July 18, 2021
Accepted: September 1, 2021
Article in press: September 1, 2021
Published online: September 28, 2021

P-Reviewer: Ferraioli G, Gupta MK, Skok K
S-Editor: Gao CC
L-Editor: A
P-Editor: Yuan YY

and ultimately liver-related mortality. The inaccessibility of regular clinical and sonographic monitoring systems has caused difficulties in the treatment of patients with chronic liver disease (CLD) and has prevented prompt hepatocellular carcinoma detection and treatment. A dramatic reduction in the number of liver donors and the transformation of numerous transplantation centers into COVID-19 units drastically decreased the rate of orthotopic liver transplantation. The indirect, unavoidable effects of the COVID-19 pandemic in the following years have yet to be determined. Substantial efforts in the management of patients with liver disease in order to overcome the inevitable COVID-19-related morbidity and mortality that will follow have yet to be initiated. Several questions regarding the impact of the COVID-19 pandemic on liver disease remain. The most important question for general CLD patients is: How will the modification of clinical practice during this pandemic affect the outcomes of CLD patients? This article reviews the influence of COVID-19 on patients with liver disease during the pandemic, with particular emphasis on the disease course associated with pandemic resolution.

Key Words: COVID-19; Pandemic; Chronic liver disease; Management; Impact; Liver-related mortality

©The Author(s) 2021. Published by Baishideng Publishing Group Inc. All rights reserved.

Core Tip: The global social, economic and political crises related to coronavirus disease 2019 (COVID-19) presumably cause more indirect than direct negative impacts on the health system. Drastic lifestyle changes, social isolation and distancing, and individual and global financial crises resulted in a robust population forfeiting healthy habits and seeking comfort in alcoholic beverages, drugs and unhealthy diets. The inevitable consequence is the increasing incidence of liver disease, liver cirrhosis decompensation and ultimately liver-related mortality. The indirect unavoidable effects of the COVID-19 pandemic in the following years have yet to be determined.

Citation: Mikolasevic I, Bozic D, Pavić T, Ruzic A, Hauser G, Radic M, Radic-Kristo D, Razov-Radas M, Puljiz Z, Milic S. Liver disease in the era of COVID-19: Is the worst yet to come? *World J Gastroenterol* 2021; 27(36): 6039-6052
URL: https://www.wjgnet.com/1007-9327/full/v27/i36/6039.htm
DOI: https://dx.doi.org/10.3748/wjg.v27.i36.6039

INTRODUCTION

The coronavirus disease 2019 (COVID-19) pandemic has spread rapidly worldwide and poses a serious threat to healthcare systems globally. It is common to encounter patients with both COVID-19 and abnormal liver function. Because COVID-19 is a newly discovered disease, additional data are needed to improve our understanding of its impact on the liver and of the appropriate management of such patients[1-15]. Information on how COVID-19 infection affects the liver and the relevance of pre-existing liver disease in acquiring the infection or developing severe disease is increasing, although we still do not know the exact mechanism. Additionally, considerations with regard to liver transplant patients, those with hepatocellular carcinoma (HCC) and those under immunosuppressive therapy are being analyzed as information is being generated. Various treatments for COVID-19 are currently under study but some of these may be potentially hepatotoxic[4-6,15].

The first and most evident consequence of the COVID-19 pandemic is its impact on the routine care of patients with chronic liver disease (CLD). The COVID-19 pandemic shifted our perception of ambulatory patient care from face-to-face examinations to virtual patient management[15-18]. Expert recommendations guiding clinicians in the treatment of patients with CLD and of transplanted patients during the pandemic are available in the form of guidelines published by the European Association for the Study of the Liver (EASL) and the American Association for the Study of Liver

Diseases (AASLD)[16-18].

Although patients with CLD are not at higher risk of acquiring the infection, whether COVID-19 and the underlying liver disease will follow an unfavorable course remains to be answered[19]. Nonetheless, questions regarding the treatment of patients with CLD following resolution of the COVID-19 pandemic remain unknown. One must consider that a considerable number of patients with CLD did not attend regular appointments, prevented by fear of acquiring the infection. Preventive, surgical and transplant programs have become secondary focuses. In light of the present circumstances, it is evident that the burdens of the pandemic-related consequences have yet to be elucidated, not only regarding global economics but also global health[19].

This article reviews the effects of COVID-19 in patients with liver disease during the pandemic, with particular emphasis on the disease course associated with pandemic resolution (Figure 1). We performed a PubMed search using the keywords "chronic liver disease" and "COVID-19". When using this algorithm there were 396 results. In this review, 74 articles with particular emphasis on COVID-19 and liver disease were analyzed.

PRE-EXISTING CLD AND COVID-19

The reported prevalence of patients with CLD in cohorts of patients with COVID-19 does not exceed 1%, suggesting that the risk of infection acquisition is similar to that in the general population[18,20]. However, the risk of a severe course of disease might be increased due to the etiology of the underlying liver disease along with the degree of liver fibrosis[18].

Liver test abnormalities

According to reports from regular and intensive care units, elevated liver enzymes, lactate dehydrogenase, creatinine kinase and myoglobin, as well as prolonged prothrombin time, are found in more than one-third of patients during COVID-19 progression[21]. A retrospective Chinese study revealed a dynamic pattern of liver molecules regardless of the severity of infection: Aspartate aminotransferase (AST) increased, followed by an increase in alanine aminotransferase (ALT) concurrent with mild oscillations in bilirubin levels. AST levels were significantly associated with mortality risk in this group of patients[22]. Another comprehensive Chinese review also reported elevated AST and ALT levels in 6%-22% and 21%-28% of patients, respectively[23]. Compared to other Chinese regions in which 16% of patients had AST elevation, studies from Wuhan reported a higher percentage, ranging from 24% to 37%. Studies have revealed a high prevalence of liver test abnormalities in men and elderly individuals[23,24]. A large American study including 5700 patients reported that 58.4% of patients had elevated AST levels (> 40 U/L) and 39% had elevated ALT levels (> 60 U/L)[25]. Two percent of patients developed acute hepatic injury and the majority of this subgroup (95%) did not survive[25]. A severe cholestatic pattern has not been reported as correlating with COVID-19 but studies have reported hyperbilirubinemia in 11%-18% of cases[21].

Several pathological mechanisms are considered to be involved in liver injury, including direct viral infection of liver cells, drug hepatotoxicity, cytokine storm and pneumonia-associated hypoxia[15,26,27]. According to several studies, the expression of ACE2 receptors on liver cells facilitates SARS CoV-2 entrance; expression is increased in bile duct cells, whose destruction appears to be primarily responsible for COVID-19-related liver injury[15,26]. Studies clarifying the exact mechanisms of liver injury are warranted[15,27-30].

It must be considered that elevated aminotransferases might be of cardiac or muscular origin and that abnormalities in liver tests are frequently transient. On the other hand, studies have reported an increased risk of severe disease in patients who present with liver injury on admission[15,28]. The severity of liver dysfunction seems to be closely associated with the severity of COVID-19[15]. As predicted by multiple studies, the usual culprits of pathological biochemical liver abnormalities are underlying CLD, sepsis-related cholestasis and drug hepatotoxicity[6]. We must not ignore the fact that the frequency and severity of liver injury in asymptomatic individuals and patients under out-of-hospital treatment remains unknown[6]. Therefore, further investigations are needed to strengthen conclusions.

Finally, the most crucial question for clinicians treating COVID-19 patients is in whom and how often to perform liver function tests. The optimal interval has not yet

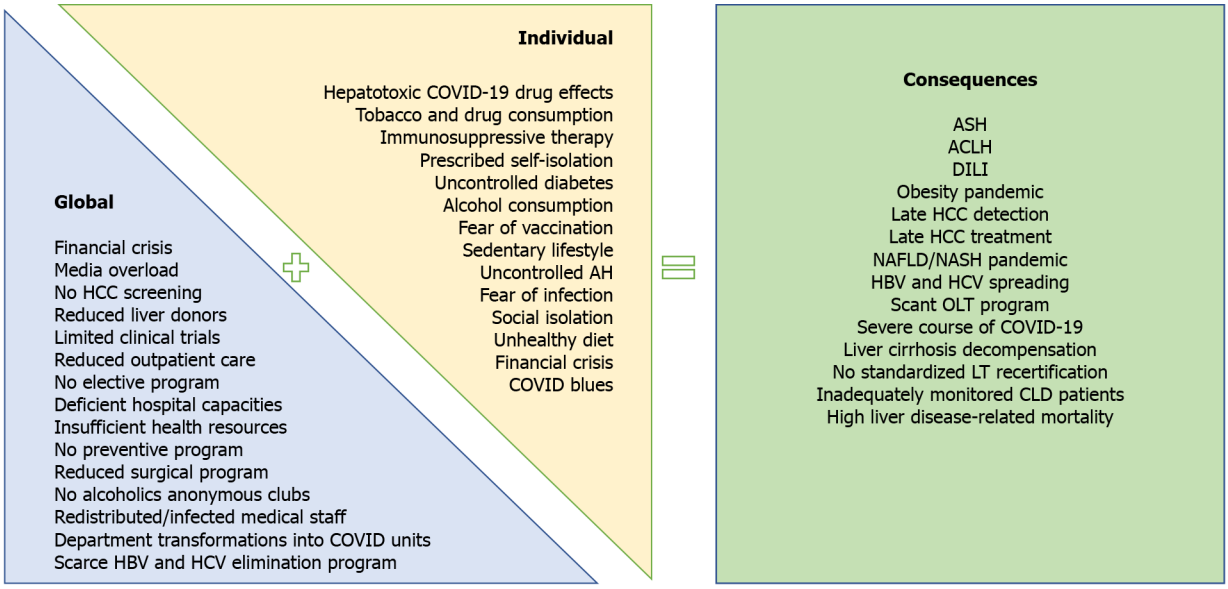


Figure 1 Global and individual effects of the coronavirus disease 2019 pandemic on liver-related morbidity and mortality. ACLF: Acute-on-chronic liver failure; AH: Arterial hypertension; ASH: Alcoholic steatohepatitis; CLD: Chronic liver disease; COVID-19: Coronavirus disease 2019; DILI: Drug-induced liver injury; HBV: Hepatitis B virus; HCC: Hepatocellular carcinoma; HCV: Hepatitis C virus; NAFLD: Non-alcoholic fatty liver disease; NASH: Non-alcoholic steatohepatitis; OLT: Orthotopic liver transplantation.

been defined, but physicians should certainly be attentive when treating severely ill patients and individuals taking novel antiviral drugs such as remdesivir or tocilizumab[6].

Nonalcoholic fatty liver disease and COVID-19

Nonalcoholic fatty liver disease (NAFLD), also known as metabolic dysfunction-associated fatty liver disease, is a common manifestation of metabolic syndrome and is remarkably prevalent in Western industrialized countries[21]. It is usually comorbid with obesity, which represents a significant risk factor for severe COVID-19 pneumonia[3,18,31]. The assumed mechanism relies on the immunological properties of adipose tissue, which also plays a role as a viral reservoir[3,18,25]. Additional risk factors accompanying NAFLD, such as arterial hypertension, obesity and diabetes, are also commonly observed in patients with a severe COVID-19 course[3,18,25].

As predicted in several studies, patients with NAFLD seem to have a longer period of viral replication and dispersion[32] and experience progression to the severe form of disease, with worsening dyspnea, hypoxia and typical radiological findings [32], even in younger patients without other comorbidities[33,34]. Among patients with NAFLD, the underlying liver fibrosis seems to correlate with severe COVID-19 presentation, regardless of other metabolic comorbidities[11,21,35]. Targher *et al*[35] also found an interrelation between advanced liver fibrosis (defined as increased Fibrosis 4 and NAFLD fibrosis scores) and severe COVID-19 presentation in a subgroup of 94 (30.3%) patients with NAFLD. However, Lopez-Mendez *et al*[36] did not confirm these findings. According to their study, although the prevalence of NAFLD and significant liver fibrosis was high in COVID-19 patients, it was not associated with worse clinical outcomes.

The exact mechanism of NAFLD-associated liver fibrosis leading to an undesired COVID-19 course has not yet been defined but presumably is potentiated by the hepatic release of multiple proinflammatory cytokines, exacerbating the severe acute respiratory syndrome coronavirus 2 (SARS-CoV-2)-induced cytokine storm[35]. On the other hand, virus-related cytokines might increase the risk of liver inflammation. This interplay of cytokine-related events forms a vicious cycle, making the NAFLD population at very high risk of COVID-19 complications[11,21].

Additional large-scale analyses are needed to determine whether NAFLD is an independent risk factor for severe COVID-19 or whether confounding factors are responsible for the previously published results. Studies based on other available noninvasive methods, including transient elastography and acoustic radiation force impulse-based techniques, are also warranted.

It is also important to note the increased predisposition for drug-induced liver injury in patients with liver steatosis[6]. Antiretrovirals such as lopinavir/ritonavir, antibiotics, antifungal agents and other drugs required to treat acute respiratory distress syndrome and systemic inflammation may induce drug-induced liver injury [37]. The possible mechanism of increased susceptibility in this group of patients is associated with oxidative stress, diminished activity of xenobiotic-metabolizing enzymes, mitochondrial malfunction and changes in lipid homeostasis[37-39]. Caution must be taken with steatogenic drugs such as amiodarone, sodium valproate, tamoxifen, methotrexate and frequently used glucocorticoids because they may induce steatohepatitis in predisposed individuals[40].

Finally, the effect of the COVID-19 pandemic on the social aspects of an individual's daily routine is the last but not least important undesirable sequela. A sedentary lifestyle, social isolation and increased consumption of processed foods are all metabolic antagonists that are especially unfavorable in patients with NAFLD[18]. The COVID-19 "blues" associated with lockdowns, loss of income and deterioration of socioeconomic status might lead to unhealthy lifestyles and consequently the promotion of obesity and associated metabolic diseases[41]. Therefore, COVID-19 will presumably be an indirect cause of expansion of the NAFLD epidemic[42]. In light of the global psychosociological COVID-19 burden, the Mayo Clinic advocates increased caution against NAFLD-promoting behaviors[42,43].

Increases in body mass index uncontrollable arterial hypertension and underregulated diabetes will certainly contribute to the worsening of NAFLD. It is therefore mandatory to treat associated metabolic comorbidities in these patients[18]. In addition, the deleterious effects of delayed detection of HCC in hepatic steatosis patients are the consequences of missed routine ultrasound examinations.

In conclusion, the EASL suggests considering early admission for all patients with NAFLD and COVID-19[18]. Encouraged by the AASLD guidelines, we recommend regular monitoring of liver function in all hospitalized COVID-19 patients[17,21]. Governments and policy makers should implement certain interventions in response to the increase in NAFLD that will insidiously follow after the COVID-19 pandemic [41]. Finally, when contemplating the introduction of lockdown in the future, the potential consequences on metabolic health should be considered[41].

Autoimmune liver disease and COVID-19

Evidence of the influence of immunosuppressive regimens on the acquisition of COVID-19 is still scarce. However, observational studies have suggested an association between glucocorticoid therapy and a severe COVID-19 course[18,44]. When treating autoimmune hepatitis (AIH) flares, the EASL suggests the administration of budesonide rather than systemic corticosteroid therapy in patients without liver cirrhosis[18]. In the clinical setting of a chronic immunosuppressive regimen it is recommended to continue treatment, except in cases of severe COVID-19, superinfections or lymphopenia that frequently follow SARS-CoV-2 infection[16]. According to the largest study of patients with AIH and COVID-19 infection there were no significant differences in the incidence of major adverse COVID-19 outcomes between patients with AIH and those with other CLD[10]. However, in this study, independent risk factors for adverse events (*i.e.*, death) in these patients were age and baseline liver disease severity. In this study, the use of immunosuppression was not associated with death in AIH patients[10]. Additional studies are needed to determine whether AIH per se or adjacent immunosuppressive treatment affect COVID-19 outcomes[18].

Alcoholic liver disease and COVID-19

Patients with alcohol use disorder (AUD) and alcohol-associated liver disease (ALD) are exemplars of the wide range of potentially negative impacts of COVID-19[45]. Primarily, social isolation and the unavailability of professional help may lead to psychological decompensation and an increased risk of relapse[45]. Depressed immune systems and other underlying comorbidities, including renal failure, obesity, chronic viral hepatitis, sarcopenia, alcoholic cardiomyopathy, tobacco use disorder and many others, make these patients easy targets for viral infection. Finally, according to published data, these patients are more prone to developing interstitial pneumonia and acute respiratory distress syndrome secondary to SARS-CoV-2 infection than their counterparts[18]. Case series of ALD individuals reported a rapid disease course, including bilobar pneumonia and acute respiratory distress syndrome requiring mechanical ventilation, with unfavorable outcomes including cardiopulmonary insufficiency and multiorgan failure[46,47]. Patients admitted for acute alcoholic steatohepatitis (ASH) are usually assessed using Maddrey's discriminant function (DF) score, with DF > 32 predicting a higher mortality rate[46]. The usual

treatment of ASH in patients with DF > 32 using the classical prednisone regimen is an additional risk factor for a severe course of COVID-19 and is therefore not recommended for patients who are self-isolating or considered at high risk of acquiring SARS-CoV-2 infection[45]. Liver impairment is frequently observed in patients with COVID-19[46]. It is also well known that ASH increases the risk of hepatorenal syndrome development, especially after contrast agent application. Cytokine damage, inadequate organ perfusion, nephrotoxic drug effects and nosocomial infections all potentiate the acute kidney injury, usually resulting in the need for continuous renal replacement therapy[47].

In order to obviate the described critical disease course with severe consequences and high mortality rate, we should focus on two main aspects in the care of ALD patients. The primary focus is the prevention, of infection by following strict epidemiologic recommendations, as well as the prevention of AUD relapse by implementing vigorous social and psychiatric care by telephone. The unavailability of support groups such as Alcoholics Anonymous should be bridged using individual or smaller group treatment[47]. The secondary focus is the prevention of a deleterious disease course using vigilant intrahospital clinical care and timely recognition of hepatobiliary, renal and respiratory complications[18].

Viral hepatitis and COVID-19

Whether chronic viral hepatitis specifically affects the COVID-19 course remains unknown. In a retrospective Italian multicenter study that included 50 patients with liver cirrhosis and SARS-CoV-2 infection, 28% had hepatitis C virus (HCV)-related cirrhosis and 10% had hepatitis B virus (HBV)-related cirrhosis. The patients were either HCV-RNA negative after anti-HCV treatment or on long-term anti-HBV treatment. The severity of liver disease was an independent predictor of mortality[29]. The same conclusion was derived from an international registry that included 152 patients with CLD and COVID-19, among which 22.5% of the CLD was due to chronic HBV or HCV infection[30].

In the last year, the COVID-19 outbreak has redirected attention from other morbidities, including viral hepatitis: as a consequence of this pandemic, most viral hepatitis elimination programs have diminished or stopped altogether[14,19,48,49]. The World Health Organization's goal of eliminating HBV and HCV and thus significantly reducing the associated mortality until 2030 has therefore been put on hold. Elimination programs are already scarce, as well as involvement by liver disease societies, epidemiologists, infection specialists and general practitioners, despite the WHO Global Hepatitis Report 2017 stating that the viral hepatitis global mortality is 1.5 million per year[19,48,49]. Preventing mother-to-child transmission and promoting blood safety are presumably the only intact weapons in the battle against HBV and HCV[19,48]. Although we will realize the full impact of reducing or delaying programs targeting hepatitis elimination in the near future, there are some mathematical models that can predict the possible impact on the global burden of viral hepatitis and hepatitis-associated morbidity and mortality that will result as a consequence of program delay[49]. A recent study used certain mathematical models to analyze the impact of delayed programs on viral hepatitis elimination[49]. The authors reported that a 1-year delay in viral hepatitis diagnosis and treatment will result in an additional 44800 HCC cases as well as 72300 deaths from HCV globally in the next 10 years[49].

If we cannot make progress in achieving the aforementioned elimination goals due to the COVID-19 crisis, then education campaigns, extensive screening, diagnostic tests, vaccination programs and treatment should at least be maintained at the former level[19,48,49].

Liver cirrhosis and COVID-19

Patients with liver cirrhosis, particularly decompensated cirrhosis, are by far the most vulnerable liver disease patients. Immune dysfunction makes them prone to any kind of infection, including SARS-CoV-2, with potentially deleterious effects on the disease course. Data suggest that the course of COVID-19 is directly connected to the degree of liver disease defined by the Child-Pugh (CP) and Model for End Stage Liver Disease scores[18].

An international registry including 103 patients with liver cirrhosis reported a 40% mortality rate, strongly correlated with the grade of liver failure: 23.9% mortality in patients with CP class A, 43.3% mortality in patients with CP class B and 63.0% mortality in patients with CP class C cirrhosis[50]. Similarly, an Italian study involving 50 patients with liver cirrhosis suffering from COVID-19 found a 30-d mortality rate of 34%, among which 71% of patients died due to COVID-related respiratory failure[51].

The largest published study to date was based on two international registries and included 745 patients with CLD (among which 52% had liver cirrhosis) and acute COVID-19 infection. When compared to the data of non-CLD patients with SARS-CoV-2 infection in a UK hospital network, a statistically significant difference in mortality ($P < 0.001$) was reported: 32% in patients with liver cirrhosis compared to 8% in those without[52]. The main cause of death was respiratory failure, with acute decompensation of liver cirrhosis occurring in 46% of patients. The authors concluded that the CP score and ALD were independent risk factors for death due to COVID-19 [52].

A prospective American multicenter study by Singh and Khan[53] compared patients with both liver cirrhosis and COVID-19 to patients with only COVID-19 and found a significant difference in the outcome (30% *vs* 13%, $P = 0.03$). However, the fact that there was no significant difference in the outcomes of patients with liver cirrhosis regarding COVID-19 infection is intriguing. It seems important to emphasize that the proportion of SARS-CoV-2-positive cirrhosis patients in this study was approximately three times lower than that in the other two subgroups.

In summary, in patients suffering from COVID-19, mortality is significantly greater in those with liver cirrhosis than in those without and is directly related to the stage of liver failure[18]. However, it remains unclear whether COVID-19-related mortality is higher than that related to other causes of decompensation that are often also infective in origin[18].

Liver cirrhosis causes 2 million deaths globally per year. Prevention of liver decompensation and prompt diagnosis and treatment of cirrhosis-related complications are of the utmost importance[54,55]. Management with endoscopic variceal screening, primary and secondary prophylaxis, implementation of telecommunication and electronic communication in drug titration, especially regarding beta-blockers and diuretic therapies, is warranted. HCC screening and diagnostic persuasion, including radiologic methods and liver biopsy, as well as therapeutic treatments ranging from radiofrequency ablation to liver transplantation (LT), should be preserved despite scarce resources, physician burnout and lack of hospital capacity[54,55].

Tapper and Asrani[55] proposed a three-wave theory to explain the effects of the COVID-19 pandemic on liver cirrhosis from the current period to future years. The first wave describes the period of physical distancing and is defined by high-acuity care and delayed elective procedures[55]. For example, patients with esophageal varices are admitted only for bleeding episodes, and elective endoscopic band ligation (EBL) is not performed due to fear of viral spread and limited healthcare resources. The direct consequence of the first phase is the second wave, appearing after the resolution of physical distancing and characterized by a high frequency of cirrhosis decompensation[55]. Continuing with the given example, a substantial number of patients with indefinitely delayed or skipped EBL procedures will begin to experience variceal bleeding episodes, leading to cirrhosis decompensation or even acute-on-chronic liver failure. Accessible, inexpensive, processed foods rich in salt, as well as alcoholic beverages, both highly consumed during pandemics, will result in the exacerbation of volume overload and also potentiate sarcopenia, which is a well-known risk factor for cirrhosis-associated morbidity and mortality[55]. The third wave will presumably comprise long-term complications. Delayed diagnosis of hepatobiliary malignancies, progression of HCC reaching the Milan criteria and the consequent elimination of patients from transplant lists, insidious deterioration of renal function, no standardized recertification of patients awaiting LT and many more complications are to be encountered. As Tapper and Asrani[55] stated, the curable will be transformed into the incurable.

HCC and COVID-19

Although there are no specific data on the outcomes of patients with HCC and COVID-19 infection, it is assumed that HCC patients will have poor outcomes, similar to those in other oncology patients[15]. However, we know that most HCC patients have pre-existing CLD and in comparison to other patients with cancers we can assume that such patients are more susceptible to the effects of COVID-19: that is, hepatic injury caused by COVID-19 can complicate existing CLD in most patients with HCC. The COVID-19 pandemic has greatly limited the medical care of HCC patients, with effects ranging from early diagnosis to treatment. As ultrasound screening examinations have mostly been delayed indefinitely, without precise upcoming appointment dates and resulting in prolonged periods without control, the risk of discovering HCC at a later stage increased in approximately 25% of patients with the biologically aggressive type of disease[55,56].

Elective hospital admissions were also delayed in the peak of the COVID-19 pandemic due to low hospital capacity and the fear of viral spread. Outpatient ambulatory care was unavailable for a certain time. Subsequently, a substantial number of patients were afraid to visit medical facilities. Therefore, diagnostic procedures such as contrast-enhanced ultrasound, multislice computed tomography, magnetic resonance imaging and liver biopsies have been delayed. Additionally, treatment options have been insufficiently maintained. Surgical resection and LT are the most affected due to a shortage of anesthetists and other medical personnel[6]. Procedures such as transarterial (chemo)embolization (TACE/TAE) and radiofrequency ablation are therefore the most important tools in treating patients with HCC. Data on the impact of COVID-19 on HCC patient care are underrepresented[56,57]. A colleague from an Italian center managed HCC patients with the goal of minimizing the impact of COVID-19 and reported their experience from February 24 to March 20, 2020, regarding the treatment of HCC patients in comparison to the same period during 2019[57]. The authors found that 11% of patients had delayed treatment of HCC for 2 mo or longer. The delayed treatment modalities comprised transarterial procedures in eight HCC patients, thermal ablation in three HCC patients and systemic therapy in two patients. Thermal ablation in the three patients was performed as an alternative procedure to surgical treatment. The results of this study represent the best efforts of clinicians to manage HCC during the COVID-19 pandemic[57].

In the case of early-stage HCC, the capacity of most hospitals for surgical treatment (resection) is limited due to the limited number of anesthesiologists as well as shortages in intensive care unit beds. Clinicians can select some patients who have been prioritized for resection and have a relatively low disease burden. Treatment modalities such as radiofrequency and microwave ablation, upfront transarterial treatment and systemic therapy may be considered as alternative methods according to the guidelines for each treatment modality[56,58]. Additionally, during the pandemic, the number of LTs were reduced or reached zero for some time due to reduced anesthetic capacity as well as a shortage of donors[56,58]. In the case of intermediate-stage HCC, a more selective approach can be used with respect to TACE in hospitals that are greatly affected by the COVID-19 pandemic. Additionally, if a specific center cannot perform TACE, systemic therapy or adequate surveillance, then imaging could be an alternative approach[56,58]. Finally, in the case of advanced-stage HCC, HCC patients who receive oral multitargeted tyrosine kinase inhibitors could be followed by clinicians for prolonged intervals or monitored by telephone or another telemedicine interface, depending on the patient's tolerance and clinical status during the COVID-19 pandemic[56,58]. The impact on the long-term outcomes of HCC due to these modifications in treatment options, as well as the delays in treatment, will soon be realized[57].

The decision to treat HCC during the pandemic should consider the availability of medical staff, risk of infection and the risk-benefit ratio for an individual patient. The management of HCC in patients is complex because it relies heavily on multidisciplinary approaches involving gastroenterologists, radiologists, hepatobiliary surgeons and oncologists, who are significantly burdened during this pandemic[15,56]. Extra coordination among different specialties is necessary to maintain clinical services for patients with HCC. It is recommended that the care and treatment of HCC patients is maintained according to the guidelines by using alternative methods of communication whenever possible in order to minimize the COVID-19 exposure risk to medical staff[15]. Widely available SARS-CoV-2 polymerase chain reaction testing is recommended before elective hospital admission, although there can never be a definite guarantee for medical personnel because a patient may be in the incubation phase of infection or the patient may contract the infection in the hospital. If the patient is acutely infected, it is reasonable to defer HCC treatment for a few weeks until after recovery from COVID-19[6].

LT AND COVID-19

LT programs have been weakened globally, even in regions where the COVID-19 prevalence has been low[59-61]. During this period of readjustment no specific guidelines were offered; however, multiple organizations released recommendations for medical personnel involved in solid organ transplantation[59-66].

Primarily, obtaining an organ from a SARS-CoV-2-infected patient is contraindicated. Moreover, screening of deceased donors, as well as recipients, is highly recommended[59-66]. In the case of unidentified infection, the donor could spread the

virus to multiple recipients, which would presumably have an unfavorable or even lethal course under severe immunosuppression[6,62].

As the risk of contracting the virus is high, even under hospital conditions, it would be appropriate to limit the number of face-to-face contacts for patients at risk of severe COVID-19. They should be advised against travel and should strictly practice physical distancing[6]. Due to cirrhosis-associated immune dysfunction, the aforementioned recommendations apply to all patients awaiting transplantation.

A further challenge is related to the staff involved in LT, who cannot be easily replaced. Quarantined, infected or redistributed personnel can prevent program realization for a certain period of time, which can have deleterious effects on potential LT recipients[59]. Therefore, splitting the team involved in LT and postoperative care into smaller subteams, as well as screening and segregating staff working with immediate post-LT patients, is recommended[59]. Compared to some other solid organ transplantations, LT is performed to preserve life. In contrast, although renal transplantation reduces dialysis morbidity and future medical costs, it is not directly lifesaving and can therefore be postponed[62]. Lifesaving transplantations, such as liver, heart and lung, have far more urgent indications and postponement may have deleterious consequences. Accordingly, it is of utmost importance that LT centers worldwide aim to restore their transplantation services.

Finally, according to preliminary data, age and comorbidity are key to determining the outcome from SARS-CoV-2 infection in LT patients[6,9].

Whether to receive vaccination is currently an unavoidable global question potentiated by substantial social media involvement. Three vaccines were approved by February 2021. Two of these, the BNT162b2 (Pfizer-BioNTech) and mRNA-1273 (Moderna) vaccines, are based on mRNAs that encode variants of the SARS-CoV-2-spiked glycoprotein[63]. Both must be administered twice, 21-28 d apart. The third approved vaccine is AZD1222, also known as the Oxford-AstraZeneca vaccine. This is an adenovirus vector that contains the full-length, codon-optimized gene that encodes the SARS-CoV-2 spike protein and should also be administered in two doses, with the second dose administered 4-12 wk after the first dose[63]. The EASL position paper recommends vaccination against SARS-CoV-2 in patients with CLD, hepatobiliary cancer and LT[63].

Post-transplant patients and COVID-19

Patients taking immunosuppressive drugs after transplantation are at increased risk of infection or viral reactivation. The exact influence of the SARS-CoV-2 virus in post-LT patients is unclear[15].

Regarding the disease course in post-transplant patients, it seems that immunosuppression might have favorable effects by disabling cytokine release syndrome, characterized by increased serum levels of interleukin (IL)-6, IL-8 and tumor necrosis factor [15,64]. A Spanish study analyzed 111 LT patients diagnosed with COVID-19[65]. During a median follow-up of approximately 3 wk, 86.5% of patients were admitted to hospital, among which 19.8% required respiratory support[65]. Surprisingly, their mortality rate (18%) was lower than in the complementary general population. Mycophenolate mofetil (MMF) administered at a dose of > 1000 mg/d was an independent predictor of severe COVID-19[65]. In contrast, treatment with calcineurin inhibitors and the mammalian target of rapamycin (mTOR) inhibitor everolimus were not associated with a severe COVID-19 course. Complete withdrawal of immunosuppression showed no benefit[65]. Therefore, MMF withdrawal or transient conversion to calcineurin inhibitors or everolimus could be beneficial for hospitalized patients until the COVID-19 resolves[65].

Vaccination in post-LT patients is recommended at approximately 3-6 mo after transplantation when immunosuppression can be reduced. This is because the immune system is too suppressed to mount the proper vaccination response in the early post-transplant period. Accordingly, vaccination of household members and of healthcare professionals caring for immunocompromised patients is advocated[63].

LIVER DISEASE AND COVID-19 IN CHILDREN

A recent review by Di Giorgio *et al*[67] nicely summarizes the current data from 105 studies on the association among pre-existing CLD and COVID-19 infection in children. According to the data, the most common liver manifestation was an elevation of transaminases[67]. The authors found that children with CLD, including those on immunosuppressive therapy (autoimmune liver disease and LT), actually do not have

a higher risk for a severe disease course of COVID-19. Additionally, they have little or no liver dysfunction[67]. As mentioned earlier, we still do not know the exact pathogenetic mechanism of liver damage in either adults or children, therefore we still do not fully understand the clinical outcomes of patients with CLD infected with COVID-19. Furthermore, there are no clear data on infectivity rates in children with CLD or regarding the presence of asymptomatic carriage of the virus in children[67]. Finally, there are no data regarding the long-term outcome of COVID-19 infection in this group of immunocompromised children[67]. Thus, further data are needed.

CURRENT STUDIES AND FUTURE DIRECTIONS

The COVID-19 pandemic has caused serious damage to the global health system and prevented the anticipation, recruitment or completion of numerous clinical trials. However, according to ClinicaTrials.gov, there are currently more than 1500 studies related to 'liver disease' in the recruitment phase[68]. In line with active clinical research and databases including patients with NAFLD and CLD, it is evident that this remains a trending topic, despite the COVID-19 pandemonium. The utilization of noninvasive methods in the assessment of liver and spleen stiffness and indirect prediction of portal hypertension remains the desired goal in the field of CLD. At the same time, clinicians worldwide are determined to find a proper therapy for NAFLD. The effects of glucagon-like peptide agonist (GLP-1) semaglutide, peroxisome proliferator-activated receptor (PPAR) agonist lanifibranor, thiazolidinediones, sodium-glucose cotransporter 2 inhibitors, prebiotics and probiotics are currently being tested in clinical trials[69-73]. Furthermore, the impact of fecal microbiota transplantation on obese patients with NAFLD is being researched on participants in India[74]. A selective thyroid hormone receptor-β agonist, resmetirom (MGL-3196), is in its third trial phase and the mitochondrial-derived peptide (MOTS-c) analog CB4211 is in its 1a/1b phase of evaluation among the NAFLD population[75,76]. Considering the global proportion of obese patients suffering from NAFLD, whose number under the COVID-19-created environment will undoubtedly grow, extension of the mentioned research and anticipation of future studies is encouraged.

CONCLUSION

The global social, economic and political crises related to the COVID-19 pandemic presumably had more indirect than direct negative impacts on health systems. Drastic lifestyle changes, social isolation and distancing, and individual and global financial crises resulted in a robust population forfeiting healthy habits and seeking comfort in alcoholic beverages, drugs and unhealthy diets[19,41]. The inevitable consequences are the rising incidence of NAFLD, viral hepatitis, acute alcoholic hepatitis, liver cirrhosis decompensation and ultimately liver-related mortality[19].

The inaccessibility of regular clinical and sonographic examinations has resulted in difficulties in the treatment of patients with CLD or prompt HCC detection and treatment. A dramatic reduction in the number of liver donors and the transformation of numerous transplantation centers into COVID-19 units have greatly reduced the rate of orthotopic LT.

The indirect unavoidable effects of the COVID-19 pandemic in the following years have yet to be determined[19]. Although the health system has been tremendously challenged, resulting in overwhelming damage that is continuously being revealed, focus should remain on the current and upcoming periods involving patients with uncontrolled chronic diseases[16,19]. Swift resumption of care practices, especially for patients with HCC or individuals requiring LT, must be initiated while simultaneously maintaining social distancing and balancing inadequate hospital resources[16,19].

Substantial efforts should be initiated for the management of patients with liver disease in order to prevent and control the inevitable COVID-19-related morbidity and mortality that will follow.

Several questions regarding the impact of the COVID-19 pandemic on liver disease remain. One of the most important questions is: What will be the effect of long-term anticoagulants on liver disease? The main question for general CLD patients is: How will the modification of clinical practice during this pandemic affect outcomes in CLD patients.

REFERENCES

1 **Téllez L**, Martín Mateos RM. COVID-19 and liver disease: An update. *Gastroenterol Hepatol* 2020; **43**: 472-480 [PMID: 32727662 DOI: 10.1016/j.gastrohep.2020.06.006]

2 **Lax SF**, Skok K, Zechner P, Kessler HH, Kaufmann N, Koelblinger C, Vander K, Bargfrieder U, Trauner M. Pulmonary Arterial Thrombosis in COVID-19 With Fatal Outcome : Results From a Prospective, Single-Center, Clinicopathologic Case Series. *Ann Intern Med* 2020; **173**: 350-361 [PMID: 32422076 DOI: 10.7326/M20-2566]

3 **Williamson EJ**, Walker AJ, Bhaskaran K, Bacon S, Bates C, Morton CE, Curtis HJ, Mehrkar A, Evans D, Inglesby P, Cockburn J, McDonald HI, MacKenna B, Tomlinson L, Douglas IJ, Rentsch CT, Mathur R, Wong AYS, Grieve R, Harrison D, Forbes H, Schultze A, Croker R, Parry J, Hester F, Harper S, Perera R, Evans SJW, Smeeth L, Goldacre B. Factors associated with COVID-19-related death using OpenSAFELY. *Nature* 2020; **584**: 430-436 [PMID: 32640463 DOI: 10.1038/s41586-020-2521-4]

4 **Nardo AD**, Schneeweiss-Gleixner M, Bakail M, Dixon ED, Lax SF, Trauner M. Pathophysiological mechanisms of liver injury in COVID-19. *Liver Int* 2021; **41**: 20-32 [PMID: 33190346 DOI: 10.1111/liv.14730]

5 **Sonzogni A**, Previtali G, Seghezzi M, Grazia Alessio M, Gianatti A, Licini L, Morotti D, Zerbi P, Carsana L, Rossi R, Lauri E, Pellegrinelli A, Nebuloni M. Liver histopathology in severe COVID 19 respiratory failure is suggestive of vascular alterations. *Liver Int* 2020; **40**: 2110-2116 [PMID: 32654359 DOI: 10.1111/liv.14601]

6 **Wong GL**, Wong VW, Thompson A, Jia J, Hou J, Lesmana CRA, Susilo A, Tanaka Y, Chan WK, Gane E, Ong-Go AK, Lim SG, Ahn SH, Yu ML, Piratvisuth T, Chan HL; Asia-Pacific Working Group for Liver Derangement during the COVID-19 Pandemic. Management of patients with liver derangement during the COVID-19 pandemic: an Asia-Pacific position statement. *Lancet Gastroenterol Hepatol* 2020; **5**: 776-787 [PMID: 32585136 DOI: 10.1016/S2468-1253(20)30190-4]

7 **Cevik M**, Bamford CGG, Ho A. COVID-19 pandemic-a focused review for clinicians. *Clin Microbiol Infect* 2020; **26**: 842-847 [PMID: 32344166 DOI: 10.1016/j.cmi.2020.04.023]

8 **Cha MH**, Regueiro M, Sandhu DS. Gastrointestinal and hepatic manifestations of COVID-19: A comprehensive review. *World J Gastroenterol* 2020; **26**: 2323-2332 [PMID: 32476796 DOI: 10.3748/wjg.v26.i19.2323]

9 **Webb GJ**, Moon AM, Barnes E, Barritt AS 4th, Marjot T. Age and comorbidity are central to the risk of death from COVID-19 in liver transplant recipients. *J Hepatol* 2021; **75**: 226-228 [PMID: 33556419 DOI: 10.1016/j.jhep.2021.01.036]

10 **Marjot T**, Buescher G, Sebode M, Barnes E, Barritt AS 4th, Armstrong MJ, Baldelli L, Kennedy J, Mercer C, Ozga AK, Casar C, Schramm C; contributing Members and Collaborators of ERN RARE-LIVER/COVID-Hep/SECURE-Cirrhosis, Moon AM, Webb GJ, Lohse AW. SARS-CoV-2 infection in patients with autoimmune hepatitis. *J Hepatol* 2021; **74**: 1335-1343 [PMID: 33508378 DOI: 10.1016/j.jhep.2021.01.021]

11 **Portincasa P**, Krawczyk M, Smyk W, Lammert F, Di Ciaula A. COVID-19 and non-alcoholic fatty liver disease: Two intersecting pandemics. *Eur J Clin Invest* 2020; **50**: e13338 [PMID: 32589264 DOI: 10.1111/eci.13338]

12 **Pedersen SF**, Ho YC. SARS-CoV-2: a storm is raging. *J Clin Invest* 2020; **130**: 2202-2205 [PMID: 32217834 DOI: 10.1172/JCI137647]

13 **Mehta P**, McAuley DF, Brown M, Sanchez E, Tattersall RS, Manson JJ; HLH Across Speciality Collaboration, UK. COVID-19: consider cytokine storm syndromes and immunosuppression. *Lancet* 2020; **395**: 1033-1034 [PMID: 32192578 DOI: 10.1016/S0140-6736(20)30628-0]

14 **Samarasekera U**. COVID-19 hits viral hepatitis care for vulnerable populations. *Lancet Gastroenterol Hepatol* 2021; **6**: 166 [PMID: 33581759 DOI: 10.1016/S2468-1253(21)00029-7]

15 **Ridruejo E**, Soza A. The liver in times of COVID-19: What hepatologists should know. *Ann Hepatol* 2020; **19**: 353-358 [PMID: 32425991 DOI: 10.1016/j.aohep.2020.05.001]

16 **Bollipo S**, Kapuria D, Rabiee A, Ben-Yakov G, Lui RN, Lee HW, Kumar G, Siau K, Turnes J, Dhanasekaran R. One world, one pandemic, many guidelines: management of liver diseases during COVID-19. *Gut* 2020; **69**: 1369-1372 [PMID: 32499304 DOI: 10.1136/gutjnl-2020-321553]

17 **Fix OK**, Hameed B, Fontana RJ, Kwok RM, McGuire BM, Mulligan DC, Pratt DS, Russo MW, Schilsky ML, Verna EC, Loomba R, Cohen DE, Bezerra JA, Reddy KR, Chung RT. Clinical Best Practice Advice for Hepatology and Liver Transplant Providers During the COVID-19 Pandemic: AASLD Expert Panel Consensus Statement. *Hepatology* 2020; **72**: 287-304 [PMID: 32298473 DOI: 10.1002/hep.31281]

18 **Boettler T**, Newsome PN, Mondelli MU, Maticic M, Cordero E, Cornberg M, Berg T. Care of patients with liver disease during the COVID-19 pandemic: EASL-ESCMID position paper. *JHEP Rep* 2020; **2**: 100113 [PMID: 32289115 DOI: 10.1016/j.jhepr.2020.100113]

19 **Pawlotsky JM**. COVID-19 and the liver-related deaths to come. *Nat Rev Gastroenterol Hepatol* 2020; **17**: 523-525 [PMID: 32528138 DOI: 10.1038/s41575-020-0328-2]

20 **CDC COVID-19 Response Team**. Preliminary Estimates of the Prevalence of Selected Underlying Health Conditions Among Patients with Coronavirus Disease 2019 - United States, February 12-March 28, 2020. *MMWR Morb Mortal Wkly Rep* 2020; **69**: 382-386 [PMID: 32240123 DOI: 10.15585/mmwr.mm6913e2]

21 **Portincasa P**, Krawczyk M, Machill A, Lammert F, Di Ciaula A. Hepatic consequences of COVID-

19 infection. Lapping or biting? *Eur J Intern Med* 2020; **77**: 18-24 [PMID: 32507608 DOI: 10.1016/j.ejim.2020.05.035]
22 **Lei F**, Liu YM, Zhou F, Qin JJ, Zhang P, Zhu L, Zhang XJ, Cai J, Lin L, Ouyang S, Wang X, Yang C, Cheng X, Liu W, Li H, Xie J, Wu B, Luo H, Xiao F, Chen J, Tao L, Cheng G, She ZG, Zhou J, Wang H, Lin J, Luo P, Fu S, Ye P, Xiao B, Mao W, Liu L, Yan Y, Chen G, Huang X, Zhang BH, Yuan Y. Longitudinal Association Between Markers of Liver Injury and Mortality in COVID-19 in China. *Hepatology* 2020; **72**: 389-398 [PMID: 32359177 DOI: 10.1002/hep.31301]
23 **Feng G**, Zheng KI, Yan QQ, Rios RS, Targher G, Byrne CD, Poucke SV, Liu WY, Zheng MH. COVID-19 and Liver Dysfunction: Current Insights and Emergent Therapeutic Strategies. *J Clin Transl Hepatol* 2020; **8**: 18-24 [PMID: 32274342 DOI: 10.14218/JCTH.2020.00018]
24 **Fan Z**, Chen L, Li J, Cheng X, Yang J, Tian C, Zhang Y, Huang S, Liu Z, Cheng J. Clinical Features of COVID-19-Related Liver Functional Abnormality. *Clin Gastroenterol Hepatol* 2020; **18**: 1561-1566 [PMID: 32283325 DOI: 10.1016/j.cgh.2020.04.002]
25 **Richardson S**, Hirsch JS, Narasimhan M, Crawford JM, McGinn T, Davidson KW; the Northwell COVID-19 Research Consortium, Barnaby DP, Becker LB, Chelico JD, Cohen SL, Cookingham J, Coppa K, Diefenbach MA, Dominello AJ, Duer-Hefele J, Falzon L, Gitlin J, Hajizadeh N, Harvin TG, Hirschwerk DA, Kim EJ, Kozel ZM, Marrast LM, Mogavero JN, Osorio GA, Qiu M, Zanos TP. Presenting Characteristics, Comorbidities, and Outcomes Among 5700 Patients Hospitalized With COVID-19 in the New York City Area. *JAMA* 2020; **323**: 2052-2059 [PMID: 32320003 DOI: 10.1001/jama.2020.6775]
26 **Xu L**, Liu J, Lu M, Yang D, Zheng X. Liver injury during highly pathogenic human coronavirus infections. *Liver Int* 2020; **40**: 998-1004 [PMID: 32170806 DOI: 10.1111/liv.14435]
27 **Zhang C**, Shi L, Wang FS. Liver injury in COVID-19: management and challenges. *Lancet Gastroenterol Hepatol* 2020; **5**: 428-430 [PMID: 32145190 DOI: 10.1016/S2468-1253(20)30057-1]
28 **Cai Q**, Huang D, Yu H, Zhu Z, Xia Z, Su Y, Li Z, Zhou G, Gou J, Qu J, Sun Y, Liu Y, He Q, Chen J, Liu L, Xu L. COVID-19: Abnormal liver function tests. *J Hepatol* 2020; **73**: 566-574 [PMID: 32298767 DOI: 10.1016/j.jhep.2020.04.006]
29 **Iavarone M**, D'Ambrosio R, Soria A, Triolo M, Pugliese N, Del Poggio P, Perricone G, Massironi S, Spinetti A, Buscarini E, Viganò M, Carriero C, Fagiuoli S, Aghemo A, Belli LS, Lucà M, Pedaci M, Rimondi A, Rumi MG, Invernizzi P, Bonfanti P, Lampertico P. High rates of 30-day mortality in patients with cirrhosis and COVID-19. *J Hepatol* 2020; **73**: 1063-1071 [PMID: 32526252 DOI: 10.1016/j.jhep.2020.06.001]
30 **Sun J**, Aghemo A, Forner A, Valenti L. COVID-19 and liver disease. *Liver Int* 2020; **40**: 1278-1281 [PMID: 32251539 DOI: 10.1111/liv.14470]
31 **Docherty AB**, Harrison EM, Green CA, Hardwick HE, Pius R, Norman L, Holden KA, Read JM, Dondelinger F, Carson G, Merson L, Lee J, Plotkin D, Sigfrid L, Halpin S, Jackson C, Gamble C, Horby PW, Nguyen-Van-Tam JS, Ho A, Russell CD, Dunning J, Openshaw PJ, Baillie JK, Semple MG; ISARIC4C investigators. Features of 20 133 UK patients in hospital with covid-19 using the ISARIC WHO Clinical Characterisation Protocol: prospective observational cohort study. *BMJ* 2020; **369**: m1985 [PMID: 32444460 DOI: 10.1136/bmj.m1985]
32 **Ji D**, Qin E, Xu J, Zhang D, Cheng G, Wang Y, Lau G. Non-alcoholic fatty liver diseases in patients with COVID-19: A retrospective study. *J Hepatol* 2020; **73**: 451-453 [PMID: 32278005 DOI: 10.1016/j.jhep.2020.03.044]
33 **Zhou YJ**, Zheng KI, Wang XB, Yan HD, Sun QF, Pan KH, Wang TY, Ma HL, Chen YP, George J, Zheng MH. Younger patients with MAFLD are at increased risk of severe COVID-19 illness: A multicenter preliminary analysis. *J Hepatol* 2020; **73**: 719-721 [PMID: 32348790 DOI: 10.1016/j.jhep.2020.04.027]
34 **Gao F**, Zheng KI, Wang XB, Yan HD, Sun QF, Pan KH, Wang TY, Chen YP, George J, Zheng MH. Metabolic associated fatty liver disease increases coronavirus disease 2019 disease severity in nondiabetic patients. *J Gastroenterol Hepatol* 2021; **36**: 204-207 [PMID: 32436622 DOI: 10.1111/jgh.15112]
35 **Targher G**, Mantovani A, Byrne CD, Wang XB, Yan HD, Sun QF, Pan KH, Zheng KI, Chen YP, Eslam M, George J, Zheng MH. Risk of severe illness from COVID-19 in patients with metabolic dysfunction-associated fatty liver disease and increased fibrosis scores. *Gut* 2020; **69**: 1545-1547 [PMID: 32414813 DOI: 10.1136/gutjnl-2020-321611]
36 **Lopez-Mendez I**, Aquino-Matus J, Gall SM, Prieto-Nava JD, Juarez-Hernandez E, Uribe M, Castro-Narro G. Association of liver steatosis and fibrosis with clinical outcomes in patients with SARS-CoV-2 infection (COVID-19). *Ann Hepatol* 2021; **20**: 100271 [PMID: 33099028 DOI: 10.1016/j.aohep.2020.09.015]
37 **Ferron PJ**, Gicquel T, Mégarbane B, Clément B, Fromenty B. Treatments in Covid-19 patients with pre-existing metabolic dysfunction-associated fatty liver disease: A potential threat for drug-induced liver injury? *Biochimie* 2020; **179**: 266-274 [PMID: 32891697 DOI: 10.1016/j.biochi.2020.08.018]
38 **Huang C**, Wang Y, Li X, Ren L, Zhao J, Hu Y, Zhang L, Fan G, Xu J, Gu X, Cheng Z, Yu T, Xia J, Wei Y, Wu W, Xie X, Yin W, Li H, Liu M, Xiao Y, Gao H, Guo L, Xie J, Wang G, Jiang R, Gao Z, Jin Q, Wang J, Cao B. Clinical features of patients infected with 2019 novel coronavirus in Wuhan, China. *Lancet* 2020; **395**: 497-506 [PMID: 31986264 DOI: 10.1016/S0140-6736(20)30183-5]
39 **Gao B**, Tsukamoto H. Inflammation in Alcoholic and Nonalcoholic Fatty Liver Disease: Friend or Foe? *Gastroenterology* 2016; **150**: 1704-1709 [PMID: 26826669 DOI: 10.1053/j.gastro.2016.01.025]
40 **Boeckmans J**, Rodrigues RM, Demuyser T, Piérard D, Vanhaecke T, Rogiers V. COVID-19 and

drug-induced liver injury: a problem of plenty or a petty point? *Arch Toxicol* 2020; **94**: 1367-1369 [PMID: 32266419 DOI: 10.1007/s00204-020-02734-1]

41 **Clemmensen C**, Petersen MB, Sørensen TIA. Will the COVID-19 pandemic worsen the obesity epidemic? *Nat Rev Endocrinol* 2020; **16**: 469-470 [PMID: 32641837 DOI: 10.1038/s41574-020-0387-z]

42 **Stanfield D**, Lucey MR. The Heightened Risk of Fatty Liver Disorders in the Time of COVID-19. *Mayo Clin Proc* 2020; **95**: 2580-2581 [PMID: 33276827 DOI: 10.1016/j.mayocp.2020.10.020]

43 **Peeraphatdit TB**, Ahn JC, Choi DH, Allen AM, Simonetto DA, Kamath PS, Shah VH. A Cohort Study Examining the Interaction of Alcohol Consumption and Obesity in Hepatic Steatosis and Mortality. *Mayo Clin Proc* 2020; **95**: 2612-2620 [PMID: 33276835 DOI: 10.1016/j.mayocp.2020.04.046]

44 **Merli M**, Perricone G, Lauterio A, Prosperi M, Travi G, Roselli E, Petrò L, De Carlis L, Belli L, Puoti M. Coronaviruses and Immunosuppressed Patients: The Facts During the Third Epidemic. *Liver Transpl* 2020; **26**: 1543-1544 [PMID: 32475054 DOI: 10.1002/lt.25806]

45 **Da BL**, Im GY, Schiano TD. Coronavirus Disease 2019 Hangover: A Rising Tide of Alcohol Use Disorder and Alcohol-Associated Liver Disease. *Hepatology* 2020; **72**: 1102-1108 [PMID: 32369624 DOI: 10.1002/hep.31307]

46 **Wiśniewska H**, Skowron M, Bander D, Hornung M, Jurczyk K, Karpińska E, Laurans Ł, Socha Ł, Czajkowski Z, Wawrzynowicz-Syczewska M. Nosocomial COVID-19 Infection and Severe COVID-19 Pneumonia in Patients Hospitalized for Alcoholic Liver Disease: A Case Report. *Am J Case Rep* 2020; **21**: e927452 [PMID: 32973125 DOI: 10.12659/AJCR.927452]

47 **Kapuria D**, Upadhyay S, Shekhar R, Torrazza-Perez E. Alcoholic Liver Disease and COVID-19 Pneumonia: A Case Series. *J Clin Transl Hepatol* 2020; **8**: 463-466 [PMID: 33447531 DOI: 10.14218/JCTH.2020.00053]

48 **Karimi-Sari H**, Rezaee-Zavareh MS. COVID-19 and viral hepatitis elimination programs: Are we stepping backward? *Liver Int* 2020; **40**: 2042 [PMID: 32319207 DOI: 10.1111/liv.14486]

49 **Blach S**, Kondili LA, Aghemo A, Cai Z, Dugan E, Estes C, Gamkrelidze I, Ma S, Pawlotsky JM, Razavi-Shearer D, Razavi H, Waked I, Zeuzem S, Craxi A. Impact of COVID-19 on global HCV elimination efforts. *J Hepatol* 2021; **74**: 31-36 [PMID: 32777322 DOI: 10.1016/j.jhep.2020.07.042]

50 **Moon AM**, Webb GJ, Aloman C, Armstrong MJ, Cargill T, Dhanasekaran R, Genescà J, Gill US, James TW, Jones PD, Marshall A, Mells G, Perumalswami PV, Qi X, Su F, Ufere NN, Barnes E, Barritt AS, Marjot T. High mortality rates for SARS-CoV-2 infection in patients with pre-existing chronic liver disease and cirrhosis: Preliminary results from an international registry. *J Hepatol* 2020; **73**: 705-708 [PMID: 32446714 DOI: 10.1016/j.jhep.2020.05.013]

51 **Hunt RH**, East JE, Lanas A, Malfertheiner P, Satsangi J, Scarpignato C, Webb GJ. COVID-19 and Gastrointestinal Disease: Implications for the Gastroenterologist. *Dig Dis* 2021; **39**: 119-139 [PMID: 33040064 DOI: 10.1159/000512152]

52 **Marjot T**, Moon AM, Cook JA, Abd-Elsalam S, Aloman C, Armstrong MJ, Pose E, Brenner EJ, Cargill T, Catana MA, Dhanasekaran R, Eshraghian A, García-Juárez I, Gill US, Jones PD, Kennedy J, Marshall A, Matthews C, Mells G, Mercer C, Perumalswami PV, Avitabile E, Qi X, Su F, Ufere NN, Wong YJ, Zheng MH, Barnes E, Barritt AS 4th, Webb GJ. Outcomes following SARS-CoV-2 infection in patients with chronic liver disease: An international registry study. *J Hepatol* 2021; **74**: 567-577 [PMID: 33035628 DOI: 10.1016/j.jhep.2020.09.024]

53 **Singh S**, Khan A. Clinical Characteristics and Outcomes of Coronavirus Disease 2019 Among Patients With Preexisting Liver Disease in the United States: A Multicenter Research Network Study. *Gastroenterology* 2020; **159**: 768-771.e3 [PMID: 32376408 DOI: 10.1053/j.gastro.2020.04.064]

54 **Asrani SK**, Devarbhavi H, Eaton J, Kamath PS. Burden of liver diseases in the world. *J Hepatol* 2019; **70**: 151-171 [PMID: 30266282 DOI: 10.1016/j.jhep.2018.09.014]

55 **Tapper EB**, Asrani SK. The COVID-19 pandemic will have a long-lasting impact on the quality of cirrhosis care. *J Hepatol* 2020; **73**: 441-445 [PMID: 32298769 DOI: 10.1016/j.jhep.2020.04.005]

56 **Chan SL**, Kudo M. Impacts of COVID-19 on Liver Cancers: During and after the Pandemic. *Liver Cancer* 2020; **9**: 491-502 [PMID: 33078127 DOI: 10.1159/000510765]

57 **Iavarone M**, Sangiovanni A, Carrafiello G, Rossi G, Lampertico P. Management of hepatocellular carcinoma in the time of COVID-19. *Ann Oncol* 2020; **31**: 1084-1085 [PMID: 32330540 DOI: 10.1016/j.annonc.2020.04.007]

58 **European Association for the Study of the Liver**. EASL Clinical Practice Guidelines: Management of hepatocellular carcinoma. *J Hepatol* 2018; **69**: 182-236 [PMID: 29628281 DOI: 10.1016/j.jhep.2018.03.019]

59 **Niriella MA**, Siriwardana RC, Perera MTPR, Narasimhan G, Chan SC, Dassanayake AS. Challenges for Liver Transplantation During Recovery From the COVID-19 Pandemic: Insights and Recommendations. *Transplant Proc* 2020; **52**: 2601-2606 [PMID: 32586665 DOI: 10.1016/j.transproceed.2020.05.032]

60 **Di Maira T**, Berenguer M. COVID-19 and liver transplantation. *Nat Rev Gastroenterol Hepatol* 2020; **17**: 526-528 [PMID: 32651555 DOI: 10.1038/s41575-020-0347-z]

61 **Ritschl PV**, Nevermann N, Wiering L, Wu HH, Moroder P, Brandl A, Hillebrandt K, Tacke F, Friedersdorff F, Schlomm T, Schöning W, Öllinger R, Schmelzle M, Pratschke J. Solid organ transplantation programs facing lack of empiric evidence in the COVID-19 pandemic: A By-proxy Society Recommendation Consensus approach. *Am J Transplant* 2020; **20**: 1826-1836 [PMID: 32323460 DOI: 10.1111/ajt.15933]

62 **Kumar D**, Manuel O, Natori Y, Egawa H, Grossi P, Han SH, Fernández-Ruiz M, Humar A. COVID-19: A global transplant perspective on successfully navigating a pandemic. *Am J Transplant* 2020; **20**: 1773-1779 [PMID: 32202064 DOI: 10.1111/ajt.15876]

63 **Cornberg M**, Buti M, Eberhardt CS, Grossi PA, Shouval D. EASL position paper on the use of COVID-19 vaccines in patients with chronic liver diseases, hepatobiliary cancer and liver transplant recipients. *J Hepatol* 2021; **74**: 944-951 [PMID: 33563499 DOI: 10.1016/j.jhep.2021.01.032]

64 **D'Antiga L**. Coronaviruses and Immunosuppressed Patients: The Facts During the Third Epidemic. *Liver Transpl* 2020; **26**: 832-834 [PMID: 32196933 DOI: 10.1002/lt.25756]

65 **Colmenero J**, Rodríguez-Perálvarez M, Salcedo M, Arias-Milla A, Muñoz-Serrano A, Graus J, Nuño J, Gastaca M, Bustamante-Schneider J, Cachero A, Lladó L, Caballero A, Fernández-Yunquera A, Loinaz C, Fernández I, Fondevila C, Navasa M, Iñarrairaegui M, Castells L, Pascual S, Ramírez P, Vinaixa C, González-Dieguez ML, González-Grande R, Hierro L, Nogueras F, Otero A, Álamo JM, Blanco-Fernández G, Fábrega E, García-Pajares F, Montero JL, Tomé S, De la Rosa G, Pons JA. Epidemiological pattern, incidence, and outcomes of COVID-19 in liver transplant patients. *J Hepatol* 2021; **74**: 148-155 [PMID: 32750442 DOI: 10.1016/j.jhep.2020.07.040]

66 **Qin J**, Wang H, Qin X, Zhang P, Zhu L, Cai J, Yuan Y, Li H. Perioperative Presentation of COVID-19 Disease in a Liver Transplant Recipient. *Hepatology* 2020; **72**: 1491-1493 [PMID: 32220017 DOI: 10.1002/hep.31257]

67 **Di Giorgio A**, Hartleif S, Warner S, Kelly D. COVID-19 in Children With Liver Disease. *Front Pediatr* 2021; **9**: 616381 [PMID: 33777864 DOI: 10.3389/fped.2021.616381]

68 **U.S. National Library of Medicine**. Identifier NCT00287391. [cited 27 Feb 2021]. In: ClinicalTrials.gov [Internet]. 2000 Feb 29 - . [about 15 screens]. Available from: URL: https://clinicaltrials.gov/ct2/results?cond=liver+disease&Search=Apply&recrs=a&age_v=&gndr=&type=&rslt=

69 **Erlandson K**, Lake JE. Study of Semaglutide for Non-Alcoholic Fatty Liver Disease (NAFLD), a Metabolic Syndrome With Insulin Resistance, Increased Hepatic Lipids, and Increased Cardiovascular Disease Risk (The SLIM LIVER Study). [accessed 2021 Feb 27]. In: ClinicalTrials.gov [Internet]. Birmingham (AL): U.S. National Library of Medicine. Available from: https://clinicaltrials.gov/ct2/show/NCT04216589?recrs=a&cond=liver+disease&draw=3&rank=58 ClinicalTrials.gov Identifier: NCT04216589

70 **Rotman Y**. Non-Alcoholic Fatty Liver Disease, the Hepatic Response to Oral Glucose, and the Effect of Semaglutide (NAFLD HEROES). [accessed 2021 Feb 27]. In: ClinicalTrials.gov [Internet]. Bethesda (MD): U.S. National Library of Medicine. Available from: https://clinicaltrials.gov/ct2/show/NCT03884075?recrs=a&cond=liver+disease&draw=3&rank=44 ClinicalTrials.gov Identifier: NCT03884075

71 **Cha BS**. Comparison of The Effects of Thiazolidinediones(TZD), Sodium- Glucose Cotransporter 2 Inhibitors(SGLT2i) Alone and TZD / SGLT2i Combination Therapy on Non-alcoholic Fatty Liver Disease in Type 2 Diabetic Patients With Fatty Liver. [accessed 2021 Feb 27]. In: ClinicalTrials.gov [Internet]. Seoul: U.S. National Library of Medicine. Available from: https://clinicaltrials.gov/ct2/show/NCT03646292?recrs=a&cond=liver+disease&draw=3&rank=47 ClinicalTrials.gov Identifier: NCT03646292

72 **Ahuja K**, Sheflin-Findling S. Role of Probiotics in Treatment of Pediatric NAFLD Patients by Assessing With Fibroscan. [accessed 2021 Feb 27]. In: ClinicalTrials.gov [Internet]. New Hyde Park (NY): U.S. National Library of Medicine. Available from: https://clinicaltrials.gov/ct2/show/NCT04671186?recrs=a&cond=liver+disease&draw=3&rank=60 ClinicalTrials.gov Identifier: NCT04671186

73 **Cusi K**. Lanifibranor in Patients With Type 2 Diabetes & Nonalcoholic Fatty Liver Disease. [accessed 2021 Feb 27]. In: ClinicalTrials.gov [Internet]. Gainesville (FL): U.S. National Library of Medicine. Available from: https://clinicaltrials.gov/ct2/show/NCT03459079?recrs=a&cond=liver+disease&draw=3&rank=53 ClinicalTrials.gov Identifier: NCT03459079

74 **Kar PS**. Effects of Fecal Microbiota Transplantation on Weight in Obese Patients With Non-alcoholic Fatty Liver Disease. [accessed 2021 Feb 27]. In: ClinicalTrials.gov [Internet]. New Delhi: U.S. National Library of Medicine. Available from: https://clinicaltrials.gov/ct2/show/NCT04594954?recrs=a&cond=liver+disease&draw=3&rank=26 ClinicalTrials.gov Identifier: NCT04594954

75 **Taub R**. A Phase 3 Study to Evaluate the Safety and Biomarkers of Resmetirom (MGL-3196) in Non Alcoholic Fatty Liver Disease (NAFLD) Patients (MAESTRO-NAFLD1). [accessed 2021 Feb 27]. In: ClinicalTrials.gov [Internet]. Birmingham (AL): U.S. National Library of Medicine. Available from: https://clinicaltrials.gov/ct2/show/NCT04197479?recrs=a&cond=liver+disease&draw=3&rank=24 ClinicalTrials.gov Identifier: NCT04197479

76 **CohBar, Inc**. A Phase 1a/1b Study of CB4211 in Healthy Non-obese Subjects and Subjects With Nonalcoholic Fatty Liver Disease. [accessed 2021 Feb 27]. In: ClinicalTrials.gov [Internet]. Chula Vista (CA): U.S. National Library of Medicine. Available from: https://clinicaltrials.gov/ct2/show/NCT03998514?recrs=a&cond=liver+disease&draw=3 ClinicalTrials.gov Identifier: NCT03998514

World Journal of Gastroenterology

Submit a Manuscript: https://www.f6publishing.com

World J Gastroenterol 2021 September 28; 27(36): 6053-6063

DOI: 10.3748/wjg.v27.i36.6053

ISSN 1007-9327 (print) ISSN 2219-2840 (online)

MINIREVIEWS

Treatment of hepatitis B virus infection in children and adolescents

Mariangela Stinco, Chiara Rubino, Sandra Trapani, Giuseppe Indolfi

ORCID number: Mariangela Stinco 0000-0003-3970-5000; Chiara Rubino 0000-0001-7480-3613; Sandra Trapani 0000-0003-1105-1500; Giuseppe Indolfi 0000-0003-3830-9823.

Author contributions: Stinco M and Indolfi G wrote the paper; Rubino C and Trapani S reviewed it critically for significant intellectual content.

Conflict-of-interest statement: The authors declare that they have no competing interests.

Open-Access: This article is an open-access article that was selected by an in-house editor and fully peer-reviewed by external reviewers. It is distributed in accordance with the Creative Commons Attribution NonCommercial (CC BY-NC 4.0) license, which permits others to distribute, remix, adapt, build upon this work non-commercially, and license their derivative works on different terms, provided the original work is properly cited and the use is non-commercial. See: http://creativecommons.org/Licenses/by-nc/4.0/

Manuscript source: Invited manuscript

Specialty type: Gastroenterology and hepatology

Country/Territory of origin: Italy

Peer-review report's scientific

Mariangela Stinco, Chiara Rubino, Sandra Trapani, Department of Health Sciences, Pediatric Section, Meyer Children's University Hospital, Florence 50139, Italy

Giuseppe Indolfi, Department Neurofarba, University of Florence and Meyer Children's University Hospital, Florence 50139, Italy

Corresponding author: Giuseppe Indolfi, MD, Professor, Department Neurofarba, University of Florence and Meyer Children's University Hospital, 6 Gaetano Pieraccini, Florence 50139, Italy. giuseppe.indolfi@meyer.it

Abstract

Hepatitis B virus (HBV) infection is one of the main causes of morbidity and mortality worldwide. Most children acquire the infection perinatally or during early childhood and develop a chronic hepatitis characterized by a high viral replication and a low-inflammation phase of infection, with normal or only slightly raised aminotransferases. Although a conservative approach in children is usually recommended, different therapies exist and different therapeutic approaches are possible. The main goals of antiviral treatment for children with chronic HBV infection are to suppress viral replication and to warn the disease progression to cirrhosis and hepatocellular carcinoma, although these complications are rare in children. Both United States Food and Drug Administration (US-FDA) and European Medicines Agency (EMA) have approved interferon alfa-2b for children aged 1 year and older, pegylated interferon alfa-2a and lamivudine for children aged 3 years and older, entecavir for use in children aged 2 years and older, and adefovir for use in those 12 years of age and older. Tenofovir disoproxil fumarate is approved by EMA for children aged 2 years and older and by US-FDA for treatment in children aged 12 years and older. Finally, EMA has approved the use of tenofovir alafenamide for treatment of children aged 12 years and older or for children weighing more than 35 kg independent of age. This narrative review will provide the framework for summarizing indications to antiviral therapy in the management of chronic HBV infection in children and adolescents.

Key Words: Hepatitis B; Children; Adolescents; Antiviral therapy; Tenofovir disoproxil fumarate; Entecavir; Interferon

©The Author(s) 2021. Published by Baishideng Publishing Group Inc. All rights reserved.

quality classification
Grade A (Excellent): 0
Grade B (Very good): B
Grade C (Good): C
Grade D (Fair): 0
Grade E (Poor): 0

Received: April 17, 2021
Peer-review started: April 17, 2021
First decision: June 3, 2021
Revised: June 30, 2021
Accepted: August 13, 2021
Article in press: August 13, 2021
Published online: September 28, 2021

P-Reviewer: Kayesh MEH, Kishida Y
S-Editor: Gong ZM
L-Editor: Filipodia
P-Editor: Li JH

Core Tip: Hepatitis B virus (HBV) is a major cause of acute and chronic liver disease. During childhood, asymptomatic chronic hepatitis B is the most common outcome of the infection, and a conservative approach is usually recommended. In selected patients there is a strict indication for treatment. Different drugs have been approved by United States Food and Drug Administration and European Medicines Agency for treatment of children and adolescents with chronic HBV infection. The main goal of the treatment is to reduce the risk of progression to cirrhosis and hepatocellular carcinoma through the suppression of HBV replication.

Citation: Stinco M, Rubino C, Trapani S, Indolfi G. Treatment of hepatitis B virus infection in children and adolescents. *World J Gastroenterol* 2021; 27(36): 6053-6063
URL: https://www.wjgnet.com/1007-9327/full/v27/i36/6053.htm
DOI: https://dx.doi.org/10.3748/wjg.v27.i36.6053

INTRODUCTION

Hepatitis B virus (HBV) infection is one of the major causes of acute and chronic liver disease and associated morbidity and mortality worldwide. In 2015, 257 million people were estimated as being chronically infected by the World Health Organization (WHO), with a global prevalence of 3%-5%, and 887,000 people died due to chronic HBV infection (CHB)[1].

Hepatitis B is a vaccine-preventable disease but, despite the availability of effective vaccine and vaccination programs, it remains a global health problem[2]. It has been estimated that annually there are almost 2 million new infections in children younger than 5 years of age. Most of the infected children acquire the infection around the time of birth through vertical transmission or during early childhood through horizontal transmission[3-5].

NATURAL HISTORY OF HBV INFECTION IN CHILDREN

The natural history and the long-term outcome of HBV infection acquired in childhood vary depending upon the age at infection. CHB is the most common outcome (90%) of the infection acquired vertically in neonates and infants. The risk of CHB is reduced to 30% when infection occurs during the first 5 years of life and < 5% for older immunocompetent children and adults[5].

HBV infection is usually asymptomatic during childhood, but sometimes acute infection could present with severe symptoms and fulminant hepatitis both in adult and children[6]. The development of complications of CHB, such as cirrhosis, hepatocellular carcinoma, and extrahepatic manifestations, is manly observed in adulthood but can also present in infancy and early childhood[7-10].

In 2017 the European Association for the Study of the Liver (EASL) proposed a new nomenclature for CHB that is no more based on the concept of immune-tolerant, immune-active, immune-control, and immune-escape, which have been previously used to describe the different phases of infection[7]. The new nomenclature emphasizes the distinction between infection and active hepatitis (defined basing on the presence of normal or raised alanine aminotransferase levels, respectively) and is based on Hepatitis B e Antigen (HBeAg) status, HBV viremia, and liver histology (Table 1)[11].

Another biomarker to monitoring HBV infection is the covalently closed circular DNA (ccc-DNA), a new biomarker related to viral replication and persistence of infection. A "complete cure" of HBV infection requires also the clearance of ccc-DNA, as well as HBsAg loss and undetectable serum HBV DNA (otherwise it is defined "functional cure")[12].

TREATMENT FOR CHRONIC HBV INFECTION

The common and main goals of antiviral treatment for adults, adolescents, and

Table 1 Patients' categories and phases in natural history of chronic hepatitis B virus infection defined by European Association for the Study of the Liver guidelines 2017[11]

	HBeAg positive	HBeAg negative	HBsAg negative
HBV infection (normal ALT)	High HBsAg	Low HBsAg	HBcAb-positive with/without positive HBsAb
	HBV DNA > 10^7 IU/mL	HBV DNA < 2000 IU/mL	HBV DNA usually undetectable
	None/minimal liver disease	No liver disease	No liver disease
	Old terminology: Immune-tolerant	Old terminology: Inactive carrier/immune control	Old terminology: Occult HBV infection
Hepatitis B (abnormal ALT)	High or intermediate HBsAg	Intermediate HBsAg	
	HBV DNA 10^4-10^7 IU/mL	HBV DNA > 2000 IU/mL	
	Moderate to severe liver disease	Moderate to severe liver disease	
	Old terminology: immune-active	Old terminology: immune escape	

HBV: Hepatitis B virus; ALT: Alanine aminotransferase levels; HBeAg: Hepatitis B e antigen; HBsAg: Hepatitis B s antigen; DNA: Deoxyribonucleic acid; HBcAb: Hepatitis B c antibodies.

children with chronic HBV infection are the effective and sustained suppression of HBV replication and consequently to decrease the risk of disease progression to cirrhosis and hepatocellular carcinoma[13-15]. Guidelines for treatment of children and adolescents have been issued by the European Society for Pediatric Gastroenterology Hepatology and Nutrition (ESPGHAN), EASL, American Association for the Study of Liver Diseases (AASLD), and Asian Pacific Association for the Study of the Liver (APASL)[11,16-18].

The aim of this narrative review is to summarize the available evidence on the use of drugs for treatment of CHB in children and adolescents, to summarize the main recommendations for treatment, and to highlight research gaps.

Interferon alfa-2b

Interferon alfa-2b has both antiviral and immunomodulatory actions. Binding to the specific transmembrane receptor, it activates intracellular signaling and gene transcription, resulting in the reduction of viral DNA level and viral injury. Furthermore, it directly stimulates the cell-mediated immune response against HBV-infected hepatocytes, thus reducing the number of cells containing ccc-DNA[19].

Interferon alfa-2b for subcutaneous injection is approved by European Medicines Agency (EMA) and United States Food and Drug Administration (US-FDA) for treatment of children and adolescents (1-17 years of age) with CHB. Treatment duration is 16 to 24 wk. The recommended dose is 6 million IU/m^2 three times a week (Table 2).

A large open-label, multinational randomized controlled trial evaluated the safety and efficacy of interferon alfa-2b[20]. Interferon alfa-2b was started at a dose of 3 million IU/m^2 of body surface area three times a week for 1 week. The dose was increased to 6 million IU/m^2 of body surface area at the second week, and this was continued for a minimum of 16 wk and a maximum of 24 wk based on results of virological testing for evidence of response (treatment was stopped at 16 or 20 wk if HBeAg was undetectable on two serum determinations taken 1 month apart). One hundred and forty-nine children were enrolled, 144 were evaluable of whom 70 received the treatment and 77 were untreated controls. Patients in the treatment arm had a better response (loss of HBV DNA and HBeAg at 24 wk of follow-up) compared to the untreated controls (26% *vs* 11%, P = 0.02). Loss of HBsAg occurred in 7 treated children (10%) but in only 1 untreated child (1.2%) (P = 0.03). Patients with lower baseline HBV DNA (< 50 pg/mL) were more likely to respond to interferon alfa-2b therapy than patients with a baseline HBV DNA greater than 200 pg/mL (41% *vs* 7%, respectively). All children in the treatment group reported at least one adverse event, the most common being influenza-like symptoms (100%), irritability, sleep disturbance and depression (40%), nausea or vomiting (40%), diarrhea or gastrointestinal distress (46%), alopecia (17%), and neutropenia (19%). The dose of interferon alfa-2b was reduced in 17 children (23%), most commonly because of neutropenia, thrombocytopenia, and fever. Three children discontinued treatment because of an adverse event. Subsequent studies confirmed the same efficacy and safety results[21-23].

Table 2 Antiviral drugs approved for children and adolescents with chronic hepatitis B virus infection[14]

	Ages approved for drug administration	Drug dosage	Drug formulations
Interferon alfa-2b	≥ 1 yr	6 million UI/m^2 three times a week	Subcutaneous injection
Peginterferon alfa-2a	≥ 3 yr	180 μg/1.73 m^2 once a week	Subcutaneous injection
Lamivudine	≥ 3 yr	3 mg/kg daily (maximum 100 mg)	Oral solution (5 mg/mL) or tablets (100 mg)
Entecavir	≥ 2 yr	10-30 kg: 0.015 mg/kg daily (maximum 0.5 mg)	Oral solution (0.05 mg/mL) or tablets (0.5 mg and 1 mg)
		> 30 kg: 0.5 mg daily	
Adefovir	≥ 12 yr	10 mg daily	Tablets (10 mg)
Tenofovir disoproxil fumarate	≥ 2 yr[1]	8 mg/kg daily (maximum 300 mg)	Oral powder (40 mg per 1 g) or tablets (150 mg, 200 mg, 250 mg and 300 mg)
	≥ 12 yr[1]	300 mg daily	
Tenofovir alafenamide	≥ 12 yr[2]	25 mg daily	Tablet (25 mg)

[1]Approved for ≥ 2 yr by the European Medicines Agency and ≥ 12 yr by the United States Food and Drug Administration.
[2]Approved independent of age for weight > 35 kg.

Peginterferon alfa

Peginterferon alfa comprises an inert, branched, 40 kD polyethylene glycol molecule attached to interferon alfa. Through the direct stimulation of immune system, it is effective in the achievement of serological response and reduction of ccc-DNA level [19].

Peginterferon alfa-2a

Peginterferon alfa-2a for subcutaneous injection is approved by EMA and US-FDA for treatment of children and adolescents (3-17 years of age) with CHB. Treatment duration is 16 to 24 wk. The recommended dose is 180 μg/1.73 m^2 once a week (Table 2).

The efficacy and safety of peginterferon alfa-2a treatment in children with CHB was assessed in the PEG-B-ACTIVE study, a phase III randomized, controlled, open-label, multicenter study[24]. Peginterferon alfa-2a was prescribed at a dose of 180 μg/1.73 m^2 once a week and was continued for a minimum of 48 wk. One hundred and sixty-one HBeAg-positive children with raised aminotransferase levels without advanced fibrosis or cirrhosis were enrolled. One hundred and fifty-one were evaluable, of whom 101 received the treatment and 50 were untreated controls. Twenty-four weeks after the end of treatment, patients who received peginterferon alfa-2a had a better response compared to untreated controls with higher HBeAg seroconversion rates (25.7% *vs* 6%, $P = 0.0043$), higher rates of hepatitis B surface antigen (HBsAg) clearance (8.9% *vs* 0%, $P = 0.03$), HBV DNA < 2000 IU/mL (28.7% *vs* 2%, $P < 0.001$) or undetectable (16.8% *vs* 2.0%, $P = 0.0069$), and alanine aminotransferase (ALT) normalization (51.5% *vs* 12%, $P < 0.001$). Loss of HBsAg occurred in 9 treated children (8.9%) and in none of those who were untreated. The most common adverse events included fever (49%), headache (30%), abdominal pain (19%), and neuropsychiatric disorder (12%). Laboratory abnormalities reported during treatment were ALT flares (53%) and neutropenia (10%) and were managed without dose modification. Short-term effects on growth appeared minimal. The study highlighted the efficacy and positive benefit/risk profile of peginterferon alfa-2a for the treatment in children and adolescents with CHB, consistent with the extensive data available in adults.

Peginterferon alfa-2b

Peginterferon alfa-2b is not approved by the US-FDA or EMA for treatment of children or adolescents with CHB but is approved for treatment of chronic hepatitis C for children 3 years of age or older (Table 2)[25-30].

Lamivudine

Lamivudine is a synthetic nucleoside analogue (analogue of cytidine) that inhibits viral replication in human cells by interfering with the DNA polymerase enzyme of HBV, and it acts as a chain terminator of DNA synthesis. If the nucleoside analogue is

incorporated in the DNA chain, it prevents the formation of the 5' to 3' phosphodiester linkage essential for DNA chain elongation, consequently terminating viral DNA growth[31].

Lamivudine is approved by EMA and US-FDA for treatment of children and adolescents (3-17 years of age) with CHB. The recommended dose is 3 mg/kg daily, oral (maximum 100 mg; Table 2).

The efficacy and safety of lamivudine treatment in children with CHB was originally assessed in one randomized, double-blind, placebo-controlled study[32]. Children and adolescents aged between 2 and 17 years received either oral lamivudine (n = 191) or placebo (n = 97) once daily for 52 wk. This study demonstrated that treatment with lamivudine was safe, efficacious, and superior to placebo, consistent with the results observed in adults with CHB. Virologic response defined by the loss of serum HBeAg and by the reduction of serum HBV DNA to undetectable levels occurred by week 52 in 23% of the children in the treatment group, as compared with 13% of children in the placebo group (P = 0.04). The rate of virologic response increased with higher baseline ALT values and scores on the histologic activity index. Loss of HBsAg occurred in 3 treated children (2%) and in none of those who were untreated. The treatment was highly safe and the nature, incidence, and severity of adverse clinical events and abnormal laboratory values in patients receiving lamivudine were similar to those receiving placebo. The emergence of YMDD-variant HBV was detected in 19% of patients who received lamivudine for 52 wk. YMDD-variant HBV may reverse the response in some patients and has been considered a limitation of lamivudine therapy.

The efficacy of lamivudine was explored in other studies. According to a recent systematic review with meta-analysis, lamivudine, when compared to placebo, was associated with significantly higher likelihood of ALT normalization, HBeAg clearance or loss, and HBV DNA suppression but not HBeAg seroconversion or HBsAg clearance after 48 wk of treatment[33-35].

Although lamivudine is a safe drug, it has low barrier to resistance.

Entecavir

Entecavir is a nucleoside analogue (analogue of deoxyguanosine). In the intracellular environment, it is rapidly phosphorylated to the active intracellular 50-triphosphate form; this active metabolite competes with the natural substrate (*i.e.*, deoxyguanosine triphosphate) of HBV polymerase and inhibits HBV replication[36].

Entecavir is approved by US-FDA and EMA for treatment of children and adolescents aged 2 years and older with CHB. The recommended treatment dose is 0.015 mg/kg daily (maximum 0.5 mg; weight > 30 kg: 0.5 mg daily; Table 2).

The efficacy and safety of entecavir were studied in a randomized, double-blind, multicenter study including children and adolescents (2 to < 18 years) with CHB[37]. Blinded treatment was administered for a minimum of 48 wk. One hundred and seventeen patients received entecavir treatment, and 56 received placebo. Patients who achieved HBeAg seroconversion continued blinded treatment while those who did not (n = 50) were switched to open-label entecavir up to week 96 of treatment. Response rates for the combined endpoint of HBeAg seroconversion and HBV DNA < 50 IU/mL at treatment week 48 occurred in 24.2% in the entecavir group, as compared with 3.3% in the placebo group (P = 0.0008). After 48 wk of treatment, patients who received entecavir had a better response compared to untreated controls with higher rates of virological suppression (49.2% *vs* 3.3%, P < 0.0001), ALT normalization (67.5% *vs* 23.3%, P < 0.0001), and HBeAg seroconversion (24.2% *vs* 10, P = 0.02). At week 96, loss of HBsAg occurred in 7 treated children (5.8%) and in none of those who were untreated. The rate of virologic response increased with low baseline HBV DNA (< 8 Log_{10} IU/mL) and high baseline ALT (> 2 × upper limit of normal). The cumulative probability of emergent entecavir resistance through years 1 and 2 of entecavir was 0.6% and 2.6%, respectively. The treatment was well tolerated with no observed differences in adverse events or changes in growth compared with placebo. A subsequent study confirmed the same efficacy and safety results[38].

Adefovir

Adefovir is an acyclic nucleotide analogue (analogue of deoxyadenosine-5´-monophosphate). It is converted by adenylate kinase to adefovir diphosphate, an active derivate that selectively inhibits the HBV polymerase. Adefovir diphosphate competes with deoxyadenosine-5´-triphosphate during HBV DNA synthesis, and, when incorporated into the HBV DNA chain, it discontinues further elongation of DNA chain, stopping HBV replication[39].

Adefovir is approved by US-FDA and EMA for treatment adolescents aged 12 years and older with CHB. The recommended treatment dose is 10 mg daily (Table 2).

The efficacy and safety of adefovir were studied in a randomized, double-blind, multicenter study including children and adolescents (2 to < 18 years) with CHB[40]. Treatment was administered for 48 wk. One hundred and eighteen patients have received adefovir treatment and 58 received placebo. Response rates for the combined endpoint of HBV DNA < 1000 copies/mL and normal ALT at treatment week 48 occurred in 19.1% in the adefovir group, as compared with 1.7% in the placebo group ($P < 0.001$). This result was primarily due to response in the 12 to 17 years age group as in the younger children, although there were apparent differences in response to those treated with adefovir compared to those who received placebo, they did not reach statistical significance. After 48 wk of treatment, patients who received tenofovir had a better response compared to untreated controls with higher rates of ALT normalization (56% *vs* 21%, $P < 0.0001$) and HBeAg seroconversion (15.9% *vs* 5.3%). More patients treated with adefovir met the combined endpoint of HBeAg seroconversion and HBV DNA < 1000 copies/mL plus normal ALT (10.6% *vs* 0/57, $P = 0.009$). Only 1 patient in the adefovir group achieved HBsAg seroconversion. The rate of virologic response increased with low baseline HBV DNA (< 8.8 Log_{10} IU/mL) and high baseline ALT (> 2.3 X upper limit of normal). No subject developed the rtA181V or rtN236T mutation associated with adefovir resistance by treatment week 48. The treatment was well tolerated with no observed differences in adverse events compared with placebo.

A subsequent study confirmed the same efficacy and safety results[41].

Tenofovir disoproxil fumarate

Tenofovir disoproxil fumarate (DF) is an inhibitor of DNA polymerase. *In vivo* it is converted by diester hydrolysis to tenofovir, an acyclic nucleotide analogue (analogue of deoxyadenosine-5´-monophosphate), and after two phosphorylation steps to its active metabolite, tenofovir diphosphate. In this form, tenofovir binds to active site of enzyme, avoiding the attaching of the natural substrate deoxyadenosine-5´-triphosphate, and inhibits the HBV DNA polymerase activity[42].

Tenofovir DF is approved by EMA for children aged 2 years and older and by US-FDA for treatment of children aged 12 years and older with CHB. The recommended treatment dose is 8 mg/kg daily (maximum 300 mg) for younger children and 300 mg daily for those older than 12 years (Table 2).

The efficacy and safety profile of tenofovir DF were studied in a randomized, double-blind, multicenter study including adolescents (12 to < 18 years) with CHB [43]. Blinded treatment was administered for 72 wk. One hundred six patients were enrolled, and 101 completed 72 wk of treatment. Fifty-two patients have received tenofovir DF treatment and 54 received placebo. Virologic response (HBV DNA < 400 copies/mL) at treatment week 72 was observed in 89% of patients who received tenofovir DF and none of those who received placebo ($P < 0.001$). The treatment was well tolerated with no observed differences in adverse events compared with placebo. No resistance to tenofovir DF developed through week 72.

Tenofovir alafenamide

Tenofovir alafenamide is a pro-drug of tenofovir diphosphate, thus it presents the same action mechanism of tenofovir DF causing causes viral DNA chain termination and preventing viral DNA transcription[42].

Tenofovir alafenamide is approved by EMA for treatment of children aged 12 years and older and, independent of age, for children weighing more than 35 kg. The recommended treatment dose is 25 mg daily. Tenofovir alafenamide was approved on the basis of studies in children with human immunodeficiency virus infection[44,45].

Telbivudine

Telbivudine is not approved by the FDA or EMA for pediatric use.

Pros and cons of anti-HBV treatment

Overall interferon based treatments are associated with higher HBeAg and HBsAg seroconversion rates and could be used for treatment of finite duration. Concerns are present with regard to tolerance and safety, and recently the availability of the drug on the market has been questioned. Furthermore, interferon and peginterferon treatments have the disadvantage of subcutaneous administration that is relevant for treatment of children.

Nucleot(s)ide analogues have been classified as having low (lamivudine, adefovir, telbivudine) and high (tenofovir, entecavir) genetic barrier to resistance and are generally used for oral treatment of indefinite duration, with an overall good safety profile[14,15].

New prospective antiviral treatment strategies

Recently, there is a growing interest in some new therapeutic strategies, targeting viral life cycle or improving antiviral immune response, that could eliminate all replicative intermediates, including ccc-DNA. The drugs targeting different steps of HBV life cycle include entry inhibitors; polymerase inhibitors; core protein (nucleocapsid) inhibitors; HBsAg release inhibitors; RNA silencers. On the other hand, the new therapies to improve anti-HBV immunity response include therapeutic vaccines, generating "new" T cells; toll-like receptor 7 and toll-like receptor 8 agonists, stimulating antiviral effector cells; retinoic acid-inducible gene I agonist; anti-HBV antibodies; checkpoint inhibitors; programmed cell death protein 1 (PD1) and PD1 ligand inhibitors, rescuing the T-cell exhaustion that can be observed in chronic HBV infection. Results of preclinical and early clinical studies are promising; thus, soon, these treatment options could be available and could potentially transform the future indications for hepatitis B treatment[46-49].

INDICATION FOR TREATMENT

The decision to start treatment in a child with CHB is based on the combined assessment of stage of liver disease, HBV DNA and ALT concentrations, and HBeAg status. Presence of other features, such as a family history of hepatocellular carcinoma, human immunodeficiency virus coinfection or other concomitant liver disease, is an additional factor to support treatment initiation. Regardless of age, all guidelines recommend treatment for children with cirrhosis, histological evidence of necroinflammation and fibrosis (active hepatitis), and fulminant or severe acute hepatitis B infection and for those undergoing immunosuppression or chemotherapy with evidence of past or ongoing HBV infection[11,13,16-18].

There are some differences between recommendations provided by the available guidelines for the treatment of CHB in children not satisfying the above treatment criteria that are highlighted in Table 3[14].

Interferon, entecavir, and tenofovir DF are recommended for treatment of chronic HBV infection in children by ESPGHAN, AASLD, and APASL. Entecavir is recommended for children aged 2–12 years in WHO guidelines while interferon is not included because its use in resource limited settings is often not feasible as a result of its high cost, requirement for injection, and high rate of adverse effects that require careful monitoring. The advantages of interferon and peginterferon as compared with nucleoside and nucleotide analogues are the absence of viral resistance and the predictable finite duration of treatment. However, the use of interferon and peginterferon requires subcutaneous injections and is associated with a high risk of adverse events. Tenofovir (tenofovir DF or tenofovir alafenamide) or entecavir have high genetic barrier and are recommended as preferred initial therapies for adults by EASL, AASLD, and WHO.

CONCLUSION

Treatment guidelines provided by the different major scientific international societies (ESPGHAN, AASLD, APASL, EASL) clearly agree on treating all patients with advanced liver disease (cirrhosis) and histological features of active hepatitis and patients with fulminant or severe acute hepatitis B infection, preventing uncontrolled HBV replication and serious complications such as cirrhosis and hepatocellular carcinoma in young adult life. The guidelines also recommended antiviral therapy for children and adolescents with HBV infection (immune-tolerant patients) undergoing immunosuppressive therapy, such as those patients who will be receiving chemotherapy or stem cell or solid organ transplantation.

All others HBV infected children who not satisfy the above treatment criteria are not typically candidates for treatment. For these patients a tight clinical, biochemical and no invasive imaging (abdominal ultrasound) follow-up will be important to monitoring the natural course of HBV infection, to identify patients undergoing

Table 3 Differences among recommendations and indications for treatment of chronic hepatitis B virus infection in adults, adolescents, and children from five professional societies or international organizations

Organization	
ESPGHAN[16]	HBeAg-positive adolescents and children with persistent alanine aminotransferase elevation for at least 6 mo
	HBeAg-negative adolescents and children with persistent alanine aminotransferase elevation for at least 6 mo for at least 12 mo
	HBV DNA > 2000 IU/mL and either
	Moderate necroinflammation or fibrosis
	Mild inflammation or fibrosis with a family history of hepatocellular carcinoma
AASLD[17]	HBeAg-positive adolescents and children with both elevated alanine aminotransferase and measurable HBV DNA concentrations
	Therapy should be deferred when HBV DNA is < 10000 IU/mL, until spontaneous HBeAg seroconversion is excluded
APASL[18]	Non-cirrhotic HBeAg-positive adolescents and children when HBV DNA level is higher than 20000 IU/mL and alanine aminotransferase is more than twice the upper limit of normal for more than 12 mo
	Non-cirrhotic HBeAg-positive adolescents and children either HBV DNA > 20000 IU/mL and ALT more than two times ULN for more than 12 mo, or a family history of hepatocellular carcinoma or cirrhosis and moderate-to-severe inflammation or pronounced fibrosis
	Non-cirrhotic, HBeAg-positive chronic HBV infection, HBV DNA < 20000 IU/mL and moderate to severe inflammation or pronounced fibrosis
	Non-cirrhotic, HBeAg-negative chronic HBV infection, HBV DNA > 2000 IU/mL, and ALT more than two times ULNNon-cirrhotic, HBeAg-negative chronic HBV infection and moderate to severe inflammation or pronounced fibrosis, regardless of HBV DNA concentration
EASL[11]	A conservative approach is warranted

ESPGHAN: European Society for Paediatric Gastroenterology Hepatology and Nutrition; HBeAg: Hepatitis B e antigen; HBV: Hepatitis B virus; DNA: Deoxyribonucleic acid; AASLD: American Association for the Study of Liver Diseases; APASL: Asian Pacific Association for the Study of the Liver; ALT: Alanine aminotransferase levels; ULN: Upper limit of normal; EASL: European Association for the Study of the Liver.

spontaneous HBeAg seroconversion, and above all to recognize rapidly those children with chronic HBV infection who may benefit from treatment (*e.g.*, patients with persistently abnormal ALT levels).

The establishment of pediatric treatment registries and of new international associations would be the most important strategy to inform best practices for the management, care, and treatment of children with HBV infection and to promote collaborative research.

REFERENCES

1 **World Health Organization**. Global hepatitis report 2017. [cited 17 April 2021]. Available from: https://www.who.int/publications/i/item/global-hepatitis-report-2017

2 B vaccines: WHO position paper – July 2017. *Wkly Epidemiol Rec* 2017; **92**: 369-392 [PMID: 28685564]

3 **Schweitzer A**, Horn J, Mikolajczyk RT, Krause G, Ott JJ. Estimations of worldwide prevalence of chronic hepatitis B virus infection: a systematic review of data published between 1965 and 2013. *Lancet* 2015; **386**: 1546-1555 [PMID: 26231459 DOI: 10.1016/S0140-6736(15)61412-X]

4 **Polaris Observatory Collaborators**. Global prevalence, treatment, and prevention of hepatitis B virus infection in 2016: a modelling study. *Lancet Gastroenterol Hepatol* 2018; **3**: 383-403 [PMID: 29599078 DOI: 10.1016/S2468-1253(18)30056-6]

5 **McMahon BJ**, Alward WL, Hall DB, Heyward WL, Bender TR, Francis DP, Maynard JE. Acute hepatitis B virus infection: relation of age to the clinical expression of disease and subsequent development of the carrier state. *J Infect Dis* 1985; **151**: 599-603 [PMID: 3973412 DOI: 10.1093/infdis/151.4.599]

6 **Tseng YR**, Wu JF, Kong MS, Hu FC, Yang YJ, Yeung CY, Huang FC, Huang IF, Ni YH, Hsu HY, Chang MH, Chen HL. Infantile hepatitis B in immunized children: risk for fulminant hepatitis and long-term outcomes. *PLoS One* 2014; **9**: e111825 [PMID: 25380075 DOI: 10.1371/journal.pone.0111825]

7 **McMahon BJ**. The natural history of chronic hepatitis B virus infection. *Hepatology* 2009; **49**: S45-S55 [PMID: 19399792 DOI: 10.1002/hep.22898]

8 **Nguyen VT**, Law MG, Dore GJ. Hepatitis B-related hepatocellular carcinoma: epidemiological characteristics and disease burden. *J Viral Hepat* 2009; **16**: 453-463 [PMID: 19302335 DOI: 10.1111/j.1365-2893.2009.01117.x]

9 **Sun YH**, Lei XY, Sai YP, Chen JH, Sun YC, Gao X. Relationship between genotypes and clinical manifestation, pathology, and cccDNA in Chinese children with hepatitis B virus-associated glomerulonephritis. *World J Pediatr* 2016; **12**: 347-352 [PMID: 27059747 DOI: 10.1007/s12519-016-0015-0]

10 **Arnone OC**, Serranti D, Bartolini E, Mastrangelo G, Stinco M, Trapani S, Ricci S, Resti M, Indolfi G. Chronic hepatitis B in children, report of a single-centre longitudinal study on 152 children. *J Viral Hepat* 2020; **27**: 1344-1351 [PMID: 32853482 DOI: 10.1111/jvh.13382]

11 **European Association for the Study of the Liver**. EASL 2017 Clinical Practice Guidelines on the management of hepatitis B virus infection. *J Hepatol* 2017; **67**: 370-398 [PMID: 28427875 DOI: 10.1016/j.jhep.2017.03.021]

12 **Allweiss L**, Dandri M. The Role of cccDNA in HBV Maintenance. *Viruses* 2017; **9** [PMID: 28635668 DOI: 10.3390/v9060156]

13 **World Health Organization**. Guidelines for the prevention, care and treatment of persons with chronic hepatitis B infection. 2015 [cited 17 April 2021]. Available from: https://www.who.int/publications/i/item/9789241549059

14 **Indolfi G**, Easterbrook P, Dusheiko G, Siberry G, Chang MH, Thorne C, Bulterys M, Chan PL, El-Sayed MH, Giaquinto C, Jonas MM, Meyers T, Walsh N, Wirth S, Penazzato M. Hepatitis B virus infection in children and adolescents. *Lancet Gastroenterol Hepatol* 2019; **4**: 466-476 [PMID: 30982722 DOI: 10.1016/S2468-1253(19)30042-1]

15 **Jonas MM**, Lok AS, McMahon BJ, Brown RS Jr, Wong JB, Ahmed AT, Farah W, Mouchli MA, Singh S, Prokop LJ, Murad MH, Mohammed K. Antiviral therapy in management of chronic hepatitis B viral infection in children: A systematic review and meta-analysis. *Hepatology* 2016; **63**: 307-318 [PMID: 26566163 DOI: 10.1002/hep.28278]

16 **Sokal EM**, Paganelli M, Wirth S, Socha P, Vajro P, Lacaille F, Kelly D, Mieli-Vergani G; European Society of Pediatric Gastroenterology, Hepatology and Nutrition. Management of chronic hepatitis B in childhood: ESPGHAN clinical practice guidelines: consensus of an expert panel on behalf of the European Society of Pediatric Gastroenterology, Hepatology and Nutrition. *J Hepatol* 2013; **59**: 814-829 [PMID: 23707367 DOI: 10.1016/j.jhep.2013.05.016]

17 **Terrault NA**, Lok ASF, McMahon BJ, Chang KM, Hwang JP, Jonas MM, Brown RS Jr, Bzowej NH, Wong JB. Update on prevention, diagnosis, and treatment of chronic hepatitis B: AASLD 2018 hepatitis B guidance. *Hepatology* 2018; **67**: 1560-1599 [PMID: 29405329 DOI: 10.1002/hep.29800]

18 **Sarin SK**, Kumar M, Lau GK, Abbas Z, Chan HL, Chen CJ, Chen DS, Chen HL, Chen PJ, Chien RN, Dokmeci AK, Gane E, Hou JL, Jafri W, Jia J, Kim JH, Lai CL, Lee HC, Lim SG, Liu CJ, Locarnini S, Al Mahtab M, Mohamed R, Omata M, Park J, Piratvisuth T, Sharma BC, Sollano J, Wang FS, Wei L, Yuen MF, Zheng SS, Kao JH. Asian-Pacific clinical practice guidelines on the management of hepatitis B: a 2015 update. *Hepatol Int* 2016; **10**: 1-98 [PMID: 26563120 DOI: 10.1007/s12072-015-9675-4]

19 **Yeh ML**, Huang JF, Dai CY, Yu ML, Chuang WL. Pharmacokinetics and pharmacodynamics of pegylated interferon for the treatment of hepatitis B. *Expert Opin Drug Metab Toxicol* 2019; **15**: 779-785 [PMID: 31593639 DOI: 10.1080/17425255.2019.1678584]

20 **Sokal EM**, Conjeevaram HS, Roberts EA, Alvarez F, Bern EM, Goyens P, Rosenthal P, Lachaux A, Shelton M, Sarles J, Hoofnagle J. Interferon alfa therapy for chronic hepatitis B in children: a multinational randomized controlled trial. *Gastroenterology* 1998; **114**: 988-995 [PMID: 9558288 DOI: 10.1016/s0016-5085(98)70318-x]

21 **Hu Y**, Ye YZ, Ye LJ, Wang XH, Yu H. Efficacy and safety of interferon alpha-2b versus pegylated interferon alpha-2a monotherapy in children with chronic hepatitis B: a real-life cohort study from Shanghai, China. *World J Pediatr* 2019; **15**: 595-600 [PMID: 31487005 DOI: 10.1007/s12519-019-00303-w]

22 **van Zonneveld M**, Flink HJ, Verhey E, Senturk H, Zeuzem S, Akarca US, Cakaloglu Y, Simon C, So TM, Gerken G, de Man RA, Hansen BE, Schalm SW, Janssen HL; HBV 99-01 Study Group. The safety of pegylated interferon alpha-2b in the treatment of chronic hepatitis B: predictive factors for dose reduction and treatment discontinuation. *Aliment Pharmacol Ther* 2005; **21**: 1163-1171 [PMID: 15854180 DOI: 10.1111/j.1365-2036.2005.02453.x]

23 **Zhao H**, Si CW, Wei L, Wan MB, Ying YK, Hou JL, Niu JQ. [A multicenter, randomized, open-label study of the safety and effectiveness of pegylated interferon alpha 2b and interferon alpha 2b in treating HBeAg positive chronic hepatitis B patients]. *Zhonghua Gan Zang Bing Za Zhi* 2006; **14**: 323-326 [PMID: 16732903]

24 **Wirth S**, Zhang H, Hardikar W, Schwarz KB, Sokal E, Yang W, Fan H, Morozov V, Mao Q, Deng H, Huang Y, Yang L, Frey N, Nasmyth-Miller C, Pavlovic V, Wat C. Efficacy and Safety of Peginterferon Alfa-2a (40KD) in Children With Chronic Hepatitis B: The PEG-B-ACTIVE Study. *Hepatology* 2018; **68**: 1681-1694 [PMID: 29689122 DOI: 10.1002/hep.30050]

25 **Wirth S**, Ribes-Koninckx C, Calzado MA, Bortolotti F, Zancan L, Jara P, Shelton M, Kerkar N, Galoppo M, Pedreira A, Rodriguez-Baez N, Ciocca M, Lachaux A, Lacaille F, Lang T, Kullmer U, Huber WD, Gonzalez T, Pollack H, Alonso E, Broue P, Ramakrishna J, Neigut D, Valle-Segarra AD, Hunter B, Goodman Z, Xu CR, Zheng H, Noviello S, Sniukiene V, Brass C, Albrecht JK. High sustained virologic response rates in children with chronic hepatitis C receiving peginterferon alfa-2b

plus ribavirin. *J Hepatol* 2010; **52**: 501-507 [PMID: 20189674 DOI: 10.1016/j.jhep.2010.01.016]
26 **Indolfi G**, Bailey H, Serranti D, Giaquinto C, Thorne C; PENTAHep Study Group. Treatment and monitoring of children with chronic hepatitis C in the Pre-DAA era: A European survey of 38 paediatric specialists. *J Viral Hepat* 2019; **26**: 961-968 [PMID: 30980773 DOI: 10.1111/jvh.13111]
27 **Indolfi G**, Easterbrook P, Dusheiko G, El-Sayed MH, Jonas MM, Thorne C, Bulterys M, Siberry G, Walsh N, Chang MH, Meyers T, Giaquinto C, Wirth S, Chan PL, Penazzato M. Hepatitis C virus infection in children and adolescents. *Lancet Gastroenterol Hepatol* 2019; **4**: 477-487 [PMID: 30982721 DOI: 10.1016/S2468-1253(19)30046-9]
28 **Indolfi G**, Nebbia G, Cananzi M, Maccabruni A, Zaramella M, D'Antiga L, Grisotto L, Azzari C, Resti M; Italian Study Group for Treatment of Chronic Hepatitis C in Children. Kinetic of Virologic Response to Pegylated Interferon and Ribavirin in Children With Chronic Hepatitis C Predicts the Effect of Treatment. *Pediatr Infect Dis J* 2016; **35**: 1300-1303 [PMID: 27636721 DOI: 10.1097/INF.0000000000001325]
29 **Bortolotti F**, Indolfi G, Zancan L, Giacchino R, Verucchi G, Cammà C, Barbera C, Resti M, Marazzi MG, Guido M. Management of chronic hepatitis C in childhood: the impact of therapy in the clinical practice during the first 2 decades. *Dig Liver Dis* 2011; **43**: 325-329 [PMID: 21111693 DOI: 10.1016/j.dld.2010.10.008]
30 **Serranti D**, Indolfi G, Nebbia G, Cananzi M, D'Antiga L, Ricci S, Stagi S, Azzari C, Resti M; Italian Study Group for Treatment of Chronic Hepatitis C in Children. Transient Hypothyroidism and Autoimmune Thyroiditis in Children With Chronic Hepatitis C Treated With Pegylated-interferon-α -2b and Ribavirin. *Pediatr Infect Dis J* 2018; **37**: 287-291 [PMID: 28953189 DOI: 10.1097/INF.0000000000001791]
31 **Porche D**. Treatment review: lamivudine. *JANAC* 1996; **7**: 51-53
32 **Jonas MM**, Mizerski J, Badia IB, Areias JA, Schwarz KB, Little NR, Greensmith MJ, Gardner SD, Bell MS, Sokal EM; International Pediatric Lamivudine Investigator Group. Clinical trial of lamivudine in children with chronic hepatitis B. *N Engl J Med* 2002; **346**: 1706-1713 [PMID: 12037150 DOI: 10.1056/NEJMoa012452]
33 **Figlerowicz M**, Kowala-Piaskowska A, Filipowicz M, Bujnowska A, Mozer-Lisewska I, Służewski W. Efficacy of lamivudine in the treatment of children with chronic hepatitis B. *Hepatol Res* 2005; **31**: 217-222 [PMID: 15799860 DOI: 10.1016/j.hepres.2005.02.003]
34 **Luo A**, Jiang X, Ren H. Lamivudine therapy for chronic hepatitis B in children: a meta-analysis. *Virol J* 2019; **16**: 88 [PMID: 31272463 DOI: 10.1186/s12985-019-1193-x]
35 **Jonas MM**, Little NR, Gardner SD; International Pediatric Lamivudine Investigator Group. Long-term lamivudine treatment of children with chronic hepatitis B: durability of therapeutic responses and safety. *J Viral Hepat* 2008; **15**: 20-27 [PMID: 18088241 DOI: 10.1111/j.1365-2893.2007.00891.x]
36 **Robinson DM**, Scott LJ, Plosker GL. Entecavir: a review of its use in chronic hepatitis B. *Drugs* 2006; **66**: 1605-22; discussion 1623 [PMID: 16956310 DOI: 10.2165/00003495-200666120-00009]
37 **Jonas MM**, Chang MH, Sokal E, Schwarz KB, Kelly D, Kim KM, Ling SC, Rosenthal P, Oraseanu D, Reynolds L, Thiry A, Ackerman P. Randomized, controlled trial of entecavir versus placebo in children with hepatitis B envelope antigen-positive chronic hepatitis B. *Hepatology* 2016; **63**: 377-387 [PMID: 26223345 DOI: 10.1002/hep.28015]
38 **Lee KJ**, Choe BH, Choe JY, Kim JY, Jeong IS, Kim JW, Yang HR, Chang JY, Kim KM, Moon JS, Ko JS. A Multicenter Study of the Antiviral Efficacy of Entecavir Monotherapy Compared to Lamivudine Monotherapy in Children with Nucleos(t)ide-naïve Chronic Hepatitis B. *J Korean Med Sci* 2018; **33**: e63 [PMID: 29441755 DOI: 10.3346/jkms.2018.33.e63]
39 **Hadziyannis SJ**, Papatheodoridis GV. Adefovir dipivoxil in the treatment of chronic hepatitis B virus infection. *Expert Rev Anti Infect Ther* 2004; **2**: 475-483 [PMID: 15482214 DOI: 10.1586/14787210.2.4.475]
40 **Jonas MM**, Kelly D, Pollack H, Mizerski J, Sorbel J, Frederick D, Mondou E, Rousseau F, Sokal E. Safety, efficacy, and pharmacokinetics of adefovir dipivoxil in children and adolescents (age 2 to <18 years) with chronic hepatitis B. *Hepatology* 2008; **47**: 1863-1871 [PMID: 18433023 DOI: 10.1002/hep.22250]
41 **Jonas MM**, Kelly D, Pollack H, Mizerski J, Sorbel J, Frederick D, Mondou E, Rousseau F, Sokal E. Efficacy and safety of long-term adefovir dipivoxil therapy in children with chronic hepatitis B infection. *Pediatr Infect Dis J* 2012; **31**: 578-582 [PMID: 22466329 DOI: 10.1097/INF.0b013e318255ffe7]
42 **Grim SA**, Romanelli F. Tenofovir disoproxil fumarate. *Ann Pharmacother* 2003; **37**: 849-859 [PMID: 12773076 DOI: 10.1345/aph.1C388]
43 **Murray KF**, Szenborn L, Wysocki J, Rossi S, Corsa AC, Dinh P, McHutchison J, Pang PS, Luminos LM, Pawlowska M, Mizerski J. Randomized, placebo-controlled trial of tenofovir disoproxil fumarate in adolescents with chronic hepatitis B. *Hepatology* 2012; **56**: 2018-2026 [PMID: 22544804 DOI: 10.1002/hep.25818]
44 **Gaur AH**, Kizito H, Prasitsueubsai W, Rakhmanina N, Rassool M, Chakraborty R, Batra J, Kosalaraksa P, Luesomboon W, Porter D, Shao Y, Myers M, Ting L, SenGupta D, Quirk E, Rhee MS. Safety, efficacy, and pharmacokinetics of a single-tablet regimen containing elvitegravir, cobicistat, emtricitabine, and tenofovir alafenamide in treatment-naive, HIV-infected adolescents: a single-arm, open-label trial. *Lancet HIV* 2016; **3**: e561-e568 [PMID: 27765666 DOI: 10.1016/S2352-3018(16)30121-7]

45 **Lockman S**, Brummel SS, Ziemba L, Stranix-Chibanda L, McCarthy K, Coletti A, Jean-Philippe P, Johnston B, Krotje C, Fairlie L, Hoffman RM, Sax PE, Moyo S, Chakhtoura N, Stringer JS, Masheto G, Korutaro V, Cassim H, Mmbaga BT, João E, Hanley S, Purdue L, Holmes LB, Momper JD, Shapiro RL, Thoofer NK, Rooney JF, Frenkel LM, Amico KR, Chinula L, Currier J; IMPAACT 2010/VESTED Study Team and Investigators. Efficacy and safety of dolutegravir with emtricitabine and tenofovir alafenamide fumarate or tenofovir disoproxil fumarate, and efavirenz, emtricitabine, and tenofovir disoproxil fumarate HIV antiretroviral therapy regimens started in pregnancy (IMPAACT 2010/VESTED): a multicentre, open-label, randomised, controlled, phase 3 trial. *Lancet* 2021; **397**: 1276-1292 [PMID: 33812487 DOI: 10.1016/S0140-6736(21)00314-7]

46 **Gane EJ**. Future anti-HBV strategies. *Liver Int* 2017; **37** Suppl 1: 40-44 [PMID: 28052637 DOI: 10.1111/liv.13304]

47 **Testoni B**, Durantel D, Zoulim F. Novel targets for hepatitis B virus therapy. *Liver Int* 2017; **37** Suppl 1: 33-39 [PMID: 28052622 DOI: 10.1111/liv.13307]

48 **Lin CL**, Yang HC, Kao JH. Hepatitis B virus: new therapeutic perspectives. *Liver Int* 2016; **36** Suppl 1: 85-92 [PMID: 26725903 DOI: 10.1111/liv.13003]

49 **Soriano V**, Barreiro P, Benitez L, Peña JM, de Mendoza C. New antivirals for the treatment of chronic hepatitis B. *Expert Opin Investig Drugs* 2017; **26**: 843-851 [PMID: 28521532 DOI: 10.1080/13543784.2017.1333105]

World Journal of Gastroenterology

Submit a Manuscript: https://www.f6publishing.com

World J Gastroenterol 2021 September 28; 27(36): 6064-6078

DOI: 10.3748/wjg.v27.i36.6064

ISSN 1007-9327 (print) ISSN 2219-2840 (online)

ORIGINAL ARTICLE

Basic Study

CircRNA_0084927 promotes colorectal cancer progression by regulating miRNA-20b-3p/glutathione S-transferase mu 5 axis

Feng Liu, Xiao-Li Xiao, Yu-Jing Liu, Ruo-Hui Xu, Wen-Jun Zhou, Han-Chen Xu, Ai-Guang Zhao, Yang-Xian Xu, Yan-Qi Dang, Guang Ji

ORCID number: Feng Liu 0000-0001-9370-7512; Xiao-Li Xiao 0000-0002-4053-0802; Yu-Jing Liu 0000-0002-9879-4413; Ruo-Hui Xu 0000-0003-1621-2326; Wen-Jun Zhou 0000-0003-4167-0337; Han-Chen Xu 0000-0003-2335-5421; Ai-Guang Zhao 0000-0002-8185-6171; Yang-Xian Xu 0000-0001-8738-3291; Yan-Qi Dang 0000-0001-8651-6937; Guang Ji 0000-0003-0842-3676.

Author contributions: Liu F and Xiao XL contributed equally to this work. Ji G and Dang YQ should be regarded as co-corresponding authors; Ji G and Dang YQ conceived, designed, and supervised the study; Dang YQ, Xu YX, and Xu HC collected the samples; Liu F, Xiao XL, Liu YJ, and Xu RH performed the experiments; Dang YQ, Liu F, and Zhou WJ analyzed the data; Dang YQ and Liu F wrote the paper; Zhou WJ, Zhao AG, and Ji G revised the manuscript; all authors reviewed and approved the final manuscript.

Supported by the National Natural Science Foundation of China, No. 81804018 and No. 81874206; and the Key Project of the Shanghai 3-Year Plan, No. ZY[2018-2020]CCCX-2002-01.

Institutional review board

Feng Liu, Xiao-Li Xiao, Yu-Jing Liu, Ruo-Hui Xu, Wen-Jun Zhou, Han-Chen Xu, Yan-Qi Dang, Guang Ji, Institute of Digestive Diseases, Longhua Hospital, China-Canada Center of Research for Digestive Diseases (ccCRDD), Shanghai University of Traditional Chinese Medicine, Shanghai 200032, China

Feng Liu, Ai-Guang Zhao, Department of Oncology, Longhua Hospital, Shanghai University of Traditional Chinese Medicine, Shanghai 200032, China

Yang-Xian Xu, Department of General Surgery, Longhua Hospital, Shanghai University of Traditional Chinese Medicine, Shanghai 200032, China

Corresponding author: Guang Ji, MD, PhD, Professor, Institute of Digestive Diseases, Longhua Hospital, China-Canada Center of Research for Digestive Diseases (ccCRDD), Shanghai University of Traditional Chinese Medicine, No. 725 South Wanping Road, Shanghai 200032, China. jiliver@vip.sina.com

Abstract

BACKGROUND

Colorectal cancer (CRC) is the third most common cancer and the second most common cause of cancer-related death worldwide. The 5-year survival rate of patients with early-stage CRC could reach 90%, but it is very low in patients with advanced-stage CRC. Recent studies have shown that circular RNAs play important roles in regulating the migration and invasion of CRC cells.

AIM

To elucidate the role of circRNA_0084927 (circ_0084927) in the migration and invasion of CRC cells and its underlying mechanism.

METHODS

Clinical tissue samples and cells were collected, and the expression of circ_0084927 was detected by quantitative polymerase chain reaction (qPCR). The diagnostic performance of circ_0084927 was assessed by receiver operating characteristic curve analysis. The role of circ_0084927 in CRC cell proliferation, migration, and invasion was determined using cell counting kit-8 assay, wound healing assay, and transwell assay, respectively. The regulatory relationship among circ_0084927, miRNA-20b-3p (miR-20b-3p), and glutathione S-transferase mu 5 (GSTM5) was identified using databases, luciferase reporter assay, qPCR,

statement: The study was reviewed and approved by the Medical Ethics Committee of Longhua Hospital Affiliated to Shanghai University of Traditional Chinese Medicine (No. 2019LCSY020).

Conflict-of-interest statement: The authors have no conflicts of interest to declare.

Data sharing statement: The original data of this study will be available upon request from corresponding author.

Open-Access: This article is an open-access article that was selected by an in-house editor and fully peer-reviewed by external reviewers. It is distributed in accordance with the Creative Commons Attribution NonCommercial (CC BY-NC 4.0) license, which permits others to distribute, remix, adapt, build upon this work non-commercially, and license their derivative works on different terms, provided the original work is properly cited and the use is non-commercial. See: http://creativecommons.org/Licenses/by-nc/4.0/

Manuscript source: Unsolicited manuscript

Specialty type: Oncology

Country/Territory of origin: China

Peer-review report's scientific quality classification

Grade A (Excellent): 0
Grade B (Very good): B
Grade C (Good): 0
Grade D (Fair): 0
Grade E (Poor): 0

Received: March 3, 2021
Peer-review started: March 3, 2021
First decision: June 3, 2021
Revised: June 4, 2021
Accepted: August 9, 2021
Article in press: August 9, 2021
Published online: September 28, 2021

P-Reviewer: Lomperta K
S-Editor: Wu YXJ
L-Editor: Wang TQ

and Western blot analysis. AKT-mTOR signaling was also verified after circ_0084927 knockdown or miR-20b-3p mimic treatment.

RESULTS

The expression of circ_0084927 was significantly increased in CRC tissues and cells, and it was higher in advanced-stage CRC compared with early-stage CRC. The area under the curve (AUC) of circ_0084927 was 0.806 [95% confidence interval (CI): 0.683-0.896]. In addition, the AUC was 0.874 (95%CI: 0.738-0.956) in patients with advanced-stage CRC and 0.713 (95%CI: 0.555-0.840) in those with early-stage CRC. Knockdown of circ_0084927 inhibited the migration and invasion of HCT116 cells. Moreover, circ_0084927 was found to act as a sponge of miR-20b-3p. MiR-20b-3p activation reduced the circ_0084927 level, whereas miR-20b-3p inhibition increased the circ_0084927 level. But the effect was not found after circ_0084927 mutation. In addition, miR-20b-3p expression in CRC patients was also reduced and negatively correlated with circ_0084927 expression. The function of circ_0084927 in HCT116 cells with circ_0084927 knockdown was rescued by miR-20b-3p. Moreover, GSTM5 expression was significantly decreased after overexpressing miR-20b-3p or inhibiting circ_0084927, but its expression was rescued when circ_0084927 and miR-20b-3p were both inhibited. Finally, AKT-mTOR signaling was markedly regulated by circ_0084927 and miR-20b-3p.

CONCLUSION

The expression of circ_0084927 is significantly increased in CRC and higher in advanced-stage CRC than in early-stage CRC. Moreover, circ_0084927 potentially regulates CRC cell migration and invasion *via* the miR-20b-3p/GSTM5/AKT/mTOR pathway.

Key Words: Colorectal cancer; CircRNA_0084927; MiRNA-20b-3p; Glutathione S-transferase mu 5; Migration; Invasion

©The Author(s) 2021. Published by Baishideng Publishing Group Inc. All rights reserved.

Core Tip: The 5-year survival rate of patients with early-stage colorectal cancer (CRC) could reach 90%, but it is very low in patients with advanced-stage CRC. Recent studies have shown that circular RNAs play important roles in regulating the migration and invasion of CRC cells. To elucidate the role of circRNA_0084927 (circ_0084927) in the migration and invasion of CRC cells and the underlying mechanism, this study was performed. The expression of circ_0084927 was significantly increased in CRC tissues and cells, and it was markedly higher in advanced-stage CRC compared with early-stage CRC. Knockdown of circ_0084927 inhibited the migration and invasion of HCT116 cells. Moreover, circ_0084927 potentially regulates CRC migration and invasion *via* the miRNA-20b-3p/glutathione S-transferase mu 5 pathway.

Citation: Liu F, Xiao XL, Liu YJ, Xu RH, Zhou WJ, Xu HC, Zhao AG, Xu YX, Dang YQ, Ji G. CircRNA_0084927 promotes colorectal cancer progression by regulating miRNA-20b-3p/glutathione S-transferase mu 5 axis. *World J Gastroenterol* 2021; 27(36): 6064-6078
URL: https://www.wjgnet.com/1007-9327/full/v27/i36/6064.htm
DOI: https://dx.doi.org/10.3748/wjg.v27.i36.6064

INTRODUCTION

Colorectal cancer (CRC) is the third most common cancer and the second most common cause of cancer-related death worldwide, and the numbers of new cases and deaths in 2018 were 1.8 million and 881000, respectively[1]. With the development of diagnostic and therapeutic technologies, the 5-year survival rate for CRC patients has reached 65%[2] and can reach 90% in early-stage CRC patients. However, the 5-year survival rate of patients with advanced-stage CRC is very low due to tumor metastasis and other complications. Although colonoscopy is the gold standard of CRC screening, approximately 60% of CRC patients are diagnosed at an advanced stage

P-Editor: Liu JH

given the rate of missed lesions and incomplete colonoscopy coverage[3-5]. Therefore, it is urgent to elucidate the pathogenesis and molecular mechanism of CRC with metastasis.

Circular RNAs (circRNAs), as important regulatory noncoding RNAs, have become a new research hotspot following microRNAs (miRNAs) and long noncoding RNAs. Researchers have demonstrated that circRNAs play important roles in tumors, including CRC[6-9], and their functions are completed in a variety of ways, such as acting as sponges of miRNAs[6,7], acting as transcriptional regulators[10,11], and translating proteins by combining with RNA binding proteins[12-15]. However, to date, the functions of circRNAs in CRC remain largely unknown, especially in CRC with metastasis. Further study to elucidate the function of circRNAs in CRC with metastasis is needed.

In this study, we first verified the differential expression of circRNA_0084927 (circ_0084927) according to previous circRNA sequencing data[16] and further found that circ_0084927 was associated with the pathological stage of CRC. Then, we demonstrated that knockdown of circ_0084927 markedly inhibited HCT116 cell migration and invasion. Regarding the regulatory mechanism of circ_0084927, it acts as a sponge of miRNA-20b-3p (miR-20b-3p), regulating glutathione S-transferase mu 5 (GSTM5) and the AKT-mTOR pathway. Therefore, our findings elucidated the role of circ_0084927 and provided a new treatment strategy for CRC with metastasis.

MATERIALS AND METHODS

Clinical tissue specimens

Thirty pairs of CRC tissues and adjacent normal tissues (normal) were obtained during surgery at the Longhua Hospital Affiliated to Shanghai University of Traditional Chinese Medicine (Shanghai, China). The diagnosis of CRC was confirmed based on pathological evidence. Tissues were snap-frozen in liquid nitrogen and stored at -80 °C before detection. The study was approved by the Ethics Committee of Longhua Hospital (No. 2019LCSY020), and informed consent was obtained from all participants.

Cell culture and transfection

Normal colon cells (FHC) and CRC cells (HCT116, HT29, SW480, and SW620) (Shanghai Cell Bank, shanghai, China) were cultured in Dulbecco's modified Eagle's medium supplemented with 10% fetal bovine serum and penicillin/streptomycin (100 U/mL) (Gibco, Carlsbad, United States) in an incubator with 5% CO_2 at 37 °C. In addition, human embryonic kidney 293T (HEK-293T) cells obtained from American Type Culture Collection (ATCC) (Manassas, United States) were cultured in Roswell Park Memorial Institute 1640 medium with 10% fetal bovine serum and penicillin/streptomycin (100 U/mL). Short hairpin circ_0084927 plasmid (sh-circ_0084927; GeneChem, China) and miR-20b-3p mimic/inhibitor or negative control (NC, Genomeditech, China; 200 nM) were transfected using FuGene HD transfection reagent (Promega, United States) according to previous studies[17,18].

Cell counting kit-8 assay

After transfection, HCT116 cells were seeded into 96-well plates at a concentration of 1 × 10^4 cells and cultured for 0 h, 24 h, 48 h, and 72 h. Then, 10 μL of cell counting kit-8 reagent was added to each well. After incubation at 37 °C for 1 h, the absorbance value was detected at 450 nm.

Wound healing assay

After transfection, HCT116 cells were seeded in a 6-well dish with a culture insert (Ibidi, Germany) at a concentration of 3 × 10^4 cells. After 24 h, the culture insert was removed, and the cells were washed twice with polybutylene succinate. Two milliliters of serum-free medium were added to each dish for 48 h. Images were captured, and the wound area was measured using Image J software (National Institutes of Health, United States).

Cell migration invasion assay

Six-well plates with 8-μm chambers (Corning, United States) were used to assess cellular migration (without Matrigel) or invasion (with Matrigel). Briefly, transfected HCT116 cells were seeded in 6-well plates at a concentration of 1 × 10^5 cells. Two

hundred microliters of serum-free medium was added to the upper chamber, and six hundred microliters of medium with 30% fetal bovine serum was added to the lower chamber for 48 h. Then, the cells were fixed with 4% paraformaldehyde for 30 min and stained with 0.1% crystal violet solution for 15 min. Four fields were randomly selected to calculate the number of migrating or invading cells and to evaluate the ability of cell migration or invasion.

Quantitative polymerase chain reaction

Total RNA was extracted using TRIzol reagent (Ambion, United States). For circRNA and mRNA analysis, cDNA was synthesized using an EVM-MLV reverse transcription kit (Aikeri Biotech, Hunan, China). For miRNA analysis, cDNA was synthesized using a miRNA cDNA synthesis kit (Sangon Biotech, Shanghai, China). The amplification reaction was performed using the SYBR-Green quantitative polymerase chain reaction (qPCR) kit (Thermo Fisher Scientific, MA, United States) or the miRNA fluorescence quantitative PCR kit (Sangon Biotech). Gene expression was normalized using β-actin or U6. The primers are listed in Table 1.

Western blot analysis

Cells were collected and lysed. Protein concentration was determined using a protein assay kit (Beyotime, China). The protein was separated and transferred to a polyvinylidene fluoride membrane followed by incubation with 5% milk at room temperature for 1 h. The membrane was incubated at 4 °C overnight with the following antibodies: GSTM5 (GTX108776, Genetex, United States), PI3 kinase p85 (PI3K, 4292S, CST, United States), phospho-PI3K (BS-3332R, Bioss, China), Akt (4685S, CST), phospho-Akt (4060S, CST), mTOR (2983S, CST), phospho-mTOR (5536S, CST), and β-actin (4970s, CST). Then, the secondary antibody was added and incubated at room temperature for 2 h, and protein expression was observed using a chemiluminescence gel imaging system (Tanon 5200, China).

Double luciferase reporter assay

HEK-293T cells were seeded in 24-well plates and transfected using FuGene HD transfection reagent (Promega, United States) according to previous studies[17,18]. Briefly, HEK-293T cells were transfected using circ_0084927 wild type (circ_0084927-WT; Genomeditech, China) or circ_0084927 mutant (circ_0084927-Mut; Genomeditech) plasmid with or without miR-20b-3p mimic/inhibitor. After transfection for 22 h, luciferase activity was detected using the dual-luciferase reporter system (Promega).

Statistical analysis

Statistical analyses were conducted using SPSS 24.0 software. Data were assessed using Student's *t*-test or one-way ANOVA. Pearson correlation was used to analyze the correlation between circRNA and miRNA. Receiver operating characteristic (ROC) curve analysis was performed to evaluate the diagnostic value using MedCalc software. $P < 0.05$ was considered statistically significant. Dr. Ming Yang from the Good Clinical Practice Office, Longhua Hospital, Shanghai University of Traditional Chinese Medicine reviewed the statistical methods of this study before submission.

RESULTS

Circ_0084927 is markedly increased in CRC and associated with the pathological stage of CRC

Our previous study has proved that circRNAs play important roles in the transition of adenoma into CRC[16], but the function of circRNAs in advanced-stage CRC remains largely undetermined. According to previous circRNA sequencing data[16], five differentially expressed circRNAs were chosen and verified. The results showed that circ_0084927 expression was significantly increased in the CRC group compared with the normal group and was higher in advanced-stage CRC compared with early-stage CRC (Figure 1A and B). The other four circRNAs were not significantly different (Supplementary Figure 1). In addition, circ_0084927 expression in CRC cells (HCT116, HT29, and SW620) was also increased (Figure 1C). ROC curve analysis was used to evaluate the diagnostic performance of circ_0084927 in CRC. The area under the curve (AUC) of circ_0084927 was 0.806 (95%CI: 0.683 to 0.896) ($P < 0.001$). In addition, the AUC was 0.874 (95%CI: 0.738-0.956) in patients with advanced-stage CRC and 0.713 (95%CI: 0.555-0.840) in those with early-stage CRC, indicating that circ_0084927 had

Table 1 Sequence of primers used in the study

Gene name	Forward (5'→3')	Reverse (5'→3')
β-actin	GGCTGTATTCCCCTCCATCG	CCAGTTGGTAACAATGCCATGT
circRNA_0084927	AGCACTACAGAGGCACAAACATC	GTGCCCTGACTACGGTGTTATC
circRNA_0138996	CTGATCCCAATGGATTGCATC	GTCCTCCCGTTCCTCTTCG
circRNA_0110477	CGAATCAAAGCAGCCTATCAAG	TGCCACATAGAATTTGGGTGTC
circRNA_0133544	CATGAGGTTAGGCAGTTGTATCG	TGTTTTTAGCCTTTTCTCCATCTC
circRNA_0002867	AACCAGAGCACATTAGCCAAAG	CAAACTCGGCGTGTTCTTCTC
GSTM5	GAAGATGGGAGGGAGGAG	CCTTGGGGAAGAGAAGAGA
U6	AGAGAAGATTAGCATGGCCCCTG	ATCCAGTGCAGGGTCCGAGG
miRNA-20b-3p	ACTGTAGTATGGGCACTTCCAG	ATCCAGTGCAGGGTCCGAGG

GSTM5: Glutathione S-transferase mu 5; U6: U6 small nuclear RNA 1.

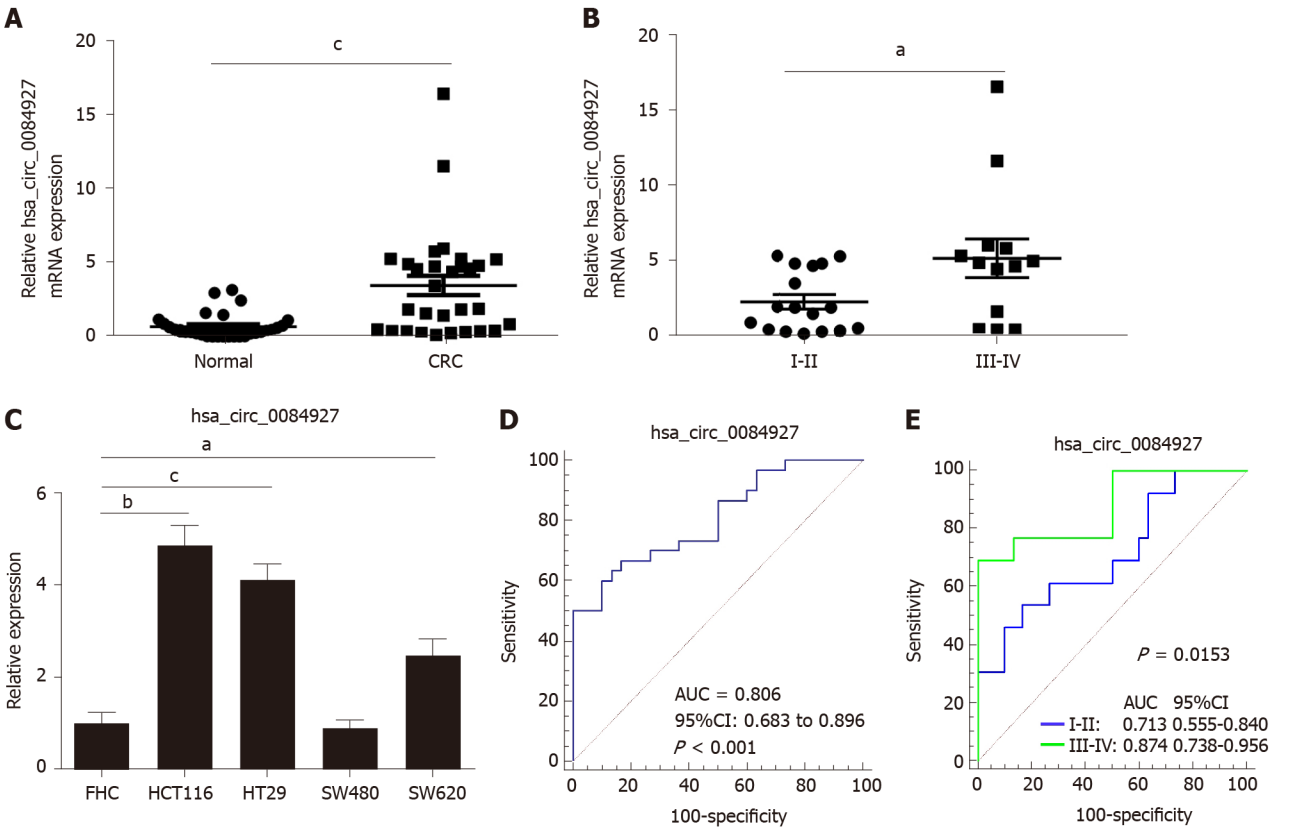


Figure 1 CircRNA_0084927 expression is markedly increased in colorectal cancer. A: Expression of circRNA_0084927 (circ_0084927) in colorectal cancer (CRC); B: Expression of circ_0084927 in advanced-stage and early-stage CRC; C: Expression of circ_0084927 in CRC cells; D: Receiver operating characteristic (ROC) curve analysis of circ_0084927; E: ROC analysis of circ_0084927 in advanced-stage and early-stage CRC. Data are presented as the mean ± SEM. $^{a}P < 0.05$; $^{b}P < 0.01$; $^{c}P < 0.001$. Circ_0084927: CircRNA_0084927; Normal: Adjacent normal tissues; CRC: Colorectal cancer; ROC: Receiver operating characteristic; AUC: Area under the curve.

higher diagnostic performance in advanced-stage CRC ($P = 0.0153$) (Figure 1D and E).

Knockdown of circ_0084927 inhibits HCT116 cell migration and invasion

To explore the function of circ_0084927 in CRC, circ_0084927 expression was inhibited in HCT116 cells using shRNA plasma (Figure 2A), and circ_0084927 knockdown markedly inhibited HCT116 cell proliferation at 48 h and 72 h (Figure 2B). In addition, circ_0084927 knockdown also significantly inhibited HCT116 cell migration and invasion (Figure 2C-G). These results demonstrated that circ_0084927 is an oncogene

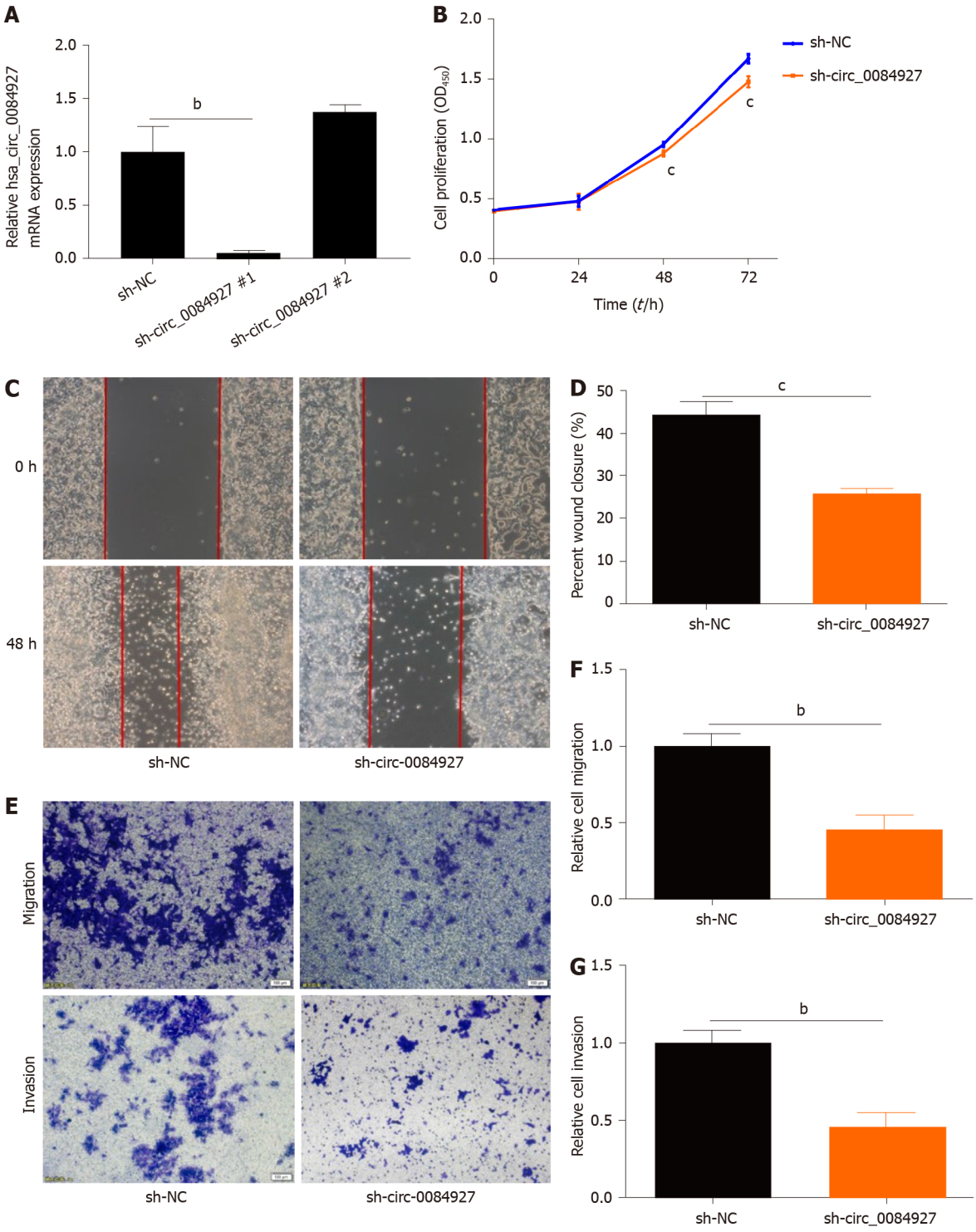


Figure 2 Knockdown of circRNA_0084927 inhibits the migration and invasion of HCT116 cells. A: Knockdown of circRNA_0084927 (circ_0084927); B: Vability of HCT116 cells after circ_0084927 knockdown; C-G: Migration and invasion of HCT116 cells tested by wound healing assay (C and D) and transwell assay (E-G). Data are presented as the mean ± SEM. $^{b}P < 0.01$; $^{c}P < 0.001$. Circ_0084927: CircRNA_0084927; Sh-circ_0084927: Short hairpin circ_0084927 plasmid; Sh-NC: Short hairpin negative control plasmid.

that promotes CRC function.

Circ_0084927 acts as a sponge of miR-20b-3p in CRC

The biological function of circRNAs mainly involves acting as a sponge of miRNAs [19]. In this study, circ_0084927 may act as a sponge of miR-20b-3p as demonstrated by bioinformatics analysis (Figure 3A). The miR-20b-3p mimic markedly reduced the luciferase activity of circ_0084927, whereas the miR-20b-3p inhibitor markedly increased the luciferase activity of circ_0084927, but had no effect on circ_0084927-Mut (Figure 3B and C). qPCR results also indicated that knockdown of circ_0084927

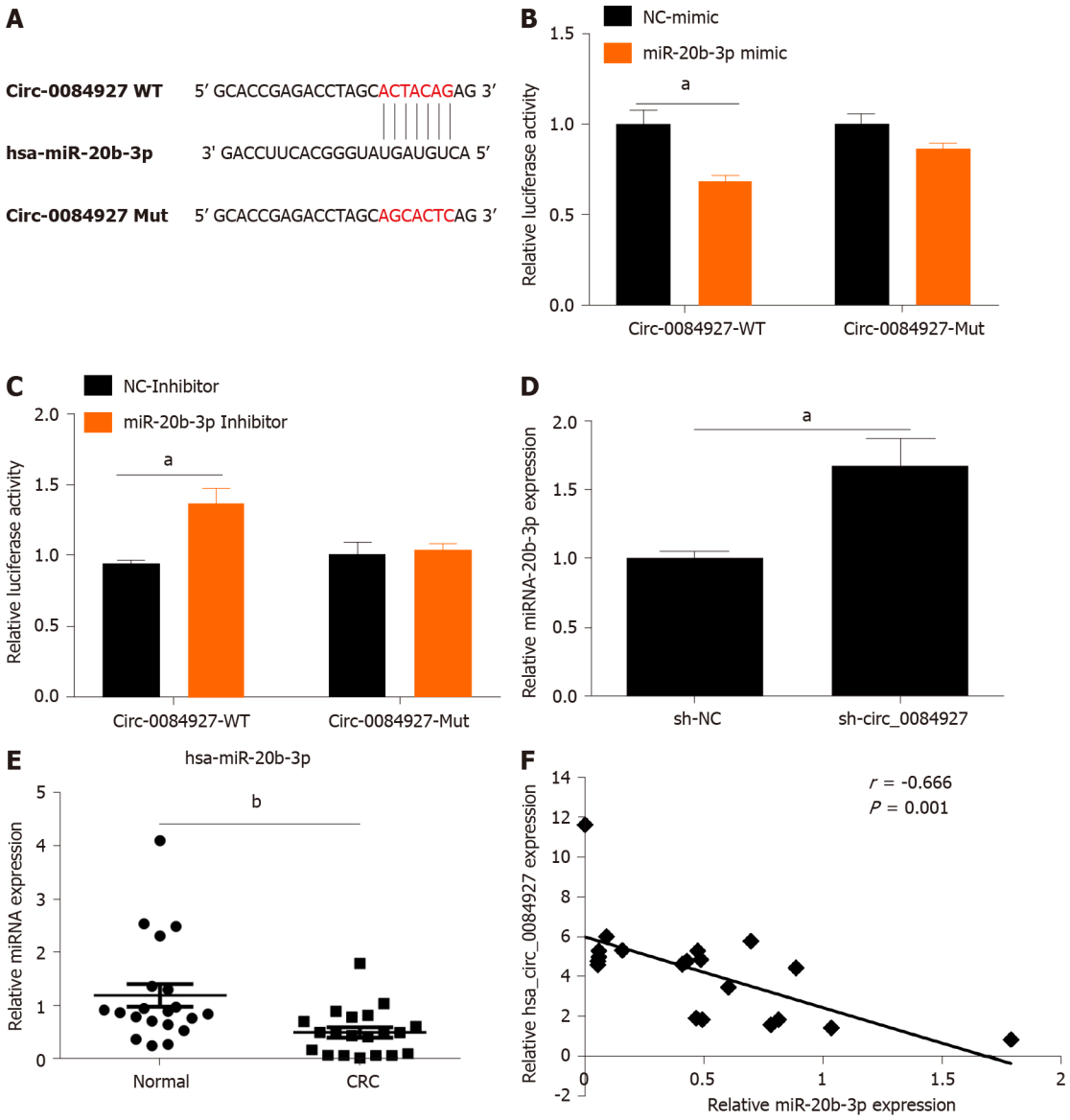


Figure 3 CircRNA_0084927 acts as a sponge of miRNA-20b-3p in colorectal cancer. A: CircRNA_0084927 (Circ_0084927) potentially acts as a sponge of miRNA-20b-3p (miR-20b-3p) in database; B: miR-20b-3p mimic could markedly reduce the luciferase activity of circ_0084927; C: miR-20b-3p inhibitor could markedly increase the luciferase activity of circ_0084927; D: circ_0084927 knockdown markedly increased the level of miR-20b-3p; E: Expression of miR-20b-3p in colorectal cancer (CRC); F: Correlation of circ_0084927 and miR-20b-3p. Data are presented as the mean ± SEM. $^{a}P < 0.05$; $^{b}P < 0.01$. Circ_0084927: CircRNA_0084927; MiR-20b-3p: MiRNA-20b-3p; NC: Negative control; CRC: Colorectal cancer; Normal: Adjacent normal tissues; Circ_0084927-WT: CircRNA_0084927 wild type; Circ_0084927-Mut: CircRNA_0084927 mutant; Sh-circ_0084927: Short hairpin circ_0084927 plasmid; Sh-NC: Short hairpin negative control plasmid.

promoted the expression of miR-20b-3p (Figure 3D). We also tested the expression of miR-20b-3p in CRC tissue samples, and its expression was significantly reduced (Figure 3E). Spearman correlation coefficient analysis revealed that circ_0084927 was negatively correlated with miR-20b-3p (Figure 3F). All of the data suggested that circ_0084927 acts as a sponge of miR-20b-3p.

The function of circ_0084927 in HCT116 cells with circ_0084927 knockdown is rescued by miR-20b-3p

To assess whether the function of circ_0084927 in HCT116 cells is mediated by miR-20b-3p, HCT116 cells with circ_0084927 knockdown was transfected with or without miR-20b-3p inhibitor (Figure 4A). The CCK-8 assay showed that circ_0084927 knockdown inhibited the proliferation of HCT116 cells, while the effect was rescued by the miR-20b-3p inhibitor (Figure 4B). Wound healing and transwell assays showed that circ_0084927 knockdown inhibited the migration and invasion of HCT116 cells, whereas miR-20b-3p inhibition rescued this effect (Figure 4C-G).

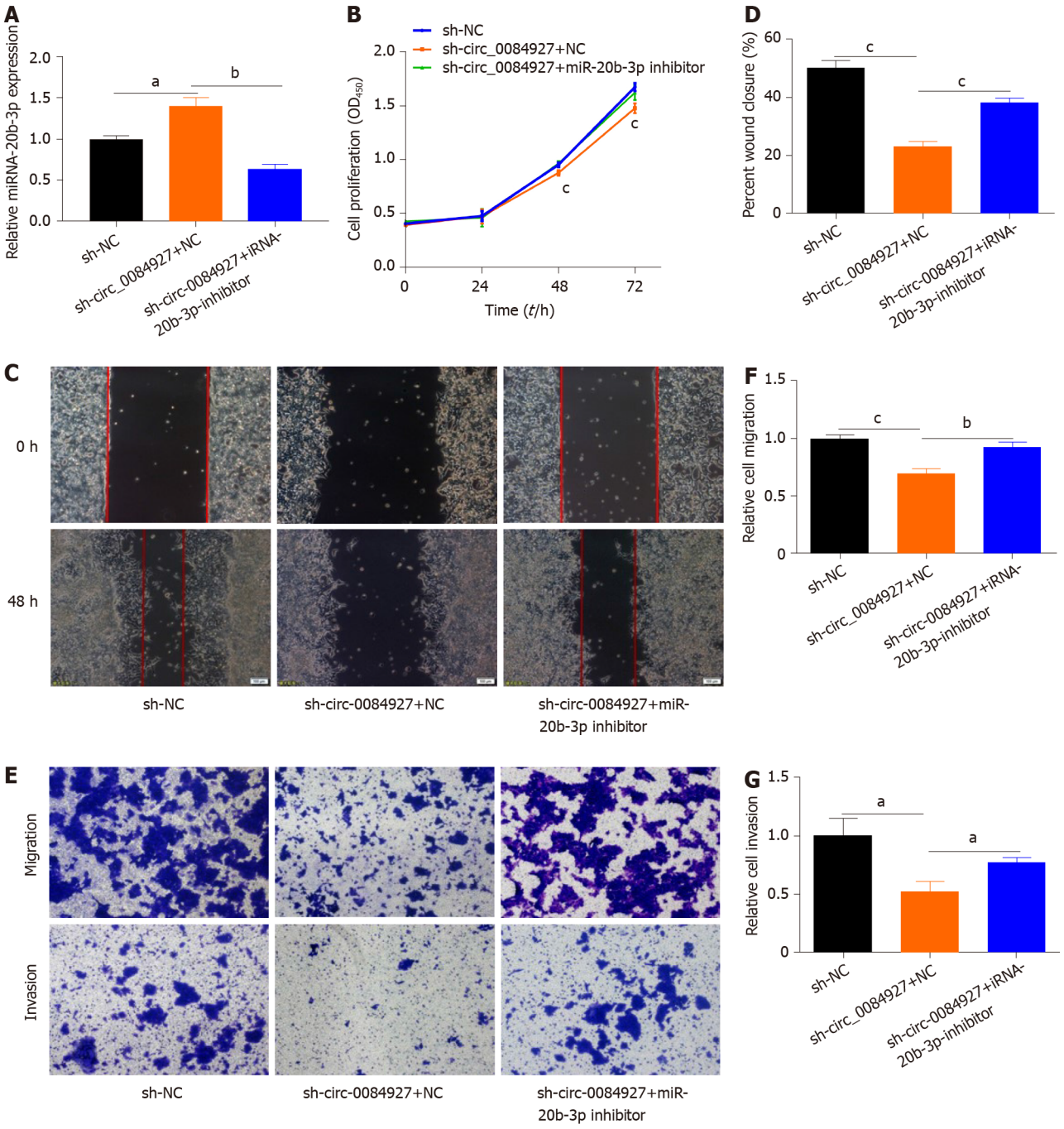


Figure 4 The function of circRNA_0084927 in HCT116 cells with circRNA_0084927 knockdown is rescued by miRNA-20b-3p. A: Expression of miRNA-20b-3p (miR-20b-3p); B: Viability of HCT116 cells detected after transfecting circRNA_0084927 (circ_0084927) or miR-20b-3p inhibitor; C-G: Migration and invasion of HCT116 cells tested by wound healing assay (C and D) and transwell assay (E-G) after transfecting sh-circ_0084927 plasmid or miR-20b-3p inhibitor. Data are presented as the mean ± SEM. $^{a}P < 0.05$; $^{b}P < 0.01$; $^{c}P < 0.001$. Sh-circ_0084927: Short hairpin circ_0084927 plasmid; Sh-NC: Short hairpin negative control plasmid; miR-20b-3p: miRNA-20b-3p.

GSTM5 is a target of miR-20b-3p

According to bioinformatics analysis, we found that GSTM5 is a target of miR-20b-3p. We then assessed GSTM5 expression after overexpressing miR-20b-3p. The results showed that *GSTM5* mRNA expression was significantly reduced after overexpressing miR-20b-3p (Figure 5A). GSTM5 protein level was consistent with its mRNA level (Figure 5B). Moreover, GSTM5 mRNA and protein expression was also markedly reduced after silencing circ_0084927 (Figure 5C and D). After transfecting the miR-20b-3p inhibitor into HCT116 cells with circ_0084927 knockdown, GSTM5 mRNA and protein expression was rescued (Figure 5E and F). The survival curve results using The Cancer Genome Atlas (TCGA) data also showed that patients with high GSTM5 levels had a poor survival, indicating that GSTM5 was negatively correlated with CRC

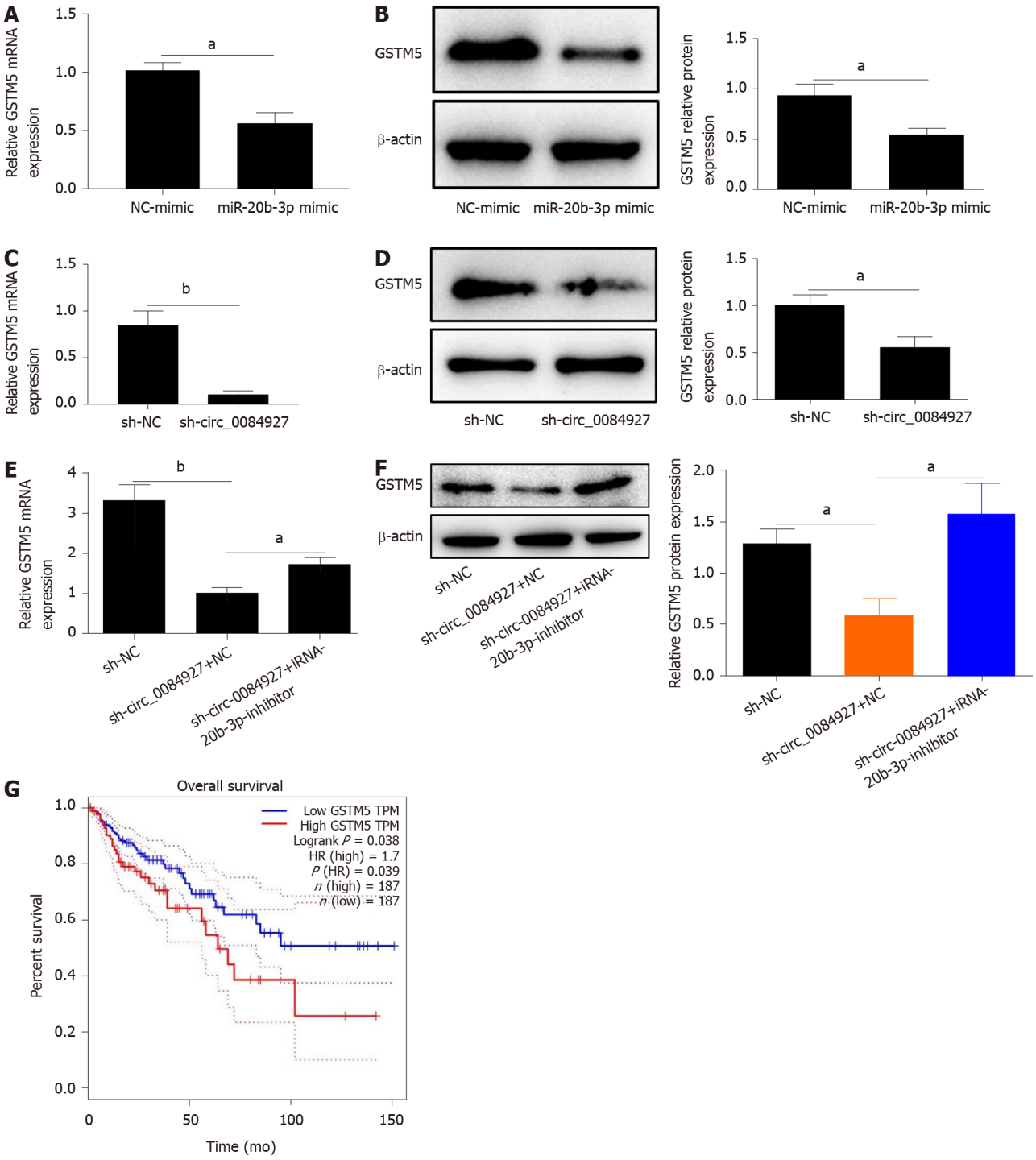
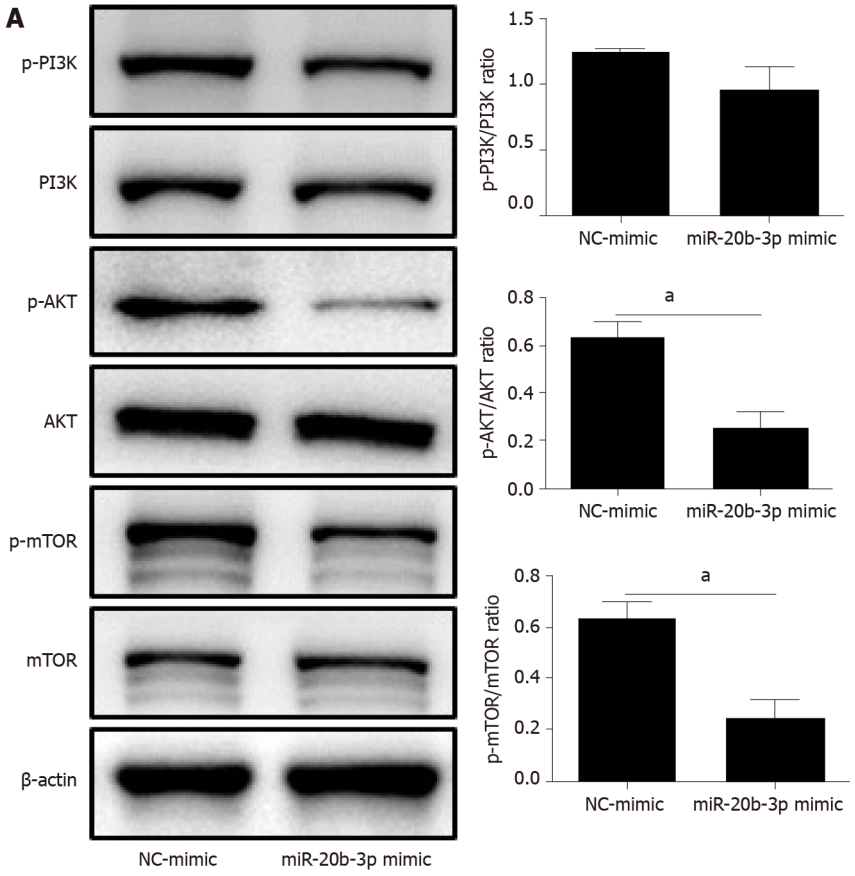


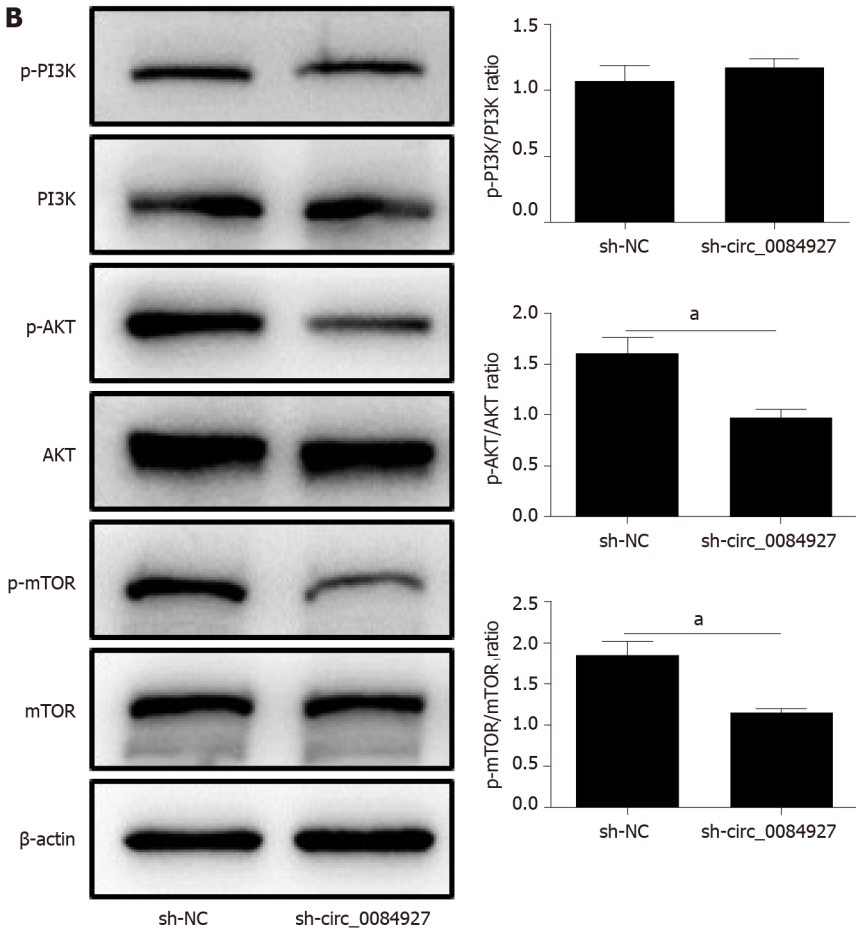
Figure 5 Glutathione S-transferase mu 5 is a target of miRNA-20b-3p. A and B: Expression of glutathione S-transferase mu 5 (GSTM5) after transfecting miRNA-20b-3p (miR-20b-3p) mimic; C and D: Expression of GSTM5 after transfecting circRNA_0084927 (circ_0084927); E and F: Expression of GSTM5 after transfecting sh-circ_0084927 plasmid and miR-20b-3p inhibitor; G: Overall survival by GSTM5 expression. Data are presented as the mean ± SEM. $^{a}P < 0.05$, $^{b}P < 0.01$. NC mimic: Negative control mimic; GSTM5: Glutathione S-transferase mu 5; miR-20b-3p: miRNA-20b-3p; Sh-circ_0084927: Short hairpin circ_0084927 plasmid; Sh-NC: Short hairpin negative control plasmid.

patient survival (Figure 5G).

The AKT-mTOR pathway is inactivated by circ_0084927 knockdown and rescued by miR-20b-3p

Further experiments found that circ_0084927 knockdown or miR-20b-3p overexpression both reduced the phosphorylation levels of AKT and mTOR (Figure 6A and B). In addition, AKT and mTOR phosphorylation levels were rescued after inhibiting miR-20b-3p in HCT116 cells with circ_0084927 knockdown (Figure 6C). These results showed that circ_0084927 regulated CRC migration and invasion *via* the miR-20b-


A
p-PI3K
PI3K
p-AKT
AKT
p-mTOR
mTOR
β-actin
NC-mimic
miR-20b-3p mimic
p-PI3K/PI3K ratio
1.5
1.0
0.5
0.0
NC-mimic
miR-20b-3p mimic
p-AKT/AKT ratio
a
0.8
0.6
0.4
0.2
0.0
NC-mimic
miR-20b-3p mimic
p-mTOR/mTOR ratio
a
0.8
0.6
0.4
0.2
0.0
NC-mimic
miR-20b-3p mimic


B
p-PI3K
PI3K
p-AKT
AKT
p-mTOR
mTOR
β-actin
sh-NC
sh-circ_0084927
p-PI3K/PI3K ratio
1.5
1.0
0.5
0.0
sh-NC
sh-circ_0084927
p-AKT/AKT ratio
a
2.0
1.5
1.0
0.5
0.0
sh-NC
sh-circ_0084927
p-mTOR/mTOR ratio
a
2.5
2.0
1.5
1.0
0.5
0.0
sh-NC
sh-circ_0084927

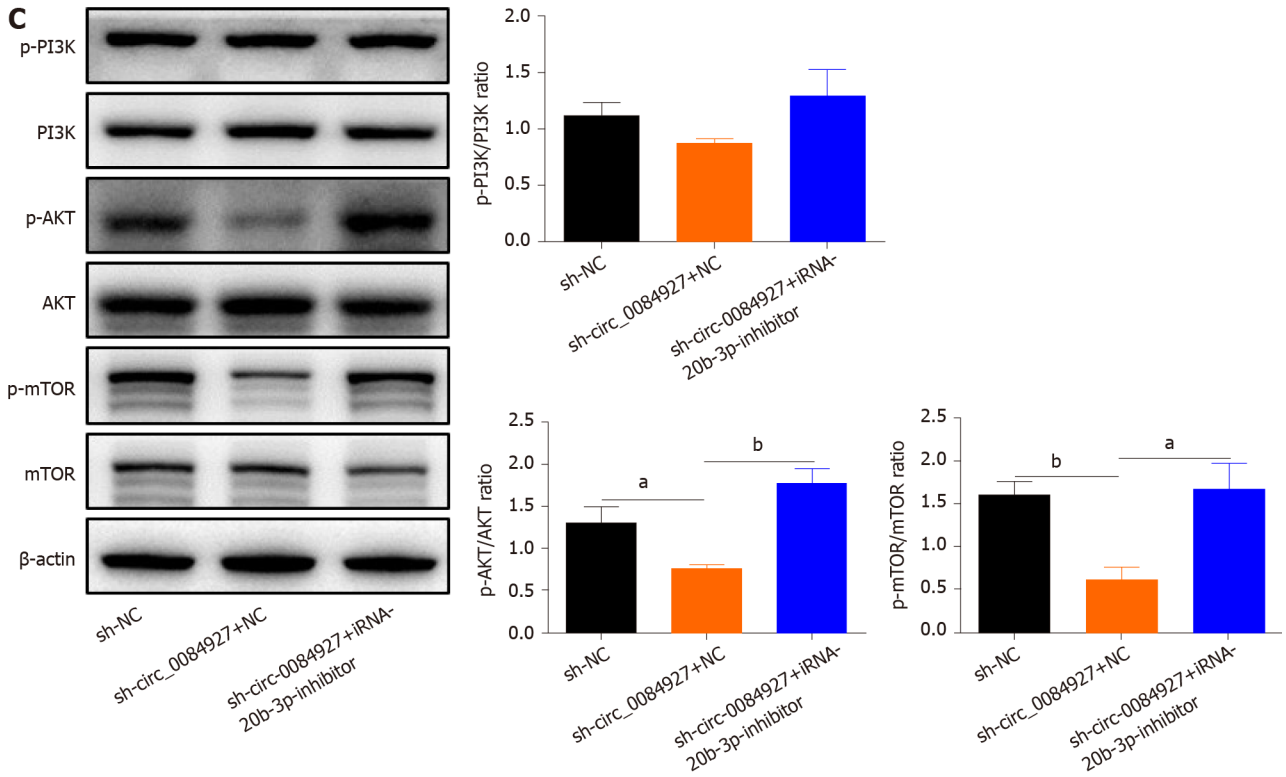


Figure 6 AKT-mTOR pathway is inactivated by circRNA_0084927 knockdown and rescued by miRNA-20b-3p. A: Expression of AKT-mTOR pathway molecules after transfecting miRNA-20b-3p (miR-20b-3p) mimic; B: Expression of AKT-mTOR pathway molecules after transfecting circRNA_0084927 (circ_0084927); C: Expression of AKT-mTOR pathway molecules after transfecting sh-circ_0084927 plasmid and miR-20b-3p inhibitor. Data are presented as the mean ± SEM. $^{a}P < 0.05$; $^{b}P < 0.01$. Sh-circ_0084927: Short hairpin circ_0084927 plasmid; Sh-NC: Short hairpin negative control plasmid; NC mimic: Negative control mimic.

3p/GSTM5/AKT-mTOR pathway.

DISCUSSION

As a malignant tumor, the incidence of CRC has recently increased. Although the 5-year survival rate of CRC patients is 65%[2], it is very low in patients with advanced-stage CRC. Therefore, it is urgent to develop techniques for the early diagnosis of CRC, which would improve patient survival. Moreover, new treatment strategies for advanced-stage CRC are also very important. Studies have indicated that circRNAs are very stable and not easily degraded due to loop properties[20] and have demonstrated the specificity of their expression in particular tissues and tumor developmental stages[20-23]. Therefore, circRNAs, such as serum exosomal hsa-circ-0004771 and circ-PNN[24,25], could act as biomarkers for the diagnosis of CRC. In addition, circRNAs could promote the progression of CRC and act as therapeutic targets[6,8,26,27]. Circ_0084927 originates from epithelial splicing regulatory protein 1 (ESRP1), which is upregulated in CRC (Supplementary Figure 2) and associated with the pathogenesis of CRC[28]. Studies have demonstrated that circ_0084927 facilitates cervical cancer advancement[29-31], but its function in CRC is unclear. In this study, we found that circ_0084927 expression was significantly increased in CRC tissues and cells, and was higher in advanced-stage CRC than in early-stage CRC. Further studies indicated that knockdown of circ_0084927 inhibited the migration and invasion of CRC cells, showing that circ_0084927 played an important role in CRC progression.

CircRNAs perform biological functions by acting as sponges of miRNAs[6,7]. In cervical cancer, miRNAs related to circ_0084927 mainly include miR-142-3p, miR-634, and miR-1179[29-31]. Our study found that circ_0084927 acts as a sponge of miR-20b-3p in CRC. In addition, miR-20b-3p activation reduced circ_0084927 level, whereas miR-20b-3p inhibition increased circ_0084927 level. The expression of circ_0084927 was not altered after the binding site with miR-20b-3p was mutated. In addition, miR-20b-3p expression in CRC patients was also reduced and was negatively correlated with circ_0084927. Studies have shown that miR-20b-3p is related to temozolomide

resistance in glioblastoma[32] and diabetic retinopathy progression[33], but the function of miR-20b-3p in CRC has not been reported. In this study, we demonstrated that miR-20b-3p rescued the effect of circ_0084927 on CRC cells, indicating the role of miR-20b-3p in CRC.

Further studies found that GSTM5 is a target of miR-20b-3p. GSTM5 expression was significantly reduced after overexpressing miR-20b-3p or silencing circ_0084927. However, GSTM5 expression was rescued after silencing circ_0084927 and inhibiting miR-20b-3p. Studies have demonstrated that glutathione S-transferases are pro-carcinogenic in CRC[34]. AS a glutathione S-transferase, GSTM5 is also involved in various tumors, including breast cancer[35,36], prostate cancer[36], ovarian carcinoma [37], and CRC[38,39]. Although previous studies have demonstrated that glutathione metabolism is involved in the progression of tumors[40-42] and GSTM5 could be a prognostic and predictive marker in CRC[38,39], the regulatory mechanism is unknown. In this study, we demonstrated that circ_0084927 regulated the migration and invasion of CRC by the miR-20b-3p/GSTM5 axis and finally regulated the AKT-mTOR pathway, which plays an important role in CRC[43-45]. Therefore, our results revealed that circ_0084927 regulated the progression of CRC *via* the miR-20b-3p/GSTM5/AKT-mTOR pathway.

CONCLUSION

In summary, we have demonstrated that circ_0084927 expression is significantly increased in CRC and is higher in advanced-stage CRC than in early-stage CRC. Mechanistically, circ_0084927 regulates the migration and invasion of CRC cells *via* the miR-20b-3p/GSTM5/AKT-mTOR pathway. This is the first study to demonstrate the role of circ_0084927 in CRC, and these findings provide a new perspective for targeted therapy of CRC with metastasis.

ARTICLE HIGHLIGHTS

Research background

Colorectal cancer (CRC) is the third most common cancer and the second most common cause of cancer-related death worldwide. Recent studies have shown that circular RNAs play important roles in regulating the progression of CRC. However, the biological role and underlying mechanism of circRNA_0084927 (circ_0084927) in CRC remain unclear.

Research motivation

Due to tumor metastasis and other complications, the 5-year survival rate of patients with advanced-stage CRC is very low. We hope to provide a new treatment strategy for CRC with metastasis.

Research objectives

The present study aimed to investigate the role and mechanism of circ_0084927 in regulating the progression of CRC.

Research methods

Clinical tissue samples and cells were collected, and the expression of circ_0084927 was detected by quantitative polymerase chain reaction (qPCR) The diagnostic performance of circ_0084927 was assessed by receiver operating characteristic curve analysis. The role of circ_0084927 in proliferation, migration, and invasion was determined using cell counting kit-8 assay, wound healing assay, and transwell assay, respectively. The regulatory relationship among circ_0084927, miRNA-20b-3p (miR-20b-3p), and glutathione S-transferase mu 5 (GSTM5) was identified using databases, luciferase reporter assays, qPCR, and Western blot analysis. AKT-mTOR signaling was also verified after circ_0084927 knockdown or miR-20b-3p mimic treatment.

Research results

The expression of circ_0084927 was significantly increased in CRC tissues and cells, and was increased in advanced-stage CRC compared with in early-stage CRC. The area under the curve (AUC) of circ_0084927 was 0.806 (95%CI: 0.683 to 0.896). In

addition, the AUC was 0.874 (95%CI: 0.738-0.956) in patients with advanced-stage CRC and 0.713 (95%CI: 0.555-0.840) in those with early-stage CRC. Knockdown of circ_0084927 inhibited the migration and invasion of HCT116 cells. Moreover, circ_0084927 was found to act as a sponge of miR-20b-3p. MiR-20b-3p activation reduced the circ_0084927 level, whereas miR-20b-3p inhibition increased the circ_0084927 level. But the effect was not found after circ_0084927 mutation. In addition, miR-20b-3p expression in CRC patients was also reduced and negatively correlated with circ_0084927 expression. The function of circ_0084927 in HCT116 cells with circ_0084927 knockdown was rescued by miR-20b-3p. Moreover, GSTM5 expression was significantly decreased after overexpressing miR-20b-3p or inhibiting circ_0084927, but its expression was rescued when circ_0084927 and miR-20b-3p were both inhibited. Finally, AKT-mTOR signaling was markedly regulated by circ_0084927 and miR-20b-3p.

Research conclusions

The expression of circ_0084927 is significantly increased in CRC and higher in advanced-stage CRC than in early-stage CRC. Moreover, circ_0084927 potentially regulates CRC migration and invasion *via* the miR-20b-3p/GSTM5/AKT/mTOR pathway.

Research perspectives

Circ_0084927 could promote CRC progression and provide a new treatment strategy for CRC with metastasis.

REFERENCES

1 **Bray F**, Ferlay J, Soerjomataram I, Siegel RL, Torre LA, Jemal A. Global cancer statistics 2018: GLOBOCAN estimates of incidence and mortality worldwide for 36 cancers in 185 countries. *CA Cancer J Clin* 2018; **68**: 394-424 [PMID: 30207593 DOI: 10.3322/caac.21492]

2 **Burgers K**, Moore C, Bednash L. Care of the Colorectal Cancer Survivor. *Am Fam Physician* 2018; **97**: 331-336 [PMID: 29671505]

3 **Zauber AG**, Winawer SJ, O'Brien MJ, Lansdorp-Vogelaar I, van Ballegooijen M, Hankey BF, Shi W, Bond JH, Schapiro M, Panish JF, Stewart ET, Waye JD. Colonoscopic polypectomy and long-term prevention of colorectal-cancer deaths. *N Engl J Med* 2012; **366**: 687-696 [PMID: 22356322 DOI: 10.1056/NEJMoa1100370]

4 **Zhao S**, Wang S, Pan P, Xia T, Chang X, Yang X, Guo L, Meng Q, Yang F, Qian W, Xu Z, Wang Y, Wang Z, Gu L, Wang R, Jia F, Yao J, Li Z, Bai Y. Magnitude, Risk Factors, and Factors Associated With Adenoma Miss Rate of Tandem Colonoscopy: A Systematic Review and Meta-analysis. *Gastroenterology* 2019; **156**: 1661-1674.e11 [PMID: 30738046 DOI: 10.1053/j.gastro.2019.01.260]

5 **Miller KD**, Nogueira L, Mariotto AB, Rowland JH, Yabroff KR, Alfano CM, Jemal A, Kramer JL, Siegel RL. Cancer treatment and survivorship statistics, 2019. *CA Cancer J Clin* 2019; **69**: 363-385 [PMID: 31184787 DOI: 10.3322/caac.21565]

6 **Jian X**, He H, Zhu J, Zhang Q, Zheng Z, Liang X, Chen L, Yang M, Peng K, Zhang Z, Liu T, Ye Y, Jiao H, Wang S, Zhou W, Ding Y, Li T. Hsa_circ_001680 affects the proliferation and migration of CRC and mediates its chemoresistance by regulating BMI1 through miR-340. *Mol Cancer* 2020; **19**: 20 [PMID: 32005118 DOI: 10.1186/s12943-020-1134-8]

7 **Shang A**, Gu C, Wang W, Wang X, Sun J, Zeng B, Chen C, Chang W, Ping Y, Ji P, Wu J, Quan W, Yao Y, Zhou Y, Sun Z, Li D. Exosomal circPACRGL promotes progression of colorectal cancer *via* the miR-142-3p/miR-506-3p- TGF-β1 axis. *Mol Cancer* 2020; **19**: 117 [PMID: 32713345 DOI: 10.1186/s12943-020-01235-0]

8 **Li XN**, Wang ZJ, Ye CX, Zhao BC, Li ZL, Yang Y. RNA sequencing reveals the expression profiles of circRNA and indicates that circDDX17 acts as a tumor suppressor in colorectal cancer. *J Exp Clin Cancer Res* 2018; **37**: 325 [PMID: 30591054 DOI: 10.1186/s13046-018-1006-x]

9 **Yang H**, Li X, Meng Q, Sun H, Wu S, Hu W, Liu G, Yang Y, Chen R. CircPTK2 (hsa_circ_0005273) as a novel therapeutic target for metastatic colorectal cancer. *Mol Cancer* 2020; **19**: 13 [PMID: 31973707 DOI: 10.1186/s12943-020-1139-3]

10 **Ashwal-Fluss R**, Meyer M, Pamudurti NR, Ivanov A, Bartok O, Hanan M, Evantal N, Memczak S, Rajewsky N, Kadener S. circRNA biogenesis competes with pre-mRNA splicing. *Mol Cell* 2014; **56**: 55-66 [PMID: 25242144 DOI: 10.1016/j.molcel.2014.08.019]

11 **Li Z**, Huang C, Bao C, Chen L, Lin M, Wang X, Zhong G, Yu B, Hu W, Dai L, Zhu P, Chang Z, Wu Q, Zhao Y, Jia Y, Xu P, Liu H, Shan G. Exon-intron circular RNAs regulate transcription in the nucleus. *Nat Struct Mol Biol* 2015; **22**: 256-264 [PMID: 25664725 DOI: 10.1038/nsmb.2959]

12 **Shang Q**, Yang Z, Jia R, Ge S. The novel roles of circRNAs in human cancer. *Mol Cancer* 2019; **18**: 6 [PMID: 30626395 DOI: 10.1186/s12943-018-0934-6]

13 **Yang Y**, Gao X, Zhang M, Yan S, Sun C, Xiao F, Huang N, Yang X, Zhao K, Zhou H, Huang S, Xie

B, Zhang N. Novel Role of FBXW7 Circular RNA in Repressing Glioma Tumorigenesis. *J Natl Cancer Inst* 2018; **110** [PMID: 28903484 DOI: 10.1093/jnci/djx166]

14 **Zhang M**, Huang N, Yang X, Luo J, Yan S, Xiao F, Chen W, Gao X, Zhao K, Zhou H, Li Z, Ming L, Xie B, Zhang N. A novel protein encoded by the circular form of the SHPRH gene suppresses glioma tumorigenesis. *Oncogene* 2018; **37**: 1805-1814 [PMID: 29343848 DOI: 10.1038/s41388-017-0019-9]

15 **Wesselhoeft RA**, Kowalski PS, Anderson DG. Engineering circular RNA for potent and stable translation in eukaryotic cells. *Nat Commun* 2018; **9**: 2629 [PMID: 29980667 DOI: 10.1038/s41467-018-05096-6]

16 **Zhu M**, Dang Y, Yang Z, Liu Y, Zhang L, Xu Y, Zhou W, Ji G. Comprehensive RNA Sequencing in Adenoma-Cancer Transition Identified Predictive Biomarkers and Therapeutic Targets of Human CRC. *Mol Ther Nucleic Acids* 2020; **20**: 25-33 [PMID: 32145677 DOI: 10.1016/j.omtn.2020.01.031]

17 **Dang Y**, Hu D, Xu J, Li C, Tang Y, Yang Z, Liu Y, Zhou W, Zhang L, Xu H, Xu Y, Ji G. Comprehensive analysis of 5-hydroxymethylcytosine in zw10 kinetochore protein as a promising biomarker for screening and diagnosis of early colorectal cancer. *Clin Transl Med* 2020; **10**: e125 [PMID: 32628818 DOI: 10.1002/ctm2.125]

18 **Dang Y**, Xu J, Zhu M, Zhou W, Zhang L, Ji G. Gan-Jiang-Ling-Zhu decoction alleviates hepatic steatosis in rats by the miR-138-5p/CPT1B axis. *Biomed Pharmacother* 2020; **127**: 110127 [PMID: 32325349 DOI: 10.1016/j.biopha.2020.110127]

19 **Hansen TB**, Jensen TI, Clausen BH, Bramsen JB, Finsen B, Damgaard CK, Kjems J. Natural RNA circles function as efficient microRNA sponges. *Nature* 2013; **495**: 384-388 [PMID: 23446346 DOI: 10.1038/nature11993]

20 **Memczak S**, Jens M, Elefsinioti A, Torti F, Krueger J, Rybak A, Maier L, Mackowiak SD, Gregersen LH, Munschauer M, Loewer A, Ziebold U, Landthaler M, Kocks C, le Noble F, Rajewsky N. Circular RNAs are a large class of animal RNAs with regulatory potency. *Nature* 2013; **495**: 333-338 [PMID: 23446348 DOI: 10.1038/nature11928]

21 **Li X**, Yang L, Chen LL. The Biogenesis, Functions, and Challenges of Circular RNAs. *Mol Cell* 2018; **71**: 428-442 [PMID: 30057200 DOI: 10.1016/j.molcel.2018.06.034]

22 **Chen LL**. The biogenesis and emerging roles of circular RNAs. *Nat Rev Mol Cell Biol* 2016; **17**: 205-211 [PMID: 26908011 DOI: 10.1038/nrm.2015.32]

23 **Cui X**, Wang J, Guo Z, Li M, Liu S, Liu H, Li W, Yin X, Tao J, Xu W. Emerging function and potential diagnostic value of circular RNAs in cancer. *Mol Cancer* 2018; **17**: 123 [PMID: 30111313 DOI: 10.1186/s12943-018-0877-y]

24 **Pan B**, Qin J, Liu X, He B, Wang X, Pan Y, Sun H, Xu T, Xu M, Chen X, Xu X, Zeng K, Sun L, Wang S. Identification of Serum Exosomal hsa-circ-0004771 as a Novel Diagnostic Biomarker of Colorectal Cancer. *Front Genet* 2019; **10**: 1096 [PMID: 31737058 DOI: 10.3389/fgene.2019.01096]

25 **Xie Y**, Li J, Li P, Li N, Zhang Y, Binang H, Zhao Y, Duan W, Chen Y, Wang Y, Du L, Wang C. RNA-Seq Profiling of Serum Exosomal Circular RNAs Reveals Circ-PNN as a Potential Biomarker for Human Colorectal Cancer. *Front Oncol* 2020; **10**: 982 [PMID: 32626660 DOI: 10.3389/fonc.2020.00982]

26 **Zeng K**, Chen X, Xu M, Liu X, Hu X, Xu T, Sun H, Pan Y, He B, Wang S. CircHIPK3 promotes colorectal cancer growth and metastasis by sponging miR-7. *Cell Death Dis* 2018; **9**: 417 [PMID: 29549306 DOI: 10.1038/s41419-018-0454-8]

27 **Chen LY**, Wang L, Ren YX, Pang Z, Liu Y, Sun XD, Tu J, Zhi Z, Qin Y, Sun LN, Li JM. The circular RNA circ-ERBIN promotes growth and metastasis of colorectal cancer by miR-125a-5p and miR-138-5p/4EBP-1 mediated cap-independent HIF-1α translation. *Mol Cancer* 2020; **19**: 164 [PMID: 33225938 DOI: 10.1186/s12943-020-01272-9]

28 **Mager LF**, Koelzer VH, Stuber R, Thoo L, Keller I, Koeck I, Langenegger M, Simillion C, Pfister SP, Faderl M, Genitsch V, Tcymbarevich I, Juillerat P, Li X, Xia Y, Karamitopoulou E, Lyck R, Zlobec I, Hapfelmeier S, Bruggmann R, McCoy KD, Macpherson AJ, Müller C, Beutler B, Krebs P. The ESRP1-GPR137 axis contributes to intestinal pathogenesis. *Elife* 2017; **6** [PMID: 28975893 DOI: 10.7554/eLife.28366]

29 **Chen L**, Zhang X, Wang S, Lin X, Xu L. Circ_0084927 Facilitates Cervical Cancer Development *via* Sponging miR-142-3p and Upregulating ARL2. *Cancer Manag Res* 2020; **12**: 9271-9283 [PMID: 33061617 DOI: 10.2147/CMAR.S263596]

30 **Qu X**, Zhu L, Song L, Liu S. circ_0084927 promotes cervical carcinogenesis by sponging miR-1179 that suppresses CDK2, a cell cycle-related gene. *Cancer Cell Int* 2020; **20**: 333 [PMID: 32699532 DOI: 10.1186/s12935-020-01417-2]

31 **Shi P**, Zhang X, Lou C, Xue Y, Guo R, Chen S. Hsa_circ_0084927 Regulates Cervical Cancer Advancement *via* Regulation of the miR-634/TPD52 Axis. *Cancer Manag Res* 2020; **12**: 9435-9448 [PMID: 33061631 DOI: 10.2147/CMAR.S272478]

32 **Wu P**, Cai J, Chen Q, Han B, Meng X, Li Y, Li Z, Wang R, Lin L, Duan C, Kang C, Jiang C. Lnc-TALC promotes O^6-methylguanine-DNA methyltransferase expression *via* regulating the c-Met pathway by competitively binding with miR-20b-3p. *Nat Commun* 2019; **10**: 2045 [PMID: 31053733 DOI: 10.1038/s41467-019-10025-2]

33 **Wang S**, Du S, Lv Y, Wang W, Zhang F. Elevated microRNA-20b-3p and reduced thioredoxin-interacting protein ameliorate diabetic retinopathy progression by suppressing the NLRP3 inflammasomes. *IUBMB Life* 2020; **72**: 1433-1448 [PMID: 32150340 DOI: 10.1002/iub.2267]

34 **Gorukmez O**, Yakut T, Gorukmez O, Sag SO, Topak A, Sahinturk S, Kanat O. Glutathione S-transferase T1, M1 and P1 Genetic Polymorphisms and Susceptibility to Colorectal Cancer in Turkey.

Asian Pac J Cancer Prev 2016; **17**: 3855-3859 [PMID: 27644629]

35 **Yu KD**, Fan L, Di GH, Yuan WT, Zheng Y, Huang W, Chen AX, Yang C, Wu J, Shen ZZ, Shao ZM. Genetic variants in GSTM3 gene within GSTM4-GSTM2-GSTM1-GSTM5-GSTM3 cluster influence breast cancer susceptibility depending on GSTM1. *Breast Cancer Res Treat* 2010; **121**: 485-496 [PMID: 19856098 DOI: 10.1007/s10549-009-0585-9]

36 **Sun C**, Gu Y, Chen G, Du Y. Bioinformatics Analysis of Stromal Molecular Signatures Associated with Breast and Prostate Cancer. *J Comput Biol* 2019; **26**: 1130-1139 [PMID: 31180245 DOI: 10.1089/cmb.2019.0045]

37 **Wang Y**, Lei L, Chi YG, Liu LB, Yang BP. A comprehensive understanding of ovarian carcinoma survival prognosis by novel biomarkers. *Eur Rev Med Pharmacol Sci* 2019; **23**: 8257-8264 [PMID: 31646556 DOI: 10.26355/eurrev_201910_19136]

38 **Sun YL**, Zhang Y, Guo YC, Yang ZH, Xu YC. A Prognostic Model Based on Six Metabolism-Related Genes in Colorectal Cancer. *Biomed Res Int* 2020; **2020**: 5974350 [PMID: 32953885 DOI: 10.1155/2020/5974350]

39 **Kap EJ**, Seibold P, Scherer D, Habermann N, Balavarca Y, Jansen L, Zucknick M, Becker N, Hoffmeister M, Ulrich A, Benner A, Ulrich CM, Burwinkel B, Brenner H, Chang-Claude J. SNPs in transporter and metabolizing genes as predictive markers for oxaliplatin treatment in colorectal cancer patients. *Int J Cancer* 2016; **138**: 2993-3001 [PMID: 26835885 DOI: 10.1002/ijc.30026]

40 **Yu D**, Liu Y, Zhou Y, Ruiz-Rodado V, Larion M, Xu G, Yang C. Triptolide suppresses IDH1-mutated malignancy *via* Nrf2-driven glutathione metabolism. *Proc Natl Acad Sci USA* 2020; **117**: 9964-9972 [PMID: 32312817 DOI: 10.1073/pnas.1913633117]

41 **Xiao Y**, Meierhofer D. Glutathione Metabolism in Renal Cell Carcinoma Progression and Implications for Therapies. *Int J Mol Sci* 2019; **20** [PMID: 31357507 DOI: 10.3390/ijms20153672]

42 **Miess H**, Dankworth B, Gouw AM, Rosenfeldt M, Schmitz W, Jiang M, Saunders B, Howell M, Downward J, Felsher DW, Peck B, Schulze A. The glutathione redox system is essential to prevent ferroptosis caused by impaired lipid metabolism in clear cell renal cell carcinoma. *Oncogene* 2018; **37**: 5435-5450 [PMID: 29872221 DOI: 10.1038/s41388-018-0315-z]

43 **Duan S**, Huang W, Liu X, Chen N, Xu Q, Hu Y, Song W, Zhou J. IMPDH2 promotes colorectal cancer progression through activation of the PI3K/AKT/mTOR and PI3K/AKT/FOXO1 signaling pathways. *J Exp Clin Cancer Res* 2018; **37**: 304 [PMID: 30518405 DOI: 10.1186/s13046-018-0980-3]

44 **Weng ML**, Chen WK, Chen XY, Lu H, Sun ZR, Yu Q, Sun PF, Xu YJ, Zhu MM, Jiang N, Zhang J, Zhang JP, Song YL, Ma D, Zhang XP, Miao CH. Fasting inhibits aerobic glycolysis and proliferation in colorectal cancer *via* the Fdft1-mediated AKT/mTOR/HIF1α pathway suppression. *Nat Commun* 2020; **11**: 1869 [PMID: 32313017 DOI: 10.1038/s41467-020-15795-8]

45 **Tan X**, Zhang Z, Yao H, Shen L. Tim-4 promotes the growth of colorectal cancer by activating angiogenesis and recruiting tumor-associated macrophages *via* the PI3K/AKT/mTOR signaling pathway. *Cancer Lett* 2018; **436**: 119-128 [PMID: 30118845 DOI: 10.1016/j.canlet.2018.08.012]

World Journal of Gastroenterology

Submit a Manuscript: https://www.f6publishing.com

World J Gastroenterol 2021 September 28; 27(36): 6079-6092

DOI: 10.3748/wjg.v27.i36.6079

ISSN 1007-9327 (print) ISSN 2219-2840 (online)

ORIGINAL ARTICLE

Basic Study

Exosomal microRNA-588 from M2 polarized macrophages contributes to cisplatin resistance of gastric cancer cells

Hai-Yan Cui, Jian-Sheng Rong, Ju Chen, Jie Guo, Jia-Qin Zhu, Mei Ruan, Rong-Rong Zuo, Shuang-Shuang Zhang, Jun-Mei Qi, Bao-Hua Zhang

ORCID number: Hai-Yan Cui 0000-0001-7701-2999; Jian-Sheng Rong 0000-0002-4408-3325; Ju Chen 0000-0002-8036-7835; Jie Guo 0000-0002-5245-2856; Jia-Qin Zhu 0000-0002-3829-2956; Mei Ruan 0000-0001-6700-0687; Rong-Rong Zuo 0000-0001-6975-6015; Shuang-Shuang Zhang 0000-0002-3322-433X; Jun-Mei Qi 0000-0001-9552-8200; Bao-Hua Zhang 0000-0003-2789-6348.

Author contributions: Cui HY, Rong JS, and Chen J designed the study; Guo J, Zhu JQ, and Ruan M performed the experiments; Zuo RR and Zhang SS collected and analysed the data; Qi JM and Zhang BH wrote the manuscript.

Institutional review board statement: This study was reviewed and approved by the Zibo Central Hospital.

Institutional animal care and use committee statement: All animal experiments in this study were approved by the Zibo Central Hospital.

Conflict-of-interest statement: The authors declare no conflict of interest for this manuscript.

Data sharing statement: No additional data are available.

ARRIVE guidelines statement: The

Hai-Yan Cui, Rong-Rong Zuo, Shuang-Shuang Zhang, Jun-Mei Qi, Department of Pathology, The Fourth People's Hospital of Zibo City, Zibo 255000, Shandong Province, China

Jian-Sheng Rong, Bao-Hua Zhang, Department of Pathology, Zibo Central Hospital, Zibo 255036, Shandong Province, China

Ju Chen, Department of Ultrasound Medicine, Zibo Central Hospital, Zibo 255036, Shandong Province, China

Jie Guo, Department of Health, The Fourth People's Hospital of Zibo City, Zibo 255000, Shandong Province, China

Jia-Qin Zhu, Department of Gastroenterology, The Fourth People's Hospital of Zibo City, Zibo 255000, Shandong Province, China

Mei Ruan, Department of Oncology, The Fourth People's Hospital of Zibo City, Zibo 255000, Shandong Province, China

Corresponding author: Bao-Hua Zhang, MSc, Chief Physician, Department of Pathology, Zibo Central Hospital, No. 54 Gongqingtuan West Road, Zhangdian District, Zibo 255036, Shandong Province, China. zhangbaohua314@163.com

Abstract

BACKGROUND

Gastric cancer is a prevalent malignant cancer with a high incidence and significantly affects the health of modern people globally. Cisplatin (DDP) is one of the most common and effective chemotherapies for patients with gastric cancer, but DDP resistance remains a severe clinical challenge.

AIM

To explore the function of M2 polarized macrophages-derived exosomal microRNA (miR)-588 in the modulation of DDP resistance of gastric cancer cells.

METHODS

M2 polarized macrophages were isolated and identified by specific markers using flow cytometry analysis. The exosomes from M2 macrophages were identified by transmission electron microscopy and related markers. The uptake of the PKH67-

authors have read the ARRIVE guidelines, and the manuscript was prepared and revised according to the ARRIVE guidelines.

Open-Access: This article is an open-access article that was selected by an in-house editor and fully peer-reviewed by external reviewers. It is distributed in accordance with the Creative Commons Attribution NonCommercial (CC BY-NC 4.0) license, which permits others to distribute, remix, adapt, build upon this work non-commercially, and license their derivative works on different terms, provided the original work is properly cited and the use is non-commercial. See: http://creativecommons.org/Licenses/by-nc/4.0/

Manuscript source: Unsolicited manuscript

Specialty type: Gastroenterology and hepatology

Country/Territory of origin: China

Peer-review report's scientific quality classification

Grade A (Excellent): 0
Grade B (Very good): B
Grade C (Good): C, C
Grade D (Fair): 0
Grade E (Poor): 0

Received: April 23, 2021
Peer-review started: April 23, 2021
First decision: May 27, 2021
Revised: June 7, 2021
Accepted: August 11, 2021
Article in press: August 11, 2021
Published online: September 28, 2021

P-Reviewer: Tanabe S, Yashiro M
S-Editor: Wu YXJ
L-Editor: Wang TQ
P-Editor: Li JH

labelled M2 macrophages-derived exosomes was detected in SGC7901 cells. The function and mechanism of exosomal miR-588 from M2 macrophages in the modulation of DDP resistance of gastric cancer cells was analyzed by CCK-8 assay, apoptosis analysis, colony formation assay, Western blot analysis, qPCR analysis, and luciferase reporter assay in SGC7901 and SGC7901/DDP cells, and by tumorigenicity analysis in nude mice.

RESULTS

M2 polarized macrophages were isolated from mouse bone marrow stimulated with interleukin (IL)-13 and IL-4. Co-cultivation of gastric cancer cells with M2 polarized macrophages promoted DDP resistance. M2 polarized macrophages-derived exosomes could transfer in gastric cancer cells to enhance DDP resistance. Exosomal miR-588 from M2 macrophages contributed to DDP resistance of gastric cancer cells. miR-588 promoted DDP-resistant gastric cancer cell growth *in vivo*. miR-588 was able to target cylindromatosis (CYLD) in gastric cancer cells. The depletion of CYLD reversed miR-588 inhibition-regulated cell proliferation and apoptosis of gastric cancer cells exposed to DDP.

CONCLUSION

In conclusion, we uncovered that exosomal miR-588 from M2 macrophages contributes to DDP resistance of gastric cancer cells by partly targeting CYLD. miR-588 may be applied as a potential therapeutic target for the treatment of gastric cancer.

Key Words: Gastric cancer; Cisplatin resistance; M2 polarized macrophages; Exosome; miR-588; Cylindromatosis

©The Author(s) 2021. Published by Baishideng Publishing Group Inc. All rights reserved.

Core Tip: In this study, we uncovered that exosomal miR-588 from M2 macrophages contributes to cisplatin resistance of gastric cancer cells by partly targeting cylindromatosis. miR-588 may be applied as a potential therapeutic target for the treatment of gastric cancer.

Citation: Cui HY, Rong JS, Chen J, Guo J, Zhu JQ, Ruan M, Zuo RR, Zhang SS, Qi JM, Zhang BH. Exosomal microRNA-588 from M2 polarized macrophages contributes to cisplatin resistance of gastric cancer cells. *World J Gastroenterol* 2021; 27(36): 6079-6092
URL: https://www.wjgnet.com/1007-9327/full/v27/i36/6079.htm
DOI: https://dx.doi.org/10.3748/wjg.v27.i36.6079

INTRODUCTION

Gastric cancer belongs to the most common malignant tumors and is the third cause of cancer-related death throughout the world[1]. Patients diagnosed with gastric cancer are usually at an advanced or late stage, which makes chemotherapy a prevalent strategy over the past decades[2]. Among the clinical chemotherapy agents, cisplatin (DDP) is capable of disrupting DNA repairment, which further causes DNA damage and apoptosis of cancer cells[3]. However, the developed therapeutic resistance makes the chemotherapy far less satisfactory in clinical application, which makes it urgent to decipher the mechanisms underlying this chemoresistance[4].

Tumor-associated macrophage (TAMs) are macrophages that participate in the tumor microenvironment function, and play a critical role in tumor development, including growth, metastasis, angiogenesis, and therapeutic resistance[5]. Recent studies have proposed that TAMs were capable of communicating with neighboring or distant cells *via* secreting exosomes[6,7]. Exosomes are membrane-derived transporting vesicles secreted by almost all types of cells, usually defined with a diameter ranging from 40 nm to 100 nm[8]. It is widely recognized that exosomes act as a communicator between cells through transporting various cargos such as mRNA, lipid, proteins, as well as microRNAs (miRNAs), and hence are related to various

functions of targeted cells[9,10]. miRNAs are endogenous short noncoding RNAs that play pivotal roles in the regulation of cancer development by directly targeting mRNA [11]. Besides, miRNAs are recently proposed to be involved in drug resistance of cancer cells[12-14]. Among which, miR-588 is upregulated in human prostate cancer with prognostic significance and notably facilitates the proliferation of prostate cancer cells[15]. Importantly, it has been reported that miR-588 serves as a promising prognostic marker for gastric cancer[16]. However, the role of miR-588 in DDP resistance of gastric cancer cells is still unknown. Accordingly, we were interested in the correlation of TAM-derived exosomes with miR-588 and its role in the modulation of DDP resistance of gastric cancer cells.

Cylindromatosis (CYLD) is a representative deubiquitinating enzyme that could counteract the E3 ubiquitin ligases-mediated protein ubiquitination[17]. It plays an important role in multiple cellular processes during tumorigenesis, such as cell apoptosis, cell cycle, cell migration, and DNA damage[17]. Mechanistically, CYLD is profoundly related to multiple critical signaling transduction pathways, especially the NF-κB signaling pathway, and acts as a tumor suppressor[18]. It has been extensively demonstrated that CYLD could negatively regulate the activation of NF-kB through deubiquitinating its upstream K63, which further inhibits the activation of NF-kB-related pro-survival signaling and promotes caspase-8-induced cell apoptosis[19]. It is noteworthy that recent studies also proposed that loss of CYLD could trigger DDP resistance in several cancers, including gastric cancer and oral squamous cell carcinoma[20,21].

In this study, we adopted a M2-polarized macrophage model to mimic TAM function, and testified that TAM-derived exosomes conferred DDP resistance in gastric cancer. We showed that the exosomes secreted by TAM contained miR-588, which directly interacts with the 3′ untranslated region of *CYLD* to suppress its expression and its tumor-suppressing function. This process subsequently hindered cell apoptosis and promoted the proliferation as well as DDP resistance of gastric cancer cells. Our study illustrated the connection between TAM and DDP resistance of gastric cancer cells, providing a potential target for gastric cancer therapy.

MATERIALS AND METHODS

Cell culture and treatment

Gastric cancer cell line SGC7901, purchased from ATCC, was maintained in DMEM containing 10% fetal bovine serum (FBS) and 1% penicillin and streptomycin (Sigma, United States) at 37 °C with 5% CO2. DDP-resistant SGC7901/DDP cells were developed from the parental SGC7901 cells that were subjected to persistent gradient exposure to DDP for about 12 mo, through increasing DDP concentration from 0.05 μg/mL until the cells acquired resistance to 1 μg/mL[22]. Mouse bone marrow cells (MBMCs) were purchased from Chinese Academy of Sciences Cell Bank of Type Culture Collection, and cultured in a normal DMEM:F12 medium containing 10% FBS and macrophage colony-stimulating factor (Sigma). To achieve polarization to M2, MBMCs were stimulated with interleukin (IL)-4 and IL-13 (30 ng/mL, Sigma) for 2 d. A transwell chamber assay was adopted to perform co-culture experiments, in which polarized macrophages were placed in the upper tanswell chamber and gastric cancer cells were cultured in the bottom well.

Flow cytometry

The M2 polarization was determined by staining for critical biomarkers and detection by flow cytometry. Briefly, cells were collected and incubated with fluorescence probe-conjugated antibodies against CD86, CD68, CD11b, CD80, CD206, CD163, and F4/80 at 4 °C for 30 min. Next, the cells were washed with PBS and analyzed by flow cytometry (BD Biosciences, United States). The antibodies used in this experiment were purchased from Abcam (United States).

For cell apoptosis, cells were processed with an apoptosis detection kit (Solarbio, China). Briefly, cells were collected and suspended in binding buffer, followed by staining with PI and Annexin V at room temperature for 20 min in dark. Next, the stained cells were collected and resuspended in binding buffer for analysis by flow cytometry.

Exosome isolation and analysis

Macrophages were cultured in medium containing 10% exosome-free FBS for 48 h. The medium was collected for extraction of exosomes with an exoEasy Maxi Kit (QIAGEN,

Germany) following the manufacturer's instruction.

To determine exosome internalization, the exosomes were labeled with PKH67 (Sigma) according to the manufacturer's protocol. Subsequently, the labeled exosomes were used to incubate with cells in each experiment, and observed using a confocal microscope (Carl Zeiss, Germany).

Transmission electron microscopy

The images of exosomes were captured by transmission electron microscopy (TEM). In brief, the samples were dropped on cleaned cooper grids coated with carbon, and washed with Milli-Q water to remove extra samples, followed by 1-min staining with uranyl acetate and air dry. Then, the samples were observed and pictured with a transmission electron microscope (Carl Zeiss).

Cell transfection

SGC7901 cells were placed in 6-well plate at a density of 3×10^5 cells per well. After incubation for 12 h, miR-588 mimic (RiboBio, China), miR-588 inhibitor (RiboBio, China), or negative control (RiboBio, China) was mixed with lipofectamine 200 (Invitrogen, United States) in Opti-MEM medium (Sigma, United States) for 20 min and added into cell culture medium. Eight hours after transfection, the medium was replaced with fresh DMEM containing 10% FBS to incubate for another 24 h. Then, the cells were used for further experiments.

Cell viability and colony formation assay

Cell viability was determined with a CCK-8 kit (Beyotime, China). MFC cells and SGC7901 cells were seeded in 96-well plates at a density of 3×10^3 cells/well and processed accordingly. Twenty-four hours after incubation, the CCK-8 reagent was added into each well. The absorbance values were detected at 450 nm at 24 h, 48 h, and 72 h, respectively.

For colony formation experiment, SGC7901 cells transfected with miR-588 inhibitor or negative control were placed in a 6-well plate (1000 cells per well), and incubated in complete medium for 2 wk to form visible colonies. Subsequently, the colonies were washed, stained with crystal violet, and captured with a microscope (Carl Zeiss).

RNA extraction and quantitative real-time PCR

Total RNA was extracted with TRIzol reagent (Takara, Japan) and reversely transcribed to cDNA with an EasyScript Reverse Transcriptase kit (TransGen, China). The quantification of cDNA was performed by using a TransStart Green qPCR SuperMix kit (TransGen), and PCR was performed on a Real-Time PCR System (BD bioscience). For detection of miR-588, the extracted RNA was processed with a poly(A) tailing kit (Invitrogen) before reverse transcription. For normalization of mRNA and miRNA, *GAPDH* and *U6* were used as the internal controls, respectively. The quantification of cDNA was analyzed by the $2^{-\Delta\Delta Ct}$ method. The sequences of primers are as follows: *GAPDH* sense, 5′- ACAACTTTGGTATCGTGGAAGG-3′ and antisense, 5′-GCCATCACGCCACAGTTTC-3′; *U6* sense, 5′-AGTAAGCCCTTGCTGTCAGTG-3′ and antisense, 5′-CCTGGGTCTGATAATGCTGGG-3′; *Arg1* sense, 5′-GTGGAAACT-TGCATGGACAAC-3′ and antisense, 5′-AATCCTGGCACATCGGGAATC-3′; *IL-10* sense, 5′-GTACCACAGCAATGGCTACC-3 and antisense, 5′-TGTTGGTGACG-GTCCAGTTG-3′; *TGF-β* sense, 5′-CTAATGGTGGAAACCCACAACG-3′ and antisense, 5′-TATCGCCAGGAATTGTTGCTG-3′; miR-588, 5′-CCGCTATTGCACAT-TACTAAGTTGCA-3

Western blot analysis

SGC7901 cells were placed in a 6-well plate at a density of 3×10^5 cells per well and transfected with miR-588 inhibitor. Total protein was extracted by using ice-cold RIPA buffer, separated by SDS-PAGE, and transferred to a nitrocellulose membrane. The membrane was then blocked by 5% non-fat milk at room temperature for 1 h, and incubated with specific primary antibodies against CD63 (1:1000, Abcam), CD9 (1:1000, Abcam), CD81 (1:1000, Abcam), HSP70 (1:500, Abcam), GAPDH (1:1000, Proteintech), Bax (1:1000, CST), pro-caspase-3 (1:2000, CST), cleaved caspase-3 (1:1000, CST), pro-caspase-9 (1:1000, CST), cleaved caspase-9 (1:1000, CST), CYLD (1:1000, Proteintech), and β-actin (1:2000, Proteintech) at 4 °C overnight. Next day, the blots were washed and incubated with secondary antibodies at room temperature for 2 h. The blots were visualized by using an ECL reagent and a gel imaging system (BD Bioscience).

Xenograft tumor model

C57 nude mice aged 5 wk were purchased from Shanghai Laboratory Animal Center of China. SGC7901 cells were transfected with miR-588 inhibitor or negative control, and suspended in saline at a density of 1 × 10^7 cells/mL. A total of 200 μL of SGC7901 cell suspension was subcutaneously injected to the left back of mice. A week after tumor cell inoculation, the mice were intraperitoneally injected with 15 mg/kg DDP. The mice were euthanized at day 30, and the tumors were isolated, weighted, and processed for subsequent analysis. Tumor size was measured every 5 d and calculated using the following formula: Width^2 × length/2.

Statistical analysis

All experiments in this study were performed at least three times independently. All data are presented as the mean ± SD and analyzed with GraphPad Prism 6.0 software. The statistical difference between two groups or multiples groups was analyzed by Student's *t*-test or one-way ANOVA, and was considered significant at $P < 0.05$.

RESULTS

M2 polarized macrophages-derived exosomes can transfer in gastric cancer cells to enhance DDP resistance

To evaluate the effect of M2 polarized macrophages on DDP resistance of gastric cancer cells, M2 polarized macrophages were isolated from murine bone marrow induced with IL-13 and IL-4 and were identified by the M2 specific marker CD206 (Figure 1A). Meanwhile, we found that the expression of M1 polarized marker iNOS was not chanced but the M2 markers, such as Arg1, IL-10, and TGF-β, were enhanced in M2 polarized macrophages compared with inactivated macrophages (Figure 1B). Then, the exosomes were isolated from M2 polarized macrophages and analyzed by TEM and identified by the expression of CD63, CD9, CD81, and HSP70 (Figure 1C and D). Moreover, the delivery of PKH67-labelled exosomes from M2 polarized macrophages was found in SGC7901 cells (Figure 1E). Significantly, M2 macrophages-derived conditioned medium and exosomes enhanced the cell survival of SGC7901 cells exposed to DDP (Figure 1F). The exosomes from M2 polarized macrophages repressed DDP-treated SGC7901 cell apoptosis (Figure 1G).

Co-culture of gastric cancer cells with M2 polarized macrophages promotes DDP resistance

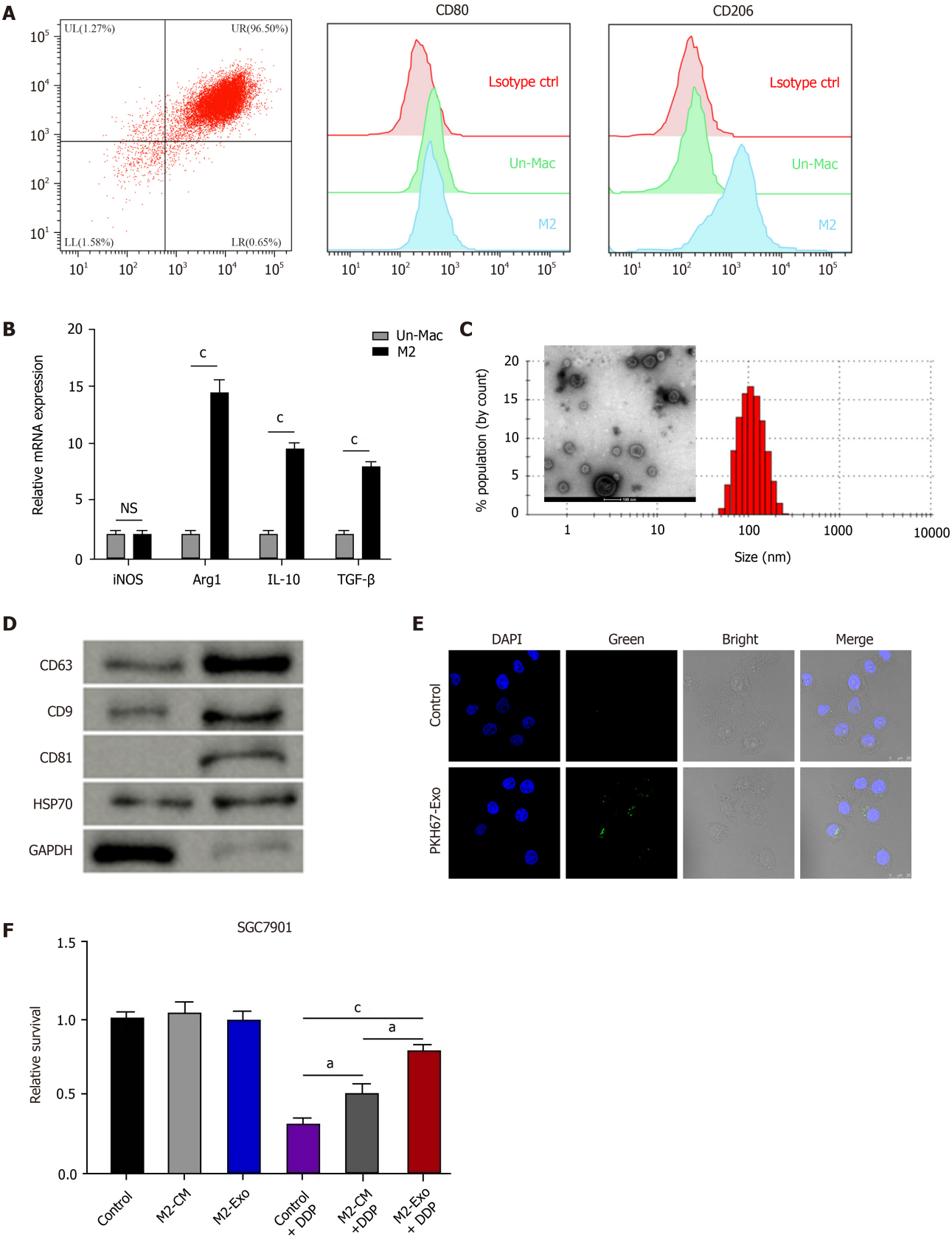
Next, we found that DDP treatment reduced the proliferation of SGC7901 cells in a time-dependent manner (Figure 2A). The co-culture of inactivated macrophages inhibited apoptosis of DDP-treated SGC7901 cells, while the co-culture of M2 polarized macrophages further reduced the cell apoptosis (Figure 2B and C).

Exosomal miR-588 from M2 macrophages contributes to DDP resistance of gastric cancer cells

We then observed that the expression of miR-588 was elevated in the exosomes from M2 macrophages compared with inactivated macrophages (Figure 3A). The miR-588 expression was enhanced in macrophages relative to SGC7901 cells, especially in the M2 polarized macrophages (Figure 3B). Meanwhile, the expression of miR-588 was increased in the DDP-resistant SGC7901 cells co-cultured with M2 macrophages or exosomes from M2 macrophages (Figure 3C). Moreover, we found that the inhibition of miR-588 by inhibitor repressed colony formation of DDP-resistant SGC7901 cells (Figure 3D). The repression of miR-588 induced DDP-resistant SGC7901 cell apoptosis (Figure 3E). The expression of Bax, cleaved caspase-3, and cleaved caspase-9 was enhanced by miR-588 inhibitor in DDP-resistant SGC7901 cells (Figure 3F). Moreover, the IC_{50} of DDP in the inhibition of SGC7901 cell viability was inhibited by miR-588 inhibitor (Figure 4A). Treatment with DDP induced apoptosis of SGC7901 cells, in which miR-588 inhibitor reinforced this effect (Figure 4B and C).

miR-588 can target CYLD in gastric cancer cells

We then identified the binding site for miR-588 in *CYLD* in the bioinformatic analysis (Figure 5A). The luciferase activity and mRNA expression of *CYLD* were significantly repressed by miR-588 mimic in the DDP-resistant SGC7901 cells (Figure 5B and C). Similarly, the protein levels of CYLD were inhibited by miR-588 mimic in DDP-


A
UL(1.27%)
UR(96.50%)
LL(1.58%)
LR(0.65%)
CD80
CD206
Lsotype ctrl
Un-Mac
M2
B
Relative mRNA expression
Un-Mac
M2
NS
c
iNOS
Arg1
IL-10
TGF-β
C
% population (by count)
Size (nm)
D
CD63
CD9
CD81
HSP70
GAPDH
E
DAPI
Green
Bright
Merge
Control
PKH67-Exo
F
SGC7901
Relative survival
a
Control
M2-CM
M2-Exo
Control + DDP
M2-CM +DDP
M2-Exo + DDP

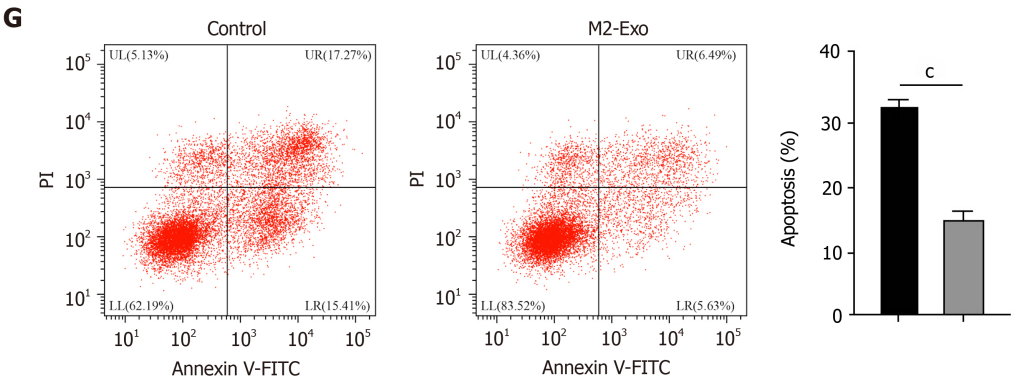


Figure 1 M2 polarized macrophages-derived exosomes can transfer in gastric cancer cells to enhance cisplatin resistance. A and B: Flow cytometry for identifying the M2 polarized macrophages isolated from murine bone marrow induced with interleukin (IL)-13 and IL-4. The M2 specific marker CD206 was identified. Un-Mac represents inactivated macrophages and M2 represents macrophages activated by IL-13 and IL-4. The mRNA expression of *iNOS*, *Arg1*, *IL-10*, and *TGF-β* was detected by qPCR in Un-Mac and M2 macrophages; C: Identification of exosomes from M2 macrophages by transmission electron microscopy; D: Detection of expression of CD63, CD9, CD81, HSP70, and GAPDH by Western blot analysis; E: Detection of uptake of the PKH67-labelled M2 exosomes (M2-Exo) in SGC7901 cells; F: Analysis of cell viability by CCK-8 assay. M2 macrophages-derived conditioned medium and M2-Exo were used to treat SGC7901 cells exposed to cisplatin (DDP) for 48 h; G: Analysis of cell apoptosis by flow cytometry SGC7901 cells were co-treated with DDP and M2-Exo. Data shown are the mean ± SD. ^{a}P <0.05; ^{c}P < 0.001. DDP: Cisplatin; Un-Mac: Inactivated macrophages; M2-Exo: M2 exosomes.

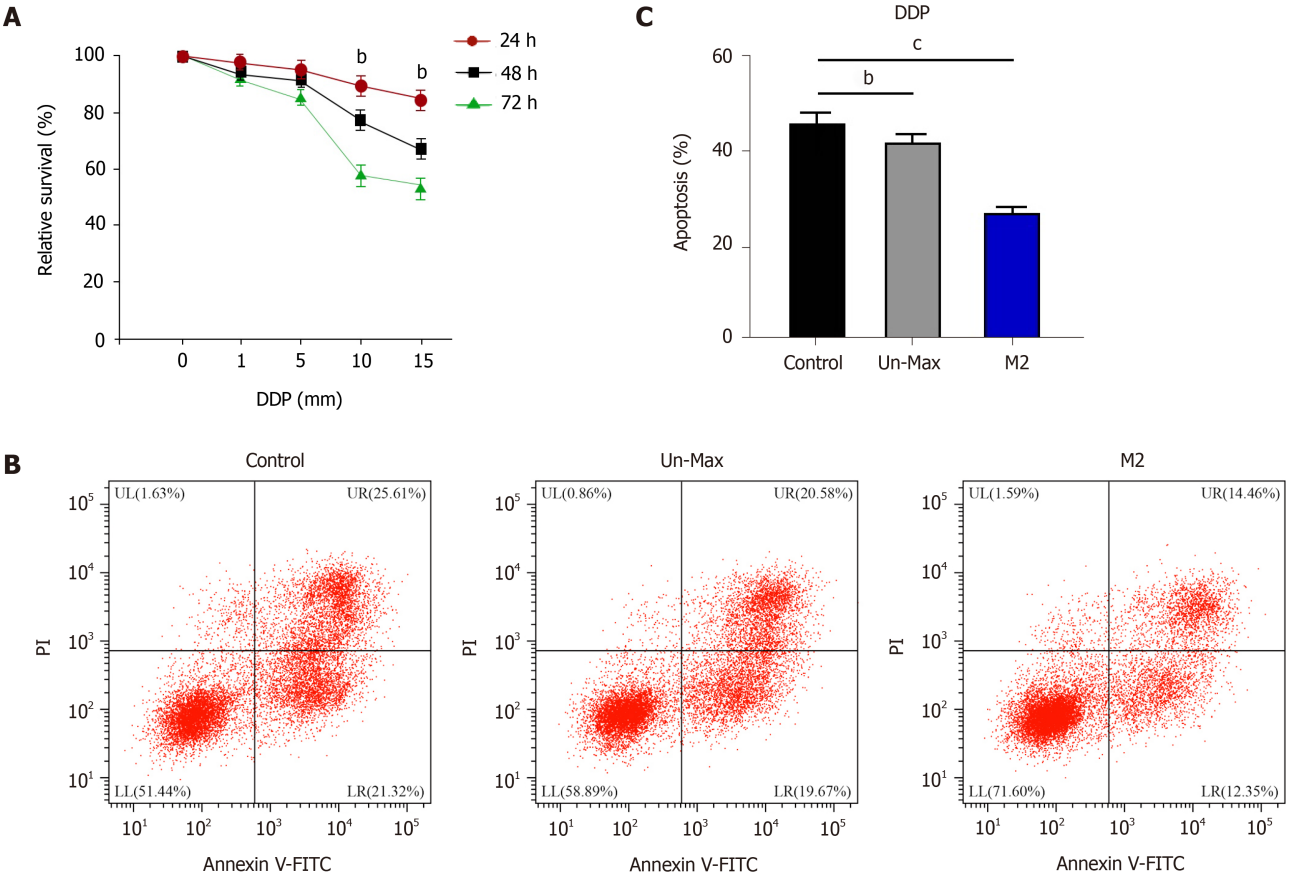


Figure 2 Co-culture of gastric cancer cells with M2 polarized macrophages promotes cisplatin resistance. A: Detection of cell viability by CCK-8 assay in SGC7901 cells treated with cisplatin (DDP); B and C: Analysis of cell apoptosis by flow cytometry in SGC7901 cells co-cultured with inactivated macrophages and M2 macrophages exposed to DDP for 48 h. Data shown are the mean ± SD. ^{b}P < 0.01; ^{c}P <0.001. DDP: Cisplatin.

resistant SGC7901 cells (Figure 5D).

miR-588/CYLD axis regulates DDP resistance of gastric cancer cells

Next, we evaluated the effect of miR-588/CYLD axis on DDP resistance of gastric cancer cells. Our data showed that treatment with DDP inhibited SGC7901 cell proliferation; miR-588 inhibitor enhanced the function of DDP, while the depletion of CYLD

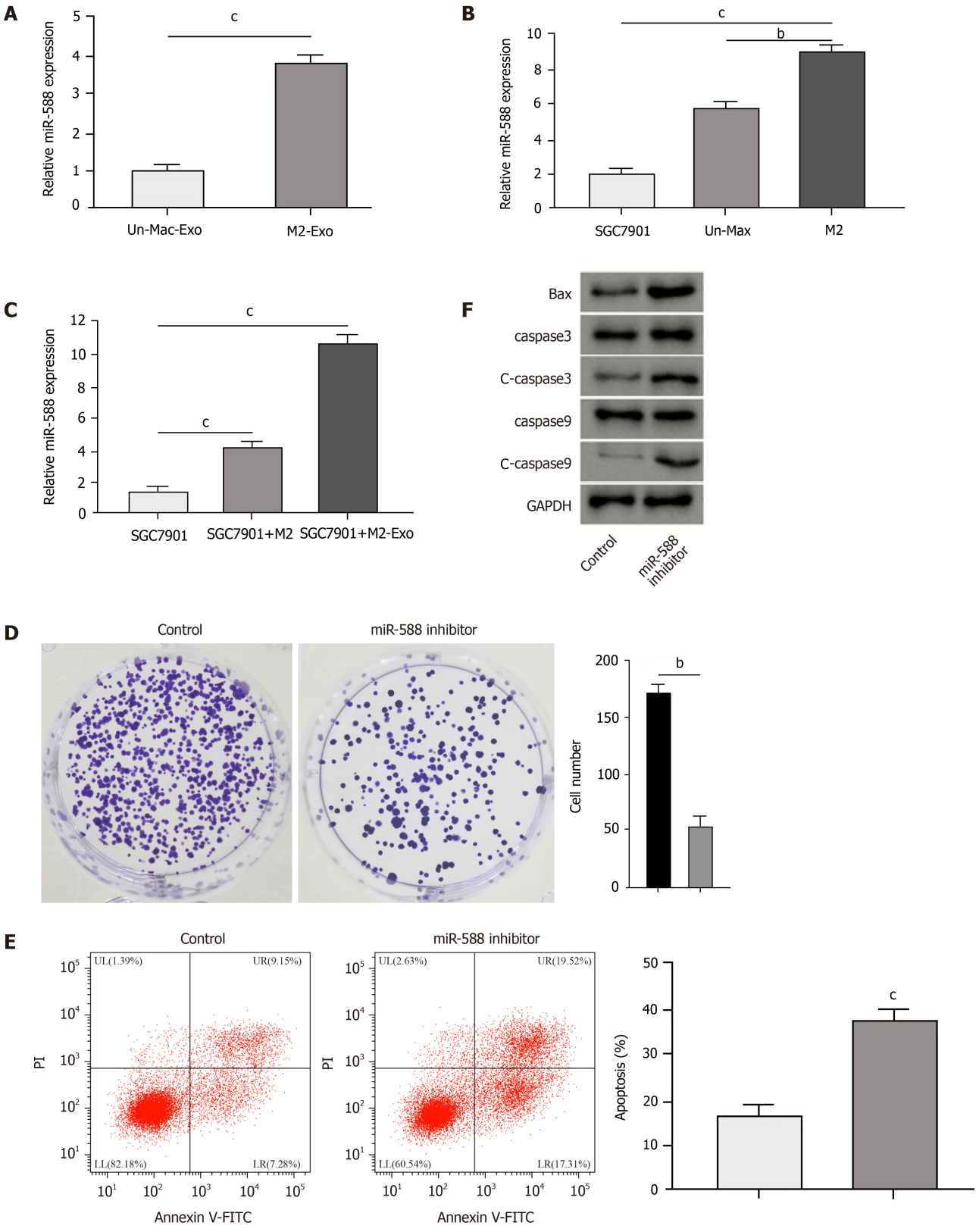
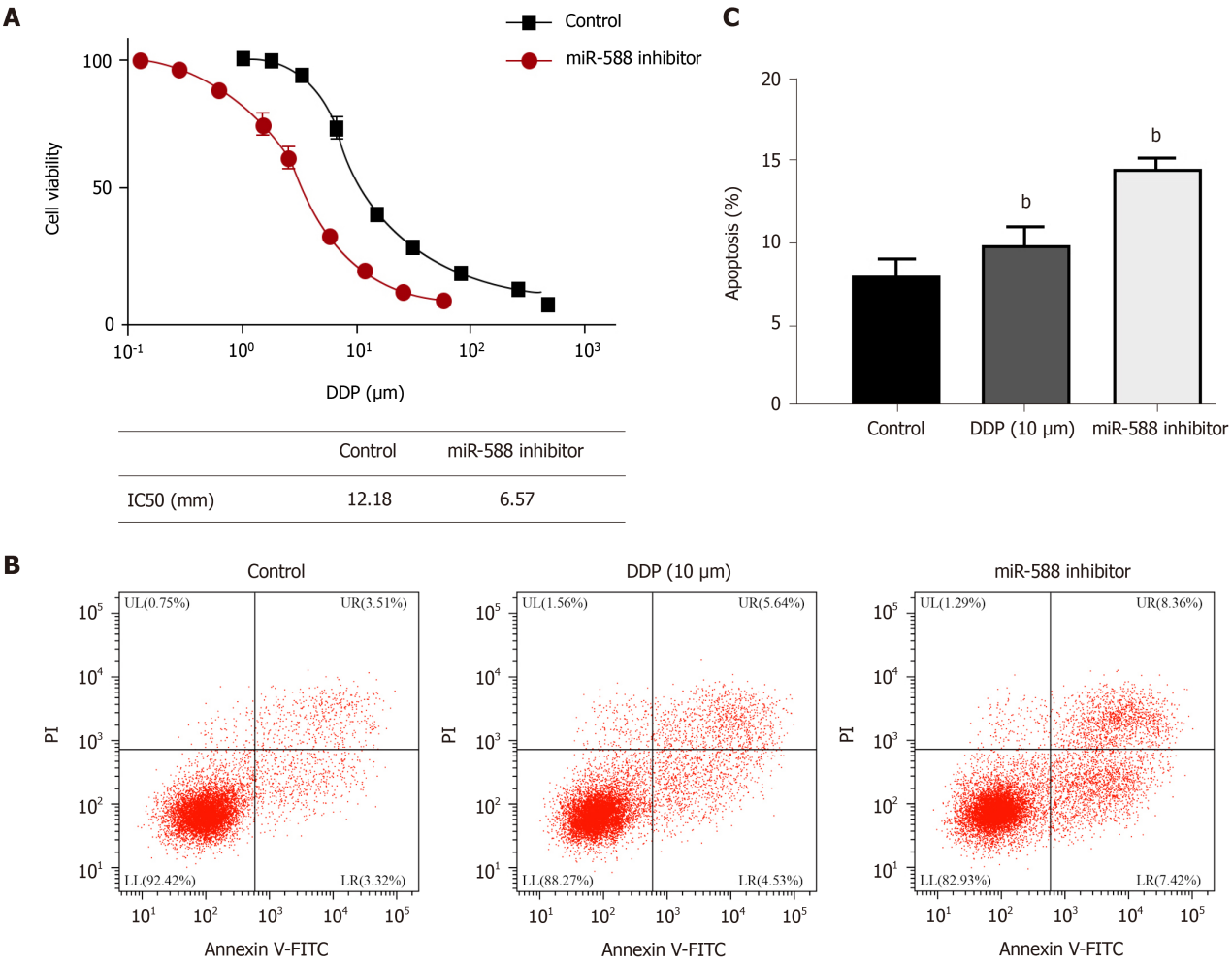


Figure 3 Exosomal miR-588 from M2 macrophages contributes to cisplatin resistance of gastric cancer cells. A: Detection of expression of miR-588 by qPCR in the exosomes from M2 macrophages and inactivated macrophages; B: Detection of expression of miR-588 by qPCR in cisplatin (DDP)-resistant SGC7901 cells, M2 macrophages, and inactivated macrophages; C: Detection of expression of miR-588 by qPCR in DDP-resistant SGC7901 cells co-cultured with M2 macrophages or exosomes from M2 macrophages; D-F: Analysis of cell proliferation by colony formation assay (D), cell apoptosis by flow cytometry (E), and expression of Bax, capase-3, caspase-9, cleaved caspase-3 (c-caspase-3), and cleaved caspase 9 (c-caspase-9) by Western blot analysis (F) in DDP-resistant SGC7901 cells treated with miR-588 inhibitor. Data shown are the mean ± SD, $^{b}P < 0.01$; $^{c}P < 0.001$.



	Control	miR-588 inhibitor
IC50 (mm)	12.18	6.57

Figure 4 miR-588 contributes to cisplatin resistance of gastric cancer cells. A: Detection of cell viability by CCK-8 assay in SGC7901 cells treated with miR-588 inhibitor and exposed to cisplatin (DDP) at the indicated doses; B and C: Detection of cell apoptosis by flow cytometry in DDP-resistant SGC7901 cells co-treated with DDP and miR-588 inhibitor. Data shown are the mean ± SD, $^{b}P < 0.01$. DDP: Cisplatin.

by siRNA reversed the effect of miR-588 inhibition (Figure 6A). Moreover, treatment with DDP induced apoptosis of SGC7901 cells; miR-588 inhibitor further enhanced the cell apoptosis, while CYLD knockdown reversed the effect of miR-588 inhibitor (Figure 6B). Moreover, tumorigenicity analysis in nude mice demonstrated that miR-588 inhibitor suppressed the tumor growth *in vivo* (Figure 7A-D). Meanwhile, we validated that the overexpression of CYLD or treatment with miR-588 inhibitor repressed the tumor growth in nude mice, while the depletion of CYLD rescued miR-588 inhibitor-reduced tumor growth in the model (Figure 7E and F).

DISCUSSION

Gastric cancer is a common malignant cancer with a high death rate and limited therapeutic strategies. DDP is widely applied in the treatment of gastric cancer patients with significant effectiveness, but DDP resistance remains a critical clinical issue. In this study, we identified that M2 polarized macrophages-derived exosomal miR-588 contributes to DDP resistance of gastric cancer cells.

Previous investigations have shown that M2 polarized macrophages-derived exosomes are involved in the modulation of cancer development. It has been reported that tumor-related macrophages-derived exosomes contribute to gastric cancer cell invasion *via* apolipoprotein E[23]. Macrophage-derived exosomal miR-21 regulates DDP resistance of gastric cancer cells[24]. M2 macrophages-derived exosomes promote metastasis of hepatocarcinoma by delivering αMβ2 integrin[25]. These studies have shown the critical function of macrophages-derived exosomal miRNAs in the modulation of cancer development. Meanwhile, miR-588 is a widely reported cancer regulator in previous studies. It has been found that miR-588 is enhanced in prostate

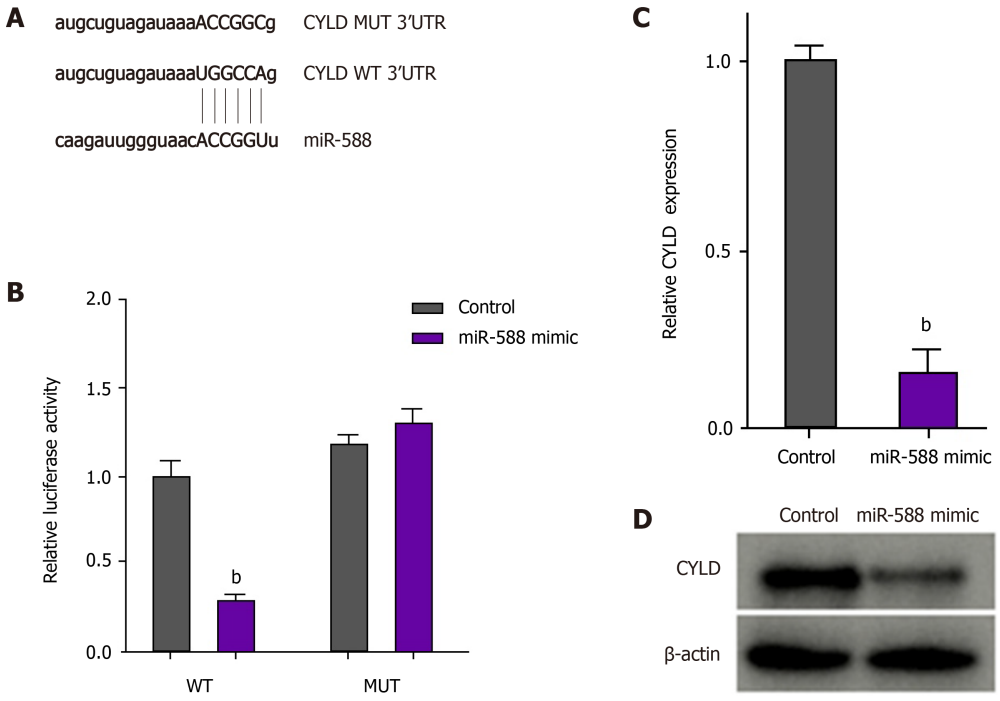


Figure 5 miR-588 can target cylindromatosis in gastric cancer cells. A: The binding site of miR-588 and cylindromatosis (CYLD) was predicted in TargetScan database; B-D: After cisplatin (DDP)-resistant SGC7901 cells were treated with miR-588 mimic, the luciferase activity of CYLD was measured by luciferase reporter assays (B); the expression of CYLD was determined by qPCR (C); and the expression of CYLD was measured by Western blot analysis (D). Data shown are the mean ± SD. $^{b}P < 0.01$. CYLD: Cylindromatosis.

cancer and is correlated with a poor prognosis[15]. miR-588 modulates epithelial-mesenchymal transition, migration, and invasion of gastric cancer cells by targeting EIF5A2 signaling[26]. The PICSAR/miR-588/EIF6 axis contributes to the regulation of hepatocellular carcinoma progression by targeting AKT/mTOR signaling[27]. Moreover, it has been reported that miR-588 serves as a prognosis biomarker for gastric cancer[16]. In previous reports, miR-588 has not been prominently implicated in gastric cancer through interaction between tumor and the surrounding microenvironment. We were interested in the function of M2 macrophages-derived exosomes in cancer development and noticed the potential function of miR-588 in gastric cancer. Therefore, we explored the correlation of M2 macrophage-derived exosomes with miR-588 and their function in gastric cancer. Our data showed that co-cultivation of gastric cancer cells with M2 polarized macrophages promoted DDP resistance. M2 polarized macrophages-derived exosomes could transfer in gastric cancer cells to enhance DDP resistance. Exosomal miR-588 from M2 macrophages contributed to DDP resistance of gastric cancer cells. miR-588 promoted DDP-resistant gastric cancer cell growth *in vivo*. These data not only provide new evidence of the critical function of M2 polarized macrophages-derived exosomes in regulating cancer progression, but also indicate the innovative role of miR-588 in gastric cancer. The correlation of M2 polarized macrophages-derived exosomal miR-588 and miR-588 in the cancer cells in regulating cancer development is an interesting scientific issue, which is needed to explore in the future. Besides, the function of other pivotal miRNAs that have been described as crucial regulators in exosomes-mediated cellular communication should be explored by more investigations. Meanwhile, the mechanisms of miR-588 transfer from macrophage to gastric cancer cells remain unclear. According to previous studies, the communications between macrophages and gastric cancer cells can be mediated by exosomes, which can engulf local tissues immediately or swarm into body fluid to affect distant target organs through endocytosis[7,24,28]. The mechanisms of miR-588 transfer from macrophage to gastric cancer cells should be confirmed by more complicated investigations in future.

Moreover, it has been reported that inhibition of CYLD enhances IFN-γ-regulated PD-L1 expression in thymic epithelial cancer[29]. LINC01260 serves as a tumor inhibitor by regulating the miR-562/CYLD axis in lung cancer[30]. CYLD enhances nasopharyngeal carcinoma cells apoptosis by modulating NDRG1[31]. MiR-454 contributes to oxaliplatin resistance and cell proliferation by targeting CYLD in gastric cancer[32]. These reports have identified the tumor suppressive function of CYLD in

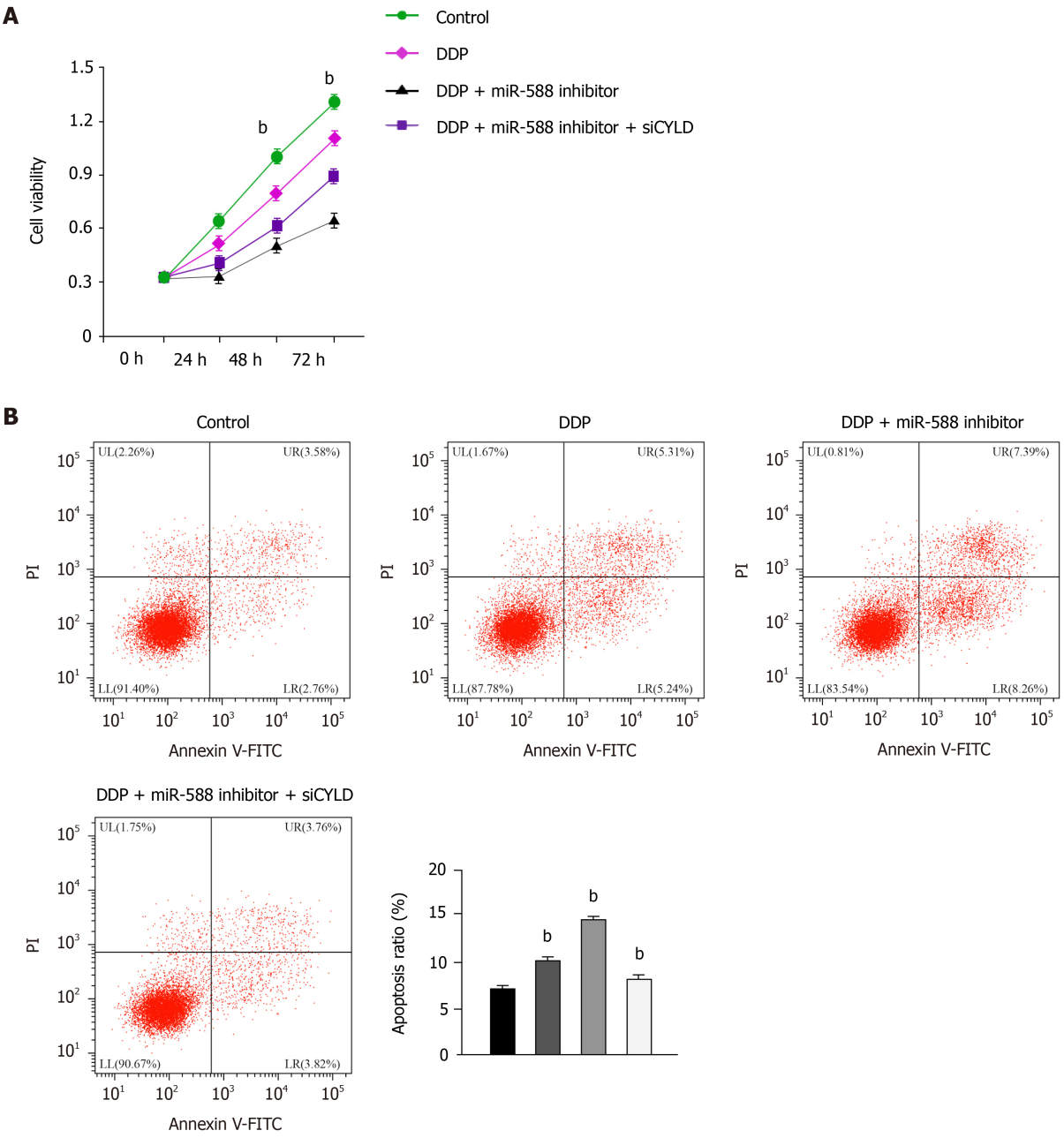


Figure 6 miR-588/cylindromatosis axis regulates cisplatin resistance of gastric cancer cells. A: Cell viability detected by CCK-8 assay; B: Cell apoptosis analyzed by flow cytometry. The SGC7901 cells were treated with cisplatin (DDP), or co-treated with DDP and miR-588 inhibitor with or without cylindromatosis siRNA. Data shown are the mean ± SD. $^{b}P < 0.01$. DDP: Cisplatin; CYLD: Cylindromatosis.

cancer progression. Our mechanical investigation showed that miR-588 targeted CYLD in gastric cancer cells and miR-588/CYLD axis contributed to the progression of gastric cancer. It presents a crucial mechanism underlying miR-588-mediated cancer development. CYLD may not be the only downstream factor underlying miR-588-mediatde tumorigenesis. Other regulators in miR-588-modulated cancer pathogenesis and their crosstalk may be investigated further in future. Targeting exosomal miR-588 from M2 macrophages may be a promising therapeutic strategy for gastric cancer and the clinical translation should be explored in future investigations.

CONCLUSION

In conclusion, we uncovered that exosomal miR-588 from M2 macrophages contributes to DDP resistance of gastric cancer cells by partly targeting CYLD. miR-588 may be applied as a potential therapeutic target for the treatment of gastric cancer.

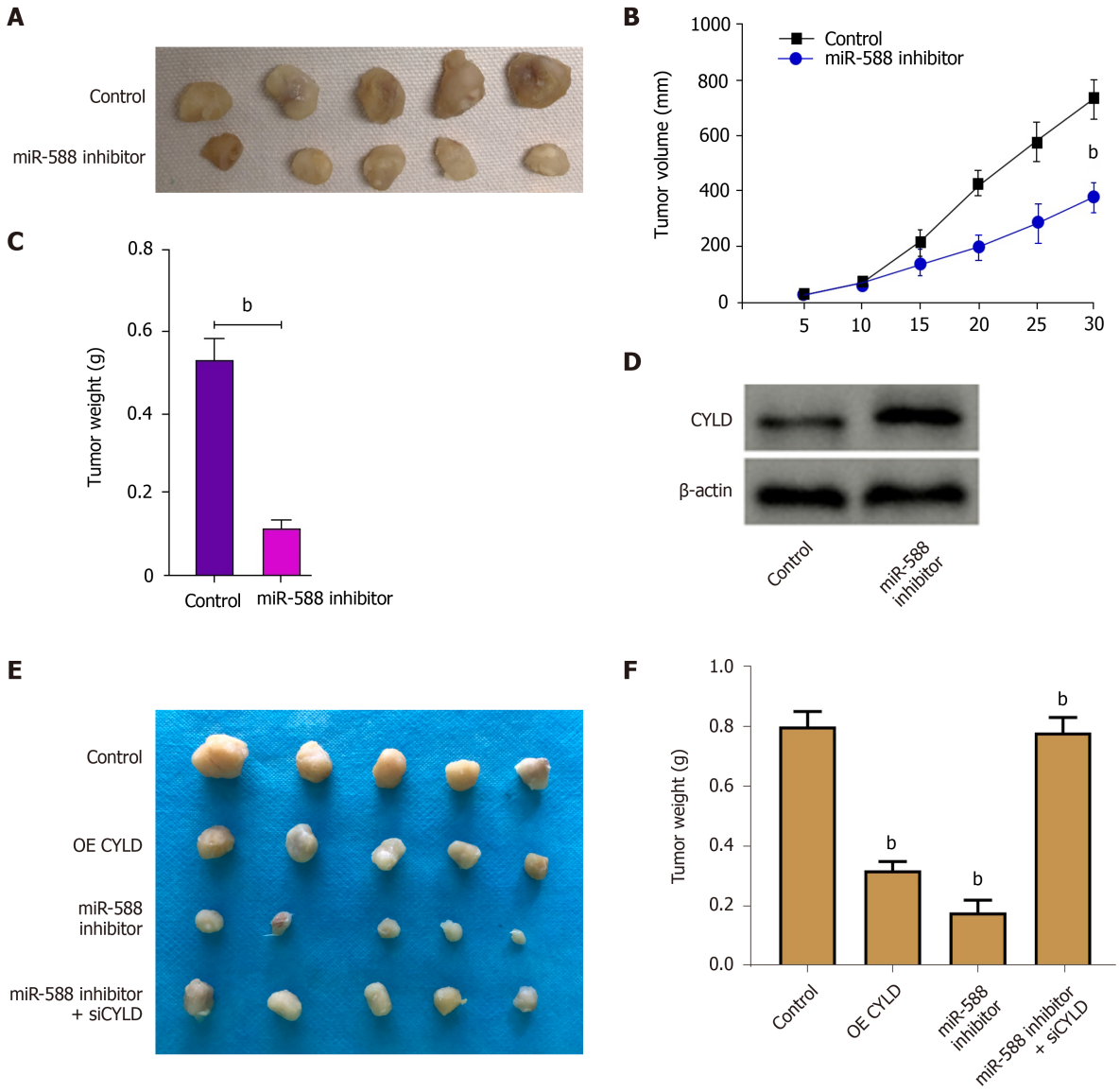


Figure 7 miR-588/cylindromatosis axis modulates cisplatin-resistant gastric cancer cell growth *in vivo*. A-D: The nude mice were injected with SGC7901 cells treated with miR-588 inhibitor, the tumor tissues (A), tumor volume (B), and tumor weight (C) were measured, and the expression of cylindromatosis (CYLD) was detected by Western blot analysis in the tumor tissues (D); E and F: The nude mice were injected with SGC7901 cells treated with CYLD overexpressing plasmid or miR-588 inhibitor, or co-treated with miR-588 inhibitor and CYLD siRNA, and the tumor tissues (E) and tumor weight (F) were measured. Data shown are the mean ± SD (n = 5). $^{b}P < 0.01$. CYLD: Cylindromatosis.

ARTICLE HIGHLIGHTS

Research background

Gastric cancer is a prevalent malignant cancer with a high incidence and significantly affects the health of modern people globally. Cisplatin (DDP) is one of the most common and effective chemotherapies for patients with gastric cancer, but DDP resistance remains a severe clinical challenge.

Research motivation

To identify the function of M2 polarized macrophages-derived exosomal miR-588 in gastric cancer cells.

Research objectives

To explore the effect of M2 polarized macrophages-derived exosomal miR-588 on DDP resistance of gastric cancer cells.

Research methods

M2 polarized macrophages were isolated and identified by specific markers using flow cytometry analysis. The exosomes from M2 macrophages were identified by TEM and related markers. The uptake of the PKH67-labelled M2 macrophages-derived exosomes was detected in SGC7901 cells. The function and mechanism of exosomal miR-588 from M2 macrophages in the modulation of DDP resistance of gastric cancer cell was analyzed by CCK-8 assay, apoptosis analysis, colony formation assay, Western blot analysis, qPCR analysis, and luciferase reporter assay in SGC7901 and SGC7901/DDP cells, and by tumorigenicity analysis in nude mice.

Research results

Polarized macrophages were isolated from mouse bone marrow stimulated with interleukin (IL)-13 and IL-4. Co-culture of gastric cancer cells with M2 polarized macrophages promoted DDP resistance. M2 polarized macrophage-derived exosomes could transfer in gastric cancer cells to enhance DDP resistance. Exosomal miR-588 from M2 macrophages contributed to DDP resistance of gastric cancer cells. miR-588 promoted DDP-resistant gastric cancer cell growth *in vivo*. miR-588 was able to target cylindromatosis (CYLD) in gastric cancer cells. The depletion of CYLD reversed miR-588 inhibition-regulated cell proliferation and apoptosis of gastric cancer cells exposed to DDP.

Research conclusions

In conclusion, we uncovered that exosomal miR-588 from M2 macrophages contributes to DDP resistance of gastric cancer cells by partly targeting CYLD.

Research perspectives

miR-588 may be applied as a potential therapeutic target for the treatment of gastric cancer.

REFERENCES

1 **Smyth EC**, Nilsson M, Grabsch HI, van Grieken NC, Lordick F. Gastric cancer. *Lancet* 2020; **396**: 635-648 [PMID: 32861308 DOI: 10.1016/S0140-6736(20)31288-5]

2 **Johnston FM**, Beckman M. Updates on Management of Gastric Cancer. *Curr Oncol Rep* 2019; **21**: 67 [PMID: 31236716 DOI: 10.1007/s11912-019-0820-4]

3 **Ghosh S**. Cisplatin: The first metal based anticancer drug. *Bioorg Chem* 2019; **88**: 102925 [PMID: 31003078 DOI: 10.1016/j.bioorg.2019.102925]

4 **Shen DW**, Pouliot LM, Hall MD, Gottesman MM. Cisplatin resistance: a cellular self-defense mechanism resulting from multiple epigenetic and genetic changes. *Pharmacol Rev* 2012; **64**: 706-721 [PMID: 22659329 DOI: 10.1124/pr.111.005637]

5 **Ngambenjawong C**, Gustafson HH, Pun SH. Progress in tumor-associated macrophage (TAM)-targeted therapeutics. *Adv Drug Deliv Rev* 2017; **114**: 206-221 [PMID: 28449873 DOI: 10.1016/j.addr.2017.04.010]

6 **Dai E**, Han L, Liu J, Xie Y, Kroemer G, Klionsky DJ, Zeh HJ, Kang R, Wang J, Tang D. Autophagy-dependent ferroptosis drives tumor-associated macrophage polarization *via* release and uptake of oncogenic KRAS protein. *Autophagy* 2020; **16**: 2069-2083 [PMID: 31920150 DOI: 10.1080/15548627.2020.1714209]

7 **Lan J**, Sun L, Xu F, Liu L, Hu F, Song D, Hou Z, Wu W, Luo X, Wang J, Yuan X, Hu J, Wang G. M2 Macrophage-Derived Exosomes Promote Cell Migration and Invasion in Colon Cancer. *Cancer Res* 2019; **79**: 146-158 [PMID: 30401711 DOI: 10.1158/0008-5472.CAN-18-0014]

8 **Kalluri R**. The biology and function of exosomes in cancer. *J Clin Invest* 2016; **126**: 1208-1215 [PMID: 27035812 DOI: 10.1172/JCI81135]

9 **Zhang L**, Yu D. Exosomes in cancer development, metastasis, and immunity. *Biochim Biophys Acta Rev Cancer* 2019; **1871**: 455-468 [PMID: 31047959 DOI: 10.1016/j.bbcan.2019.04.004]

10 **Wortzel I**, Dror S, Kenific CM, Lyden D. Exosome-Mediated Metastasis: Communication from a Distance. *Dev Cell* 2019; **49**: 347-360 [PMID: 31063754 DOI: 10.1016/j.devcel.2019.04.011]

11 **Bartel DP**. MicroRNAs: genomics, biogenesis, mechanism, and function. *Cell* 2004; **116**: 281-297 [PMID: 14744438 DOI: 10.1016/s0092-8674(04)00045-5]

12 **Bach DH**, Hong JY, Park HJ, Lee SK. The role of exosomes and miRNAs in drug-resistance of cancer cells. *Int J Cancer* 2017; **141**: 220-230 [PMID: 28240776 DOI: 10.1002/ijc.30669]

13 **Bayraktar R**, Van Roosbroeck K. miR-155 in cancer drug resistance and as target for miRNA-based therapeutics. *Cancer Metastasis Rev* 2018; **37**: 33-44 [PMID: 29282605 DOI: 10.1007/s10555-017-9724-7]

14 **Gao ZQ**, Wang JF, Chen DH, Ma XS, Yang W, Zhe T, Dang XW. Long non-coding RNA GAS5 antagonizes the chemoresistance of pancreatic cancer cells through down-regulation of miR-181c-5p.

Biomed Pharmacother 2018; **97**: 809-817 [PMID: 29112934 DOI: 10.1016/j.biopha.2017.10.157]
15 **Zhao N**, Lin T, Zhao C, Zhao S, Zhou S, Li Y. MicroRNA-588 is upregulated in human prostate cancer with prognostic and functional implications. *J Cell Biochem* 2017 [PMID: 28980707 DOI: 10.1002/jcb.26417]
16 **Chen Y**, Zhang J, Gong W, Dai W, Xu X, Xu S. miR-588 is a prognostic marker in gastric cancer. *Aging (Albany NY)* 2020; **13**: 2101-2117 [PMID: 33323542 DOI: 10.18632/aging.202212]
17 **Sun SC**. CYLD: a tumor suppressor deubiquitinase regulating NF-kappaB activation and diverse biological processes. *Cell Death Differ* 2010; **17**: 25-34 [PMID: 19373246 DOI: 10.1038/cdd.2009.43]
18 **Lork M**, Verhelst K, Beyaert R. CYLD, A20 and OTULIN deubiquitinases in NF-κB signaling and cell death: so similar, yet so different. *Cell Death Differ* 2017; **24**: 1172-1183 [PMID: 28362430 DOI: 10.1038/cdd.2017.46]
19 **Brummelkamp TR**, Nijman SM, Dirac AM, Bernards R. Loss of the cylindromatosis tumour suppressor inhibits apoptosis by activating NF-kappaB. *Nature* 2003; **424**: 797-801 [PMID: 12917690 DOI: 10.1038/nature01811]
20 **Suenaga N**, Kuramitsu M, Komure K, Kanemaru A, Takano K, Ozeki K, Nishimura Y, Yoshida R, Nakayama H, Shinriki S, Saito H, Jono H. Loss of Tumor Suppressor CYLD Expression Triggers Cisplatin Resistance in Oral Squamous Cell Carcinoma. *Int J Mol Sci* 2019; **20** [PMID: 31635163 DOI: 10.3390/ijms20205194]
21 **Wang Z**, Wang Q, Xu G, Meng N, Huang X, Jiang Z, Chen C, Zhang Y, Chen J, Li A, Li N, Zou X, Zhou J, Ding Q, Wang S. The long noncoding RNA CRAL reverses cisplatin resistance *via* the miR-505/CYLD/AKT axis in human gastric cancer cells. *RNA Biol* 2020; **17**: 1576-1589 [PMID: 31885317 DOI: 10.1080/15476286.2019.1709296]
22 **Xu W**, Chen Q, Wang Q, Sun Y, Wang S, Li A, Xu S, Røe OD, Wang M, Zhang R, Yang L, Zhou J. JWA reverses cisplatin resistance *via* the CK2-XRCC1 pathway in human gastric cancer cells. *Cell Death Dis* 2014; **5**: e1551 [PMID: 25476899 DOI: 10.1038/cddis.2014.517]
23 **Zheng P**, Luo Q, Wang W, Li J, Wang T, Wang P, Chen L, Zhang P, Chen H, Liu Y, Dong P, Xie G, Ma Y, Jiang L, Yuan X, Shen L. Tumor-associated macrophages-derived exosomes promote the migration of gastric cancer cells by transfer of functional Apolipoprotein E. *Cell Death Dis* 2018; **9**: 434 [PMID: 29567987 DOI: 10.1038/s41419-018-0465-5]
24 **Zheng P**, Chen L, Yuan X, Luo Q, Liu Y, Xie G, Ma Y, Shen L. Exosomal transfer of tumor-associated macrophage-derived miR-21 confers cisplatin resistance in gastric cancer cells. *J Exp Clin Cancer Res* 2017; **36**: 53 [PMID: 28407783 DOI: 10.1186/s13046-017-0528-y]
25 **Wu J**, Gao W, Tang Q, Yu Y, You W, Wu Z, Fan Y, Zhang L, Wu C, Han G, Zuo X, Zhang Y, Chen Z, Ding W, Li X, Lin F, Shen H, Tang J, Wang X. M2 Macrophage-Derived Exosomes Facilitate HCC Metastasis by Transferring $\alpha_M \beta_2$ Integrin to Tumor Cells. *Hepatology* 2021; **73**: 1365-1380 [PMID: 32594528 DOI: 10.1002/hep.31432]
26 **Zhou X**, Xu M, Guo Y, Ye L, Long L, Wang H, Tan P. MicroRNA-588 regulates invasion, migration and epithelial-mesenchymal transition *via* targeting EIF5A2 pathway in gastric cancer. *Cancer Manag Res* 2018; **10**: 5187-5197 [PMID: 30464616 DOI: 10.2147/CMAR.S176954]
27 **Liu Z**, Mo H, Sun L, Wang L, Chen T, Yao B, Liu R, Niu Y, Tu K, Xu Q, Yang N. Long noncoding RNA PICSAR/miR-588/EIF6 axis regulates tumorigenesis of hepatocellular carcinoma by activating PI3K/AKT/mTOR signaling pathway. *Cancer Sci* 2020; **111**: 4118-4128 [PMID: 32860321 DOI: 10.1111/cas.14631]
28 **Binenbaum Y**, Fridman E, Yaari Z, Milman N, Schroeder A, Ben David G, Shlomi T, Gil Z. Transfer of miRNA in Macrophage-Derived Exosomes Induces Drug Resistance in Pancreatic Adenocarcinoma. *Cancer Res* 2018; **78**: 5287-5299 [PMID: 30042153 DOI: 10.1158/0008-5472.CAN-18-0124]
29 **Umemura S**, Zhu J, Chahine JJ, Kallakury B, Chen V, Kim IK, Zhang YW, Goto K, He Y, Giaccone G. Downregulation of CYLD promotes IFN-γ mediated PD-L1 expression in thymic epithelial tumors. *Lung Cancer* 2020; **147**: 221-228 [PMID: 32738418 DOI: 10.1016/j.lungcan.2020.07.018]
30 **Chen Y**, Lei Y, Lin J, Huang Y, Zhang J, Chen K, Sun S, Lin X. The LINC01260 Functions as a Tumor Suppressor *via* the miR-562/CYLD/NF-κB Pathway in Non-Small Cell Lung Cancer. *Onco Targets Ther* 2020; **13**: 10707-10719 [PMID: 33116647 DOI: 10.2147/OTT.S253730]
31 **Lin Y**, Wang L, Luo W, Zhou X, Chen Y, Yang K, Liao J, Wu D, Cai L. CYLD Promotes Apoptosis of Nasopharyngeal Carcinoma Cells by Regulating NDRG1. *Cancer Manag Res* 2020; **12**: 10639-10649 [PMID: 33149672 DOI: 10.2147/CMAR.S268216]
32 **Huang C**, Liu J, Pan X, Peng C, Xiong B, Feng M, Yang X. miR-454 promotes survival and induces oxaliplatin resistance in gastric carcinoma cells by targeting CYLD. *Exp Ther Med* 2020; **19**: 3604-3610 [PMID: 32346424 DOI: 10.3892/etm.2020.8655]

World Journal of Gastroenterology

Submit a Manuscript: https://www.f6publishing.com

World J Gastroenterol 2021 September 28; 27(36): 6093-6109

DOI: 10.3748/wjg.v27.i36.6093

ISSN 1007-9327 (print) ISSN 2219-2840 (online)

ORIGINAL ARTICLE

Case Control Study

Evaluation of biomarkers, genetic mutations, and epigenetic modifications in early diagnosis of pancreatic cancer

Bilal Rah, Manzoor Ahmad Banday, Gh Rasool Bhat, Omar J Shah, Humira Jeelani, Fizalah Kawoosa, Tahira Yousuf, Dil Afroze

ORCID number: Bilal Rah 0000-0003-3673-5044; Manzoor Ahmad Banday 0000-0002-9495-845X; Gh Rasool Bhat 0000-0002-5223-4875; Omar J Shah 0000-0001-9207-7440; Humira Jeelani 0000-0001-5545-3283; Fizalah Kawoosa 0000-0002-2669-6128; Tahira Yousuf 0000-0002-6983-2716; Dil Afroze 0000-0002-0724-8899.

Author contributions: Rah B performed data analysis and manuscript writing; Banday MA contributed to study design, data analysis and gave directions; Bhat GR contributed to data analysis and proofreading; Shah OJ contributed by providing patient samples; Jeelani H contributed to manuscript writing; Kawoosa F contributed to sample collection and experimentation; Yousuf T contributed to manuscript writing; and Afroze D contributed to study design, data analysis and gave directions; All authors gave the final approval of the current version of the manuscript for publication and agreed to be accountable for the current work.

Institutional review board statement: The study was reviewed and approved by the Institutional Ethics committee (IEC), Sher-i-Kashmir Institute of

Bilal Rah, Gh Rasool Bhat, Humira Jeelani, Tahira Yousuf, Dil Afroze, Advanced Centre for Human Genetics, Sher-i-Kashmir Institute of Medical Sciences, Srinagar 190011, Jammu and Kashmir, India

Manzoor Ahmad Banday, Department of Medical Oncology, Sher-i-Kashmir Institute of Medical Sciences, Srinagar 190011, Jammu and Kashmir, India

Omar J Shah, Department of Surgical Gastroenterology, Sher-i-Kashmir Institute of Medical Sciences, Srinagar 190011, Jammu and Kashmir, India

Fizalah Kawoosa, Department of Immunology and Molecular Medicine, Sher-i-Kashmir Institute of Medical Science, Srinagar 190011, Jammu and Kashmir, India

Corresponding author: Dil Afroze, PhD, Full Professor, Advanced Centre for Human Genetics, Sher-i-Kashmir Institute of Medical Sciences, Main Road, Srinagar 190011, Jammu and Kashmir, India. afrozedil@gmail.com

Abstract

BACKGROUND

Pancreatic cancer (PC) is one of the deadliest malignancies with an alarming mortality rate. Despite significant advancement in diagnostics and therapeutics, early diagnosis remains elusive causing poor prognosis, marred by mutations and epigenetic modifications in key genes which contribute to disease progression.

AIM

To evaluate the various biological tumor markers collectively for early diagnosis which could act as prognostic biomarkers and helps in future therapeutics of PC in Kashmir valley.

METHODS

A total of 50 confirmed PC cases were included in the study to evaluate the levels of carbohydrate antigen 19-9 (CA 19-9), tissue polypeptide specific antigen (TPS), carcinoembryonic antigen (CEA), vascular endothelial growth factor-A (VEGF-A), and epidermal growth factor receptor (EGFR). Mutational analysis was performed to evaluate the mutations in Kirsten rat sarcoma (*KRAS*), Breast cancer type 2 (*BRCA-2*), and deleted in pancreatic cancer-4 (*DPC-4*) genes. However, epigenetic modifications (methylation of CpG islands) were performed in the promoter

Medical Sciences, Srinagar, Jammu and Kashmir, India

Conflict-of-interest statement: The authors declare no conflicts of interest.

Data sharing statement: No additional data are available

STROBE statement: The authors have read the STROBE Statement, and the manuscript was prepared and revised according to the STROBE Statement.

Open-Access: This article is an open-access article that was selected by an in-house editor and fully peer-reviewed by external reviewers. It is distributed in accordance with the Creative Commons Attribution NonCommercial (CC BY-NC 4.0) license, which permits others to distribute, remix, adapt, build upon this work non-commercially, and license their derivative works on different terms, provided the original work is properly cited and the use is non-commercial. See: http://creativecommons.org/Licenses/by-nc/4.0/

Manuscript source: Unsolicited manuscript

Specialty type: Gastroenterology and hepatology

Country/Territory of origin: India

Peer-review report's scientific quality classification

Grade A (Excellent): 0
Grade B (Very good): 0
Grade C (Good): C
Grade D (Fair): 0
Grade E (Poor): 0

Received: April 7, 2021
Peer-review started: April 7, 2021
First decision: May 27, 2021
Revised: June 10, 2021
Accepted: July 13, 2021
Article in press: July 13, 2021
Published online: September 28, 2021

P-Reviewer: Shafqat S
S-Editor: Ma YJ
L-Editor: Filipodia

regions of cyclin-dependent kinase inhibitor 2A (*p16; CDKN2A*), MutL homolog 1 (*hMLH1*), and Ras association domain-containing protein 1(*RASSF1A*) genes.

RESULTS

We found significantly elevated levels of biological markers CA 19-9 ($P \leq 0.05$), TPS ($P \leq 0.05$), CEA ($P \leq 0.001$), and VEGF ($P \leq 0.001$). Molecular genetic analysis revealed that *KRAS* gene mutation is predominant in codon 12 (16 subjects, $P \leq 0.05$), and 13 (12 subjects, $P \leq 0.05$). However, we did not find a mutation in *DPC-4* (1203G > T) and *BRCA-2* (617delT) genes. Furthermore, epigenetic modification revealed that CpG methylation in 21 ($P \leq 0.05$) and 4 subjects in the promoter regions of the *p16* and *hMLH1* gene, respectively.

CONCLUSION

In conclusion, CA 19-9, TPS, CEA, and VEGF levels were significantly elevated and collectively have potential as diagnostic and prognostic markers in PC. Global data of mutation in the *KRAS* gene commonly in codon 12 and rare in codon 13 could augment the predisposition towards PC. Additionally, methylation of the *p16* gene could also modulate transcription of genes thereby increasing the predisposition and susceptibility towards PC.

Key Words: Pancreatic cancer; Genetic mutations; Epigenetic modifications; Biomarkers; Risk factors; Diagnostics

©The Author(s) 2021. Published by Baishideng Publishing Group Inc. All rights reserved.

Core Tip: This study demonstrates that the collective evaluation of genetic mutations, epigenetic modifications in key genes and elevated levels of serum carbohydrate antigen 19-9, tissue polypeptide specific antigen, carcinoembryonic antigen, and vascular endothelial growth factor-A could be used as predictive biomarkers for diagnostics and prognostics in pancreatic cancer patients of the ethnic Kashmiri population. This could be useful to track the disease status of pancreatic cancer patients who are on a different regimen of chemotherapeutic interventions. To validate these results in the ethnic Kashmiri population, future studies need comprehensive, cohort, and replicative studies with large sample size.

Citation: Rah B, Banday MA, Bhat GR, Shah OJ, Jeelani H, Kawoosa F, Yousuf T, Afroze D. Evaluation of biomarkers, genetic mutations, and epigenetic modifications in early diagnosis of pancreatic cancer. *World J Gastroenterol* 2021; 27(36): 6093-6109
URL: https://www.wjgnet.com/1007-9327/full/v27/i36/6093.htm
DOI: https://dx.doi.org/10.3748/wjg.v27.i36.6093

INTRODUCTION

Pancreatic cancer (PC) is one of the deadliest malignancies among several solid malignancies. It is the 15th leading cancer in the world with an overall estimated incidence of 277000 new cases which is being diagnosed every year[1]. In the United States, PC is the fourth leading cause of death with a 5-year survival rate of less than 5%[2]. PC is mostly found in elderly people and has been reported to be associated with several risk factors[3]. The predominant risk factors include age, cigarette smoking, a high-fat diet, decreased serum levels of folate, diabetes mellitus, obesity, and chronic pancreatitis[4,5]. The familial history of pancreatitis increases the probability of developing PC by around 40%[6]. PC has the lowest prognosis among several solid-type tumors, mainly because almost 80% of PC patients are diagnosed when the disease is in the advanced or metastatic stage[7]. Owing to the lack of specific biological biomarkers used in clinical practice for the detection of PC and its nonspecific symptomology at the initial stage of the malignancy, the early diagnosis is extremely critical to detect and analyze disease progression[8]. Therefore, it is vital to identify specific biomarkers that play a key role in early diagnosis thereby improving the management and therapeutic outcome in PC.

P-Editor: Xing YX

Tumor biomarker(s) are the substances that can be examined in body fluids (blood, urine, and other fluids), synthesized and excreted by malignant cells within the tumor tissue besides exceeding the normal level potentiating its use for cancer diagnosis and/or prognosis[9]. Thus, ideally, the tumor markers should have high sensitivity and specificity, however, none of the tumor biomarkers have attained such precision [10]. Recent reports suggest that commonly used biomarkers for various malignancies include carbohydrate antigen 19-9 (CA 19-9), tissue polypeptide specific antigen (TPS), carcinoembryonic antigen (CEA), vascular endothelial growth factor-A (VEGF-A), and epidermal growth factor receptor (EGFR)[11]. The CA 19-9 and CEA are high molecular weight glycoproteins attached to the surface of tumor cells predominantly used in the diagnosis and prognosis of gut-associated cancers. However, marred by low sensitivity and specificity, they far from qualify for the diagnosis of other cancers [12]. The group of intermediate filament proteins to which TPS belongs is mainly used to measure cytokeratin 18 and 19 and expected to reflect the tumor progression. A few studies have examined TPS expression in PC; however, the findings are contentious. Although, individually TPS expression in PC may not provide significant information about the disease progression; in concert with other tumor biological markers it is worthwhile to evaluate its role for early diagnosis, prognosis, and to predict metastatic growth of PC[13]. A predominant dimeric, heparin-associated glycoprotein, VEGF-A has powerful pro-angiogenic and mitogenic activity. Elevated expression of VEGF-A enhances vascular permeability of endothelial cells and is reported to be involved in PC-associated angiogenesis[14], thus potentiates as a predictive biomarker. EGFR is a transmembrane protein that regulates cell growth and development. Mutation or elevated expression of EGFR is a key event in the pathogenesis of various malignancies such as glioblastoma, lung and oral carcinomas. There are reports of EGFR-mediated signaling associated with EGFR mutation in PC patients[15]. Consequently, these reports suggest that evaluation of serum EGFR levels in PC can be a promising putative biomarker for early diagnosis and prognosis to monitor the disease status post-therapeutic interventions. Although, individually the tumor biomarkers could aid in diagnostic and prognostic evaluation to a certain level, however, collectively, they can be more beneficial to track tumor progression and could be more useful to monitor disease status. Therefore, the current study aims to evaluate the collective role of various tumor biomarkers in PC patients for their potential role in early diagnosis and application in prognosis to examine post-treatment disease status in the ethnic Kashmiri population.

Genetic mutations play a pivotal role in tumor progression and genetic markers are critically important for the detection of malignant changes in PC[16]. Approximately, 97% of PC patients have alterations in genes that either follow the germline inheritance mode of transmission or occur sporadically[17]. These mutations could be either oncogenic (gain of function) or diminish tumor suppressor activity (loss of function). Gain-of-function in Kirsten rat sarcoma (*KRAS)* a proto-oncogene that encodes guanosine triphosphatase (GTPase), is one of the prominent mediators in signal transduction pathways that are implicated in neoplastic transformation and inflammation[18]. Approximately 95% of all cancers including PC are reported to harbor a *KRAS* gene mutation which is a key event in early tumorigenesis. The major *KRAS* activating gene mutations reportedly occur at codon 12 and less commonly at codon 13 and codon 61. Therefore, evaluation of genetic mutational analysis at the hotspot regions of the *KRAS* gene could help in early diagnosis and prognosis in PC. Breast cancer type 2 *(BRCA-2)*, a tumor suppressor gene is associated with the maintenance of the genome by enhancing homologous recombination of a double-stranded break. Around 80% of *BRCA-2* mutations are either frameshift or nonsense mutations that result in the formation of premature stop codons to encode non-functional BRCA-2 protein[19]. Almost 7.3% of PC patients have a hereditary mutation in the *BRCA-2* gene which increases the risk of developing PC by approximately 20-fold[20] implicating a critical role of *BRCA-2* in the early diagnosis of PC. Another vital gene, 'deleted in pancreatic cancer-4' *(DPC-4)* also known as SMAD family member 4, mothers against decapentaplegic homolog 4 (*SMAD-4)* is a tumor suppressor gene involved in the regulation of gene transcription. DPC-4 protein a downstream target of transforming growth factor-beta (TGF-β) pathway plays a critical role in the activation of TGF-β signaling thereby promotes neoplastic growth. It is reported that 30% of PC cases develop due to homozygous mutations in the *DPC-4* gene[21,22]. Thus, mutational analysis of the *DPC-4* gene could be a promising factor for the early diagnosis and prognosis of PC.

Besides genetic mutations, recent evidence suggests the epigenetic modifications such as DNA methylation plays a critical role in the pathogenesis of PC. In the recent past, reports suggest that methylation at the promoter regions of key tumor

suppressor genes induces gene silencing and contributes to the development and progression of tumorigenesis[23]. Various tumor suppressor genes were inactivated by epigenetic modifications. Cyclin-dependent kinase inhibitor 2A (*p16; CDKN2A*), a tumor suppressor gene that encodes a member of cyclin-dependent kinase inhibitor which arrests the G_1-S phase of the cell cycle to prevent tumor cell progression. Loss of the *p16* gene is reported in 70% of cancers and around 10%-15% of the loss was due to promoter methylation[24]. Thus, screening of epigenetic modifications at the promoter region of the *p16* gene could help in the early diagnosis of PC. MutL homolog 1 (*hMLH1)* a tumor suppressor gene that belongs to the mismatched repair gene family and prevents DNA damage by radiations and other associated mechanisms. *hMLH1* is also reported to be inactivated epigenetically by promoter methylation which leads to DNA damage. The accumulation of mismatched and damaged DNA promotes tumor cell progression[25]. Ras association domain-containing protein 1*(RASSF1A)* is another tumor suppressor gene inactivated by promoter methylation. It is a component of RAS/PI3K/AKT and RAS/MAPK pathways. Recent reports suggest that epigenetic modifications in the *RASSF1A* promoter region promote tumor progression in various cancers including kidney, breast, lung, prostate, and thyroid[26]. Recent evidence suggests that 64% of pancreatic adenocarcinoma patients have *RASSF1A* hypermethylation at the promoter region, indicating that analysis of hypermethylation of *RASSF1A* at promoter region could be a promising approach for early diagnosis of PC. To summarize, these studies suggest that genetic mutations, epigenetic modulations, and elevated levels of serum biological markers play a critical role in the early diagnosis, therapeutics, and prognosis of various cancer. Therefore, keeping in consideration the documented role of tumor biomarkers, genetic mutations, and DNA methylation of tumor suppressor/protooncogenes in various malignancies including PC. The current study aimed to evaluate the serum levels of various biological tumor markers, genetic mutations, and epigenetic modifications of some key regulatory genes in PC. This would prove immensely helpful in the early diagnosis of PC, which helps in the identification of high-risk PC and may enable their development as biomarkers for future diagnostics, therapeutic interventions, and prognostics in the ethnic Kashmiri population.

MATERIALS AND METHODS

In this study, a total of 50 patients with pancreatic carcinoma and 50 healthy controls were included.

Inclusion criteria

Only the patients with histologically confirmed pancreatic carcinoma were included in this study. Written consent was taken at the very beginning from all the patients and healthy controls that were included in the study.

Exclusion criteria

The patients with a history of other malignancies and those who were not willing to comply with pre-requisite protocol were excluded from the study.

Physical examination and lifestyle habits

The study was designed and approved by the institutional review board of the Sher-i-Kashmir Institute of Medical Sciences (SKIMS), and informed consent was obtained from all participants. A comprehensive physical/clinical examination was performed in the Department of Medical Oncology, SKIMS, and the patients were evaluated for Jaundice (by examining features like yellowing of eyes and skin), pruritis (by examining features like redness, bumps, spots or blisters, dry/cracked skin and leathery/scaly skin), muscle wasting (by evaluating features like weakness or numbness in the limbs, loss of muscle coordination, tingling or weakness of the extremities, impaired balance while walking, fatigue and a general illness, facial weakness, progressive weakness, gradual memory loss and liver enlargement (were examined by features like abdominal pain, nausea/vomiting, fatigue, whitening of eyes and yellowing of the skin).

Besides the physical examination, lifestyle activities of the PC patients were also recorded which included smoking status, salt tea consumption, spicy and non-spicy food intake, dried vegetable consumption, mutton, and beef consumption, fish consumption, oil intake, urine habits, bowel habits, and daily physical activity were also recorded.

Laboratory findings

The basic clinical laboratory findings were performed by using automated analyzers. The laboratory findings are liver function test (like aspartate transaminase-AST, alanine transaminase-ALT, bilirubin, and alkaline phosphatase-ALP), diabetic status (hyperglycemia) by measuring glucose levels, and anemia by measuring red blood cell (RBC) count.

Diagnostic imaging

For any other malignancy PC patients were initially screened by using multiphase multidetector computed tomography (CT) scan, magnetic resonance imaging (MRI), ultrasonography (USG), endoscopic ultrasound (EUS), and chest X-ray (CXR).

Sample collection

A total of 5 mL blood sample was collected in clot activator and Ethylenediaminetetraacetic acid (EDTA) vial from PC patients. The serum was separated from the clot activator vials using centrifugation and was stored at -80 °C for further analysis. EDTA vials contain blood was stored at -20 °C for DNA extraction. A tissue chunk (12-50 µm thick tumor tissue section) was obtained from the PC patient by endoscopy using USG-guided probes for mutational analysis and epigenetic modifications.

Tumor biomarkers

Tumor markers including CA19-9, TPS, CEA, VEGF-A, and EGFR were estimated in the serum obtained from blood collected from the PC patients. Measurement of CA 19-9, CEA, VEGF-A, and EGFR levels in serum were performed by using a modular E-170 analyzer. However, TPS levels in the serum were measured by using an Immulite instrument.

Genetic mutation analysis

Genomic DNA was extracted by the phenol-chloroform method from mononuclear cells. Hypaque density gradient centrifugation was performed to extract leucocytes from blood and tissue samples obtained from PC patients. The quantity and quality control analysis of genomic DNA was performed by carrying out UV spectrophotometer (Eppendorf Biospectrometer®, Hamburg Germany) analysis and Gel electrophoresis, respectively. However, polymerase chain reaction (PCR) was carried out with a different set of primers for *KRAS*, *DPC-4*, and *BRACA-2* genes under different PCR conditions. The PCR products obtained were subjected to Restriction Fragment Length Polymorphism (RFLP) using restriction enzymes BstN1 and BglI for mutational analysis of *KRAS* codon 12 and 13, respectively. GGA→TGA in exon 8, codon 358 of *DPC-4* gene was analyzed by using MnlI restriction enzyme. 6174delT of *BRCA-2* was analyzed by using allele-specific PCR technique and polyacrylamide gel electrophoresis (PAGE) was carried out to study any change in the *BRCA-2* gene.

Epigenetic analysis

The epigenetic analysis was performed by examining the methylation status of the promoter and exon regions of genes including *p16*, *RASSF1A*, and *hMLH1*. The methylation status of *p16*, *RASSF1A*, and *hMLH1* genes was determined by methylation-specific (MSP) PCR. Briefly, DNA extracted from tissue samples was first subjected to bisulfite conversion using EZ direct methylation kit. The bisulfite-converted DNA was then subjected to PCR using methylated and unmethylated primers specific for the respective genes. The results were analyzed on 2% agarose gel.

Statistical analysis

Numerical data collected from experiments for statistical analysis were performed by using non-parametrical statistical analysis tools which are the Kruskal-Wallis test and Mann-Whitney *U* test.

RESULTS

The current study included 50 PC patients with a mean age of 47.82 years at the time of diagnosis for the evaluation of various tumor biological markers for the PC diagnosis. Radio-diagnostics such as USG and CT, confirmed that all 50 patients had PC. Further, histopathological analysis supported the radio-diagnostic results and revealed that out of 50 confirmed PC patients, 47 PC patients had characterized to

have adenocarcinoma whereas the remaining 3 PC patients have neuroendocrine carcinoma in the pancreas as shown in Figure 1. The other demographic parameters and daily activities of all confirmed 50 PC patients are presented in Table 1.

Owing to have relative ease in blood collection and non-invasive, it is preferred to evaluate the biological tumor markers in serum. Therefore, we also intended to evaluate the biological tumor markers which included CA 19-9, TPS, CEA, VEGF-A, and EGFR levels in the blood collected from PC patients. Our results demonstrated that the levels of serum biological tumor markers CA 19-9, CEA, VEGF-A, TPS, EGFR of PC patients were significantly raised in 33 (66%), 32 (64%), 48 (96%), 48 (96%) and 0 out of 50 PC patients, respectively (Table 2) and Figure 2.

Although the PC progression is a heterogeneous and complex process that includes cell proliferation of intraepithelial and dysplasia to form a mass of cells, followed by an invasion of cells to neighboring tissues. Subsequently, one of the important driving factors of PC progression is genetic mutations of protooncogenes (gain-of-function) and tumor suppressor genes (loss-of-function). Among genetic mutations, *KRAS* mutation is the key point mutation followed by deletion mutation in tumor suppressor genes *BRCA-2, DPC-4,* and *p16* in PC. To evaluate whether the PC patients in our study harbor these mutations, we sought to perform mutational analysis of *KRAS* hotspot codons (codon 12 and codon 13), *DPC-4* (1203G>T), and *BRCA-2* mutation (6174delT) in our PC subjects. Our mutational analysis results revealed that out of 50 PC patients, 16 and 12 PC patients had *KRAS* mutation at codons 12 and 13, respectively. However, we could not find mutation(s) at codons 12 and 13 of the *KRAS* gene in the remaining 34 and 38 PC patients, respectively Figure 3. The representative agarose gel picture of the amplification product of codons 12 and 13 of the *KRAS* gene and their RFLP pattern is shown in Figures 4 and 5. Subsequently, the mutational analysis of tumor suppressor gene *DPC-4* (1203G>T) and *BRCA-2* (6174delT) were also evaluated in all PC subjects. Interestingly, we did not find any mutations in *DPC-4* and *BRCA-2* mutation at (1203G>T) (6174delT) sites, respectively Figure 3. The representative agarose gel picture of *DPC-4* (1203G>T) amplification and RFLP pattern is shown in Figure 6, respectively, and that of amplification and RFLP pattern of *BRCA-2* (6174delT) is shown in Figure 7. The results obtained from the genetic mutation analysis are summarized in Table 3.

Epigenetic alterations have been documented to play a crucial role in PC progression. The *p16, RASSF1A,* and *hMLH1* are key tumor suppressor genes regulating mismatch repair to minimize DNA damage and are frequently inactivated by epigenetic modification in various malignancies. Therefore, we intended to investigate the epigenetic modification (methylation of CpG islands) of *p16, RASSF1A,* and *hMLH1* genes by determining the methylation in their respective promoter regions in all PC subjects. Our epigenetic modification results demonstrated that 21 out of 50 PC subjects were found methylated in the CpG islands of the promoter region of the *p16* gene while the remaining 29 were unmethylated. However, the CpG islands in the promoter region of *RASSF1A* were found to be unmethylated in all 50 PC patients. Additionally, we observed that 4 out of 50 PC patients showed methylation patterns in the promoter region of the *hMLH1* gene, whereas the remaining 46 PC patients had the *hMLH1* gene unmethylated in their promoter regions. The representative agarose gel pic of MS-PCR for *hMLH1* and *RASSF1A* is shown in Figure 8. The methylation and unmethylation status as observed in the present study for *p16, hMLH1,* and *RASSF1A* are summarized in Table 4 and Figure 9.

DISCUSSION

Despite new therapeutic approaches to improve the outcome of PC patients by the introduction of molecular target approaches and combinatorial therapy, there is an unmet need to find the prospective biomarkers for early diagnosis of PC[27]. Therefore, the aim of the current study was to collective evaluation of tumor biological markers, mutational status, and epigenetic modulations in PC patients of the ethnic Kashmiri population for early diagnosis. Our findings revealed the elevated levels of serum biomarkers CA 19-9, TPS, CEA, and VEGF-A, in the blood samples of PC patients, however, EGFR levels were found to be in the normal range. The mutational analysis demonstrated that the *KRAS* gene mutation which is the major driver in PC progression was found in codons 12 (16 subjects) and 13 (12 subjects). Furthermore, DNA of CpG islands of 21 subjects was found significantly methylated in the promoter regions of the *p16* gene. Collectively, these results suggest that in combination with mutational analysis and epigenetic modulations (CpG methylation), the biological

Table 1 Characteristics and clinical presentations of cases in the present study, *n* (%)

Patient characteristics	Cases, *n* = 50	*P* value
Age in yr		
≤ 50	28 (56.0)	0.0377
> 50	22 (44.0)	
Gender		
Male	29 (58.0)	0.031
Female	21 (42.0)	
Family history		
Smoker		
Yes	22 (44.0)	0.034
No	28 (56.0)	
Lifestyle		
Active	44 (88.0)	0.001
Sedentary	06 (12.0)	
Residence		
Rural	40 (80.0)	0.01
Urban	10 (20.0)	
Dietary habits		
Salt tea		
Yes	47 (94.0)	0.01
No	03 (06.0)	
Spicy food		
Yes	28 (56.0)	0.043
No	22 (44.0)	
Appetite		
Yes	25 (50.0)	0.05
No	25 (50.0)	
Vegetables		
Yes	48 (100.0)	0.001
No	02 (00.0)	
Non-veg.		
Yes	47 (100.0)	0.001
No	03 (00.0)	
Edible oil		
Saturated	43 (86.0)	0.01
Unsaturated	07 (17.0)	
Urine habits		
Normal	28 (56.0)	0.05
Disturbed	22 (44.0)	
Bowel habits		
Normal	30 (60.0)	0.05
Disturbed	20 (40.0)	

Table 2 Analysis of tumor biological marker in the serum of pancreatic cancer patients

Tumor marker	Normal level	PC patients with elevated levels of tumor markers	PC patients with normal levels of tumor markers	*P* value for PC patients with elevated levels *vs* normal levels
CA19-9	< 37 U/mL	33	17	0.05
TPS	< 80 U/L	32	18	0.05
CEA	< 5 ng/mL	48	02	0.003
VEGF-A	31.2-2000 pg/mL	48	02	0.003
EGFR	62.5-4000 pg/mL	0	50	0.001

PC: Pancreatic cancer; CA19-9: Carbohydrate antigen 19-9; TPS: Tissue polypeptide specific antigen; CEA: Carcinoembryonic antigen; VEGF-A: Vascular endothelial growth factor-A; EGFR: Epidermal growth factor receptor.

Table 3 Mutational analysis of *KRAS* (Codon 12 and 13), *DPC-4*, and *BRCA-2* gene mutations within pancreatic cancer subjects

Key genes in PC patients evaluated for mutational analysis	Mutation's present	Mutation's absent	*P* value for mutations present *vs* absent
KRAS mutation (codon 12)	16	34	0.05
KRAS mutation (codon 13)	12	38	0.05
DPC-4 mutation (1203G>T)	0	50	0.001
BRCA-2 mutation (6174delT)	0	50	0.001

KRAS: Kirsten rat sarcoma; *DPC-4*: Deleted in pancreatic cancer-4; *BRCA-2*: Breast cancer type 2.

Table 4 Methylation and unmethylation status in the promoter region of *p16*, *RASSF1A*, and *hMLH1*within pancreatic cancer subjects

Genes	Promoter methylation analysis status	Promoter unmethylation analysis status	*P* value for promoter methylation *vs* ummethylation
p16	21	29	0.05
RASSF1A	0	50	0.001
hMLH1	4	46	0.165

tumor markers evaluated in PC subjects could be valuable for early diagnostics and could strongly predict the PC prognostics. Additionally, these types of studies could further strengthen the validation of biological tumor markers and have a promising perspective for the predisposition and susceptibility towards PC.

A biological tumor marker is an entity in the body that gives information about a diagnosis, prognosis, and therapeutic modalities for a particular disease. The preferred entity to be eligible as a biomarker should be available in body fluids and non-invasive [28]. One of the important tumor biomarkers used in various malignancies is a high molecular weight glycoprotein CA 19-9. Biochemically, a carbohydrate antigen, CA19-9 is mainly expressed by the cells of the pancreaticobiliary system. Previous studies suggest that CA 19-9 levels were elevated in gut-associated malignancies such as gastric, bile duct, colorectal, and ovarian cancers. Owing to its relatively higher sensitivity and specificity among other biomarkers in PC patients, CA 19-9 is an important and valuable biomarker in the diagnostics of PC[29]. Although reports suggest a significant progress in overall survival and reduction in CA19-9 levels in PC, however, a recent study by Hess *et al*[30] did not support these findings. O'Brien *et al* [31] reported that CA 19-9 levels were raised in PC patients and may act as a better biomarker for the early diagnosis of PC. Besides, the levels of CA 19-9 were found directly associated with tumor size, tumor burden, and stage of tumorigenesis in PC, the pre-and post-operative levels of CA 19-9 in PC patients could be used as a prognosticator. Consistent with these findings, our results revealed that out of 50 PC

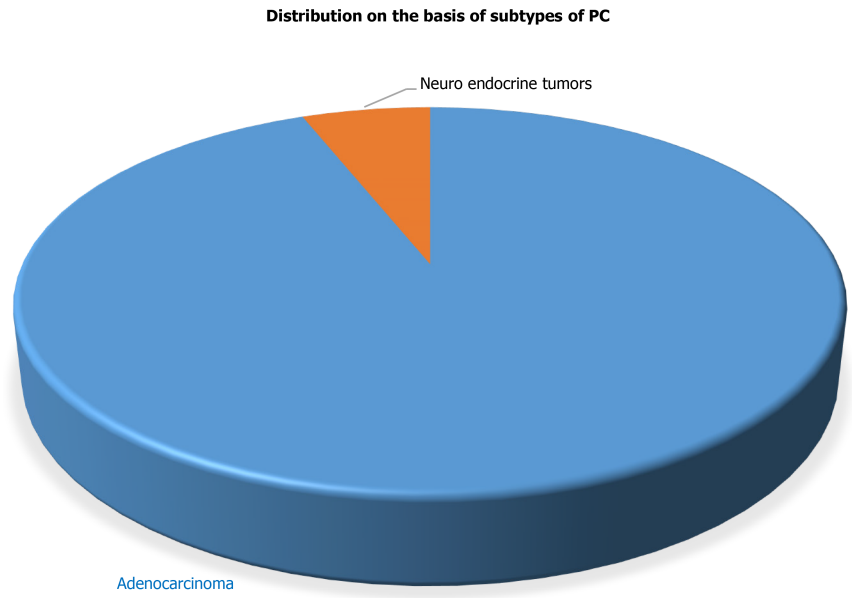


Figure 1 Distribution of samples (cases) based on subtypes of pancreatic cancer. PC: Pancreatic cancer.

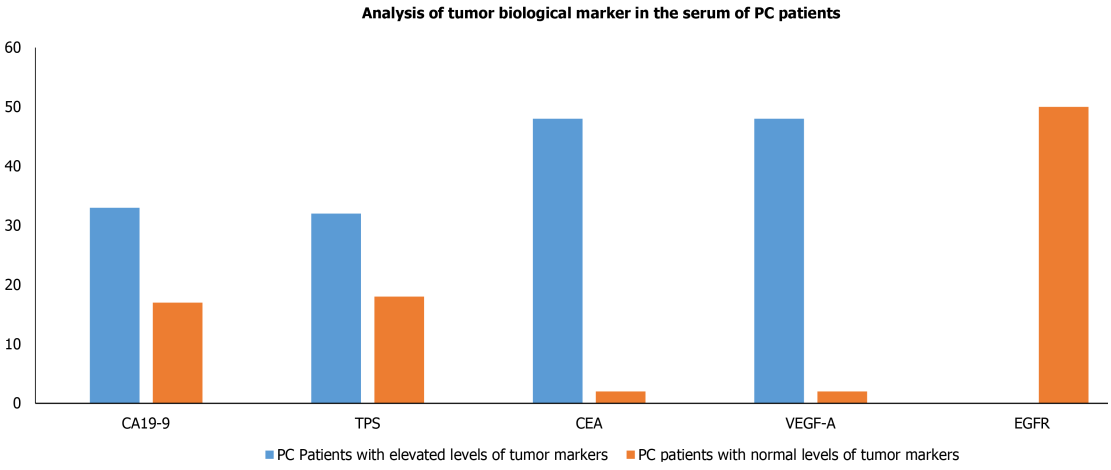


Figure 2 Analysis of tumor biological marker (carbohydrate antigen 19-9, tissue polypeptide specific antigen, carcinoembryonic antigen, vascular endothelial growth factor-A, and epidermal growth factor receptor) in the serum of pancreatic cancer patients. PC: Pancreatic cancer; CA19-9: Carbohydrate antigen 19-9; TPS: Tissue polypeptide specific antigen; CEA: Carcinoembryonic antigen; VEGF-A: Vascular endothelial growth factor-A; EGFR: Epidermal growth factor receptor.

patients 33 had significantly elevated levels of CA 19-9 in their blood samples, which indicates that more studies with a large cohort size are needed in the future to validate CA 19-9 as a better early diagnostic biomarker in PC.

Another valuable biomarker used in the diagnosis of various malignancies is TPS. It is essentially an antigen that binds to the epitope of soluble cytokeratin 18 fragments. The striking feature of TPS is to differentiate between PC and chronic pancreatitis and it is a better marker than CA 19-9 for differentiating PC and pancreatitis[32]. Previous studies suggested that serum TPS levels have a better correlation with gastric, colorectal, and pancreatic cancer than CA 19-9, CA 195, or CEA biomarkers[33,34]. Consistent with the previous studies, our results revealed that 48 out of 50 confirmed PC patients had significantly elevated levels of TPS, which suggests that elevated levels of serum TPS are better correlated with PC than CA 19-9 and could act as a better diagnostic and prognostic biomarker in PC. CEA, a glycoprotein, first identified in 1965, is present normally in the fetal pancreas, gastrointestinal tract, and liver. In the adolescent stage, it is found in lesser quantity in endodermal tissue and colon. CEA was used as a diagnostic marker of PC decades before and is now replaced by markers that have greater sensitivity for the detection of PC[35]. Elevated serum levels of CEA

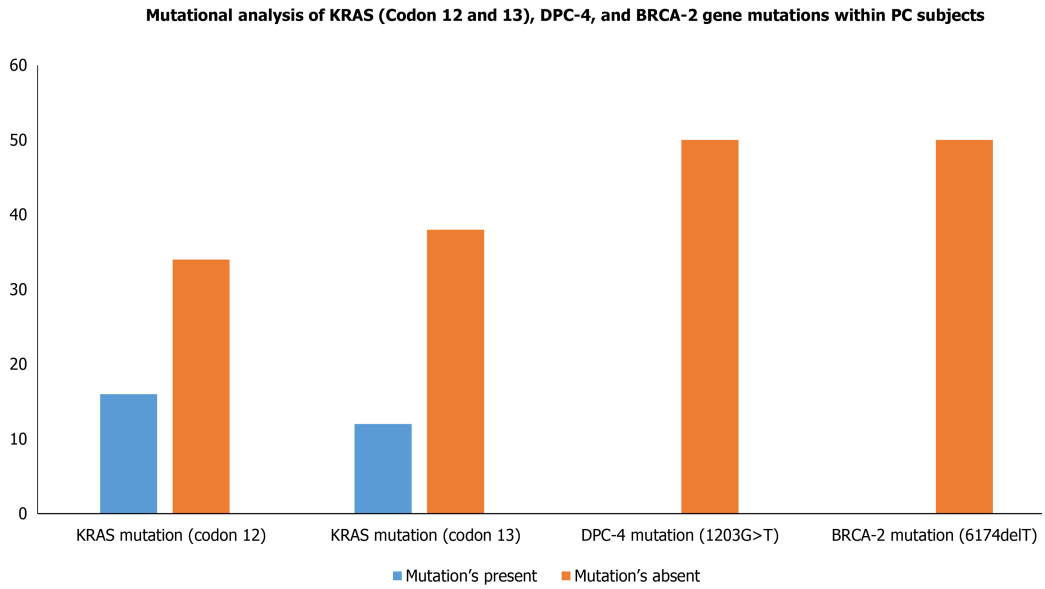


Figure 3 Mutational analysis of *KRAS* (Codon 12 and 13), *DPC-4*, and *BRCA-2* gene mutations within pancreatic cancer cases. KRAS: Kirsten rat sarcoma; DPC-4: Deleted in pancreatic cancer-4; BRCA-2: Breast cancer type 2.

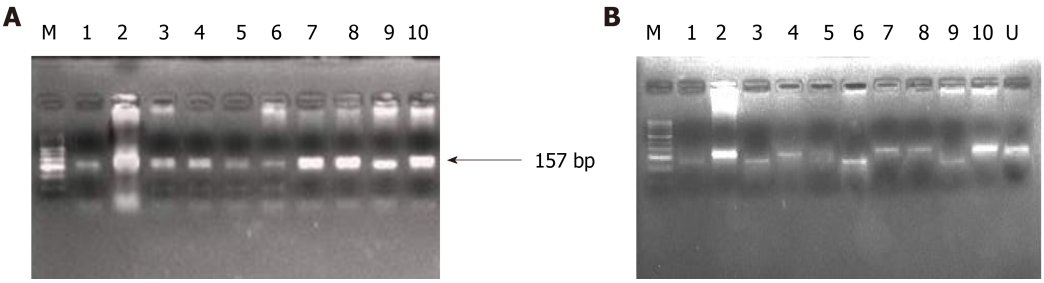


Figure 4 Representative agarose gel picture of polymerase chain reaction amplification (A) and restriction fragment length polymorphism using BstN1 (B) for *KRAS* codon 12. The arrow represents the 157 bp amplicon and M denotes the DNA marker (50 bp). Lane M represents a DNA marker (50 bp). Lanes 2, 4, 7, 8, and 10 represent the mutant band (undigested) of 157 bp. Lane 1, 3, 6, and 9 represent the wild band (digested) of 128 bp. U represents the undigested band used as mutant control.

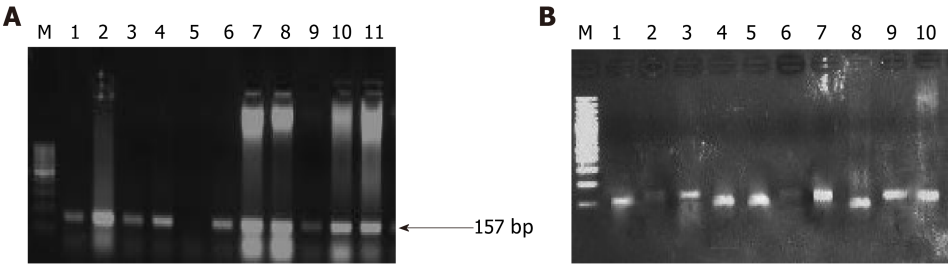


Figure 5 Representative gel picture of polymerase chain reaction amplification (A) and restriction fragment length polymorphism using BglI (B) for *K-RAS* codon 13. The arrow represents the 157 bp amplicon and M denotes the DNA marker (100 bp). Lane M represents a DNA marker (100 bp). Lanes 2, 3, 6, 7, 8, 9, 10, and 11 represent the mutant band (undigested) of 157 bp. Lanes 1, 4, 5, and 8 represent a wild band (digested) of 125 bp.

have been documented in more than 60% of cases of PC. Consistent with previous findings, our results demonstrated that 64% of patients (32 out of 50 confirmed PC) had elevated levels of serum CEA. However, if used with other biomarkers for early diagnostics, CEA could be adding up great value to early diagnostics of PC[36]. High expression of VEGF-A is associated with tumor size and progression. Overexpression of VEGF-A has been reported in head and neck, non-small cell lung, ovarian, endometrial, osteosarcoma, bladder, B cell lymphoma, ocular adnexal lymphoma, papillary renal cell carcinoma, and pancreatic cancers. VEGF-A is reported to have an

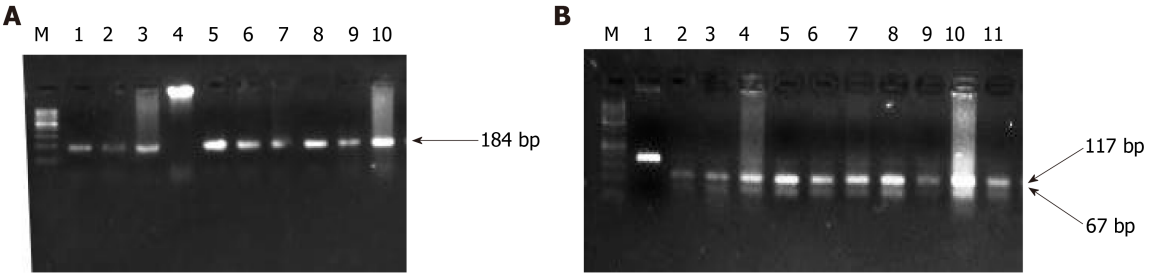


Figure 6 Representative gel picture of polymerase chain reaction amplification and restriction fragment length polymorphism using MnlI of *DPC-4*. The arrow represents the 184bp amplicon and M denotes the DNA marker (100 bp). Lane M represents a DNA marker (50 bp). 117 bp and 67 bp represent the wild bands (digested). U represents the mutant control band of 184 bp (undigested).

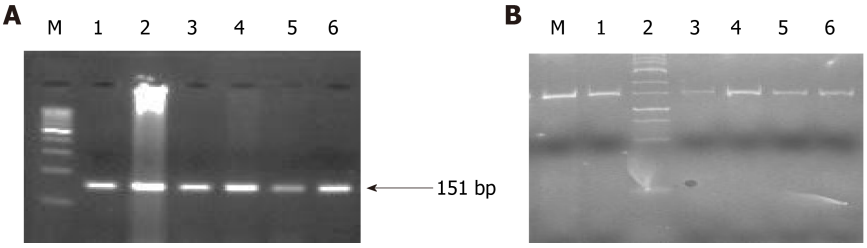


Figure 7 Representative agarose gel picture of AS-polymerase chain reaction amplification (A) and gel picture representing polyacrylamide gel electrophoresis (20% gel) (B) of *BRCA-2*. All the lanes show 151 bp amplicon which is the wild band and M denotes the DNA marker (100 bp). M is the marker lane (25 bp). Here also, the only wild band (151 bp) is observed in all the lanes.

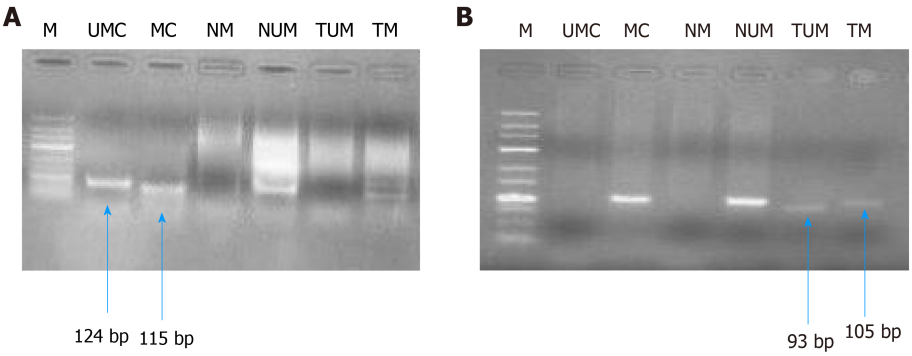


Figure 8 Gel picture representing MS-polymerase chain reaction for *hMLH1* (A, 100 bp) and *RASSF1A* (B, 25 bp). M represents DNA marker; UMC represents unmethylated control; MC represents methylated control; NM represents normal methylated; NUM represents normal unmethylated; TUM represents tumor unmethylated; TM represents tumor methylation.

80 gene loci whose alterations are reported in hepatocarcinoma, lung, pancreatic, and endometrial cancers[36]. A study conducted by Seo *et al*[37] demonstrated that 93% of ductal pancreatic adenocarcinomas showed high expression of VEGF-A protein. In the recent past, around 77% of VEGF-A expression was observed in PC tissues whereas only 15% of VEGF-A expression was found in the normal range[38]. Consistent with these findings, our results showed that out of 50 confirmed PC subjects, 48 cases had elevated levels of VEGF-A expression, which indicates that VEGF-A plays a critical role and had a strong causal association with PC progression, thus could act as a valuable tumor biomarker in combination with other biomarkers for early diagnosis of PC.

Besides, the currently available biomarkers for PC diagnostics, it is worthy to introduce genetic markers to develop more sophisticated tools for early detection of PC. PC is a disease that harbors somatic as well as hereditary mutations. Approximately, 5%-10% of the familial PC is caused by a mutation in a myriad of genes and surges the predisposition to PC by several-fold[24]. Previous studies reported that several genes showed a strong causal association with PC progression, among these most important are *KRAS, DPC-4,* and *BRCA-2* which in turn are associated with

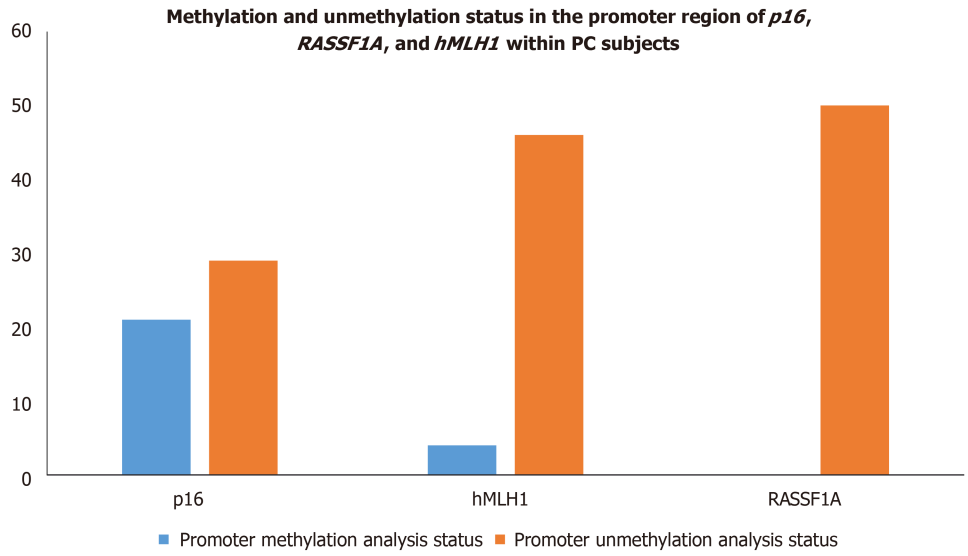


Figure 9 Methylation and unmethylation status in the promoter region of *p16*, *RASSF1A*, and *hMLH1* within pancreatic cancer subjects.
PC: Pancreatic cancer.

different other genes using different interactions like physical interaction, genetic interaction, shared protein interaction, *etc.* as depicted in Figure 10[39]. The most common mutation reported in PC is *KRAS* mutation and is the earliest recognizable event in its pathogenesis. Studies have reported that mutations in the *KRAS* gene are mainly limited to codon 12 and rarely on codon 13[40,41]. The pathological mutation in *KRAS* encodes constitutive Ras protein which belongs to GTP binding protein family. The constitute Ras protein facilitates the oncogenic signaling pathway which leads to inflammation, deregulated cellular growth, cell motility, and remodeling of the cytoskeletal elements. *KRAS* gene mutations are known to be driver mutations that occur sporadically. It accounts for 30% of early neoplasms of the pancreas and nearly 100% in pancreatic adenocarcinomas. Besides PC, a mutation in the *KRAS* gene is adequate to promote lung cancer, colon cancer, breast cancer, and other cancers as well [42,43]. Recent clinical data suggest that *KRAS* mutations act as significant prognostic biomarker to predict therapeutic intervention for PC management. Kim *et al*[44] demonstrated that out of 136 PC patients, 70 PC patients harbored point mutation in codon 12 of the *KRAS* gene, and these patients have shown dismal response to gemcitabine-based chemotherapy compared to those who had wild type allele for *KRAS* gene[44]. Another study revealed that out of 173 PC patients, 121 were found to harbor point mutations in codon 12 of the *KRAS* gene, and among them are nonresponders to erlotinib. However, patients with wild-type alleles displayed a promising overall survival rate[45]. Consistent with these studies, our mutational analysis results revealed that 16 PC patients had *KRAS* point mutation at codon 12, interestingly we observe point mutation in the *KRAS* gene at codon 13. These findings suggest that further studies are needed to validate the high frequency of point mutation in codon 13 of the *KRAS gene. BRCA-1 and BRCA-2* germline mutations substantially increase the lifetime risk of breast cancer tumorigenesis. Recent reports suggest that the mutations in these genes also have a strong causal association with other cancers including PC[46]. The primary role of the *BRCA-2* gene is the maintenance of the genome by enhancing homologous recombination of a double-stranded break. Approximately, 80% of *BRCA-2* mutations are either frameshift or non-sense mutations which result in the formation of premature stop codons to encode non-functional BRCA-2 protein. *BRCA-2* mutations have been found in 7.3% of familial PC patients which indicates an increased risk of cancers by about 20-fold[47]. *DPC-4* (*SMAD-4)* is a tumor suppressor gene intricated in the regulatory mechanisms of gene transcription. Approximately, 30% of PC cases have been reported to harbor homozygous mutations in the *DPC-4* gene[21]. The mutated *DPC-4* gene-encoded hyperactivated Smad-4 protein leads to the activation of TGF-β pathways thereby promote cell proliferation and tumor growth. Mutations in the *DPC-4* gene have been reported in approximately 50% of PCs and serves as a leading cause of protein inactivation[48]. Inconsistent with previous studies, our mutational analysis of *BRCA-2* and *DPC-4* genes revealed a zero frequency of *DPC-4* 1203 G>T and *BRCA-2* 6174 deletion in PC patients. Collectively, these findings suggest that a larger sample size is

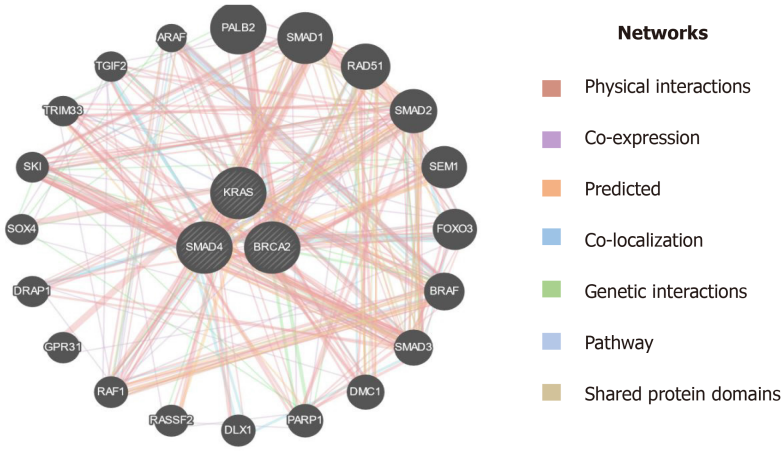


Figure 10 Interaction of *KRAS*, *SMAD4* (*DPC4*), and *BRCA2* with other genes based on various parameters. KRAS: Kirsten rat sarcoma; DPC-4: Deleted in pancreatic cancer-4; BRCA-2: Breast cancer type 2.

needed to validate our results in the ethnic Kashmiri population.

Epigenetic modulations play a critical role in tumorigenesis. Change in DNA methylation of tumor suppressor genes has indispensable importance in therapeutics and could serve as biomarkers for diagnostics and prognostics in various cancers[49]. *p16* is a tumor suppressor gene that encodes cyclin-dependent kinase inhibitors to arrest the cellular growth of malignant cells. Besides point mutations and homozygous deletions in the *p16* gene, recent evidence suggests that methylation of CpG islands in the promoter regions of *p16* stimulates transcriptional silencing of the *p16* gene and contributes to PC progression. In the recent past, hypermethylation in the promoter region of *p16* is significantly raised in chronic pancreatitis compared to normal; suggesting that hypermethylation in the promoter region of the *p16* gene might deregulate cell cycle kinetics and could promote PC progression. Further, reports demonstrated that *p16* hypermethylation in chronic pancreatitis might increase the risk of PC development many-fold[48]. Moore *et al*[50] demonstrated the role of *p16* promoter hypermethylation and associated molecular pathways involved in exocrine and endocrine development of PC. Further, studies suggest that the reduction in overall survival rate associated with *p16* alterations signifies the fact that *p16* could act as an important diagnostic and prognostic biomarker in resected ductal PC patients [51]. *RASSF1A* is another tumor suppressor and an important component of RAS/PI3K/AKT and RAS/RAF/MEK/ERK pathways that have been epigenetically inactivated in various sporadic human malignancies. A higher frequency of promoter methylation status of *RASSF1A* has been implicated in several cancers. The highest frequency of *RASSF1A* promoter hypermethylation was reported in prostate cancer (99%), followed by lung cancer (95%) and breast cancer (88%)[52]. Recent reports suggest that a low frequency of *hMLH1* hypermethylation was detected in PC. The loss of the *hMLH1* gene which encodes for Mut L protein homology 1 is common in various cancers. Further, whole-genome sequencing revealed that somatic *hMLH1* mutations are rare in cancers with an observed frequency of < 1%[53]. In the present study, we carried out epigenetic modifications (CpG methylation) of promoter regions of *p16*, *RASSF1A*, and *hMLH1* genes. Our results demonstrate that significant hypermethylation (CpG islands) was reported in the promoter regions of the *p16* gene in PC patients. However, we observed an extremely low frequency of methylation in the promoter region of the *hMLH1* gene in PC patients. Interestingly, the CpG methylation in the promoter region of the *RASSF1A* gene was completely absent in PC patients. Additionally, *in-silico* analysis suggest that plethora of genes are associated through various interactions with the key genes (*hMLH1*, *RASSF1A*, and *CDKN2A*) as in Figure 11, which could play a key role in the progression of PC[39]. Together, these results suggest that a cohort and comprehensive study with larger sample size is needed to document our findings in the ethnic Kashmiri population.

CONCLUSION

In conclusion, the present study strongly suggests that the elevated levels of serum CA

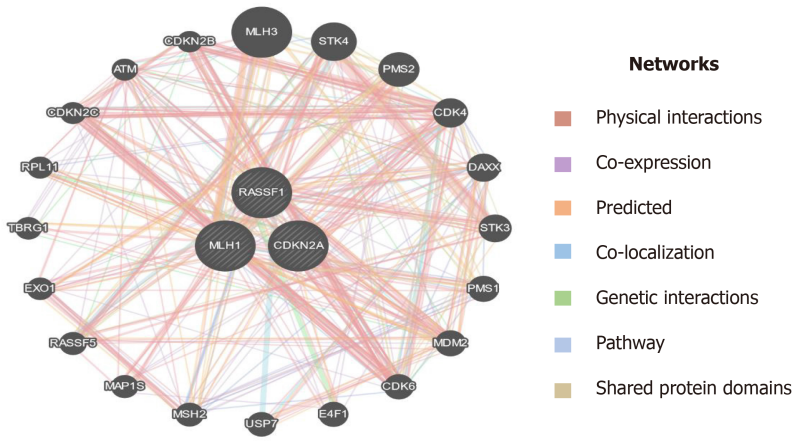


Figure 11 Interaction of *MLH1*, *RASSF1*, and *CDKN2A* (*p16*) with other important genes which have a role in the progression of pancreatic cancer.

19-9, TPS, CEA, and VEGF-A can be used as predictive biomarkers in PC patients of the ethnic Kashmiri population and may act as prognostic biomarkers to benefit the patients who are on a different regimen of chemotherapeutic interventions. Further, mutational analysis data suggest that besides harboring point mutation in codon 12 of *KRAS* gene, the PC patients of the current study significantly harbored codon 13-point mutation as well, which is very rarely reported in the previous studies. This may act as a genetic risk predictor in the development of PC. Additionally, considerable hypermethylation (CpG islands) in the promoter region of the *p16* gene in the current study may lead to silencing of the *p16* gene and could also increase the predisposition towards PC. However, we could not find the association of *DPC*-4G>T and *BRCA*-2 6174 deletion mutations and hypermethylation of CpG islands in the promoter region of *RASSF1A* and *hMLH1* gene towards the risk of PC. To validate these results in the Kashmiri population the future studies need to be comprehensive and with larger sample sizes.

ARTICLE HIGHLIGHTS

Research background

Pancreatic cancer (PC) is one of the deadliest malignancies with an alarming mortality rate. Despite significant advancement in diagnostics and therapeutics, early diagnosis remains elusive causing poor prognosis, marred by mutations and epigenetic modifications in key genes which contribute to disease progression.

Research motivation

To explore the various biological tumor markers collectively and mutational analysis of key regulatory genes for early diagnosis and prognosis of PC.

Research objectives

To evaluate various biological tumor markers collectively in PC and their association with genetic mutation and epigenetic modification of key regulatory genes that could act as early diagnostic and prognostic biomarkers and will help in future therapeutics of PC in Kashmir valley.

Research methods

The current study includes 50 confirmed PC cases to evaluate the levels of carbohydrate antigen 19-9 (CA 19-9), tissue polypeptide specific antigen (TPS), carcinoembryonic antigen (CEA), vascular endothelial growth factor-A (VEGF-A), and epidermal growth factor receptor (EGFR) by enzyme-linked immunosorbent assay (ELISA) method. Mutational analysis of key genes Kirsten rat sarcoma (*KRAS*), Breast cancer type 2 (*BRCA*-2), and deleted in pancreatic cancer-4 (*DPC*-4) genes was performed to evaluate the mutations at hotspot regions. Furthermore, epigenetic modifications were performed in the promoter regions of cyclin-dependent kinase

inhibitor 2A (*p16; CDKN2A*), MutL homolog 1 (*hMLH1*), and Ras association domain-containing protein 1 (*RASSF1A*) genes.

Research results

Besides significant elevation in levels of tumor markers CA 19-9 ($P \leq 0.05$), TPS ($P \leq 0.05$), CEA ($P \leq 0.001$), and VEGF ($P \leq 0.001$), our mutational analysis observed that *KRAS* gene mutation is predominant in codon 12 (16 subjects, $P \leq 0.05$), and 13 (12 subjects, $P \leq 0.05$). Additionally, epigenetic modification analysis suggests that CpG methylation was observed in 21 ($P \leq 0.05$) and 4 subjects in the promoter regions of the *p16* and *hMLH1* gene, respectively.

Research conclusions

The study revealed the significant elevation of serum biological markers in PC patients and the causal association of hotspot mutations and epigenetic modification of key with PC pathogenesis thus indicates the potential of biological markers, mutational status, and epigenetic modifications of key genes collectively for predisposition, susceptibility as well as diagnostics and prognostics of PC.

Research perspectives

The study strongly suggests that the elevated levels of serum CA 19-9, TPS, CEA, and VEGF-A can be used as predictive biomarkers in PC subjects. Additionally, mutational analysis epigenetic modifications in the promoter region of key genes may act as prognostic biomarkers to benefit the patients who are on a different regimen of chemotherapeutic interventions. Further to validate these results, future studies need comprehensive, cohort, and explicative studies with large sample sizes.

ACKNOWLEDGEMENTS

The authors extend their appreciation to the State Department of Science and Technology, Jammu and Kashmir, India.

REFERENCES

1 **Hadden M**, Mittal A, Samra J, Zreiqat H, Sahni S, Ramaswamy Y. Mechanically stressed cancer microenvironment: Role in pancreatic cancer progression. *BiochimBiophysActa Rev Cancer* 2020; **1874**: 188418 [PMID: 32827581 DOI: 10.1016/j.bbcan.2020.188418]

2 **Saad AM**, Turk T, Al-Husseini MJ, Abdel-Rahman O. Trends in pancreatic adenocarcinoma incidence and mortality in the United States in the last four decades; a SEER-based study. *BMC Cancer* 2018; **18**: 688 [PMID: 29940910 DOI: 10.1186/s12885-018-4610-4]

3 **Rawla P**, Sunkara T, Gaduputi V. Epidemiology of Pancreatic Cancer: Global Trends, Etiology and Risk Factors. *World J Oncol* 2019; **10**: 10-27 [PMID: 30834048 DOI: 10.14740/wjon1166]

4 **Midha S**, Chawla S, Garg PK. Modifiable and non-modifiable risk factors for pancreatic cancer: A review. *Cancer Lett* 2016; **381**: 269-277 [PMID: 27461582 DOI: 10.1016/j.canlet.2016.07.022]

5 **Avgerinos KI**, Spyrou N, Mantzoros CS, Dalamaga M. Obesity and cancer risk: Emerging biological mechanisms and perspectives. *Metabolism* 2019; **92**: 121-135 [PMID: 30445141 DOI: 10.1016/j.metabol.2018.11.001]

6 **Wang W**, Chen S, Brune KA, Hruban RH, Parmigiani G, Klein AP. PancPRO: risk assessment for individuals with a family history of pancreatic cancer. *J ClinOncol* 2007; **25**: 1417-1422 [PMID: 17416862 DOI: 10.1200/JCO.2006.09.2452]

7 **Stathis A**, Moore MJ. Advanced pancreatic carcinoma: current treatment and future challenges. *Nat Rev ClinOncol* 2010; **7**: 163-172 [PMID: 20101258 DOI: 10.1038/nrclinonc.2009.236]

8 **McGuigan A**, Kelly P, Turkington RC, Jones C, Coleman HG, McCain RS. Pancreatic cancer: A review of clinical diagnosis, epidemiology, treatment and outcomes. *World J Gastroenterol* 2018; **24**: 4846-4861 [PMID: 30487695 DOI: 10.3748/wjg.v24.i43.4846]

9 **Marrugo-Ramírez J**, Mir M, Samitier J. Blood-Based Cancer Biomarkers in Liquid Biopsy: A Promising Non-Invasive Alternative to Tissue Biopsy. *Int J MolSci* 2018; **19** [PMID: 30248975 DOI: 10.3390/ijms19102877]

10 **Kumar S**, Mohan A, Guleria R. Biomarkers in cancer screening, research and detection: present and future: a review. *Biomarkers* 2006; **11**: 385-405 [PMID: 16966157 DOI: 10.1080/13547500600775011]

11 **Brase JC**, Wuttig D, Kuner R, Sültmann H. Serum microRNAs as non-invasive biomarkers for cancer. *Mol Cancer* 2010; **9**: 306 [PMID: 21110877 DOI: 10.1186/1476-4598-9-306]

12 **Rückert F**, Pilarsky C, Grützmann R. Serum tumor markers in pancreatic cancer-recent discoveries.

Cancers (Basel) 2010; **2**: 1107-1124 [PMID: 24281109 DOI: 10.3390/cancers2021107]
13 **Barak V**, Goike H, Panaretakis KW, Einarsson R. Clinical utility of cytokeratins as tumor markers. *ClinBiochem* 2004; **37**: 529-540 [PMID: 15234234 DOI: 10.1016/j.clinbiochem.2004.05.009]
14 **van der Bilt AR**, Terwisscha van ScheltingaAG, Timmer-Bosscha H, Schröder CP, Pot L, Kosterink JG, van der Zee AG, Lub-de Hooge MN, de Jong S, de Vries EG, Reyners AK. Measurement of tumor VEGF-A levels with 89Zr-bevacizumab PET as an early biomarker for the antiangiogenic effect of everolimus treatment in an ovarian cancer xenograft model. *Clin Cancer Res* 2012; **18**: 6306-6314 [PMID: 23014526 DOI: 10.1158/1078-0432.CCR-12-0406]
15 **Lassman AB**, Roberts-Rapp L, Sokolova I, Song M, Pestova E, Kular R, Mullen C, Zha Z, Lu X, Gomez E, Bhathena A, Maag D, Kumthekar P, Gan HK, Scott AM, Guseva M, Holen KD, Ansell PJ, van den Bent MJ. Comparison of Biomarker Assays for *EGFR*: Implications for Precision Medicine in Patients with Glioblastoma. *Clin Cancer Res* 2019; **25**: 3259-3265 [PMID: 30796037 DOI: 10.1158/1078-0432.CCR-18-3034]
16 **Iacobuzio-Donahue CA**. Genetic evolution of pancreatic cancer: lessons learnt from the pancreatic cancer genome sequencing project. *Gut* 2012; **61**: 1085-1094 [PMID: 21749982 DOI: 10.1136/gut.2010.236026]
17 **Ducreux M**, Cuhna AS, CaramellaC, Hollebecque A, Burtin P, Goéré D, Seufferlein T, Haustermans K, Van Laethem JL, Conroy T, Arnold D; ESMO Guidelines Committee. Cancer of the pancreas: ESMO Clinical Practice Guidelines for diagnosis, treatment and follow-up. *Ann Oncol* 2015; **26** Suppl 5: v56-v68 [PMID: 26314780 DOI: 10.1093/annonc/mdv295]
18 **Matikas A**, Mistriotis D, Georgoulias V, Kotsakis A. Targeting KRAS mutated non-small cell lung cancer: A history of failures and a future of hope for a diverse entity. *Crit Rev OncolHematol* 2017; **110**: 1-12 [PMID: 28109399 DOI: 10.1016/j.critrevonc.2016.12.005]
19 **Blackford A**, Parmigiani G, Kensler TW, Wolfgang C, Jones S, Zhang X, Parsons DW, Lin JC, Leary RJ, Eshleman JR, Goggins M, Jaffee EM, Iacobuzio-Donahue CA, Maitra A, Klein A, Cameron JL, Olino K, Schulick R, Winter J, Vogelstein B, Velculescu VE, Kinzler KW, Hruban RH. Genetic mutations associated with cigarette smoking in pancreatic cancer. *Cancer Res* 2009; **69**: 3681-3688 [PMID: 19351817 DOI: 10.1158/0008-5472.CAN-09-0015]
20 **Reznik R**, Hendifar AE, Tuli R. Genetic determinants and potential therapeutic targets for pancreatic adenocarcinoma. *Front Physiol* 2014; **5**: 87 [PMID: 24624093 DOI: 10.3389/fphys.2014.00087]
21 **Cicenas J**, Kvederaviciute K, Meskinyte I, Meskinyte-Kausiliene E, Skeberdyte A, Cicenas J. KRAS, TP53, CDKN2A, SMAD4, BRCA1, and BRCA2 Mutations in Pancreatic Cancer. *Cancers (Basel)* 2017; **9** [PMID: 28452926 DOI: 10.3390/cancers9050042]
22 **Buscail L**, Bournet B, Cordelier P. Role of oncogenic KRAS in the diagnosis, prognosis and treatment of pancreatic cancer. *Nat Rev GastroenterolHepatol* 2020; **17**: 153-168 [PMID: 32005945 DOI: 10.1038/s41575-019-0245-4]
23 **Mishra NK**, Guda C. Genome-wide DNA methylation analysis reveals molecular subtypes of pancreatic cancer. *Oncotarget* 2017; **8**: 28990-29012 [PMID: 28423671 DOI: 10.18632/oncotarget.15993]
24 **Maitra A**, Hruban RH. Pancreatic cancer. *Annu Rev Pathol* 2008; **3**: 157-188 [PMID: 18039136 DOI: 10.1146/annurev.pathmechdis.3.121806.154305]
25 **Smith L**, Anti S, White N, Saldanha SN. The Genetics and Epigenetics of Colorectal Cancer Health Disparity. In: Epigenetic Mechanisms in Cancer. Elsevier, 2018: 87-115
26 **Wang G**, Zhao D, Spring DJ, DePinho RA. Genetics and biology of prostate cancer. *Genes Dev* 2018; **32**: 1105-1140 [PMID: 30181359 DOI: 10.1101/gad.315739.118]
27 **Herreros-Villanueva M**, Bujanda L. Non-invasive biomarkers in pancreatic cancer diagnosis: what we need *vs* what we have. *Ann Transl Med* 2016; **4**: 134 [PMID: 27162784 DOI: 10.21037/atm.2016.03.44]
28 **D'Costa JJ**, Goldsmith JC, Wilson JS, Bryan RT, Ward DG. A Systematic Review of the Diagnostic and Prognostic Value of Urinary Protein Biomarkers in Urothelial Bladder Cancer. *Bladder Cancer* 2016; **2**: 301-317 [PMID: 27500198 DOI: 10.3233/BLC-160054]
29 **Sattar Z**, Ali S, Hussain I, Sattar F, Hussain S, Ahmad S. Diagnosis of pancreatic cancer. In: Theranostic Approach for Pancreatic Cancer. Elsevier, 2019: 51-68
30 **Hess V**, Glimelius B, Grawe P, Dietrich D, Bodoky G, Ruhstaller T, Bajetta E, Saletti P, Figer A, Scheithauer W, Herrmann R. CA 19-9 tumour-marker response to chemotherapy in patients with advanced pancreatic cancer enrolled in a randomised controlled trial. *Lancet Oncol* 2008; **9**: 132-138 [PMID: 18249033 DOI: 10.1016/S1470-2045(08)70001-9]
31 **O'Brien DP**, Sandanayake NS, Jenkinson C, Gentry-Maharaj A, Apostolidou S, Fourkala EO, Camuzeaux S, Blyuss O, Gunu R, Dawnay A, Zaikin A, Smith RC, Jacobs IJ, Menon U, Costello E, Pereira SP, Timms JF. Serum CA19-9 is significantly upregulated up to 2 years before diagnosis with pancreatic cancer: implications for early disease detection. *Clin Cancer Res* 2015; **21**: 622-631 [PMID: 24938522 DOI: 10.1158/1078-0432.CCR-14-0365]
32 **Slesak B**, Harlozinska-Szmyrka A, Knast W, Sedlaczek P, van Dalen A, Einarsson R. Tissue polypeptide specific antigen (TPS), a marker for differentiation between pancreatic carcinoma and chronic pancreatitis. A comparative study with CA 19-9. *Cancer* 2000; **89**: 83-88 [PMID: 10897004 DOI: 10.1002/1097-0142(20000701)89:1<83::aid-cncr12>3.0.co;2-j]
33 **Kornek G**, Schenk T, Raderer M, Djavarnmad M, Scheithauer W. Tissue polypeptide-specific antigen (TPS) in monitoring palliative treatment response of patients with gastrointestinal tumours. *Br J Cancer* 1995; **71**: 182-185 [PMID: 7529527 DOI: 10.1038/bjc.1995.37]

34 **Jelski W**, Mroczko B. Biochemical Markers of Colorectal Cancer - Present and Future. *Cancer Manag Res* 2020; **12**: 4789-4797 [PMID: 32606968 DOI: 10.2147/CMAR.S253369]

35 **Hammarstrom S**, Shively JE, Paxton RJ, Beatty BG, Larsson A, Ghosh R, Bormer O, Buchegger F, Mach JP, Burtin P. Antigenic sites in carcinoembryonic antigen. *Cancer Res* 1989; **49**: 4852-4858 [PMID: 2474375]

36 **Wu FT**, Stefanini MO, Mac Gabhann F, Kontos CD, Annex BH, Popel AS. A systems biology perspective on sVEGFR1: its biological function, pathogenic role and therapeutic use. *J Cell Mol Med* 2010; **14**: 528-552 [PMID: 19840194 DOI: 10.1111/j.1582-4934.2009.00941.x]

37 **Seo Y**, Baba H, Fukuda T, Takashima M, Sugimachi K. High expression of vascular endothelial growth factor is associated with liver metastasis and a poor prognosis for patients with ductal pancreatic adenocarcinoma. *Cancer* 2000; **88**: 2239-2245 [PMID: 10820344 DOI: 10.1002/(sici)1097-0142(20000515)88:10<2239::aid-cncr6>3.0.co;2-v]

38 **Stacker SA**, Achen MG. The VEGF signaling pathway in cancer: the road ahead. *Chin J Cancer* 2013; **32**: 297-302 [PMID: 23419196 DOI: 10.5732/cjc.012.10319]

39 **Warde-Farley D**, Donaldson SL, Comes O, Zuberi K, Badrawi R, Chao P, Franz M, Grouios C, Kazi F, Lopes CT, Maitland A, Mostafavi S, Montojo J, Shao Q, Wright G, Bader GD, Morris Q. The GeneMANIA prediction server: biological network integration for gene prioritization and predicting gene function. *Nucleic Acids Res* 2010; **38**: W214-W220 [PMID: 20576703 DOI: 10.1093/nar/gkq537]

40 **Kim ST**, Lim DH, Jang KT, Lim T, Lee J, Choi YL, Jang HL, Yi JH, Baek KK, Park SH, Park YS, Lim HY, Kang WK, Park JO. Impact of KRAS mutations on clinical outcomes in pancreatic cancer patients treated with first-line gemcitabine-based chemotherapy. *Mol Cancer Ther* 2011; **10**: 1993-1999 [PMID: 21862683 DOI: 10.1158/1535-7163.MCT-11-0269]

41 **Ghimessy A**, Radeczky P, Laszlo V, Hegedus B, Renyi-Vamos F, Fillinger J, Klepetko W, Lang C, Dome B, Megyesfalvi Z. Current therapy of KRAS-mutant lung cancer. *Cancer Metastasis Rev* 2020; **39**: 1159-1177 [PMID: 32548736 DOI: 10.1007/s10555-020-09903-9]

42 **Hezel AF**, Kimmelman AC, Stanger BZ, Bardeesy N, Depinho RA. Genetics and biology of pancreatic ductal adenocarcinoma. *Genes Dev* 2006; **20**: 1218-1249 [PMID: 16702400 DOI: 10.1101/gad.1415606]

43 **Kodaz H**, Kostek O, Hacioglu MB, Erdogan B, Kodaz CE, Hacibekiroglu I, Turkmen E, Uzunoglu S, Cicin I. Frequency of RAS mutations (KRAS, NRAS, HRAS) in human solid cancer. *Breast Cancer* 2017; 7 [DOI: 10.14744/ejmo.2017.22931]

44 **Kim D**, Xue JY, Lito P. Targeting KRAS(G12C): From Inhibitory Mechanism to Modulation of Antitumor Effects in Patients. *Cell* 2020; **183**: 850-859 [PMID: 33065029 DOI: 10.1016/j.cell.2020.09.044]

45 **Boeck S**, Ormanns S, Haas M, Bächmann S, Laubender RP, Siveke JT, Jung A, Kirchner T, Heinemann V. Translational research in pancreatic cancer: KRAS and beyond. *Pancreas* 2014; **43**: 150-152 [PMID: 24326376 DOI: 10.1097/MPA.0b013e31829629f6]

46 **Wong W**, Raufi AG, Safyan RA, Bates SE, Manji GA. BRCA Mutations in Pancreas Cancer: Spectrum, Current Management, Challenges and Future Prospects. *Cancer Manag Res* 2020; **12**: 2731-2742 [PMID: 32368150 DOI: 10.2147/CMAR.S211151]

47 **Goggins M**, Schutte M, Lu J, Moskaluk CA, Weinstein CL, Petersen GM, Yeo CJ, Jackson CE, Lynch HT, Hruban RH, Kern SE. Germline BRCA2 gene mutations in patients with apparently sporadic pancreatic carcinomas. *Cancer Res* 1996; **56**: 5360-5364 [PMID: 8968085]

48 **Maitra A**, Kern SE, Hruban RH. Molecular pathogenesis of pancreatic cancer. *Best Pract Res ClinGastroenterol* 2006; **20**: 211-226 [PMID: 16549325 DOI: 10.1016/j.bpg.2005.10.002]

49 **van Kampen JG**, Marijnissen-van Zanten MA, Simmer F, van der Graaf WT, Ligtenberg MJ, Nagtegaal ID. Epigenetic targeting in pancreatic cancer. *Cancer Treat Rev* 2014; **40**: 656-664 [PMID: 24433955 DOI: 10.1016/j.ctrv.2013.12.002]

50 **Moore PS**, Orlandini S, Zamboni G, Capelli P, Rigaud G, Falconi M, Bassi C, Lemoine NR, Scarpa A. Pancreatic tumours: molecular pathways implicated in ductal cancer are involved in ampullary but not in exocrine nonductal or endocrine tumorigenesis. *Br J Cancer* 2001; **84**: 253-262 [PMID: 11161385 DOI: 10.1054/bjoc.2000.1567]

51 **Gerdes B**, Ramaswamy A, Ziegler A, Lang SA, Kersting M, Baumann R, Wild A, Moll R, Rothmund M, Bartsch DK. p16INK4a is a prognostic marker in resected ductal pancreatic cancer: an analysis of p16INK4a, p53, MDM2, an Rb. *Ann Surg* 2002; **235**: 51-59 [PMID: 11753042 DOI: 10.1097/00000658-200201000-00007]

52 **Dammann R**, Schagdarsurengin U, Liu L, Otto N, Gimm O, Dralle H, Boehm BO, Pfeifer GP, Hoang-Vu C. Frequent RASSF1A promoter hypermethylation and K-ras mutations in pancreatic carcinoma. *Oncogene* 2003; **22**: 3806-3812 [PMID: 12802288 DOI: 10.1038/sj.onc.1206582]

53 **Lawrence YR**, Moughan J, Magliocco AM, Klimowicz AC, Regine WF, Mowat RB, DiPetrillo TA, Small W Jr, Simko JP, Golan T, Winter KA, Guha C, Crane CH, Dicker AP. Expression of the DNA repair gene MLH1 correlates with survival in patients who have resected pancreatic cancer and have received adjuvant chemoradiation: NRG Oncology RTOG Study 9704. *Cancer* 2018; **124**: 491-498 [PMID: 29053185 DOI: 10.1002/cncr.31058]

World Journal of Gastroenterology

Submit a Manuscript: https://www.f6publishing.com

World J Gastroenterol 2021 September 28; 27(36): 6110-6127

DOI: 10.3748/wjg.v27.i36.6110

ISSN 1007-9327 (print) ISSN 2219-2840 (online)

ORIGINAL ARTICLE

Retrospective Study

Impact of radiogenomics in esophageal cancer on clinical outcomes: A pilot study

Valentina Brancato, Nunzia Garbino, Lorenzo Mannelli, Marco Aiello, Marco Salvatore, Monica Franzese, Carlo Cavaliere

ORCID number: Valentina Brancato 0000-0002-6232-7645; Nunzia Garbino 0000-0001-6863-7313; Lorenzo Mannelli 0000-0002-9102-4176; Marco Aiello 0000-0002-3676-0664; Marco Salvatore 0000-0001-9734-7702; Monica Franzese 0000-0002-6490-7694; Carlo Cavaliere 0000-0002-3297-2213.

Author contributions: Brancato V performed the research and wrote the manuscript; Franzese M, Mannelli L and Aiello M contributed to the conception and design of the study and to the acquisition and interpretation of the data; Garbino N, Franzese M and Brancato V contributed to the data curation and processing; Franzese M, Salvatore M, Aiello M and Mannelli L revised the article; Cavaliere C designed the research and approved the final version for publication.

Institutional review board statement: The study was conducted in accordance with the Declaration of Helsinki, and the study protocol was approved by the Ethics Committee of the Istituto Nazionale Tumori "Fondazione G. Pascale (protocol number 1/20).

Informed consent statement: Patients were not required to give informed consent to the study

Valentina Brancato, Nunzia Garbino, Lorenzo Mannelli, Marco Aiello, Marco Salvatore, Monica Franzese, Carlo Cavaliere, IRCCS SDN, Naples 80143, Italy

Corresponding author: Lorenzo Mannelli, MD, PhD, Professor, IRCCS SDN, Via E. Gianturco, Naples 80143, Italy. mannellilorenzo@yahoo.it

Abstract

BACKGROUND

Esophageal cancer (ESCA) is the sixth most common malignancy in the world, and its incidence is rapidly increasing. Recently, several microRNAs (miRNAs) and messenger RNA (mRNA) targets were evaluated as potential biomarkers and regulators of epigenetic mechanisms involved in early diagnosis. In addition, computed tomography (CT) radiomic studies on ESCA improved the early stage identification and the prediction of response to treatment. Radiogenomics provides clinically useful prognostic predictions by linking molecular characteristics such as gene mutations and gene expression patterns of malignant tumors with medical images and could provide more opportunities in the management of patients with ESCA.

AIM

To explore the combination of CT radiomic features and molecular targets associated with clinical outcomes for characterization of ESCA patients.

METHODS

Of 15 patients with diagnosed ESCA were included in this study and their CT imaging and transcriptomic data were extracted from The Cancer Imaging Archive and gene expression data from The Cancer Genome Atlas, respectively. Cancer stage, history of significant alcohol consumption and body mass index (BMI) were considered as clinical outcomes. Radiomic analysis was performed on CT images acquired after injection of contrast medium. In total, 1302 radiomics features were extracted from three-dimensional regions of interest by using PyRadiomics. Feature selection was performed using a correlation filter based on Spearman's correlation (ρ) and Wilcoxon-rank sum test respect to clinical outcomes. Radiogenomic analysis involved ρ analysis between radiomic features associated with clinical outcomes and transcriptomic signatures consisting of eight N6-methyladenosine RNA methylation regulators and five up-regulated

miRNA. The significance level was set at $P < 0.05$.

RESULTS

Of 25, five and 29 radiomic features survived after feature selection, considering stage, alcohol history and BMI as clinical outcomes, respectively. Radiogenomic analysis with stage as clinical outcome revealed that six of the eight mRNA regulators and two of the five up-regulated miRNA were significantly correlated with ten and three of the 25 selected radiomic features, respectively ($-0.61 < \rho < -0.60$ and $0.53 < \rho < 0.69$, $P < 0.05$). Assuming alcohol history as clinical outcome, no correlation was found between the five selected radiomic features and mRNA regulators, while a significant correlation was found between one radiomic feature and three up-regulated miRNAs ($\rho = -0.56$, $\rho = -0.64$ and $\rho = 0.61$, $P < 0.05$). Radiogenomic analysis with BMI as clinical outcome revealed that four mRNA regulators and one up-regulated miRNA were significantly correlated with 10 and two radiomic features, respectively ($-0.67 < \rho < -0.54$ and $0.53 < \rho < 0.71$, $P < 0.05$).

CONCLUSION

Our study revealed interesting relationships between the expression of eight N6-methyladenosine RNA regulators, as well as five up-regulated miRNAs, and CT radiomic features associated with clinical outcomes of ESCA patients.

Key Words: Esophageal cancer; Radiogenomics; Computed tomography; Radiomics; MicroRNAs; N6-methyladenosine

©The Author(s) 2021. Published by Baishideng Publishing Group Inc. All rights reserved.

Core Tip: This is a retrospective study aiming at investigating the relationship between the expression levels of transcriptomic features (eight N6-methyladenosine RNA methylation regulators and five up-regulated microRNAs) and radiomic features extracted from computed tomography images that were significantly associated to clinical outcomes (stage, alcohol history, body mass index) in patients with esophageal cancer . Radiogenomic analysis revealed significant correlations between the expression of the N6-methyladenosine RNA regulators, as well as five up-regulated microRNAs, and several computed tomography radiomic features associated with three investigated clinical outcomes of esophageal cancer patients.

Citation: Brancato V, Garbino N, Mannelli L, Aiello M, Salvatore M, Franzese M, Cavaliere C. Impact of radiogenomics in esophageal cancer on clinical outcomes: A pilot study. *World J Gastroenterol* 2021; 27(36): 6110-6127
URL: https://www.wjgnet.com/1007-9327/full/v27/i36/6110.htm
DOI: https://dx.doi.org/10.3748/wjg.v27.i36.6110

INTRODUCTION

Esophageal cancer (ESCA) is one of the most common malignancies and ranks sixth as a cause of lethal cancer worldwide[1]. Despite the different types of treatment, ESCA remains a devastating pathology with an overall 5-year survival rate of 15%–25%. The main issue related to ESCA is that, given the late symptoms manifestation, most patients are diagnosed with advanced-stage ESCA characterized by unresectability or metastatic disease, for which the best treatment choices are palliative interventions such as concurrent chemoradiotherapy and combination chemotherapy[2,3]. The majority of ESCAs fall into two main histologic subtypes: Esophageal adenocarcinoma and esophageal squamous cell carcinoma (ESCC)[4]. Imaging plays a key role in each step of the management of ESCA. Computed tomography (CT) plays an important role in the diagnosis, staging and treatment guidance of ESCA. This imaging technique allows to evaluate the loco-regional extension of ESCA by showing the extent of involvement of the esophageal wall by tumor, as well as the tumor invasion of the peri-esophageal fat[5]. Moreover, it is also useful to detect the presence of distant

because the analysis used anonymous clinical data that were obtained after each patient agreed to treatment by written consent.

Conflict-of-interest statement: The authors declare that there is no conflict of interest in this study.

Data sharing statement: No additional data are available.

Open-Access: This article is an open-access article that was selected by an in-house editor and fully peer-reviewed by external reviewers. It is distributed in accordance with the Creative Commons Attribution NonCommercial (CC BY-NC 4.0) license, which permits others to distribute, remix, adapt, build upon this work non-commercially, and license their derivative works on different terms, provided the original work is properly cited and the use is non-commercial. See: http://creativecommons.org/Licenses/by-nc/4.0/

Manuscript source: Unsolicited manuscript

Specialty type: Oncology

Country/Territory of origin: Italy

Peer-review report's scientific quality classification
Grade A (Excellent): A
Grade B (Very good): 0
Grade C (Good): C, C
Grade D (Fair): 0
Grade E (Poor): E

Received: March 2, 2021
Peer-review started: March 2, 2021
First decision: June 3, 2021
Revised: June 16, 2021
Accepted: July 30, 2021
Article in press: July 30, 2021
Published online: September 28, 2021

P-Reviewer: Barad AK, Endo S, Hamaya Y
S-Editor: Zhang H
L-Editor: Filipodia
P-Editor: Xing YX

metastases[6,7]. However, CT has several limitations associated with the ability to evaluate the intra-tumor heterogeneity of the ESCA, as well as in visually distinguishing the post-treatment residual tumor[8,9].

Therefore, since it is well-recognized that information arising from images may be substantially enhanced by quantitative imaging analysis, the radiomics role has rapidly increased in the last decade for cancer applications, including those related to ESCA[10-12]. Radiomics is evolving as medical technology and is currently one of the most interesting research fields. Through radiomics, quantitative data can be extrapolated from diagnostic images, and these extracted parameters (radiomic features) have the potential to identify tumor characteristics[10,11,13]. The innovative field of radiomics could provide opportunities in the management of ESCA patients for improvements in every step of ESCA management[12,14]. Recent studies on CT radiomics in ESCA analyzed CT radiomics features for several steps of ESCA management, such as preoperative stage identification[15] and prediction of response to treatment[3,16].

On the other hand, the emerging clinical relevance of genomics in cancer medicine by applying the next generation sequencing technologies has provided unprecedented opportunities to understand the biological basis of different cancer types, identify genomic biomarkers in carcinogenesis, identify potential bio-molecular targets for drug response and resistance and to guide clinical decision-making regarding the personalized medicine and the clinical practice[17,18].

Gene expression profiling can improve knowledge about the molecular alterations during carcinogenesis. Biomarkers of these molecular alterations, in turn, may be useful in diagnosing cancers, particularly early, curable cancers. Recently, results from gene expression data analyses have made it possible to investigate the complex pathological mechanisms involved in ESCA, with the aim to discover novel molecular markers for tumor diagnosis and to customize therapy based on an individual tumor genetic composition[19-21]. Several microRNA (miRNA), such as miR-93, miR-21, miR-4746 and miR-196a, were evaluated as potential biomarkers for the early diagnosis of cancer, highlighting their diagnostic values[22]. Recently, several studies also suggested that N6-methyladenosine (m6A) methylation can play a crucial role in cancer progression by regulating biological functions that affect noncoding RNA expression[23,24] In particular, a recent study[25] highlighted the role of m6A methylation regulators aberrantly expressed in ESCA to predict clinical outcomes.

Combining radiomic features with molecular and genomic characteristics can provide insights to characterize tumor phenotype[26]. In this direction, radiogenomics, as a new field that provides clinically useful prognostic predictions by linking molecular characteristics such as gene mutations and gene expression patterns of malignant tumors with medical images, could provide more opportunities in the management of patients with ESCA for improvements in staging, predicting treatment response and survival[7,21]. Based on promising results obtained from preliminary CT-based radiomics studies on ESCA[16,27] and considering the capability of miRNAs as potential biomarkers able to characterize differential expression of different cancer tissues, as well as the critical role of m6A as epigenetic regulator in cancer biology, we aimed to combine these findings in a radiogenomic study, using appropriate variables as clinical endpoints. Specifically, we used the preoperative ESCA stage as a clinical outcome, since the survival of ESCA patients with early stage (stage I−II) could be up to 85%[28]. Additionally, surgical resection, chemoradiation or other optimal therapeutic approaches depend on accurate preoperative staging. Therefore, accurate preoperative staging is important for predicting prognosis and choosing a suitable therapeutic strategy for patients with ESCA[15]. We also used the history of significant alcohol consumption as a clinical outcome, since this is considered as one of the major risk factors for ESCA[29]. Lastly, we evaluated body mass index (BMI) as a clinical outcome, due to its association with increased risk of ESCA[30,31].

Using publicly available integrated ESCA cohort from The Cancer Genome Atlas (TCGA) and The Cancer Imaging Archive (TCIA)[32,33], we aimed at investigating possible relationships between CT-radiomic features associated with the three above-mentioned clinical outcomes and correlated with esophageal up-regulated miRNAs, which were *in silic*o-validated from Zeng *et al*[22], in order to evaluate potential biomarkers for the early diagnosis of ESCA. Furthermore, we evaluated if the same CT-radiomics features could be associated with epigenetic signatures, considering m6A RNA methylation regulators-based prognostic signature for ESCA from Xu *et al* [25] in order to support important information for developing diagnostic and therapeutic strategies.

MATERIALS AND METHODS

Patient population and definition of clinical outcomes

The study was conducted in accordance with the Declaration of Helsinki, and the study protocol was approved by the Ethics Committee of the Istituto Nazionale Tumori "Fondazione G. Pascale (protocol number 1/20). Sixteen patients with diagnosed ESCA were extrapolated by combining the public databases TCIA-TCGA and included in this study[32,33]. All subjects performed CT investigation with iodized contrast medium injection. Of 16 patients, one was excluded due to the presence of artifacts on acquired images. Due to their availability for all 15 patients, the transcriptome profiling and the following clinical variables were extracted and considered as outcomes for this study: Cancer stage, history of significant alcohol consumption and BMI value. We did not perform analyses on smoking measurements (tobacco history, age at starting smoking, pack-year smoked) due to the incompleteness of these data. To perform radiogenomic analyses, we divided patients into two groups according to stages I−II or III−IV, making stage outcome binary. Refer to Table 1 for clinical characteristics and outcomes of included patients.

Image acquisition and processing

CT examinations were acquired on GE Medical Systems (9 patients) and Siemens (6 patients) CT scanner, with slice thickness ranging from 1.25 mm to 2.5 mm and pixel size varying from 0.67 to 0.9. three-dimensional (3D) regions of interest (ROIs) encompassing the tumor were manually delineated slice-by-slice by using ITK-SNAP (version 3.6.0, http://www.itksnap.org) on the post-administration of contrast agents CT images. The tumor localization was divided into three regions: 7 patients presented lesions at the middle level, 2 subjects in the middle/distal area and 6 patients in the distal esophagus.

Gray-levels normalization was not performed, since CT gray values reflect absolute world values (Hounsfield units) and should be comparable between scanners. To correct variability from parameters related to voxel size and so unify voxel size across the cohort, radiomics data were extracted from images resampled to isotropic voxels of $1 \times 1 \times 1$ mm^3 using B Spline interpolator.

Radiomic analysis

Radiomic features extraction: A total of 1302 radiomics features were extracted from segmented ROIs by using the open source Python package PyRadiomics (https://pyradiomics.readthedocs.io/en/Latest/). The extracted radiomics features were categorized into five groups: (1) Shape features (n = 14); (2) First-order features including 18 intensity statistics; (3) 74 multi-dimensional texture features including 23 gray level co-occurrence matrix (GLCM), 16 gray level size zone matrix (GLSZM), 16 gray level run length matrix (GLRLM), 14 gray level dependence matrix (GLDM) and 5 neighboring gray tone difference matrix (NGTDM) features; 1196 transformed first-order and textural features including; (4) 736 wavelet features in frequency channels LHL, LLH, HHH, HLH, HLL,HHL, LHH and LLL, where L and H are low- and high-pass filters, respectively; and (5) 460 LoG filtered features with sigma ranging from 1.0 and 5.0, with step size = 1. Features of groups (2) and (3) were grouped together and, from now on, this group will be referred to as "original features". The extracted radiomics features grouped by similarity in four categories are listed in the Supplementary Table 1. The computing algorithms can be found at www.radiomics.io and the image biomarker standardization initiative presented a document to standardize the nomenclature and definition of radiomic features[34].

Radiomic features selection: Features selection was performed separately for shape features, original features, wavelet features and LoG filtered features in two steps, followed by a third step involving the whole set of features passed through the step I and II. In the first step, a correlation filter based on the absolute values of pairwise Spearman's correlation (ρ) coefficient was used to reduce feature redundancy. Threshold for ρ was set to 0.8. Briefly, if two features had $\rho > 0.8$, the function looks at the mean absolute correlation of each variable and the variable with the largest mean absolute correlation is removed. The second step varied according to the type of outcome variables. For binary outcomes, a further feature restriction through a univariate analysis was performed by using non-parametric Wilcoxon rank-sum test to investigate the statistical significance with respect to the outcome. Statistical significance was set to $P < 0.05$. The significantly different features were then selected and further reduced in the third step. For continuous outcomes, the second step

Table 1 Characteristics of included patients

Clinical characteristic	Value
Age (mean ± SD)	56.8 ± 8.65
Sex, *n* (%)	
Male	12 (20)
Female	3 (80)
Histologic diagnosis, *n* (%)	
EAC	2 (13.3)
ESCC	13 (86.7)
Cancer stage, *n* (%)	
I-II	4 (26.7)
III-IV	11 (73.3)
TNM staging	
Primary tumor (T)	
T1	3 (20)
T2	2 (13.3)
T3	8 (53.4)
T4	2 (13.3)
Regional lymph nodes (N)	
N0	4 (26.7)
N1	6 (40)
N2	3 (20)
N3	2 (13.3)
Distant metastases (M)	
M0	12 (80)
M1	3 (20)
Alcohol history, *n* (%)	
Yes	8 (53)
No	7 (47)
Smoking history, *n* (%)	
Lifelong non-smoker	1 (6.6)
Current smoker	7 (46.6)
Current reformed smoker	2 (13.3)
Current reformed smoker for > 15 yr	1 (6.6)
NA	4 (26.6)
Age at starting smoking	
Under 18 yr old	6 (40)
Over 18 yr old	3 (20)
NA	6 (40)
Pack-year smoked	
Under 10	6 (40)
Over 10	3 (20)
NA	6 (40)

BMI (mean ± SD)	20.8 ± 3.55

BMI: Body mass index; EAC: Esophagus adenocarcinoma; ESCC: Esophagus squamous cell carcinoma; TNM: tumor, node, and metastasis classification (classification of malignant tumors).

consisted of computing ρ between each feature selected through the step I and the reference outcome. Then, all features with a significant $\rho > 0.5$ and P value < 0.05 were considered. In order to check for redundancies among features belonging to the different four groups, the third step consisted in applying the correlation filter described in step I to the whole feature set passed through step II. All steps were implemented using Matlab R2020a (The MathWorks Inc., Natick, MA, United States).

Predictive models building and analysis for stage assessment: In order to evaluate the predictive power of CT radiomic features taken by them for ESCA staging, a fourth step of feature selection was performed for features that were associated with stage. The latter step consisted in ranking the remaining features based on the mutual information (MI) between the distribution of the values of a certain feature and the membership to a particular class. Features were evaluated independently, and the final feature selection occurred by aggregating the five top ranked ones[35-37]. For the binary stage I-II/stage III-IV classification task, the reduced feature set was used to build logistic regression models of order from 1 to 5 that would best predict ESCA stage by using an imbalanced-adjusted bootstrap resampling (IABR) approach on 1000 bootstrap samples[38]. Specifically, the training set was made up 1000 bootstrap samples randomly drawn with replacement from the available dataset. The testing set consisted of the instances that did not belong to the bootstrap sample. Then, application of the imbalance-adjustment step made the probability of picking a positive and a negative instance in the bootstrap sample the same[39-41].

For each model order, the combination of features maximizing the 0.632+ area under the receiver operating characteristic curve (AUC) within 1000 bootstrap training and testing samples was identified. Finally, IABR on 1000 samples was performed again for all models to assess prediction performances[38,42].

Additional analyses were performed starting from the first two, three and four features surviving after the MI-based feature selection step (which was used to build logistic regression models of order from 1 to 2, 1 to 3 and 1 to 4, respectively) that would best predict ESCA stage. Moreover, given that the overall stage is determined after the cancer is assigned categories describing the tumor (T), node (N) and metastasis (M) categories, we tested the capability of these features for predicting T and N status. Analyses assuming M status as clinical outcome were not performed due to the extremely unbalanced sample. Patients were divided into two groups according to T1-T2 or T3−T4 tumor status, making T stage outcome binary. Similarly, we evaluated if CT radiomic features could assess N status by dividing patients into two groups according to the absence (N0) or presence (N1-N2-N3) lymph node status[43].

Transcriptomic data collection

RNA-Seq and miRNA-Seq data of esophageal carcinoma of tumor tissues were downloaded from the GDC Data Portal (https://gdc-portal.nci.nih.gov/) considering for TCGA-ESCA project only patients with associated imaging data from TCIA database (see Supplementary Tables 2 and 3 for Clinical and Transcriptomic data, respectively). The mRNAs expression levels were considered as read count based on gene length and the total number of mapped reads (FPKM values). Moreover, miRNA expression quantification was downloaded and normalized counts in reads-per-million-miRNA-mapped were considered.

Radiogenomic analysis

An integrative study design was defined (see Figure 1 for the flowchart reporting the organization of data and analyses in the study) and reported as radiogenomic workflow in Figure 2 in order to evaluate potential association between significant radiomic features according to selected clinical variables (stage, history of significant alcohol consumption and BMI) with biomarkers and RNA regulators characterizing esophageal cancer. For this purpose, a Spearman's correlation analysis was investigated between radiomic features selected after the three features selection steps described above and transcriptomic signatures suggested by Zeng *et al*[22] and Xu *et al*[25]. Specifically, we calculated ρ between the whole selected feature set and the eight

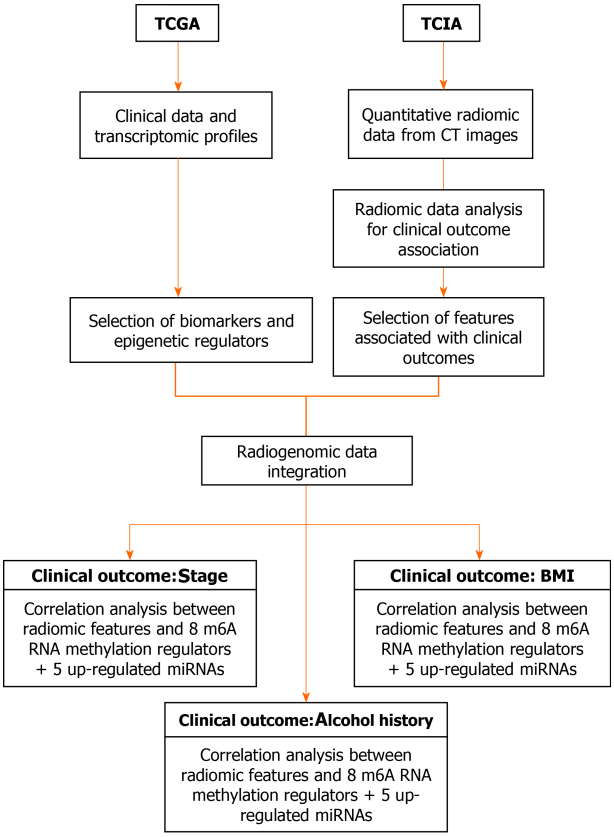


Figure 1 Flowchart reporting the organization of data and analyses in the study. BMI: Body mass index; CT: Computed tomography; TCGA: The Cancer Genome Atlas; TCIA: The Cancer Imaging Archive.

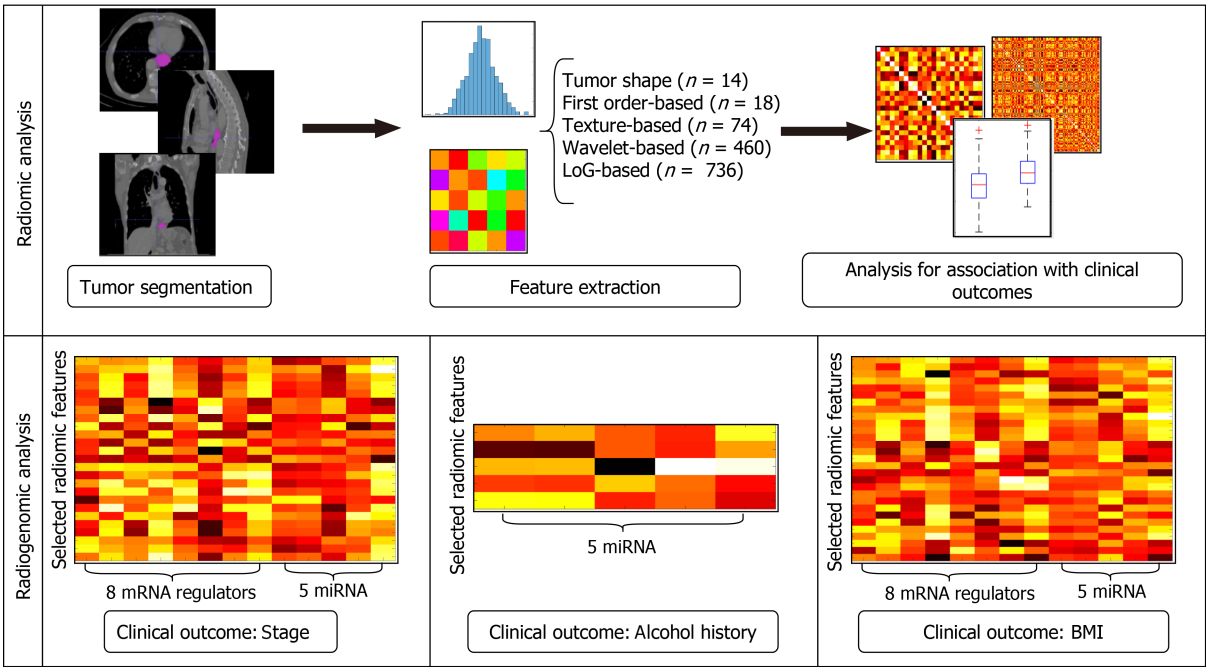


Figure 2 Workflow of radiogenomic analysis implemented in the study. On the first row the radiomic analysis steps. On the second row the radiogenomic analysis for each clinical outcome. BMI: Body mass index; miRNA: MicroRNA; mRNA: Messenger RNA.

m6A RNA methylation regulators (KIAA1429, HNRNPC, RBM15, METTL3, WTAP, YTHDF1, YTHDC1, YTHDF2), as well as ρ between the whole selected feature set and the five up-regulated miRNAs (miRNA-93, miRNA-21, miRNA-4746, miRNA-196a-1, miRNA-196a-2). The significance level was set to 0.05. All analyses were performed

using Matlab R2020a. The statistical methods of this study were reviewed by our bioinformatics and biostatistics group of our research support center.

RESULTS

Radiomic analysis

Radiomic feature selection: None of the 14 shape features passed the step II of features selection, both considering binary outcomes (namely stage and alcohol history) and BMI. So, radiogenomic analysis was not performed for this feature group. Concerning original, wavelet and Log sigma feature groups, the step I of feature selection reduced the feature sets from 92, 736 and 460 to 23, 127 and 65, respectively. Concerning stage analysis, Wilcoxon rank-sum test used in step II of feature selection revealed significant results for 26 radiomic features, of which 25 belonging to the wavelet feature set and the remaining one was the original first order maximum value. However, the latter feature did not pass the second correlation filter of step III (refer to Table 2). Considering the presence of alcoholic history as clinical outcome, Wilcoxon rank-sum test revealed significant results for five features, of which one belonging to original feature set (Kurtosis) and the remaining ones to wavelet feature set. These five features passed step III, since Kurtosis showed a correlation lower than 0.8 with all four wavelet features (refer to Table 2). Lastly, considering BMI as the clinical outcome, 26 wavelet and three LoG sigma features were selected due to a significant $\rho > 0.5$ ($P < 0.05$) with BMI. In total, 29 radiomic features (see Table 3) survived after the second correlation filter and were associated with the three examined clinical outcomes.

Predictive models building and analysis for stage assessment: The top five features selected after the MI-based feature selection step were wavelet LLH GLDM high gray level emphasis, LLH NGTDM complexity, HHH GLCM joint entropy, HLH entropy and HLL GLCM cluster prominence. Prediction performances of multivariable logistic regression models for the stage I-II/stage III-IV classification task were very high for both five model orders. However, by inspecting prediction performances values in Table 4, we determined that the simplest multivariable model with the best prediction performances were reached by the second order model (AUC = 87%, sensitivity = 64%, specificity = 83% and accuracy = 79%), which was based on wavelet LLH NGTDM complexity and HHH GLCM joint entropy. These results were also confirmed by additional analyses (Supplementary Tables 4-6). The top five features were also found to be able to predict T and N staging, with best AUCs (0.79 and 0.80, respectively) reached by second order models (see Supplementary Tables 7 and 8 for analyses involving five features). Results of additional analyses for T and N prediction by using two, three and four features are reported in Supplementary Tables 9-11 (T staging) and Supplementary Tables 12-14 (N staging).

Radiogenomic analysis

Stage: Overall, radiogenomic analysis revealed that six of the eight mRNA regulators were significantly correlated with 10 of the 25 selected radiomic features, which were all belonging to the wavelet group. In particular, HRNPC and WTAP were positively correlated with wavelet HHL NGTDM strength ($\rho = 0.61$, $\rho = 0.61$, $P < 0.05$, respectively); METTL3 was positively correlated with wavelet LHL GLDM high gray level emphasis, HLL GLRLM gray level variance, HLL GLDM dependence entropy and LLL GLDM small dependence high gray level emphasis ($\rho = 0.54$, $\rho = 0.53$, $\rho = 0.56$, $\rho = 0.6$, $P < 0.05$, respectively) and negatively correlated with wavelet HLL GLCM inverse variance ($\rho = -0.6$, $P < 0.05$); YTHDF1 reported a positive and significant correlation with the wavelet feature HLL GLCM maximum probability ($\rho = 0.6$, $P < 0.05$) and a negative correlation with HLL 90th percentile ($\rho = -0.61$, $P < 0.05$); YTHDF2 was positively correlated with the wavelet feature HHH GLCM contrast and HHH GLSZM zone percentage ($\rho = 0.57$, $\rho = 0.56$, $P < 0.05$, respectively); the latter feature was also positively correlated with YTHDC1 ($\rho = 0.6$, $P < 0.05$). Moreover, correlation analysis with the five up-regulated miRNA revealed a significant positive correlation between miRNA-93 and two radiomic features, namely wavelet LHL GLDM high gray level emphasis ($\rho = 0.69$, $P < 0.05$) and HHH GLCM joint entropy ($\rho = 0.58$, $P < 0.05$). Notably, HHH GLCM joint entropy contributed to building the best predictive models for stage assessment, as well as T and N assessment. Finally, a positive correlation between miRNA-4746 and HHL GLCM cluster shade was found ($\rho = 0.53$, $P < 0.05$). The radiogenomic results for stage are shown through a heatmap in the Figure 3.

Table 2 Selected radiomic features after the three feature selection steps for binary outcomes

Selected radiomic features, stage	Stage I-II, mean ± SD	Stage III-IV, mean ± SD	*P* value
Wavelet-HLH first order entropy	0.62 ± 0.13	0.21 ± 0.31	0.031
Wavelet-LHL GLDM high gray level emphasis	0.59 ± 0.32	0.21 ± 0.21	0.044
Wavelet-HLL GLDM high gray level run emphasis	0.67 ± 0.37	0.2 ± 0.18	0.019
Wavelet-HLL GLDM gray level variance	0.74 ± 0.29	0.22 ± 0.29	0.007
Wavelet-HLL GLDM cluster prominence	0.59 ± 0.36	0.14 ± 0.3	0.019
Wavelet-HLL GLDM inverse variance	0.27 ± 0.3	0.68 ± 0.23	0.028
Wavelet-HLL GLDM maximum probability	0.14 ± 0.17	0.58 ± 0.32	0.042
Wavelet-HLL GLDM dependence entropy	0.78 ± 0.18	0.42 ± 0.25	0.028
Wavelet-HLL GLDM dependence variance	0.2 ± 0.21	0.48 ± 0.26	0.044
Wavelet-HLL GLSZM size zone non uniformity	0.69 ± 0.39	0.15 ± 0.15	0.028
Wavelet-HLL GLSZM small area low gray level emphasis	0.02 ± 0.03	0.24 ± 0.33	0.041
Wavelet-HLL first order 90 percentile	0.55 ± 0.39	0.17 ± 0.16	0.029
Wavelet-HHH GLRLM gray level non uniformity normalized	0.39 ± 0.27	0.87 ± 0.19	0.007
Wavelet-HHH GLCM joint entropy	0.68 ± 0.22	0.2 ± 0.27	0.021
Wavelet-HHH GLCM Contrast	0.78 ± 0.19	0.45 ± 0.25	0.021
Wavelet-HHH GLSZM gray level variance	0.91 ± 0.11	0.3 ± 0.39	0.021
Wavelet-HHH GLSZM zone percentage	0.83 ± 0.13	0.35 ± 0.34	0.029
Wavelet-HHH first order 10 percentile	0.11 ± 0.08	0.46 ± 0.35	0.029
Wavelet-HHL NGTDM strength	0.66 ± 0.3	0.28 ± 0.3	0.044
Wavelet-HHL GLCM cluster shade	0.51 ± 0.49	0.04 ± 0.03	0.007
Wavelet-HHL first order Entropy	0.68 ± 0.33	0.27 ± 0.21	0.029
Wavelet-HHL first order mean absolute deviation	0.66 ± 0.35	0.25 ± 0.18	0.029
Wavelet-LLH NGTDM complexity	0.23 ± 0.13	0.13 ± 0.29	0.044
Wavelet-LLH GLDM high gray level emphasis	0.34 ± 0.23	0.14 ± 0.29	0.044
Wavelet-LLL GLDM small dependence high gray level emphasis	0.67 ± 0.32	0.25 ± 0.22	0.029
Selected radiomic features (alcohol history)	**No alcohol history (mean ± SD)**	**Alcohol history (mean ± SD)**	***P* value**
Original first order kurtosis	0.37 ± 0.32	0.12 ± 0.12	0.037
Wavelet-LHH first order interquartile range	0.24 ± 0.24	0.5 ± 0.25	0.049
Wavelet-LHH first order mean	0.94 ± 0.04	0.75 ± 0.31	0.013
Wavelet-HHL first order median	0.62 ± 0.2	0.37 ± 0.19	0.026
Wavelet-LLH first order uniformity	0.68 ± 0.27	0.41 ± 0.26	0.037

The first column includes the two binary clinical outcomes investigated in this study (stage, alcohol history). GLCM: Gray level co-occurrence matrix; GLDM: Gray level dependence matrix; GLRLM: Gray level run length matrix; GLSZM: Gray level size zone matrix; H: High-pass filter; L: Low-pass filter; NGTDM: Neighboring gray tone difference matrix; SD: Standard deviation.

Alcohol history: From the integrated analysis, none of the five selected radiomic features was significantly correlated with any of eight RNA regulators (data not shown). Conversely, correlation analysis with the five up-regulated miRNA revealed a significant correlation between the wavelet feature LHH first order Mean and three up-regulated miRNA, namely miRNA-21 ($\rho = -0.56$, $P < 0.05$), miRNA-4746 ($\rho = 0.64$, $P < 0.05$) and miRNA-93 ($\rho = 0.61$, $P < 0.05$), as reported in the heatmap in Figure 4.

Table 3 Selected radiomic features after the three feature selection steps for body mass index

Selected radiomic features	mean ± SD	ρ	*P* value
Wavelet-HLH GLCM IMC2	0.46 ± 0.31	0.6	0.017
Wavelet-HLH GLCM MCC	0.33 ± 0.27	0.67	0.006
Wavelet-HLH first order median	0.59 ± 0.28	-0.56	0.029
Wavelet-HLH first order entropy	0.32 ± 0.33	0.63	0.013
Wavelet-HLH first order root mean squared	0.44 ± 0.31	0.71	0.003
Wavelet-HLH first order skewness	0.5 ± 0.33	0.52	0.049
Wavelet-HLH first order mean absolute deviation	0.54 ± 0.29	0.62	0.013
Wavelet-LHL GLCM IDN	0.77 ± 0.29	0.58	0.023
Wavelet-LHL GLDM high gray level emphasis	0.31 ± 0.29	0.54	0.039
Wavelet-HLL GLRLM high gray level run emphasis	0.32 ± 0.32	0.54	0.038
Wavelet-HLL GLRLM gray level variance	0.36 ± 0.37	0.62	0.014
Wavelet-HLL GLCM cluster prominence	0.26 ± 0.36	0.6	0.018
Wavelet-HLL GLCM inverse variance	0.57 ± 0.3	-0.58	0.022
Wavelet-HLL GLCM maximum probability	0.47 ± 0.35	-0.53	0.043
Wavelet-HLL GLDM dependence variance	0.41 ± 0.27	-0.6	0.018
Wavelet-HLL GLSZM size zone non uniformity	0.29 ± 0.33	0.57	0.028
Wavelet-HHH GLRLM gray level non uniformity normalized	0.74 ± 0.3	-0.54	0.039
Wavelet-HHH GLCM difference average	0.64 ± 0.31	0.56	0.03
Wavelet-HHH GLCM contrast	0.53 ± 0.28	0.64	0.009
Wavelet-HHH GLSZM small area emphasis	0.55 ± 0.33	0.69	0.005
Wavelet-HHH GLSZM small area low gray level emphasis	0.55 ± 0.33	0.59	0.022
Wavelet-HHL first order entropy	0.38 ± 0.3	0.57	0.025
Wavelet-HHL first order mean	0.64 ± 0.28	0.59	0.02
Wavelet-HHL first order mean absolute deviation	0.36 ± 0.29	0.55	0.032
Wavelet-LLH NGTDM complexity	0.16 ± 0.26	0.53	0.044
Wavelet-LLL GLDM small dependence high gray level emphasis	0.36 ± 0.3	0.56	0.031
Log-sigma-1-0-mm-3D first order root mean squared	0.43 ± 0.26	-0.51	0.049
Log-sigma-5-0-mm-3D GLRLM short run low gray level emphasis	0.22 ± 0.25	-0.52	0.047
Log-sigma-5-0-mm-3D first order 10 percentile	0.48 ± 0.39	-0.59	0.02

GLCM: Gray level co-occurrence matrix; GLDM: Gray level dependence matrix; GLRLM: Gray level run length matrix; GLSZM: Gray level size zone matrix; H: High-pass filter; L: Low-pass filter; NGTDM: Neighboring gray tone difference matrix; SD: Standard deviation.

BMI: Overall, radiogenomic analysis revealed that four of the eight mRNA regulators were significantly correlated with 10 of the 29 selected radiomic features, of which five belonging to wavelet group and three belonging to LoG sigma group as reported in Figure 5. In particular, METTL3 was positively correlated with HLH median, LHL GLDM high gray level emphasis, HLL GLRLM gray level variance and LLL GLDM small dependence high gray level emphasis ($\rho = 0.71$, $\rho = 0.54$, $\rho = 0.53$, $\rho = 0.6$, $P < 0.05$, respectively) and negatively correlated with HLL GLCM inverse variance and LoG sigma 10th percentile calculated with sigma = 5.0 ($\rho = -0.6$, $\rho = -0.66$, $P < 0.05$, respectively); YTHDF1 was positively correlated with wavelet feature HLL GLCM maximum probability ($\rho = 0.6$, $P < 0.05$), whereas YTHDC1 was positively correlated with the wavelet HHH GLCM difference average ($\rho = 0.67$, $P < 0.05$) and inversely

Table 4 Results of multivariate analysis for the stage I-II/stage III-IV classification task

Model order	Features involved	AUC ± SE	Sens ± SE	Spec ± SE	ACC ± SE
1	Wavelet-HHH GLCM joint entropy	0.896 ± 0.005	0.513 ± 0.021	0.865 ± 0.007	0.77 ± 0.006
2	Wavelet-LLH NGTDM complexity; Wavelet-HHH GLCM joint entropy	0.869 ± 0.008	0.643 ± 0.021	0.834 ± 0.008	0.79 ± 0.006
3	Wavelet-LLH NGTDM complexity; Wavelet-HHH GLCM joint entropy; Wavelet-HLH first order entropy	0.826 ± 0.009	0.523 ± 0.023	0.815 ± 0.009	0.744 ± 0.006
4	Wavelet-HLL GLCM cluster prominence; Wavelet-HHH GLCM joint entropy; Wavelet-LLH NGTDM complexity; Wavelet-HLH first order entropy	0.799 ± 0.009	0.668 ± 0.022	0.766 ± 0.009	0.752 ± 0.007
5	Wavelet-LLH GLDM high gray level emphasis; Wavelet-HHH GLCM joint entropy; Wavelet HLL GLCM cluster prominence; Wavelet HLH entropy; Wavelet LLH NGTDM complexity	0.724 ± 0.011	0.516 ± 0.025	0.762 ± 0.01	0.708 ± 0.008

For each model (from order 1 to 5), area under the receiver operating characteristic curve, sensitivity, specificity and accuracy were reported with the standard error on a 95%CI over all bootstrap sample. AUC: Area under the receiver operating characteristic curve; GLCM: Gray level co-occurrence matrix; GLDM: Gray level dependence matrix; GLRLM: Gray level run length matrix; GLSZM: Gray level size zone matrix; H: High-pass filter; L: Low-pass filter; NGTDM: Neighboring gray tone difference matrix; SE: Standard error.

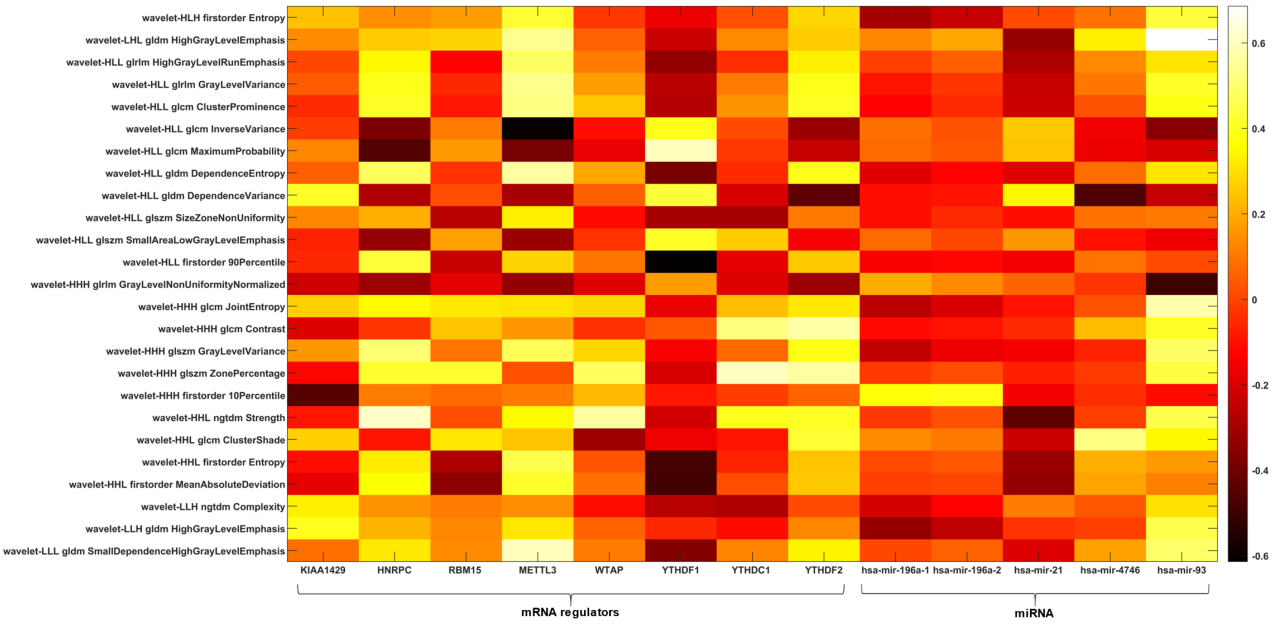


Figure 3 Radiogenomic analysis using stage as clinical outcome. Heatmap depicting the correlation matrix between transcriptomic features and radiomic features significantly associated with stage. GLCM: Gray level co-occurrence matrix; GLDM: Gray level dependence matrix; GLRLM: Gray level run length matrix; GLSZM: Gray level size zone matrix; H: High-pass filter; L: Low-pass filter; NGTDM: Neighboring gray tone difference matrix.

correlated with and LoG sigma root mean squared calculated with sigma = 1.0 (ρ = -0.67, P < 0.05); similarly, YTHDF2 was positively correlated with the wavelet HHH GLCM contrast (ρ = 0.57, P < 0.05) and inversely with the LoG sigma 10th percentile calculated with sigma = 5.0 (ρ = -0.56, P < 0.05). Moreover, correlation analysis with the five up-regulated miRNA revealed a significant correlation only between miRNA-93 and two radiomic features as reported in Figure 5 and in particular with the wavelet feature LHL GLRLM high gray level run emphasis (ρ = 0.69, P < 0.05) and the LoG sigma 10th percentile calculated with sigma = 5.0 (ρ = -0.54, P < 0.05).

DISCUSSION

Several studies reported that some miRNAs, such as miR-21, miR-183, miR-574-5p and miR-601, can regulate the pathways in esophageal carcinogenesis by their altered

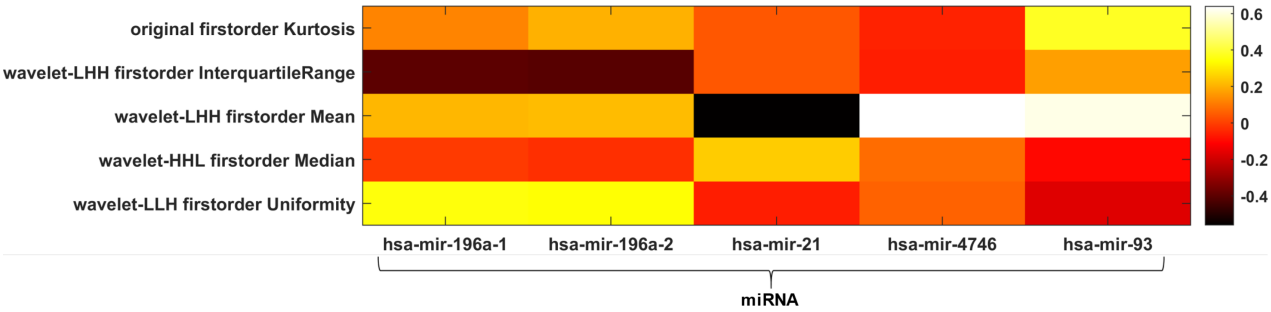


Figure 4 Radiogenomic analysis using alcohol history as clinical outcome. Heatmap depicting the correlation matrix between transcriptomic features and radiomic features significantly associated with alcohol history. H: High-pass filter; L: Low-pass filter; miRNA: MicroRNA.

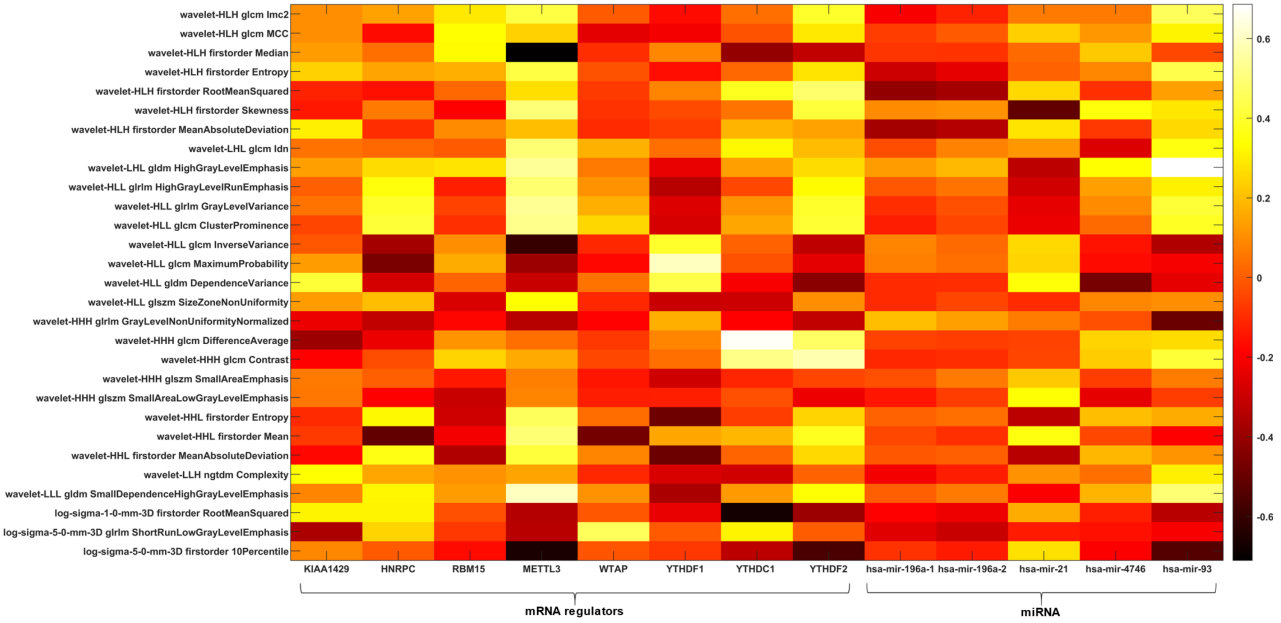


Figure 5 Radiogenomic analysis using body mass index as clinical outcome. Heatmap depicting the correlation matrix between transcriptomic features and radiomic features significantly associated with body mass index. GLCM: Gray level co-occurrence matrix; GLDM: Gray level dependence matrix; GLRLM: Gray level run length matrix; GLSZM: Gray level size zone matrix; H: High-pass filter; L: Low-pass filter; miRNA: MicroRNA; mRNA: Messenger RNA; NGTDM: Neighboring gray tone difference matrix.

expression associated with the increasing of risks factors, including dietary, smoking and drinking habits[44]. Moreover, a recent study, through an integrated approach, evaluated how dysregulated miRNAs by regulating RNA targets changed the relative miRNA-mRNA expression to survival and clinical characteristics[45]. In addition, miRNAs, more generally noncoding RNAs, have the ability to regulate m6A modifications, thereby affecting gene expression in cancer progression. Previous studies highlighted a strong relation between RNA methylation and breast cancer. In particular, Zhang *et al*[46] reported significant difference in expression levels and prognostic value of five m6RNA regulators (YTHDF3, ZC3H13, LRPPRC, METTL16, RBM15B) in breast cancer. Furthermore, in a recent study, Zhao *et al*[47] showed that m6A regulator genomic aberration is associated with prognosis of ESCA patients.

It is recognized that the use of CT radiomics is rapidly increasing in the field of ESCA management, playing an important role in preoperative nodal staging, diagnosis and prognosis and for predicting treatment response to chemoradiotherapy [3,48-52]. Wu *et al*[15] showed that CT radiomic features were able to discriminate between stage I-II and III-IV ESCA. In a study by Yang *et al*[45], predictive models based on CT radiomic features were able to predict complete pathologic response after neoadjuvant chemoradiotherapy of ESCA patients. CT texture features were also found to be independent predictors of survival[48], while CT wavelet features were associated with the 3-year overall survival after chemoradiotherapy in a study involving 165 patients performed by Larue *et al*[51].

In our pilot study, we examined the relationship between the expression levels of eight m6A RNA methylation regulators (KIAA1429, HNRNPC, RBM15, METTL3, WTAP, YTHDF1, YTHDC1, YTHDF2), as well as five up-regulated miRNAs (miRNA-93, miRNA-21, miRNA-4746, miRNA-196a-1 and miRNA-196a-2) and radiomic features extracted from CT images that were significantly associated to clinical outcomes (stage, alcohol history, BMI) in patients with ESCA belonging to the public integrated datasets TCGA/TCIA. We decided to evaluate by combining radiomic and transcriptomic data the above-mentioned m6A RNA methylation regulators and up-regulated miRNA since previous studies on gene expression in ESCA found interesting results on specific mRNAs associated with tumor stage through epigenetic regulation and miRNAs signature as a prognostic biomarker[22,25].

Interestingly, both considering binary clinical outcomes (namely stage and alcohol history) and BMI, CT radiomic features that survived after radiomic feature selection were mostly belonging to the wavelet group, while only histogram Kurtosis and three LoG sigma features (one textural and two histogram features) survived after feature selection for alcohol history and BMI analysis, respectively. Wavelet features were also able to differentiate between stage I-II and III-IV ESCA, with an AUC superior to 80%. Similar performances were achieved when using the same features for predicting T and N, and this could be because T and N assignments contribute to determine the overall ESCA stage[43]. These results are in line with those found by Liu *et al*[53], even if they did not include textural features from wavelet CT images.

These results were in line with previous radiomics studies, in which CT imaging features describing tumor heterogeneity also were shown to have prognostic value in esophageal cancer[51,54]. Wavelet radiomic features from pretreatment CT were found to be useful to predict overall survival of ESCA patients after chemoradiotherapy in a study by Larue *et al*[51]. Moreover, in the work by Qiu *et al*[54], wavelet features resulted predominant in the radiomic-based predictive model developed to estimate recurrence-free survival in ESCA patients achieving a pathologic complete response.

Radiogenomic analysis performed for stage assessment revealed significant correlations between 10 wavelet textural features and six of the eight m6A RNA methylation regulators (HRNPC, WTAP, METTL3, YTHDF1, YTHDF2, YTHDC1). Moreover, correlation analysis with the five up-regulated miRNA revealed a significant positive correlation between miRNA-93 and two radiomic wavelet features, namely LHL GLDM high gray level emphasis and HHH GLCM joint entropy. It is worth to note that the wavelet feature HHH GLCM joint entropy was positively correlated with miRNA-93 and contributed to building the best predictive models for the overall stage assessment and for the assessment of the T and N categories. From the literature, miR-93 is reported to be associated in various tumors and it is recently found to regulate mechanisms of drug resistance in triple negative breast cancer[55]. Moreover, Ansari *et al*[56] evaluated miR-93 as potential deregulated biomarker for early detection of ESCA. Based on these considerations, combining genomic features with radiomic ones might be of further added value for ESCA staging, thereby influencing the personalized medicine workflow in the field of ESCA. Concerning radiogenomic analysis performed using alcohol history as clinical outcome, there were no significant associations between selected CT features and the eight m6A RNA methylation regulators, while the correlation analysis with the five up-regulated miRNA revealed a significant correlation between the wavelet feature LHH first order mean and three up-regulated miRNA, namely miRNA-21, miRNA-4746 and miRNA-93. Finally, the radiogenomic analysis on BMI revealed a significant correlation between wavelet and LoG sigma features and METTL3, YTHDF1, YTHDC1 and YTHDF2. Wavelet and LoG sigma features were also associated with miRNA-93 in radiogenomic analysis involving the five up-regulated miRNAs.

In addition, a recent study has experimentally verified that overexpression of METTL3 in tumor tissues of ESCA patients compared with normal condition from adjacent tissues is associated with metabolic status, highlighting a significant correlation with tumor size and histological differentiation; this result suggests that MTLL3 may become a possible pathological index for diagnosis and a potential therapeutic target[57].

However, to our knowledge, this is the first ESCA radiogenomic study investigating the association with clinical staging and potential risk factors. Although previous radiogenomic studies were performed on ESCA[21,49,58], the strength of our study was that this is the first radiogenomic study investigating the association with stage, alcohol history, and BMI. Moreover, is not to be neglected that it is a radiogenomic study on an unexplored cancer type such as ESCA.

However, several limitations are worth noting. First, due to the extremely small sample size and the retrospective nature of the study, our results remain to be validated with a larger and prospective patient sample in the future. Second, the small sample size may have affected also prediction model performances. Therefore, a larger and more balanced study group is needed to conduct better a radiomic analysis and build more robust prediction models. In particular, although the IABR strategy we used for model building is a common reliable approach in case of small and imbalanced datasets, a larger sample size would allow using part of the dataset for the training and part for testing and validating the performance of the classifier with external datasets. In addition, it should be considered that the availability of the eight m6A RNA methylation regulators and the five up-regulated miRNAs only for a small population has prevented us from investigating other clinical outcomes, which were missing for the investigated patients. It would have been interesting to perform similar analyses considering smoking variables as clinical outcomes. In fact, in addition to alcohol, tobacco is an established risk factor for ESCA and has been proven to act synergically with alcohol to increase the risk of ESCA[59,60]. However, we could not perform analyses involving outcomes associated with smoking due to the incompleteness of these data for the included patients' cohort.

CONCLUSION

In conclusion, our preliminary study revealed interesting relationships between the expression levels of eight m6A RNA methylation regulators, as well as the five up-regulated miRNAs, and CT radiomic features that were significantly associated with clinical outcomes. Our results strengthen the role of miRNA overexpression and the possible characterization of biomarkers from liquid biopsy for ESCA assessment and staging, introducing new insights for omics integration toward a personalized medicine approach. Further prospective and retrospective studies involving larger groups of patients are essential to validate obtained results and perform in-depth analyses.

ARTICLE HIGHLIGHTS

Research background

Esophageal cancer (ESCA) is the sixth most common malignancy in the world, and its incidence is rapidly increasing. Radiogenomics provides clinically useful prognostic predictions by linking molecular characteristics such as gene mutations and gene expression patterns of malignant tumors with medical images and could provide more opportunities in the management of patients with ESCA.

Research motivation

Recently, several microRNAs (miRNAs) and messenger (RNA) targets were evaluated as potential biomarkers and regulators of epigenetic mechanisms involved in ESCA. In addition, the use of computed tomography (CT) radiomics is rapidly increasing in the field of ESCA and plays an important role in different ESCA management steps. Moreover, there are no previous radiogenomic studies on ESCA investigating the association with clinical staging and potential risk factors. This has motivated us to investigate on the relationship between the expression levels of eight N6-methyl-adenosine (m6A) RNA methylation regulators, as well as the five up-regulated miRNAs, and radiomic features extracted from CT images that were significantly associated to clinical outcomes.

Research objectives

To explore the combination of CT radiomic features and molecular targets associated with clinical outcomes for characterization of ESCA patients.

Research methods

Fifteen patients with diagnosed ESCA were included in this study, and their CT imaging and transcriptomic data were extracted from The Cancer Imaging Archive and gene expression data from The Cancer Genome Atlas, respectively. Cancer stage, history of significant alcohol consumption and body mass index (BMI) were

considered as clinical outcomes. Radiomic analysis was performed on CT images acquired after injection of contrast medium. In total, 1302 radiomics features were extracted from three-dimensional regions of interest by using PyRadiomics. Radiogenomic analysis involved Spearman's correlation (ρ) analysis between radiomic features associated with clinical outcomes and transcriptomic signatures consisting in eight m6A RNA methylation regulators and five up-regulated miRNA.

Research results

Radiogenomic analysis with stage as clinical outcome revealed that six of the eight mRNA regulators and two of the five up-regulated miRNA were significantly correlated with 10 and three of the 25 selected radiomic features, respectively. Assuming alcohol history as clinical outcome, no correlation was found between the five selected radiomic features and mRNA regulators, while a significant correlation was found between one radiomic feature and three up-regulated miRNA. Radiogenomic analysis with BMI as clinical outcome revealed that four mRNA regulators and one up-regulated miRNA were significantly correlated with 10 and two radiomic features, respectively.

Research conclusions

Our study revealed interesting relationships between the expression of eight m6a RNA regulators, as well as five up-regulated miRNAs, and CT radiomic features associated with clinical outcomes of ESCA patients.

Research perspectives

This preliminary study revealed interesting associations between m6a RNA regulators, as well as miRNAs, and CT radiomic features associated with clinical outcomes of ESCA patients. Further investigations on different ESCA omics data are required. Moreover, multimodal data combined with artificial intelligence techniques characteristics are desirable.

ACKNOWLEDGEMENTS

All results shown here are in whole or part based upon data generated by the TCGA Research Network: https://www.cancer.gov/tcga.

REFERENCES

1 **Bray F**, Ferlay J, Soerjomataram I, Siegel RL, Torre LA, Jemal A. Global cancer statistics 2018: GLOBOCAN estimates of incidence and mortality worldwide for 36 cancers in 185 countries. *CA Cancer J Clin* 2018; **68**: 394-424 [PMID: 30207593 DOI: 10.3322/caac.21492]

2 **Ahmad NR**, Goosenberg EB, Frucht H, Coia LR. Palliative Treatment of Esophageal Cancer. *Semin Radiat Oncol* 1994; **4**: 202-214 [PMID: 10717108 DOI: 10.1053/SRAO00400192]

3 **Yang Z**, He B, Zhuang X, Gao X, Wang D, Li M, Lin Z, Luo R. CT-based radiomic signatures for prediction of pathologic complete response in esophageal squamous cell carcinoma after neoadjuvant chemoradiotherapy. *J Radiat Res* 2019; **60**: 538-545 [PMID: 31111948 DOI: 10.1093/jrr/rrz027]

4 **Napier KJ**, Scheerer M, Misra S. Esophageal cancer: A Review of epidemiology, pathogenesis, staging workup and treatment modalities. *World J Gastrointest Oncol* 2014; **6**: 112-120 [PMID: 24834141 DOI: 10.4251/wjgo.v6.i5.112]

5 **Milsom JW**, Senagore A, Walshaw RK, Mostosky UV, Wang P, Johnson W, Chaudry IH. Preoperative radiation therapy produces an early and persistent reduction in colorectal anastomotic blood flow. *J Surg Res* 1992; **53**: 464-469 [PMID: 1434596 DOI: 10.1016/0022-4804(92)90091-d]

6 **Tirumani H**, Rosenthal MH, Tirumani SH, Shinagare AB, Krajewski KM, Ramaiya NH. Esophageal Carcinoma: Current Concepts in the Role of Imaging in Staging and Management. *Can Assoc Radiol J* 2015; **66**: 130-139 [PMID: 25770628 DOI: 10.1016/j.carj.2014.08.006]

7 **Elsherif SB**, Andreou S, Virarkar M, Soule E, Gopireddy DR, Bhosale PR, Lall C. Role of precision imaging in esophageal cancer. *J Thorac Dis* 2020; **12**: 5159-5176 [PMID: 33145093 DOI: 10.21037/jtd.2019.08.15]

8 **Umeoka S**, Koyama T, Togashi K, Saga T, Watanabe G, Shimada Y, Imamura M. Esophageal cancer: evaluation with triple-phase dynamic CT--initial experience. *Radiology* 2006; **239**: 777-783 [PMID: 16621930 DOI: 10.1148/radiol.2393050222]

9 **Sultan R**, Haider Z, Chawla TU. Diagnostic accuracy of CT scan in staging resectable esophageal cancer. *J Pak Med Assoc* 2016; **66**: 90-92 [PMID: 26712189]

10 **Lambin P**, Rios-Velazquez E, Leijenaar R, Carvalho S, van Stiphout RG, Granton P, Zegers CM,

Gillies R, Boellard R, Dekker A, Aerts HJ. Radiomics: extracting more information from medical images using advanced feature analysis. *Eur J Cancer* 2012; **48**: 441-446 [PMID: 22257792 DOI: 10.1016/j.ejca.2011.11.036]

11 **Gillies RJ**, Kinahan PE, Hricak H. Radiomics: Images Are More than Pictures, They Are Data. *Radiology* 2016; **278**: 563-577 [PMID: 26579733 DOI: 10.1148/radiol.2015151169]

12 **van Rossum PSN**, Xu C, Fried DV, Goense L, Court LE, Lin SH. The emerging field of radiomics in esophageal cancer: current evidence and future potential. *Transl Cancer Res* 2016; **5**: 410-423 [PMID: 30687593 DOI: 10.21037/tcr.2016.06.19]

13 **Rizzo S**, Botta F, Raimondi S, Origgi D, Fanciullo C, Morganti AG, Bellomi M. Radiomics: the facts and the challenges of image analysis. *Eur Radiol Exp* 2018; **2**: 36 [PMID: 30426318 DOI: 10.1186/s41747-018-0068-z]

14 **Hou T-C**, Huang W-C, Tai H-C, Chen Y-J. Integrated radiomic model for predicting the prognosis of esophageal squamous cell carcinoma patients undergoing neoadjuvant chemoradiation. *Ther Radiol Oncol* 2019; **3**: 28 [DOI: 10.21037/tro.2019.07.03]

15 **Wu L**, Wang C, Tan X, Cheng Z, Zhao K, Yan L, Liang Y, Liu Z, Liang C. Radiomics approach for preoperative identification of stages I-II and III-IV of esophageal cancer. *Chin J Cancer Res* 2018; **30**: 396-405 [PMID: 30210219 DOI: 10.21147/j.issn.1000-9604.2018.04.02]

16 **Jin X**, Zheng X, Chen D, Jin J, Zhu G, Deng X, Han C, Gong C, Zhou Y, Liu C, Xie C. Prediction of response after chemoradiation for esophageal cancer using a combination of dosimetry and CT radiomics. *Eur Radiol* 2019; **29**: 6080-6088 [PMID: 31028447 DOI: 10.1007/s00330-019-06193-w]

17 **Hyman DM**, Taylor BS, Baselga J. Implementing Genome-Driven Oncology. *Cell* 2017; **168**: 584-599 [PMID: 28187282 DOI: 10.1016/j.cell.2016.12.015]

18 **Berger MF**, Mardis ER. The emerging clinical relevance of genomics in cancer medicine. *Nat Rev Clin Oncol* 2018; **15**: 353-365 [PMID: 29599476 DOI: 10.1038/s41571-018-0002-6]

19 **Guo W**, Jiang YG. Current gene expression studies in esophageal carcinoma. *Curr Genomics* 2009; **10**: 534-539 [PMID: 20514215 DOI: 10.2174/138920209789503888]

20 **Visser E**, Franken IA, Brosens LA, Ruurda JP, van Hillegersberg R. Prognostic gene expression profiling in esophageal cancer: a systematic review. *Oncotarget* 2017; **8**: 5566-5577 [PMID: 27852047 DOI: 10.18632/oncotarget.13328]

21 **Hoshino I**, Yokota H, Ishige F, Iwatate Y, Takeshita N, Nagase H, Uno T, Matsubara H. Radiogenomics predicts the expression of microRNA-1246 in the serum of esophageal cancer patients. *Sci Rep* 2020; **10**: 2532 [PMID: 32054931 DOI: 10.1038/s41598-020-59500-7]

22 **Zeng JH**, Xiong DD, Pang YY, Zhang Y, Tang RX, Luo DZ, Chen G. Identification of molecular targets for esophageal carcinoma diagnosis using miRNA-seq and RNA-seq data from The Cancer Genome Atlas: a study of 187 cases. *Oncotarget* 2017; **8**: 35681-35699 [PMID: 28415685 DOI: 10.18632/oncotarget.16051]

23 **Ma S**, Chen C, Ji X, Liu J, Zhou Q, Wang G, Yuan W, Kan Q, Sun Z. The interplay between m6A RNA methylation and noncoding RNA in cancer. *J Hematol Oncol* 2019; **12**: 121 [PMID: 31757221 DOI: 10.1186/s13045-019-0805-7]

24 **Lan Q**, Liu PY, Haase J, Bell JL, Hüttelmaier S, Liu T. The Critical Role of RNA m^6A Methylation in Cancer. *Cancer Res* 2019; **79**: 1285-1292 [PMID: 30894375 DOI: 10.1158/0008-5472.CAN-18-2965]

25 **Xu LC**, Pan JX, Pan HD. Construction and Validation of an m6A RNA Methylation Regulators-Based Prognostic Signature for Esophageal Cancer. *Cancer Manag Res* 2020; **12**: 5385-5394 [PMID: 32753956 DOI: 10.2147/CMAR.S254870]

26 **Sah BR**, Owczarczyk K, Siddique M, Cook GJR, Goh V. Radiomics in esophageal and gastric cancer. *Abdom Radiol (NY)* 2019; **44**: 2048-2058 [PMID: 30116873 DOI: 10.1007/s00261-018-1724-8]

27 **Klaassen R**, Larue RTHM, Mearadji B, van der Woude SO, Stoker J, Lambin P, van Laarhoven HWM. Feasibility of CT radiomics to predict treatment response of individual liver metastases in esophagogastric cancer patients. *PLoS One* 2018; **13**: e0207362 [PMID: 30440002 DOI: 10.1371/journal.pone.0207362]

28 **Wu R**, Zhuang H, Mei YK, Sun JY, Dong T, Zhao LL, Fan ZN, Liu L. Systematic identification of key functional modules and genes in esophageal cancer. *Cancer Cell Int* 2021; **21**: 134 [PMID: 33632229 DOI: 10.1186/s12935-021-01826-x]

29 **Peng Q**, Chen H, Huo JR. Alcohol consumption and corresponding factors: A novel perspective on the risk factors of esophageal cancer. *Oncol Lett* 2016; **11**: 3231-3239 [PMID: 27123096 DOI: 10.3892/ol.2016.4401]

30 **Long E**, Beales IL. The role of obesity in oesophageal cancer development. *Therap Adv Gastroenterol* 2014; **7**: 247-268 [PMID: 25364384 DOI: 10.1177/1756283X14538689]

31 **Turati F**, Tramacere I, La Vecchia C, Negri E. A meta-analysis of body mass index and esophageal and gastric cardia adenocarcinoma. *Ann Oncol* 2013; **24**: 609-617 [PMID: 22898040 DOI: 10.1093/annonc/mds244]

32 **Lucchesi FR**, Aredes ND. Radiology Data from The Cancer Genome Atlas Esophageal Carcinoma [TCGA-ESCA] collection. *The Cancer Imaging Archive* 2016 [DOI: 10.7937/K9/TCIA.2016.VPTNRGFY]

33 **Clark K**, Vendt B, Smith K, Freymann J, Kirby J, Koppel P, Moore S, Phillips S, Maffitt D, Pringle M, Tarbox L, Prior F. The Cancer Imaging Archive (TCIA): maintaining and operating a public information repository. *J Digit Imaging* 2013; **26**: 1045-1057 [PMID: 23884657 DOI: 10.1007/s10278-013-9622-7]

34 **Zwanenburg A**, Vallières M, Abdalah MA, Aerts HJWL, Andrearczyk V, Apte A, Ashrafinia S, Bakas S, Beukinga RJ, Boellaard R, Bogowicz M, Boldrini L, Buvat I, Cook GJR, Davatzikos C, Depeursinge A, Desseroit MC, Dinapoli N, Dinh CV, Echegaray S, El Naqa I, Fedorov AY, Gatta R, Gillies RJ, Goh V, Götz M, Guckenberger M, Ha SM, Hatt M, Isensee F, Lambin P, Leger S, Leijenaar RTH, Lenkowicz J, Lippert F, Losnegård A, Maier-Hein KH, Morin O, Müller H, Napel S, Nioche C, Orlhac F, Pati S, Pfaehler EAG, Rahmim A, Rao AUK, Scherer J, Siddique MM, Sijtsema NM, Socarras Fernandez J, Spezi E, Steenbakkers RJHM, Tanadini-Lang S, Thorwarth D, Troost EGC, Upadhaya T, Valentini V, van Dijk LV, van Griethuysen J, van Velden FHP, Whybra P, Richter C, Löck S. The Image Biomarker Standardization Initiative: Standardized Quantitative Radiomics for High-Throughput Image-based Phenotyping. *Radiology* 2020; **295**: 328-338 [PMID: 32154773 DOI: 10.1148/radiol.2020191145]

35 **Vergara JR**, Estévez PA. A review of feature selection methods based on mutual information. *Neural Comput Applic* 2014; **24**: 175-186 [DOI: 10.1007/s00521-013-1368-0]

36 **Zaffalon M**, Hutter M. Robust Feature Selection by Mutual Information Distributions. 2014 Preprint. Available from: arXiv: 1408.1487v1

37 **Roffo G**. Feature Selection Library (MATLAB Toolbox). 2018 Preprint. Available from: arXiv: 1607.01327v5

38 **Vallières M**, Freeman CR, Skamene SR, El Naqa I. A radiomics model from joint FDG-PET and MRI texture features for the prediction of lung metastases in soft-tissue sarcomas of the extremities. *Phys Med Biol* 2015; **60**: 5471-5496 [PMID: 26119045 DOI: 10.1088/0031-9155/60/14/5471]

39 **Efron B**. Bootstrap Methods: Another Look at the Jackknife. *Ann Statist* 1979; **7**: 1-26 [DOI: 10.1214/aos/1176344552]

40 **Efron B**, Tibshirani R. Improvements on Cross-Validation: The .632+ Bootstrap Method. *J Am Stat Assoc* 1997; **92**: 548 [DOI: 10.2307/2965703]

41 **Brancato V**, Aiello M, Basso L, Monti S, Palumbo L, Di Costanzo G, Salvatore M, Ragozzino A, Cavaliere C. Evaluation of a multiparametric MRI radiomic-based approach for stratification of equivocal PI-RADS 3 and upgraded PI-RADS 4 prostatic lesions. *Sci Rep* 2021; **11**: 643 [PMID: 33436929 DOI: 10.1038/s41598-020-80749-5]

42 **Sahiner B**, Chan HP, Hadjiiski L. Classifier performance prediction for computer-aided diagnosis using a limited dataset. *Med Phys* 2008; **35**: 1559-1570 [PMID: 18491550 DOI: 10.1118/1.2868757]

43 **Berry MF**. Esophageal cancer: staging system and guidelines for staging and treatment. *J Thorac Dis* 2014; **6** Suppl 3: S289-S297 [PMID: 24876933 DOI: 10.3978/j.issn.2072-1439.2014.03.11]

44 **Stánitz É**, Juhász K, Gombos K, Gőcze K, Tóth C, Kiss I. Alteration of miRNA expression correlates with lifestyle, social and environmental determinants in esophageal carcinoma. *Anticancer Res* 2015; **35**: 1091-1097 [PMID: 25667498]

45 **Yang H**, Su H, Hu N, Wang C, Wang L, Giffen C, Goldstein AM, Lee MP, Taylor PR. Integrated analysis of genome-wide miRNAs and targeted gene expression in esophageal squamous cell carcinoma (ESCC) and relation to prognosis. *BMC Cancer* 2020; **20**: 388 [PMID: 32375686 DOI: 10.1186/s12885-020-06901-6]

46 **Zhang B**, Gu Y, Jiang G. Expression and Prognostic Characteristics of m^6 A RNA Methylation Regulators in Breast Cancer. *Front Genet* 2020; **11**: 604597 [PMID: 33362863 DOI: 10.3389/fgene.2020.604597]

47 **Zhao H**, Xu Y, Xie Y, Zhang L, Gao M, Li S, Wang F. m6A Regulators Is Differently Expressed and Correlated With Immune Response of Esophageal Cancer. *Front Cell Dev Biol* 2021; **9**: 650023 [PMID: 33748145 DOI: 10.3389/fcell.2021.650023]

48 **Ganeshan B**, Skogen K, Pressney I, Coutroubis D, Miles K. Tumour heterogeneity in oesophageal cancer assessed by CT texture analysis: preliminary evidence of an association with tumour metabolism, stage, and survival. *Clin Radiol* 2012; **67**: 157-164 [PMID: 21943720 DOI: 10.1016/j.crad.2011.08.012]

49 **Hu Y**, Xie C, Yang H, Ho JWK, Wen J, Han L, Chiu KWH, Fu J, Vardhanabhuti V. Assessment of Intratumoral and Peritumoral Computed Tomography Radiomics for Predicting Pathological Complete Response to Neoadjuvant Chemoradiation in Patients With Esophageal Squamous Cell Carcinoma. *JAMA Netw Open* 2020; **3**: e2015927 [PMID: 32910196 DOI: 10.1001/jamanetworkopen.2020.15927]

50 **Piazzese C**, Foley K, Whybra P, Hurt C, Crosby T, Spezi E. Discovery of stable and prognostic CT-based radiomic features independent of contrast administration and dimensionality in oesophageal cancer. *PLoS One* 2019; **14**: e0225550 [PMID: 31756181 DOI: 10.1371/journal.pone.0225550]

51 **Larue RTHM**, Klaassen R, Jochems A, Leijenaar RTH, Hulshof MCCM, van Berge Henegouwen MI, Schreurs WMJ, Sosef MN, van Elmpt W, van Laarhoven HWM, Lambin P. Pre-treatment CT radiomics to predict 3-year overall survival following chemoradiotherapy of esophageal cancer. *Acta Oncol* 2018; **57**: 1475-1481 [PMID: 30067421 DOI: 10.1080/0284186X.2018.1486039]

52 **Hou Z**, Yang Y, Li S, Yan J, Ren W, Liu J, Wang K, Liu B, Wan S. Radiomic analysis using contrast-enhanced CT: predict treatment response to pulsed low dose rate radiotherapy in gastric carcinoma with abdominal cavity metastasis. *Quant Imaging Med Surg* 2018; **8**: 410-420 [PMID: 29928606 DOI: 10.21037/qims.2018.05.01]

53 **Liu S**, Zheng H, Pan X, Chen L, Shi M, Guan Y, Ge Y, He J, Zhou Z. Texture analysis of CT imaging for assessment of esophageal squamous cancer aggressiveness. *J Thorac Dis* 2017; **9**: 4724-4732 [DOI: 10.21037/jtd.2017.06.46]

54 **Qiu Q**, Duan J, Deng H, Han Z, Gu J, Yue NJ, Yin Y. Development and Validation of a Radiomics

Nomogram Model for Predicting Postoperative Recurrence in Patients With Esophageal Squamous Cell Cancer Who Achieved pCR After Neoadjuvant Chemoradiotherapy Followed by Surgery. *Front Oncol* 2020; **10**: 1398 [PMID: 32850451 DOI: 10.3389/fonc.2020.01398]

55 **Qattan A**, Al-Tweigeri T, Alkhayal W, Suleman K, Tulbah A, Amer S. Clinical Identification of Dysregulated Circulating microRNAs and Their Implication in Drug Response in Triple Negative Breast Cancer (TNBC) by Target Gene Network and Meta-Analysis. *Genes* 2021; **12**: 549 [DOI: 10.3390/genes12040549]

56 **Ansari MH**, Irani S, Edalat H, Amin R, Mohammadi Roushandeh A. Deregulation of miR-93 and miR-143 in human esophageal cancer. *Tumor Biol* 2016; **37**: 3097-3103 [DOI: 10.1007/s13277-015-3987-9]

57 **Liu XS**, Yuan LL, Gao Y, Zhou LM, Yang JW, Pei ZJ. Overexpression of METTL3 associated with the metabolic status on ^{18}F-FDG PET/CT in patients with Esophageal Carcinoma. *J Cancer* 2020; **11**: 4851-4860 [PMID: 32626532 DOI: 10.7150/jca.44754]

58 **Hu Y**, Xie C, Yang H, Ho JWK, Wen J, Han L, Lam KO, Wong IYH, Law SYK, Chiu KWH, Vardhanabhuti V, Fu J. Computed tomography-based deep-learning prediction of neoadjuvant chemoradiotherapy treatment response in esophageal squamous cell carcinoma. *Radiother Oncol* 2021; **154**: 6-13 [PMID: 32941954 DOI: 10.1016/j.radonc.2020.09.014]

59 **Prabhu A**, Obi KO, Rubenstein JH. The synergistic effects of alcohol and tobacco consumption on the risk of esophageal squamous cell carcinoma: a meta-analysis. *Am J Gastroenterol* 2014; **109**: 822-827 [PMID: 24751582 DOI: 10.1038/ajg.2014.71]

60 **Dong J**, Thrift AP. Alcohol, smoking and risk of oesophago-gastric cancer. *Best Pract Res Clin Gastroenterol* 2017; **31**: 509-517 [PMID: 29195670 DOI: 10.1016/j.bpg.2017.09.002]

World Journal of Gastroenterology

Submit a Manuscript: https://www.f6publishing.com

World J Gastroenterol 2021 September 28; 27(36): 6128-6141

DOI: 10.3748/wjg.v27.i36.6128

ISSN 1007-9327 (print) ISSN 2219-2840 (online)

ORIGINAL ARTICLE

Retrospective Study

Clinicopathological characteristics and longterm survival of patients with synchronous multiple primary gastrointestinal stromal tumors: A propensity score matching analysis

Hao Wu, Chen Li, Han Li, Liang Shang, Hai-Yan Jing, Jin Liu, Zhen Fang, Feng-Ying Du, Yang Liu, Meng-Di Fu, Ke-Wei Jiang, Le-Ping Li

ORCID number: Hao Wu 0000-0001-9222-2521; Chen Li 0000-0003-3556-2719; Han Li 0000-0002-0699-673X; Liang Shang 0000-0002-9542-7650; Hai-Yan Jing 0000-0003-0913-6898; Jin Liu 0000-0001-7959-1541; Zhen Fang 0000-0002-7073-8997; Feng-Ying Du 0000-0002-2767-1301; Yang Liu 0000-0001-7167-7439; Meng-Di Fu 0000-0002-4172-6794; Ke-Wei Jiang 0000-0002-6706-4741; Le-Ping Li 0000-0003-2329-6791.

Author contributions: All authors helped to perform the research; Wu H and Li C were involved equally in the conception and design; Li H provided clinical advice; Fu MD was involved in the follow-up of patients; Fang Z was involved in preliminary medical record screening and entry; Liu Y was involved in the verification of the included data; Du FY was involved in the drafting of the paper or revising it critically for intellectual content; Jing HY and Jiang KW provided pathology images and supervised the report; Shang L and Li LP were involved in the final approval of the version to be published; All authors agreed to be accountable for all aspects of the work.

Supported by Key Research and

Hao Wu, Liang Shang, Zhen Fang, Feng-Ying Du, Yang Liu, Le-Ping Li, Department of Gastroenterological Surgery, Shandong Provincial Hospital, Cheeloo College of Medicine, Shandong University, Jinan 250021, Shandong Province, China

Chen Li, Ke-Wei Jiang, Department of Gastroenterological Surgery, Peking University People's Hospital, Beijing 100044, China

Han Li, Department of General Surgery, The First Affiliated Hospital of Shandong First Medical University, Jinan 250021, Shandong Province, China

Liang Shang, Le-Ping Li, Department of Digestive Tumor Translational Medicine, Engineering Laboratory of Shandong Province, Shandong Provincial Hospital, Jinan 250021, Shandong Province, China

Liang Shang, Le-Ping Li, Medical Science and Technology Innovation Center, Shandong First Medical University & Shandong Academy of Medical Sciences, Jinan 250021, Shandong Province, China

Hai-Yan Jing, Department of Pathology, Shandong Provincial Hospital, Cheeloo College of Medicine, Shandong University, Jinan 250021, Shandong Province, China

Jin Liu, Department of Gastroenterology, Shandong Provincial Hospital, Cheeloo College of Medicine, Shandong University, Jinan 250021, Shandong Province, China

Meng-Di Fu, Department of Clinical Medicine, Cheeloo College of Medicine, Shandong University, Jinan 250021, Shandong Province, China

Corresponding author: Le-Ping Li, MD, Full Professor, Department of Gastroenterological Surgery, Shandong Provincial Hospital, Cheeloo College of Medicine, Shandong University, No. 324 Jingwuweiqi road, Huaiyin District, Jinan 250021, Shandong Province, China. lileping@sdu.edu.cn

Abstract

BACKGROUND

Multiple gastrointestinal stromal tumors (MGISTs) are specific and rare. Little is

Development Program of Shandong Province, No. 2019JZZY010104 and No. 2019GSF108146; Special Foundation for Taishan Scholars Program of Shandong Province, No. ts20190978; and Academic Promotion Programme of Shandong First Medical University, No. 2019QL021.

Institutional review board statement: This study was designed in compliance with the Helsinki Declaration and approved by the Ethics Committee of Shandong Provincial Hospital (SWYX: No. 2021-035).

Informed consent statement: Patients were not required to give informed consent to the study because the analysis used anonymous clinical data that were obtained after each patient agreed to treatment by written consent.

Conflict-of-interest statement: We have no financial relationships to disclose.

Open-Access: This article is an open-access article that was selected by an in-house editor and fully peer-reviewed by external reviewers. It is distributed in accordance with the Creative Commons Attribution NonCommercial (CC BY-NC 4.0) license, which permits others to distribute, remix, adapt, build upon this work non-commercially, and license their derivative works on different terms, provided the original work is properly cited and the use is non-commercial. See: http://creativecommons.org/Licenses/by-nc/4.0/

Manuscript source: Unsolicited manuscript

Specialty type: Gastroenterology and hepatology

Country/Territory of origin: China

Peer-review report's scientific quality classification

Grade A (Excellent): 0
Grade B (Very good): B
Grade C (Good): 0
Grade D (Fair): 0

known about the impact of MGISTs on the survival of patients with gastrointestinal stromal tumors (GIST). The diagnosis, treatment and follow-up strategies of MGISTs is not specifically described in guidelines.

AIM

To compare the clinicopathological characteristics and prognosis of MGISTs and solitary GISTs (SGISTs)

METHODS

Patients diagnosed with primary GISTs from March 2010 to January 2020 were included. Due to the inhomogeneous distribution of several baseline characteristics and uneven MGIST and SGIST group sizes, propensity score matching was performed according to comorbidities, body mass index, tumor location, mitotic index, sex, age and American Society of Anesthesiologists score. Differences in clinicopathological characteristics and prognosis between patients with MGISTs and patients with SGISTs were compared.

RESULTS

Among the entire cohort of 983 patients, the incidence of MGISTs was 4.17%. Before matching, patients with MGISTs and those with SGISTs had disparities in body mass index, surgical approach, tumor size and mitotic index. After 1:4 ratio matching, the clinical baseline data were comparable. The 5-year progression-free survival rate was 52.17% in the MGIST group and 75.00% in the SGIST group (P = 0.031). On multivariate analysis, tumor location, tumor size, mitotic index, imatinib treatment and MGISTs (hazard ratio = 2.431, 95% confidence interval = 1.097-5.386, P = 0.029) were identified as independent prognostic factors of progression-free survival. However, overall survival was similar between the SGIST and MGIST groups.

CONCLUSION

Patients with MGISTs had poorer progression-free survival than patients with SGISTs. Risk criteria and diagnostic and treatment strategies should be developed to achieve personalized precision therapy and maximize the survival benefit.

Key Words: Gastrointestinal stromal tumors; Synchronous; Multiple tumors; Solitary tumor; Propensity score matching; Prognosis

©The Author(s) 2021. Published by Baishideng Publishing Group Inc. All rights reserved.

Core Tip: Whether the clinicopathological characteristics and long-term survival of patients with multiple gastrointestinal stromal tumors are different from those of patients with solitary gastrointestinal stromal tumors is unclear. This is the first study to compare and describe these features. For accuracy and clarity, propensity score matching was used to balance the differences to explore the prognostic factors for patients with multiple gastrointestinal stromal tumors. To date, this study has the most detailed data and the largest number of patients, which may bring new insight to the diagnosis and treatment of multiple gastrointestinal stromal tumors.

Citation: Wu H, Li C, Li H, Shang L, Jing HY, Liu J, Fang Z, Du FY, Liu Y, Fu MD, Jiang KW, Li LP. Clinicopathological characteristics and longterm survival of patients with synchronous multiple primary gastrointestinal stromal tumors: A propensity score matching analysis. *World J Gastroenterol* 2021; 27(36): 6128-6141
URL: https://www.wjgnet.com/1007-9327/full/v27/i36/6128.htm
DOI: https://dx.doi.org/10.3748/wjg.v27.i36.6128

INTRODUCTION

As one of the most common mesenchymal tumors with an incidence of approximately 10 per million population, gastrointestinal stromal tumors (GISTs) are receiving

Grade E (Poor): 0

Received: June 19, 2021
Peer-review started: June 19, 2021
First decision: July 14, 2021
Revised: July 26, 2021
Accepted: August 13, 2021
Article in press: August 13, 2021
Published online: September 28, 2021

P-Reviewer: Vij M
S-Editor: Yan JP
L-Editor: Filipodia
P-Editor: Li JH



increasing attention[1-3]. GISTs are commonly located in the stomach and small intestine and rarely found in the esophagus, colon and rectum[4].

Multiple GISTs (MGISTs) refer to GISTs with two or more synchronous tumors in the gastrointestinal tract[5]. With the rapid advancement of precise diagnostic techniques and detailed pathological examinations, the detection and reporting of MGISTs have increased gradually. MGISTs accounted for nearly 2% of all GISTs in a multicenter study in China from 2001 to 2014[6]. However, due to the low incidence, there is currently no large-scale demographic survey showing the incidence of MGISTs.

Whether the clinical and pathological features of MGISTs are different from those of solitary GISTs (SGISTs) also remains unclear. Additionally, little is known about the impact of MGISTs on the survival of patients with GISTs. The diagnosis, treatment and follow-up strategies for MGISTs are not specifically described in the guidelines from the National Comprehensive Cancer Network, European Society for Medical Oncology and other academic institutions. Thus, we analyzed the clinicopathological characteristics and long-term survival of a large cohort of patients with MGISTs. It is urgent to gain insight into these questions to achieve personalized precision therapy in the future.

MATERIALS AND METHODS

Study design and approval

This retrospective cohort study was performed based on a prospectively collected database of GISTs at our hospital. All relevant procedures were approved by the Institutional Review Board. This study was designed in compliance with the Declaration of Helsinki and approved by the Ethics Committee of our hospital. The Reporting and Guidelines in propensity score analysis were also followed[7].

Patients

A total of 1163 consecutive patients diagnosed with GISTs and undergoing resection at our hospital between March 2010 and January 2020 were initially pooled; of whom, 1054 were classified as having primary GISTs (Figure 1). All oncological resections with curative intent were performed by senior surgeons specialized in achieving the rigorous standard at our institution. The inclusion criteria were: (1) Age > 18 years; (2) Pathological diagnosis of GIST; (3) No evidence of recurrent GIST or distant metastasis before treatment; and (4) Physiological status based on an Eastern Cooperative Oncology Group score < 3 points. The exclusion criteria were: (1) Any previous or concurrent malignancies; (2) First operation performed in other institutions; (3) Missing or illegible baseline information; and (4) Missing follow-up data. Finally, 983 patients with regular follow-up were included and analyzed. The follow-up was performed every 3 mo for the first 3 years, then every 6 mo up to 5 years, and then every year or until death in the following years. The latest follow-up date was December 2020.

Data collection

The following clinicopathological characteristics were routinely collected from the GIST database: Age, sex, tobacco and alcohol use, body mass index (BMI), comorbidities, chief complaint, tumor location, tumor size, mitotic index (per 50 high power fields), American Society of Anesthesiologists score, modified National Institutes of Health risk category, surgical approach, intraoperative blood transfusion, operation time, postoperative complications, hospitalization time, postoperative imatinib, immunohistochemistry results and hematological indices. BMI was classified into the following categories: < 18.5, 18.5-24.9 and ≥ 25 kg/m2, based on the World Health Organization classification. The comorbidities analyzed comprised hypertension, diabetes mellitus, anemia, pulmonary disease (asthma, pneumonia, chronic obstructive pulmonary disease, *etc*.), heart disease (arrhythmia, coronary atherosclerotic heart disease, *etc*.), liver disease (hepatitis, cirrhosis, *etc*.), renal disease (nephritis, chronic kidney disease, *etc*.) and central nervous system disease (cerebrovascular disease, neurodegenerative disease, *etc*.).

The primary outcome was progression-free survival (PFS), which was defined as the interval between the date of resection and the date of confirmed disease progression or death. The secondary outcome was overall survival (OS), which was calculated from the date of surgery until the date of death. Patients were censored at the date of the last follow-up without the above event.

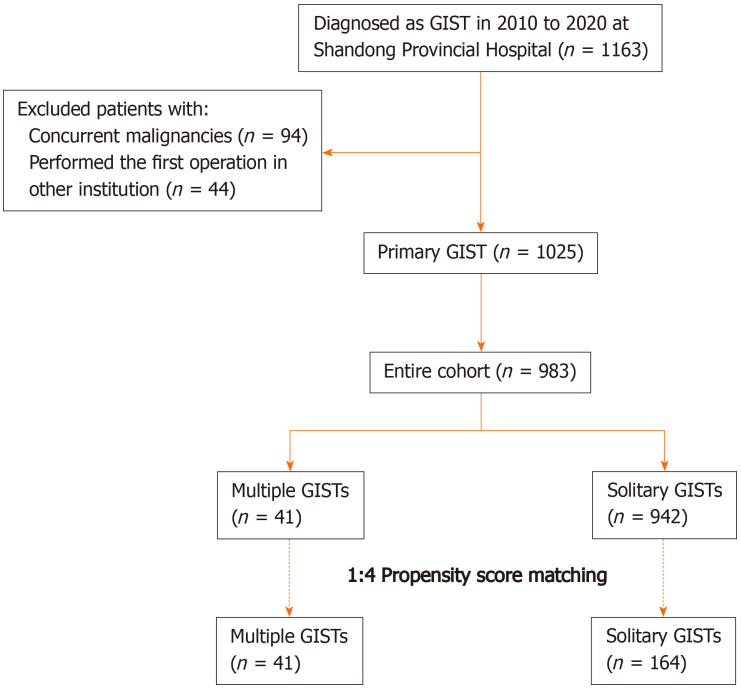


Figure 1 Flow chart of the of this study. GIST: Gastrointestinal stromal tumors; MGIST: Multiple gastrointestinal stromal tumors.

Definition of MGISTs

There is currently no authoritative and recognized definition of MGISTs. With reference to the criteria for multiple other cancers[8-11], especially multiple gastric cancers[12], we defined MGISTs as follows: (1) Each lesion must be pathologically proven; (2) All lesions must be separated microscopically; and (3) The possibility that one of the lesions represents a local extension of a metastatic tumor must be ruled out beyond reasonable doubt. It is because of the above criteria that all patients with any GIST outside the digestive tract (such as the omentum) were excluded. We defined MGISTs as two or more GISTs in the digestive tract. When MGISTs were different in size and mitotic index, the tumor was recorded according to the most advanced tumor. Similarly, in clinical practice, a modified National Institutes of Health risk category was also defined and assessed according to the most advanced tumor.

Statistical analysis

Categorical variables were analyzed using Pearson's χ^2 test or Fisher's exact test, according to the expected values. The Mann–Whitney *U* test was utilized to compare continuous variables, which are presented as medians and interquartile ranges and as the mean ± SD. The Kaplan–Meier method and log-rank test were performed to conduct survival analyses and evaluate differences in survival time, respectively. Univariate and multivariate analyses were performed using the Cox proportional hazards model. Univariate analysis was primarily performed, and variables with $P < 0.2$ were subsequently input into the multivariate analysis to determine the independent prognostic factors. Hazard ratios with their 95% confidence intervals were also derived. Statistical significance was defined as $P < 0.05$. SPSS version 26.0 (IBM, Armonk, NY, United States) and R version 3.5.3 (The R Foundation for Statistical Computing, Vienna, Austria) were used for statistical analysis.

Propensity score matching

Due to the inhomogeneous distribution of several baseline characteristics and uneven group sizes between patients with MGISTs and SGISTs, propensity score matching was performed. First, a propensity score was calculated using a logistic regression model in which the MGIST group was regressed as a dependent variable on relevant baseline parameters. The propensity score matching ratio was set to a 1:4 ratio to minimize the differences due to comorbidities, BMI, tumor location, mitotic index, sex, age and American Society of Anesthesiologist score with the nearest neighbor method. The assessment of propensity score matching is shown in Supplementary Figure 1.

RESULTS

Patient characteristics

The flow chart for the study is shown in Figure 1. Of the 983 consecutive patients who were pooled into the entire cohort between March 2010 and January 2020 at our institution, 41 (4.17%) with MGISTs were identified.

The preoperative clinical characteristics are described in Table 1. Before matching, most of the baseline characteristics were similar between the two groups, with significant differences only in BMI (P = 0.010). Regarding surgical and postoperative pathological characteristics and treatment of the SGISTs and MGISTs (Table 2), there were significant differences in surgical approach (P = 0.028), tumor size (P = 0.007), mitotic index (P = 0.009) and modified National Institutes of Health risk category (P = 0.044).

After propensity score matching at a 1:4 ratio, all baseline characteristics of the 41 patients in the MGIST group were compared with those of the 164 patients in the SGIST group (Tables 1 and 2). Supplementary pathological characteristics and blood indicators are shown in Supplementary Table 1. We also listed the clinical characteristics of patients with multiple tumors in detail (Supplementary Table 2) and showed several pathological images from these patients (Supplementary Figure 2).

Impact of MGISTs on PFS and OS

The median follow-up time of the entire matched cohort was 1468 d (IQR, 938-2225 d), and the 1-, 3- and 5-year PFS rates were 96.06%, 83.66% and 70.09%, respectively. For the patients with MGISTs, the 1-, 3- and 5-year PFS rates were 90.00%, 74.19% and 52.17%, respectively and compared with the 1-, 3- and 5-year PFS rates of 97.55%, 86.78% and 75.00% for the patients with SGISTs (P = 0.031) (Figure 2). We continued to explore the impact of MGISTs on OS. The 1-, 3- and 5-year OS rates were 98.16%, 92.50% and 83.75% for patients with SGISTs compared with 100%, 86.67% and 60.00% for patients with MGISTs, respectively, with no significant differences (P = 0.085) (Figure 3).

Univariate and multivariate analyses

Univariate analysis identified the following prognostic factors for PFS: age (P = 0.069), tumor location (P < 0.001), tumor size (P = 0.001), mitotic index (P < 0.001), blood transfusion (P = 0.018), intraoperative tumor rupture (P = 0.011), imatinib treatment (P = 0.133) and MGISTs (P = 0.035). On multivariate analysis, tumor location (P = 0.002), tumor size (P = 0.035), mitotic index (P = 0.001), imatinib treatment (P < 0.001) and MGISTs (P = 0.029) were eventually identified as independent prognostic factors for PFS (Table 3).

Univariate analysis revealed that tumor location (P < 0.001), tumor size (P = 0.021), mitotic index (P < 0.001), blood transfusion (P = 0.008), intraoperative tumor rupture (P = 0.113), imatinib treatment (P = 0.030) and MGISTs (P = 0.092) were correlated with OS. Subsequent multivariate analysis showed that tumor location (P = 0.003), mitotic index (P= 0.015) and imatinib treatment (P < 0.001) could be identified as independent risk factors for OS (Table 4). OS of patients with MGISTs (P = 0.106) was similar to that of patients with a single GIST.

DISCUSSION

MGISTs are often found in clinical treatment but ignored or misinterpreted as recurrence or metastasis. With the current lack of convincing results from large-scale studies based on demographics or clinicopathological characteristics, this is the first study to analyze the clinicopathological differences between patients with MGISTs and those with SGISTs. For accuracy and clarity, propensity score matching was used to balance the differences to explore the prognostic factors for patients with MGISTs.

A total of 983 patients were included in the cohort, including 41 with MGISTs. MGISTs accounted for approximately 4.17% of all GISTs in our study. With a median age of 60 years, patients with MGISTs had a similar age at initial diagnosis as patients with SGISTs. The incidence of GISTs is almost equal in men and women[13]; however, in our study, a male predisposition (M/F=27/14) was observed.

The BMI of patients with MGISTs was significantly lower than that of patients with SGISTs, which was pointed out for the first time, but the reason for this finding is not clear. Smoking and alcohol consumption did not affect the occurrence of MGISTs. There were no significant differences in American Society of Anesthesiologists classi-

Table 1 Preoperative clinical characteristics of solitary gastrointestinal stromal tumors and multiple gastrointestinal stromal tumors in the entire cohort and after propensity score matching

Parameters	Entire cohort, before matching		*P* value	Propensity score matched cohort		*P* value
	SGIST, *n* (%)	MGIST, *n* (%)		SGIST, *n* (%)	MGIST, *n* (%)	
All cases	942	41		164	41	
Age (yr)			0.450			0.889
≤ 60	516 (54.78)	20 (48.78)		82 (50.00)	20 (48.78)	
> 60	426 (45.22)	21 (51.22)		82 (50.00)	21 (51.22)	
Gender			0.060			0.596
Male	479 (50.85)	27 (65.85)		115 (70.12)	27 (65.85)	
Female	463 (49.15)	14 (34.15)		49 (29.88)	14 (34.15)	
BMI (kg/m^2)			**0.010**			0.193
BMI < 18.5	41 (4.35)	6 (14.63)		11 (6.71)	6 (14.63)	
18.5 ≤ BMI < 25	501 (53.18)	19 (46.34)		94 (57.32)	19 (46.34)	
BMI ≥ 25	400 (42.46)	16 (39.02)		59 (35.98)	16 (39.02)	
Tobacco use			0.899			0.093
No	704 (74.73)	31 (75.61)		101 (61.59)	31 (75.61)	
Yes	238 (25.27)	10 (24.39)		63 (38.41)	10 (24.39)	
Alcohol use			0.514			0.768
No	687 (72.93)	28 (60.98)		108 (65.85)	28 (60.98)	
Yes	255 (27.07)	13 (31.71)		56 (34.15)	13 (31.71)	
ASA score			0.443			0.868
I/II	779 (82.70)	32 (78.05)		126 (74.83)	32 (78.05)	
III/IV	163 (17.30)	9 (21.95)		38 (23.17)	9 (21.85)	
Comorbidities[1]			0.236			1.000
Present	417 (44.27)	22 (53.66)		88 (53.66)	22 (53.66)	
Absent	525 (55.73)	19 (46.34)		76 (46.34)	19 (46.34)	
Location			0.450			0.884
Gastric	650 (69.00)	26 (63.41)		106 (64.63)	26 (63.41)	
Non-gastric	292 (31.00)	15 (36.58)		58 (35.37)	15 (36.58)	
Chief complaint						
Abdominal pain	303 (32.17)	15 (36.58)	0.554	54 (32.93)	15 (36.58)	0.657
Abdominal distention	149 (15.82)	9 (21.95)	0.295	23 (14.02)	9 (21.95)	0.211
Hematemesis	42 (4.46)	3 (7.32)	0.429	9 (5.49)	3 (7.32)	0.710
Hematochezia	167 (17.72)	9 (21.95)	0.490	34 (20.73)	9 (21.95)	0.864
Medical examination	275 (29.19)	11 (26.83)	0.744	42 (25.61)	11 (26.83)	0.906
Other	96 (10.19)	2 (4.88)	0.266	17 (10.37)	2 (4.88)	0.278

[1]Comorbidities: comprised of hypertension, diabetes mellitus, anemia, pulmonary disease (asthma, pneumonia, chronic obstructive pulmonary disease, *etc.*), heart disease (arrhythmia, coronary atherosclerotic heart disease, *etc.*), liver disease (hepatitis, cirrhosis, *etc.*), renal disease (nephritis, chronic kidney disease, *etc.*) and central nervous system disease (cerebrovascular disease, neurodegenerative disease, *etc.*). Bold values indicate $P < 0.05$. ASA: American Society of Anesthesiologists; BMI: Body mass index; MGIST: Multiple gastrointestinal stromal tumors; SGIST: Solitary gastrointestinal stromal tumors.

fication or comorbidities, which means that the patients were in similar physical conditions at the time of diagnosis.

Table 2 Surgical and postoperative pathological characteristics and treatment of the solitary gastrointestinal stromal tumors and multiple gastrointestinal stromal tumors of the entire cohort and after propensity score matching

Parameters	Entire cohort, before matching		*P* value	Propensity score matched cohort		*P* value
	SGIST, *n* (%)	MGIST, *n* (%)		SGIST, *n* (%)	MGIST, *n* (%)	
All cases	942	41		164	41	
Surgical approach			**0.028**			0.361
Open	458 (48.62)	27 (65.85)		94 (57.32)	27 (65.85)	
Laparoscopic	255 (27.07)	11 (26.83)		43 (26.22)	11 (26.83)	
Endoscopic	229 (24.31)	3 (7.32)		27 (14.63)	3 (7.32)	
Blood transfusion			0.161			1.000
Yes	171 (18.15)	11 (26.83)		44 (26.83)	11 (26.83)	
No	771 (81.85)	30 (73.17)		120 (73.17)	30 (73.17)	
Tumor size (cm)			**0.007**			0.200
Length ≤ 5	575 (61.04)	15 (36.59)		74 (45.12)	15 (36.59)	
5 < Length ≤ 10	239 (25.37)	16 (39.02)		41 (25.00)	16 (39.02)	
Length > 10	128 (13.59)	10 (24.39)		49 (29.88)	10 (24.39)	
Mitotic index (per 50 HPF)			**0.009**			0.715
0-5	724 (76.86)	27 (65.85)		101 (61.59)	27 (65.85)	
6-10	127 (13.48)	4 (9.76)		24 (14.63)	4 (9.76)	
> 10	91 (9.66)	10 (24.39)		39 (23.78)	10 (24.39)	
Modified NIH risk			**0.044**			0.486
Very low	210 (22.29)	4 (9.76)		29 (17.68)	4 (9.76)	
Low	291 (30.89)	9 (21.95)		30 (18.29)	9 (21.95)	
Intermediate	147 (15.61)	8 (19.51)		22 (13.41)	8 (19.51)	
High	294 (31.21)	20 (48.78)		83 (50.61)	20 (48.78)	
Operate time (min)			0.336			0.627
mean ± SD	139 ± 78	151 ± 63		145 ± 67	151 ± 63	
Median (IQR)	120 (80-180)	150 (120-180)		140 (90-190)	150 (120-180)	
Intraoperative tumor rupture			0.376			0.490
Yes	10 (1.06)	1 (2.44)		2 (1.22)	1 (2.44)	
No	932 (98.94)	40 (97.56)		162 (98.78)	40 (97.56)	
Hospitalization time in d			0.226			0.442
mean ± SD	13.55 ± 6.32	14.78 ± 7.66		13.96 ± 5.69	14.78 ± 7.66	
Median (IQR)	12 (10-15)	14 (9-16)		13 (11-16)	14 (9-16)	
Postoperative complications			0.391			0.610
Present	179 (19.00)	10 (24.39)		34 (20.73)	10 (24.39)	
Absent	763 (81.00)	31 (73.61)		130 (79.27)	31 (73.61)	
Imatinib treatment			0.187			0.832
Yes	298 (31.63)	17 (41.46)		71 (43.29)	17 (41.46)	
No	644 (68.37)	24 (58.54)		93 (56.71)	24 (58.54)	

Bold values indicate $P < 0.05$. HPF: High power field; IQR: Interquartile range; MGIST: Multiple gastrointestinal stromal tumors; NIH: National Institutes of Health; SD: SD; SGIST: Solitary gastrointestinal stromal tumors.

There was no significant difference in the chief complaint, which also implies

Table 3 Univariate and multivariate of the clinicopathological factors for progression-free survival

Characteristics	Univariate analysis		Multivariate analysis	
	HR (95%CI)	*P* value	HR (95%CI)	*P* value
Age in yr				
≤ 60	Reference		Reference	
> 60	1.845 (0.953-3.571)	0.069	1.525 (0.740-3.143)	0.252
Sex				
Female	Reference			
Male	0.913 (0.460-1.809)	0.793		
Comorbidities				
Absent	Reference			
Present	1.147 (0.606-2.172)	0.673		
Tumor location				
Gastric	Reference		Reference	
Non-gastric	3.548 (1.847-6.818)	**< 0.001**	3.176 (1.526-6.607)	**0.002**
Tumor size in cm		**0.001**		**0.035**
Length ≤ 5	Reference		Reference	
5 < Length ≤ 10	3.022 (1.117-8.179)	**0.029**	2.180 (0.716-6.642)	0.170
Length > 10	5.848 (2.359-14.499)	**< 0.001**	4.071 (1.375-12.052)	**0.011**
Mitotic index, per 50 HPF		**< 0.001**		**0.001**
0-5	Reference		Reference	
6-10	4.094 (1.555-10.777)	**0.004**	4.108 (1.309-12.897)	**0.015**
> 10	7.859 (3.676-16.799)	**< 0.001**	6.577 (2.540-17.029)	**< 0.001**
Surgical approach		0.251		
Open	Reference			
Laparoscopic	0.449 (0.174-1.154)	0.096		
Endoscopic	0 (0-1.006E+230)	0.961		
Blood transfusion				
No	Reference		Reference	
Yes	2.176 (1.143-4.145)	**0.018**	1.569 (0.739-3.332)	0.241
Intraoperative tumor rupture				
No	Reference		Reference	
Yes	6.383 (1.524-26.726)	**0.011**	4.458 (0.863-23.015)	0.074
Imatinib treatment				
Yes	Reference		Reference	
No	0.584 (0.290-1.178)	0.133	4.608 (2.030-10.461)	**< 0.001**
MGIST				
Absent	Reference		Reference	
Present	2.091 (1.055-4.145)	**0.035**	2.431 (1.097-5.386)	**0.029**

Bold values indicate $P < 0.05$. CI: Confidence interval; HPF: High power field; HR: Hazard ratio; MGIST: Multiple gastrointestinal stromal tumors.

difficulty in clinical diagnosis. MGISTs are often reported to be associated with type 1 neurofibromatosis[14], the Carney triad[15] and Carney–Stratakis syndrome[16]. In the records of our medical center, there was only one patient with neurofibromatosis, who

Table 4 Univariate and multivariate analysis of the clinicopathological factors for overall survival

Characteristics	Univariate analysis		Multivariate analysis	
	HR (95%CI)	*P* value	HR (95%CI)	*P* value
Age in yr				
≤ 65	Reference			
> 65	1.665 (0.754-3.676)	0.207		
Gender				
Female	Reference			
Male	1.099 (0.461-2.616)	0.832		
Comorbidities				
Absent	Reference			
Present	1.061 (0.491-2.291)	0.881		
Tumor location				
Gastric	Reference		Reference	
Non-gastric	4.428 (1.967-9.965)	**< 0.001**	3.812 (1.577-9.213)	**0.003**
Tumor size in cm		**0.021**		0.556
Length ≤ 5	Reference		Reference	
5 < Length ≤ 10	2.279 (0.722-7.189)	0.160	1.381 (0.346-5.519)	0.648
Length > 10	4.159 (1.498-11.549)	**0.006**	2.070 (0.539-7.959)	0.290
Mitotic index, per 50 HPF		**< 0.001**		**0.015**
0-5	Reference		Reference	
6-10	3.120 (0.913-10.669)	0.070	4.129 (0.963-17.707)	0.056
> 10	7.515 (3.045-18.548)	**< 0.001**	6.051 (1.762-20.778)	**0.004**
Surgical approach		0.684		
Open	Reference			
Laparoscopic	0.621 (0.213-1.815)	0.384		
Endoscopic	0 (0-3.609E+275)	0.968		
Blood transfusion				
No	Reference		Reference	
Yes	2.832 (1.312-6.113)	**0.008**	1.298 (0.547-3.082)	0.554
Intraoperative tumor rupture				
No	Reference		Reference	
Yes	5.094 (0.682-38.043)	0.113	3.264 (0.355-30.022)	0.296
Imatinib treatment				
Yes	Reference		Reference	
No	2.952 (1.113-7.831)	**0.030**	7.841 (2.677-22.693)	**< 0.001**
MGIST				
Absent	Reference		Reference	
Present	2.050 (0.889-4.726)	0.092	2.404 (0.830-6.966)	0.106

Bold values indicate $P < 0.05$. CI: Confidence interval; HPF: High power field; HR: Hazard ratio; MGIST: Multiple gastrointestinal stromal tumors.

has been reported in our previous study[17]. However, this patient was not included in this cohort because of concurrent colon cancer. Familial and pediatric GISTs are also associated with multicentric risk[18]. However, these types of MGISTs were not found

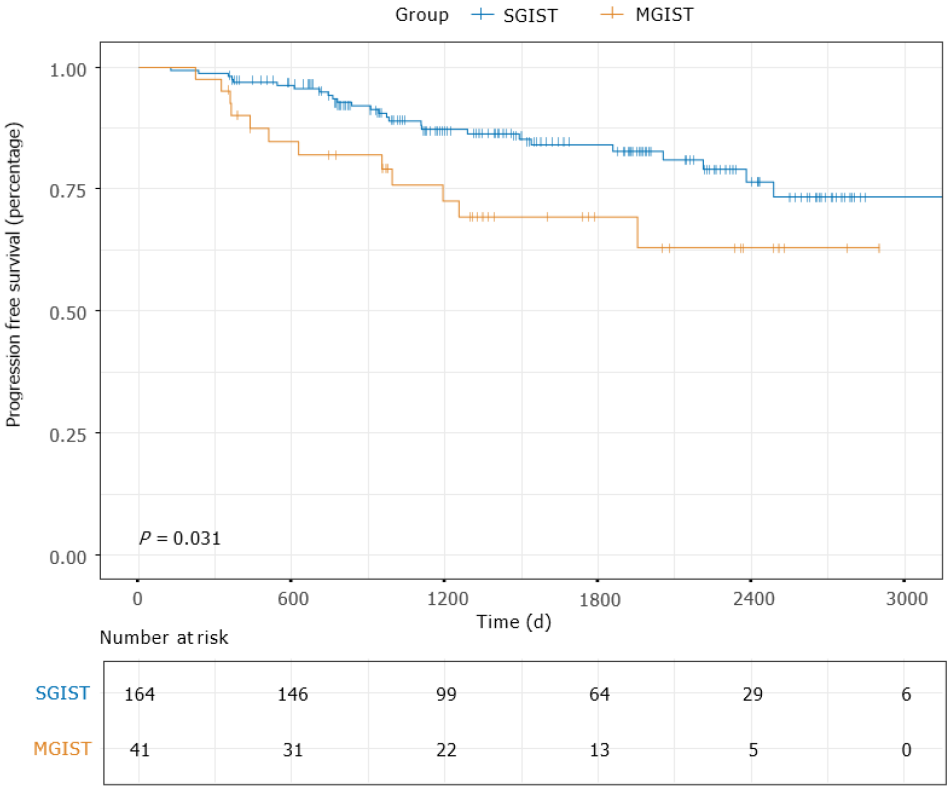


Figure 2 Kaplan–Meier survival analysis of progression-free survival. MGIST: Multiple gastrointestinal stromal tumors; SGIST: Solitary gastrointestinal stromal tumors.

in our study. This may be due to bias in the publication of case reports on these particular patients or the fact that the examination strategy has not been perfected so that such patients are missed by our colleagues. In addition, all cases of GISTs predominantly affected a single organ, and we should still pay attention to patients with multiorgan involvement to prevent misdiagnosis.

Imaging examination is an important basis for diagnosis[19]. Computed tomography or enhanced computed tomography is currently recommended but does not play an adequate role in the diagnosis of MGISTs. Of the 41 MGIST patients in our hospital, 38 underwent computed tomography examination, but only four were diagnosed accordingly. None of the MGISTs < 1 cm were detected, but this may be due to the large size of the major tumor or insufficient imaging evidence to diagnose the small tumor. For endoscopic examination, 8 of the 26 patients were suspected to have MGISTs before surgery, but endoscopy only revealed the tumor growing into the intestinal cavity, and none of the 15 cases of small intestinal MGISTs was detected. No case of MGISTs was diagnosed by B-ultrasonography or upper digestive tract radiography. Magnetic resonance imaging might be useful for diagnosis but is seldom used in ordinary examinations. Micro-GISTs, with low or no mitotic activity and little clinical significance, are common in the stomach (20%-35%)[20,21] and can transform to clinical GISTs by unknown mechanisms. Therefore, the development or modification of an examination method for preoperative screening of MGISTs can develop a more appropriate treatment plan for patients and obtain a greater survival benefit.

Heterogeneous morphology could be observed and the common growth patterns of MGISTs manifest a satellite phenomenon, that is, one or more main tumors surrounded by several small tumors. Of course, homogeneous morphology was still present in some tumors of MGISTs. Almost all gastric MGISTs consisted of two tumors and grew inside. On the contrary, small intestinal GISTs, especially in the jejunum, almost always had more than two tumors, and most of them grew outside. Unfortunately, the phenomenon has rarely been described in other studies, and it is difficult to determine whether it is a general finding. It is possible that MGISTs have different growth patterns and prognoses from SGISTs, and further research is needed.

The cellular types of the tumors were similar. Before propensity score matching, there was a significant difference in tumor necrosis. In addition, the proportion of calcification and cystic degeneration of MGISTs was higher than that of SGISTs, but

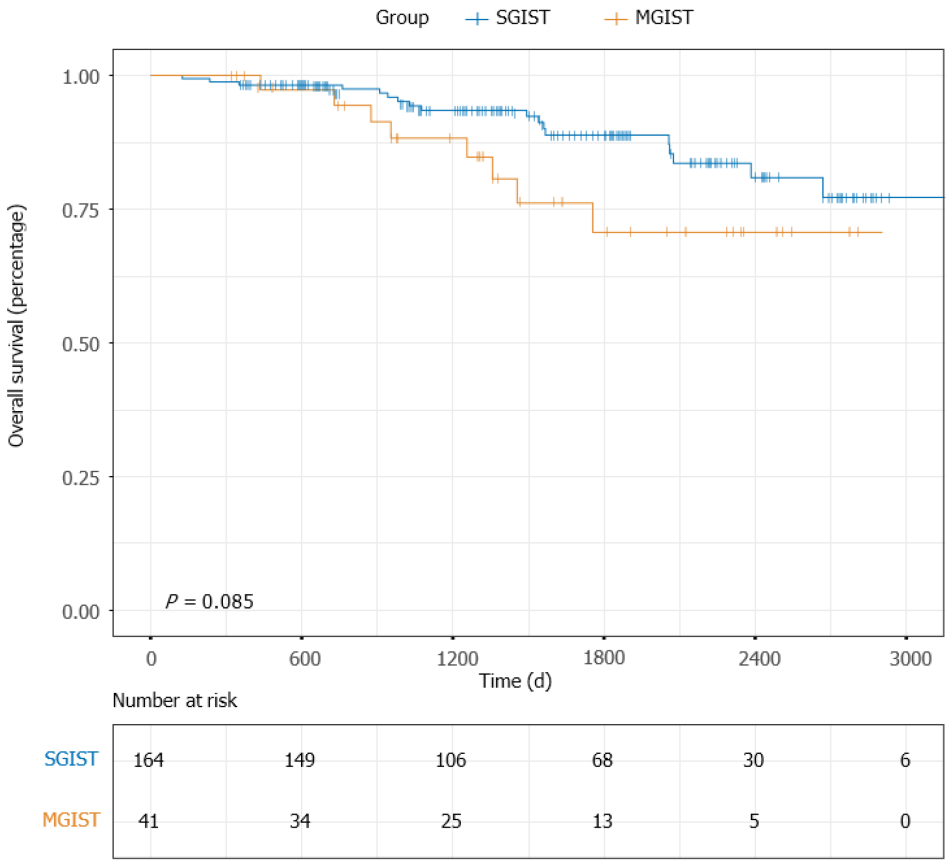


Figure 3 Kaplan–Meier survival analysis of overall survival. MGIST: Multiple gastrointestinal stromal tumors; SGIST: Solitary gastrointestinal stromal tumors.

the difference was not significant. In the propensity score matched cohort, all the above characteristics of MGISTs were compared with those of SGISTs.

For blood parameters, except for prealbumin, no significant differences were found. Immunohistochemical staining for Ki-67 antigen is often used, although this score is relatively subjective[22]. With regard to immunohistochemical markers, KIT (CD117) and ANO1 (DOG1) are two of the most sensitive and specific for GISTs[23]. S-100 and CD34 can also be used as auxiliary diagnostic indicators[24]. Unfortunately, there was no significant difference in these indicators between the patients with MGISTs and those with SGISTs.

The tumor mitotic rate is the most significant independent prognostic factor for GIST recurrence after surgery for both the stomach[25] and small intestine[26]. In our cohort, patients with MGISTs had larger tumors and a higher mitotic index, which also contributed to more advanced tumor stages.

The main treatment strategy for GISTs > 2 cm is surgical resection, and this is also the case for MGISTs. R0 resection, minimally invasive surgery and regular imaging surveillance are required to ensure perioperative and postoperative safety of patients. MGISTs may involve many segments of the gastrointestinal tract, so extensive resection is more common than with SGISTs. Therefore, consultation with experienced specialists is required to assess surgical extension and perioperative adjuvant therapy. In the practice of our medical center, the rate of open surgery for MGISTs is significantly higher than that for SGISTs. Imatinib was used for KIT/PDGFRA mutated GISTs[27] and is usually recommended for high-risk patients after surgery.

Of the 41 patients evaluated, 11 received intraoperative blood transfusions, which is higher than the rate for other operations and should compel surgeons to conduct a thorough preoperative evaluation and develop appropriate protocols. However, there was only a slight increase in operation time, intraoperative tumor rupture, postoperative hospital stays and postoperative complications in patients with MGISTs, and the difference was not significant.

After propensity score matching, all the above parameters were well balanced. We then tried to evaluate the clinical, perioperative and therapeutic factors associated with OS through Cox univariate and multivariate hazard ratio models.

There have been few studies related to the prognosis of patients with MGISTs[28]. Our study demonstrated that PFS of patients with MGISTs was significantly poorer than that of patients with SGISTs and that MGISTs were an independent risk factor for poor PFS. However, OS was similar between patients with SGISTs and those with MGISTs. This may be related to the characteristics of patients with MGISTs, suggesting that clinicians should closely monitor the condition of these patients, and it may be necessary to improve the risk classification of MGIST patients.

Given the lack of clinical trials, SGIST therapy has conflicting results in MGIST patients with regard to factors such as surgical excision and perioperative adjuvant therapy. This study suggests that more attention should be paid to such patients to explore more suitable treatment strategies. Gene detection and molecular biological experiments are also needed to explain specific manifestations[29,30].

There were some shortcomings in our research. First, as a single-center design with a small sample size, the statistical power of our findings might have been weakened. Moreover, due to the high cost, few of these patients had undergone gene detection. Last, there may have been a possibility of missed diagnoses, which could have led to an underestimation of the incidence of MGISTs.

To date, this study has the most detailed data and the largest number of patients, which may bring new insight to the diagnosis and treatment of MGISTs.

CONCLUSION

Patients with MGISTs may have demographic characteristics and immunohistochemical markers that are similar to those of patients with SGISTs, but MGIST patients also have unique tumor features. In this study, we found that MGISTs were an independent factor for PFS after propensity score matching analysis; however, OS was similar. The perioperative and long-term prognosis of patients remains of concern and requires multicenter, large sample, long-term follow-up, prospective studies. Most importantly, risk criteria, diagnostic strategies and treatment procedures suitable for this disease of lower morbidity should be developed to achieve personalized precision therapy and maximize the survival benefit of these patients.

ARTICLE HIGHLIGHTS

Research background

Synchronous primary multiple gastrointestinal stromal tumors (MGISTs) are specific and rare. The diagnosis, treatment and follow-up strategies of MGISTs are not specifically described in guidelines.

Research motivation

Due to the low incidence, there is currently no large-scale demographic survey showing the incidence of MGISTs. Additionally, little is known about the impact of MGISTs on the survival of patients with gastrointestinal stromal tumors (GISTs).

Research objectives

This study aimed to compare the clinicopathological characteristics and prognoses of patients with MGISTs and patients with solitary GISTs (SGISTs).

Research methods

Due to the inhomogeneous distribution of several baseline characteristics and uneven MGIST and SGIST group sizes, propensity score matching was performed according to comorbidities, body mass index, tumor location, mitotic index, sex, age and American Society of Anesthesiologists score.

Research results

Among the entire cohort, the incidence of MGISTs was 4.17%. Patients with MGISTs and those with SGISTs had disparities in body mass index, surgical approach, tumor size and mitotic index. Tumor location, tumor size, mitotic index, imatinib treatment and MGISTs were identified as independent prognostic factors of progression-free survival. However, overall survival was similar between the SGIST and MGIST groups.

Research conclusions

Patients with MGISTs may have demographic characteristics and immunohistochemical markers that are similar to those of patients with SGISTs, but MGIST patients also have unique tumor features. Without specific diagnostic indicators and symptoms, patients with MGISTs were identified as having a poorer progression-free survival than patients with SGISTs.

Research perspectives

Risk criteria, diagnostic strategies and treatment procedures suitable for these tumors of lower morbidity should be developed to achieve personalized precision therapy and maximize the survival benefit of these patients.

ACKNOWLEDGEMENTS

We extend our thanks to all patients involved in the study. We would also like to thank the Medical Records Department of Shandong Provincial Hospital for providing data support and the efforts of medical workers over the past decades.

REFERENCES

1 **Joensuu H**, Hohenberger P, Corless CL. Gastrointestinal stromal tumour. *Lancet* 2013; **382**: 973-983 [PMID: 23623056 DOI: 10.1016/S0140-6736(13)60106-3]
2 **Ma GL**, Murphy JD, Martinez ME, Sicklick JK. Epidemiology of gastrointestinal stromal tumors in the era of histology codes: results of a population-based study. *Cancer Epidemiol Biomarkers Prev* 2015; **24**: 298-302 [PMID: 25277795 DOI: 10.1158/1055-9965.EPI-14-1002]
3 **Serrano C**, George S. Gastrointestinal Stromal Tumor: Challenges and Opportunities for a New Decade. *Clin Cancer Res* 2020; **26**: 5078-5085 [PMID: 32601076 DOI: 10.1158/1078-0432.CCR-20-1706]
4 **Nilsson B**, Bümming P, Meis-Kindblom JM, Odén A, Dortok A, Gustavsson B, Sablinska K, Kindblom LG. Gastrointestinal stromal tumors: the incidence, prevalence, clinical course, and prognostication in the preimatinib mesylate era--a population-based study in western Sweden. *Cancer* 2005; **103**: 821-829 [PMID: 15648083 DOI: 10.1002/cncr.20862]
5 **Gasparotto D**, Rossi S, Bearzi I, Doglioni C, Marzotto A, Hornick JL, Grizzo A, Sartor C, Mandolesi A, Sciot R, Debiec-Rychter M, Dei Tos AP, Maestro R. Multiple primary sporadic gastrointestinal stromal tumors in the adult: an underestimated entity. *Clin Cancer Res* 2008; **14**: 5715-5721 [PMID: 18779314 DOI: 10.1158/1078-0432.CCR-08-0622]
6 **Zhang X**, Ning L, Hu Y, Zhao S, Li Z, Li L, Dai Y, Jiang L, Wang A, Chu X, Li Y, Yang D, Lu C, Yao L, Cui G, Lin H, Chen G, Cui Q, Guo H, Zhang H, Lun Z, Xia L, Su Y, Han G, Hui X, Wei Z, Sun Z, Shen S, Zhou Y. Prognostic Factors for Primary Localized Gastrointestinal Stromal Tumors After Radical Resection: Shandong Gastrointestinal Surgery Study Group, Study 1201. *Ann Surg Oncol* 2020; **27**: 2812-2821 [PMID: 32040699 DOI: 10.1245/s10434-020-08244-9]
7 **Yao XI**, Wang X, Speicher PJ, Hwang ES, Cheng P, Harpole DH, Berry MF, Schrag D, Pang HH. Reporting and Guidelines in Propensity Score Analysis: A Systematic Review of Cancer and Cancer Surgical Studies. *J Natl Cancer Inst* 2017; **109** [PMID: 28376195 DOI: 10.1093/jnci/djw323]
8 **He W**, Zheng C, Wang Y, Dan J, Zhu M, Wei M, Wang J, Wang Z. Prognosis of synchronous colorectal carcinoma compared to solitary colorectal carcinoma: a matched pair analysis. *Eur J Gastroenterol Hepatol* 2019; **31**: 1489-1495 [PMID: 31441800 DOI: 10.1097/MEG.0000000000001487]
9 **Bos ACRK**, Matthijsen RA, van Erning FN, van Oijen MGH, Rutten HJT, Lemmens VEPP. Treatment and Outcome of Synchronous Colorectal Carcinomas: A Nationwide Study. *Ann Surg Oncol* 2018; **25**: 414-421 [PMID: 29159744 DOI: 10.1245/s10434-017-6255-y]
10 **Otowa Y**, Nakamura T, Takiguchi G, Yamamoto M, Kanaji S, Imanishi T, Oshikiri T, Suzuki S, Tanaka K, Kakeji Y. Safety and benefit of curative surgical resection for esophageal squamous cell cancer associated with multiple primary cancers. *Eur J Surg Oncol* 2016; **42**: 407-411 [PMID: 26733367 DOI: 10.1016/j.ejso.2015.11.012]
11 **Yu YC**, Hsu PK, Yeh YC, Huang CS, Hsieh CC, Chou TY, Hsu HS, Wu YC, Huang BS, Hsu WH. Surgical results of synchronous multiple primary lung cancers: similar to the stage-matched solitary primary lung cancers? *Ann Thorac Surg* 2013; **96**: 1966-1974 [PMID: 24021769 DOI: 10.1016/j.athoracsur.2013.04.142]
12 **Moertel CG**, Bargen JA, Soule EH. Multiple gastric cancers; review of the literature and study of 42 cases. *Gastroenterology* 1957; **32**: 1095-1103 [PMID: 13438166]
13 **Rubin BP**, Heinrich MC, Corless CL. Gastrointestinal stromal tumour. *Lancet* 2007; **369**: 1731-1741 [PMID: 17512858 DOI: 10.1016/s0140-6736(07)60780-6]
14 **Miettinen M**, Fetsch JF, Sobin LH, Lasota J. Gastrointestinal stromal tumors in patients with

neurofibromatosis 1: a clinicopathologic and molecular genetic study of 45 cases. *Am J Surg Pathol* 2006; **30**: 90-96 [PMID: 16330947 DOI: 10.1097/01.pas.0000176433.81079.bd]

15 **Zhang L**, Smyrk TC, Young WF Jr, Stratakis CA, Carney JA. Gastric stromal tumors in Carney triad are different clinically, pathologically, and behaviorally from sporadic gastric gastrointestinal stromal tumors: findings in 104 cases. *Am J Surg Pathol* 2010; **34**: 53-64 [PMID: 19935059 DOI: 10.1097/PAS.0b013e3181c20f4f]

16 **Pasini B**, McWhinney SR, Bei T, Matyakhina L, Stergiopoulos S, Muchow M, Boikos SA, Ferrando B, Pacak K, Assie G, Baudin E, Chompret A, Ellison JW, Briere JJ, Rustin P, Gimenez-Roqueplo AP, Eng C, Carney JA, Stratakis CA. Clinical and molecular genetics of patients with the Carney-Stratakis syndrome and germline mutations of the genes coding for the succinate dehydrogenase subunits SDHB, SDHC, and SDHD. *Eur J Hum Genet* 2008; **16**: 79-88 [PMID: 17667967 DOI: 10.1038/sj.ejhg.5201904]

17 **Shang L**, Fang Z, Liu J, Du F, Jing H, Xu Y, Dong K, Zhang X, Wu H, Jing C, Li L. Case report of ascending colon cancer and multiple jejunal GISTs in a patient with neurofibromatosis type 1 (NF1). *BMC Cancer* 2019; **19**: 1196 [PMID: 31805970 DOI: 10.1186/s12885-019-6375-9]

18 **Haller F**, Schulten HJ, Armbrust T, Langer C, Gunawan B, Füzesi L. Multicentric sporadic gastrointestinal stromal tumors (GISTs) of the stomach with distinct clonal origin: differential diagnosis to familial and syndromal GIST variants and peritoneal metastasis. *Am J Surg Pathol* 2007; **31**: 933-937 [PMID: 17527083 DOI: 10.1097/01.pas.0000213440.78407.27]

19 **Vernuccio F**, Taibbi A, Picone D, LA Grutta L, Midiri M, Lagalla R, Lo Re G, Bartolotta TV. Imaging of Gastrointestinal Stromal Tumors: From Diagnosis to Evaluation of Therapeutic Response. *Anticancer Res* 2016; **36**: 2639-2648 [PMID: 27272772]

20 **Kawanowa K**, Sakuma Y, Sakurai S, Hishima T, Iwasaki Y, Saito K, Hosoya Y, Nakajima T, Funata N. High incidence of microscopic gastrointestinal stromal tumors in the stomach. *Hum Pathol* 2006; **37**: 1527-1535 [PMID: 16996566 DOI: 10.1016/j.humpath.2006.07.002]

21 **Agaimy A**, Wünsch PH, Hofstaedter F, Blaszyk H, Rümmele P, Gaumann A, Dietmaier W, Hartmann A. Minute gastric sclerosing stromal tumors (GIST tumorlets) are common in adults and frequently show c-KIT mutations. *Am J Surg Pathol* 2007; **31**: 113-120 [PMID: 17197927 DOI: 10.1097/01.pas.0000213307.05811.f0]

22 **Liang YM**, Li XH, Li WM, Lu YY. Prognostic significance of PTEN, Ki-67 and CD44s expression patterns in gastrointestinal stromal tumors. *World J Gastroenterol* 2012; **18**: 1664-1671 [PMID: 22529697 DOI: 10.3748/wjg.v18.i14.1664]

23 **Novelli M**, Rossi S, Rodriguez-Justo M, Taniere P, Seddon B, Toffolatti L, Sartor C, Hogendoorn PC, Sciot R, Van Glabbeke M, Verweij J, Blay JY, Hohenberger P, Flanagan A, Dei Tos AP. DOG1 and CD117 are the antibodies of choice in the diagnosis of gastrointestinal stromal tumours. *Histopathology* 2010; **57**: 259-270 [PMID: 20716168 DOI: 10.1111/j.1365-2559.2010.03624.x]

24 **Riddle ND**, Gonzalez RJ, Bridge JA, Antonia S, Bui MM. A CD117 and CD34 immunoreactive sarcoma masquerading as a gastrointestinal stromal tumor: diagnostic pitfalls of ancillary studies in sarcoma. *Cancer Control* 2011; **18**: 152-159 [PMID: 21666577 DOI: 10.1177/107327481101800302]

25 **Miettinen M**, Sobin LH, Lasota J. Gastrointestinal stromal tumors of the stomach: a clinicopathologic, immunohistochemical, and molecular genetic study of 1765 cases with long-term follow-up. *Am J Surg Pathol* 2005; **29**: 52-68 [PMID: 15613856 DOI: 10.1097/01.pas.0000146010.92933.de]

26 **Miettinen M**, Makhlouf H, Sobin LH, Lasota J. Gastrointestinal stromal tumors of the jejunum and ileum: a clinicopathologic, immunohistochemical, and molecular genetic study of 906 cases before imatinib with long-term follow-up. *Am J Surg Pathol* 2006; **30**: 477-489 [PMID: 16625094 DOI: 10.1097/00000478-200604000-00008]

27 **Li K**, Tjhoi W, Shou C, Yang W, Zhang Q, Liu X, Yu J. Multiple gastrointestinal stromal tumors: analysis of clinicopathologic characteristics and prognosis of 20 patients. *Cancer Manag Res* 2019; **11**: 7031-7038 [PMID: 31413638 DOI: 10.2147/CMAR.S197560]

28 **Li C**, Yang KL, Wang Q, Tian JH, Li Y, Gao ZD, Yang XD, Ye YJ, Jiang KW. Clinical features of multiple gastrointestinal stromal tumors: A pooling analysis combined with evidence and gap map. *World J Gastroenterol* 2020; **26**: 7550-7567 [PMID: 33384554 DOI: 10.3748/wjg.v26.i47.7550]

29 **Nguyen V**, Banerjee S, Sicklick JK. Moving gastrointestinal stromal tumours towards truly personalised precision therapy. *Lancet Oncol* 2020; **21**: 865-867 [PMID: 32615099 DOI: 10.1016/S1470-2045(20)30335-1]

30 **Li J**, Shen L. The current status of and prospects in research regarding gastrointestinal stromal tumors in China. *Cancer* 2020; **126** Suppl 9: 2048-2053 [PMID: 32293728 DOI: 10.1002/cncr.32684]

World Journal of Gastroenterology

Submit a Manuscript: https://www.f6publishing.com

World J Gastroenterol 2021 September 28; 27(36): 6142-6153

DOI: 10.3748/wjg.v27.i36.6142

ISSN 1007-9327 (print) ISSN 2219-2840 (online)

ORIGINAL ARTICLE

Observational Study

Urotensin II levels in patients with inflammatory bowel disease

Damir Alicic, Dinko Martinovic, Doris Rusic, Piero Marin Zivkovic, Ivana Tadin Hadjina, Marino Vilovic, Marko Kumric, Daria Tokic, Daniela Supe-Domic, Slaven Lupi-Ferandin, Josko Bozic

ORCID number: Damir Alicic 0000-0002-5354-6299; Dinko Martinovic 0000-0003-2060-5130; Doris Rusic 0000-0002-7018-4947; Piero Marin Zivkovic 0000-0001-5649-698X; Ivana Tadin Hadjina 0000-0002-4443-5896; Marino Vilovic 0000-0002-5433-5063; Marko Kumric 0000-0002-9696-3359; Daria Tokic 0000-0001-9508-4160; Daniela Supe-Domic 0000-0002-5584-3182; Slaven Lupi-Ferandin 0000-0003-0220-5256; Josko Bozic 0000-0003-1634-0635.

Author contributions: Bozic J was the guarantor and designed the study; Alicic D, Martinovic D, Rusic D, Zivkovic PM, Tadin Hadjina I, Vilovic M, Kumric M, Tokic D, Lupi-Ferandin S and Supe-Domic D participated in the acquisition, analysis, and interpretation of the data and drafted the initial manuscript; Bozic J, Alicic D and Martinovic D revised the article critically for important intellectual content.

Institutional review board statement: The study was approved by the Ethics Committee of University Hospital of Split, No. 500-03/17-01/86.

Informed consent statement: All study participants, or their legal guardian, provided informed written consent prior to study enrollment.

Damir Alicic, Piero Marin Zivkovic, Ivana Tadin Hadjina, Department of Gastroenterology, University Hospital of Split, Split 21000, Croatia

Dinko Martinovic, Marino Vilovic, Marko Kumric, Josko Bozic, Department of Pathophysiology, University of Split School of Medicine, Split 21000, Croatia

Doris Rusic, Department of Pharmacy, University of Split School of Medicine, Split 21000, Croatia

Daria Tokic, Department of Anesthesiology and Intensive care, University Hospital of Split, Split 21000, Croatia

Daniela Supe-Domic, Department of Health Studies, University of Split, Split 21000, Croatia

Slaven Lupi-Ferandin, Department of Maxillofacial Surgery, University Hospital of Split, Split 21000, Croatia

Corresponding author: Josko Bozic, MD, PhD, Associate Professor, Department of Pathophysiology, University of Split School of Medicine, Soltanska 2, Split 21000, Croatia. josko.bozic@mefst.hr

Abstract

BACKGROUND

Patients with inflammatory bowel disease (IBD) are associated with increased cardiovascular risk and have increased overall cardiovascular burden. On the other hand, urotensin II (UII) is one of the most potent vascular constrictors with immunomodulatory effect that is connected with a number of different cardiometabolic disorders as well. Furthermore, patients with ulcerative colitis have shown increased expression of urotensin II receptor in comparison to healthy controls. Since the features of IBD includes chronic inflammation and endothelial dysfunction as well, it is plausible to assume that there is connection between increased cardiac risk in IBD and UII.

AIM

To determine serum UII levels in patients with IBD and to compare them to control subjects, as well as investigate possible associations with relevant clinical and biochemical parameters.

METHODS

This cross sectional study consecutively enrolled 50 adult IBD patients (26 with

Conflict-of-interest statement: There are no conflict of interest to report.

Data sharing statement: No additional data are available.

STROBE statement: The authors have read the STROBE Statement-checklist of items, and the manuscript was prepared and revised according to the STROBE Statement-checklist of items.

Open-Access: This article is an open-access article that was selected by an in-house editor and fully peer-reviewed by external reviewers. It is distributed in accordance with the Creative Commons Attribution NonCommercial (CC BY-NC 4.0) license, which permits others to distribute, remix, adapt, build upon this work non-commercially, and license their derivative works on different terms, provided the original work is properly cited and the use is non-commercial. See: http://creativecommons.org/Licenses/by-nc/4.0/

Manuscript source: Invited manuscript

Specialty type: Gastroenterology and hepatology

Country/Territory of origin: Croatia

Peer-review report's scientific quality classification

Grade A (Excellent): 0
Grade B (Very good): B
Grade C (Good): 0
Grade D (Fair): 0
Grade E (Poor): 0

Received: April 27, 2021
Peer-review started: April 27, 2021
First decision: June 13, 2021
Revised: June 17, 2021
Accepted: August 19, 2021
Article in press: August 19, 2021
Published online: September 28, 2021

P-Reviewer: Sassaki LY
S-Editor: Wu YXJ
L-Editor: Filipodia
P-Editor: Yuan YY

Crohn's disease and 24 with ulcerative colitis) and 50 age and gender matched controls. Clinical assessment was performed by the same experienced gastroenterologist according to the latest guidelines. Ulcerative Colitis Endoscopic Index of Severity and Simple Endoscopic Score for Crohn's Disease were used for endoscopic evaluation. Serum levels of UII were determined using the enzyme immunoassay kit for human UII, according to the manufacturer's instructions.

RESULTS

IBD patients have significantly higher concentrations of UII when compared to control subjects (7.57 ± 1.41 *vs* 1.98 ± 0.69 ng/mL, $P < 0.001$), while there were no significant differences between Crohn's disease and ulcerative colitis patients (7.49 ± 1.42 *vs* 7.65 ± 1.41 ng/mL, $P = 0.689$). There was a significant positive correlation between serum UII levels and high sensitivity C reactive peptide levels ($r = 0.491$, $P < 0.001$) and a significant negative correlation between serum UII levels and total proteins ($r = -0.306$, $P = 0.032$). Additionally, there was a significant positive correlation between serum UII levels with both systolic ($r = 0.387$, $P = 0.005$) and diastolic ($r = 0.352$, $P = 0.012$) blood pressure. Moreover, serum UII levels had a significant positive correlation with Ulcerative Colitis Endoscopic Index of Severity ($r = 0.425$, $P = 0.048$) and Simple Endoscopic Score for Crohn's Disease ($r = 0.466$, $P = 0.028$) scores. Multiple linear regression analysis showed that serum UII levels retained significant association with high sensitivity C reactive peptide (β ± standard error, 0.262 ± 0.076, $P < 0.001$) and systolic blood pressure (0.040 ± 0.017, $P = 0.030$).

CONCLUSION

It is possible that UII is involved in the complex pathophysiology of cardiovascular complications in IBD patients, and its purpose should be investigated in further studies.

Key Words: Inflammatory bowel disease; Crohn's disease; Ulcerative colitis; Urotensin II; Cardiovascular risk; Endoscopic activity

©The Author(s) 2021. Published by Baishideng Publishing Group Inc. All rights reserved.

Core Tip: Urotensin II (UII) is a potent vasoconstrictor with an immunomodulatory effect that is connected to various cardiovascular disorders. On the other hand, patients with inflammatory bowel disease (IBD) have increased cardiovascular burden as well as increased expression of UII receptors. It is plausible that UII is involved in the complex pathophysiology of IBD complications. In the current study, we investigated UII levels in the IBD population and compared it to matched control subjects, as well as connection of UII with relevant clinical and biochemical parameters. The results of this study showed that serum UII levels are higher in IBD patients in comparison with the control group.

Citation: Alicic D, Martinovic D, Rusic D, Zivkovic PM, Tadin Hadjina I, Vilovic M, Kumric M, Tokic D, Supe-Domic D, Lupi-Ferandin S, Bozic J. Urotensin II levels in patients with inflammatory bowel disease. *World J Gastroenterol* 2021; 27(36): 6142-6153
URL: https://www.wjgnet.com/1007-9327/full/v27/i36/6142.htm
DOI: https://dx.doi.org/10.3748/wjg.v27.i36.6142

INTRODUCTION

Inflammatory bowel disease (IBD) is a relapsing chronic inflammation of the gastrointestinal tract with an unpredictable course[1]. It can be divided into two disorders: Crohn's disease (CD) and ulcerative colitis (UC). Although the two disorders have a similar clinical manifestation, they differ in the location and the depth of the inflammation. The etiology of the disease is considered to be multifactorial as a complex interrelation between extrinsic factors, genetic predisposition, immunological

imbalance and microbiota disturbances. Furthermore, IBD can exhibit a wide range of extraintestinal manifestations that affect the kidneys, eyes, joints, liver, skin, heart and blood circulation[2-6].

Urotensin II (UII) is a pleotropic peptide originally found 40 years ago in the neurosecretory system of the teleost fish, while in the meantime its activity was also found in humans. UII is considered to be the most potent vasoconstrictor discovered so far, with the effect 10-fold stronger than that of endothelin-1[7]. Furthermore, its expression was found distributed in most organs and tissues, including both the central nervous and cardiovascular systems, as well as the lungs, kidneys, spleen, hypophysis, adrenal glands, stomach, pancreas, ovaries and liver[8,9]. UII activity is regulated through the urotensin receptor (UTR), which after activation induces calcium mobilization in cellular plasma, smooth muscle cells proliferation and collagen synthesis[10]. Due to the wide range of functions, UII has an extensive effect on most of the organ systems in the body, and consequently it is also associated with numerous diseases and disorders[11-13]. Moreover, recent studies are pointing to possible UII immunomodulatory effects, as it was shown that UII is involved in the regulation of the inflammation process[14,15].

In the last few decades, the extraintestinal manifestations and complications of IBD are a major issue that is increasingly investigated for an improvement of both diagnostic and treatment criteria. It is well-established that patients with IBD are associated with a high cardiovascular risk, and it was shown that they have a higher prevalence cardiovascular diseases[16-18]. However, a Danish cohort study showed that patients with IBD have a lower prevalence of the traditional cardiovascular risk factors in comparison to the general population, while on the other hand they had a higher cardiovascular burden[19]. This ambiguity is well-established, yet it is unclear what are the factors that contribute to high cardiovascular risk in patients with IBD. Since UII is one of the most potent vasoconstrictors known, and it is well-known that it is associated with cardiovascular diseases, it is reasonable to presume that there is a possible connection between cardiovascular risk in IBD patients and UII[20,21]. Moreover, seeing that recent studies are pointing to UII immunomodulatory effect and since the hallmark of IBD is the chronic inflammation, this further suggests the need to investigate clinically the possible association between them[14,15]. Additionally, a recent study conducted on patients with UC showed that they have an increased expression of UTR compared to healthy controls[22]. Moreover, that expression was found to be increased in both disease lesions and healthy tissue biopsies.

Hence, the aim of this study was to evaluate serum UII levels in patients with IBD and to compare them with healthy, gender and age matched controls. Moreover, we further investigated the possible association between UII levels and the relevant clinical and biochemical parameters.

MATERIALS AND METHODS

Study design and ethical considerations

This cross-sectional study was conducted at the University Hospital of Split and the University of Split School of Medicine during the period from January 2018 to March 2019.

Before the start of the study, every participant was informed about the aim, course and procedures involved, and they all signed an informed written consent. The study was conducted in accordance with all ethical principles of the Seventh Revision of the Helsinki Declaration, and it was approved by the Ethics Committee of University Hospital of Split (date of approval: November 23, 2017).

Subjects

This study included 50 adult patients with pre-diagnosed IBD (24 patients with UC and 26 patients with CD) and 50 healthy, age and gender matched controls. The diagnosis of UC and CD was established on clinical, radiological, endoscopic and histological traits in accordance with the European Consensus on Crohn's Disease and Ulcerative Colitis[23]. Inclusion criteria were: Disease duration of at least 1 year, stable disease activity in the past 3 mo and age between 18 and 65 years. Exclusion criteria were: Diabetes, obesity, arterial hypertension, use of statins, cardiovascular disorders, therapy with corticosteroids during 3 mo prior to study onset, substance abuse and consumption of alcohol more than 40 g/d.

Additionally, we checked medical records of the control subjects regarding gastrointestinal conditions, and additionally we performed screening for abdominal pain presence, symptoms related to defecation and change in frequency and form of stool according to the Rome IV criteria for irritable bowel syndrome[24], as well as any other symptoms that could suggest gluten and lactose intolerance. If any of these conditions were present, we excluded the subject from the control group. Furthermore, all potential control group subjects underwent detailed physical examination along with laboratory analysis of the complete blood count and biochemical parameters. We excluded all participants who showed any sign of inflammation in any of these steps.

Disease severity assessment

Disease activity evaluation was performed using clinical and endoscopic indices. The assessment was conducted by the same experienced gastroenterologist according to the latest guidelines, and the colonoscopy needed for the evaluation of the disease activity was performed within 2 wk of blood sampling. We used endoscopic indices for the evaluation of the disease activity since they have an advantage before clinical indices according to the European Consensus on Crohn's Disease and Ulcerative Colitis guidelines[25]. Moreover, all IBD patients had their high sensitivity C reactive peptide (hsCRP) and fecal calprotectin evaluated to assess further the activity of the disease.

Ulcerative Colitis Endoscopic Index of Severity (UCEIS) is a quantitative grading system used for the evaluation of UC activity. Depending on the score, there are four possible grades for disease activity: (0-1)–remission; (2-4)–mild; (5-6)–moderate and (7-8)–severe activity[26].

Simple Endoscopic Score for CD (SES-CD) is a quantitative grading system used for the evaluation of CD activity. According to the majority of studies, the threshold values for interpretation of the results are: (0-2)–remission; (3-6)–mild activity; (7-15)–moderate activity and (≥ 16)–severe disease[27].

Blood sampling and laboratory analysis

All blood samples were taken from the cubital vein after 12-h fasting. After extraction, all samples were processed in the same day except for the UII samples, which were centrifuged and stored at -80 °C for further analysis. All the procedures were conducted according to the international standards, in the same laboratory and by the same experienced medical biochemist who was blinded to the subjects group in the study. Serum levels of UII were determined using the enzyme immunoassay kit for human UII (Phoenix Pharmaceuticals, Burlingame, CA, United States), according to the manufacturer's instructions. Concentration of the analyzed quality control sample that arrived from the manufacturer was within predefined acceptable deviation. The linear range of the assay was 0.06-8.2 ng/mL, and sensitivity was 0.06 ng/mL. Coefficient of variation within the probe was less than 10% and between probes was less than 15%. Other biochemical parameters were analyzed according to standard laboratory procedures.

Stool samples were received by a trained laboratory technician in sterile containers within 3 d of sampling. Fecal extraction and analyses were performed by an experienced medical biochemist.

Anthropometric and clinical assessment

All participants were subjected to detailed anamnesis, physical examination and measurements of anthropometric characteristics - body weight, body height and body mass index (BMI). For measurement of body weight and height, a calibrated medical scale with built-in heights (Seca, Birmingham, United Kingdom) was used. BMI was calculated according to the formula = [body weight (kg)]/[height per square (m^2)].

Statistical analysis

Collected data were analyzed with statistical software MedCalc (version 17.4.1; MedCalc Software, Ostend, Belgium,). Quantitative data were expressed as mean ± SD or median and interquartile range, while qualitative data were expressed as whole number and percentage. Kolmogorov-Smirnov test was used to estimate the normality of data distribution. Comparison of serum UII levels and other parameters between patients with IBD and control subjects was done by Student *t*-test for independent samples or Mann-Whitney *U* test. For comparison of qualitative variables, Chi-squared test was used. Pearson's correlation or Spearman's correlation was used to estimate the correlation between biochemical, anthropometric and clinical parameters with serum UII levels. Furthermore, multiple linear regression analysis was used to determine

significant independent predictors of serum UII levels, with reporting corresponding *P* values with unstandardized β-coefficients, standard error and t-values. The level of statistical significance was set at $P < 0.05$.

RESULTS

Baseline characteristics of the study population

There were no statistically significant differences regarding age, gender and anthropometric features between the IBD patients and healthy controls (Table 1). Laboratory analyses showed that the IBD group compared to the control group had significantly lower erythrocytes (4.7 ± 0.5 *vs* 5.0 ± 0.4 × 10^{12}/L, $P = 0.020$), hemoglobin (140.4 ± 17.3 *vs* 148.1 ± 13.7 g/L, $P = 0.015$) and albumins (39.5 ± 5.1 *vs* 43.7 ± 2.4 g/L, $P < 0.001$), while they had significantly higher hsCRP levels (3.4 ± 2.6 *vs* 1.2 ± 1.1 mg/L, $P < 0.001$) (Table 2).

Serum urotensin II levels

Serum UII levels were significantly higher in the IBD group compared to the control group (7.26 ± 1.67 *vs* 1.98 ± 0.68 ng/mL, $P < 0.001$) (Figure 1A). Furthermore, there were no statistically significant differences in serum UII levels between the patients with UC and patients with CD (7.15 ± 1.63 *vs* 7.36 ± 1.73 ng/mL, $P = 0.672$) (Figure 1B).

Correlations between urotensin II and other biochemical, anthropometric and clinical parameters

There was a significant positive correlation between serum UII levels and hsCRP levels ($r = 0.491$, $P < 0.001$) and a significant negative correlation between serum UII levels and total proteins ($r = -0.306$, $P = 0.032$). There were no significant correlations with other biochemical parameters (Table 3).

There was a significant positive correlation between serum UII levels with both systolic ($r = 0.387$, $P = 0.005$) and diastolic ($r = 0.352$, $P = 0.012$) blood pressure. Moreover, serum UII levels had a significant positive correlation with UCEIS ($r = 0.425$, $P = 0.048$) and SES-CD ($r = 0.466$, $P = 0.028$) scores (Table 3).

Multiple linear regression

Multiple linear regression analysis showed that serum UII levels retained significant association with hsCRP (β ± standard error, 0.262 ± 0.076, $P < 0.001$) and systolic blood pressure (0.040 ± 0.017, $P = 0.030$) after model adjustment for age, gender, BMI and diastolic blood pressure, with serum UII levels as a dependent variable (Table 4).

DISCUSSION

The results of this study showed that serum UII levels are higher in patients with IBD compared to the healthy controls, while there was no significant difference between patients with UC and patients with CD. To the best of our knowledge, this is the first clinical study to investigate serum UII levels in both UC and CD.

Association between UII and IBD was only explored in a recent experimental pilot study that investigated expression of the UII receptor UTR in patients with UC[22]. They measured UTR expression from biopsies of the UC lesions and healthy colon tissue, and their outcomes determined that UTR expression was significantly higher in both the UC lesions and healthy tissue of the UC patients compared to the control group biopsies. Furthermore, a Chinese animal study conducted on mice with dextran sulfate sodium induced colitis explored the mechanisms of UTR in colonic inflammation[28]. They administrated the mice with urantide, a special antagonist of UTR that consequently alleviated rectal bleeding, tissue injury and production of interleukin (IL)-17 and tumor necrosis factor alpha (TNF-α). Furthermore, they showed that the inhibition of UTR reduced the activation of the nuclear factor-κB both *in vitro* and *in vivo*. Similarly, a study conducted on mice with induced acute liver failure assessed UTR expression and mechanisms involved[15]. They found that mice treated with urantide and consequent UTR downregulation expressed prevention of pro-inflammatory cytokines increase. TNF-α, IL-1β and interferon-γ were significantly lower compared to the mice with induced acute liver failure that were not treated with urantide. Additionally, a recent study explored UTR effects in acute liver failure by using Kupffer cells as a model system[29]. They found that UTR mediates production

Table 1 Baseline characteristics of the inflammatory bowel disease group and the control group

Parameter	IBD group (*n* = 50)	Control group (*n* = 50)	*P* value[1]
Male gender, *n* (%)	31 (62)	29 (58)	0.838
Age (yr)	44.3 ± 14.8	40.6 ± 12.3	0.181
Body weight (kg)	78.4 ± 14.0	81.1 ± 15.0	0.356
Body height (cm)	176.9 ± 9.8	179.6 ± 7.9	0.130
Body mass index (kg/m^2)	23.9 ± 3.7	24.9 ± 3.4	0.136
SBP (mmHg)	119.5 ± 11.2	116.6 ± 9.2	0.156
DBP (mmHg)	77.7 ± 8.3	75.0 ± 8.6	0.112
Smoking, *n* (%)	12 (24.0)	9 (18.4)	0.660
Disease duration (yr)[2]	6.0 (3.0-11.0)	-	-
UCEIS (score)	6.0 (5.0-7.0)	-	-
SES-CD (score)	9.2 (6.6-12.0)	-	-
Aminosalycilates	32 (64.0%)	-	-
DMARD	15 (30.0%)	-	-
Monoclonal antibodies	29 (58.0%)	-	-

[1]Chi-square test or t-test for independent samples.
[2]Time period since the initial diagnosis.
DBP: Diastolic blood pressure; DMARD: Disease-modifying antirheumatic drug; SBP: Systolic blood pressure; SES-CD: Simple endoscopic score for Crohn's disease; UCEIS: Ulcerative colitis index of severity. Data are presented as whole number (percentage), mean ± SD or median (interquartile range).

Table 2 Laboratory parameters of the inflammatory bowel disease group and the control group

Parameter	IBD group (*n* = 50)	Control group (*n* = 50)	*P* value[1]
Erythrocytes (× 10^{12}/L)	4.7 ± 0.5	5.0 ± 0.4	0.020
Hemoglobin (g/L)	140.4 ± 17.3	148.1 ± 13.7	0.015
Fasting glucose (mmol/L)	5.1 ± 0.9	5.0 ± 0.6	0.653
Urea (mmol/L)	4.7 ± 1.5	5.6 ± 1.6	0.004
Creatinine (μmol/L)	71.4 ± 15.3	75.9 ± 14.7	0.134
Total proteins (g/L)	71.2 ± 6.6	72.1 ± 3.9	0.394
Albumins (g/L)	39.5 ± 5.1	43.7 ± 2.4	< 0.001
hsCRP (mg/L)	3.4 ± 2.6	1.2 ± 1.1	< 0.001
Triglycerides (mmol/L)	1.3 ± 0.9	1.1 ± 0.6	0.311
Total cholesterol (mmol/L)	4.8 ± 1.3	5.2 ± 1.2	0.091
HDL cholesterol (mmol/L)	1.3 ± 0.4	1.4 ± 0.3	0.447
LDL cholesterol (mmol/L)	2.6 (2.1-3.4)	3.2 (2.4-3.9)	0.018
FC (μg/g)	231 (61.5-619.2)	-	-

[1]*t*-test for independent samples or Mann-Whitney *U* test.
FC: Fecal calprotectin; HDL: High-density lipoprotein; HsCRP: High sensitivity C-reactive protein; LDL: Low-density lipoprotein. Data are presented as mean ± SD and median (interquartile range).

and release of proinflammatory cytokines TNF-α, IL-1β and interferon-γ by using the inflammatory pathway nuclear factor-κB. All of these aforementioned studies point to the possibility that UII, besides the already well-established vasoconstriction, is also involved in the development and enhancement of the inflammatory response.

Table 3 Correlation analysis between serum urotensin II levels and different biochemical, anthropometric and clinical parameters in the inflammatory bowel disease group (*n* = 50)

Parameter	*r*[1]	*P* value
hsCRP (mg/L)	0.491	< 0.001
Total proteins (g/L)	-0.306	0.032
Albumins (g/L)	-0.182	0.210
Triglycerides (mmol/L)	0.057	0.698
Total cholesterol (mmol/L)	-0.114	0.439
HDL (mmol/L)	-0.153	0.298
LDL (mmol/L)	-0.103[3]	0.487
Urea (mmol/L)	0.013	0.928
Creatinine (μmol/L)	0.133	0.356
Age (yr)	-0.072	0.614
Body mass index (kg/m^2)	-0.037	0.800
SBP (mmHg)	0.387	0.005
DBP (mmHg)	0.352	0.012
IBD duration (yr)[2]	0.045[3]	0.751
FC (μg/g)	0.048[3]	0.812
UCEIS (score)	0.425[3]	0.048
SES-CD (score)	0.466[3]	0.028

[1]Pearson's correlation coefficient.
[2]Time period before the initial diagnosis.
[3]Spearman's rank correlation coefficient.
DBP: Diastolic blood pressure; FC: Fecal calprotectin; hsCRP: High sensitivity C-reactive protein; SBP: Systolic blood pressure; SES-CD: Simple endoscopic score for Crohn's disease; UCEIS: Ulcerative colitis index of severity.

Table 4 Multiple linear regression model of independent predictors for serum urotensin II levels

Variable	B[1]	SE	*t* value	*P* value
Age	0.009	0.015	0.570	0.571
Gender	-0.740	0.405	-1.825	0.075
BMI	-0.106	0.059	-1.793	0.080
SBP	0.040	0.017	2.243	0.030
DBP	0.039	0.025	1.535	0.132
hsCRP	0.262	0.076	3.469	< 0.001

[1]Unstandardized coefficient β.
BMI: Body mass index; DBP: Diastolic blood pressure; hsCRP: High sensitivity C-reactive protein; SBP: Systolic blood pressure; SE: Standard error.

According to these results, it could be hypothesized that in IBD, among other mechanisms, higher UII levels and consequently greater UTR activity can be associated with elevated TNF-α concentrations, which cause the development of the aberrant inflammatory response[30]. It is well established that IBD is linked with elevated TNF-α levels in the mucosa of the gastrointestinal tract and consequently an abnormal inflammatory response that is associated with the dysregulation of mucosal immune cells and tissue injury[31]. Moreover, TNF-α contributes to inflammation through disruption of the epithelial barrier, stimulation of villous epithelial cells apoptosis and secretion of chemokines from intestinal epithelium[32]. This possibility is further supported by our results that UII is in a significant positive association with

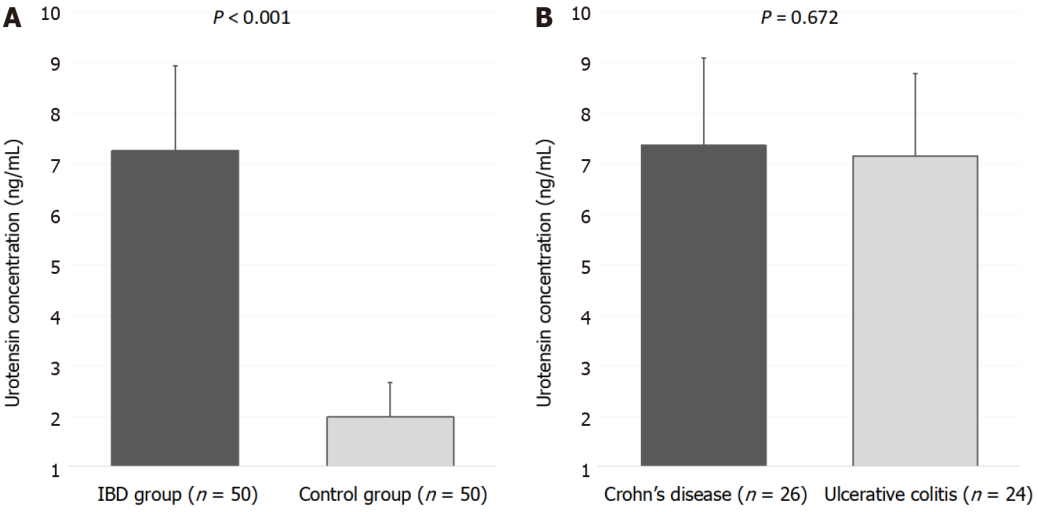


Figure 1 Serum urotensin II levels. A: Comparison between the inflammatory bowel disease group and the control group. B: Comparison between patients with Crohn's disease and patients with ulcerative colitis.

hsCRP, which was additionally supported with multiple linear regression, and clinical indices of IBD activity as well. These results implicate that disease activity could be closely related to UII levels.

Moreover, it is important to highlight that the previous studies have shown that high TNF-α levels play a major role in the disruption of macro and microvascular circulation[33]. It induces the production of reactive oxygen species, which results in endothelial dysfunction, while several studies presented that the administration of anti-TNF-α therapy to patients with IBD results in a significant improvement of endothelial dysfunction[32,34]. It is possible that functional and structural changes of the vascular endothelium due to chronic inflammation consequently results in higher cardiovascular risk in IBD patients[35]. Furthermore, with more severe disease activity and consequent greater inflammation, the resulting endothelial dysfunction that accompanies these changes is more advanced. It was presented by two recent studies that heart dysfunction, as well as fibrosis and cell hypertrophy, were significantly decreased in experimental heart models treated with UTR antagonists[36,37]. Moreover, a recent study showed that elevated UII levels are associated with the severity of cardiovascular risk factors[38].

In the last 2 decades, it has become clear that chronic systemic inflammation plays a major part in the initiation and progression of atherosclerosis[39,40]. Circulating UII was reported to promote increase of reactive oxygen species levels, which are important molecules in the initiation of atherosclerosis[41]. In a Chinese animal study, urantide administration reduced the proportion of the macrophage lesion area as well as improved the plaque characteristics in hyperlipidemic rabbits by increasing the collagen content[42]. Even though UTR antagonist downregulated proinflammatory cytokines, it did not significantly change the lipid profile. In summary, although the UTR antagonist did not change the progression of atherosclerosis, it significantly affected composition of atherosclerotic plaque. These results imply that UII is associated with the process of atherosclerosis, but the downregulation of its receptor UTR only affects the properties of the atherosclerotic plaque, while it does not stop its actual progression.

Our results also determined a significant positive correlation between serum UII levels with systolic and diastolic blood pressure. This is in alignment with several other clinical and experimental studies that have found an association between UII and arterial pressure, probably present due to its established vasoconstrictive effect[43,44]. Moreover, studies have shown that IBD patients have a lower incidence of some of the traditional risk factors for cardiovascular diseases, including hypertension[19]. In a current scenario, it is still questionable why IBD patients have lower incidence of hypertension, although UII levels are elevated in comparison with healthy subjects. It is hard to hypothesize from our results what are the possible reasons for this ambiguity, and further studies are needed to elaborate this issue. However, it is possible that UII vasoconstriction effect is diminished by other factors that are present in IBD patients.

This study had several limitations. It was a single center study with a cross-sectional design. Moreover, our sample size was relatively low, and we were not able to eliminate completely all possible confounding effects.

CONCLUSION

In conclusion, this study showed that patients with IBD have a higher serum level of UII compared to the control group. This implied association with IBD was further supported with the positive correlation between UII and hsCRP, UCEIS and SES-CD. All of these results suggest that UII could be involved in the pathophysiology of IBD, especially in the inflammation severity and disease activity. However, future studies need to clarify these connections.

ARTICLE HIGHLIGHTS

Research background

Patients with inflammatory bowel disease (IBD) are associated with increased cardiovascular risk and have increased overall cardiovascular burden. On the other hand, urotensin II (UII) is one of the most potent vascular constrictors with immunomodulatory effect that is connected with a number of different cardiometabolic disorders as well. Since the features of IBD includes chronic inflammation and endothelial dysfunction, it is plausible to assume that there is connection between increased cardiac risk in IBD and UII.

Research motivation

While a recent study showed that patients with ulcerative colitis (UC) have increased expression of urotensin II receptor in comparison to healthy controls, a larger clinical study regarding UII serum levels in patients with IBD is still missing.

Research objectives

The aim of this study was to compare serum levels of UII between patients with IBD and healthy controls. The additional goal was to investigate the association of serum UII levels with the anthropometric, clinical and biochemical parameters.

Research methods

This study included 50 adult patients with pre-diagnosed IBD (24 patients with UC and 26 patients with Crohn's disease (CD) and 50 healthy, age and gender matched controls. Serum levels of UII were determined using the enzyme immunoassay kit for human UII, according to the manufacturer's instructions. Other parameters were analyzed according to the standard laboratory procedures.

Research results

Analysis has shown that IBD patients have significantly higher concentrations of UII when compared to control subjects (7.57 ± 1.41 *vs* 1.98 ± 0.69 ng/mL, $P < 0.001$), while there were no significant differences between CD and UC patients (7.49 ± 1.42 *vs* 7.65 ± 1.41 ng/mL, $P = 0.689$). There was a significant positive correlation between serum UII levels and high sensitivity C reactive peptide levels ($r = 0.491$, $P < 0.001$), UC Endoscopic Index of Severity ($r = 0.425$, $P = 0.048$) and Simple Endoscopic Score for CD ($r = 0.466$, $P = 0.028$) scores.

Research conclusions

Our clinical results suggest that UII could be involved in the pathophysiology of IBD, especially in the inflammation severity and disease activity.

Research perspectives

Future larger scale multicenter studies need to clarify the connection between UII and IBD.

ACKNOWLEDGEMENTS

The authors would like to thank to Behmen D, MA for her careful language assistance.

REFERENCES

1 **Zhang YZ**, Li YY. Inflammatory bowel disease: pathogenesis. *World J Gastroenterol* 2014; **20**: 91-99 [PMID: 24415861 DOI: 10.3748/wjg.v20.i1.91]
2 **Brnic D**, Martinovic D, Zivkovic PM, Tokic D, Vilovic M, Rusic D, Tadin Hadjina I, Libers C, Glumac S, Supe-Domic D, Tonkic A, Bozic J. Inactive matrix Gla protein is elevated in patients with inflammatory bowel disease. *World J Gastroenterol* 2020; **26**: 4866-4877 [PMID: 32921963 DOI: 10.3748/wjg.v26.i32.4866]
3 **Brnić D**, Martinovic D, Zivkovic PM, Tokic D, Tadin Hadjina I, Rusic D, Vilovic M, Supe-Domic D, Tonkic A, Bozic J. Serum adropin levels are reduced in patients with inflammatory bowel diseases. *Sci Rep* 2020; **10**: 9264 [PMID: 32518265 DOI: 10.1038/s41598-020-66254-9]
4 **Fragoulis GE**, Liava C, Daoussis D, Akriviadis E, Garyfallos A, Dimitroulas T. Inflammatory bowel diseases and spondyloarthropathies: From pathogenesis to treatment. *World J Gastroenterol* 2019; **25**: 2162-2176 [PMID: 31143068 DOI: 10.3748/wjg.v25.i18.2162]
5 **Filimon AM**, Negreanu L, Doca M, Ciobanu A, Preda CM, Vinereanu D. Cardiovascular involvement in inflammatory bowel disease: Dangerous liaisons. *World J Gastroenterol* 2015; **21**: 9688-9692 [PMID: 26361415 DOI: 10.3748/wjg.v21.i33.9688]
6 **Cheng K**, Faye AS. Venous thromboembolism in inflammatory bowel disease. *World J Gastroenterol* 2020; **26**: 1231-1241 [PMID: 32256013 DOI: 10.3748/wjg.v26.i12.1231]
7 **Svistunov AA**, Tarasov VV, Shakhmardanova SA, Sologova SS, Bagaturiya ET, Chubarev VN, Galenko-Yaroshevsky PA, Avila-Rodriguez MF, Barreto GE, Aliev G. Urotensin II: Molecular Mechanisms of Biological Activity. *Curr Protein Pept Sci* 2018; **19**: 924-934 [PMID: 28875851 DOI: 10.2174/1389203718666170829162335]
8 **Federico A**, Zappavigna S, Dallio M, Misso G, Merlino F, Loguercio C, Novellino E, Grieco P, Caraglia M. Urotensin-II Receptor: A Double Identity Receptor Involved in Vasoconstriction and in the Development of Digestive Tract Cancers and other Tumors. *Curr Cancer Drug Targets* 2017; **17**: 109-121 [PMID: 27338741 DOI: 10.2174/1568009616666160621101248]
9 **Pereira-Castro J**, Brás-Silva C, Fontes-Sousa AP. Novel insights into the role of urotensin II in cardiovascular disease. *Drug Discov Today* 2019; **24**: 2170-2180 [PMID: 31430542 DOI: 10.1016/j.drudis.2019.08.005]
10 **Castel H**, Desrues L, Joubert JE, Tonon MC, Prézeau L, Chabbert M, Morin F, Gandolfo P. The G Protein-Coupled Receptor UT of the Neuropeptide Urotensin II Displays Structural and Functional Chemokine Features. *Front Endocrinol (Lausanne)* 2017; **8**: 76 [PMID: 28487672 DOI: 10.3389/fendo.2017.00076]
11 **Eyre HJ**, Speight T, Glazier JD, Smith DM, Ashton N. Urotensin II in the development and progression of chronic kidney disease following ⅝ nephrectomy in the rat. *Exp Physiol* 2019; **104**: 421-433 [PMID: 30575177 DOI: 10.1113/EP087366]
12 **Khan K**, Albanese I, Yu B, Shalal Y, Al-Kindi H, Alaws H, Tardif JC, Gourgas O, Cerutti M, Schwertani A. Urotensin II, urotensin-related peptide, and their receptor in aortic valve stenosis. *J Thorac Cardiovasc Surg* 2019 [PMID: 31679703 DOI: 10.1016/j.jtcvs.2019.09.029]
13 **Chen X**, Yin L, Jia WH, Wang NQ, Xu CY, Hou BY, Li N, Zhang L, Qiang GF, Yang XY, Du GH. Chronic Urotensin-II Administration Improves Whole-Body Glucose Tolerance in High-Fat Diet-Fed Mice. *Front Endocrinol (Lausanne)* 2019; **10**: 453 [PMID: 31379736 DOI: 10.3389/fendo.2019.00453]
14 **Sun SL**, Liu LM. Urotensin II: an inflammatory cytokine. *J Endocrinol* 2019 [PMID: 30601760 DOI: 10.1530/joe-18-0505]
15 **Liang DY**, Liu LM, Ye CG, Zhao L, Yu FP, Gao DY, Wang YY, Yang ZW. Inhibition of UII/UTR system relieves acute inflammation of liver through preventing activation of NF-κB pathway in ALF mice. *PLoS One* 2014; **8**: e64895 [PMID: 23755157 DOI: 10.1371/journal.pone.0064895]
16 **Bigeh A**, Sanchez A, Maestas C, Gulati M. Inflammatory bowel disease and the risk for cardiovascular disease: Does all inflammation lead to heart disease? *Trends Cardiovasc Med* 2020; **30**: 463-469 [PMID: 31653485 DOI: 10.1016/j.tcm.2019.10.001]
17 **Singh S**, Kullo IJ, Pardi DS, Loftus EV Jr. Epidemiology, risk factors and management of cardiovascular diseases in IBD. *Nat Rev Gastroenterol Hepatol* 2015; **12**: 26-35 [PMID: 25446727 DOI: 10.1038/nrgastro.2014.202]
18 **Zivkovic PM**, Matetic A, Tadin Hadjina I, Rusic D, Vilovic M, Supe-Domic D, Borovac JA, Mudnic I, Tonkic A, Bozic J. Serum Catestatin Levels and Arterial Stiffness Parameters Are Increased in Patients with Inflammatory Bowel Disease. *J Clin Med* 2020; **9** [PMID: 32110996 DOI: 10.3390/jcm9030628]
19 **Kristensen SL**, Ahlehoff O, Lindhardsen J, Erichsen R, Jensen GV, Torp-Pedersen C, Nielsen OH, Gislason GH, Hansen PR. Disease activity in inflammatory bowel disease is associated with increased risk of myocardial infarction, stroke and cardiovascular death--a Danish nationwide cohort study. *PLoS One* 2013; **8**: e56944 [PMID: 23457642 DOI: 10.1371/journal.pone.0056944]

20 **Ahmed AH**, Maulood IM. Endothelin-1 and angiotensin-II modulate urotensin-II vasoconstriction in rat aorta exposed to mercury. *Bratisl Lek Listy* 2018; **119**: 444-449 [PMID: 30160135 DOI: 10.4149/BLL_2018_081]

21 **Jumaah S**, Çelekli A, Sucu M. The role of human urotensin-II in patients with hypertrophic cardiomyopathy. *J Immunoassay Immunochem* 2018; **39**: 150-162 [PMID: 28686108 DOI: 10.1080/15321819.2017.1344130]

22 **Gravina AG**, Dallio M, Tuccillo C, Martorano M, Abenavoli L, Luzza F, Stiuso P, Lama S, Grieco P, Merlino F, Caraglia M, Loguercio C, Federico A. Urotensin II receptor expression in patients with ulcerative colitis: a pilot study. *Minerva Gastroenterol Dietol* 2020; **66**: 23-28 [PMID: 31293119 DOI: 10.23736/S1121-421X.19.02602-3]

23 **Magro F**, Gionchetti P, Eliakim R, Ardizzone S, Armuzzi A, Barreiro-de Acosta M, Burisch J, Gecse KB, Hart AL, Hindryckx P, Langner C, Limdi JK, Pellino G, Zagórowicz E, Raine T, Harbord M, Rieder F; European Crohn's and Colitis Organisation [ECCO]. Third European Evidence-based Consensus on Diagnosis and Management of Ulcerative Colitis. Part 1: Definitions, Diagnosis, Extra-intestinal Manifestations, Pregnancy, Cancer Surveillance, Surgery, and Ileo-anal Pouch Disorders. *J Crohns Colitis* 2017; **11**: 649-670 [PMID: 28158501 DOI: 10.1093/ecco-jcc/jjx008]

24 **Schmulson MJ**, Drossman DA. What Is New in Rome IV. *J Neurogastroenterol Motil* 2017; **23**: 151-163 [PMID: 28274109 DOI: 10.5056/jnm16214]

25 **Sturm A**, Maaser C, Calabrese E, Annese V, Fiorino G, Kucharzik T, Vavricka SR, Verstockt B, van Rheenen P, Tolan D, Taylor SA, Rimola J, Rieder F, Limdi JK, Laghi A, Krustiņš E, Kotze PG, Kopylov U, Katsanos K, Halligan S, Gordon H, González Lama Y, Ellul P, Eliakim R, Castiglione F, Burisch J, Borralho Nunes P, Bettenworth D, Baumgart DC, Stoker J; European Crohn's and Colitis Organisation [ECCO] and the European Society of Gastrointestinal and Abdominal Radiology [ESGAR]. ECCO-ESGAR Guideline for Diagnostic Assessment in IBD Part 2: IBD scores and general principles and technical aspects. *J Crohns Colitis* 2019; **13**: 273-284 [PMID: 30137278 DOI: 10.1093/ecco-jcc/jjy114]

26 **Travis SP**, Schnell D, Krzeski P, Abreu MT, Altman DG, Colombel JF, Feagan BG, Hanauer SB, Lichtenstein GR, Marteau PR, Reinisch W, Sands BE, Yacyshyn BR, Schnell P, Bernhardt CA, Mary JY, Sandborn WJ. Reliability and initial validation of the ulcerative colitis endoscopic index of severity. *Gastroenterology* 2013; **145**: 987-995 [PMID: 23891974 DOI: 10.1053/j.gastro.2013.07.024]

27 **Daperno M**, D'Haens G, Van Assche G, Baert F, Bulois P, Maunoury V, Sostegni R, Rocca R, Pera A, Gevers A, Mary JY, Colombel JF, Rutgeerts P. Development and validation of a new, simplified endoscopic activity score for Crohn's disease: the SES-CD. *Gastrointest Endosc* 2004; **60**: 505-512 [PMID: 15472670 DOI: 10.1016/s0016-5107(04)01878-4]

28 **Yang Y**, Zhang J, Chen X, Wu T, Xu X, Cao G, Li H, Li Y. UII/GPR14 is involved in NF-κB-mediated colonic inflammation *in vivo* and in vitro. *Oncol Rep* 2016; **36**: 2800-2806 [PMID: 27600191 DOI: 10.3892/or.2016.5069]

29 **Liu LM**, Liang DY, Ye CG, Tu WJ, Zhu T. The UII/UT system mediates upregulation of proinflammatory cytokines through p38 MAPK and NF-κB pathways in LPS-stimulated Kupffer cells. *PLoS One* 2015; **10**: e0121383 [PMID: 25803040 DOI: 10.1371/journal.pone.0121383]

30 **Lichtenstein GR**. Comprehensive review: antitumor necrosis factor agents in inflammatory bowel disease and factors implicated in treatment response. *Therap Adv Gastroenterol* 2013; **6**: 269-293 [PMID: 23814608 DOI: 10.1177/1756283X13479826]

31 **Friedrich M**, Pohin M, Powrie F. Cytokine Networks in the Pathophysiology of Inflammatory Bowel Disease. *Immunity* 2019; **50**: 992-1006 [PMID: 30995511 DOI: 10.1016/j.immuni.2019.03.017]

32 **Schinzari F**, Armuzzi A, De Pascalis B, Mores N, Tesauro M, Melina D, Cardillo C. Tumor necrosis factor-alpha antagonism improves endothelial dysfunction in patients with Crohn's disease. *Clin Pharmacol Ther* 2008; **83**: 70-76 [PMID: 17507924 DOI: 10.1038/sj.clpt.6100229]

33 **Zhang H**, Park Y, Wu J, Chen Xp, Lee S, Yang J, Dellsperger KC, Zhang C. Role of TNF-alpha in vascular dysfunction. *Clin Sci (Lond)* 2009; **116**: 219-230 [PMID: 19118493 DOI: 10.1042/CS20080196]

34 **Zanoli L**, Inserra G, Cappello M, Ozturk K, Castellino P. Aortic Stiffness in Patients With Inflammatory Bowel Disease Reduced After Anti-Tumor Necrosis Factor Therapy. *J Am Coll Cardiol* 2019; **73**: 981-982 [PMID: 30819367 DOI: 10.1016/j.jacc.2018.12.032]

35 **Cibor D**, Domagala-Rodacka R, Rodacki T, Jurczyszyn A, Mach T, Owczarek D. Endothelial dysfunction in inflammatory bowel diseases: Pathogenesis, assessment and implications. *World J Gastroenterol* 2016; **22**: 1067-1077 [PMID: 26811647 DOI: 10.3748/wjg.v22.i3.1067]

36 **Park CH**, Lee JH, Lee MY, Lee BH, Oh KS. A novel role of G protein-coupled receptor kinase 5 in urotensin II-stimulated cellular hypertrophy in H9c2$_{UT}$ cells. *Mol Cell Biochem* 2016; **422**: 151-160 [PMID: 27613164 DOI: 10.1007/s11010-016-2814-y]

37 **Oh KS**, Lee JH, Yi KY, Lim CJ, Park BK, Seo HW, Lee BH. A novel urotensin II receptor antagonist, KR-36996, improved cardiac function and attenuated cardiac hypertrophy in experimental heart failure. *Eur J Pharmacol* 2017; **799**: 94-102 [PMID: 28163023 DOI: 10.1016/j.ejphar.2017.02.003]

38 **Demirpence M**, Guler A, Yilmaz H, Sayin A, Pekcevik Y, Turkon H, Colak A, Ari EM, Aslanipour B, Kocabas GU, Calan M. Is elevated urotensin II level a predictor for increased cardiovascular risk in subjects with acromegaly? *J Endocrinol Invest* 2019; **42**: 207-215 [PMID: 29804270 DOI: 10.1007/s40618-018-0905-1]

39 **Chistiakov DA**, Grechko AV, Myasoedova VA, Melnichenko AA, Orekhov AN. The role of monocytosis and neutrophilia in atherosclerosis. *J Cell Mol Med* 2018; **22**: 1366-1382 [PMID: 29364567 DOI: 10.1111/jcmm.13462]

40 **Koelwyn GJ**, Corr EM, Erbay E, Moore KJ. Regulation of macrophage immunometabolism in atherosclerosis. *Nat Immunol* 2018; **19**: 526-537 [PMID: 29777212 DOI: 10.1038/s41590-018-0113-3]

41 **Mohammadi A**, Najar AG, Khoshi A. Effect of urotensin II on apolipoprotein B100 and apolipoprotein A-I expression in HepG2 cell line. *Adv Biomed Res* 2014; **3**: 22 [PMID: 24600602 DOI: 10.4103/2277-9175.124661]

42 **Yu QQ**, Cheng DX, Xu LR, Li YK, Zheng XY, Liu Y, Li YF, Liu HL, Bai L, Wang R, Fan JL, Liu EQ, Zhao SH. Urotensin II and urantide exert opposite effects on the cellular components of atherosclerotic plaque in hypercholesterolemic rabbits. *Acta Pharmacol Sin* 2020; **41**: 546-553 [PMID: 31685976 DOI: 10.1038/s41401-019-0315-8]

43 **Watanabe T**, Kanome T, Miyazaki A, Katagiri T. Human urotensin II as a link between hypertension and coronary artery disease. *Hypertens Res* 2006; **29**: 375-387 [PMID: 16940699 DOI: 10.1291/hypres.29.375]

44 **Debiec R**, Christofidou P, Denniff M, Bloomer LD, Bogdanski P, Wojnar L, Musialik K, Charchar FJ, Thompson JR, Waterworth D, Song K, Vollenweider P, Waeber G, Zukowska-Szczechowska E, Samani NJ, Lambert D, Tomaszewski M. Urotensin-II system in genetic control of blood pressure and renal function. *PLoS One* 2013; **8**: e83137 [PMID: 24391740 DOI: 10.1371/journal.pone.0083137]

World Journal of Gastroenterology

Submit a Manuscript: https://www.f6publishing.com

World J Gastroenterol 2021 September 28; 27(36): 6154-6160

DOI: 10.3748/wjg.v27.i36.6154

ISSN 1007-9327 (print) ISSN 2219-2840 (online)

CASE REPORT

Inverted Meckel's diverticulum diagnosed using capsule endoscopy: A case report

Ismael El Hajra Martínez, Marta Calvo, José Luis Martínez-Porras, Lucia Gomez-Pimpollo Garcia, Jose L Rodriguez, Carmen Leon, José Luis Calleja Panero

ORCID number: Ismael El Hajra Martínez 0000-0002-7802-0920; Marta Calvo 0000-0003-0744-8636; José Luis Martínez-Porras 0000-0003-0560-9213; Lucia Gomez-Pimpollo Garcia 0000-0001-8914-8500; Jose L Rodriguez 0000-0003-0513-1707; Carmen Leon 0000-0003-1971-9253; José Luis Calleja Panero 0000-0002-2265-6591.

Author contributions: El Hajra Martínez I and Calvo M contributed to the manuscript design and drafting, and reviewed the literature; Martínez-Porras JL performed capsule endoscopy, and interpretation and revision of the manuscript; Gomez-Pimpollo Garcia L contributed to analysis and interpretation of the imaging findings, and revision of the manuscript; Rodriguez JL contributed to pathological examination and revision of the manuscript; Leon C performed laparoscopic surgery and manuscript drafting; Calleja Panero JL and Calvo M were responsible for revision of the manuscript for important intellectual content; All authors issued final approval for the version to be submitted.

Informed consent statement: The patient provided informed written consent prior to treatment.

Ismael El Hajra Martínez, Marta Calvo, José Luis Martínez-Porras, Department of Gastroenterology, Hospital Universitario Puerta de Hierro, Madrid 28222, Spain

Lucia Gomez-Pimpollo Garcia, Department of Radiology, Hospital Universitario Puerta de Hierro, Madrid 28222, Spain

Jose L Rodriguez, Department of Diagnostic Pathology, Hospital Universitario Puerta de Hierro, Madrid 28222, Spain

Carmen Leon, Department of Surgery, Hospital Universitario Puerta de Hierro, Madrid 28222, Spain

José Luis Calleja Panero, Department of Gastroenterology, Hospital Universitario Puerta de Hierro, Madrid 28222, Spain

Corresponding author: Marta Calvo, PhD, Doctor, Department of Gastroenterology, Hospital Universitario Puerta de Hierro, Calle Joaquín Rodrigo, 1, Majadahonda, Madrid 28222, Spain. calvo.marta@gmail.com

Abstract

BACKGROUND

Meckel's diverticulum is a common asymptomatic congenital gastrointestinal anomaly. However, its presentation as an inverted Meckel's diverticulum is a rare complication, of which few cases have been reported in the literature.

CASE SUMMARY

Here, we report the case of a 33-year-old man with iron deficiency anemia without manifestation of gastrointestinal bleeding. An upper gastrointestinal endoscopy and total colonoscopy were performed, but no abnormalities were found within the observed area. Finally, a capsule endoscopy was performed and offered us a clue to subsequently confirm the diagnosis of inverted Meckel's diverticulum *via* computed tomography scan. Laparoscopic intestinal resection surgery was performed. The final pathology report described a Meckel's diverticulum.

CONCLUSION

Since inverted Meckel's diverticulum is an uncommon disease and its clinical presentation is not specific, it may go undetected by capsule endoscopy.

Conflict-of-interest statement: The authors declare having no conflicts of interest.

CARE Checklist (2016) statement: The authors have read the CARE Checklist (2016), and the manuscript was prepared and revised according to the CARE Checklist (2016).

Open-Access: This article is an open-access article that was selected by an in-house editor and fully peer-reviewed by external reviewers. It is distributed in accordance with the Creative Commons Attribution NonCommercial (CC BY-NC 4.0) license, which permits others to distribute, remix, adapt, build upon this work non-commercially, and license their derivative works on different terms, provided the original work is properly cited and the use is non-commercial. See: http://creativecommons.org/Licenses/by-nc/4.0/

Manuscript source: Unsolicited manuscript

Specialty type: Gastroenterology and hepatology

Country/Territory of origin: Spain

Peer-review report's scientific quality classification

Grade A (Excellent): 0
Grade B (Very good): B, B, B
Grade C (Good): 0
Grade D (Fair): 0
Grade E (Poor): 0

Received: February 25, 2021
Peer-review started: February 25, 2021
First decision: April 29, 2021
Revised: May 13, 2021
Accepted: August 16, 2021
Article in press: August 16, 2021
Published online: September 28, 2021

P-Reviewer: Camí MM, Racz I, Sulbaran MN
S-Editor: Wang JL
L-Editor: Filipodia
P-Editor: Li JH

Successful diagnosis and treatment of this disease requires a high index of clinical suspicion.

Key Words: Inverted Meckel's diverticulum; Capsule endoscopy; Anemia study; Small bowel tumor; Case report

©The Author(s) 2021. Published by Baishideng Publishing Group Inc. All rights reserved.

Core Tip: Inverted Meckel's diverticulum is an uncommon disease with a wide spectrum of accompanying nonspecific symptoms. We present, here, a case of iron deficiency anemia with negative endoscopic study, in which capsule endoscopy played a key role in confirming the diagnosis. Since inverted Meckel's diverticulum is an uncommon disease with few cases described in the literature, this report aims to contribute more information concerning the clinical characteristics as well as radiological and capsule endoscopy findings of inverted Meckel's diverticulum that can help clinicians make the correct diagnosis.

Citation: El Hajra Martínez I, Calvo M, Martínez-Porras JL, Gomez-Pimpollo Garcia L, Rodriguez JL, Leon C, Calleja Panero JL. Inverted Meckel's diverticulum diagnosed using capsule endoscopy: A case report. *World J Gastroenterol* 2021; 27(36): 6154-6160
URL: https://www.wjgnet.com/1007-9327/full/v27/i36/6154.htm
DOI: https://dx.doi.org/10.3748/wjg.v27.i36.6154

INTRODUCTION

Meckel's diverticulum is a common congenital gastrointestinal anomaly which is a remanent of the omphalomesenteric duct[1]. It is often within 100 cm of the ileocecal valve and located in the antimesenteric surface of the ileum[2]. According to autopsy studies, this condition is found in 0.3%-2% of the general population[3,4].

Patients with Meckel's diverticulum are usually asymptomatic. However, up to 6.4% develop complications that require surgery[5]. The most common complications are gastrointestinal bleeding in association with ectopic gastric and/or pancreatic mucosa, intestinal obstruction, intussusceptions, diverticulitis or volvulus. The inversion of Meckel's diverticulum is a rare complication with a pathophysiology not clearly understood, that can be a clinical challenge given its diagnostic difficulty. Moreover, the clinical presentation is nonspecific, the most frequent mode of presentation being intussusception, abdominal pain, anemia or gastrointestinal bleeding[6].

Although Meckel's diverticulum is the most common congenital anomaly of the small bowel, inversion or invagination of the diverticulum is a rare occurrence. To date, there are only around 100 cases in the literature that demonstrate the presence of inverted Meckel's diverticulum.

Herein, we present the case of iron deficiency anemia without manifestation of gastrointestinal bleeding, in which capsule endoscopy played a key role in the final diagnosis of inverted Meckel's diverticulum.

CASE PRESENTATION

Chief complaints

A 33-year-old male with no significant medical history presented to the emergency room with progressive weakness, easy fatigability and headache. He had no evidence of lower or upper gastrointestinal bleeding and he reported no abdominal pain, nausea, vomiting, anorexia, fever or weight loss.

History of present illness

The patient's symptoms started 3 wk prior and had worsened over the last 4 d.

History of past illness
There was no significant medical history.

Personal and family history
There was no significant medical history.

Physical examination
In the emergency room, the patient was clinically stable, with a normal temperature (36.7 °C). The patient exhibited an oxygen saturation level of 97% while he was breathing ambient air. His blood pressure was 102/61 mmHg and his heart rate was 91 beats per minute. The patient was awake, alert, and fully oriented. Physical examination revealed signs of pallor and an absence of lymphadenopathy, hepatosplenomegaly, bone tenderness or jaundice. Examination of the rectum revealed a few external hemorrhoids, but there was no blood or melena in the rectal vault; there were no skin tags, fissures or palpable masses.

Laboratory examinations
The initial laboratory findings showed low hemoglobin levels (7 g/dL), a white blood cell count of 11250 per mm^3, a platelet count of 221000 per mm^3 and a C-reactive protein of 1.31 mg/dL. Two pints of packed red blood cells were therefore transfused and the patient was admitted to the gastroenterology department. Electrocardiography (ECG) showed sinus rhythm at 93 beats per minute and the results of the patient's chest radiography were normal.

The patient's next blood test, showed a mean corpuscular volume of 72.5 fl, a mean corpuscular hemoglobin of 25.6 pg, and a reticulocyte count of 1%. The patient's iron level was 38 μg/dL, his ferritin level was 17 ng/mL, and his transferrin saturation was 9%. The hemolysis study was negative. Hence, the patient's anemia was classified as iron deficiency anemia.

Imaging examinations
During this period, an upper gastrointestinal endoscopy and a colonoscopy were performed to study the patient's anemia. The colonoscopy revealed internal hemorrhoids without any other relevant findings while the upper gastrointestinal endoscopy showed no abnormalities. The patient remained stable and was discharged and the study was completed on an outpatient basis with oral iron treatment.

During his visit to the outpatient clinic 3 wk later, the patient remained anemic, with a hemoglobin level of 8.8 g/dL. The anemia study was completed with a capsule endoscopy, which revealed a lifted erosion and mild bulge in the ileum of approximately 8-9 mm in size (Figure 1). These findings of appearance of a subepithelial bulge in the ileum suggested an inverted Meckel diverticulum. Normal intestinal mucosa was seen on the surface of the tumor with a longer small intestine transit time suggestive of Meckel's diverticulum. A technetium-99m pertechnetate radioisotope scintigraphy (Meckel's scan) was performed and was negative. The patient subsequently underwent an ultrasound examination, which revealed no pathological findings. Finally, an abdominal computed tomography (CT) was performed and showed a central area of fat attenuation surrounded by a thick collar of soft tissue attenuation (Figure 2) suggestive of inverted Meckel's diverticulum.

FINAL DIAGNOSIS
The patient was diagnosed with an inverted Meckel's diverticulum and underwent a laparoscopic surgery. A large intraluminal polyp-like mass in the mid-ileum was observed. The remainder of the small bowel was normal to the level of the ligament of Treitz. A segmentary resection of the small bowel with adequate margin was performed and side-to-side anastomosis was carried out using a stapling device.

On gross examination, the specimen consisted of a segmental resection of the small bowel of 8 cm × 4 cm × 2.6 cm with a sausage-shaped polypoid lesion.

Histological examination (Figure 3) showed a polypoid lesion, with a central fatty and collagenous core lined with an intestinal type mucosa. A central area of ulceration was seen, with no presence of gastric or pancreatic heterotopia. The final pathology report described a Meckel's diverticulum.

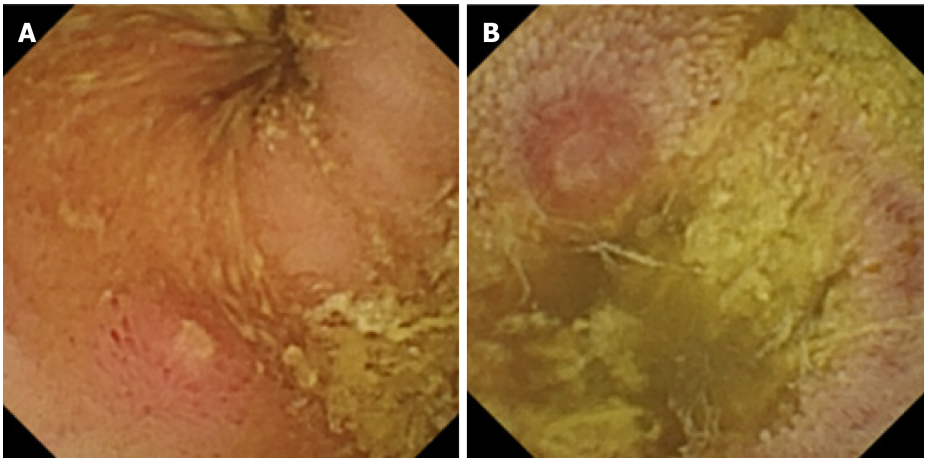


Figure 1 Capsule endoscopy with protruding lesion. A: Capsule endoscopy with protruding lesion, with a depressed erosion at the tip suggestive of Meckel's diverticulum; B: Capsule endoscopy with protruding lesion suggestive of Meckel's diverticulum.



Figure 2 Abdominal computed tomography scan revealed a central area of fat attenuation surrounded by a thick collar of soft tissue attenuation suggestive of Meckel's diverticulum.

TREATMENT

The patient was diagnosed with an inverted Meckel's diverticulum and underwent a laparoscopic surgery. A large intraluminal polyp-like mass in the mid-ileum was observed. The remainder of the small bowel was normal to the level of the ligament of Treitz. A segmentary resection of the small bowel with adequate margin was performed and side-to-side anastomosis was carried out using a stapling device.

OUTCOME AND FOLLOW-UP

The patient had an uneventful postoperative course and was discharged 4 d after surgery.

DISCUSSION

Meckel's diverticulum is the most common congenital anomaly in the gastrointestinal tract[1] and is often incidentally discovered during evaluations performed for other reasons, as it is usually an asymptomatic condition. However, complications can occur in up to 6.4% of patients[7]. These are more frequent in the pediatric population and mainly involve bowel obstruction with or without intussusception, gastrointestinal hemorrhage, diverticulitis and inflammation, and Littre hernia (hernia involving the

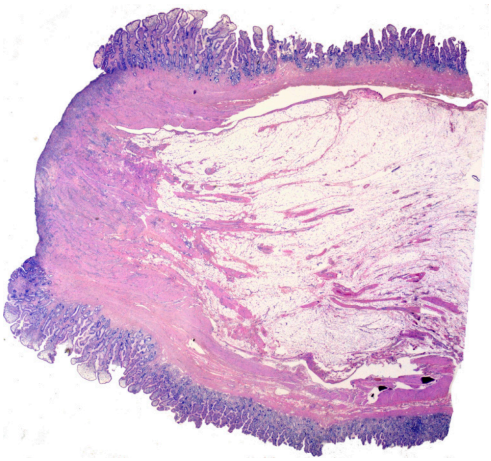


Figure 3 Low power histologic examination of a polypoid lesion lined by an intestinal type mucosa with a central ulcerated area. No gastric or pancreatic heterotopic tissue can be found.

bowel segment bearing Meckel's)[4,7].

Inverted Meckel's diverticulum is an unusual condition that is not yet clearly understood and there are no more than 100 cases reported in literature.

It has been proposed that the mechanism that could produce the inversion is an abnormal peristaltic movement around an ulceration or ectopic tissue. Nevertheless, no ectopic tissue was found in 41% of patients with inverted Meckel's diverticulum[6]. In this regard, tc-99m pertechnetate scintigraphy can help detect ectopic gastric mucosa and has been used for years as a diagnostic method for Meckel's diverticulum, especially in children, with a sensitivity of 92.1% and a specificity of 95.4%[8]. In adults, the sensitivity of this method is significantly less (54%)[9]. No cases of diagnosis of inverted Meckel's diverticulum by scintigraphy have been described, while there is only 1 case with gastric and pancreatic mucosa in the histopathological sample where the scintigraphy was negative[10]. Our patient's scintigraphy was negative. Therefore, this suggests that a negative scan does not preclude the presence of ectopic mucosa and the diagnosis of possible inverted Meckel's diverticulum.

This inversion of the Meckel's diverticulum can lead to a complete intussusception of the bowel or compromise blood flow to that bowel, ulceration and then gastrointestinal bleeding. The bleeding can also be explained by repetitive mechanical trauma to the mucosa from the reversible intussusception.

As in our patient, anemia or gastrointestinal bleeding are the most frequent clinical manifestations, found in up to 80% of patients[6]. This usually leads to an upper and lower gastrointestinal endoscopy, where the cause of the bleeding cannot be found.

Other clinical manifestations which can occur are abdominal pain (68%) and intussusception (39%). The median age of presentation is 27.7 years, younger than that reported for Meckel's diverticulum, which has been 33, with a male to female ratio of approximately 2.33:1[6].

Regarding the diagnostic tools, abdominal ultrasonography can contribute to the diagnosis, but often shows nonspecific findings such as thickened intestinal wall, fluid fille target or distended loops of bowel[11,12]. In our case, abdominal ultrasonography revealed no pathological findings.

One of the most useful tools is a CT scan. It usually shows a thickened small intestinal wall, with an elongated, intraluminal, fat-attenuating lesion[13], as in our case. In the case of intussusceptions, a CT scan is especially useful as it can reveal the characteristic "target sign". Inverted Meckel's diverticulum is sometimes confused with a lipoma on CT scans because it also consists of macroscopic fatty tissue. However, in most cases, abdominal CT scans provide useful information for the diagnosis and treatment of inverted Meckel's diverticulum[6].

Capsule endoscopy has recently been considered a useful diagnostic tool for diagnosing Meckel's diverticulum[9,14,15]. However, the role of capsule endoscopy in the identification of Meckel's diverticulum is not yet clear, with only a few case reports and case series available. Furthermore, in the case of inverted Meckel's diverticulum, the information is very limited, represented by only 2 case reports[16,17]. The capsule findings compatible with inverted Meckel's diverticulum were described as an elevated lesion with normal mucosa[16] or as pedunculated polyp[17].

In our case, the capsule endoscopy images were similar (a subepithelial protruding lesion in the ileum with the presence of blood, hematin, ulcer or erosion) and offered us a clue to subsequently confirm the diagnosis of inverted Meckel's diverticulum. In addition, the clinical suspicion due to the clinical characteristics (such as the fact that the patient was a young man with anemia) and a negative endoscopic study was of great importance for the diagnosis of inverted Meckel's diverticulum.

Regarding the risk of possible intestinal obstruction of the endoscopic capsule due to Meckel's diverticulum, no events have been described.

Surgery is the treatment of choice for symptomatic Meckel's diverticulum. The general consensus is that it should be treated with resection. In the case of asymptomatic Meckel's diverticulum, there is some debate. Resection is generally recommended for patients younger than 40-years-old, with diverticulum longer than 2 cm, diverticula with narrow necks, fibrous bands, and/or ectopic gastric tissue, and/or when the diverticulum appears thickened and inflamed[4,6,18].

It is important to note that in cases of anemia without abdominal pain, like that of our patient, it may take a long time for the patient to be diagnosed with inverted Meckel's diverticulum, given that it is an unusual condition with a nonspecific clinical presentation. Capsule endoscopy is usually performed in those patients with anemia with a normal upper and lower gastrointestinal endoscopy. However, if clinicians are unaware of the characteristics of this lesion, it may go undetected since it is an uncommon disease. Therefore, this report aims to contribute more information concerning the clinical characteristics, radiological findings and especially, the capsule endoscopy findings of inverted Meckel's diverticulum that can help clinicians suspect that this disease is present and enable them to establish a definitive diagnosis.

CONCLUSION

To date, inverted Meckel's diverticulum is a pathology that is still not completely well known, with few cases described in the literature. Its clinical presentation is not specific, its most frequent symptoms being anemia or lower gastrointestinal bleeding. Patients are often given an upper and lower gastrointestinal endoscopy which reveals no abnormalities and a subsequent capsule endoscopy. Therefore, increased awareness of the disease and a greater understanding of the features of this lesion in capsule endoscopy findings could ultimately help clinicians make the correct diagnosis.

REFERENCES

1 **Sagar J**, Kumar V, Shah DK. Meckel's diverticulum: a systematic review. *J R Soc Med* 2006; **99**: 501-505 [PMID: 17021300 DOI: 10.1258/jrsm.99.10.501]

2 **Karadeniz Cakmak G**, Emre AU, Tascilar O, Bektaş S, Uçan BH, Irkorucu O, Karakaya K, Ustundag Y, Comert M. Lipoma within inverted Meckel's diverticulum as a cause of recurrent partial intestinal obstruction and hemorrhage: a case report and review of literature. *World J Gastroenterol* 2007; **13**: 1141-1143 [PMID: 17373755 DOI: 10.3748/wjg.v13.i7.1141]

3 **WEINSTEIN EC**, CAIN JC, REMINE WH. Meckel's diverticulum: 55 years of clinical and surgical experience. *JAMA* 1962; **182**: 251-253 [PMID: 13999637 DOI: 10.1001/jama.1962.03050420027007]

4 **Park JJ**, Wolff BG, Tollefson MK, Walsh EE, Larson DR. Meckel diverticulum: the Mayo Clinic experience with 1476 patients (1950-2002). *Ann Surg* 2005; **241**: 529-533 [PMID: 15729078 DOI: 10.1097/01.sla.0000154270.14308.5f]

5 **Cullen JJ**, Kelly KA, Moir CR, Hodge DO, Zinsmeister AR, Melton LJ 3rd. Surgical management of Meckel's diverticulum. An epidemiologic, population-based study. *Ann Surg* 1994; **220**: 564-8; discussion 568 [PMID: 7944666 DOI: 10.1097/00000658-199410000-00014]

6 **Rashid OM**, Ku JK, Nagahashi M, Yamada A, Takabe K. Inverted Meckel's diverticulum as a cause of occult lower gastrointestinal hemorrhage. *World J Gastroenterol* 2012; **18**: 6155-6159 [PMID: 23155346 DOI: 10.3748/wjg.v18.i42.6155]

7 **Hansen CC**, Søreide K. Systematic review of epidemiology, presentation, and management of Meckel's diverticulum in the 21st century. *Medicine (Baltimore)* 2018; **97**: e12154 [PMID: 30170459 DOI: 10.1097/MD.0000000000012154]

8 **Hosseinnezhad T**, Shariati F, Treglia G, Kakhki VR, Sadri K, Kianifar HR, Sadeghi R. 99mTc-Pertechnetate imaging for detection of ectopic gastric mucosa: a systematic review and meta-analysis of the pertinent literature. *Acta Gastroenterol Belg* 2014; **77**: 318-327 [PMID: 25509203]

9 **Krstic SN**, Martinov JB, Sokic-Milutinovic AD, Milosavljevic TN, Krstic MN. Capsule endoscopy is useful diagnostic tool for diagnosing Meckel's diverticulum. *Eur J Gastroenterol Hepatol* 2016; **28**: 702-707 [PMID: 26854797 DOI: 10.1097/MEG.0000000000000603]

10 **Dujardin M**, de Beeck BO, Osteaux M. Inverted Meckel's diverticulum as a leading point for

ileoileal intussusception in an adult: case report. *Abdom Imaging* 2002; **27**: 563-565 [PMID: 12172999 DOI: 10.1007/s00261-001-0070-3]

11 **El-Dhuwaib Y**, O'Shea S, Ammori BJ. Laparoscopic reduction of an ileoileal intussusception and resection of an inverted Meckel's diverticulum in an adult. *Surg Endosc* 2003; **17**: 1157 [PMID: 12728389 DOI: 10.1007/s00464-002-4284-4]

12 **Karahasanoglu T**, Memisoglu K, Korman U, Tunckale A, Curgunlu A, Karter Y. Adult intussusception due to inverted Meckel's diverticulum: laparoscopic approach. *Surg Laparosc Endosc Percutan Tech* 2003; **13**: 39-41 [PMID: 12598757 DOI: 10.1097/00129689-200302000-00009]

13 **Takagaki K**, Osawa S, Ito T, Iwaizumi M, Hamaya Y, Tsukui H, Furuta T, Wada H, Baba S, Sugimoto K. Inverted Meckel's diverticulum preoperatively diagnosed using double-balloon enteroscopy. *World J Gastroenterol* 2016; **22**: 4416-4420 [PMID: 27158212 DOI: 10.3748/wjg.v22.i17.4416]

14 **Wu J**, Huang Z, Wang Y, Tang Z, Lai L, Xue A, Huang Y. Clinical features of capsule endoscopy in 825 children: A single-center, retrospective cohort study. *Medicine (Baltimore)* 2020; **99**: e22864 [PMID: 33120825 DOI: 10.1097/MD.0000000000022864]

15 **Lin L**, Liu K, Liu H, Wu J, Zhang Y. Capsule endoscopy as a diagnostic test for Meckel's diverticulum. *Scand J Gastroenterol* 2019; **54**: 122-127 [PMID: 30638099 DOI: 10.1080/00365521.2018.1553353]

16 **Ibuka T**, Araki H, Sugiyama T, Takada J, Kubota M, Shirakami Y, Shiraki M, Shimizu M, Suzui N, Miyazaki T. [A case of an elderly patient with inverted Meckel's diverticulum with small intestinal bleeding detected using capsule and double-balloon endoscopies]. *Nihon Shokakibyo Gakkai Zasshi* 2017; **114**: 2005-2011 [PMID: 29109349 DOI: 10.11405/nisshoshi.114.2005]

17 **Payeras Capó MA**, Ambrona Zafra D, Garrido Durán C. Inverted Meckel's diverticulum in an adult patient diagnosed *via* capsule endoscopy. *Rev Esp Enferm Dig* 2018; **110**: 210-211 [PMID: 29368940 DOI: 10.17235/reed.2018.5347/2017]

18 **Lequet J**, Menahem B, Alves A, Fohlen A, Mulliri A. Meckel's diverticulum in the adult. *J Visc Surg* 2017; **154**: 253-259 [PMID: 28698005 DOI: 10.1016/j.jviscsurg.2017.06.006]

Published by **Baishideng Publishing Group Inc**
7041 Koll Center Parkway, Suite 160, Pleasanton, CA 94566, USA
Telephone: +1-925-3991568
E-mail: bpgoffice@wjgnet.com
Help Desk: https://www.f6publishing.com/helpdesk
https://www.wjgnet.com

© 2021 Baishideng Publishing Group Inc. All rights reserved.

ISSN 1007-9327 (print)
ISSN 2219-2840 (online)

World Journal of *Gastroenterology*

World J Gastroenterol 2021 October 7; 27(37): 6161-6347



Published by Baishideng Publishing Group Inc

World Journal of Gastroenterology

Contents

Weekly Volume 27 Number 37 October 7, 2021

FRONTIER

6161 Significance of gut microbiota in alcoholic and non-alcoholic fatty liver diseases

Sharma SP, Suk KT, Kim DJ

OPINION REVIEW

6180 Surveillance for hepatocellular carcinoma at the community level: Easier said than done

Del Poggio P, Mazzoleni M, Lazzaroni S, D'Alessio A

REVIEW

6191 Challenges and opportunities in the application of artificial intelligence in gastroenterology and hepatology

Christou CD, Tsoulfas G

MINIREVIEWS

6224 Impact of *Helicobacter pylori* infection on gut microbiota

Iino C, Shimoyama T

6231 Therapeutic drug monitoring in inflammatory bowel disease: The dawn of reactive monitoring

Albader F, Golovics PA, Gonczi L, Bessissow T, Afif W, Lakatos PL

ORIGINAL ARTICLE

Basic Study

6248 Increased systemic RNA oxidative damage and diagnostic value of RNA oxidative metabolites during *Shigella flexneri*-induced intestinal infection

Nie JJ, Pian YY, Hu JH, Fan GQ, Zeng LT, Ouyang QG, Gao ZX, Liu Z, Wang CC, Liu Q, Cai JP

Retrospective Cohort Study

6262 Hepatitis B virus persistent infection-related single nucleotide polymorphisms in HLA regions are associated with viral load in hepatoma families

Hsieh AR, Fann CSJ, Lin HC, Tai J, Hsieh SY, Tai DI

Retrospective Study

6277 Recently acquired hepatitis C virus infection among people living with human immunodeficiency virus at a university hospital in Taiwan

Huang MH, Sun HY, Ho SY, Chang SY, Hsieh SM, Sheng WH, Chuang YC, Huang YS, Su LH, Liu WC, Su YC, Hung CC

World Journal of Gastroenterology

Weekly Volume 27 Number 37 October 7, 2021

Contents

Observational Study

6290 *Helicobacter pylori* in gastric cancer: Features of infection and their correlations with long-term results of treatment

Senchukova MA, Tomchuk O, Shurygina EI

SYSTEMATIC REVIEWS

6306 Determination of gluten immunogenic peptides for the management of the treatment adherence of celiac disease: A systematic review

Coto L, Mendia I, Sousa C, Bai JC, Cebolla A

CASE REPORT

6322 Pancreatic paraganglioma diagnosed by endoscopic ultrasound-guided fine needle aspiration: A case report and review of literature

Lanke G, Stewart JM, Lee JH

6332 Abdominal cocoon in children: A case report and review of literature

Keese D, Schmedding A, Saalabian K, Lakshin G, Fiegel H, Rolle U

LETTER TO THE EDITOR

6345 Gastrointestinal symptoms in patients with COVID-19: Is there a relationship with mortality and new variations of SARS-CoV-2?

Ribeiro IB, de Moura DTH, de Moura EGH

ABOUT COVER

Editorial Board Member of *World Journal of Gastroenterology*, Yoichi Matsuo, MD, PhD, Professor, Department of Gastroenterological Surgery, Nagoya City University Graduate School of Medical Sciences, Kawasumi 1, Mizuho-cho, Mizuho-ku, Nagoya 4678601, Japan. nukemat0328@gmail.com

AIMS AND SCOPE

The primary aim of *World Journal of Gastroenterology* (*WJG*, *World J Gastroenterol*) is to provide scholars and readers from various fields of gastroenterology and hepatology with a platform to publish high-quality basic and clinical research articles and communicate their research findings online. *WJG* mainly publishes articles reporting research results and findings obtained in the field of gastroenterology and hepatology and covering a wide range of topics including gastroenterology, hepatology, gastrointestinal endoscopy, gastrointestinal surgery, gastrointestinal oncology, and pediatric gastroenterology.

INDEXING/ABSTRACTING

The *WJG* is now indexed in Current Contents®/Clinical Medicine, Science Citation Index Expanded (also known as SciSearch®), Journal Citation Reports®, Index Medicus, MEDLINE, PubMed, PubMed Central, and Scopus. The 2021 edition of Journal Citation Report® cites the 2020 impact factor (IF) for *WJG* as 5.742; Journal Citation Indicator: 0.79; IF without journal self cites: 5.590; 5-year IF: 5.044; Ranking: 28 among 92 journals in gastroenterology and hepatology; and Quartile category: Q2. The *WJG*'s CiteScore for 2020 is 6.9 and Scopus CiteScore rank 2020: Gastroenterology is 19/136.

RESPONSIBLE EDITORS FOR THIS ISSUE

Production Editor: *Ying-Yi Yuan*; **Production Department Director:** *Xiang Li*; **Editorial Office Director:** *Ze-Mao Gong*.

NAME OF JOURNAL
World Journal of Gastroenterology

ISSN
ISSN 1007-9327 (print) ISSN 2219-2840 (online)

LAUNCH DATE
October 1, 1995

FREQUENCY
Weekly

EDITORS-IN-CHIEF
Andrzej S Tarnawski, Subrata Ghosh

EDITORIAL BOARD MEMBERS
http://www.wjgnet.com/1007-9327/editorialboard.htm

PUBLICATION DATE
October 7, 2021

COPYRIGHT
© 2021 Baishideng Publishing Group Inc

INSTRUCTIONS TO AUTHORS
https://www.wjgnet.com/bpg/gerinfo/204

GUIDELINES FOR ETHICS DOCUMENTS
https://www.wjgnet.com/bpg/GerInfo/287

GUIDELINES FOR NON-NATIVE SPEAKERS OF ENGLISH
https://www.wjgnet.com/bpg/gerinfo/240

PUBLICATION ETHICS
https://www.wjgnet.com/bpg/GerInfo/288

PUBLICATION MISCONDUCT
https://www.wjgnet.com/bpg/gerinfo/208

ARTICLE PROCESSING CHARGE
https://www.wjgnet.com/bpg/gerinfo/242

STEPS FOR SUBMITTING MANUSCRIPTS
https://www.wjgnet.com/bpg/GerInfo/239

ONLINE SUBMISSION
https://www.f6publishing.com

© 2021 Baishideng Publishing Group Inc. All rights reserved. 7041 Koll Center Parkway, Suite 160, Pleasanton, CA 94566, USA

E-mail: bpgoffice@wjgnet.com https://www.wjgnet.com

World Journal of Gastroenterology

Submit a Manuscript: https://www.f6publishing.com

World J Gastroenterol 2021 October 7; 27(37): 6161-6179

DOI: 10.3748/wjg.v27.i37.6161

ISSN 1007-9327 (print) ISSN 2219-2840 (online)

FRONTIER

Significance of gut microbiota in alcoholic and non-alcoholic fatty liver diseases

Satya Priya Sharma, Ki Tae Suk, Dong Joon Kim

ORCID number: Satya Priya Sharma 0000-0001-5994-8179; Ki Tae Suk 0000-0002-9206-9245; Dong Joon Kim 0000-0002-5792-1500.

Author contributions: Suk KT and Kim DJ equally contributed on this manuscript; Sharma SP and Suk KT contributed to manuscript preparation and writing; Sharma SP, Suk KT and Kim DJ conceptualize and design the manuscript, fulfill the authorship criteria established by the International Committee of Medical Journal Editors and verify the validity of the results reported; and the final draft of the manuscript is read and approved by all the authors.

Supported by Basic Science Research Program (National Research Foundation of Korea), No. 2020R1A6A1A03043026.

Conflict-of-interest statement: The authors declare that they have no conflict of interest.

Open-Access: This article is an open-access article that was selected by an in-house editor and fully peer-reviewed by external reviewers. It is distributed in accordance with the Creative Commons Attribution NonCommercial (CC BY-NC 4.0) license, which permits others to distribute, remix, adapt, build

Satya Priya Sharma, Ki Tae Suk, Dong Joon Kim, Institute for Liver and Digestive Diseases, Hallym University College of Medicine, Chuncheon 24252, South Korea

Corresponding author: Dong Joon Kim, MD, Professor, Institute for Liver and Digestive Diseases, Hallym University College of Medicine, Chuncheon 24252, South Korea. djkim@hallym.ac.kr

Abstract

Liver-gut communication is vital in fatty liver diseases, and gut microbes are the key regulators in maintaining liver homeostasis. Chronic alcohol abuse and persistent overnutrition create dysbiosis in gut ecology, which can contribute to fatty liver disease. In this review, we discuss the gut microbial compositional changes that occur in alcoholic and nonalcoholic fatty liver diseases and how this gut microbial dysbiosis and its metabolic products are involved in fatty liver disease pathophysiology. We also summarize the new approaches related to gut microbes that might help in the diagnosis and treatment of fatty liver disease.

Key Words: Fatty liver disease; Alcoholic fatty liver disease; Non-alcoholic fatty liver disease; Gut microbiome; Dysbiosis

©The Author(s) 2021. Published by Baishideng Publishing Group Inc. All rights reserved.

Core Tip: In this review, we compare the gut microbial composition in two different fatty liver diseases: Alcoholic fatty liver and nonalcoholic fatty liver. This review enables readers to recognize the gut microbiota compositional differences that occur in these two histopathologically analogous conditions and to explore these gut microbial compositional variations in their research. Additionally, this review will also be helpful in the design of new experiments aiming to develop new diagnostic and/or therapeutic methodologies.

Citation: Sharma SP, Suk KT, Kim DJ. Significance of gut microbiota in alcoholic and non-alcoholic fatty liver diseases. *World J Gastroenterol* 2021; 27(37): 6161-6179

URL: https://www.wjgnet.com/1007-9327/full/v27/i37/6161.htm

DOI: https://dx.doi.org/10.3748/wjg.v27.i37.6161

upon this work non-commercially, and license their derivative works on different terms, provided the original work is properly cited and the use is non-commercial. See: http://creativecommons.org/Licenses/by-nc/4.0/

Manuscript source: Invited manuscript

Specialty type: Gastroenterology and hepatology

Country/Territory of origin: South Korea

Peer-review report's scientific quality classification

Grade A (Excellent): A
Grade B (Very good): B
Grade C (Good): 0
Grade D (Fair): 0
Grade E (Poor): 0

Received: May 21, 2021
Peer-review started: May 21, 2021
First decision: June 22, 2021
Revised: July 5, 2021
Accepted: August 31, 2021
Article in press: August 31, 2021
Published online: October 7, 2021

P-Reviewer: Chattopadhyay S, Prysyazhnyuk V
S-Editor: Yan JP
L-Editor: A
P-Editor: Guo X

INTRODUCTION

Significant increases in mortality and morbidity due to chronic fatty liver disease have raised great global health concerns. Alcoholic fatty liver disease (AFLD) and nonalcoholic fatty liver disease (NAFLD) are the most common chronic fatty liver illnesses in the Western world, with prevalences of 6% and 25%, respectively[1], and are the leading causes of liver transplantation[2,3]. Both AFLD and NAFLD start with fat accumulation in the liver, known as benign or simple steatosis, which leads to inflammation identified as steatohepatitis. Advanced disease includes fibrosis and cirrhosis, which can lead to a more severe state, including hepatocellular carcinoma and liver failure, and ultimately can cause death. Only 20% of patients with AFLD and NAFLD develop progressive liver disease[4,5]. In addition to fat accumulation, increased inflammation, and alcohol consumption, other causes, such as an altered gut microbial composition, gut microbial metabolites, or gut barrier function, are associated with the exacerbation of chronic liver disease[6,7].

The recent increase in the understanding of the microbiota and its metabolites has changed the perspectives of various chronic diseases[8]. The human gut microbiota represents a complex ecosystem with various species of microbes that are approximately 1-2 kg in weight in total[9,10]. The gut microbiota maintains homeostasis by interacting with the host and has important functions, including metabolism, digestion, vitamin production, mucosal immune reaction, and the translocation of microbial-associated molecular patterns[11-14]. Importantly, the gut microbiota is known to have a significant role in liver disease progression, but the associated mechanisms are still not fully established.

The liver is the first organ exposed to gut microbial metabolites through portal vein blood. Therefore, the gut microbial community has a vital role in liver homeostasis, and dysbiosis in gut microbial ecology can produce microbial metabolites and components that can have a direct impact on the liver[15-19]. Similarly, the liver also influences gut microbial ecology, particularly in the intestine, through primary bile acids[20-22]. In this way, the liver and gut share a close bidirectional relationship. Interestingly, fecal microbiota transplantation (FMT) studies showed a proof of concept in alcohol-associated and metabolic disease generation and establishment[19,23,24].

Although AFLD and NAFLD have similar histopathological characteristics, they have different etiologies[25]. Thus, gut microbial composition in AFLD and NAFLD could have some commonalities as well as dissimilarities at various classification levels[16,26]. These gut microbial compositional similarities in AFLD and NAFLD could help not only establish common pathophysiological pathways but also increase the chance of finding common treatments. Conversely, gut microbial compositional variations in AFLD and NAFLD could be helpful for the development of specific disease-based signatural gut microbiota profiles. Additionally, these disease-specific gut microbiota profiles could be valuable for the design of gut-microbiota-based therapies such as probiotics[27], synbiotics[28], postbiotics[29] and/or FMT[30] to ameliorate liver disease. These microbial therapeutics also could provide access for developing personalized patient-based treatments to restore liver functions in AFLD and/or NAFLD. AFLD and/or NAFLD-specific gut microbiota profiles could also be useful in the future as diagnostic biomarker tools for the early diagnosis of these diseases.

Considering the importance of the disease-specific gut microbial signature in AFLD and/or NAFLD, herein, we review the gut microbial compositions related to AFLD and/or NAFLD development, especially focusing on the relationship of these compositions with the progression of both diseases, particularly in humans. We also explicitly focus on the microbial signature pertaining to AFLD and/or NAFLD and common microbes in both fatty liver conditions. This review also helps in the understanding of the deep association between the gut microbiota and fatty liver diseases, which can also be considered microbiota-associated fatty liver diseases.

GUT MICROBIAL COMMUNITY EUBIOSIS

The gut microbiota is an endogenous ecosystem that coevolves with the host as a symbiotic organ and regulates the normal physiological functions of the gut, such as food digestion and nutrient absorption, and provides essential micronutrients to the host[31]. The gut microbial ecosystem maintains a balance between the microbial species living inside the gut known as "eubiosis" that is crucial for good health.

Microbial colonization in the gastrointestinal tract starts immediately after birth and is dominated by the *Bifidobacterium* genus, and a decline in this dominance is observed in the first year of life[32]. The infant gut microbiota is changeable, as this microbial colonization is affected by multiple external factors, such as the mode of delivery, medications, nourishment[33,34], age, genetic background, and cultural/geographic influence[32,35,36]. Similarly, breastfed infants have a less diverse gut microbiota than formula-fed infants, which is the best possible explanation for the difference in gut microbial composition between United States infants and non-United States infants, as United States infants have 28 operational taxonomic units dominated by the *Prevotella* genus[32]. As children start consuming solid foods, the gut microbiota becomes more diverse and starts stabilizing[32,35,37,38]. Fecal samples collected from different geographical regions showed that the gut microbiota composition took shape toward an adult-like configuration until 3 years of age[32], after which the gut composition became more persistent[39].

Primarily, the *Firmicutes* and *Bacteroidetes* phyla dominated the adult human gut microbial composition, and *Actinobacteria*, *Proteobacteria* and *Verrucomicrobia* were found in lesser abundance. Fecal metagenomic analysis from 4 different countries identified well-classified robust gut microbial communities, named enterotypes, represented through multiple numbers of 3 genera: *Prevotella*, *Ruminococcus* and *Bacteroides*[40], and this classification of enterotype was independent of nationality, age, body mass index (BMI), and sex. However, this enterotype-based classification remains a topic of debate because external factors such as diet are considered primary regulators of gut microbiota composition and functions[41,42] and fail to be identified in healthy and elderly individuals[43]. In addition to diet, aging is also a considerable factor that changes the gut microbiota composition. Bacteria belonging to the *Bacteroidaceae*, *Lachnospiraceae* and *Ruminococcaceae* families are negatively correlated with aging independent of geographical region, lifestyle, and dietary habits[44-46]. Moreover, healthy aging showed increased microbial richness and higher numbers of *Bifidobacterium*, *Oscillospira*, *Akkermansia*, and *Christensenellaceae*[45]. Emerging metagenomic empirical evidence suggests that a healthier gut always has a more diverse microbiota population and that a healthy gut is essential to maintain human health[47,48].

GUT MICROBIAL COMMUNITY DYSBIOSIS

A change or alteration in gut microbial composition, which can be related to diseased conditions, is termed "dysbiosis"[49]. Gut microbiota composition varies from birth to death[50] and is influenced by various environmental factors[51-54]. Gut microbial dysbiosis also has a close connection with AFLD and NAFLD.

Gut microbiota alteration in AFLD

Persistent high intake of ethanol is the root cause of AFLD[55], as it disrupts the multilayered intestinal defense system involving physical, immunological, and humoral components[56]. Normally, the liver enzyme alcohol dehydrogenase and the ethanol-oxidizing system convert ethanol to acetaldehyde, which is toxic to hepatic cells. Acetaldehyde is immediately metabolized to acetate, released into the bloodstream, and used as a biological fuel by cells for energy production. In a persistently elevated ethanol consumption state, the accumulation of toxic acetaldehyde is increased in the liver, which leads to the production of highly reactive molecules that generate an oxidative stress milieu and contribute to liver injuries[16]. An increase in the flow of ethanol in the liver alters SIRT1 signaling and initiates fat accumulation in hepatocytes[57]. Ethanol reduces SIRT1 expression in the liver, which leads to the fat accumulation in liver cells by disrupting multiple SIRT1-dependent transcription factors and cofactors, such as peroxisome proliferator-activated receptor α, PPARγ coactivator-1α, AMP-activated kinase, lipin-1, β-catenin, forkhead transcription factor O1, sterol regulatory element-binding protein 1, nuclear factor activated T cells c4, and nuclear transcription factor-κB[57-59]. Ethanol facilitates the inhibition of SIRT1, which leads to various signaling network disruptions that increase the accumulation of fat in hepatocytes by decreasing β-oxidation and lipolysis, boosting lipogenesis and inflammation, and collectively leading to AFLD. Recently, human and animal models suggested that even a small intake of alcohol can harm intestinal barrier integrity and raise microbial byproduct levels in the circulation[60,61]. Moreover, there is adequate experimental evidence proving that the interrelationship between alterations in the intestinal microbiota and alcohol abuse and acute and

chronic alcohol exposure is primarily responsible for gut microbiota dysbiosis and can lead to AFLD through various pathways, as shown in Figure 1[62]. Animal model-based studies explain that alcohol-induced microbial dysbiosis in the intestine changes homeostasis in the gut-liver axis and that this altered intestinal microbiota plays a crucial role as a mediator in the production of the many negative effects of alcohol.

Animal studies have shown that 3 weeks of alcohol exposure causes a 'leaky gut', which increases the number of *Bacteroidetes* and *Verrucomicrobia* and decreases the growth of bacteria with anti-inflammatory activity, such as *Firmicutes* (genera such as *Lactobacillus, Lactococcus, Leuconostoc* and *Pediococcus*), in the cecum[63]. Another rodent alcohol-based model showed that changes in intestinal permeability associated with intestinal microbial alterations are related to the decreased expression of hypoxia-induced factor 1α. These studies showed a relative increase in *Actinobacteria* and *Proteobacteria* and a decline in the *Firmicutes* phylum. Moreover, these changes were restored by treatment with probiotic *Lactobacillus rhamnosus* (*L. rhamnosus*) GG therapy[64-67].

Interestingly, gnotobiotic animals have become an imperative alcoholic model to explore the relationship between the gut and the liver. A comparative study of gnotobiotic and wild-type rats showed less proinflammatory cytokine release and inflammation in gnotobiotic rats than in wild-type rats when treated with alcohol for one week. Moreover, fecal transplantation from alcohol-fed wild-type rats in gnotobiotic animals increased hepatic and intestinal inflammation, indicating the involvement of the intestinal microbiota in AFLD[68]. Chronic alcohol intake also changes the intestinal mucus composition, and mucin knockout animals have less bacterial overgrowth, minimal translocation of the bacteria and reduced intestinal inflammation when administered alcohol[69]. In other studies, the bacterial species *Akkermansia muciniphila* (*A. muciniphila*) from the *Verrucomicrobia* phylum showed potential anti-inflammatory properties in AFLD[70], and the depletion of *A. muciniphila* species was noticed in alcoholic animal models[71,72]. *A. muciniphila* improves intestinal markers such as gut barrier function and mucus thickness and diminishes the liver damage produced by alcohol[73]. Cumulatively, animal studies strongly indicate that alcohol intake considerably changes the intestinal microbial composition (as shown in Table 1), which can be responsible for producing early-onset AFLD by inducing proinflammatory changes, translocating the bacteria and bacterial material by reducing mucus thickness and increasing intestinal permeability.

Likewise, human studies also support the close association between alcohol intake and intestinal microbial dysbiosis in the onset of AFLD, similar to animal models. Prolonged alcohol intake markedly decreases the *Bacteroidetes* population and increases *Proteobacteria*, which leads to compromised intestinal permeability and an increase in the level of bacterial materials such lipopolysaccharides (LPS) and endotoxins in the hepatic circulation and ultimately causes liver injuries[74]. The families *Ruminococcaceae* and *Lachnospiraceae* and their ratio are considered to be protective, whereas *Enterobacteriaceae* to *Bacteroidaceae* and their ratio are believed to be potential pathobionts in the intestine, especially in those with a liver disease with an alcoholic etiology. Therefore, the overgrowth of potentially pathogenic species in the gut in chronic alcohol abuse conditions is related to the initiation of liver injuries[74-76]. The effect of these microbial alterations in the gut is not yet completely understood. However, the administration of *L. rhamnosus* GG improves the *Lachnospiraceae* population and limits the growth of *Enterobacteriaceae,* which leads to a decline in proinflammatory cytokines[77]. A reduction in *A. muciniphila* was observed in patients with alcoholic steatohepatitis compared with healthy controls, and this decline in *A. muciniphila* seems to be related to the severity of liver injuries[73]. Additionally, *A. muciniphila* was considered a health-boosting bacterial species along with *Bifidobacterium* spp., *Roseburia hominis*, and *Feacalibacterium prausnitzii*[78]. However, human and animal empirical data hinted that alcohol-induced gut microbial dysbiosis, especially ethanol consumption, but that some alcoholic beverages, such as red wine, could exert a positive impact on gut microbial ecology. A human crossover study demonstrated that red wine consumption increased the number of *Bacteroides, Enterococcus*, and *Bifidobacterium*[79].

Alterations in the gut microbiota due to persistent alcoholic intake are not restricted to bacterial species; the fungal composition also changes. Remarkably, alcoholic liver disease (ALD) patients have a high risk of bacterial infection, and patients with advanced cirrhosis are more prone to fungal infections. Moreover, fungal infections increased the mortality rate in cirrhosis and alcoholic hepatitis patients[80-82]. In an alcoholic murine model, increased fungal growth, particularly *Candida* spp., was observed and was related to an increase in liver damage[83]. The study results showed that liver inflammation was induced by β-glucan, which is a fungal cell wall component. β-Glucan binds with Kupffer cell C-type lectin-like receptor and

Table 1 Representative studies presenting gut microbial dysbiosis in alcoholic fatty liver disease

Ref.	Sequencing method	Overgrown microbes	Depleted microbes	Model
Yan *et al*[63] (2011)	Pyrosequencing	↑*Bacteroidales*	↓*Lactococcus*	Murine
		↑*Bacteroides*	↓*Pediococcus*	
		↑*Porphyromonadaceae*	↓*Lactobacillus*	
			↓*Leuconostoc*	
Otterson *et al*[64] (2013)	Pyrosequencing	↑*Corynebacterium*	↓*Bacteroides*	Murine
		↑*Alcaligenes*	↓*Tannerella*	
		↑*Listeria*	↓*unclassified Lachnospiraceae*	
		↑*Acetivibrio*	↓*undefined Ruminococcaceae*	
		↑*Allobaculum*		
Lowe *et al*[71] (2017)	16S rDNA	↑*Actinobacteria*	↓*Tenericutes*	Murine
		↑*Eubacteriaceae*	↓*Verrucomicrobia*	
			↓*Lachnospiraceae*	
			↓*Moraxellaceae*	
			↓*Akkermansia*	
Grander *et al*[73] (2018)	Illumina MiSeq	↑*Olsenella*	↓*Acinetobacter*	Murine
		↑*Eubacterium*	↓*Anaerotruncus*	
		↑*Acetivibrio*	↓*Akkermansia*	
			↓*Blautia*	
Kakiyama *et al*[74] (2013)	Pyrosequencing	↑*Enterobacteriaceae*	↓*Blautia*	Human
		↑*Veillonellaceae*	↓*Ruminococcaceae*	
			↓*Lachnospiraceae*	
			↓*Rikenellaceae*	
Bajaj *et al*[75] (2014)	Pyrosequencing	↑*Enterococcaeae*	↓*Clostridiales XIV*	Human
		↑*Staphylococcaceae*	↓*Ruminococcaceae*	
		↑*Enterobacteriaceae*	↓*Lachnospiraceae*	
Yang *et al*[83] (2017)	Illumina MiSeq	↑*Candida* spp.	↓*Epicoccum*	Human
		↑*Candida albicans*	↓*Unclassified fungi*	
		↑*Candida dubliniensis*	↓*Galactomyces*	
			↓*Debaryomyces*	
Ferrere *et al*[144] (2017)	Illumina MiSeq	↑*Actinobacteria*	↓*Bacteroidetes*	Murine
		↑*Firmicutes*	↓*Proteobacteria*	
		↑*Coriobacteriaceae*		
		↑*Odoribacteriacea*		
		↑*Clostridiaceae*		
		↑*Dorea*		
Wang *et al*[145] (2019)	Illumina MiSeq	↑*Verrucomicrobia*	↓*Bacteroidetes*	Monkey
		↑*Proteobacteria*	↓*Cytophagales*	
		↑*Optitutus*	↓*Flavobacteriales*	
		↑*Botrytis*	↓*Sphingobacteriales*	
		↑*Sporothrix*	↓*Lactobacillales*	
			↓*Nitrosomonadales*	

			↓*Opitutales*	
			↓*Helotiales*	
			↓*Ophiostomatales*	
Zhong *et al*[146] (2021)	Illumina MiSeq	↑*Proteobacteria*	↓*Ruminococcaceae*	Human
		↑*Fusobacteria*	↓*Faecalibacterium*	
		↑*Fusobacteriaceae*	↓*Lachnospira*	
		↑*Enterobacteriaceae*	↓*Agathobacter*	
		↑*Burkholderiaceae*	↓*Ruminococcus*	
		↑*Fusobacterium*		
		↑*Escherichia-Shigella*		

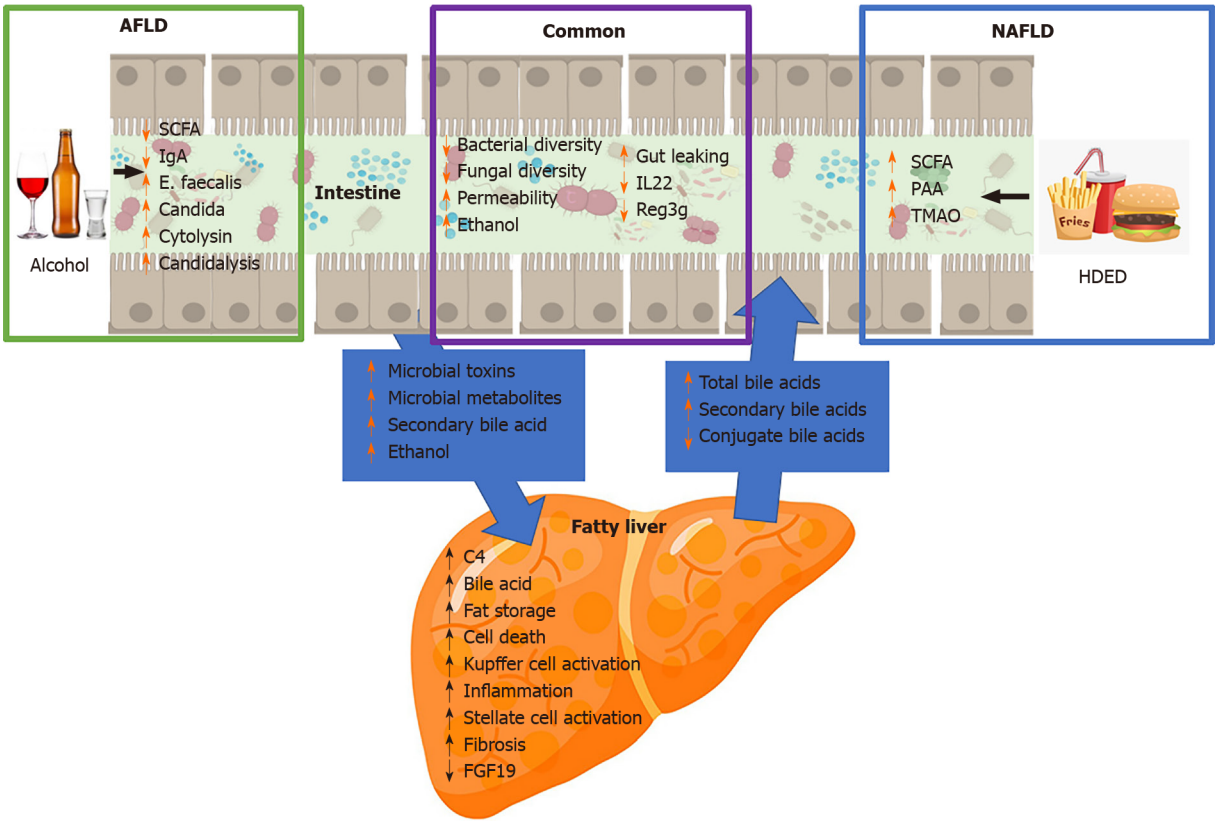


Figure 1 Gut microbiota role in alcoholic fatty liver disease and non-alcoholic fatty liver disease pathogenesis. Intestinal microbes have the potential relationship with fatty liver disease progression. Regular intake of alcohol and overnutrition altered the gut microbial composition which influence the various pathways and induce the liver injuries and produce the alcoholic fatty liver disease (AFLD) and non-alcoholic fatty liver disease (NAFLD). There are some common pathways found in both AFLD and NAFLD diseases (in the purple box) and others are specifically related to a particular disease. AFLD: Alcoholic fatty liver disease; NAFLD: Non-alcoholic fatty liver disease; HDED: High dense energy diet; SCFA: Short chain fatty acids; IgA: Immunoglobulin A; IL22: Interleukin 22; Reg3g: Regenerating islet-derived protein 3 gamma; C4: Precursor 7α-hydroxy-4-cholesten-3-one; FGF19: Fibroblast growth factor 19; PAA: Phenylacetic acid; TMAO: Trimethylamine N-oxide.

upregulates IL-1β. Similarly, ALD patients also showed an increased immune response to intestinal fungi compared to healthy controls. These findings suggest that the composition of nonbacterial gut microbes, such fungi, can also affect AFLD generation, progression, and final outcomes in patients with AFLD.

Gut microbiota alterations in NAFLD

The gut microbiota exacerbates and/or alleviates NAFLD conditions through several pathways (Figure 1). Animal and human studies have presented a causal involvement of the gut microbiota in NAFLD establishment[84-86] and its severity[87-89]; however, a robust correlation between the gut microbiota and NAFLD advancement has not yet been established. Differences in gut microbial composition at various hierarchical

levels have been recorded in NAFLD patients compared with healthy controls[90,91]. In NAFLD, alterations in the gut microbial community have been shown to start at the phylum level, where increased Proteobacteria have been reported in many studies[90,92,93]. Likewise, altered composition has also been observed at the family level, where an overgrowth of *Enterobacteriaceae*[84,92] and suppression of *Rikenellaceae*[84,94] and *Ruminococcaceae*[91,92,95] have been reported. Moreover, genera such as *Escherichia*[84,90], *Dorea*[94,95], and *Peptoniphilus*[84,94] were overpopulated, and *Anaerosporobacter* [91], *Coprococcus*[84,90,91], *Eubacterium*[84,90], *Faecalibacterium*[84] and *Prevotella*[90,96] were less populated.

In a comparative study, Wang *et al*[91] showed a higher proportion of gram-negative bacteria, including *Bacteroidetes*, and decreased *Firmicutes* in NAFLD patients when the gut microbiota was compared with lean healthy subjects. The decline in *Firmicutes* is associated with short-chain fatty acid (SCFA)-producing bacteria such as *Lactobacillaceae*, *Lachnospiraceae*, and *Ruminococcaceae*. An overgrowth of gram-negative bacterial species was seen in children with NAFLD, with an increased ratio of Gammaproteobacteria and Epsilonproteobacteria compared to their obese and lean counterparts[97]. In contrast, bacteria from the *Firmicutes* phylum (such as *Lactobacillus*, *Roseburia, Dorea*, and *Robinsoniella*) were found to be increased in the population of NAFLD patients in another study[95]. However, contradictory results were reported in other studies that showed increases in *Dorea* and *Ruminococcus* in NAFLD patients[94,98]. Variability in gut microbial composition was observed with different levels of NAFLD severity. Bacteria belonging to *Firmicutes* were more dominant in moderate NAFLD, while the prevalence of *Proteobacteria* was noted to be associated with the severity of disease, as in fibrosis[93]. The bacterial species that were dominant in mild NAFLD compared to severe NAFLD conditions were *Eubacterium rectale* and *Ruminococcus obeum*[93]. These human study results reflect the conflicting gut microbiota composition in NAFLD, which needs to be evaluated further by implementing a greater number of NAFLD patient-based gut microbial compositional studies.

The gut microbial composition was also assessed in severe NAFLD conditions such as fibrosis and/or in nonalcoholic steatohepatitis (NASH) to examine the functional role of gut microbial dysbiosis in fibrosis progression. The results of these comparative studies exhibited a decline in gram-negative bacterial abundance. Comparative analysis of the gut microbiota between individuals with severe NAFLD and healthy or less severe NAFLD conditions showed a decrease in the *Fusobacteria* phylum population and an increase in *Enterobacteriaceae* family bacteria such as the genera *Shigella*, *Ruminococcin* and *Bacteroides*[92,96]. Similarly, gram-positive bacteria from the *Firmicutes* phylum, the family *Prevotellaceae* and the genus *Prevotella* also showed increases in severe NAFLD conditions[93]. Recently, a study presented a significant alteration based on fibrosis severity in nonobese patients but not in obese patients, where *Ruminococcaceae* and *Veillonellaceae* were the leading microbes related to fibrosis severity in nonobese subjects[99]. Interestingly, oral microbes, including *Streptococcus* [76,100,101], *Veillonella*[91,100], and *Prevotella*[100,102], are discriminatory microbes for advanced NAFLD conditions (especially cirrhosis). Additionally, some microbe representations were constant in NAFLD patients compared with healthy individuals, but some showed conflicting tendencies[103]. Conclusively, microbial composition in NAFLD patients presented a drastic shift in taxonomic group composition by showing an increased ratio of pathogenic microbes and a decline in microbes that are considered metabolically beneficial microbes. Subsequently, this compositional shift in microbial composition might be responsible for NAFLD pathogenesis and exacerbate the severity of the disease from simple steatosis to NASH and from NASH to cirrhosis. Summarized information on gut microbial dysbiosis in NAFLD is listed in Table 2, which provides details regarding the increased and decreased populations of bacteria in NAFLD.

The gut microbiota composition in NAFLD presented a considerable contradiction, where some microbial taxa showed variability in their occurrence, as shown in Table 2. The underlying reasoning behind these contradictory compositional variabilities might be related to study design, clinical study end points, result interpretation, *etc*. Moreover, these underlying reasons could be fundamental restraints in the process of establishing a robust relationship between the gut and NAFLD. Thus, to determine the pathophysiological association between the gut and liver, these fundamental limitations should be resolved.

Table 2 Representative studies presenting gut microbial dysbiosis in non-alcoholic fatty liver disease

Ref.	Sequencing method	Overgrown microbes	Depleted microbes	Model
Michail *et al*[97] (2015)	Ion torrent	↑*Actinobacteria*	↓*Erysipelotrichia*	Human
		↑*Prevotella*	↓*Alphaproteobacteria*	
		↑*Clostridia*	↓*Verrucomicrobia*	
		↑*Fusobacteria*		
		↑*Epsilonproteobacteria*		
		↑*Gammaproteobacteria*		
Wang *et al*[91] (2016)	Pyrosequencing	↑*Bacteroidaceae*	↓*Lachnospiraceae*	Human
		↑*Prevotellaceae*	↓*Ruminococcaceae*	
			↓*Lactobacillaceae*	
Raman *et al*[95] (2013)	Pyrosequencing	↑*Alphaproteobacteria*	↓*Ruminococcaceae*	Human
		↑*Lactobacillaceae*	↓*Oscillibacter*	
		↑*Lachnospiraceae*	↓*Porphyromonadaceae*	
		↑*Veillonellaceae*		
Chierico *et al*[94] (2017)	Pyrosequencing	↑*Actinobacteria*	↓*Bacteroidetes*	Human
		↑*Bradyrhizobium*	↓*Oscillospira*	
		↑*Anaerococcus*	↓*Rikenellaceae*	
		↑*Peptoniphilus*		
		↑*Propionibacterium acnes*		
		↑*Dorea*		
		↑*Ruminococcus*		
Hoyles *et al*[90] (2018)	Shotgun	↑*Proteobacteria*	↓*Firmicutes*	Human
		↑*Actinobacteria*	↓*Euryarchaeota*	
		↑*Verrucomicrobia*		
Shen *et al*[92] (2017)	16S rDNA	↑*Proteobacteria*	↓*Bacteroidetes*	Human
		↑*Fusobacteria*	↓*Prevotellaceae*	
		↑*Lachnospiraceae*	↓*Ruminococcaceae*	
		↑*Enterobacteriaceae*	↓*Prevotella*	
		↑*Erysipelotrichaceae*		
		↑*Streptococcaceae*		
		↑*Escherichia Shigella*		
Zhu *et al*[84] (2013)	Pyrosequencing	↑*Bacteroidetes*	↓*Actinobacteria*	Human
		↑*Proteobacteria*	↓*Bifidobacteriaceae*	
		↑*Alcaligenaceae*	↓*Clostridiales family XI*	
		↑*Campylobacteraceae*	↓*Lachnospiraceae*	
		↑*Enterobacteriaceae*		
Chierico *et al*[94] (2017)	Pyrosequencing	↑*Coriobacteriaceae*	↓*Porphyromonadaceae*	Human
		↑*Bacteroidaceae*	↓*Rikenellaceae*	
Minicis *et al*[147] (2014)	Pyrosequencing	↑*Firmicutes*	↓*Bacteroidetes*	Murine
		↑*Actinobacteria*		
Lee *et al*[148] (2020)	16S rDNA	↑*Firmicutes*	↓*Bacteroidetes*	Murine
		↑*Deferribacters*	↓*Lactobacillus murinus*	

	↑*Helicobacter japonicus*
	↑*Mucispirillum schaedleri*
	↑*Flintibacter butyricus*

GUT ROLE IN FATTY LIVER

Trillions of microorganisms reside in the gut, including bacteria, archaea, fungi, and viruses, but liver-disease-related research primarily targets the bacterial community, which includes more than 10 bacterial phyla[104,105]. The gut microbiota includes more than 3 million genes collectively, in comparison to the 23000 genes of the human genome; however, human cells and gut bacterial cells are roughly equal in number [106]. This gut microbial genetic material certainly has a defining role in human pathophysiology through multiple mechanisms, especially in liver disease, due to its close relationship with the gut[6,107,108].

Gut microbial dysbiosis

Generally, the gut microbiota starts to be shaped at birth and becomes stable in early childhood. This balanced and stable gut microbiota acquires a unique quotient for each microbial species in a healthy state[38]. As discussed above, gut microbial dysbiosis, defined by diminished microbial diversity and distorted gut microbial composition, is observed in both AFLD and NAFLD patients compared to healthy controls[18,103]. Alcohol abuse and overnutrition deplete several bacterial species and shift the microbial composition toward gram-negative bacteria. Microbial species depleted in liver diseases are considered beneficial microbes, and overgrown microbial species are associated with liver pathophysiology and known as pathobionts[109]. Alcohol consumption is linked with diminished fungal diversity generated by an increased number of *Candida* species[83,110,111]. Moreover, gut viruses are the most abundant gut microbes; nonetheless, they have not yet been characterized in liver disease.

This gut compositional proclivity toward gram-negative bacterial species influences multiple pathways directly or indirectly that contribute to AFLD and NAFLD establishment[16,91,92]. The distorted gut microbiota alters various metabolic processes, such as bile acids, short-chain fatty acids, and energy harvesting, which leads to the initiation of fatty liver disease[112]. The distorted gut microbiota also damages gut barrier function, through which microbes and their metabolites can translocate and activate the inflammasome in the liver and cause fatty liver[112]. The detailed role of the gut microbiota in fatty liver pathogenesis is presented in Figure 1.

Leaky gut syndrome

In the intestine, there are multiple layers of barriers, including physical, biochemical, and immunological barriers, that restrict the translocation of microbes and their products. Chronic alcohol abuse causes gut barrier dysfunction by altering the gut microbial composition[113]. Thus, pathogen-associated molecular patterns, such as LPS, are able to translocate from the lumen of the intestine to the liver *via* the portal vein and are recognized by inflammasomes such as Toll-like receptors in the liver to stimulate hepatic inflammation, which leads to hepatocyte injuries and liver fibrosis [112]. Likewise, similar pathophysiological pathways are involved in NAFLD progression, but gut disruption and inflammation are stimulated by dietary factors other than alcohol[112]. Other types of inflammasomes, including NOD-like receptor protein 3 (NLRP3), also respond to LPS and cause liver inflammation. The activation of NLRP3 triggers the caspase 1 pathway and produces interleukin-1β and several other inflammatory cytokines, which cause apoptosis and fibrosis. Higher levels of inflammasomes such NLRP3 and others were found in severe fatty liver conditions induced by both alcohol and overnutrition[114,115]. The translocation of the microbial metabolites from the intestine to the liver because of the dysfunction of intestinal barriers and increased intestinal permeability could be the contributing factor for AFLD and NAFLD, but more studies are required to establish robust associations.

Bile acid dysregulation

Bile acid synthesis and secretion are essential functions performed by liver cells. Importantly, bile acids not only are crucial for dietary fat emulsification but also act as ligands for nuclear and G-protein coupled receptors and regulate various metabolic functions, including glucose and fat metabolism[116]. Therefore, smooth regulation of bile acids is important for maintaining a healthy metabolic profile, but gut microbial

dysbiosis is associated with bile acid dysregulation and is associated with fatty liver pathogenesis through metabolites[117].

Normally, conjugated bile acids are released from hepatocytes, carried by the biliary duct, and secreted into the intestine. After lipid emulsification, the remaining bile acids (primary, hydrophilic, and conjugated) are reabsorbed in the terminal ileum. Bile acid secretion from hepatocytes is primarily regulated by the farnesoid X receptor (FXR) negative feedback mechanism[118]. The release of primary bile acids in the intestine activates intestinal FXR, which precedes the transcription of fibroblast growth factor 19 (FGF19). The ileal hormone FGF19 is carried to the liver *via* the portal vein, where FGF19 suppresses CYP7A1 expression and controls bile acid secretion[119]. The disruption of bile acid homeostasis is the leading cause of fatty liver[119-121].

The change in the gut microbial composition induced by alcohol abuse and a high intake of energy-dense food cause the dysregulation of the bile acid system and instigate fatty liver diseases (AFLD and NAFLD)[122,123]. In AFLD and NAFLD, pathobionts increased in number and were responsible for the conversion of secondary bile acids from primary bile acids and reduced FXR signaling. This downregulation of FXR expression increased insulin resistance and altered glucose and lipid metabolism, which are the key regulatory pathways in AFLD and NAFLD generation. Moreover, AFLD and NAFLD patients showed higher levels of secondary bile acids than primary bile acids in feces and blood. Similarly, the dysregulation of FXR signaling and FGF19 is increased with the severity of the disease in both AFLD and NAFLD[124-127]. These outcomes suggest that FXR and bile acid compositional dysregulation are the metabolic features of AFLD and NAFLD and that the dysregulation of both metabolic factors (FXR and bile acids) increases with the severity of AFLD and NAFLD.

Although gut bacteria control bile acid metabolism, the involvement of intestinal bacteria or other gut microbes (including archaea, fungi, and viruses) in bile acid dysregulation in fatty liver patients is not completely understood, and more experimental evidence is required to fill the fundamental gaps.

Short-chain fatty acid dysregulation

Nondigestible carbohydrates in food are fermented by gut bacteria, and SCFAs are produced. Butyrate, acetate, and propionate are the most abundant SCFAs found in the intestine. SCFAs have many beneficial effects, including being used as an energy source by colonocytes and enterocytes, maintaining gut barrier function, suppressing hepatic cell proliferation, reducing inflammation, and lowering food intake by increasing satiety[128]. Considering the beneficial function of SCFAs in regulating metabolic pathways, their level in the body is crucial to maintain good health.

Chronic alcohol abuse is related to reduced SCFA levels in the stool[129]. The SCFA concentration and SCFA-producing bacterial concentration are decreased in the feces of alcoholic hepatitis patients[109]. The low circulatory butyrate level is also associated with serum endotoxin, inflammation, and more advanced liver diseases[130]. In contrast, a higher level of SCFAs and an increased number of SCFA-producing bacteria were found in NASH patients; however, the study population was small[131]. Additionally, increasing levels of SCFAs are related to immune regulation and NAFLD progression[131]. Higher fecal concentrations of propionate and butyrate were observed in mild to severe NAFLD patients, whereas higher fecal concentrations of acetate and formate were found in advanced fibrosis patients[132,133]. There is an insufficient amount of empirical proof to establish a concrete relationship between SCFAs and fatty liver diseases, and more studies are required to determine the association between SCFAs and fatty liver diseases.

Endogenous ethanol production

Microbial fermentation of dietary sugar increases the endogenous alcohol level in pediatric NASH patients[84]. Recently, a *Klebsiella pneumonia* strain was identified in a NASH patient fecal sample and was responsible for producing endogenous ethanol and increasing the blood ethanol level without alcohol consumption[134]. FMT from NASH patients to animals results in liver damage, and the elimination of alcohol-producing *Klebsiella pneumoniae* strains reduces liver damage. Additionally, NASH patient weight reduction was also related to a reduced ability to produce ethanol in the gut microbiome[134]. Another study focusing on comparing the gut microbial profile in pediatric NAFLD patients showed higher circulatory ethanol levels in diseased patients, which was related to the higher number of *Prevotella* and Gammaproteobacteria[97]. The results from another study showed that a higher circulatory level of ethanol in NAFLD patients could be the end result of ethanol dehydrogenase activity in insulin-dependent impairment conditions[135]. Thus, gut

microbial dysbiosis, which can lead to an increasing level of endogenous ethanol in the body, could be an underlying cause of NAFLD and could be responsible for producing the same histopathological characteristics as AFLD. However, some inconsistencies in the results were observed, and establishing an association between this endogenous ethanol phenomenon and NAFLD generation needs more experimental proof[16,136,137].

Gut microbial virulence factors

Virulence factors are microbial proteins and peptides that help pathobionts colonize and are associated with disease generation. A recent study recognized that cytolysin, a protein secreted (exotoxin) by *E. faecalis*, damages hepatocytes and is highly associated with increased mortality in alcoholic hepatitis patients[18,138]. Unfortunately, few studies have shown any further toxins or other proteins related to gut microbiota that can be associated with liver disease.

FUTURE PERSPECTIVES

Fatty liver disease (both AFLD and NAFLD) is intricately linked with the gut microbiota and its dysbiosis. Recent advancements in gut microbiome-based metagenomics studies related to liver disease have shown that an increase in and/or depletion of the specific microbial content could contribute greatly to liver injuries and is possibly the key regulator in fatty liver disease establishment and progression[112]. Growing evidence regarding the role of the gut microbiota in fatty liver disease generation and progression turns this noncommunicable disease into a communicable disease[139]. Therefore, targeting the gut microbiota through various techniques may be an approach for the management of liver disease in the future.

Prognostic and/or diagnostic biomarkers

As discussed above, the microbial composition in fatty liver diseases is different from that in healthy individuals. Gut microbes themselves or their microbial metabolites might be useful as prognostic and/or diagnostic tools for the early detection of fatty liver conditions. Generally, constant alcohol intake of more than 60 g per day leads to alcoholic hepatic steatosis, which also presents with higher levels of liver enzymes, such aspartate aminotransferase (AST) and alanine aminotransferase (ALT), and in NAFLD, daily alcohol intake is approximately 30 g per day. Typically, two to three times higher serum AST levels have been observed compared to serum ALT due to alcoholic liver injuries. Patients with AFLD also have higher serum gamma-glutamyl-transpeptidase levels[140]. Similarly, NAFLD also has noninvasive biomarker detection protocols, such as the NAFLD fibrosis score (including age, BMI, the AST-to-ALT ratio, impaired fasting glucose and diabetes, albumin and platelets), FIB-4 index (including age, ALT, AST, and platelets), and FibroTest (including total bilirubin, α2-macroglobulin, γ-glutamyl transferase, haptoglobin, and apolipoprotein A1 corrected for sex and age)[141]. These are the common diagnostic parameters used for AFLD and NAFLD diagnosis. However, there is a lack of conclusive biomarkers that can help in the early diagnosis of hepatic steatosis, and the repertoire of gut microbes and their metabolite profiles might help to fill this gap. Interestingly, a set of gut bacteria combined with age and BMI was used to identify liver disease, and a much more accurate diagnosis was able to be made with its use in patients with advanced fibrosis [93]. The gut microbes used as a marker in this study were first identified from NAFLD and advanced fibrosis patients *via* metagenomics analysis and then further used for diagnostic purposes[93]. In a separate study, the combination of metagenomic signature microbes with age and serum albumin levels precisely identified cirrhosis in patients with geographically different origins. Additionally, adding serum aspartate aminotransferase levels to these diagnostic tools increased diagnostic efficacy even in the early stage of fibrosis[142]. In other studies, gut-microbe-derived metabolites showed great potential as diagnostic markers for fatty liver diseases and other liver conditions[18,90,143].

Although gut microbes and their metabolites have the potential to be noninvasive prognostic and/or diagnostic tools for fatty liver and other liver diseases, larger population-based studies are still required to eliminate constraints related to geographical factors, ethnicity, and dietary factors. Further studies are also warranted to compare the diagnostic ability of gut microbes and their metabolites with contemporary in-use investigative practices such as biopsy and image-based approaches.

CONCLUSION

Gut microbiota is crucial in fatty liver diseases (in both AFLD and NAFLD), thus relevance of fatty liver disease specific gut microbial signatures should be further explored in longitudinal human studies. Where, a team of clinician and researchers can prospectively correlate the deterioration of liver with the alteration in the gut microbiota community. Merging fatty liver disease specific gut microbiota with microbial derived metabolites can be helpful in the future to diagnose and treat the AFLD and NAFLD patients.

REFERENCES

1 **Xiao J**, Wang F, Wong NK, He J, Zhang R, Sun R, Xu Y, Liu Y, Li W, Koike K, He W, You H, Miao Y, Liu X, Meng M, Gao B, Wang H, Li C. Global liver disease burdens and research trends: Analysis from a Chinese perspective. *J Hepatol* 2019; **71**: 212-221 [PMID: 30871980 DOI: 10.1016/j.jhep.2019.03.004]

2 **Wong RJ**, Aguilar M, Cheung R, Perumpail RB, Harrison SA, Younossi ZM, Ahmed A. Nonalcoholic steatohepatitis is the second leading etiology of liver disease among adults awaiting liver transplantation in the United States. *Gastroenterology* 2015; **148**: 547-555 [PMID: 25461851 DOI: 10.1053/j.gastro.2014.11.039]

3 **Lee BP**, Vittinghoff E, Dodge JL, Cullaro G, Terrault NA. National Trends and Long-term Outcomes of Liver Transplant for Alcohol-Associated Liver Disease in the United States. *JAMA Intern Med* 2019; **179**: 340-348 [PMID: 30667468 DOI: 10.1001/jamainternmed.2018.6536]

4 **Parker R**, Aithal GP, Becker U, Gleeson D, Masson S, Wyatt JI, Rowe IA; WALDO study group. Natural history of histologically proven alcohol-related liver disease: A systematic review. *J Hepatol* 2019; **71**: 586-593 [PMID: 31173814 DOI: 10.1016/j.jhep.2019.05.020]

5 **Loomba R**, Adams LA. The 20% Rule of NASH Progression: The Natural History of Advanced Fibrosis and Cirrhosis Caused by NASH. *Hepatology* 2019; **70**: 1885-1888 [PMID: 31520407 DOI: 10.1002/hep.30946]

6 **Acharya C**, Bajaj JS. Chronic Liver Diseases and the Microbiome-Translating Our Knowledge of Gut Microbiota to Management of Chronic Liver Disease. *Gastroenterology* 2021; **160**: 556-572 [PMID: 33253686 DOI: 10.1053/j.gastro.2020.10.056]

7 **Reuter B**, Bajaj JS. Microbiome: Emerging Concepts in Patients with Chronic Liver Disease. *Clin Liver Dis* 2020; **24**: 493-520 [PMID: 32620285 DOI: 10.1016/j.cld.2020.04.006]

8 **Jiang W**, Wu N, Wang X, Chi Y, Zhang Y, Qiu X, Hu Y, Li J, Liu Y. Dysbiosis gut microbiota associated with inflammation and impaired mucosal immune function in intestine of humans with non-alcoholic fatty liver disease. *Sci Rep* 2015; **5**: 8096 [PMID: 25644696 DOI: 10.1038/srep08096]

9 **Cui X**, Ye L, Li J, Jin L, Wang W, Li S, Bao M, Wu S, Li L, Geng B, Zhou X, Zhang J, Cai J. Metagenomic and metabolomic analyses unveil dysbiosis of gut microbiota in chronic heart failure patients. *Sci Rep* 2018; **8**: 635 [PMID: 29330424 DOI: 10.1038/s41598-017-18756-2]

10 **Kundu P**, Blacher E, Elinav E, Pettersson S. Our Gut Microbiome: The Evolving Inner Self. *Cell* 2017; **171**: 1481-1493 [PMID: 29245010 DOI: 10.1016/j.cell.2017.11.024]

11 **Lindheim L**, Bashir M, Münzker J, Trummer C, Zachhuber V, Leber B, Horvath A, Pieber TR, Gorkiewicz G, Stadlbauer V, Obermayer-Pietsch B. Alterations in Gut Microbiome Composition and Barrier Function Are Associated with Reproductive and Metabolic Defects in Women with Polycystic Ovary Syndrome (PCOS): A Pilot Study. *PLoS One* 2017; **12**: e0168390 [PMID: 28045919 DOI: 10.1371/journal.pone.0168390]

12 **Prakash S**, Tomaro-Duchesneau C, Saha S, Cantor A. The gut microbiota and human health with an emphasis on the use of microencapsulated bacterial cells. *J Biomed Biotechnol* 2011; **2011**: 981214 [PMID: 21772792 DOI: 10.1155/2011/981214]

13 **Lynch SV**, Pedersen O. The Human Intestinal Microbiome in Health and Disease. *N Engl J Med* 2016; **375**: 2369-2379 [PMID: 27974040 DOI: 10.1056/NEJMra1600266]

14 **Fouhy F**, Ross RP, Fitzgerald GF, Stanton C, Cotter PD. Composition of the early intestinal microbiota: knowledge, knowledge gaps and the use of high-throughput sequencing to address these gaps. *Gut Microbes* 2012; **3**: 203-220 [PMID: 22572829 DOI: 10.4161/gmic.20169]

15 **Mazagova M**, Wang L, Anfora AT, Wissmueller M, Lesley SA, Miyamoto Y, Eckmann L, Dhungana S, Pathmasiri W, Sumner S, Westwater C, Brenner DA, Schnabl B. Commensal microbiota is hepatoprotective and prevents liver fibrosis in mice. *FASEB J* 2015; **29**: 1043-1055 [PMID: 25466902 DOI: 10.1096/fj.14-259515]

16 **Lang S**, Schnabl B. Microbiota and Fatty Liver Disease-the Known, the Unknown, and the Future. *Cell Host Microbe* 2020; **28**: 233-244 [PMID: 32791115 DOI: 10.1016/j.chom.2020.07.007]

17 **Bajaj JS**, Hylemon PB. Gut-liver axis alterations in alcoholic liver disease: Are bile acids the answer? *Hepatology* 2018; **67**: 2074-2075 [PMID: 29272041 DOI: 10.1002/hep.29760]

18 **Duan Y**, Llorente C, Lang S, Brandl K, Chu H, Jiang L, White RC, Clarke TH, Nguyen K, Torralba M, Shao Y, Liu J, Hernandez-Morales A, Lessor L, Rahman IR, Miyamoto Y, Ly M, Gao B, Sun W, Kiesel R, Hutmacher F, Lee S, Ventura-Cots M, Bosques-Padilla F, Verna EC, Abraldes JG, Brown

RS Jr, Vargas V, Altamirano J, Caballería J, Shawcross DL, Ho SB, Louvet A, Lucey MR, Mathurin P, Garcia-Tsao G, Bataller R, Tu XM, Eckmann L, van der Donk WA, Young R, Lawley TD, Stärkel P, Pride D, Fouts DE, Schnabl B. Bacteriophage targeting of gut bacterium attenuates alcoholic liver disease. *Nature* 2019; **575**: 505-511 [PMID: 31723265 DOI: 10.1038/s41586-019-1742-x]

19 **Llopis M**, Cassard AM, Wrzosek L, Boschat L, Bruneau A, Ferrere G, Puchois V, Martin JC, Lepage P, Le Roy T, Lefèvre L, Langelier B, Cailleux F, González-Castro AM, Rabot S, Gaudin F, Agostini H, Prévot S, Berrebi D, Ciocan D, Jousse C, Naveau S, Gérard P, Perlemuter G. Intestinal microbiota contributes to individual susceptibility to alcoholic liver disease. *Gut* 2016; **65**: 830-839 [PMID: 26642859 DOI: 10.1136/gutjnl-2015-310585]

20 **Tilg H**, Cani PD, Mayer EA. Gut microbiome and liver diseases. *Gut* 2016; **65**: 2035-2044 [PMID: 27802157 DOI: 10.1136/gutjnl-2016-312729]

21 **Di Ciaula A**, Garruti G, Lunardi Baccetto R, Molina-Molina E, Bonfrate L, Wang DQ, Portincasa P. Bile Acid Physiology. *Ann Hepatol* 2017; **16**: s4-s14 [PMID: 29080336 DOI: 10.5604/01.3001.0010.5493]

22 **Duca FA**, Lam TKT. Bye, bye, bile: how altered bile acid composition changes small intestinal lipid sensing. *Gut* 2020; **69**: 1549-1550 [PMID: 32303610 DOI: 10.1136/gutjnl-2020-320873]

23 **Le Roy CI**, Bowyer RCE, Castillo-Fernandez JE, Pallister T, Menni C, Steves CJ, Berry SE, Spector TD, Bell JT. Dissecting the role of the gut microbiota and diet on visceral fat mass accumulation. *Sci Rep* 2019; **9**: 9758 [PMID: 31278309 DOI: 10.1038/s41598-019-46193-w]

24 **Boulangé CL**, Neves AL, Chilloux J, Nicholson JK, Dumas ME. Impact of the gut microbiota on inflammation, obesity, and metabolic disease. *Genome Med* 2016; **8**: 42 [PMID: 27098727 DOI: 10.1186/s13073-016-0303-2]

25 **Cohen JC**, Horton JD, Hobbs HH. Human fatty liver disease: old questions and new insights. *Science* 2011; **332**: 1519-1523 [PMID: 21700865 DOI: 10.1126/science.1204265]

26 **Jiang L**, Schnabl B. Gut Microbiota in Liver Disease: What Do We Know and What Do We Not Know? *Physiology (Bethesda)* 2020; **35**: 261-274 [PMID: 32490750 DOI: 10.1152/physiol.00005.2020]

27 **Koutnikova H**, Genser B, Monteiro-Sepulveda M, Faurie JM, Rizkalla S, Schrezenmeir J, Clément K. Impact of bacterial probiotics on obesity, diabetes and non-alcoholic fatty liver disease related variables: a systematic review and meta-analysis of randomised controlled trials. *BMJ Open* 2019; **9**: e017995 [PMID: 30928918 DOI: 10.1136/bmjopen-2017-017995]

28 **Sáez-Lara MJ**, Robles-Sanchez C, Ruiz-Ojeda FJ, Plaza-Diaz J, Gil A. Effects of Probiotics and Synbiotics on Obesity, Insulin Resistance Syndrome, Type 2 Diabetes and Non-Alcoholic Fatty Liver Disease: A Review of Human Clinical Trials. *Int J Mol Sci* 2016; **17** [PMID: 27304953 DOI: 10.3390/ijms17060928]

29 **Sharpton SR**, Schnabl B, Knight R, Loomba R. Current Concepts, Opportunities, and Challenges of Gut Microbiome-Based Personalized Medicine in Nonalcoholic Fatty Liver Disease. *Cell Metab* 2021; **33**: 21-32 [PMID: 33296678 DOI: 10.1016/j.cmet.2020.11.010]

30 **Acharya C**, Bajaj JS. Transmitting Diet-Related Microbial Benefit through Fecal Microbiota Transplant in NASH: Can Microbiota Cut Through the Fat? *Hepatol Commun* 2020; **4**: 1559-1561 [PMID: 33163828 DOI: 10.1002/hep4.1596]

31 **Brestoff JR**, Artis D. Commensal bacteria at the interface of host metabolism and the immune system. *Nat Immunol* 2013; **14**: 676-684 [PMID: 23778795 DOI: 10.1038/ni.2640]

32 **Yatsunenko T**, Rey FE, Manary MJ, Trehan I, Dominguez-Bello MG, Contreras M, Magris M, Hidalgo G, Baldassano RN, Anokhin AP, Heath AC, Warner B, Reeder J, Kuczynski J, Caporaso JG, Lozupone CA, Lauber C, Clemente JC, Knights D, Knight R, Gordon JI. Human gut microbiome viewed across age and geography. *Nature* 2012; **486**: 222-227 [PMID: 22699611 DOI: 10.1038/nature11053]

33 **Bokulich NA**, Chung J, Battaglia T, Henderson N, Jay M, Li H, D Lieber A, Wu F, Perez-Perez GI, Chen Y, Schweizer W, Zheng X, Contreras M, Dominguez-Bello MG, Blaser MJ. Antibiotics, birth mode, and diet shape microbiome maturation during early life. *Sci Transl Med* 2016; **8**: 343ra82 [PMID: 27306664 DOI: 10.1126/scitranslmed.aad7121]

34 **Dominguez-Bello MG**, Costello EK, Contreras M, Magris M, Hidalgo G, Fierer N, Knight R. Delivery mode shapes the acquisition and structure of the initial microbiota across multiple body habitats in newborns. *Proc Natl Acad Sci U S A* 2010; **107**: 11971-11975 [PMID: 20566857 DOI: 10.1073/pnas.1002601107]

35 **Bäckhed F**, Roswall J, Peng Y, Feng Q, Jia H, Kovatcheva-Datchary P, Li Y, Xia Y, Xie H, Zhong H, Khan MT, Zhang J, Li J, Xiao L, Al-Aama J, Zhang D, Lee YS, Kotowska D, Colding C, Tremaroli V, Yin Y, Bergman S, Xu X, Madsen L, Kristiansen K, Dahlgren J, Wang J. Dynamics and Stabilization of the Human Gut Microbiome during the First Year of Life. *Cell Host Microbe* 2015; **17**: 852 [PMID: 26308884 DOI: 10.1016/j.chom.2015.05.012]

36 **Hill CJ**, Lynch DB, Murphy K, Ulaszewska M, Jeffery IB, O'Shea CA, Watkins C, Dempsey E, Mattivi F, Tuohy K, Ross RP, Ryan CA, O' Toole PW, Stanton C. Evolution of gut microbiota composition from birth to 24 weeks in the INFANTMET Cohort. *Microbiome* 2017; **5**: 4 [PMID: 28095889 DOI: 10.1186/s40168-016-0213-y]

37 **Tsuji H**, Oozeer R, Matsuda K, Matsuki T, Ohta T, Nomoto K, Tanaka R, Kawashima M, Kawashima K, Nagata S, Yamashiro Y. Molecular monitoring of the development of intestinal microbiota in Japanese infants. *Benef Microbes* 2012; **3**: 113-125 [PMID: 22683836 DOI:

10.3920/BM2011.0038]
38 **Cheng J**, Ringel-Kulka T, Heikamp-de Jong I, Ringel Y, Carroll I, de Vos WM, Salojärvi J, Satokari R. Discordant temporal development of bacterial phyla and the emergence of core in the fecal microbiota of young children. *ISME J* 2016; **10**: 1002-1014 [PMID: 26430856 DOI: 10.1038/ismej.2015.177]
39 **Zmora N**, Zilberman-Schapira G, Suez J, Mor U, Dori-Bachash M, Bashiardes S, Kotler E, Zur M, Regev-Lehavi D, Brik RB, Federici S, Cohen Y, Linevsky R, Rothschild D, Moor AE, Ben-Moshe S, Harmelin A, Itzkovitz S, Maharshak N, Shibolet O, Shapiro H, Pevsner-Fischer M, Sharon I, Halpern Z, Segal E, Elinav E. Personalized Gut Mucosal Colonization Resistance to Empiric Probiotics Is Associated with Unique Host and Microbiome Features. *Cell* 2018; **174**: 1388-1405.e21 [PMID: 30193112 DOI: 10.1016/j.cell.2018.08.041]
40 **Arumugam M**, Raes J, Pelletier E, Le Paslier D, Yamada T, Mende DR, Fernandes GR, Tap J, Bruls T, Batto JM, Bertalan M, Borruel N, Casellas F, Fernandez L, Gautier L, Hansen T, Hattori M, Hayashi T, Kleerebezem M, Kurokawa K, Leclerc M, Levenez F, Manichanh C, Nielsen HB, Nielsen T, Pons N, Poulain J, Qin J, Sicheritz-Ponten T, Tims S, Torrents D, Ugarte E, Zoetendal EG, Wang J, Guarner F, Pedersen O, de Vos WM, Brunak S, Doré J; MetaHIT Consortium, Antolín M, Artiguenave F, Blottiere HM, Almeida M, Brechot C, Cara C, Chervaux C, Cultrone A, Delorme C, Denariaz G, Dervyn R, Foerstner KU, Friss C, van de Guchte M, Guedon E, Haimet F, Huber W, van Hylckama-Vlieg J, Jamet A, Juste C, Kaci G, Knol J, Lakhdari O, Layec S, Le Roux K, Maguin E, Mérieux A, Melo Minardi R, M'rini C, Muller J, Oozeer R, Parkhill J, Renault P, Rescigno M, Sanchez N, Sunagawa S, Torrejon A, Turner K, Vandemeulebrouck G, Varela E, Winogradsky Y, Zeller G, Weissenbach J, Ehrlich SD, Bork P. Enterotypes of the human gut microbiome. *Nature* 2011; **473**: 174-180 [PMID: 21508958 DOI: 10.1038/nature09944]
41 **David LA**, Maurice CF, Carmody RN, Gootenberg DB, Button JE, Wolfe BE, Ling AV, Devlin AS, Varma Y, Fischbach MA, Biddinger SB, Dutton RJ, Turnbaugh PJ. Diet rapidly and reproducibly alters the human gut microbiome. *Nature* 2014; **505**: 559-563 [PMID: 24336217 DOI: 10.1038/nature12820]
42 **Muegge BD**, Kuczynski J, Knights D, Clemente JC, González A, Fontana L, Henrissat B, Knight R, Gordon JI. Diet drives convergence in gut microbiome functions across mammalian phylogeny and within humans. *Science* 2011; **332**: 970-974 [PMID: 21596990 DOI: 10.1126/science.1198719]
43 **Claesson MJ**, Jeffery IB, Conde S, Power SE, O'Connor EM, Cusack S, Harris HM, Coakley M, Lakshminarayanan B, O'Sullivan O, Fitzgerald GF, Deane J, O'Connor M, Harnedy N, O'Connor K, O'Mahony D, van Sinderen D, Wallace M, Brennan L, Stanton C, Marchesi JR, Fitzgerald AP, Shanahan F, Hill C, Ross RP, O'Toole PW. Gut microbiota composition correlates with diet and health in the elderly. *Nature* 2012; **488**: 178-184 [PMID: 22797518 DOI: 10.1038/nature11319]
44 **Biagi E**, Franceschi C, Rampelli S, Severgnini M, Ostan R, Turroni S, Consolandi C, Quercia S, Scurti M, Monti D, Capri M, Brigidi P, Candela M. Gut Microbiota and Extreme Longevity. *Curr Biol* 2016; **26**: 1480-1485 [PMID: 27185560 DOI: 10.1016/j.cub.2016.04.016]
45 **Kong F**, Hua Y, Zeng B, Ning R, Li Y, Zhao J. Gut microbiota signatures of longevity. *Curr Biol* 2016; **26**: R832-R833 [PMID: 27676296 DOI: 10.1016/j.cub.2016.08.015]
46 **Wang N**, Li R, Lin H, Fu C, Wang X, Zhang Y, Su M, Huang P, Qian J, Jiang F, Wang H, Jiang L, Yu X, Liu J, Chen Y, Jiang Q. Enriched taxa were found among the gut microbiota of centenarians in East China. *PLoS One* 2019; **14**: e0222763 [PMID: 31639130 DOI: 10.1371/journal.pone.0222763]
47 **Bajinka O**, Tan Y, Abdelhalim KA, Özdemir G, Qiu X. Extrinsic factors influencing gut microbes, the immediate consequences and restoring eubiosis. *AMB Express* 2020; **10**: 130 [PMID: 32710186 DOI: 10.1186/s13568-020-01066-8]
48 **Ruan W**, Engevik MA, Spinler JK, Versalovic J. Healthy Human Gastrointestinal Microbiome: Composition and Function After a Decade of Exploration. *Dig Dis Sci* 2020; **65**: 695-705 [PMID: 32067143 DOI: 10.1007/s10620-020-06118-4]
49 **Hooks KB**, O'Malley MA. Dysbiosis and Its Discontents. *mBio* 2017; **8** [PMID: 29018121 DOI: 10.1128/mBio.01492-17]
50 **Rodríguez JM**, Murphy K, Stanton C, Ross RP, Kober OI, Juge N, Avershina E, Rudi K, Narbad A, Jenmalm MC, Marchesi JR, Collado MC. The composition of the gut microbiota throughout life, with an emphasis on early life. *Microb Ecol Health Dis* 2015; **26**: 26050 [PMID: 25651996 DOI: 10.3402/mehd.v26.26050]
51 **Vandeputte D**, Falony G, Vieira-Silva S, Tito RY, Joossens M, Raes J. Stool consistency is strongly associated with gut microbiota richness and composition, enterotypes and bacterial growth rates. *Gut* 2016; **65**: 57-62 [PMID: 26069274 DOI: 10.1136/gutjnl-2015-309618]
52 **Rothschild D**, Weissbrod O, Barkan E, Kurilshikov A, Korem T, Zeevi D, Costea PI, Godneva A, Kalka IN, Bar N, Shilo S, Lador D, Vila AV, Zmora N, Pevsner-Fischer M, Israeli D, Kosower N, Malka G, Wolf BC, Avnit-Sagi T, Lotan-Pompan M, Weinberger A, Halpern Z, Carmi S, Fu J, Wijmenga C, Zhernakova A, Elinav E, Segal E. Environment dominates over host genetics in shaping human gut microbiota. *Nature* 2018; **555**: 210-215 [PMID: 29489753 DOI: 10.1038/nature25973]
53 **Wu GD**, Chen J, Hoffmann C, Bittinger K, Chen YY, Keilbaugh SA, Bewtra M, Knights D, Walters WA, Knight R, Sinha R, Gilroy E, Gupta K, Baldassano R, Nessel L, Li H, Bushman FD, Lewis JD. Linking long-term dietary patterns with gut microbial enterotypes. *Science* 2011; **334**: 105-108 [PMID: 21885731 DOI: 10.1126/science.1208344]

54 **Bajaj JS**, Idilman R, Mabudian L, Hood M, Fagan A, Turan D, White MB, Karakaya F, Wang J, Atalay R, Hylemon PB, Gavis EA, Brown R, Thacker LR, Acharya C, Heuman DM, Sikaroodi M, Gillevet PM. Diet affects gut microbiota and modulates hospitalization risk differentially in an international cirrhosis cohort. *Hepatology* 2018; **68**: 234-247 [PMID: 29350768 DOI: 10.1002/hep.29791]

55 **Seitz HK**, Bataller R, Cortez-Pinto H, Gao B, Gual A, Lackner C, Mathurin P, Mueller S, Szabo G, Tsukamoto H. Alcoholic liver disease. *Nat Rev Dis Primers* 2018; **4**: 16 [PMID: 30115921 DOI: 10.1038/s41572-018-0014-7]

56 **Wiest R**, Albillos A, Trauner M, Bajaj JS, Jalan R. Targeting the gut-liver axis in liver disease. *J Hepatol* 2017; **67**: 1084-1103 [PMID: 28526488 DOI: 10.1016/j.jhep.2017.05.007]

57 **You M**, Jogasuria A, Taylor C, Wu J. Sirtuin 1 signaling and alcoholic fatty liver disease. *Hepatobiliary Surg Nutr* 2015; **4**: 88-100 [PMID: 26005675 DOI: 10.3978/j.issn.2304-3881.2014.12.06]

58 **Ding RB**, Bao J, Deng CX. Emerging roles of SIRT1 in fatty liver diseases. *Int J Biol Sci* 2017; **13**: 852-867 [PMID: 28808418 DOI: 10.7150/ijbs.19370]

59 **Liang X**, Hu M, Rogers CQ, Shen Z, You M. Role of SIRT1-FoxO1 signaling in dietary saturated fat-dependent upregulation of liver adiponectin receptor 2 in ethanol-administered mice. *Antioxid Redox Signal* 2011; **15**: 425-435 [PMID: 21194380 DOI: 10.1089/ars.2010.3780]

60 **Bala S**, Marcos M, Gattu A, Catalano D, Szabo G. Acute binge drinking increases serum endotoxin and bacterial DNA levels in healthy individuals. *PLoS One* 2014; **9**: e96864 [PMID: 24828436 DOI: 10.1371/journal.pone.0096864]

61 **Voigt RM**, Forsyth CB, Shaikh M, Zhang L, Raeisi S, Aloman C, Preite NZ, Donohue TM Jr, Fogg L, Keshavarzian A. Diurnal variations in intestinal barrier integrity and liver pathology in mice: implications for alcohol binge. *Am J Physiol Gastrointest Liver Physiol* 2018; **314**: G131-G141 [PMID: 29074484 DOI: 10.1152/ajpgi.00103.2017]

62 **Leung C**, Rivera L, Furness JB, Angus PW. The role of the gut microbiota in NAFLD. *Nat Rev Gastroenterol Hepatol* 2016; **13**: 412-425 [PMID: 27273168 DOI: 10.1038/nrgastro.2016.85]

63 **Yan AW**, Fouts DE, Brandl J, Stärkel P, Torralba M, Schott E, Tsukamoto H, Nelson KE, Brenner DA, Schnabl B. Enteric dysbiosis associated with a mouse model of alcoholic liver disease. *Hepatology* 2011; **53**: 96-105 [PMID: 21254165 DOI: 10.1002/hep.24018]

64 **Bull-Otterson L**, Feng W, Kirpich I, Wang Y, Qin X, Liu Y, Gobejishvili L, Joshi-Barve S, Ayvaz T, Petrosino J, Kong M, Barker D, McClain C, Barve S. Metagenomic analyses of alcohol induced pathogenic alterations in the intestinal microbiome and the effect of Lactobacillus rhamnosus GG treatment. *PLoS One* 2013; **8**: e53028 [PMID: 23326376 DOI: 10.1371/journal.pone.0053028]

65 **Wang Y**, Kirpich I, Liu Y, Ma Z, Barve S, McClain CJ, Feng W. Lactobacillus rhamnosus GG treatment potentiates intestinal hypoxia-inducible factor, promotes intestinal integrity and ameliorates alcohol-induced liver injury. *Am J Pathol* 2011; **179**: 2866-2875 [PMID: 22093263 DOI: 10.1016/j.ajpath.2011.08.039]

66 **Chen P**, Torralba M, Tan J, Embree M, Zengler K, Stärkel P, van Pijkeren JP, DePew J, Loomba R, Ho SB, Bajaj JS, Mutlu EA, Keshavarzian A, Tsukamoto H, Nelson KE, Fouts DE, Schnabl B. Supplementation of saturated long-chain fatty acids maintains intestinal eubiosis and reduces ethanol-induced liver injury in mice. *Gastroenterology* 2015; **148**: 203-214.e16 [PMID: 25239591 DOI: 10.1053/j.gastro.2014.09.014]

67 **Shao T**, Zhao C, Li F, Gu Z, Liu L, Zhang L, Wang Y, He L, Liu Y, Liu Q, Chen Y, Donde H, Wang R, Jala VR, Barve S, Chen SY, Zhang X, McClain CJ, Feng W. Intestinal HIF-1α deletion exacerbates alcoholic liver disease by inducing intestinal dysbiosis and barrier dysfunction. *J Hepatol* 2018; **69**: 886-895 [PMID: 29803899 DOI: 10.1016/j.jhep.2018.05.021]

68 MCC, Lacerda NL, Ferreira CM, Goncalves JL, Almeida D, Gamba C, Cassali G, Pedroso SH, Moreira C, Martins FS, Nicoli JR, Teixeira MM, Godard ALB, Vieira AT. Comparing the effects of acute alcohol consumption in germ-free and conventional mice: the role of the gut microbiota. *BMC Microbiol* 2014; **14**: 240 [PMID: 25223989 DOI: 10.1186/s12866-014-0240-4]

69 **Hartmann P**, Chen P, Wang HJ, Wang L, McCole DF, Brandl K, Stärkel P, Belzer C, Hellerbrand C, Tsukamoto H, Ho SB, Schnabl B. Deficiency of intestinal mucin-2 ameliorates experimental alcoholic liver disease in mice. *Hepatology* 2013; **58**: 108-119 [PMID: 23408358 DOI: 10.1002/hep.26321]

70 **Derrien M**, Belzer C, de Vos WM. Akkermansia muciniphila and its role in regulating host functions. *Microb Pathog* 2017; **106**: 171-181 [PMID: 26875998 DOI: 10.1016/j.micpath.2016.02.005]

71 **Lowe PP**, Gyongyosi B, Satishchandran A, Iracheta-Vellve A, Ambade A, Kodys K, Catalano D, Ward DV, Szabo G. Alcohol-related changes in the intestinal microbiome influence neutrophil infiltration, inflammation and steatosis in early alcoholic hepatitis in mice. *PLoS One* 2017; **12**: e0174544 [PMID: 28350851 DOI: 10.1371/journal.pone.0174544]

72 **Lowe PP**, Gyongyosi B, Satishchandran A, Iracheta-Vellve A, Ambade A, Cho Y, Kodys K, Catalano D, Ward DV, Szabo G. Correction: Alcohol-related changes in the intestinal microbiome influence neutrophil infiltration, inflammation and steatosis in early alcoholic hepatitis in mice. *PLoS One* 2017; **12**: e0179070 [PMID: 28562651 DOI: 10.1371/journal.pone.0179070]

73 **Grander C**, Adolph TE, Wieser V, Lowe P, Wrzosek L, Gyongyosi B, Ward DV, Grabherr F, Gerner RR, Pfister A, Enrich B, Ciocan D, Macheiner S, Mayr L, Drach M, Moser P, Moschen AR, Perlemuter G, Szabo G, Cassard AM, Tilg H. Recovery of ethanol-induced *Akkermansia*

muciniphila depletion ameliorates alcoholic liver disease. *Gut* 2018; **67**: 891-901 [PMID: 28550049 DOI: 10.1136/gutjnl-2016-313432]

74 **Kakiyama G**, Pandak WM, Gillevet PM, Hylemon PB, Heuman DM, Daita K, Takei H, Muto A, Nittono H, Ridlon JM, White MB, Noble NA, Monteith P, Fuchs M, Thacker LR, Sikaroodi M, Bajaj JS. Modulation of the fecal bile acid profile by gut microbiota in cirrhosis. *J Hepatol* 2013; **58**: 949-955 [PMID: 23333527 DOI: 10.1016/j.jhep.2013.01.003]

75 **Bajaj JS**, Heuman DM, Hylemon PB, Sanyal AJ, White MB, Monteith P, Noble NA, Unser AB, Daita K, Fisher AR, Sikaroodi M, Gillevet PM. Altered profile of human gut microbiome is associated with cirrhosis and its complications. *J Hepatol* 2014; **60**: 940-947 [PMID: 24374295 DOI: 10.1016/j.jhep.2013.12.019]

76 **Chen Y**, Yang F, Lu H, Wang B, Chen Y, Lei D, Wang Y, Zhu B, Li L. Characterization of fecal microbial communities in patients with liver cirrhosis. *Hepatology* 2011; **54**: 562-572 [PMID: 21574172 DOI: 10.1002/hep.24423]

77 **Bajaj JS**, Heuman DM, Hylemon PB, Sanyal AJ, Puri P, Sterling RK, Luketic V, Stravitz RT, Siddiqui MS, Fuchs M, Thacker LR, Wade JB, Daita K, Sistrun S, White MB, Noble NA, Thorpe C, Kakiyama G, Pandak WM, Sikaroodi M, Gillevet PM. Randomised clinical trial: Lactobacillus GG modulates gut microbiome, metabolome and endotoxemia in patients with cirrhosis. *Aliment Pharmacol Ther* 2014; **39**: 1113-1125 [PMID: 24628464 DOI: 10.1111/apt.12695]

78 **Bressa C**, Bailén-Andrino M, Pérez-Santiago J, González-Soltero R, Pérez M, Montalvo-Lominchar MG, Maté-Muñoz JL, Domínguez R, Moreno D, Larrosa M. Differences in gut microbiota profile between women with active lifestyle and sedentary women. *PLoS One* 2017; **12**: e0171352 [PMID: 28187199 DOI: 10.1371/journal.pone.0171352]

79 **Queipo-Ortuño MI**, Boto-Ordóñez M, Murri M, Gomez-Zumaquero JM, Clemente-Postigo M, Estruch R, Cardona Diaz F, Andrés-Lacueva C, Tinahones FJ. Influence of red wine polyphenols and ethanol on the gut microbiota ecology and biochemical biomarkers. *Am J Clin Nutr* 2012; **95**: 1323-1334 [PMID: 22552027 DOI: 10.3945/ajcn.111.027847]

80 **Bajaj JS**, Reddy RK, Tandon P, Wong F, Kamath PS, Biggins SW, Garcia-Tsao G, Fallon M, Maliakkal B, Lai J, Vargas HE, Subramanian RM, Thuluvath P, Thacker LR, O'Leary JG. Prediction of Fungal Infection Development and Their Impact on Survival Using the NACSELD Cohort. *Am J Gastroenterol* 2018; **113**: 556-563 [PMID: 29257141 DOI: 10.1038/ajg.2017.471]

81 **Lahmer T**, Messer M, Schwerdtfeger C, Rasch S, Lee M, Saugel B, Schmid RM, Huber W. Invasive mycosis in medical intensive care unit patients with severe alcoholic hepatitis. *Mycopathologia* 2014; **177**: 193-197 [PMID: 24710759 DOI: 10.1007/s11046-014-9740-x]

82 **Gustot T**, Maillart E, Bocci M, Surin R, Trépo E, Degré D, Lucidi V, Taccone FS, Delforge ML, Vincent JL, Donckier V, Jacobs F, Moreno C. Invasive aspergillosis in patients with severe alcoholic hepatitis. *J Hepatol* 2014; **60**: 267-274 [PMID: 24055548 DOI: 10.1016/j.jhep.2013.09.011]

83 **Yang AM**, Inamine T, Hochrath K, Chen P, Wang L, Llorente C, Bluemel S, Hartmann P, Xu J, Koyama Y, Kisseleva T, Torralba MG, Moncera K, Beeri K, Chen CS, Freese K, Hellerbrand C, Lee SM, Hoffman HM, Mehal WZ, Garcia-Tsao G, Mutlu EA, Keshavarzian A, Brown GD, Ho SB, Bataller R, Stärkel P, Fouts DE, Schnabl B. Intestinal fungi contribute to development of alcoholic liver disease. *J Clin Invest* 2017; **127**: 2829-2841 [PMID: 28530644 DOI: 10.1172/JCI90562]

84 **Zhu L**, Baker SS, Gill C, Liu W, Alkhouri R, Baker RD, Gill SR. Characterization of gut microbiomes in nonalcoholic steatohepatitis (NASH) patients: a connection between endogenous alcohol and NASH. *Hepatology* 2013; **57**: 601-609 [PMID: 23055155 DOI: 10.1002/hep.26093]

85 **Mouzaki M**, Comelli EM, Arendt BM, Bonengel J, Fung SK, Fischer SE, McGilvray ID, Allard JP. Intestinal microbiota in patients with nonalcoholic fatty liver disease. *Hepatology* 2013; **58**: 120-127 [PMID: 23401313 DOI: 10.1002/hep.26319]

86 **Jennison E**, Byrne CD. The role of the gut microbiome and diet in the pathogenesis of non-alcoholic fatty liver disease. *Clin Mol Hepatol* 2021; **27**: 22-43 [PMID: 33291863 DOI: 10.3350/cmh.2020.0129]

87 **Eslamparast T**, Eghtesad S, Poustchi H, Hekmatdoost A. Recent advances in dietary supplementation, in treating non-alcoholic fatty liver disease. *World J Hepatol* 2015; **7**: 204-212 [PMID: 25729475 DOI: 10.4254/wjh.v7.i2.204]

88 **Eslamparast T**, Poustchi H, Zamani F, Sharafkhah M, Malekzadeh R, Hekmatdoost A. Synbiotic supplementation in nonalcoholic fatty liver disease: a randomized, double-blind, placebo-controlled pilot study. *Am J Clin Nutr* 2014; **99**: 535-542 [PMID: 24401715 DOI: 10.3945/ajcn.113.068890]

89 **Rahimlou M**, Ahmadnia H, Hekmatdoost A. Dietary supplements and pediatric non-alcoholic fatty liver disease: Present and the future. *World J Hepatol* 2015; **7**: 2597-2602 [PMID: 26557952 DOI: 10.4254/wjh.v7.i25.2597]

90 **Hoyles L**, Fernández-Real JM, Federici M, Serino M, Abbott J, Charpentier J, Heymes C, Luque JL, Anthony E, Barton RH, Chilloux J, Myridakis A, Martinez-Gili L, Moreno-Navarrete JM, Benhamed F, Azalbert V, Blasco-Baque V, Puig J, Xifra G, Ricart W, Tomlinson C, Woodbridge M, Cardellini M, Davato F, Cardolini I, Porzio O, Gentileschi P, Lopez F, Foufelle F, Butcher SA, Holmes E, Nicholson JK, Postic C, Burcelin R, Dumas ME. Molecular phenomics and metagenomics of hepatic steatosis in non-diabetic obese women. *Nat Med* 2018; **24**: 1070-1080 [PMID: 29942096 DOI: 10.1038/s41591-018-0061-3]

91 **Wang B**, Jiang X, Cao M, Ge J, Bao Q, Tang L, Chen Y, Li L. Altered Fecal Microbiota Correlates with Liver Biochemistry in Nonobese Patients with Non-alcoholic Fatty Liver Disease. *Sci Rep* 2016; **6**: 32002 [PMID: 27550547 DOI: 10.1038/srep32002]

92 **Shen F**, Zheng RD, Sun XQ, Ding WJ, Wang XY, Fan JG. Gut microbiota dysbiosis in patients with non-alcoholic fatty liver disease. *Hepatobiliary Pancreat Dis Int* 2017; **16**: 375-381 [PMID: 28823367 DOI: 10.1016/S1499-3872(17)60019-5]

93 **Loomba R**, Seguritan V, Li W, Long T, Klitgord N, Bhatt A, Dulai PS, Caussy C, Bettencourt R, Highlander SK, Jones MB, Sirlin CB, Schnabl B, Brinkac L, Schork N, Chen CH, Brenner DA, Biggs W, Yooseph S, Venter JC, Nelson KE. Gut Microbiome-Based Metagenomic Signature for Non-invasive Detection of Advanced Fibrosis in Human Nonalcoholic Fatty Liver Disease. *Cell Metab* 2017; **25**: 1054-1062.e5 [PMID: 28467925 DOI: 10.1016/j.cmet.2017.04.001]

94 **Del Chierico F**, Nobili V, Vernocchi P, Russo A, De Stefanis C, Gnani D, Furlanello C, Zandonà A, Paci P, Capuani G, Dallapiccola B, Miccheli A, Alisi A, Putignani L. Gut microbiota profiling of pediatric nonalcoholic fatty liver disease and obese patients unveiled by an integrated meta-omics-based approach. *Hepatology* 2017; **65**: 451-464 [PMID: 27028797 DOI: 10.1002/hep.28572]

95 **Raman M**, Ahmed I, Gillevet PM, Probert CS, Ratcliffe NM, Smith S, Greenwood R, Sikaroodi M, Lam V, Crotty P, Bailey J, Myers RP, Rioux KP. Fecal microbiome and volatile organic compound metabolome in obese humans with nonalcoholic fatty liver disease. *Clin Gastroenterol Hepatol* 2013; **11**: 868-75.e1 [PMID: 23454028 DOI: 10.1016/j.cgh.2013.02.015]

96 **Boursier J**, Mueller O, Barret M, Machado M, Fizanne L, Araujo-Perez F, Guy CD, Seed PC, Rawls JF, David LA, Hunault G, Oberti F, Calès P, Diehl AM. The severity of nonalcoholic fatty liver disease is associated with gut dysbiosis and shift in the metabolic function of the gut microbiota. *Hepatology* 2016; **63**: 764-775 [PMID: 26600078 DOI: 10.1002/hep.28356]

97 **Michail S**, Lin M, Frey MR, Fanter R, Paliy O, Hilbush B, Reo NV. Altered gut microbial energy and metabolism in children with non-alcoholic fatty liver disease. *FEMS Microbiol Ecol* 2015; **91**: 1-9 [PMID: 25764541 DOI: 10.1093/femsec/fiu002]

98 **Jiang C**, Xie C, Li F, Zhang L, Nichols RG, Krausz KW, Cai J, Qi Y, Fang ZZ, Takahashi S, Tanaka N, Desai D, Amin SG, Albert I, Patterson AD, Gonzalez FJ. Intestinal farnesoid X receptor signaling promotes nonalcoholic fatty liver disease. *J Clin Invest* 2015; **125**: 386-402 [PMID: 25500885 DOI: 10.1172/JCI76738]

99 **Lee G**, You HJ, Bajaj JS, Joo SK, Yu J, Park S, Kang H, Park JH, Kim JH, Lee DH, Lee S, Kim W, Ko G. Distinct signatures of gut microbiome and metabolites associated with significant fibrosis in non-obese NAFLD. *Nat Commun* 2020; **11**: 4982 [PMID: 33020474 DOI: 10.1038/s41467-020-18754-5]

100 **Qin N**, Yang F, Li A, Prifti E, Chen Y, Shao L, Guo J, Le Chatelier E, Yao J, Wu L, Zhou J, Ni S, Liu L, Pons N, Batto JM, Kennedy SP, Leonard P, Yuan C, Ding W, Hu X, Zheng B, Qian G, Xu W, Ehrlich SD, Zheng S, Li L. Alterations of the human gut microbiome in liver cirrhosis. *Nature* 2014; **513**: 59-64 [PMID: 25079328 DOI: 10.1038/nature13568]

101 **Caussy C**, Tripathi A, Humphrey G, Bassirian S, Singh S, Faulkner C, Bettencourt R, Rizo E, Richards L, Xu ZZ, Downes MR, Evans RM, Brenner DA, Sirlin CB, Knight R, Loomba R. A gut microbiome signature for cirrhosis due to nonalcoholic fatty liver disease. *Nat Commun* 2019; **10**: 1406 [PMID: 30926798 DOI: 10.1038/s41467-019-09455-9]

102 **Chen Y**, Ji F, Guo J, Shi D, Fang D, Li L. Dysbiosis of small intestinal microbiota in liver cirrhosis and its association with etiology. *Sci Rep* 2016; **6**: 34055 [PMID: 27687977 DOI: 10.1038/srep34055]

103 **Aron-Wisnewsky J**, Vigliotti C, Witjes J, Le P, Holleboom AG, Verheij J, Nieuwdorp M, Clément K. Gut microbiota and human NAFLD: disentangling microbial signatures from metabolic disorders. *Nat Rev Gastroenterol Hepatol* 2020; **17**: 279-297 [PMID: 32152478 DOI: 10.1038/s41575-020-0269-9]

104 **Sender R**, Fuchs S, Milo R. Are We Really Vastly Outnumbered? *Cell* 2016; **164**: 337-340 [PMID: 26824647 DOI: 10.1016/j.cell.2016.01.013]

105 **Sender R**, Fuchs S, Milo R. Revised Estimates for the Number of Human and Bacteria Cells in the Body. *PLoS Biol* 2016; **14**: e1002533 [PMID: 27541692 DOI: 10.1371/journal.pbio.1002533]

106 **Schroeder BO**, Bäckhed F. Signals from the gut microbiota to distant organs in physiology and disease. *Nat Med* 2016; **22**: 1079-1089 [PMID: 27711063 DOI: 10.1038/nm.4185]

107 **Wang R**, Tang R, Li B, Ma X, Schnabl B, Tilg H. Gut microbiome, liver immunology, and liver diseases. *Cell Mol Immunol* 2021; **18**: 4-17 [PMID: 33318628 DOI: 10.1038/s41423-020-00592-6]

108 **Seo YS**, Shah VH. The role of gut-liver axis in the pathogenesis of liver cirrhosis and portal hypertension. *Clin Mol Hepatol* 2012; **18**: 337-346 [PMID: 23323248 DOI: 10.3350/cmh.2012.18.4.337]

109 **Smirnova E**, Puri P, Muthiah MD, Daitya K, Brown R, Chalasani N, Liangpunsakul S, Shah VH, Gelow K, Siddiqui MS, Boyett S, Mirshahi F, Sikaroodi M, Gillevet P, Sanyal AJ. Fecal Microbiome Distinguishes Alcohol Consumption From Alcoholic Hepatitis But Does Not Discriminate Disease Severity. *Hepatology* 2020; **72**: 271-286 [PMID: 32056227 DOI: 10.1002/hep.31178]

110 **Chu H**, Duan Y, Lang S, Jiang L, Wang Y, Llorente C, Liu J, Mogavero S, Bosques-Padilla F, Abraldes JG, Vargas V, Tu XM, Yang L, Hou X, Hube B, Stärkel P, Schnabl B. The Candida albicans exotoxin candidalysin promotes alcohol-associated liver disease. *J Hepatol* 2020; **72**: 391-400 [PMID: 31606552 DOI: 10.1016/j.jhep.2019.09.029]

111 **Lang S**, Duan Y, Liu J, Torralba MG, Kuelbs C, Ventura-Cots M, Abraldes JG, Bosques-Padilla F, Verna EC, Brown RS Jr, Vargas V, Altamirano J, Caballería J, Shawcross D, Lucey MR, Louvet A, Mathurin P, Garcia-Tsao G, Ho SB, Tu XM, Bataller R, Stärkel P, Fouts DE, Schnabl B. Intestinal

Fungal Dysbiosis and Systemic Immune Response to Fungi in Patients With Alcoholic Hepatitis. *Hepatology* 2020; **71**: 522-538 [PMID: 31228214 DOI: 10.1002/hep.30832]

112 **Tripathi A**, Debelius J, Brenner DA, Karin M, Loomba R, Schnabl B, Knight R. The gut-liver axis and the intersection with the microbiome. *Nat Rev Gastroenterol Hepatol* 2018; **15**: 397-411 [PMID: 29748586 DOI: 10.1038/s41575-018-0011-z]

113 **Leclercq S**, Matamoros S, Cani PD, Neyrinck AM, Jamar F, Stärkel P, Windey K, Tremaroli V, Bäckhed F, Verbeke K, de Timary P, Delzenne NM. Intestinal permeability, gut-bacterial dysbiosis, and behavioral markers of alcohol-dependence severity. *Proc Natl Acad Sci U S A* 2014; **111**: E4485-E4493 [PMID: 25288760 DOI: 10.1073/pnas.1415174111]

114 **Wree A**, McGeough MD, Peña CA, Schlattjan M, Li H, Inzaugarat ME, Messer K, Canbay A, Hoffman HM, Feldstein AE. NLRP3 inflammasome activation is required for fibrosis development in NAFLD. *J Mol Med (Berl)* 2014; **92**: 1069-1082 [PMID: 24861026 DOI: 10.1007/s00109-014-1170-1]

115 **Voican CS**, Njiké-Nakseu M, Boujedidi H, Barri-Ova N, Bouchet-Delbos L, Agostini H, Maitre S, Prévot S, Cassard-Doulcier AM, Naveau S, Perlemuter G. Alcohol withdrawal alleviates adipose tissue inflammation in patients with alcoholic liver disease. *Liver Int* 2015; **35**: 967-978 [PMID: 24766056 DOI: 10.1111/liv.12575]

116 **Molinaro A**, Wahlström A, Marschall HU. Role of Bile Acids in Metabolic Control. *Trends Endocrinol Metab* 2018; **29**: 31-41 [PMID: 29195686 DOI: 10.1016/j.tem.2017.11.002]

117 **Molinero N**, Ruiz L, Sánchez B, Margolles A, Delgado S. Intestinal Bacteria Interplay With Bile and Cholesterol Metabolism: Implications on Host Physiology. *Front Physiol* 2019; **10**: 185 [PMID: 30923502 DOI: 10.3389/fphys.2019.00185]

118 **Jia W**, Xie G, Jia W. Bile acid-microbiota crosstalk in gastrointestinal inflammation and carcinogenesis. *Nat Rev Gastroenterol Hepatol* 2018; **15**: 111-128 [PMID: 29018272 DOI: 10.1038/nrgastro.2017.119]

119 **Arora T**, Bäckhed F. The gut microbiota and metabolic disease: current understanding and future perspectives. *J Intern Med* 2016; **280**: 339-349 [PMID: 27071815 DOI: 10.1111/joim.12508]

120 **Chow MD**, Lee YH, Guo GL. The role of bile acids in nonalcoholic fatty liver disease and nonalcoholic steatohepatitis. *Mol Aspects Med* 2017; **56**: 34-44 [PMID: 28442273 DOI: 10.1016/j.mam.2017.04.004]

121 **Arab JP**, Karpen SJ, Dawson PA, Arrese M, Trauner M. Bile acids and nonalcoholic fatty liver disease: Molecular insights and therapeutic perspectives. *Hepatology* 2017; **65**: 350-362 [PMID: 27358174 DOI: 10.1002/hep.28709]

122 **Kakiyama G**, Hylemon PB, Zhou H, Pandak WM, Heuman DM, Kang DJ, Takei H, Nittono H, Ridlon JM, Fuchs M, Gurley EC, Wang Y, Liu R, Sanyal AJ, Gillevet PM, Bajaj JS. Colonic inflammation and secondary bile acids in alcoholic cirrhosis. *Am J Physiol Gastrointest Liver Physiol* 2014; **306**: G929-G937 [PMID: 24699327 DOI: 10.1152/ajpgi.00315.2013]

123 **Jiao N**, Baker SS, Chapa-Rodriguez A, Liu W, Nugent CA, Tsompana M, Mastrandrea L, Buck MJ, Baker RD, Genco RJ, Zhu R, Zhu L. Suppressed hepatic bile acid signalling despite elevated production of primary and secondary bile acids in NAFLD. *Gut* 2018; **67**: 1881-1891 [PMID: 28774887 DOI: 10.1136/gutjnl-2017-314307]

124 **Brandl K**, Hartmann P, Jih LJ, Pizzo DP, Argemi J, Ventura-Cots M, Coulter S, Liddle C, Ling L, Rossi SJ, DePaoli AM, Loomba R, Mehal WZ, Fouts DE, Lucey MR, Bosques-Padilla F, Mathurin P, Louvet A, Garcia-Tsao G, Verna EC, Abraldes JG, Brown RS Jr, Vargas V, Altamirano J, Caballería J, Shawcross D, Stärkel P, Ho SB, Bataller R, Schnabl B. Dysregulation of serum bile acids and FGF19 in alcoholic hepatitis. *J Hepatol* 2018; **69**: 396-405 [PMID: 29654817 DOI: 10.1016/j.jhep.2018.03.031]

125 **Nobili V**, Alisi A, Mosca A, Della Corte C, Veraldi S, De Vito R, De Stefanis C, D'Oria V, Jahnel J, Zohrer E, Scorletti E, Byrne CD. Hepatic farnesoid X receptor protein level and circulating fibroblast growth factor 19 concentration in children with NAFLD. *Liver Int* 2018; **38**: 342-349 [PMID: 28746779 DOI: 10.1111/liv.13531]

126 **Mouzaki M**, Wang AY, Bandsma R, Comelli EM, Arendt BM, Zhang L, Fung S, Fischer SE, McGilvray IG, Allard JP. Bile Acids and Dysbiosis in Non-Alcoholic Fatty Liver Disease. *PLoS One* 2016; **11**: e0151829 [PMID: 27203081 DOI: 10.1371/journal.pone.0151829]

127 **Caussy C**, Hsu C, Singh S, Bassirian S, Kolar J, Faulkner C, Sinha N, Bettencourt R, Gara N, Valasek MA, Schnabl B, Richards L, Brenner DA, Hofmann AF, Loomba R. Serum bile acid patterns are associated with the presence of NAFLD in twins, and dose-dependent changes with increase in fibrosis stage in patients with biopsy-proven NAFLD. *Aliment Pharmacol Ther* 2019; **49**: 183-193 [PMID: 30506692 DOI: 10.1111/apt.15035]

128 **Schwenger KJ**, Clermont-Dejean N, Allard JP. The role of the gut microbiome in chronic liver disease: the clinical evidence revised. *JHEP Rep* 2019; **1**: 214-226 [PMID: 32039372 DOI: 10.1016/j.jhepr.2019.04.004]

129 **Couch RD**, Dailey A, Zaidi F, Navarro K, Forsyth CB, Mutlu E, Engen PA, Keshavarzian A. Alcohol induced alterations to the human fecal VOC metabolome. *PLoS One* 2015; **10**: e0119362 [PMID: 25751150 DOI: 10.1371/journal.pone.0119362]

130 **Juanola O**, Ferrusquía-Acosta J, García-Villalba R, Zapater P, Magaz M, Marín A, Olivas P, Baiges A, Bellot P, Turon F, Hernández-Gea V, González-Navajas JM, Tomás-Barberán FA, García-Pagán JC, Francés R. Circulating levels of butyrate are inversely related to portal hypertension, endotoxemia, and systemic inflammation in patients with cirrhosis. *FASEB J* 2019; **33**: 11595-11605

[PMID: 31345057 DOI: 10.1096/fj.201901327R]

131 **Rau M**, Rehman A, Dittrich M, Groen AK, Hermanns HM, Seyfried F, Beyersdorf N, Dandekar T, Rosenstiel P, Geier A. Fecal SCFAs and SCFA-producing bacteria in gut microbiome of human NAFLD as a putative link to systemic T-cell activation and advanced disease. *United European Gastroenterol J* 2018; **6**: 1496-1507 [PMID: 30574320 DOI: 10.1177/2050640618804444]

132 **Loomba R**, Seguritan V, Li W, Long T, Klitgord N, Bhatt A, Dulai PS, Caussy C, Bettencourt R, Highlander SK, Jones MB, Sirlin CB, Schnabl B, Brinkac L, Schork N, Chen CH, Brenner DA, Biggs W, Yooseph S, Venter JC, Nelson KE. Gut Microbiome-Based Metagenomic Signature for Non-invasive Detection of Advanced Fibrosis in Human Nonalcoholic Fatty Liver Disease. *Cell Metab* 2019; **30**: 607 [PMID: 31484056 DOI: 10.1016/j.cmet.2019.08.002]

133 **Chu H**, Duan Y, Yang L, Schnabl B. Small metabolites, possible big changes: a microbiota-centered view of non-alcoholic fatty liver disease. *Gut* 2019; **68**: 359-370 [PMID: 30171065 DOI: 10.1136/gutjnl-2018-316307]

134 **Yuan J**, Chen C, Cui J, Lu J, Yan C, Wei X, Zhao X, Li N, Li S, Xue G, Cheng W, Li B, Li H, Lin W, Tian C, Zhao J, Han J, An D, Zhang Q, Wei H, Zheng M, Ma X, Li W, Chen X, Zhang Z, Zeng H, Ying S, Wu J, Yang R, Liu D. Fatty Liver Disease Caused by High-Alcohol-Producing Klebsiella pneumoniae. *Cell Metab* 2019; **30**: 675-688.e7 [PMID: 31543403 DOI: 10.1016/j.cmet.2019.08.018]

135 **Engstler AJ**, Aumiller T, Degen C, Dürr M, Weiss E, Maier IB, Schattenberg JM, Jin CJ, Sellmann C, Bergheim I. Insulin resistance alters hepatic ethanol metabolism: studies in mice and children with non-alcoholic fatty liver disease. *Gut* 2016; **65**: 1564-1571 [PMID: 26006114 DOI: 10.1136/gutjnl-2014-308379]

136 **Chen X**, Zhang Z, Li H, Zhao J, Wei X, Lin W, Zhao X, Jiang A, Yuan J. Endogenous ethanol produced by intestinal bacteria induces mitochondrial dysfunction in non-alcoholic fatty liver disease. *J Gastroenterol Hepatol* 2020; **35**: 2009-2019 [PMID: 32150306 DOI: 10.1111/jgh.15027]

137 **Dai X**, Hou H, Zhang W, Liu T, Li Y, Wang S, Wang B, Cao H. Microbial Metabolites: Critical Regulators in NAFLD. *Front Microbiol* 2020; **11**: 567654 [PMID: 33117316 DOI: 10.3389/fmicb.2020.567654]

138 **Lang S**, Demir M, Duan Y, Martin A, Schnabl B. Cytolysin-positive Enterococcus faecalis is not increased in patients with non-alcoholic steatohepatitis. *Liver Int* 2020; **40**: 860-865 [PMID: 31943701 DOI: 10.1111/liv.14377]

139 **Finlay BB**; CIFAR Humans; Microbiome. Are noncommunicable diseases communicable? *Science* 2020; **367**: 250-251 [PMID: 31949069 DOI: 10.1126/science.aaz3834]

140 **Crabb DW**, Im GY, Szabo G, Mellinger JL, Lucey MR. Diagnosis and Treatment of Alcohol-Associated Liver Diseases: 2019 Practice Guidance From the American Association for the Study of Liver Diseases. *Hepatology* 2020; **71**: 306-333 [PMID: 31314133 DOI: 10.1002/hep.30866]

141 **Stefan N**, Häring HU, Cusi K. Non-alcoholic fatty liver disease: causes, diagnosis, cardiometabolic consequences, and treatment strategies. *Lancet Diabetes Endocrinol* 2019; **7**: 313-324 [PMID: 30174213 DOI: 10.1016/S2213-8587(18)30154-2]

142 **Oh TG**, Kim SM, Caussy C, Fu T, Guo J, Bassirian S, Singh S, Madamba EV, Bettencourt R, Richards L, Yu RT, Atkins AR, Huan T, Brenner DA, Sirlin CB, Downes M, Evans RM, Loomba R. A Universal Gut-Microbiome-Derived Signature Predicts Cirrhosis. *Cell Metab* 2020; **32**: 878-888.e6 [PMID: 32610095 DOI: 10.1016/j.cmet.2020.06.005]

143 **Caussy C**, Hsu C, Lo MT, Liu A, Bettencourt R, Ajmera VH, Bassirian S, Hooker J, Sy E, Richards L, Schork N, Schnabl B, Brenner DA, Sirlin CB, Chen CH, Loomba R; Genetics of NAFLD in Twins Consortium. Link between gut-microbiome derived metabolite and shared gene-effects with hepatic steatosis and fibrosis in NAFLD. *Hepatology* 2018; **68**: 918-932 [PMID: 29572891 DOI: 10.1002/hep.29892]

144 **Ferrere G**, Wrzosek L, Cailleux F, Turpin W, Puchois V, Spatz M, Ciocan D, Rainteau D, Humbert L, Hugot C, Gaudin F, Noordine ML, Robert V, Berrebi D, Thomas M, Naveau S, Perlemuter G, Cassard AM. Fecal microbiota manipulation prevents dysbiosis and alcohol-induced liver injury in mice. *J Hepatol* 2017; **66**: 806-815 [PMID: 27890791 DOI: 10.1016/j.jhep.2016.11.008]

145 **Wang H**, Yan Y, Yi X, Duan Y, Wang J, Li S, Luo L, Huang T, Inglis B, Li X, Ji W, Tan T, Si W. Histopathological Features and Composition of Gut Microbiota in Rhesus Monkey of Alcoholic Liver Disease. *Front Microbiol* 2019; **10**: 165 [PMID: 30800107 DOI: 10.3389/fmicb.2019.00165]

146 **Zhong X**, Cui P, Jiang J, Ning C, Liang B, Zhou J, Tian L, Zhang Y, Lei T, Zuo T, Ye L, Huang J, Chen H. *Streptococcus*, the Predominant Bacterium to Predict the Severity of Liver Injury in Alcoholic Liver Disease. *Front Cell Infect Microbiol* 2021; **11**: 649060 [PMID: 33816353 DOI: 10.3389/fcimb.2021.649060]

147 **De Minicis S**, Rychlicki C, Agostinelli L, Saccomanno S, Candelaresi C, Trozzi L, Mingarelli E, Facinelli B, Magi G, Palmieri C, Marzioni M, Benedetti A, Svegliati-Baroni G. Dysbiosis contributes to fibrogenesis in the course of chronic liver injury in mice. *Hepatology* 2014; **59**: 1738-1749 [PMID: 23959503 DOI: 10.1002/hep.26695]

148 **Lee NY**, Joung HC, Kim BK, Kim BY, Park TS, Suk KT. *Lactobacillus lactis* CKDB001 ameliorate progression of nonalcoholic fatty liver disease through of gut microbiome: addendum. *Gut Microbes* 2020; **12**: 1829449 [PMID: 33131411 DOI: 10.1080/19490976.2020.1829449]

World Journal of Gastroenterology

Submit a Manuscript: https://www.f6publishing.com

World J Gastroenterol 2021 October 7; 27(37): 6180-6190

DOI: 10.3748/wjg.v27.i37.6180

ISSN 1007-9327 (print) ISSN 2219-2840 (online)

OPINION REVIEW

Surveillance for hepatocellular carcinoma at the community level: Easier said than done

Paolo Del Poggio, Marzio Mazzoleni, Sergio Lazzaroni, Andrea D'Alessio

ORCID number: Paolo Del Poggio 0000-0002-9387-8909; Marzio Mazzoleni 0000-0003-4295-0904; Sergio Lazzaroni 0000-0002-7369-8476; Andrea D'Alessio 0000-0002-6797-0410.

Author contributions: All authors equally contributed to this paper with conception and design of the study, literature review, drafting, critical revision and editing; they all have approved the final version.

Conflict-of-interest statement: The authors declare that they have no conflicting interests.

Open-Access: This article is an open-access article that was selected by an in-house editor and fully peer-reviewed by external reviewers. It is distributed in accordance with the Creative Commons Attribution NonCommercial (CC BY-NC 4.0) license, which permits others to distribute, remix, adapt, build upon this work non-commercially, and license their derivative works on different terms, provided the original work is properly cited and the use is non-commercial. See: http://creativecommons.org/Licenses/by-nc/4.0/

Manuscript source: Invited manuscript

Specialty type: Gastroenterology

Paolo Del Poggio, Sergio Lazzaroni, Unità di Epatologia, Policlinico San Marco Zingonia GSD University and Research Hospital Unità Epatologia, Osio Sotto 24040, Bergamo, Italy

Marzio Mazzoleni, Primary Care Physician, ASST Bergamo, Osio Sotto 24040, Bergamo, Italy

Andrea D'Alessio, Department of Medicine, Policlinico San Marco Zingonia, GSD University and Research Hospital, Osio Sotto 24040, Bergamo, Italy

Corresponding author: Paolo Del Poggio, MD, Consultant Physician-Scientist, Unità di Epatologia, Policlinico San Marco Zingonia GSD University and Research Hospital Unità Epatologia, Corso Europa Unita 7, Osio Sotto 24040, Bergamo, Italy.
paolo.delpoggio51@gmail.com

Abstract

Surveillance for hepatocellular carcinoma (HCC) in high-risk patients with semiannual ultrasound examinations is advocated by all international guidelines. However, as long as the identification of the population to be screened and the surveillance programs are not well implemented, the real-life impact of HCC surveillance in reducing mortality for HCC cannot be known. We propose a new approach that promotes the identification of cirrhotic patients by primary care physicians (PCPs) and referral of patients to the hepatologist for surveillance. Surveillance should be incorporated, when feasible, in a hub and spoke model of comprehensive hepatology care. Training PCPs to identify cirrhotic patients and performing surveillance in a subspecialist setting are equally important to improve the effectiveness of real-life surveillance and to decrease HCC mortality over time.

Key Words: Hepatocellular carcinoma; Cirrhosis; Ultrasound surveillance; Primary health care

©The Author(s) 2021. Published by Baishideng Publishing Group Inc. All rights reserved.

Core Tip: Ultrasound surveillance for hepatocellular carcinoma is recommended by all official guidelines for high-risk patients, but its uptake at the community level is low. We discuss the obstacles hampering its implementation and propose a hub and spoke

and hepatology

Country/Territory of origin: Italy

Peer-review report's scientific quality classification
Grade A (Excellent): 0
Grade B (Very good): B, B
Grade C (Good): 0
Grade D (Fair): 0
Grade E (Poor): 0

Received: March 2, 2021
Peer-review started: March 2, 2021
First decision: April 17, 2021
Revised: April 24, 2021
Accepted: August 10, 2021
Article in press: August 10, 2021
Published online: October 7, 2021

P-Reviewer: Cojocariu C, Zhang L
S-Editor: Fan JR
L-Editor: Filipodia
P-Editor: Wu RR

model network for the effective delivery of surveillance in the real world setting.

Citation: Del Poggio P, Mazzoleni M, Lazzaroni S, D'Alessio A. Surveillance for hepatocellular carcinoma at the community level: Easier said than done. *World J Gastroenterol* 2021; 27(37): 6180-6190
URL: https://www.wjgnet.com/1007-9327/full/v27/i37/6180.htm
DOI: https://dx.doi.org/10.3748/wjg.v27.i37.6180

INTRODUCTION

Primary liver cancer is the third leading cause of cancer related mortality worldwide [1]. It includes hepatocellular carcinoma (HCC), comprising of 75%-85% cases, intrahepatic cholangiocarcinoma (10%-15%), and other rare types[1]. The HCC death toll is the highest in East Asia and Africa, with an annual mortality rate greater than 20/100000 people[2]. Mortality is lower in Western Europe and in the United States (12-12.7/100000) but it has increased rapidly in the last decade[3]. On the other hand, Eastern Europe, Scandinavia, and India have the lowest mortality rate (less than 4/100.000). The great majority of HCC cases in the Western world are diagnosed in cirrhotic patients, while in Asia and Central Africa the most significant risk factor for HCC is chronic hepatitis B virus infection with or without cirrhosis. Therefore, patients with those risk factors (cirrhosis and/or chronic hepatitis B infection) should undergo surveillance, with the goal of identifying the tumor at an early stage when curative treatments are feasible. A randomized study of chronic hepatitis B patients in China [4], several longitudinal cohort studies in patients affected by cirrhosis of any etiology [5-7], and a meta-analysis[8] have demonstrated the benefit of ultrasound surveillance (US) in improving survival. In addition, several studies have shown that US is cost effective for the surveillance of patients affected by chronic hepatitis B and of cirrhotic patients. Indeed, HCC incidence in those populations is 0.2% and 1.5% per year respectively, which is considered acceptable to define cost effectiveness[9-11]. On the other hand, the effectiveness of US is still uncertain in young Non-Asian inactive carriers of hepatitis B surface antigen (HBsAg), in patients with chronic hepatitis C infection with advanced fibrosis, and by those with nonalcoholic fatty liver disease (NAFLD) without cirrhosis. For those reasons, the three most important international guidelines advocate periodic abdominal ultrasound scans with or without alpha-fetoprotein (AFP) in all cirrhotics and chronic hepatitis B patients, irrespective of antiviral treatment[2,12,13] as a cost effective and noninvasive surveillance modality. According to the guidelines, US should be performed on a semiannual basis, with the exclusion of decompensated cirrhotics not listed for liver transplantation, in which surveillance is considered futile.

Despite the recommendations, real-life implementation of surveillance programs is far from optimal. It has recently been shown that, in addition to an increase in the proportion of HCC diagnosed at an early stage, 64% of the cases detected in the United States between 2006 and 2012 were diagnosed at an intermediate or an advanced stage [14]. That is probably the result of the low implementation of surveillance programs, with less than 20% of cirrhotics undergoing regular surveillance[15]. Surveillance is hindered by several issues, insufficient identification of patients at risk, failure to order surveillance, failure to perform surveillance with effective tools, poor patient adherence to the surveillance program, failure to establish a care-unit network to provide effective treatment. This review aims to analyze these steps one-by-one in order to identify the obstacles hampering the implementation of surveillance in real life.

FAILURE TO IDENTIFY THE PATIENTS AT RISK

One of the most important factors responsible for the low uptake of surveillance is the failure of primary care physicians (PCPs) to identify patients at risk to be enrolled in surveillance programs. In two web-based surveys, PCPs reported lack of knowledge of current guidelines. They could not correctly identify the at-risk categories and ordered random surveillance of chronic liver disease patients[16,17]. It is noteworthy that cirrhosis is widely under diagnosed and that increased identification and surveillance

of cirrhotic patients would be very cost effective in detecting HCC at an early stage. As an example, assuming an ultrasound sensitivity of 65% for early-stage HCC[18], an increase in the detection rate of cirrhotic patients from 50% to 75% would result in a significant increase of early-stage HCC diagnosed by abdominal ultrasound. Thanks to the identification of high-risk patients, ultrasound screening would thus allow the identification of a number of early-stage HCC comparable to magnetic resonance imaging (MRI) use, which has a higher sensitivity (90%) but is more expensive and has a higher false-positive rate. Another negative consequence of the failure to identify cirrhotic patients is that the cause of liver damage is not treated, and consequently HCC would often be diagnosed in a critical patient not eligible for radical treatment anymore.

Fortunately, the performance of PCPs can be improved by training interventions[19] and by participation in specialist networks, as shown by the French experience in hepatitis C[20]. To address the problem, in 2006 we started an education program targeting 120 PCPs, aimed at the identification of cirrhotic patients and their surveillance for HCC[21]. The program was started in the southern part of the Province of Bergamo in two hospitals, Policlinico S. Marco, Zingonia, and Azienda Ospedaliera di Treviglio, that have hepatology clinics providing medium-complexity specialist care. More complex cases are referred to a tertiary care hospital in Bergamo, which has a liver transplant center. Two hepatologists had established a network of collaboration with PCPs for the management and referral of patients with liver disease, but also provided care for patients from the nearby provinces, where no specific network had been implemented. The training program consisted of a 1-year intensive course in 2006, followed by annual refreshers from 2007 to December 2013. PCPs were instructed to perform screening of all patients at risk of liver cirrhosis, *i.e.* hepatitis C virus (HCV) infection, HBsAg positivity, alcohol abuse (> 60 g/d in women and > 80 g/d in men), body mass index > 30 kg/m^2, and to refer them to the liver specialist for diagnostic confirmation and US planning[20]. Abdominal ultrasound was performed, and the data were analyzed, by hepatologists or by radiologists who worked at the same hospital and had strong expertise in liver cancer detection.

The results showed that 6 years after training PCPs, there was a significant increase in the number of HCC patients detected by US at an early stage and suitable for radical treatment (Figure 1). As a consequence, 3- and 5-year survival of HCC patients improved significantly from 35% to 48% and 20% to 40%, respectively ($P < 0.05$) after training. In contrast, both the proportion of HCCs detected by US, and patient survival did not change in areas where PCPs were not trained. The study has some limitations. Firstly, PCPs did not record the number of cirrhotic patients who were identified, but only the number of HCC patients who were diagnosed. Secondly, the cirrhosis criteria used by PCPs to refer the patient to the hepatologist were mainly ultrasound based using two of the following ultrasound criteria, liver surface nodularity, nonhomogeneous liver texture, left lobe or caudate lobe hypertrophy, distorted hepatic veins, spleen longitudinal diameter > 12 cm or one ultrasound criterion plus a platelet count < 130.000/mL. Currently, those criteria are obsolete, as the availability of new proprietary (*e.g.*, Fibrotest, Enhanced Liver Fibrosis, and Fibrometer) and nonproprietary biochemical scores (fibrosis-4, aspartate transaminase to platelet ratio index), and NAFLD fibrosis scores) have improved diagnostic accuracy. Nonetheless, the study showed that it is essential to establish a collaboration network among hepatologists and PCPs, and that strengthening PCP skills in identifying and referring suspected cirrhotic patients may result in an increased number of HCCs diagnosed at an early stage and improved patient survival. In the following years, the network of collaboration was extended to the whole province of Bergamo, and specific training aimed at the diagnosis of cirrhosis was incorporated into a comprehensive hepatology education program that involved 900 PCPs. The program consists of specific courses organized every 3 years by the local health authority and annual symposia organized by the tertiary care hospital of Bergamo. The percentage of HCCs diagnosed at an early stage in the following years was still high, indicating that the positive effect of training persisted in time. Indeed, 166 (77%) of 202 HCCs diagnosed in cirrhotic patients at Policlinico S. Marco Hospital from January 2014 through December 2020, were found at an early stage and could be effectively treated. It is worth noting that only 14 HCCs were diagnosed in noncirrhotic patients, seven with chronic hepatitis B and currently under surveillance, six were detected at an early stage, five had chronic hepatitis C infection, and two had noncirrhotic nonalcoholic steatohepatitis (NASH). Therefore, our real-life data confirm the adequacy of the official guidelines recommending US only in patients affected by cirrhosis or chronic hepatitis B.

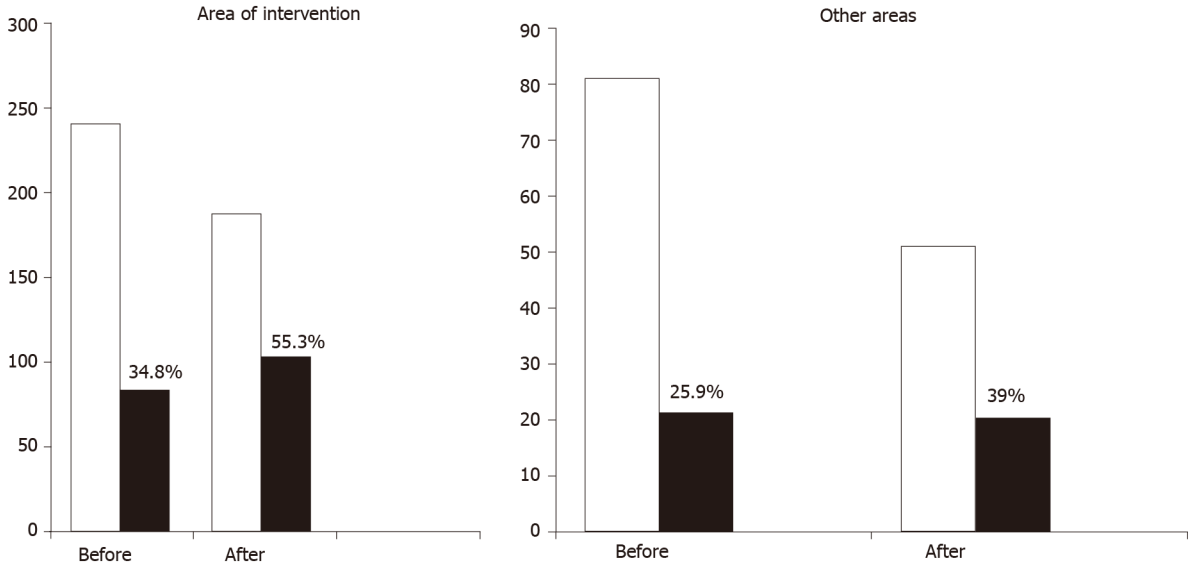


Figure 1 Hepatocellular carcinoma diagnosis before and after implementation of the training program in the area where primary care physicians were trained and in other areas where primary care physicians were not trained. White bars indicate the total number of hepatocellular carcinomas. Black bars indicate hepatocellular carcinomas diagnosed by surveillance. In the intervention area the diagnoses under surveillance increased from 85 of 244 (34.8%) to 105 of 190 (55%) after training (Δ = + 20.5%, $P < 0.001$). The diagnoses increased from 21 of 81 (25.9%) to 20 of 51 (39%) in other areas (Δ = + 13.1%, $P = 0.11$, not significant).

FAILURE TO ORDER SURVEILLANCE

The identification of cirrhotic patients for surveillance does not imply that surveillance will be effectively performed. In fact, surveillance is sometimes carried out by the PCP and ultrasound scans are performed by radiologists without specific expertise in liver disease. In that case, the patient is referred to the hepatologist or gastroenterologist only if a focal lesion is detected, a scenario called "population-based surveillance". In Italy and other countries, thanks to the widespread diffusion of ultrasound equipment and the motivation of an active medical sonography society, US is directly performed by hepatologists with sonographic skills and able to perform the examinations by themselves (*i.e.* specialist or subspecialist surveillance). Population-based surveillance is mainly implemented in the United States, while specialist surveillance is more widespread in Europe and Asia. A systematic review and meta-analysis comparing the two US modalities reported a much higher effectiveness of surveillance in the specialist setting (73.7%) rather than in population-based cohorts (8.8 %), with the lowest effectiveness in patients with alcoholic and NASH cirrhosis[22]. There are many reasons for the difference. PCPs and radiologists without specific expertise in liver disease may have limited knowledge of the international guidelines[17,23]. Concerns of other serious comorbidities, logistic problems such as poor accessibility of ultrasound facilities, and difficulties in the scheduling process. Consequently, the need to access low-cost, affordable ultrasound facilities may result in delays or absence of PCP surveillance[24]. Several interventions can be introduced to improve US programs, namely the use of automatic reminders for PCPs or the implementation of protocols that can be carried out by nurses or pharmacists[22]. Beste *et al*[25] reported that a primary care-oriented clinical reminder integrated into clinical records improved PCP surveillance from 18.2% to 27.6%[25], whereas no improvement was observed in the control sites (from 16.1% to 17.5%). Similarly, in a large study of 1800 cirrhotic patients, Singal *et al*[26] observed that mailed outreach invitations increased surveillance from 24% to a staggering 44.5% with no benefit seen by the addition of patient navigation [26]. Overall, it can be concluded that surveillance performed in subspecialist settings, if feasible, would be preferable to population surveillance. In the latter case, decreased use of US could be expected, and even after the interventions mentioned above (*i.e.* internal modalities such as medical reminders, nurse-based protocols, and patient navigation and outreach modalities such as mailed invitations), it was only slightly improved. Therefore, it is essential to ensure that PCPs are aware of the importance of appropriate specialist surveillance and to reinforce the need of specific education programs addressed to them.

FAILURE TO USE THE APPROPRIATE SURVEILLANCE TOOL

Liver ultrasound

Liver sonography is recommended by all existent guidelines as the standard HCC surveillance test to be used. A meta-analysis of 15 studies of cirrhotic patients showed that abdominal ultrasound had good sensitivity (84%) and excellent specificity (91%) for the detection of HCC at any stage[27]. However, the pooled sensitivity for the detection of early-stage HCC was as low as 47%, with only marginal improvement (53%) after exclusion of the studies performed before the introduction of high-density crystal probes and harmonic imaging. It is noteworthy that the sensitivity of ultrasound is characterized by a wide range of variation (from 21% to 81%), reflecting the operator dependency of US scans. In fact, in a single study performed at a university-based tertiary care center, the sensitivity of abdominal ultrasound was 82% [28]. Similarly, in a large Italian cohort study, where examinations were performed in both outside facilities and hospital wards, the sensitivity rose to 66%[18]. It is important to consider that ultrasound examinations in the United States were performed by technicians who recorded the images, which were subsequently reviewed and interpreted by radiologists. That can affect the accuracy of the examinations reported in those studies, as real-time interpretation of ultrasound findings is of paramount importance in ensuring the adequacy of the examination, especially in patients who are difficult to examine. In conclusion, it seems that pooled study results underestimate the sensitivity of ultrasound for the detection of early-stage HCC. It is more likely that the sensitivity of ultrasound carried out with high quality scanners and by well-trained doctors in a real-time manner, would be as high as 70%. Admittedly, even in optimal conditions, US fails to detect early-stage HCC in approximately one-third of the patients[18]. Two studies have addressed the causes of surveillance failure. Overall, both studies found that male sex, obesity, and advanced liver disease were associated with failure to detect HCC at an early stage[18,29]. Fatty liver, often associated with obesity and more frequently observed in males, may hinder good visualization of the liver, while advanced liver disease may produce a coarse echo pattern that masks early-stage tumors. It is important to distinguish poor visibility of the tumor by abdominal ultrasound, which represents a true limitation of this technology, from biologically aggressive tumors, which may show an infiltrative or rapidly growing pattern that may be difficult to detect regardless of the diagnostic tool.

Computed tomography and magnetic resonance imaging

The use of CT or MRI can obviate the above-mentioned technical limitations of ultrasound, but they rarely can identify an aggressive tumor at an early stage. In one study, 20% of the ultrasound examinations were considered technically inadequate for excluding HCC[29]. In another study, 32% of HCCs were detected beyond the early stage by semiannual US, 12% of them showing biologically aggressive features, *i.e.*, AFP > 1000 ng/mL, vascular thrombosis, distant metastasis, or infiltrative pattern[18]. Therefore, technical limitations of US to detect early-stage HCC can be deemed to be around 20%, hence it is important that ultrasound reports include a statement about the quality of the examination and the potential recommendation to perform second-level imaging (CT or MRI). MRI has a sensitivity of 83.7% for the detection of early-stage HCC[30] and should be preferred to CT, which has lower sensitivity (62.5%), similar to that of ultrasound[31]. However, it is noticeable that biologically aggressive tumors are poorly detected by MRI (16% failure to detect HCC) as well as by US (12% failure). Those tumors thus represent a hardcore of HCCs eluding both kinds of imaging surveillance. The good news is that only a small percentage of HCCs have those characteristics. However, it should be recognized that the pattern of HCC growth is heterogeneous[32] and many indolent tumors can develop an aggressive pattern with time, as shown by an increase of the percentage of biologically aggressive tumors detected by annual compared with semiannual surveillance, (*i.e.* 28% *vs* 12%) [18]. The possibility that indolent HCCs might transform into more aggressive tumors with time has raised some concerns of the common real-life practice of performing annual instead of semiannual MRI to reduce surveillance cost

Contrast-enhanced ultrasound

Contrast-enhanced US with intravascular agents (*e.g.*, Levovist, Sonovue) has a limited role in surveillance as it is impossible to scan the whole liver in the arterial phase when small tumors are detected[33]. On the other hand, perfluorocarbon (Sonazoid) seems to a promising agent[34], as it is taken up and retained by Kupffer cells for 60 min after

bolus injection, allowing a scan of the entire liver in the late phase when HCC appears as a black hole. Sonazoid-enhanced US might therefore be useful to detect HCC developing in livers with a coarse echotexture, but it cannot be of any advantage in obese patients or severe fatty livers, where CT or MRI remain the only option to accurately exclude HCC.

AFP

The sensitivity of AFP to detect early-stage HCC is too low to be used alone as a surveillance tool[35]. Only the Asian-Pacific Guidelines recommend the use of AFP in surveillance programs, with a cutoff of 200 ng/mL[2]. This cutoff is highly specific but reduces AFP sensitivity to a level as low as 22%[12]. However, new and effective pharmacological treatment of hepatitis B and C may remove false-positive AFP results caused by necro-inflammatory activity and enable the use of lower cutoff levels, providing better AFP sensitivity without compromising its specificity. Another method to improve AFP diagnostic accuracy is to monitor its changes over time[36]. An algorithm including AFP variations has been created and was tested in the Hepatitis C Antiviral Long-Term Treatment Against Cirrhosis Trial cohort, with good results in identifying patients at increased risk of HCC[37]. A recent meta-analysis showed that the addition of AFP levels to abdominal ultrasound improved the overall sensitivity for the detection of early-stage HCC from 45% to 63%[27], but as pointed out before, the low sensitivity of US in the meta-analysis raises doubts on the quality of the ultrasound examinaions. It therefore remains an open question whether AFP can improve the performance of properly executed sonography. It is important to stress that the addition of AFP screening to abdominal sonography could adversely affect the already low level of surveillance application by PCPs because of the logistic and financial burden introduced by duplicating the surveillance tool. In our real-life practice we assess AFP levels alongside abdominal US only in patients with cured hepatitis C or well-controlled chronic hepatitis B and optimal adherence to follow-up visits. A change in AFP values over time prompts performing second-level imaging, particularly in cases with a coarse echo pattern on sonography. On the other hand, stable AFP levels permit advising the continuation of standard US, avoiding additional cost.

New biochemical markers

In recent years, new markers have been proposed for the diagnosis of early HCC. Each of them by itself does not seem to confer any benefit in diagnostic accuracy compared with US with or without AFP[35]. However, a combination of AFP-L3, AFP, and des-gamma-carboxy prothrombin was tested in a large study and proved to have a sensitivity greater than 60% for early HCC, which is similar to the sensitivity of currently approved surveillance tools[38]. The algorithm is interesting, and if confirmed could be used as an alternative to ultrasound in the setting of population surveillance, especially where ultrasound scanners are not available or not accessible.

THE PROBLEM OF ADHERENCE

Patient adherence is key to the effectiveness of the surveillance program. Racial and ethnic minorities have poor awareness of surveillance programs, probably because of their low socioeconomic status. Patients also report difficulties scheduling surveillance ultrasound, concerns of the cost, need of off-work days, and difficulties reaching the facilities where the exam is performed[39]. The difficulties have a greater impact on subspecialty-based than on population-based surveillance, and should be addressed by appropriate interventions. In our hospital, the great majority of examinations are performed by hepatologists (PD and SL) and each appointment is directly booked by the specialist, thus making the scheduling process much easier. Visits and US examinations are reimbursed by the National Health Care System, with no additional cost for the patient. They are both performed at the same time to minimize off-work time, and if the patient is under antiviral treatment, the drug can be collected from the hospital pharmacy on the same day. Table 1 shows adherence to surveillance in 362 cirrhotic patients followed from January 2013 through December 2020 in our outpatient clinic. Adherence was defined as the performance of regular annual or semiannual ultrasound examinations in the last 24 months. Overall adherence to surveillance was rather good and only slightly lower than that observed in studies from other subspecialty clinics, (*i.e.* 65% *vs* 73%)[22]. It should be highlighted that in 2020 Northern Italy was heavily hit by the coronavirus disease 2019 pandemic and that the liver clinic was

Table 1 Adherence to surveillance by 362 cirrhotic patients followed from January 2013 through December 2020 at the hepatology unit of Policlinico S. Marco

Etiology of cirrhosis	Adherent	Semiannual	Annual	Nonadherent
Alcoholic (103)	55 (52%)	31 (56%)	24 (44%)	48 (46%)
HBV (53)	39 (73%)	35 (90%)	4 (10%)	14 (27%)
HCV (164)	119 (72%)	101 (85%)	18 (15%)	45 (28%)
NAFLD (42)	24 (57%)	17 (71%)	7 (29%)	18 (43%)
Total: 362	237 (65%)	184 (77%)	53 (23%)	125 (35%)

Adherence was defined as the performance of regular annual or semiannual ultrasound examinations in the previous 24 mo. HBV: Hepatitis B virus; HCV: Hepatitis C virus; NAFLD: Nonalcoholic fatty liver disease.

closed down for 2 months until April 2020. The restrictions and the fear of being infected and contracting the disease might have induced patients to avoid medical appointments, as observed for other screening programs during the pandemic. Despite that, nearly two-thirds of the patients continued surveillance, which in 77% of the cases was semiannual and in line with the official recommendations. It should be emphasized that the definition of adherence is not unequivocal, as some investigators used restrictive definitions while others, as we did, use operational definitions. Patients who underwent at least 1 or 2 surveillance exams in the last 12 months were considered adherent to the surveillance program. Moreover, as adherence decreases over time, studies with longer follow-up show lower adherence rates and cannot be compared with studies that have a shorter follow-up. To solve this conundrum it has been proposed to define adherence to the surveillance program as the proportion of time up-to-date with screening[22], although in retrospective studies complete patient data are often lacking, and this parameter may be difficult to achieve. In accord with other studies, we found a lower adherence to surveillance programs in alcoholic and metabolic cirrhotic patients (NAFLD). In those patients, the time interval between screening exams was more frequently annual than semiannual. On the other hand, patients affected by cirrhosis secondary to hepatitis B and C, had a higher adherence to the surveillance programs (72% and 73% respectively) and exams were almost exclusively performed with semiannual periodicity. The reasons for the low adherence in the former categories are multifactorial. Lack of family support and low socio-economic status are important and can hinder the access to the health care system as well as social stigma associated with alcohol abuse and obesity. It is well known that marginalized and stigmatized patients are more dependent on a good relationship with the healthcare provider than on getting the right information from scientific sources or mail reminders. They may also overestimate the prescription of drugs compared with regular screening tests, and perceive the periodicity of ultrasound examinations as a mere waste of time. It is therefore important to establish an empathic nonjudgmental relationship with those patients. The ultrasound examination should be integrated with the hepatologist consultation, a longer time for the visit should be scheduled, medical issues should be discussed, and drugs prescribed if necessary. It is important to make the patient understand that surveillance is essential to take care of their liver disease. For that purpose, it would be helpful to establish a close collaboration with Alcoholics Anonymous or other self-help groups, that could help the patients to be actively involved and aware of the importance of surveillance.

CONCLUSION

In conclusion, despite generalized consensus of all scientific guidelines on the utility of surveillance for HCC in high-risk patients, the implementation of surveillance at the community level is far from ideal. Low access to surveillance programs is associated with a lower number of HCC diagnosed at an early stage and decreased survival. Therefore, it is important to study the obstacles hampering the adherence to surveillance of the high-risk population in order to implement appropriate interventions.

Adherence to surveillance programs is higher in hospital/subspecialty-based surveillance compared with population-based surveillance, in which tests are ordered by PCPs and performed by general radiologists. Subspecialty-based surveillance should therefore be the first choice when feasible. However, the geographic location of the facilities and the distance from the hospital may result in population surve-illance as the only available choice. In both cases, lack of identification of the at-risk categories by PCPs, (*i.e.* cirrhotic patients and chronic hepatitis B patients), is the most important issue hindering implementation of adequate surveillance. Education programs targeted to PCPs to improve their skills in identifying the patients at risk can facilitate prompt referral to the hepatologist/gastroenterologist for US. PCPs should be encouraged to use biochemical scores to raise the suspicion of cirrhosis, and if feasible, portable elastography scanners. Once the diagnosis of cirrhosis has been established by transient elastography, acoustic radiation force impulse elastography, or other modalities, the patient should be followed up in a specialty setting. Regarding the surveillance tools, real-life experience confirms that semiannual ultrasound examination with the addition of sequential AFP monitoring in selected cases is the most appropriate method, with a sensitivity of about 70%. Ultrasound examinations should be of high quality and hence preferably performed by radiologists with good expertise in liver imaging, or when feasible, by the hepatologist himself. When ultrasound examinations are unsatisfactory (about 20% of cases), it should be explicitly noted in the sonographic report and the patient preferably surveilled with an annual MRI, which brings the total detection rate of early-stage HCC up to 85%. Fifteen percent of HCCs are aggressive tumors that cannot be diagnosed at an early stage with the currently available tools. Adherence to scheduled examinations is still a problem, particularly in some categories of patients, *i.e.* alcoholic and NAFLD cirrhotic patients. In order to improve patient adherence, a less complex approach that reducing the number of visits to the hospital and reducing bureaucratic procedures should be used. Once a diagnosis of HCC is made. It should be promptly treated in the appropriate setting, with evaluation of the necessity to refer the patient to a tertiary care hospital for more advanced treatments or to be evaluated for liver transplantation. Figure 2 shows the hub and spoke model of care of cirrhotic patients implemented in our province. According to the model, cirrhotic patients are identified by PCPs using appropriate screening tests. The patients are then referred to the liver clinics of general hospitals (Spokes) for diagnosis confirmation and implementation of surveillance programs. Therapeutic interventions are performed locally when feasible or the patient is referred to the tertiary referral hospital (Hub) for further treatment.

KEY TAKE AWAY MESSAGES

Surveillance for HCC in cirrhotic patients and chronic hepatitis B patients allows detection of the tumor at an early stage and improves survival.

International guidelines recommend semiannual ultrasound with or without AFP monitoring in these patients, but surveillance implementation at the community level is low.

Education programs targeting PCP and aiming at improving the identification and referral of patients at risk of HCC should be implemented.

Subspecialty-based surveillance performed by the hepatologist or gastroenterologist in the setting of the liver clinic of a general hospital is the preferred model, when feasible.

Ultrasound and MRI should be used sequentially in case of inadequate sonography.

Surveillance should be incorporated into the specific care and follow-up provided by the liver clinic to enhance adherence.

The liver clinic of the general hospital should be integrated into a hub and spoke model of care alongside PCPs and tertiary referral hospitals to ensure proper access to care.

ACKNOWLEDGMENTS

We thank Dr. Francesca De Martini for scientific and language revision of the English text.

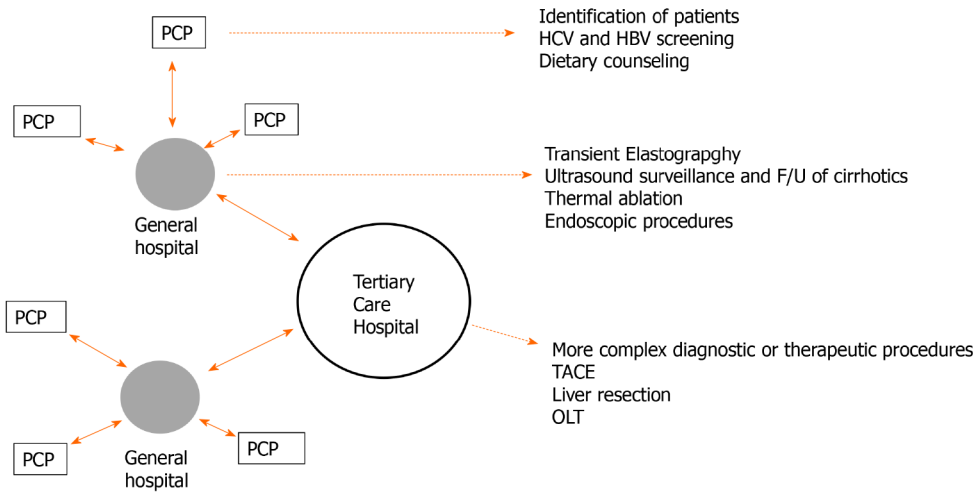


Figure 2 Hub and spoke model for the diagnosis and follow-up of cirrhotic patients by primary care physicians in the province of Bergamo. In the model, ultrasound surveillance and follow-up of cirrhotics are performed by hepatologists in general hospitals. HBV: Hepatitis B virus; HCV: Hepatitis C virus; OLT: Orthotopic liver transplantation; PCP: Primary care physicians.

REFERENCES

1 **Sung H**, Ferlay J, Siegel RL, Laversanne M, Soerjomataram I, Jemal A, Bray F. Global Cancer Statistics 2020: GLOBOCAN Estimates of Incidence and Mortality Worldwide for 36 Cancers in 185 Countries. *CA Cancer J Clin* 2021; **71**: 209-249 [PMID: 33538338 DOI: 10.3322/caac.21660]

2 **Omata M**, Cheng AL, Kokudo N, Kudo M, Lee JM, Jia J, Tateishi R, Han KH, Chawla YK, Shiina S, Jafri W, Payawal DA, Ohki T, Ogasawara S, Chen PJ, Lesmana CRA, Lesmana LA, Gani RA, Obi S, Dokmeci AK, Sarin SK. Asia-Pacific clinical practice guidelines on the management of hepatocellular carcinoma: a 2017 update. *Hepatol Int* 2017; **11**: 317-370 [PMID: 28620797 DOI: 10.1007/s12072-017-9799-9]

3 **Tapper EB**, Parikh ND. Mortality due to cirrhosis and liver cancer in the United States, 1999-2016: observational study. *BMJ* 2018; **362**: k2817 [PMID: 30021785 DOI: 10.1136/bmj.k2817]

4 **Zhang BH**, Yang BH, Tang ZY. Randomized controlled trial of screening for hepatocellular carcinoma. *J Cancer Res Clin Oncol* 2004; **130**: 417-422 [PMID: 15042359 DOI: 10.1007/s00432-004-0552-0]

5 **El-Serag HB**, Kramer JR, Chen GJ, Duan Z, Richardson PA, Davila JA. Effectiveness of AFP and ultrasound tests on hepatocellular carcinoma mortality in HCV-infected patients in the USA. *Gut* 2011; **60**: 992-997 [PMID: 21257990 DOI: 10.1136/gut.2010.230508]

6 **Pateron D**, Ganne N, Trinchet JC, Aurousseau MH, Mal F, Meicler C, Coderc E, Reboullet P, Beaugrand M. Prospective study of screening for hepatocellular carcinoma in Caucasian patients with cirrhosis. *J Hepatol* 1994; **20**: 65-71 [PMID: 7515408 DOI: 10.1016/s0168-8278(05)80468-4]

7 **Trevisani F**, De Notariis S, Rapaccini G, Farinati F, Benvegnù L, Zoli M, Grazi GL, Del PP, Di N, Bernardi M; Italian Liver Cancer Group. Semiannual and annual surveillance of cirrhotic patients for hepatocellular carcinoma: effects on cancer stage and patient survival (Italian experience). *Am J Gastroenterol* 2002; **97**: 734-744 [PMID: 11922571 DOI: 10.1111/j.1572-0241.2002.05557.x]

8 **Singal AG**, Pillai A, Tiro J. Early detection, curative treatment, and survival rates for hepatocellular carcinoma surveillance in patients with cirrhosis: a meta-analysis. *PLoS Med* 2014; **11**: e1001624 [PMID: 24691105 DOI: 10.1371/journal.pmed.1001624]

9 **Sarasin FP**, Giostra E, Hadengue A. Cost-effectiveness of screening for detection of small hepatocellular carcinoma in western patients with Child-Pugh class A cirrhosis. *Am J Med* 1996; **101**: 422-434 [PMID: 8873514 DOI: 10.1016/S0002-9343(96)00197-0]

10 **Lin OS**, Keeffe EB, Sanders GD, Owens DK. Cost-effectiveness of screening for hepatocellular carcinoma in patients with cirrhosis due to chronic hepatitis C. *Aliment Pharmacol Ther* 2004; **19**: 1159-1172 [PMID: 15153169 DOI: 10.1111/j.1365-2036.2004.01963.x]

11 **Thompson Coon J**, Rogers G, Hewson P, Wright D, Anderson R, Cramp M, Jackson S, Ryder S, Price A, Stein K. Surveillance of cirrhosis for hepatocellular carcinoma: systematic review and economic analysis. *Health Technol Assess* 2007; **11**: 1-206 [PMID: 17767898 DOI: 10.3310/hta11340]

12 **European Association for the Study of the Liver**. EASL Clinical Practice Guidelines: Management of hepatocellular carcinoma. *J Hepatol* 2018; **69**: 182-236 [PMID: 29628281 DOI: 10.1016/j.jhep.2018.03.019]

13 **Heimbach JK**, Kulik LM, Finn RS, Sirlin CB, Abecassis MM, Roberts LR, Zhu AX, Murad MH, Marrero JA. AASLD guidelines for the treatment of hepatocellular carcinoma. *Hepatology* 2018; **67**: 358-380 [PMID: 28130846 DOI: 10.1002/hep.29086]

14 **Noone A**, Howlader N, Krapcho M. Cancer statistics review, 1975-2015. Bethesda, MD: National

Cancer Insitute, 2018

15 **Singal AG**, Yopp A, S Skinner C, Packer M, Lee WM, Tiro JA. Utilization of hepatocellular carcinoma surveillance among American patients: a systematic review. *J Gen Intern Med* 2012; **27**: 861-867 [PMID: 22215266 DOI: 10.1007/s11606-011-1952-x]

16 **Simmons OL**, Feng Y, Parikh ND, Singal AG. Primary Care Provider Practice Patterns and Barriers to Hepatocellular Carcinoma Surveillance. *Clin Gastroenterol Hepatol* 2019; **17**: 766-773 [PMID: 30056183 DOI: 10.1016/j.cgh.2018.07.029]

17 **Dalton-Fitzgerald E**, Tiro J, Kandunoori P, Halm EA, Yopp A, Singal AG. Practice patterns and attitudes of primary care providers and barriers to surveillance of hepatocellular carcinoma in patients with cirrhosis. *Clin Gastroenterol Hepatol* 2015; **13**: 791-8.e1 [PMID: 25019694 DOI: 10.1016/j.cgh.2014.06.031]

18 **Del Poggio P**, Olmi S, Ciccarese F, Di Marco M, Rapaccini GL, Benvegnù L, Borzio F, Farinati F, Zoli M, Giannini EG, Caturelli E, Chiaramonte M, Trevisani F; Italian Liver Cancer (ITA. LI.CA) Group. Factors that affect efficacy of ultrasound surveillance for early stage hepatocellular carcinoma in patients with cirrhosis. *Clin Gastroenterol Hepatol* 2014; **12**: 1927-33.e2 [PMID: 24582947 DOI: 10.1016/j.cgh.2014.02.025]

19 **Cozzolongo R**, Cuppone R, Petruzzi J, Stroffolini T, Manghisi OG. Approach of primary care physicians to hepatitis C: an educational survey from a Southern Italian area. *J Infect* 2005; **51**: 396-400 [PMID: 16321651 DOI: 10.1016/j.jinf.2004.12.004]

20 **Delarocque-Astagneau E**, Meffre C, Dubois F, Pioche C, Le Strat Y, Roudot-Thoraval F, Hillon P, Silvain C, Dhumeaux D, Desenclos JC; Hepatitis C Surveillance System Committee; Scientific Committee for the National Prevalence Survey of Hepatitis B and C Markers. The impact of the prevention programme of hepatitis C over more than a decade: the French experience. *J Viral Hepat* 2010; **17**: 435-443 [PMID: 19780936 DOI: 10.1111/j.1365-2893.2009.01196.x]

21 **Del Poggio P**, Olmi S, Ciccarese F, Mazzoleni M, Jazzetti M, Jamoletti C, Mattiello M, Del Poggio A, Portugali V, Stroffolini T. A training program for primary care physicians improves the effectiveness of ultrasound surveillance of hepatocellular carcinoma. *Eur J Gastroenterol Hepatol* 2015; **27**: 1103-1108 [PMID: 26049705 DOI: 10.1097/MEG.0000000000000404]

22 **Wolf E**, Rich NE, Marrero JA, Parikh ND, Singal AG. Use of Hepatocellular Carcinoma Surveillance in Patients With Cirrhosis: A Systematic Review and Meta-Analysis. *Hepatology* 2021; **73**: 713-725 [PMID: 32383272 DOI: 10.1002/hep.31309]

23 **McGowan CE**, Edwards TP, Luong MU, Hayashi PH. Suboptimal surveillance for and knowledge of hepatocellular carcinoma among primary care providers. *Clin Gastroenterol Hepatol* 2015; **13**: 799-804 [PMID: 25117773 DOI: 10.1016/j.cgh.2014.07.056]

24 **Farvardin S**, Patel J, Khambaty M, Yerokun OA, Mok H, Tiro JA, Yopp AC, Parikh ND, Marrero JA, Singal AG. Patient-reported barriers are associated with lower hepatocellular carcinoma surveillance rates in patients with cirrhosis. *Hepatology* 2017; **65**: 875-884 [PMID: 27531684 DOI: 10.1002/hep.28770]

25 **Beste LA**, Ioannou GN, Yang Y, Chang MF, Ross D, Dominitz JA. Improved surveillance for hepatocellular carcinoma with a primary care-oriented clinical reminder. *Clin Gastroenterol Hepatol* 2015; **13**: 172-179 [PMID: 24813175 DOI: 10.1016/j.cgh.2014.04.033]

26 **Singal AG**, Tiro JA, Murphy CC, Marrero JA, McCallister K, Fullington H, Mejias C, Waljee AK, Pechero Bishop W, Santini NO, Halm EA. Mailed Outreach Invitations Significantly Improve HCC Surveillance Rates in Patients With Cirrhosis: A Randomized Clinical Trial. *Hepatology* 2019; **69**: 121-130 [PMID: 30070379 DOI: 10.1002/hep.30129]

27 **Tzartzeva K**, Obi J, Rich NE, Parikh ND, Marrero JA, Yopp A, Waljee AK, Singal AG. Surveillance Imaging and Alpha Fetoprotein for Early Detection of Hepatocellular Carcinoma in Patients With Cirrhosis: A Meta-analysis. *Gastroenterology* 2018; **154**: 1706-1718.e1 [PMID: 29425931 DOI: 10.1053/j.gastro.2018.01.064]

28 **Bolondi L**, Sofia S, Siringo S, Gaiani S, Casali A, Zironi G, Piscaglia F, Gramantieri L, Zanetti M, Sherman M. Surveillance programme of cirrhotic patients for early diagnosis and treatment of hepatocellular carcinoma: a cost effectiveness analysis. *Gut* 2001; **48**: 251-259 [PMID: 11156649 DOI: 10.1136/gut.48.2.251]

29 **Simmons O**, Fetzer DT, Yokoo T, Marrero JA, Yopp A, Kono Y, Parikh ND, Browning T, Singal AG. Predictors of adequate ultrasound quality for hepatocellular carcinoma surveillance in patients with cirrhosis. *Aliment Pharmacol Ther* 2017; **45**: 169-177 [PMID: 27862091 DOI: 10.1111/apt.13841]

30 **Kim SY**, An J, Lim YS, Han S, Lee JY, Byun JH, Won HJ, Lee SJ, Lee HC, Lee YS. MRI With Liver-Specific Contrast for Surveillance of Patients With Cirrhosis at High Risk of Hepatocellular Carcinoma. *JAMA Oncol* 2017; **3**: 456-463 [PMID: 27657493 DOI: 10.1001/jamaoncol.2016.3147]

31 **Pocha C**, Dieperink E, McMaken KA, Knott A, Thuras P, Ho SB. Surveillance for hepatocellular cancer with ultrasonography vs. computed tomography -- a randomised study. *Aliment Pharmacol Ther* 2013; **38**: 303-312 [PMID: 23750991 DOI: 10.1111/apt.12370]

32 **Rich NE**, John BV, Parikh ND, Rowe I, Mehta N, Khatri G, Thomas SM, Anis M, Mendiratta-Lala M, Hernandez C, Odewole M, Sundaram LT, Konjeti VR, Shetty S, Shah T, Zhu H, Yopp AC, Hoshida Y, Yao FY, Marrero JA, Singal AG. Hepatocellular Carcinoma Demonstrates Heterogeneous Growth Patterns in a Multicenter Cohort of Patients With Cirrhosis. *Hepatology* 2020; **72**: 1654-1665 [PMID: 32017165 DOI: 10.1002/hep.31159]

33 **Lencioni R**, Piscaglia F, Bolondi L. Contrast-enhanced ultrasound in the diagnosis of hepatocellular

carcinoma. *J Hepatol* 2008; **48**: 848-857 [PMID: 18328590 DOI: 10.1016/j.jhep.2008.02.005]

34 **Kudo M**, Hatanaka K, Kumada T, Toyoda H, Tada T. Double-contrast ultrasound: a novel surveillance tool for hepatocellular carcinoma. *Am J Gastroenterol* 2011; **106**: 368-370 [PMID: 21301463 DOI: 10.1038/ajg.2010.432]

35 **Kanwal F**, Singal AG. Surveillance for Hepatocellular Carcinoma: Current Best Practice and Future Direction. *Gastroenterology* 2019; **157**: 54-64 [PMID: 30986389 DOI: 10.1053/j.gastro.2019.02.049]

36 **Lee E**, Edward S, Singal AG, Lavieri MS, Volk M. Improving screening for hepatocellular carcinoma by incorporating data on levels of α-fetoprotein, over time. *Clin Gastroenterol Hepatol* 2013; **11**: 437-440 [PMID: 23247324 DOI: 10.1016/j.cgh.2012.11.029]

37 **Tayob N**, Lok AS, Do KA, Feng Z. Improved Detection of Hepatocellular Carcinoma by Using a Longitudinal Alpha-Fetoprotein Screening Algorithm. *Clin Gastroenterol Hepatol* 2016; **14**: 469-475.e2 [PMID: 26260109 DOI: 10.1016/j.cgh.2015.07.049]

38 **Berhane S**, Toyoda H, Tada T, Kumada T, Kagebayashi C, Satomura S, Schweitzer N, Vogel A, Manns MP, Benckert J, Berg T, Ebker M, Best J, Dechêne A, Gerken G, Schlaak JF, Weinmann A, Wörns MA, Galle P, Yeo W, Mo F, Chan SL, Reeves H, Cox T, Johnson P. Role of the GALAD and BALAD-2 Serologic Models in Diagnosis of Hepatocellular Carcinoma and Prediction of Survival in Patients. *Clin Gastroenterol Hepatol* 2016; **14**: 875-886.e6 [PMID: 26775025 DOI: 10.1016/j.cgh.2015.12.042]

39 **Wong RJ**, Ahmed A; Hepatocellular Carcinoma Research Committee of the Chronic Liver Disease Foundation. Understanding Gaps in the Hepatocellular Carcinoma Cascade of Care: Opportunities to Improve Hepatocellular Carcinoma Outcomes. *J Clin Gastroenterol* 2020; **54**: 850-856 [PMID: 33030855 DOI: 10.1097/MCG.0000000000001422]

World Journal of Gastroenterology

Submit a Manuscript: https://www.f6publishing.com

World J Gastroenterol 2021 October 7; 27(37): 6191-6223

DOI: 10.3748/wjg.v27.i37.6191

ISSN 1007-9327 (print) ISSN 2219-2840 (online)

REVIEW

Challenges and opportunities in the application of artificial intelligence in gastroenterology and hepatology

Chrysanthos D Christou, Georgios Tsoulfas

ORCID number: Chrysanthos D Christou 0000-0002-5417-8686; Georgios Tsoulfas 0000-0001-5043-7962.

Author contributions: Christou CD performed the screening of articles for eligibility and drafted the manuscript; Tsoulfas G performed the screening of articles for eligibility and edited the manuscript.

Conflict-of-interest statement: The authors declare no conflict of interest for this article.

Open-Access: This article is an open-access article that was selected by an in-house editor and fully peer-reviewed by external reviewers. It is distributed in accordance with the Creative Commons Attribution NonCommercial (CC BY-NC 4.0) license, which permits others to distribute, remix, adapt, build upon this work non-commercially, and license their derivative works on different terms, provided the original work is properly cited and the use is non-commercial. See: http://creativecommons.org/Licenses/by-nc/4.0/

Manuscript source: Invited manuscript

Specialty type: Gastroenterology and hepatology

Chrysanthos D Christou, Georgios Tsoulfas, Organ Transplant Unit, Hippokration General Hospital, Aristotle University of Thessaloniki, Thessaloniki 54622, Greece

Corresponding author: Georgios Tsoulfas, FACS, FICS, MD, Associate Professor, Organ Transplant Unit, Hippokration General Hospital, Aristotle University of Thessaloniki, 66 Tsimiski Street, Thessaloniki 54622, Greece. tsoulfasg@gmail.com

Abstract

Artificial intelligence (AI) is an umbrella term used to describe a cluster of interrelated fields. Machine learning (ML) refers to a model that learns from past data to predict future data. Medicine and particularly gastroenterology and hepatology, are data-rich fields with extensive data repositories, and therefore fruitful ground for AI/ML-based software applications. In this study, we comprehensively review the current applications of AI/ML-based models in these fields and the opportunities that arise from their application. Specifically, we refer to the applications of AI/ML-based models in prevention, diagnosis, management, and prognosis of gastrointestinal bleeding, inflammatory bowel diseases, gastrointestinal premalignant and malignant lesions, other nonmalignant gastrointestinal lesions and diseases, hepatitis B and C infection, chronic liver diseases, hepatocellular carcinoma, cholangiocarcinoma, and primary sclerosing cholangitis. At the same time, we identify the major challenges that restrain the widespread use of these models in healthcare in an effort to explore ways to overcome them. Notably, we elaborate on the concerns regarding intrinsic biases, data protection, cybersecurity, intellectual property, liability, ethical challenges, and transparency. Even at a slower pace than anticipated, AI is infiltrating the healthcare industry. AI in healthcare will become a reality, and every physician will have to engage with it by necessity.

Key Words: Artificial intelligence; Machine learning; Gastroenterology; Hepatology; Artificial neural networks; Support vector machine

©The Author(s) 2021. Published by Baishideng Publishing Group Inc. All rights reserved.

Core Tip: The opportunities that arise from the application of artificial intelligence/machine learning-based models in gastroenterology and hepatology include the

Country/Territory of origin: Greece

Peer-review report's scientific quality classification
Grade A (Excellent): 0
Grade B (Very good): 0
Grade C (Good): C
Grade D (Fair): 0
Grade E (Poor): 0

Received: January 31, 2021
Peer-review started: January 31, 2021
First decision: March 14, 2021
Revised: May 6, 2021
Accepted: August 31, 2021
Article in press: August 31, 2021
Published online: October 7, 2021

P-Reviewer: Atsawarungruangkit A
S-Editor: Liu M
L-Editor: A
P-Editor: Liu JH

establishment of targeted screening programs through the identification of patients prone to develop cancer, the development of non-invasive diagnostic tools, the improvement of the diagnostic accuracy, the development of treatment allocation frameworks based on predictions of outcomes for different treatment modalities, the development of models to ensure cost-effective use of resources, the development of triage tools for higher levels of care and decision-making tools for further treatment, based on individualized patient outcome predictions, and finally the development of predictive models of prognosis for patient and family counseling.

Citation: Christou CD, Tsoulfas G. Challenges and opportunities in the application of artificial intelligence in gastroenterology and hepatology. *World J Gastroenterol* 2021; 27(37): 6191-6223
URL: https://www.wjgnet.com/1007-9327/full/v27/i37/6191.htm
DOI: https://dx.doi.org/10.3748/wjg.v27.i37.6191

INTRODUCTION

Artificial intelligence (AI) is an umbrella term to describe any application where computer systems are used to perform tasks normally associated with human intelligence[1,2]. AI is a cluster of interrelated fields, including machine learning (ML) and probabilistic reasoning, planning and decision making, fuzzy systems, computer vision, natural language processing, knowledge representation, and neural networks (NN)[1]. Despite their differences, these fields are all driven by advancements in computing power and Big Data.

ML could be described as a model that learns from past data in order to predict future data[3]. The application of ML in healthcare was catalyzed by several healthcare trends, such as electronic healthcare records and patient summaries, genomic analyses and biomedical research, routine imaging, and telemedicine, that have transformed the healthcare industry into a data-rich science with data as an omnipresent concept[4-6]. Specifically, while in 2013, the healthcare industry produced 153 exabytes (10^{18} gigabytes) of data, it has been projected to reach 2314 exabytes in 2020[7]. Therefore, the healthcare industry generates an enormous amount of data that conform with the features that define Big Data: Volume, high-velocity, high-variety, and veracity, which cannot be analyzed or managed by traditional software[5,8,9]. AI promises to process and analyze these extensive repositories of data and turn them into meaningful insights.

Several studies have described AI as the potential solution to long-standing healthcare challenges such as increasing diagnostic accuracy, enhancing telemedicine, providing substantial cost reduction, promoting evidence-based medicine, facilitating targeted literature search, and delivering individualized care[10-14]. More importantly, AI could substantially alleviate the burden of diseases by reducing the associated mortality and morbidity through optimizing patient outcomes[15,16].

In gastroenterology and hepatology, physicians handle large amounts of clinical data and an extensive repository of imaging data generated from endoscopy, ultrasound, and computed tomography (CT). Therefore gastroenterology and hepatology are data-rich fields, and thus fruitful ground for AI applications with extensive research conducted in these fields, particularly regarding the prevention, diagnosis, management, and prognosis of diseases[17,18]. We aim to comprehensively review the applications of AI in gastroenterology and hepatology and identify the current challenges of utilizing AI in healthcare in an effort to explore ways to overcome them.

SEARCH STRATEGY

We conducted a comprehensive literature review of the Medline, Cochrane, and Scopus databases using the following algorithm: [(artificial intelligence OR machine learning OR deep learning OR neural networks OR support vector machine OR computer-assisted OR computer-aided) AND (gastroenterology OR hepatology OR

esophageal OR small bowel OR large bowel OR gastric cancer OR capsule endoscopy OR polyps OR colonoscopy OR colorectal cancer OR gastrointestinal bleeding OR inflammatory bowel disease OR Crohn's disease OR celiac disease OR ulcers OR hepatocellular carcinoma OR cholangiocarcinoma OR liver fibrosis OR fatty liver OR chronic liver disease OR cirrhosis)]. Articles were reviewed for eligibility by the two authors independently (CC, GT), and disagreements were solved by a discussion between the two authors. Finally, the reference lists of eligible articles were reviewed to identify further related literature, including articles, books, and other forms of publication. We excluded studies written in a language other than English and publications of abstracts. The review of the literature was completed on January 27, 2021.

AI CLASSIFIERS

Before discussing AI's current applications and challenges in gastroenterology and hepatology, we briefly describe the AI classifiers in ML models that we identified as the most commonly used among the eligible articles. Specifically, we describe the basic features of the support vector machine (SVM), the artificial NN (ANN), and the convolutional NN (CNN). ML is divided into supervised and unsupervised based on whether the training data is labeled or not[19]. In other words, through supervised ML, a new data set is classified for an outcome based on previous data sets that trained the ML model, while in unsupervised ML, there is no outcome but rather an attempt to detect unknown patterns and correlations within the data[20].

SVMs are supervised learning models with associated learning algorithms trained to assign classes to new cases. SVMs require a training set of data where each case is pre-labeled regarding the outcome classification. The data points of the features of each case are treated as points in a high-dimensional space[21]. Based on these mapped points, separating hyperplanes are drawn, aiming to distinguish these points upon their labeled class[22]. The hyperplane with the maximum distance from the mapped data points, known as the maximum functional margin, is selected since it provides the SMV's full potential to classify new examples correctly[21,22]. SVMs typically perform linear classification analysis. For non-linear analysis, kernel function could introduce additional dimensions to the raw data; and thus turning a non-linear problem into a linear problem in a higher-dimensional space[23].

An ANN is an ML model inspired by the human brain's neuronal connections that consist of an input layer, an output layer, and a hidden layer between them[18]. ANNs are applied both in supervised and unsupervised ML[24]. When multiple hidden layers are inserted between the input and output layers, and the network's architecture becomes more complex with multiple interconnections, the concept of deep NN (DNN) emerges[24,25]. During DNN training, the model adjusts the weighted correlations between the nodes of the input layer and the nodes of the multiple hidden layers[18,20]. Within DNN, CNNs are biologically variants inspired by multi-layer perceptrons[26]. CNNs have been extensively applied for medical image analysis[17,18]. During the CNN model development, the images are preprocessed using multiple filters, and multiple feature maps are created in a process called convolution[26].

APPLICATIONS OF AI IN GASTROENTEROLOGY

AI/ML-based models have been extensively applied in the prevention, diagnostics, management, and prognosis of gastrointestinal (GI) diseases, including GI bleeding (GIB), inflammatory bowel diseases (IBDs), malignant and premalignant lesions, and other nonmalignant lesions/diseases such as gastroesophageal reflux, *Helicobacter pylori* (*H. pylori*) infection, ulcers, celiac disease, and intestinal hookworms.

Prevention

Table 1 summarizes the findings of the identified studies applying AI/ML models in the prevention of gastroenterological diseases. AI/ML-based software could be used in screening programs to identify high-risk patients not currently identified by standard screening guidelines. In a recent study, researchers developed seven different AI/ML models to identify patients at high risk of developing gastric cancer following the eradication of *H. pylori* infection[27]. The extreme gradient boosting (GB) model demonstrated the highest performance[27]. A CNN was developed in a different study to classify patients at low, moderate, and high risk of developing gastric cancer using

Table 1 Artificial intelligence applications in gastroenterology: Prevention

Ref.	Parameters employed	AI classifier	Sizes of the training/validation sets	Outcomes	Performance
Leung *et al* [27]	Laboratory results, clinicopathological parameters	Several	64238/25330 patients	Risk of gastric cancer development following *H.pylori* eradication	0.53-0.97[2,6], 59.3-98.1[3,6], 51.5-93.6[4,6]
Nakahira *et al*[28]	Laboratory results, clinicopathological parameters, endoscopic images	CNN	7826/454 patients	Stratify risk of gastric cancer development	---
Taninaga *et al*[29]	Laboratory results, clinicopathological parameters, endoscopic images	CART	1144/287	Prediction of future gastric cancer	63.4-94.8[1,6], 0.736-0.874[2,6]
Goshen *et al*[31]	Laboratory results, clinicopathological parameters	DT, RF, GB	688 flagged patients	High risk of CRC development	----

[1]Accuracy (%).
[2]Area under the receiver operating curve or c-index.
[3]Sensitivity (%).
[4]Specificity (%).
[5]Training.
[6]Internal validation.
[7]External validation/testing. CART: Classification and regression tree; CNN: Convolutional neural network; CRC: Colorectal cancer; DT: Decision tree; GB: Gradient boosting; RF: Random forest.

endoscopic images[28]. A similar study used multiple classification and regression trees (CART) to develop a model that predicts future gastric cancer development[29]. Another notable example is the ColonFlag test, an ML algorithm that uses age, sex, and complete blood count data to identify patients at high risk of developing colorectal cancer[30,31]. In a recent study, among 254 individuals who underwent colonoscopy, 19 cancers (7.5%) and 22 (8.7%) advanced adenomas were identified in a population of patients who would otherwise have avoided screening[31]. These studies demonstrate how AI/ML-based models could be used in a real clinical setting to establish targeted screening programs.

Diagnostics

Table 2 summarizes the findings of the identified studies applying AI/ML models to diagnose gastroenterological diseases. AI/ML-based software is applied in Computed Aided Detection or Diagnosis (CAD) systems used in radiology to augment medical images' interpretation accuracy. A CAD typically includes the stages of preprocessing, extraction of features, and feature selection and classification[32]. CAD systems could also aid endoscopists in navigating through the different anatomical locations of the GI tract. Specifically, a model based on a CNN employed esophagogastroduodenoscopy images to recognize the anatomical locations with outstanding performance[33].

Regarding the diagnosis of gastroesophageal reflux, an ANN model was developed as a non-invasive diagnostic tool by employing only clinical data[34]. For patients with Barrett's esophagus, a deep learning-based (DL) CAD system was developed to differentiate patients with malignant from patients with nondysplastic Barret's esophagus [35]. The CAD system also identified the optimal site to perform a biopsy with an accuracy between 92% and 97%[35]. An SVM model was developed in another study employing white-light endoscopic imaging to identify early neoplastic lesions[36]. In a recent study, images from volumetric laser endomicroscopy were used to develop a CAD system to detect neoplastic lesions for patients with Barret's esophagus[37]. A similar study using volumetric laser endomicroscopy developed an ML model for detecting neoplastic lesions[38]. Notably, the model outperformed the experts in volumetric laser endomicroscopy[38]. Finally, to diagnose esophageal squamous cell carcinoma, a CNN model was developed by employing endocytoscopic images as an alternative to biopsy[39].

For diagnosing patients with *H. pylori* infection, a CNN was developed in a study employing gastroscopic images[40]. A different CNN for *H. pylori* diagnosis was developed in a prospective pilot study analyzing images taken from the stomach's lesser curvature using either white light imaging, blue light imaging, or linked color imaging[41]. Notably, employing blue light and linked color imaging yielded significantly higher performance than white light imaging[41]. In a similar study, a

Table 2 Artificial intelligence applications in gastroenterology: Diagnosis

Ref.	Diagnostic Modality	AI classifier	Sizes of the training/validation sets	Outcomes	Performance
Takiyama *et al* [33]	Esophago-gastro-duodenoscopy imaging	CNN	1750/435[7]	Anatomical classification among larynx, esophagus, stomach, and duodenum	0.99-1.00[2,7]
Pace *et al*[34]	Laboratory results, clinicopathological parameters	ANN	159 patients	Diagnosis of gastroesophageal reflux disease	67.86-100[1,6]
de Groof *et al* [35]	Esophageal endoscopic images	DNN	1247/297[6]/80[7]/80[7] patients	Classification of malignant from nondysplastic Barret's esophagus	88.2[1,6], 87.5-88.8[1,7], 87.6[3,6], 90.0-92.5[3,7], 88.6[4,6], 82.5-87.5[4,7]
van der Sommen *et al*[36]	White-light endoscopic imaging	SVM	44 patients with Barret's esophagus	Diagnosis of early neoplastic lesions	Per image: 62-90[3,6], 65-90[4,6], Per patient: 52-100[3,6], 74-96[4,6]
Struyvenberg *et al*[37]	Volumetric laser endomicroscopy imaging	Several	29 patients with Barret's esophagus	Diagnosis of neoplastic lesions	0.83-0.94[2,6]
Swager *et al*[38]	Volumetric laser endomicroscopy imaging	Several	60 images	Diagnosis of neoplastic lesions	0.89-0.95[2,6]
Kumagai *et al* [39]	Endocytoscopic imaging	CNN	4715/1520[7]	Diagnosis of esophageal squamous cell carcinoma	90.9[1,7], 0.72-0.90[2,7], 39.4-46.4[3,7], 98.2-98.4[4,7]
Zheng *et al*[40]	Endoscopic images	CNN	1507/452 patients	Diagnosis of *H.pylori* infection	84.5-93.8[1,6], 0.93-0.97[2,6], 81.4-91.6[3,6], 90.1-98.6[4,6]
Nakashima *et al* [41]	Endoscopic images	CNN	162/60 patients	Diagnosis of *H.pylori* infection	0.66-0.96[2,6]
Itoh *et al*[42]	Endoscopic images	CNN	149/30 images	Diagnosis of *H.pylori* infection	0.956[2,6], 86.7[3,6], 86.7[4,6]
Shichijo *et al*[43]	Endoscopic images	CNN	32308/11481[7]	Diagnosis of *H.pylori* infection	83.1-87.7[1,7], 81.9-88.9[3,7], 83.4-87.4[4,7]
Kanesaka *et al* [45]	NBI	SVM	126/81 NBI images	Diagnosis of gastric cancer	96.3[1,6], 96.7[3,6], 95.0[4,6]
Hirasawa *et al* [46]	Endoscopic images	CNN	13584/2296[7]	Diagnosis of gastric cancer	92.2[3,7]
Zhu *et al*[47]	Laboratory results, clinicopathological parameters, cancer biomarkers	GB/DT	496/213 patients	Diagnosis of gastric cancer	85.9[1,5], 831[,6], 0.91[2,6], 88[3,5], 87[3,6], 83.4[4,5], 84.1[4,6]
Tenório *et al*[48]	Laboratory results, clinicopathological parameters	Several	178/38	Diagnosis of celiac disease	71.5-80[1,6], 0.71-0.84[2,6], 69-82[3,6], 67-80[4,6]
Caetano Dos Santos *et al*[49]	Endomysial autoantibody test for IgA-class antibodies images	SVM	2597 images (training:validation = 7:3)	Diagnosis of celiac disease	96.8-98.85[1,6], 82.84-98.91[3,6], 98.81-99.40[4,6]
Hujoel *et al*[50]	Laboratory results, clinicopathological parameters	Several	408 undiagnosed patients	Diagnosis of celiac disease	0.49-0.53[2,6]
Manandhar *et al* [51]	Gut microbiome data	RF	1429 fecal 16S metagenomic data subjects	Diagnosis of IBD	0.80-0.82[2,6]
Wei *et al*[52]	Single nucleotide polymorphisms data	Several	60828 samples	Classification of CD and UC	0.782-0.866[2,6]
Mossotto *et al* [53]	Capsule endoscopy, histologic imaging	SVM	239/48[7] pediatric patients	Classification of CD, UC, and unclassified IBD	71-82.7[1,5], 0.78-0.87[2,5], 83.3[1,7], 83-85[3,7]
Xia *et al*[58]	Capsule endoscopy imaging	CNN	697/100[7] patients, 822590/201365[7], images	Classification among different types of gastric lesions	77.1-86[1,7], 0.80-0.90[2,7], 96.2-100[3,7], 56.5-76.2[4,7]
Seguí *et al*[59]	Capsule endoscopy imaging	CNN	50 videos	Classification of small bowel mobility events	96[1,6]
Park *et al*[60]	Capsule endoscopy imaging	CNN	139 videos, 200000 images (training:validation:test = 6:2:2)	Small bowel lesion identification	80.29-98.34[1,6], 0.999[2,5], 0.998[2,6,7]

Hwang *et al*[61]	Capsule endoscopy imaging	CNN	7556/5760[7] images	Classification of hemorrhagic and ulcerative lesions	96.62-96.83[1,7], 95.07-97.61[3,7], 96.04-98.18[4,7]
Otani *et al*[62]	Capsule endoscopy imaging	DNN	167/40[7] patients	Classification among different types of small bowel lesions	0.950-0.996[2,6], 0.884-0.928[2,7]
Yuan *et al*[63]	Capsule endoscopy imaging	SVM	20 patients, 340 images (training:validation = 8:2)	Diagnosis of peptic ulcers	92.65[1,6], 94.12[3,6], 91.18[4,6]
Karargyris *et al*[64]	Capsule endoscopy imaging	SVM	80 frames	Diagnosis of peptic ulcers	75[3,6], 73.3[4,6]
He *et al*[65]	Capsule endoscopy imaging	CNN	11 patients, 440000 images	Diagnosis of intestinal hookworms	88.5[1,6], 0.895[2,6], 84.6[3,6], 88.6[4,6]
Leenhardt *et al*[66]	Capsule endoscopy imaging	CNN	600/600 images	Diagnosis of gastrointestinal angiectasia	100[3,6], 96[4,6]
Zhou *et al*[67]	Capsule endoscopy imaging	CNN	21 videos	Diagnosis of celiac disease	100[3,6], 100[4,6]
Yamada *et al*[68]	Colon capsule endoscopy imaging	CNN	15933/4784[7]	Diagnosis of colorectal neoplasias	83.9[7], 0.902[2,7], 79[3,7], 87[4,7]
Wang *et al*[69]	Colonoscopy imaging	CNN	5545 images/27113[7] images/612[7] images/138[7] videos/54[7] videos	Identification of colorectal polyps	0.984[2,7], 88.24-100[3,7], 95.40-95.92[2,7]
Misawa *et al*[70]	Colonoscopy imaging	CNN	411/35 short videos	Identification of colorectal polyps	76.5[1,6], 0.87[2,6], 90[3,6], 63.3[4,6]
Urban G *et al*[71]	Colonoscopy imaging	CNN	8641 images/20[7] videos	Identification of colorectal polyps	96.4[1,7], 0.991[2,7]
Ozawa *et al*[72]	Colonoscopy imaging	CNN	20431/7077[7] images	Identification of colorectal polyps, Classification of colorectal polyps	90-97[3,7], 47-98[1,7]
Mori *et al*[73]	NBI and methylene blue staining images	SVM	466 diminutive polyps	Classification of diminutive rectosigmoid adenomas	NPV(%): 93.7-96.5
Tischendorf *et al*[74]	NBI	SVM	209 colorectal polyps	Classification of colorectal polyps	90[3,6], 70.2[4,6]
Gross *et al*[75]	NBI	SVM	434 colorectal polyps	Classification of small colorectal polyps	93.1[1,6], 95.0[3,6], 90.3[4,6]
Kominami *et al*[76]	NBI	SVM	118 colorectal polyps	Classification of colorectal polyps	93.2[1,6], 93.0[3,6], 93.3[4,6]
Misawa *et al*[77]	NBI endocytoscopy	SVM	979/100 endocytoscopy, images	Classification of colorectal polyps	90[1,6], 84.5[3,6], 97.6[4,6]
Takeda *et al*[78]	NBI endocytoscopy	SVM	5543/200 endocytoscopy, images	Diagnosis of invasive CRC	94.1[1,6], 89.4[3,6], 98.9[4,6]
Chen *et al*[79]	NBI	CNN	2157/284[7]	Classification neoplastic from hyperplastic polyps	96.3[3,7], 78.1[4,7], NPV(%): 91.5[7]
Komeda *et al*[80]	NBI	CNN	1200/600 images	Classification of adenomatous from non-adenomatous polyps	75.1[1,6]
Byrne *et al*[81]	NBI	CNN	223/40[7] videos	Classification of adenomas from hyperplastic polyps	94[1,7], 0.95[2,7], 98[3,7], 83[4,7], NPV(%): 97[7]

[1]Accuracy (%).
[2]Area under the receiver operating curve or c-index.
[3]Sensitivity (%).
[4]Specificity (%).
[5]Training.
[6]Internal validation.
[7]External validation/testing. ANN: Artificial neural network; CD: Chron's disease; CNN: Convolutional neural network; CRC: Colorectal cancer; DNN: Deep neural network; DT: Decision tree; GB: Gradient boosting; IBD: Inflammatory bowel disease; NBI: Narrow-band imaging; NPV: Negative predictive value; RF: Random forest; SVM: Support vector machine; UC: Ulcerative colitis.

CNN model employed images from upper GI endoscopy to detect *H. pylori* infection

[42]. Finally, Shichijo *et al*[43] developed two different CNN models to diagnose *H. pylori* infection. The first, a 22-layered deep CNN, performed comparably with endoscopists, while the second, which classified images based on their location in the stomach, performed comparably with endoscopists in terms of sensitivity and specificity but demonstrated a significantly higher accuracy[43]. The time needed to analyze all the images was 3 min and 18 s and 3 min and 14 s for the two CNNs, while for endoscopists, the average time needed was 230.1 min[43]. A recent meta-analysis evaluating the performance of CNNs to diagnose infection with *H. pylori* concluded that it is currently equivalent to physicians[44].

Regarding the diagnosis of gastric cancer, an SVM-based CAD model was developed to identify early gastric cancer features in narrow-band imaging (NBI) gastroscopy[45]. In a different retrospective study, a CNN was developed to detect gastric cancer from endoscopic images. Even though the model managed to correctly classify 71 of the 77 gastric cancer lesions (92.2% sensitivity), it also falsely identified 161 non-cancerous lesions as gastric cancer, yielding a low positive predictive value of 30.6%[46]. Approximately half of these lesions were gastritis with an irregular mucosal surface or changes in color tone[46]. Finally, in a recent study, a non-invasive GB/decision tree (DT) model employing only nonendoscopic parameters was developed to diagnose gastric cancer[47].

Regarding the diagnosis of celiac disease, five different AI/ML-based models were developed in a study using clinical data as a base for non-invasively diagnosing celiac disease[48]. Interestingly, the models were tested using 13 different algorithms and different input variables variations, resulting in 270 different tested models[48]. Among them, a model based on the Bayesian classifier demonstrated the highest performance[48]. A different study developed an SVM that employed images from the endomysial autoantibody test for IgA-class antibodies to classify patients with celiac disease[49]. Finally, in a different study, the authors aimed to develop several AI/ML-based models, which employ clinical data, to predict celiac disease in a group of patients who remained undiagnosed[50]. The models were unsuccessful, with only two models slightly outperforming random chance in predicting celiac disease[50].

In the diagnosis of IBDs, a recent study developed five different AI/ML-based models using data from the gut microbiome to classify patients with IBD[51]. The Random Forest (RF) model demonstrated the highest performance with AUROCs of 0.80 when bacterial taxa were used and 0.82 when operational taxonomic features were used[51]. Finally, the models were tested in distinguishing between Chron's disease (CD) and ulcerative colitis (UC), with the RF model demonstrating an AUROC > 0.9[51]. A multicentered, genome-wide association study used data from single-nucleotide polymorphisms to develop several AI/ML-based models to classify patients with CD and UC[52]. For pediatric IBDs, an SVM-based model employed data from histologic and endoscopic images to classify pediatric patients with CD, UC, or unclassified IBD[53]. Other studies have employed images from wireless capsule endoscopy to build SVM models that identify patients with CD with reported accuracies between 80.2% and 100%[54-57].

Focusing on capsule endoscopy, in a recent study, magnetically controlled capsule endoscopy imaging was employed to develop a CNN that provides an automatic detection and classification system for gastric lesions[58]. These lesions included erosions, polyps, ulcers, submucosal tumors, normal mucosa, and xanthomas[58]. A different study used images generated by a wireless capsule to develop a CNN able to classify the small bowel motility among six distinct intestinal motility events[59]. In a recent study, an AI-assisted capsule endoscopy reading model was developed to assist lesion identification[60]. Notably, the model significantly shortened the reading time of images by trainees[60].

To distinguish between hemorrhagic and ulcerative lesions, a CNN was developed using images from small bowel capsule endoscopy[61]. In a similar, recent study, a DNN model used capsule endoscopy images to classify different small bowel lesions (erosions, ulcers, tumors, and vascular lesions)[62]. SVM-based models were developed in two other studies employing images from capsule endoscopy to identify peptic ulcers[63,64]. In three different studies, CNNs have been developed, employing images from capsule endoscopy to diagnose intestinal hookworms, GI angiectasia, and celiac disease[65-67]. Finally, a CNN was developed in a recent study to detect colorectal neoplasias in images from colon capsule endoscopy[68].

Regarding the identification of colorectal polyps in coloscopy, a CNN model was designed to analyze colonoscopy images and videos and identify colorectal polyps [69]. Interestingly, the model's sensitivity to identify flat isochromatic, less than 0.5 cm polyps, which are typically associated with a higher missing rate, was estimated at 91.65% per image[69]. A different study, employing short videos from colonoscopies,

developed a CNN model that identifies colorectal polyps[70]. In another study, a CNN was developed employing videos and images from coloscopy to detect colorectal polyps in real-time[71]. Interestingly, when experts reviewed the colonoscopy videos, they managed to identify additional non-removed polyps with the assistance of the CNN model[71]. In a recent study, an automated polyp detection model based on CNN was developed to identify and then classify colorectal polyps into adenomas, hyperplastic, sessile serrated adenomas, and cancer[72]. The model managed to process the images at a speed of 20 m per frame[72].

Specifically for colorectal polyps classification, in a prospective study, an SVM-based model was developed using NBI and methylene blue staining images to classify diminutive rectosigmoid adenomas in real-time[73]. A prospective pilot study developed an SVM model that employed NBI images to detect and classify colorectal polyps based on vascularization features as neoplastic and non-neoplastic[74]. In a comparative study, an SVM model demonstrated comparable performance at classifying the neoplastic nature of diminutive polyps (< 10 mm) to that of experts in NBI colonoscopy but surpassed the performance of non-experts[75]. Two other studies developed SVM models that employed NBI images to classify colorectal lesions (neoplastic or non-neoplastic)[76,77]. Finally, an SVM model was developed in a retrospective study to diagnose invasive colorectal cancer based on NBI endocytoscopy images[78].

Except for SVMs, several studies employed CNNs for colorectal polyps classification. One comparative study developed a CNN employing NBI colonoscopy images to classify neoplastic polyps[79]. Notably, the model's performance was found comparable to that of experts but superior to the performance of non-experts[79]. In another study focusing on NBI colonoscopy, a CNN model was developed to classify adenomatous from non-adenomatous polyps[80]. A different study developed a CNN model to classify adenomas from hyperplastic polyps during NBI colonoscopy[81].

The performances reported by the majority of the AI/ML-based models surpass both the NPV threshold recommended by the American Society of Gastrointestinal Endoscopy (90%) for adenoma detection and the estimated pooled NPV reported in a meta-analysis conducted by the society (91%)[82,83]. Finally, we should mention that currently, the majority of the CAD systems that we reported have the shortcoming of manual segmentations of lesions. The endoscopists should identify the areas of interest before the model could analyze and attempt to classify. This weakness has been acknowledged by the European Society of Gastrointestinal Endoscopy[84]. Other obstacles to developing CAD systems constitute the lack of large datasets and the lack of variability in images. A recent study aimed to resolve this by developing a CNN that "adds" polyps to the images to increase the repository of images for training and advance the development of automated polyp detection models[85].

Management

Table 3 summarizes the findings of the identified studies applying AI/ML models for the management of gastroenterological diseases. In a recent study, data from baseline impedance, nocturnal baseline impedance, and acid exposure time were used as a base for a DT model to predict the treatment response with proton pump inhibitors for patients with gastroesophageal reflux disease[86]. The aim was to establish a decision-making framework for treatment allocation[86].

AI/ML-based models have been used in the management of malignant GI lesions. Regarding gastric cancer, a CNN has been developed to predict whether the early gastric cancer has invaded the mucosa and submucosa layers of the stomach and act as a decision tool for endoscopic resection[87]. Interestingly, the CNN model outperformed endoscopists[87]. In the same concept, a DNN was developed to classify gastric cancer based on invasion depth as a basis for treatment allocation[88]. Specifically, the model demonstrated accuracy for predicting T1, T1a, T1b T2, T3, T4, and an overall accuracy of 77.2%, 68.9%, 63.6%, 49.1%, 51.0%, 55.3%, and 64.7%, respectively[88]. In colorectal cancer, the identification of microsatellite instability significantly impacts the treatment allocation process. A DL model was developed to identify microsatellite instability directly from hematoxylin and eosin-stained whole slide image[89]. Notably, the model outperformed a group of pathologists[89]. Finally, an SVM model that predicted the lymph node metastasis status of patients with colorectal cancer was designed as a tool to identify patients who would benefit from additional treatment following the endoscopic resection of T1 tumors[90]. Notably, the model outperformed the staging systems endorsed by current guidelines[90].

Regarding the management of GIB, in a recent study, an ML model was developed using data from patients admitted to the intensive care unit (ICU) following a GIB to predict the need for transfusion[91]. The authors suggested that it could potentially be

Table 3 Artificial intelligence applications in gastroenterology: Treatment

Ref.	Parameters employed	AI classifier	Sizes of the training/validation sets	Outcomes	Performance
Rogers *et al* [86]	Data from baseline impedance, nocturnal baseline impedance, and acid exposure time	DT	335 patients	Prediction of treatment response with proton pump inhibitors for patients with gastroesophageal reflux disease	0.31-0.938[2,6]
Zhu *et al* [87]	Endoscopic images	CNN	790/203[7] images	Invasion of gastric cancer at the mucosa and submucosa layers of the stomach	89.16[1,7], 0.94[2,7], 76.47[3,7], 95.56[4,7]
Kubota *et al* [88]	Endoscopic images	DNN	800/90 images	Invasion depth of gastric cancer	64.7[1,6]
Yamashita *et al*[89]	Hematoxylin and eosin-stained WSI	DNN	100/15[6]/484[7]	Identificication of CRC microsatellite instability	0.931[2,6], 0.779[2,7], 76[3,7], 66.6[4,7]
Ichimasa *et al*[90]	Laboratory results, clinicopathological parameters	SVM	590/100[7]	Prediction of lymph node metastasis status	69[1,7], 0.821[2,7], 100[3,7], 66[4,7]
Levi *et al* [91]	Laboratory results, clinicopathological parameters	RFE	14620 patients	Prediction of the need for transfusion following GIB	50.21-74.88[1,6], 0.7858-0.8141[2,6], 69.17-92.77[3,6], 35.02-79.82[4,6]
Chu *et al* [92]	Laboratory results, clinicopathological parameters	Several	122/67 patients	Prediction of the source of GIB	69.7-94.3[1,6], 0.658-0.999[2,6], 90.1-98.0[3,6], 89-100[4,6]
				Prediction of the need for blood resuscitatio	64.7-94.1[1,6], 0.381-0.993[2,6], 90.3-93.9[3,6], 18.4-95.5[4,6]
				Prediction of the need for emergent endoscopy	62.7-83.3[1,6], 0.404-0.913[2,6], 80.1-89.1[3,6], 13.8-85.7[4,6]
				Prediction of disposition	58.4-89.7[1,6], 0.324-0.972[2,6], 81.9-92.9[3,6], 18.4-90.9[4,6]
Das *et al*[93]	Laboratory results, clinicopathological parameters	ANN	194/193[6]/200[7] patients	Prediction of major stigmata of recent hemorrhage	89[1,3,4,6], 77[1,7], 96[3,7], 63[4,7]
				Prediction of the need for emergent endoscopy	81[1,3,6], 61[1,7], 94[3,6], 82[4,6], 48[4,7]
Augustin *et al*[94]	Laboratory results, clinicopathological parameters	CART	164/103[7] patients	Stratification of risk of rebleeding and mortality following acute variceal hemorrhage	0.81-0.83[2,7]
Loftus *et al* [95]	Laboratory results, clinicopathological parameters	ANN	103/44 patients	Prediction of severe lower GIB	0.979[2]
				Prediction of the need for surgical intervention	0.954[2,6]
Ayaru *et al* [96]	Laboratory results, clinicopathological parameters	GB	170/130[7]	Prediction of severe lower GIB	78[1,6], 83[1,7]
				Prediction of recurrent bleeding	88[1,6], 88[1,7]
				Prediction of the need for intervention	88[1,6], 91[1,7]

[1]Accuracy (%).
[2]Area under the receiver operating curve or c-index.
[3]Sensitivity (%).
[4]Specificity (%).
[5]Training.
[6]Internal validation.
[7]External validation/testing. ANN: Artificial neural network; CART: Classification and regression tree; CNN: Convolutional neural network; CRC: Colorectal cancer; DT: Decision tree; DNN: Deep neural network; GB: Gradient boosting; GIB: Gastrointestinal bleeding; RFE: Recursive feature elimination; WSI: Whole-slide image.

used as a decision-making tool to triage patients to the ICU or the ward[91]. A different study developed several AI/ML models for patients with acute GIB to predict four different outputs: The source of bleeding, the need for urgent blood transfusion, the need for urgent endoscopy, and the disposition[92]. The study aimed to establish a decision-making framework for the efficient management of GIB. The RF model outperformed all seven other models for all four outputs[92].

Focusing on the upper GIB, an ANN model was developed as a non-invasive triage tool for patients with upper GIB[93]. In the external cohort, the ANN performed similarly to the complete Rockall Score (includes endoscopic variables) in predicting stigmata of recent hemorrhage[93]. A different study developed a CART model regarding acute variceal hemorrhage to predict rebleeding and mortality and achieved the discrimination of three distinct prognostic groups of low, intermediate, and high risk[94]. Its performance was significantly superior to Child-Pugh and Model for End-Stage Disease (MELD) but comparable to a conventional logistic regression (LR) model [94].

Focusing on the lower GIB, two different ANN models were developed in a study aiming to predict severe acute lower GIB and the need for surgical intervention[95]. The first ANN significantly outperformed the Strate prediction rule for predicting severe bleeding (AUROCs: 0.98 *vs* 0.66)[95]. A different study employed nonendoscopic variables to develop a model based on a GB classifier to predict severe lower GIB, recurrent bleeding, and the need for clinical intervention[96]. On external validation, the model was found equally accurate to a conventional LR model for recurrent bleeding and the need for clinical intervention but superior in predicting severe lower GIB[96].

Prognosis

Table 4 summarizes the findings of the identified studies applying AI/ML models regarding the prognosis of gastroenterological diseases. Several SVM-based nomograms were developed in a study to predict distant metastasis for operated patients with oesophageal squamous cell carcinoma[97]. A different study employed clinicopathological data to develop an ANN model to predict the survival of patients with esophageal cancer operated with curative intends[98]. The model surpassed the Tumor–Node–Metastasis (TNM) model[98]. Regarding gastric cancer, a recent study developed five different AI/ML-based models to predict recurrence in operated patients[99]. Among the models, the RF demonstrated the best performance[99].

An ANN model was developed for patients with IBD, which used meteorological data to predict seasonal variations of onset and relapse in patients with CD and UC [100]. In the validation cohort, the model predicted the onset frequency and the frequency of relapse of the IBD with a mean absolute percentage error of 37.58% and 17.1%, respectively[100]. A study focusing on CD developed an ANN model to predict mucosal remission for patients treated with azathioprine 16 wk following treatment [101]. In a study focusing on UC, an ANN was developed employing clinical data to predict the patients with UC treated with cytoapheresis, who will eventually require operation[102].

Regarding the prognosis of GIB, a CART model was developed to predict in-hospital mortality of cirrhotic patients presenting with upper GIB[103]. In a multicentered study, an ANN model was developed employing pre-endoscopic variables to predict 30-d mortality in patients with non-variceal upper GIB[104]. Similarly, a prospective, multicentered study employed pre-endoscopic variables to develop an ANN model that predicts 30-d mortality in patients with non-variceal upper GIB[105]. The ANN significantly outperformed the Rockall scoring system (AUROCs: 0.95 *vs* 0.67)[105].

Regarding colorectal cancer, a recent study developed several ML models to predict the RAS and BRAF mutation status for patients with advanced colorectal cancer[106]. Notably, the ANN demonstrated the best performance[106]. In a different study employing clinicopathologic variables and data generated from immunochemistry, a least absolute shrinkage and selection operator regression model was developed to predict the lymph node metastasis status in a cohort of operated patients for T1 colorectal cancer[107].

Opportunities of AI application in gastroenterology

Therefore, the opportunities that arise from applying AI/ML-based software in gastroenterology include:

AI/ML models could be developed and integrated into the clinical setting to employ routinely collected data directly from the patient's electronic health records and flag patients at high risk of developing certain GI diseases in real-time. Current efforts include the prevention of gastric[27-29] and colorectal cancer[30,31]. Such ML models could become the basis for tailoring targeted screening programs.

Endoscopy is the gold standard for the diagnosis of a plethora of GI diseases. AI/ML models employing non-invasive parameters that provide reliably accurate diagnosis could substitute endoscopy or significantly minimize its use, thus ameliorating the impact of endoscopy-related complications, significantly decreasing

Table 4 Artificial intelligence applications in gastroenterology: Prognosis

Ref.	Parameters employed	AI classifier	Sizes of the training/validation sets	Outcomes	Performance
Yang *et al*[97]	Laboratory results, immunomarkers, clinicopathological parameters	SVM	319/164 patients	Distant metastasis of oesophageal squamous cell carcinoma following surgery	69.5-80.1[1,6], 44.7-67.2[3,6], 81.6-97.7[4,6]
Sato *et al*[98]	Laboratory results, clinicopathological parameters, tumor characteristics	ANN	395 patients (training:validation:test = 53:27:20)	1-year and 5-year survival of patients with esophageal cancer following surgery	0.883-0.884[2,7], 78.1-80.7[3,7], 84.7-86.5[4,7]
Zhou *et al*[99]	Laboratory results, clinicopathological parameters, tumor characteristics	Several	2012 patients (training:validation = 8:2)	Recurrence of gastric cancer following surgery	0.790-0.962[2,5], 0.771-0.795[2,6]
Peng *et al*[100]	Meteorological data	ANN	901 patients	Variations of onset and relapse of IBDs	----
Hardalaç *et al* [101]	Clinicopathological parameters, treatment data	ANN	129 patients (training:validation:test = 80:10:10)	Prediction of mucosal remission for CD patients treated with azathioprine	58.1-79.1[1,6], 0.527-0.883[2,6]
Takayama *et al*[102]	Clinicopathological parameters, treatment data	ANN	54/36 patients	Prediction of the need for operation for UC patients treated with cytoapheresis	96[3,6], 97[4,6]
Lyles *et al* [103]	Laboratory results, clinicopathological parameters	CART	884 patients	Prediction of in-hospital mortality of upper GIB in cirrhotic patients	----
Grossi *et al* [104]	Laboratory results, clinicopathological parameters	ANN	807 patients	30-d mortality of patients with non-variceal upper GIB	81.2-89.0[1,6], 0.87[2,6], 81.5-93.3[3,6], 80.9-84.7[4,6]
Rotondano *et al*[105]	Laboratory results, clinicopathological parameters	ANN	2380 patients	30-d mortality of patients with non-variceal upper GIB	96.8[1,6], 0.95[2,6], 83.8[3,6], 97.5[4,6]
Shi *et al*[106]	CT radiomics	Several	124/35 patients	Prediction of the presence of RAS and BRAF mutations in CRC	ANN: 87[1,5], 71[1,6], 0.90-0.95[2,5], 0.79[2,6]
Kang *et al* [107]	Laboratory results, immunomarkers, clinicopathological parameters, tumor characteristics	LASSO	221/95 patients	Prediction of lymph node metastasis status in operated patients for T1 CRC	0.795[2,5], 0.765[2,6]

[1]Accuracy (%).
[2]Area under the receiver operating curve or c-index.
[3]Sensitivity (%).
[4]Specificity (%).
[5]Training.
[6]Internal validation.
[7]External validation/testing. ANN: Artificial neural network; CART: Classification and regression tree; CD: Chron's disease; CRC: Colorectal cancer; CT: Computed tomography; GIB: Gastrointestinal bleeding; IBD: Inflammatory bowel disease; LASSO: Least absolute shrinkage and selection operator; SVM: Support vector machine; UC: Ulcerative colitis.

the cost for diagnosis, and providing an alternative to an unpleasant intervention for the patient. Current efforts include the diagnosis of gastroesophageal reflux disease [34], gastric cancer[47], celiac disease[48,50], and IBDs[51].

Expect from replacing endoscopy; AI/ML models could also improve its efficacy. CAD systems could facilitate navigating the GI tract and serve as the second "observer" for the endoscopist, an "observer" non-susceptible to distraction, which identifies lesions missed by the endoscopist. Particularly for capsule endoscopy, a CAD system that automatically detects and classifies lesions could significantly decrease the time required to evaluate the images by endoscopists while increasing diagnostic accuracy. Current efforts include the diagnosis of IBDs[53-57], gastric lesions[58], small bowel mobility disorders[59], small bowel lesions such as hemorrhagic and ulcerative lesions[60-64], intestinal hookworms[65], GI angiectasia[66], celiac disease[67], and colorectal cancer[68].

Physicians could use CADs to augment the accuracy of classifying polyps based on their neoplastic nature. As a result, the morbidity and mortality associated with failing to remove a neoplastic polyp could be lessened. At the same time, the complications related to removing a non-neoplastic polyp could be avoided. Therefore, CADs could significantly increase the cost-effectiveness of polyp management. Current efforts include the development of SVMs[73-76] and CNNs[79-81] for the classification of the neoplastic nature of colorectal polyps during NBI colonoscopy.

AI/ML models that accurately predict the response to different treatments could be used as a basis for individualized treatment allocation. Current efforts include the response of treatment with proton pump inhibitors for patients with gastroesophageal reflux disease[86], the mucosal remission for CD patients treated with azathioprine [101], and the need for operation for UC patients treated with cytoapheresis[102].

Particularly for GIB management, AI/ML models could be used to identify the source of bleeding[92] and as frameworks for decision-making, including the need to transfuse patients[92], perform emergent endoscopy[92,93] or emergent surgery[95, 96], and finally, triage patients with severe GIB to the ICU[95,96].

Finally, AI/ML models could be used as predictive tools that stratify the risk of complications and predict overall survival and recurrence following treatment. Such models could be used to tailor individualized follow-up schedules and for patient and family counseling. Current efforts include the prediction of overall survival for patients with esophageal cancer[98], the risk of recurrence of operated patients with gastric cancer[99], and 30-d mortality of patients with non-variceal GIB[104,105].

APPLICATIONS OF AI IN HEPATOLOGY

Prevention

Table 5 summarizes the findings of the identified studies applying AI/ML models for the prevention of disease in the field of hepatology. In a recent study, a prospective cohort of apparently healthy volunteers was enrolled in a study, which developed a DT-based model to classify patients based on their risk of developing non-alcoholic fatty liver disease (NAFLD) and liver fibrosis[108]. A similar study used routinely collected laboratory and clinical parameters to develop several AI/ML-based models to identify patients with NAFLD in the general population[109]. In a different study, several AI/ML models were developed as potential tools for targeted screening for NAFLD[110]. The Bayesian network model demonstrated the highest accuracy, followed by an SVM model[110]. Notably, an LR model outperformed all the models. These studies are examples of how AI/ML-based models could be used in primary care as tools for detecting chronic liver diseases. In a different study, multiple AI/ML models were developed as a basis for a non-invasive tool for assessing the level of fibrosis progression in NAFLD patients[111]. Notably, the RF model demonstrated the highest performance[111]. A different study managed to develop an ML model for patients at high risk of developing NAFLD to classify patients with non-alcoholic fatty liver (NAFL) and non-alcoholic steatohepatitis (NASH)[112]. Several AI/ML models were developed in a different study to classify healthy individuals from patients with NAFL and NASH[113]. Among them, a GB tree model demonstrated the highest performance, followed by an RF model[113]. In another study, four different AI/ML-based models were developed utilizing data from biochemical and enzyme-linked immunosorbent assays to classify patients with NAFLD and alcoholic liver disease with or without cirrhosis[114].

AI/ML models that utilize data directly from the electronic health records from patients infected with hepatitis B (HBV) and hepatitis C (HCV) could be used as the basis for targeted screening tools for liver carcinomas. A GB model was developed in a study using only serum markers aiming to predict fibrosis and classify the stage of fibrosis in two cohorts of patients with HBV and HCV[115]. An ANN model was developed in another study that employed only routine clinical data to predict significant fibrosis for patients with HBV[116]. In a similar study, an ANN model was developed by employing only routine laboratory data from HBV patients to identify patients with cirrhotic liver[117]. A different study developed an ANN model employing only non-invasive data to predict advanced liver fibrosis in HCV patients [118]. A similar study developed several AI/ML-based models to develop a non-invasive tool for identifying HCV patients with advanced fibrosis[119]. Among the developed models, a model based on alternating DTs demonstrated the highest performance[119]. These studies demonstrate how AI/ML models using routine clinical data could be used to identify patients who will benefit from a sustained

Table 5 Artificial intelligence applications in hepatology: Prevention

Ref.	Parameters employed	AI classifier	Sizes of the training/validation sets	Outcomes	Performance
Goldman *et al*[108]	National database of routine annual health check-ups	DT-based	12019 patients	Risk of NAFLD and cirrhosis	84.50-85.73[1,6], 0.7740-0.8486[2,6]
Yip *et al*[109]	Laboratory results, clinicopathological parameters	Several	500/422	Identify patients with NAFLD	0.87-0.90[2,5], 0.78-0.88[2,6], 55.48-94.52[3,5], 51.69-92.37[3,6], 58.47-91.53[4,5], 50.99-90.46[4,6]
Ma *et al*[110]	Laboratory results, clinicopathological parameters	Several	10508 patients (training:validation = 9:1)	Identify patients with NAFLD	49.47-82.92[1,6], 20.2-68.0[3,6], 54.4-94.6[4,6]
Sowa *et al* [111]	Laboratory results, clinicopathological parameters	Several	126 morbidly obese patients (training:validation = 9:1)	Fibrosis in NAFLD patients	79[1,6], 30.8-60.0[3,6], 77.0-92.2[4,6]
Canbay *et al* [112]	Laboratory results, clinicopathological parameters	EFS	164/122 obese patients	Classification of NAFLD and NASH	0.7339[2,5], 0.7028[2,6]
Fialoke *et al* [113]	National database of routine annual health check-ups	Several	108139 patients (training:validation = 4:1)	Classification among healthy, NAFLD, and NASH	77.2-79.7[1,6], 0.842-0.876[2,6], 74.5-77.4[3,6]
Sowa *et al* [114]	Data from biochemical and enzyme-linked immunosorbent assays	Several	133 patients (training:validation = 9:1)	Classification of NAFLD and ALD	DT: 89.02-95.1[1,6], 74.19-94.12[3,6], 96.08-98.04[4,6], RF: 0.8932-0.9846[2,6], SVM: 0.9058-0.9118[2,6]
Wei *et al* [115]	Laboratory results, clinicopathological parameters	GB	576 HBV patients, (training:validation = 7:3), 368[7] HCV patients	Classification of fibrosis/cirrhosis in HBV patients	0.904-0.974[2,5], 0.871-0.918[2,6], 79-88[3,5], 78-84[3,6], 86-92[4,5], 85[4,6]
				Classification of fibrosis/cirrhosis in HCV patients	0.797-0.849[2,7]
Wang *et al* [116]	Laboratory results, clinicopathological parameters	ANN	226/113[6]/116[7] HBV patients	Classification of significant fibrosis	0.883[2,5], 0.884[2,6], 0.920[2,7]
Raoufy *et al* [117]	Laboratory results, clinicopathological parameters	ANN	86/58 HBV patients	Classification of liver cirrhosis	91.38[1,6], 0.898[2,6], 87.5[3,6], 92[4,6]
Piscaglia *et al*[118]	Laboratory results, clinicopathological parameters	ANN	414/96 HCV patients	Classification of significant fibrosis	45.8-86.5[1,6], 0.87[2,5], 0.93[2,6], 30.4-100[3,6], 30.1-98.6[4,6]
Hashem *et al* [119]	Laboratory results, clinicopathological parameters	Several	22690/16877 HCV patients	Classification of significant fibrosis	66.3-84.4[1,6], 0.73-0.76[2,6]
Ioannou *et al* [120]	Clinical/laboratory data extracted directly from electronic health records	DNN	48151 patients with HCV-related cirrhosis (training:validation = 9:1)	HCC development in HCV cirrhosis	0.759-0.806[2,6]
Emu *et al* [121]	Laboratory results, clinicopathological parameters	Several	1385 patients HCV (training:validation = 4:1)	Stage of liver cirrhosis	97.228-97.831[1,6]

[1]Accuracy (%).
[2]Area under the receiver operating curve or c-index.
[3]Sensitivity (%).
[4]Specificity (%).
[5]Training.
[6]Internal validation.
[7]External validation/testing. ALD: Alcoholic liver disease; ANN: Artificial neural network; DNN: Deep neural network; DT: Decision tree; EFS: Ensemble feature selection; GB: Gradient boosting; HBV: Hepatitis B; HCC: Hepatocellular carcinoma; HCV: Hepatitis C; NAFLD: Non-alcoholic fatty liver disease; NASH: Non-alcoholic steatohepatitis RF: Random forest; SVM: Support vector machine.

virological response (SVR) to delay chronic liver disease progression.

Regarding the development of HCC, a recent study investigated if a DNN could outperform conventional LR models in predicting HCC development in patients with HCV[120]. A different study using variables including demographic, laboratory results, and clinical findings, developed RF, DNN, and LR models to reliably predict

the stage of liver cirrhosis in patients infected with HCV[121]. Accurately predicting patients with HCV prone to develop HCC could help identify patients who would be benefited from a targeted screening and are in a greater need of antiviral treatment to achieve an SVR.

Diagnostics

Table 6 summarizes the findings of the identified studies applying AI/ML models for diagnosis in the field of hepatology. Regarding chronic liver disease, a study used CT imaging data of patients with a confirmed liver fibrosis diagnosis to develop a CNN model for the staging of liver fibrosis[122]. Notably, the model outperformed the radiologists' interpretation[122]. A different study employed ultrasound imaging of patients with fatty liver disease to develop an SVM model and an extreme learning machine model (a type of ANN) for diagnosis and risk stratification[123]. A different study that employed ultrasound shear wave elastography features developed an SVM model to identify patients with chronic liver disease[124]. Another study used images from real-time tissue elastography to develop four different AI/ML-based models to classify liver fibrosis[125]. Notably, the RF model outperformed the rest, followed by the KNN and the SVM models[125].

In a study, CT imaging was employed to develop an ANN model that differentiates between HCC, intrahepatic peripheral cholangiocarcinoma (CCA), hemangioma, and metastasis[126]. Interestingly, when radiologists evaluated the images, their performance significantly increased when they considered the ANN's output, from an AUROC of 0.888 to one of 0.934[126]. Focusing on HCC diagnosis, a recent retrospective study developed a CNN that employed MRI images of patients with HCC. The model was trained with a combination of images that met the Liver Imaging Reporting and Data System (typical) and with images that did not (atypical)[127]. In a multicenter, retrospective study, a CNN was developed that employed MRI scans to identify HCC lesions[128]. Notably, the model surpassed the performance of less experienced radiologists in the diagnosis of small HCC lesions[128]. The model was able to analyze 100 images in just 3.4 s[128]. Finally, a different study aimed to develop a non-invasive ANN model that predicts the presence of microscopic vascular invasion and the tumor grade of HCC[129].

Regarding diagnosis of CCA and pancreatic adenocarcinoma, a study developed an ANN model using data generated by metabolomic and proteomic analyses of bile from patients undergoing endoscopic retrograde cholangiopancreatography aiming to classify patients with and without cancer[130]. A different study used data from the plasma levels of bile acids to develop six different AI/ML-based models to classify patients as having CCA or a benign biliary disease[131]. Among the six developed models, a model based on the Naive Bayes classifier demonstrated the highest performance[131]. Finally, in another study, an ANN model was designed to analyze images from magnetic resonance cholangiopancreatography to diagnose CCA with a reported accuracy of 92.8%[132].

Management

Table 7 summarizes the findings of the identified studies applying AI/ML models to manage hepatic diseases. With the guidance of AI/ML-based software trained by data generated from gene mutation biomarkers, serum markers, imaging, and the clinical setting, high-quality, evidence-based, and individualized treatments could be employed regarding chemotherapy, radiotherapy, and immunotherapy. In HBV management, a recent study developed several AI/ML-based models that use soluble immune markers to predict early virological relapse after discontinuation of nucleoside analogs treatment[133]. The model could be used to exclude patients at high risk of virological relapse from treatment cessation. In HCV management, a study utilized data from full-length HCV genome sequencing of variants of HCV to develop multiple AI/ML-based models that classify HCV anti-viral resistance variants[134]. Notably, the SVM model demonstrated the highest performance[134].

In HCC management, a recent study used data from DNA methylation profiling to develop an RF-based model that predicts 6-mo progression-free survival. Such models could be used to personalize patient surveillance[135]. In an international, multi-institutional study, a CART model was developed that aimed to create a framework beyond the Barcelona-Clinic-Liver-Cancer (BCLC) staging system, which is currently endorsed by guidelines for treatment allocation[136,137]. The model defined six distinct prognostic groups of patients based on predictive factors of overall survival that could be used as a framework for treatment allocation[137]. Notably, the radiologic tumor burden score, which is not integrated into the BCLC staging system, was found as the best predictor of long-term outcome for BCLC stage B patients[137].

Table 6 Artificial intelligence applications in hepatology: Diagnosis

Ref.	Diagnostic Modality	AI classifier	Sizes of the training/validation sets	Outcomes	Performance
Choi *et al*[122]	CT imaging	CNN	7461/421[6]/298[7]/172[7] patients	Liver fibrosis staging (F0-F4)	83.1[1,5], 80.8[1,6], 74.4-80.2[1,7]
				Classification among significant fibrosis, advanced fibrosis, and cirrhosis	92.1-95.0[1,6,7], 0.95-0.97[2,6,7], 84.6-95.5[3,6,7], 89.9-96.6[4,6,7]
Kuppili *et al*[123]	US imaging	ELM, SVM	63 patients	Diagnosis of FLD	ELM: 81.7-92.4[1,6], 0.81-0.92[2,6], 85.10-91.30[3,6], 78.52-92.10[4,6], SVM: 76.14-86.42[1,6], 0.74-0.86[2,6], 76.80-88.20[3,6], 74.52-86.30[4,6]
Gatos *et al*[124]	US shear wave elastography imaging	SVM	126 patients	Classification of chronic liver disease from healthy patients	87.3[1,6], 0.87[2,6], 93.5[3,6], 81.2[4,6]
Chen *et al*[125]	Real-time tissue elastography imaging, age, sex	Several	513 patient (training:validation = 3:1)	Classification of liver fibrosis	80.44-82.87[1,6], 79.67-92.97[3,6], 46.25-82.50[4,6]
Matake *et al*[126]	Clinicopathological parameters, CT imaging	ANN	120 patients	Classification among four types of focal liver lesions	0.961[2,6]
Oestmann *et al*[127]	Multiphasic MRI scans	CNN	150/10 patients	Classification of HCC and non-HCC lesions	94.1[1,5], 87.3[1,6], 0.912[2,6]
					For HCC: 92.7[3,6], 82.0[4,6]
					For non-HCC: 82.0[3,6], 92.7[4,6]
Kim *et al*[128]	MRI scans	CNN	455[5,6]/54[7] patients	HCC detection	0.97[2,6], 94[3,6], 99[4,6], 0.90[2,7], 87[3,7], 93[4,7]
Cucchetti *et al*[129]	Laboratory results, clinicopathological parameters, radiological data, histological data	ANN	175/75 patients	MVI	0.92[2,5], 91.0[1,6]
				Histopathological Grade	0.94[2,5], 93.3[1,6]
Urman *et al*[130]	Metabolomic and proteomic analyses of bile	Several	139 patients	Classification of CCA and pancreatic adenocarcinoma	0.98-1.00[2,6], 88-94.1[3,6], 92.3-100[4,6]
Negrini *et al*[131]	Plasma bile acids profiles	Several	112 patients (training:validation = 4:1)	Classification of CCA and benign biliary disease	68.2-86.4[1,6], 0.77-0.95[2,6], 64-79[3,6], 63-100[4,6]
Logeswaran[132]	MRCP	MLP	55/593[7] images	CCA diagnosis	92.8-96.3[1,6], 83.64-90.14[1,7]

[1]Accuracy (%).
[2]Area under the receiver operating curve or c-index.
[3]Sensitivity (%).
[4]Specificity (%).
[5]Training.
[6]Internal validation.
[7]External validation/testing. ANN: Artificial neural network; CCA: Cholangiocarcinoma; CNN: Convolutional neural network; CT: Computed tomography; ELM: Extreme learning machine; FLD: Fatty liver disease; HCC: Hepatocellular carcinoma; MLP: Multi-layer perceptron; MRCP: Magnetic resonance cholangiopancreatography MRI: Magnetic resonance imaging; MVI: Microvascular invasion; SVM: Support vector machine; US: Ultrasound.

These findings could help us reevaluate HCC management into a multidisciplinary, individualized approach that goes beyond the BCLC criteria[138].

In the management of patients with CCA, in an international study, a CART model was developed with solely preoperative variables to identify patients who would be more likely to benefit from surgery[139]. The model managed to isolate four distinct prognostic groups of patients with similar patient outcomes[139]. The authors concluded that this model could be used to inform presurgical decisions-for example, the use of neoadjuvant therapy for patients with poor prognoses[139]. In a different study, the researchers developed a DNN model to establish an AI framework through which specific prognostic groups could be used to identify which patients were more likely to benefit from different treatment modalities such as neoadjuvant chemotherapy or transarterial chemoembolization[140]. The framework was found to be

Table 7 Artificial intelligence applications in hepatology: Treatment

Ref.	Parameters employed	AI classifier	Sizes of the training/validation sets	Outcomes	Performance
Wübbolding *et al*[133]	Analyze soluble immune markers	Several	28/49[7] HBV patients	Prediction of early virological relapse	0.73-0.89[2,6], 0.59-0.67[2,7]
Haga *et al*[134]	WGS of HCV	Several	86/87 HCV patients	Classification of HCV variants resistant to antiviral drugs	0.5-0.937[2,5], 0.597-0.954[2,6]
Bedon *et al*[135]	DNA methylation profiling	RF-based	300/74 HCC specimens	6-mo progression-free survival	67.1-80.6[1,5], 64.8-80.2[1,7]
Tsilimigras *et al* [137]	Laboratory results, clinicopathological parameters, tumor characteristics	CART	976 HCC patients	Determining factors of prognostic weigh preoperatively within the BCLC staging system	---
Tsilimigras *et al* [139]	Laboratory results, clinicopathological parameters, tumor characteristics	CART	1146 CCA patients	Determining factors of prognostic weigh preoperatively	---
Jeong *et al*[140]	Laboratory results, clinicopathological parameters	DNN	1421/234[7]	Intrahepatic CCA susceptible to adjuvant therapy following resection	0.84[2,5], 0.78[2,7]
Shao *et al*[141]	Clinicopathological parameters	ANN	288 CCA patients (training:validation = 8:2)	Predict early occlusion following bilateral plastic stent placement	0.9648[2,5], 0.9544[2,6]

[1]Accuracy (%).
[2]Area under the receiver operating curve or c-index.
[3]Sensitivity (%).
[4]Specificity (%).
[5]Training.
[6]Internal validation.
[7]External validation/testing. ANN: Artificial neural network; BCLC: Barcelona clinic liver cancer; CART: Classification and regression tree; CCA: Cholangiocarcinoma; DNN: Deep neural network; HCC: Hepatocellular carcinoma; HCV: Hepatitis C; RF: Random forest; WGS: Whole-genome sequencing.

significantly more accurate than the current guidelines of the American Joint Committee of Cancer[140]. Finally, a study developed an ANN to predict which patients with inoperable hilar CCA will develop early occlusion following a bilateral plastic stent placement[141].

Prognosis

Table 8 summarizes the findings of the identified studies applying AI/ML models regarding prognosis in the field of hepatology. An ANN model was developed in a study to identify patients with HBV cirrhosis at a high risk of developing esophageal varices[142]. In a different study, two different RF models were created using clinical data, the first to identify esophageal varices and the second to classify patients with esophageal varices that require treatment[143].

Regarding HCC, several studies have focused on developing AI/ML-based models that would reliably predict patient outcomes (survival and recurrence). A retrospective study compared the performance among an ANN, an LR model, and a DT to predict the 1-, 3-, and 5-year disease-free survival in patients with HCC following resection [144]. A similar study used a nationwide database to compare an ANN and an LR model in predicting the 5-year survival of patients with HCC following hepatic resection and concluded that the ANN model surpassed the performance of the LR model[145]. In a different study by the same department, an ANN model and an LR model were compared, but instead, the outcome was in-hospital mortality, and the ANN was found superior to the LR model[146]. Interestingly, the study reported that the surgeon volume was the best single predictor of in-hospital mortality[146]. Regarding predictors, a different study comparing ANN and LR models reported that the ANN model identified a greater number of significant predictors than the LR model, except for outperforming it in survival predictions[147]. In a prospective study that aimed to compare an ANN model's performance to the performance of traditional staging systems in predicting survival for patients with early HCC, the ANN model outperformed the Hepato-Pancreato-Biliary Association's, the TNM 6th, and the BCLC staging systems with higher reported AUROCs in all training, internal validation, and external validation cohorts[148]. In a recent study, a GB survival classifier-based

Table 8 Artificial intelligence applications in hepatology: Prognosis

Ref.	Parameters employed	AI classifier	Sizes of the training/validation sets	Outcomes	Performance
Hong *et al* [142]	Laboratory results, clinicopathological parameters	ANN	197 HBV patients (training:validation = 4:1)	Development of esophageal varices in HBV cirrhosis	87.82[1,6], 93.75[3,6], 71.70[4,6]
Dong *et al* [143]	Laboratory results, clinicopathological parameters	RF	238/109[7]	Identification of esophageal varices	0.84[2,5], 0.82[2,7]
				Classification of esophageal varices requiring treatment	0.74[2,5], 0.75[2,7]
Ho *et al*[144]	Laboratory results, clinicopathological parameters, surgery parameters	ANN, DT	427, 354, and 297 patients for 1-, 3-, and 5-year survival (training:validation = 8:2)	1-, 3-, and 5-year disease-free survival Following surgical resection	ANN: 0.963-0.989[2,5], 93.5-96.3[3,5], 91.6-97.9[4,5], 0.774-0.864[2,6], 70.0-78.7[3,6], 54.2-92.7[4,6]
					DT: 0.675-0.825[2,5], 19.6-94.8[3,5], 45.8-97.9[4,5], 0.561-0.718[2,6], 0-88.5[3,6], 37.5-96.4[4,6]
Shi *et al*[145]	Laboratory results, clinicopathological parameters, tumor characteristics	ANN	22926 patients	5-year survival following surgical resection	96.57[1,6], 0.885[2,6], 97.43[1,7], 0.871[2,7], 74.23[3,7],
Shi *et al*[146]	Laboratory results, clinicopathological parameters, surgery parameters	ANN	22926 hepatectomies	In-hospital mortality following surgical resection	97.28[1,6], 0.84[2,6], 95.93[1,7], 0.82[2,7], 78.40[3,7], 94.57[4,7]
Chiu *et al* [147]	Laboratory results, clinicopathological parameters, tumor characteristics	ANN	434, 341, and 264 patients for 1-, 3-, and 5-year survival, (training:validation = 8:2)	1-, 3-, and 5-year overall survival, following surgical resection	98.5-99.5[1,5], 0.980-0.993[2,5], 99.7-100[3,5], 96.2-99.2[4,5], 72.1-85.1[1,6], 0.798-0.875[2,6], 71.4-88.6[3,6], 50.0-82.1[4,6]
Qiao *et al* [148]	Laboratory results, clinicopathological parameters, tumor characteristics	ANN	362/181[6]/104[7] patients	Survival following surgical resection	0.855[2,5], 80.00[3,5], 73.40[4,5], 0.832[2,6], 78.67[3,6], 75.70[4,6], 0.829[2,7], 77.42[3,7], 78.08[4,7]
Liu *et al*[149]	Laboratory results, data from immunochemistry of peripheral blood mononuclear cells, tumor characteristics	GB survival classifier	136/56[6]/105[7]	Risk of HCC-related death	0.844[2,5], 0.827[2,6], 0.806[2,7]
Zhong *et al* [150]	ALBI/CTP stage	ANN	319 / 61[7] / 124[7]	Survival of patients treated with chemoembolization and sorafenib	ALBI-based: 0.716[2,7], 0.823[2,7]
					CTP-based: 0.779[2,7], 0.693[2,7]
Divya and Radha[152]	Laboratory results, clinicopathological parameters, tumor characteristics	APO, SVM, RF	152 patients	Recurrence following RFA	95.5[1,6], 95.1[3,6], 95.8[4,6]
Yamashita *et al*[153]	Hematoxylin and eosin-stained WSI	CNN	299 / 53[6]/198[7] WSIs	Recurrence following Surgical Resection	0.724[2,6], 0.683[2,7]
Liang *et al* [154]	Laboratory results, clinicopathological parameters	SVM	83 patients	Recurrence following RFA	73-82[1,6], 0.60-0.69[2,6], 77-86[3,6], 73-82[4,6]
Eaton *et al* [155]	Laboratory results, clinicopathological parameters	GB-based	509/278 patients with primary sclerosing cholangitis	Classify risk of primary sclerosing cholangitis-related complications	0.96[2,6], 0.90[2,7]
Andres *et al* [156]	Laboratory results, clinicopathological parameters, donor characteristics	PSSP system	2769 patients	Survival following transplantation for primary sclerosing cholangitis	----
Rodriguez-Luna *et al* [157]	Genotyping data from microsatellite mutations/deletions	ANN	19 transplated patients	Post-transplant HCC recurrence	89.5[1,6]
Lau *et al*[158]	Laboratory results, clinicopathological parameters, donor characteristics	ANN, RF	90/90 transplants	Graft failure/primary nonfunction	ANN: 0.734-0.835[2,6]
					RF: 0.787-0.818[2,6]
				3-mo graft failure	ANN: 0.559[2,6], R6: 0.715[2,6]
Briceño *et al* [160]	Laboratory results, clinicopathological parameters,	ANN	1003 liver transplants	3-mo graft failure	0.806-0.821[2,6]

	surgical parameters, donor characteristics

[1]Accuracy (%).
[2]Area under the receiver operating curve or c-index.
[3]Sensitivity (%).
[4]Specificity (%).
[5]Training.
[6]Internal validation.
[7]External validation/testing. ALBI: Albumin-bilirubin; ANN: Artificial neural network; APO: Artificial plant optimization; CNN: Convolutional neural network; CTP: Child–Turcotte–Pugh; DT: Decision tree; GB: Gradient boosting; HBV: Hepatitis B; HCC: Hepatocellular carcinoma; PSSP: Patient-specific survival prediction; RF: Random forest; RFA: Radiofrequency ablation; SVM: Support vector machine; WSI: Whole-slide image.

model was developed to stratify the risk of an HCC-related death into three distinct categories[149]. Finally, in another recent study, an ANN identified albumin-bilirubin grade as the most important prognostic factor for the survival of patients with HCC treated with the combination of transarterial chemoembolization and sorafenib as initial treatment[150]. A systematic review aimed to compare the performance of AI/ML-based software and that of traditional linear prediction models in predicting survival for patients with HCC concluded that AI/ML models provided enhanced accuracy[151].

Except for survival, other studies have developed AI/ML models to predict the recurrence of HCC following therapeutical treatment. An interesting study employed several AI/ML methods, including Artificial Plant Optimization, SVM, and RF to predict HCC recurrence following radiofrequency ablation[152]. A recent study developed a CNN employing histopathologic images to predict recurrence in operated HCC patients[153]. A different study developed an SVM model to predict the recurrence in a group of patients who underwent radiofrequency ablation[154].

Regarding primary sclerosing cholangitis, a team of researchers derived and validated a risk estimate tool based on GB algorithms to predict the outcomes of the disease[155]. In a different study, an ML model was developed to predict survival curves for patients with primary sclerosing cholangitis following liver transplantation [156]. The P value of the χ^2 test of the distributional calibration was 1, indicating excellent calibration of the model[156].

Focusing on liver transplantation, a team developed an ANN model combined with genotyping for microsatellite mutations/deletion to predict HCC recurrence in a cohort of patients receiving a liver transplant[157]. Several other studies have focused on the survival of individual liver grafts following transplantation[158-160]. In a multi-centered study, the authors developed an ANN model to predict the 3-mo graft survival and loss[160]. Interestingly, their model outperformed all extensively validated scores, including the MELD, the donor risk index (DRI), the survival outcome following liver transplantation, and the balance of risk, with their performance significantly lower (AUROCs range: 0.42-0.67)[160]. In a different study, an RF model was developed to predict the 30-d failure graft. Notably, this model too outperformed MELD and DRI[158]. These findings could help reevaluate our thinking regarding the current models of recipient-donor matching.

Opportunities of AI application in hepatology

Therefore, the opportunities that arise from applying AI/ML-based software in hepatology include:

Regarding primary care, ML models could be integrated into the clinical setting and flag individuals in the general population at high risk of developing chronic liver disease in real-time by employing routinely collected data from the electronic health records. Current efforts include models that identify patients at high risk to develop NAFLD, NASH, fibrosis, and cirrhosis[108-114]. These models could be used to design targeted screening programs.

Particularly for patients with chronic HBV and HCV infection, AI/ML models could be used to stratify each individual's risk to progress through the several stages of cirrhosis and develop HCC. Multiple studies have been conducted in this regard for both HBV-related[115-117] and HCV-related[115,118-121] cirrhosis. Such models could be used to identify patients in greater need of SVR and tailor individualized follow-up schedules.

In diagnosis, AI/ML models provide the opportunity for increased diagnostic accuracy of various hepatic diseases and in multiple diagnostic modalities (such as

US/CT/MRI imaging and histologic images). Current efforts include CAD models for the diagnosis of chronic liver disease, HCC[127-129], and CCA[130-132].

AI/ML models that accurately and reliably predict the response to specific treatments could be used to tailor evidence-based frameworks for individualized treatment allocation. Current efforts include the development of frameworks for the management of HCC[136,137] and CCA[139,140].

Regarding prognosis, AI/ML models could be used to reliably predict complications, in-hospital mortality, overall survival, and recurrence following treatment. Current efforts include the prediction of in-hospital and HCC-related death[146,149], of overall survival of HCC patients following surgery[144,145,147,148], and HCC recurrence following surgery or RFA[152-154]. Such models could be used to tailor individualized follow-up schedules and for patient and family counseling.

Particularly for liver transplantation, AI/ML models could be used to predict graft failure or cancer recurrence for patients transplanted for cancer. Such models could be used to reevaluate and optimize our current practices regarding recipient-donor matching for graft allocation[157-160].

CURRENT CHALLENGES OF AI APPLICATIONS

Intrinsic bias and accuracy

The level of accuracy of AI systems is mostly dependent on the quality of the training dataset. Existing biases and prejudices in the training data set will inadvertently be built into the algorithms limiting the AI/ML-based software's accuracy[161]. Discrepancies in the data collection process, imperfections of standardization, and incorrectly labeled cases become part of the algorithms' training and are thus integrated into the end product. Two of the most common biases found in these models are: (1) Spectrum bias; and (2) Overfitting. Spectrum bias occurs when the patients (whose generated data were used during the training and internal validation of these models) do not constitute a representative sample of the target population[162]. On the other hand, overfitting refers to the tendency of models to be customized for the training data [162]. The performance of the model is thus exaggerated for the training dataset but is significantly inferior in new datasets[162]. CNNs, which are extensively used in gastroenterology and hepatology, are particularly vulnerable to overfitting[26]. Another substantial bias source is that physicians often misrecord data in the electronic health records, sometimes even the chief complaint[163]. These biases significantly impact the performance of AI/ML-based models and undermine their applications. A measure to alleviate the impact of biases is the standardization of data collection methods while establishing evaluation systems that scrutinize underlying biases and check data accuracy[15,164]. Another crucial step to tackle these biases is the external validation of models, in a clinical setting, from data generated from patients prospectively enrolled in the study[165]. Initial implementation of AI/ML-based models in the clinical setting should occur on a small scale, similar to phase I and phase II of the clinical trials[166]. Existing tools, such as the PROBAST tool, could be used during the development of AI/ML-based models to comprehensively assess the risk of bias[164,167]. The American Medical Association has recently acknowledged the need to identify and address bias in data when testing or deploying AI/ML-based software to avoid introducing or exacerbating health care disparities [168]. Therefore, the real challenge is to develop an AI/ML-based software that taps into the true potential hidden by the data without picking up the biases.

Several other limitations affect the performance of these models. An example is the limited resolution of capsule endoscopy images compared to other types of endoscopy [18]. A different limitation is the in silico nature of most of the currently developed models, which significantly impacts the expectations of similar performances in a real clinical setting. Another limitation of these algorithms is that they utilize a series of variables that in the real clinical setting are derived in a series of careful decisions made by physicians and are not readily available as a complete set of data. Therefore, these variables' presence or absence could become a significant shortcoming of these models in a real clinical setting, making them impractical to use. Finally, there is a lack of consistency in the metrics used to assess performance (sensitivity, specificity, AUROC, accuracy, *etc.*), limiting the ability to draw meaningful comparisons between the models[17].

Data protection and cybersecurity

Similarly, with all patient data, those utilized in AI/ML-based software should

conform with the seven principles described in Article 5 of the General Data Protection Regulation. Specifically, the personal data are required to: (1) Be processed fairly, lawfully, and transparently; (2) Be relevant, adequate, and limited to the intended purpose; (3) Be collected for explicit, specific, and lawful purposes; (4) Be accurate and up to date; (5) Permit identification for only as long as necessary; (6) Ensure appropriate security; and (7) Demonstrate compliance and accountability[169]. A particular challenge for AI is the resistance to the concept of utterly electronic tracking of healthcare records due to the belief that it exposes the vast amount of stored sensitive health record data to massive disclosures[170]. These concerns are not entirely unjustifiable if one considers examples such as the transfer of data from 1.6 million patient records from the Royal Free Nathional Health Service Foundation Trust to Google DeepMind, which was later ruled illegal[171]. Nevertheless, any effort or policy towards paper-based data due to data protection concerns could substantially undermine the application of AI modes in healthcare.

The healthcare industry is a particularly attractive target for cyberattacks as it contains sensitive personal data and financial information. Several physical and technical safeguards have been implemented under the Health Insurance Portability and Accountability Act to protect against the breach of sensitive patient data[172]. However, from the application of AI technology in the healthcare industry, new vulnerabilities and dangers emerge except traditional cybersecurity concerns. If ML models can learn from data, they could also be fooled by data. Data could be introduced malevolently in the algorithms to manipulate the developed AI/ML models into making wrong decisions with currently unknown ramifications to patient outcomes[173]. In a recent study, the authors demonstrated how attackers could use DL to add or remove lung cancer tumors in CT scans[174]. This study demonstrated how both a group of radiologists and a state-of-the-art deep AI model were particularly susceptible to the attack[174]. How could we, therefore, be confident that the AI/ML model has not been compromised? Evidently, healthcare facilities will have to develop additional information technology infrastructure to shield the healthcare system from these new threats.

Intellectual property

The Food and Drug Administration (FDA) recently acknowledged that it receives a high volume of submissions regarding AI/ML-based software marketing, with the list of already approved algorithms increasing rapidly[175,176]. A challenging point will be determining the law framework and regulatory standards that AI/ML-based software should follow. The key is classifying AI/ML software as "medical device", "service", or as "product", and achieving this requires a careful evaluation of the intentive use of AI/ML-based software. AI/ML-based software that aims to assist physicians in diagnosing, interpreting, and treatment decisions could be classified as medical devices and fall under the respective regulations[12]. In 2019, the FDA announced its aim to review AI/ML-based software regulation and has recently published the AI/ML– Based Software as a Medical Device Action Plan[175,177]. The action plan published by the FDA focuses on five pillars aimed to facilitate innovation and advance AI/ML-based software that are classified as medical devices. These include: (1) A tailored regulatory framework; (2) Good ML practice that could be achieved by consensus standards efforts; (3) A patient-centered approach incorporating transparency to users that takes into account usability, trust, equity, and accountability; (4) Regulatory science methods related to algorithm bias and robustness, and finally; and (5) Real-world performance[175]. When it comes to law and regulation, the real challenge is finding the golden snitch between too much regulation that strangles innovation and creation and too little regulation, which could have unexpected and devastating consequences for healthcare, and by extension, the well-being of patients.

Another interesting point regarding intellectual property and safety is the substantial divergence of the AI/ML-based software from the original product years after its approval and distribution[178]. What are the rights of developers on the product following its purchase? Since the original product constantly changes by learning from the clinical setting's data, the deviated model years after the purchase and the original software could be seen as two entirely different products. The first is protected under copyright law. However, the latter has now produced intellectual property on its own since it encompasses data generated by the healthcare facility [173]. Who could therefore claim legal rights over the final product? Also, who ensures the credibility and safety of the model as it deviates from the original product? Clearly, there is a need for lifecycle regulation of AI/ML-based software that ensures postapproval guardrails such as built-in audits[165]. Alternatively, time-limited authoriz-

ations could be employed to allow the FDA to perform periodic audits to review the accumulated modifications to the initial product[165].

Liability

Except for intellectual property, another legal challenge that arises from applying AI/ML-based software in the clinical setting is liability. A quite intriguing concept is that AI's findings and decisions could become legally binding in the future. As AI/ML-based models evolve and become more sophisticated, it is fair to assume that they will eventually surpass physicians, at least in specific tasks. How could then, the physicians justify ignoring the decision presented by AI? Especially when their decisions are made solemnly based on data and lack any sense of subjectivity. And who is liable when the followed decision made by the model causes injury? Currently, there is no legal precedent that assigns liability in a case where the injury was inflicted on a patient due to an erroneous output generated by AI/ML-based software[179].

To avoid malpractice liability, a physician is required to provide medical care at the same level as a competent physician of the same specialty while considering the available resources[180]. However, when an AI/ML-based software recommendation is involved, the concept of liability becomes more complicated. In an insightful recent legal analysis, the authors provide eight scenarios based on the combinations of whether the AI recommendation follows standard care and/or is accurate, the physician follows or rejects that recommendation, and whether a medical injury occurs [179]. The authors conclude that since current law shields physicians from liability when the standard care is followed, it also incentivizes physicians to minimize AI's actual usefulness, transforming AI into a confirmatory tool rather than a tool to augment the level of care[179]. Until a comprehensive legal framework regarding liability is developed, healthcare facilities would justifiably hesitate to adopt AI technologies due to the fear and unawareness of how they will expose the facility and its staff to liability[181].

Ethical challenges and transparency

AI could become the third participant in the physician-patient relationship and potentially undermine the trust between them. First, the idea that data are shared with third parties for AI model development could lead patients to withhold information from physicians and become less transparent[182]. Second, AI/ML-based models cannot act like compassionate human beings, which is an integral part of a physician's clinical life. Therefore, AI-driven decision-making neither encompasses an understanding of the patient's needs nor respects the patient's wishes nor demonstrates empathy, nor realizes when a patient feels discomfort or requires some rest or a hand to hold on to. Therefore, retaining the trust in the physician-patient relationship could be proven challenging in the AI era.

Another challenge is patient consent in AI applications. Clearly, it is practically impossible to acquire informed consent from each and every patient whose data are used during the development and validation of AI/ML-based software. In any case, we cannot predict how the algorithms would use specific data points during the training of the model and whether data of a specific patient have any significant impact on the model as a whole[183]. However, when AI/ML-based models are used in the clinical setting, especially for patient recording (in computer vision), patients should be adequately informed, and explicit consent should be acquired[184].

Achieving equilibrium between ensuring a high level of care and avoiding privacy encroachment could be challenging. For example, with computer vision advancement, monitoring could be used to detect any deviations from the optimal bedside practices such as patient mobilization and hand hygiene practices, which leaves patients vulnerable to identification[185,186]. Practices such as data minimization (collecting the least data needed) could address these challenges[185].

Changing the physicians' and patients' stance towards AI technologies could be proven a herculean task. Currently, around 2/3 of the population feels uncomfortable using their data to improve care quality and are unfavorable to AI/ML-based software performing tasks typically performed by physicians[183]. There are justifiable concerns that certain biases included in the training data due to racism, sexism, and socioeconomic inequality would be integrated into the AI/ML-based software. A notorious example is the COMPAS algorithm, which was found to falsely flag black people as likely to re-offend[187]. This was aggravated when developers made the argument that the algorithm was protected under intellectual property law and thus is not open to scrutiny[187]. These examples could erroneously undermine the trust towards AI altogether. A trustworthy AI/ML-based software should be built around the principles of transparency, credibility, auditability, reliability, and recoverability

[188].

The last but not least challenge in applying AI/ML-based software in healthcare is the lack of transparency, which is currently a major concern. The lack of transparency is demonstrated by the non-interpretability associated with these algorithms, described as a "black-box", where the inner logic is hidden[18]. This violates a fundamental tenet of medical ethics that physicians should comprehend at least the basic features of the devices they use and could undermine the trustworthiness of these technologies[189]. Thus, those who develop AI/ML-based models and physicians should collaborate to reach at least a degree of explainability on how AI/ML-based algorithms reach decisions. Attention maps and saliency region are examples of methods that could lessen the lack of interpretability of these models[190]. A slightly different and intriguing point of view is that withholding the widespread application of AI/ML-based software, due to their opacity, when their application could significantly benefit patients is, in fact, unethical[183]. With most of the population being prejudiced against AI, developing trust for these technologies would require several steps, including addressing bias, increasing transparency, communicating with the patients their role in provided care, protecting data privacy, and developing a robust regulatory framework.

CONCLUSION

Even though multiple efforts for AI's integration into healthcare have been made, they all originate from high-income countries[191]. Understandably, since all AI/ML-based software is data-driven, the opportunities to participate in the AI ecosystem for low- and middle-income countries, where the healthcare system does not generate extensive electronic, standardized data, are significantly limited. Not being included in the development of these models would introduce a significant spectrum bias, which could undermine these models' application in low- and middle-income countries. Thus, despite being described as the key to healthcare equity, AI could become another brick in the wall of inequality. A challenge for the future would be to include low- and middle-income countries in AI model development initiatives.

Even though these AI/ML-based software's central idea is that they could surpass physicians in performing certain tasks, the existing literature comparing AI/ML-based models and physicians' performance is limited[192]. A recent meta-analysis, which included multidisciplinary comparative studies, identified only 25 studies meeting their inclusion criteria from all medical specialties[193]. The authors concluded that currently, DL models' diagnostic performance in detecting diseases from medical imaging is equivalent to that of healthcare professionals[193]. Clearly, there is a contrast between the abundance of studies developing and validating ML algorithms and the lack of studies comparing these models' performance to physicians' performance at the investigated task. Thus, there is a crystalline need for further comparative studies in the clinical setting.

Another challenge for the future would be to combine AI with other emerging fields, such as 3D printing and bioprinting, augmented reality, novel biomarkers such as microRNAs, and robotics[194-198]. Envision a world where all these technologies and their applications are unified and integrated into everyday clinical practice. AI could be the means through which this new sophisticated, complex clinical setting is handled. The future AI clinician rejects oversimplifying an inherently complex field but instead embraces the complexity.

AI can outperform physicians in the ability to precisely quantify correlations even in domains where physicians possess in-depth knowledge[173]. However, AI models are simply tools like any other and should be treated as such. Tools with their accuracy, sensitivity, and specificity in performing certain tasks, tools that carry biases, and whose findings should be evaluated in conjunction with other clinical and paraclinical findings. Reliance on AI should not exclude non-quantifiable information from decision-making[183]. Clinical reasoning and critical thinking should not be subsumed by AI at the altar of technological advancement. AI's integration into healthcare should not replace the physicians' intelligence but rather augment it. Thus, we should aim for AI-assisted and not AI-driven clinical practice[14]. Finally, AI systems should be applied in healthcare along with equally advanced evaluation systems, which properly assess their ramifications within the clinical practice environment, investigate their unintended consequences, and, most notably, evaluate their impact on patient outcomes[163]. An example of an evaluative initiative is the Digital Health Innovation Action Plan launched by the FDA that aims to assess medical software under

development based on five excellence criteria: product quality, patient safety, clinical responsibility, cybersecurity responsibility, and proactive culture[199].

Despite being on the front line for several decades, AI still comes short of delivering the presumable solutions to long-standing healthcare problems. AI winters, where AI funding is significantly reduced, demonstrate the frustration that AI is not evolving at a pace investors would feel comfortable sustaining the funding[1]. AI may seem like a field that constantly overpromises but usually underdelivers, given its current impact on healthcare. In this review, we have highlighted the current challenges that we believe restrain the extensive application of AI in healthcare in an attempt to explore ways to overcome them.

Nevertheless, even at a slower pace, AI will eventually "infiltrate" not only the hospital setting but rather the healthcare industry as a whole, from central healthcare facilities to private practice and telemedicine, from medical schools and teaching hospitals to pharmaceutical companies, and even healthcare policy-makers in government. AI will become a reality; everyone will have to conform with, to avoid becoming obsolete. Therefore, sooner or later, physicians will have to engage with the field of AI by necessity. The role of physicians in this upcoming "revolution", however, remains to be seen. Will we be shaping this "revolution", or will we be mere observers?

Limitations

Finally, our review has few limitations. First, our study is a narrative review, and despite our best effort to follow a carefully designed search strategy to provide a comprehensive review of the current literature, our study is prone to selection bias due to its nature. Second, each study described in our study carries its own risk of bias and faces several limitations described in each study. We did not use any bias risk assessment tool to systematically evaluate if a study was worth inclusion rather than the followed search strategy and our judgment. Again this makes our review prone to selection bias. In addition, the majority of our included studies were performed in silico, and the performances reported could deviate substantially when the models are applied in a real clinical setting. Finally, with few exceptions, the majority of results report a superior or at least equivalent performance of AI/ML-based algorithms compared to the performance of conventional statistic models, widely used staging systems, extensively investigated and validated scores, and physician knowledge and reasoning, which have dominated decision-making in healthcare for decades. Thus, at least in the concept of publication bias, our findings should be interpreted with caution.

REFERENCES

1 **Jayabalasingham B**. Artificial Intelligence: How knowledge is created, transferred, and used. Elsevier, 2019
2 **Russell SJ**. Artificial intelligence: a modern approach. Harlow: Pearson, 2016
3 **Cruz JA**, Wishart DS. Applications of machine learning in cancer prediction and prognosis. *Cancer Inform* 2007; **2**: 59-77 [PMID: 19458758]
4 **Raghupathi W**, Raghupathi V. Big data analytics in healthcare: promise and potential. *Health Inf Sci Syst* 2014; **2**: 3 [PMID: 25825667 DOI: 10.1186/2047-2501-2-3]
5 **Pastorino R**, De Vito C, Migliara G, Glocker K, Binenbaum I, Ricciardi W, Boccia S. Benefits and challenges of Big Data in healthcare: an overview of the European initiatives. *Eur J Public Health* 2019; **29**: 23-27 [PMID: 31738444 DOI: 10.1093/eurpub/ckz168]
6 **Dash S**, Shakyawar SK, Sharma M, Kaushik S. Big data in healthcare: management, analysis and future prospects. *J Big Data* 2019; **6**: 54 [DOI: 10.1186/s40537-019-0217-0]
7 **Statista**. Healthcare data volume globally 2020 forecast. [cited 20 December 2020]. Available from: https://www.statista.com/statistics/1037970/global-healthcare-data-volume/
8 **McAfee A**, Brynjolfsson E. Big data: the management revolution. *Harv Bus Rev* 2012; **90**: 60-66, 68, 128 [PMID: 23074865]
9 **Beyer MA**, Laney D. The importance of 'big data: a definition. *CT Gart* 2012; 2014
10 Computational Technology for Effective Health Care: Immediate Steps and Strategic Directions. Stead WW, Lin HS, editors. Washington (DC): National Academies Press (US), 2009
11 **Matheny ME**, Whicher D, Thadaney Israni S. Artificial Intelligence in Health Care: A Report From the National Academy of Medicine. *JAMA* 2020; **323**: 509-510 [PMID: 31845963 DOI: 10.1001/jama.2019.21579]
12 **Sugawara E**, Nikaido H. Properties of AdeABC and AdeIJK efflux systems of Acinetobacter baumannii compared with those of the AcrAB-TolC system of Escherichia coli. *Antimicrob Agents Chemother* 2014; **58**: 7250-7257 [PMID: 25246403 DOI: 10.1128/AAC.03728-14]
13 **Lai-Hung Wong G**, Sung JJ. The emerging role of big data in gastroenterology and hepatology. *J*

Gastroenterol Hepatol 2019; **34**: 307-308 [PMID: 30698322 DOI: 10.1111/jgh.14606]
14 **Ruffle JK**, Farmer AD, Aziz Q. Artificial Intelligence-Assisted Gastroenterology- Promises and Pitfalls. *Am J Gastroenterol* 2019; **114**: 422-428 [PMID: 30315284 DOI: 10.1038/s41395-018-0268-4]
15 **Loftus TJ**, Tighe PJ, Filiberto AC, Efron PA, Brakenridge SC, Mohr AM, Rashidi P, Upchurch GR Jr, Bihorac A. Artificial Intelligence and Surgical Decision-making. *JAMA Surg* 2020; **155**: 148-158 [PMID: 31825465 DOI: 10.1001/jamasurg.2019.4917]
16 **Rumsfeld JS**, Joynt KE, Maddox TM. Big data analytics to improve cardiovascular care: promise and challenges. *Nat Rev Cardiol* 2016; **13**: 350-359 [PMID: 27009423 DOI: 10.1038/nrcardio.2016.42]
17 **Le Berre C**, Sandborn WJ, Aridhi S, Devignes MD, Fournier L, Smaïl-Tabbone M, Danese S, Peyrin-Biroulet L. Application of Artificial Intelligence to Gastroenterology and Hepatology. *Gastroenterology* 2020; **158**: 76-94 [PMID: 31593701 DOI: 10.1053/j.gastro.2019.08.058]
18 **Yang YJ**, Bang CS. Application of artificial intelligence in gastroenterology. *World J Gastroenterol* 2019; **25**: 1666-1683 [PMID: 31011253 DOI: 10.3748/wjg.v25.i14.1666]
19 **Huang S**, Cai N, Pacheco PP, Narrandes S, Wang Y, Xu W. Applications of Support Vector Machine (SVM) Learning in Cancer Genomics. *Cancer Genomics Proteomics* 2018; **15**: 41-51 [PMID: 29275361 DOI: 10.21873/cgp.20063]
20 **Deo RC**. Machine Learning in Medicine. *Circulation* 2015; **132**: 1920-1930 [PMID: 26572668 DOI: 10.1161/CIRCULATIONAHA.115.001593]
21 **Noble WS**. What is a support vector machine? *Nat Biotechnol* 2006; **24**: 1565-1567 [PMID: 17160063 DOI: 10.1038/nbt1206-1565]
22 **Guo CY**, Chou YC. A novel machine learning strategy for model selections - Stepwise Support Vector Machine (StepSVM). *PLoS One* 2020; **15**: e0238384 [PMID: 32853243 DOI: 10.1371/journal.pone.0238384]
23 **Aizerman M**, Braverman E, Rozonoer L. Theoretical foundations of the potential function method in pattern recognition learning. *Autom Remote Control* 1964; **25**: 821-837
24 **Kriegeskorte N**, Golan T. Neural network models and deep learning. *Curr Biol* 2019; **29**: R231-R236 [PMID: 30939301 DOI: 10.1016/j.cub.2019.02.034]
25 **LeCun Y**, Bengio Y, Hinton G. Deep learning. *Nature* 2015; **521**: 436-444 [PMID: 26017442 DOI: 10.1038/nature14539]
26 **Anwar SM**, Majid M, Qayyum A, Awais M, Alnowami M, Khan MK. Medical Image Analysis using Convolutional Neural Networks: A Review. *J Med Syst* 2018; **42**: 226 [PMID: 30298337 DOI: 10.1007/s10916-018-1088-1]
27 **Leung WK**, Cheung KS, Li B, Law SYK, Lui TKL. Applications of machine learning models in the prediction of gastric cancer risk in patients after Helicobacter pylori eradication. *Aliment Pharmacol Ther* 2021; **53**: 864-872 [PMID: 33486805 DOI: 10.1111/apt.16272]
28 **Nakahira H**, Ishihara R, Aoyama K, Kono M, Fukuda H, Shimamoto Y, Nakagawa K, Ohmori M, Iwatsubo T, Iwagami H, Matsuno K, Inoue S, Matsuura N, Shichijo S, Maekawa A, Kanesaka T, Yamamoto S, Takeuchi Y, Higashino K, Uedo N, Matsunaga T, Tada T. Stratification of gastric cancer risk using a deep neural network. *JGH Open* 2020; **4**: 466-471 [PMID: 32514455 DOI: 10.1002/jgh3.12281]
29 **Taninaga J**, Nishiyama Y, Fujibayashi K, Gunji T, Sasabe N, Iijima K, Naito T. Prediction of future gastric cancer risk using a machine learning algorithm and comprehensive medical check-up data: A case-control study. *Sci Rep* 2019; **9**: 12384 [PMID: 31455831 DOI: 10.1038/s41598-019-48769-y]
30 **Kinar Y**, Kalkstein N, Akiva P, Levin B, Half EE, Goldshtein I, Chodick G, Shalev V. Development and validation of a predictive model for detection of colorectal cancer in primary care by analysis of complete blood counts: a binational retrospective study. *J Am Med Inform Assoc* 2016; **23**: 879-890 [PMID: 26911814 DOI: 10.1093/jamia/ocv195]
31 **Goshen R**, Choman E, Ran A, Muller E, Kariv R, Chodick G, Ash N, Narod S, Shalev V. Computer-Assisted Flagging of Individuals at High Risk of Colorectal Cancer in a Large Health Maintenance Organization Using the ColonFlag Test. *JCO Clin Cancer Inform* 2018; **2**: 1-8 [PMID: 30652563 DOI: 10.1200/CCI.17.00130]
32 **Mosquera-Lopez C**, Agaian S, Velez-Hoyos A, Thompson I. Computer-Aided Prostate Cancer Diagnosis From Digitized Histopathology: A Review on Texture-Based Systems. *IEEE Rev Biomed Eng* 2015; **8**: 98-113 [PMID: 25055385 DOI: 10.1109/RBME.2014.2340401]
33 **Takiyama H**, Ozawa T, Ishihara S, Fujishiro M, Shichijo S, Nomura S, Miura M, Tada T. Automatic anatomical classification of esophagogastroduodenoscopy images using deep convolutional neural networks. *Sci Rep* 2018; **8**: 7497 [PMID: 29760397 DOI: 10.1038/s41598-018-25842-6]
34 **Pace F**, Buscema M, Dominici P, Intraligi M, Baldi F, Cestari R, Passaretti S, Bianchi Porro G, Grossi E. Artificial neural networks are able to recognize gastro-oesophageal reflux disease patients solely on the basis of clinical data. *Eur J Gastroenterol Hepatol* 2005; **17**: 605-610 [PMID: 15879721 DOI: 10.1097/00042737-200506000-00003]
35 **de Groof AJ**, Struyvenberg MR, van der Putten J, van der Sommen F, Fockens KN, Curvers WL, Zinger S, Pouw RE, Coron E, Baldaque-Silva F, Pech O, Weusten B, Meining A, Neuhaus H, Bisschops R, Dent J, Schoon EJ, de With PH, Bergman JJ. Deep-Learning System Detects Neoplasia in Patients With Barrett's Esophagus With Higher Accuracy Than Endoscopists in a Multistep Training and Validation Study With Benchmarking. *Gastroenterology* 2020; **158**: 915-929.e4

[PMID: 31759929 DOI: 10.1053/j.gastro.2019.11.030]
36 **van der Sommen F**, Zinger S, Curvers WL, Bisschops R, Pech O, Weusten BL, Bergman JJ, de With PH, Schoon EJ. Computer-aided detection of early neoplastic lesions in Barrett's esophagus. *Endoscopy* 2016; **48**: 617-624 [PMID: 27100718 DOI: 10.1055/s-0042-105284]
37 **Struyvenberg MR**, van der Sommen F, Swager AF, de Groof AJ, Rikos A, Schoon EJ, Bergman JJ, de With PHN, Curvers WL. Improved Barrett's neoplasia detection using computer-assisted multiframe analysis of volumetric laser endomicroscopy. *Dis Esophagus* 2020; **33**: doz065 [PMID: 31364700 DOI: 10.1093/dote/doz065]
38 **Swager AF**, van der Sommen F, Klomp SR, Zinger S, Meijer SL, Schoon EJ, Bergman JJGHM, de With PH, Curvers WL. Computer-aided detection of early Barrett's neoplasia using volumetric laser endomicroscopy. *Gastrointest Endosc* 2017; **86**: 839-846 [PMID: 28322771 DOI: 10.1016/j.gie.2017.03.011]
39 **Kumagai Y**, Takubo K, Kawada K, Aoyama K, Endo Y, Ozawa T, Hirasawa T, Yoshio T, Ishihara S, Fujishiro M, Tamaru JI, Mochiki E, Ishida H, Tada T. Diagnosis using deep-learning artificial intelligence based on the endocytoscopic observation of the esophagus. *Esophagus* 2019; **16**: 180-187 [PMID: 30547352 DOI: 10.1007/s10388-018-0651-7]
40 **Zheng W**, Zhang X, Kim JJ, Zhu X, Ye G, Ye B, Wang J, Luo S, Li J, Yu T, Liu J, Hu W, Si J. High Accuracy of Convolutional Neural Network for Evaluation of Helicobacter pylori Infection Based on Endoscopic Images: Preliminary Experience. *Clin Transl Gastroenterol* 2019; **10**: e00109 [PMID: 31833862 DOI: 10.14309/ctg.0000000000000109]
41 **Nakashima H**, Kawahira H, Kawachi H, Sakaki N. Artificial intelligence diagnosis of *Helicobacter pylori* infection using blue laser imaging-bright and linked color imaging: a single-center prospective study. *Ann Gastroenterol* 2018; **31**: 462-468 [PMID: 29991891 DOI: 10.20524/aog.2018.0269]
42 **Itoh T**, Kawahira H, Nakashima H, Yata N. Deep learning analyzes Helicobacter pylori infection by upper gastrointestinal endoscopy images. *Endosc Int Open* 2018; **6**: E139-E144 [PMID: 29399610 DOI: 10.1055/s-0043-120830]
43 **Shichijo S**, Nomura S, Aoyama K, Nishikawa Y, Miura M, Shinagawa T, Takiyama H, Tanimoto T, Ishihara S, Matsuo K, Tada T. Application of Convolutional Neural Networks in the Diagnosis of Helicobacter pylori Infection Based on Endoscopic Images. *EBioMedicine* 2017; **25**: 106-111 [PMID: 29056541 DOI: 10.1016/j.ebiom.2017.10.014]
44 **Mohan BP**, Khan SR, Kassab LL, Ponnada S, Mohy-Ud-Din N, Chandan S, Dulai PS, Kochhar GS. Convolutional neural networks in the computer-aided diagnosis of *Helicobacter pylori* infection and non-causal comparison to physician endoscopists: a systematic review with meta-analysis. *Ann Gastroenterol* 2021; **34**: 20-25 [PMID: 33414617 DOI: 10.20524/aog.2020.0542]
45 **Kanesaka T**, Lee TC, Uedo N, Lin KP, Chen HZ, Lee JY, Wang HP, Chang HT. Computer-aided diagnosis for identifying and delineating early gastric cancers in magnifying narrow-band imaging. *Gastrointest Endosc* 2018; **87**: 1339-1344 [PMID: 29225083 DOI: 10.1016/j.gie.2017.11.029]
46 **Hirasawa T**, Aoyama K, Tanimoto T, Ishihara S, Shichijo S, Ozawa T, Ohnishi T, Fujishiro M, Matsuo K, Fujisaki J, Tada T. Application of artificial intelligence using a convolutional neural network for detecting gastric cancer in endoscopic images. *Gastric Cancer* 2018; **21**: 653-660 [PMID: 29335825 DOI: 10.1007/s10120-018-0793-2]
47 **Zhu SL**, Dong J, Zhang C, Huang YB, Pan W. Application of machine learning in the diagnosis of gastric cancer based on noninvasive characteristics. *PLoS One* 2020; **15**: e0244869 [PMID: 33382829 DOI: 10.1371/journal.pone.0244869]
48 **Tenório JM**, Hummel AD, Cohrs FM, Sdepanian VL, Pisa IT, de Fátima Marin H. Artificial intelligence techniques applied to the development of a decision-support system for diagnosing celiac disease. *Int J Med Inform* 2011; **80**: 793-802 [PMID: 21917512 DOI: 10.1016/j.ijmedinf.2011.08.001]
49 **Caetano Dos Santos FL**, Michalek IM, Laurila K, Kaukinen K, Hyttinen J, Lindfors K. Automatic classification of IgA endomysial antibody test for celiac disease: a new method deploying machine learning. *Sci Rep* 2019; **9**: 9217 [PMID: 31239486 DOI: 10.1038/s41598-019-45679-x]
50 **Hujoel IA**, Murphree DH Jr, Van Dyke CT, Choung RS, Sharma A, Murray JA, Rubio-Tapia A. Machine Learning in Detection of Undiagnosed Celiac Disease. *Clin Gastroenterol Hepatol* 2018; **16**: 1354-1355.e1 [PMID: 29253540 DOI: 10.1016/j.cgh.2017.12.022]
51 **Manandhar I**, Alimadadi A, Aryal S, Munroe PB, Joe B, Cheng X. Gut microbiome-based supervised machine learning for clinical diagnosis of inflammatory bowel diseases. *Am J Physiol Gastrointest Liver Physiol*2021epub ahead of print [PMID: 33439104 DOI: 10.1152/ajpgi.00360.2020]
52 **Wei Z**, Wang W, Bradfield J, Li J, Cardinale C, Frackelton E, Kim C, Mentch F, Van Steen K, Visscher PM, Baldassano RN, Hakonarson H; International IBD Genetics Consortium. Large sample size, wide variant spectrum, and advanced machine-learning technique boost risk prediction for inflammatory bowel disease. *Am J Hum Genet* 2013; **92**: 1008-1012 [PMID: 23731541 DOI: 10.1016/j.ajhg.2013.05.002]
53 **Mossotto E**, Ashton JJ, Coelho T, Beattie RM, MacArthur BD, Ennis S. Classification of Paediatric Inflammatory Bowel Disease using Machine Learning. *Sci Rep* 2017; **7**: 2427 [PMID: 28546534 DOI: 10.1038/s41598-017-02606-2]
54 **Charisis VS**, Hadjileontiadis LJ. Potential of hybrid adaptive filtering in inflammatory lesion detection from capsule endoscopy images. *World J Gastroenterol* 2016; **22**: 8641-8657 [PMID: 27818583 DOI: 10.3748/wjg.v22.i39.8641]

55 **Jebarani W**, Daisy VJ. Assessment of Crohn's disease lesions in Wireless Capsule Endoscopy images using SVM based classification. Signal Processing Image Processing & Pattern Recognition (ICSIPR); Semantic Scholar, 2013: 303-307 [DOI: 10.1109/ICSIPR.2013.6497945]

56 **Girgis HZ**, Mitchell BR, Dassopoulos T, Mullin G, Hager G. An intelligent system to detect Crohn's disease inflammation in Wireless Capsule Endoscopy videos. 2010 IEEE International Symposium on Biomedical Imaging: From Nano to Macro; 2010 Apr 14-17; Rotterdam, Netherlands. IEEE, 2010 [DOI: 10.1109/ISBI.2010.5490253]

57 **Kumar R**, Zhao Q, Seshamani S, Mullin G, Hager G, Dassopoulos T. Assessment of Crohn's disease lesions in wireless capsule endoscopy images. *IEEE Trans Biomed Eng* 2012; **59**: 355-362 [PMID: 22020661 DOI: 10.1109/TBME.2011.2172438]

58 **Xia J**, Xia T, Pan J, Gao F, Wang S, Qian YY, Wang H, Zhao J, Jiang X, Zou WB, Wang YC, Zhou W, Li ZS, Liao Z. Use of artificial intelligence for detection of gastric lesions by magnetically controlled capsule endoscopy. *Gastrointest Endosc* 2021; **93**: 133-139.e4 [PMID: 32470426 DOI: 10.1016/j.gie.2020.05.027]

59 **Seguí S**, Drozdzal M, Pascual G, Radeva P, Malagelada C, Azpiroz F, Vitrià J. Generic feature learning for wireless capsule endoscopy analysis. *Comput Biol Med* 2016; **79**: 163-172 [PMID: 27810622 DOI: 10.1016/j.compbiomed.2016.10.011]

60 **Park J**, Hwang Y, Nam JH, Oh DJ, Kim KB, Song HJ, Kim SH, Kang SH, Jung MK, Jeong Lim Y. Artificial intelligence that determines the clinical significance of capsule endoscopy images can increase the efficiency of reading. *PLoS One* 2020; **15**: e0241474 [PMID: 33119718 DOI: 10.1371/journal.pone.0241474]

61 **Hwang Y**, Lee HH, Park C, Tama BA, Kim JS, Cheung DY, Chung WC, Cho YS, Lee KM, Choi MG, Lee S, Lee BI. Improved classification and localization approach to small bowel capsule endoscopy using convolutional neural network. *Dig Endosc* 2021; **33**: 598-607 [PMID: 32640059 DOI: 10.1111/den.13787]

62 **Otani K**, Nakada A, Kurose Y, Niikura R, Yamada A, Aoki T, Nakanishi H, Doyama H, Hasatani K, Sumiyoshi T, Kitsuregawa M, Harada T, Koike K. Automatic detection of different types of small-bowel lesions on capsule endoscopy images using a newly developed deep convolutional neural network. *Endoscopy* 2020; **52**: 786-791 [PMID: 32557474 DOI: 10.1055/a-1167-8157]

63 **Yuan Y**, Wang J, Li B, Meng MQ. Saliency based ulcer detection for wireless capsule endoscopy diagnosis. *IEEE Trans Med Imaging* 2015; **34**: 2046-2057 [PMID: 25850085 DOI: 10.1109/TMI.2015.2418534]

64 **Karargyris A**, Bourbakis N. Identification of ulcers in Wireless Capsule Endoscopy videos. 2009 IEEE International Symposium on Biomedical Imaging: From Nano to Macro. 2009 Jun 28-Jul 1; Boston, MA, USA. IEEE, 2009 [DOI: 10.1109/ISBI.2009.5193107]

65 **He JY**, Wu X, Jiang YG, Peng Q, Jain R. Hookworm Detection in Wireless Capsule Endoscopy Images With Deep Learning. *IEEE Trans Image Process* 2018; **27**: 2379-2392 [PMID: 29470172 DOI: 10.1109/TIP.2018.2801119]

66 **Leenhardt R**, Vasseur P, Li C, Saurin JC, Rahmi G, Cholet F, Becq A, Marteau P, Histace A, Dray X; CAD-CAP Database Working Group. A neural network algorithm for detection of GI angiectasia during small-bowel capsule endoscopy. *Gastrointest Endosc* 2019; **89**: 189-194 [PMID: 30017868 DOI: 10.1016/j.gie.2018.06.036]

67 **Zhou T**, Han G, Li BN, Lin Z, Ciaccio EJ, Green PH, Qin J. Quantitative analysis of patients with celiac disease by video capsule endoscopy: A deep learning method. *Comput Biol Med* 2017; **85**: 1-6 [PMID: 28412572 DOI: 10.1016/j.compbiomed.2017.03.031]

68 **Yamada A**, Niikura R, Otani K, Aoki T, Koike K. Automatic detection of colorectal neoplasia in wireless colon capsule endoscopic images using a deep convolutional neural network. *Endoscopy* 2021; **53**: 832-836 [PMID: 32947623 DOI: 10.1055/a-1266-1066]

69 **Wang P**, Xiao X, Glissen Brown JR, Berzin TM, Tu M, Xiong F, Hu X, Liu P, Song Y, Zhang D, Yang X, Li L, He J, Yi X, Liu J, Liu X. Development and validation of a deep-learning algorithm for the detection of polyps during colonoscopy. *Nat Biomed Eng* 2018; **2**: 741-748 [PMID: 31015647 DOI: 10.1038/s41551-018-0301-3]

70 **Misawa M**, Kudo SE, Mori Y, Cho T, Kataoka S, Yamauchi A, Ogawa Y, Maeda Y, Takeda K, Ichimasa K, Nakamura H, Yagawa Y, Toyoshima N, Ogata N, Kudo T, Hisayuki T, Hayashi T, Wakamura K, Baba T, Ishida F, Itoh H, Roth H, Oda M, Mori K. Artificial Intelligence-Assisted Polyp Detection for Colonoscopy: Initial Experience. *Gastroenterology* 2018; **154**: 2027-2029.e3 [PMID: 29653147 DOI: 10.1053/j.gastro.2018.04.003]

71 **Urban G**, Tripathi P, Alkayali T, Mittal M, Jalali F, Karnes W, Baldi P. Deep Learning Localizes and Identifies Polyps in Real Time With 96% Accuracy in Screening Colonoscopy. *Gastroenterology* 2018; **155**: 1069-1078.e8 [PMID: 29928897 DOI: 10.1053/j.gastro.2018.06.037]

72 **Ozawa T**, Ishihara S, Fujishiro M, Kumagai Y, Shichijo S, Tada T. Automated endoscopic detection and classification of colorectal polyps using convolutional neural networks. *Therap Adv Gastroenterol* 2020; **13**: 1756284820910659 [PMID: 32231710 DOI: 10.1177/1756284820910659]

73 **Mori Y**, Kudo SE, Misawa M, Saito Y, Ikematsu H, Hotta K, Ohtsuka K, Urushibara F, Kataoka S, Ogawa Y, Maeda Y, Takeda K, Nakamura H, Ichimasa K, Kudo T, Hayashi T, Wakamura K, Ishida F, Inoue H, Itoh H, Oda M, Mori K. Real-Time Use of Artificial Intelligence in Identification of Diminutive Polyps During Colonoscopy: A Prospective Study. *Ann Intern Med* 2018; **169**: 357-366 [PMID: 30105375 DOI: 10.7326/M18-0249]

74 **Tischendorf JJ**, Gross S, Winograd R, Hecker H, Auer R, Behrens A, Trautwein C, Aach T, Stehle

T. Computer-aided classification of colorectal polyps based on vascular patterns: a pilot study. *Endoscopy* 2010; **42**: 203-207 [PMID: 20101564 DOI: 10.1055/s-0029-1243861]

75 **Gross S**, Trautwein C, Behrens A, Winograd R, Palm S, Lutz HH, Schirin-Sokhan R, Hecker H, Aach T, Tischendorf JJ. Computer-based classification of small colorectal polyps by using narrow-band imaging with optical magnification. *Gastrointest Endosc* 2011; **74**: 1354-1359 [PMID: 22000791 DOI: 10.1016/j.gie.2011.08.001]

76 **Kominami Y**, Yoshida S, Tanaka S, Sanomura Y, Hirakawa T, Raytchev B, Tamaki T, Koide T, Kaneda K, Chayama K. Computer-aided diagnosis of colorectal polyp histology by using a real-time image recognition system and narrow-band imaging magnifying colonoscopy. *Gastrointest Endosc* 2016; **83**: 643-649 [PMID: 26264431 DOI: 10.1016/j.gie.2015.08.004]

77 **Misawa M**, Kudo SE, Mori Y, Nakamura H, Kataoka S, Maeda Y, Kudo T, Hayashi T, Wakamura K, Miyachi H, Katagiri A, Baba T, Ishida F, Inoue H, Nimura Y, Mori K. Characterization of Colorectal Lesions Using a Computer-Aided Diagnostic System for Narrow-Band Imaging Endocytoscopy. *Gastroenterology* 2016; **150**: 1531-1532.e3 [PMID: 27072671 DOI: 10.1053/j.gastro.2016.04.004]

78 **Takeda K**, Kudo SE, Mori Y, Misawa M, Kudo T, Wakamura K, Katagiri A, Baba T, Hidaka E, Ishida F, Inoue H, Oda M, Mori K. Accuracy of diagnosing invasive colorectal cancer using computer-aided endocytoscopy. *Endoscopy* 2017; **49**: 798-802 [PMID: 28472832 DOI: 10.1055/s-0043-105486]

79 **Chen PJ**, Lin MC, Lai MJ, Lin JC, Lu HH, Tseng VS. Accurate Classification of Diminutive Colorectal Polyps Using Computer-Aided Analysis. *Gastroenterology* 2018; **154**: 568-575 [PMID: 29042219 DOI: 10.1053/j.gastro.2017.10.010]

80 **Komeda Y**, Handa H, Watanabe T, Nomura T, Kitahashi M, Sakurai T, Okamoto A, Minami T, Kono M, Arizumi T, Takenaka M, Hagiwara S, Matsui S, Nishida N, Kashida H, Kudo M. Computer-Aided Diagnosis Based on Convolutional Neural Network System for Colorectal Polyp Classification: Preliminary Experience. *Oncology* 2017; **93** Suppl 1: 30-34 [PMID: 29258081 DOI: 10.1159/000481227]

81 **Byrne MF**, Chapados N, Soudan F, Oertel C, Linares Pérez M, Kelly R, Iqbal N, Chandelier F, Rex DK. Real-time differentiation of adenomatous and hyperplastic diminutive colorectal polyps during analysis of unaltered videos of standard colonoscopy using a deep learning model. *Gut* 2019; **68**: 94-100 [PMID: 29066576 DOI: 10.1136/gutjnl-2017-314547]

82 **ASGE Technology Committee**, Abu Dayyeh BK, Thosani N, Konda V, Wallace MB, Rex DK, Chauhan SS, Hwang JH, Komanduri S, Manfredi M, Maple JT, Murad FM, Siddiqui UD, Banerjee S. ASGE Technology Committee systematic review and meta-analysis assessing the ASGE PIVI thresholds for adopting real-time endoscopic assessment of the histology of diminutive colorectal polyps. *Gastrointest Endosc* 2015; **81**: 502.e1-502.e16 [PMID: 25597420 DOI: 10.1016/j.gie.2014.12.022]

83 **Rex DK**, Kahi C, O'Brien M, Levin TR, Pohl H, Rastogi A, Burgart L, Imperiale T, Ladabaum U, Cohen J, Lieberman DA. The American Society for Gastrointestinal Endoscopy PIVI (Preservation and Incorporation of Valuable Endoscopic Innovations) on real-time endoscopic assessment of the histology of diminutive colorectal polyps. *Gastrointest Endosc* 2011; **73**: 419-422 [PMID: 21353837 DOI: 10.1016/j.gie.2011.01.023]

84 **East JE**, Vleugels JL, Roelandt P, Bhandari P, Bisschops R, Dekker E, Hassan C, Horgan G, Kiesslich R, Longcroft-Wheaton G, Wilson A, Dumonceau JM. Advanced endoscopic imaging: European Society of Gastrointestinal Endoscopy (ESGE) Technology Review. *Endoscopy* 2016; **48**: 1029-1045 [PMID: 27711949 DOI: 10.1055/s-0042-118087]

85 **de Almeida Thomaz V**, Sierra-Franco CA, Raposo AB. Training data enhancements for improving colonic polyp detection using deep convolutional neural networks. *Artif Intell Med* 2021; **111**: 101988 [PMID: 33461694 DOI: 10.1016/j.artmed.2020.101988]

86 **Rogers B**, Samanta S, Ghobadi K, Patel A, Savarino E, Roman S, Sifrim D, Gyawali CP. Artificial intelligence automates and augments baseline impedance measurements from pH-impedance studies in gastroesophageal reflux disease. *J Gastroenterol* 2021; **56**: 34-41 [PMID: 33151406 DOI: 10.1007/s00535-020-01743-2]

87 **Zhu Y**, Wang QC, Xu MD, Zhang Z, Cheng J, Zhong YS, Zhang YQ, Chen WF, Yao LQ, Zhou PH, Li QL. Application of convolutional neural network in the diagnosis of the invasion depth of gastric cancer based on conventional endoscopy. *Gastrointest Endosc* 2019; **89**: 806-815.e1 [PMID: 30452913 DOI: 10.1016/j.gie.2018.11.011]

88 **Kubota K**, Kuroda J, Yoshida M, Ohta K, Kitajima M. Medical image analysis: computer-aided diagnosis of gastric cancer invasion on endoscopic images. *Surg Endosc* 2012; **26**: 1485-1489 [PMID: 22083334 DOI: 10.1007/s00464-011-2036-z]

89 **Yamashita R**, Long J, Longacre T, Peng L, Berry G, Martin B, Higgins J, Rubin DL, Shen J. Deep learning model for the prediction of microsatellite instability in colorectal cancer: a diagnostic study. *Lancet Oncol* 2021; **22**: 132-141 [PMID: 33387492 DOI: 10.1016/S1470-2045(20)30535-0]

90 **Ichimasa K**, Kudo SE, Mori Y, Misawa M, Matsudaira S, Kouyama Y, Baba T, Hidaka E, Wakamura K, Hayashi T, Kudo T, Ishigaki T, Yagawa Y, Nakamura H, Takeda K, Haji A, Hamatani S, Mori K, Ishida F, Miyachi H. Artificial intelligence may help in predicting the need for additional surgery after endoscopic resection of T1 colorectal cancer. *Endoscopy* 2018; **50**: 230-240 [PMID: 29272905 DOI: 10.1055/s-0043-122385]

91 **Levi R**, Carli F, Arévalo AR, Altinel Y, Stein DJ, Naldini MM, Grassi F, Zanoni A, Finkelstein S,

Vieira SM, Sousa J, Barbieri R, Celi LA. Artificial intelligence-based prediction of transfusion in the intensive care unit in patients with gastrointestinal bleeding. *BMJ Health Care Inform* 2021; **28**: e100245 [PMID: 33455913 DOI: 10.1136/bmjhci-2020-100245]

92 **Chu A**, Ahn H, Halwan B, Kalmin B, Artifon EL, Barkun A, Lagoudakis MG, Kumar A. A decision support system to facilitate management of patients with acute gastrointestinal bleeding. *Artif Intell Med* 2008; **42**: 247-259 [PMID: 18063351 DOI: 10.1016/j.artmed.2007.10.003]

93 **Das A**, Ben-Menachem T, Farooq FT, Cooper GS, Chak A, Sivak MV Jr, Wong RC. Artificial neural network as a predictive instrument in patients with acute nonvariceal upper gastrointestinal hemorrhage. *Gastroenterology* 2008; **134**: 65-74 [PMID: 18061180 DOI: 10.1053/j.gastro.2007.10.037]

94 **Augustin S**, Muntaner L, Altamirano JT, González A, Saperas E, Dot J, Abu-Suboh M, Armengol JR, Malagelada JR, Esteban R, Guardia J, Genescà J. Predicting early mortality after acute variceal hemorrhage based on classification and regression tree analysis. *Clin Gastroenterol Hepatol* 2009; **7**: 1347-1354 [PMID: 19699816 DOI: 10.1016/j.cgh.2009.08.011]

95 **Loftus TJ**, Brakenridge SC, Croft CA, Smith RS, Efron PA, Moore FA, Mohr AM, Jordan JR. Neural network prediction of severe lower intestinal bleeding and the need for surgical intervention. *J Surg Res* 2017; **212**: 42-47 [PMID: 28550920 DOI: 10.1016/j.jss.2016.12.032]

96 **Ayaru L**, Ypsilantis PP, Nanapragasam A, Choi RC, Thillanathan A, Min-Ho L, Montana G. Prediction of Outcome in Acute Lower Gastrointestinal Bleeding Using Gradient Boosting. *PLoS One* 2015; **10**: e0132485 [PMID: 26172121 DOI: 10.1371/journal.pone.0132485]

97 **Yang HX**, Feng W, Wei JC, Zeng TS, Li ZD, Zhang LJ, Lin P, Luo RZ, He JH, Fu JH. Support vector machine-based nomogram predicts postoperative distant metastasis for patients with oesophageal squamous cell carcinoma. *Br J Cancer* 2013; **109**: 1109-1116 [PMID: 23942069 DOI: 10.1038/bjc.2013.379]

98 **Sato F**, Shimada Y, Selaru FM, Shibata D, Maeda M, Watanabe G, Mori Y, Stass SA, Imamura M, Meltzer SJ. Prediction of survival in patients with esophageal carcinoma using artificial neural networks. *Cancer* 2005; **103**: 1596-1605 [PMID: 15751017 DOI: 10.1002/cncr.20938]

99 **Zhou C**, Hu J, Wang Y, Ji MH, Tong J, Yang JJ, Xia H. A machine learning-based predictor for the identification of the recurrence of patients with gastric cancer after operation. *Sci Rep* 2021; **11**: 1571 [PMID: 33452440 DOI: 10.1038/s41598-021-81188-6]

100 **Peng JC**, Ran ZH, Shen J. Seasonal variation in onset and relapse of IBD and a model to predict the frequency of onset, relapse, and severity of IBD based on artificial neural network. *Int J Colorectal Dis* 2015; **30**: 1267-1273 [PMID: 25976931 DOI: 10.1007/s00384-015-2250-6]

101 **Hardalaç F**, Başaranoğlu M, Yüksel M, Kutbay U, Kaplan M, Özderin Özin Y, Kılıç ZM, Demirbağ AE, Coşkun O, Aksoy A, Gangarapu V, Örmeci N, Kayaçetin E. The rate of mucosal healing by azathioprine therapy and prediction by artificial systems. *Turk J Gastroenterol* 2015; **26**: 315-321 [PMID: 26039001 DOI: 10.5152/tjg.2015.0199]

102 **Takayama T**, Okamoto S, Hisamatsu T, Naganuma M, Matsuoka K, Mizuno S, Bessho R, Hibi T, Kanai T. Computer-Aided Prediction of Long-Term Prognosis of Patients with Ulcerative Colitis after Cytoapheresis Therapy. *PLoS One* 2015; **10**: e0131197 [PMID: 26111148 DOI: 10.1371/journal.pone.0131197]

103 **Lyles T**, Elliott A, Rockey DC. A risk scoring system to predict in-hospital mortality in patients with cirrhosis presenting with upper gastrointestinal bleeding. *J Clin Gastroenterol* 2014; **48**: 712-720 [PMID: 24172184 DOI: 10.1097/MCG.0000000000000014]

104 **Grossi E**, Marmo R, Intraligi M, Buscema M. Artificial Neural Networks for Early Prediction of Mortality in Patients with Non Variceal Upper GI Bleeding (UGIB). *Biomed Inform Insights* 2008; **1**: 7-19 [PMID: 27429551 DOI: 10.4137/bii.s814]

105 **Rotondano G**, Cipolletta L, Grossi E, Koch M, Intraligi M, Buscema M, Marmo R; Italian Registry on Upper Gastrointestinal Bleeding (Progetto Nazionale Emorragie Digestive). Artificial neural networks accurately predict mortality in patients with nonvariceal upper GI bleeding. *Gastrointest Endosc* 2011; **73**: 218-226 [PMID: 21295635 DOI: 10.1016/j.gie.2010.10.006]

106 **Shi R**, Chen W, Yang B, Qu J, Cheng Y, Zhu Z, Gao Y, Wang Q, Liu Y, Li Z, Qu X. Prediction of KRAS, NRAS and BRAF status in colorectal cancer patients with liver metastasis using a deep artificial neural network based on radiomics and semantic features. *Am J Cancer Res* 2020; **10**: 4513-4526 [PMID: 33415015]

107 **Kang J**, Choi YJ, Kim IK, Lee HS, Kim H, Baik SH, Kim NK, Lee KY. LASSO-Based Machine Learning Algorithm for Prediction of Lymph Node Metastasis in T1 Colorectal Cancer. *Cancer Res Treat* 2021; **53**: 773-783 [PMID: 33421980 DOI: 10.4143/crt.2020.974]

108 **Goldman O**, Ben-Assuli O, Rogowski O, Zeltser D, Shapira I, Berliner S, Zelber-Sagi S, Shenhar-Tsarfaty S. Non-alcoholic Fatty Liver and Liver Fibrosis Predictive Analytics: Risk Prediction and Machine Learning Techniques for Improved Preventive Medicine. *J Med Syst* 2021; **45**: 22 [PMID: 33426569 DOI: 10.1007/s10916-020-01693-5]

109 **Yip TC**, Ma AJ, Wong VW, Tse YK, Chan HL, Yuen PC, Wong GL. Laboratory parameter-based machine learning model for excluding non-alcoholic fatty liver disease (NAFLD) in the general population. *Aliment Pharmacol Ther* 2017; **46**: 447-456 [PMID: 28585725 DOI: 10.1111/apt.14172]

110 **Ma H**, Xu CF, Shen Z, Yu CH, Li YM. Application of Machine Learning Techniques for Clinical Predictive Modeling: A Cross-Sectional Study on Nonalcoholic Fatty Liver Disease in China. *Biomed Res Int* 2018; **2018**: 4304376 [PMID: 30402478 DOI: 10.1155/2018/4304376]

111 **Sowa JP**, Heider D, Bechmann LP, Gerken G, Hoffmann D, Canbay A. Novel algorithm for non-

invasive assessment of fibrosis in NAFLD. *PLoS One* 2013; **8**: e62439 [PMID: 23638085 DOI: 10.1371/journal.pone.0062439]

112 **Canbay A**, Kälsch J, Neumann U, Rau M, Hohenester S, Baba HA, Rust C, Geier A, Heider D, Sowa JP. Non-invasive assessment of NAFLD as systemic disease-A machine learning perspective. *PLoS One* 2019; **14**: e0214436 [PMID: 30913263 DOI: 10.1371/journal.pone.0214436]

113 **Fialoke S**, Malarstig A, Miller MR, Dumitriu A. Application of Machine Learning Methods to Predict Non-Alcoholic Steatohepatitis (NASH) in Non-Alcoholic Fatty Liver (NAFL) Patients. *AMIA Annu Symp Proc* 2018; **2018**: 430-439 [PMID: 30815083]

114 **Sowa JP**, Atmaca Ö, Kahraman A, Schlattjan M, Lindner M, Sydor S, Scherbaum N, Lackner K, Gerken G, Heider D, Arteel GE, Erim Y, Canbay A. Non-invasive separation of alcoholic and non-alcoholic liver disease with predictive modeling. *PLoS One* 2014; **9**: e101444 [PMID: 24988316 DOI: 10.1371/journal.pone.0101444]

115 **Wei R**, Wang J, Wang X, Xie G, Wang Y, Zhang H, Peng CY, Rajani C, Kwee S, Liu P, Jia W. Clinical prediction of HBV and HCV related hepatic fibrosis using machine learning. *EBioMedicine* 2018; **35**: 124-132 [PMID: 30100397 DOI: 10.1016/j.ebiom.2018.07.041]

116 **Wang D**, Wang Q, Shan F, Liu B, Lu C. Identification of the risk for liver fibrosis on CHB patients using an artificial neural network based on routine and serum markers. *BMC Infect Dis* 2010; **10**: 251 [PMID: 20735842 DOI: 10.1186/1471-2334-10-251]

117 **Raoufy MR**, Vahdani P, Alavian SM, Fekri S, Eftekhari P, Gharibzadeh S. A novel method for diagnosing cirrhosis in patients with chronic hepatitis B: artificial neural network approach. *J Med Syst* 2011; **35**: 121-126 [PMID: 20703578 DOI: 10.1007/s10916-009-9348-8]

118 **Piscaglia F**, Cucchetti A, Benlloch S, Vivarelli M, Berenguer J, Bolondi L, Pinna AD, Berenguer M. Prediction of significant fibrosis in hepatitis C virus infected liver transplant recipients by artificial neural network analysis of clinical factors. *Eur J Gastroenterol Hepatol* 2006; **18**: 1255-1261 [PMID: 17099373 DOI: 10.1097/01.meg.0000243885.55562.7e]

119 **Hashem S**, Esmat G, Elakel W, Habashy S, Raouf SA, Elhefnawi M, Eladawy M, ElHefnawi M. Comparison of Machine Learning Approaches for Prediction of Advanced Liver Fibrosis in Chronic Hepatitis C Patients. *IEEE/ACM Trans Comput Biol Bioinform* 2018; **15**: 861-868 [PMID: 28391204 DOI: 10.1109/TCBB.2017.2690848]

120 **Ioannou GN**, Tang W, Beste LA, Tincopa MA, Su GL, Van T, Tapper EB, Singal AG, Zhu J, Waljee AK. Assessment of a Deep Learning Model to Predict Hepatocellular Carcinoma in Patients With Hepatitis C Cirrhosis. *JAMA Netw Open* 2020; **3**: e2015626 [PMID: 32870314 DOI: 10.1001/jamanetworkopen.2020.15626]

121 **Emu M**, Kamal FB, Choudhury S, Alves de Oliveira TE. Assisting the Non-invasive Diagnosis of Liver Fibrosis Stages using Machine Learning Methods. *Annu Int Conf IEEE Eng Med Biol Soc* 2020; **2020**: 5382-5387 [PMID: 33019198 DOI: 10.1109/EMBC44109.2020.9176542]

122 **Choi KJ**, Jang JK, Lee SS, Sung YS, Shim WH, Kim HS, Yun J, Choi JY, Lee Y, Kang BK, Kim JH, Kim SY, Yu ES. Development and Validation of a Deep Learning System for Staging Liver Fibrosis by Using Contrast Agent-enhanced CT Images in the Liver. *Radiology* 2018; **289**: 688-697 [PMID: 30179104 DOI: 10.1148/radiol.2018180763]

123 **Kuppili V**, Biswas M, Sreekumar A, Suri HS, Saba L, Edla DR, Marinho RT, Sanches JM, Suri JS. Extreme Learning Machine Framework for Risk Stratification of Fatty Liver Disease Using Ultrasound Tissue Characterization. *J Med Syst* 2017; **41**: 152 [PMID: 28836045 DOI: 10.1007/s10916-017-0797-1]

124 **Gatos I**, Tsantis S, Spiliopoulos S, Karnabatidis D, Theotokas I, Zoumpoulis P, Loupas T, Hazle JD, Kagadis GC. A Machine-Learning Algorithm Toward Color Analysis for Chronic Liver Disease Classification, Employing Ultrasound Shear Wave Elastography. *Ultrasound Med Biol* 2017; **43**: 1797-1810 [PMID: 28634041 DOI: 10.1016/j.ultrasmedbio.2017.05.002]

125 **Chen Y**, Luo Y, Huang W, Hu D, Zheng RQ, Cong SZ, Meng FK, Yang H, Lin HJ, Sun Y, Wang XY, Wu T, Ren J, Pei SF, Zheng Y, He Y, Hu Y, Yang N, Yan H. Machine-learning-based classification of real-time tissue elastography for hepatic fibrosis in patients with chronic hepatitis B. *Comput Biol Med* 2017; **89**: 18-23 [PMID: 28779596 DOI: 10.1016/j.compbiomed.2017.07.012]

126 **Matake K**, Yoshimitsu K, Kumazawa S, Higashida Y, Irie H, Asayama Y, Nakayama T, Kakihara D, Katsuragawa S, Doi K, Honda H. Usefulness of artificial neural network for differential diagnosis of hepatic masses on CT images. *Acad Radiol* 2006; **13**: 951-962 [PMID: 16843847 DOI: 10.1016/j.acra.2006.04.009]

127 **Oestmann PM**, Wang CJ, Savic LJ, Hamm CA, Stark S, Schobert I, Gebauer B, Schlachter T, Lin M, Weinreb JC, Batra R, Mulligan D, Zhang X, Duncan JS, Chapiro J. Deep learning-assisted differentiation of pathologically proven atypical and typical hepatocellular carcinoma (HCC) *vs* non-HCC on contrast-enhanced MRI of the liver. *Eur Radiol* 2021; **31**: 4981-4990 [PMID: 33409782 DOI: 10.1007/s00330-020-07559-1]

128 **Kim J**, Min JH, Kim SK, Shin SY, Lee MW. Detection of Hepatocellular Carcinoma in Contrast-Enhanced Magnetic Resonance Imaging Using Deep Learning Classifier: A Multi-Center Retrospective Study. *Sci Rep* 2020; **10**: 9458 [PMID: 32527998 DOI: 10.1038/s41598-020-65875-4]

129 **Cucchetti A**, Piscaglia F, Grigioni AD, Ravaioli M, Cescon M, Zanello M, Grazi GL, Golfieri R, Grigioni WF, Pinna AD. Preoperative prediction of hepatocellular carcinoma tumour grade and micro-vascular invasion by means of artificial neural network: a pilot study. *J Hepatol* 2010; **52**: 880-888 [PMID: 20409605 DOI: 10.1016/j.jhep.2009.12.037]

130 **Urman JM**, Herranz JM, Uriarte I, Rullán M, Oyón D, González B, Fernandez-Urién I, Carrascosa

J, Bolado F, Zabalza L, Arechederra M, Alvarez-Sola G, Colyn L, Latasa MU, Puchades-Carrasco L, Pineda-Lucena A, Iraburu MJ, Iruarrizaga-Lejarreta M, Alonso C, Sangro B, Purroy A, Gil I, Carmona L, Cubero FJ, Martínez-Chantar ML, Banales JM, Romero MR, Macias RIR, Monte MJ, Marín JJG, Vila JJ, Corrales FJ, Berasain C, Fernández-Barrena MG, Avila MA. Pilot Multi-Omic Analysis of Human Bile from Benign and Malignant Biliary Strictures: A Machine-Learning Approach. *Cancers (Basel)* 2020; **12**: 1644 [PMID: 32575903 DOI: 10.3390/cancers12061644]

131 **Negrini D**, Zecchin P, Ruzzenente A, Bagante F, De Nitto S, Gelati M, Salvagno GL, Danese E, Lippi G. Machine Learning Model Comparison in the Screening of Cholangiocarcinoma Using Plasma Bile Acids Profiles. *Diagnostics (Basel)* 2020; **10**: 551 [PMID: 32748848 DOI: 10.3390/diagnostics10080551]

132 **Logeswaran R**. Cholangiocarcinoma--an automated preliminary detection system using MLP. *J Med Syst* 2009; **33**: 413-421 [PMID: 20052894 DOI: 10.1007/s10916-008-9203-3]

133 **Wübbolding M**, Lopez Alfonso JC, Lin CY, Binder S, Falk C, Debarry J, Gineste P, Kraft ARM, Chien RN, Maasoumy B, Wedemeyer H, Jeng WJ, Meyer Hermann M, Cornberg M, Höner Zu Siederdissen C. Pilot Study Using Machine Learning to Identify Immune Profiles for the Prediction of Early Virological Relapse After Stopping Nucleos(t)ide Analogues in HBeAg-Negative CHB. *Hepatol Commun* 2021; **5**: 97-111 [PMID: 33437904 DOI: 10.1002/hep4.1626]

134 **Haga H**, Sato H, Koseki A, Saito T, Okumoto K, Hoshikawa K, Katsumi T, Mizuno K, Nishina T, Ueno Y. A machine learning-based treatment prediction model using whole genome variants of hepatitis C virus. *PLoS One* 2020; **15**: e0242028 [PMID: 33152046 DOI: 10.1371/journal.pone.0242028]

135 **Bedon L**, Dal Bo M, Mossenta M, Busato D, Toffoli G, Polano M. A Novel Epigenetic Machine Learning Model to Define Risk of Progression for Hepatocellular Carcinoma Patients. *Int J Mol Sci* 2021; **22**: 1075 [PMID: 33499054 DOI: 10.3390/ijms22031075]

136 **European Association for the Study of the Liver**. EASL Clinical Practice Guidelines: Management of hepatocellular carcinoma. *J Hepatol* 2018; **69**: 182-236 [PMID: 29628281 DOI: 10.1016/j.jhep.2018.03.019]

137 **Tsilimigras DI**, Mehta R, Moris D, Sahara K, Bagante F, Paredes AZ, Farooq A, Ratti F, Marques HP, Silva S, Soubrane O, Lam V, Poultsides GA, Popescu I, Grigorie R, Alexandrescu S, Martel G, Workneh A, Guglielmi A, Hugh T, Aldrighetti L, Endo I, Pawlik TM. Utilizing Machine Learning for Pre- and Postoperative Assessment of Patients Undergoing Resection for BCLC-0, A and B Hepatocellular Carcinoma: Implications for Resection Beyond the BCLC Guidelines. *Ann Surg Oncol* 2020; **27**: 866-874 [PMID: 31696396 DOI: 10.1245/s10434-019-08025-z]

138 **Christou CD**, Tooulias A, Tsolakidis A, Papayiannis V, Pianetcki-Tsiantzi B, Tsoulfas G, Papadopoulos VN. Management of Hepatocellular Carcinoma in the Era of Individualized Therapy: The Experience of a Greek Tertiary Center. *Ochsner J* 2020; **20**: 272-278 [PMID: 33071659 DOI: 10.31486/toj.19.0092]

139 **Tsilimigras DI**, Mehta R, Moris D, Sahara K, Bagante F, Paredes AZ, Moro A, Guglielmi A, Aldrighetti L, Weiss M, Bauer TW, Alexandrescu S, Poultsides GA, Maithel SK, Marques HP, Martel G, Pulitano C, Shen F, Soubrane O, Koerkamp BG, Endo I, Pawlik TM. A Machine-Based Approach to Preoperatively Identify Patients with the Most and Least Benefit Associated with Resection for Intrahepatic Cholangiocarcinoma: An International Multi-institutional Analysis of 1146 Patients. *Ann Surg Oncol* 2020; **27**: 1110-1119 [PMID: 31728792 DOI: 10.1245/s10434-019-08067-3]

140 **Jeong S**, Ge Y, Chen J, Gao Q, Luo G, Zheng B, Sha M, Shen F, Cheng Q, Sui C, Liu J, Wang H, Xia Q, Chen L. Latent Risk Intrahepatic Cholangiocarcinoma Susceptible to Adjuvant Treatment After Resection: A Clinical Deep Learning Approach. *Front Oncol* 2020; **10**: 143 [PMID: 32140448 DOI: 10.3389/fonc.2020.00143]

141 **Shao F**, Huang Q, Wang C, Qiu L, Hu YG, Zha SY. Artificial Neural Networking Model for the Prediction of Early Occlusion of Bilateral Plastic Stent Placement for Inoperable Hilar Cholangiocarcinoma. *Surg Laparosc Endosc Percutan Tech* 2018; **28**: e54-e58 [PMID: 29252936 DOI: 10.1097/SLE.0000000000000502]

142 **Hong WD**, Ji YF, Wang D, Chen TZ, Zhu QH. Use of artificial neural network to predict esophageal varices in patients with HBV related cirrhosis. *Hepat Mon* 2011; **11**: 544-547 [PMID: 22087192]

143 **Dong TS**, Kalani A, Aby ES, Le L, Luu K, Hauer M, Kamath R, Lindor KD, Tabibian JH. Machine Learning-based Development and Validation of a Scoring System for Screening High-Risk Esophageal Varices. *Clin Gastroenterol Hepatol* 2019; **17**: 1894-1901.e1 [PMID: 30708109 DOI: 10.1016/j.cgh.2019.01.025]

144 **Ho WH**, Lee KT, Chen HY, Ho TW, Chiu HC. Disease-free survival after hepatic resection in hepatocellular carcinoma patients: a prediction approach using artificial neural network. *PLoS One* 2012; **7**: e29179 [PMID: 22235270 DOI: 10.1371/journal.pone.0029179]

145 **Shi HY**, Lee KT, Wang JJ, Sun DP, Lee HH, Chiu CC. Artificial neural network model for predicting 5-year mortality after surgery for hepatocellular carcinoma: a nationwide study. *J Gastrointest Surg* 2012; **16**: 2126-2131 [PMID: 22878787 DOI: 10.1007/s11605-012-1986-3]

146 **Shi HY**, Lee KT, Lee HH, Ho WH, Sun DP, Wang JJ, Chiu CC. Comparison of artificial neural network and logistic regression models for predicting in-hospital mortality after primary liver cancer surgery. *PLoS One* 2012; **7**: e35781 [PMID: 22563399 DOI: 10.1371/journal.pone.0035781]

147 **Chiu HC**, Ho TW, Lee KT, Chen HY, Ho WH. Mortality predicted accuracy for hepatocellular

carcinoma patients with hepatic resection using artificial neural network. *Scientific World Journal* 2013; **2013**: 201976 [PMID: 23737707 DOI: 10.1155/2013/201976]

148 **Qiao G**, Li J, Huang A, Yan Z, Lau WY, Shen F. Artificial neural networking model for the prediction of post-hepatectomy survival of patients with early hepatocellular carcinoma. *J Gastroenterol Hepatol* 2014; **29**: 2014-2020 [PMID: 24989634 DOI: 10.1111/jgh.12672]

149 **Liu X**, Lu J, Zhang G, Han J, Zhou W, Chen H, Zhang H, Yang Z. A Machine Learning Approach Yields a Multiparameter Prognostic Marker in Liver Cancer. *Cancer Immunol Res* 2021; **9**: 337-347 [PMID: 33431375 DOI: 10.1158/2326-6066.CIR-20-0616]

150 **Zhong BY**, Yan ZP, Sun JH, Zhang L, Hou ZH, Yang MJ, Zhou GH, Wang WS, Li Z, Huang P, Zhang S, Zhu XL, Ni CF. Prognostic Performance of Albumin-Bilirubin Grade With Artificial Intelligence for Hepatocellular Carcinoma Treated With Transarterial Chemoembolization Combined With Sorafenib. *Front Oncol* 2020; **10**: 525461 [PMID: 33392064 DOI: 10.3389/fonc.2020.525461]

151 **Lai Q**, Spoletini G, Mennini G, Laureiro ZL, Tsilimigras DI, Pawlik TM, Rossi M. Prognostic role of artificial intelligence among patients with hepatocellular cancer: A systematic review. *World J Gastroenterol* 2020; **26**: 6679-6688 [PMID: 33268955 DOI: 10.3748/wjg.v26.i42.6679]

152 **R D**, P R. An Optimized HCC Recurrence Prediction Using APO Algorithm Multiple Time Series Clinical Liver Cancer Dataset. *J Med Syst* 2019; **43**: 193 [PMID: 31115780 DOI: 10.1007/s10916-019-1265-x]

153 **Yamashita R**, Long J, Saleem A, Rubin DL, Shen J. Deep learning predicts postsurgical recurrence of hepatocellular carcinoma from digital histopathologic images. *Sci Rep* 2021; **11**: 2047 [PMID: 33479370 DOI: 10.1038/s41598-021-81506-y]

154 **Liang JD**, Ping XO, Tseng YJ, Huang GT, Lai F, Yang PM. Recurrence predictive models for patients with hepatocellular carcinoma after radiofrequency ablation using support vector machines with feature selection methods. *Comput Methods Programs Biomed* 2014; **117**: 425-434 [PMID: 25278224 DOI: 10.1016/j.cmpb.2014.09.001]

155 **Eaton JE**, Vesterhus M, McCauley BM, Atkinson EJ, Schlicht EM, Juran BD, Gossard AA, LaRusso NF, Gores GJ, Karlsen TH, Lazaridis KN. Primary Sclerosing Cholangitis Risk Estimate Tool (PREsTo) Predicts Outcomes of the Disease: A Derivation and Validation Study Using Machine Learning. *Hepatology* 2020; **71**: 214-224 [PMID: 29742811 DOI: 10.1002/hep.30085]

156 **Andres A**, Montano-Loza A, Greiner R, Uhlich M, Jin P, Hoehn B, Bigam D, Shapiro JAM, Kneteman NM. A novel learning algorithm to predict individual survival after liver transplantation for primary sclerosing cholangitis. *PLoS One* 2018; **13**: e0193523 [PMID: 29543895 DOI: 10.1371/journal.pone.0193523]

157 **Rodriguez-Luna H**, Vargas HE, Byrne T, Rakela J. Artificial neural network and tissue genotyping of hepatocellular carcinoma in liver-transplant recipients: prediction of recurrence. *Transplantation* 2005; **79**: 1737-1740 [PMID: 15973178 DOI: 10.1097/01.tp.0000161794.32007.d1]

158 **Lau L**, Kankanige Y, Rubinstein B, Jones R, Christophi C, Muralidharan V, Bailey J. Machine-Learning Algorithms Predict Graft Failure After Liver Transplantation. *Transplantation* 2017; **101**: e125-e132 [PMID: 27941428 DOI: 10.1097/TP.0000000000001600]

159 **Cruz-Ramírez M**, Hervás-Martínez C, Fernández JC, Briceño J, de la Mata M. Multi-objective evolutionary algorithm for donor–recipient decision system in liver transplants. *Eur J Oper Res* 2012; 317-327 [DOI: 10.1016/j.ejor.2012.05.013]

160 **Briceño J**, Cruz-Ramírez M, Prieto M, Navasa M, Ortiz de Urbina J, Orti R, Gómez-Bravo MÁ, Otero A, Varo E, Tomé S, Clemente G, Bañares R, Bárcena R, Cuervas-Mons V, Solórzano G, Vinaixa C, Rubín A, Colmenero J, Valdivieso A, Ciria R, Hervás-Martínez C, de la Mata M. Use of artificial intelligence as an innovative donor-recipient matching model for liver transplantation: results from a multicenter Spanish study. *J Hepatol* 2014; **61**: 1020-1028 [PMID: 24905493 DOI: 10.1016/j.jhep.2014.05.039]

161 **Crawford K**, Calo R. There is a blind spot in AI research. *Nature* 2016; **538**: 311-313 [PMID: 27762391 DOI: 10.1038/538311a]

162 **Park SH**, Han K. Methodologic Guide for Evaluating Clinical Performance and Effect of Artificial Intelligence Technology for Medical Diagnosis and Prediction. *Radiology* 2018; **286**: 800-809 [PMID: 29309734 DOI: 10.1148/radiol.2017171920]

163 **Patel VL**, Shortliffe EH, Stefanelli M, Szolovits P, Berthold MR, Bellazzi R, Abu-Hanna A. The coming of age of artificial intelligence in medicine. *Artif Intell Med* 2009; **46**: 5-17 [PMID: 18790621 DOI: 10.1016/j.artmed.2008.07.017]

164 **Parikh RB**, Teeple S, Navathe AS. Addressing Bias in Artificial Intelligence in Health Care. *JAMA* 2019; **322**: 2377-2378 [PMID: 31755905 DOI: 10.1001/jama.2019.18058]

165 **Hwang TJ**, Kesselheim AS, Vokinger KN. Lifecycle Regulation of Artificial Intelligence- and Machine Learning-Based Software Devices in Medicine. *JAMA* 2019; **322**: 2285-2286 [PMID: 31755907 DOI: 10.1001/jama.2019.16842]

166 **Shortliffe EH**, Sepúlveda MJ. Clinical Decision Support in the Era of Artificial Intelligence. *JAMA* 2018; **320**: 2199-2200 [PMID: 30398550 DOI: 10.1001/jama.2018.17163]

167 **Wolff RF**, Moons KGM, Riley RD, Whiting PF, Westwood M, Collins GS, Reitsma JB, Kleijnen J, Mallett S; PROBAST Group†. PROBAST: A Tool to Assess the Risk of Bias and Applicability of Prediction Model Studies. *Ann Intern Med* 2019; **170**: 51-58 [PMID: 30596875 DOI: 10.7326/M18-1376]

168 **American Medical Association**. AMA passes first policy recommendations on augmented

intelligence. 2018 Jun 14 [cited 20 December 2020]. Available from: https://www.ama-assn.org/press-center/press-releases/ama-passes-first-policy-recommendations-augmented-intelligence

169 **Chico V**. The impact of the General Data Protection Regulation on health research. *Br Med Bull* 2018; **128**: 109-118 [PMID: 30445448 DOI: 10.1093/bmb/ldy038]

170 **Council NR**. For the Record: Protecting Electronic Health Information. Washington, DC: The National Academies Press, 1997

171 **The Guardian**. Royal Free breached UK data law in 1.6m patient deal with Google's DeepMind. [cited 20 December 2020]. Available from: https://www.theguardian.com/technology/2017/jul/03/google-deepmind-16m-patient-royal-free-deal-data-protection-act

172 **U.S. Department of Labor**. Health Insurance Portability and Accountability Act (HIPAA). 2004 [cited 20 December 2020]. Available from: https://www.dol.gov/agencies/ebsa/laws-and-regulations/laws/hipaa

173 **National Academies of Sciences, Engineering, and Medicine**. Artificial Intelligence and Machine Learning to Accelerate Translational Research: Proceedings of a Workshop-in Brief. Washington (DC): National Academies Press, 2018 [PMID: 30048078 DOI: 10.17226/25197]

174 **Mirsky Y**, Mahler T, Shelef I, Elovici Y. CT-GAN: Malicious tampering of 3D medical imagery using deep learning. Proceedings of the 28th USENIX Security Symposium (USENIX Security 2019). arXiv, 2019: 461–478

175 **U.S. Food and Drug**. Software as a Medical Device (SaMD) Action Plan. 2021 [cited 2021 January 23]. Available from: Available from: https://www.fda.gov/medical-devices/software-medical-device-samd/artificial-intelligence-and-machine-learning-software-medical-device

176 **Topol EJ**. High-performance medicine: the convergence of human and artificial intelligence. *Nat Med* 2019; **25**: 44-56 [PMID: 30617339 DOI: 10.1038/s41591-018-0300-7]

177 **U.S. Food and Drug**. Proposed Regulatory Framework for Modifications to Artificial Intelligence / Machine Learning (AI / ML) -Based Software as a Medical Device (SaMD) - Discussion Paper and Request for Feedback. 2019 [cited 20 January 23]. Available from: Available from: https://www.fda.gov/files/medical%20devices/published/US-FDA-Artificial-Intelligence-and-Machine-Learning-Discussion-Paper.pdf

178 **Institute of Medicine**. Medical devices and the public's health: the FDA(k) 510 clearance process at 35 years. Washington: the National Academies Press, 2011

179 **Price WN 2nd**, Gerke S, Cohen IG. Potential Liability for Physicians Using Artificial Intelligence. *JAMA* 2019; **322**: 1765-1766 [PMID: 31584609 DOI: 10.1001/jama.2019.15064]

180 **Froomkin AM**, Kerr I, Pineau J. When ais outperform doctors: confronting the challenges of a tort-induced over-reliance on machine learning. *Ariz L Rev* 2018; **61**

181 **Cohen IG**, Lynch HF, Vayena E, Gasser U. Big data, health law, and bioethics. New York, NY: Cambridge University Press, 2018

182 **Nundy S**, Montgomery T, Wachter RM. Promoting Trust Between Patients and Physicians in the Era of Artificial Intelligence. *JAMA* 2019; **322**: 497-498 [PMID: 31305873 DOI: 10.1001/jama.2018.20563]

183 **Future Advocacy**. Ethical, Social, and political challenges of artificial intelligence in health. [cited 20 December 2020]. Available from: https://wellcome.org/sites/default/files/ai-in-health-ethical-social-political-challenges.pdf

184 **Gerke S**, Yeung S, Cohen IG. Ethical and Legal Aspects of Ambient Intelligence in Hospitals. *JAMA* 2020; **323**: 601-602 [PMID: 31977033 DOI: 10.1001/jama.2019.21699]

185 **Yeung S**, Rinaldo F, Jopling J, Liu B, Mehra R, Downing NL, Guo M, Bianconi GM, Alahi A, Lee J, Campbell B, Deru K, Beninati W, Fei-Fei L, Milstein A. A computer vision system for deep learning-based detection of patient mobilization activities in the ICU. *NPJ Digit Med* 2019; **2**: 11 [PMID: 31304360 DOI: 10.1038/s41746-019-0087-z]

186 **Yeung S**, Downing NL, Fei-Fei L, Milstein A. Bedside Computer Vision - Moving Artificial Intelligence from Driver Assistance to Patient Safety. *N Engl J Med* 2018; **378**: 1271-1273 [PMID: 29617592 DOI: 10.1056/NEJMp1716891]

187 **ProPublica**. Machine Bias. [cited 2021 January 23]. Available from: https://www.propublica.org/article/machine-bias-risk-assessments-in-criminal-sentencing

188 **Al'Aref SJ**, Singh G, Baskaran L, Metaxas D. Machine Learning in Cardiovascular Medicine. 2020 [cited 2021 January 23]. Available from: http://public.eblib.com/choice/PublicFullRecord.aspx?p=6404325

189 **Vayena E**, Blasimme A, Cohen IG. Machine learning in medicine: Addressing ethical challenges. *PLoS Med* 2018; **15**: e1002689 [PMID: 30399149 DOI: 10.1371/journal.pmed.1002689]

190 **Park SH**. Artificial Intelligence in Medicine: Beginners Guide. *DOAJ* 2018; **78**: 301-308 [DOI: 10.3348/jksr.2018.78.5.301]

191 **Zhang L**, Wang H, Li Q, Zhao MH, Zhan QM. Big data and medical research in China. *BMJ* 2018; **360**: j5910 [PMID: 29437562 DOI: 10.1136/bmj.j5910]

192 **Cook TS**. Human *vs* machine in medicine: can scientific literature answer the question? *Lancet Digit Health* 2019; **1**: e246-e247 [PMID: 33323246 DOI: 10.1016/S2589-7500(19)30124-4]

193 **Liu X**, Faes L, Kale AU, Wagner SK, Fu DJ, Bruynseels A, Mahendiran T, Moraes G, Shamdas M, Kern C, Ledsam JR, Schmid MK, Balaskas K, Topol EJ, Bachmann LM, Keane PA, Denniston AK.

A comparison of deep learning performance against health-care professionals in detecting diseases from medical imaging: a systematic review and meta-analysis. *Lancet Digit Health* 2019; **1**: e271-e297 [PMID: 33323251 DOI: 10.1016/S2589-7500(19)30123-2]

194 **Christou CD**, Tsoulfas G. The Role of microRNA in Hepatic Ischemia/Reperfusion Injury. *Microrna* 2020; **9**: 248-254 [PMID: 31995027 DOI: 10.2174/2211536609666200129162531]

195 **Panesar S**, Cagle Y, Chander D, Morey J, Fernandez-Miranda J, Kliot M. Artificial Intelligence and the Future of Surgical Robotics. *Ann Surg* 2019; **270**: 223-226 [PMID: 30907754 DOI: 10.1097/SLA.0000000000003262]

196 **Kassahun Y**, Yu B, Tibebu AT, Stoyanov D, Giannarou S, Metzen JH, Vander Poorten E. Surgical robotics beyond enhanced dexterity instrumentation: a survey of machine learning techniques and their role in intelligent and autonomous surgical actions. *Int J Comput Assist Radiol Surg* 2016; **11**: 553-568 [PMID: 26450107 DOI: 10.1007/s11548-015-1305-z]

197 **Wang DD**, Qian Z, Vukicevic M, Engelhardt S, Kheradvar A, Zhang C, Little SH, Verjans J, Comaniciu D, O'Neill WW, Vannan MA. 3D Printing, Computational Modeling, and Artificial Intelligence for Structural Heart Disease. *JACC Cardiovasc Imaging* 2021; **14**: 41-60 [PMID: 32861647 DOI: 10.1016/j.jcmg.2019.12.022]

198 **Volonté F**, Pugin F, Bucher P, Sugimoto M, Ratib O, Morel P. Augmented reality and image overlay navigation with OsiriX in laparoscopic and robotic surgery: not only a matter of fashion. *J Hepatobiliary Pancreat Sci* 2011; **18**: 506-509 [PMID: 21487758 DOI: 10.1007/s00534-011-0385-6]

199 **U.S. Food and Drug**. Developing a Software Precertification Program: A Working Model. 2018 [cited 2021 January 23]. Available from: https://www.fda.gov/media/113802/download

World Journal of Gastroenterology

Submit a Manuscript: https://www.f6publishing.com

World J Gastroenterol 2021 October 7; 27(37): 6224-6230

DOI: 10.3748/wjg.v27.i37.6224

ISSN 1007-9327 (print) ISSN 2219-2840 (online)

MINIREVIEWS

Impact of *Helicobacter pylori* infection on gut microbiota

Chikara Iino, Tadashi Shimoyama

ORCID number: Chikara Iino 0000-0001-6844-4415; Tadashi Shimoyama 0000-0001-9615-0000.

Author contributions: Iino C and Shimoyama T designed the review; Iino C interpreted the data and drafted the manuscript; Shimoyama T critically revised the paper.

Conflict-of-interest statement: The authors declare that there are no conflicts of interest regarding the publication of this paper.

Open-Access: This article is an open-access article that was selected by an in-house editor and fully peer-reviewed by external reviewers. It is distributed in accordance with the Creative Commons Attribution NonCommercial (CC BY-NC 4.0) license, which permits others to distribute, remix, adapt, build upon this work non-commercially, and license their derivative works on different terms, provided the original work is properly cited and the use is non-commercial. See: http://creativecommons.org/Licenses/by-nc/4.0/

Manuscript source: Invited manuscript

Specialty type: Gastroenterology and hepatology

Country/Territory of origin: Japan

Peer-review report's scientific

Chikara Iino, Tadashi Shimoyama, Department of Gastroenterology, Hirosaki University Graduate School of Medicine, Hirosaki 036-8562, Japan

Tadashi Shimoyama, Department of Internal Medicine, Aomori General Health Examination Center, Aomori 030-0962, Japan

Corresponding author: Tadashi Shimoyama, FACG, MD, PhD, Director, Department of Internal Medicine, Aomori General Health Examination Center, 2-19-12 Tsukuda, Aomori 030-0962, Japan. tsimo@hirosaki-u.ac.jp

Abstract

A number of studies have revealed the association between *Helicobacter pylori* (*H. pylori*) infection and the gut microbiota. More than half of the investigations on the impact of *H. pylori* on the gut microbiota have been the sub-analyses of the influence of eradication therapy. It was observed that *H. pylori* eradication altered gut microbiota within a short period after eradication, and majority of the alterations took a long period of time to reverse back to the original. Changes in the gut microbiota within a short period after eradication may be attributed to antibiotics and proton pump inhibitors. Modification of gastric acidity in the stomach caused by a long-term *H. pylori* infection alters the gut microbiota. Analysis of the gut microbiota should be conducted in a large population, adjusting for considerable biases associated with the composition of the gut microbiota, such as age, sex, body mass index, diet and the virulence of *H. pylori*.

Key Words: *Helicobacter pylori*; Gut microbiota; Atrophic gastritis; Eradication; Proton pump inhibitor

©The Author(s) 2021. Published by Baishideng Publishing Group Inc. All rights reserved.

Core Tip: *Helicobacter pylori* (*H. pylori*) eradication alters gut microbiota within a short period after eradication; this is attributed to antibiotics and proton pump inhibitors. However, most of these alterations reverse back to baseline levels over a long period of time. Modification of acidity in the stomach with mucosal atrophy caused by *H. pylori* infection alters the gut microbiota. As the human gut microbiome is diverse among individuals, a large population size is needed to study. Adjustment of biases associated with the composition of the gut microbiota is also crucial for accurate evaluation of the association between *H. pylori* infection and the gut microbiota.

quality classification
Grade A (Excellent): 0
Grade B (Very good): B
Grade C (Good): 0
Grade D (Fair): 0
Grade E (Poor): 0

Received: March 16, 2021
Peer-review started: March 16, 2021
First decision: April 29, 2021
Revised: May 13, 2021
Accepted: September 2, 2021
Article in press: September 2, 2021
Published online: October 7, 2021

P-Reviewer: Dong XS
S-Editor: Gao CC
L-Editor: A
P-Editor: Yuan YY



Citation: Iino C, Shimoyama T. Impact of *Helicobacter pylori* infection on gut microbiota. *World J Gastroenterol* 2021; 27(37): 6224-6230
URL: https://www.wjgnet.com/1007-9327/full/v27/i37/6224.htm
DOI: https://dx.doi.org/10.3748/wjg.v27.i37.6224

INTRODUCTION

In recent years, a number of studies related to gut microbiota have been published, shedding light on the association between gut microbiota and human health. The human microbiota consists of as many as 10-100 trillion symbiotic microbial cells harbored in the intestinal tract of every person[1]. The gut microbiota plays a pivotal role of in the metabolic, physiological, and immunological systems of the human body [2], and its structure is closely associated with an individual's health and past illnesses [3].

Accordingly, research on the association between *Helicobacter pylori* (*H. pylori*) infection and the microbiota has also increased[4]. Most of the studies, including our previous studies that revealed the influence of *H. pylori* infection on the gut microbiota, have focused on the gastric microbiota, while only a few studies have investigated the gut microbiota harbored in the intestinal tract of patients with *H. pylori* infection[5,6]. Subsequently, some published studies have revealed new findings and have improved our understanding of this phenomenon. Therefore, the current review aims to summarize the recent evidence on the influence of *H. pylori* infection on the gut microbiota, while focusing on the gut microbiota in the intestinal tract, and to discuss the mechanisms underlying the *H. pylori* mediated alterations in the gut microbiota.

H. PYLORI AND GUT MICROBIOTA

More than half of the investigations on the impact of *H. pylori* on the gut microbiota have been the sub-analyses of the influence of eradication therapy on the gut microbiota[7-11] (Table 1). Two earlier studies were based on in situ hybridization and bacterial culturing using fecal samples. A study showed that the gut microbiota of *H. pylori*-positive patients was characterized by an increase in the growth of acid-tolerant *Lactobacillus acidophilus*[7]. Another study found that the total amount of *Anaerobes* and *Clostridia* present in *H. pylori*-positive patients was significantly lower as compared to that of *H. pylori*-negative subjects[8]. Subsequent studies were based on the analysis of the fecal 16S rRNA. The analysis of the fecal 16S rRNA from 70 *H. pylori*-positive subjects and 35 *H. pylori*-negative subjects showed a decrease in the abundance of *Clostridia* as well as total anaerobes in the fecal samples of *H. pylori*-positive individuals[9]. In a study on young adults, the microbial diversity of the gut microbiota was higher in patients infected with *H. pylori* than in healthy controls. Moreover, at the phylum level, the relative abundance of *Proteobacteria* significantly increased in patients infected with *H. pylori*[10]. In contrast, only the study by Martín-Núñez *et al*[11] revealed that in comparison with uninfected individuals, the alpha diversity of gut microbiota was significantly lower in patients infected with *H. pylori*. In these studies, the composition of the gut microbiota between subjects infected and uninfected was not the primary endpoint. Moreover, the number of subjects taken into consideration was relatively small. As the diversity of the human gut microbiome varies among individuals, a large population size is needed.

A few studies have been conducted to investigate the influence of *H. pylori* infection on the gut microbiota[5,6,12,13]. Our large population study performed using 16S rRNA amplification from fecal samples revealed that *Lactobacillus* in the human gut microbiota may be influenced by *H. pylori* infection[5]. In a small-sample study, Dash *et al*[12] showed that the gut microbiota of *H. pylori*-infected individuals were enriched with members of *Succinivibrio*, *Coriobacteriaceae*, *Enterococcaceae*, and *Rikenellaceae* families. Furthermore, several studies have suggested that the composition of the human gut microbiota changes with age, body mass index (BMI), and sex[14-16]. Therefore, we excluded the influence of these factors using the propensity score matching, which has not been considered in previous studies. We compared 214 *H. pylori*-positive subjects and 214 matched *H. pylori*-negative subjects from a large population study and found a higher gut microbial diversity and a different gut microbiota composition in subjects with *H. pylori*[6]. Furthermore, at the genus level,

Table 1 Studies for the influence of *Helicobacter pylori* infection on gut microbiota

Ref.	Study groups *H. pylori* (+) *vs* (-)	Aim	Main findings for *H. pylori* positive subject
Bühling *et al*[7], 2001	51 *vs* 27	Sub analysis for eradication study	*L. acidophilus* ↑
Myllyluoma *et al* [8], 2007	39 *vs* 19	Sub analysis for eradication study	*Clostridia* ↓, *Anaerobes* ↓
Chen *et al*[9], 2018	70 *vs* 35	Sub analysis for eradication study	Diversity ↑, *Nitrospirae* ↓, the relative abundance of 19 pathways were significantly different between *H. pylori*-negative and *H. pylori*-positive patients
Iino *et al*[5], 2018	226 *vs* 524	Analysis of microbiota without eradication	*Lactobacillus* ↑
He *et al*[10], 2019	10 *vs* 7	Sub analysis for eradication study	Diversity ↑, *Proteobacteria* ↑
Iino *et al*[6], 2020	214 *vs* 214	Analysis of microbiota without eradication	Diversity ↑, *Haemophilusu* ↑, *Streptococcus* ↑, *Gemella* ↑, *Actinomyces* ↑
Martín-Núñez *et al* [11], 2019	40 *vs* 20	Sub analysis for eradication study	Diversity ↓, *Oscillospira* ↓
Dash *et al*[12], 2019	12 *vs* 48	Analysis of microbiota without eradication	Diversity ↑, *Succinivibrio* ↑, *Coriobacteriaceae* ↑, *Enterococcaceae* ↑, *Rikenellaceae* ↑, *Candida glabrata* ↑
Frost *et al*[13], 2019	212 *vs* 212	Analysis of microbiota without eradication	Diversity ↑, *Prevotella* ↑, *Bacteroidetes* ↓, *Parasutterella* ↑, *Holdemanella* ↑, *Betaproteobacteria* ↑, *Pseudoflavonifractor* ↓, *Alisonella* ↑, *Howardella* ↑

Helicobacter pylori: *H. pylori*.

the abundance of *Actinomyces*, *Gemella*, *Streptococcus*, and *Haemophilus* was significantly higher in the gut microbiota of *H. pylori*-infected subjects. Another recent study conducted by Frost *et al*[13] assessed the microbiota composition of 212 *H. pylori*-positive subjects and 212 matched negative controls. Similar to our study, all control samples were matched with respect to age, sex, BMI, alcohol consumption, smoking, proton pump inhibitor (PPI) usage, history of peptic ulcer disease, and dietary habits. This study demonstrated that *H. pylori* infection was associated with alterations in fecal microbiota and an overall increase in fecal microbial diversity. A later study on the long-term effects of *H. pylori* eradication demonstrated that the structure of the gut microbiota is more closely associated with subject-specific parameters, such as age or BMI, than with the eradication therapy itself[17]. Therefore, adjusting for biases associated with the composition of the gut microbiota is crucial for accurate evaluation of its composition. Diet is a key modifiable factor affecting the composition of the gut microbiota[18]. However, only one study has addressed this parameter[13].

THE INFLUENCE OF *H. PYLORI* ERADICATION ON GUT MICROBIOTA

A number of published studies have investigated the changes in the gut microbiota after *H. pylori* eradication. A recent systematic review of 24 articles examining the effect of *H. pylori* eradication on the gut microbiota revealed that most studies identified a significant decrease in the alpha diversity of the gut microbiota within a short period after eradication but no further alterations were observed for over 6 mo after *H. pylori* eradication[19]. Additionally, the abundance of *Proteobacteria* increased during a short-term follow-up whereas that of *Lactobacillus* decreased; *Enterobacteriaceae* and *Enterococcus* increased during the short-term and interim follow-up. Moreover, a more recent study evaluating the long-term effects of *H. pylori* eradication found out that the composition of the gut microbiota was restored to baseline status over the 2 years after eradication, and the relative abundances of the microbial species at the genus level before and after eradication did not differ significantly[17]. However, modest differences in the taxonomic composition were observed before and after eradication. The findings of this study where diversity of the microbiota tends to decrease in the short period after eradication and returns to baseline thereafter, it was consistent with the findings of most studies[9,10,20-26]. However, the taxonomic composition before and after eradication varied among the studies[21,22]. Some studies demonstrated that the relative abundance of all genera was restored to baseline

levels. Other studies revealed notable changes at the genus level[10,24-26]. Thus, it may be assumed that after the microbial diversity returns to baseline, the levels of each strain might demonstrate minor variations following the eradication of *H. pylori*.

THE MECHANISMS UNDERLYING *H. PYLORI* INFECTION INDUCED GUT MICROBIOTA

Although the mechanisms underlying *H. pylori* infection associated alterations in gut microbiota are still unknown, some studies have suggested possible contributing factors; these included host immune responses, virulence factors, physical contact and modification of gastric acidity[4,27]. A previous study performed using a transgenic *Drosophila* model revealed that the virulence factor, cytotoxin-associated gene A (CagA), of *H. pylori* may contribute to gut microbiota dysbiosis[28]. CagA, which is translocated into host epithelial cells after bacterial attachment, impairs cell polarity and affects host signaling pathways, thereby promoting inflammation[29]. Vacuolating cytotoxin A (VacA) is also an important virulence factor of *H. pylori*. VacA is a secreted toxin that lead to damages of gastric epithelial cells, and promotes cell death[30]. CagA and VacA counter-regulate each other to manipulate host cell responses[31]. CagA and VacA can alter the gastric microbiota and immune phenotypes previously attributed to *H. pylori* infection in the stomach[28]. Therefore, CagA and VacA have been associated with important requirements for long-term sequelae in humans. As such, ongoing crosstalk between *H. pylori* and gastric commensal microbiota may affect the host immune response. The altered host immune response may also modulate the gut microbiota[9,32]. A previous review suggested the possibility of a direct interaction of *H. pylori,* which migrates from the stomach towards the intestinal tract, with the local gut microbiota[4]. However, this hypothesis is yet to be proven. In fact, in our previous study, the presence of *H. pylori* in the intestinal tract was found to be rare even in subjects with *H. pylori* infection[6]. Therefore, the influence of *H. pylori* in the intestine on gut microbiota seems to be limited.

Modification of gastric acidity as a result of *H. pylori* infection is one of the variable effects on altered gut microbiota. PPIs, which decrease gastric acidity, affect the gut microbiota[33,34]. Reduced gastric acid promotes the passage of acid-sensitive bacteria and changes the intestinal environment[35]. Similar to the interference with the action of PPIs, *H. pylori* can regulate gastric luminal acidity. *H. pylori* infection is generally acquired during childhood and persists for life unless eradicated by treatment. In the initial stages of *H. pylori* infection, acute gastritis temporarily leads to impaired gastric acid secretion[36]. In later stages, a significant decrease in gastric acid secretion is observed in individuals who develop severe atrophic gastritis[36,37]. Previous studies investigating the gut microbiota following PPI administration detected an increase in the *Lactobacillus* population in the gut microbiota[33,34]. We evaluated *Lactobacillus* according to the degree of gastric atrophy in subjects with and without *H. pylori* infection[5]. The relative abundance of *Lactobacillus* in the human gut microbiota significantly increased after the development of severe atrophic gastritis. In another study, after adjusting for biases, we demonstrated that among *H. pylori*-infected subjects, a significant increase in the abundance of the genus *Streptococcus* was observed in subjects with severe atrophic gastritis[6]. These results support the hypothesis that severe atrophic gastritis reduces gastric acid secretion and affects the composition of the gut microbiota, similar to the results of PPI administration. Most previous studies examining the association between *H. pylori* infection and gut microbiota have not considered the influence of gastric mucosal atrophy. However, atrophic gastritis may be an important mechanism associated with the changes in the gut microbiota induced by *H. pylori* infection.

In previous studies, although *H. pylori* eradication was observed to alter gut microbiota within a short period, most of the changes induced tended to return to baseline levels over a long periods after eradication therapy[9,10,20-26]. The changes in the gut microbiota within a short period after eradication may be attributed to antibiotics and PPIs that were administered for *H. pylori* eradication. This finding was represented by a study that demonstrated a decrease in gut microbial diversity within a short period after eradication therapy in both patients with and without successful eradication[38]. The changes in the diversity within a short period after eradication may be attributed to the eradication therapy itself. Hence, the influence of eradication therapy on the gut microbiota would diminish over a long period of time. After eradication, the influence of host immune responses towards *H. pylori,* virulence factors, and physical contact with *H. pylori* could decrease or disappear. In contrast, the

modification of gastric acidity depends on the degree of mucosal atrophy. Hence, after *H. pylori* eradication, gastric acid secretion gradually improves in patients without gastric mucosal atrophy[39]. However, this improvement is not observed in patients with severe atrophic gastritis[40]. Further studies demonstrating minor changes in the gut microbiota over a long period need to be conducted using a large number of subjects with severe atrophic gastritis. Especially after *H. pylori* eradication, mechanisms other than gastric acid modification would not have a significant impact on the gut microbiota.

CONCLUSION

Although all the studies demonstrated a compositional change in the gut microbiota of *H. pylori*-infected patients, the results of these studies were not consistent with each other. This incompatibility may be attributed to several factors. Although remarkable variations are observed in the gut microbiota among individuals, the sample size considered in these studies was relatively small, and subjects were included regardless of biases associated with the composition of the gut microbiota, such as, age, gender, BMI and diet. Therefore, an analysis of gut microbiota in a large population should be conducted while adjusting to considerable biases. Particularly, it is necessary to evaluate of the degree of atrophic gastritis, which is associated with gastric acid production, when investigating the influence of *H. pylori* infection on the gut microbiota. Additionally, the virulence of *H. pylori* differs depending on the status of CagA. The prevalence of CagA-positive *H. pylori* infection varies, and the prevalence of the most virulent strain, eliciting the East Asian-type CagA phenotype, is dependent on geographical area[41]. Therefore, the investigation of the influence of *H. pylori* infection on the gut microbiota may yield different results depending on the area in which the study is conducted. Future studies should consider these points and predict the mechanisms underlying *H. pylori* infection induced changes in the gut microbiota.

REFERENCES

1 **Ursell LK**, Metcalf JL, Parfrey LW, Knight R. Defining the human microbiome. *Nutr Rev* 2012; **70** Suppl 1: S38-S44 [PMID: 22861806 DOI: 10.1111/j.1753-4887.2012.00493.x]

2 **Jandhyala SM**, Talukdar R, Subramanyam C, Vuyyuru H, Sasikala M, Nageshwar Reddy D. Role of the normal gut microbiota. *World J Gastroenterol* 2015; **21**: 8787-8803 [PMID: 26269668 DOI: 10.3748/wjg.v21.i29.8787]

3 **Gerritsen J**, Smidt H, Rijkers GT, de Vos WM. Intestinal microbiota in human health and disease: the impact of probiotics. *Genes Nutr* 2011; **6**: 209-240 [PMID: 21617937 DOI: 10.1007/s12263-011-0229-7]

4 **Tao ZH**, Han JX, Fang JY. Helicobacter pylori infection and eradication: Exploring their impacts on the gastrointestinal microbiota. *Helicobacter* 2020; **25**: e12754 [PMID: 32876377 DOI: 10.1111/hel.12754]

5 **Iino C**, Shimoyama T, Chinda D, Arai T, Chiba D, Nakaji S, Fukuda S. Infection of *Helicobacter pylori* and Atrophic Gastritis Influence *Lactobacillus* in Gut Microbiota in a Japanese Population. *Front Immunol* 2018; **9**: 712 [PMID: 29681906 DOI: 10.3389/fimmu.2018.00712]

6 **Iino C**, Shimoyama T, Chinda D, Sakuraba H, Fukuda S, Nakaji S. Influence of Helicobacter pylori Infection and Atrophic Gastritis on the Gut Microbiota in a Japanese Population. *Digestion* 2020; **101**: 422-432 [PMID: 31394526 DOI: 10.1159/000500634]

7 **Bühling A**, Radun D, Müller WA, Malfertheiner P. Influence of anti-Helicobacter triple-therapy with metronidazole, omeprazole and clarithromycin on intestinal microflora. *Aliment Pharmacol Ther* 2001; **15**: 1445-1452 [PMID: 11552917 DOI: 10.1046/j.1365-2036.2001.01033.x]

8 **Myllyluoma E**, Ahlroos T, Veijola L, Rautelin H, Tynkkynen S, Korpela R. Effects of anti-Helicobacter pylori treatment and probiotic supplementation on intestinal microbiota. *Int J Antimicrob Agents* 2007; **29**: 66-72 [PMID: 17141481 DOI: 10.1016/j.ijantimicag.2006.08.034]

9 **Chen L**, Xu W, Lee A, He J, Huang B, Zheng W, Su T, Lai S, Long Y, Chu H, Chen Y, Wang L, Wang K, Si J, Chen S. The impact of Helicobacter pylori infection, eradication therapy and probiotic supplementation on gut microenvironment homeostasis: An open-label, randomized clinical trial. *EBioMedicine* 2018; **35**: 87-96 [PMID: 30145102 DOI: 10.1016/j.ebiom.2018.08.028]

10 **He C**, Peng C, Wang H, Ouyang Y, Zhu Z, Shu X, Zhu Y, Lu N. The eradication of Helicobacter pylori restores rather than disturbs the gastrointestinal microbiota in asymptomatic young adults. *Helicobacter* 2019; **24**: e12590 [PMID: 31124220 DOI: 10.1111/hel.12590]

11 **Martín-Núñez GM**, Cornejo-Pareja I, Coin-Aragüez L, Roca-Rodríguez MDM, Muñoz-Garach A, Clemente-Postigo M, Cardona F, Moreno-Indias I, Tinahones FJ. H. pylori eradication with antibiotic treatment causes changes in glucose homeostasis related to modifications in the gut microbiota. *PLoS*

One 2019; **14**: e0213548 [PMID: 30870471 DOI: 10.1371/journal.pone.0213548]
12 **Dash NR**, Khoder G, Nada AM, Al Bataineh MT. Exploring the impact of Helicobacter pylori on gut microbiome composition. *PLoS One* 2019; **14**: e0218274 [PMID: 31211818 DOI: 10.1371/journal.pone.0218274]
13 **Frost F**, Kacprowski T, Rühlemann M, Bang C, Franke A, Zimmermann K, Nauck M, Völker U, Völzke H, Biffar R, Schulz C, Mayerle J, Weiss FU, Homuth G, Lerch MM. Helicobacter pylori infection associates with fecal microbiota composition and diversity. *Sci Rep* 2019; **9**: 20100 [PMID: 31882864 DOI: 10.1038/s41598-019-56631-4]
14 **Hasan N**, Yang H. Factors affecting the composition of the gut microbiota, and its modulation. *PeerJ* 2019; **7**: e7502 [PMID: 31440436 DOI: 10.7717/peerj.7502]
15 **Borgo F**, Garbossa S, Riva A, Severgnini M, Luigiano C, Benetti A, Pontiroli AE, Morace G, Borghi E. Body Mass Index and Sex Affect Diverse Microbial Niches within the Gut. *Front Microbiol* 2018; **9**: 213 [PMID: 29491857 DOI: 10.3389/fmicb.2018.00213]
16 **Odamaki T**, Kato K, Sugahara H, Hashikura N, Takahashi S, Xiao JZ, Abe F, Osawa R. Age-related changes in gut microbiota composition from newborn to centenarian: a cross-sectional study. *BMC Microbiol* 2016; **16**: 90 [PMID: 27220822 DOI: 10.1186/s12866-016-0708-5]
17 **Gudra D**, Pupola D, Skenders G, Leja M, Radovica-Spalvina I, Gorskis H, Vangravs R, Fridmanis D. Lack of significant differences between gastrointestinal tract microbial population structure of Helicobacter pylori-infected subjects before and 2 years after a single eradication event. *Helicobacter* 2020; **25**: e12748 [PMID: 32776403 DOI: 10.1111/hel.12748]
18 **Leeming ER**, Johnson AJ, Spector TD, Le Roy CI. Effect of Diet on the Gut Microbiota: Rethinking Intervention Duration. *Nutrients* 2019; **11** [PMID: 31766592 DOI: 10.3390/nu11122862]
19 **Huang R**, Ju Z, Zhou PK. A gut dysbiotic microbiota-based hypothesis of human-to-human transmission of non-communicable diseases. *Sci Total Environ* 2020; **745**: 141030 [PMID: 32726703 DOI: 10.1016/j.scitotenv.2020.141030]
20 **Yanagi H**, Tsuda A, Matsushima M, Takahashi S, Ozawa G, Koga Y, Takagi A. Changes in the gut microbiota composition and the plasma ghrelin level in patients with *Helicobacter pylori*-infected patients with eradication therapy. *BMJ Open Gastroenterol* 2017; **4**: e000182 [PMID: 29225907 DOI: 10.1136/bmjgast-2017-000182]
21 **Hsu PI**, Pan CY, Kao JY, Tsay FW, Peng NJ, Kao SS, Chen YH, Tsai TJ, Wu DC, Tsai KW. Short-term and long-term impacts of Helicobacter pylori eradication with reverse hybrid therapy on the gut microbiota. *J Gastroenterol Hepatol* 2019; **34**: 1968-1976 [PMID: 31115933 DOI: 10.1111/jgh.14736]
22 **Hsu PI**, Pan CY, Kao JY, Tsay FW, Peng NJ, Kao SS, Wang HM, Tsai TJ, Wu DC, Chen CL, Tsai KW; Taiwan Acid-related Disease (TARD) Study Group. Helicobacter pylori eradication with bismuth quadruple therapy leads to dysbiosis of gut microbiota with an increased relative abundance of Proteobacteria and decreased relative abundances of Bacteroidetes and Actinobacteria. *Helicobacter* 2018; **23**: e12498 [PMID: 29897654 DOI: 10.1111/hel.12498]
23 **Martín-Núñez GM**, Cornejo-Pareja I, Roca-Rodríguez MDM, Clemente-Postigo M, Cardona F, Fernández-García JC, Moreno-Indias I, Tinahones FJ. *H. pylori* Eradication Treatment Causes Alterations in the Gut Microbiota and Blood Lipid Levels. *Front Med (Lausanne)* 2020; **7**: 417 [PMID: 32850910 DOI: 10.3389/fmed.2020.00417]
24 **Liou JM**, Lee YC, Wu MS. Treatment of Helicobacter pylori infection and its long-term impacts on gut microbiota. *J Gastroenterol Hepatol* 2020; **35**: 1107-1116 [PMID: 31984532 DOI: 10.1111/jgh.14992]
25 **Liou JM**, Chen CC, Chang CM, Fang YJ, Bair MJ, Chen PY, Chang CY, Hsu YC, Chen MJ, Lee JY, Yang TH, Luo JC, Chen CY, Hsu WF, Chen YN, Wu JY, Lin JT, Lu TP, Chuang EY, El-Omar EM, Wu MS; Taiwan Gastrointestinal Disease and Helicobacter Consortium. Long-term changes of gut microbiota, antibiotic resistance, and metabolic parameters after Helicobacter pylori eradication: a multicentre, open-label, randomised trial. *Lancet Infect Dis* 2019; **19**: 1109-1120 [PMID: 31559966 DOI: 10.1016/S1473-3099(19)30272-5]
26 **Jakobsson HE**, Jernberg C, Andersson AF, Sjölund-Karlsson M, Jansson JK, Engstrand L. Short-term antibiotic treatment has differing long-term impacts on the human throat and gut microbiome. *PLoS One* 2010; **5**: e9836 [PMID: 20352091 DOI: 10.1371/journal.pone.0009836]
27 **Ye Q**, Shao X, Shen R, Chen D, Shen J. Changes in the human gut microbiota composition caused by Helicobacter pylori eradication therapy: A systematic review and meta-analysis. *Helicobacter* 2020; **25**: e12713 [PMID: 32515529 DOI: 10.1111/hel.12713]
28 **Jones TA**, Hernandez DZ, Wong ZC, Wandler AM, Guillemin K. The bacterial virulence factor CagA induces microbial dysbiosis that contributes to excessive epithelial cell proliferation in the Drosophila gut. *PLoS Pathog* 2017; **13**: e1006631 [PMID: 29049360 DOI: 10.1371/journal.ppat.1006631]
29 **Hatakeyama M**. Helicobacter pylori CagA and gastric cancer: a paradigm for hit-and-run carcinogenesis. *Cell Host Microbe* 2014; **15**: 306-316 [PMID: 24629337 DOI: 10.1016/j.chom.2014.02.008]
30 **Isomoto H**, Moss J, Hirayama T. Pleiotropic actions of Helicobacter pylori vacuolating cytotoxin, VacA. *Tohoku J Exp Med* 2010; **220**: 3-14 [PMID: 20046046 DOI: 10.1620/tjem.220.3]
31 **Abreu MT**, Peek RM Jr. Gastrointestinal malignancy and the microbiome. *Gastroenterology* 2014; **146**: 1534-1546.e3 [PMID: 24406471 DOI: 10.1053/j.gastro.2014.01.001]
32 **Peek RM Jr**, Fiske C, Wilson KT. Role of innate immunity in Helicobacter pylori-induced gastric

malignancy. *Physiol Rev* 2010; **90**: 831-858 [PMID: 20664074 DOI: 10.1152/physrev.00039.2009]

33 **Imhann F**, Bonder MJ, Vich Vila A, Fu J, Mujagic Z, Vork L, Tigchelaar EF, Jankipersadsing SA, Cenit MC, Harmsen HJ, Dijkstra G, Franke L, Xavier RJ, Jonkers D, Wijmenga C, Weersma RK, Zhernakova A. Proton pump inhibitors affect the gut microbiome. *Gut* 2016; **65**: 740-748 [PMID: 26657899 DOI: 10.1136/gutjnl-2015-310376]

34 **Jackson MA**, Goodrich JK, Maxan ME, Freedberg DE, Abrams JA, Poole AC, Sutter JL, Welter D, Ley RE, Bell JT, Spector TD, Steves CJ. Proton pump inhibitors alter the composition of the gut microbiota. *Gut* 2016; **65**: 749-756 [PMID: 26719299 DOI: 10.1136/gutjnl-2015-310861]

35 **Heimesaat MM**, Fischer A, Plickert R, Wiedemann T, Loddenkemper C, Göbel UB, Bereswill S, Rieder G. Helicobacter pylori induced gastric immunopathology is associated with distinct microbiota changes in the large intestines of long-term infected Mongolian gerbils. *PLoS One* 2014; **9**: e100362 [PMID: 24941045 DOI: 10.1371/journal.pone.0100362]

36 **Waldum HL**, Kleveland PM, Sørdal ØF. *Helicobacter pylori* and gastric acid: an intimate and reciprocal relationship. *Therap Adv Gastroenterol* 2016; **9**: 836-844 [PMID: 27803738 DOI: 10.1177/1756283x16663395]

37 **Kusters JG**, van Vliet AH, Kuipers EJ. Pathogenesis of Helicobacter pylori infection. *Clin Microbiol Rev* 2006; **19**: 449-490 [PMID: 16847081 DOI: 10.1128/cmr.00054-05]

38 **Guo Y**, Zhang Y, Gerhard M, Gao JJ, Mejias-Luque R, Zhang L, Vieth M, Ma JL, Bajbouj M, Suchanek S, Liu WD, Ulm K, Quante M, Li ZX, Zhou T, Schmid R, Classen M, Li WQ, You WC, Pan KF. Effect of *Helicobacter pylori* on gastrointestinal microbiota: a population-based study in Linqu, a high-risk area of gastric cancer. *Gut* 2020; **69**: 1598-1607 [PMID: 31857433 DOI: 10.1136/gutjnl-2019-319696]

39 **Haruma K**, Mihara M, Okamoto E, Kusunoki H, Hananoki M, Tanaka S, Yoshihara M, Sumii K, Kajiyama G. Eradication of Helicobacter pylori increases gastric acidity in patients with atrophic gastritis of the corpus-evaluation of 24-h pH monitoring. *Aliment Pharmacol Ther* 1999; **13**: 155-162 [PMID: 10102944 DOI: 10.1046/j.1365-2036.1999.00459.x]

40 **Iijima K**, Sekine H, Koike T, Imatani A, Ohara S, Shimosegawa T. Long-term effect of Helicobacter pylori eradication on the reversibility of acid secretion in profound hypochlorhydria. *Aliment Pharmacol Ther* 2004; **19**: 1181-1188 [PMID: 15153171 DOI: 10.1111/j.1365-2036.2004.01948.x]

41 **Sahara S**, Sugimoto M, Vilaichone RK, Mahachai V, Miyajima H, Furuta T, Yamaoka Y. Role of Helicobacter pylori cagA EPIYA motif and vacA genotypes for the development of gastrointestinal diseases in Southeast Asian countries: a meta-analysis. *BMC Infect Dis* 2012; **12**: 223 [PMID: 22994150 DOI: 10.1186/1471-2334-12-223]

World Journal of Gastroenterology

Submit a Manuscript: https://www.f6publishing.com

World J Gastroenterol 2021 October 7; 27(37): 6231-6247

DOI: 10.3748/wjg.v27.i37.6231

ISSN 1007-9327 (print) ISSN 2219-2840 (online)

MINIREVIEWS

Therapeutic drug monitoring in inflammatory bowel disease: The dawn of reactive monitoring

Farah Albader, Petra Anna Golovics, Lorant Gonczi, Talat Bessissow, Waqqas Afif, Peter Laszlo Lakatos

ORCID number: Farah Albader 0000-0003-2657-4558; Petra Anna Golovics 0000-0003-3195-183X; Lorant Gonczi 0000-0002-8819-6460; Talat Bessissow 0000-0003-2610-1910; Waqqas Afif 0000-0001-6869-0982; Peter Laszlo Lakatos 0000-0002-3948-6488.

Author contributions: All authors contributed equally to this paper with regards to the conception and structure of the paper in addition to the literature review, drafting and revision with unanimous approval of the final version.

Conflict-of-interest statement: Authors declare no conflict of interest.

Open-Access: This article is an open-access article that was selected by an in-house editor and fully peer-reviewed by external reviewers. It is distributed in accordance with the Creative Commons Attribution NonCommercial (CC BY-NC 4.0) license, which permits others to distribute, remix, adapt, build upon this work non-commercially, and license their derivative works on different terms, provided the original work is properly cited and the use is non-commercial. See: http://creativecommons.org/Licenses/by-nc/4.0/

Manuscript source: Invited

Farah Albader, Department of Internal Medicine, McGill University, Montreal H3G1A4, Quebec, Canada

Petra Anna Golovics, Division of Gastroenterology, Hungarian Defence Forces, Medical Centre, Budapest H-1062, Hungary

Petra Anna Golovics, Waqqas Afif, Peter Laszlo Lakatos, Division of Gastroenterology, McGill University, Montreal H3G 1A4, Quebec, Canada

Lorant Gonczi, First Department of Medicine, Semmelweis University, Budapest H-1083, Hungary

Talat Bessissow, Division of Gastroenterology, McGill University Health Centre, Montreal H3G 1A4, Quebec, Canada

Corresponding author: Peter Laszlo Lakatos, MD, PhD, Professor, Staff Physician, Division of Gastroenterology, McGill University, 1650 Cedar Avenue, Montreal H3G 1A4, Quebec, Canada. kislakpet99@gmail.com

Abstract

Inflammatory bowel disease (IBD) is a chronic condition that significantly affects the quality of life of its patients. Biologic drugs have been the mainstay treatment in the management of IBD patients but despite their significant contribution, there remains a proportion of patients that do not respond or lose response to treatment. Therapeutic drug monitoring (TDM) involves measuring levels of serum drug concentrations and anti-drug antibodies. TDM of biologic drugs initially emerged to understand treatment failure in other immune mediated inflammatory diseases. This was then introduced in IBD to rationalize primary non-response or secondary loss of response, given that low serum drug concentrations or the formation of anti-drug antibodies are variably associated with treatment failure. The aim of this narrative review is to provide an overview regarding the current use of TDM in clinical practice and to present the evidence available regarding its use in both proactive and reactive clinical settings in preventing and managing treatment failure. This review also presents the existing evidence regarding the association of various clinical outcomes with specific thresholds of drug concentrations, in everyday practice. A narrative review of published articles and conference abstracts regarding the use of TDM in IBD management, through an electronic search using PubMed and ScienceDirect. TDM has proven to be superior and more cost effective in guiding management of

manuscript

Specialty type: Gastroenterology and hepatology

Country/Territory of origin: Canada

Peer-review report's scientific quality classification

Grade A (Excellent): 0
Grade B (Very good): B
Grade C (Good): 0
Grade D (Fair): 0
Grade E (Poor): 0

Received: March 19, 2021
Peer-review started: March 19, 2021
First decision: May 1, 2021
Revised: May 8, 2021
Accepted: August 31, 2021
Article in press: August 31, 2021
Published online: October 7, 2021

P-Reviewer: Schoenenberger-Arnaiz JA
S-Editor: Fan JR
L-Editor: A
P-Editor: Xing YX

patients with treatment failure compared to empiric dose escalation or change in treatment. Despite a trend towards an association between clinical outcomes and drug concentrations, proactive TDM based strategies have not been shown to achieve clear benefit in long-term outcomes. In the clinical setting, TDM has proven to be useful in managing IBD patients, and its use in the reactive setting, as an additional tool to help manage patients with treatment failure, is being promoted as newer guidelines and consensus groups implement TDM as part of the management plan.

Key Words: Therapeutic drug monitoring; Inflammatory bowel disease; Biologic therapies; Loss of response; Reactive; Proactive

©The Author(s) 2021. Published by Baishideng Publishing Group Inc. All rights reserved.

Core Tip: In this review, we discuss the existing studies that looked at both proactive and reactive therapeutic drug monitoring (TDM) and concluded that in current practice, reactive TDM has been shown to be useful. When used as an adjunct to clinical assessment and biomarkers in patients with treatment failure, TDM has proven to be a valuable tool for subsequent management.

Citation: Albader F, Golovics PA, Gonczi L, Bessissow T, Afif W, Lakatos PL. Therapeutic drug monitoring in inflammatory bowel disease: The dawn of reactive monitoring. *World J Gastroenterol* 2021; 27(37): 6231-6247
URL: https://www.wjgnet.com/1007-9327/full/v27/i37/6231.htm
DOI: https://dx.doi.org/10.3748/wjg.v27.i37.6231

INTRODUCTION

The management of patients with inflammatory bowel disease (IBD) has changed dramatically over the past decade, more so since the use of biologic agents[1]. Biologics such as anti-tumor necrosis factor (anti-TNF) agents have revolutionized the treatment of patients with IBD during this time in addition to newer classes of biologic agents, such as selective adhesion molecule and interleukin 12 and 23 inhibitors that are also being used. Furthermore, with advances in the treatment of IBD, goals of therapy have also changed as specialists worldwide have adopted the 'treat to target' approach in the management of IBD[2]. Despite these advances, treatment failure still occurs in a significant proportion of IBD patients[3], prompting a need in dose intensification or discontinuation of therapy with a change to another class of drug[4,5]. In the past, treatment failure in IBD, defined as either a primary non-response (PNR) or secondary loss of response (sLOR) to a drug, has been difficult to explain and predict. But as a result of a better understanding of the pharmacodynamics (PD) and pharmacokinetics (PK) of biologic drugs, the idea of therapeutic drug monitoring (TDM) emerged as an important tool. It plays a role in not only identifying the mechanism of loss of response but also in guiding clinicians in their treatment approach[6,7].

TDM is defined as the measurement of serum drug and/or anti-drug antibody (ADA) concentrations. ADAs refer to antibodies that are formed in response to the immune system's recognition of biologic drugs. In several studies, ADAs have been found to be associated with treatment failure because of an up-regulated clearance of the drug[8,9]. Another mechanism of treatment failure relates to a non-immune mediated clearance, resulting in sub-therapeutic levels of the drug.

Over the years, TDM was initially used in the reactive setting for patients, when there was a suspected loss of response to a biologic drug, mainly the anti-TNF agents. Based on the serum drug levels and/or presence of ADAs, the management was changed with the aim of optimizing their current treatment, thus avoiding unnecessary dose intensification or targeted switching between anti-TNF agents or out of class. However, preliminary results from recently published data have shown that TDM used in the proactive setting, by preemptively targeting specific thresholds of serum drug levels, may in fact result in more favorable clinical outcomes[10-17]. Despite growing evidence supporting the use TDM in IBD, there still exist limitations

of its use, such as when to use it and how best to apply it. This is evident in the fact that routine use of TDM in the management of IBD patients is not recommended in guidelines, but rather made as suggestions by organizations when faced with a patient with suspected treatment failure[18-22].

This review article summarizes the latest evidence with regards to the use of TDM in both the reactive and proactive settings in addition to its limitations and how it is currently being used in clinical practice.

BACKGROUND OF TDM

The idea of TDM involves measuring the serum concentration of a drug, to maintain an adequate dose that would ensure drug efficacy and to avoid drug toxicity[23]. Use of TDM in clinical practice has existed for many years, even before the development of biologics. In the past, TDM was used for a variety of medications, such as antibiotics and immunosuppressants. More recently, it has been applied to biologics mainly to monitor drug efficacy and to guide management in suspected treatment failure for IBD patients on biologics. In IBD, TDM involves the measurement serum drug levels, in addition to the measurement of ADAs, both of which are related to drug efficacy[8,9]. Although many studies have proved its utility, many issues exist such as timing of TDM, identification of target thresholds for serum drug levels and ADAs, and the practical application of the results. Data looking into this shows that there is considerable variability in target thresholds because of multiple factors that come to play, such as the different methods and assays used in TDM measurements, or the desired clinical outcome.

Lastly, given that the first class of biologics were anti-TNF agents, the use of TDM was first applied for patients who were treated with either infliximab or adalimumab, thus most studies looking into TDM revolved around anti-TNFs. With time, as newer classes of biologics emerged for their use in IBD, more studies were done regarding the application of TDM with vedolizumab or ustekinumab.

OVERVIEW OF TECHNICAL ASPECTS OF TDM

In TDM, the measurement of serum drug levels involves measuring the trough level (TL), meaning the lowest concentration of the drug just before the next dose. With the TL, the goal is to maintain a level sufficient enough for the drug to reach its maximal efficacy[24], and this is where the issue of target thresholds comes to play[25]. Before discussing the clinical relevance of these targets, it is important to know the technical aspects of TL and ADA measurements.

Assays used for TDM

Current tests for TL and ADA concentrations include various commercially available assays such as enzyme-linked immunoassay (ELISA), radioimmunoassay, high pressure liquid chromatography based homogeneous mobility assay, with ELISA being the most commonly used[26,27]. Drug assays use the drug as a calibrator while ADA assays use a monoclonal ADA as a calibrator, with titers often expressed as milligrams *per* liter. Several studies comparing various drug assays showed good correlation, however since assay methodologies and sensitivities differ, it is best to use the same assay when applying TDM[28]. Additionally, it is important to note that in the case of ELISA assays, the presence of the drug in the serum interferes with the detection of ADAs, thus not adequately quantifying ADA concentrations[29,30]. Various modified ELISA methods have been constructed to circumvent this problem, *e.g.*, by improved puffer technologies, labeled 'drug resistant' assays for ADA detection.

Additionally, other factors that may influence results include human factors such as appropriate collection, handling, and storage. Newer studies looking into improving TDM have suggested the idea of point of care (POC) testing in the near future, where TDM measurements are made available on spot, without the need for a laboratory-based testing method[30].

MECHANISMS OF TREATMENT FAILURE IN IBD

To better comprehend the application of TDM in IBD, it is essential to understand the idea of drug PD and PK, as they are significant in understanding the mechanism of treatment failure[24]. Various factors affect a patient's response to treatment, including low or sub-therapeutic drug levels related to increased clearance, whether it is immune or non-immune mediated in addition to the underlying pathway targeted by the drug.

PNR vs sLOR

Biologic agents, namely anti-TNF drugs, have significantly advanced the management of IBD patients. However, despite this, up to 30% of IBD patients fail to show an initial response after the induction period, also known as PNR, and up to 50% showing sLOR during the maintenance phase, especially during the first year 3-5]. Those with sLOR are patients who had initially responded after the induction phase, but then started to develop symptoms of disease activity, suggestive of treatment failure. Pharmacokinetic mechanisms underlining PNR and sLOR are thought to be due to inadequate serum drug concentrations as evidence has shown that those with low serum drug concentrations during induction or maintenance are less likely to achieve clinical response[31,32].

One study that signified this is the personalized anti-TNF therapy in Crohn's disease (CD) study (PANTS), which was a prospective observational study carried out in the United Kingdom that included 955 patients with active luminal CD[33]. Results of the study revealed that anti-TNF failure is highly dependent on low drug concentration and that this was associated with immunogenicity and the development of ADAs, especially during induction[33]. This finding mimics other studies that also revealed that higher drug concentrations early on is associated with a reduced risk of PNR and in preventing sLOR[34,35].

Clinical relevance of ADAs

One important aspect of treatment failure in IBD revolves around the idea of immunogenicity, which is an important downside of biologics. Immunogenicity deals with the fact that the immune system recognizes protein aspects of the drug as foreign and forms antibodies in response. These antibodies then form complexes with the drug, resulting in increased drug clearance and lower concentrations of the drug, rendering it ineffective[30]. However, it is important to note that not all antibodies work in the same way. In fact, two types of antibodies exist, neutralizing (NAb) *vs* non-neutralizing antibodies (non-NAb). Although they both bind to the drug, each render it ineffective in a different way[36]. NAb inhibits the pharmacological function of the drug, thus preventing target binding, whereas non-NAb promotes increased clearance of the drug[37]. This is relevant to the understanding of TDM since there is evidence pointing to a correlation between ADA formation and low serum drug levels[38-40].

One study that evaluated the clinical significance of ADAs was by Baert *et al*[32] that looked at a cohort of 125 CD patients receiving episodic infusions of infliximab. Results of this study revealed an association between the development of antibodies against infliximab response to treatment, as low trough infliximab level and high ADA level was found in 83% (10/12) with complete loss of response to infliximab. This finding reflects results of other studies that have also shown that ADA association was independently associated with LOR. There was also a large proportion of patients (61%) that had detectable ADAs and that there was an inverse relationship between ADA titers and duration of response ($P < 0.0001$)[32]. Moreover, they also noted that the median duration of clinical response was longer in patients with low ADA concentrations compared to those with higher ADA concentrations (71 d *vs* 35 d; $P < 0.001$). Similar conclusions were drawn in a study by Reinhold *et al*[41], where 16/104 (14%) patients had positive ADA titers and 15 of them had sub-therapeutic TLs, reflecting the increased drug clearance effect of ADAs[41].

As explained, ADAs play a significant role in treatment failure of IBD patients on biologics as antibodies neutralize the effect of the biologic agent, but the evidence linking ADA to LOR is not straightforward. This was demonstrated in a prospective study by Gonczi *et al*[42] that followed 112 IBD patients who were on therapy with adalimumab. Results of this study revealed that ADA positivity was significantly associated with LOR ($P = 0.007$), but the association between low TL and ADA positivity was not statistically significant ($P = 0.054$). They concluded that despite the development of ADA, low TL was not associated with LOR and that mainly ADA development should be considered a predictor for treatment failure[42]. This reiterates

the significance of NAb in that they inhibit the pharmacological function of the drug resulting in clinical non-response. As opposed to non-NAb, which affect drug efficacy by increased drug clearance thus resulting in low drug levels. For this reason, interpretation of ADA and TL when dealing with LOR should be made with caution.

Another clinically relevant aspect involves patients who develop infusion reactions. These are often found in those with persistently low drug concentrations and a significant concentration of ADAs[32,43], and this was demonstrated in the same study by Reinhold *et al*[41]. In this retrospective study that followed 104 IBD patients treated with infliximab or adalimumab, the authors delineated a positive correlation between the presence of ADAs and the development of infusions reactions as 44% (7/13) of patients with infusion reactions had positive ADA titers[41].

In conclusion, it has become clear that different ADAs exist and that not all types of antibodies affect drug clearance. Available data suggests that the presence of ADAs has a potential negative impact on clinical outcomes. Additionally, the relationship between ADA and treatment failure is not clear cut and that the impact of ADAs, may be more relevant to certain biologics than others[44-46].

ASSOCIATION OF SERUM DRUG CONCENTRATIONS WITH CLINICAL OUTCOMES

Numerous studies have demonstrated an association between drug levels and favorable outcomes[33,47-50]. Additionally, recent data has shown that higher serum drug concentrations during induction especially, is strongly associated with positive outcomes[34]. However, it is important to note that serum drug concentrations of different biologics vary as a result of many factors, such as patient demographics (age and body size), degree of underlying inflammation, and severity of disease[51]. As a result, there exists a large variation in target thresholds of TLs for each biologic drug. Current thresholds for serum drug concentrations are determined from observational studies and post HOC analyses, by looking at a variety of drug concentrations that have been found to be associated with specific outcomes; these can be seen in Table 1 [48,52-56].

In a retrospective multi-center study carried out by Juncadella *et al*[47], 98 IBD patients on therapy with adalimumab, underwent TDM and were followed to determine factors associated with outcomes such as biochemical, endoscopic, and histological remission. Results revealed that higher drug concentration during maintenance associated with good clinical outcomes and drug concentration > 12 μg/mL were associated with endoscopic (P = 0.003) and histological remission (P = 0.012) in CD[47]. Similar results were found in another retrospective study by Ungar *et al*[57], where serum drug levels of both infliximab and adalimumab were significantly higher in patients with mucosal healing compared to those with active disease on endoscopy (P = 0.002 for infliximab and P = 0.01 for adalimumab)[57].

Moreover, results of the PANTS study, showed that the only factor independently associated with PNR was a low infliximab (IFX) concentration at week 14 and that drug concentrations values associated with remission at weeks 14 and 54 were > 7 μg/mL for infliximab and > 12 μg/mL for adalimumab[33].

In terms of disease severity, for CD patients with peri-anal fistula, current evidence supports the idea of targeting higher serum drug concentrations in those patients compared to those without fistulizing disease[56,58,59]. A study by Davidov *et al*[56], showed a positive association between infliximab TLs during induction and closure of perianal fistula in CD patients, further suggesting that those patients may benefit from a drug level guided treatment.

Interestingly, despite evidence that shows a positive association of higher serum drug levels with clinical outcomes, preliminary results from the SERENE CD and SERENE ulcerative colitis (UC) trials did not show an added benefit. In both trials, patients with CD and UC, were randomized to either induction by standard dosing (SIR) of adalimumab or by an intensified dosing regimen (HIR). Results of both trials revealed that there was no added benefit from those who underwent an intensified regimen even though that subset of patients had higher serum drug concentrations[60,61]. Additionally, in terms of primary endpoints, the rates of clinical and endoscopic remission were similar among both groups.

Table 1 Association between various thresholds for serum drug concentrations and clinical outcomes

Drug	Serum drug level	Clinical outcome
Infliximab (IFX)		
IFX	< 2 μg/mL for CD/UC at week 14	Increased incidence of IFX antibodies[52]
IFX	> 2.1 μg/mL at week 14 in UC	Associated with mucosal healing[53]
IFX	≥ 3 μg/mL during maintenance	Clinical remission[48]
IFX	> 3 μg/mL at week 14 or 22 in CD	Sustained response[54]
IFX	3-7 μg/mL during maintenance	Remission[16]
IFX	≥ 7 μg/mL during maintenance	Mucosal healing[48]
IFX	< 7 μg/mL at week 14 in luminal CD	Absence of primary response[53]
IFX	> 9.2 μg/mL at induction week 2 in CD	Fistula response at weeks 14 and 30[56]
IFX	≥ 10 μg/mL at induction week 6	Clinical response[48]
IFX	> 15 μg/mL at week 6 in UC	Associated with mucosal healing[53]
IFX	≥ 20 μg/mL at induction week 2	Clinical response[48]
IFX	≥ 22 μg/mL at week 6 in UC	Clinical response at week 8[55]
IFX	≥ 25 μg/mL at induction week 2	Mucosal healing[48]
Adalimumab (Ada.)		
Ada.	≥ 3 μg/mL during maintenance	Clinical response[48]
Ada.	≥ 5 μg/mL post induction (week 14)	Clinical response[48]
Ada.	≥ 7 μg/mL post induction (week 14)	Mucosal healing[48]
Ada.	≥ 8 μg/mL during maintenance	Mucosal healing[48]
Ada.	< 12 μg/mL at week 14 in luminal CD	Absence of primary response[53]
Ustekinumab (UST)		
UST	≥ 1 μg/mL during maintenance	Clinical response[48]
UST	≥ 3.5 μg/mL post induction (week 8)	Clinical response[48]
UST	≥ 4.5 μg/mL during maintenance	Mucosal healing[48]
Vedolizumab (VDZ)		
VDZ	≥ 12 μg/mL during maintenance	Clinical response[48]
VDZ	≥ 14 μg/mL during maintenance	Mucosal healing[48]
VDZ	≥ 15 μg/mL post induction (week 14)	Clinical response[48]
VDZ	≥ 17 μg/mL post induction (week 14)	Mucosal healing[48]
VDZ	≥ 24 μg/mL at induction (week 6)	Clinical response[48]
VDZ	≥ 28 μg/mL at induction (week 2)	Clinical response[48]

Many studies that looked at exposure response relationship studies of anti-tumor necrosis factor drugs have demonstrated that specific drug concentration thresholds are associated with certain clinical outcomes, such as clinical response, improvement in biochemical markers, endoscopic remission, and mucosal healing.

MANAGEMENT OF TREATMENT FAILURE IN IBD USING A TDM BASED STRATEGY-REACTIVE TDM

Prior to TDM, the standard of care for suspected treatment failure, after exclusion of secondary causes such as infections and non-compliance, was either by empiric dose escalation, change to an alternative anti-TNF, or change to a different class of biologic.

The empiric approach of managing loss of response is considered frequently suboptimal and may lead to additional costs. The TDM-based strategy, by applying measurements of anti-TNF drug levels and anti-drug antibodies at the time of treatment failure offers an alternative. With time, more studies looking into benefits of

TDM emerged. These studies highlighted that TDM may be a useful adjunct to optimize the treatment of IBD patients, more cost effective than the standard of practice of empiric changes in management and can be useful in identifying patients who may be supra-therapeutic and instead, may benefit from dose reduction[6,62-64].

A multi-center study carried out by Guidi *et al*[65], was one of the first prospective studies carried out in a clinical practice setting that compared the management of sLOR by a TDM based algorithm to empiric dose escalations for IBD patients on infliximab. Results of their study demonstrated that the group of patients who underwent TDM based management of LOR resulted in lower rates of dose escalations with similar rates of clinical response, in addition to the fact that the TDM approach was more cost-effective[65]. Another study that reflected similar results was a randomized controlled study (RCT) carried out by Steenholdt *et al*[66], which recruited 69 Danish patients with CD on treatment with infliximab, who had developed sLOR. Patients were randomized to either routine infliximab dose or TDM based interventions. Rates of clinical response, measured by CD activity index were the same in both groups, 53% *vs* 58% ($P = 0.81$) respectively, however the costs *per* patients was 34% lower in TDM based group ($P < 0.001$)[66].

An important study that supported the use of reactive monitoring was by Afif *et al*[67], which looked at measurements of serum drug and ADA levels of 155 IBD patients who were on treatment with infliximab. Results of this study highlighted the importance of TDM in the management of partial or loss of response, as it provided insight into who might benefit from a change in drug or dose escalation. In this study, it can be seen that in ADA positive patients, the decision to change to another anti-TNF resulted in a complete or partial response in 92% of patients compared to 17% for those who underwent dose escalation. Additionally, with regards to drug levels, those who underwent dose escalation because of sub-therapeutic drug levels had a higher rate of complete or partial response compared to those who changed to an alternate drug[67]. Similarly, Yanai *et al*[6] demonstrated the utility of TDM in managing loss of response, as results from their study showed that patients with high ADA levels had longer duration to response when there was a drug change compared to dose escalation ($P = 0.03$) and that dose escalation was found to be more effective for those with low or undetectable ADA levels[6].

Additionally, in a study carried out by Kelly *et al*[63], which followed primary responders on infliximab who initially presented with clinical disease activity, authors revealed that those who underwent TDM based escalation had significantly higher clinical response ($P < 0.01$) and lower rates of hospitalization (22% TDM *vs* 35% non-TDM, $P = 0.025$) compared to the non-TDM based group[63].

A study by Ungar and colleagues that looked at infliximab levels during induction, brought to light an important finding that may help better manage patients with acute severe UC. Results of their study indicated that at day 14, those with acute severe UC had lower serum drug levels compared to patients with moderately severe UC. This is significant as it suggests that patients with acute severe UC may benefit from an intensified regimen as drug efficacy may have been affected by the high degree of inflammation[68].

In terms of cost-effectiveness, Steenholdt *et al*[66] was able to demonstrate that an individualized approach using reactive TDM was in fact more effective[66]. Results of this multi-center RCT showed that the costs for the intention to treat patients were substantially lower in the TDM based group compared to various infliximab dosing regimens (€ 6038 *vs* € 9178, $P < 0.001$). Similar results were also replicated in a study by Velayos *et al*[62], again demonstrating that dose adjustments made based on a TDM based algorithmic approach is more cost effective than empiric dose escalation[62].

The key recommendations at sLOR regarding the clinical scenarios of different combinations of TL and ADA level results at TDM are consistent based on the above studies. The suggested therapeutic algorithm for the optimal management of anti-TNF treatment failure based on TDM results is summarized in Figure 1[69].

As mentioned earlier, TDM can be approached in one of two ways, either in the reactive or proactive setting. Although much debate exists around the many issues surrounding the use of TDM, in current practice, it is mainly used in the reactive setting. Prior to TDM, standard of practice for the management of treatment failure in IBD is through empiric dose escalation. But with growing evidence highlighting the utility of reactive TDM in guiding subsequent management and that it may in fact be more cost effective, more specialists are using it in their practice[62,66].

As a result of numerous exposure-response relationships linking target TLs to therapeutic outcomes, the idea of proactive approach emerged in the hopes of targeting a specific threshold to avoid PNR or sLOR.

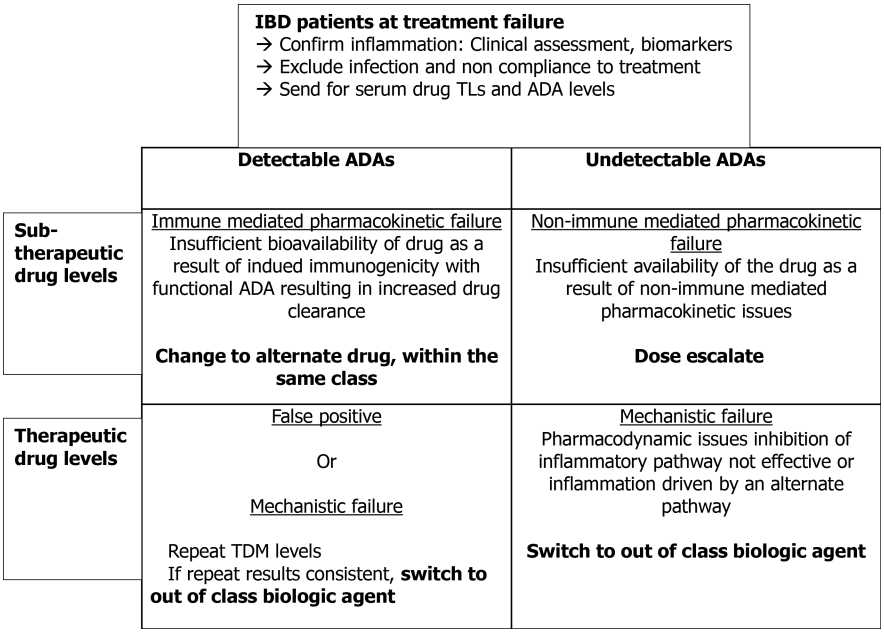


Figure 1 Therapeutic drug monitoring based approach to treatment failure. IBD: Inflammatory bowel disease; ADA: Anti-drug antibody.

PROACTIVE TDM

The idea of using a proactive approach stemmed from preliminary data revealing that targeting a specific drug concentration at various intervals is associated with better clinical outcomes, compared to empiric dose escalation and TDM done in the reactive setting[13,16,47-50]. A pivotal trial that demonstrated the potential benefits of proactive TDM is the landmark TAXIT trial (Trough Level Adapted Infliximab Treatment). This was a single center RCT of 263 IBD patients on infliximab, whose progress was followed to compare clinical benefit and cost effectiveness of concentration *vs* clinical based approach. As a result of the design study, the primary end point, of clinical and biochemical remission after 1 year, was not met. However, important findings included lower rates of undetectable drug levels and disease relapse in the proactive group[16].

More recently, Fernandes *et al*[15] carried out a prospective study of 205 IBD patients with results strongly supporting the proactive approach. Patients were randomized to two groups, those who were treated with IFX without TDM (data collected retrospectively) and those who underwent proactive TDM. In terms of outcomes, they looked at mucosal healing, need for hospitalization, and surgery. Results demonstrated that there were higher rates of treatment escalation in the TDM group ($P < 0.001$) with less need for surgery in addition to higher rates of mucosal healing ($P < 0.0001$), concluding that the proactive approach significantly decreased odds of reaching any unfavorable outcomes[15].

In a multi-center, retrospective cohort study of 102 IBD patients on infliximab, Papamichael and colleagues compared outcomes associated between those who underwent reactive *vs* proactive drug monitoring. The study demonstrated that those who underwent proactive testing after initial reactive testing was associated with greater drug persistence in addition to fewer IBD related hospitalizations (HR 0.18, CI 0.05-0.99; $P = 0.007$)[10].

Another multi-center study carried out by Papamichael *et al*[11], involving IBD patients on adalimumab also showed promising results with regards to the proactive approach as results also demonstrated that those who underwent proactive TDM had a reduced risk of treatment failure compared to the standard of care[11].

A recent study that strongly supports the proactive approach is the PAILOT study (Pediatric CD Adalimumab-Level based Optimization Treatment) by Assa *et al*[14]. This was a RCT of 78 children with CD who were on treatment with adalimumab and their primary end point was sustained steroid free remission. Authors of the study reached their primary endpoint with 82% in the proactive *vs* 48% in the reactive ($P = 0.002$) in addition to lower biochemical markers in the proactive group ($P = 0.003$)[14]. This study is considered a step forward supporting proactive TDM as this was the first proactive RCT whose primary endpoint was reached.

The TAILORIX trial (Tailored Treatment with Infliximab for Active CD) by D'Haens *et al*[12], was another important proactive trial carried out with the aim of promoting the treat to trough approach. This trial followed 122 biologic naïve patients with active CD who received induction with infliximab and were randomized to three different groups of maintenance infliximab. The three various groups comprised of various dose intensifications based on clinical assessment, biomarkers and/or serum infliximab levels with the primary outcome being sustained corticosteroid free clinical remission at one year. In the end, this trial failed to show the benefit of the proactive approach as results demonstrated that increasing infliximab dose based on combination of symptoms, biomarkers, and drug concentrations does not lead to increased rates of steroid free remission (P = 0.50) compared to dose escalation based on symptoms alone[12]. Interestingly, it is worth noting that less than 50% of patients in each group failed to reach the primary endpoint of corticosteroid free remission in addition to the fact that dose optimization was only carried out at week 14.

Interestingly, new evidence looking at proactive TDM was revealed through several studies including both the SERENE-CD and SERENE-UC trials. In the post induction phase of both trials, authors followed patients into the maintenance phase following induction with high dose *vs* standard dose adalimumab in the treatment of patients with moderate to severe CD and UC[60,70]. In the maintenance phase of SERENE-CD study, clinical responders from the induction phase were recruited and the authors explored outcomes after 44 wk on adalimumab using a clinical based assessment with the use of biomarkers or through proactive TDM with specified target thresholds. Preliminary results presented at United European Gastroenterology conference (UEG) showed that in terms of efficacy endpoints, the rates were the same in both arms and that the addition of TDM as a criteria showed no added benefit as the rates of clinical response, steroid free clinical remission, and endoscopic remission were similar[70]. A study by Bossuyt *et al*[71], presented at UEG 2020, showed similar results in terms of clinical endpoints, by comparing outcomes of two groups, ultra-proactive TDM *vs* reactive TDM. In this study, at the end of one year, there was no difference noted between both groups in terms of composite endpoints of: IBD related hospitalizations, IBD related surgeries, and change of treatment[71].

On the other hand, the SERENE-UC trial looked at outcomes of patients who were randomized to either a high dose or standard dose adalimumab maintenance regimen. Colombel *et al*[60], concluded that there was a higher number of patients who achieved clinical remission at week 52 in the high dose group, compared to the standard dose group. However, despite the clear numerical difference, it was not statistically significant. Here, the hypothesis was that with an intensified regimen, there would be higher drug bioavailability, which could result in positive outcomes. This theory was based on a previous trial that an intensive regimen in patients with severe UC resulted in lower rates of patients requiring colectomy[72]. Although drug levels were higher in the intensified regimen in both trials, the rates of clinical endpoints were the same.

Although more studies are demonstrating results in favor of proactive TDM, the range of studies remain limited in that the majority are retrospective in nature. Additionally, even with the current use of TDM, used by IBD specialists in the reactive setting, multiple factors are considered in the subsequent management of treatment failure, and not simply by a treat to trough concentration approach.

TDM IN CLINICAL PRACTICE

Despite the issues surrounding the application of TDM involving how and when it should be used, it has proven to be a valuable tool. The current use of TDM as one of many tools of clinical assessment has helped in advancing the care of these patients. As such, the use of TDM has been recommended in certain guidelines and by consensus groups as an adjunct to manage patients with suspected treatment failure. Furthermore, because of the lack of evidence from proactive trials to support the idea of improved clinical outcomes associated with this approach, many support the use of TDM in the reactive setting. For further information, refer to Table 2 for a list of the main TDM based trials including both reactive and proactive[6,10-12,14-16,66,67,70,71,73-77].

As evident, the debate over when to apply TDM is still ongoing because of limited prospective large trial studies. For this reason, TDM has not been fully incorporated into guidelines but rather hinted at as suggestions to help guide treatment in those with suspected treatment failure. One example is the guideline by the American

Table 2 A list of the main trials looking at both reactive and proactive therapeutic drug monitoring

Ref.	Study design; *n*	Population studied	Type of intervention	Primary outcome	Results
Vande Casteele *et al*[16], 2015 (Proactive)	Prospective single center study RCT, *n* = 263	Adults with mod to severe UC responders to infliximab (IFX)	IFX. Target 3-7 μg/mL during maintenance phase. Clinical *vs* concentration-based dose escalation	Clinical and biochemical remission	Fewer flares in concentration-based group. No difference in remission rates at 1 yr
Papamichael *et al*[73], 2017 (Proactive)	Retrospective multi-center RCT, *n* = 264	Adults with CD + UC	IFX 5-10 μg/mL	Treatment failureNeed for IBD related hospitalization or surgery. Adverse events	Proactive was associated with better clinical outcomes, including greater drug durability, less need for IBD-related surgery or hospitalization
Perinbasekar *et al*[74], 2017 (Proactive)	Retrospective single center study, *n* = 127	Adult IBD patients initiating treatment with either IFX or adalimumab (Ada)	IFX target ≥ 3 μg/mL; Ada target ≥ 5 μg/mL	Clinical response at 1 yr. Endoscopic response. Persistence with anti-TNF at 1 yr	Persistence with therapy and clinical and endoscopic response were superior for proactive compared to control patients treated with infliximab
Bernardo *et al* [75], 2017 (Proactive)	Retrospective single center study, *n* = 117	Adult IBD patients on treatment with infliximab	Clinical based *vs* proactive TDM. (1) Target IFX CD 3-7 μg/mL; (2) Target IFX UC 5-10 μg/mL; (3) Target Ada CD 5-7 μg/mL; and (4) Target Ada UC 7-9 μg/mL	At 48 wk (1) Clinical remission; (2) Rates of hospitalizations; (3) Rates of surgery; and (4) Therapeutic failure	No difference noted in relation to outcomes. Higher rates of drug escalation in proactive group. Longer period of remission in proactive group
D'Haens *et al* [12], 2018 (Proactive)	Prospective multi-center RCT, *n* = 122	Adults with mod to severe luminal CD biologic naïve on infliximab maintenance	Dose escalation using combined approach of clinical + TDM *vs* symptom-based approach. IFX target > 3 μg/mL during maintenance phase	Sustained steroid-free clinical remission at weeks 22-54 and mucosal healing at week 54	No difference in terms of rates of steroid-free remission
Papamichael *et al*[10], 2018 (Proactive *vs* reactive)	Retrospective multicenter study, *n* = 102	Adult IBD patients on infliximab	Reactive TDM followed by subsequent proactive TDM *vs* reactive testing IFX target 5-10 μg/mL	Treatment failure. IBD related hospitalization and surgery	Proactive monitoring after reactive testing associated with greater drug persistence and fever IBD related hospitalizations
Papamichael *et al*[11], 2019 (Proactive)	Retrospective multicenter study, *n* = 382	IBD patients on maintenance therapy with adalimumab	Proactive *vs* reactive TDM. Ada > 10 μg/mL	Treatment failure	Proactive associated with lower risk of treatment failure
Assa *et al*[14], 2019 (Proactive)	Prospective multi-center RCT, *n* = 78	Ages 6-17 yr with CD with response to adalimumab	Ada target trough levels ≥ 5 μg/mL	Sustained steroid-free clinical remission (weeks 8-72)	Higher rates of steroid free clinical remission in proactive group
Strik *et al*[76], 2019 (Proactive)	Retrospective multi-center RCT, *n* = 80	UC + CD in clinical remission on infliximab maintenance therapy	Dashboard driven dose escalation with TDM *vs* non TDM. IFX level > 3 μg/mL	Clinical remission	Dashboard-guided dosing resulted in a significant higher proportion of patients who maintained clinical remission during 1 yr of treatment
Danese *et al* [70], 2020 (Proactive)	Prospective multi-center RCT, *n* = 184	Clinical responders from induction phase of SERENE-CD	Clinical based group *vs* proactive TDM (TL 5-10 μg/mL) adalimumab every week or every other week	Clinical remission and endoscopic response and remission at 1 yr	No difference in terms of clinical end points
Fernandes *et al* [15], 2020 (Proactive)	Prospective study, *n* = 205	IBD patients completing infliximab induction therapy	Prospective arm (TDM-based dose escalation) *vs* retrospective arm (non-TDM). IFX levels 3-7 μg/mL CD; IFX levels 5-10 μg/mL UC	Need for surgery, hospital admission, treatment endrates of mucosal healing at 2 yr of treatment	Proactive TDM associated with fewer surgeries and higher rates of mucosal healing
Bossuyt *et al* [71], 2020 (Proactive *vs* reactive)	Prospective multi-center RCT	All IBD patients on infliximab therapy > week 14	Using point of care testing at the time of infusion > proactive *vs* reactive TDM	Clinical remissionDiscontinuation of infliximab. Composite end points of IBD related hospitalizations and surgeries, change of treatment	No difference in terms of rate of clinical remission or treatment discontinuationUltra-proactive not superior to reactive
Afif *et al*[67], 2010 (Reactive)	Retrospective study, *n* =155	IBD patients who had infliximab	Measurements of human anti-chimeric antibodies	Loss of response. Change in treatment	Measurement of both antibody and drug levels lead to

			(HACAs) and infliximab concentrations		improved response
Steenholdt *et al* [66], 2014 (Reactive)	Prospective RCT, *n* = 69	CD patients failing on infliximab therapy	Infliximab intensification *vs* algorithm defined using TDM	Clinical and economic outcomes at week 20	Lower healthcare costs in algorithm-based group. Similar rates of clinical response and remission
Kelly *et al*[63], 2017 (Reactive)	Retrospective study, *n* = 312	Primary responders on infliximab who underwent dose escalation	TDM *vs* clinical based dose escalation of infliximab	Endoscopic remissionClinical response	Higher rates of endoscopic remission with TDM
Pouillon *et al* [77], 2018 (Reactive)	Retrospective single center study, *n* = 226	IBD patients who completed maintenance phase of TAXIT	Clinical based *vs* trough concentration-based dosing of infliximab, infliximab level 3-7 μg/mL	IBD related hospitalization and surgery. Steroid use. Mucosal healing	Similar rates of mucosal healing in both groups. Higher rates of treatment discontinuation in clinic-based group

TDM: Therapeutic drug monitoring; TNF: Tumor necrosis factor; IBD: Inflammatory bowel disease; RCT: Randomized controlled study; IFX: Infliximab; Ada: Adalimumab.

Gastroenterological Association, in which the use of TDM is suggested for patients with active IBD on anti-TNFs but not recommended for those with quiescent IBD[18]. Table 3 lists the various recommendations and statements made by various gastroenterology guidelines and consensus groups[18-22].

PRACTICAL ASPECTS-HOW BEST TO APPLY TDM

Although much evidence exists supporting the use of TDM in the proactive setting, it has become clear that current evidence has not supported its use as routine practice in the management of IBD patients. Instead of dividing TDM into two separate entities, TDM should be considered as a useful tool in the management of IBD patients. As clinicians, we treat patients as a whole, in the sense that we treat their conditions by looking at various aspects including their clinical assessment in addition to biomarkers. Therefore, TDM should be considered as another adjunct that will help guide management as opposed to looking at it as the sole means of ensuring clinical response and remission.

Given the fact that various thresholds for serum drug levels and ADAs exist, it can be difficult to choose which one to target, especially since another variable that complicates this is the type of assay used for these measurements. However, despite the wide range, in current practice, certain thresholds have been followed to ensure clinical response in IBD patients who are on biologic agents. An example of these thresholds to target during maintenance therapy can be seen clearly in Table 4[16,41,78,79] The values listed in the table have been determined by a panel of IBD specialists that have carefully looked at existing literature relating to TDM[79]. Interestingly, the cut-off values listed by this group differs from the suggestions put forth in the AGA 2017 guideline[18]. It is important to note that these cut-off values are not absolute and should always be made in context with the clinical picture and that higher values might be needed for more rigorous clinical outcomes[48]. In the end, optimal TLs are difficult to define because of the multiple factors discussed above and because of the limited data from observational studies and post HOC analyses, thus it is important to be aware that the idea of 'one size' fits all may not be appropriate.

LIMITATIONS OF TDM

In research, RCTs are considered the gold standard in providing evidence for causal relationships and to support changes to clinical practice, and this seems to be lacking with regards to TDM. Thus, the majority of data available regarding TDM has been based mainly on prospective and retrospective observational studies or post HOC analyses. In addition to the timing of TDM and how often it should be carried out, other issues around TDM have to do with how to best interpret the results given the difficulty in obtaining results in a timely manner and being able to implement changes immediately[79]. Also, the bulk of evidence supporting TDM revolves mainly around

Table 3 Recommendations and statements made by various gastroenterology guidelines and consensus groups

Guideline/Consensus group	Recommendation
AGA[18,19]	Active IBD with anti-TNF → suggest use of reactive TDM
	Quiescent IBD with anti-TNF → not recommended
Inflammatory bowel disease Sydney/Australian Inflammatory bowel disease consensus working group (2017)[20]	Use of TDM preferred in (1) Upon suspected treatment failure; (2) Following successful induction; and (3) When completed drug holiday
	For those in clinical remission, consider TDM periodically only if it will change management
British guidelines (2019)[21]	Good practice recommendation → ALL IBD patients should be reviewed 2-4 wk post loading dose to assess response and check drug levels and anti-drug antibodies
	Use of serum drug trough & anti-drug antibody concentrations to be incorporated when deciding in change of therapy (dose escalation *vs* switch to other anti-TNF drug or out of class change)
ECCO (2020)[22]	CD in remission on anti-TNF → insufficient evidence to recommend FOR or AGAINST TDM
	CD patients who have lost response → insufficient evidence

AGA: American Gastroenterology Association; ECCO: European Colitis & Crohn's Organization; TDM: Therapeutic drug monitoring; TNF: Tumor necrosis factor; IBD: Inflammatory bowel disease.

Table 4 Therapeutic drug monitoring thresholds used in current practice (Using enzyme-linked immunoassay)

Drug	Cut-off for serum drug concentration	Cut-off for detectable ADA
Infliximab	> 3 μg/mL	Present if > 10 μg/mL
Adalimumab	> 5 μg/mL	Present if > 10 μg/mL
Certolizumab	> 15 μg/mL	-
Ustekinumab	Insufficient evidence to make a suggestion	-
Vedolizumab	Insufficient evidence to make a suggestion	-

ADA: Anti-drug antibody.

anti-TNF and less so with the other biologics such as vedolizumab and ustekinumab [80-82]. These newer biologics are now being used more in IBD thus it is imperative that well designed studies are done looking into outcomes associated with TDM based approach using these drugs.

Nonetheless, results from recent trials are promising and provide hope that more guidance may come soon. One example of such trials, is the PRECISION trial by Strik *et al*[76], which was the first prospective trial that demonstrated clinical benefit of a more personalized approach involving a dashboard system that incorporates patient features and TDM[76]. The ultra-proactive trial put forth by Bossuyt *et al*[71] is another example, making it one of the first studies to involve the use of POC testing, suggesting that this technology may be feasible to facilitate future research and the application of TDM. Lastly, the NOR-DRUM study also brings hope as this will be the first large sized RCT looking at the safety and effectiveness of TDM in patients receiving anti-TNF for a range of immune-mediated diseases, including IBD[83].

CONCLUSION

In the end, despite its issues, TDM has evolved the management of IBD patients and is being used more in clinical practice in the hopes of preventing loss of response and to ensure maximal use of biologic drugs. Even though more studies are showing results that support proactive TDM usage, many of them have methodological issues, making their data less reliable to be able to implement changes in clinical practice. Hence making it difficult to prove that proactive TDM is associated with better therapeutic outcomes. At present, TDM has been shown to be a useful tool in managing patients

suspected of loss of response and although it has not been fully implemented in guidelines, its usefulness in current practice brings hope that this might soon change.

REFERENCES

1 **Akobeng AA**, Sandborn WJ, Bickston SJ, Chande N, Shackelton LM, Nelson S, Feagan BG. Tumor necrosis factor-alpha antagonists twenty years later: what do Cochrane reviews tell us? *Inflamm Bowel Dis* 2014; **20**: 2132-2141 [PMID: 25299543 DOI: 10.1097/MIB.0000000000000218]

2 **Peyrin-Biroulet L**, Sandborn W, Sands BE, Reinisch W, Bemelman W, Bryant RV, D'Haens G, Dotan I, Dubinsky M, Feagan B, Fiorino G, Gearry R, Krishnareddy S, Lakatos PL, Loftus EV Jr, Marteau P, Munkholm P, Murdoch TB, Ordás I, Panaccione R, Riddell RH, Ruel J, Rubin DT, Samaan M, Siegel CA, Silverberg MS, Stoker J, Schreiber S, Travis S, Van Assche G, Danese S, Panes J, Bouguen G, O'Donnell S, Pariente B, Winer S, Hanauer S, Colombel JF. Selecting Therapeutic Targets in Inflammatory Bowel Disease (STRIDE): Determining Therapeutic Goals for Treat-to-Target. *Am J Gastroenterol* 2015; **110**: 1324-1338 [PMID: 26303131 DOI: 10.1038/ajg.2015.233]

3 **Ben-Horin S**, Chowers Y. Review article: loss of response to anti-TNF treatments in Crohn's disease. *Aliment Pharmacol Ther* 2011; **33**: 987-995 [PMID: 21366636 DOI: 10.1111/j.1365-2036.2011.04612.x]

4 **Gisbert JP**, Panés J. Loss of response and requirement of infliximab dose intensification in Crohn's disease: a review. *Am J Gastroenterol* 2009; **104**: 760-767 [PMID: 19174781 DOI: 10.1038/ajg.2008.88]

5 **Billioud V**, Sandborn WJ, Peyrin-Biroulet L. Loss of response and need for adalimumab dose intensification in Crohn's disease: a systematic review. *Am J Gastroenterol* 2011; **106**: 674-684 [PMID: 21407178 DOI: 10.1038/ajg.2011.60]

6 **Yanai H**, Lichtenstein L, Assa A, Mazor Y, Weiss B, Levine A, Ron Y, Kopylov U, Bujanover Y, Rosenbach Y, Ungar B, Eliakim R, Chowers Y, Shamir R, Fraser G, Dotan I, Ben-Horin S. Levels of drug and antidrug antibodies are associated with outcome of interventions after loss of response to infliximab or adalimumab. *Clin Gastroenterol Hepatol* 2015; **13**: 522-530.e2 [PMID: 25066837 DOI: 10.1016/j.cgh.2014.07.029]

7 **Volk N**, Siegel CA. Defining Failure of Medical Therapy for Inflammatory Bowel Disease. *Inflamm Bowel Dis* 2019; **25**: 74-77 [PMID: 30016434 DOI: 10.1093/ibd/izy238]

8 **Seow CH**, Newman A, Irwin SP, Steinhart AH, Silverberg MS, Greenberg GR. Trough serum infliximab: a predictive factor of clinical outcome for infliximab treatment in acute ulcerative colitis. *Gut* 2010; **59**: 49-54 [PMID: 19651627 DOI: 10.1136/gut.2009.183095]

9 **Karmiris K**, Paintaud G, Noman M, Magdelaine-Beuzelin C, Ferrante M, Degenne D, Claes K, Coopman T, Van Schuerbeek N, Van Assche G, Vermeire S, Rutgeerts P. Influence of trough serum levels and immunogenicity on long-term outcome of adalimumab therapy in Crohn's disease. *Gastroenterology* 2009; **137**: 1628-1640 [PMID: 19664627 DOI: 10.1053/j.gastro.2009.07.062]

10 **Papamichael K**, Vajravelu RK, Vaughn BP, Osterman MT, Cheifetz AS. Proactive Infliximab Monitoring Following Reactive Testing is Associated With Better Clinical Outcomes Than Reactive Testing Alone in Patients With Inflammatory Bowel Disease. *J Crohns Colitis* 2018; **12**: 804-810 [PMID: 29590345 DOI: 10.1093/ecco-jcc/jjy039]

11 **Papamichael K**, Juncadella A, Wong D, Rakowsky S, Sattler LA, Campbell JP, Vaughn BP, Cheifetz AS. Proactive Therapeutic Drug Monitoring of Adalimumab Is Associated With Better Long-term Outcomes Compared With Standard of Care in Patients With Inflammatory Bowel Disease. *J Crohns Colitis* 2019; **13**: 976-981 [PMID: 30689771 DOI: 10.1093/ecco-jcc/jjz018]

12 **D'Haens G**, Vermeire S, Lambrecht G, Baert F, Bossuyt P, Pariente B, Buisson A, Bouhnik Y, Filippi J, Vander Woude J, Van Hootegem P, Moreau J, Louis E, Franchimont D, De Vos M, Mana F, Peyrin-Biroulet L, Brixi H, Allez M, Caenepeel P, Aubourg A, Oldenburg B, Pierik M, Gils A, Chevret S, Laharie D; GETAID. Increasing Infliximab Dose Based on Symptoms, Biomarkers, and Serum Drug Concentrations Does Not Increase Clinical, Endoscopic, and Corticosteroid-Free Remission in Patients With Active Luminal Crohn's Disease. *Gastroenterology* 2018; **154**: 1343-1351.e1 [PMID: 29317275 DOI: 10.1053/j.gastro.2018.01.004]

13 **Vaughn BP**, Martinez-Vazquez M, Patwardhan VR, Moss AC, Sandborn WJ, Cheifetz AS. Proactive therapeutic concentration monitoring of infliximab may improve outcomes for patients with inflammatory bowel disease: results from a pilot observational study. *Inflamm Bowel Dis* 2014; **20**: 1996-2003 [PMID: 25192499 DOI: 10.1097/MIB.0000000000000156]

14 **Assa A**, Matar M, Turner D, Broide E, Weiss B, Ledder O, Guz-Mark A, Rinawi F, Cohen S, Topf-Olivestone C, Shaoul R, Yerushalmi B, Shamir R. Proactive Monitoring of Adalimumab Trough Concentration Associated With Increased Clinical Remission in Children With Crohn's Disease Compared With Reactive Monitoring. *Gastroenterology* 2019; **157**: 985-996.e2 [PMID: 31194979 DOI: 10.1053/j.gastro.2019.06.003]

15 **Fernandes SR**, Bernardo S, Simões C, Gonçalves AR, Valente A, Baldaia C, Moura Santos P, Correia LA, Tato Marinho R. Proactive Infliximab Drug Monitoring Is Superior to Conventional Management in Inflammatory Bowel Disease. *Inflamm Bowel Dis* 2020; **26**: 263-270 [PMID: 31247074 DOI: 10.1093/ibd/izz131]

16 **Vande Casteele N**, Ferrante M, Van Assche G, Ballet V, Compernolle G, Van Steen K, Simoens S, Rutgeerts P, Gils A, Vermeire S. Trough concentrations of infliximab guide dosing for patients with inflammatory bowel disease. *Gastroenterology* 2015; **148**: 1320-9.e3 [PMID: 25724455 DOI: 10.1053/j.gastro.2015.02.031]

17 **Martins CdA**, Moss AC, Sobrado CW, Queiroz NSF. Practical Aspects of Proactive TDM for Anti-TNF Agents in IBD: Defining Time Points and Thresholds to Target. *Crohns Colitis 360* 2019; 1 [DOI: 10.1093/crocol/otz049]

18 **Feuerstein JD**, Nguyen GC, Kupfer SS, Falck-Ytter Y, Singh S; American Gastroenterological Association Institute Clinical Guidelines Committee. American Gastroenterological Association Institute Guideline on Therapeutic Drug Monitoring in Inflammatory Bowel Disease. *Gastroenterology* 2017; **153**: 827-834 [PMID: 28780013 DOI: 10.1053/j.gastro.2017.07.032]

19 **Vande Casteele N**, Herfarth H, Katz J, Falck-Ytter Y, Singh S. American Gastroenterological Association Institute Technical Review on the Role of Therapeutic Drug Monitoring in the Management of Inflammatory Bowel Diseases. *Gastroenterology* 2017; **153**: 835-857.e6 [PMID: 28774547 DOI: 10.1053/j.gastro.2017.07.031]

20 **Mitrev N**, Vande Casteele N, Seow CH, Andrews JM, Connor SJ, Moore GT, Barclay M, Begun J, Bryant R, Chan W, Corte C, Ghaly S, Lemberg DA, Kariyawasam V, Lewindon P, Martin J, Mountifield R, Radford-Smith G, Slobodian P, Sparrow M, Toong C, van Langenberg D, Ward MG, Leong RW; IBD Sydney Organisation and the Australian Inflammatory Bowel Diseases Consensus Working Group. Review article: consensus statements on therapeutic drug monitoring of anti-tumour necrosis factor therapy in inflammatory bowel diseases. *Aliment Pharmacol Ther* 2017; **46**: 1037-1053 [PMID: 29027257 DOI: 10.1111/apt.14368]

21 **Lamb CA**, Kennedy NA, Raine T, Hendy PA, Smith PJ, Limdi JK, Hayee B, Lomer MCE, Parkes GC, Selinger C, Barrett KJ, Davies RJ, Bennett C, Gittens S, Dunlop MG, Faiz O, Fraser A, Garrick V, Johnston PD, Parkes M, Sanderson J, Terry H; IBD guidelines eDelphi consensus group, Gaya DR, Iqbal TH, Taylor SA, Smith M, Brookes M, Hansen R, Hawthorne AB. British Society of Gastroenterology consensus guidelines on the management of inflammatory bowel disease in adults. *Gut* 2019; **68**: s1-s106 [PMID: 31562236 DOI: 10.1136/gutjnl-2019-318484]

22 **Torres J**, Bonovas S, Doherty G, Kucharzik T, Gisbert JP, Raine T, Adamina M, Armuzzi A, Bachmann O, Bager P, Biancone L, Bokemeyer B, Bossuyt P, Burisch J, Collins P, El-Hussuna A, Ellul P, Frei-Lanter C, Furfaro F, Gingert C, Gionchetti P, Gomollon F, González-Lorenzo M, Gordon H, Hlavaty T, Juillerat P, Katsanos K, Kopylov U, Krustins E, Lytras T, Maaser C, Magro F, Marshall JK, Myrelid P, Pellino G, Rosa I, Sabino J, Savarino E, Spinelli A, Stassen L, Uzzan M, Vavricka S, Verstockt B, Warusavitarne J, Zmora O, Fiorino G. ECCO Guidelines on Therapeutics in Crohn's Disease: Medical Treatment. *J Crohns Colitis* 2020; **14**: 4-22 [PMID: 31711158 DOI: 10.1093/ecco-jcc/jjz180]

23 **Cheifetz A**. Overview of Therapeutic Drug Monitoring of Biologic Agents in Patients With Inflammatory Bowel Disease. *Gastroenterol Hepatol (N Y)* 2017; **13**: 556-559 [PMID: 29038648]

24 **Lobo ED**, Hansen RJ, Balthasar JP. Antibody pharmacokinetics and pharmacodynamics. *J Pharm Sci* 2004; **93**: 2645-2668 [PMID: 15389672 DOI: 10.1002/jps.20178]

25 **Vaughn BP**, Sandborn WJ, Cheifetz AS. Biologic concentration testing in inflammatory bowel disease. *Inflamm Bowel Dis* 2015; **21**: 1435-1442 [PMID: 25590953 DOI: 10.1097/MIB.0000000000000312]

26 **Gils A**, Vande Casteele N, Poppe R, Van de Wouwer M, Compernolle G, Peeters M, Brouwers E, Vermeire S, Geukens N, Declerck PJ. Development of a universal anti-adalimumab antibody standard for interlaboratory harmonization. *Ther Drug Monit* 2014; **36**: 669-673 [PMID: 24906181 DOI: 10.1097/FTD.0000000000000074]

27 **Bendtzen K**, Ainsworth M, Steenholdt C, Thomsen OØ, Brynskov J. Individual medicine in inflammatory bowel disease: monitoring bioavailability, pharmacokinetics and immunogenicity of anti-tumour necrosis factor-alpha antibodies. *Scand J Gastroenterol* 2009; **44**: 774-781 [PMID: 19140087 DOI: 10.1080/00365520802699278]

28 **Dreesen E**, Bossuyt P, Mulleman D, Gils A, Pascual-Salcedo D. Practical recommendations for the use of therapeutic drug monitoring of biopharmaceuticals in inflammatory diseases. *Clin Pharmacol* 2017; **9**: 101-111 [PMID: 29042821 DOI: 10.2147/CPAA.S138414]

29 **Cassinotti A**, Travis S. Incidence and clinical significance of immunogenicity to infliximab in Crohn's disease: a critical systematic review. *Inflamm Bowel Dis* 2009; **15**: 1264-1275 [PMID: 19235918 DOI: 10.1002/ibd.20899]

30 **Vermeire S**, Dreesen E, Papamichael K, Dubinsky MC. How, When, and for Whom Should We Perform Therapeutic Drug Monitoring? *Clin Gastroenterol Hepatol* 2020; **18**: 1291-1299 [PMID: 31589978 DOI: 10.1016/j.cgh.2019.09.041]

31 **Nanda KS**, Cheifetz AS, Moss AC. Impact of antibodies to infliximab on clinical outcomes and serum infliximab levels in patients with inflammatory bowel disease (IBD): a meta-analysis. *Am J Gastroenterol* 2013; **108**: 40-47; quiz 48 [PMID: 23147525 DOI: 10.1038/ajg.2012.363]

32 **Baert F**, Noman M, Vermeire S, Van Assche G, D' Haens G, Carbonez A, Rutgeerts P. Influence of immunogenicity on the long-term efficacy of infliximab in Crohn's disease. *N Engl J Med* 2003; **348**: 601-608 [PMID: 12584368 DOI: 10.1056/NEJMoa020888]

33 **Kennedy NA**, Heap GA, Green HD, Hamilton B, Bewshea C, Walker GJ, Thomas A, Nice R, Perry MH, Bouri S, Chanchlani N, Heerasing NM, Hendy P, Lin S, Gaya DR, Cummings JRF, Selinger CP, Lees CW, Hart AL, Parkes M, Sebastian S, Mansfield JC, Irving PM, Lindsay J, Russell RK,

McDonald TJ, McGovern D, Goodhand JR, Ahmad T; UK Inflammatory Bowel Disease Pharmacogenetics Study Group. Predictors of anti-TNF treatment failure in anti-TNF-naive patients with active luminal Crohn's disease: a prospective, multicentre, cohort study. *Lancet Gastroenterol Hepatol* 2019; **4**: 341-353 [PMID: 30824404 DOI: 10.1016/S2468-1253(19)30012-3]

34 **Brandse JF**, Mathôt RA, van der Kleij D, Rispens T, Ashruf Y, Jansen JM, Rietdijk S, Löwenberg M, Ponsioen CY, Singh S, van den Brink GR, D'Haens GR. Pharmacokinetic Features and Presence of Antidrug Antibodies Associate With Response to Infliximab Induction Therapy in Patients With Moderate to Severe Ulcerative Colitis. *Clin Gastroenterol Hepatol* 2016; **14**: 251-8.e1 [PMID: 26545802 DOI: 10.1016/j.cgh.2015.10.029]

35 **Brandse JF**, Mould D, Smeekes O, Ashruf Y, Kuin S, Strik A, van den Brink GR, D'Haens GR. A Real-life Population Pharmacokinetic Study Reveals Factors Associated with Clearance and Immunogenicity of Infliximab in Inflammatory Bowel Disease. *Inflamm Bowel Dis* 2017; **23**: 650-660 [PMID: 28195852 DOI: 10.1097/MIB.0000000000001043]

36 **Gunn GR 3rd**, Sealey DC, Jamali F, Meibohm B, Ghosh S, Shankar G. From the bench to clinical practice: understanding the challenges and uncertainties in immunogenicity testing for biopharmaceuticals. *Clin Exp Immunol* 2016; **184**: 137-146 [PMID: 26597698 DOI: 10.1111/cei.12742]

37 **Shankar G**, Arkin S, Cocea L, Devanarayan V, Kirshner S, Kromminga A, Quarmby V, Richards S, Schneider CK, Subramanyam M, Swanson S, Verthelyi D, Yim S; American Association of Pharmaceutical Scientists. Assessment and reporting of the clinical immunogenicity of therapeutic proteins and peptides-harmonized terminology and tactical recommendations. *AAPS J* 2014; **16**: 658-673 [PMID: 24764037 DOI: 10.1208/s12248-014-9599-2]

38 **Ainsworth MA**, Bendtzen K, Brynskov J. Tumor necrosis factor-alpha binding capacity and anti-infliximab antibodies measured by fluid-phase radioimmunoassays as predictors of clinical efficacy of infliximab in Crohn's disease. *Am J Gastroenterol* 2008; **103**: 944-948 [PMID: 18028512 DOI: 10.1111/j.1572-0241.2007.01638.x]

39 **Allez M**, Karmiris K, Louis E, Van Assche G, Ben-Horin S, Klein A, Van der Woude J, Baert F, Eliakim R, Katsanos K, Brynskov J, Steinwurz F, Danese S, Vermeire S, Teillaud JL, Lémann M, Chowers Y. Report of the ECCO pathogenesis workshop on anti-TNF therapy failures in inflammatory bowel diseases: definitions, frequency and pharmacological aspects. *J Crohns Colitis* 2010; **4**: 355-366 [PMID: 21122530 DOI: 10.1016/j.crohns.2010.04.004]

40 **Weisshof R**, Ungar B, Blatt A, Dahan A, Pressman S, Waterman M, Kopylov U, Ben-Horin S, Chowers Y. Anti-infliximab Antibodies with Neutralizing Capacity in Patients with Inflammatory Bowel Disease: Distinct Clinical Implications Revealed by a Novel Assay. *Inflamm Bowel Dis* 2016; **22**: 1655-1661 [PMID: 27120567 DOI: 10.1097/MIB.0000000000000797]

41 **Reinhold I**, Blümel S, Schreiner J, Boyman O, Bögeholz J, Cheetham M, Rogler G, Biedermann L, Scharl M. Clinical Relevance of Anti-TNF Antibody Trough Levels and Anti-Drug Antibodies in Treating Inflammatory Bowel Disease Patients. *Inflamm Intest Dis* 2021; **6**: 38-47 [PMID: 33850838 DOI: 10.1159/000511296]

42 **Gonczi L**, Kurti Z, Rutka M, Vegh Z, Farkas K, Lovasz BD, Golovics PA, Gecse KB, Szalay B, Molnar T, Lakatos PL. Drug persistence and need for dose intensification to adalimumab therapy; the importance of therapeutic drug monitoring in inflammatory bowel diseases. *BMC Gastroenterol* 2017; **17**: 97 [PMID: 28789636 DOI: 10.1186/s12876-017-0654-1]

43 **Ben-Horin S**, Chowers Y. Tailoring anti-TNF therapy in IBD: drug levels and disease activity. *Nat Rev Gastroenterol Hepatol* 2014; **11**: 243-255 [PMID: 24393836 DOI: 10.1038/nrgastro.2013.253]

44 **Bian S**, Dreesen E, Tang HT, Compernolle G, Peeters M, Van Assche G, Ferrante M, Vermeire S, Gils A. Antibodies Toward Vedolizumab Appear from the First Infusion Onward and Disappear Over Time. *Inflamm Bowel Dis* 2017; **23**: 2202-2208 [PMID: 29140943 DOI: 10.1097/MIB.0000000000001255]

45 **Chiu HY**, Chu TW, Cheng YP, Tsai TF. The Association between Clinical Response to Ustekinumab and Immunogenicity to Ustekinumab and Prior Adalimumab. *PLoS One* 2015; **10**: e0142930 [PMID: 26566272 DOI: 10.1371/journal.pone.0142930]

46 **Strand V**, Balsa A, Al-Saleh J, Barile-Fabris L, Horiuchi T, Takeuchi T, Lula S, Hawes C, Kola B, Marshall L. Immunogenicity of Biologics in Chronic Inflammatory Diseases: A Systematic Review. *BioDrugs* 2017; **31**: 299-316 [PMID: 28612180 DOI: 10.1007/s40259-017-0231-8]

47 **Juncadella A**, Papamichael K, Vaughn BP, Cheifetz AS. Maintenance Adalimumab Concentrations Are Associated with Biochemical, Endoscopic, and Histologic Remission in Inflammatory Bowel Disease. *Dig Dis Sci* 2018; **63**: 3067-3073 [PMID: 30006816 DOI: 10.1007/s10620-018-5202-5]

48 **Papamichael K**, Cheifetz AS. Therapeutic drug monitoring in inflammatory bowel disease: for every patient and every drug? *Curr Opin Gastroenterol* 2019; **35**: 302-310 [PMID: 30973355 DOI: 10.1097/MOG.0000000000000536]

49 **Roblin X**, Marotte H, Rinaudo M, Del Tedesco E, Moreau A, Phelip JM, Genin C, Peyrin-Biroulet L, Paul S. Association between pharmacokinetics of adalimumab and mucosal healing in patients with inflammatory bowel diseases. *Clin Gastroenterol Hepatol* 2014; **12**: 80-84.e2 [PMID: 23891927 DOI: 10.1016/j.cgh.2013.07.010]

50 **Paul S**, Moreau AC, Del Tedesco E, Rinaudo M, Phelip JM, Genin C, Peyrin-Biroulet L, Roblin X. Pharmacokinetics of adalimumab in inflammatory bowel diseases: a systematic review and meta-analysis. *Inflamm Bowel Dis* 2014; **20**: 1288-1295 [PMID: 24831559 DOI: 10.1097/MIB.0000000000000037]

51 **Dirks NL**, Meibohm B. Population pharmacokinetics of therapeutic monoclonal antibodies. *Clin Pharmacokinet* 2010; **49**: 633-659 [PMID: 20818831 DOI: 10.2165/11535960-000000000-00000]

52 **Vande Casteele N**, Gils A, Singh S, Ohrmund L, Hauenstein S, Rutgeerts P, Vermeire S. Antibody response to infliximab and its impact on pharmacokinetics can be transient. *Am J Gastroenterol* 2013; **108**: 962-971 [PMID: 23419382 DOI: 10.1038/ajg.2013.12]

53 **Papamichael K**, Van Stappen T, Vande Casteele N, Gils A, Billiet T, Tops S, Claes K, Van Assche G, Rutgeerts P, Vermeire S, Ferrante M. Infliximab Concentration Thresholds During Induction Therapy Are Associated With Short-term Mucosal Healing in Patients With Ulcerative Colitis. *Clin Gastroenterol Hepatol* 2016; **14**: 543-549 [PMID: 26681486 DOI: 10.1016/j.cgh.2015.11.014]

54 **Bortlik M**, Duricova D, Malickova K, Machkova N, Bouzkova E, Hrdlicka L, Komarek A, Lukas M. Infliximab trough levels may predict sustained response to infliximab in patients with Crohn's disease. *J Crohns Colitis* 2013; **7**: 736-743 [PMID: 23200919 DOI: 10.1016/j.crohns.2012.10.019]

55 **Adedokun OJ**, Sandborn WJ, Feagan BG, Rutgeerts P, Xu Z, Marano CW, Johanns J, Zhou H, Davis HM, Cornillie F, Reinisch W. Association between serum concentration of infliximab and efficacy in adult patients with ulcerative colitis. *Gastroenterology* 2014; **147**: 1296-1307.e5 [PMID: 25173754 DOI: 10.1053/j.gastro.2014.08.035]

56 **Davidov Y**, Ungar B, Bar-Yoseph H, Carter D, Haj-Natour O, Yavzori M, Chowers Y, Eliakim R, Ben-Horin S, Kopylov U. Association of Induction Infliximab Levels With Clinical Response in Perianal Crohn's Disease. *J Crohns Colitis* 2017; **11**: 549-555 [PMID: 28453755 DOI: 10.1093/ecco-jcc/jjw182]

57 **Ungar B**, Levy I, Yavne Y, Yavzori M, Picard O, Fudim E, Loebstein R, Chowers Y, Eliakim R, Kopylov U, Ben-Horin S. Optimizing Anti-TNF-α Therapy: Serum Levels of Infliximab and Adalimumab Are Associated With Mucosal Healing in Patients With Inflammatory Bowel Diseases. *Clin Gastroenterol Hepatol* 2016; **14**: 550-557.e2 [PMID: 26538204 DOI: 10.1016/j.cgh.2015.10.025]

58 **Strik AS**, Löwenberg M, Buskens CJ, B Gecse K, I Ponsioen C, Bemelman WA, D'Haens GR. Higher anti-TNF serum levels are associated with perianal fistula closure in Crohn's disease patients. *Scand J Gastroenterol* 2019; **54**: 453-458 [PMID: 31032686 DOI: 10.1080/00365521.2019.1600014]

59 **Bouguen G**, Siproudhis L, Gizard E, Wallenhorst T, Billioud V, Bretagne JF, Bigard MA, Peyrin-Biroulet L. Long-term outcome of perianal fistulizing Crohn's disease treated with infliximab. *Clin Gastroenterol Hepatol* 2013; **11**: 975-81.e1 [PMID: 23376316 DOI: 10.1016/j.cgh.2012.12.042]

60 **Colombel F**, Panés J, D'Haens G, Schreiber S, Panaccione R, Peyrin-Biroulet L, Loftus E, Danese S, Louis E, Armuzzi A, Ferrante M, Vogelsang H, Lefebvre J, Doan T, Xie W, Huang B, Petersson J, Kalabic J, Robinson A, Sandborn W. OP01 Higher vs. standard adalimumab maintenance regimens in patients with moderately to severely active ulcerative colitis: Results from the SERENE-UC maintenance study. *J Crohns Colitis* 2020; **14**: S001-S001 [DOI: 10.1093/ecco-jcc/jjz203.000]

61 **D'Haens G SW**, Loftus Jr E, Hanauer SB, Peyrin-Biroulet L, Panaccione R, Panes J, Colombel JF, Ferrante M, Louis E, Armuzzi A, Zhou Q, Huang B, Kwatra NV, Mostafa NM, Doan T, Petersson J, Song A, Anne M. High vs standard adalimumab induction dosing regimens in patients with moderately to severely active Crohn's disease: results from the SERENE-CD induction study. *United European Gastroenterol J* 2019; **7** [DOI: 10.14309/01.ajg.0000704640.35342.ed]

62 **Velayos FS**, Kahn JG, Sandborn WJ, Feagan BG. A test-based strategy is more cost effective than empiric dose escalation for patients with Crohn's disease who lose responsiveness to infliximab. *Clin Gastroenterol Hepatol* 2013; **11**: 654-666 [PMID: 23357488 DOI: 10.1016/j.cgh.2012.12.035]

63 **Kelly OB**, Donnell SO, Stempak JM, Steinhart AH, Silverberg MS. Therapeutic Drug Monitoring to Guide Infliximab Dose Adjustment is Associated with Better Endoscopic Outcomes than Clinical Decision Making Alone in Active Inflammatory Bowel Disease. *Inflamm Bowel Dis* 2017; **23**: 1202-1209 [PMID: 28498155 DOI: 10.1097/MIB.0000000000001126]

64 **Restellini S**, Chao CY, Lakatos PL, Aruljothy A, Aziz H, Kherad O, Bitton A, Wild G, Afif W, Bessissow T. Therapeutic Drug Monitoring Guides the Management of Crohn's Patients with Secondary Loss of Response to Adalimumab. *Inflamm Bowel Dis* 2018; **24**: 1531-1538 [PMID: 29668893 DOI: 10.1093/ibd/izy044]

65 **Guidi L**, Pugliese D, Panici Tonucci T, Berrino A, Tolusso B, Basile M, Cantoro L, Balestrieri P, Civitelli F, Bertani L, Marzo M, Felice C, Gremese E, Costa F, Viola F, Cicala M, Kohn A, Gasbarrini A, Rapaccini GL, Ruggeri M, Armuzzi A. Therapeutic Drug Monitoring is More Cost-Effective than a Clinically Based Approach in the Management of Loss of Response to Infliximab in Inflammatory Bowel Disease: An Observational Multicentre Study. *J Crohns Colitis* 2018; **12**: 1079-1088 [PMID: 29860436 DOI: 10.1093/ecco-jcc/jjy076]

66 **Steenholdt C**, Brynskov J, Thomsen OØ, Munck LK, Fallingborg J, Christensen LA, Pedersen G, Kjeldsen J, Jacobsen BA, Oxholm AS, Kjellberg J, Bendtzen K, Ainsworth MA. Individualised therapy is more cost-effective than dose intensification in patients with Crohn's disease who lose response to anti-TNF treatment: a randomised, controlled trial. *Gut* 2014; **63**: 919-927 [PMID: 23878167 DOI: 10.1136/gutjnl-2013-305279]

67 **Afif W**, Loftus EV Jr, Faubion WA, Kane SV, Bruining DH, Hanson KA, Sandborn WJ. Clinical utility of measuring infliximab and human anti-chimeric antibody concentrations in patients with inflammatory bowel disease. *Am J Gastroenterol* 2010; **105**: 1133-1139 [PMID: 20145610 DOI: 10.1038/ajg.2010.9]

68 **Ungar B**, Mazor Y, Weisshof R, Yanai H, Ron Y, Goren I, Waizbard A, Yavzori M, Fudim E, Picard O, Loebstein R, Kopylov U, Dotan I, Chowers Y, Eliakim R, Ben-Horin S. Induction infliximab

levels among patients with acute severe ulcerative colitis compared with patients with moderately severe ulcerative colitis. *Aliment Pharmacol Ther* 2016; **43**: 1293-1299 [PMID: 27091119 DOI: 10.1111/apt.13631]

69 **Ma C**, Battat R, Jairath V, Vande Casteele N. Advances in Therapeutic Drug Monitoring for Small-Molecule and Biologic Therapies in Inflammatory Bowel Disease. *Curr Treat Options Gastroenterol* 2019; **17**: 127-145 [PMID: 30680599 DOI: 10.1007/s11938-019-00222-9]

70 **Danese S SW**, Loftus EV, Hanauer S, Schreiber S, Peyrin-Biroulet L, Panaccione R, Panes J, Baert F, Colombel JF, Ferrante M, Louis E, Armuzzi A, Goteti VS, Mostafa N, Doan T, Petersson J, Robinson A, Song A, D'Haens GR. Clinically Adjusted vs Therapeutic Drug Monitoring Dosing Regimens With Adalimumab in Patients With Moderately to Severely Active Crohn's Disease: Results From the SERENE-CD Maintenance Study. *United European Gastroenterol* 2020 [DOI: 10.14309/01.ajg.0000704640.35342.ed]

71 **Bossuyt P**, Pouillon L, Claeys S, D'Haens S, Hoefkens E, Strubbe B, Marichal D, Peeters H. Ultra-proactive therapeutic drug monitoring of infliximab based on point-of-care-testing in inflammatory bowel disease: results of a pragmatic trial. *J Crohns Colitis* 2021; **23**: jjab127 [PMID: 34297099 DOI: 10.1093/ecco-jcc/jjab127]

72 **Govani S**, Waljee A, Stidham R, Higgins P, Hardiman K. 516 Accelerated Dosing of Infliximab Prevents Colectomy Within 90 Days in Only Half of Patients With Severe Ulcerative Colitis. *Gastroenterology* 2016; **150**: S106 [DOI: 10.1016/s0016-5085(16)30462-0]

73 **Papamichael K**, Chachu KA, Vajravelu RK, Vaughn BP, Ni J, Osterman MT, Cheifetz AS. Improved Long-term Outcomes of Patients With Inflammatory Bowel Disease Receiving Proactive Compared With Reactive Monitoring of Serum Concentrations of Infliximab. *Clin Gastroenterol Hepatol* 2017; **15**: 1580-1588.e3 [PMID: 28365486 DOI: 10.1016/j.cgh.2017.03.031]

74 **Perinbasekar R**, Brown S, Syed N, Lonsako S, Cross R. Proactive Monitoring of Infliximab (IFX) and Adalimumab (ADA) Using LabCorp's Electrochemiluminescence Assay (ECLIA) in Inflammatory Bowel Disease Patients: 719. *Official J the Am College Gastroenterol* 2017; **112**: S397

75 **Bernardo S**, Fernandes S, Gonçalves AR, Baldaia C, Valente A, Santos P, Araújo-Correia L, Velosa J. P453 Efficacy of therapeutic drug monitoring of anti-TNF therapy in the control of patients with inflammatory bowel disease. *J Crohns Colitis* 2017; **11**: S308-S309 [DOI: 10.1093/ecco-jcc/jjx002.578]

76 **Strik A**, Berends S, Mould D, Mathôt R, Ponsioen C, van den Brande J, Jansen J, Hoekman D, Brandse J, Löwenberg M, D'Haens G. DOP56 Dashboard driven vs. conventional dosing of infliximab in inflammatory bowel disease patients: the PRECISION trial. *J Crohns Colitis* 2019; **13(Supplement_1)**: S063-S063 [DOI: 10.1093/ecco-jcc/jjy222.090]

77 **Pouillon L**, Ferrante M, Van Assche G, Rutgeerts P, Noman M, Sabino J, Vande Casteele N, Gils A, Vermeire S. Mucosal Healing and Long-term Outcomes of Patients With Inflammatory Bowel Diseases Receiving Clinic-Based vs Trough Concentration-Based Dosing of Infliximab. *Clin Gastroenterol Hepatol* 2018; **16**: 1276-1283.e1 [PMID: 29203225 DOI: 10.1016/j.cgh.2017.11.046]

78 **Roblin X**, Rinaudo M, Del Tedesco E, Phelip JM, Genin C, Peyrin-Biroulet L, Paul S. Development of an algorithm incorporating pharmacokinetics of adalimumab in inflammatory bowel diseases. *Am J Gastroenterol* 2014; **109**: 1250-1256 [PMID: 24913041 DOI: 10.1038/ajg.2014.146]

79 **Papamichael K**, Cheifetz AS, Melmed GY, Irving PM, Vande Casteele N, Kozuch PL, Raffals LE, Baidoo L, Bressler B, Devlin SM, Jones J, Kaplan GG, Sparrow MP, Velayos FS, Ullman T, Siegel CA. Appropriate Therapeutic Drug Monitoring of Biologic Agents for Patients With Inflammatory Bowel Diseases. *Clin Gastroenterol Hepatol* 2019; **17**: 1655-1668.e3 [PMID: 30928454 DOI: 10.1016/j.cgh.2019.03.037]

80 **Ward MG**, Sparrow MP, Roblin X. Therapeutic drug monitoring of vedolizumab in inflammatory bowel disease: current data and future directions. *Therap Adv Gastroenterol* 2018; **11**: 1756284818772786 [PMID: 29774052 DOI: 10.1177/1756284818772786]

81 **Berends S**, Löwenberg M, Baert F, Mathôt R, Clasquin E, Woude C, Hoentjen F, Bossuyt P, Franchimont D, Rispens T, de Vries A, Vermeire S, D'Haens G. DOP046 Higher serum concentrations of vedolizumab are associated with superior endoscopic outcomes in Crohn's disease: data from the LOVE-CD trial. *J Crohns Colitis* 2018; **12**: S063-S063 [DOI: 10.1093/ecco-jcc/jjx180.083]

82 **Löwenberg M**, Vermeire S, Mostafavi N, Hoentjen F, Franchimont D, Bossuyt P, Hindryckx P, Rispens T, de Vries A, van der Woude CJ, Berends S, Ambarus CA, Mathot R, Clasquin E, Baert F, D'Haens G. Vedolizumab Induces Endoscopic and Histologic Remission in Patients With Crohn's Disease. *Gastroenterology* 2019; **157**: 997-1006.e6 [PMID: 31175865 DOI: 10.1053/j.gastro.2019.05.067]

83 **Syversen SW**, Goll GL, Jørgensen KK, Olsen IC, Sandanger Ø, Gehin JE, Warren DJ, Sexton J, Mørk C, Jahnsen J, Kvien TK, Bolstad N, Haavardsholm EA. Therapeutic drug monitoring of infliximab compared to standard clinical treatment with infliximab: study protocol for a randomised, controlled, open, parallel-group, phase IV study (the NOR-DRUM study). *Trials* 2020; **21**: 13 [PMID: 31907007 DOI: 10.1186/s13063-019-3734-4]

World Journal of Gastroenterology

Submit a Manuscript: https://www.f6publishing.com

World J Gastroenterol 2021 October 7; 27(37): 6248-6261

DOI: 10.3748/wjg.v27.i37.6248

ISSN 1007-9327 (print) ISSN 2219-2840 (online)

ORIGINAL ARTICLE

Basic Study

Increased systemic RNA oxidative damage and diagnostic value of RNA oxidative metabolites during *Shigella flexneri*-induced intestinal infection

Jing-Jing Nie, Ya-Ya Pian, Ji-Hong Hu, Guo-Qing Fan, Lv-Tao Zeng, Qiu-Geng Ouyang, Zhen-Xiang Gao, Zhen Liu, Chen-Chen Wang, Qian Liu, Jian-Ping Cai

ORCID number: Jing-Jing Nie 0000-0002-6563-1175; Ya-Ya Pian 0000-0002-1519-3947; Ji-Hong Hu 0000-0002-5433-954X; Guo-Qing Fan 0000-0001-9122-5149; Lv-Tao Zeng 0000-0002-2252-5110; Qiu-Geng Ouyang 0000-0001-6348-5066; Zhen-Xiang Gao 0000-0001-7037-206X; Zhen Liu 0000-0003-4672-7515; Chen-Chen Wang 0000-0001-5763-7174; Qian Liu 0000-0003-4610-2531; Jian-Ping Cai 0000-0003-2793-9221.

Author contributions: Cai JP provided the research concept; Cai JP, Hu JH, and Nie JJ designed the study; Nie JJ and Pian YY performed the majority of the experiments; Fan GQ, Zeng LT, Ouyang QG, Wang CC, Liu Q, Liu Z, and Gao ZX helped to perform part of the experiments; Nie JJ performed the statistical analysis; Nie JJ and Cai JP wrote the manuscript; all authors approved the final version of the article; Nie JJ and Pian YY contributed equally to this work.

Supported by the National Key R&D Program of China, No. 2018YFC2000300; and CAMS Innovation Fund for Medical Sciences, No. 2018-I2M-1-002.

Jing-Jing Nie, Ya-Ya Pian, Ji-Hong Hu, Zhen-Xiang Gao, Department of Microbiology, National Center for Clinical Laboratories, Beijing Hospital, National Center of Gerontology, Institute of Geriatric Medicine, Chinese Academy of Medical Sciences, Beijing 100730, China

Guo-Qing Fan, Lv-Tao Zeng, Zhen Liu, Qian Liu, Jian-Ping Cai, The Key Laboratory of Geriatrics, Beijing Institute of Geriatrics, Beijing Hospital, National Center of Gerontology, National Health Commission, Institute of Geriatric Medicine, Chinese Academy of Medical Sciences, Beijing 100730, China

Qiu-Geng Ouyang, Chen-Chen Wang, Department of Pharmacy, Wenzhou Medical University, Wenzhou 325035, Zhejiang Province, China

Corresponding author: Jian-Ping Cai, PhD, Professor, The Key Laboratory of Geriatrics, Beijing Institute of Geriatrics, Beijing Hospital, National Center of Gerontology, National Health Commission, Institute of Geriatric Medicine, Chinese Academy of Medical Sciences, No. 1 Dahua Road, Dongcheng District, Beijing 100730, China. caijp61@vip.sina.com

Abstract

BACKGROUND

Shigella flexneri (*S. flexneri*) is a major pathogen causing acute intestinal infection, but the systematic oxidative damage incurred during the course of infection has not been investigated.

AIM

To investigate the incurred systemic RNA oxidative damage and the diagnostic value of RNA oxidative metabolites during *S. flexneri*-induced intestinal infection.

METHODS

In this study, a Sprague-Dawley rat model of acute intestinal infection was established by oral gavage with *S. flexneri* strains. The changes in white blood cells (WBCs) and cytokine levels in blood and the inflammatory response in the colon were investigated. We also detected the RNA and DNA oxidation in urine and tissues.

RESULTS

Institutional animal care and use committee statement: This study was approved by the Ethical Committee of the Institute of Medical Biotechnology, Chinese Academy of Medical Sciences (approval number: IMB-201803140206).

Conflict-of-interest statement: The authors declare no conflicts of interest in association with the present study.

Data sharing statement: No additional data are available.

ARRIVE guidelines statement: The authors have read the ARRIVE guidelines, and the manuscript was prepared and revised according to the ARRIVE guidelines.

Open-Access: This article is an open-access article that was selected by an in-house editor and fully peer-reviewed by external reviewers. It is distributed in accordance with the Creative Commons Attribution NonCommercial (CC BY-NC 4.0) license, which permits others to distribute, remix, adapt, build upon this work non-commercially, and license their derivative works on different terms, provided the original work is properly cited and the use is non-commercial. See: http://creativecommons.org/Licenses/by-nc/4.0/

Manuscript source: Invited manuscript

Specialty type: Gastroenterology and hepatology

Country/Territory of origin: China

Peer-review report's scientific quality classification

Grade A (Excellent): 0
Grade B (Very good): B, B
Grade C (Good): 0
Grade D (Fair): 0
Grade E (Poor): 0

Received: March 2, 2021
Peer-review started: March 2, 2021
First decision: April 17, 2021
Revised: April 29, 2021

S. flexneri infection induced an increase in WBCs, C-reactive protein, interleukin (IL)-6, IL-10, IL-1β, IL-4, IL-17a, IL-10, and tumor necrosis factor α (TNF-α) in blood. Of note, a significant increase in urinary 8-oxo-7,8-dihydroguanosine (8-oxo-Gsn), an important marker of total RNA oxidation, was detected after intestinal infection (P = 0.03). The urinary 8-oxo-Gsn level returned to the baseline level after recovery from infection. In addition, the results of a correlation analysis showed that urinary 8-oxo-Gsn was positively correlated with the WBC count and the cytokines IL-6, TNF-α, IL-10, IL-1β, and IL-17α. Further detection of the oxidation in different tissues showed that *S. flexneri* infection induced RNA oxidative damage in the colon, ileum, liver, spleen, and brain.

CONCLUSION

Acute infection induced by *S. flexneri* causes increased RNA oxidative damage in various tissues (liver, spleen, and brain) and an increase of 8-oxo-Gsn, a urinary metabolite. Urinary 8-oxo-Gsn may be useful as a biomarker for evaluating the severity and prognosis of infection.

Key Words: 8-oxo-7,8-dihydroguanosine; *Shigella flexneri*; Infection; Oxidative damage

©The Author(s) 2021. Published by Baishideng Publishing Group Inc. All rights reserved.

Core Tip: *Shigella flexneri* (*S. flexneri*) is a major pathogen causing acute intestinal infection, but the systematic oxidative damage incurred during the course of infection has not been investigated. By establishing a Sprague-Dawley rat model with *S. flexneri* infection in the intestine, we found that 8-oxo-7,8-dihydroguanosine (8-oxo-Gsn) levels were markedly increased in the colon, ileum, liver, spleen, and brain after infection, showing that *S. flexneri* can exacerbate systemic RNA oxidation. The changing trend in levels of urinary 8-oxo-Gsn (as the RNA oxidative metabolites) was consistent with the changes in the white blood cell count, C-reactive protein level, and cytokine levels during infection. Urinary 8-oxo-Gsn may be useful as a biomarker for evaluating the severity and prognosis of infection.

Citation: Nie JJ, Pian YY, Hu JH, Fan GQ, Zeng LT, Ouyang QG, Gao ZX, Liu Z, Wang CC, Liu Q, Cai JP. Increased systemic RNA oxidative damage and diagnostic value of RNA oxidative metabolites during *Shigella flexneri*-induced intestinal infection. *World J Gastroenterol* 2021; 27(37): 6248-6261
URL: https://www.wjgnet.com/1007-9327/full/v27/i37/6248.htm
DOI: https://dx.doi.org/10.3748/wjg.v27.i37.6248

INTRODUCTION

Shigella infection is a major public health concern around the world, causing acute diarrhea, known as shigellosis or bacillary dysentery. There are almost 165 million cases of diarrhea caused by *Shigella* each year, of which 163 million occur in developing countries[1]. People of all ages can be infected by *Shigella*, but children under five years old are most susceptible[2].

Shigella flexneri (*S. flexneri*) is the most frequently isolated *Shigella* species worldwide [2]. The pathogenesis of *S. flexneri* involves invasion of the mucosa by bacteria, which replicate within and spread between the mucosal epithelial cells, resulting in a subsequent severe inflammatory response and epithelial destruction in the colon tissue. However, the oxidative damage in the colon during *S. flexneri*-induced infection has not been investigated. In the present study, the oxidative stress changes in the intestine during *S. flexneri*-induced acute intestinal infection were investigated.

Shigella infection can cause inflammatory responses in the intestine, which is also a potential source of inflammation-related cytokines[3]. Researchers have established cell models/animal models and observed the infected patients to investigate the inflammation-related cytokine production. In cell models, *S. flexneri* was able to cause an increase in interleukin (IL)-1, IL-10, and tumor necrosis factor α (TNF-α) in macrophage-like cells[4]. Outer membrane protein A of *S. flexneri* can trigger B cells to

Accepted: August 9, 2021
Article in press: August 9, 2021
Published online: October 7, 2021

P-Reviewer: Kashyap MK, Scarfi S
S-Editor: Zhang H
L-Editor: Wang TQ
P-Editor: Li JH

secret the cytokines IL-6 and IL-10[5]. The production of the cytokines IL-4, IL-6, and IL-8 is increased in HeLa cells with *S. flexneri* infection[6]. Researchers also found that the TNFα and IL-1β production is reduced in mouse macrophages with an *S. flexneri msbB* gene mutation[7]. In mouse models, *S. flexneri* infection can cause an increase in the IL-1β production[8]. In *S. flexneri*-infected patients, the TNF-α, IL-1, IL-4, IL-6, and interferon-γ levels increased significantly after infection[3].

In the present study, we established an *S. flexneri*-infected rat model to explore the changes in the levels of the above-mentioned cytokines (IL-1, IL-6, IL-10, and TNF-α) as well as IL-17α, which plays important roles in host immunity against intracellular pathogens.

Urinary 8-oxo-7,8-dihydroguanosine (8-oxo-Gsn) and 8-oxo-7,8-dihydro-2-deoxyguanosine (8-oxo-dGsn) are oxidative stress by-products of RNA and DNA, respectively, which are widely used as markers of oxidative stress[9,10]. Previous studies have reported their utility as biomarkers for predicting aging-related diseases[11] and neurodegenerative diseases[12]. Our lab found that 8-oxo-Gsn may have potential utility as a marker for evaluating the severity of *Salmonella*-related infection[13]. The present study investigated the diagnostic value of 8-oxo-Gsn and 8-oxo-dGsn in intestinal infection induced by *S. flexneri*. In addition, we investigated the correlation between cytokine levels and oxidative production of 8-oxo-Gsn.

Accumulating evidence suggests that intestinal infection caused by Gram-negative bacteria may also influence other organs. For example, the Gram-negative bacterium *Escherichia coli* can form extracellular amyloid, which may play a role in causing sporadic Alzheimer's disease[14]. *S. dysenteriae*, a causative agent of bloody diarrhea, may cause diarrhea-associated hemolytic uremic syndrome and neurological disorders [15]. Acute intestinal infection induced by *Salmonella* can cause oxidative damage to the intestine, liver, and spleen[13]. However, the effects of *Shigella*-induced intestinal infection on other tissues have not been reported.

We hope that the rat infection model established in the present study will help improve our understanding of how vertebrates regulate their response to *S. flexneri* infection. We further intended to explore whether or not *S. flexneri* infection in the intestine can cause oxidative damage to other organs, such as the liver, spleen, and brain.

MATERIALS AND METHODS

Bacterial strains

The *S. flexneri* strain used in this study (CICC 21534) was purchased from the China Center of Industrial Culture Collection (CICC; Beijing, China). The source of the CICC 21534 strain was Guizhou Health and Epidemic Prevention Station, China. The serotype of CICC 21534 was F1a.

S. flexneri strain CICC 21534 was stored at -80 °C. The isolate was subcultured on blood agar plates twice and then suspended in Trypticase Soy Broth (bioMérieux SA, 69280 Marcy I'Etoile, France). The bacterial concentration was measured spectrophotometrically and confirmed by serial dilution on blood agar.

Animal experimental design

Twenty-four 4-wk-old healthy male Sprague-Dawley (SD) rats were purchased from Vital River (Beijing, China). All appropriate measures were taken to minimize the pain or discomfort of the rats. The rats were housed in a temperature-controlled room (24 ± 2 °C). Drinking water and food were provided *ad libitum*. There were three rats in each cage. The rats were not pretreated with any antibiotics and were all healthy before treatment, with normal white blood cell (WBC) counts and a normal flora in the feces.

The rats were divided randomly into either an infection group or a control group. In the infection group (n = 12), rats were infected by gavage with 1 dose of 1×10^9 colony-forming units (CFU) of the *S. flexneri* strain. In the control group (n = 12), rat gavage was performed with phosphate-buffered saline (PBS). On days 1, 5, 9, and 18, three rats per group were euthanized by intraperitoneal injection of pentobarbital sodium (200 mg/kg), and tissues were obtained.

For the establishment of the infection model, before infection, the rats were starved overnight. To neutralize the gastric acid, 400 μL of 3% $NaHCO_3$ was administered orally 15 min before infection. The rats in the infection group were then orally administered with 1×10^9 CFU of *S. flexneri* in a volume of 1 mL. The establishment of infection was verified by the continuous detection of *S. flexneri* in feces, an increased WBC count, and obvious lymphocyte infiltration in the colon. In the control group,

rats were also starved overnight and administered with 3% $NaHCO_3$ orally 15 min before PBS administration.

We took care of and sacrificed the animals strictly according to animal welfare laws and regulations. This study was approved by the Ethical Committee of the Institute of Medical Biotechnology, Chinese Academy of Medical Sciences (approval number: IMB-201803140206).

Body temperature and body weight of rats

The body temperature (rectal temperature) and body weight of the rats were measured every morning.

Microbiological detection

For the qualitative detection, conventional bacterial culture methods were used to detect *S. flexneri* in feces. Samples were collected and inoculated onto blood agar, China blue agar plates (Jinzhang Science and Technology Development Co. Ltd, Tianjin 300190, China), and Salmonella-Shigella (bioMérieux SA, 69280 Marcy I'Etoile, France) agar plates within 2 h of collection. *S. flexneri* was identified using morphologic observation on the selective medium, combined with triple-iron slants and Vitek 2 (bioMérieux, Inc., NC, United States) detection.

For the quantitative detection of *S. flexneri*, the feces and tissues were weighed after collection and then diluted in 1 mL of PBS and homogenized with a tissue homogenizer (PRO Scientific Inc., CT, United States). After centrifugation, the supernatant was diluted and inoculated onto Salmonella-Shigella (bioMérieux SA, Marcy I'Etoile, France) agar plates. The plates were incubated at 37 °C overnight. The number of *Shigella* colonies was counted on each plate. *Shigella* was quantitatively detected in the infection and control groups at fixed time points on days 1, 3, 5, 7, 9, 13, 15, and 18.

White blood cell count

WBCs in blood samples were counted manually. A 20-μL blood sample was added to 380 μL of 2% ethanoic acid solution. Then, WBCs were counted in a hemacytometer using a conventional light microscope.

C-reactive protein and cytokine detection

Blood samples were collected by the tail vein sampling method. Serum C-reactive protein (CRP) levels were detected with a Rat CRP ELISA kit (Immunology Consultants Laboratory, Inc., OR, United States). The CRP test kit is a highly sensitive two-site ELISA for measuring CRP in rat biological samples. The assay for quantification of CRP in samples requires that each test sample be diluted before use. For the serum samples of the rats in our study, 1/12000 dilution was appropriate for detection. The dilution ratio was determined based on the data provided by the kit and the data of the preliminary experiment.

The cytokines TNF-α, IL-6, IL-10, IL-1β, IL-4, and IL-17α were measured using a commercially available MILLIPLEX MAP Kit (Rat Cytokine/Chemokine Magnetic Bead Panel, 96-Well Plate Assay, Cat. #RECYTMAG-65K, RECYMAG65K27PMX, RECYMAG-65PMX27BK; Millipore Corporation, MA, United States) according to the manufacturer's protocol. In this study, 1/2 dilution of serum was appropriate for detection. A Luminex 200 System (Luminex Corporation, TX, United States) was used for quantification.

Detection of urinary 8-oxo-dGsn and 8-oxo-Gsn levels

The manual bladder expression method was used to collect the urine samples of rats. Urine samples were stored at -80 °C. Urinary 8-oxo-dGsn and 8-oxo-Gsn were detected by the liquid chromatography with tandem mass spectrometry method as reported [13]. In brief, all urine samples were analyzed using an Agilent 1290 Infinity UHPLC instrument equipped with an Agilent 6490 triple-quadrupole mass spectrometer with a Jet Stream ESI source and iFunnel (Agilent, United States; parameters are shown in Supplementary Tables 1-3). The concentrations of 8-oxo-dGsn and 8-oxo-Gsn were then normalized by urinary creatinine to correct for the impact of water intake/excretion on urine. The results are presented as the ratio of the concentrations of nucleosides (8-oxo-dGsn and 8-oxo-Gsn) and creatinine.

Hematoxylin and eosin staining of tissues

Histopathological tests were performed using standard laboratory procedures. Tissue samples were fixed in 10% neutral-buffered formalin and embedded in paraffin. The paraffin-embedded tissue was then sliced into 4-μm-thick sections with a microtome

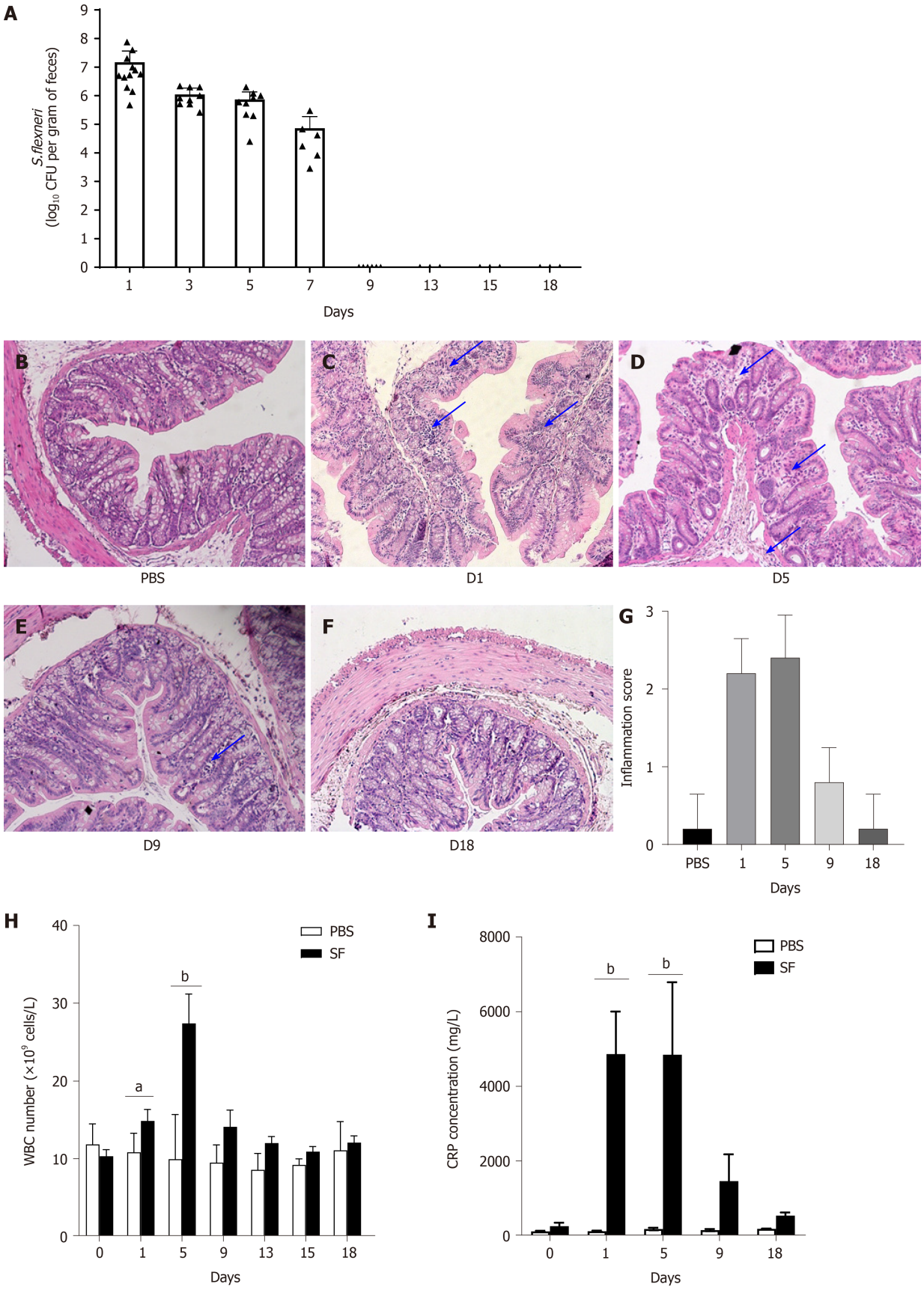


Figure 1 Pathogen colonization, intestinal inflammation, and changes in the white blood cell count and C-reactive protein level after *Shigella flexneri* infection in rats. A: Quantitative detection of *Shigella flexneri* (*S. flexneri*) in feces of Sprague-Dawley rats after infection; B-G: Representative hematoxylin & eosin (H&E) staining (100 × magnification) of colon tissue from control and *S. flexneri*-infected groups; B: H&E staining of normal colon tissue in the control group; C: H&E staining of colon tissue after *S. flexneri* infection at day 1; D: H&E staining of colon tissue on day 5; E: H&E staining of colon tissue on day 9; F: H&E staining of colon tissue on day 18; G: Inflammation scores of the control and infection groups at different time points; H: White blood cells counts in the *S.*

flexneri infection and control groups; I: C-reactive protein in the *S. flexneri* infection and control groups. [a]*P* < 0.05; [b]*P* < 0.01; and [c]*P* < 0.001. Scale bar, 100 μm. Black arrows indicate inflammatory cell infiltration. PBS: Phosphate-buffered saline; WBC: White blood cell; CRP: C-reactive protein; CFU: Colony-forming units; *S. flexneri*: *Shigella flexneri*.

and placed onto glass slides for further experiments. The tissue sections were deparaffinized with xylene, hydrated through an alcohol series, and then stained with hematoxylin and eosin (H&E). After dehydration and clearing, the mounting tissue sections were observed under a light microscope. H&E Stain kit was purchased from ZSGB-BIO (Beijing, China).

Immunohistochemical detection of 8-oxo-Gsn and 8-oxo-dGsn

Immunohistochemical staining was performed to detect the expression of 8-oxo-Gsn in the ileum, colon, liver, spleen, and brain. In brief, paraffin-embedded tissue sections were deparaffinized in xylene and rehydrated through a series of graded alcohols. Antigen retrieval was performed in citric acid buffer at 95 °C for 40 min. DNase I (TaKaRa Biotechnology Co., Ltd., Dalian, China) was added to slides to remove genomic DNA from samples. The slides were washed with 1 × PBS, and 3% hydrogen peroxide was added to eliminate endogenous peroxidases. Slides were then blocked with goat serum working solution. Primary monoclonal 15A3 antibody (ab62623; Abcam, Cambridge, United Kingdom) was added, and slides were incubated at 37 °C for 2 h (antibody dilutions: Colon, 1:700; ileum, 1:2000; liver, 1:700; spleen, 1:700; brain, 1:2000). The sections were incubated with HRP-conjugated secondary antibody (PV-6002; ZSGB-BIO) for 20 min. Coloration was performed with DAB (ZSGB-BIO), and the sections were observed under a microscope[16].

To detect the expression of 8-oxo-dGsn in tissue, tissue sections were treated with RNase A (TaKaRa Biotechnology Co., Ltd.) to remove RNA from samples. The primary monoclonal antibody was N45.1 (ab48508; Abcam). The dilutions of primary antibody were 1:2000 for the colon, 1:3000 for the ileum, 1:3000 for the liver, 1:500 for the spleen, and 1:2000 for the brain.

Statistical analysis

The SPSS 16.0 software program was used for the statistical analyses. Quantitative data are expressed as the mean ± SD and were analyzed by a *t*-test or one-way analysis of variance (ANOVA) after the normality test. Pearson's correlation coefficient (*r*) was used when comparing the linear relationship between the variables with a normal distribution. An area under the receiver operating characteristic (ROC) curve was created to assess the predictive value of urinary 8-oxo-Gsn and cytokines for the presence of infection. The results were considered significant only when $P < 0.05$.

RESULTS

Orally administered S. flexneri can provoke pathogen colonization and intestinal inflammation in rats

The body temperature showed no significant changes during the infection progression. Furthermore, the body weight increase of the rats was not significantly different between the infection and control groups.

After the intragastric administration of *S. flexneri*, serial fecal cultures were performed at fixed time points (days 1, 3, 5, 7, 9, 13, 15, and 18) in the two groups. In the control group, *S. flexneri* was undetectable during the experiment. In the infection group, *S. flexneri* was detectable in the feces of all infected rats after infection (day 1) and remained until day 7, whereas it was undetectable on day 9 (Figure 1A). In the intestine, liver, and spleen, *S. flexneri* was detectable on days 1 and/or 5. *S. flexneri* was undetectable in the brain at all time points.

Shigella can invade the colonic epithelial cells and provoke an intense inflammatory response. Compared with the control group (Figure 1B), obvious leukocyte infiltration was observed in the colonic mucosa on day 1 ($P < 0.001$ *vs* control; Figure 1C and G) and day 5 ($P < 0.001$ *vs* control; Figure 1D and G) after infection with *S. flexneri*, as detected by H&E staining. Intestinal inflammation was decreased on day 9 (Figure 1E), which was accompanied by pathogen elimination. By day 18, the colonic mucosa had returned to normal (Figure 1F).

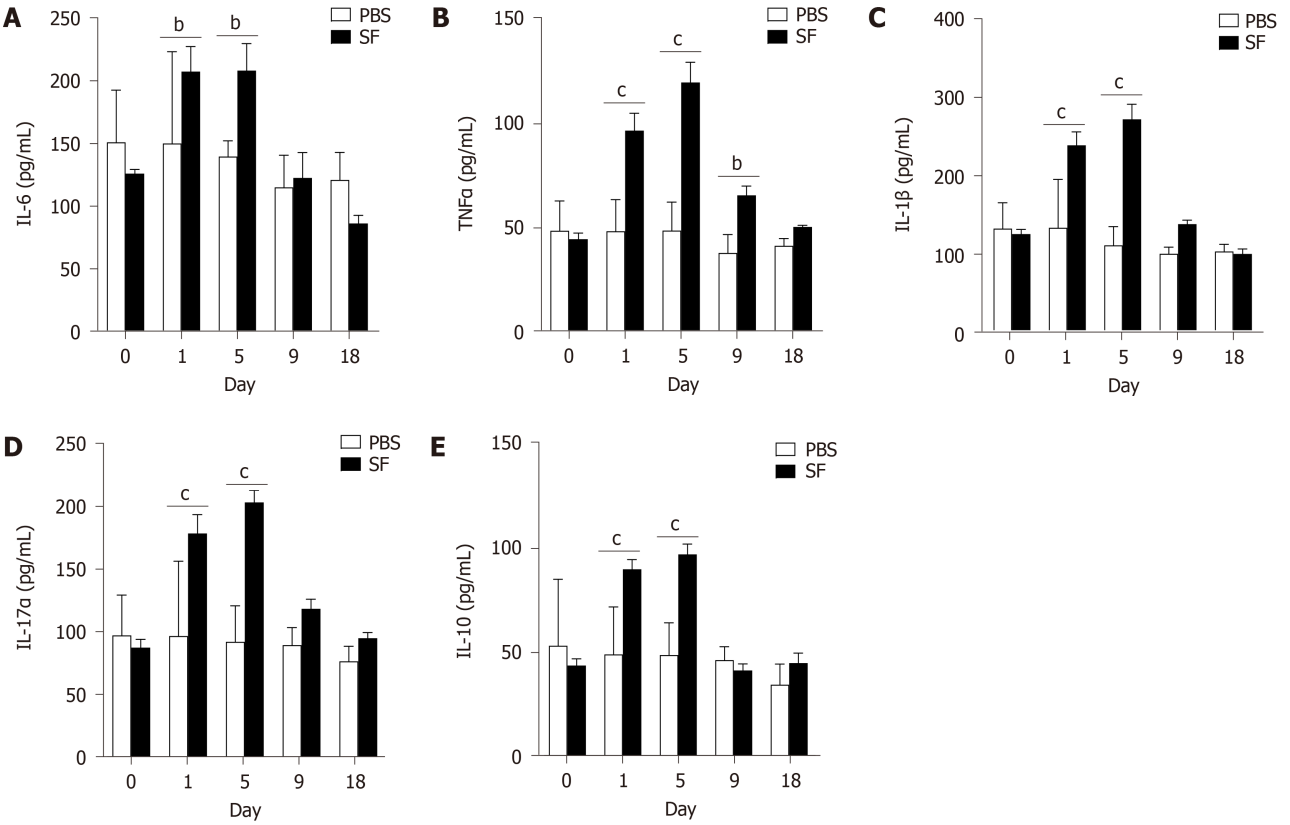


Figure 2 Inflammatory cytokines interleukin-6, tumor necrosis factor-α, interleukin-1β, interleukin-17α, and interleukin-10 detected in serum samples of *Shigella flexneri* infected rats. A: Interleukin (IL)-6; B: Tumor necrosis factor-α; C: IL-1β; D: IL-17α; E: IL-10. 0: Before infection. 1-18: The number of days after the establishment of the *Shigella flexneri* infection model. n = 12 per group on day 0 and day 1; n = 9 per group on day 5; n = 6 per group on day 9; n = 3 per group on day 18. Data are presented as the mean ± SEM. $^{a}P < 0.05$; $^{b}P < 0.01$; and $^{c}P < 0.001$ (two-tailed unpaired Student's t-test). PBS: Phosphate-buffered saline; IL: Interleukin; TNF: Tumor necrosis factor.

Changes in WBC count and CRP levels during the course of infection

The WBC count is often used to assess bacterial infections. The changes in the WBC count after the establishment of intestinal infection are shown in Figure 1H. The WBC count increased after oral exposure to *S. flexneri* and peaked on day 5 ($P < 0.0001$, $WBC_{day5} = 27.42 \pm 3.77 \times 10^9$ cells/L). The WBC count then decreased and returned to baseline after day 13. In the control group, there were no significant changes in the WBC count during the experiment.

Furthermore, it was shown that the level of CRP, an acute-phase response protein commonly used as a marker of inflammation, was significantly increased after exposure to *S. flexneri* on day 1 (CRP = $4.87 \pm 1.59 \times 10^3$ mg/L, $P = 0.005$), and the level remained high when it was detected on day 5 (CRP = $4.85 \pm 1.41 \times 10^3$ mg/L, $P = 0.002$). The CRP level then decreased and returned to baseline on day 18 (Figure 1I).

Induction of inflammatory cytokine production

The expression of IL-6, an important mediator of the acute-phase response, was significantly increased in the infection group on day 1 (207.26 ± 19.93 pg/mL, $P = 0.02$) and remained high when detected on day 5 (207.99 ± 21.49 pg/mL, $P = 0.01$; Figure 2A). After pathogen clearance on day 9, the levels of IL-6 decreased and returned to baseline.

The expression of TNF-α, a cell-signaling protein involved in systemic inflammation and one of the cytokines that make up the acute phase reaction, was also significantly increased after infection (day 1: 96.07 ± 8.29 pg/mL, $P < 0.001$) and peaked on day 5 (119.11 ± 9.69 pg/mL, $P < 0.001$). The TNF-α level then decreased and returned to the baseline at the end of the experiment (Figure 2B).

Consistent with this trend, increased levels of proinflammatory IL-1β (Figure 2C) and IL-17α (Figure 2D) were observed after infection and peaked on day 5. IL-10, a cytokine with multiple, pleiotropic effects in immunoregulation and inflammation, was also significantly produced after bacterial infection (Figure 2E).

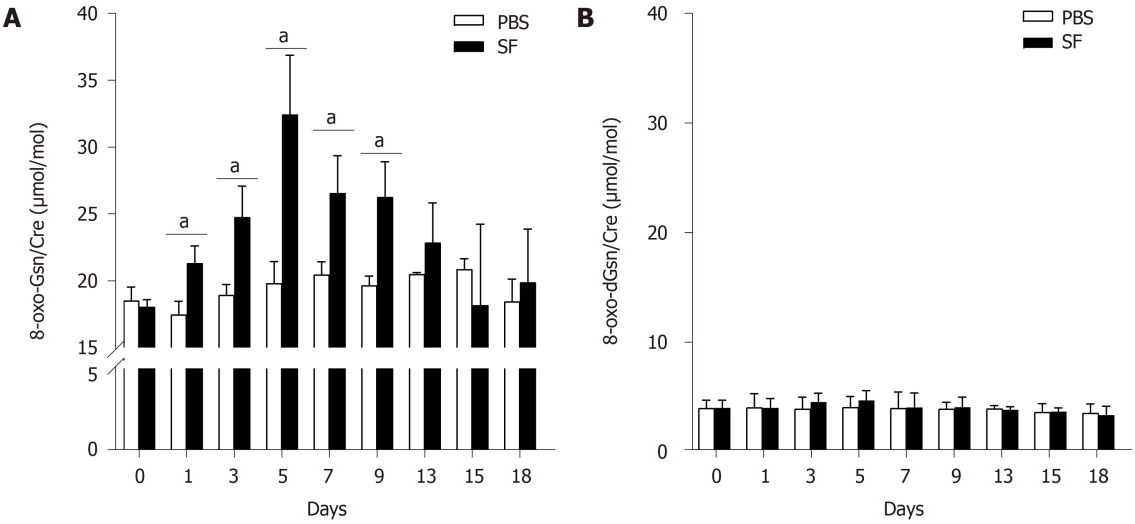


Figure 3 Liquid chromatography-tandem mass spectrometry measurement of 8-oxo-7,8-dihydroguanosine and 8-oxo-7,8-dihydro-2-deoxyguanosine in the urine of Sprague-Dawley rats. A: Urinary 8-oxo-7,8-dihydroguanosine; B: Urinary 8-oxo-7,8-dihydro-2-deoxyguanosine. *n* = 12 per group on day 0 and day 1; *n* = 9 per group on day 3 and day 5; *n* = 6 per group on day 9; *n* = 3 per group on day 13, day 15, and day 18. 0: Before infection. 1-18: The number of days after the establishment of the *Shigella flexneri* infection model. [a]*P* < 0.05. 8-oxo-Gsn: 8-oxo-7,8-dihydroguanosine; 8-oxo-dGsn: 8-oxo-7,8-dihydro-2-deoxyguanosine.

High levels of oxidized guanosine in urine after Shigella infection

8-oxo-Gsn levels were increased after oral exposure to *S. flexneri*. Compared with the control group, significantly increased levels of 8-oxo-Gsn were observed from day 1 to day 9 ($P < 0.05$), with the level peaking on day 5 ($P = 0.017$). After day 5, the level of 8-oxo-Gsn began to decrease and returned to baseline on day 15 (Figure 3A). The trends in the changes in the urinary 8-oxo-Gsn level were consistent with the changes in colonic tissue inflammation, the WBC count, and the CRP level, suggesting that urinary 8-oxo-Gsn may serve as a biomarker for assessing the severity of the infection.

In the control group, no significant changes in the 8-oxo-Gsn level were observed at any time point. For 8-oxo-dGsn, no significant changes were observed at any time point (Figure 3B).

Shigella infection leads to RNA oxidative damage in tissues

Immunohistochemical staining showed that the 8-oxo-Gsn staining intensity in the infected colon tissue was significantly altered compared with normal colon tissue ($P < 0.05$; Figure 4A). In infected colon tissues, antibodies directed against the RNA damage marker 8-oxo-Gsn produced more intense staining than uninfected colon tissues, thereby indicating a general increase in oxidative stress and RNA damage. Although 8-oxo-Gsn was more highly expressed on day 1 than on day 5, the difference between the two time points was not statistically significant. In the ileum (Figure 4B), liver (Figure 4C), spleen (Figure 4D), and brain tissues (Figure 4E), the expression of 8-oxo-Gsn was significantly higher on days 1 and day 5 than that in uninfected tissues.

The levels of the DNA damage marker 8-oxo-dGsn were significantly increased in the colon and brain tissues after infection (Figure 5A and E). In the infection group, there was no significant change in the 8-oxo-dGsn expression in the ileum, liver, or spleen (Figure 5B-D).

Correlation of 8-oxo-Gsn with WBC, CRP, and inflammatory cytokines

The 8-oxo-Gsn concentration in the urine of the infection group was positively correlated with the WBC count ($r = 0.652$, $P < 0.001$) and levels of IL-6 ($r = 0.461$, $P = 0.005$), TNF-α ($r = 0.541$, $P = 0.001$), IL-10 ($r = 0.359$, $P = 0.032$), IL-1β ($r = 0.402$, $P = 0.017$), and IL-17α ($r = 0.431$, $P = 0.009$). No significant correlation was found between 8-oxo-Gsn and CRP ($r = 0.289$, $P = 0.203$).

HE staining and fecal discharge are the gold standards for diagnosing the presence of infection. The predictive value of 8-oxo-Gsn in identifying the presence of intestinal infection was assessed using a ROC curve. The area under the ROC curve of urinary 8-oxo-Gsn was 0.750 (95%CI, 0.615–0.885, $P = 0.001$) (Figure 6A).

The predictive value of the WBC count and CRP for identifying intestinal infection was also assessed using a ROC curve. The area under the ROC of the WBC count was

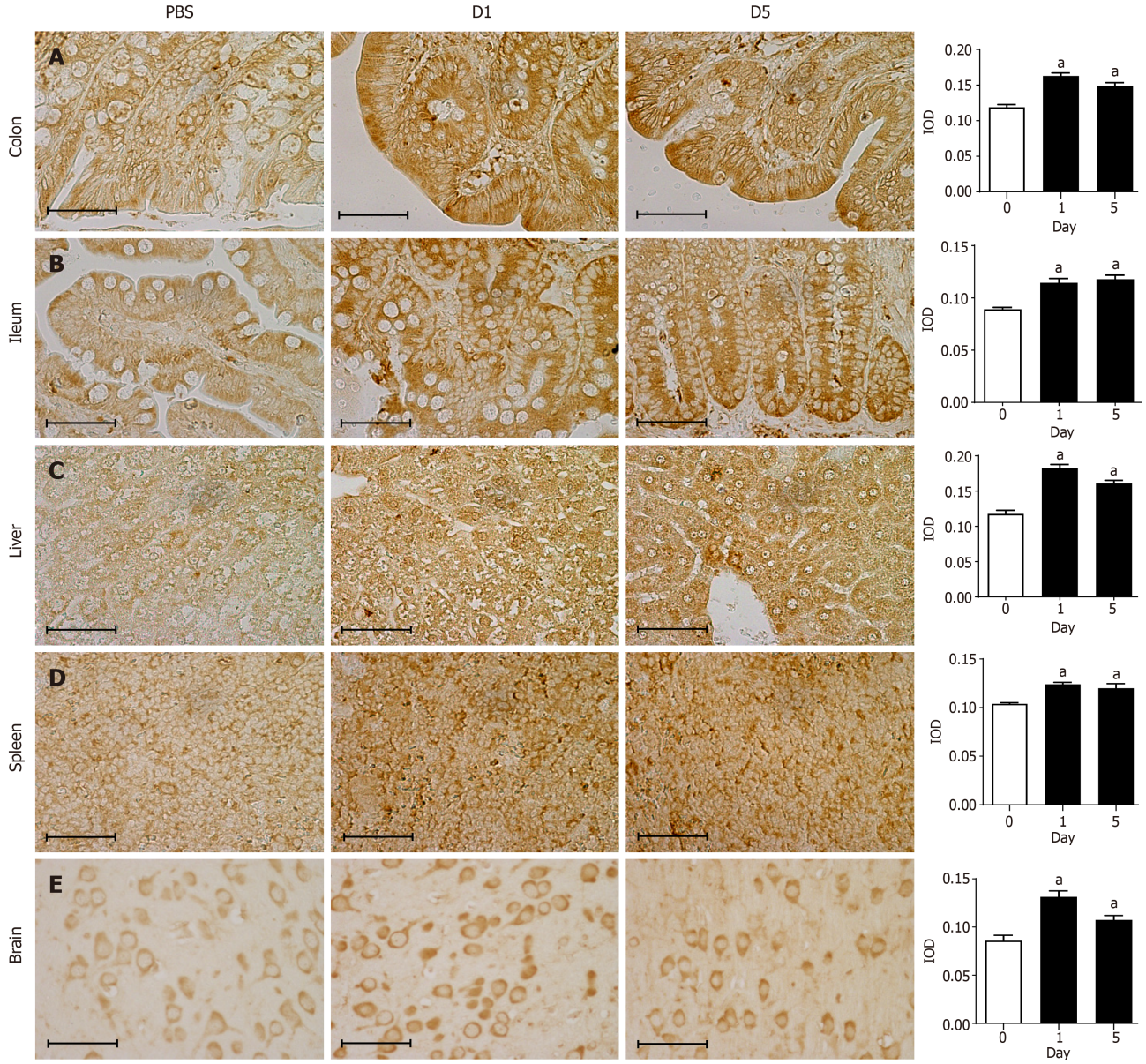


Figure 4 Immunohistochemical staining for 8-oxo-7,8-dihydroguanosine in tissues. A: Representative images showing immunohistochemical staining (400 × magnification) of 8-oxo-7,8-dihydroguanosine (8-oxo-Gsn) in paraffin-embedded colon sections from rats. Left panel images (PBS) indicate the results of the control group. Middle panel images (D1) indicate the results one day after *Shigella flexneri* (*S. flexneri*) infection. Right panel images (D5) indicate the results five days after *S. flexneri* infection; B: Immunohistochemical staining for 8-oxo-Gsn in ileum sections; C: Immunohistochemical staining for 8-oxo-Gsn in liver sections; D: Immunohistochemical staining for 8-oxo-Gsn in spleen sections; E: Immunohistochemical staining for 8-oxo-Gsn in brain sections. Histogram: The quantitative analysis of immunohistochemical staining of 8-oxo-Gsn in tissues of the infection and control groups. Scale bar, 50 μm. $^{a}P < 0.05$. The immunohistochemical images were analyzed using the Image Pro-Plus (IPP) software. The integrated optical density (IOD) is a representative parameter for assessing the immunostaining quantification in the IPP analyses, and it indicates the total amount of staining material in that area. IOD: Integrated optical density.

0.792 (95%CI, 0.674–0.911, $P < 0.001$) (Figure 6B), and that for CRP was 0.733 (95%CI, 0.544–0.923, $P = 0.014$) (Figure 6C).

For inflammatory cytokines, the area under the ROC of IL-6 (Figure 6D), TNF-α (Figure 6E), IL-1β (Figure 6F), IL-17α (Figure 6G), and IL-10 (Figure 6H) was 0.838 (95%CI, 0.698–0.978, $P = 0.003$), 0.980 (95%CI, 0.948–1.012, $P < 0.001$), 0.948 (95%CI, 0.882–1.014, $P < 0.001$), 0.964 (95%CI, 0.917–1.012, $P < 0.001$), and 0.864 (95%CI, 0.752–0.977, $P < 0.001$), respectively.

DISCUSSION

The present findings suggested that urinary 8-oxo-Gsn can be used to identify the presence of infection and to assess the severity of infection. In this study, *Shigella* infection in the gastrointestinal tract induced significant increases in the 8-oxo-Gsn

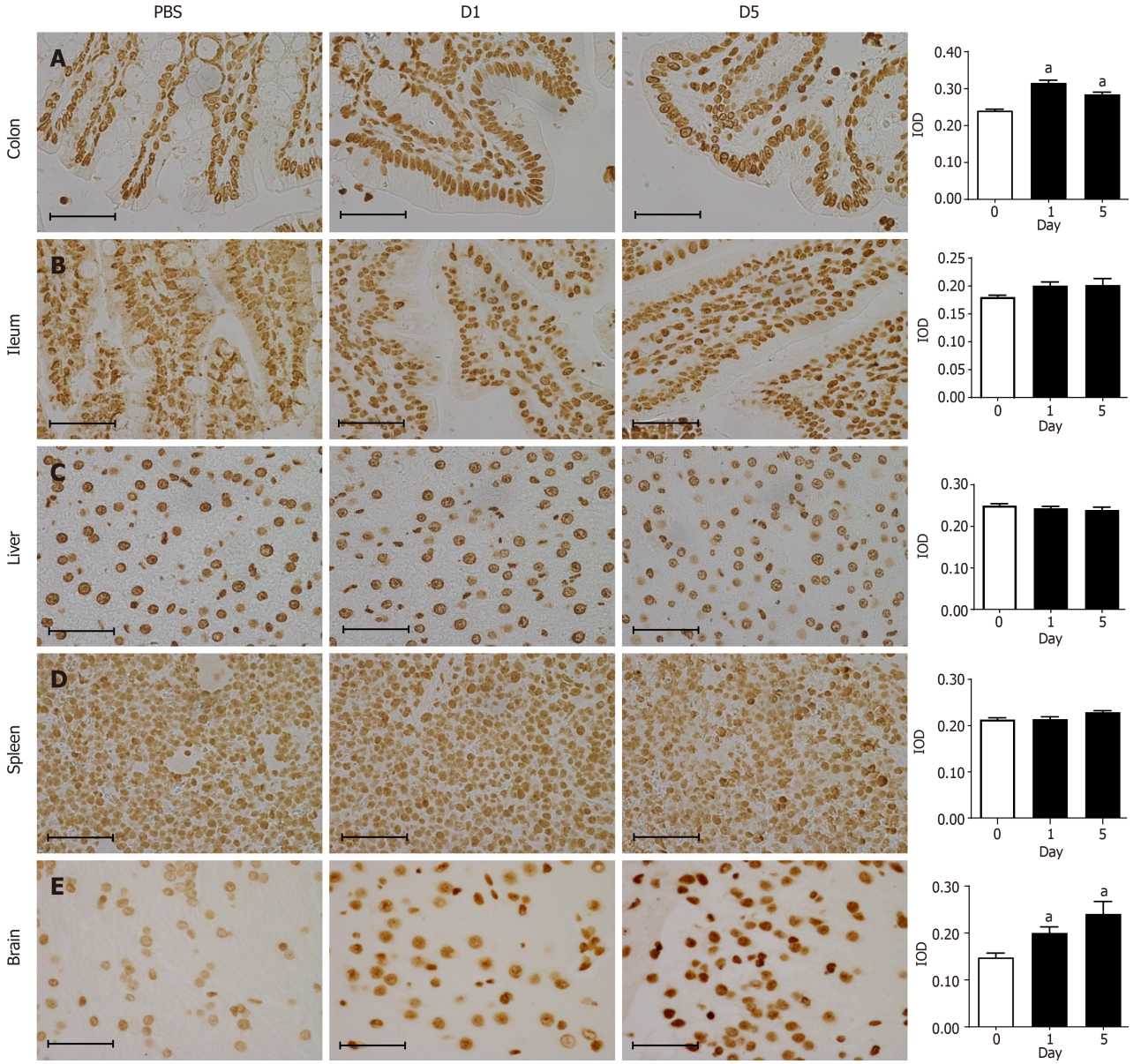


Figure 5 Immunohistochemical staining for 8-oxo-7,8-dihydro-2-deoxyguanosine in tissues. A: Representative images showing immunohistochemical staining (400 × magnification) of 8-oxo-7,8-dihydro-2-deoxyguanosine (8-oxo-dGsn; a DNA oxidative damage marker) in colon sections of rats. Left panel images (PBS) indicate the results of the control group. Middle panel images (D1) indicate the results one day after *Shigella flexneri* (*S. flexneri*) infection. Right panel images (D5) indicate the results five days after *S. flexneri* infection; B: Immunohistochemical staining for 8-oxo-dGsn in ileum sections; C: Immunohistochemical staining for 8-oxo-dGsn in liver sections; D: Immunohistochemical staining for 8-oxo-dGsn in spleen sections; E: Immunohistochemical staining for 8-oxo-dGsn in brain sections. Histogram: The quantitative analysis of immunohistochemical staining of 8-oxo-dGsn in tissues from the infection and control groups. Scale bar, 50 μm. $^{a}P < 0.05$. IOD: Integrated optical density.

concentration, the WBC count, and the CRP level. The WBC count is widely used to evaluate the severity of bacterial infections. CRP, an acute-phase protein of hepatic origin, is a non-specific marker of inflammation and one of the most sensitive acute-phase reactants.

The levels of 8-oxo-Gsn, a marker of oxidative stress, as well as the WBC count and the CRP level, which are markers of inflammation, were all increased significantly on day 1 and peaked on day 5. Following the clearance of the pathogen, the values for these biomarkers returned to the baseline level.

The correlation analysis showed that 8-oxo-Gsn was positively correlated with the WBC count. Although no significant correlation was found between 8-oxo-Gsn and CRP, the trend of the urinary 8-oxo-Gsn concentration was consistent with the changes of the WBC count and CRP level. The sharp increase in the CRP level on day 1 (20 times higher than that on day 0) may be the reason for the absence of a significant correlation. The predictive value of the 8-oxo-Gsn concentration, WBC count, and CRP level for differentiating between infection and non-infection was assessed using the

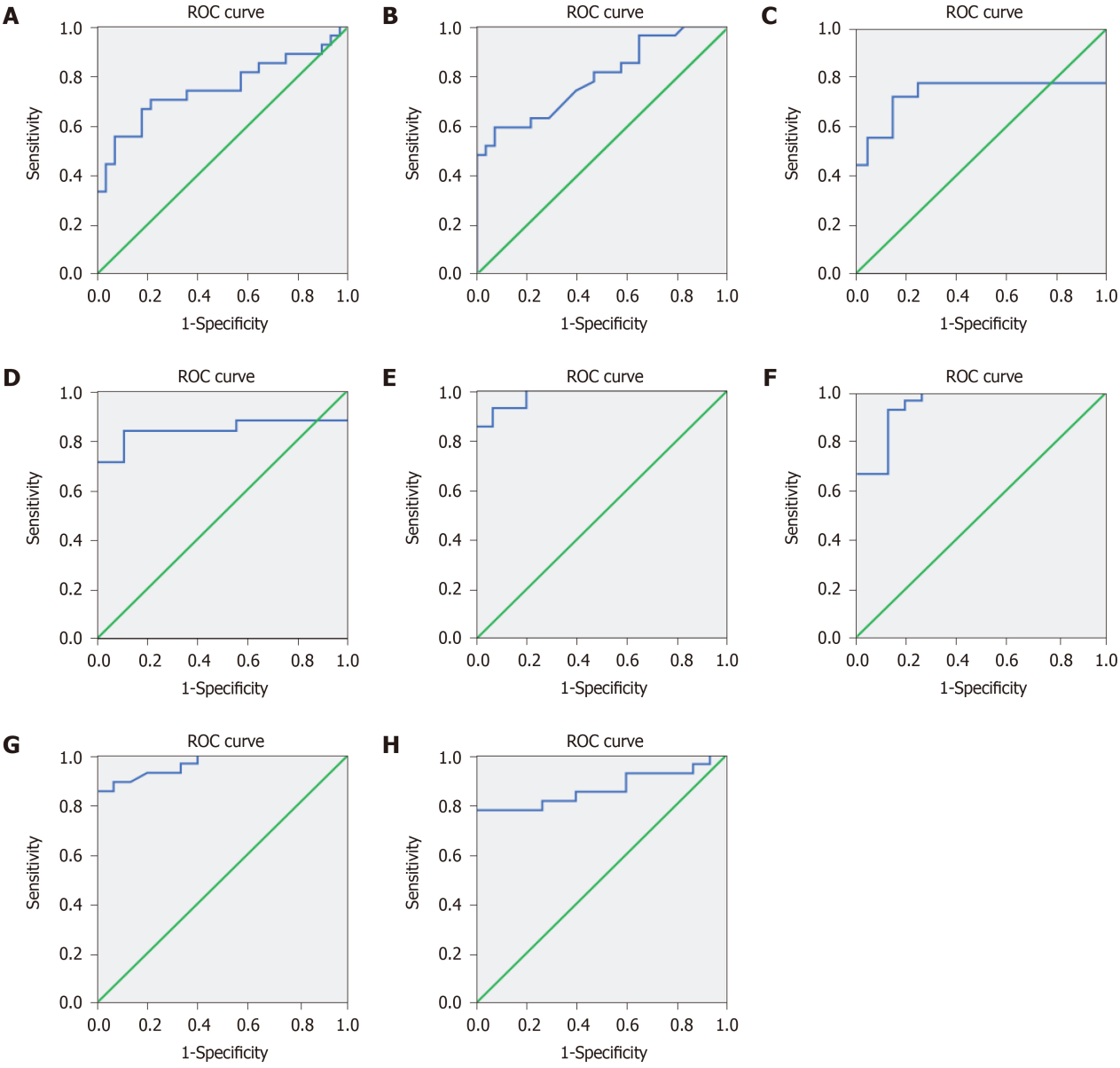


Figure 6 Receiver operator characteristic curves of 8-oxo-7,8-dihydroguanosine, white blood cell count, C-reactive protein, interleukin-6, tumor necrosis factor α, interleukin-1β, interleukin-17α, and interleukin-10 for assessing the infection status. A: Receiver operator characteristic (ROC) curve of urinary 8-oxo-7,8-dihydroguanosine; B: ROC curve of white blood cell count; C: ROC curve of C-reactive protein; D: ROC curve of interleukin (IL)-6; E: ROC curve of tumor necrosis factor α; F: ROC curve of IL-1β; G: ROC curve of IL-17α; H: ROC curve of IL-10. ROC: Receiver operator characteristic.

ROC curve. The results showed that 8-oxo-Gsn achieved a fair accuracy in classifying subjects as infected or uninfected. When the area under the ROC curve for the 8-oxo-Gsn concentration was compared to those of the WBC count and CRP level, all values ranged from 0.70 to 0.80, indicating that these diagnostic markers have a similar discrimination ability for the infection status[17]. Furthermore, urinary 8-oxo-Gsn is a noninvasive biomarker and can be measured more frequently than blood biomarkers, such as the WBC and CRP.

The immunohistochemistry results showed that in addition to intestinal tract tissue, 8-oxo-Gsn (RNA oxidative product) levels were increased in the liver, spleen, and brain tissues. Previous studies have shown that *Shigella* has a predilection to infect and colonize the large bowel[2,18]. The increased oxidative stress in other tissues might be induced by endo- or exotoxin produced by *Shigella* strains, according to previous studies[14,15,19]. Our study suggested that diarrhea caused by *Shigella* bacteria could induce a transient elevation in systemic oxidative stress.

The levels of the DNA oxidative product 8-oxo-dGsn showed no significant changes in urine, ileum, liver, or spleen tissues. The increase was only detected in the colon and brain. The results suggested that DNA oxidative damage occurred less frequently than

RNA oxidative damage in the course of acute infection. This might be because DNA molecules have a double-stranded structure, which is protected by histones and the cell nucleus[11]. All of these protections reduce the DNA oxidative damage during acute infection. Previous studies have shown that, in the course of chronic infection, DNA oxidative damage occurred more frequently, which helps promote inflammation-mediated carcinogenesis[20,21].

The present study showed that the levels of the cytokines IL-6, TNF-α, IL-1β, IL-17α and IL-10 were significantly increased after infection. Previous studies also showed that *S. flexneri* induced the release of both inflammatory (IL6, IL-8, and IL1β) and anti-inflammatory cytokines (IL-10)[22-24]. However, changes in the levels of IL-17α in *S. flexneri*-related infection have not been investigated. IL-17 has emerged as a central player in the mammalian immune system[25]. To promote inflammation, IL-17 acts in concert with IL-1β and TNF-α[26], with IL-1β being required to mediate inflammation in *S. flexneri* infection[8]. The present results suggested that *S. flexneri* infection activates inflammatory cytokines. Our findings also showed that the cytokine levels were positively correlated with the concentration of 8-oxo-Gsn, a marker of RNA oxidation, which proved again that 8-oxo-Gsn was useful as a diagnostic biomarker in infection.

CONCLUSION

In summary, during the early stage of *Shigella* infection, tissue inflammation occurs at the site of pathogen colonization, accompanied by an increase in reactive oxygen species (ROS) and the release of inflammatory cytokines. With the clearance of *Shigella*, the levels of oxidative stress markers and inflammatory cytokines decline, and the tissue inflammation recovers. The results suggested that although an increase in ROS can induce RNA oxidative damage in the colon and various tissues, this is temporary and differs from DNA oxidative damage, which occurs more frequently under conditions of chronic infection[20]. Thus, the combination of oxidative stress and inflammatory cytokines promotes infection recovery. A previous study showed that the RNA oxidative nucleic acid 8-oxoGTP increased protein variation[27]. The influence of various mutated proteins in infection, especially in the course of chronic infection, should be investigated in future studies.

ARTICLE HIGHLIGHTS

Research background

Shigella infection is a major public health concern around the world. *Shigella flexneri* (*S. flexneri*) is a major pathogen causing acute intestinal infection and is more frequently fatal than other *Shigella* species. The white blood cell (WBC) count and levels of C-reactive protein (CRP) and cytokines have always been used to evaluate the severity of *Shigella*-induced infection. Because RNA oxidation plays a substantial role in the progression of multiple diseases, the RNA oxidative product 8-oxo-7,8-dihydroguanosine (8-oxo-Gsn) may be useful as a biomarker for predicting infectious disease progression and severity.

Research motivation

There is no information regarding the diagnostic value of urinary 8-oxo-Gsn and 8-oxo-7,8-dihydro-2-deoxyguanosine (8-oxo-dGsn) in intestinal infection induced by *S. flexneri*. In addition, the correlation of blood inflammatory-related cytokines with RNA oxidative metabolites is unclear. Furthermore, the systematic tissue oxidative damage during *Shigella*-induced intestinal infection has not been investigated.

Research objectives

To determine the systemic RNA oxidative damage incurred in *S. flexneri*-induced intestinal infection and to evaluate the diagnostic value of the RNA oxidative metabolites 8-oxo-Gsn in urine.

Research methods

Sprague-Dawley rats were used to establish an acute intestinal infection model by oral gavage of *S. flexneri* strains. The CRP level was measured by ELISA, and cytokines

were detected using the MILLIPLEX MAP Kit according to the manufacturer's protocol. Hematoxylin and eosin staining was performed to detect tissue inflammation. Liquid chromatography with tandem mass spectrometry was used to determine the 8-oxo-dGsn and 8-oxo-Gsn levels in urine. Immunohistochemical staining was performed to detect the expression of 8-oxo-Gsn and 8-oxo-dGsn in the ileum, colon, liver, spleen, and brain.

Research results

Intestinal infection induced by *S. flexneri* caused an increase in inflammation-related markers in the blood [WBCs, CRP, tumor necrosis factor α (TNF-α), interleukin (IL)-6, IL-10, IL-1β, IL-4, and IL-17a] and RNA oxidative damage-related markers in the urine (8-oxo-Gsn). The urinary 8-oxo-Gsn level increased after infection and returned to the baseline level after recovery from infection. A correlation analysis showed that urinary 8-oxo-Gsn was positively correlated with the WBC count and the cytokines IL-6, TNF-α, IL-10, IL-1β, and IL-17α. The evaluation of oxidation in different tissues showed that intestinal infection caused by *S. flexneri* induced an increase in RNA oxidative damage in various tissues, including the intestine, liver, spleen, and brain.

Research conclusions

This study demonstrated that acute intestinal infection induced by *S. flexneri* not only causes RNA oxidative damage in the intestine but also other tissues as well (liver, spleen, and brain). Furthermore, the urinary metabolite of RNA oxidation 8-oxo-Gsn was shown to be useful as a diagnostic index to evaluate the infection status.

Research perspectives

Urinary 8-oxo-Gsn can be used as a noninvasive diagnostic biomarker to evaluate the severity and prognosis of infection in clinical practice.

ACKNOWLEDGEMENTS

We are grateful to the members of the Institute of Geriatrics of the Ministry of Health for advice and assistance.

REFERENCES

1 **Sheikh AF**, Moosavian M, Abdi M, Heidary M, Shahi F, Jomehzadeh N, Seyed-Mohammadi S, Saki M, Khoshnood S. Prevalence and antimicrobial resistance of *Shigella* species isolated from diarrheal patients in Ahvaz, southwest Iran. *Infect Drug Resist* 2019; **12**: 249-253 [PMID: 30774392 DOI: 10.2147/IDR.S187861]

2 **Jennison AV**, Verma NK. Shigellaflexneri infection: pathogenesis and vaccine development. *FEMS Microbiol Rev* 2004; **28**: 43-58 [PMID: 14975529 DOI: 10.1016/j.femsre.2003.07.002]

3 **Raqib R**, Lindberg AA, Wretlind B, Bardhan PK, Andersson U, Andersson J. Persistence of local cytokine production in shigellosis in acute and convalescent stages. *Infect Immun* 1995; **63**: 289-296 [PMID: 7806368 DOI: 10.1128/IAI.63.1.289-296.1995]

4 **Bando SY**, Moreno AC, Albuquerque JA, Amhaz JM, Moreira-Filho CA, Martinez MB. Expression of bacterial virulence factors and cytokines during *in vitro* macrophage infection by enteroinvasive Escherichia coli and Shigella flexneri: a comparative study. *Mem Inst Oswaldo Cruz* 2010; **105**: 786-791 [PMID: 20944993 DOI: 10.1590/s0074-02762010000600009]

5 **Bhowmick R**, Pore D, Chakrabarti MK. Outer membrane protein A (OmpA) of Shigella flexneri 2a induces TLR2-mediated activation of B cells: involvement of protein tyrosine kinase, ERK and NF-κB. *PLoS One* 2014; **9**: e109107 [PMID: 25286253 DOI: 10.1371/journal.pone.0109107]

6 **García-Weber D**, Dangeard AS, Cornil J, Thai L, Rytter H, Zamyatina A, Mulard LA, Arrieumerlou C. ADP-heptose is a newly identified pathogen-associated molecular pattern of *Shigella flexneri*. *EMBO Rep* 2018; **19** [PMID: 30455202 DOI: 10.15252/embr.201846943]

7 **Ranallo RT**, Kaminski RW, George T, Kordis AA, Chen Q, Szabo K, Venkatesan MM. Virulence, inflammatory potential, and adaptive immunity induced by Shigella flexneri msbB mutants. *Infect Immun* 2010; **78**: 400-412 [PMID: 19884336 DOI: 10.1128/IAI.00533-09]

8 **Sansonetti PJ**, Phalipon A, Arondel J, Thirumalai K, Banerjee S, Akira S, Takeda K, Zychlinsky A. Caspase-1 activation of IL-1beta and IL-18 are essential for Shigella flexneri-induced inflammation. *Immunity* 2000; **12**: 581-590 [PMID: 10843390 DOI: 10.1016/s1074-7613(00)80209-5]

9 **Halliwell B**. Why and how should we measure oxidative DNA damage in nutritional studies? *Am J Clin Nutr* 2000; **72**: 1082-1087 [PMID: 11063432 DOI: 10.1093/ajcn/72.5.1082]

10 **Poulsen HE**, Specht E, Broedbaek K, Henriksen T, Ellervik C, Mandrup-Poulsen T, Tonnesen M,

Nielsen PE, Andersen HU, Weimann A. RNA modifications by oxidation: a novel disease mechanism? *Free Radic Biol Med* 2012; **52**: 1353-1361 [PMID: 22306201 DOI: 10.1016/j.freeradbiomed.2012.01.009]

11 **Nie B**, Gan W, Shi F, Hu GX, Chen LG, Hayakawa H, Sekiguchi M, Cai JP. Age-dependent accumulation of 8-oxoguanine in the DNA and RNA in various rat tissues. *Oxid Med Cell Longev* 2013; **2013**: 303181 [PMID: 23738036 DOI: 10.1155/2013/303181]

12 **Isobe C**, Abe T, Terayama Y. Homocysteine may contribute to pathogenesis of RNA damage in brains with Alzheimer's disease. *Neurodegener Dis* 2009; **6**: 252-257 [PMID: 19940460 DOI: 10.1159/000262443]

13 **Hu JH**, Nie JJ, Gao ZX, Weng QH, Wang ZH, Li CB, Pian YY, Zhang R, Jiang ZL, Xia MM, Cai JP. Oxidative DNA and RNA damage and their prognostic values during Salmonella enteritidis-induced intestinal infection in rats. *Free Radic Res* 2018; **52**: 961-969 [PMID: 30422023 DOI: 10.1080/10715762.2018.1500022]

14 **Zhan X**, Stamova B, Sharp FR. Lipopolysaccharide Associates with Amyloid Plaques, Neurons and Oligodendrocytes in Alzheimer's Disease Brain: A Review. *Front Aging Neurosci* 2018; **10**: 42 [PMID: 29520228 DOI: 10.3389/fnagi.2018.00042]

15 **Lee MS**, Tesh VL. Roles of Shiga Toxins in Immunopathology. *Toxins (Basel)* 2019; **11** [PMID: 30970547 DOI: 10.3390/toxins11040212]

16 **Zheng JD**, Hei AL, Zuo PP, Dong YL, Song XN, Takagi Y, Sekiguchi M, Cai JP. Age-related alterations in the expression of MTH2 in the hippocampus of the SAMP8 mouse with learning and memory deterioration. *J Neurol Sci* 2009; **287**: 188-196 [PMID: 19735921 DOI: 10.1016/j.jns.2009.07.027]

17 **Li F**, He H. Assessing the Accuracy of Diagnostic Tests. *Shanghai Arch Psychiatry* 2018; **30**: 207-212 [PMID: 30858674 DOI: 10.11919/j.issn.1002-0829.218052]

18 **Schroeder GN**, Hilbi H. Molecular pathogenesis of Shigella spp.: controlling host cell signaling, invasion, and death by type III secretion. *Clin Microbiol Rev* 2008; **21**: 134-156 [PMID: 18202440 DOI: 10.1128/CMR.00032-07]

19 **Obata F**, Tohyama K, Bonev AD, Kolling GL, Keepers TR, Gross LK, Nelson MT, Sato S, Obrig TG. Shiga toxin 2 affects the central nervous system through receptor globotriaosylceramide localized to neurons. *J Infect Dis* 2008; **198**: 1398-1406 [PMID: 18754742 DOI: 10.1086/591911]

20 **Ohnishi S**, Ma N, Thanan R, Pinlaor S, Hammam O, Murata M, Kawanishi S. DNA damage in inflammation-related carcinogenesis and cancer stem cells. *Oxid Med Cell Longev* 2013; **2013**: 387014 [PMID: 24382987 DOI: 10.1155/2013/387014]

21 **Tsukiyama-Kohara K**. Role of oxidative stress in hepatocarcinogenesis induced by hepatitis C virus. *Int J Mol Sci* 2012; **13**: 15271-15278 [PMID: 23203124 DOI: 10.3390/ijms131115271]

22 **Marteyn B**, Gazi A, Sansonetti P. Shigella: a model of virulence regulation in vivo. *Gut Microbes* 2012; **3**: 104-120 [PMID: 22356862 DOI: 10.4161/gmic.19325]

23 **Liu G**, Pilla G, Tang CM. Shigella host: Pathogen interactions: Keeping bacteria in the loop. *Cell Microbiol* 2019; **21**: e13062 [PMID: 31134722 DOI: 10.1111/cmi.13062]

24 **Samandari T**, Kotloff KL, Losonsky GA, Picking WD, Sansonetti PJ, Levine MM, Sztein MB. Production of IFN-gamma and IL-10 to Shigella invasins by mononuclear cells from volunteers orally inoculated with a Shiga toxin-deleted Shigella dysenteriae type 1 strain. *J Immunol* 2000; **164**: 2221-2232 [PMID: 10657678 DOI: 10.4049/jimmunol.164.4.2221]

25 **Onishi RM**, Gaffen SL. Interleukin-17 and its target genes: mechanisms of interleukin-17 function in disease. *Immunology* 2010; **129**: 311-321 [PMID: 20409152 DOI: 10.1111/j.1365-2567.2009.03240.x]

26 **Gaffen SL**. An overview of IL-17 function and signaling. *Cytokine* 2008; **43**: 402-407 [PMID: 18701318 DOI: 10.1016/j.cyto.2008.07.017]

27 **Dai DP**, Gan W, Hayakawa H, Zhu JL, Zhang XQ, Hu GX, Xu T, Jiang ZL, Zhang LQ, Hu XD, Nie B, Zhou Y, Li J, Zhou XY, Zhang TM, He Q, Liu DG, Chen HB, Yang N, Zuo PP, Zhang ZX, Yang HM, Wang Y, Wilson SH, Zeng YX, Wang JY, Sekiguchi M, Cai JP. Transcriptional mutagenesis mediated by 8-oxoG induces translational errors in mammalian cells. *Proc Natl Acad Sci USA* 2018; **115**: 4218-4222 [PMID: 29610342 DOI: 10.1073/pnas.1718363115]

World Journal of Gastroenterology

Submit a Manuscript: https://www.f6publishing.com

World J Gastroenterol 2021 October 7; 27(37): 6262-6276

DOI: 10.3748/wjg.v27.i37.6262

ISSN 1007-9327 (print) ISSN 2219-2840 (online)

ORIGINAL ARTICLE

Retrospective Cohort Study

Hepatitis B virus persistent infection-related single nucleotide polymorphisms in HLA regions are associated with viral load in hepatoma families

Ai-Ru Hsieh, Cathy S J Fann, Hung-Chun Lin, Jennifer Tai, Sen-Yung Hsieh, Dar-In Tai

ORCID number: Ai-Ru Hsieh 0000-0003-3900-9101; Cathy S J Fann 0000-0001-9025-2276; Hung-Chun Lin 0000-0002-6978-5702; Jennifer Tai 0000-0002-0500-8867; Sen-Yung Hsieh 0000-0002-1723-7261; Dar-In Tai 0000-0003-1054-1583.

Author contributions: Tai DI is the guarantor and designed the study; Hsieh AR and Fann CSJ participated in the statistical analysis and data interpretation; Lin HC, Tai J, Hsieh SY and Tai DI participated in the data acquisition; Fann CSJ revised the manuscript critically for important intellectual content.

Supported by Chang Gung Memorial Hospital, No. CMRPG3C0701; and National Science Council, No. NSC101-2314-B-182A-025-MY3 and No. MOST 107-2314-B-039-059.

Institutional review board statement: The study was approved by the institutional review board of Chang Gung Memorial Hospital, Taiwan (IRB 104-2596).

Informed consent statement: Written informed consent was obtained from all participants before the study. All experiments

Ai-Ru Hsieh, Department of Statistics, Tamkang University, New Taipei City 25137, Taiwan

Cathy S J Fann, Institute of Biomedical Sciences, Academia Sinica, Nankang, Taipei 11529, Taiwan

Hung-Chun Lin, Jennifer Tai, Sen-Yung Hsieh, Dar-In Tai, Division of Hepatology, Department of Gastroenterology and Hepatology, Chang Gung Memorial Hospital, Linkou Medical Center, Taoyuan 33305, Taiwan

Corresponding author: Dar-In Tai, MD, PhD, Professor, Division of Hepatology, Department of Gastroenterology and Hepatology, Chang Gung Memorial Hospital, Linkou Medical Center, No. 5 Fuxing Street, Guishan District, Taoyuan 33305, Taiwan. tai48978@cgmh.org.tw

Abstract

BACKGROUND

Genome-wide association studies from Asia indicate that HLA-DP and HLA-DQ loci are important in persistent hepatitis B virus (HBV) infections. One of the key elements for HBV-related carcinogenesis is persistent viral replication and inflammation.

AIM

To examine genetic and nongenetic factors with persistent HBV infection and viral load in families with hepatocellular carcinoma (HCC).

METHODS

The HCC families included 301 hepatitis B surface antigen (HBsAg) carriers and 424 noncarriers born before the nationwide vaccination program was initiated in 1984. Five HBV-related single nucleotide polymorphisms (SNPs) — rs477515, rs9272105, rs9276370, rs7756516, and rs9277535 — were genotyped. Factors associated with persistent HBV infection and viral load were analyzed by a generalized estimating equation.

RESULTS

In the first-stage persistent HBV study, all SNPs except rs9272105 were associated with persistent infection. A significantly higher area under the reciprocal operating characteristic curve for nongenetic factors *vs* genetic factors ($P < 0.001$)

suggests that the former play a major role in persistent HBV infection. In the second-stage viral load study, we added 8 HBsAg carriers born after 1984. The 309 HBsAg carriers were divided into low (n = 162) and high viral load (n = 147) groups with an HBV DNA cutoff of 10^5 cps/mL. Sex, relationship to the index case, rs477515, rs9272105, and rs7756516 were associated with viral load. Based on the receiver operating characteristic curve analysis, genetic and nongenetic factors affected viral load equally in the HCC family cohort (P = 0.3117).

CONCLUSION

In these east Asian adults, the mechanism of persistent HBV infection-related SNPs was a prolonged viral replication phase.

Key Words: Generalized estimating equation; Genetic polymorphism; Genome-wide association study; Hepatitis B surface antigen; Hepatitis B virus; Replication

©The Author(s) 2021. Published by Baishideng Publishing Group Inc. All rights reserved.

Core Tip: Hepatitis B virus (HBV)-related single nucleotide polymorphisms (SNPs) have been identified in East Asians. We evaluated five SNPs and nongenetic factors associated with HBV infection in a hepatocellular carcinoma family cohort. The factors were correlated with hepatitis B surface antigen (HBsAg) in the first-stage and with HBV viral load in the second-stage. The SNPs, sex, generation, and index case HBsAg contributed to persistent HBV infection. Neonatal tolerance and SNPs in the HLA loci were both independently associated with persistent HBV infection. A prolonged HBV replication phase in parents could be the main mechanism of persistent HBV infection in children in East Asia.

Citation: Hsieh AR, Fann CSJ, Lin HC, Tai J, Hsieh SY, Tai DI. Hepatitis B virus persistent infection-related single nucleotide polymorphisms in HLA regions are associated with viral load in hepatoma families. *World J Gastroenterol* 2021; 27(37): 6262-6276
URL: https://www.wjgnet.com/1007-9327/full/v27/i37/6262.htm
DOI: https://dx.doi.org/10.3748/wjg.v27.i37.6262

INTRODUCTION

Chronic hepatitis B is a global disease, with the highest prevalence in Africa and Asia [1,2]. Hepatitis B virus (HBV) is highly infectious[3,4], and those who are infected early in life are likely to develop a persistent infection[5-7]. Intra-familial spread of infection is common, resulting in the clustering of chronic hepatitis B surface antigen (HBsAg) carriers and hepatocellular carcinoma (HCC) in families[8-10]. Recent genome-wide association studies (GWASs) in Japan, Korea, Saudi Arabia, China, and Taiwan have consistently shown that single nucleotide polymorphisms (SNPs) at the HLA-DP and HLA-DQ loci play important roles in persistent HBV infection[11-19]. However, risk alleles of HBV-related SNPs are not present in the majority of Africans[20,21], so the high prevalence of HBsAg carriers in Africa cannot be completely explained by the SNPs.

It is well known that clearance of the hepatitis B e antigen (HBeAg) occurs earlier in African than in Asian HBsAg carriers[22-25]. In east Asia, the annual HBeAg seroconversion rate is < 2% in children younger than 3 years of age and around 5% in children older than 3 years of age[22,23]. On the contrary, an HBeAg annual clearance rate of 14%-16% has been found in Euro-Mediterranean and African children[24,25]. HBeAg clearance is associated with a decreased viral load and results in a decrease of perinatal infections and the development of chronic persistent HBV infection[7,23]. We propose that persistent HBV infection-related SNPs may be one of the reasons for the prolonged HBV replication phase in east Asians. To evaluate this hypothesis, we analyzed the HBV-related SNP and demographic data obtained from HCC families. HCC families are known to have higher perinatal transmission and a longer HBV replication phase than the general population[9,10]. We expect that the genetic and nongenetic factors characteristic of HCC families may help us to understand the

and data comparisons were carried out in compliance with relevant laws and guidelines, and in accord with the ethical standards of the Declaration of Helsinki.

Conflict-of-interest statement: The authors declare that they have no conflicting interests.

Data sharing statement: No additional data are available.

STROBE statement: The authors have read the STROBE Statement-checklist of items, and the manuscript was prepared and revised according to the STROBE Statement-checklist of items.

Open-Access: This article is an open-access article that was selected by an in-house editor and fully peer-reviewed by external reviewers. It is distributed in accordance with the Creative Commons Attribution NonCommercial (CC BY-NC 4.0) license, which permits others to distribute, remix, adapt, build upon this work non-commercially, and license their derivative works on different terms, provided the original work is properly cited and the use is non-commercial. See: http://creativecommons.org/Licenses/by-nc/4.0/

Manuscript source: Invited manuscript

Specialty type: Gastroenterology and hepatology

Country/Territory of origin: Taiwan

Peer-review report's scientific quality classification

Grade A (Excellent): A
Grade B (Very good): 0
Grade C (Good): 0
Grade D (Fair): 0
Grade E (Poor): 0

Received: April 8, 2021
Peer-review started: April 8, 2021
First decision: June 26, 2021
Revised: July 6, 2021
Accepted: September 1, 2021
Article in press: September 1, 2021
Published online: October 7, 2021

P-Reviewer: Wang L

S-Editor: Gao CC
L-Editor: A
P-Editor: Liu JH

nature of persistent HBV infection.

MATERIALS AND METHODS

Ethics statement

Our study was approved by the institutional review board of Chang Gung Memorial Hospital, Taiwan (IRB 104-2596). Written informed consent was obtained from all participants. All experiments and data comparisons were carried out in compliance with relevant laws and guidelines, and complied with the ethical standards of the Declaration of Helsinki.

Study participants

Patients with HCC who were diagnosed at Chang Gung Memorial Hospital, Lin-Kou Medical Center were included as index cases. From 2003 to 2007, relatives of the patients were prospectively invited to complete a liver disease survey. The details of the survey can be seen in our previous report[10]. Briefly, after confirmation of their relation to the index HCC patient, the relatives received a structured questionnaire and underwent assessments of their liver biochemistry, alpha-fetoprotein, viral markers, and HBV genotyping. Peripheral blood samples were collected for host genome analysis.

Study size

We calculated sample sizes and statistical power to detect genetic effects in the study. The calculation considered the impact the minor allele frequency (MAF, from 0.1 to 0.4), odds ratio (OR, from 1.05 to 3), statistical power (from 0.5 to 0.9) and measurement error (type I error = 0.05) have on sample size. Power calculations were performed with QUANTO power calculator, version 1.2.4 (https://preventivemedicine.usc.edu/download-quanto/).

SNP selection and genotyping

Four genetic variants (rs477515, rs9276370, rs7756516, rs9277535) associated with persistent HBV infection that were previously identified[17] were included in the analysis. One additional HCC-related SNP (rs9272105) previously identified in China was also included[26]. Genomic DNA was extracted from peripheral blood cells using MagNA Pure LC DNA isolation kits with automated DNA isolation instruments (MagNA Pure LC II; Roche Diagnostics, Mannheim, Germany). Triple-SNP (rs477515, rs9272105, rs9277535) genotyping was performed with *Taq*Man Genotyping assays (Applied Biosystems, Foster City, CA, United States). Two SNPs (rs7756516, rs9276370) were genotyped with a Sequenom MassARRAY System (Sequenom, San Diego, CA, United States). The *Taq*Man assays were carried out by Vita Genomics (New Taipei City, Taiwan), and the Sequenom MassARRAY assays were performed by the Academia Sinica National Genotyping Center (Taipei, Taiwan). The overall genotype call rate was > 95%.

Statistical analysis

The statistical analyses were performed with SAS version 8.2 for UNIX (SAS Institute, Cary, NC, United States), PLINK (http://zzz.bwh.harvard.edu/plink/) (http://zzz.bwh.harvard.edu/plink/summary.shtml), R 2.15.1 (http://www.r-project.org/), and the Family-Based Association Test software (http://www.biostat.harvard.edu/~fbat/fbat.htm)[27]. A two-tailed P value < 0.05 was considered statistically significant. All associations were controlled for confounding factors. SNP data was quality controlled using the following criteria: (1) Call rate > 0.95; (2) MAF > 0.01; and (3) Deviation from Hardy-Weinberg equilibrium P > 0.001.

Individual locus analysis: We assessed the association of SNPs with persistent HBV infection or viral load in an additive genetic model using univariate and multivariate logistic regression of the data from unrelated male participants. In the family analysis, relatives included individuals living in the same household. First- and second-stage analyses were conducted with a generalized estimating equation (GEE) that included data correlated with a binary response (*e.g.*, to HBsAg status and HBV DNA level) using an exchangeable working correlation structure[28,29]. Univariate and multivariate analysis of the first- and second-stage results were assessed using the GEE method combined with the PROC GENMOD procedure in SAS 9.3 (SAS Institute). ORs were reported with 95% confidence intervals (CIs).

Weighted genetic risk score calculation: The weighted genetic risk score (WGRS) was calculated for the SNPs that were significantly associated with persistent infection or viral load. We assumed that each SNP was independently associated with risk according to an additive genetic model. The WGRS was calculated by multiplying the number of risk alleles at each polymorphic locus (0, 1, or 2) by each person for the corresponding relative logarithm of the OR (w_i) from the multivariate individual locus analysis and rescaling it with the factor $m/\sum_i w_i$, as follows: $WGRS = (m/\sum_i w_i) \cdot \sum w_i n_i$, where m is the number of statistically significant SNPs and n_i is the number of risk alleles for SNPi[30]. We divided the continuous WGRS into quartiles (Q1-4) and compared the risks among them.

Evaluation of genetic and nongenetic factors: We analyzed factors associated with persistent HBV infection or viral load using the logistic regression model unrelated participants and the GEE method for family data. Three prediction models were used: (1) The genetic model included only SNPs and WGRS; (2) The nongenetic model included only demographic data; and (3) The mixed model included both genetic and nongenetic variables. The contribution of the WGRS was evaluated using the area under the receiver operating characteristic curve (AUC), net reclassification improvement (NRI) method[31], and integrated discrimination improvement (IDI)[32] with the prediction model with and without the WGRS. To assess the demographic impact of including the WGRS in the model, an AUC of 0.5 indicated no discrimination and an AUC of 1 indicated perfect discrimination. The NRI indicated the proportion of subjects reclassified correctly (NRI > 0) or incorrectly (NRI < 0) into the various risk categories. An IDI > 0 indicated a statistically significant prediction of improvement as a result of adding variables to the model.

RESULTS

The HCC family cohort included 835 participants (Figure 1), of whom 301 HBsAg-positive and 424 of HBsAg-negative family members were selected for the first-stage HBV infection-persistence analysis. We excluded those born after the nationwide vaccination program was initiated in 1984. In the second-stage viral load study, we added 8 HBsAg carriers born after 1984 (Figure 1). A cohort of 309 HBsAg carriers was divided into high (n = 147) and low (n = 162) viral load groups using an HBV DNA cutoff of 10^5 cps/mL.

First stage: Factors associated with persistent HBV infection

Risk factors associated with being an HBsAg carrier were identified in the first-stage analysis. Demographic factors, which included age, sex, index case sex, relation to the index case, index HBsAg, and maternal HBsAg, are shown in Table 1. Age (OR = 1.018, P = 0.0013), sex (OR = 1.641, P = 0.0001), relation to the index case (OR = 3.203, P < 0.0001; index generation compared with children and grandchildren), index HBsAg (OR = 4.913, P < 0.0001), maternal HBsAg (OR = 3.31, P < 0.0001), and serum glutamic pyruvic transaminase (SGPT) (OR = 1.017, P < 0.0001) were significantly associated with persistent HBV infection. The associations remained significant after controlling for sex and age.

The SNPs rs477515 (OR = 1.377, P = 0.0274), rs9276370 (OR = 1.790, P = 0.0012), rs7756516 (OR = 1.654, P = 0.0048), and rs9277535 (OR = 1.519, P = 0.0004) were significantly associated with chronic HBV infection (Table 1). The ORs remained statistically significant after controlling for sex and age. HCC families carrying more risk alleles had an increased OR (Table 2, upper panel). Compared with participants with a WGRS in Q1, those with scores in Q2 and Q3–4 had higher risks of HBsAg positivity (Q2 OR = 1.878, P = 0.0014; Q3-4 OR = 2.538, P < 0.0001).

Results of the multivariate GEE analysis of the risk factors associated with persistent HBV infection are shown in Table 3. In the nongenetic model, sex, index generation, and index and maternal index HBsAg were associated with persistent HBV infection. In the genetic model, rs9277535 and WGRS were associated with persistent HBV infection. In the mixed model, all the risk factors were significant (male sex P = 0.0205; index generation P = 0.0001; index HBsAg P < 0.0001; maternal HBsAg P = 0.0072; rs9277535 P = 0.0029; WGRS P = 0.0012; Table 3).

The AUC for persistent HBV infection (Table 3) was 0.786 (P < 0.0001) in the nongenetic model and 0.620 (P < 0.0001) in the genetic model. Although the SNPs were identified by GWAS in unrelated subjects, the AUC data suggest that nongenetic factors were more important than genetic factors for the development of persistent

Table 1 Factors associated with persistent hepatitis B virus infection in the hepatocellular carcinoma family cohort

	HBsAg					
Category	**Positive**	**Negative**	**OR (95%CI)**	**Adjusted OR (95%CI)[1]**	***P* value**	**Adjusted *P* value[2]**
Total family members, *n*	301	424				
Age in yr, mean ± SD	44.23 ± 13.84	41.25 ± 14.97	1.018 (1.007-1.03)	1.017 (1.006-1.028)	0.0013	0.0030
Sex, *n* (%)						
Male	182 (60.47)	203 (47.88)	1.641 (1.279-2.107)	1.57 (1.225-2.011)	0.0001	0.0004
Female	119 (39.53)	221 (52.12)	1	1		
Index sex, *n* (%)						
Male	226 (75.08)	309 (72.88)	1.207 (0.726-2.006)	1.147 (0.681-1.93)	0.4685	0.6061
Female	75 (24.92)	115 (27.12)	1	1		
Relation to index, *n* (%)						
Children and grandchildren	146 (48.50)	319 (75.24)	1	1		
Parent generation	7 (2.33)	15 (3.54)	0.7 (0.302-1.622)	1.472 (0.533-4.065)	0.4059	0.4559
Index generation	148 (49.17)	90 (21.23)	3.203 (2.282-4.498)	4.861 (2.923-8.083)	< 0.0001	< 0.0001
Index status, *n* (%)						
HBsAg-	70 (23.26)	257 (60.61)	1	1		
HBsAg+	231 (76.74)	167 (39.39)	4.913 (3.209-7.522)	5.928 (3.747-9.377)	< 0.0001	< 0.0001
Mother's status, *n* (%)						
HBsAg-	85 (28.24)	239 (56.37)	1	1		
HBsAg+	91 (30.23)	45 (10.61)	3.31 (1.894-5.783)	3.296 (1.891-5.746)	< 0.0001	< 0.0001
Unknown	125 (41.53)	140 (33.02)	2.305 (1.568-3.39)	1.87 (1.202-2.91)	<.0001	0.0055
SGPT, mean ± SD	49.98 ± 65.39	25.83 ± 24.92	1.017 (1.011-1.022)	1.015 (1.009-1.020)	< 0.0001	< 0.0001
rs477515 (MAF = 0.1552) Chr6: 32601914[1]						
TT (reference)	5 (1.66)	20 (4.72)				
TC	59 (19.60)	116 (27.36)				
CC	237 (78.74)	288 (67.92)	1.377 (1.036-1.831)	1.38 (1.034-1.842)	0.0274	0.0285
rs9272105 (MAF = 0.4282) Chr6: 32632222[1]						
GG (reference)	54 (17.94)	84 (19.86)				
GA	137 (45.51)	207 (48.94)				
AA	110 (36.54)	132 (31.21)	1.054 (0.859-1.293)	1.031 (0.844-1.261)	0.6126	0.7639
rs9276370 (MAF = 0.1159) Chr6: 32739518[1]						
GG (reference)	3 (1.00)	13 (3.07)				
GT	39 (12.96)	97 (22.88)				
TT	259 (86.05)	314 (74.06)	1.790 (1.258-2.547)	1.759 (1.228-2.519)	0.0012	0.0021
rs7756516 (MAF = 0.1166) Chr6: 32756140[1]						
CC (reference)	3 (1.00)	13 (3.07)				
CT	42 (13.95)	95 (22.41)				
TT	256 (85.05)	316 (74.53)	1.654 (1.166-2.346)	1.612 (1.123-2.313)	0.0048	0.0096
rs9277535 (MAF = 0.3234) Chr6: 33087084[1]						
AA (reference)	21 (6.98)	61 (14.39)				
AG	114 (37.87)	191 (45.05)				
GG	166 (55.15)	172 (40.57)	1.519 (1.204-1.916)	1.493 (1.182-1.886)	0.0004	0.0008

[1]Genome build GRCH38.
[2]Adjusted for sex and age. HBsAg: Hepatitis B surface antigen; MAF: Minor allele frequency; SGPT: Serum glutamic pyruvic transaminase; CI: Confidence interval; OR: Odds ratio.

Table 2 Cumulative effect of the genetic-risk alleles associated with hepatitis B viral load or persistent hepatitis B virus infection

Study	WGRS quartile	OR (95%CI)	*P* value
Family first stage: Persistent HBV infection	Q1 (WGRS ≤ 6.166)	1	
	Q2 (WGRS = 6.166-7.083)	1.878 (1.277-2.762)	0.0014
	Q3,4 (WGRS > 7.083)[1]	2.538 (1.742-3.698)	< 0.0001
	Cochran-Armitage trend test		< 0.0001
Family second stage: Viral load	Q1 (WGRS ≤ 4.583)	1	
	Q2 (WGRS = 4.583-5.291)	2.204 (1.253-3.878)	0.0061
	Q3,4 (WGRS > 5.291)[2]	3.156 (1.780-5.595)	< 0.0001
	Cochran-Armitage trend test		< 0.0001

[1]The number of hepatitis B surface antigen negative individuals in Q4 was < 5, so Q3 and Q4 were combined.
[2]The number of individuals with hepatitis B virus DNA < 10^5 cps/mL in Q4 was < 1, so Q3 and Q4 were combined. The cumulative effect was calculated from: Four single nucleotide polymorphisms (SNPs) (rs9272105, rs9276370, rs7756516, and s9277535) in unrelated male hepatitis B surface antigen (HBsAg) carriers; four SNPs (rs477515, rs9276370, rs7756516, and rs9277535) in the first-stage hepatocellular carcinoma (HCC) family cohort analysis; and three SNPs (rs477515, rs9272105, and rs7756516) in HBsAg-positive carriers in the second-stage HCC family cohort analysis. CI: Confidence interval; OR: Odds ratio; Q: Quartile; WGRS: Weighted genetic risk score; HBV: Hepatitis B virus.

HBV infection (P < 0.0001; Figure 2). The combination of genetic and nongenetic factors resulted in an AUC of 0.795 (P < 0.0001; Figure 2 and Table 3). The IDI was 0.017 (95%CI: 0.009-0.026, P < 0.0001) and the NRI was 0.330 (95%CI: 0.192-0.467, P < 0.0001). The IDI and NRI values indicated statistically significant predicted improvement in the mixed, relative to the nongenetic model (Table 3).

Second stage: Factors associated with HBV viral load in HBsAg-positive HCC families

Factors associated with the HBV viral load were evaluated in HBsAg-positive families (Table 4). In that group, male sex (OR = 1.922, P = 0.0078), relation to the index case (OR = 2.033, P = 0.0029), index HBsAg (OR = 2.508, P = 0.0036), and SGPT (OR = 1.010, P = 0.0105) were significantly associated with the HBV viral load. The associations remained statistically significant after controlling for sex. HBV genotypes were also evaluated in HCC families, and of the participants with known HBV genotypes, the prevalence of genotype C was higher in those with high viral loads (41/143, 28.7%) than in those with low viral loads (15/90, 16.7%, P = 0.0431). The difference was marginally significant in multivariate analysis (P = 0.0515; Table 4).

Of the five SNPs included in the analysis, rs477515 (OR = 3.107, P = 0.0002), rs9272105 (OR = 1.747, P = 0.0009), and rs7756516 (OR = 1.951, P = 0.0272) were significantly associated with HBV viral load. The associations remained significant after controlling for sex (Table 4). Participants carrying more risk alleles had higher ORs for HBV viral load (Table 2, lower panel) and compared with patients having a WGRS in Q1, those in Q2 (OR = 2.204, P = 0.0061) and Q3-4 (OR = 3.156, P < 0.0001) had higher odds of having an HBV viral load.

The results of multivariate GEE analysis of factors associated with the HBV viral load in the genetic, nongenetic, and mixed models are shown in Table 5. In the nongenetic model, the risk of HBV viral load was higher in males (OR = 1.955, P = 0.0162) and in those with index HBsAg positivity (OR = 2.219, P = 0.0187). In the genetic model, the risk allele rs477515 (OR = 2.246, P = 0.0159) and the WGRS (OR = 1.644, P < 0.0001) were significantly different between the groups with high and low viral loads. In the mixed model, sex, rs477515, and WGRS were significantly different in the groups with high and low viral loads (Table 5).

The AUC of the HBV viral load was 0.674 (P < 0.0001) for the nongenetic model, 0.632 (P < 0.0001) for the genetic model, and 0.704 (P < 0.0001) for the mixed model (Figure 3 and Table 5). The results suggest that both genetic and nongenetic factors

Table 3 Multivariate generalized estimating equation and area under the curve for hepatitis B surface antigen status in the hepatocellular carcinoma family cohort

	Nongenetic model		Mixed model	
Variable	**OR (95%CI)**	***P* value**	**OR (95%CI)**	***P* value**
Sex, male	1.458 (1.048-2.027)	0.0250	1.514 (1.075-2.133)[1]/1.487 (1.063-2.081)[2]	0.0177[1]/0.0205[2]
Index sex, male	0.915 (0.532-1.573)	0.7475	0.853 (0.496-1.466)[1]/0.838 (0.488-1.442)[2]	0.5648[1]/0.5238[2]
Age in yr	1.001 (0.984-1.018)	0.9392	1.000 (0.982-1.017)[1]/0.998 (0.981-1.016)[2]	0.9608[1]/0.8582[2]
Relation to index				
Parent generation	0.523 (0.176-1.555)	0.2434	0.560 (0.182-1.719)[1]/0.603 (0.198-1.833)[2]	0.3108[1]/0.3726[2]
Index generation	3.385 (1.836-6.239)	< 0.0001	3.344 (1.766-6.331)[1]/3.493 (1.860-6.559)[2]	0.0002[1]/0.0001[2]
Index's HBsAg+	5.077 (3.103-8.308)	< 0.0001	4.919 (2.980-8.119)[1]/4.756 (2.912-7.766)[2]	< 0.0001[1]/< 0.0001[2]
Mother's status				
HBsAg+	2.597 (1.332-5.064)	0.0051	2.459 (1.270-4.760)[1]/2.517 (1.284-4.933)[2]	0.0076[1]/0.0072[2]
Unknown	1.395 (0.788-2.469)	0.2538	1.412 (0.790-2.522)[1]/1.413 (0.795-2.511)[2]	0.2444[1]/0.2387[2]
AUC (95%CI)	0.786 (0.752-0.820)	< 0.0001		
	Genetic model			
rs477515	1.303 (0.969-1.753)	0.0802	1.121 (0.770-1.631)	0.5507
rs9276370	2.741 (0.766-9.812)	0.1211	3.040 (0.623-14.839)	0.1693
rs7756516	0.592 (0.171-2.042)	0.4064	0.516 (0.104-2.554)	0.4177
rs9277535	1.575 (1.244-1.995)	0.0002	1.535 (1.157-2.035)	0.0029
AUC (95%CI)	0.632 (0.593-0.671)	< 0.0001	0.798 (0.765-0.831)	< 0.0001
WGRS	1.322 (1.162-1.505)	< 0.0001	1.269 (1.099-1.465)	0.0012
AUC (95%CI)	0.620 (0.580-0.660)	< 0.0001	0.795 (0.762-0.829)	< 0.0001
IDI (95%CI)			0.017 (0.009-0.026)	< 0.0001
NRI (95%CI)			0.330 (0.192-0.467)	< 0.0001

[1]Each single nucleotide polymorphism was included in the mixed model.
[2]The weighted genetic risk score was added in the mixed model. AUC: Area under the receiver operating characteristic curve; CI: Confidence interval; OR: Odds ratio; GEE: Generalized estimating equation; IDI: Integrated discrimination improvement; NRI: Net reclassification improvement; WGRS: Weighted genetic risk score.

had an effect on HBV viral load. Both the IDI (0.042, 95%CI: 0.019-0.065, $P = 0.0003$) and the NRI (0.440, 95%CI: 0.236–0.644, $P < 0.0001$) indicated that the mixed model represented a significant improvement (Table 5).

DISCUSSION

In this HCC family cohort, we found that both genetic and nongenetic factors were significantly associated with persistent HBV infection. In addition, HBV-related SNPs in the HLA-DP and HLA-DQ regions were associated with HBV viral load. GWASs conducted in diverse Asian populations have revealed that the HLA-DP and -DP loci play roles in persistent HBV infection[10-19]. We evaluated persistent HBV infection in the first-stage HCC family study. Expression of four of the five HBV-related SNPs differed significantly between the HBsAg carriers and the noncarriers. When only the risk alleles of the four SNPs were included in the univariate analysis, the OR for

Table 4 Factors associated with hepatitis B viral load in a hepatitis B surface antigen-positive hepatocellular carcinoma family cohort

	HBV DNA					
Category	**≥ 10^5 cps/mL**	**< 10^5 cps/mL**	**OR (95%CI)**	**Adjusted OR (95% CI)[2]**	***P* value**	**Adjusted *P* value[2]**
Total members	147	162				
Age in yr, mean ± SD	45.03 ± 14.18	41.82 ± 14.21	1.017 (1-1.035)	1.017 (0.999-1.035)	0.0538	0.0668
Sex, *n* (%)						
Male	100 (68.03)	88 (54.32)	1.922 (1.188-3.111)	1.914 (1.187-3.087)	0.0078	0.0078
Female	47 (31.97)	74 (45.68)	1	1		
Relation to index, *n* (%)						
Children and grandchildren generation	58 (39.46)	95 (58.64)	1	1		
Parent generation	5 (3.4)	2 (1.23)	3.683 (0.866-15.656)	5.056 (1.259-20.3)	0.0775	0.0223
Index generation	84 (57.14)	65 (40.12)	2.033 (1.274-3.246)	1.845 (1.144-2.977)	0.0029	0.0121
Index's status, *n* (%)						
HBsAg-	21 (14.29)	49 (30.25)	1	1		
HBsAg+	126 (85.71)	113 (69.75)	2.508 (1.351-4.657)	2.492 (1.324-4.692)	0.0036	0.0047
Mother's status, *n* (%)						
HBsAg-	43 (29.25)	43 (26.54)	1	1		
HBsAg+	46 (31.29)	51 (31.48)	0.874 (0.467-1.634)	0.91 (0.485-1.707)	0.6724	0.7693
Unknown	58 (39.46)	68 (41.98)	0.855 (0.491-1.49)	0.857 (0.488-1.503)	0.5804	0.5898
HBV genotype (BGT230), *n* (%)						
Unknown[3]	3 (2.05)	72 (44.44)	0.03 (0.009-0.104)	0.029 (0.008-0.1)	< 0.0001	< 0.0001
B	102 (69.86)	75 (46.3)	1	1		
C	41 (28.08)	15 (9.26)	2.042 (1.023-4.079)	2.066 (0.995-4.288)	0.0431	0.0515
SGPT, mean ± SD	63.92 ± 79.63	37.02 ± 45.22	1.010 (1.002-1.018)	1.009 (1.001-1.017)	0.0105	0.0260
rs477515 (MAF = 0.1149) Chr6: 32601914[1]						
TT (reference)	1 (0.68)	4 (2.47)				
TC	15 (10.2)	46 (28.4)				
CC	131 (89.12)	112 (69.14)	3.107 (1.708-5.653)	3.195 (1.746-5.847)	0.0002	0.0002
rs9272105 (MAF = 0.4078) Chr6: 32632222[1]						
GG (reference)	20 (13.61)	36 (22.22)				
GA	59 (40.14)	81 (50)				
AA	68 (46.26)	45 (27.78)	1.747 (1.256-2.428)	1.75 (1.247-2.456)	0.0009	0.0012
rs9276370 (MAF = 0.07605) Chr6: 32739518[1]						
GG (reference)	1 (0.68)	3 (1.85)				
GT	14 (9.52)	25 (15.43)				
TT	132 (89.8)	134 (82.72)	1.747 (0.933-3.272)	1.679 (0.901-3.131)	0.0811	0.1029
rs7756516 (MAF = 0.08091) Chr6: 32756140[1]						
CC (reference)	0 (0)	4 (2.47)				
CT	16 (10.88)	26 (16.05)				
TT	131 (89.12)	132 (81.48)	1.951 (1.078-3.53)	1.875 (1.029-3.417)	0.0272	0.0400
rs9277535 (MAF = 0.2589) Chr6: 33087084[1]						
AA (reference)	13 (8.84)	8 (4.94)				
AG	45 (30.61)	73 (45.06)				

GG	89 (60.54)	81 (50)	1.235 (0.849-1.797)	1.303 (0.888-1.911)	0.2703	0.1767

[1]Genome Build ARCH38.
[2]Adjusted by sex.
[3]Eight cases not tested. CI: Confidence interval; HBsAg: Hepatitis B surface antigen; OR: Odds ratio; HBV: Hepatitis B virus.

Table 5 Multivariate generalized estimating equation and area under the curve hepatitis B viral loads in a hepatocellular family cohort

	Nongenetic model		Mixed model	
Variable	**OR (95%CI)**	***P* value**	**OR (95%CI)**	***P* value**
SNP				
Sex, male	1.955 (1.132-3.376)	0.0162	1.918 (1.101-3.341)[1]/1.911 (1.097-3.328)[2]	0.0214[1]/0.0223[2]
Index sex, male	0.903 (0.481-1.699)	0.7527	0.914 (0.488-1.713)[1]/0.912 (0.482-1.725)[2]	0.7786[1]/0.7771[2]
Age in yr	1.012 (0.987-1.037)	0.3363	1.007 (0.983-1.032)[1]/1.008 (0.983-1.033)[2]	0.5658[1]/0.5426[2]
Relation to index				
Parent generation	4.182 (0.68-25.731)	0.1228	4.343 (0.81-23.285)[1]/4.091 (0.75-22.316)[2]	0.0866[1]/0.1036[2]
Index generation	1.7 (0.844-3.423)	0.1372	1.851 (0.912-3.756)[1]/1.797 (0.894-3.611)[2]	0.0881[1]/0.0999[2]
Index HBsAg+	2.219 (1.142-4.31)	0.0187	1.734 (0.853-3.526)[1]/1.816 (0.907-3.636)[2]	0.1283[1]/0.0918[2]
Mother's status				
HBsAg+	0.828 (0.407-1.684)	0.6021	0.766 (0.361-1.623)[1]/0.763 (0.360-1.619)[2]	0.4862[1]/0.4814[2]
Unknown	0.537 (0.275-1.045)	0.0673	0.549 (0.272-1.107)[1]/0.559 (0.278-1.125)[2]	0.094[1]/0.1030[2]
AUC (95%CI)	0.674 (0.614-0.734)	< 0.0001		
	Genetic model			
rs477515	2.246 (1.164-4.333)	0.0159	2.242 (1.113-4.515)	0.0238
rs9272105	1.386 (0.965-1.991)	0.0775	1.266 (0.866-1.849)	0.2232
rs7756516	1.385 (0.765-2.509)	0.2826	1.379 (0.753-2.524)	0.2977
AUC (95%CI)	0.638 (0.579-0.698)	< 0.0001	0.705 (0.648-0.763)	< 0.0001
WGRS	1.644 (1.317-2.052)	< 0.0001	1.567 (1.250-1.965)	< 0.0001
AUC (95%CI)	0.632 (0.573-0.692)	< 0.0001	0.704 (0.646-0.761)	< 0.0001
IDI (95%CI)			0.042 (0.019-0.065)	0.0003
NRI (95%CI)			0.440 (0.236-0.644)	< 0.0001

[1]Each single nucleotide polymorphism was added in the mixed model.
[2]The weighted genetic risk score was added in the mixed model. AUC: Area under the receiver operating characteristic curve; GEE: Generalized estimating equation; IDI: Integrated discrimination improvement; NRI: Net reclassification improvement; CI: Confidence interval; HBsAg: Hepatitis B surface antigen; OR: Odds ratio.

persistence was significant if the WGRS was > 7 (Table 2, upper panel). In the genetic model, multivariate GEE analysis found that expression of one SNP (rs9277535) and the WGRS were significantly different between HBsAg carriers and noncarriers, and the differences remained significant in the presence of nongenetic factors (Table 3). Regression analysis showed that HBV-related SNPs were associated with persistent HBV infection in these HCC families. This is the first study to confirm that SNPs identified by GWAS were associated with persistent HBV infection in a family cohort.

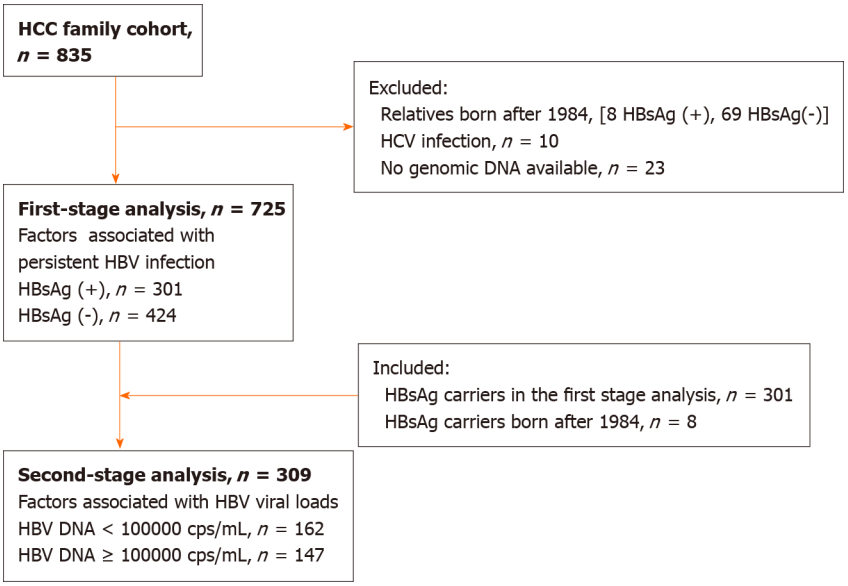


Figure 1 Study flow chart. Hepatitis B virus persistent infection and viral load were analyzed in a hepatocellular carcinoma family cohort. HCC: Hepatocellular carcinoma; HBV: Hepatitis B virus; HCV: Hepatitis C virus; HBsAg: Hepatitis B surface antigen.

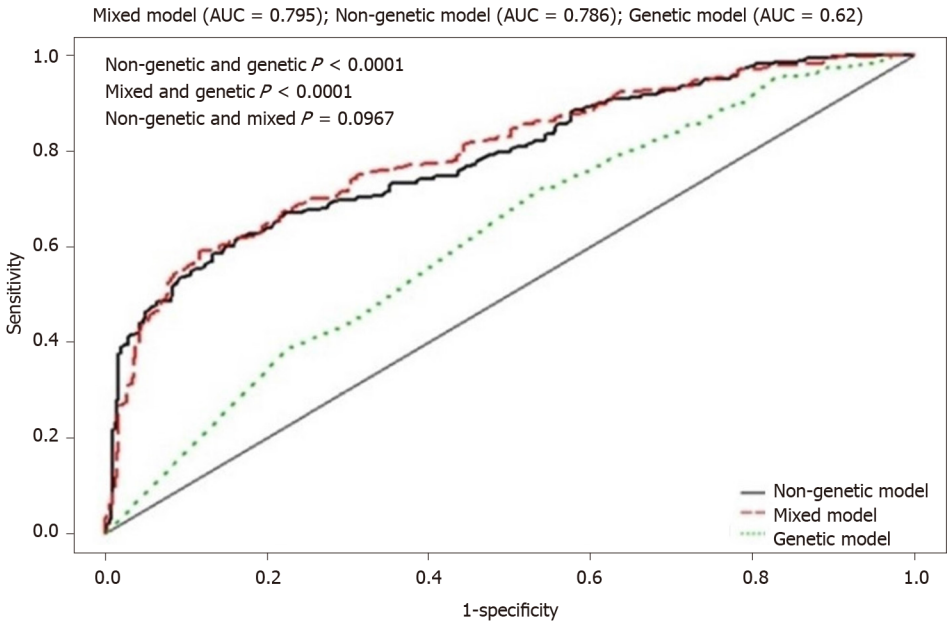


Figure 2 First-stage persistent hepatitis B virus infection. Genetic, nongenetic, and combined risk factors for persistent hepatitis B virus (HBV) infection were evaluated by area under the receiver operating characteristic curves derived from generalized estimating equation regression models. Significantly higher areas under the curve for nongenetic compared with genetic factors ($P < 0.001$) suggest that nongenetic factors played a major role in persistent HBV infection. AUC: Area under the receiver operating characteristic curve.

Nongenetic factors also affected persistent HBV infection. Age, sex, generation, index HBsAg status, and maternal HBsAg status all differed significantly between HBsAg carriers and noncarriers (Table 1). The AUC was 0.786 in the nongenetic model, 0.620 in the genetic model, and 0.795 in the mixed model (Table 3). The ROC analysis thus implied that nongenetic factors contributed more to persistent HBV infection than genetic factors did (genetic *vs* nongenetic factors $P < 0.0001$ and mixed *vs* nongenetic factors $P < 0.0001$; Figure 2). The results are consistent with exposure to HBV early in life and an important influence on the persistence of HBV infection[5-7]. Our overall findings indicate that the HCC family members may have been exposed to HBV early in life because of the high HBsAg prevalence in the index cases and/or their mothers. Accounting for both genetic and nongenetic cofactors, the prevalence of HBsAg was 41.5% (301/725) in this HCC family cohort.

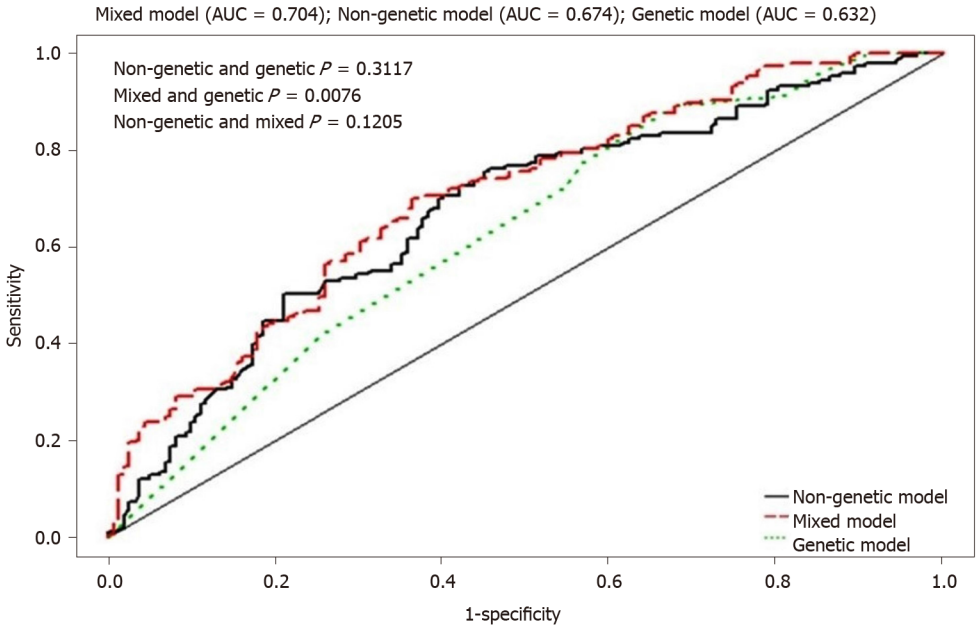


Figure 3 Second-stage hepatitis B virus viral load. The genetic, nongenetic, and combined risk factors for hepatitis B virus (HBV) viral load were evaluated by area under the receiver operating characteristic curves derived from generalized estimating equation regression models. The difference between the receiver operating characteristic curves of genetic and nongenetic factors was not significant (P = 0.3117). The finding suggests that both factors contributed to the HBV viral load. AUC: Area under the receiver operating characteristic curve.

In the presence of SNPs identified in a GWAS, nongenetic factors remain important in persistent HBV infection. The persistence of infection induced by the SNPs might depend on a delay in clearance of the HBeAg. It is known that in HBsAg carriers, HBeAg clearance occurs earlier in African than in Asian populations[22-25]. That means East Asians of reproductive age are likely to have higher HBV viral loads and a higher rate of perinatal HBV infection of their babies[7,10,22,23]. Perinatal infection usually persists as a chronic infection[7,23]. As African women usually clear HBeAg before reproductive age[24,25], the viral load during pregnancy is likely to be lower than that in East Asians, which would decrease the chance of perinatal HBV infection [24]. We suspect that a prolonged HBV replication phase in parents could be the mechanism of persistent HBV infection associated with SNPs.

Univariate analysis of the factors associated with HBV viral load in the HCC family cohort revealed that three of the five SNPs (rs477515, rs9272105, rs7756516) differed significantly between the high and low viral load groups (Table 4). The cumulative effect of the WGRS was also greater in the high viral load group (Table 3, lower panel). Multivariate GEE analysis found that the rs477515 SNP (OR = 2.242, P = 0.0238) and WGRS (OR = 1.567, P < 0.0001) were independently associated with a high viral load in the mixed model (Table 5). Our data thus support the prevailing view that the SNPs associated with persistent HBV infection promote persistent HBV replication. The mean ages of our study groups ranged from 41.25-45.03 years (Tables 1 and 4). Persistent high viral loads in these age groups were likely to have resulted in perinatal transmission of chronic HBV infection during the reproductive age.

Our previous study demonstrated that nongenetic factors influenced the HBV viral load in HCC families[10]. In this study, we observed that sex, generation, and index HBsAg cases were associated with a high viral load in the nongenetic model (Table 4). We also compared the relative contributions of genetic and nongenetic factors associated with viral load in the HCC family cohort. The AUCs of the viral load were 0.674 in the nongenetic model and 0.632 in the genetic model. The AUC in the mixed model was up to 0.704 (Table 5). Therefore, both genetic and nongenetic factors were associated with HBV viral load in the HCC family cohort. It should be noted that we included only SNPs in the HLA region. The association of other loci, such as polymorphisms of interferon gamma, complement factor B, CD40, and INST10, which have also been reported to be associated with HBV viral load, was not investigated[33-35].

One of the five SNPs we evaluated, rs9277535, was reported by Tao *et al*[36] to be associated with more aggressive liver disease, but it was reported by Li *et al*[37] not to be associated with disease progression. Our previous GWAS revealed that rs9276370 was associated with HBV therapeutic response[17]. Univariate analysis found that the

two SNPs were not significantly associated with viral load in this HCC family cohort. Two previous studies found that rs477515 was associated with HBV vaccine response [38,39], and that SNP was found to be associated with viral load in this cohort. Li *et al* [26] reported that rs9272105 was associated with HCC in a GWAS, and univariate analysis found that it was associated with viral load in this HCC family cohort. All these previous reports suggest that a single SNP provides a small contribution to HBV viral loads. Persistent HBV replication seems to be determined by multiple genetic and nongenetic risk factors.

This study provides information that may help to establish more accurate models of disease through the incorporation of genetic and nongenetic factors, but it was limited by the relatively small number of HCC families. Another limitation was that HBV genotype studies were not available in patients with low viral loads. HBV genotype C has been associated with a lower HBeAg clearance rate than genotype B[40]. We found a high adjusted OR (2.066, P = 0.0515) for the association of genotype C with a high viral load relative to a low viral load in this HCC family cohort (Table 4).

CONCLUSION

We conclude that SNPs associated with persistent HBV infection prolong the replication phase in the parent generation and increase the burden of persistent infection in the offspring generation.

ARTICLE HIGHLIGHTS

Research background

Genome-wide association studies (GWASs) in Asian populations indicate that the HLA-DP and HLA-DQ loci are involved in the persistence of hepatitis B virus (HBV) infections. Persistent viral replication and inflammation are key influencers in HBV-related carcinogenesis.

Research motivation

HBV-related single nucleotide polymorphisms (SNPs) have been identified in east Asian populations but are uncommon in African populations. Different mechanisms may drive persistent infection in those regions.

Research objectives

We examined genetic and nongenetic factors associated with persistent HBV infection and viral load in families with hepatocellular carcinoma (HCC).

Research methods

HCC families were enrolled. Five HBV-related SNPs (rs477515, rs9272105, rs9276370, rs7756516, and rs9277535) were genotyped. Factors associated with persistent HBV infection and viral load were identified with the use of generalized estimating equations.

Research results

In the first-stage persistent HBV study, all SNPs except rs9272105 were associated with persistent infection. A significantly higher contribution of nongenetic than genetic factors (P < 0.001) to persistent HBV infection was found. In the second-stage viral load study, sex, relationship with index case, rs477515, rs9272105, and rs7756516 were associated with viral load. Receiver operating characteristic curve, and genetic and nongenetic factors had equal effects on viral load in the HCC family cohort (P = 0.3117).

Research conclusions

GWAS identified SNPs that have roles in persistent HBV infection and HBV viral loads in an HCC family cohort. Nongenetic factors were more important than genetic factors in persistent HBV infection but had equal contributions to HBV viral load. HBV-related SNPs resulting in high viral loads in parents may drive persistent infection in East Asian populations. The mechanism of persistent HBV infection-related SNPs involves a prolonged viral replication phase in East Asian adults.

Research perspectives

Termination of the HBV replication phase before pregnancy will be a therapeutic goal in East Asian countries.

REFERENCES

1 **Schweitzer A**, Horn J, Mikolajczyk RT, Krause G, Ott JJ. Estimations of worldwide prevalence of chronic hepatitis B virus infection: a systematic review of data published between 1965 and 2013. *Lancet* 2015; **386**: 1546-1555 [PMID: 26231459 DOI: 10.1016/S0140-6736(15)61412-X]

2 **Hou J**, Liu Z, Gu F. Epidemiology and Prevention of Hepatitis B Virus Infection. *Int J Med Sci* 2005; **2**: 50-57 [PMID: 15968340 DOI: 10.7150/ijms.2.50]

3 **Kingsley LA**, Rinaldo CR Jr, Lyter DW, Valdiserri RO, Belle SH, Ho M. Sexual transmission efficiency of hepatitis B virus and human immunodeficiency virus among homosexual men. *JAMA* 1990; **264**: 230-234 [PMID: 2192096]

4 **Kane A**, Lloyd J, Zaffran M, Simonsen L, Kane M. Transmission of hepatitis B, hepatitis C and human immunodeficiency viruses through unsafe injections in the developing world: model-based regional estimates. *Bull World Health Organ* 1999; **77**: 801-807 [PMID: 10593027]

5 **Beasley RP**. Rocks along the road to the control of HBV and HCC. *Ann Epidemiol* 2009; **19**: 231-234 [PMID: 19344859 DOI: 10.1016/j.annepidem.2009.01.017]

6 **Edmunds WJ**, Medley GF, Nokes DJ, Hall AJ, Whittle HC. The influence of age on the development of the hepatitis B carrier state. *Proc Biol Sci* 1993; **253**: 197-201 [PMID: 8397416 DOI: 10.1098/rspb.1993.0102]

7 **Burk RD**, Hwang LY, Ho GY, Shafritz DA, Beasley RP. Outcome of perinatal hepatitis B virus exposure is dependent on maternal virus load. *J Infect Dis* 1994; **170**: 1418-1423 [PMID: 7995980 DOI: 10.1093/infdis/170.6.1418]

8 **Sung JL**, Chen DS. Geographical distribution of the subtype of hepatitis B surface antigen in Chinese. *Gastroenterol Jpn* 1977; **12**: 58-63 [PMID: 196971 DOI: 10.1007/BF02773627]

9 **Liu X**, Baecker A, Wu M, Zhou JY, Yang J, Han RQ, Wang PH, Jin ZY, Liu AM, Gu X, Zhang XF, Wang XS, Su M, Hu X, Sun Z, Li G, Fu A, Jung SY, Mu L, He N, Li L, Zhao JK, Zhang ZF. Family history of liver cancer may modify the association between HBV infection and liver cancer in a Chinese population. *Liver Int* 2019; **39**: 1490-1503 [PMID: 31228882 DOI: 10.1111/liv.14182]

10 **Hsieh AR**, Fann CS, Yeh CT, Lin HC, Wan SY, Chen YC, Hsu CL, Tai J, Lin SM, Tai DI. Effects of sex and generation on hepatitis B viral load in families with hepatocellular carcinoma. *World J Gastroenterol* 2017; **23**: 876-884 [PMID: 28223732 DOI: 10.3748/wjg.v23.i5.876]

11 **Kamatani Y**, Wattanapokayakit S, Ochi H, Kawaguchi T, Takahashi A, Hosono N, Kubo M, Tsunoda T, Kamatani N, Kumada H, Puseenam A, Sura T, Daigo Y, Chayama K, Chantratita W, Nakamura Y, Matsuda K. A genome-wide association study identifies variants in the HLA-DP locus associated with chronic hepatitis B in Asians. *Nat Genet* 2009; **41**: 591-595 [PMID: 19349983 DOI: 10.1038/ng.348]

12 **Mbarek H**, Ochi H, Urabe Y, Kumar V, Kubo M, Hosono N, Takahashi A, Kamatani Y, Miki D, Abe H, Tsunoda T, Kamatani N, Chayama K, Nakamura Y, Matsuda K. A genome-wide association study of chronic hepatitis B identified novel risk locus in a Japanese population. *Hum Mol Genet* 2011; **20**: 3884-3892 [PMID: 21750111 DOI: 10.1093/hmg/ddr301]

13 **Hu Z**, Liu Y, Zhai X, Dai J, Jin G, Wang L, Zhu L, Yang Y, Liu J, Chu M, Wen J, Xie K, Du G, Wang Q, Zhou Y, Cao M, Liu L, He Y, Wang Y, Zhou G, Jia W, Lu J, Li S, Yang H, Shi Y, Zhou W, Shen H. New loci associated with chronic hepatitis B virus infection in Han Chinese. *Nat Genet* 2013; **45**: 1499-1503 [PMID: 24162738 DOI: 10.1038/ng.2809]

14 **Nishida N**, Sawai H, Matsuura K, Sugiyama M, Ahn SH, Park JY, Hige S, Kang JH, Suzuki K, Kurosaki M, Asahina Y, Mochida S, Watanabe M, Tanaka E, Honda M, Kaneko S, Orito E, Itoh Y, Mita E, Tamori A, Murawaki Y, Hiasa Y, Sakaida I, Korenaga M, Hino K, Ide T, Kawashima M, Mawatari Y, Sageshima M, Ogasawara Y, Koike A, Izumi N, Han KH, Tanaka Y, Tokunaga K, Mizokami M. Genome-wide association study confirming association of HLA-DP with protection against chronic hepatitis B and viral clearance in Japanese and Korean. *PLoS One* 2012; **7**: e39175 [PMID: 22737229 DOI: 10.1371/journal.pone.0039175]

15 **Kim YJ**, Kim HY, Lee JH, Yu SJ, Yoon JH, Lee HS, Kim CY, Cheong JY, Cho SW, Park NH, Park BL, Namgoong S, Kim LH, Cheong HS, Shin HD. A genome-wide association study identified new variants associated with the risk of chronic hepatitis B. *Hum Mol Genet* 2013; **22**: 4233-4238 [PMID: 23760081 DOI: 10.1093/hmg/ddt266]

16 **Al-Qahtani AA**, Al-Anazi MR, Abdo AA, Sanai FM, Al-Hamoudi W, Alswat KA, Al-Ashgar HI, Khalaf NZ, Eldali AM, Viswan NA, Al-Ahdal MN. Association between HLA variations and chronic hepatitis B virus infection in Saudi Arabian patients. *PLoS One* 2014; **9**: e80445 [PMID: 24465366 DOI: 10.1371/journal.pone.0080445]

17 **Chang SW**, Fann CS, Su WH, Wang YC, Weng CC, Yu CJ, Hsu CL, Hsieh AR, Chien RN, Chu CM, Tai DI. A genome-wide association study on chronic HBV infection and its clinical progression in male Han-Taiwanese. *PLoS One* 2014; **9**: e99724 [PMID: 24940741 DOI: 10.1371/journal.pone.0099724]

18 **Huang YH**, Liao SF, Khor SS, Lin YJ, Chen HY, Chang YH, Huang YH, Lu SN, Lee HW, Ko WY,

Huang C, Liu PC, Chen YJ, Wu PF, Chu HW, Wu PE, Tokunaga K, Shen CY, Lee MH. Large-scale genome-wide association study identifies HLA class II variants associated with chronic HBV infection: a study from Taiwan Biobank. *Aliment Pharmacol Ther* 2020; **52**: 682-691 [PMID: 32573827 DOI: 10.1111/apt.15887]

19 **Zeng Z**, Liu H, Xu H, Lu H, Yu Y, Xu X, Yu M, Zhang T, Tian X, Xi H, Guan L, Zhang J, O'Brien SJ; HBVstudy consortium. Genome-wide association study identifies new loci associated with risk of HBV infection and disease progression. *BMC Med Genomics* 2021; **14**: 84 [PMID: 33736632 DOI: 10.1186/s12920-021-00907-0]

20 **Tai DI**, Jeng WJ, Lin CY. A global perspective on hepatitis B-related single nucleotide polymorphisms and evolution during human migration. *Hepatol Commun* 2017; **1**: 1005-1013 [PMID: 29404438 DOI: 10.1002/hep4.1113]

21 **Tai DI**, Tai J. The role of genetic factors in HBV-related HCC: perspectives from local genetic backgrounds and clinical epidemiology. *Hepatoma Res* 2020; **6**: 74 [DOI: 10.20517/2394-5079.2020.54]

22 **Chang MH**, Hsu HY, Hsu HC, Ni YH, Chen JS, Chen DS. The significance of spontaneous hepatitis B e antigen seroconversion in childhood: with special emphasis on the clearance of hepatitis B e antigen before 3 years of age. *Hepatology* 1995; **22**: 1387-1392 [PMID: 7590652]

23 **Chang MH**, Sung JL, Lee CY, Chen CJ, Chen JS, Hsu HY, Lee PI, Chen DS. Factors affecting clearance of hepatitis B e antigen in hepatitis B surface antigen carrier children. *J Pediatr* 1989; **115**: 385-390 [PMID: 2769497 DOI: 10.1016/s0022-3476(89)80836-4]

24 **Hadziyannis SJ**. Natural history of chronic hepatitis B in Euro-Mediterranean and African countries. *J Hepatol* 2011; **55**: 183-191 [PMID: 21238520 DOI: 10.1016/j.jhep.2010.12.030]

25 **Iorio R**, Giannattasio A, Cirillo F, D' Alessandro L, Vegnente A. Long-term outcome in children with chronic hepatitis B: a 24-year observation period. *Clin Infect Dis* 2007; **45**: 943-949 [PMID: 17879906 DOI: 10.1086/521864]

26 **Li S**, Qian J, Yang Y, Zhao W, Dai J, Bei JX, Foo JN, McLaren PJ, Li Z, Yang J, Shen F, Liu L, Li S, Pan S, Wang Y, Li W, Zhai X, Zhou B, Shi L, Chen X, Chu M, Yan Y, Wang J, Cheng S, Shen J, Jia W, Liu J, Wen Z, Li A, Zhang Y, Zhang G, Luo X, Qin H, Chen M, Wang H, Jin L, Lin D, Shen H, He L, de Bakker PI, Zeng YX, Wu M, Hu Z, Shi Y, Zhou W. GWAS identifies novel susceptibility loci on 6p21.32 and 21q21.3 for hepatocellular carcinoma in chronic hepatitis B virus carriers. *PLoS Genet* 2012; **8**: e1002791 [PMID: 22807686 DOI: 10.1371/journal.pgen.1002791]

27 **Horvath S**, Xu X, Laird NM. The family based association test method: strategies for studying general genotype--phenotype associations. *Eur J Hum Genet* 2001; **9**: 301-306 [PMID: 11313775 DOI: 10.1038/sj.ejhg.5200625]

28 **Miyake K**, Yang W, Hara K, Yasuda K, Horikawa Y, Osawa H, Furuta H, Ng MC, Hirota Y, Mori H, Ido K, Yamagata K, Hinokio Y, Oka Y, Iwasaki N, Iwamoto Y, Yamada Y, Seino Y, Maegawa H, Kashiwagi A, Wang HY, Tanahashi T, Nakamura N, Takeda J, Maeda E, Yamamoto K, Tokunaga K, Ma RC, So WY, Chan JC, Kamatani N, Makino H, Nanjo K, Kadowaki T, Kasuga M. Construction of a prediction model for type 2 diabetes mellitus in the Japanese population based on 11 genes with strong evidence of the association. *J Hum Genet* 2009; **54**: 236-241 [PMID: 19247372 DOI: 10.1038/jhg.2009.17]

29 **Song YM**, Sung J, Yang S, Choe YH, Chang YS, Park WS. Factors associated with immunoprophylaxis failure against vertical transmission of hepatitis B virus. *Eur J Pediatr* 2007; **166**: 813-818 [PMID: 17120036 DOI: 10.1007/s00431-006-0327-5]

30 **Ding K**, Bailey KR, Kullo IJ. Genotype-informed estimation of risk of coronary heart disease based on genome-wide association data linked to the electronic medical record. *BMC Cardiovasc Disord* 2011; **11**: 66 [PMID: 22151179 DOI: 10.1186/1471-2261-11-66]

31 **Pencina MJ**, D'Agostino RB Sr, Steyerberg EW. Extensions of net reclassification improvement calculations to measure usefulness of new biomarkers. *Stat Med* 2011; **30**: 11-21 [PMID: 21204120 DOI: 10.1002/sim.4085]

32 **Pencina MJ**, D'Agostino RB Sr, D'Agostino RB Jr, Vasan RS. Evaluating the added predictive ability of a new marker: from area under the ROC curve to reclassification and beyond. *Stat Med* 2008; **27**: 157-172; discussion 207-212 [PMID: 17569110 DOI: 10.1002/sim.2929]

33 **Ben Selma W**, Laribi AB, Alibi S, Boukadida J. Association of an IFN-γ variant with susceptibility to chronic hepatitis B by the enhancement of HBV DNA replication. *Cytokine* 2021; **143**: 155525 [PMID: 33896709 DOI: 10.1016/j.cyto.2021.155525]

34 **Jiang DK**, Ma XP, Yu H, Cao G, Ding DL, Chen H, Huang HX, Gao YZ, Wu XP, Long XD, Zhang H, Zhang Y, Gao Y, Chen TY, Ren WH, Zhang P, Shi Z, Jiang W, Wan B, Saiyin H, Yin J, Zhou YF, Zhai Y, Lu PX, Gu X, Tan A, Wang JB, Zuo XB, Sun LD, Liu JO, Yi Q, Mo Z, Zhou G, Liu Y, Sun J, Shugart YY, Zheng SL, Zhang XJ, Xu J, Yu L. Genetic variants in five novel loci including CFB and CD40 predispose to chronic hepatitis B. *Hepatology* 2015; **62**: 118-128 [PMID: 25802187 DOI: 10.1002/hep.27794]

35 **Li Y**, Si L, Zhai Y, Hu Y, Hu Z, Bei JX, Xie B, Ren Q, Cao P, Yang F, Song Q, Bao Z, Zhang H, Han Y, Wang Z, Chen X, Xia X, Yan H, Wang R, Zhang Y, Gao C, Meng J, Tu X, Liang X, Cui Y, Liu Y, Wu X, Li Z, Wang H, Hu B, He M, Gao Z, Xu X, Ji H, Yu C, Sun Y, Xing B, Yang X, Tan A, Wu C, Jia W, Li S, Zeng YX, Shen H, He F, Mo Z, Zhou G. Genome-wide association study identifies 8p21.3 associated with persistent hepatitis B virus infection among Chinese. *Nat Commun* 2016; **7**: 11664 [PMID: 27244555 DOI: 10.1038/ncomms11664]

36 **Tao J**, Su K, Yu C, Liu X, Wu W, Xu W, Jiang B, Luo R, Yao J, Zhou J, Zhan Y, Ye C, Yuan W,

Jiang X, Cui W, Li MD, Li L. Fine mapping analysis of HLA-DP/DQ gene clusters on chromosome 6 reveals multiple susceptibility loci for HBV infection. *Amino Acids* 2015; **47**: 2623-2634 [PMID: 26197724 DOI: 10.1007/s00726-015-2054-6]

37 **Li J**, Yang D, He Y, Wang M, Wen Z, Liu L, Yao J, Matsuda K, Nakamura Y, Yu J, Jiang X, Sun S, Liu Q, Song Q, Chen M, Yang H, Tang F, Hu X, Wang J, Chang Y, He X, Chen Y, Lin J. Associations of HLA-DP variants with hepatitis B virus infection in southern and northern Han Chinese populations: a multicenter case-control study. *PLoS One* 2011; **6**: e24221 [PMID: 21904616 DOI: 10.1371/journal.pone.0024221]

38 **Pan L**, Zhang L, Zhang W, Wu X, Li Y, Yan B, Zhu X, Liu X, Yang C, Xu J, Zhou G, Xu A, Li H, Liu Y. A genome-wide association study identifies polymorphisms in the HLA-DR region associated with non-response to hepatitis B vaccination in Chinese Han populations. *Hum Mol Genet* 2014; **23**: 2210-2219 [PMID: 24282030 DOI: 10.1093/hmg/ddt586]

39 **Deng Y**, Li P, Liu W, Pu R, Yang F, Song J, Yin J, Han X, Li C, Zhao J, Wang H, Cao G. The genetic polymorphism down-regulating HLA-DRB1 enhancer activity facilitates HBV persistence, evolution and hepatocarcinogenesis in the Chinese Han population. *J Viral Hepat* 2020; **27**: 1150-1161 [PMID: 32568442 DOI: 10.1111/jvh.13353]

40 **Kao JH**, Chen PJ, Lai MY, Chen DS. Hepatitis B virus genotypes and spontaneous hepatitis B e antigen seroconversion in Taiwanese hepatitis B carriers. *J Med Virol* 2004; **72**: 363-369 [PMID: 14748059 DOI: 10.1002/jmv.10534]

World Journal of Gastroenterology

Submit a Manuscript: https://www.f6publishing.com

World J Gastroenterol 2021 October 7; 27(37): 6277-6289

DOI: 10.3748/wjg.v27.i37.6277

ISSN 1007-9327 (print) ISSN 2219-2840 (online)

ORIGINAL ARTICLE

Retrospective Study

Recently acquired hepatitis C virus infection among people living with human immunodeficiency virus at a university hospital in Taiwan

Miao-Hui Huang, Hsin-Yun Sun, Shu-Yuan Ho, Sui-Yuan Chang, Szu-Min Hsieh, Wang-Huei Sheng, Yu-Chung Chuang, Yu-Shan Huang, Li-Hsin Su, Wen-Chun Liu, Yi-Ching Su, Chien-Ching Hung

ORCID number: Miao-Hui Huang 0000-0001-8961-1104; Hsin-Yun Sun 0000-0003-0074-7721; Shu-Yuan Ho 0000-0002-9657-7239; Sui-Yuan Chang 0000-0002-6009-6724; Szu-Min Hsieh 0000-0002-1879-4086; Wang-Huei Sheng 0000-0002-5605-7853; Yu-Chung Chuang 0000-0003-3094-8276; Yu-Shan Huang 0000-0002-9047-5709; Li-Hsin Su 0000-0002-1879-2216; Wen-Chun Liu 0000-0002-0356-9898; Yi-Ching Su 0000-0002-0187-1348; Chien-Ching Hung 0000-0001-7345-0836.

Author contributions: Huang MH designed and performed the research; Sun HY and Hung CC designed the research and supervised the report; Ho SY and Chang SY provided laboratory support; Hung CC, Sun HY, Hsieh SM, Sheng WH, Chuang YC, Huang YS, Su LH, Liu WC, and Su YC were involved in the collection and assembly of clinical data; Huang MH and Hung CC participated in the data analysis and drafted the report; All authors reviewed and approved the final version of the report.

Supported by National Taiwan University Hospital, Taipei, Taiwan, No. NTUH106-003347 (to Sun HY).

Miao-Hui Huang, Department of Internal Medicine, Hualien Tzu Chi Hospital, Buddhist Tzu Chi Medical Foundation and Tzu Chi University, Hualien 970410, Taiwan

Hsin-Yun Sun, Szu-Min Hsieh, Wang-Huei Sheng, Yu-Chung Chuang, Yu-Shan Huang, Li-Hsin Su, Wen-Chun Liu, Yi-Ching Su, Chien-Ching Hung, Department of Internal Medicine, National Taiwan University Hospital and National Taiwan University College of Medicine, Taipei 100008, Taiwan

Shu-Yuan Ho, Sui-Yuan Chang, Department of Laboratory Medicine, National Taiwan University Hospital and National Taiwan University College of Medicine, Taipei 100008, Taiwan

Sui-Yuan Chang, Department of Clinical Laboratory Sciences and Medical Biotechnology, National Taiwan University College of Medicine, Taipei 100233, Taiwan

Chien-Ching Hung, Department of Tropical Medicine and Parasitology, National Taiwan University College of Medicine, Taipei 100233, Taiwan

Chien-Ching Hung, Department of Medical Research, China Medical University Hospital and China Medical University, Taichung 404394, Taiwan

Corresponding author: Chien-Ching Hung, MD, PhD, Professor, Department of Internal Medicine, National Taiwan University Hospital and National Taiwan University College of Medicine, No. 7 Chung-Shan South Road, Taipei 100008, Taiwan. hcc0401@ntu.edu.tw

Abstract

BACKGROUND

Little is known about the engagement in hepatitis C virus (HCV) care and completion of HCV treatment in people living with human immunodeficiency virus (HIV) (PLWH) who have HCV coinfection in the Asia-Pacific region. Examining the HCV care cascade can identify barriers to the completion of HCV treatment and facilitate achievement of HCV micro-elimination in PLWH.

AIM

To investigate the care cascade of incident HCV infections among PLWH in

Institutional review board statement: This retrospective study was approved by the Research Ethics Committee of National Taiwan University Hospital (registration number: 201605103RINC and 201605128RINC).

Informed consent statement: Written informed consents were obtained from all included participants prior to study inclusion.

Conflict-of-interest statement: The authors have no competing interest to disclose.

Data sharing statement: The datasets generated and/or analyzed during the current study are available from the corresponding author upon reasonable request.

Open-Access: This article is an open-access article that was selected by an in-house editor and fully peer-reviewed by external reviewers. It is distributed in accordance with the Creative Commons Attribution NonCommercial (CC BY-NC 4.0) license, which permits others to distribute, remix, adapt, build upon this work non-commercially, and license their derivative works on different terms, provided the original work is properly cited and the use is non-commercial. See: http://creativecommons.org/Licenses/by-nc/4.0/

Manuscript source: Invited manuscript

Specialty type: Gastroenterology and hepatology

Country/Territory of origin: Taiwan

Peer-review report's scientific quality classification

Grade A (Excellent): 0
Grade B (Very good): 0
Grade C (Good): C, C, C
Grade D (Fair): 0
Grade E (Poor): 0

Received: April 5, 2021
Peer-review started: April 5, 2021
First decision: July 3, 2021

Taiwan.

METHODS

PLWH with incident HCV infections, defined as HCV seroconversion, were retrospectively identified by sequential anti-HCV testing of all archived blood samples at National Taiwan University Hospital between 2011 and 2018. All PLWH with incident HCV infections were followed until December 31, 2019. The care cascade of HCV examined included all incident HCV-infected patients, the percentages of anti-HCV antibodies detected by HIV-treating physicians in clinical care, plasma HCV RNA load tested, HCV RNA positivity diagnosed, referral to treatment assessment made, anti-HCV treatment initiated, and sustained virologic response achieved. Those who had HCV seroconversion during the interferon (IFN) era (2011–2016) and the direct-acting antiviral (DAA) era (2017–2018) were analyzed separately. The duration of HCV viremia—from the date of seroconversion to viral clearance by treatments or until the end of observation—and the incidence of sexually transmitted infections (STIs) during the HCV viremic period were estimated.

RESULTS

During the study period, 287 of 3495 (8.2%) PLWH (92.3% being men who have sex with men) who were HCV-seronegative at baseline developed HCV seroconversion by retrospective testing of all archived blood samples. Of the 287 incident HCV infections, 277 (96.5%) had anti-HCV antibodies detected by HIV-treating physicians, 270 (94.1%) had plasma HCV RNA determined and 251 (87.5%) tested positive for HCV RNA. Of those with HCV viremia, 226 (78.7%) were referred to treatment assessment, 215 (74.9%) initiated anti-HCV treatment, and 202 (70.4%) achieved viral clearance. Compared with that in the IFN era, the median interval from HCV seroconversion by retrospective testing to detection of HCV seropositivity by HIV-treating physicians was significantly shorter in the DAA era {179 d [interquartile range (IQR) 87-434] *vs* 92 d (IQR 57-173); $P < 0.001$}. The incidence rate of STIs in the DAA *vs* the IFN era was 50.5 per 100 person-years of follow-up (PYFU) and 38.5 per 100 PYFU, respectively, with an incidence rate ratio of 1.31 (95% confidence interval 0.96-1.77), while the duration of HCV viremia was 380 d (IQR 274-554) and 735 d (IQR 391-1447) ($P < 0.001$), respectively.

CONCLUSION

While anti-HCV therapies are effective in achieving viral clearance, our study suggests more efforts are needed to expedite the linkage of PLWH diagnosed with incident HCV infections to HCV treatment.

Key Words: Recent hepatitis C virus infection; Cascade of care; Direct-acting antivirals; People living with human immunodeficiency virus; Sustained virologic response; Sexually transmitted infections

©The Author(s) 2021. Published by Baishideng Publishing Group Inc. All rights reserved.

Core Tip: We examined the hepatitis C virus (HCV) care cascade among people living with human immunodeficiency virus who acquired incident HCV infections at a university hospital in Taiwan between 2011 and 2018. We observed high rates of linkage to HCV care and retention in care in both interferon (IFN, 2011 to 2016) and direct-acting antiviral (DAA, 2017 to 2018) eras. The rate of referral to treatment assessment had increased from the IFN era to the DAA era. Moreover, the duration of HCV viremia was markedly shortened because of early diagnosis and linkage to effective treatment in the DAA era compared to that in the IFN era.

Citation: Huang MH, Sun HY, Ho SY, Chang SY, Hsieh SM, Sheng WH, Chuang YC, Huang YS, Su LH, Liu WC, Su YC, Hung CC. Recently acquired hepatitis C virus infection among people living with human immunodeficiency virus at a university hospital in Taiwan. *World J Gastroenterol* 2021; 27(37): 6277-6289
URL: https://www.wjgnet.com/1007-9327/full/v27/i37/6277.htm

Revised: July 13, 2021
Accepted: September 2, 2021
Article in press: September 2, 2021
Published online: October 7, 2021

P-Reviewer: Mohamed SY, Zarębska-Michaluk D
S-Editor: Ma YJ
L-Editor: A
P-Editor: Wu RR



DOI: https://dx.doi.org/10.3748/wjg.v27.i37.6277

INTRODUCTION

Viral hepatitis is a major public health threat and approximately 2.3 million people living with human immunodeficiency virus (HIV) (PLWH) are coinfected with hepatitis C virus (HCV) globally[1-3]. Injection drug users (IDUs) have been the major contributors to HCV transmission[4]. In Asia-Pacific region, the prevalence of HCV coinfection among PLWH ranges from 3.8% to 42.6%, and may be as high as 80.8% to 98.5% among IDUs[5,6]. Since 2000, incident HCV infections among PLWH who are MSM have continued to increase in the United States, European countries, and Australia[7-9]. Similar increasing trends were observed among PLWH who are MSM in Asia-Pacific region[10,11]. The causes of the increases of HCV transmission among MSM are multifactorial and are related to concurrent sexually transmitted infections (STIs), unprotected anal intercourse, traumatic sexual contacts, and use of recreational drugs by inhalation or injection[12].

The evolution of HCV treatment from interferon (IFN)-based therapy to IFN-free direct-acting antivirals (DAAs) has significantly improved tolerability and effectiveness in achieving viral clearance[13]. The rates of viral clearance with DAAs are similarly high for HCV-monoinfected patients and HCV/HIV-coinfected patients in clinical trials and real-world experience[14-18]. With the introduction of effective DAAs, ending the HCV epidemic is considered an achievable goal by scaling up diagnosis and treatment of HCV infection[1]. Among the interventional strategies proposed to achieve hepatitis elimination, the continuum assessed by the "cascade of care" on the population level is suggested to evaluate the status of hepatitis treatment services and the level of engagement in care[19,20]. The proportion of patients in each step of the cascade—infected, tested, status confirmed, engagement in care, treatment initiated, cured, and followed up for chronic care—reflects the coverage of diagnosis, access to treatment, and quality of care.

In Taiwan, pegylated IFN plus ribavirin (PEG-IFN/RBV) has become the standard anti-HCV treatment regimen since 2004 and has been fully reimbursed by the National Health Insurance (NHI) since 2009[21,22]. DAAs were not available until 2017, when the regimens were restricted to individuals with chronic HCV infection with evidence of significant hepatic fibrosis. Generic versions of patented DAAs could be purchased for individual use from Bangladesh[23]. Before 2019, referral to a hepatologist for hepatitis C evaluation and treatment was required according to NHI regulations. The reimbursement restrictions on the use of DAAs were lifted in January of 2019 by allowing HCV viremic patients to initiate DAAs regardless of liver fibrosis status. Subsequently, PLWH with HCV viremia could be evaluated and DAAs initiated by HIV-treating physicians at infectious disease clinics.

In this study, we aimed to examine the HCV care cascade among PLWH who received a diagnosis of incident HCV infection at a university hospital in Taiwan.

MATERIALS AND METHODS

Study design and data collection

We retrospectively reviewed the medical records of all PLWH aged 18 years or older seeking medical care for HIV at the National Taiwan University Hospital (NTUH), the largest designated hospital for HIV inpatient and outpatient care in Taiwan, from January 2011 to December 2018; and those included were followed until death, loss to follow-up, transfer of care, or the end of the study on December 31, 2019, whichever occurred first. The study period (2011-2018) spanned two different eras of anti-HCV treatment, from the IFN/RBV era (2011-2016) to the DAA era (2017-2018) before restricted access to HCV treatments were completely lifted in early 2019. In this study, the IFN-based regimen was PEG-IFN plus weight-based RBV with response-guided treatment duration. From 2016 to 2018, generic versions of patent IFN-free DAAs (sofosbuvir/velpatasvir) were used for treatment of recently acquired HCV infection.

Anti-HCV antibodies were detected using a fourth-generation enzyme immunoassay (Dia.Pro Diagnostic Bioprobes Srl. Italy)[11] and the HCV serostatus of the first available blood samples during the study period were regarded as the baseline serostatus. For those with a negative anti-HCV status at baseline, anti-HCV testing of

all their archived blood samples were performed retrospectively on an annual basis to detect HCV seroconversion. Patients who developed HCV seroconversion within the past 12 mo were identified as having recently acquired HCV infection and were included in this study.

The date of HCV seroconversion was arbitrarily assigned as the mid-point between the dates of the first positive and the last negative anti-HCV test. Using a standardized case record form, we collected data on patient demographics, HIV transmission risk groups, and laboratory test results, including CD4 lymphocyte count and plasma HIV RNA load (PVL), hepatitis B surface antigen (HBsAg), rapid plasma reagin (RPR) titer, plasma HCV RNA load and genotype when HCV viremia was detected.

The study was approved by the Research Ethics Committee of the hospital (registration number: 201605103RINC and 201605128RINC) and informed consent was obtained from all the participants.

Definitions

The HCV care cascade comprised the following steps of care: (1) "HCV infected" included all seroconverters in the past 12 mo identified by testing of archived blood samples; (2) "antibody detected" defined as a confirmed anti-HCV-positive test identified by HIV-treating physicians and documented in the medical records; (3) "HCV RNA tested" as the performance of a plasma HCV RNA test either after a positive anti-HCV test or when HCV viremia is detected during an acute infection with a negative anti-HCV test; (4) "HCV RNA positivity" as detectable plasma HCV RNA at the time of testing; (5) "Referred to treatment assessment" as successful referral of HCV-infected individuals to a hepatology clinic for evaluation of liver fibrosis or HCV treatment; or completion of pretreatment blood testing in infectious disease clinics as required by NHI regulation in 2019, including evaluation of liver fibrosis, renal function, HCV genotype, and plasma HCV RNA load[16]; (6) "Treatment initiated" as patients who had been prescribed HCV treatment medications; and (7) "Sustained virologic response (SVR) achieved" as the state of persistently undetectable HCV RNA until 24 wk after completion of IFN-based regimens and 12 wk after completion of DAA treatments.

The durations between two consecutive steps of the care cascade were recorded. Those who had HCV seroconversion during the IFN era (2011–2016) and the DAA era (2017–2018) were analyzed separately for comparison of the proportion of patients attaining each step and the interval between two consecutive steps of the cascade. The total duration of HCV viremia was defined as the interval between the estimated date of HCV seroconversion to the end of HCV treatment in those with undetectable HCV RNA; those who did not achieve SVR were followed until the completion of re-treatment with undetectable HCV RNA, the end of observation, or loss to follow-up, whichever occurred first.

The number of STIs, including syphilis (defined as a four-fold increase of RPR titers, consistent clinical symptoms, or administration of syphilis treatment), and gonorrhea (defined as culture-confirmed *Neisseria gonorrhoeae* infection or consistent clinical symptoms and administration of gonorrhea treatment), during the defined intervals of HCV viremia was calculated. We used occurrences of STIs as surrogate markers for unprotected sex contacts of the included PLWH during the HCV viremic period without effective treatment to indicate the risk for onward transmission of HCV.

Statistical analysis

The cascade of care after diagnosis of recently acquired HCV infection was examined by each step using descriptive analysis. Comparisons of categorical variables were performed by chi-square analysis and those of continuous variables by a Mann-Whitney *U* Test. The incidence rate of STIs during HCV viremia was calculated as the number of STIs per 100 PYFU. All analyses were two-tailed, and a $P < 0.05$ was considered statistically significant. All statistical analyses were performed using Stata/SE, version 14.0. The statistical methods of this study were reviewed by the staff of National Taiwan University Hospital–Statistical Consulting Unit (NTUH-SCU).

RESULTS

Between January 2011 and December 2018, 3,495 PLWH had a negative anti-HCV antibody test at baseline (Figure 1) and HCV seroconversion was detected in 294 (8.4%) PLWH. After excluding 7 PLWH who were lost to follow-up when seroconversion occurred, a total of 287 PLWH were included in the analysis of the HCV care

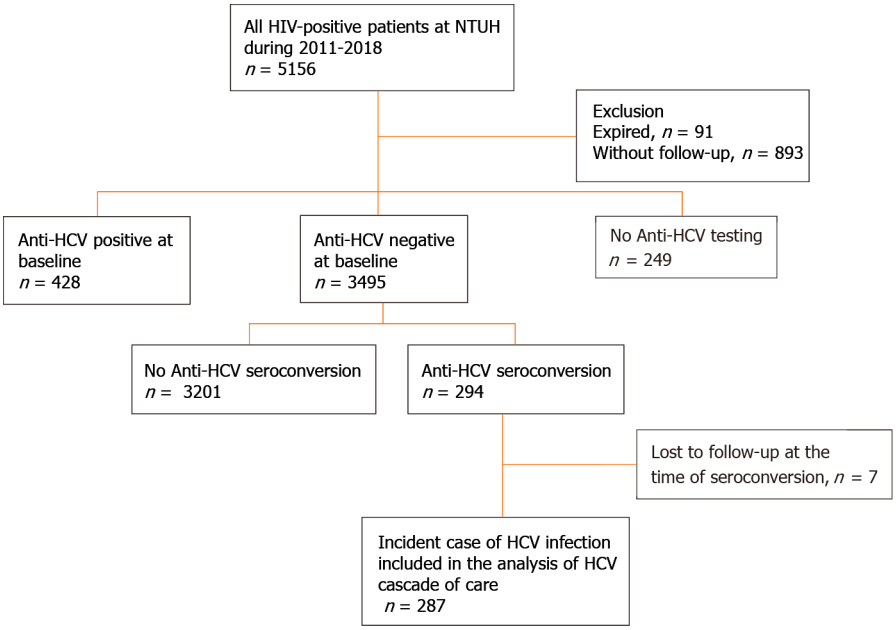


Figure 1 Patient flow. Between 2011 and 2018, 3495 people living with human immunodeficiency virus (HIV) (PLWH) had negative anti-hepatitis C virus (HCV) antibody tests at baseline and HCV seroconversion was detected in 294 (8.4%) PLWH. After excluding 7 PLWH who were lost to follow-up when HCV seroconversion occurred, a total of 287 PLWH were included in the analysis of the care cascade of incident HCV infections. HIV: Human immunodeficiency virus; NTUH: National Taiwan University Hospital; HCV: Hepatitis C virus.

cascade.

The clinical characteristics of the included 287 PLWH with recently acquired HCV infection are shown in Table 1. All of them were male, with a mean age of 34.5 years [standard deviation (SD) 7.6]. The mean PVL was 1.72 $\log_{10}$ copies/mL (SD 1.09) and mean CD4 count was 597.7 cells/mm^3 (SD 251.1) at the time of HCV seroconversion. The HBsAg seropositivity rate was 14.9% and active or previous syphilis was present in 89.2%. The risk groups of HIV acquisition included 265 (92.3%) MSM, 5 (1.8%) heterosexuals, 4 (1.4%) IDUs, and 13 (4.5%) unknown. The mean plasma HCV RNA load was 5.72 $\log_{10}$ copies/mL (SD 1.50). Twenty-two (7.7%), 84 (29.3%), 119 (41.5%), 6 (2.1%), and 34 (11.8%) PLWH had infection with HCV genotypes 1a, 1b, 2a, 3, and 6, respectively, and 3 (1%) had mixed infections of genotypes 1b and 2.

Of the 287 PLWH, 277 (96.5%) were found to have HCV seroconversions by HIV-treating physicians, including 8 diagnosed at the stage of acute infection with positive HCV RNA and negative anti-HCV antibody. Plasma HCV RNA load was determined in 270 (94.1%) PLWH after seroconversion, with 19 (12.5%) clearing viremia spontaneously and 251 (87.5%) remaining viremic (Table 2). Overall, 226 (78.7%) PLWH were referred to hepatology clinics for treatment assessment, and anti-HCV treatments were initiated in 215 (74.9%) PLWH, of whom 202 (70.4%) achieved SVR (Table 2).

Compared with PLWH who had HCV seroconversion in the IFN era (2011–2016), those who seroconverted in the DAA era (2017–2018) had higher achievement rates of all sequential steps of the care cascade (Figure 2), though not reaching statistical significance. The rate of antibody diagnosis within one year of HCV seroconversion was significantly higher in the DAA era than that in the IFN era (88.2% *vs* 69.5%; $P < 0.001$) (Figure 2). In the IFN era, the major gap of engagement in care was from HCV RNA positivity to referral for assessment and treatment, which resulted in a loss of 11.8% of those found to be HCV viremic.

The median interval from seroconversion to detection of HCV seropositivity by HIV-treating physicians was 130 d [interquartile range (IQR), 80-295], which was significantly shorter in the DAA era than in the IFN era [92 d (IQR, 57-173) *vs* 179 d (IQR 87-434); $P < 0.001$] (Table 2, Figure 3). From detection of HCV seropositivity to HCV RNA testing, the interval was 21 d (IQR 6-39) and 12 d (IQR 6-68) in the IFN and DAA eras, respectively ($P = 0.19$). The intervals from HCV RNA testing to treatment assessment and from assessment to treatment initiation were longer in the DAA era compared with those in the IFN era, 81 d (IQR 14-169) *vs* 26 d (IQR 7-208), and 42 d (IQR 18-84) *vs* 35 d (IQR 27-90), which were not statistically significantly different ($P = 0.25$ and $P = 0.55$, respectively). The duration of viremia was 735 d (IQR 391-1447) in the IFN era, which was significantly longer than that in the DAA era (380 d; IQR 274-

Table 1 Clinical characteristics of people living with human immunodeficiency virus who had incident hepatitis C virus infection from 2011 to 2018

Clinical characteristics	*n* = 287
Age, mean ± SD, yr	34.5 ± 7.6
Male sex, *n* (%)	287 (100)
Risk group, *n* (%)	
Men who have sex with men	265 (92.3)
Heterosexuals	5 (1.8)
Injecting drug users	4 (1.4)
Unknown	13 (4.5)
HIV PVL, mean ± SD, log_{10} copies/mL	1.72 ± 1.09
CD4 count, mean ± SD, cells/mm^3	597.7 ± 251.1
HBsAg-positive, *n* (%)	42 (14.9)
Syphilis, *n* (%)	256 (89.2)
Plasma HCV RNA, mean ± SD, log_{10} copies/mL	5.72 ± 1.50)
HCV genotype, *n* (%)	
1a	22 (7.7)
1b	84 (29.3)
2a	119 (41.5)
3	6 (2.1)
6	34 (11.8)
Mixed genotype 1b+2	3 (1.0)
No data	19 (6.6)
Year of seroconversion, *n* (%)	
2011	23 (8.0)
2012	28 (9.8)
2013	27 (9.4)
2014	24 (8.4)
2015	31 (10.8)
2016	43 (14.9)
2017	54 (18.8)
2018	57 (19.9)

HBsAg: Hepatitis B surface antigen; HCV: Hepatitis C virus; HIV: Human immunodeficiency virus; PVL: Plasma viral load; RNA: Ribonucleic acid.

554; $P < 0.001$).

Among the HCV seroconverters in the IFN era, a total of 165 episodes of STIs were observed in the entire HCV viremic duration of 428.2 PYFU, resulting in an incidence rate of 38.5 per 100 PYFU. In the DAA era, the HCV seroconverters acquired a total of 55 episodes of STIs during 108.8 PYFU of viremia, leading to an incidence rate of 50.5 per 100 PYFU. The incidence rate ratio (IRR) of STIs in the DAA era *vs* the IFN era was 1.31 (95%CI 0.96-1.77).

Figure 4 demonstrates the breakdown of HCV treatment uptake by year. The annual number of PLWH with HCV viremia who received IFN-based therapy was unchanged from 2012 to 2016. With the introduction of DAAs in 2016, the number of PLWH receiving DAA treatment increased year by year, especially in 2019, when restrictions on DAA reimbursement were lifted and all HCV viremic patients could be treated with DAAs.

Table 2 Care cascade of incident hepatitis C infections among people living with human immunodeficiency virus in the interferon and direct-acting antiviral eras

	Total 2011-2018, *n* = 287	Seroconversion in		*P* value
		2011-2016 IFN era, *n* = 176	2017-2018DAA era, *n* = 111	
Antibody detected, *n* (%)[1]	277 (96.5)	167 (94.9)	110 (99.1)	0.09
HCV RNA tested, *n* (%)[1]	270 (97.5)	162 (97.0)	108 (98.2)	0.08
HCV RNA positivity, *n* (%)[1]	251 (93.0)	152 (93.8)	99 (91.7)	0.48
Referred to treatment assessment, *n* (%)[1]	226 (90.0)	134 (88.2)	92 (92.9)	0.17
Treatment initiated, *n* (%)[1]	215 (95.1)	131 (97.8)	84 (91.3)	0.81
SVR achieved, *n* (%)[1]	202 (94)	120 (91.6)	82 (97.6)	0.19
Interval between each step, median days (IQR)				
Seroconversion to antibody detected	130 (80-295)	179 (87-434)	92 (57-173)	< 0.001
Antibody detected to HCV RNA tested	19 (6-81)	21 (6-93)	12 (6-68)	0.19
HCV RNA tested to treatment assessment	43 (11-181)	26 (7-208)	81 (14-169)	0.25
Treatment assessment to treatment initiation	36 (21-90)	35 (27-90)	42 (18-84)	0.55
Duration of viremia[2]	502 (325-945)	735 (391-1447)	380 (274-554)	< 0.001
Events of STIs during HCV viremia	220	165	55	< 0.001
Incidence rate of STIs during HCV viremia, (per 100-PYFU)	41.0	38.5	50.5	0.09

[1]Percentage that moved from the previous step to current step of care cascade.

[2]From the time of seroconversion to end of treatment. DAA: Direct-acting antiviral; IFN: Interferon; IQR; Interquartile range; PYFU: Person-years of follow-up; STIs: Sexually transmitted infections; SVR: Sustained virologic response.

DISCUSSION

In this study, we observed high rates of linkage to HCV care and retention in the care system among PLWH at our institution, in both the IFN and DAA eras. The retention rates between each step of the care cascade after detection of incident HCV infection primarily exceeded 90% (Figure 2). A major barrier noted in the IFN era was referral to treatment assessment (88.2%) after detection of HCV viremia, while this gap seemed diminished in the DAA era. In addition, the duration of HCV viremia, from seroconversion to completion of HCV treatment, was markedly shortened in the DAA era compared to that in the IFN era (380 d *vs* 735 d; $P < 0.001$). The improvement was mainly due to early diagnosis of recently acquired HCV infection by HIV-treating physicians because the diagnostic rate within one year after seroconversion increased from 69.5% (116/167) to 88.2% (97/110), and the median time from seroconversion to antibody diagnosis was shortened from 179 d to 92 d ($P < 0.001$).

The occurrence of STIs during HCV viremia represented risky sexual behavior, potentially resulting in onward transmission of HCV to their contacts. The incidence rate of STIs observed in the DAA era was higher than that in the IFN era, though not reaching statistical significance (50.5 *vs* 38.5 per 100 PYFU; IRR 1.31, 95%CI 0.96-1.77). In contrast, the total number of STI episodes was far fewer in the DAA era *vs* the IFN era (55 episodes among 111 patients *vs* 165 episodes among 176 patients, respectively), likely due to a shorter duration of HCV viremia. The curtailing of HCV viremia with the initiation of effective DAAs may indicate reduced opportunities to transmit HCV during the viremic period.

There are limited data to describe the care cascade after incident HCV infections were diagnosed both in the general population and in HCV-coinfected PLWH in the Asia-Pacific region. In our study, we tested archived blood samples to include all patients who had recent HCV infections in the previous year and estimated the time of seroconversion. In doing so, we could assess the rate of antibody diagnosis of HCV infection by treating physicians, the interval of delay in clinical diagnosis, and the duration of HCV viremia before effective anti-HCV treatments were initiated. Prior population-level studies of the care cascade either estimated the seroprevalence of

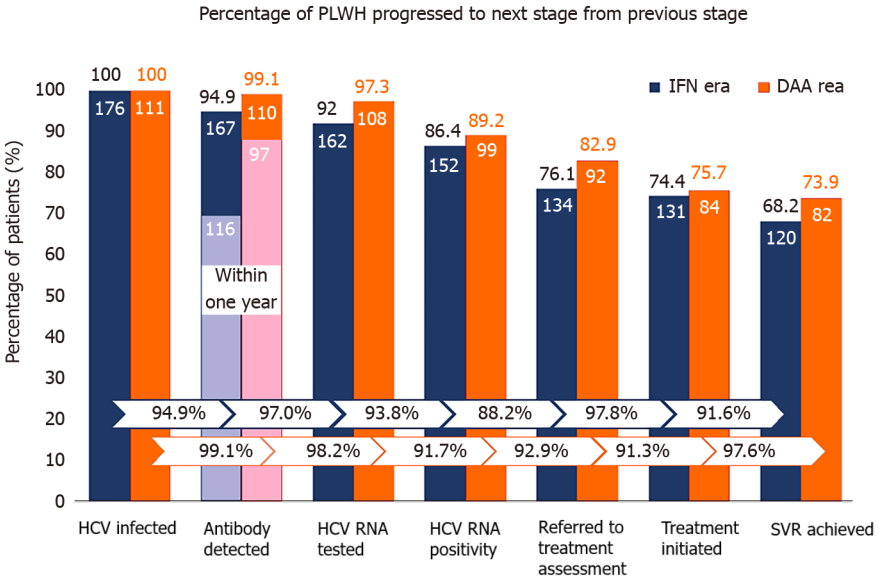


Figure 2 Care cascade of incident hepatitis C virus infections in the interferon and direct-acting antiviral eras. In the interferon era (blue columns), 176 people living with human immunodeficiency virus (HIV) (PLWH) had incident hepatitis C virus (HCV) infections by retrospective testing of all archive blood samples; 167 (94.9%) were found to have HCV seroconversion by HIV-treating physicians; and the diagnostic rate within one year after seroconversion was 69.4% (116 out of 167). Plasma HCV RNA was tested in 162 (97.0%) PLWH after seroconversion, of which 152 (93.8%) were viremic. A total of 134 (88.2%) viremic PLWH were referred to hepatology clinics; anti-HCV treatments were initiated in 131 (97.8%), and 120 (91.6% of all treated PLWH) achieved sustained virologic response (SVR). In the direct-acting antiviral era (orange columns), 111 PLWH had incident HCV infections; 110 (99.1%) were found to have HCV seroconversion by HIV-treating physicians; and the diagnostic rate within one year after seroconversion was 88.2% (97 out of 110). Plasma HCV RNA was detected in 108 (98.2%) PLWH after seroconversion and 99 (91.7%) were viremic. A total of 92 (92.9%) viremic PLWH received treatment assessment, anti-HCV treatments were initiated in 84 (91.3%), and 82 (97.6% of all treated patients) achieved SVR. IFN: Interferon; DAA: Direct-acting antiviral; HCV: Hepatitis C virus; PLWH: People living with human immunodeficiency virus.

HCV[24,25] or described the cascade since the diagnosis of anti-HCV positivity[26]. In single-center studies focusing on HCV-coinfected PLWH, the actual numbers of HCV infections were not shown in the care cascade[27,28].

Previous population-based care cascade assessments for HCV infection in the IFN era revealed low rates of retention in care and treatment initiation, probably related to concerns about inconvenience, lower effectiveness, intolerability, and higher rates of adverse effects with IFN/RBV treatment. The antibody diagnostic rate was 50% to 75%; HCV RNA testing was performed in 30 to 50% of patients; less than 20% of patients received HCV treatment; and the final SVR rate was lower than 10%[24,25]. At our institution during the IFN era, the antibody diagnosis, HCV RNA testing, treatment initiation, and SVR rates were 94.9%, 92.0%, 74.4%, and 68.2%, respectively, much higher than those of previous population-level studies. We believe that regularly scheduled follow-up visits for fully-reimbursed HIV antiretroviral treatments in the majority of PLWH might have provided an opportunity to facilitate HCV testing and increase engagement of HCV care[29,30]. However, mandatory referrals to a hepatologist for HCV pretreatment assessment and management may have raised the barrier to anti-HCV treatment initiation and achievement of viral clearance, as such a requirement negatively impacts convenience and costs, thereby potentially increasing the risk of dropout from HCV care. This barrier has diminished since 2019 when NHI approved HIV-treating physicians to participate in HCV assessment and treatment for PLWH at infectious disease clinics. The rate of treatment assessment after HCV RNA positivity increased from 88.2% (134/152) in the IFN era to 92.9% (92/99) in the DAA era.

The introduction of DAAs has been shown to improve engagement of HCV care and treatment uptake. The British Columbia Hepatitis Tester Cohort demonstrated improvement of the care cascade in the DAA era. Of the patients who tested anti-HCV-positive, 83% had HCV RNA testing done; and, of those who were HCV viremic and were genotyped, 61% received DAA therapy, with 90% achieving SVR[31]. In a report from seven HCV elimination studies among PLWH in the early DAA era, the average treatment uptake increased to 48% and treatment completion rates reached 96%[32]. Our current study showed a significantly higher rate of linkage to care, with > 90% of PLWH consistently advancing from each cascade step to the next in the DAA era, which resulted in a total of 84.8% (84/99) viremic patients initiating anti-HCV

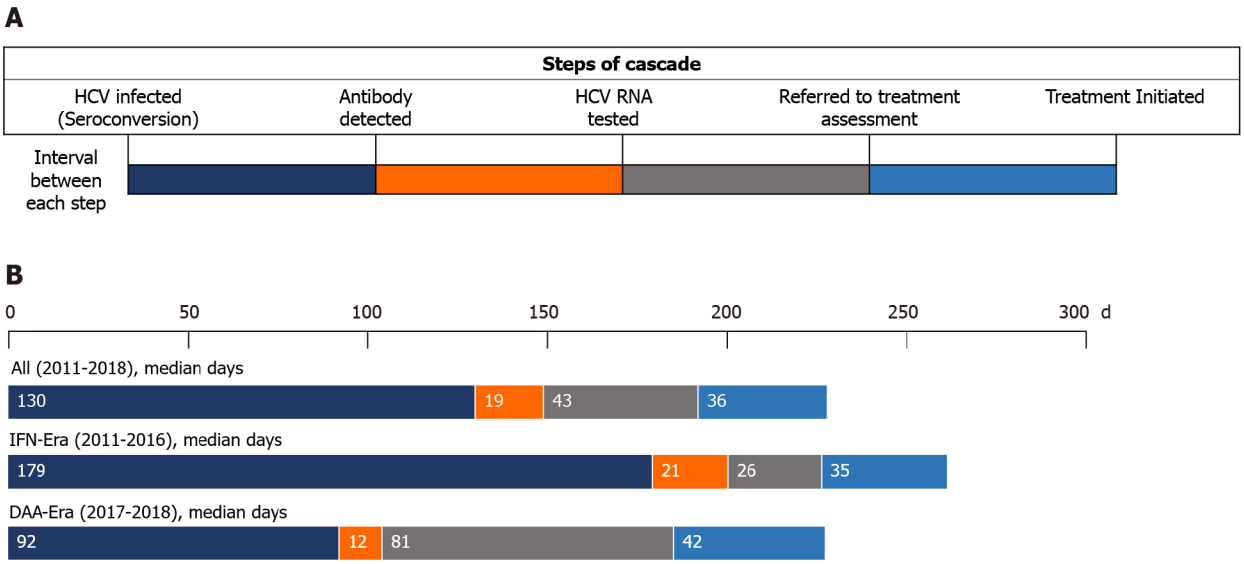


Figure 3 Intervals between steps of the care cascade of incident hepatitis C virus infections. A: Demonstration of the intervals between each step of the care cascade; B: In all included people living with human immunodeficiency virus (HIV) (PLWH), the median interval from seroconversion to detection of hepatitis C virus (HCV) seropositivity by HIV-treating physicians was 130 days, which was significantly shorter in the direct-acting antiviral (DAA) era (median 92 d) than that in the interferon (IFN) era (median 179 d) ($P < 0.001$). In the IFN era, the median interval from detection of HCV seropositivity to HCV RNA testing was 21 d, that from RNA testing to referral to treatment assessment was 26 d, and that from assessment to treatment initiation was 35 d. In the DAA era, the median interval from detection of HCV seropositivity to HCV RNA testing was 12 d, that from RNA testing to referral to treatment assessment was 81 d, and that from assessment to treatment initiation was 42 d. The differences in the intervals after antibody diagnosis were not statistically significant between PLWH included in the IFN era and those in the DAA era. HCV: Hepatitis C virus; IFN: Interferon; DAA: Direct-acting antiviral.

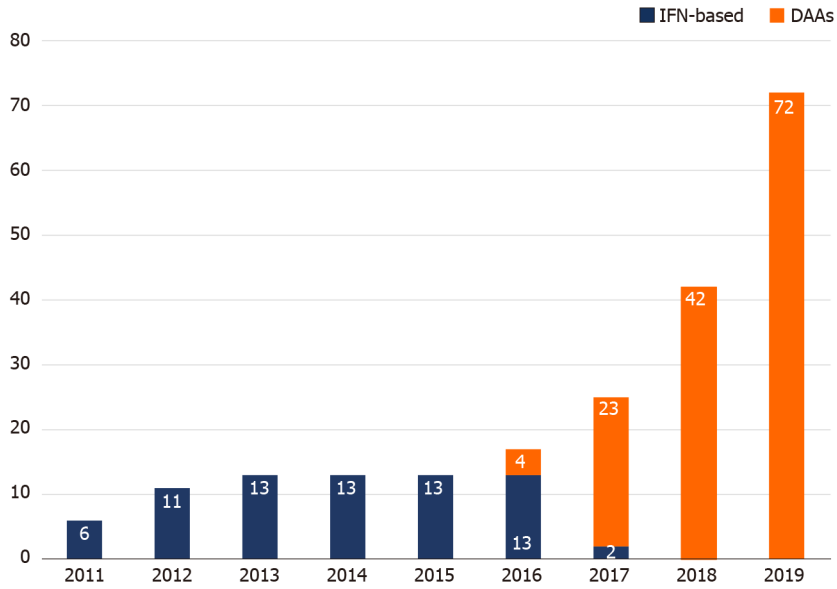


Figure 4 Hepatitis C virus treatment uptake by year from 2011 to 2019. The annual numbers of people living with human immunodeficiency virus (PLWH) who received interferon-based therapy were unchanged from 2012 to 2016. With the introduction of direct-acting antivirals (DAAs) since 2016, the number of PLWH receiving DAAs increased annually, especially in 2019, when the restrictions on the DAA reimbursement were lifted and all hepatitis C virus viremic patients could be treated with DAAs. DAA: Direct-acting antiviral; IFN: Interferon.

treatments, and 97.6% (82/84) achieving SVR. In the Swiss HIV Cohort Study, the treatment incidence increased from 4.5 per 100 PYFU before the availability of DAAs, to 22.4 per 100 PYFU after the introduction of second-generation DAAs[33]. These findings were in line with observations from our study. While the annual number of IFN-based therapy remained unchanged from 2012 to 2016, the number of DAA treatment initiated progressively increased from 2016 to 2018, which further rocketed in 2019, when the restriction on DAA reimbursement was lifted (Figure 4). During the period between 2016 and 2018, when access to DAA through NHI reimbursement

remained limited, generic DAAs could be purchased overseas by PLWH themselves; however, accessibility was limited by the cost incurred. During this period, we found that the median intervals from HCV RNA testing to referral to treatment assessment, and those from referral to treatment initiation were longer than those in the IFN era, though not reaching statistical significance (Table 2 and Figure 3).

There are several limitations in this study. First, the cascade of HCV care from this single-center study might not be generalizable to other institutions in Taiwan, given that discrepancies in the patients' demographic and clinical characteristics and socio-economic status may exist. At our institution, PLWH with recent HCV infection were mainly MSM, accounting for more than 90% of the included patients, while the percentages of heterosexual and IDUs were both lower than 2%. Prior studies suggested from an assessment of the HCV care cascade in IDUs that active drug users had poorer treatment adherence, resulting in lower rates of viral clearance[34-36]. Second, our study did not investigate factors that may be associated with failure of engagement in the HCV care cascade. Third, HCV reinfection, which can occur in this high-risk group[37-39], were not included in the analyses of the HCV care cascade.

CONCLUSION

In conclusion, we describe the HCV care cascade at a referral hospital in Taiwan from the IFN era to the DAA era. The rates of engagement in each step of the HCV care cascade were high in both eras and the barriers to referral and reimbursement diminished over time. However, given both the longer intervals of HCV viremia observed in the DAA era and a higher incidence of STIs potentially contributing to onward transmission of HCV, more efforts are needed to expedite the linkage of PLWH diagnosed with incident HCV infections to HCV treatment.

ARTICLE HIGHLIGHTS

Research background

Recently acquired hepatitis C virus (HCV) infections are increasingly reported in people living with human immunodeficiency virus (HIV) (PLWH) who are men who have sex with men. With availability of highly effective direct-acting antivirals (DAAs) for the treatment of HCV, microelimination HCV is considered an achievable goal in this at-risk population.

Research motivation

To achieve microelimination of HCV in PLWH, each step of the continuum of HCV care, from diagnosis, linkage to and engagement in care, initiation of anti-HCV treatment, treatment completion, to prevention against reinfection, is crucial. Examining the HCV care cascade can identify barriers to the completion of HCV treatment and facilitate achievement of HCV micro-elimination in PLWH.

Research objectives

The study aimed to evaluate the care cascade of PLWH with recently acquired HCV infections at a university hospital designated for HIV care in Taiwan.

Research methods

The authors retrospectively reviewed the medical records of all PLWH testing negative for anti-HCV at baseline who developed anti-HCV seroconversion between 2011 to 2018 and were observed till the end of 2019. The number of people in each step of HCV care cascade was assessed and the duration between two sequential steps was estimated.

Research results

A total of 287 PLWH recently acquired HCV infections during the study period. High rates of linkage to HCV care and retention in the care were observed in our cohort. Compared with the interferon (IFN, 2011-2016) era, the barrier of referral to anti-HCV treatment assessment was diminished and the total duration of HCV viremia marked decreased in the direct-acting antiviral (DAA, 2017-2018) era.

Research conclusions

The achievement rates of engagement in each step of the HCV care cascade were high in both IFN and DAA eras and the barriers to referral and treatment initiation diminished over time.

Research perspectives

The impact of scale-up of HCV testing and DAA treatment after lifting the restriction on DAA reimbursement on the trends of incident HCV infections in PLWH warrants more long-term observation.

ACKNOWLEDGEMENTS

The authors would like to express their gratitude to the staff of National Taiwan University Hospital-Statistical Consulting Unit (NTUH-SCU) for statistical consultation and analyses.

REFERENCES

1 **Thomas DL**. Global Elimination of Chronic Hepatitis. *N Engl J Med* 2019; **380**: 2041-2050 [PMID: 31116920 DOI: 10.1056/NEJMra1810477]
2 **Platt L**, Easterbrook P, Gower E, McDonald B, Sabin K, McGowan C, Yanny I, Razavi H, Vickerman P. Prevalence and burden of HCV co-infection in people living with HIV: a global systematic review and meta-analysis. *Lancet Infect Dis* 2016; **16**: 797-808 [PMID: 26922272 DOI: 10.1016/S1473-3099(15)00485-5]
3 **Cooke GS**, Andrieux-Meyer I, Applegate TL, Atun R, Burry JR, Cheinquer H, Dusheiko G, Feld JJ, Gore C, Griswold MG, Hamid S, Hellard ME, Hou J, Howell J, Jia J, Kravchenko N, Lazarus JV, Lemoine M, Lesi OA, Maistat L, McMahon BJ, Razavi H, Roberts T, Simmons B, Sonderup MW, Spearman CW, Taylor BE, Thomas DL, Waked I, Ward JW, Wiktor SZ; Lancet Gastroenterology & Hepatology Commissioners. Accelerating the elimination of viral hepatitis: a Lancet Gastroenterology & Hepatology Commission. *Lancet Gastroenterol Hepatol* 2019; **4**: 135-184 [PMID: 30647010 DOI: 10.1016/S2468-1253(18)30270-X]
4 **Trickey A**, Fraser H, Lim AG, Peacock A, Colledge S, Walker JG, Leung J, Grebely J, Larney S, Martin NK, Hickman M, Degenhardt L, May MT, Vickerman P. The contribution of injection drug use to hepatitis C virus transmission globally, regionally, and at country level: a modelling study. *Lancet Gastroenterol Hepatol* 2019; **4**: 435-444 [PMID: 30981685 DOI: 10.1016/S2468-1253(19)30085-8]
5 **Martinello M**, Amin J, Matthews GV, Dore GJ. Prevalence and Disease Burden of HCV Coinfection in HIV Cohorts in the Asia Pacific Region: A Systematic Review and Meta-Analysis. *AIDS Rev* 2016; **18**: 68-80 [PMID: 27196354]
6 **Zhou J**, Dore GJ, Zhang F, Lim PL, Chen YM; TREAT Asia HIV Observational Database. Hepatitis B and C virus coinfection in The TREAT Asia HIV Observational Database. *J Gastroenterol Hepatol* 2007; **22**: 1510-1518 [PMID: 17645479 DOI: 10.1111/j.1440-1746.2007.05062.x]
7 **van de Laar T**, Pybus O, Bruisten S, Brown D, Nelson M, Bhagani S, Vogel M, Baumgarten A, Chaix ML, Fisher M, Gotz H, Matthews GV, Neifer S, White P, Rawlinson W, Pol S, Rockstroh J, Coutinho R, Dore GJ, Dusheiko GM, Danta M. Evidence of a large, international network of HCV transmission in HIV-positive men who have sex with men. *Gastroenterology* 2009; **136**: 1609-1617 [PMID: 19422083 DOI: 10.1053/j.gastro.2009.02.006]
8 **Wandeler G**, Gsponer T, Bregenzer A, Günthard HF, Clerc O, Calmy A, Stöckle M, Bernasconi E, Furrer H, Rauch A; Swiss HIV Cohort Study. Hepatitis C virus infections in the Swiss HIV Cohort Study: a rapidly evolving epidemic. *Clin Infect Dis* 2012; **55**: 1408-1416 [PMID: 22893583 DOI: 10.1093/cid/cis694]
9 **Boesecke C**, Grint D, Soriano V, Lundgren JD, d'Arminio Monforte A, Mitsura VM, Chentsova N, Hadziosmanovic V, Kirk O, Mocroft A, Peters L, Rockstroh JK; EuroSIDA in EuroCoord. Hepatitis C seroconversions in HIV infection across Europe: which regions and patient groups are affected? *Liver Int* 2015; **35**: 2384-2391 [PMID: 25875966 DOI: 10.1111/liv.12848]
10 **Sun HY**, Uemura H, Wong NS, Chan DP, Wong BC, Lin PH, Su LH, Hung CC, Oka S, Chang SY, Lee SS. Molecular epidemiology of acute HCV infection in HIV-positive patients from Hong Kong, Taipei, Tokyo. *Liver Int* 2019; **39**: 1044-1051 [PMID: 30770636 DOI: 10.1111/liv.14073]
11 **Ho SY**, Su LH, Sun HY, Huang YS, Chuang YC, Huang MH, Liu WC, Su YC, Lin PH, Chang SY, Hung CC. Trends of recent hepatitis C virus infection among HIV-positive men who have sex with men in Taiwan, 2011-2018. *EClinicalMedicine* 2020; **24**: 100441 [PMID: 32637905 DOI: 10.1016/j.eclinm.2020.100441]
12 **Chan DP**, Sun HY, Wong HT, Lee SS, Hung CC. Sexually acquired hepatitis C virus infection: a review. *Int J Infect Dis* 2016; **49**: 47-58 [PMID: 27270138 DOI: 10.1016/j.ijid.2016.05.030]

13 **Sikavi C**, Chen PH, Lee AD, Saab EG, Choi G, Saab S. Hepatitis C and human immunodeficiency virus coinfection in the era of direct-acting antiviral agents: No longer a difficult-to-treat population. *Hepatology* 2018; **67**: 847-857 [PMID: 29108121 DOI: 10.1002/hep.29642]

14 **Brown RS Jr**, Buti M, Rodrigues L, Chulanov V, Chuang WL, Aguilar H, Horváth G, Zuckerman E, Carrion BR, Rodriguez-Perez F, Urbánek P, Abergel A, Cohen E, Lovell SS, Schnell G, Lin CW, Zha J, Wang S, Trinh R, Mensa FJ, Burroughs M, Felizarta F. Glecaprevir/pibrentasvir for 8 weeks in treatment-naïve patients with chronic HCV genotypes 1-6 and compensated cirrhosis: The EXPEDITION-8 trial. *J Hepatol* 2020; **72**: 441-449 [PMID: 31682879 DOI: 10.1016/j.jhep.2019.10.020]

15 **Rockstroh JK**, Lacombe K, Viani RM, Orkin C, Wyles D, Luetkemeyer AF, Soto-Malave R, Flisiak R, Bhagani S, Sherman KE, Shimonova T, Ruane P, Sasadeusz J, Slim J, Zhang Z, Samanta S, Ng TI, Gulati A, Kosloski MP, Shulman NS, Trinh R, Sulkowski M. Efficacy and Safety of Glecaprevir/Pibrentasvir in Patients Coinfected With Hepatitis C Virus and Human Immunodeficiency Virus Type 1: The EXPEDITION-2 Study. *Clin Infect Dis* 2018; **67**: 1010-1017 [PMID: 29566246 DOI: 10.1093/cid/ciy220]

16 **Wyles D**, Bräu N, Kottilil S, Daar ES, Ruane P, Workowski K, Luetkemeyer A, Adeyemi O, Kim AY, Doehle B, Huang KC, Mogalian E, Osinusi A, McNally J, Brainard DM, McHutchison JG, Naggie S, Sulkowski M; ASTRAL-5 Investigators. Sofosbuvir and Velpatasvir for the Treatment of Hepatitis C Virus in Patients Coinfected With Human Immunodeficiency Virus Type 1: An Open-Label, Phase 3 Study. *Clin Infect Dis* 2017; **65**: 6-12 [PMID: 28369210 DOI: 10.1093/cid/cix260]

17 **Liu CH**, Sun HY, Hsieh SM, Liu WC, Sheng WH, Liu CJ, Su TH, Tseng TC, Chen PJ, Hung CC, Kao JH. Evolution of estimated glomerular filtration rate in human immunodeficiency virus and hepatitis C virus-coinfected patients receiving sofosbuvir-based direct-acting antivirals and antiretroviral therapy. *J Viral Hepat* 2021; **28**: 887-896 [PMID: 33759290 DOI: 10.1111/jvh.13502]

18 **Liu CH**, Chen PY, Chen JJ, Lo CC, Su WW, Tseng KC, Liu CJ, Huang CS, Huang KJ, Yang SS, Peng CY, Tsai MC, Kao WY, Chang CY, Shih YL, Fang YJ, Chen CY, Lee PL, Huang JJ, Su PY, Tseng CW, Hung CC, Chang CH, Huang YJ, Lai HC, Chang CC, Lee FJ, Hsieh TY, Kao JH. Sofosbuvir/velpatasvir for patients with chronic hepatitis C virus infection and compensated liver disease: real-world data in Taiwan. *Hepatol Int* 2021; **15**: 338-349 [PMID: 33677787 DOI: 10.1007/s12072-021-10158-x]

19 **Rockstroh J**, Boesecke C. Treatment of acute hepatitis C in HIV coinfection: Is this a chance for achieving microelimination? *United European Gastroenterol J* 2019; **7**: 465-466 [PMID: 31065363 DOI: 10.1177/2050640619843735]

20 **Heffernan A**, Cooke GS, Nayagam S, Thursz M, Hallett TB. Scaling up prevention and treatment towards the elimination of hepatitis C: a global mathematical model. *Lancet* 2019; **393**: 1319-1329 [PMID: 30704789 DOI: 10.1016/S0140-6736(18)32277-3]

21 **Kao JH**. Hepatitis C virus infection in Taiwan: Past, present, and future. *J Formos Med Assoc* 2016; **115**: 65-66 [PMID: 26228687 DOI: 10.1016/j.jfma.2015.06.012]

22 **Liu CH**, Sheng WH, Sun HY, Hsieh SM, Lo YC, Liu CJ, Su TH, Yang HC, Liu WC, Chen PJ, Chen DS, Hung CC, Kao JH. Peginterferon plus Ribavirin for HIV-infected Patients with Treatment-Naïve Acute or Chronic HCV Infection in Taiwan: A Prospective Cohort Study. *Sci Rep* 2015; **5**: 17410 [PMID: 26616669 DOI: 10.1038/srep17410]

23 **Liu CH**, Sun HY, Liu CJ, Sheng WH, Hsieh SM, Lo YC, Liu WC, Su TH, Yang HC, Hong CM, Tseng TC, Chen PJ, Chen DS, Hung CC, Kao JH. Generic velpatasvir plus sofosbuvir for hepatitis C virus infection in patients with or without human immunodeficiency virus coinfection. *Aliment Pharmacol Ther* 2018; **47**: 1690-1698 [PMID: 29665069 DOI: 10.1111/apt.14647]

24 **Janjua NZ**, Kuo M, Yu A, Alvarez M, Wong S, Cook D, Wong J, Grebely J, Butt ZA, Samji H, Ramji A, Tyndall M, Krajden M. The Population Level Cascade of Care for Hepatitis C in British Columbia, Canada: The BC Hepatitis Testers Cohort (BC-HTC). *EBioMedicine* 2016; **12**: 189-195 [PMID: 27596150 DOI: 10.1016/j.ebiom.2016.08.035]

25 **Yehia BR**, Schranz AJ, Umscheid CA, Lo Re V 3rd. The treatment cascade for chronic hepatitis C virus infection in the United States: a systematic review and meta-analysis. *PLoS One* 2014; **9**: e101554 [PMID: 24988388 DOI: 10.1371/journal.pone.0101554]

26 **Simmons R**, Ireland G, Irving W, Hickman M, Sabin C, Ijaz S, Ramsay M, Lattimore S, Mandal S. Establishing the cascade of care for hepatitis C in England-benchmarking to monitor impact of direct acting antivirals. *J Viral Hepat* 2018; **25**: 482-490 [PMID: 29239130 DOI: 10.1111/jvh.12844]

27 **Cachay ER**, Hill L, Wyles D, Colwell B, Ballard C, Torriani F, Mathews WC. The hepatitis C cascade of care among HIV infected patients: a call to address ongoing barriers to care. *PLoS One* 2014; **9**: e102883 [PMID: 25036553 DOI: 10.1371/journal.pone.0102883]

28 **Zuckerman A**, Douglas A, Nwosu S, Choi L, Chastain C. Increasing success and evolving barriers in the hepatitis C cascade of care during the direct acting antiviral era. *PLoS One* 2018; **13**: e0199174 [PMID: 29912944 DOI: 10.1371/journal.pone.0199174]

29 **Lazarus JV**, Safreed-Harmon K, Thursz MR, Dillon JF, El-Sayed MH, Elsharkawy AM, Hatzakis A, Jadoul M, Prestileo T, Razavi H, Rockstroh JK, Wiktor SZ, Colombo M. The Micro-Elimination Approach to Eliminating Hepatitis C: Strategic and Operational Considerations. *Semin Liver Dis* 2018; **38**: 181-192 [PMID: 29986353 DOI: 10.1055/s-0038-1666841]

30 **Busschots D**, Kremer C, Koc ÖM, Heyens L, Bielen R, Apers L, Florence E, Messiaen P, Van Laethem K, Van Wijngaerden E, Nevens F, Hens N, Robaeys G. The hepatitis C cascade of care in the Belgian HIV population: One step closer to elimination. *Int J Infect Dis* 2021; **105**: 217-223

[PMID: 33610786 DOI: 10.1016/j.ijid.2021.02.068]

31 **Bartlett SR**, Yu A, Chapinal N, Rossi C, Butt Z, Wong S, Darvishian M, Gilbert M, Wong J, Binka M, Alvarez M, Tyndall M, Krajden M, Janjua NZ. The population level care cascade for hepatitis C in British Columbia, Canada as of 2018: Impact of direct acting antivirals. *Liver Int* 2019; **39**: 2261-2272 [PMID: 31444846 DOI: 10.1111/liv.14227]

32 **Sacks-Davis R**, Doyle JS, Rauch A, Beguelin C, Pedrana AE, Matthews GV, Prins M, van der Valk M, Klein MB, Saeed S, Lacombe K, Chkhartishvili N, Altice FL, Hellard ME. Linkage and retention in HCV care for HIV-infected populations: early data from the DAA era. *J Int AIDS Soc* 2018; **21** Suppl 2: e25051 [PMID: 29633559 DOI: 10.1002/jia2.25051]

33 **Béguelin C**, Suter A, Bernasconi E, Fehr J, Kovari H, Bucher HC, Stoeckle M, Cavassini M, Rougemont M, Schmid P, Wandeler G, Rauch A; Swiss HIV Cohort Study. Trends in HCV treatment uptake, efficacy and impact on liver fibrosis in the Swiss HIV Cohort Study. *Liver Int* 2018; **38**: 424-431 [PMID: 28741901 DOI: 10.1111/liv.13528]

34 **Iversen J**, Grebely J, Catlett B, Cunningham P, Dore GJ, Maher L. Estimating the cascade of hepatitis C testing, care and treatment among people who inject drugs in Australia. *Int J Drug Policy* 2017; **47**: 77-85 [PMID: 28578863 DOI: 10.1016/j.drugpo.2017.05.022]

35 **Morris MD**, Mirzazadeh A, Evans JL, Briceno A, Coffin P, Hahn JA, Page KA. Treatment cascade for hepatitis C virus in young adult people who inject drugs in San Francisco: Low number treated. *Drug Alcohol Depend* 2019; **198**: 133-135 [PMID: 30921649 DOI: 10.1016/j.drugalcdep.2019.02.008]

36 **Ireland G**, Simmons R, Hickman M, Eastwood B, Ramsay M, Mandal S. Mapping the hepatitis C cascade of care in people attending drug treatment services in England: A data linkage study. *Int J Drug Policy* 2019; **72**: 55-60 [PMID: 31257040 DOI: 10.1016/j.drugpo.2019.06.006]

37 **Newsum AM**, Matser A, Schinkel J, van der Valk M, Brinkman K, van Eeden A, Lauw FN, Rijnders BJA, van de Laar TJW, van de Kerkhof M, Smit C, Boyd A, Arends JE, Prins M; MSM Observational Study of Acute Infection with hepatitis C (MOSAIC) study group. Incidence of HCV Reinfection Among HIV-Positive MSM and Its Association With Sexual Risk Behavior: A Longitudinal Analysis. *Clin Infect Dis* 2021; **73**: 460-467 [PMID: 32459339 DOI: 10.1093/cid/ciaa645]

38 **Huang MH**, Chang SY, Liu CH, Cheng A, Su LH, Liu WC, Su YC, Sun HY, Hung CC, Chang SC. HCV reinfections after viral clearance among HIV-positive patients with recent HCV infection in Taiwan. *Liver Int* 2019; **39**: 1860-1867 [PMID: 31343813 DOI: 10.1111/liv.14199]

39 **Ingiliz P**, Martin TC, Rodger A, Stellbrink HJ, Mauss S, Boesecke C, Mandorfer M, Bottero J, Baumgarten A, Bhagani S, Lacombe K, Nelson M, Rockstroh JK; NEAT study group. HCV reinfection incidence and spontaneous clearance rates in HIV-positive men who have sex with men in Western Europe. *J Hepatol* 2017; **66**: 282-287 [PMID: 27650285 DOI: 10.1016/j.jhep.2016.09.004]

World Journal of Gastroenterology

Submit a Manuscript: https://www.f6publishing.com

World J Gastroenterol 2021 October 7; 27(37): 6290-6305

DOI: 10.3748/wjg.v27.i37.6290

ISSN 1007-9327 (print) ISSN 2219-2840 (online)

ORIGINAL ARTICLE

Observational Study

Helicobacter pylori in gastric cancer: Features of infection and their correlations with long-term results of treatment

Marina A Senchukova, Olesya Tomchuk, Elena I Shurygina

ORCID number: Marina A Senchukova 0000-0001-8371-740X; Olesya Tomchuk 0000-0003-4065-620X; Elena I Shurygina 0000-0002-0571-2803.

Author contributions: Senchukova MA wrote the paper; Tomchuk O and Shurygina EI perfomed the collected the data.

Institutional review board statement: The study was reviewed and approved by the Institutional Review Board of the Orenburg State Medical University.

Informed consent statement: All patients provided written informed consent.

Conflict-of-interest statement: The authors declare no conflicts of interests related to the publication of this study.

Data sharing statement: No additional data are available.

STROBE statement: The authors have read the STROBE Statement—checklist of items, and the manuscript was prepared and revised according to the STROBE Statement—checklist of items.

Open-Access: This article is an open-access article that was

Marina A Senchukova, Department of Oncology, Orenburg State Medical University, Orenburg 460000, Russia

Olesya Tomchuk, Department of Histology, Cytology, Embryology, Orenburg State Medical University, Orenburg 460000, Russia

Elena I Shurygina, Department of Pathology, Orenburg State Medical University, Orenburg 460000, Russia

Corresponding author: Marina A Senchukova, MD, PhD, Professor, Department of Oncology, Orenburg State Medical University, Sovetskaya Street 6, Orenburg 460000, Russia. masenchukova@yandex.com

Abstract

BACKGROUND

Helicobacter pylori (*H. pylori*) is a spiral-shaped bacterium responsible for the development of chronic gastritis, gastric ulcer, gastric cancer (GC), and MALT-lymphoma of the stomach. *H. pylori* can be present in the gastric mucosa (GM) in both spiral and coccoid forms. However, it is not known whether the severity of GM contamination by various vegetative forms of *H. pylori* is associated with clinical and morphological characteristics and long-term results of GC treatment.

AIM

To establish the features of *H. pylori* infection in patients with GC and their correlations with clinical and morphological characteristics of diseases and long-term results of treatment.

METHODS

Of 109 patients with GC were included in a prospective cohort study. *H. pylori* in the GM and tumor was determined by rapid urease test and by immunohistochemically using the antibody to *H. pylori*. The results obtained were compared with the clinical and morphological characteristics and prognosis of GC. Statistical analysis was performed using the Statistica 10.0 software.

RESULTS

H. pylori was detected in the adjacent to the tumor GM in 84.5% of cases, of which a high degree of contamination was noted in 50.4% of the samples. Coccoid forms of *H. pylori* were detected in 93.4% of infected patients, and only coccoid-in 68.9%.

selected by an in-house editor and fully peer-reviewed by external reviewers. It is distributed in accordance with the Creative Commons Attribution NonCommercial (CC BY-NC 4.0) license, which permits others to distribute, remix, adapt, build upon this work non-commercially, and license their derivative works on different terms, provided the original work is properly cited and the use is non-commercial. See: http://creativecommons.org/Licenses/by-nc/4.0/

Manuscript source: Invited manuscript

Specialty type: Gastroenterology and hepatology

Country/Territory of origin: Russia

Peer-review report's scientific quality classification

Grade A (Excellent): 0
Grade B (Very good): B
Grade C (Good): 0
Grade D (Fair): 0
Grade E (Poor): 0

Received: April 30, 2021
Peer-review started: April 30, 2021
First decision: June 17, 2021
Revised: June 21, 2021
Accepted: August 31, 2021
Article in press: August 31, 2021
Published online: October 7, 2021

P-Reviewer: Modun D
S-Editor: Fan JR
L-Editor: A
P-Editor: Guo X

It was found that a high degree of GM contamination by the coccoid forms of *H. pylori* was observed significantly more often in diffuse type of GC (P = 0.024), in poorly differentiated GC (P = 0.011), in stage T3-4 (P = 0.04) and in N1 (P = 0.011). In cases of moderate and marked concentrations of *H. pylori* in GM, a decrease in 10-year relapse free and overall survival from 55.6% to 26.3% was observed (P = 0.02 and P = 0.07, respectively). The relationship between the severity of the GM contamination by the spiral-shaped forms of *H. pylori* and the clinical and morphological characteristics and prognosis of GC was not revealed.

CONCLUSION

The data obtained indicates that *H. pylori* may be associated not only with induction but also with the progression of GC.

Key Words: Gastric cancer; *Helicobacter pylori*; Coccoid and spiral forms of bacteria; Rapid urease test; Relapse free survival; Overall survival

©The Author(s) 2021. Published by Baishideng Publishing Group Inc. All rights reserved.

Core Tip: The role of *Helicobacter pylori* (*H. pylori*) in the progression of gastric cancer (GC) is not well understood. Our results indicate that in GC, a high degree of gastric mucosa contamination by coccoid forms of *H. pylori* is associated with advanced stages of the disease and deterioration of long-term results of treatment.

Citation: Senchukova MA, Tomchuk O, Shurygina EI. *Helicobacter pylori* in gastric cancer: Features of infection and their correlations with long-term results of treatment. *World J Gastroenterol* 2021; 27(37): 6290-6305
URL: https://www.wjgnet.com/1007-9327/full/v27/i37/6290.htm
DOI: https://dx.doi.org/10.3748/wjg.v27.i37.6290

INTRODUCTION

Gastric cancer (GC) continues to be one of the most common malignant diseases in the world[1,2]. Despite a decreasing trend in the incidence of GC in most countries of the world, the treatment results of this pathology cannot be considered satisfactory. In the structure of mortality from malignant neoplasms, this pathology firmly occupies 2nd place in most developed countries of the world, and the 5-year survival rate of radically operated patients does not exceed 15%-30%[3,4].

It is important to note that it is impossible to improve the long-term results of malignant neoplasms treatment without knowledge of the mechanisms associated with their progression[3]. Clinical studies in recent years indicate that inflammatory infiltration of the tumor stroma and surrounding tissues can have an important prognostic value and affect the long-term results of malignant neoplasm treatment[5-9]. A number of studies have shown that inflammatory infiltration of the tumor stroma is associated with the body's adequate immune response to the tumor, and may be a favorable prognosis factor in various malignant neoplasms[10,11], including GC[12,13]. At the same time, the data obtained by other researchers indicates that pronounced inflammatory infiltration of the tumor stroma, especially T-reg lymphocytes and macrophages, may be a factor contributing to the progression of malignant neoplasms[14,15]. There was a decrease in the overall survival (OS) and relapse-free survival (RFS) of GC patients with a high content of Foxp3 + T-reg in the tumor stroma and regional metastases[16-18] and macrophages[16,19]. It is believed that inflammatory infiltration of the tumor stroma can contribute to tumor progression by activating the mechanisms of angiogenesis, expression of E- and L-selectins, formation of the products of lipid peroxidation and free radicals, destruction of connective tissue matrix and basement membranes of epithelia by proteolytic enzymes, and activation of epithelial-mesenchymal transformation[20-23].

When studying the role of inflammation in the progression of GC, it is impossible to ignore the problem of *Helicobacter pylori* (*H. pylori*) infection. *H. pylori* is a gram-negative, spiral-shaped bacterium, the habitat of which is the gastric mucosa (GM) and

duodenum. *H. pylori* differs from other bacteria in a set of properties that make it possible to colonize the GM and persist for a long time under conditions that are unfavorable for other microorganisms[24,25]. These include: (1) The ability to produce a special enzyme-urease; (2) Synthesis of lytic enzymes that cause the depolymerization and dissolution of gastric mucus, consisting mainly of mucin; (3) The mobility of the bacterium, which is ensured by the presence of 5-6 flagella; (4) The high adhesiveness of bacteria to GM epithelial cells of the GM and elements of connective tissue due to the interaction of bacterial ligands with the corresponding cells receptors; (5) Production of various exotoxins (VacA, CagA, and others); (6) Instability of the *H. pylori* genome; (7) The presence of vegetative and coccoid forms of bacteria; and (8) possibility of intracellular persistence and translocation outside the GM [26-29].

It should be noted that despite the huge number of studies devoted to *H. pylori*, it is still not clear whether *H. pylori* is involved only in the initiation of the tumor process in the stomach, or whether it can affect the mechanisms of tumor progression. The relationship between the severity of *H. pylori* infection and the clinical and morphological characteristics of GC and long-term results of this pathology treatment remains poorly studied, and in this connection, the question of the expediency of anti-Helicobacter therapy in patients with invasive GC remains open.

Objective

To assess the features of *H. pylori* infection in patients with Stage I-IIIB GC and their correlation with the clinical and morphological characteristics of the disease, the presence of antibiotic therapy (AT) before surgery, and long-term treatment results.

MATERIALS AND METHODS

The patients

One hundred and nine patients with GC who had undergone radical surgery (R0) between May 2007 and March 2010 at the Orenburg Regional Clinical Oncology Center, were included in this prospective cohort pilot study. Study inclusion criteria were: Histologically proven invasive GC; no evidence of distant metastases; radical surgery (R0); no prior gastric surgery; no previous chemotherapy or radiotherapy. The study did not include patients with decompensation of cardiovascular and renal diseases, exacerbation of chronic inflammatory processes, severe allergic processes, or who received glucocorticoids, antihistamines, and non-steroidal anti-inflammatory drugs. The study was performed in accordance with the Helsinki Declaration and internationally recognized guidelines, and the privacy of patients was protected by decoding the data according to the privacy regulations of the Orenburg Regional Clinical Oncologic Center (Russia, Orenburg). All patients provided written informed consent. The protocol was approved by the Institutional Review Board of the Orenburg State Medical University (Russia, Orenburg).

Clinical and pathological data including age, tumor localization, stage, type of surgery, histology, the presence of AT before surgery, postoperative therapy, and long-term results of treatment were retrieved from the routine reports for analyses. The distribution of patients according to the clinical and pathological characteristics of GC is presented in Table 1.

When interviewing patients, it was found that 45 patients received AT before admission to the clinic due to a preliminary wrong diagnosis of gastric ulcer or chronic gastritis. The following combinations of antibacterial drugs were most commonly ordered: Amoxicillin + clarithromycin (34 patients), amoxicillin + clarithromycin + metronidazole (6 patients), amoxicillin + metronidazole (3 patients), other drugs (2 patients). Information about the antibacterial drugs, the timing and duration of their intake was entered into the primary patient documentation and then taken into account in the analysis. We considered only those patients who underwent AT in the period from 1 to 1.5 mo before the operation, lasting at least seven days, and using two or more antibacterial drugs.

The long-term results of treatment were assessed for the period from May 12, 2007 to April 12, 2021. The median follow-up period was 86.2 mo. As of April 12, 2021, 26 (24.5%) patients were alive, 54 (50.9%) had died from the progression of GC, 20 (18.9%) had died from causes other than GC, and six (5.6%) left the region at different follow-up periods. Malignant tumors of other localizations were diagnosed in 8 patients at different times after the operation: Non-Hodgkin's lymphomas-in three, prostate cancer-in one, lung cancer-in two, laryngeal cancer-in one, and breast cancer-in one patient. With the exception of one patient with non-Hodgkin's lymphoma, the other

Table 1 The distribution of patients according to the clinical and pathological characteristics of gastric cancer

Characteristics of gastric cancer	*n*	Percent
Age	61.7 ± 1.03 years (from 24 to 81 years, the median–was 61 years)	
Sex		
Men	72	66.1
Women	37	33.9
Tumor localization		
Upper third	18	16.5
Middle third	32	29.4
Lower third	57	52.3
Total gastric cancer	2	1.8
T status		
T1	12	11
T2	30	27.5
T3	62	56.9
T4	5	4.6
N status		
N0	57	52.3
N1	20	18.3
N2	32	29.3
TNM		
T1-2N0M0	40	36.7
T3N0M0	17	15.6
T3-4N1M0	20	18.3
T3-4N2M0	32	29.3
Types of GC		
Intestinal type	50	45.9
Diffuse-types	59	54.1
Grade (histolology)		
G1	31	28.4
G2	19	17.4
G3	33	30.3
Signet ring cell carcinoma	26	23.9
Type sugery		
Subtotal distal resection	85	78
Subtotal proximal resection	18	16.5
Gastrectomy	7	6.4

GC: Gastric cancer.

patients died from the progression of these diseases. The causes of death were not associated with malignant tumors for the other patients. During the period 2020-2021, seven patients contracted coronavirus disease-19, one of whom died from the disease, but the rest are alive.

Detection H. pylori infection

H. pylori in the GM and tumor was determined by rapid urease test (RUT) and by immunohistochemically (IHC) using the antibody to *H. pylori*.

RUT

After removal of the stomach (within 30 min) a greater curvature of the organ was opened and biopsy samples were taken from the tumor and the adjacent macroscopically non-tumorous GM at a distance of 3-5 cm from the tumor margin. The samples were placed on test strips (HELPIL–test, "AMA", Russia) for three minutes. The presence and the severity of the infection were evaluated by the color change of the indicator from yellow to blue.

According to the intensity and the time of the appearance of a blue color, we distinguished three degrees of infection: 3+: Marked (+++)-bright staining in the first minute of the study; 2+: Moderate (++)–for an average intensity of staining for 2 min and 1+ mild (+)-weak staining for three minutes. If the color of the indicator did not change, or became dirty gray, and if after repeated research the same result was received, the test was evaluated as negative. The same samples were later used for histological analysis and IGH.

Immunohistochemistry

The presence and features of *H. pylori* infection were studied in samples of the GM adjacent to the tumor, in the tumor tissue, in the omentum, and regional lymph nodes of 46 patients, by immunohistochemistry.

The sections for IGH were dewaxed and rehydrated by sequential immersion in xylene and graded ethanol and water. For antigen retrieval, the sections boiling for 10 min in citrate buffer (pH 6) and endogenous peroxidase activity was blocked with 30 mL/L hydrogen peroxide solution. Slides were incubated at room temperature with the anti-*H. pylori* (RB-9070, Thermo Fisher Scientific, the immunogen is purified *H. pylori*) rabbit polyclonal antibodies in diluted at 1:1000 for 30 min.

The visualization system included DAB (UltraVision LP Detection System HRP Polymer & DAB Plus Chromogen) and hematoxylin counterstaining. For negative control sections, the primary antibody was replaced with phosphate-buffered saline and processed in the same manner.

The concentration of *H. pylori* in the GM detected by IGH was graded as 1+ for mild, 2+ for moderate, and 3+ for marked according to the Sydney system[30]. The presence of point inclusions giving a positive reaction with antibodies to *H. pylori* in the cytoplasm of epithelial cells of deep gastric glands and of the lymphoid cells of the lamina propria of GM as well as in omentum and lymph node, were taken into account.

All sections were carefully and completely scanned by two of the authors (MS and OT) without knowledge of the clinical and pathological data.

The data obtained was compared with clinical features of GC: Stage, localization, histology, the presence of AT before surgery, and 10-year OS and RFS.

Statistics

Statistical analysis was performed using the Statistica 10.0 software. The correlations between different data were evaluated using the nonparametric Spearman's rank correlation or gamma correlation. Chi-square tests were carried out to analyze the difference of distribution among the categorized data. Mann–Whitney U nonparametric test was used to compare the value of the quantitative data. The survival was analyzed using the Kaplan-Meier method. The log-rank test was used to compare survival curves between subgroups of patients. A value of $P < 0.05$ was considered statistically significant.

RESULTS

The features of H. pylori infection in GC

Of 93 patients (84.5%) demonstrated positive RUT. According to RUT the concentration of *H. pylori* in GM was mild (1+) in 38 (34.8%) patients, moderate (2+)-in 37 (33.9%) and marked (3+)–in 8 (16.5%). RUT was negative in 16 patients (14.7%).

It was found that urease activity 2+ and 3+ were significantly more frequent in GM than in tumors (in 55.5% and 13.3% of cases, respectively, $P = 0.01$). In more than half the cases (53.3%), the urease activity in the tumor was lower than in the adjacent GM.

Forty-six samples of GM were stained by IHC. The coccoid forms of *H. pylori* were found to prevail in GM adjacent to the tumor (Figure 1A). Coccoid forms of *H. pylori* only were identified in 31 (63.1%) patients, and coccoid and spiral in 12 (30.4%) patients (Figure 1B). No signs of infection were found in 3 (6.5%) patients. The concentration of coccoid and spiral forms of *H. pylori* in GM according to IGH was 1+ in 24 (52.2%) and 1 (19.6%) patients, 2+-in 11 (23.9%) and 4 (8.7%), and 3+-in 8 (17.4%) and 1 (2.2%) patients. A positive correlation between the concentration of coccoid and spiral forms of *H. pylori* (gamma = 0.642, $P < 0.0001$) was noted.

The localization of *H. pylori* in GM was observed not only in the surface mucous gel layer of the stomach (Figure 1C) but also within the cytoplasm of the gastric superficial-foveolar epithelium (Figure 1D). The point inclusions giving a positive reaction with antibodies to *H. pylori* were also revealed in the cytoplasm of the epithelial cells of deep gastric glands (in 41.3% samples) and of the immune cells (Figure 1E) of the lamina propria of GM (in 43.5% samples), as well as of the intraepithelial lymphocytes (Figure 1F). The close relationship between the presence of point inclusions in immune cells and epithelial cells (gamma = 0.642, $P < 0.0001$) was noted. The individual cocci or their small clusters, and sometimes the short rod bacterium, were also often detected in the lamina propria of the GM. We also found bacteria in the omentum and lymph nodes. In the omentum the bacteria were presented predominantly by cocci between 0.5 and 1 μm in diameter (Figure 2A). Cocci were arranged most commonly by the small compact groups up to 10-15 cells in the immediate vicinity of the LN capsule. The bacteria were located mainly between the adipocytes. However, it was not clear whether bacteria were outside of the cells or in a narrow rim of cytoplasm of the fat cells.

In the tissue of lymph nodes we usually observed the small accumulations of cocci between 10 and 15 cells (Figure 2B). Bacteria were located between lymphocytes of the paracortical area, but not so compact, as in the omentum. Quite often the concentration of bacteria was observed around the nuclei of cells that can testify to their intracellular localization.

Correlations of clinical and pathological characteristics of GC with the severity of H. pylori infection according to RUT data

The gamma correlation coefficient test (gamma) showed that the severity of *H. pylori* in GM according to RUT positively correlated with the T status (gamma = 0.537, $P < 0.00001$), N status (gamma = 0.371, $P = 0.0007$) and stage (gamma = 0.520, $P < 0.00001$), and negatively correlated with the presence of AT in anamnesis (gamma = -0.418, $P = 0.003$). The marked (+++) and moderate (++) degrees of *H. pylori* infection were more often observed in Grade 2 and Grade 3, in T3-4 status, in N1 status, in the T3-4N1-2 stage, and in the absence of AT in anamnesis (Table 2). Correlations of *H. pylori* concentration in GM according to RUT with 10-year OS and RFS of GC patients were not determined.

It is important to note that the presence in AT 1-1.5 mo before surgery was associated with a significant improvement in RFS and OS (Figure 3), however, this applied only to patients with local GC (T1-3N0). In advanced GC (T3-4N1 and T3-4N2) there were no significant differences in patient survival (Figure 4).

Correlations of clinical and pathological characteristics of GC with the concentration of spiral and coccoid forms of H. pylori in the GM

It is important to note that correlations between the clinical and pathological characteristics of GC and the concentration of *H. pylori* spiral forms in GM were not found. However, the concentration of *H. pylori* coccoid forms correlated with age ($\rho = -0.502$, $P = 0.0006$), histology (gamma = 0.550, $P = 0.0004$), T status (gamma = 0.709, $P = 0.0001$), N status (gamma = 0.509, $P = 0.002$) stage (gamma = 0.636, $P = 0.0002$), and 10-year RFS (gamma = -0.521, $P = 0.008$) and OS (gamma = -0.500, $P = 0.044$). In cases with a moderate and marked concentration (2+ or 3+) of *H. pylori* coccoid forms in GM compared to cases with a low concentration (1+ or without infection) the patients were younger (57.9 ± 2.5 years *vs* 66.2 ± 1.4 years, respectively, $P = 0.004$) and the diffuse type of GC, poorly differentiated tumors (G3), T3-4 stage and N1 stage of GC were more often observed (Table 3). In cases of moderate and marked concentrations of *H. pylori* in GM, a decrease in 10-year progression-free survival (PFS) and OS survival from 55.6% to 26.3% was observed ($P = 0.02$ and $P = 0.07$, respectively). PFS and OS curves, depending on the concentration of coccoid forms of *H. pylori* in GM, are presented in Figure 5.

Table 2 Clinical and pathological characteristics of gastric cancer depending on the data rapid urease test

Characteristics of gastric cancer	Degrees of infection according to RUT test				*P* value
	No or mild, *n* (%)		Moderate or marked, *n* (%)		
Age	63.8 ± 10.1		58.8 ± 11.2		0.008
T status					
T1	9	75	3	25	0.01
T2	20	66.7	10	33.3	
T3	24	38.7	38	61.3	
T4	1	20	4	80	
N status					
N0	37	64.9	20	35.1	0.0001
N1	2	10	18	90	
N2	15	46.9	17	53.1	
TNM					
T1-2N0M0	28	70	12	30	0.002
T3N0M0	9	52.9	8	47.1	
T3-4N1-2	17	32.7	35	67.3	
Types of GC					
Intestinal type	27	54	23	46	0.39
Diffuse-types	27	45.8	32	54.2	
Grade (histolology)					
G1	22	70	9	30	0.005
G2	5	26.3	14	73.7	
G3	12	36.4	21	63.6	
Signet ring cell carcinoma	15	57.6	11	42.3	
Antibiotic therapy before surgery					
No	25	41.2	37	68.5	0.025
Presence	28	52.8	17	31.5	

RUT: Rapid urease test; GC: Gastric cancer.

There were no correlations between the presence of point inclusions in the cytoplasm of epithelial cells of deep gastric glands, in the stroma immune cells, and in the intraepithelial lymphocytes with the clinical and pathological characteristics of GC.

DISCUSSION

A large amount of clinical and experimental data testifies to the important role of *H. pylori* in the occurrence of GC[31-34], but, there is less research into the features of *H. pylori* infection in patients with GC and its role in tumor progression, and the results are quite contradictory. These contradictions relate to many aspects, such as: (1) The frequency of infection in patients with GC. This data varies widely and ranges from 36% to 100%[35-40]; (2) The relation of infection with GC prognosis. Some researchers have noted an improvement in the long-term results of GC treatment in infected patients[41,42], while others, on the contrary, found that the presence of H. pylori infection was associated with a decrease in patient survival[43,44]; and (3) The connection between the infection and a histologic type of GC. In some studies, it was noted that patients with an intestinal type of GC are more often infected with *H. pylori* than patients with the diffuse type of GC[45,46]. Other researchers did not find a

Table 3 Clinical and pathological characteristics of gastric cancer depending on the concentration of *Helicobacter pylori* coccoid forms in the gastric mucosa

Characteristics of gastric cancer	Degrees of infection according to RUT test				*P* value
	No or mild, *n* (%)		Moderate or marked, *n* (%)		
Age	66.2 ± 1.4		57.9 ± 2.5		0.004
T status					
T1	6	85.7	1	14.3	0.04
T2	9	81.8	2	18.2	
T3	12	44.4	15	55.6	
T4	0	0	1	100	
N status					
N0	18	78.3	5	21.7	0.01
N1	1	16.7	5	83.8	
N2	8	47.1	9	52.9	
TNM					
T1-2N0M0	14	82.3	3	17.6	0.02
T3N0M0	4	66.7	2	33.3	
T3-4N1-2	9	39.1	14	60.9	
Types of GC					
WIntestinal type	18	75	6	25	0.02
Diffuse-types	9	40.9	13	59.1	
Grade (histolology)					
G1	14	93.3	1	6.7	0.008
G2	4	44.4	5	55.6	
G3	2	28.3	5	71.4	
Signet ring cell carcinoma	7	46.7	8	53.3	
Antibiotic therapy before surgery					
No	16	64.5	10	38.5	0.655
Presence	11	55	9	45	

RUT: Rapid urease test; GC: Gastric cancer.

difference in *H. pylori* infection in patients with different histological types of tumors [47].

It is believed that the differences noted are associated with the fact that to reveal the infection the authors used the methods that were significantly different in their sensitivity, and primarily, to coccoid forms of bacteria. Most of the studies were carried out without considering coccoid forms of *H. pylori* and the concentration of bacteria in GM. The use of the biochemical method for the detection of urease activity and immunohistochemistry for visualization of bacteria in our study allowed us not only to assess the presence of infection in patients with GC, but also to mark some of its features associated with the localization of bacteria in the stomach, with a ratio of cocci and spiral forms, and the degree of bacterial contamination of GM.

Our data for the Orenburg region recorded a high rate of *H. pylori* infection in patients with GC (84.5%). The coccoid forms of *H. pylori*, preserving a high degree of urease activity, dominated in GM in patients with GC. They were found in 93.4% of infected patients, with only coccoid forms of *H. pylori*-in 68.9%.

It is known that the coccoid forms of *H. pylo*ri can arise in response to unfavorable environmental factors, such as AT [47,48]. These forms are resistant to AT[49,50] and are able to form biofilms[51] and avoid the immune system[50]. They express a higher rate of cagE mRNA than their spiral counterparts[52], and by increasing the synthesis

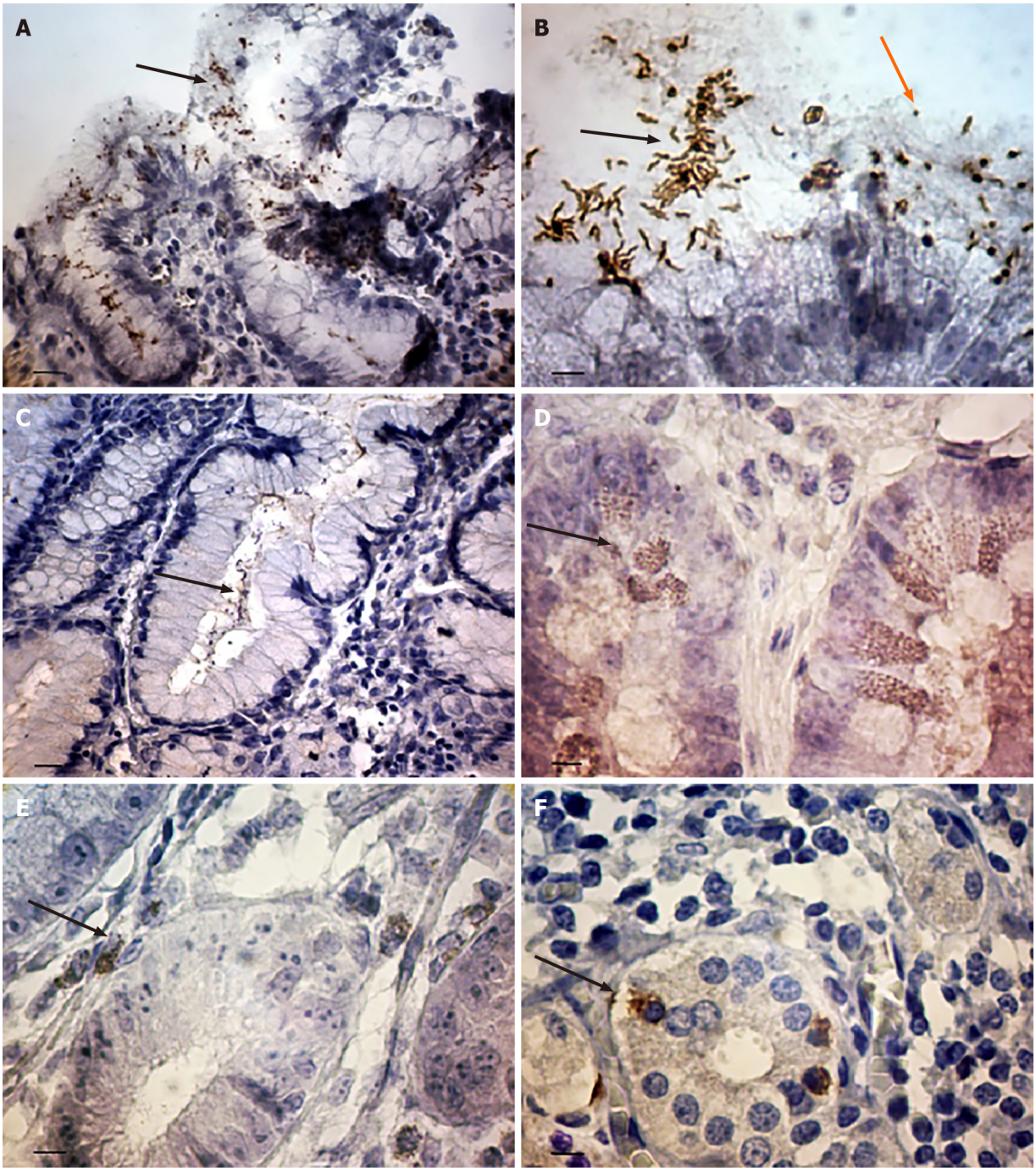


Figure 1 The features of *Helicobacter pylori* localization in gastric mucosa in patients with gastric cancer. A: Coccoid forms of *Helicobacter pylori* (*H. pylori*) in the gastric pit. The some bacteria within the cytoplasm of epithelium cells (arrows); B: The spiral (black arrows) and coccoid (orange arrows) forms of *H. pylori* on the surface of superficial-foveolar gastric epithelium; C: The bacteria in the surface mucous gel layer of stomach (arrows); D: The point inclusions giving a positive reaction with antibodies to *H. pylori* within the cytoplasm of epithelial cells of deep gastric glands (arrows); E: The point inclusions giving a positive reaction with antibodies to *H. pylori* within the cytoplasm of the immune cells of the lamina propria of gastric mucosa (arrows); F: The point inclusions giving a positive reaction with antibodies to *H. pylori* within the cytoplasm of intraepithelial lymphocytes (arrows). Immunoperoxidase staining with anti-*H. pylori* antibody, immersion. Bars: A: 20 μm; B: 10 μm; C: 20 μm; D-F: 10 μm.

of tumor necrosis factor-alpha (TNF-α)-inducing protein (Hps), which is introduced into the cytosol and cell nuclei, they can activate nuclear factor-kappaB (NF-κB) and the expression of TNF-α and other cytokines involved in carcinogenesis[53,54]. The effect on the proliferation of gastric epithelial cells in the *H. pylori* coccoid forms is also stronger than in the helical forms[55], and they can induce the expression of VEGF-A and transforming growth factor-β[56]. The ability to transform into coccoid forms was also found to be characteristic of the most virulent strains of *H. pylori*[50,54].

It should be noted that the higher infection by coccoid forms of *H. pylori* in patients with GC, compared to patients with gastritis or gastric ulcer, had been mentioned by

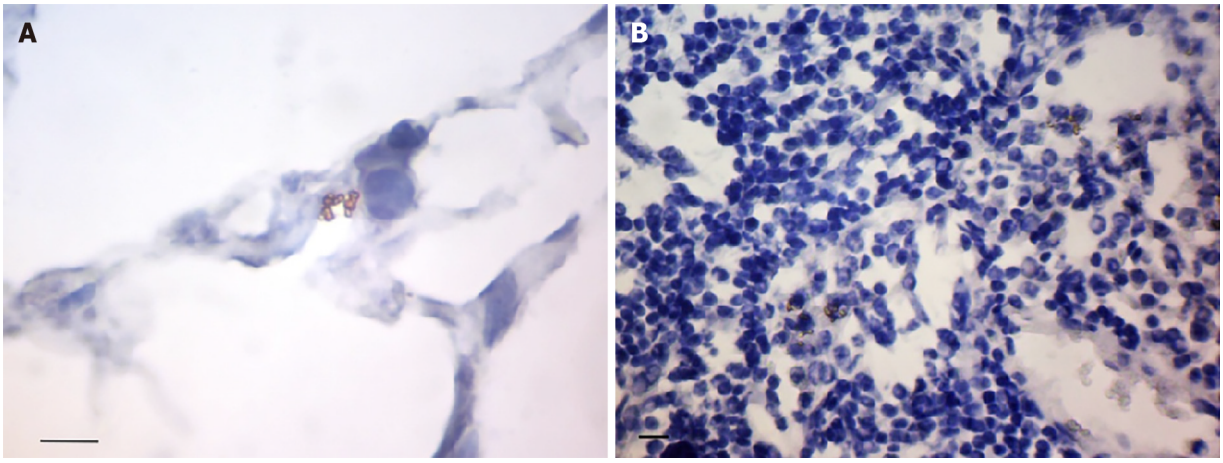


Figure 2 The features of *Helicobacter pylori* localization in omentum and lymph node in patients with gastric cancer. A: The small group of cocci located in the central part of the omentum adipocyte; B: The congestions of bacteria around the nucleus of lymphocytes in the paracortical area of lymph node. Immunoperoxidase staining with anti-*Helicobacter pylori* antibody, immersion, Bars: 10 μm.

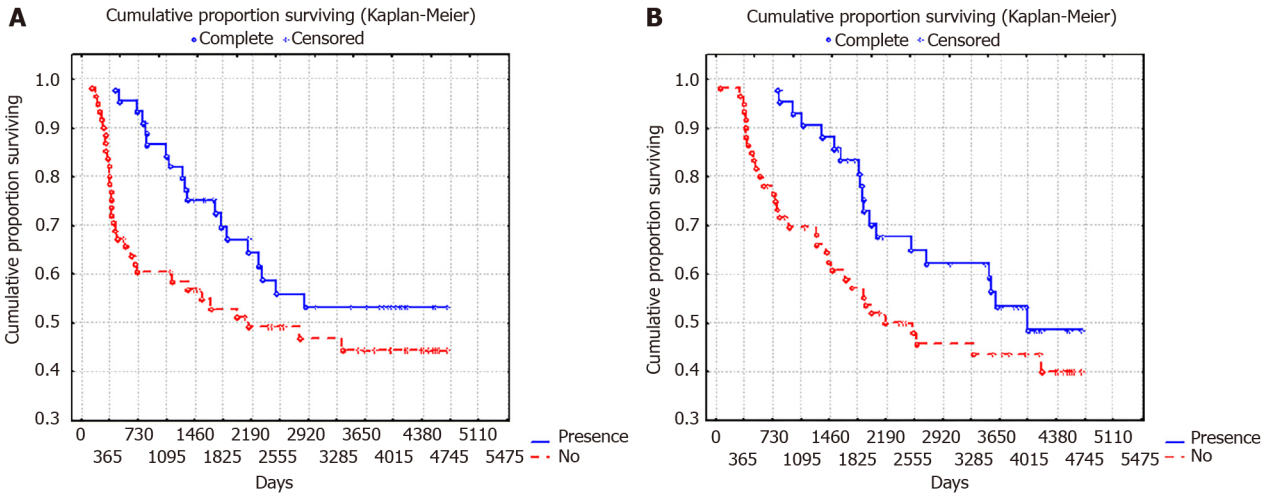


Figure 3 10-year overall surviving and relapse-free surviving of patients with gastric cancer depending on the presence of antibiotic therapy 1-1.5 mo before surgery (*P* = 0.02). A: 10-year overall surviving; B: Relapse-free surviving.

other researchers[57]. A number of studies have shown that coccoid forms of *H. pylori* retained urease activity[58] and the expression of such antigens as CagA, UreA, porin, components of the Cag type IV secretion system (TFSS), antigen-binding adhesin of the blood group BabA and others[59,60].

The use of immunohistochemistry in this study made it possible to detect the bacteria not only in the gastric mucus and on the surface of epithelial cells, but also within the cytoplasm of epithelial and immune cells of GM. Such intracellular expression was characterized by point inclusions giving a specific reaction with antibodies to *H. pylori*.

The intracellular persistence of *H. pylori* has been demonstrated by many investigators. They found *H. pylori* in the cytoplasm of epithelial cells, intercellular spaces, in the lamina propria of GM, and in the lumen of small vessels[61-63]. We assume that the point inclusions in the cytoplasm of epithelial and immune cells giving a positive reaction with antibodies to *H. pylori* is similar to those particle-rich cytoplasmic structure (PaCS) described earlier in the human superficial-foveolar epithelium and its metaplastic or dysplastic foci[64]. The authors found that the PaCS are a colocalization of VacA, CagA, urease, and outer membrane proteins with NOD1 receptor, ubiquitin-activating enzyme E1, polyubiquitinated proteins, proteasome components, and potentially oncogenic proteins like SHP2 and ERKs[64]. They believe that PaCS is a novel, proteasome-enriched structure arising in ribosome-rich cytoplasm at sites of *H. pylori* product accumulation.

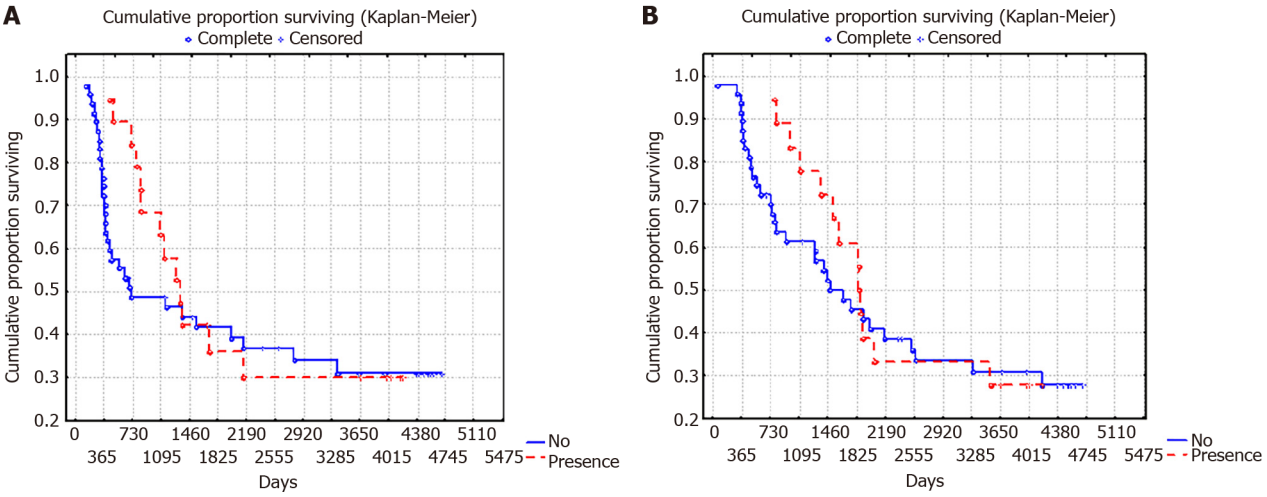


Figure 4 10-year overall surviving and relapse-free surviving of patients with T3-4N1-2M0 stages of gastric cancer depending on the presence of antibiotic therapy 1-1.5 mo before surgery (*P* = 0.78). A: 10-year overall surviving; B: Relapse-free surviving.

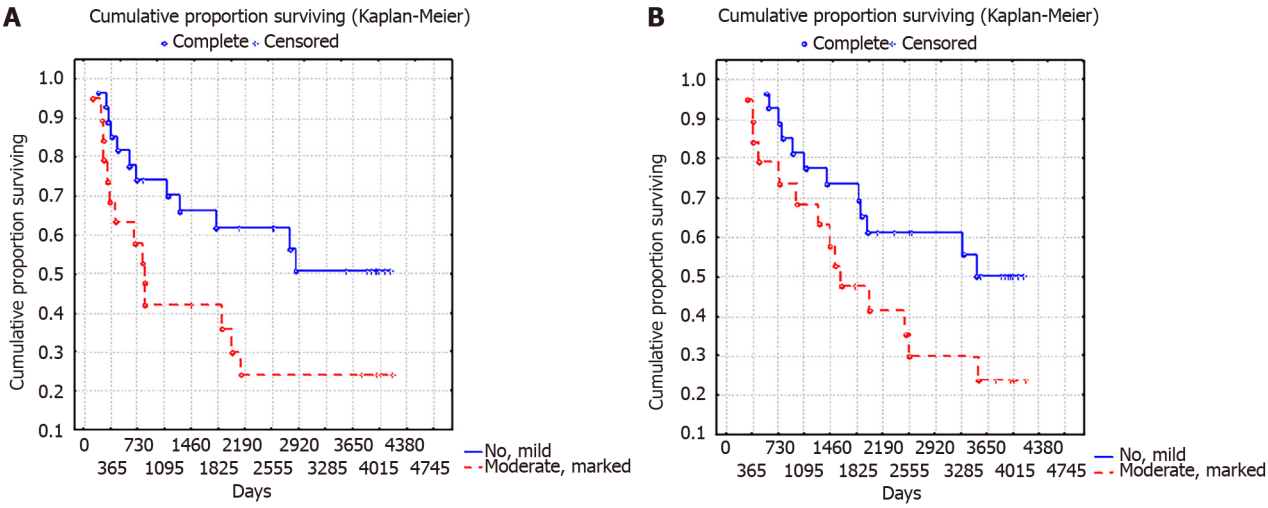


Figure 5 10-year overall surviving and relapse-free surviving of patients with gastric cancer depending on the concentration of *Helicobacter pylori* coccoid forms in the gastric mucosa (*P* = 0.02). A: 10-year overall surviving; B: Relapse-free surviving.

We believe that the immune cells with point inclusions in the lamina propria of GM are likely to be macrophages. The data obtained by several researchers suggests this conclusion[65,66]. It is noted that even the absorbed bacteria retains their viability in macrophages, which may be associated with the violation of the phagosome maturation[66-68]. The use of confocal microscopy enabled the localization of the bacteria within the cells to be associated with the endosomal and lysosomal markers, and found that *H. pylori* could use the vesicles of autophagosomes (autophagic vesicles) for its own replication[63,69].

The study found that the concentration of *H. pylori* coccoid forms in GM was the most significant clinical factor. This factor was associated with the tumor histology, T status, N status, stage, 10-year PFS, and OS. The moderate and marked concentrations of coccoid forms of *H. pylori* were more often found in the diffuse type of GC (P = 0.024) and T3-4 (P = 0.04) stage. Interestingly, the high concentration of *H. pylori* is more frequent in Stage N1 than in N2 (at 90.0% and 53.1%, respectively, P = 0.024).

The moderate and marked concentrations of coccoid forms of *H. pylori* represented a prognostic factor associated with the decrease of 10-year RFS and OS from 55.6% to 26.3% (P = 0.02 and P = 0.07, respectively).

It should be noted that the results of this study do not allow us to unambiguously judge the effect of *H. pylori* on GC progression. A decrease in OS and DFS in patients with moderate and marked concentrations of *H. pylori* coccoid forms in the GM may be due to the fact that these patients had more advanced stages and more aggressive

forms of GC. Meanwhile, there are more and more studies showing that *H. pylori* infection can promote GC progression by activating the NF-κB signaling pathway and induction of interleukin-8 secretion[70], the activation of epithelial-mesenchymal transformation[71-74] and angiogenesis[75,76], as well as increasing the invasive properties of tumor cells[77]. It can be assumed that the administration of AT before surgery contributes to the reduction of the inflammatory process activity and normalization of the adhesive properties of tumour cells, which in turn decreases metastasis risk and improves the long-term results of the treatment of GC. The data literature on the improvement of the long-term results of malignant tumours treatment when using antibacterial drugs testify in favour of this hypothesis[78-80].

CONCLUSION

The data obtained indicates that *H. pylori* may be associated not only with induction but also with the progression of GC. It can be assumed that the prevalence of coccoid forms of bacteria and their intracellular persistence can affect the mechanisms of tumor progression. Further appropriate studies regarding the role of *H. pylori* in the progression of GC are obviously advisable.

ARTICLE HIGHLIGHTS

Research background

Gastric cancer (GC) continues to be one of the most common malignant diseases in the world. It is known that *Helicobacter pylori* (*H. pylori*) infection, initiating the development of a chronic inflammatory process in the gastric mucosa (GM), is the leading risk factor for GC. At the same time, clinical studies indicate that inflammatory infiltration of the tumor stroma and surrounding tissues can have an important prognostic value and affect the long-term results of malignant neoplasm treatment.

Research motivation

It is still not clear whether *H. pylori* is involved only in the initiation of the tumor process in the stomach, or whether it can affect the mechanisms of tumor progression.

Research objectives

The aim of this study was to establish the features of *H. pylori* infection in patients with GC and their correlations with clinical and morphological characteristics of diseases and long-term results of treatment.

Research methods

In this prospective observational study, we included all patients with GC who had undergone radical surgery (R0) between May 2007 and March 2010 at the Orenburg Regional Clinical Oncology Center. Features of the *H. pylori* infection and its severity was determined by rapid urease test and by immunohistochemically using the antibody to *H. pylori*. The data obtained we compared with clinical features of GC: Stage, localization, histology, the presence of antibiotic therapy (AT) before surgery, and 10-year overall and disease-free survival.

Research results

We found *H. pylori* infection in the adjacent to the tumor GM in 84.5% of cases. We have established that the coccoid forms of *H. pylori* predominate in the GM of patients with GC. A high rate of infection by coccoid forms of *H. pylori* has been associated with more aggressive type of GC, advanced stage, and decline of a 10-year overall and disease-free survival. The presence of AT 1-1.5 mo before the operation was associated with an improvement in the 10-year survival rate of patients with local (T1-3N0M0), but not advanced (T3-4N1-2M0) stages of GC.

Research conclusions

These results indicate that *H. pylori* may be associated not only with induction but also with the progression of GC.

Research perspectives

The results obtained do not allow one to draw unambiguous conclusions about the role of *H. pylori* in the progression of GC. Further appropriate prospective studies regarding the role of *H. pylori* in the progression of GC are obviously advisable.

REFERENCES

1 **Thrift AP**, El-Serag HB. Burden of Gastric Cancer. *Clin Gastroenterol Hepatol* 2020; **18**: 534-542 [PMID: 31362118 DOI: 10.1016/j.cgh.2019.07.045]

2 **Bray F**, Ferlay J, Soerjomataram I, Siegel RL, Torre LA, Jemal A. Global cancer statistics 2018: GLOBOCAN estimates of incidence and mortality worldwide for 36 cancers in 185 countries. *CA Cancer J Clin* 2018; **68**: 394-424 [PMID: 30207593 DOI: 10.3322/caac.21492]

3 **Baniak N**, Senger JL, Ahmed S, Kanthan SC, Kanthan R. Gastric biomarkers: a global review. *World J Surg Oncol* 2016; **14**: 212 [PMID: 27514667 DOI: 10.1186/s12957-016-0969-3]

4 **Siegel RL**, Miller KD, Jemal A. Cancer statistics, 2015. *CA Cancer J Clin* 2015; **65**: 5-29 [PMID: 25559415 DOI: 10.3322/caac.21254]

5 **Jairath NK**, Farha MW, Jairath R, Harms PW, Tsoi LC, Tejasvi T. Prognostic value of intratumoral lymphocyte-to-monocyte ratio and M0 macrophage enrichment in tumor immune microenvironment of melanoma. *Melanoma Manag* 2020; **7**: MMT51 [PMID: 33318782 DOI: 10.2217/mmt-2020-0019]

6 **Farha M**, Jairath NK, Lawrence TS, El Naqa I. Characterization of the Tumor Immune Microenvironment Identifies M0 Macrophage-Enriched Cluster as a Poor Prognostic Factor in Hepatocellular Carcinoma. *JCO Clin Cancer Inform* 2020; **4**: 1002-1013 [PMID: 33136432 DOI: 10.1200/CCI.20.00077]

7 **Man YG**, Stojadinovic A, Mason J, Avital I, Bilchik A, Bruecher B, Protic M, Nissan A, Izadjoo M, Zhang X, Jewett A. Tumor-infiltrating immune cells promoting tumor invasion and metastasis: existing theories. *J Cancer* 2013; **4**: 84-95 [PMID: 23386907 DOI: 10.7150/jca.5482]

8 **Wang M**, Li Z, Peng Y, Fang J, Fang T, Wu J, Zhou J. Identification of immune cells and mRNA associated with prognosis of gastric cancer. *BMC Cancer* 2020; **20**: 206 [PMID: 32164594 DOI: 10.1186/s12885-020-6702-1]

9 **Li W**, Li M, Wang H, Peng Y, Dong S, Lu Y, Wang F, Xu F, Liu L, Zhao Q. Infiltrating Immune Cells in Gastric Cancer: A Novel Predicting Model for Prognosis. *J Cancer* 2021; **12**: 965-975 [PMID: 33442396 DOI: 10.7150/jca.51079]

10 **Stanton SE**, Disis ML. Clinical significance of tumor-infiltrating lymphocytes in breast cancer. *J Immunother Cancer* 2016; **4**: 59 [PMID: 27777769 DOI: 10.1186/s40425-016-0165-6]

11 **Öjlert ÅK**, Halvorsen AR, Nebdal D, Lund-Iversen M, Solberg S, Brustugun OT, Lingjaerde OC, Helland Å. The immune microenvironment in non-small cell lung cancer is predictive of prognosis after surgery. *Mol Oncol* 2019; **13**: 1166-1179 [PMID: 30854794 DOI: 10.1002/1878-0261.12475]

12 **Wang M**, Huang YK, Kong JC, Sun Y, Tantalo DG, Yeang HXA, Ying L, Yan F, Xu D, Halse H, Di Costanzo N, Gordon IR, Mitchell C, Mackay LK, Busuttil RA, Neeson PJ, Boussioutas A. High-dimensional analyses reveal a distinct role of T-cell subsets in the immune microenvironment of gastric cancer. *Clin Transl Immunology* 2020; **9**: e1127 [PMID: 32377339 DOI: 10.1002/cti2.1127]

13 **Shin SJ**, Kim SY, Choi YY, Son T, Cheong JH, Hyung WJ, Noh SH, Park CG, Kim HI. Mismatch Repair Status of Gastric Cancer and Its Association with the Local and Systemic Immune Response. *Oncologist* 2019; **24**: e835-e844 [PMID: 30894409 DOI: 10.1634/theoncologist.2018-0273]

14 **Takeuchi Y**, Nishikawa H. Roles of regulatory T cells in cancer immunity. *Int Immunol* 2016; **28**: 401-409 [PMID: 27160722 DOI: 10.1093/intimm/dxw025]

15 **Barua S**, Fang P, Sharma A, Fujimoto J, Wistuba I, Rao AUK, Lin SH. Spatial interaction of tumor cells and regulatory T cells correlates with survival in non-small cell lung cancer. *Lung Cancer* 2018; **117**: 73-79 [PMID: 29409671 DOI: 10.1016/j.lungcan.2018.01.022]

16 **Jiang W**, Liu K, Guo Q, Cheng J, Shen L, Cao Y, Wu J, Shi J, Cao H, Liu B, Tao K, Wang G, Cai K. Tumor-infiltrating immune cells and prognosis in gastric cancer: a systematic review and meta-analysis. *Oncotarget* 2017; **8**: 62312-62329 [PMID: 28977947 DOI: 10.18632/oncotarget.17602]

17 **Kindlund B**, Sjöling Å, Yakkala C, Adamsson J, Janzon A, Hansson LE, Hermansson M, Janson P, Winqvist O, Lundin SB. $CD4^+$ regulatory T cells in gastric cancer mucosa are proliferating and express high levels of IL-10 but little TGF-β. *Gastric Cancer* 2017; **20**: 116-125 [PMID: 26782287 DOI: 10.1007/s10120-015-0591-z]

18 **Yuan XL**, Chen L, Li MX, Dong P, Xue J, Wang J, Zhang TT, Wang XA, Zhang FM, Ge HL, Shen LS, Xu D. Elevated expression of Foxp3 in tumor-infiltrating Treg cells suppresses T-cell proliferation and contributes to gastric cancer progression in a COX-2-dependent manner. *Clin Immunol* 2010; **134**: 277-288 [PMID: 19900843 DOI: 10.1016/j.clim.2009.10.005]

19 **Yang S**, Liu T, Cheng Y, Bai Y, Liang G. Immune cell infiltration as a biomarker for the diagnosis and prognosis of digestive system cancer. *Cancer Sci* 2019; **110**: 3639-3649 [PMID: 31605436 DOI: 10.1111/cas.14216]

20 **Chang WJ**, Du Y, Zhao X, Ma LY, Cao GW. Inflammation-related factors predicting prognosis of gastric cancer. *World J Gastroenterol* 2014; **20**: 4586-4596 [PMID: 24782611 DOI: 10.3748/wjg.v20.i16.4586]

21 **Greten FR**, Grivennikov SI. Inflammation and Cancer: Triggers, Mechanisms, and Consequences. *Immunity* 2019; **51**: 27-41 [PMID: 31315034 DOI: 10.1016/j.immuni.2019.06.025]

22 **Suarez-Carmona M**, Lesage J, Cataldo D, Gilles C. EMT and inflammation: inseparable actors of cancer progression. *Mol Oncol* 2017; **11**: 805-823 [PMID: 28599100 DOI: 10.1002/1878-0261.12095]

23 **Roy S**, Glaser S, Chakraborty S. Inflammation and Progression of Cholangiocarcinoma: Role of Angiogenic and Lymphangiogenic Mechanisms. *Front Med (Lausanne)* 2019; **6**: 293 [PMID: 31921870 DOI: 10.3389/fmed.2019.00293]

24 **de Brito BB**, da Silva FAF, Soares AS, Pereira VA, Santos MLC, Sampaio MM, Neves PHM, de Melo FF. Pathogenesis and clinical management of *Helicobacter pylori* gastric infection. *World J Gastroenterol* 2019; **25**: 5578-5589 [PMID: 31602159 DOI: 10.3748/wjg.v25.i37.5578]

25 **Šterbenc A**, Jarc E, Poljak M, Homan M. *Helicobacter pylori* virulence genes. *World J Gastroenterol* 2019; **25**: 4870-4884 [PMID: 31543679 DOI: 10.3748/wjg.v25.i33.4870]

26 **Gu H**. Role of Flagella in the Pathogenesis of Helicobacter pylori. *Curr Microbiol* 2017; **74**: 863-869 [PMID: 28444418 DOI: 10.1007/s00284-017-1256-4]

27 **Ansari S**, Yamaoka Y. *Helicobacter pylori* Virulence Factors Exploiting Gastric Colonization and its Pathogenicity. *Toxins (Basel)* 2019; **11** [PMID: 31752394 DOI: 10.3390/toxins11110677]

28 **Necchi V**, Candusso ME, Tava F, Luinetti O, Ventura U, Fiocca R, Ricci V, Solcia E. Intracellular, intercellular, and stromal invasion of gastric mucosa, preneoplastic lesions, and cancer by Helicobacter pylori. *Gastroenterology* 2007; **132**: 1009-1023 [PMID: 17383424 DOI: 10.1053/j.gastro.2007.01.049]

29 **Semino-Mora C**, Doi SQ, Marty A, Simko V, Carlstedt I, Dubois A. Intracellular and interstitial expression of Helicobacter pylori virulence genes in gastric precancerous intestinal metaplasia and adenocarcinoma. *J Infect Dis* 2003; **187**: 1165-1177 [PMID: 12695995 DOI: 10.1086/368133]

30 **Dixon MF**, Genta RM, Yardley JH, Correa P. Classification and grading of gastritis. The updated Sydney System. International Workshop on the Histopathology of Gastritis, Houston 1994. *Am J Surg Pathol* 1996; **20**: 1161-1181 [PMID: 8827022 DOI: 10.1097/00000478-199610000-00001]

31 **Servetas SL**, Bridge DR, Merrell DS. Molecular mechanisms of gastric cancer initiation and progression by Helicobacter pylori. *Curr Opin Infect Dis* 2016; **29**: 304-310 [PMID: 26779778 DOI: 10.1097/QCO.0000000000000248]

32 **Tsuda M**, Asaka M, Kato M, Matsushima R, Fujimori K, Akino K, Kikuchi S, Lin Y, Sakamoto N. Effect on Helicobacter pylori eradication therapy against gastric cancer in Japan. *Helicobacter* 2017; **22** [PMID: 28771894 DOI: 10.1111/hel.12415]

33 **Franco AT**, Johnston E, Krishna U, Yamaoka Y, Israel DA, Nagy TA, Wroblewski LE, Piazuelo MB, Correa P, Peek RM Jr. Regulation of gastric carcinogenesis by Helicobacter pylori virulence factors. *Cancer Res* 2008; **68**: 379-387 [PMID: 18199531 DOI: 10.1158/0008-5472.CAN-07-0824]

34 **Noto JM**, Gaddy JA, Lee JY, Piazuelo MB, Friedman DB, Colvin DC, Romero-Gallo J, Suarez G, Loh J, Slaughter JC, Tan S, Morgan DR, Wilson KT, Bravo LE, Correa P, Cover TL, Amieva MR, Peek RM Jr. Iron deficiency accelerates Helicobacter pylori-induced carcinogenesis in rodents and humans. *J Clin Invest* 2013; **123**: 479-492 [PMID: 23257361 DOI: 10.1172/JCI64373]

35 **Arif M**, Syed S. Association of Helicobacter pylori with carcinoma of stomach. *J Pak Med Assoc* 2007; **57**: 337-341 [PMID: 17867254]

36 **Gong EJ**, Lee JY, Bae SE, Park YS, Choi KD, Song HJ, Lee GH, Jung HY, Jeong WJ, Cheon GJ, Yook JH, Kim BS. Characteristics of non-cardia gastric cancer with a high serum anti-Helicobacter pylori IgG titer and its association with diffuse-type histology. *PLoS One* 2018; **13**: e0195264 [PMID: 29621300 DOI: 10.1371/journal.pone.0195264]

37 **Cho SJ**, Choi IJ, Kim CG, Lee JY, Kook MC, Seong MW, Park SR, Lee JS, Kim YW, Ryu KW, Lee JH, Nam BH, Park YI. Helicobacter pylori Seropositivity Is Associated with Gastric Cancer Regardless of Tumor Subtype in Korea. *Gut Liver* 2010; **4**: 466-474 [PMID: 21253294 DOI: 10.5009/gnl.2010.4.4.466]

38 **Sarker KK**, Kabir MJ, Bhuyian AKMMU, Alam MS, Chowdhury FR, Ahad MA, Rahman MA, Rahman MM. *H. pylori* infection and gastric cancer in Bangladesh: a case-control study. *Int J Surg Oncol (N Y)* 2017; **2**: e44 [PMID: 29177209 DOI: 10.1097/IJ9.0000000000000044]

39 **Fang WL**, Huang KH, Chang SC, Lin CH, Chen MH, Chao Y, Lo SS, Li AF, Wu CW, Shyr YM. Comparison of the Clinicopathological Characteristics and Genetic Alterations Between Patients with Gastric Cancer with or Without *Helicobacter pylori* Infection. *Oncologist* 2019; **24**: e845-e853 [PMID: 30796154 DOI: 10.1634/theoncologist.2018-0742]

40 **Khan MR**, Farooqi NB, Shahzad N. Is Proximal Gastric Cancer A Different Entity From Distal Gastric Cancer? *J Ayub Med Coll Abbottabad* 2020; **32**: 194-197 [PMID: 32583993]

41 **Fang X**, Liu K, Cai J, Luo F, Yuan F, Chen P. Positive *Helicobacter pylori* status is associated with better overall survival for gastric cancer patients: evidence from case-cohort studies. *Oncotarget* 2017; **8**: 79604-79617 [PMID: 29108340 DOI: 10.18632/oncotarget.18758]

42 **Li G**, Yu S, Xu J, Zhang X, Ye J, Wang Z, He Y. The prognostic role of Helicobacter pylori in gastric cancer patients: A meta-analysis. *Clin Res Hepatol Gastroenterol* 2019; **43**: 216-224 [PMID: 30361060 DOI: 10.1016/j.clinre.2018.08.012]

43 **Wang J**, Liu X. Correlation Analysis between *Helicobacter pylori* Infection Status and Tumor Clinical Pathology as Well as Prognosis of Gastric Cancer Patients. *Iran J Public Health* 2018; **47**: 1529-1536 [PMID: 30524983]

44 **Li G**, Wang Z, Xu J, Cui J, Cai S, Zhan W, He Y. Gastric cancer patients with Helicobacter pylori

infection have a poor prognosis. *J Surg Oncol* 2013; **108**: 421-426 [PMID: 24037736 DOI: 10.1002/jso.23417]

45 **Zhang XY**, Zhang PY, Aboul-Soud MA. From inflammation to gastric cancer: Role of *Helicobacter pylori*. *Oncol Lett* 2017; **13**: 543-548 [PMID: 28356927 DOI: 10.3892/ol.2016.5506]

46 **Marsh AM**, Buicko JL. Gastric Resection. 2021 Jul 30. In: StatPearls [Internet]. Treasure Island (FL): StatPearls Publishing; 2021 Jan– [PMID: 32809595]

47 **Reshetnyak VI**, Reshetnyak TM. Significance of dormant forms of *Helicobacter pylori* in ulcerogenesis. *World J Gastroenterol* 2017; **23**: 4867-4878 [PMID: 28785141 DOI: 10.3748/wjg.v23.i27.4867]

48 **Ierardi E**, Losurdo G, Mileti A, Paolillo R, Giorgio F, Principi M, Di Leo A. The Puzzle of Coccoid Forms of *Helicobacter pylori*: Beyond Basic Science. *Antibiotics (Basel)* 2020; **9** [PMID: 32486473 DOI: 10.3390/antibiotics9060293]

49 **Kadkhodaei S**, Siavoshi F, Akbari Noghabi K. Mucoid and coccoid Helicobacter pylori with fast growth and antibiotic resistance. *Helicobacter* 2020; **25**: e12678 [PMID: 31880001 DOI: 10.1111/hel.12678]

50 **Krzyżek P**, Grande R. Transformation of *Helicobacter pylori* into Coccoid Forms as a Challenge for Research Determining Activity of Antimicrobial Substances. *Pathogens* 2020; **9** [PMID: 32143312 DOI: 10.3390/pathogens9030184]

51 **Percival SL**, Suleman L. Biofilms and Helicobacter pylori: Dissemination and persistence within the environment and host. *World J Gastrointest Pathophysiol* 2014; **5**: 122-132 [PMID: 25133015 DOI: 10.4291/wjgp.v5.i3.122]

52 **Poursina F**, Faghri J, Moghim S, Zarkesh-Esfahani H, Nasr-Esfahani B, Fazeli H, Hasanzadeh A, Safaei HG. Assessment of cagE and babA mRNA expression during morphological conversion of Helicobacter pylori from spiral to coccoid. *Curr Microbiol* 2013; **66**: 406-413 [PMID: 23263256 DOI: 10.1007/s00284-012-0280-7]

53 **Loke MF**, Ng CG, Vilashni Y, Lim J, Ho B. Understanding the dimorphic lifestyles of human gastric pathogen Helicobacter pylori using the SWATH-based proteomics approach. *Sci Rep* 2016; **6**: 26784 [PMID: 27222005 DOI: 10.1038/srep26784]

54 **Gladyshev N**, Taame M, Kravtsov V. Clinical and laboratory importance of detecting *Helicobacter pylori* coccoid forms for the selection of treatment. *Prz Gastroenterol* 2020; **15**: 294-300 [PMID: 33777268 DOI: 10.5114/pg.2020.101557]

55 **Li N**, Han L, Chen J, Lin X, Chen H, She F. Proliferative and apoptotic effects of gastric epithelial cells induced by coccoid Helicobacter pylori. *J Basic Microbiol* 2013; **53**: 147-155 [PMID: 22581720 DOI: 10.1002/jobm.201100370]

56 **Prevete N**, Rossi FW, Rivellese F, Lamacchia D, Pelosi C, Lobasso A, Necchi V, Solcia E, Fiocca R, Ceppa P, Staibano S, Mascolo M, D'Argenio G, Romano M, Ricci V, Marone G, De Paulis A. Helicobacter pylori HP(2-20) induces eosinophil activation and accumulation in superficial gastric mucosa and stimulates VEGF-alpha and TGF-beta release by interacting with formyl-peptide receptors. *Int J Immunopathol Pharmacol* 2013; **26**: 647-662 [PMID: 24067461 DOI: 10.1177/039463201302600308]

57 **Chan WY**, Hui PK, Leung KM, Chow J, Kwok F, Ng CS. Coccoid forms of Helicobacter pylori in the human stomach. *Am J Clin Pathol* 1994; **102**: 503-507 [PMID: 7524304 DOI: 10.1093/ajcp/102.4.503]

58 **Can F**, Karahan C, Dolapci I, Demirbilek M, Tekeli A, Arslan H. Urease activity and urea gene sequencing of coccoid forms of H. pylori induced by different factors. *Curr Microbiol* 2008; **56**: 150-155 [PMID: 18167027 DOI: 10.1007/s00284-007-9047-y]

59 **Hirukawa S**, Sagara H, Kaneto S, Kondo T, Kiga K, Sanada T, Kiyono H, Mimuro H. Characterization of morphological conversion of Helicobacter pylori under anaerobic conditions. *Microbiol Immunol* 2018; **62**: 221-228 [PMID: 29446491 DOI: 10.1111/1348-0421.12582]

60 **Morales-Espinosa R**, Delgado G, Serrano LR, Castillo E, Santiago CA, Hernández-Castro R, Gonzalez-Pedraza A, Mendez JL, Mundo-Gallardo LF, Manzo-Merino J, Ayala S, Cravioto A. High expression of Helicobacter pylori VapD in both the intracellular environment and biopsies from gastric patients with severity. *PLoS One* 2020; **15**: e0230220 [PMID: 32163505 DOI: 10.1371/journal.pone.0230220]

61 **Ozbek A**, Ozbek E, Dursun H, Kalkan Y, Demirci T. Can Helicobacter pylori invade human gastric mucosa?: an *in vivo* study using electron microscopy, immunohistochemical methods, and real-time polymerase chain reaction. *J Clin Gastroenterol* 2010; **44**: 416-422 [PMID: 19904218 DOI: 10.1097/MCG.0b013e3181c21c69]

62 **Dudley J**, Wieczorek T, Selig M, Cheung H, Shen J, Odze R, Deshpande V, Zukerberg L. Clinicopathological characteristics of invasive gastric Helicobacter pylori. *Hum Pathol* 2017; **61**: 19-25 [PMID: 27771376 DOI: 10.1016/j.humpath.2016.09.029]

63 **Huang Y**, Wang QL, Cheng DD, Xu WT, Lu NH. Adhesion and Invasion of Gastric Mucosa Epithelial Cells by *Helicobacter pylori*. *Front Cell Infect Microbiol* 2016; **6**: 159 [PMID: 27921009 DOI: 10.3389/fcimb.2016.00159]

64 **Necchi V**, Sommi P, Ricci V, Solcia E. In vivo accumulation of Helicobacter pylori products, NOD1, ubiquitinated proteins and proteasome in a novel cytoplasmic structure. *PLoS One* 2010; **5**: e9716 [PMID: 20300534 DOI: 10.1371/journal.pone.0009716]

65 **Ito T**, Kobayashi D, Uchida K, Takemura T, Nagaoka S, Kobayashi I, Yokoyama T, Ishige I, Ishige Y, Ishida N, Furukawa A, Muraoka H, Ikeda S, Sekine M, Ando N, Suzuki Y, Yamada T, Suzuki T,

Eishi Y. Helicobacter pylori invades the gastric mucosa and translocates to the gastric lymph nodes. *Lab Invest* 2008; **88**: 664-681 [PMID: 18475258 DOI: 10.1038/labinvest.2008.33]

66 **Keep S**, Borlace G, Butler R, Brooks D. Role of immune serum in the killing of Helicobacter pylori by macrophages. *Helicobacter* 2010; **15**: 177-183 [PMID: 20557358 DOI: 10.1111/j.1523-5378.2010.00750.x]

67 **Sit WY**, Chen YA, Chen YL, Lai CH, Wang WC. Cellular evasion strategies of Helicobacter pylori in regulating its intracellular fate. *Semin Cell Dev Biol* 2020; **101**: 59-67 [PMID: 32033828 DOI: 10.1016/j.semcdb.2020.01.007]

68 **Pagliari M**, Munari F, Toffoletto M, Lonardi S, Chemello F, Codolo G, Millino C, Della Bella C, Pacchioni B, Vermi W, Fassan M, de Bernard M, Cagnin S. *Helicobacter pylori* Affects the Antigen Presentation Activity of Macrophages Modulating the Expression of the Immune Receptor CD300E through miR-4270. *Front Immunol* 2017; **8**: 1288 [PMID: 29085364 DOI: 10.3389/fimmu.2017.01288]

69 **Chu YT**, Wang YH, Wu JJ, Lei HY. Invasion and multiplication of Helicobacter pylori in gastric epithelial cells and implications for antibiotic resistance. *Infect Immun* 2010; **78**: 4157-4165 [PMID: 20696835 DOI: 10.1128/IAI.00524-10]

70 **Zhang X**, Zhang J, Lin Y, Xu K, Li N, Chen H, She F. Analysis of the relationship between invasive capability of Helicobacter pylori and gastroduodenal diseases. *J Med Microbiol* 2015; **64**: 498-506 [PMID: 25752851 DOI: 10.1099/jmm.0.000049]

71 **Sougleri IS**, Papadakos KS, Zadik MP, Mavri-Vavagianni M, Mentis AF, Sgouras DN. Helicobacter pylori CagA protein induces factors involved in the epithelial to mesenchymal transition (EMT) in infected gastric epithelial cells in an EPIYA- phosphorylation-dependent manner. *FEBS J* 2016; **283**: 206-220 [PMID: 26907789 DOI: 10.1111/febs.13592]

72 **Choi YJ**, Kim N, Chang H, Lee HS, Park SM, Park JH, Shin CM, Kim JM, Kim JS, Lee DH, Jung HC. Helicobacter pylori-induced epithelial-mesenchymal transition, a potential role of gastric cancer initiation and an emergence of stem cells. *Carcinogenesis* 2015; **36**: 553-563 [PMID: 25784376 DOI: 10.1093/carcin/bgv022]

73 **Krzysiek-Maczka G**, Targosz A, Szczyrk U, Wrobel T, Strzalka M, Brzozowski T, Czyz J, Ptak-Belowska A. Long-Term *Helicobacter pylori* Infection Switches Gastric Epithelium Reprogramming Towards Cancer Stem Cell-Related Differentiation Program in *Hp*-Activated Gastric Fibroblast-TGFβ Dependent Manner. *Microorganisms* 2020; **8** [PMID: 33023180 DOI: 10.3390/microorganisms8101519]

74 **Molina-Castro S**, Ramírez-Mayorga V, Alpízar-Alpízar W. Priming the seed: *Helicobacter pylori* alters epithelial cell invasiveness in early gastric carcinogenesis. *World J Gastrointest Oncol* 2018; **10**: 231-243 [PMID: 30254719 DOI: 10.4251/wjgo.v10.i9.231]

75 **Tafreshi M**, Guan J, Gorrell RJ, Chew N, Xin Y, Deswaerte V, Rohde M, Daly RJ, Peek RM Jr, Jenkins BJ, Davies EM, Kwok T. *Helicobacter pylori* Type IV Secretion System and Its Adhesin Subunit, CagL, Mediate Potent Inflammatory Responses in Primary Human Endothelial Cells. *Front Cell Infect Microbiol* 2018; **8**: 22 [PMID: 29468142 DOI: 10.3389/fcimb.2018.00022]

76 **Liu N**, Zhou N, Chai N, Liu X, Jiang H, Wu Q, Li Q. Helicobacter pylori promotes angiogenesis depending on Wnt/beta-catenin-mediated vascular endothelial growth factor *via* the cyclooxygenase-2 pathway in gastric cancer. *BMC Cancer* 2016; **16**: 321 [PMID: 27198692 DOI: 10.1186/s12885-016-2351-9]

77 **Li H**, Xu CX, Gong RJ, Chi JS, Liu P, Liu XM. How does *Helicobacter pylori* cause gastric cancer through connexins: An opinion review. *World J Gastroenterol* 2019; **25**: 5220-5232 [PMID: 31558869 DOI: 10.3748/wjg.v25.i35.5220]

78 **Takemori N**, Ooi HK, Imai G, Hoshino K, Saio M. Possible mechanisms of action of clarithromycin and its clinical application as a repurposing drug for treating multiple myeloma. *Ecancermedicalscience* 2020; **14**: 1088 [PMID: 33014130 DOI: 10.3332/ecancer.2020.1088]

79 **Zhou B**, Xia M, Wang B, Thapa N, Gan L, Sun C, Guo E, Huang J, Lu Y, Cai H. Clarithromycin synergizes with cisplatin to inhibit ovarian cancer growth *in vitro* and in vivo. *J Ovarian Res* 2019; **12**: 107 [PMID: 31703731 DOI: 10.1186/s13048-019-0570-9]

80 **Van Nuffel AM**, Sukhatme V, Pantziarka P, Meheus L, Sukhatme VP, Bouche G. Repurposing Drugs in Oncology (ReDO)-clarithromycin as an anti-cancer agent. *Ecancermedicalscience* 2015; **9**: 513 [PMID: 25729426 DOI: 10.3332/ecancer.2015.513]

World Journal of Gastroenterology

Submit a Manuscript: https://www.f6publishing.com

World J Gastroenterol 2021 October 7; 27(37): 6306-6321

DOI: 10.3748/wjg.v27.i37.6306

ISSN 1007-9327 (print) ISSN 2219-2840 (online)

SYSTEMATIC REVIEWS

Determination of gluten immunogenic peptides for the management of the treatment adherence of celiac disease: A systematic review

Laura Coto, Irati Mendia, Carolina Sousa, Julio César Bai, Angel Cebolla

ORCID number: Laura Coto 0000-0002-3883-2027; Irati Mendia 0000-0001-9584-7885; Carolina Sousa 0000-0002-9235-9496; Julio César Bai 0000-0003-4159-0185; Angel Cebolla 0000-0002-6976-4522.

Author contributions: Coto L, Mendia I, Sousa C, Bai JC and Cebolla A contributed equally to the revision of the literature, wrote the draft, and/or revised the final manuscript for intellectual content.

Supported by Ministerio de Ciencia e Innovación, No. DI-16-08943 and No. DI-17-09627.

Conflict-of-interest statement: Angel Cebolla is the founder and current CEO of Biomedal S.L., Angel Cebolla and Carolina Sousa are inventors of the patent "Detecting gluten peptides in human fluids" (No. WO/2016/005643), Laura Coto and Irati Mendia are employees at Biomedal S.L., Julio César Bai declares no conflict of interest.

PRISMA 2009 Checklist statement: The authors have read the PRISMA 2009 Checklist, and the manuscript was prepared and revised according to the PRISMA 2009 Checklist.

Open-Access: This article is an open-access article that was selected by an in-house editor and

Laura Coto, Irati Mendia, Angel Cebolla, Research and Development, Biomedal, Camas 41900, Seville, Spain

Laura Coto, Human Nutrition and Food Science Doctoral Program, University of Granada, Granada 18011, Spain

Irati Mendia, Molecular Biology, Biomedicine and Clinical Research Doctoral Program, University of Seville, Seville 41012, Spain

Carolina Sousa, Department of Microbiology and Parasitology, University of Seville, Seville 41013, Spain

Julio César Bai, Department of Gastroenterology, Dr. Carlos Bonorino Udaondo Gastroenterology Hospital, Buenos Aires 1264, Argentina

Julio César Bai, Research Institutes, Universidad del Salvador, Buenos Aires 1050, Argentina

Corresponding author: Julio César Bai, MD, Professor, Department of Gastroenterology, Dr. Carlos Bonorino Udaondo Gastroenterology Hospital, Av. Caseros 2061, Buenos Aires 1264, Argentina. jbai@intramed.net

Abstract

BACKGROUND

Gluten is a complex mixture of proteins with immunogenic peptide sequences triggering the autoimmune activity in patients with celiac disease (CeD). Gluten immunogenic peptides (GIP) are resistant to gastrointestinal digestion and are then excreted *via* the stool and urine. Most common detection methods applied in the follow-up visits for CeD patients such as serology tests, dietetic interviews, questionnaires, and duodenal biopsy have been proved to be inefficient, invasive, or inaccurate for evaluating gluten-free diet (GFD) compliance. Determination of excreted GIP in stool and urine has been developed as a non-invasive, direct, and specific test for GFD monitoring.

AIM

To summarize published literature about the clinical utility of GIP determination in comparison to the tools employed for GFD monitoring.

METHODS

PubMed and Web of Science searches were performed using the keywords "gluten immunogenic peptides" or "gluten immunogenic peptide" and a

fully peer-reviewed by external reviewers. It is distributed in accordance with the Creative Commons Attribution-NonCommercial (CC BY-NC 4.0) license, which permits others to distribute, remix, adapt, build upon this work non-commercially, and license their derivative works on different terms, provided the original work is properly cited and the use is non-commercial. See: http://creativecommons.org/Licenses/by-nc/4.0/

Manuscript source: Invited manuscript

Specialty type: Gastroenterology and hepatology

Country/Territory of origin: Argentina

Peer-review report's scientific quality classification

Grade A (Excellent): 0
Grade B (Very good): B, B
Grade C (Good): 0
Grade D (Fair): 0
Grade E (Poor): 0

Received: March 22, 2021
Peer-review started: March 22, 2021
First decision: June 14, 2021
Revised: June 28, 2021
Accepted: September 2, 2021
Article in press: September 2, 2021
Published online: October 7, 2021

P-Reviewer: Ciacci C, Stein J
S-Editor: Ma YJ
L-Editor: A
P-Editor: Wu RR

combination of the previous terms with "feces", "stools", "urine", "celiac disease", "gluten-free diet", and "adherence" to identify relevant clinical studies published in English and Spanish between 2012 to January 2021. Reference lists from the articles were reviewed to identify additional pertinent articles. Published articles and abstracts reporting the clinical use of GIP determination in stool and/or urine for the follow-up of patients with CeD in comparison with other tools in use were included. Case reports, commentaries, reviews, conference papers, letters, and publications that did not focus on the aims of this review were excluded.

RESULTS

Total of 15 publications were found that involved the use of GIP determination in stool and/or urine to monitor the adherence to the GFD in comparison to other tools. Studies included both children and adults diagnosed with CeD and healthy volunteers. Overall, these preliminary studies indicated that this novel technique was highly sensitive for the detection of GFD transgressions and therefore could facilitate the follow-up of patients with CeD. Tools identified in this work included the CeD-specific serology, dietetic questionnaires, symptomatology, and the duodenal biopsy. Review of the literature revealed that the rates of GFD adherence may vary between 30%-93% using either stool or urine GIP determination, 49%-96% by the serology, 59%-94% using the dietetic questionnaires, 56%-95% by the reported symptoms and 44%-76% with the duodenal biopsy. In addition, the association between the different methods and histological abnormalities (Marsh II-III) was found to be 33%-100% for GIP determination (stool and urine), 25%-39% for CeD-specific serology, 3%-50% for dietetic questionnaires, and 22%-28% for the symptomatology.

CONCLUSION

Excreted GIP detection is the precise approach for determining voluntary or involuntary gluten consumption in CeD patients preventing future complications arising from gluten exposure.

Key Words: Celiac disease; Gluten-free diet; Gluten immunogenic peptides; Immunoassays; Stool; Urine

©The Author(s) 2021. Published by Baishideng Publishing Group Inc. All rights reserved.

Core Tip: A strict gluten-free diet (GFD) is the only available treatment for celiac disease. However, treatment adherence is difficult due to the ubiquitous nature of gluten, hurting patients' quality of life. Despite several tests to evaluate GFD compliance, it has been proven to be invasive or inefficient. The determination of gluten immunogenic peptides (GIP) in stool and urine has been developed as a non-invasive, direct, and specific test for GFD monitoring. We herein summarized the current available literature meeting the clinical utility of GIP determination compared to the available tools in use.

Citation: Coto L, Mendia I, Sousa C, Bai JC, Cebolla A. Determination of gluten immunogenic peptides for the management of the treatment adherence of celiac disease: A systematic review. *World J Gastroenterol* 2021; 27(37): 6306-6321
URL: https://www.wjgnet.com/1007-9327/full/v27/i37/6306.htm
DOI: https://dx.doi.org/10.3748/wjg.v27.i37.6306

INTRODUCTION

Gluten is a heterologous polymorphic mixture of proteins called prolamins. Wheat prolamins are termed gliadins and glutenins. Prolamins provide food products with special functional properties such as elasticity as well as extensibility and are characterized by high proline and glutamine content, allowing for the more efficiently

packing of proteins but also complicating the enzyme-mediated hydrolysis of their tight structures[1]. Consequently, many of these proteins are insufficiently degraded by gastric and pancreatic enzymes in the gastrointestinal tract. Therefore, after the ingestion of gluten-containing foods, some gluten peptides can enter the intestinal epithelium and trigger an immune response in genetically predisposed individuals suffering from celiac disease (CeD)[2-4].

Evidence suggests that gluten can cross the intestinal barrier *via* the transcellular pathway perpetuating intestinal inflammation in the context of gluten intolerance[5, 6]. The α-gliadin 33-mer peptide has been described as one of the most immunodominant gluten peptides, harboring several T cell epitopes[2]. Another three gluten peptides have been shown to trigger high immunogenicity observed in most CeD patients[7]. Thus, most of the immune response against gluten may be accounted for by a limited group of gluten epitopes[7]. The anti- α-gliadin 33-mer antibodies A1 and G12 could specifically and sensitively detect excreted gluten immunogenic peptides (GIP) in stool and urine[8,9], confirming the resistance of GIP to human gastrointestinal digestion as well as their absorption into the bloodstream.

CeD is a systemic disease, involving well-known key immune factors, including the human leukocyte antigen (HLA-DQ2 and HLA-DQ8), the anti-tissue transglutaminase (anti-tTG) antibodies, and gluten[10]. As a systemic disease, there are intestinal and extraintestinal symptoms that can be presented individually or in combination. In addition, patients may also be completely asymptomatic[11]. Intestinal presentation of CeD is common in both the pediatric and adult patient population and is characterized by diarrhea, loss of appetite, abdominal distention, bloating, pain, constipation, or weight loss[12,13]. The most common extraintestinal symptoms are iron deficiency anemia, osteopenia or osteoporosis, hypertransaminasemia, neurological afflictions, or changes in reproductive function[10]. Nevertheless, a relevant proportion of patients present atypical symptoms or remain asymptomatic despite damage to the intestinal mucosa and elevated CeD-specific serum antibodies, which may delay diagnosis or even be undiagnosed[14].

Following CeD diagnosis, patients must follow a strict, life-long gluten-free diet (GFD), the only treatment currently available, which not only reduces disease symptoms but also allows for the healing of the intestinal epithelia and prevents long-term complications[15-17]. However, following a strict GFD is challenging and requires substantial daily effort, hurting the quality of life in addition to psychological problems and fear of involuntary gluten intake, even in patients considering themselves to be strictly adherent[15,18-20]. Gluten-free food availability, inadequate food labeling regulations, cost, and safety are the main barriers related to GFD[18,21, 22]. Therefore, the frequency of voluntary and involuntary transgressions is high. It was reported that at least 50% of adult patients are not fully adherent to the GFD in a daily or weekly period of observation[8,9,23,24]. In addition, 36%-55% of patients who expressed their complete adherence to a GFD did not achieve histological remission, potentially from inadvertent lapses in their daily gluten intake[24-27]. Inadvertent gluten ingestion was suggested to be more frequent than intentional intake, not only when eating out, but also at home[28-30]. A systematic review recently reported adherence rates ranging from 23% to 98% in the pediatric population, determined by using all available methods for evaluating adherence[31].

Although continuous patient monitoring is expected to improve GFD adherence, there is no consensus on how frequent and which tools to use in the patient follow-up [32-35]. All available guidelines recommended clinical and dietary evaluation as well as serology tests at least once a year or every two years to confirm the GFD adherence in addition to detecting possible complications[14]. However, monitoring approaches have not been comprehensively assessed with a clear lack of a gold standard for comparisons[36-38]. Thus, various questions often arise among caregivers and patients regarding the best approach for detecting gluten exposure. GFD follow-up through the detection of excreted GIP has the benefits of being non-invasive, objective, and specific, highlighting its potential as a complementary technique for monitoring CeD treatment[8,9].

Despite the increasing number of studies on the use of GIP excretion determination for the assessment of GFD compliance, there are limited reference guidelines on the detection of GIP in stool and urine for monitoring the treatment in patients diagnosed with CeD. The purpose of this systematic review is to compile insights from studies that tackled the practical issues related to the clinical utility of the available methods for GIP determination compared to current GFD adherence monitoring methods.

MATERIALS AND METHODS

Literature search strategy

PubMed and Web of Science searches were performed using the search terms "gluten immunogenic peptides" or "gluten immunogenic peptide" and a combination of the previous terms with "feces", "stools", "urine", "celiac disease", "gluten-free diet", and "adherence" using the Boolean AND operator, which allows the establishments of logical relations among concepts. References of included full-text articles were scrutinized for additional studies.

Inclusion and exclusion criteria

The eligibility criteria were based on the PICOS (Participants, Intervention, Comparison, Outcomes, Study design) acronym. Articles eligible to be included in this review were required to meet the following criteria: (1) The study reported both children and adult patients diagnosed with CeD, since it would be more useful for readers as the evidence available about the use of this tool is limited; (2) The intervention was the use of GIP determination in stool and/or urine as a tool for monitoring the rate of adherence to the GFD in comparison with the current tools in use, like the serology, dietetic questionnaires, symptomatology, and duodenal biopsy; (3) It was a prospective cohort/cross-sectional/case-control study; (4) The article was written in English or Spanish language; and (5) The article was published between 2012 and January 2021.

We excluded publications that did not focus on the aim of this review. If a full-text paper could not be obtained, but the abstract presented sufficient data, the publication was included. Case reports, commentaries, reviews, conference papers, and letters were excluded.

Retrieved manuscripts were reviewed by the authors, and the data were extracted and described.

RESULTS

Through the literature review, our searches yielded 67 results after the removal of duplicates. In total, 52 entries were excluded for different reasons: 23 did not respond to the aim of this publication, 28 were reviews, case reports, or conference papers, and one had not abstract or full-text available. After screening, 15 publications were eligible for further study. Of these, 14 had a full text in English and one had an English abstract. Two publications reported complementary data about the same study (Figure 1).

The 15 publications included both children and adults diagnosed with CeD. Healthy adult and pediatric volunteers were also included in many of the studies. The articles were published between 2016 and 2021. The characteristics of included studies are summarized in Table 1[8,9,22-24,29,30,39-46].

DISCUSSION

Methods for the determination of excreted GIP

Analytical methods require a standard analyte for quantitative determination. The main issue is the selection of a standard gluten peptide in the huge heterogeneity of the gluten proteins and the countless number of gluten hydrolyzed fragments. The a-gliadin 33-mer peptide (LQLQPFPQPQLPYPQPQLPYPQPQLPYPQPQPF) is resistant to hydrolysis *via* gastric, pancreatic, and intestinal brush-border membrane proteases, which allows for its detection in human excretions. This peptide is considered one of the most immunodominant gluten peptides for CeD patients, as it contains three overlapping T cell epitopes, repetitions of p57-68[2,47,48]. Monoclonal antibodies A1 and G12 were generated against the α-2-gliadin 33-mer peptide specifically and sensitively detecting significant amounts of excreted GIP in stool and urine[8,9]. The reactive epitope profile may thus play an important role in the detection of excreted GIP. Even though there are a variety of antibodies on the market that allow for gluten detection in food, such as R5, 401.21, α20, 14G11, and 13F6, only G12 and/or A1 are useful for gluten peptide sensitive detection in stool and urine[8,9,49-52].

Urine samples are highly heterogeneous matrices with low protein content, making complicating the development of immunoassays for biomarkers detection. Urine

Table 1 Studies that have used gluten immunogenic peptides determination in stool and/or urine for gluten-free diet monitoring

Ref.	Design	Study population	Intervention	Main results
Comino *et al* [8]	Prospective, multicenter, observational study	184 adult and pediatric CeD patients	Fecal GIP ELISA, serology, questionnaires, and symptoms to evaluate adherence to the GFD	GIP-positive results were found in 12%-28% of children < 12 years-old, 30% in > 13 years-old females and 60% in > 13 years-old males. Low correlation of anti-tTG and anti-DGP markers and poor adherence to the GFD
Moreno *et al* [9]	Randomized controlled study	58 adult and pediatric CeD patients and 76 healthy controls	Urine GIP LFIA test, serology, and duodenal biopsy to evaluate adherence to the GFD	About 50% CeD patients were GIP-positive. High correlation of GIP quantifiable concentration in urine with persistent villus atrophy in treated CeD patients (n = 25). No correlation between serology and mucosal damage
Gerasimidis *et al*[39]	Cross-sectional study cohort for a subgroup	63 pediatric CeD patients	Fecal ELISA GIP test, serology, and questionnaires to evaluate gluten intake during diagnosis and adherence to the GFD after diagnosis	GIP-positive results in 95% of de novo patients with CeD during diagnosis. GIP-positive results were found in 17% and 27% of patients after 6 and 12 months of the beginning of the GFD, respectively. GIP-positive results were found in 16%, 16%, and 14% of patients considered compliant according to the Biagi score, tTG, and clinical assessment, respectively
Comino *et al* [40]	Prospective, multicenter, observational study	64 pediatric CeD patients	Fecal GIP ELISA, serology, questionnaires, and symptoms to evaluate adherence to the GFD after diagnosis	Most children (97%) were GIP-positive at diagnosis. A decrease of GIP detection was observed on a GFD, but the rate of GIP-positive results increased from 13% at 6 months to 25% at 24 months. Anti-tTG antibody levels showed low sensitivity to identify patients with GIP-positive results. Dietitian assessment was only moderately correlated with GIP detection
Costa *et al*[41]	Cross-sectional study and prospective cohort	44 adult CeD patients	Fecal GIP ELISA, stool and urine LFIA GIP tests, serology, questionnaires, and symptoms to evaluate adherence to the GFD	25% of patients had at least one GIP-positive test, 32% in asymptomatic patients and 15.8% in symptomatic patients. Dietary assessment estimated gluten intake in only 50% of GIP-positive samples. Anti-tTG and anti-DGP positive results in 3/12 and 6/12 of GIP-positive cases, respectively
Silvester *et al* [29,30]	Prospective longitudinal study	18 adult CeD patients	Monitoring GFD adherence by collection of daily food, stool, and urine samples for the analysis of GIP content, and relationship with duodenal biopsy, serology, questionnaires, and symptoms	GIP were detected in 66,7% patients. No significant correlation was found between gluten ingestion and non-invasive measures of GFD adherence. Most patients with normal anti-tTG had ≥ 1 GIP-positive sample (64%), 2/3 of these had persistent villous atrophy (Marsh 3a) and 2/3 of those with all GIP-negative samples had normal villous architecture (Marsh 0-1) but 4/6 with Marsh 0 had detectable gluten in ≥ 1 sample
Ruiz-Carnicer *et al* [23]	Prospective observational study	22 newly diagnosed CeD patients, 77 CeD patients following a GFD and 13 healthy volunteers	Urine LFIA GIP test to evaluate adherence to the GFD and comparison with serology, clinical manifestations, dietary questionnaire, and histological results	Mucosal damage (Marsh II-III) was found in 24% of CeD patients, 94%of these had ≥ 1 GIP urine sample. 60-80% of these were asymptomatic, had negative serologic results and were compliant with treatment regarding the dietary questionnaire. GIP-negative results were found in 97% of the patients without mucosal damage
Fernandez-Miaja *et al*[22]	Cross-sectional study	80 pediatric CeD patients	Relationship of fecal LFIA GIP for GFD monitoring GFD with CDAT, serology and sociodemographic and clinical data	Acceptable agreement was found between GIP detection and CDAT questionnaire (92.5% and 86.3% adherence rate, respectively). Most patients (83.3%) with GIP-positive results had negative anti-tTG antibodies
Porcelli *et al* [42]	Cross-sectional study	25 CeD patients	Assessment of compliance with the GFD using Fecal GIP ELISA testing, the Biagi questionnaire, evaluation of symptoms and serology	GIP-positive results were found in 4 patients, 2 of these complied with the GFD according to the Biagi questionnaire. All GIP-negative patients were asymptomatic. Levels of anti-tTG antibodies were significantly higher in GIP-positive patients than in GIP-negative patients
Roca *et al*[43]	Prospective, cross-sectional study	43 pediatric CeD patients at follow-up (Group 1) and 18 at diagnosis (Group 2)	Fecal GIP ELISA and LFIA analysis to monitor in real life the adherence to GFD Comparison to food record questionnaire and serology	Group 1: GIP-positive results were found in of 34.9% patients by ELISA (46,7% also by LFIA). 48.8% of patients had positive anti-tTG antibodies (4 reported symptoms) and 10 of these had GIP-positive results by ELISA (70% also by LFIA) (2 reported symptoms). All the transgressions detected by food record were also detected with GIP
Porcelli *et al* [44]	Cross-sectional study	55 CeD patients: 27 adults and 28 children	Assessment of compliance with the GFD using Fecal GIP ELISA, the Biagi questionnaire, evaluation of symptoms and serology	GIP-positive results were found in 8 patients, 71.4% of these were asymptomatic and 37.5% had raised anti-tTG antibodies. A significant association was found between the Biagi score and GIP-positive results but according to the Biagi score, 57.1% of GIP-positive patients followed the diet strictly and 5.4% of GIP-negative subjects did not comply with the diet

Laserna-Mendieta *et al* [45]	Prospective observational study	97 adolescent and adult CeD patients	Evaluation of the sensitivity and specificity of fecal GIP LFIA test to detect duodenal lesions in CeD patients on a GFD and comparison to serology and questionnaires	Compared to the duodenal histology, GIP LFIA test showed similar sensitivity (33%) and specificity (81%) to anti-tTG antibodies. No relationship was found between GIP and questionnaires but an association between GIP and patients' self-reported gluten consumption was seen
Stefanolo *et al* [24]	Prospective observational study	53 adult CeD patients	Fecal GIP ELISA and urine LFIA GIP test, anti-tTG, anti-DGP, and questionnaires to evaluate adherence to the GFD in symptomatic and asymptomatic patients	At least one GIP-positive result in 88.7% of patients for the 4 wk period. Patients who had symptoms had elevated GIP levels for more weeks than patients who did not have these symptoms ($P < 0.05$). Correlation was found between GIP and anti-DGP antibodies but not with levels of anti-tTG antibodies
Fernández-Bañares *et al* [46]	Multicenter prospective observational study	76 adult CeD patients	Fecal GIP ELISA, anti-tTG, questionnaires and symptomatology to evaluate villous atrophy persistence after 2 years on a GFD	Persistent villous atrophy was present in 53% of patients at follow-up, 72% of these were asymptomatic and 75% had negative anti-tTG antibodies. Most patients were adherent to the GFD according to the dietary evaluation. In contrast, GIP-positive results were found in ≥ 1 fecal sample of 77% of patients with villous atrophy and in 60% of patients with mucosal recovery

GIP: Gluten immunogenic peptides; LFIA: Lateral flow immunoassay; GFD: Gluten-free diet; CeD: Celiac disease; anti-tTG: Anti-tissue transglutaminase; anti-DGP: Anti-deamidated gluten peptide; CDAT: Celiac disease adherence test.

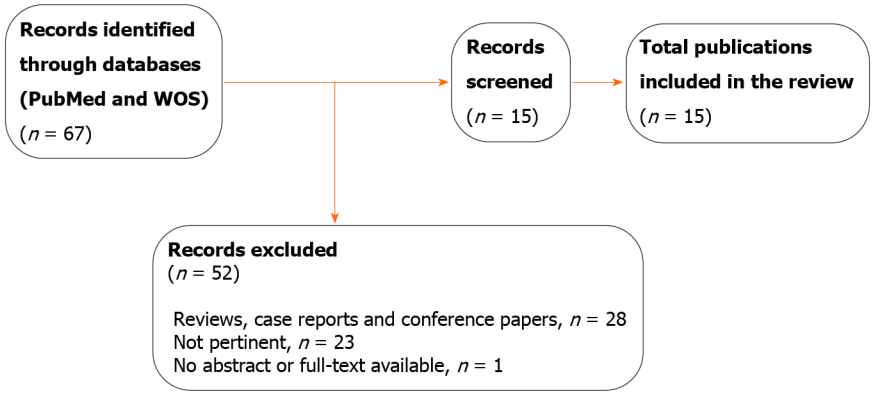


Figure 1 Flow-chart of the publications search and selection.

contains organic molecules such as urea, creatinine, and uric acid, inorganic ions such as K^+, Na^+, Cl^-, and Ca^{2+}, cells, as well as peptides of more than 1500 proteins[53]. The concentration of these compounds and the pH usually exhibit considerable variability not only among individuals but also between different urine samples taken from the same individual[54]. The complex composition of these samples and its variability, in addition to the high frequency of matrix interferences, complicate the reproducibility and robustness of urine immunoassays. Chatziharalambous *et al*[53] evaluated 11 commercial ELISA assays for the detection of urine biomarkers, reporting that only three of them met the requirements of FDA validation guidelines[55].

The currently available tests for GIP detection in stool and/or urine (Table 2) are immunoassays adapted from those used for gluten detection in foods to maximize sensitivity. Lateral flow immunoassay (LFIA) tests can detect GIP from concentrations of 0.15 μg GIP/g in stool and 2.2 ng GIP/mL in urine after less than 30 minutes, showing both tests a high sensitivity (98.5% and 97%, respectively) and specificity of 100%[9,56]. While these tests provide qualitative data, semiquantitative results could also be obtained in urine samples using the LFIA coupled with a lateral flow reader [9]. A quantitative G12-based sandwich ELISA test for stools was developed to increase the sensitivity and quantitative determinations. The analytical sensitivity of the assay was 0.16 μg GIP/g stool (limit of quantification), and it was validated in a multicenter clinical study, showing a diagnostic sensitivity and specificity of 98.5% and 100%, respectively[8].

Estimation of the time and amount of ingested gluten

Although a significant correlation between gluten intake and excreted GIP concentration was reported, high variability is usually observed among subjects[9,29,30,43]. Interindividual diversity (weight, sex, age, gut microbiota, *etc.*), the type of gluten-

Table 2 Available immunomethods to detect gluten immunogenic peptides in stool and urine

Technique	Antibodies	Sample	Analytical sensitivity	Diagnostic sensitivity	Diagnostic specificity	Ref.
ELISA	G12/G12	Stool	0.16 μg/g	0.98	1	[8]
LFIA	G12/A1	Stool	0.15 μg/g	0.97	1	[56]
LFIA	G12/A1	Urine	2.2 ng/mL (LOD), 6.25 ng/mL (LOQ)	0.91	0.99	[9]

ELISA: Enzyme-like immunosorbent assay; LFIA: Lateral flow immunoassay; LOD: Limit of detection; LOQ: Limit of quantification.

containing food (beer, pasta, bread, cookies, *etc.*), the amount of daily liquid intake, and the accompanying diet may have a considerable impact on the resulting GIP concentration as well as the excretion time in urine and stool samples, especially when the gluten exposure is not regular[9,29,30,43].

It appears difficult to predict the specific time and amount of gluten intake with high accuracy based on excreted GIP concentration and even considering the time of sample collection. However, some constraints regarding the expected time for GIP detection and the limits of detection could have been determined in different studies (Table 3).

It was observed that after consuming normal gluten containing diet, a negative result in both urine and stool samples was rarely observed in the following 6-12 h and 3-5 days, respectively, after the last gluten-containing meal[9,43]. Moreover, in individuals with multiple regular transgressions, the interval between gluten ingestion and urine sample collection for maximal sensitivity of detection was generally consistent between 4 and 24 h[29,30].

Despite the variability of GIP concentrations found among individuals in most studies, a significantly low GIP content was typically observed in patients with CeD compared to healthy individuals with no diet restrictions[8,9].

Clinical utility of GIP determination in urine or stools

Fecal immunoassays were first suggested as a novel method for the detection of gluten intake during diagnosis and GFD monitoring[57]. Two different methods could be used to estimate the amount of ingested gluten depending on the situation: LFIA test for either clinical laboratories or point-of-care settings due to its simplicity, while ELISA would be more suitable when a quantitative analysis and/or high throughput are convenient[58,59]. In a prospective, nonrandomized, partially-blinded, multicenter study GFD compliance of CeD children and adults was examined by measuring fecal GIP (determined by ELISA), a dietary questionnaire, celiac serology, and clinical response, as markers of diet adherence[8]. Their results revealed detectable amounts of GIP in the stools of about 30% of the analyzed patients on a GFD for at least one year in comparison to the 18% found when assessing by dietary questionnaire or by determination of anti-tTG antibodies in the serum alone. Indeed, less GIP-positive results were found in those declared non-compliant by the food questionnaire, while 70% of patients who did not declare any gluten intake had positive levels of GIP in stools[8].

Then, Moreno *et al*[9] demonstrated that urine samples could be used to monitor GFD compliance *via* an LFIA test. These tests revealed a high level of GFD infringement in patients on long-term treatment (48% and 45% in adults and children, respectively)[9]. Thus, several studies have compared GIP detection results in stool and urine for GFD monitoring, with information obtained *via* CeD-specific serology, dietary questionnaires, symptomatology, and duodenal biopsies, revealing the limitations of all these methods used to evaluate GFD transgressions and the concordance between them (Table 4).

A branch of the first study with newly diagnosed pediatric CeD patients (n = 64) showed that the percentage of diet adherence decreased on follow-up at 6, 12, and 24 mo, as the rate of GIP-positive stools increased from 13% to 25%[40]. Meanwhile, anti-deamidated gliadin peptide (anti-DGP) antibodies normalized by 24 mo, and anti-tTG antibodies were elevated in 20% of the patients. Some children, particularly the older ones, were reported to have a propensity for GFD non-compliance, and 46% of non-adherent participants had at least two GIP-positive stools during follow-up[40]. Similar data were reported by other groups[22,44]. Patients with higher levels of gluten exposure exhibited prolonged ascension of anti-tTG antibodies (P < 0.05) than those with GIP-negative results.

Table 3 Parametrical features of the gluten immunogenic peptides excretion using lateral flow immunoassay and enzyme-like immunosorbent assay methods

Specifications for the determination of GIP excretion after gluten intake	Sample	Time ranges (h)	Gluten source (amount)	Method
Shortest time to detect GIP	Urine	3-9	GCD (> 2 g)	LFIA [9,29,30]
	Stool→	< 24	GCD (> 2 g)	LFIA; ELISA[43]
Longest time to detect GIP	Urine	36	GCD (> 2 g)	LFIA[9,29,30]
	Stool	> 72	GCD (> 2 g)	LFIA; ELISA[29,30,43]
Minimal gluten intake to detect excreted GIP	Urine		> 40-500 mg/d; 25-50 mg	LFIA; SPE + LFIA[9,41]
	Stool		> 40 mg/d	ELISA, LFIA[41,43]

GIP: Gluten immunogenic peptides; GCD: Gluten containing diet including different food types; LFIA: Lateral flow immunoassay; ELISA: Enzyme-like immunosorbent assay; SPE: Solid phase extraction.

Table 4 Determination of gluten-free diet non-adherence using different tools, *n* (%)

Ref.	Stool GIP+	Urine GIP+	anti-tTG+	anti-DGP+	Questionnaires[1]	Symptoms	Duodenal biopsy (Marsh II/III)
Comino *et al*[8]	56 (30)	-	32 (18)	11 (6)	25 (18)	9 (5)	-
Moreno *et al*[9]	-	12 (48)	4 (16)		-	-	7 (28)
Gerasimidis *et al*[39]	11 (19)	-	12 (20)	-	4 (6)	-	-
Comino *et al*[40]	6 (25)	-	7 (20)	0 (0)	-	-	-
Costa *et al*[41]	11 (25)	3 (7)	9 (21)	18 (45)	18 (41)	19 (43)	-
Silvester *et al*[29,30]	5 (28)	8 (44)	7 (39)	-	4 (22)	8 (44)	10 (56)
Ruiz-Carnicer *et al*[23]	-	44 (58)	9 (12)	-	14 (23)	18 (23)	18 (24)
Fernández-Miaja *et al*[22]	6 (8)	-	3 (4)	-	10 (13)	-	-
Roca *et al*[43]	15 (35)	-	22 (51)	-	4 (9)	4 (9)	-
Porcelli *et al*[44]	8 (15)	-	3 (6)	-	5 (11)	16 (34)	-
Laserna-Mendieta *et al*[45]	22 (23)	-	11 (12)	-	17 (18)	-	6 (28)
Stefanolo *et al*[24]	33 (62)	37 (70)	22 (42)	25 (47)	-	18 (34)	-
Fernández-Bañares *et al*[46]	53 (70)	-	17 (22)	-	6 (8)	15 (20)	40 (53)

[1]Questionnaires used were Celiac Disease Adherence Test (CDAT), Biagi Score and standard food records evaluated by dietitians.
GFD: Gluten-free diet; GIP: Gluten immunogenic peptides; anti-tTG: Anti-tissue transglutaminase; anti-DGP: Anti-deamidated gluten peptide; -: Not available.

In agreement with these data, Gerasimidis *et al*[39] found that most patients following a GFD had GIP-negative results, while 18% exhibited recent gluten exposure, which was not detected by using anti-tTG antibodies and the Biagi score. These findings confirmed the limitations of dietary evaluation and serology in adult patients with CeD on a GFD. A quarter of patients considered adherent by those methods had detectable GIP, using both LFIA and ELISA tests, in at least one of two independent tests during the 2 wk of the study. A 65,9% of concordance was observed between dietary reports and GIP results. Only four patients had high serum antibody values and two of them confirmed dietary non-compliance, in agreement with GIP results[41].

Recent research demonstrated that both ELISA and LFIA methods confirmed suspected and unsuspected dietary exposure in stool samples of CeD children and adolescent patients on a long-term GFD. However, no significant association was found between longer GFD duration, and the amount of GIP recovered in stool[43].

GIP-positive results were obtained from 35% of patients by ELISA (47% of these were also confirmed by LFIA). However, based on the dietary questionnaire, 90.7% of patients were compliant with the treatment. All the patients revealed as non-adherent by the questionnaire had GIP-positive stools. Furthermore, anti-tTG antibodies were detected in five patients, three of whom were also GIP-positive. However, the authors suggested that these elevated levels may be related to the short length of treatment (< 12 mo) and a lack of GFD adherence, as a patient with negative serology and GIP-negative stools was identified.

Differences in diet compliance rates based on a GIP LIFA test in stools and a validated adherence questionnaire (CDAT) (92.5% *vs* 86.3%, respectively) were observed among 80 CeD children and adolescent patients[22]. Nevertheless, the methods exhibited acceptable concordance (Kappa: 0.31, $P = 0.004$). Of those patients with good adherence using CDAT ($n = 66$), three had GIP-positive results. Porcelli *et al* [44] also found a significant association between strict diet adherence estimated by the Biagi score and fecal GIP detection. According to the Biagi score, 94.6% of GIP-negative patients exhibited good adherence. However, the questionnaire failed in the identification of 57.1% of GIP-positive patients, while GIP detection did not recognize 5.4% of gluten exposures declared *via* the questionnaire. In this study, 62.5% of GIP-positive patients exhibited negative anti-tTG antibodies levels.

The results from the DOGGIE BAG study[29,30] also confirmed that diet transgressions in patients with CeD were frequent despite efforts made to strictly follow the GFD. In this prospective longitudinal study, the food consumed by patients, in addition to their urine and stool samples, were analyzed for gluten intake and GIP excretion, respectively, throughout 10 days before a biopsy at 24 mo after the diagnosis. Gluten was found in the food of 9/18 participants at concentrations as high as 200 ppm, and GIP-positive results were obtained in 12/18 participants reporting good adherence to the GFD (8 of these had positive urine samples, and five had positive stool samples). No correlation was observed between gluten exposure and commonly used non-invasive measures of GFD adherence. Most of the participants (73%) who suspected a gluten exposure had at least one positive food, stool, or urine sample. Among the remaining participants who did not suspect any gluten intake, four of them resulted positive for GIP[29,30]. Other authors also found a significant association between patient self-reported gluten consumption and GIP detection. GIP was detected in 52.9% of patients who suspected gluten intake in the last month in comparison to 16.3% for those who were not aware of any gluten exposure[45].

On the other hand, several studies examined the association between the available tools for GFD monitoring and the duodenal biopsy, currently considered the gold standard (Table 5). Moreno *et al*[9] assessed the correlation between duodenal biopsies and GIP concentration in urine samples. Analysis of duodenal biopsies revealed that all the adult patients with small intestine damage (Marsh II/III) had GIP-positive urine samples ($n = 7$). In addition, there was a significant correlation between the absence of GIP in urine and the absence of villus atrophy in the gut intestinal epithelium. In agreement with other publications[60-62], this study confirmed the poor correlation of serological tests with mucosal healing as well as the limitations of dietary history questionnaires in the assessment of GFD adherence.

In addition, a comprehensive study with a cohort of 77 participants under treatment with a GFD for ≥ 24 mo revealed that 58% had detectable GIP in their urine in at least one sample of three collected during the week[23]. Among the patients with GIP-negative results, 97% of them did not present histological abnormalities (Marsh 0–I), while among patients with GIP-positive results, 17 of 44 (39%) had histological damage in the intestinal epithelial (Marsh II-III), with only 16% presenting positive serological results. Significant differences were found in GIP concentrations between participants with Marsh II–III and Marsh 0–I. The highest sensitivity was observed when at least one of three urine samples tested GIP-positive (94.4%). However, this combination exhibited low specificity (53.4%). In contrast, the optimal specificity was obtained when a single urine sample was collected on the visit day (84.2%). Then, it was expected that one GIP-positive urine sample on the day of the visit would reveal a regular habit of GFD non-compliance not-restrained by the medical supervision. The authors did not observe concordance between gluten exposure measured by GIP and serology, or through a CDAT questionnaire and symptomatology, all of which exhibited low sensitivity for mucosal damage (38.9%, 22.2%, and 42.9%, respectively).

About the association of duodenal biopsy and GIP in fecal samples, Fernández-Bañares *et al*[46] found that most of CeD patients (77%) with persistent villous atrophy obtained a GIP-positive result in at least 1 stool sample after 2 years under GFD. In contrast, dietary evaluation failed to detect most of these gluten exposures, considering these cases as excellent or good adherent to the diet. In addition, 72.5% of

Table 5 Rate of transgressions in the gluten-free diet using different tools in presence/absence of mucosal atrophy by duodenal biopsy, *n* (%)

Ref.	GIP+ (Stool and/or urine)	Serology+	Questionnaires[1]	Symptoms
Duodenal biopsy (Marsh II/III)				
Moreno *et al*[9]	7 (100)	2 (29)	-	-
Silvester *et al*[29,30]	8 (80)	-	-	-
Ruiz-Carnicer *et al*[23]	17 (94)	7 (39)	6 (43)	4 (22)
Laserna-Mendieta *et al*[45]	2 (33)	2 (33)	3 (50)	-
Fernández-Bañares *et al*[46]	31 (78)	10 (25)	1 (3)	11 (28)
Duodenal biopsy (Marsh 0/I)				
Moreno *et al*[9]	5 (28)	2 (11)	-	-
Silvester *et al*[29,30]	4 (50)	-	-	-
Ruiz-Carnicer *et al*[23]	27 (47)	2 (3)	8 (17)	14 (24)
Laserna-Mendieta *et al*[45]	20 (22)	9 (10)	77 (85)	-
Fernández-Bañares *et al*[46]	22 (61)	7 (19)	5 (14)	4 (11)

[1]Questionnaires used were Celiac Disease Adherence Test (CDAT), Biagi Score and standard food records evaluated by dietitians.
GFD: Gluten-free diet; GIP: Gluten immunogenic peptides; -: Not available.

those patients were asymptomatic, and 75% of them obtained negative anti-tTG antibodies. Despite GIP-positive results were also found in 60% of patients with mucosal recovery, no significant differences were found in the amount of GIP between patients with persistent villous atrophy and recovered patients[46].

Other authors reported a weaker association between evident gluten exposure, as measured by GIP detection in urine and stool, and persistent villous atrophy[29,30,45]. In the DOGGIE BAG study referred to above, at least one GIP-positive sample was found in 7 of 11 patients with normal serology, and 2/3 of them had persistent villous atrophy (Marsh IIIa) after 24 mo of follow-up. Further, 2/3 of patients with GIP-negative results for all samples were Marsh 0-I, showing significant mucosal recovery [29,30]. A possible explanation for the discordance described before is that occasional or low gluten exposure may be sufficient for GIP detection but not enough to induce mucosal damage in some patients with CeD[23,29,30,45]. A delay of intestinal mucosal recovery[29,30,45] and improved compliance of participants during the study was also considered[29,30]. Besides, Laserna-Mendieta *et al*[45] reported a low sensitivity but acceptable specificity of GIP for the detection of mucosal damage, however for the calculation they included in the same group Marsh 1 patients (n = 21), who do not present mucosal damage but lymphocytic infiltration, and Marsh 2 and 3 patients (n = 6). Moreover, in this study, weak GIP-positive results were discarded for analysis and duodenal biopsies were performed in two hospitals with different pathologists, entailing a risk of interobserver variability[63,64]. Hence, with these results, the introduction of GIP detection as a non-invasive and sensitive assessment approach for GFD adherence may reduce the need for endoscopy and could identify potential intestinal mucosal damage not detectable *via* serological tests or dietary questionnaires. In addition, intestinal mucosal recovery could be predicted based on recurring negative GIP tests.

Regarding the relationship between symptoms and GIP excretion, only a small percentage of CeD patients reported symptoms in the studies with the highest number of celiac volunteers, although a score system for symptomatology was not used[8]. Roca *et al*[43] detected GIP in samples from 22.7% of asymptomatic pediatric patients negative for anti-tTG antibodies. In contrast, Costa *et al*[41] reported that most adult patients with gluten transgressions determined *via* GIP detection were asymptomatic, although the difference was not statistically significant due to the low number of cases enrolled. Similar data were published by Porcelli *et al*[44] wherein the rate of asymptomatic patients with GIP-positive results was 71.4%.

A recent publication[24] studied the relationship of stool and urine GIP results with gastrointestinal symptoms in CeD adult patients for 4 wk to represent a real-life scenario. 62% of the patients were found to have at least one GIP-positive stool test,

and 69.9% had positive urine samples. The results suggested that symptoms in CeD patients under a GFD are the consequence of gluten exposure. A significantly higher rate of GIP-positive stool samples was observed in symptomatic compared to asymptomatic patients (77.8% *vs* 54.3%, respectively). However, a group of asymptomatic patients also had the highest number of GIP-positive urine samples per patient. This observation highlights the importance of distinguishing asymptomatic patients due to no gluten consumption from those patients consuming gluten because they were asymptomatic.

Considering that avoiding symptoms is the main motivation for adhering to a GFD, GIP content could be a useful indicator for the identification of asymptomatic patients with considerable immunogenic gluten exposure preventing gut mucosal recovery. Furthermore, GIP detection may help in symptomatic patients with CeD to determine whether non-responsive celiac disease or refractory celiac disease occurs due to recurrent gluten exposure or due to additional factors inducing persistent symptoms, such as the consumption of FODMAPs or intestinal dysbiosis[40,41,65,66].

CONCLUSION

Excreted GIP detection in either stool or urine is a precise approach for determining voluntary or involuntary gluten consumption. However, isolated GIP measurements might not identify intermittent compliance, unless punctual transgressions took place close to the moment of sample collection. It appears that the use of multiple samples (at least two) contributes to higher sensitivity and specificity of GIP detection[23,24]. In a considerable number of studies, biopsies and recurrent excretion of GIP indicated that serological tests, symptoms, and dietary questionnaires were not sufficient indicators of GFD adherence[9,23,29-31]. However, anti-tTG antibodies and clinical dietary assessment have been recently suggested as complementary tools in the evaluation of GFD adherence[44,45]. In this context, Porcelli *et al*[44] proposed the use of the Biagi score in combination with fecal GIP tests using a binary logistic regression model. In contrast, other groups did not find anti-tTG levels to be a relevant marker of adherence even though anti-DGP antibodies levels have been shown to significantly correlate with the quantity and frequency of GIP excretion in stools[24,41].

Regarding which method is more appropriate, Roca *et al*[43,67] proposed GIP testing of fecal samples as a non-invasive method that allows patient empowerment for self-managing the disease. ELISA is to be used for the laboratory quantification of GIP, while LFIA strips should be used for patient self-control following suspected involuntary infringements. Even though GIP evaluation may represent an extra cost for CeD patients monitoring, its inclusion in the pursuing of strict GFD adherence would reduce health expenditure by preventing future complications arising from gluten exposure in overlooked asymptomatic patients and would improve the self-esteem or "peace of mind" of patients adhering to the GFD, decreasing the need for additional assessment and endoscopy in non-responsive celiac disease or refractory celiac disease, especially in children.

Some authors have already proposed algorithms for the application of the determination of GIP in stools[39] and urine[23] for the follow-up of patients with CeD. It is expected that the application of those protocols with some variations will be progressively introduced in the guidelines to assess the adherence of patients to the GFD. Future studies may also determine the utility of GIP excretion analysis for other applications, such as the confirmation that sufficient gluten has been ingested before diagnosis or to discover unknown aspects of gluten protein metabolism.

ARTICLE HIGHLIGHTS

Research background

A lifelong strict gluten-free diet (GFD) is the only available treatment for celiac disease (CeD), which reduces symptoms and allows the healing of the intestinal mucosa, preventing long-term complications. However, total exclusion of gluten is difficult to achieve in practice and voluntary and involuntary transgressions are highly frequent.

Research motivation

Gluten immunogenic peptides (GIP) detection in stool and urine is becoming increasingly apparent as a noninvasive and reliable marker for close and efficient GFD

monitoring in patients with CeD.

Research objectives

The authors aimed to summarize published data regarding the performance of GIP determination in stool and urine in comparison to other available tools in assessing GFD adherence in patients with CeD.

Research methods

The authors conducted a systematic review searching in PubMed and Web of Science clinical studies that reported the performance of GIP determination in stool and/or urine with other biomarkers for the evaluation of treatment adherence in adult and pediatric patients with CeD.

Research results

The authors screened 67 articles and 15 articles were included for full-text analysis. In the selected publications GIP determination in stool and/or urine were compared with at least one of the following markers: levels of CeD-specific serology, results from CeD-specific non-specific questionnaires, symptomatology, and duodenal biopsy. Fecal determination by ELISA was the most investigated GIP marker, followed by urine rapid test and stool rapid test. Variability was seen in the concordance between the different tools among the studies reviewed due to the differences found in the study design, the target population, and the methods used. One of the main outcome measures reviewed was the diagnostic accuracy of these tools in assessing mucosal healing. An association of mucosal status and GIP detection was observed in some publications, where serology, questionnaires, and symptomatology showed lower sensitivity. Furthermore, GIP detection may help in symptomatic patients to determine whether non-responsive CeD or refractory CeD occurs due to recurrent gluten exposure or due to additional factors.

Research conclusions

The introduction of GIP detection in stool and/or urine as a non-invasive marker for GFD monitoring in patients with CeD may reduce health expenditure by preventing future complications arising from gluten exposure not detectable by other tools in use. Stool and urine rapid tests may be an option for disease self-managing by the patient, while fecal ELISA test could be used for GIP quantification in the laboratory.

Research perspectives

The introduction of algorithms for GIP determination within the follow-up of patients with CeD in guidelines will allow its routine use in clinical practice. In addition, future studies may also determine their utility for other applications such as the confirmation of gluten consumption during the diagnosis process or the investigation of gluten metabolism.

ACKNOWLEDGEMENTS

This paper will be part of Laura Coto's doctorate that is being carried out within the context of "Human Nutrition Program" at the University of Granada.

REFERENCES

1 **Shewry PR**, Halford NG, Belton PS, Tatham AS. The structure and properties of gluten: an elastic protein from wheat grain. *Philos Trans R Soc Lond B Biol Sci* 2002; **357**: 133-142 [PMID: 11911770 DOI: 10.1098/rstb.2001.1024]

2 **Shan L**, Molberg Ø, Parrot I, Hausch F, Filiz F, Gray GM, Sollid LM, Khosla C. Structural basis for gluten intolerance in celiac sprue. *Science* 2002; **297**: 2275-2279 [PMID: 12351792 DOI: 10.1126/science.1074129]

3 **Fasano A**, Catassi C. Clinical practice. Celiac disease. *N Engl J Med* 2012; **367**: 2419-2426 [PMID: 23252527 DOI: 10.1056/NEJMcp1113994]

4 **Abadie V**, Sollid LM, Barreiro LB, Jabri B. Integration of genetic and immunological insights into a model of celiac disease pathogenesis. *Annu Rev Immunol* 2011; **29**: 493-525 [PMID: 21219178 DOI: 10.1146/annurev-immunol-040210-092915]

5 **Loeff T**, Araya M, Pérez-Bravo F. Frequency of MYO9B polymorphisms in celiac patients and

controls. *Rev Esp Enferm Dig* 2012; **104**: 566-571 [PMID: 23368647 DOI: 10.4321/s1130-01082012001100003]

6 **Wapenaar MC**, Monsuur AJ, van Bodegraven AA, Weersma RK, Bevova MR, Linskens RK, Howdle P, Holmes G, Mulder CJ, Dijkstra G, van Heel DA, Wijmenga C. Associations with tight junction genes PARD3 and MAGI2 in Dutch patients point to a common barrier defect for coeliac disease and ulcerative colitis. *Gut* 2008; **57**: 463-467 [PMID: 17989107 DOI: 10.1136/gut.2007.133132]

7 **Tye-Din JA**, Stewart JA, Dromey JA, Beissbarth T, van Heel DA, Tatham A, Henderson K, Mannering SI, Gianfrani C, Jewell DP, Hill AV, McCluskey J, Rossjohn J, Anderson RP. Comprehensive, quantitative mapping of T cell epitopes in gluten in celiac disease. *Sci Transl Med* 2010; **2**: 41ra51 [PMID: 20650871 DOI: 10.1126/scitranslmed.3001012]

8 **Comino I**, Fernández-Bañares F, Esteve M, Ortigosa L, Castillejo G, Fambuena B, Ribes-Koninckx C, Sierra C, Rodríguez-Herrera A, Salazar JC, Caunedo Á, Marugán-Miguelsanz JM, Garrote JA, Vivas S, Lo Iacono O, Nuñez A, Vaquero L, Vegas AM, Crespo L, Fernández-Salazar L, Arranz E, Jiménez-García VA, Antonio Montes-Cano M, Espín B, Galera A, Valverde J, Girón FJ, Bolonio M, Millán A, Cerezo FM, Guajardo C, Alberto JR, Rosinach M, Segura V, León F, Marinich J, Muñoz-Suano A, Romero-Gómez M, Cebolla Á, Sousa C. Fecal Gluten Peptides Reveal Limitations of Serological Tests and Food Questionnaires for Monitoring Gluten-Free Diet in Celiac Disease Patients. *Am J Gastroenterol* 2016; **111**: 1456-1465 [PMID: 27644734 DOI: 10.1038/ajg.2016.439]

9 **Moreno ML**, Cebolla Á, Muñoz-Suano A, Carrillo-Carrion C, Comino I, Pizarro Á, León F, Rodríguez-Herrera A, Sousa C. Detection of gluten immunogenic peptides in the urine of patients with coeliac disease reveals transgressions in the gluten-free diet and incomplete mucosal healing. *Gut* 2017; **66**: 250-257 [PMID: 26608460 DOI: 10.1136/gutjnl-2015-310148]

10 **Caio G**, Volta U, Sapone A, Leffler DA, De Giorgio R, Catassi C, Fasano A. Celiac disease: a comprehensive current review. *BMC Med* 2019; **17**: 142 [PMID: 31331324 DOI: 10.1186/s12916-019-1380-z]

11 **Leonard MM**, Sapone A, Catassi C, Fasano A. Celiac Disease and Nonceliac Gluten Sensitivity: A Review. *JAMA* 2017; **318**: 647-656 [PMID: 28810029 DOI: 10.1001/jama.2017.9730]

12 **Vivas S**, Ruiz de Morales JM, Fernandez M, Hernando M, Herrero B, Casqueiro J, Gutierrez S. Age-related clinical, serological, and histopathological features of celiac disease. *Am J Gastroenterol* 2008; **103**: 2360-2365; quiz 2366 [PMID: 18702652 DOI: 10.1111/j.1572-0241.2008.01977.x]

13 **Reilly NR**, Aguilar K, Hassid BG, Cheng J, Defelice AR, Kazlow P, Bhagat G, Green PH. Celiac disease in normal-weight and overweight children: clinical features and growth outcomes following a gluten-free diet. *J Pediatr Gastroenterol Nutr* 2011; **53**: 528-531 [PMID: 21670710 DOI: 10.1097/MPG.0b013e3182276d5e]

14 **Lindfors K**, Ciacci C, Kurppa K, Lundin KEA, Makharia GK, Mearin ML, Murray JA, Verdu EF, Kaukinen K. Coeliac disease. *Nat Rev Dis Primers* 2019; **5**: 3 [PMID: 30631077 DOI: 10.1038/s41572-018-0054-z]

15 **Lebwohl B**, Granath F, Ekbom A, Smedby KE, Murray JA, Neugut AI, Green PH, Ludvigsson JF. Mucosal healing and risk for lymphoproliferative malignancy in celiac disease: a population-based cohort study. *Ann Intern Med* 2013; **159**: 169-175 [PMID: 23922062 DOI: 10.7326/0003-4819-159-3-201308060-00006]

16 **Elli L**, Ferretti F, Orlando S, Vecchi M, Monguzzi E, Roncoroni L, Schuppan D. Management of celiac disease in daily clinical practice. *Eur J Intern Med* 2019; **61**: 15-24 [PMID: 30528262 DOI: 10.1016/j.ejim.2018.11.012]

17 **Therrien A**, Kelly CP, Silvester JA. Celiac Disease: Extraintestinal Manifestations and Associated Conditions. *J Clin Gastroenterol* 2020; **54**: 8-21 [PMID: 31513026 DOI: 10.1097/MCG.0000000000001267]

18 **See JA**, Kaukinen K, Makharia GK, Gibson PR, Murray JA. Practical insights into gluten-free diets. *Nat Rev Gastroenterol Hepatol* 2015; **12**: 580-591 [PMID: 26392070 DOI: 10.1038/nrgastro.2015.156]

19 **Leinonen H**, Kivelä L, Lähdeaho ML, Huhtala H, Kaukinen K, Kurppa K. Daily Life Restrictions are Common and Associated with Health Concerns and Dietary Challenges in Adult Celiac Disease Patients Diagnosed in Childhood. *Nutrients* 2019; **11** [PMID: 31349675 DOI: 10.3390/nu11081718]

20 **Troncone R**, Auricchio R, Granata V. Issues related to gluten-free diet in coeliac disease. *Curr Opin Clin Nutr Metab Care* 2008; **11**: 329-333 [PMID: 18403932 DOI: 10.1097/MCO.0b013e3282f795f8]

21 **Vriezinga SL**, Schweizer JJ, Koning F, Mearin ML. Coeliac disease and gluten-related disorders in childhood. *Nat Rev Gastroenterol Hepatol* 2015; **12**: 527-536 [PMID: 26100369 DOI: 10.1038/nrgastro.2015.98]

22 **Fernández Miaja M**, Díaz Martín JJ, Jiménez Treviño S, Suárez González M, Bousoño García C. [Study of adherence to the gluten-free diet in coeliac patients]. *An Pediatr (Barc)* 2021; **94**: 377-384 [PMID: 32830086 DOI: 10.1016/j.anpedi.2020.06.017]

23 **Ruiz-Carnicer Á**, Garzón-Benavides M, Fombuena B, Segura V, García-Fernández F, Sobrino-Rodríguez S, Gómez-Izquierdo L, Montes-Cano MA, Rodríguez-Herrera A, Millán R, Rico MC, González-Naranjo C, Bozada-García JM, Díaz J, Coronel-Rodríguez C, Espín B, Romero-Gómez M, Cebolla Á, Sousa C, Comino I, Argüelles F, Pizarro Á. Negative predictive value of the repeated absence of gluten immunogenic peptides in the urine of treated celiac patients in predicting mucosal healing: new proposals for follow-up in celiac disease. *Am J Clin Nutr* 2020; **112**: 1240-1251 [PMID: 32692806 DOI: 10.1093/ajcn/nqaa188]

24 **Stefanolo JP**, Tálamo M, Dodds S, de la Paz Temprano M, Costa AF, Moreno ML, Pinto-Sánchez MI, Smecuol E, Vázquez H, Gonzalez A, Niveloni SI, Mauriño E, Verdu EF, Bai JC. Real-World Gluten Exposure in Patients With Celiac Disease on Gluten-Free Diets, Determined From Gliadin Immunogenic Peptides in Urine and Fecal Samples. *Clin Gastroenterol Hepatol* 2021; **19**: 484-491.e1 [PMID: 32217152 DOI: 10.1016/j.cgh.2020.03.038]

25 **Stoven S**, Murray JA, Marietta E. Celiac disease: advances in treatment *via* gluten modification. *Clin Gastroenterol Hepatol* 2012; **10**: 859-862 [PMID: 22728383 DOI: 10.1016/j.cgh.2012.06.005]

26 **Tio M**, Cox MR, Eslick GD. Meta-analysis: coeliac disease and the risk of all-cause mortality, any malignancy and lymphoid malignancy. *Aliment Pharmacol Ther* 2012; **35**: 540-551 [PMID: 22239821 DOI: 10.1111/j.1365-2036.2011.04972.x]

27 **Hall NJ**, Rubin GP, Charnock A. Intentional and inadvertent non-adherence in adult coeliac disease. A cross-sectional survey. *Appetite* 2013; **68**: 56-62 [PMID: 23623778 DOI: 10.1016/j.appet.2013.04.016]

28 **Muhammad H**, Reeves S, Jeanes YM. Identifying and improving adherence to the gluten-free diet in people with coeliac disease. *Proc Nutr Soc* 2019; **78**: 418-425 [PMID: 30630540 DOI: 10.1017/S002966511800277X]

29 **Silvester JA**, Comino I, Rigaux LN, Segura V, Green KH, Cebolla A, Weiten D, Dominguez R, Leffler DA, Leon F, Bernstein CN, Graff LA, Kelly CP, Sousa C, Duerksen DR. Exposure sources, amounts and time course of gluten ingestion and excretion in patients with coeliac disease on a gluten-free diet. *Aliment Pharmacol Ther* 2020; **52**: 1469-1479 [PMID: 32981131 DOI: 10.1111/apt.16075]

30 **Silvester JA**, Comino I, Kelly CP, Sousa C, Duerksen DR; DOGGIE BAG Study Group. Most Patients With Celiac Disease on Gluten-Free Diets Consume Measurable Amounts of Gluten. *Gastroenterology* 2020; **158**: 1497-1499.e1 [PMID: 31866245 DOI: 10.1053/j.gastro.2019.12.016]

31 **Myléus A**, Reilly NR, Green PHR. Rate, Risk Factors, and Outcomes of Nonadherence in Pediatric Patients With Celiac Disease: A Systematic Review. *Clin Gastroenterol Hepatol* 2020; **18**: 562-573 [PMID: 31173891 DOI: 10.1016/j.cgh.2019.05.046]

32 **Villafuerte-Galvez J**, Vanga RR, Dennis M, Hansen J, Leffler DA, Kelly CP, Mukherjee R. Factors governing long-term adherence to a gluten-free diet in adult patients with coeliac disease. *Aliment Pharmacol Ther* 2015; **42**: 753-760 [PMID: 26206401 DOI: 10.1111/apt.13319]

33 **Bebb JR**, Lawson A, Knight T, Long RG. Long-term follow-up of coeliac disease--what do coeliac patients want? *Aliment Pharmacol Ther* 2006; **23**: 827-831 [PMID: 16556185 DOI: 10.1111/j.1365-2036.2006.02824.x]

34 **Haines ML**, Anderson RP, Gibson PR. Systematic review: The evidence base for long-term management of coeliac disease. *Aliment Pharmacol Ther* 2008; **28**: 1042-1066 [PMID: 18671779 DOI: 10.1111/j.1365-2036.2008.03820.x]

35 **Herman ML**, Rubio-Tapia A, Lahr BD, Larson JJ, Van Dyke CT, Murray JA. Patients with celiac disease are not followed up adequately. *Clin Gastroenterol Hepatol* 2012; **10**: 893-899.e1 [PMID: 22610009 DOI: 10.1016/j.cgh.2012.05.007]

36 **Catassi C**, Fabiani E, Iacono G, D'Agate C, Francavilla R, Biagi F, Volta U, Accomando S, Picarelli A, De Vitis I, Pianelli G, Gesuita R, Carle F, Mandolesi A, Bearzi I, Fasano A. A prospective, double-blind, placebo-controlled trial to establish a safe gluten threshold for patients with celiac disease. *Am J Clin Nutr* 2007; **85**: 160-166 [PMID: 17209192 DOI: 10.1093/ajcn/85.1.160]

37 **Walker MM**, Murray JA. An update in the diagnosis of coeliac disease. *Histopathology* 2011; **59**: 166-179 [PMID: 21054494 DOI: 10.1111/j.1365-2559.2010.03680.x]

38 **Catassi C**. Protocollo per la diagnosi ed il follow-up della malattia celiaca. *Encicl del Dirit* 2015; 263-358

39 **Gerasimidis K**, Zafeiropoulou K, Mackinder M, Ijaz UZ, Duncan H, Buchanan E, Cardigan T, Edwards CA, McGrogan P, Russell RK. Comparison of Clinical Methods With the Faecal Gluten Immunogenic Peptide to Assess Gluten Intake in Coeliac Disease. *J Pediatr Gastroenterol Nutr* 2018; **67**: 356-360 [PMID: 29916953 DOI: 10.1097/MPG.0000000000002062]

40 **Comino I**, Segura V, Ortigosa L, Espín B, Castillejo G, Garrote JA, Sierra C, Millán A, Ribes-Koninckx C, Román E, Rodríguez-Herrera A, Díaz J, Silvester JA, Cebolla Á, Sousa C. Prospective longitudinal study: use of faecal gluten immunogenic peptides to monitor children diagnosed with coeliac disease during transition to a gluten-free diet. *Aliment Pharmacol Ther* 2019; **49**: 1484-1492 [PMID: 31074004 DOI: 10.1111/apt.15277]

41 **Costa AF**, Sugai E, Temprano MP, Niveloni SI, Vázquez H, Moreno ML, Domínguez-Flores MR, Muñoz-Suano A, Smecuol E, Stefanolo JP, González AF, Cebolla-Ramirez A, Mauriño E, Verdú EF, Bai JC. Gluten immunogenic peptide excretion detects dietary transgressions in treated celiac disease patients. *World J Gastroenterol* 2019; **25**: 1409-1420 [PMID: 30918433 DOI: 10.3748/wjg.v25.i11.1409]

42 **Porcelli B**, Ferretti F, Cinci F, Biviano I, Santini A, Grande E, Quagliarella F, Terzuoli L, Bacarelli MR, Bizzaro N, Vascotto M, Marini M. Fecal gluten immunogenic peptides as indicators of dietary compliance in celiac patients. *Minerva Gastroenterol Dietol* 2020; **66**: 201-207 [PMID: 32218420 DOI: 10.23736/S1121-421X.20.02662-8]

43 **Roca M**, Donat E, Masip E, Crespo-Escobar P, Cañada-Martínez AJ, Polo B, Ribes-Koninckx C. Analysis of gluten immunogenic peptides in feces to assess adherence to the gluten-free diet in pediatric celiac patients. *Eur J Nutr* 2021; **60**: 2131-2140 [PMID: 33057793 DOI: 10.1007/s00394-020-02404-z]

44 **Porcelli B**, Ferretti F, Biviano I, Santini A, Cinci F, Vascotto M, Grande E, Quagliarella F, Terzuoli

L, Bizzaro N, Marini M, Rentini S. Testing for fecal gluten immunogenic peptides: a useful tool to evaluate compliance with gluten-free diet by celiacs. *Ann Gastroenterol* 2020; **33**: 631-637 [PMID: 33162739 DOI: 10.20524/aog.2020.0530]

45 **Laserna-Mendieta EJ**, Casanova MJ, Arias Á, Arias-González L, Majano P, Mate LA, Gordillo-Vélez CH, Jiménez M, Angueira T, Tébar-Romero E, Carrillo-Ramos MJ, Tejero-Bustos MÁ, Gisbert JP, Santander C, Lucendo AJ. Poor Sensitivity of Fecal Gluten Immunogenic Peptides and Serum Antibodies to Detect Duodenal Mucosal Damage in Celiac Disease Monitoring. *Nutrients* 2020; **13** [PMID: 33396719 DOI: 10.3390/nu13010098]

46 **Fernández-Bañares F**, Beltrán B, Salas A, Comino I, Ballester-Clau R, Ferrer C, Molina-Infante J, Rosinach M, Modolell I, Rodríguez-Moranta F, Arau B, Segura V, Fernández-Salazar L, Santolaria S, Esteve M, Sousa C; CADER study group. Persistent Villous Atrophy in De Novo Adult Patients With Celiac Disease and Strict Control of Gluten-Free Diet Adherence: A Multicenter Prospective Study (CADER Study). *Am J Gastroenterol* 2021; **116**: 1036-1043 [PMID: 33491958 DOI: 10.14309/ajg.0000000000001139]

47 **Qiao SW**, Bergseng E, Molberg O, Jung G, Fleckenstein B, Sollid LM. Refining the rules of gliadin T cell epitope binding to the disease-associated DQ2 molecule in celiac disease: importance of proline spacing and glutamine deamidation. *J Immunol* 2005; **175**: 254-261 [PMID: 15972656 DOI: 10.4049/jimmunol.175.1.254]

48 **Camarca A**, Anderson RP, Mamone G, Fierro O, Facchiano A, Costantini S, Zanzi D, Sidney J, Auricchio S, Sette A, Troncone R, Gianfrani C. Intestinal T cell responses to gluten peptides are largely heterogeneous: implications for a peptide-based therapy in celiac disease. *J Immunol* 2009; **182**: 4158-4166 [PMID: 19299713 DOI: 10.4049/jimmunol.0803181]

49 **Skerritt JH**, Hill AS. Monoclonal antibody sandwich enzyme immunoassays for determination of gluten in foods. *J Agric Food Chem* 1991; **38**: 1771-1778 [DOI: 10.1021/jf00098a029]

50 **Valdés I**, García E, Llorente M, Méndez E. Innovative approach to low-level gluten determination in foods using a novel sandwich enzyme-linked immunosorbent assay protocol. *Eur J Gastroenterol Hepatol* 2003; **15**: 465-474 [PMID: 12702901 DOI: 10.1097/01.meg.0000059119.41030.df]

51 **van den Broeck HC**, de Jong HC, Salentijn EM, Dekking L, Bosch D, Hamer RJ, Gilissen LJ, van der Meer IM, Smulders MJ. Presence of celiac disease epitopes in modern and old hexaploid wheat varieties: wheat breeding may have contributed to increased prevalence of celiac disease. *Theor Appl Genet* 2010; **121**: 1527-1539 [PMID: 20664999 DOI: 10.1007/s00122-010-1408-4]

52 **Zhang J**, Portela SB, Horrell JB, Leung A, Weitmann DR, Artiuch JB, Wilson SM, Cipriani M, Slakey LK, Burt AM, Dias Lourenco FJ, Spinali MS, Ward JR, Seit-Nebi A, Sundvor SE, Yates SN. An integrated, accurate, rapid, and economical handheld consumer gluten detector. *Food Chem* 2019; **275**: 446-456 [PMID: 30724219 DOI: 10.1016/j.foodchem.2018.08.117]

53 **Chatziharalambous D**, Lygirou V, Latosinska A, Stravodimos K, Vlahou A, Jankowski V, Zoidakis J. Analytical Performance of ELISA Assays in Urine: One More Bottleneck towards Biomarker Validation and Clinical Implementation. *PLoS One* 2016; **11**: e0149471 [PMID: 26889680 DOI: 10.1371/journal.pone.0149471]

54 **Adachi J**, Kumar C, Zhang Y, Olsen JV, Mann M. The human urinary proteome contains more than 1500 proteins, including a large proportion of membrane proteins. *Genome Biol* 2006; **7**: R80 [PMID: 16948836 DOI: 10.1186/gb-2006-7-9-R80]

55 **U.S. Department of Health and Human Services FDA**. Bioanalytical Method Validation Guidance for Industry. 2018; 1–41. Available from: https://www.fda.gov/regulatory-information/search-fda-guidance-documents/bioanalytical-method-validation-guidance-industry

56 **Biomedal**. iVYCHECK GIP Stool. [cited 15 June 2021]. Available from: https://ivydal.biomedal.com/tests-de-uso-profesional/ivycheck-gip-stool/

57 **Auricchio S**. An innovative approach to measure compliance to a gluten-free diet. *Am J Clin Nutr* 2012; **95**: 537-538 [PMID: 22301934 DOI: 10.3945/ajcn.111.032888]

58 **Bethune MT**, Crespo-Bosque M, Bergseng E, Mazumdar K, Doyle L, Sestak K, Sollid LM, Khosla C. Noninflammatory gluten peptide analogs as biomarkers for celiac sprue. *Chem Biol* 2009; **16**: 868-881 [PMID: 19716477 DOI: 10.1016/j.chembiol.2009.07.009]

59 **Ehren J**, Morón B, Martin E, Bethune MT, Gray GM, Khosla C. A food-grade enzyme preparation with modest gluten detoxification properties. *PLoS One* 2009; **4**: e6313 [PMID: 19621078 DOI: 10.1371/journal.pone.0006313]

60 **Sharkey LM**, Corbett G, Currie E, Lee J, Sweeney N, Woodward JM. Optimising delivery of care in coeliac disease - comparison of the benefits of repeat biopsy and serological follow-up. *Aliment Pharmacol Ther* 2013; **38**: 1278-1291 [PMID: 24117503 DOI: 10.1111/apt.12510]

61 **Tursi A**, Brandimarte G, Giorgetti GM. Lack of usefulness of anti-transglutaminase antibodies in assessing histologic recovery after gluten-free diet in celiac disease. *J Clin Gastroenterol* 2003; **37**: 387-391 [PMID: 14564185 DOI: 10.1097/00004836-200311000-00007]

62 **Rashtak S**, Ettore MW, Homburger HA, Murray JA. Comparative usefulness of deamidated gliadin antibodies in the diagnosis of celiac disease. *Clin Gastroenterol Hepatol* 2008; **6**: 426-432; quiz 370 [PMID: 18304884 DOI: 10.1016/j.cgh.2007.12.030]

63 **Arguelles-Grande C**, Tennyson CA, Lewis SK, Green PH, Bhagat G. Variability in small bowel histopathology reporting between different pathology practice settings: impact on the diagnosis of coeliac disease. *J Clin Pathol* 2012; **65**: 242-247 [PMID: 22081783 DOI: 10.1136/jclinpath-2011-200372]

64 **Ravelli A**, Villanacci V. Tricks of the trade: How to avoid histological pitfalls in celiac disease.

Pathol Res Pract 2012; **208**: 197-202 [PMID: 22417775 DOI: 10.1016/j.prp.2012.01.008]

65 **Gibson PR**, Muir JG, Newnham ED. Other Dietary Confounders: FODMAPS *et al*. *Dig Dis* 2015; **33**: 269-276 [PMID: 25925934 DOI: 10.1159/000371401]

66 **Wacklin P**, Kaukinen K, Tuovinen E, Collin P, Lindfors K, Partanen J, Mäki M, Mättö J. The duodenal microbiota composition of adult celiac disease patients is associated with the clinical manifestation of the disease. *Inflamm Bowel Dis* 2013; **19**: 934-941 [PMID: 23478804 DOI: 10.1097/MIB.0b013e31828029a9]

67 **Roca M**, Donat E, Masip E, Crespo Escobar P, Fornes-Ferrer V, Polo B, Ribes-Koninckx C. Detection and quantification of gluten immunogenic peptides in feces of infants and their relationship with diet. *Rev Esp Enferm Dig* 2019; **111**: 106-110 [PMID: 30318895 DOI: 10.17235/reed.2018.5549/2018]

World Journal of Gastroenterology

Submit a Manuscript: https://www.f6publishing.com

World J Gastroenterol 2021 October 7; 27(37): 6322-6331

DOI: 10.3748/wjg.v27.i37.6322

ISSN 1007-9327 (print) ISSN 2219-2840 (online)

CASE REPORT

Pancreatic paraganglioma diagnosed by endoscopic ultrasound-guided fine needle aspiration: A case report and review of literature

Gandhi Lanke, John M Stewart, Jeffrey H Lee

ORCID number: Gandhi Lanke 0000-0002-5577-2257; John M Stewart 0000-0002-9589-8508; Jeffrey H Lee 0000-0001-6740-3670.

Author contributions: Lanke G composed and drafted the paper; Stewart JM provided path images, revised, and edited the draft; Lee JH conceptualized, designed, revised, and edited the draft.

Informed consent statement: All study participants, or their legal guardian, provided informed written consent prior to study enrollment.

Conflict-of-interest statement: None of the authors have any potential conflicts (financial, professional, or personal) that are relevant to the manuscript.

CARE Checklist (2016) statement: The authors have read the CARE Checklist (2016), and the manuscript was prepared and revised according to the CARE Checklist (2016).

Open-Access: This article is an open-access article that was selected by an in-house editor and fully peer-reviewed by external reviewers. It is distributed in accordance with the Creative Commons Attribution NonCommercial (CC BY-NC 4.0) license, which permits others to

Gandhi Lanke, Department of Gastroenterology, Hepatology and Nutrition, MD Anderson Cancer Center, Lubbock, TX 79407, United States

John M Stewart, Pathology-lab Medicine Division, MD Anderson Cancer Center, Houston, TX 77030, United States

Jeffrey H Lee, Department of Gastroenterology, Hepatology and Nutrition, MD Anderson Cancer Center, Houston, TX 77030, United States

Corresponding author: Jeffrey H Lee, AGAF, FACG, FASGE, MD, Director, Professor, Department of Gastroenterology, Hepatology and Nutrition, MD Anderson Cancer Center, 1515 Holcombe Blvd, Unit 1466, Houston, TX 77030, United States. jefflee@mdanderson.org

Abstract

BACKGROUND

Pancreatic paragangliomas (PPGL) are rare benign neuroendocrine neoplasms but malignancy can occur. PPGL are often misdiagnosed as pancreatic neuroendocrine tumor or pancreatic adenocarcinoma.

CASE SUMMARY

We reviewed 47 case reports of PPGL published in PubMed to date. Fifteen patients (15/47) with PPGL underwent endoscopic ultrasound-guided fine needle aspiration (EUS-FNA). Only six (6/15) were correctly diagnosed as PPGL. All patients with PPGL underwent surgical resection except three (one patient surgery was aborted because of hypertensive crisis, two patients had metastasis or involvement of major vessels). Our patient remained on close surveillance as she was asymptomatic.

CONCLUSION

Accurate preoperative diagnosis of PPGL can be safely achieved by EUS-FNA with immunohistochemistry. Multidisciplinary team approach should be considered to bring the optimal results in the management of PPGL.

Key Words: Pancreatic paraganglioma; Endoscopic ultrasound-guided fine needle aspiration; Meta-iodobenzylguanidine scan; Metanephrines; GATA-3; Immunohistochemistry; Case report

©The Author(s) 2021. Published by Baishideng Publishing Group Inc. All rights reserved.

distribute, remix, adapt, build upon this work non-commercially, and license their derivative works on different terms, provided the original work is properly cited and the use is non-commercial. See: http://creativecommons.org/Licenses/by-nc/4.0/

Manuscript source: Invited manuscript

Specialty type: Gastroenterology and hepatology

Country/Territory of origin: United States

Peer-review report's scientific quality classification
Grade A (Excellent): 0
Grade B (Very good): B
Grade C (Good): 0
Grade D (Fair): 0
Grade E (Poor): 0

Received: April 6, 2021
Peer-review started: April 6, 2021
First decision: June 17, 2021
Revised: June 28, 2021
Accepted: September 3, 2021
Article in press: September 3, 2021
Published online: October 7, 2021

P-Reviewer: Zhou Y
S-Editor: Gao CC
L-Editor: A
P-Editor: Ma YJ



Core Tip: The morphologic overlap between pancreatic paraganglioma and neuroendocrine tumor is significant. An accurate diagnosis by endoscopic ultrasound-guided fine needle aspiration requires firstly that the possibility of paraganglioma is considered and secondly that a cell block is available for immunohistochemical stains. A patient-centered approach supported by a multidisciplinary team of radiologists, advanced endoscopists, endocrinologists, pathologists, oncologists, and surgeons is paramount in the management of pancreatic paraganglioma.

Citation: Lanke G, Stewart JM, Lee JH. Pancreatic paraganglioma diagnosed by endoscopic ultrasound-guided fine needle aspiration: A case report and review of literature. *World J Gastroenterol* 2021; 27(37): 6322-6331
URL: https://www.wjgnet.com/1007-9327/full/v27/i37/6322.htm
DOI: https://dx.doi.org/10.3748/wjg.v27.i37.6322

INTRODUCTION

Paragangliomas are rare neuroendocrine neoplasms arising from the sympathetic and parasympathetic paraganglia. This tumor is called pheochromocytoma in the adrenal medulla and elsewhere is known as extra-adrenal paraganglioma or simply as paraganglioma. The malignant potential of these tumors is difficult to predict. Most behave in a benign manner, but metastasis, which best defines malignant paraganglioma, may occur in 15%-20%[1]. When found in or around the pancreas this tumor is often misdiagnosed as pancreatic neuroendocrine tumor (PNET) or even pancreatic adenocarcinoma. In this study, we report a case of pancreatic paraganglioma diagnosed by endoscopic ultrasound-guided fine needle aspiration (EUS-FNA) and review of the literature on pancreatic paraganglioma.

CASE PRESENTATION

Chief complaints

A 73-year-old female presented with a chief complaint for evaluation of an incidental finding of peripancreatic lymph node.

History of present illness

She underwent computed tomography (CT) of the abdomen and pelvis as part of her routine surveillance for extranodal marginal zone B-cell lymphoma of mucosa-associated lymphoid tissue (MALT-lymphoma) of the lung and was found to have peripancreatic lymph node. She denied any abdominal pain, change in bowel habit, weight loss, nausea, or vomiting.

History of past illness

Her medical history was significant for MALT-lymphoma, invasive lobular breast carcinoma, hypertension, atrial fibrillation, mitral valve prolapse, mitral valve stenosis, and actinic keratosis. Her surgical history included a mastectomy with sentinel lymph node dissection, laparoscopic cholecystectomy, tonsillectomy, left knee replacement, and bilateral carpal tunnel repair.

Personal and family history

Her family history was significant for colon cancer in maternal grandmother at the age of 65 years, prostate cancer in brother at the age of 63 years, and melanoma in mother. She had no history of alcohol or tobacco abuse. She has 2 children and attained menopause at the age of 52 years. Her medications included aspirin, furosemide, carvedilol, rosuvastatin, amiodarone, digoxin, anastrozole, and Eliquis.

Physical examination

Her physical examination was unremarkable, and her abdomen was soft nontender, nondistended with no palpable mass.

Laboratory examinations

Laboratory exam including fractionated metanephrines, chromogranin, and gastrin were negative.

Imaging examinations

CT of the abdomen and pelvis showed 2 cm × 1.1 cm lymph node adjacent to the pancreatic head (Figure 1A).

Endoscopy

EUS showed a 19 mm × 11.5 mm hypoechoic lesion near the pancreatic head (Figure 1B). Two FNA passes using a 25-gauge needle were performed *via* trans-duodenal approach (Figure 1C).

Pathology

Direct FNA smears showed tumor with neuroendocrine features. Initial immunoperoxidase stains performed on cell block sections were positive for synaptophysin and chromogranin, which seemed to confirm the morphologic impression of PNET. The pathologist was subsequently informed about the peripancreatic location and lack of a definite pancreatic lesion.

FINAL DIAGNOSIS

After additional testing showed the tumor to be positive for GATA-3 and negative for keratin with low expression of Ki-67 (less than 1%), the FNA diagnosis was revised to paraganglioma.

TREATMENT

Our patient was referred to endocrine surgery team after the FNA diagnosis of paraganglioma. After a thorough discussion with the patient on the benefits and risks of surgical resection, the patient elected to remain on close surveillance since she was asymptomatic with a 2-cm, nonfunctioning paraganglioma.

OUTCOME AND FOLLOW-UP

After a 1-year follow up, patient was found to have stable asymptomatic peripancreatic paraganglioma with no increase in size.

DISCUSSION

Paragangliomas are non-epithelial neuroendocrine neoplasms arising in close association with components of the parasympathetic and sympathetic nervous systems [2]. Most parasympathetic paragangliomas are nonfunctional and located along the glossopharyngeal and vagal nerves in the neck and base of the skull[3]. Sympathetic paraganglia secrete catecholamines (functional) and they are commonly located in the paravertebral ganglia of thorax, abdomen, and pelvis[3]. The incidence of extra-adrenal paraganglioma is unclear as these are often described with pheochromocytoma. In the United States, approximately 500-1600 cases are diagnosed every year and the combined annual incidence of pheochromocytoma/paraganglioma is approximately 0.8 per 100000 person-years[4,5]. Pancreatic paragangliomas are more common in women than men (2:1) and the mean age of incidence is 52 years (19-85 years)[6].

Patients with functional paragangliomas can experience hypertension, headache, sweating, and palpitations due to the excessive secretion of catecholamines[7]. Nonsecretory paragangliomas may present with abdominal mass with or without abdominal pain, but most are found incidentally on imaging studies[8,9]. CT has a sensitivity of approximately 90% in the identification of extra-adrenal paragangliomas, which frequently appear as highly vascular structures with areas of intralesional hemorrhage and necrosis[8,10]. The CT findings of pancreatic paragangliomas differ from those of pancreatic ductal adenocarcinoma by their location at the pancreatic

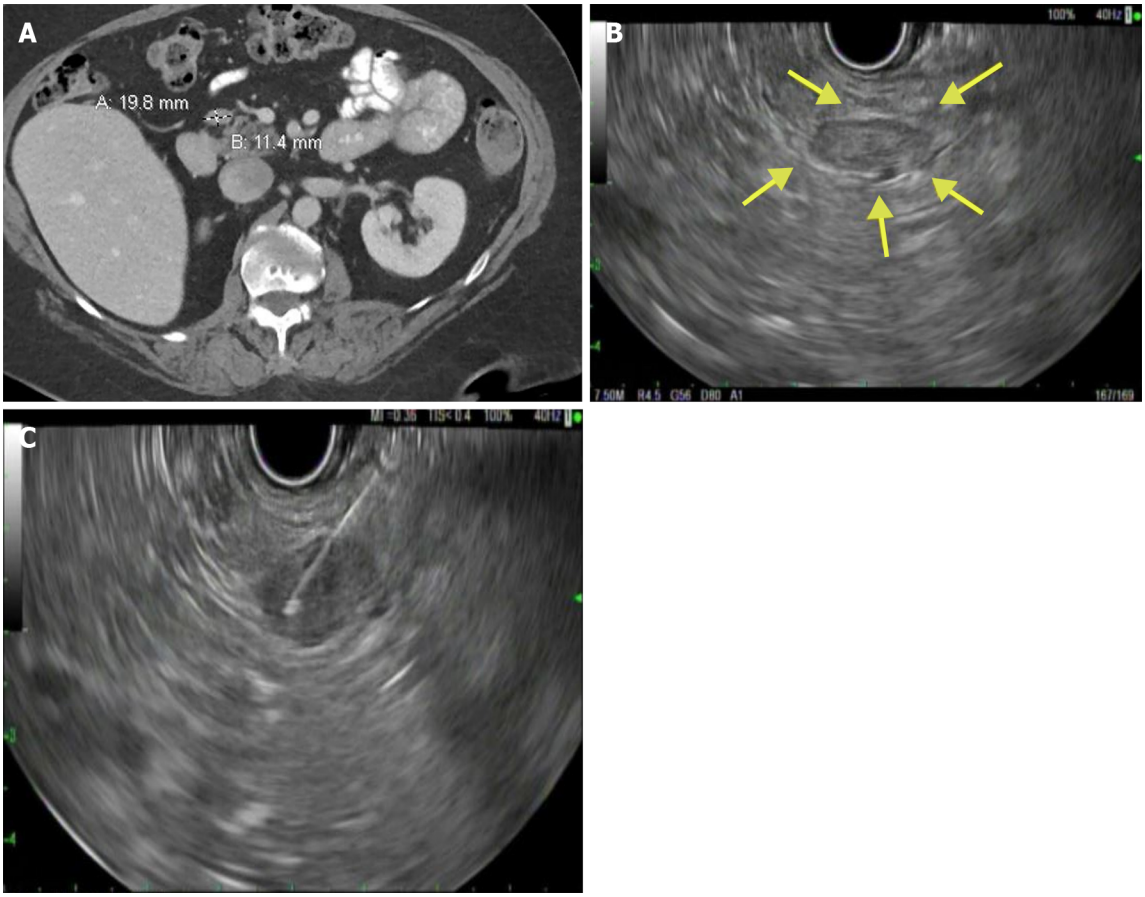


Figure 1 Computed tomography and endoscopy examinations. A: Computed tomography of abdomen pelvis showing a peripancreatic lymph node adjacent to the pancreatic head; B: Endoscopic ultrasonography showing a hypoechoic lesion near the pancreatic head; C: Endoscopic ultrasound-guided fine needle aspiration of the peripancreatic lesion.

head and absence of biliary dilation, although mild pancreatic duct dilatation is sometimes seen[11]. Paragangliomas are also differentiated from nonfunctioning islet cell tumor of the pancreas by observation of early contrast filling of the prominent draining veins of the tumor and the portal vein[12]. Magnetic resonance imaging (MRI) provides tissue characterization superior to CT without radiation[13]. Working synergistically, meta-iodobenzylguanidine (MIBG, I^{123} or I^{131}) scan is useful in differentiating functional from nonfunctional paragangliomas as well as in the detection of tumors in unusual locations, multiple primary tumors, and metastasis[13]. MIBG scan has a sensitivity of 85% and specificity of 95%-100% in the detection of extra-adrenal paragangliomas. Plasma or urinary metanephrines can be used to further establish the diagnosis of functional paragangliomas[13,14].

While most paragangliomas are solitary and sporadic, they can be multicentric and hereditary. Genetic testing should be considered in all patients diagnosed with paraganglioma as nearly 40% (pheochromocytoma and paraganglioma) carry germline mutations. Genetic testing allows for the identification of simultaneous cancers in hereditary syndromes and assists with screening family members at high risk[15]. The most common genetic mutations associated with paragangliomas are *RET* gene in multiple endocrine neoplasia type 2A and 2B, *VHL* in von Hippel-Lindau disease, *NF1* in neurofibromatosis type 1, and succinate dehydrogenase (*SDH*) B, D, C genes[15].

One of the most valuable tools that can assist in establishing the diagnosis of paraganglioma is EUS, which both enables localization of the mass and acquisition of tissue samples for cytology *via* FNA. When not considered in the differential diagnosis, pancreatic paragangliomas can be easily misdiagnosed on EUS-FNA cytology as pancreatic neuroendocrine tumor (NET)[16,17]. Some authors suggest that EUS-FNA should not be done in functional paragangliomas as it can trigger the secretion of catecholamines[18]. In our case, the diagnosis was not established before EUS-FNA and there were no complications during and after the procedure.

On cytology, the cells of paragangliomas are relatively uniform in size, epithelioid in appearance with round to oval nuclei, and arranged in loosely cohesive clusters

Table 1 Reported cases of pancreatic paraganglioma in the literature

No.	Ref.	Age	Gender	Size	Location	EUS-FNA	Preop-diagnosis	Surgery	Postop diagnosis
1	Fujino *et al* [21]	61	Male	2.5 cm	Uncinate process	No	PNET	Pancreaticoduodenectomy	PPGL
2	Ohkawara *et al*[33]	72	Female	4 cm	Head	No	NET	Surgical resection of head	PPGL
3	Perrot *et al* [34]	41	Female	4.3 cm	Tail	No	PPGL	Tumor resection	PPGL
4	Tsukada *et al* [35]	51	Male	2.5 cm	Uncinate	No	PNET	Surgical resection	PPGL
5	Kim *et al*[12]	57	Female	7 cm	Head	No	Non-functioning islet cell tumor	Pancreaticoduodenectomy	PPGL
6	Paik[36]	70	Female	4.2 cm	Tail	No	None	Distal pancreatectomy	PPGL
7	He *et al*[37]	40	Female	4.5 cm	Uncinate	No	None	Surgical resection	PPGL
8	Higa and Kapur[38]	65	Female	2.1 cm	Uncinate	No	None	Pancreaticoduodenectomy	PPGL
9	Al-jiffry *et al* [39]	19	Female	9.5 cm	Head and neck	No	Sarcoma	Pancreaticoduodenectomy	PPGL
10	Zhang *et al* [27]	50	Female	6 cm	Head	Yes	Functional PPGL	Chemotherapy	PPGL
11	Zhang *et al* [27]	63	Female	4 cm	Head	No	Functional PPGL	Surgical resection	PPGL
12	Borgohain *et al*[40]	55	Female	19 cm	Tail	No	Pancreatic cancer	Surgical resection	PPGL
13	Straka *et al* [41]	53	Female	Not mentioned	Head	No	None	Surgical resection	PPGL
14	Meng *et al* [11]	54	Female	3 cm	Head	No	None	Surgical resection	PPGL
15	Meng *et al* [11]	41	Female	6.2 cm	Head	No	None	Surgical resection	PPGL
16	Misumi *et al* [42]	47	Female	1.5 cm	Head	EUS only	PNET	Pancreaticoduodenectomy	PPGL
17	Bartley *et al* [43]	75	Female	15 cm	Tail	No	Pancreatic cyst	Not available	PPGL
18	Bartley *et al* [43]	70	Female	3 cm	Head	No	Pancreatic cyst	Not available	PPGL
19	Cope *et al* [44]	72	Female	14 cm	Head	No	Cystadenoma	Not available	PPGL
20	Zamir *et al* [45]	47	Male	10 cm	Body	No	Pancreatic cyst	Not available	PPGL
21	Parithivel *et al*[46]	85	Male	6 cm	Head	No	NET	Surgical resection	PPGL
22	Wang *et al* [32]	30	Female	6.4 cm	Tail	No	None	No surgery	PPGL
23	Ganc *et al*[18]	37	Female	4.8 cm	Head	Yes	NET	Pancreatico duodenectomy	PPGL
24	Tumuluru *et al*[47]	62	Female	2.9 cm	Body	Yes	NET	Distal pancreatectomy/splenectomy	PPGL
25	Ginesu *et al* [48]	55	Male	2.5 cm	Uncinate	No	NET	pancreaticoduodenectomy	PPGL
26	Liang and Xu[6]	41	Male	6.4 cm	Uncinate	No	NET	pancreaticoduodenectomy	PPGL
27	Lin *et al*[3]	42	Female	6.3 cm	Body	No	NET	Middlesegment pancreatectomy	PPGL

28	Nguyen *et al* [23]	70	Female	5.8 cm	Tail	Yes	PPGL	Surgical resection	PPGL
29	Zeng *et al*[19]	58	Female	6.5 cm	Head	Yes	NET	Surgical resection	PPGL
30	Zeng *et al*[19]	53	Female	2.5 cm	Head	Yes	NET	Surgical resecion	PPGL
31	Singhi *et al* [16]	61	Female	14 cm	Tail	Yes	Pseudocyst	Surgical resection	PPGL
32	Singhi *et al* [16]	52	Female	14 cm	Body	Yes	PPGL	Not performed	PPGL
33	Singhi *et al* [16]	54	Female	6.5 cm	Head	Yes	PPGL	Surgical resection	PPGL
34	Singhi *et al* [16]	40	Male	5.1 cm	Body	Yes	NET	Surgical resection	PPGL
35	Singhi *et al* [16]	78	Female	17 cm	Body	Yes	Spindle cell neoplasm	Surgical resection	PPGL
36	Singhi *et al* [16]	44	Male	5.5 cm	Head	Yes	PPGL	Surgical resection	PPGL
37	Singhi *et al* [16]	38	Male	15 cm	Body	No	None	Surgical resection	PPGL
38	Singhi *et al* [16]	47	Male	7.5 cm	Body	No	NET	Surgical resection	PPGL
39	Singhi *et al* [16]	37	Female	5.7 cm	Tail	No	NET	Surgical resection	PPGL
40	Fite and Maleki[49]	40	Male	5.1 cm	Peripancreatic	No	NET	Surgical resection	PPGL
41	Fite and Maleki[49]	23	Female	7.0 cm	Peripancreatic	No	NET	Surgical resection	PPGL
42	Malthouse *et al*[50]	58	Male	8 cm	Head	No	NET	Not available	PPGL
43	Malthouse *et al*[50]	45	Female	8 cm	Head	No	Retro peritoneal tumor	Not available	PPGL
44	Sangster *et al* [10]	50	Male	Not available	Head	Yes	Poorly differentiatedcarcinoma	Radiation treatment	PPGL
45	Lightfoot *et al*[51]	66	Male	6 cm	Head/uncinate	No	None	Pancreaticoduodenectomy	PPGL
46	Abbasi *et al* [52]	61	Female	7.2 cm	Head/uncinate	Yes	NET	Pancreaticoduodenenctomy	PPGL
47	Present case	73	Female	2 cm	Head	Yes	PPGL	No surgery	PPGL

PPGL: Pancreatic paraganglioma; PNET: Pancreatic Neuroendocrine tumor; EUS-FNA: Endoscopic ultrasound-guided fine needle aspiration.

[19]. Morphological patterns like acinar/glandular architecture and rosette-like arrangements can be observed in paragangliomas[20]. In histologic sections, the tumor is typically composed of nests of cells separated by a highly vascularized network[21].

Although the morphologic overlap between paraganglioma and NET is significant, the distinction can be confidently made with immunoperoxidase stains, which require a cell block preparation. Both pancreatic paragangliomas and NETs readily express neuroendocrine markers like synaptophysin and chromogranin[19]. While most NETs are immunoreactive to pancytokeratins (AE1/AE3 and CAM 5.2) but not vimentin, paragangliomas show the opposite profile[19]. GATA-3 and PAX-8 can also be used to distinguish paragangliomas from NETs. Paragangliomas from any anatomic site are immunoreactive to GATA-3 in approximately 55% of the cases, but NETs are always nonreactive[22]. Of note, GATA-3 can be positive in cells of breast, urothelial, and pancreatic origin[23]. PAX-8 has a sensitivity of 88% and specificity of 74% for primary pancreatic NETs, but paragangliomas have weak or negative immunoreactivity to PAX -8[24-26]. In our case, FNA smears with Papanicolaou stain showed abundant, tangled cellular processes and relatively uniform nuclei with finely granular chromatin and indistinct nucleoli (Figure 2). FNA cell block with hematoxylin and eosin stain (Figure 3A), diffuse cytoplasmic staining with chromogranin (Figure 3B),

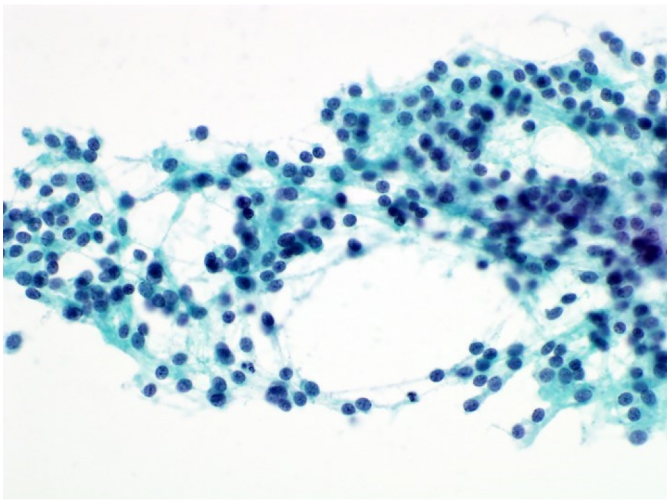


Figure 2 Fine needle aspiration direct smear. Papanicolaou stain, × 400.

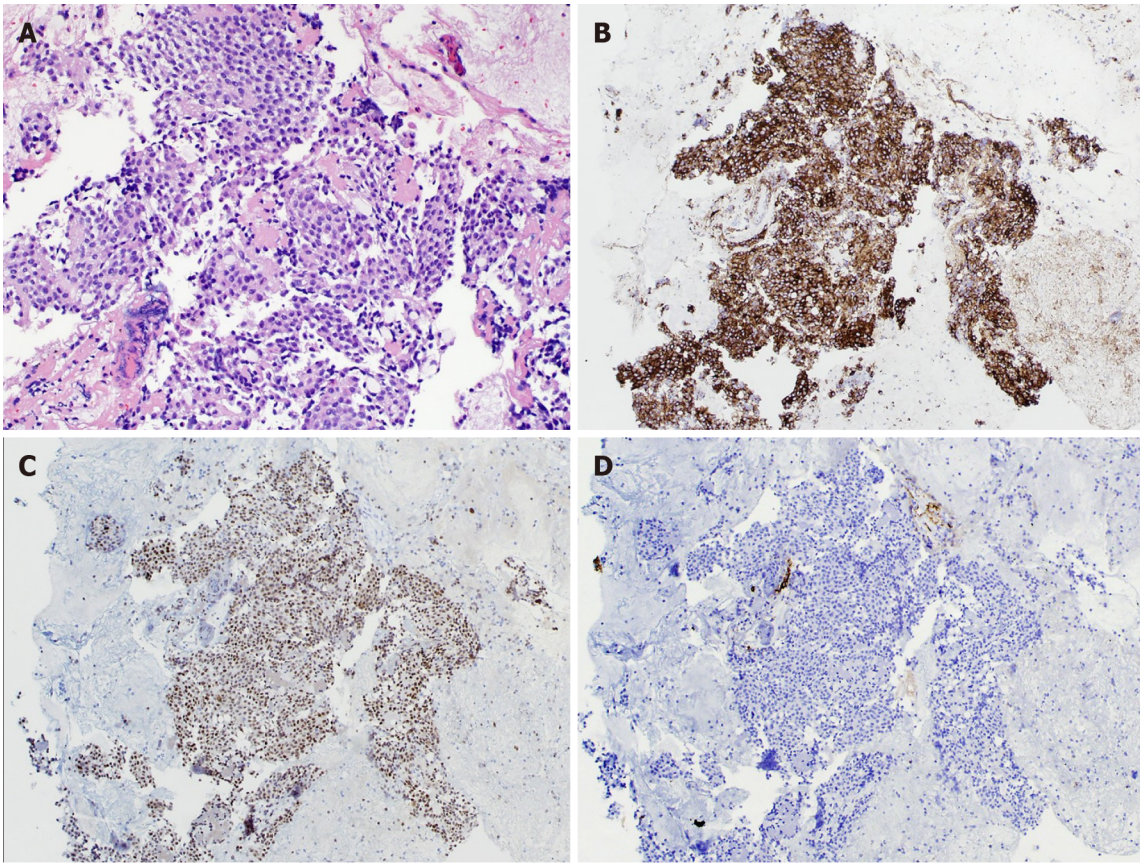


Figure 3 Fine needle aspiration cell block. A: Hematoxylin and eosin stain, × 200; B: Diffuse cytoplasmic staining, chromogranin (× 100); C: Diffuse nuclear staining, GATA-3, (× 100); D: No staining, keratin cocktail (× 100).

diffuse nuclear staining with GATA-3 (Figure 3C), and no staining with keratin cocktail (Figure 3D).

Since there are no definitive criteria for the diagnosis of malignancy in paraganglioma apart from metastasis, the treatment of choice for paraganglioma is surgical resection. For functional paragangliomas, preoperative administration of α-adrenergic receptor blocker can help prevent a hypertensive crisis during the surgery[27]. The most common sites of metastasis include the regional lymph nodes, bone, lung, and liver, and the dissemination usually occurs through blood or lymph nodes[28]. When surgery is not feasible, radiation therapy can be considered[29]. For malignant paragangliomas, treatment with I^{131} MIBG or combination chemotherapy (cyclophos-

phamide, vincristine, and dacarbazine) is effective[30]. Octreotide is also useful in inoperable paragangliomas[31].

Our review of the literature in the English language found 47 case reports of pancreatic paragangliomas published in PubMed to date (Table 1). Fifteen patients with pancreatic paragangliomas underwent EUS-FNA; six were correctly diagnosed as paraganglioma; six were misdiagnosed as NET; one had no diagnosis; one was diagnosed as spindle cell neoplasm; and one was diagnosed as pseudocyst. All patients with a pancreatic paraganglioma underwent surgery except three: one patient who developed a hypertensive crisis during the surgery (thus surgery was aborted) [32]; and two patients with metastasis or involvement of the major vessels[10,16].

Our case illustrates that accurate preoperative diagnosis of paraganglioma can be safely made by EUS-FNA. When paragangliomas are small and asymptomatic, it would be reasonable to follow them with periodic imaging studies.

CONCLUSION

Pancreatic paragangliomas are rare and EUS-FNA is a valuable tool in establishing the diagnosis. When assessing a lesion in the pancreas, paraganglioma should be included in the differential diagnoses along with PNET and pancreatic ductal adenocarcinoma. As EUS-FNA can trigger a hypertensive crisis in functional pancreatic paragangliomas, pre-procedure use of alpha-adrenergic blocker should be considered. To bring the optimal result in the management of paraganglioma, it is imperative to have a multidisciplinary team approach involving radiologists, advanced endoscopists, endocrinologists, pathologists, oncologists, and surgeons.

REFERENCES

1 **Lenders JW**, Eisenhofer G, Mannelli M, Pacak K. Phaeochromocytoma. *Lancet* 2005; **366**: 665-675 [PMID: 16112304 DOI: 10.1016/S0140-6736(05)67139-5]

2 **Asa SL**, Ezzat S, Mete O. The Diagnosis and Clinical Significance of Paragangliomas in Unusual Locations. *J Clin Med* 2018; **7** [PMID: 30217041 DOI: 10.3390/jcm7090280]

3 **Lin S**, Peng L, Huang S, Li Y, Xiao W. Primary pancreatic paraganglioma: a case report and literature review. *World J Surg Oncol* 2016; **14**: 19 [PMID: 26801079 DOI: 10.1186/s12957-016-0771-2]

4 **Beard CM**, Sheps SG, Kurland LT, Carney JA, Lie JT. Occurrence of pheochromocytoma in Rochester, Minnesota, 1950 through 1979. *Mayo Clin Proc* 1983; **58**: 802-804 [PMID: 6645626]

5 **Chen H**, Sippel RS, O'Dorisio MS, Vinik AI, Lloyd RV, Pacak K; North American Neuroendocrine Tumor Society (NANETS). The North American Neuroendocrine Tumor Society consensus guideline for the diagnosis and management of neuroendocrine tumors: pheochromocytoma, paraganglioma, and medullary thyroid cancer. *Pancreas* 2010; **39**: 775-783 [PMID: 20664475 DOI: 10.1097/MPA.0b013e3181ebb4f0]

6 **Liang W**, Xu S. CT and MR Imaging Findings of Pancreatic Paragangliomas: A Case Report. *Medicine (Baltimore)* 2016; **95**: e2959 [PMID: 26945413 DOI: 10.1097/MD.0000000000002959]

7 **Lack EE**, Cubilla AL, Woodruff JM, Lieberman PH. Extra-adrenal paragangliomas of the retroperitoneum: A clinicopathologic study of 12 tumors. *Am J Surg Pathol* 1980; **4**: 109-120 [PMID: 7377461 DOI: 10.1097/00000478-198004000-00002]

8 **Kaltsas GA**, Besser GM, Grossman AB. The diagnosis and medical management of advanced neuroendocrine tumors. *Endocr Rev* 2004; **25**: 458-511 [PMID: 15180952 DOI: 10.1210/ER.2003-0014]

9 **Elder EE**, Elder G, Larsson C. Pheochromocytoma and functional paraganglioma syndrome: no longer the 10% tumor. *J Surg Oncol* 2005; **89**: 193-201 [PMID: 15719371 DOI: 10.1002/jso.20177]

10 **Sangster G**, Do D, Previgliano C, Li B, LaFrance D, Heldmann M. Primary retroperitoneal paraganglioma simulating a pancreatic mass: a case report and review of the literature. *HPB Surg* 2010; **2010**: 645728 [PMID: 21188160 DOI: 10.1155/2010/645728]

11 **Meng L**, Wang J, Fang SH. Primary pancreatic paraganglioma: a report of two cases and literature review. *World J Gastroenterol* 2015; **21**: 1036-1039 [PMID: 25624744 DOI: 10.3748/wjg.v21.i3.1036]

12 **Kim SY**, Byun JH, Choi G, Yu E, Choi EK, Park SH, Lee MG. A case of primary paraganglioma that arose in the pancreas: the Color Doppler ultrasonography and dynamic CT features. *Korean J Radiol* 2008; **9** Suppl: S18-S21 [PMID: 18607119 DOI: 10.3348/kjr.2008.9.s.s18]

13 **van Gils AP**, Falke TH, van Erkel AR, Arndt JW, Sandler MP, van der Mey AG, Hoogma RP. MR imaging and MIBG scintigraphy of pheochromocytomas and extraadrenal functioning paragangliomas. *Radiographics* 1991; **11**: 37-57 [PMID: 1671719 DOI: 10.1148/radiographics.11.1.1671719]

14 **Plouin PF**, Gimenez-Roqueplo AP. Initial work-up and long-term follow-up in patients with

phaeochromocytomas and paragangliomas. *Best Pract Res Clin Endocrinol Metab* 2006; **20**: 421-434 [PMID: 16980203 DOI: 10.1016/j.beem.2006.07.004]
15 **Dahia PL**. Pheochromocytoma and paraganglioma pathogenesis: learning from genetic heterogeneity. *Nat Rev Cancer* 2014; **14**: 108-119 [PMID: 24442145 DOI: 10.1038/nrc3648]
16 **Singhi AD**, Hruban RH, Fabre M, Imura J, Schulick R, Wolfgang C, Ali SZ. Peripancreatic paraganglioma: a potential diagnostic challenge in cytopathology and surgical pathology. *Am J Surg Pathol* 2011; **35**: 1498-1504 [PMID: 21921779 DOI: 10.1097/PAS.0b013e3182281767]
17 **Jiménez-Heffernan JA**, Vicandi B, López-Ferrer P, González-Peramato P, Pérez-Campos A, Viguer JM. Cytologic features of pheochromocytoma and retroperitoneal paraganglioma: a morphologic and immunohistochemical study of 13 cases. *Acta Cytol* 2006; **50**: 372-378 [PMID: 16900997 DOI: 10.1159/000325975]
18 **Ganc RL**, Castro AC, Colaiacovo R, Vigil R, Rossini LG, Altenfelder R. Endoscopic ultrasound-guided fine needle aspiration for the diagnosis of nonfunctional paragangliomas: a case report and review of the literature. *Endosc Ultrasound* 2012; **1**: 108-109 [PMID: 24949346 DOI: 10.7178/eus.02.009]
19 **Zeng J**, Simsir A, Oweity T, Hajdu C, Cohen S, Shi Y. Peripancreatic paraganglioma mimics pancreatic/gastrointestinal neuroendocrine tumor on fine needle aspiration: Report of two cases and review of the literature. *Diagn Cytopathol* 2017; **45**: 947-952 [PMID: 28560856 DOI: 10.1002/dc.23761]
20 **Gong Y**, DeFrias DV, Nayar R. Pitfalls in fine needle aspiration cytology of extraadrenal paraganglioma. A report of 2 cases. *Acta Cytol* 2003; **47**: 1082-1086 [PMID: 14674085 DOI: 10.1159/000326652]
21 **Fujino Y**, Nagata Y, Ogino K, Watahiki H, Ogawa H, Saitoh Y. Nonfunctional paraganglioma of the pancreas: report of a case. *Surg Today* 1998; **28**: 209-212 [PMID: 9525014 DOI: 10.1007/s005950050108]
22 **Weissferdt A**, Kalhor N, Liu H, Rodriguez J, Fujimoto J, Tang X, Wistuba II, Moran CA. Thymic neuroendocrine tumors (paraganglioma and carcinoid tumors): a comparative immunohistochemical study of 46 cases. *Hum Pathol* 2014; **45**: 2463-2470 [PMID: 25294372 DOI: 10.1016/j.humpath.2014.08.013]
23 **Nguyen E**, Nakasaki M, Lee TK, Lu D. Diagnosis of paraganglioma as a pancreatic mass: A case report. *Diagn Cytopathol* 2018; **46**: 804-806 [PMID: 29882285 DOI: 10.1002/dc.23974]
24 **Sangoi AR**, Ohgami RS, Pai RK, Beck AH, McKenney JK. PAX8 expression reliably distinguishes pancreatic well-differentiated neuroendocrine tumors from ileal and pulmonary well-differentiated neuroendocrine tumors and pancreatic acinar cell carcinoma. *Mod Pathol* 2011; **24**: 412-424 [PMID: 20890270 DOI: 10.1038/modpathol.2010.176]
25 **Koo J**, Mertens RB, Mirocha JM, Wang HL, Dhall D. Value of Islet 1 and PAX8 in identifying metastatic neuroendocrine tumors of pancreatic origin. *Mod Pathol* 2012; **25**: 893-901 [PMID: 22388755 DOI: 10.1038/modpathol.2012.34]
26 **Long KB**, Srivastava A, Hirsch MS, Hornick JL. PAX8 Expression in well-differentiated pancreatic endocrine tumors: correlation with clinicopathologic features and comparison with gastrointestinal and pulmonary carcinoid tumors. *Am J Surg Pathol* 2010; **34**: 723-729 [PMID: 20414099 DOI: 10.1097/PAS.0b013e3181da0a20]
27 **Zhang L**, Liao Q, Hu Y, Zhao Y. Paraganglioma of the pancreas: a potentially functional and malignant tumor. *World J Surg Oncol* 2014; **12**: 218 [PMID: 25030833 DOI: 10.1186/1477-7819-12-218]
28 **Verma A**, Pandey D, Akhtar A, Arsia A, Singh N. Non-functional paraganglioma of retroperitoneum mimicking pancreatic mass with concurrent urinary bladder paraganglioma: an extremely rare entity. *J Clin Diagn Res* 2015; **9**: XD09-XD11 [PMID: 25859512 DOI: 10.7860/JCDR/2015/11156.5570]
29 **Yang JH**, Bae SJ, Park S, Park HK, Jung HS, Chung JH, Min YK, Lee MS, Kim KW, Lee MK. Bilateral pheochromocytoma associated with paraganglioma and papillary thyroid carcinoma: report of an unusual case. *Endocr J* 2007; **54**: 227-231 [PMID: 17264467 DOI: 10.1507/endocrj.k06-068]
30 **Fitzgerald PA**, Goldsby RE, Huberty JP, Price DC, Hawkins RA, Veatch JJ, Dela Cruz F, Jahan TM, Linker CA, Damon L, Matthay KK. Malignant pheochromocytomas and paragangliomas: a phase II study of therapy with high-dose 131I-metaiodobenzylguanidine (131I-MIBG). *Ann N Y Acad Sci* 2006; **1073**: 465-490 [PMID: 17102115 DOI: 10.1196/annals.1353.050]
31 **Tonyukuk V**, Emral R, Temizkan S, Sertçelik A, Erden I, Corapçioğlu D. Case report: patient with multiple paragangliomas treated with long acting somatostatin analogue. *Endocr J* 2003; **50**: 507-513 [PMID: 14614206 DOI: 10.1507/endocrj.50.507]
32 **Wang ZL**, Fu L, Zhang Y, Babu SR, Tian B. An asymptomatic pheochromocytoma originating from the tail of the pancreas. *Pancreas* 2012; **41**: 165-167 [PMID: 22173833 DOI: 10.1097/MPA.0b013e31822362d0]
33 **Ohkawara T**, Naruse H, Takeda H, Asaka M. Primary paraganglioma of the head of pancreas: contribution of combinatorial image analyses to the diagnosis of disease. *Intern Med* 2005; **44**: 1195-1196 [PMID: 16357461 DOI: 10.2169/internalmedicine.44.1195]
34 **Perrot G**, Pavic M, Milou F, Crozes C, Faucompret S, Vincent E. [Difficult diagnosis of a pancreatic paraganglioma]. *Rev Med Interne* 2007; **28**: 701-704 [PMID: 17618712 DOI: 10.1016/j.revmed.2007.06.001]
35 **Tsukada A**, Ishizaki Y, Nobukawa B, Kawasaki S. Paraganglioma of the pancreas: a case report and review of the literature. *Pancreas* 2008; **36**: 214-216 [PMID: 18376320 DOI: 10.1097/01.MPA.0000311841.35183.45]

36 **Paik KY**. [Paraganglioma of the pancreas metastasized to the adrenal gland: a case report]. *Korean J Gastroenterol* 2009; **54**: 409-412 [PMID: 20026898 DOI: 10.4166/kjg.2009.54.6.409]

37 **He J**, Zhao F, Li H, Zhou K, Zhu B. Pancreatic paraganglioma: A case report of CT manifestations and literature review. *Quant Imaging Med Surg* 2011; **1**: 41-43 [PMID: 23256053 DOI: 10.3978/j.issn.2223-4292.2011.08.02]

38 **Higa B**, Kapur U. Malignant paraganglioma of the pancreas. *Pathology* 2012; **44**: 53-55 [PMID: 22157694 DOI: 10.1097/PAT.0b013e32834e42b6]

39 **Al-Jiffry BO**, Alnemary Y, Khayat SH, Haiba M, Hatem M. Malignant extra-adrenal pancreatic paraganglioma: case report and literature review. *BMC Cancer* 2013; **13**: 486 [PMID: 24138700 DOI: 10.1186/1471-2407-13-486]

40 **Borgohain M**, Gogoi G, Das D, Biswas M. Pancreatic paraganglioma: An extremely rare entity and crucial role of immunohistochemistry for diagnosis. *Indian J Endocrinol Metab* 2013; **17**: 917-919 [PMID: 24083178 DOI: 10.4103/2230-8210.117217]

41 **Straka M**, Soumarova R, Migrova M, Vojtek C. Pancreatic paraganglioma - a rare and dangerous entity. Vascular anatomy and impact on management. *J Surg Case Rep* 2014; **2014** [PMID: 25056378 DOI: 10.1093/jscr/rju074]

42 **Misumi Y**, Fujisawa T, Hashimoto H, Kagawa K, Noie T, Chiba H, Horiuchi H, Harihara Y, Matsuhashi N. Pancreatic paraganglioma with draining vessels. *World J Gastroenterol* 2015; **21**: 9442-9447 [PMID: 26309372 DOI: 10.3748/wjg.v21.i31.9442]

43 **Bartley O**, Ekdahl PH, Hultén L. Paraganglioma simulating pancreatic cyst. *Acta Chir Scand* 1966; **132**: 289-297 [PMID: 5929097]

44 **Cope C**, Greenberg SH, Vidal JJ, Cohen EA. Nonfunctioning nonchromaffin paraganglioma of the pancreas. *Arch Surg* 1974; **109**: 440-442 [PMID: 4368962 DOI: 10.1001/ARCHSURG.1974.01360030092024]

45 **Zamir O**, Amir G, Lernau O, Ne'eman Z, Nissan S. Nonfunctional paraganglioma of the pancreas. *Am J Gastroenterol* 1984; **79**: 761-763 [PMID: 6486113]

46 **Parithivel VS**, Niazi M, Malhotra AK, Swaminathan K, Kaul A, Shah AK. Paraganglioma of the pancreas: literature review and case report. *Dig Dis Sci* 2000; **45**: 438-441 [PMID: 10711464 DOI: 10.1023/a:1005401718763]

47 **Tumuluru S**, Mellnick V, Doyle M, Goyal B. Pancreatic Paraganglioma: A Case Report. *Case Rep Pancreat Cancer* 2016; **2**: 79-83 [PMID: 30631823 DOI: 10.1089/crpc.2016.0016]

48 **Ginesu GC**, Barmina M, Paliogiannis P, Trombetta M, Cossu ML, Feo CF, Addis F, Porcu A. Nonfunctional paraganglioma of the head of the pancreas: A rare case report. *Int J Surg Case Rep* 2016; **28**: 81-84 [PMID: 27689525 DOI: 10.1016/j.ijscr.2016.09.012]

49 **Fite JJ**, Maleki Z. Paraganglioma: Cytomorphologic features, radiologic and clinical findings in 12 cases. *Diagn Cytopathol* 2018; **46**: 473-481 [PMID: 29575826 DOI: 10.1002/dc.23928]

50 **Malthouse SR**, Robinson L, Rankin SC. Ultrasonic and computed tomographic appearances of paraganglioma simulating pancreatic mass. *Clin Radiol* 1992; **45**: 271-272 [PMID: 1395386 DOI: 10.1016/s0009-9260(05)80013-3]

51 **Lightfoot N**, Santos P, Nikfarjam M. Paraganglioma mimicking a pancreatic neoplasm. *JOP* 2011; **12**: 259-261 [PMID: 21546704]

52 **Abbasi A**, Wakeman KM, Pillarisetty VG. Pancreatic paraganglioma mimicking pancreatic neuroendocrine tumor. *Rare Tumors* 2020; **12**: 2036361320982799 [PMID: 33425308 DOI: 10.1177/2036361320982799]

World Journal of Gastroenterology

Submit a Manuscript: https://www.f6publishing.com

World J Gastroenterol 2021 October 7; 27(37): 6332-6344

DOI: 10.3748/wjg.v27.i37.6332

ISSN 1007-9327 (print) ISSN 2219-2840 (online)

CASE REPORT

Abdominal cocoon in children: A case report and review of literature

Daniel Keese, Andrea Schmedding, Kerstin Saalabian, Georgy Lakshin, Henning Fiegel, Udo Rolle

ORCID number: Daniel Keese 0000-0001-6951-5641; Andrea Schmedding 0000-0002-7796-3329; Kerstin Saalabian 0000-0001-6513-4614; Georgy Lakshin 0000-0003-2894-0021; Henning Fiegel 0000-0001-5411-4335; Udo Rolle 0000-0002-1268-6092.

Author contributions: Keese D, Schmedding A, Saalabian K, and Rolle U contributed to the study conception and design, acquisition, analysis, and interpretation of the data, and final approval of the version of the article to be published; Keese D drafted the article; Lakshin G, Fiegel H, and Rolle U contributed to critical revisions related to the intellectual content of the manuscript.

Informed consent statement: All study participants, or their legal guardian, provided informed written consent prior to study enrolment.

Conflict-of-interest statement: None of the authors has a conflict of interest.

CARE Checklist (2016) statement: The authors have read the CARE Checklist (2016), and the manuscript was prepared and revised according to the CARE Checklist (2016).

Open-Access: This article is an open-access article that was selected by an in-house editor and

Daniel Keese, Andrea Schmedding, Kerstin Saalabian, Georgy Lakshin, Henning Fiegel, Udo Rolle, Goethe-University Frankfurt, Department of Paediatric Surgery and Paediatric Urology, University Hospital, Frankfurt 60590, Germany

Corresponding author: Udo Rolle, FRCS (Hon), MD, MSc, Chairman, Dean, Director, Professor, Goethe-University Frankfurt, Department of Paediatric Surgery and Paediatric Urology, University Hospital, Theodor-Stern-Kai 7, Frankfurt 60590, Germany.
udo.rolle@kgu.de

Abstract

BACKGROUND

Abdominal cocoon or "encapsulating peritoneal sclerosis" (EPS) is an uncommon and rare cause of intestinal obstruction. Only a few cases have been reported in paediatric patients. Typically, EPS is described as the primary form in young adolescent girls from tropical and subtropical countries because of viral peritonitis due to retrograde menstruation or a history of peritoneal dialysis. Most patients are asymptomatic or present with abdominal pain, which is likely to occur secondary to subacute bowel obstruction. Findings at imaging, such as ultrasound, computed tomography, and magnetic resonance imaging, are often nonspecific. When diagnosed, EPS is characterized by total or partial encasement of the bowel within a thick fibrocollagenous membrane that envelopes the small intestine in the form of a cocoon because of chronic intraabdominal fibroinflammatory processes. The membrane forms a fibrous tissue sheet that covers, fixes, and finely constricts the gut, compromising its motility.

CASE SUMMARY

We present a case of EPS in a 12-year-old boy 8 wk after primary surgery for resection of symptomatic jejunal angiodysplasia. There was no history of peritoneal dialysis or drug intake.

CONCLUSION

In this report, we sought to highlight the diagnostic, surgical, and histopathological characteristics and review the current literature on EPS in paediatric patients.

Key Words: Abdominal cocoon; Peritoneal encapsulation; Encapsulating peritoneal sclerosis; Intestinal obstruction; Children; Case report

©The Author(s) 2021. Published by Baishideng Publishing Group Inc. All rights reserved.

fully peer-reviewed by external reviewers. It is distributed in accordance with the Creative Commons Attribution NonCommercial (CC BY-NC 4.0) license, which permits others to distribute, remix, adapt, build upon this work non-commercially, and license their derivative works on different terms, provided the original work is properly cited and the use is non-commercial. See: http://creativecommons.org/Licenses/by-nc/4.0/

Manuscript source: Unsolicited manuscript

Specialty type: Surgery

Country/Territory of origin: Germany

Peer-review report's scientific quality classification

Grade A (Excellent): A
Grade B (Very good): B
Grade C (Good): 0
Grade D (Fair): 0
Grade E (Poor): 0

Received: February 18, 2021
Peer-review started: February 18, 2021
First decision: April 18, 2021
Revised: April 30, 2021
Accepted: August 20, 2021
Article in press: August 20, 2021
Published online: October 7, 2021

P-Reviewer: Mayr J, Wani I
S-Editor: Liu M
L-Editor: Filipodia
P-Editor: Liu JH



Core Tip: Abdominal cocoon syndrome is rare in children. Cases with no history of previous peritoneal dialysis are practically nonexistent. Our report of a 12-year-old boy reveals that abdominal surgery can be a trigger for the development of encapsulating peritoneal sclerosis (EPS). Indications for surgery for EPS are usually due to mechanical ileus, and the final diagnosis is made intraoperatively. Surgical therapy for EPS is the first choice, and total intestinal enterolysis of EPS seems to be the best approach. The long-term prognosis for children is good.

Citation: Keese D, Schmedding A, Saalabian K, Lakshin G, Fiegel H, Rolle U. Abdominal cocoon in children: A case report and review of literature. *World J Gastroenterol* 2021; 27(37): 6332-6344
URL: https://www.wjgnet.com/1007-9327/full/v27/i37/6332.htm
DOI: https://dx.doi.org/10.3748/wjg.v27.i37.6332

INTRODUCTION

Encapsulating bowel disease is a very rare but serious condition. The differentiation between congenital peritoneal encapsulation (CPE) and encapsulating peritoneal sclerosis (EPS) is obvious. CPE, reported for the first time in 1868 by Cleland[1], is the result of an embryological intestinal malformation that occurs when the yolk sac returns to the abdominal cavity, creating an accessory membrane covering the bowel. This is to be distinguished from EPS, which is far more common than CPE and was first described in 1907 by Owtschinnikow[2] with the term "peritonitis chronica fibrosa incapsulata". In 1987, Foo *et al*[3] used the term "abdominal cocoon" for primary or idiopathic EPS in cases where no established cause could be identified.

EPS has been recognized to occur in various geographically and ethnically diverse locations. In addition to various terms, such as "peritoneal sclerosis, peritoneal fibrosis, sclerosing peritonitis, sclerotic thickening of the peritoneal membrane, sclerosing obstructive peritonitis or encapsulating peritonitis", EPS is the most common name[4]. Because inflammatory features are not always apparent, the use of the word peritonitis, as in the general terminology, is not preferred. ESP has been proposed as the appropriate term by the International Society for Peritoneal Dialysis when peritoneal dialysis is the reason for the ubiquitous inflammatory processes that cause cocoon formations. Today, most authors use the term abdominal cocoon not only for the primary or idiopathic form but also for the secondary form of EPS[5-8] (Figure 1). The primary type is classically described in young adolescent girls from tropical and subtropical countries, which is mostly idiopathic in nature. A few of the etiopathogenesis proposed for the primary form are viral peritonitis, retrograde menstruation with superimposed viral infection, and gynecological infection-inducing cell-mediated immunological tissue damage. However, these theories may not explain the etiopathogenesis in all patients, as this condition is also seen in men, premenstrual women, and children. The secondary form can occur secondary to multiple predisposing factors in addition to peritoneal dialysis, *e.g.*, peritoneum inflammation with fibroblastic proliferation, systemic lupus erythematosus, liver cirrhosis, endometriotic cyst, abdominal trauma/surgery, abdominal tuberculosis, or malignancy[9,10].

EPS is characterized by total or partial encasement of the bowel within a thick fibrocollagenous membrane that envelopes the small intestine in the form of a cocoon as a result of chronic intraabdominal fibroinflammatory processes[11]. The result is the formation of fibrous tissue sheets that cover, fix, and ultimately constrict the gut, compromising its motility. Most patients are asymptomatic or present with (recurrent) abdominal pain, which is likely to occur secondary to partial/complete bowel obstruction. Usually, patients have had prior episodes with similar symptoms that have resolved spontaneously. With the development of complete sclerosis due to the formation of a cocoon, there are overt signs of mechanical ileus.

Clinically, the abdomen is often soft at palpation. A soft nontender mass may be palpable in the central part of the abdomen, which represents clumped-up bowel loops. Imaging findings seen on ultrasound (US), computed tomography (CT), and magnetic resonance imaging (MRI) are often nonspecific[7]. Other imaging modalities, such as barium studies or positron emission tomography studies, have been discussed and have not revealed any appreciable advantage in the diagnosis of EPS. Therefore,

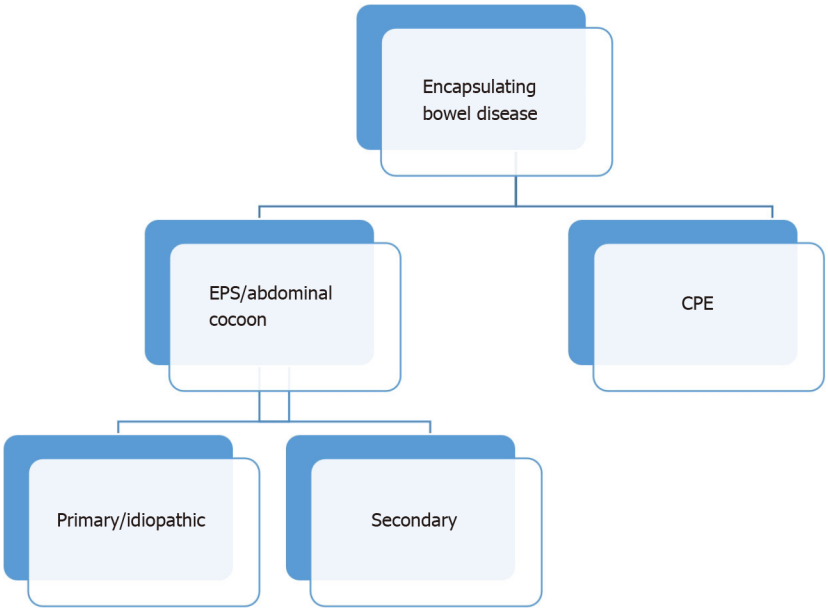


Figure 1 Flow chart and classification for encapsulating bowel diseases. EPS: Encapsulating peritoneal sclerosis; CPE: Congenital peritoneal encapsulation.

this condition is often only diagnosed intraoperatively, followed by histological analysis[12].

EPS has a clearly different histology than CPE. The thin membrane on the visceral peritoneum contributes to the formation of the intestinal encapsulation of EPS. Histologically, the membrane is comprised mainly of organized fibrin, probably derived from plasma exudation from the peritoneal microvasculature. Peritoneal fibroblasts appear swollen and exhibit an increased level of cellularity, accompanied by the expression of various activation and proliferation markers. Persistent inflammatory changes are also predictive of the onset of EPS[4].

The development of EPS has been divided, taking into account clinical and pathological findings in four stages, as proposed by Nakamoto[13]. The pre-EPS stage is characterized by the presence of ultrafiltration failure and/or altered solute transport status; this is followed by inflammatory, encapsulating, and obstructive phases, the last of which is characterized by intestinal obstruction and the formation of an "abdominal cocoon". A staging system has been proposed in the peritoneal catheter (PD)-associated EPS literature based on a combination of clinical, laboratory, and radiographic findings. Nakamoto[13] categorized patients with EPS into Stage 1 (pre-EPS), Stage 2 (inflammatory), Stage 3 (encapsulating), and Stage 4 (chronic) based on abdominal symptoms, inflammation, encapsulation, and intestinal findings (Figure 2). Different conservative therapeutic approaches have been proposed depending on the stage of the disease, which include nutritional support, immunosuppression with corticosteroids as the best studied, colchicine, azathioprine, mycophenolate mofetil, cyclosporine, and mammalian target of rapamycin. Furthermore, antifibrotics such as tamoxifen can increase the efficiency of immunosuppressive drugs.

The division into four disease stages enables stage-appropriate therapy for EPS. Table 1 shows the stage-dependent therapy of EPS according to Nakamoto[13]. For a long time, surgical treatment of EPS was not considered appropriate due to the high perioperative mortality rate of up to 70%. On the other hand, several studies showed that, independent of the therapy procedure, the overall mortality in EPS patients was 67%. In a recent study, the mortality in surgically treated patients was only 42%. This reduction in mortality can only be achieved by timely and adequate surgical therapy. However, to date, there is neither a uniform surgical therapy concept nor standardized perioperative management.

To our knowledge, there has been no prior definitive, systematic review of EPS in children without a history of PD. Due to the assumption that younger patients are at greater risk for EPS, it is important to highlight the age groups of the patients.

In the following, we present a case of a 12-year-old boy with EPS 8 wk after primary laparotomy. We report his medical history, clinical presentation at admission, laboratory values, preoperative diagnostic and intraoperative findings, histological results, and days until discharge (short-term outcomes). The main objective of the

Table 1 Summary of therapy options of encapsulating peritoneal sclerosis according to the staging system

Stage	Therapy options
Stage 1/pre-EPS	Discontinuation of pertioneal dialysis
	("Sedation" of the peritoneum)
	Peritoneal lavage
	Glucocorticoids
Stage 2	Glucocorticoids
Stage 3	Glucocorticoids
	Total parenteral nutrition
Stage 4	Operation

EPS: Encapsulating peritoneal sclerosis.

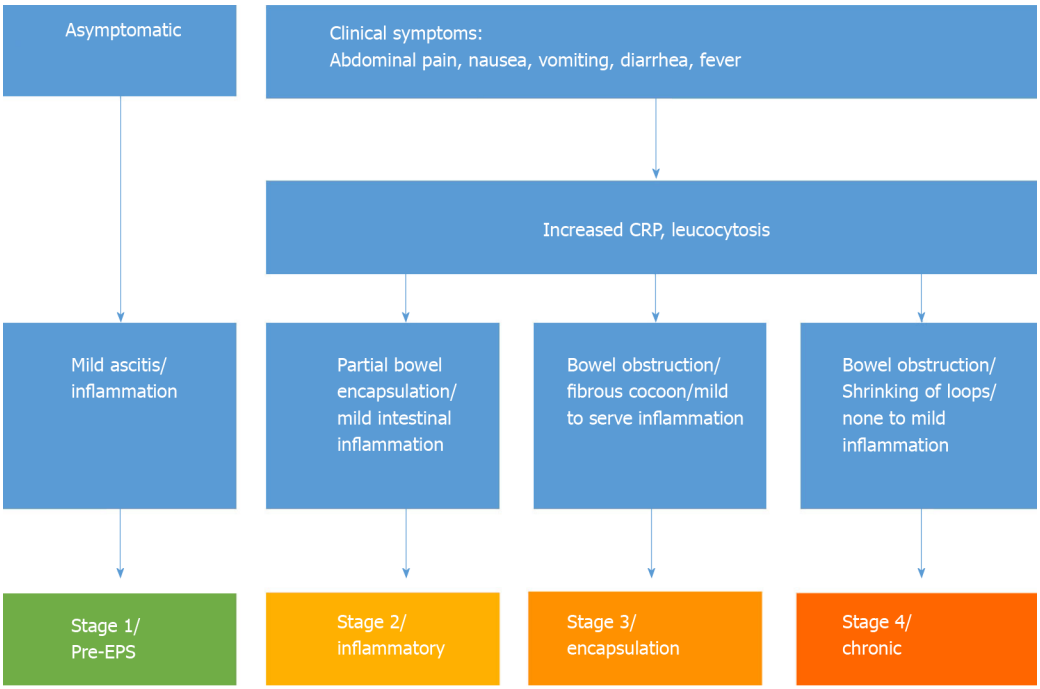


Figure 2 Stages of encapsulating peritoneal sclerosis with associated clinical, serologic, and intestinal findings. EPS: Encapsulating peritoneal sclerosis; CRP: C-reactive protein.

present study was to perform a systematic review of the literature to identify studies on EPS/abdominal cocoons in children. For review, we scanned PubMed, Medline, and Google Scholar search engines for articles containing the terms "EPS", "abdominal cocoon", "abdominal cocoon syndrome", "encapsulating bowel disease", and "SEP", children and paediatric" published from January 1990 to January 2020. Terms were entered alone or in combinations.

We included all articles reporting case series or case reports in the English and German languages. All series and case reports reporting patients younger than 18 years were included (quantitative screening). Further eligibility criteria were a report of the clinical presentation, sex and age, operation as the treatment, and histopathological findings (qualitative screening). Data for all clinical, diagnostic, therapeutic, and etiologic findings were collected from the different databases. We included primary (idiopathic) and secondary forms [abdominal surgery, abdominal trauma, abdominal tuberculosis, peritoneal shunts, liver transplantation, recurrent peritonitis, beta-blocker treatment (practolol or propranolol), chemotherapy, gastrointestinal malignancy, systemic lupus erythaematosus, or parasitic infection] of EPS with the exception of EPS due to PD. We excluded PD-associated EPS because, as mentioned above, in these cases, ESP is the appropriate term with inflammatory processes in the

cocoon, such as formation of the bowel. We then created a PRISMA flow chart showing the results of the literature search (Figure 3).

CASE PRESENTATION

Chief complaints

A 12-year-old boy with Xq24 deletion syndrome presented with symptoms of intermittent intestinal obstruction 8 wk after primary surgery.

History of present illness

The child was symptomatic with a distended abdomen, refusal of feeds, and episodes of abdominal pain. Furthermore, he presented with large gastric residuals that became bilious in the next week.

History of past illness

Eight weeks previously, he presented with suspected intestinal bleeding without further symptoms. US, abdominal MRI, endoscopy, and laparoscopy did not reveal the cause of the chronic bleeding. Specialized angiographic MRI was suspicious for a small intraluminal vascular tumour in the ileum. Limited laparotomy and meticulous palpation of the small bowel enabled the identification of the tumour in the lower ileum. Limited small bowel resection and primary anastomosis were performed. Further clinical investigation of the whole small and large bowel did not reveal any further pathological findings. Histopathological examination showed a venous malformation (2.5 cm × 2.0 cm) at the transition of the jejunum to the ileum. The following clinical course was uneventful. The boy was discharged on the 5th postoperative day.

Personal and family history

Except for Xq24 deletion syndrome, there was no other personal or family history of acute or chronic disease.

Physical examination

On physical examination, the patient showed a distended abdomen and abdominal pain. The examination of the heart, lungs, and further organ status showed no abnormalities. Due to his Xq24 deletion syndrome, he showed psychomotor delay, intellectual disability, and a characteristic craniofacial dysmorphism.

Laboratory examinations

Laboratory findings showed slightly elevated C-reactive protein (0.3 mg/dL) and normal findings across the rest of the blood panel.

Imaging examinations

The abdominal US showed pendulum peristalsis and free fluid in the abdominal cavity, and a plain abdominal X-ray showed some air fluid levels (Figure 4A). A gastrointestinal contrast study was performed, which revealed distended small bowel loops (maximum diameter of 50 mm) and narrow segments of the large intestine. There was appropriate intestinal transit, with the presence of contrast in the jejunal and ileal loops after 1 h of administration. The contrast agent arrived at the terminal ileum and caecum at 2 h of intestinal transit. Due to the inconclusive results, we performed MRI, which revealed a distended duodenum and small bowel loops with multiple intraluminal air fluid levels and thickened walls but with no signs of obstruction (Figure 4B).

FINAL DIAGNOSIS

Due to the clinical symptoms of obstructive bowel disease and inconclusive radiological signs, the patient underwent relaparotomy. Intraoperatively, we found a completely encapsulated small bowel (Figure 5). The massive, fibroconnective membrane encapsulated the bowel from the ligament of Treitz to the ileocecal junction. The thick, firm, and white membrane was not attached to the parietal peritoneum. Microscopic findings showed partially mesothelium-covered, predom-

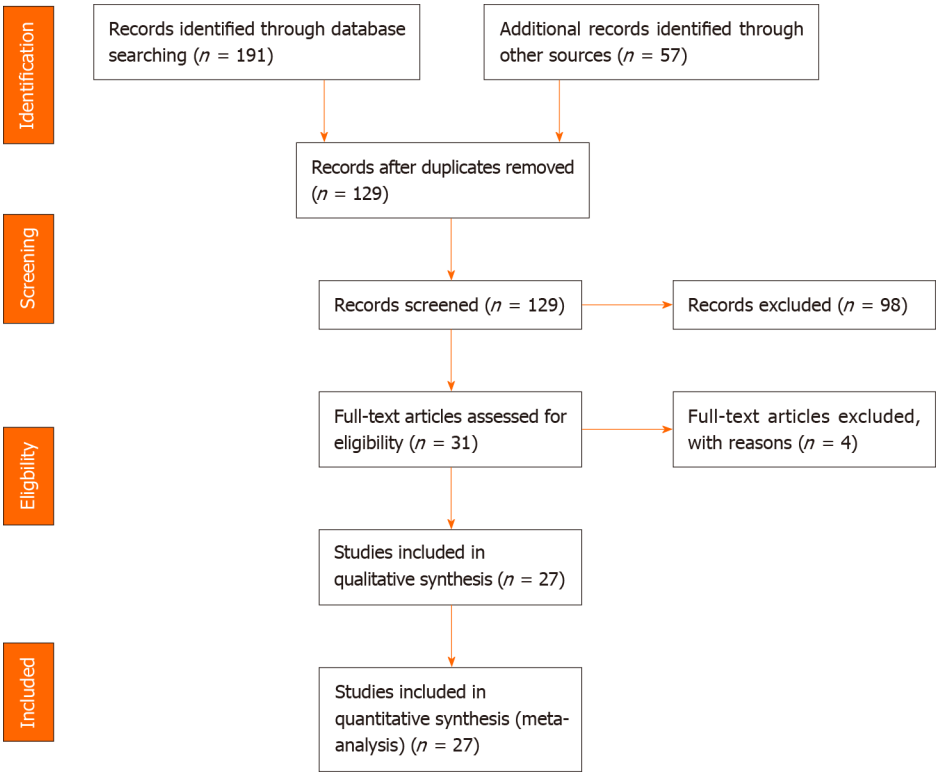


Figure 3 PRSIMA Flow chart showing the results of the literature search.

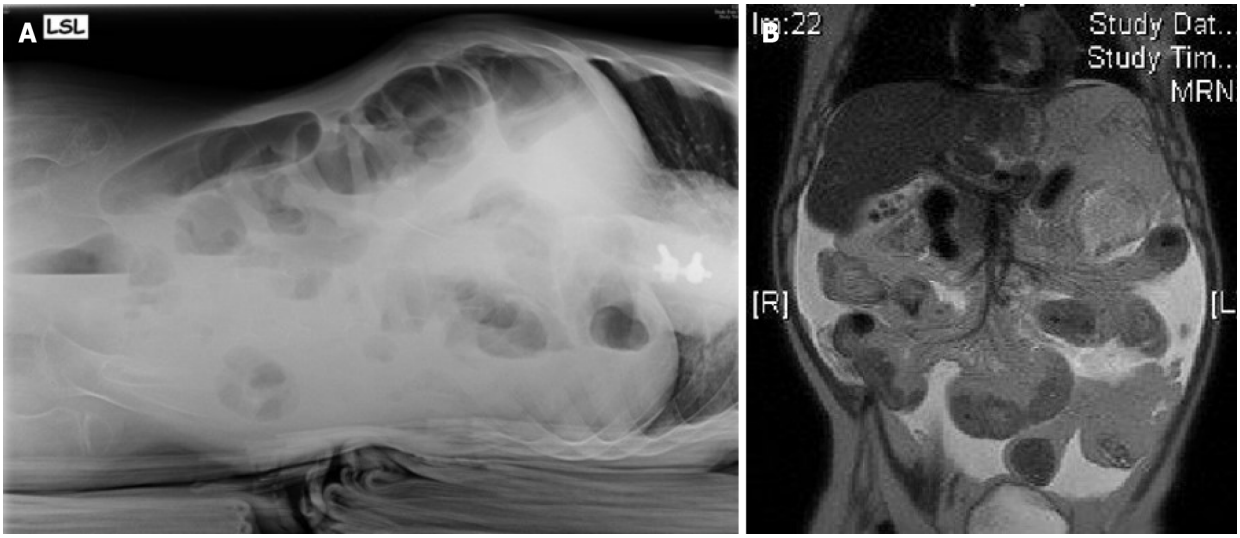


Figure 4 Diagnostic imaging. A: X-ray with lateral abdominal view showing some air fluid levels; B: Magnetic resonance imaging in coronal plane with distended duodenum and small bowel loops with multiple intraluminal air fluid levels and thickened walls.

inantly edematous loosened fibre-rich connective tissue with prominent, predominantly small vessels with a prominent endothelial lining with hyperchromatic oval nuclei, mostly positive for CD31 and CD34. No evidence of malignancy was found (Figure 6).

TREATMENT

We performed extensive adhesiolysis by peeling the fibrous pseudocapsulae from the small bowel. This resulted in freeing of the small bowel but also in multiple serosal injuries with diffuse bleeding. No bowel perforation occurred.



Figure 5 The small bowel is shortened, considerably thickened, and covered with a fibrous membrane, which separates and constricts the entire small intestine from approximately 10 cm distal to Treitz's ligament to approximately 5 cm proximal to the ileocecal junction.

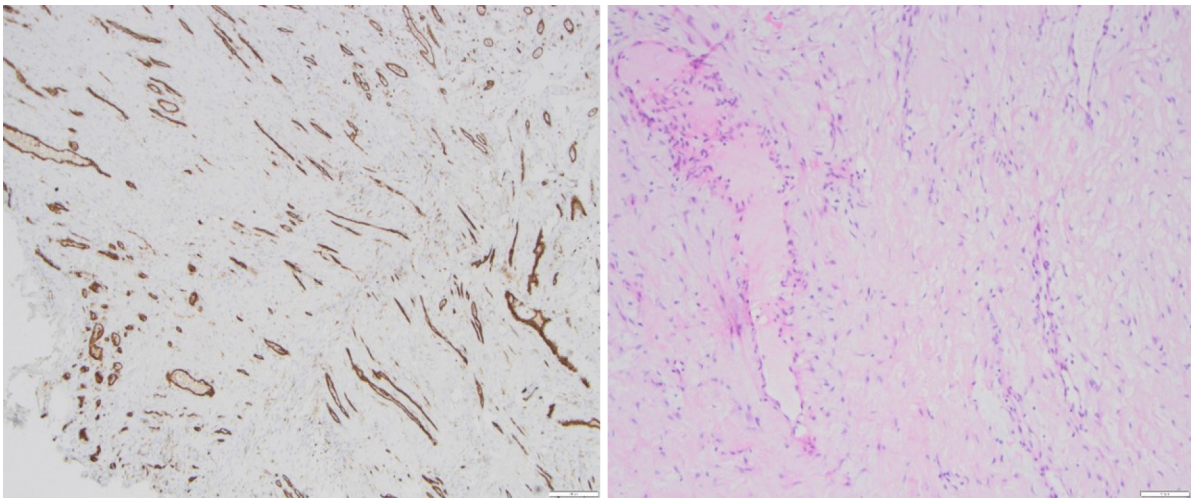


Figure 6 Microscopic findings showed partially mesothelium-covered, predominantly edematous loosened fiber-rich connective tissue with prominent, predominantly small vessels with prominent endothelial lining with hyperchromatic oval nuclei.

OUTCOME AND FOLLOW-UP

The following clinical course was prolonged due to peritonitis, massive ascites, and paralytic ileus. Eventually, 2 wk after surgery, the first feeds could be established, and the child was discharged on the 23rd postoperative day. The follow-up is now 12 mo and uneventful. A summary of the most relevant aspects of the case is listed in Table 2.

DISCUSSION

Literature review

Articles identified after reviewing and applying the inclusion criteria are listed in Table 3. No comparable case could be found in children presenting with EPS after surgery. Sahoo *et al*[14] reported EPS as an idiopathic form in a case series of 4 patients (3 boys, 1 girl) between 6 and 8 years of age, and Mehta *et al*[15] and Bassiouny *et al*[16] reported EPS in a 7-year-old boy without underlying disease. Ahmad *et al*[17] mentioned a case report of EPS in a newborn as a consequence of meconium peritonitis. In total, 27 articles could be found reporting 33 patients (Table 3). Among these patients, 24 were girls and 9 were boys. Their ages ranged from 2 d to 17 years.

Table 2 Summery of our patient data

Age	Clinical symptoms	Labatory findings	Intraoperive findings	Histology
11 yr	Abdominal pain; Distended abdomen; Vomiting (bilious)	CRP: 0.3 mg/dL	Complete; encapsulation of the small bowel	Fibrous connective tissue with prominent vas-cularization, predomi-nantly from the venous type

CRP: C-reactive protein.

Especially in older patients (≥ 10 years of age), EPS was detected more often in girls (f:m = 22:2). Various radiological modalities for diagnosis (singly or in addition) were reported, such as abdominal X-rays (n = 21), US (n = 18), contrast studies (n = 8), and CT scans (n = 11). In three cases, no diagnostic tool was mentioned. Thirty-two patients underwent surgery (laparotomy), while 1 patient underwent conservative treatment with antitubercular medications. When laparotomy was performed, adhesiolysis and excision was the treatment of the choice (n = 32). Two patients underwent appendectomy simultaneously, and two patients underwent temporary enterostomy due to pronounced bowel inflammation. In 3 patients, limited bowel resection, including the ileocecal region, was performed since it was too difficult to incise and release the envelope without injuring the intestines. In all reported cases with surgical treatment, the operation and postoperative period were uneventful.

Discussion

The clinical picture of EPS is largely unknown in the medical world[18]. The embryonal condition is characterized by an accessory peritoneal sac derived from the peritoneum of the yolk sac as it is withdrawn into the abdominal cavity during the 12th week of gestation[3]. Only a few risk factors are known[9]. This disease can occur as a late consequence of long-term peritoneal dialysis[19-23]. However, even this is not necessarily always the case, since cases are known in which EPS is already visible shortly after initiation of PD therapy[11]. In these cases, the mortality depends on the duration of PD, ranging between 30% and 60%. In other cases where EPS is not associated with PD, various reports have reported beta blockers as the cause of EPS [10]. In animal models, practolol inhibits the release of surfactant from type II pneumocytes, resulting in damage to the abdominal serosa[24]. Tumours with peritoneal dissemination and infectious peritonitis are other frequently mentioned risk factors for EPS, supported by epidemiological data. Pathogens significantly increase the risk, highlighting *Staphylococcus aureus*, fungi, *Pseudomonas* spp., and *Haemophilus influenza*[3,4,10]. Fowler *et al*[25] suggested echovirus infection as an etiologic factor, and Foo *et al*[3] thought tuberculosis could be involved.

Several theories have been formulated about the pathogenesis of idiopathic EPS [26], for example, retrograde menstruation due to virus infection or pelvic peritonitis with tissue damage incurred by cell-mediated immunity[3,5,11]. Retrograde menstruation explains the relatively high number of adolescent girls with idiopathic abdominal cocoons (Table 3). Moreover, several tumour entities and/or abdominal operations may lead to adhesions and peritoneal fibrosis[27-29]. Therefore, overall, the most common theory is developing a membrane in the form of sclerosis secondary to peritonitis[17,18]. Prospectively controlled randomized studies are lacking, and most studies on EPS present small patient collections over a long period of time[10-13].

The presented case is very unusual because of the child's young age, the atypical geographical region, and a very rare cause (secondary to abdominal surgery). Most of the other publications with paediatric patient collections are secondary forms after tuberculosis infection or after prolonged PD. The short time interval to the primary laparotomy in our patient is a special feature that has not been described in the literature thus far. EPS after kidney transplantation (as an abdominal surgical intervention) has been reported in case reports; however, these patients also had a history of PD or chronic kidney diseases[30]. In many cases of idiopathic EPS, no correlation can be detected with any potential risk factor[4,31-33]. Nevertheless, two considerations are important: First, in these forms, peritoneal disorders are often associated with general connective tissue damage, particularly of the serous membranes, such as abdominal trauma; this indicates a major role of immunopathogenesis in EPS. The second factor can be a genetic predisposition, which is suggested due to the high frequency of EPS in women from subtropical regions and familial forms such as multifocal family fibrosclerosis.

Table 3 Systematic literature review-patient data

Ref.	Age/sex	Clinical presantation	Diagnostic	Etiology	Treatment
Ahmad *et al*[17], 2013	2 d/m	Polyhydramnion, vomiting, abdominal distension, failure to pass meconium	US, X-ray	Meconium peritonitis	Surgery
Sahoo *et al*[14] 1996	6 yr/m	Abdominal pain, bilious vomiting	US, X-ray, BMFT	Idiopathic	Surgery
Mehta *et al*[15], 1994	7 yr/m	Colicky periumbilical pain, vomiting, constipation	US, X-ray	Idiopathic	Surgery
Bassiouny *et al*[16], 2011	7 yr/m	Crampy abdominal pain	X-ray, contrast enema	Idiopathic	Surgery
Sahoo *et al*[14], 1996	6 yr/m	Constipation, on-and-off vomiting	US, X-ray, BMFT	Idiopathic	Surgery
Tolstrup *et al*[35], 2017	8 yr/f	Signs of enteritis	CT	Idiopathic	Surgery
Sahoo *et al*[14], 1996	8 yr/f	Intermittent bilious vomiting, abdominal distension	BMFT	Idiopathic	Surgery
Sahoo *et al*[14], 1996	8 yr/m	Colicky abdominal pain, vomiting, constipation	X-ray	Idiopathic	Surgery
Kaushik *et al*[10], 2006	9 yr/m	Abdominal pain, vomiting, constipation	-	Abdominal tuberculosis	Surgery (with temp. enterostomy)
Okobia *et al*[37], 2001	10 yr/f	Abdominal pain, abdominal distension, weight loss	X-ray	Idiopathic	Surgery (with appendectomy)
Bassiouny *et al*[16], 2011	12 yr/f	Colicky abdominal pain, vomiting	US, X-ray	Idiopathic	Surgery
Okobia *et al*[37], 2001	12 yr/f	Colicky abdominal pain, abdominal distension	US, X-ray	Idiopathic	Surgery (with appendectomy)
Dehn *et al*[29], 1985	12 yr/f	Abdominal pain, bilious vomiting	US, X-ray	Idiopathic	Surgery
Kayastha *et al*[23], 2012	13 yr/f	Abdominal pain in tright iliac region, vomiting	US	Idiopathic	Surgery
Sreevathsa *et al*[33], 2013	13 yr/f	Colicky central abdominal pain	US, X-ray, BMFT	Idiopathic	Surgery (with ileocaecal resection)
Pillai *et al*[26], 2006	13 yr/f	Abdominal pain, vomiting	US, X-ray, CT	Idiopathic	Surgery
Chatura *et al*[40], 2012	14 yr/f	Colicky abdominal pain	US	Idiopathic	Surgery (with ileocolectomy)
Ibrahim *et al*[41], 2009	14 yr/m	Colicky abdominal pain, vomiting, constipation	X-ray	Idiopathic	Surgery (with appendectomy)
Calvo *et al*[42], 2015	14 yr/f	Colicky abdominal pain, bilious vomiting, weight loss	US, CT	Idiopathic	Surgery
Shah *et al*[43], 2013	14 yr/f	Colicky abdominal pain, vomiting	CT / BMFT	Idiopathic	Surgery
Sreevathsa *et al*[33], 2013	14 yr/f	Colicky central abdominal pain	US, X-ray, BMFT	Idiopathic	Surgery (with ileocaecal resection)
Kumar *et al*[44], 2012	14 yr/f	Colicky abdominal pain, vomiting	US, CT	Idiopathic	Conservatively
Yucel *et al*[53], 2011	15 yr/f	Abdominal pain	X-ray, CT	Idiopathic	Surgery
Raju[45], 2004	15 yr/f	Recurrent abdominal pain	X-ray, contrast study	Idiopathic	Surgery
Ndiaye *et al*[46], 2012	15 yr/f	Subocclusive obstruction, loss of weight (11kg)	CT	Idiopathic	Surgery
Choudhury *et al*[47], 2009	15 yr/f	Crampy abdominal pain right abdomen, weight loss	-	Idiopathic	Surgery (with partial ileocolic resection)
Mordehai *et al*[48], 2001	15 yr/f	Crampy abdominal pain	US, X-ray	Idiopathic	Surgery
Mohanty *et al*[49], 2009	15 yr/f	Colicky abdominal pain, vomiting	US, X-ray, CT	Idiopathic	Surgery
Kumar *et al*[36], 2009	16 yr/f	Abdominal pain in the left lower abdomen, vomiting	US, X-ray, CT	Idiopathic	Surgery
Jayant *et al*[50], 2011	16 yr/f	Small bowel obstruction	CT	Idiopathic	Surgery

Kaushik *et al*[10], 2006	17 yr/m	Abdominal pain, vomiting, constipation	-	Abdominal tuberculosis	Surgery (with temp. enterostomy)
Naniwadekar *et al* [51], 2014	17 yr/f	Abdominal pain, vomiting, constipation	US, X-ray, GI scopy	Idiopathic	Surgery
Kaur *et al*[52], 2012	17 yr/f	Recurrent abdominal pain	US, X-ray, CT	Idiopathic	Surgery

BMFT: Barium meal follow-through; CT: Computer tomography; f: Female; GI: Gastrointestinal; m: Male; US: Ultrasound.

In reports including patients with long-term PD, pathogenesis is often described with the "two-hit"-hypothesis[3,4] when disruption of normal peritoneal/mesothelial physiology is a result of extensive PD over a period of years and predisposes the individual to a second hit that triggers the process. This second hit may take the form of an episode of peritonitis, discontinuing PD, or an acute intra-abdominal event. In our case, this hypothesis is unlikely because he was a non-PD patient, and there was a very short period between the two events. Therefore, the reason for the development of EPS in our patient must be found in the previous operation with resection of lymphangioma as an abdominal trauma and trigger for sclerosis. Another reason for developing EPS could be cystic lymphangioma of the small bowel itself as a benign vascular tumour with peritoneal dissemination. Garosi[19] and Célicout *et al*[34] described different tumour entities in connection with EPS in patients without PD, including histiocytic lymphoma, gastric, ovarian, pancreatic and renal cell carcinoma, and oedematous polyposis of the colon. Cystic lymphangioma as a trigger for EPS could not be found in the literature thus far. Because the lymphangioma was resected in total during the first operation, we believe that primary abdominal surgery was the trigger for EPS in our patient.

Diagnostic modalities

Because the early clinical features are often nonspecific[35,36], it is difficult to make a definite preoperative diagnosis of EPS. There are no specific serological markers for EPS. Ultrasonography may show dilated small bowel loops, ascites with or without parietal loculations, and a membrane covering the small bowel loops with occasional formation of a mass of bowel loops and adhesions[37]. Abdominal X-rays have a low sensitivity, showing mostly dilated small bowel loops with multiple air fluid levels. Peritoneal and bowel wall calcification has also been reported. Abdominal CT has a higher sensitivity (70%-90%) to detect the etiology of high-grade small bowel obstruction but should be used cautiously due to radiation risks in young patients. In our search of the literature, MRI has not been reported in paediatric patients with abdominal cocoons. Nevertheless, MRI has been recently reported as another useful modality in diagnosing EPS and may be a preferred technique in children.

Surgical procedures

In the international literature, two surgical therapy approaches for EPS have been described but were only reported in studies within adult patient collections. In 1998, C élicout *et al*[34] published a study in which 3 of 32 patients had dialysis-associated EPS. In the remaining patients, the EPS was the result of a malignancy (14 of 32) or due to b-blocker intake (5 of 32). The indication for the operation was, in all cases, the ultima ratio after long-lasting ileus disease. Japanese reports are based on studies that only included PD patients[38]. The intraoperative approach in Japan includes removal of the interenteric adhesions and the detachment of the encapsulating small intestinal membranes. The occlusive membranes on the intestine are dissected through longitudinal incisions. However, peritoneal sclerosis makes it difficult to identify the "right" layer, so special attention must be paid to serosa lesions. These are insidious because they can lead to occult perforations postoperatively with an increase in small bowel motility and the resulting increased pressure. In case of doubt, any altered segments of the small intestine are therefore resected. In Japan, in suitable cases, solitary stenoses are dilated with a Miller-Abott probe from the intraluminal side. Thus, even tandem stenoses can be corrected without resection. The balloon is deflated after completion of the dilatation and left *in situ* for splinting of the intestine. Usually, the probe is removed after 1 wk. In the opinion of the Japanese authors, the Noble plicature can prevent reobstruction by kinking as well as the reoccurrence of adhesions or entrapment of the small intestine in the Douglas cavity or in the excavation rectovesicalis, respectively.

The use of probes for intestinal splinting and the methods of plication have been discussed very controversially in Germany and have only historical significance. In our opinion, these methods, which carry their own risk, are not reliable enough to prevent the recurrence of ileus disease. In an international comparison, Japan has the most experience with EPS.

In addition to total intestinal enterolysis, which was performed in all cases with surgical treatment, deserosation, and decapsulation, peritonectomies, fibrin membranectomy, and omentectomies were performed in accordance with the findings. Additionally, an opening of the bursa omentalis for the decompression of fluid or for complete unleashing of the stomach may be essential.

There are hardly any reports from the Anglo-American region regarding surgical therapy for EPS. Studies from Australia[39] and Canada[8] mostly refer to conservative therapy for the disease. The surgical procedure is only mentioned as laparotomy and adhesiolysis. Therefore, our strategy was like the international approach with the avocation of extensive enterolysis and detachment of the encapsulating small intestinal membranes.

Postoperative complications

In work published in 1998 by Célicout *et al*[34], the authors showed a mortality rate of 19% and an anastomosis failure rate of 12%. The total complication rate of 38% was the lowest at that time in the literature but was still considered too high[21]. Ten years later, Kawaguchi *et al*[5] published a retrospective study that included 130 surgically treated EPS patients. The reported mortality was 6.9%. However, the recurrence rate was very high (25.4%). Of the 130 patients, 33 had to be reoperated on for recurrence or postoperative ileus, and some patients underwent reoperations up to six times. In our reported case, as well as in the reports with paediatric patients, there were no complications after the operation, and no recurrence was described.

Histological examination

A few histological features, such as fibrin deposits, fibroblast swelling, angiogenesis, and mononuclear inflammatory infiltrate, differentiate peritoneal fibrosis from actual EPS. Since this means that even fewer predictive histological features are available, the German Peritoneal Biopsy Register was established at the initiative of the German Society of Nephrology. Here, we present prospective histomorphology characteristics of peritoneal biopsies with the aim of analysing the pathogenesis of the disease and producing reproducible algorithms for histological diagnosis confirmation. Therefore, the histological evaluation of EPS can now be increasingly based on standardized criteria. The Institute of Pathology at the Robert Bosch Hospital has become the reference centre for the histomorphology evaluation of peritoneal biopsies of the "European EPS Working Group". Our histological results showed fibrous connective tissue with prominent vascularization, predominantly from the venous type, matching an early form of EPS.

CONCLUSION

The diagnosis of EPS is mainly made intraoperatively, and surgery is often indicated due to symptomatic ileus. A history of abdominal trauma, surgery, or abdominal tumour can be a trigger for developing EPS. Surgery, including adhesiolysis and excision, is the first choice of treatment. Total intestinal enterolysis of EPS is the best surgical approach. The long-term prognosis for children is good.

REFERENCES

1 **Cleland**. On an Abnormal Arrangement of the Peritoneum, with Remarks on the Development of the Mesocolon. *J Anat Physiol* 1868; **2**: 201-206 [PMID: 17230753]

2 **Owtschinnikow PJ**. Peritonitis chronica fibrosa incapsulata. *Arch für Klinische Chirurgie* 1907; **83**: 623-634

3 **Foo KT**, Ng KC, Rauff A, Foong WC, Sinniah R. Unusual small intestinal obstruction in adolescent girls: the abdominal cocoon. *Br J Surg* 1978; **65**: 427-430 [PMID: 656764 DOI: 10.1002/bjs.1800650617]

4 **Allam H**, Al Yahri O, Mathew S, Darweesh A, Suliman AN, Abdelaziem S, Khairat M, Toro A, Di Carlo I. The enigma of primary and secondary encapsulating peritoneal sclerosis. *BMC Surg* 2016; **16**: 81 [PMID: 27964725 DOI: 10.1186/s12893-016-0198-2]

5 **Kawaguchi Y**, Kawanishi H, Mujais S, Topley N, Oreopoulos DG. Encapsulating peritoneal sclerosis: definition, etiology, diagnosis, and treatment. International Society for Peritoneal Dialysis Ad Hoc Committee on Ultrafiltration Management in Peritoneal Dialysis. *Perit Dial Int* 2000; **20** Suppl 4: S43-S55 [PMID: 11098928]

6 **Kirshtein B**, Mizrahi S, Sinelnikov I, Lantsberg L. Abdominal cocoon as a rare cause of small bowel obstruction in an elderly man: report of a case and review of the literature. *Indian J Surg* 2011; **73**: 73-75 [PMID: 22211046 DOI: 10.1007/s12262-010-0200-7]

7 **Varun**, Arunagiri. An Observational study of patients undergoing conservative Vs surgical management for adhesive small bowel obstruction. Masters thesis, Kilpauk Medical College, 2014

8 **Devabalan TK**, Nadarajan AR, Roopavathana B, Chase S, Nayak S, Eapen A. Primary and secondary abdominal cocoon- diagnostic and management challenges: retrospective study. *Int Surg J* 2019; **6**: 1360-1367 [DOI: 10.18203/2349-2902.isj20191278]

9 **Brown MC**, Simpson K, Kerssens JJ, Mactier RA; Scottish Renal Registry. Encapsulating peritoneal sclerosis in the new millennium: a national cohort study. *Clin J Am Soc Nephrol* 2009; **4**: 1222-1229 [PMID: 19541815 DOI: 10.2215/CJN.01260209]

10 **Kaushik R**, Punia RP, Mohan H, Attri AK. Tuberculous abdominal cocoon--a report of 6 cases and review of the Literature. *World J Emerg Surg* 2006; **1**: 18 [PMID: 16800898 DOI: 10.1186/1749-7922-1-18]

11 **Mandavdhare HS**, Kumar A, Sharma V, Rana SS. Abdominal cocoon: An enigmatic entity. *Tropical Gastroenterol* 2016; **37**: 156-167 [DOI: 10.7869/tg.349]

12 **Singhal M**, Krishna S, Lal A, Narayanasamy S, Bal A, Yadav TD, Kochhar R, Sinha SK, Khandelwal N, Sheikh AM. Encapsulating Peritoneal Sclerosis: The Abdominal Cocoon. *Radiographics* 2019; **39**: 62-77 [PMID: 30526331 DOI: 10.1148/rg.2019180108]

13 **Nakamoto H**. Encapsulating peritoneal sclerosis--a clinician's approach to diagnosis and medical treatment. *Perit Dial Int* 2005; **25** Suppl 4: S30-S38 [PMID: 16300270]

14 **Sahoo SP**, Gangopadhyay AN, Gupta DK, Gopal SC, Sharma SP, Dash RN. Abdominal cocoon in children: a report of four cases. *J Pediatr Surg* 1996; **31**: 987-988 [PMID: 8811577 DOI: 10.1016/s0022-3468(96)90431-5]

15 **Mehta MH**, Patel RV, Patel CK, Balar NN. Peritoneal encapsulation and abdominal cocoon in a male child. *Pediatr Surg Int* 1994; **9**: 415-416 [DOI: 10.1007/BF01686021]

16 **Bassiouny IE**, Abbas TO. Small bowel cocoon: a distinct disease with a new developmental etiology. *Case Rep Surg* 2011; **2011**: 940515 [PMID: 22606598 DOI: 10.1155/2011/940515]

17 **Ahmad S**, Kayastha K, Javed S, Wasti A. Abdominal cocoon secondary to meconium peritonitis in a neonate: a case report. *J Neonatal Surg* 2013; **2**: 12 [PMID: 26023432]

18 **Cai J**, Wang Y, Xuan Z, Hering J, Helton S, Espat NJ. The abdominal cocoon: a rare cause of intestinal obstruction in two patients. *Am Surg* 2007; **73**: 1133-1135 [PMID: 18092648]

19 **Garosi G**. Different aspects of peritoneal sclerosis. *Contrib Nephrol* 2003; 18-29 [PMID: 12800340 DOI: 10.1159/000071385]

20 **Nomoto Y**, Kawaguchi Y, Kubo H, Hirano H, Sakai S, Kurokawa K. Sclerosing encapsulating peritonitis in patients undergoing continuous ambulatory peritoneal dialysis: a report of the Japanese Sclerosing Encapsulating Peritonitis Study Group. *Am J Kidney Dis* 1996; **28**: 420-427 [PMID: 8804242 DOI: 10.1016/s0272-6386(96)90501-6]

21 **Nakayama M**, Yamamoto H, Ikeda M, Hasegawa T, Kato N, Takahashi H, Otsuka Y, Yokoyama K, Yamamoto R, Kawaguchi Y, Hosoya T. Risk factors and preventive measures for encapsulating peritoneal sclerosis--Jikei experience 2002. *Adv Perit Dial* 2002; **18**: 144-148 [PMID: 12402607]

22 **Akbulut S**. Accurate definition and management of idiopathic sclerosing encapsulating peritonitis. *World J Gastroenterol* 2015; **21**: 675-687 [PMID: 25593498 DOI: 10.3748/wjg.v21.i2.675]

23 **Kayastha K**, Mirza B. Abdominal cocoon simulating acute appendicitis. *APSP J Case Rep* 2012; **3**: 8 [PMID: 22953302]

24 **Xia J**, Xie W, Chen L, Liu D. Abdominal cocoon with early postoperative small bowel obstruction: A case report and review of literature in China. *Medicine (Baltimore)* 2018; **97**: e11102 [PMID: 29924005 DOI: 10.1097/MD.0000000000011102]

25 **Fowler R**. Primary peritonitis: changing aspects 1956-1970. *Aust Paediatr J* 1971; **7**: 73-83 [PMID: 5093237]

26 **Pillai J**, Kumar S, Praneena. Idiopathic abdominal cocoon. *Indian J Radiol Imaging* 2006; **16**: 483-485 [DOI: 10.4103/0971-3026.32251]

27 **Marusawa H**, Katsurada A, Takaya H, Kumegawa Y, Kajimura K, Yamashita Y. A case of encapsulating peritonitis associated with pancreatic ascites induced by carcinoma of the pancreas. *Nihon Shokakibyo Gakkai Zasshi* 1996; **93**: 932-936 [PMID: 8986086]

28 **Stenram U**. Sclerosing peritonitis in a case of benign cystic ovarian teratoma. A case report. *APMIS* 1997; **105**: 414-416 [PMID: 9201244 DOI: 10.1111/j.1699-0463.1997.tb00589.x]

29 **Dehn TC**, Lucas MG, 39Wood RF. Idiopathic sclerosing peritonitis. *Postgrad Med J* 1985; **61**: 841-842 [PMID: 4059150 DOI: 10.1136/pgmj.61.719.841]

30 **Sufrin G**, Chasan S, Golio A, Murphy GP. Paraneoplastic and serologic syndromes of renal adenocarcinoma. *Semin Urol* 1989; **7**: 158-171 [PMID: 2690260]

31 **Dehner LP**, Coffin CM. Idiopathic fibrosclerotic disorders and other inflammatory pseudotumors. *Semin Diagn Pathol* 1998; **15**: 161-173 [PMID: 9606807]

32 **Saied GA**, Hassan AZ, Ossip M. Idiopathic sclerosing encapsulating peritonitis. Case report and

review of literature. *European Surg* 2010; **42**: 103-106 [DOI: 10.1007/s10353-010-0506-5]
33 **Sreevathsa MR**, Harsha AH. Chronic encapsulating peritonitis or cocoon abdomen. *Trop Gastroenterol* 2013; **34**: 204-206 [PMID: 24851542]
34 **Célicout B**, Levard H, Hay J, Msika S, Fingerhut A, Pelissier E. Sclerosing encapsulating peritonitis: early and late results of surgical management in 32 cases. French Associations for Surgical Research. *Dig Surg* 1998; **15**: 697-702 [PMID: 9845640 DOI: 10.1159/000018681]
35 **Tolstrup J**, Lauritsen ML. [Abdominal cocoon syndrome in an eigth-year-old girl caused acute bowel obstruction]. *Ugeskr Laeger* 2017; **179**: V05170380 [PMID: 29260698]
36 **Kumar A**, Ramakrishnan TS, Sahu S, Mishra KB. Idiopathic sclerosing encapsulating peritonitis--is a preoperative diagnosis possible? *Surg Today* 2009; **39**: 610-614 [PMID: 19562451 DOI: 10.1007/s00595-008-3890-8]
37 **Okobia Evbuomwan NM**, Osime U, Okonofua FE. The abdominal Cocoon – A report of three cases and reviews of literature. *Nigerian J Clin Practice* 2001; **4**: 100-103
38 **Kawaguchi Y**, Saito A, Kawanishi H, Nakayama M, Miyazaki M, Nakamoto H, Tranaeus A. Recommendations on the management of encapsulating peritoneal sclerosis in Japan, 2005: diagnosis, predictive markers, treatment, and preventive measures. *Perit Dial Int* 2005; **25** Suppl 4: S83-S95 [PMID: 16300277]
39 **Rigby RJ**, Hawley CM. Sclerosing peritonitis: the experience in Australia. *Nephrol Dial Transplant* 1998; **13**: 154-159 [PMID: 9481732 DOI: 10.1093/ndt/13.1.154]
40 **Chatura RK**, Nayak VJ. Abdominal cocoon: case report of a rare cause of intestinal obstruction. *Indian J Pathol Microbiol* 2012; **55**: 379-380 [PMID: 23032838 DOI: 10.4103/0377-4929.101751]
41 **Ibrahim NA**, Oludara MA. Abdominal cocoon in an adolescent male patient. *Trop Doct* 2009; **39**: 254-256 [PMID: 19762590 DOI: 10.1258/td.2009.090104]
42 **Calvo PA**, Marta DDS, Isnard Blanchara RM, Ojanguren Sabánb I, Castellví Gil A. Abdominal cocoon syndrome: A diagnostic and therapeutic challenge. Case report. *Cir Esp* 2015; **93**: e61-e62 [DOI: 10.1016/j.ciresp.2013.04.016]
43 **Shah MY**, Gedam BS, Sonarkar R, Gopinath KS. Abdominal cocoon: an unusual cause of subacute intestinal obstruction. *Indian J Surg* 2013; **75**: 391-393 [PMID: 24426626 DOI: 10.1007/s12262-012-0582-9]
44 **Kumar J**, Garg A, Chowdhury V, Prakash A, Singh S. Abdominal cocoon--a rare case of intestinal obstruction. A report of two cases. *Arab J Gastroenterol* 2012; **13**: 188-190 [PMID: 23432990 DOI: 10.1016/j.ajg.2012.08.007]
45 **Raju GS**. Abdominal cocoon due to primary peritonitis: barium meal is valuable in diagnosis. *Trop Gastroenterol* 2004; **25**: 80-81 [PMID: 15471322]
46 **Ndiaye AR**, Mbengue A, Soko TO, Diémé EP, Diagne NM, Diouf CT, Fall A, Fall F, Diop Y, Diakhaté IC. Idiopathic sclerosing encapsulating peritonitis: a case in an adolescent girl. *Diagn Interv Imaging* 2012; **93**: 629-631 [PMID: 22749202 DOI: 10.1016/j.diii.2012.03.017]
47 **Choudhury T**, Kamal M. Abdominal Cocoon - A Case Report with Short Review of Literature. *BSMMU J* 2009; **2**: 81-84 [DOI: 10.3329/bsmmuj.v2i2.4763]
48 **Mordehai J**, Kleiner O, Kirshtein B, Barki Y, Mares AJ. Peritoneal encapsulation: a rare cause of bowel obstruction in children. *J Pediatr Surg* 2001; **36**: 1059-1061 [PMID: 11431778 DOI: 10.1053/jpsu.2001.24746]
49 **Mohanty D**, Jain BK, Agrawal J, Gupta A, Agrawal V. Abdominal cocoon: clinical presentation, diagnosis, and management. *J Gastrointest Surg* 2009; **13**: 1160-1162 [PMID: 18649113 DOI: 10.1007/s11605-008-0595-7]
50 **Jayant M**, Kaushik R. Cocoon within an abdominal cocoon. *J Surg Case Rep* 2011; **2011**: 7 [PMID: 24950587 DOI: 10.1093/jscr/2011.5.7]
51 **Naniwadekar RG**, Kulkarni SR, Bane P, Agrarwal S, Garje A. Abdominal cocoon: an unusual presentation of small bowel obstruction. *J Clin Diagn Res* 2014; **8**: 173-174 [PMID: 24701524 DOI: 10.7860/JCDR/2014/6514.4049]
52 **Kaur R**, Chauhan D, Dalal U, Khurana U. Abdominal cocoon with small bowel obstruction: two case reports. *Abdom Imaging* 2012; **37**: 275-278 [PMID: 21643736 DOI: 10.1007/s00261-011-9754-5]
53 **Yucel AF**, Kocakusak A, Arikan S, Demirbag N, Tarlaci A, Batur S. A rare cause of acute abdomen: perforated primary sarcomatoid carcinoma of the small intestine - report of a case, with a brief review of the literature. *J Cancer Res Ther* 2011; **7**: 348-350 [PMID: 22044822 DOI: 10.4103/0973-1482.87005]

World Journal of Gastroenterology

Submit a Manuscript: https://www.f6publishing.com

World J Gastroenterol 2021 October 7; 27(37): 6345-6347

DOI: 10.3748/wjg.v27.i37.6345

ISSN 1007-9327 (print) ISSN 2219-2840 (online)

LETTER TO THE EDITOR

Gastrointestinal symptoms in patients with COVID-19: Is there a relationship with mortality and new variations of SARS-CoV-2?

Igor Braga Ribeiro, Diogo Turiani Hourneaux de Moura, Eduardo Guimarães Hourneaux de Moura

ORCID number: Igor Braga Ribeiro 0000-0003-1844-8973; Diogo Turiani Hourneaux de Moura 0000-0002-7446-0355; Eduardo Guimarães Hourneaux de Moura 0000-0003-1215-5731.

Author contributions: Ribeiro IB conceptualized the study and wrote the manuscript; de Moura DTH and de Moura EGH performed the critical final review of manuscript.

Conflict-of-interest statement: There is nothing to disclose.

Open-Access: This article is an open-access article that was selected by an in-house editor and fully peer-reviewed by external reviewers. It is distributed in accordance with the Creative Commons Attribution NonCommercial (CC BY-NC 4.0) license, which permits others to distribute, remix, adapt, build upon this work non-commercially, and license their derivative works on different terms, provided the original work is properly cited and the use is non-commercial. See: http://creativecommons.org/Licenses/by-nc/4.0/

Manuscript source: Invited manuscript

Specialty type: Gastroenterology and hepatology

Igor Braga Ribeiro, Diogo Turiani Hourneaux de Moura, Eduardo Guimarães Hourneaux de Moura, Departamento de Gastroenterologia, Serviço de Endoscopia Gastrointestinal do Hospital das Clínicas HCFMUSP, Faculdade de Medicina, Universidade de Sao Paulo, Sao Paulo 05403-010, Brazil

Corresponding author: Igor Braga Ribeiro, MD, Associate Research Scientist, Surgeon, Departamento de Gastroenterologia, Serviço de Endoscopia Gastrointestinal do Hospital das Clínicas HCFMUSP, Faculdade de Medicina, Universidade de Sao Paulo, Av. Dr Enéas de Carvalho Aguiar, 225, 6o andar, bloco 3, Sao Paulo 05403-010, Brazil. igorbraga1@gmail.com

Abstract

Coronavirus disease 2019 (COVID-19) is caused by the severe acute respiratory syndrome coronavirus 2 (SARS-CoV-2). Although, respiratory symptoms are typical the digestive system is also a susceptible target with gastrointestinal symptoms present even in the absence of respiratory symptoms. The gastrointestinal symptoms of COVID-19 include diarrhea, abdominal pain, anorexia, and nausea among other symptoms. Some questions that remain to be answered include: Do patients with gastrointestinal symptoms have a higher mortality? SARS-CoV-2 variants are already a global reality: Do these variants present with a greater prevalence of gastrointestinal symptoms? Do patients with these symptoms warrant more intensive care unit care?

Key Words: COVID-19; SARS-CoV-2; Gastrointestinal symptoms; Intensive care unit; Variant

©The Author(s) 2021. Published by Baishideng Publishing Group Inc. All rights reserved.

Core Tip: With the emergence of new variants of severe acute respiratory syndrome coronavirus 2 (SARS-CoV-2) and its clinical manifestations, the following questions have arisen: are gastrointestinal symptoms and complications the same as the other variants or are they different? And are these related to severity of the disease? In this letter to the editor, we discuss the relationship between the new SARS-CoV-2 variants with gastrointestinal manifestations and the severity of disease with the new variants.

Citation: Ribeiro IB, de Moura DTH, de Moura EGH. Gastrointestinal symptoms in patients

Country/Territory of origin: Brazil

Peer-review report's scientific quality classification

Grade A (Excellent): 0
Grade B (Very good): B
Grade C (Good): 0
Grade D (Fair): D
Grade E (Poor): 0

Received: June 29, 2021
Peer-review started: June 29, 2021
First decision: July 13, 2021
Revised: July 14, 2021
Accepted: August 25, 2021
Article in press: August 25, 2021
Published online: October 7, 2021

P-Reviewer: Kumar A, Zhang H
S-Editor: Fan JR
L-Editor: Filipodia
P-Editor: Li X

with COVID-19: Is there a relationship with mortality and new variations of SARS-CoV-2? *World J Gastroenterol* 2021; 27(37): 6345-6347
URL: https://www.wjgnet.com/1007-9327/full/v27/i37/6345.htm
DOI: https://dx.doi.org/10.3748/wjg.v27.i37.6345

TO THE EDITOR

We read with interest the article by Cao *et al*[1] titled "Coronavirus disease 2019 (COVID-19) and its effects on the digestive system."

In 2020, our team conducted a cohort study[2] evaluating 400 patients diagnosed with COVID-19 that, even though it is the largest study in Latin America, unfortunately, was not included in the author's review. In our study, 33.25% of patients reported one or more gastrointestinal symptoms, with diarrhea being the most common, representing approximately 17% of the total. This data corroborates the author's review. It was also found that when these patients had gastrointestinal symptoms, they had a greater tendency to have other concomitant symptoms, especially myalgia and fatigue ($P < 0.05$).

It was also observed that patients with chronic kidney disease ($P < 0.05$), using chronic immunosuppressants, or chronic use of angiotensin receptor blockers or angiotensin-converting enzyme inhibitors had a higher prevalence of gastrointestinal symptoms. Admission to the intensive care unit (ICU), need for mechanical ventilation, length of stay in the ICU, length of hospital stay, need for vasopressor support, laboratory results, and hospital mortality did not differ based on the presence of gastrointestinal symptoms ($P > 0.05$). Regression analyzes showed that immunosuppression [odds ratio (OR): 2.60 (95% confidence interval (CI): 1.20-5.63)], male sex [OR: 1.94 (95%CI: 1.12-3.36)], and older age [OR: 1.04 (95%CI: 1.02-1.06)] were associated with increased mortality.

As described above, our study[2] demonstrated, before the emergence of the new variants of severe acute respiratory syndrome coronavirus 2 (SARS-CoV-2)[3,4], that gastrointestinal symptoms were not associated with a greater need for ICU admission or the severity of the disease in patients in Latin America.

This is a very controversial topic; some studies suggest a less severe clinical evolution in patients with gastrointestinal symptoms[5,6], whereas in the study by Redd *et al*[7], there was no statistical difference.

The study by Leal *et al*[8], evaluating 234 European patients with digestive symptoms, also had a more favorable and non-severe prognosis.

In a review carried out by Wang *et al*[9], it was observed that pancreatic damage or mesenteric ischemia/thrombosis could increase mortality.

In the pediatric population, in the study by de Paula *et al*[10], logistic regression analysis identified that laboratory-confirmed COVID-19 pediatric patients with gastrointestinal symptoms had an increased risk of cardiac abnormalities confirmed by echocardiogram (OR: 6316; 95%CI: 1.717-79043; $P = 0.012$).

We emphasize that in all these studies there was no distinction regarding the variety of SARS-CoV-2 studied.

It is currently known that the high expression of angiotensin-converting enzyme 2 in the lung and the intestinal tract makes the small bowel and colon highly susceptible to SARS-CoV-2 infection, which offers a potential explanation for diarrhea observed in many COVID-19 patients. Since tryptophan absorption requires angiotensin-converting enzyme 2, its deficiency can alter the intestinal microbiota and cause intestinal inflammation[11].

Given the above, we believe a more realistic discussion to be made, and we ask the authors the following: (1) Do patients with gastrointestinal symptoms have more severe disease outcomes or not? (2) Do SARS-CoV-2 variants have a greater gastrointestinal involvement? (3) Do SARS-CoV-2 variants have a relationship between gastrointestinal symptoms and/or disease severity? and (4) Do these patients have a greater need for admission to ICUs?

Finally, we would like to congratulate and thank the authors on the level of shared evidence.

ACKNOWLEDGMENTS

We would like to thank Dr. Sergio A. Sánchez-Luna for reviewing the English translation of this article.

REFERENCES

1 **Cao TT**, Zhang GQ, Pellegrini E, Zhao Q, Li J, Luo LJ, Pan HQ. COVID-19 and its effects on the digestive system. *World J Gastroenterol* 2021; **27**: 3502-3515 [PMID: 34239265 DOI: 10.3748/wjg.v27.i24.3502]

2 **Moura DTH**, Proença IM, McCarty TR, Sagae VMT, Ribeiro IB, Oliveira GHP, Souza GMV, Hirsch BS, Scatimburgo MVCV, Thompson CC, Carrilho FJ, Cecconello I, Moura EGH. Gastrointestinal Manifestations and Associated Health Outcomes of COVID-19: A Brazilian Experience From the Largest South American Public Hospital. *Clinics (Sao Paulo)* 2020; **75**: e2271 [PMID: 33146362 DOI: 10.6061/clinics/2020/e2271]

3 **SeyedAlinaghi S**, Mirzapour P, Dadras O, Pashaei Z, Karimi A, MohsseniPour M, Soleymanzadeh M, Barzegary A, Afsahi AM, Vahedi F, Shamsabadi A, Behnezhad F, Saeidi S, Mehraeen E, Shayesteh Jahanfar. Characterization of SARS-CoV-2 different variants and related morbidity and mortality: a systematic review. *Eur J Med Res* 2021; **26**: 51 [PMID: 34103090 DOI: 10.1186/s40001-021-00524-8]

4 **Harvey WT**, Carabelli AM, Jackson B, Gupta RK, Thomson EC, Harrison EM, Ludden C, Reeve R, Rambaut A; COVID-19 Genomics UK (COG-UK) Consortium, Peacock SJ, Robertson DL. SARS-CoV-2 variants, spike mutations and immune escape. *Nat Rev Microbiol* 2021; **19**: 409-424 [PMID: 34075212 DOI: 10.1038/s41579-021-00573-0]

5 **Mao R**, Qiu Y, He JS, Tan JY, Li XH, Liang J, Shen J, Zhu LR, Chen Y, Iacucci M, Ng SC, Ghosh S, Chen MH. Manifestations and prognosis of gastrointestinal and liver involvement in patients with COVID-19: a systematic review and meta-analysis. *Lancet Gastroenterol Hepatol* 2020; **5**: 667-678 [PMID: 32405603 DOI: 10.1016/S2468-1253(20)30126-6]

6 **Aghemo A**, Piovani D, Parigi TL, Brunetta E, Pugliese N, Vespa E, Omodei PD, Preatoni P, Lleo A, Repici A, Voza A, Cecconi M, Malesci A, Bonovas S, Danese S; Humanitas COVID-19 Task Force. COVID-19 Digestive System Involvement and Clinical Outcomes in a Large Academic Hospital in Milan, Italy. *Clin Gastroenterol Hepatol* 2020; **18**: 2366-2368.e3 [PMID: 32437870 DOI: 10.1016/j.cgh.2020.05.011]

7 **Redd WD**, Zhou JC, Hathorn KE, McCarty TR, Bazarbashi AN, Thompson CC, Shen L, Chan WW. Prevalence and Characteristics of Gastrointestinal Symptoms in Patients With Severe Acute Respiratory Syndrome Coronavirus 2 Infection in the United States: A Multicenter Cohort Study. *Gastroenterology* 2020; **159**: 765-767.e2 [PMID: 32333911 DOI: 10.1053/j.gastro.2020.04.045]

8 **Leal T**, Costa E, Arroja B, Gonçalves R, Alves J. Gastrointestinal manifestations of COVID-19: results from a European centre. *Eur J Gastroenterol Hepatol* 2021; **33**: 691-694 [PMID: 33787540 DOI: 10.1097/MEG.0000000000002152]

9 **Wang MK**, Yue HY, Cai J, Zhai YJ, Peng JH, Hui JF, Hou DY, Li WP, Yang JS. COVID-19 and the digestive system: A comprehensive review. *World J Clin Cases* 2021; **9**: 3796-3813 [PMID: 34141737 DOI: 10.12998/wjcc.v9.i16.3796]

10 **de Paula CSY**, Palandri GG, Fonseca TS, Vendramini TCA, Farhat SCL, Pereira MFB, Litvinov N, Toma RK, de Sá FVM, Rodrigues KR, Schvartsman C, Forsait S, Sakita NK, Kanunfre KA, Rocha MC, Dos Santos EH, Okay TS, Pinho JRR, de Carvalho WB, Carneiro-Sampaio M, Almeida Silva CA, Marques HHS; Pediatric COVID HC-FMUSP Study Group. Gastrointestinal manifestations are associated with severe pediatric COVID-19: A study in tertiary hospital. *J Infect* 2021; **83**: e22-e25 [PMID: 33940088 DOI: 10.1016/j.jinf.2021.04.030]

11 **Ma C**, Cong Y, Zhang H. COVID-19 and the Digestive System. *Am J Gastroenterol* 2020; **115**: 1003-1006 [PMID: 32618648 DOI: 10.14309/ajg.0000000000000691]

Published by **Baishideng Publishing Group Inc**
7041 Koll Center Parkway, Suite 160, Pleasanton, CA 94566, USA
Telephone: +1-925-3991568
E-mail: bpgoffice@wjgnet.com
Help Desk: https://www.f6publishing.com/helpdesk
https://www.wjgnet.com

© 2021 Baishideng Publishing Group Inc. All rights reserved.

ISSN 1007-9327 (print)
ISSN 2219-2840 (online)

World Journal of *Gastroenterology*

World J Gastroenterol 2021 October 14; 27(38): 6348-6514



Published by Baishideng Publishing Group Inc

World Journal of Gastroenterology

Contents

Weekly Volume 27 Number 38 October 14, 2021

EDITORIAL

6348 Biomarkers for gastrointestinal adverse events related to thiopurine therapy

Zudeh G, Franca R, Stocco G, Decorti G

REVIEW

6357 Fully covered metal biliary stents: A review of the literature

Lam R, Muniraj T

6374 Intraoperative use of indocyanine green fluorescence imaging in rectal cancer surgery: The state of the art

Peltrini R, Podda M, Castiglioni S, Di Nuzzo MM, D'Ambra M, Lionetti R, Sodo M, Luglio G, Mucilli F, Di Saverio S, Bracale U, Corcione F

MINIREVIEWS

6387 Transcription factors specificity protein and nuclear receptor 4A1 in pancreatic cancer

Safe S, Shrestha R, Mohankumar K, Howard M, Hedrick E, Abdelrahim M

6399 Artificial intelligence for the early detection of colorectal cancer: A comprehensive review of its advantages and misconceptions

Viscaino M, Torres Bustos J, Muñoz P, Auat Cheein C, Cheein FA

6415 Faecal immunochemical test outside colorectal cancer screening?

Pin-Vieito N, Puga M, Fernández-de-Castro D, Cubiella J

ORIGINAL ARTICLE

Basic Study

6430 Fecal metabolomic profiles: A comparative study of patients with colorectal cancer *vs* adenomatous polyps

Nannini G, Meoni G, Tenori L, Ringressi MN, Taddei A, Niccolai E, Baldi S, Russo E, Luchinat C, Amedei A

Retrospective Cohort Study

6442 High total Joule heat increases the risk of post-endoscopic submucosal dissection electrocoagulation syndrome after colorectal endoscopic submucosal dissection

Ochi M, Kawagoe R, Kamoshida T, Hamano Y, Ohkawara H, Ohkawara A, Kakinoki N, Yamaguchi Y, Hirai S, Yanaka A, Tsuchiya K

Retrospective Study

6453 Effects of acute kidney injury on acute pancreatitis patients' survival rate in intensive care unit: A retrospective study

Shi N, Sun GD, Ji YY, Wang Y, Zhu YC, Xie WQ, Li NN, Han QY, Qi ZD, Huang R, Li M, Yang ZY, Zheng JB, Zhang X, Dai QQ, Hou GY, Liu YS, Wang HL, Gao Y

6465 Magnetic resonance imaging-radiomics evaluation of response to chemotherapy for synchronous liver metastasis of colorectal cancer

Ma YQ, Wen Y, Liang H, Zhong JG, Pang PP

Observational Study

6476 Deep learning *vs* conventional learning algorithms for clinical prediction in Crohn's disease: A proof-of-concept study

Con D, van Langenberg DR, Vasudevan A

6489 Serum soluble suppression of tumorigenicity 2 as a novel inflammatory marker predicts the severity of acute pancreatitis

Zhang Y, Cheng B, Wu ZW, Cui ZC, Song YD, Chen SY, Liu YN, Zhu CJ

CASE REPORT

6501 Monomorphic epitheliotropic intestinal T-cell lymphoma presenting as melena with long-term survival: A case report and review of literature

Ozaka S, Inoue K, Okajima T, Tasaki T, Ariki S, Ono H, Ando T, Daa T, Murakami K

CORRECTION

6511 Correction to "Effect of probiotic Lactobacillus plantarum Dad-13 powder consumption on the gut microbiota and intestinal health of overweight adults". *World J Gastroenterol* 2021; 27(1): 107-128 [PMID: 33505154 DOI: 10.3748/wjg.v27.i1.107]

Rahayu ES

LETTER TO THE EDITOR

6513 Preservation of the superior rectal artery in laparoscopic colectomy for slow transit constipation: Is it really associated with better outcomes?

Parra RS, Feres O, Rocha JJR

ABOUT COVER

Editorial Board Member of *World Journal of Gastroenterology*, Veerapol Kukongviriyapan, PhD, Professor, Department of Pharmacology, Faculty of Medicine, Khon Kaen University, 123 Moo 16, Mittraphap Road, Muang District, Khon Kaen 40002, Thailand. veerapol@kku.ac.th

AIMS AND SCOPE

The primary aim of *World Journal of Gastroenterology* (*WJG*, *World J Gastroenterol*) is to provide scholars and readers from various fields of gastroenterology and hepatology with a platform to publish high-quality basic and clinical research articles and communicate their research findings online. *WJG* mainly publishes articles reporting research results and findings obtained in the field of gastroenterology and hepatology and covering a wide range of topics including gastroenterology, hepatology, gastrointestinal endoscopy, gastrointestinal surgery, gastrointestinal oncology, and pediatric gastroenterology.

INDEXING/ABSTRACTING

The *WJG* is now indexed in Current Contents®/Clinical Medicine, Science Citation Index Expanded (also known as SciSearch®), Journal Citation Reports®, Index Medicus, MEDLINE, PubMed, PubMed Central, and Scopus. The 2021 edition of Journal Citation Report® cites the 2020 impact factor (IF) for *WJG* as 5.742; Journal Citation Indicator: 0.79; IF without journal self cites: 5.590; 5-year IF: 5.044; Ranking: 28 among 92 journals in gastroenterology and hepatology; and Quartile category: Q2. The *WJG*'s CiteScore for 2020 is 6.9 and Scopus CiteScore rank 2020: Gastroenterology is 19/136.

RESPONSIBLE EDITORS FOR THIS ISSUE

Production Editor: *Ji-Hong Liu*; **Production Department Director:** *Yu-Jie Ma*; **Editorial Office Director:** *Ze-Mao Gong*.

NAME OF JOURNAL
World Journal of Gastroenterology

ISSN
ISSN 1007-9327 (print) ISSN 2219-2840 (online)

LAUNCH DATE
October 1, 1995

FREQUENCY
Weekly

EDITORS-IN-CHIEF
Andrzej S Tarnawski, Subrata Ghosh

EDITORIAL BOARD MEMBERS
http://www.wjgnet.com/1007-9327/editorialboard.htm

PUBLICATION DATE
October 14, 2021

COPYRIGHT
© 2021 Baishideng Publishing Group Inc

INSTRUCTIONS TO AUTHORS
https://www.wjgnet.com/bpg/gerinfo/204

GUIDELINES FOR ETHICS DOCUMENTS
https://www.wjgnet.com/bpg/GerInfo/287

GUIDELINES FOR NON-NATIVE SPEAKERS OF ENGLISH
https://www.wjgnet.com/bpg/gerinfo/240

PUBLICATION ETHICS
https://www.wjgnet.com/bpg/GerInfo/288

PUBLICATION MISCONDUCT
https://www.wjgnet.com/bpg/gerinfo/208

ARTICLE PROCESSING CHARGE
https://www.wjgnet.com/bpg/gerinfo/242

STEPS FOR SUBMITTING MANUSCRIPTS
https://www.wjgnet.com/bpg/GerInfo/239

ONLINE SUBMISSION
https://www.f6publishing.com

© 2021 Baishideng Publishing Group Inc. All rights reserved. 7041 Koll Center Parkway, Suite 160, Pleasanton, CA 94566, USA

E-mail: bpgoffice@wjgnet.com https://www.wjgnet.com

World Journal of Gastroenterology

Submit a Manuscript: https://www.f6publishing.com

World J Gastroenterol 2021 October 14; 27(38): 6348-6356

DOI: 10.3748/wjg.v27.i38.6348

ISSN 1007-9327 (print) ISSN 2219-2840 (online)

EDITORIAL

Biomarkers for gastrointestinal adverse events related to thiopurine therapy

Giulia Zudeh, Raffaella Franca, Gabriele Stocco, Giuliana Decorti

ORCID number: Giulia Zudeh 0000-0001-6168-5662; Raffaella Franca 0000-0001-8569-2023; Gabriele Stocco 0000-0003-0964-5879; Giuliana Decorti 0000-0002-9714-6246.

Author contributions: Zudeh G and Franca R wrote, revised, and edited the manuscript; Stocco G conceptualized, edited, and revised the manuscript; Decorti G conceptualized, wrote, revised, edited, and supervised the manuscript; all authors read and approved the final manuscript.

Conflict-of-interest statement: All authors declare no conflicts of interest for this manuscript.

Open-Access: This article is an open-access article that was selected by an in-house editor and fully peer-reviewed by external reviewers. It is distributed in accordance with the Creative Commons Attribution NonCommercial (CC BY-NC 4.0) license, which permits others to distribute, remix, adapt, build upon this work non-commercially, and license their derivative works on different terms, provided the original work is properly cited and the use is non-commercial. See: http://creativecommons.org/Licenses/by-nc/4.0/

Manuscript source: Invited

Giulia Zudeh, Gabriele Stocco, Department of Life Sciences, University of Trieste, Trieste 34127, Italy

Raffaella Franca, Giuliana Decorti, Department of Medical, Surgical and Health Sciences, University of Trieste, Trieste 34149, Italy

Giuliana Decorti, Institute for Maternal and Child Health I.R.C.C.S Burlo Garofolo, Trieste 34137, Italy

Corresponding author: Gabriele Stocco, PhD, Associate Professor, Department of Life Sciences, University of Trieste, Via Fleming 22, Trieste 34127, Italy. stoccog@units.it

Abstract

Thiopurines are immunomodulators used in the treatment of acute lymphoblastic leukemia and inflammatory bowel diseases. Adverse reactions to these agents are one of the main causes of treatment discontinuation or interruption. Myelosuppression is the most frequent adverse effect; however, approximately 5%-20% of patients develop gastrointestinal toxicity. The identification of biomarkers able to prevent and/or monitor these adverse reactions would be useful for clinicians for the proactive management of long-term thiopurine therapy. In this editorial, we discuss evidence supporting the use of *PACSIN2*, *RAC1*, and *ITPA* genes, in addition to *TPMT* and *NUDT15*, as possible biomarkers for thiopurine-related gastrointestinal toxicity.

Key Words: Thiopurines; Gastrointestinal adverse effects; Biomarkers; *PACSIN2*; *RAC1*; *ITPA*

©The Author(s) 2021. Published by Baishideng Publishing Group Inc. All rights reserved.

Core Tip: Adverse reactions to thiopurines are one of the main causes of treatment discontinuation or interruption. In addition to myelosuppression, approximately 5–20% of patients develop gastrointestinal toxicity; the identification of biomarkers to prevent and/or monitor these adverse reactions is important for the proactive management of long-term thiopurine therapy. In this editorial, we discuss evidence supporting the use of *PACSIN2*, *RAC1*, and *ITPA* genes, in addition to *TPMT* and *NUDT15*, as possible

manuscript

Specialty type: Gastroenterology and hepatology

Country/Territory of origin: Italy

Peer-review report's scientific quality classification

Grade A (Excellent): 0
Grade B (Very good): B
Grade C (Good): 0
Grade D (Fair): 0
Grade E (Poor): 0

Received: March 12, 2021
Peer-review started: March 12, 2021
First decision: April 17, 2021
Revised: April 29, 2021
Accepted: September 3, 2021
Article in press: September 3, 2021
Published online: October 14, 2021

P-Reviewer: Dahiya DS
S-Editor: Gao CC
L-Editor: Wang TQ
P-Editor: Yu HG



biomarkers for thiopurine-related gastrointestinal toxicity.

Citation: Zudeh G, Franca R, Stocco G, Decorti G. Biomarkers for gastrointestinal adverse events related to thiopurine therapy. *World J Gastroenterol* 2021; 27(38): 6348-6356
URL: https://www.wjgnet.com/1007-9327/full/v27/i38/6348.htm
DOI: https://dx.doi.org/10.3748/wjg.v27.i38.6348

INTRODUCTION

Mechanisms of action and adverse effects of thiopurine

Thiopurines, such as mercaptopurine (MP) and its prodrug azathioprine (AZA), are immunomodulatory drugs used in the treatment of pediatric acute lymphoblastic leukemia (ALL) and nonmalignant conditions, such as inflammatory bowel diseases (IBDs)[1,2]. These immunomodulators undergo a complex biotransformation that leads to the production of different thionucleotides (TGNs), such as thioguanosine mono-, di-, and triphosphate (tGMP, tGDP, and tGTP) and deoxythioguanosine mono-, di-, and triphosphate (tdGMP, tdGDP, and tdGTP) (Figure 1). These purine antimetabolites exert their cytotoxic activity through different mechanisms, such as inhibition of *de novo* purine synthesis, interference with the incorporation of guanosine nucleotides into DNA and RNA, and induction of apoptosis due to inhibition of the Ras-related C3 botulinum toxin substrate 1 (Rac-1) protein, a Rho-GTPase[3]. Under physiological conditions, Rac-1-GTP activates the MEKK/IκB/NF-κB and STAT3 survival pathways in activated lymphocytes, resulting in an increase in the antiapoptotic protein Bcl-xL, whereas during thiopurine treatment, the binding of tGTP to Rac-1 impairs these pathways, enhancing apoptosis[3]. Thiopurines are also processed through catabolic pathways, in which xanthine oxidase and thiopurine methyltransferase (TPMT) are the main enzymes involved, producing inactive metabolites such as thiouric acid and methylmercaptopurine, respectively. TPMT also catalyzes the S-methylation of intermediates resulting from MP conversion to TGN, leading to the production of secondary methylated nucleotides (MMPNs) (Figure 1). The role of MMPN metabolites is not fully characterized; however, they could contribute to the inhibition of *de novo* purine synthesis. Factors affecting the TGN/MMPN ratio could influence thiopurine efficacy and toxicity. For example, the amount of TGN in white blood cells is responsible for the immunosuppressive effects; when TPMT activity is compromised, TGN levels increase, leading to dangerous myelosuppression[3].

Thiopurines have a narrow therapeutic index, with an increased risk of severe toxicity and treatment discontinuation[4]. Direct cytotoxic damage can occur in proliferating cells of different tissues and organs. In particular, thiopurines have been associated with the dose-dependent hematological toxicity observed in approximately 80% of ALL cases; in IBD patients, the incidence of bone marrow toxicity is lower (approximately 10%)[5,6]. Neutropenia and leukopenia are the most frequent outcomes of myelosuppression, related to an increased risk of infection, and the main reasons for therapy discontinuation or interruption that can lead to disease aggravation in both ALL and IBD[7-9]. Thiopurine-induced gastrointestinal (GI) toxicity occurs in approximately 5%-20% of ALL and IBD patients; the main symptoms are nausea, vomiting, stomatitis, abdominal pain or cramping, gastritis, gastric ulcer, GI bleeding, and diarrhea[10,11]. Moreover, these immunosuppressors are associated with the risk of neurological complications, hepatotoxicity, pancreatitis, arthralgia, and skin rush[10,12-16].

In the clinic, white blood cell counting is commonly performed to monitor the immunosuppressive effects of these drugs; however, recently, pharmacogenetic biomarkers for predicting thiopurine-induced hematological adverse events have been identified. From a pharmacogenetic point of view, *TPMT* is one of the best characterized genes[17]. Both TPMT protein expression and enzymatic activity are affected by the presence of variants in the *TPMT* gene. More than 44 *TPMT* variant alleles have been described; *TPMT**2 (rs1800462, 238G>C, pAla80Pro), *TPMT* **3B* (rs1800460, 460G>A, p. Ala154Thr), *TPMT***3C* (rs1142345, 719A>G, p. Tyr240Cys), and *TPMT***3A* (rs1800460 and rs1142345 haplotypes) are the most frequent variants in Europeans and can explain up to 95% of TPMT deficiencies[18-20]. As reported above, decreased TPMT activity leads to higher TGN levels and lower MMPN in white blood cells; these

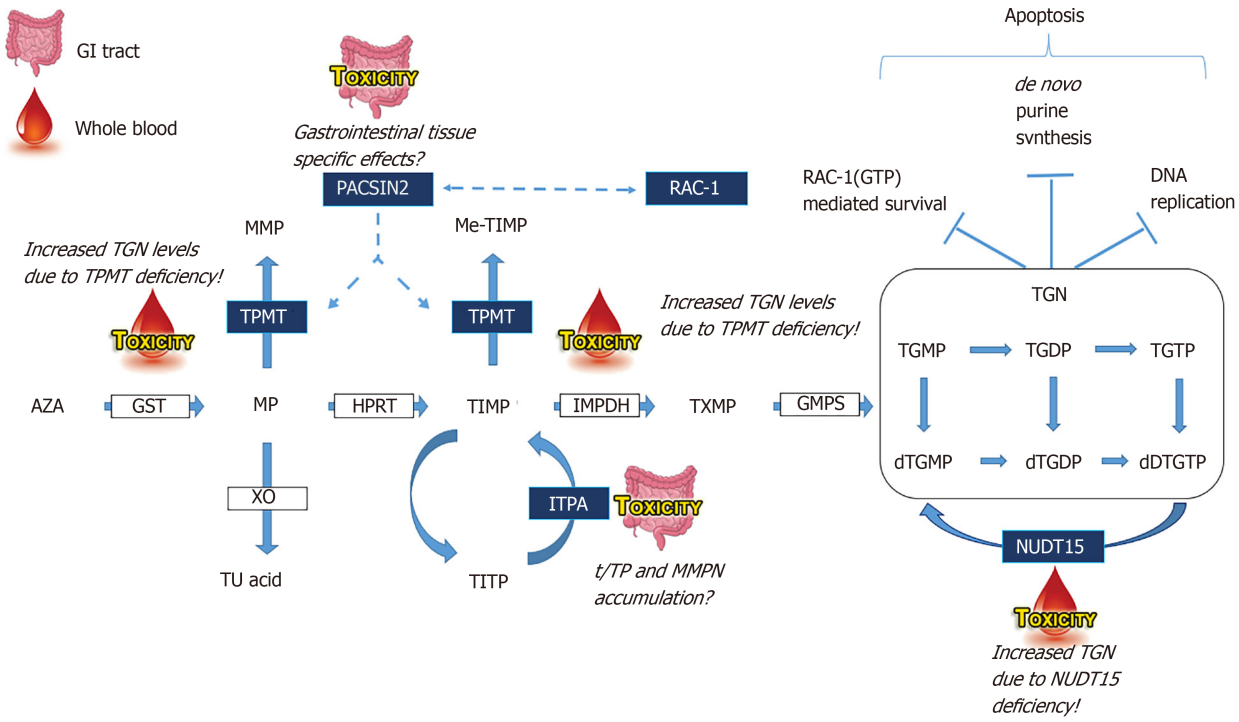


Figure 1 Thiopurine metabolic pathway and possible biomarkers for drug-related toxicity. Dashed arrows indicate the impact of PACSIN2 on TPMT activity and the interaction between PACSIN2 and Rac-1. AZA: Azathioprine; ITPA: Inosine triphosphate pyrophosphatase; IMPDH: Inosine-5'-monophosphate dehydrogenase; GMPS: GMP synthase; GST: Glutathione-S-transferase; Me-TIMP: Methyl-thioinosine monophosphate; Me-TITP: Methyl-thioinosinetriphosphate; MP: Mercaptopurine; MMP: Methyl-mercaptopurine; NUDT15: Nudix hydrolase 15; PACSIN2: Protein kinase C and casein kinase substrate in neurons protein 2; TGDP: Thioguanine diphosphate; TGMP: Thioguanine monophosphate; TGTP: Thioguanine triphosphate; TIMP: Thioinosine monophosphate; TITP: Thioinosine triphosphate; TNG: 6-Thioguanine nucleotide; TPMT: Thiopurine S-methyltransferase; TXMP: Thioxanthine monophosphate; 6-TU acid: Thiouric acid; XO: Xanthine oxidase.

variants are indeed associated with a higher risk of myelosuppression[21]. Variable number tandem repeats (VNTRs) in the *TPMT* promoter are associated with reduced *TPMT* expression levels and a higher risk of MP hematological toxicity[22]. Furthermore, genetic variants in nudix hydrolase 15 (*NUDT15*) have been identified as additional pharmacogenetic markers for the prediction of thiopurine-induced toxicities, especially in Asian individuals. NUDT15 removes a pyrophosphate group by canonical GTP and drug-derived tGTP active metabolites. The most studied *NUDT15* variants are rs116855232 (c.415C> T, p. Arg139Cys), rs147390019 (G>A, p. Arg139His), rs186364861 (G>A, p. Val18Ile), and rs746071566 (36_37insGGAGTC insertion, p.Val18_Val19insGlyVal). Variant alleles encode NUDT15 with compromised activity, leading to a higher tGTP/tGMP ratio and incorporation of TGN into DNA[23,24]. Indeed, these variants have been associated with MP and AZA intolerance[23,25]. On these bases, different guidelines for thiopurine dose adjustment based on *TPMT* and *NUDT15* genotypes have been released to reduce the occurrence of drug-related side effects[26].

In addition to pharmacogenetic markers, TGN levels could be monitored in erythrocytes to avoid severe myelosuppression during therapy. In particular, TGN levels higher than 450 pmol/8 × 10^8 red blood cells (RBCs) and higher than 1000 pmol/8 × 10^8 RBCs have been shown to be associated with myelotoxicity in IBD and ALL patients, respectively, while levels of MMPN above 5700 pmol/8 × 10^8 RBCs have been shown to be related to a higher hepatotoxicity risk in IBD patients[27,28].

BIOMARKERS FOR THIOPURINE-INDUCED GASTROINTESTINAL ADVERSE EVENTS

Although genome-wide association studies (GWAS) have indicated that TPMT activity is predominantly a monogenic trait[29], a percentage of wild-type *TPMT* carriers present reduced TPMT activity, suggesting the existence of other regulatory mechanisms able to modulate its function[30,31]. In 2012, Stocco *et al*[32] demonstrated

that the expression levels and the single nucleotide polymorphism (SNP) rs2413739 of the protein kinase C and casein kinase substrate in neurons 2 (*PACSIN2*) gene were associated with TPMT activity in HapMap cell lines and in a cohort of ALL pediatric patients enrolled at St. Jude Research Children Hospital (SJRCH, Memphis, United States), suggesting a possible role of *PACSIN2* as a TPMT modulator[32]. The authors found that the intronic variant rs2413739 (C>T) was associated with an increased risk of severe GI toxicity during consolidation therapy in two independent cohorts of ALL pediatric patients treated according to the SJRCH Total 13B protocol and to the Associazione Italiana Ematologia Oncologia Pediatrica/Berlin-Frankfurt-Münster (AIEOP-BFM) 2000 protocol[32]. Patients received 75 mg/m^2 MP daily and 2 g/m^2 high-dose methotrexate (HD-MTX) i.v. twice a week for 2 wk at SJRCH, whereas those undergoing the AIEOP-BFM 2000 protocol were treated daily with 25 mg/m^2 MP and received four HD-MTX (2-5 g/m^2) infusions once every 2 wk. To further validate these results, Franca *et al*[33] investigated the possible role of *PACSIN2* rs2413739 in an additional cohort of ALL pediatric patients treated according to the AIEOP-BFM 2009 protocol, with the same consolidation phase as AIEOP-BFM ALL 2000, and in a cohort of IBD pediatric patients undergoing AZA therapy. In the ALL cohort, the *PACSIN2* T allele was associated with decreased TPMT activity during maintenance therapy, particularly in patients heterozygous for *TPMT* rs1142345 and rs1800460. Moreover, the *PACSIN2* TT genotype was associated with a higher risk of GI toxicity during the consolidation phase. The latter association was borderline, likely because of the limited number of clinical data available (n = 81); however, it was in line with the findings of Stocco *et al*[32]. Far more complex to understand is thiopurine-induced GI toxicities in IBD patients, where the occurrence of adverse effects can overlap with clinical manifestations of the disease. Interestingly, Franca *et al*[33] showed that IBD patients carrying the *PACSIN2* T allele and undergoing AZA treatment presented a more active disease, measured as pediatric ulcerative colitis activity/pediatric Crohn's disease activity (PUCAI/PCDAI) indices > 10, according to standard clinical practice. No association between the rs2413739 variant and either TPMT activity or TGN/MMPN levels was found, suggesting a thiopurine-independent effect on the clinical phenotype [33]. Enzymatic activity was significantly higher in the ALL patients than in the IBD patients[33]. The different impact of *PACSIN2* SNP rs2413739 on TPMT activity could be partially explained by patient age: The ALL cohort comprised children under 10 years, while the IBD patients were mainly teenagers. The authors hypothesized that the *PACSIN2* genetic impact on TPMT activity could be more evident in younger patients, who seemed to have increased TPMT activity[34,35]. Moreover, concomitant treatment with MTX in the ALL cohort could contribute to discrepancies in the results; MTX could impact S-adenosyl methionine levels, a TPMT cofactor responsible for the stability of the protein[36]. Since Franca *et al*[33] did not detect significant changes in TGN levels in *PACSIN2* T allele carriers, they hypothesized a thiopurine-independent effect of PACSIN2 on GI toxicity and a tissue-specific role of *PACSIN2* in the intestine. Notably, the Genotype-Tissue Expression Portal (GTEx) shows that *PACSIN2* and *TPMT* expression levels are increased in blood and in the esophageal mucosa of healthy *PACSIN2* rs2413739 T allele carriers but not in the small intestine and colon of these subjects, supporting the idea that the enhanced GI toxicity observed in TT patients is not related to differential expression of *TPMT* in the GI tract[37]. Other evidence regarding PACSIN2 suggests its role as a regulator of intestinal mucosal homeostasis and inflammation. Intriguingly, an underinvestigated mechanism of IBD pathogenesis is VE-cadherin-directed vascular barrier disruption[38], and PACSIN2 has been recognized as a regulator of cell–cell adhesion in the endothelium through the inhibition of asymmetric VE-cadherin internalization from adherens junctions[39]. Stocco *et al*[32] performed an agnostic gene expression analysis in the human B leukemia cell line NALM6 and identified autophagy as one of the pathways significantly affected by *PACSIN2* knockdown, thus suggesting a possible role of this gene in autophagy, another mechanism involved in IBD pathogenesis[32,40,41]. Moreover, the human protein ATLAS report shows that lower levels of PACSIN2 are related to a reduced survival probability in colorectal adenocarcinoma patients, leaving open the question of whether PACSIN2 is a marker of therapeutic response or a contributing factor to intestinal cancer progression[42]. Dedicated studies to clarify the issue of PACSIN2 and GI pathology are needed; however, all this evidence supports the hypothesis that PACSIN2 could be a susceptibility factor for intestinal tissue damage.

Thiopurine-derived tGTPs are able to compete with GTP on Rac-1, a Rho-GTPase involved in cellular proliferation. It can be hypothesized that factors reducing Rac-1 expression or activity could influence cell susceptibility to cytotoxic stimuli, thus contributing to thiopurine efficacy and toxicity. Interestingly, Rac-1 was able to bind

PACSIN2 through a physical interaction[3]; this protein–protein interaction seemed to be responsible for reciprocal regulation: Rac-1 activity controlled PACSIN2 cellular distribution, whereas PACSIN2 could negatively modulate Rac-1 activity[43]. *In vitro* data showed decreased activity of Rac-1 in the presence of the rs34932801 (G>C) SNP in the *RAC1* promoter, and interestingly, this polymorphism was associated with MP hematologic toxicity in a cohort of European IBD patients[44]. Another study reported that Rac-1 expression levels decreased during thiopurine maintenance therapy in IBD patients and that MP responders presented lower Rac-1 expression and activity levels, whereas in nonresponders, these parameters were increased. On these bases, Rac-1 was proposed as a potential biomarker of thiopurine effectiveness in IBD[45]. Intriguingly, conditional disruption of Rac-1 in phagocytes of mice resulted in protection from colitis[46]. In contrast, Rac-1 and STAT3 signaling have been considered contributing factors to IBD development[47], and it was found that both the expression and activity levels of Rac-1 were directly related to colon inflammation grade[46]. Sustained Rac-1-GTP activity in lamina propria T lymphocytes could be more difficult to counteract by thiopurines and lead to resistance of T lymphocytes to apoptosis and thus to their unrestrained accumulation, which subsequently results in the amplification of the inflammatory response in the GI tract. In this sense, in IBD patients, Rac-1 could represent a biomarker of thiopurine-induced GI toxicity and of disease severity and progression, without a clear discrimination between the two clinical phenotypes.

Another potential biomarker for thiopurine GI toxicity is the inosine triphosphate pyrophosphatase (*ITPA*) gene. ITPA is one of the enzymes involved in the thiopurine metabolic pathway. By hydrolyzing inosine triphosphate (ITP) and xanthosine triphosphate nucleotides (XTP) into their monophosphate derivatives (IMP and XMP, respectively), ITPA prevents the accumulation of these noncanonical metabolites in cells and their incorporation into DNA or RNA, where they can interact with DNA/RNA polymerase activity[48]. The thioinosine analog (tIMP), an intermediate of MP conversion to TGN, is converted to tITP, which is also an ITPA substrate (Figure 1). A study performed on a large childhood ALL cohort (n = 511), treated according to the AIEOP-BFM-2000 protocol, showed that the missense variant rs1127354 (C>A, p. Pro32Thr) in *ITPA* was associated with a higher risk of severe GI toxicity during induction/consolidation therapy[10]. This missense variant partially reduces ITPA enzymatic activity in heterozygotes and completely reduces ITPA enzymatic activity in variant homozygotes[49,50], stimulating the accumulation of unusual tITP with the potential to cause adverse metabolic effects[51]. Other studies in pediatric ALL patients showed contradictory results on the *ITPA* rs1127354 association with myelotoxicity[52-54]. Stocco *et al*[53] found significantly higher concentrations of MMPN in patients with the nonfunctional *ITPA* allele. The association between the *ITPA* polymorphism and MP metabolism or neutropenia in ALL patients treated with an MP dose adjusted on the basis of the *TPMT* genotype underlined the important role of this gene in thiopurine toxicity.

CLINICAL IMPLEMENTATIONS

The *PACSIN2* rs2413739 SNP could be considered a potential biomarker for thiopurine-related GI toxicity, being associated with this clinical phenotype in three independent ALL cohorts and with increased active disease in a cohort of IBD patients. Further investigations are needed to understand the molecular basis of this genetic effect and the functional role of the PACSIN2 protein in the healthy and damaged GI epithelium before its possible translation into the clinic. Additionally, the contribution of *RAC1* and *ITPA* SNPs, as potential biomarkers for thiopurine-related GI toxicity, requires further validation in patients undergoing therapy with these drugs. Currently, there are no clinical trials focusing on the role of these genes/proteins in GI toxicity in ALL and IBD patients.

If these candidates would be confirmed as markers for GI toxicity, several applications could be speculated in clinical practice. For example, in patients treated with thiopurines, clinicians could be warned of the patients' genetic predisposition to GI damage (*e.g.*, patients carrying the *PACSIN2* rs2413739 or *ITPA* rs1127354 homozygous variant genotypes). Pharmacogenetic information could be used as an alert for physicians, identifying patients who need intensive monitoring for adverse effects or those who should undergo supportive care earlier, even when less severe episodes of toxicity occur.

CONCLUSION

While highly effective, thiopurines are responsible for serious toxicities in ALL and IBD. This scenario points out the importance of identifying predictive biomarkers for detecting and monitoring the tissue-specific side effects of thiopurine. Data reported in this editorial underline the complexity of thiopurine pharmacokinetic mechanisms, which could be influenced by multiple genes and nongenetic factors able to exert their function on the whole body or through a tissue-specific mechanism of action.

REFERENCES

1 **Cooper SL**, Brown PA. Treatment of pediatric acute lymphoblastic leukemia. *Pediatr Clin North Am* 2015; **62**: 61-73 [PMID: 25435112 DOI: 10.1016/j.pcl.2014.09.006]

2 **Chande N**, Patton PH, Tsoulis DJ, Thomas BS, MacDonald JK. Azathioprine or 6-mercaptopurine for maintenance of remission in Crohn's disease. *Cochrane Database Syst Rev* 2015; CD000067 [PMID: 26517527 DOI: 10.1002/14651858.CD000067.pub3]

3 **Tiede I**, Fritz G, Strand S, Poppe D, Dvorsky R, Strand D, Lehr HA, Wirtz S, Becker C, Atreya R, Mudter J, Hildner K, Bartsch B, Holtmann M, Blumberg R, Walczak H, Iven H, Galle PR, Ahmadian MR, Neurath MF. CD28-dependent Rac1 activation is the molecular target of azathioprine in primary human CD4+ T lymphocytes. *J Clin Invest* 2003; **111**: 1133-1145 [PMID: 12697733 DOI: 10.1172/JCI16432]

4 **Coulthard S**, Hogarth L. The thiopurines: an update. *Invest New Drugs* 2005; **23**: 523-532 [PMID: 16267626 DOI: 10.1007/s10637-005-4020-8]

5 **Hindorf U**, Lindqvist M, Peterson C, Söderkvist P, Ström M, Hjortswang H, Pousette A, Almer S. Pharmacogenetics during standardised initiation of thiopurine treatment in inflammatory bowel disease. *Gut* 2006; **55**: 1423-1431 [PMID: 16543290 DOI: 10.1136/gut.2005.074930]

6 **An Q**, Fan CH, Xu SM. Current views of common pediatric cancers - an update. *Eur Rev Med Pharmacol Sci* 2017; **21**: 20-24 [PMID: 29165770]

7 **de Boer NKH**, Peyrin-Biroulet L, Jharap B, Sanderson JD, Meijer B, Atreya I, Barclay ML, Colombel JF, Lopez A, Beaugerie L, Marinaki AM, van Bodegraven AA, Neurath MF. Thiopurines in Inflammatory Bowel Disease: New Findings and Perspectives. *J Crohns Colitis* 2018; **12**: 610-620 [PMID: 29293971 DOI: 10.1093/ecco-jcc/jjx181]

8 **Lennard L**, Rees CA, Lilleyman JS, Maddocks JL. Childhood leukaemia: a relationship between intracellular 6-mercaptopurine metabolites and neutropenia. *Br J Clin Pharmacol* 1983; **16**: 359-363 [PMID: 6578834 DOI: 10.1111/j.1365-2125.1983.tb02178.x]

9 **Goel RM**, Blaker P, Mentzer A, Fong SC, Marinaki AM, Sanderson JD. Optimizing the use of thiopurines in inflammatory bowel disease. *Ther Adv Chronic Dis* 2015; **6**: 138-146 [PMID: 25954498 DOI: 10.1177/2040622315579063]

10 **Franca R**, Rebora P, Bertorello N, Fagioli F, Conter V, Biondi A, Colombini A, Micalizzi C, Zecca M, Parasole R, Petruzziello F, Basso G, Putti MC, Locatelli F, d'Adamo P, Valsecchi MG, Decorti G, Rabusin M. Pharmacogenetics and induction/consolidation therapy toxicities in acute lymphoblastic leukemia patients treated with AIEOP-BFM ALL 2000 protocol. *Pharmacogenomics J* 2017; **17**: 4-10 [PMID: 26644204 DOI: 10.1038/tpj.2015.83]

11 **Heckmann JM**, Lambson EM, Little F, Owen EP. Thiopurine methyltransferase (TPMT) heterozygosity and enzyme activity as predictive tests for the development of azathioprine-related adverse events. *J Neurol Sci* 2005; **231**: 71-80 [PMID: 15792824 DOI: 10.1016/j.jns.2005.01.003]

12 **Franca R**, Zudeh G, Lucafò M, Rabusin M, Decorti G, Stocco G. Genome wide association studies for treatment-related adverse effects of pediatric acute lymphoblastic leukemia. *Wiley Interdiscip Rev Syst Biol Med* 2020; e1509 [PMID: 33016644 DOI: 10.1002/wsbm.1509]

13 **Gisbert JP**, González-Lama Y, Maté J. Thiopurine-induced liver injury in patients with inflammatory bowel disease: a systematic review. *Am J Gastroenterol* 2007; **102**: 1518-1527 [PMID: 17391318 DOI: 10.1111/j.1572-0241.2007.01187.x]

14 **Toksvang LN**, Schmidt MS, Arup S, Larsen RH, Frandsen TL, Schmiegelow K, Rank CU. Hepatotoxicity during 6-thioguanine treatment in inflammatory bowel disease and childhood acute lymphoblastic leukaemia: A systematic review. *PLoS One* 2019; **14**: e0212157 [PMID: 31125338 DOI: 10.1371/journal.pone.0212157]

15 **Chande N**, Townsend CM, Parker CE, MacDonald JK. Azathioprine or 6-mercaptopurine for induction of remission in Crohn's disease. *Cochrane Database Syst Rev* 2016; **10**: CD000545 [PMID: 27783843 DOI: 10.1002/14651858.CD000545.pub5]

16 **Nygaard U**, Toft N, Schmiegelow K. Methylated metabolites of 6-mercaptopurine are associated with hepatotoxicity. *Clin Pharmacol Ther* 2004; **75**: 274-281 [PMID: 15060506 DOI: 10.1016/j.clpt.2003.12.001]

17 **Zhou S**. Clinical pharmacogenomics of thiopurine S-methyltransferase. *Curr Clin Pharmacol* 2006; **1**: 119-128 [PMID: 18666383 DOI: 10.2174/157488406784111627]

18 **Appell ML**, Berg J, Duley J, Evans WE, Kennedy MA, Lennard L, Marinaki T, McLeod HL, Relling MV, Schaeffeler E, Schwab M, Weinshilboum R, Yeoh AE, McDonagh EM, Hebert JM, Klein TE,

Coulthard SA. Nomenclature for alleles of the thiopurine methyltransferase gene. *Pharmacogenet Genomics* 2013; **23**: 242-248 [PMID: 23407052 DOI: 10.1097/FPC.0b013e32835f1cc0]

19 **Spire-Vayron de la Moureyre C**, Debuysere H, Mastain B, Vinner E, Marez D, Lo Guidice JM, Chevalier D, Brique S, Motte K, Colombel JF, Turck D, Noel C, Flipo RM, Pol A, Lhermitte M, Lafitte JJ, Libersa C, Broly F. Genotypic and phenotypic analysis of the polymorphic thiopurine S-methyltransferase gene (TPMT) in a European population. *Br J Pharmacol* 1998; **125**: 879-887 [PMID: 9831928 DOI: 10.1038/sj.bjp.0702152]

20 **Chouchana L**, Narjoz C, Roche D, Golmard JL, Pineau B, Chatellier G, Beaune P, Loriot MA. Interindividual variability in TPMT enzyme activity: 10 years of experience with thiopurine pharmacogenetics and therapeutic drug monitoring. *Pharmacogenomics* 2014; **15**: 745-757 [PMID: 24897283 DOI: 10.2217/pgs.14.32]

21 **Lennard L**, Cartwright CS, Wade R, Richards SM, Vora A. Thiopurine methyltransferase genotype-phenotype discordance and thiopurine active metabolite formation in childhood acute lymphoblastic leukaemia. *Br J Clin Pharmacol* 2013; **76**: 125-136 [PMID: 23252716 DOI: 10.1111/bcp.12066]

22 **Burgueño-Rodríguez G**, Méndez Y, Olano N, Dabezies A, Bertoni B, Souto J, Castillo L, da Luz J, Soler AM. Ancestry and TPMT-VNTR Polymorphism: Relationship with Hematological Toxicity in Uruguayan Patients with Acute Lymphoblastic Leukemia. *Front Pharmacol* 2020; **11**: 594262 [PMID: 33424606 DOI: 10.3389/fphar.2020.594262]

23 **Moriyama T**, Nishii R, Perez-Andreu V, Yang W, Klussmann FA, Zhao X, Lin TN, Hoshitsuki K, Nersting J, Kihira K, Hofmann U, Komada Y, Kato M, McCorkle R, Li L, Koh K, Najera CR, Kham SK, Isobe T, Chen Z, Chiew EK, Bhojwani D, Jeffries C, Lu Y, Schwab M, Inaba H, Pui CH, Relling MV, Manabe A, Hori H, Schmiegelow K, Yeoh AE, Evans WE, Yang JJ. NUDT15 polymorphisms alter thiopurine metabolism and hematopoietic toxicity. *Nat Genet* 2016; **48**: 367-373 [PMID: 26878724 DOI: 10.1038/ng.3508]

24 **Suiter CC**, Moriyama T, Matreyek KA, Yang W, Scaletti ER, Nishii R, Hoshitsuki K, Singh M, Trehan A, Parish C, Smith C, Li L, Bhojwani D, Yuen LYP, Li CK, Li CH, Yang YL, Walker GJ, Goodhand JR, Kennedy NA, Klussmann FA, Bhatia S, Relling MV, Kato M, Hori H, Bhatia P, Ahmad T, Yeoh AEJ, Stenmark P, Fowler DM, Yang JJ. Massively parallel variant characterization identifies *NUDT15* alleles associated with thiopurine toxicity. *Proc Natl Acad Sci U S A* 2020; **117**: 5394-5401 [PMID: 32094176 DOI: 10.1073/pnas.1915680117]

25 **Moriyama T**, Nishii R, Lin TN, Kihira K, Toyoda H, Jacob N, Kato M, Koh K, Inaba H, Manabe A, Schmiegelow K, Yang JJ, Hori H. The effects of inherited NUDT15 polymorphisms on thiopurine active metabolites in Japanese children with acute lymphoblastic leukemia. *Pharmacogenet Genomics* 2017; **27**: 236-239 [PMID: 28445187 DOI: 10.1097/FPC.0000000000000282]

26 **Relling MV**, Schwab M, Whirl-Carrillo M, Suarez-Kurtz G, Pui CH, Stein CM, Moyer AM, Evans WE, Klein TE, Antillon-Klussmann FG, Caudle KE, Kato M, Yeoh AEJ, Schmiegelow K, Yang JJ. Clinical Pharmacogenetics Implementation Consortium Guideline for Thiopurine Dosing Based on TPMT and NUDT15 Genotypes: 2018 Update. *Clin Pharmacol Ther* 2019; **105**: 1095-1105 [PMID: 30447069 DOI: 10.1002/cpt.1304]

27 **Dubinsky MC**, Lamothe S, Yang HY, Targan SR, Sinnett D, Théorêt Y, Seidman EG. Pharmacogenomics and metabolite measurement for 6-mercaptopurine therapy in inflammatory bowel disease. *Gastroenterology* 2000; **118**: 705-713 [PMID: 10734022 DOI: 10.1016/s0016-5085(00)70140-5]

28 **Adam de Beaumais T**, Fakhoury M, Medard Y, Azougagh S, Zhang D, Yakouben K, Jacqz-Aigrain E. Determinants of mercaptopurine toxicity in paediatric acute lymphoblastic leukemia maintenance therapy. *Br J Clin Pharmacol* 2011; **71**: 575-584 [PMID: 21395650 DOI: 10.1111/j.1365-2125.2010.03867.x]

29 **Liu C**, Yang W, Pei D, Cheng C, Smith C, Landier W, Hageman L, Chen Y, Yang JJ, Crews KR, Kornegay N, Karol SE, Wong FL, Jeha S, Sandlund JT, Ribeiro RC, Rubnitz JE, Metzger ML, Pui CH, Evans WE, Bhatia S, Relling MV. Genomewide Approach Validates Thiopurine Methyltransferase Activity Is a Monogenic Pharmacogenomic Trait. *Clin Pharmacol Ther* 2017; **101**: 373-381 [PMID: 27564568 DOI: 10.1002/cpt.463]

30 **McLeod HL**, Krynetski EY, Relling MV, Evans WE. Genetic polymorphism of thiopurine methyltransferase and its clinical relevance for childhood acute lymphoblastic leukemia. *Leukemia* 2000; **14**: 567-572 [PMID: 10764140 DOI: 10.1038/sj.leu.2401723]

31 **Fakhoury M**, Andreu-Gallien J, Mahr A, Medard Y, Azougagh S, Vilmer E, Jacqz-Aigrain E. Should TPMT genotype and activity be used to monitor 6-mercaptopurine treatment in children with acute lymphoblastic leukaemia? *J Clin Pharm Ther* 2007; **32**: 633-639 [PMID: 18021342 DOI: 10.1111/j.1365-2710.2007.00858.x]

32 **Stocco G**, Yang W, Crews KR, Thierfelder WE, Decorti G, Londero M, Franca R, Rabusin M, Valsecchi MG, Pei D, Cheng C, Paugh SW, Ramsey LB, Diouf B, McCorkle JR, Jones TS, Pui CH, Relling MV, Evans WE. PACSIN2 polymorphism influences TPMT activity and mercaptopurine-related gastrointestinal toxicity. *Hum Mol Genet* 2012; **21**: 4793-4804 [PMID: 22846425 DOI: 10.1093/hmg/dds302]

33 **Franca R**, Stocco G, Favretto D, Giurici N, Del Rizzo I, Locatelli F, Vinti L, Biondi A, Colombini A, Fagioli F, Barisone E, Pelin M, Martellossi S, Ventura A, Decorti G, Rabusin M. PACSIN2 rs2413739 influence on thiopurine pharmacokinetics: validation studies in pediatric patients. *Pharmacogenomics J* 2020; **20**: 415-425 [PMID: 31792371 DOI: 10.1038/s41397-019-0130-0]

34 **McLeod HL**, Krynetski EY, Wilimas JA, Evans WE. Higher activity of polymorphic thiopurine S-

methyltransferase in erythrocytes from neonates compared to adults. *Pharmacogenetics* 1995; **5**: 281-286 [PMID: 8563768 DOI: 10.1097/00008571-199510000-00003]

35 **Pettersson B**, Almer S, Albertioni F, Söderhäll S, Peterson C. Differences between children and adults in thiopurine methyltransferase activity and metabolite formation during thiopurine therapy: possible role of concomitant methotrexate. *Ther Drug Monit* 2002; **24**: 351-358 [PMID: 12021625 DOI: 10.1097/00007691-200206000-00005]

36 **Karas-Kuželički N**, Šmid A, Tamm R, Metspalu A, Mlinarič-Raščan I. From pharmacogenetics to pharmacometabolomics: SAM modulates TPMT activity. *Pharmacogenomics* 2014; **15**: 1437-1449 [PMID: 25303295 DOI: 10.2217/pgs.14.84]

37 **GTEx Portal**. Genotype-Tissue Expression (GTEx) Portal. [cited 30 August 2021]. In: GTEx Portal [Internet]. Available from: https://gtexportal.org/home/

38 **Langer V**, Vivi E, Regensburger D, Winkler TH, Waldner MJ, Rath T, Schmid B, Skottke L, Lee S, Jeon NL, Wohlfahrt T, Kramer V, Tripal P, Schumann M, Kersting S, Handtrack C, Geppert CI, Suchowski K, Adams RH, Becker C, Ramming A, Naschberger E, Britzen-Laurent N, Stürzl M. IFN-γ drives inflammatory bowel disease pathogenesis through VE-cadherin-directed vascular barrier disruption. *J Clin Invest* 2019; **129**: 4691-4707 [PMID: 31566580 DOI: 10.1172/JCI124884]

39 **Dorland YL**, Malinova TS, van Stalborch AM, Grieve AG, van Geemen D, Jansen NS, de Kreuk BJ, Nawaz K, Kole J, Geerts D, Musters RJ, de Rooij J, Hordijk PL, Huveneers S. The F-BAR protein pacsin2 inhibits asymmetric VE-cadherin internalization from tensile adherens junctions. *Nat Commun* 2016; **7**: 12210 [PMID: 27417273 DOI: 10.1038/ncomms12210]

40 **Iida T**, Onodera K, Nakase H. Role of autophagy in the pathogenesis of inflammatory bowel disease. *World J Gastroenterol* 2017; **23**: 1944-1953 [PMID: 28373760 DOI: 10.3748/wjg.v23.i11.1944]

41 **Haq S**, Grondin J, Banskota S, Khan WI. Autophagy: roles in intestinal mucosal homeostasis and inflammation. *J Biomed Sci* 2019; **26**: 19 [PMID: 30764829 DOI: 10.1186/s12929-019-0512-2]

42 **Uhlén M**, Fagerberg L, Hallström BM, Lindskog C, Oksvold P, Mardinoglu A, Sivertsson Å, Kampf C, Sjöstedt E, Asplund A, Olsson I, Edlund K, Lundberg E, Navani S, Szigyarto CA, Odeberg J, Djureinovic D, Takanen JO, Hober S, Alm T, Edqvist PH, Berling H, Tegel H, Mulder J, Rockberg J, Nilsson P, Schwenk JM, Hamsten M, von Feilitzen K, Forsberg M, Persson L, Johansson F, Zwahlen M, von Heijne G, Nielsen J, Pontén F. Proteomics. Tissue-based map of the human proteome. *Science* 2015; **347**: 1260419 [PMID: 25613900 DOI: 10.1126/science.1260419]

43 **de Kreuk BJ**, Nethe M, Fernandez-Borja M, Anthony EC, Hensbergen PJ, Deelder AM, Plomann M, Hordijk PL. The F-BAR domain protein PACSIN2 associates with Rac1 and regulates cell spreading and migration. *J Cell Sci* 2011; **124**: 2375-2388 [PMID: 21693584 DOI: 10.1242/jcs.080630]

44 **Bourgine J**, Garat A, Allorge D, Crunelle-Thibaut A, Lo-Guidice JM, Colombel JF, Broly F, Billaut-Laden I. Evidence for a functional genetic polymorphism of the Rho-GTPase Rac1. Implication in azathioprine response? *Pharmacogenet Genomics* 2011; **21**: 313-324 [PMID: 21372752 DOI: 10.1097/FPC.0b013e3283449200]

45 **Seinen ML**, van Nieuw Amerongen GP, de Boer NK, Mulder CJ, van Bezu J, van Bodegraven AA. Rac1 as a Potential Pharmacodynamic Biomarker for Thiopurine Therapy in Inflammatory Bowel Disease. *Ther Drug Monit* 2016; **38**: 621-627 [PMID: 27465973 DOI: 10.1097/FTD.0000000000000326]

46 **Muise AM**, Walters T, Xu W, Shen-Tu G, Guo CH, Fattouh R, Lam GY, Wolters VM, Bennitz J, van Limbergen J, Renbaum P, Kasirer Y, Ngan BY, Turner D, Denson LA, Sherman PM, Duerr RH, Cho J, Lees CW, Satsangi J, Wilson DC, Paterson AD, Griffiths AM, Glogauer M, Silverberg MS, Brumell JH. Single nucleotide polymorphisms that increase expression of the guanosine triphosphatase RAC1 are associated with ulcerative colitis. *Gastroenterology* 2011; **141**: 633-641 [PMID: 21684284 DOI: 10.1053/j.gastro.2011.04.057]

47 **Atreya R**, Atreya I, Neurath MF. Novel signal transduction pathways: analysis of STAT-3 and Rac-1 signaling in inflammatory bowel disease. *Ann N Y Acad Sci* 2006; **1072**: 98-113 [PMID: 17057193 DOI: 10.1196/annals.1326.001]

48 **Sakumi K**, Abolhassani N, Behmanesh M, Iyama T, Tsuchimoto D, Nakabeppu Y. ITPA protein, an enzyme that eliminates deaminated purine nucleoside triphosphates in cells. *Mutat Res* 2010; **703**: 43-50 [PMID: 20601097 DOI: 10.1016/j.mrgentox.2010.06.009]

49 **Shipkova M**, Lorenz K, Oellerich M, Wieland E, von Ahsen N. Measurement of erythrocyte inosine triphosphate pyrophosphohydrolase (ITPA) activity by HPLC and correlation of ITPA genotype-phenotype in a Caucasian population. *Clin Chem* 2006; **52**: 240-247 [PMID: 16384889 DOI: 10.1373/clinchem.2005.059501]

50 **Arenas M**, Duley J, Sumi S, Sanderson J, Marinaki A. The ITPA c.94C>A and g.IVS2+21A>C sequence variants contribute to missplicing of the ITPA gene. *Biochim Biophys Acta* 2007; **1772**: 96-102 [PMID: 17113761 DOI: 10.1016/j.bbadis.2006.10.006]

51 **Marinaki AM**, Ansari A, Duley JA, Arenas M, Sumi S, Lewis CM, Shobowale-Bakre el-M, Escuredo E, Fairbanks LD, Sanderson JD. Adverse drug reactions to azathioprine therapy are associated with polymorphism in the gene encoding inosine triphosphate pyrophosphatase (ITPase). *Pharmacogenetics* 2004; **14**: 181-187 [PMID: 15167706 DOI: 10.1097/00008571-200403000-00006]

52 **Hareedy MS**, El Desoky ES, Woillard JB, Thabet RH, Ali AM, Marquet P, Picard N. Genetic variants in 6-mercaptopurine pathway as potential factors of hematological toxicity in acute lymphoblastic leukemia patients. *Pharmacogenomics* 2015; **16**: 1119-1134 [PMID: 26237184 DOI: 10.2217/PGS.15.62]

53 **Stocco G**, Cheok MH, Crews KR, Dervieux T, French D, Pei D, Yang W, Cheng C, Pui CH, Relling

MV, Evans WE. Genetic polymorphism of inosine triphosphate pyrophosphatase is a determinant of mercaptopurine metabolism and toxicity during treatment for acute lymphoblastic leukemia. *Clin Pharmacol Ther* 2009; **85**: 164-172 [PMID: 18685564 DOI: 10.1038/clpt.2008.154]

54 **Chiengthong K**, Ittiwut C, Muensri S, Sophonphan J, Sosothikul D, Seksan P, Suppipat K, Suphapeetiporn K, Shotelersuk V. NUDT15 c.415C>T increases risk of 6-mercaptopurine induced myelosuppression during maintenance therapy in children with acute lymphoblastic leukemia. *Haematologica* 2016; **101**: e24-e26 [PMID: 26405151 DOI: 10.3324/haematol.2015.134775]

World Journal of Gastroenterology

Submit a Manuscript: https://www.f6publishing.com

World J Gastroenterol 2021 October 14; 27(38): 6357-6373

DOI: 10.3748/wjg.v27.i38.6357

ISSN 1007-9327 (print) ISSN 2219-2840 (online)

REVIEW

Fully covered metal biliary stents: A review of the literature

Robert Lam, Thiruvengadam Muniraj

ORCID number: Robert Lam 0000-0000-0001-0001; Thiruvengadam Muniraj 0000-0002-4904-2645.

Author contributions: Lam R and Muniraj T equally contributed to the work; All authors have read and approved the final manuscript.

Conflict-of-interest statement: None of the authors have any conflicts of interest to disclose.

Open-Access: This article is an open-access article that was selected by an in-house editor and fully peer-reviewed by external reviewers. It is distributed in accordance with the Creative Commons Attribution NonCommercial (CC BY-NC 4.0) license, which permits others to distribute, remix, adapt, build upon this work non-commercially, and license their derivative works on different terms, provided the original work is properly cited and the use is non-commercial. See: http://creativecommons.org/Licenses/by-nc/4.0/

Manuscript source: Invited manuscript

Specialty type: Gastroenterology and hepatology

Country/Territory of origin: United States

Peer-review report's scientific quality classification

Robert Lam, Thiruvengadam Muniraj, Department of Medicine, Yale University School of Medicine, New Haven, CT 06520, United States

Corresponding author: Thiruvengadam Muniraj, FRCP, MD, PhD, Assistant Professor, Department of Medicine, Yale University School of Medicine, 333 Cedar Street, 1080 LMP, New Haven, CT 06520, United States. thiruvengadam.muniraj@yale.edu

Abstract

Fully covered self-expandable metal stents (FCSEMS) represent the latest advancement of metal biliary stents used to endoscopically treat a variety of obstructive biliary pathology. A large stent diameter and synthetic covering over the tubular mesh prolong stent patency and reduce risk for tissue hyperplasia and tumor ingrowth. Additionally, FCSEMS can be easily removed. All these features address issues faced by plastic and uncovered metal stents. The purpose of this paper is to comprehensively review the application of FCSEMS in benign and malignant biliary strictures, biliary leak, and post-sphincterotomy bleeding.

Key Words: Fully covered self-expandable metal stents; Plastic stents; Endoscopy; Chronic pancreatitis; Biliary stricture; Biliary leak; Stent migration

©The Author(s) 2021. Published by Baishideng Publishing Group Inc. All rights reserved.

Core Tip: Fully covered self-expandable metal stents (FCSEMS) are composed of a metal alloy tubular mesh with a synthetic covering to minimize tumor ingrowth. They have a broad range of biliary endoscopic applications, including the treatment of strictures, biliary leak, and post-sphincterotomy bleeding. Novel anchoring designs have been effective at addressing the common problem of stent migration with FCSEMS.

Citation: Lam R, Muniraj T. Fully covered metal biliary stents: A review of the literature. *World J Gastroenterol* 2021; 27(38): 6357-6373

URL: https://www.wjgnet.com/1007-9327/full/v27/i38/6357.htm

DOI: https://dx.doi.org/10.3748/wjg.v27.i38.6357

Grade A (Excellent): 0
Grade B (Very good): 0
Grade C (Good): C
Grade D (Fair): 0
Grade E (Poor): 0

Received: March 30, 2021
Peer-review started: March 30, 2021
First decision: June 23, 2021
Revised: July 9, 2021
Accepted: August 27, 2021
Article in press: August 27, 2021
Published online: October 14, 2021

P-Reviewer: Kosuga T
S-Editor: Ma YJ
L-Editor: A
P-Editor: Xing YX

INTRODUCTION

Recent advances in endoscopic stenting have enabled the treatment of a wide range of obstructive biliary pathologies previously requiring surgical and percutaneous intervention[1]. Early randomized control studies found that endoscopic stenting compared to surgical or percutaneous intervention was associated with decreased 30 d morbidity and mortality, decreased complications rates, lower overall cost, and higher quality of life[2-4]. Plastic stents were the earliest stent type used, and metal stents were introduced later in the 1980s[5]. The purpose of this report is to review the current applications of fully covered self-expandable metal stents (FCSEMS) for biliary strictures, biliary leak, and post-sphincterotomy bleeding.

PLASTIC STENTS

Plastic stents are commonly used because of their efficacy, easy insertion and removal, and low cost[1,6,7] (Figure 1A). Plastic biliary stents come in various shapes and can be made of Teflon, polyethylene or polyurethane materials. Standard diameters of plastic biliary stents are 7.0 Fr, 8.5 Fr, 10.0 Fr and 11.5 Fr, and standard lengths range from 5 cm to 18 cm. Appropriate stent length is determined using a graduated guide wire and guiding catheter. Initial placement is guided using a radio-opaque guidewire. Plastic stents are equipped with side holes that allow for drainage even when the ends are impacted against the biliary or digestive tract wall, or clogged with debris. Additionally, plastic stents may have anchoring flaps to prevent stent migration. Multiple plastic stents (MPS) can be inserted during each endoscopic retrograde cholangiopancreatography (ERCP) session.

A major disadvantage of plastic stents is the tendency for occlusion due to the formation of a bacterial biofilm, leading to recurrent jaundice and pruritis[8,9]. Acute cholangitis may develop in up to 20%-40% of cases requiring the need for stent exchange[10]. Stent occlusion rates and complications of acute cholangitis are lower with large stent diameters of 10 Fr and 11.5 Fr compared to 7 Fr or 8.5 Fr stents, likely due to a higher biliary flow rate[11]. However, a retrospective study of 33 patients comparing the efficacy and complications of 10 Fr biliary stents to 11.5 Fr stents for use in malignant and benign biliary tract disease found no significant differences in success rates or complications[12]. Median patency for 10 Fr plastic stents is an estimated 4-5 mo[13]. Moreover, a special therapeutic duodenoscope with a wide working channel of 4.2 mm diameter is needed to use 11.5 Fr plastic stents.

SELF-EXPANDABLE METAL STENTS

Self-expandable metal stents (SEMS) were designed with a larger luminal diameter than plastic stents to prolong stent patency and address occlusion complications faced by plastic stents[14-16]. The core structure of a SEMS comprises a 4-12 cm long tubular mesh made up of metal alloys, including stainless steel, Nitinol, Elgiloy and Platinol [17] (Figure 1B). Metal alloys allow adequate radial expansible force without compromising on flexibility inside the duct. Each metal stent is more expensive than a plastic stent. However, SEMS have a lower risk of recurrent biliary obstruction compared to plastic stents. Overall, SEMS is more cost-effective than plastic stents over time, especially when life expectancy exceeds 4 mo[18-22]. Comparisons between plastic stents and different types of SEMS are summarized in Table 1.

SEMS are constrained by an 8-8.5 Fr surrounding sheath while it is inserted through a channel in the duodenoscope. Deployment occurs when the sheath is retracted, expanding the stent to a maximal diameter of 10 mm.

Mechanisms of SEMS occlusion differ from plastic stents *via* the following: (1) Tissue in-growth through the stent mesh; (2) Tumor overgrowth around the proximal or distal end of the stent; (3) Mucosal hyperplasia into the stent because of a chronic inflammatory reaction to the stent mesh; and, less commonly; and (4) Biliary sludge [23-26]. In contrast to plastic stents, occluded SEMS with tumor or tissue in-growth or over-growth are often difficult to reposition or remove once deployed[27]. Treatment of a SEMS occlusion involves insertion of new plastic stents or deployment of another SEMS within the initial stent. Mechanical cleaning with an extraction balloon may also be helpful[28]. Additional complications of SEMS include duodenal wall erosion by the stent, which may lead to duodenal perforation and acute bleeding[29].

Table 1 Strengths and disadvantages of plastic stents and self-expandable metal stents

	Strengths	Disadvantages
Plastic stents	Easy placement, removal, and exchange; Cost-effective for use < 4 mo; Variety of shapes and sizes	Tendency for stent occlusion after several months
Uncovered self-expandable metal stents (USEMS)	Long stent patency due to large luminal diameter; Stent malposition is rare	Cost-effective for use > 4 mo; High risk for tissue ingrowth or tumor overgrowth; Risk for duodenal wall erosion; Biliary leakage possible; Difficult to reposition or remove
Partially covered self-expandable metal stents (PCSEMS)	Long stent patency due to large luminal diameter; Biliary leakage is rare	Cost-effective for use > 4 mo; Intermediate risk for tissue ingrowth or tumor overgrowth; Risk for duodenal wall erosion; Difficult to reposition or remove; Side branch obstruction possible
Fully covered self-expandable metal stents (FCSEMS)	Long stent patency due to large luminal diameter, covering inhibits tissue/tumor in-growth through mesh; No biliary leakage	Cost-effective for use > 4 mo; Risk for duodenal wall erosion; Difficult to reposition or remove; High risk of stent migration; Side branch obstruction possible

Stent designs continue to evolve to overcome these factors. Silicone, polyurethane, and expanded polytetrafluoroethylene coverings may be applied over a part (partly-covered) or entire (fully-covered) length of SEMS to prevent tumor in-growth through the mesh[27,30] (Figures 1C, 1D, and 1E). Additionally, the covering allows for easier SEMS removal compared to bare-metal stents[31].

BENIGN BILIARY STRICTURES

Benign biliary strictures (BBS) form after an initial insult to the biliary duct that leads to inflammation, collagen deposition, fibrosis, and bile duct narrowing[32]. Common causes include post-operative injury, chronic pancreatitis (CP), and chronic inflammatory cholangiopathies (Table 2)[33]. BBS may present with pain, jaundice, pruritis, and/or elevated liver function tests[34]. A combination of magnetic resonance cholangiopancreatography (MRCP) and/or endoscopic (ERCP) retrograde cholangiopancreatography may be used during the evaluation process to elucidate biliary ductal anatomy[35]. Tissue sampling *via* endoluminal biopsy or biliary brushings will confirm non-malignant tissue and determine the primary etiology. ERCP is the therapeutic modality of choice for BBS because of its efficacy, safety, and noninvasive nature[36-38].

Post-operative BBS

The most common causes of post-operative BBS occur after cholecystectomy and biliary duct surgery[39,40]. An effective means of therapeutic decompression using plastic stents can be achieved with the placement of MPS side-by-side across the stricture[41]. Plastic stents used for up to 1 year with interval replacement in 3-4 mo intervals have demonstrated excellent safety, high clinical success rates, and low rates of stricture recurrence[42]. Plastic stent occlusion within 4-5 mo requiring endoscopic stent exchange is a major limitation because of overall cost and requirement for patient compliance[13,43].

In contrast, FCSEMS can expand to a large stent diameter equivalent to three 10 Fr stents, and its chemical covering limits tissue hyperplasia and in-growth. A single FCSEMS can remain in place for a prolonged period without the need for repeated stent exchange prior to removal[44,45].

In a retrospective study of 69 patients comparing the efficacy and safety of FCSEMS and plastic stents for postsurgical BBS, findings revealed a similar technical success rate (100% in both groups) and stricture recurrence (16% in the PS group and 22% in the FCSEMS group)[46]. However, the median duration of stenting in the FCSEMS group (5.2 mo) was significantly lower than that of the PS group (10.7 mo), requiring multiple stent exchanges. In fact, the FCSEMS group had a shorter total operation and fluoroscopy time because only one metal stent needed to be deployed compared to 2-5 plastic stents in the PS group. The study highlighted the use of FCSEMS as a practical and effective alternative means to the endoscopic treatment of post-surgical BBS with plastic stents.

A prospective, nonrandomized study of 18 patients also evaluated the 6-12 mo temporary use of FCSEMS for symptomatic post-cholecystectomy BBS, including a 5 year follow-up time period[47]. Successful FCSEMS placement deployment and

Table 2 Etiology of benign biliary strictures

Extrinsic	Intrinsic
Chronic pancreatitis	Post-operative (*i.e.*, post-liver transplantation and post-cholecystectomy)
Pancreatic fluid collection	Primary sclerosing cholangitis
Cholecystitis	IgG Cholangiopathy

IgG: Immunoglobin G.

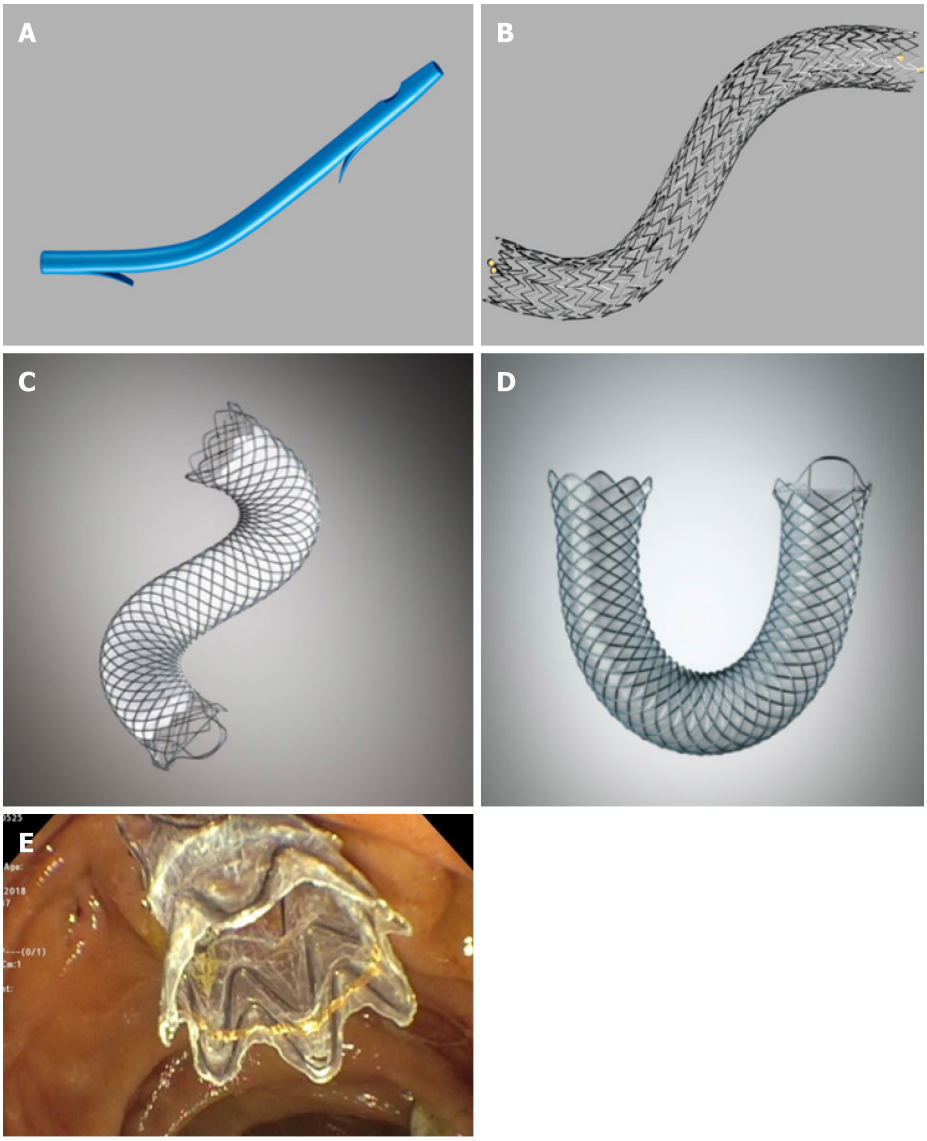


Figure 1 Various types of plastic and metal stents for endoscopic treatment. A: Plastic biliary stent (10 Fr with flaps); B: Uncovered metal biliary stent; C: Partially covered metal biliary stent; D: Fully covered self-expandable metal biliary stent; E: Fully covered self-expandable metal biliary stent with anti-migration fins (Images B-D courtesy of Boston Scientific Corporation, Boston, United States).

removal was achieved in 83% of patients with a median indwell time of 11 mo. As well, 72% of patients achieved stricture resolution at the end of the FCSEMS indwell period. Kaplan Meier analysis predicted 61% probability of remaining stent-free among patients who received FCSEMS. Complications included spontaneous stent migration (17%) and stent-related adverse events, including cholangitis (33%) and pancreatitis (6%). Despite a large sample size and absence of a control group, the study showcased that temporary 1-year placement of FCSEMS can maintain long-term stricture resolution. Table 3 highlights differences in study outcomes between plastic stents and FCSEMS for use in post-operative BBS.

Table 3 Comparison of study outcomes of plastic stents and fully covered self-expandable metal stents for treatment of post-operative benign biliary strictures

Ref.	Methods	Patients	Stent placement	Followup time(mo)	Clinical success[1] (%)	Recurrence (%)
Bergman *et al*[42]	Retrospective, single center	57	Two 10F plastic stents	24	77	20
Costamagna *et al*[41]	Retrospective, single center	154	Multiple plastic stents	108	96.7	12
Chaput *et al*[44]	Retrospective, single center	92	FCSEMS	12	84.9	21.9
Tringali *et al*[47]	Prospective, mult-center	187	FCSEMS	60	83.3	15.4

[1]Clinical success defined as removal of stent for resolution of benign biliary stricture. FCSEMS: Fully covered self-expandable metal stents.

Anastomotic biliary strictures from orthostatic liver transplantation

Anastomotic biliary strictures (AS) are responsible for nearly 80% of biliary strictures after orthostatic liver transplantation (OLT)[48,49]. They typically occur within 1-2 mo of surgery, and are characterized as single BBS short in length. Existing strategies to treat AS associated BBS include balloon dilatation and endoscopic stenting[50]. While the use of MPS is the gold standard similar to the treatment post-cholecystectomy BBS, premature stent occlusion is a major limitation[51-53].

In the only meta-analysis to date comparing FCSEMS to plastic stents in the use of post-OLT AS, there was no significant difference in stricture resolution, complications, and recurrence[54]. However, FCSEMS use was associated with reduced treatment time (mean difference of -3.58 mo). Complications of pancreatitis and post-procedural pain were more common in FCSEMS. While prior studies have identified FCSEMS with stent migration rates as high as 33%, this adverse event could not be compared in the metanalysis because it was inconsistently reported across the 7 included studies [55,56].

Novel FCSEMS designs with antimigration properties have been developed to address shortcomings with stent migration. A retrospective multicenter Australian study evaluated the use of a novel FCSEMS in 36 patients for treatment of AS after OLT. Some of the patients within the cohort had failed the MPS approach[57]. The Niti-S FCSEMS biliary stent (Taewoong Medical Co Ltd., South Korea) used had an antimigration waist, short stent length, and a removable string for easy removal. Average duration of indwell treatment time was 3.8 mo. Stricture resolution was achieved in 100% of patients and all stents were removed without any difficulty. Only 2.8% of patients experienced stent migration. Nearly 75% of patients remained free of AS recurrence. Excellent clinical and technical success in this study with low rates of stent migration was a major breakthrough in the use of FCSEMS with anti-migration features for AS.

A more recent British retrospective study also evaluated the same type of antimigration FCSEMS (Taewoong Medical Co Ltd., South Korea) in a cohort of 62 patients[58]. Approximately 96% of patients had immediate stricture resolution after 12 wk indwell time. Furthermore, 72% of patients continued to maintain long-term resolution of the AS with a mean follow up period of 548 d. No stent migration occurred in any of the patients. Complication rates were low at 15%, and were primarily stent and procedure-related, such as pancreatitis, cholangitis and wire-guided perforation.

Overall, study findings using FCSEMS with new antimigration designs have shown promise in their application for post-OLT AS treatment. Larger cohort and randomized controlled studies should compare these novel FCSEMS to plastic stents. Alternative antimigration designs should be considered to maximize safe indwell time of stents.

CP

CP-associated BBS are a consequence of recurrent inflammation and subsequent fibrosis. Stricture formation occurs in up to 30% to 40% of cases[59]. Endoscopic intervention is focused on draining the main pancreatic duct to provide pancreatic decompression[60]. Historically, the strictures were treated *via* balloon dilation and endoscopic plastic stent placement, requiring up to 3 or more ERCP sessions[61].

Current recommendations from the Asia-Pacific guidelines recommend the use of FCSEMS or MPS for the endoscopic treatment of CP-associated BBS[62]. To date, the WallFlex Biliary RX Fully Covered Stent (Boston Scientific, United States) is the only FCSEMS approved by the United States Food and Drug Administration for treatment of BBS due to CP for indwell time up to 12 mo[63].

Existing retrospective and case series studies have supported the use of FCSEMS for the treatment of refractory pancreatic duct strictures: clinical and technical success rates have been as high as 90%-100% with a shorter indwell time compared to plastic stents[64-66]. The largest and longest prospective study to date investigated long-term outcomes after 10-12 mo indwell of a single FCSEMS for CP-associated BBS[67]. The cohort consisted of 118 patients, most of whom had failed previous treated with plastic stents. Patients were regularly followed for 5 years after FCSEMS removal. Approximately 80% of patients had stricture resolution at the time of stent removal. Nearly 62% of patients remained stent-free following 75 mo of FCSEMS placement. The success rate was relatively high compared to traditional outcomes with a single plastic stent, which faces issues of short occlusion time[68,69]. In fact, 78% of patients who had a resolved BBS post-indwell continued to remain stent free for 5 years. Of note, 23% of patients experienced serious adverse events that were mostly stent-related, including cholangitis, pancreatitis, and cholecystitis. This study was important in further demonstrating the single-use application of FCSEMS for CP BBS with long term stricture-free durability. This is notable in CP BBS, which notoriously has a poor response to endoscopic intervention with high risks of recurrence.

MALIGNANT BILIARY STRICTURES

Malignant biliary strictures (MBS) are most commonly caused by pancreatic cancer, but can also be caused by cholangiocarcinoma and metastatic disease[70,71]. Clinical presentation is consistent with biliary duct obstruction, including jaundice and cholestatic pattern of transaminase elevation. While MBS shares the same diagnostic evaluation as BBS with MRCP and/or ERCP modalities, tissue sampling will be the differentiating factor with findings of malignancy. Prognosis is poor 5-year survival rates for pancreatic cancer and cholangiocarcinoma are 8% and 10% respectively[72,73].

Non-hilar MBS

Among the 30% of MBS cases which are surgically resectable, endoscopic intervention may be considered to provide preoperative biliary decompression (PBD) (Figures 2A and 2B). PBD decompression is an area of great controversy because of the risks for serious complications, including pancreatitis and cholangitis. A landmark randomized control trial of 202 patients with a pancreatic head cancer compared the outcomes of preoperative biliary drainage for 5 wk to 6 wk preceding surgery to surgery alone. The biliary drainage group had significantly higher (74%) rates of complications than the surgery alone group (39%). Mortality or hospital length of stay did not differ between both groups[74]. Metanalyses investigating the benefits of preoperative biliary drainage has found similar results–length of hospital stay and mortality rate are comparable in preoperative biliary drainage and surgery alone groups[75,76]. Currently, preoperative biliary drainage is indicated for patients with MBS with concurrent severe symptomology (*i.e.*, severe pruritis, cholangitis), elevated bilirubin > 250 μmol/L, or patients undergoing neoadjuvant chemotherapy[77,78].

Nearly 70% of MBS are surgically unresectable at the initial presentation[79]. Endoscopic palliative stent placement for symptom relief is one approach to management. SEMS placement is preferred over plastic stents, especially when life expectancy is greater than 4-6 mo – SEMS have lower rates of stent dysfunction, reintervention, and cholangitis, and higher survival and stent patency rates[80-82].

Outcomes of FCSEMS compared to uncovered self-expandable metal stents (USEMS) in patients with unresectable MBS have also been extensively studied. A randomized controlled trial (RCT) of 749 patients with MBS investigated the outcomes of FCSMES *vs* USEMS placement. No significant difference was found between both groups for patency or survival rates[83]. Tumor ingrowth was higher in the USEMS group compared to the FCSEMS group. However, patients in the FCSEMS were more prone to stent migration and acute pancreatitis. Another recent RCT compared the use of FCSEMS to USEMS in 158 patients with nonresectable MBS. Surprisingly, median stent patency was lower for the FCSEMS (240 d) than the USEMS (541 d) group[84]. Consistent with the other study, FCSEMS had a significantly higher rate of migration,

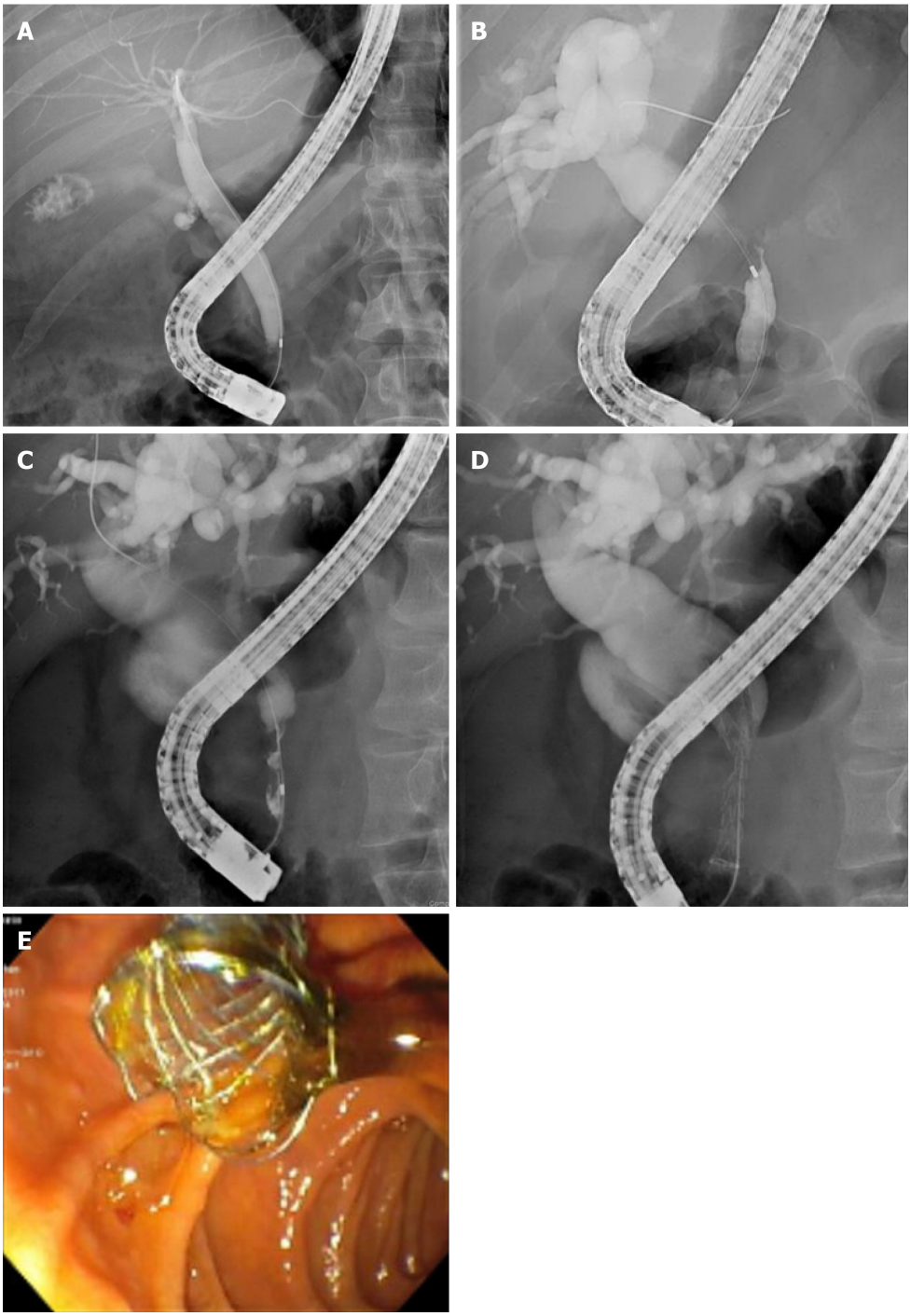


Figure 2 Endoscopic retrograde cholangiopancreatography showing cholangiocarcinoma in mid and distal common bile duct compared to normal anatomy. A: Normal anatomy demomonstrating patent cystic, common bile, and intrahepatic ducts; B: Mid common bile duct biliary stricture with dilated common bile duct and intrahepatic ducts; C: Distal common bile duct biliary stricture with dilated common bile duct and intrahepaptic ducts; D: Fully covered self-expandable metal stent (FCSEMS) placement in the common bile duct; E: Endoscopic view of FCSEMS placed in the distal common bile duct.

with no difference in overall survival between both groups[84]. To explain the stent patency finding in the FCSEMS group, the study proposed that occlusion may not be due to tumor ingrowth per se. The specific NitiS FCSEMS stent chosen for the study may promote an inflammatory reaction causing tissue hyperplasia. Thus, this finding may not be generalizable to all FCSEMS.

Metanalyses have also investigated this topic with mixed results, including studies with partly covered SEMS. A metanalysis involving 5 RCTs with 781 patients showed that CSEMS had superior patency rates compared with UCSEMS for MBS[85]. However, another metanalysis involving 9 RCTs with 1061 patients found no difference in stent patency between both groups[86].

Overall, there is no consensus regarding the superiority of FCSEMS or USEMS for palliative decompression of MBS. FCSEMS may be preferred for ease of removal or in circumstances where tumor ingrowth risk is high, such as in pancreatic cancer or cholangiocarcinoma. However, the problem of stent migration should be factored into the management decision. UCSEMS should be considered when there is short survival time or where likelihood of tumor in growth is low.

Hilar MBS

Malignant Hilar Strictures (MHS) are most commonly unresectable at presentation[87] (Figure 2C). MHS are classified by the Bismuth-Corlette classification, which accounts for the extent of involvement of the hilum and/or left or right main hepatic ducts[88]. The goal of management is to provide palliative decompression to improve quality of life, reduce jaundice, and decrease risk of cholangitis[89]. As with other MBS, metal stents are preferred over plastic ones because of superior patient survival, drainage rate, and stent patency[90]. Stent placement in the hilar region is technically difficult, and can be managed by unilateral or bilateral stenting (Figures 2D and 2E). Bilateral stenting can be approached *via* stent in stent or side by side approach[91].

A RCT involving 159 patients with malignant hilar biliary obstruction showed that patients with unilateral stenting (88.6%) had significantly higher rate of technical success than bilateral stenting (76.9%)[92]. Additionally, the bilateral stent group (16.6%) had significantly higher rates of early cholangitis. Study findings suggested that unilateral drainage was superior to bilateral stenting with lower risk of adverse complications. However, a more recent multicenter RCT found no significant difference in the technical success rate between bilateral (95.5%) and unilateral groups (100%). The median stent patency was higher in the bilateral group (252 d) than the unilateral (139 d), with fewer reinterventions needed for the bilateral group[93]. A metanalysis with 1292 patients found higher success rate in the unilateral group (97%) than the bilateral group (89%)[94]. Other retrospective studies have found comparable rates of technical success between both groups[95-98]. Overall, there is no clear consensus whether the unilateral or bilateral approach is superior. Unilateral approach may be preferred given the technical difficulty of bilateral placement.

Y-shaped bilateral SEMS devices have also been designed, which offers an effective and safe approach for unresectable MHS[98,99]. However, they are yet to be practiced routinely across endoscopic centers.

BILIARY LEAK

Biliary leak occurs due to traumatic injury or iatrogenic injury to the biliary duct from cholecystectomy, ERCP, liver resection, or orthostatic liver transplantation[100-103]. Biliary leak tends to present within 1 wk postoperatively, and are commonly located at the end of the cystic duct stump or duct of Luschka[104]. Minor bile duct leaks are characterized by low drain output and self-resolve without intervention[105]. In contrast, complex bile leaks are characterized by the persistent biliary discharge from an open T-tube or drain[106,107]. Standard of care involves plastic stent placement with or without sphincterotomy to reduce transpapillary pressure gradient[108]. As a result, bile drainage will preferentially drain into the duodenum and bypass the site of bile leak. Complex bile leaks commonly occur in anastomotic bile leaks following orthostatic liver transplantation or cholecystectomy, and may be refractory to plastic stent intervention[103,109]. FCSEMS have been investigated for use in these situations because of the larger expansile diameter and membrane coating, which theoretically provides an effective seal at the site of the leak (Figures 3A and 3B).

In a retrospective study investigating patients with complex post-OLT bile leaks treated with CSEMS placement, successful deployment and long-term leakage control was achieved using FCSEMS with fins (77.8% of patients) and FCSEMS with flared ends (70%)[110]. A concerning finding was that large number of patients who received FCSEMS with fins (35%) experienced post-stent removal biliary strictures. This likely occurred due to stent-induced biliary duct compression and ischemia, which highlights one of the major risks of FCSEMS use for biliary leak.

Another US-based study evaluated the use of Viabil FCSEMS (Gore, United States) placement for 5 patients with bile leaks[111]. All patients had successfully sealed bile leaks confirmed with cholangiogram. Most patients did not have any complications. However, 1 patient developed a hepatic abscess and sepsis. Another patient had stent occlusion after being lost to followup for 8.5 mo, but post-ERCP removal of the occluded stent revealed a sealed bile leak on cholangiogram.

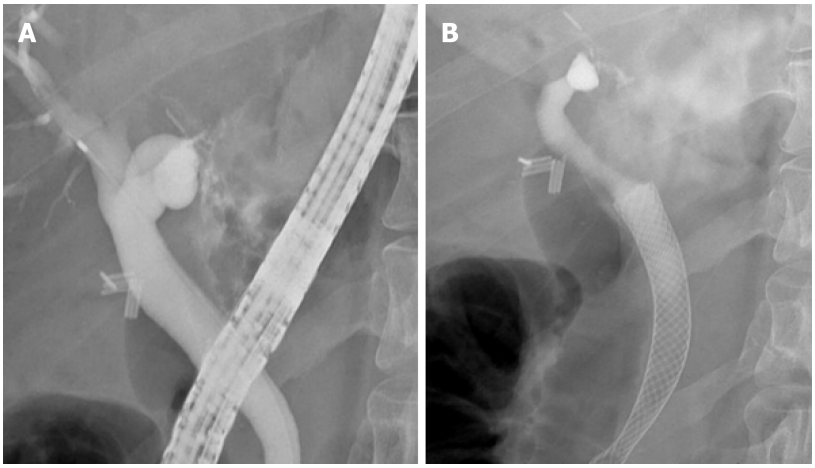


Figure 3 Endoscopic treatment of biliary leak after donor liver transplantation. A: Extravasation of contrast at site of biliary leak; B: Resolution of biliary leak after placement of a fully covered self-expandable metal stent.

A pilot study consisted of 16 patients who underwent CSEMS placement for a biliary leak. These patients either failed to respond to conventional ERCP or had severe comorbidities that prevented multiple procedures[112]. Nearly all (15/16 patients) of the patients had complete resolution of the leak confirmed with cholangiogram. Only 1 proximal and distal migration complication was documented.

In summary, existing studies have demonstrated proof of successful bile leak closure using FCSEMS (Table 4). However, complications, including stent migration and post-removal strictures, make the widespread use of FCSEMS for complex biliary leaks debatable. Future studies should investigate this topic using larger cohort sizes.

POST-SPHINCTEROTOMY BLEEDING

Biliary endoscopic sphincterotomy (ES) refers to the resection of the biliary sphincter and intraduodenal segment of the common bile duct. It is an essential procedure for ERCP in the treatment for a variety of biliary and papillary disease, including choledocholithiasis, bile leak, and biliary strictures[113]. Post-endoscopic bleeding is a major complication of biliary sphincterotomy[114]. Most post-ES bleeds are small and resolve spontaneously[115]. Other cases present with significant bleeding requiring blood transfusion support and urgent endoscopic intervention. While existing methods include injection, balloon tamponade, and mechanical (*e.g.*, embolization) approaches, endoscopic hemostasis can also be achieved by tamponade effect *via* FCSEMS deployment[113].

The largest retrospective study to date evaluated 67 patients with post-ES bleeding, and compared the use of FCSEMS treatment *vs* non-FCSEMS treatment (*e.g.*, balloon tamponade, sclerotherapy, epinephrine injection, thermal cautery or clip placement) [116]. At 72 h post intervention, the study found that the FCSEMS group (0.66 g/dL) had a significantly lower bleeding rate than the non-FCSEMS group (1.98 g/dL) even though the proportion of patients determined to be at high risk for post-ES bleeding was higher in the FCSEMS treatment group (40%) *vs* non-FCSEMS treatment group (9%). All patients in the FCSEMS group achieved hemostasis, and no adverse events were documented. The study findings supported the use of FCSEMS in patients with severe or immediate bleeding not responsive to initial endoscopic treatment.

Smaller-sized retrospective and case studies have demonstrated similar success with complete hemostasis using FCSEMS for difficult-control post-ES bleeding[117,118]. No studies to date have investigated the use of FCSEMS as primary post-ES treatment therapy. Larger perspective and randomized controlled studies should be conducted to evaluate the optimal timing for FCSEMS removal after achieving hemostasis.

COMPLICATIONS

Stent migration is the most frequent complication of FCSEMS, which occurs in 20%-40% of cases[119,120]. Proximal stent migration refers to FCSEMS migration into the

Table 4 Comparison of study outcomes usng fully covered self-expanding metal stents for treatment of biliary leak

Ref.	Methods	Patients	Type, duration of stent placement (mo)	Follow-up time (mo)	Clinical success rate[1] (%)
Martins *et al* [110]	Restrospective, single center	31	PCSEMS (3), FCSEMS with fins (3.3), FCSEMS with flare ends (3)	PCSEMS (44), FCSEMS with fins (27), FCSEMS with flare ends (6.6)	PCSEMS (100), FCSEMS with fins (77.8), FCSEMS with flare ends (70)
Lalezari *et al*[111]	Retrospective, single center	5	FCSEMS with fins (3)	26	100
Kahaleh *et al*[112]	Retrospective single, center	16	FCSEMS (3)	9	94

[1]Clinical success rate defined as resolution of biliary leak confirmed with imaging. PCSEMS: Partially covered self-expandable metal stents; FCSEMS: Fully covered self-expandable metal stents.

biliary duct, while distal stent migration refers to migration to the duodenum or bowel. Endoscopic intervention is needed to remove and replace the displaced stent. A prospective study comparing the temporary use of FCSEMS with unflared ends to flared ends in patients with CP-related BBS revealed the migration rate was 100% for unflared FCSEMS compared to 40% of flared FCSEMS[121]. FCSEMS designed with anchoring flaps or flared ends are preferred as they reduce the risk of migration. A multicenter, prospective study of compared the antimigration effects and efficacy of FCSEMS with an anchoring flap to a flared end at the proximal end. After a median followup time of 6 mo, none of the patients in the anchoring flap had stent migration compared to 33% of patients in the flared end, suggesting that the anchoring flap design was superior to the flared end design. Both types of FCSEMS were able to be removed in all of the patients[122]. Overall, new stent designs including anchoring flaps, flared ends, and additional anchoring plastic stents have been validated in studies to reduce migration risk[123-125].

Cholecystitis is another complication associated with FCSEMS use most commonly in MBS. The pathophysiological mechanism is thought to be obstruction of biliary flow if the cystic duct orifice is obstructed by the synthetic covering of the FCSEMS[126, 127].

Stent occlusion may occur from tumor ingrowth, tissue overgrowth, or sludge, predisposing to the development of cholangitis[23-26]. However, time to and rate of occlusion is considerably less compared to plastic stents[128]. Factors such as FCSEMS location and treatment indication dictate different levels of risk[129].

CONCLUSION

FCSEMS represents the latest development of SEMS used by endoscopists treat a variety of benign and malignant biliary pathology, including biliary leak, post-sphincterotomy bleeding, and strictures. A chemical covering reduces the risk of tissue hyperplasia and tumor ingrowth, prolonging stent patency. The studies examined in our review have shown that FCSEMS can be clinically effective for a variety of endoscopic applications. However, FCSEMS commonly face problems of stent migration, which can be addressed with modifications including flared ends and anchoring flaps. Future areas of research will continue to expand the interventional applications using FCSEMS, and design new modifications to reduce complications.

REFERENCES

1 **Mangiavillano B**, Pagano N, Baron TH, Arena M, Iabichino G, Consolo P, Opocher E, Luigiano C. Biliary and pancreatic stenting: Devices and insertion techniques in therapeutic endoscopic retrograde cholangiopancreatography and endoscopic ultrasonography. *World J Gastrointest Endosc* 2016; **8**: 143-156 [PMID: 26862364 DOI: 10.4253/wjge.v8.i3.143]

2 **Brandabur JJ**, Kozarek RA, Ball TJ, Hofer BO, Ryan JA Jr, Traverso LW, Freeny PC, Lewis GP. Nonoperative versus operative treatment of obstructive jaundice in pancreatic cancer: cost and survival analysis. *Am J Gastroenterol* 1988; **83**: 1132-1139 [PMID: 2458678]

3 **Raikar GV**, Melin MM, Ress A, Lettieri SZ, Poterucha JJ, Nagorney DM, Donohue JH. Cost-effective analysis of surgical palliation versus endoscopic stenting in the management of

unresectable pancreatic cancer. *Ann Surg Oncol* 1996; **3**: 470-475 [PMID: 8876889 DOI: 10.1007/bf02305765]

4 **Luman W**, Cull A, Palmer KR. Quality of life in patients stented for malignant biliary obstructions. *Eur J Gastroenterol Hepatol* 1997; **9**: 481-484 [PMID: 9187881 DOI: 10.1097/00042737-199705000-00013]

5 **Obuch JC**, Wagh MS. Endoscopic therapy for benign biliary strictures: evaluation of metal *vs.* plastic biliary stents. *Hepatobiliary Surg Nutr* 2017; **6**: 268-271 [PMID: 28848751 DOI: 10.21037/hbsn.2017.05.04]

6 **Yeoh KG**, Zimmerman MJ, Cunningham JT, Cotton PB. Comparative costs of metal versus plastic biliary stent strategies for malignant obstructive jaundice by decision analysis. *Gastrointest Endosc* 1999; **49**: 466-471 [PMID: 10202060 DOI: 10.1016/s0016-5107(99)70044-1]

7 **ASGE Technology Assessment Committee**, Pfau PR, Pleskow DK, Banerjee S, Barth BA, Bhat YM, Desilets DJ, Gottlieb KT, Maple JT, Siddiqui UD, Tokar JL, Wang A, Song LM, Rodriguez SA. Pancreatic and biliary stents. *Gastrointest Endosc* 2013; **77**: 319-327 [PMID: 23410693 DOI: 10.1016/j.gie.2012.09.026]

8 **Vaishnavi C**, Samanta J, Kochhar R. Characterization of biofilms in biliary stents and potential factors involved in occlusion. *World J Gastroenterol* 2018; **24**: 112-123 [PMID: 29358888 DOI: 10.3748/wjg.v24.i1.112]

9 **Sung JJ**. Bacterial biofilm and clogging of biliary stents. *J Ind Microbiol* 1995; **15**: 152-155 [PMID: 8519471 DOI: 10.1007/BF01569819]

10 **Lee TH**, Lee SJ, Moon JH, Park SH. Technical tips and issues of biliary stenting, focusing on malignant hilar obstruction. *Minerva Gastroenterol Dietol* 2014; **60**: 135-149 [PMID: 24780948]

11 **Speer AG**, Cotton PB, MacRae KD. Endoscopic management of malignant biliary obstruction: stents of 10 French gauge are preferable to stents of 8 French gauge. *Gastrointest Endosc* 1988; **34**: 412-417 [PMID: 2460394 DOI: 10.1016/s0016-5107(88)71407-8]

12 **Kadakia SC**, Starnes E. Comparison of 10 French gauge stent with 11.5 French gauge stent in patients with biliary tract diseases. *Gastrointest Endosc* 1992; **38**: 454-459 [PMID: 1511821 DOI: 10.1016/s0016-5107(92)70476-3]

13 **Donelli G**, Guaglianone E, Di Rosa R, Fiocca F, Basoli A. Plastic biliary stent occlusion: factors involved and possible preventive approaches. *Clin Med Res* 2007; **5**: 53-60 [PMID: 17456835 DOI: 10.3121/cmr.2007.683]

14 **Huibregtse K**, Cheng J, Coene PP, Fockens P, Tytgat GN. Endoscopic placement of expandable metal stents for biliary strictures--a preliminary report on experience with 33 patients. *Endoscopy* 1989; **21**: 280-282 [PMID: 2482170 DOI: 10.1055/s-2007-1012969]

15 **Neuhaus H**, Hagenmüller F, Classen M. Self-expanding biliary stents: preliminary clinical experience. *Endoscopy* 1989; **21**: 225-228 [PMID: 2792016 DOI: 10.1055/s-2007-1012954]

16 **Irving JD**, Adam A, Dick R, Dondelinger RF, Lunderquist A, Roche A. Gianturco expandable metallic biliary stents: results of a European clinical trial. *Radiology* 1989; **172**: 321-326 [PMID: 2664861 DOI: 10.1148/radiology.172.2.2664861]

17 **Chun HJ**, Kim ES, Hyun JJ, Kwon YD, Keum B, Kim CD. Gastrointestinal and biliary stents. *J Gastroenterol Hepatol* 2010; **25**: 234-243 [PMID: 20136988 DOI: 10.1111/j.1440-1746.2009.06152.x]

18 **Davids PH**, Groen AK, Rauws EA, Tytgat GN, Huibregtse K. Randomised trial of self-expanding metal stents versus polyethylene stents for distal malignant biliary obstruction. *Lancet* 1992; **340**: 1488-1492 [PMID: 1281903 DOI: 10.1016/0140-6736(92)92752-2]

19 **Knyrim K**, Wagner HJ, Pausch J, Vakil N. A prospective, randomized, controlled trial of metal stents for malignant obstruction of the common bile duct. *Endoscopy* 1993; **25**: 207-212 [PMID: 8519239 DOI: 10.1055/s-2007-1010294]

20 **Kaassis M**, Boyer J, Dumas R, Ponchon T, Coumaros D, Delcenserie R, Canard JM, Fritsch J, Rey JF, Burtin P. Plastic or metal stents for malignant stricture of the common bile duct? *Gastrointest Endosc* 2003; **57**: 178-182 [PMID: 12556780 DOI: 10.1067/mge.2003.66]

21 **Prat F**, Chapat O, Ducot B, Ponchon T, Pelletier G, Fritsch J, Choury AD, Buffet C. A randomized trial of endoscopic drainage methods for inoperable malignant strictures of the common bile duct. *Gastrointest Endosc* 1998; **47**: 1-7 [PMID: 9468416 DOI: 10.1016/s0016-5107(98)70291-3]

22 **Wagner HJ**, Knyrim K, Vakil N, Klose KJ. Plastic endoprostheses versus metal stents in the palliative treatment of malignant hilar biliary obstruction. A prospective and randomized trial. *Endoscopy* 1993; **25**: 213-218 [PMID: 7686100 DOI: 10.1055/s-2007-1010295]

23 **Lee MJ**, Dawson SL, Mueller PR, Krebs TL, Saini S, Hahn PF. Palliation of malignant bile duct obstruction with metallic biliary endoprostheses: technique, results, and complications. *J Vasc Interv Radiol* 1992; **3**: 665-671 [PMID: 1280177 DOI: 10.1016/s1051-0443(92)72920-0]

24 **Hausegger KA**, Kleinert R, Lammer J, Klein GE, Flückiger F. Malignant biliary obstruction: histologic findings after treatment with self-expandable stents. *Radiology* 1992; **185**: 461-464 [PMID: 1410354 DOI: 10.1148/radiology.185.2.1410354]

25 **Silvis SE**, Sievert CE Jr, Vennes JA, Abeyta BK, Brennecke LH. Comparison of covered versus uncovered wire mesh stents in the canine biliary tract. *Gastrointest Endosc* 1994; **40**: 17-21 [PMID: 8163131 DOI: 10.1016/s0016-5107(94)70004-4]

26 **Levy MJ**, Baron TH, Gostout CJ, Petersen BT, Farnell MB. Palliation of malignant extrahepatic biliary obstruction with plastic versus expandable metal stents: An evidence-based approach. *Clin Gastroenterol Hepatol* 2004; **2**: 273-285 [PMID: 15067620 DOI: 10.1016/s1542-3565(04)00055-2]

27 **Nam HS**, Kang DH. Current Status of Biliary Metal Stents. *Clin Endosc* 2016; **49**: 124-130 [PMID: 26911896 DOI: 10.5946/ce.2016.023]

28 **Tham TC**, Carr-Locke DL, Vandervoort J, Wong RC, Lichtenstein DR, Van Dam J, Ruymann F, Chow S, Bosco JJ, Qaseem T, Howell D, Pleskow D, Vannerman W, Libby ED. Management of occluded biliary Wallstents. *Gut* 1998; **42**: 703-707 [PMID: 9659168 DOI: 10.1136/gut.42.5.703]

29 **Miller G**, Yim D, Macari M, Harris M, Shamamian P. Retroperitoneal perforation of the duodenum from biliary stent erosion. *Curr Surg* 2005; **62**: 512-515 [PMID: 16125609 DOI: 10.1016/j.cursur.2005.03.011]

30 **Seo DW**, Sherman S, Dua KS, Slivka A, Roy A, Costamagna G, Deviere J, Peetermans J, Rousseau M, Nakai Y, Isayama H, Kozarek R; Biliary SEMS During Neoadjuvant Therapy Study Group. Covered and uncovered biliary metal stents provide similar relief of biliary obstruction during neoadjuvant therapy in pancreatic cancer: a randomized trial. *Gastrointest Endosc* 2019; **90**: 602-612.e4 [PMID: 31276674 DOI: 10.1016/j.gie.2019.06.032]

31 **Familiari P**, Bulajic M, Mutignani M, Lee LS, Spera G, Spada C, Tringali A, Costamagna G. Endoscopic removal of malfunctioning biliary self-expandable metallic stents. *Gastrointest Endosc* 2005; **62**: 903-910 [PMID: 16301035 DOI: 10.1016/j.gie.2005.08.051]

32 **Shimada H**, Endo I, Shimada K, Matsuyama R, Kobayashi N, Kubota K. The current diagnosis and treatment of benign biliary stricture. *Surg Today* 2012; **42**: 1143-1153 [PMID: 23001533 DOI: 10.1007/s00595-012-0333-3]

33 **Ma MX**, Jayasekeran V, Chong AK. Benign biliary strictures: prevalence, impact, and management strategies. *Clin Exp Gastroenterol* 2019; **12**: 83-92 [PMID: 30858721 DOI: 10.2147/CEG.S165016]

34 **Costamagna G**, Boškoski I. Current treatment of benign biliary strictures. *Ann Gastroenterol* 2013; **26**: 37-40 [PMID: 24714594]

35 **Shanbhogue AK**, Tirumani SH, Prasad SR, Fasih N, McInnes M. Benign biliary strictures: a current comprehensive clinical and imaging review. *AJR Am J Roentgenol* 2011; **197**: W295-W306 [PMID: 21785056 DOI: 10.2214/AJR.10.6002]

36 **Kahaleh M**, Brijbassie A, Sethi A, Degaetani M, Poneros JM, Loren DE, Kowalski TE, Sejpal DV, Patel S, Rosenkranz L, McNamara KN, Raijman I, Talreja JP, Gaidhane M, Sauer BG, Stevens PD. Multicenter trial evaluating the use of covered self-expanding metal stents in benign biliary strictures: time to revisit our therapeutic options? *J Clin Gastroenterol* 2013; **47**: 695-699 [PMID: 23442836 DOI: 10.1097/MCG.0b013e31827fd311]

37 **Wagh MS**, Chavalitdhamrong D, Moezardalan K, Chauhan SS, Gupte AR, Nosler MJ, Forsmark CE, Draganov PV. Effectiveness and safety of endoscopic treatment of benign biliary strictures using a new fully covered self expandable metal stent. *Diagn Ther Endosc* 2013; **2013**: 183513 [PMID: 23956613 DOI: 10.1155/2013/183513]

38 **Cahen DL**, Rauws EA, Gouma DJ, Fockens P, Bruno MJ. Removable fully covered self-expandable metal stents in the treatment of common bile duct strictures due to chronic pancreatitis: a case series. *Endoscopy* 2008; **40**: 697-700 [PMID: 18704837 DOI: 10.1055/s-2008-1077353]

39 **Machado NO**. Biliary complications postlaparoscopic cholecystectomy: mechanism, preventive measures, and approach to management: a review. *Diagn Ther Endosc* 2011; **2011**: 967017 [PMID: 21822368 DOI: 10.1155/2011/967017]

40 **Lillemoe KD**, Melton GB, Cameron JL, Pitt HA, Campbell KA, Talamini MA, Sauter PA, Coleman J, Yeo CJ. Postoperative bile duct strictures: management and outcome in the 1990s. *Ann Surg* 2000; **232**: 430-441 [PMID: 10973393 DOI: 10.1097/00000658-200009000-00015]

41 **Costamagna G**, Tringali A, Perri V, Familiari P, Boškoski I, Barbaro F, Landi R. Endotherapy of postcholecystectomy biliary strictures with multiple plastic stents: long-term results in a large cohort of patients. *Gastrointest Endosc* 2020; **91**: 81-89 [PMID: 31175873 DOI: 10.1016/j.gie.2019.05.042]

42 **Bergman JJ**, Burgemeister L, Bruno MJ, Rauws EA, Gouma DJ, Tytgat GN, Huibregtse K. Long-term follow-up after biliary stent placement for postoperative bile duct stenosis. *Gastrointest Endosc* 2001; **54**: 154-161 [PMID: 11474383 DOI: 10.1067/mge.2001.116455]

43 **Costamagna G**, Tringali A, Mutignani M, Perri V, Spada C, Pandolfi M, Galasso D. Endotherapy of postoperative biliary strictures with multiple stents: results after more than 10 years of follow-up. *Gastrointest Endosc* 2010; **72**: 551-557 [PMID: 20630514 DOI: 10.1016/j.gie.2010.04.052]

44 **Chaput U**, Vienne A, Audureau E, Bauret P, Bichard P, Coumaros D, Napoléon B, Ponchon T, Duchmann JC, Laugier R, Lamouliatte H, Védrenne B, Gaudric M, Chaussade S, Robin F, Leblanc S, Prat F. Temporary placement of fully covered self-expandable metal stents for the treatment of benign biliary strictures. *United European Gastroenterol J* 2016; **4**: 403-412 [PMID: 27403307 DOI: 10.1177/2050640615606550]

45 **García-Cano J**. Use of fully covered self-expanding metal stents in benign biliary diseases. *World J Gastrointest Endosc* 2012; **4**: 142-147 [PMID: 22523615 DOI: 10.4253/wjge.v4.i4.142]

46 **Wu J**, Zhou DX, Wang TT, Gao DJ, Hu B. A New Fully Covered Self-Expandable Metal Stent for the Treatment of Postsurgical Benign Biliary Strictures. *Dig Dis Sci* 2017; **62**: 2550-2557 [PMID: 28776138 DOI: 10.1007/s10620-017-4698-4]

47 **Tringali A**, Reddy DN, Ponchon T, Neuhaus H, Lladó FG, Navarrete C, Bruno MJ, Kortan PP, Lakhtakia S, Peetermans J, Rousseau M, Carr-Locke D, Devière J, Costamagna G; Benign Biliary Stenoses Working Group. Treatment of post-cholecystectomy biliary strictures with fully-covered self-expanding metal stents - results after 5 years of follow-up. *BMC Gastroenterol* 2019; **19**: 214 [PMID: 31830897 DOI: 10.1186/s12876-019-1129-3]

48 **Balderramo D**, Navasa M, Cardenas A. Current management of biliary complications after liver

transplantation: emphasis on endoscopic therapy. *Gastroenterol Hepatol* 2011; **34**: 107-115 [PMID: 20692731 DOI: 10.1016/j.gastrohep.2010.05.008]

49 **Villa NA**, Harrison ME. Management of Biliary Strictures After Liver Transplantation. *Gastroenterol Hepatol (N Y)* 2015; **11**: 316-328 [PMID: 27482175]

50 **Ryu CH**, Lee SK. Biliary strictures after liver transplantation. *Gut Liver* 2011; **5**: 133-142 [PMID: 21814591 DOI: 10.5009/gnl.2011.5.2.133]

51 **Tabibian JH**, Asham EH, Han S, Saab S, Tong MJ, Goldstein L, Busuttil RW, Durazo FA. Endoscopic treatment of postorthotopic liver transplantation anastomotic biliary strictures with maximal stent therapy (with video). *Gastrointest Endosc* 2010; **71**: 505-512 [PMID: 20189508 DOI: 10.1016/j.gie.2009.10.023]

52 **Rerknimitr R**, Sherman S, Fogel EL, Kalayci C, Lumeng L, Chalasani N, Kwo P, Lehman GA. Biliary tract complications after orthotopic liver transplantation with choledochocholedochostomy anastomosis: endoscopic findings and results of therapy. *Gastrointest Endosc* 2002; **55**: 224-231 [PMID: 11818927 DOI: 10.1067/mge.2002.120813]

53 **Holt AP**, Thorburn D, Mirza D, Gunson B, Wong T, Haydon G. A prospective study of standardized nonsurgical therapy in the management of biliary anastomotic strictures complicating liver transplantation. *Transplantation* 2007; **84**: 857-863 [PMID: 17984838 DOI: 10.1097/01.tp.0000282805.33658.ce]

54 **Facciorusso A**, Rosca EC, Ashimi A, Ugoeze KC, Pathak U, Infante V, Muscatiello N. Management of anastomotic biliary stricture after liver transplantation: metal versus plastic stent. *Ann Gastroenterol* 2018; **31**: 728-734 [PMID: 30386124 DOI: 10.20524/aog.2018.0297]

55 **Tarantino I**, Mangiavillano B, Di Mitri R, Barresi L, Mocciaro F, Granata A, Masci E, Curcio G, Di Pisa M, Marino A, Traina M. Fully covered self-expandable metallic stents in benign biliary strictures: a multicenter study on efficacy and safety. *Endoscopy* 2012; **44**: 923-927 [PMID: 22893134 DOI: 10.1055/s-0032-1310011]

56 **Cantù P**, Tarantino I, Baldan A, Mutignani M, Tringali A, Lombardi G, Cerofolini A, Di Sario A, Catalano G, Bertani H, Ghinolfi D, Boarino V, Masci E, Bulajic M, Pisani A, Fantin A, Ligresti D, Barresi L, Traina M, Ravelli P, Forti E, Barbaro F, Costamagna G, Rodella L, Maroni L, Salizzoni M, Conigliaro R, Filipponi F, Merighi A, Staiano T, Monteleone M, Mazzaferro V, Zucchi E, Zilli M, Nadal E, Rosa R, Santi G, Parzanese I, De Carlis L, Donato MF, Lampertico P, Maggi U, Caccamo L, Rossi G, Vecchi M, Penagini R. Endo-therapies for biliary duct-to-duct anastomotic stricture after liver transplantation: Outcomes of a nationwide survey. *Liver Int* 2019; **39**: 1355-1362 [PMID: 30500104 DOI: 10.1111/liv.14010]

57 **Aepli P**, St John A, Gupta S, Hourigan LF, Vaughan R, Efthymiou M, Kaffes A. Success and complications of an intra-ductal fully covered self-expanding metal stent (ID-FCSEMS) to treat anastomotic biliary strictures (AS) after orthotopic liver transplantation (OLT). *Surg Endosc* 2017; **31**: 1558-1563 [PMID: 27572066 DOI: 10.1007/s00464-016-5138-9]

58 **Warner B**, Harrison P, Farman M, Devlin J, Reffitt D, El-Sherif Y, Khorsandi SE, Prachalias A, Cerisuelo MC, Menon K, Jassem W, Srinivasan P, Vilca-Melendez H, Heneghan M, Heaton N, Joshi D. A unique type of fully covered metal stent for the management of post liver transplant biliary anastomotic strictures. *BMC Gastroenterol* 2020; **20**: 329 [PMID: 33028218 DOI: 10.1186/s12876-020-01479-6]

59 **Wilson C**, Auld CD, Schlinkert R, Hasan AH, Imrie CW, MacSween RN, Carter DC. Hepatobiliary complications in chronic pancreatitis. *Gut* 1989; **30**: 520-527 [PMID: 2714685 DOI: 10.1136/gut.30.4.520]

60 **Mangiavillano B**, Pagano N, Baron TH, Luigiano C. Outcome of stenting in biliary and pancreatic benign and malignant diseases: A comprehensive review. *World J Gastroenterol* 2015; **21**: 9038-9054 [PMID: 26290631 DOI: 10.3748/wjg.v21.i30.9038]

61 **Arslanlar S**, Jain R. Benign biliary strictures related to chronic pancreatitis: balloons, stents, or surgery. *Curr Treat Options Gastroenterol* 2007; **10**: 369-375 [PMID: 17897575 DOI: 10.1007/s11938-007-0037-8]

62 **Hu B**, Sun B, Cai Q, Wong Lau JY, Ma S, Itoi T, Moon JH, Yasuda I, Zhang X, Wang HP, Ryozawa S, Rerknimitr R, Li W, Kutsumi H, Lakhtakia S, Shiomi H, Ji M, Li X, Qian D, Yang Z, Zheng X. Asia-Pacific consensus guidelines for endoscopic management of benign biliary strictures. *Gastrointest Endosc* 2017; **86**: 44-58 [PMID: 28283322 DOI: 10.1016/j.gie.2017.02.031]

63 **Poley JW**, Ponchon T, Puespoek A, Bruno M, Roy A, Peetermans J, Rousseau M, Lépilliez V, Dolak W, Tringali A, Blero D, Carr-Locke D, Costamagna G, Devière J; Benign Biliary Stenoses Working Group. Fully covered self-expanding metal stents for benign biliary stricture after orthotopic liver transplant: 5-year outcomes. *Gastrointest Endosc* 2020; **92**: 1216-1224 [PMID: 32417298 DOI: 10.1016/j.gie.2020.04.078]

64 **Sharaiha RZ**, Novikov A, Weaver K, Marfatia P, Buscaglia JM, DiMaio CJ, Diehl D, Gabr MM, Gaidhane M, Siddiqui A, Kahaleh M. Fully covered self-expanding metal stents for refractory pancreatic duct strictures in symptomatic chronic pancreatitis, US experience. *Endosc Int Open* 2019; **7**: E1419-E1423 [PMID: 31673613 DOI: 10.1055/a-0858-2169]

65 **Moon SH**, Kim MH, Park DH, Song TJ, Eum J, Lee SS, Seo DW, Lee SK. Modified fully covered self-expandable metal stents with antimigration features for benign pancreatic-duct strictures in advanced chronic pancreatitis, with a focus on the safety profile and reducing migration. *Gastrointest Endosc* 2010; **72**: 86-91 [PMID: 20493483 DOI: 10.1016/j.gie.2010.01.063]

66 **Park DH**, Kim MH, Moon SH, Lee SS, Seo DW, Lee SK. Feasibility and safety of placement of a

newly designed, fully covered self-expandable metal stent for refractory benign pancreatic ductal strictures: a pilot study (with video). *Gastrointest Endosc* 2008; **68**: 1182-1189 [PMID: 19028228 DOI: 10.1016/j.gie.2008.07.027]

67 **Lakhtakia S**, Reddy N, Dolak W, Ponchon T, Bruno MJ, Bourke MJ, Neuhaus H, Roy A, González-Huix Lladó F, Kortan PP, Peetermans J, Rousseau M, Costamagna G, Devière J; Benign Biliary Stenoses Working Group. Long-term outcomes after temporary placement of a self-expanding fully covered metal stent for benign biliary strictures secondary to chronic pancreatitis. *Gastrointest Endosc* 2020; **91**: 361-369.e3 [PMID: 31494135 DOI: 10.1016/j.gie.2019.08.037]

68 **Kahl S**, Zimmermann S, Genz I, Glasbrenner B, Pross M, Schulz HU, Mc Namara D, Schmidt U, Malfertheiner P. Risk factors for failure of endoscopic stenting of biliary strictures in chronic pancreatitis: a prospective follow-up study. *Am J Gastroenterol* 2003; **98**: 2448-2453 [PMID: 14638347 DOI: 10.1111/j.1572-0241.2003.08667.x]

69 **Smits ME**, Rauws EA, van Gulik TM, Gouma DJ, Tytgat GN, Huibregtse K. Long-term results of endoscopic stenting and surgical drainage for biliary stricture due to chronic pancreatitis. *Br J Surg* 1996; **83**: 764-768 [PMID: 8696734 DOI: 10.1002/bjs.1800830612]

70 **Dorrell R**, Pawa S, Pawa R. Endoscopic Management of Malignant Biliary Stricture. *Diagnostics (Basel)* 2020; **10** [PMID: 32532018 DOI: 10.3390/diagnostics10060390]

71 **Kapoor BS**, Mauri G, Lorenz JM. Management of Biliary Strictures: State-of-the-Art Review. *Radiology* 2018; **289**: 590-603 [PMID: 30351249 DOI: 10.1148/radiol.2018172424]

72 **Goodman MT**, Yamamoto J. Descriptive study of gallbladder, extrahepatic bile duct, and ampullary cancers in the United States, 1997-2002. *Cancer Causes Control* 2007; **18**: 415-422 [PMID: 17264972 DOI: 10.1007/s10552-006-0109-4]

73 **Pinter M**, Hucke F, Zielonke N, Waldhör T, Trauner M, Peck-Radosavljevic M, Sieghart W. Incidence and mortality trends for biliary tract cancers in Austria. *Liver Int* 2014; **34**: 1102-1108 [PMID: 24119058 DOI: 10.1111/liv.12325]

74 **van der Gaag NA**, Rauws EA, van Eijck CH, Bruno MJ, van der Harst E, Kubben FJ, Gerritsen JJ, Greve JW, Gerhards MF, de Hingh IH, Klinkenbijl JH, Nio CY, de Castro SM, Busch OR, van Gulik TM, Bossuyt PM, Gouma DJ. Preoperative biliary drainage for cancer of the head of the pancreas. *N Engl J Med* 2010; **362**: 129-137 [PMID: 20071702 DOI: 10.1056/NEJMoa0903230]

75 **Moole H**, Bechtold M, Puli SR. Efficacy of preoperative biliary drainage in malignant obstructive jaundice: a meta-analysis and systematic review. *World J Surg Oncol* 2016; **14**: 182 [PMID: 27400651 DOI: 10.1186/s12957-016-0933-2]

76 **Sewnath ME**, Karsten TM, Prins MH, Rauws EJ, Obertop H, Gouma DJ. A meta-analysis on the efficacy of preoperative biliary drainage for tumors causing obstructive jaundice. *Ann Surg* 2002; **236**: 17-27 [PMID: 12131081 DOI: 10.1097/00000658-200207000-00005]

77 **Dumonceau JM**, Tringali A, Papanikolaou IS, Blero D, Mangiavillano B, Schmidt A, Vanbiervliet G, Costamagna G, Devière J, García-Cano J, Gyökeres T, Hassan C, Prat F, Siersema PD, van Hooft JE. Endoscopic biliary stenting: indications, choice of stents, and results: European Society of Gastrointestinal Endoscopy (ESGE) Clinical Guideline - Updated October 2017. *Endoscopy* 2018; **50**: 910-930 [PMID: 30086596 DOI: 10.1055/a-0659-9864]

78 **ASGE Standards of Practice Committee**, Eloubeidi MA, Decker GA, Chandrasekhara V, Chathadi KV, Early DS, Evans JA, Fanelli RD, Fisher DA, Foley K, Hwang JH, Jue TL, Lightdale JR, Pasha SF, Saltzman JR, Sharaf R, Shergill AK, Cash BD, DeWitt JM. The role of endoscopy in the evaluation and management of patients with solid pancreatic neoplasia. *Gastrointest Endosc* 2016; **83**: 17-28 [PMID: 26706297 DOI: 10.1016/j.gie.2015.09.009]

79 **Fernandez Y Viesca M**, Arvanitakis M. Early Diagnosis And Management Of Malignant Distal Biliary Obstruction: A Review On Current Recommendations And Guidelines. *Clin Exp Gastroenterol* 2019; **12**: 415-432 [PMID: 31807048 DOI: 10.2147/CEG.S195714]

80 **Zorrón Pu L**, de Moura EG, Bernardo WM, Baracat FI, Mendonça EQ, Kondo A, Luz GO, Furuya Júnior CK, Artifon EL. Endoscopic stenting for inoperable malignant biliary obstruction: A systematic review and meta-analysis. *World J Gastroenterol* 2015; **21**: 13374-13385 [PMID: 26715823 DOI: 10.3748/wjg.v21.i47.13374]

81 **Moole H**, Jaeger A, Cashman M, Volmar FH, Dhillon S, Bechtold ML, Puli SR. Are self-expandable metal stents superior to plastic stents in palliating malignant distal biliary strictures? *Med J Armed Forces India* 2017; **73**: 42-48 [PMID: 28123244 DOI: 10.1016/j.mjafi.2016.08.014]

82 **Yuan TW**, Liu HQ, Wang SB, Cao J. Comparison of plastic stents with self-expandable metal stents in palliative treatment of malignant biliary obstruction: a meta-analysis. *Eur Rev Med Pharmacol Sci* 2017; **21**: 2847-2857 [PMID: 28682432]

83 **Lee JH**, Krishna SG, Singh A, Ladha HS, Slack RS, Ramireddy S, Raju GS, Davila M, Ross WA. Comparison of the utility of covered metal stents versus uncovered metal stents in the management of malignant biliary strictures in 749 patients. *Gastrointest Endosc* 2013; **78**: 312-324 [PMID: 23591331 DOI: 10.1016/j.gie.2013.02.032]

84 **Conio M**, Mangiavillano B, Caruso A, Filiberti RA, Baron TH, De Luca L, Signorelli S, Crespi M, Marini M, Ravelli P, Conigliaro R, De Ceglie A. Covered versus uncovered self-expandable metal stent for palliation of primary malignant extrahepatic biliary strictures: a randomized multicenter study. *Gastrointest Endosc* 2018; **88**: 283-291.e3 [PMID: 29653120 DOI: 10.1016/j.gie.2018.03.029]

85 **Saleem A**, Leggett CL, Murad MH, Baron TH. Meta-analysis of randomized trials comparing the patency of covered and uncovered self-expandable metal stents for palliation of distal malignant bile

duct obstruction. *Gastrointest Endosc* 2011; **74**: 321-327.e1 [PMID: 21683354 DOI: 10.1016/j.gie.2011.03.1249]

86 **Almadi MA**, Barkun AN, Martel M. No benefit of covered *vs* uncovered self-expandable metal stents in patients with malignant distal biliary obstruction: a meta-analysis. *Clin Gastroenterol Hepatol* 2013; **11**: 27-37.e1 [PMID: 23103324 DOI: 10.1016/j.cgh.2012.10.019]

87 **Jarnagin W**, Winston C. Hilar cholangiocarcinoma: diagnosis and staging. *HPB (Oxford)* 2005; **7**: 244-251 [PMID: 18333200 DOI: 10.1080/13651820500372533]

88 **Bismuth H**, Majno PE. Biliary strictures: classification based on the principles of surgical treatment. *World J Surg* 2001; **25**: 1241-1244 [PMID: 11596882 DOI: 10.1007/s00268-001-0102-8]

89 **Abraham NS**, Barkun JS, Barkun AN. Palliation of malignant biliary obstruction: a prospective trial examining impact on quality of life. *Gastrointest Endosc* 2002; **56**: 835-841 [PMID: 12447294 DOI: 10.1067/mge.2002.129868]

90 **Lee TH**, Moon JH, Park SH. Bilateral metallic stenting in malignant hilar obstruction. *Clin Endosc* 2014; **47**: 440-446 [PMID: 25325005 DOI: 10.5946/ce.2014.47.5.440]

91 **Hong W**, Chen S, Zhu Q, Chen H, Pan J, Huang Q. Bilateral stenting methods for hilar biliary obstructions. *Clinics (Sao Paulo)* 2014; **69**: 647-652 [PMID: 25318098 DOI: 10.6061/clinics/2014(09)12]

92 **De Palma GD**, Galloro G, Siciliano S, Iovino P, Catanzano C. Unilateral versus bilateral endoscopic hepatic duct drainage in patients with malignant hilar biliary obstruction: results of a prospective, randomized, and controlled study. *Gastrointest Endosc* 2001; **53**: 547-553 [PMID: 11323577 DOI: 10.1067/mge.2001.113381]

93 **Lee TH**, Kim TH, Moon JH, Lee SH, Choi HJ, Hwangbo Y, Hyun JJ, Choi JH, Jeong S, Kim JH, Park DH, Han JH, Park SH. Bilateral *vs* unilateral placement of metal stents for inoperable high-grade malignant hilar biliary strictures: a multicenter, prospective, randomized study (with video). *Gastrointest Endosc* 2017; **86**: 817-827 [PMID: 28479493 DOI: 10.1016/j.gie.2017.04.037]

94 **Aghaie Meybodi M**, Shakoor D, Nanavati J, Ichkhanian Y, Vosoughi K, Brewer Gutierrez OI, Kalloo AN, Singh V, Kumbhari V, Ngamruengphong S, Khashab MA. Unilateral versus bilateral endoscopic stenting in patients with unresectable malignant hilar obstruction: a systematic review and meta-analysis. *Endosc Int Open* 2020; **8**: E281-E290 [PMID: 32118102 DOI: 10.1055/a-1067-4326]

95 **Staub J**, Siddiqui A, Murphy M, Lam R, Parikh M, Pleskow D, Papachristou G, Sharaiha R, Iqbal U, Loren D, Kowalski T, Noor A, Mumtaz T, Yasuda I, Thomas S, Hsaeeb A, Herrick J, Greene T, Adler DG. Unilateral versus bilateral hilar stents for the treatment of cholangiocarcinoma: a multicenter international study. *Ann Gastroenterol* 2020; **33**: 202-209 [PMID: 32127742 DOI: 10.20524/aog.2020.0451]

96 **Chang WH**, Kortan P, Haber GB. Outcome in patients with bifurcation tumors who undergo unilateral versus bilateral hepatic duct drainage. *Gastrointest Endosc* 1998; **47**: 354-362 [PMID: 9609426 DOI: 10.1016/s0016-5107(98)70218-4]

97 **Naitoh I**, Ohara H, Nakazawa T, Ando T, Hayashi K, Okumura F, Okayama Y, Sano H, Kitajima Y, Hirai M, Ban T, Miyabe K, Ueno K, Yamashita H, Joh T. Unilateral versus bilateral endoscopic metal stenting for malignant hilar biliary obstruction. *J Gastroenterol Hepatol* 2009; **24**: 552-557 [PMID: 19220678 DOI: 10.1111/j.1440-1746.2008.05750.x]

98 **Chang G**, Xia FF, Li HF, Niu S, Xu YS. Unilateral versus bilateral stent insertion for malignant hilar biliary obstruction. *Abdom Radiol (NY)* 2017; **42**: 2745-2751 [PMID: 28477177 DOI: 10.1007/s00261-017-1174-8]

99 **Lee JH**, Kang DH, Kim JY, Lee SM, Kim DH, Park CW, Cho HS, Kim GH, Kim TO, Heo J, Song GA, Cho M, Kim S, Kim CW, Lee JW. Endoscopic bilateral metal stent placement for advanced hilar cholangiocarcinoma: a pilot study of a newly designed Y stent. *Gastrointest Endosc* 2007; **66**: 364-369 [PMID: 17643714 DOI: 10.1016/j.gie.2006.12.061]

100 **Connor S**, Garden OJ. Bile duct injury in the era of laparoscopic cholecystectomy. *Br J Surg* 2006; **93**: 158-168 [PMID: 16432812 DOI: 10.1002/bjs.5266]

101 **Pachter HL**, Hofstetter SR. The current status of nonoperative management of adult blunt hepatic injuries. *Am J Surg* 1995; **169**: 442-454 [PMID: 7694987 DOI: 10.1016/s0002-9610(99)80194-9]

102 **Carrillo EH**, Spain DA, Wohltmann CD, Schmieg RE, Boaz PW, Miller FB, Richardson JD. Interventional techniques are useful adjuncts in nonoperative management of hepatic injuries. *J Trauma* 1999; **46**: 619-22; discussion 622 [PMID: 10217224 DOI: 10.1097/00005373-199904000-00010]

103 **Kapoor S**, Nundy S. Bile duct leaks from the intrahepatic biliary tree: a review of its etiology, incidence, and management. *HPB Surg* 2012; **2012**: 752932 [PMID: 22645406 DOI: 10.1155/2012/752932]

104 **Nawaz H**, Papachristou GI. Endoscopic treatment for post-cholecystectomy bile leaks: update and recent advances. *Ann Gastroenterol* 2011; **24**: 161-163 [PMID: 24713786]

105 **Kitami M**, Murakami G, Suzuki D, Takase K, Tsuboi M, Saito H, Takahashi S. Heterogeneity of subvesical ducts or the ducts of Luschka: a study using drip-infusion cholangiography-computed tomography in patients and cadaver specimens. *World J Surg* 2005; **29**: 217-223 [PMID: 15650797 DOI: 10.1007/s00268-004-7652-5]

106 **Trondsen E**, Ruud TE, Nilsen BH, Mårvik R, Myrvold HE, Buanes T, Viste A, Jørgensen PF, Jacobsen T, Rosseland AR. Complications during the introduction of laparoscopic cholecystectomy in Norway. A prospective multicentre study in seven hospitals. *Eur J Surg* 1994; **160**: 145-151

[PMID: 8003567]
107 **Barkun AN**, Rezieg M, Mehta SN, Pavone E, Landry S, Barkun JS, Fried GM, Bret P, Cohen A. Postcholecystectomy biliary leaks in the laparoscopic era: risk factors, presentation, and management. McGill Gallstone Treatment Group. *Gastrointest Endosc* 1997; **45**: 277-282 [PMID: 9087834 DOI: 10.1016/s0016-5107(97)70270-0]
108 **Shah JN**. Endoscopic treatment of bile leaks: current standards and recent innovations. *Gastrointest Endosc* 2007; **65**: 1069-1072 [PMID: 17531644 DOI: 10.1016/j.gie.2007.02.022]
109 **Canena J**, Horta D, Coimbra J, Meireles L, Russo P, Marques I, Ricardo L, Rodrigues C, Capela T, Carvalho D, Loureiro R, Dias AM, Ramos G, Coutinho AP, Romão C, Veiga PM. Outcomes of endoscopic management of primary and refractory postcholecystectomy biliary leaks in a multicentre review of 178 patients. *BMC Gastroenterol* 2015; **15**: 105 [PMID: 26285593 DOI: 10.1186/s12876-015-0334-y]
110 **Martins FP**, Phillips M, Gaidhane MR, Schmitt T, Kahaleh M. Biliary leak in post-liver-transplant patients: is there any place for metal stent? *HPB Surg* 2012; **2012**: 684172 [PMID: 22619479 DOI: 10.1155/2012/684172]
111 **Lalezari D**, Singh I, Reicher S, Eysselein VE. Evaluation of fully covered self-expanding metal stents in benign biliary strictures and bile leaks. *World J Gastrointest Endosc* 2013; **5**: 332-339 [PMID: 23858377 DOI: 10.4253/wjge.v5.i7.332]
112 **Kahaleh M**, Sundaram V, Condron SL, De La Rue SA, Hall JD, Tokar J, Friel CM, Foley EF, Adams RB, Yeaton P. Temporary placement of covered self-expandable metallic stents in patients with biliary leak: midterm evaluation of a pilot study. *Gastrointest Endosc* 2007; **66**: 52-59 [PMID: 17324415 DOI: 10.1016/j.gie.2006.07.036]
113 **Li ZH**, Chen M, Liu JK, Ding J, Dong JH. Endoscopic sphincterotomy in the treatment of cholangiopancreatic diseases. *World J Gastroenterol* 2005; **11**: 2678-2680 [PMID: 15849834 DOI: 10.3748/wjg.v11.i17.2678]
114 **Lin WC**, Lin HH, Hung CY, Shih SC, Chu CH. Clinical endoscopic management and outcome of post-endoscopic sphincterotomy bleeding. *PLoS One* 2017; **12**: e0177449 [PMID: 28545082 DOI: 10.1371/journal.pone.0177449]
115 **Ferreira LE**, Baron TH. Post-sphincterotomy bleeding: who, what, when, and how. *Am J Gastroenterol* 2007; **102**: 2850-2858 [PMID: 18042116 DOI: 10.1111/j.1572-0241.2007.01563.x]
116 **Cochrane J**, Schlepp G. Comparing endoscopic intervention against fully covered self-expanding metal stent placement for post-endoscopic sphincterotomy bleed (CEASE Study). *Endosc Int Open* 2016; **4**: E1261-E1264 [PMID: 27995186 DOI: 10.1055/s-0042-118227]
117 **Shah JN**, Marson F, Binmoeller KF. Temporary self-expandable metal stent placement for treatment of post-sphincterotomy bleeding. *Gastrointest Endosc* 2010; **72**: 1274-1278 [PMID: 20951987 DOI: 10.1016/j.gie.2010.08.012]
118 **Itoi T**, Yasuda I, Doi S, Mukai T, Kurihara T, Sofuni A. Endoscopic hemostasis using covered metallic stent placement for uncontrolled post-endoscopic sphincterotomy bleeding. *Endoscopy* 2011; **43**: 369-372 [PMID: 21360425 DOI: 10.1055/s-0030-1256126]
119 **Majmudar K**, Murad F. Fully-Covered Self-Expandable Metal Stents May Increase the Risk of Cholecystitis in Patients With Intact Gallbladders Compared to Uncovered Self-Expandable Metal Stents When Placed for Malignant Biliary Obstruction: 7. *Am J Gastroenterol* 2018; **113** [DOI: 10.14309/00000434-201810001-00007]
120 **Haseeb A**, Siddiqui A, Taylor LJ, Mills A, Kowalski TE, Loren DE, Dahmus J, Yalamanchili S, Cao C, Canakis A, Mumtaz T, Parikh M, Adler DG. Use of fully covered self-expanding metal stents for benign biliary etiologies: a large multi-center experience. *Minerva Gastroenterol Dietol* 2018; **64**: 111-116 [PMID: 28875690 DOI: 10.23736/S1121-421X.17.02428-X]
121 **Perri V**, Boškoski I, Tringali A, Familiari P, Mutignani M, Marmo R, Costamagna G. Fully covered self-expandable metal stents in biliary strictures caused by chronic pancreatitis not responding to plastic stenting: a prospective study with 2 years of follow-up. *Gastrointest Endosc* 2012; **75**: 1271-1277 [PMID: 22464813 DOI: 10.1016/j.gie.2012.02.002]
122 **Park DH**, Lee SS, Lee TH, Ryu CH, Kim HJ, Seo DW, Park SH, Lee SK, Kim MH, Kim SJ. Anchoring flap *vs* flared end, fully covered self-expandable metal stents to prevent migration in patients with benign biliary strictures: a multicenter, prospective, comparative pilot study (with videos). *Gastrointest Endosc* 2011; **73**: 64-70 [PMID: 21184871 DOI: 10.1016/j.gie.2010.09.039]
123 **Katsinelos P**, Lazaraki G, Gkagkalis S, Chatzimavroudis G, Anastasiadou K, Georgakis N, Giouleme O, Zavos C, Kountouras J. A fully covered self-expandable metal stent anchored by a 10-Fr double pigtail plastic stent: an effective anti-migration technique. *Ann Gastroenterol* 2017; **30**: 114-117 [PMID: 28042247 DOI: 10.20524/aog.2016.0089]
124 **Kahaleh M**, Talreja JP, Loren DE, Kowalski TE, Poneros JM, Degaetani M, Raijman I, Sejpal DV, Patel S, Rosenkranz L, McNamara KN, Brijbassie A, Wang AY, Gaidhane M, Sethi A, Stevens PD. Evaluation of a fully covered self-expanding metal stent with flared ends in malignant biliary obstruction: a multicenter study. *J Clin Gastroenterol* 2013; **47**: e96-100 [PMID: 23933803 DOI: 10.1097/MCG.0b013e3182951a32]
125 **Paik WH**, Woo SM, Chun JW, Song BJ, Lee WJ, Ahn DW, Lee YS, Choi YH, Ryu JK, Kim YT, Lee SH. Efficacy of an internal anchoring plastic stent to prevent migration of a fully covered metal stent in malignant distal biliary strictures: a randomized controlled study. *Endoscopy* 2021; **53**: 578-585 [PMID: 32886935 DOI: 10.1055/a-1256-0571]
126 **Isayama H**, Komatsu Y, Tsujino T, Sasahira N, Hirano K, Toda N, Nakai Y, Yamamoto N, Tada M,

Yoshida H, Shiratori Y, Kawabe T, Omata M. A prospective randomised study of "covered" versus "uncovered" diamond stents for the management of distal malignant biliary obstruction. *Gut* 2004; **53**: 729-734 [PMID: 15082593 DOI: 10.1136/gut.2003.018945]

127 **Jang S**, Stevens T, Parsi M, Lopez R, Zuccaro G, Dumot J, Vargo JJ. Association of covered metallic stents with cholecystitis and stent migration in malignant biliary stricture. *Gastrointest Endosc* 2018; **87**: 1061-1070 [PMID: 28867074 DOI: 10.1016/j.gie.2017.08.024]

128 **Gardner TB**, Spangler CC, Byanova KL, Ripple GH, Rockacy MJ, Levenick JM, Smith KD, Colacchio TA, Barth RJ, Zaki BI, Tsapakos MJ, Gordon SR. Cost-effectiveness and clinical efficacy of biliary stents in patients undergoing neoadjuvant therapy for pancreatic adenocarcinoma in a randomized controlled trial. *Gastrointest Endosc* 2016; **84**: 460-466 [PMID: 26972022 DOI: 10.1016/j.gie.2016.02.047]

129 **Motte S**, Deviere J, Dumonceau JM, Serruys E, Thys JP, Cremer M. Risk factors for septicemia following endoscopic biliary stenting. *Gastroenterology* 1991; **101**: 1374-1381 [PMID: 1936809 DOI: 10.1016/0016-5085(91)90091-x]

World Journal of Gastroenterology

Submit a Manuscript: https://www.f6publishing.com

World J Gastroenterol 2021 October 14; 27(38): 6374-6386

DOI: 10.3748/wjg.v27.i38.6374

ISSN 1007-9327 (print) ISSN 2219-2840 (online)

REVIEW

Intraoperative use of indocyanine green fluorescence imaging in rectal cancer surgery: The state of the art

Roberto Peltrini, Mauro Podda, Simone Castiglioni, Maria Michela Di Nuzzo, Michele D'Ambra, Ruggero Lionetti, Maurizio Sodo, Gaetano Luglio, Felice Mucilli, Salomone Di Saverio, Umberto Bracale, Francesco Corcione

ORCID number: Roberto Peltrini 0000-0003-0445-2269; Mauro Podda 0000-0001-9941-0883; Simone Castiglioni 0000-0001-5540-8642; Maria Michela Di Nuzzo 0000-0002-3000-3769; Michele D'Ambra 0000-0001-5450-5280; Ruggero Lionetti 0000-0003-1165-2576; Maurizio Sodo 0000-0002-7469-4661; Gaetano Luglio 0000-0002-5931-9599; Felice Mucilli 0000-0003-1591-0325; Salomone Di Saverio 0000-0001-5685-5022; Umberto Bracale 0000-0002-9868-0889; Francesco Corcione 0000-0002-7157-5157.

Author contributions: Peltrini R, Castiglioni S, Di Nuzzo MM, Bracale U, Crocione F designed the study; Peltrini R, Castiglioni S, Di Nuzzo MM, Podda M, D'Ambra M, Lionetti R, Sodo M, Luglio acquired and interpreted the data; Peltrini R, Podda M, Castiglioni S, Di Nuzzo MM wrote the manuscript; Peltrini R, Podda M, Sodo M, Luglio G, Mucilli F, Di Saverio S, Bracale U, Corcione F made critical revisions; All authors approved the final version.

Conflict-of-interest statement: Authors declare no conflict of interests for this article.

Open-Access: This article is an open-access article that was selected by an in-house editor and

Roberto Peltrini, Maria Michela Di Nuzzo, Michele D'Ambra, Ruggero Lionetti, Maurizio Sodo, Gaetano Luglio, Umberto Bracale, Francesco Corcione, Department of Public Health, University of Naples Federico II, Napoli 80131, Italy

Mauro Podda, Department of Emergency Surgery, Cagliari University Hospital "Duilio Casula", Azienda Ospedaliero-Universitaria di Cagliari, Cagliari 09100, Italy

Simone Castiglioni, Felice Mucilli, Department of Medical, Oral and Biotechnological Sciences, University G. D'Annunzio Chieti-Pescara, Pescara 65100, Italy

Salomone Di Saverio, Department of General Surgery, University of Insubria, ASST Sette Laghi, Varese 21100, Italy

Corresponding author: Roberto Peltrini, MD, Surgeon, Department of Public Health, University of Naples Federico II, Via Pansini 5, Napoli 80131, Italy. roberto.peltrini@gmail.com

Abstract

Indocyanine green (ICG) fluorescence imaging is widely used in abdominal surgery. The implementation of minimally invasive rectal surgery using new methods like robotics or a transanal approach required improvement of optical systems. In that setting, ICG fluorescence optimizes intraoperative vision of anatomical structures by improving blood and lymphatic flow. The purpose of this review was to summarize all potential applications of this upcoming technology in rectal cancer surgery. Each type of use has been separately addressed and the evidence was investigated. During rectal resection, ICG fluorescence angiography is mainly used to evaluate the perfusion of the colonic stump in order to reduce the risk of anastomotic leaks. In addition, ICG fluorescence imaging allows easy visualization of organs such as the ureter or urethra to protect them from injury. This intraoperative technology is a valuable tool for conducting lymph node dissection along the iliac lymphatic chain or to better identifying the rectal dissection planes when a transanal approach is performed. This is an overview of the applications of ICG fluorescence imaging in current surgical practice and a synthesis of the results obtained from the literature. Although further studies are need to investigate the real clinical benefits, these findings may enhance use of ICG fluorescence in current clinical practice and stimulate future research on new applications.

fully peer-reviewed by external reviewers. It is distributed in accordance with the Creative Commons Attribution NonCommercial (CC BY-NC 4.0) license, which permits others to distribute, remix, adapt, build upon this work non-commercially, and license their derivative works on different terms, provided the original work is properly cited and the use is non-commercial. See: http://creativecommons.org/Licenses/by-nc/4.0/

Manuscript source: Unsolicited manuscript

Specialty type: Surgery

Country/Territory of origin: Italy

Peer-review report's scientific quality classification

Grade A (Excellent): 0
Grade B (Very good): B
Grade C (Good): 0
Grade D (Fair): 0
Grade E (Poor): 0

Received: April 18, 2021
Peer-review started: April 18, 2021
First decision: June 30, 2021
Revised: June 30, 2021
Accepted: August 18, 2021
Article in press: August 18, 2021
Published online: October 14, 2021

P-Reviewer: Wu A
S-Editor: Wu YXJ
L-Editor: Filipodia
P-Editor: Xing YX



Key Words: Indocyanine green; Fluorescence imaging; Near infrared; Rectal cancer; Total mesorectal excision; Anastomotic leakage

©The Author(s) 2021. Published by Baishideng Publishing Group Inc. All rights reserved.

Core Tip: There is growing interest in real-time fluorescence-guided surgery. The intraoperative use of indocyanine green (ICG) during rectal cancer surgery has found many applications over time. Given the wide availability in current practice, it is important for clinicians to be aware of all potential uses of ICG fluorescence technology in order to facilitate the procedures, limit injuries, and improve outcomes. Herein, we provide a concise overview of the literature regarding the use of ICG fluorescence imaging in this setting.

Citation: Peltrini R, Podda M, Castiglioni S, Di Nuzzo MM, D'Ambra M, Lionetti R, Sodo M, Luglio G, Mucilli F, Di Saverio S, Bracale U, Corcione F. Intraoperative use of indocyanine green fluorescence imaging in rectal cancer surgery: The state of the art. *World J Gastroenterol* 2021; 27(38): 6374-6386
URL: https://www.wjgnet.com/1007-9327/full/v27/i38/6374.htm
DOI: https://dx.doi.org/10.3748/wjg.v27.i38.6374

INTRODUCTION

Colorectal carcinoma is the third most common cancer for both men and women and the second leading cause of cancer-related deaths[1]. Primary rectal localization occurs in 35% of cases[2]. Although multidisciplinary management of rectal cancer is the standard of care, surgery remains the cornerstone of curative treatment. Total mesorectal excision (TME), described for the first time by Heald *et al*[3,4], should now be performed routinely in cases of middle and lower rectal tumors after neoadjuvant therapy for locally advanced cancer (T3-4 and/or N+)[5]. Respect for the principles of surgical oncology, including complete TME, and negative distal and circumferential resection margins is mandatory to achieve improved survival. Also, much effort has been made to achieve faster and enhanced recovery[6,7] and better quality of life after rectal cancer surgery[8] over time. Advances in oncology research[9] have resulted in increasing roles for the latest technologies in surgery. Enhanced video/camera systems [10], robotic technology[11], powered staplers[12], and specialized operating platforms for natural orifice transluminal endoscopic surgery[13] are just a few examples of surgical innovations in colorectal surgery introduced in the last decades. In this setting, laser fluorescence using indocyanine green (ICG) dye is a promising and widespread real-time technology because of its easy accessibility, accuracy and cost-effectiveness.

The concept of ICG intraoperative angiography is based on the ability of ICG to absorb near-infrared light (NIR) at 800 nm and to emit fluorescence at a wavelength of 830 nm. Albumin is the most important intravascular binding-protein for ICG so that tissue microperfusion is revealed by the presence of fluorescence. In brief, a bolus of ICG is injected into the patient intravenously, NIR light is then absorbed by ICG in the tissue, and the resulting fluorescence is a reflection of perfusion. After the introduction of ICG angiography in clinical practice in 1989 to evaluate choroidal circulation[14], fluorescence imaging technology has been used in hepatobiliary[15,16], gastric cancer [17], gynecologic cancer[18], breast cancer[19] and transplantation surgery[20]. Furthermore, many colorectal surgeons routinely use ICG imaging to assess bowel viability during colorectal anastomosis. However, several applications of ICG angiography have been described in colorectal surgery with increasing interest for rectal cancer resection. In fact, the implementation of minimally invasive rectal surgery using new approaches (*e.g.*, robotic, and transanal) required the improvement of optical systems. In that regard, ICG fluorescence has optimized the intraoperative vision of anatomical structures by the enhancement of blood and lymph flow. The aim of this review is to identify and synthesize data from original research evaluating any possible application of ICG fluorescence imaging in rectal cancer surgery. In the last 5 years, the use of ICG fluorescence in rectal cancer surgery has attracted great interest.

The items regarding different intraoperative applications are summarized below.

ASSESSMENT OF VASCULAR PERFUSION AT THE ANASTOMOTIC SITE

Anastomotic leakage (AL) is the most feared complication after TME because it is associated with increased mortality, reoperation, and definitive stoma formation[21,22]. Additionally, the relationship between AL and local recurrence has been found to lead to significant differences in long-term outcomes[23]. It has a significant impact on postoperative functional outcome[24] and increases the economic burden of public health systems[25]. That easily explains the importance of developing prevention strategies in order to reduce the amount of related complications affecting survival and quality of life. The AL rate after anterior rectal resection ranges from 3% to 23%[26,27]. AL is defined by the International Study Group of Rectal cancer as a defect at the level of the anastomotic site that allows communication between the intraluminal and extraluminal compartments identified through clinical evaluation with digital rectal exploration, endoscopic examination, computed tomography radiological evidence of contrast leakage through the suture gap or the presence of perianastomotic hydro-aerial collection. It is also classified as grade A if it does not affect the postoperative course, grade B when conservative management antibiotic therapy or percutaneous/transanal drainage is required, and grace C when surgical revision is required[26,28].

Various risk factors are associated with AL, but insufficient blood perfusion is generally considered as one of the main causes[29,30]. ICG is a water soluble, tricarbocyanine dye that provides real-time visualization of vascular structures by emitting fluorescence when stimulated by polarized light[31]. The evaluation of perfusion of the supposed proximal section line starts within 60 s of an intravenous bolus injection of ICG. An NIR camera detects the fluorescence of the microcirculation of the colonic wall receiving adequate vascularization. Therefore, ICG fluorescence reflects the colonic stump perfusion allowing the choice of the most appropriate site for the final section and then for the anastomosis (Figure 1). A second check can be also performed after the anastomosis construction both by injecting a second bolus of ICG to verify fluorescence of the stumps and by transanal endoscopic suture line visualization. Some limitations of the technique are related to its being, once again, a subjective evaluation by the surgeon of the intensity of the emitted infrared light. Furthermore, it is not a completely standardized technique as there are variables related to the dose of injected ICG (0.013-0.89 mg/kg), the proximity of the laparoscope to the colic wall, the number and type of checks performed, and differences in the equipment available on the market[32-34].

Kudszus was the first to show the usefulness of ICG fluorescence angiography (FA) in colorectal surgery[35]. The study reported that ICG FA led to a change in the location of the planned proximal resection line in 13.9% of patients. ICG FA significantly reduced AL by 4% compared with the control group. Furthermore, Jafari *et al*[36] assessed the utility of ICG FA in left colectomy and anterior resection in the PILLAR II study. The incidence of AL in their study was 1.4%, with a change in the surgical strategy in 8% of patients. Boni *et al*[37] reported that ICG FA could be safely and effectively performed in rectal surgery. The use of IGC-FA changed the surgical plan in 4.7% of their patients and AL did not occur in the ICG group, compared with an incidence of 5.2% in the control group. However, the differences were not statistically significant. The studies agree on the safety and feasibility of the technique and demonstrate its usefulness in the assessment of tissue perfusion.

Several comparative retrospective and prospective studies investigated the relationship between the use of ICG and the 30-d AL rate as the primary outcome[31,33,38-40]. They showed a statistically significant correlation between ICG FA and reduction in the risk of AL associated with the modification of the proximal section line. In a propensity score-matched analysis[41], AL rates of Clavien-Dindo grade ≥ II and ≥ III were 10.4% (22/211) and 9.5% (20/211) in the non-ICG FA group and 4.7% (10/211) and 2.8% (6/211) in the ICG FA group, respectively. Similarly, Foo *et al*[42] demonstrated that the use of ICG FA was significantly associated with a lower AL rate in TME (4.7% *vs* 11.6%; P = 0.043) but not non-TME resections. However, not all studies agree on the results. Two propensity score-matched studies failed to demonstrate a statistically significant difference in the rate of AL between the two compared groups, although both reported a change in the proximal section after ICG injection of 27.1% and 18.18%, respectively[43,44]. Most of the studies had limitations such as a small sample size or their retrospective nature. Only two randomized

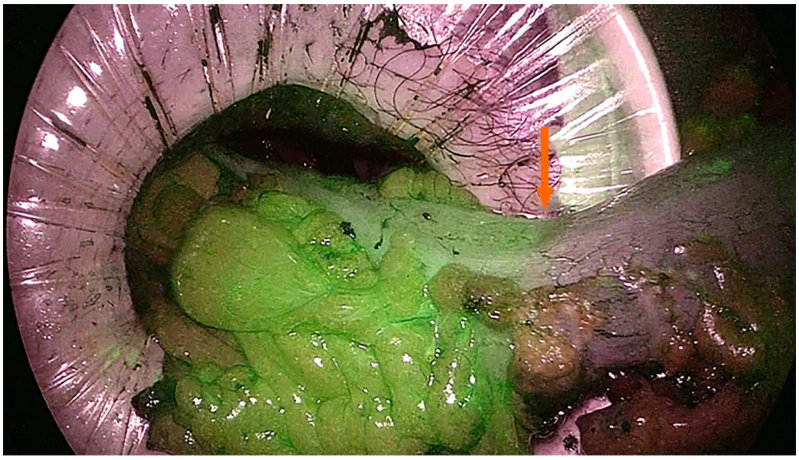


Figure 1 Evaluation of intestinal perfusion after intravenous injection of indocyanine green during total mesorectal excision allows identification of the section line before anastomosis construction (orange arrow).

controlled trials (RCTs) were published. In the first one[45], differences in AL or reoperation rates between ICG and the control group (5% *vs* 9% and 6.7% *vs* 6.5%) were not significant. Although the authors confirmed the efficacy of ICG in bowel viability assessment during left colectomy or anterior resection, a real advantage related to AL was not demonstrated. The FLAG trial[46] involved 377 patients who underwent anterior rectal resection, 187 in the ICG FA group and 190 in the control group. The results showed that changes in the transection line were performed in almost 20% of patients. A decrease in AL was achieved using ICG FA, but the difference was statistically significant only in cases with low rectal anastomosis (14.4% with ICG FA *vs* 25.7% without ICG FA; $P = 0.04$). Two recent meta-analyses assessed the role of ICG FA imaging on the incidence of AL after rectal cancer surgery[34,47]. In a pooled analysis of 2088 patients, the AL rate in the ICG group was significantly lower than that in the control group, and the intraoperative use of ICG was associated with a decreased overall complication rate and reduced reoperation rate. However, both analyses suffer from the same limitations as the studies taken into consideration and the lack of RCTs in the analysis.

Finally, evaluation of bowel perfusion by ICG FA was reported exclusively after transanal total mesorectal excision (TaTME) by Mizrahi *et al*[48]. In their retrospective cohort of 54 patients who received a very low anastomosis, a check was performed before proximal transection and at the completion of anastomosis. In 18.5% of the cases the surgeon changed the proximal resection margin because of impaired fluorescence. All those anastomoses were shown to be successful at the second control. Two patients (3.7%) suffered from AL, and in neither of them was the splenic flexure mobilized. Furthermore, ICG FA improved clinical outcomes also after robotic sphincter-saving rectal resections[49]. In conclusion, the use of fluorescent angiography with ICG injection has proven to be a safe and feasible method to evaluate bowel perfusion whatever the surgical approach for rectal resection. At the time of the construction of the anastomosis, ICG FA can influence decision making by reconsidering the resection line. Several studies have found a significant decrease in the rate of AL after ICG FA imaging, and that has had a large impact on recovery. Future high quality trials should confirm the impact on AL rates and standardize the technique.

URETHRA VISUALIZATION DURING TRANSANAL TME

TaTME is a relatively new procedure[50] for the curative resection of rectal tumors. It was developed to overcome the difficult dissection at the lower third of the rectum, especially in obese male patients and/or bulky tumors. Some retrospective series have reported that enhanced visualization of the dissection plane allowed better nerve preservation, improved resection margins, and improved functional outcomes compared with laparoscopic TME[51,52]. However, the bottom-up transanal approach is not without complications. Incidence of iatrogenic urethral injuries has been reported, ranging from 1% to 6.7% during TaTME procedures[53]. An international inquiry reported 34 urethral injuries from 32 surgical teams worldwide between 2010

and 2017, resulting in a significant postoperative morbidity rate of 26%[50]. However, there is still concern that urologic injuries during TaTME may be underreported and that their incidence might be related to surgeon experience. Therefore, enhancement of urethral visualization should be considered useful and advantageous in the early learning experience. Several bioimaging modalities exist that can improve urethral identification, including ICG NIR fluorescence[54]. Different systems have been successfully used to detect the urethra by ICG fluorescence imaging such as the IRIS ureteral kit (Stryker, Kalamazoo, MI, United States)[55] or the PINPOINT laparoscopic system (Stryker, United States)[56] with intraurethral ICG injection or infiltration adjacent to the catheter in the urethra, respectively. Experimental studies demonstrated that direct ICG instillation into the urethra or through a urine catheter for NIR fluorescence imaging seem to be easily applicable and clinically reproducible during TaTME[55-57]. Although an open-label clinical feasibility study (NCT03204201) with intraoperative direct instillation of ICG into the urethra for low rectal cancers was terminated because of technique failures, implementation of the technique has been described by some authors. Barnes *et al*[58] evaluated the efficacy of two novel methods in cadaveric models. In the first, ICG mixed with silicone was infiltrated into 10-Fr one-way Foley catheter and allowed to set for 1 wk. In the second, new preclinical IRDye 800BK (LI-COR Biosciences®, Lincoln, Nebraska, United States) was infiltrated directly into the urethra *via* the urethral meatus prior to dissection. Both methods were effective in identifying the fluorescence located only within the urethra. IRDye 800BK provided a greater depth of penetration than the ICG-silicone mix, suggesting it could be a more satisfactory alternative to ICG. In addition, Barberio *et al*[59] demonstrated the superior brightness of near-infrared coating of equipment (NICE) coated catheter compared with ICG-based solutions in cadaveric experiments by exhibiting a higher fluorescence intensity than urinary catheters filled with ICG. In conclusion, no final specific recommendations can be drawn from the clinical use of ICG fluorescence imaging to identify and prevent urethral injuries during TaTME procedures because of the very limited data available. However, future studies will have to take into account that fluorescence technology plays a major role in this setting.

URETER IDENTIFICATION

The incidence of iatrogenic urethral injuries (IUI) ranges from 0.24% to 1.95% in colorectal surgery, and rectal cancer is considered a risk factor for IUI because of the close proximity of the ureters to the dissection plane[60], similar to the risk with deep pelvic endometriosis[61,62]. Despite its low incidence, IUI significantly affects postoperative morbidity, mortality, length of stay and hospital charges[60]. Visualization of the ureters is thus advocated during pelvic surgery by the visible peristalsis that occurs when the ureter is gently pressed (Kelly's sign). However, adhesions, obesity, and an incorrect plane of dissection contribute to the lack of or incorrect recognition of the ureter, which can jeopardize its integrity. For that reason, a selective use of prophylactic urethral stents in high risk procedures is commonly accepted, but there is no sufficient evidence to support a decrease in IUI or intraoperative identification[63,64]. In that setting, interest in fluorescence imaging has been increasing over time. While contrasting results were found for intravenous administration of methylene blue dye to urethral detection in colorectal surgery[65,66], ICG FA proved to be a viable alternative to real-time ureter identification and IUI prevention. Before surgery, a 6-Fr catheter is placed into the urethral orifice by cystoscopy. As ICG binds to the proteins of the ureteric epithelium[67], a retrograde injection of 5 mg ICG diluted in 2 mL of distilled water is made, and infrared emission is captured by the filtered lens system and electronically converted into green color visualizing ureter location. The technique has proven to be safe and helpful to identify the ureter in several small case-series who underwent minimally invasive pelvic surgery[68-72]. As a catheter insertion of only 1 cm is required, there is a lower risk of IUI during catheterization than during conventional endoscopic stenting procedures, thus avoiding additional cystoscopies to remove the catheter. Furthermore, ICG urethral instillation is less expensive than other fluorescence-based systems such as illuminated catheters [68].

White *et al*[73] recently evaluated the safety and efficacy of intraurethral ICG FA along with any potential benefit related to the technique during colorectal robotic surgery. In their experience involving 16 patients, there were short procedure times, low morbidity, and reliable urethral identification and avoidance. The United States

Food and Drug Administration approval of ICG is limited to intravenous use[74]. Therefore, disclosure of intraurethral off-label use would be needed. In contrast, new intravenous fluorescent dyes with renal clearance, such as fluorescein sodium[75] and IRDye® 800-BK[76] have been used in experimental models to test the penetration of fluorescence in the ureters, with promising results for surgical practice. Additionally, the formulation of ICG in a liposome-based delivery system allows its excretion in urine in animal models and seems a promising fluorophore solution[77,78]. In conclusion, evidence supporting the use of intraurethral ICG instillation in order to improve intraoperative ureter detection is based on few noncomparative feasibility studies involving mixed pelvic surgeries. Despite the efficacy demonstrated in ordinary or complex situations, no study exclusively focused on rectal cancer resections exists to date. It remains to be proven whether this innovation significantly affects surgical procedures and provides clinical benefits by reducing IUI.

LYMPH NODE MAPPING

Lateral pelvic lymph node dissection (LLND) allows the removal of the nodal compartment along the common iliac, internal iliac, and obturator arteries. The lymphatic stations are considered a major cause of locoregional recurrence in rectal cancer and are treated with preoperative chemoradiotherapy and curative resection [79]. While it is widely accepted to perform LLND in selected patients with rectal cancer and lateral lymph nodes that are clinically positive[5], the Japanese Society for Cancer of the Colon and Rectum guidelines[80] recommend LLND even when lateral lymph node metastasis is not detected by preoperative or intraoperative diagnosis. Indeed, LLND is associated with a lower rate of local recurrence compared with TME alone despite no significant differences in either overall survival or local recurrence-free survival[81].

As ICG fluorescence imaging has proven to be a useful tool for identifying lymphatic drainage in colorectal surgery[82,83], ICG-enhanced NIR fluorescence-guided imaging has been used to improve the accuracy and the completeness of LLND. In such cases, ICG fluorescence imaging is carried out the injection of ICG dye into the submucosal layer on the distal side of the tumor through the anus immediately before surgery. In a comparative retrospective series of 42 mid and low rectal cancer patients, the ICG group experienced a significantly lower intraoperative blood loss and a larger number of harvested lateral pelvic lymph nodes[84]. The use of ICG may improve the safety of LLND that is affected by the technical difficulties of the procedure, complicated pelvic wall anatomy, and the effects of preoperative radiation on the tissues. In that setting, real-time identification of lateral pelvic nodes could help to distinguish lymphatic tissue from vascular and nervous structures, thus avoiding postoperative genitourinary dysfunction and providing better surgical staging. However, evidence is still limited[85-87] and additional studies are needed to address the real clinical advantages and standardization of this technique.

A sentinel node (SN) is defined as the first node in the regional peritumoral area that drains the tumor. SN biopsy, in addition to conventional resection, may add clinically significant prognostic information in colorectal surgery[88-90]. NIR laparoscopy with ICG mapping allowed easy intraoperative identification of mesocolic lymphatic drainage and SN during colorectal oncologic resections[91]. Similarly Noura *et al*[92] described the detection of SN by ICG with an NIR system in 25 patients who had no preoperative diagnosis of metastatic lateral pelvic lymph nodes. The success rate of detecting the lateral SN was 92%, and 100% concordance was observed between SN and dissected lateral lymph nodes status. That preliminary study highlighted the feasibility and reliability of lateral SN biopsy as a potential discriminator to perform LLND, but the sensitivity may be compromised by preoperative neoadjuvant chemoradiotherapy[93,94].

TUMOR LOCALIZATION

Several reports have described the intraoperative identification of colonic tumors by NIR with ICG fluorescence imaging, with satisfactory results[95-98]. Accurate identification of the location of colorectal tumors is crucial in minimally invasive surgery because of the lack of tactile perception, especially for cancer at an early stage because of its small size or location on a movable part of the colon. As for rectal cancer, precise tumor site localization allows achieving a clear and safe distal resection margin, which

may affect not only oncological outcomes but also bowel function and quality of life. In that setting, endoscopic tattooing of rectal tumors, both with a high-definition fluorescence imaging system (Karl Storz GmbH & Co. KG, Tuttlingen, Germany)[93] and the PINPOINT® endoscopic fluorescence imaging system (PINPOINT system; Novadaq Technologies Inc., Mississauga, ON, Canada)[99], is feasible and has clinical advantages. In a comparative retrospective series, 342 patients scheduled for laparoscopic colorectal resection were enrolled after propensity score matching[100]. The tumor was tattooed in 114 patients. In a subgroup analysis of 160 patients who underwent anterior resection, the tattooed group had a significantly shorter operative time (unlike right and left colectomy), less blood loss, and a shorter hospital stay than the non-tattooed group. In addition, Goo *et al*[101] compared 200 tattooed colorectal cancer patients (44 rectal cancers) with 879 non-tattooed patients (300 rectal cancers) to evaluate the effect of preoperative colonoscopic tattooing with ICG on adequate lymph node harvest in colorectal cancer. They found that preoperative tattooing in T1 colorectal cancer significantly improved adequate lymph node harvest, with a higher number of retrieved lymph nodes in rectal cancer than in colon cancer.

Fluorescence technology to localize rectal tumors has been developed not only in the field of imaging systems[99], but also by ICG formulation. Fenestrated peritumoral capillaries and impaired lymphatic drainage delay the washout of large molecules from tumors, which has been described as the enhanced permeability and retention effect[102]. The formulation of ICG as a liposome-based delivery system improved tumor-specific localization in experimental models, with the advantages of intravenous injection and better results than free ICG[103,104]. Finally, there are limited data on the role of ICG in the detection of peritoneal carcinomatosis of colorectal origin. Cytoreductive surgery followed by hyperthermic intraperitoneal chemotherapy is the only potentially curative option in patients with limited peritoneal metastases[105]. Intraoperative injection of ICG seems a useful tool to identify peritoneal metastases and detect additional subclinical malignant peritoneal nodules, resulting in modification of the planned surgery in 29% of patients[106]. However, further investigations are required to draw firm conclusions.

OTHER USES

Peritumoral injection of ICG may help the surgeon to perform an adequate dissection along the embryological surgical planes and visualize the relationship with surrounding structures during TaTME[107], conventional laparoscopic TME[108], and abdominoperineal resection (APR)[109]. Omentoplasty is a well-known method to fill the pelvic cavity after APR or in case of complications after rectal cancer surgery. A pilot study of the intraoperative value of NIR fluorescence imaging with ICG to assess omental perfusion after the creation of a pedicled omentoplasty found that a change in decision making occurred in 80% of the cases[110], and a positive impact on the nonhealing rates of patients undergoing salvage surgery for chronic pelvic sepsis was also observed[111].

CONCLUSION

The adoption of ICG fluorescence imaging in rectal cancer surgery and its multiple applications has increased over time. The major field of application is the evaluation of bowel perfusion at the time of anastomosis construction along with a better intraoperative identification of anatomical structures such as the ureter, urethra, lymph nodes, and tumor location. These objectives are relevant because they aim to improve patient safety by avoiding or reducing the risk of complications. However, further investigations are needed to assess the impact of intraoperative ICG fluorescence imaging on clinical, oncological and cost-effective outcomes.

REFERENCES

1 **Siegel RL**, Miller KD, Jemal A. Cancer statistics, 2020. *CA Cancer J Clin* 2020; **70**: 7-30 [PMID: 31912902 DOI: 10.3322/caac.21590]

2 **Glynne-Jones R**, Wyrwicz L, Tiret E, Brown G, Rödel C, Cervantes A, Arnold D; ESMO Guidelines Committee. Rectal cancer: ESMO Clinical Practice Guidelines for diagnosis, treatment

and follow-up. *Ann Oncol* 2017; **28**: iv22-iv40 [PMID: 28881920 DOI: 10.1093/annonc/mdx224]
3 **Heald RJ**. A new approach to rectal cancer. *Br J Hosp Med* 1979; **22**: 277-281 [PMID: 391315]
4 **Heald RJ**, Husband EM, Ryall RD. The mesorectum in rectal cancer surgery--the clue to pelvic recurrence? *Br J Surg* 1982; **69**: 613-616 [PMID: 6751457 DOI: 10.1002/bjs.1800691019]
5 **You YN**, Hardiman KM, Bafford A, Poylin V, Francone TD, Davis K, Paquette IM, Steele SR, Feingold DL; On Behalf of the Clinical Practice Guidelines Committee of the American Society of Colon and Rectal Surgeons. The American Society of Colon and Rectal Surgeons Clinical Practice Guidelines for the Management of Rectal Cancer. *Dis Colon Rectum* 2020; **63**: 1191-1222 [PMID: 33216491 DOI: 10.1097/DCR.0000000000001762]
6 **EuroSurg Collaborative**. Safety and efficacy of non-steroidal anti-inflammatory drugs to reduce ileus after colorectal surgery. *Br J Surg* 2020; **107**: e161-e169 [PMID: 31595986 DOI: 10.1002/bjs.11326]
7 **Peltrini R**, Cantoni V, Green R, Greco PA, Calabria M, Bucci L, Corcione F. Efficacy of transversus abdominis plane (TAP) block in colorectal surgery: a systematic review and meta-analysis. *Tech Coloproctol* 2020; **24**: 787-802 [PMID: 32253612 DOI: 10.1007/s10151-020-02206-9]
8 **Peltrini R**, Luglio G, Cassese G, Amendola A, Caruso E, Sacco M, Pagano G, Sollazzo V, Tufano A, Giglio MC, Bucci L, Palma GD. Oncological Outcomes and Quality of Life After Rectal Cancer Surgery. *Open Med (Wars)* 2019; **14**: 653-662 [PMID: 31565674 DOI: 10.1515/med-2019-0075]
9 **De Palma FDE**, Luglio G, Tropeano FP, Pagano G, D'Armiento M, Kroemer G, Maiuri MC, De Palma GD. The Role of Micro-RNAs and Circulating Tumor Markers as Predictors of Response to Neoadjuvant Therapy in Locally Advanced Rectal Cancer. *Int J Mol Sci* 2020; **21** [PMID: 32987896 DOI: 10.3390/ijms21197040]
10 **Corcione F**, Silvestri V, Merola G, Dambra M, Lionetti R, Pirozzi N, Peltrini R, Pontecorvi E, Bracale U. Use of the ORBEYE™ Exoscope in General Surgery: The Advent of Video-Assisted Open Surgery. *Surg Innov* 2021; **28**: 79-84 [PMID: 33054634 DOI: 10.1177/1553350620965344]
11 **Tejedor P**, Sagias F, Khan JS. The Use of Enhanced Technologies in Robotic Surgery and Its Impact on Outcomes in Rectal Cancer: A Systematic Review. *Surg Innov* 2020; **27**: 384-391 [PMID: 32484427 DOI: 10.1177/1553350620928277]
12 **Herzig DO**, Ogilvie JW, Chudzinski A, Ferrara A, Ashraf SQ, Jimenez-Rodriguez RM, Van der Speeten K, Kinross J, Schimmelpenning H, Sagar PM, Cannon JA, Schwiers ML, Singleton DW, Waggoner JR, Fryrear R 2nd, Sylla P. Assessment of a circular powered stapler for creation of anastomosis in left-sided colorectal surgery: A prospective cohort study. *Int J Surg* 2020; **84**: 140-146 [PMID: 33176211 DOI: 10.1016/j.ijsu.2020.11.001]
13 **Karimyan V**, Sodergren M, Clark J, Yang GZ, Darzi A. Navigation systems and platforms in natural orifice translumenal endoscopic surgery (NOTES). *Int J Surg* 2009; **7**: 297-304 [PMID: 19481186 DOI: 10.1016/j.ijsu.2009.05.007]
14 **Destro M**, Puliafito CA. Indocyanine green videoangiography of choroidal neovascularization. *Ophthalmology* 1989; **96**: 846-853 [PMID: 2472588 DOI: 10.1016/s0161-6420(89)32826-0]
15 **Dip F**, LoMenzo E, Sarotto L, Phillips E, Todeschini H, Nahmod M, Alle L, Schneider S, Kaja L, Boni L, Ferraina P, Carus T, Kokudo N, Ishizawa T, Walsh M, Simpfendorfer C, Mayank R, White K, Rosenthal RJ. Randomized Trial of Near-infrared Incisionless Fluorescent Cholangiography. *Ann Surg* 2019; **270**: 992-999 [PMID: 30614881 DOI: 10.1097/SLA.0000000000003178]
16 **Wang X**, Teh CSC, Ishizawa T, Aoki T, Cavallucci D, Lee SY, Panganiban KM, Perini MV, Shah SR, Wang H, Xu Y, Suh KS, Kokudo N. Consensus Guidelines for the Use of Fluorescence Imaging in Hepatobiliary Surgery. *Ann Surg* 2021; **274**: 97-106 [PMID: 33351457 DOI: 10.1097/SLA.0000000000004718]
17 **He M**, Jiang Z, Wang C, Hao Z, An J, Shen J. Diagnostic value of near-infrared or fluorescent indocyanine green guided sentinel lymph node mapping in gastric cancer: A systematic review and meta-analysis. *J Surg Oncol* 2018; **118**: 1243-1256 [PMID: 30380146 DOI: 10.1002/jso.25285]
18 **Koual M**, Benoit L, Nguyen-Xuan HT, Bentivegna E, Azaïs H, Bats AS. Diagnostic value of indocyanine green fluorescence guided sentinel lymph node biopsy in vulvar cancer: A systematic review. *Gynecol Oncol* 2021; **161**: 436-441 [PMID: 33551201 DOI: 10.1016/j.ygyno.2021.01.031]
19 **Goonawardena J**, Yong C, Law M. Use of indocyanine green fluorescence compared to radioisotope for sentinel lymph node biopsy in early-stage breast cancer: systematic review and meta-analysis. *Am J Surg* 2020; **220**: 665-676 [PMID: 32115177 DOI: 10.1016/j.amjsurg.2020.02.001]
20 **Gerken ALH**, Nowak K, Meyer A, Weiss C, Krüger B, Nawroth N, Karampinis I, Heller K, Apel H, Reissfelder C, Schwenke K, Keese M, Lang W, Rother U. Quantitative Assessment of Intraoperative Laser Fluorescence Angiography with Indocyanine Green Predicts Early Graft Function after Kidney Transplantation. *Ann Surg* 2020; Publish Ahead of Print [PMID: 33394595 DOI: 10.1097/SLA.0000000000004529]
21 **Peeters KC**, Tollenaar RA, Marijnen CA, Klein Kranenbarg E, Steup WH, Wiggers T, Rutten HJ, van de Velde CJ; Dutch Colorectal Cancer Group. Risk factors for anastomotic failure after total mesorectal excision of rectal cancer. *Br J Surg* 2005; **92**: 211-216 [PMID: 15584062 DOI: 10.1002/bjs.4806]
22 **Matthiessen P**, Hallböök O, Andersson M, Rutegård J, Sjödahl R. Risk factors for anastomotic leakage after anterior resection of the rectum. *Colorectal Dis* 2004; **6**: 462-469 [PMID: 15521937 DOI: 10.1111/j.1463-1318.2004.00657.x]

23 **Mirnezami A**, Mirnezami R, Chandrakumaran K, Sasapu K, Sagar P, Finan P. Increased local recurrence and reduced survival from colorectal cancer following anastomotic leak: systematic review and meta-analysis. *Ann Surg* 2011; **253**: 890-899 [PMID: 21394013 DOI: 10.1097/SLA.0b013e3182128929]

24 **Kverneng Hultberg D**, Svensson J, Jutesten H, Rutegård J, Matthiessen P, Lydrup ML, Rutegård M. The Impact of Anastomotic Leakage on Long-term Function After Anterior Resection for Rectal Cancer. *Dis Colon Rectum* 2020; **63**: 619-628 [PMID: 32032197 DOI: 10.1097/DCR.0000000000001613]

25 **Ashraf SQ**, Burns EM, Jani A, Altman S, Young JD, Cunningham C, Faiz O, Mortensen NJ. The economic impact of anastomotic leakage after anterior resections in English NHS hospitals: are we adequately remunerating them? *Colorectal Dis* 2013; **15**: e190-e198 [PMID: 23331871 DOI: 10.1111/codi.12125]

26 **Rahbari NN**, Weitz J, Hohenberger W, Heald RJ, Moran B, Ulrich A, Holm T, Wong WD, Tiret E, Moriya Y, Laurberg S, den Dulk M, van de Velde C, Büchler MW. Definition and grading of anastomotic leakage following anterior resection of the rectum: a proposal by the International Study Group of Rectal Cancer. *Surgery* 2010; **147**: 339-351 [PMID: 20004450 DOI: 10.1016/j.surg.2009.10.012]

27 **Peltrini R**, Imperatore N, Carannante F, Cuccurullo D, Capolupo GT, Bracale U, Caricato M, Corcione F. Age and comorbidities do not affect short-term outcomes after laparoscopic rectal cancer resection in elderly patients. A multi-institutional cohort study in 287 patients. *Updates Surg* 2021; **73**: 527-537 [PMID: 33586089 DOI: 10.1007/s13304-021-00990-z]

28 **Kulu Y**, Ulrich A, Bruckner T, Contin P, Welsch T, Rahbari NN, Büchler MW, Weitz J; International Study Group of Rectal Cancer. Validation of the International Study Group of Rectal Cancer definition and severity grading of anastomotic leakage. *Surgery* 2013; **153**: 753-761 [PMID: 23623834 DOI: 10.1016/j.surg.2013.02.007]

29 **Attard JA**, Raval MJ, Martin GR, Kolb J, Afrouzian M, Buie WD, Sigalet DL. The effects of systemic hypoxia on colon anastomotic healing: an animal model. *Dis Colon Rectum* 2005; **48**: 1460-1470 [PMID: 15909070 DOI: 10.1007/s10350-005-0047-3]

30 **Vignali A**, Gianotti L, Braga M, Radaelli G, Malvezzi L, Di Carlo V. Altered microperfusion at the rectal stump is predictive for rectal anastomotic leak. *Dis Colon Rectum* 2000; **43**: 76-82 [PMID: 10813128 DOI: 10.1007/BF02237248]

31 **Impellizzeri HG**, Pulvirenti A, Inama M, Bacchion M, Marrano E, Creciun M, Casaril A, Moretto G. Near-infrared fluorescence angiography for colorectal surgery is associated with a reduction of anastomotic leak rate. *Updates Surg* 2020; **72**: 991-998 [PMID: 32253688 DOI: 10.1007/s13304-020-00758-x]

32 **Boni L**, David G, Dionigi G, Rausei S, Cassinotti E, Fingerhut A. Indocyanine green-enhanced fluorescence to assess bowel perfusion during laparoscopic colorectal resection. *Surg Endosc* 2016; **30**: 2736-2742 [PMID: 26487209 DOI: 10.1007/s00464-015-4540-z]

33 **Losurdo P**, Mis TC, Cosola D, Bonadio L, Giudici F, Casagranda B, Bortul M, de Manzini N. Anastomosis Leak: Is There Still a Place for Indocyanine Green Fluorescence Imaging in Colon-Rectal Surgery? *Surg Innov* 2020; 1553350620975258 [PMID: 33236661 DOI: 10.1177/1553350620975258]

34 **Shen Y**, Yang T, Yang J, Meng W, Wang Z. Intraoperative indocyanine green fluorescence angiography to prevent anastomotic leak after low anterior resection for rectal cancer: a meta-analysis. *ANZ J Surg* 2020; **90**: 2193-2200 [PMID: 32159273 DOI: 10.1111/ans.15809]

35 **Kudszus S**, Roesel C, Schachtrupp A, Höer JJ. Intraoperative laser fluorescence angiography in colorectal surgery: a noninvasive analysis to reduce the rate of anastomotic leakage. *Langenbecks Arch Surg* 2010; **395**: 1025-1030 [PMID: 20700603 DOI: 10.1007/s00423-010-0699-x]

36 **Jafari MD**, Wexner SD, Martz JE, McLemore EC, Margolin DA, Sherwinter DA, Lee SW, Senagore AJ, Phelan MJ, Stamos MJ. Perfusion assessment in laparoscopic left-sided/anterior resection (PILLAR II): a multi-institutional study. *J Am Coll Surg* 2015; **220**: 82-92.e1 [PMID: 25451666 DOI: 10.1016/j.jamcollsurg.2014.09.015]

37 **Boni L**, Fingerhut A, Marzorati A, Rausei S, Dionigi G, Cassinotti E. Indocyanine green fluorescence angiography during laparoscopic low anterior resection: results of a case-matched study. *Surg Endosc* 2017; **31**: 1836-1840 [PMID: 27553790 DOI: 10.1007/s00464-016-5181-6]

38 **Hasegawa H**, Tsukada Y, Wakabayashi M, Nomura S, Sasaki T, Nishizawa Y, Ikeda K, Akimoto T, Ito M. Impact of intraoperative indocyanine green fluorescence angiography on anastomotic leakage after laparoscopic sphincter-sparing surgery for malignant rectal tumors. *Int J Colorectal Dis* 2020; **35**: 471-480 [PMID: 31907595 DOI: 10.1007/s00384-019-03490-0]

39 **Otero-Piñeiro AM**, de Lacy FB, Van Laarhoven JJ, Martín-Perez B, Valverde S, Bravo R, Lacy AM. The impact of fluorescence angiography on anastomotic leak rate following transanal total mesorectal excision for rectal cancer: a comparative study. *Surg Endosc* 2021; **35**: 754-762 [PMID: 32072284 DOI: 10.1007/s00464-020-07442-6]

40 **Benčurik V**, Škrovina M, Martínek L, Bartoš J, Macháčková M, Dosoudil M, Štěpánová E, Přibylová L, Briš R, Vomáčková K. Intraoperative fluorescence angiography and risk factors of anastomotic leakage in mini-invasive low rectal resections. *Surg Endosc* 2021; **35**: 5015-5023 [PMID: 32970211 DOI: 10.1007/s00464-020-07982-x]

41 **Watanabe J**, Ishibe A, Suwa Y, Suwa H, Ota M, Kunisaki C, Endo I. Indocyanine green fluorescence imaging to reduce the risk of anastomotic leakage in laparoscopic low anterior resection

for rectal cancer: a propensity score-matched cohort study. *Surg Endosc* 2020; **34**: 202-208 [PMID: 30877565 DOI: 10.1007/s00464-019-06751-9]

42 **Foo CC**, Ng KK, Tsang J, Wei R, Chow F, Chan TY, Lo O, Law WL. Colonic perfusion assessment with indocyanine-green fluorescence imaging in anterior resections: a propensity score-matched analysis. *Tech Coloproctol* 2020; **24**: 935-942 [PMID: 32385673 DOI: 10.1007/s10151-020-02232-7]

43 **Bonadio L**, Iacuzzo C, Cosola D, Cipolat Mis T, Giudici F, Casagranda B, Biloslavo A, de Manzini N. Indocyanine green-enhanced fluorangiography (ICGf) in laparoscopic extraperitoneal rectal cancer resection. *Updates Surg* 2020; **72**: 477-482 [PMID: 32072407 DOI: 10.1007/s13304-020-00725-6]

44 **Wada T**, Kawada K, Hoshino N, Inamoto S, Yoshitomi M, Hida K, Sakai Y. The effects of intraoperative ICG fluorescence angiography in laparoscopic low anterior resection: a propensity score-matched study. *Int J Clin Oncol* 2019; **24**: 394-402 [PMID: 30406482 DOI: 10.1007/s10147-018-1365-5]

45 **De Nardi P**, Elmore U, Maggi G, Maggiore R, Boni L, Cassinotti E, Fumagalli U, Gardani M, De Pascale S, Parise P, Vignali A, Rosati R. Intraoperative angiography with indocyanine green to assess anastomosis perfusion in patients undergoing laparoscopic colorectal resection: results of a multicenter randomized controlled trial. *Surg Endosc* 2020; **34**: 53-60 [PMID: 30903276 DOI: 10.1007/s00464-019-06730-0]

46 **Alekseev M**, Rybakov E, Shelygin Y, Chernyshov S, Zarodnyuk I. A study investigating the perfusion of colorectal anastomoses using fluorescence angiography: results of the FLAG randomized trial. *Colorectal Dis* 2020; **22**: 1147-1153 [PMID: 32189424 DOI: 10.1111/codi.15037]

47 **Song M**, Liu J, Xia D, Yao H, Tian G, Chen X, Liu Y, Jiang Y, Li Z. Assessment of intraoperative use of indocyanine green fluorescence imaging on the incidence of anastomotic leakage after rectal cancer surgery: a PRISMA-compliant systematic review and meta-analysis. *Tech Coloproctol* 2021; **25**: 49-58 [PMID: 32885328 DOI: 10.1007/s10151-020-02335-1]

48 **Mizrahi I**, de Lacy FB, Abu-Gazala M, Fernandez LM, Otero A, Sands DR, Lacy AM, Wexner SD. Transanal total mesorectal excision for rectal cancer with indocyanine green fluorescence angiography. *Tech Coloproctol* 2018; **22**: 785-791 [PMID: 30430309 DOI: 10.1007/s10151-018-1869-z]

49 **Kim JC**, Lee JL, Park SH. Interpretative Guidelines and Possible Indications for Indocyanine Green Fluorescence Imaging in Robot-Assisted Sphincter-Saving Operations. *Dis Colon Rectum* 2017; **60**: 376-384 [PMID: 28267004 DOI: 10.1097/DCR.0000000000000782]

50 **Sylla P**, Rattner DW, Delgado S, Lacy AM. NOTES transanal rectal cancer resection using transanal endoscopic microsurgery and laparoscopic assistance. *Surg Endosc* 2010; **24**: 1205-1210 [PMID: 20186432 DOI: 10.1007/s00464-010-0965-6]

51 **de'Angelis N**, Portigliotti L, Azoulay D, Brunetti F. Transanal total mesorectal excision for rectal cancer: a single center experience and systematic review of the literature. *Langenbecks Arch Surg* 2015; **400**: 945-959 [PMID: 26497544 DOI: 10.1007/s00423-015-1350-7]

52 **Chen CC**, Lai YL, Jiang JK, Chu CH, Huang IP, Chen WS, Cheng AY, Yang SH. Transanal Total Mesorectal Excision Versus Laparoscopic Surgery for Rectal Cancer Receiving Neoadjuvant Chemoradiation: A Matched Case-Control Study. *Ann Surg Oncol* 2016; **23**: 1169-1176 [PMID: 26597369 DOI: 10.1245/s10434-015-4997-y]

53 **Al-Taher M**, Knapen B, Barberio M, Felli E, Gioux S, Bouvy ND, Stassen LPS, Marescaux J, Diana M. Near infrared fluorescence imaging of the urethra: a systematic review of the literature. *Minim Invasive Ther Allied Technol* 2020; 1-8 [PMID: 33000653 DOI: 10.1080/13645706.2020.1826974]

54 **Atallah S**, Mabardy A, Volpato AP, Chin T, Sneider J, Monson JRT. Surgery beyond the visible light spectrum: theoretical and applied methods for localization of the male urethra during transanal total mesorectal excision. *Tech Coloproctol* 2017; **21**: 413-424 [PMID: 28589242 DOI: 10.1007/s10151-017-1641-9]

55 **Nitta T**, Tanaka K, Kataoka J, Ohta M, Ishii M, Ishibashi T, Okuda J. Novel technique with the IRIS U kit to prevent urethral injury in patients undergoing transanal total mesorectal excision. *Ann Med Surg (Lond)* 2019; **46**: 1-3 [PMID: 31463048 DOI: 10.1016/j.amsu.2019.08.002]

56 **Barnes TG**, Penna M, Hompes R, Cunningham C. Fluorescence to highlight the urethra: a human cadaveric study. *Tech Coloproctol* 2017; **21**: 439-444 [PMID: 28560481 DOI: 10.1007/s10151-017-1615-y]

57 **Ohta S**, Nishi M, Tokunaga T, Yoshikawa K, Higashijima J, Miyatani T, Kashihara H, Takasu C, Ishikawa D, Shimada M. Usefulness of an ICG fluorescence catheter system in TaTME for avoiding intraoperative urethral injury. *J Med Invest* 2020; **67**: 285-288 [PMID: 33148903 DOI: 10.2152/jmi.67.285]

58 **Barnes TG**, Volpi D, Cunningham C, Vojnovic B, Hompes R. Improved urethral fluorescence during low rectal surgery: a new dye and a new method. *Tech Coloproctol* 2018; **22**: 115-119 [PMID: 29460054 DOI: 10.1007/s10151-018-1757-6]

59 **Barberio M**, Al-Taher M, Forgione A, Hoskere Ashoka A, Felli E, Agnus V, Marescaux J, Klymchenko A, Diana M. A novel method for near-infrared fluorescence imaging of the urethra during perineal and transanal surgery: demonstration in a cadaveric model. *Colorectal Dis* 2020; **22**: 1749-1753 [PMID: 32443182 DOI: 10.1111/codi.15156]

60 **Halabi WJ**, Jafari MD, Nguyen VQ, Carmichael JC, Mills S, Pigazzi A, Stamos MJ. Ureteral

injuries in colorectal surgery: an analysis of trends, outcomes, and risk factors over a 10-year period in the United States. *Dis Colon Rectum* 2014; **57**: 179-186 [PMID: 24401879 DOI: 10.1097/DCR.0000000000000033]

61 **Azioni G**, Bracale U, Scala A, Capobianco F, Barone M, Rosati M, Pignata G. Laparoscopic ureteroneocystostomy and vesicopsoas hitch for infiltrative ureteral endometriosis. *Minim Invasive Ther Allied Technol* 2010; **19**: 292-297 [PMID: 20868303 DOI: 10.3109/13645706.2010.507345]

62 **Bracale U**, Azioni G, Rosati M, Barone M, Pignata G. Deep pelvic endometriosis (Adamyan IV stage): multidisciplinary laparoscopic treatments. *Acta Chir Iugosl* 2009; **56**: 41-46 [PMID: 19504988 DOI: 10.2298/aci0901041b]

63 **Croghan SM**, Zaborowski A, Mohan HM, Mulvin D, McGuire BB, Murphy M, Galvin DJ, Lennon G, Quinlan D, Winter DC. The sentinel stent? *Int J Colorectal Dis* 2019; **34**: 1161-1178 [PMID: 31175421 DOI: 10.1007/s00384-019-03314-1]

64 **Speicher PJ**, Goldsmith ZG, Nussbaum DP, Turley RS, Peterson AC, Mantyh CR. Ureteral stenting in laparoscopic colorectal surgery. *J Surg Res* 2014; **190**: 98-103 [PMID: 24656474 DOI: 10.1016/j.jss.2014.02.025]

65 **Yeung TM**, Volpi D, Tullis ID, Nicholson GA, Buchs N, Cunningham C, Guy R, Lindsey I, George B, Jones O, Wang LM, Hompes R, Vojnovic B, Hamdy F, Mortensen NJ. Identifying Ureters In Situ Under Fluorescence During Laparoscopic and Open Colorectal Surgery. *Ann Surg* 2016; **263**: e1-e2 [PMID: 26672509 DOI: 10.1097/SLA.0000000000001513]

66 **Al-Taher M**, van den Bos J, Schols RM, Bouvy ND, Stassen LP. Fluorescence Ureteral Visualization in Human Laparoscopic Colorectal Surgery Using Methylene Blue. *J Laparoendosc Adv Surg Tech A* 2016; **26**: 870-875 [PMID: 27575463 DOI: 10.1089/Lap.2016.0264]

67 **Frangioni JV**. In vivo near-infrared fluorescence imaging. *Curr Opin Chem Biol* 2003; **7**: 626-634 [PMID: 14580568 DOI: 10.1016/j.cbpa.2003.08.007]

68 **Mandovra P**, Kalikar V, Patankar RV. Real-Time Visualization of Ureters Using Indocyanine Green During Laparoscopic Surgeries: Can We Make Surgery Safer? *Surg Innov* 2019; **26**: 464-468 [PMID: 30734638 DOI: 10.1177/1553350619827152]

69 **Siddighi S**, Yune JJ, Hardesty J. Indocyanine green for intraoperative localization of ureter. *Am J Obstet Gynecol* 2014; **211**: 436.e1-436.e2 [PMID: 24835212 DOI: 10.1016/j.ajog.2014.05.017]

70 **Foppa C**, Spinelli A. Ureteric identification with indocyanine green fluorescence in laparoscopic redo pouch surgery. *Tech Coloproctol* 2018; **22**: 627-628 [PMID: 30167911 DOI: 10.1007/s10151-018-1838-6]

71 **Kanabur P**, Chai C, Taylor J. Use of Indocyanine Green for Intraoperative Ureteral Identification in Nonurologic Surgery. *JAMA Surg* 2020; **155**: 520-521 [PMID: 32186665 DOI: 10.1001/jamasurg.2020.0094]

72 **Lee Z**, Moore B, Giusto L, Eun DD. Use of indocyanine green during robot-assisted ureteral reconstructions. *Eur Urol* 2015; **67**: 291-298 [PMID: 25220372 DOI: 10.1016/j.eururo.2014.08.057]

73 **White LA**, Joseph JP, Yang DY, Kelley SR, Mathis KL, Behm K, Viers BR. Intraureteral indocyanine green augments ureteral identification and avoidance during complex robotic-assisted colorectal surgery. *Colorectal Dis* 2021; **23**: 718-723 [PMID: 33064915 DOI: 10.1111/codi.15407]

74 **Yellinek S**, Krizzuk D, J Nogueras J, D Wexner S. Ureteral Injury During Colorectal Surgery: Two Case Reports and a Literature Review. *J Anus Rectum Colon* 2018; **2**: 71-76 [PMID: 31559346 DOI: 10.23922/jarc.2017-052]

75 **Dip FD**, Nahmod M, Anzorena FS, Moreira A, Sarotto L, Ampudia C, Kalaskar SN, Ferraina P, Rosenthal RJ, Wexner SD. Novel technique for identification of ureters using sodium fluorescein. *Surg Endosc* 2014; **28**: 2730-2733 [PMID: 24737531 DOI: 10.1007/s00464-014-3519-5]

76 **Al-Taher M**, van den Bos J, Schols RM, Kubat B, Bouvy ND, Stassen LPS. Evaluation of a novel dye for near-infrared fluorescence delineation of the ureters during laparoscopy. *BJS Open* 2018; **2**: 254-261 [PMID: 30079395 DOI: 10.1002/bjs5.59]

77 **Portnoy E**, Nizri E, Golenser J, Shmuel M, Magdassi S, Eyal S. Imaging the urinary pathways in mice by liposomal indocyanine green. *Nanomedicine* 2015; **11**: 1057-1064 [PMID: 25791809 DOI: 10.1016/j.nano.2015.02.019]

78 **Friedman-Levi Y**, Larush L, Diana M, Marchegiani F, Marescaux J, Goder N, Lahat G, Klausner J, Eyal S, Magdassi S, Nizri E. Optimization of liposomal indocyanine green for imaging of the urinary pathways and a proof of concept in a pig model. *Surg Endosc* 2018; **32**: 963-970 [PMID: 28779247 DOI: 10.1007/s00464-017-5773-9]

79 **Kim TH**, Jeong SY, Choi DH, Kim DY, Jung KH, Moon SH, Chang HJ, Lim SB, Choi HS, Park JG. Lateral lymph node metastasis is a major cause of locoregional recurrence in rectal cancer treated with preoperative chemoradiotherapy and curative resection. *Ann Surg Oncol* 2008; **15**: 729-737 [PMID: 18057989 DOI: 10.1245/s10434-007-9696-x]

80 **Hashiguchi Y**, Muro K, Saito Y, Ito Y, Ajioka Y, Hamaguchi T, Hasegawa K, Hotta K, Ishida H, Ishiguro M, Ishihara S, Kanemitsu Y, Kinugasa Y, Murofushi K, Nakajima TE, Oka S, Tanaka T, Taniguchi H, Tsuji A, Uehara K, Ueno H, Yamanaka T, Yamazaki K, Yoshida M, Yoshino T, Itabashi M, Sakamaki K, Sano K, Shimada Y, Tanaka S, Uetake H, Yamaguchi S, Yamaguchi N, Kobayashi H, Matsuda K, Kotake K, Sugihara K; Japanese Society for Cancer of the Colon and Rectum. Japanese Society for Cancer of the Colon and Rectum (JSCCR) guidelines 2019 for the treatment of colorectal cancer. *Int J Clin Oncol* 2020; **25**: 1-42 [PMID: 31203527 DOI: 10.1007/s10147-019-01485-z]

81 **Fujita S**, Mizusawa J, Kanemitsu Y, Ito M, Kinugasa Y, Komori K, Ohue M, Ota M, Akazai Y,

Shiozawa M, Yamaguchi T, Bandou H, Katsumata K, Murata K, Akagi Y, Takiguchi N, Saida Y, Nakamura K, Fukuda H, Akasu T, Moriya Y; Colorectal Cancer Study Group of Japan Clinical Oncology Group. Mesorectal Excision With or Without Lateral Lymph Node Dissection for Clinical Stage II/III Lower Rectal Cancer (JCOG0212): A Multicenter, Randomized Controlled, Noninferiority Trial. *Ann Surg* 2017; **266**: 201-207 [PMID: 28288057 DOI: 10.1097/SLA.0000000000002212]

82 **Watanabe J**, Ota M, Suwa Y, Ishibe A, Masui H, Nagahori K. Real-Time Indocyanine Green Fluorescence Imaging-Guided Complete Mesocolic Excision in Laparoscopic Flexural Colon Cancer Surgery. *Dis Colon Rectum* 2016; **59**: 701-705 [PMID: 27270525 DOI: 10.1097/DCR.0000000000000608]

83 **Park SY**, Park JS, Kim HJ, Woo IT, Park IK, Choi GS. Indocyanine Green Fluorescence Imaging-Guided Laparoscopic Surgery Could Achieve Radical D3 Dissection in Patients With Advanced Right-Sided Colon Cancer. *Dis Colon Rectum* 2020; **63**: 441-449 [PMID: 31996582 DOI: 10.1097/DCR.0000000000001597]

84 **Zhou SC**, Tian YT, Wang XW, Zhao CD, Ma S, Jiang J, Li EN, Zhou HT, Liu Q, Liang JW, Zhou ZX, Wang XS. Application of indocyanine green-enhanced near-infrared fluorescence-guided imaging in laparoscopic lateral pelvic lymph node dissection for middle-low rectal cancer. *World J Gastroenterol* 2019; **25**: 4502-4511 [PMID: 31496628 DOI: 10.3748/wjg.v25.i31.4502]

85 **Kim HJ**, Park JS, Choi GS, Park SY, Lee HJ. Fluorescence-guided Robotic Total Mesorectal Excision with Lateral Pelvic Lymph Node Dissection in Locally Advanced Rectal Cancer: A Video Presentation. *Dis Colon Rectum* 2017; **60**: 1332-1333 [PMID: 29112571 DOI: 10.1097/DCR.0000000000000936]

86 **Kawada K**, Yoshitomi M, Inamoto S, Sakai Y. Indocyanine Green Fluorescence-Guided Laparoscopic Lateral Lymph Node Dissection for Rectal Cancer. *Dis Colon Rectum* 2019; **62**: 1401 [PMID: 31596765 DOI: 10.1097/DCR.0000000000001475]

87 **Kazanowski M**, Al Furajii H, Cahill RA. Near-infrared laparoscopic fluorescence for pelvic side wall delta mapping in patients with rectal cancer--'PINPOINT' nodal assessment. *Colorectal Dis* 2015; **17** Suppl 3: 32-35 [PMID: 26394741 DOI: 10.1111/codi.13030]

88 **van der Pas MH**, Meijer S, Hoekstra OS, Riphagen II, de Vet HC, Knol DL, van Grieken NC, Meijerink WJ. Sentinel-lymph-node procedure in colon and rectal cancer: a systematic review and meta-analysis. *Lancet Oncol* 2011; **12**: 540-550 [PMID: 21549638 DOI: 10.1016/S1470-2045(11)70075-4]

89 **Joosten JJ**, Strobbe LJ, Wauters CA, Pruszczynski M, Wobbes T, Ruers TJ. Intraoperative lymphatic mapping and the sentinel node concept in colorectal carcinoma. *Br J Surg* 1999; **86**: 482-486 [PMID: 10215818 DOI: 10.1046/j.1365-2168.1999.01051.x]

90 **Nastro P**, Sodo M, Dodaro CA, Gargiulo S, Acampa W, Bracale U, Renda A. Intraoperative radiochromoguided mapping of sentinel lymph node in colon cancer. *Tumori* 2002; **88**: 352-353 [PMID: 12400991]

91 **Cahill RA**, Anderson M, Wang LM, Lindsey I, Cunningham C, Mortensen NJ. Near-infrared (NIR) laparoscopy for intraoperative lymphatic road-mapping and sentinel node identification during definitive surgical resection of early-stage colorectal neoplasia. *Surg Endosc* 2012; **26**: 197-204 [PMID: 21853392 DOI: 10.1007/s00464-011-1854-3]

92 **Noura S**, Ohue M, Seki Y, Tanaka K, Motoori M, Kishi K, Miyashiro I, Ohigashi H, Yano M, Ishikawa O, Miyamoto Y. Feasibility of a lateral region sentinel node biopsy of lower rectal cancer guided by indocyanine green using a near-infrared camera system. *Ann Surg Oncol* 2010; **17**: 144-151 [PMID: 19774415 DOI: 10.1245/s10434-009-0711-2]

93 **Handgraaf HJ**, Boogerd LS, Verbeek FP, Tummers QR, Hardwick JC, Baeten CI, Frangioni JV, van de Velde CJ, Vahrmeijer AL. Intraoperative fluorescence imaging to localize tumors and sentinel lymph nodes in rectal cancer. *Minim Invasive Ther Allied Technol* 2016; **25**: 48-53 [PMID: 25950124 DOI: 10.3109/13645706.2015.1042389]

94 **Braat AE**, Oosterhuis JW, Moll FC, de Vries JE, Wiggers T. Sentinel node detection after preoperative short-course radiotherapy in rectal carcinoma is not reliable. *Br J Surg* 2005; **92**: 1533-1538 [PMID: 16231281 DOI: 10.1002/bjs.5169]

95 **Nagata J**, Fukunaga Y, Akiyoshi T, Konishi T, Fujimoto Y, Nagayama S, Yamamoto N, Ueno M. Colonic Marking With Near-Infrared, Light-Emitting, Diode-Activated Indocyanine Green for Laparoscopic Colorectal Surgery. *Dis Colon Rectum* 2016; **59**: e14-e18 [PMID: 26734978 DOI: 10.1097/DCR.0000000000000542]

96 **Zako T**, Ito M, Hyodo H, Yoshimoto M, Watanabe M, Takemura H, Kishimoto H, Kaneko K, Soga K, Maeda M. Extra-luminal detection of assumed colonic tumor site by near-infrared laparoscopy. *Surg Endosc* 2016; **30**: 4153-4159 [PMID: 26659227 DOI: 10.1007/s00464-015-4669-9]

97 **Watanabe M**, Tsunoda A, Narita K, Kusano M, Miwa M. Colonic tattooing using fluorescence imaging with light-emitting diode-activated indocyanine green: a feasibility study. *Surg Today* 2009; **39**: 214-218 [PMID: 19280280 DOI: 10.1007/s00595-008-3849-9]

98 **Miyoshi N**, Ohue M, Noura S, Yano M, Sasaki Y, Kishi K, Yamada T, Miyashiro I, Ohigashi H, Iishi H, Ishikawa O, Imaoka S. Surgical usefulness of indocyanine green as an alternative to India ink for endoscopic marking. *Surg Endosc* 2009; **23**: 347-351 [PMID: 18443867 DOI: 10.1007/s00464-008-9938-4]

99 **Watanabe M**, Murakami M, Ozawa Y, Yoshizawa S, Matsui N, Aoki T. Intraoperative Identification of Colonic Tumor Sites Using a Near-Infrared Fluorescence Endoscopic Imaging

System and Indocyanine Green. *Dig Surg* 2017; **34**: 495-501 [PMID: 28219066 DOI: 10.1159/000458450]

100 **Park JH**, Moon HS, Kwon IS, Yun GY, Lee SH, Park DH, Kim JS, Kang SH, Lee ES, Kim SH, Sung JK, Lee BS, Jeong HY. Usefulness of colonic tattooing using indocyanine green in patients with colorectal tumors. *World J Clin Cases* 2018; **6**: 632-640 [PMID: 30430118 DOI: 10.12998/wjcc.v6.i13.632]

101 **Goo JJ**, Ryu DG, Kim HW, Park SB, Kang DH, Choi CW, Kim SJ, Nam HS, Kim HS, Son GM, Park BS. Efficacy of preoperative colonoscopic tattooing with indocyanine green on lymph node harvest and factors associated with inadequate lymph node harvest in colorectal cancer. *Scand J Gastroenterol* 2019; **54**: 666-672 [PMID: 31071272 DOI: 10.1080/00365521.2019.1612940]

102 **Matsumura Y**, Maeda H. A new concept for macromolecular therapeutics in cancer chemotherapy: mechanism of tumoritropic accumulation of proteins and the antitumor agent smancs. *Cancer Res* 1986; **46**: 6387-6392 [PMID: 2946403]

103 **Magdassi S**, Bar-David S, Friedman-Levi Y, Zigmond E, Varol C, Lahat G, Klausner J, Eyal S, Nizri E. Intraoperative Localization of Rectal Tumors Using Liposomal Indocyanine Green. *Surg Innov* 2017; **24**: 139-144 [PMID: 28152672 DOI: 10.1177/1553350617690310]

104 **Bar-David S**, Larush L, Goder N, Aizic A, Zigmond E, Varol C, Klausner J, Magdassi S, Nizri E. Size and lipid modification determine liposomal Indocyanine green performance for tumor imaging in a model of rectal cancer. *Sci Rep* 2019; **9**: 8566 [PMID: 31189986 DOI: 10.1038/s41598-019-45038-w]

105 **Glockzin G**, Zeman F, Croner RS, Königsrainer A, Pelz J, Ströhlein MA, Rau B, Arnold D, Koller M, Schlitt HJ, Piso P. Perioperative Systemic Chemotherapy, Cytoreductive Surgery, and Hyperthermic Intraperitoneal Chemotherapy in Patients With Colorectal Peritoneal Metastasis: Results of the Prospective Multicenter Phase 2 COMBATAC Trial. *Clin Colorectal Cancer* 2018; **17**: 285-296 [PMID: 30131226 DOI: 10.1016/j.clcc.2018.07.011]

106 **Liberale G**, Vankerckhove S, Caldon MG, Ahmed B, Moreau M, Nakadi IE, Larsimont D, Donckier V, Bourgeois P; Group R&D for the Clinical Application of Fluorescence Imaging of the Jules Bordet's Institute. Fluorescence Imaging After Indocyanine Green Injection for Detection of Peritoneal Metastases in Patients Undergoing Cytoreductive Surgery for Peritoneal Carcinomatosis From Colorectal Cancer: A Pilot Study. *Ann Surg* 2016; **264**: 1110-1115 [PMID: 27828822 DOI: 10.1097/SLA.0000000000001618]

107 **Dapri G**, Cahill R, Bourgeois P, Liberale G, Galdon Gomez M, Cadière GB. Peritumoural injection of indocyanine green fluorescence during transanal total mesorectal excision to identify the plane of dissection - a video vignette. *Colorectal Dis* 2017; **19**: 599-600 [PMID: 28467625 DOI: 10.1111/codi.13698]

108 **Ismael G**, Al Furajji H, Cahill RA. Near-infrared laparoscopic fluorescence to guide fascial plane identification in total mesorectal excision for rectal cancer: A Video Vignette. *Colorectal Dis* 2015; **17** Suppl 3: 36 [PMID: 26394742 DOI: 10.1111/codi.13089]

109 **Kawada K**, Hida K, Yoshitomi M, Sakai Y. A novel use of indocyanine green to identify the plane of dissection during abdominoperineal resection by the transperineal approach - a video vignette. *Colorectal Dis* 2018; **20**: 455-456 [PMID: 29512858 DOI: 10.1111/codi.14065]

110 **Slooter MD**, Blok RD, Wisselink DD, Buskens CJ, Bemelman WA, Tanis PJ, Hompes R. Near-infrared fluorescence angiography for intra-operative assessment of pedicled omentoplasty for filling of a pelvic cavity: a pilot study. *Tech Coloproctol* 2019; **23**: 723-728 [PMID: 31432336 DOI: 10.1007/s10151-019-02048-0]

111 **Slooter MD**, Blok RD, de Krom MA, Buskens CJ, Bemelman WA, Tanis PJ, Hompes R. Optimizing omentoplasty for management of chronic pelvic sepsis by intra-operative fluorescence angiography: a comparative cohort study. *Colorectal Dis* 2020; **22**: 2252-2259 [PMID: 32683788 DOI: 10.1111/codi.15276]

World Journal of Gastroenterology

Submit a Manuscript: https://www.f6publishing.com

World J Gastroenterol 2021 October 14; 27(38): 6387-6398

DOI: 10.3748/wjg.v27.i38.6387

ISSN 1007-9327 (print) ISSN 2219-2840 (online)

MINIREVIEWS

Transcription factors specificity protein and nuclear receptor 4A1 in pancreatic cancer

Stephen Safe, Rupesh Shrestha, Kumaravel Mohankumar, Marcell Howard, Erik Hedrick, Maen Abdelrahim

ORCID number: Stephen Safe 0000-0002-2115-3060; Rupesh Shrestha 0000-0002-6785-2932; Kumaravel Mohankumar 0000-0002-6159-8080; Marcell Howard 0000-0002-0000-359X; Erik Hedrick 0000-0002-0667-0991; Maen Abdelrahim 0000-0002-6631-5035.

Author contributions: Safe S, Abdelrahim M and Hedrick E substantial contributions to conception and design of the study, acquisition of data, or analysis and interpretation of data; Shrestha R and Howard M drafting the article or making critical revisions related to important intellectual content of the manuscript; Safe S, Mohankumar K and Shrestha R final approval of the version of the article to be published.

Supported by Houston Methodist Cancer Center Innovation Award.

Conflict-of-interest statement: Authors declare no conflict of interests for this article.

Open-Access: This article is an open-access article that was selected by an in-house editor and fully peer-reviewed by external reviewers. It is distributed in accordance with the Creative Commons Attribution NonCommercial (CC BY-NC 4.0) license, which permits others to

Stephen Safe, Kumaravel Mohankumar, Marcell Howard, Department of Veterinary Physiology and Pharmacology, Texas A&M University, College Station, TX 77845, United States

Rupesh Shrestha, Department of Biochemistry and Biophysics, Texas A&M University, College Station, TX 77845, United States

Erik Hedrick, Cancer Institute, Cleveland Clinic, Cleveland, OH 44195, United States

Maen Abdelrahim, Department of Medical Oncology, Houston Methodist Hospital Cancer Center, Houston, TX 77030, United States

Corresponding author: Stephen Safe, PhD, Full Professor, Department of Veterinary Physiology and Pharmacology, Texas A&M University, 4466 TAMU, College Station, TX 77845, United States. ssafe@cvm.tamu.edu

Abstract

Specificity protein (Sp) transcription factors (TFs) Sp1, Sp3 and Sp4, and the orphan nuclear receptor 4A1 (NR4A1) are highly expressed in pancreatic tumors and Sp1 is a negative prognostic factor for pancreatic cancer patient survival. Results of knockdown and overexpression of Sp1, Sp3 and Sp4 in pancreatic and other cancer lines show that these TFs are individually pro-oncogenic factors and loss of one Sp TF is not compensated by other members. NR4A1 is also a pro-oncogenic factor and both NR4A1 and Sp TFs exhibit similar functions in pancreatic cancer cells and regulate cell growth, survival, migration and invasion. There is also evidence that Sp TFs and NR4A1 regulate some of the same genes including survivin, epidermal growth factor receptor, PAX3-FOXO1, α5- and α6-integrins, β1-, β3- and β4-integrins; this is due to NR4A1 acting as a cofactor and mediating NR4A1/Sp1/4-regulated gene expression through GC-rich gene promoter sites. Several studies show that drugs targeting Sp downregulation or NR4A1 antagonists are highly effective inhibitors of Sp/NR4A1-regulated pathways and genes in pancreatic and other cancer cells, and the triterpenoid celastrol is a novel dual-acting agent that targets both Sp TFs and NR4A1.

Key Words: Specificity protein; Nuclear receptor 4A1; Pancreatic cancer; Transcription factors; Ligand inhibitors; Nuclear receptor 4A antagonists

©The Author(s) 2021. Published by Baishideng Publishing Group Inc. All rights reserved.

distribute, remix, adapt, build upon this work non-commercially, and license their derivative works on different terms, provided the original work is properly cited and the use is non-commercial. See: http://creativecommons.org/Licenses/by-nc/4.0/

Manuscript source: Invited manuscript

Specialty type: Gastroenterology and hepatology

Country/Territory of origin: United States

Peer-review report's scientific quality classification
Grade A (Excellent): A
Grade B (Very good): 0
Grade C (Good): C, C
Grade D (Fair): D
Grade E (Poor): 0

Received: January 14, 2021
Peer-review started: January 14, 2021
First decision: March 29, 2021
Revised: April 30, 2021
Accepted: September 6, 2021
Article in press: September 6, 2021
Published online: October 14, 2021

P-Reviewer: Li JT, Matsuo Y, Uhlmann D
S-Editor: Gao CC
L-Editor: A
P-Editor: Liu JH



Core Tip: Specificity protein (Sp), transcription factors (TFs), Sp1, Sp3 and Sp4, and nuclear receptor 4A1 (NR4A1, Nur77) are highly expressed in pancreatic cancer cells and tumors. Results of gene silencing studies show that Sp TFs and NR4A1 are pro-oncogenic and regulate pathways/genes associated with cell proliferation, survival and migration/invasion. Bis-indole derived ligands (CDIMs) that bind NR4A1 act as NR4A1 antagonists and we discuss an important mechanism of gene regulation by NR4A1/Sp complexes which can be inhibited by NR4A1 antagonists.

Citation: Safe S, Shrestha R, Mohankumar K, Howard M, Hedrick E, Abdelrahim M. Transcription factors specificity protein and nuclear receptor 4A1 in pancreatic cancer. *World J Gastroenterol* 2021; 27(38): 6387-6398
URL: https://www.wjgnet.com/1007-9327/full/v27/i38/6387.htm
DOI: https://dx.doi.org/10.3748/wjg.v27.i38.6387

INTRODUCTION

Pancreatic cancer is a devastating disease and it is estimated that in 2020, the number of diagnosed cases in the United States will be 57600 and 47050 will die because of this disease[1]. Despite advances in treating pancreatic cancer with surgical intervention and various therapeutic regimens, the five-year survival rate from pancreatic cancer is < 10%[1] and this is due, in part to the late detection of the tumors due to lack of symptoms and lack of early biomarkers of this cancer. There are many risk factors for pancreatic cancer and this includes pancreatitis, obesity and metabolic syndrome; due to the obesity crisis in many countries, it is estimated that by 2030, pancreatic cancer will be the second leading cause of cancer deaths[2]. Development of pancreatic cancer is associated with the temporal increases in expression of various oncogenes and inactivation of tumor suppressor genes resulting in enhanced cancer cell proliferation, survival, migration, invasion and metastasis[3-6]. Gemcitabine has largely replaced 5-fluorouracil as the major cytotoxic drug for treatment of pancreatic cancer and many other mechanism-based drugs targeting critical genes associated with various pro-oncogenic pathways in pancreatic cancer are being developed or are in clinical trials[7, 8]. The success of these agents in combination therapies targeting one or more pro-oncogenic pathways has been limited but promising. For example, one study using the vascular endothelial growth factor inhibitor bevacizumab in combination with leucovorin, nab-paclitaxel, oxiplatin and 5-fluorouracil and this resulted in a one-year survival of 82% for the treated patients[9]. In this review, we will focus on three transcription factors (TFs), namely specificity proteins (Sps) Sp1, Sp3 and Sp4, and nuclear receptor 4A1 (NR4A1, TR3, Nur77) and their overlapping pro-oncogenic roles in pancreatic cancers. We will also highlight an interesting convergence of these TFs and outline approaches for simultaneous targeting NR4A1 and Sp TFs by mechanism-based agents resulting in inhibition of cancer cell growth, survival, migration and invasion.

Sp and NR4A1: Background

Sp TFs are members of the Sp-Kruppel-like factor family (Sp/KLF) of TFs which includes 9 Sp TFs and 17 KLF proteins[10-14]. Sp1-Sp4 genes have a similar domain structure, however, it is evident that among other Sp/KLF family of TFs, their domain structures are highly diverse with the most common features being the zinc finger DNA binding domain and its subsequent interactions with GC/GT-rich gene promoter sequences[10-14]. Sp1 was the first TF identified and characterized[15] and Sp1 knockout mouse embryos exhibited retarded development and other abnormalities, and embryolethality is observed (day 11)[11]. Comparable studies on other Sp family members indicate that these TFs play important roles in early development and differentiation by their regulation of key genes involved in these functions. A detailed analysis of the age-dependent expression of individual Sp TFs is not available, however, there is evidence that for Sp1, there is an age-dependent decrease in expression in both rodent and human tissues[16-19]. Presumably the functions of Sp1 in aging animals are replaced by other TFs. The concern and subsequent focus on Sp1 and other Sp TFs (Sp3 and Sp4) in cancer emerged from studies showing that Sp1, Sp3 and Sp4 were overexpressed in cancer cells and tumors

[20]. These TFs were also identified as negative prognostic factors for cancer patient survival from several cancers and functional studies demonstrated the pro-oncogenic activity for Sp TFs[20]. The overexpression and prognostic value of Sp TFs have primarily focused on Sp1 and one of the first studies showed that Sp1 was overexpressed in patients with pancreatic tumors and was a negative prognostic factor for patient survival[21]. Most studies on cancer patients have reported that Sp1 or Sp3 is overexpressed and/or is a negative prognostic factor for glioma, astrocytoma, colon, gastric, liver, prostate and head and neck cancers; in lung and breast cancers; in addition, there are some conflicting results[22-40]. An important linkage between Sp1 and cancer was observed in studies showing that carcinogen- or oncogene- induced transformation of human fibroblasts into fibrosarcomas was accompanied by an 8-18-fold increase in expression of Sp1. Moreover, the ability of fibrosarcoma cells to form tumors in athymic nude mice was abrogated after Sp1 knockdown[41]. Subsequent studies show that Sp TFs are pro-oncogenic and regulate pathways and genes associated with cell growth, survival, migration and invasion (Figure 1).

NR4A1 and two related receptors NR4A2 (Nurr1) and NR4A3 (Nor1) are orphan nuclear receptors with structures and endogenous functions that differ significantly from Sp TFs[42,43]. NR4A1 and NR4A3 knockout mice are viable whereas NR4A2$^{-/-}$ mice exhibit early mortality due to dopaminergic and other neuronal deficits[44-48]. Endogenous ligands for NR4A have not been identified, however, NR4A bind structurally diverse synthetic compounds and these receptors interact with nerve growth factor β response elements (NBREs: AAAGGTCA) and Nur response elements [NuRE: AAAT(GA)C/T/CA] as monomers and dimers respectively[49-51]. In addition, NR4A1 and NR4A2 form a heterodimer with retinoid X receptor and bind a DR5 motif[52,53]. NR4As are immediate early genes induced by diverse stressors and they play important roles in maintaining cellular homeostasis and in pathophysiology [42,43,54]. NR4A1 and Sp TFs are remarkably distinct in their structures and functions in maintaining cellular homeostasis, however, in pancreatic cancer and other tumor types, their functions are similar. Like Sp1, NR4A1 is overexpressed in solid tumors from patients with pancreatic, breast, liver, glioblastoma, ovarian, colon, melanoma, endometrial, cervical, rhabdomyosarcoma and gastric cancer[55-64]. Moreover, high expression of NR4A1 in tumors is a negative prognostic factor for lung, breast, colon and ovarian cancer patients[58-60,63]. The negative prognostic significance of NR4A1 overexpression is paralleled by studies showing that like Sp TFs, NR4A1 is pro-oncogenic and regulates pathways comparable to that described for Sp TFs (Figure 1). Thus, there is an interesting parallel in the expression, functions and prognostic values of Sp TFs (primarily Sp1) and NR4A1 in multiple tumor types. This review will focus on the individual roles and interactions of Sp TFs and NR4A1 in pancreatic cancer and this will include genes commonly regulated by NR4A1/Sp complex in which NR4A1/Sp1 and NR4A1/Sp4 interact at GC-rich gene promoter sites that bind Sp.

Sp TFs and pancreatic cancer

Shi *et al*[65] first reported the overexpression of Sp1 in pancreatic cancer cell lines and in pancreatic tumors compared to non-tumor tissue and subsequent studies showed that Sp1, Sp3 and Sp4 were co-expressed in most pancreatic cancer cells[66]. The three structurally related TFs target similar GC-rich sequences in gene promoters and there is evidence for some genes, that Sp3 acts as a transcriptional repressor. A systematic study of the functions of Sp1, Sp3 and Sp4 was investigated in Panc1, MiaPaCa2 and L3.6pL pancreatic cancer cells and also in cell lines derived from lung, colon, kidney and breast tumors[66]. Figure 1 illustrates the functional effects of Sp1 knockdown which resulted in decreased pancreatic cancer cell growth, induced Annexin V staining (apoptosis) and decreased migration and this was accompanied by PARP cleavage, another marker of apoptosis. These results were somewhat surprising since it might be expected that the loss of Sp1 would be compensated for by Sp3 and Sp4. The functional properties of Sp3 and Sp4 were also determined in Panc1, L3.6pL and MiaPaca2 cells by knockdown and the results showed that like Sp1, knockdown of Sp3 or Sp4 decreased cell proliferation, induced apoptosis (increased Annexin V staining and cleaved PARP) and decreased cell invasion and similar results were observed in lung, breast, kidney and colon cancer cell lines[66]. These results indicated the importance of all three Sp TFs as independent pro-oncogenic factors that regulate pancreatic cell growth, survival and invasion, and related genes and it was suggested that Sp TFs were non-oncogene addiction genes[66].

Genomic analysis of altered gene expression after individual knockdown of Sp1, Sp3 and Sp4 in Panc1 pancreatic cancer cells further demonstrated their pro-oncogenic functions and unique effects of Sp1, Sp3 and Sp4 in this cell line. Figure 2A illustrates the total number of genes that are changed after individual knockdown of Sp1, Sp3

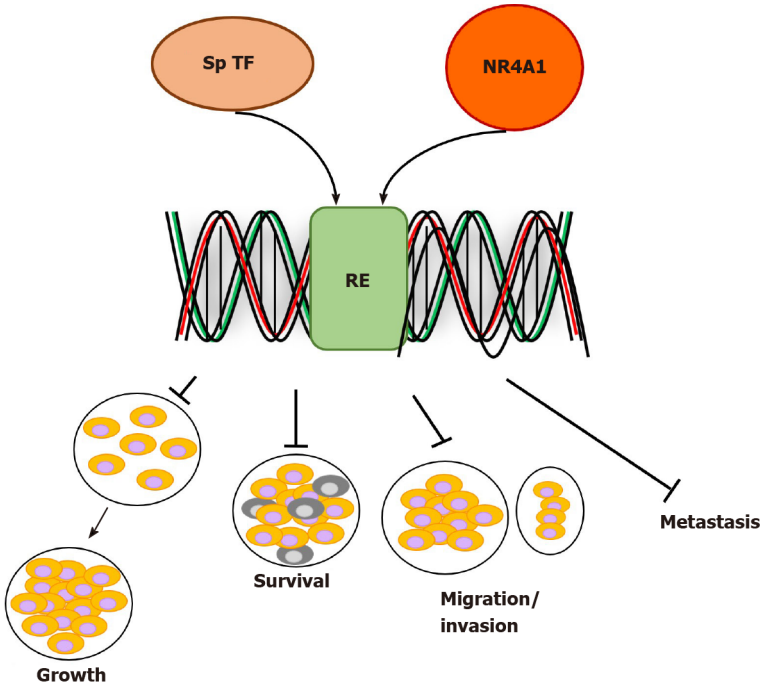


Figure 1 Common functional properties of specificity protein transcription factors and nuclear receptor 4A1 in pancreatic and other cancer cells. Specificity protein (Sp) transcription factors (TFs) (Sp1, Sp3 and Sp4) bind GC-rich gene promoter sequences to activate gene expression associated with enhanced cell proliferation, survival, migration, invasion and metastasis. Nuclear receptor 4A1 (NR4A1) binds as monomer or homodimers to NBRE and NuRE promoter elements and NR4A1 also acts as a cofactor for Sp1 and Sp4-regulated genes and NR4A1/Sp binds GC-rich promoter sequences. Sp: Specificity protein; TFs: Transcription factors; NR4A1: Nuclear receptor 4A1.

and Sp4, the number of uniquely modified genes and the number of genes commonly repressed or induced by Sp1-Sp3, Sp1-Sp4 and Sp3-Sp4. Knockdown of Sp3 and Sp4 resulted in the highest number (and percentage) of commonly induced or repressed genes. Causal Ingenuity Pathway Analysis (IPA) of the genes affected by knockdown were sorted into functional groups and Figure 2B-D illustrate the overlap in affected genes in the Sp1-Sp3, Sp1-Sp4 and Sp3-Sp4 groups associated cell growth, survival and cellular movement (migration and invasion). The overall number and percentage of commonly induced or repressed genes was highest for Sp3 and Sp4 in each functional category and this was similar to that observed for the total number of commonly induced or repressed genes (Figure 2A). Quantitative results from the causal IPA confirmed that the genomic changes observed in the array data were consistent with the functional changes observed after individual knockdown of Sp1, Sp3 and Sp4. This study also confirmed that knockdown of Sp1 alone or Sp1/3/4 (combination) in L3.6pL pancreatic cancer cells also decreased the growth of tumors in athymic nude mice bearing L3.6pL cells as xenografts[66].

In addition to the array studies noted above, there are a number of studies on Sp knockdown or overexpression in pancreatic cancer cells that have identified other Sp-regulated genes that contribute to the pro-oncogenic functions of Sp1, Sp3 and Sp4, and this includes regulation of pro-oncogenic long non-coding RNAs (MALAT1) and microRNAs (Table 1)[20,66-69]. These data were obtained only in pancreatic cancer cells; however, similar results for many of these genes have also been observed in other cancer cell lines[20]. Results summarized in Table 1 were observed in multiple pancreatic cancer cell lines and for some genes, their regulation by Sp TFs is cell context-dependent and there are also differences in the roles of Sp1, Sp3 and Sp4. Some studies used a combination of oligonucleotides targeting the 3 TFs (siSp1/3/4) and the combined knockdown of Sp1, Sp3 and Sp4 by RNA interference in Panc28 and L3.6pL pancreatic cancer cells decreased expression of NFkB-p65 and NFkB-p50 proteins[70]. In the former cell line, individual knockdown of Sp1, Sp3 or Sp4 partially decreased expression of both NFkB subunits. In L3.6pL cells, Sp1 and to a lesser extent Sp3, but not Sp4 knockdown decreased NFkB-p65 whereas Sp4 knockdown was primarily responsible for decreased expression of NFkB-p50 protein.

NR4A1 and pancreatic cancer

The pro-oncogenic role of NR4A1 has been investigated in multiple solid tumor

Table 1 Specificity protein regulated genes in pancreatic cancer cells

Functional	Sp-regulated gene
Cell proliferation and cell cycle progression	*EGFR, IGFR, cyclin D1, PIK3R1, pmTOR, 4-EBP, pS6RP, STAT3, pSTAT3, NFkB-p65/950*
Survival and apoptosis	*Survivin, bcl-2, PARP cleavage, APAF1, ATM, TNFRSF25, COX2, NFkB-p65/5*
Cell migration/movement EMT	*B1-integrin, α2-integrin, MTSS1, vimentin*
Angiogenesis	*VEGF, VEGFR1, VEGFR2, COX2*
Other pro-oncogenic factors	*TNFα, BRCA1, ARHGEF2, Ajuba, MALAT-1, RAS-6TP, FAS*

A detailed analysis of specificity protein (Sp)-regulated genes (Sp1, Sp3 and Sp4) in Panc1 cells based on RNAseq after Sp knockdown has been reported [66] and reviewed[20]. Sp: Specificity protein; EMT: Epithelial-mesenchymal transition.

derived cancer cell lines (rev. in 70), however, the number of publications on the functions of NR4A1 in pancreatic cancer is limited[55,71,72]. Knockdown of NR4A1 in pancreatic cancer cells inhibits cancer cell and tumor growth in athymic nude mouse xenograft studies, induces apoptosis and inhibits migration/invasion. Thus, the pro-oncogenic functions of NR4A1 and Sp TFs in pancreatic cancer cell lines are similar (Figure 1) and comparable results were obtained after their knockdown. For example, knockdown of NR4A1 by RNA interference in pancreatic cancer cells decreased expression of bcl-2 and survivin and this was accompanied by markers of apoptosis including increased TUNEL staining, caspase-3 and PARP cleavage[55,71]. Proteome analysis confirmed that loss of NR4A1 enhanced cell death and decreased gene products associated with cell proliferation and this was accompanied by increased reactive oxygen species (ROS) and ROS-induced endoplasmic reticulum (ER) stress genes including CHOP, Grp78, ATF4 and XBP-1s[71]. In addition, genes such as thioredoxin domain containing 5 (TXNDC5) and isocitrate dehydrogenase 1 (IDH1) that maintain high reductant levels are also NR4A1 regulated genes and their loss after receptor knockdown triggers the ROS-ER stress response. Knockdown of NR4A1 also decreased cell migration and expression of β1- and α5-integrins which play a role in NR4A1-regulated pancreatic cancer cell migration[72]. Thus, there is overlap between the function of Sp TFs and NR4A1 in pancreatic cancer cell lines and studies in other cancer cell lines show that many of the Sp-regulated genes summarized in Table 1 are also regulated by NR4A1[70]. Regulation of the same genes by Sp TFs and NR4A1 was recently reported in breast cancer cells where knockdown of Sp4 or NR4A1 decreased expression of α6- and β1-integrins in MDA-MB-231 and SKBR3 breast cancer cells. The effects of Sp3 and Sp1 knockdown on expression of these integrins was gene- and cell context-specific.

Mechanistic convergence of NR4A1 and Sp TFs

Both NR4A1 and Sp TFs are nuclear proteins that interact with defined cis-elements in their target gene promoters. Mechanistic studies showing cooperative activation of common genes by NR4A1 and Sp1 was first observed in pancreatic cancer cells and subsequently investigated and confirmed in other cancer cell lines[55,72]. The survivin gene has a GC-rich promoter that binds Sp TFs and has been extensively characterized as an Sp-regulated gene[73,74]. Knockdown of NR4A1 or treatment with NR4A1 antagonists decreased expression of survivin protein and mRNA and also decreased luciferase activity in pancreatic cancer cells transfected with GC-rich survivin promoter-luciferase constructs[55]. Further analysis of survivin regulation in pancreatic cancer cells showed that survivin is regulated by a p300/NR4A1/Sp1 complex where Sp1 binds the GC-rich survivin promoter, NR4A1 acts as a cofactor/coactivator and p300 is also part of the complex. The identification of this functional NR4A1/Sp complex is consistent with previous reports showing many other nuclear receptors also activate gene expression through interactions with Sp1. Studies in other cancer cell lines have identified other NR4A1-regulated genes that are regulated by NR4A1/Sp1, NR4A1/Sp4 or NR4A1/Sp1/4 and these include β1-, β3- and β4-integrins, α5- and α6-integrins, TXNDC5 and the PAX3-FOX01 fusion oncogene and the checkpoint gene PD-L1 (rev. in 70). Thus, like Ajuba[75], NR4A1 acts as a cofactor for Sp TFs in pancreatic and other cancer cell lines and they coregulate some of the same genes (EGFR, survivin and IGF1R). The possible interactions of NR4A1 and Ajuba, a coregulator of Sp-regulated genes needs to be further investigated.

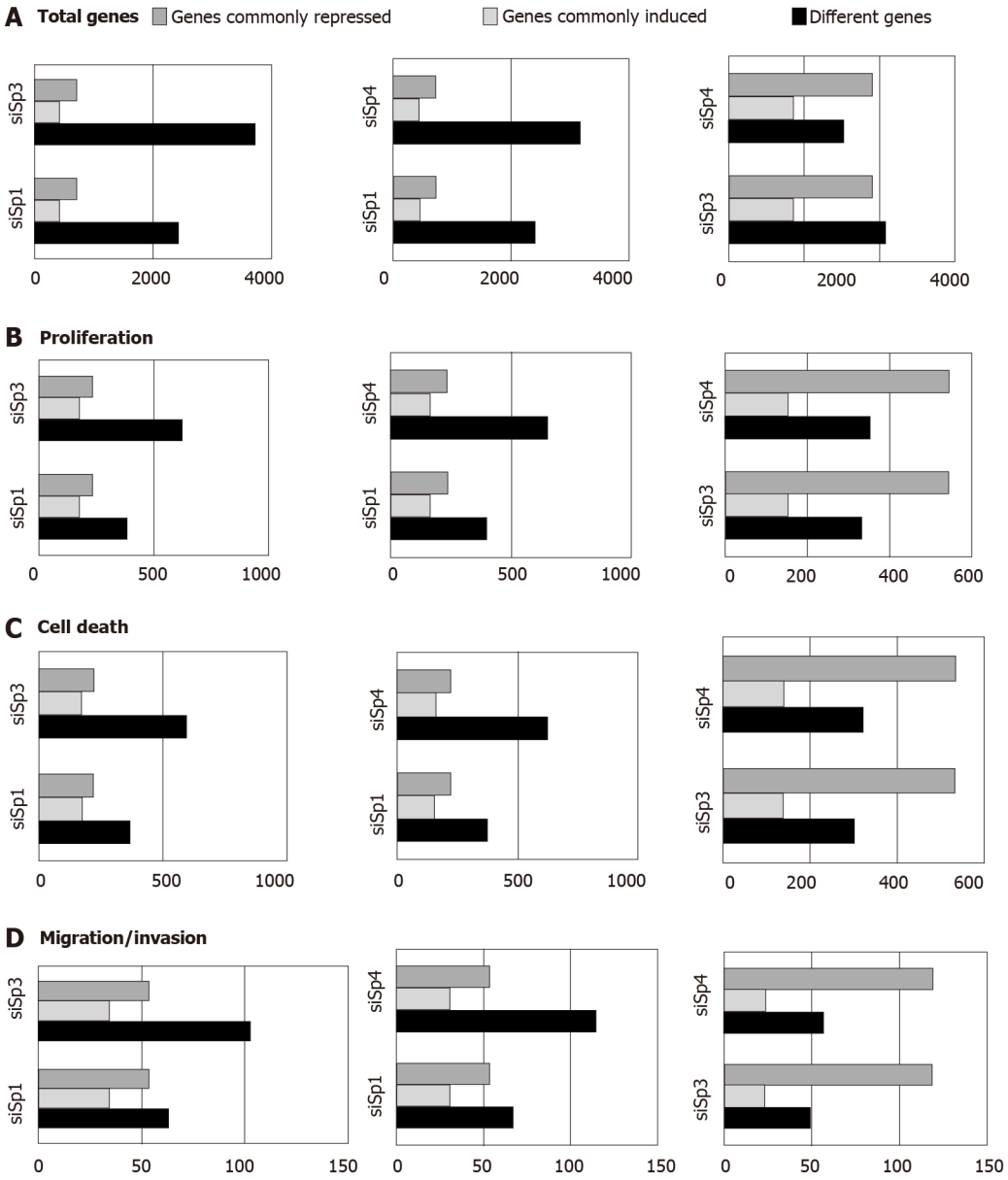


Figure 2 Genomic analysis of Sp1, Sp3 and Sp4 regulated genes in pancreatic cancer cells. A: The number of total genes regulated by specificity protein (Sp) transcription factors (TFs) in Panc1 cell was determined by individual Sp knockdown (siSp1, siSp3 and siSp4) and the number of unique (Different genes) and commonly repressed (Genes commonly repressed) and induced (Genes commonly induced) genes are indicated; B-D: Ingenuity Pathway Analysis analysis of genes that regulate cell proliferation (B), cell death (C) and migration/invasion (D) compares the number of unique and commonly repressed/induced genes by Sp1 and Sp3, Sp1 and Sp4 and Sp3 and Sp4 as described[66].

DRUGS THAT TARGET SP TFS AND NR4A1

Several drugs that target Sp TFs in pancreatic cancer cells have been identified and these include tolfenamic acid and structurally related compounds, COX2 inhibitors curcumin, metformin, piperlongumine, methyl 2-cyano-3,12-dioxooleana-1,9-dien-28-oate (CDDO-Me), benzylisothiocyanate (BITC) and phenethylisothiocyanate (PEITC) (Figure 3)[20]. All of these compounds downregulate Sp1, Sp3 and Sp4 through different pathways. For example, tolfenamic acid and COX2 inhibitors induce proteasome-dependent degradation of Sp1, Sp3 and Sp4 whereas metformin induces the dual specificity phosphatases MPK-1 and MPK-5 which are important for Sp downregulation. The phosphatases downregulate miR-27a which results in upregulation of ZBTB10, a Sp repressor which competitively displaces Sp TFs from GC-rich sites resulting in gene inactivation since ZBTB10 Lacks a transactivation domain. ROS-inducers including PEITC, BITC, piperlongumine, CDDO-Me and curcumin also decrease Sp-regulated gene expression through an ROS-mediated pathway which also involves induction of Sp repressors namely ZBTB4, ZBTB10 and ZBTB34[20] (Figure 4). This pathway involves ROS-dependent remodeling of repressor complexes

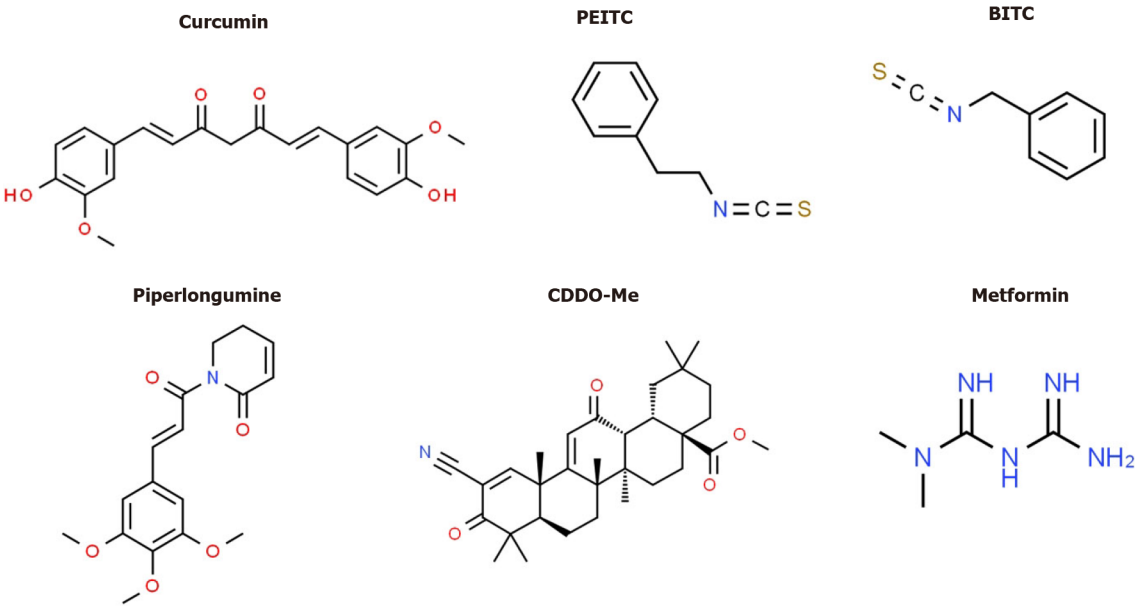


Figure 3 Structures of agents that target downregulation of Sp1, Sp3 and Sp4 in pancreatic and other cancer cell lines[68]. The structurally diverse compounds act through multiple pathways in different cancer cell lines.

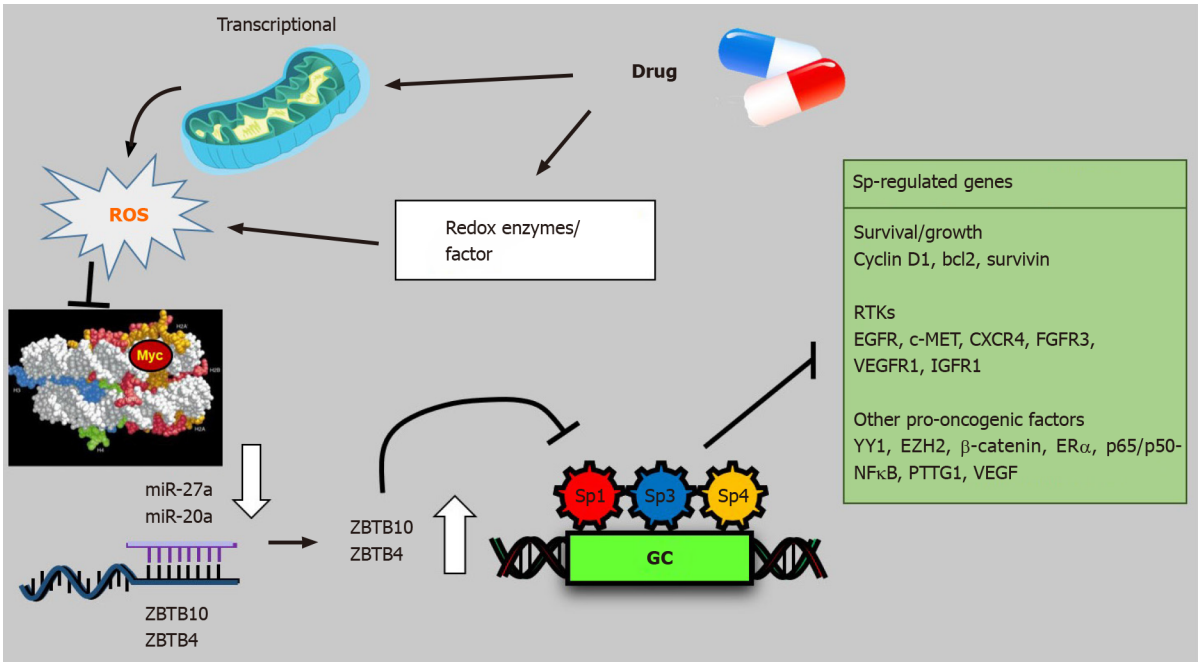


Figure 4 Mechanism of reactive oxygen species-dependent downregulation of specificity protein transcription factors. Induction of reactive oxygen species results in epigenetic suppression of Myc, downregulation of microRNAs, induction of ZBTB suppressors and decreased expression of specificity protein (Sp) transcription factors and Sp-regulated genes[20]. ROS: Reactive oxygen species; Sp: Specificity protein.

which results in downregulation of cMyc and cMyc-dependent microRNAs (miR-27a, miR-17-92) and induction of ZBTBs. These compounds (Figure 4) and others induce similar patterns and mechanisms of Sp downregulation in other cancer cell lines[20], however, there are compound-specific differences in mechanisms that are cell context-dependent.

Bis (3'-indolyl)-1-(p-hydroxyphenyl) methane (DIM-C-pPhOH) (Figure 5) was identified as an NR4A1 Ligand that acts as a receptor antagonist and mimics the effects of NR4A1 knockdown in pancreatic and other cancer cell lines[70]. DIM-C-pPhOH and several 3,5-disubstituted phenyl analogs are inhibitors of cell proliferation, survival and migration/invasion and they inhibit expression of NR4A1/Sp- and other NR4A1-regulated genes. Moreover, many of the 3,5-disubstituted analogs of

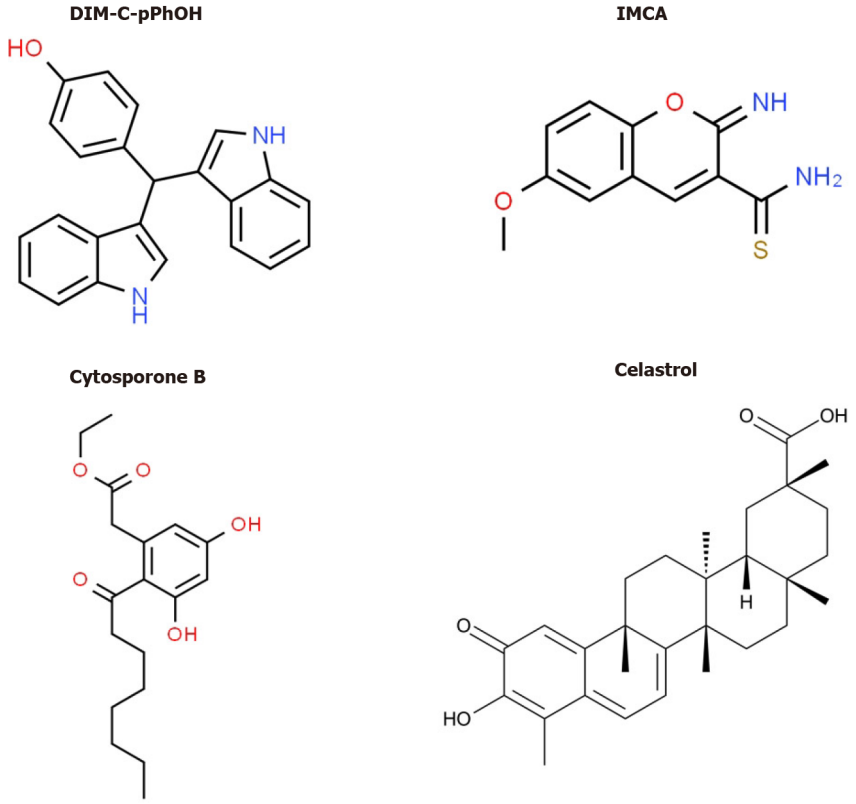


Figure 5 Nuclear receptor 4A1 ligands. Structures of compounds that directly bind nuclear receptor 4A1 include DIM-C-pPhOH, IMCA, cytosporone B and celastrol[76-80].

DIM-C-pPhOH inhibit tumor growth in mouse xenograft models at doses < 5 mg/kg per day and ongoing studies have identified ligands that inhibit tumor growth at doses < 1mg/kg per day. Interestingly, several other classes of compounds bind and modulate NR4A1-dependent pathways/genes and these include cytosporone B and structurally related compounds, IMCA (2-imino-6-methoxy-2H-chromene-3-carbothiomide) and the triterpenoid celastrol and analogs[76-80] (Figure 5). Fascinatingly, celastrol also activates ROS-dependent downregulation of Sp1, Sp3 and Sp4 in bladder cancer cells[80] (*e.g.*, Figure 4) and uniquely acts as a bifunctional agent targeting both Sp TFs and NR4A1. Ongoing studies in this laboratory have identified other dual targeting agents with potential for clinical applications for pancreatic cancer therapy.

CONCLUSION

In summary, it is evident that both Sp TFs and NR4A1 are pro-oncogenic factors that regulate pancreatic cancer cell and tumor growth and interactions of NR4A1 and Sp TFs are also important for regulating many critical genes (Figure 1) involved in pro-oncogenic functions. Although the functional importance of NR4A1/Sp regulated genes in cancer cell growth, survival, migration and invasion has been established in pancreatic and other cancers, clinical applications of drugs targeting Sp and NR4A1 are lacking. Several compounds have been identified that induce Sp downregulation or inhibit/antagonize NR4A1. Current studies in our laboratories are focused on identifying agents like celastrol that act simultaneously as NR4A1 antagonists and Sp downregulators as a new class of drugs that will enhance the effectiveness of current chemotherapies used for clinical treatment of pancreatic and other cancers.

REFERENCES

1 **Siegel RL**, Miller KD, Jemal A. Cancer statistics, 2020. *CA Cancer J Clin* 2020; **70**: 7-30 [PMID: 31912902 DOI: 10.3322/caac.21590]

2 **Zhang Y**, Yang C, Cheng H, Fan Z, Huang Q, Lu Y, Fan K, Luo G, Jin K, Wang Z, Liu C, Yu X. Novel agents for pancreatic ductal adenocarcinoma: emerging therapeutics and future directions. *J Hematol Oncol* 2018; **11**: 14 [PMID: 29386069 DOI: 10.1186/s13045-017-0551-7]

3 **Karandish F**, Mallik S. Biomarkers and Targeted Therapy in Pancreatic Cancer. *Biomark Cancer* 2016; **8**: 27-35 [PMID: 27147897 DOI: 10.4137/BiC.s34414]

4 **Michael JV**, Goldfinger LE. Concepts and advances in cancer therapeutic vulnerabilities in RAS membrane targeting. *Semin Cancer Biol* 2019; **54**: 121-130 [PMID: 29203271 DOI: 10.1016/j.semcancer.2017.11.021]

5 **Eser S**, Schnieke A, Schneider G, Saur D. Oncogenic KRAS signalling in pancreatic cancer. *Br J Cancer* 2014; **111**: 817-822 [PMID: 24755884 DOI: 10.1038/bjc.2014.215]

6 **Jones S**, Zhang X, Parsons DW, Lin JC, Leary RJ, Angenendt P, Mankoo P, Carter H, Kamiyama H, Jimeno A, Hong SM, Fu B, Lin MT, Calhoun ES, Kamiyama M, Walter K, Nikolskaya T, Nikolsky Y, Hartigan J, Smith DR, Hidalgo M, Leach SD, Klein AP, Jaffee EM, Goggins M, Maitra A, Iacobuzio-Donahue C, Eshleman JR, Kern SE, Hruban RH, Karchin R, Papadopoulos N, Parmigiani G, Vogelstein B, Velculescu VE, Kinzler KW. Core signaling pathways in human pancreatic cancers revealed by global genomic analyses. *Science* 2008; **321**: 1801-1806 [PMID: 18772397 DOI: 10.1126/science.1164368]

7 **Qian Y**, Gong Y, Fan Z, Luo G, Huang Q, Deng S, Cheng H, Jin K, Ni Q, Yu X, Liu C. Molecular alterations and targeted therapy in pancreatic ductal adenocarcinoma. *J Hematol Oncol* 2020; **13**: 130 [PMID: 33008426 DOI: 10.1186/s13045-020-00958-3]

8 **Stoica AF**, Chang CH, Pauklin S. Molecular Therapeutics of Pancreatic Ductal Adenocarcinoma: Targeted Pathways and the Role of Cancer Stem Cells. *Trends Pharmacol Sci* 2020; **41**: 977-993 [PMID: 33092892 DOI: 10.1016/j.tips.2020.09.008]

9 **Isacoff WH**, Reber HA, Bedford R, Hoos W, Rahib L, Upfill-Brown A, Donahue T, Hines OJ. Low-Dose Continuous 5-Fluorouracil Combined with Leucovorin, nab-Paclitaxel, Oxaliplatin, and Bevacizumab for Patients with Advanced Pancreatic Cancer: A Retrospective Analysis. *Target Oncol* 2018; **13**: 461-468 [PMID: 29882102 DOI: 10.1007/s11523-018-0572-3]

10 **Suske G**, Bruford E, Philipsen S. Mammalian SP/KLF transcription factors: bring in the family. *Genomics* 2005; **85**: 551-556 [PMID: 15820306 DOI: 10.1016/j.ygeno.2005.01.005]

11 **Marin M**, Karis A, Visser P, Grosveld F, Philipsen S. Transcription factor Sp1 is essential for early embryonic development but dispensable for cell growth and differentiation. *Cell* 1997; **89**: 619-628 [PMID: 9160753 DOI: 10.1016/s0092-8674(00)80243-3]

12 **Vizcaíno C**, Mansilla S, Portugal J. Sp1 transcription factor: A long-standing target in cancer chemotherapy. *Pharmacol Ther* 2015; **152**: 111-124 [PMID: 25960131 DOI: 10.1016/j.pharmthera.2015.05.008]

13 **Beishline K**, Azizkhan-Clifford J. Sp1 and the 'hallmarks of cancer'. *FEBS J* 2015; **282**: 224-258 [PMID: 25393971 DOI: 10.1111/febs.13148]

14 **Kim CK**, He P, Bialkowska AB, Yang VW. SP and KLF Transcription Factors in Digestive Physiology and Diseases. *Gastroenterology* 2017; **152**: 1845-1875 [PMID: 28366734 DOI: 10.1053/j.gastro.2017.03.035]

15 **Kadonaga JT**, Carner KR, Masiarz FR, Tjian R. Isolation of cDNA encoding transcription factor Sp1 and functional analysis of the DNA binding domain. *Cell* 1987; **51**: 1079-1090 [PMID: 3319186 DOI: 10.1016/0092-8674(87)90594-0]

16 **Oh JE**, Han JA, Hwang ES. Downregulation of transcription factor, Sp1, during cellular senescence. *Biochem Biophys Res Commun* 2007; **353**: 86-91 [PMID: 17161377 DOI: 10.1016/j.bbrc.2006.11.118]

17 **Adrian GS**, Seto E, Fischbach KS, Rivera EV, Adrian EK, Herbert DC, Walter CA, Weaker FJ, Bowman BH. YY1 and Sp1 transcription factors bind the human transferrin gene in an age-related manner. *J Gerontol A Biol Sci Med Sci* 1996; **51**: B66-B75 [PMID: 8548503 DOI: 10.1093/gerona/51a.1.b66]

18 **Park SC**. Nuclear barrier hypothesis of aging as mechanism for trade-off growth to survival. *Adv Exp Med Biol* 2011; **720**: 3-13 [PMID: 21901614 DOI: 10.1007/978-1-4614-0254-1_1]

19 **Kim SY**, Kang HT, Han JA, Park SC. The transcription factor Sp1 is responsible for aging-dependent altered nucleocytoplasmic trafficking. *Aging Cell* 2012; **11**: 1102-1109 [PMID: 23013401 DOI: 10.1111/acel.12012]

20 **Safe S**, Abbruzzese J, Abdelrahim M, Hedrick E. Specificity Protein Transcription Factors and Cancer: Opportunities for Drug Development. *Cancer Prev Res (Phila)* 2018; **11**: 371-382 [PMID: 29545399 DOI: 10.1158/1940-6207.CAPR-17-0407]

21 **Jiang NY**, Woda BA, Banner BF, Whalen GF, Dresser KA, Lu D. Sp1, a new biomarker that identifies a subset of aggressive pancreatic ductal adenocarcinoma. *Cancer Epidemiol Biomarkers Prev* 2008; **17**: 1648-1652 [PMID: 18628415 DOI: 10.1158/1055-9965.EPI-07-2791]

22 **Kong LM**, Liao CG, Fei F, Guo X, Xing JL, Chen ZN. Transcription factor Sp1 regulates expression of cancer-associated molecule CD147 in human lung cancer. *Cancer Sci* 2010; **101**: 1463-1470 [PMID: 20384626 DOI: 10.1111/j.1349-7006.2010.01554.x]

23 **Li L**, Gao P, Li Y, Shen Y, Xie J, Sun D, Xue A, Zhao Z, Xu Z, Zhang M, Li B, Jiang J. JMJD2A-dependent silencing of Sp1 in advanced breast cancer promotes metastasis by downregulation of DIRAS3. *Breast Cancer Res Treat* 2014; **147**: 487-500 [PMID: 25193278 DOI: 10.1007/s10549-014-3083-7]

24 **Wang XB**, Peng WQ, Yi ZJ, Zhu SL, Gan QH. [Expression and prognostic value of transcriptional

factor sp1 in breast cancer]. *Ai Zheng* 2007; **26**: 996-1000 [PMID: 17927860]
25 **Kim JY**, Jung HH, Ahn S, Bae S, Lee SK, Kim SW, Lee JE, Nam SJ, Ahn JS, Im YH, Park YH. The relationship between nuclear factor (NF)-κB family gene expression and prognosis in triple-negative breast cancer (TNBC) patients receiving adjuvant doxorubicin treatment. *Sci Rep* 2016; **6**: 31804 [PMID: 27545642 DOI: 10.1038/srep31804]
26 **Wang L**, Wei D, Huang S, Peng Z, Le X, Wu TT, Yao J, Ajani J, Xie K. Transcription factor Sp1 expression is a significant predictor of survival in human gastric cancer. *Clin Cancer Res* 2003; **9**: 6371-6380 [PMID: 14695137]
27 **Lee HS**, Park CK, Oh E, Erkin ÖC, Jung HS, Cho MH, Kwon MJ, Chae SW, Kim SH, Wang LH, Park MJ, Lee SY, Yang HB, Jia L, Choi YL, Shin YK. Low SP1 expression differentially affects intestinal-type compared with diffuse-type gastric adenocarcinoma. *PLoS One* 2013; **8**: e55522 [PMID: 23437057 DOI: 10.1371/journal.pone.0055522]
28 **Yao JC**, Wang L, Wei D, Gong W, Hassan M, Wu TT, Mansfield P, Ajani J, Xie K. Association between expression of transcription factor Sp1 and increased vascular endothelial growth factor expression, advanced stage, and poor survival in patients with resected gastric cancer. *Clin Cancer Res* 2004; **10**: 4109-4117 [PMID: 15217947 DOI: 10.1158/1078-0432.CCR-03-0628]
29 **Guan H**, Cai J, Zhang N, Wu J, Yuan J, Li J, Li M. Sp1 is upregulated in human glioma, promotes MMP-2-mediated cell invasion and predicts poor clinical outcome. *Int J Cancer* 2012; **130**: 593-601 [PMID: 21469139 DOI: 10.1002/ijc.26049]
30 **Dong Q**, Cai N, Tao T, Zhang R, Yan W, Li R, Zhang J, Luo H, Shi Y, Luan W, Zhang Y, You Y, Wang Y, Liu N. An axis involving SNAI1, microRNA-128 and SP1 modulates glioma progression. *PLoS One* 2014; **9**: e98651 [PMID: 24959930 DOI: 10.1371/journal.pone.0098651]
31 **Maurer GD**, Leupold JH, Schewe DM, Biller T, Kates RE, Hornung HM, Lau-Werner U, Post S, Allgayer H. Analysis of specific transcriptional regulators as early predictors of independent prognostic relevance in resected colorectal cancer. *Clin Cancer Res* 2007; **13**: 1123-1132 [PMID: 17317820 DOI: 10.1158/1078-0432.CCR-06-1668]
32 **Chen YT**, Tsai HP, Wu CC, Chen CY, Chai CY, Kwan AL. High-level Sp1 is Associated with Proliferation, Invasion, and Poor Prognosis in Astrocytoma. *Pathol Oncol Res* 2019; **25**: 1003-1013 [PMID: 29948615 DOI: 10.1007/s12253-018-0422-8]
33 **Liu L**, Ji P, Qu N, Pu WL, Jiang DW, Liu WY, Li YQ, Shi RL. The impact of high co-expression of Sp1 and HIF1α on prognosis of patients with hepatocellular cancer. *Oncol Lett* 2016; **12**: 504-512 [PMID: 27347172 DOI: 10.3892/ol.2016.4634]
34 **Kong LM**, Yao L, Lu N, Dong YL, Zhang J, Wang YQ, Liu L, Zhang HL, Huang JG, Liao CG. Interaction of KLF6 and Sp1 regulates basigin-2 expression mediated proliferation, invasion and metastasis in hepatocellular carcinoma. *Oncotarget* 2016; **7**: 27975-27987 [PMID: 27057625 DOI: 10.18632/oncotarget.8564]
35 **Hu J**, Hu H, Hang JJ, Yang HY, Wang ZY, Wang L, Chen DH, Wang LW. Simultaneous high expression of PLD1 and Sp1 predicts a poor prognosis for pancreatic ductal adenocarcinoma patients. *Oncotarget* 2016; **7**: 78557-78565 [PMID: 27713167 DOI: 10.18632/oncotarget.12447]
36 **Zhang HW**, Wang EW, Li LX, Yi SH, Li LC, Xu FL, Wang DL, Wu YZ, Nian WQ. A regulatory loop involving miR-29c and Sp1 elevates the TGF-β1 mediated epithelial-to-mesenchymal transition in lung cancer. *Oncotarget* 2016; **7**: 85905-85916 [PMID: 27829234 DOI: 10.18632/oncotarget.13137]
37 **Zhang J**, Zhu ZG, Ji J, Yuan F, Yu YY, Liu BY, Lin YZ. Transcription factor Sp1 expression in gastric cancer and its relationship to long-term prognosis. *World J Gastroenterol* 2005; **11**: 2213-2217 [PMID: 15818728 DOI: 10.3748/wjg.v11.i15.2213]
38 **Essafi-Benkhadir K**, Grosso S, Puissant A, Robert G, Essafi M, Deckert M, Chamorey E, Dassonville O, Milano G, Auberger P, Pagès G. Dual role of Sp3 transcription factor as an inducer of apoptosis and a marker of tumour aggressiveness. *PLoS One* 2009; **4**: e4478 [PMID: 19212434 DOI: 10.1371/journal.pone.0004478]
39 **Bedolla RG**, Gong J, Prihoda TJ, Yeh IT, Thompson IM, Ghosh R, Kumar AP. Predictive value of Sp1/Sp3/FLIP signature for prostate cancer recurrence. *PLoS One* 2012; **7**: e44917 [PMID: 23028678 DOI: 10.1371/journal.pone.0044917]
40 **Hsu TI**, Wang MC, Chen SY, Yeh YM, Su WC, Chang WC, Hung JJ. Sp1 expression regulates lung tumor progression. *Oncogene* 2012; **31**: 3973-3988 [PMID: 22158040 DOI: 10.1038/onc.2011.568]
41 **Lou Z**, O'Reilly S, Liang H, Maher VM, Sleight SD, McCormick JJ. Down-regulation of overexpressed sp1 protein in human fibrosarcoma cell lines inhibits tumor formation. *Cancer Res* 2005; **65**: 1007-1017 [PMID: 15705902]
42 **Maxwell MA**, Muscat GE. The NR4A subgroup: immediate early response genes with pleiotropic physiological roles. *Nucl Recept Signal* 2006; **4**: e002 [PMID: 16604165 DOI: 10.1621/nrs.04002]
43 **Pearen MA**, Muscat GE. Minireview: Nuclear hormone receptor 4A signaling: implications for metabolic disease. *Mol Endocrinol* 2010; **24**: 1891-1903 [PMID: 20392876 DOI: 10.1210/me.2010-0015]
44 **Lee SL**, Wesselschmidt RL, Linette GP, Kanagawa O, Russell JH, Milbrandt J. Unimpaired thymic and peripheral T cell death in mice lacking the nuclear receptor NGFI-B (Nur77). *Science* 1995; **269**: 532-535 [PMID: 7624775 DOI: 10.1126/science.7624775]
45 **Zetterström RH**, Solomin L, Jansson L, Hoffer BJ, Olson L, Perlmann T. Dopamine neuron agenesis in Nurr1-deficient mice. *Science* 1997; **276**: 248-250 [PMID: 9092472 DOI: 10.1126/science.276.5310.248]

46 **Saucedo-Cardenas O**, Quintana-Hau JD, Le WD, Smidt MP, Cox JJ, De Mayo F, Burbach JP, Conneely OM. Nurr1 is essential for the induction of the dopaminergic phenotype and the survival of ventral mesencephalic late dopaminergic precursor neurons. *Proc Natl Acad Sci U S A* 1998; **95**: 4013-4018 [PMID: 9520484 DOI: 10.1073/pnas.95.7.4013]

47 **Cheng LE**, Chan FK, Cado D, Winoto A. Functional redundancy of the Nur77 and Nor-1 orphan steroid receptors in T-cell apoptosis. *EMBO J* 1997; **16**: 1865-1875 [PMID: 9155013 DOI: 10.1093/emboj/16.8.1865]

48 **Woronicz JD**, Calnan B, Ngo V, Winoto A. Requirement for the orphan steroid receptor Nur77 in apoptosis of T-cell hybridomas. *Nature* 1994; **367**: 277-281 [PMID: 8121493 DOI: 10.1038/367277a0]

49 **Wilson TE**, Fahrner TJ, Johnston M, Milbrandt J. Identification of the DNA binding site for NGFI-B by genetic selection in yeast. *Science* 1991; **252**: 1296-1300 [PMID: 1925541 DOI: 10.1126/science.1925541]

50 **Maira M**, Martens C, Philips A, Drouin J. Heterodimerization between members of the Nur subfamily of orphan nuclear receptors as a novel mechanism for gene activation. *Mol Cell Biol* 1999; **19**: 7549-7557 [PMID: 10523643 DOI: 10.1128/mcb.19.11.7549]

51 **Philips A**, Lesage S, Gingras R, Maira MH, Gauthier Y, Hugo P, Drouin J. Novel dimeric Nur77 signaling mechanism in endocrine and lymphoid cells. *Mol Cell Biol* 1997; **17**: 5946-5951 [PMID: 9315652 DOI: 10.1128/mcb.17.10.5946]

52 **Perlmann T**, Jansson L. A novel pathway for vitamin A signaling mediated by RXR heterodimerization with NGFI-B and NURR1. *Genes Dev* 1995; **9**: 769-782 [PMID: 7705655 DOI: 10.1101/gad.9.7.769]

53 **Zetterström RH**, Solomin L, Mitsiadis T, Olson L, Perlmann T. Retinoid X receptor heterodimerization and developmental expression distinguish the orphan nuclear receptors NGFI-B, Nurr1, and Nor1. *Mol Endocrinol* 1996; **10**: 1656-1666 [PMID: 8961274 DOI: 10.1210/mend.10.12.8961274]

54 **Kurakula K**, Koenis DS, van Tiel CM, de Vries CJ. NR4A nuclear receptors are orphans but not lonesome. *Biochim Biophys Acta* 2014; **1843**: 2543-2555 [PMID: 24975497 DOI: 10.1016/j.bbamcr.2014.06.010]

55 **Lee SO**, Abdelrahim M, Yoon K, Chintharlapalli S, Papineni S, Kim K, Wang H, Safe S. Inactivation of the orphan nuclear receptor TR3/Nur77 inhibits pancreatic cancer cell and tumor growth. *Cancer Res* 2010; **70**: 6824-6836 [PMID: 20660371 DOI: 10.1158/0008-5472.CAN-10-1992]

56 **Lacey A**, Rodrigues-Hoffman A, Safe S. PAX3-FOXO1A Expression in Rhabdomyosarcoma Is Driven by the Targetable Nuclear Receptor NR4A1. *Cancer Res* 2017; **77**: 732-741 [PMID: 27864345 DOI: 10.1158/0008-5472.CAN-16-1546]

57 **Smith AG**, Lim W, Pearen M, Muscat GE, Sturm RA. Regulation of NR4A nuclear receptor expression by oncogenic BRAF in melanoma cells. *Pigment Cell Melanoma Res* 2011; **24**: 551-563 [PMID: 21362156 DOI: 10.1111/j.1755-148X.2011.00843.x]

58 **Wang JR**, Gan WJ, Li XM, Zhao YY, Li Y, Lu XX, Li JM, Wu H. Orphan nuclear receptor Nur77 promotes colorectal cancer invasion and metastasis by regulating MMP-9 and E-cadherin. *Carcinogenesis* 2014; **35**: 2474-2484 [PMID: 25064356 DOI: 10.1093/carcin/bgu157]

59 **Zhou F**, Drabsch Y, Dekker TJ, de Vinuesa AG, Li Y, Hawinkels LJ, Sheppard KA, Goumans MJ, Luwor RB, de Vries CJ, Mesker WE, Tollenaar RA, Devilee P, Lu CX, Zhu H, Zhang L, Dijke PT. Nuclear receptor NR4A1 promotes breast cancer invasion and metastasis by activating TGF-β signalling. *Nat Commun* 2014; **5**: 3388 [PMID: 24584437 DOI: 10.1038/ncomms4388]

60 **Delgado E**, Boisen MM, Laskey R, Chen R, Song C, Sallit J, Yochum ZA, Andersen CL, Sikora MJ, Wagner J, Safe S, Elishaev E, Lee A, Edwards RP, Haluska P, Tseng G, Schurdak M, Oesterreich S. High expression of orphan nuclear receptor NR4A1 in a subset of ovarian tumors with worse outcome. *Gynecol Oncol* 2016; **141**: 348-356 [PMID: 26946093 DOI: 10.1016/j.ygyno.2016.02.030]

61 **Zhu B**, Yang JR, Jia Y, Zhang P, Shen L, Li XL, Li J, Wang B. Overexpression of NR4A1 is associated with tumor recurrence and poor survival in non-small-cell lung carcinoma. *Oncotarget* 2017; **8**: 113977-113986 [PMID: 29371962 DOI: 10.18632/oncotarget.23048]

62 **Muscat GE**, Eriksson NA, Byth K, Loi S, Graham D, Jindal S, Davis MJ, Clyne C, Funder JW, Simpson ER, Ragan MA, Kuczek E, Fuller PJ, Tilley WD, Leedman PJ, Clarke CL. Research resource: nuclear receptors as transcriptome: discriminant and prognostic value in breast cancer. *Mol Endocrinol* 2013; **27**: 350-365 [PMID: 23292282 DOI: 10.1210/me.2012-1265]

63 **Hu Y**, Chau T, Liu HX, Liao D, Keane R, Nie Y, Yang H, Wan YJ. Bile acids regulate nuclear receptor (Nur77) expression and intracellular location to control proliferation and apoptosis. *Mol Cancer Res* 2015; **13**: 281-292 [PMID: 25232032 DOI: 10.1158/1541-7786.MCR-14-0230]

64 **Cho HJ**, Zhao J, Jung SW, Ladewig E, Kong DS, Suh YL, Lee Y, Kim D, Ahn SH, Bordyuh M, Kang HJ, Sa JK, Seo YJ, Kim ST, Lim DH, Dho YS, Lee JI, Seol HJ, Choi JW, Park WY, Park CK, Rabadan R, Nam DH. Distinct genomic profile and specific targeted drug responses in adult cerebellar glioblastoma. *Neuro Oncol* 2019; **21**: 47-58 [PMID: 30085274 DOI: 10.1093/neuonc/noy123]

65 **Shi Q**, Le X, Abbruzzese JL, Peng Z, Qian CN, Tang H, Xiong Q, Wang B, Li XC, Xie K. Constitutive Sp1 activity is essential for differential constitutive expression of vascular endothelial growth factor in human pancreatic adenocarcinoma. *Cancer Res* 2001; **61**: 4143-4154 [PMID: 11358838]

66 **Hedrick E**, Cheng Y, Jin UH, Kim K, Safe S. Specificity protein (Sp) transcription factors Sp1, Sp3 and Sp4 are non-oncogene addiction genes in cancer cells. *Oncotarget* 2016; **7**: 22245-22256 [PMID:

26967243 DOI: 10.18632/oncotarget.7925]
67 **Kent OA**, Mendell JT, Rottapel R. Transcriptional Regulation of miR-31 by Oncogenic KRAS Mediates Metastatic Phenotypes by Repressing RASA1. *Mol Cancer Res* 2016; **14**: 267-277 [PMID: 26747707 DOI: 10.1158/1541-7786.MCR-15-0456]
68 **Li S**, Wang Q, Qiang Q, Shan H, Shi M, Chen B, Zhao S, Yuan L. Sp1-mediated transcriptional regulation of MALAT1 plays a critical role in tumor. *J Cancer Res Clin Oncol* 2015; **141**: 1909-1920 [PMID: 25773124 DOI: 10.1007/s00432-015-1951-0]
69 **Tan Y**, Yin H, Zhang H, Fang J, Zheng W, Li D, Li Y, Cao W, Sun C, Liang Y, Zeng J, Zou H, Fu W, Yang X. Sp1-driven up-regulation of miR-19a decreases RHOB and promotes pancreatic cancer. *Oncotarget* 2015; **6**: 17391-17403 [PMID: 26041879 DOI: 10.18632/oncotarget.3975]
70 **Safe S**, Karki K. The Paradoxical Roles of Orphan Nuclear Receptor 4A (NR4A) in Cancer. *Mol Cancer Res* 2021; **19**: 180-191 [PMID: 33106376 DOI: 10.1158/1541-7786.MCR-20-0707]
71 **Lee SO**, Jin UH, Kang JH, Kim SB, Guthrie AS, Sreevalsan S, Lee JS, Safe S. The orphan nuclear receptor NR4A1 (Nur77) regulates oxidative and endoplasmic reticulum stress in pancreatic cancer cells. *Mol Cancer Res* 2014; **12**: 527-538 [PMID: 24515801 DOI: 10.1158/1541-7786.MCR-13-0567]
72 **Hedrick E**, Lee SO, Safe S. The nuclear orphan receptor NR4A1 regulates β1-integrin expression in pancreatic and colon cancer cells and can be targeted by NR4A1 antagonists. *Mol Carcinog* 2017; **56**: 2066-2075 [PMID: 28418095 DOI: 10.1002/mc.22662]
73 **Stauber RH**, Mann W, Knauer SK. Nuclear and cytoplasmic survivin: molecular mechanism, prognostic, and therapeutic potential. *Cancer Res* 2007; **67**: 5999-6002 [PMID: 17616652 DOI: 10.1158/0008-5472.CAN-07-0494]
74 **Wu J**, Ling X, Pan D, Apontes P, Song L, Liang P, Altieri DC, Beerman T, Li F. Molecular mechanism of inhibition of survivin transcription by the GC-rich sequence-selective DNA binding antitumor agent, hedamycin: evidence of survivin down-regulation associated with drug sensitivity. *J Biol Chem* 2005; **280**: 9745-9751 [PMID: 15637054 DOI: 10.1074/jbc.M409350200]
75 **Zhang B**, Song L, Cai J, Li L, Xu H, Li M, Wang J, Shi M, Chen H, Jia H, Hou Z. The LIM protein Ajuba/SP1 complex forms a feed forward loop to induce SP1 target genes and promote pancreatic cancer cell proliferation. *J Exp Clin Cancer Res* 2019; **38**: 205 [PMID: 31101117 DOI: 10.1186/s13046-019-1203-2]
76 **Zhan Y**, Du X, Chen H, Liu J, Zhao B, Huang D, Li G, Xu Q, Zhang M, Weimer BC, Chen D, Cheng Z, Zhang L, Li Q, Li S, Zheng Z, Song S, Huang Y, Ye Z, Su W, Lin SC, Shen Y, Wu Q. Cytosporone B is an agonist for nuclear orphan receptor Nur77. *Nat Chem Biol* 2008; **4**: 548-556 [PMID: 18690216 DOI: 10.1038/nchembio.106]
77 **Wang WJ**, Wang Y, Chen HZ, Xing YZ, Li FW, Zhang Q, Zhou B, Zhang HK, Zhang J, Bian XL, Li L, Liu Y, Zhao BX, Chen Y, Wu R, Li AZ, Yao LM, Chen P, Zhang Y, Tian XY, Beermann F, Wu M, Han J, Huang PQ, Lin T, Wu Q. Orphan nuclear receptor TR3 acts in autophagic cell death *via* mitochondrial signaling pathway. *Nat Chem Biol* 2014; **10**: 133-140 [PMID: 24316735 DOI: 10.1038/nchembio.1406]
78 **Zhang L**, Liu W, Wang Q, Li Q, Wang H, Wang J, Teng T, Chen M, Ji A, Li Y. New Drug Candidate Targeting the 4A1 Orphan Nuclear Receptor for Medullary Thyroid Cancer Therapy. *Molecules* 2018; **23** [PMID: 29498706 DOI: 10.3390/molecules23030565]
79 **Hu M**, Luo Q, Alitongbieke G, Chong S, Xu C, Xie L, Chen X, Zhang D, Zhou Y, Wang Z, Ye X, Cai L, Zhang F, Chen H, Jiang F, Fang H, Yang S, Liu J, Diaz-Meco MT, Su Y, Zhou H, Moscat J, Lin X, Zhang XK. Celastrol-Induced Nur77 Interaction with TRAF2 Alleviates Inflammation by Promoting Mitochondrial Ubiquitination and Autophagy. *Mol Cell* 2017; **66**: 141-153.e6 [PMID: 28388439 DOI: 10.1016/j.molcel.2017.03.008]
80 **Chen Z**, Zhang D, Yan S, Hu C, Huang Z, Li Z, Peng S, Li X, Zhu Y, Yu H, Lian B, Kang Q, Li M, Zeng Z, Zhang XK, Su Y. SAR study of celastrol analogs targeting Nur77-mediated inflammatory pathway. *Eur J Med Chem* 2019; **177**: 171-187 [PMID: 31132532 DOI: 10.1016/j.ejmech.2019.05.009]

World Journal of Gastroenterology

Submit a Manuscript: https://www.f6publishing.com

World J Gastroenterol 2021 October 14; 27(38): 6399-6414

DOI: 10.3748/wjg.v27.i38.6399

ISSN 1007-9327 (print) ISSN 2219-2840 (online)

MINIREVIEWS

Artificial intelligence for the early detection of colorectal cancer: A comprehensive review of its advantages and misconceptions

Michelle Viscaino, Javier Torres Bustos, Pablo Muñoz, Cecilia Auat Cheein, Fernando Auat Cheein

ORCID number: Michelle Viscaino 0000-0001-6693-7865; Javier Torres Bustos 0000-0003-1333-3894; Pablo Muñoz 0000-0001-5007-7864; Cecilia Auat Cheein 0000-0003-2042-6108; Fernando Auat Cheein 0000-0002-6347-7696.

Author contributions: Viscaino M performed the majority of the writing and prepared the figures and tables; Torres Bustos J performed the writing; Muñoz P provided the medical input in writing the paper; Auat Cheein C performed the writing and made critical revisions related to the medical content of the manuscript; Auat Cheein F designed the outline, edited, and reviewed the final version of the article and managed the funding; all authors read and approved the final manuscript.

Supported by Chilean National Agency for Research and Development (ANID), No. FB0008; and CONICYT-PCHA/Doctorado Nacional, No. 2018-21181420.

Conflict-of-interest statement: The authors deny any conflict of interest.

Open-Access: This article is an open-access article that was selected by an in-house editor and fully peer-reviewed by external reviewers. It is distributed in

Michelle Viscaino, Javier Torres Bustos, Department of Electronic Engineering, Universidad Tecnica Federico Santa Maria, Valpaiso 2340000, Chile

Pablo Muñoz, Hospital Clinico, University of Chile, Santiago 8380456, Chile

Cecilia Auat Cheein, Facultad de Medicina, Universidad Nacional de Santiago del Estero, Santiago del Estero 4200, Argentina

Fernando Auat Cheein, Department of Electronic Engineering, Universidad Técnica Federico Santa María, Valparaiso 2340000, Chile

Corresponding author: Fernando Auat Cheein, PhD, Associate Professor, Department of Electronic Engineering, Universidad Técnica Federico Santa María, Av. España 1680, Valparaiso 2340000, Chile. fernando.auat@usm.cl

Abstract

Colorectal cancer (CRC) was the second-ranked worldwide type of cancer during 2020 due to the crude mortality rate of 12.0 per 100000 inhabitants. It can be prevented if glandular tissue (adenomatous polyps) is detected early. Colonoscopy has been strongly recommended as a screening test for both early cancer and adenomatous polyps. However, it has some limitations that include the high polyp miss rate for smaller (< 10 mm) or flat polyps, which are easily missed during visual inspection. Due to the rapid advancement of technology, artificial intelligence (AI) has been a thriving area in different fields, including medicine. Particularly, in gastroenterology AI software has been included in computer-aided systems for diagnosis and to improve the assertiveness of automatic polyp detection and its classification as a preventive method for CRC. This article provides an overview of recent research focusing on AI tools and their applications in the early detection of CRC and adenomatous polyps, as well as an insightful analysis of the main advantages and misconceptions in the field.

Key Words: Artificial intelligence; Machine learning; Deep learning; Medical images; Colorectal cancer; Colorectal polyps

©The Author(s) 2021. Published by Baishideng Publishing Group Inc. All rights reserved.

accordance with the Creative Commons Attribution NonCommercial (CC BY-NC 4.0) license, which permits others to distribute, remix, adapt, build upon this work non-commercially, and license their derivative works on different terms, provided the original work is properly cited and the use is non-commercial. See: http://creativecommons.org/Licenses/by-nc/4.0/

Manuscript source: Unsolicited manuscript

Specialty type: Engineering, biomedical

Country/Territory of origin: Chile

Peer-review report's scientific quality classification

Grade A (Excellent): A
Grade B (Very good): 0
Grade C (Good): 0
Grade D (Fair): 0
Grade E (Poor): 0

Received: February 28, 2021
Peer-review started: February 28, 2021
First decision: March 27, 2021
Revised: April 26, 2021
Accepted: September 14, 2021
Article in press: September 14, 2021
Published online: October 14, 2021

P-Reviewer: Ryan E
S-Editor: Gong ZM
L-Editor: A
P-Editor: Li JH

Core Tip: Artificial intelligence-based (AI) methods have demonstrated high performance in classification, object detection, and segmentation tasks. Through multidisciplinary and collaborative work between clinicians and technicians, the advantages of AI have been successfully applied in automatic polyp detection and classification. The new AI-based systems present a better polyp detection rate and contribute to better clinical decision-making for preventing colorectal cancer (CRC). This article provides an overview of recent research focusing on AI and its applications in the early detection of CRC and adenomatous polyps.

Citation: Viscaino M, Torres Bustos J, Muñoz P, Auat Cheein C, Cheein FA. Artificial intelligence for the early detection of colorectal cancer: A comprehensive review of its advantages and misconceptions. *World J Gastroenterol* 2021; 27(38): 6399-6414
URL: https://www.wjgnet.com/1007-9327/full/v27/i38/6399.htm
DOI: https://dx.doi.org/10.3748/wjg.v27.i38.6399

INTRODUCTION

Colorectal cancer (CRC) is a common malignancy. Worldwide, in 2020, it ranked third among neoplasms, with incidences of 1931590 cases, representing 10% of neoplasms. However, in terms of mortality, it ranked second for the same year after lung cancer due to the crude mortality rate of 12.0 per 100000 inhabitants, prevailing in the male population[1].

Although CRC remains among the ten most frequent cancers, in a retrospective description, it was observed that at a global level, between 2000 and 2019 its ranking was stable in high-income countries, in which it maintained second place as a cause of death from neoplasia. However, in the remaining countries, it gradually increased; hence, in 2019, CRC was the 3rd leading cause of cancer death in upper-middle-income countries, the 4th leading cause in lower-middle-income countries, and the 5th leading cause in countries where income was low[2]. It is expected that by 2035, in those countries where it remains stable, the CRC mortality rate will decrease due to the application of early detection programs that are being implemented, the active participation of the population, and the prioritization of education on this matter. Nevertheless, it is expected that by 2035, in countries with low incomes, the mortality rate will continue to increase due mainly to late diagnosis and limited access to treatment if these indicators are not strategically addressed in time[3].

The risk of CRC in the general population is not uniform, and it is associated with factors such as a family history of CRC, lifestyles and eating habits and above all, the presence of polyps, either isolated or associated with genetic polyposis syndromes[4]. CRC can then be prevented by modifying diet and lifestyle, as well as early detection and timely treatment. Various studies have shown that screening tests facilitate the detection of precursor lesions in early stages. This, added to their subsequent elimination, promotes a reduction in CRC incidence and mortality[5-7].

Colonoscopy is the gold standard procedure for the diagnosis of large intestine (colon) and rectal diseases. The World Gastroenterology Organization establishes that both the sensitivity and the specificity of colonoscopy for the detection of polyps and colon cancer is 95%[4]. The United States Preventive Services Task Force determined that colonoscopy has a sensitivity between 89% and 98% for detecting adenomas of 10 mm and larger. For adenomas of 6 mm or more, the sensitivity ranges from 75% to 93%, while the specificity found was 89%[8], in which case a screening test for CRC is recommended. Additionally, in joint work between the American Cancer Society, the United States Multisocial Working Group and the American College of Radiology in 2008, colonoscopy was strongly recommended as a screening test designed to detect both early cancer and adenomatous polyps if resources were available and patients were willing to undergo an invasive test[5]. Similarly, the National Comprehensive Cancer Network recommends and promotes the application of colonoscopy for the detection of adenomatous polyps and early stages of CRC[9]. It should be noted that colonoscopy is a procedure that depends fundamentally on physician observation. In recent decades, technology has been incorporated into the inspection procedure, known as computer-aided systems.

Computer-aided detection/diagnosis systems (CADe/CADx) have been proposed, developed, and clinically used since 1966, especially in thoracic and breast imaging as well as in the cancer risk assessment[10]. The progress of computational resources and medical imaging devices has enabled CADe/CADx systems to support tasks in other areas, such as endoscopic examination[11]. CADe aims to find or localize abnormal or suspicious regions, increasing the detection rate while reducing the false negative rate (FNR). Additionally, CADx provides a second objective opinion regarding the assessment of a disease from image-based information. In the early stages of both systems, their algorithms were predominantly based on feature extraction methods engineered by domain experts[12]. However, the widespread progress of diseases and variability of cases have rendered these methods obsolete and have opened the research to new and improved methods. In particular, artificial intelligence (AI) has provided tools and algorithms capable of achieving high performance in terms of accuracy, sensitivity, and specificity to face tasks related to feature extraction, classification, detection, and region segmentation.

This work focuses on the main contributions of AI in gastroenterology, in particular, to the early detection of CRC through polyp detection and classification. We focus on those works that enhance the performance of endoscopic tests, which allow for direct visualization of existing lesions in the mucosa of the colon and rectum. With the numerous applications of AI and the growing interest in AI-related topics, some misconceptions have been discovered that are worth analysing.

WORLD OF AI

Since the term AI was first used in 1956, it has been a thriving field with relevant applications in several areas, including medicine[10]. The term AI refers to technology that allows computer systems to perform tasks that normally require human skills. The field of AI is broad and includes different fields, such as robotics, computer vision, natural language processing and machine learning, as shown in Figure 1. Often, such areas overlap to deliver more advanced features and capabilities. In medicine, robotic devices are increasingly being used in minimally invasive surgical procedures, such as robotic-assisted surgery for patients with CRC[13]. Natural language processing is another crucial AI area used to make the machine read, understand, and interpret human language. In the treatment of CRC, natural language processing has been useful for extracting relevant clinical information from scanned colonoscopy and pathology reports that would otherwise have to be extracted manually[14]. Computer vision and image processing have also been helpful in colonoscopy exploration, enhancing the visualization of lesion tissues[15]. However, from all AI fields, machine learning is the most widely used in three areas of medicine: Early detection and diagnosis, treatment, and outcome prediction and prognosis evaluation[16]. Gastrointestinal endoscopy has advanced in all three areas, but there is a clear trend in the detection and classification of polyps (see Wang *et al*[11], Nogueira-Rodríguez *et al*[17] and the references therein).

The following subsections focus on analysing the most prominent AI-based works on endoscopic tests without ignoring a brief review of the most commonly used machine learning algorithms (including deep neural networks) and evaluation metrics.

MACHINE LEARNING

Machine learning, a subset of AI, refers to a set of computer algorithms that learn from the input data provided, adjust a model through a training process, and perform predictions in novel situations by using the trained model[18]. According to the type of learning strategy, machine learning algorithms can be classified into two categories: Supervised and unsupervised learning. In supervised learning, a training set that contains the input data with the correct response (targets) must be previously available. The model is trained using the training set until it is generalized to respond correctly to all possible inputs. In the case of unsupervised learning, the correct answers are not provided, and the model attempts to group the data into categories identifying similarities between such data[19,20]. In medicine, supervised learning is the most commonly applied strategy because the goal is predicting a known outcome by mimicking a physician or health professional.

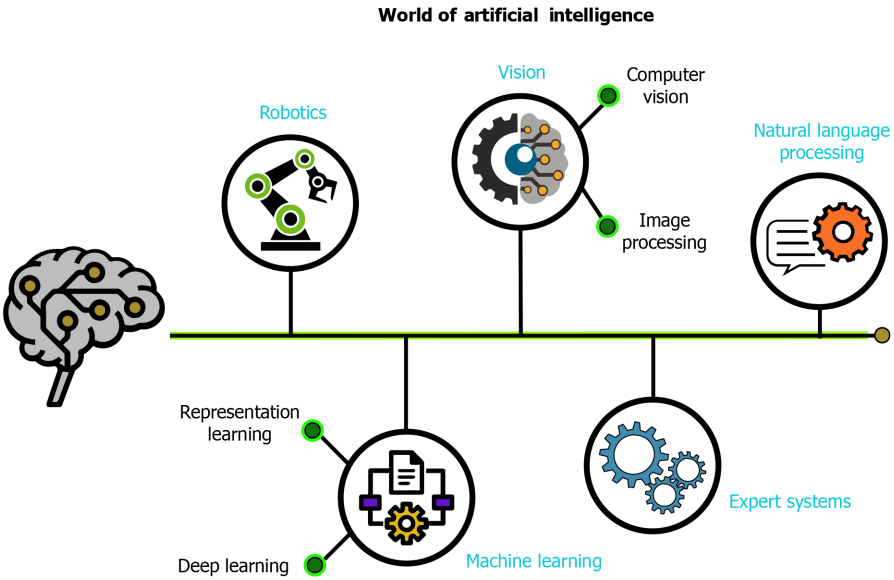


Figure 1 Artificial intelligence is a set of fields that are combining to improve tasks that involve human cognitive functions such as learning, reasoning and self-correction.

In the context of machine learning, healthcare data can be categorized as structured and unstructured. Imaging, genetic data, and electrophysiological data are some examples of structured data, whereas physical examination notes or clinical laboratory results that contain large portions of narrative texts are unstructured data[19]. The major digital data sources in medicine are images resulting from the development and improvement of different medical imaging techniques (*e.g.*, computer tomography, magnetic resonance imaging, ultrasound, X-ray and endoscopy)[10].

In gastroenterology, most computer-aided diagnosis/detection systems use images or videos, enabling the use of machine learning techniques to enhance their outcomes. In early works, CADe/x systems combined feature extractor methods and classical machine learning techniques such as random forest, decision trees, and support vector machines[21-23]. More recent works have shown applications that use deep learning algorithms such as convolutional neural networks (CNNs), in part due to the high performance and low latency of the systems[20].

The selection of one machine learning algorithm over another should be guided by analysing the available data as well as the task to be performed with it. Table 1 summarizes the main characteristics of the algorithms used in the last 5 years of state-of-the-art polyp detection and/or classification. We narrowed the analysis to the four most commonly used methods according to the Scopus and PubMed databases applied to medicine namely, support vector machines, random forest, decision trees and deep neural networks. Both support vector machines and random forests present high performance even if the data have high dimensionality. However, support vector machines are not recommended when the database is large because they increase training and inference time without improving performance[24]. Conversely, random forest presents high performance when working with large databases[25]. Deep neural networks outperform classical machine learning algorithms in almost all criteria but require large quantities of labelled data that may not be available, or the acquisition and labelling process may be very expensive or time consuming.

EVALUATION METRICS OF MACHINE LEARNING ALGORITHMS

Evaluation metrics are tied to the tasks (*e.g.*, classification, detection, localization, and segmentation) performed by the machine learning models. In gastroenterology in applications such as automatic polyp detection or classification, the evaluation metrics can be computed considering different levels: Video sequence, image, or region (pixel level).

Table 2 summarizes the terms and formulation of metrics commonly used for performance evaluation of machine learning models. In particular, those used in AI-based applications for colonoscopy. Some terms are key to understanding the

Table 1 Comparison between different types of machine learning approaches used in studies focused on polyp detection and classification

Characteristics	Support vector machine	Random forest	Decision trees	Deep neural networks	Context	Ref.
High dimensional data	High	High	Moderate	High	Performance	Shen *et al*[12]; Goodfellow *et al*[26]
Overlapped classes	Low	Low	Low	High		
Imbalance datasets	Moderate	High	Low	Moderate		
Non-linear data	Moderate	High	Moderate	High		
Larger dataset	Moderate[1]	High[1]	Low	High		
Outliers	Moderate	Moderate	Low	High	Robustness	Shen *et al*[12]; Yu *et al*[20]
Over-fitting	Moderate	High	Low	High		
Handling of missing values	Poor	Good	Good	Good		
Reproducibility	High	High	High	Moderate	Complexity	Yu *et al*[20]
Interpretability	Moderate	Moderate	High	Low		

[1]Consider that it leads to slow response time.

Table 2 Most common evaluation metrics found in the state of the art for detection, segmentation and classification tasks

Term	Symbol	Description
Positive	P	Number of real positive cases in the data
Negative	N	Number of real negative cases in the data
True positive	TP	Number of correct positive cases classified/detected
True negative	TN	Number of correct negative cases classified/detected
False positive	FP	Instances incorrectly classified/detected as positive
False negative	FN	Instances incorrectly classified/detected as negative
Area under curve	AUC	Area under the ROC plot
Term	**Task**	**Formulation**
Accuracy	C, D, S	(TP + TN)/(TP + TN + FN + FP)
Precision/PPV	C, D, S	TP/(TP + FP)
Sensitivity/Recall/TPR	C, D, S	TP/(TP + FN)
Specificity/TNR	C, D, S	TN/(TN + FP)
FPR	C, D, S	FP/(TN + FP)
FNR	C, D, S	FN/(TP + FN)
f1-score/DICE index	C, D, S	2 · (precision · recall)/(precision + recall)
f2-score	C, D, S	4 · (precision·recall)/(4·precision + recall)
IoU/Jaccard index	D, S	(target ∩ prediction)/(target ∪ prediction)
AAC	D, S	(detected area ∩ real area)/(real area)

C: Classification; D: Detection; S: Segmentation. PPV: Positive predictive value; TPR: True positive rate; TNR: True negative rate. AAC: Annotated area covered.

evaluation metrics in algorithms used for automatic polyp detection and/or classification. There are two well-defined cases: Images with polyps (positive cases) and images without polyps (negative cases). In both cases, some authors[15,27,28] define a true positive (TP) when the algorithm output finds the correct region of the polyp

(detection) or labels the image as a polyp (classification). In the case of detection, only one TP is considered per polyp, avoiding over-detection. Any detection or classification as a positive case outside the region of polyp or images without polyps is considered false positive. The absence of positive output in detection or classification in images with a polyp is considered a false negative. If the algorithm does not provide any positive output in images without polyps, it is considered a true negative. Positive polyp detection is a common evaluation metric that can be computed as a true positive rate (see Table 2) or polyp-based analysis by defining a threshold of the positive frame-level predictions[29].

The most widely used evaluation metric is accuracy (see formulation in Table 2). It works well in datasets with an equal number of samples belonging to each class (*i.e.*, balanced dataset), but it is not recommended for imbalanced datasets[30]. Evaluation metrics such as sensitivity, specificity, and positive predictive value are not dependent on the class distribution; therefore, they are not biased by imbalanced datasets[31]. The use of evaluation metrics also depends on the task to be performed. In detection tasks, metrics such as the f1-score (or DICE index) and f2-score of the Jaccard index are widely used[17]. We analyse each evaluation metric below.

Accuracy represents the overall effectiveness of the algorithm when comparing the number of correctly classified/detected samples with the total number of samples[17].

Precision (positive predictive value) represents the proportion of predicted positive cases that are real positives[17].

Sensitivity (recall or true positive rate) measures the ability of the algorithm to correctly identify the positive cases[17].

Specificity (true negative rate) measures the ability of the algorithm to correctly identify the negative cases[17].

The false positive rate (FPR) represents the proportion of negative cases incorrectly identified as positive cases in the data. In statistics, the FPR is equivalent to the type I error[26].

The FNR represents the proportion of positive cases incorrectly identified as negative cases in the data. In statistics, the FPR is equivalent to the type II error[26].

The DICE index (f1-score) determines the similarity between two different areas whether the algorithm is performing segmentation or detection tasks. In classification, the f1-score is a metric to evaluate a trade-off between precision and recall[32].

The f2-score is a metric to evaluate a trade-off between precision and recall but lowers the importance of precision and increases the importance of recall[17].

The Jaccard index (IoU) is a metric mostly used in detection/segmentation algorithms and quantifies overlap between the target area and the area predicted by the algorithm[32].

Annotated area covered is an evaluation metric mostly used in detection or segmentation tasks. It represents the proportion of the real area detected/segmented by the algorithm[33].

The area under the curve (AUC) is a metric obtained from the receiver operating characteristic curve that relates to the sensitivity *vs* specificity of a binary classifier[31]. The best classifier is the one with the AUC closest to 1.

ENHANCING COLONOSCOPY OUTCOMES *VIA* AI

Colonoscopy exploration is performed through a flexible tube (endoscope) that contains a tiny video camera at the tip. The camera allows the physician to see the inside of the entire colon by displaying the image on a digital screen, as shown in Figure 2. During the process, the physician detects (or not) the presence of lesions on the colon and polyps, and then, depending on the shape, colour and texture of the polyp, determines whether to remove it[15]. The outcome of colonoscopy exploration depends on several factors. On the one hand, the procedure is intrinsically dependent on the technology used, such as the camera resolution, screen size and resolution, frame rate, and capability to deal with blurriness, among other issues[15]. On the other hand, the results can be affected by the cognitive capabilities of the physician (*e.g.*, tiredness, fatigue or concentration) during the exploration procedure[34]. Other factors, such as bowel preparation and the percentage of the colon explored, can also affect the outcome of the exploration[35].

Traditional colonoscopy has been shown to be successful when detecting polyps larger than 10 mm, which are easily detected by physicians during inspection. However, the miss rate of polyp detection increases with smaller sized and/or flat polyps[36]. There are both clinical and technical efforts to improve colonoscopy

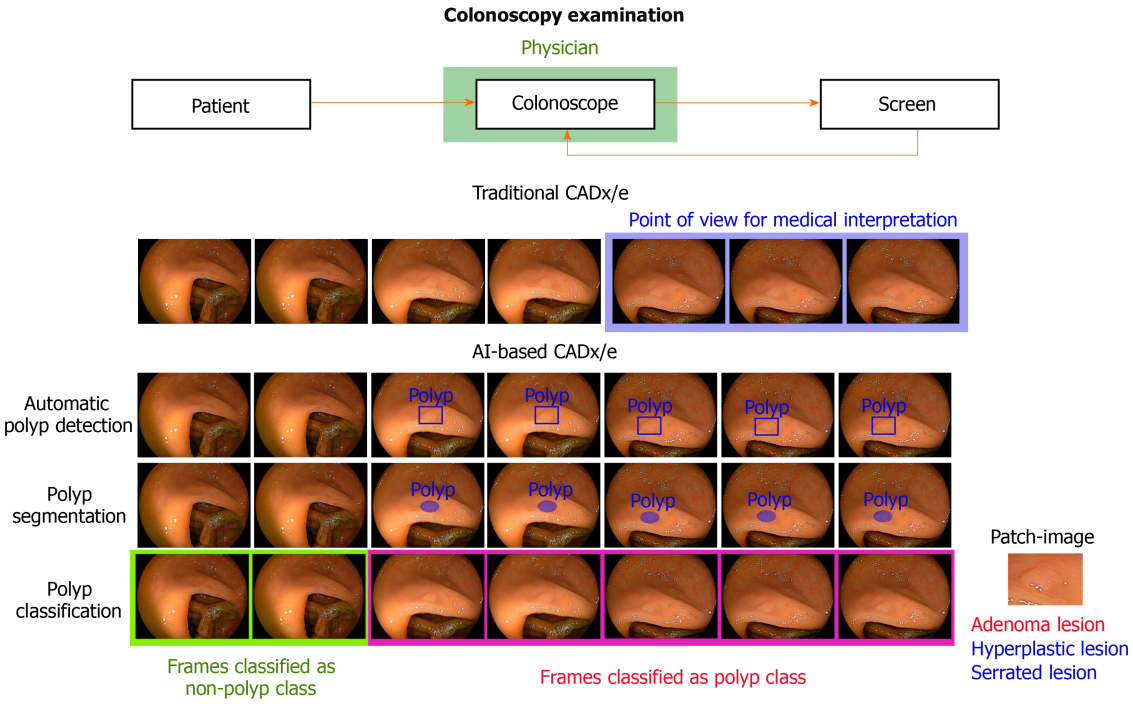


Figure 2 Comparison of traditional and AI-based computer-aided systems on colonoscopy examination.

results. For example, continuous improvement of the skills of physicians through training and practice[37] and the improvement of image/video acquisition devices combined with the development of clinically applicable CADx/e systems have been reported. Another technique used to make fine details of the mucosal surface more visible (evidencing small or slight lesions) on endoscopy tests is chromoscopy (also known as chromoendoscopy or chromocolonoscopy)[38].

Initially, chromoscopy consisted of spraying contrast dyes on the mucosa with the aim of outlining the mucosal morphology (dye-based chromoendoscopy DCE)[39]. The most frequent contrast dye used is indigo-carmine in concentrations varying from 0.2% to 2%[38]. DCE has been demonstrated to be a useful tool for endoscopists to detect and characterize lesions more accurately. A study presented by Brown *et al*[38] found that the rate of detection of small polyps was improved by DCE by approximately 90%. Such analysis was conducted on 2727 patients and showed that the detection of small polyps that could potentially develop into cancer was increased by 30% when chromoscopy was used. Although the DCE technique is simple to use and safe, it is labour intensive and time consuming, and the outcomes highly depend on bowel preparation[38,39]. Over the years, with the introduction of electronics and the improvement in technology, a new era of chromoscopy called virtual chromoendoscopy (VCE) has been adopted. VCE includes pre-processing optical imaging techniques, such as Olympus' narrow-band imaging (NBI) and autofluorescence imaging, as well as the post-processing techniques Pentax's i-SCAN and Fujinon intelligent chromoendoscopy[15]. Of all VCE techniques, NBI has been studied most frequently for assessing gastroenterology diseases[40]. This pre-processing technique uses light of specific wavelengths (green - 540 nm and blue -415 nm) to enhance detail on the mucosal surface. Although VCE techniques such as NBI can detect small-size or flat polyps, they suffer from some drawbacks, such as interobserver and intraobserver variability[41]. Such drawbacks refer to expertise, levels of distraction, or stress. However, the use of CADx/e systems may increase standardization in the process and, perhaps most importantly, more widespread adoption by non-experts in the field [41].

In this context, the new developments of CADx/e systems have focused on systems to assist in the detection and/or localization of polyps and the classification of the different types of polyps, both fundamental tasks to help clinicians at all stages of CRC diagnosis. AI has emerged as a powerful tool in two well-differentiated tasks: Polyp detection (including localization and segmentation) and polyp classification. By including an AI-based algorithm in the CADx/e systems that attend colonoscopy exploration, they can predict whether there are one (or more) polyps in a given video frame using white light alone, without the aid of advanced endoscopic imaging

modalities. If the purpose is also to locate the polyp, the algorithm predicts the position of the polyp in the image, as shown in Figure 2. If the physician requires a finer analysis, segmentation tools can allow isolation of the polyp region at the pixel level on the image. Once a polyp is detected, polyp classification aims to catalogue the type of polyp. The latter is particularly important because it allows the clinician to make a better decision as to whether to remove the polyp depending on whether it seems to be a benign, pre-malignant, or malignant polyp. Currently, to confirm if a polyp is malignant, the suspected polyp must be removed, and then a pathology test must be performed. However, an expected advance in the future is that AI can assist clinicians in differentiating polyps.

Colorectal polyps are anatomically pathologically classified as adenomatous, hyperplastic, or serrated and inflammatory, hamartomatous, juvenile, the latter being synthesized terminologically as miscellaneous, given their low prevalence (10%-20%) [42]. Adenomatous polyps are the most frequent (60%-70%). Depending on their histological characteristics, they can be tubular, villous, or tubulovillous. They can be of different degrees of dysplasia, which constitutes one of the elements for the diagnosis or the presumption of CRC[8,42]. Hyperplastic polyps have a prevalence between 10% and 30%. Although they are not usually neoplastic, there is a type of serrated polyp, the sessile serrated adenoma, which is considered a CRC precursor lesion through what is known as the serrated pathway of carcinogenesis[8,42,43].

ADVANCES IN AI FOR DETECTING AND CLASSIFYING COLORECTAL POLYPS

Automatic polyp detection—including classification and segmentation—in colonoscopy videos has been an active research topic during the last two decades. After analysing approaches reported in the literature, there are three well-defined methods: Hand-crafted, feature-based machine learning, and end-to-end learning approaches. Each method is discussed in more detail below. At the end of the analysis, we summarize the works in Table 3, showing the screening test, imaging modality and contribution for each one.

Hand-crafted approach

Hand-crafted methods refer to those based on exploiting low-level image processing techniques to obtain candidate polyp boundaries. This method considers the polyp as a protruding surface, with its boundaries detected using intensity valleys[37], Hessian filters[44], or the Hough transform[45].

Feature-based machine learning approach

Feature-based methods encompass the first era of machine learning: Designing a feature extractor and then training a classifier to predict a given class (*e.g.*, polyps or non-polyps). In early works, a texture descriptor was used to provide relevant features about the region of the image containing polyps using wavelet sub-band information in the work of Wimmer *et al*[46], Haralick co-occurrence matrix in the work of Hu *et al* [21], or Gaussian-kernel low pass filtering in the work of Mamanov *et al*[47]. Other features, such as shape, colour, and edge geometry, have also been used to create more robust detection systems that include polyp segmentation[32]. Glasmachers[33] proposed a CAD system that combines context-based image information to remove non-polyp information and shape features to reliably localize polyps.

After generating a feature vector using descriptors of texture, colour and/or shape, a classifier is required to predict whether polyps are present in the colonoscopy image, distinguishing between the different types of polyps or whether the region characterized on the image is a polyp (localization). The most commonly used classifiers are k-nearest neighbours[46], decision trees[22], random forests[22,32], and support vector machine[23].

End-to-end learning approach

The end-to-end (E2E) learning approach refers to training a learning system represented by a single model (generally a deep neural network)[33]. As the technology evolved and the computational capabilities increased, the use of convolutional neural networks as a key part of CADx/e systems is increasingly frequent in automatic polyp detection[48] and/or polyp classification tasks[49]. The advantage of the E2E approach is the possibility of designing more complex multitasking systems:

Table 3 Summary of studies focused on artificial intelligence applications for automatic polyp detection, classification, and segmentation

Study	Screening test	Imaging modality	Data type	AI-based algorithm	Contribution	Acc	Sen	Spe
Wimmer *et al* [46]	Colonoscopy	WL, NBI	Images	k-nearest neighbours	Polyp classification: non-neoplastic, neoplastic	80%	-	-
Tajbakhsh *et al* [22]	Colonoscopy	WL	Images	Decision trees; Random forest	Automatic polyp detection	-	88%	-
Hu *et al*[21]	CT Colonography	Greyscale	Images	Random forest	Polyp classification: non-neoplastic, neoplastic	-	-	-
Zhang *et al*[50]	Colonoscopy	WL, NBI	Images	CNN: Caffenet	Polyp detection and classification: benign from malignant	86%	88%	-
Shin *et al*[23]	Colonoscopy	WL	Images	Support vector machine	Whole image classification: polyps from non-polyps	96%	96%	96%
Sánchez-González *et al*[32]	Colonoscopy	WL	Images	Random forest; CNN: Bayesnet	Polyp segmentation	97%	76%	99%
Tan *et al*[52]	CT Colonography	Greyscale	Images	Customized CNN	Polyp classification: adenoma from adenocarcinoma	87%	90%	71%
Fonolla *et al*[51]	Colonoscopy	WL, NBI, LCI	Images	CNN: EfficientNet	Polyp classification: benign from pre-malignant	95%	96%	93%
Hwang *et al*[46]	Colonoscopy	WL	Images	Customized CNN	Polyp detection and segmentation	-	-	-
Park *et al*[53]	Colonoscopy	WL	Images	Customized CNN	Whole image classification: normal, adenoma and adenocarcinoma	94%	~94%	-
Viscaino *et al* [54]	Colonoscopy	Greyscale	Images	Support vector machine; Decision treesk-nearest neighbours; Random forest	Whole image classification: polyp and non-polyp	97%	98%	96%

WL: White light; NBI: Narrow-band imaging; LCI: Linked colour imaging; Acc: Accuracy; Sen: Sensitivity; Spe: Specificity.

Detecting polyps and then identifying whether the detected polyp is hyperplastic or adenomatous[50]. Information about whether a polyp can be malignant will assist the clinician in making a better clinical decision (to remove or not the polyp)[51].

There are other alternatives to colonoscopy; colonography or wireless capsule endoscopy are also used as screening techniques to detect polyps. Both alternatives are less invasive and do not present a risk of perforation to patients as colonoscopy does. AI-based algorithms have also been used to enhance the analysis *via* CT colonography. In particular, the use of greyscale information in the image (using a grey-level co-occurrence matrix in the work of Tan *et al*[52] or texture information in the work of Hu *et al*[21]) combined with CNN has been useful for differentiation of polyps: Adenoma from adenocarcinoma[53], non-neoplastic from neoplastic polyp[21], or images with polyps and without polyps[54].

MICCAI 2015 POLYP DETECTION CHALLENGE

MICCAI proposes a common validation and evaluation framework of new algorithms published in the field of biomedical image analysis (Bernal *et al*[15] and the references therein). Each year MICCAI launches international competitions (challenges) that allow for benchmarking algorithms on publicly released datasets and offers a basis to discuss validation strategies[22]. In 2015, the MICCAI sub-challenge on automatic polyps was launched and represented a significant advance in the area. As a result of this competition, three large endoscopic image databases were published, establishing a benchmark for new algorithms[22,37,55].

Colonoscopy datasets

To successfully train classical machine learning models, it is necessary to have reasonably sized databases[22]. However, to train deep learning models, large databases are required because the quantity of data is related to the network

performance. The most famous public databases used in computer science are ImageNet[56], with more than 14 million natural images hand-annotated in 20000 categories, or Microsoft's COCO[57], with more than 2500000 images. The state-of-the-art reports better than 90% accuracy in classification, object detection and localization tasks with deep neural networks pre-trained with these databases. In medicine, creating large databases represents a challenge because the data and the expertly annotated ground truth are required. In the case of colonoscopy, some publicly available datasets for polyp detection and classification have been released in the last few years. In particular, efforts such as the MICCA 2015 sub-challenge have prompted different groups to create and make available the databases summarized in Table 4.

Three datasets annotated for automatic polyp detection have been very popular in the scientific community: CVC-ClinicDB[37], ETIS-Larib[55], and ASU-Mayo Clinic Colonoscopy Video[22]. Both datasets CVC-ClinicDB and ETIS-Larib are composed of annotated frames, whereas the ASU-Mayo Clinic dataset is composed of 38 fully annotated videos selected to show maximum variation in colonoscopy procedures. All public databases are summarized in Table 4, as well as their characteristics.

MISCONCEPTIONS IN AI

Deep learning-based AI models offer promising results for medical image analysis. Nevertheless, a thorough understanding of the available data and its limitations and proficient curation of suitable training, testing, and validation subsets are required to successfully train these models responsibly and use them in a clinical setup, *e.g.*, as a diagnostic support tool. Following are some of the most common misconceptions.

Imbalanced datasets

In medicine, obtaining samples to create datasets can be a time consuming and expensive process[15]. This becomes even more complicated when samples are obtained from invasive procedures such as colonoscopy. Another important aspect is that as a result of data scarcity (*e.g.*, due to the low incidence of a medical condition), an intrinsic imbalance in the data can occur. Therefore, the available colonoscopy datasets mostly do not contain the same number of samples per class (also known as an imbalanced dataset)[29,63,64]. If a deep learning model is trained on such a dataset, the result will present a high risk of exhibiting bias against the minority classes and, in extreme cases, ignoring it altogether.

Moreover, the dataset structure needs to be considered when studying the performance metrics of deep learning models, such as accuracy and/or error rate, which are the most frequently used metrics when evaluating classification results. However, both are insufficient when working with an imbalanced dataset, as the relative contribution of the minority classes to these metrics is negligible[30]. Best practice is to be aware of the limitations of each metric and evaluate the performance of the algorithm with a set of complementary metrics (see Table 2).

The time and effort required to curate balanced datasets for intrinsically imbalanced problems have led researchers to develop techniques to enable AI models to be successfully trained on an imbalanced dataset[30]. Currently, the proposed methods can be grouped into data-level techniques and algorithm-level methods, which can be combined in hybrid approaches.

Data-level techniques aim to decrease the level of imbalance by modifying the class distribution within the available dataset. On the one hand, under-sampling methods voluntarily discard data from the majority classes, reducing the total information available to train the model. The simplistic approach to under-sampling is random under-sampling, which discards random samples from the majority classes. Notwithstanding, valuable information might be lost in the process. Intelligent under-sampling methods select removal candidates using more elaborated criteria, such as redundancy within each class in the majority group, known as one-sided selection[65], or their distance from minority samples, known as near-miss algorithms, as the several alternatives presented in Mani *et al*[66]. On the other hand, over-sampling methods artificially increase the quantity of available data in the minority classes. One technique, random over-sampling (ROS), which randomly duplicates samples from the minority classes, is the naive approach to over-sampling and is known to cause overfitting[67]. The model memorizes particular training samples instead of learning the underlying characteristics of the corresponding class and is then unable to generalize to novel data [26]. Several methods have been proposed to reduce over-fitting while over-sampling, such as the synthetic minority over-sampling technique introduced in Chawla *et al*[68]

Table 4 Summary of publicly available colonoscopy datasets

Dataset	Year	Description	Data type	Ground truth
CVC-ColonDB[29,58]	2012	380 sequential WL images from 15 videos	Images (574 × 500 pixels)	Binary mask to locate the polyp
CVC-PolypHD[58,59]	2012	56 WL images	Images (1920 × 1080 pixels)	Binary mask to locate the polyp
ETIS-Larib[55]	2014	196 WL images from 34 video sequences (44 different polyps)	Images (1125 × 966)	Binary mask to locate the polyp
CVC-ClinicDB[37]	2015	612 sequential WL images from 31 videos sequences (31 different polyps)	Images (388 × 284 pixels)	Binary mask to locate the polyp
ASU-Mayo[22]	2016	38 short video sequences (NBI, WL)	Video (SD and HD video)	Binary mask for 20 training videos
Colonoscopic dataset[49]	2016	76 short video sequences (NBI, WL)	Video	Labels: hyperplastic, adenoma and serrated
Kvasir-SEG[60]	2017	1000 images with polyps	Images	Binary mask to locate the polyp
CVC-ClinicVideoDB[61]	2017	18 sequences	Video (SD video)	Binary mask to locate the polyp
CP-CHILD-A, CP-CHILD-B[62]	2020	10000 images	Images (256 × 256)	Labels: polyp and non-polyp

WL: White light; NBI: Narrow-band imaging.

and its variants Han *et al*[69], Jo *et al*[70], or the cluster-based over-sampling method proposed in Jo *et al*[70].

Algorithm-level methods comprise cost-sensitive learning algorithms[71], which assign penalties to each majority class, increasing the importance of the minority classes, and decision process adjustments, which shift the decision threshold such that bias towards the minority classes is reduced.

Correlated data

Another dataset structure aspect to consider when inspecting performance metrics is the presence of correlation between dataset splits (most commonly training, testing and validation)[26]. We consider the task of analysing images obtained from a recorded colonoscopy to classify detected colorectal polyps as malignant or benign. If the training and validation dataset splits contain frames from the same video or patient, the correlation introduced by this situation will affect validation metrics, resulting in over-optimistic results and the risk of hidden generalization or over-fitting problems.

Interpretability

Machine learning, and more broadly AI, are essentially statistical models. During the training process, a set of parameters that define the specific behaviour of the base model is adjusted so that model predictions match expert annotations for elements in the database. Notwithstanding, commonly used models do not consider domain-specific expert knowledge in their predictions. Hence, it is possible for the trained model to learn features that are undesirable or incorrect, such as unintended patterns or visual artefacts present in the database, instead of constraining the feature space to medically relevant features only. To avoid this problem, manual assessment of the database elements is advised, along with internal feature visualization techniques[72]. See Deng *et al*[73] for a review of different strategies proposed to incorporate expert knowledge as prior information to machine learning (ML)/AI models.

FUTURE PROSPECTS

The results obtained from AI-based models are promising and establish an advantage compared to traditional methods. However, there are some limitations to be overcome by future research to propose clinically useful methods.

Overcoming real-time constraints: Videos in a colonoscopy exploration are generally acquired at 25 frames per second[15], which means that the maximum time

available to process each image (frame) must be less than 40 ms.

Increasing the variability of polyp cases, including studies with data from multiple medical centres if possible. However, given the scarcity of data on less common lesions (serrated adenomas) and knowing that deep learning approaches require vast numbers of labelled training samples, new research may include techniques such as few-shot learning introduced by Vinyals *et al*[74]. This technique focuses on learning a class from one or a few labelled samples and has been successfully applied in other medical areas, such as cervical cancer cell classification[75], breast cancer classification [76], and metastatic tumour classification[77].

Including in the polyp detection scheme the ability to detect other elements such as folds or blood vessels that can appear in a real exploration and can affect current methods' performance.

Tests were performed on complete video sequences to analyse the performance of the model under temporal consistency constraints and high variability in polyp appearance due to camera progression. Both conditions might impact the models' performance in a real clinical environment.

The ability to obtain uncertainty estimates from ML/AI model predictions is key to a responsible adoption of these techniques in clinical setups, as biased recommendations from CADx/e can have adverse effects on the final diagnosis. Bayesian deep learning has been proposed as a framework to address this problem, where deep learning models can deliver uncertainty information along with classification results [78] at the expense of an increased number of training parameters (and hence more training data required) or a more restricted model structure, *e.g.*, the need to incorporate dropout units within the mode architecture, as in Gal *et al*[79] 2016. Both of the abovementioned techniques have been successfully combined with active learning algorithms that enable incremental dataset labelling and/or training of the model parameters as new data become available (see Gal *et al*[80], 2017, and Woodward *et al* [81], 2016).

CONCLUSION

AI is a promising area in gastroenterology. With the processing power and high performance of algorithms such as deep learning, a new era of AI-based computer-aided systems can assist physicians in essential tasks such as colorectal polyp detection and classification. To achieve clinically useful systems, both clinicians and technicians must cooperate to mitigate AI drawbacks. Although most of the current technological effort has been focused on creating more precise polyp detection and classification tools, it remains a long path to be covered before adopting AI-based technology into the physician's daily work as an assistive tool for diagnosis decisions.

REFERENCES

1 **Ferlay J**, Ervik M, Lam F, Colombet M, Mery L, Piñeros M, Znaor A, Soerjomataram I, Bray F. Global Cancer Observatory: Cancer Today [Internet]. Lyon, Francia: International Agency for Research on Cancer; 2020. Available from: https://gco.iarc.fr/today

2 **World Health Organization**. Global Health Estimates 2019: Deaths by Cause, Age, Sex, by Country and by Region, 2000-2019. [Internet]. Geneva; 2020. Available from: https://www.who.int/data/gho/data/themes/mortality-and-global-health-estimates

3 **Araghi M**, Soerjomataram I, Jenkins M, Brierley J, Morris E, Bray F, Arnold M. Global trends in colorectal cancer mortality: projections to the year 2035. *Int J Cancer* 2019; **144**: 2992-3000 [PMID: 30536395 DOI: 10.1002/ijc.32055]

4 **Winawer S**, Classen M, Lambert R, Fried M, Dite P, Goh KL, Guarner F, Lieberman D, Eliakim R, Levin B, Saenz R, Khan AG, Khalif I, Lanas A, Lindberg G, O'Brien MJ, Young G, Krabshuis J, Smith R, Schmiegel W, Rex D, Amrani N, Zauber A. Colorectal cancer screening World Gastroenterology Organisation/International Digestive Cancer Alliance Practice Guidelines. *South African Gastroenterol Rev* 2008; **6**: 13-20 [DOI: 10.4314/sagr.v6i1.30745]

5 **Levin B**, Lieberman DA, McFarland B, Smith RA, Brooks D, Andrews KS, Dash C, Giardiello FM, Glick S, Levin TR, Pickhardt P, Rex DK, Thorson A, Winawer SJ; American Cancer Society Colorectal Cancer Advisory Group; US Multi-Society Task Force; American College of Radiology Colon Cancer Committee. Screening and surveillance for the early detection of colorectal cancer and adenomatous polyps, 2008: a joint guideline from the American Cancer Society, the US Multi-Society Task Force on Colorectal Cancer, and the American College of Radiology. *CA Cancer J Clin* 2008; **58**: 130-160 [PMID: 18322143 DOI: 10.3322/CA.2007.0018]

6 **Wolf AMD**, Fontham ETH, Church TR, Flowers CR, Guerra CE, LaMonte SJ, Etzioni R, McKenna

MT, Oeffinger KC, Shih YT, Walter LC, Andrews KS, Brawley OW, Brooks D, Fedewa SA, Manassaram-Baptiste D, Siegel RL, Wender RC, Smith RA. Colorectal cancer screening for average-risk adults: 2018 guideline update from the American Cancer Society. *CA Cancer J Clin* 2018; **68**: 250-281 [PMID: 29846947 DOI: 10.3322/caac.21457]

7 **Walsh JM**, Terdiman JP. Colorectal cancer screening: scientific review. *JAMA* 2003; **289**: 1288-1296 [PMID: 12633191 DOI: 10.1001/jama.289.10.1288]

8 **Lin JS**, Piper MA, Perdue LA, Rutter C, Webber EM, O'Connor E, Smith N, Whitlock EP. Screening for Colorectal Cancer: A Systematic Review for the U.S. Preventive Services Task Force [Internet]. 2016. Rockville (MD): Agency for Healthcare Research and Quality (US); 2016 Jun. Report No.: 14-05203-EF-1 [PMID: 27441328]

9 **National Comprehensive Cancer Network**. NCCN Clinical Practice Guidelines in Oncology (NCCN Guidelines): Colorectal cancer screening. National Comprehensive Cancer Network; 2013

10 **Giger ML**. Machine Learning in Medical Imaging. *J Am Coll Radiol* 2018; **15**: 512-520 [PMID: 29398494 DOI: 10.1016/j.jacr.2017.12.028]

11 **Wang KW**, Dong M. Potential applications of artificial intelligence in colorectal polyps and cancer: Recent advances and prospects. *World J Gastroenterol* 2020; **26**: 5090-5100 [PMID: 32982111 DOI: 10.3748/wjg.v26.i34.5090]

12 **Shen D**, Wu G, Suk HI. Deep Learning in Medical Image Analysis. *Annu Rev Biomed Eng* 2017; **19**: 221-248 [PMID: 28301734 DOI: 10.1146/annurev-bioeng-071516-044442]

13 **Schootman M**, Hendren S, Ratnapradipa K, Stringer L, Davidson NO. Adoption of Robotic Technology for Treating Colorectal Cancer. *Dis Colon Rectum* 2016; **59**: 1011-1018 [PMID: 27749475 DOI: 10.1097/DCR.0000000000000688]

14 **Laique SN**, Hayat U, Sarvepalli S, Vaughn B, Ibrahim M, McMichael J, Qaiser KN, Burke C, Bhatt A, Rhodes C, Rizk MK. Application of optical character recognition with natural language processing for large-scale quality metric data extraction in colonoscopy reports. *Gastrointest Endosc* 2021; **93**: 750-757 [PMID: 32891620 DOI: 10.1016/j.gie.2020.08.038]

15 **Bernal J**, Tajkbaksh N, Sanchez FJ, Matuszewski BJ, Hao Chen, Lequan Yu, Angermann Q, Romain O, Rustad B, Balasingham I, Pogorelov K, Sungbin Choi, Debard Q, Maier-Hein L, Speidel S, Stoyanov D, Brandao P, Cordova H, Sanchez-Montes C, Gurudu SR, Fernandez-Esparrach G, Dray X, Jianming Liang, Histace A. Comparative Validation of Polyp Detection Methods in Video Colonoscopy: Results From the MICCAI 2015 Endoscopic Vision Challenge. *IEEE Trans Med Imaging* 2017; **36**: 1231-1249 [PMID: 28182555 DOI: 10.1109/TMI.2017.2664042]

16 **Jiang F**, Jiang Y, Zhi H, Dong Y, Li H, Ma S, Wang Y, Dong Q, Shen H. Artificial intelligence in healthcare: past, present, and future. Stroke and vascular neurology 2017; 2: 230-243 [DOI: 10.1136/svn-2017-000101]

17 **Nogueira-Rodríguez A**, Domínguez-Carbajales R, López-Fernández H, Iglesias Á, Cubiella J, Fdez-Riverola F, Reboiro-Jato M, Glez-Peña D. Deep Neural Networks approaches for detecting and classifying colorectal polyps. *Neurocomputing* 2021; **423**: 721-734 [DOI: 10.1016/j.neucom.2020.02.123]

18 **Deo RC**. Machine Learning in Medicine. *Circulation* 2015; **132**: 1920-1930 [PMID: 26572668 DOI: 10.1161/CIRCULATIONAHA.115.001593]

19 **Ravi D**, Wong C, Deligianni F, Berthelot M, Andreu-Perez J, Lo B, Yang GZ. Deep Learning for Health Informatics. *IEEE J Biomed Health Inform* 2017; **21**: 4-21 [PMID: 28055930 DOI: 10.1109/JBHI.2016.2636665]

20 **Yu KH**, Beam AL, Kohane IS. Artificial intelligence in healthcare. *Nat Biomed Eng* 2018; **2**: 719-731 [PMID: 31015651 DOI: 10.1038/s41551-018-0305-z]

21 **Hu Y**, Liang Z, Song B, Han H, Pickhardt PJ, Zhu W, Duan C, Zhang H, Barish MA, Lascarides CE. Texture Feature Extraction and Analysis for Polyp Differentiation *via* Computed Tomography Colonography. *IEEE Trans Med Imaging* 2016; **35**: 1522-1531 [PMID: 26800530 DOI: 10.1109/TMI.2016.2518958]

22 **Tajbakhsh N**, Gurudu SR, Liang J. Automated Polyp Detection in Colonoscopy Videos Using Shape and Context Information. *IEEE Trans Med Imaging* 2016; **35**: 630-644 [PMID: 26462083 DOI: 10.1109/TMI.2015.2487997]

23 **Shin Y**, Balasingham I. Automatic polyp frame screening using patch based combined feature and dictionary learning. *Comput Med Imaging Graph* 2018; **69**: 33-42 [PMID: 30172091 DOI: 10.1016/j.compmedimag.2018.08.001]

24 **Nalepa J**, Kawulok M. Selecting training sets for support vector machines: a review. *Artificial Intelligence Review* 2019; **52**: 857-900 [DOI: 10.1007/s10462-017-9611-1]

25 **Breiman L**. Random Forests. *Machine Learning* 2001; **45**: 5-32 [DOI: 10.1023/A:1010933404324]

26 **Goodfellow I**, Bengio Y, Courville A. Chapter 5: Machine Learning Basics. In: Goodfellow I, Bengio Y, Courville A. Deep Learning. The MIT Press 2016: 96-161

27 **Qadir HA**, Balasingham I, Solhusvik J, Bergsland J, Aabakken L, Shin Y. Improving Automatic Polyp Detection Using CNN by Exploiting Temporal Dependency in Colonoscopy Video. *IEEE J Biomed Health Inform* 2020; **24**: 180-193 [PMID: 30946683 DOI: 10.1109/JBHI.2019.2907434]

28 **Patel K**, Li K, Tao K, Wang Q, Bansal A, Rastogi A, Wang G. A comparative study on polyp classification using convolutional neural networks. *PLoS One* 2020; **15**: e0236452 [PMID: 32730279 DOI: 10.1371/journal.pone.0236452]

29 **Misawa M**, Kudo SE, Mori Y, Cho T, Kataoka S, Yamauchi A, Ogawa Y, Maeda Y, Takeda K, Ichimasa K, Nakamura H, Yagawa Y, Toyoshima N, Ogata N, Kudo T, Hisayuki T, Hayashi T,

Wakamura K, Baba T, Ishida F, Itoh H, Roth H, Oda M, Mori K. Artificial Intelligence-Assisted Polyp Detection for Colonoscopy: Initial Experience. *Gastroenterology* 2018; **154**: 2027-2029.e3 [PMID: 29653147 DOI: 10.1053/j.gastro.2018.04.003]

30 **Johnson JM**, Khoshgoftaar TM. Survey on deep learning with class imbalance. *J Big Data* 2019; **6**: 1-54 [DOI: 10.1186/s40537-019-0192-5]

31 **Viscaino M**, Maass JC, Delano PH, Torrente M, Stott C, Auat Cheein F. Computer-aided diagnosis of external and middle ear conditions: A machine learning approach. *PLoS One* 2020; **15**: e0229226 [PMID: 32163427 DOI: 10.1371/journal.pone.0229226]

32 **Sánchez-González A**, García-Zapirain B, Sierra-Sosa D, Elmaghraby A. Automatized colon polyp segmentation *via* contour region analysis. *Comput Biol Med* 2018; **100**: 152-164 [PMID: 30015012 DOI: 10.1016/j.compbiomed.2018.07.002]

33 **Glasmachers T**. Limits of End-to-End Learning. Proceedings of the Ninth Asian Conference on Machine Learning. *PMLR* 2017; **77**: 17-32

34 **Lee SH**, Chung IK, Kim SJ, Kim JO, Ko BM, Hwangbo Y, Kim WH, Park DH, Lee SK, Park CH, Baek IH, Park DI, Park SJ, Ji JS, Jang BI, Jeen YT, Shin JE, Byeon JS, Eun CS, Han DS. An adequate level of training for technical competence in screening and diagnostic colonoscopy: a prospective multicenter evaluation of the learning curve. *Gastrointest Endosc* 2008; **67**: 683-689 [PMID: 18279862 DOI: 10.1016/j.gie.2007.10.018]

35 **Lebwohl B**, Kastrinos F, Glick M, Rosenbaum AJ, Wang T, Neugut AI. The impact of suboptimal bowel preparation on adenoma miss rates and the factors associated with early repeat colonoscopy. *Gastrointest Endosc* 2011; **73**: 1207-1214 [PMID: 21481857 DOI: 10.1016/j.gie.2011.01.051]

36 **Leufkens AM**, van Oijen MG, Vleggaar FP, Siersema PD. Factors influencing the miss rate of polyps in a back-to-back colonoscopy study. *Endoscopy* 2012; **44**: 470-475 [PMID: 22441756 DOI: 10.1055/s-0031-1291666]

37 **Bernal J**, Sánchez FJ, Fernández-Esparrach G, Gil D, Rodríguez C, Vilariño F. WM-DOVA maps for accurate polyp highlighting in colonoscopy: Validation vs. saliency maps from physicians. *Comput Med Imaging Graph* 2015; **43**: 99-111 [PMID: 25863519 DOI: 10.1016/j.compmedimag.2015.02.007]

38 **Brown SR**, Baraza W, Din S, Riley S. Chromoscopy *vs* conventional endoscopy for the detection of polyps in the colon and rectum. *Cochrane Database Syst Rev* 2016; **4**: CD006439 [PMID: 27056645 DOI: 10.1002/14651858.CD006439.pub4]

39 **Singh R**, Chiam KH, Leiria F, Pu LZCT, Choi KC, Militz M. Chromoendoscopy: role in modern endoscopic imaging. *Transl Gastroenterol Hepatol* 2020; **5**: 39 [PMID: 32632390 DOI: 10.21037/tgh.2019.12.06]

40 **van der Laan JJH**, van der Waaij AM, Gabriëls RY, Festen EAM, Dijkstra G, Nagengast WB. Endoscopic imaging in inflammatory bowel disease: current developments and emerging strategies. *Expert Rev Gastroenterol Hepatol* 2021; **15**: 115-126 [PMID: 33094654 DOI: 10.1080/17474124.2021.1840352]

41 **Alagappan M**, Brown JRG, Mori Y, Berzin TM. Artificial intelligence in gastrointestinal endoscopy: The future is almost here. *World J Gastrointest Endosc* 2018; **10**: 239-249 [PMID: 30364792 DOI: 10.4253/wjge.v10.i10.239]

42 **Moreira L**, Castells A, Castelvi S. Pólipos y poliposis colorrectales. In: Montoro MA, García Pagán JC: Gastroenterología y Hepatología Problemas comunes en la práctica clínica. 2nd ed. Madrid: Asociación Española de Gastroenterología; 2012: 607-616

43 **East JE**, Saunders BP, Jass JR. Sporadic and syndromic hyperplastic polyps and serrated adenomas of the colon: classification, molecular genetics, natural history, and clinical management. *Gastroenterol Clin North Am* 2008; **37**: 25-46, v [PMID: 18313538 DOI: 10.1016/j.gtc.2007.12.014]

44 **Iwahori Y**, Hattori A, Adachi Y, Bhuyan MK, Woodham RJ, Kasugai K. Automatic Detection of Polyp Using Hessian Filter and HOG Features. *Procedia Computer Sci* 2015; **60**: 730-739 [DOI: 10.1016/j.procs.2015.08.226]

45 **Ruiz L**, Guayacán L, Martínez F. Automatic polyp detection from a regional appearance model and a robust dense Hough coding. In: 2019 XXII Symposium on Image, Signal Processing and Artificial Vision (STSIVA) Bucaramanga, Colombia 2019: 1-5 [DOI: 10.1109/STSIVA.2019.8730270]

46 **Wimmer G**, Tamaki T, Tischendorf JJ, Häfner M, Yoshida S, Tanaka S, Uhl A. Directional wavelet based features for colonic polyp classification. *Med Image Anal* 2016; **31**: 16-36 [PMID: 26948110 DOI: 10.1016/j.media.2016.02.001]

47 **Mamonov AV**, Figueiredo IN, Figueiredo PN, Tsai YH. Automated polyp detection in colon capsule endoscopy. *IEEE Trans Med Imaging* 2014; **33**: 1488-1502 [PMID: 24710829 DOI: 10.1109/TMI.2014.2314959]

48 **Hwang M**, Wang D, Kong XX, Wang Z, Li J, Jiang WC, Hwang KS, Ding K. An automated detection system for colonoscopy images using a dual encoder-decoder model. *Comput Med Imaging Graph* 2020; **84**: 101763 [PMID: 32805673 DOI: 10.1016/j.compmedimag.2020.101763]

49 **Mesejo P**, Pizarro D, Abergel A, Rouquette O, Beorchia S, Poincloux L, Bartoli A. Computer-Aided Classification of Gastrointestinal Lesions in Regular Colonoscopy. *IEEE Trans Med Imaging* 2016; **35**: 2051-2063 [PMID: 28005009 DOI: 10.1109/TMI.2016.2547947]

50 **Zhang R**, Zheng Y, Mak TW, Yu R, Wong SH, Lau JY, Poon CC. Automatic Detection and Classification of Colorectal Polyps by Transferring Low-Level CNN Features From Nonmedical Domain. *IEEE J Biomed Health Inform* 2017; **21**: 41-47 [PMID: 28114040 DOI: 10.1109/JBHI.2016.2635662]

51 **Fonollà R**, van der Zander QWE, Schreuder RM, Masclee A, Schoon EJ, van der Sommen S, de With PHN. A CNN CADx System for Multimodal Classification of Colorectal Polyps Combining WL, BLI, and LCI Modalities. *Appl Sci* 2020; **10**: 5040 [DOI: 10.3390/app10155040]

52 **Tan J**, Gao Y, Liang Z, Cao W, Pomeroy MJ, Huo Y, Li L, Barish MA, Abbasi AF, Pickhardt PJ. 3D-GLCM CNN: A 3-Dimensional Gray-Level Co-Occurrence Matrix-Based CNN Model for Polyp Classification *via* CT Colonography. *IEEE Trans Med Imaging* 2020; **39**: 2013-2024 [PMID: 31899419 DOI: 10.1109/TMI.2019.2963177]

53 **Park HC**, Kim YJ, Lee SW. Adenocarcinoma recognition in endoscopy images using optimized convolutional neural networks. *Appl Sci* 2020; **10**: 1650 [DOI: 10.3390/app10051650]

54 **Viscaino M**, Cheein FA. Machine learning for computer-aided polyp detection using wavelets and content-based image. In: 2019 41st Annual International Conference of the IEEE Engineering in Medicine and Biology Society (EMBC) 2019; 23: 961-965 [DOI: 10.1109/EMBC.2019.8857831]

55 **Silva J**, Histace A, Romain O, Dray X, Granado B. Toward embedded detection of polyps in WCE images for early diagnosis of colorectal cancer. *Int J Comput Assist Radiol Surg* 2014; **9**: 283-293 [PMID: 24037504 DOI: 10.1007/s11548-013-0926-3]

56 **Deng J**, Dong W, Socher R, Li LJ, Li K, Li FF. ImageNet: A large-scale hierarchical image database. In: 2009 IEEE Conference on Computer Vision and Pattern Recognition. Miami, Florida. 2009: 248-255 [DOI: 10.1109/CVPR.2009.5206848]

57 **Lin TY**, Maire M, Belongie S, Bourdev L, Girshick R, Hays J, Perona P, Ramanan D, Zitnick CL, Dollár P. Microsoft COCO: Common Objects in Context; 2015. [cited 10 January 2021] Available from: http://arxiv.org/abs/1405.0312

58 **Vázquez D**, Bernal J, Sánchez FJ, Fernández-Esparrach G, López AM, Romero A, Drozdzal M, Courville A. A Benchmark for Endoluminal Scene Segmentation of Colonoscopy Images. *J Healthc Eng* 2017; **2017**: 4037190 [PMID: 29065595 DOI: 10.1155/2017/4037190]

59 **Bernal J**, Sánchez J, Vilariño F. Towards automatic polyp detection with a polyp appearance model. *Pattern Recogn* 2012; **45**: 3166-3182 [DOI: 10.1016/j.patcog.2012.03.002]

60 **Pogorelov K**, Schmidt PT, Riegler M, Halvorsen P, Randel KR, Griwodz C. KVASIR: A Multi-Class Image Dataset for Computer Aided Gastrointestinal Disease Detection. In: Proceedings of the 8th ACM on Multimedia Systems. 2017 [DOI: 10.1145/3083187.3083212]

61 **Angermann Q**, Bernal J, Sánchez-Montes C, Hammami M, Fernández-Esparrach G, Dray X, Romain O, Sánchez FJ, Histace A. Towards real-time polyp detection in colonoscopy videos: Adapting still frame-based methodologies for video sequences analysis. In: Computer Assisted and Robotic Endoscopy and Clinical Image-Based Procedures, 2017: 29-41 [DOI: 10.1007/978-3-319-67543-5_3]

62 **Wang W**, Tian J, Zhang C, Luo Y, Wang X, Li J. An improved deep learning approach and its applications on colonic polyp images detection. *BMC Med Imaging* 2020; **20**: 83 [PMID: 32698839 DOI: 10.1186/s12880-020-00482-3]

63 **Chen PJ**, Lin MC, Lai MJ, Lin JC, Lu HH, Tseng VS. Accurate Classification of Diminutive Colorectal Polyps Using Computer-Aided Analysis. *Gastroenterology* 2018; **154**: 568-575 [PMID: 29042219 DOI: 10.1053/j.gastro.2017.10.010]

64 **Lui TKL**, Wong KKY, Mak LLY, Ko MKL, Tsao SKK, Leung WK. Endoscopic prediction of deeply submucosal invasive carcinoma with use of artificial intelligence. *Endosc Int Open* 2019; **7**: E514-E520 [PMID: 31041367 DOI: 10.1055/a-0849-9548]

65 **Kubat M**, Matwin S. Addressing the Curse of Imbalanced Training Sets: One-Sided Selection. In: ICML; 1997; 97: 179-186

66 **Zhang J**, Mani I. KNN Approach to Unbalanced Data Distributions: A Case Study Involving Information Extraction. In: Proceedings of workshop on learning from imbalanced datasets. 2003

67 **Van Hulse J**, Khoshgoftaar TM, Napolitano A. Experimental perspectives on learning from imbalanced data. In: Proceedings of the 24th international conference on machine learning, New York, USA. 2007: 935-942 [DOI: 10.1145/1273496.1273614]

68 **Chawla NV**, Bowyer KW, Hall LO, Kegelmeyer WP. Smote: synthetic minority over-sampling technique. *J Artif Int Res* 2002; 321-57 [DOI: 10.1613/jair.953]

69 **Han H**, Wang W-Y, Mao B-H. Borderline-smote: a new over-sampling method in imbalanced data sets learning. In: Huang DS, Zhang XP, Huang GB, editors. Advances in Intelligent Computing. Berlin: Springer 2005; 878-887 [DOI: 10.1007/11538059_91]

70 **Jo T**, Japkowicz N. Class imbalances vs small disjuncts. ACM SIGKDD Explorations Newsletter. 2004; 6: 40-49 [DOI: 10.1145/1007730.1007737]

71 **Thai-Nghe N**, Gantner Z, Schmidt-Thieme L. Cost-sensitive learning methods for imbalanced data. The 2010 International Joint Conference on Neural Networks (IJCNN); 2010. Barcelona. Spain: 1-8 [DOI: 10.1109/IJCNN.2010.5596486]

72 **Mahendran A**, Vedaldi A. Understanding deep image representations by inverting them. In: Proceedings of the IEEE conference on computer vision and pattern recognition; Boston, USA, 2015: 5188-5196 [DOI: 10.1109/CVPR.2015.7299155]

73 **Deng C**, Ji X, Rainey C, Zhang J, Lu W. Integrating Machine Learning with Human Knowledge. *iScience* 2020; **23**: 101656 [PMID: 33134890 DOI: 10.1016/j.isci.2020.101656]

74 **Vinyals O**, Blundell C, Lillicrap T, Kavukcuoglu K, Wierstra D. Matching Networks for One Shot Learning. Part of Advances in Neural Information Processing Systems 29 (NIPS 2016)

75 **Yarlagadda DVK**, Rao P, Rao D, Tawfik O. A system for one-shot learning of cervical cancer cell classification in histopathology images. Proc. SPIE 10956, Medical Imaging 2019: Digital Pathology;

2019: 1095611 2019 [DOI: 10.1117/12.2512963]

76 **Cano F**, Cruz-Roa A. An exploratory study of one-shot learning using Siamese convolutional neural network for histopathology image classification in breast cancer from few data examples. In: 15th International Symposium on Medical Information Processing and Analysis 2020; 11330: 113300A [DOI: 10.1117/12.2546488]

77 **Mostavi M**, Chiu YC, Chen Y, Huang Y. CancerSiamese: one-shot learning for primary and metastatic tumor classification. *bioRxiv* 2020; Preprint [DOI: 10.1101/2020.09.07.286583]

78 **Kendall A**, Gal Y. What uncertainties do we need in bayesian deep learning for computer vision? NIPS'17: Proceedings of the 31st International Conference on Neural Information Processing Systems 2017: 5580-5590

79 **Gal Y**, Ghahramani Z. Dropout as a Bayesian Approximation: Representing Model Uncertainty in Deep Learning. In: Proceedings of the 33rd International Conference on Machine Learning, New York, NY, USA. *PMLR* 2016; **48**: 1050-1059

80 **Gal Y**, Islam R, Ghahramani Z. Deep Bayesian Active Learning with Image Data. In: Proceedings of the 34th International Conference on Machine Learning. *PMLR* 2017; **70**: 1183-1192

81 **Woodward M**, Finn C. Active One-shot Learning. In: NIPS 2016, Deep Reinforcement Learning Workshop, Barcelona, Spain. 2016

World Journal of Gastroenterology

Submit a Manuscript: https://www.f6publishing.com

World J Gastroenterol 2021 October 14; 27(38): 6415-6429

DOI: 10.3748/wjg.v27.i38.6415

ISSN 1007-9327 (print) ISSN 2219-2840 (online)

MINIREVIEWS

Faecal immunochemical test outside colorectal cancer screening?

Noel Pin-Vieito, Manuel Puga, Daniel Fernández-de-Castro, Joaquín Cubiella

ORCID number: Noel Pin-Vieito 0000-0003-0526-4104; Manuel Puga 0000-0003-4898-3889; Daniel Fernández-de-Castro 0000-0002-4510-0553; Joaquín Cubiella 0000-0002-9994-4831.

Author contributions: All authors contributed equally to the manuscript in the conception and design of the article, acquisition of data, analysis and interpretation of data; drafting the article or making critical revisions related to important intellectual content of the manuscript, and final approval of the version of the article to be published.

Supported by Spain's Carlos III Health Care Institute by Means of Project (Co-funded by European Regional Development Fund/European Social Fund "A way to make Europe"/"Investing in your future"), No. PI17/00837.

Conflict-of-interest statement: No conflict of interest.

Open-Access: This article is an open-access article that was selected by an in-house editor and fully peer-reviewed by external reviewers. It is distributed in accordance with the Creative Commons Attribution NonCommercial (CC BY-NC 4.0) license, which permits others to distribute, remix, adapt, build upon this work non-commercially, and license their derivative works

Noel Pin-Vieito, Manuel Puga, Daniel Fernández-de-Castro, Joaquín Cubiella, Department of Gastroenterology, Complexo Hospitalario Universitario de Ourense, Instituto de Investigación Sanitaria Galicia Sur, Centro de Investigación Biomédica en Red de Enfermedades Hepáticas y Digestivas (CIBERehd), Ourense 32005, Spain

Corresponding author: Joaquín Cubiella, MD, PhD, Doctor, Staff Physician, Statistician, Department of Gastroenterology, Complexo Hospitalario Universitario de Ourense, Instituto de Investigación Sanitaria Galicia Sur, Centro de Investigación Biomédica en Red de Enfermedades Hepáticas y Digestivas (CIBERehd), Rúa Ramón Puga 52-56, Ourense 32005, Spain. joaquin.cubiella.fernandez@sergas.es

Abstract

Faecal immunochemical tests (FITs) are the most widely colorectal cancer (CRC) diagnostic biomarker available. Many population screening programmes are based on this biomarker, with the goal of reducing CRC mortality. Moreover, in recent years, a large amount of evidence has been produced on the use of FIT to detect CRC in patients with abdominal symptoms in primary healthcare as well as in surveillance after adenoma resection. The aim of this review is to highlight the available evidence on these two topics. We will summarize the evidence on diagnostic yield in symptomatic patients with CRC and significant colonic lesion and the different options to use this (thresholds, brands, number of determinations, prediction models and combinations). We will include recommendations on FIT strategies in primary healthcare proposed by regulatory bodies and scientific societies and their potential effects on healthcare resources and CRC prognosis. Finally, we will show information regarding FIT-based surveillance as an alternative to endoscopic surveillance after high-risk polyp resection. To conclude, due to the coronavirus disease 2019 pandemic, FIT-based strategies have become extremely relevant since they enable a reduction of colonoscopy demand and access to the healthcare system by selecting individuals with the highest risk of CRC.

Key Words: Adenoma; Colorectal cancer; Diagnostic performance; Faecal biomarkers; Faecal haemoglobin; Faecal immunochemical test; Primary healthcare

©The Author(s) 2021. Published by Baishideng Publishing Group Inc. All rights reserved.

Core Tip: Faecal immunochemical test (FIT) is a colorectal cancer (CRC) diagnostic

on different terms, provided the original work is properly cited and the use is non-commercial. See: http://creativecommons.org/Licenses/by-nc/4.0/

Manuscript source: Invited manuscript

Specialty type: Gastroenterology and hepatology

Country/Territory of origin: Spain

Peer-review report's scientific quality classification

Grade A (Excellent): 0
Grade B (Very good): 0
Grade C (Good): C
Grade D (Fair): 0
Grade E (Poor): 0

Received: April 7, 2021
Peer-review started: April 7, 2021
First decision: June 26, 2021
Revised: June 27, 2021
Accepted: August 16, 2021
Article in press: August 16, 2021
Published online: October 14, 2021

P-Reviewer: Cai ZZ
S-Editor: Gao CC
L-Editor: Filipodia
P-Editor: Liu JH

biomarker used widely in CRC screening programmes. In recent years, a large body of evidence has appeared that enables recommending its use in different scenarios. For the evaluation of symptomatic patients in primary healthcare, FIT improves use of available endoscopic resources, avoiding unnecessary colonoscopies, predicts the risk of CRC and may have an impact on prognosis. Furthermore, although endoscopic surveillance after adenoma resection is widely extended, there are relevant doubts over its efficiency in the context of high-quality baseline colonoscopies and a FIT-based surveillance strategy could be an alternative.

Citation: Pin-Vieito N, Puga M, Fernández-de-Castro D, Cubiella J. Faecal immunochemical test outside colorectal cancer screening? *World J Gastroenterol* 2021; 27(38): 6415-6429
URL: https://www.wjgnet.com/1007-9327/full/v27/i38/6415.htm
DOI: https://dx.doi.org/10.3748/wjg.v27.i38.6415

INTRODUCTION

Colorectal cancer (CRC) is a relevant health problem in the Western world. In 2018, almost half a million new cases were diagnosed in Europe and 250000 patients died due to CRC[1]. Health authorities have devised two main strategies to reduce the impact of CRC: screening in average- and high-risk populations and early detection in symptomatic patients[2-4].

All preventive and diagnostic strategies are based either on invasive or non-invasive techniques. Colonoscopy is the cornerstone of all techniques, due to its diagnostic yield, the capacity of histological sampling, and especially, its ability to perform therapeutic procedures. However, colonoscopy is time and resource consuming, there is limited capacity with potential waiting lists and it is associated with side effects. Among the non-invasive techniques either imaging techniques or several diagnostic biomarkers have been evaluated[5].

Faecal occult blood tests (FOBTs) are the most widely CRC diagnostic biomarker available. FOBTs detect either blood or blood products (such as globin) in faeces with different methods. There are two main types of FOBTs: Chemical (cFOBT) or immunological (faecal immunochemical test, FIT). cFOBTs demonstrated its effect on reducing CRC mortality in CRC screening in large-scale randomized controlled trials[5]. However, they have been gradually replaced by semiquantitative FITs due to their advantages. FITs are based on the reaction of monoclonal or polyclonal antibodies specific for human faecal haemoglobin (f-Hb), albumin, or other faecal blood components. Thus, they do not require any dietary or pharmacological restriction, as long as they do not react with blood from the upper digestive tract or with any food component. The greatest advantage is determined by its ability to detect and quantify f-Hb concentrations 7 to 15 times lower than those detected by chemical tests. This significantly improves CRC and advanced adenoma detection sensitivity. Moreover, FITs enable reliable and accurate automated analyses, which prevents subjective interpretation[6]. For this reason, most CRC mass screening programmes have opted for FIT. Moreover, there is a large amount of evidence on the diagnostic accuracy of FITs for CRC and adenoma detection in asymptomatic patients[7].

In recent years, a large amount of evidence has been produced on the use of FITs to detect CRC in patients with abdominal symptoms[8-10] as well as in the surveillance of high-risk subjects (surveillance after adenoma resection)[11,12]. Furthermore, due to the coronavirus disease 2019 (COVID-19) pandemic, FIT has become extremely relevant due to the limited endoscopic resources available and access to healthcare systems[13]. The aim of this review is, therefore, to update the evidence and recommendations available on use of FIT outside the scope of CRC screening. This topic is structured into the following sections: Evidence on FIT in the evaluation of symptomatic patients; risk prediction models for CRC incorporating FIT in symptomatic patients; a combination of FIT with other non-invasive biomarkers in patients with abdominal symptoms; recommendations on the use of FIT in primary healthcare; effect of FIT on CRC prognosis; and FIT for surveillance after adenoma resection.

EVIDENCE ON FIT IN THE EVALUATION OF SYMPTOMATIC PATIENTS

Despite the implementation of CRC screening programmes, most CRC cases are still diagnosed after symptomatic presentation[14]. A large number of studies have been performed on the effectiveness of FIT for triaging referrals; also in symptomatic patients, which have been summarized in a number of recent systematic reviews[8-10, 15]. The first systematic review assessing the value of immunochemical-based FOBTs as first-line investigation in symptomatic patients was completed in 2008[15]. This review included nine studies evaluating several FIT assays using different methods and reported that FIT had better diagnostic performance than cFOBTs. However, the studies included had a small sample size and a high degree of clinical heterogeneity (*i.e.* different populations, use of quantitative and qualitative FITs), which limits the conclusions of the meta-analysis.

This work was supplemented by another systematic review[10], conducted to inform the development of a new National Institute for Health and Care Excellence (NICE) diagnostics guidance (DG) 30[16]. This review included nine studies, which provided data about clinical evaluations of three quantitative FIT assays and showed that when the FIT result is based on a single sample with a cut-off point of 10 μg Hb/g of faeces, the sensitivity for detecting CRC was 92.1% (95% confidence interval [CI]: 86.9-95.3) and 100% (95%CI: 71.5-100) for OC-Sensor (Eiken Chemical Co. Ltd., Tokyo, Japan) and HM-JACKarc (Kyowa-Medex Co. Ltd., Tokyo, Japan) FIT assays, respectively, indicating that both could be useful to rule out CRC. In that review, specificity was estimated to be 85.8% (95%CI: 78.3-91) and 76.6% (95%CI: 72.6-80.3) for OC-Sensor and HM-JACKarc FIT assays, respectively. The systematic review also included results from a study evaluating the diagnostic accuracy of the FOB Gold (Sentinel Diagnostics, Milan, Italy) FIT assay to detect a significant colonic lesion (SCL) using a f-Hb cut-off of 9 μg Hb/g faeces, defined as bleeding, cancer or polyp (sensitivity 45.2%; specificity 92.3%). As a result of this evidence,[10] NICE recommended use of the OC Sensor®, HMJACKarc®, and FOB Gold® FIT assays in primary healthcare to assess people who have accounted low risk symptoms (without rectal bleeding) who do not meet the criteria for a suspected cancer pathway referral, using a threshold of 10 μg Hb/g faeces[16,17]. However, important clinical concerns have been raised related to this recommendation[18].

Applicability of quantitative FITs in the assessment of patients with abdominal symptoms in primary healthcare

The systematic review supporting DG 30 only included one study performed in a primary healthcare setting[19], and none of the reviewed studies assessed FIT accuracy in real practice. Hence, the assessment of FIT accuracy to detect CRC in a cohort of symptomatic patients recruited from primary healthcare could lead to different results when compared to another comprised by symptomatic patients referred to secondary healthcare[8]. This could happen for reasons unrelated to CRC prevalence[20]. In this sense, high-risk symptoms (*i.e.* rectal bleeding) are shared between CRC and other benign conditions (*i.e.* anorectal disease, diverticular disease, colorectal polyps, inflammatory bowel disease or non-steroidal anti-inflammatory drug related enteropathy) which are more prevalent, thus reducing FIT specificity to detect CRC[21].

A subsequent meta-analysis was aimed at solving these problems[8]. The authors performed subgroup analyses according to the characteristics of the studies (100% symptomatic cohorts/mixed cohorts of symptomatic/asymptomatic subjects) and CRC prevalence. In this respect, the pooled estimates of sensitivity for studies comprised solely by symptomatic patients and studies made up of mixed cohorts was 94.1% (95%CI: 90.0-96.6) and 85.5% (95%CI: 76.5-91.4), respectively. Conversely, there were no statistically significant differences between the pooled sensitivity of studies with CRC prevalence < 2.5% (84.9%, 95%CI: 73.4-92.0) and ≥ 2.5% (91.7%, 95%CI: 83.3-96.1).

Since then, many studies assessing the diagnostic accuracy of FIT have been performed in primary healthcare. However, some have limitations, mainly due to their retrospective nature[9] or the criteria used for CRC diagnosis. Several studies have not used colonoscopy or a sufficient follow-up time (at least 2 years) to detect incident CRC. These two criteria have been used as "reference tests" in the systematic reviews available to select high-quality studies[8,10,15,22]. Furthermore, they have been confirmed in a different meta-analysis which detected similar diagnostic accuracy among the studies that used these criteria[7]. This evidence has been summarized in a recently published meta-analysis that has evaluated the diagnostic accuracy of FIT in patients presenting lower abdominal symptoms in primary healthcare. The results

confirmed previous findings. Twenty-three studies (69536 participants) were included with a CRC prevalence ranging between 0.3% and 6.2%. Six studies (n = 34691) evaluated FIT as rule in test (threshold of ≥ 150 μg Hb/g faeces) showing moderate sensitivity (64.1%, 95%CI: 57.8-69.9) and high specificity (95.0%, 95%CI: 91.2-97.2). A threshold of 10 μg/g (15 studies; n = 48872) resulted in sensitivity and specificity of 87.2% (95%CI: 81.0-91.6) and 84.4% (95%CI: 79.4-88.3) for CRC, respectively[9].

In this meta-analysis, the number needed to scope to detect a CRC as well as the number of missed CRC per 1000 patients according to expected CRC prevalence in primary care was calculated. The number of missed CRC per 1000 patients if a patient has a 'negative' FIT result in a population with a CRC prevalence of 2% is expected to increase from four to five when using the threshold of 20 μg Hb/g faeces instead of 10 μg Hb/g faeces. However, at the same CRC prevalence, the number needed to scope is expected to decrease from 10 to 4 if the 150 μg Hb/g faeces threshold is used instead of 10 μg Hb/g faeces[9].

Accuracy of FIT in detecting SCL and gastrointestinal cancer in patients with abdominal symptoms

As previously discussed, abdominal symptoms are non-specific and shared among benign and malignant diseases. Thus, the aim of a physician is not only to rule out CRC as long as other benign conditions may also present with the same symptoms and may benefit from diagnosis. In this sense, a previous meta-analysis revealed that FIT may not be sensitive enough to rule out all SCL[8]. Unfortunately, there is a high degree of heterogeneity among the studies evaluated due to the FIT brands used, the threshold selected, and especially, the differences in SCL definitions. The definitions used vary among inflammatory bowel disease, cancer, or high-risk adenoma; plus any type of colitis; plus any advanced adenoma, polyposis, complicated diverticular disease, colonic ulcer and bleeding angiodysplasia or even any colonic lesion detection regardless of its importance[8]. In a recently published meta-analysis, the overall pooled sensitivity and specificity of FITs for SCL for studies that used the limit of detection as a threshold (seven studies; n = 22624 patients) was 70.4% (95%CI: 68.4-72.3) and 78.4% (95%CI: 77.8-78.9), respectively. At the ≥ 10 μg Hb/g faeces threshold (seven studies; n = 20407 patients), the sensitivity and specificity were 69.1% (95%CI: 60.5-76.5) and 87.2% (95%CI: 83.4-90.2), respectively. Furthermore, three studies (n = 20528 patients) evaluated the diagnostic accuracy of FIT with a threshold of ≥ 150 μg Hb/g faeces showing sensitivity and specificity of 35.9% (95%CI: 33.8-38.1) and 97.5% (95%CI: 97.3-97.8), respectively[9].

Gastrointestinal (GI) symptoms are non-specific and could be related to different GI diseases. A relevant question is whether symptomatic patients with a completely normal colonoscopy after a positive FIT require further evaluation. In a recently published study, the risk of GI cancer detection (upper GI cancer and CRC) after a complete colonoscopy without CRC was evaluated according to the FIT result (threshold 10 μg Hb/g faeces). During a mean time of 45.5 ± 20.0 mo, GI cancer was detected in 57 (2.1%) patients: upper GI cancer in 35 (1.3%) and CRC in 14 (0.5%). FIT-positive subjects revealed a higher CRC risk (hazard ratio [HR] 3.8, 95%CI: 1.2-11.9] with no differences in GI (HR 1.5, 95%CI: 0.8-2.7) or upper GI cancer risk (HR 1.0, 95%CI: 0.5-2.2). Upper GI cancer was detected in 22 (0.8%) patients during the first year. Two variables were independently associated: anaemia (odds ratio [OR] 5.6, 95%CI: 2.2-13.9) and age ≥ 70 years (OR 2.7, 95%CI: 1.1-7.0)[23].

Does one sample with a cut-off point of 10 μg Hb/g of faeces fit everybody?

NICE recommends a single f-Hb cut-off of 10 μg Hb/g faeces to be used in the evaluation of symptomatic patients at all ages regardless of sex. However, using FIT with the same cut-off for asymptomatic populations has been associated with a higher accuracy for advanced adenoma detection in males[24]. However, a recently published meta-analysis on the diagnostic accuracy for CRC detection in asymptomatic patients did not show any differences between males and females[7]. These variations may be related to the differences in advanced adenoma prevalence and location as well as colonic transit.

One key question is what threshold is used to determine a positive result in the evaluation of symptomatic patients. Most studies have evaluated the 10 μg Hb/g of faeces threshold to triage symptomatic patients as this cut-off approximates to the quantitation limit documented by the manufacturers of most FIT analytical systems[8, 10]. Nonetheless, a recent study showed that using a cut-off point of 20 μg Hb/g of faeces could reduce the number of colonoscopy examinations without missing more than 1 CRC per 1000 patients evaluated belonging to the low-risk group defined by

NICE DG 30[9]. Moreover, other thresholds have also been proposed: limit of determination, and recently, 150 μg Hb/g of faeces[25]. Thus, while patients with a concentration below the limit of determination had a risk of detecting a CRC less than 0.2%; in patients with a Hb greater than 150 μg/g of faeces the risk of detecting a CRC was greater than 31.1%.

In fact, the choice of threshold is a trade-off among the number of patients required to be referred to colonoscopy, the number of missing CRC, and CRC prevalence. In our meta-analysis, we calculated the number needed to scope to detect a CRC as well as the number of missed CRC per 1000 patients according to expected CRC prevalence in primary care. The number of missed CRC per 1000 patients if a patient has a 'negative' FIT result in a population with a CRC prevalence of 2% is expected to increase from four to five when using the threshold of 20 μg Hb/g faeces instead of 10 μg Hb/g faeces. However, at the same CRC prevalence, the number needed to scope is expected to decrease from 10 to 4 if the 150 μg Hb/g faeces threshold is used instead of 10 μg Hb/g faeces[9]. With respect to colonoscopy, we must take into account not only the resources required to evaluate patients and waiting lists but also the risks associated with colonoscopy. In a recently published meta-analysis, they were estimated at 5.8 perforations per 10000 colonoscopies (95%CI: 5.7-6.0) and 2.4 cases of relevant bleeding per 1000 colonoscopies (95%CI: 2.4-2.5)[26]. In this sense, it also seems reasonable to use a higher cut-off than that recommended by NICE, if there is well-planned safety netting to evaluate symptomatic patients with a negative result if symptoms persist. Furthermore, results could also be closely monitored locally to enable the rapid adjustment of cut-offs to optimize each area's resources[27]. However, because f-Hb correlates directly with the severity of colorectal lesions, raising the f-Hb cut-off will lead to losing a higher number of SCLs. However, those are less urgent for diagnosis and could easily be subsequently rescued in an environment whose colonoscopy resources are preserved through the appropriate use of FIT as a first line triage test.

There is the option of using more than one FIT determination. Two studies included in a previous meta-analysis[8,10] examined the utility of one *vs* two faecal samples for detecting advanced neoplasia (CRC plus advanced adenoma). The diagnostic yield of the two samples using a cut-off of 20 μg Hb/g faeces was attained with only one sample using a cut-off of 10 μg Hb/g faeces. This highlights the need for further investigation to verify the efficiency of using different strategies to triage not only advanced adenoma but also any SCL, if the use of a higher cut-off than that recommended by NICE (10 μg Hb/g faeces) is conditioned to a "safety netting", which requires more than one FIT sample.

RISK PREDICTION MODELS FOR CRC INCORPORATING FIT IN SYMPTOMATIC PATIENTS

A number of predictive models have been developed to improve clinical judgement in patients with abdominal symptoms, and some have included quantitative FITs[28]. In recent years, two prediction models (COLONPREDICT and the FAST score) have been developed and were externally validated, not only to identify people at higher risk of CRC but also to define a subgroup whose CRC risk is so low that we can ensure that no further evaluation is required[29,30]. For that purpose, both prediction models defined two cut-offs. The first (COLONPREDICT< 3.50 and FAST score < 2.12 respectively) was evaluated to identify a low-risk population with a negative predictive value (NPV) of having CRC higher than 99%. In this subgroup, no further evaluation should be recommended as the risk of performing a colonoscopy is similar to the risk of severe complications associated with this exploration[26]. A second cut-off (COLONPREDICT ≥ 5.60, FAST score ≥ 4.50) was calculated to define a high-risk subgroup in which at least 90% of CRC would be detected.

Despite COLONPREDICT, the model has shown a high diagnostic performance, with an area under the curve (AUC) of 0.92 in both derivation and validation cohorts, it has been criticized as too complex for routine primary healthcare practice due to considering too many clinical (age, sex, acetylsalicylic acid treatment, previous colonoscopy, rectal mass, benign anorectal lesion, rectal bleeding and change in bowel habit) and laboratory (serum carcinoembryonic antigen, faecal and blood haemoglobin) variables[29]. Conversely, the FAST score combines only three variables (f-Hb, sex and age). In addition to being easier, this model has also shown high accuracy to predict the individual risk of CRC and SCL in symptomatic patients (AUC = 0.88)[30]. To date, none of these prediction models have been validated in primary

healthcare.

A similar risk score was developed by Rodríguez-Alonso *et al*[31] for advanced neoplasia detection. A score between 0 and 11 is calculated for each patient according to three variables (sex, age, and FIT), and a risk score ≥ 5 is considered the optimal cut-off point for colonoscopy referral. More recently, the COLONOFIT score aims to assess the risk of advanced neoplasia (CRC plus advanced adenoma) in symptomatic patients with indication of a fast-track colonoscopy[32]. This model is based on age, colonoscopy (in the previous 5 years), tobacco use, and variables related to FIT (maximum f-Hb value and number of samples with FIT > 4 μg Hb/g faeces). A COLONOFIT score > 10 points enables diagnosis of 98% of CRC (NPV = 99.7%) and 77% of advanced adenomas, and has been shown to classify patients 3% to 4% better than the FAST score in this study. However, COLONFIT needs the submission of three FIT samples, which could reduce adherence and compromise its successful implementation in primary healthcare.

COMBINATION OF FIT WITH OTHER NON-INVASIVE BIOMARKERS IN PATIENTS WITH ABDOMINAL SYMPTOMS

Although many biomarkers have been evaluated for the detection of CRC in a screening setting[33], they have shown little applicability in clinical practice. A few studies have explored the possibility of improving the diagnostic performance of FIT in combination with other non-invasive biomarkers, mainly faecal calprotectin, M2-piruvate kinase and volatile organic compounds, in symptomatic patients[19,34-36]. In general, adding a second biomarker either improves sensitivity reducing specificity and increasing the number of patients referred to colonoscopy, or by contrast, increases specificity reducing sensitivity and the number of patients with a positive result. Only one study has evaluated the concomitant analysis of FIT and faecal calprotectin. This has shown mixed results, presumably due to heterogeneity of both targets, FIT assays, and cut-offs used. Mowat *et al*[19] reported the diagnostic accuracy of FIT (OC-Sensor®) and faecal calprotectin to detect SCL (CRC plus higher risk adenoma plus inflammatory bowel disease) using different cut-offs. The sensitivity of one sample of the OC-Sensor to detect CRC and SCL was 89.3% and 68.6% respectively (cut-off 10 μg Hb/g faeces). Furthermore, when using the limit of haemoglobin detection as a cut-off, the sensitivity to detect CRC and SCL improved by 100% and 88.2%, respectively. Finally, when adding the measurement of faecal calprotectin, the sensitivity to detect SCL increased by 91.2% and 96.1% using the 200 μg Hb/g faeces and 50 μg Hb/g faeces cut-offs, respectively[19].

RECOMMENDATIONS ON USE OF FIT IN PRIMARY HEALTHCARE

Not many international clinical guidelines have opted for the potential advantages of introducing FIT in daily clinical practice. The available literature was reviewed by van Melle *et al*[37], which identified a limited number of countries with clinical guidelines that explicitly recommended use of FIT in symptomatic patients: Australia[38], Spain [5], United Kingdom[16,17] and Denmark (limited to specialized healthcare). We searched most guidelines mentioned by van Melle *et al*[37], in addition to others such as the Italian[39], Colombian[40] and English versions of the Chinese guideline[41]. However, only the 2019 update of the Scottish guideline[42] raised the possibility of including FIT, after completion of several pilot studies currently being developed in Scotland (Table 1).

As previously noted, the NICE recommended that FIT be performed in primary healthcare in symptomatic patients with a positive predictive value below 3%[16,17] after performing a systematic review[10]. Specifically, in the National Institute for Health and Care Excellence guideline, 12 FIT is recommended in patients without rectal bleeding aged under 60 with altered bowel habits or iron deficiency anaemia, patients without rectal bleeding aged over 50 with abdominal pain or weight loss (in which the combination of both symptoms would have been a fast-track criterion); and patients older than 60 with anaemia[17]. Patients with a positive FIT should be referred through the fast-track pathway for further evaluation. In the DG 30, FIT is recommended in any symptomatic patient that does not meet any of the fast-track criteria[18]. The Australian guideline[38] includes the indications of the NICE guidelines to recommend FIT in patients aged under 60 without overt bleeding with a

Table 1 Clinical guidelines and recommendations on colorectal cancer diagnosis that include the use of faecal immunochemical test in primary healthcare

Guideline	Year	Criteria to use FIT
NICE DG 30 United Kingdom [16]	2017	People without rectal bleeding who have unexplained symptoms but do not meet the criteria for a suspected cancer pathway referral outlined in NICE's guideline on suspected cancer
Australia[38]	2018	In people with symptoms other than overt rectal bleeding, FIT can be used as part of the diagnostic assessment in primary healthcare. It is of particular use in the following circumstances to support diagnostic assessment and notify the urgency of colonoscopy: people over 50 yr with either unexplained weight loss or abdominal pain; and people under 60 yr with either altered bowel habit or anaemia
Spain[5]	2018	Patients with lower gastrointestinal symptoms of recent onset who do not meet criteria for referral without delay to a specialist service due to high suspicion of CRC (rectal or abdominal mass, rectal bleeding or iron-deficiency anaemia) should undergo a FIT
NICE NG12 United Kingdom [17]	2021	Offer FIT to assess for CRC in adults without rectal bleeding who: Are aged 50 and over with unexplained abdominal pain or weight loss, or are aged under 60 with changes in their bowel habit, or iron-deficiency anaemia, or are aged 60 and over and have anaemia even in the absence of iron deficiency

CRC: Colorectal cancer; DG: Diagnostics guidance; FIT: Faecal immunochemical test; NG: National Institute for Health and Care Excellence guideline; NICE: National Institute for Health and Care Excellence.

change in bowel habit or anaemia; and in those over 50 with abdominal pain or weight loss. Based on the article published by Mowat *et al*[19], the recommendation justified performing FIT to rule out SCL.

The Spanish guideline on CRC diagnosis and prevention[5] is based on the NICE DG 30 (including the 10 μg Hb/g of faeces cut-off) and the systematic review performed by Westwood *et al*[10]. FIT is recommended for the evaluation of any patient with lower GI symptoms if they do not meet the criteria for urgent referral to colonoscopy (tumour or mass on examination or imaging tests, rectal bleeding associated with CRC or iron deficiency anaemia). Therefore, this guide includes non-suspicious rectal bleeding as a FIT application criterion. In the event of a positive result, the guide recommends requesting a colonoscopy and in case of negative result, to monitor symptoms and refer the patient to a specialized level if symptoms persist.

On the other hand, guidelines that do not recommend FIT in primary healthcare generally propose referral to specialized healthcare for all high-risk symptoms and only recommend observation in patients with low-risk symptoms such as loss of appetite, constipation or mucus in the faeces[37]. The specialist will probably finally request the colonoscopy and decide priority himself. The New Zealand guide, updated in 2014[43], explicitly advises against its use, due to the lack of evidence in its favour and compares it with carcinoembryonic antigen. The Ontario clinical guidelines[44] withdrew the recommendations that included cFOBTs in 2017, to avoid a possible conflict with its screening programme. In 2019, this exclusion was extended to FITs. Other clinical guidelines only contemplate cFOBTs[45].

EFFECT OF A FIT-BASED STRATEGY ON RESOURCES

As we have seen, the guidelines that recommend FIT in primary healthcare are intended to identify a subgroup of patients at high risk of CRC detection despite presenting mild symptoms. Otherwise, these patients would not have been included in the fast-track colonoscopy. However, a negative FIT result in these patients would reduce the number of colonoscopies performed with no relevant findings[10]. This strategy may avoid colonoscopy-related risks in subjects with a low CRC risk and facilitate better prioritization on colonoscopy waiting lists. In this sense, an estimation performed based on the results obtained in the Pin-Vieito study[8] with a 3% CRC estimated prevalence and 10 μg Hb/g and 20 μg Hb/g of faeces cut-off (cohorts 100% symptomatic) highlights that FIT will avoid approximately 2/3 of the colonoscopy with two missed CRC out of 1000 patients evaluated (Figure 1). If we take the SCL into consideration with 12% and 10 μg Hb/g of faeces cut-off, the positive predictive value would be 24.8%, and the number of undetected SCL would be 24 out of 1000 subjects, mainly advanced adenomas.

Due to the COVID-19 pandemic, the risk stratification of subjects with GI symptoms has become of the utmost relevance. A modelling study has recently been published.

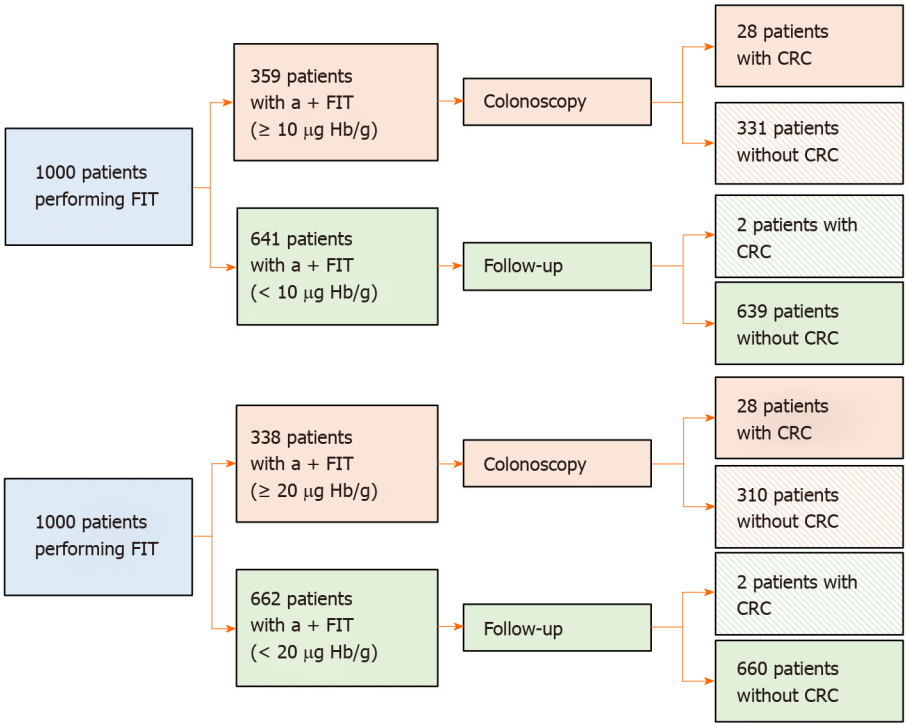


Figure 1 Estimation of the number of patients who need to be referred for colonoscopy, and the diagnostic yield for colorectal cancer in the 10 and 20 μg Hb/g of faeces thresholds[8]. CRC: Colorectal cancer; FIT: Faecal immunochemical test.

This model evaluated the effect of delays for colonoscopy on CRC mortality due to lack of endoscopic capacity and prioritization of colonoscopy in patients with a f-Hb ≥ 10 μg Hb/g of faeces. A delay higher than 6 mo would lead to 2250 attributable deaths and loss of 32799 life-years. In contrast, using FIT to stratify only 18% of symptomatic patients would be referred to colonoscopy; 89% of these deaths would be avoided and the requirements for colonoscopy would be reduced by > 80%[13]. This information has been confirmed in a recently published retrospective study in primary healthcare with a sample size of 14487 consecutive patients who underwent a FIT due to low-risk symptoms without fast-track criteria[46]. Using a ≥ 10 μg Hb/g faeces threshold, 10% of adults would be investigated to detect 91% of cancers with a number needed to scope of ten to detect one cancer and three to detect a SCL. Only 12 CRCs (< 2/1000 subjects) would be missed in the subjects evaluated. This proportion is similar to the colonoscopy-associated side effects[26] and CRC prevalence in asymptomatic adults aged 50-69[47].

A relevant topic is the strategy in subjects with a negative FIT result. Unfortunately, the information is limited. Hypothetically, symptoms in patients with CRC and a negative FIT will persist or even worsen, so they would require additional medical healthcare. In the Spanish guidelines, follow-up and request for colonoscopy are recommended if symptoms persist[5]. The results of the study performed by Nicholson *et al*[46] support this strategy because seven out of the 12 FIT-negative CRC were detected within 1 mo after FIT. A better understanding of the characteristics of patients with false negative results and their clinical course, is key to guide the most effective diagnostic tests to perform during follow-up.

Westwood *et al*[10] published a cost-effectiveness analysis to inform NICE about the use of FIT in symptomatic patients. For the effectiveness analysis, a meta-analysis was performed and for the cost analysis, a model based on quality-of-life-adjusted life years (QALYs) was devised. Researchers compared three strategies: triage with FIT, triage with cFOBT and no triage (direct referral to colonoscopy). The cost of a colonoscopy and the FIT was estimated at £372 and £4.53, respectively. The differences in QALYs between the three strategies were minimal. The triage strategy using FIT demonstrated a higher cost, but also higher efficacy and cost-effectiveness than cFOBT. It would only be surpassed in cost-effectiveness by placing the cut-off point at the detection threshold of 2 μg/g of Hb in faeces. The FIT also demonstrated greater cost-effectiveness compared to no triage, with an incremental cost of £258.09 per patient. Taking into account the lost QALYs due to FIT false-negatives, saving of £2578.543 per lost QALY was calculated using triage with FIT.

EFFECT OF FIT ON CRC PROGNOSIS

The main objective of any diagnostic strategy is to improve the prognosis of the disease detected. We have evidence that FIT-based CRC screening improves CRC prognosis through early detection[48]. However, the information regarding CRC prognosis detected after a positive FIT in symptomatic subjects is still limited. In this sense, a Polish retrospective analysis of 535 CRC detected in symptomatic subjects evaluated the effect of the pathway to CRC diagnosis on prognosis. CRC detected after a positive FIT (HemCheck-1) result revealed better prognosis than CRC detected on the basis of clinical evaluation (40 ± 47 mo *vs* 25 ± 38 mo; $P < 0.001$)[49].

In a recently published Spanish population-based study[14], a significantly longer 3-year survival was observed in patients with CRC diagnosed after a positive FIT in comparison with CRC detected after a negative result or without a FIT (HR 1.50; 95%CI: 1.22-1.84). These differences in prognosis were related to an earlier CRC stage at diagnosis in the positive FIT group. The reason for these findings is unclear; it is hypothesized that requesting a FIT could reduce diagnostic delay. However, there is a risk of bias, since in one-third of the positives the reason for the FIT request could not be confirmed and they could be related to opportunistic CRC screening.

Although these two retrospective studies have limitations and risk of bias (ignorance of comorbidities, circumstances of the CRC diagnosis, indications for FIT, single-centre, *etc.*), they support the hypothesis that evaluation of symptomatic patients with FIT could modify CRC prognosis. The causes of these differences are not clear and may include diagnostic delay, severity of the onset symptoms and characteristics of the general practitioner. Prospective studies need to be performed that evaluate the effect of a FIT-based diagnostic strategy on CRC prognosis to fully identify the strengths and weaknesses and thus find their ideal place in clinical practice guidelines.

FIT IN SURVEILLANCE AFTER ADENOMA RESECTION

Colorectal polyps are precursor lesions for CRC. Therefore, their removal during colonoscopy reduces CRC risk[5]. These patients have an increased risk of developing more polyps and eventually CRC over the years, so adopting surveillance strategies is recommended[5]. In recent years, mainly motivated by the implementation of the CRC populations screening programmes, there has been an increase in the number of patients with resected colorectal polyps that require surveillance. This has meant that colonoscopies have also undergone a major increase, which require large amounts of resources and highlights the currently overloaded endoscopy services[50,51]. However, we must keep in mind that colonoscopy is an invasive and expensive procedure, with a risk of adverse events, associated both with the procedure itself and with the sedation necessary for it to be performed correctly[26]. For these reasons, it seems reasonable that surveillance colonoscopy for patients after polyp removal should be targeted at those most likely to benefit[51].

The aim of surveillance after colorectal polyp resection is to reduce CRC incidence [51]. In order to make decisions on surveillance, there are two questions that need to be answered: what is the long term (10 years) risk of CRC without surveillance, and does endoscopic surveillance reduce CRC risk compared with no surveillance/participation in a CRC screening programme?

Until recently, the information available was limited and referred to the short-term risk of advanced adenoma detection, an intermediate lesion[52]. Several long-term studies with CRC incidence as the main endpoint have recently been published (Table 2)[53-58]. They reveal that subjects with low-risk lesions (mainly 1-2 non-advanced adenomas or serrated lesions) have a long-term CRC risk similar to the control group (general population or subjects with normal colonoscopy). In contrast, CRC risk is increased in subjects with high-risk lesions (mainly advanced adenomas/serrated lesions and/or multiple adenomas). Taking into account these results, the available practice guidelines recommend in the low-risk group a surveillance strategy equivalent to that recommended in the general population: participation in a CRC screening programme[2,5,59-61].

However, the evidence regarding the benefits of endoscopic surveillance in high-risk lesions is limited to cohort studies. In the study published by Cottet *et al*[62] in 2012, the standardized incidence ratio was 1.10 (95%CI: 0.62-1.82) and 4.26 (95%CI: 2.89-6.04) in those patients with and without colonoscopy follow-up, respectively. In a recently published study including 6239 patients with high-risk lesions, endoscopic

Table 2 Colorectal cancer risk in patients with high risk adenomas or low risk adenomas

Ref.	Patients	Follow-up in yr	Comparison group	High risk lesions	Low risk lesions
Løberg *et al*[53], 2014	40826	7.7	General population	SIR 1.62 (95%CI: 1.50-1.75)	SIR 0.98 (95%CI: 0.89-1.08)
Click *et al*[56], 2018	15935	12.9	No adenoma group	RR 2.7 (95%CI: 1.9-3.7)	RR 1.2 (95%CI: 0.8-1.7)
Lee *et al*[54], 2020	64422	8.1	No adenoma group	HR 2.61 (95%CI: 1.87-3.63)	HR 1.29 (95%CI: 0.89-1.88)
Wieszczy *et al*[55], 2020	236089	7.1	General population	SIR 0.65 (95%CI: 0.51-0.82)	SIR 0.35 (95%CI: 0.26-0.45)
He *et al*[58], 2020	122899	10	No adenoma group	HR 4.07 (95%CI: 2.89-5.72)	HR 1.21 (95%CI: 0.68-2.16)
Cross *et al*[57], 2021	21318	10.1	General population	SIR 1.30 (95%CI: 1.03-1.62)	SIR 0.75 (95%CI: 0.63- 0.88)

HR: Hazard ratio; RR: Rate ratio; SIR: Standardized incidence ratio.

surveillance was associated with a reduction in CRC risk (HR 0.71, 95%CI: 0.49-1.03 for 1 visit; 0.44, 0.28-0.70 for ≥ 2 visits)[57]. Atkin *et al*[63] also showed in a study including 12000 patients with high-risk lesions (1-2 adenomas ≥ 10 mm or 3-4 adenomas < 10 mm), that performing at least one endoscopic surveillance reduces the incidence of CRC (HR 0.57, 95%CI: 0.40-0.80). However, this risk reduction was limited to a subgroup of patients: low-quality colonoscopy, large (≥ 20 mm), high-grade dysplasia and proximal adenomas. In this respect, available guidelines recommend performing baseline colonoscopy with full exploration of the colonic mucosa and resection of all polyps detected[2,5,59-61]. CRC detection during surveillance depends not only on the characteristics of the polyps but also on the endoscopist's technical ability. A recently published Polish study revealed that long-term risk of CRC is increased (HR 2.69, 95%CI: 1.62-4.47) if baseline colonoscopy is performed by low-performing endoscopists (adenoma detection rate < 20%)[64].

One limitation of FIT is its limited diagnostic accuracy for adenomas at a single determination. In asymptomatic subjects, at a single determination FIT detects 31% and 21% of advanced adenomas at the 10 μg Hb/g and 20 μg Hb/g of faeces thresholds, respectively, with specificity higher than 90%[7]. There are several characteristics of the adenomas associated with a positive FIT: number, location, morphology and size[5]. However, the strength of a FIT-based CRC screening is that it is based on periodic (annual or biennial) determination. Furthermore, the threshold used can be tailored according to colonoscopy capacity and long-term objective. The evidence available on a FIT-based surveillance is limited. A prospective British study published in 2019 investigated whether faecal FIT could reduce the surveillance burden on patients and endoscopy services. The study population was patients with intermediate risk of CRC after polyp removal (1-2 adenomas ≥ 10 mm or 3-4 adenomas < 10 mm). Subjects were offered an annual FIT and all subjects underwent a 3-year scheduled colonoscopy. The number of patients that required work-up colonoscopy using the 10 μg Hb/g threshold was 28.8%. The 3-year programme sensitivity for CRC and advanced adenoma was 72.4% and 56.6% with a specificity of 71.1% and 73.7%, respectively. Incremental cost-effectiveness of colonoscopy *vs* FIT surveillance was £7354 per additional advanced adenoma detected and £180778 per additional CRC detected[11].

Similar results were obtained in a diagnostic accuracy study that evaluated FIT (2 μg Hb/g) in a cohort of high-risk patients who underwent endoscopic surveillance. A total of 593 patients were included, including 41 (6.9%) with advanced neoplasia (4 CRC, 37 higher-risk adenoma). Of the 238 patients (40.1%) who had detectable FIT, 31 (13.0%) had advanced neoplasia (2 CRC, 29 higher-risk adenoma) compared with 10 (2.8%) with undetectable FIT (2 CRC, 8 higher-risk adenoma). A detectable FIT gave NPV of 99.4% for CRC and 97.2% for CRC plus higher-risk adenoma. According to these results, a FIT determination can provide an objective estimate of the risk of advanced neoplasia, and could enable tailored scheduling of colonoscopy[65].

In the absence of results from randomized clinical trials evaluating a FIT-based surveillance strategy, we have information from a simulation study[66]. This study evaluated the additional benefit in terms of cost-effectiveness of adding colonoscopy surveillance to a CRC screening programme. Based on the information obtained from the Dutch CRC screening programme, FIT screening without colonoscopy surveillance after adenoma removal reduces CRC mortality by 50.4% compared with no screening or surveillance. Adding colonoscopy surveillance after adenoma resection to FIT screening would reduce mortality by an additional 1.7% to 52.1% but would increase

lifetime colonoscopy demand by 62% at an additional cost of €68000, for an increase of 0.9 life-year. Despite the reduction in mortality provided by endoscopic surveillance compared to FIT follow-up, this study concludes that it is not a cost-effective strategy based on the incremental cost-effectiveness ratios, which exceeds the Dutch willingness-to-pay threshold of €36602 per life-year gained and also substantially increases colonoscopy demand[66].

CONCLUSION

In conclusion, we have enough evidence to recommend use of FIT to triage symptomatic patients in primary healthcare. FIT improves use of available endoscopic resources, avoids unnecessary colonoscopies, accurately predicts the risk of CRC and may have an impact on CRC prognosis. On the other hand, although endoscopic surveillance after adenoma resection is widely extended, there are relevant doubts about its efficiency in the context of high-quality baseline colonoscopies. Moreover, in terms of evaluating the effect on CRC incidence, endoscopic surveillance should be compared with participation in a CRC screening programme. In this sense, we require a randomized controlled trial comparing endoscopic with FIT-based surveillance after high-risk polyp resection.

REFERENCES

1 **World Health Organization**. Cancer Today. International Agency for Research on Cancer. [cited 23 May 2020]. In: World Health Organization [Internet]. Available from: https://gco.iarc.fr/today/home

2 **Atkin WS**, Valori R, Kuipers EJ, Hoff G, Senore C, Segnan N, Jover R, Schmiegel W, Lambert R, Pox C; International Agency for Research on Cancer. European guidelines for quality assurance in colorectal cancer screening and diagnosis. First Edition--Colonoscopic surveillance following adenoma removal. *Endoscopy* 2012; **44** Suppl 3: SE151-SE163 [PMID: 23012119 DOI: 10.1055/s-0032-1309821]

3 **Hamilton W**. Five misconceptions in cancer diagnosis. *Br J Gen Pract* 2009; **59**: 441-445, 447; discussion 446 [PMID: 19520027 DOI: 10.3399/bjgp09X420860]

4 **National Collaborating Centre for Cancer (UK)**. Suspected Cancer: Recognition and Referral. London: National Institute for Health and Care Excellence (NICE); 2015 Jun. National Institute for Health and Care Excellence: Clinical Guidelines [PMID: 26180880]

5 **Cubiella J**, Marzo-Castillejo M, Mascort-Roca JJ, Amador-Romero FJ, Bellas-Beceiro B, Clofent-Vilaplana J, Carballal S, Ferrándiz-Santos J, Gimeno-García AZ, Jover R, Mangas-Sanjuán C, Moreira L, Pellisè M, Quintero E, Rodríguez-Camacho E, Vega-Villaamil P; Sociedad Española de Medicina de Familia y Comunitaria y Asociación Española de Gastroenterología. Clinical practice guideline. Diagnosis and prevention of colorectal cancer. 2018 Update. *Gastroenterol Hepatol* 2018; **41**: 585-596 [PMID: 30245076 DOI: 10.1016/j.gastrohep.2018.07.012]

6 **Quintero E**. [Chemical or immunological tests for the detection of fecal occult blood in colorectal cancer screening? *Gastroenterol Hepatol* 2009; **32**: 565-576 [PMID: 19577340 DOI: 10.1016/j.gastrohep.2009.01.179]

7 **Selby K**, Levine EH, Doan C, Gies A, Brenner H, Quesenberry C, Lee JK, Corley DA. Effect of Sex, Age, and Positivity Threshold on Fecal Immunochemical Test Accuracy: A Systematic Review and Meta-analysis. *Gastroenterology* 2019; **157**: 1494-1505 [PMID: 31472152 DOI: 10.1053/j.gastro.2019.08.023]

8 **Pin Vieito N**, Zarraquiños S, Cubiella J. High-risk symptoms and quantitative faecal immunochemical test accuracy: Systematic review and meta-analysis. *World J Gastroenterol* 2019; **25**: 2383-2401 [PMID: 31148909 DOI: 10.3748/wjg.v25.i19.2383]

9 **Pin-Vieito N**, Tejido-Sandoval C, de Vicente-Bielza N, Sánchez-Gómez C, Cubiella J. Faecal immunochemical tests safely enhance rational use of resources during the assessment of suspected symptomatic colorectal cancer in primary care: systematic review and meta-analysis. *Gut* 2021 [PMID: 34108236 DOI: 10.1136/gutjnl-2021-324856]

10 **Westwood M**, Corro Ramos I, Lang S, Luyendijk M, Zaim R, Stirk L, Al M, Armstrong N, Kleijnen J. Faecal immunochemical tests to triage patients with lower abdominal symptoms for suspected colorectal cancer referrals in primary care: a systematic review and cost-effectiveness analysis. *Health Technol Assess* 2017; **21**: 1-234 [PMID: 28643629 DOI: 10.3310/hta21330]

11 **Cross AJ**, Wooldrage K, Robbins EC, Kralj-Hans I, MacRae E, Piggott C, Stenson I, Prendergast A, Patel B, Pack K, Howe R, Swart N, Snowball J, Duffy SW, Morris S, von Wagner C, Halloran SP, Atkin WS. Faecal immunochemical tests (FIT) *vs* colonoscopy for surveillance after screening and polypectomy: a diagnostic accuracy and cost-effectiveness study. *Gut* 2019; **68**: 1642-1652 [PMID: 30538097 DOI: 10.1136/gutjnl-2018-317297]

12 **Dai C**, Jiang M, Sun MJ, Cao Q. Fecal immunochemical test for predicting mucosal healing in

ulcerative colitis patients: A systematic review and meta-analysis. *J Gastroenterol Hepatol* 2018; **33**: 990-997 [PMID: 29427297 DOI: 10.1111/jgh.14121]

13 **Loveday C**, Sud A, Jones ME, Broggio J, Scott S, Gronthound F, Torr B, Garrett A, Nicol DL, Jhanji S, Boyce SA, Williams M, Barry C, Riboli E, Kipps E, McFerran E, Muller DC, Lyratzopoulos G, Lawler M, Abulafi M, Houlston RS, Turnbull C. Prioritisation by FIT to mitigate the impact of delays in the 2-week wait colorectal cancer referral pathway during the COVID-19 pandemic: a UK modelling study. *Gut* 2021; **70**: 1053-1060 [PMID: 32855306 DOI: 10.1136/gutjnl-2020-321650]

14 **Gutierrez-Stampa MA**, Aguilar V, Sarasqueta C, Cubiella J, Portillo I, Bujanda L. Impact of the faecal immunochemical test on colorectal cancer survival. *BMC Cancer* 2020; **20**: 616 [PMID: 32611328 DOI: 10.1186/s12885-020-07074-y]

15 **Jellema P**, van der Windt DA, Bruinvels DJ, Mallen CD, van Weyenberg SJ, Mulder CJ, de Vet HC. Value of symptoms and additional diagnostic tests for colorectal cancer in primary care: systematic review and meta-analysis. *BMJ* 2010; **340**: c1269 [PMID: 20360221 DOI: 10.1136/bmj.c1269]

16 **National Institute for Health and Care Excellence**. Quantitative faecal immunochemical tests to guide referral for colorectal cancer in primary care. [cited 16 Mar 2021]. In: National Institute for Health and Care Excellence [Internet]. Available from: https://www.nice.org.uk/guidance/dg30

17 **National Institute for Health and Care Excellence**. Suspected cancer: recognition and referral NICE guideline [NG12]. [cited 16 Mar 2021]. In: National Institute for Health and Care Excellence [Internet]. Available from: https://www.nice.org.uk/guidance/ng12

18 **Fraser CG**. Faecal immunochemical tests for haemoglobin (FIT) in the assessment of patients with lower abdominal symptoms: current controversies. *Gastroenterol Hepatol* 2019; **42**: 263-270 [PMID: 30459060 DOI: 10.1016/j.gastrohep.2018.09.007]

19 **Mowat C**, Digby J, Strachan JA, Wilson R, Carey FA, Fraser CG, Steele RJ. Faecal haemoglobin and faecal calprotectin as indicators of bowel disease in patients presenting to primary care with bowel symptoms. *Gut* 2016; **65**: 1463-1469 [PMID: 26294695 DOI: 10.1136/gutjnl-2015-309579]

20 **Leeflang MM**, Rutjes AW, Reitsma JB, Hooft L, Bossuyt PM. Variation of a test's sensitivity and specificity with disease prevalence. *CMAJ* 2013; **185**: E537-E544 [PMID: 23798453 DOI: 10.1503/cmaj.121286]

21 **Hamilton W**, Walter FM, Rubin G, Neal RD. Improving early diagnosis of symptomatic cancer. *Nat Rev Clin Oncol* 2016; **13**: 740-749 [PMID: 27458007 DOI: 10.1038/nrclinonc.2016.109]

22 **Lee JK**, Liles EG, Bent S, Levin TR, Corley DA. Accuracy of fecal immunochemical tests for colorectal cancer: systematic review and meta-analysis. *Ann Intern Med* 2014; **160**: 171 [PMID: 24658694 DOI: 10.7326/M13-1484]

23 **Pin-Vieito N**, Iglesias MJ, Remedios D, Rodríguez-Alonso L, Rodriguez-Moranta F, Álvarez-Sánchez V, Fernández-Bañares F, Boadas J, Martínez-Bauer E, Campo R, Bujanda L, Ferrandez Á, Piñol V, Rodríguez-Alcalde D, Guardiola J, Cubiella J, On Behalf Of The Colonpredict Study Investigators. Risk of gastrointestinal cancer in a symptomatic cohort after a complete colonoscopy: Role of faecal immunochemical test. *World J Gastroenterol* 2020; **26**: 70-85 [PMID: 31933515 DOI: 10.3748/wjg.v26.i1.70]

24 **Grobbee EJ**, Wieten E, Hansen BE, Stoop EM, de Wijkerslooth TR, Lansdorp-Vogelaar I, Bossuyt PM, Dekker E, Kuipers EJ, Spaander MC. Fecal immunochemical test-based colorectal cancer screening: The gender dilemma. *United European Gastroenterol J* 2017; **5**: 448-454 [PMID: 28507758 DOI: 10.1177/2050640616659998]

25 **D'Souza N**, Georgiou Delisle T, Chen M, Benton S, Abulafi M; NICE FIT Steering Group. Faecal immunochemical test is superior to symptoms in predicting pathology in patients with suspected colorectal cancer symptoms referred on a 2WW pathway: a diagnostic accuracy study. *Gut* 2021; **70**: 1130-1138 [PMID: 33087488 DOI: 10.1136/gutjnl-2020-321956]

26 **Kothari ST**, Huang RJ, Shaukat A, Agrawal D, Buxbaum JL, Abbas Fehmi SM, Fishman DS, Gurudu SR, Khashab MA, Jamil LH, Jue TL, Law JK, Lee JK, Naveed M, Qumseya BJ, Sawhney MS, Thosani N, Yang J, DeWitt JM, Wani S; ASGE Standards of Practice Committee Chair. ASGE review of adverse events in colonoscopy. *Gastrointest Endosc* 2019; **90**: 863-876.e33 [PMID: 31563271 DOI: 10.1016/j.gie.2019.07.033]

27 **Toes-Zoutendijk E**, van Leerdam ME, Dekker E, van Hees F, Penning C, Nagtegaal I, van der Meulen MP, van Vuuren AJ, Kuipers EJ, Bonfrer JMG, Biermann K, Thomeer MGJ, van Veldhuizen H, Kroep S, van Ballegooijen M, Meijer GA, de Koning HJ, Spaander MCW, Lansdorp-Vogelaar I; Dutch National Colorectal Cancer Screening Working Group. Real-Time Monitoring of Results During First Year of Dutch Colorectal Cancer Screening Program and Optimization by Altering Fecal Immunochemical Test Cut-Off Levels. *Gastroenterology* 2017; **152**: 767-775.e2 [PMID: 27890769 DOI: 10.1053/j.gastro.2016.11.022]

28 **Grigore B**, Lewis R, Peters J, Robinson S, Hyde CJ. Development, validation and effectiveness of diagnostic prediction tools for colorectal cancer in primary care: a systematic review. *BMC Cancer* 2020; **20**: 1084 [PMID: 33172448 DOI: 10.1186/s12885-020-07572-z]

29 **Cubiella J**, Vega P, Salve M, Díaz-Ondina M, Alves MT, Quintero E, Álvarez-Sánchez V, Fernández-Bañares F, Boadas J, Campo R, Bujanda L, Clofent J, Ferrandez Á, Torrealba L, Piñol V, Rodríguez-Alcalde D, Hernández V, Fernández-Seara J; COLONPREDICT study investigators. Development and external validation of a faecal immunochemical test-based prediction model for colorectal cancer detection in symptomatic patients. *BMC Med* 2016; **14**: 128 [PMID: 27580745 DOI: 10.1186/s12916-016-0668-5]

30 **Cubiella J**, Digby J, Rodríguez-Alonso L, Vega P, Salve M, Díaz-Ondina M, Strachan JA, Mowat C,

McDonald PJ, Carey FA, Godber IM, Younes HB, Rodriguez-Moranta F, Quintero E, Álvarez-Sánchez V, Fernández-Bañares F, Boadas J, Campo R, Bujanda L, Garayoa A, Ferrandez Á, Piñol V, Rodríguez-Alcalde D, Guardiola J, Steele RJ, Fraser CG; COLONPREDICT study investigators. The fecal hemoglobin concentration, age and sex test score: Development and external validation of a simple prediction tool for colorectal cancer detection in symptomatic patients. *Int J Cancer* 2017; **140**: 2201-2211 [PMID: 28187494 DOI: 10.1002/ijc.30639]

31 **Rodríguez-Alonso L**, Rodríguez-Moranta F, Ruiz-Cerulla A, Lobatón T, Arajol C, Binefa G, Moreno V, Guardiola J. An urgent referral strategy for symptomatic patients with suspected colorectal cancer based on a quantitative immunochemical faecal occult blood test. *Dig Liver Dis* 2015; **47**: 797-804 [PMID: 26055489 DOI: 10.1016/j.dld.2015.05.004]

32 **Fernández-Bañares F**, Clèries R, Boadas J, Ribes J, Oliva JC, Alsius A, Sanz X, Martínez-Bauer E, Galter S, Pujals M, Pujol M, Del Pozo P, Campo R. Prediction of advanced colonic neoplasm in symptomatic patients: a scoring system to prioritize colonoscopy (COLONOFIT study). *BMC Cancer* 2019; **19**: 734 [PMID: 31345180 DOI: 10.1186/s12885-019-5926-4]

33 **Loktionov A**. Biomarkers for detecting colorectal cancer non-invasively: DNA, RNA or proteins? *World J Gastrointest Oncol* 2020; **12**: 124-148 [PMID: 32104546 DOI: 10.4251/wjgo.v12.i2.124]

34 **Parente F**, Marino B, Ilardo A, Fracasso P, Zullo A, Hassan C, Moretti R, Cremaschini M, Ardizzoia A, Saracino I, Perna F, Vaira D. A combination of faecal tests for the detection of colon cancer: a new strategy for an appropriate selection of referrals to colonoscopy? *Eur J Gastroenterol Hepatol* 2012; **24**: 1145-1152 [PMID: 22735608 DOI: 10.1097/MEG.0b013e328355cc79]

35 **Widlak MM**, Neal M, Daulton E, Thomas CL, Tomkins C, Singh B, Harmston C, Wicaksono A, Evans C, Smith S, Savage RS, Covington JA, Arasaradnam RP. Risk stratification of symptomatic patients suspected of colorectal cancer using faecal and urinary markers. *Colorectal Dis* 2018; **20**: O335-O342 [PMID: 30248228 DOI: 10.1111/codi.14431]

36 **Arasaradnam RP**, McFarlane MJ, Ryan-Fisher C, Westenbrink E, Hodges P, Thomas MG, Chambers S, O'Connell N, Bailey C, Harmston C, Nwokolo CU, Bardhan KD, Covington JA. Detection of colorectal cancer (CRC) by urinary volatile organic compound analysis. *PLoS One* 2014; **9**: e108750 [PMID: 25268885 DOI: 10.1371/journal.pone.0108750]

37 **van Melle M**, Yep Manzano SIS, Wilson H, Hamilton W, Walter FM, Bailey SER. Faecal immunochemical test to triage patients with abdominal symptoms for suspected colorectal cancer in primary care: review of international use and guidelines. *Fam Pract* 2020; **37**: 606-615 [PMID: 32377668 DOI: 10.1093/fampra/cmaa043]

38 **Cancer Council**. Cancer Council Australia Colorectal Cancer Guidelines Working Party. Clinical Practice Guidelines for the Prevention, Early Detection and Management of Colorectal Cancer. [cited 17 Mar 2021]. In: Cancer Council [Internet]. Available from: https://wiki.cancer.org.au/australia/Guidelines:Colorectal_cancer

39 **Association of Medical Oncology**. Linee Guida AIOM 2020 neoplasie del retto e ano. [cited 16 Sep 2021]. In: Association of Medical Oncology [Internet]. Available from: https://www.aiom.it/wp-content/uploads/2021/01/2020_LG_AIOM_-Retto_e_Ano.pdf

40 **Ministerio de Salud y Protección Social**. Guía de Práctica Clínica para la detección temprana, diagnóstico, tratamiento integral, seguimiento y rehabilitación del cáncer de colon y recto. Sistema General de Seguridad Social en Salud – Colombia Guía No 20 – Segunda edición Guía para professional. [cited 16 Mar 2021]. In: Ministerio de Salud y Protección Social [Internet]. Available from: http://gpc.minsalud.gov.co/gpc_sites/Repositorio/Conv_500/GPC_cancer_colon/GPC_Ca_colon_Profesionales2daEd.pdf

41 **National Health Commission of The People's Republic of China**. National guidelines for diagnosis and treatment of colorectal cancer 2020 in China (English version). *Chin J Cancer Res* 2020; **32**: 415-445 [PMID: 32965276 DOI: 10.21147/j.issn.1000-9604.2020.04.01]

42 **Scottish Government**. Scottish referral guidelines for suspected cancer. [cited 16 Mar 2021]. In: Scottish Government [Internet]. Available from: https://www.gov.scot/binaries/content/documents/govscot/publications/advice-and-guidance/2019/01/scottish-referral-guidelines-suspected-cancer-january-2019/documents/scottish-referral-guidelines-suspected-cancer/scottish-referral-guidelines-suspected-cancer

43 **New Zealand Guidelines Group**. Suspected Cancer in Primary Care: Guidelines for Investigation, Referral and Reducing Ethnic Disparities. [cited 17 Mar 2021]. In: New Zealand Guidelines Group [Internet]. Available from: https://www.health.govt.nz/system/files/documents/publications/suspected-cancer-guideline-sep09.pdf

44 **The Colorectal Cancer Referral Expert Panel**. Referral of Patients with Suspected Colorectal Cancer by Family Physicians and Other Primary Care Providers. [cited 17 Mar 2021]. In: The Colorectal Cancer Referral Expert Panel [Internet]. Available from: https://www.cancercareontario.ca/sites/ccocancercare/files/guidelines/summary/pebc24-1s.pdf

45 **Del Giudice ME**, Vella ET, Hey A, Simunovic M, Harris W, Levitt C. Guideline for referral of patients with suspected colorectal cancer by family physicians and other primary care providers. *Can Fam Physician* 2014; **60**: 717-723, e383 [PMID: 25122815]

46 **Nicholson BD**, James T, Paddon M, Justice S, Oke JL, East JE, Shine B. Faecal immunochemical testing for adults with symptoms of colorectal cancer attending English primary care: a retrospective cohort study of 14 487 consecutive test requests. *Aliment Pharmacol Ther* 2020; **52**: 1031-1041 [PMID: 32677733 DOI: 10.1111/apt.15969]

47 **Quintero E**, Castells A, Bujanda L, Cubiella J, Salas D, Lanas Á, Andreu M, Carballo F, Morillas JD, Hernández C, Jover R, Montalvo I, Arenas J, Laredo E, Hernández V, Iglesias F, Cid E, Zubizarreta R, Sala T, Ponce M, Andrés M, Teruel G, Peris A, Roncales MP, Polo-Tomás M, Bessa X, Ferrer-Armengou O, Grau J, Serradesanferm A, Ono A, Cruzado J, Pérez-Riquelme F, Alonso-Abreu I, de la Vega-Prieto M, Reyes-Melian JM, Cacho G, Díaz-Tasende J, Herreros-de-Tejada A, Poves C, Santander C, González-Navarro A; COLONPREV Study Investigators. Colonoscopy *vs* fecal immunochemical testing in colorectal-cancer screening. *N Engl J Med* 2012; **366**: 697-706 [PMID: 22356323 DOI: 10.1056/NEJMoa1108895]

48 **Parente F**, Vailati C, Boemo C, Bonoldi E, Ardizzoia A, Ilardo A, Tortorella F, Cereda D, Cremaschini M, Moretti R. Improved 5-year survival of patients with immunochemical faecal blood test-screen-detected colorectal cancer *vs* non-screening cancers in northern Italy. *Dig Liver Dis* 2015; **47**: 68-72 [PMID: 25306524 DOI: 10.1016/j.dld.2014.09.015]

49 **Banaszkiewicz Z**, Budzyński J, Tojek K, Jarmocik P, Frasz J, Mrozowski M, Świtoński M, Jawień A. The fecal occult blood test as a tool for improved outpatient qualification for colonoscopy. A single-center experience and 10-year follow-up survey. *Adv Med Sci* 2017; **62**: 171-176 [PMID: 28282604 DOI: 10.1016/j.advms.2016.08.003]

50 **Hull MA**, Rees CJ, Sharp L, Koo S. A risk-stratified approach to colorectal cancer prevention and diagnosis. *Nat Rev Gastroenterol Hepatol* 2020; **17**: 773-780 [PMID: 33067592 DOI: 10.1038/s41575-020-00368-3]

51 **Rutter MD**, Bretthauer M, Hassan C, Jover R; WEO Surveillance Working Group. Principles for Evaluation of Surveillance After Removal of Colorectal Polyps: Recommendations From the World Endoscopy Organization. *Gastroenterology* 2020; **158**: 1529-1533.e4 [PMID: 32240700 DOI: 10.1053/j.gastro.2019.12.052]

52 **Martínez ME**, Baron JA, Lieberman DA, Schatzkin A, Lanza E, Winawer SJ, Zauber AG, Jiang R, Ahnen DJ, Bond JH, Church TR, Robertson DJ, Smith-Warner SA, Jacobs ET, Alberts DS, Greenberg ER. A pooled analysis of advanced colorectal neoplasia diagnoses after colonoscopic polypectomy. *Gastroenterology* 2009; **136**: 832-841 [PMID: 19171141 DOI: 10.1053/j.gastro.2008.12.007]

53 **Løberg M**, Kalager M, Holme Ø, Hoff G, Adami HO, Bretthauer M. Long-term colorectal-cancer mortality after adenoma removal. *N Engl J Med* 2014; **371**: 799-807 [PMID: 25162886 DOI: 10.1056/NEJMoa1315870]

54 **Lee JK**, Jensen CD, Levin TR, Doubeni CA, Zauber AG, Chubak J, Kamineni AS, Schottinger JE, Ghai NR, Udaltsova N, Zhao WK, Fireman BH, Quesenberry CP, Orav EJ, Skinner CS, Halm EA, Corley DA. Long-term Risk of Colorectal Cancer and Related Death After Adenoma Removal in a Large, Community-based Population. *Gastroenterology* 2020; **158**: 884-894.e5 [PMID: 31589872 DOI: 10.1053/j.gastro.2019.09.039]

55 **Wieszczy P**, Kaminski MF, Franczyk R, Loberg M, Kobiela J, Rupinska M, Kocot B, Rupinski M, Holme O, Wojciechowska U, Didkowska J, Ransohoff D, Bretthauer M, Kalager M, Regula J. Colorectal Cancer Incidence and Mortality After Removal of Adenomas During Screening Colonoscopies. *Gastroenterology* 2020; **158**: 875-883.e5 [PMID: 31563625 DOI: 10.1053/j.gastro.2019.09.011]

56 **Click B**, Pinsky PF, Hickey T, Doroudi M, Schoen RE. Association of Colonoscopy Adenoma Findings With Long-term Colorectal Cancer Incidence. *JAMA* 2018; **319**: 2021-2031 [PMID: 29800214 DOI: 10.1001/jama.2018.5809]

57 **Cross AJ**, Robbins EC, Pack K, Stenson I, Patel B, Rutter MD, Veitch AM, Saunders BP, Duffy SW, Wooldrage K. Colorectal cancer risk following polypectomy in a multicentre, retrospective, cohort study: an evaluation of the 2020 UK post-polypectomy surveillance guidelines. *Gut* 2021 [PMID: 33674342 DOI: 10.1136/gutjnl-2020-323411]

58 **He X**, Hang D, Wu K, Nayor J, Drew DA, Giovannucci EL, Ogino S, Chan AT, Song M. Long-term Risk of Colorectal Cancer After Removal of Conventional Adenomas and Serrated Polyps. *Gastroenterology* 2020; **158**: 852-861.e4 [PMID: 31302144 DOI: 10.1053/j.gastro.2019.06.039]

59 **Rutter MD**, East J, Rees CJ, Cripps N, Docherty J, Dolwani S, Kaye PV, Monahan KJ, Novelli MR, Plumb A, Saunders BP, Thomas-Gibson S, Tolan DJM, Whyte S, Bonnington S, Scope A, Wong R, Hibbert B, Marsh J, Moores B, Cross A, Sharp L. British Society of Gastroenterology/Association of Coloproctology of Great Britain and Ireland/Public Health England post-polypectomy and post-colorectal cancer resection surveillance guidelines. *Gut* 2020; **69**: 201-223 [PMID: 31776230 DOI: 10.1136/gutjnl-2019-319858]

60 **Hassan C**, Antonelli G, Dumonceau JM, Regula J, Bretthauer M, Chaussade S, Dekker E, Ferlitsch M, Gimeno-Garcia A, Jover R, Kalager M, Pellisé M, Pox C, Ricciardiello L, Rutter M, Helsingen LM, Bleijenberg A, Senore C, van Hooft JE, Dinis-Ribeiro M, Quintero E. Post-polypectomy colonoscopy surveillance: European Society of Gastrointestinal Endoscopy (ESGE) Guideline - Update 2020. *Endoscopy* 2020; **52**: 687-700 [PMID: 32572858 DOI: 10.1055/a-1185-3109]

61 **Gupta S**, Lieberman D, Anderson JC, Burke CA, Dominitz JA, Kaltenbach T, Robertson DJ, Shaukat A, Syngal S, Rex DK. Recommendations for Follow-Up After Colonoscopy and Polypectomy: A Consensus Update by the US Multi-Society Task Force on Colorectal Cancer. *Am J Gastroenterol* 2020; **115**: 415-434 [PMID: 32039982 DOI: 10.14309/ajg.0000000000000544]

62 **Cottet V**, Jooste V, Fournel I, Bouvier AM, Faivre J, Bonithon-Kopp C. Long-term risk of colorectal cancer after adenoma removal: a population-based cohort study. *Gut* 2012; **61**: 1180-1186 [PMID: 22110052 DOI: 10.1136/gutjnl-2011-300295]

63 **Atkin W**, Wooldrage K, Brenner A, Martin J, Shah U, Perera S, Lucas F, Brown JP, Kralj-Hans I, Greliak P, Pack K, Wood J, Thomson A, Veitch A, Duffy SW, Cross AJ. Adenoma surveillance and colorectal cancer incidence: a retrospective, multicentre, cohort study. *Lancet Oncol* 2017; **18**: 823-834 [PMID: 28457708 DOI: 10.1016/S1470-2045(17)30187-0]

64 **Wieszczy P**, Waldmann E, Løberg M, Regula J, Rupinski M, Bugajski M, Gray K, Kalager M, Ferlitsch M, Kaminski MF, Bretthauer M. Colonoscopist Performance and Colorectal Cancer Risk After Adenoma Removal to Stratify Surveillance: Two Nationwide Observational Studies. *Gastroenterology* 2021; **160**: 1067-1074.e6 [PMID: 33065063 DOI: 10.1053/j.gastro.2020.10.009]

65 **Digby J**, Cleary S, Gray L, Datt P, Goudie DR, Steele RJC, Strachan JA, Humphries A, Fraser CG, Mowat C. Faecal haemoglobin can define risk of colorectal neoplasia at surveillance colonoscopy in patients at increased risk of colorectal cancer. *United European Gastroenterol J* 2020; **8**: 559-566 [PMID: 32213041 DOI: 10.1177/2050640620913674]

66 **Greuter MJE**, de Klerk CM, Meijer GA, Dekker E, Coupé VMH. Screening for Colorectal Cancer With Fecal Immunochemical Testing With and Without Postpolypectomy Surveillance Colonoscopy: A Cost-Effectiveness Analysis. *Ann Intern Med* 2017; **167**: 544-554 [PMID: 28973514 DOI: 10.7326/M16-2891]

World Journal of Gastroenterology

Submit a Manuscript: https://www.f6publishing.com

World J Gastroenterol 2021 October 14; 27(38): 6430-6441

DOI: 10.3748/wjg.v27.i38.6430

ISSN 1007-9327 (print) ISSN 2219-2840 (online)

ORIGINAL ARTICLE

Basic Study

Fecal metabolomic profiles: A comparative study of patients with colorectal cancer *vs* adenomatous polyps

Giulia Nannini, Gaia Meoni, Leonardo Tenori, Maria Novella Ringressi, Antonio Taddei, Elena Niccolai, Simone Baldi, Edda Russo, Claudio Luchinat, Amedeo Amedei

ORCID number: Giulia Nannini 0000-0002-6481-6864; Gaia Meoni 0000-0002-8608-4641; Leonardo Tenori 0000-0001-6438-059X; Maria Novella Ringressi 0000-0002-1644-0583; Antonio Taddei 0000-0003-2963-4085; Elena Niccolai 0000-0002-9205-8079; Simone Baldi 0000-0002-5151-2618; Edda Russo 0000-0003-3141-1091; Claudio Luchinat 0000-0003-2271-8921; Amedeo Amedei 0000-0002-6797-9343.

Author contributions: Nannini G and Meoni G equally contributed to drafting the manuscript; Nannini G, Meoni G, Tenori L, Luchinat C, and Amedei A designed and coordinated the study; Nannini G and Meoni G performed the research; Niccolai E, Ringressi MN, and Taddei A contributed to providing patients' clinical information; Niccolai E, Baldi S, and Russo E collected the biological samples; Meoni G and Tenori L analyzed the data; Luchinat C and Amedei A coordinated the research; Nannini G and Meoni G drafted the manuscript; Tenori L, Luchinat C, and Amedei A revised the manuscript.

Institutional review board statement: The study was reviewed and approved by the Comitato Etico Regionale per la

Giulia Nannini, Maria Novella Ringressi, Antonio Taddei, Elena Niccolai, Simone Baldi, Edda Russo, Amedeo Amedei, Department of Clinical and Experimental Medicine, University of Florence, Florence 50134, Italy

Gaia Meoni, Leonardo Tenori, Department of Chemistry "Ugo Schiff", University of Florence, Florence 50134, Italy

Claudio Luchinat, Department of Chemistry & Magnetic Resonance Center (CERM), University of Florence, Florence 50134, Italy

Corresponding author: Amedeo Amedei, BSc, Reader (Associate Professor), Department of Clinical and Experimental Medicine, University of Florence, Largo Brambilla 3, Florence 50134, Italy. aamedei@unifi.it

Abstract

BACKGROUND

Colorectal cancer (CRC), the third most common cause of death in both males and females worldwide, shows a positive response to therapy and usually a better prognosis when detected at an early stage. However, the survival rate declines when the diagnosis is late and the tumor spreads to other organs. Currently, the measures widely used in the clinic are fecal occult blood test and evaluation of serum tumor markers, but the lack of sensitivity and specificity of these markers restricts their use for CRC diagnosis. Due to its high sensitivity and precision, colonoscopy is currently the gold-standard screening technique for CRC, but it is a costly and invasive procedure. Therefore, the implementation of custom-made methodologies including those with minimal invasiveness, protection, and reproducibility is highly desirable. With regard to other screening methods, the screening of fecal samples has several benefits, and metabolomics is a successful method to classify the metabolite shift in living systems as a reaction to pathophysiological influences, genetic modifications, and environmental factors.

AIM

To characterize the variation groups and potentially recognize some diagnostic markers, we compared with healthy controls (HCs) the fecal nuclear magnetic resonance (NMR) metabolomic profiles of patients with CRC or adenomatous polyposis (AP).

Sperimentazione Clinica della Regione Toscana, Sezione AREA VASTA CENTRO Institutional Review Board (CE: 11166_spe and 13080_oss).

Conflict-of-interest statement: All other authors have nothing to disclose.

Data sharing statement: No additional data are available.

Open-Access: This article is an open-access article that was selected by an in-house editor and fully peer-reviewed by external reviewers. It is distributed in accordance with the Creative Commons Attribution NonCommercial (CC BY-NC 4.0) license, which permits others to distribute, remix, adapt, build upon this work non-commercially, and license their derivative works on different terms, provided the original work is properly cited and the use is non-commercial. See: http://creativecommons.org/Licenses/by-nc/4.0/

Manuscript source: Invited manuscript

Specialty type: Gastroenterology and hepatology

Country/Territory of origin: Italy

Peer-review report's scientific quality classification

Grade A (Excellent): 0
Grade B (Very good): 0
Grade C (Good): C
Grade D (Fair): 0
Grade E (Poor): 0

Received: March 9, 2021
Peer-review started: March 9, 2021
First decision: May 1, 2021
Revised: May 17, 2021
Accepted: August 25, 2021
Article in press: August 25, 2021
Published online: October 14, 2021

P-Reviewer: Wang KW
S-Editor: Wu YXJ
L-Editor: Filipodia
P-Editor: Liu JH

METHODS

Proton nuclear magnetic resonance spectroscopy was used in combination with multivariate and univariate statistical approaches, to define the fecal metabolic profiles of 32 CRC patients, 16 AP patients, and 38 HCs well matched in age, sex, and body mass index.

RESULTS

NMR metabolomic analyses revealed that fecal sample profiles differed among CRC patients, AP patients, and HCs, and some discriminatory metabolites including acetate, butyrate, propionate, 3-hydroxyphenylacetic acid, valine, tyrosine and leucine were identified.

CONCLUSION

In conclusion, we are confident that our data can be a forerunner for future studies on CRC management, especially the diagnosis and evaluation of the effectiveness of treatments.

Key Words: Colorectal cancer; Adenomatous polyps; Nuclear magnetic resonance metabolomics; Fecal samples; Fecal metabolomics

©The Author(s) 2021. Published by Baishideng Publishing Group Inc. All rights reserved.

Core Tip: Colorectal cancer (CRC) is the third leading cause of cancer-related death worldwide. Fecal occult blood and serum tumor markers are indicators currently used in the clinic, but their lack of sensitivity and precision limit their use for CRC diagnosis. Colonoscopy is the gold-standard screening technique for CRC, but it is costly and invasive. Using readily accessible biological samples such as stool specimens, in conjunction with high-throughput molecular profiling techniques, could significantly contribute to diagnosing and understanding the patient's relationship with CRC. We compared with healthy subjects the fecal nuclear magnetic resonance metabolomic profiles of patients with CRC or adenomatous polyposis.

Citation: Nannini G, Meoni G, Tenori L, Ringressi MN, Taddei A, Niccolai E, Baldi S, Russo E, Luchinat C, Amedei A. Fecal metabolomic profiles: A comparative study of patients with colorectal cancer *vs* adenomatous polyps. *World J Gastroenterol* 2021; 27(38): 6430-6441
URL: https://www.wjgnet.com/1007-9327/full/v27/i38/6430.htm
DOI: https://dx.doi.org/10.3748/wjg.v27.i38.6430

INTRODUCTION

Colorectal cancer (CRC) is globally the third most common cause of cancer-related death in both men and women[1]. Many CRC cases are attributable to changeable (and therefore potentially preventable)[2] risk factors including diet, smoking, high alcohol consumption, physical inactivity, and being overweight. If diagnosed at an early stage, CRC shows a good response to therapy and usually a better prognosis, while survival decreases when the diagnosis is late, and the tumor spreads to other organs[3]. In addition, it is well documented that about 95% of CRCs are adenocarcinomas and begin as colonic adenomatous polyps (AP)[4] or adenomas. A series of molecular alterations and mutations induce CRC development. Tumors can be prevented with polyps excision and adequate treatment[5]. The fecal occult blood test and evaluation of serum tumor markers are commonly used in the clinic[6]; however, the lack of sensitivity and specificity of these markers limits their application in CRC diagnosis[6-8]. Currently, colonoscopy represents the gold-standard screening procedure for CRC due to its high sensitivity and specificity, but it is an expensive and especially invasive procedure[9,10]. Therefore, it is highly desirable to introduce custom-made methodologies combining minimal invasiveness, safety, and reproducibility. The screening of fecal samples has many advantages with respect to other screening techniques. In fact, stool screening is certainly non-invasive and primarily reflects the colorectal status. Moreover, the use of easily accessible and non-invasive biological samples, such as

stool specimens, combined with high-throughput molecular profiling techniques, can significantly contribute to the diagnosis of CRC and to the understanding of its interaction with the patient.

Metabolomics is an omics science that is an efficient approach to characterizing the change of metabolites in living systems as a response to pathophysiological stimuli, genetic modifications, and environmental factors. Metabolites are low molecular weight organic molecules that take part (as substrates or products) in the biochemical processes essential for sustaining life. Thus, the comprehensive evaluation of metabolites and their changes are fundamental to observe and measure the response of the organism to diverse conditions.

Nuclear magnetic resonance (NMR) spectroscopy is one of the most useful high-throughput techniques to obtain metabolomics information from biological samples [11,12]. NMR-based metabolomics has been successfully applied for disease classification[13-18] and prognosis. Starting from these premises, we compared the fecal NMR metabolomic profiles of patients with CRC or AP with those of healthy controls (HCs) to characterize the differences among the groups and possibly identify diagnostic markers.

MATERIALS AND METHODS

Patients and biological samples

A total of 86 patients including 32 CRC patients, 16 AP patients, and 38 HCs were enrolled for different studies between January 2016 and February 2019 at the Careggi Hospital and University of Florence, Italy. The Ethics Committee Area Vasta Toscana Centro (Italy) approved the studies. All fecal samples were taken at diagnosis, before starting any treatment (*e.g.*, surgical resection, chemotherapy, probiotic intake). Moreover, patients with evidence of serious illness, immunodeficit, autoimmune or infectious diseases were excluded. CRC patients, AP patients, and HCs were well matched in age, sex and body mass index. Table 1 summarizes the clinical characteristics of the enrolled patients.

Stool samples were collected in pre-labeled collection cups. Fecal water was extracted to ratios of 1:2 (g/mL, weight of unthawed feces-to-buffer) in 0.75 M phosphate-buffered saline (PBS, pH 7.4)[19]. The buffered samples where homogenized by whirl mixing for 30 s and sonicated for 15 min. Then each sample was centrifuged at 10000 g for 10 min at 4 °C, and 700 μL supernatant was transferred to 1.5 mL Eppendorf tubes and centrifuged again at 14000 rpm for 5 min at 4 °C. The clear supernatant was used for NMR analyses.

NMR sample preparation and analyses

A total of 70 μL buffer solution (1.5 M KH_2PO_4/d_2O, pH 7.4; 2 mmol/L NaN_3; 0.1% TMSP) was added to 630 μL of each fresh fecal water sample, and a total of 600 μL of this mixture was transferred to a 5 mm NMR tube.

One-dimensional proton NMR (^{1}H-NMR) spectra for all samples were acquired using the Bruker 600 MHz spectrometer (Bruker BioSpin srl; Rheinstetten, Germany) operating at 600.13 MHz proton Larmor frequency and equipped with a 5 mm PATXI ^{1}H-^{13}C-^{15}N and ^{2}H-decoupling probe including a *z* axis gradient coil, an automatic tuning-matching, and an automatic and refrigerated sample changer (SampleJet, Bruker BioSpin srl; Rheinstetten).

The BTO 2000 thermocouple served for temperature stabilization at the level of approximately 0.1 K at the sample. Before measurement, samples were kept for at least 3 min inside the NMR probe head for temperature equilibration.

Two one-dimensional ^{1}H-NMR spectra, namely one-dimensional (1D) NOESY and Carr-Purcell-Meiboom-Gill (CPMG), were acquired at 310 K with different pulse sequences: a standard nuclear Overhauser effect spectroscopy pulse sequence 1D NOESY PRESAT (noesygppr1d.comp; Bruker BioSpin) pulse sequence, using 64 scans, 98304 data points, a spectral width of 18028 Hz, an acquisition time of 2.7 s, a relaxation delay of 4 s, and a mixing time of 0.1 s; and a standard spin echo CPMG[20] (cpmgpr1d.comp; Bruker BioSpin) pulse sequence applied to a standard 1D sequence, with 64 scans, 73728 data points, a spectral width of 12019 Hz, and a relaxation delay of 4 s.

Spectral processing and statistical analysis

Free induction decays were multiplied by an exponential function equivalent to 0.3 Hz line-broadening factor before applying Fourier transform. Transformed spectra were

Table 1 Clinical characteristics of colorectal cancer patients, adenomatous patients, and healthy controls

Code	Gender ratio M/F	Median age, yr	Range of age, yr	Tumor staging T0/T1/T2/T3/T4 (*n* of patients)	Diet	Race
CRC	22 M-10 F; M/F = 2, 2	72	36-85	2/6/10/6/8	Mediterranean	Caucasian
AP	9M-7F; M/F = 1, 3	59	41-79	-	Mediterranean	Caucasian
HS	28M-10F; M/F = 2,8	47	27-68	-	Mediterranean	Caucasian

AP: Adenomatous patients; CRC: Colorectal cancer; HCs: Healthy controls.

automatically corrected for phase and baseline distortions and fecal spectra calibrated to TMSP singlet at 0 ppm using the TopSpin version 4.1.0 (Bruker BioSpin GmbH).

NMR spectra were segmented into bins of 0.02 ppm in the spectral range between 0.2 and 10.00 ppm. Regions containing residual water signal (between 4.6 and 4.9 ppm) were removed from the binning. The spectral intensity within each bin was integrated using Assure NMR 2.2, and the corresponding area was calculated to obtain the variable used as input for the statistical methods.

Before analysis of the generated data matrix, probabilistic quotient normalization [21] normalization and mean centering of the variables were performed.

Statistical analyses of the data were performed using R[22]. On processed NMR spectra, multivariate data analyses were performed. Principal component analysis (PCA) was used as unsupervised technique for exploratory analyses to check the homogeneity of the acquired spectra and to visualize the presence of outliers. As a supervised technique, orthogonal projections to latent structures-discriminant analysis (OPLS-DA) was applied. The OPLS-DA method is a multivariate projection approach that is commonly used to model spectroscopic data. Compared to PCA or partial least squares projection to latent structures (PLS), OPLS is able to distinguish between "response-related" and "response-orthogonal" fluctuations in data, delivering benefits in terms of model interpretation[23]. All of the accuracies reported and the confusion matrix for different classifications were assessed by means of 100 cycles of the Monte Carlo cross-validation scheme (MCCV, R script developed in-house). In this case, 90% of the data were randomly chosen at each iteration as a training set to build the model. Then the remaining 10% was tested, and the sensitivity, specificity, and accuracy of the classification were assessed. Metabolite identification was performed manually based on previous literature[19,24], the human metabolome database public database, and a library of pure organic compounds (BBIOREFCODE; Bruker BioSpin). The relative metabolite concentrations (expressed in arbitrary units) were calculated integrating and calculating the peaks area[25].

To determine the discriminating molecules among all classes under study, the Wilcoxon test was chosen to infer differences between two groups of subjects[26]. False discovery rate (FDR) correction was applied using the Benjamini & Hochberg method, and adjusted $P < 0.05$ was considered statistically significant[27]. The effect size, using the Cliff's delta (Cd) formulation[28], was also calculated to aid in the identification of the meaningful signals giving an estimation of the magnitude of the separation between the different groups. The magnitude was assessed using the thresholds provided in Romano and Coll[29], *i.e.* $|Cd| < 0.147$ "negligible," $|Cd| < 0.33$ "small," $|Cd| < 0.474$ "medium,"and otherwise "large."

Changes in metabolite levels were calculated as the $\log_2$ (fold change) ratio of the normalized median intensities of the corresponding signals in the spectra of the two groups. MetaboAnalyst 4.0 free online software was used for pathway analysis[30].

RESULTS

Metabolic fingerprint of CRC and AP patients

The NMR spectra of 86 fecal extract samples (32 CRC, 16 AP, and 38 HC) were acquired. Because of the suboptimal shimming quality of 7 spectra, only 79 spectra (1D NOESY: 26 CRC, 15 AP and 38 HCs; CPMG: 27 CRC, 14 AP, and 38 HCs) were used in subsequent analyses.

PCA was initially carried out to generate an overview of the variation among the different groups of patients (CRC, AP, and HCs) using bucketed spectra of fecal extracts. Some trends could be detected in the score plots of the first two principal components as shown in Supplementary Figure 1. Indeed, both score plots reveal that

CRC and AP patient groups tend to spread in the plots more than HCs that are more grouped. However, no net clustering seems to appear in the metabolomic profiles of the groups of patients neither with respect to HCs using this unsupervised approach.

Comparative analyses among the groups have been performed to test the capability of ^{1}H-NMR fecal water spectra to classify the samples of the patients according to the diagnosis. Several models have been built using a MC cross-validated supervised OPLS-DA approach. First, all three groups (CRC, AP, and HCs) were used in the same model to test the accuracy of the approach in the prediction of the healthy or the patho-logical state using a single bucketed NMR fecal spectrum (Supplementary Figure 2). As is shown in the score plots of Supplementary Figure 2, the AP samples occupied the middle metabolomic space between HCs and CRC. Indeed, the resulting true AP-positive percentages of the OPLS-DA NOESY and CPMG models were 37.7% and 18%, respectively (Supplementary Figure 2), and most of the AP patients were misclassified within the metabolomic space of HCs or CRC.

Prognostic data about patients are not available therefore was impossible to assess whether the AP patients predicted within the metabolomic space of CRC were more predisposed to developing cancer.

The capability to correctly classify HCs provides another important challenge for clinical screening. Indeed, other OPLS-DA models have been attempted to distinguish the fecal water spectra of HCs compared to AP + CRC patients yielding an overall predictive accuracy of 85.3% using 1D NOESY binned spectra (Table 2, Supplementary Figure 3A).

Furthermore, separated models were established comparing separately the ^{1}HNMR binned spectra of HCs *vs* CRC, HCs *vs* AP, and CRC *vs* AP patients (Table 2, Supplementary Figure 3B-D). As reported in Table 2, all models built on 1D NOESY bucketed spectra are better performing than those built on CPMG spectra. Supplementary Figure 3 shows the score plots related to the higher predictive accuracy among the models listed in Table 2. The reported models suggest the existence of a metabolomic fingerprint in fecal extracts of CRC and AP compared with HCs, confirming what was previously suggested by PCA and the literature available[24,31-33].

In most biofluids, low mass metabolites coexist with high mass biomolecules such as lipids, proteins, and lipoproteins. Here, two NMR pulse sequences were used to selectively observe the different components: 1D NOESY pulse sequence yields a spectrum in which both signals of metabolites and high molecular weight molecules (*e.g.*, lipids, lipoproteins, and albumin) are visible; the CPMG pulse sequence enables the selective observation of small molecule components in solutions containing macromolecules (*via* T2 filtering). Representative one-dimensional ^{1}H-NMR spectra of fecal extracts obtained with the mentioned pulse sequences are shown in Supplementary Figure 4. Indeed, NOESY experiments, which are sensitive to both low and high molecular weight compounds, resulted more accurate classifiers of all of the cases considered in this study and are described in Table 2 (HCs *vs* AP and CRC: sensitivity 84.9%, specificity 85.7%, predictive accuracy 85.3%; HCs *vs* CRC: sensitivity 85.0%, specificity 88.6%, accuracy 86.8%; HCs *vs* AP: sensitivity 71.7.8%, specificity 83.8%, predictive accuracy 77.8%: AP *vs* CRC: sensitivity 87.4%, specificity 71.6%, predictive accuracy 79.5%).

Metabolic profiles of CRC and AP patients

With the aim of identifying metabolite-level variations characteristic for each group, univariate analyses were applied to the identified fecal metabolites. Marked changes were observed in the metabolic profiles of fecal samples between CRC patients and HCs. Indeed, the first were characterized by a significantly lower content of 3-hydroxyphenylacetate, methanol, galactose, acetate, xylose and isobutyrate and a higher content of glycerol and phenylalanine (Figure 1A). Compared to HCs, AP patients had significantly lower amounts of 3-hydroxyphelylacetate, butyrate, acetate, propionate, isobutyrate and lactate+threonine (considered together because of the overlapping doublets at 1.33 ppm) as reported in Figure 1C. In CRC fecal extract profiles, when compared to AP patients, only leucine, tyrosine, and valine remained statistically significant and were present in higher amounts (Figure 1B). The complete list of fecal extract metabolites identified is reported in Supplementary Table 1. The most relevant pathways identified are reported in Table 3 and Supplementary Figure 5.

The top six identified metabolomic pathways in CRC ($P < 0.05$) were aminoacyl-tRNA biosynthesis, phenylalanine, tyrosine and tryptophan biosynthesis, valine, leucine and isoleucine biosynthesis, phenylalanine and galactose metabolism and valine, leucine and isoleucine degradation. Among them, valine, leucine and isoleucine biosynthesis, aminoacyl-tRNA biosynthesis, valine, leucine and isoleucine

Table 2 Summary of orthogonal projections to latent structures-discriminant analysis models built fecal water spectra acquired using selective one-dimensional proton nuclear magnetic resonance pulse sequences, sensitivity (%), specificity (%) and predictive accuracy (%) assessed following 100 runs of Monte Carlo cross-validation are reported for each model

	^{1}H NMR fecal extract spectra OPLS-DA cv models			
Group (*n* of samples)	Pulse sequences	Sensitivity (%)	Specificity (%)	Predictive accuracy (%)
HS (38) *vs* AP&CRC (41)	1D noesy; CPMG	84.9	85.7	85.3
HS (38) *vs* AP&CRC (41)		77.5	83.8	80.5
HS (38) *vs* CRC (26)	1D noesy; CPMG	94.2	90.2	93.7
HS (38) *vs* CRC (27)		97.3	85.2	91.0
HS (38) *vs* AP (15)	1D noesy; CPMG	90.8	76.6	87.0
HS (38) *vs* AP (14)		69.0	67.6	81.1
AP (15) *vs* CRC (26)	1D noesy; CPMG	77.0	90.4	79.3
AP (14) *vs* CRC (27)		67.5	74.0	72.7

AP: Adenomatous patients; CPMG: Carr-Purcell-Meiboom-Gill; CRC: Colorectal cancer.
^{1}HNMR: One-dimensional proton nuclear magnetic resonance; HCs: Healthy controls; OPLS-DA: Orthogonal projections to latent structures-discriminant analysis.

Table 3 Identified pathways from fecal water metabolites

Pathway analyses fecal water samples						
Fecal metabolites		Metabolites	*P*	Holm *P*	FDR	Impact
AP	Valine, leucine and isoleucine biosynthesis	Leucine, valine	8.25×10^{-4}	0.069	0.069	0.0
	Aminoacyl-tRNA biosynthesis	Valine, leucine, tyrosine	0.002	0.17	0.08	0.0
	Valine, leucine and isoleucine degradation	Leucine, valine	0.02	1	0.48	0.0
	Phenylalanine, tyrosine and tryptophan biosynthesis	Tyrosine	0.02	1	0.48	0.5
CRC	Aminoacyl-tRNA biosynthesis	Phenylalanine, valine, leucine, tyrosine	2.3×10^{-4}	0.019	0.01	0
	Phenylalanine, tyrosine and tryptophan biosynthesis	Phenylalanine, tyrosine	2.7×10^{-4}	0.022	0.035	1
	Valine, leucine and isoleucine biosynthesis	Leucine, valine	0.0012	0.1	0.035	0.0
	Phenylalanine metabolism	Phenylalanine, tyrosine	0.0019	0.16	0.041	0.36
	Galactose metabolism	Galactose, glycerol	0.014	1.0	0.2	0.05
	Valine, leucine and isoleucine degradation	Valine, leucine	0.03	1.0	0.43	0.0

An integrated analysis based on MetaboAnalyst 4.0 software built on significantly altered metabolites in colorectal cancer (CRC); and adenomatous patients (AP): View of most contributing pathways; *P* is the original *P* value calculated from the enrichment analysis; Holm *P* is the *P* value adjusted by Holm-Bonferroni method; the false discovery rate is the *P* value adjusted using false discovery rate (FDR); Impact is the pathway impact value calculated from pathway topology analysis.

degradation and phenylalanine, tyrosine and tryptophan biosynthesis pathways were also altered in AP patients (Table 3).

DISCUSSION

In this study, we evaluated the fecal metabolomic profiles of CRC and AP patients

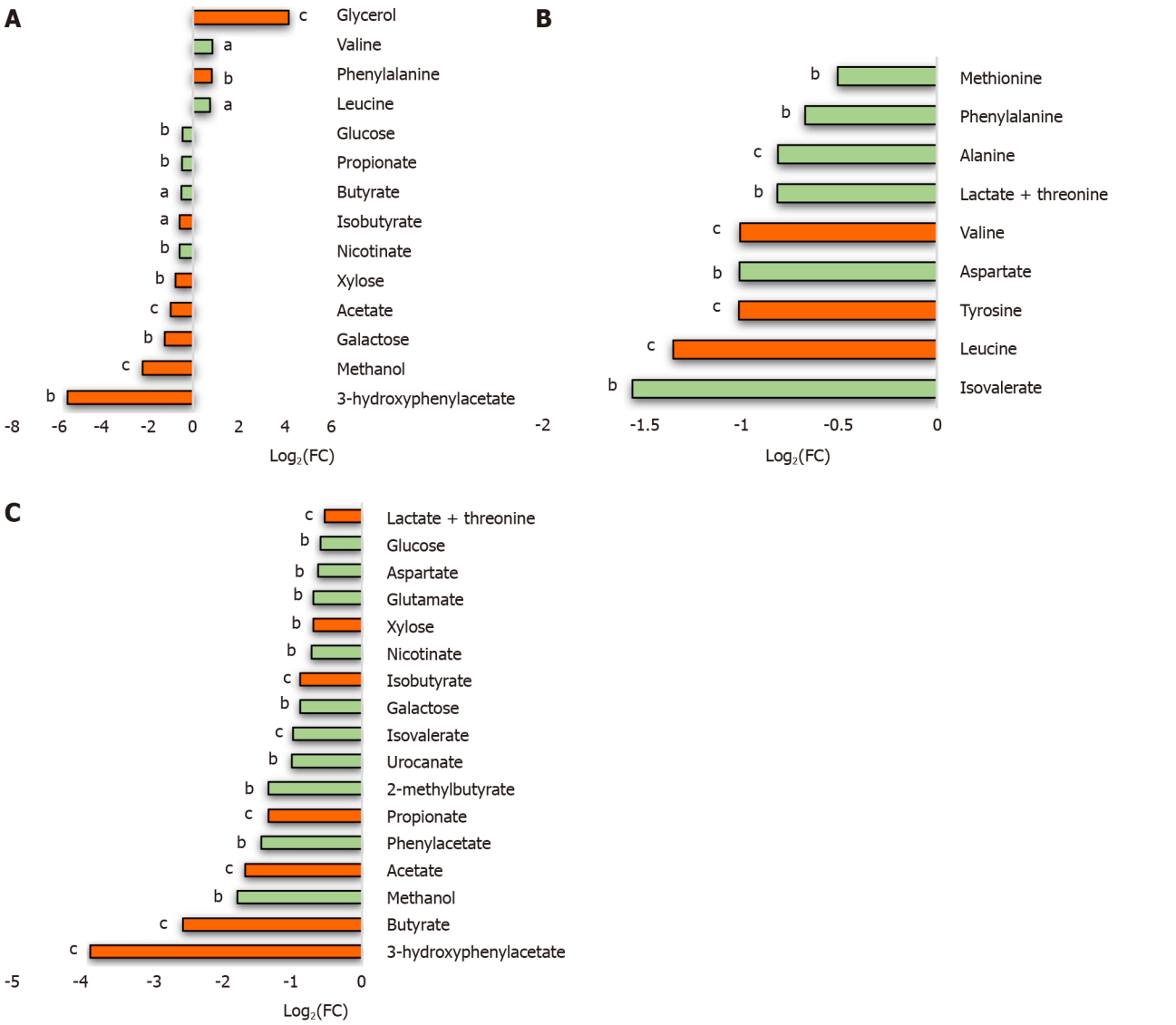


Figure 1 Fecal water metabolite levels of colorectal cancer, polyps' patients and healthy controls. Boxplots of fold-change (FC) values for the significantly altered metabolites. Red bars represent metabolites levels that remain significant after the false discovery rate (FDR) correction (FDR $P < 0.05$), green bars are the metabolites that are no more significant after the FDR correction ($P < 0.05$). Cliff's delta effect size is also reported for each metabolites in the comparisons (a: Small effect, b: Medium effect, c: Large effect). A: Comparison between healthy controls (HCs) and colorectal cancer (CRC) patients, negative $\log_2$ (FC) values mean lower metabolite levels in CRC fecal samples, positive $\log_2$(FC) values report higher content in CRC compared to HCs; B: Negative $\log_2$(FC) represent higher metabolite levels in CRC patients compared to polyp patients; C: Comparison between HCs and polyp patient-negative $\log_2$(FC) values mean lower metabolite levels in polyp patients fecal water.

with respect to HCs using NMR spectroscopy. The metabolome is a quantitative collection of low molecular weight compounds generated by metabolism[34]. Metabolomics is an emerging field of research downstream from genomics, proteomics, and transcriptomics. The metabolic screening of stool samples, which reflects the colorectal status, might contribute to the development of non-invasive screening tests[35,36]. The power of metabolomics consists in the capacity to detect and characterize tumors because cellular metabolism alterations represent a key hallmark of cancer[37]. To date, studies evaluating fecal metabolic changes associated with CRC are still lacking. Notably, no study has described fecal metabolomic changes associated with adenoma. Despite the high variability in fecal water profiles, reliable metabolic differences between patients and HCs were observed by preliminary analyses of the spectra. First, the PCA of the ^{1}H-NMR spectral data was carried out to identify some trends and outliers, showing some separation among cancer, adenoma, and HC groups. However, this unsupervised approach does not seem to clearly characterize the groups. These results were not surprising in light of the inter-individual variability introduced with diet, lifestyle, sex *etc.*

To optimize the separation among groups, we used OPLS-DA MCCV models, which were effective in discriminating the fecal metabolomic fingerprints of CRC patients and HCs (overall predictive accuracy of 93.7%). From the above analyses we can conclude that both low and high molecular weight molecules, visible using the 1D NOESY pulse sequence, are important to characterize at metabolic level the two pathological profiles. Moreover, the capability to accurately predict HCs when compared to patients with colonic AP or adenomas and CRC patients (showed predictive accuracy of 85.3%) using ^{1}H-NMR fecal water spectra, could be tested on a larger number of subjects to develop fast screening following a positive fecal occult blood test in order to spare colonoscopy in some patients who have bleeding due to other reasons[38,39].

In detail, the short-chain fatty acids (SCFAs) were found to be significantly decreased in CRC and AP patients, and in particular, lower levels of acetate were observed with respect to the HCs. SCFAs are microbial-derived metabolites, produced through gut bacteria fermentation of complex carbohydrates. SCFAs can be absorbed by the colonic epithelium, suppling energy and playing a crucial role in the regulation of fatty acids, glucose, and cholesterol metabolism[40-43]. A decrease in SCFA abundance is strictly linked to an unhealthy gut microbiota status, and alterations in the fecal SCFA profile may be the result of gut microbiota dysbiosis, inflammatory changes, or both[44]. Our data confirmed what has been previously reported by other studies. In particular, the analyses by Lin *et al*[45] demonstrated a high diagnostic performance of fecal acetate in CRC patients with respect to HCs.

In contrast with previous data, we did not find decreased levels of butyric acid in CRC patients with respect to HCs; however, we observed significantly decreased levels in AP. Butyric acid has an important homeostatic role in the human colon, and *in vitro* and *in vivo* studies have demonstrated its ability in preventing CRC[46-48]. However, other studies have showed contrasting results, suggesting a pro-cancer role of butyric acid, and low levels of butyrate usually seem to be linked with CRC development[31,35]. This double-edged role is named "butyrate paradox"[49,50]. Our results could be very interesting in this respect, suggesting that low levels of butyric acid in adenoma could lead to CRC development, while "normal" levels of butyrate in CRC could support cancer progression and promote the differentiation of regulatory T cells, which show a pro- tumorigenic role[51], especially in advanced CRC.

In addition, we found significantly low levels of 3-hydroxyphenylacetic (3-HPAA) acid in both CRC and AP patients. 3-HPAA acid is a weak acid and one of the most abundant products of polyphenol degradation in the large intestine[52,53]. Food polyphenols are broken down into other phenolic compounds by colonic bacteria action. In this way, poorly absorbable large-size polyphenols are converted to small-sized bioavailable metabolites, including 3-HPAA, which could be more biologically active[54,53]. Polyphenolic colon metabolites could be important endogenous antioxidants able to scavenge excess of free radicals, suppressing their effects on protein, lipid, and DNA damage[55]. A recent study demonstrated that polyphenol metabolites produced by colonic microbiota reduce some enzymatic activities involved in human tumorigenesis[56]. 3-HPAA can act as a CRC preventive agent by inhibition of cyclooxygenase-2 (COX-2)[57], a mediator of inflammation that is significantly overexpressed in a variety of human malignancies. Moreover, some studies have reported that COX-2 inhibitors not only prevent tumor formation but also decrease the number of already established polyps in patients with familial AP[58]. Accordingly, our results suggest that low levels of 3-HPAA are insufficient to inhibit COX-2, and consequently COX-2 expression can promote the development, tumor growth, immune suppression, angiogenesis, and metastasis of cancer cells.

Furthermore, higher amounts of amino acids such as leucine, tyrosine and valine, were present in the stool of CRC patients (compared to AP), probably resulting from malabsorption due to large epithelial inflammation and damage associated with CRC [59]. Previous metabolomic studies on fecal water have suggested that amino acid concentrations mirror the malabsorption of nutrients caused by the malfunction of epithelium barrier protection[60]. In agreement with previous studies, we documented higher levels of amino acids in the fecal water of CRC patients[31,35,61]. Alterations of amino acid levels can be associated with altered cancer cell activities, including the synthesis of proteins or catabolism to provide energy and/or other metabolite substrates.

CONCLUSION

In summary, our NMR metabolomics investigation revealed for the first time that fecal sample profiles can discriminate among CRC AP, AP patients and HCs, and some discriminatory metabolites were identified including acetate, butyrate, propionate, 3-HPAA acid, valine, tyrosine, and leucine. These altered metabolites suggest that changes in CRC and adenoma are associated with different pathway perturbations including valine, leucine and isoleucine biosynthesis, aminoacyl-tRNA biosynthesis, valine, leucine and isoleucine degradation phenylalanine, tyrosine and tryptophan biosynthesis, phenylalanine metabolism and galactose metabolism. In conclusion, we are confident that our data can be a forerunner for future studies on CRC management, especially the diagnostics and evaluation of the effectiveness of the treatments.

ARTICLE HIGHLIGHTS

Research background

Colorectal cancer (CRC) is globally the third most common cause of death. If diagnosed at an early stage, CRC shows a good response to therapy and usually a better prognosis. Unfortunately, despite its invasiveness, colonoscopy represents the gold-standard screening procedure for CRC.

Research motivation

Considering that colonoscopy is an expensive and invasive procedure, it seems to be essential to introduce custom-made methodologies combining minimal invasiveness, safety, and reproducibility. Fecal sample screening has many advantages with respect to other screening techniques.

Research objectives

The main objective of our study was to compare with HCs (HCs) the fecal nuclear magnetic resonance (NMR) metabolomic profiles of patients with CRC or adenomatous polyposis (AP) to characterize the variations among the groups and potentially identify some diagnostic markers.

Research methods

In order to define the fecal metabolic profile of 32 CRC, 16 AP patients and 38 HCs we used proton nuclear magnetic resonance spectroscopy in combination with multivariate and univariate statistical approaches.

Research results

The NMR spectra of 86 fecal extract samples have been acquired. With the aim of identifying metabolite level variations characteristic for each group, univariate analyses were applied to the identified fecal metabolites. The most marked changes were observed in the metabolic profiles of fecal samples of CRC patient *vs* HCs. AP patients, compared to HCs show significant lower amount of 3-hydroxyphelylacetate, butyrate, acetate, propionate, isobutyrate and lactate+threonine. In CRC fecal extract profiles, when compared to AP patients, only leucine, tyrosine, and valine remained statistically significant and present in higher amounts.

Research conclusions

The metabolic screening of stool samples might contribute to the development of non-invasive screening tests. To date, studies evaluating fecal metabolic changes associated with CRC are still lacking. Furthermore, no study has described fecal metabolomic changes associated with adenoma. The short-chain fatty acids were found to be significantly decreased in CRC and AP patients, and in particular, lower levels of acetate were observed with respect to HCs. In contrast with previous data, we did not find decreased levels of butyric acid in CRC patients compared to HCs; however, we observed significantly decreased levels in AP patients. We showed significantly low levels of 3-hydroxyphenylacetic (3-HPAA) acid in both CRC and AP patients. Finally, higher amounts of amino acids such as leucine, tyrosine, and valine were present in the stool of CRC patients (compared to AP), probably resulting from malabsorption due to large epithelial inflammation and damage.

Research perspectives

For the first time, we showed that fecal sample profiles can discriminate among CRC patients, AP patients and HCs, and some discriminatory metabolites were identified including acetate, butyrate, propionate, 3-HPAA acid, valine, tyrosine, and leucine. We believe that our data will be a starting point for future studies on CRC management, especially the diagnostics and evaluation of the effective of the treatments.

REFERENCES

1 **Rawla P**, Sunkara T, Barsouk A. Epidemiology of colorectal cancer: incidence, mortality, survival, and risk factors. *Prz Gastroenterol* 2019; **14**: 89-103 [PMID: 31616522 DOI: 10.5114/pg.2018.81072]

2 **Islami F**, Goding Sauer A, Miller KD, Siegel RL, Fedewa SA, Jacobs EJ, McCullough ML, Patel AV, Ma J, Soerjomataram I, Flanders WD, Brawley OW, Gapstur SM, Jemal A. Proportion and number of cancer cases and deaths attributable to potentially modifiable risk factors in the United States. *CA Cancer J Clin* 2018; **68**: 31-54 [PMID: 29160902 DOI: 10.3322/caac.21440]

3 **The Lancet**. Toward better control of colorectal cancer. *Lancet* 2014; **383**: 1437 [PMID: 24766949 DOI: 10.1016/S0140-6736(14)60699-1]

4 **Manne U**, Shanmugam C, Katkoori VR, Bumpers HL, Grizzle WE. Development and progression of colorectal neoplasia. *Cancer Biomark* 2010; **9**: 235-265 [PMID: 22112479 DOI: 10.3233/CBM-2011-0160]

5 **Yang L**, Wang S, Lee JJ, Lee S, Lee E, Shinbrot E, Wheeler DA, Kucherlapati R, Park PJ. An enhanced genetic model of colorectal cancer progression history. *Genome Biol* 2019; **20**: 168 [PMID: 31416464 DOI: 10.1186/s13059-019-1782-4]

6 **Nannini G**, Meoni G, Amedei A, Tenori L. Metabolomics profile in gastrointestinal cancers: Update and future perspectives. *World J Gastroenterol* 2020; **26**: 2514-2532 [PMID: 32523308 DOI: 10.3748/wjg.v26.i20.2514]

7 **Weitz J**, Koch M, Debus J, Höhler T, Galle PR, Büchler MW. Colorectal cancer. *Lancet* 2005; **365**: 153-165 [PMID: 15639298 DOI: 10.1016/S0140-6736(05)17706-X]

8 **Huerta S**. Recent advances in the molecular diagnosis and prognosis of colorectal cancer. *Expert Rev Mol Diagn* 2008; **8**: 277-288 [PMID: 18598107 DOI: 10.1586/14737159.8.3.277]

9 **Issa IA**, Noureddine M. Colorectal cancer screening: An updated review of the available options. *World J Gastroenterol* 2017; **23**: 5086-5096 [PMID: 28811705 DOI: 10.3748/wjg.v23.i28.5086]

10 **Young PE**, Womeldorph CM. Colonoscopy for colorectal cancer screening. *J Cancer* 2013; **4**: 217-226 [PMID: 23459594 DOI: 10.7150/jca.5829]

11 **Zhang A**, Sun H, Wang P, Han Y, Wang X. Recent and potential developments of biofluid analyses in metabolomics. *J Proteomics 2012***75**: 1079-1088 [PMID: 22079244 DOI: 10.1016/j.jprot.2011.10.027]

12 **Vignoli A**, Ghini V, Meoni G, Licari C, Takis PG, Tenori L, Turano P, Luchinat C. High-Throughput Metabolomics by 1D NMR. *Angew Chem Int Ed Engl* 2019; **58**: 968-994 [PMID: 29999221 DOI: 10.1002/anie.201804736]

13 **Singh MP**, Saxena M, Saimbi CS, Siddiqui MH, Roy R. Post-periodontal surgery propounds early repair salivary biomarkers by 1 H NMR based metabolomics. *Metabolomics* 2019; **15**: 141 [PMID: 31612356 DOI: 10.1007/s11306-019-1593-3]

14 **Meoni G**, Lorini S, Monti M, Madia F, Corti G, Luchinat C, Zignego AL, Tenori L, Gragnani L. The metabolic fingerprints of HCV and HBV infections studied by Nuclear Magnetic Resonance Spectroscopy. *Sci Rep* 2019; **9**: 4128 [PMID: 30858406 DOI: 10.1038/s41598-019-40028-4]

15 **Obi AT**, Stringer KA, Diaz JA, Finkel MA, Farris DM, Yeomans L, Wakefield T, Myers DD Jr. 1D-^{1}H-nuclear magnetic resonance metabolomics reveals age-related changes in metabolites associated with experimental venous thrombosis. *J Vasc Surg Venous Lymphat Disord* 2016; **4**: 221-230 [PMID: 26993871 DOI: 10.1016/j.jvsv.2015.09.010]

16 **Debik J**, Euceda LR, Lundgren S, Gythfeldt HVL, Garred Ø, Borgen E, Engebraaten O, Bathen TF, Giskeødegård GF. Assessing Treatment Response and Prognosis by Serum and Tissue Metabolomics in Breast Cancer Patients. *J Proteome Res* 2019; **18**: 3649-3660 [PMID: 31483662 DOI: 10.1021/acs.jproteome.9b00316]

17 **Hao J**, Yang T, Zhou Y, Gao GY, Xing F, Peng Y, Tao YY, Liu CH. Serum Metabolomics Analysis Reveals a Distinct Metabolic Profile of Patients with Primary Biliary Cholangitis. *Sci Rep.* 2017; **7**: 784. [PMID: 28400566 DOI: 10.1038/s41598-017-00944-9]

18 **Fulghesu AM**, Piras C, Dessì A, Succu C, Atzori L, Pintus R, Gentile C, Angioni S, Fanos V. Urinary Metabolites Reveal Hyperinsulinemia and Insulin Resistance in Polycystic Ovarian Syndrome (PCOS). *Metabolites* 2021; **11** [PMID: 34357331 DOI: 10.3390/METABO11070437]

19 **Lamichhane S**, Yde CC, Schmedes MS, Jensen HM, Meier S, Bertram HC. Strategy for Nuclear-Magnetic-Resonance-Based Metabolomics of Human Feces. *Anal Chem* 2015; **87**: 5930-5937 [PMID: 25985090 DOI: 10.1021/acs.analchem.5b00977]

20 **Meiboom S**, Gill D, Modified Spin-Echo Method for Measuring Nuclear Relaxation Times. Rev Sci Instru 2004; 29: 688 [DOI: 10.1063/1.1716296]

21 **Dieterle F**, Ross A, Schlotterbeck G, Senn H. Probabilistic quotient normalization as robust method to account for dilution of complex biological mixtures. Application in 1H NMR metabonomics. *Anal Chem* 2006; **78**: 4281-4290 [PMID: 16808434 DOI: 10.1021/ac051632c]

22 **Ihaka R**, Gentleman R, R: A Language for Data Analysis and Graphics. J Comput Graph Stat 1996; 5: 299 [DOI: 10.2307/1390807]

23 **Westerhuis JA**, van Velzen EJ, Hoefsloot HC, Smilde AK. Multivariate paired data analysis: multilevel PLSDA *vs* OPLSDA. *Metabolomics* 2010; **6**: 119-128 [PMID: 20339442 DOI: 10.1007/s11306-009-0185-z]

24 **Bertini I**, Cacciatore S, Jensen BV, Schou JV, Johansen JS, Kruhøffer M, Luchinat C, Nielsen DL, Turano P. Metabolomic NMR fingerprinting to identify and predict survival of patients with metastatic colorectal cancer. *Cancer Res* 2012; **72**: 356-364 [PMID: 22080567 DOI: 10.1158/0008-5472.CAN-11-1543]

25 **Onitilo AA**, Kio E, Doi SA. Tumor-related hyponatremia. *Clin Med Res* 2007; **5**: 228-237 [PMID: 18086907 DOI: 10.3121/cmr.2007.762]

26 **Wilcoxon F**. Individual Comparisons by Ranking Methods. *Biom Bull* 1945; **1**: 80 [DOI: 10.2307/3001968]

27 **Benjamini Y**, Hochberg Y. On the Adaptive Control of the False Discovery Rate in Multiple Testing With Independent Statistics. *J Educ Behav Stat* 2000; **25**: 60-83 [DOI: 10.3102/10769986025001060]

28 **Cliff N**. Ordinal Methods for Behavioral Data Analysis. *Psychology* 1996; In press

29 **Romano JS**, Kromrey J, Coraggio J. Appropriate statistics for ordinal level data: Should we really be using t-test and Cohen'sd for evaluating group differences on the NSSE and other surveys? Annual Meeting of the Florida Association of Institutional Research. 2006: 1-3

30 **Chong J**, Yamamoto M, Xia J. MetaboAnalystR 2.0: From Raw Spectra to Biological Insights. *Metabolites* 2019; **9** [PMID: 30909447 DOI: 10.3390/metabo9030057]

31 **Lin Y**, Ma C, Liu C, Wang Z, Yang J, Liu X, Shen Z, Wu R. NMR-based fecal metabolomics fingerprinting as predictors of earlier diagnosis in patients with colorectal cancer. *Oncotarget* 2016; **7**: 29454-29464 [PMID: 27107423 DOI: 10.18632/oncotarget.8762]

32 **Farshidfar F**, Weljie AM, Kopciuk KA, Hilsden R, McGregor SE, Buie WD, MacLean A, Vogel HJ, Bathe OF. A validated metabolomic signature for colorectal cancer: exploration of the clinical value of metabolomics. *Br J Cancer* 2016; **115**: 848-857 [PMID: 27560555 DOI: 10.1038/bjc.2016.243]

33 **Gu J**, Xiao Y, Shu D, Liang X, Hu X, Xie Y, Lin D, Li H. Metabolomics Analysis in Serum from Patients with Colorectal Polyp and Colorectal Cancer by ^{1}H-NMR Spectrometry. *Dis Markers* 2019; **2019**: 3491852 [PMID: 31089393 DOI: 10.1155/2019/3491852]

34 **Claudino WM**, Quattrone A, Biganzoli L, Pestrin M, Bertini I, Di Leo A. Metabolomics: available results, current research projects in breast cancer, and future applications. *J Clin Oncol* 2007; **25**: 2840-2846 [PMID: 17502626 DOI: 10.1200/JCO.2006.09.7550]

35 **Monleón D**, Morales JM, Barrasa A, López JA, Vázquez C, Celda B. Metabolite profiling of fecal water extracts from human colorectal cancer. *NMR Biomed* 2009; **22**: 342-348 [PMID: 19006102 DOI: 10.1002/nbm.1345]

36 **Wang C**, Ke C, Wang X, Chi C, Guo L, Luo S, Guo Z, Xu G, Zhang F, Li E. Noninvasive detection of colorectal cancer by analysis of exhaled breath. *Anal Bioanal Chem* 2014; **406**: 4757-4763 [PMID: 24820062 DOI: 10.1007/s00216-014-7865-x]

37 **García-Cañaveras JC**, Lahoz A. Tumor Microenvironment-Derived Metabolites: A Guide to Find New Metabolic Therapeutic Targets and Biomarkers. *Cancers (Basel)* 2021; **13** [PMID: 34203535 DOI: 10.3390/CANCERS13133230]

38 **Bardhan PK**, Beltinger J, Beltinger RW, Hossain A, Mahalanabis D, Gyr K. Screening of patients with acute infectious diarrhoea: evaluation of clinical features, faecal microscopy, and faecal occult blood testing. *Scand J Gastroenterol* 2000; **35**: 54-60 [PMID: 10672835 DOI: 10.1080/003655200750024533]

39 **Harewood GC**, Ahlquist DA. Fecal occult blood testing for iron deficiency: a reappraisal. *Dig Dis* 2000; **18**: 75-82 [PMID: 11060470 DOI: 10.1159/000016968]

40 **Moos WH**, Faller DV, Harpp DH, Kanara I, Pernokas J, Powers WR, Steliou K. Microbiota and Neurological Disorders: A Gut Feeling. *BioResearch* 2016; **5**: 137-145 [DOI: 10.1089/biores.2016.0010]

41 **Davis CD**, Milner JA. Gastrointestinal microflora, food components and colon cancer prevention. *J Nutr Biochem* 2009; **20**: 743-752 [PMID: 19716282 DOI: 10.1016/j.jnutbio.2009.06.001]

42 **Kasubuchi M**, Hasegawa S, Hiramatsu T, Ichimura A, Kimura I. Dietary gut microbial metabolites, short-chain fatty acids, and host metabolic regulation. *Nutrients* 2015; **7**: 2839-2849 [PMID: 25875123 DOI: 10.3390/nu7042839]

43 **Natarajan N**, Pluznick JL. From microbe to man: the role of microbial short chain fatty acid metabolites in host cell biology. *Am J Physiol Cell Physiol* 2014; **307**: C979-C985 [PMID: 25273884 DOI: 10.1152/ajpcell.00228.2014]

44 **Feng W**, Ao H, Peng C. Gut Microbiota, Short-Chain Fatty Acids, and Herbal Medicines. *Front Pharmacol* 2018; **9**: 1354 [PMID: 30532706 DOI: 10.3389/fphar.2018.01354]

45 **Lin Y**, Ma C, Bezabeh T, Wang Z, Liang J, Huang Y, Zhao J, Liu X, Ye W, Tang W, Ouyang T, Wu R. ^{1} H NMR-based metabolomics reveal overlapping discriminatory metabolites and metabolic pathway disturbances between colorectal tumor tissues and fecal samples. *Int J Cancer* 2019; **145**: 1679-1689 [PMID: 30720869 DOI: 10.1002/ijc.32190]

46 **Zhang M**, Zhou Q, Dorfman RG, Huang X, Fan T, Zhang H, Zhang J, Yu C. Butyrate inhibits

interleukin-17 and generates Tregs to ameliorate colorectal colitis in rats. *BMC Gastroenterol* 2016; **16**: 84 [PMID: 27473867 DOI: 10.1186/s12876-016-0500-x]

47 **Zeng H**, Taussig DP, Cheng WH, Johnson LK, Hakkak R. Butyrate Inhibits Cancerous HCT116 Colon Cell Proliferation but to a Lesser Extent in Noncancerous NCM460 Colon Cells. *Nutrients* 2017; **9** [PMID: 28045428 DOI: 10.3390/nu9010025]

48 **Singh N**, Gurav A, Sivaprakasam S, Brady E, Padia R, Shi H, Thangaraju M, Prasad PD, Manicassamy S, Munn DH, Lee JR, Offermanns S, Ganapathy V. Activation of Gpr109a, receptor for niacin and the commensal metabolite butyrate, suppresses colonic inflammation and carcinogenesis. *Immunity* 2014; **40**: 128-139 [PMID: 24412617 DOI: 10.1016/j.immuni.2013.12.007]

49 **Belcheva A**, Irrazabal T, Robertson SJ, Streutker C, Maughan H, Rubino S, Moriyama EH, Copeland JK, Surendra A, Kumar S, Green B, Geddes K, Pezo RC, Navarre WW, Milosevic M, Wilson BC, Girardin SE, Wolever TMS, Edelmann W, Guttman DS, Philpott DJ, Martin A. Gut microbial metabolism drives transformation of MSH2-deficient colon epithelial cells. *Cell* 2014; **158**: 288-299 [PMID: 25036629 DOI: 10.1016/j.cell.2014.04.051]

50 **Niccolai E**, Baldi S, Ricci F, Russo E, Nannini G, Menicatti M, Poli G, Taddei A, Bartolucci G, Calabrò AS, Stingo FC, Amedei A. Evaluation and comparison of short chain fatty acids composition in gut diseases. *World J Gastroenterol* 2019; **25**: 5543-5558 [PMID: 31576099 DOI: 10.3748/wjg.v25.i36.5543]

51 **Niccolai E**, Ricci F, Russo E, Nannini G, Emmi G, Taddei A, Ringressi MN, Melli F, Miloeva M, Cianchi F, Bechi P, Prisco D, Amedei A. The Different Functional Distribution of "Not Effector" T Cells (Treg/Tnull) in Colorectal Cancer. *Front Immunol* 2017; **8**: 1900 [PMID: 29375559 DOI: 10.3389/fimmu.2017.01900]

52 **Halliwell B**, Rafter J, Jenner A. Health promotion by flavonoids, tocopherols, tocotrienols, and other phenols: direct or indirect effects? *Am J Clin Nutr* 2005; **81**: 268S-276S [PMID: 15640490 DOI: 10.1093/ajcn/81.1.268S]

53 **Henning SM**, Wang P, Abgaryan N, Vicinanza R, de Oliveira DM, Zhang Y, Lee RP, Carpenter CL, Aronson WJ, Heber D. Phenolic acid concentrations in plasma and urine from men consuming green or black tea and potential chemopreventive properties for colon cancer. *Mol Nutr Food Res* 2013; **57**: 483-493 [PMID: 23319439 DOI: 10.1002/mnfr.201200646]

54 **Selma MV**, Espín JC, Tomás-Barberán FA. Interaction between phenolics and gut microbiota: role in human health. *J Agric Food Chem* 2009; **57**: 6485-6501 [PMID: 19580283 DOI: 10.1021/jf902107d]

55 **Amić A**, Marković Z, Marković JMD, Jeremić S, Lučić B, Amić D. Free radical scavenging and COX-2 inhibition by simple colon metabolites of polyphenols: A theoretical approach. *Comput Biol Chem* 2016; **65**: 45-53 [PMID: 27750207 DOI: 10.1016/j.compbiolchem.2016.09.013]

56 **Miene C**, Weise A, Glei M. Impact of polyphenol metabolites produced by colonic microbiota on expression of COX-2 and GSTT2 in human colon cells (LT97). *Nutr Cancer* 2011; **63**: 653-662 [PMID: 21598179 DOI: 10.1080/01635581.2011.552157]

57 **Karlsson PC**, Huss U, Jenner A, Halliwell B, Bohlin L, Rafter JJ. Human fecal water inhibits COX-2 in colonic HT-29 cells: role of phenolic compounds. *J Nutr* 2005; **135**: 2343-2349 [PMID: 16177193 DOI: 10.1093/jn/135.10.2343]

58 **Rostom A**, Dubé C, Lewin G, Tsertsvadze A, Barrowman N, Code C, Sampson M, Moher D; U. S. Preventive Services Task Force. Nonsteroidal anti-inflammatory drugs and cyclooxygenase-2 inhibitors for primary prevention of colorectal cancer: a systematic review prepared for the U.S. Preventive Services Task Force. *Ann Intern Med* 2007; **146**: 376-389 [PMID: 17339623 DOI: 10.7326/0003-4819-146-5-200703060-00010]

59 **Trinchieri G**. Cancer and inflammation: an old intuition with rapidly evolving new concepts. *Annu Rev Immunol* 2012; **30**: 677-706 [PMID: 22224761 DOI: 10.1146/annurev-immunol-020711-075008]

60 **Marchesi JR**, Holmes E, Khan F, Kochhar S, Scanlan P, Shanahan F, Wilson ID, Wang Y. Rapid and noninvasive metabonomic characterization of inflammatory bowel disease. *J Proteome Res* 2007; **6**: 546-551 [PMID: 17269711 DOI: 10.1021/pr060470d]

61 **Weir TL**, Manter DK, Sheflin AM, Barnett BA, Heuberger AL, Ryan EP. Stool microbiome and metabolome differences between colorectal cancer patients and healthy adults. *PLoS One* 2013; **8**: e70803 [PMID: 23940645 DOI: 10.1371/journal.pone.0070803]

World Journal of Gastroenterology

Submit a Manuscript: https://www.f6publishing.com

World J Gastroenterol 2021 October 14; 27(38): 6442-6452

DOI: 10.3748/wjg.v27.i38.6442

ISSN 1007-9327 (print) ISSN 2219-2840 (online)

ORIGINAL ARTICLE

Retrospective Cohort Study

High total Joule heat increases the risk of post-endoscopic submucosal dissection electrocoagulation syndrome after colorectal endoscopic submucosal dissection

Masanori Ochi, Ryosuke Kawagoe, Toshiro Kamoshida, Yukako Hamano, Haruka Ohkawara, Atsushi Ohkawara, Nobushige Kakinoki, Yuji Yamaguchi, Shinji Hirai, Akinori Yanaka, Kiichiro Tsuchiya

ORCID number: Masanori Ochi 0000-0003-0850-6076; Ryosuke Kawagoe 0000-0001-5283-2384; Toshiro Kamoshida 0000-0003-4930-1018; Yukako Hamano 0000-0003-3491-310X; Haruka Ohkawara 0000-0001-8427-5826; Atsushi Ohkawara 0000-0003-1764-565X; Nobushige Kakinoki 0000-0002-1522-2226; Yuji Yamaguchi 0000-0002-4084-0827; Shinji Hirai 0000-0001-7141-0240; Akinori Yanaka 0000-0001-7967-5665; Kiichiro Tsuchiya 0000-0002-1977-8707.

Author contributions: Ochi M, Kawagoe R, Kamoshida T, Hamano Y, Ohkawara A, Ohkawara H, Kakinoki N, Yamaguchi Y, Hirai S, Yanaka A and Tsuchiya K contributed equally to this work; Ochi M and Kawagoe R collected and analyzed the data; Ochi M and Kawagoe R drafted the manuscript; Ochi M, Kawagoe R and Kamoshida T designed and supervised the study; Hamano Y, Ohkawara A, Ohkawara H, Kakinoki N, Yamaguchi Y, Hirai S, Yanaka A and Tsuchiya K offered technical or material support; all authors have read and approved the final version to be published.

Institutional review board

Masanori Ochi, Toshiro Kamoshida, Yukako Hamano, Haruka Ohkawara, Atsushi Ohkawara, Nobushige Kakinoki, Yuji Yamaguchi, Shinji Hirai, Department of Gastroenterology, Hitachi General Hospital, Hitachi City 317-0077, Ibaraki, Japan

Ryosuke Kawagoe, Akinori Yanaka, Kiichiro Tsuchiya, Department of Gastroenterology, Faculty of Medicine, University of Tsukuba, Tsukuba 305-8576, Ibaraki, Japan

Corresponding author: Masanori Ochi, MD, Doctor, Department of Gastroenterology, Hitachi General Hospital, 2-1-1, Jonancho, Hitachi City, Hitachi City 317-0077, Ibaraki, Japan.
maochi-tei@umin.ac.jp

Abstract

BACKGROUND

We hypothesized that thermal damage accumulation during endoscopic submucosal dissection (ESD) causes the pathogenesis of post-ESD electrocoagulation syndrome (PECS).

AIM

To determine the association between Joule heat and the onset of PECS.

METHODS

We performed a retrospective cohort study in patients who underwent colorectal ESD from May 2013 to March 2021 in Japan. We developed a novel device that measures swift coagulation time with a sensor adjacent to the electrosurgical coagulation unit foot switch, which enabled us to calculate total Joule heat. PECS was defined as localized abdominal pain (visual analogue scale ≥ 30 mm during hospitalization or increased by ≥ 20 mm from the baseline) and fever (temperature ≥ 37.5 degrees or white blood cell count ≥ 10000 μ/L). Patients exposed to more or less than the median Joule heat value were assigned to the high and low Joule heat groups, respectively. Statistical analyses included Mann-Whitney U and chi-square tests and logistic regression and receiver operating characteristic curve (ROC) analyses.

RESULTS

We evaluated 151 patients. The PECS incidence was 10.6% (16/151 cases), and all

patients were followed conservatively and discharged without severe complications. In multivariate analysis, high Joule heat was an independent PECS risk factor. The area under the ROC curve showing the correlation between PECS and total Joule heat was high [0.788 (95% confidence interval: 0.666-0.909)].

CONCLUSION

Joule heat accumulation in the gastrointestinal wall is involved in the onset of PECS. ESD-related thermal damage to the peeled mucosal surface is probably a major component of the mechanism underlying PECS.

Key Words: Post-endoscopic submucosal dissection electrocoagulation syndrome; Joule heat; Colorectal endoscopic submucosal dissection; Colorectal neoplasms; Electrocoagulation; Gastrointestinal tract

©The Author(s) 2021. Published by Baishideng Publishing Group Inc. All rights reserved.

Core Tip: We investigated the association between Joule heat and the onset of post-endoscopic submucosal dissection electrocoagulation syndrome (PECS), using originally developed a device to measure swift coagulation time with a sensor adjacent to the electrosurgical coagulation unit foot switch which enabled us to calculate total Joule heat. High Joule heat was an independent PECS risk factor. Moreover, the area under the operating characteristic curve showing the correlation between PECS and total Joule heat was high. Joule heat accumulation is involved in the onset of PECS. endoscopic submucosal dissection-related thermal damage of the peeled mucosal surface is probably a major component of the mechanism underlying PECS.

Citation: Ochi M, Kawagoe R, Kamoshida T, Hamano Y, Ohkawara H, Ohkawara A, Kakinoki N, Yamaguchi Y, Hirai S, Yanaka A, Tsuchiya K. High total Joule heat increases the risk of post-endoscopic submucosal dissection electrocoagulation syndrome after colorectal endoscopic submucosal dissection. *World J Gastroenterol* 2021; 27(38): 6442-6452
URL: https://www.wjgnet.com/1007-9327/full/v27/i38/6442.htm
DOI: https://dx.doi.org/10.3748/wjg.v27.i38.6442

INTRODUCTION

Colorectal endoscopic submucosal dissection (ESD), a minimally invasive operation, is the best endoscopic procedure for *en bloc* resection of superficial colorectal tumors[1-4]. However, ESD is associated with severe complications, with rates of perforation and bleeding of 2% to 14% and 0.7% to 3.1%, respectively[4-10]. Post-ESD electrocoagulation syndrome (PECS) is another notable adverse event that can occur after colorectal ESD. The incidence of PECS is 9% to 40%, although most cases improve with conservative therapy[11-15]. In addition, PECS sometimes manifests as a delayed perforation. Therefore, physicians require clinically useful PECS predictors to identify patients who are at risk[12,16].

Currently, two main hypotheses explain the mechanism underlying PECS. One suggests that ESD exposes the mucosa, which is then infected by intestinal bacteria, resulting in inflammation[13,17]. The other proposes that the peeled mucosal surface is inflamed by thermal damage during ESD[13,18]. Interestingly, a clipping closure method performed to prevent intestinal bacteria from infecting the exposed mucosa did not reduce the onset of PECS[19]. In contrast, few studies have examined the impact of thermal damage during ESD on the onset of PECS.

We have often encountered patients with PECS who underwent a lengthy colorectal ESD, and previous studies of PECS risk factors implicated prolonged ESD procedures [20,21]. We hypothesized that electrocoagulation is associated with Joule heat capable of causing thermal damage to the gastrointestinal wall during long ESD operations. Therefore, we aimed to determine the association between Joule heat and the onset of PECS.

statement: The Hitachi General Hospital Institutional Review Board approved this study (2019-97, 2020-1), and it was performed according to the ethical guidelines of the 1964 Declaration of Helsinki and its later amendments.

Informed consent statement: Informed consent was obtained using an opt-out option on the Hitachi General Hospital's website (see institution website uniform resource locators: http://www.hitachi.co.jp/hospital/hitachi/infor/opto-out/index.html).

Conflict-of-interest statement: All the authors have no conflict of interest related to the manuscript.

Data sharing statement: The original anonymous dataset is available on request from the corresponding author at maochi-tei@umin.ac.jp.

STROBE statement: The authors have read the STROBE Statement - checklist of items, and the manuscript was prepared and revised according to the STROBE Statement -checklist of items.

Open-Access: This article is an open-access article that was selected by an in-house editor and fully peer-reviewed by external reviewers. It is distributed in accordance with the Creative Commons Attribution NonCommercial (CC BY-NC 4.0) license, which permits others to distribute, remix, adapt, build upon this work non-commercially, and license their derivative works on different terms, provided the original work is properly cited and the use is non-commercial. See: http://creativecommons.org/Licenses/by-nc/4.0/

Manuscript source: Unsolicited manuscript

Specialty type: Gastroenterology and hepatology

Country/Territory of origin: Japan

Peer-review report's scientific quality classification

Grade A (Excellent): 0

Grade B (Very good): B
Grade C (Good): 0
Grade D (Fair): 0
Grade E (Poor): 0

Received: May 24, 2021
Peer-review started: May 24, 2021
First decision: June 22, 2021
Revised: July 17, 2021
Accepted: September 10, 2021
Article in press: September 10, 2021
Published online: October 14, 2021

P-Reviewer: Li YY
S-Editor: Liu M
L-Editor: A
P-Editor: Yuan YY

MATERIALS AND METHODS

Study design and patient selection

We performed a retrospective study in patients who underwent colorectal ESD at Hitachi General Hospital in Japan from May 2013 to March 2021. Case selection was according to the indications for colorectal ESD established by the Japan Gastroenterological Endoscopy Society guidelines[22]. Therefore, our inclusion criteria were as follows: (1) Laterally spreading tumors of the non-granular type with the Vi-type pit pattern, carcinomas with shallow T1 submucosal (SM) invasion, large depressed-type tumors, and large protruded-type tumors that are difficult to remove en bloc by endoscopic mucosal resection; and (2) Mucosal tumors with SM fibrosis. Patients with multiple colorectal neoplasms or apparent deeply invasive T1 SM carcinoma were excluded. R0 resection was defined as no cancer cells seen microscopically at the primary tumor site. We converted the swift-coagulation mode time, measured by an electrosurgical-coagulation unit with a high-frequency generator (VIO 300D, ERBE Co. Ltd., Tubingen, Germany), to Joule heat.

The Hitachi General Hospital Institutional Review Board approved the study (No. 2019-97, 2020-1), and our research was performed according to the ethical guidelines of the 1964 Declaration of Helsinki and its later amendments. The study is registered on the University Hospital Medical Information Network (ID: UMIN000038704, UMIN 000041580). Although our ethics committee waived the requirement for informed consent from each patient because we used anonymized data, we obtained informed consent using an opt-out option on our facility's website (uniform resource locator below).

PECS definition

PECS was defined as localized abdominal pain and fever without apparent perforation after colorectal ESD. We used a visual analog scale (VAS) to evaluate localized abdominal pain. Nurses who were not research participants administered the VAS. The pain criteria were defined as a score ≥ 30 mm from the postoperative day (POD) 1 to discharge or increased by ≥ 20 mm from the hospital admission VAS score. Our fever criteria were body temperature ≥ 37.5 degrees or white blood cell count ≥ 10000 μ/L from POD 1 to discharge.

Colorectal ESD procedures

All patients underwent bowel preparation (polyethylene glycol, 2 L) before colorectal ESD. Then, the patients were sedated in the endoscopy room using intravenous injections of pentazocine (15-30 mg/kg body weight). We added midazolam (1-3 mg/session) if pentazocine was insufficient for sedation. Electrocardiogram monitoring was performed in each case. The procedures were performed by 10 endoscopists (one expert colorectal endoscopic surgeon and 9 less experienced colorectal endoscopic surgeons). An expert was defined as an endoscopist who performed more than 40 colorectal ESDs[23]. We used a water-jet system colonoscope (PCF-Q260JI, Olympus Corporation, Tokyo, Japan) with a transparent hood (DH-29CR for scope tip, Fujifilm, Tokyo, Japan) attached to the scope tip. Marking, mucosal incision, and mucosal detachment were performed with a dual knife (KD-655Q, Olympus Corporation). We injected 0.4% sodium hyaluronate acid diluted in physiological saline into the SM layer directly below the lesion before mucosal detachment. A coagrasper (FD-411QR, Olympus Corporation) and an endoscopic clip (HX-610-090, Olympus Corporation) were used to obtain hemostasis.

Calculating Joule heat

We used the electrosurgical-coagulation unit to detach the lesion's colorectal mucosa. We changed the setting mode according to the procedure step and used dry-cut, swift-coagulation, and soft-coagulation modes. We calculated the power applied using the diagram in the manufacturer's technical manual that shows the relationship between resistance (Ω) and power (W) in the swift-coagulation mode (Supplementary material). As human internal resistance is 1000-1600 Ω[24], the lesion resistance was defined as 1300 Ω. Thus, lesions are detached while the electrosurgical-coagulation unit automatically adjusts the power output. However, this automatic power adjustment is difficult to monitor.

The curve describing the relationship between power (vertical axis) and resistance (horizontal axis) in the manufacturer's technical diagram (we used effect 4 in our study) showed that the power corresponding to 1300 Ω is 50 W (Supplementary material). Therefore, we obtained the formula: power consumption (J) = power (W) ×

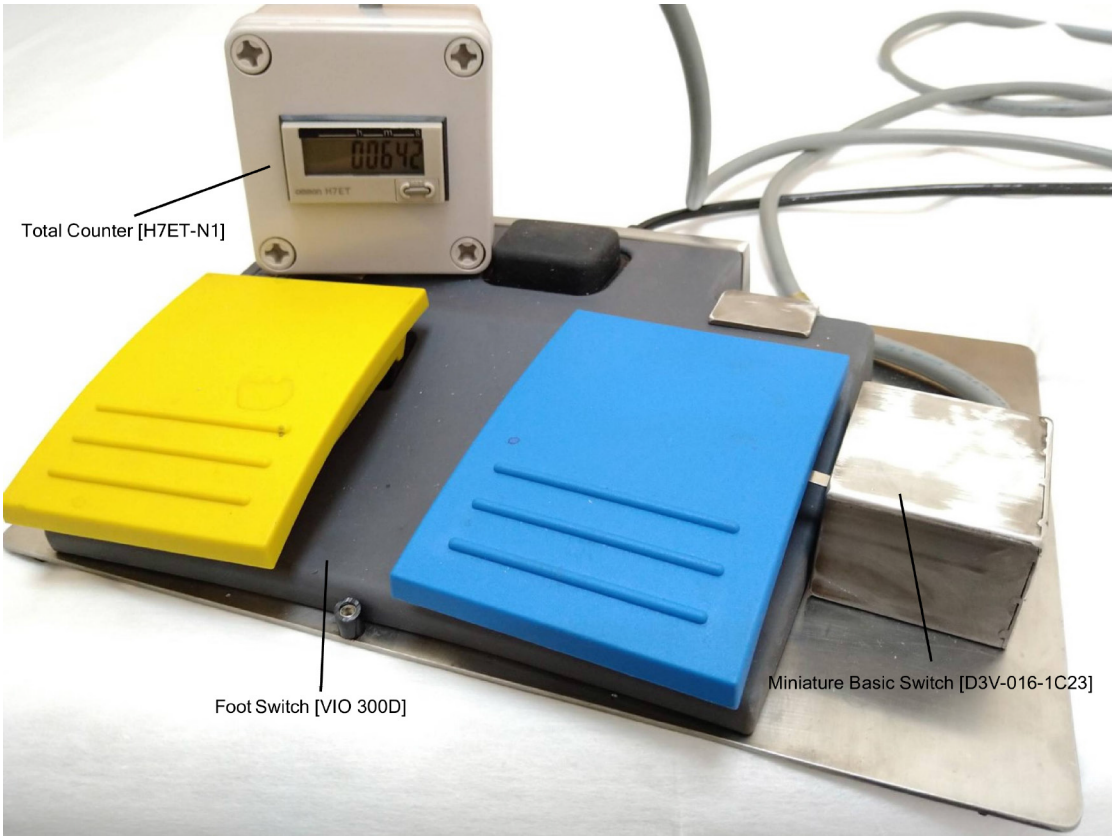


Figure 1 A novel device for measuring the swift-coagulation mode time with a sensor adjacent to the foot switch of the electrosurgical coagulation unit.

time (s) from the relationship between power and power consumption. We used this formula to calculate the total Joule heat applied to the lesion.

We developed a novel device to measure the swift coagulation time with a sensor [Miniature Basic Switch (D3V-016-1C23), OMRON Corporation, Kyoto, Japan] adjacent to the foot switch of the electrosurgical coagulation unit (Figure 1). This sensor was activated when the operator stepped down on the foot switch, and the swift-coagulation mode time was recorded by a counter [Total Counter (H7ET-N1), OMRON Corporation]. In cases where the swift-coagulation time was not measured, we retrospectively calculated the time using the data (swift-coagulation mode time/procedure time: Mean 3%) obtained from the measured cases. Patients exposed to more or less than the median Joule heat value (8460 J) were assigned to the high and low Joule heat groups, respectively.

Post-ESD hospitalization

In all patients, on POD 1, the vital signs and a blood sample were examined to check for bleeding, the pain VAS was administered, and radiography was performed to check for free air. We considered a fever, localized abdominal pain, or increased C-reactive protein suspicious for delayed perforation associated with PECS. If the pain or fever criteria were satisfied, we performed computed tomography. In the absence of adverse findings, patients resumed eating, starting with dinner on POD 1. If no fever, localized abdominal pain, or bleeding occurred after eating resumed, patients were discharged on POD 6.

Statistical analysis

We analyzed continuous and categorical variables using Mann-Whitney U and chi-square tests, respectively. In our multivariate analysis, we performed logistic regression analyses using important factors identified by univariate analysis. We determined the cutoff of the total Joule heat value that predicted the onset of PECS using receiver operating characteristic (ROC) curve analysis. A P value less than 0.05 was considered statistically significant. All statistical analyses were performed using SPSS software (version 26, IBM Corp., Armonk, NY, United States). The statistical methods of this study were reviewed by Masanori Ochi from the Department of

Gastroenterology, Hitachi General Hospital, Japan.

RESULTS

Baseline characteristics

Of 170 patients admitted for colorectal ESD, 19 met the exclusion criteria (multiple lesions, *n* = 6; post-ESD infection, *n* = 2; perforation during ESD, *n* = 7; ESD discontinuation, *n* = 4) (Figure 2). We analyzed the remaining 151 patients [mean age, 67.3 years (range 39-92); male, 62.3%]. Tumors occurred in the right colon (*n* = 59, 39.1%), left colon (*n* = 41, 27.2%), and rectum (*n* = 51, 33.8%); R0 and *en bloc* resections were achieved in 115 patients (76.2%) and 135 patients (89.4%), respectively; and PECS occurred in 16 patients (10.6 %) (Table 1).

Primary outcome

The high (*n* = 76) and low (*n* = 75) Joule heat groups showed no statistically significant difference in sex; tumor morphology, location, or depth of pathological invasion; R0 resection rate; or incidence of SM fibrosis (Table 2). Univariate analyses revealed that patient age was significantly greater, and the PECS incidence was significantly higher in the high Joule group than in the low Joule group; the specimen size was also significantly larger in the high Joule group. Compared to the low Joule heat group, the high Joule heat group included more patients who had undergone ESD performed by a trainee, and the difference was significant. In addition, the R0 resection rate was significantly higher in the low Joule group. Multivariate analysis showed that the R0 resection rate [odds ratio (OR), 3.27; 95% confidence interval (CI): 1.26-8.45; $P = 0.01$] and PECS incidence (OR, 4.83; 95%CI: 1.08-21.50; $P = 0.03$) were significantly higher and the specimen size (OR, 1.07; 95%CI: 1.03-1.11; $P < 0.01$) and number of ESD procedures performed by a trainee (OR, 5.30; 95%CI: 2.32-12.10; $P < 0.01$) were significantly larger in the high Joule heat group than in the low Joule heat group (Table 3).

PECS and Joule heat correlation analysis

The area under the ROC curve showing the correlation between PECS and total Joule heat was 0.788 (95%CI: 0.666-0.909), and the PECS onset cutoff value was 15390 J (sensitivity, 0.625; specificity, 0.822) (Figure 3).

DISCUSSION

To our knowledge, this study, performed using our novel device, is the first to indicate high total Joule heat exposure during colorectal ESD as a PECS risk factor. Additionally, PECS and Joule heat were highly correlated, and the Joule heat cutoff value where PECS occurred was 15390 J.

PECS is a state of temporary inflammation resulting from transmission of electrocoagulation heat to the resection site muscle layer and serous membrane during endoscopic therapy[18,25,26]. Previously reported PECS risk factors include tumor location[11,13,20,27], SM fibrosis[27], long procedure time[20,21], and specimen diameter[11,13]. Long procedures lead to the occurrence of PECS due to increased electrical current load on the gastrointestinal wall[11]. Additionally, ischemic changes occur in the gastrointestinal wall due to excessive current during incision, dissection, and hemostasis[28]. These reports suggest that Joule heat of the peeled mucosal surface is associated with the occurrence of PECS.

A study of lengthy procedures (mean, 90 min) demonstrated that long procedure time is a PECS risk factor[20]. However, several studies that did not include long procedure time as a PECS risk factor showed that the procedures were short (range, 52-67 min)[11,28,29]. Our study revealed that ESD procedures performed by trainees are associated with the onset of PECS. A previous study showed that ESD procedures performed by trainees are longer than those performed by experienced endoscopists [23]. Because the swift-coagulation mode time probably increases as the procedure time lengthens, high Joule heat accumulation is likely to occur during long ESDs, causing severe damage to the peeled mucosal surface, leading to PECS. Previous studies were limited in that they did not consider the impact of the ESD procedure time on the Joule heat delivered to the lesion. In this study, measurement of swift-coagulation mode time allowed us to investigate the association between PECS and

Table 1 Characteristics of patients who underwent endoscopic submucosal dissection, *n* (%)

Patient features	*n* (%)
Number of patients	151
Male	94 (62.3)
Age (yr), mean ± SD	67.3 ± 10.9
BMI (kg/m^2), mean ± SD	22.9 ± 3.0
Specimen size	
< 40 mm	132 (87.4)
≥ 40 mm	19 (12.6)
Total Joule heat	
< 8460 J[1]	75 (49.7)
≥ 8460 J	76 (50.3)
Tumor location	
Right colon	59 (39.1)
Left colon	41 (27.1)
Rectum	51 (33.8)
Tumor morphology	
0-Is/Ip	29 (19.2)
LST-G	75 (49.7)
LST-NG (0-IIc)	47 (31.1)
Depth of pathological invasion	
Tis (M)	130 (86.1)
T1 (SM)	21 (13.9)
Histological diagnosis	
Adenoma	67 (44.4)
Adenocarcinoma	80 (53.0)
Other	4 (2.6)
ECOG performance status after ESD	
0	144 (95.4)
≥1	7 (4.6)
R0 resection	115 (76.2)
ESD procedure performed by trainees	52 (34.4)
Additional endoscopic therapy after ESD	2 (1.3)
Additional surgery after ESD	12 (7.9)
En bloc resection	135 (89.4)
Intraoperative perforation or penetration	7 (4.6)
Submucosal fibrosis	45 (29.8)
PECS	16 (10.6)

[1]Patients exposed to more or less than the median Joule heat value (8460 J) were assigned to the high and low Joule heat groups, respectively.
BMI: Body mass index; Is: Sessile type; Ip: Pedunculated type; LST-G: Lateral spreading tumor granular type; LST-NG: Lateral spreading tumor non-granular type; IIc: Superficial depressed type; Tis (M): Carcinoma in situ or intramucosal carcinoma; T1 (SM): Tumor invades submucosa; R0: Microscopically margin-negative; ESD: Endoscopic submucosal dissection; PECS: Post-endoscopic submucosal dissection electrocoagulation syndrome; SD: Standard deviation; ECOG performance status: Eastern Cooperative Oncology Group performance status.

total Joule heat. Our study revealed that the total Joule heat applied to the peeled

Table 2 Clinicopathological factors in the high and low Joule heat groups, *n* (%)

	High Joule heat	Low Joule heat	*P* value
	n = 76	*n* = 75	
Sex			0.54
Male	45 (59.2)	49 (65.3)	
Female	31 (40.8)	26 (34.7)	
Age (yr), mean ± SD	69 ± 11.5	66 ± 10.2	< 0.01
BMI (kg/m^2), mean ± SD	22.8 ± 2.3	23.0 ± 3.2	0.77
Specimen size			< 0.01
< 40 mm	60 (78.9)	73 (97.3)	
≥ 40 mm	16 (21.1)	2 (2.7)	
Tumor location			0.84
Right colon	28 (36.9)	31 (41.3)	
Left colon	21 (27.6)	20 (26.7)	
Rectum	27 (35.5)	24 (32.0)	
Tumor morphology			0.56
0-Is/Ip	18 (23.7)	21 (28.0)	
LST-G	36 (47.4)	29 (38.7)	
LST-NG (0-IIc)	22 (28.9)	25 (33.3)	
Depth of pathological invasion			0.66
Tis (M)	64 (84.2)	66 (88.0)	
T1 (SM)	12 (15.8)	9 (12.0)	
Histological diagnosis			0.12
Adenoma	34 (44.7)	33 (44.0)	
Adenocarcinoma	42 (55.3)	38 (50.7)	
Other	0 (0.0)	4 (5.3)	
Performance status after ESD			0.45
0	71 (93.4)	73 (97.3)	
≥ 1	5 (6.6)	2 (2.7)	
R0 resection	50 (65.8)	65 (86.7)	< 0.01
ESD procedure performed by trainees	37 (55.3)	15 (13.3)	< 0.01
Additional endoscopic therapy after ESD	1 (1.3)	1 (1.3)	0.999
Additional surgery after ESD	8 (10.5)	4 (5.3)	0.38
En bloc resection	69 (90.8)	73 (97.3)	0.18
Submucosal fibrosis	27 (35.5)	18 (24.0)	0.17
PECS	13 (17.1)	3 (4.0)	0.02

BMI: Body mass index; Is: Sessile type; Ip: Pedunculated type; LST-G: Lateral spreading tumor granular type; LST-NG: Lateral spreading tumor non-granular type; IIc: Superficial depressed type; Tis (M): Carcinoma in situ or intramucosal carcinoma; T1 (SM): Tumor invades submucosa; R0: Microscopically margin-negative; ESD: Endoscopic submucosal dissection; PECS: Post-endoscopic submucosal dissection electrocoagulation syndrome; SD: Standard deviation.

surface is involved in the development of PECS. Furthermore, using the total Joule heat cutoff value of PECS occurrence could allow the introduction of PECS prevention measures, including online measurement of swift-coagulation mode time during colorectal ESD. For example, an online PECS alert system is promising.

Table 3 Multivariate analysis of risk factors associated with high Joule heat accumulation

	Odds ratio	95%CI	*P* value
Age	1.03	0.99-1.06	0.17
R0 resection	3.27	1.26-8.45	0.01
Specimen size	1.07	1.03-1.11	< 0.01
ESD procedure performed by trainees	5.30	2.32-12.10	< 0.01
PECS	4.83	1.08-21.50	0.03

PECS: Post-endoscopic submucosal dissection electrocoagulation syndrome; R0: Microscopically margin-negative; 95% CI: 95% confidence interval.

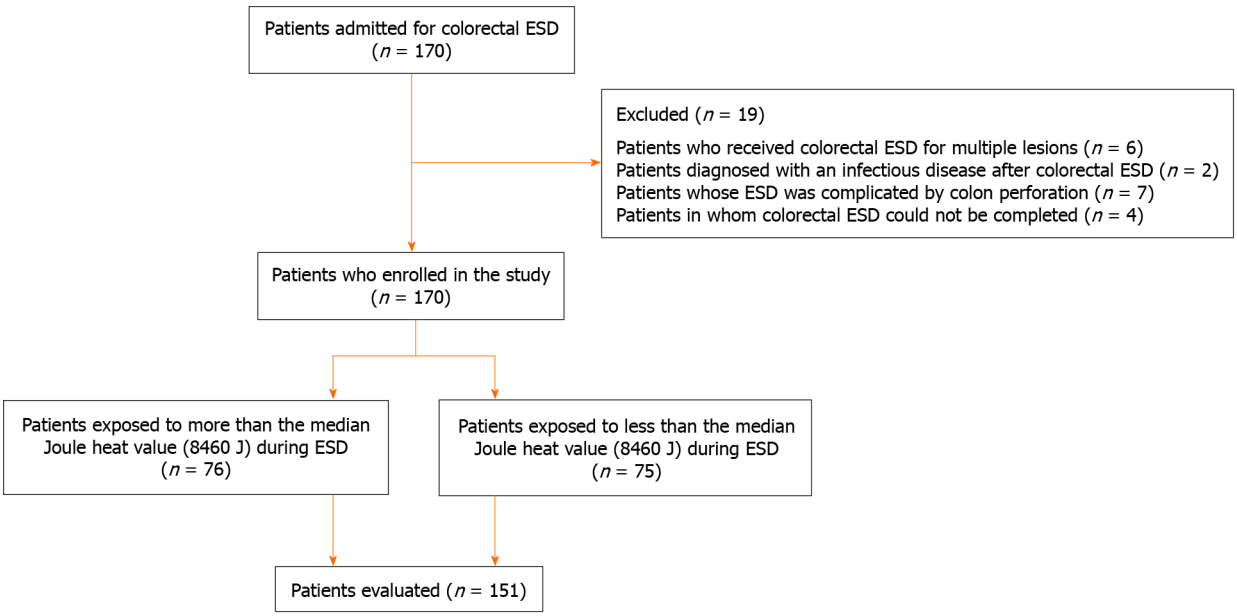


Figure 2 Study flowchart. ESD: Endoscopic submucosal dissection.

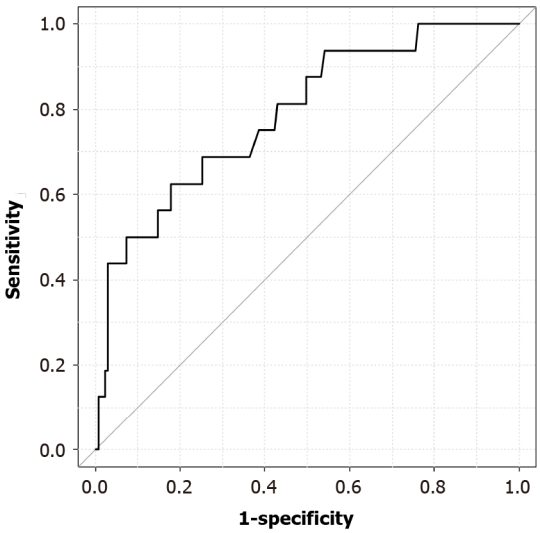


Figure 3 Receiver-operating characteristic curve showing the correlation between post-endoscopic submucosal dissection electrocoagulation syndrome and total Joule heat [area under the curve = 0.788 (95% confidence interval: 0.666-0.909)].

Limits of the study

First, because this was a retrospective cohort study, we could not rule out poor endoscope operability as a confounding factor. Second, as this was a single-center study, selection bias cannot be excluded. Nevertheless, we imposed strict inclusion and exclusion criteria to mitigate selection bias to the greatest extent possible. Last, the sample size was small. In the future, a prospective study should be performed to establish the validity of our results.

CONCLUSION

We found that Joule heat accumulation within the gastrointestinal wall is involved in the onset of PECS. ESD-related thermal damage to the mucosal peeled surface is probably a major component of the mechanism underlying PECS.

ARTICLE HIGHLIGHTS

Research background

Few studies have examined the impact of endoscopic submucosal dissection (ESD)-related thermal damage on the onset of post-ESD electrocoagulation syndrome (PECS).

Research motivation

We hypothesized that electrocoagulation is associated with Joule heat capable of causing thermal damage to the gastrointestinal wall during long ESD operations.

Research objectives

We aimed to determine the association between high Joule heat and the onset of PECS.

Research methods

We developed a novel device to measure the swift coagulation time with a sensor adjacent to the electrosurgical coagulation unit foot switch, which enabled us to calculate total Joule heat. PECS was defined as localized abdominal pain (visual analogue scale ≥ 30 mm during hospitalization or increased by ≥ 20 mm from the baseline) and fever (temperature ≥ 37.5 degrees or white blood cell count ≥ 10000 μ/L). Patients exposed to more or less than the median Joule heat value were assigned to the high and low Joule heat groups, respectively.

Research results

We evaluated 151 patients. The PECS incidence was 10.6% (16/151 cases), and all patients were followed conservatively and discharged without severe complications. In multivariate analysis, high Joule heat was an independent PECS risk factor. The area under the ROC curve showing the correlation between PECS and total Joule heat was high [0.788 (95% confidence interval: 0.666-0.909)].

Research conclusions

Joule heat accumulation in the gastrointestinal wall is involved in the onset of PECS. ESD-related thermal damage of the peeled mucosal surface is probably a major component of the mechanism underlying PECS.

Research perspectives

Future prospective studies should be performed to establish the validity of our results.

REFERENCES

1 **Puli SR**, Kakugawa Y, Saito Y, Antillon D, Gotoda T, Antillon MR. Successful complete cure *en-bloc* resection of large nonpedunculated colonic polyps by endoscopic submucosal dissection: a meta-analysis and systematic review. *Ann Surg Oncol* 2009; **16**: 2147-2151 [PMID: 19479308 DOI: 10.1245/s10434-009-0520-7]

2 **Saito Y**, Fukuzawa M, Matsuda T, Fukunaga S, Sakamoto T, Uraoka T, Nakajima T, Ikehara H, Fu KI, Itoi T, Fujii T. Clinical outcome of endoscopic submucosal dissection versus endoscopic mucosal

resection of large colorectal tumors as determined by curative resection. *Surg Endosc* 2010; **24**: 343-352 [PMID: 19517168 DOI: 10.1007/s00464-009-0562-8]

3 **Saito Y**, Uraoka T, Yamaguchi Y, Hotta K, Sakamoto N, Ikematsu H, Fukuzawa M, Kobayashi N, Nasu J, Michida T, Yoshida S, Ikehara H, Otake Y, Nakajima T, Matsuda T, Saito D. A prospective, multicenter study of 1111 colorectal endoscopic submucosal dissections (with video). *Gastrointest Endosc* 2010; **72**: 1217-1225 [PMID: 21030017 DOI: 10.1016/j.gie.2010.08.004]

4 **Kobayashi N**, Yoshitake N, Hirahara Y, Konishi J, Saito Y, Matsuda T, Ishikawa T, Sekiguchi R, Fujimori T. Matched case-control study comparing endoscopic submucosal dissection and endoscopic mucosal resection for colorectal tumors. *J Gastroenterol Hepatol* 2012; **27**: 728-733 [PMID: 22004124 DOI: 10.1111/j.1440-1746.2011.06942.x]

5 **Nakajima T**, Saito Y, Tanaka S, Iishi H, Kudo SE, Ikematsu H, Igarashi M, Saitoh Y, Inoue Y, Kobayashi K, Hisasbe T, Matsuda T, Ishikawa H, Sugihara K. Current status of endoscopic resection strategy for large, early colorectal neoplasia in Japan. *Surg Endosc* 2013; **27**: 3262-3270 [PMID: 23508817 DOI: 10.1007/s00464-013-2903-x]

6 **Wada Y**, Kudo SE, Tanaka S, Saito Y, Iishii H, Ikematsu H, Igarashi M, Saitoh Y, Inoue Y, Kobayashi K, Hisabe T, Tsuruta O, Kashida H, Ishikawa H, Sugihara K. Predictive factors for complications in endoscopic resection of large colorectal lesions: a multicenter prospective study. *Surg Endosc* 2015; **29**: 1216-1222 [PMID: 25159643 DOI: 10.1007/s00464-014-3799-9]

7 **Fujishiro M**, Yahagi N, Kakushima N, Kodashima S, Muraki Y, Ono S, Yamamichi N, Tateishi A, Oka M, Ogura K, Kawabe T, Ichinose M, Omata M. Outcomes of endoscopic submucosal dissection for colorectal epithelial neoplasms in 200 consecutive cases. *Clin Gastroenterol Hepatol* 2007; **5**: 678-683 [PMID: 17466600 DOI: 10.1016/j.cgh.2007.01.006]

8 **Isomoto H**, Nishiyama H, Yamaguchi N, Fukuda E, Ishii H, Ikeda K, Ohnita K, Nakao K, Kohno S, Shikuwa S. Clinicopathological factors associated with clinical outcomes of endoscopic submucosal dissection for colorectal epithelial neoplasms. *Endoscopy* 2009; **41**: 679-683 [PMID: 19670135 DOI: 10.1055/s-0029-1214979]

9 **Watabe H**, Yamaji Y, Okamoto M, Kondo S, Ohta M, Ikenoue T, Kato J, Togo G, Matsumura M, Yoshida H, Kawabe T, Omata M. Risk assessment for delayed hemorrhagic complication of colonic polypectomy: polyp-related factors and patient-related factors. *Gastrointest Endosc* 2006; **64**: 73-78 [PMID: 16813806 DOI: 10.1016/j.gie.2006.02.054]

10 **Okamoto K**, Watanabe T, Komeda Y, Kono T, Takashima K, Okamoto A, Kono M, Yamada M, Arizumi T, Kamata K, Minaga K, Yamao K, Nagai T, Asakuma Y, Takenaka M, Sakurai T, Matsui S, Nishida N, Chikugo T, Kashida H, Kudo M. Risk Factors for Postoperative Bleeding in Endoscopic Submucosal Dissection of Colorectal Tumors. *Oncology* 2017; **93** Suppl 1: 35-42 [PMID: 29258069 DOI: 10.1159/000481228]

11 **Jung D**, Youn YH, Jahng J, Kim JH, Park H. Risk of electrocoagulation syndrome after endoscopic submucosal dissection in the colon and rectum. *Endoscopy* 2013; **45**: 714-717 [PMID: 23990482 DOI: 10.1055/s-0033-1344555]

12 **Hong MJ**, Kim JH, Lee SY, Sung IK, Park HS, Shim CS. Prevalence and clinical features of coagulation syndrome after endoscopic submucosal dissection for colorectal neoplasms. *Dig Dis Sci* 2015; **60**: 211-216 [PMID: 25502119 DOI: 10.1007/s10620-014-3484-9]

13 **Yamashina T**, Takeuchi Y, Uedo N, Hamada K, Aoi K, Yamasaki Y, Matsuura N, Kanesaka T, Akasaka T, Yamamoto S, Hanaoka N, Higashino K, Ishihara R, Iishi H. Features of electrocoagulation syndrome after endoscopic submucosal dissection for colorectal neoplasm. *J Gastroenterol Hepatol* 2016; **31**: 615-620 [PMID: 26202127 DOI: 10.1111/jgh.13052]

14 **Lee SP**, Sung IK, Kim JH, Lee SY, Park HS, Shim CS, Ki HK. A randomized controlled trial of prophylactic antibiotics in the prevention of electrocoagulation syndrome after colorectal endoscopic submucosal dissection. *Gastrointest Endosc* 2017; **86**: 349-357.e2 [PMID: 27899322 DOI: 10.1016/j.gie.2016.11.022]

15 **Lee SP**, Kim JH, Sung IK, Lee SY, Park HS, Shim CS, Han HS. Effect of submucosal fibrosis on endoscopic submucosal dissection of colorectal tumors: pathologic review of 173 cases. *J Gastroenterol Hepatol* 2015; **30**: 872-878 [PMID: 25641510 DOI: 10.1111/jgh.12886]

16 **Hirasawa K**, Sato C, Makazu M, Kaneko H, Kobayashi R, Kokawa A, Maeda S. Coagulation syndrome: Delayed perforation after colorectal endoscopic treatments. *World J Gastrointest Endosc* 2015; **7**: 1055-1061 [PMID: 26380051 DOI: 10.4253/wjge.v7.i12.1055]

17 **Mori H**, Kobara H, Rafiq K, Nishiyama N, Fujihara S, Oryu M, Masaki T. Effects of gastric irrigation on bacterial counts before endoscopic submucosal dissection: a randomized case control prospective study. *PLoS One* 2013; **8**: e65377 [PMID: 23762354 DOI: 10.1371/journal.pone.0065377]

18 **Christie JP**, Marrazzo J 3rd. "Mini-perforation" of the colon--not all postpolypectomy perforations require laparotomy. *Dis Colon Rectum* 1991; **34**: 132-135 [PMID: 1993410 DOI: 10.1007/BF02049986]

19 **Nomura S**, Shimura T, Katano T, Iwai T, Mizuno Y, Yamada T, Ebi M, Hirata Y, Nishie H, Mizushima T, Nojiri Y, Togawa S, Shibata S, Kataoka H. A multicenter, single-blind randomized controlled trial of endoscopic clipping closure for preventing coagulation syndrome after colorectal endoscopic submucosal dissection. *Gastrointest Endosc* 2020; **91**: 859-867.e1 [PMID: 31785275 DOI: 10.1016/j.gie.2019.11.030]

20 **Arimoto J**, Higurashi T, Kato S, Fuyuki A, Ohkubo H, Nonaka T, Yamaguchi Y, Ashikari K, Chiba H, Goto S, Taguri M, Sakaguchi T, Atsukawa K, Nakajima A. Risk factors for post-colorectal

endoscopic submucosal dissection (ESD) coagulation syndrome: a multicenter, prospective, observational study. *Endosc Int Open* 2018; **6**: E342-E349 [PMID: 29527556 DOI: 10.1055/s-0044-101451]

21 **Lee H**, Cheoi KS, Chung H, Park JC, Shin SK, Lee SK, Lee YC. Clinical features and predictive factors of coagulation syndrome after endoscopic submucosal dissection for early gastric neoplasm. *Gastric Cancer* 2012; **15**: 83-90 [PMID: 21761134 DOI: 10.1007/s10120-011-0073-x]

22 **Tanaka S**, Kashida H, Saito Y, Yahagi N, Yamano H, Saito S, Hisabe T, Yao T, Watanabe M, Yoshida M, Saitoh Y, Tsuruta O, Sugihara KI, Igarashi M, Toyonaga T, Ajioka Y, Kusunoki M, Koike K, Fujimoto K, Tajiri H. Japan Gastroenterological Endoscopy Society guidelines for colorectal endoscopic submucosal dissection/endoscopic mucosal resection. *Dig Endosc* 2020; **32**: 219-239 [PMID: 31566804 DOI: 10.1111/den.13545]

23 **Hotta K**, Oyama T, Shinohara T, Miyata Y, Takahashi A, Kitamura Y, Tomori A. Learning curve for endoscopic submucosal dissection of large colorectal tumors. *Dig Endosc* 2010; **22**: 302-306 [PMID: 21175483 DOI: 10.1111/j.1443-1661.2010.01005.x]

24 **Freiberger H**. Der elektrische widerstand des menschlichen körpers gegen technischen gleich- und wechselstrom. Berlin: Verlag von Julius Springer, 1934

25 **Waye JD**, Lewis BS, Yessayan S. Colonoscopy: a prospective report of complications. *J Clin Gastroenterol* 1992; **15**: 347-351 [PMID: 1294644]

26 **Cha JM**, Lim KS, Lee SH, Joo YE, Hong SP, Kim TI, Kim HG, Park DI, Kim SE, Yang DH, Shin JE. Clinical outcomes and risk factors of post-polypectomy coagulation syndrome: a multicenter, retrospective, case-control study. *Endoscopy* 2013; **45**: 202-207 [PMID: 23381948 DOI: 10.1055/s-0032-1326104]

27 **Ito S**, Hotta K, Imai K, Yamaguchi Y, Kishida Y, Takizawa K, Kakushima N, Tanaka M, Kawata N, Yoshida M, Ishiwatari H, Matsubayashi H, Ono H. Risk factors of post-endoscopic submucosal dissection electrocoagulation syndrome for colorectal neoplasm. *J Gastroenterol Hepatol* 2018; **33**: 2001-2006 [PMID: 29864790 DOI: 10.1111/jgh.14302]

28 **Hanaoka N**, Uedo N, Ishihara R, Higashino K, Takeuchi Y, Inoue T, Chatani R, Hanafusa M, Tsujii Y, Kanzaki H, Kawada N, Iishi H, Tatsuta M, Tomita Y, Miyashiro I, Yano M. Clinical features and outcomes of delayed perforation after endoscopic submucosal dissection for early gastric cancer. *Endoscopy* 2010; **42**: 1112-1115 [PMID: 21120780 DOI: 10.1055/s-0030-1255932]

29 **Kobayashi R**, Hirasawa K, Sato C, Makazu M, Kaneko H, Ikeda R, Fukuchi T, Sawada A, Ozeki Y, Taguri M, Takebayashi S, Maeda S. Utility of multi-detector computed tomography scans after colorectal endoscopic submucosal dissection: a prospective study. *Gastrointest Endosc* 2018; **87**: 818-826 [PMID: 29122602 DOI: 10.1016/j.gie.2017.10.038]

World Journal of Gastroenterology

Submit a Manuscript: https://www.f6publishing.com

World J Gastroenterol 2021 October 14; 27(38): 6453-6464

DOI: 10.3748/wjg.v27.i38.6453

ISSN 1007-9327 (print) ISSN 2219-2840 (online)

ORIGINAL ARTICLE

Retrospective Study

Effects of acute kidney injury on acute pancreatitis patients' survival rate in intensive care unit: A retrospective study

Ni Shi, Guo-Dong Sun, Yuan-Yuan Ji, Ying Wang, Yu-Cheng Zhu, Wan-Qiu Xie, Na-Na Li, Qiu-Yuan Han, Zhi-Dong Qi, Rui Huang, Ming Li, Zhen-Yu Yang, Jun-Bo Zheng, Xing Zhang, Qing-Qing Dai, Gui-Ying Hou, Yan-Song Liu, Hong-Liang Wang, Yang Gao

ORCID number: Ni Shi 0000-0002-8172-7468; Guo-Dong Sun 0000-0003-2289-2524; Yuan-Yuan Ji 0000-0002-4448-4196; Ying Wang 0000-0002-1716-5974; Yu-Cheng Zhu 0000-0002-0447-9894; Wan-Qiu Xie 0000-0003-0825-8092; Na-Na Li 0000-0002-0683-3439; Qiu-Yuan Han 0000-0003-2786-9729; Zhi-Dong Qi 0000-0002-0799-3784; Rui Huang 0000-0002-7633-1274; Ming Li 0000-0003-1672-281X; Zhen-Yu Yang 0000-0002-1782-0772; Jun-Bo Zheng 0000-0001-9547-6172; Xing Zhang 0000-0002-0007-0768; Qing-Qing Dai 0000-0002-7062-4463; Gui-Ying Hou 0000-0001-8353-3117; Yan-Song Liu 0000-0001-7828-0733; Hong-Liang Wang 0000-0002-1407-0072; Yang Gao 0000-0002-0612-0818.

Author contributions: Shi N and Gao Y carried out the conception, design, definition of intellectual content, literature search, data acquisition, data analysis, and manuscript preparation; all authors participated in data acquisition, data analysis; Sun GD, Ji YY, Wang Y, Zhu YC, Xie WQ, Li NN, Han QY, Qi ZD, Huang R, Li M, Yang ZY, Zheng JB, Zhang X, Dai QQ, Hou GY, Liu YS, and Wang HL provided assistance for statistical analysis; Shi N, Wang HL, and Gao Y carried out literature search and manuscript editing; Wang HL, Sun

Ni Shi, Qiu-Yuan Han, Zhi-Dong Qi, Rui Huang, Ming Li, Zhen-Yu Yang, Jun-Bo Zheng, Xing Zhang, Qing-Qing Dai, Gui-Ying Hou, Yan-Song Liu, Hong-Liang Wang, Department of Critical Care Medicine, The Second Affiliated Hospital of Harbin Medical University, Harbin 150086, Heilongjiang Province, China

Guo-Dong Sun, Yuan-Yuan Ji, Wan-Qiu Xie, Na-Na Li, Department of Critical Care Medicine, The First Affiliated Hospital of Harbin Medical University, Harbin 150001, Heilongjiang Province, China

Ying Wang, Department of Critical Care Medicine, The First People Hospital of Mudanjiang city, Mudanjiang 157000, Heilongjiang Province, China

Yu-Cheng Zhu, Department of Critical Care Medicine, The Hongxinglong Hospital of Beidahuang Group, Shuangyashan 155811, Heilongjiang Province, China

Yang Gao, Department of Critical Care Medicine, The Sixth Affiliated Hospital of Harbin Medical University, Harbin 150028, Heilongjiang Province, China

Corresponding author: Yang Gao, MD, Department of Critical Care Medicine, The Sixth Affiliated Hospital of Harbin Medical University, Zhongyuan Avenue, Harbin 150028, Heilongjiang Province, China. gaoyang0312@126.com

Abstract

BACKGROUND

Acute kidney injury (AKI) is one of the most common acute pancreatitis (AP)-associated complications that has a significant effect on AP, but the factors affecting the AP patients' survival rate remains unclear.

AIM

To assess the influences of AKI on the survival rate in AP patients.

METHODS

A total of 139 AP patients were included in this retrospective study. Patients were divided into AKI group (n = 72) and non-AKI group (n = 67) according to the occurrence of AKI. Data were collected from medical records of hospitalized patients. Then, these data were compared between the two groups and further

GD, and Gao Y performed manuscript review; All authors have read and approved the content of the manuscript; and Shi N and Sun GD contributed equally to this work.

Supported by the Scientific Research Project of Heilongjiang Health and Family Planning Commission, No. 2018086 and No. 2018392.

Institutional review board statement: This study was approved by the Ethics Committee of The Second Affiliated Hospital of Harbin Medical University.

Informed consent statement: Due to the nature of retrospective study, the written informed consent of this study was waived.

Conflict-of-interest statement: The authors declare that there is no conflict of interest.

Data sharing statement: No additional data are available.

Open-Access: This article is an open-access article that was selected by an in-house editor and fully peer-reviewed by external reviewers. It is distributed in accordance with the Creative Commons Attribution NonCommercial (CC BY-NC 4.0) license, which permits others to distribute, remix, adapt, build upon this work non-commercially, and license their derivative works on different terms, provided the original work is properly cited and the use is non-commercial. See: http://creativecommons.org/Licenses/by-nc/4.0/

Manuscript source: Unsolicited manuscript

Specialty type: Gastroenterology and hepatology

Country/Territory of origin: China

Peer-review report's scientific quality classification

Grade A (Excellent): A
Grade B (Very good): B
Grade C (Good): 0
Grade D (Fair): 0

analysis was performed.

RESULTS

AKI is more likely to occur in male AP patients (P = 0.009). AP patients in AKI group exhibited a significantly higher acute physiologic assessment and chronic health evaluation II score, higher Sequential Organ Failure Assessment score, lower Glasgow Coma Scale score, and higher demand for mechanical ventilation, infusion of vasopressors, and renal replacement therapy than AP patients in non-AKI group (P < 0.01, P < 0.01, P = 0.01, P = 0.001, P < 0.01, P < 0.01, respectively). Significant differences were noted in dose of norepinephrine and adrenaline, duration of mechanical ventilation, maximum and mean values of intra-peritoneal pressure (IPP), maximum and mean values of procalcitonin, maximum and mean serum levels of creatinine, minimum platelet count, and length of hospitalization. Among AP patients with AKI, the survival rate of surgical intensive care unit and in-hospital were only 23% and 21% of the corresponding rates in AP patients without AKI, respectively. The factors that influenced the AP patients' survival rate included body mass index (BMI), mean values of IPP, minimum platelet count, and hospital day, of which mean values of IPP showed the greatest impact.

CONCLUSION

AP patients with AKI had a lower survival rate and worse relevant clinical outcomes than AP patients without AKI, which necessitates further attention to AP patients with AKI in surgical intensive care unit.

Key Words: Acute kidney injury; Acute pancreatitis; Surgical intensive care unit; Survival rate; Risk factors; Intra-peritoneal pressure

©The Author(s) 2021. Published by Baishideng Publishing Group Inc. All rights reserved.

Core Tip: Acute pancreatitis (AP) has become a common gastrointestinal disorder in surgical intensive care unit, and excessive secretion and/or poor drainage of pancreatic juice are the essence of AP onset. Acute kidney injury (AKI) is a common complication of AP, which is ordinarily associated with adverse outcomes. Among AP patients with AKI, the survival rate of surgical intensive care unit and in-hospital were only 23% and 21% of the corresponding rates in AP patients without AKI, respectively. The factors that influenced the AP patients' survival rate included body mass index (BMI), mean values of intra-peritoneal pressure, minimum platelet count, and hospital day, of which mean values of intra-peritoneal pressure showed the greatest impact.

Citation: Shi N, Sun GD, Ji YY, Wang Y, Zhu YC, Xie WQ, Li NN, Han QY, Qi ZD, Huang R, Li M, Yang ZY, Zheng JB, Zhang X, Dai QQ, Hou GY, Liu YS, Wang HL, Gao Y. Effects of acute kidney injury on acute pancreatitis patients' survival rate in intensive care unit: A retrospective study. *World J Gastroenterol* 2021; 27(38): 6453-6464
URL: https://www.wjgnet.com/1007-9327/full/v27/i38/6453.htm
DOI: https://dx.doi.org/10.3748/wjg.v27.i38.6453

INTRODUCTION

Acute pancreatitis (AP) is an excessive inflammatory response caused by digestion of the pancreas itself, which can further lead to local and distant organ damage, or even single or multiple organ failure. In the wake of continuous in-depth understanding of pathophysiological mechanism of AP and improvement of treatment measures, AP-related mortality rate is annually declining, whereas AP-associated hospitalization rises year-by-year worldwide[1,2]. In clinical practice, about 80% of the common etiologies are attributed to gallstones and alcohol consumption[3], however, the proportion of different etiologies significantly varies among different countries. In addition, hypertriglyceridemia is a high-risk factor for AP, and may lead to direct damage to pancreas and pancreatic exocrine function[4,5]. Thus, identification of

Grade E (Poor): 0

Received: March 4, 2021
Peer-review started: March 4, 2021
First decision: April 5, 2021
Revised: April 15, 2021
Accepted: August 23, 2021
Article in press: August 23, 2021
Published online: October 14, 2021

P-Reviewer: Deepak P, Zimmerman M
S-Editor: Yan JP
L-Editor: Filipodia
P-Editor: Xing YX



etiologies is highly essential to manage better AP patients. AP can be categorized into mild acute pancreatitis (MAP), moderately severe acute pancreatitis (MSAP), and severe acute pancreatitis (SAP) according to the presence and duration of organ failure presented in the revised Atlanta classification (2013)[6]. The mortality rate is high among SAP patients, reaching 15%-30% or even higher[7], due to persistent organ failure. Therefore, earlier identification and appropriate use of intensive care support can be conducive to prevent further disease progression, thereby improving AP patients' prognosis[8].

Acute kidney injury (AKI) is one of the most common AP-associated complications, resulting from uncontrolled inflammatory response, release of pancreatic amylase, hypovolemia, insufficient renal perfusion, micro-circulatory disturbance, intra-abdominal hypertension, and reactive oxygen species[9]. At present, AKI is mainly diagnosed based on the criteria presented by the Kidney Disease Improving Global Outcomes (KIDGO) guidelines[10,11]. The incidence of AKI has gradually, while steadily, increased year-by-year worldwide[12]. AKI can deteriorate AP patient's medical status and is an independent risk factor for increased mortality and development of chronic kidney disease (CKD). When AKI and AP occur simultaneously, a worse clinical prognosis is expected[13,14], involving longer period of hospitalization and higher mortality rate. However, in clinical practice, there is no an effective therapeutic approach for AKI except for renal replacement therapy (RRT)[15]. AKI has imposed a huge medical burden in China as well as in the world. Therefore, development of early detection and prevention measures is highly significant to avoid adverse outcomes associated with AKI[16].

Although previous studies have confirmed that concurrent AKI is associated with a poor prognosis[17], there is no reliable research assessing the influences of AKI on Chinese AP patients' survival rate who were hospitalized at surgical intensive care unit (SICU). Hence, to address this scientific gap, the current retrospective study was conducted.

MATERIALS AND METHODS

Study design

This retrospective study enrolled 139 AP patients who were admitted to the SICU of The Second Affiliated Hospital of Harbin Medical University (Harbin, Heilongjiang Province, China) between January 2014 and March 2019. Baseline and clinical data were collected during hospitalization. The enrolled AP patients were divided into AKI group (n = 72) and non-AKI group (n = 67) according to occurrence of AKI. This study was approved by the Ethics Committee of The Second Affiliated Hospital of Harbin Medical University.

Study population

The inclusion criteria for this retrospective study were as follows: Patients who were admitted to the SICU of The Second Affiliated Hospital of Harbin Medical University; patients who were diagnosed with AP; patients' age > 18-years-old. The exclusion criteria were as follows: Pregnant or breastfeeding women; patients with CKD; patients with recurrent pancreatitis; patients who received renal transplantation; incomplete medical data.

Diagnosis of AP

A combination of medical history, symptoms and physical examinations, laboratory tests, and radiographic examinations (*e.g.*, abdominal ultrasound, contrast-enhanced computed tomography, or magnetic resonance imaging) was applied to confirm the diagnosis of AP. A limited number of diagnosed AP patients were eventually confirmed by undergoing exploratory laparotomy.

Diagnosis and classification of AKI

Diagnosis and classification of AKI were conducted based on the criteria presented by the KIDGO guidelines (2012)[18], in which serum creatinine criteria was defined as an increased absolute value in serum creatinine level of ≥ 0.3 mg/dL (≥ 26.4 μmol/L) or a percentage increase in serum creatinine level of ≥ 50% within 48 h. Baseline serum creatinine level was defined as the lowest serum creatinine level measured within 2 d prior to admission to SICU. If no serum creatinine level was measured, the serum creatinine level recorded in the first measurement within 2 d after admission to SICU

was considered as baseline serum creatinine level.

RRT

In the present study, all AP patients who needed to undergo RRT were managed with continuous veno-venous hemofiltration (CVVH), anti-coagulation with heparin, and fixed pre- and post-dilution strategies. Blood flow rates, amount of substitute fluid, and dehydration volume were individually adjusted according to each patient's medical status.

Measurement of serum procalcitonin level and intra-peritoneal pressure

Serum procalcitonin (PCT) level was intermittently measured after AP patients' admission to SICU through Mini-VIDAS (Hain Lifescience GmbH; Nehren, Germany). Intra-peritoneal pressure (IPP) was indirectly reflected *via* measuring intravesical pressure with Freund's catheter.

Data collection

Baseline and clinical data, including patients' age, gender, body mass index (BMI), Acute Physiologic Assessment and Chronic Health Evaluation II (APACHE II) score, Sequential Organ Failure Assessment (SOFA) score, Glasgow Coma Scale (GCS) score, duration of mechanical ventilation (MV), abdominal puncture drainage, gallbladder puncture drainage, infusion of vasopressors, demand of RRT, IPP, body temperature, PCT, creatinine, platelet count, hospital day, and prognosis were collected from medical records of hospitalized patients. APACHE II score and SOFA score were calculated by the first 24 h clinical data after SICU admission.

Statistical analysis

Variables conforming to normal distribution were described as mean ± SD, while those abnormally distributed variables were expressed as median (range). Normality analysis was applied to continuous data. SPSS 22.0 software (IBM, Armonk, NY, United Sates) was used to carry out statistical analyses. Independent-samples *t*-test was used to perform inter-group comparison for normally distributed data, while Mann-Whitney *U* test was employed for inter-group comparison for abnormally distributed data. Classification data were expressed by the number of samples, and χ^2 test was adopted. The prognosis of AP patients who were admitted to SICU was analyzed by binary logistic regression analysis, while the remaining indicators were analyzed by the *t*-test or Mann-Whitney *U* test. P value < 0.05 was considered statistically significant.

RESULTS

Patients' baseline and clinical data

A total of 139 AP patients were enrolled in this retrospective study. The enrolled AP patients were divided into AKI group (n = 72) and non-AKI group (n = 67) according to occurrence of AKI. As shown in Table 1, AKI was more likely to occur in male AP patients (P = 0.009). AP patients with AKI exhibited a significantly higher APACHE II score, higher SOFA score, lower GCS score, and higher demand for MV, infusion of vasopressors, and RRT than non-AKI AP patients (P < 0.01, P < 0.01, P = 0.01, P = 0.001, P < 0.01, P < 0.01, respectively). No significant difference was observed in the remaining baseline and clinical data, including patients' age, BMI, proportion of abdominal puncture drainage, and gallbladder puncture drainage.

Vasopressor infusion

There were significant differences in types of vasopressors and proportion of norepinephrine, adrenaline, and vasopressor infusion between the two groups (Table 2).

Analysis of prognostic indicators

Significant differences were noted in dose of norepinephrine and adrenaline, duration of MV, maximum and mean values of IPP, maximum and mean values of PCT, maximum and mean serum levels of creatinine, minimum platelet count, prognosis of AP patients admitted to SICU, and hospital day between the two groups (Table 3). Among AP patients with AKI, the survival rates of SICU and in-hospital were only 23% and 21% of the corresponding rates in AP patients without AKI, respectively.

Table 1 Baseline and clinical data of patients

	AKI (*n* = 72)	Non-AKI (*n* = 67)	Z/χ^2	*P* value
Age	45.00 (17.50)	44.00 (21.00)	-0.07	0.94
Gender			6.745	0.009
Male	50	32		
Female	22	35		
BMI	24.45 (2.38)	23.80 (2.60)	-1.20	0.23
APACHE II Score	18.00 (7.75)	9.00 (7.00)	-7.47	< 0.01
SOFA Score	9.00 (6.00)	4.00 (4.00)	-6.50	< 0.01
GCS Score	15.00 (3.00)	15.00 (0.00)	-2.71	0.01
MV			10.94	0.001
Yes	46	24		
No	26	43		
Abdominal puncture drainage			0.19	0.66
Yes	36	36		
No	36	31		
Gallbladder puncture drainage			2.36	0.12
Yes	17	9		
No	55	58		
Vasopressor infusion			26.84	< 0.01
Yes	21	18		
No	51	49		
RRT				
Yes	44	20	13.651	< 0.01
No	28	47		

AKI: Acute kidney injury; APACHE II: Acute Physiology and Chronic Health Evaluation II; BMI: Body mass index; GCS: Glasgow Coma Scale; MV: Mechanical ventilation; RRT: Renal replacement therapy; SOFA: Sequential Organ Failure Assessment.

Analysis of the related factors influencing AP patients' survival rate

The factors influencing the AP patients' survival rate who were hospitalized at SICU included BMI, mean values of IPP, minimum platelet count, and hospital day. Among these factors, mean values of IPP showed the greatest effect (Table 4). The values of area under the receiver operating characteristic (ROC) curve for the four factors related to patients with or without AKI were calculated to predict the AP patients' survival rate, and were 0.896 and 0.891, respectively (Figure 1 and Table 5; $P > 0.5$). However, there was no significant different in values of the area under the two ROC curves. The sensitivity and specificity of the two ROC curves were approximately the same [sensitivity (80.6%) *vs* specificity (88.0%)].

Risk thresholds of the related factors

Risk thresholds of BMI, mean values of IPP, minimum platelet count, and hospital day were ≥ 24, ≥ 23, ≤ 77, and ≤ 4, respectively, which indicated that BMI ≥ 24, mean values of IPP ≥ 23, minimum platelet count ≤ 77, and hospital day ≤ 4 were risk factors for AP patients' survival rate who were hospitalized at SICU.

DISCUSSION

Excessive secretion and/or poor drainage of pancreatic juice are the essence of AP onset. With the increasing incidence of gallstones and alcohol abuse, AP had become a

Table 2 Vasopressor infusion

	AKI, *n* = 72	Non-AKI, *n* = 67	χ^2	*P* value
Types of vasopressors			27.44	< 0.01
No	21	49		
1	34	14		
≥ 2	17	4		
Norepinephrine infusion			35.35	< 0.01
Yes	49	17		
No	23	50		
Adrenaline infusion			12.75	< 0.01
Yes	15	1		
No	57	66		
Vasopressor infusion			26.84	< 0.01
Yes	51	18		
No	21	49		

AKI: Acute kidney injury.

common gastrointestinal disorder. The majority of cases with AP are MAP characterized by no new onset of organ dysfunction, whereas SAP not only leads to new onset of organ dysfunction, but also lasts for more than 48 h[6]. With aggravation of the condition from MAP to SAP, the length of stay at SICU and mortality rate significantly increased. Hence, SAP patients should be managed in SICU for multiple organ support therapy and surgical interventions to avoid further disease progression [19]. When AP happens, hemodynamic status should be assessed immediately to avoid hypovolemia or volume overload caused by excessive fluid resuscitation[20], which might cause detrimental influences[21]. Routine use of prophylactic antibiotics in SAP or necrotizing pancreatitis was not clinically recommended in the guidelines [22], because of no mortality benefit or reduction in the incidence of infected necrosis [23]. The ability to penetrate pancreatic necrotic tissue is of great significance in the selection of antibiotics. Less than 50% of necrotizing pancreatitis patients need surgical interventions, in which step-up approach and minimally invasive strategies were advocated[24-27], involving endoscopic nasobiliary drainage, percutaneous transhepatic gallbladder drainage, percutaneous transhepatic biliary drainage, endoscopic retrograde cholangiopancreatography, endoscopic transgastric/transduodenal drainage, and video-assisted retroperitoneal debridement.

During AP, kidney is the most vulnerable organ and is typically sacrificed to protect other important organs, such as heart, lung, brain, and liver. As a consequence, AKI is a common complication of AP, which is ordinarily associated with adverse outcomes, including risk of subsequent CKD, end-stage renal disease, RRT dependence, in-hospital and post-discharge mortality, and even healthcare cost-containment concerns [28-30]. It was generally believed that the incidence of AKI was about 20% in critically ill adult patients[31]. More than 50% of SAP patients would develop into AKI according to previous literature[3,17,32]. Different organs interact with each other in the whole body, and the deteriorated kidney function can inevitably cause or aggravate damage to other organs without early intervention. Diuretics had been demonstrated to be an independent risk factor for AKI[33], and thus, were no longer recommended for routine use in clinical practice. When RRT is required, the mortality rate may even exceed 75%[34]. Compared with developed countries, AKI is typically substantial underdiagnoses and undertreatment in developing countries[35], especially in African countries, which may be partially explained as seriously inadequate repeated serum creatinine assay[36].

At present, about 20% of AKI patients require to undergo RRT[37], and this rate continues to increase worldwide. Some eligible patients for RRT may decline to undergo this intervention because of resource constraints, high costs of therapy, or severe comorbidities[38], which significantly increase mortality rate compared with those cases who received it[39]. RRT involves different treatment modalities, such as

Table 3 Analysis of prognostic indicators

	AKI, *n* = 72	Non-AKI, *n* = 67	*Z/t/Wald*	*P* value	OR
Prognosis of SICU			9.54	0.002	0.23
cure	48	60			
other	24	7			
Prognosis of in-hospital			11.33	0.001	0.21
cure	46	60			
other	26	7			
Duration of MV	34.00 (87.75)	0.00 (18.00)	-3.92	< 0.01	
Maximum values of IPP	24.50 (10.00)	18.00 (10.00)	-5.39	< 0.01	
Mean values of IPP	21.40 (6.82)	15.29 (4.73)	6.175	< 0.01	
Maximum values of body temperature	37.80 (1.20)	37.50 (1.00)	-2.00	0.05	
Mean values of body temperature	37.00 (0.50)	37.00 (0.30)	-0.59	0.56	
Maximum values of PCT	16.28 (21.12)	2.87 (9.28)	-5.96	< 0.01	
Mean values of PCT	8.52 (11.52)	1.58 (4.20)	-6.42	< 0.01	
Maximum serum levels of creatinine	284.35 (215.73)	87.60 (47.80)	-9.94	< 0.01	
Mean serum levels of creatinine	197.45 (172.10)	65.60 (29.60)	-9.48	< 0.01	
Minimum platelet count	93.00 (87.75)	137.00 (73.00)	-3.18	< 0.01	
Mean platelet count	174.40 (112.15)	198.00 (103.60)	-1.64	0.10	
Hospital day	9.00 (12.75)	8.00 (11.00)	-0.07	0.94	
Dose of norepinephrine	16.00 (52.00)	0.00 (4.00)	-5.11	< 0.01	
Dose of adrenaline	0.00 (0.00)	0.00 (0.00)	-3.58	< 0.01	

AKI: Acute kidney injury; MV: Mechanical ventilation; IPP: Intra-peritoneal pressure; OR: Odds ratio; PCT: Procalcitonin; SICU: Surgical intensive care unit.

Table 4 Analysis of the related factors influencing acute pancreatitis patients' survival rate

	B	SE	Wald	*df*	*P* value	Exp (B)
BMI	1.4904	0.6467	5.3105	1.0000	0.0212	4.4387
Mean values of IPP	2.6477	0.6217	18.1355	1.0000	0.0000	14.1211
Minimum platelet count	-1.2285	0.6125	4.0237	1.0000	0.0449	0.2927
Hospital day	-1.8571	0.5965	9.6913	1.0000	0.0019	0.1561
Constant	-0.9863	0.8689	1.2883	1.0000	0.2564	0.3730

BMI: Body mass index; IPP: Intra-peritoneal pressure; SE: Standard error.

hemodialysis, hemofiltration, hemodiafiltration, and peritoneal dialysis. It has been suggested that continuous RRT has several advantages over intermittent RRT, including better hemodynamic stability (blood pressure control and blood circulation), improved survival, and greater likelihood of renal recovery[38,40,41]. Thus, CVVH had occupied the mainstream of RRT, particularly for AP patients who were hospitalized at SICU, because of its outstanding effectiveness and safety. Although it has been suggested that early application of RRT in patients with severe sepsis, irrespective of the presence of renal failure, might be beneficial, CVVH did not limit further organ damage and even prolonged the need for organ support. RRT is a non-selective method, which can simultaneously remove detrimental and beneficial substances. In clinical practice, in spite of great advances in RRT development, there is still a lack of uniform standards for RRT-associated strategies, such as optimal timing

Table 5 Area under the receiver operating characteristic curve

Variables	Area	SE	Asymptotic, *P* value	Asymptotic 95%CI	
				Lower bound	Upper bound
With AKI	0.896	0.033	0	0.831	0.961
Without AKI	0.891	0.037	0	0.819	0.963

AKI: Acute kidney injury; CI: Confidence interval; SE: Standard error.

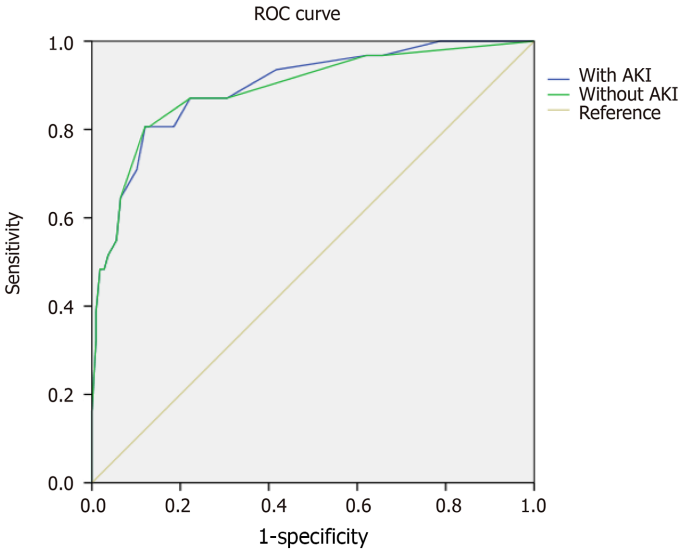


Figure 1 The receiver operating characteristic curve of these four factors related to acute pancreatitis patients without or with acute kidney injury. AKI: Acute kidney injury; ROC: Receiver operating characteristic.

for initiation of RRT, anti-coagulation, and optimal dosage[42,43].

Among several scoring systems, APACHE II score and SOFA score are commonly used to reflect timely and accurately illness severity and predict prognosis of AP patients[44]. It is well known that GCS score is a simple and valuable tool for indication of nervous system function and prediction of short- and long-term mortality [45], in which its discriminative power is similar to other more complex scoring systems[46]. Therefore, these three scoring systems were selected to assess the severity of AP in the present research. A number of scholars pointed out that demand for MV, infusion of vasopressors, and RRT could be risk factors for increased mortality in AP patients[47]. PCT level may contribute to earlier and better stratification of septic patients who are at risk of death and admitted to SICU[48]. To our knowledge, the increased IPP and decreased platelet count are closely associated with the severity and prognosis of AP in clinical practice[49]. Hence, the above-mentioned indicators were employed in the current study.

The present retrospective study provided a comprehensive description about the influences of AKI on AP patients' survival rate who were hospitalized at SICU in accordance with the criteria presented by the KIDGO guidelines. Our findings revealed that AP patients with AKI had more severe degree of illness than AP patients without AKI, as evidenced by higher APACHE II score, higher SOFA score, and lower GCS score, and the survival rates of SICU and in-hospital were only 23% and 21% of the corresponding rates in AP patients without AKI, respectively, which were roughly consistent with previously reported rates[10,31]. These gaps can be partially explained by the increased emphasis placed on AP and improvement of diagnostic methods and standardized therapeutic bundles. For AP patients with AKI, other influences were found to be associated with demand for MV, infusion of vasopressors and RRT, dosages of norepinephrine and adrenaline, duration of MV, maximum and mean values of IPP, maximum and mean values of PCT, maximum and mean serum levels of creatinine, and minimum platelet count. It was revealed that AKI negatively and seriously affected AP patients who were hospitalized at SICU.

The factors that influenced AP patients' survival rate who were hospitalized at SICU included BMI, mean values of IPP, minimum platelet count, and hospital day. With every unit change in BMI, mean values of IPP, minimum platelet count, and hospital day, the AP patients' survival rate was 4.4387, 14.1211, 0.1561, and 0.3730 of the original rates, respectively. Therefore, mean values of IPP had the greatest influence on the AP patients' survival rate who were hospitalized at SICU. Risk thresholds of BMI, mean values of IPP, minimum platelet count, and hospital day were ≥ 24, ≥ 23, ≤ 77, and ≤ 4, respectively, which indicated that BMI ≥ 24, mean values of IPP ≥ 23, minimum platelet count ≤ 77, and hospital day ≤ 4 were risk factors for the AP patients' survival rate who were hospitalized at SICU.

The present study contains a number of limitations. First, although significant differences were detected, this was only a small sample-size, single-center, retrospective study, which might reduce the reliability of our conclusion and its application to AP patients in clinical practice. Second, clinical data were obtained only on the basis of the medical records during hospitalization, which might lead to research bias. Last but not least, the etiology of AP had not been further differentiated. It is noteworthy that different etiologies may induce different clinical manifestations and prognosis, necessitating conducting further studies in the future.

CONCLUSION

In conclusion, this study attempted to clarify the influence of AKI on AP patients' survival rate who were hospitalized at SICU. Results showed that AP patients with AKI exhibited lower survival rate and worse relevant clinical outcomes than AP patients without AKI. Besides, BMI, mean values of IPP, minimum platelet count, and hospital day may play significant roles in predicting the AP patients' survival rate who were hospitalized at SICU. Our findings suggest that prevention of AKI is clinically important.

ARTICLE HIGHLIGHTS

Research background

Acute kidney injury (AKI) is common in acute pancreatitis (AP) patients, but the risk factors are not clear.

Research motivation

This study tried to explore the associated risk factors of AKI in AP patients.

Research objectives

This study aimed to assess the influences of AKI on the survival rate in AP patients.

Research methods

Patients were divided into two groups based on AKI status, and comparisons between the groups were calculated for diverse variables.

Research results

AKI is more likely to occur in male AP patients.

Research conclusions

AP patients with AKI exhibited lower survival rate and worse relevant clinical outcomes than AP patients without AKI in SICU.

Research perspectives

This study provided clinical evidence for prevention of AKI in AP patients.

ACKNOWLEDGEMENTS

We highly appreciate the contribution of participants and co-workers from surgical intensive care unit of The Second and First Affiliated Hospital of Harbin Medical

University to this research.

REFERENCES

1 **Krishna SG**, Kamboj AK, Hart PA, Hinton A, Conwell DL. The Changing Epidemiology of Acute Pancreatitis Hospitalizations: A Decade of Trends and the Impact of Chronic Pancreatitis. *Pancreas* 2017; **46**: 482-488 [PMID: 28196021 DOI: 10.1097/MPA.0000000000000783]

2 **Russell PS**, Mittal A, Brown L, McArthur C, Phillips AJR, Petrov M, Windsor JA. Admission, management and outcomes of acute pancreatitis in intensive care. *ANZ J Surg* 2017; **87**: E266-E270 [PMID: 27018076 DOI: 10.1111/ans.13498]

3 **Pavlidis P**, Crichton S, Lemmich Smith J, Morrison D, Atkinson S, Wyncoll D, Ostermann M. Improved outcome of severe acute pancreatitis in the intensive care unit. *Crit Care Res Pract* 2013; **2013**: 897107 [PMID: 23662207 DOI: 10.1155/2013/897107]

4 **Weiss FU**, Laemmerhirt F, Lerch MM. Etiology and Risk Factors of Acute and Chronic Pancreatitis. *Visc Med* 2019; **35**: 73-81 [PMID: 31192240 DOI: 10.1159/000499138]

5 **Kopecky K**, Moreland A, Hebert C, Colbert GB. Plasmapheresis for recurrent acute pancreatitis from hypertriglyceridemia. *Proc (Bayl Univ Med Cent)* 2017; **30**: 358-359 [PMID: 28670087 DOI: 10.1080/08998280.2017.11929648]

6 **Banks PA**, Bollen TL, Dervenis C, Gooszen HG, Johnson CD, Sarr MG, Tsiotos GG, Vege SS; Acute Pancreatitis Classification Working Group. Classification of acute pancreatitis--2012: revision of the Atlanta classification and definitions by international consensus. *Gut* 2013; **62**: 102-111 [PMID: 23100216 DOI: 10.1136/gutjnl-2012-302779]

7 **Karakayali FY**. Surgical and interventional management of complications caused by acute pancreatitis. *World J Gastroenterol* 2014; **20**: 13412-13423 [PMID: 25309073 DOI: 10.3748/wjg.v20.i37.13412]

8 **Jacob AO**, Stewart P, Jacob O. Early surgical intervention in severe acute pancreatitis: Central Australian experience. *ANZ J Surg* 2016; **86**: 805-810 [PMID: 24890051 DOI: 10.1111/ans.12707]

9 **Petejova N**, Martinek A. Acute kidney injury following acute pancreatitis: A review. *Biomed Pap Med Fac Univ Palacky Olomouc Czech Repub* 2013; **157**: 105-113 [PMID: 23774848 DOI: 10.5507/bp.2013.048]

10 **Luo X**, Jiang L, Du B, Wen Y, Wang M, Xi X; Beijing Acute Kidney Injury Trial (BAKIT) workgroup. A comparison of different diagnostic criteria of acute kidney injury in critically ill patients. *Crit Care* 2014; **18**: R144 [PMID: 25005361 DOI: 10.1186/cc13977]

11 **Pan HC**, Chien YS, Jenq CC, Tsai MH, Fan PC, Chang CH, Chang MY, Tian YC, Fang JT, Yang CW, Chen YC. Acute Kidney Injury Classification for Critically Ill Cirrhotic Patients: A Comparison of the KDIGO, AKIN, and RIFLE Classifications. *Sci Rep* 2016; **6**: 23022 [PMID: 26983372 DOI: 10.1038/srep23022]

12 **Rhee C**, Dantes R, Epstein L, Murphy DJ, Seymour CW, Iwashyna TJ, Kadri SS, Angus DC, Danner RL, Fiore AE, Jernigan JA, Martin GS, Septimus E, Warren DK, Karcz A, Chan C, Menchaca JT, Wang R, Gruber S, Klompas M; CDC Prevention Epicenter Program. Incidence and Trends of Sepsis in US Hospitals Using Clinical *vs* Claims Data, 2009-2014. *JAMA* 2017; **318**: 1241-1249 [PMID: 28903154 DOI: 10.1001/jama.2017.13836]

13 **Lin HY**, Lai JI, Lai YC, Lin PC, Chang SC, Tang GJ. Acute renal failure in severe pancreatitis: A population-based study. *Ups J Med Sci* 2011; **116**: 155-159 [PMID: 21250932 DOI: 10.3109/03009734.2010.547636]

14 **Li H**, Qian Z, Liu Z, Liu X, Han X, Kang H. Risk factors and outcome of acute renal failure in patients with severe acute pancreatitis. *J Crit Care* 2010; **25**: 225-229 [PMID: 19781906 DOI: 10.1016/j.jcrc.2009.07.009]

15 **Gao Y**, Kang K, Liu H, Kong W, Han Q, Zhang X, Huang R, Qu J, Wang H, Wang S, Liu R, Liu Y, Yu K. GTS-21 attenuates LPS-induced renal injury *via* the cholinergic anti-inflammatory pathway in mice. *Am J Transl Res* 2017; **9**: 4673-4681 [PMID: 29118926]

16 **Li PK**, Burdmann EA, Mehta RL; World Kidney Day Steering Committee 2013. Acute kidney injury: global health alert. *Kidney Int* 2013; **83**: 372-376 [PMID: 23302721 DOI: 10.1038/ki.2012.427]

17 **Zhou J**, Li Y, Tang Y, Liu F, Yu S, Zhang L, Zeng X, Zhao Y, Fu P. Effect of acute kidney injury on mortality and hospital stay in patient with severe acute pancreatitis. *Nephrology (Carlton)* 2015; **20**: 485-491 [PMID: 25726708 DOI: 10.1111/nep.12439]

18 **Kellum JA**, Lameire N; KDIGO AKI Guideline Work Group. Diagnosis, evaluation, and management of acute kidney injury: a KDIGO summary (Part 1). *Crit Care* 2013; **17**: 204 [PMID: 23394211 DOI: 10.1186/cc11454]

19 **Tenner S**, Baillie J, DeWitt J, Vege SS; American College of Gastroenterology. American College of Gastroenterology guideline: management of acute pancreatitis. *Am J Gastroenterol* 2013; **108**: 1400-15; 1416 [PMID: 23896955 DOI: 10.1038/ajg.2013.218]

20 **Ekinci C**, Karabork M, Siriopol D, Dincer N, Covic A, Kanbay M. Effects of Volume Overload and Current Techniques for the Assessment of Fluid Status in Patients with Renal Disease. *Blood Purif* 2018; **46**: 34-47 [PMID: 29649794 DOI: 10.1159/000487702]

21 **de-Madaria E**, Soler-Sala G, Sánchez-Payá J, Lopez-Font I, Martínez J, Gómez-Escolar L, Sempere L, Sánchez-Fortún C, Pérez-Mateo M. Influence of fluid therapy on the prognosis of acute

pancreatitis: a prospective cohort study. *Am J Gastroenterol* 2011; **106**: 1843-1850 [PMID: 21876561 DOI: 10.1038/ajg.2011.236]

22 **Crockett SD**, Wani S, Gardner TB, Falck-Ytter Y, Barkun AN; American Gastroenterological Association Institute Clinical Guidelines Committee. American Gastroenterological Association Institute Guideline on Initial Management of Acute Pancreatitis. *Gastroenterology* 2018; **154**: 1096-1101 [PMID: 29409760 DOI: 10.1053/j.gastro.2018.01.032]

23 **Bai Y**, Gao J, Zou DW, Li ZS. Prophylactic antibiotics cannot reduce infected pancreatic necrosis and mortality in acute necrotizing pancreatitis: evidence from a meta-analysis of randomized controlled trials. *Am J Gastroenterol* 2008; **103**: 104-110 [PMID: 17925000 DOI: 10.1111/j.1572-0241.2007.01575.x]

24 **Hollemans RA**, Bakker OJ, Boermeester MA, Bollen TL, Bosscha K, Bruno MJ, Buskens E, Dejong CH, van Duijvendijk P, van Eijck CH, Fockens P, van Goor H, van Grevenstein WM, van der Harst E, Heisterkamp J, Hesselink EJ, Hofker S, Houdijk AP, Karsten T, Kruyt PM, van Laarhoven CJ, Laméris JS, van Leeuwen MS, Manusama ER, Molenaar IQ, Nieuwenhuijs VB, van Ramshorst B, Roos D, Rosman C, Schaapherder AF, van der Schelling GP, Timmer R, Verdonk RC, de Wit RJ, Gooszen HG, Besselink MG, van Santvoort HC; Dutch Pancreatitis Study Group. Superiority of Step-up Approach *vs* Open Necrosectomy in Long-term Follow-up of Patients With Necrotizing Pancreatitis. *Gastroenterology* 2019; **156**: 1016-1026 [PMID: 30391468 DOI: 10.1053/j.gastro.2018.10.045]

25 **Rashid MU**, Hussain I, Jehanzeb S, Ullah W, Ali S, Jain AG, Khetpal N, Ahmad S. Pancreatic necrosis: Complications and changing trend of treatment. *World J Gastrointest Surg* 2019; **11**: 198-217 [PMID: 31123558 DOI: 10.4240/wjgs.v11.i4.198]

26 **Jones JD**, Clark CJ, Dyer R, Case LD, Mishra G, Pawa R. Analysis of a Step-Up Approach Versus Primary Open Surgical Necrosectomy in the Management of Necrotizing Pancreatitis: Experience in a Cohort of Patients at a US Academic Medical Center. *Pancreas* 2018; **47**: 1317-1321 [PMID: 30211807 DOI: 10.1097/MPA.0000000000001154]

27 **Koutroumpakis E**, Slivka A, Furlan A, Dasyam AK, Dudekula A, Greer JB, Whitcomb DC, Yadav D, Papachristou GI. Management and outcomes of acute pancreatitis patients over the last decade: A US tertiary-center experience. *Pancreatology* 2017; **17**: 32-40 [PMID: 28341116 DOI: 10.1016/j.pan.2016.10.011]

28 **Zeng X**, McMahon GM, Brunelli SM, Bates DW, Waikar SS. Incidence, outcomes, and comparisons across definitions of AKI in hospitalized individuals. *Clin J Am Soc Nephrol* 2014; **9**: 12-20 [PMID: 24178971 DOI: 10.2215/CJN.02730313]

29 **Lewington AJ**, Cerdá J, Mehta RL. Raising awareness of acute kidney injury: a global perspective of a silent killer. *Kidney Int* 2013; **84**: 457-467 [PMID: 23636171 DOI: 10.1038/ki.2013.153]

30 **Horkan CM**, Purtle SW, Mendu ML, Moromizato T, Gibbons FK, Christopher KB. The association of acute kidney injury in the critically ill and postdischarge outcomes: a cohort study*. *Crit Care Med* 2015; **43**: 354-364 [PMID: 25474534 DOI: 10.1097/CCM.0000000000000706]

31 **Susantitaphong P**, Cruz DN, Cerda J, Abulfaraj M, Alqahtani F, Koulouridis I, Jaber BL; Acute Kidney Injury Advisory Group of the American Society of Nephrology. World incidence of AKI: a meta-analysis. *Clin J Am Soc Nephrol* 2013; **8**: 1482-1493 [PMID: 23744003 DOI: 10.2215/CJN.00710113]

32 **Wajda J**, Dumnicka P, Maraj M, Ceranowicz P, Kuźniewski M, Kuśnierz-Cabala B. Potential Prognostic Markers of Acute Kidney Injury in the Early Phase of Acute Pancreatitis. *Int J Mol Sci* 2019; **20** [PMID: 31366007 DOI: 10.3390/ijms20153714]

33 **Nisula S**, Kaukonen KM, Vaara ST, Korhonen AM, Poukkanen M, Karlsson S, Haapio M, Inkinen O, Parviainen I, Suojaranta-Ylinen R, Laurila JJ, Tenhunen J, Reinikainen M, Ala-Kokko T, Ruokonen E, Kuitunen A, Pettilä V; FINNAKI Study Group. Incidence, risk factors and 90-day mortality of patients with acute kidney injury in Finnish intensive care units: the FINNAKI study. *Intensive Care Med* 2013; **39**: 420-428 [PMID: 23291734 DOI: 10.1007/s00134-012-2796-5]

34 **Nassar TI**, Qunibi WY. AKI Associated with Acute Pancreatitis. *Clin J Am Soc Nephrol* 2019; **14**: 1106-1115 [PMID: 31118209 DOI: 10.2215/CJN.13191118]

35 **Singh TB**, Rathore SS, Choudhury TA, Shukla VK, Singh DK, Prakash J. Hospital-acquired acute kidney injury in medical, surgical, and intensive care unit: A comparative study. *Indian J Nephrol* 2013; **23**: 24-29 [PMID: 23580801 DOI: 10.4103/0971-4065.107192]

36 **Yang L**, Xing G, Wang L, Wu Y, Li S, Xu G, He Q, Chen J, Chen M, Liu X, Zhu Z, Yang L, Lian X, Ding F, Li Y, Wang H, Wang J, Wang R, Mei C, Xu J, Li R, Cao J, Zhang L, Wang Y, Bao B, Liu B, Chen H, Zha Y, Luo Q, Chen D, Shen Y, Liao Y, Zhang Z, Wang X, Zhang K, Liu L, Mao P, Guo C, Li J, Wang Z, Bai S, Shi S, Liu Z, Wang F, Huang D, Wang S, Ge S, Shen Q, Zhang P, Wu L, Pan M, Zou X, Zhu P, Zhao J, Zhou M, Hu W, Zhang T, Han J, Wen T, Zhao M; ISN AKF 0by25 China Consortiums. Acute kidney injury in China: a cross-sectional survey. *Lancet* 2015; **386**: 1465-1471 [PMID: 26466051 DOI: 10.1016/S0140-6736(15)00344-X]

37 **Hoste EA**, Bagshaw SM, Bellomo R, Cely CM, Colman R, Cruz DN, Edipidis K, Forni LG, Gomersall CD, Govil D, Honoré PM, Joannes-Boyau O, Joannidis M, Korhonen AM, Lavrentieva A, Mehta RL, Palevsky P, Roessler E, Ronco C, Uchino S, Vazquez JA, Vidal Andrade E, Webb S, Kellum JA. Epidemiology of acute kidney injury in critically ill patients: the multinational AKI-EPI study. *Intensive Care Med* 2015; **41**: 1411-1423 [PMID: 26162677 DOI: 10.1007/s00134-015-3934-7]

38 **Clark WR**, Ding X, Qiu H, Ni Z, Chang P, Fu P, Xu J, Wang M, Yang L, Wang J, Ronco C. Renal

replacement therapy practices for patients with acute kidney injury in China. *PLoS One* 2017; **12**: e0178509 [PMID: 28692694 DOI: 10.1371/journal.pone.0178509]

39 **Wang F**, Hong D, Wang Y, Feng Y, Wang L, Yang L; ISN AKF 0 by 25 China Consortium. Renal replacement therapy in acute kidney injury from a Chinese cross-sectional study: patient, clinical, socioeconomic and health service predictors of treatment. *BMC Nephrol* 2017; **18**: 152 [PMID: 28472927 DOI: 10.1186/s12882-017-0567-9]

40 **Schneider AG**, Bellomo R, Bagshaw SM, Glassford NJ, Lo S, Jun M, Cass A, Gallagher M. Choice of renal replacement therapy modality and dialysis dependence after acute kidney injury: a systematic review and meta-analysis. *Intensive Care Med* 2013; **39**: 987-997 [PMID: 23443311 DOI: 10.1007/s00134-013-2864-5]

41 **Heung M**, Yessayan L. Renal Replacement Therapy in Acute Kidney Injury: Controversies and Consensus. *Crit Care Clin* 2017; **33**: 365-378 [PMID: 28284300 DOI: 10.1016/j.ccc.2016.12.003]

42 **Gao Y**, Qi ZD, Liu RJ, Liu HT, Han QY, Zhang X, Huang R, Li M, Yang ZY, Zheng JB, Qu JD, Wang SC, Liu YS, Wang HL, Yu KJ. A multi-center cross-sectional study on blood purification among adult patients in intensive care unit in China: a study protocol. *Chin Med J (Engl)* 2019; **132**: 1208-1211 [PMID: 30882465 DOI: 10.1097/CM9.0000000000000180]

43 **Zhang X**, Cao Y, Pan CK, Han QY, Guo YQ, Song T, Qi ZD, Huang R, Li M, Yang ZY, Zheng JB, Hou GY, Li JY, Wang SC, Liu YS, Liu RJ, Gao Y, Wang HL. Effect of initiation of renal replacement therapy on mortality in acute pancreatitis patients. *Medicine (Baltimore)* 2020; **99**: e23413 [PMID: 33217887 DOI: 10.1097/MD.0000000000023413]

44 **Mikó A**, Vigh É, Mátrai P, Soós A, Garami A, Balaskó M, Czakó L, Mosdósi B, Sarlós P, Erőss B, Tenk J, Rostás I, Hegyi P. Computed Tomography Severity Index vs. Other Indices in the Prediction of Severity and Mortality in Acute Pancreatitis: A Predictive Accuracy Meta-analysis. *Front Physiol* 2019; **10**: 1002 [PMID: 31507427 DOI: 10.3389/fphys.2019.01002]

45 **Handschu R**, Haslbeck M, Hartmann A, Fellgiebel A, Kolominsky-Rabas P, Schneider D, Berrouschot J, Erbguth F, Reulbach U. Mortality prediction in critical care for acute stroke: Severity of illness-score or coma-scale? *J Neurol* 2005; **252**: 1249-1254 [PMID: 15917980 DOI: 10.1007/s00415-005-0853-5]

46 **Huang KB**, Ji Z, Wu YM, Wang SN, Lin ZZ, Pan SY. The prediction of 30-day mortality in patients with primary pontine hemorrhage: a scoring system comparison. *Eur J Neurol* 2012; **19**: 1245-1250 [PMID: 22524995 DOI: 10.1111/j.1468-1331.2012.03724.x]

47 **Fischer AJ**, Andreottola F, Lenz P, Lebiedz P. [Acute pancreatitis in intensive care medicine: Which risk score is useful? *Med Klin Intensivmed Notfmed* 2017; **112**: 717-723 [PMID: 28144728 DOI: 10.1007/s00063-017-0260-6]

48 **Jain S**, Sinha S, Sharma SK, Samantaray JC, Aggrawal P, Vikram NK, Biswas A, Sood S, Goel M, Das M, Vishnubhatla S, Khan N. Procalcitonin as a prognostic marker for sepsis: a prospective observational study. *BMC Res Notes* 2014; **7**: 458 [PMID: 25034373 DOI: 10.1186/1756-0500-7-458]

49 **Kefeli A**, Basyigit S, Özgür Yeniova A, Küçükazman M, Nazligül Y, Aktas B. Platelet Number and Indexes during Acute Pancreatitis. *Euroasian J Hepatogastroenterol* 2014; **4**: 67-69 [PMID: 29699350 DOI: 10.5005/ip-journals-10018-1104]

World Journal of Gastroenterology

Submit a Manuscript: https://www.f6publishing.com

World J Gastroenterol 2021 October 14; 27(38): 6465-6475

DOI: 10.3748/wjg.v27.i38.6465

ISSN 1007-9327 (print) ISSN 2219-2840 (online)

ORIGINAL ARTICLE

Retrospective Study

Magnetic resonance imaging-radiomics evaluation of response to chemotherapy for synchronous liver metastasis of colorectal cancer

Yan-Qing Ma, Yang Wen, Hong Liang, Jian-Guo Zhong, Pei-Pei Pang

ORCID number: Yan-Qing Ma 0000-0002-6131-3284; Yang Wen 0000-0003-3961-4328; Hong Liang 0000-0003-1598-2409; Jian-Guo Zhong 0000-0001-6344-2883; Pei-Pei Pang 0000-0001-9318-6315.

Author contributions: Ma YQ designed the retrospective study and wrote the original article; Wen Y directed and coordinated the study; Zhong JG and Liang H performed a part of the study; Pang PP analyzed the data; All authors have read and approve the final manuscript.

Supported by The fund of Medical and Health Research Projects of Health Commission of Zhejiang Province, No. 2019KY035.

Institutional review board statement: The study was reviewed and approved by the Institutional Review Board of Zhejiang Provincial People's Hospital, No. 2020QT251.

Informed consent statement: For the characteristics of retrospective study, formal written consent is not applicable.

Conflict-of-interest statement: The author declare that they have no conflict of interest.

Data sharing statement: Technical

Yan-Qing Ma, Yang Wen, Jian-Guo Zhong, Department of Radiology, Zhejiang Provincial People's Hospital, Affiliated People's Hospital of Hangzhou Medical College, Hangzhou 310000, Zhejiang Province, China

Hong Liang, Department of Radiology, Hangzhou Medical College, Hangzhou 310000, Zhejiang Province, China

Pei-Pei Pang, Department of Pharmaceuticals Diagnosis, GE Healthcare, Hangzhou 310000, Zhejiang Province, China

Corresponding author: Yang Wen, MD, Chief Doctor, Department of Radiology, Zhejiang Provincial People's Hospital, Affiliated People's Hospital of Hangzhou Medical College, No. 158 Shangtang Road, Hangzhou 310000, Zhejiang Province, China. 13989454104@163.com

Abstract

BACKGROUND

Synchronous liver metastasis (SLM) is an indicator of poor prognosis for colorectal cancer (CRC). Nearly 50% of CRC patients develop hepatic metastasis, with 15%-25% of them presenting with SLM. The evaluation of SLM in CRC is crucial for precise and personalized treatment. It is beneficial to detect its response to chemotherapy and choose an optimal treatment method.

AIM

To construct prediction models based on magnetic resonance imaging (MRI)-radiomics and clinical parameters to evaluate the chemotherapy response in SLM of CRC.

METHODS

A total of 102 CRC patients with 223 SLM lesions were identified and divided into disease response (DR) and disease non-response (non-DR) to chemotherapy. After standardizing the MRI images, the volume of interest was delineated and radiomics features were calculated. The MRI-radiomics logistic model was constructed after methods of variance/Mann-Whitney *U* test, correlation analysis, and least absolute shrinkage and selection operator in feature selecting. The radiomics score was calculated. The receiver operating characteristics curves by the DeLong test were analyzed with MedCalc software to compare the validity of all models. Additionally, the area under curves (AUCs) of DWI, T2WI, and portal phase of contrast-enhanced sequences radiomics model (Ra-DWI, Ra-T2WI, and

appendix, statistical code, and dataset available from the corresponding author at email address. Participants informed consent was not obtained but the presented data are anonymized and risk of identification is low.

Open-Access: This article is an open-access article that was selected by an in-house editor and fully peer-reviewed by external reviewers. It is distributed in accordance with the Creative Commons Attribution NonCommercial (CC BY-NC 4.0) license, which permits others to distribute, remix, adapt, build upon this work non-commercially, and license their derivative works on different terms, provided the original work is properly cited and the use is non-commercial. See: http://creativecommons.org/Licenses/by-nc/4.0/

Manuscript source: Unsolicited manuscript

Specialty type: Gastroenterology and hepatology

Country/Territory of origin: China

Peer-review report's scientific quality classification

Grade A (Excellent): 0
Grade B (Very good): B
Grade C (Good): 0
Grade D (Fair): 0
Grade E (Poor): 0

Received: April 25, 2021
Peer-review started: April 25, 2021
First decision: June 3, 2021
Revised: June 5, 2021
Accepted: August 27, 2021
Article in press: August 27, 2021
Published online: October 14, 2021

P-Reviewer: Soucisse ML
S-Editor: Wu YXJ
L-Editor: Filipodia
P-Editor: Yuan YY

Ra-portal phase of contrast-enhanced sequences) were calculated. The radiomics-clinical nomogram was generated by combining radiomics features and clinical characteristics of CA19-9 and clinical N staging.

RESULTS

The AUCs of the MRI-radiomics model were 0.733 and 0.753 for the training (156 lesions with 68 non-DR and 88 DR) and the validation (67 lesions with 29 non-DR and 38 DR) set, respectively. Additionally, the AUCs of the training and the validation set of Ra-DWI were higher than those of Ra-T2WI and Ra-portal phase of contrast-enhanced sequences (training set: 0.652 *vs* 0.628 and 0.633, validation set: 0.661 *vs* 0.575 and 0.543). After chemotherapy, the top four of twelve delta-radiomics features of Ra-DWI in the DR group belonged to gray-level run-length matrices radiomics parameters. The radiomics-clinical nomogram containing radiomics score, CA19-9, and clinical N staging was built. This radiomics-clinical nomogram can effectively discriminate the patients with DR from non-DR with a higher AUC of 0.809 (95% confidence interval: 0.751-0.858).

CONCLUSION

MRI-radiomics is conducive to predict chemotherapeutic response in SLM patients of CRC. The radiomics-clinical nomogram, involving radiomics score, CA19-9, and clinical N staging is more effective in predicting chemotherapeutic response.

Key Words: Radiomics; Synchronous liver metastasis; Colorectal cancer; Chemotherapy; Magnetic resonance; Nomogram

©The Author(s) 2021. Published by Baishideng Publishing Group Inc. All rights reserved.

Core Tip: Synchronous liver metastasis (SLM) indicates poor prognosis for colorectal cancer. Nearly 50% of colorectal cancer patients develop hepatic metastasis, with 15%-25% of them presenting with SLM. It is beneficial to detect the response of SLM to chemotherapy. Magnetic resonance imaging-radiomics could provide a non-invasive approach to predict the risk of SLM. The logistic model of DWI sequence behaved the best in evaluating the chemotherapeutic response in SLM compared with T2WI, DWI, and portal phase of contrast-enhanced sequences. Moreover, the radiomics-clinical nomogram containing radiomics score, CA19-9, and clinical N staging is more effective in predicting the chemotherapeutic response of SLM patients.

Citation: Ma YQ, Wen Y, Liang H, Zhong JG, Pang PP. Magnetic resonance imaging-radiomics evaluation of response to chemotherapy for synchronous liver metastasis of colorectal cancer. *World J Gastroenterol* 2021; 27(38): 6465-6475
URL: https://www.wjgnet.com/1007-9327/full/v27/i38/6465.htm
DOI: https://dx.doi.org/10.3748/wjg.v27.i38.6465

INTRODUCTION

Colorectal cancer (CRC) is the fourth most common malignancy worldwide[1], accounting for approximately one-third of cancer related deaths in western countries [2]. Nearly 50% of CRC patients developed hepatic metastasis throughout the course of disease, and 15%-25% of them were associated synchronous liver metastasis (SLM) [3]. SLM is confirmed as an indicator of poor prognosis for CRC, which was defined as a lesion identified within 90 d after the diagnosis of the primary tumor[4]. Currently, the standard guideline for the treatment of CRC patients with SLM remains undetermined. Conventional treatment for this condition is colectomy, followed by chemotherapy and liver resection[5]. Preoperative chemotherapy has superiority on early treatment of metastatic disease, which may help to achieve a negative resection margin[6] and reduce the risk of local recurrence[1]. However, liver injuries can be induced by chemotherapy, such as vascular changes and chemotherapy-associated steatohepatitis[7]. Previous studies have reported that administration of more than 12

cycles of preoperative chemotherapy increased the risk of re-operation and prolonged hospital stay[8]. Excessive cycles of preoperative chemotherapy may result in increased damage to the liver and lost potential opportunity to receive surgery[7] since progression of chemotherapy is irreversible. Therefore, precise and non-invasive assessment of the response of SLM patients to preoperative chemotherapy is a critical step in individualized treatment. In addition, SLM patients who were predicted as non-responders could benefit from alternative therapies to avoid dispensable chemotherapy.

Radiomics is a promising and non-invasive method to analyze conventional imaging features and incorporate them into predictive models to evaluate tumor behaviors[9]. Previous work has concluded that the nomogram combining radiomics and clinical factors exhibited favorable ability and accuracy in evaluating metastatic pulmonary nodules in CRC patients[10]. Analysis of liver texture is potentially a supplement to routine computed tomography examination and may provide prognostic markers for CRC patients[11]. A radiomics signature was validated to be a complementary predictor for preoperative staging of CRC patients[12]. It has been suggested that magnetic resonance imaging (MRI)-radiomics of CRC patients could provide a non-invasive approach to predict the risk of SLM[13].

To the best of our knowledge, little attention has been paid to predict the response of chemotherapy in SLM patients. This retrospective study examined the emerging role of MRI-radiomics signature in order to detect the prediction efficiency of models in chemotherapeutic response of SLM patients and avoid ineffective chemotherapy.

MATERIALS AND METHODS

Patient selection

This retrospective study was approved by the institutional review board of our hospital. For the characteristics of retrospective study, formal written consent is not applicable. Research methods were carried out in accordance with the Declaration of Helsinki.

A total of 102 CRC patients with 223 SLM lesions were identified from 2017 to 2020 in our hospital. SLM was a histopathologically confirmed intrahepatic lesion within 90 d of the diagnosis of CRC[4]. Inclusion criteria included: (1) Patients were histopathologically diagnosed as classical adenocarcinoma in CRC, excluding mucinous and signet ring adenocarcinoma[14]; (2) Patients have at least one SLM lesion; (3) For patients with multiple SLM lesions, the top three largest ones were selected to analyze; (4) Patients underwent baseline and 3 mo follow-up MRI examination after the start of chemotherapy; and (5) Patients underwent mFOLFOX7 chemotherapy regimen. Exclusion criteria included: (1) Patients underwent anti-tumor treatments such as chemotherapy, radiotherapy, or transarterial chemoembolization before baseline MRI examinations; (2) Patients were diagnosed with CRC with biopsy but not with surgery; (3) History of other malignancies; and (4) Patients were diagnosed as mucinous or signet ring adenocarcinoma. The general characteristics involved gender, age, tumor markers, and clinical T/N staging were recorded. The tumor markers encompassed alpha-fetoprotein (normal range: 0.0-20.0 μg/L), carcinoembryonic antigen (normal range: 0.0-5.0 μg/L), and CA19-9 (normal range: 0.0-37.0 U/mL) that all were divided into normal and abnormal subgroups.

The response to chemotherapy was assessed after 3 mo from the start of chemotherapy by MRI examinations. The response of lesions was categorized into four subgroups according to the Response Evaluation Criteria in Solid Tumors (version 1.1) criterion[15]: (1) Complete response refers that all target lesions disappeared; (2) Partial response is defined as lesions having at least a 30% decrease in the sum diameters of lesions; (3) Progressive disease is defined as lesions having at least a 20% increase in the sum diameters of lesions; and (4) Stable disease is defined as tumors with neither sufficient shrinkage nor sufficient increase in the lesions. None of the patients in this study belonged to complete response. Patients with partial response were classified as disease response (DR) group (Figure 1), while patients with progressive or stable disease were merged into disease non-response (non-DR) group.

MRI examination and image processing

All examinations were performed using 3.0-T MRI (Discovery 750, GE Healthcare, Waukesha, WI, United States). The axial T2WI, DWI, and portal phase of contrast-enhanced sequences (CE_{PP}) were taken. CE-MRI was performed with gadobenate dimeglumine being injected *via* a dual head pressure injector at a rate of 2 mL/s and

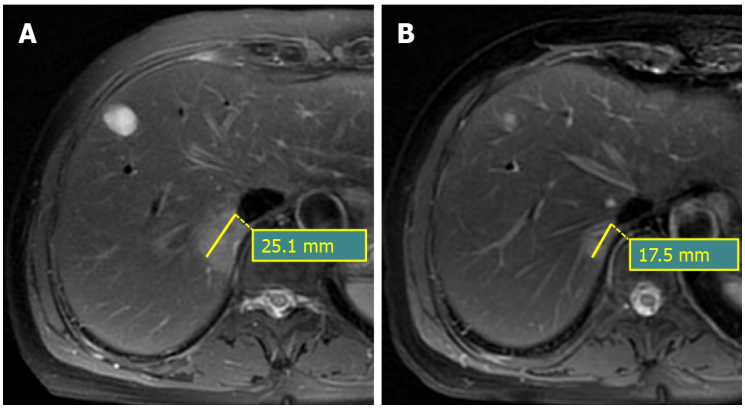


Figure 1 Magnetic resonance imaging examinations. A: A 48-year-old female had a synchronous liver metastasis with baseline long diameter of 25.1 mm; B: After chemotherapy, the lesion a had 30.3% decrease in long diameter of 17.5 mm, which belonged to the disease response group for analysis.

followed by 20 mL saline flush at the same rate. Post-contrast image acquisition was done in the axial plane in arterial phase (AP), PP, and equilibrium phases (EP). The imaging parameters were as follows: T2WI (TR 10000-12000 ms, TE 85 ms; FOV 36 cm × 40 cm, matix 320 × 320, thickness 5.0 mm, interval 1.0 mm), CE (TR 3.7 ms, TE 2.2 ms; FA 12°, matix 260 × 260, thickness 5.0 mm, interval 1.0 mm, 0.2 mL/Kg), and DWI (TR 3500 ms, TE 75 ms; FOV 32 cm × 32 cm, matix 128 × 128, thickness 3.0 mm, interval 0.6 mm, *b* value 0 and 800 s/mm^2).

The process of image standardization included resampling images into a 1.0 mm × 1.0 mm × 1.0 mm voxel size of X/Y/Z-spacing, denoising images by Gaussian, and normalizing the gray level of images to a scale from 1 to 32, which is automatically performed with the software of AK (Artificial Intelligence Kit, version 3.0.0, GE Healthcare).

Then, the three-dimensional volume of interest (VOI) was manually delineated in all the images by software of "ITK-SNAP" (version 3.4.0, http://www.itksnap.org/) by two radiologists with 9 and 12 years of experience in MRI diagnosis, respectively. Finally, the radiomics features of two radiologists were automatically calculated in AK software.

MRI-radiomics signature construction

A total of 396 radiomics features were automatically calculated by AK software, including 42 histogram parameters, 54 texture parameters, 9 form factor parameters, 100 gray-level co-occurrence matrices parameters, 180 gray-level run-length matrices parameters (RLM), and 11 gray-level size zone matrices parameters. The specific description of radiomics features is presented in the Supplemental Material. These radiomics features have underlying relationships with pathophysiological characteristics[16], intracellular heterogeneity[17], as well as genotypes[18], and so on.

Five steps were carried out to select radiomics features. First, the intra-class correlation coefficient (ICC) for all features by two radiologists was analyzed. Features with ICC greater than 0.80 were selected[19], and the mean values of radiomics features from two radiologists were calculated as robust features for further analysis. Second, we normalized the selected radiomics features by replacing the abnormal values with mean and converting the features into non-dimensional values *via* subtracting by mean and dividing by standard deviation value to eliminate discrepancies. Third, we randomly grouped the cohort into a training set and a validation set with a proportion of 7:3 (156 lesions in the training set with 68 non-DR and 88 DR lesions, 67 lesions in the validation set with 29 non-DR and 38 DR lesions). Fourth, we applied analysis of variance/Mann-Whitney *U* test, correlation analysis, and least absolute shrinkage and selection operator to select optimal features. The specific explanation of the methods to select radiomics features is summarized in the Supplemental Material. Last, the MRI-radiomics logistic model to differentiate DR and non-DR patients was constructed in the training set and verified by the validation set. The workflow of the radiomics signature in differentiating DR and non-DR patients was illustrated in Figure 2.

The calibration curves were depicted to compare the consistency between predicted and actual ability to evaluate response to chemotherapy, accompanied by Hosmer-Lemeshow test. The receiver operating characteristic curve was constructed by DeLong test, and the area under curve (AUC) was calculated to evaluate the validity of

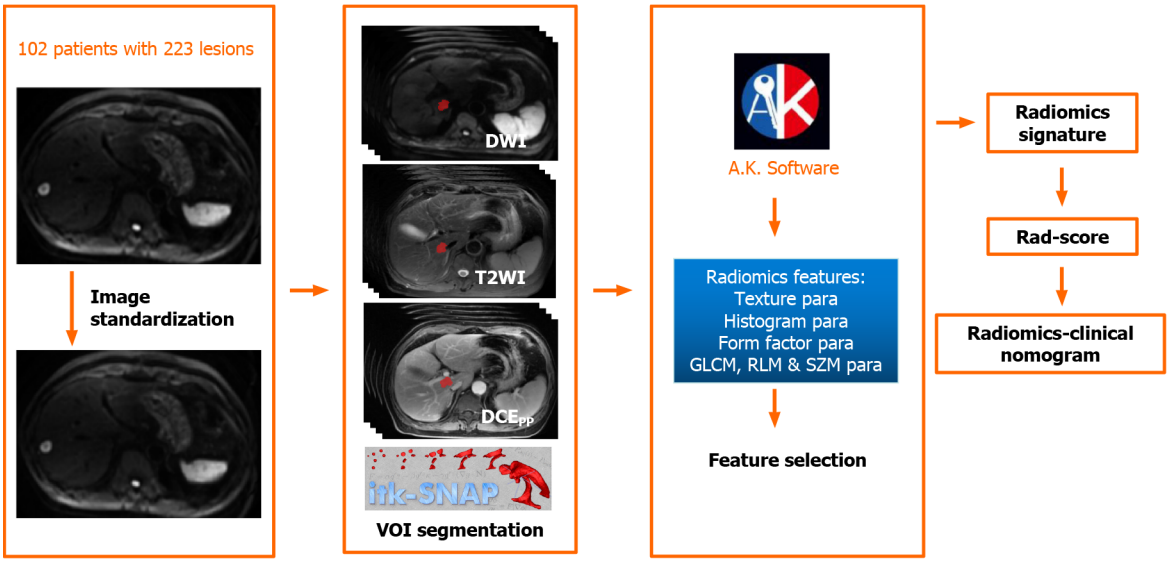


Figure 2 The workflow of radiomics signature in differentiating the responses of synchronous liver metastasis patients to chemotherapy.
VOI: Volume of interest; GLCM: Gray-level co-occurrence matrices; RLM: Run-length matrices; SZM: Size zone matrices; Rad-score: Radiomics score.

MRI-radiomics logistic models.

Statistical analysis

Analysis of variance/Mann-Whitney *U* test /MW, correlation analysis, least absolute shrinkage and selection operator, the logistic model construction, the calibration curve establishment, and radiomics-clinical nomogram development were performed with R software V4.0.1 to select features that potentially predict chemotherapeutic response. The calibration curves were depicted with Hosmer-Lemeshow test to compare the consistency between predicted and actual ability of evaluating response of chemotherapy. The receiver operating characteristic curves were constructed to calculate the AUC with a 95% confidence interval (CI), and the DeLong test was made to evaluate the validity of models in MedCalc V18.2.1. The general information, such as gender, age, tumor index, and T/N stage, was analyzed with IBM SPSS V22.0, using χ^2 or independent samples *t*-test. A two-tailed $P < 0.05$ was considered statistically significant.

RESULTS

Patients' general information

General information of patients were listed in Table 1. A total of 102 patients with 223 lesions were enrolled. There were 53 patients with 97 lesions in the non-DR group and 49 patients with 126 lesions in the DR group. The mean age of non-DR was 63.2 ± 9.5-years-old, and that of DR was 59.9 ± 11.6-years-old. In general, baseline demographics and tumor characteristics were balanced in the DR and non-DR groups, with exceptions of CA19-9 ($P = 0.045$) and clinical N staging ($P = 0.030$). Higher ratios of patients with normal CA19-9 levels were enrolled in the non-DR group (non-DR was 56.6% *vs* DR was 36.7%). In regard to clinical N staging, patients in the non-DR group primarily were staged to be N1 (52.8%), while stage N2 (73.5%) ranked the top in the DR group.

MRI-radiomics logistic model construction

Among the total 1188 radiomics features from T2WI, DWI, and CE_{PP} sequences of MRI examination, 893 features with ICC greater than 0.80 between two radiologists remained for the following analysis. After decreasing redundant features with the methods of analysis of variance/Mann-Whitney *U* test, correlation analysis, and least absolute shrinkage and selection operator, 12 features were selected to construct the MRI-radiomics logistic model for predicting responses of chemotherapy (Figure 3) and the radiomics score (rad-score) was calculated accordingly. The 12 optimal features included four DWI features , six T2WI features , and two CE_{PP} features. The AUC of

Table 1 Baseline patient characteristics

General characteristics	non-DR, *n* = 53	DR, *n* = 49	*P* value
Demographics			
Gender (female/male)	28/25	17/32	0.065
Age (mean ± SD)	63.3 ± 11.1/63.2 ± 7.5	58.6 ± 11.2/59.7 ± 14.1	0.117
Tumor markers			
AFP (normal/abnormal)	51/2	47/2	0.936
CEA (normal/abnormal)	14/39	14/35	0.807
CA19-9 (normal/abnormal)	30/23	18/31	0.045
Clinical T/N staging			
T1/T2/T3/T4	0/1/48/4	0/10/33/6	0.136
N0/N1/N2	3/28/22	5/8/36	0.030

The characteristics of age and clinical T/N staging were analyzed by independent-samples *t*-test. The data of gender and tumor markers of AFP/CEA/CA19-9 were analyzed by Pearson χ^2. A $P < 0.05$ was viewed as statistically significant. Non-DR: Disease non-response group; DR: Disease response group; SD: Standard deviation; AFP: Alpha-fetoprotein; CEA: Carcinoembryonic antigen.

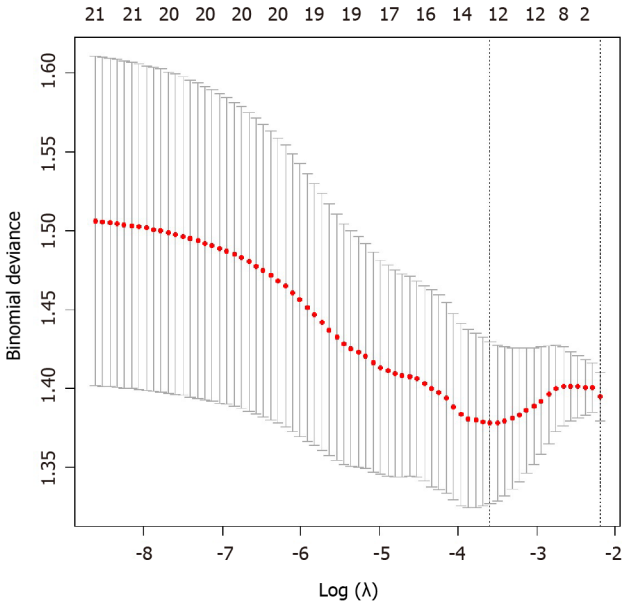


Figure 3 The feature selection method of least absolute shrinkage and selection operator. A total of 12 optimal features were selected.

this model was 0.733 (95%CI, 0.656-0.800) in the training set and was 0.753 (95%CI, 0.633-0.849) in the validation set. The calibration curves showed good consistency in the predicted and the actual ability to evaluate chemotherapy responses in both training and validation sets. The non-significant Hosmer-Lemeshow test suggested goodness-of-fit for the MRI-radiomics logistic models in the training ($P = 0.858$) and validation ($P = 0.374$) set.

Furthermore, we also compared prediction efficiency in chemotherapeutic response between different radiomics models of single DWI, T2WI, or CE_{PP} sequence (Ra-DWI, Ra-T2WI, Ra-CE_{PP}). The AUCs of these models were listed in Table 2. The AUCs of the training set and validation set of Ra-DWI were 0.652 (95%CI, 0.571-0.726) and 0.661 (95%CI, 0.536-0.772), which were higher than those of Ra-T2WI and Ra-CE_{PP} (Table 2). Then we compared the radiomics features of DWI between the baseline and after chemotherapy in the DR group. There were 105 lesions enrolled, as the post-chemotherapy images of another 21 lesions were not satisfactory. By features selection, 11 significant delta-radiomics features were left. The remaining features included histogram (Quantile 0.025), texture (ClusterShade_angle90_offset1), gray-level co-occurrence matrices Entropy (GLCMEntropy_angle135_offset7/_angle90_offset1, and

Table 2 The area under the curve of radiomics model of DWI sequence, radiomics model of T2WI sequence, and radiomics model of portal phase of contrast-enhanced sequences models in the training set and the validation set

Sequence	Training set	*P* value	Validation set	*P* value
Ra-DWI	0.652 (95%CI, 0.571-0.726)	0.001	0.661 (95%CI, 0.536-0.772)	0.018
Ra-T2WI	0.628 (95%CI, 0.547-0.704)	0.005	0.575 (95%CI, 0.450-0.695)	0.291
Ra-CE_{PP}	0.633 (95%CI, 0.552-0.709)	0.003	0.543 (95%CI, 0.418-0.664)	0.544

A $P < 0.05$ of the DeLong test was considered statistically significant. The DeLong test of validation set in radiomics model of T2WI sequence and radiomics model of portal phase of contrast-enhanced sequences had no statistical significance. Ra-DWI: Radiomics model of DWI sequence; Ra-T2WI: Radiomics model of T2WI sequence; Ra-CE_{PP}: Radiomics model of portal phase of contrast-enhanced sequences; CI: Confidence interval.

differenceEntropy), RLM (LongRunHighGreyLevelEmphasis_AllDirection_offset1_SD/_angle45_offset7, ShortRun Emphasis_angle45/90_offset1/HighGreyLevelEmphasis_angle90_offset7), and size zone variability. The top 4 of the 11 delta-radiomics features belonged to RLM parameters.

Radiomics-clinical nomogram analysis

For clinical characteristics, tumor marker CA19-9 ($P = 0.045$) and clinical N staging ($P = 0.030$) were demonstrated to be statistically different between DR and non-DR groups. Thus, CA19-9 and clinical N staging, together with rad-score were integrated into the logistic model to construct the radiomics-clinical nomogram (Figure 4). The formula of the logistic model was: Y = -2.141 + 1.018 × [rad-score] + 0.893 × [CA19-9] + 1.042 × [N staging]. The AUC of the radiomics-clinical nomogram was 0.809 (95%CI, 0.751-0.858).

DISCUSSION

The standardized treatment for SLM patients is unascertained, and early detection of patients with DR or non-DR is crucial for personalized treatment planning. In order to predict patients' responses to chemotherapy, we generated a MRI-radiomics based model in this study. The AUC of this model was 0.733 in the training set and was 0.753 in the validation set. Non-significant Hosmer-Lemeshow test and the calibration curve of the MRI-radiomics model showed good consistency between the predicted and actual probability. Although the AUC value was not ideal enough, the non-invasive MRI examination is still beneficial to differentiate non-DR and DR in clinical practice. There were 156 lesions with 68 non-DR and 88 DR lesions in the training set and 12 radiomics features to construct MR-radiomics logistic model. The sample size of the logistic model often relies on an events per predictor variable[20]. Vittinghoff *et al*[21] conducted a large simulation study of other influences on relative bias, confidence interval coverage, and type I error and found that the events per predictor variable between 5 to 9 could achieve acceptable results. In our study, the events per predictor variable were 5.7 in non-DR group and were 7.3 in the DR group, which were both in the range of 5 to 9. Therefore we believed that the MRI-radiomics model based on 156 lesions in the training set was valid.

As for the selection of MRI sequences, a recent investigation in reproducibility and robustness of MRI radiomics has suggested that caution should be taken in the interpretation of clinical studies using T1WI features to delineate VOI[22]. Meanwhile, after making some attempt in the exploration stage, we realized that it was difficult and inaccurate to depict VOI in AP and EP of CE sequence. Thus, we selected DWI, T2WI, and PP of CE sequences to do future research. Features with ICC more than 0.80 identified by two radiologists were selected, and the mean values of selected features were calculated as robust features for further analysis. After comparing the predictive efficiency between Ra-DWI, Ra-T2WI, and Ra-CE_{PP}, Ra-DWI demonstrated outstanding predictive value compared with Ra-T2WI and Ra-CE_{PP} (AUCs in the training set: 0.652 *vs* 0.628, 0.633; AUCs in the validation set: 0.661 *vs* 0.575, 0.543). We should think highly of DWI due to its potential for evaluating DR and non-DR in clinical practice. As has been investigated that delta-radiomics analysis explored the change of radiomics features between baseline and follow-up computed tomography images can improve the differentiation of pre-invasive ground glass nodules from invasive ground glass nodules[23].

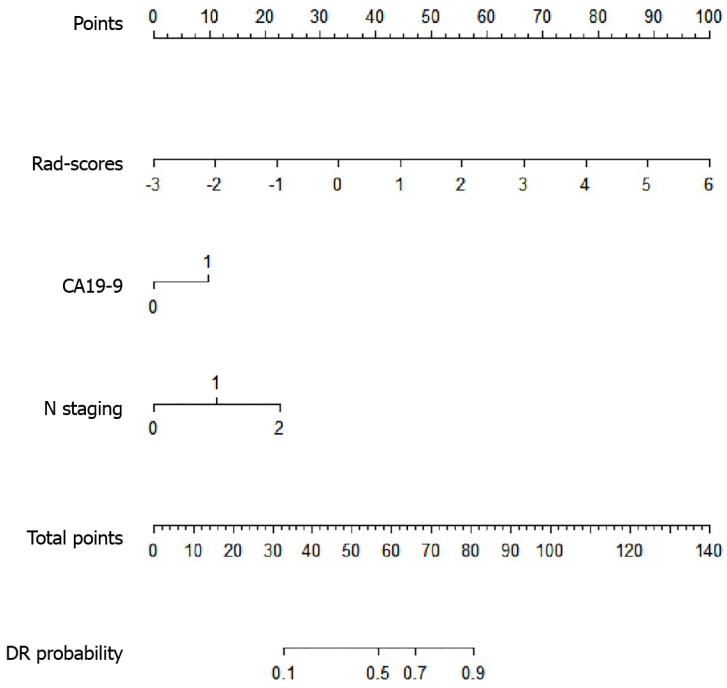


Figure 4 The nomogram of radiomics-clinical analysis to differentiate patients with disease non-response group from disease response group. The zero in CA19-9 represented normal and one referred to abnormal. DR: Disease response group; Rad-score: Radiomics score.

After comparing the delta-radiomics of DR between baseline and post-chemotherapy MRI examination, we obtained the top 4 of 11 delta-radiomics features of post-chemotherapy belonging to RLM parameters. Kim *et al*[24] analyzed the association between pathological characteristics and gray-level run-length matrices features of pancreatic cancer and revealed that gray-level non-uniformity values of RLM were powerful indicators for prognosis. RLM is more sensitive to reflect changes of regional heterogeneity since it analyzes radiomics changes through the whole length of the run [25]. These results suggested that DWI helped to discriminate patients with DR from non-DR in clinical practice.

The nomogram of incorporated independent risk factors for clinical events, such as differentiation[26], survival[27], and recurrence[28], has been widely applied in the field of oncology. The radiomics-clinical nomogram contained rad-score, CA19-9, and clinical N staging demonstrated better predictive accuracy compared with MRI-radiomics signature (AUC: 0.809 *vs* 0.733 in the training set, and 0.753 in the validation set). In patients with SLM, elevation of CA19-9 and carcinoembryonic antigen is a prognostic indicator and can predict response to treatment[29]. A previous study identified that CA19-9 was the best prognostic indicator of metastatic CRC[30] and also was a significant prognostic indicator for CRC patients treated with neoadjuvant chemoradiotherapy[29]. Similar to a previous study[31], we demonstrated that more patients (63.3%) with DR had elevated levels of CA19-9 than those with non-DR (43.4%), suggesting that CA19-9 was a promising indicator for predicting response to chemotherapy ($P < 0.05$). A study by Märkl *et al*[32] illustrated that lymph node staging played a significant role in prognosis evaluation and treatment stratification for CRC. In the current study, we confirmed that clinical N staging had a correlation to chemotherapeutic response. Taken together, the proposed radiomics-clinical nomogram is beneficial in estimating the chemotherapeutic response and in selecting appropriate patients to receive chemotherapy.

Our study had several limitations. First, we only took PP of CE for analysis since the lesions in AP and EP of CE sequence were not visible enough for VOI segmentation. An automatic segmentation method to deal with the AP/EP images remains to be developed. Second, this is a single center study, and the prediction models should be further verified in other centers and in a larger cohort. Third, the inevitable flaw may occur in this retrospective study since the histopathological grade and clinical characteristics of selected patients may be unbalanced. Fourth, as for the criteria for evaluating the response of chemotherapy, we chose the Response Evaluation Criteria in Solid Tumors criterion instead of considering histopathological evidence, which may be complementary to the results of the radiomics. Therefore, our results should be further validated in future multiangle and multiclassification sample studies.

CONCLUSION

In conclusion, our study indicated that the MRI-radiomics logistic model was a helpful and non-invasive predictor for differentiating patients with non-DR from DR. Ra-DWI was more efficient in distinguishing patients with non-DR from DR than that of Ra-T2WI and Ra-CE_{PP}, and the RLM parameter of Ra-DWI was superior in reflecting the delta-radiomics after chemotherapy. Furthermore, the radiomics-clinical nomogram based on the MRI-radiomics signature and clinical factors of CA19-9 and clinical N staging is conducive to better predict non-DR and DR of SLM patients and provides a theoretical and practical basis for the choice of treatment strategies.

ARTICLE HIGHLIGHTS

Research background

Synchronous liver metastasis (SLM) frequently occurs in colorectal cancer (CRC). Nearly 50% of CRC patients develop hepatic metastasis, with 15%-25% of them presenting with SLM. The evaluation of SLM in CRC is crucial for a precise and personalized treatment.

Research motivation

To construct prediction models based on magnetic resonance imaging (MRI)-radiomics and clinical parameters to evaluate the chemotherapy response in SLM patients in the context of CRC.

Research objectives

A total of 102 patients with 223 SLM lesions were identified and divided into disease response (DR) and disease non-response (non-DR) to chemotherapy.

Research methods

The MRI-radiomics logistic models containing T2WI, DWI, and portal phase of dynamic contrast-enhanced sequences radiomics models (Ra-T2WI, Ra-DWI and Ra-portal phase of dynamic contrast-enhanced sequences) were constructed after methods of feature dimension, and the respective radiomics score was calculated. Then radiomics-clinical nomogram was generated by combining radiomics score, CA19-9, and clinical N staging.

Research results

The AUCs of the training and validation set of Ra-DWI were 0.652 and 0.661, which were higher than those of Ra-T2WI and Ra-portal phase of dynamic contrast-enhanced sequences. After chemotherapy, the top four delta-radiomics features of Ra-DWI in DR group belonged to gray-level run-length matrices parameters. The radiomics-clinical nomogram was built with an AUC of 0.809 and can effectively discriminate the patients with DR from non-DR.

Research conclusions

MRI-radiomics is conducive to predict chemotherapeutic response in SLM patients. The Ra-DWI logistic model behaved the best in differentiating DR and non-DR. Run-length matrices parameters of Ra-DWI were more sensitive to reflect the delta-radiomics after chemotherapy. The radiomics-clinical nomogram is more effective in predicting chemotherapeutic response.

Research perspectives

This study provides new insights into the potential ability of MRI-radiomics in evaluating chemotherapeutic response in SLM patents. The MRI-radiomics features combined with clinical characteristics is more effective in evaluation.

REFERENCES

1 **Song JH**, Jeong JU, Lee JH, Kim SH, Cho HM, Um JW, Jang HS; Korean Clinical Practice Guideline for Colon and Rectal Cancer Committee. Preoperative chemoradiotherapy *vs* postoperative chemoradiotherapy for stage II-III resectable rectal cancer: a meta-analysis of randomized controlled

trials. *Radiat Oncol J* 2017; **35**: 198-207 [PMID: 29037017 DOI: 10.3857/roj.2017.00059]
2 **Siegel RL**, Miller KD, Jemal A. Cancer Statistics, 2017. *CA Cancer J Clin* 2017; **67**: 7-30 [PMID: 28055103 DOI: 10.3322/caac.21387]
3 **Manfredi S**, Lepage C, Hatem C, Coatmeur O, Faivre J, Bouvier AM. Epidemiology and management of liver metastases from colorectal cancer. *Ann Surg* 2006; **244**: 254-259 [PMID: 16858188 DOI: 10.1097/01.sla.0000217629.94941.cf]
4 **Conrad C**, Vauthey JN, Masayuki O, Sheth RA, Yamashita S, Passot G, Bailey CE, Zorzi D, Kopetz S, Aloia TA, You YN. Individualized Treatment Sequencing Selection Contributes to Optimized Survival in Patients with Rectal Cancer and Synchronous Liver Metastases. *Ann Surg Oncol* 2017; **24**: 3857-3864 [PMID: 28929463 DOI: 10.1245/s10434-017-6089-7]
5 **Tsoulfas G**, Pramateftakis MG. Management of rectal cancer and liver metastatic disease: which comes first? *Int J Surg Oncol* 2012; **2012**: 196908 [PMID: 22778934 DOI: 10.1155/2012/196908]
6 **Gall TM**, Basyouny M, Frampton AE, Darzi A, Ziprin P, Dawson P, Paraskeva P, Habib NA, Spalding DR, Cleator S, Lowdell C, Jiao LR. Neoadjuvant chemotherapy and primary-first approach for rectal cancer with synchronous liver metastases. *Colorectal Dis* 2014; **16**: O197-O205 [PMID: 24344746 DOI: 10.1111/codi.12534]
7 **Nordlinger B**, Benoist S. Benefits and risks of neoadjuvant therapy for liver metastases. *J Clin Oncol* 2006; **24**: 4954-4955 [PMID: 17075112 DOI: 10.1200/JCO.2006.07.9244]
8 **Aloia T**, Sebagh M, Plasse M, Karam V, Lévi F, Giacchetti S, Azoulay D, Bismuth H, Castaing D, Adam R. Liver histology and surgical outcomes after preoperative chemotherapy with fluorouracil plus oxaliplatin in colorectal cancer liver metastases. *J Clin Oncol* 2006; **24**: 4983-4990 [PMID: 17075116 DOI: 10.1200/JCO.2006.05.8156]
9 **Alahmari SS**, Cherezov D, Goldgof D, Hall L, Gillies RJ, Schabath MB. Delta Radiomics Improves Pulmonary Nodule Malignancy Prediction in Lung Cancer Screening. *IEEE Access* 2018; **6**: 77796-77806 [PMID: 30607311 DOI: 10.1109/ACCESS.2018.2884126]
10 **Hu T**, Wang S, Huang L, Wang J, Shi D, Li Y, Tong T, Peng W. A clinical-radiomics nomogram for the preoperative prediction of lung metastasis in colorectal cancer patients with indeterminate pulmonary nodules. *Eur Radiol* 2019; **29**: 439-449 [PMID: 29948074 DOI: 10.1007/s00330-018-5539-3]
11 **Miles KA**, Ganeshan B, Griffiths MR, Young RC, Chatwin CR. Colorectal cancer: texture analysis of portal phase hepatic CT images as a potential marker of survival. *Radiology* 2009; **250**: 444-452 [PMID: 19164695 DOI: 10.1148/radiol.2502071879]
12 **Liang C**, Huang Y, He L, Chen X, Ma Z, Dong D, Tian J, Liang C, Liu Z. The development and validation of a CT-based radiomics signature for the preoperative discrimination of stage I-II and stage III-IV colorectal cancer. *Oncotarget* 2016; **7**: 31401-31412 [PMID: 27120787 DOI: 10.18632/oncotarget.8919]
13 **Shu Z**, Fang S, Ding Z, Mao D, Cai R, Chen Y, Pang P, Gong X. MRI-based Radiomics nomogram to detect primary rectal cancer with synchronous liver metastases. *Sci Rep* 2019; **9**: 3374 [PMID: 30833648 DOI: 10.1038/s41598-019-39651-y]
14 **Nitsche U**, Zimmermann A, Späth C, Müller T, Maak M, Schuster T, Slotta-Huspenina J, Käser SA, Michalski CW, Janssen KP, Friess H, Rosenberg R, Bader FG. Mucinous and signet-ring cell colorectal cancers differ from classical adenocarcinomas in tumor biology and prognosis. *Ann Surg* 2013; **258**: 775-782; discussion 782-783 [PMID: 23989057 DOI: 10.1097/SLA.0b013e3182a69f7e]
15 **Eisenhauer EA**, Therasse P, Bogaerts J, Schwartz LH, Sargent D, Ford R, Dancey J, Arbuck S, Gwyther S, Mooney M, Rubinstein L, Shankar L, Dodd L, Kaplan R, Lacombe D, Verweij J. New response evaluation criteria in solid tumours: revised RECIST guideline (version 1.1). *Eur J Cancer* 2009; **45**: 228-247 [PMID: 19097774 DOI: 10.1016/j.ejca.2008.10.026]
16 **Delgado AF**, Fahlström M, Nilsson M, Berntsson SG, Zetterling M, Libard S, Alafuzoff I, van Westen D, Lätt J, Smits A, Larsson EM. Diffusion Kurtosis Imaging of Gliomas Grades II and III - A Study of Perilesional Tumor Infiltration, Tumor Grades and Subtypes at Clinical Presentation. *Radiol Oncol* 2017; **51**: 121-129 [PMID: 28740446 DOI: 10.1515/raon-2017-0010]
17 **Gillies RJ**, Kinahan PE, Hricak H. Radiomics: Images Are More than Pictures, They Are Data. *Radiology* 2016; **278**: 563-577 [PMID: 26579733 DOI: 10.1148/radiol.2015151169]
18 **Bowen L**, Xiaojing L. Radiogenomics of Clear Cell Renal Cell Carcinoma: Associations Between mRNA-Based Subtyping and CT Imaging Features. *Acad Radiol* 2019; **26**: e32-e37 [PMID: 30064916 DOI: 10.1016/j.acra.2018.05.002]
19 **Kraemer HC**. Correlation coefficients in medical research: from product moment correlation to the odds ratio. *Stat Methods Med Res* 2006; **15**: 525-545 [PMID: 17260922 DOI: 10.1177/0962280206070650]
20 **van Smeden M**, Moons KG, de Groot JA, Collins GS, Altman DG, Eijkemans MJ, Reitsma JB. Sample size for binary logistic prediction models: Beyond events per variable criteria. *Stat Methods Med Res* 2019; **28**: 2455-2474 [PMID: 29966490 DOI: 10.1177/0962280218784726]
21 **Vittinghoff E**, McCulloch CE. Relaxing the rule of ten events per variable in logistic and Cox regression. *Am J Epidemiol* 2007; **165**: 710-718 [PMID: 17182981 DOI: 10.1093/aje/kwk052]
22 **Baeßler B**, Weiss K, Pinto Dos Santos D. Robustness and Reproducibility of Radiomics in Magnetic Resonance Imaging: A Phantom Study. *Invest Radiol* 2019; **54**: 221-228 [PMID: 30433891 DOI: 10.1097/RLI.0000000000000530]
23 **Ma Y**, Ma W, Xu X, Cao F. How Does the Delta-Radiomics Better Differentiate Pre-Invasive GGNs From Invasive GGNs? *Front Oncol* 2020; **10**: 1017 [PMID: 32766129 DOI:

10.3389/fonc.2020.01017]

24 **Kim HS**, Kim YJ, Kim KG, Park JS. Preoperative CT texture features predict prognosis after curative resection in pancreatic cancer. *Sci Rep* 2019; **9**: 17389 [PMID: 31757989 DOI: 10.1038/s41598-019-53831-w]

25 **Loh HH**, Leu JG. The analysis of natural textures using run length features. *IEEE Trans Indus Elec* 1988; **35**: 323-328 [DOI: 10.1109/41.192665]

26 **Roemeling S**, Roobol MJ, Kattan MW, van der Kwast TH, Steyerberg EW, Schröder FH. Nomogram use for the prediction of indolent prostate cancer: impact on screen-detected populations. *Cancer* 2007; **110**: 2218-2221 [PMID: 17893906 DOI: 10.1002/cncr.23029]

27 **Peeters KC**, Kattan MW, Hartgrink HH, Kranenbarg EK, Karpeh MS, Brennan MF, van de Velde CJ. Validation of a nomogram for predicting disease-specific survival after an R0 resection for gastric carcinoma. *Cancer* 2005; **103**: 702-707 [PMID: 15641033 DOI: 10.1002/cncr.20783]

28 **Kattan MW**, Wheeler TM, Scardino PT. Postoperative nomogram for disease recurrence after radical prostatectomy for prostate cancer. *J Clin Oncol* 1999; **17**: 1499-1507 [PMID: 10334537 DOI: 10.1200/JCO.1999.17.5.1499]

29 **Kouri M**, Pyrhönen S, Kuusela P. Elevated CA19-9 as the most significant prognostic factor in advanced colorectal carcinoma. *J Surg Oncol* 1992; **49**: 78-85 [PMID: 1738240 DOI: 10.1002/jso.2930490204]

30 **Wang WS**, Lin JK, Chiou TJ, Liu JH, Fan FS, Yen CC, Lin TC, Jiang JK, Yang SH, Wang HS, Chen PM. CA19-9 as the most significant prognostic indicator of metastatic colorectal cancer. *Hepatogastroenterology* 2002; **49**: 160-164 [PMID: 11941943]

31 **Zhou W**, Yang F, Peng J, Wang F, Lin Y, Jiang W, Yang X, Li L, Lu Z, Wan D, Pan Z, Fan W. High pretreatment serum CA19-9 level predicts a poor prognosis for patients with stage III colon cancer after curative resection and adjuvant chemotherapy. *J Cancer* 2019; **10**: 3810-3818 [PMID: 31333798 DOI: 10.7150/jca.31375]

32 **Märkl B**. Stage migration *vs* immunology: The lymph node count story in colon cancer. *World J Gastroenterol* 2015; **21**: 12218-12233 [PMID: 26604632 DOI: 10.3748/wjg.v21.i43.12218]

World Journal of Gastroenterology

Submit a Manuscript: https://www.f6publishing.com

World J Gastroenterol 2021 October 14; 27(38): 6476-6488

DOI: 10.3748/wjg.v27.i38.6476

ISSN 1007-9327 (print) ISSN 2219-2840 (online)

ORIGINAL ARTICLE

Observational Study

Deep learning *vs* conventional learning algorithms for clinical prediction in Crohn's disease: A proof-of-concept study

Danny Con, Daniel R van Langenberg, Abhinav Vasudevan

ORCID number: Danny Con 0000-0002-4983-6103; Daniel R van Langenberg 0000-0003-3662-6307; Abhinav Vasudevan 0000-0001-5026-9014.

Author contributions: Con D contributed conceptualization, data collection, statistical analysis, data interpretation, manuscript drafting; van Langenberg DR contributed conceptualization, data interpretation, reviewing of manuscript critically for important intellectual content; Vasudevan A contributed conceptualization, data collection, data interpretation, reviewing of manuscript critically for important intellectual content; all authors approved the final version of the manuscript.

Institutional review board statement: This study was reviewed and approved by the Eastern Health Office of Research & Ethics (approval number: LR 61/2015).

Informed consent statement: Patients were not required to give informed consent to the study because the analysis used anonymous clinical data that were obtained retrospectively.

Conflict-of-interest statement: Con D has no relevant conflicts of interest to declare. AV has received

Danny Con, Daniel R van Langenberg, Abhinav Vasudevan, Department of Gastroenterology and Hepatology, Eastern Health, Box Hill 3128, Victoria, Australia

Daniel R van Langenberg, Abhinav Vasudevan, Faculty of Medicine, Nursing and Health Sciences, Monash University, Box Hill 3128, Victoria, Australia

Corresponding author: Danny Con, MD, Doctor, Statistician, Department of Gastroenterology and Hepatology, Eastern Health, 8 Arnold Street, Box Hill 3128, Victoria, Australia. dannycon302@gmail.com

Abstract

BACKGROUND

Traditional methods of developing predictive models in inflammatory bowel diseases (IBD) rely on using statistical regression approaches to deriving clinical scores such as the Crohn's disease (CD) activity index. However, traditional approaches are unable to take advantage of more complex data structures such as repeated measurements. Deep learning methods have the potential ability to automatically find and learn complex, hidden relationships between predictive markers and outcomes, but their application to clinical prediction in CD and IBD has not been explored previously.

AIM

To determine and compare the utility of deep learning with conventional algorithms in predicting response to anti-tumor necrosis factor (anti-TNF) therapy in CD.

METHODS

This was a retrospective single-center cohort study of all CD patients who commenced anti-TNF therapy (either adalimumab or infliximab) from January 1, 2010 to December 31, 2015. Remission was defined as a C-reactive protein (CRP) < 5 mg/L at 12 mo after anti-TNF commencement. Three supervised learning algorithms were compared: (1) A conventional statistical learning algorithm using multivariable logistic regression on baseline data only; (2) A deep learning algorithm using a feed-forward artificial neural network on baseline data only; and (3) A deep learning algorithm using a recurrent neural network on repeated data. Predictive performance was assessed using area under the receiver operator characteristic curve (AUC) after 10× repeated 5-fold cross-validation.

financial support to attend educational meetings from Ferring. van Langenberg DR has served as a speaker and/or received travel support from Takeda, Ferring and Shire. He has consultancy agreements with Abbvie, Janssen and Pfizer. He received research funding grants for investigator-driven studies from Ferring, Shire and AbbVie.

Data sharing statement: No additional data are available.

STROBE statement: The authors have read the STROBE Statement-checklist of items, and the manuscript was prepared and revised according to the STROBE Statement-checklist of items.

Open-Access: This article is an open-access article that was selected by an in-house editor and fully peer-reviewed by external reviewers. It is distributed in accordance with the Creative Commons Attribution NonCommercial (CC BY-NC 4.0) license, which permits others to distribute, remix, adapt, build upon this work non-commercially, and license their derivative works on different terms, provided the original work is properly cited and the use is non-commercial. See: http://creativecommons.org/Licenses/by-nc/4.0/

Manuscript source: Invited manuscript

Specialty type: Gastroenterology and hepatology

Country/Territory of origin: Australia

Peer-review report's scientific quality classification

Grade A (Excellent): 0
Grade B (Very good): B
Grade C (Good): C
Grade D (Fair): 0
Grade E (Poor): 0

Received: March 5, 2021
Peer-review started: March 5, 2021
First decision: April 17, 2021
Revised: April 26, 2021
Accepted: September 6, 2021

RESULTS

A total of 146 patients were included (median age 36 years, 48% male). Concomitant therapy at anti-TNF commencement included thiopurines (68%), methotrexate (18%), corticosteroids (44%) and aminosalicylates (33%). After 12 mo, 64% had CRP < 5 mg/L. The conventional learning algorithm selected the following baseline variables for the predictive model: Complex disease behavior, albumin, monocytes, lymphocytes, mean corpuscular hemoglobin concentration and gamma-glutamyl transferase, and had a cross-validated AUC of 0.659, 95% confidence interval (CI): 0.562-0.756. A feed-forward artificial neural network using only baseline data demonstrated an AUC of 0.710 (95%CI: 0.622-0.799; P = 0.25 *vs* conventional). A recurrent neural network using repeated biomarker measurements demonstrated significantly higher AUC compared to the conventional algorithm (0.754, 95%CI: 0.674-0.834; P = 0.036).

CONCLUSION

Deep learning methods are feasible and have the potential for stronger predictive performance compared to conventional model building methods when applied to predicting remission after anti-TNF therapy in CD.

Key Words: Machine learning; Artificial intelligence; Precision medicine; Personalized medicine; Deep learning

©The Author(s) 2021. Published by Baishideng Publishing Group Inc. All rights reserved.

Core Tip: Deep learning has vast potential, but its clinical utility in predicting outcomes in Crohn's disease (CD) has not been explored. This study showed that deep learning algorithms (a recurrent neural network) using a more complex information structure including repeated biomarker measurements had a better predictive performance compared to a conventional statistical algorithm using only baseline data. This proof-of-concept study therefore paves the way for further research in the use of deep learning methods in clinical prediction in CD.

Citation: Con D, van Langenberg DR, Vasudevan A. Deep learning *vs* conventional learning algorithms for clinical prediction in Crohn's disease: A proof-of-concept study. *World J Gastroenterol* 2021; 27(38): 6476-6488
URL: https://www.wjgnet.com/1007-9327/full/v27/i38/6476.htm
DOI: https://dx.doi.org/10.3748/wjg.v27.i38.6476

INTRODUCTION

Crohn's disease (CD) is a heterogeneous chronic inflammatory bowel disease (IBD) that is characterized by intermittent flares, medication changes, the potential need for surgery and substantial psychological morbidity[1,2]. As with many chronic conditions, predicting disease trajectory, outcomes and response to therapies in CD are key components of clinical practice where management is tailored to the individual [3]. Precision medicine has been in part driven by the vast expansion of available electronic health data, genomic data and novel disease biomarkers[3]. However, deciphering the complex relationships between large amounts of information and multiple data types presents new analytical challenges.

Traditional approaches to constructing prediction models rely on multivariable regression approaches, typically logistic regression for classification or proportional hazards regression for longitudinal prediction[4]. The resulting predictive models are thus typically only linear combinations of the included predictors and may have limited ability to learn more complex relationships within the data. The advantage of machine learning and artificial intelligence over traditional predictive tools is the potential ability for computational algorithms to automatically find and learn complex, hidden relationships between predictive markers and outcomes[5,6]. This is especially true for deep learning or artificial neural network (ANN) methods, although their 'black box' approach has been criticized for an inability to produce a causal

Article in press: September 6, 2021
Published online: October 14, 2021

P-Reviewer: Jin B, Yu C
S-Editor: Gao CC
L-Editor: A
P-Editor: Liu JH



explanation between predictors and outcomes[6].

Despite some limitations, there is much interest in developing and testing machine learning and deep learning tools to aid decision making[5,7]. In luminal gastroenterology, machine learning is gaining traction but its use has been relatively limited to automatic image recognition in endoscopy[8-11] as well as feature selection in genomic and microbiomics data[12,13]. Although there has been great interest in predicting clinical outcomes in CD such as response to therapeutics including biologics[14-18] and immunomodulators[19,20], studies investigating the utility of machine learning models for such predictive tasks have been more limited[21-23]. In particular, the utility of deep learning or ANNs specifically in clinical prediction of CD remains unknown[7].

We aimed to evaluate the utility of deep learning algorithms compared with conventional statistical learning algorithms for clinical prediction in this proof-of-concept study. In particular, we aimed to compare these algorithms as methods of learning and prediction in a general sense, rather than to develop any specific predictive model or score.

MATERIALS AND METHODS

Study design

This proof-of-concept study utilized a retrospective longitudinal cohort at a tertiary health network comprising three acute hospitals in Melbourne, Australia. The focus of the study was to compare the ability of two supervised learning algorithms (conventional statistical learning *vs* deep learning) to predict remission after 12 mo of treatment using clinical variables and biomarkers available at baseline. The performance of each algorithm was evaluated using cross-validation. The emphasis of the study was to compare the predictive performance of the two methods of learning rather than any specific model itself. This study was approved by the Eastern Health Office of Research & Ethics (approval number: LR 61/2015).

Study cohort

All adult patients > 18 years with confirmed CD according to standard criteria[24] were included if they were commenced on treatment with an anti-tumor necrosis factor (anti-TNF) agent (adalimumab or infliximab) for luminal CD and received at least one dose of the drug between January 2010 and December 2015. Patients receiving anti-TNF for perianal disease without luminal disease were excluded. Patients were followed up for 12 mo to determine rates of biochemical remission.

Outcomes

Response to anti-TNF was defined as having achieved biochemical remission as per serum C-reactive protein (CRP) < 5 mg/L at 12 mo. This endpoint was chosen because CRP is an accepted biomarker to reflect disease activity and predict outcomes in CD [25,26]. Additionally, normalization of CRP predicts better outcomes in CD patients in remission[27,28]. The first CRP measurement after 12 mo and before 18 mo was used. Patients who did not have a CRP measurement in this time period were excluded.

Data collection and pre-processing

Baseline characteristics were collected *via* hospital and clinic records, including Montreal classification, concomitant baseline therapies, prior anti-TNF exposure and prior surgeries. Biomarker data were collected at two time points: (1) A baseline measurement defined as the most proximate measurement prior to commencing anti-TNF, up to 3 mo before commencement; and (2) A prior measurement defined as the second most proximate measurement, up to 12 mo before commencement. Only patients with complete baseline data were included, while missing prior values were imputed with the respective baseline value. The following variables were log-transformed to correct skewness: serum bilirubin, alanine aminotransferase, alkaline phosphatase and gamma-glutamyl transferase (GGT). The data underlying this article cannot be shared publicly due to privacy and ethical concerns. The data will be shared upon reasonable request to the corresponding author.

Statistical learning algorithm (conventional approach)

The conventional approach to developing a predictive clinical model is to run univariable and multivariable regression analysis to find useful and preferably

independent predictors of the outcome of interest (see Figure 1). Criteria for variable selection usually involves significance testing (*P* values) or likelihood-based information criterion (such as the Akaike information criterion). In this study, logistic regression was used given the dichotomous nature of the outcome (CRP < 5 mg/L *vs* CRP ≥ 5 mg/L). The conventional approach typically only uses data from a single time-point, therefore we used baseline data only (the most proximate measurement for all biomarkers). For this conventional approach, we employed the following modelling algorithm: (1) Perform univariable logistic regression on each variable and retain all variables with $P < 0.5$; (2) Run backwards stepwise selection on all retained variables with removal criterion $P > 0.2$; and (3) Use the regression coefficients in the remaining multivariable model to derive the predictive score.

Deep learning algorithms (experimental approach)

A basic deep learning algorithm is a feed-forward ANN[6]. An ANN is composed of layers: an input layer (consisting of all the input predictor variables), an output layer (the prediction), and a number of 'hidden' layers (see Figure 1). Nodes within a hidden layer are called 'neurons'. The hidden layers allow an ANN to learn complex, non-linear relationships between input variables and the outcome of interest. The influence of nodes in a layer on other nodes in subsequent layers is 'trained' or fitted using a mathematical function and ultimately determines how information is propagated through the ANN — this is analogous to fitting a regression line on data in conventional statistics. An ANN with only an input and output layer, without hidden layers, can be analogous to simple logistic regression, although they are not equivalent.

However, like the conventional statistical algorithm, a basic feed-forward ANN is still only able to model relationships between predictors at a single time-point. A recurrent neural network (RNN) is a more advanced deep learning algorithm that is able to model repeated measurements over time. Like a feed-forward ANN, information is propagated from the input layer to the output layer. However, instead of only allowing the information to pass through once, information is fed to the RNN sequentially, or 'recurrently' — that is, each set of repeated measurements is inputted once at a time allowing the RNN to update its knowledge of the relationship between the predictors and the outcome. Therefore, the algorithm is additionally able to learn and utilize the dynamics of biomarkers over time, in a way that cannot be achieved by conventional statistical learning methods.

We tested the feed-forward ANN and the RNN in three separate experiments: (1) Using all baseline clinical data in a feed-forward ANN; (2) Using only baseline biomarker data in a feed-forward ANN; and (3) Using repeated biomarker data in an RNN. In this study after hyper-parameter tuning, we used a feed-forward ANN architecture of 3 hidden layers, each with 64 neurons, and an RNN architecture of 1 hidden layer with 64 neurons.

Comparison of algorithms

The predictive performances of the conventional statistical algorithm and the experimental deep learning algorithm (ANN) was defined as their ability to correctly classify 12-mo CRP < 5 mg/L measured using the area under the receiver operator characteristic curve (AUC). Because the learning ability of an ANN can be arbitrarily increased, an overly powerful ANN that is trained such that it has near-perfect prediction on the original training cohort, would suffer from poor predictive ability in an external cohort (this is called 'over-fitting', a well-known phenomenon). Similarly, the same conventional statistical learning algorithm might result in models with different variables when applied to different cohorts. Therefore, it is important to evaluate the ability of a learning algorithm to predict outcomes in patients that are not included in the original training cohort (external validity).

In the absence of external testing cohorts to assess external validity, cross-validation is an internal validation procedure that is suited to this purpose[4]. During cross-validation, the cohort is randomly divided into *k* equally sized sub-cohorts, known as 'folds' (where *k* is often 5 or 10 by convention). Then, one fold is set aside to be used to test the algorithm, after the algorithm is first trained on the remaining *k*-1 folds (see Figure 2). This allows the algorithms to be tested on patients that were not used during training. The process is then repeated for each fold (where each fold takes turns in being the test fold). The average AUC after repeating *k* times gives the cross-validated AUC. However, this procedure is not free from error, because the partitioning process may have randomly resulted in a better (or worse) than usual performance. Thus it is important to repeat the whole process a number of times, to reduce this error[29].

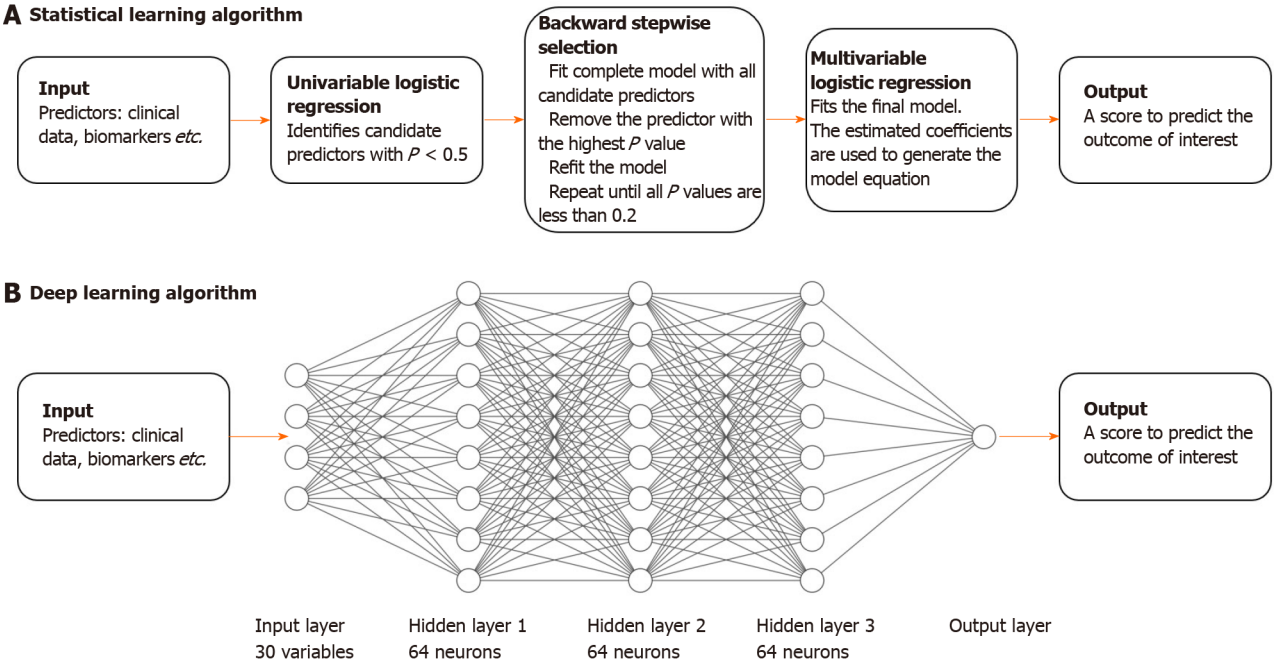


Figure 1 Comparison of the predictive modelling process using two supervised learning algorithms. A: Conventional statistical learning; B: Deep learning.

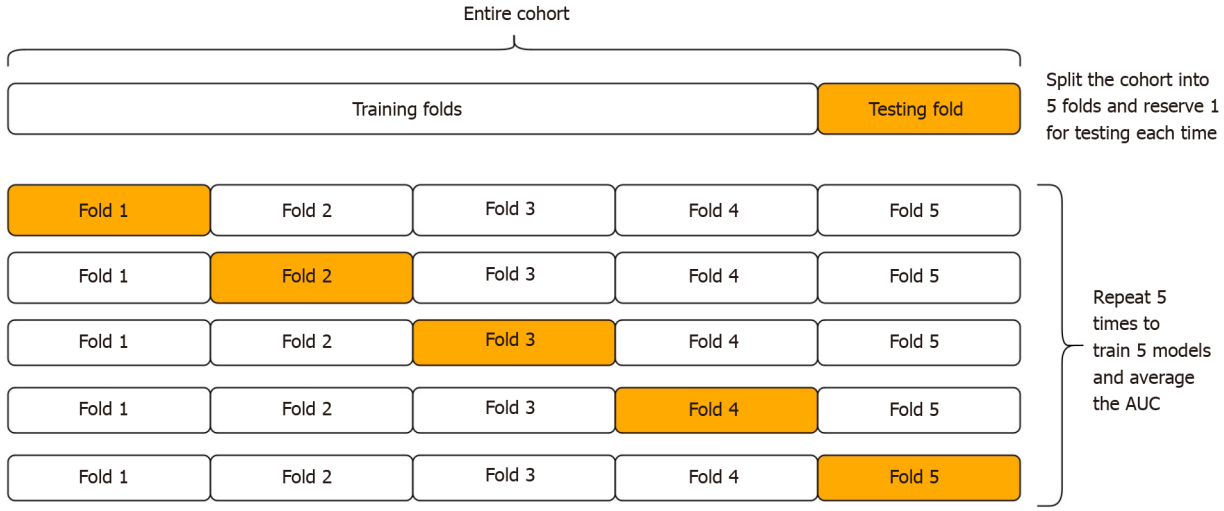


Figure 2 Schematic diagram of *k*-fold cross validation procedure for *k* = 5. This method is considered more reliable than a random train-test split, which would be analogous to training only one model, instead of the average of *k* models. AUC: Area under the receiver operator characteristic curve.

For this study, we used 5-fold cross-validation repeated 10 times to estimate the generalizability of each algorithm on unseen data. Statistical comparison of the cross-validated AUCs of each learning algorithm was made using the variance-corrected repeated *k*-fold *t* test instead of a conventional paired *t* test because of the independency violation from repeated partitioning of the same dataset[29]. For comparison, the naïve or apparent AUC of each model after training and testing on the same entire cohort was given, however this is non-informative. Sample size calculations were conducted only as a guide given the exploratory nature of the study and without prior similar studies on which to base AUC assumptions. The target sample size to detect a 10% difference in AUC with 80% power and 95% significance assuming an AUC variance of 10% was n = 157[30]. To instead detect a 15% difference in AUC under the same conditions, a sample size of n = 70 was required. The Python 3.8.4 programming language with the open-source module PyTorch was used to create the deep learning algorithm. Stata/IC 16 (Texas, United States, 2020) was used to create the statistical learning algorithm.

RESULTS

Baseline characteristics

A total of 146 CD patients were included (see Table 1). Their median age was 36 years [inter-quartile range (IQR) 25-50], 48% were male and median disease duration since diagnosis was 5 years (IQR 1-12). The anti-TNF commenced was infliximab in 58% and adalimumab in 42%. Concomitant therapy at anti-TNF commencement included thiopurines (68%), methotrexate (18%), corticosteroids (44%) and aminosalicylates (33%). Over a quarter of patients (28%) had prior intestinal surgery, while 15% had prior exposure to anti-TNF. After 12 mo, 94 (64%) patients were in biochemical remission (CRP < 5 mg/L).

Statistical learning algorithm

Univariable analysis: Baseline factors associated with biochemical remission at 12 mo on univariable testing included non-complex disease behavior (B1), higher albumin and mean corpuscular hemoglobin concentration (MCHC), and lower platelets, lymphocytes and monocytes (each $P < 0.05$; see Table 2), while lower neutrophil count was nearly significant ($P = 0.06$). There was no significant association with age, sex, disease location or baseline medical therapies (see Table 2).

Multivariable analysis: After backward stepwise selection, the following variables remained in the final multivariable model: Complex disease, baseline albumin, monocytes, lymphocytes, MCHC and GGT (see Table 2). The resulting prediction model was given by the following equation (coefficients correct to two significant figures): Score = 0.079 × (albumin, g/L) + 0.050 × (MCHC, mg/L) - 1.1 × (monocytes, 10^9/L) - 0.43 × (lymphocytes, 10^9/L) - 1.0 × (complex disease, y=1 | n=0) - 0.69 × $\log_e$ (GGT, IU/L).

Outcome prediction: After 10× 5-fold cross validation, the average AUC of the statistical learning algorithm was 0.659 [95% confidence interval (CI): 0.562-0.756]. This suggests the statistical learning algorithm is expected to accurately classify 65.9% of patients in external cohorts who have similar characteristics to the study cohort (see Table 3). The algorithm performed better than chance (AUC > 0.5) 94% of the time and had an AUC > 0.7 in 38% of occasions (see Figure 3). The apparent naïve AUC (when trained and tested on the same data) of the model was 0.771.

Deep learning algorithms

Feed-forward ANN with complete baseline data: The feed-forward ANN with complete baseline data had a cross-validated AUC of 0.710 (95%CI: 0.622-0.799) (see Figure 3 and Table 3). This difference was not statistically significant using the variance corrected t test ($P = 0.25$). The algorithm performed better than chance 100% of the time and had good performance (AUC > 0.7) 54% of the time (see Figure 3). For comparison, the naïve AUC of the model was 0.857.

Feed-forward ANN with baseline biomarker data only: The same feed-forward ANN using only baseline biomarker data had a similar cross-validated AUC of 0.706 (95%CI: 0.621-0.791), which was again not significantly different compared to the conventional algorithm ($P = 0.33$) (see Table 3). The algorithm performed better than chance 100% of the time and had good performance (AUC > 0.7) 58% of the time (see Figure 3). The naïve AUC of the model was 0.776.

RNN with repeated biomarker data: The same feed-forward ANN using only baseline biomarker data had a similar cross-validated AUC of 0.754 (95%CI: 0.674-0.834), which was significantly higher than the AUC of the conventional algorithm ($P = 0.036$) (see Table 3). This suggests the RNN is expected to accurately classify 75.4% of patients in external cohorts who have similar characteristics to the study cohort. The RNN algorithm performed better than chance 100% of the time and had good performance (AUC > 0.7) 72% of the time (see Figure 3). For comparison, the naïve AUC of the model was 0.892.

DISCUSSION

The rapid expansion of available health data has motivated the development of machine learning and deep learning tools to predict useful outcomes in clinical medicine[5,6]. The advent of machine learning and data science techniques is

Table 1 Baseline characteristics of study cohort (*n* = 146)

Characteristic	*n* (%)
Age, years, median (IQR)	36 (25-50)
Sex	
Female	76 (52)
Male	70 (48)
Smoker (active)	33 (23)
CD behavior	
B1: Non-stricturing, non-penetrating	75 (51)
B2: Stricturing	56 (38)
B3: Penetrating/fistulizing	15 (10)
CD location	
L1: Ileal	41 (28)
L2: Colonic	43 (29)
L3: Ileocolonic	62 (42)
L4: Isolated UGI	0 (0)
Perianal involvement	20 (21)
Initial anti-TNF commenced	
Infliximab	84 (58)
Adalimumab	62 (42)
Baseline thiopurine	99 (68)
Baseline methotrexate	27 (18)
Baseline corticosteroids	64 (44)
Baseline aminosalicylates	48 (33)
Prior anti-TNF	22 (15)
Prior intestinal surgery	41 (28)
Disease duration, yr, median (IQR)	5 (1-12)
Baseline investigations	
CRP, mg/L, median (IQR)	3 (2-8)
Albumin, g/L, median (IQR)	37 (36-41)

IQR: Inter-quartile range; CD: Crohn's disease; CRP: C-reactive protein; TNF: Tumor necrosis factor; UGI: Upper gastrointestinal.

especially applicable to IBD due to the heterogeneity and chronic nature of such conditions and the repeated measures of disease activity over time which provides data that may be more suitable for complex modelling techniques. For instance, those with CD typically present with a wide array of disparate disease phenotypes and underlying pathogeneses, and their response to treatment and the trajectory of their disease course varies substantially and changes based on their response[31]. This study has exhibited the potential of deep learning algorithms in predicting response to anti-TNF therapy in patients with CD. The ability to predict the likelihood of response to a given treatment is crucial for risk-benefit assessment, which in turn is crucial to facilitate shared decision making between clinicians and patients[32]. Further, although biologic therapies have revolutionized management in IBD[31], medical therapy is now the principal driver of healthcare costs[33,34] and health economic considerations will inevitably affect treatment choice. Ideally, patients should receive therapies that are both likely to work and cost-effective. Therefore, there can be no 'one-size-fits-all' strategy to management, and precision and personalized medicine are key objectives.

Table 2 Estimated odds ratios with 95% confidence intervals on univariable and multivariable logistic regression analysis

Predictor	Univariable		Multivariable	
	OR (95%CI)	*P* value	Adj. OR (95%CI)	*P* value
Age, per year	0.98 (0.96-1.00)	0.10	-	-
Male (*vs* female)	1.42 (0.72-2.82)	0.31	-	-
CD behavior				
B1	1.0		Not included	
B2	0.45 (0.22-0.94)	0.034	Not included	
B3	0.42 (0.13-1.29)	0.13	Not included	
CD location				
L1: ileal	1.0		Not included	
L2: colonic	1.33 (0.54-3.31)	0.54	Not included	
L3: ileocolonic	0.91 (0.40-2.06)	0.83	Not included	
Ileal location (L1)	0.94 (0.45-2.00)	0.88	Not included	
Complex disease (B2/B3)	0.44 (0.22-0.89)	0.021	0.36 (0.16-0.80)	0.012
Active smoker	0.76 (0.40-1.47)	0.42	-	-
Perianal involvement	1.14 (0.49-2.65)	0.77	Not included	
Anti-TNF type: infliximab (*vs* adalimumab)	1.12 (0.56-2.22)	0.75	Not included	
Baseline immunomodulator	1.24 (0.47-3.27)	0.66	Not included	
Baseline corticosteroids	1.10 (0.56-2.18)	0.78	Not included	
Baseline aminosalicylates	1.16 (0.56-2.40)	0.69	Not included	
Prior anti-TNF	0.96 (0.37-2.47)	0.94	Not included	
Prior intestinal surgery	0.71 (0.34-1.48)	0.36	-	-
Disease duration, per $\log_e$ year	0.83 (0.65-1.06)	0.14	-	-
Albumin, per g/L	1.12 (1.03-1.22)	0.006	1.08 (0.98-1.20)	0.12
Hemoglobin, per g/L	1.01 (0.99-1.04)	0.32	-	-
HCT, per %	0.91 (0.71-1.16)	0.44	-	-
RCC, per 10^9/L	1.07 (0.84-1.36)	0.60	Not included	
MCV, per fL	1.01 (0.96-1.07)	0.64	Not included	
MCH, per pg/cell	1.15 (0.99-1.32)	0.06	-	-
MCHC, per mg/L	1.05 (1.02-1.08)	0.002	1.05 (1.02-1.09)	0.004
Platelets, per 100 × 10^9/L	0.63 (0.43-0.93)	0.020	-	-
Neutrophils, per 10^9/L	0.91 (0.82-1.00)	0.06	-	-
Lymphocytes, per 10^9/L	0.66 (0.46-0.93)	0.019	0.65 (0.41-1.02)	0.06
Monocytes, per 10^9/L	0.23 (0.08-0.63)	0.004	0.34 (0.10-1.16)	0.09
Eosinophils, per 10^9/L	0.61 (0.08-4.77)	0.64	Not included	
Basophils, per 0.01 × 10^9/L	0.92 (0.80-1.06)	0.24	-	-
Bilirubin, per $\log_e$ μmol/L	1.38 (0.70-2.72)	0.36	-	-
ALT, per $\log_e$ IU/L	1.04 (0.60-1.80)	0.90	Not included	
ALP, per $\log_e$ IU/L	0.55 (0.18-1.64)	0.28	-	-
GGT, per $\log_e$ IU/L	0.71 (0.46-1.09)	0.12	0.69 (0.43-1.11)	0.13

Variables excluded after univariable regression are in grey; variables excluded after stepwise selection are marked with a dash. CI: Confidence interval; OR: Odds ratio; CD: Crohn's disease; TNF: tumor necrosis factor; HCT: Hematocrit; RCC: Red cell count; MCV: Mean corpuscular volume; MCH: Mean corpuscular hemoglobin; MCHC: Mean corpuscular hemoglobin concentration; ALP: Alkaline phosphatase; ALT: Alanine aminotransferase; GGT: Gamma-glutamyl transferase.

Table 3 Comparison of learning algorithms during cross-validation experiments

Algorithm	Dataset[1]	AUC (%)		*P* value[2]
		Mean	SD	
Conventional statistics	Baseline clinical + biomarker data	65.9	9.5	-
Feed-forward ANN	Baseline clinical + biomarker data	71.0	8.7	0.25
Feed-forward ANN	Baseline biomarker data only	70.6	8.3	0.33
Recurrent neural network	Baseline and prior biomarker data	75.4	7.8	0.036

[1]Clinical data refers to non-biochemical data such as age, sex, disease characteristics and concurrent treatments. Biomarker data refers to complete blood count, liver function tests and albumin.
[2]*P* value for comparison against conventional statistical algorithm, using the variance-corrected repeated *k*-fold *t* test. AUC: Area under the receiver operator characteristic curve; ANN: Artificial neural network.

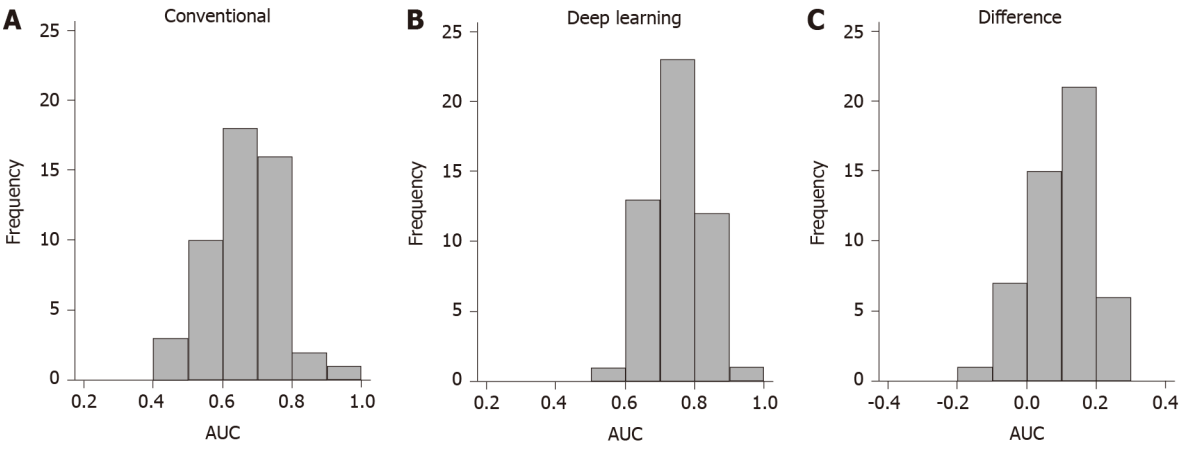


Figure 3 Distribution of area under the receiver operator characteristic curve after 10 × 5 fold cross validation. A: Conventional statistical learning algorithm (mean 0.659, SD 0.095); B: Recurrent neural network (mean 0.754, SD 0.078); C: Head-to-head comparison, matched at each fold and repetition (mean difference, + 0.095, *P* = 0.036). AUC: Area under the receiver operator characteristic curve.

Conventional statistical learning algorithms have generated many useful clinical scores, including the CD activity index[35], the simple endoscopic score for CD[36], scores to predict response to biologic therapies[16], and scores to differentiate CD from intestinal tuberculosis[37]. The advantage of conventional scores is often their simplicity and interpretability. A simple score can be memorized and calculated at the bed side and are intuitive as they utilize important risk factors of the outcome of interest. Yet clinical scores can only apply to a rather generic subgroup of patients and are never specific to any individual, as they utilize relatively few variables. Further, conventional methods are not readily able to model more complex, non-linear or time-dependent health states. With new genomic and microbiomic profiling, as well as the rapid uptake of comprehensive electronic medical records with mass data linkage, the ability of conventional learning algorithms to select useful predictive factors may become redundant[38].

Although the advantages of deep learning for the analysis of non-numerical data types is obvious, such as image data in endoscopy[39-41] and text or speech data in natural language processing[42], the utility of deep learning for the analysis of numerical data is less clear but remains promising. A recent study has demonstrated the utility of machine learning in predicting anti-TNF response in rheumatoid arthritis, but relied on genetic markers in addition to clinical data[43]. Another recent study

used machine learning to predict whether patients with ankylosing spondylitis required anti-TNF therapy, but did not evaluate whether response to therapy could be predicted[44]. It is anticipated that new data science and machine learning techniques are required to handle large amounts of data for use in clinical practice, although the optimal algorithms for this task remain unknown. Nevertheless, with the provision of comprehensive training data, machine learning tools have the potential to aid in individualized risk prediction, although no such model exists in IBD currently. In our cohort, the RNN deep learning algorithm was able to outperform the conventional algorithm after incorporating repeated biomarker measurements and thus additionally learn the non-linear temporal dynamics of the respective biomarkers — a feat that is not possible with conventional prediction models. It is expected that with enough training data, deep learning methods such as the RNN will be able to incorporate the time series data from multiple repeated health states of an individual patient over time. The clear trade-off with deep learning methods is the need for more data coordination and software to execute. However, the continued uptake of automated medical records in routine clinical practice may mitigate this limitation in future. Further, with the ever increasing breadth and volume of information from sources including comprehensive previous medical history, serum and fecal biomarkers, imaging and endoscopic data as well as genetics, the role of machine learning in prediction in chronic diseases including IBD is likely to expand.

This study has also demonstrated the importance of applying model validation techniques during model development[29]. ANNs and other powerful algorithms have the ability to learn intricate differences in data, yet poorly specified models that focus only on learning power have the propensity to learn the random variations or artefacts in the data, which are present only due to chance. This is evidenced by the RNN in this study achieving excellent AUC during training, but a reduced AUC when tested on unseen data (naïve AUC 0.892; cross-validated AUC 0.754). The same phenomenon occurred with the statistical learning algorithm but to a somewhat lesser extent (naïve AUC 0.771; cross-validated AUC 0.659). Therefore, studies developing predictive models should take care to avoid naïvely assessing predictive performance and ensure that effective cross-validation or bootstrapping methods are used for appropriate interval validation[4]. If available, external validation of predictive models in entirely new and different cohorts is the gold standard for model validation[4].

The dataset used in this study was retrospective and from a single center which subjects the results to information bias and limits their external validity. The outcome used was biochemical remission as this is a readily available as a repeated measure which allowed demonstration of more conventional and machine learning models, however it is acknowledged that clinical symptoms and/or mucosal healing are more clinically relevant end-points. Nevertheless, the goal of this study was to demonstrate the feasibility of deep learning methods in clinical prediction in this proof-of-concept study, rather than to develop a specific predictive model. Further, in practice, much larger cohorts will be required to properly train and calibrate deep learning models to maximize their utility in the real world. In future, all studies investigating specific predictive models should be subject to prospective controlled validation prior their application in clinical practice, specifically having shown that outcomes are improved after using predictive models to guide management.

CONCLUSION

In conclusion, we have demonstrated the feasibility of deep learning algorithms for clinical prediction in CD, which demonstrated an improved predictive performance compared to conventional methods. However, conventional statistical methods retain the advantage of simplicity and intuitiveness, allowing their use at the bedside. Yet with the rapid expansion of available health data, machine learning models have the potential to supersede currently conventional methods and greatly improve the development of tools for the clinical prediction of patient outcomes.

ARTICLE HIGHLIGHTS

Research background

Machine learning and artificial intelligence have the potential to revolutionize precision care in inflammatory bowel diseases. The greatest area of interest has been

the application of deep learning methods in automatic tumor detection during endoscopy, yet the application of such techniques in clinical outcome prediction has been lacking.

Research motivation

Traditional approaches to clinical prediction rely on conventional statistical algorithms such as regression, which are not suitable for more complex data such as repeated biomarker measurements.

Research objectives

To determine and compare the utility of deep learning with conventional algorithms in predicting response to anti-tumor necrosis factor (anti-TNF) therapy in Crohn's disease (CD).

Research methods

A retrospective cohort of CD patients commenced on anti-TNF therapy was used to experimentally develop and cross-validate three supervised learning algorithms: (1) Statistical learning algorithm; (2) Feed-forward artificial neural network; and (3) Recurrent neural network with repeated data. Predictive utility was quantified using the area under the receiver operator characteristic curve (AUC).

Research results

Within our cohort of 146 patients, the conventional statistical learning algorithm had the weakest performance [AUC 0.659, 95% confidence interval (CI): 0.562-0.756], compared to the feed-forward artificial neural network (AUC 0.710, 95%CI: 0.622-0.799; P = 0.25 *vs* conventional) and the recurrent neural network using repeated biomarker measurements (AUC 0.754, 95%CI: 0.674-0.834; P = 0.036 *vs* conventional).

Research conclusions

Deep learning methods are feasible and have the potential for stronger predictive performance compared to conventional model building methods when applied to predicting remission after anti-TNF therapy in CD.

Research perspectives

This has been the first study to investigate the utility of deep neural networks in predicting clinical outcomes using repeated clinical data in inflammatory bowel disease. Future studies should incorporate additional data types such as genetic, imaging and endoscopic factors.

REFERENCES

1 **Podolsky DK**. Inflammatory bowel disease. *N Engl J Med* 2002; **347**: 417-429 [PMID: 12167685 DOI: 10.1056/NEJMra020831]

2 **Jackson BD**, Con D, Gorelik A, Liew D, Knowles S, De Cruz P. Examination of the relationship between disease activity and patient-reported outcome measures in an inflammatory bowel disease cohort. *Intern Med J* 2018; **48**: 1234-1241 [PMID: 29663629 DOI: 10.1111/imj.13937]

3 **Denson LA**, Curran M, McGovern DPB, Koltun WA, Duerr RH, Kim SC, Sartor RB, Sylvester FA, Abraham C, de Zoeten EF, Siegel CA, Burns RM, Dobes AM, Shtraizent N, Honig G, Heller CA, Hurtado-Lorenzo A, Cho JH. Challenges in IBD Research: Precision Medicine. *Inflamm Bowel Dis* 2019; **25**: S31-S39 [PMID: 31095701 DOI: 10.1093/ibd/izz078]

4 **Moons KG**, Altman DG, Reitsma JB, Ioannidis JP, Macaskill P, Steyerberg EW, Vickers AJ, Ransohoff DF, Collins GS. Transparent Reporting of a multivariable prediction model for Individual Prognosis or Diagnosis (TRIPOD): explanation and elaboration. *Ann Intern Med* 2015; **162**: W1-73 [PMID: 25560730 DOI: 10.7326/M14-0698]

5 **Chen H**, Sung JJY. Potentials of AI in medical image analysis in Gastroenterology and Hepatology. *J Gastroenterol Hepatol* 2021; **36**: 31-38 [PMID: 33140875 DOI: 10.1111/jgh.15327]

6 **Le Berre C**, Sandborn WJ, Aridhi S, Devignes MD, Fournier L, Smaïl-Tabbone M, Danese S, Peyrin-Biroulet L. Application of Artificial Intelligence to Gastroenterology and Hepatology. *Gastroenterology* 2020; **158**: 76-94.e2 [PMID: 31593701 DOI: 10.1053/j.gastro.2019.08.058]

7 **Kohli A**, Holzwanger EA, Levy AN. Emerging use of artificial intelligence in inflammatory bowel disease. *World J Gastroenterol* 2020; **26**: 6923-6928 [PMID: 33311940 DOI: 10.3748/wjg.v26.i44.6923]

8 **Takenaka K**, Ohtsuka K, Fujii T, Negi M, Suzuki K, Shimizu H, Oshima S, Akiyama S, Motobayashi M, Nagahori M, Saito E, Matsuoka K, Watanabe M. Development and Validation of a

Deep Neural Network for Accurate Evaluation of Endoscopic Images From Patients With Ulcerative Colitis. *Gastroenterology* 2020; **158**: 2150-2157 [PMID: 32060000 DOI: 10.1053/j.gastro.2020.02.012]

9 **Otani K**, Nakada A, Kurose Y, Niikura R, Yamada A, Aoki T, Nakanishi H, Doyama H, Hasatani K, Sumiyoshi T, Kitsuregawa M, Harada T, Koike K. Automatic detection of different types of small-bowel lesions on capsule endoscopy images using a newly developed deep convolutional neural network. *Endoscopy* 2020; **52**: 786-791 [PMID: 32557474 DOI: 10.1055/a-1167-8157]

10 **Klang E**, Barash Y, Margalit RY, Soffer S, Shimon O, Albshesh A, Ben-Horin S, Amitai MM, Eliakim R, Kopylov U. Deep learning algorithms for automated detection of Crohn's disease ulcers by video capsule endoscopy. *Gastrointest Endosc* 2020; **91**: 606-613.e2 [PMID: 31743689 DOI: 10.1016/j.gie.2019.11.012]

11 **Sze SF**, Cheung WI, Wong WC, Hui YT, Lam JTW. AmplifEYE assisted colonoscopy *vs* standard colonoscopy: A randomized controlled study. *J Gastroenterol Hepatol* 2021; **36**: 376-382 [PMID: 33141979 DOI: 10.1111/jgh.15331]

12 **Abbas M**, Matta J, Le T, Bensmail H, Obafemi-Ajayi T, Honavar V, El-Manzalawy Y. Biomarker discovery in inflammatory bowel diseases using network-based feature selection. *PLoS One* 2019; **14**: e0225382 [PMID: 31756219 DOI: 10.1371/journal.pone.0225382]

13 **Bodein A**, Chapleur O, Droit A, Lê Cao KA. A Generic Multivariate Framework for the Integration of Microbiome Longitudinal Studies With Other Data Types. *Front Genet* 2019; **10**: 963 [PMID: 31803221 DOI: 10.3389/fgene.2019.00963]

14 **Matsuoka K**, Hamada S, Shimizu M, Nanki K, Mizuno S, Kiyohara H, Arai M, Sugimoto S, Iwao Y, Ogata H, Hisamatsu T, Naganuma M, Kanai T, Mochizuki M, Hashiguchi M. Factors predicting the therapeutic response to infliximab during maintenance therapy in Japanese patients with Crohn's disease. *PLoS One* 2018; **13**: e0204632 [PMID: 30286108 DOI: 10.1371/journal.pone.0204632]

15 **Ding NS**, Malietzis G, Lung PFC, Penez L, Yip WM, Gabe S, Jenkins JT, Hart A. The body composition profile is associated with response to anti-TNF therapy in Crohn's disease and may offer an alternative dosing paradigm. *Aliment Pharmacol Ther* 2017; **46**: 883-891 [PMID: 28881017 DOI: 10.1111/apt.14293]

16 **Barber GE**, Yajnik V, Khalili H, Giallourakis C, Garber J, Xavier R, Ananthakrishnan AN. Genetic Markers Predict Primary Non-Response and Durable Response To Anti-TNF Biologic Therapies in Crohn's Disease. *Am J Gastroenterol* 2016; **111**: 1816-1822 [PMID: 27596696 DOI: 10.1038/ajg.2016.408]

17 **Ward MG**, Warner B, Unsworth N, Chuah SW, Brownclarke C, Shieh S, Parkes M, Sanderson JD, Arkir Z, Reynolds J, Gibson PR, Irving PM. Infliximab and adalimumab drug levels in Crohn's disease: contrasting associations with disease activity and influencing factors. *Aliment Pharmacol Ther* 2017; **46**: 150-161 [PMID: 28481014 DOI: 10.1111/apt.14124]

18 **Mortensen JH**, van Haaften WT, Karsdal MA, Bay-Jensen AC, Olinga P, Grønbæk H, Hvas CL, Manon-Jensen T, Dijkstra G, Dige A. The Citrullinated and MMP-degraded Vimentin Biomarker (VICM) Predicts Early Response to Anti-TNFα Treatment in Crohn's Disease. *J Clin Gastroenterol* 2021; **55**: 59-66 [PMID: 32301833 DOI: 10.1097/MCG.0000000000001341]

19 **Con D**, Parthasarathy N, Bishara M, Luber RP, Joshi N, Wan A, Rickard JA, Long T, Connoley DJ, Sparrow MP, Gibson PR, van Langenberg DR, Vasudevan A. Development of a Simple, Serum Biomarker-based Model Predictive of the Need for Early Biologic Therapy in Crohn's Disease. *J Crohns Colitis* 2021; **15**: 583-593 [PMID: 32949458 DOI: 10.1093/ecco-jcc/jjaa194]

20 **Cornish JS**, Wirthgen E, Däbritz J. Biomarkers Predictive of Response to Thiopurine Therapy in Inflammatory Bowel Disease. *Front Med (Lausanne)* 2020; **7**: 8 [PMID: 32064265 DOI: 10.3389/fmed.2020.00008]

21 **Waljee AK**, Wallace BI, Cohen-Mekelburg S, Liu Y, Liu B, Sauder K, Stidham RW, Zhu J, Higgins PDR. Development and Validation of Machine Learning Models in Prediction of Remission in Patients With Moderate to Severe Crohn Disease. *JAMA Netw Open* 2019; **2**: e193721 [PMID: 31074823 DOI: 10.1001/jamanetworkopen.2019.3721]

22 **Waljee AK**, Lipson R, Wiitala WL, Zhang Y, Liu B, Zhu J, Wallace B, Govani SM, Stidham RW, Hayward R, Higgins PDR. Predicting Hospitalization and Outpatient Corticosteroid Use in Inflammatory Bowel Disease Patients Using Machine Learning. *Inflamm Bowel Dis* 2017; **24**: 45-53 [PMID: 29272474 DOI: 10.1093/ibd/izx007]

23 **Noh SM**, Oh EH, Park SH, Lee JB, Kim JY, Park JC, Kim J, Ham NS, Hwang SW, Yang DH, Byeon JS, Myung SJ, Yang SK, Ye BD. Association of Faecal Calprotectin Level and Combined Endoscopic and Radiological Healing in Patients With Crohn's Disease Receiving Anti-tumour Necrosis Factor Therapy. *J Crohns Colitis* 2020; **14**: 1231-1240 [PMID: 32157278 DOI: 10.1093/ecco-jcc/jjaa042]

24 **Maaser C**, Sturm A, Vavricka SR, Kucharzik T, Fiorino G, Annese V, Calabrese E, Baumgart DC, Bettenworth D, Borralho Nunes P, Burisch J, Castiglione F, Eliakim R, Ellul P, González-Lama Y, Gordon H, Halligan S, Katsanos K, Kopylov U, Kotze PG, Krustinš E, Laghi A, Limdi JK, Rieder F, Rimola J, Taylor SA, Tolan D, van Rheenen P, Verstockt B, Stoker J; European Crohn's and Colitis Organisation [ECCO] and the European Society of Gastrointestinal and Abdominal Radiology [ESGAR]. ECCO-ESGAR Guideline for Diagnostic Assessment in IBD Part 1: Initial diagnosis, monitoring of known IBD, detection of complications. *J Crohns Colitis* 2019; **13**: 144-164 [PMID: 30137275 DOI: 10.1093/ecco-jcc/jjy113]

25 **Porter AC**, Aubrecht J, Birch C, Braun J, Cuff C, Dasgupta S, Gale JD, Hinton R, Hoffmann SC, Honig G, Linggi B, Schito M, Casteele NV, Sauer JM. Biomarkers of Crohn's Disease to Support the

Development of New Therapeutic Interventions. *Inflamm Bowel Dis* 2020; **26**: 1498-1508 [PMID: 32840322 DOI: 10.1093/ibd/izaa215]

26 **Ma C**, Battat R, Parker CE, Khanna R, Jairath V, Feagan BG. Update on C-reactive protein and fecal calprotectin: are they accurate measures of disease activity in Crohn's disease? *Expert Rev Gastroenterol Hepatol* 2019; **13**: 319-330 [PMID: 30791776 DOI: 10.1080/17474124.2019.1563481]

27 **Lin X**, Qiu Y, Feng R, Chen B, He Y, Zeng Z, Zhang S, Chen M, Mao R. Normalization of C-Reactive Protein Predicts Better Outcome in Patients With Crohn's Disease With Mucosal Healing and Deep Remission. *Clin Transl Gastroenterol* 2020; **11**: e00135 [PMID: 32463625 DOI: 10.14309/ctg.0000000000000135]

28 **Click B**, Vargas EJ, Anderson AM, Proksell S, Koutroubakis IE, Ramos Rivers C, Hashash JG, Regueiro M, Watson A, Dunn MA, Schwartz M, Swoger J, Baidoo L, Barrie A 3rd, Binion DG. Silent Crohn's Disease: Asymptomatic Patients with Elevated C-reactive Protein Are at Risk for Subsequent Hospitalization. *Inflamm Bowel Dis* 2015; **21**: 2254-2261 [PMID: 26197446 DOI: 10.1097/MIB.0000000000000516]

29 **Bouckaert RR**, Frank E. Evaluating the Replicability of Significance Tests for Comparing Learning Algorithms, in Advances in Knowledge Discovery and Data Mining. In: Dai H, Srikant R, Zhang C. Lecture Notes in Computer Science. Springer: Berlin, Heidelberg, 2004

30 **Hajian-Tilaki K**. Sample size estimation in diagnostic test studies of biomedical informatics. *J Biomed Inform* 2014; **48**: 193-204 [PMID: 24582925 DOI: 10.1016/j.jbi.2014.02.013]

31 **Torres J**, Mehandru S, Colombel JF, Peyrin-Biroulet L. Crohn's disease. *Lancet* 2017; **389**: 1741-1755 [PMID: 27914655 DOI: 10.1016/S0140-6736(16)31711-1]

32 **Con D**, Jackson B, Gray K, De Cruz P. eHealth for inflammatory bowel disease self-management - the patient perspective. *Scand J Gastroenterol* 2017; **52**: 973-980 [PMID: 28598210 DOI: 10.1080/00365521.2017.1333625]

33 **van der Valk ME**, Mangen MJ, Severs M, van der Have M, Dijkstra G, van Bodegraven AA, Fidder HH, de Jong DJ, van der Woude CJ, Romberg-Camps MJ, Clemens CH, Jansen JM, van de Meeberg PC, Mahmmod N, van der Meulen-de Jong AE, Ponsioen CY, Bolwerk C, Vermeijden JR, Siersema PD, Leenders M, Oldenburg B; COIN study group and the Dutch Initiative on Crohn and Colitis. Evolution of Costs of Inflammatory Bowel Disease over Two Years of Follow-Up. *PLoS One* 2016; **11**: e0142481 [PMID: 27099937 DOI: 10.1371/journal.pone.0142481]

34 **Jackson B**, Con D, Ma R, Gorelik A, Liew D, De Cruz P. Health care costs associated with Australian tertiary inflammatory bowel disease care. *Scand J Gastroenterol* 2017; **52**: 851-856 [PMID: 28509590 DOI: 10.1080/00365521.2017.1323117]

35 **Best WR**, Becktel JM, Singleton JW, Kern F Jr. Development of a Crohn's disease activity index. National Cooperative Crohn's Disease Study. *Gastroenterology* 1976; **70**: 439-444 [PMID: 1248701]

36 **Daperno M**, D'Haens G, Van Assche G, Baert F, Bulois P, Maunoury V, Sostegni R, Rocca R, Pera A, Gevers A, Mary JY, Colombel JF, Rutgeerts P. Development and validation of a new, simplified endoscopic activity score for Crohn's disease: the SES-CD. *Gastrointest Endosc* 2004; **60**: 505-512 [PMID: 15472670 DOI: 10.1016/s0016-5107(04)01878-4]

37 **Limsrivilai J**, Pausawasdi N. Intestinal tuberculosis or Crohn's disease: a review of the diagnostic models designed to differentiate between these two gastrointestinal diseases. *Intest Res* 2021; **19**: 21-32 [PMID: 32311862 DOI: 10.5217/ir.2019.09142]

38 **Sung JJ**, Stewart CL, Freedman B. Artificial intelligence in health care: preparing for the fifth Industrial Revolution. *Med J Aust* 2020; **213**: 253-255.e1 [PMID: 32892395 DOI: 10.5694/mja2.50755]

39 **Iwagami H**, Ishihara R, Aoyama K, Fukuda H, Shimamoto Y, Kono M, Nakahira H, Matsuura N, Shichijo S, Kanesaka T, Kanzaki H, Ishii T, Nakatani Y, Tada T. Artificial intelligence for the detection of esophageal and esophagogastric junctional adenocarcinoma. *J Gastroenterol Hepatol* 2021; **36**: 131-136 [PMID: 32511793 DOI: 10.1111/jgh.15136]

40 **East JE**, Rittscher J. Artificial intelligence for colonoscopic polyp detection: High performance *vs* human nature. *J Gastroenterol Hepatol* 2020; **35**: 1663-1664 [PMID: 33043510 DOI: 10.1111/jgh.15262]

41 **Parasher G**, Wong M, Rawat M. Evolving role of artificial intelligence in gastrointestinal endoscopy. *World J Gastroenterol* 2020; **26**: 7287-7298 [PMID: 33362384 DOI: 10.3748/wjg.v26.i46.7287]

42 **Shung D**, Tsay C, Laine L, Chang D, Li F, Thomas P, Partridge C, Simonov M, Hsiao A, Tay JK, Taylor A. Early identification of patients with acute gastrointestinal bleeding using natural language processing and decision rules. *J Gastroenterol Hepatol* 2021; **36**: 1590-1597 [PMID: 33105045 DOI: 10.1111/jgh.15313]

43 **Guan Y**, Zhang H, Quang D, Wang Z, Parker SCJ, Pappas DA, Kremer JM, Zhu F. Machine Learning to Predict Anti-Tumor Necrosis Factor Drug Responses of Rheumatoid Arthritis Patients by Integrating Clinical and Genetic Markers. *Arthritis Rheumatol* 2019; **71**: 1987-1996 [PMID: 31342661 DOI: 10.1002/art.41056]

44 **Lee S**, Eun Y, Kim H, Cha HS, Koh EM, Lee J. Machine learning to predict early TNF inhibitor users in patients with ankylosing spondylitis. *Sci Rep* 2020; **10**: 20299 [PMID: 33219239 DOI: 10.1038/s41598-020-75352-7]

World Journal of Gastroenterology

Submit a Manuscript: https://www.f6publishing.com

World J Gastroenterol 2021 October 14; 27(38): 6489-6500

DOI: 10.3748/wjg.v27.i38.6489

ISSN 1007-9327 (print) ISSN 2219-2840 (online)

ORIGINAL ARTICLE

Observational Study

Serum soluble suppression of tumorigenicity 2 as a novel inflammatory marker predicts the severity of acute pancreatitis

Yan Zhang, Bo Cheng, Zhong-Wei Wu, Zong-Chao Cui, Yao-Dong Song, San-Yang Chen, Yan-Na Liu, Chang-Ju Zhu

ORCID number: Yan Zhang 0000-0002-3657-4255; Bo Cheng 0000-0001-9474-9861; Zhong-Wei Wu 0000-0002-1983-9274; Zong-Chao Cui 0000-0001-8167-5437; Yao-Dong Song 0000-0002-9586-7963; San-Yang Chen 0000-0003-1949-4680; Yan-Na Liu 0000-0003-4788-3085; Chang-Ju Zhu 0000-0002-5811-7936.

Author contributions: Zhu CJ conceived and designed the study; Zhang Y, Cheng B, Liu YN and Wang QF performed the research; Wu ZW contributed the data acquisition; Zhang Y and Cui ZC conducted data analysis/interpretation; Song YD contributed statistical analysis; Zhang Y and Chen SY wrote the manuscript; All authors have read and approved the final manuscript.

Supported by Henan Province Education Department for Henan Province University Key Scientific Research Project, No. 20A320018 and No. 20A320064.

Institutional review board statement: The study was reviewed and approved by the First Affiliated Hospital of Zhengzhou University Institutional Review Board [(Approval No. 2018-KY-140)].

Informed consent statement: All

Yan Zhang, Bo Cheng, Zhong-Wei Wu, Zong-Chao Cui, Yao-Dong Song, San-Yang Chen, Yan-Na Liu, Chang-Ju Zhu, Department of Emergency, the First Affiliated Hospital of Zhengzhou University, Zhengzhou 450052, Henan Province, China

Corresponding author: Chang-Ju Zhu, PhD, Chief Doctor, Chief Physician, Director, Doctor, Professor, Department of Emergency, the First Affiliated Hospital of Zhengzhou University, No. 1 Eastern Jianshe Road, Zhengzhou 450052, Henan Province, China.
zhuchangju98@163.com

Abstract

BACKGROUND

Acute pancreatitis (AP) is an inflammatory disease in which the regulatory pathway is complex and not well understood. Soluble suppression of tumorigenicity 2 (sST2) protein receptor functions as a decoy receptor for interleukin (IL)-33 to prevent IL-33/suppression of tumorigenicity 2L (ST2L)-pathway-mediated T helper (Th)2 immune responses.

AIM

To investigate the role of sST2 in AP.

METHODS

We assessed the association between sST2 and severity of AP in 123 patients enrolled in this study. The serum levels of sST2, C-reactive protein (CRP) and Th1- and Th2-related cytokines, including interferon (IFN)-γ, tumor necrosis factor (TNF)-α, IL-2, IL-4, IL-5 and IL-13, were measured by highly sensitive ELISA, and the severity of AP in patients was evaluated by the 2012 Atlanta Classification Criteria.

RESULTS

Serum sST2 levels were significantly increased in AP patients, and further, these levels were significantly elevated in severe AP (SAP) patients compared to moderately severe AP (MSAP) and mild AP (MAP) patients. Logistic regression showed sST2 was a predictor of SAP [odds ratio (OR): 1.003 (1.001–1.006), P = 0.000]. sST2 cutoff point was 1190 pg/mL, and sST2 above this cutoff was associated with SAP. sST2 was also a predictor of any organ failure and mortality during AP [OR: 1.006 (1.003–1.009), P = 0.000, OR: 1.002 (1.001–1.004), P = 0.012,

respectively]. Additionally, the Th1-related cytokines IFN-γ and TNF-α in the SAP group were higher and the Th2-related cytokine IL-4 in the SAP group was significantly lower than those in MSAP and MAP groups.

CONCLUSION

sST2 may be used as a novel inflammatory marker in predicting AP severity and may regulate the function and differentiation of IL-33/ST2-mediated Th1 and Th2 Lymphocytes in AP homeostasis.

Key Words: Acute pancreatitis; Soluble suppression of tumorigenicity 2; T-helper 1 cells; T-helper 2 cells; Interleukin-33; Biomarker

©The Author(s) 2021. Published by Baishideng Publishing Group Inc. All rights reserved.

Core Tip: Acute pancreatitis (AP) is an inflammatory disease in which the regulatory pathway is complex and not well understood. The interleukin (IL)-33/ suppression of tumorigenicity 2L (ST2L) functional pathway is involved in the pathological process of AP. Soluble suppression of tumorigenicity 2 protein (sST2) is a soluble receptor, which is released in the circulation acts as a decoy receptor by binding IL-33. However, sST2 as one of the most promising disease biomarker, has not been studied in the development of AP. In this study we studied the role of sST2 as an inflammatory marker for predicting the severity of acute pancreatitis.

Citation: Zhang Y, Cheng B, Wu ZW, Cui ZC, Song YD, Chen SY, Liu YN, Zhu CJ. Serum soluble suppression of tumorigenicity 2 as a novel inflammatory marker predicts the severity of acute pancreatitis. *World J Gastroenterol* 2021; 27(38): 6489-6500
URL: https://www.wjgnet.com/1007-9327/full/v27/i38/6489.htm
DOI: https://dx.doi.org/10.3748/wjg.v27.i38.6489

INTRODUCTION

Acute pancreatitis (AP) is caused by activation of pancreatic enzymes induced by a variety of etiologies, resulting in autodigestion, hemorrhage, edema, and even necrosis of pancreatic tissue, with or without other organ function changes. The clinical severity of AP is related to its prognosis. Severe AP (SAP) has a poor prognosis, and can cause severe disorders of multiple organ functions, and the mortality can reach 30%[1]. Excessive activation of inflammatory cells and their cytokines is one of the main mechanisms of pathogenesis of AP. The development and outcome of AP are closely related to immune function[2]. Research on changes in inflammatory mediators in patients with different clinical severity of AP is important clinically. A better understanding of the regulatory inflammatory pathways in AP is beneficial for discovery of new therapeutic targets.

Suppression of tumorigenicity 2 protein (ST2) is a member of the interleukin (IL)-1 receptor family with transmembrane (ST2L) and soluble (sST2) isoforms. The ligand of ST2 is IL-33, which can produce nuclear signal transduction and immunomodulatory functions in various cells when combined with ST2L. IL-33 is mainly produced by epithelial and endothelial cells. After exposure to pathogens, stress or necrosis caused by injury, IL-33 can signal the presence of tissue damage to local immune cells, thereby acting as a danger signal or alarm protein[3]. ST2L can form a heterodimer with IL-1R-related protein, which is widely present in the membranes of mast cells, T helper (Th)2 cells, dendritic cells, basophils, and macrophages[4,5]. The importance and role of the IL-33/ST2L axis have been evaluated and confirmed in several inflammatory and cardiac diseases and cancer. sST2, as a soluble receptor that is released in the circulation, acts as a decoy receptor by binding IL-33, and, thus, sST2 is involved as the counterbalance/response on IL-33/ST2L axis activation by inhibiting its signal transduction through ST2L.

The IL-33/ST2L functional pathway is involved in coxsackievirus B5 (CVB5)-induced pancreatitis[6]. Mice deficient in ST2L develop significantly more severe pancreatitis. Conversely, wild-type mice treated with recombinant IL-33 develop

study participants, or their legal guardian, provided informed written consent prior to study enrollment.

Conflict-of-interest statement: All the authors have no potential conflict of interest to disclose.

Data sharing statement: Technical appendix, statistical code, and dataset available from the corresponding author at zhuchangju98@163.com. No additional data are available.

STROBE statement: The authors have read the STROBE Statement—checklist of items, and the manuscript was prepared and revised according to the STROBE Statement—checklist of items.

Open-Access: This article is an open-access article that was selected by an in-house editor and fully peer-reviewed by external reviewers. It is distributed in accordance with the Creative Commons Attribution NonCommercial (CC BY-NC 4.0) license, which permits others to distribute, remix, adapt, build upon this work non-commercially, and license their derivative works on different terms, provided the original work is properly cited and the use is non-commercial. See: http://creativecommons.org/Licenses/by-nc/4.0/

Manuscript source: Unsolicited manuscript

Specialty type: Gastroenterology and hepatology

Country/Territory of origin: China

Peer-review report's scientific quality classification
Grade A (Excellent): 0
Grade B (Very good): B
Grade C (Good): C, C
Grade D (Fair): 0
Grade E (Poor): 0

Received: April 4, 2021
Peer-review started: April 4, 2021
First decision: May 27, 2021
Revised: June 10, 2021
Accepted: August 27, 2021
Article in press: August 27, 2021

Published online: October 14, 2021

P-Reviewer: Barauskas G, Pezzilli R
S-Editor: Ma YJ
L-Editor: Filipodia
P-Editor: Liu JH

significantly lower viral titers, and pancreatitis is attenuated, indicating that IL-33/ST2L is involved in the pathological process of AP. SAP can cause severe disorders of multiple organ, including AP-related myocardial, kidney, or lung injury. In clinical studies, sST2 is recognized as an important marker for monitoring treatment in heart failure patients and higher sST2 is associated with worse right ventricular dysfunction and higher mean pulmonary and right atrial pressures[7-9]. sST2 is also recognized as an important prognostic marker in patients with kidney injury, where specific characteristics of sST2 enable better assessment of the risk of end-stage renal disease patients on dialysis[10]. It has been also found to be relevant in pulmonary diseases, sepsis, trauma, and gastrointestinal diseases[11-14]. sST2 can be used as a biomarker in heart, lung and kidney injury, and may also be served as biomarker in the severity of AP. However, sST2, as one of the most promising disease biomarkers, has not been studied in the development of AP.

The IL-33/ST2L pathway promotes $CD4^+$ T-cell differentiation to an atypical Th2 phenotype[15]. $CD4^+$ T cells play a major role in the pathogenesis of pancreatitis[16]. In this study, we investigated whether and how the IL-33/ST2L pathway was involved in AP in patients with different clinical severity of AP.

MATERIALS AND METHODS

Patients

A total of 123 hospitalized AP patients were recruited between January 2018 and August 2020 in the Emergency Surgery Department, Emergency Internal Medicine Department, and Comprehensive Intensive Care Unit (ICU) in the First Affiliated Hospital of Zhengzhou University. Inclusion criteria for subject enrollment included: (1) age 18–90 years; (2) clinically and radiographically confirmed AP; and (3) syndrome onset < 24 h prior to study enrollment. Exclusion criteria were: (1) Pregnancy or patients with immunodeficiency, acute and chronic hepatitis, end-stage liver and kidney disease, malignant tumors, or trauma; (2) Patients who have used hormones or immunosuppressive agents within the past 3 mo; and (3) Patients with chronic pancreatitis. This study complied with medical ethics standards and was approved by the hospital Ethics Committee. All participants provided written informed consent.

Demographic and clinical data

Demographic and clinical data were collected, including age, sex, ethnicity, body mass index (BMI), etiology, and comorbidities. According to the 2012 Atlanta Classification Criteria, patients were divided into: (1) Mild AP (MAP): No organ failure and local and systemic complications; (2) Moderately severe AP (MSAP): Local and/or systemic complications and/or transient organ failure (< 48 h); and (3) SAP: Persistent organ failure (> 48 h), with or without local complications.

Measurement of serum sST2, interferon-γ, tumor necrosis factor-α, IL-2, IL-4, IL-5, IL-13 and C-reactive protein

For serum preparation, peripheral venous blood samples (4 mL) were collected from each patient within 24 h after symptom onset and allowed to clot for 2 h at room temperature prior to centrifugation at 1500 rpm for 20 min. Serum was aliquoted and stored at -80 °C until further testing. The laboratory technicians were blinded to the baseline data and AP severity of the patients. Serum sST2 Levels were measured using a human sST2 ELISA kit (Elabscience, Wuhan, China). Serum C-reactive protein (CRP) and levels of Th1-cell-related inflammatory factors interferon (IFN)-γ, tumor necrosis factor (TNF)-α and IL-2 and Th2-cell-related inflammatory factors IL-4, IL-5 and IL-13 were measured in duplicate using an ELISA kit from Elabscience.

Statistical analysis

The Shapiro–Wilk test was used to test the normality of the data, and the Levene test was used to analyze the homogeneity of the data. Normally distributed measurement data are expressed as mean ± SE, and data were compared between groups by Student's *t* test and analysis of variance. Non-normally distributed measurement data are represented by median and interquartile range [M (IQR)], and comparison of data between groups used the Kruskal–Wallis test, and the nonparametric Mann–Whitney *U* test was used for comparison between the two groups. The *Z* value was used for the statistic. Categorical variables were described as frequencies with percentages, and

chi-square test was used to examine significant differences between categorical variables. The influence of serum sST2 levels on severity was assessed using univariate and multivariate binary logistic regression analysis, with significant confounding factors tested in the adjusted univariate analysis. Results were expressed as adjusted odds ratios (ORs) with the corresponding 95% confidence intervals (CIs). Optimal sST2 cutoff points were obtained using receiver operating characteristic (ROC) curve analysis. Additionally, IFN-γ, TNF-α, IL-2, IL-4, IL-5, and IL-13 data were logarithmically transformed for analysis. The relationships between sST2, IFN-γ, TNF-α, IL-2, IL-4, IL-5, and IL-13 and total length of hospital stay and ICU hospital stay were analyzed using Spearman's rank correlation. $P < 0.05$ was considered statistically significant. All statistical analyses were performed using SPSS version 21.0.

RESULTS

Patient characteristics

We enrolled 123 patients: 55 (45%) with MAP, 37 (30%) with MSAP, and 31 (25%) with SAP. The etiology of AP was biliary stones (74.8%), alcohol (8.9%), laparoscopic retrograde cholangiopancreatography (1.6%), alcohol and biliary stones (8.1%) and metabolic factors (2.5%), drug-induced (0.8%), and idiopathic pancreatitis (3.3%). The etiology did not differ significantly among the groups. The incidence of acute pancreatitis with acute cholecystitis is 4.8%. Three patients had accompanying cholecystitis in the MAP group, one patient had cholecystitis in MSAP group, and two patients in the SAP group. There was no significant difference between the groups for cholecystitis.

The BMI of the healthy control group was lower than that of the MAP, MSAP, and SAP groups, and the difference was significant ($Z = -3.15$, $P = 0.002$, $Z = -3.16$, $P = 0.002$, $Z = -5.046$, $P = 0.000$). There was no significant difference in BMI between the MAP and MSAP groups ($Z = -2.27$, $P = 0.820$). The BMI of the MAP and MSAP groups was lower than that of the SAP group ($Z = -2.767$, $P = 0.006$, $Z = -2.452$, $P = 0.014$, respectively).

In the MAP group, three patients had accompanying hypertension, three were complicated by diabetes, and three were complicated by coronary heart disease. In the MSAP group, two patients had hypertension, three were complicated by diabetes, and one was complicated by coronary heart disease. Two patients in the SAP group had hypertension, five were complicated with diabetes, and one with coronary heart disease. There was no significant difference between the groups for co-morbidity, hypertension, diabetes, and coronary heart disease. None of the 123 patients were taking immunosuppressive agents. After statistical analysis, there was no significant difference in age, gender, or ethnicity between the AP groups. Patients in the AP groups had no significant difference in age, gender, or ethnicity compared with the healthy control group (Table 1).

sST2 Levels elevated in SAP patients

To identify the involvement of the IL-33/ST2L pathway in AP, we examined expression of IL-33 and sST2 in the serum after AP. The level of IL-33 was extremely low in the blood of all AP patients. Almost all samples were under the detection limit of the IL-33 ELISA, and only seven patients showed higher values. In addition, the low, almost undetectable levels of IL-33 were unlikely to be associated with worsening clinical outcomes. Nevertheless, we tested the levels of sST2 at the same time.

The sST2 content of the AP group and the healthy control group conformed to a normal distribution and uniformity of variance. We observed increased levels of sST2 in AP patients compared to healthy controls (1115.4 *vs* 211.1 pg/mL, $t = 9.355$, $P = 0.000$) (Figure 1). The sST2 value of the three AP groups did not conform to a normal distribution, and the nonparametric Kruskal–Wallis *H* test was used for comparison among multiple groups. The level of sST2 was significantly higher in the SAP group compared with MSAP and MAP groups ($Z = -3.510$, $P = 0.000$, $Z = -7.305$, $P = 0.000$, respectively). The level of sST2 in the MSAP group was significantly higher than in the MAP group ($Z = -6.489$, $P = 0.000$). The data are shown in Figure 2 and Table 2. The level of CRP in the SAP group was significantly higher than in the MSAP and MAP groups ($Z = -5.634$, $P = 0.000$, $Z = -7.150$, $P = 0.000$, respectively). The level of CRP in the MSAP group was higher than in the MAP group ($Z = -2.891$, $P = 0.000$) (Figure 3). This suggested that sST2 expression was increased in the SAP group, and that IL-33 signaling played a role in regulating the inflammatory response during AP.

Table 1 Demographic and clinical data of acute pancreatitis patients and health controls

	MAP (*n* = 55)	MSAP (*n* = 37)	SAP (*n* = 31)	Control (*n* = 42)	χ^2/t	*P* value
Age, yr	45.16 ± 1.74	50.35 ± 2.54	51.94 ± 2.42	45.60 ± 1.75	2.173	0.093
Gender					4.418	0.220
Male	34 (61.8)	21 (56.8)	14 (45.2)	18 (42.9)		
Female	21 (38.2)	16 (43.2)	17 (54.8)	24 (57.1)		
BMI, kg/m^2	25.63 (2.15)	25.81 (1.97)	26.54 (1.22)	24.61 (2.09)	28.518	0.000
Ethnicity					1.7	0.721
Han nationality	52 (94.5)	36 (97.3)	31 (100.0)	41 (97.6)		
Minority	3 (5.5)	1 (2.7)	0 (0.0)	1 (2.4)		
Etiology					9.374	0.677
Biliary stones	45 (81.8)	27 (73.0)	20 (64.5)			
Alcoholic	4 (7.3)	4 (10.8)	3 (9.7)			
ERCP	1 (1.8)	0 (0.0)	1 (3.2)			
Metabolic	1 (1.8)	1 (2.7)	1 (3.2)			
Mixed (alcohol + biliary stones)	2 (3.7)	3 (8.1)	5 (16.2)			
Drug-induced idiopathic	1 (1.8)	0 (0.0)	0 (0.0)			
Co-morbidity	1 (1.8)	2 (5.4)	1 (3.2)			
Hypertension	3 (5.5)	2 (5.4)	2 (6.5)		0.044	0.978
Diabetes	3 (5.5)	3 (8.1)	5 (16.1)		2.691	0.283
Coronary heart disease	3 (5.5)	1 (2.7)	1 (3.2)		0.515	0.860
Cholecystitis	3 (5.5)	1 (2.7)	2 (6.5)		0.582	0.747

Normally distributed continuous variables are represented by the mean ± SE, non-normally distributed continuous variables are represented by the median (interquartile range), and categorical variables are represented by the number of cases and percentages. AP: Acute pancreatitis; BMI: Body mass index; ERCP: Endoscopic retrograde cholangiopancreatography; MAP: Mild acute pancreatitis; MSAP: Moderately severe acute pancreatitis; SAP: Severe acute pancreatitis.

Table 2 Levels of Serum soluble suppression of tumorigenicity 2 and C-reactive protein in different acute pancreatitis groups

	MAP (*n* = 55)	MSAP (*n* = 37)	SAP (*n* = 31)	χ^2	*P* value
	Median (IQR)	Median (IQR)	Median (IQR)		
sST2 (pg/mL)	540 (385)	1250 (700)[b]	1890 (812)[b,d]	74.899	0.000
CRP 48 h (mg/L)	59.37 (32.92)	76.54 (31.79)[b]	120.78 (56.66)[b,d]	59.403	0.000

[b]$P < 0.001$ *vs* mild acute pancreatitis group.
[d]$P < 0.001$ *vs* moderately severe acute pancreatitis group. AP: Acute pancreatitis; MAP: Mild AP; MSAP: Moderately severe AP; SAP: Severe AP; sST2: Soluble suppression of tumorigenicity 2; CRP: C- reactive protein.

sST2 has predictive value for severity of AP

We conducted a multivariate analysis to evaluate whether the relationship of sST2 with SAP was really independent. Logistic regression showed that sST2 levels at admission [OR: 1.003 (1.001–1.006), $P = 0.000$] was a predictor of SAP. With the ROC curve, the optimal cut-off value of serum sST2 levels as an indicator for prediction of SAP was projected to be 1190 pg/mL, which yielded a sensitivity of 90.3% and specificity of 76.1%, with the area under the curve 0.889 (95%CI: 0.829–0.949; $P = 0.000$) (Figure 4).

sST2 was also a predictor of any organ failure and mortality during AP [OR: 1.006 (1.003–1.009), $P = 0.000$, OR: 1.002 (1.000–1.004), $P = 0.012$, respectively]. BMI and CRP

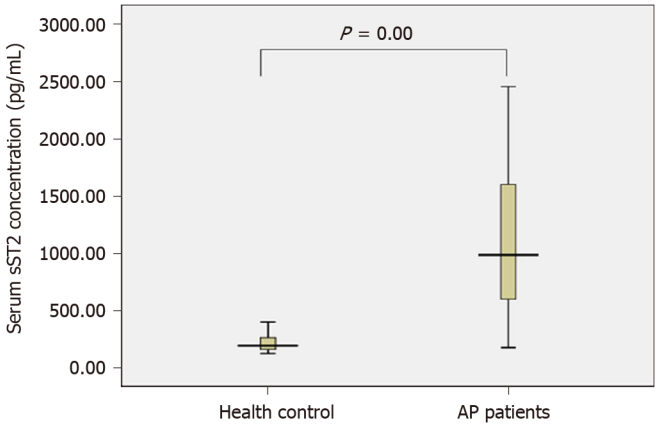


Figure 1 Serum soluble suppression of tumorigenicity 2 level in acute pancreatitis patients and health control. AP: Acute pancreatitis; sST2: Soluble suppression of tumorigenicity 2.

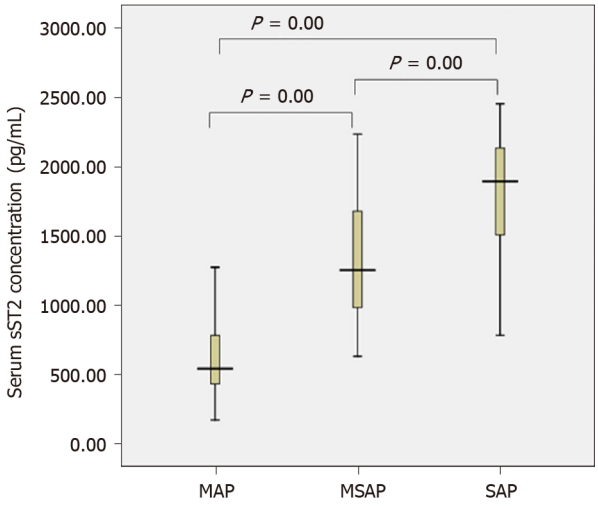


Figure 2 Serum soluble suppression of tumorigenicity 2 level in acute pancreatitis patients. AP: Acute pancreatitis; MAP: Mild acute pancreatitis; MSAP: Moderately severe acute pancreatitis; SAP: Severe acute pancreatitis; sST2: Soluble suppression of tumorigenicity 2.

were also predictors of SAP at admission [OR: 2.629 (1.075–6.429), P = 0.034, OR: 1.066 (1.031–1.101), P =0.002, respectively]. However, there was no value of BMI and CRP for predicting organ failure and mortality. sST2, CRP, age, BMI, and gender were not predictive of necrosis. The data are shown in Table 3. Furthermore, there was a significant correlation between the level of sST2 and total hospital stay and length of stay in ICU (r = 0.463, P = 0.000, r = 0.673, P = 0.000) (Table 4).

Relationship between levels of serum inflammatory factors of Th1 and Th2 cells and severity of AP

To further explore the biological mechanism of AP, we examined the production of Th1-related cytokines IFN-γ, TNF-α and IL-2 and Th2-related cytokines IL-4, IL-5 and IL-13 in the serum to clarify the role of the inflammatory process in the pathogenesis of AP. The concentration of inflammatory factors measured after logarithmic conversion was in accordance with the normal distribution. Statistical analysis showed that the serum levels of IFN-γ and TNF-α in the SAP and MSAP groups were higher than those in the MAP group, and the difference was significant. There was no significant difference in IFN-γ and TNF-α between the SAP and MSAP groups. IL-4 expression in the SAP group was significantly lower than that in the MAP and MSAP groups, but there was no significant difference between the MAP and MSAP groups. There was no significant difference in the expression of IL-2, IL-5 and IL-13 between the MAP, MSAP and SAP groups (Table 5).

Expression of Th1-cell-associated inflammatory factor IFN-γ and TNF-α was positively correlated with the length of total hospital stay and total ICU stay, while

Table 3 Multivariate binary regressions in acute pancreatitis patients showing association between soluble suppression of tumorigenicity 2 levels on admission and severity, necrosis, organ failure and mortality

Variables	OR (95%CI)	*P* value	Variables	OR (95%CI)	*P* value
MAP/MSAP and SAP			Necrosis		
Age	1.031 (0.969-1.097)	0.330	Age	1.019 (0.990-1.049)	0.209
BMI	2.629 (1.075-6.429)	0.034	BMI	0.973 (0.695-1.362)	0.847
Gender	1.096 (1.001-1.006)	0.910	Gender	0.529 (0.234-1.198)	0.127
CRP	1.066 (1.031-1.101)	0.002	CRP	1.009 (0.995-1.023)	0.209
sST2	1.003 (1.001-1.006)	0.000	sST2	1.000 (0.999-1.001)	0.837
Any organ failure			Mortality		
Age	1.017 (0.963-1.074)	0.546	Age	1.024 (0.967-1.085)	0.411
BMI	1.407 (0.788-2.511)	0.248	BMI	1.685 (0.731-3.883)	0.220
Gender	0.246 (0.050-1.202)	0.083	Gender	0.249 (0.040-1.563)	0.138
CRP	1.030 (0.991-1.071)	0.128	CRP	1.009 (0.987-1.032)	0.415
sST2	1.006 (1.003-1.009)	0.000	sST2	1.002 (1.000-1.004)	0.012

AP: Acute pancreatitis; MAP: Mild AP; MSAP: Moderately severe AP; SAP: Severe AP; BMI: Body mass index; CRP: C-reactive protein; sST2: Soluble suppression of tumorigenicity 2.

Table 4 Correlation between serum inflammatory factor and total hospital stay and intensive care unit stay

sST2/LN (Inflammatory factors, pg/mL)	Total hospital stay		Total ICU stay	
	r	*P* value	*r*	*P* value
sST2	0.463[b]	0.000	0.673[b]	0.000
LN (IFN-γ)	0.430[b]	0.000	0.700[b]	0.000
LN (TNF-α)	0.341[b]	0.000	0.652[b]	0.000
LN (IL-2)	-0.043	0.638	-0.082	0.366
LN (IL-4)	-0.483[b]	0.000	-0.440[b]	0.000
LN (IL-5)	-0.123	0.174	0.062	0.494
LN (IL-13)	-0.006	0.946	-0.139	0.126

[b]$P < 0.001$. sST2: Soluble suppression of tumorigenicity 2; ICU: Intensive care unit; IFN-γ: Interferon-γ; TNF-α: Tumor necrosis factor-α; IL: Interleukin.

expression of Th2-cell-associated inflammatory factor IL-4 was negatively correlated with the length of total hospital stay and total ICU stay (Table 4).

DISCUSSION

The results of our study showed that the levels of sST2 were significantly increased in SAP patients, and there were significant increases in Th1-related cytokines IFN-γ and TNF-α, and a decrease in Th2-related cytokine IL-4. This suggested an insufficient IL-33-driven Th2-type inflammatory response was involved in the pathophysiological process of AP. sST2 is a secreted form of the ST2 receptor and acts as a decoy receptor for IL-33, thus inactivating the functions of IL-33. sST2 expression increases in response to proinflammatory cytokines[17]. Our data were in line with a previous study showing elevated levels of sST2 in AP[18]. Importantly, in our study the levels of sST2 predicted the total hospital stay and length of stay in the ICU, as well as predicted organ failure and mortality during AP. These data support the findings of our study showing that SAP patients more frequently had higher serum levels of sST2 compared with MAP and MSAP patients, and that the early elevated levels of sST2

Table 5 Serum inflammatory factor levels in patients with acute pancreatitis

LN (inflammatory factors pg/mL)	MAP, mean ± SE	MSAP, mean ± SE	SAP, mean ± SE	*F*	*P* value
LN (IFN-γ)	1.98 ± 0.07	2.57 ± 0.08[b]	3.08 ± 0.07[b]	53.393	0.000
LN (TNF-α)	1.63 ± 0.04	2.07 ± 0.05[b]	2.33 ± 0.05[b,d]	45.369	0.000
LN (IL-2)	1.06 ± 0.05	1.05 ± 0.06	0.99 ± 0.05	0.362	0.697
LN (IL-4)	1.02 ± 0.03	0.99 ± 0.04	0.64 ± 0.03[b,d]	23.195	0.000
LN (IL-5)	0.10 ± 0.05	0.10 ± 0.07	0.13 ± 0.08	0.043	0.958
LN (IL-13)	0.76 ± 0.03	0.68 ± 0.06	0.63 ± 0.07	1.703	0.187

Due to the logarithmic transformation of the data, some data are displayed as negative values. The data are expressed as mean ± SE.
[b]$P < 0.001$ *vs* mild acute pancreatitis group.
[d]$P < 0.001$ *vs* moderately severe acute pancreatitis group. AP: Acute pancreatitis; MAP: Mild AP; MSAP: Moderately severe AP; SAP: Severe AP; IFN-γ: Interferon-γ; TNF-α: Tumor necrosis factor-α; IL: Interleukin.

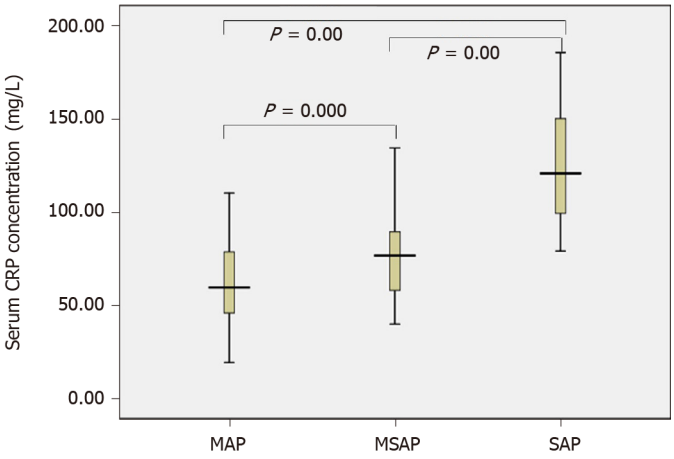


Figure 3 Serum C-reactive protein level in acute pancreatitis patients. AP: Acute pancreatitis; CRP: C-reactive protein; MAP: Mild acute pancreatitis; MSAP: Moderately severe acute pancreatitis; SAP: Severe acute pancreatitis.

correlated with worsened outcome of AP. Thus, the normal function of IL-33 may be inhibited in AP.

SAP can cause severe systemic inflammation and multiple organ dysfunction. It is reported that endogenous danger signals, such as tissue damage or necrosis, and exogenous danger signals, such as microbial pathogens and endotoxins, can enhance the production of sST2 and stimulate the secretion of inflammatory cytokines, thereby weakening the immune response of organs exposed to the danger signals and leading to adverse outcomes[19]. It has been suggested that serum levels of sST2 are significantly increased in inflammatory diseases and serve as a prognostic biomarker of multiple organ dysfunction syndrome (MODS), cardiovascular events, heart failure, acute hypoxemic respiratory failure, and progression of kidney failure. A study based on cardiopulmonary resuscitation showed that plasma levels of sST2 were associated with higher risk of MODS and early death[20]. A role of sST2 in acute hypoxemic respiratory failure indicates that using sST2 concentrations to guide ventilator management may more accurately reflect underlying lung injury and outperform traditional measures of readiness for ventilator liberation[21]. Higher sST2 Levels predict mortality in severe sepsis[12]. These findings agree with our results showing that sST2 was a predictor of any organ failure and mortality during AP.

The IL-33/ST2L pathway has been shown to mediate the modulation of inflammation in different diseases by promoting Th2 response and inhibiting Th1 response [22,23]. Mice that lack IL-33 signaling develop significantly more severe pancreatitis [6]. Based on the regulatory effect of the IL-33/ST2 signaling pathway on Th1 and Th2 cells, we further measured the function of Th1 and Th2 cells in patients with AP. An important finding in our study was the relationship between Th1- and Th2-related cytokines and the severity of AP. Cytokine levels in Th1 cells in patients with SAP were significantly higher than those in patients with MAP and MSAP, and cytokines in

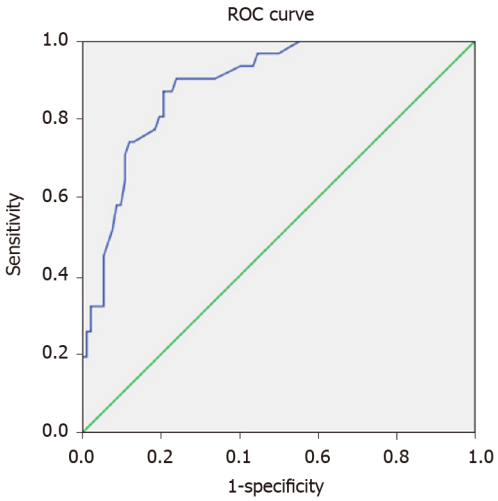


Figure 4 Receiver operating characteristic curve demonstrating sensitivity as a function of 1 – specificity for predicting severe acute pancreatitis based on serum soluble suppression of tumorigenicity 2 levels. ROC: Receiver operating characteristic.

Th2 cells in patients with MAP and MSAP were significantly increased compared with patients with SAP. In our study, we observed that both sST2 and the Th1 cytokines IFN-γ and TNF-α were increased and the Th2 cytokine IL-4 was decreased in SAP. We speculate that increased sST2 in SAP might cause increases in IFN-γ and TNF-α, and decreases in IL-4 by antagonizing the IL-33/ST2 signaling pathway, whereas this inference still needs to be verified by further animal research in the future.

The serum levels of Th1-related cytokines IFN-γ and TNF-α in the SAP group were higher than those in the MAP and MSAP groups, and expression of Th2-related cytokine IL-4 in the SAP group was significantly lower than in the MAP and MSAP groups. The expression of Th1-related inflammatory factors IFN-γ and TNF-α was positively correlated with the length of total hospital stay and total ICU stay, and Th2-cell-associated inflammatory factor IL-4 expression was negatively correlated with the length of hospital and ICU stays. The results suggested that Th1-cell-related immune response was an important factor that aggravated the development of AP, and Th2 cells might have a protective role in the development of AP. Our findings indicate that Th1 and Th2 cells were involved in cytokine-dependent pathways in severity of AP. The results proved that a change in immune response played an important role in the pathogenesis of AP.

In this study, we found an immune imbalance in patients with SAP. Th1-cell-related cytokines IFN-γ and TNF-α in the serum of patients with SAP were higher than those in patients with MSAP. We also found that the expression levels of Th1-cell-associated inflammatory factors IFN-γ and TNF-α were positively correlated with the length of total hospital stay and total ICU stay. This finding is consistent with the latest research showing that inflammatory factors play a consistent role in the pathogenesis of AP[24-26]. IFN-γ and TNF-α could stimulate B cells to produce antibodies, activate macrophages and $CD8^+$ T cells, promote cell-mediated immunity and cytotoxic T cell responses[27], and could induce Th1 cell differentiation and inhibit Th2 cell proliferation. Previous research findings and the present study suggest that Th1 cells are involved in the pathogenesis of AP, especially in the development of SAP. Th1 cells exacerbate the pathophysiological process of AP by releasing Th1-related inflammatory factors.

In humans, serum concentrations of sST2 are increased in several diseases, such as heart disease, pulmonary disease, burn injury, and graft-versus-host disease[28-33]. Few studies have reported the influence of the IL-33/ST2 signaling pathway on the development of AP[6,34-36] and less attention has been paid to Th1 and Th2 cells in the pathogenesis of AP[24]. In this study, we found that the expression of the Th2-related cytokine IL-4 in SAP was significantly lower than that in MAP and MSAP. Expression of the Th2-related inflammatory factor IL-4 was negatively correlated with the length of hospital and ICU hospital stays, suggesting that Th2 cells are involved in the pathogenesis of AP with the tendency to improve symptoms of acute pancreatitis. Collectively, Th2 cells might have a protective effect in the development of AP, tending to delay its development.

Our research had some limitations. Firstly, the main limitation was the small sample size, which may have reduced the statistical power, the accuracy, and effectiveness of identifying true positive results. In future, the results need to be confirmed with larger sample sizes. Secondly, this study was a single-center study, which might have resulted in selection bias. Thirdly, in cases of pancreatitis combined with cholecystitis, cholecystitis might affect the results of the study. Fourthly, we did not examine the numbers of Th1 and Th2 cells. Finally, establishing the initial relationship between AP and elevated sST2 concentrations in our study is novel and useful, but it is necessary to determine the long-term predictive value of sST2 for the prognosis of AP in subsequent longitudinal studies.

CONCLUSION

In conclusion, sST2 may be used as a novel inflammatory marker in predicting AP severity and may regulate the function and differentiation of IL-33/ST2-mediated Th1 and Th2 Lymphocytes in AP homeostasis.

ARTICLE HIGHLIGHTS

Research background

The clinical severity of acute pancreatitis (AP) is related to its prognosis. Excessive activation of inflammatory cells and their cytokines is one of the main mechanisms of pathogenesis of AP. Research on changes in inflammatory mediators in patients with different clinical severity of AP is important clinically. The interleukin (IL)-33/ST2L functional pathway is involved in the pathological process of AP. Soluble suppression of tumorigenicity 2 (sST2) is a secreted form of the ST2 receptor and acts as a decoy receptor for IL-33. In this study, we investigated whether the sST2 could serve as a novel inflammatory marker predicting the severity of acute pancreatitis.

Research motivation

In this study, the authors focused on the function of sST2 in predicting the severity of AP. The key issue to be solved is the association between IL-33/ST2L pathway and AP. The significance of solving these problems may constitute a new therapeutic target for regulating immune activation during the AP inflammatory storm.

Research objectives

The objective of this study was to investigate the role of sST2 in AP.

Research methods

The authors assessed the association between sST2 and severity of AP in 123 patients enrolled in this study. The serum levels of sST2, C-reactive protein (CRP) and Th1- and Th2-related cytokines interferon (IFN)-γ, tumor necrosis factor (TNF)-α ,IL-2, IL-4, IL-5 and IL-13 were measured by highly sensitive ELISA and the severity of AP patients was evaluated by the 2012 Atlanta Classification Criteria.

Research results

The serum sST2 Level was significantly increased in AP patients and significantly elevated in severe acute pancreatitis (SAP) patients compared to moderate severe acute pancreatitis and mild acute pancreatitis patients. The cutoff point of sST2 at 1190pg/mL was associated with SAP.

Research conclusions

This study suggests that sST2 may be used as a novel inflammatory marker in predicting the severity of acute pancreatitis and that sST2 might regulate the function and differentiation of IL-33/ST2L mediated Th1 and Th2 lymphocytes in the homeostasis of acute pancreatitis.

Research perspectives

It is necessary to determine the long-term predictive value of sST2 for the prognosis of AP in subsequent longitudinal studies. Additionally, the role of IL-33/ST2L in acute pancreatitis needs to be further verified in both *in vivo* and *in vitro* experiments.

ACKNOWLEDGEMENTS

We thank the study participants and the clinical staff for their contribution to this study.

REFERENCES

1 **Muniraj T**, Gajendran M, Thiruvengadam S, Raghuram K, Rao S, Devaraj P. Acute pancreatitis. *Dis Mon* 2012; **58**: 98-144 [PMID: 22370054 DOI: 10.1016/j.disamonth.2012.01.005]
2 **Minkov GA**, Halacheva KS, Yovtchev YP, Gulubova MV. Pathophysiological mechanisms of acute pancreatitis define inflammatory markers of clinical prognosis. *Pancreas* 2015; **44**: 713-717 [PMID: 26061557 DOI: 10.1097/MPA.0000000000000329]
3 **Pascual-Figal DA**, Januzzi JL. The biology of ST2: the International ST2 Consensus Panel. *Am J Cardiol* 2015; **115**: 3B-7B [PMID: 25665766 DOI: 10.1016/j.amjcard.2015.01.034]
4 **Schmitz J**, Owyang A, Oldham E, Song Y, Murphy E, McClanahan TK, Zurawski G, Moshrefi M, Qin J, Li X, Gorman DM, Bazan JF, Kastelein RA. IL-33, an interleukin-1-like cytokine that signals *via* the IL-1 receptor-related protein ST2 and induces T helper type 2-associated cytokines. *Immunity* 2005; **23**: 479-490 [PMID: 16286016 DOI: 10.1016/j.immuni.2005.09.015]
5 **Barksby HE**, Lea SR, Preshaw PM, Taylor JJ. The expanding family of interleukin-1 cytokines and their role in destructive inflammatory disorders. *Clin Exp Immunol* 2007; **149**: 217-225 [PMID: 17590166 DOI: 10.1111/j.1365-2249.2007.03441.x]
6 **Sesti-Costa R**, Silva GK, Proença-Módena JL, Carlos D, Silva ML, Alves-Filho JC, Arruda E, Liew FY, Silva JS. The IL-33/ST2 pathway controls coxsackievirus B5-induced experimental pancreatitis. *J Immunol* 2013; **191**: 283-292 [PMID: 23733876 DOI: 10.4049/jimmunol.1202806]
7 **Emdin M**, Aimo A, Vergaro G, Bayes-Genis A, Lupón J, Latini R, Meessen J, Anand IS, Cohn JN, Gravning J, Gullestad L, Broch K, Ueland T, Nymo SH, Brunner-La Rocca HP, de Boer RA, Gaggin HK, Ripoli A, Passino C, Januzzi JL Jr. sST2 Predicts Outcome in Chronic Heart Failure Beyond NT-proBNP and High-Sensitivity Troponin T. *J Am Coll Cardiol* 2018; **72**: 2309-2320 [PMID: 30384887 DOI: 10.1016/j.jacc.2018.08.2165]
8 **Aimo A**, Januzzi JL Jr, Bayes-Genis A, Vergaro G, Sciarrone P, Passino C, Emdin M. Clinical and Prognostic Significance of sST2 in Heart Failure: JACC Review Topic of the Week. *J Am Coll Cardiol* 2019; **74**: 2193-2203 [PMID: 31648713 DOI: 10.1016/j.jacc.2019.08.1039]
9 **O'Meara E**, Prescott MF, Claggett B, Rouleau JL, Chiang LM, Solomon SD, Packer M, McMurray JJV, Zile MR. Independent Prognostic Value of Serum Soluble ST2 Measurements in Patients With Heart Failure and a Reduced Ejection Fraction in the PARADIGM-HF Trial (Prospective Comparison of ARNI With ACEI to Determine Impact on Global Mortality and Morbidity in Heart Failure). *Circ Heart Fail* 2018; **11**: e004446 [PMID: 29748349 DOI: 10.1161/CIRCHEARTFAILURE.117.004446]
10 **Homsak E**, Ekart R. ST2 as a novel prognostic marker in end-stage renal disease patients on hemodiafiltration. *Clin Chim Acta* 2018; **477**: 105-112 [PMID: 29221927 DOI: 10.1016/j.cca.2017.12.006]
11 **Shieh JM**, Tseng HY, Jung F, Yang SH, Lin JC. Elevation of IL-6 and IL-33 Levels in Serum Associated with Lung Fibrosis and Skeletal Muscle Wasting in a Bleomycin-Induced Lung Injury Mouse Model. *Mediators Inflamm* 2019; **2019**: 7947596 [PMID: 31049028 DOI: 10.1155/2019/7947596]
12 **Hoogerwerf JJ**, Tanck MW, van Zoelen MA, Wittebole X, Laterre PF, van der Poll T. Soluble ST2 plasma concentrations predict mortality in severe sepsis. *Intensive Care Med* 2010; **36**: 630-637 [PMID: 20151106 DOI: 10.1007/s00134-010-1773-0]
13 **Billiar IM**, Guardado J, Abdul-Malak O, Vodovotz Y, Billiar TR, Namas RA. Elevations in Circulating sST2 Levels Are Associated With In-Hospital Mortality and Adverse Clinical Outcomes After Blunt Trauma. *J Surg Res* 2019; **244**: 23-33 [PMID: 31279260 DOI: 10.1016/j.jss.2019.05.057]
14 **Boga S**, Alkim H, Koksal AR, Ozagari AA, Bayram M, Tekin Neijmann S, Sen I, Alkim C. Serum ST2 in inflammatory bowel disease: a potential biomarker for disease activity. *J Investig Med* 2016; **64**: 1016-1024 [PMID: 27001944 DOI: 10.1136/jim-2016-000062]
15 **Lu J**, Kang J, Zhang C, Zhang X. The role of IL-33/ST2L signals in the immune cells. *Immunol Lett* 2015; **164**: 11-17 [PMID: 25662624 DOI: 10.1016/j.imlet.2015.01.008]
16 **Schmidt AI**, Kühlbrey C, Lauch R, Wolff-Vorbeck G, Chikhladze S, Hopt UT, Wittel UA. The predominance of a naive T helper cell subset in the immune response of experimental acute pancreatitis. *Pancreatology* 2017; **17**: 209-218 [PMID: 28258935 DOI: 10.1016/j.pan.2017.02.011]
17 **Mildner M**, Storka A, Lichtenauer M, Mlitz V, Ghannadan M, Hoetzenecker K, Nickl S, Dome B, Tschachler E, Ankersmit HJ. Primary sources and immunological prerequisites for sST2 secretion in humans. *Cardiovasc Res* 2010; **87**: 769-777 [PMID: 20363761 DOI: 10.1093/cvr/cvq104]
18 **Ouziel R**, Gustot T, Moreno C, Arvanitakis M, Degré D, Trépo E, Quertinmont E, Vercruysse V, Demetter P, Le Moine O, McKenzie AN, Delhaye M, Devière J, Lemmers A. The ST2 pathway is involved in acute pancreatitis: a translational study in humans and mice. *Am J Pathol* 2012; **180**: 2330-2339 [PMID: 22542450 DOI: 10.1016/j.ajpath.2012.03.009]
19 **Griesenauer B**, Paczesny S. The ST2/IL-33 Axis in Immune Cells during Inflammatory Diseases. *Front Immunol* 2017; **8**: 475 [PMID: 28484466 DOI: 10.3389/fimmu.2017.00475]

20 **Ristagno G**, Varpula T, Masson S, Greco M, Bottazzi B, Milani V, Aleksova A, Sinagra G, Assandri R, Tiainen M, Vaahersalo J, Kurola J, Barlera S, Montanelli A, Latini R, Pettilä V, Bendel S, Skrifvars MB; FINNRESUSCI Study Group. Elevations of inflammatory markers PTX3 and sST2 after resuscitation from cardiac arrest are associated with multiple organ dysfunction syndrome and early death. *Clin Chem Lab Med* 2015; **53**: 1847-1857 [PMID: 25993733 DOI: 10.1515/cclm-2014-1271]

21 **Alladina J**, Levy SD, Cho JL, Brait KL, Rao SR, Camacho A, Hibbert KA, Harris RS, Medoff BD, Januzzi JL, Thompson BT, Bajwa EK. Plasma Soluble Suppression of Tumorigenicity-2 Associates with Ventilator Liberation in Acute Hypoxemic Respiratory Failure. *Am J Respir Crit Care Med* 2021; **203**: 1257-1265 [PMID: 33400890 DOI: 10.1164/rccm.202005-1951OC]

22 **Akimoto M**, Maruyama R, Takamaru H, Ochiya T, Takenaga K. Soluble IL-33 receptor sST2 inhibits colorectal cancer malignant growth by modifying the tumour microenvironment. *Nat Commun* 2016; **7**: 13589 [PMID: 27882929 DOI: 10.1038/ncomms13589]

23 **Mahmutovic Persson I**, Menzel M, Ramu S, Cerps S, Akbarshahi H, Uller L. IL-1β mediates lung neutrophilia and IL-33 expression in a mouse model of viral-induced asthma exacerbation. *Respir Res* 2018; **19**: 16 [PMID: 29361942 DOI: 10.1186/s12931-018-0725-z]

24 **Rodriguez-Nicolas A**, Martínez-Chamorro A, Jiménez P, Matas-Cobos AM, Redondo-Cerezo E, Ruiz-Cabello F. TH1 and TH2 Cytokine Profiles as Predictors of Severity in Acute Pancreatitis. *Pancreas* 2018; **47**: 400-405 [PMID: 29517628 DOI: 10.1097/MPA.0000000000001006]

25 **Nieminen A**, Maksimow M, Mentula P, Kyhälä L, Kylänpää L, Puolakkainen P, Kemppainen E, Repo H, Salmi M. Circulating cytokines in predicting development of severe acute pancreatitis. *Crit Care* 2014; **18**: R104 [PMID: 24886762 DOI: 10.1186/cc13885]

26 **Gunjaca I**, Zunic J, Gunjaca M, Kovac Z. Circulating cytokine levels in acute pancreatitis-model of SIRS/CARS can help in the clinical assessment of disease severity. *Inflammation* 2012; **35**: 758-763 [PMID: 21826480 DOI: 10.1007/s10753-011-9371-z]

27 **Romagnani S**. The increased prevalence of allergy and the hygiene hypothesis: missing immune deviation, reduced immune suppression, or both? *Immunology* 2004; **112**: 352-363 [PMID: 15196202 DOI: 10.1111/j.1365-2567.2004.01925.x]

28 **Jiang M**, Tao S, Zhang S, Wang J, Zhang F, Li F, Ding J. Type 2 innate lymphoid cells participate in IL-33-stimulated Th2-associated immune response in chronic obstructive pulmonary disease. *Exp Ther Med* 2019; **18**: 3109-3116 [PMID: 31572551 DOI: 10.3892/etm.2019.7924]

29 **Kriechbaum SD**, Wiedenroth CB, Peters K, Barde MA, Ajnwojner R, Wolter JS, Haas M, Roller FC, Guth S, Rieth AJ, Rolf A, Hamm CW, Mayer E, Keller T, Liebetrau C. Galectin-3, GDF-15, and sST2 for the assessment of disease severity and therapy response in patients suffering from inoperable chronic thromboembolic pulmonary hypertension. *Biomarkers* 2020; **25**: 578-586 [PMID: 32901511 DOI: 10.1080/1354750X.2020.1821776]

30 **Kula AJ**, Katz R, Zelnick LR, Soliman E, Go A, Shlipak M, Deo R, Ky B, DeBoer I, Anderson A, Christenson R, Seliger SL, Defilippi C, Feldman HI, Wolf M, Kusek J, Shafi T, He J, Bansal N. Association of circulating cardiac biomarkers with electrocardiographic abnormalities in chronic kidney disease. *Nephrol Dial Transplant* 2020 [PMID: 33367652 DOI: 10.1093/ndt/gfaa296]

31 **Li X**, Chen T, Gao Q, Zhang W, Xiao Y, Zhu W, Zeng L, Li Z, Yang S, Wang R, Wang X, Feng Y, Zhang X. A panel of 4 biomarkers for the early diagnosis and therapeutic efficacy of aGVHD. *JCI Insight* 2019; **4** [PMID: 31434801 DOI: 10.1172/jci.insight.130413]

32 **Watson CJ**, Gallagher J, Wilkinson M, Russell-Hallinan A, Tea I, James S, O'Reilly J, O'Connell E, Zhou S, Ledwidge M, McDonald K. Biomarker profiling for risk of future heart failure (HFpEF) development. *J Transl Med* 2021; **19**: 61 [PMID: 33563287 DOI: 10.1186/s12967-021-02735-3]

33 **Zhang Y**, Xiao Y, Liu Y, Fang Q, Tian Z, Li J, Zhou D, Xie Z, Dong R, Zhang S. Prognostic Value of Circulating sST2 for the Prediction of Mortality in Patients With Cardiac Light-Chain Amyloidosis. *Front Cardiovasc Med* 2020; **7**: 597472 [PMID: 33553254 DOI: 10.3389/fcvm.2020.597472]

34 **Kempuraj D**, Twait EC, Williard DE, Yuan Z, Meyerholz DK, Samuel I. The novel cytokine interleukin-33 activates acinar cell proinflammatory pathways and induces acute pancreatic inflammation in mice. *PLoS One* 2013; **8**: e56866 [PMID: 23418608 DOI: 10.1371/journal.pone.0056866]

35 **Hara A**, Watanabe T, Minaga K, Yoshikawa T, Kamata K, Kudo M. Biomarkers in autoimmune pancreatitis and immunoglobulin G4-related disease. *World J Gastroenterol* 2021; **27**: 2257-2269 [PMID: 34040320 DOI: 10.3748/wjg.v27.i19.2257]

36 **Minaga K**, Watanabe T, Hara A, Kamata K, Omoto S, Nakai A, Otsuka Y, Sekai I, Yoshikawa T, Yamao K, Takenaka M, Chiba Y, Kudo M. Identification of serum IFN-α and IL-33 as novel biomarkers for type 1 autoimmune pancreatitis and IgG4-related disease. *Sci Rep* 2020; **10**: 14879 [PMID: 32938972 DOI: 10.1038/s41598-020-71848-4]

World Journal of Gastroenterology

Submit a Manuscript: https://www.f6publishing.com

World J Gastroenterol 2021 October 14; 27(38): 6501-6510

DOI: 10.3748/wjg.v27.i38.6501

ISSN 1007-9327 (print) ISSN 2219-2840 (online)

CASE REPORT

Monomorphic epitheliotropic intestinal T-cell lymphoma presenting as melena with long-term survival: A case report and review of literature

Sotaro Ozaka, Kunimitsu Inoue, Tomoya Okajima, Takako Tasaki, Shimpei Ariki, Hideki Ono, Takeaki Ando, Tsutomu Daa, Kazunari Murakami

ORCID number: Sotaro Ozaka 0000-0002-6283-7012; Kunimitsu Inoue 0000-0001-9102-2472; Tomoya Okajima 0000-0001-9230-5212; Takako Tasaki 0000-0002-6293-682X; Shimpei Ariki 0000-0001-9516-9906; Hideki Ono 0000-0001-6217-2084; Takeaki Ando 0000-0002-7110-0733; Tsutomu Daa 0000-0001-5060-9883; Kazunari Murakami 0000-0003-2668-5039.

Author contributions: Ozaka S cared for the patient, performed endoscopic treatment, and wrote and corrected the manuscript; Inoue K, Okajima T, Tasaki T, Ariki S, and Ono H cared for the patient and reviewed and corrected the manuscript; Daa T interpreted the pathological findings and contributed to manuscript drafting; Ando T performed the chemotherapy and contributed to manuscript drafting; Murakami K provided oversight for the manuscript and revised it for important intellectual content; all authors issued final approval for the version to be submitted.

Informed consent statement: Informed consent was obtained from the patient for publication of this report and any accompanying images.

Sotaro Ozaka, Shimpei Ariki, Kazunari Murakami, Department of Gastroenterology, Faculty of Medicine, Oita University, Oita 879-5593, Japan

Kunimitsu Inoue, Tomoya Okajima, Takako Tasaki, Hideki Ono, Department of Gastroenterology, Almeida Memorial Hospital, Oita 870-1195, Japan

Takeaki Ando, Department of Hematology, Almeida Memorial Hospital, Oita 870-1195, Japan

Tsutomu Daa, Department of Diagnostic Pathology, Oita University, Oita 879-5593, Japan

Corresponding author: Sotaro Ozaka, MD, Staff Physician, Department of Gastroenterology, Faculty of Medicine, Oita University, 1-1 Idaigaoka, Hasama, Oita 879-5593, Japan. ozakaso@oita-u.ac.jp

Abstract

BACKGROUND

Monomorphic epitheliotropic intestinal T-cell lymphoma (MEITL) is a rare primary intestinal T-cell lymphoma, previously known as enteropathy-associated T-cell lymphoma type II. MEITL is an aggressive T-cell lymphoma with a poor prognosis and high mortality rate. The known major complications of MEITL are intestinal perforation and obstruction. Here, we present a case of MEITL that was diagnosed following upper gastrointestinal bleeding from an ulcerative duodenal lesion, with recurrence-free survival for 5 years.

CASE SUMMARY

A 68-year-old female was admitted to our hospital with melena and mild anemia. An urgent esophagogastroduodenoscopy (EGD) revealed bleeding from an ulcerative lesion in the transverse part of the duodenum, for which hemostatic treatment was performed. MEITL was diagnosed following repeated biopsies of the lesion, and cyclophosphamide, doxorubicin, vincristine, and prednisone (CHOP) chemotherapy was administered. She achieved complete remission after eight full cycles of CHOP therapy. At the last follow-up examination, EGD revealed a scarred ulcer and ^{18}Fluorodeoxyglucose (^{18}FDG) positron emission tomography/computed tomography showed no abnormal FDG accumulation. The patient has been in complete remission for 68 mo after initial diagnosis.

Conflict-of-interest statement: The authors declare that they have no conflict of interest.

CARE Checklist (2016) statement: The authors have read the CARE Checklist (2016), and the manuscript was prepared and revised according to the CARE Checklist (2016).

Open-Access: This article is an open-access article that was selected by an in-house editor and fully peer-reviewed by external reviewers. It is distributed in accordance with the Creative Commons Attribution NonCommercial (CC BY-NC 4.0) license, which permits others to distribute, remix, adapt, build upon this work non-commercially, and license their derivative works on different terms, provided the original work is properly cited and the use is non-commercial. See: http://creativecommons.org/Licenses/by-nc/4.0/

Manuscript source: Unsolicited manuscript

Specialty type: Gastroenterology and Hepatology

Country/Territory of origin: Japan

Peer-review report's scientific quality classification

Grade A (Excellent): 0
Grade B (Very good): B
Grade C (Good): 0
Grade D (Fair): 0
Grade E (Poor): 0

Received: April 9, 2021
Peer-review started: April 9, 2021
First decision: May 24, 2021
Revised: June 1, 2021
Accepted: September 6, 2021
Article in press: September 6, 2021
Published online: October 14, 2021

P-Reviewer: Strainiene S
S-Editor: Wang JL
L-Editor: A
P-Editor: Xing YX

CONCLUSION
To rule out MEITL, it is important to carefully perform histological examination when bleeding from a duodenal ulcer is observed.

Key Words: Monomorphic epitheliotropic intestinal T-cell lymphoma; Enteropathy-associated T-cell lymphoma type II; Gastrointestinal bleeding; Intestinal lymphoma; Duodenal ulcer; Case report

©The Author(s) 2021. Published by Baishideng Publishing Group Inc. All rights reserved.

Core Tip: Monomorphic epitheliotropic intestinal T-cell lymphoma (MEITL) is a primary intestinal T-cell lymphoma with the known major complications of intestinal perforation and obstruction. We experienced a case of MEITL that was diagnosed after gastrointestinal bleeding from an ulcerative duodenal lesion, who survived for a long time after treatment. MEITL can present as gastrointestinal bleeding. In addition, although MEITL has a poor prognosis, patients with MEITL might survive for a long time if effective treatment is administered at an early stage. Therefore, it is important to perform thorough histological examination for the early diagnosis of MEITL in cases with bleeding duodenal ulcers.

Citation: Ozaka S, Inoue K, Okajima T, Tasaki T, Ariki S, Ono H, Ando T, Daa T, Murakami K. Monomorphic epitheliotropic intestinal T-cell lymphoma presenting as melena with long-term survival: A case report and review of literature. *World J Gastroenterol* 2021; 27(38): 6501-6510
URL: https://www.wjgnet.com/1007-9327/full/v27/i38/6501.htm
DOI: https://dx.doi.org/10.3748/wjg.v27.i38.6501

INTRODUCTION

Monomorphic epitheliotropic intestinal T-cell lymphoma (MEITL) is a rare primary intestinal T-cell lymphoma newly defined by the 2016 revision of the World Health Organization, that was previously known as enteropathy-associated T-cell lymphoma (EATL) type II[1]. It arises from intestinal intraepithelial T lymphocytes and tends to behave aggressively[2]. EATL was originally categorized into two major groups, EATL type I and EATL type II. EATL type I is now simply classified as EATL, and it is strongly associated with celiac disease and occurs in Western countries. In this type, tumor cells are positive for CD3 and CD30 on immunohistochemistry staining, but negative for CD8 and CD56. On the other hand, EATL type II has been renamed MEITL, shows no definite association with celiac disease, and occurs in an Asian population. In this type of malignancy, tumor cells are positive for CD3, CD8 and CD56, but negative for CD30[3,4]. MEITL is most frequently found in the jejunum and ileum[5,6], and often presents with gastrointestinal perforation or obstruction[2]. MEITL is known to have a very poor prognosis due to treatment resistance and perforation or obstruction of the bowel at diagnosis or during the course of treatment [7]. Herein, we present a case of MEITL that was diagnosed following upper gastrointestinal bleeding from an ulcerative duodenal lesion, and who enjoyed recurrence-free survival for 5 years following treatment.

CASE PRESENTATION

Chief complaints

A 68-year-old female presented to the emergency department with melena.

History of present illness

The melena started a day before she consulted us. She had no past history of chronic abdominal symptoms suggesting the presence of celiac disease.

History of past illness
The patient had a history of hypertension and hyperlipidemia.

Personal and family history
She had no significant personal and family history.

Physical examination
Her body temperature was 36.4 °C, blood pressure was 128/85 mmHg, and heart rate was 98 bpm with sinus rhythm. She had mild abdominal tenderness, but there was no obvious hepatosplenomegaly or lymphadenopathy. Digital rectal examination revealed melena.

Laboratory examinations
Laboratory tests indicated a hemoglobin level of 11.3 g/dL, blood urea nitrogen level of 26.0 mg/dL, and creatinine level of 1.64 mg/dL. Her serum lactate dehydrogenase level was 232 U/L (106- 211 U/L) and soluble interleukin-2 receptor level was 213 U/mL (145- 519 U/mL) (Table 1).

Imaging examinations
Urgent esophagogastroduodenoscopy (EGD) showed an ulcerative lesion with fresh blood clots in the transverse part of the duodenum (Figure 1A). Based on the location and shape of the lesion, we suspected not only a peptic ulcer, but also an ulcer caused by vascular malformation or malignancy. Therefore, we decided to interrupt the endoscopy and perform contrast-enhanced computed tomography (CT) scan, which showed slight localized contrast enhancement on the wall of the transverse part of the duodenum in the early phase of contrast injection (Figure 1B). No vascular lesions were observed, and there was no extravasation of contrast agent in the delayed phase. EGD was immediately resumed again for further observation of the lesion. When we removed the blood clots, a protruding vessel was seen at the base of the ulcer, which was coagulated using hemostatic forceps (Coagrasper; Olympus Corp., Tokyo, Japan) (Figure 1C).

Further diagnostic work-up
Following this hemostatic treatment, the patient was discharged from the hospital without re-bleeding. The lesion that caused the bleeding was suspected to be a malignant tumor of the duodenum based on its location. EGDs, including forceps biopsies from the ulcerative lesion, were performed three times after the initial hemostatic treatment. While the first and second biopsies revealed no malignancy, the third biopsy showed findings suggestive of malignant lymphoma. On pathological evaluation, diffuse proliferation of atypical medium-sized lymphoid cells was seen in the entire mucosa, along with a few intraepithelial lesions (Figure 2A and B). No necrosis was observed. Immunohistochemical analysis revealed that the cells were positive for CD3 and CD56, and negative for CD4, CD5, CD8, CD20 and EBER (Figure 2C-E).

At this point, MEITL was suspected, and examinations for systemic lesions were subsequently performed. No abnormal lymphocytes were found on iliac bone marrow examination. ^{18}Fluorodeoxyglucose (^{18}FDG) positron emission tomography/CT (^{18}FDG-PET/CT) showed nodular FDG accumulation in the wall of the transverse part of the duodenum, consistent with the findings of contrast-enhanced CT (Figure 3). There was no abnormal FDG accumulation in the systemic lymph nodes or other parts of the gastrointestinal tract. The results of total colonoscopy and random biopsies of the gastrointestinal tract were unremarkable.

MULTIDISCIPLINARY EXPERT CONSULTATION

Ayako Gamachi, MD, PhD, Chief of the Department of Diagnostic Pathology, Almeida Memorial Hospital; and Tsutomu Daa, MD, PhD, Professor, Department of Diagnostic Pathology, Oita University
Pathological evaluations of the duodenal biopsy samples were performed by expert pathologists. The results of immunostaining of the duodenal biopsy specimen were consistent with MEITL.

Table 1 Laboratory data on admission

Items	Data	Reference	Items	Data	Reference	Items	Data	Reference
WBC	6720 /μL	3500-9100	TP	7.5 g/dL	6.4-8.4	γ-GTP	12 U/L	16-73
RBC	393 × 10^4 /μL	376-500	Alb	4.5 g/dL	3.6-5.2	Na	140 mEq/L	135-146
Hb	11.3 g/dL	11.3-15.2	BUN	26.0 mg/dL	6-22	Cl	107 mEq/L	96-108
Hct	34.2%	33.4-44.9	Cre	0.81 mg/dL	0.40-0.80	K	4.4 mEq/L	3.5-5.0
MCV	87.0 fL	79-100	T-bil	0.5 mg/dL	0.2-1.2	CRP	0.08 mg/dL	0-0.23
MCHC	33.0%	13.0-36.9	CK	140 U/L	43-165	sIL-2R	213 U/mL	145-519
Plt	21.4 × 10^4 /μL	13.0-16.9	AST	31 U/L	13-33	HBs Ag	(-)	(-)
PT	68%	70-130	ALT	12 U/L	6-30	HCV Ab	(-)	(-)
APTT	38.5 s	24-39	LDH	232 U/L	106-211	HTLV-1 Ab	(-)	(-)
			ALP	220 U/L	100-340			

WBC: White blood cell; RBC: Red blood cell; Hb: Hemoglobin; Hct: Hematocrit; MCV: Mean corpuscular volume; MCHC: Mean corpuscular hemoglobin concentration; Plt: Platelets; PT: Prothrombin; APTT: Activated partial thromboplastin time; TP: Total protein; Alb: Albumin; BUN: Blood urea nitrogen; Cre: Creatinine; T-bil: Total bilirubin; CK: Creatine Kinase; AST: Aspartate transaminase; ALT: Alanine transferase; LDH: Lactate dehydrogenase; ALP: Alkaline phosphatase; γ-GTP: γ-glutamyl transpeptidase; Na: Sodium; Cl: Chloride; K: Potassium; CRP: C-reactive protein; sIL-2R: Soluble interleukin-2 receptor; HBs Ag: HBs antigen; HCV Ab: HCV antibody; HTLV-1 Ab: HTLV-1 antibody.

FINAL DIAGNOSIS

Based on the clinical course, features of the tumor and imaging evaluations, we diagnosed MEITL (previously EATL type II) confined to the duodenum.

TREATMENT

Cyclophosphamide, doxorubicin, vincristine, and prednisone (CHOP) chemotherapy was administered without a dosage reduction.

OUTCOME AND FOLLOW-UP

EGD performed after three cycles of CHOP therapy clearly showed that the ulcerative lesion in the duodenum had reduced in size (Figure 4A), and no atypical lymphoid cells were detected in biopsy specimens taken from the lesion. The patient tolerated the chemotherapy well and received eight full cycles of CHOP chemotherapy. ^{18}FDG-PET/CT after the final cycle revealed no abnormal FDG accumulation in the transverse part of the duodenum. Therefore, we concluded that the patient had achieved complete remission (CR). EGD at the last follow-up examination revealed a scarred ulcer (Figure 4B), and ^{18}FDG-PET/CT showed no abnormal FDG accumulation (Figure 5). The patient has been in CR for 68 mo after the initial diagnosis.

DISCUSSION

Our experience in this case highlights two important clinical points. First, MEITL can present as gastrointestinal bleeding, and not just as intestinal perforation and obstruction. Second, patients with MEITL can survive for a long time if effective treatment is administered early.

MEITL is a primary intestinal T-cell lymphoma previously known as EATL type II [1]. It is a rare intestinal tumor, accounting for 1.7% of all malignant lymphomas[8] and less than 10%-16% of gastrointestinal lymphomas[9]. MEITL differs from EATL (previously EATL type I) in that it predominantly affects Asian populations and is not associated with celiac disease[10]. Histologically, it consists of monomorphic small- to

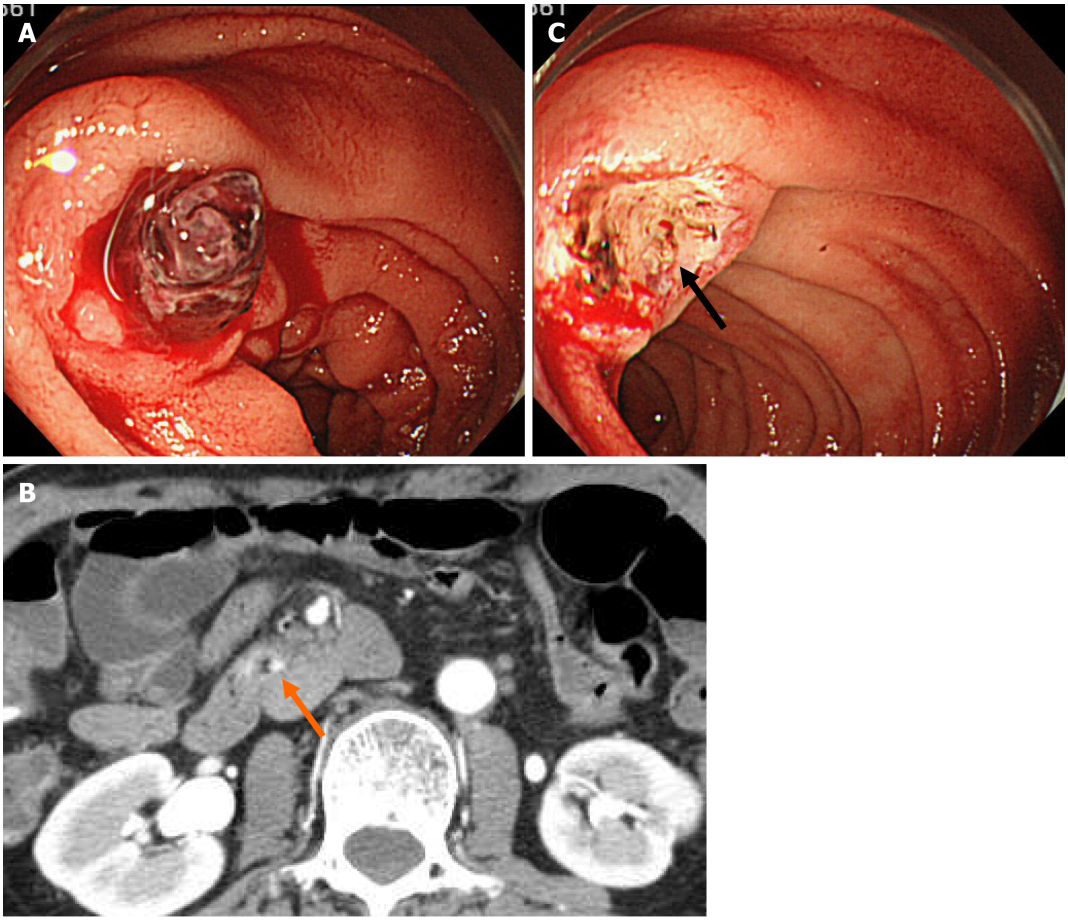


Figure 1 Endoscopic images and abdominal contrast-enhanced computed tomography scan images on initial examination. A: Esophagogastroduodenoscopy showed an ulcerative lesion with fresh blood clots in the transverse part of the duodenum; B: Contrast-enhanced computed tomography scan showed a slight localized contrast effect on the wall of the transverse part of the duodenum (arrow); C: When the blood clots were removed, a protruding vessel was observed at the base of the ulcer (arrow).

medium-sized cells that usually express CD3, CD8 and CD56, but not CD30[3,4]. Positive rates for CD8 and CD56 were reported to be 63-79% and 73-95%, respectively [8,11]. The present case had no past history of chronic abdominal symptoms suggestive of the presence of celiac disease. Histopathological examination revealed an infiltration of atypical medium-sized lymphoid cells in the entire mucosa, along with intraepithelial lesions, and immunostaining was positive for CD3 and CD56 and negative for CD5 and CD8, leading to the diagnosis of MEITL.

Our MEITL patient presented with gastrointestinal bleeding and not intestinal perforation or obstruction. More than 50% of MEITL cases are diagnosed as a result of intestinal perforation or obstruction, and emergency surgery is required in about 40% of them[9,12]. In contrast, MEITL is less frequently detected as a result of gastrointestinal bleeding. A search of the PubMed database found four case reports of MEITL or EATL that presented with gastrointestinal bleeding at the first diagnosis[13-16] (Table 2). There was a male preponderance (80%) among the five cases, and all the patients were aged above 60 years including our patient. Two cases had lesions in the jejunum, two in the stomach, and only our case had a lesion in the duodenum. Most of them showed ulcerative lesions. Only one case had a perforated lesion. Four of the five patients were diagnosed with MEITL and one with EATL. Chemotherapy was administered in four cases, and surgery was performed in two cases. To the best of our knowledge, this is the first case of MEITL that was treated with an endoscopic procedure for upper gastrointestinal bleeding. In terms of the outcomes, two cases, including our case, survived for more than 24 mo, and the two cases with gastric involvement died at 13 mo. Although it was previously reported that the median overall survival of all types of MEITL is 7 mo[11,17], the cases diagnosed after gastrointestinal bleeding had a relatively good prognosis.

In a histopathological study of a case of MEITL with perforation, tumor cells positive for TIA-1 or Granzyme B, a cytotoxic molecule, were reported to have markedly infiltrated all layers of the intestinal wall[18,19]. This suggests that MEITL

Table 2 Case reports of enteropathy-associated T-cell lymphoma and monomorphic epitheliotropic intestinal T-cell lymphoma presenting gastrointestinal bleeding

Case	Ref.	Age/Sex	Symptom	Location	Macroscopic finding	Perforation	Diagnosis	Treatment	Outcome
1	[13]	76/M	Gastrointestinal bleeding	Jejunum	Ulcer	Yes	EATL	Operation → chemotherapy	24 mo/alive
2	[14]	77/M	Positive for fecal occult bleeding	Jejunum	Ulcer, stenosis	No	MEITL	Operation	NA
3	[15]	68/M	Melena	Stomach	Ulcer (type 3 tumor)	No	MEITL	Chemotherapy	13 mo/death
4	[16]	65/M	Gastrointestinal bleeding	Stomach	NA	No	MEITL	Chemotherapy	13 mo/death
5	Our case	68/F	Melena	Duodenum	Ulcer	No	MEITL	Chemotherapy	66 mo/alive

NA: Not available; MEITL: Monomorphic epitheliotropic intestinal T-cell lymphoma; EATL: Enteropathy-associated T-cell lymphoma.

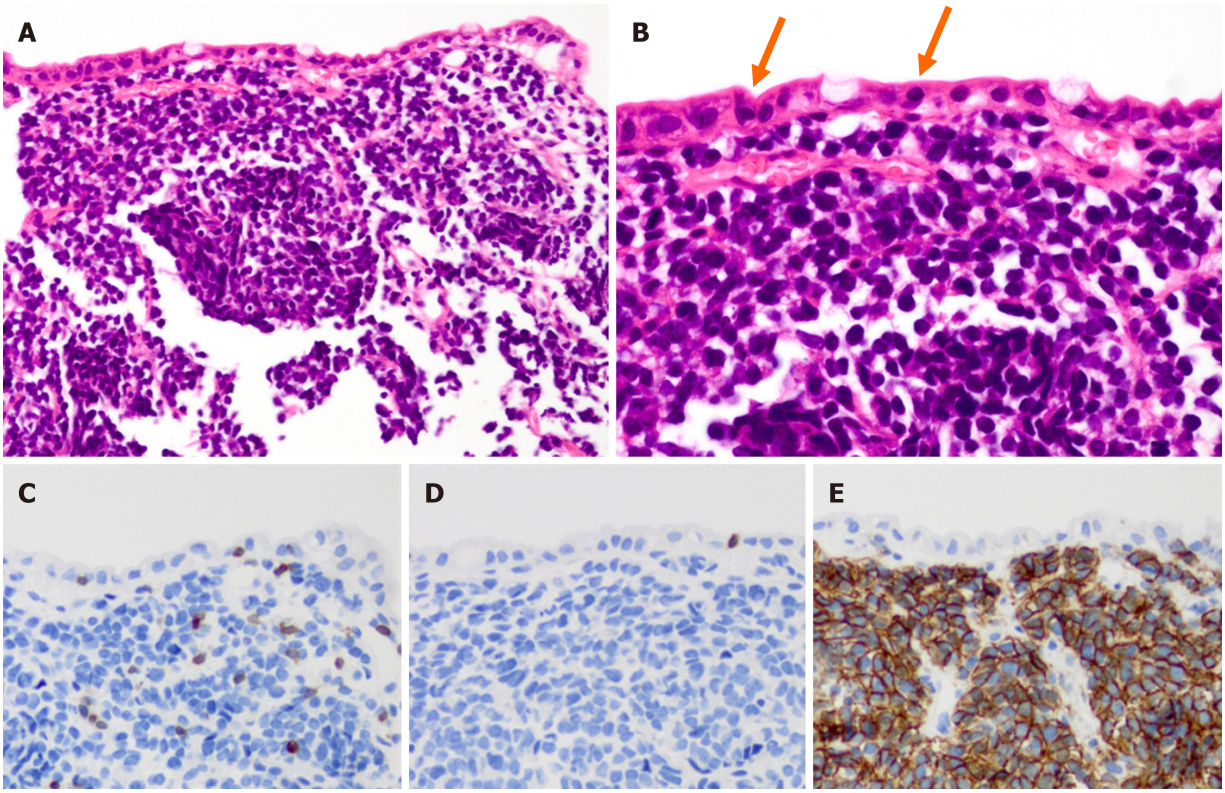


Figure 2 Histological and immunohistochemical analyses. A: Hematoxylin-eosin staining showed infiltration of medium-size atypical lymphoid cells in the mucosa; B: Lymphoid cell infiltration was also observed in the epithelium (arrow); C: Lymphoid cells expressed CD3; D: The lymphoid cells were CD8 negative; E: Lymphoid cells were CD56 positive. Magnification 200× (A, C-E) and 400× (B).

easily penetrates the gastrointestinal tract by growing destructively through all its layers, resulting in a relatively lower incidence of gastrointestinal bleeding.

Our case suggests that patients with MEITL might survive for a long time if effective treatment is administered at an early stage. MEITL is an aggressive T-cell lymphoma with a very poor prognosis and high mortality rate[20]. The median overall survival was previously reported as 7 mo[11,17], and the 5-year survival rate was reported as 20%, with a 5-year failure-free survival rate of 4%[8]. Surgery, chemotherapy and radiotherapy are all used to treat MEITL, although these treatments have shown poor overall outcomes[21]. Although several studies have demonstrated the benefit of autologous stem cell transplantation[22-25], there is no standardized treatment strategy. Moreover, MEITL often requires emergency surgery due to

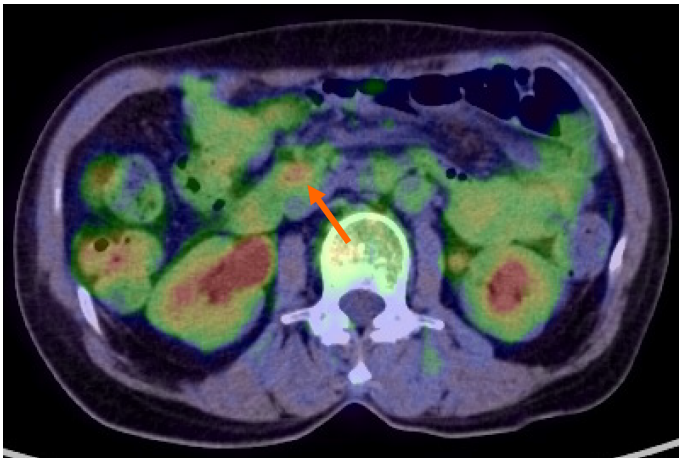


Figure 3 Pre-treatment ^{18}Fluorodeoxyglucose positron emission tomography/computed tomography images. ^{18}Fluorodeoxyglucose positron emission tomography/computed tomography showed abnormal nodular accumulation in the wall of the transverse part of the duodenum (arrow).

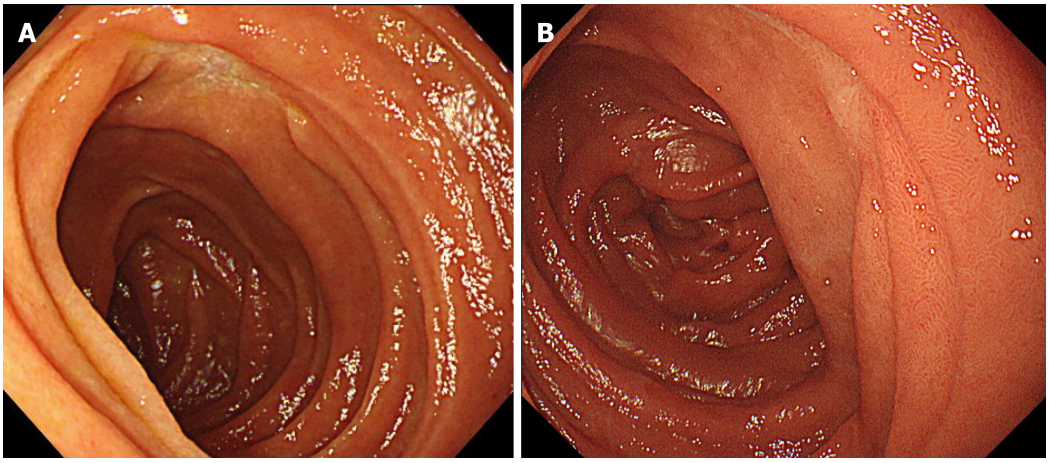


Figure 4 Follow-up endoscopic examinations. A: Esophagogastroduodenoscopy (EGD) after three cycles of cyclophosphamide, doxorubicin, vincristine, and prednisone therapy revealed that the ulcerative lesion had clearly reduced in size; B: EGD performed 60 mo after complete remission showed a scarred ulcer.

intestinal perforation or obstruction, and the lesion has usually spread before it is diagnosed[26]. Unfortunately, most patients are unable to receive effective chemotherapy due to their poor performance status and severe malnutrition at the time of diagnosis[27]. On the other hand, in a study of 26 patients with MEITL, the prognosis of non-perforated cases was significantly better than that of perforated cases, suggesting that early treatment before perforation might improve the prognosis of MEITL[28]. The present case has shown the most favorable prognosis to date, because we were able to diagnose MEITL at an early stage due to her presentation with upper gastrointestinal bleeding, and hence performed chemotherapy while the patient was in good general condition. In the previously reported cases shown in Table 2, as well, the prognosis tended to be relatively good in cases that were diagnosed after hemorrhage. This is probably because the lesion was perforated in only one case and the other cases were able to start chemotherapy before perforation. This suggests that gastrointestinal bleeding is an important sign that can lead to early diagnosis and treatment of MEITL.

So far, only one other case of MEITL with a failure-free survival for more than 5 years has been reported[29]. This case was diagnosed early by the finding of only chorionic changes (white villi) without a mass or ulcer, and CHOP therapy was started before perforation. Ishibashi *et al*[30] reported that edematous and granular mucosae with or without villous atrophy are characteristic findings of prodromal lesions of MEITL in the small intestine or duodenum. Even in the absence of obvious masses or ulcers, it is important not to overlook such micro-changes in the gastrointestinal mucosa to facilitate the early diagnosis of MEITL.

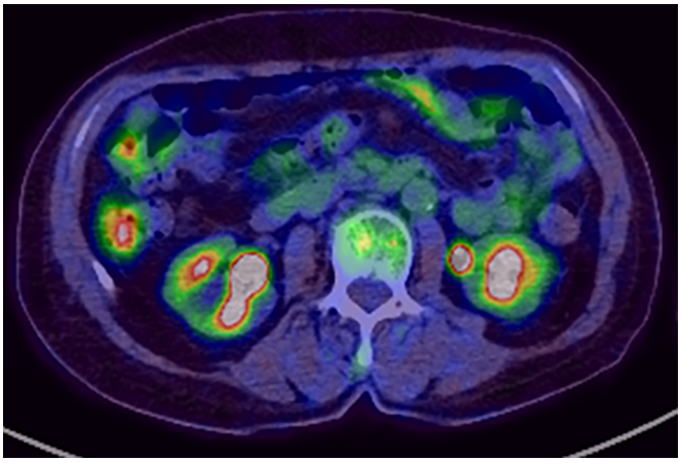


Figure 5 Follow-up ^{18}Fluorodeoxyglucose positron emission tomography/computed tomography at 60 mo after complete remission. ^{8}Fluorodeoxyglucose positron emission tomography/computed tomography showed no abnormal fluorodeoxyglucose accumulation.

Another point to note is that the diagnostic ratio of intestinal T-cell lymphoma (ITCL) by endoscopy, including tissue biopsy, is low. Sun *et al*[31] reported that out of 34 ITCL patients who underwent endoscopy, eight patients (23.5%) were definitively diagnosed with ITCL by histology. Daum *et al*[32] also reported that only 21% of intestinal non-Hodgkin lymphomas were diagnosed endoscopically. In the present case as well, a total of three tissue biopsies were required before the final diagnosis of MEITL. The following are some of the reasons for this: (1) Tissue specimens from endoscopic biopsy are usually not sufficiently large to allow correct diagnosis; (2) ITCL is known to be primarily located in the submucosa and smooth muscle, and it is difficult to detect the lesion from biopsy specimens through the mucosal layer; and (3) The disease is easy to overlook because of its rarity. Hence, a tissue biopsy of ulcerative gastrointestinal lesions should be performed carefully from the base of the ulcer, while considering the possibility of malignant lymphoma.

CONCLUSION

We report a case of MEITL diagnosed after upper gastrointestinal bleeding from an ulcerative duodenal lesion, with recurrence-free survival for 5 years after chemotherapy. MEITL can present as gastrointestinal bleeding, and not only as intestinal perforation and obstruction. In addition, although MEITL is an aggressive T-cell lymphoma with a poor prognosis, patients with MEITL can survive for a long time if effective treatment is administered early. Therefore, it is important to carefully perform histological examination to rule out MEITL when bleeding from a duodenal ulcer is observed.

ACKNOWLEDGEMENTS

We thank Dr. Ayako Gamachi (Chief of the Department of Diagnostic Pathology, Almeida Memorial Hospital) for providing histopathological images of the duodenal biopsy.

REFERENCES

1 **Swerdlow SH**, Campo E, Pileri SA, Harris NL, Stein H, Siebert R, Advani R, Ghielmini M, Salles GA, Zelenetz AD, Jaffe ES. The 2016 revision of the World Health Organization classification of lymphoid neoplasms. *Blood* 2016; **127**: 2375-2390 [PMID: 26980727 DOI: 10.1182/blood-2016-01-643569]

2 **van de Water JM**, Cillessen SA, Visser OJ, Verbeek WH, Meijer CJ, Mulder CJ. Enteropathy associated T-cell lymphoma and its precursor lesions. *Best Pract Res Clin Gastroenterol* 2010; **24**: 43-56 [PMID: 20206108 DOI: 10.1016/j.bpg.2009.11.002]

3 **van Vliet C**, Spagnolo DV. T- and NK-cell lymphoproliferative disorders of the gastrointestinal tract:

review and update. *Pathology* 2020; **52**: 128-141 [PMID: 31727264 DOI: 10.1016/j.pathol.2019.10.001]
4 **Takeshita M**, Nakamura S, Kikuma K, Nakayama Y, Nimura S, Yao T, Urabe S, Ogawara S, Yonemasu H, Matsushita Y, Karube K, Iwashita A. Pathological and immunohistological findings and genetic aberrations of intestinal enteropathy-associated T cell lymphoma in Japan. *Histopathology* 2011; **58**: 395-407 [PMID: 21323966 DOI: 10.1111/j.1365-2559.2011.03768.x]
5 **Ferreri AJ**, Zinzani PL, Govi S, Pileri SA. Enteropathy-associated T-cell lymphoma. *Crit Rev Oncol Hematol* 2011; **79**: 84-90 [PMID: 20655757 DOI: 10.1016/j.critrevonc.2010.06.006]
6 **Liu Z**, He L, Jiao Y, Wang H, Suo J. Type II enteropathy-associated T cell lymphoma in the duodenum: A rare case report. *Medicine (Baltimore)* 2020; **99**: e20050 [PMID: 32501967 DOI: 10.1097/MD.0000000000020050]
7 **Nijeboer P**, Malamut G, Mulder CJ, Cerf-Bensussan N, Sibon D, Bouma G, Cellier C, Hermine O, Visser O. Enteropathy-associated T-cell lymphoma: improving treatment strategies. *Dig Dis* 2015; **33**: 231-235 [PMID: 25925928 DOI: 10.1159/000369542]
8 **Delabie J**, Holte H, Vose JM, Ullrich F, Jaffe ES, Savage KJ, Connors JM, Rimsza L, Harris NL, Müller-Hermelink K, Rüdiger T, Coiffier B, Gascoyne RD, Berger F, Tobinai K, Au WY, Liang R, Montserrat E, Hochberg EP, Pileri S, Federico M, Nathwani B, Armitage JO, Weisenburger DD. Enteropathy-associated T-cell lymphoma: clinical and histological findings from the international peripheral T-cell lymphoma project. *Blood* 2011; **118**: 148-155 [PMID: 21566094 DOI: 10.1182/blood-2011-02-335216]
9 **Tse E**, Gill H, Loong F, Kim SJ, Ng SB, Tang T, Ko YH, Chng WJ, Lim ST, Kim WS, Kwong YL. Type II enteropathy-associated T-cell lymphoma: a multicenter analysis from the Asia Lymphoma Study Group. *Am J Hematol* 2012; **87**: 663-668 [PMID: 22641357 DOI: 10.1002/ajh.23213]
10 **Afzal A**, Esmaeili A, Ibrahimi S, Farooque U, Gehrs B. Monomorphic Epitheliotropic Intestinal T-Cell Lymphoma With Extraintestinal Areas of Peripheral T-Cell Lymphoma Involvement. *Cureus* 2020; **12**: e10021 [PMID: 32983716 DOI: 10.7759/cureus.10021]
11 **Yi JH**, Lee GW, Do YR, Jung HR, Hong JY, Yoon DH, Suh C, Choi YS, Yi SY, Sohn BS, Kim BS, Oh SY, Park J, Jo JC, Lee SS, Oh YH, Kim SJ, Kim WS. Multicenter retrospective analysis of the clinicopathologic features of monomorphic epitheliotropic intestinal T-cell lymphoma. *Ann Hematol* 2019; **98**: 2541-2550 [PMID: 31493002 DOI: 10.1007/s00277-019-03791-y]
12 **Zettl A**, deLeeuw R, Haralambieva E, Mueller-Hermelink HK. Enteropathy-type T-cell lymphoma. *Am J Clin Pathol* 2007; **127**: 701-706 [PMID: 17511112 DOI: 10.1309/nw2bk1dxb0eqg55h]
13 **Kinaci E**, Gunes ME, Huq GE. An unusual presentation of EATL type 1: Emergency surgery due to life-threatening gastrointestinal bleeding. *Int J Surg Case Rep* 2013; **4**: 961-964 [PMID: 24055918 DOI: 10.1016/j.ijscr.2013.08.007]
14 **Ho HC**, Nagar AB, Hass DJ. Obscure gastrointestinal bleeding and video capsule retention due to enteropathy-associated T-cell lymphoma. *Gastroenterol Hepatol (N Y)* 2013; **9**: 536-538 [PMID: 24719605]
15 **Lu S**, Zhou G, Chen M, Liu W, Zhao S. Monomorphic Epitheliotropic Intestinal T-cell Lymphoma of the Stomach: Two Case Reports and a Literature Review. *Int J Surg Pathol* 2021; **29**: 410-419 [PMID: 32856508 DOI: 10.1177/1066896920953906]
16 **Chan TSY**, Lee E, Khong PL, Tse EWC, Kwong YL. Positron emission tomography computed tomography features of monomorphic epitheliotropic intestinal T-cell lymphoma. *Hematology* 2018; **23**: 10-16 [PMID: 28581364 DOI: 10.1080/10245332.2017.1335979]
17 **Olmos-Alpiste F**, Vázquez I, Gallardo F, Sánchez-Gonzalez B, Colomo L, Pujol RM. Monomorphic Epitheliotropic Intestinal T-Cell Lymphoma With Secondary Cutaneous Involvement: A Diagnostic Challenge. *Am J Dermatopathol* 2021; **43**: 300-304 [PMID: 33264131 DOI: 10.1097/DAD.0000000000001855]
18 **Yamamura K**, Ishigure K, Ishida N. [Enteropathy-type T-cell lymphoma triggering perforated peritonitis successfully treated with comprehensive therapy]. *J Ipn Surg Assoc* 2011; **72**: 821-827
19 **Abouyabis AN**, Shenoy PJ, Lechowicz MJ, Flowers CR. Incidence and outcomes of the peripheral T-cell lymphoma subtypes in the United States. *Leuk Lymphoma* 2008; **49**: 2099-2107 [PMID: 19021052 DOI: 10.1080/10428190802455867]
20 **Tan SY**, Chuang SS, Tang T, Tan L, Ko YH, Chuah KL, Ng SB, Chng WJ, Gatter K, Loong F, Liu YH, Hosking P, Cheah PL, Teh BT, Tay K, Koh M, Lim ST. Type II EATL (epitheliotropic intestinal T-cell lymphoma): a neoplasm of intra-epithelial T-cells with predominant CD8αα phenotype. *Leukemia* 2013; **27**: 1688-1696 [PMID: 23399895 DOI: 10.1038/leu.2013.41]
21 **Gentille C**, Qin Q, Barbieri A, Ravi PS, Iyer S. Use of PEG-asparaginase in monomorphic epitheliotropic intestinal T-cell lymphoma, a disease with diagnostic and therapeutic challenges. *Ecancermedicalscience* 2017; **11**: 771 [PMID: 29062389 DOI: 10.3332/ecancer.2017.771]
22 **Ikebe T**, Miyazaki Y, Abe Y, Urakami K, Ohtsuka E, Saburi Y, Saburi M, Ando T, Kohno K, Ogata M, Kadota J. Successful treatment of refractory enteropathy-associated T-cell lymphoma using high-dose chemotherapy and autologous stem cell transplantation. *Intern Med* 2010; **49**: 2157-2161 [PMID: 20930447 DOI: 10.2169/internalmedicine.49.3409]
23 **Sieniawski M**, Angamuthu N, Boyd K, Chasty R, Davies J, Forsyth P, Jack F, Lyons S, Mounter P, Revell P, Proctor SJ, Lennard AL. Evaluation of enteropathy-associated T-cell lymphoma comparing standard therapies with a novel regimen including autologous stem cell transplantation. *Blood* 2010; **115**: 3664-3670 [PMID: 20197551 DOI: 10.1182/blood-2009-07-231324]
24 **Jantunen E**, Boumendil A, Finel H, Luan JJ, Johnson P, Rambaldi A, Haynes A, Duchosal MA,

Bethge W, Biron P, Carlson K, Craddock C, Rudin C, Finke J, Salles G, Kroschinsky F, Sureda A, Dreger P; Lymphoma Working Party of the EBMT. Autologous stem cell transplantation for enteropathy-associated T-cell lymphoma: a retrospective study by the EBMT. *Blood* 2013; **121**: 2529-2532 [PMID: 23361910 DOI: 10.1182/blood-2012-11-466839]

25 **Nijeboer P**, de Baaij LR, Visser O, Witte BI, Cillessen SA, Mulder CJ, Bouma G. Treatment response in enteropathy associated T-cell lymphoma; survival in a large multicenter cohort. *Am J Hematol* 2015; **90**: 493-498 [PMID: 25716069 DOI: 10.1002/ajh.23992]

26 **Chandesris MO**, Malamut G, Verkarre V, Meresse B, Macintyre E, Delarue R, Rubio MT, Suarez F, Deau-Fischer B, Cerf-Bensussan N, Brousse N, Cellier C, Hermine O. Enteropathy-associated T-cell lymphoma: a review on clinical presentation, diagnosis, therapeutic strategies and perspectives. *Gastroenterol Clin Biol* 2010; **34**: 590-605 [PMID: 21050687 DOI: 10.1016/j.gcb.2010.09.008]

27 **Gale J**, Simmonds PD, Mead GM, Sweetenham JW, Wright DH. Enteropathy-type intestinal T-cell lymphoma: clinical features and treatment of 31 patients in a single center. *J Clin Oncol* 2000; **18**: 795-803 [PMID: 10673521 DOI: 10.1200/JCO.2000.18.4.795]

28 **Kikuma K**, Yamada K, Nakamura S, Ogami A, Nimura S, Hirahashi M, Yonemasu H, Urabe S, Naito S, Matsuki Y, Sadahira Y, Takeshita M. Detailed clinicopathological characteristics and possible lymphomagenesis of type II intestinal enteropathy-associated T-cell lymphoma in Japan. *Hum Pathol* 2014; **45**: 1276-1284 [PMID: 24746558 DOI: 10.1016/j.humpath.2013.10.038]

29 **Kakugawa Y**, Terasaka S, Watanabe T, Tanaka S, Taniguchi H, Saito Y. Enteropathy-associated T-cell lymphoma in small intestine detected by capsule endoscopy. *Leuk Lymphoma* 2012; **53**: 1623-1624 [PMID: 22242819 DOI: 10.3109/10428194.2012.656633]

30 **Ishibashi H**, Nimura S, Kayashima Y, Takamatsu Y, Aoyagi K, Harada N, Kadowaki M, Kamio T, Sakisaka S, Takeshita M. Multiple lesions of gastrointestinal tract invasion by monomorphic epitheliotropic intestinal T-cell lymphoma, accompanied by duodenal and intestinal enteropathy-like lesions and microscopic lymphocytic proctocolitis: a case series. *Diagn Pathol* 2016; **11**: 66 [PMID: 27457239 DOI: 10.1186/s13000-016-0519-x]

31 **Sun ZH**, Zhou HM, Song GX, Zhou ZX, Bai L. Intestinal T-cell lymphomas: a retrospective analysis of 68 cases in China. *World J Gastroenterol* 2014; **20**: 296-302 [PMID: 24415885 DOI: 10.3748/wjg.v20.i1.296]

32 **Daum S**, Ullrich R, Heise W, Dederke B, Foss HD, Stein H, Thiel E, Zeitz M, Riecken EO. Intestinal non-Hodgkin's lymphoma: a multicenter prospective clinical study from the German Study Group on Intestinal non-Hodgkin's Lymphoma. *J Clin Oncol* 2003; **21**: 2740-2746 [PMID: 12860953 DOI: 10.1200/JCO.2003.06.026]

World Journal of Gastroenterology

Submit a Manuscript: https://www.f6publishing.com

World J Gastroenterol 2021 October 14; 27(38): 6511-6512

DOI: 10.3748/wjg.v27.i38.6511

ISSN 1007-9327 (print) ISSN 2219-2840 (online)

CORRECTION

Correction to "Effect of probiotic Lactobacillus plantarum Dad-13 powder consumption on the gut microbiota and intestinal health of overweight adults". *World J Gastroenterol* 2021; 27(1): 107-128 [PMID: 33505154 DOI: 10.3748/wjg.v27.i1.107]

Endang Sutriswati Rahayu

ORCID number: Endang Sutriswati Rahayu 0000-0002-6101-3433.

Author contributions: Rahayu ES contributed to this correction.

Conflict-of-interest statement: The author declares that there is no conflicts of interest.

Open-Access: This article is an open-access article that was selected by an in-house editor and fully peer-reviewed by external reviewers. It is distributed in accordance with the Creative Commons Attribution NonCommercial (CC BY-NC 4.0) license, which permits others to distribute, remix, adapt, build upon this work non-commercially, and license their derivative works on different terms, provided the original work is properly cited and the use is non-commercial. See: http://creativecommons.org/Licenses/by-nc/4.0/

Manuscript source: Unsolicited manuscript

Specialty type: Food science and technology

Country/Territory of origin: Indonesia

Endang Sutriswati Rahayu, Food and Agricultural Product Technology, Universitas Gadjah Mada, Yogyakarta 55281, Indonesia

Corresponding author: Endang Sutriswati Rahayu, PhD, Professor, Food and Agricultural Product Technology, Universitas Gadjah Mada, Jl. Flora Bulaksumur No.1, Yogyakarta 55281, Indonesia. endangsrahayu@ugm.ac.id

Abstract

We corrected the wrong name of the primers used in this study. The correct name should be Bakt_341F (5′-CGCTCTTCCGATCTCTGCCTACGGGNGGCWGCAG-3′) and Bakt_805R (5′-TGCTCTTCCGATCTGACGACTACHVGGGTATCT-AATCC-3′).

Key Words: Correction; Primers; Wrong name; Error; Suggestions

©The Author(s) 2021. Published by Baishideng Publishing Group Inc. All rights reserved.

Core Tip: This revision includes correction of the name of primer used in the study and added content based on reviewer suggestion, such as title revision, commentary on female group's weight loss, and explanations regarding the reduced average daily energy intake in the last month of ingestion period.

Citation: Rahayu ES. Correction to "Effect of probiotic Lactobacillus plantarum Dad-13 powder consumption on the gut microbiota and intestinal health of overweight adults". *World J Gastroenterol* 2021; 27(1): 107-128 [PMID: 33505154 DOI: 10.3748/wjg.v27.i1.107]. *World J Gastroenterol* 2021; 27(38): 6511-6512

URL: https://www.wjgnet.com/1007-9327/full/v27/i38/6511.htm

DOI: https://dx.doi.org/10.3748/wjg.v27.i38.6511

Peer-review report's scientific quality classification

Grade A (Excellent): 0
Grade B (Very good): B, B
Grade C (Good): 0
Grade D (Fair): 0
Grade E (Poor): 0

Received: May 27, 2021
Peer-review started: May 27, 2021
First decision: June 17, 2021
Revised: June 29, 2021
Accepted: August 27, 2021
Article in press: August 27, 2021
Published online: October 14, 2021

P-Reviewer: Lazea C, Pirojsakul K
S-Editor: Ma YJ
L-Editor: A
P-Editor: Liu JH

TO THE EDITOR

Correction to: Rahayu ES, Mariyatun M, Putri Manurung NE, Hasan PN, Therdtatha P, Mishima R, Komalasari H, Mahfuzah NA, Pamungkaningtyas FH, Yoga WK, Nurfiana DA, Liwan SY, Juffrie M, Nugroho AE, Utami T. "Effect of probiotic Lactobacillus plantarum Dad-13 powder consumption on the gut microbiota and intestinal health of overweight adults". *World J Gastroenterol* 2021; 27(1): 107-128 [PMID: 33505154 DOI: 10.3748/wjg.v27.i1.107].

The name of the primers used in this study[1], Bakt_341F (5′-CGCTCTTCCGATCTCTGCCTACGGGGGGGCWGCAG-355) GGCTATICCCACCATTCCCCATTCCACCACCACCACCACCACCACCACCACCAUTAA was spelled incorrectly. The correct name should be Bakt_341F (5′-CGCTCTTCCGATCTCTGCCTACGGGNGGCWGCAG-3′) and Bakt_805R (5′-TGCTCTTCCGATCTGACGACTACHVGGGTATCTAATCC-3′). We apologize for this error.

The title of this article[1] was "Effect of probiotic Lactobacillus plantarum Dad-13 powder consumption on the gut microbiota and intestinal health of overweight adults". As the focus of the manuscript was on Lombok, Indonesia, the title should be "Effect of probiotic Lactobacillus plantarum Dad-13 powder consumption on the gut microbiota and intestinal health of Indonesian overweight adults".

Regarding the weight loss in females, it may be caused by probiotics influence. This finding also found in the study conducted by Sanchez *et al*[2] that the *Lactobacillus rhamnosus* CGMCC1.3724 (LPR) supplementation was significantly reduce weight on female subjects and had no effect on male subjects.

About the reduced average daily energy intake in the last month of ingestion period, we did not know the exact cause of this case. When the study was carried out, we let the subjects ate as their usual diet. There was no emphasis on reducing the daily intake from us.

We express our gratitude toward reviewer for these suggestions.

REFERENCES

1 **Rahayu ES**, Mariyatun M, Putri Manurung NE, Hasan PN, Therdtatha P, Mishima R, Komalasari H, Mahfuzah NA, Pamungkaningtyas FH, Yoga WK, Nurfiana DA, Liwan SY, Juffrie M, Nugroho AE, Utami T. Effect of probiotic *Lactobacillus plantarum* Dad-13 powder consumption on the gut microbiota and intestinal health of overweight adults. *World J Gastroenterol* 2021; **27**: 107-128 [PMID: 33505154 DOI: 10.3748/wjg.v27.i1.107]

2 **Sanchez M**, Darimont C, Drapeau V, Emady-Azar S, Lepage M, Rezzonico E, Ngom-Bru C, Berger B, Philippe L, Ammon-Zuffrey C, Leone P, Chevrier G, St-Amand E, Marette A, Doré J, Tremblay A. Effect of Lactobacillus rhamnosus CGMCC1.3724 supplementation on weight loss and maintenance in obese men and women. *Br J Nutr* 2014; **111**: 1507-1519 [PMID: 24299712 DOI: 10.1017/S0007114513003875]

World Journal of Gastroenterology

Submit a Manuscript: https://www.f6publishing.com

World J Gastroenterol 2021 October 14; 27(38): 6513-6514

DOI: 10.3748/wjg.v27.i38.6513

ISSN 1007-9327 (print) ISSN 2219-2840 (online)

LETTER TO THE EDITOR

Preservation of the superior rectal artery in laparoscopic colectomy for slow transit constipation: Is it really associated with better outcomes?

Rogério Serafim Parra, Omar Feres, José Joaquim Ribeiro Rocha

ORCID number: Rogério Serafim Parra 0000-0002-5566-9284; Omar Feres 0000-0003-3593-0526; José Joaquim Ribeiro Rocha 0000-0001-7118-0545.

Author contributions: Parra RS wrote the manuscript; Feres O and Rocha JJR wrote and revised the manuscript; All authors contributed to the revision of the manuscript for important intellectual content, granted final approval of the version to be published and agreed to be accountable for all aspects of the work in ensuring that questions related to the accuracy or integrity of any part of the work are appropriately investigated and resolved.

Conflict-of-interest statement: The author(s) declared no potential conflicts of interest with respect to the research, authorship and/or publication of this article.

Open-Access: This article is an open-access article that was selected by an in-house editor and fully peer-reviewed by external reviewers. It is distributed in accordance with the Creative Commons Attribution NonCommercial (CC BY-NC 4.0) license, which permits others to

Rogério Serafim Parra, Omar Feres, José Joaquim Ribeiro Rocha, Department of Surgery and Anatomy, Ribeirao Preto Medical School, University of São Paulo, Ribeirao Preto 14048900, Brazil

Corresponding author: Rogério Serafim Parra, MD, PhD, Assistant Professor, Staff Physician, Department of Surgery and Anatomy, Ribeirao Preto Medical School, University of São Paulo, Ribeirao Preto 14048900, Brazil. rsparra@hcrp.usp.br

Abstract

Few patients with slow-transit constipation refractory to conservative treatment can benefit with a subtotal colectomy with ileorectal anastomosis with the preservation of the superior rectal artery. In this letter to the editor some important issues were discussed. First, the study did not include a comparison group. Second, they did not present the functional results in the short or long term related to the bowel function of these patients after surgery. Finally, the authors showed that this surgical procedure was safe, and no cases of leakage were found.

Key Words: Laparoscopy; Colorectal surgery; Constipation; Colectomy

©The Author(s) 2021. Published by Baishideng Publishing Group Inc. All rights reserved.

Core Tip: Subtotal colectomy remains a treatment option for few patients with slow-transit constipation (STC) refractory to conservative treatment. A careful patient selection is important to improve benefits and reduce risk of adverse outcomes. Laparoscopically assisted subtotal colectomy with ileorectal anastomosis and preservation of the superior rectal artery may be effective for STC and can be the best surgical option in these situation.

Citation: Parra RS, Feres O, Rocha JJR. Preservation of the superior rectal artery in laparoscopic colectomy for slow transit constipation: Is it really associated with better outcomes? *World J Gastroenterol* 2021; 27(38): 6513-6514

URL: https://www.wjgnet.com/1007-9327/full/v27/i38/6513.htm

DOI: https://dx.doi.org/10.3748/wjg.v27.i38.6513

distribute, remix, adapt, build upon this work non-commercially, and license their derivative works on different terms, provided the original work is properly cited and the use is non-commercial. See: http://creativecommons.org/Licenses/by-nc/4.0/

Manuscript source: Unsolicited manuscript

Specialty type: Gastroenterology and hepatology

Country/Territory of origin: Brazil

Peer-review report's scientific quality classification

Grade A (Excellent): 0
Grade B (Very good): 0
Grade C (Good): C
Grade D (Fair): 0
Grade E (Poor): 0

Received: June 22, 2021
Peer-review started: June 22, 2021
First decision: August 19, 2021
Revised: August 20, 2021
Accepted: September 15, 2021
Article in press: September 15, 2021
Published online: October 14, 2021

P-Reviewer: Carannante F
S-Editor: Ma YJ
L-Editor: A
P-Editor: Yu HG

TO THE EDITOR

Wu *et al*[1] recently published an observational study on the largest patient sample with vascular preservation with slow transit constipation (STC) who were submitted to laparoscopically assisted subtotal colectomy with ileorectal anastomosis and preservation of the superior rectal artery (SRA). The authors concluded that this surgical approach could significantly improve bowel function with careful patient selection and that sparing the SRA may protect against anastomosis leakage. Despite the relevant information described in the study, some important issues need to be discussed.

First, the study did not include a comparison group, *e.g.*, patients undergoing the same surgical laparoscopic procedure without SRA preservation, to find out whether one procedure is advantageous over the other. Would the SRA preservation status affect the length of hospital stay, first time to flatus, leakage volume, or postoperative complication rate? Second, based on the results, the authors cannot state that the surgery "can significantly improve bowel function with careful patient selection". The authors did not present the functional results in the short or long term related to the bowel function of these patients after surgery, as other authors have[2]. Third, they cannot state that sparing the SRA may protect against anastomosis leakage. What the authors showed is that this surgery was safe, and no cases of leakage were found. Finally, why did the surgeons make a 4-5 cm Pfannenstiel incision and bring out the mobilized bowel segment? The key limitation of the work was the absence of a control group, which would enrich the important and relevant findings of their study. In our clinical practice, we try to preserve the SRA in nononcological procedures, such as for endometriosis, diverticular disease and STC, as described by other authors[3]. However, we remove the surgical specimen using a trocar in the lower right abdominal quadrant. In the other aspects of the manuscript, we agree with the authors and believe that the best surgical option in STC could be laparoscopic subtotal colectomy with ileorectal anastomosis with preservation of the SRA.

REFERENCES

1 **Wu CW**, Pu TW, Kang JC, Hsiao CW, Chen CY, Hu JM, Lin KH, Lin TC. Preservation of superior rectal artery in laparoscopically assisted subtotal colectomy with ileorectal anastomosis for slow transit constipation. *World J Gastroenterol* 2021; **27**: 3121-3129 [PMID: 34168413 DOI: 10.3748/wjg.v27.i22.3121]

2 **Vergara-Fernandez O**, Mejía-Ovalle R, Salgado-Nesme N, Rodríguez-Dennen N, Pérez-Aguirre J, Guerrero-Guerrero VH, Sánchez-Robles JC, Valdovinos-Díaz MA. Functional outcomes and quality of life in patients treated with laparoscopic total colectomy for colonic inertia. *Surg Today* 2014; **44**: 34-38 [PMID: 23686591 DOI: 10.1007/s00595-012-0464-6]

3 **Sohn M**, Schlitt HJ, Hornung M, Zülke C, Hochrein A, Moser C, Agha A. Preservation of the superior rectal artery: influence of surgical technique on anastomotic healing and postoperative morbidity in laparoscopic sigmoidectomy for diverticular disease. *Int J Colorectal Dis* 2017; **32**: 955-960 [PMID: 28378155 DOI: 10.1007/s00384-017-2792-x]

Published by **Baishideng Publishing Group Inc**
7041 Koll Center Parkway, Suite 160, Pleasanton, CA 94566, USA
Telephone: +1-925-3991568
E-mail: bpgoffice@wjgnet.com
Help Desk: https://www.f6publishing.com/helpdesk
https://www.wjgnet.com

© 2021 Baishideng Publishing Group Inc. All rights reserved.

ISSN 1007-9327 (print)
ISSN 2219-2840 (online)

World Journal of *Gastroenterology*

World J Gastroenterol 2021 October 21; 27(39): 6515-6736



Published by Baishideng Publishing Group Inc

World Journal of Gastroenterology

Contents

Weekly Volume 27 Number 39 October 21, 2021

EDITORIAL

6515 Importance of *BRCA* mutation for the current treatment of pancreatic cancer beyond maintenance

Martínez-Galán J, Rodriguez I, Caba O

FRONTIER

6522 Acetyl-CoA carboxylase inhibitors in non-alcoholic steatohepatitis: Is there a benefit?

Neokosmidis G, Cholongitas E, Tziomalos K

REVIEW

6527 Therapeutic resistance in pancreatic ductal adenocarcinoma: Current challenges and future opportunities

Jain A, Bhardwaj V

6551 Evaluation of botanicals as potential COVID-19 symptoms terminator

Caliskan UK, Karakus MM

MINIREVIEWS

6572 Current and emerging therapeutic strategies in pancreatic cancer: Challenges and opportunities

Manrai M, Tilak TVSVGK, Dawra S, Srivastava S, Singh A

6590 Cathepsin L, transmembrane peptidase/serine subfamily member 2/4, and other host proteases in COVID-19 pathogenesis – with impact on gastrointestinal tract

Berdowska I, Matusiewicz M

6601 Endoscopic anti-reflux therapy for gastroesophageal reflux disease

Rodríguez de Santiago E, Albéniz E, Estremera-Arevalo F, Teruel Sanchez-Vegazo C, Lorenzo-Zúñiga V

ORIGINAL ARTICLE

Basic Study

6615 Cold exposure and capsaicin promote 1,2-dimethylhyrazine-induced colon carcinogenesis in rats correlates with extracellular matrix remodeling

Qin JC, Yu WT, Li HX, Liang YQ, Nong FF, Wen B

6631 Detection and analysis of common pathogenic germline mutations in Peutz-Jeghers syndrome

Gu GL, Zhang Z, Zhang YH, Yu PF, Dong ZW, Yang HR, Yuan Y

World Journal of Gastroenterology

Weekly Volume 27 Number 39 October 21, 2021

Contents

Clinical and Translational Research

6647 Validation of the Italian translation of the perceived stigma scale and resilience assessment in inflammatory bowel disease patients

Cococcia S, Lenti MV, Mengoli C, Klersy C, Borrelli de Andreis F, Secco M, Ghorayeb J, Delliponti M, Corazza GR, Di Sabatino A

Retrospective Cohort Study

6659 Prognostic factors of minimally invasive surgery for gastric cancer: Does robotic gastrectomy bring oncological benefit?

Nakauchi M, Suda K, Shibasaki S, Nakamura K, Kadoya S, Kikuchi K, Inaba K, Uyama I

Observational Study

6673 Diagnostic usefulness of selected proteases and acute phase factors in patients with colorectal adenocarcinoma

Sebzda T, Gnus J, Dziadkowiec B, Latka M, Gburek J

6689 Impact of a colorectal cancer screening program implantation on delays and prognosis of non-screening detected colorectal cancer

Cubiella J, Lorenzo M, Baiocchi F, Tejido C, Conde A, Sande-Meijide M, Castro M

Prospective Study

6701 Standard liver weight model in adult deceased donors with fatty liver: A prospective cohort study

Li B, Chen PY, Tan YF, Huang H, Jiang M, Wu ZR, Jiang CH, Zheng DF, He D, Shi YJ, Luo Y, Yang JY

SYSTEMATIC REVIEWS

6715 Microbiota shaping – the effects of probiotics, prebiotics, and fecal microbiota transplant on cognitive functions: A systematic review

Baldi S, Mundula T, Nannini G, Amedei A

LETTER TO THE EDITOR

6733 Impact of COVID-19 pandemic on the neuropsychiatric status of Wilson's disease

Lanza G, Godani M, Ferri R, Raggi A

ABOUT COVER

Editorial Board Member of *World Journal of Gastroenterology*, José B Cotter, MD, PhD, Chief Doctor, Professor, Department of Gastroenterology, Hospital da Senhora da Oliveira, Rua dos Cutileiros, Creixomil, Guimarães 4835-044, Portugal. jcotter@hospitaldeguimaraes.min-saude.pt

AIMS AND SCOPE

The primary aim of *World Journal of Gastroenterology* (*WJG*, *World J Gastroenterol*) is to provide scholars and readers from various fields of gastroenterology and hepatology with a platform to publish high-quality basic and clinical research articles and communicate their research findings online. *WJG* mainly publishes articles reporting research results and findings obtained in the field of gastroenterology and hepatology and covering a wide range of topics including gastroenterology, hepatology, gastrointestinal endoscopy, gastrointestinal surgery, gastrointestinal oncology, and pediatric gastroenterology.

INDEXING/ABSTRACTING

The *WJG* is now indexed in Current Contents®/Clinical Medicine, Science Citation Index Expanded (also known as SciSearch®), Journal Citation Reports®, Index Medicus, MEDLINE, PubMed, PubMed Central, and Scopus. The 2021 edition of Journal Citation Report® cites the 2020 impact factor (IF) for *WJG* as 5.742; Journal Citation Indicator: 0.79; IF without journal self cites: 5.590; 5-year IF: 5.044; Ranking: 28 among 92 journals in gastroenterology and hepatology; and Quartile category: Q2. The *WJG*'s CiteScore for 2020 is 6.9 and Scopus CiteScore rank 2020: Gastroenterology is 19/136.

RESPONSIBLE EDITORS FOR THIS ISSUE

Production Editor: *Yan-Xia Xing*; **Production Department Director:** *Xiang Li*; **Editorial Office Director:** *Ze-Mao Gong*.

NAME OF JOURNAL
World Journal of Gastroenterology

ISSN
ISSN 1007-9327 (print) ISSN 2219-2840 (online)

LAUNCH DATE
October 1, 1995

FREQUENCY
Weekly

EDITORS-IN-CHIEF
Andrzej S Tarnawski, Subrata Ghosh

EDITORIAL BOARD MEMBERS
http://www.wjgnet.com/1007-9327/editorialboard.htm

PUBLICATION DATE
October 21, 2021

COPYRIGHT
© 2021 Baishideng Publishing Group Inc

INSTRUCTIONS TO AUTHORS
https://www.wjgnet.com/bpg/gerinfo/204

GUIDELINES FOR ETHICS DOCUMENTS
https://www.wjgnet.com/bpg/GerInfo/287

GUIDELINES FOR NON-NATIVE SPEAKERS OF ENGLISH
https://www.wjgnet.com/bpg/gerinfo/240

PUBLICATION ETHICS
https://www.wjgnet.com/bpg/GerInfo/288

PUBLICATION MISCONDUCT
https://www.wjgnet.com/bpg/gerinfo/208

ARTICLE PROCESSING CHARGE
https://www.wjgnet.com/bpg/gerinfo/242

STEPS FOR SUBMITTING MANUSCRIPTS
https://www.wjgnet.com/bpg/GerInfo/239

ONLINE SUBMISSION
https://www.f6publishing.com

© 2021 Baishideng Publishing Group Inc. All rights reserved. 7041 Koll Center Parkway, Suite 160, Pleasanton, CA 94566, USA

E-mail: bpgoffice@wjgnet.com https://www.wjgnet.com

World Journal of Gastroenterology

Submit a Manuscript: https://www.f6publishing.com

World J Gastroenterol 2021 October 21; 27(39): 6515-6521

DOI: 10.3748/wjg.v27.i39.6515

ISSN 1007-9327 (print) ISSN 2219-2840 (online)

EDITORIAL

Importance of *BRCA* mutation for the current treatment of pancreatic cancer beyond maintenance

Joaquina Martínez-Galán, Isabel Rodriguez, Octavio Caba

ORCID number: Joaquina Martínez-Galán 0000-0002-6814-2748; Isabel Rodriguez 0000-0003-4292-8731; Octavio Caba 0000-0003-3426-8294.

Author contributions: Martinez-Galan J designed the overall concept and outline of the manuscript; Caba O contributed to the discussion, and carried out the design of the manuscript; Martinez-Galan J and Rodriguez I contributed to the writing and editing of the manuscript and review of the literature.

Supported by Junta de Andalucía, No. PC-0498-2017 and No. PC-0549-2017.

Conflict-of-interest statement: Joaquina Martinez-Galan, Isabel Rodriguez, and Octavio Caba have nothing to disclose.

Open-Access: This article is an open-access article that was selected by an in-house editor and fully peer-reviewed by external reviewers. It is distributed in accordance with the Creative Commons Attribution NonCommercial (CC BY-NC 4.0) license, which permits others to distribute, remix, adapt, build upon this work non-commercially, and license their derivative works on different terms, provided the original work is properly cited and the use is non-commercial. See: htt

Joaquina Martínez-Galán, Isabel Rodriguez, Department of Medical Oncology, Virgen de las Nieves University Hospital, Granada 18014, Spain

Octavio Caba, Institute of Biopathology and Regenerative Medicine (IBIMER), University of Granada, Granada 18016, Spain

Corresponding author: Octavio Caba, PhD, Professor, Institute of Biopathology and Regenerative Medicine (IBIMER), University of Granada, Avenida del Conocimiento s/n, Granada 18016, Spain. ocaba@ugr.es

Abstract

In this editorial, we comment on pancreatic cancer (PC), one of the most aggressive and lethal cancers. Only minimal improvements in survival rates have been achieved over recent years. Available chemotherapeutic regimens have little impact, and surgical resection remains the only reliable curative approach. We address current treatment options for these patients, focusing on the usefulness of *breast cancer (BRCA)* gene mutation as a prognostic biomarker and predictor of response to chemotherapy. Superior survival outcomes have been reported in patients with PC and mutant *BRCA* gene treated with first-line platinum-based chemotherapy. Therefore, it appears appropriate to include *BRCA* gene status among clinical criteria used to select the chemotherapy regimen. In addition, maintenance treatment with poly(ADP-ribose) polymerase inhibitors has been found to improve progression-free survival in patients with PC and mutated *BRCA* whose disease does not progress after first-line platinum-based chemotherapy. This combination has therefore been proposed as the optimal treatment regimen for these patients.

Key Words: Pancreatic cancer; Treatment; *BRCA*; Mutation; Poly(ADP-ribose) polymerase inhibitor; Maintenance

©The Author(s) 2021. Published by Baishideng Publishing Group Inc. All rights reserved.

Core Tip: Pancreatic cancer remains one of the most lethal malignant neoplasms, and available treatments have several limitations. Genetic studies are not currently recommended to support treatment selection. However, *breast cancer (BRCA)* gene

p://creativecommons.org/Licenses/by-nc/4.0/

Manuscript source: Invited manuscript

Specialty type: Gastroenterology and hepatology

Country/Territory of origin: Spain

Peer-review report's scientific quality classification

Grade A (Excellent): 0
Grade B (Very good): B, B, B
Grade C (Good): 0
Grade D (Fair): 0
Grade E (Poor): 0

Received: March 16, 2021
Peer-review started: March 16, 2021
First decision: May 1, 2021
Revised: May 10, 2021
Accepted: September 3, 2021
Article in press: September 3, 2021
Published online: October 21, 2021

P-Reviewer: Nemunaitis J, Shimada S, Wang WQ
S-Editor: Fan JR
L-Editor: Filipodia
P-Editor: Xing YX

mutation has been associated with superior survival outcomes in patients treated with platinum-based chemotherapy. Hence, it appears appropriate to consider the *BRCA* gene status of patients with this cancer among clinical criteria for the selection of first-line chemotherapy regimen.

Citation: Martínez-Galán J, Rodriguez I, Caba O. Importance of *BRCA* mutation for the current treatment of pancreatic cancer beyond maintenance. *World J Gastroenterol* 2021; 27(39): 6515-6521
URL: https://www.wjgnet.com/1007-9327/full/v27/i39/6515.htm
DOI: https://dx.doi.org/10.3748/wjg.v27.i39.6515

INTRODUCTION

Pancreatic cancer (PC) continues to be one of the most lethal malignant neoplasms, with a 5-year survival rate of only 5%[1]. It currently represents the third cause of cancer-related mortality and is expected to be the second by 2030[2]. Surgery is considered the sole potentially curative treatment; however, only 20% of patients diagnosed with PC are candidates for surgery at the time of diagnosis, and surgical resection is frequently followed by recurrence and therapeutic resistance[3].

There have been only limited advances in PC treatment over the past few decades. However, progress in basic research has recently generated increased molecular information on PC, improving knowledge of its biology and helping to explain the poor effectiveness of current therapies and the therapeutic resistance observed[4]. For instance, *KRAS*[5], *breast cancer* (*BRCA)*[6], and *ataxia-telangiectasia mutated*[7] genes play a major role in the prognosis and response to treatment of patients with advanced PC. Hence, the identification of patients with mutations in these genes can support the design of individualized therapies that may improve survival outcomes.

In this article, we evaluate the usefulness of *BRCA* gene mutation as a prognostic and predictive biomarker of the response to chemotherapy in PC patients, beyond their maintenance treatment.

CURRENT ADVANCED PC TREATMENT

Two first-line chemotherapy options are currently available for advanced PC, FOLFIRINOX and gemcitabine+nab-paclitaxel (GEM+Nab-P)[8]. These have both demonstrated superior overall survival (OS), progression-free survival (PFS), and response rates (RRs) compared to patients receiving monotherapy with gemcitabine. Specifically, the PRODIGE4/ACCORD11 study reported improved OS (11.1 *vs* 6.8 mo, respectively), PFS (6.4 *vs* 3.3 mo), and RR (31.6% *vs* 9.4%) in the FOLFIRINOX *vs* gemcitabine arm[9]. The MPACT study also reported improved OS (8.7 *vs* 6.6 mo), PFS (5.5 *vs* 3.7 mo), and RR (23% *vs* 7%) with GEM+Nab-P *vs* gemcitabine alone[10]. The higher percentage improvements obtained in the PRODIGE4/ACCORD11 study may be explained by the more favorable prognosis of the participants, who were less representative of the real-life clinical setting compared to those in the MPACT study. Specifically, the functional Eastern Cooperative Oncology Group score was 0 in 37% of PRODIGE4/ACCORD11 study participants *vs* 16% of MPACT study participants, the pancreatic head was tumor site in < 40% of the former *vs* 44% of the latter (60%-65% in clinical practice), the mean number of metastatic sites was two in the former *vs* three in the latter, the carbohydrate antigen 19-9 marker was elevated in 42% of the former *vs* 52% of the latter, and no patient over the age of 76 years participated in the former study. It should be noted that the higher survival and RRs in the PRODIGE4/ACCORD11 study were accompanied by a significant increase in hematologic and non-hematologic toxicity. This explains why FOLFIRINOX is frequently administered at a reduced dose or in modified form in the clinical setting. Finally, no randomized trials have been undertaken to compare these options, hampering evaluation of the optimal first-line treatment of PC. The only published studies have a retrospective or non-randomized prospective design, and the results have been contradictory[11-13]. Consequently, the choice of chemotherapy regimen largely depends on clinical variables, such as the performance status and previous comorbidities of patients[14,

15].

There are currently no recommendations for genetic studies to support the selection of PC treatments. One promising approach is the identification of mutations in genes involved in response mechanisms to DNA damage, such as *BRCA*, whose mutation has been associated with superior OS outcomes in PC patients treated with platinum-based chemotherapy[16]. This evidence is based on multiple *in vitro* studies and is supported by the longer OS observed in patients with advanced PC treated with platinum-based regimens who were *BRCA* mutation carriers than in those who were not (14 mo *vs* 5 mo; hazard ratio [HR] = 0.58; P = 0.08); however, this clinical trial was retrospective and only included 12 patients[17].

ROLE OF POLY(ADP-RIBOSE) POLYMERASE AND ITS IMPORTANCE IN MUTATED *BRCA*

Mutations in the genetic code must be detected and repaired to preserve genome integrity, avoiding the uncontrolled proliferation of healthy cells and possible development of cancer[18]. One DNA repair pathway detects single-strand DNA breaks. If defective, another pathway is involved in the detection of double-strand DNA breaks followed by their homologous recombination repair (HRR), using sister chromatids to restore the original DNA sequence in a high-fidelity mechanism[19]. Nuclear enzyme poly(ADP-ribose) polymerase (PARP) is responsible for detecting DNA damage and facilitating its repair. Specifically, PARP1, the main member of the PARP family, binds to and repairs both single- and double-strand DNA breaks[20]. Conversely, PARP1 inhibition results in persistent single-strand DNA breaks that lead to replication bifurcations and double-strand DNA breaks[21].

About 7% of PC patients possess *BRCA* mutations[22]. In these patients, the inhibition of PARP and resulting loss by the tumor of functional DNA repair pathways can synergically interact and produce the specific death of tumor cells. Studies in patients with ovarian, prostate, or breast cancer found that PARP inhibition enhances the activity of cytotoxic DNA agents including alkylating agents, topoisomerase inhibitors, and radiotherapeutic agents[23]. Hence, it appears plausible to assume distinct biological behaviors and responses to therapy in patients with advanced PC who have *BRCA* mutations, especially germline mutations. This has implications for the treatment selection and suggests that *BRCA* mutations may be a useful biomarker to predict the response to first-line treatment with platinum.

PLATINUM-BASED CHEMOTHERAPY IN PATIENTS WITH PC AND MUTATED *BRCA* GENE

Tumors with *BRCA* mutations are phenotypically characterized by their susceptibility to platinum-based chemotherapy, as noted above. *BRCA*-deficient cells accumulate double-strand DNA breaks, generating genomic instability and a greater predisposition to malignant transformation and progression. This is because the loss of HRR and PARP1 pathways leads to so-called synthetic lethality during DNA replication [24].

Patients with ovarian cancer who had mutated *BRCA*, either of somatic or germline origin, respond better to platinum-based chemotherapy regimens, with a superior prognosis and survival rate compared to those without this mutation[25]. In a study of 549 patients with metastatic PC, 78% of whom had at least one family member with a history of cancer, a median OS (mOS) of 8.1 mo (95% confidence interval [CI]: 7.5-9.0) was achieved by platinum-based chemotherapy, and 31% remained alive at 1 year. The mOS was higher in the patients with a family history of breast or ovarian cancer (8.5 mo; HR = 0.76; P = 0.042) and even higher in those with a family history of pancreatic and breast or ovarian cancer (14.8 mo; HR = 0. 43; P = 0.0003)[17]. According to these findings, a substantial subpopulation of patients with PC could benefit from platinum-based regimens. However, the underlying molecular mechanisms have not yet been elucidated, and further research is warranted in patients with *BRCA* mutant/deficient profiles. Other studies of PC patients receiving platinum-based chemotherapy have described a longer OS in those with a family history of breast, ovarian, or PC than in those with no family history of these cancers [26].

Cells with mutated *BRCA* are more susceptible to platinum and anthracyclines, which are selectively lethal in cells with HRR defects[27]. In a retrospective study of 36 PC patients treated with FOLFIRINOX, multivariate analyses confirmed a significantly longer mOS in patients with *vs* without homologous repair gene mutations (odds ratio [OR] = 1.47; 95%CI: 1.04-2.06; P = 0.04)[17]. In a study by Lowery *et al*[28] of 15 patients with advanced PC and germline *BRCA* mutation (*BRCA1* in 4 [27%] and *BRCA2* in 11 [73%]), 6 received platinum chemotherapy as first-line treatment, and 5 of these had a radiological partial response according to RECIST criteria, while the remaining patient had a complete response to the infusion of 5-fluorouracil, leucovorin, oxaliplatin, and irinotecan[28]. A study by Golan *et al*[26] of 71 patients with PC and a mutation in *BRCA1* (n = 21), *BRCA2* (n = 49), or both (n = 1) reported a longer mOS in patients treated with platinum than in those receiving other agents (22 *vs* 4.4 mo, respectively); the authors concluded that outcomes are more favorable in patients with PC who have *BRCA1* or *BRCA2* mutations than in those who do not[26].

USEFULNESS OF IPARP IN PC WITH MUTATED *BRCA*

In the highly influential POLO study[29], 154 patients with PC and germline *BRCA* mutation who showed no disease progression after at least 16 wk with FOLFIRINOX were randomly assigned to a group receiving maintenance therapy with olaparib, a PARP inhibitor (iPARP), or to a group receiving no maintenance treatment. Patients in the olaparib group showed a statistically significant improvement in PFS (7.4 mo *vs* 3.8 mo; HR = 0.53; 95%CI: 0.35-0.82), and 22% of them remained progression-free at 2 years compared to 9.6% in the untreated group, although there was no between-group difference in OS (18.9 *vs* 18.1 mo, respectively). Accordingly, the United States Food and Drug Administration approved olaparib as maintenance therapy for patients with advanced PC and germline *BRCA* mutation who show no disease progression after at least 16 wk of first-line treatment with platinum-based chemotherapy. In this regard, it has been reported that the iPARP-associated response does not depend on the germline or somatic origin of the *BRCA* mutation. Thus, one meta-analysis[22] describes eight studies that reported a response to PARPi in 24/43 (55.8%) patients with somatic *BRCA* mutation *vs* 69/157 (43.9%) patients with germline *BCRA* mutation, a non-significant difference (P = 0.399). In addition, five studies in the meta-analysis found no difference in PFS between patients with somatic *vs* germline *BCRA* mutations. The authors concluded that the response to iPARP therapy is similar between these types of patient.

Platinum-based chemotherapy has been combined with the administration of iPARP. An open-label, randomized, multicenter phase II trial was conducted on the efficacy of cisplatin plus gemcitabine with *vs* without veliparib in 50 patients with PC and germline-mutated *BRCA*. The RR was 74.1% for cisplatin plus gemcitabine with veliparib *vs* 65.2% for cisplatin plus gemcitabine alone (P = 0.55), obtaining a disease control rate of 100% with the former regimen *vs* 78.3% with the latter (P = 0.02). According to the authors, cisplatin plus gemcitabine is effective in advanced germline-mutated *BRCA* PC, and the addition of veliparib offers no improvement in therapeutic response[30-32]. These results support the selection of platinum-based chemotherapy as first-line treatment for patients with PC and germline *BRCA* mutation.

Various clinical trials are currently exploring the combination of iPARP with different chemotherapy and immunotherapy regimens (Table 1). It has been proposed that PARP inhibition induces tumor immunogenicity by increasing the tumor antigen load and the expression of programmed death-ligand 1 in tumor tissue, thereby increasing the susceptibility of patients with *BRCA* mutations to immunotherapy, as already demonstrated in breast cancer[33], small cell lung cancer[34], and ovarian cancer[35].

In summary, current studies suggest that *BRCA* mutation status may be a useful prognostic and predictive biomarker of the response to platinum in patients with PC, identifying those who may benefit from platinum-based chemotherapy as standard first-line treatment.

CLINICAL IMPLICATIONS

PC is associated with a poor prognosis and high resistance to chemotherapy. Few cytotoxic agents have demonstrated activity against this tumor, including platinum-based (FOLFIRINOX) and gemcitabine-based (GEM+Nab-P) regimens, and they

Table 1 Clinical trials on the combination of poly(ADP-ribose) polymerase inhibitor with chemotherapy and immunotherapy

Identifier	Phase	iPARP	Title	Status
NCT04548752	II	Olaparib	Randomized Phase II Clinical Trial of Olaparib + Pembrolizumab *vs* Olaparib Alone as Maintenance Therapy in Metastatic Pancreatic Cancer Patients with Germline BRCA1 or BRCA2 Mutations	Recruiting
NCT02890355	II	Veliparib	Randomized Phase II Study of 2nd Line FOLFIRI *vs* Modified FOLFIRI With PARP Inhibitor ABT-888 (Veliparib) (NSC-737664) in Metastatic Pancreatic Cancer	Active, not recruiting
NCT01585805	II	Veliparib	A Randomized Phase II Study of Gemcitabine, Cisplatin +/- Veliparib in Patients with Pancreas Adenocarcinoma and known BRCA/ PALB2 Mutation (Part I) and a Phase II Single Arm Study of Single-Agent Veliparib in Previously Treated Pancreas Adenocarcinoma (Part II)	Active, not recruiting
NCT01489865	I/II	ABT-888	A Phase I/II Study of ABT-888 in combination with 5-fluorouracil and Oxaliplatin (Modified FOLFOX-6) in Patients with Metastatic Pancreatic Cancer	Active, not recruiting
NCT03404960	I/II	Niraparib + Nivolumab Niraparib + Ipilimumab	PARPVAX: A Phase 1b/2, Open Label Study of Niraparib Plus either Ipilimumab or Nivolumab in Patients with Advanced Pancreatic Cancer whose disease has not progressed on Platinum-based Therapy	Recruiting
NCT03553004	II	Niraparib	Niraparib in Metastatic Pancreatic Cancer after previous Chemotherapy (NIRA-PANC)	Recruiting

iPARP: Poly(ADP-ribose) polymerase inhibitor.

deliver very modest benefits to the patient. There has been no comparative study of these agents to determine which is more appropriate as a first-line treatment, and this decision relies on the clinical characteristics and comorbidities of the patients. Two important issues must still be resolved: the best regimen for the personalization and optimization of first-line chemotherapy in patients with PC; and the ideal sequencing of chemotherapy lines, taking into account the accumulated toxicity and the molecular profile of the cancer.

As noted above, the *BRCA* gene encodes proteins essential for repairing double-strand DNA damage *via* the HRR pathway, and its mutation has been found to predict the response to first-line chemotherapy with platinum plus iPARP in patients with PC [26]. Thus, patients with advanced PC and germline *BRCA* mutation lived significantly longer when treated with platinum *vs* other cytotoxic agents[17]. In addition, maintenance treatment with iPARP has been found to improve the PFS of patients with PC and mutated *BRCA* whose disease does not progress after first-line platinum-based chemotherapy. Taken together, these findings support the selection of platinum-based regimens as first-line treatment of patients with PC and germline *BRCA* mutation[30-32].

Given the lack of evidence on the optimal treatment of patients with PC, it appears appropriate to consider the presence/absence of *BRCA* mutation among clinical criteria for the selection of first-line chemotherapy regimen.

CONCLUSION

An appreciable number of patients with PC have a mutated *BRCA* gene, and the ongoing development of drugs that target DNA repair pathways may offer relevant therapeutic benefits to this little-studied but clinically important sub-population. This defect in DNA repair pathways has the potential to improve outcomes in patients undergoing platinum-based chemotherapy, assisting individualized selection of the optimal first-line regimen.

ACKNOWLEDGEMENTS

The authors are grateful to Richard Davies for assistance with the English version.

REFERENCES

1 **Siegel RL**, Miller KD, Jemal A. Cancer statistics, 2020. *CA Cancer J Clin* 2020; **70**: 7-30 [PMID:

31912902 DOI: 10.3322/caac.21590]
2 **Rahib L**, Smith BD, Aizenberg R, Rosenzweig AB, Fleshman JM, Matrisian LM. Projecting cancer incidence and deaths to 2030: the unexpected burden of thyroid, liver, and pancreas cancers in the United States. *Cancer Res* 2014; **74**: 2913-2921 [PMID: 24840647 DOI: 10.1158/0008-5472.CAN-14-0155]
3 **Martin-Perez E**, Domínguez-Muñoz JE, Botella-Romero F, Cerezo L, Matute Teresa F, Serrano T, Vera R. Multidisciplinary consensus statement on the clinical management of patients with pancreatic cancer. *Clin Transl Oncol* 2020; **22**: 1963-1975 [PMID: 32318964 DOI: 10.1007/s12094-020-02350-6]
4 **Zeng S**, Pöttler M, Lan B, Grützmann R, Pilarsky C, Yang H. Chemoresistance in Pancreatic Cancer. *Int J Mol Sci* 2019; **20** [PMID: 31514451 DOI: 10.3390/ijms20184504]
5 **Buscail L**, Bournet B, Cordelier P. Role of oncogenic KRAS in the diagnosis, prognosis and treatment of pancreatic cancer. *Nat Rev Gastroenterol Hepatol* 2020; **17**: 153-168 [PMID: 32005945 DOI: 10.1038/s41575-019-0245-4]
6 **Luo G**, Lu Y, Jin K, Cheng H, Guo M, Liu Z, Long J, Liu C, Ni Q, Yu X. Pancreatic cancer: BRCA mutation and personalized treatment. *Expert Rev Anticancer Ther* 2015; **15**: 1223-1231 [PMID: 26402249 DOI: 10.1586/14737140.2015.1086271]
7 **Armstrong SA**, Schultz CW, Azimi-Sadjadi A, Brody JR, Pishvaian MJ. ATM Dysfunction in Pancreatic Adenocarcinoma and Associated Therapeutic Implications. *Mol Cancer Ther* 2019; **18**: 1899-1908 [PMID: 31676541 DOI: 10.1158/1535-7163.MCT-19-0208]
8 **Neoptolemos JP**, Kleeff J, Michl P, Costello E, Greenhalf W, Palmer DH. Therapeutic developments in pancreatic cancer: current and future perspectives. *Nat Rev Gastroenterol Hepatol* 2018; **15**: 333-348 [PMID: 29717230 DOI: 10.1038/s41575-018-0005-x]
9 **Conroy T**, Desseigne F, Ychou M, Bouché O, Guimbaud R, Bécouarn Y, Adenis A, Raoul JL, Gourgou-Bourgade S, de la Fouchardière C, Bennouna J, Bachet JB, Khemissa-Akouz F, Péré-Vergé D, Delbaldo C, Assenat E, Chauffert B, Michel P, Montoto-Grillot C, Ducreux M; Groupe Tumeurs Digestives of Unicancer; PRODIGE Intergroup. FOLFIRINOX *vs* gemcitabine for metastatic pancreatic cancer. *N Engl J Med* 2011; **364**: 1817-1825 [PMID: 21561347 DOI: 10.1056/NEJMoa1011923]
10 **Von Hoff DD**, Ervin T, Arena FP, Chiorean EG, Infante J, Moore M, Seay T, Tjulandin SA, Ma WW, Saleh MN, Harris M, Reni M, Dowden S, Laheru D, Bahary N, Ramanathan RK, Tabernero J, Hidalgo M, Goldstein D, Van Cutsem E, Wei X, Iglesias J, Renschler MF. Increased survival in pancreatic cancer with nab-paclitaxel plus gemcitabine. *N Engl J Med* 2013; **369**: 1691-1703 [PMID: 24131140 DOI: 10.1056/NEJMoa1304369]
11 **Kim S**, Signorovitch JE, Yang H, Patterson-Lomba O, Xiang CQ, Ung B, Parisi M, Marshall JL. Comparative Effectiveness of nab-Paclitaxel Plus Gemcitabine *vs* FOLFIRINOX in Metastatic Pancreatic Cancer: A Retrospective Nationwide Chart Review in the United States. *Adv Ther* 2018; **35**: 1564-1577 [PMID: 30209750 DOI: 10.1007/s12325-018-0784-z]
12 **Tempero MA**, Malafa MP, Chiorean EG, Czito B, Scaife C, Narang AK, Fountzilas C, Wolpin BM, Al-Hawary M, Asbun H, Behrman SW, Benson AB, Binder E, Cardin DB, Cha C, Chung V, Dillhoff M, Dotan E, Ferrone CR, Fisher G, Hardacre J, Hawkins WG, Ko AH, LoConte N, Lowy AM, Moravek C, Nakakura EK, O'Reilly EM, Obando J, Reddy S, Thayer S, Wolff RA, Burns JL, Zuccarino-Catania G. Pancreatic Adenocarcinoma, Version 1.2019. *J Natl Compr Canc Netw* 2019; **17**: 202-210 [PMID: 30865919 DOI: 10.6004/jnccn.2019.0014]
13 **Williet N**, Saint A, Pointet AL, Tougeron D, Pernot S, Pozet A, Bechade D, Trouilloud I, Lourenco N, Hautefeuille V, Locher C, Desrame J, Artru P, Thirot Bidault A, Le Roy B, Pezet D, Phelip JM, Taieb J. Folfirinox *versus* gemcitabine/nab-paclitaxel as first-line therapy in patients with metastatic pancreatic cancer: a comparative propensity score study. *Therap Adv Gastroenterol* 2019; **12**: 1756284819878660 [PMID: 31598136 DOI: 10.1177/1756284819878660]
14 **Pavel M**, Öberg K, Falconi M, Krenning EP, Sundin A, Perren A, Berruti A; ESMO Guidelines Committee. Gastroenteropancreatic neuroendocrine neoplasms: ESMO Clinical Practice Guidelines for diagnosis, treatment and follow-up. *Ann Oncol* 2020; **31**: 844-860 [PMID: 32272208 DOI: 10.1016/j.annonc.2020.03.304]
15 **Hidalgo M**, Álvarez R, Gallego J, Guillén-Ponce C, Laquente B, Macarulla T, Muñoz A, Salgado M, Vera R, Adeva J, Alés I, Arévalo S, Blázquez J, Calsina A, Carmona A, de Madaria E, Díaz R, Díez L, Fernández T, de Paredes BG, Gallardo ME, González I, Hernando O, Jiménez P, López A, López C, López-Ríos F, Martín E, Martínez J, Martínez A, Montans J, Pazo R, Plaza JC, Peiró I, Reina JJ, Sanjuanbenito A, Yaya R, Carrato A. Consensus guidelines for diagnosis, treatment and follow-up of patients with pancreatic cancer in Spain. *Clin Transl Oncol* 2017; **19**: 667-681 [PMID: 27995549 DOI: 10.1007/s12094-016-1594-x]
16 **Mylavarapu S**, Das A, Roy M. Role of BRCA Mutations in the Modulation of Response to Platinum Therapy. *Front Oncol* 2018; **8**: 16 [PMID: 29459887 DOI: 10.3389/fonc.2018.00016]
17 **Sehdev A**, Gbolahan O, Hancock BA, Stanley M, Shahda S, Wan J, Wu HH, Radovich M, O'Neil BH. Germline and Somatic DNA Damage Repair Gene Mutations and Overall Survival in Metastatic Pancreatic Adenocarcinoma Patients Treated with FOLFIRINOX. *Clin Cancer Res* 2018; **24**: 6204-6211 [PMID: 30131383 DOI: 10.1158/1078-0432.CCR-18-1472]
18 **Lord CJ**, Ashworth A. PARP inhibitors: Synthetic lethality in the clinic. *Science* 2017; **355**: 1152-1158 [PMID: 28302823 DOI: 10.1126/science.aam7344]
19 **Hoeijmakers JH**. Genome maintenance mechanisms for preventing cancer. *Nature* 2001; **411**: 366-

374 [PMID: 11357144 DOI: 10.1038/35077232]
20 **Alemasova EE**, Lavrik OI. Poly(ADP-ribosyl)ation by PARP1: reaction mechanism and regulatory proteins. *Nucleic Acids Res* 2019; **47**: 3811-3827 [PMID: 30799503 DOI: 10.1093/nar/gkz120]
21 **Mateo J**, Lord CJ, Serra V, Tutt A, Balmaña J, Castroviejo-Bermejo M, Cruz C, Oaknin A, Kaye SB, de Bono JS. A decade of clinical development of PARP inhibitors in perspective. *Ann Oncol* 2019; **30**: 1437-1447 [PMID: 31218365 DOI: 10.1093/annonc/mdz192]
22 **Mohyuddin GR**, Aziz M, Britt A, Wade L, Sun W, Baranda J, Al-Rajabi R, Saeed A, Kasi A. Similar response rates and survival with PARP inhibitors for patients with solid tumors harboring somatic *vs* Germline BRCA mutations: a Meta-analysis and systematic review. *BMC Cancer* 2020; **20**: 507 [PMID: 32493233 DOI: 10.1186/s12885-020-06948-5]
23 **Kamel D**, Gray C, Walia JS, Kumar V. PARP Inhibitor Drugs in the Treatment of Breast, Ovarian, Prostate and Pancreatic Cancers: An Update of Clinical Trials. *Curr Drug Targets* 2018; **19**: 21-37 [PMID: 28699513 DOI: 10.2174/1389450118666170711151518]
24 **Hu Y**, Guo M. Synthetic lethality strategies: Beyond BRCA1/2 mutations in pancreatic cancer. *Cancer Sci* 2020; **111**: 3111-3121 [PMID: 32639661 DOI: 10.1111/cas.14565]
25 **Ray-Coquard I**, Pautier P, Pignata S, Pérol D, González-Martín A, Berger R, Fujiwara K, Vergote I, Colombo N, Mäenpää J, Selle F, Sehouli J, Lorusso D, Guerra Alía EM, Reinthaller A, Nagao S, Lefeuvre-Plesse C, Canzler U, Scambia G, Lortholary A, Marmé F, Combe P, de Gregorio N, Rodrigues M, Buderath P, Dubot C, Burges A, You B, Pujade-Lauraine E, Harter P; PAOLA-1 Investigators. Olaparib plus Bevacizumab as First-Line Maintenance in Ovarian Cancer. *N Engl J Med* 2019; **381**: 2416-2428 [PMID: 31851799 DOI: 10.1056/NEJMoa1911361]
26 **Golan T**, Kanji ZS, Epelbaum R, Devaud N, Dagan E, Holter S, Aderka D, Paluch-Shimon S, Kaufman B, Gershoni-Baruch R, Hedley D, Moore MJ, Friedman E, Gallinger S. Overall survival and clinical characteristics of pancreatic cancer in BRCA mutation carriers. *Br J Cancer* 2014; **111**: 1132-1138 [PMID: 25072261 DOI: 10.1038/bjc.2014.418]
27 **Tung NM**, Garber JE. BRCA1/2 testing: therapeutic implications for breast cancer management. *Br J Cancer* 2018; **119**: 141-152 [PMID: 29867226 DOI: 10.1038/s41416-018-0127-5]
28 **Lowery MA**, Kelsen DP, Stadler ZK, Yu KH, Janjigian YY, Ludwig E, D'Adamo DR, Salo-Mullen E, Robson ME, Allen PJ, Kurtz RC, O'Reilly EM. An emerging entity: pancreatic adenocarcinoma associated with a known BRCA mutation: clinical descriptors, treatment implications, and future directions. *Oncologist* 2011; **16**: 1397-1402 [PMID: 21934105 DOI: 10.1634/theoncologist.2011-0185]
29 **Golan T**, Locker GY, Kindler HL. Maintenance Olaparib for Metastatic Pancreatic Cancer. Reply. *N Engl J Med* 2019; **381**: 1492-1493 [PMID: 31597029 DOI: 10.1056/NEJMc1911185]
30 **O'Reilly EM**, Lee JW, Zalupski M, Capanu M, Park J, Golan T, Tahover E, Lowery MA, Chou JF, Sahai V, Brenner R, Kindler HL, Yu KH, Zervoudakis A, Vemuri S, Stadler ZK, Do RKG, Dhani N, Chen AP, Kelsen DP. Randomized, Multicenter, Phase II Trial of Gemcitabine and Cisplatin With or Without Veliparib in Patients With Pancreas Adenocarcinoma and a Germline *BRCA/PALB2* Mutation. *J Clin Oncol* 2020; **38**: 1378-1388 [PMID: 31976786 DOI: 10.1200/JCO.19.02931]
31 **Fazio N**. Cisplatin Plus Gemcitabine as Standard of Care for Germline *BRCA/PALB2*-Mutated Pancreatic Adenocarcinoma: Are We Moving Too Fast? *J Clin Oncol* 2020; **38**: 2466-2467 [PMID: 32407212 DOI: 10.1200/JCO.20.00419]
32 **O'Reilly EM**, Park W, Kelsen DP. Reply to N. Fazio. *J Clin Oncol* 2020; **38**: 2467-2468 [PMID: 32407214 DOI: 10.1200/JCO.20.00833]
33 **Jiao S**, Xia W, Yamaguchi H, Wei Y, Chen MK, Hsu JM, Hsu JL, Yu WH, Du Y, Lee HH, Li CW, Chou CK, Lim SO, Chang SS, Litton J, Arun B, Hortobagyi GN, Hung MC. PARP Inhibitor Upregulates PD-L1 Expression and Enhances Cancer-Associated Immunosuppression. *Clin Cancer Res* 2017; **23**: 3711-3720 [PMID: 28167507 DOI: 10.1158/1078-0432.CCR-16-3215]
34 **Sen T**, Rodriguez BL, Chen L, Corte CMD, Morikawa N, Fujimoto J, Cristea S, Nguyen T, Diao L, Li L, Fan Y, Yang Y, Wang J, Glisson BS, Wistuba II, Sage J, Heymach JV, Gibbons DL, Byers LA. Targeting DNA Damage Response Promotes Antitumor Immunity through STING-Mediated T-cell Activation in Small Cell Lung Cancer. *Cancer Discov* 2019; **9**: 646-661 [PMID: 30777870 DOI: 10.1158/2159-8290.CD-18-1020]
35 **Rocconi RP**, Monk BJ, Walter A, Herzog TJ, Galanis E, Manning L, Bognar E, Wallraven G, Stanbery L, Aaron P, Senzer N, Coleman RL, Nemunaitis J. Gemogenovatucel-T (Vigil) immunotherapy demonstrates clinical benefit in homologous recombination proficient (HRP) ovarian cancer. *Gynecol Oncol* 2021; **161**: 676-680 [PMID: 33715892 DOI: 10.1016/j.ygyno.2021.03.009]

World Journal of Gastroenterology

Submit a Manuscript: https://www.f6publishing.com

World J Gastroenterol 2021 October 21; 27(39): 6522-6526

DOI: 10.3748/wjg.v27.i39.6522

ISSN 1007-9327 (print) ISSN 2219-2840 (online)

FRONTIER

Acetyl-CoA carboxylase inhibitors in non-alcoholic steatohepatitis: Is there a benefit?

Georgios Neokosmidis, Evangelos Cholongitas, Konstantinos Tziomalos

ORCID number: Georgios Neokosmidis 0000-0003-1858-9098; Evangelos Cholongitas 0000-0002-3645-582X; Konstantinos Tziomalos 0000-0002-3172-1594.

Author contributions: Neokosmidis G drafted the editorial; Cholongitas E and Tziomalos K critically revised the draft.

Conflict-of-interest statement: We have no conflict of interest to declare.

Open-Access: This article is an open-access article that was selected by an in-house editor and fully peer-reviewed by external reviewers. It is distributed in accordance with the Creative Commons Attribution NonCommercial (CC BY-NC 4.0) license, which permits others to distribute, remix, adapt, build upon this work non-commercially, and license their derivative works on different terms, provided the original work is properly cited and the use is non-commercial. See: http://creativecommons.org/Licenses/by-nc/4.0/

Manuscript source: Invited manuscript

Specialty type: Gastroenterology and hepatology

Country/Territory of origin: Greece

Georgios Neokosmidis, Konstantinos Tziomalos, First Propedeutic Department of Internal Medicine, Medical School, Aristotle University of Thessaloniki, AHEPA Hospital, Thessaloniki 54636, Greece

Evangelos Cholongitas, First Department of Internal Medicine, Medical School, National and Kapodistrian University of Athens, Laiko General Hospital, Athens 11527, Greece

Corresponding author: Konstantinos Tziomalos, MD, MSc, PhD, Associate Professor, First Propedeutic Department of Internal Medicine, Medical School, Aristotle University of Thessaloniki, AHEPA Hospital, 1 Stilponos Kyriakidi street, Thessaloniki 54636, Greece. ktziomalos@yahoo.com

Abstract

De novo lipogenesis (DNL) plays an important role in the pathogenesis of hepatic steatosis and also appears to be implicated in hepatic inflammation and fibrosis. Accordingly, the inhibition of acetyl-CoA carboxylase, which catalyzes the rate-limiting step of DNL, might represent a useful approach in the management of patients with nonalcoholic fatty liver disease (NAFLD). Animal studies and preliminary data in patients with NAFLD consistently showed an improvement in steatosis with the use of these agents. However, effects on fibrosis were variable and an increase in plasma triglyceride levels was observed. Therefore, more long-term studies are needed to clarify the role of these agents in NAFLD and to determine their risk/benefit profile.

Key Words: Acetyl-CoA carboxylase inhibitors; Non-alcoholic steatohepatitis; Fibrosis; Steatosis; Firsocostat

©The Author(s) 2021. Published by Baishideng Publishing Group Inc. All rights reserved.

Core Tip: Acetyl-CoA carboxylase inhibitors suppress de novo lipogenesis resulting in improvement in hepatic steatosis in both animal models and in patients with nonalcoholic fatty liver disease. However, the effects of these agents on hepatic fibrosis are inconsistent and they increase plasma triglyceride levels, casting doubt on their risk/benefit profile.

Peer-review report's scientific quality classification
Grade A (Excellent): 0
Grade B (Very good): 0
Grade C (Good): C
Grade D (Fair): 0
Grade E (Poor): 0

Received: March 28, 2021
Peer-review started: March 28, 2021
First decision: June 14, 2021
Revised: June 28, 2021
Accepted: September 22, 2021
Article in press: September 22, 2021
Published online: October 21, 2021

P-Reviewer: Ocker M
S-Editor: Wang LL
L-Editor: A
P-Editor: Yuan YY

Citation: Neokosmidis G, Cholongitas E, Tziomalos K. Acetyl-CoA carboxylase inhibitors in non-alcoholic steatohepatitis: Is there a benefit? *World J Gastroenterol* 2021; 27(39): 6522-6526
URL: https://www.wjgnet.com/1007-9327/full/v27/i39/6522.htm
DOI: https://dx.doi.org/10.3748/wjg.v27.i39.6522

INTRODUCTION

Non-alcoholic fatty liver disease (NAFLD) is the commonest chronic liver disease in high-income countries, affecting 17%-46% of the general population[1]. NAFLD includes non-alcoholic fatty liver, characterized by isolated hepatic steatosis, and non-alcoholic steatohepatitis (NASH), where variable degrees of hepatic inflammation and fibrosis coexist with steatosis[2]. NASH is associated with increased risk for cirrhosis, hepatocellular cancer (HCC) and cardiovascular disease[3,4]. Diet and exercise, aiming at weight loss, is the cornerstone of management of NAFLD, but only a minority of patients achieves and maintains weight loss > 5%, which is essential for improvement in liver histology[2,5]. Several pharmacological agents have been evaluated in patients with NAFLD but none is currently licensed for use in this disease[2]. Therefore, there is an unmet need for safe and effective treatments in patients with NASH.

NON-ALCOHOLIC FATTY LIVER DISEASE

The pathogenesis of NASH is complex and multiple pathways, including insulin resistance, inflammation, oxidative stress and apoptosis are implicated[6]. De novo lipogenesis (DNL), defined as the synthesis of fatty acids from non-lipid sources, is pivotal in the development and progression of NASH. DNL is increased in patients with NAFLD and appears to be responsible for up to 38% of intrahepatic triglyceride content in this population[7]. In addition to its contribution to the development of hepatic steatosis, DNL also promotes fibrosis by activating hepatic stellate cells (HSC), which are the principal contributors to liver fibrosis[8,9]. Acetyl-CoA carboxylase (ACC) catalyzes the ATP-dependent carboxylation of acetyl-coenzyme A (CoA) to form malonyl-CoA, which is the rate-limiting and key regulatory step in DNL[10]. ACC exists as two isoenzymes that are encoded by two different genes; ACC1 is cytosolic whereas ACC2 is located at the mitochondrial membrane[10].

Given the central role of ACC in DNL and the implication of the latter in the pathogenesis of NAFLD, ACC might represent an attractive therapeutic target in this disease. Indeed, early studies showed that liver-specific, genetic inactivation of ACC protects against the development of hepatic steatosis[11,12]. More recently, several orally available, liver-specific, dual ACC1/ACC2 inhibitors have been developed and are being evaluated in the management of NAFLD (Table 1). Perhaps the most promising is firsocostat, formerly known as GS-0976. In mice with NASH, this agent improved hepatic steatosis and also reduced hepatic inflammation[13,14]. However, an increase in serum triglyceride, glucose and insulin levels as well in total body fat mass was observed[13,14]. In another study, a structural analog of GS-0976 reduced hepatic steatosis and hepatic insulin resistance in high-fructose-fed rats[15]. However, a 30%-130% increase in plasma triglyceride levels was again observed, which was attributed to an increase in very low density lipoprotein production and a decrease in triglyceride clearance by lipoprotein lipase[15]. Other ACC inhibitors also showed promise in ameliorating hepatic steatosis in rodent models of NASH. ND-630 reduced hepatic steatosis in Zucker diabetic fatty rats[16]. In addition, PF-05221304 not only improved liver steatosis in a rat model of NASH but also reduced hepatic inflammation[17].

In addition to the reduction in hepatic steatosis, ACC inhibition also appears to ameliorate hepatic fibrosis (Table 1), which is the strongest predictor of mortality in NASH[18-20]. In recent studies, firsocostat and a structural analog of this agent inhibited the activation of HSCs and reduced hepatic fibrosis both *in vitro* and in animal models of NASH[9,13,14]. PF-05221304 also prevented the activation of primary HSCs to myofibroblasts *in vitro* and reduced fibrosis in choline-deficient, high-fat-fed rats[17]. In contrast, MK-4074 did not affect fibrosis in a rat model of NASH, suggesting that the effect of ACC inhibition on fibrosis might be agent-specific [21]. On the other hand, another liver-specific, dual ACC1/ACC2 inhibitor, ND-654,

Table 1 Major findings of preclinical and clinical studies that evaluated the effects of acetyl-CoA carboxylase inhibitors in non-alcoholic steatohepatitis

Population	ACC inhibitor	Major findings	Ref.
Mice with NASH	Firsocostat (GS-0976)	↓ Hepatic steatosis, inflammation and fibrosis	[13, 14]
High-fructose-fed rats	A structural analog of firsocostat	↓ Hepatic steatosis; ↓ hepatic insulin resistance	[15]
Zucker diabetic fatty rats	ND-630	↓ Hepatic steatosis	[16]
Rat model of NASH	PF-05221304	↓ Hepatic steatosis, inflammation and fibrosis	[17]
Rat model of NASH	MK-4074	No effect on hepatic fibrosis	[21]
Rat model of NASH	ND-654	↓ Hepatic steatosis; Delayed progression of hepatocellular cancer	[22]
10 patients with NASH	Firsocostat	↓ Hepatic steatosis and fibrosis	[23]
126 patients with NASH	Firsocostat	↓ Hepatic steatosis and tissue inhibitor of metalloproteinase-1 levels	[24]
392 patients with NASH and bridging fibrosis or compensated cirrhosis (F3-F4)	Firsocostat	↓ Hepatic steatosis and stiffness	[25]
Healthy subjects	PF-05221304	Dose-dependent suppression of de novo lipogenesis	[26]
Overweight and/or obese adult males	ND-630	Suppression of de novo lipogenesis	[27]
30 patients with non-alcoholic fatty liver	MK-4074	↓ Hepatic steatosis	[28]

not only reduced hepatic steatosis but also delayed the progression of HCC in a rat model[22].

Preliminary studies suggest that ACC inhibition might also be effective in patients with NAFLD (Table 1). In a pilot, open-label, prospective study in 10 patients with NASH, administration of firsocostat for 12 wk reduced hepatic steatosis, assessed with magnetic resonance imaging (MRI), and fibrosis, assessed with both magnetic resonance elastography (MRE) and serum levels of tissue inhibitor of metalloproteinase 1 (TIMP-1)[23]. However, serum alanine aminotransferase levels did not change[23]. In a phase 2, randomized study in 126 patients with NASH, treatment with GS-0976 for 12 wk reduced hepatic steatosis, assessed with MRI, and TIMP-1 Levels more than placebo[24]. However, changes in MRE-measured liver stiffness did not differ among groups and an 11%-13% increase in serum triglyceride levels was observed in patients treated with GS-0976[24]. In a larger, phase 2b, randomized trial in 392 patients with NASH and bridging fibrosis or compensated cirrhosis (F3-F4), the incidence of the primary endpoint (a ≥ 1-stage improvement in fibrosis without worsening of NASH) did not differ between firsocostat and placebo[25]. However, firsocostat improved steatosis, increased the proportion of patients with ≥ 1-grade improvement in liver histology and improved liver stiffness evaluated by transient elastography and the Enhanced Liver Fibrosis Test compared with placebo[25]. Notably, serum glucose and insulin levels as well as body weight did not change in patients treated with firsocostat [25]. On the other hand, a mean increase in serum triglyceride levels by 42 mg/dL was observed in the firsocostat group[25].

Other ACC inhibitors also showed promising results in pilot clinical studies (Table 1). In healthy subjects, PF-05221304 dose-dependently suppressed DNL and was well-tolerated[26]. With doses yielding ≥ 90% DNL inhibition, asymptomatic increases in serum triglyceride levels and declines in platelet count occurred but these were not observed at ≤ 80% DNL inhibition[26]. A single dose of ND-630 was also shown to suppress DNL in overweight and/or obese but otherwise healthy adult males and was well tolerated[27]. Finally, in a randomized study in 30 patients with NAFL, treatment with MK-4074 for 4 wk decreased hepatic fat more than pioglitazone and placebo[28]. However, a 2-fold increase in plasma triglyceride levels was observed in patients treated with MK-4074 and not in the other groups[28]. It was shown that inhibition of ACC results in reduced intrahepatic content of polyunsaturated fatty acids, which in turn activates sterol regulatory element-binding protein-1c that increases hepatic production of very low density lipoprotein and therefore plasma triglyceride levels[28].

CONCLUSION

In conclusion, ACC inhibitors appear to represent a promising tool for ameliorating hepatic steatosis. The effect of these agents on hepatic fibrosis is less consistent and more studies are needed to assess their impact on NASH. In addition, given the high cardiovascular risk of patients with NASH, the increase in triglyceride levels during treatment with ACC inhibitors is a cause of concern and should be also be factored in the decision to administer them in this population.

REFERENCES

1 **Vernon G**, Baranova A, Younossi ZM. Systematic review: the epidemiology and natural history of non-alcoholic fatty liver disease and non-alcoholic steatohepatitis in adults. *Aliment Pharmacol Ther* 2011; **34**: 274-285 [PMID: 21623852 DOI: 10.1111/j.1365-2036.2011.04724.x]

2 **European Association for the Study of the Liver (EASL)**; European Association for the Study of Diabetes (EASD); European Association for the Study of Obesity (EASO). EASL-EASD-EASO Clinical Practice Guidelines for the management of non-alcoholic fatty liver disease. *J Hepatol* 2016; **64**: 1388-1402 [PMID: 27062661 DOI: 10.1016/j.jhep.2015.11.004]

3 **Haflidadottir S**, Jonasson JG, Norland H, Einarsdottir SO, Kleiner DE, Lund SH, Björnsson ES. Long-term follow-up and liver-related death rate in patients with non-alcoholic and alcoholic related fatty liver disease. *BMC Gastroenterol* 2014; **14**: 166 [PMID: 25260964 DOI: 10.1186/1471-230X-14-166]

4 **Targher G**, Day CP, Bonora E. Risk of cardiovascular disease in patients with nonalcoholic fatty liver disease. *N Engl J Med* 2010; **363**: 1341-1350 [PMID: 20879883 DOI: 10.1056/NEJMra0912063]

5 **Vilar-Gomez E**, Martinez-Perez Y, Calzadilla-Bertot L, Torres-Gonzalez A, Gra-Oramas B, Gonzalez-Fabian L, Friedman SL, Diago M, Romero-Gomez M. Weight Loss Through Lifestyle Modification Significantly Reduces Features of Nonalcoholic Steatohepatitis. *Gastroenterology* 2015; **149**: 367-78.e5; quiz e14-5 [PMID: 25865049 DOI: 10.1053/j.gastro.2015.04.005]

6 **Robinson KE**, Shah VH. Pathogenesis and pathways: nonalcoholic fatty liver disease & alcoholic liver disease. *Transl Gastroenterol Hepatol* 2020; **5**: 49 [PMID: 33073044 DOI: 10.21037/tgh.2019.12.05]

7 **Smith GI**, Shankaran M, Yoshino M, Schweitzer GG, Chondronikola M, Beals JW, Okunade AL, Patterson BW, Nyangau E, Field T, Sirlin CB, Talukdar S, Hellerstein MK, Klein S. Insulin resistance drives hepatic de novo lipogenesis in nonalcoholic fatty liver disease. *J Clin Invest* 2020; **130**: 1453-1460 [PMID: 31805015 DOI: 10.1172/JCI134165]

8 **Mederacke I**, Hsu CC, Troeger JS, Huebener P, Mu X, Dapito DH, Pradere JP, Schwabe RF. Fate tracing reveals hepatic stellate cells as dominant contributors to liver fibrosis independent of its aetiology. *Nat Commun* 2013; **4**: 2823 [PMID: 24264436 DOI: 10.1038/ncomms3823]

9 **Bates J**, Vijayakumar A, Ghoshal S, Marchand B, Yi S, Kornyeyev D, Zagorska A, Hollenback D, Walker K, Liu K, Pendem S, Newstrom D, Brockett R, Mikaelian I, Kusam S, Ramirez R, Lopez D, Li L, Fuchs BC, Breckenridge DG. Acetyl-CoA carboxylase inhibition disrupts metabolic reprogramming during hepatic stellate cell activation. *J Hepatol* 2020; **73**: 896-905 [PMID: 32376414 DOI: 10.1016/j.jhep.2020.04.037]

10 **Carotti S**, Aquilano K, Valentini F, Ruggiero S, Alletto F, Morini S, Picardi A, Antonelli-Incalzi R, Lettieri-Barbato D, Vespasiani-Gentilucci U. An overview of deregulated lipid metabolism in nonalcoholic fatty liver disease with special focus on lysosomal acid lipase. *Am J Physiol Gastrointest Liver Physiol* 2020; **319**: G469-G480 [PMID: 32812776 DOI: 10.1152/ajpgi.00049.2020]

11 **Mao J**, DeMayo FJ, Li H, Abu-Elheiga L, Gu Z, Shaikenov TE, Kordari P, Chirala SS, Heird WC, Wakil SJ. Liver-specific deletion of acetyl-CoA carboxylase 1 reduces hepatic triglyceride accumulation without affecting glucose homeostasis. *Proc Natl Acad Sci U S A* 2006; **103**: 8552-8557 [PMID: 16717184 DOI: 10.1073/pnas.0603115103]

12 **Choi CS**, Savage DB, Abu-Elheiga L, Liu ZX, Kim S, Kulkarni A, Distefano A, Hwang YJ, Reznick RM, Codella R, Zhang D, Cline GW, Wakil SJ, Shulman GI. Continuous fat oxidation in acetyl-CoA carboxylase 2 knockout mice increases total energy expenditure, reduces fat mass, and improves insulin sensitivity. *Proc Natl Acad Sci U S A* 2007; **104**: 16480-16485 [PMID: 17923673 DOI: 10.1073/pnas.0706794104]

13 **Gapp B**, Jourdain M, Bringer P, Kueng B, Weber D, Osmont A, Zurbruegg S, Knehr J, Falchetto R, Roma G, Dietrich W, Valdez R, Beckmann N, Nigsch F, Sanyal AJ, Ksiazek I. Farnesoid X Receptor Agonism, Acetyl-Coenzyme A Carboxylase Inhibition, and Back Translation of Clinically Observed Endpoints of *De Novo* Lipogenesis in a Murine NASH Model. *Hepatol Commun* 2020; **4**: 109-125 [PMID: 31909359 DOI: 10.1002/hep4.1443]

14 **Matsumoto M**, Yashiro H, Ogino H, Aoyama K, Nambu T, Nakamura S, Nishida M, Wang X, Erion DM, Kaneko M. Acetyl-CoA carboxylase 1 and 2 inhibition ameliorates steatosis and hepatic fibrosis in a MC4R knockout murine model of nonalcoholic steatohepatitis. *PLoS One* 2020; **15**: e0228212 [PMID: 31990961 DOI: 10.1371/journal.pone.0228212]

15 **Goedeke L**, Bates J, Vatner DF, Perry RJ, Wang T, Ramirez R, Li L, Ellis MW, Zhang D, Wong KE,

Beysen C, Cline GW, Ray AS, Shulman GI. Acetyl-CoA Carboxylase Inhibition Reverses NAFLD and Hepatic Insulin Resistance but Promotes Hypertriglyceridemia in Rodents. *Hepatology* 2018; **68**: 2197-2211 [PMID: 29790582 DOI: 10.1002/hep.30097]

16 **Harriman G**, Greenwood J, Bhat S, Huang X, Wang R, Paul D, Tong L, Saha AK, Westlin WF, Kapeller R, Harwood HJ Jr. Acetyl-CoA carboxylase inhibition by ND-630 reduces hepatic steatosis, improves insulin sensitivity, and modulates dyslipidemia in rats. *Proc Natl Acad Sci U S A* 2016; **113**: E1796-E1805 [PMID: 26976583 DOI: 10.1073/pnas.1520686113]

17 **Ross TT**, Crowley C, Kelly KL, Rinaldi A, Beebe DA, Lech MP, Martinez RV, Carvajal-Gonzalez S, Boucher M, Hirenallur-Shanthappa D, Morin J, Opsahl AC, Vargas SR, Bence KK, Pfefferkorn JA, Esler WP. Acetyl-CoA Carboxylase Inhibition Improves Multiple Dimensions of NASH Pathogenesis in Model Systems. *Cell Mol Gastroenterol Hepatol* 2020; **10**: 829-851 [PMID: 32526482 DOI: 10.1016/j.jcmgh.2020.06.001]

18 **Ekstedt M**, Hagström H, Nasr P, Fredrikson M, Stål P, Kechagias S, Hultcrantz R. Fibrosis stage is the strongest predictor for disease-specific mortality in NAFLD after up to 33 years of follow-up. *Hepatology* 2015; **61**: 1547-1554 [PMID: 25125077 DOI: 10.1002/hep.27368]

19 **Vilar-Gomez E**, Calzadilla-Bertot L, Wai-Sun Wong V, Castellanos M, Aller-de la Fuente R, Metwally M, Eslam M, Gonzalez-Fabian L, Alvarez-Quiñones Sanz M, Conde-Martin AF, De Boer B, McLeod D, Hung Chan AW, Chalasani N, George J, Adams LA, Romero-Gomez M. Fibrosis Severity as a Determinant of Cause-Specific Mortality in Patients With Advanced Nonalcoholic Fatty Liver Disease: A Multi-National Cohort Study. *Gastroenterology* 2018; **155**: 443-457.e17 [PMID: 29733831 DOI: 10.1053/j.gastro.2018.04.034]

20 **Dulai PS**, Singh S, Patel J, Soni M, Prokop LJ, Younossi Z, Sebastiani G, Ekstedt M, Hagstrom H, Nasr P, Stal P, Wong VW, Kechagias S, Hultcrantz R, Loomba R. Increased risk of mortality by fibrosis stage in nonalcoholic fatty liver disease: Systematic review and meta-analysis. *Hepatology* 2017; **65**: 1557-1565 [PMID: 28130788 DOI: 10.1002/hep.29085]

21 **Zhang J**, Muise ES, Han S, Kutchukian PS, Costet P, Zhu Y, Kan Y, Zhou H, Shah V, Huang Y, Saigal A, Akiyama TE, Shen XL, Cai TQ, Shah K, Carballo-Jane E, Zycband E, Yi L, Tian Y, Chen Y, Imbriglio J, Smith E, Devito K, Conway J, Ma LJ, Hoek M, Sebhat IK, Peier AM, Talukdar S, McLaren DG, Previs SF, Jensen KK, Pinto S. Molecular Profiling Reveals a Common Metabolic Signature of Tissue Fibrosis. *Cell Rep Med* 2020; **1**: 100056 [PMID: 33205063 DOI: 10.1016/j.xcrm.2020.100056]

22 **Lally JSV**, Ghoshal S, DePeralta DK, Moaven O, Wei L, Masia R, Erstad DJ, Fujiwara N, Leong V, Houde VP, Anagnostopoulos AE, Wang A, Broadfield LA, Ford RJ, Foster RA, Bates J, Sun H, Wang T, Liu H, Ray AS, Saha AK, Greenwood J, Bhat S, Harriman G, Miao W, Rocnik JL, Westlin WF, Muti P, Tsakiridis T, Harwood HJ Jr, Kapeller R, Hoshida Y, Tanabe KK, Steinberg GR, Fuchs BC. Inhibition of Acetyl-CoA Carboxylase by Phosphorylation or the Inhibitor ND-654 Suppresses Lipogenesis and Hepatocellular Carcinoma. *Cell Metab* 2019; **29**: 174-182.e5 [PMID: 30244972 DOI: 10.1016/j.cmet.2018.08.020]

23 **Lawitz EJ**, Coste A, Poordad F, Alkhouri N, Loo N, McColgan BJ, Tarrant JM, Nguyen T, Han L, Chung C, Ray AS, McHutchison JG, Subramanian GM, Myers RP, Middleton MS, Sirlin C, Loomba R, Nyangau E, Fitch M, Li K, Hellerstein M. Acetyl-CoA Carboxylase Inhibitor GS-0976 for 12 Weeks Reduces Hepatic De Novo Lipogenesis and Steatosis in Patients With Nonalcoholic Steatohepatitis. *Clin Gastroenterol Hepatol* 2018; **16**: 1983-1991.e3 [PMID: 29705265 DOI: 10.1016/j.cgh.2018.04.042]

24 **Loomba R**, Kayali Z, Noureddin M, Ruane P, Lawitz EJ, Bennett M, Wang L, Harting E, Tarrant JM, McColgan BJ, Chung C, Ray AS, Subramanian GM, Myers RP, Middleton MS, Lai M, Charlton M, Harrison SA. GS-0976 Reduces Hepatic Steatosis and Fibrosis Markers in Patients With Nonalcoholic Fatty Liver Disease. *Gastroenterology* 2018; **155**: 1463-1473.e6 [PMID: 30059671 DOI: 10.1053/j.gastro.2018.07.027]

25 **Loomba R**, Noureddin M, Kowdley KV, Kohli A, Sheikh A, Neff G, Bhandari BR, Gunn N, Caldwell SH, Goodman Z, Wapinski I, Resnick M, Beck AH, Ding D, Jia C, Chuang JC, Huss RS, Chung C, Subramanian GM, Myers RP, Patel K, Borg BB, Ghalib R, Kabler H, Poulos J, Younes Z, Elkhashab M, Hassanein T, Iyer R, Ruane P, Shiffman ML, Strasser S, Wong VW, Alkhouri N; ATLAS Investigators. Combination Therapies Including Cilofexor and Firsocostat for Bridging Fibrosis and Cirrhosis Attributable to NASH. *Hepatology* 2021; **73**: 625-643 [PMID: 33169409 DOI: 10.1002/hep.31622]

26 **Bergman A**, Carvajal-Gonzalez S, Tarabar S, Saxena AR, Esler WP, Amin NB. Safety, Tolerability, Pharmacokinetics, and Pharmacodynamics of a Liver-Targeting Acetyl-CoA Carboxylase Inhibitor (PF-05221304): A Three-Part Randomized Phase 1 Study. *Clin Pharmacol Drug Dev* 2020; **9**: 514-526 [PMID: 32065514 DOI: 10.1002/cpdd.782]

27 **Stiede K**, Miao W, Blanchette HS, Beysen C, Harriman G, Harwood HJ Jr, Kelley H, Kapeller R, Schmalbach T, Westlin WF. Acetyl-coenzyme A carboxylase inhibition reduces de novo lipogenesis in overweight male subjects: A randomized, double-blind, crossover study. *Hepatology* 2017; **66**: 324-334 [PMID: 28470676 DOI: 10.1002/hep.29246]

28 **Kim CW**, Addy C, Kusunoki J, Anderson NN, Deja S, Fu X, Burgess SC, Li C, Ruddy M, Chakravarthy M, Previs S, Milstein S, Fitzgerald K, Kelley DE, Horton JD. Acetyl CoA Carboxylase Inhibition Reduces Hepatic Steatosis but Elevates Plasma Triglycerides in Mice and Humans: A Bedside to Bench Investigation. *Cell Metab* 2017; **26**: 394-406.e6 [PMID: 28768177 DOI: 10.1016/j.cmet.2017.07.009]

World Journal of Gastroenterology

Submit a Manuscript: https://www.f6publishing.com

World J Gastroenterol 2021 October 21; 27(39): 6527-6550

DOI: 10.3748/wjg.v27.i39.6527

ISSN 1007-9327 (print) ISSN 2219-2840 (online)

REVIEW

Therapeutic resistance in pancreatic ductal adenocarcinoma: Current challenges and future opportunities

Aditi Jain, Vikas Bhardwaj

ORCID number: Aditi Jain 0000-0001-9383-7501; Vikas Bhardwaj 0000-0003-3364-8711.

Author contributions: Jain A and Bhardwaj V decided on topics, compiled information, wrote and reviewed the manuscript.

Conflict-of-interest statement: The authors declare no conflict of interests for this article.

Open-Access: This article is an open-access article that was selected by an in-house editor and fully peer-reviewed by external reviewers. It is distributed in accordance with the Creative Commons Attribution NonCommercial (CC BY-NC 4.0) license, which permits others to distribute, remix, adapt, build upon this work non-commercially, and license their derivative works on different terms, provided the original work is properly cited and the use is non-commercial. See: http://creativecommons.org/Licenses/by-nc/4.0/

Manuscript source: Invited manuscript

Specialty type: Gastroenterology and hepatology

Country/Territory of origin: United States

Peer-review report's scientific

Aditi Jain, The Jefferson Pancreas, Biliary and Related Cancer Center, Department of Surgery, Sidney Kimmel Cancer Center, Thomas Jefferson University, Philadelphia, PA 19107, United States

Vikas Bhardwaj, Department of Pharmaceutical Sciences, Jefferson College of Pharmacy, Thomas Jefferson University, Philadelphia, PA 19107, United States

Corresponding author: Vikas Bhardwaj, PhD, Assistant Professor, Department of Pharmaceutical Sciences, Jefferson College of Pharmacy, Thomas Jefferson University, 130 South 9th Street, Philadelphia, PA 19107, United States. vikas.bhardwaj@jefferson.edu

Abstract

Pancreatic ductal adenocarcinoma (PDAC) is the third leading cause of cancer-related deaths in the United States. Although chemotherapeutic regimens such as gemcitabine+ nab-paclitaxel and FOLFIRINOX (FOLinic acid, 5-Fluroruracil, IRINotecan, and Oxaliplatin) significantly improve patient survival, the prevalence of therapy resistance remains a major roadblock in the success of these agents. This review discusses the molecular mechanisms that play a crucial role in PDAC therapy resistance and how a better understanding of these mechanisms has shaped clinical trials for pancreatic cancer chemotherapy. Specifically, we have discussed the metabolic alterations and DNA repair mechanisms observed in PDAC and current approaches in targeting these mechanisms. Our discussion also includes the lessons learned following the failure of immunotherapy in PDAC and current approaches underway to improve tumor's immunological response.

Key Words: Pancreatic cancer; Metabolism; DNA repair; Therapy-resistance; Immunotherapy

©The Author(s) 2021. Published by Baishideng Publishing Group Inc. All rights reserved.

Core Tip: With a five-year survival rate of 10%, pancreatic adenocarcinomas are one of the most aggressive forms of cancer. Despite extensive efforts, only a few drug combinations have been found to be effective in improving patient outcomes. The drug-resistant mechanisms active in pancreatic ductal adenocarcinoma contribute to the

quality classification
Grade A (Excellent): A
Grade B (Very good): B
Grade C (Good): 0
Grade D (Fair): 0
Grade E (Poor): 0

Received: May 6, 2021
Peer-review started: May 6, 2021
First decision: June 12, 2021
Revised: June 22, 2021
Accepted: August 30, 2021
Article in press: August 30, 2021
Published online: October 21, 2021

P-Reviewer: Li CG, Reshkin SJ
S-Editor: Gao CC
L-Editor: A
P-Editor: Yuan YY

ineffectiveness of therapies. Through this review, we discuss key mechanisms that contribute to the development of resistant phenotype in pancreatic tumors and how these mechanisms are being sought as a target to treat this cancer.

Citation: Jain A, Bhardwaj V. Therapeutic resistance in pancreatic ductal adenocarcinoma: Current challenges and future opportunities. *World J Gastroenterol* 2021; 27(39): 6527-6550
URL: https://www.wjgnet.com/1007-9327/full/v27/i39/6527.htm
DOI: https://dx.doi.org/10.3748/wjg.v27.i39.6527

INTRODUCTION

Pancreatic ductal adenocarcinoma (PDAC) is a highly aggressive tumor, with a 5-year overall survival of 10%. As the cause of approximately 47000 deaths annually, it is the third leading cause of cancer-related mortality in the United States and is expected to be the second primary cause of cancer-related deaths by 2030[1,2]. Surgical resection of the tumor remains the only curative option for patients with PDAC. However, due to late diagnosis, only a limited number of patients qualify for it. Relapse is common and often observed as early as two months post-surgery. Therefore, adjuvant chemotherapy is often prescribed to improve patient outcomes. For over a decade, gemcitabine was the mainstay for chemotherapy for resectable PDACs. The drug advanced the patient survival to 5.65 mo compared with 4.41 mo with 5-fluorouracil[3]. Recently, a combination therapy FOLFIRINOX (FOLinic acid, 5-Fluroruracil, IRINotecan, and Oxaliplatin) displayed better patient outcomes than gemcitabine[4]. The four-drug cocktail, although toxic, significantly improved survival in PDAC patients and is currently approved for both resectable and metastatic PDAC[5-9] (Table 1).

The complex pancreatic cancer biology is often attributed as the underlying cause of the poor chemotherapeutic response. This review will highlight the current knowledge of the therapeutic resistance mechanisms prevalent in PDAC and the opportunities PDAC tumor biology provides for its efficient targeting.

CURRENT THERAPIES IN PDAC

Gemcitabine

Gemcitabine has been a mainstay for PDAC treatment since 1997, when it was found to improve median and overall survival compared to 5-fluorouracil[3]. Gemcitabine (2′, 2′- difluorodeoxycytidine) is a difluoro analog of deoxycytidine which inhibits DNA synthesis through (1) inhibition of ribonucleotide reductase (RR), (2) inhibition of DNA polymerase (*via* diphosphate analog), or (3) mis-incorporation into the DNA, thus preventing chain elongation (*via* triphosphate analog)[10,11]. The inhibition of RR by the diphosphate analog depletes the deoxy-ribonucleotide pool essential for DNA synthesis.

Numerous mechanisms for gemcitabine inactivity have been demonstrated. Although resistance can be divided into innate and acquired forms, we will present evidence referring to both as "resistance" for this review.

The first interaction of gemcitabine with the cells occurs at the nucleotide transporter level. These transporters-concentrative nucleoside transporters (hCNTs) and equilibrative nucleoside transporters (hENTs) allow the transport of gemcitabine into the cells[12]. Evidence of the importance of nucleotide transporters for gemcitabine activity includes the observation that, in the absence of hENT1, PDAC patients treated with gemcitabine have reduced survival[13]. The enzyme deoxycytidine kinase (dCK) is the rate-limiting enzyme that converts gemcitabine into di-fluoro deoxycytidine mono-phosphate and is essential for gemcitabine-induced cytotoxicity[14]. Acquired resistant models demonstrate reduced expression of dCK in cells that do not respond to gemcitabine[14,15]. However, a recent analysis of the patient-derived xenograft PDAC model found no change in dCK levels in the gemcitabine-resistant tumors[16], indicating that mechanisms independent of dCK contribute to poor response to gemcitabine.

Table 1 Landmark trials for approved pancreatic ductal adenocarcinoma therapies

Treatment	Tumor characteristic	Primary endpoint	Ref.
Gemcitabine	Advanced PDAC	Median survival, 5.65 mo	Burris *et al*[3]
Gemcitabine + Erlotinib *vs* Gemcitabine	Locally Advanced or metastatic PDAC	Overall survival (OS), 6.24 mo *vs* 5.91 mo	Hoffmann *et al*[59]
FOLFIRINOX *vs* Gemcitabine	Metastatic PDAC	OS, 11.1 mo *vs* 6.8 mo	Conroy *et al*[4]
Gemcitabine + nab-paclitaxel *vs* Gemcitabine	Metastatic PDAC	OS, 8.5 mo *vs* 6.7 mo	Couvelard *et al*[60]
Gemcitabine + Capacitabine *vs* Gemcitabine	Resectable PDAC	OS, 28 mo *vs* 25.5 mo	Neoptolemos *et al*[8]

PDAC: Pancreatic ductal adenocarcinoma.

As mentioned earlier, when gemcitabine inhibits RR, the deoxy-ribonucleotide pool of the cells becomes depleted, leading to cell death. Overexpression of M1 and M2 isoforms, namely RRM1 and RRM2, is associated with reduced cellular response to gemcitabine[16-18]. Micro RNAs such as miR20a-5 and miR211 have been shown to downregulate RR, enhancing pancreatic cancer's sensitivity to gemcitabine and inhibiting cellular invasion[19,20]. Similarly, natural product, small molecule, and miRNA-based inhibition of RR sensitizes PDAC cells to gemcitabine[19-21-24]. Although strong *in vitro* data indicate RRM1/RRM2 play a key role in gemcitabine sensitivity, conflicting clinical outcomes have limited the utility of these enzymes for PDAC prognosis[25-28].

Other cellular processes such as epithelial-mesenchymal transition (EMT), mitogenic signaling, and tumor-stroma interaction also contribute to gemcitabine resistance [29]. Analysis of PDAC lines revealed that the EMT gene expression profile differs considerably between drug-sensitive and -resistant cells[30]. The drug-resistant cells showed reduced response to gemcitabine, 5-fluorouracil, and cisplatin, and expressed elevated levels of EMT marker Zeb1[30]. In addition, suppression of EMT enhanced the sensitivity of PDAC to gemcitabine by regulating the expression of nucleoside transporters[31].

5-Fluorouracil

Similar to gemcitabine, 5-fluorouracil belongs to the antimetabolite class of anti-cancer agents. 5-Fluorouracil inhibits the enzyme thymidylate synthetase (TS), which is responsible for methylation of deoxyuridine mono-phosphate to deoxythymidine mono-phosphate, a precursor for DNA synthesis. 5-Fluorouracil was the first drug to be approved as PDAC adjuvant therapy[32,33]. Although no longer used as monotherapy, 5-fluorouracil forms a part of the PDAC chemotherapeutic regimen FOLFIRINOX. Compared to gemcitabine therapy, combination therapy with FOLFIRINOX improved the overall survival and median progression-free survival of patients with metastatic PDAC[4]. Although any improvement in PDAC patient outcomes should be observed as a positive sign, the high toxicity of the drug regimen, limited patient eligibility for FOLFIRINOX, and prevalence of 5-fluorouracil resistant mechanisms may further limit the use this combination therapy in PDAC[34-38]. Multiple mechanisms have demonstrated to contribute to 5-fluorouracil resistance, such as alteration in (1) 5-fluorouracil metabolizing enzymes, (2) membrane transporters, and (3) pro-survival/ pro-apoptotic pathways. High TS expression is associated with poor survival in PDAC patients, however, the difference in survival is more significant in patients that received 5-fluorouracil based therapy[39,40]. The enzyme dihydropyrimidine dehydrogenase (DPD) catabolizes the 5-fluorouracil in the liver. In colorectal cancer patients receiving 5-fluorouracil based therapy, high DPD levels was associated with significantly shorter disease-free survival and overall survival[41]. In vitro analysis of PDAC cells lines and 5-fluorouracil-resistant sub-lines revealed that high expression of TS and DPDY is associated with poor 5-fluorouracil response[42].

Targeted therapies in PDAC

Comprehensive genetic analysis has revealed that pancreatic cancers are a host of numerous genetic mutations[43]. Mutation of *K-ras* is the most frequent genetic alteration observed in more than 90% of pancreatic cancer cases[44]. K-ras protein is a downstream signaling molecule activated by various transmembrane receptor tyrosine kinases, such as the epidermal growth factor receptor (EGFR), insulin-like growth factor receptor, and c-met. EGFR, overexpressed in more than 40% of pancreatic

cancers, is associated with poor disease prognosis, invasion, and aggressive clinical behavior[45,46]. Given its importance, therapies targeting EGFR have been tested to determine their ability to improve the outcomes of PDAC patients. In one phase III trial, the addition of erlotinib (EGFR tyrosine kinase inhibitor) to gemcitabine-based therapy significantly improved the overall survival of PDAC patients[47]. A recent clinical trial compared the efficacy of gemcitabine + erlotinib in rash-positive pancreatic cancer patients and found similar one-year survival and better quality of life compared to patients on FOLFIRINOX[48]. Some trials however, have failed to show the clinical benefit of adding EGFR targeting drugs to PDAC chemotherapy[49-52]. Therapies targeting other molecular mechanisms active in pancreatic cancer have not shown beneficial effects, and EGFR targeting may have a place in PDAC therapy as precision medicine[53-57].

FUTURE OPPORTUNITIES TO TARGET PDAC

Pancreatic tumor metabolism

Pancreatic cancer is characterized by a dense stroma surrounding the tumor. This dense stromal region limits vascularization, creating an environment limiting oxygen and nutrient supply[58,59]. Limited oxygen gives rise to hypoxia that is associated with poor patient prognosis[59-61]. In an abundance of oxygen, the non-malignant cells produce most of their energy from mitochondrial oxidative phosphorylation (OXPHOS) while cancer cells exhibit an altered metabolism, first observed in the 1920s by Warburg[62], in which they produce most of their energy from glycolysis. Further, Warburg[62] observed that the majority of the glucose taken up by the cancer cells is converted to lactate rather than CO_2, an observation that has since been witnessed and verified by various researchers in various tumors, including PDAC[63-70]. Pancreatic cancer shows upregulation in glycolysis, pentose phosphate pathway (PPP), fatty acid synthesis, and purine/pyrimidine synthesis, and downregulation of enzymes involved in Kreb's cycle and the OXPHOS.

Analysis of the pancreatic cancer progression model revealed that the metabolic alterations precede tumor formation[71]. Metabolic rewiring in the early stages involves upregulated glycolytic and PPP. The altered metabolic profile allows quick ATP production and provides nucleotides and other metabolic intermediates required for proliferating cancer cells[72]. However, the suppression of OXPHOS can lead to excessive acid build-up within the cancer cells in the form of lactate. To circumvent this, pancreatic cancers express monocarboxylate transporters (MCT1 and MCT4) to efflux out lactate[73,74]. These metabolic adaptations, aided by the upregulation of glucose transporters GLUT1, allow the cancer cells to utilize glucose for their energy and biosynthetic needs. In addition, the molecular biology of pancreatic cancers, such as mutation of KRAS and P53, contribute to the so-called "glycolytic switch" in the PDACs by regulating genes like hexokinase-2, glucose transporters GLUT-1, and PKM2, and by promoting anabolic processes[75-78].

Altered tumor metabolism is also associated with poor therapy response in pancreatic tumors. Acquired gemcitabine-resistant models of pancreatic cancer show a marked increase in aerobic glycolysis that maintains the EMT phenotype and reduced responsiveness to the therapeutic agent[79]. The resistant cells exhibit elevated glycolytic enzymes HK2, LDHA and PKM2, and glucose transporter GLUT1. Below we discuss the central carbon metabolic pathways — namely, glycolysis, tricarboxylic acid (TCA) cycle, and the PPP — as therapeutic targets in pancreatic cancer.

Glycolysis as therapeutic target: Analysis of pancreatic tumors reveals that HK2 expression is upregulated in localized tumors as well as metastatic tumors compared to non-malignant tissues[80]. Since HK2 plays a crucial role in pancreatic tumors, efforts have been made to evaluate HK2 as a therapeutic target for pancreatic cancers. We were among the first to show that inhibition of glycolytic enzymes HK2 inhibits the growth and pro-survival signaling in pancreatic cancers[81]. In addition, inhibition of HK2 in pancreatic cancer cells suppresses their anchorage-independent growth and invasion[80]. The role of HK2 has also been implicated in gemcitabine resistance, as HK2 dimerization is enhanced in cells that do not respond to gemcitabine[82]. *In vitro* and *in vivo* analysis revealed that inhibition of HK2 enhanced the sensitivity of PDAC to gemcitabine. Similarly, in another study, inhibition of HK2 using chemical inhibitor 2-deoxyglucose enhanced resistant cells' sensitivity to gemcitabine[79].

PKM2: Pyruvate kinase (PK) is a glycolytic enzyme that catalyzes the conversion of phosphoenol pyruvate and ADP into pyruvate and ATP. Four isoforms of the enzyme

exist in vertebrates: PKR in erythrocytes; PKL in liver and kidney; PKM1 in adult muscle, brain, and heart; and PKM2 in most adult tissues and fetal tissues[83]. Phosphorylation of PKM2 at tyrosine residue 105 (Y105) is associated with reduced PKM2 activity and enhanced tumor growth[84,85]. Analyses of PKM isoform show abundance of isoform M2 in tumor cells compared to high levels of M1 in normal tissues[52,53]. In cancer cell lines, high PKM2 Levels are associated with proliferation, metastasis, and angiogenesis[54-56]. The role of PKM2 in pancreatic tumors is, however, controversial. Using the mice model of PDAC, a recent report demonstrated that although PKM2 expression is elevated in PDAC, the loss of PKM2 does not significantly affect the size of tumors or the survival of mice bearing PDAC[86]. Surgical specimens from 115 PDAC patients show that PKM2 expression is associated with better overall survival[87]. However, others have shown that high PKM2 expression correlates with poor patient outcomes[88,89]. Considering several observations demonstrating a vital role of PKM2 in pancreatic cancer survival, invasion, angiogenesis, metastasis, and drug resistance, we believe the PKM2 serves as an attractive target for the treatment of PDAC, even though its role in pancreatic cancer tumorigenesis is still unproven[90-95].

Lactate dehydrogenase (LDH): LDH is an enzyme that exists as a tetramer and catalyzes the conversion of pyruvate to lactate and *vice versa*. LDHA (LDH gene product) regulates pyruvate's conversion to lactate, thus preventing the entry of pyruvate into the TCA cycle. Deregulated expression of LDHA is observed in various tumors, including pancreatic, gastric, bladder, cholangiocarcinoma, lung, and endometrial cancers[96-102]. Numerous oncogenic signaling molecules, namely, HIF1 alpha, myc, FOXM1, and tyrosine kinase receptors, can regulate the level or the activity of LDH[96,103-106]. Elevated levels of LDH are associated with unfavorable prognoses for PDAC patient survival, chemotherapy response, and recurrence[107-112]. Preclinical studies have revealed that inhibition of LDH reduces the survival of PDAC cells[113,114].

PPP as therapeutic target: The PPP branches from glycolysis and contributes to the cancer phenotype through (1) synthesis of NADPH (oxidative PPP), which is important for redox regulation and fatty acid synthesis, and (2) supplying the proliferating cells with pentose sugar (non-oxidative PPP) for nucleic acid biosynthesis [115]. Accumulating evidence indicates that PPP plays a vital role in pancreatic tumor survival, metastasis, and therapy resistance. Our lab and others have shown that MYC regulates the activity of both oxidative and non-oxidative PPP through the regulation of G6PD and the RPIA (non-oxidative PPP) gene[78,116,117]. The regulation of RPIA *via* MYC appears to be under the directive of KRAS. The MAPK-MYC-RPIA-nucleotide biosynthesis pathway is shown to be important for KRAS-mediated maintenance of PDAC[78,116]. Considering that most PDAC patients (90%) express mutant KRAS, inhibition of PPP is an attractive strategy for developing more efficient pancreatic cancer therapies that would target KRAS-induced metabolic abnormalities. Our recent results found that pancreatic cancer cells resistant to erlotinib express elevated levels of G6PD. The upregulated G6PD prevents the induction of ROS in response to erlotinib, thus protecting the cells from drug-induced cytotoxicity[117]. The non-oxidative PPP has also been implicated in PDAC therapy resistance. Shukla *et al*[118] found that gemcitabine-resistant cells express enhanced carbon flux into the non-oxidative PPP, aided by elevated non-oxidative PPP enzyme levels. This alteration in metabolic flux allows elevated pyrimidine synthesis that contributes to gemcitabine resistance[118].

TCA cycle and OXPHOS as therapeutic target: Although cancer cells exhibit an elevated flux of glycolytic intermediate into branched pathways, the TCA cycle is still functional. The TCA cycle continues to provide proliferating cancer cells with energy, macromolecules and maintain the cellular redox balance. Recent reports have demonstrated the importance of the TCA cycle and OXPHOS in pancreatic cancer survival[119-123]. Due to their critical roles, the TCA cycle and OXPHOS have been tested as a therapeutic target for PDAC therapy. Three major approaches have been sought to this end: (1) Targeting TCA cycle enzyme/intermediates; (2) Targeting glutamine-dependent anaplerosis; and (3) Targeting the OXPHOS.

Glutamine, a non-essential amino acid, is considered an important energy source for PDAC along with glucose[124,125]. Accumulating evidence demonstrates that glutamine plays a vital role in PDAC proliferation, invasion, maintenance of redox balance, chemotherapy, and radiotherapy resistance, underlining glutamine metabolism as a potential therapeutic target[126-132]. However, conflicting results show that the presence of glutamine suppresses PDAC growth and invasion, dampening

enthusiasm for targeting glutamine metabolism[133-135]. A current clinical trial (NCT04634539) is analyzing whether adding glutamine improves efficacy and reduces the toxicity of PDAC chemotherapy. The results from this trial will shed light on the effect of glutamine on PDAC chemotherapy.

Two additional approaches, targeting the OXPHOS and the TCA cycle, have shown promise in preclinical evaluations, and agents targeting them are currently in clinical trials (Table 2). IACS-010759 inhibits mitochondrial complex one and has recently completed a phase I study in different tumor types, including advanced pancreatic cancers (Table 2). Although the preclinical data regarding the effect of IACS-010759 on pancreatic tumors is lacking, inhibition of OXPHOS complex one appears to be a promising strategy for overcoming drug resistance[136-139]. The anti-diabetic drug metformin has been tested and continues to be tested for its efficacy in PDAC (NCT01210911, NCT02336087, and NCT01666730). Although the experience with metformin in clinical settings has not resulted in improved patient outcomes, a recent meta-analysis indicated survival benefits in patients with PDAC and concurrent diabetes mellitus, highlighting a need for a personalized therapeutic approach for the success of this therapy[140-142].

CPI-613 or Demivistat (Table 2) is a TCA cycle targeting agent that inhibits the activity of pyruvate dehydrogenase and α- ketoglutarate dehydrogenase. In a phase 1 trial, 61% of patients achieved an objective response, and 3 (17%) patients achieved a complete response after receiving CPI-613[143].

Targeting PDAC DNA repair

Activating KRAS mutations are major drivers of malignant growth in PDAC and have remained undruggable until recent promising developments. Oncogenic KRAS-induced DNA replication stress drives genomic instability and tumorigenesis in PDAC. Genomic analysis have also revealed that modifications in "DNA damage control" is a prominent genetic alteration observed in PDAC[43]. Recently, genetic alterations in PDAC have been classified into four sub-types by Waddell *et al*[144]: (1) Stable; (2) Locally rearranged; (3) Scattered; and (4) Unstable. The "unstable" phenotype harbors mutations in the DNA damage repair (DDR), such as BRCA1, BRCA2, PALB2, and ATM. Mutations in ATM account for the most frequently occurring somatic mutations in approximately 4% of PDAC cases, followed by BRCA2, STK11, and BRCA1[144-147]. Given the important role these DDR genes play in a significant proportion of human PDACs, patients are likely to benefit from tailored, targeted therapies, including platinums, directed against specific DDR (Table 3). The following paragraphs will discuss these therapies.

Platinums: Platinum agents (cisplatin, oxaliplatin) cause DNA damage by forming platinum adducts on the DNA and causing DNA interstrand crosslinks[148]. Oxaliplatin is a component of the standard of care FOLFIRINOX, and platinum compounds alone are well suited in cancers that have a deficiency in the homologous repair (HR) pathway. Many studies have highlighted the advantageous use of platinum compounds for HR-deficient PDAC. Golan *et al*[149] showed a survival benefit (22 mo *vs* 9 mo) in platinum-treated *vs* platinum-naïve BRCA1/2 mutated advanced PDAC. Similarly, platinum improved overall survival in patients with HR-deficient PDACs and in patients with germline BRCA1, BRCA2, and PALB2 mutations[150,151]. Hence careful patient selection depending on the genetic make-up of the tumor would be essential for platinums to succeed.

Poly (ADP-ribose) glycohydrolase: Poly (ADP-ribose) glycohydrolase (PARG) is a macrodomain protein with exo- and endo-glycohydrolase activity[152,153]. It critically regulates DNA damage responses by removing poly (ADP-ribose) molecules (PARylation) on modified proteins during the DNA repair process. It is the primary PAR degrading enzyme and reverses poly (ADP ribose) polymerase (PARP) functions by hydrolyzing the ribose-ribose bonds present in PAR molecules. By preventing cytoplasmic PAR accumulation, PARG prevents PAR-mediated apoptosis, termed as parthanatos[154]. Inhibiting PARG causes DNA replication fork collapse, which leads to irreparable DNA damage and cell death. Recent studies have highlighted the benefits of selectively targeting PARG as an anti-cancer therapeutic strategy alone or in combination with other genotoxic therapies[155-157]. Targeting PARG was shown to enhance chemotherapeutic effects of DNA damaging agents, like oxaliplatin and 5-fluorouracil in PDAC, and was also synergistic with mitotic kinase, Wee-1 inhibition. In a siRNA screen with DNA replication factors, PARG inhibition was shown to be synergistic with TIMELESS, HUS1, MCM2, CHK1, and RFC2 proteins in an ovarian cancer model, indicating that combinations of PARGi and DNA replication stress

Table 2 Pancreatic ductal adenocarcinoma trials involving agents that target tumor metabolism

Drug	Target	Trial description	NCI trial number
IACS-010759	OXPHOS inhibitor	Phase I, in advanced cancers	NCT03291938
CPI-613	PDH/alpha KDH inhibitor	Phase I, combination with Gem + nab-paclitaxel	NCT03435289
CPI-613	PDH/alpha KDH inhibitor	Phase II, combination with FOLFIRINOX	NCT03699319
CPI-613	PDH/alpha KDH inhibitor	Phase III, combination with modified FOLFIRINOX	NCT03504423
Metformin and atorvastatin	Metabolic inhibitors	Metformin + Atorvastatin + Doxycycline + Mebendazole in cancers	NCT02201381
L-glutamine	Glutamine analog	Phase I, combination with Gem + nab-paclitaxel	NCT04634539

OXPHOS: Oxidative phosphorylation; PDH: Pyruvate dehydrogenase; KDH: Ketoglutarate dehydrogenase.

Table 3 Pancreatic ductal adenocarcinoma trials involving agents that target DNA repair

Drug	Target	Trial description	NCI trial number
M6620 (VX-970)	ATR	Phase I, M6620 and irinotecan hydrochloride in treating patients with solid tumors that are metastatic or cannot be removed by surgery	NCT02595931
AZD6738/olaparib	ATR/PARP	Phase II, Phase II trial of AZD6738 alone and in combination with olaparib	NCT03682289
BAY1895344	ATR	Phase I, testing the addition of an anti-cancer drug, BAY 1895344 ATR inhibitor, to the chemotherapy treatment (Gemcitabine) for advanced solid tumors, pancreatic cancer, and ovarian cancer	NCT04616534
Olaparib	PARP	Phase II, a study of pembrolizumab and olaparib for people with metastatic pancreatic ductal adenocarcinoma and homologous recombination deficiency or exceptional treatment response to platinum-based therapy	NCT04666740
Olaparib	PARP	Phase I, targeted PARP or MEK/ERK inhibition in patients with pancreatic cancer	NCT04005690
Olaparib	PARP	Phase II, a phase 2 study of cediranib in combination with olaparib in advanced solid tumors	NCT02498613
Olaparib	PARP	Phase II, olaparib in treating patients with stage IV pancreatic cancer	NCT02677038
Talazoparib	PARP	Phase II, measuring the effects of talazoparib in patients with advanced cancer and DNA repair variations	NCT04550494
Talazoparib	PARP	Phase I/II, a study of avelumab, binimetinib and talazoparib in patients with locally advanced or metastatic RAS-mutant solid tumors	NCT03637491
Niraparib	PARP	Phase II, niraparib in metastatic pancreatic cancer after previous chemotherapy (NIRA-PANC): A phase 2 trial	NCT03553004
Niraparib	PARP	Phase II, niraparib in patients with pancreatic cancer	NCT03601923
Rucaparib	PARP	Phase II, maintenance rucaparib in BRCA1, BRCA2 or PALB2 mutated pancreatic cancer that has not progressed on platinum-based therapy	NCT03140670
MK1775	WEE1	Phase I/II, a phase i and randomized phase II study of nab-paclitaxel/gemcitabine with or without AZD1775 for treatment of metastatic adenocarcinoma of the pancreas	NCT02194829

PARP: Poly (ADP ribose) polymerase.

inducers should be evaluated as potential therapeutic strategies for PDAC treatment [158]. A synthetic lethal relationship with PARG inhibition and DDR proteins like BRCA1, BRCA2, ABRAXAS, BARD1, and PALB2 was reported in an MCF7 breast cancer model[159]. Since genomic screens in PDAC have revealed alterations/mutations in similar DDR proteins, it is valuable to target PARG in such DDR-deficient PDAC tumors.

Wee-1: WEE1 kinase is an important cell cycle regulator of the G2-M checkpoint and is overexpressed in various cancers, including glioblastoma, breast cancer, osteosarcoma, and hepatocellular carcinoma[160-163]. It phosphorylates and inactivates CDK1 to allow for the repair of damaged DNA before entering mitosis. Wee-1 has regulatory roles in DNA replication stress and HR mechanisms[164-166]. In PDAC, Wee-1 expression is upregulated by a post-transcriptional mechanism regulated by RNA

binding protein, HuR[167], and its inhibition has been found to be effective in DNA repair-deficient PDAC cells[168]. In one study, Wee-1 inhibition was found to sensitize PDAC cells to gemcitabine chemo-radiation therapy[165]. Another study showed Wee-1 inhibition was synergistic with gemcitabine in p53-deficient PDAC xenografts[169]. Co-targeting WEE1 and ATM was shown to synergistically reduce cell proliferation and migration *via* downregulation of PDL-1 expression in pancreatic cancers[170]. Recently, it was also published that a combination of Wee-1 with another DNA repair target, PARG, enhances DNA damage and decreases cell survival in PDAC cells[171].

PARP: PARP is a DNA repair enzyme that plays a role in inflammation, regulation of cell death, transcription, and modulation of post-transcriptional gene expression. In response to DNA damage, PARP-1 could either promote cell survival and DNA repair or cause cell death when the damage is high[172]. PARP covalently adds Poly (ADP ribose) (PAR) chains onto its target proteins by consuming beta nicotinamide adenine dinucleotide (β NAD+). PAR further recruits other DNA repair proteins in the process of damage repair. Chemical competitive inhibitors of PARP enzymatic activity have gained interest as treatment options for many cancers, like ovarian, breast, uterine, and prostate[173], specifically for patients with tumors harboring somatic or germline defects/mutations in HR genes like *BRCA1/2*. Recent whole-genome sequencing studies done in patients with familial pancreatic cancer show that mutations in *BRCA2* gene accounts for 5%-10% of familial pancreatic cancers. In the Ashkenazi Jewish population with PDAC, this percentage increases to 13.7% and represents a major subgroup of PDAC cases that could benefit from PARP inhibitor (PARPi) therapy. In the context of synthetic lethality, impairment of two DNA repair pathways induces cell death and thus targeting HR deficient cells (*BRCA1/2* mutants or others) with PARP inhibitors was found to be lethal[174,175]. Following the success of POLO trial (Pancreas Cancer Olaparib Ongoing), in 2019 FDA approved olaparib (PARPi) as a maintenance therapy in patients with a germline BRCA mutated metastatic PDAC that had not progressed on first-line platinum therapy[174]. An increasing amount of ongoing preclinical and clinical studies suggest that PARPi in combination with either conventional chemotherapeutics (gemcitabine/nab-paclitaxel) or radiation therapy could benefit patients in the long run[176]. However, recent research suggests that although these respond greatly to PARP inhibitors, there is still 40%-70% of BRCA1/2-mutated cancers that fail to respond to PARPi therapy and in those settings PARPi cannot be used. Novel efforts to create a 'BRCAness-tumors harboring mutations in HR beyond BRCA1/2' phenotype in the cells by use of other small molecule inhibitors and their combination with PARPi is now being exploited. Bagnolini *et al*[174] discovered a small molecule disruptor of RAD51-BRCA2 interaction synergizes with olaparib in pancreatic cancer cells. Another study showed synthetic lethaility with PARPi therapy and FGFR1 blockade in pancreatic cancer[177]. Failure of PARPi therapy can also be attributed to acquired resistance mechanisms[178]. A study in pancreatic cancer showed a secondary mutation in BRCA2 emerged after the patient's exceptional response to platinum and PARPi therapy, which likely restored BRCA2 function in PARP inhibitor-resistant tumor cells[179]. Thus, careful evaluation and design of PARPi therapy should be pursued, and novel targets for PARPi beyond BRCA1/2 should be explored.

Other inhibitors of DDR pathway: Ataxia telangiectasia mutated (ATM) and RAD-3 related (ATR) are serine/threonine protein kinases that are involved in double/single-strand break repair and modulate DNA replication stress and DDR signaling[180-182]. ATM is one of the most commonly mutated DDR genes, and many whole genomic sequencing studies in PDAC have reported both somatic or germline ATM loss-of-function mutations. ATM loss drives pancreatic cancer progression, angiogenesis, epithelial-to-mesenchymal transition, and stemness[183]. Radiosensitization of cells with ATM loss/inhibition has been well documented in many tumor types, including pancreatic cancers[184-186]. ATM loss can also synergize with platinums and PARP inhibitor therapies, emphasizing its role in DNA repair. Specific to PDAC, two studies have shown that patients with ATM/ATR mutated tumors respond well to oxaliplatin-based chemotherapy, experiencing either improved progression-free survival or a stable disease[187,188]. Based on these data, multiple ongoing clinical trials (Phase I/II) involving ATM-deficient solid tumors have been initiated with DNA damage agents like PARP inhibitor therapies (olaparib, talazoparib, and niraparib), some of which accept pancreatic cancer patients. Chemical inhibition of ATM *via* small molecule inhibitors (AZD0156, AZD1390) is also being tested in combination with other agents in early stage clinical trials in patients with advanced solid tumors and brain tumors (NCT02588105, NCT03423628). Lack of ATM function may lead to

increased dependence on ATR for DDR, and thus ATR inhibition may be particularly potent in PDACs with somatic mutations in ATM. A recent study employing a multi-DDR interference strategy that included an ATR inhibitor and PARP and DNA-PKC inhibitor was shown to inhibit FOLFIRINOX-induced invasive clones in ATM-deficient PDAC tumors[189]. In 2012, a study tested VX-970, an ATR inhibitor, and found it sensitizes PDAC cells to radiation therapy *in vivo* and *in vitro*[190]. Another study found that a combination treatment of AZD6738 (ATR inhibitor) and gemcitabine induces PDAC regression by preventing checkpoint activation by gemcitabine[191]. The ATR inhibitors (VX-970, AZD6738, BAY18953[43]) are currently in the early stages of clinical development, like ATM inhibitors in patients with advanced solid tumors and lymphomas (NCT03188965, NCT03682289, NCT02595931, and NCT03718091), with or without other chemotherapeutic agents. Although these appear to be promising therapies, their clinical activity in PDAC patients is yet to be shown[183].

Immunotherapy

Immunotherapy has achieved promising outcomes in certain cancers, however is yet to be realized in PDAC[192-194]. Tumors with high tumor mutation burden (TMB, approximate mutations per megabase), such as melanomas and NSCLC, have shown to respond better to immunotherapy[195-197]. These TMBs are generally associated with mismatch repair (MMR) deficiency. PDACs intrinsically have low MMR deficiencies, which may explain the lower response to immunotherapy approaches such as immune checkpoint inhibitors (ICI)[198]. The immunosuppressive nature and "*T cell exhaustion*" further contributes to the poor response of PDAC to immunotherapy.

The PDAC is characterized by the presence of dense stroma in the tumor microenvironment. The stromal components include T cells (cytotoxic and regulatory) and myeloid cells such as tumor-associated macrophages (TAM). Infiltration with macrophages is observed in early PDAC tumor development stages and is associated with poor prognosis in PDAC patients[199-201]. These macrophages secrete immunosuppressive factors such as arginase and TGFβ, and thereby regulate T-cell mediated cytotoxicity and surveillance[200]. The myeloid-derived suppressor cells are immature myeloid cells that suppress T cell proliferation and promote ROS-induced T cell apoptosis[202,203]. The term "T cell exhaustion" is used for T cells' differentiation state in chronic antigen exposure. The exhaustion stage is driven by persistent T cell receptor signaling leading to ineffective T cell functioning[204-206]. Recent evidence has shown that the T cells present in the PDAC tumor microenvironment are defective in the production of interferon and tumor necrosis factors following peptide recognition[207,208]. However, the T cells with identical peptide specificity in the spleen retain functionality in tumor-bearing animals[209].

Some approaches that are currently under investigation for improving the immunological response of PDAC include as follow.

Cancer vaccines and immune checkpoint blockade: Monotherapies targeting programmed cell death 1 (PD-1) and programmed cell death ligand 1 (PD-L1) have not shown promising responses in PDAC. However, the therapy showed tumor regression and disease stabilization in other advanced cancers such as NSCLC, melanoma, and renal cancers[193]. Similarly, inhibition of PD-1 or PD-L1 failed to demonstrate a positive response in PDAC animal models[207,210-212]. Similar to ICI inhibitors, vaccine trials using vaccine-GVAX pancreas (granulocyte-macrophage colony-stimulating factor-secreting allogeneic pancreatic tumor cells) failed to improve overall survival in PDAC patients compared to single-agent chemotherapy[213]. Since the vaccines were able to recruit T cells, one approach to improve their efficacy would be to promote the activation of T cells, which may be achieved through the combination of vaccines with ICI[214]. Currently, clinical trials are underway for establishing the safety and efficacy of these GVAX with ICIs (NCT03153410, NCT02451982, and NCT02648282).

Targeting tumor associated macrophages: Another way to improve the efficacy of immunotherapies is to inhibit the immunosuppressive signaling that originates from the tumor microenvironment. For this, one strategy being tested is to inhibit myeloid cells. Researchers found that CD11b agonist reduces the total number of myeloid cells and improves survival in PDAC mice. In addition, when CD11b was combined with anti-PD-1, anti-CLTA-4, and gemcitabine, enhanced infiltration of tumor with CD8 T cells was observed[212]. Similarly, other studies have confirmed that targeting TAMs improves therapeutic and T-cell checkpoint immunotherapy response in PDAC models[215-217]. Blockade of Csf1/Csf1R (macrophage colony-stimulating factor

1/receptor) reduces collagen deposits and enhances CD8 T cell infiltration in the PDAC mice model[218]. Currently, a phase II trial is underway to determine the efficacy of cabralizumab (CSF1R inhibitor) in combination with nivolumab and chemotherapy in PDAC (NCT03336216).

Adoptive T cell therapy

Adoptive T cell therapy involves isolating T cells from tumors and then engineering, expanding, and infusing them back into the patients[219]. The chimeric antigen receptor (CAR) T cell therapy is an example of adoptive T cell therapy wherein the T cells are manipulated to express CAR to assist tumor recognition[220]. Antigen targets that are being tested for PDAC include mesothelin, prostate stem cell antigen, CEA, MUC1, and HER2[221]. However, the immunosuppressive microenvironment remains a hindrance in CAR-T cell therapy's success in PDAC[222,223]. Other barrier to the success of adoptive T cell therapy in PDAC include antigen selection and toxicities [224-226]. Still, a few promising outcomes have sustained hope for the use of this approach in PDAC. A phase 1 trial found that treatment of PDAC patients with mesothelin-targeting-CART-T cells stabilized disease in 2 out of 6 patients[227]. Similarly, analysis of efficacy and safety of MUC1-targeting CART-T cells found the therapy to be safe and successfully elevated the levels of CD4+ and CD8+ T cells at the tumor[228]. Currently, clinical trials are underway to determine MUC-1-targeted CAR-T cell therapy's efficacy and safety in patients with solid tumors, including PDAC (NCT02587689 and NCT02617134).

CONCLUSION

The PDAC remains an intractable disease that is slated to be the second leading cause of cancer-related deaths by 2030. Although surgical resection remains the only curative treatment option, late diagnosis, in addition to the patient's performance status, limits the scope of surgical intervention. Chemotherapeutic regimens such as gemcitabine+nab-paclitaxel and FOLFIRINOX has shown promise in improving patient survival; however, drug resistance remains a continuing challenge that has limited their efficacy. Two approaches that may improve PDAC patient outcomes include inhibiting the mechanism(s) that promote therapy resistance and targeting the key pathways essential for PDAC survival. The altered metabolism provides the PDAC cells with energy (ATP) and macromolecules essential for tumor growth. Additionally, studies have shown that metabolism plays a key role in PDAC therapy resistance. Similarly, PARP targeting therapies' success has once again brought the importance of DNA repair mechanisms in PDAC into the center. The limited success of immunotherapy has dampened the enthusiasm for targeting PDAC using this approach. However, the uncovering of mechanisms contributing to poor PDAC's response to immunotherapy has provided opportunities to test newer approaches. Even though the strategies mentioned above have shown promising pre-clinical results individually, a regimen targeting multiple aspects of PDAC will likely deliver a better clinical outcome in this deadly disease.

ACKNOWLEDGEMENTS

We thank Wilson J (Thomas Jefferson University, Philadelphia, PA, United States) for her support in editing this manuscript.

REFERENCES

1 **Siegel RL**, Miller KD, Jemal A. Cancer statistics, 2020. *CA Cancer J Clin* 2020; **70**: 7-30 [PMID: 31912902 DOI: 10.3322/caac.21590]

2 **Rahib L**, Smith BD, Aizenberg R, Rosenzweig AB, Fleshman JM, Matrisian LM. Projecting cancer incidence and deaths to 2030: the unexpected burden of thyroid, liver, and pancreas cancers in the United States. *Cancer Res* 2014; **74**: 2913-2921 [PMID: 24840647 DOI: 10.1158/0008-5472.CAN-14-0155]

3 **Burris HA 3rd**, Moore MJ, Andersen J, Green MR, Rothenberg ML, Modiano MR, Cripps MC, Portenoy RK, Storniolo AM, Tarassoff P, Nelson R, Dorr FA, Stephens CD, Von Hoff DD. Improvements in survival and clinical benefit with gemcitabine as first-line therapy for patients with

advanced pancreas cancer: a randomized trial. *J Clin Oncol* 1997; **15**: 2403-2413 [PMID: 9196156 DOI: 10.1200/JCO.1997.15.6.2403]

4 **Conroy T**, Desseigne F, Ychou M, Bouché O, Guimbaud R, Bécouarn Y, Adenis A, Raoul JL, Gourgou-Bourgade S, de la Fouchardière C, Bennouna J, Bachet JB, Khemissa-Akouz F, Péré-Verger D, Delbaldo C, Assenat E, Chauffert B, Michel P, Montoto-Grillot C, Ducreux M; Groupe Tumeurs Digestives of Unicancer; PRODIGE Intergroup. FOLFIRINOX *vs* gemcitabine for metastatic pancreatic cancer. *N Engl J Med* 2011; **364**: 1817-1825 [PMID: 21561347 DOI: 10.1056/NEJMoa1011923]

5 **Labori KJ**, Katz MH, Tzeng CW, Bjørnbeth BA, Cvancarova M, Edwin B, Kure EH, Eide TJ, Dueland S, Buanes T, Gladhaug IP. Impact of early disease progression and surgical complications on adjuvant chemotherapy completion rates and survival in patients undergoing the surgery first approach for resectable pancreatic ductal adenocarcinoma - A population-based cohort study. *Acta Oncol* 2016; **55**: 265-277 [PMID: 26213211 DOI: 10.3109/0284186X.2015.1068445]

6 **Oettle H**, Post S, Neuhaus P, Gellert K, Langrehr J, Ridwelski K, Schramm H, Fahlke J, Zuelke C, Burkart C, Gutberlet K, Kettner E, Schmalenberg H, Weigang-Koehler K, Bechstein WO, Niedergethmann M, Schmidt-Wolf I, Roll L, Doerken B, Riess H. Adjuvant chemotherapy with gemcitabine *vs* observation in patients undergoing curative-intent resection of pancreatic cancer: a randomized controlled trial. *JAMA* 2007; **297**: 267-277 [PMID: 17227978 DOI: 10.1001/jama.297.3.267]

7 **Neoptolemos JP**, Stocken DD, Bassi C, Ghaneh P, Cunningham D, Goldstein D, Padbury R, Moore MJ, Gallinger S, Mariette C, Wente MN, Izbicki JR, Friess H, Lerch MM, Dervenis C, Oláh A, Butturini G, Doi R, Lind PA, Smith D, Valle JW, Palmer DH, Buckels JA, Thompson J, McKay CJ, Rawcliffe CL, Büchler MW; European Study Group for Pancreatic Cancer. Adjuvant chemotherapy with fluorouracil plus folinic acid *vs* gemcitabine following pancreatic cancer resection: a randomized controlled trial. *JAMA* 2010; **304**: 1073-1081 [PMID: 20823433 DOI: 10.1001/jama.2010.1275]

8 **Neoptolemos JP**, Palmer DH, Ghaneh P, Psarelli EE, Valle JW, Halloran CM, Faluyi O, O'Reilly DA, Cunningham D, Wadsley J, Darby S, Meyer T, Gillmore R, Anthoney A, Lind P, Glimelius B, Falk S, Izbicki JR, Middleton GW, Cummins S, Ross PJ, Wasan H, McDonald A, Crosby T, Ma YT, Patel K, Sherriff D, Soomal R, Borg D, Sothi S, Hammel P, Hackert T, Jackson R, Büchler MW; European Study Group for Pancreatic Cancer. Comparison of adjuvant gemcitabine and capecitabine with gemcitabine monotherapy in patients with resected pancreatic cancer (ESPAC-4): a multicentre, open-label, randomised, phase 3 trial. *Lancet* 2017; **389**: 1011-1024 [PMID: 28129987 DOI: 10.1016/S0140-6736(16)32409-6]

9 **Dreyer SB**, Chang DK, Bailey P, Biankin AV. Pancreatic Cancer Genomes: Implications for Clinical Management and Therapeutic Development. *Clin Cancer Res* 2017; **23**: 1638-1646 [PMID: 28373362 DOI: 10.1158/1078-0432.CCR-16-2411]

10 **Mini E**, Nobili S, Caciagli B, Landini I, Mazzei T. Cellular pharmacology of gemcitabine. *Ann Oncol* 2006; **17** Suppl 5: v7-12 [PMID: 16807468 DOI: 10.1093/annonc/mdj941]

11 **Heinemann V**, Hertel LW, Grindey GB, Plunkett W. Comparison of the cellular pharmacokinetics and toxicity of 2',2'-difluorodeoxycytidine and 1-beta-D-arabinofuranosylcytosine. *Cancer Res* 1988; **48**: 4024-4031 [PMID: 3383195]

12 **Mackey JR**, Mani RS, Selner M, Mowles D, Young JD, Belt JA, Crawford CR, Cass CE. Functional nucleoside transporters are required for gemcitabine influx and manifestation of toxicity in cancer cell lines. *Cancer Res* 1998; **58**: 4349-4357 [PMID: 9766663]

13 **Spratlin J**, Sangha R, Glubrecht D, Dabbagh L, Young JD, Dumontet C, Cass C, Lai R, Mackey JR. The absence of human equilibrative nucleoside transporter 1 is associated with reduced survival in patients with gemcitabine-treated pancreas adenocarcinoma. *Clin Cancer Res* 2004; **10**: 6956-6961 [PMID: 15501974 DOI: 10.1158/1078-0432.CCR-04-0224]

14 **Ohhashi S**, Ohuchida K, Mizumoto K, Fujita H, Egami T, Yu J, Toma H, Sadatomi S, Nagai E, Tanaka M. Down-regulation of deoxycytidine kinase enhances acquired resistance to gemcitabine in pancreatic cancer. *Anticancer Res* 2008; **28**: 2205-2212 [PMID: 18751396]

15 **Saiki Y**, Yoshino Y, Fujimura H, Manabe T, Kudo Y, Shimada M, Mano N, Nakano T, Lee Y, Shimizu S, Oba S, Fujiwara S, Shimizu H, Chen N, Nezhad ZK, Jin G, Fukushige S, Sunamura M, Ishida M, Motoi F, Egawa S, Unno M, Horii A. DCK is frequently inactivated in acquired gemcitabine-resistant human cancer cells. *Biochem Biophys Res Commun* 2012; **421**: 98-104 [PMID: 22490663 DOI: 10.1016/j.bbrc.2012.03.122]

16 **Miller AL**, Garcia PL, Gamblin TL, Vance RB, Yoon KJ. Development of gemcitabine-resistant patient-derived xenograft models of pancreatic ductal adenocarcinoma. *Cancer Drug Resist* 2020; **3**: 572-585 [PMID: 33073205 DOI: 10.20517/cdr.2020.35]

17 **Wang C**, Zhang W, Fu M, Yang A, Huang H, Xie J. Establishment of human pancreatic cancer gemcitabineresistant cell line with ribonucleotide reductase overexpression. *Oncol Rep* 2015; **33**: 383-390 [PMID: 25394408 DOI: 10.3892/or.2014.3599]

18 **Nakahira S**, Nakamori S, Tsujie M, Takahashi Y, Okami J, Yoshioka S, Yamasaki M, Marubashi S, Takemasa I, Miyamoto A, Takeda Y, Nagano H, Dono K, Umeshita K, Sakon M, Monden M. Involvement of ribonucleotide reductase M1 subunit overexpression in gemcitabine resistance of human pancreatic cancer. *Int J Cancer* 2007; **120**: 1355-1363 [PMID: 17131328 DOI: 10.1002/ijc.22390]

19 **Maftouh M**, Avan A, Funel N, Frampton AE, Fiuji H, Pelliccioni S, Castellano L, Galla V, Peters

GJ, Giovannetti E. miR-211 modulates gemcitabine activity through downregulation of ribonucleotide reductase and inhibits the invasive behavior of pancreatic cancer cells. *Nucleosides Nucleotides Nucleic Acids* 2014; **33**: 384-393 [PMID: 24940696 DOI: 10.1080/15257770.2014.891741]

20 **Lu H**, Lu S, Yang D, Zhang L, Ye J, Li M, Hu W. MiR-20a-5p regulates gemcitabine chemosensitivity by targeting RRM2 in pancreatic cancer cells and serves as a predictor for gemcitabine-based chemotherapy. *Biosci Rep* 2019; **39** [PMID: 30777929 DOI: 10.1042/BSR20181374]

21 **Xia G**, Wang H, Song Z, Meng Q, Huang X. Gambogic acid sensitizes gemcitabine efficacy in pancreatic cancer by reducing the expression of ribonucleotide reductase subunit-M2 (RRM2). *J Exp Clin Cancer Res* 2017; **36**: 107 [PMID: 28797284 DOI: 10.1186/s13046-017-0579-0]

22 **Vena F**, Li Causi E, Rodriguez-Justo M, Goodstal S, Hagemann T, Hartley JA, Hochhauser D. The MEK1/2 Inhibitor Pimasertib Enhances Gemcitabine Efficacy in Pancreatic Cancer Models by Altering Ribonucleotide Reductase Subunit-1 (RRM1). *Clin Cancer Res* 2015; **21**: 5563-5577 [PMID: 26228206 DOI: 10.1158/1078-0432.CCR-15-0485]

23 **Roman NO**, Samulitis BK, Wisner L, Landowski TH, Dorr RT. Imexon enhances gemcitabine cytotoxicity by inhibition of ribonucleotide reductase. *Cancer Chemother Pharmacol* 2011; **67**: 183-192 [PMID: 20339847 DOI: 10.1007/s00280-010-1306-0]

24 **Mitsuno M**, Kitajima Y, Ohtaka K, Kai K, Hashiguchi K, Nakamura J, Hiraki M, Noshiro H, Miyazaki K. Tranilast strongly sensitizes pancreatic cancer cells to gemcitabine *via* decreasing protein expression of ribonucleotide reductase 1. *Int J Oncol* 2010; **36**: 341-349 [PMID: 20043067 DOI: 10.3892/ijo_00000505]

25 **Hwang DW**, Shin E, Cho JY, Han HS, Yoon YS. Human equilibrative nucleoside transporter-1 (hENT1) and ribonucleotide reductase regulatory subunit M1 (RRM1) expression; do they have survival impact to pancreatic cancer? *Ann Hepatobiliary Pancreat Surg* 2020; **24**: 127-136 [PMID: 32457256 DOI: 10.14701/ahbps.2020.24.2.127]

26 **Han QL**, Zhou YH, Lyu Y, Yan H, Dai GH. Effect of ribonucleotide reductase M1 expression on overall survival in patients with pancreatic cancer receiving gemcitabine chemotherapy: A literature-based meta-analysis. *J Clin Pharm Ther* 2018; **43**: 163-169 [PMID: 29214667 DOI: 10.1111/jcpt.12655]

27 **Aoyama T**, Miyagi Y, Murakawa M, Yamaoku K, Atsumi Y, Shiozawa M, Ueno M, Morimoto M, Oshima T, Yukawa N, Yoshikawa T, Rino Y, Masuda M, Morinaga S. Clinical implications of ribonucleotide reductase subunit M1 in patients with pancreatic cancer who undergo curative resection followed by adjuvant chemotherapy with gemcitabine. *Oncol Lett* 2017; **13**: 3423-3430 [PMID: 28521448 DOI: 10.3892/ol.2017.5935]

28 **Elander NO**, Aughton K, Ghaneh P, Neoptolemos JP, Palmer DH, Cox TF, Campbell F, Costello E, Halloran CM, Mackey JR, Scarfe AG, Valle JW, McDonald AC, Carter R, Tebbutt NC, Goldstein D, Shannon J, Dervenis C, Glimelius B, Deakin M, Charnley RM, Anthoney A, Lerch MM, Mayerle J, Oláh A, Büchler MW, Greenhalf W; European Study Group for Pancreatic Cancer. Intratumoural expression of deoxycytidylate deaminase or ribonuceotide reductase subunit M1 expression are not related to survival in patients with resected pancreatic cancer given adjuvant chemotherapy. *Br J Cancer* 2018; **118**: 1084-1088 [PMID: 29523831 DOI: 10.1038/s41416-018-0005-1]

29 **Zeng S**, Pöttler M, Lan B, Grützmann R, Pilarsky C, Yang H. Chemoresistance in Pancreatic Cancer. *Int J Mol Sci* 2019; **20** [PMID: 31514451 DOI: 10.3390/ijms20184504]

30 **Arumugam T**, Ramachandran V, Fournier KF, Wang H, Marquis L, Abbruzzese JL, Gallick GE, Logsdon CD, McConkey DJ, Choi W. Epithelial to mesenchymal transition contributes to drug resistance in pancreatic cancer. *Cancer Res* 2009; **69**: 5820-5828 [PMID: 19584296 DOI: 10.1158/0008-5472.CAN-08-2819]

31 **Zheng X**, Carstens JL, Kim J, Scheible M, Kaye J, Sugimoto H, Wu CC, LeBleu VS, Kalluri R. Epithelial-to-mesenchymal transition is dispensable for metastasis but induces chemoresistance in pancreatic cancer. *Nature* 2015; **527**: 525-530 [PMID: 26560028 DOI: 10.1038/nature16064]

32 **Kalser MH**, Ellenberg SS. Pancreatic cancer. Adjuvant combined radiation and chemotherapy following curative resection. *Arch Surg* 1985; **120**: 899-903 [PMID: 4015380 DOI: 10.1001/archsurg.1985.01390320023003]

33 **Moertel CG**, Frytak S, Hahn RG, O'Connell MJ, Reitemeier RJ, Rubin J, Schutt AJ, Weiland LH, Childs DS, Holbrook MA, Lavin PT, Livstone E, Spiro H, Knowlton A, Kalser M, Barkin J, Lessner H, Mann-Kaplan R, Ramming K, Douglas HO Jr, Thomas P, Nave H, Bateman J, Lokich J, Brooks J, Chaffey J, Corson JM, Zamcheck N, Novak JW. Therapy of locally unresectable pancreatic carcinoma: a randomized comparison of high dose (6000 rads) radiation alone, moderate dose radiation (4000 rads + 5-fluorouracil), and high dose radiation + 5-fluorouracil: The Gastrointestinal Tumor Study Group. *Cancer* 1981; **48**: 1705-1710 [PMID: 7284971 DOI: 10.1002/1097-0142(19811015)48:8<1705::aid-cncr2820480803>3.0.co;2-4]

34 **Chevalier H**, Vienot A, Lièvre A, Edeline J, El Hajbi F, Peugniez C, Vernerey D, Meurisse A, Hammel P, Neuzillet C, Borg C, Turpin A. FOLFIRINOX De-Escalation in Advanced Pancreatic Cancer: A Multicenter Real-Life Study. *Oncologist* 2020; **25**: e1701-e1710 [PMID: 32886823 DOI: 10.1634/theoncologist.2020-0577]

35 **Foschini F**, Napolitano F, Servetto A, Marciano R, Mozzillo E, Carratù AC, Santaniello A, De Placido P, Cascetta P, Butturini G, Frigerio I, Regi P, Silvestris N, Delcuratolo S, Vasile E, Vivaldi C, Bianco C, De Placido S, Formisano L, Bianco R. FOLFIRINOX after first-line gemcitabine-based

chemotherapy in advanced pancreatic cancer: a retrospective comparison with FOLFOX and FOLFIRI schedules. *Ther Adv Med Oncol* 2020; **12**: 1758835920947970 [PMID: 33062062 DOI: 10.1177/1758835920947970]

36 **Jung JH**, Shin DW, Kim J, Lee JC, Hwang JH. Primary Granulocyte Colony-Stimulating Factor Prophylaxis in Metastatic Pancreatic Cancer Patients Treated with FOLFIRINOX as the First-Line Treatment. *Cancers (Basel)* 2020; **12** [PMID: 33120908 DOI: 10.3390/cancers12113137]

37 **Kang SP**, Saif MW. Pharmacogenomics and pancreatic cancer treatment. Optimizing current therapy and individualizing future therapy. *JOP* 2008; **9**: 251-266 [PMID: 18469437]

38 **Zhang N**, Yin Y, Xu SJ, Chen WS. 5-Fluorouracil: mechanisms of resistance and reversal strategies. *Molecules* 2008; **13**: 1551-1569 [PMID: 18794772 DOI: 10.3390/molecules13081551]

39 **Hu YC**, Komorowski RA, Graewin S, Hostetter G, Kallioniemi OP, Pitt HA, Ahrendt SA. Thymidylate synthase expression predicts the response to 5-fluorouracil-based adjuvant therapy in pancreatic cancer. *Clin Cancer Res* 2003; **9**: 4165-4171 [PMID: 14519641]

40 **Jenh CH**, Geyer PK, Baskin F, Johnson LF. Thymidylate synthase gene amplification in fluorodeoxyuridine-resistant mouse cell lines. *Mol Pharmacol* 1985; **28**: 80-85 [PMID: 2991733]

41 **Ciaparrone M**, Quirino M, Schinzari G, Zannoni G, Corsi DC, Vecchio FM, Cassano A, La Torre G, Barone C. Predictive role of thymidylate synthase, dihydropyrimidine dehydrogenase and thymidine phosphorylase expression in colorectal cancer patients receiving adjuvant 5-fluorouracil. *Oncology* 2006; **70**: 366-377 [PMID: 17179731 DOI: 10.1159/000098110]

42 **Kurata N**, Fujita H, Ohuchida K, Mizumoto K, Mahawithitwong P, Sakai H, Onimaru M, Manabe T, Ohtsuka T, Tanaka M. Predicting the chemosensitivity of pancreatic cancer cells by quantifying the expression levels of genes associated with the metabolism of gemcitabine and 5-fluorouracil. *Int J Oncol* 2011; **39**: 473-482 [PMID: 21617862 DOI: 10.3892/ijo.2011.1058]

43 **Jones S**, Zhang X, Parsons DW, Lin JC, Leary RJ, Angenendt P, Mankoo P, Carter H, Kamiyama H, Jimeno A, Hong SM, Fu B, Lin MT, Calhoun ES, Kamiyama M, Walter K, Nikolskaya T, Nikolsky Y, Hartigan J, Smith DR, Hidalgo M, Leach SD, Klein AP, Jaffee EM, Goggins M, Maitra A, Iacobuzio-Donahue C, Eshleman JR, Kern SE, Hruban RH, Karchin R, Papadopoulos N, Parmigiani G, Vogelstein B, Velculescu VE, Kinzler KW. Core signaling pathways in human pancreatic cancers revealed by global genomic analyses. *Science* 2008; **321**: 1801-1806 [PMID: 18772397 DOI: 10.1126/science.1164368]

44 **Smit VT**, Boot AJ, Smits AM, Fleuren GJ, Cornelisse CJ, Bos JL. KRAS codon 12 mutations occur very frequently in pancreatic adenocarcinomas. *Nucleic Acids Res* 1988; **16**: 7773-7782 [PMID: 3047672 DOI: 10.1093/nar/16.16.7773]

45 **Lemoine NR**, Hughes CM, Barton CM, Poulsom R, Jeffery RE, Klöppel G, Hall PA, Gullick WJ. The epidermal growth factor receptor in human pancreatic cancer. *J Pathol* 1992; **166**: 7-12 [PMID: 1538276 DOI: 10.1002/path.1711660103]

46 **Boeck S**, Jung A, Laubender RP, Neumann J, Egg R, Goritschan C, Vehling-Kaiser U, Winkelmann C, Fischer von Weikersthal L, Clemens MR, Gauler TC, Märten A, Klein S, Kojouharoff G, Barner M, Geissler M, Greten TF, Mansmann U, Kirchner T, Heinemann V. EGFR pathway biomarkers in erlotinib-treated patients with advanced pancreatic cancer: translational results from the randomised, crossover phase 3 trial AIO-PK0104. *Br J Cancer* 2013; **108**: 469-476 [PMID: 23169292 DOI: 10.1038/bjc.2012.495]

47 **Moore MJ**, Goldstein D, Hamm J, Figer A, Hecht JR, Gallinger S, Au HJ, Murawa P, Walde D, Wolff RA, Campos D, Lim R, Ding K, Clark G, Voskoglou-Nomikos T, Ptasynski M, Parulekar W; National Cancer Institute of Canada Clinical Trials Group. Erlotinib plus gemcitabine compared with gemcitabine alone in patients with advanced pancreatic cancer: a phase III trial of the National Cancer Institute of Canada Clinical Trials Group. *J Clin Oncol* 2007; **25**: 1960-1966 [PMID: 17452677 DOI: 10.1200/JCO.2006.07.9525]

48 **Haas M**, Siveke JT, Schenk M, Lerch MM, Caca K, Freiberg-Richter J, Fischer von Weikersthal L, Kullmann F, Reinacher-Schick A, Fuchs M, Kanzler S, Kunzmann V, Ettrich TJ, Kruger S, Westphalen CB, Held S, Heinemann V, Boeck S. Efficacy of gemcitabine plus erlotinib in rash-positive patients with metastatic pancreatic cancer selected according to eligibility for FOLFIRINOX: A prospective phase II study of the 'Arbeitsgemeinschaft Internistische Onkologie'. *Eur J Cancer* 2018; **94**: 95-103 [PMID: 29549862 DOI: 10.1016/j.ejca.2018.02.008]

49 **Van Cutsem E**, Li CP, Nowara E, Aprile G, Moore M, Federowicz I, Van Laethem JL, Hsu C, Tham CK, Stemmer SM, Lipp R, Zeaiter A, Fittipaldo A, Csutor Z, Klughammer B, Meng X, Ciuleanu T. Dose escalation to rash for erlotinib plus gemcitabine for metastatic pancreatic cancer: the phase II RACHEL study. *Br J Cancer* 2014; **111**: 2067-2075 [PMID: 25247318 DOI: 10.1038/bjc.2014.494]

50 **Philip PA**, Benedetti J, Corless CL, Wong R, O'Reilly EM, Flynn PJ, Rowland KM, Atkins JN, Mirtsching BC, Rivkin SE, Khorana AA, Goldman B, Fenoglio-Preiser CM, Abbruzzese JL, Blanke CD. Phase III study comparing gemcitabine plus cetuximab *vs* gemcitabine in patients with advanced pancreatic adenocarcinoma: Southwest Oncology Group-directed intergroup trial S0205. *J Clin Oncol* 2010; **28**: 3605-3610 [PMID: 20606093 DOI: 10.1200/JCO.2009.25.7550]

51 **Katopodis O**, Souglakos J, Stathopoulos E, Christopoulou A, Kontopodis E, Kotsakis A, Kalbakis K, Kentepozidis N, Polyzos A, Hatzidaki D, Georgoulias V. Frontline treatment with gemcitabine, oxaliplatin and erlotinib for the treatment of advanced or metastatic pancreatic cancer: a multicenter phase II study of the Hellenic Oncology Research Group (HORG). *Cancer Chemother Pharmacol* 2014; **74**: 333-340 [PMID: 24930058 DOI: 10.1007/s00280-014-2509-6]

52 **Heinemann V**, Vehling-Kaiser U, Waldschmidt D, Kettner E, Märten A, Winkelmann C, Klein S, Kojouharoff G, Gauler TC, von Weikersthal LF, Clemens MR, Geissler M, Greten TF, Hegewisch-Becker S, Rubanov O, Baake G, Höhler T, Ko YD, Jung A, Neugebauer S, Boeck S. Gemcitabine plus erlotinib followed by capecitabine *vs* capecitabine plus erlotinib followed by gemcitabine in advanced pancreatic cancer: final results of a randomised phase 3 trial of the 'Arbeitsgemeinschaft Internistische Onkologie' (AIO-PK0104). *Gut* 2013; **62**: 751-759 [PMID: 22773551 DOI: 10.1136/gutjnl-2012-302759]

53 **Rich TA**, Winter K, Safran H, Hoffman JP, Erickson B, Anne PR, Myerson RJ, Cline-Burkhardt VJ, Perez K, Willett C. Weekly paclitaxel, gemcitabine, and external irradiation followed by randomized farnesyl transferase inhibitor R115777 for locally advanced pancreatic cancer. *Onco Targets Ther* 2012; **5**: 161-170 [PMID: 22977306 DOI: 10.2147/OTT.S33560]

54 **Kindler HL**, Niedzwiecki D, Hollis D, Sutherland S, Schrag D, Hurwitz H, Innocenti F, Mulcahy MF, O'Reilly E, Wozniak TF, Picus J, Bhargava P, Mayer RJ, Schilsky RL, Goldberg RM. Gemcitabine plus bevacizumab compared with gemcitabine plus placebo in patients with advanced pancreatic cancer: phase III trial of the Cancer and Leukemia Group B (CALGB 80303). *J Clin Oncol* 2010; **28**: 3617-3622 [PMID: 20606091 DOI: 10.1200/JCO.2010.28.1386]

55 **Kindler HL**, Ioka T, Richel DJ, Bennouna J, Létourneau R, Okusaka T, Funakoshi A, Furuse J, Park YS, Ohkawa S, Springett GM, Wasan HS, Trask PC, Bycott P, Ricart AD, Kim S, Van Cutsem E. Axitinib plus gemcitabine *vs* placebo plus gemcitabine in patients with advanced pancreatic adenocarcinoma: a double-blind randomised phase 3 study. *Lancet Oncol* 2011; **12**: 256-262 [PMID: 21306953 DOI: 10.1016/S1470-2045(11)70004-3]

56 **Infante JR**, Somer BG, Park JO, Li CP, Scheulen ME, Kasubhai SM, Oh DY, Liu Y, Redhu S, Steplewski K, Le N. A randomised, double-blind, placebo-controlled trial of trametinib, an oral MEK inhibitor, in combination with gemcitabine for patients with untreated metastatic adenocarcinoma of the pancreas. *Eur J Cancer* 2014; **50**: 2072-2081 [PMID: 24915778 DOI: 10.1016/j.ejca.2014.04.024]

57 **Chung V**, McDonough S, Philip PA, Cardin D, Wang-Gillam A, Hui L, Tejani MA, Seery TE, Dy IA, Al Baghdadi T, Hendifar AE, Doyle LA, Lowy AM, Guthrie KA, Blanke CD, Hochster HS. Effect of Selumetinib and MK-2206 *vs* Oxaliplatin and Fluorouracil in Patients With Metastatic Pancreatic Cancer After Prior Therapy: SWOG S1115 Study Randomized Clinical Trial. *JAMA Oncol* 2017; **3**: 516-522 [PMID: 27978579 DOI: 10.1001/jamaoncol.2016.5383]

58 **Mahadevan D**, Von Hoff DD. Tumor-stroma interactions in pancreatic ductal adenocarcinoma. *Mol Cancer Ther* 2007; **6**: 1186-1197 [PMID: 17406031 DOI: 10.1158/1535-7163.MCT-06-0686]

59 **Hoffmann AC**, Mori R, Vallbohmer D, Brabender J, Klein E, Drebber U, Baldus SE, Cooc J, Azuma M, Metzger R, Hoelscher AH, Danenberg KD, Prenzel KL, Danenberg PV. High expression of HIF1a is a predictor of clinical outcome in patients with pancreatic ductal adenocarcinomas and correlated to PDGFA, VEGF, and bFGF. *Neoplasia* 2008; **10**: 674-679 [PMID: 18592007 DOI: 10.1593/neo.08292]

60 **Couvelard A**, O'Toole D, Leek R, Turley H, Sauvanet A, Degott C, Ruszniewski P, Belghiti J, Harris AL, Gatter K, Pezzella F. Expression of hypoxia-inducible factors is correlated with the presence of a fibrotic focus and angiogenesis in pancreatic ductal adenocarcinomas. *Histopathology* 2005; **46**: 668-676 [PMID: 15910598 DOI: 10.1111/j.1365-2559.2005.02160.x]

61 **Büchler P**, Reber HA, Lavey RS, Tomlinson J, Büchler MW, Friess H, Hines OJ. Tumor hypoxia correlates with metastatic tumor growth of pancreatic cancer in an orthotopic murine model. *J Surg Res* 2004; **120**: 295-303 [PMID: 15234226 DOI: 10.1016/j.jss.2004.02.014]

62 **Warburg O**. On the origin of cancer cells. *Science* 1956; **123**: 309-314 [PMID: 13298683 DOI: 10.1126/science.123.3191.309]

63 **Cairns RA**, Harris IS, Mak TW. Regulation of cancer cell metabolism. *Nat Rev Cancer* 2011; **11**: 85-95 [PMID: 21258394 DOI: 10.1038/nrc2981]

64 **Christofk HR**, Vander Heiden MG, Harris MH, Ramanathan A, Gerszten RE, Wei R, Fleming MD, Schreiber SL, Cantley LC. The M2 splice isoform of pyruvate kinase is important for cancer metabolism and tumour growth. *Nature* 2008; **452**: 230-233 [PMID: 18337823 DOI: 10.1038/nature06734]

65 **Dong X**, Li Y, Chang P, Tang H, Hess KR, Abbruzzese JL, Li D. Glucose metabolism gene variants modulate the risk of pancreatic cancer. *Cancer Prev Res (Phila)* 2011; **4**: 758-766 [PMID: 21411499 DOI: 10.1158/1940-6207.CAPR-10-0247]

66 **Dong X**, Tang H, Hess KR, Abbruzzese JL, Li D. Glucose metabolism gene polymorphisms and clinical outcome in pancreatic cancer. *Cancer* 2011; **117**: 480-491 [PMID: 20845477 DOI: 10.1002/cncr.25612]

67 **Markovets AA**, Herman D. Analysis of cancer metabolism with high-throughput technologies. *BMC Bioinformatics* 2011; **12** Suppl 10: S8 [PMID: 22166000 DOI: 10.1186/1471-2105-12-S10-S8]

68 **Wei Z**, Cui L, Mei Z, Liu M, Zhang D. miR-181a mediates metabolic shift in colon cancer cells *via* the PTEN/AKT pathway. *FEBS Lett* 2014; **588**: 1773-1779 [PMID: 24685694 DOI: 10.1016/j.febslet.2014.03.037]

69 **Mikuriya K**, Kuramitsu Y, Ryozawa S, Fujimoto M, Mori S, Oka M, Hamano K, Okita K, Sakaida I, Nakamura K. Expression of glycolytic enzymes is increased in pancreatic cancerous tissues as evidenced by proteomic profiling by two-dimensional electrophoresis and liquid chromatography-mass spectrometry/mass spectrometry. *Int J Oncol* 2007; **30**: 849-855 [PMID: 17332923 DOI: 10.3892/ijo.30.4.849]

70 **Zhou W**, Capello M, Fredolini C, Piemonti L, Liotta LA, Novelli F, Petricoin EF. Proteomic analysis of pancreatic ductal adenocarcinoma cells reveals metabolic alterations. *J Proteome Res* 2011; **10**: 1944-1952 [PMID: 21309613 DOI: 10.1021/pr101179t]

71 **Vernucci E**, Abrego J, Gunda V, Shukla SK, Dasgupta A, Rai V, Chaika N, Buettner K, Illies A, Yu F, Lazenby AJ, Swanson BJ, Singh PK. Metabolic Alterations in Pancreatic Cancer Progression. *Cancers (Basel)* 2019; **12** [PMID: 31861288 DOI: 10.3390/cancers12010002]

72 **Martinez-Outschoorn UE**, Peiris-Pagés M, Pestell RG, Sotgia F, Lisanti MP. Cancer metabolism: a therapeutic perspective. *Nat Rev Clin Oncol* 2017; **14**: 11-31 [PMID: 27141887 DOI: 10.1038/nrclinonc.2016.60]

73 **Wu DH**, Liang H, Lu SN, Wang H, Su ZL, Zhang L, Ma JQ, Guo M, Tai S, Yu S. miR-124 Suppresses Pancreatic Ductal Adenocarcinoma Growth by Regulating Monocarboxylate Transporter 1-Mediated Cancer Lactate Metabolism. *Cell Physiol Biochem* 2018; **50**: 924-935 [PMID: 30355947 DOI: 10.1159/000494477]

74 **Kong SC**, Nøhr-Nielsen A, Zeeberg K, Reshkin SJ, Hoffmann EK, Novak I, Pedersen SF. Monocarboxylate Transporters MCT1 and MCT4 Regulate Migration and Invasion of Pancreatic Ductal Adenocarcinoma Cells. *Pancreas* 2016; **45**: 1036-1047 [PMID: 26765963 DOI: 10.1097/MPA.0000000000000571]

75 **Feldmann G**, Beaty R, Hruban RH, Maitra A. Molecular genetics of pancreatic intraepithelial neoplasia. *J Hepatobiliary Pancreat Surg* 2007; **14**: 224-232 [PMID: 17520196 DOI: 10.1007/s00534-006-1166-5]

76 **Shen L**, Sun X, Fu Z, Yang G, Li J, Yao L. The fundamental role of the p53 pathway in tumor metabolism and its implication in tumor therapy. *Clin Cancer Res* 2012; **18**: 1561-1567 [PMID: 22307140 DOI: 10.1158/1078-0432.CCR-11-3040]

77 **Schwartzenberg-Bar-Yoseph F**, Armoni M, Karnieli E. The tumor suppressor p53 down-regulates glucose transporters GLUT1 and GLUT4 gene expression. *Cancer Res* 2004; **64**: 2627-2633 [PMID: 15059920 DOI: 10.1158/0008-5472.can-03-0846]

78 **Ying H**, Kimmelman AC, Lyssiotis CA, Hua S, Chu GC, Fletcher-Sananikone E, Locasale JW, Son J, Zhang H, Coloff JL, Yan H, Wang W, Chen S, Viale A, Zheng H, Paik JH, Lim C, Guimaraes AR, Martin ES, Chang J, Hezel AF, Perry SR, Hu J, Gan B, Xiao Y, Asara JM, Weissleder R, Wang YA, Chin L, Cantley LC, DePinho RA. Oncogenic Kras maintains pancreatic tumors through regulation of anabolic glucose metabolism. *Cell* 2012; **149**: 656-670 [PMID: 22541435 DOI: 10.1016/j.cell.2012.01.058]

79 **Zhao H**, Duan Q, Zhang Z, Li H, Wu H, Shen Q, Wang C, Yin T. Up-regulation of glycolysis promotes the stemness and EMT phenotypes in gemcitabine-resistant pancreatic cancer cells. *J Cell Mol Med* 2017; **21**: 2055-2067 [PMID: 28244691 DOI: 10.1111/jcmm.13126]

80 **Anderson M**, Marayati R, Moffitt R, Yeh JJ. Hexokinase 2 promotes tumor growth and metastasis by regulating lactate production in pancreatic cancer. *Oncotarget* 2017; **8**: 56081-56094 [PMID: 28915575 DOI: 10.18632/oncotarget.9760]

81 **Bhardwaj V**, Rizvi N, Lai MB, Lai JC, Bhushan A. Glycolytic enzyme inhibitors affect pancreatic cancer survival by modulating its signaling and energetics. *Anticancer Res* 2010; **30**: 743-749 [PMID: 20392992]

82 **Fan K**, Fan Z, Cheng H, Huang Q, Yang C, Jin K, Luo G, Yu X, Liu C. Hexokinase 2 dimerization and interaction with voltage-dependent anion channel promoted resistance to cell apoptosis induced by gemcitabine in pancreatic cancer. *Cancer Med* 2019; **8**: 5903-5915 [PMID: 31426130 DOI: 10.1002/cam4.2463]

83 **Dayton TL**, Jacks T, Vander Heiden MG. PKM2, cancer metabolism, and the road ahead. *EMBO Rep* 2016; **17**: 1721-1730 [PMID: 27856534 DOI: 10.15252/embr.201643300]

84 **Anastasiou D**, Poulogiannis G, Asara JM, Boxer MB, Jiang JK, Shen M, Bellinger G, Sasaki AT, Locasale JW, Auld DS, Thomas CJ, Vander Heiden MG, Cantley LC. Inhibition of pyruvate kinase M2 by reactive oxygen species contributes to cellular antioxidant responses. *Science* 2011; **334**: 1278-1283 [PMID: 22052977 DOI: 10.1126/science.1211485]

85 **Hitosugi T**, Kang S, Vander Heiden MG, Chung TW, Elf S, Lythgoe K, Dong S, Lonial S, Wang X, Chen GZ, Xie J, Gu TL, Polakiewicz RD, Roesel JL, Boggon TJ, Khuri FR, Gilliland DG, Cantley LC, Kaufman J, Chen J. Tyrosine phosphorylation inhibits PKM2 to promote the Warburg effect and tumor growth. *Sci Signal* 2009; **2**: ra73 [PMID: 19920251 DOI: 10.1126/scisignal.2000431]

86 **Hillis AL**, Lau AN, Devoe CX, Dayton TL, Danai LV, Di Vizio D, Vander Heiden MG. PKM2 is not required for pancreatic ductal adenocarcinoma. *Cancer Metab* 2018; **6**: 17 [PMID: 30386596 DOI: 10.1186/s40170-018-0188-1]

87 **Lockney NA**, Zhang M, Lu Y, Sopha SC, Washington MK, Merchant N, Zhao Z, Shyr Y, Chakravarthy AB, Xia F. Pyruvate Kinase Muscle Isoenzyme 2 (PKM2) Expression Is Associated with Overall Survival in Pancreatic Ductal Adenocarcinoma. *J Gastrointest Cancer* 2015; **46**: 390-398 [PMID: 26385349 DOI: 10.1007/s12029-015-9764-6]

88 **Mohammad GH**, Olde Damink SW, Malago M, Dhar DK, Pereira SP. Pyruvate Kinase M2 and Lactate Dehydrogenase A Are Overexpressed in Pancreatic Cancer and Correlate with Poor Outcome. *PLoS One* 2016; **11**: e0151635 [PMID: 26989901 DOI: 10.1371/journal.pone.0151635]

89 **Ogawa H**, Nagano H, Konno M, Eguchi H, Koseki J, Kawamoto K, Nishida N, Colvin H, Tomokuni A, Tomimaru Y, Hama N, Wada H, Marubashi S, Kobayashi S, Mori M, Doki Y, Ishii H. The combination of the expression of hexokinase 2 and pyruvate kinase M2 is a prognostic marker in patients with pancreatic cancer. *Mol Clin Oncol* 2015; **3**: 563-571 [PMID: 26137268 DOI:

10.3892/mco.2015.490]
90 **Azoitei N**, Becher A, Steinestel K, Rouhi A, Diepold K, Genze F, Simmet T, Seufferlein T. PKM2 promotes tumor angiogenesis by regulating HIF-1α through NF-κB activation. *Mol Cancer* 2016; **15**: 3 [PMID: 26739387 DOI: 10.1186/s12943-015-0490-2]
91 **Calabretta S**, Bielli P, Passacantilli I, Pilozzi E, Fendrich V, Capurso G, Fave GD, Sette C. Modulation of PKM alternative splicing by PTBP1 promotes gemcitabine resistance in pancreatic cancer cells. *Oncogene* 2016; **35**: 2031-2039 [PMID: 26234680 DOI: 10.1038/onc.2015.270]
92 **Chen S**, Chen X, Shan T, Ma J, Lin W, Li W, Kang Y. MiR-21-mediated Metabolic Alteration of Cancer-associated Fibroblasts and Its Effect on Pancreatic Cancer Cell Behavior. *Int J Biol Sci* 2018; **14**: 100-110 [PMID: 29483829 DOI: 10.7150/ijbs.22555]
93 **Cheng TY**, Yang YC, Wang HP, Tien YW, Shun CT, Huang HY, Hsiao M, Hua KT. Pyruvate kinase M2 promotes pancreatic ductal adenocarcinoma invasion and metastasis through phosphorylation and stabilization of PAK2 protein. *Oncogene* 2018; **37**: 1730-1742 [PMID: 29335522 DOI: 10.1038/s41388-017-0086-y]
94 **Kim DJ**, Park YS, Kang MG, You YM, Jung Y, Koo H, Kim JA, Kim MJ, Hong SM, Lee KB, Jang JJ, Park KC, Yeom YI. Pyruvate kinase isoenzyme M2 is a therapeutic target of gemcitabine-resistant pancreatic cancer cells. *Exp Cell Res* 2015; **336**: 119-129 [PMID: 26112218 DOI: 10.1016/j.yexcr.2015.05.017]
95 **Li C**, Zhao Z, Zhou Z, Liu R. PKM2 Promotes Cell Survival and Invasion Under Metabolic Stress by Enhancing Warburg Effect in Pancreatic Ductal Adenocarcinoma. *Dig Dis Sci* 2016; **61**: 767-773 [PMID: 26500118 DOI: 10.1007/s10620-015-3931-2]
96 **Cui J**, Shi M, Xie D, Wei D, Jia Z, Zheng S, Gao Y, Huang S, Xie K. FOXM1 promotes the warburg effect and pancreatic cancer progression *via* transactivation of LDHA expression. *Clin Cancer Res* 2014; **20**: 2595-2606 [PMID: 24634381 DOI: 10.1158/1078-0432.CCR-13-2407]
97 **Giatromanolaki A**, Sivridis E, Gatter KC, Turley H, Harris AL, Koukourakis MI; Tumour and Angiogenesis Research Group. Lactate dehydrogenase 5 (LDH-5) expression in endometrial cancer relates to the activated VEGF/VEGFR2(KDR) pathway and prognosis. *Gynecol Oncol* 2006; **103**: 912-918 [PMID: 16837029 DOI: 10.1016/j.ygyno.2006.05.043]
98 **Jiang W**, Zhou F, Li N, Li Q, Wang L. FOXM1-LDHA signaling promoted gastric cancer glycolytic phenotype and progression. *Int J Clin Exp Pathol* 2015; **8**: 6756-6763 [PMID: 26261559]
99 **Kobari M**, Hisano H, Matsuno S, Sato T, Kan M, Tachibana T. Establishment of six human pancreatic cancer cell lines and their sensitivities to anti-tumor drugs. *Tohoku J Exp Med* 1986; **150**: 231-248 [PMID: 3547771 DOI: 10.1620/tjem.150.231]
100 **Koukourakis MI**, Kakouratos C, Kalamida D, Bampali Z, Mavropoulou S, Sivridis E, Giatromanolaki A. Hypoxia-inducible proteins HIF1α and lactate dehydrogenase LDH5, key markers of anaerobic metabolism, relate with stem cell markers and poor post-radiotherapy outcome in bladder cancer. *Int J Radiat Biol* 2016; **92**: 353-363 [PMID: 27010533 DOI: 10.3109/09553002.2016.1162921]
101 **Thonsri U**, Seubwai W, Waraasawapati S, Sawanyawisuth K, Vaeteewoottacharn K, Boonmars T, Cha'on U. Overexpression of lactate dehydrogenase A in cholangiocarcinoma is correlated with poor prognosis. *Histol Histopathol* 2017; **32**: 503-510 [PMID: 27615379 DOI: 10.14670/HH-11-819]
102 **Yu C**, Hou L, Cui H, Zhang L, Tan X, Leng X, Li Y. LDHA upregulation independently predicts poor survival in lung adenocarcinoma, but not in lung squamous cell carcinoma. *Future Oncol* 2018; **14**: 2483-2492 [PMID: 29756998 DOI: 10.2217/fon-2018-0177]
103 **Semenza GL**, Jiang BH, Leung SW, Passantino R, Concordet JP, Maire P, Giallongo A. Hypoxia response elements in the aldolase A, enolase 1, and lactate dehydrogenase A gene promoters contain essential binding sites for hypoxia-inducible factor 1. *J Biol Chem* 1996; **271**: 32529-32537 [PMID: 8955077 DOI: 10.1074/jbc.271.51.32529]
104 **Shim H**, Dolde C, Lewis BC, Wu CS, Dang G, Jungmann RA, Dalla-Favera R, Dang CV. c-Myc transactivation of LDH-A: implications for tumor metabolism and growth. *Proc Natl Acad Sci U S A* 1997; **94**: 6658-6663 [PMID: 9192621 DOI: 10.1073/pnas.94.13.6658]
105 **Li SS**, Pan YE, Sharief FS, Evans MJ, Lin MF, Clinton GM, Holbrook JJ. Cancer-associated lactate dehydrogenase is a tyrosylphosphorylated form of human LDH-A, skeletal muscle isoenzyme. *Cancer Invest* 1988; **6**: 93-101 [PMID: 3365574 DOI: 10.3109/07357908809077032]
106 **Liu J**, Chen G, Liu Z, Liu S, Cai Z, You P, Ke Y, Lai L, Huang Y, Gao H, Zhao L, Pelicano H, Huang P, McKeehan WL, Wu CL, Wang C, Zhong W, Wang F. Aberrant FGFR Tyrosine Kinase Signaling Enhances the Warburg Effect by Reprogramming LDH Isoform Expression and Activity in Prostate Cancer. *Cancer Res* 2018; **78**: 4459-4470 [PMID: 29891507 DOI: 10.1158/0008-5472.CAN-17-3226]
107 **Faloppi L**, Bianconi M, Giampieri R, Sobrero A, Labianca R, Ferrari D, Barni S, Aitini E, Zaniboni A, Boni C, Caprioni F, Mosconi S, Fanello S, Berardi R, Bittoni A, Andrikou K, Cinquini M, Torri V, Scartozzi M, Cascinu S; Italian Group for the Study of Digestive Tract Cancer (GISCAD). The value of lactate dehydrogenase serum levels as a prognostic and predictive factor for advanced pancreatic cancer patients receiving sorafenib. *Oncotarget* 2015; **6**: 35087-35094 [PMID: 26397228 DOI: 10.18632/oncotarget.5197]
108 **Gan J**, Wang W, Yang Z, Pan J, Zheng L, Yin L. Prognostic value of pretreatment serum lactate dehydrogenase level in pancreatic cancer patients: A meta-analysis of 18 observational studies. *Medicine (Baltimore)* 2018; **97**: e13151 [PMID: 30431587 DOI: 10.1097/MD.0000000000013151]
109 **Ji F**, Fu SJ, Guo ZY, Pang H, Ju WQ, Wang DP, Hua YP, He XS. Prognostic value of combined

preoperative lactate dehydrogenase and alkaline phosphatase levels in patients with resectable pancreatic ductal adenocarcinoma. *Medicine (Baltimore)* 2016; **95**: e4065 [PMID: 27399091 DOI: 10.1097/MD.0000000000004065]

110 **Mann JR**, Pearson D, Barrett A, Raafat F, Barnes JM, Wallendszus KR. Results of the United Kingdom Children's Cancer Study Group's malignant germ cell tumor studies. *Cancer* 1989; **63**: 1657-1667 [PMID: 2467734 DOI: 10.1002/1097-0142(19900501)63:9<1657::aid-cncr2820630902>3.0.co;2-8]

111 **Tas F**, Aykan F, Alici S, Kaytan E, Aydiner A, Topuz E. Prognostic factors in pancreatic carcinoma: serum LDH levels predict survival in metastatic disease. *Am J Clin Oncol* 2001; **24**: 547-550 [PMID: 11801751 DOI: 10.1097/00000421-200112000-00003]

112 **Xiao Y**, Chen W, Xie Z, Shao Z, Xie H, Qin G, Zhao N. Prognostic relevance of lactate dehydrogenase in advanced pancreatic ductal adenocarcinoma patients. *BMC Cancer* 2017; **17**: 25 [PMID: 28056913 DOI: 10.1186/s12885-016-3012-8]

113 **Annas D**, Cheon SY, Yusuf M, Bae SJ, Ha KT, Park KH. Synthesis and initial screening of lactate dehydrogenase inhibitor activity of 1,3-benzodioxole derivatives. *Sci Rep* 2020; **10**: 19889 [PMID: 33199724 DOI: 10.1038/s41598-020-77056-4]

114 **Moir JAG**, Long A, Haugk B, French JJ, Charnley RM, Manas DM, Wedge SR, Mann J, Robinson SM, White SA. Therapeutic Strategies Toward Lactate Dehydrogenase Within the Tumor Microenvironment of Pancreatic Cancer. *Pancreas* 2020; **49**: 1364-1371 [PMID: 33122526 DOI: 10.1097/MPA.0000000000001689]

115 **Stanton RC**. Glucose-6-phosphate dehydrogenase, NADPH, and cell survival. *IUBMB Life* 2012; **64**: 362-369 [PMID: 22431005 DOI: 10.1002/iub.1017]

116 **Santana-Codina N**, Roeth AA, Zhang Y, Yang A, Mashadova O, Asara JM, Wang X, Bronson RT, Lyssiotis CA, Ying H, Kimmelman AC. Oncogenic KRAS supports pancreatic cancer through regulation of nucleotide synthesis. *Nat Commun* 2018; **9**: 4945 [PMID: 30470748 DOI: 10.1038/s41467-018-07472-8]

117 **Sharma N**, Bhushan A, He J, Kaushal G, Bhardwaj V. Metabolic plasticity imparts erlotinib-resistance in pancreatic cancer by upregulating glucose-6-phosphate dehydrogenase. *Cancer Metab* 2020; **8**: 19 [PMID: 32974013 DOI: 10.1186/s40170-020-00226-5]

118 **Shukla SK**, Purohit V, Mehla K, Gunda V, Chaika NV, Vernucci E, King RJ, Abrego J, Goode GD, Dasgupta A, Illies AL, Gebregiworgis T, Dai B, Augustine JJ, Murthy D, Attri KS, Mashadova O, Grandgenett PM, Powers R, Ly QP, Lazenby AJ, Grem JL, Yu F, Matés JM, Asara JM, Kim JW, Hankins JH, Weekes C, Hollingsworth MA, Serkova NJ, Sasson AR, Fleming JB, Oliveto JM, Lyssiotis CA, Cantley LC, Berim L, Singh PK. MUC1 and HIF-1alpha Signaling Crosstalk Induces Anabolic Glucose Metabolism to Impart Gemcitabine Resistance to Pancreatic Cancer. *Cancer Cell* 2017; **32**: 71-87.e7 [PMID: 28697344 DOI: 10.1016/j.ccell.2017.06.004]

119 **Viale A**, Pettazzoni P, Lyssiotis CA, Ying H, Sánchez N, Marchesini M, Carugo A, Green T, Seth S, Giuliani V, Kost-Alimova M, Muller F, Colla S, Nezi L, Genovese G, Deem AK, Kapoor A, Yao W, Brunetto E, Kang Y, Yuan M, Asara JM, Wang YA, Heffernan TP, Kimmelman AC, Wang H, Fleming JB, Cantley LC, DePinho RA, Draetta GF. Oncogene ablation-resistant pancreatic cancer cells depend on mitochondrial function. *Nature* 2014; **514**: 628-632 [PMID: 25119024 DOI: 10.1038/nature13611]

120 **Sancho P**, Burgos-Ramos E, Tavera A, Bou Kheir T, Jagust P, Schoenhals M, Barneda D, Sellers K, Campos-Olivas R, Graña O, Viera CR, Yuneva M, Sainz B Jr, Heeschen C. MYC/PGC-1α Balance Determines the Metabolic Phenotype and Plasticity of Pancreatic Cancer Stem Cells. *Cell Metab* 2015; **22**: 590-605 [PMID: 26365176 DOI: 10.1016/j.cmet.2015.08.015]

121 **Kovalenko I**, Glasauer A, Schöckel L, Sauter DR, Ehrmann A, Sohler F, Hägebarth A, Novak I, Christian S. Identification of KCa3.1 Channel as a Novel Regulator of Oxidative Phosphorylation in a Subset of Pancreatic Carcinoma Cell Lines. *PLoS One* 2016; **11**: e0160658 [PMID: 27494181 DOI: 10.1371/journal.pone.0160658]

122 **Dey P**, Baddour J, Muller F, Wu CC, Wang H, Liao WT, Lan Z, Chen A, Gutschner T, Kang Y, Fleming J, Satani N, Zhao D, Achreja A, Yang L, Lee J, Chang E, Genovese G, Viale A, Ying H, Draetta G, Maitra A, Wang YA, Nagrath D, DePinho RA. Genomic deletion of malic enzyme 2 confers collateral lethality in pancreatic cancer. *Nature* 2017; **542**: 119-123 [PMID: 28099419 DOI: 10.1038/nature21052]

123 **Zarei M**, Lal S, Parker SJ, Nevler A, Vaziri-Gohar A, Dukleska K, Mambelli-Lisboa NC, Moffat C, Blanco FF, Chand SN, Jimbo M, Cozzitorto JA, Jiang W, Yeo CJ, Londin ER, Seifert EL, Metallo CM, Brody JR, Winter JM. Posttranscriptional Upregulation of IDH1 by HuR Establishes a Powerful Survival Phenotype in Pancreatic Cancer Cells. *Cancer Res* 2017; **77**: 4460-4471 [PMID: 28652247 DOI: 10.1158/0008-5472.CAN-17-0015]

124 **Nishi K**, Suzuki M, Yamamoto N, Matsumoto A, Iwase Y, Yamasaki K, Otagiri M, Yumita N. Glutamine Deprivation Enhances Acetyl-CoA Carboxylase Inhibitor-induced Death of Human Pancreatic Cancer Cells. *Anticancer Res* 2018; **38**: 6683-6689 [PMID: 30504377 DOI: 10.21873/anticanres.13036]

125 **Son J**, Lyssiotis CA, Ying H, Wang X, Hua S, Ligorio M, Perera RM, Ferrone CR, Mullarky E, Shyh-Chang N, Kang Y, Fleming JB, Bardeesy N, Asara JM, Haigis MC, DePinho RA, Cantley LC, Kimmelman AC. Glutamine supports pancreatic cancer growth through a KRAS-regulated metabolic pathway. *Nature* 2013; **496**: 101-105 [PMID: 23535601 DOI: 10.1038/nature12040]

126 **Chakrabarti G**, Moore ZR, Luo X, Ilcheva M, Ali A, Padanad M, Zhou Y, Xie Y, Burma S,

Scaglioni PP, Cantley LC, DeBerardinis RJ, Kimmelman AC, Lyssiotis CA, Boothman DA. Targeting glutamine metabolism sensitizes pancreatic cancer to PARP-driven metabolic catastrophe induced by ß-lapachone. *Cancer Metab* 2015; **3**: 12 [PMID: 26462257 DOI: 10.1186/s40170-015-0137-1]

127 **Chen R**, Lai LA, Sullivan Y, Wong M, Wang L, Riddell J, Jung L, Pillarisetty VG, Brentnall TA, Pan S. Disrupting glutamine metabolic pathways to sensitize gemcitabine-resistant pancreatic cancer. *Sci Rep* 2017; **7**: 7950 [PMID: 28801576 DOI: 10.1038/s41598-017-08436-6]

128 **Jia C**, Li H, Fu D, Lan Y. GFAT1/HBP/O-GlcNAcylation Axis Regulates *β*-Catenin Activity to Promote Pancreatic Cancer Aggressiveness. *Biomed Res Int* 2020; **2020**: 1921609 [PMID: 32149084 DOI: 10.1155/2020/1921609]

129 **Li D**, Fu Z, Chen R, Zhao X, Zhou Y, Zeng B, Yu M, Zhou Q, Lin Q, Gao W, Ye H, Zhou J, Li Z, Liu Y. Inhibition of glutamine metabolism counteracts pancreatic cancer stem cell features and sensitizes cells to radiotherapy. *Oncotarget* 2015; **6**: 31151-31163 [PMID: 26439804 DOI: 10.18632/oncotarget.5150]

130 **Lyssiotis CA**, Son J, Cantley LC, Kimmelman AC. Pancreatic cancers rely on a novel glutamine metabolism pathway to maintain redox balance. *Cell Cycle* 2013; **12**: 1987-1988 [PMID: 23759579 DOI: 10.4161/cc.25307]

131 **Raho S**, Capobianco L, Malivindi R, Vozza A, Piazzolla C, De Leonardis F, Gorgoglione R, Scarcia P, Pezzuto F, Agrimi G, Barile SN, Pisano I, Reshkin SJ, Greco MR, Cardone RA, Rago V, Li Y, Marobbio CMT, Sommergruber W, Riley CL, Lasorsa FM, Mills E, Vegliante MC, De Benedetto GE, Fratantonio D, Palmieri L, Dolce V, Fiermonte G. KRAS-regulated glutamine metabolism requires UCP2-mediated aspartate transport to support pancreatic cancer growth. *Nat Metab* 2020; **2**: 1373-1381 [PMID: 33230296 DOI: 10.1038/s42255-020-00315-1]

132 **Wang J**, Wang B, Ren H, Chen W. miR-9-5p inhibits pancreatic cancer cell proliferation, invasion and glutamine metabolism by targeting GOT1. *Biochem Biophys Res Commun* 2019; **509**: 241-248 [PMID: 30591220 DOI: 10.1016/j.bbrc.2018.12.114]

133 **Jeong SM**, Hwang S, Park K, Yang S, Seong RH. Enhanced mitochondrial glutamine anaplerosis suppresses pancreatic cancer growth through autophagy inhibition. *Sci Rep* 2016; **6**: 30767 [PMID: 27477484 DOI: 10.1038/srep30767]

134 **Recouvreux MV**, Moldenhauer MR, Galenkamp KMO, Jung M, James B, Zhang Y, Lowy A, Bagchi A, Commisso C. Glutamine depletion regulates Slug to promote EMT and metastasis in pancreatic cancer. *J Exp Med* 2020; **217** [PMID: 32510550 DOI: 10.1084/jem.20200388]

135 **Roux C**, Riganti C, Borgogno SF, Curto R, Curcio C, Catanzaro V, Digilio G, Padovan S, Puccinelli MP, Isabello M, Aime S, Cappello P, Novelli F. Endogenous glutamine decrease is associated with pancreatic cancer progression. *Oncotarget* 2017; **8**: 95361-95376 [PMID: 29221133 DOI: 10.18632/oncotarget.20545]

136 **Bao B**, Wang Z, Ali S, Ahmad A, Azmi AS, Sarkar SH, Banerjee S, Kong D, Li Y, Thakur S, Sarkar FH. Metformin inhibits cell proliferation, migration and invasion by attenuating CSC function mediated by deregulating miRNAs in pancreatic cancer cells. *Cancer Prev Res (Phila)* 2012; **5**: 355-364 [PMID: 22086681 DOI: 10.1158/1940-6207.CAPR-11-0299]

137 **Cheng G**, Zielonka J, Ouari O, Lopez M, McAllister D, Boyle K, Barrios CS, Weber JJ, Johnson BD, Hardy M, Dwinell MB, Kalyanaraman B. Mitochondria-Targeted Analogues of Metformin Exhibit Enhanced Antiproliferative and Radiosensitizing Effects in Pancreatic Cancer Cells. *Cancer Res* 2016; **76**: 3904-3915 [PMID: 27216187 DOI: 10.1158/0008-5472.CAN-15-2534]

138 **Masoud R**, Reyes-Castellanos G, Lac S, Garcia J, Dou S, Shintu L, Abdel Hadi N, Gicquel T, El Kaoutari A, Diémé B, Tranchida F, Cormareche L, Borge L, Gayet O, Pasquier E, Dusetti N, Iovanna J, Carrier A. Targeting Mitochondrial Complex I Overcomes Chemoresistance in High OXPHOS Pancreatic Cancer. *Cell Rep Med* 2020; **1**: 100143 [PMID: 33294863 DOI: 10.1016/j.xcrm.2020.100143]

139 **Rajeshkumar NV**, Yabuuchi S, Pai SG, De Oliveira E, Kamphorst JJ, Rabinowitz JD, Tejero H, Al-Shahrour F, Hidalgo M, Maitra A, Dang CV. Treatment of Pancreatic Cancer Patient-Derived Xenograft Panel with Metabolic Inhibitors Reveals Efficacy of Phenformin. *Clin Cancer Res* 2017; **23**: 5639-5647 [PMID: 28611197 DOI: 10.1158/1078-0432.CCR-17-1115]

140 **Kordes S**, Pollak MN, Zwinderman AH, Mathôt RA, Weterman MJ, Beeker A, Punt CJ, Richel DJ, Wilmink JW. Metformin in patients with advanced pancreatic cancer: a double-blind, randomised, placebo-controlled phase 2 trial. *Lancet Oncol* 2015; **16**: 839-847 [PMID: 26067687 DOI: 10.1016/S1470-2045(15)00027-3]

141 **Reni M**, Dugnani E, Cereda S, Belli C, Balzano G, Nicoletti R, Liberati D, Pasquale V, Scavini M, Maggiora P, Sordi V, Lampasona V, Ceraulo D, Di Terlizzi G, Doglioni C, Falconi M, Piemonti L. (Ir)relevance of Metformin Treatment in Patients with Metastatic Pancreatic Cancer: An Open-Label, Randomized Phase II Trial. *Clin Cancer Res* 2016; **22**: 1076-1085 [PMID: 26459175 DOI: 10.1158/1078-0432.CCR-15-1722]

142 **Shi YQ**, Zhou XC, Du P, Yin MY, Xu L, Chen WJ, Xu CF. Relationships are between metformin use and survival in pancreatic cancer patients concurrent with diabetes: A systematic review and meta-analysis. *Medicine (Baltimore)* 2020; **99**: e21687 [PMID: 32925714 DOI: 10.1097/MD.0000000000021687]

143 **Alistar A**, Morris BB, Desnoyer R, Klepin HD, Hosseinzadeh K, Clark C, Cameron A, Leyendecker J, D'Agostino R Jr, Topaloglu U, Boteju LW, Boteju AR, Shorr R, Zachar Z, Bingham PM, Ahmed T, Crane S, Shah R, Migliano JJ, Pardee TS, Miller L, Hawkins G, Jin G, Zhang W, Pasche B.

Safety and tolerability of the first-in-class agent CPI-613 in combination with modified FOLFIRINOX in patients with metastatic pancreatic cancer: a single-centre, open-label, dose-escalation, phase 1 trial. *Lancet Oncol* 2017; **18**: 770-778 [PMID: 28495639 DOI: 10.1016/S1470-2045(17)30314-5]

144 **Waddell N**, Pajic M, Patch AM, Chang DK, Kassahn KS, Bailey P, Johns AL, Miller D, Nones K, Quek K, Quinn MC, Robertson AJ, Fadlullah MZ, Bruxner TJ, Christ AN, Harliwong I, Idrisoglu S, Manning S, Nourse C, Nourbakhsh E, Wani S, Wilson PJ, Markham E, Cloonan N, Anderson MJ, Fink JL, Holmes O, Kazakoff SH, Leonard C, Newell F, Poudel B, Song S, Taylor D, Waddell N, Wood S, Xu Q, Wu J, Pinese M, Cowley MJ, Lee HC, Jones MD, Nagrial AM, Humphris J, Chantrill LA, Chin V, Steinmann AM, Mawson A, Humphrey ES, Colvin EK, Chou A, Scarlett CJ, Pinho AV, Giry-Laterriere M, Rooman I, Samra JS, Kench JG, Pettitt JA, Merrett ND, Toon C, Epari K, Nguyen NQ, Barbour A, Zeps N, Jamieson NB, Graham JS, Niclou SP, Bjerkvig R, Grützmann R, Aust D, Hruban RH, Maitra A, Iacobuzio-Donahue CA, Wolfgang CL, Morgan RA, Lawlor RT, Corbo V, Bassi C, Falconi M, Zamboni G, Tortora G, Tempero MA; Australian Pancreatic Cancer Genome Initiative, Gill AJ, Eshleman JR, Pilarsky C, Scarpa A, Musgrove EA, Pearson JV, Biankin AV, Grimmond SM. Whole genomes redefine the mutational landscape of pancreatic cancer. *Nature* 2015; **518**: 495-501 [PMID: 25719666 DOI: 10.1038/nature14169]

145 **Bailey P**, Chang DK, Nones K, Johns AL, Patch AM, Gingras MC, Miller DK, Christ AN, Bruxner TJ, Quinn MC, Nourse C, Murtaugh LC, Harliwong I, Idrisoglu S, Manning S, Nourbakhsh E, Wani S, Fink L, Holmes O, Chin V, Anderson MJ, Kazakoff S, Leonard C, Newell F, Waddell N, Wood S, Xu Q, Wilson PJ, Cloonan N, Kassahn KS, Taylor D, Quek K, Robertson A, Pantano L, Mincarelli L, Sanchez LN, Evers L, Wu J, Pinese M, Cowley MJ, Jones MD, Colvin EK, Nagrial AM, Humphrey ES, Chantrill LA, Mawson A, Humphris J, Chou A, Pajic M, Scarlett CJ, Pinho AV, Giry-Laterriere M, Rooman I, Samra JS, Kench JG, Lovell JA, Merrett ND, Toon CW, Epari K, Nguyen NQ, Barbour A, Zeps N, Moran-Jones K, Jamieson NB, Graham JS, Duthie F, Oien K, Hair J, Grützmann R, Maitra A, Iacobuzio-Donahue CA, Wolfgang CL, Morgan RA, Lawlor RT, Corbo V, Bassi C, Rusev B, Capelli P, Salvia R, Tortora G, Mukhopadhyay D, Petersen GM; Australian Pancreatic Cancer Genome Initiative, Munzy DM, Fisher WE, Karim SA, Eshleman JR, Hruban RH, Pilarsky C, Morton JP, Sansom OJ, Scarpa A, Musgrove EA, Bailey UM, Hofmann O, Sutherland RL, Wheeler DA, Gill AJ, Gibbs RA, Pearson JV, Waddell N, Biankin AV, Grimmond SM. Genomic analyses identify molecular subtypes of pancreatic cancer. *Nature* 2016; **531**: 47-52 [PMID: 26909576 DOI: 10.1038/nature16965]

146 **Hoadley KA**, Yau C, Hinoue T, Wolf DM, Lazar AJ, Drill E, Shen R, Taylor AM, Cherniack AD, Thorsson V, Akbani R, Bowlby R, Wong CK, Wiznerowicz M, Sanchez-Vega F, Robertson AG, Schneider BG, Lawrence MS, Noushmehr H, Malta TM; Cancer Genome Atlas Network, Stuart JM, Benz CC, Laird PW. Cell-of-Origin Patterns Dominate the Molecular Classification of 10,000 Tumors from 33 Types of Cancer. *Cell* 2018; **173**: 291-304.e6 [PMID: 29625048 DOI: 10.1016/j.cell.2018.03.022]

147 **Witkiewicz AK**, McMillan EA, Balaji U, Baek G, Lin WC, Mansour J, Mollaee M, Wagner KU, Koduru P, Yopp A, Choti MA, Yeo CJ, McCue P, White MA, Knudsen ES. Whole-exome sequencing of pancreatic cancer defines genetic diversity and therapeutic targets. *Nat Commun* 2015; **6**: 6744 [PMID: 25855536 DOI: 10.1038/ncomms7744]

148 **Johnstone TC**, Park GY, Lippard SJ. Understanding and improving platinum anticancer drugs--phenanthriplatin. *Anticancer Res* 2014; **34**: 471-476 [PMID: 24403503]

149 **Golan T**, Kanji ZS, Epelbaum R, Devaud N, Dagan E, Holter S, Aderka D, Paluch-Shimon S, Kaufman B, Gershoni-Baruch R, Hedley D, Moore MJ, Friedman E, Gallinger S. Overall survival and clinical characteristics of pancreatic cancer in BRCA mutation carriers. *Br J Cancer* 2014; **111**: 1132-1138 [PMID: 25072261 DOI: 10.1038/bjc.2014.418]

150 **Pishvaian MJ**, Blais EM, Brody JR, Rahib L, Lyons E, De Arbeloa P, Hendifar A, Mikhail S, Chung V, Sohal DPS, Leslie S, Mason K, Tibbets L, Madhavan S, Matrisian LM, Petricoin E. Outcomes in Patients With Pancreatic Adenocarcinoma With Genetic Mutations in DNA Damage Response Pathways: Results From the Know Your Tumor Program. *JCO Precis Oncol* 2019; 1-10 [DOI: 10.1200/po.19.00115]

151 **Yu S**, Agarwal P, Mamtani R, Symecko H, Spielman K, O'Hara M, O'Dwyer PJ, Schneider C, Teitelbaum U, Nathanson KL, Domchek SM, Reiss KA. Retrospective Survival Analysis of Patients With Resected Pancreatic Ductal Adenocarcinoma and a Germline BRCA or PALB2 Mutation. *JCO Precis Oncol* 2018; 1-11 [DOI: 10.1200/po.18.00271]

152 **Rack JG**, Perina D, Ahel I. Macrodomains: Structure, Function, Evolution, and Catalytic Activities. *Annu Rev Biochem* 2016; **85**: 431-454 [PMID: 26844395 DOI: 10.1146/annurev-biochem-060815-014935]

153 **Barkauskaite E**, Jankevicius G, Ladurner AG, Ahel I, Timinszky G. The recognition and removal of cellular poly(ADP-ribose) signals. *FEBS J* 2013; **280**: 3491-3507 [PMID: 23711178 DOI: 10.1111/febs.12358]

154 **Harrision D**, Gravells P, Thompson R, Bryant HE. Poly(ADP-Ribose) Glycohydrolase (PARG) vs. Poly(ADP-Ribose) Polymerase (PARP) - Function in Genome Maintenance and Relevance of Inhibitors for Anti-cancer Therapy. *Front Mol Biosci* 2020; **7**: 191 [PMID: 33005627 DOI: 10.3389/fmolb.2020.00191]

155 **Lear AL**, Perkins HR. O-acetylation of peptidoglycan in Neisseria gonorrhoeae. Investigation of lipid-linked intermediates and glycan chains newly incorporated into the cell wall. *J Gen Microbiol*

1986; **132**: 2413-2420 [PMID: 3098911 DOI: 10.1099/00221287-132-9-2413]

156 **Shirai H**, Poetsch AR, Gunji A, Maeda D, Fujimori H, Fujihara H, Yoshida T, Ogino H, Masutani M. PARG dysfunction enhances DNA double strand break formation in S-phase after alkylation DNA damage and augments different cell death pathways. *Cell Death Dis* 2013; **4**: e656 [PMID: 23744356 DOI: 10.1038/cddis.2013.133]

157 **Gravells P**, Neale J, Grant E, Nathubhai A, Smith KM, James DI, Bryant HE. Radiosensitization with an inhibitor of poly(ADP-ribose) glycohydrolase: A comparison with the PARP1/2/3 inhibitor olaparib. *DNA Repair (Amst)* 2018; **61**: 25-36 [PMID: 29179156 DOI: 10.1016/j.dnarep.2017.11.004]

158 **Pillay N**, Tighe A, Nelson L, Littler S, Coulson-Gilmer C, Bah N, Golder A, Bakker B, Spierings DCJ, James DI, Smith KM, Jordan AM, Morgan RD, Ogilvie DJ, Foijer F, Jackson DA, Taylor SS. DNA Replication Vulnerabilities Render Ovarian Cancer Cells Sensitive to Poly(ADP-Ribose) Glycohydrolase Inhibitors. *Cancer Cell* 2019; **35**: 519-533.e8 [PMID: 30889383 DOI: 10.1016/j.ccell.2019.02.004]

159 **Gravells P**, Grant E, Smith KM, James DI, Bryant HE. Specific killing of DNA damage-response deficient cells with inhibitors of poly(ADP-ribose) glycohydrolase. *DNA Repair (Amst)* 2017; **52**: 81-91 [PMID: 28254358 DOI: 10.1016/j.dnarep.2017.02.010]

160 **Iorns E**, Lord CJ, Grigoriadis A, McDonald S, Fenwick K, Mackay A, Mein CA, Natrajan R, Savage K, Tamber N, Reis-Filho JS, Turner NC, Ashworth A. Integrated functional, gene expression and genomic analysis for the identification of cancer targets. *PLoS One* 2009; **4**: e5120 [PMID: 19357772 DOI: 10.1371/journal.pone.0005120]

161 **Masaki T**, Shiratori Y, Rengifo W, Igarashi K, Yamagata M, Kurokohchi K, Uchida N, Miyauchi Y, Yoshiji H, Watanabe S, Omata M, Kuriyama S. Cyclins and cyclin-dependent kinases: comparative study of hepatocellular carcinoma *vs* cirrhosis. *Hepatology* 2003; **37**: 534-543 [PMID: 12601350 DOI: 10.1053/jhep.2003.50112]

162 **Mir SE**, De Witt Hamer PC, Krawczyk PM, Balaj L, Claes A, Niers JM, Van Tilborg AA, Zwinderman AH, Geerts D, Kaspers GJ, Peter Vandertop W, Cloos J, Tannous BA, Wesseling P, Aten JA, Noske DP, Van Noorden CJ, Würdinger T. In silico analysis of kinase expression identifies WEE1 as a gatekeeper against mitotic catastrophe in glioblastoma. *Cancer Cell* 2010; **18**: 244-257 [PMID: 20832752 DOI: 10.1016/j.ccr.2010.08.011]

163 **Wang H**, Huang M, Zhang DY, Zhang F. Global profiling of signaling networks: study of breast cancer stem cells and potential regulation. *Oncologist* 2011; **16**: 966-979 [PMID: 21665913 DOI: 10.1634/theoncologist.2010-0230]

164 **Dreyer SB**, Upstill-Goddard R, Paulus-Hock V, Paris C, Lampraki EM, Dray E, Serrels B, Caligiuri G, Rebus S, Plenker D, Galluzzo Z, Brunton H, Cunningham R, Tesson M, Nourse C, Bailey UM, Jones M, Moran-Jones K, Wright DW, Duthie F, Oien K, Evers L, McKay CJ, McGregor GA, Gulati A, Brough R, Bajrami I, Pettitt S, Dziubinski ML, Candido J, Balkwill F, Barry ST, Grützmann R, Rahib L; Glasgow Precision Oncology Laboratory,; Australian Pancreatic Cancer Genome Initiative, Johns A, Pajic M, Froeling FEM, Beer P, Musgrove EA, Petersen GM, Ashworth A, Frame MC, Crawford HC, Simeone DM, Lord C, Mukhopadhyay D, Pilarsky C, Tuveson DA, Cooke SL, Jamieson NB, Morton JP, Sansom OJ, Bailey PJ, Biankin AV, Chang DK. Targeting DNA Damage Response and Replication Stress in Pancreatic Cancer. *Gastroenterology* 2021; **160**: 362-377.e13 [PMID: 33039466 DOI: 10.1053/j.gastro.2020.09.043]

165 **Kausar T**, Schreiber JS, Karnak D, Parsels LA, Parsels JD, Davis MA, Zhao L, Maybaum J, Lawrence TS, Morgan MA. Sensitization of Pancreatic Cancers to Gemcitabine Chemoradiation by WEE1 Kinase Inhibition Depends on Homologous Recombination Repair. *Neoplasia* 2015; **17**: 757-766 [PMID: 26585231 DOI: 10.1016/j.neo.2015.09.006]

166 **Saini P**, Li Y, Dobbelstein M. Wee1 is required to sustain ATR/Chk1 signaling upon replicative stress. *Oncotarget* 2015; **6**: 13072-13087 [PMID: 25965828 DOI: 10.18632/oncotarget.3865]

167 **Lal S**, Burkhart RA, Beeharry N, Bhattacharjee V, Londin ER, Cozzitorto JA, Romeo C, Jimbo M, Norris ZA, Yeo CJ, Sawicki JA, Winter JM, Rigoutsos I, Yen TJ, Brody JR. HuR posttranscriptionally regulates WEE1: implications for the DNA damage response in pancreatic cancer cells. *Cancer Res* 2014; **74**: 1128-1140 [PMID: 24536047 DOI: 10.1158/0008-5472.CAN-13-1915]

168 **Lal S**, Zarei M, Chand SN, Dylgjeri E, Mambelli-Lisboa NC, Pishvaian MJ, Yeo CJ, Winter JM, Brody JR. WEE1 inhibition in pancreatic cancer cells is dependent on DNA repair status in a context dependent manner. *Sci Rep* 2016; **6**: 33323 [PMID: 27616351 DOI: 10.1038/srep33323]

169 **Rajeshkumar NV**, De Oliveira E, Ottenhof N, Watters J, Brooks D, Demuth T, Shumway SD, Mizuarai S, Hirai H, Maitra A, Hidalgo M. MK-1775, a potent Wee1 inhibitor, synergizes with gemcitabine to achieve tumor regressions, selectively in p53-deficient pancreatic cancer xenografts. *Clin Cancer Res* 2011; **17**: 2799-2806 [PMID: 21389100 DOI: 10.1158/1078-0432.CCR-10-2580]

170 **Jin MH**, Nam AR, Park JE, Bang JH, Bang YJ, Oh DY. Therapeutic Co-targeting of WEE1 and ATM Downregulates PD-L1 Expression in Pancreatic Cancer. *Cancer Res Treat* 2020; **52**: 149-166 [PMID: 31291716 DOI: 10.4143/crt.2019.183]

171 **Agostini LC**, Jain A, Shupp A, Nevler A, McCarthy G, Bussard KM, Yeo CJ, Brody JR. Combined Targeting of PARG and Wee1 Causes Decreased Cell Survival and DNA Damage in an S-Phase-Dependent Manner. *Mol Cancer Res* 2021; **19**: 207-214 [PMID: 33257507 DOI: 10.1158/1541-7786.MCR-20-0708]

172 **Krishnakumar R**, Kraus WL. The PARP side of the nucleus: molecular actions, physiological

outcomes, and clinical targets. *Mol Cell* 2010; **39**: 8-24 [PMID: 20603072 DOI: 10.1016/j.molcel.2010.06.017]

173 **Rouleau M**, Patel A, Hendzel MJ, Kaufmann SH, Poirier GG. PARP inhibition: PARP1 and beyond. *Nat Rev Cancer* 2010; **10**: 293-301 [PMID: 20200537 DOI: 10.1038/nrc2812]

174 **Bagnolini G**, Milano D, Manerba M, Schipani F, Ortega JA, Gioia D, Falchi F, Balboni A, Farabegoli F, De Franco F, Robertson J, Pellicciari R, Pallavicini I, Peri S, Minucci S, Girotto S, Di Stefano G, Roberti M, Cavalli A. Synthetic Lethality in Pancreatic Cancer: Discovery of a New RAD51-BRCA2 Small Molecule Disruptor That Inhibits Homologous Recombination and Synergizes with Olaparib. *J Med Chem* 2020; **63**: 2588-2619 [PMID: 32037829 DOI: 10.1021/acs.jmedchem.9b01526]

175 **Farmer H**, McCabe N, Lord CJ, Tutt AN, Johnson DA, Richardson TB, Santarosa M, Dillon KJ, Hickson I, Knights C, Martin NM, Jackson SP, Smith GC, Ashworth A. Targeting the DNA repair defect in BRCA mutant cells as a therapeutic strategy. *Nature* 2005; **434**: 917-921 [PMID: 15829967 DOI: 10.1038/nature03445]

176 **Miller AL**, Garcia PL, Yoon KJ. Developing effective combination therapy for pancreatic cancer: An overview. *Pharmacol Res* 2020; **155**: 104740 [PMID: 32135247 DOI: 10.1016/j.phrs.2020.104740]

177 **Lai SW**, Bamodu OA, Chen JH, Wu AT, Lee WH, Chao TY, Yeh CT. Targeted PARP Inhibition Combined with FGFR1 Blockade is Synthetically Lethal to Malignant Cells in Patients with Pancreatic Cancer. *Cells* 2020; **9** [PMID: 32276472 DOI: 10.3390/cells9040911]

178 **Noordermeer SM**, van Attikum H. PARP Inhibitor Resistance: A Tug-of-War in BRCA-Mutated Cells. *Trends Cell Biol* 2019; **29**: 820-834 [PMID: 31421928 DOI: 10.1016/j.tcb.2019.07.008]

179 **Pishvaian MJ**, Biankin AV, Bailey P, Chang DK, Laheru D, Wolfgang CL, Brody JR. BRCA2 secondary mutation-mediated resistance to platinum and PARP inhibitor-based therapy in pancreatic cancer. *Br J Cancer* 2017; **116**: 1021-1026 [PMID: 28291774 DOI: 10.1038/bjc.2017.40]

180 **Hsieh HJ**, Peng G. Cellular responses to replication stress: Implications in cancer biology and therapy. *DNA Repair (Amst)* 2017; **49**: 9-20 [PMID: 27908669 DOI: 10.1016/j.dnarep.2016.11.002]

181 **Maréchal A**, Zou L. DNA damage sensing by the ATM and ATR kinases. *Cold Spring Harb Perspect Biol* 2013; **5** [PMID: 24003211 DOI: 10.1101/cshperspect.a012716]

182 **Ubhi T**, Brown GW. Exploiting DNA Replication Stress for Cancer Treatment. *Cancer Res* 2019; **79**: 1730-1739 [PMID: 30967400 DOI: 10.1158/0008-5472.CAN-18-3631]

183 **Russell R**, Perkhofer L, Liebau S, Lin Q, Lechel A, Feld FM, Hessmann E, Gaedcke J, Güthle M, Zenke M, Hartmann D, von Figura G, Weissinger SE, Rudolph KL, Möller P, Lennerz JK, Seufferlein T, Wagner M, Kleger A. Loss of ATM accelerates pancreatic cancer formation and epithelial-mesenchymal transition. *Nat Commun* 2015; **6**: 7677 [PMID: 26220524 DOI: 10.1038/ncomms8677]

184 **Moding EJ**, Lee CL, Castle KD, Oh P, Mao L, Zha S, Min HD, Ma Y, Das S, Kirsch DG. Atm deletion with dual recombinase technology preferentially radiosensitizes tumor endothelium. *J Clin Invest* 2014; **124**: 3325-3338 [PMID: 25036710 DOI: 10.1172/JCI73932]

185 **Cowell IG**, Durkacz BW, Tilby MJ. Sensitization of breast carcinoma cells to ionizing radiation by small molecule inhibitors of DNA-dependent protein kinase and ataxia telangiectsia mutated. *Biochem Pharmacol* 2005; **71**: 13-20 [PMID: 16293233 DOI: 10.1016/j.bcp.2005.09.029]

186 **Ayars M**, Eshleman J, Goggins M. Susceptibility of ATM-deficient pancreatic cancer cells to radiation. *Cell Cycle* 2017; **16**: 991-998 [PMID: 28453388 DOI: 10.1080/15384101.2017.1312236]

187 **Kondo T**, Kanai M, Kou T, Sakuma T, Mochizuki H, Kamada M, Nakatsui M, Uza N, Kodama Y, Masui T, Takaori K, Matsumoto S, Miyake H, Okuno Y, Muto M. Association between homologous recombination repair gene mutations and response to oxaliplatin in pancreatic cancer. *Oncotarget* 2018; **9**: 19817-19825 [PMID: 29731985 DOI: 10.18632/oncotarget.24865]

188 **Aguirre AJ**, Nowak JA, Camarda ND, Moffitt RA, Ghazani AA, Hazar-Rethinam M, Raghavan S, Kim J, Brais LK, Ragon D, Welch MW, Reilly E, McCabe D, Marini L, Anderka K, Helvie K, Oliver N, Babic A, Da Silva A, Nadres B, Van Seventer EE, Shahzade HA, St Pierre JP, Burke KP, Clancy T, Cleary JM, Doyle LA, Jajoo K, McCleary NJ, Meyerhardt JA, Murphy JE, Ng K, Patel AK, Perez K, Rosenthal MH, Rubinson DA, Ryou M, Shapiro GI, Sicinska E, Silverman SG, Nagy RJ, Lanman RB, Knoerzer D, Welsch DJ, Yurgelun MB, Fuchs CS, Garraway LA, Getz G, Hornick JL, Johnson BE, Kulke MH, Mayer RJ, Miller JW, Shyn PB, Tuveson DA, Wagle N, Yeh JJ, Hahn WC, Corcoran RB, Carter SL, Wolpin BM. Real-time Genomic Characterization of Advanced Pancreatic Cancer to Enable Precision Medicine. *Cancer Discov* 2018; **8**: 1096-1111 [PMID: 29903880 DOI: 10.1158/2159-8290.CD-18-0275]

189 **Roger E**, Gout J, Arnold F, Beutel AK, Müller M, Abaei A, Barth TFE, Rasche V, Seufferlein T, Perkhofer L, Kleger A. Maintenance Therapy for ATM-Deficient Pancreatic Cancer by Multiple DNA Damage Response Interferences after Platinum-Based Chemotherapy. *Cells* 2020; **9** [PMID: 32948057 DOI: 10.3390/cells9092110]

190 **Fokas E**, Prevo R, Pollard JR, Reaper PM, Charlton PA, Cornelissen B, Vallis KA, Hammond EM, Olcina MM, Gillies McKenna W, Muschel RJ, Brunner TB. Targeting ATR *in vivo* using the novel inhibitor VE-822 results in selective sensitization of pancreatic tumors to radiation. *Cell Death Dis* 2012; **3**: e441 [PMID: 23222511 DOI: 10.1038/cddis.2012.181]

191 **Wallez Y**, Dunlop CR, Johnson TI, Koh SB, Fornari C, Yates JWT, Bernaldo de Quirós Fernández S, Lau A, Richards FM, Jodrell DI. The ATR Inhibitor AZD6738 Synergizes with Gemcitabine *In Vitro* and *In Vivo* to Induce Pancreatic Ductal Adenocarcinoma Regression. *Mol Cancer Ther* 2018;

17: 1670-1682 [PMID: 29891488 DOI: 10.1158/1535-7163.MCT-18-0010]

192 **Rosenberg SA**, Restifo NP. Adoptive cell transfer as personalized immunotherapy for human cancer. *Science* 2015; **348**: 62-68 [PMID: 25838374 DOI: 10.1126/science.aaa4967]

193 **Brahmer JR**, Tykodi SS, Chow LQ, Hwu WJ, Topalian SL, Hwu P, Drake CG, Camacho LH, Kauh J, Odunsi K, Pitot HC, Hamid O, Bhatia S, Martins R, Eaton K, Chen S, Salay TM, Alaparthy S, Grosso JF, Korman AJ, Parker SM, Agrawal S, Goldberg SM, Pardoll DM, Gupta A, Wigginton JM. Safety and activity of anti-PD-L1 antibody in patients with advanced cancer. *N Engl J Med* 2012; **366**: 2455-2465 [PMID: 22658128 DOI: 10.1056/NEJMoa1200694]

194 **Royal RE**, Levy C, Turner K, Mathur A, Hughes M, Kammula US, Sherry RM, Topalian SL, Yang JC, Lowy I, Rosenberg SA. Phase 2 trial of single agent Ipilimumab (anti-CTLA-4) for locally advanced or metastatic pancreatic adenocarcinoma. *J Immunother* 2010; **33**: 828-833 [PMID: 20842054 DOI: 10.1097/CJI.0b013e3181eec14c]

195 **Le DT**, Uram JN, Wang H, Bartlett BR, Kemberling H, Eyring AD, Skora AD, Luber BS, Azad NS, Laheru D, Biedrzycki B, Donehower RC, Zaheer A, Fisher GA, Crocenzi TS, Lee JJ, Duffy SM, Goldberg RM, de la Chapelle A, Koshiji M, Bhaijee F, Huebner T, Hruban RH, Wood LD, Cuka N, Pardoll DM, Papadopoulos N, Kinzler KW, Zhou S, Cornish TC, Taube JM, Anders RA, Eshleman JR, Vogelstein B, Diaz LA Jr. PD-1 Blockade in Tumors with Mismatch-Repair Deficiency. *N Engl J Med* 2015; **372**: 2509-2520 [PMID: 26028255 DOI: 10.1056/NEJMoa1500596]

196 **Alexandrov LB**, Nik-Zainal S, Wedge DC, Aparicio SA, Behjati S, Biankin AV, Bignell GR, Bolli N, Borg A, Børresen-Dale AL, Boyault S, Burkhardt B, Butler AP, Caldas C, Davies HR, Desmedt C, Eils R, Eyfjörd JE, Foekens JA, Greaves M, Hosoda F, Hutter B, Ilicic T, Imbeaud S, Imielinski M, Jäger N, Jones DT, Jones D, Knappskog S, Kool M, Lakhani SR, López-Otín C, Martin S, Munshi NC, Nakamura H, Northcott PA, Pajic M, Papaemmanuil E, Paradiso A, Pearson JV, Puente XS, Raine K, Ramakrishna M, Richardson AL, Richter J, Rosenstiel P, Schlesner M, Schumacher TN, Span PN, Teague JW, Totoki Y, Tutt AN, Valdés-Mas R, van Buuren MM, van 't Veer L, Vincent-Salomon A, Waddell N, Yates LR; Australian Pancreatic Cancer Genome Initiative; ICGC Breast Cancer Consortium; ICGC MMML-Seq Consortium; ICGC PedBrain, Zucman-Rossi J, Futreal PA, McDermott U, Lichter P, Meyerson M, Grimmond SM, Siebert R, Campo E, Shibata T, Pfister SM, Campbell PJ, Stratton MR. Signatures of mutational processes in human cancer. *Nature* 2013; **500**: 415-421 [PMID: 23945592 DOI: 10.1038/nature12477]

197 **Yarchoan M**, Hopkins A, Jaffee EM. Tumor Mutational Burden and Response Rate to PD-1 Inhibition. *N Engl J Med* 2017; **377**: 2500-2501 [PMID: 29262275 DOI: 10.1056/NEJMc1713444]

198 **Humphris JL**, Patch AM, Nones K, Bailey PJ, Johns AL, McKay S, Chang DK, Miller DK, Pajic M, Kassahn KS, Quinn MC, Bruxner TJ, Christ AN, Harliwong I, Idrisoglu S, Manning S, Nourse C, Nourbakhsh E, Stone A, Wilson PJ, Anderson M, Fink JL, Holmes O, Kazakoff S, Leonard C, Newell F, Waddell N, Wood S, Mead RS, Xu Q, Wu J, Pinese M, Cowley MJ, Jones MD, Nagrial AM, Chin VT, Chantrill LA, Mawson A, Chou A, Scarlett CJ, Pinho AV, Rooman I, Giry-Laterriere M, Samra JS, Kench JG, Merrett ND, Toon CW, Epari K, Nguyen NQ, Barbour A, Zeps N, Jamieson NB, McKay CJ, Carter CR, Dickson EJ, Graham JS, Duthie F, Oien K, Hair J, Morton JP, Sansom OJ, Grützmann R, Hruban RH, Maitra A, Iacobuzio-Donahue CA, Schulick RD, Wolfgang CL, Morgan RA, Lawlor RT, Rusev B, Corbo V, Salvia R, Cataldo I, Tortora G, Tempero MA; Australian Pancreatic Cancer Genome Initiative, Hofmann O, Eshleman JR, Pilarsky C, Scarpa A, Musgrove EA, Gill AJ, Pearson JV, Grimmond SM, Waddell N, Biankin AV. Hypermutation In Pancreatic Cancer. *Gastroenterology* 2017; **152**: 68-74.e2 [PMID: 27856273 DOI: 10.1053/j.gastro.2016.09.060]

199 **Tsujikawa T**, Kumar S, Borkar RN, Azimi V, Thibault G, Chang YH, Balter A, Kawashima R, Choe G, Sauer D, El Rassi E, Clayburgh DR, Kulesz-Martin MF, Lutz ER, Zheng L, Jaffee EM, Leyshock P, Margolin AA, Mori M, Gray JW, Flint PW, Coussens LM. Quantitative Multiplex Immunohistochemistry Reveals Myeloid-Inflamed Tumor-Immune Complexity Associated with Poor Prognosis. *Cell Rep* 2017; **19**: 203-217 [PMID: 28380359 DOI: 10.1016/j.celrep.2017.03.037]

200 **Clark CE**, Hingorani SR, Mick R, Combs C, Tuveson DA, Vonderheide RH. Dynamics of the immune reaction to pancreatic cancer from inception to invasion. *Cancer Res* 2007; **67**: 9518-9527 [PMID: 17909062 DOI: 10.1158/0008-5472.CAN-07-0175]

201 **Diaz-Montero CM**, Salem ML, Nishimura MI, Garrett-Mayer E, Cole DJ, Montero AJ. Increased circulating myeloid-derived suppressor cells correlate with clinical cancer stage, metastatic tumor burden, and doxorubicin-cyclophosphamide chemotherapy. *Cancer Immunol Immunother* 2009; **58**: 49-59 [PMID: 18446337 DOI: 10.1007/s00262-008-0523-4]

202 **Siret C**, Collignon A, Silvy F, Robert S, Cheyrol T, André P, Rigot V, Iovanna J, van de Pavert S, Lombardo D, Mas E, Martirosyan A. Deciphering the Crosstalk Between Myeloid-Derived Suppressor Cells and Regulatory T Cells in Pancreatic Ductal Adenocarcinoma. *Front Immunol* 2019; **10**: 3070 [PMID: 32038621 DOI: 10.3389/fimmu.2019.03070]

203 **Stromnes IM**, DelGiorno KE, Greenberg PD, Hingorani SR. Stromal reengineering to treat pancreas cancer. *Carcinogenesis* 2014; **35**: 1451-1460 [PMID: 24908682 DOI: 10.1093/carcin/bgu115]

204 **Blank CU**, Haining WN, Held W, Hogan PG, Kallies A, Lugli E, Lynn RC, Philip M, Rao A, Restifo NP, Schietinger A, Schumacher TN, Schwartzberg PL, Sharpe AH, Speiser DE, Wherry EJ, Youngblood BA, Zehn D. Defining 'T cell exhaustion'. *Nat Rev Immunol* 2019; **19**: 665-674 [PMID: 31570879 DOI: 10.1038/s41577-019-0221-9]

205 **Martinez GJ**, Pereira RM, Äijö T, Kim EY, Marangoni F, Pipkin ME, Togher S, Heissmeyer V, Zhang YC, Crotty S, Lamperti ED, Ansel KM, Mempel TR, Lähdesmäki H, Hogan PG, Rao A. The

transcription factor NFAT promotes exhaustion of activated CD8$^+$ T cells. *Immunity* 2015; **42**: 265-278 [PMID: 25680272 DOI: 10.1016/j.immuni.2015.01.006]

206 **Pauken KE**, Sammons MA, Odorizzi PM, Manne S, Godec J, Khan O, Drake AM, Chen Z, Sen DR, Kurachi M, Barnitz RA, Bartman C, Bengsch B, Huang AC, Schenkel JM, Vahedi G, Haining WN, Berger SL, Wherry EJ. Epigenetic stability of exhausted T cells limits durability of reinvigoration by PD-1 blockade. *Science* 2016; **354**: 1160-1165 [PMID: 27789795 DOI: 10.1126/science.aaf2807]

207 **Burrack AL**, Spartz EJ, Raynor JF, Wang I, Olson M, Stromnes IM. Combination PD-1 and PD-L1 Blockade Promotes Durable Neoantigen-Specific T Cell-Mediated Immunity in Pancreatic Ductal Adenocarcinoma. *Cell Rep* 2019; **28**: 2140-2155.e6 [PMID: 31433988 DOI: 10.1016/j.celrep.2019.07.059]

208 **Stromnes IM**, Schmitt TM, Hulbert A, Brockenbrough JS, Nguyen H, Cuevas C, Dotson AM, Tan X, Hotes JL, Greenberg PD, Hingorani SR. T Cells Engineered against a Native Antigen Can Surmount Immunologic and Physical Barriers to Treat Pancreatic Ductal Adenocarcinoma. *Cancer Cell* 2015; **28**: 638-652 [PMID: 26525103 DOI: 10.1016/j.ccell.2015.09.022]

209 **Burrack AL**, Rollins MR, Spartz EJ, Mesojednik TD, Schmiechen ZC, Raynor JF, Wang IX, Kedl RM, Stromnes IM. CD40 Agonist Overcomes T Cell Exhaustion Induced by Chronic Myeloid Cell IL-27 Production in a Pancreatic Cancer Preclinical Model. *J Immunol* 2021; **206**: 1372-1384 [PMID: 33558374 DOI: 10.4049/jimmunol.2000765]

210 **Ma Y**, Li J, Wang H, Chiu Y, Kingsley CV, Fry D, Delaney SN, Wei SC, Zhang J, Maitra A, Yee C. Combination of PD-1 Inhibitor and OX40 Agonist Induces Tumor Rejection and Immune Memory in Mouse Models of Pancreatic Cancer. *Gastroenterology* 2020; **159**: 306-319.e12 [PMID: 32179091 DOI: 10.1053/j.gastro.2020.03.018]

211 **Mirlekar B**, Michaud D, Searcy R, Greene K, Pylayeva-Gupta Y. IL35 Hinders Endogenous Antitumor T-cell Immunity and Responsiveness to Immunotherapy in Pancreatic Cancer. *Cancer Immunol Res* 2018; **6**: 1014-1024 [PMID: 29980536 DOI: 10.1158/2326-6066.CIR-17-0710]

212 **Panni RZ**, Herndon JM, Zuo C, Hegde S, Hogg GD, Knolhoff BL, Breden MA, Li X, Krisnawan VE, Khan SQ, Schwarz JK, Rogers BE, Fields RC, Hawkins WG, Gupta V, DeNardo DG. Agonism of CD11b reprograms innate immunity to sensitize pancreatic cancer to immunotherapies. *Sci Transl Med* 2019; **11** [PMID: 31270275 DOI: 10.1126/scitranslmed.aau9240]

213 **Le DT**, Picozzi VJ, Ko AH, Wainberg ZA, Kindler H, Wang-Gillam A, Oberstein P, Morse MA, Zeh HJ 3rd, Weekes C, Reid T, Borazanci E, Crocenzi T, LoConte NK, Musher B, Laheru D, Murphy A, Whiting C, Nair N, Enstrom A, Ferber S, Brockstedt DG, Jaffee EM. Results from a Phase IIb, Randomized, Multicenter Study of GVAX Pancreas and CRS-207 Compared with Chemotherapy in Adults with Previously Treated Metastatic Pancreatic Adenocarcinoma (ECLIPSE Study). *Clin Cancer Res* 2019; **25**: 5493-5502 [PMID: 31126960 DOI: 10.1158/1078-0432.CCR-18-2992]

214 **Kinkead HL**, Hopkins A, Lutz E, Wu AA, Yarchoan M, Cruz K, Woolman S, Vithayathil T, Glickman LH, Ndubaku CO, McWhirter SM, Dubensky TW Jr, Armstrong TD, Jaffee EM, Zaidi N. Combining STING-based neoantigen-targeted vaccine with checkpoint modulators enhances antitumor immunity in murine pancreatic cancer. *JCI Insight* 2018; **3** [PMID: 30333318 DOI: 10.1172/jci.insight.122857]

215 **Nywening TM**, Belt BA, Cullinan DR, Panni RZ, Han BJ, Sanford DE, Jacobs RC, Ye J, Patel AA, Gillanders WE, Fields RC, DeNardo DG, Hawkins WG, Goedegebuure P, Linehan DC. Targeting both tumour-associated CXCR2$^+$ neutrophils and CCR2$^+$ macrophages disrupts myeloid recruitment and improves chemotherapeutic responses in pancreatic ductal adenocarcinoma. *Gut* 2018; **67**: 1112-1123 [PMID: 29196437 DOI: 10.1136/gutjnl-2017-313738]

216 **Steele CW**, Karim SA, Leach JDG, Bailey P, Upstill-Goddard R, Rishi L, Foth M, Bryson S, McDaid K, Wilson Z, Eberlein C, Candido JB, Clarke M, Nixon C, Connelly J, Jamieson N, Carter CR, Balkwill F, Chang DK, Evans TRJ, Strathdee D, Biankin AV, Nibbs RJB, Barry ST, Sansom OJ, Morton JP. CXCR2 Inhibition Profoundly Suppresses Metastases and Augments Immunotherapy in Pancreatic Ductal Adenocarcinoma. *Cancer Cell* 2016; **29**: 832-845 [PMID: 27265504 DOI: 10.1016/j.ccell.2016.04.014]

217 **Zhu Y**, Knolhoff BL, Meyer MA, Nywening TM, West BL, Luo J, Wang-Gillam A, Goedegebuure SP, Linehan DC, DeNardo DG. CSF1/CSF1R blockade reprograms tumor-infiltrating macrophages and improves response to T-cell checkpoint immunotherapy in pancreatic cancer models. *Cancer Res* 2014; **74**: 5057-5069 [PMID: 25082815 DOI: 10.1158/0008-5472.CAN-13-3723]

218 **Candido JB**, Morton JP, Bailey P, Campbell AD, Karim SA, Jamieson T, Lapienyte L, Gopinathan A, Clark W, McGhee EJ, Wang J, Escorcio-Correia M, Zollinger R, Roshani R, Drew L, Rishi L, Arkell R, Evans TRJ, Nixon C, Jodrell DI, Wilkinson RW, Biankin AV, Barry ST, Balkwill FR, Sansom OJ. CSF1R$^+$ Macrophages Sustain Pancreatic Tumor Growth through T Cell Suppression and Maintenance of Key Gene Programs that Define the Squamous Subtype. *Cell Rep* 2018; **23**: 1448-1460 [PMID: 29719257 DOI: 10.1016/j.celrep.2018.03.131]

219 **Stromnes IM**, Schmitt TM, Chapuis AG, Hingorani SR, Greenberg PD. Re-adapting T cells for cancer therapy: from mouse models to clinical trials. *Immunol Rev* 2014; **257**: 145-164 [PMID: 24329795 DOI: 10.1111/imr.12141]

220 **Liu J**, Zhong JF, Zhang X, Zhang C. Allogeneic CD19-CAR-T cell infusion after allogeneic hematopoietic stem cell transplantation in B cell malignancies. *J Hematol Oncol* 2017; **10**: 35 [PMID: 28143567 DOI: 10.1186/s13045-017-0405-3]

221 **Ali AI**, Oliver AJ, Samiei T, Chan JD, Kershaw MH, Slaney CY. Genetic Redirection of T Cells for the Treatment of Pancreatic Cancer. *Front Oncol* 2019; **9**: 56 [PMID: 30809507 DOI: 10.3389/fonc.2019.00056]

222 **Akce M**, Zaidi MY, Waller EK, El-Rayes BF, Lesinski GB. The Potential of CAR T Cell Therapy in Pancreatic Cancer. *Front Immunol* 2018; **9**: 2166 [PMID: 30319627 DOI: 10.3389/fimmu.2018.02166]

223 **Wu AA**, Jaffee E, Lee V. Current Status of Immunotherapies for Treating Pancreatic Cancer. *Curr Oncol Rep* 2019; **21**: 60 [PMID: 31101991 DOI: 10.1007/s11912-019-0811-5]

224 **Morgan RA**, Yang JC, Kitano M, Dudley ME, Laurencot CM, Rosenberg SA. Case report of a serious adverse event following the administration of T cells transduced with a chimeric antigen receptor recognizing ERBB2. *Mol Ther* 2010; **18**: 843-851 [PMID: 20179677 DOI: 10.1038/mt.2010.24]

225 **Parkhurst MR**, Yang JC, Langan RC, Dudley ME, Nathan DA, Feldman SA, Davis JL, Morgan RA, Merino MJ, Sherry RM, Hughes MS, Kammula US, Phan GQ, Lim RM, Wank SA, Restifo NP, Robbins PF, Laurencot CM, Rosenberg SA. T cells targeting carcinoembryonic antigen can mediate regression of metastatic colorectal cancer but induce severe transient colitis. *Mol Ther* 2011; **19**: 620-626 [PMID: 21157437 DOI: 10.1038/mt.2010.272]

226 **Thistlethwaite FC**, Gilham DE, Guest RD, Rothwell DG, Pillai M, Burt DJ, Byatte AJ, Kirillova N, Valle JW, Sharma SK, Chester KA, Westwood NB, Halford SER, Nabarro S, Wan S, Austin E, Hawkins RE. The clinical efficacy of first-generation carcinoembryonic antigen (CEACAM5)-specific CAR T cells is limited by poor persistence and transient pre-conditioning-dependent respiratory toxicity. *Cancer Immunol Immunother* 2017; **66**: 1425-1436 [PMID: 28660319 DOI: 10.1007/s00262-017-2034-7]

227 **Beatty GL**, O'Hara MH, Lacey SF, Torigian DA, Nazimuddin F, Chen F, Kulikovskaya IM, Soulen MC, McGarvey M, Nelson AM, Gladney WL, Levine BL, Melenhorst JJ, Plesa G, June CH. Activity of Mesothelin-Specific Chimeric Antigen Receptor T Cells Against Pancreatic Carcinoma Metastases in a Phase 1 Trial. *Gastroenterology* 2018; **155**: 29-32 [PMID: 29567081 DOI: 10.1053/j.gastro.2018.03.029]

228 **You F**, Jiang L, Zhang B, Lu Q, Zhou Q, Liao X, Wu H, Du K, Zhu Y, Meng H, Gong Z, Zong Y, Huang L, Lu M, Tang J, Li Y, Zhai X, Wang X, Ye S, Chen D, Yuan L, Qi L, Yang L. Phase 1 clinical trial demonstrated that MUC1 positive metastatic seminal vesicle cancer can be effectively eradicated by modified Anti-MUC1 chimeric antigen receptor transduced T cells. *Sci China Life Sci* 2016; **59**: 386-397 [PMID: 26961900 DOI: 10.1007/s11427-016-5024-7]

World Journal of Gastroenterology

Submit a Manuscript: https://www.f6publishing.com

World J Gastroenterol 2021 October 21; 27(39): 6551-6571

DOI: 10.3748/wjg.v27.i39.6551

ISSN 1007-9327 (print) ISSN 2219-2840 (online)

REVIEW

Evaluation of botanicals as potential COVID-19 symptoms terminator

Ufuk Koca Caliskan, Methiye Mancak Karakus

ORCID number: Ufuk Koca Caliskan 0000-0002-5216-7588; Methiye Mancak Karakus 0000-0002-0085-7552.

Author contributions: Caliskan UK and Karakus MM equally contributed to collect data and to write the paper; both authors read and approved the final manuscript.

Conflict-of-interest statement: Authors declare that they have no conflicts of interest for this article.

Open-Access: This article is an open-access article that was selected by an in-house editor and fully peer-reviewed by external reviewers. It is distributed in accordance with the Creative Commons Attribution NonCommercial (CC BY-NC 4.0) license, which permits others to distribute, remix, adapt, build upon this work non-commercially, and license their derivative works on different terms, provided the original work is properly cited and the use is non-commercial. See: http://creativecommons.org/Licenses/by-nc/4.0/

Manuscript source: Invited manuscript

Specialty type: Gastroenterology and hepatology

Country/Territory of origin: Turkey

Peer-review report's scientific quality classification

Ufuk Koca Caliskan, Methiye Mancak Karakus, Department of Pharmacognosy and Pharmaceutical Botany, Gazi University, Ankara 06500, Turkey

Corresponding author: Ufuk Koca Caliskan, PhD, Professor, Department of Pharmacognosy and Pharmaceutical Botany, Gazi University, Faculty of Pharmacy, Ankara 06500, Turkey. ukoca@gazi.edu.tr

Abstract

Information about the coronavirus disease 2019 (COVID-19) pandemic is still evolving since its appearance in December 2019 and has affected the whole world. Particularly, a search for an effective and safe treatment for COVID-19 continues. Botanical mixtures contain secondary metabolites (such as flavonoids, phenolics, alkaloids, essential oils *etc.*) with many therapeutic effects. In this study, the use of herbal treatments against COVID-19 was evaluated. Medical synthetic drugs focus mainly on respiratory symptoms, however herbal therapy with plant extracts may be useful to relieve overall symptoms of COVID-19 due to the variety of bioactive ingredients. Since COVID-19 is a virus that affects the respiratory tract, the antiviral effects of botanicals/plants against respiratory viruses have been examined through clinical studies. Data about COVID-19 patients revealed that the virus not only affects the respiratory system but different organs including the gastrointestinal (GI) system. As GI symptoms seriously affect quality of life, herbal options that might eliminate these problems were also evaluated. Finally, computer modeling studies of plants and their active compounds on COVID-19 were included. In summary, herbal therapies were identified as potential options for both antiviral effects and control of COVID-19 symptoms. Further data will be needed to enlighten all aspects of COVID-19 pathogenesis, before determining the effects of plants on severe acute respiratory syndrome coronavirus 2.

Key Words: COVID-19; Herbal therapies; Plant; SARS-CoV-2; Antiviral; Symptom

©The Author(s) 2021. Published by Baishideng Publishing Group Inc. All rights reserved.

Core Tip: To stop the coronavirus disease 2019 (COVID-19) pandemic, extensive search is ongoing to develop effective and safe drugs against severe acute respiratory syndrome coronavirus 2. COVID-19 in a major way affects the respiratory system, but many patients also have gastrointestinal (GI) symptoms. Plants have beneficial effects

Grade A (Excellent): 0
Grade B (Very good): B
Grade C (Good): 0
Grade D (Fair): 0
Grade E (Poor): 0

Received: March 16, 2021
Peer-review started: March 16, 2021
First decision: May 1, 2021
Revised: May 1, 2021
Accepted: September 14, 2021
Article in press: September 14, 2021
Published online: October 21, 2021

P-Reviewer: Wang X
S-Editor: Fan JR
L-Editor: A
P-Editor: Xing YX



on various systems with their varied array of metabolites. In our study, the potential effects of herbal treatments against COVID-19 were examined. Their antiviral effects, their effects on the respiratory system, GI system, and other COVID-19 symptoms were investigated.

Citation: Caliskan UK, Karakus MM. Evaluation of botanicals as potential COVID-19 symptoms terminator. *World J Gastroenterol* 2021; 27(39): 6551-6571
URL: https://www.wjgnet.com/1007-9327/full/v27/i39/6551.htm
DOI: https://dx.doi.org/10.3748/wjg.v27.i39.6551

INTRODUCTION

New coronavirus disease 2019 (COVID-19), which emerged in Wuhan in December 2019, spread rapidly and affected the whole world. The emergence, epidemiology, origin and evolution of COVID-19 has been extensively studied by Sun *et al*[1].

Severe acute respiratory syndrome coronavirus 2 (SARS-CoV-2) has been shown to carry out viral replication in the human host mainly through three main proteins and enzymes: 3-chymotrypsin-like protease (3CLpro), angiotensin-converting enzyme-2 (ACE2) and spike protein (TMPRSS2)[2,3]. ACE2 receptors are found in the body not only in the lungs but also in tissues such as the endothelium, heart, kidney and intestine[2]. This distribution makes many organs a target of COVID-19. The significance of ACE2, which is found in intestinal tissues, especially for amino acid uptake from foods, has been emphasized and it has been suggested that the intestine may be an important entry site for SARS-CoV-2[2-4] Azithromycin, chloroquine, lopinavir, remdesivir, ritonavir are options used in treatment and whose effects are evaluated[5]. Effective and safe drugs and vaccines are sought all over the world to prevent novel coronavirus. Minerals, herbs, herbal products, probiotics and vitamins are the main natural resources, whose effectiveness and also the usability of herbal medicines in COVID-19 were investigated and benefit, risk assessments were evaluated[6-8]. Truly, since the beginning of the COVID-19, herbal medicines have been used in China. A study has shown that 90% of the 214 patients were treated with the traditional herbal medicine, moreover, it is reported that some of them prevented COVID-19 infection in healthy individuals and enhanced the health state of patients with mild or severe symptoms[9,10]. Health scientists from the Zhongnan Hospital of Wuhan University included the use of traditional medicines in the guidelines for the treatment and prevention of COVID-19. The experts recommended using medicinal plants for the prevention of COVID-19, additionally, the use of different herbal mixtures were recommended according to the disease-stage[11].

Herbs and herbal products provide generous sources of primary and mostly secondary metabolites, which are valuable compounds (phenolics, flavonoids, tannins, alkaloids, essential oils, *etc.*) for prophylactic and chronical therapeutic purposes. Some of these metabolites in herbs and herbal mixtures have high chemical variety than the synthetics in stopping viral proliferations, and having antiviral activities[12]. Thus, botanicals can both show antiviral effects and relieve the symptoms of COVID-19 thanks to the different substance groups, which demonstrate different biological effects that will not be possible to achieve with a single synthetic drug. Based on this understanding, in this review, we offer all the potential interventions for COVID-19 infection according to previous and recently found antiviral effects of herbals. Considering the major transmission routes of COVID-19, where mostly ACE2 receptors found and the symptoms, the plants have been handled especially with their effects on the mostly respiratory and also gastrointestinal (GI) systems. Although ACE2, is typically expressed in epithelial cells of the airways, various GI symptoms in COVID-19 might be explained by the high expression of ACE2 in the digestive tract. Additionally, liver tests abnormalities, active viral replication in GI tract and patients' manifestations with GI symptoms (abdominal pain, diarrhea, nausea, vomiting) and possible fecal-oral transmission reveal the GI involvement in COVID-19[13].

Recent findings demonstrated that early blocking of COVID-19 with ACE2 inhibitors was one of the mechanisms used by novel drugs[14], on the other hand diabetes mellitus and hypertension enhanced the risk of COVID-19 infection, in spite of using ACE2 inhibitors[15-17]. Furthermore, unpredicted ACE2 upregulation by

ACE2 inhibitors, ibuprofen and angiotensin II type-I receptor blockers lead to need of identifying/using alternative ACE2 blockers[18]. Consequently, botanicals or natural products might be alternatively and selectively might block the ACE2 receptors without inhibiting the enzyme activity in order to treat and/or prevent COVID-19 spread in humans without increasing ACE2 expression in patients and therefore increased risk for COVID-19[19].

Clinical human studies showing the effect of plants on respiratory infections are presented as a table. Based on the pharmacological properties of plants, their practicality on COVID-19 symptoms have been evaluated. In the last part of the article, plants that inhibit ACE receptors, the research studies and their active compounds on COVID-19 also included and it is aimed to examine the plants from a broad perspective.

ANTIVIRAL EFFECTS OF HERBAL THERAPIES

Most of the respiratory diseases (approximately 80%) are caused by viral agents[20]. Viral respiratory diseases are responsible for high mortality and morbidity, especially in disadvantaged and sensitive elderlies and immunocompromised individuals[21, 22]. The main respiratory viruses are adenovirus, coronavirus, influenza virus, respiratory syncytial virus and rhinovirus[20]. Plants with antiviral effects and studies showing the effects of these on respiratory viruses are given in Table 1. Human clinical studies showing the effects of plants on respiratory tract infections are presented in Table 2.

EFFECTS OF HERBAL TREATMENT ON COVID-19 SYMPTOMS

Cough and fever are common symptoms in patients with COVID-19, including fatigue, shortness of breath, headache, muscle pain, sore throat, sputum, hemoptysis, diarrhea, dyspnea, rhinorrhea, chest pain, nausea, and vomiting[23]. COVID-19 symptoms in children are similar to those in adults and are relatively mild[24].

Although, the current synthetic drugs focus on mainly respiratory symptoms, herbal therapy can be used to relieve overall symptoms of COVID-19 with their bioactive ingredients[25]. The meta-analysis study, which included randomized controlled trial studies, found significant effects of the combination of western medicine and herbal therapies. Combined treatment has been effective in cough, fever, dry and sore throat, fatigue and overall GI symptoms. The combined therapy significantly improved the disappearance rate of cough and sputum production[26]. In another meta-analysis, it was found that the addition of Chinese herbal medicine for standard care improved the symptoms and signs of COVID-19 as well as decreased levels of C-reactive protein[27]. The effects of plants that can alleviate the symptoms of COVID-19 are summarized in Table 3. In addition, plants regarded as ACE inhibitors are shown in Table 4.

THE EFFECTS OF HERBS AND THEIR ACTIVE COMPOUNDS ON COVID-19

In recent years, artificial intelligence has often been used to discover natural products as medicine[28,29]. After the outbreak of COVID-19, computer models were used to investigate the effect of many plants and their components on SARS-CoV-2. Khaerunnisa *et al*[30], determined the COVID-19 Main Protease (Mpro) inhibitor effects of medicinal plant components in a molecular docking study. They suggested apigenin-7-glucoside, curcumin, catechin, demethoxycurcumin, epicatechin-gallate, luteolin-7-glucoside, and oleuropein, as potential inhibitors of COVID-19 Mpro. In a similar molecular docking study using sixty-seven molecules of natural origin, crocin, digitoxigenin and b-eudesmol were proposed as inhibitors against coronavirus[31]. Another study was carried out using one hundred seventy-one essential oil components. The study determined the best docking ligands for the SARS-CoV target proteins were (E)--farnesene, (E,E)--farnesene and (E,E)-farnesol, thereby suggesting essential oil components may act synergistically with other antiviral agents, or they may provide some relief of COVID-19 symptoms[32]. Computer modeling studies and clinical studies against SARS-CoV-2 in some prominent plants/products and their

Table 1 Antiviral effects of plants on respiratory viruses

Plant name	Preparation	Susceptible viruses	Ref.
Allium sativum (Garlic)	Aqueous extracts	Influenza A (H9N2)	Rasool *et al*[53], 2017
	Extract	Infectious bronchitis virus	Mohajer Shojai *et al*[54], 2016
	Ethanolic extract	Influenza A (H1N1)	Chavan *et al*[55], 2016
	Garlic oil	Influenza A (H1N1)	Choi[56], 2018
	Fresh extract	Influenza A (H1N1)	Mehrbod *et al*[57], 2013
	Aqueous extract	Adenovirus (ADV3 and ADV41)	Chen *et al*[58], 2011
Aloe vera (Aloe)	Aloe anthraquinones and several derivatives (3-O-tetraacetoglupiranosil)	Influenza A	Borges-Argáez *et al*[59], 2019
	Aloe-emodin	Influenza A	Li *et al*[60], 2014
Astragalus mongholicus (Astragalus)	*Astragalus* polysaccharides	Avian infectious bronchitis virus	Zhang *et al*[61], 2018
	Astragalus polysaccharide	Influenza A (H9N2)	Kallon *et al*[62], 2013
Camellia sinensis (Green tea)	Catechins -EGCG	Adenovirus	Weber *et al*[63], 2003
	Catechin	Influenza A	Kuzuhara *et al*[64], 2009
	Catechins	Influenza A (H5N1)	Liu *et al*[65], 2012
	Polyphenols	Influenza A; Influenza B	Yang *et al*[66], 2014
Curcuma longa (Turmeric)	Curcumin	Influenza A virus	Chen *et al*[67], 2013
			Dai *et al*[68], 2018
	Curcumin	Influenza A (H1N1, H6N1)	Chen *et al*[69], 2010
	Curcumin	RSV	Obata *et al*[70], 2013
Echinacea purpurea (Purple coneflower)	*E. purpurea* fresh herb and root tinctures	Influenza	Vimalanathan *et al*[71], 2013
	Standardized *E. purpurea* extract	Influenza A (H5N1, H7N7, H1N1)	Pleschka *et al*[72], 2009
	Standardized *E. purpurea* extract	Rhinoviruses, RSV	Hudson *et al*[73], 2011
Eucalyptus globulus (Eucalyptus)	Essential oil- vapor phase	Influenza	Vimalanathan *et al*[74], 2014
Ginkgo biloba (Ginkgo)	Leaf extract	Influenza A (H1N1, H3N2)	Haruyama *et al*[75], 2013
Glycyrrhiza sp. (Licorice)	Water extract of licorice (*Glycyrrhiza uralensis*)	RSV	Feng Yeh *et al*[76], 2013
	Glycyrrhizic acid derivatives	SARS-CoV	Hoever *et al*[77], 2005
	Extract of *Glycyrrhiza inflata*	Influenza A (H1N1)	Dao *et al*[78], 2011
	Glycyrrhizin	Influenza A	Wolkerstorfer *et al*[79], 2009
	Glycyrrhizin	Influenza A (H5N1)	Michaelis *et al*[80], 2010
Lepidium meyenii (Maca)	Extracted with methanol	Influenza A; Influenza B	Del Valle Mendoza *et al* [81], 2014
Melaleuca alternifolia (Tea tree)	Tea tree oil	Influenza A (H1N1)	Garozzo *et al*[82], 2011
	Aerosol and vapor of tea tree oil	Influenza A (H11N9)	Usachev *et al*[83], 2013
	Tea tree oil	Influenza A (H11N9)	Pyankov *et al*[84], 2012
Melissa officinalis (Lemon balm)	Essential oil	Influenza A (H9N2)	Pourghanbari *et al*[85], 2016
	Extract	Avian infectious bronchitis	Lelešius *et al*[86], 2019
Mentha piperita (Peppermint)	Ethanol extract	RSV	Li *et al*[87], 2017
	Extract	Avian infectious bronchitis	Lelešius *et al*[86], 2019

Nigella sativa (Black cumin)	Ethanol extracts of	Influenza A (H5N1)	Dorra *et al*[88], 2019
	Ethanol extracts of	Influenza A (H9N2)	Umar *et al*[89], 2016
	Extract	Coronavirus	Ulasli *et al*[90], 2014
Panax ginseng (Ginseng)	Root of plant *Panax ginseng*	RSV	Lee *et al*[91], 2014
	Panax Korean red ginseng extract	RSV	Lee *et al*[92], 2014
	Red ginseng extract and polysaccharide and saponin fractions	Influenza A (H1N1)	Yin *et al*[93], 2013
	Korean red ginseng extract	Influenza A (H1N1, H3N2)	Yoo *et al*[94], 2012
Pelargonium sidoides (Pelargonium)	*Pelargonium sidoides* radix extract EPs® 7630	Rhinovirus	Roth *et al*[95], 2019
	EPs® 7630	Respiratory viruses	Michaelis *et al*[96], 2011
	EPs® 7630	Influenza A (H1N1, H3N2)	Theisen *et al*[97], 2012
Sambucus nigra (Black elder)	Extract	Infectious bronchitis virus	Chen *et al*[98], 2014
	Standardized elderberry liquid extract	Influenza A; Influenza B	Krawitz *et al*[99], 2011
	Concentrated juice of elderberry	Influenza A	Kinoshita *et al*[100], 2012
	Elderberry flavonoids	Influenza A (H1N1)	Roschek *et al*[101], 2009
Scutellaria baicalensis (Chinese skullcap)	Chemical constituents	Influenza A (H1N1)	Ji *et al*[102], 2015
	Baicalin	SARS-CoV	Chen *et al*[103], 2004
Torreya nucifera (Japanese nutmeg yew)	Ethanol extract	SARS-CoV	Ryu *et al*[104], 2010
Thymus vulgaris (Thyme)	Essential oil- liquid phase	Influenza	Vimalanathan *et al*[74], 2014
	Extract	Avian infectious bronchitis	Lelešius *et al*[86], 2019
Withania somnifera (Ashwagandha)	Withaferin A	Influenza A (H1N1)	Cai *et al*[105], 2015
Zingiber officinalis (Ginger)	Aqueous extracts	Influenza A (H9N2)	Rasool *et al*[53], 2017
	Ethanol extracts	Influenza A- (H5N1)	Dorra *et al*[88], 2019
	Fresh ginger	RSV	Chang *et al*[106], 2013

Influenza A strains: H1N1, H3N2, H5N1, H6N1, H7N7, H9N2, H11N9; RSV: Respiratory syncytial virus; H1N1: Influenza A; SARS-CoV: Severe acute respiratory syndrome coronavirus.

metabolites are given below.

Curcuma longa

Utomo and Meiyanto[33] revealed the potential of several compounds of *Curcuma longa* against SARS-CoV-2 by binding to three protein receptors (*RBD-S*, *PD-ACE2*, *SARS-CoV-2 protease*). They showed that *Curcuma* sp. compounds can bind to target receptors, thus, have potential inhibitory effects on SARS-CoV-2 infectivity. Rajagopal *et al*[34] showed in their *in silico* docking study that *Curcuma longa* components could be effective against COVID-19 by inhibiting the SARS-CoV-2 Mpro enzyme. Morever, cyclocurcumin and curcumin possess significant binding at the active site of SARS-CoV-2 Mpro when compared to hydroxychloroquine and nelfinavir. When compared to remdesivir, cyclocurcumin is significantly more active [Glide score: Cyclocurcumin (−6.77); remdesivir (−6.38); curcumin (−6.13); nelfinavir (−5.93); hydroxychloroquine (− 5.47)]. In a similar study, diacetylcurcuminin was more effective on COVID-19 (Mpro) than nelfinavir[35]. Another study suggested the use of curcumin with hydroxychloroquine to destabilize the SARS-CoV2 receptor proteins[36]. Gonzalez-Paz *et al*[37] showed that curcumin strongly binds to 3CL-protease of COVID-19 Curcumin caused enzyme folding and structural changes in viral protease. Moreover, curcumin bound more strongly to the enzyme than chloroquine.

Eucalyptus globulus

Sharma[38] suggested that eucalyptus essential oil active compounds are potential inhibitors of COVID-19 Mpro. They conducted a molecular docking study to evaluate

Table 2 Human clinical studies showing the effect of plants on respiratory infections

Plant	Disease state	Participant	Dosage	Study design	Results
Aged garlic extract[107]	Cold andflu illness	120 healthy subjects, 2 groups (21-50 yr)	4 capsules/d (2.56 g); 90 d	Double-blind, randomized, placebo-controlled parallel intervention	Increase in γδ-T cell and NK cell. Reduction in cold and flu severity; decrease in symptom days
E. purpurea and *E. angustifolia* root[108]	New-onset common cold	719 patients, 4 parallel groups (12-80 yr)	First 24 h: Equivalent of 10.2 g of root. Next 4 d: 5.1 g	Randomized, controlled trial	Disease duration and severity are not statistically significantly changed
Echinacea purpurea alcohol extract (Echinaforce®) [109]	Common cold	755 healthy subjects, 2 groups (≥ 18 yr)	Illness prevention: 3 × 0.9 mL. Acute stages of colds: 5 × 0.9 mL	Randomized, double-blind, placebo-controlled trial	Reduction of the total number of cold episodes, cumulated episode days, and pain-killer medicated episodes. Inhibited virally confirmed colds and especially prevented enveloped virus infections. Maximal effects on recurrent infections. Prophylactic intake of *E. purpurea* over a period of 4 mo to provide a positive risk/benefit ratio
Echinacea root extract[110]	Respiratory symptoms	175 adults, 2 groups (18–65 yr)	Tablets: 112.5 mg *E. purpurea* 6:1 extract (equivalent to 675 mg dry root) and 150 mg *E. angustifolia* 4:1 extract (equivalent to 600 mg dry root) 3 × 1 tablet, if required: 3 × 2 tablets	Randomized, double blind, placebo-controlled trial	Lower respiratory symptom scores. Preventive effect against the development of respiratory symptoms during travel, including long-haul flights
Green tea catechins and theanine[111]	Influenza	200 healthcare workers, 2 groups	Capsules: Green tea catechins (378 mg/d) and theanine (210 mg/d). 5 m	Randomized, double-blind, placebo-controlled trial	Lower incidence of influenza infection in the catechin/theanine group
Ivy leaf extract[112]	Acute or chronic bronchial inflammatory disease	9657 patients (5181 children)	Ivy leaves extract [drug-to-extract ratio: 5-7.5:1; extraction solvent: ethanol 30% (w/w)]. 0–5 yr: 3 × 2.5 mL; 6–12 yr: 3 × 5 mL; 12 yr and adults: 3 × 5–7.5 mL. 7 d	Prospective, open, multicenter post marketing study	Healing or improvement in 95% of symptoms. Effective and well tolerated
Ivy extract (Hedelix®) [113]	Acute respiratory catarrh and/or chronic recidivating inflammatory bronchial disease	268 children, 2 groups (syrup and drops groups) (0-12 yr)	0-1 yr: 1 × 2.5 mL syrup or 3 × 5 drops, 1-4 yr: 3 × 2.5 mL syrup or 3 × 16 drops, 4-10 yr: 4 × 2.5 mL syrup or 3 × 21 drops, 10-12 yr: 3 × 5 mL syrup or 3 × 31 drops. 14 d	Independent open, non-interventional studies	Effective and safe treatment of cough. Reduction in symptoms (especially rhinitis, cough and viscous mucus)
Ivy leaves dry extract (Prospan ®) [114]	Bronchial asthma	30 children (suffering from partial or uncontrolled mild persistent allergic asthma despite long-term treatment with 400 μg budesonide equivalent), 2 groups (6–11 yr)	2 × 5 mL (corresponding to 70 mg extract) 28–30 d	Randomized, double blind, placebo-controlled, cross-over study	Improvement of MEF75-25, MEF25 and VC
Korean red ginseng extract[115]	Influenza-like illness	100 healthy adults, 2 groups (30-70 yr)	9 capsules/d. 3 m	Placebo-controlled trial	Reduced the incidence of influenza-like illness
Modified ginseng extracts (GS-3K8 and GINST)[116]	Acute respiratory illness	45 healthy applicants, 3 groups (39-65 yr)	Capsules: 500 mg; 6 capsules/d; 8 wk	Randomized, double-blind, placebo-controlled pilot study	Reduction in acute respiratory illness development and symptom duration
Panax quinquefolius extract CVT-E002[117]	Acute respiratory illness and Chronic Lymphocytic Leukemia	293 patients, 2 groups (≥ 18 yr)	2 × 200 mg extract. 3 m	Randomized, double-blind, placebo-controlled study	Reduction intense acute respiratory illness and moderately-severe sore throat. Increased antibody responses.

Panax ginseng [118]	Chronic obstructive pulmonary disease	14 participants, 2 groups (57–73 yr)	2 × 200 mg 4 wk	Clinical trial protocol and pilot study	One participant in *P. ginseng* group reported events of sore throat, cough and fever
Panax ginseng root extract [119]	Chronic obstructive pulmonary disease	168 participants, 2 groups	2 × 100 mg capsules. 24 wk	Randomized, multi-center, double-blind, placebo controlled	Reduction in symptoms
Pelargonium sidoides extract EPs® 7630 [120]	Chronic obstructive pulmonary disease	199 adults, 2 groups (18 yr and older)	30 drops. 24 wk	Randomized, double-blind, placebo-controlled, parallel group trial	Improvement in HRQoL (health-related quality-of-life) and PRO (Patient-reported outcomes)
Pelargonium sidoides extract EPs® 7630 [121]	Acute bronchitis	220 patients (1-18 yr)	1-6 yr: 3 × 10 drops; 6–12 yr: 3 × 20 drops; 12-18 yr: 3 × 30 drops; 7 d	Randomized, double-blind, placebo-controlled clinical trial	Reduction in the total score of bronchitis-specific symptoms (especially cough and rales at auscultation)
Pelargonium sidoides extract EPs® 7630 [122]	Upper respiratory tract infections	28 children with a diagnosed transient hypogammaglobulinemia of infancy (1-5 yr)	3 × 10 drops; 7 d	Randomized, placebo controlled, prospective, monocentric pilot study	Increased appetite. Reduction of nasal congestion
Pelargonium sidoides root extract EPs® 7630[123]	Upper respiratory tract- asthma attacks	61 children (1–14 yr)	1–5 yr: 3 × 10 drops; 6–12 yr: 3 × 20 drops; 12 yr and above: 3 × 30 drops; 5 d	Randomized, placebo controlled	Reduction the severity of symptoms (especially cough and nasal congestion). Shortening of the duration of upper respiratory viral infections. Reduction asthma attack frequency
Pelargonium sidoides preparation EPs® 7630 [124]	Acute non-streptococcal tonsillopharyngitis	126 children, 2 groups (6–10 yr)	3 × 20 drops. 6 d	Double-blind, placebo-controlled clinical trial	Decrease in tonsillitis severity score compared to placebo in the EPs® 7630 group after 4 d of treatment
Pelargonium sidoides extract EPs® 7630 [125]	Common cold	207 adults (18-55 yr)	SD: 3 × 30 drops; HD: 3 × 60 drops; 10 d	Prospective, double-blind, parallel-group, placebo-controlled, phase 3, 2 parts, 2-arm, clinical trial	After 10 d, clinical treatment in 90.4% of the active drug group. Reduction the severity of symptoms and short the duration of the disease. Higher full recovery rates or greater recovery for HD treatment on day 5
Sambucus nigra extract [126]	Influenza	64 patients (16-60 yr)	Lozenge: 175 mg extract; 4 lozenges/d; 2 d	Randomized, double-blind, placebo-controlled, pilot clinical trials	Significant improvement in most symptoms within 24 h (fever, headache, muscle aches and nasal congestion). Significant improvement in all investigated symptoms within 48 h (cough and mucus discharge)
Sambucus nigra extract [127]	Respiratory health	312 adults, 2 groups	Capsules: 300 mg. Before travel: 2 capsules/d. During travel and after arrival: 3 capsules/d. 14 d	Randomized, double-blind placebo-controlled clinical trial	Reduction of cold duration and severity in air travelers. Low symptom score

SD: Standard dose; HD: High dose.

the effect of eucalyptol (1.8 cineol), which is a component of eucalyptus essential oil, on Mpro. They showed that eucalyptol/Mpro complexes produce hydrophobic interactions, strong ionic interactions, hydrogen bond interactions, and eucalyptol may be a potential inhibitor of COVID-19 Mpro. Similarly, M pro/3CL pro/eucalyptol complexes have been shown to form hydrophobic interactions[39]. In another study, Sharma and Kaur[40] suggested jensenone, the component of eucalyptus essential oil, as a potential COVID-19 Mpro inhibitor. In a molecular docking study of 12 active ingredients of eucalyptus essential oil, all of these ingredients were found to bind effectively to the COVID-19 S-protein. Especially the toruatone component was effectively bound and the Spike (S) protein/Toruatone complexes formed hydrogen and hydrophobic interactions[41]. Muhammad *et al*[42], in a study of the molecular

Table 3 Plants that can have an impact on coronavirus disease 2019 symptoms

Plant name	Effects	Ref.
Allium sativum (Garlic)	Analgesic	Dehghani *et al*[128], 2018
	Anti-inflammatory	Arreola *et al*[129], 2015
	Anti-platelet	Hiyasat *et al*[130], 2009
	Heart protection	Sultana *et al*[131], 2016
	Hepatic protection	Aprioku *et al*[132], 2017
	Improving GI function	Chen *et al*[133], 2018
	Renal protection	Seckiner *et al*[134], 2014
Curcuma longa (Turmeric)	Analgesic	Henrotin *et al*[135], 2020
		Eke-Okoro *et al*[136], 2018
	Antiemetic	Liu *et al*[137], 2018
	Antifatigue	Huang *et al*[138], 2015
	Anti-inflammatory	Shimizu *et al*[139], 2019
	Antifibrotic	Gouda *et al*[140], 2019
	Antipyretic	Haider *et al*[141], 2013
	Bronchodilator	Ram *et al*[142], 2003
	GI protection	Haider *et al*[141], 2013
		Dulbecco and Savarino[143], 2013
	Hepatic protection	Dulbecco and Savarino[143], 2013
Glycyrrhiza glabra (Licorice)	Antitussives	Nosalova *et al*[144], 2013
		Kuang *et al*[145], 2018
	Anti-inflammatory	Kao *et al*[146], 2010
	Respiratory system protection	Shi *et al*[147], 2011
Nigella sativa (Black cumin)	Analgesic	Rushmi *et al*[148], 2017
	Anticoagulant	Muralidharan-Chari *et al*[149], 2016
	Antihistaminic	Ansari *et al*[150], 2010
		Alsamarai *et al*[151], 2014
	Anti-inflammatory	Majdalawieh and Fayyad[152], 2015
		Mahdavi *et al*[153], 2016
	Bronchodilation	Boskabady *et al*[154], 2010
		Salem *et al*[155], 2017
Panax ginseng (Ginseng)	Adaptogenic	Ratan *et al*[156], 2021
Pelargonium sidoides (Pelargonium)	Antitussives	Bao *et al*[157], 2015
	Secretolytic activity	Bao *et al*[157], 2015
Scutellaria baicalensis (Chinese skullcap)	Antiemetic	Aung *et al*[158], 2005
	Anti-inflammatory	Hong *et al*[159], 2013
	GI protection	Mehendale *et al*[160], 2007
		Cui *et al*[161], 2021
	Hepatic protection	Thanh *et al*[162], 2015
	Neuroprotective	Dai *et al*[163], 2013
	Regulation of histamine release-Anti allergic	Bui *et al*[164], 2017
Thymus vulgaris (Thyme)	Analgesic	Laub[165], 2018

		Salmalian *et al*[166], 2014
	Anticoagulant	Okazaki *et al*[167], 2002
	Anti-inflammatory	Habashy *et al*[168], 2018
Withania somnifera (Ashwagandha)	Adaptogenic	Salve *et al*[169], 2019
	Analgesic	Murthy *et al*[170], 2019
	Anticoagulant, antithrombotic	Ku *et al*[171], 2014
	Anti-inflammatory	Gupta and Singh[172], 2014
	Antitussives	Nosalova *et al*[144], 2013
	Stress-relieving	Lopresti *et al*[173], 2019
Zingiber officinale (Ginger)	Analgesic	Maghbooli *et al*[174], 2014
		Bartels *et al*[175], 2015
	Antiemetic	Tóth *et al*[176], 2018
	Anti-inflammatory	Khan *et al*[177], 2015
	Antiplatelet, antithrombotic	Lee *et al*[178], 2017
	Antitussives	Bera *et al*[179], 2016
	GI protection	Nanjundaiah *et al*[180], 2011
	Hepatic protection	Ajith *et al*[181], 2007
	Nephroprotective	Ajith *et al*[182], 2007

insertion of eucalyptus active ingredients into Mpro, showed that the α-gurjune of eucalyptus, aromadene and allo-aromadene components have strong binding energy.

Glycyrrhiza glabra

Sinha *et al*[43] conducted molecular docking simulation studies of two antiviral drugs (lopinavir and ribavirin) and 20 compounds of *Glycyrrhiza glabra*. Two protein targets from COVID-19 have been identified: Non-structural protein-15 endoribonuclease and spike glycoprotein. Glycyrrhizic acid prevented the virus from entering the host cell, due to its bulky structure. Gliasperin A showed high affinity to Nsp15 endoribonuclease and inhibited its activity. The authors suggested that glycyrrhizic acid disrupts the connection of the virus with the ACE2 receptor at the input level, and Gliasperin A inhibits the replication process of the virus after it enters the host cell. Another study showed that glycyrrhizin can be highly bound to Mpro[44].

Scutellaria baicalensis

Liu *et al*[45] investigated the *in vitro* effect of *Scutellaria baicalensis* and its components on COVID-19. Baicalein (its main ingredient) and the ethanol extract of the plant inhibited the 3CLpro activity and replication of COVID-19. The ethanol extract also inhibited viral entry. Udrea *et al*[46] suggested the benefit *Scutellaria baicalensis* flavones (especially baicalein) against respiratory damage caused by COVID-19. Flavones bound to 3CLpro. strongly bound to wogonin flavone, nitric oxide synthase and cyclooxygenase 2. In addition, norwogonin and baicalein arachidonate modulated 15-lipoxygenase and lysine-specific demethylase 4D analogue.

Thymus vulgaris

In a randomized clinical study conducted on patients suffering from COVID-19, it was found that *Thymus vulgaris* strengthens the immune system and can be used to reduce COVID-19 symptoms. In the study, 83 COVID-19 patients were randomly divided into the control group and the group receiving thyme (TRG). TRG was given as thyme essential oil three times a day for seven days. A questionnaire asking about symptoms such as fever, cough, fatigue, and loss of appetite was completed before and at the end of treatment to determine the effect of thyme on symptoms. Thyme essential oil significantly reduced the severity of symptoms such as fever, cough, shortness of breath, dizziness, muscle pain, anorexia, weakness and lethargy and fatigue. Additionally, thyme increased lymphocyte count and calcium while decreasing blood urea nitrogen and neutrophil count[47]. Carvacrol, a component of thyme, has been

Table 4 Angiotensin-converting enzyme inhibitor plant

Plants	The compound under study	Results	Ref.
Ammoides verticillata essential oil	Isothymol	SARS-CoV-2/ACE2 inhibition	Abdelli *et al*[183], 2021
Allium sativum essential oil	Organosulfur compounds (99.4% of its essential oil)	SARS-CoV-2/ACE2 inhibition. Garlic essential oil can prevent protein maturation of the virus and the spread of infection	Thuy *et al*[184], 2020
Apium graveolens	Apigenin	Kidneys of spontaneous hypertensive rats/Regulation in ACE2 expression	Sui *et al*[185], 2010
Camellia sinensis	Black tea; Dark tea; Green tea; Oolong tea; White tea	ACE inhibition: Green < oolong < white < black < dark teas	Dong *et al*[186], 2011
Citrus aurantium *Erigeron breviscapus* *Glycine max* *Glycyrrhiza radix* *Scutellaria baicalensis*	Hesperetin. Scutellarin. Nicotianamine. Glycyrrhizin. Baicalin	SARS-CoV-2/Connecting to ACE2 and blocking the SARS-CoV-2 input	Chen and Du[187], 2020
Geranium and lemon essential oils	Citronellol and limonene	SARS-CoV-2/ACE2 inhibition	Senthil Kumar *et al*[188], 2020
Ginseng *Glycyrrhiza uralensis*	Ginsenoside Rg6; Ginsenoside F1; Monoammonium glycyrrhizinate; Glycyrrhizic acid methyl ester	SARS-CoV-2/ACE2 kinase inhibition	Zi *et al*[189], 2020
Glycine max (soybean)	Nicotianamine	ACE2 inhibition	Takahashi *et al*[190], 2015
Glycyrrhiza glabra	Glycyrrhizic acid	SARS-CoV-2/Glycyrrhizic acid disrupts the connection of the virus with the ACE2 receptor at the entry level	Sinha *et al*[43], 2021
Hibiscus sabdariffa anthocyanins	Delphinidin- and cyanidin-3-O-sambubiosides	ACE inhibition	Ojeda *et al*[191], 2010
Linum usitatissimum (Flaxseed)	Secoisolariciresinol diglucoside	ACE inhibition	Prasad *et al*[192], 2013
Melaleuca cajuputi essential oil	Components (70.9% of the oil)	SARS-CoV-2/ACE2 and PDB6LU7 proteins inhibition	My *et al*[193], 2020
Nicotiana benthamiana	Recombinant ACE2-Fc fusion protein produced from *N. benthamiana*	SARS-CoV-2/Strong binding to the RBD of SARS-CoV-2 and inhibition	Siriwattananon *et al*[194], 2020
Withania somnifera	Withanone	SARS-CoV-2/Docking to the connector interface of the AEC2-RBD complex	Balkrishna *et al*[51], 2020

ACE: Angiotensin-converting enzyme; RBD: Receptor binding domain; SARS-CoV-2: Severe acute respiratory syndrome coronavirus 2; ACE2: Angiotensin-converting enzyme-2.

shown to inhibit Mpro by *in silico* study. It can be a potential inhibitor of controlling viral replication[48].

Withania somnifera

W. somnifera components withanolides have potential antiviral properties on COVID-19[49]. Patel *et al*[50] demonstrated that *W. somnifera*'s Withanoside VI components have positive interactions at the binding site of protein targets of SARS-CoV-2. Withanone reduced the electrostatic interaction between ACE2 and receptor binding domain[51]. Withaferin A, which is found in the *W. somnifera* plant, has been shown to interact with Mpro and Glucose regulated protein 78 (GRP78) receptor[52].

CONCLUSION

In this study, the concept of "being effective against COVID-19" for herbal treatments was discussed from the angles of antiviral effect and control of symptoms, specifically related to GI system.

Antiviral effects on COVID-19

Since COVID-19 is a virus that mainly affects the respiratory tract, the antiviral effects of medicinal plants against respiratory viruses have been examined firstly. The structure similarities of SARS-CoV-2 have been found with SARS-CoV and Middle East respiratory syndrome coronavirus. Therefore, it can be suggested that plants and their compounds affecting these viruses may also be potential treatment options for COVID-19. Here firstly, clinical studies supporting antiviral effects of 22 plant on respiratory viruses has been reviewed which determined that glycyrrhizic acid derivatives obtained from *Glycyrrhiza* sp, *Nigella sativa*, *Scutellaria baicalensis* and *Torreya nucifera* have anti-COVID-19 effects. Plants such as *Allium sativum*, *Glycyrrhiza glabra*, *Melaleuca* sp, *Withania somnifera* have been shown to bind to ACE2 receptors that are imperative for COVID-19 replication. Focusing on these plants might be a logical way to go for herbal treatment against COVID-19.

This review also showed the antiviral effects of essential oils obtained from plants have the potential to affect COVID-19. The treatment involves using inhaled steam supplemented by essential oils possessing natural antimicrobial properties, oropharyngeal sanitization, as well as they are remedies for symptomatic relief. Inhalation of antimicrobial essential oils may help attenuate the virus in the nasal cavity, nasopharynx, oropharynx, and laryngopharynx. Antiseptic mouthwashes and gargles can also help to sanitize the oral cavity and oropharynx, whereas antiseptic lozenges can help to sanitize the oro- and laryngopharynx as well. The steam will carry the tiny particles of the antimicrobial constituents from these essential oils into the respiratory tract and is likely to improve the efficacy of the steam treatment. The steam supplemented by antimicrobial volatile oils may help to provide a local antimicrobial effect within the airways.

There are computer model studies showing that some botanicals and active ingredients are effective in COVID-19. *Allium sativum*, *Curcuma longa*, *Eucalyptus globulus*, *Glycyrrhiza glabra*, *Melaleuca* sp, *Thymus vulgaris*, *Withania somnifera* is among these plants. These studies with commonly found plants will guide future studies to develop effective supplements or drugs for COVID-19.

Symptomatic treatment of COVID-19

Since the symptoms of COVID-19 seriously affect the quality of life, herbal options to eliminate them were also evaluated in this review. Previously, herbs such as garlic, echinacea and ginseng were found to reduce the symptoms of cold in healthy individuals. Plants with their pharmacological effects are natural options for eliminating the symptoms of COVID-19. Based on the effects described in Table 3, *Allium sativum*, *Curcuma longa*, *Scutellaria baicalensis* and *Zingiber officinale* are easily found as prominent plants to eliminate the GI symptoms of COVID-19. For example, ginger can eliminate the negative effects of COVID-19 on the GI system with its antiemetic and hepatic protective properties. A clinical study was conducted with thyme essential oil on COVID-19. Thyme essential oil was found to significantly reduce COVID-19 symptoms. This revealed an option that thyme and essential oil have potential effects for consideration in treatment of COVID-19. Studies on more essential oils of eucalyptus reveal more effects of eucalyptus on respiratory system symptoms. *Eucalyptus globulus*, *Hedera helix*, *Pelargonium sidoides*, *Sambucus nigra*, *Thymus vulgaris* can be recommended for relief of respiratory symptoms. ACE2 receptors are found in tissues other than the lung, such as the intestine. Based on this fact, we concluded that the use of herbs binding to ACE2 receptors can eliminate the side effects that may occur in variety of organs including GI tract. As shown in Table 4 these plants are *Ammoides verticillate*, *Allium sativum*, *Apium graveolens*, *Camellia sinensis*, *Citrus aurantium*, *Erigeron breviscapus*, *Glycine max*, *Glycyrrhiza glabra*, *Hibiscus sabdariffa*, *Linum usitatissimum*, *Melaleuca* sp., *Nicotiana benthamiana*, *Withania somnifera*.

Based on these studies, herbal treatments offer several potential treatments of COVID-19. Plants may be an option for the treatment of COVID-19 and its symptoms, as well as protection from COVID-19. Even though these data point to good outcomes there is always the possibility of interaction between drugs used and these herbs. For instance, herbs such as ginger with antithrombotic effects can be beneficial on COVID-19 symptoms, but one might be cautious about escalated risk of bleeding when it is used together with antithrombotic or anticoagulant drugs. Therefore, it is extremely important to avoid the indiscriminate use of plants.

For a plant to be used as a medicine, its effect must be supported by clinical studies. COVID-19 is just emerging, and more research are needed for its treatment. Yet, herbal therapies are potential options for both antiviral effects and the control of COVID-19 symptoms. Since plants with multiple pharmacological effects can affect many systems

(respiratory, GI, and nervous), herbs might be more effective against COVID-19 than synthetic drugs. But first, all aspects of SARS-CoV-2 need to be examined. Then, the effects of plants on this virus should be determined by further studies.

The strengths and weaknesses of this review

Unlike other studies, in this report, the effect of plants on COVID-19 was evaluated in several ways. Preclinical studies, clinical studies and silico studies are included in this review. Moreover, the efficacy on COVID-19 symptoms has been addressed by including different systems. On the other hand, the focus is on the respiratory and GI systems. The effects, not only of botanicals but also active metabolites of have been studied.

The biggest limitation of this study is the lack of sufficient studies on the efficacy of botanicals. Since botanical studies are generally preclinical studies, results may vary due to conducting and including clinical studies. In clinical studies showing the effects of the plants in Table 2 on respiratory tract infections, the results were generally obtained with questionnaire studies. Placebo effects and breadth of study may be effective in positive results.

REFERENCES

1 **Sun J**, He WT, Wang L, Lai A, Ji X, Zhai X, Li G, Suchard MA, Tian J, Zhou J, Veit M, Su S. COVID-19: Epidemiology, Evolution, and Cross-Disciplinary Perspectives. *Trends Mol Med* 2020; **26**: 483-495 [PMID: 32359479 DOI: 10.1016/j.molmed.2020.02.008]

2 **Zhang H**, Penninger JM, Li Y, Zhong N, Slutsky AS. Angiotensin-converting enzyme 2 (ACE2) as a SARS-CoV-2 receptor: Molecular mechanisms and potential therapeutic target. *Intensive Care Med* 2020; **46**: 586-590 [PMID: 32125455 DOI: 10.1007/s00134-020-05985-9]

3 **Hoffmann M**, Kleine-Weber H, Schroeder S, Krüger N, Herrler T, Erichsen S, Schiergens TS, Herrler G, Wu NH, Nitsche A, Müller MA, Drosten C, Pöhlmann S. SARS-CoV-2 Cell Entry Depends on ACE2 and TMPRSS2 and Is Blocked by a Clinically Proven Protease Inhibitor. *Cell* 2020; **181**: 271-280.e8 [PMID: 32142651 DOI: 10.1016/j.cell.2020.02.052]

4 **Hashimoto T**, Perlot T, Rehman A, Trichereau J, Ishiguro H, Paolino M, Sigl V, Hanada T, Hanada R, Lipinski S, Wild B, Camargo SM, Singer D, Richter A, Kuba K, Fukamizu A, Schreiber S, Clevers H, Verrey F, Rosenstiel P, Penninger JM. ACE2 links amino acid malnutrition to microbial ecology and intestinal inflammation. *Nature* 2012; **487**: 477-481 [PMID: 22837003 DOI: 10.1038/nature11228]

5 **Felsenstein S**, Herbert JA, McNamara PS, Hedrich CM. COVID-19: Immunology and treatment options. *Clin Immunol* 2020; **215**: 108448 [PMID: 32353634 DOI: 10.1016/j.clim.2020.108448]

6 **Singh R**, Shaik L, Mehra I, Kashyap R, Surani S. Novel and Controversial Therapies in COVID-19. *Open Respir Med J* 2020; **14**: 79-86 [PMID: 33717367 DOI: 10.2174/1874306402014010079]

7 **Silveira D**, Prieto-Garcia JM, Boylan F, Estrada O, Fonseca-Bazzo YM, Jamal CM, Magalhães PO, Pereira EO, Tomczyk M, Heinrich M. COVID-19: Is There Evidence for the Use of Herbal Medicines as Adjuvant Symptomatic Therapy? *Front Pharmacol* 2020; **11**: 581840 [PMID: 33071794 DOI: 10.3389/fphar.2020.581840]

8 **Panyod S**, Ho CT, Sheen LY. Dietary therapy and herbal medicine for COVID-19 prevention: A review and perspective. *J Tradit Complement Med* 2020; **10**: 420-427 [PMID: 32691006 DOI: 10.1016/j.jtcme.2020.05.004]

9 **DU HZ**, Hou XY, Miao YH, Huang BS, Liu DH. Traditional Chinese Medicine: an effective treatment for 2019 novel coronavirus pneumonia (NCP). *Chin J Nat Med* 2020; **18**: 206-210 [PMID: 32245590 DOI: 10.1016/S1875-5364(20)30022-4]

10 **Xu K**, Cai H, Shen Y, Ni Q, Chen Y, Hu S, Li J, Wang H, Yu L, Huang H, Qiu Y, Wei G, Fang Q, Zhou J, Sheng J, Liang T, Li L. [Management of corona virus disease-19 (COVID-19): the Zhejiang experience]. *Zhejiang Da Xue Xue Bao Yi Xue Ban* 2020; **49**: 147-157 [PMID: 32096367 DOI: 10.3785/j.issn.1008-9292.2020.02.02]

11 **Jin YH**, Cai L, Cheng ZS, Cheng H, Deng T, Fan YP, Fang C, Huang D, Huang LQ, Huang Q, Han Y, Hu B, Hu F, Li BH, Li YR, Liang K, Lin LK, Luo LS, Ma J, Ma LL, Peng ZY, Pan YB, Pan ZY, Ren XQ, Sun HM, Wang Y, Wang YY, Weng H, Wei CJ, Wu DF, Xia J, Xiong Y, Xu HB, Yao XM, Yuan YF, Ye TS, Zhang XC, Zhang YW, Zhang YG, Zhang HM, Zhao Y, Zhao MJ, Zi H, Zeng XT, Wang XH; , for the Zhongnan Hospital of Wuhan University Novel Coronavirus Management and Research Team, Evidence-Based Medicine Chapter of China International Exchange and Promotive Association for Medical and Health Care (CPAM). A rapid advice guideline for the diagnosis and treatment of 2019 novel coronavirus (2019-nCoV) infected pneumonia (standard version). *Mil Med Res* 2020; **7**: 4 [PMID: 32029004 DOI: 10.1186/s40779-020-0233-6]

12 **Naithani R**, Mehta RG, Shukla D, Chandersekera SN, Moriarty RM. Antiviral activity of phytochemicals: A current perspective. In Dietary Components and Immune Function. Totowa, NJ, Humana Press, 2010: 421-468

13 **Vespa E**, Pugliese N, Colapietro F, Aghemo A. Stay (GI) Healthy: COVID-19 and Gastrointestinal Manifestations. *Tech Innov Gastrointest Endosc* 2021; **23**: 179-189 [PMID: 33521703 DOI: 10.1016/j.tige.2021.01.006]

14 **Adedeji AO**, Severson W, Jonsson C, Singh K, Weiss SR, Sarafianos SG. Novel inhibitors of severe acute respiratory syndrome coronavirus entry that act by three distinct mechanisms. *J Virol* 2013; **87**: 8017-8028 [PMID: 23678171 DOI: 10.1128/JVI.00998-13]

15 **Guan WJ**, Ni ZY, Hu Y, Liang WH, Ou CQ, He JX, Liu L, Shan H, Lei CL, Hui DSC, Du B, Li LJ, Zeng G, Yuen KY, Chen RC, Tang CL, Wang T, Chen PY, Xiang J, Li SY, Wang JL, Liang ZJ, Peng YX, Wei L, Liu Y, Hu YH, Peng P, Wang JM, Liu JY, Chen Z, Li G, Zheng ZJ, Qiu SQ, Luo J, Ye CJ, Zhu SY, Zhong NS; China Medical Treatment Expert Group for Covid-19. Clinical Characteristics of Coronavirus Disease 2019 in China. *N Engl J Med* 2020; **382**: 1708-1720 [PMID: 32109013 DOI: 10.1056/NEJMoa2002032]

16 **Yang X**, Yu Y, Xu J, Shu H, Xia J, Liu H, Wu Y, Zhang L, Yu Z, Fang M, Yu T, Wang Y, Pan S, Zou X, Yuan S, Shang Y. Clinical course and outcomes of critically ill patients with SARS-CoV-2 pneumonia in Wuhan, China: a single-centered, retrospective, observational study. *Lancet Respir Med* 2020; **8**: 475-481 [PMID: 32105632 DOI: 10.1016/S2213-2600(20)30079-5]

17 **Zhang JJ**, Dong X, Cao YY, Yuan YD, Yang YB, Yan YQ, Akdis CA, Gao YD. Clinical characteristics of 140 patients infected with SARS-CoV-2 in Wuhan, China. *Allergy* 2020; **75**: 1730-1741 [PMID: 32077115 DOI: 10.1111/all.14238]

18 **Fang L**, Karakiulakis G, Roth M. Are patients with hypertension and diabetes mellitus at increased risk for COVID-19 infection? *Lancet Respir Med* 2020; **8**: e21 [PMID: 32171062 DOI: 10.1016/S2213-2600(20)30116-8]

19 **Benarba B**, Pandiella A. Medicinal Plants as Sources of Active Molecules Against COVID-19. *Front Pharmacol* 2020; **11**: 1189 [PMID: 32848790 DOI: 10.3389/fphar.2020.01189]

20 **Mahony JB**, Petrich A, Smieja M. Molecular diagnosis of respiratory virus infections. *Crit Rev Clin Lab Sci* 2011; **48**: 217-249 [PMID: 22185616 DOI: 10.3109/10408363.2011.640976]

21 **Talbot HK**, Falsey AR. The diagnosis of viral respiratory disease in older adults. *Clin Infect Dis* 2010; **50**: 747-751 [PMID: 20121411 DOI: 10.1086/650486]

22 **Englund J**, Feuchtinger T, Ljungman P. Viral infections in immunocompromised patients. *Biol Blood Marrow Transplant* 2011; **17**: S2-S5 [PMID: 21195305 DOI: 10.1016/j.bbmt.2010.11.008]

23 **Chen N**, Zhou M, Dong X, Qu J, Gong F, Han Y, Qiu Y, Wang J, Liu Y, Wei Y, Xia J, Yu T, Zhang X, Zhang L. Epidemiological and clinical characteristics of 99 cases of 2019 novel coronavirus pneumonia in Wuhan, China: a descriptive study. *Lancet* 2020; **395**: 507-513 [PMID: 32007143 DOI: 10.1016/S0140-6736(20)30211-7]

24 **Xia W**, Shao J, Guo Y, Peng X, Li Z, Hu D. Clinical and CT features in pediatric patients with COVID-19 infection: Different points from adults. *Pediatr Pulmonol* 2020; **55**: 1169-1174 [PMID: 32134205 DOI: 10.1002/ppul.24718]

25 **Geier MR**, Geier DA. Respiratory conditions in coronavirus disease 2019 (COVID-19): Important considerations regarding novel treatment strategies to reduce mortality. *Med Hypotheses* 2020; **140**: 109760 [PMID: 32344310 DOI: 10.1016/j.mehy.2020.109760]

26 **Ang L**, Song E, Lee HW, Lee MS. Herbal Medicine for the Treatment of Coronavirus Disease 2019 (COVID-19): A Systematic Review and Meta-Analysis of Randomized Controlled Trials. *J Clin Med* 2020; **9** [PMID: 32456123 DOI: 10.3390/jcm9051583]

27 **Fan AY**, Gu S, Alemi SF; Research Group for Evidence-based Chinese Medicine. Chinese herbal medicine for COVID-19: Current evidence with systematic review and meta-analysis. *J Integr Med* 2020; **18**: 385-394 [PMID: 32792254 DOI: 10.1016/j.joim.2020.07.008]

28 **Chen Y**, de Bruyn Kops C, Kirchmair J. Data Resources for the Computer-Guided Discovery of Bioactive Natural Products. *J Chem Inf Model* 2017; **57**: 2099-2111 [PMID: 28853576 DOI: 10.1021/acs.jcim.7b00341]

29 **Yang YJ**, Bang CS. Application of artificial intelligence in gastroenterology. *World J Gastroenterol* 2019; **25**: 1666-1683 [PMID: 31011253 DOI: 10.3748/wjg.v25.i14.1666]

30 **Khaerunnisa S**, Kurniawan H, Awaluddin R, Suhartati S, Soetjipto S. Potential inhibitor of COVID-19 main protease (Mpro) from several medicinal plant compounds by molecular docking study. 2020 Preprint. Available from: 20944 [DOI: 10.20944/preprints202003.0226.v1]

31 **Aanouz I**, Belhassan A, El-Khatabi K, Lakhlifi T, El-Ldrissi M, Bouachrine M. Moroccan Medicinal plants as inhibitors against SARS-CoV-2 main protease: Computational investigations. *J Biomol Struct Dyn* 2021; **39**: 2971-2979 [PMID: 32306860 DOI: 10.1080/07391102.2020.1758790]

32 **Silva JKRD**, Figueiredo PLB, Byler KG, Setzer WN. Essential Oils as Antiviral Agents. Potential of Essential Oils to Treat SARS-CoV-2 Infection: An *In-Silico* Investigation. *Int J Mol Sci* 2020; **21** [PMID: 32408699 DOI: 10.3390/ijms21103426]

33 **Utomo RY**, Meiyanto E. Revealing the potency of citrus and galangal constituents to halt SARS-CoV-2 infection. 2020 Preprint. Available from: 2020030214 [DOI: 10.20944/preprints202003.0214.v1]

34 **Rajagopal K**, Varakumar P, Baliwada A, Byran G. Activity of phytochemical constituents of *Curcuma longa* (turmeric) and *Andrographis paniculata* against coronavirus (COVID-19): an in silico approach. *Futur J Pharm Sci* 2020; **6**: 104 [PMID: 33215042 DOI: 10.1186/s43094-020-00126-x]

35 **Adem S**, Eyupoglu V, Sarfraz I, Rasul A, Ali M. Identification of potent COVID-19 main protease (Mpro) inhibitors from natural polyphenols: An in silico strategy unveils a hope against corona. 2020

Preprint. Available from: 2020030333 [DOI: 10.20944/preprints202003.0333.v1]
36 **Srivastava A**, Singh D. Destabilizing the structural integrity of SARS-CoV2 receptor proteins by curcumin along with hydroxychloroquine: An in silico approach for a combination therapy. 2020 Preprint. Available from: chemrxiv:12090438 [DOI: 10.26434/chemrxiv.12090438]
37 **Gonzalez-Paz LA**, Lossada CA, Moncayo LS, Romero F, Paz JL, Vera-Villalobos J, Pérez AE, San-Blas E, Alvarado YJ. Theoretical molecular docking study of the structural disruption of the viral 3CL-protease of COVID19 induced by binding of capsaicin, piperine and curcumin part 1: A comparative study with chloroquine and hydrochloroquine two antimalaric drugs. 2020 Preprint. Available from: rs-21206 [DOI: 10.21203/rs.3.rs-21206/v1]
38 **Sharma AD**. Eucalyptol (1, 8 cineole) from eucalyptus essential oil a potential inhibitor of COVID 19 corona virus infection by molecular docking studies. 2020 Preprint. Available from: 2020030455
39 **Sharma AD**, Inderjeet KAUR. Molecular docking and pharmacokinetic screening of eucalyptol (1, 8 cineole) from eucalyptus essential oil against SARS-CoV-2. *Not Sci Biol* 2020; **12**: 536-545 [DOI: 10.15835/nsb12210711]
40 **Sharma AD**, Kaur I. Molecular docking studies on jensenone from eucalyptus essential oil as a potential inhibitor of COVID 19 corona virus infection. 2020 Preprint. Available from: arXiv:2004.00217
41 **Sharma AD**, Kaur I. Eucalyptus essential oil bioactive molecules from against SARS-CoV-2 spike protein: Insights from computational studies. 2021 Preprint. Available from: rs-140069 [DOI: 10.21203/rs.3.rs-140069/v1]
42 **Muhammad IA**, Muangchoo K, Muhammad A, Ajingi YUS, Muhammad IY, Umar ID, Muhammad AB. A computational study to ıdentify potential inhibitors of SARS-CoV-2 main protease (Mpro) from Eucalyptus active compounds. *Computation* 2020; **8**: 79 [DOI: 10.3390/computation8030079]
43 **Sinha SK**, Prasad SK, Islam MA, Gurav SS, Patil RB, AlFaris NA, Aldayel TS, AlKehayez NM, Wabaidur SM, Shakya A. Identification of bioactive compounds from *Glycyrrhiza glabra* as possible inhibitor of SARS-CoV-2 spike glycoprotein and non-structural protein-15: a pharmacoinformatics study. *J Biomol Struct Dyn* 2021; **39**: 4686-4700 [PMID: 32552462 DOI: 10.1080/07391102.2020.1779132]
44 **Narkhede RR**, Pise AV, Cheke RS, Shinde SD. Recognition of Natural Products as Potential Inhibitors of COVID-19 Main Protease (Mpro): In-Silico Evidences. *Nat Prod Bioprospect* 2020; **10**: 297-306 [PMID: 32557405 DOI: 10.1007/s13659-020-00253-1]
45 **Liu H**, Ye F, Sun Q, Liang H, Li C, Li S, Lu R, Huang B, Tan W, Lai L. *Scutellaria baicalensis* extract and baicalein inhibit replication of SARS-CoV-2 and its 3C-like protease *in vitro*. *J Enzyme Inhib Med Chem* 2021; **36**: 497-503 [PMID: 33491508 DOI: 10.1080/14756366.2021.1873977]
46 **Udrea AM**, Mernea M, Buiu C, Avram S. *Scutellaria baicalensis* flavones as potent drugs against acute respiratory injury during SARS-CoV-2 infection: Structural biology approaches. *Processes* 2020; **8**: 1468 [DOI: 10.3390/pr8111468]
47 **Sardari S**, Mobaiend A, Ghassemifard L, Kamali K, Khavasi N. Therapeutic effect of thyme (*Thymus vulgaris*) essential oil on patients with COVID19: A randomized clinical trial. *J Adv Med* 2021; **29**: 83-91 [DOI: 10.30699/jambs.29.133.83]
48 **Kumar A**, Choudhir G, Shukla SK, Sharma M, Tyagi P, Bhushan A, Rathore M. Identification of phytochemical inhibitors against main protease of COVID-19 using molecular modeling approaches. *J Biomol Struct Dyn* 2021; **39**: 3760-3770 [PMID: 32448034 DOI: 10.1080/07391102.2020.1772112]
49 **Dhawan M**, Parmar M, Sharun K, Tiwari R, Bilal M, Dhama K. Medicinal and therapeutic potential of withanolides from *Withania somnifera* against COVID-19. *J Appl Pharm Sci* 2021; **11**: 6-13 [DOI: 10.7324/JAPS.2021.110402]
50 **Patel CN**, Goswami D, Jaiswal DG, Parmar RM, Solanki HA, Pandya HA. Pinpointing the potential hits for hindering interaction of SARS-CoV-2 S-protein with ACE2 from the pool of antiviral phytochemicals utilizing molecular docking and molecular dynamics (MD) simulations. *J Mol Graph Model* 2021; **105**: 107874 [PMID: 33647752 DOI: 10.1016/j.jmgm.2021.107874]
51 **Balkrishna A**, Pokhrel S, Singh J, Varshney A. Withanone from Withania somnifera may inhibit novel coronavirus (COVID-19) entry by disrupting interactions between viral S-protein receptor binding domain and host ACE2 receptor. 2020 Preprint. Available from: rs-17806 [DOI: 10.21203/rs.3.rs-17806/v1]
52 **Sudeep HV**, Gouthamchandra K, Shyamprasad K. Molecular docking analysis of Withaferin A from *Withania somnifera* with the Glucose regulated protein 78 (GRP78) receptor and the SARS-CoV-2 main protease. *Bioinformation* 2020; **16**: 411-417 [PMID: 32831523 DOI: 10.6026/97320630016411]
53 **Rasool A**, Khan MU, Ali MA, Anjum AA, Ahmed I, Aslam A, Mustafa G, Masood S, Nawaz M. Anti-avian influenza virus H9N2 activity of aqueous extracts of *Zingiber officinalis* (Ginger) and *Allium sativum* (Garlic) in chick embryos. *Pak J Pharm Sci* 2017; **30**: 1341-1344 [PMID: 29039335]
54 **Mohajer Shojai T**, Ghalyanchi Langeroudi A, Karimi V, Barin A, Sadri N. The effect of *Allium sativum* (Garlic) extract on infectious bronchitis virus in specific pathogen free embryonic egg. *Avicenna J Phytomed* 2016; **6**: 458-267 [PMID: 27516987]
55 **Chavan RD**, Shinde P, Girkar K, Madage R, Chowdhary A. Assessment of Anti-Influenza Activity and Hemagglutination Inhibition of *Plumbago indica* and *Allium sativum* Extracts. *Pharmacognosy Res* 2016; **8**: 105-111 [PMID: 27034600 DOI: 10.4103/0974-8490.172562]

56 **Choi HJ**. Chemical Constituents of Essential Oils Possessing Anti-Influenza A/WS/33 Virus Activity. *Osong Public Health Res Perspect* 2018; **9**: 348-353 [PMID: 30584499 DOI: 10.24171/j.phrp.2018.9.6.09]

57 **Mehrbod P**, Aini I, Amini E, Eslami M, Torabi A, Bande F, Kheiri MT. Assessment of direct immunofluorescence assay in detection of antiviral effect of garlic extract on influenza virus. *Afr J Microbiol Res* 2013; **7**: 2608-2612 [DOI: 10.5897/ajmr12.2329]

58 **Chen CH**, Chou TW, Cheng LH, Ho CW. *In vitro* anti-adenoviral activity of five *Allium* plants. *Taiwan Huaxuegongchengshi Xuehui Xuebao* 2011; **42**: 228-232 [DOI: 10.1016/j.jtice.2010.07.011]

59 **Borges-Argáez R**, Chan-Balan R, Cetina-Montejo L, Ayora-Talavera G, Sansores-Peraza P, Gómez-Carballo J, Cáceres-Farfán M. *In vitro* evaluation of anthraquinones from *Aloe vera* (*Aloe barbadensis* Miller) roots and several derivatives against strains of influenza virus. *Ind Crops Prod* 2019; **132**: 468-475 [PMID: 32288269 DOI: 10.1016/j.indcrop.2019.02.056]

60 **Li SW**, Yang TC, Lai CC, Huang SH, Liao JM, Wan L, Lin YJ, Lin CW. Antiviral activity of aloe-emodin against influenza A virus *via* galectin-3 up-regulation. *Eur J Pharmacol* 2014; **738**: 125-132 [PMID: 24877694 DOI: 10.1016/j.ejphar.2014.05.028]

61 **Zhang P**, Liu X, Liu H, Wang W, Li X, Wu X. *Astragalus* polysaccharides inhibit avian infectious bronchitis virus infection by regulating viral replication. *Microb Pathog* 2018; **114**: 124-128 [PMID: 29170045 DOI: 10.1016/j.micpath.2017.11.026]

62 **Kallon S**, Li X, Ji J, Chen C, Xi Q, Chang S, Xue C, Ma J, Xie Q, Zhang Y. *Astragalus* polysaccharide enhances immunity and inhibits H9N2 avian influenza virus *in vitro* and *in vivo*. *J Anim Sci Biotechnol* 2013; **4**: 22 [PMID: 23786718 DOI: 10.1186/2049-1891-4-22]

63 **Weber JM**, Ruzindana-Umunyana A, Imbeault L, Sircar S. Inhibition of adenovirus infection and adenain by green tea catechins. *Antiviral Res* 2003; **58**: 167-173 [PMID: 12742577 DOI: 10.1016/s0166-3542(02)00212-7]

64 **Kuzuhara T**, Iwai Y, Takahashi H, Hatakeyama D, Echigo N. Green tea catechins inhibit the endonuclease activity of influenza A virus RNA polymerase. *PLoS Curr* 2009; **1**: RRN1052 [PMID: 20025206 DOI: 10.1371/currents.rrn1052]

65 **Liu J**, Yang Z, Wang S, Liu L, Chen G, Wang L. Exploring the molecular basis of H5N1 hemagglutinin binding with catechins in green tea: A flexible docking and molecular dynamics study. *J Theor Comput Chem* 2012; **11**: 111-125 [DOI: 10.1142/s0219633612500071]

66 **Yang ZF**, Bai LP, Huang WB, Li XZ, Zhao SS, Zhong NS, Jiang ZH. Comparison of in vitro antiviral activity of tea polyphenols against influenza A and B viruses and structure-activity relationship analysis. *Fitoterapia* 2014; **93**: 47-53 [PMID: 24370660 DOI: 10.1016/j.fitote.2013.12.011]

67 **Chen TY**, Chen DY, Wen HW, Ou JL, Chiou SS, Chen JM, Wong ML, Hsu WL. Inhibition of enveloped viruses infectivity by curcumin. *PLoS One* 2013; **8**: e62482 [PMID: 23658730 DOI: 10.1371/journal.pone.0062482]

68 **Dai J**, Gu L, Su Y, Wang Q, Zhao Y, Chen X, Deng H, Li W, Wang G, Li K. Inhibition of curcumin on influenza A virus infection and influenzal pneumonia *via* oxidative stress, TLR2/4, p38/JNK MAPK and NF-κB pathways. *Int Immunopharmacol* 2018; **54**: 177-187 [PMID: 29153953 DOI: 10.1016/j.intimp.2017.11.009]

69 **Chen DY**, Shien JH, Tiley L, Chiou SS, Wang SY, Chang TJ, Lee YJ, Chan KW, Hsu WL. Curcumin inhibits influenza virus infection and haemagglutination activity. *Food Chem* 2010; **119**: 1346-1351 [DOI: 10.1016/j.foodchem.2009.09.011]

70 **Obata K**, Kojima T, Masaki T, Okabayashi T, Yokota S, Hirakawa S, Nomura K, Takasawa A, Murata M, Tanaka S, Fuchimoto J, Fujii N, Tsutsumi H, Himi T, Sawada N. Curcumin prevents replication of respiratory syncytial virus and the epithelial responses to it in human nasal epithelial cells. *PLoS One* 2013; **8**: e70225 [PMID: 24058438 DOI: 10.1371/journal.pone.0070225]

71 **Vimalanathan S**, Schoop R, Hudson J. High-potency anti-influenza therapy by a combination of *Echinacea purpurea* fresh herb and root tinctures. *J App Pharmac Sci* 2013; **3**: 001-005 [DOI: 10.1055/s-0033-1352301]

72 **Pleschka S**, Stein M, Schoop R, Hudson JB. Anti-viral properties and mode of action of standardized *Echinacea purpurea* extract against highly pathogenic avian influenza virus (H5N1, H7N7) and swine-origin H1N1 (S-OIV). *Virol J* 2009; **6**: 197 [PMID: 19912623 DOI: 10.1186/1743-422X-6-197]

73 **Hudson J**, Vimalanathan S. Echinacea—A source of potent antivirals for respiratory virus infections. *Pharmaceuticals* 2011; **4**: 1019-1031 [DOI: 10.3390/ph4071019]

74 **Vimalanathan S**, Hudson J. Anti-influenza virus activity of essential oils and vapors. *Am J Essent Oil* 2014; **2**: 47-53 [DOI: 10.7324/japs.2012.2734]

75 **Haruyama T**, Nagata K. Anti-influenza virus activity of *Ginkgo biloba* leaf extracts. *J Nat Med* 2013; **67**: 636-642 [PMID: 23179317 DOI: 10.1007/s11418-012-0725-0]

76 **Feng Yeh C**, Wang KC, Chiang LC, Shieh DE, Yen MH, San Chang J. Water extract of licorice had anti-viral activity against human respiratory syncytial virus in human respiratory tract cell lines. *J Ethnopharmacol* 2013; **148**: 466-473 [PMID: 23643542 DOI: 10.1016/j.jep.2013.04.040]

77 **Hoever G**, Baltina L, Michaelis M, Kondratenko R, Tolstikov GA, Doerr HW, Cinatl J Jr. Antiviral activity of glycyrrhizic acid derivatives against SARS-coronavirus. *J Med Chem* 2005; **48**: 1256-1259 [PMID: 15715493 DOI: 10.1021/jm0493008]

78 **Dao TT**, Nguyen PH, Lee HS, Kim E, Park J, Lim SI, Oh WK. Chalcones as novel influenza A (H1N1) neuraminidase inhibitors from *Glycyrrhiza inflata*. *Bioorg Med Chem Lett* 2011; **21**: 294-

298 [PMID: 21123068 DOI: 10.1016/j.bmcl.2010.11.016]
79 **Wolkerstorfer A**, Kurz H, Bachhofner N, Szolar OH. Glycyrrhizin inhibits influenza A virus uptake into the cell. *Antiviral Res* 2009; **83**: 171-178 [PMID: 19416738 DOI: 10.1016/j.antiviral.2009.04.012]
80 **Michaelis M**, Geiler J, Naczk P, Sithisarn P, Ogbomo H, Altenbrandt B, Leutz A, Doerr HW, Cinatl J Jr. Glycyrrhizin inhibits highly pathogenic H5N1 influenza A virus-induced pro-inflammatory cytokine and chemokine expression in human macrophages. *Med Microbiol Immunol* 2010; **199**: 291-297 [PMID: 20386921 DOI: 10.1007/s00430-010-0155-0]
81 **Del Valle Mendoza J**, Pumarola T, Gonzales LA, Del Valle LJ. Antiviral activity of maca (*Lepidium meyenii*) against human influenza virus. *Asian Pac J Trop Med* 2014; **7S1**: S415-S420 [PMID: 25312160 DOI: 10.1016/S1995-7645(14)60268-6]
82 **Garozzo A**, Timpanaro R, Stivala A, Bisignano G, Castro A. Activity of *Melaleuca alternifolia* (tea tree) oil on Influenza virus A/PR/8: Study on the mechanism of action. *Antiviral Res* 2011; **89**: 83-88 [PMID: 21095205 DOI: 10.1016/j.antiviral.2010.11.010]
83 **Usachev EV**, Pyankov OV, Usacheva OV, Agranovski IE. Antiviral activity of tea tree and eucalyptus oil aerosol and vapour. *J Aerosol Sci* 2013; **59**: 22-30 [DOI: 10.1016/j.jaerosci.2013.01.004]
84 **Pyankov OV**, Usachev EV, Pyankova O, Agranovski IE. Inactivation of airborne influenza virus by tea tree and eucalyptus oils. *Aerosol Sci Technol* 2012; **46**: 1295-1302 [DOI: 10.1080/02786826.2012.708948]
85 **Pourghanbari G**, Nili H, Moattari A, Mohammadi A, Iraji A. Antiviral activity of the oseltamivir and *Melissa officinalis* L. essential oil against avian influenza A virus (H9N2). *Virusdisease* 2016; **27**: 170-178 [PMID: 27366768 DOI: 10.1007/s13337-016-0321-0]
86 **Lelešius R**, Karpovaitė A, Mickienė R, Drevinskas T, Tiso N, Ragažinskienė O, Kubilienė L, Maruška A, Šalomskas A. *In vitro* antiviral activity of fifteen plant extracts against avian infectious bronchitis virus. *BMC Vet Res* 2019; **15**: 178 [PMID: 31142304 DOI: 10.1186/s12917-019-1925-6]
87 **Li Y**, Liu Y, Ma A, Bao Y, Wang M, Sun Z. *In vitro* antiviral, anti-inflammatory, and antioxidant activities of the ethanol extract of *Mentha piperita* L. *Food Sci Biotechnol* 2017; **26**: 1675-1683 [PMID: 30263705 DOI: 10.1007/s10068-017-0217-9]
88 **Dorra N**, El-Berrawy M, Sallam S, Mahmoud R. Evaluation of antiviral and antioxidant activity of selected herbal extracts. *Public Health* 2019; **49**: 36-40 [DOI: 10.21608/jhiph.2019.29464]
89 **Umar S**, Munir MT, Subhan S, Azam T, Nisa Q, Khan MI, Umar W, Rehman Z, Saqib AS, Shah MA. Protective and antiviral activities of *Nigella sativa* against avian influenza (H9N2) in Turkeys. *J Saudi Soc Agric Sci* 2016; **10** [DOI: 10.1016/j.jssas.2016.09.004]
90 **Ulasli M**, Gurses SA, Bayraktar R, Yumrutas O, Oztuzcu S, Igci M, Igci YZ, Cakmak EA, Arslan A. The effects of *Nigella sativa* (Ns), *Anthemis hyalina* (Ah) and *Citrus sinensis* (Cs) extracts on the replication of coronavirus and the expression of TRP genes family. *Mol Biol Rep* 2014; **41**: 1703-1711 [PMID: 24413991 DOI: 10.1007/s11033-014-3019-7]
91 **Lee JS**, Ko EJ, Hwang HS, Lee YN, Kwon YM, Kim MC, Kang SM. Antiviral activity of ginseng extract against respiratory syncytial virus infection. *Int J Mol Med* 2014; **34**: 183-190 [PMID: 24756136 DOI: 10.3892/ijmm.2014.1750]
92 **Lee JS**, Cho MK, Hwang HS, Ko EJ, Lee YN, Kwon YM, Kim MC, Kim KH, Lee YT, Jung YJ, Kang SM. Ginseng diminishes lung disease in mice immunized with formalin-inactivated respiratory syncytial virus after challenge by modulating host immune responses. *J Interferon Cytokine Res* 2014; **34**: 902-914 [PMID: 25051168 DOI: 10.1089/jir.2013.0093]
93 **Yin SY**, Kim HJ. A comparative study of the effects of whole red ginseng extract and polysaccharide and saponin fractions on influenza A (H1N1) virus infection. *Biol Pharm Bull* 2013; **36**: 1002-1007 [PMID: 23727921 DOI: 10.1248/bpb.b13-00123]
94 **Yoo DG**, Kim MC, Park MK, Song JM, Quan FS, Park KM, Cho YK, Kang SM. Protective effect of Korean red ginseng extract on the infections by H1N1 and H3N2 influenza viruses in mice. *J Med Food* 2012; **15**: 855-862 [PMID: 22856395 DOI: 10.1089/jmf.2012.0017]
95 **Roth M**, Fang L, Stolz D, Tamm M. *Pelargonium sidoides* radix extract EPs 7630 reduces rhinovirus infection through modulation of viral binding proteins on human bronchial epithelial cells. *PLoS One* 2019; **14**: e0210702 [PMID: 30707726 DOI: 10.1371/journal.pone.0210702]
96 **Michaelis M**, Doerr HW, Cinatl J Jr. Investigation of the influence of EPs® 7630, a herbal drug preparation from *Pelargonium sidoides*, on replication of a broad panel of respiratory viruses. *Phytomedicine* 2011; **18**: 384-386 [PMID: 21036571 DOI: 10.1016/j.phymed.2010.09.008]
97 **Theisen LL**, Muller CP. EPs® 7630 (Umckaloabo®), an extract from *Pelargonium sidoides* roots, exerts anti-influenza virus activity *in vitro* and *in vivo*. *Antiviral Res* 2012; **94**: 147-156 [PMID: 22475498 DOI: 10.1016/j.antiviral.2012.03.006]
98 **Chen C**, Zuckerman DM, Brantley S, Sharpe M, Childress K, Hoiczyk E, Pendleton AR. *Sambucus nigra* extracts inhibit infectious bronchitis virus at an early point during replication. *BMC Vet Res* 2014; **10**: 24 [PMID: 24433341 DOI: 10.1186/1746-6148-10-24]
99 **Krawitz C**, Mraheil MA, Stein M, Imirzalioglu C, Domann E, Pleschka S, Hain T. Inhibitory activity of a standardized elderberry liquid extract against clinically-relevant human respiratory bacterial pathogens and influenza A and B viruses. *BMC Complement Altern Med* 2011; **11**: 16 [PMID: 21352539 DOI: 10.1186/1472-6882-11-16]
100 **Kinoshita E**, Hayashi K, Katayama H, Hayashi T, Obata A. Anti-influenza virus effects of elderberry juice and its fractions. *Biosci Biotechnol Biochem* 2012; **76**: 1633-1638 [PMID: 22972323

DOI: 10.1271/bbb.120112]

101 **Roschek B Jr**, Fink RC, McMichael MD, Li D, Alberte RS. Elderberry flavonoids bind to and prevent H1N1 infection in vitro. *Phytochemistry* 2009; **70**: 1255-1261 [PMID: 19682714 DOI: 10.1016/j.phytochem.2009.06.003]

102 **Ji S**, Li R, Wang Q, Miao WJ, Li ZW, Si LL, Qiao X, Yu SW, Zhou DM, Ye M. Anti-H1N1 virus, cytotoxic and Nrf2 activation activities of chemical constituents from *Scutellaria baicalensis*. *J Ethnopharmacol* 2015; **176**: 475-484 [PMID: 26578185 DOI: 10.1016/j.jep.2015.11.018]

103 **Chen F**, Chan KH, Jiang Y, Kao RY, Lu HT, Fan KW, Cheng VC, Tsui WH, Hung IF, Lee TS, Guan Y, Peiris JS, Yuen KY. *In vitro* susceptibility of 10 clinical isolates of SARS coronavirus to selected antiviral compounds. *J Clin Virol* 2004; **31**: 69-75 [PMID: 15288617 DOI: 10.1016/j.jcv.2004.03.003]

104 **Ryu YB**, Jeong HJ, Kim JH, Kim YM, Park JY, Kim D, Nguyen TT, Park SJ, Chang JS, Park KH, Rho MC, Lee WS. Biflavonoids from *Torreya nucifera* displaying SARS-CoV 3CL(pro) inhibition. *Bioorg Med Chem* 2010; **18**: 7940-7947 [PMID: 20934345 DOI: 10.1016/j.bmc.2010.09.035]

105 **Cai Z**, Zhang G, Tang B, Liu Y, Fu X, Zhang X. Promising Anti-influenza Properties of Active Constituent of *Withania somnifera* Ayurvedic Herb in Targeting Neuraminidase of H1N1 Influenza: Computational Study. *Cell Biochem Biophys* 2015; **72**: 727-739 [PMID: 25627548 DOI: 10.1007/s12013-015-0524-9]

106 **Chang JS**, Wang KC, Yeh CF, Shieh DE, Chiang LC. Fresh ginger (*Zingiber officinale*) has anti-viral activity against human respiratory syncytial virus in human respiratory tract cell lines. *J Ethnopharmacol* 2013; **145**: 146-151 [PMID: 23123794 DOI: 10.1016/j.jep.2012.10.043]

107 **Nantz MP**, Rowe CA, Muller CE, Creasy RA, Stanilka JM, Percival SS. Supplementation with aged garlic extract improves both NK and γδ-T cell function and reduces the severity of cold and flu symptoms: A randomized, double-blind, placebo-controlled nutrition intervention. *Clin Nutr* 2012; **31**: 337-344 [PMID: 22280901 DOI: 10.1016/j.clnu.2011.11.019]

108 **Barrett B**, Brown R, Rakel D, Mundt M, Bone K, Barlow S, Ewers T. Echinacea for treating the common cold: A randomized trial. *Ann Intern Med* 2010; **153**: 769-777 [PMID: 21173411 DOI: 10.7326/0003-4819-153-12-201012210-00003]

109 **Jawad M**, Schoop R, Suter A, Klein P, Eccles R. Safety and Efficacy Profile of *Echinacea purpurea* to Prevent Common Cold Episodes: A Randomized, Double-Blind, Placebo-Controlled Trial. *Evid Based Complement Alternat Med* 2012; **2012**: 841315 [PMID: 23024696 DOI: 10.1155/2012/841315]

110 **Tiralongo E**, Lea RA, Wee SS, Hanna MM, Griffiths LR. Randomised, double blind, placebo-controlled trial of echinacea supplementation in air travellers. *Evid Based Complement Alternat Med* 2012; **2012**: 417267 [PMID: 22229040 DOI: 10.1155/2012/417267]

111 **Matsumoto K**, Yamada H, Takuma N, Niino H, Sagesaka YM. Effects of green tea catechins and theanine on preventing influenza infection among healthcare workers: A randomized controlled trial. *BMC Complement Altern Med* 2011; **11**: 15 [PMID: 21338496 DOI: 10.1186/1472-6882-11-15]

112 **Fazio S**, Pouso J, Dolinsky D, Fernandez A, Hernandez M, Clavier G, Hecker M. Tolerance, safety and efficacy of *Hedera helix* extract in inflammatory bronchial diseases under clinical practice conditions: A prospective, open, multicentre postmarketing study in 9657 patients. *Phytomedicine* 2009; **16**: 17-24 [PMID: 16860549 DOI: 10.1016/j.phymed.2006.05.003]

113 **Schmidt M**, Thomsen M, Schmidt U. Suitability of ivy extract for the treatment of paediatric cough. *Phytother Res* 2012; **26**: 1942-1947 [PMID: 22532491 DOI: 10.1002/ptr.4671]

114 **Zeil S**, Schwanebeck U, Vogelberg C. Tolerance and effect of an add-on treatment with a cough medicine containing ivy leaves dry extract on lung function in children with bronchial asthma. *Phytomedicine* 2014; **21**: 1216-1220 [PMID: 24916707 DOI: 10.1016/j.phymed.2014.05.006]

115 **Ha KC**, Kim MG, Oh MR, Choi EK, Back HI, Kim SY, Park EO, Kwon DY, Yang HJ, Kim MJ, Kang HJ, Lee JH, Choi KM, Chae SW, Lee CS. A placebo-controlled trial of Korean red ginseng extract for preventing influenza-like illness in healthy adults. *BMC Complement Altern Med* 2012; **12**: 10 [PMID: 22314101 DOI: 10.1186/1472-6882-12-10]

116 **Hwang JH**, Park SH, Choi EK, Jung SJ, Pyo MK, Chae SW. A randomized, double-blind, placebo-controlled pilot study to assess the effects of protopanaxadiol saponin-enriched ginseng extract and pectinase-processed ginseng extract on the prevention of acute respiratory illness in healthy people. *J Ginseng Res* 2020; **44**: 697-703 [PMID: 32913399 DOI: 10.1016/j.jgr.2019.01.002]

117 **High KP**, Case D, Hurd D, Powell B, Lesser G, Falsey AR, Siegel R, Metzner-Sadurski J, Krauss JC, Chinnasami B, Sanders G, Rousey S, Shaw EG. A randomized, controlled trial of *Panax quinquefolius* extract (CVT-E002) to reduce respiratory infection in patients with chronic lymphocytic leukemia. *J Support Oncol* 2012; **10**: 195-201 [PMID: 22266154 DOI: 10.1016/j.suponc.2011.10.005]

118 **Wu L**, Zhang AL, Di YM, Shergis JL, Chen Y, Guo X, Wen Z, Thien F, Worsnop C, Lin L, Xue CC. *Panax ginseng* therapy for chronic obstructive pulmonary disease: A clinical trial protocol and pilot study. *Chin Med* 2014; **9**: 20 [PMID: 25161696 DOI: 10.1186/1749-8546-9-20]

119 **Xue CC**, Shergis JL, Zhang AL, Worsnop C, Fong H, Story D, Da Costa C, Thien FC. *Panax ginseng* C.A Meyer root extract for moderate chronic obstructive pulmonary disease (COPD): Study protocol for a randomised controlled trial. *Trials* 2011; **12**: 164 [PMID: 21718484 DOI: 10.1186/1745-6215-12-164]

120 **Matthys H**, Funk P. *Pelargonium sidoides* preparation EPs 7630 in COPD: Health-related quality-of-life and other patient-reported outcomes in adults receiving add-on therapy. *Curr Med Res Opin*

2018; **34**: 1245-1251 [PMID: 29231073 DOI: 10.1080/03007995.2017.1416344]
121 **Kamin W**, Ilyenko LI, Malek FA, Kieser M. Treatment of acute bronchitis with EPs 7630: Randomized, controlled trial in children and adolescents. *Pediatr Int* 2012; **54**: 219-226 [PMID: 22360575 DOI: 10.1111/j.1442-200X.2012.03598.x]
122 **Patiroglu T**, Tunc A, Eke Gungor H, Unal E. The efficacy of *Pelargonium sidoides* in the treatment of upper respiratory tract infections in children with transient hypogammaglobulinemia of infancy. *Phytomedicine* 2012; **19**: 958-961 [PMID: 22809962 DOI: 10.1016/j.phymed.2012.06.004]
123 **Tahan F**, Yaman M. Can the *Pelargonium sidoides* root extract EPs® 7630 prevent asthma attacks during viral infections of the upper respiratory tract in children? *Phytomedicine* 2013; **20**: 148-150 [PMID: 23142309 DOI: 10.1016/j.phymed.2012.09.022]
124 **Berezhnoi VV**, Heger M, Lehmacher W, Seifert G. Clinical efficacy and safety of liquid *Pelargonium sidoides* preparation (EPs 7630) in children with acute non-streptococcal tonsillopharyngitis. *J Compr Ped* 2016; **7** [DOI: 10.17795/compreped-42158]
125 **Riley DS**, Lizogub VG, Zimmermann A, Funk P, Lehmacher W. Efficacy and Tolerability of High-dose *Pelargonium* Extract in Patients with the Common Cold. *Altern Ther Health Med* 2018; **24**: 16-26 [PMID: 29055287]
126 **Kong FK**. Pilot clinical study on a proprietary elderberry extract: Efficacy in addressing influenza symptoms. *J Pharmacokinet Pharmacodyn* 2009; **5**: 32-43 [DOI: 10.1007/s10928-014-9365-1]
127 **Tiralongo E**, Wee SS, Lea RA. Elderberry Supplementation Reduces Cold Duration and Symptoms in Air-Travellers: A Randomized, Double-Blind Placebo-Controlled Clinical Trial. *Nutrients* 2016; **8**: 182 [PMID: 27023596 DOI: 10.3390/nu8040182]
128 **Dehghani S**, Alipoor E, Salimzadeh A, Yaseri M, Hosseini M, Feinle-Bisset C, Hosseinzadeh-Attar MJ. The effect of a garlic supplement on the pro-inflammatory adipocytokines, resistin and tumor necrosis factor-alpha, and on pain severity, in overweight or obese women with knee osteoarthritis. *Phytomedicine* 2018; **48**: 70-75 [PMID: 30195882 DOI: 10.1016/j.phymed.2018.04.060]
129 **Arreola R**, Quintero-Fabián S, López-Roa RI, Flores-Gutiérrez EO, Reyes-Grajeda JP, Carrera-Quintanar L, Ortuño-Sahagún D. Immunomodulation and anti-inflammatory effects of garlic compounds. *J Immunol Res* 2015; **2015**: 401630 [PMID: 25961060 DOI: 10.1155/2015/401630]
130 **Hiyasat B**, Sabha D, Grotzinger K, Kempfert J, Rauwald JW, Mohr FW, Dhein S. Antiplatelet activity of *Allium ursinum* and *Allium sativum*. *Pharmacology* 2009; **83**: 197-204 [PMID: 19174616 DOI: 10.1159/000196811]
131 **Sultana MR**, Bagul PK, Katare PB, Anwar Mohammed S, Padiya R, Banerjee SK. Garlic activates SIRT-3 to prevent cardiac oxidative stress and mitochondrial dysfunction in diabetes. *Life Sci* 2016; **164**: 42-51 [PMID: 27590611 DOI: 10.1016/j.lfs.2016.08.030]
132 **Aprioku JS**, Amah-Tariah FS. Garlic (*Allium sativum* L.) protects hepatic and renal toxicity of alloxan in rats. *Br J Pharm Res* 2017; 1-7 [DOI: 10.9734/JPRI/2017/34909]
133 **Chen YA**, Tsai JC, Cheng KC, Liu KF, Chang CK, Hsieh CW. Extracts of black garlic exhibits gastrointestinal motility effect. *Food Res Int* 2018; **107**: 102-109 [PMID: 29580467 DOI: 10.1016/j.foodres.2018.02.003]
134 **Seckiner I**, Bayrak O, Can M, Mungan AG, Mungan NA. Garlic supplemented diet attenuates gentamicin nephrotoxicity ın rats. *Int Braz J Urol* 2014; **40**: 562-567 [PMID: 25251961 DOI: 10.1590/S1677-5538.IBJU.2014.04.17]
135 **Henrotin Y**, Donneau AF, de Vlam K, Wittoek R, Luyten F. Responses to "Bio-optimized *Curcuma longa* extract is efficient on knee osteoarthritis pain: A double-blind multicenter randomized placebo controlled three-arm study": authors' reply. *Arthritis Res Ther* 2020; **22**: 23 [PMID: 32046787 DOI: 10.1186/s13075-020-2109-2]
136 **Eke-Okoro UJ**, Raffa RB, Pergolizzi JV Jr, Breve F, Taylor R Jr; NEMA Research Group. Curcumin in turmeric: Basic and clinical evidence for a potential role in analgesia. *J Clin Pharm Ther* 2018; **43**: 460-466 [PMID: 29722036 DOI: 10.1111/jcpt.12703]
137 **Liu Z**, Huang P, Law S, Tian H, Leung W, Xu C. Preventive Effect of Curcumin Against Chemotherapy-Induced Side-Effects. *Front Pharmacol* 2018; **9**: 1374 [PMID: 30538634 DOI: 10.3389/fphar.2018.01374]
138 **Huang WC**, Chiu WC, Chuang HL, Tang DW, Lee ZM, Wei L, Chen FA, Huang CC. Effect of curcumin supplementation on physiological fatigue and physical performance in mice. *Nutrients* 2015; **7**: 905-921 [PMID: 25647661 DOI: 10.3390/nu7020905]
139 **Shimizu K**, Funamoto M, Sunagawa Y, Shimizu S, Katanasaka Y, Miyazaki Y, Wada H, Hasegawa K, Morimoto T. Anti-inflammatory Action of Curcumin and Its Use in the Treatment of Lifestyle-related Diseases. *Eur Cardiol* 2019; **14**: 117-122 [PMID: 31360234 DOI: 10.15420/ecr.2019.17.2]
140 **Gouda MM**, Bhandary YP. Acute Lung Injury: IL-17A-Mediated Inflammatory Pathway and Its Regulation by Curcumin. *Inflammation* 2019; **42**: 1160-1169 [PMID: 31011925 DOI: 10.1007/s10753-019-01010-4]
141 **Haider S**, Naqvi F, Tabassum S, Saleem S, Batool Z, Sadir S, Rasheed S, Saleem D, Nawaz A, Ahmad S. Preventive effects of curcumin against drug- and starvation-induced gastric erosions in rats. *Sci Pharm* 2013; **81**: 549-558 [PMID: 23833720 DOI: 10.3797/scipharm.1207-17]
142 **Ram A**, Das M, Ghosh B. Curcumin attenuates allergen-induced airway hyperresponsiveness in sensitized guinea pigs. *Biol Pharm Bull* 2003; **26**: 1021-1024 [PMID: 12843631 DOI: 10.1248/bpb.26.1021]
143 **Dulbecco P**, Savarino V. Therapeutic potential of curcumin in digestive diseases. *World J Gastroenterol* 2013; **19**: 9256-9270 [PMID: 24409053 DOI: 10.3748/wjg.v19.i48.9256]

144 **Nosalova G**, Fleskova D, Jurecek L, Sadlonova V, Ray B. Herbal polysaccharides and cough reflex. *Respir Physiol Neurobiol* 2013; **187**: 47-51 [PMID: 23597834 DOI: 10.1016/j.resp.2013.03.015]

145 **Kuang Y**, Li B, Fan J, Qiao X, Ye M. Antitussive and expectorant activities of licorice and its major compounds. *Bioorg Med Chem* 2018; **26**: 278-284 [PMID: 29224994 DOI: 10.1016/j.bmc.2017.11.046]

146 **Kao TC**, Shyu MH, Yen GC. Glycyrrhizic acid and 18beta-glycyrrhetinic acid inhibit inflammation *via* PI3K/Akt/GSK3beta signaling and glucocorticoid receptor activation. *J Agric Food Chem* 2010; **58**: 8623-8629 [PMID: 20681651 DOI: 10.1021/jf101841r]

147 **Shi Q**, Hou Y, Yang Y, Bai G. Protective effects of glycyrrhizin against β_2-adrenergic receptor agonist-induced receptor internalization and cell apoptosis. *Biol Pharm Bull* 2011; **34**: 609-617 [PMID: 21532146 DOI: 10.1248/bpb.34.609]

148 **Rushmi ZT**, Akter N, Mow RJ, Afroz M, Kazi M, de Matas M, Rahman M, Shariare MH. The impact of formulation attributes and process parameters on black seed oil loaded liposomes and their performance in animal models of analgesia. *Saudi Pharm J* 2017; **25**: 404-412 [PMID: 28344496 DOI: 10.1016/j.jsps.2016.09.011]

149 **Muralidharan-Chari V**, Kim J, Abuawad A, Naeem M, Cui H, Mousa SA. Thymoquinone Modulates Blood Coagulation in Vitro *via* Its Effects on Inflammatory and Coagulation Pathways. *Int J Mol Sci* 2016; **17**: 474 [PMID: 27043539 DOI: 10.3390/ijms17040474]

150 **Ansari MA**, Ansari NA, Junejo SA. Montelukast vs *Nigella sativa* for management of seasonal allergic rhinitis: A single blind comparative clinical trial. *Pak J Med Sci* 2010; **26**: 249-254 [DOI: 10.1046/j.1365-2222.2002.01422.x]

151 **Alsamarai AM**, Abdulsatar M, Ahmed Alobaidi AH. Evaluation of topical black seed oil in the treatment of allergic rhinitis. *Antiinflamm Antiallergy Agents Med Chem* 2014; **13**: 75-82 [PMID: 23855426 DOI: 10.2174/18715230113129990014]

152 **Majdalawieh AF**, Fayyad MW. Immunomodulatory and anti-inflammatory action of *Nigella sativa* and thymoquinone: A comprehensive review. *Int Immunopharmacol* 2015; **28**: 295-304 [PMID: 26117430 DOI: 10.1016/j.intimp.2015.06.023]

153 **Mahdavi R**, Namazi N, Alizadeh M, Farajnia S. *Nigella sativa* oil with a calorie-restricted diet can improve biomarkers of systemic inflammation in obese women: A randomized double-blind, placebo-controlled clinical trial. *J Clin Lipidol* 2016; **10**: 1203-1211 [PMID: 27678438 DOI: 10.1016/j.jacl.2015.11.019]

154 **Boskabady MH**, Mohsenpoor N, Takaloo L. Antiasthmatic effect of *Nigella sativa* in airways of asthmatic patients. *Phytomedicine* 2010; **17**: 707-713 [PMID: 20149611 DOI: 10.1016/j.phymed.2010.01.002]

155 **Salem AM**, Bamosa AO, Qutub HO, Gupta RK, Badar A, Elnour A, Afzal MN. Effect of *Nigella sativa* supplementation on lung function and inflammatory mediatorsin partly controlled asthma: a randomized controlled trial. *Ann Saudi Med* 2017; **37**: 64-71 [PMID: 28151459 DOI: 10.5144/0256-4947.2017.64]

156 **Ratan ZA**, Youn SH, Kwak YS, Han CK, Haidere MF, Kim JK, Min H, Jung YJ, Hosseinzadeh H, Hyun SH, Cho JY. Adaptogenic effects of *Panax ginseng* on modulation of immune functions. *J Ginseng Res* 2021; **45**: 32-40 [PMID: 33437154 DOI: 10.1016/j.jgr.2020.09.004]

157 **Bao Y**, Gao Y, Koch E, Pan X, Jin Y, Cui X. Evaluation of pharmacodynamic activities of EPs® 7630, a special extract from roots of *Pelargonium sidoides*, in animals models of cough, secretolytic activity and acute bronchitis. *Phytomedicine* 2015; **22**: 504-509 [PMID: 25925973 DOI: 10.1016/j.phymed.2015.03.004]

158 **Aung H**, Mehendale S, Chang WT, Wang CZ, Xie JT, Yuan CS. *Scutellaria baicalensis* decreases ritonavir-induced nausea. *AIDS Res Ther* 2005; **2**: 12 [PMID: 16368007 DOI: 10.1186/1742-6405-2-12]

159 **Hong GE**, Kim JA, Nagappan A, Yumnam S, Lee HJ, Kim EH, Lee WS, Shin SC, Park HS, Kim GS. Flavonoids Identified from Korean *Scutellaria baicalensis* Georgi Inhibit Inflammatory Signaling by Suppressing Activation of NF- κ B and MAPK in RAW 264.7 Cells. *Evid Based Complement Alternat Med* 2013; **2013**: 912031 [PMID: 24348728 DOI: 10.1155/2013/912031]

160 **Mehendale S**, Aung H, Wang CZ, Tong R, Foo A, Xie JT, Yuan CS. *Scutellaria baicalensis* and a constituent flavonoid, baicalein, attenuate ritonavir-induced gastrointestinal side-effects. *J Pharm Pharmacol* 2007; **59**: 1567-1572 [PMID: 17976269 DOI: 10.1211/jpp.59.11.0015]

161 **Cui L**, Guan X, Ding W, Luo Y, Wang W, Bu W, Song J, Tan X, Sun E, Ning Q, Liu G, Jia X, Feng L. *Scutellaria baicalensis* Georgi polysaccharide ameliorates DSS-induced ulcerative colitis by improving intestinal barrier function and modulating gut microbiota. *Int J Biol Macromol* 2021; **166**: 1035-1045 [PMID: 33157130 DOI: 10.1016/j.ijbiomac.2020.10.259]

162 **Thanh HN**, Minh HPT, Le TA, Ly HDT, Huu TN, Duc LV, Kim TD, Thanh TB. Ethanol extracts of *Scutellaria baicalensis* protect against lipopolysaccharide-induced acute liver injury in mice. *Asian Pac J Trop Biomed* 2015; **5**: 761-767 [DOI: 10.1016/j.apjtb.2015.07.007]

163 **Dai J**, Chen L, Qiu YM, Li SQ, Xiong WH, Yin YH, Jia F, Jiang JY. Activations of GABAergic signaling, HSP70 and MAPK cascades are involved in baicalin's neuroprotection against gerbil global ischemia/reperfusion injury. *Brain Res Bull* 2013; **90**: 1-9 [PMID: 23041106 DOI: 10.1016/j.brainresbull.2012.09.014]

164 **Bui TT**, Piao CH, Song CH, Lee CH, Shin HS, Chai OH. Baicalein, wogonin, and *Scutellaria baicalensis* ethanol extract alleviate ovalbumin-induced allergic airway inflammation and mast cell-mediated anaphylactic shock by regulation of Th1/Th2 imbalance and histamine release. *Anat Cell*

Biol 2017; **50**: 124-134 [PMID: 28713616 DOI: 10.5115/acb.2017.50.2.124]

165 **Laub A**. Using species of the Lamiaceae family for musculoskeletal pain. 2018. [cited 10 January 2021]. Available from: https://www.researchgate.net/publication/335156154_Using_Species_of_the_Lamiaceae_Family_for_Musculoskeletal_Pain

166 **Salmalian H**, Saghebi R, Moghadamnia AA, Bijani A, Faramarzi M, Nasiri Amiri F, Bakouei F, Behmanesh F, Bekhradi R. Comparative effect of *Thymus vulgaris* and ibuprofen on primary dysmenorrhea: A triple-blind clinical study. *Caspian J Intern Med* 2014; **5**: 82-88 [PMID: 24778782]

167 **Okazaki K**, Kawazoe K, Takaishi Y. Human platelet aggregation inhibitors from thyme (*Thymus vulgaris* L.). *Phytother Res* 2002; **16**: 398-399 [PMID: 12112303 DOI: 10.1002/ptr.979]

168 **Habashy NH**, Serie MM, Attia WE, Abdelgaleil SA. Chemical characterization, antioxidant and anti-inflammatory properties of Greek *Thymus vulgaris* extracts and their possible synergism with Egyptian *Chlorella vulgaris*. *J Funct Foods* 2018; **40**: 317-328 [DOI: 10.1016/j.jff.2017.11.022]

169 **Salve J**, Pate S, Debnath K, Langade D. Adaptogenic and Anxiolytic Effects of Ashwagandha Root Extract in Healthy Adults: A Double-blind, Randomized, Placebo-controlled Clinical Study. *Cureus* 2019; **11**: e6466 [PMID: 32021735 DOI: 10.7759/cureus.6466]

170 **Murthy MNK**, Gundagani S, Nutalapati C, Pingali U. Evaluation of analgesic activity of standardised aqueous extract of *Withania somnifera* in healthy human volunteers using mechanical pain model. *J Clin Diagn* 2019; **13**: 1-4 [DOI: 10.7860/jcdr/2019/37590.12441]

171 **Ku SK**, Bae JS. Antiplatelet, anticoagulant, and profibrinolytic activities of withaferin A. *Vascul Pharmacol* 2014; **60**: 120-126 [PMID: 24534482 DOI: 10.1016/j.vph.2014.01.009]

172 **Gupta A**, Singh S. Evaluation of anti-inflammatory effect of *Withania somnifera* root on collagen-induced arthritis in rats. *Pharm Biol* 2014; **52**: 308-320 [PMID: 24188460 DOI: 10.3109/13880209.2013.835325]

173 **Lopresti AL**, Smith SJ, Malvi H, Kodgule R. An investigation into the stress-relieving and pharmacological actions of an ashwagandha (*Withania somnifera*) extract: A randomized, double-blind, placebo-controlled study. *Medicine (Baltimore)* 2019; **98**: e17186 [PMID: 31517876 DOI: 10.1097/MD.0000000000017186]

174 **Maghbooli M**, Golipour F, Moghimi Esfandabadi A, Yousefi M. Comparison between the efficacy of ginger and sumatriptan in the ablative treatment of the common migraine. *Phytother Res* 2014; **28**: 412-415 [PMID: 23657930 DOI: 10.1002/ptr.4996]

175 **Bartels EM**, Folmer VN, Bliddal H, Altman RD, Juhl C, Tarp S, Zhang W, Christensen R. Efficacy and safety of ginger in osteoarthritis patients: A meta-analysis of randomized placebo-controlled trials. *Osteoarthritis Cartilage* 2015; **23**: 13-21 [PMID: 25300574 DOI: 10.1016/j.joca.2014.09.024]

176 **Tóth B**, Lantos T, Hegyi P, Viola R, Vasas A, Benkő R, Gyöngyi Z, Vincze Á, Csécsei P, Mikó A, Hegyi D, Szentesi A, Matuz M, Csupor D. Ginger (*Zingiber officinale*): An alternative for the prevention of postoperative nausea and vomiting. A meta-analysis. *Phytomedicine* 2018; **50**: 8-18 [PMID: 30466995 DOI: 10.1016/j.phymed.2018.09.007]

177 **Khan AM**, Shahzad M, Raza Asim MB, Imran M, Shabbir A. *Zingiber officinale* ameliorates allergic asthma *via* suppression of Th2-mediated immune response. *Pharm Biol* 2015; **53**: 359-367 [PMID: 25420680 DOI: 10.3109/13880209.2014.920396]

178 **Lee W**, Ku SK, Kim MA, Bae JS. Anti-factor Xa activities of zingerone with anti-platelet aggregation activity. *Food Chem Toxicol* 2017; **105**: 186-193 [PMID: 28414123 DOI: 10.1016/j.fct.2017.04.012]

179 **Bera K**, Nosalova G, Sivova V, Ray B. Structural Elements and Cough Suppressing Activity of Polysaccharides from *Zingiber officinale* Rhizome. *Phytother Res* 2016; **30**: 105-111 [PMID: 26522239 DOI: 10.1002/ptr.5508]

180 **Nanjundaiah SM**, Annaiah HN, Dharmesh SM. Gastroprotective Effect of Ginger Rhizome (*Zingiber officinale*) Extract: Role of Gallic Acid and Cinnamic Acid in H(+), K(+)-ATPase/H. pylori Inhibition and Anti-Oxidative Mechanism. *Evid Based Complement Alternat Med* 2011; **2011**: 249487 [PMID: 19570992 DOI: 10.1093/ecam/nep060]

181 **Ajith TA**, Hema U, Aswathy MS. *Zingiber officinale* Roscoe prevents acetaminophen-induced acute hepatotoxicity by enhancing hepatic antioxidant status. *Food Chem Toxicol* 2007; **45**: 2267-2272 [PMID: 17637489 DOI: 10.1016/j.fct.2007.06.001]

182 **Ajith TA**, Nivitha V, Usha S. *Zingiber officinale* Roscoe alone and in combination with alpha-tocopherol protect the kidney against cisplatin-induced acute renal failure. *Food Chem Toxicol* 2007; **45**: 921-927 [PMID: 17210214 DOI: 10.1016/j.fct.2006.11.014]

183 **Abdelli I**, Hassani F, Bekkel Brikci S, Ghalem S. *In silico* study the inhibition of angiotensin converting enzyme 2 receptor of COVID-19 by *Ammoides verticillata* components harvested from Western Algeria. *J Biomol Struct Dyn* 2021; **39**: 3263-3276 [PMID: 32362217 DOI: 10.1080/07391102.2020.1763199]

184 **Thuy BTP**, My TTA, Hai NTT, Hieu LT, Hoa TT, Thi Phuong Loan H, Triet NT, Anh TTV, Quy PT, Tat PV, Hue NV, Quang DT, Trung NT, Tung VT, Huynh LK, Nhung NTA. Investigation into SARS-CoV-2 Resistance of Compounds in Garlic Essential Oil. *ACS Omega* 2020; **5**: 8312-8320 [PMID: 32363255 DOI: 10.1021/acsomega.0c00772]

185 **Sui H**, Yu Q, Zhi Y, Geng G, Liu H, Xu H. [Effects of apigenin on the expression of angiotensin-converting enzyme 2 in kidney in spontaneously hypertensive rats]. *Wei Sheng Yan Jiu* 2010; **39**: 693-696, 700 [PMID: 21351633]

186 **Dong J**, Xu X, Liang Y, Head R, Bennett L. Inhibition of angiotensin converting enzyme (ACE)

activity by polyphenols from tea (*Camellia sinensis*) and links to processing method. *Food Funct* 2011; **2**: 310-319 [PMID: 21779569 DOI: 10.1039/c1fo10023h]

187 **Chen H**, Du Q. Potential natural compounds for preventing SARS-CoV-2 (2019-nCoV) infection. 2020 Preprint. Available from: 2020010358 [DOI: 10.20944/preprints202001.0358.v3]

188 **Senthil Kumar KJ**, Gokila Vani M, Wang CS, Chen CC, Chen YC, Lu LP, Huang CH, Lai CS, Wang SY. Geranium and Lemon Essential Oils and Their Active Compounds Downregulate Angiotensin-Converting Enzyme 2 (ACE2), a SARS-CoV-2 Spike Receptor-Binding Domain, in Epithelial Cells. *Plants (Basel)* 2020; **9** [PMID: 32575476 DOI: 10.3390/plants9060770]

189 **Zi CT**, Zhang N, Yang L, Wang LX, Wu YL, Su YS, Wang XJ. Discovery of a potent angiotensin converting enzyme 2 inhibitor from Chinese medicinal and edible plant via docking-based virtual screening. 2020 Preprint. Available from: rs-32515 [DOI: 10.21203/rs.3.rs-32515/v1]

190 **Takahashi S**, Yoshiya T, Yoshizawa-Kumagaye K, Sugiyama T. Nicotianamine is a novel angiotensin-converting enzyme 2 inhibitor in soybean. *Biomed Res* 2015; **36**: 219-224 [PMID: 26106051 DOI: 10.2220/biomedres.36.219]

191 **Ojeda D**, Jiménez-Ferrer E, Zamilpa A, Herrera-Arellano A, Tortoriello J, Alvarez L. Inhibition of angiotensin convertin enzyme (ACE) activity by the anthocyanins delphinidin- and cyanidin-3-O-sambubiosides from *Hibiscus sabdariffa*. *J Ethnopharmacol* 2010; **127**: 7-10 [PMID: 19808084 DOI: 10.1016/j.jep.2009.09.059]

192 **Prasad K**. Secoisolariciresinol Diglucoside (SDG) Isolated from Flaxseed, an Alternative to ACE Inhibitors in the Treatment of Hypertension. *Int J Angiol* 2013; **22**: 235-238 [PMID: 24436618 DOI: 10.1055/s-0033-1351687]

193 **My TTA**, Loan HTP, Hai NTT, Hieu LT, Hoa TT, Thuy BTP, Quang DT, Triet NT, Anh TTV, Dieu NTX, Trung NT, Hue NV, Tat PV, Tung VT, Nhung NTA. Evaluation of the Inhibitory Activities of COVID-19 of *Melaleuca cajuputi* Oil Using Docking Simulation. *Chemistry Select* 2020; **5**: 6312-6320 [PMID: 32572383 DOI: 10.1002/slct.202000822]

194 **Siriwattananon K**, Manopwisedjaroen S, Kanjanasirirat P, Budi Purwono P, Rattanapisit K, Shanmugaraj B, Smith DR, Borwornpinyo S, Thitithanyanont A, Phoolcharoen W. Development of Plant-Produced Recombinant ACE2-Fc Fusion Protein as a Potential Therapeutic Agent Against SARS-CoV-2. *Front Plant Sci* 2020; **11**: 604663 [PMID: 33584747 DOI: 10.3389/fpls.2020.604663]

World Journal of Gastroenterology

Submit a Manuscript: https://www.f6publishing.com

World J Gastroenterol 2021 October 21; 27(39): 6572-6589

DOI: 10.3748/wjg.v27.i39.6572

ISSN 1007-9327 (print) ISSN 2219-2840 (online)

MINIREVIEWS

Current and emerging therapeutic strategies in pancreatic cancer: Challenges and opportunities

Manish Manrai, T V S V G K Tilak, Saurabh Dawra, Sharad Srivastava, Anupam Singh

ORCID number: Manish Manrai 0000-0002-5805-033X; TVSVGK Tilak 0000-0002-1380-8346; Saurabh Dawra 0000-0002-7679-9491; Sharad Srivastava 0000-0003-3269-5989; Anupam Singh 0000-0002-7610-1807.

Author contributions: Manrai M conceptualized the review and with Tilak TVSVGK, Dawra S was involved with resources, formal analysis, data curation, writing, review, and editing; Srivastava S was involved with resources and analysis; Singh A was involved with review and editing.

Conflict-of-interest statement: The authors have no conflict-of-interest for this manuscript.

Open-Access: This article is an open-access article that was selected by an in-house editor and fully peer-reviewed by external reviewers. It is distributed in accordance with the Creative Commons Attribution NonCommercial (CC BY-NC 4.0) license, which permits others to distribute, remix, adapt, build upon this work non-commercially, and license their derivative works on different terms, provided the original work is properly cited and the use is non-commercial. See: http://creativecommons.org/Licenses/by-nc/4.0/

Manuscript source: Invited

Manish Manrai, T V S V G K Tilak, Department of Internal Medicine, Armed Forces Medical College, Pune 411040, Maharashtra, India

Saurabh Dawra, Sharad Srivastava, Department of Internal Medicine, Command Hospital, Pune 411040, Maharashtra, India

Anupam Singh, Department of Gastroenterology, Post Graduate Institute of Medical Education and Research, Chandigarh 160011, India

Corresponding author: Manish Manrai, MBBS, MD, Professor, Department of Internal Medicine, Armed Forces Medical College, Solapur Road, Pune 411040, Maharashtra, India. manishmanrai@yahoo.com

Abstract

Pancreatic carcinoma (PC) is one of the leading causes of cancer-related deaths worldwide. Despite early detection and advances in therapeutics, the prognosis remains dismal. The outcome and therapeutic approach are dependent on the stage of PC at the time of diagnosis. The standard of care is surgery, followed by adjuvant chemotherapy. The advent of newer drugs has changed the landscape of adjuvant therapy. Moreover, recent trials have highlighted the role of neoadjuvant therapy and chemoradiotherapy for resectable and borderline resectable PC. As we progress towards a better understanding of tumor biology, genetics, and microenvironment, novel therapeutic strategies and targeted agents are now on the horizon. We have described the current and emerging therapeutic strategies in PC.

Key Words: Resectable pancreatic carcinoma; Borderline resectable pancreatic carcinoma; Locally advanced pancreatic carcinoma; Adjuvant therapy; Neoadjuvant therapy; Newer advances in pancreatic carcinoma

©The Author(s) 2021. Published by Baishideng Publishing Group Inc. All rights reserved.

Core Tip: An improved understanding of the natural history of pancreatic carcinoma, genetics, and tumor biology has highlighted the role of novel therapeutic strategies. However, despite recent advances in the management of pancreatic carcinoma, the

manuscript

Specialty type: Gastroenterology and hepatology

Country/Territory of origin: India

Peer-review report's scientific quality classification

Grade A (Excellent): A
Grade B (Very good): 0
Grade C (Good): 0
Grade D (Fair): 0
Grade E (Poor): 0

Received: January 28, 2021
Peer-review started: January 28, 2021
First decision: May 2, 2021
Revised: May 9, 2021
Accepted: August 16, 2021
Article in press: August 16, 2021
Published online: October 21, 2021

P-Reviewer: Zeng C
S-Editor: Gao CC
L-Editor: Filipodia
P-Editor: Liu JH

prognosis remains poor. We have attempted to conceptualize the current therapeutic strategies in light of recent advances.

Citation: Manrai M, Tilak TVSVGK, Dawra S, Srivastava S, Singh A. Current and emerging therapeutic strategies in pancreatic cancer: Challenges and opportunities. *World J Gastroenterol* 2021; 27(39): 6572-6589
URL: https://www.wjgnet.com/1007-9327/full/v27/i39/6572.htm
DOI: https://dx.doi.org/10.3748/wjg.v27.i39.6572

INTRODUCTION

World over, new cases of pancreatic carcinoma (PC) add up close to three lakh each year[1,2]. There hasn't been a significant increase in the long-term survival rates, with the 5-year survival rates increasing to 5%-6% over the last 30 years, despite early detection and advances in therapeutics for pancreatic cancer[3,4]. The estimates of leading causes of cancer deaths suggest that PC may become the second, next only to lung cancer in the United States over the next decade[1].

Pancreatic ductal adenocarcinoma (PDAC) is exemplified by abundant genetic mutations, germline or acquired. Among the common ones are *CDK2NA* and *KRAS* seen in nearly 90%, *TP53* in 75%-90%, and *SMAD4/DPC4* in about 50%[5,6]. Additionally, genomic and epigenetic alterations are present, which have ignited research for targeted therapy. The desmoplastic stroma and the tumor microenvironment have been the focus of clinical explorations.

The outcomes of PC depend on the stage at diagnosis. Nearly half the cases are diagnosed as metastatic, wherein the survival ranges from 7-11 mo, at best[7,8]. In cases where the disease is non-metastatic but unresectable, there is a modest increase of survival, of nearly 6 months over the metastatic disease. The peculiarity of resectable PC lies in the poor overall survival, of approximately 2 years with adjuvant therapy. This is in stark contrast to most of the other resectable cancers.

The standard of care of resectable PC is surgery followed by adjuvant chemotherapy (CT). The benefit for this approach was established by the European Study Group for Pancreatic Cancer 1 (ESPAC-1) and the CONKO-001 trials, using 5-fluorouracil (5-FU)/leucovorin and gemcitabine respectively[7-9]. The phase III randomized PRODIGE 24 trial using 5-FU/leucovorin with irinotecan and oxaliplatin (FOLFIRINOX) and APACT trial with nab-paclitaxel with gemcitabine changed the landscape of adjuvant therapy following their success noticed in the metastatic setting [10,11]. The role of chemoradiotherapy (CRT) in the adjuvant setting is yet to see the final statement based on the existing literature. Following the lack of survival benefit with CRT in the ESPAC-1 and European Organization for Research and Treatment of Cancer (EORTC) trials and contrasting results with two registry data showing survival benefit of CRT compared to CT, one large series compared the three modalities of systemic CT, CRT or CRT followed by CT. There was a significant survival benefit with CT and CRT followed by CT than in the CRT in patients with stage III disease. This benefit was however not seen in patients with stage I/II disease[12-16].

The management of borderline resectable pancreatic adenocarcinomas (BRPCs) has seen the emergence of adjuvant regimes in the 'neoadjuvant' or 'induction therapy' role with FOLFIRINOX and nab-paclitaxel with gemcitabine[17,18]. There is no robust data to suggest the survival benefit of these protocols so far; however, there has been demonstrable tolerability and increased resection rates. A clinical challenge has been to offer adjuvant therapy to patients receiving induction therapy. The results of phase II ESPAC-5F trial, presented at the 2020 virtual ASCO meeting, comparing four arms-frontline surgery, induction therapy with gemcitabine and capecitabine, or modified FOLFIRINOX and CRT. The study revealed similar outcomes between the frontline and induction treatment[19].

The metastatic setting is seeing numerous trials with conventional CT as well as targeted agents as the biology and tumor microenvironment, genetics, and molecular concepts are being better understood. This has led to a search for novel therapeutic strategies for managing PC. This review attempts to address the challenge faced by the practicing clinician in optimal sequencing of the available modalities in the various stages of the illness.

MANAGEMENT OF RESECTABLE PANCREATIC CANCER

A resectable adenocarcinoma does not have metastases to a distant organ or distant lymph nodes; there is no vascular involvement [characterized by absence of superior mesenteric vein (SMV) or portal vein (PV) involvement], tumor thrombosis, or venous encasement > 180°. Also, the fat planes around the celiac axis (CA), hepatic artery (HA), and superior mesenteric artery (SMA) ought to be clear[20].

Surgery

Surgery is the only treatment option that offers a cure for PDAC. Surgery aims to completely resect the tumor and achieve a microscopically negative tumor margin (R0). R0 dissection is defined as clearance of > 1 mm *i.e.*, the margin of healthy tissue around the removed tumor should be > 1 mm. The various surgical options include pancreaticoduodenectomy (Whipple's procedure) and distal pancreatectomy. Pancreaticoduodenectomy with SMA first approach is the standard of care for adenocarcinoma localized to the head of the pancreas (HOP). The surgery should involve dissection of greater than 15 lymph nodes and skeletonization of SMA down to adventitia of anterior, left lateral and posterior borders[21,22]. A sampling of paraaortic lymph nodes with an examination of the frozen section is an additional option. For PDAC involving the body and tail of the pancreas, distal pancreatectomy along with splenectomy is the treatment option. This involves dissection of greater than 15 lymph nodes[23,24].

Minimally invasive techniques for pancreatic resection beginning with laparoscopic distal pancreatectomy have been attempted. They offer advantages in the form of reduced blood loss and decreased hospital stay. However, the rate of achieving positive resection margin, morbidity, and mortality of the procedure remains the same as that of an open procedure. The use of robotic techniques in Whipple's procedure has shown reduced rates of post-procedure complications[25]. Traditionally preoperative biliary drainage has been advised for patients who present with obstructive jaundice. Recent evidence, however, points towards a higher rate of perioperative complications among those undergoing pre-operative drainage *vs* those undergoing upfront surgery[26].

The risk of developing tumor recurrence among those patients who undergo curative resection for PC varies from 69%-75% at 2 years to 80%-90% at 5 years post-surgery[27]. Tumor recurrence occurs secondary to locoregional occurrence in a majority of cases. This led to the hypothesis that the use of adjuvant therapy may reduce locoregional tumor recurrence.

Post-operative complications may reduce a patients' access to adjuvant CT and overall survival. Hence, it becomes imperative to screen patients who are at high risk of post-operative complications, like elderly patients, patients with poor performance status, or higher comorbidity profiles. Preoperative pancreatic resection score (PREPARE) and Surgical results analysis and search (SOAR) are validated and useful scoring systems for assessing the risk of developing complications post-operatively[28,29].

Adjuvant CT

The gold standard treatment for resectable PC is surgery followed by adjuvant CT. The era of adjuvant CT gained prominence when the results of the European Group for Pancreatic Cancer (ESPAC-1) trial showed significant improved median survival and 5-year survival in patients who received adjuvant CT of fluorouracil and folinic acid *vs* those who underwent surgery alone (20.1 mo *vs* 15.5 mo, respectively; $P = 0.009$). This was followed by the CONKO-001 (Charité Onkologietrial) trial, using adjuvant gemcitabine, which showed a median disease-free survival of 13.4 mo and 5-year survival of 20.7% *vs* 10.4% *vs* 6.9 mo respectively in the surgery alone group. The efficacy of these two treatment regimens was compared in the ESPAC-3 trial. Results of this study showed no survival benefit of one treatment regimen over the other, however, the treatment-related adverse effects were higher in the fluorouracil and folinic acid group.

To further improve the therapeutic outcome with adjuvant CT, a concept of combination systemic therapy has evolved. Several agents have been studied in various trials (Table 1). Among those of note are the ESPAC-4, PRODIGE and APACT studies. The ESPAC-4 trial carried out a comparison of gemcitabine *vs* a combination of gemcitabine plus capecitabine, which showed favorable overall survival benefit while using combination therapy [hazard ratio (HR): 0.82, 95% confidence interval (CI): 0.68-0.98; $P = 0.032$]. However, no significant recurrence-free survival benefit was seen in 2 years of follow-up of these patients (HR: 0.86, 95%CI: 0.73-1.02; $P = 0.082$).

Table 1 Landmark trials on adjuvant treatment in pancreatic adenocarcinoma

Study	No. of patients	Treatment arms	Median DFS in mo	Median OS in mo
GITSG[33]	43	Observation	NR	20.0
		Radiotherapy + 5-FU f/b adjuvant 5-FU	NR	10.9
ESPAC-1[34]	289	Observation	NR	15.5
		Chemoradiotherapy	NR	13.9
		5-FU/folinic acid	NR	20.1
		Chemoradiotherapy + 5-FU/folinic acid	NR	19.9
CONKO-001[9]	354	Observation	6.7	20.2
		Gemcitabine	13.4	22.8
ESPAC-3[35]	1088	5-FU/folinic acid	14.1	23.0
		Gemcitabine	14.3	23.6
ESPAC-4[36]	730	Gemcitabine	13.1	25.5
		Gemcitabine + Capecitabine	13.9	28.0
CONKO-005[30]	436	Gemcitabine	11.4	26.5
		Gemcitabine + Erlotinib	11.4	24.6
PRODIGE 24-PA6[37]	493	Gemcitabine	12.8	35.0
		FOLFIRINOX	21.6	54.4
APACT[11]	866	Gemcitabine	18.8	36.2
		Gemcitabine + nab-paclitaxel	19.4	40.5

5-FU: 5-Fluorouracil; CONKO: Charité Onkologie; DFS: Disease-free survival; ESPAC: European Group for Pancreatic Cancer; GITSG: Gastrointestinal Tumor Study Group; NR: Not reported; OS: Overall survival; PRODIGE: Partenariat de Recherche en Oncologie DIGEstive.

The Partenariat de Recherche en Oncologie Digestive (PRODIGE 24-PA6) trial highlighted the successful use of FOLFIRINOX (oxaliplatin + irinotecan + leucovorin) *vs* gemcitabine in patients with good performance status (Eastern Cooperative Oncology Group, ECOG: 0-1). The median disease-free survival in patients with combination therapy was 21.6 mo *vs* 12.8 mo in the gemcitabine group. The latest in series is the Nab-paclitaxel and Gemcitabine *vs* Gemcitabine Alone as Adjuvant Therapy for Patients with Resected Pancreatic Cancer (APACT) study, which has shown encouraging results of using combination therapy of gemcitabine plus nanoparticle albumin-bound paclitaxel (nab-paclitaxel). Median disease-free survival was not statistically significant in the two arms (19.4 mo in combination arm *vs* 18.8 mo in gemcitabine only arm). Overall survival favored the combination CT group (HR: 0.82, 95%CI: 0.68-0.996; $P = 0.045$)[27].

Another concept is the use of targeted agents (erlotinib or sorafenib) or immunotherapy (algenpantucel-L) in combination with gemcitabine. However, to date, none of these agents have shown any favorable survival outcome *vs* the use of gemcitabine alone[30-32].

Adjuvant CRT

Adjuvant CRT aims to prevent locoregional tumor recurrence. Amongst the first trials to assess the efficacy of CRT in PC was the EORTC trial, which showed no significant survival benefit amongst patients of PDAC who received CRT (40 Gy + continuous infusion of fluorouracil)[13]. This was followed by the ESPAC-1 trial, which employed the following three different adjuvant therapy designs: CRT, CT alone, and CRT followed by adjuvant CT. Patients undergoing adjuvant CT were found to have poor survival benefits after a median follow-up of 47 mo (HR: 1.28, 95%CI: 0.99-1.66; $P = 0.05$)[34]. The RTOG 9704 trial was carried out to assess the benefit of adding gemcitabine to postoperative radiation + fluorouracil *vs* adjuvant therapy with fluorouracil. The trial showed no survival benefit in either of the two treatment groups [38].

Although these trials failed to prove any survival benefit, they nevertheless provided useful information on the feasibility and tolerability of these treatment options. Analysis of the US National Cancer Database which included patients of pancreatic adenocarcinoma who underwent curative resection followed by adjuvant CT showed survival benefit (median overall survival with CT + radiation: 22.3 mo and adjuvant CT alone: 20.0 mo; $P = 0.001$)[14].

Timing of adjuvant CT

There are definite gaps in our knowledge regarding the optimal timing of initiating CT following surgery and follow-up of patients undergoing adjuvant therapy for curable PC. Delay in initiating as well as non-initiation of adjuvant treatment is not uncommon. Post-operative morbidity adversely impacts the initiation of adjuvant treatment. It has been estimated that approximately 20% of patients become ineligible for adjuvant CT. The ESPAC-3 trial aimed to analyze the outcome among those who were initiated on CT within 8 wk of surgery and those who were initiated on CT after 8 wk of surgery. There was no survival benefit in either of the two arms, while successful completion of six cycles of CT was found to be an independent predictor of survival[39]. Similar results have been put forward by analyzing multi-institutional retrospective data of patients who had undergone curative resection for PDAC. Thus, the evidence so far suggests that patients who receive adjuvant therapy more than 12 wk following surgery are still good candidates for adjuvant CT[40].

Therefore, in summary, the standard of care in resectable pancreatic adenocarcinoma is surgical resection followed by adjuvant CT. Single-agent (5-FU) is preferred for periampullary tumors of pancreatic origin. Patients with adenocarcinoma in the head, body, or tail of the pancreas may be treated with FOLFIRINOX (patients with good post-operative performance status, ECOG: 0-1) and combination therapy of gemcitabine+ capecitabine in those with poor performance status postoperatively (Figure 1).

Neoadjuvant therapy

Conceptually, the use of neoadjuvant therapy in resectable PC gained prominence when this approach was shown to have improved survival benefit in other gastrointestinal malignancies[41]. It offers the following theoretical advantages: reduction of circulating tumor cells and micrometastasis before surgery, and avoiding surgery in those who experience disease progression while on neoadjuvant therapy, thus, reducing surgical mortality and morbidity. Of particular interest is the ability of neoadjuvant treatment to achieve tumor downsizing or downstaging (lower T and N stages, reducing the rates of vascular, lymphatic, and perineural invasion, and the ability to achieve better R0 resection post-surgery). Moreover, individuals who receive neoadjuvant CT are more likely to be able to access the entire therapeutic sequence[42, 43].

The preoperative or postoperative CT for resectable pancreatic adenocarcinoma (PACT-15) trial has shown the efficacy of neoadjuvant CT in patients with resectable PDAC[44]. One of the first published phase III trials assessing the role of neoadjuvant gemcitabine followed by gemcitabine and radiation before surgery is the PREOPANC trial. Although it has not shown statistically significant survival benefit in patients using neoadjuvant CT + CRT (overall survival of 16 mo for neoadjuvant therapy *vs* 14.3 mo for initial surgery), better R0 resection rates, locoregional disease-free survival, and lower rates of vascular and perineural invasion favor neoadjuvant CT[45]. Analyses of 'US National Cancer Database data have shown a favorable survival using perioperative CT in patients with early PC as compared with upfront surgery. Another similar cohort study by Mokdad and colleagues[46] demonstrated statistically significant median overall survival in the neoadjuvant group *vis a vis* upfront surgery group (26 mo *vs* 23 mo respectively; $P = 0.01$). Many other phase III trials are being conducted to have a better understanding of this therapeutic aspect[27] (Table 2). Neoadjuvant treatment is well tolerated. The risk of postoperative pancreatic fistula formation (3%-11%), risk of postoperative infections (3%-7%) and mortality (0%-4%) compared to those who have undergone surgery alone[47].

MANAGEMENT OF BRPC

The National Comprehensive Cancer Network has defined BRPC based on the following radiological criteria: Contrast-enhanced computerized tomographic (CECT) scan using the pancreatic protocol, the relationship of tumor with the surrounding

Table 2 Landmark trails on use of neoadjuvant chemotherapy

Study	No. of patients	Treatment arms	Resection rate, %	R0	Median DFS in mo	Median OS in mo
PACT-15[44]	93 Resectable	Surgery + gemcitabine	85	27	4.7	20.4
		Surgery + 6 PEXG	90	37	12.4	26.4
		3PEXG + surgery + 3 PEXG	84	63	16.9	16.9
PREOPANC-01[48]	248 Resectable + BRPC	26Gy/15fr + gemcitabine	60	63	9.9	17.1
		Surgery	72	31	7.9	13.7

BRPC: Borderline resectable pancreatic cancer; DFS: Disease-free survival; OS: Overall survival; PEXG: Cisplatin, epirubicin, gemcitabine, and capecitabine.

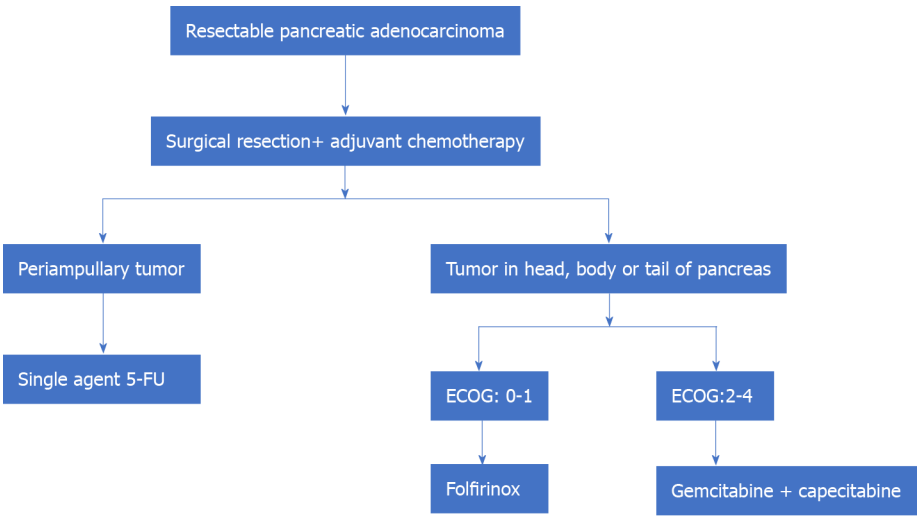


Figure 1 Management of resectable pancreatic adenocarcinoma. 5-FU: 5-Fluorouracil; ECOG: Eastern Cooperative Oncology Group.

vasculature, and the absence/presence of metastasis.

Thus, a BRPC localized to the HOP is one where the tumor is in contact with the common HA but without extension to the CA or artery bifurcation and variant arterial anatomy, contact with the SMA < 180°, contact with the SMV or PV < 180° without venous contour irregularity or thrombosis, which allows for safe and complete arterial and venous resection and reconstruction[20].

Borderline resectable PDAC in the pancreatic body or tail is 'the solid tumor in contact with the CA of < 180° or contact with the CA > 180° without the involvement of the aorta and gastroduodenal artery to allow a 'modified Appleby surgery'[20]. Another definition, the Anderson classification for BRPC, classifies it into the following three different groups: Group A includes patients with a tumor that abuts visceral arteries or causes short-segment occlusion of SMV; group B, have findings suggestive of metastasis; and group C patients are those who have marginal performance status[49].

Historically, therapeutic options for BRPC consist of upfront surgery, surgery followed by adjuvant CT/CRT, and neoadjuvant CT. The standard surgical options remain Whipple procedure, total pancreatectomy, or distal pancreatectomy, based on the tumor localization. An approach favoring upfront surgery carries with itself the risk of early failure, which has often been attributed to the poor pre-operative staging of tumor radiologically, inability to carry out a radical surgery, and the aggressive tumor behavior owing to variations in tumor biology. This has brought about an interest in considering neoadjuvant CT for patients with BRPC.

A meta-analysis carried out by the Dutch Pancreatic Cancer Group has shown a median survival of 19.2 mo in patients undergoing neoadjuvant CT *vs* 12.8 mo in those undergoing upfront surgery[50]. A peculiar problem in comparing different groups arises when different CT/CRT regimens are being compared. A recent patient-level meta-analysis has analyzed the efficacy of neoadjuvant FOLFIRINOX in BRPC, finding a favorable trend using FOLFIRINOX (median overall survival of 22 mo and median disease progression-free survival of 18.0 mo)[18].

A recent randomized control trial has assessed the use of CRT as neoadjuvant therapy for BRPC. The investigators combined 54 Gy in 30 fractions + weekly gemcitabine followed by adjuvant gemcitabine. Results have shown a better resection rate in the neoadjuvant group *vs* the surgery only group (51.8% *vs* 26.1% respectively) as well as a statistically significant 2-year survival (40.7% *vs* 26%; $P = 0.028$)[51]. The preoperative CRT *vs* immediate surgery for resectable and borderline resectable pancreatic cancer (PREOPANC-1) trial has used intention-to-treat analysis to study the efficacy of neoadjuvant CRT (gemcitabine-based) *vs* upfront surgery in BRPC. Patients in the neoadjuvant CRT group had a lower resection rate (60%) *vs* those in the upfront surgery group (72%; $P = 0.065$). R0 resection rate was statistically higher in the neoadjuvant group *vs* the upfront surgery group (61% *vs* 31%; $P < 0.001$). To add to the benefits, patients receiving neoadjuvant CRT had a longer median time till recurrence *vs* the surgery only group (9.9 mo *vs* 7.9 mo; $P = 0.023$)[48].

Results of these trials have shown the efficacy of both neoadjuvant CT as well as for CRT in BRPC. Several ongoing trials are being carried out to study the efficacy of induction therapy in improving overall survival in BRPC and which of the two therapeutic strategies (CT/CRT) is better suited for the same.

MANAGEMENT OF LOCALLY ADVANCED PC

The concept of locally advanced PC (LAPC) has evolved based on the development of radiological criteria of resectability and the availability of neoadjuvant therapy. Practically, the pancreatic tumors which are not metastatic and are unresectable due to 'irreversible' vascular invasion (encasement of aorta, invasion of PV or SMV, involvement of the SMA or celiac trunk by > 180°) are considered as LAPC[52,53]. The median survival has been variably reported from 10 mo to 30 mo.

The standard treatment for LAPC is gemcitabine-based CT. For patients with good performance status (ECOG0-1), the FOLFIRINOX-based regimen and for those with ECOG0-2, the nab-paclitaxel-gemcitabine-based regimen may be considered[53]. Some observational studies and pooled analyses of different approaches have advocated induction treatment with either FOLFIRINOX or nab-paclitaxel–gemcitabine followed by CRT. Using this approach median survival of 24.2 mo and disease progression-free survival of 15 mo has been reported[54]. However, the use of either upfront radiation therapy or following induction treatment with gemcitabine is not beneficial for patients with LAPC. Recently published meta-analysis has reported similar overall survival and drug-related side effects of CRT and CT in the setting of LAPC[55]. CRT using capecitabine as a radiosensitizer, however, has been tried for improvement of local control of disease in a subset of patients with LAPC. Since this is not a standard treatment approach, it has been proposed that this may be offered to only a select group of individuals[56].

Ongoing trials in LAPC are trying to assess the efficacy of FOLFIRINOC *vs* gemcitabine as induction therapy (NEOPAN; NCT02539537), use of nab-paclitaxel-gemcitabine for induction regimen + radiation therapy *vs* continuous CT, and use of activation of the *DPC4* gene (RTOG 1201; NCT01921751).

An interesting recent concept that has emerged in the management of LAPC is the role of surgery. This was proposed by researchers from the Medical College of Wisconsin based on the observation that those with an initially unresectable disease as per radiological criteria may convert to the resectable tumor after induction CT ± CRT. They have proposed the classification of patients with LAPC into the following two distinct categories: Type A, tumors that may be considered for resection following induction CT; and type B: Definitively unresectable tumors (> 270° encasement of the SMA, > 180° encasement of the CA, encasement of the aorta, and > 180° encasement of the HA with extension beyond the bifurcation of the proper HA into right and left HA)[52]. Thus, patients with LAPC type A, who have completed induction CT should be considered for surgical exploration. This is especially pertinent as the specificity of a CECT scan to determine tumor staging, operability, and R0 resectability for HOP carcinoma decrease following induction therapy. In such a setting, surgical exploration is the ideal modality to prove/ rule out vascular involvement[57]. Resected patients who have received CT preoperatively can also be considered for an additional course of CT following surgery[58] (Figure 2).

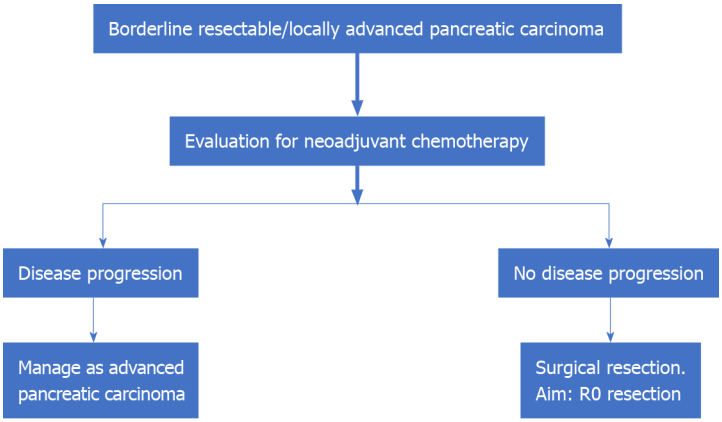


Figure 2 Management of borderline resectable/locally advance pancreatic carcinoma.

MANAGEMENT OF ADVANCED METASTATIC PC

CT forms the backbone of therapeutic regimens for the management of metastatic PC. Till the advent of gemcitabine, fluorouracil was the only approved drug in the management of APC. The use of gemcitabine has brought about benefits of disease progression-free survival, and overall survival (from 4.4 mo to 5.7 mo, $P = 0.0025$) with similar drug-related side effects as compared to fluorouracil[59]. This was followed by trials that analyzed the survival benefit of adding another cytotoxic drug or targeted therapy to gemcitabine. Use of erlotinib to gemcitabine-based regimen has shown median overall survival benefit (5.91 mo to 6.24 mo, $P = 0.038$) and 1-year survival benefit (17% to 23%, $P = 0.023$)[60]. A combination regimen consisting of cisplatin, epirubicin, fluorouracil, and gemcitabine (PEFG) *vs* gemcitabine has shown 'four-month progression-free survival' of 60% *vs* 28% in gemcitabine alone arm, $P = 0.001$ with no difference in overall survival[44]. A combination of gemcitabine + nab-paclitaxel in patients with ECOG0-2 has shown an improvement of 'median overall survival' *vs* gemcitabine alone (8.5 mo *vs* 6.7 mo, $P < 0.001$). The PRODIGE 4-ACCORD11 trial is a landmark trial that has shown the overall survival benefit of using FOLFIRINOX (median survival: 11.1 mo) in patients with APC *vs* gemcitabine (6.8 mo, $P < 0.001$)[10]. FOLFIRINOX has not been compared to nab-paclitaxel + gemcitabine in any prospective trial to date. Thus, the FOLFIRINOX regimen is now the standard of care for patients of APC with ECOG: 0-1, normal serum bilirubin, and no underlying cardiac pathology. The limiting step in the FOLFIRINOX regimen happens to be the performance status of the individual and comorbidity profile with the elderly or low-profile patients likely to have a poorer outcome. Other prognostic factors are the number of metastases, and liver metastases, presence of genetic mutations such as *DNA damage response* (*DDR*) gene mutations and *BRCA* tumor suppressor gene mutations[61-63]. Modified FOLFIRINOX has been tried with similar efficacy and better tolerance profile as compared to the standard FOLFIRINOX regimen. This regimen includes fluorouracil bolus suppression or a dose reduction of irinotecan (or both)[64].

Progress of disease in patients with first-line CT regimens presents a particular challenge with around 50% of patients being eligible for second-line CT[65]. Combination regimens like gemcitabine-platinum and fluoropyrimidine-platinum have shown disease progression-free survival of 2.5 mo *vs* 1.9 mo for single agents ($P = 0.169$) but no improvement in overall survival (5.1 mo *vs* 4.3 mo, $P = 0.169$)[66]. The various combination regimens that have been tried on the failure of first- and second-line regimens are oxaliplatin, folinic acid, and 5-FU (OFF regimen), and nanoliposomal irinotecan (MM-398), 5-FU, and folinic acid regimen. The CONKO-003 trial has shown overall survival benefit of using the OFF regimen over the 5-FU–folinic acid (FF regimen); the median survival was 5.9 mo *vs* 3.3 mo respectively ($P = 0.01$)[67]. The disease progression-free survival with use of nanoliposomal irinotecan (MM-398), 5-FU, and folinic acid regimen after failure of the FOLFIRINOX regimen has been reported to be 5.1 mo with overall survival of 8.8 mo[68]. The results of using targeted agents, namely the Jak1 and Jak2 tyrosine kinase inhibitor ruxolitinib and glufosfamide, have been rather disappointing. However, patients with metastatic solid tumors (including 8 patients with pancreatic tumors), with deficient mismatch repair and failed first-line therapy have shown response to the PD-1 immune checkpoint

inhibitor (ICI) pembrolizumab (disease control rate: 77%, objective response: 53% and complete radiological recovery: 21%)[69]. Mutation in the *BRCA* gene has been reported in around 5% of patients with APC. Targeted therapy in patients with *BRCA* gene mutation using 'poly ADP-ribose polymerase (PARP) inhibitors' is being actively investigated[70] (Figure 3).

Palliative treatment

Palliative treatment aims to allay patients' symptoms and improve their quality of life. Pain management, symptomatic relief, and psychological support are the pillars of this strategy.

Gastric outlet obstruction (GOO), extrahepatic biliary obstruction (EHBO), and abdominal pain are the three most common disabling symptoms in APC which adversely affect an individual's quality of life besides being a major source of 'caregiver fatigue'. GOO, presenting as nausea, vomiting, dehydration, and weight loss, is seen in 10%-25% of all APC cases. Palliative surgery with open gastrojejunostomy (GJ) is the traditional approach to managing a malignant GOO. Placement of endoscopic duodenal stents and laparoscopic GJ has been tried, with varying degrees of success. Surgical procedures offer good functional outcomes at the cost of increased mortality[71]. EHBO can present with obstructive jaundice. Endoscopic retrograde cholangiopancreatography (ERCP)-guided biliary stent placement is the accepted gold standard approach for the management of malignant EHBO. Both plastic and self-expanding metal stents (SEMSs) have been used, with literature favoring the use of covered SEMSs. Failure of ERCP-guided biliary drainage may warrant drainage through the percutaneous route or an endoscopic ultrasonography-guided biliary drainage (EUS BD)[72]. Hepaticojejunostomy with a Roux-en-Y reconstruction and cholecystectomy is the favored palliative surgical procedure for palliation of EHBO secondary to PC. Laparoscopic biliary bypass and robot-assisted laparoscopic hepaticojejunostomy have been technically successful with satisfactory surgical outcomes[73,74]. Thus, patients with good performance status may benefit from a palliative surgical procedure while those with poor performance status warrant endoscopic biliary drainage.

Malignant infiltration of celiac or mesenteric nerve plexus in patients of APC may cause abdominal and back pain. This may adversely affect an individual's quality of life. Multimodal drug therapy encompassing the use of non-steroidal anti-inflammatory drugs and or opioid analgesics in various combinations form the bedrock of pain management. Intraoperative celiac block using ethanol or a local anesthetic using either laparoscopic or open approach and EUS-guided neurolysis of celiac plexus, have all been tried[71] (Figure 4).

NEWER MODALITIES FOR PANCREATIC CANCER

Immunotherapy for pancreatic cancer

The tumor microenvironment of PC is responsible for aggressiveness as well as chemoresistance. This makes the case for utilizing immunotherapy in the advanced and metastatic settings. However, the approval for ICI is currently for patients with mismatch repair-deficient cases[69]. The updated results of the Keynote-158, using pembrolizumab in patients with advanced PDAC revealed an overall response rate (ORR) of 18.2%, median progression-free survival of 2.1 mo, and median overall survival of 4.0 mo[75]. The results are not very encouraging despite this, due to fewer driver mutations, variable expression of PD-1/PD-L1 and neoantigen burden in the tumor tissue, and absence of DDR, which are hallmarks of this malignancy[76].

Targeted therapy

The highly actionable mutations detected in molecular profiling of the Know Your Tumor initiative were 27%, of which the common ones involved the *KRAS, TP53, MLL3, CDKN2A, SMAD4, TGFBR2, ARID1A,* and *SF3B1* genes. These mutations, however, do not have any therapeutic modality to target[77,78]. *Neurotrophic receptor tyrosine kinase* (*NTRK*) gene fusions have been detected in about 6% of pancreatic adenocarcinomas. Larotrectinib and entrectinib are two newer agents receiving accelerated approval for use in metastatic tumors with *NTRK* gene biomarker with tissue agnostic indication[79,80]. Three single-arm trials, namely LOXO-TRK-14001, SCOUT and NAVIGATE, had a total of 55 patients with *NTRK* fusions and had an ORR of 55% with Larotrectinib[81]. The median progression-free survival was not achieved after a median duration of 9.9 mo. Similarly, in three other single-arm trials,

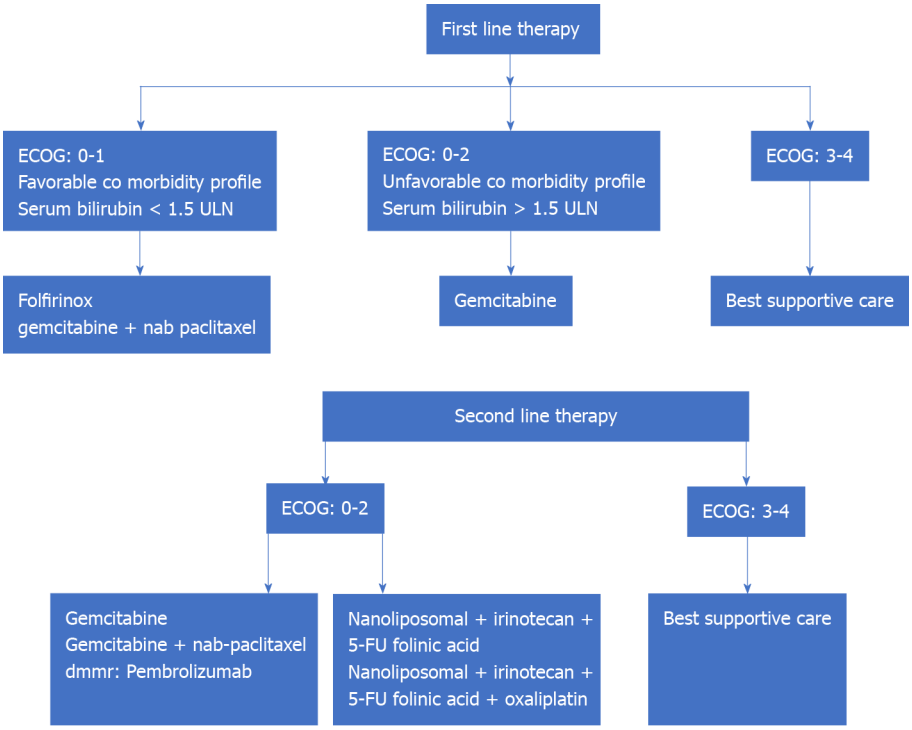


Figure 3 Management of advanced metastatic pancreatic carcinoma. ECOG: Eastern Cooperative Oncology Group; ULN: Upper limit of normal.

including ALKA-372-001, STARTRK-1 and STARTRK-2, with 60 patients in total, the patients with *NTRK* fusion had an ORR of 100%[82].

Germline *BRCA1/2* mutations and homologous recombination deficiency enable the utility of platinum agents as well as poly (adenosine diphosphate-ribose) polymerase (PARP) inhibition as a novel therapeutic modality. Olaparib, a PARP inhibitor was approved by the United States' Food and Drug Administration in December 2019 for patients with advanced metastatic malignancy having germline *BRCA1/2* mutation. The phase III POLO trial utilizing olaparib in PAC, progressing after platinum-based therapy revealed median progression-free survival of 7.4 mo *vs* 3.8 in the control arm (HR: 0.53, 95%CI: 0.35-0.82; P = 0.004). This did not translate into an overall survival benefit[83].

Macrophage-targeted therapy

Macrophages residing in the tumor environment are labeled as tumor-associated macrophages. CD 51 is a marker of macrophages that promotes the stemness of PDAC cells by regulating the TGF-β1/smad2/3 pathway. As a result, CD 51- targeted therapy is evolving as a newer therapeutic modality. Similarly, CD 40 activation, which promotes anti-tumor T-cell responses has been targeted by using anti-CD 40 antibody, CP-870893 along with gemcitabine, providing initial results of response[84].

Cancer vaccines

The ability of cancer vaccines to stimulate dendritic cell responses and activate the adaptive immune responses has been harnessed for many cancers, including PC. The expression of murine enzyme alpha-1,3-galactosyltransferase (alpha-GT) by genetic engineering on PC cell lines HAPa1 and HAPa2 lead to anti-alpha-Gal antibody responses in humans[85]. Algenpanteucel-L was used in a phase II study and phase III (IMPRESS Trial). When algenpanteucel-L was given after gemcitabine and 5-FU based CRT, 81%-86% 1-year disease-free survival and 96% 1-year overall survival were observed[86,87].

GVAX, a line of engineered pancreatic tumor cells secreting GM-CSF has been tested in phase I study along with cyclophosphamide (Cy) with early results of tolerability and survival. In a phase II study, GVAX/Cy was tested against a GVAX/Cy followed by CRS 207 (a live-attenuated *Listeria* strain that induces tumor-associated antigens) and resulted in better overall survival in the latter arm (6.1 mo *vs* 3.9 mo, P = 0.02)[88].

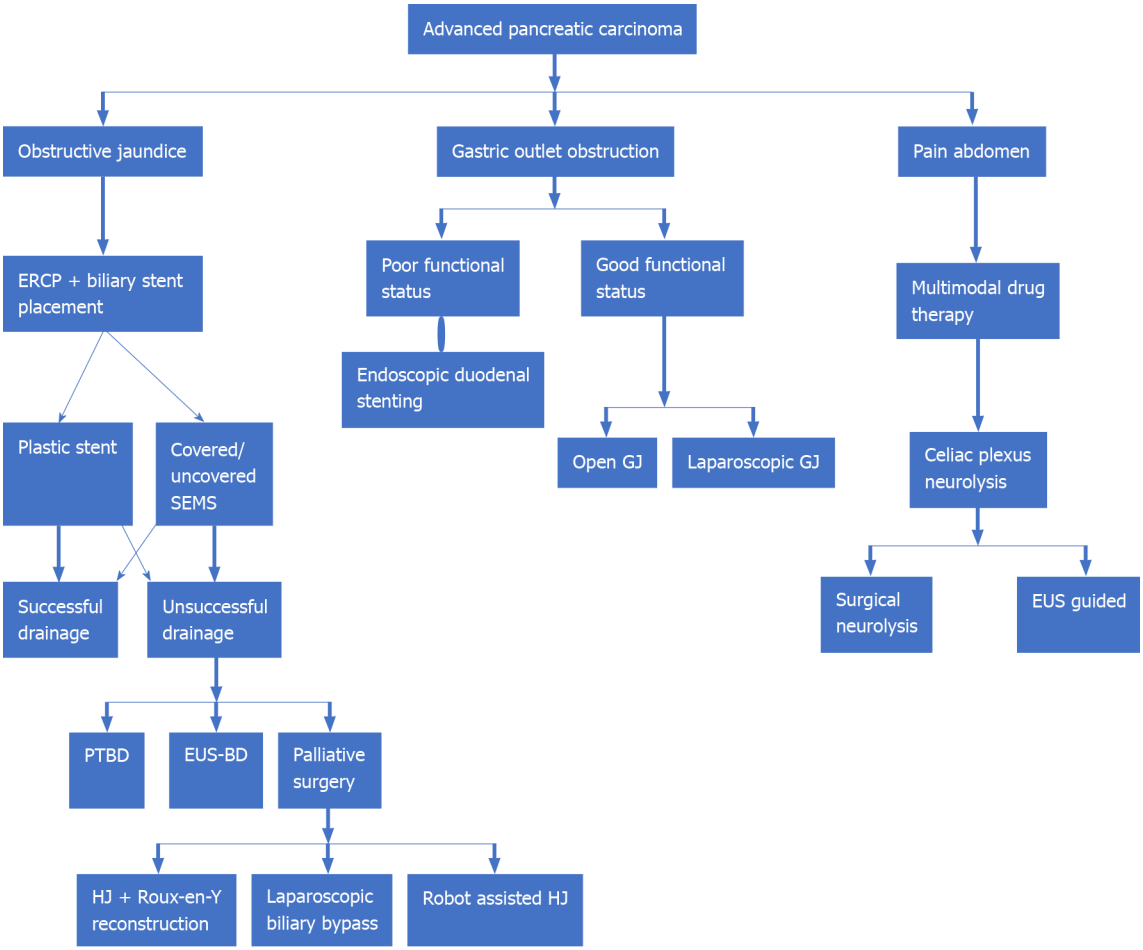


Figure 4 Palliative management in metastatic pancreatic carcinoma. ERCP: Endoscopic retrograde cholangiopancreatography; EUS: Endoscopic ultrasound; EUS-BD: Endoscopic ultrasound guided biliary drainage; GJ: Gastrojejunostomy; HJ: Hepaticojejunostomy; PTBD: Percutaneous transhepatic biliary drainage; SEMS: Self-expanding metal stent.

Other membranous and intracytoplasmic targets

There have been numerous trials using targets like vascular endothelial growth factor (VEGF) and VEGF-receptor, RAS-RAF-MEK-ERK pathway, *etc.* but none have shown robust survival data[89,90]. The rapamycin-insensitive companion of mTOR (RICTOR) expression was found to have a survival benefit in resected PAC patients, with those having a lower expression doubling the survival as compared to the high expressers [91].

CONCLUSION

We have attempted to provide an inclusive version of the management of PC, with special emphasis on current strategies and the road ahead with emerging modalities of therapy. Of course, there are certain gaps in the understanding of this disease and the evolution of treatment options is always challenging. For times to come, newer modalities appear promising; however, there is no substitute for early diagnosis and management for disease-free survival.

REFERENCES

1 **Siegel RL**, Miller KD, Jemal A. Cancer statistics, 2019. *CA Cancer J Clin* 2019; **69**: 7-34 [PMID: 30620402 DOI: 10.3322/caac.21551]
2 **Ferlay J**, Soerjomataram I, Dikshit R, Eser S, Mathers C, Rebelo M, Parkin DM, Forman D, Bray F. Cancer incidence and mortality worldwide: sources, methods and major patterns in GLOBOCAN 2012. *Int J Cancer* 2015; **136**: E359-E386 [PMID: 25220842 DOI: 10.1002/ijc.29210]
3 **Bosetti C**, Bertuccio P, Malvezzi M, Levi F, Chatenoud L, Negri E, La Vecchia C. Cancer mortality

in Europe, 2005-2009, and an overview of trends since 1980. *Ann Oncol* 2013; **24**: 2657-2671 [PMID: 23921790 DOI: 10.1093/annonc/mdt301]

4 **Bosetti C**, Bertuccio P, Negri E, La Vecchia C, Zeegers MP, Boffetta P. Pancreatic cancer: overview of descriptive epidemiology. *Mol Carcinog* 2012; **51**: 3-13 [PMID: 22162227 DOI: 10.1002/mc.20785]

5 **Rozenblum E**, Schutte M, Goggins M, Hahn SA, Panzer S, Zahurak M, Goodman SN, Sohn TA, Hruban RH, Yeo CJ, Kern SE. Tumor-suppressive pathways in pancreatic carcinoma. *Cancer Res* 1997; **57**: 1731-1734 [PMID: 9135016]

6 **Moore PS**, Orlandini S, Zamboni G, Capelli P, Rigaud G, Falconi M, Bassi C, Lemoine NR, Scarpa A. Pancreatic tumours: molecular pathways implicated in ductal cancer are involved in ampullary but not in exocrine nonductal or endocrine tumorigenesis. *Br J Cancer* 2001; **84**: 253-262 [PMID: 11161385 DOI: 10.1054/bjoc.2000.1567]

7 **Oettle H**, Post S, Neuhaus P, Gellert K, Langrehr J, Ridwelski K, Schramm H, Fahlke J, Zuelke C, Burkart C, Gutberlet K, Kettner E, Schmalenberg H, Weigang-Koehler K, Bechstein WO, Niedergethmann M, Schmidt-Wolf I, Roll L, Doerken B, Riess H. Adjuvant chemotherapy with gemcitabine *vs* observation in patients undergoing curative-intent resection of pancreatic cancer: a randomized controlled trial. *JAMA* 2007; **297**: 267-277 [PMID: 17227978 DOI: 10.1001/jama.297.3.267]

8 **Abdel-Rahman O**, Elsayed Z, Elhalawani H. Gemcitabine-based chemotherapy for advanced biliary tract carcinomas. *Cochrane Database Syst Rev* 2018; **4**: CD011746 [PMID: 29624208 DOI: 10.1002/14651858.CD011746.pub2]

9 **Oettle H**, Neuhaus P, Hochhaus A, Hartmann JT, Gellert K, Ridwelski K, Niedergethmann M, Zülke C, Fahlke J, Arning MB, Sinn M, Hinke A, Riess H. Adjuvant chemotherapy with gemcitabine and long-term outcomes among patients with resected pancreatic cancer: the CONKO-001 randomized trial. *JAMA* 2013; **310**: 1473-1481 [PMID: 24104372 DOI: 10.1001/jama.2013.279201]

10 **Conroy T**, Desseigne F, Ychou M, Bouché O, Guimbaud R, Bécouarn Y, Adenis A, Raoul JL, Gourgou-Bourgade S, de la Fouchardière C, Bennouna J, Bachet JB, Khemissa-Akouz F, Péré-Vergé D, Delbaldo C, Assenat E, Chauffert B, Michel P, Montoto-Grillot C, Ducreux M; Groupe Tumeurs Digestives of Unicancer; PRODIGE Intergroup. FOLFIRINOX *vs* gemcitabine for metastatic pancreatic cancer. *N Engl J Med* 2011; **364**: 1817-1825 [PMID: 21561347 DOI: 10.1056/NEJMoa1011923]

11 **Tempero MA**, Reni M, Riess H, Pelzer U, O'Reilly EM, Winter JM, Oh DY, Li CP, Tortora G, Chang HM, Lopez CD, Tabernero J, Van Cutsem E, Philip PA, Goldstein D, Berlin J, Ferrara S, Li M, Lu BD, Biankin A. APACT: phase III, multicenter, international, open-label, randomized trial of adjuvant nab-paclitaxel plus gemcitabine (nab-P/G) *vs* gemcitabine (G) for surgically resected pancreatic adenocarcinoma. *J Clin Oncol* 2019; **37**: 15

12 **Neoptolemos JP**, Stocken DD, Friess H, Bassi C, Dunn JA, Hickey H, Beger H, Fernandez-Cruz L, Dervenis C, Lacaine F, Falconi M, Pederzoli P, Pap A, Spooner D, Kerr DJ, Büchler MW; European Study Group for Pancreatic Cancer. A randomized trial of chemoradiotherapy and chemotherapy after resection of pancreatic cancer. *N Engl J Med* 2004; **350**: 1200-1210 [PMID: 15028824 DOI: 10.1056/NEJMoa032295]

13 **Klinkenbijl JH**, Jeekel J, Sahmoud T, van Pel R, Couvreur ML, Veenhof CH, Arnaud JP, Gonzalez DG, de Wit LT, Hennipman A, Wils J. Adjuvant radiotherapy and 5-fluorouracil after curative resection of cancer of the pancreas and periampullary region: phase III trial of the EORTC gastrointestinal tract cancer cooperative group. *Ann Surg* 1999; **230**: 776-782; discussion 782 [PMID: 10615932 DOI: 10.1097/00000658-199912000-00006]

14 **Rutter CE**, Park HS, Corso CD, Lester-Coll NH, Mancini BR, Yeboa DN, Johung KL. Addition of radiotherapy to adjuvant chemotherapy is associated with improved overall survival in resected pancreatic adenocarcinoma: An analysis of the National Cancer Data Base. *Cancer* 2015; **121**: 4141-4149 [PMID: 26280559 DOI: 10.1002/cncr.29652]

15 **Hsieh MC**, Chang WW, Yu HH, Lu CY, Chang CL, Chow JM, Chen SU, Cheng Y, Wu SY. Adjuvant radiotherapy and chemotherapy improve survival in patients with pancreatic adenocarcinoma receiving surgery: adjuvant chemotherapy alone is insufficient in the era of intensity modulation radiation therapy. *Cancer Med* 2018; **7**: 2328-2338 [PMID: 29665327 DOI: 10.1002/cam4.1479]

16 **You MS**, Ryu JK, Huh G, Chun JW, Paik WH, Lee SH, Kim YT. Comparison of efficacy between adjuvant chemotherapy and chemoradiation therapy for pancreatic cancer: AJCC stage-based approach. *World J Clin Oncol* 2020; **11**: 747-760 [PMID: 33033696 DOI: 10.5306/wjco.v11.i9.747]

17 **Cascinu S**, Berardi R, Bianco R, Bilancia D, Zaniboni A, Ferrari D, Mosconi S, Spallanzani A, Cavanna L, Leo S, Negri F, Beretta GD, Sobrero A, Banzi M, Morabito A, Bittoni A, Marciano R, Ferrara D, Noventa S, Piccirillo MC. Nab-paclitaxel (Nab) plus gemcitabine (G) is more effective than G alone in locally advanced, unresectable pancreatic cancer (LAUPC): The GAP trial, a GISCAD phase II comparative randomized trial. *Ann Oncol* 2019; **30**: v253-v254 [DOI: 10.1093/annonc/mdz247.001]

18 **Janssen QP**, Buettner S, Suker M, Beumer BR, Addeo P, Bachellier P, Bahary N, Bekaii-Saab T, Bali MA, Besselink MG, Boone BA, Chau I, Clarke S, Dillhoff M, El-Rayes BF, Frakes JM, Grose D, Hosein PJ, Jamieson NB, Javed AA, Khan K, Kim KP, Kim SC, Kim SS, Ko AH, Lacy J, Margonis GA, McCarter MD, McKay CJ, Mellon EA, Moorcraft SY, Okada KI, Paniccia A, Parikh PJ, Peters NA, Rabl H, Samra J, Tinchon C, van Tienhoven G, van Veldhuisen E, Wang-Gillam A, Weiss MJ,

Wilmink JW, Yamaue H, Homs MYV, van Eijck CHJ, Katz MHG, Groot Koerkamp B. Neoadjuvant FOLFIRINOX in Patients With Borderline Resectable Pancreatic Cancer: A Systematic Review and Patient-Level Meta-Analysis. *J Natl Cancer Inst* 2019; **111**: 782-794 [PMID: 31086963 DOI: 10.1093/jnci/djz073]

19 **Ghaneh P**, Palmer HP, Cicconi S, Halloran C, Psarelli EE, Rawcliffe CL, Sripadam R, Mukherjee S, Wadsley J, Al-Mukhtar A, Jiao LR, Wasan HS, Carter R, Graham JS, Ammad F, Evans J, Tjaden C, Hackert T, Buchler MW, Neoptolemos JP; European Study Group for Pancreatic Cancer (ESPAC). ESPAC-5F: Four-arm, prospective, multicenter, international randomized phase II trial of immediate surgery compared with neoadjuvant gemcitabine plus capecitabine (GEMCAP) or FOLFIRINOX or chemoradiotherapy (CRT) in patients with borderline resectable pancreatic cancer. *J Clin Oncol* 2020; **15**: 4505 [DOI: 10.1200/JCO.2020.38.15_suppl.4505]

20 **Tempero MA**, Malafa MP, Chiorean EG, Czito B, Scaife C, Narang AK, Fountzilas C, Wolpin BM, Al-Hawary M, Asbun H, Behrman SW, Benson AB, Binder E, Cardin DB, Cha C, Chung V, Dillhoff M, Dotan E, Ferrone CR, Fisher G, Hardacre J, Hawkins WG, Ko AH, LoConte N, Lowy AM, Moravek C, Nakakura EK, O'Reilly EM, Obando J, Reddy S, Thayer S, Wolff RA, Burns JL, Zuccarino-Catania G. Pancreatic Adenocarcinoma, Version 1.2019. *J Natl Compr Canc Netw* 2019; **17**: 202-210 [PMID: 30865919 DOI: 10.6004/jnccn.2019.0014]

21 **Strasberg SM**, Linehan DC, Hawkins WG. Radical antegrade modular pancreatosplenectomy procedure for adenocarcinoma of the body and tail of the pancreas: ability to obtain negative tangential margins. *J Am Coll Surg* 2007; **204**: 244-249 [PMID: 17254928 DOI: 10.1016/j.jamcollsurg.2006.11.002]

22 **Malleo G**, Maggino L, Ferrone CR, Marchegiani G, Mino-Kenudson M, Capelli P, Rusev B, Lillemoe KD, Bassi C, Fernàndez-Del Castillo C, Salvia R. Number of Examined Lymph Nodes and Nodal Status Assessment in Distal Pancreatectomy for Body/Tail Ductal Adenocarcinoma. *Ann Surg* 2019; **270**: 1138-1146 [PMID: 29672406 DOI: 10.1097/SLA.0000000000002781]

23 **Delpero JR**, Bachellier P, Regenet N, Le Treut YP, Paye F, Carrere N, Sauvanet A, Autret A, Turrini O, Monges-Ranchin G, Boher JM. Pancreaticoduodenectomy for pancreatic ductal adenocarcinoma: a French multicentre prospective evaluation of resection margins in 150 evaluable specimens. *HPB (Oxford)* 2014; **16**: 20-33 [PMID: 23464850 DOI: 10.1111/hpb.12061]

24 **Negoi I**, Hostiuc S, Runcanu A, Negoi RI, Beuran M. Superior mesenteric artery first approach *vs* standard pancreaticoduodenectomy: a systematic review and meta-analysis. *Hepatobiliary Pancreat Dis Int* 2017; **16**: 127-138 [PMID: 28381375 DOI: 10.1016/s1499-3872(16)60134-0]

25 **McGuigan A**, Kelly P, Turkington RC, Jones C, Coleman HG, McCain RS. Pancreatic cancer: A review of clinical diagnosis, epidemiology, treatment and outcomes. *World J Gastroenterol* 2018; **24**: 4846-4861 [PMID: 30487695 DOI: 10.3748/wjg.v24.i43.4846]

26 **van der Gaag NA**, Rauws EA, van Eijck CH, Bruno MJ, van der Harst E, Kubben FJ, Gerritsen JJ, Greve JW, Gerhards MF, de Hingh IH, Klinkenbijl JH, Nio CY, de Castro SM, Busch OR, van Gulik TM, Bossuyt PM, Gouma DJ. Preoperative biliary drainage for cancer of the head of the pancreas. *N Engl J Med* 2010; **362**: 129-137 [PMID: 20071702 DOI: 10.1056/NEJMoa0903230]

27 **Lambert A**, Schwarz L, Borbath I, Henry A, Van Laethem JL, Malka D, Ducreux M, Conroy T. An update on treatment options for pancreatic adenocarcinoma. *Ther Adv Med Oncol* 2019; **11**: 1758835919875568 [PMID: 31598142 DOI: 10.1177/1758835919875568]

28 **Uzunoglu FG**, Reeh M, Vettorazzi E, Ruschke T, Hannah P, Nentwich MF, Vashist YK, Bogoevski D, König A, Janot M, Gavazzi F, Zerbi A, Todaro V, Malleo G, Uhl W, Montorsi M, Bassi C, Izbicki JR, Bockhorn M. Preoperative Pancreatic Resection (PREPARE) score: a prospective multicenter-based morbidity risk score. *Ann Surg* 2014; **260**: 857-863; discussion 863 [PMID: 25243549 DOI: 10.1097/SLA.0000000000000946]

29 **Ragulin-Coyne E**, Carroll JE, Smith JK, Witkowski ER, Ng SC, Shah SA, Zhou Z, Tseng JF. Perioperative mortality after pancreatectomy: a risk score to aid decision-making. *Surgery* 2012; **152**: S120-S127 [PMID: 22766367 DOI: 10.1016/j.surg.2012.05.018]

30 **Sinn M**, Bahra M, Liersch T, Gellert K, Messmann H, Bechstein W, Waldschmidt D, Jacobasch L, Wilhelm M, Rau BM, Grützmann R, Weinmann A, Maschmeyer G, Pelzer U, Stieler JM, Striefler JK, Ghadimi M, Bischoff S, Dörken B, Oettle H, Riess H. CONKO-005: Adjuvant Chemotherapy With Gemcitabine Plus Erlotinib Versus Gemcitabine Alone in Patients After R0 Resection of Pancreatic Cancer: A Multicenter Randomized Phase III Trial. *J Clin Oncol* 2017; **35**: 3330-3337 [PMID: 28817370 DOI: 10.1200/JCO.2017.72.6463]

31 **Sinn M**, Liersch T, Gellert K, Riess H, Stübs P, Waldschmidt DT, Pelzer U, Stieler J, Striefler JK, Bahra M, Dörken B, Oettle H. LBA18 - Conko-006: a Randomized Double-Blinded Phase Iib-Study of Adjuvant Therapy with Gemcitabine + Sorafenib/Placebo for Patients with R1-Resection of Pancreatic Cancer. *Ann Oncol* 2014; **25**: v1 [DOI: 10.1093/annonc/mdu438.18]

32 **Yoshitomi H**, Togawa A, Kimura F, Ito H, Shimizu H, Yoshidome H, Otsuka M, Kato A, Nozawa S, Furukawa K, Miyazaki M; Pancreatic Cancer Chemotherapy Program of the Chiba University Department of General Surgery Affiliated Hospital Group. A randomized phase II trial of adjuvant chemotherapy with uracil/tegafur and gemcitabine *vs* gemcitabine alone in patients with resected pancreatic cancer. *Cancer* 2008; **113**: 2448-2456 [PMID: 18823024 DOI: 10.1002/cncr.23863]

33 Further evidence of effective adjuvant combined radiation and chemotherapy following curative resection of pancreatic cancer. Gastrointestinal Tumor Study Group. *Cancer* 1987; **59**: 2006-2010 [PMID: 3567862 DOI: 10.1002/1097-0142(19870615)59:12<2006::aid-cncr2820591206>3.0.co;2-b]

34 **Neoptolemos JP**, Dunn JA, Stocken DD, Almond J, Link K, Beger H, Bassi C, Falconi M, Pederzoli

P, Dervenis C, Fernandez-Cruz L, Lacaine F, Pap A, Spooner D, Kerr DJ, Friess H, Büchler MW; European Study Group for Pancreatic Cancer. Adjuvant chemoradiotherapy and chemotherapy in resectable pancreatic cancer: a randomised controlled trial. *Lancet* 2001; **358**: 1576-1585 [PMID: 11716884 DOI: 10.1016/s0140-6736(01)06651-x]

35 **Neoptolemos JP**, Stocken DD, Bassi C, Ghaneh P, Cunningham D, Goldstein D, Padbury R, Moore MJ, Gallinger S, Mariette C, Wente MN, Izbicki JR, Friess H, Lerch MM, Dervenis C, Oláh A, Butturini G, Doi R, Lind PA, Smith D, Valle JW, Palmer DH, Buckels JA, Thompson J, McKay CJ, Rawcliffe CL, Büchler MW; European Study Group for Pancreatic Cancer. Adjuvant chemotherapy with fluorouracil plus folinic acid *vs* gemcitabine following pancreatic cancer resection: a randomized controlled trial. *JAMA* 2010; **304**: 1073-1081 [PMID: 20823433 DOI: 10.1001/jama.2010.1275]

36 **Neoptolemos JP**, Palmer DH, Ghaneh P, Psarelli EE, Valle JW, Halloran CM, Faluyi O, O'Reilly DA, Cunningham D, Wadsley J, Darby S, Meyer T, Gillmore R, Anthoney A, Lind P, Glimelius B, Falk S, Izbicki JR, Middleton GW, Cummins S, Ross PJ, Wasan H, McDonald A, Crosby T, Ma YT, Patel K, Sherriff D, Soomal R, Borg D, Sothi S, Hammel P, Hackert T, Jackson R, Büchler MW; European Study Group for Pancreatic Cancer. Comparison of adjuvant gemcitabine and capecitabine with gemcitabine monotherapy in patients with resected pancreatic cancer (ESPAC-4): a multicentre, open-label, randomised, phase 3 trial. *Lancet* 2017; **389**: 1011-1024 [PMID: 28129987 DOI: 10.1016/S0140-6736(16)32409-6]

37 **Conroy T**, Hammel P, Hebbar M, Ben Abdelghani M, Wei AC, Raoul JL, Choné L, Francois E, Artru P, Biagi JJ, Lecomte T, Assenat E, Faroux R, Ychou M, Volet J, Sauvanet A, Breysacher G, Di Fiore F, Cripps C, Kavan P, Texereau P, Bouhier-Leporrier K, Khemissa-Akouz F, Legoux JL, Juzyna B, Gourgou S, O'Callaghan CJ, Jouffroy-Zeller C, Rat P, Malka D, Castan F, Bachet JB; Canadian Cancer Trials Group and the Unicancer-GI–PRODIGE Group. FOLFIRINOX or Gemcitabine as Adjuvant Therapy for Pancreatic Cancer. *N Engl J Med* 2018; **379**: 2395-2406 [PMID: 30575490 DOI: 10.1056/NEJMoa1809775]

38 **Regine WF**, Winter KA, Abrams RA, Safran H, Hoffman JP, Konski A, Benson AB, Macdonald JS, Kudrimoti MR, Fromm ML, Haddock MG, Schaefer P, Willett CG, Rich TA. Fluorouracil *vs* gemcitabine chemotherapy before and after fluorouracil-based chemoradiation following resection of pancreatic adenocarcinoma: a randomized controlled trial. *JAMA* 2008; **299**: 1019-1026 [PMID: 18319412 DOI: 10.1001/jama.299.9.1019]

39 **Valle JW**, Palmer D, Jackson R, Cox T, Neoptolemos JP, Ghaneh P, Rawcliffe CL, Bassi C, Stocken DD, Cunningham D, O'Reilly D, Goldstein D, Robinson BA, Karapetis C, Scarfe A, Lacaine F, Sand J, Izbicki JR, Mayerle J, Dervenis C, Oláh A, Butturini G, Lind PA, Middleton MR, Anthoney A, Sumpter K, Carter R, Büchler MW. Optimal duration and timing of adjuvant chemotherapy after definitive surgery for ductal adenocarcinoma of the pancreas: ongoing lessons from the ESPAC-3 study. *J Clin Oncol* 2014; **32**: 504-512 [PMID: 24419109 DOI: 10.1200/JCO.2013.50.7657]

40 **Xia BT**, Ahmad SA, Al Humaidi AH, Hanseman DJ, Ethun CG, Maithel SK, Kooby DA, Salem A, Cho CS, Weber SM, Stocker SJ, Talamonti MS, Bentrem DJ, Abbott DE. Time to Initiation of Adjuvant Chemotherapy in Pancreas Cancer: A Multi-Institutional Experience. *Ann Surg Oncol* 2017; **24**: 2770-2776 [PMID: 28600732 DOI: 10.1245/s10434-017-5918-z]

41 **Newton AD**, Datta J, Loaiza-Bonilla A, Karakousis GC, Roses RE. Neoadjuvant therapy for gastric cancer: current evidence and future directions. *J Gastrointest Oncol* 2015; **6**: 534-543 [PMID: 26487948 DOI: 10.3978/j.issn.2078-6891.2015.047]

42 **Gillen S**, Schuster T, Meyer Zum Büschenfelde C, Friess H, Kleeff J. Preoperative/neoadjuvant therapy in pancreatic cancer: a systematic review and meta-analysis of response and resection percentages. *PLoS Med* 2010; **7**: e1000267 [PMID: 20422030 DOI: 10.1371/journal.pmed.1000267]

43 **Schorn S**, Demir IE, Reyes CM, Saricaoglu C, Samm N, Schirren R, Tieftrunk E, Hartmann D, Friess H, Ceyhan GO. The impact of neoadjuvant therapy on the histopathological features of pancreatic ductal adenocarcinoma - A systematic review and meta-analysis. *Cancer Treat Rev* 2017; **55**: 96-106 [PMID: 28342938 DOI: 10.1016/j.ctrv.2017.03.003]

44 **Reni M**, Balzano G, Zanon S, Zerbi A, Rimassa L, Castoldi R, Pinelli D, Mosconi S, Doglioni C, Chiaravalli M, Pircher C, Arcidiacono PG, Torri V, Maggiora P, Ceraulo D, Falconi M, Gianni L. Safety and efficacy of preoperative or postoperative chemotherapy for resectable pancreatic adenocarcinoma (PACT-15): a randomised, open-label, phase 2-3 trial. *Lancet Gastroenterol Hepatol* 2018; **3**: 413-423 [PMID: 29625841 DOI: 10.1016/S2468-1253(18)30081-5]

45 **O'Reilly EM**, Ferrone C. Neoadjuvant or Adjuvant Therapy for Resectable or Borderline Resectable Pancreatic Cancer: Which Is Preferred? *J Clin Oncol* 2020; **38**: 1757-1759 [PMID: 32119598 DOI: 10.1200/JCO.19.03318]

46 **Mokdad AA**, Minter RM, Zhu H, Augustine MM, Porembka MR, Wang SC, Yopp AC, Mansour JC, Choti MA, Polanco PM. Neoadjuvant Therapy Followed by Resection Versus Upfront Resection for Resectable Pancreatic Cancer: A Propensity Score Matched Analysis. *J Clin Oncol* 2017; **35**: 515-522 [PMID: 27621388 DOI: 10.1200/JCO.2016.68.5081]

47 **Verma V**, Li J, Lin C. Neoadjuvant Therapy for Pancreatic Cancer: Systematic Review of Postoperative Morbidity, Mortality, and Complications. *Am J Clin Oncol* 2016; **39**: 302-313 [PMID: 26950464 DOI: 10.1097/COC.0000000000000278]

48 **Versteijne E**, Suker M, Groothuis K, Akkermans-Vogelaar JM, Besselink MG, Bonsing BA, Buijsen J, Busch OR, Creemers GM, van Dam RM, Eskens FALM, Festen S, de Groot JWB, Groot Koerkamp B, de Hingh IH, Homs MYV, van Hooft JE, Kerver ED, Luelmo SAC, Neelis KJ, Nuyttens J, Paardekooper GMRM, Patijn GA, van der Sangen MJC, de Vos-Geelen J, Wilmink JW, Zwinderman

AH, Punt CJ, van Eijck CH, van Tienhoven G; Dutch Pancreatic Cancer Group. Preoperative Chemoradiotherapy Versus Immediate Surgery for Resectable and Borderline Resectable Pancreatic Cancer: Results of the Dutch Randomized Phase III PREOPANC Trial. *J Clin Oncol* 2020; **38**: 1763-1773 [PMID: 32105518 DOI: 10.1200/JCO.19.02274]

49 **Katz MH**, Pisters PW, Evans DB, Sun CC, Lee JE, Fleming JB, Vauthey JN, Abdalla EK, Crane CH, Wolff RA, Varadhachary GR, Hwang RF. Borderline resectable pancreatic cancer: the importance of this emerging stage of disease. *J Am Coll Surg* 2008; **206**: 833-846; discussion 846 [PMID: 18471707 DOI: 10.1016/j.jamcollsurg.2007.12.020]

50 **Versteijne E**, Vogel JA, Besselink MG, Busch ORC, Wilmink JW, Daams JG, van Eijck CHJ, Groot Koerkamp B, Rasch CRN, van Tienhoven G; Dutch Pancreatic Cancer Group. Meta-analysis comparing upfront surgery with neoadjuvant treatment in patients with resectable or borderline resectable pancreatic cancer. *Br J Surg* 2018; **105**: 946-958 [PMID: 29708592 DOI: 10.1002/bjs.10870]

51 **Jang JY**, Han Y, Lee H, Kim SW, Kwon W, Lee KH, Oh DY, Chie EK, Lee JM, Heo JS, Park JO, Lim DH, Kim SH, Park SJ, Lee WJ, Koh YH, Park JS, Yoon DS, Lee IJ, Choi SH. Oncological Benefits of Neoadjuvant Chemoradiation With Gemcitabine Versus Upfront Surgery in Patients With Borderline Resectable Pancreatic Cancer: A Prospective, Randomized, Open-label, Multicenter Phase 2/3 Trial. *Ann Surg* 2018; **268**: 215-222 [PMID: 29462005 DOI: 10.1097/SLA.0000000000002705]

52 **Evans DB**, George B, Tsai S. Non-metastatic Pancreatic Cancer: Resectable, Borderline Resectable, and Locally Advanced-Definitions of Increasing Importance for the Optimal Delivery of Multimodality Therapy. *Ann Surg Oncol* 2015; **22**: 3409-3413 [PMID: 26122369 DOI: 10.1245/s10434-015-4649-2]

53 **Neuzillet C**, Gaujoux S, Williet N, Bachet JB, Bauguion L, Colson Durand L, Conroy T, Dahan L, Gilabert M, Huguet F, Marthey L, Meilleroux J, de Mestier L, Napoléon B, Portales F, Sa Cunha A, Schwarz L, Taieb J, Chibaudel B, Bouché O, Hammel P; Thésaurus National de Cancérologie Digestive (TNCD); Société Nationale Française de Gastroentérologie (SNFGE); Fédération Francophone de Cancérologie Digestive (FFCD); Groupe Coopérateur multidisciplinaire en Oncologie (GERCOR); Fédération Nationale des Centres de Lutte Contre le Cancer (UNICANCER); Société Française de Chirurgie Digestive (SFCD); Société Française d'Endoscopie Digestive (SFED); Société Française de Radiothérapie Oncologique (SFRO); Association de Chirurgie Hépato-Bilio-Pancréatique et Transplantation (ACHBT); Association Française de Chirurgie (AFC). Pancreatic cancer: French clinical practice guidelines for diagnosis, treatment and follow-up (SNFGE, FFCD, GERCOR, UNICANCER, SFCD, SFED, SFRO, ACHBT, AFC). *Dig Liver Dis* 2018; **50**: 1257-1271 [PMID: 30219670 DOI: 10.1016/j.dld.2018.08.008]

54 **Suker M**, Beumer BR, Sadot E, Marthey L, Faris JE, Mellon EA, El-Rayes BF, Wang-Gillam A, Lacy J, Hosein PJ, Moorcraft SY, Conroy T, Hohla F, Allen P, Taieb J, Hong TS, Shridhar R, Chau I, van Eijck CH, Koerkamp BG. FOLFIRINOX for locally advanced pancreatic cancer: a systematic review and patient-level meta-analysis. *Lancet Oncol* 2016; **17**: 801-810 [PMID: 27160474 DOI: 10.1016/S1470-2045(16)00172-8]

55 **Wang C**, Liu X, Wang X, Wang Y, Cha N. Effects of chemoradiotherapy and chemotherapy on survival of patients with locally advanced pancreatic cancer: A meta-analysis of randomized controlled trials. *Medicine (Baltimore)* 2018; **97**: e12260 [PMID: 30200163 DOI: 10.1097/MD.0000000000012260]

56 **Mukherjee S**, Hurt CN, Bridgewater J, Falk S, Cummins S, Wasan H, Crosby T, Jephcott C, Roy R, Radhakrishna G, McDonald A, Ray R, Joseph G, Staffurth J, Abrams RA, Griffiths G, Maughan T. Gemcitabine-based or capecitabine-based chemoradiotherapy for locally advanced pancreatic cancer (SCALOP): a multicentre, randomised, phase 2 trial. *Lancet Oncol* 2013; **14**: 317-326 [PMID: 23474363 DOI: 10.1016/S1470-2045(13)70021-4]

57 **Bockhorn M**, Uzunoglu FG, Adham M, Imrie C, Milicevic M, Sandberg AA, Asbun HJ, Bassi C, Büchler M, Charnley RM, Conlon K, Cruz LF, Dervenis C, Fingerhutt A, Friess H, Gouma DJ, Hartwig W, Lillemoe KD, Montorsi M, Neoptolemos JP, Shrikhande SV, Takaori K, Traverso W, Vashist YK, Vollmer C, Yeo CJ, Izbicki JR; International Study Group of Pancreatic Surgery. Borderline resectable pancreatic cancer: a consensus statement by the International Study Group of Pancreatic Surgery (ISGPS). *Surgery* 2014; **155**: 977-988 [PMID: 24856119 DOI: 10.1016/j.surg.2014.02.001]

58 **Khorana AA**, Mangu PB, Berlin J, Engebretson A, Hong TS, Maitra A, Mohile SG, Mumber M, Schulick R, Shapiro M, Urba S, Zeh HJ, Katz MHG. Potentially Curable Pancreatic Cancer: American Society of Clinical Oncology Clinical Practice Guideline Update. *J Clin Oncol* 2017; **35**: 2324-2328 [PMID: 28398845 DOI: 10.1200/JCO.2017.72.4948]

59 **Burris HA 3rd**, Moore MJ, Andersen J, Green MR, Rothenberg ML, Modiano MR, Cripps MC, Portenoy RK, Storniolo AM, Tarassoff P, Nelson R, Dorr FA, Stephens CD, Von Hoff DD. Improvements in survival and clinical benefit with gemcitabine as first-line therapy for patients with advanced pancreas cancer: a randomized trial. *J Clin Oncol* 1997; **15**: 2403-2413 [PMID: 9196156 DOI: 10.1200/JCO.1997.15.6.2403]

60 **Moore K**. Endothelin and vascular function in liver disease. *Gut* 2004; **53**: 159-161 [PMID: 14724140 DOI: 10.1136/gut.2003.024703]

61 **Tabernero J**, Chiorean EG, Infante JR, Hingorani SR, Ganju V, Weekes C, Scheithauer W, Ramanathan RK, Goldstein D, Penenberg DN, Romano A, Ferrara S, Von Hoff DD. Prognostic factors of survival in a randomized phase III trial (MPACT) of weekly nab-paclitaxel plus

gemcitabine *vs* gemcitabine alone in patients with metastatic pancreatic cancer. *Oncologist* 2015; **20**: 143-150 [PMID: 25582141 DOI: 10.1634/theoncologist.2014-0394]

62 **Sehdev A**, Gbolahan O, Hancock BA, Stanley M, Shahda S, Wan J, Wu HH, Radovich M, O'Neil BH. Germline and Somatic DNA Damage Repair Gene Mutations and Overall Survival in Metastatic Pancreatic Adenocarcinoma Patients Treated with FOLFIRINOX. *Clin Cancer Res* 2018; **24**: 6204-6211 [PMID: 30131383 DOI: 10.1158/1078-0432.CCR-18-1472]

63 **Fogelman D**, Sugar EA, Oliver G, Shah N, Klein A, Alewine C, Wang H, Javle M, Shroff R, Wolff RA, Abbruzzese JL, Laheru D, Diaz LA Jr. Family history as a marker of platinum sensitivity in pancreatic adenocarcinoma. *Cancer Chemother Pharmacol* 2015; **76**: 489-498 [PMID: 26126726 DOI: 10.1007/s00280-015-2788-6]

64 **Kang H**, Jo JH, Lee HS, Chung MJ, Bang S, Park SW, Song SY, Park JY. Comparison of efficacy and safety between standard-dose and modified-dose FOLFIRINOX as a first-line treatment of pancreatic cancer. *World J Gastrointest Oncol* 2018; **10**: 421-430 [PMID: 30487953 DOI: 10.4251/wjgo.v10.i11.421]

65 **Walker EJ**, Ko AH. Beyond first-line chemotherapy for advanced pancreatic cancer: an expanding array of therapeutic options? *World J Gastroenterol* 2014; **20**: 2224-2236 [PMID: 24605022 DOI: 10.3748/wjg.v20.i9.2224]

66 **Nagrial AM**, Chin VT, Sjoquist KM, Pajic M, Horvath LG, Biankin AV, Yip D. Second-line treatment in inoperable pancreatic adenocarcinoma: A systematic review and synthesis of all clinical trials. *Crit Rev Oncol Hematol* 2015; **96**: 483-497 [PMID: 26481952 DOI: 10.1016/j.critrevonc.2015.07.007]

67 **Oettle H**, Riess H, Stieler JM, Heil G, Schwaner I, Seraphin J, Görner M, Mölle M, Greten TF, Lakner V, Bischoff S, Sinn M, Dörken B, Pelzer U. Second-line oxaliplatin, folinic acid, and fluorouracil *vs* folinic acid and fluorouracil alone for gemcitabine-refractory pancreatic cancer: outcomes from the CONKO-003 trial. *J Clin Oncol* 2014; **32**: 2423-2429 [PMID: 24982456 DOI: 10.1200/JCO.2013.53.6995]

68 **Portal A**, Pernot S, Tougeron D, Arbaud C, Bidault AT, de la Fouchardière C, Hammel P, Lecomte T, Dréanic J, Coriat R, Bachet JB, Dubreuil O, Marthey L, Dahan L, Tchoundjeu B, Locher C, Lepère C, Bonnetain F, Taieb J. Nab-paclitaxel plus gemcitabine for metastatic pancreatic adenocarcinoma after Folfirinox failure: an AGEO prospective multicentre cohort. *Br J Cancer* 2015; **113**: 989-995 [PMID: 26372701 DOI: 10.1038/bjc.2015.328]

69 **Le DT**, Durham JN, Smith KN, Wang H, Bartlett BR, Aulakh LK, Lu S, Kemberling H, Wilt C, Luber BS, Wong F, Azad NS, Rucki AA, Laheru D, Donehower R, Zaheer A, Fisher GA, Crocenzi TS, Lee JJ, Greten TF, Duffy AG, Ciombor KK, Eyring AD, Lam BH, Joe A, Kang SP, Holdhoff M, Danilova L, Cope L, Meyer C, Zhou S, Goldberg RM, Armstrong DK, Bever KM, Fader AN, Taube J, Housseau F, Spetzler D, Xiao N, Pardoll DM, Papadopoulos N, Kinzler KW, Eshleman JR, Vogelstein B, Anders RA, Diaz LA Jr. Mismatch repair deficiency predicts response of solid tumors to PD-1 blockade. *Science* 2017; **357**: 409-413 [PMID: 28596308 DOI: 10.1126/science.aan6733]

70 **Domchek SM**, Hendifar AE, McWilliams RR, Geva R, Epelbaum R, Biankin A, Vonderheide RH, Wolff RA, Alberts SR, Giordano H, Goble S, Lin KK, Shroff RT. RUCAPANC: An open-label, phase 2 trial of the PARP inhibitor rucaparib in patients (pts) with pancreatic cancer (PC) and a known deleterious germline or somatic BRCA mutation. *J Clin Oncol* 2016; **15**: 34

71 **Perinel J**, Adham M. Palliative therapy in pancreatic cancer-palliative surgery. *Transl Gastroenterol Hepatol* 2019; **4**: 28 [PMID: 31231695 DOI: 10.21037/tgh.2019.04.03]

72 **Dumonceau JM**, Tringali A, Papanikolaou IS, Blero D, Mangiavillano B, Schmidt A, Vanbiervliet G, Costamagna G, Devière J, García-Cano J, Gyökeres T, Hassan C, Prat F, Siersema PD, van Hooft JE. Endoscopic biliary stenting: indications, choice of stents, and results: European Society of Gastrointestinal Endoscopy (ESGE) Clinical Guideline - Updated October 2017. *Endoscopy* 2018; **50**: 910-930 [PMID: 30086596 DOI: 10.1055/a-0659-9864]

73 **Berti S**, Ferrarese A, Feleppa C, Francone E, Martino V, Bianchi C, Falco E. Laparoscopic perspectives for distal biliary obstruction. *Int J Surg* 2015; **21** Suppl 1: S64-S67 [PMID: 26118614 DOI: 10.1016/j.ijsu.2015.04.092]

74 **Lai EC**, Tang CN. Robot-assisted laparoscopic hepaticojejunostomy for advanced malignant biliary obstruction. *Asian J Surg* 2015; **38**: 210-213 [PMID: 25797562 DOI: 10.1016/j.asjsur.2015.01.010]

75 **Marabelle A**, Le DT, Ascierto PA, Di Giacomo AM, De Jesus-Acosta A, Delord JP, Geva R, Gottfried M, Penel N, Hansen AR, Piha-Paul SA, Doi T, Gao B, Chung HC, Lopez-Martin J, Bang YJ, Frommer RS, Shah M, Ghori R, Joe AK, Pruitt SK, Diaz LA Jr. Efficacy of Pembrolizumab in Patients With Noncolorectal High Microsatellite Instability/Mismatch Repair-Deficient Cancer: Results From the Phase II KEYNOTE-158 Study. *J Clin Oncol* 2020; **38**: 1-10 [PMID: 31682550 DOI: 10.1200/JCO.19.02105]

76 **Banerjee K**, Kumar S, Ross KA, Gautam S, Poelaert B, Nasser MW, Aithal A, Bhatia R, Wannemuehler MJ, Narasimhan B, Solheim JC, Batra SK, Jain M. Emerging trends in the immunotherapy of pancreatic cancer. *Cancer Lett* 2018; **417**: 35-46 [PMID: 29242097 DOI: 10.1016/j.canlet.2017.12.012]

77 **Pishvaian MJ**, Bender RJ, Halverson D, Rahib L, Hendifar AE, Mikhail S, Chung V, Picozzi VJ, Sohal D, Blais EM, Mason K, Lyons EE, Matrisian LM, Brody JR, Madhavan S, Petricoin EF 3rd. Molecular Profiling of Patients with Pancreatic Cancer: Initial Results from the Know Your Tumor Initiative. *Clin Cancer Res* 2018; **24**: 5018-5027 [PMID: 29954777 DOI: 10.1158/1078-0432.CCR-18-0531]

78 **Biankin AV**, Waddell N, Kassahn KS, Gingras MC, Muthuswamy LB, Johns AL, Miller DK, Wilson PJ, Patch AM, Wu J, Chang DK, Cowley MJ, Gardiner BB, Song S, Harliwong I, Idrisoglu S, Nourse C, Nourbakhsh E, Manning S, Wani S, Gongora M, Pajic M, Scarlett CJ, Gill AJ, Pinho AV, Rooman I, Anderson M, Holmes O, Leonard C, Taylor D, Wood S, Xu Q, Nones K, Fink JL, Christ A, Bruxner T, Cloonan N, Kolle G, Newell F, Pinese M, Mead RS, Humphris JL, Kaplan W, Jones MD, Colvin EK, Nagrial AM, Humphrey ES, Chou A, Chin VT, Chantrill LA, Mawson A, Samra JS, Kench JG, Lovell JA, Daly RJ, Merrett ND, Toon C, Epari K, Nguyen NQ, Barbour A, Zeps N; Australian Pancreatic Cancer Genome Initiative, Kakkar N, Zhao F, Wu YQ, Wang M, Muzny DM, Fisher WE, Brunicardi FC, Hodges SE, Reid JG, Drummond J, Chang K, Han Y, Lewis LR, Dinh H, Buhay CJ, Beck T, Timms L, Sam M, Begley K, Brown A, Pai D, Panchal A, Buchner N, De Borja R, Denroche RE, Yung CK, Serra S, Onetto N, Mukhopadhyay D, Tsao MS, Shaw PA, Petersen GM, Gallinger S, Hruban RH, Maitra A, Iacobuzio-Donahue CA, Schulick RD, Wolfgang CL, Morgan RA, Lawlor RT, Capelli P, Corbo V, Scardoni M, Tortora G, Tempero MA, Mann KM, Jenkins NA, Perez-Mancera PA, Adams DJ, Largaespada DA, Wessels LF, Rust AG, Stein LD, Tuveson DA, Copeland NG, Musgrove EA, Scarpa A, Eshleman JR, Hudson TJ, Sutherland RL, Wheeler DA, Pearson JV, McPherson JD, Gibbs RA, Grimmond SM. Pancreatic cancer genomes reveal aberrations in axon guidance pathway genes. *Nature* 2012; **491**: 399-405 [PMID: 23103869 DOI: 10.1038/nature11547]

79 **National Institutes of Health's National Library of Medicine**. DailyMed - VITRAKVI- larotrectinib capsule VITRAKVI- larotrectinib solution, concentrate. In: National Institutes of Health's National Library of Medicine [Internet]. Available from: https://NLM/NIH/HHS/USA.gov

80 **Genentech**. Rozlytrek™ (entrectinib) - Information for Healthcare Providers. In: Genentech [Internet]. Available from: www.gene.com

81 **Drilon A**, Laetsch TW, Kummar S, DuBois SG, Lassen UN, Demetri GD, Nathenson M, Doebele RC, Farago AF, Pappo AS, Turpin B, Dowlati A, Brose MS, Mascarenhas L, Federman N, Berlin J, El-Deiry WS, Baik C, Deeken J, Boni V, Nagasubramanian R, Taylor M, Rudzinski ER, Meric-Bernstam F, Sohal DPS, Ma PC, Raez LE, Hechtman JF, Benayed R, Ladanyi M, Tuch BB, Ebata K, Cruickshank S, Ku NC, Cox MC, Hawkins DS, Hong DS, Hyman DM. Efficacy of Larotrectinib in TRK Fusion-Positive Cancers in Adults and Children. *N Engl J Med* 2018; **378**: 731-739 [PMID: 29466156 DOI: 10.1056/NEJMoa1714448]

82 **Drilon A**, Siena S, Ou SI, Patel M, Ahn MJ, Lee J, Bauer TM, Farago AF, Wheler JJ, Liu SV, Doebele R, Giannetta L, Cerea G, Marrapese G, Schirru M, Amatu A, Bencardino K, Palmeri L, Sartore-Bianchi A, Vanzulli A, Cresta S, Damian S, Duca M, Ardini E, Li G, Christiansen J, Kowalski K, Johnson AD, Patel R, Luo D, Chow-Maneval E, Hornby Z, Multani PS, Shaw AT, De Braud FG. Safety and Antitumor Activity of the Multitargeted Pan-TRK, ROS1, and ALK Inhibitor Entrectinib: Combined Results from Two Phase I Trials (ALKA-372-001 and STARTRK-1). *Cancer Discov* 2017; **7**: 400-409 [PMID: 28183697 DOI: 10.1158/2159-8290.CD-16-1237]

83 **Golan T**, Hammel P, Reni M, Van Cutsem E, Macarulla T, Hall MJ, Park JO, Hochhauser D, Arnold D, Oh DY, Reinacher-Schick A, Tortora G, Algül H, O'Reilly EM, McGuinness D, Cui KY, Schlienger K, Locker GY, Kindler HL. Maintenance Olaparib for Germline *BRCA*-Mutated Metastatic Pancreatic Cancer. *N Engl J Med* 2019; **381**: 317-327 [PMID: 31157963 DOI: 10.1056/NEJMoa1903387]

84 **Beatty GL**, Torigian DA, Chiorean EG, Saboury B, Brothers A, Alavi A, Troxel AB, Sun W, Teitelbaum UR, Vonderheide RH, O'Dwyer PJ. A phase I study of an agonist CD40 monoclonal antibody (CP-870,893) in combination with gemcitabine in patients with advanced pancreatic ductal adenocarcinoma. *Clin Cancer Res* 2013; **19**: 6286-6295 [PMID: 23983255 DOI: 10.1158/1078-0432.CCR-13-1320]

85 **Rossi GR**, Mautino MR, Unfer RC, Seregina TM, Vahanian N, Link CJ. Effective treatment of preexisting melanoma with whole cell vaccines expressing alpha(1,3)-galactosyl epitopes. *Cancer Res* 2005; **65**: 10555-10561 [PMID: 16288048 DOI: 10.1158/0008-5472.CAN-05-0627]

86 **Hardacre JM**, Mulcahy M, Small W, Talamonti M, Obel J, Krishnamurthi S, Rocha-Lima CS, Safran H, Lenz HJ, Chiorean EG. Addition of algenpantucel-L immunotherapy to standard adjuvant therapy for pancreatic cancer: a phase 2 study. *J Gastrointest Surg* 2013; **17**: 94-100; discussion p. 100 [PMID: 23229886 DOI: 10.1007/s11605-012-2064-6]

87 **Coveler AL**, Rossi GR, Vahanian NN, Link C, Chiorean EG. Algenpantucel-L immunotherapy in pancreatic adenocarcinoma. *Immunotherapy* 2016; **8**: 117-125 [PMID: 26787078 DOI: 10.2217/imt.15.113]

88 **Sahin IH**, Askan G, Hu ZI, O'Reilly EM. Immunotherapy in pancreatic ductal adenocarcinoma: an emerging entity? *Ann Oncol* 2017; **28**: 2950-2961 [PMID: 28945842 DOI: 10.1093/annonc/mdx503]

89 **Kindler HL**, Niedzwiecki D, Hollis D, Sutherland S, Schrag D, Hurwitz H, Innocenti F, Mulcahy MF, O'Reilly E, Wozniak TF, Picus J, Bhargava P, Mayer RJ, Schilsky RL, Goldberg RM. Gemcitabine plus bevacizumab compared with gemcitabine plus placebo in patients with advanced pancreatic cancer: phase III trial of the Cancer and Leukemia Group B (CALGB 80303). *J Clin Oncol* 2010; **28**: 3617-3622 [PMID: 20606091 DOI: 10.1200/JCO.2010.28.1386]

90 **Lemstrova R**, Brynychova V, Hughes DJ, Hlavac V, Dvorak P, Doherty JE, Murray HA, Crockard M, Oliverius M, Hlavsa J, Honsova E, Mazanec J, Kala Z, Lovecek M, Havlik R, Ehrmann J, Strouhal O, Soucek P, Melichar B, Mohelnikova-Duchonova B. Dysregulation of KRAS signaling in pancreatic cancer is not associated with *KRAS* mutations and outcome. *Oncol Lett* 2017; **14**: 5980-5988 [PMID: 29113235 DOI: 10.3892/ol.2017.6946]

91 **Schmidt KM**, Hellerbrand C, Ruemmele P, Michalski CW, Kong B, Kroemer A, Hackl C, Schlitt HJ, Geissler EK, Lang SA. Inhibition of mTORC2 component RICTOR impairs tumor growth in pancreatic cancer models. *Oncotarget* 2017; **8**: 24491-24505 [PMID: 28445935 DOI: 10.18632/oncotarget.15524]

World Journal of Gastroenterology

Submit a Manuscript: https://www.f6publishing.com

World J Gastroenterol 2021 October 21; 27(39): 6590-6600

DOI: 10.3748/wjg.v27.i39.6590

ISSN 1007-9327 (print) ISSN 2219-2840 (online)

MINIREVIEWS

Cathepsin L, transmembrane peptidase/serine subfamily member 2/4, and other host proteases in COVID-19 pathogenesis – with impact on gastrointestinal tract

Izabela Berdowska, Malgorzata Matusiewicz

ORCID number: Izabela Berdowska 0000-0002-0275-4522; Malgorzata Matusiewicz 0000-0003-4624-0109.

Author contributions: Berdowska I performed the literature research and wrote the manuscript; Matusiewicz M performed the literature research, created the graphs and revised the manuscript; both authors discussed, designed the general concept of the work, read and approve the final manuscript.

Conflict-of-interest statement: Dr. Matusiewicz has nothing to disclose.

Open-Access: This article is an open-access article that was selected by an in-house editor and fully peer-reviewed by external reviewers. It is distributed in accordance with the Creative Commons Attribution NonCommercial (CC BY-NC 4.0) license, which permits others to distribute, remix, adapt, build upon this work non-commercially, and license their derivative works on different terms, provided the original work is properly cited and the use is non-commercial. See: http://creativecommons.org/Licenses/by-nc/4.0/

Izabela Berdowska, Malgorzata Matusiewicz, Department of Biochemistry and Immunochemistry, Wroclaw Medical University, Wroclaw 50-368, Lower Silesia, Poland

Corresponding author: Malgorzata Matusiewicz, PhD, Senior Lecturer, Department of Biochemistry and Immunochemistry, Wroclaw Medical University, Chalubinskiego 10, Wroclaw 50-368, Lower Silesia, Poland. malgorzata.matusiewicz@umed.wroc.pl

Abstract

Severe acute respiratory syndrome coronavirus-2 (SARS-CoV-2) seems to employ two routes of entrance to the host cell; *via* membrane fusion (with the cells expressing both angiotensin converting enzyme 2 (ACE2) and transmembrane peptidase/serine subfamily member 2/4 (TMPRSS2/4)) or *via* receptor-mediated endocytosis (to the target cells expressing only ACE2). The second mode is associated with cysteine cathepsins (probably cathepsin L) involvement in the virus spike protein (S protein) proteolytic activation. Also furin might activate the virus S protein enabling it to enter cells. Gastrointestinal tract (GIT) involvement in SARS-CoV-2 infection is evident in a subset of coronavirus disease 2019 (COVID-19) patients exhibiting GIT symptoms, such as diarrhea, and presenting viral-shedding in feces. Considering the abundance and co-localization of ACE2 and TMPRSS2 in the lower GIT (especially brush-border enterocytes), these two receptors seem to be mainly involved in SARS-CoV-2 invasion of the digestive tract. Additionally, *in vitro* studies have demonstrated the virions capability of infection and replication in the human epithelial cells lining GIT. However, also furin and cysteine cathepsins (cathepsin L) might participate in the activation of SARS-CoV-2 spike protein contributing to the virus invasiveness within GIT. Moreover, cathepsin L (due to its involvement in extracellular matrix components degradation and remodeling, the processes enhanced during SARS-CoV-2-induced inflammation) might be responsible for the dysregulation of absorption/digestion functions of GIT, thus adding to the observed in some COVID-19 patients symptoms such as diarrhea.

Key Words: COVID-19; SARS-CoV-2; Angiotensin converting enzyme 2; Transmembrane peptidase/serine subfamily member 2/4; Cathepsin L; Gastrointestinal tract

©The Author(s) 2021. Published by Baishideng Publishing Group Inc. All rights reserved.

Manuscript source: Invited manuscript

Specialty type: Gastroenterology and hepatology

Country/Territory of origin: Poland

Peer-review report's scientific quality classification

Grade A (Excellent): A
Grade B (Very good): 0
Grade C (Good): C
Grade D (Fair): 0
Grade E (Poor): 0

Received: March 29, 2021
Peer-review started: March 29, 2021
First decision: June 14, 2021
Revised: June 28, 2021
Accepted: September 19, 2021
Article in press: September 19, 2021
Published online: October 21, 2021

P-Reviewer: Khachfe H, Khan MKA
S-Editor: Wang LL
L-Editor: A
P-Editor: Xing YX



Core Tip: Gastrointestinal tract (GIT) is believed to participate in severe acute respiratory syndrome coronavirus-2 (SARS-CoV-2) dissemination. The current research shows the abundance and co-localization of angiotensin converting enzyme 2 (ACE2) and transmembrane peptidase/serine subfamily member 2 receptors in the lower GIT. Furthermore, about half of coronavirus disease 2019 patients present with GIT symptoms, such as diarrhea, and exhibit viral-shedding in feces. Additionally, *in vitro* studies have demonstrated the virions capability of infection and replication in the human epithelial cells lining GIT. This paper reviews the possible routes of the virus infection with respect to the host-enzymatic systems responsible for the proteolytic priming of SARS-CoV-2.

Citation: Berdowska I, Matusiewicz M. Cathepsin L, transmembrane peptidase/serine subfamily member 2/4, and other host proteases in COVID-19 pathogenesis – with impact on gastrointestinal tract. *World J Gastroenterol* 2021; 27(39): 6590-6600
URL: https://www.wjgnet.com/1007-9327/full/v27/i39/6590.htm
DOI: https://dx.doi.org/10.3748/wjg.v27.i39.6590

INTRODUCTION

Coronaviruses may employ several host proteases for their invasion into target cells. The enzymes participating in the viruses activation include: proprotein convertases (PCs) (mainly furin), transmembrane serine proteases, especially transmembrane peptidase/serine subfamily member 2 (TMPRSS2), the lysosomal cathepsins (mainly cathepsin L), elastase, and coagulation factor Xa[1].

Severe acute respiratory syndrome coronavirus-2 (SARS-CoV-2) virus responsible for coronavirus disease 2019 (COVID-19) pandemic exhibits many similarities when compared to SARS-CoV. It employs a similar mechanism of host cells invasion; recognizes and binds the same type of angiotensin converting enzyme 2 (ACE2) receptors to enter host cells (but with higher affinity[2]), and comparable processing of spike protein (S protein) seems to be necessary for the virion fusion with the host cell membrane[3-7] (Figure 1).

Two proteolytic events need to be conducted for SARS-CoV-2 activation; initially spike protein is cut in the specific cleavage site between S1 and S2 domain, then the second cleavage within S2 domain (S2′ site) allows for the exposition of the fusion peptide, which enables membrane fusion. The first proteolytic step can happen in the producer cell, in the extracellular space, or within the host cell's endosome. This cleavage site in SARS-CoV-2 spike protein is recognized by various proteases, including furin (unlike in SARS-CoV lacking furin-cleavage site between S1 and S2)[6, 8] and TMPRSS2[3]. The second cleavage can be either performed by TMPRSS2 on the surface of the host cell, or in the endolysosomes by lysosomal proteases, most probably cathepsin L[9].

Therefore, as proposed by Pislar *et al*[10], two routes of SARS-CoV-2 entry to the host cell are likely; *via* membrane fusion with the host cells which expose both ACE2 and TMPRSS2 (and/or other transmembrane serine proteases such as TMPRSS4[11]) proteins, or *via* receptor-mediated endocytosis (RME) to the target cells expressing only ACE2 receptors. In the first case, both processing steps performed by TMPRSS2 before the virus entry enable membrane fusion, whereas in the second mechanism, the virion binding with ACE2 receptors induces endocytosis followed by spike protein activation by cathepsin L (and/or other cysteine cathepsins)[4,10]. As a result of either of these pathways, viral RNA is released in the host cell and undergoes the processes of replication (Figure 2).

TYPES OF HOST PROTEASES IN SARS-CoV-2 INVASION

The findings of several studies support the notion that, apart from ACE2 receptors, the main host peptidases involved in SARS-CoV-2 spike protein processing include: TMPRSS2 (and/or TMPRSS4), lysosomal cysteine cathepsins (mainly cathepsin L), as well as furin-like PCs. They may participate in SARS-CoV-2 activation independently,

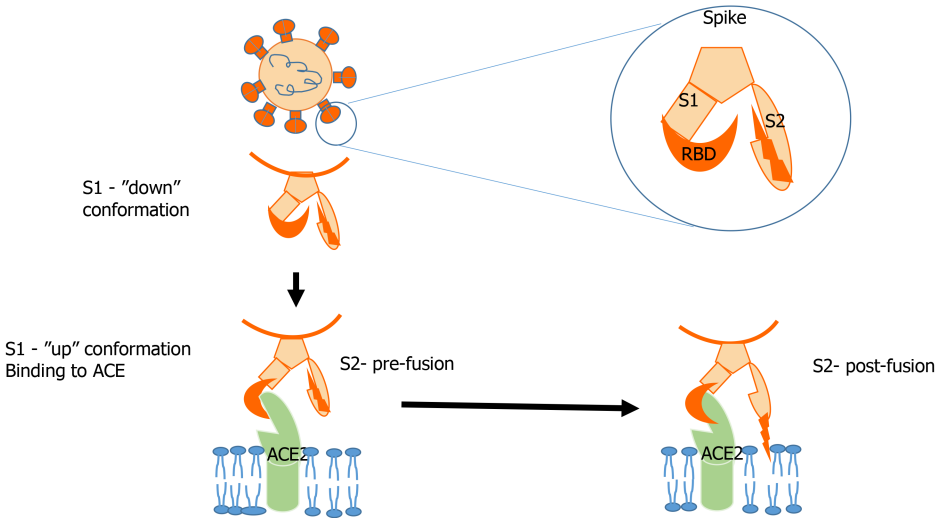


Figure 1 Alternations in spike proteins conformation upon binding to ACE 2. Spike S1 subunit contains receptor binding domain, that has to change from "down-conformation" state to "up-conformation" state to be accessible for ACE2. Changes in S1 subunit trigger conformational changes in S2 subunit, causing exposition of hydrophobic domain, changing it from "pre-fusion" to "post-fusion" state. This enables fusion of the virus with host membrane (after Zhu *et al*[7]).

or their actions may overlap or complete one another, depending on the pattern of the virion-recognized proteins exposed on the host cells (*e.g.* expressing or not TMPRSS2).

Cysteine cathepsins (CCs) in pathology

Cysteine cathepsins belonging to the papain-like family of cysteine proteases (containing cysteine in their catalytic center) comprise 11 cathepsins (B, C, F, H, K, L, O, S, V, X and W) in the human organism[12,13]. They belong to lysosomal proteases involved mainly in intracellular protein breakdown, antigen processing, MHC-II mediated immune response, and apoptosis. However, their functions go far beyond this; they participate in various physio-pathological processes not only intracellularly, but also in the extracellular matrix (ECM), because, except for their endolysosomal sequestration, they have been observed in the nucleus, cytosol, mitochondria, at the plasma membranes and in the extracellular milieu[13,14]. Their secretion is observed in physiological conditions (*e.g.* in bone remodeling – conducted by osteoclasts-secreted cathepsin K, in wound healing performed by keratinocytes-secreted cathepsin B, in prohormone processing – thyroid hormones released from thyroglobulin by cathepsins B, L and K secreted from the thyroid epithelial cells). However, an excessive secretion of cysteine cathepsins is mostly observed in pathological states associated with inflammatory processes, such as cancer diseases (cathepsins B, C, K, L, S, H, X), cardiovascular diseases (cathepsins C, K, L, S, V), joint and bone diseases (cathepsins K, B, L, S, H), inflammatory bowel disease (cathepsin L), and many other disorders (summarized in[12-15]). In these pathological states CCs typically act extracellularly, where they participate in collagen, elastin, and other ECM components degradation directly or indirectly (activating other proteases) after being secreted from recruited immune cells (mostly), as well as from inflamed tissue cells (to the lesser extent). Macrophages and other immune cells infiltrating tissues seem to be the main extracellular source of CCs whose secretion is stimulated by inflammatory factors like cytokines. However, also other cell types secrete excessive amounts of CCs, including osteoclasts or chondrocytes (oversecreting cathepsin K and/or S in arthritis and osteoporosis), or cancer cells and tumor-associated fibroblasts (oversecreting cathepsin S, L and/or B in cancer invasion)[14]. Apart from degradation of main components of ECM, also more refined processing of ECM (undergoing both intra-, and extracellularly) is ascribed to CCs. This comprises modifying and shedding cell adhesion molecules and cell membrane receptors, which affects signal transduction pathways, as well as processing cytokines and chemokines, which upregulates immune response [14]. The resulting augmentation of inflammatory processes further induces the secretion of CCs, enhancing the destruction of ECM, which eventually leads to the acceleration of the processes observed in the aforementioned disorders.

Due to their roles in multiple inflammatory-based disorders, CCs have been considered for a long time as a target for medicinal drugs design. However, because of ubiquitous expression of most CCs, their constitutive, overlapping functions, broad substrate specificities, most of the studied so far medicines have exhibited unfavorable

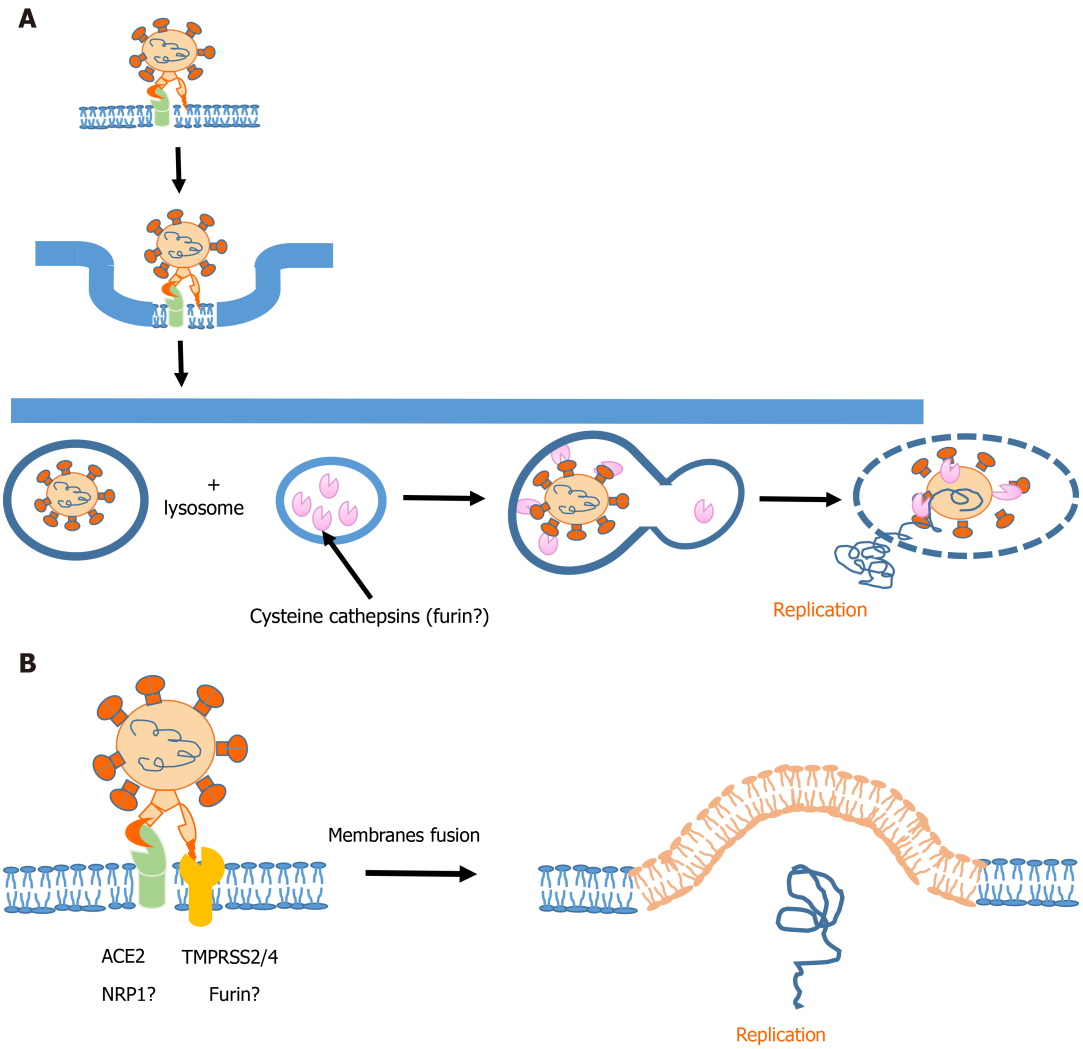


Figure 2 Two modes of virus entry. A: Receptor-mediated endocytosis of severe acute respiratory syndrome coronavirus-2. After binding to ACE2 and formation of endosome, lysosomal cathepsins activate spike protein, which leads to the release of the viral RNA into host cell. B: Membrane fusion mechanism - priming of the spike proteins is mediated by transmembrane peptidase/serine subfamily member 2/4, which leads to fusion of viral and host membranes and release of the viral RNA into host cell.

side effects, thus not surviving clinical trials. However, the attempts to construct CCs-aimed drugs, taking advantage of the newest technology, are underway. The most clinical trials have been conducted on cathepsins K and S inhibitors, also cathepsin C seems to be a promising target, whereas the remaining cathepsins inhibitors have either got stuck in the initial stages of clinical trials or their trials have been discontinued (reviewed in[14]).

Cathepsin L in inflammatory processes

Similarly to other cysteine cathepsins, cathepsin L exhibits pleiotropic activities in the human organism. One of the most evident actions of this enzyme is (beside cathepsins S, K and V) its participation in inflammatory processes associated with various pathological conditions[14-16]. For example Menzel *et al*[17] have demonstrated the up to 10-fold induction of cathepsin L expression (mRNA) in intestinal macrophages derived from inflammatory bowel disease (IBD) patients, and the clear improvement of the disorder symptoms in DSS (dextran-sulphate-sodium)-induced colitis mice mode, when a simultaneous application of cathepsins L and B inhibitors was investigated. Xu *et al*[18] have exhibited the stimulatory function of cathepsin L in microglia-mediated neuroinflammation, which accompanies many neurological disorders including Parkinson's disease. Cao *et al*[19] have shown the correlation between serum cathepsin L activity and the markers of inflammation (such as neutrophile counts and hs-CRP) in the patients with chronic kidney disease.

Cysteine cathepsins and TMPRSS2 in SARS-CoV-2 invasion

Cell line experimental systems creating the environment aimed at the inhibition of CCs have substantiated the function of these enzymes in the processes of SARS-CoV-2 activation. Raising pH in the endolysosomal compartments (with ammonium chloride and/or bafilomycin A), which inactivates lysosomal proteases working in acidic environment, or application of cysteine proteases inhibitors (such as E-64d inhibitor - inactivating cysteine cathepsins L, B, H, as well as cytosolic calpain) have significantly limited entry of SARS-CoV-2 into chosen cell lines[4]. Ou *et al*[20] (applying lentiviral pseudotype system) have demonstrated that the treatment of HEK-293/hACE2 cells with E-64d inhibitor reduced entry of SARS-CoV-2 S pseudovirions by over 90%. Further, the Authors compared the effect of two specific inhibitors of cathepsin L (SID 26681509), and cathepsin B (CA-074). Whereas the first inhibitor limited the pseudovirions entry by over 76%, the second one did not exhibit any significant effect, which suggests a prevalent function of cathepsin L in the receptor-mediated endocytosis mechanism of the virus invasion. RME mechanism in HEK- 293/hACE2 cells has been confirmed by the Authors in the experiments showing the inhibition of the SARS-CoV-2 S protein entry by blocking the factors inevitable in the process of endolysosomal trafficking (PI(3)P 5-kinase (PIKfyve) and two-pore channel subtype 2 (TPC2)[20]. The involvement of CCs has been also observed by Hoffmann *et al*[3] who demonstrated that the increase in pH (with ammonium chloride) almost completely inhibited SARS-2-S-driven entry into 293T cells expressing ACE2 but devoid of TMPRSS2. This observation is in agreement with Ou *et al*[20] findings confirming that the virus entry into these cells undergoes *via* RME with the involvement of cathepsin L in spike protein activation. In their experiments on the human colon cell line - Caco-2 cells overexpressing TMPRSS2, Hoffmann *et al*[3] exhibited the participation of both TMPRSS2 and CCs in the mechanism of the virus entry into these cells. Alkalization of the environment caused around 90% reduction in SARS-2-S-driven entry, whereas incubation with E-64d inhibited the virus entry by around 40%. On the other hand, the application of camostat mesylate (inhibitor of TMPRSS2 and other serine proteases) reduced the virus entry by about 90%, and when the Authors used both inhibitors simultaneously, they achieved nearly complete virus-entry inhibition to Caco-2 TMPRSS2 (+) cells. They also found that E-64 inhibitor significantly reduced the virus entry into Vero and 293T cells not expressing TMPRSS2, which indicates the endolysosomal pathway. However, the transduction of these cell lines with TMPRSS2 markedly reversed the effect of CCs inhibition, emphasizing the function of TMPRSS2 in the S protein priming, agreeably with Ou *et al*[20] findings that the expression of TMPRSS 2, 4, 11 A, 11D, and 11E on 293/hACE2 cells enhanced SARS-CoV-2 S protein-mediated cell–cell fusion. Moreover, the Authors noted that, however the addition of trypsin (like TMPRSS belonging to serine proteases) stimulated the formation of syncytia in 293/hACE2 cells (indicative of activated by trypsin SARS-2-S protein-stimulated cell-cell fusion), this process was also noticed in the experiments without trypsin. These findings indicate that binding with ACE2 receptors may be a sufficient event inducing cell-cell fusion (without the proteolytic priming with the extracellular protease). Nevertheless, it is possible that other host extracellular peptidases are involved in spike protein activation. The findings derived from Hoffmann *et al*[3] and Ou *et al*[20] experiments are depicted in Table 1.

Furin in SARS-CoV-2 invasion

As determined by Shang *et al*[8], another enzyme involved in SARS-CoV-2 spike protein priming is furin belonging to proprotein convertases (PCs). PCs are eukaryotic serine proteases, and ubiquitously expressed furin belongs to the PCs subfamily present in the organelles of the constitutive protein secretion pathway. These enzymes participate in the proteolytic post-translational modification of a variety of functionally important peptides and proteins, such as growth factors and hormones, both intra- and extracellularly (in the trans-Golgi network, endosomes, and pericellular environment). The amino acid sequence specifically recognized and cleaved by PCs including furin, is found in many viral surface proteins, so different viruses (like MERS-CoV) are activated by these enzymes[1]. Unlike SARS-CoV (exhibiting PC cleavage site motif only in the S2' site) [1], SARS-CoV-2 spike protein includes PCs specific motif at the S1/S2 boundary[8]. Shang *et al*[8] have performed experiments to examine whether this sequence is cut by furin. They demonstrated that PCs inhibitors reduced SARS-CoV-2 pseudovirus entry into three cell lines expressing hACE2 receptors; HeLa cells (human cervical cells), Calu-3 cells (human lung epithelial cells), and MRC-5 cells (human lung fibroblast cells). Moreover, the mutation of the PCs specific motif significantly reduced the pseudovirions entry to the studied cells. The

Table 1 Receptors/proteases involved in Severe acute respiratory syndrome coronavirus-2 invasion of human cells

Receptor/protease	Experimental model	Observation	Ref.
ACE2 and TMPRSS2/4	Human small intestinal enteroids; HEK-293T cell line transfected with ACE2, TMPRSS2, or TMPRSS4	Productive infection of SARS-CoV-2 in ACE2 (+) mature enterocytes; Correlation of ACE2, TMPRSS2 and 4 with SARS-CoV-2 invasiveness	Zang *et al*[11]
ACE2 and TMPRSS2	ACE2 and TMPRSS2 expressing C2BBe1, Caco-2, and Calu-3 cell lines	Persistent invasion and replication of SARS-CoV-2 in the cells; Correlation of TMPRSS2 (but not ACE2) with SARS-CoV-2 RNA	Lee *et al*[33]
ACE2, TMPRSS2, and CCs	HEK-293T cell line transfected with ACE2; Caco-2 cells overexpressing TMPRSS2	Inhibition of SARS-CoV-2 pseudovirus entry into HEK-293T ACE2(+)/TMPRSS2(-) by pH increase and E-64 inhibitor; Inhibition of SARS-CoV-2 pseudovirus entry into Caco-2 TMPRSS2(+) by pH increase, CCs inhibitor (E-64d), and TMPRSS2 inhibitor (camostat mesylate)	Hoffmann *et al*[3]
ACE2, TMPRSS 2, 4, 11A, 11D, 11E, and CCs (cathepsin L)	HEK-293T cell line transfected with ACE2	Inhibition of SARS-CoV-2 pseudovirus entry into the cells with CCs inhibitor (E-64d) and cathepsin L inhibitor (but not cathepsin B inhibitor); Intensification of SARS-CoV-2 S protein-mediated cell–cell fusion, caused by expression of TMPRSS 2, 4, 11A, 11D, and 11E on 293/hACE2 cells	Ou *et al*[20]
ACE2 and TMPRSS2	ACE2 and TMPRSS2 expressing Caco-2 and T84 cell lines	Persistent invasion and replication of SARS-CoV-2 in the cells	Stanifer *et al*[35]
ACE2, furin, TMPRSS2, and CCs	ACE2-expressing HeLa, Calu-3, and MRC-5 cell lines	Reduction of SARS-CoV-2 pseudovirus entry into cells by inhibitors of PCs, CCs and TMPRSS2	Shang *et al*[8]
NRP1, ACE2, and TMPRSS2	HEK-293T cell line transfected with ACE2, TMPRSS2, or NRP1	Augmentation of SARS-CoV-2 infectivity when NRP1 was coexpressed with ACE2 and TMPRSS2	Cantuti-Castelvetri *et al*[21]

ACE2: Angiotensin converting enzyme 2; NRP1: Neuropilin 1 (receptor which binds furin-cleaved substrates); TMPRSS2/4: Transmembrane peptidase/serine subfamily member 2/4; CCs: Cysteine cathepsins; HEK-293T: Human embryonic kidney 293T cells; Caco-2: Human colorectal adenocarcinoma cell line; C2BBe1: A subclone of Caco-2; T84: Human colon carcinoma cell line; HeLa: Human cervical cell line; Calu-3: Human lung epithelial cell line; MRC-5: Human lung fibroblast cell line; PCs: Proprotein convertases.

Authors detected no cleavage within the spike protein, when they packaged the pseudoviruses to HEK293T cells pretreated with furin-targeting siRNA. Additionally, they excluded the participation of matrix metalloproteinases (MMPs) in the experiment with the application of MMP inhibitor. Therefore, they confirmed the involvement of furin in SARS-CoV-2 entry into chosen cells. Additionally, furin priming of SARS-CoV-2 spike protein has been associated with the virions recognition and binding by neuropilin 1 (NRP1 - receptor which binds furin-cleaved substrates). Cantuti-Castelvetri *et al*[21] have shown that, except for ACE2, also NRP1 receptors are involved in SARS-CoV-2 invasion. Although the exact mechanism of NRP1 participation in this process is not elucidated, the Authors found the receptors to markedly enhance the virus infectivity. Apart from furin involvement, Shang *et al*[8] also observed the association of other aforementioned peptidases with SARS-CoV-2 invasion. They noticed the reduction in the pseudovirus entry to the three studied cell lines, caused by the application of both serine proteases (camostat) and cysteine cathepsins (E64) inhibitors. Furthermore, the pseudovirus entry to HeLa cells was more markedly reduced when either camostat or E64d was applied in the cells pretreated with proprotein convertases inhibitor[8]. Therefore, it might be concluded that depending on the type of target cells, TMPRSS2, lysosomal cathepsins, and furin might be involved in the activation of SARS-CoV-2 entry exhibiting cumulative/overlapping final effect (Figure 2). The observations of Shang *et al*[8] and Cantuti-Castelvetri *et al*[21] are collected in Table 1.

Cysteine cathepsins as a target in search for COVID-19 therapy

Focusing on cathepsin L expression as a target in search for an anti-Covid-19 drug, Smieszek *et al*[22] have tested an array of medications applied in clinical practice. They found amantadine (a drug used previously to treat influenza A, and now applied in neurological diseases including Parkinson's disease) to be a promising compound. Being able to accumulate in lysosomes and alkalize them, amantadine belongs to lysosomotropic agents. Such compounds inactivate lysosomal enzymes including CCs whose optimal pH lies below 5. The Authors demonstrated a significant reduction in cathepsin L gene expression using amantadine, however also other cysteine cathepsin

genes expression was inhibited, including cathepsins B and K, with the most pronounced effect observed for cathepsin H. Therefore, it might be hypothesized that this is also cathepsin H which plays an important role in the processing of the SARS-2-S spike protein. The activity of cathepsin H would have been inhibited similarly to other lysosomal cathepsins in the aforementioned experiments (raising pH and/or using E64 inhibitor), which demonstrated a significant reduction of SARS-2-S-mediated entry to the studied cells. However, in comparison with thoroughly studied cathepsins B, L, S, and K, there is much less scientific data referring to cathepsin H.

Amantadine efficiency in COVID-19 treatment has been suggested by Rejdak *et al* [23] who documented no clinical manifestations of COVID-19 infection in 22 patients in spite of the confirmation of SARS-CoV-2 presence with rRT-PCR testing in all of these individuals. The patients had been treated with either amantadine or memantine, for at least 3 months prior to the infection exposure, due to their conditions (multiple sclerosis, Parkinson's disease or cognitive impairment). Therefore, amantadine seems to be a promising treatment for COVID-19 patients. The effect of amantadine may be associated with the down-regulation of cysteine cathepsins (L and/or H) in the endolysosomal compartment and/or the disturbance of viroporin protein channel probably involved in the viral RNA release, as suggested for SARS-CoV[24].

As discussed before, the generation of anti-CCs medicinal drugs is a problematic issue (associated with the observation of unfavorable side effects). Hence, the attitude aimed at screening the already existing therapeutics, which would lower the activity of proteases involved in SARS-CoV-2 activation, seems a rational approach.

EFFECT OF SARS-CoV-2 ON GASTROINTESTINAL TRACT

Gastrointestinal symptoms and fecal virus shedding in COVID-19 patients

A significant amount of scientific evidence accumulated so far points to gastrointestinal tract (GIT), especially its lower part, as a target organ affected by SARS-CoV-2, beside the respiratory system[25]. Apart from the typical pulmonary symptoms (cough, fever, shortness of breath), some of the patients (around 4%-50% individuals) present with digestive symptoms like diarrhea, nausea, vomiting and abdominal pain[26]. Moreover, the virus mRNA presence in stool samples has been observed in some patients, often persisting long after its disappearance from the respiratory tract. Wu *et al*[27] have documented SARS-CoV-2 mRNA presence in the feces of more than half of the studied patients, with duration for up to 5 wk after its vanishing from the respiratory tract specimens. It might suggest active proliferation of the virus in the gastrointestinal tract of some patients. Similarly, Xiao *et al*[28] have observed fecal virus shedding in more than 50% of the studied patients, and in over 20% of them the duration of positive results in stool exceeded the virus presence in the respiratory samples. Additionally, the Authors detected the protein parts of the virus (as well as the presence of ACE2 receptors) in gastrointestinal epithelial cells. The virus replication in rectal tissue derived from a COVID-19 patient has been noted by Qian *et al*[29] who detected SARS-CoV-2 components in the intestinal epithelial cells (but mainly in intestinal lymphocytes and macrophages). The Authors hypothesize that, like in the case of influenza virus, it is possible for SARS-CoV-2 virions to be transported from the respiratory tract to the GIT *via* the immune cells. In the meta-analysis of 60 studies comprising over 4000 COVID-19 patients, performed by Cheung *et al*[30], 17.6% of the patients exhibited gastrointestinal symptoms, and in almost 50% (30%-70%) the virus mRNA was detected in the feces. Most of these positive stool samples (above 70%) were collected after the loss of the virus from the respiratory specimens.

However, it is still not clear, whether the virus is transmittable *via* fecal-oral route. Whereas Wang *et al*[31] detected live virus in the fecal samples, Zang *et al*[11] demonstrated the inactivation of the virions released into the intestinal lumen in the environment simulating human colonic fluid. Moreover, the Authors did not manage to recover infectious virus from the stool specimens.

Ability of SARS-CoV-2 to productively infect human GIT cells via ACE2 and TMPRSS

Several studies have demonstrated the invasion and replication of SARS-CoV-2 in the human GIT cells. Chu *et al*[32] in their ex-vivo experiments on human intestinal tissues have evidenced the ability of SARS-CoV-2 to infect, proliferate and release infectious virus particles from intestinal cells. In comparison with SARS-CoV, SARS-CoV-2 replicated less efficiently and brought about less damages in the human intestinal

epithelium, but evoked greater response of innate immune system (inducing the expression of proinflammatory mediators such as interferons and interleukins). Hence, the Authors suggested that the gastrointestinal tract might serve as an alternative route of virus dissemination. The vulnerability of the human GIT epithelial cells to SARS-CoV-2 invasion *via* ACE2 and TMPRSS-2 receptors has been confirmed in other studies with the application of intestinal cell lines models, as well as human small intestinal organoids – hSIOs[11,33-35]. Lee *et al*[33] investigated the growth of SARS-CoV-2 in a human GIT cell line model; C2BBe1 (a subclone of human epithelial colorectal adenocarcinoma cells: Caco-2). C2BBe1 (genetically and structurally resembling the brush border epithelial cells in the human GIT[36,37], and expressing moderate level of ACE2 and high level of TMPRSS2[33]) exhibited the greatest susceptibility to the virus. SARS-CoV-2 virions invaded and replicated in these cells, as well as in Caco-2[33,35] and T84 (human colon carcinoma) cells[35]. Furthermore, Stanifer *et al*[35] demonstrated SARS-CoV-2 infection of human colon organoids followed by active virions replication. These observations are in agreement with other studies on hSIOs[11,34]. Zang *et al*[11] reported productive infection of SARS-CoV-2 in $ACE2^{(+)}$ mature enterocytes, dependent on TMPRSS2 and TMPRSS4 receptors in human small intestinal enteroids. The Authors noted the role of an additional serine protease: TMPRSS4 which heightened the effect of TMPRSS2. Also, the two serine proteases enhanced SARS-CoV-2 spike protein-induced cell-cell fusion observed by the Authors.

ACE2 receptors (except for the respiratory system) are present in a variety of other organs including the gastrointestinal tract, where a great number of these proteins has been detected in the lower part of GIT[38]. Unlike in the upper segment (oral cavity, esophagus, stomach), high expression of ACE2 (both mRNA and protein) is observed in the small intestine (the greatest level), colon and rectum, as well as in the gall bladder[38,39]. Actually, ACE2 expression in the small intestine is much higher in comparison with all other organs in the human organism including the respiratory tract[11]. Specifically, ACE2 is present in the enterocyte cytoplasm and in the apical brush border, as well as in the glandular cells (in the lining epithelium of the lower GIT)[37]. The expression of ACE2 receptors has been exhibited to increase upon enterocytes differentiation. Lee *et al*[33] observed that (unlike constitutively expressed TMPRSS2), the expression of ACE2 receptors was significantly stimulated in the experiment inducing C2BBe1 enterocytes differentiation, associated with the generation of more pronounced features typical for brush border cells. Similarly, Zang *et al*[11] detected the greatest expression of ACE2 in mature brush border enterocytes, and Lamers *et al*[34] noticed around 1000-fold increase in ACE2 mRNA expression upon enterocytes differentiation. Zang *et al*[11] observed all studied receptors (ACE2, as well as TMPRSS2 and TMPRSS4) to be correlated with the virus invasiveness, similarly as Lee *et al*[33] noted a strong correlation between TMPRSS2 (although not ACE2) and viral RNA levels in the studied human epithelial cell lines (including Caco-2 and C2BBe1). Lee *et al*[33] found that the ectopic coexpression of ACE2 and TMPRSS2 in RPMI 2650 cells enhanced viral dissemination by 56.7 times (over 10-fold more in comparison with the sole ACE2 effect – 4.9 times, whereas TMPRSS2 transfection alone did not enhance the level of infectivity). It might be supposed that an effective level of ACE2 receptors is a prerequisite for the virions invasion of epithelial cells, but abundant expression of TMPRSS2 (and possibly TMPRSS4) greatly facilitates ACE2-mediated SARS-CoV-2 dissemination in the human GIT.

The involvement of both ACE2 and TMPRSS2 in SARS-CoV-2 invasion of GIT epithelial cells is in accordance with the reported co-localization of the two receptors in the lower GIT[38-40]. The most abundant expression of both proteins has been detected in the small intestine epithelial cells[38]; especially in the brush border cells [33]. Lee *et al*[39] evaluated single-cell RNA-sequencing datasets from the GIT in search for these two genes co-expression, and found the small intestine enterocytes as well as colonocytes to display the highest proportions of cells co-expressing ACE2 and TMPRSS2. Additionally, the Authors checked for the co-expression of ACE2, TMPRSS2 and TMPRSS4, and demonstrated the highest proportions of the three genes co-expression in the progenitor and stem-like epithelial cells in the small intestine. TMPRSS4 is an extra serine protease involved in SARS-CoV-2 activation and invasion, enhancing TMPRSS2 priming effect[11]. Therefore, both ACE2 and TMPRSS2 seem to be the main receptors responsible for SARS-CoV-2 invasion of GIT. The experimental data coming from Lee *et al*[33], Zang *et al*[11], and Stanifer *et al*[35] investigations are displayed in Table 1.

Putative association between SARS-CoV-2-mediated ACE2 disturbance and gastrointestinal symptoms development in COVID-19 patients

The known function of angiotensin converting enzyme 2 (ACE2) is the regulation of systemic arterial blood pressure (renin-angiotensin system). ACE2 catalyzes the conversion of Ang I to angiotensin (1–9) and angiotensin II (Ang II) to angiotensin (1–7), what counteracts the effects of Ang II, leading to decrease in blood pressure and inflammatory processes attenuation (reviewed in[41]). However, the role of ACE2 in GIT (where it is abundantly expressed) seems to be rather associated with the processes occurring in this organ. The analysis of the digestive system specific functional enrichment map for ACE2 gene suggests the involvement of ACE2 in digestion (with reference to its proteolytic activity) and transport of metabolites (the regulation of amino acid transport)[38]. In fact, ACE-2 proteins have been demonstrated to be coupled with sodium-dependent amino acids and glucose transporters. ACE2 is a chaperone for the sodium-dependent amino acid transporter B0AT1 which is involved in transport of neutral amino acids[42]. Moreover, ACE2 participates in the regulation of gut microbiota homeostasis[43,44].

Therefore, as proposed by Kumar *et al*[38], it might be hypothesized that SARS-CoV-2-associated dysregulation of ACE2 receptors in the human GIT may be involved in the mechanism of GIT symptoms development in COVID-19 patients.

CONCLUSION

In light of the presented studies, the impact of SARS-CoV-2 virus on GIT is evident, with the most substantiated involvement of ACE2 and TMPRSS2. However, except for these two receptors (and probably TMPRSS4), also other proteases might be implicated in SARS-CoV-2 invasion of GIT, as well as the development of the observed symptoms. Ubiquitously expressed furin and cathepsin L may be involved in spike protein processing, contributing to the virus invasiveness. Cathepsin L (and other CCs) might participate in the endolysosomal processing of the spike protein following ACE2-mediated endocytosis of the virion particles. Additionally, SARS-CoV-2 – induced inflammatory cytokines could stimulate the secretion of cathepsin L. Therefore, extracellular cathepsin L may contribute both to the spike protein processing, as well as degradation/remodeling of the ECM components and membrane-bound receptors including TMPRSS2/4 and ACE2. The resulting events might accelerate the inflammatory processes disturbing the digestion/absorption of nutrients yielding the observed symptoms such as diarrhea. However, more research is required, since the participation of furin and lysosomal cathepsins in SARS-CoV-2 GIT-invasion is more speculative.

REFERENCES

1 **Izaguirre G**. The Proteolytic Regulation of Virus Cell Entry by Furin and Other Proprotein Convertases. *Viruses* 2019; **11** [PMID: 31505793 DOI: 10.3390/v11090837]

2 **Wrapp D**, Wang N, Corbett KS, Goldsmith JA, Hsieh CL, Abiona O, Graham BS, McLellan JS. Cryo-EM structure of the 2019-nCoV spike in the prefusion conformation. *Science* 2020; **367**: 1260-1263 [PMID: 32075877 DOI: 10.1126/science.abb2507]

3 **Hoffmann M**, Kleine-Weber H, Schroeder S, Krüger N, Herrler T, Erichsen S, Schiergens TS, Herrler G, Wu NH, Nitsche A, Müller MA, Drosten C, Pöhlmann S. SARS-CoV-2 Cell Entry Depends on ACE2 and TMPRSS2 and Is Blocked by a Clinically Proven Protease Inhibitor. *Cell* 2020; **181**: 271-280.e8 [PMID: 32142651 DOI: 10.1016/j.cell.2020.02.052]

4 **Blaess M**, Kaiser L, Sauer M, Csuk R, Deigner HP. COVID-19/SARS-CoV-2 Infection: Lysosomes and Lysosomotropism Implicate New Treatment Strategies and Personal Risks. *Int J Mol Sci* 2020; **21** [PMID: 32668803 DOI: 10.3390/ijms21144953]

5 **Zhou P**, Yang XL, Wang XG, Hu B, Zhang L, Zhang W, Si HR, Zhu Y, Li B, Huang CL, Chen HD, Chen J, Luo Y, Guo H, Jiang RD, Liu MQ, Chen Y, Shen XR, Wang X, Zheng XS, Zhao K, Chen QJ, Deng F, Liu LL, Yan B, Zhan FX, Wang YY, Xiao GF, Shi ZL. A pneumonia outbreak associated with a new coronavirus of probable bat origin. *Nature* 2020; **579**: 270-273 [PMID: 32015507 DOI: 10.1038/s41586-020-2012-7]

6 **Walls AC**, Park YJ, Tortorici MA, Wall A, McGuire AT, Veesler D. Structure, Function, and Antigenicity of the SARS-CoV-2 Spike Glycoprotein. *Cell* 2020; **181**: 281-292.e6 [PMID: 32155444 DOI: 10.1016/j.cell.2020.02.058]

7 **Zhu G**, Zhu C, Zhu Y, Sun F. Minireview of progress in the structural study of SARS-CoV-2 proteins. *Curr Res Microb Sci* 2020; **1**: 53-61 [PMID: 33236001 DOI: 10.1016/j.crmicr.2020.06.003]

8 **Shang J**, Wan Y, Luo C, Ye G, Geng Q, Auerbach A, Li F. Cell entry mechanisms of SARS-CoV-2. *Proc Natl Acad Sci U S A* 2020; **117**: 11727-11734 [PMID: 32376634 DOI: 10.1073/pnas.2003138117]

9 **Wei J**, Alfajaro MM, DeWeirdt PC, Hanna RE, Lu-Culligan WJ, Cai WL, Strine MS, Zhang SM, Graziano VR, Schmitz CO, Chen JS, Mankowski MC, Filler RB, Ravindra NG, Gasque V, de Miguel FJ, Patil A, Chen H, Oguntuyo KY, Abriola L, Surovtseva YV, Orchard RC, Lee B, Lindenbach BD, Politi K, van Dijk D, Kadoch C, Simon MD, Yan Q, Doench JG, Wilen CB. Genome-wide CRISPR Screens Reveal Host Factors Critical for SARS-CoV-2 Infection. *Cell* 2021; **184**: 76-91.e13 [PMID: 33147444 DOI: 10.1016/j.cell.2020.10.028]

10 **Pišlar A**, Mitrović A, Sabotič J, Pečar Fonović U, Perišić Nanut M, Jakoš T, Senjor E, Kos J. The role of cysteine peptidases in coronavirus cell entry and replication: The therapeutic potential of cathepsin inhibitors. *PLoS Pathog* 2020; **16**: e1009013 [PMID: 33137165 DOI: 10.1371/journal.ppat.1009013]

11 **Zang R**, Gomez Castro MF, McCune BT, Zeng Q, Rothlauf PW, Sonnek NM, Liu Z, Brulois KF, Wang X, Greenberg HB, Diamond MS, Ciorba MA, Whelan SPJ, Ding S. TMPRSS2 and TMPRSS4 promote SARS-CoV-2 infection of human small intestinal enterocytes. *Sci Immunol* 2020; **5** [PMID: 32404436 DOI: 10.1126/sciimmunol.abc3582]

12 **Berdowska I**. Cysteine proteases as disease markers. *Clin Chim Acta* 2004; **342**: 41-69 [PMID: 15026265 DOI: 10.1016/j.cccn.2003.12.016]

13 **Vizovišek M**, Fonović M, Turk B. Cysteine cathepsins in extracellular matrix remodeling: Extracellular matrix degradation and beyond. *Matrix Biol* 2019; **75-76**: 141-159 [PMID: 29409929 DOI: 10.1016/j.matbio.2018.01.024]

14 **Vizovišek M**, Vidak E, Javoršek U, Mikhaylov G, Bratovš A, Turk B. Cysteine cathepsins as therapeutic targets in inflammatory diseases. *Expert Opin Ther Targets* 2020; **24**: 573-588 [PMID: 32228244 DOI: 10.1080/14728222.2020.1746765]

15 **Vidak E**, Javoršek U, Vizovišek M, Turk B. Cysteine Cathepsins and their Extracellular Roles: Shaping the Microenvironment. *Cells* 2019; **8** [PMID: 30897858 DOI: 10.3390/cells8030264]

16 **Gomes CP**, Fernandes DE, Casimiro F, da Mata GF, Passos MT, Varela P, Mastroianni-Kirsztajn G, Pesquero JB. Cathepsin L in COVID-19: From Pharmacological Evidences to Genetics. *Front Cell Infect Microbiol* 2020; **10**: 589505 [PMID: 33364201 DOI: 10.3389/fcimb.2020.589505]

17 **Menzel K**, Hausmann M, Obermeier F, Schreiter K, Dunger N, Bataille F, Falk W, Scholmerich J, Herfarth H, Rogler G. Cathepsins B, L and D in inflammatory bowel disease macrophages and potential therapeutic effects of cathepsin inhibition in vivo. *Clin Exp Immunol* 2006; **146**: 169-180 [PMID: 16968411 DOI: 10.1111/j.1365-2249.2006.03188.x]

18 **Xu S**, Zhang H, Yang X, Qian Y, Xiao Q. Inhibition of cathepsin L alleviates the microglia-mediated neuroinflammatory responses through caspase-8 and NF-κB pathways. *Neurobiol Aging* 2018; **62**: 159-167 [PMID: 29154036 DOI: 10.1016/j.neurobiolaging.2017.09.030]

19 **Cao Y**, Liu X, Li Y, Lu Y, Zhong H, Jiang W, Chen AF, Billiar TR, Yuan H, Cai J. Cathepsin L activity correlates with proteinuria in chronic kidney disease in humans. *Int Urol Nephrol* 2017; **49**: 1409-1417 [PMID: 28534128 DOI: 10.1007/s11255-017-1626-7]

20 **Ou X**, Liu Y, Lei X, Li P, Mi D, Ren L, Guo L, Guo R, Chen T, Hu J, Xiang Z, Mu Z, Chen X, Chen J, Hu K, Jin Q, Wang J, Qian Z. Characterization of spike glycoprotein of SARS-CoV-2 on virus entry and its immune cross-reactivity with SARS-CoV. *Nat Commun* 2020; **11**: 1620 [PMID: 32221306 DOI: 10.1038/s41467-020-15562-9]

21 **Cantuti-Castelvetri L**, Ojha R, Pedro LD, Djannatian M, Franz J, Kuivanen S, van der Meer F, Kallio K, Kaya T, Anastasina M, Smura T, Levanov L, Szirovicza L, Tobi A, Kallio-Kokko H, Österlund P, Joensuu M, Meunier FA, Butcher SJ, Winkler MS, Mollenhauer B, Helenius A, Gokce O, Teesalu T, Hepojoki J, Vapalahti O, Stadelmann C, Balistreri G, Simons M. Neuropilin-1 facilitates SARS-CoV-2 cell entry and infectivity. *Science* 2020; **370**: 856-860 [PMID: 33082293 DOI: 10.1126/science.abd2985]

22 **Smieszek SP**, Przychodzen BP, Polymeropoulos MH. Amantadine disrupts lysosomal gene expression: A hypothesis for COVID19 treatment. *Int J Antimicrob Agents* 2020; **55**: 106004 [PMID: 32361028 DOI: 10.1016/j.ijantimicag.2020.106004]

23 **Rejdak K**, Grieb P. Adamantanes might be protective from COVID-19 in patients with neurological diseases: multiple sclerosis, parkinsonism and cognitive impairment. *Mult Scler Relat Disord* 2020; **42**: 102163 [PMID: 32388458 DOI: 10.1016/j.msard.2020.102163]

24 **Torres J**, Maheswari U, Parthasarathy K, Ng L, Liu DX, Gong X. Conductance and amantadine binding of a pore formed by a lysine-flanked transmembrane domain of SARS coronavirus envelope protein. *Protein Sci* 2007; **16**: 2065-2071 [PMID: 17766393 DOI: 10.1110/ps.062730007]

25 **Sahu T**, Mehta A, Ratre YK, Jaiswal A, Vishvakarma NK, Bhaskar LVKS, Verma HK. Current understanding of the impact of COVID-19 on gastrointestinal disease: Challenges and openings. *World J Gastroenterol* 2021; **27**: 449-469 [PMID: 33642821 DOI: 10.3748/wjg.v27.i6.449]

26 **Pan L**, Mu M, Yang P, Sun Y, Wang R, Yan J, Li P, Hu B, Wang J, Hu C, Jin Y, Niu X, Ping R, Du Y, Li T, Xu G, Hu Q, Tu L. Clinical Characteristics of COVID-19 Patients With Digestive Symptoms in Hubei, China: A Descriptive, Cross-Sectional, Multicenter Study. *Am J Gastroenterol* 2020; **115**: 766-773 [PMID: 32287140 DOI: 10.14309/ajg.0000000000000620]

27 **Wu Y**, Guo C, Tang L, Hong Z, Zhou J, Dong X, Yin H, Xiao Q, Tang Y, Qu X, Kuang L, Fang X, Mishra N, Lu J, Shan H, Jiang G, Huang X. Prolonged presence of SARS-CoV-2 viral RNA in faecal samples. *Lancet Gastroenterol Hepatol* 2020; **5**: 434-435 [PMID: 32199469 DOI: 10.1016/S2468-1253(20)30083-2]

28 **Xiao F**, Tang M, Zheng X, Liu Y, Li X, Shan H. Evidence for Gastrointestinal Infection of SARS-CoV-2. *Gastroenterology* 2020; **158**: 1831-1833.e3 [PMID: 32142773 DOI: 10.1053/j.gastro.2020.02.055]

29 **Qian Q**, Fan L, Liu W, Li J, Yue J, Wang M, Ke X, Yin Y, Chen Q, Jiang C. Direct evidence of active SARS-CoV-2 replication in the intestine. *Clin Infect Dis* 2020 [PMID: 32638022 DOI: 10.1093/cid/ciaa925]

30 **Cheung KS**, Hung IFN, Chan PPY, Lung KC, Tso E, Liu R, Ng YY, Chu MY, Chung TWH, Tam AR, Yip CCY, Leung KH, Fung AY, Zhang RR, Lin Y, Cheng HM, Zhang AJX, To KKW, Chan KH, Yuen KY, Leung WK. Gastrointestinal Manifestations of SARS-CoV-2 Infection and Virus Load in Fecal Samples From a Hong Kong Cohort: Systematic Review and Meta-analysis. *Gastroenterology* 2020; **159**: 81-95 [PMID: 32251668 DOI: 10.1053/j.gastro.2020.03.065]

31 **Wang W**, Xu Y, Gao R, Lu R, Han K, Wu G, Tan W. Detection of SARS-CoV-2 in Different Types of Clinical Specimens. *JAMA* 2020; **323**: 1843-1844 [PMID: 32159775 DOI: 10.1001/jama.2020.3786]

32 **Chu H**, Chan JF, Wang Y, Yuen TT, Chai Y, Shuai H, Yang D, Hu B, Huang X, Zhang X, Hou Y, Cai JP, Zhang AJ, Zhou J, Yuan S, To KK, Hung IF, Cheung TT, Ng AT, Hau-Yee Chan I, Wong IY, Law SY, Foo DC, Leung WK, Yuen KY. SARS-CoV-2 Induces a More Robust Innate Immune Response and Replicates Less Efficiently Than SARS-CoV in the Human Intestines: An Ex Vivo Study With Implications on Pathogenesis of COVID-19. *Cell Mol Gastroenterol Hepatol* 2021; **11**: 771-781 [PMID: 33010495 DOI: 10.1016/j.jcmgh.2020.09.017]

33 **Lee S**, Yoon GY, Myoung J, Kim SJ, Ahn DG. Robust and persistent SARS-CoV-2 infection in the human intestinal brush border expressing cells. *Emerg Microbes Infect* 2020; **9**: 2169-2179 [PMID: 32969768 DOI: 10.1080/22221751.2020.1827985]

34 **Lamers MM**, Beumer J, van der Vaart J, Knoops K, Puschhof J, Breugem TI, Ravelli RBG, Paul van Schayck J, Mykytyn AZ, Duimel HQ, van Donselaar E, Riesebosch S, Kuijpers HJH, Schipper D, van de Wetering WJ, de Graaf M, Koopmans M, Cuppen E, Peters PJ, Haagmans BL, Clevers H. SARS-CoV-2 productively infects human gut enterocytes. *Science* 2020; **369**: 50-54 [PMID: 32358202 DOI: 10.1126/science.abc1669]

35 **Stanifer ML**, Kee C, Cortese M, Zumaran CM, Triana S, Mukenhirn M, Kraeusslich HG, Alexandrov T, Bartenschlager R, Boulant S. Critical Role of Type III Interferon in Controlling SARS-CoV-2 Infection in Human Intestinal Epithelial Cells. *Cell Rep* 2020; **32**: 107863 [PMID: 32610043 DOI: 10.1016/j.celrep.2020.107863]

36 **Peterson MD**, Mooseker MS. Characterization of the enterocyte-like brush border cytoskeleton of the C2BBe clones of the human intestinal cell line, Caco-2. *J Cell Sci* 1992; **102** (Pt 3): 581-600 [PMID: 1506435 DOI: 10.1242/jcs.102.3.581]

37 **Klijn C**, Durinck S, Stawiski EW, Haverty PM, Jiang Z, Liu H, Degenhardt J, Mayba O, Gnad F, Liu J, Pau G, Reeder J, Cao Y, Mukhyala K, Selvaraj SK, Yu M, Zynda GJ, Brauer MJ, Wu TD, Gentleman RC, Manning G, Yauch RL, Bourgon R, Stokoe D, Modrusan Z, Neve RM, de Sauvage FJ, Settleman J, Seshagiri S, Zhang Z. A comprehensive transcriptional portrait of human cancer cell lines. *Nat Biotechnol* 2015; **33**: 306-312 [PMID: 25485619 DOI: 10.1038/nbt.3080]

38 **Kumar A**, Faiq MA, Pareek V, Raza K, Narayan RK, Prasoon P, Kumar P, Kulandhasamy M, Kumari C, Kant K, Singh HN, Qadri R, Pandey SN, Kumar S. Relevance of SARS-CoV-2 related factors ACE2 and TMPRSS2 expressions in gastrointestinal tissue with pathogenesis of digestive symptoms, diabetes-associated mortality, and disease recurrence in COVID-19 patients. *Med Hypotheses* 2020; **144**: 110271 [PMID: 33254575 DOI: 10.1016/j.mehy.2020.110271]

39 **Lee JJ**, Kopetz S, Vilar E, Shen JP, Chen K, Maitra A. Relative Abundance of SARS-CoV-2 Entry Genes in the Enterocytes of the Lower Gastrointestinal Tract. *Genes (Basel)* 2020; **11** [PMID: 32545271 DOI: 10.3390/genes11060645]

40 **Gkogkou E**, Barnasas G, Vougas K, Trougakos IP. Expression profiling meta-analysis of ACE2 and TMPRSS2, the putative anti-inflammatory receptor and priming protease of SARS-CoV-2 in human cells, and identification of putative modulators. *Redox Biol* 2020; **36**: 101615 [PMID: 32863223 DOI: 10.1016/j.redox.2020.101615]

41 **Wiese O**, Zemlin AE, Pillay TS. Molecules in pathogenesis: angiotensin converting enzyme 2 (ACE2). *J Clin Pathol* 2021; **74**: 285-290 [PMID: 32759311 DOI: 10.1136/jclinpath-2020-206954]

42 **Singer D**, Camargo SM. Collectrin and ACE2 in renal and intestinal amino acid transport. *Channels (Austin)* 2011; **5**: 410-423 [PMID: 21814048 DOI: 10.4161/chan.5.5.16470]

43 **Camargo SM**, Singer D, Makrides V, Huggel K, Pos KM, Wagner CA, Kuba K, Danilczyk U, Skovby F, Kleta R, Penninger JM, Verrey F. Tissue-specific amino acid transporter partners ACE2 and collectrin differentially interact with hartnup mutations. *Gastroenterology* 2009; **136**: 872-882 [PMID: 19185582 DOI: 10.1053/j.gastro.2008.10.055]

44 **Hashimoto T**, Perlot T, Rehman A, Trichereau J, Ishiguro H, Paolino M, Sigl V, Hanada T, Hanada R, Lipinski S, Wild B, Camargo SM, Singer D, Richter A, Kuba K, Fukamizu A, Schreiber S, Clevers H, Verrey F, Rosenstiel P, Penninger JM. ACE2 Links amino acid malnutrition to microbial ecology and intestinal inflammation. *Nature* 2012; **487**: 477-481 [PMID: 22837003 DOI: 10.1038/nature11228]

World Journal of Gastroenterology

Submit a Manuscript: https://www.f6publishing.com

World J Gastroenterol 2021 October 21; 27(39): 6601-6614

DOI: 10.3748/wjg.v27.i39.6601

ISSN 1007-9327 (print) ISSN 2219-2840 (online)

MINIREVIEWS

Endoscopic anti-reflux therapy for gastroesophageal reflux disease

Enrique Rodríguez de Santiago, Eduardo Albéniz, Fermin Estremera-Arevalo, Carlos Teruel Sanchez-Vegazo, Vicente Lorenzo-Zúñiga

ORCID number: Enrique Rodríguez de Santiago 0000-0002-2852-6042; Eduardo Albéniz 0000-0002-9311-3746; Fermin Estremera-Arevalo 0000-0003-2676-1353; Carlos Teruel Sanchez-Vegazo 0000-0001-6626-2933; Vicente Lorenzo-Zúñiga 0000-0002-4072-3241.

Author contributions: Rodriguez de Santiago E and Lorenzo-Zuñiga V designed the research study; all authors performed the literature review; Rodriguez de Santiago E drafted the first version of the manuscript; Estremera-Arevalo F, Lorenzo-Zuñiga V, Albeniz E, and Teruel Sanchez-Vegazo C critically reviewed the manuscript; all authors have read and approved the final manuscript.

Conflict-of-interest statement: The authors declare no conflicts of interest for this article.

Open-Access: This article is an open-access article that was selected by an in-house editor and fully peer-reviewed by external reviewers. It is distributed in accordance with the Creative Commons Attribution NonCommercial (CC BY-NC 4.0) license, which permits others to distribute, remix, adapt, build upon this work non-commercially, and license their derivative works on different terms, provided the original work is properly cited and the use is non-commercial. See: htt

Enrique Rodríguez de Santiago, Carlos Teruel Sanchez-Vegazo, Department of Gastroenterology and Hepatology, Hospital Universitario Ramón y Cajal, Instituto Ramón y Cajal de Investigació n Sanitaria (IRYCIS), Madrid 28034, Spain

Eduardo Albéniz, Fermin Estremera-Arevalo, Endoscopy Unit, Gastroenterology Department, Hospital Universitario de Navarra. Gastrointestinal Endoscopy Research Unit, Navarrabiomed Biomedical Research Center. Pamplona, Spain

Vicente Lorenzo-Zúñiga, Endoscopy Unit, Gastroenterology Department, Hospital Universitari i Politècnic La Fe, Instituto de Investigación Sanitaria La Fe (IIS La Fe), Valencia 46026, Spain

Corresponding author: Enrique Rodríguez de Santiago, MD, MHSc, PhD, Consultant Physician-Scientist, Department of Gastroenterology and Hepatology, Hospital Universitario Ramón y Cajal, Instituto Ramón y Cajal de Investigación Sanitaria (IRYCIS), Ctra. de Colmenar Viejo km. 9100, Madrid 28034, Spain. enrodesan@gmail.com

Abstract

Gastroesophageal reflux disease has an increasing incidence and prevalence worldwide. A significant proportion of patients have a suboptimal response to proton pump inhibitors or are unwilling to take lifelong medication due to concerns about long-term adverse effects. Endoscopic anti-reflux therapies offer a minimally invasive option for patients unwilling to undergo surgical treatment or take lifelong medication. The best candidates are those with a good response to proton pump inhibitors and without a significant sliding hiatal hernia. Transoral incisionless fundoplication and nonablative radiofrequency are the techniques with the largest body of evidence and that have been tested in several randomized clinical trials. Band-assisted ligation techniques, anti-reflux mucosectomy, anti-reflux mucosal ablation, and new plication devices have yielded promising results in recent noncontrolled studies. Nonetheless, the role of endoscopic procedures remains controversial due to limited long-term and comparative data, and no consensus exists in current clinical guidelines. This review provides an updated summary focused on the patient selection, technical details, clinical success, and safety of current and future endoscopic anti-reflux techniques.

Key Words: Treatment; Gastroesophageal reflux; Transoral incisionless fundoplication; Anti-reflux mucosectomy; Anti-reflux mucosal ablation; Stretta

©The Author(s) 2021. Published by Baishideng Publishing Group Inc. All rights reserved.

p://creativecommons.org/Licenses/by-nc/4.0/

Manuscript source: Unsolicited manuscript

Specialty type: Gastroenterology and hepatology

Country/Territory of origin: Spain

Peer-review report's scientific quality classification

Grade A (Excellent): 0
Grade B (Very good): B
Grade C (Good): 0
Grade D (Fair): 0
Grade E (Poor): 0

Received: April 19, 2021
Peer-review started: April 19, 2021
First decision: June 23, 2021
Revised: July 1, 2021
Accepted: August 31, 2021
Article in press: August 31, 2021
Published online: October 21, 2021

P-Reviewer: Singh A
S-Editor: Gong ZM
L-Editor: Filipodia
P-Editor: Yuan YY

Core Tip: Gastroesophageal reflux disease is a common disorder that impacts quality of life. Endoscopic anti-reflux therapies are intended to offer an alternative for patients unwilling to undergo surgical treatment or take lifelong medication. Several techniques, such as transoral incisionless fundoplication, nonablative radiofrequency, plication methods, and anti-reflux mucosectomy, have shown encouraging results, but their role in the management of gastroesophageal reflux disease remains controversial. Careful patient selection and awareness of the advantages and disadvantages of each technique are essential to optimize outcomes. We herein provide an updated review of the technical aspects, clinical success, and safety of the principle endoscopic anti-reflux procedures.

Citation: Rodríguez de Santiago E, Albéniz E, Estremera-Arevalo F, Teruel Sanchez-Vegazo C, Lorenzo-Zúñiga V. Endoscopic anti-reflux therapy for gastroesophageal reflux disease. *World J Gastroenterol* 2021; 27(39): 6601-6614
URL: https://www.wjgnet.com/1007-9327/full/v27/i39/6601.htm
DOI: https://dx.doi.org/10.3748/wjg.v27.i39.6601

INTRODUCTION

Gastroesophageal reflux disease (GERD) is a condition that develops when reflux of stomach contents causes troublesome symptoms or complications in the esophagus or beyond[1,2]. GERD is very frequent worldwide, with a prevalence ranging from 7.4% in Southern Asia to 19.6% in Central America, and it affects both sexes similarly[3]. The increment in aging and obesity, both predisposing factors for GERD, may increase its impact in the near future even further[4]. Many other factors also favor GERD exacerbation, including tobacco and certain drugs, such as calcium blockers and tricyclic antidepressants[5,6]. GERD negatively affects quality of life and imposes economic and productivity loss burdens[7].

Although the cause of GERD is still incompletely understood, several underlying predisposing pathophysiological mechanisms have been described. While low esophageal sphincter (LES) basal pressure may facilitate reflux after abdominal strain or during swallowing, a more pertinent mechanism is transient LES relaxation (TLESR), which can be associated with esophageal shortening[8,9]. Gastroesophageal junction (GEJ) disruption due to a hiatal hernia (HH) constitutes an additional factor because it contributes to LES incompetence and also displaces the acid pocket closer to the esophageal mucosa[10,11]. Altered visceral sensitivity has a bidirectional effect in GERD, magnifying symptoms in patients without mucosal injury and reducing symptom awareness in Barrett's esophagus patients[12]. Esophageal hypomotility, low saliva production, and other mechanisms such as certain breathing patterns may also contribute to GERD[13].

The management of GERD is multimodal. Lifestyle modifications such as weight loss, tobacco cessation, and, in selected cases, postural advice[14] have proven efficacy and may be sufficient in mild cases. Drug therapy occupies the next level, with proton pump inhibitors (PPIs) having a huge impact on GERD treatment due to high esophagitis healing rates, surpassing the performance of histamine receptor antagonists and exhibiting high cost-efficacy[15,16]. They are the cornerstone of medical GERD treatment. Anti-reflux surgery (ARS), namely laparoscopic fundoplication, is the last step in GERD management. Its objectives are as follows: (1) LES fixation to the hiatus and intraabdominal segment length augmentation; (2) LES basal pressure increase; and (3) hiatal repair. The latter aspect appears crucial because hiatal repair itself impacts the length and pressure of the LES more than fundoplication[17]. Randomized controlled trials (RCTs) have failed to demonstrate a clear long-term superiority of ARS over PPIs[18]. Consequently, ARS is reserved for patients who do not respond to PPIs, do not tolerate them due to adverse effects, or are unwilling to maintain them in the long term.

PPI refractoriness probably constitutes the most frequent indication for surgery, although it is a confusing term and thus deserves further consideration. The same concept frequently encompasses vastly different realities. Refractoriness can be partial or complete, a distinction that is clinically relevant. Recent and major trials have defined the grade of refractoriness needed to meet inclusion criteria[19]. Subsequently,

symptoms can persist for very different reasons, such as poor adherence to medical therapies, absence of a relationship with reflux (*e.g.*, functional heartburn), or objectively proven reflux persistence despite proper medical treatment. Therefore, guidelines advise a full diagnostic workup before surgery to demonstrate as consistently as possible that the symptoms, whether refractory or not, are objectively secondary to GERD[2,20-27].

In the last 30 years, effort has been made to design endoscopic anti-reflux therapies that serve as a valuable option for GERD management, either as an alternative to ARS or as bridge therapy between pharmacological treatment and surgery. They do not thus far allow hiatal repair and constrain candidate selection to individuals without a HH. In 1979, Angelchik[28] used a silicon prosthesis as the first endoscopic treatment for GERD. Since then, numerous other treatments have emerged, with many, such as GEJ injections of bulking agents and several plication techniques, disappearing because of low efficacy or unacceptable adverse effects[29-31]. Here, we present a comprehensive review of the endoscopic approaches for the treatment of GERD that have survived the test of time or have recently been designed (Table 1).

INDICATIONS FOR ENDOSCOPIC ANTI-REFLUX THERAPY

Endoscopic therapies should be considered at least in the same scenarios as surgery and should offer some advantages over ARS. Specifically, endoscopic anti-reflux therapy should be considered in PPI nonresponders, in patients who have a contraindication to PPIs or have concerns regarding their long-term adverse effects, and in those who either do not qualify for ARS or refuse it. Ideally, endoscopic techniques should demonstrate noninferior efficacy, alongside a shorter operation time, lower complication rate, and lower secondary long-term morbidity. Finally, they should not preclude a future fundoplication in case of failure.

Laparoscopic fundoplication performed by skilled surgeons has a low short-term morbidity and mortality but can cause significant adverse effects in the medium term, such as dysphagia (in up to 24% of patients), gas-bloat syndrome, and incisional hernia, and revision surgeries are not infrequent[22]. It fails in 10%-15% of patients in the short term, and long-term studies have shown that more than 30% of patients are still on PPIs years after surgery[22,32]. This constitutes the scenario against which endoscopic therapies should be compared.

The guidelines of the main medical and surgical societies and expert consensus documents published in the last 10 years have addressed the endoscopic alternatives as well as the surgical option. Their recommendations and the level of evidence or consensus that they are based upon are summarized in Table 2[2,20-26,33-35]. Transoral incisionless fundoplication (TIF) and nonablative radiofrequency are considered appropriate in well-selected patients and situations according to recent guidelines.

CURRENT ENDOSCOPIC THERAPIES

Transoral incisionless fundoplication

The aim of TIF is to perform an endoscopic fundoplication by reestablishing the flap valve mechanism with a 3-cm high-pressure zone at the distal esophagus to durably restore LES function[36]. This procedure mirrors ARS by using an endoscopic suturing device with T-fasteners, the EsophyXâ device (EndoGastric Solutions, Inc., Redmond, WA, United States)[37]. These devices have evolved from a longitudinally oriented gastrogastric plication to one with a greater degree of rotational movement, 200° to 300° in circumference and a 2-3-cm length wrap over the distal esophagus below the diaphragm to create full-thickness serosa-to-serosa esophagogastric plications. This easier to use and more automated device can deploy about 20 fasteners without the need for visualization of the stylet/fastener deployment. The objective of the technique is to restore the integrity of the angle of His by firing stabilizing T-fasteners, deployed 2 to 3 cm above the GEJ, with a 270° esophagogastric wrap, to mimic a Toupet surgical fundoplication. The EsophyXâ device was approved in 2007 by the United States Food and Drug Administration as a single-use, two-operator device comprising a tip (tissue retractor, tissue mold and chassis, fasteners over a stylet, and the invaginator) and body (H-fasteners, helix retractor lock, vacuum connection, fastener pusher, helix retractor control, tissue mold knob, gastroscope point of insertion).

Table 1 Comparison of current endoscopic therapies for gastroesophageal reflux disease

	TIF	MUSE	Stretta®	GERDx™	ARMS/ARMA	Band ligation
Efficacy	++	+	+ -	+	+	+
Safety	+	+	++	+	+	+
Technical difficulty	++	++	+	++	+	+
Add-on device	+	+	+	+	-	-
RCT available	+	-	+	-	-	-
Maximum follow-up (yr)	10	5	10	0.25	3	1
Cost	++	++	++	++	+	+

++: Indicates the highest score; +: Indicates a moderate score or yes; -: Indicates uncertainty; TIF: Transoral incisionless fundoplication; MUSE: Medigus ultrasonic surgical endostapler; GERDx™: Endoscopic full-thickness plication device; ARMS: Anti-reflux mucosectomy; ARMA: Anti-reflux mucosal ablation; RCT: Randomized controlled trial.

Optimal candidates for TIF are patients who demonstrate LES incompetence (Hill grade II) without a concomitant HH. TIF 1.0 has been discontinued because TIF 2.0 achieves much better results[36]. The improved procedure has been evaluated in nine noncomparative studies[38-46] and in five RCTs[47-51] comprising 886 patients with moderate GERD without a large HH, Los Angeles grade C or D esophagitis, or Barrett´s esophagus (Table 3). Clinical success rates ranged from a modest 50% at 12 mo to as high as 92% at 10 years. Severe adverse events (SAEs) have been reported in 2.4% of patients[52]. A recent network meta-analysis suggested that the TIF 2.0 procedure manages symptoms and allows PPI discontinuation at rates similar to those of ARS with an improved safety profile and fewer long-term adverse events[53]. A clinical response, defined by an improvement of at least 50% in GERD health-related quality of life (GERD-HRQL) score or remission of heartburn and regurgitation, was observed in 66% of patients treated with TIF. Moreover, TIF had the highest probability of improving GERD-HRQL (0.96), followed by ARS (0.66) and PPIs (0.042). In contrast, ARS had the highest probability of increasing the percent time at pH < 4 (0.99), followed by PPIs (0.64) and TIF (0.32)[53]. A review of the published evidence supports the belief that most selected patients undergoing TIF 2.0 experience a long-term elimination of GERD symptoms with no SAEs and that this procedure is a cost-effective alternative to ARS.

Medigus ultrasonic surgical endostapler

The Medigus ultrasonic surgical endostapler (MUSE), or MUSE™ system (Medigus, Omer, Israel), combines microvisual, ultrasonic, and surgical stapling capabilities into one device, which enables a single endoscopist to perform a transoral anterior fundoplication. This flexible surgical endostapler resembles an endoscope with a rigid section holding a cartridge with five standard 4.8-mm titanium surgical staples. The distal tip contains an anvil for bending the staples, two small 21-gauge screws, and an ultrasonic transducer to measure the distance to the cartridge. This method is a three-step procedure: (1) The stapler is advanced into the stomach through an overtube and retroflex; (2) The system is retracted to 3 cm proximal to the GEJ for clamping when the tissue thickness is 1.4-1.6 mm, and the stapler is then fired; and (3) The procedure is repeated to add quintuplets of staples to create an anti-reflux barrier.

This endoscopic stapling system has been evaluated in four noncomparative studies [46,54-56] and in one two-arm case series study[57] including 209 patients with GERD without a HH larger than 3 cm (Table 3). Clinical success rates ranged from 69% to 92% with follow-up durations from 6 mo to 5 years. The risk of SAEs (empyema, hemorrhage, esophageal perforation) was 3.5%. Overall, data on the efficacy and safety of MUSE are scarce and evidence from RCTs is lacking.

Nonablative radiofrequency treatment (Stretta®)

This endoscopic-guided method involves the application of radiofrequency energy to the muscle fibers of the LES and the gastric cardia, through the Stretta® system (Restech, Houston, TX, United States). The Stretta® catheter is introduced over the guidewire and positioned sequentially at three levels: 0.5 cm proximal to the GEJ, at the GEJ, and 0.5 cm below the GEJ. At each level, the balloon basket assembly is

Table 2 Summary of guidelines and consensus recommendations and invasive gastroesophageal reflux disease therapies

Society guidelines and year of publication	Indication for surgery	Strength of recommendation, level of evidence, and grade of consensus	Endoscopic anti-reflux therapy addressed	Guideline recommendation on endoscopic anti-reflux therapy	Strength of recommendation and level of evidence
ACG guidelines for diagnosis and management of GERD, 2013[2]	Option for long-term treatment	Quality: High. Strength: Strong	Radiofrequency, bulking agents, endoscopic suturing	Not recommended	Quality: Moderate. Strength: Conditional
	Generally not recommended in PPI-unresponsive patients	Quality: High. Strength: Strong			
	Refractory patients with objective evidence of ongoing reflux as the cause of symptoms	Quality: Low. Strength: Conditional			
EAES recommendations, 2014[22]	Good response but dependent on long-term PPI therapy, after optimal risk-benefit discussion	Grade: C. Consensus: 100%	Radiofrequency (Stretta®), bulking agent injection (Enteryx®), plication (EndoCinch®, full-thickness plication, EsophyX®	Not enough evidence available to recommend any as an alternative option to surgery	Grade of recommendation: B. Expert consensus: 100%
	Total or partial refractoriness despite adequate PPI therapy in terms of dosage and intake	Grade: A. Consensus: 100%			
	Well-selected NERD patients and those with hypersensitive esophagus	Grade: C. Consensus: 100%			
American Society of Gastrointestinal Endoscopy: The role of endoscopy in the management of GERD, 2015[95]	Not provided	Not provided	Radiofrequency (Stretta®) and transoral incisionless fundoplication	Consider in highly selected patients. No details on selection criteria	Low quality
Asia-Pacific consensus on refractory GERD management, 2016[23]	Refractory symptoms with objectively documented GERD	Quality: Moderate. Strength: Strong. Consensus: 100%	None	Not applicable	Not applicable
World Gastroenterology Organisation Global Guidelines, 2017[24]	Large hiatal hernia with volume-related reflux symptoms. Refractory esophagitis. Refractory symptoms documented as caused by GERD. Medication adverse effects	Not specified	Endoscopic therapies in general	Only in the context of clinical trials	Not specified
SAGES Guidelines on GERD surgical treatment, 2010, and on endoluminal anti-reflux treatments, 2017[21,34]	Appropriately selected GERD patients	Grade A	Transoral incisionless fundoplication	Control of symptoms in appropriately selected patients in the short term; appears to lose effectiveness	Quality: Moderate. Strength: Strong
			Radiofrequency	Control of symptoms in appropriately selected patients; long-term effect in appropriately selected patients	Quality: Moderate. Strength: Strong
USA expert panel (surgeons and advanced therapeutic endoscopists) recommendations on GERD management, 2020[25]	PPI responders (complete or partial)	Appropriate. Consensus: 87%-100%	Transoral incisionless fundoplication	PPI responders (complete or partial), no hernia, any other scenario	Appropriate. Consensus: 93%
				PPI responders (complete or partial) or nonresponders, significant hernia, any other scenario	Not appropriate
	PPI nonresponder, no hernia, heartburn-hypersensitivity, or negative pH-impedance	Appropriateness uncertain		PPI nonresponder, no hernia and acid breakthrough, hypersensitivity or	Appropriate. Consensus: 80%–93%

	study			negative pH-impedance study for heartburn	
	PPI nonresponder, any other scenario	Appropriate. Consensus: 80%-100%		PPI nonresponder, regurgitation, negative pH-impedance study	Appropriateness uncertain
			Radiofrequency	PPI responders (complete or partial) or nonresponders, no hernia, any scenario	Appropriateness uncertain
				PPI responders (complete or partial) or nonresponders, significant hernia	Not appropriate
ESGE guidelines on endoscopic management of gastrointestinal motility disorders, 2020 [35]	Not applicable	Not applicable	Transoral incisionless fundoplication	Possible role in mild GERD patients who are unwilling to take PPIs or undergo surgery. Against widespread use	Quality: Moderate. Strength: Strong. Consensus: 92.8%
			Medigus Ultrasonic Surgical Endostapler	Insufficient data. Use only in clinical trials	Quality: Low. Strength: Strong. Consensus: 100%
			Radiofrequency	Can be considered in selected patients only, without erosive esophagitis and hiatal hernia	Quality: Moderate. Strength: Weak. Consensus: 92.9%
			Anti-reflux mucosectomy	Against routine use in clinical practice	Quality: Low. Strength: Strong. Consensus: 100%
ESNM/ASNM consensus paper on management of refractory GERD, 2020 [26]	Refractory GERD symptoms in patients with proven GERD	Consensus: 100%	Transoral incisionless fundoplication	Short-term benefit in improving regurgitation in carefully selected patients	Consensus: 100%
			Radiofrequency	Variable symptom improvement, limited objective improvement in acid burden or manometric esophagogastric junction features	Consensus: 100%

ACG: American College of Gastroenterology; EAES: European Association of Endoscopic Surgery; SAGES: Society of the Americans Gastrointestinal and Endoscopic Surgeons; GERD: Gastroesophageal reflux disease; ESGE: European Society of Gastrointestinal Endoscopy; ESNM: European Society of Neurogastroenterology and Motility; ASNM: American Society of Neurogastroenterology and Motility; PPIs: Proton pump inhibitors; NERD: Nonerosive reflux disease.

inflated and then four nitinol needle electrodes (22-gauge, 5.5-mm) are extended into the muscular layer to deliver a radiofrequency current and induce a thermal reaction. Next, to deliver radiofrequency energy to four additional points, the catheter is rotated 45º clockwise[58]. The pathophysiological mechanism is not fully understood, but the thermal injury is thought to promote submucosal fibrosis and muscularis propria hypertrophy, which would decrease the frequency of TLESR and GEJ compliance while increasing LES and gastric yield pressures[58].

The Stretta® procedure has been evaluated in numerous cohort studies and in five RCTs, three with sham therapy and two with PPI use[59] (Tables 1 and 3). The RCT results did not show significant changes in esophageal acid exposure at 6 mo following Stretta®, compared with the PPI group[60]. Likewise, patients treated with Stretta® presented significant improvements in heartburn symptoms and quality of life in only the short term, compared with a sham procedure, with no long-term data[61-63]. A meta-analysis including 159 patients, limited to four RCTs, confirmed the absence of significant changes in patients with GERD[64]. More recently, a second meta-analysis that included both RCTs and 24 other cohort studies with 2468 evaluated patients[65] showed a significant postprocedural improvement in quality of life and in heartburn score but no improvement in basal LES pressure. The procedure is safe and well-tolerated, and SAEs are very rare. RCTs and cohort studies reported erosions, mucosal lacerations, gastroparesis, mediastinal inflammation, pneumonia,

Table 3 Clinical success and safety of endoscopic therapies

Technique	Study design and population	Clinical success, range	Major adverse events, range
Transoral incisionless fundoplication	No. of RCTs: 5; *n* = 343 No. of nonrandomized case series: 9; *n* = 543	50%–92%	0%–4.4%
Medigus ultrasonic surgical endostapler	No. of RCTs: 0 No. of nonrandomized case series: 5; *n* = 199	69%–92%	0%–9%
Nonablative radiofrequency (Stretta®)	No. of RCTs: 5; *n* = 173 No. of nonrandomized case series: 29; *n* = 2571	15%–100%	0%–1%
Endoscopic plication device (GERDx™)	No. of RCTs: 0 No. of nonrandomized case series: 1; *n* = 40	19 out of 40 patients were off PPIs	10%
Band ligation techniques	No. of RCTs: 1; *n* = 150 No. of nonrandomized case series: 2; *n* = 73	43%–54%[1]	0%
Anti-reflux mucosectomy	No. of RCTs: 0 No. of nonrandomized case series: 12; *n* = 331	58%–100%	0%–17%
Anti-reflux mucosal ablation	No. of RCTs: 0 No. of nonrandomized case series: 3; *n* = 130	58%–89%	0%–13%

[1]Clinical success not defined in the randomized controlled trial. There was a significant reduction in gastroesophageal reflux disease health-related quality of life score and 24-h pH-metry outcomes. RCT: Randomized controlled trial; PPIs: Proton pump inhibitors.

and pleural effusion[66].

Endoscopic plication device (GERDx™)

The GERDx™ device (G-SURG GmbH, Seeon-Seebruck, Germany) uses hydraulic elements for control and requires a slim gastroscope that works as a light source. It is the advanced single-use product of the company that has acquired the Plicator technology after withdrawal of the Plicator device (Ethicon Endo-Surgery, Sommerville, NJ) from the market. The experience with GERDx™ is still minimal, with only two publications in this regard, one of which is an interim analysis by the same authors (Tables 1 and 3).

In a single-center, single-arm trial, Weitzendorfer *et al*[67,68] prospectively assessed the outcomes of 40 patients with refractory GERD treated with the GERDx™ device. Of the 40 patients, 7 underwent LARS before the 3-mo follow-up. The mean DeMeester score was reduced from 46.48 to 20.03 in the 30 patients who completed the follow-up. Of these 30 patients, 18 (60.0%) achieved normal DeMeester score levels. In addition, 3 (10.0%) stated that they were on daily PPI medication after the plication, with 8 (26.7%) taking on-demand medication and 19 (63.3%) off medication. Moderate SAEs were reported by 10% of the patients (a hematoma at the GEJ, a case of pneumonia, a suture passing through the left hepatic lobe, pleural empyema, a severe Mallory-Weiss tear). The single-study evidence, lack of a comparator arm, and the very short follow-up make this endoscopic treatment experimental at this time, necessitating new RCTs to corroborate improvements in quality of life and acid exposure and confirm procedural safety.

Anti-reflux mucosectomy and anti-reflux mucosal ablation

Anti-reflux mucosectomy (ARMS) was first devised in a patient with a Barrett's esophagus-related lesion treated by endoscopic submucosal dissection. The resulting scar improved GERD symptoms and normalized the DeMeester score[69]. This observation led to the first case series, published by Inoue *et al*[69] in 2014. In ARMS, endoscopic resection of the gastric cardiac mucosa is performed to reduce the opening

of the GEJ. Initial ARMS cases were performed by endoscopic submucosal dissection, but subsequent reports indicated that cap- or band-assisted mucosal resection is faster, easier to perform, and equally effective[70-72]. ARMS has been suggested to suppress the backflow of gastric content and enhance the GEJ flap valve mechanism, but the underlying anti-reflux mechanism is poorly understood[72]. A RCT conducted in animals found that ARMS increased the pressure and volume required to induce fluid passage from the gastric cavity to the esophagus[73]. One clinical study revealed that ARMS increased the integrated relaxation pressure and LES resting pressure but decreased GEJ distensibility, which could hypothetically reduce the frequency of TLESR[72,74].

In 2020, Inoue *et al*[75] and Hernández Mondragón *et al*[76] proposed that ablation of the gastric cardiac mucosa by argon plasma coagulation (forced mode 100 W) or a coagulation current applied by an endoknive (spray coagulation 50 W, effect 2) can also induce scar formation and yield similar clinical outcomes. This approach, named anti-reflux mucosal ablation (ARMA), is intended to simplify the procedure, reduce the risk of perforation, and facilitate the retreatment of patients who have failed ARMS.

In addition to their technical simplicity, ARMS and ARMA do not require costly add-on devices and can be performed in a standard endoscopy room[72,76]. Key points during ARMS and ARMA are adequate submucosal injection to prevent perforation and the sparing of a rim of healthy mucosa to minimize the risk of GEJ stenosis**.** The procedure is not standardized, but most authors spare the esophageal mucosa and perform a gastric cardia 270°-320° treatment or mimic a "butterfly" shape by sparing 1 cm of normal mucosa along the greater and lesser curvature[72,75-77].

In total, 15 nonrandomized studies (12 on ARMS[69-72,74,77-83] and three on ARMA[75,76,84]) comprising 461 patients have evaluated the safety and effectiveness of these techniques (Tables 1 and 3). Follow-up ranged from 2 mo to a maximum of 3 years (in two studies[72,76]). Clinical success ranged from 58% to 100% at 2-6 mo[81, 83] and from 72% to 76% at 3 years[72,76]. Dysphagia was the most common adverse event, occurring in about 5% to 10% of the patients. In contrast to what occurs with dysphagia associated with ARS[85], ARMS- and ARMA-associated dysphagia can be easily treated by small-caliber balloon dilation and does not necessarily compromise clinical success[72,76]. Gastrointestinal perforation is the most feared complication and has been reported in four patients treated with ARMS[72,77,78] and in none treated with ARMA. Given the lack of RCT and long-term data, these techniques should be viewed as experimental and reserved for patients included in research protocols.

Band ligation techniques

Three studies have assessed the outcomes of rubber band placement at the GEJ to reduce the width of the opening of the gastric cardia. Seleem *et al*[86] performed a RCT that included 150 patients with refractory GERD. The number of bands applied and the frequency of endoscopic sessions were determined according to the narrowing of the GEJ during banding. A maximum of four bands per session were allowed. Follow-up at 1 year showed a significant improvement in GERD-HRQL score and the number of reflux episodes. Mild dysphagia (25.3%) and epigastric pain (40%) were the most common adverse events, but no SAEs were recorded[86]. Hu *et al*[87] also reported favorable subjective and 24-h pH-metry outcomes in a case series of 13 patients and named the procedure "peroral endoscopic cardial constriction". The authors placed two single-band ligation devices (Fujinon, Tokyo, Japan) at the greater and lesser curvatures, close to the Z line. The first band was placed approximately 1.0 cm above the cardia along the lesser curvature, whereas the second band was delivered 1.0 cm above the greater curvature[87]. Finally, a clip was placed at the base of the bands to minimize the risk of band slippage. In 2020, another Chinese group reported favorable results with this technique in a nonrandomized study of 60 patients, with the approach now named "clip band ligation anti-reflux therapy (C-BLART)"[88] (Tables 1 and 3).

Because the above-mentioned RCT does not adhere to the Consolidated Standards of Reporting Trials quality requirements and the two case series were noncontrolled and included a limited number of patients, the technique should currently be viewed as experimental.

FUTURE DIRECTIONS

The history of endoscopic therapies for GERD is replete with encouraging preclinical studies and case series that fail to clear the hurdle of long-term and well-designed

RCTs. The main underlying reasons are the complex and multifactorial pathophysiology of GERD and the often short-lived anatomical changes induced by endoscopic therapies. Moreover, many endoscopic techniques require expensive add-on devices and cumbersome technical steps that have limited their popularization. To complicate further this issue, patient selection has been heterogeneous, and we lack consensus regarding the definition of clinical success or the admissible thresholds of cost and adverse events. Future endoscopic therapies and GERD research should bear all of this in mind.

The first consideration is that only a subset of well-selected GERD patients are good candidates for endoscopic therapies because current techniques remain unable to fix the hiatus, enhance esophageal motility, or normalize LES competence. Artificial intelligence through knowledge-based clinical decision support systems could be of help in the future for improving patient selection. Combined approaches that consider more than one GERD mechanism have been proposed to address this issue, such as a combination of ARMS with a plication method[89] or of TIF with laparoscopic HH repair[90]. Second, technical feasibility is critical for introducing a procedure into clinical practice. The learning curve of anti-reflux endoscopic therapies has not been well-described, and scientific societies have not published curricula documents to guide training. Band ligation, ARMS, and, more recently, ARMA are at very early stages but represent an attractive option from this perspective. Our group is currently performing a double-blind RCT to assess the clinical success and safety of ARMA[91]. Third, patient-reported outcomes are increasingly being recognized by clinicians, regulatory agencies, and patients as highly valuable tools to assess the impact of new interventions. Thus, we believe that studies should place symptoms and GERD-related quality of life as primary endpoints. A "black or white" perspective for clinical success does not reflect the complexity of GERD patients, and partial but significant improvements should also be taken into account. This makes anti-reflux endoscopy not only an alternative to PPIs, but also a complementary tool that can reduce their consumption and partially improve quality of life. A > 50% drop in the GERD-HRQL score or in other validated clinical questionnaires has been used in recent RCTs and appears to be a reasonable approach[52,53]. In addition, more objective GERD parameters (24-h pH-impedance testing, endoscopic esophagitis) and sham/placebo arms are needed to support subjective improvements. Outcome definitions should be in line with recent international consensus[26,27,92,93]. RCTs should include long-term follow-up as part of the trial or as a post-RCT prospective observational phase to assess durability. Finally, endoscopic therapies seem cost-effective, but we need more comparative data with PPI and surgery[94].

CONCLUSION

Endoscopic therapy for GERD aims to offer an alternative to PPIs and ARS in patients without significant diaphragmatic crura impairment. TIF, the technique with the largest body of evidence, has been proven to improve GERD symptoms and acid exposure time and reduce PPI consumption. Nonablative radiofrequency (Stretta®) is the method with the lowest rate of SAEs, but its efficacy has been called into question in recent meta-analyses. Band ligation techniques, ARMS, ARMA, and new plication devices have shown promising results in initial reports and RCTs are eagerly awaited. Careful patient selection, ongoing technical refinements, and RCTs with long-term data are the roadmap to unveil the potential of minimally invasive anti-reflux endoscopic techniques.

REFERENCES

1 **Vakil N**, van Zanten SV, Kahrilas P, Dent J, Jones R; Global Consensus Group. The Montreal definition and classification of gastroesophageal reflux disease: a global evidence-based consensus. *Am J Gastroenterol* 2006; **101**: 1900-1920; quiz 1943 [PMID: 16928254 DOI: 10.1111/j.1572-0241.2006.00630.x]

2 **Katz PO**, Gerson LB, Vela MF. Guidelines for the diagnosis and management of gastroesophageal reflux disease. *Am J Gastroenterol* 2013; **108**: 308-328; quiz 329 [PMID: 23419381 DOI: 10.1038/ajg.2012.444]

3 **Eusebi LH**, Ratnakumaran R, Yuan Y, Solaymani-Dodaran M, Bazzoli F, Ford AC. Global prevalence of, and risk factors for, gastro-oesophageal reflux symptoms: a meta-analysis. *Gut* 2018; **67**: 430-440 [PMID: 28232473 DOI: 10.1136/gutjnl-2016-313589]

4 **Diaz-Rubio M**, Moreno-Elola-Olaso C, Rey E, Locke GR 3rd, Rodriguez-Artalejo F. Symptoms of gastro-oesophageal reflux: prevalence, severity, duration and associated factors in a Spanish population. *Aliment Pharmacol Ther* 2004; **19**: 95-105 [PMID: 14687171 DOI: 10.1046/j.1365-2036.2003.01769.x]

5 **van Soest EM**, Dieleman JP, Siersema PD, Schoof L, Sturkenboom MC, Kuipers EJ. Tricyclic antidepressants and the risk of reflux esophagitis. *Am J Gastroenterol* 2007; **102**: 1870-1877 [PMID: 17511756 DOI: 10.1111/j.1572-0241.2007.01320.x]

6 **Boeckxstaens G**, El-Serag HB, Smout AJ, Kahrilas PJ. Republished: symptomatic reflux disease: the present, the past and the future. *Postgrad Med J* 2015; **91**: 46-54 [PMID: 25583739 DOI: 10.1136/postgradmedj-2013-306393rep]

7 **Gisbert JP**, Cooper A, Karagiannis D, Hatlebakk J, Agréus L, Jablonowski H, Nuevo J. Impact of gastroesophageal reflux disease on work absenteeism, presenteeism and productivity in daily life: a European observational study. *Health Qual Life Outcomes* 2009; **7**: 90 [PMID: 19835583 DOI: 10.1186/1477-7525-7-90]

8 **Holloway RH**, Dent J. Pathophysiology of gastroesophageal reflux. Lower esophageal sphincter dysfunction in gastroesophageal reflux disease. *Gastroenterol Clin North Am* 1990; **19**: 517-535 [PMID: 2228162 DOI: 10.1016/S0889-8553(21)00654-3]

9 **Iovino P**, Theron B, Prew S, Menon S, Trudgill N. The mechanisms associated with reflux episodes in ambulant subjects with gastro-esophageal reflux disease. *Neurogastroenterol Motil* 2021; **33**: e14023 [PMID: 33112052 DOI: 10.1111/nmo.14023]

10 **Ciriza-de-los-Ríos C**, Canga-Rodríguez-Valcárcel F, Castel-de-Lucas I, Lora-Pablos D, de-la-Cruz-Bértolo J, Castellano-Tortajada G. How useful is esophageal high resolution manometry in diagnosing gastroesophageal junction disruption: causes affecting this disruption and its relationship with manometric alterations and gastroesophageal reflux. *Rev Esp Enferm Dig* 2014; **106**: 22-29 [PMID: 24689712 DOI: 10.4321/s1130-01082014000100004]

11 **van Herwaarden MA**, Samsom M, Smout AJ. Excess gastroesophageal reflux in patients with hiatus hernia is caused by mechanisms other than transient LES relaxations. *Gastroenterology* 2000; **119**: 1439-1446 [PMID: 11113064 DOI: 10.1053/gast.2000.20191]

12 **Aziz Q**, Fass R, Gyawali CP, Miwa H, Pandolfino JE, Zerbib F. Functional Esophageal Disorders. *Gastroenterology* 2016 [PMID: 27144625 DOI: 10.1053/j.gastro.2016.02.012]

13 **Tack J**, Pandolfino JE. Pathophysiology of Gastroesophageal Reflux Disease. *Gastroenterology* 2018; **154**: 277-288 [PMID: 29037470 DOI: 10.1053/j.gastro.2017.09.047]

14 **Kaltenbach T**, Crockett S, Gerson LB. Are lifestyle measures effective in patients with gastroesophageal reflux disease? *Arch Intern Med* 2006; **166**: 965-971 [PMID: 16682569 DOI: 10.1001/archinte.166.9.965]

15 **Dent J**, Hetzel DJ, MacKinnon MA, Reed WD, Narielvala FM. Evaluation of omeprazole in reflux oesophagitis. *Scand J Gastroenterol Suppl* 1989; **166**: 76-82; discussion 94 [PMID: 2690334 DOI: 10.3109/00365528909091249]

16 **Weijenborg PW**, Cremonini F, Smout AJ, Bredenoord AJ. PPI therapy is equally effective in well-defined non-erosive reflux disease and in reflux esophagitis: a meta-analysis. *Neurogastroenterol Motil* 2012; **24**: 747-757, e350 [PMID: 22309489 DOI: 10.1111/j.1365-2982.2012.01888.x]

17 **Louie BE**, Kapur S, Blitz M, Farivar AS, Vallières E, Aye RW. Length and pressure of the reconstructed lower esophageal sphincter is determined by both crural closure and Nissen fundoplication. *J Gastrointest Surg* 2013; **17**: 236-243 [PMID: 23188217 DOI: 10.1007/s11605-012-2074-4]

18 **Garg SK**, Gurusamy KS. Laparoscopic fundoplication surgery versus medical management for gastro-oesophageal reflux disease (GORD) in adults. *Cochrane Database Syst Rev* 2015; CD003243 [PMID: 26544951 DOI: 10.1002/14651858.CD003243.pub3]

19 **Spechler SJ**, Hunter JG, Jones KM, Lee R, Smith BR, Mashimo H, Sanchez VM, Dunbar KB, Pham TH, Murthy UK, Kim T, Jackson CS, Wallen JM, von Rosenvinge EC, Pearl JP, Laine L, Kim AW, Kaz AM, Tatum RP, Gellad ZF, Lagoo-Deenadayalan S, Rubenstein JH, Ghaferi AA, Lo WK, Fernando RS, Chan BS, Paski SC, Provenzale D, Castell DO, Lieberman D, Souza RF, Chey WD, Warren SR, Davis-Karim A, Melton SD, Genta RM, Serpi T, Biswas K, Huang GD. Randomized Trial of Medical versus Surgical Treatment for Refractory Heartburn. *N Engl J Med* 2019; **381**: 1513-1523 [PMID: 31618539 DOI: 10.1056/NEJMoa1811424]

20 **Kahrilas PJ**, Shaheen NJ, Vaezi MF, Hiltz SW, Black E, Modlin IM, Johnson SP, Allen J, Brill JV; American Gastroenterological Association. American Gastroenterological Association Medical Position Statement on the management of gastroesophageal reflux disease. *Gastroenterology* 2008; **135**: 1383-1391, 1391.e1 [PMID: 18789939 DOI: 10.1053/j.gastro.2008.08.045]

21 **Stefanidis D**, Hope WW, Kohn GP, Reardon PR, Richardson WS, Fanelli RD; SAGES Guidelines Committee. Guidelines for surgical treatment of gastroesophageal reflux disease. *Surg Endosc* 2010; **24**: 2647-2669 [PMID: 20725747 DOI: 10.1007/s00464-010-1267-8]

22 **Fuchs KH**, Babic B, Breithaupt W, Dallemagne B, Fingerhut A, Furnee E, Granderath F, Horvath P, Kardos P, Pointner R, Savarino E, Van Herwaarden-Lindeboom M, Zaninotto G; European Association of Endoscopic Surgery (EAES). EAES recommendations for the management of gastroesophageal reflux disease. *Surg Endosc* 2014; **28**: 1753-1773 [PMID: 24789125 DOI: 10.1007/s00464-014-3431-z]

23 **Fock KM**, Talley N, Goh KL, Sugano K, Katelaris P, Holtmann G, Pandolfino JE, Sharma P, Ang TL, Hongo M, Wu J, Chen M, Choi MG, Law NM, Sheu BS, Zhang J, Ho KY, Sollano J, Rani AA,

Kositchaiwat C, Bhatia S. Asia-Pacific consensus on the management of gastro-oesophageal reflux disease: an update focusing on refractory reflux disease and Barrett's oesophagus. *Gut* 2016; **65**: 1402-1415 [PMID: 27261337 DOI: 10.1136/gutjnl-2016-311715]

24 **Hunt R**, Armstrong D, Katelaris P, Afihene M, Bane A, Bhatia S, Chen MH, Choi MG, Melo AC, Fock KM, Ford A, Hongo M, Khan A, Lazebnik L, Lindberg G, Lizarzabal M, Myint T, Moraes-Filho JP, Salis G, Lin JT, Vaidya R, Abdo A, LeMair A; Review Team:. World Gastroenterology Organisation Global Guidelines: GERD Global Perspective on Gastroesophageal Reflux Disease. *J Clin Gastroenterol* 2017; **51**: 467-478 [PMID: 28591069 DOI: 10.1097/MCG.0000000000000854]

25 **Gawron AJ**, Bell R, Abu Dayyeh BK, Buckley FP, Chang K, Dunst CM, Edmundowicz SA, Jobe B, Lipham JC, Lister D, Canto MI, Smith MS, Starpoli AA, Triadafilopoulos G, Watson TJ, Wilson E, Pandolfino JE, Kaizer A, Van De Voorde Z, Yadlapati R. Surgical and endoscopic management options for patients with GERD based on proton pump inhibitor symptom response: recommendations from an expert U.S. panel. *Gastrointest Endosc* 2020; **92**: 78-87.e2 [PMID: 32007519 DOI: 10.1016/j.gie.2020.01.037]

26 **Zerbib F**, Bredenoord AJ, Fass R, Kahrilas PJ, Roman S, Savarino E, Sifrim D, Vaezi M, Yadlapati R, Gyawali CP. ESNM/ANMS consensus paper: Diagnosis and management of refractory gastro-esophageal reflux disease. *Neurogastroenterol Motil* 2021; **33**: e14075 [PMID: 33368919 DOI: 10.1111/nmo.14075]

27 **Pauwels A**, Boecxstaens V, Andrews CN, Attwood SE, Berrisford R, Bisschops R, Boeckxstaens GE, Bor S, Bredenoord AJ, Cicala M, Corsetti M, Fornari F, Gyawali CP, Hatlebakk J, Johnson SB, Lerut T, Lundell L, Mattioli S, Miwa H, Nafteux P, Omari T, Pandolfino J, Penagini R, Rice TW, Roelandt P, Rommel N, Savarino V, Sifrim D, Suzuki H, Tutuian R, Vanuytsel T, Vela MF, Watson DI, Zerbib F, Tack J. How to select patients for antireflux surgery? *Gut* 2019; **68**: 1928-1941 [PMID: 31375601 DOI: 10.1136/gutjnl-2019-318260]

28 **Angelchik JP**, Cohen R. A new surgical procedure for the treatment of gastroesophageal reflux and hiatal hernia. *Surg Gynecol Obstet* 1979; **148**: 246-248 [PMID: 154176]

29 **Yew KC**, Chuah SK. Antireflux endoluminal therapies: past and present. *Gastroenterol Res Pract* 2013; **2013**: 481417 [PMID: 23935608 DOI: 10.1155/2013/481417]

30 **Filipi CJ**, Lehman GA, Rothstein RI, Raijman I, Stiegmann GV, Waring JP, Hunter JG, Gostout CJ, Edmundowicz SA, Dunne DP, Watson PA, Cornet DA. Transoral, flexible endoscopic suturing for treatment of GERD: a multicenter trial. *Gastrointest Endosc* 2001; **53**: 416-422 [PMID: 11275879 DOI: 10.1067/mge.2001.113502]

31 **Fockens P**, Cohen L, Edmundowicz SA, Binmoeller K, Rothstein RI, Smith D, Lin E, Nickl N, Overholt B, Kahrilas PJ, Vakil N, Abdel Aziz Hassan AM, Lehman GA. Prospective randomized controlled trial of an injectable esophageal prosthesis *vs* a sham procedure for endoscopic treatment of gastroesophageal reflux disease. *Surg Endosc* 2010; **24**: 1387-1397 [PMID: 20198491 DOI: 10.1007/s00464-009-0784-9]

32 **Oor JE**, Roks DJ, Broeders JA, Hazebroek EJ, Gooszen HG. Seventeen-year Outcome of a Randomized Clinical Trial Comparing Laparoscopic and Conventional Nissen Fundoplication: A Plea for Patient Counseling and Clarification. *Ann Surg* 2017; **266**: 23-28 [PMID: 28294958 DOI: 10.1097/SLA.0000000000002106]

33 **Falk GW**, Fennerty MB, Rothstein RI. AGA Institute medical position statement on the use of endoscopic therapy for gastroesophageal reflux disease. *Gastroenterology* 2006; **131**: 1313-1314 [PMID: 17030198 DOI: 10.1053/j.gastro.2006.08.018]

34 **Pearl J**, Pauli E, Dunkin B, Stefanidis D. SAGES endoluminal treatments for GERD. *Surg Endosc* 2017; **31**: 3783-3790 [PMID: 28643067 DOI: 10.1007/s00464-017-5639-1]

35 **Weusten BLAM**, Barret M, Bredenoord AJ, Familiari P, Gonzalez JM, van Hooft JE, Lorenzo-Zúñiga V, Louis H, Martinek J, van Meer S, Neumann H, Pohl D, Prat F, von Renteln D, Savarino E, Sweis R, Tack J, Tutuian R, Ishaq S. Endoscopic management of gastrointestinal motility disorders - part 2: European Society of Gastrointestinal Endoscopy (ESGE) Guideline. *Endoscopy* 2020; **52**: 600-614 [PMID: 32462649 DOI: 10.1055/a-1171-3174]

36 **Chang KJ**, Bell R. Transoral Incisionless Fundoplication. *Gastrointest Endosc Clin N Am* 2020; **30**: 267-289 [PMID: 32146946 DOI: 10.1016/j.giec.2019.12.008]

37 **Ihde GM**. The evolution of TIF: transoral incisionless fundoplication. *Therap Adv Gastroenterol* 2020; **13**: 1756284820924206 [PMID: 32499834 DOI: 10.1177/1756284820924206]

38 **Testoni PA**, Corsetti M, Di Pietro S, Castellaneta AG, Vailati C, Masci E, Passaretti S. Effect of transoral incisionless fundoplication on symptoms, PPI use, and ph-impedance refluxes of GERD patients. *World J Surg* 2010; **34**: 750-757 [PMID: 20091308 DOI: 10.1007/s00268-010-0394-7]

39 **Ihde GM**, Besancon K, Deljkich E. Short-term safety and symptomatic outcomes of transoral incisionless fundoplication with or without hiatal hernia repair in patients with chronic gastroesophageal reflux disease. *Am J Surg* 2011; **202**: 740-746; discussion 746-747 [PMID: 22014853 DOI: 10.1016/j.amjsurg.2011.06.035]

40 **Narsule CK**, Burch MA, Ebright MI, Hess DT, Rivas R Jr, Daly BD, Fernando HC. Endoscopic fundoplication for the treatment of gastroesophageal reflux disease: initial experience. *J Thorac Cardiovasc Surg* 2012; **143**: 228-234 [PMID: 22070927 DOI: 10.1016/j.jtcvs.2011.10.008]

41 **Bell RC**, Barnes WE, Carter BJ, Sewell RW, Mavrelis PG, Ihde GM, Hoddinott KM, Fox MA, Freeman KD, Gunsberger T, Hausmann MG, Dargis D, DaCosta Gill B, Wilson E, Trad KS. Transoral incisionless fundoplication: 2-year results from the prospective multicenter U.S. study. *Am Surg* 2014; **80**: 1093-1105 [PMID: 25347499 DOI: 10.1177/000313481408001124]

42 **Wilson EB**, Barnes WE, Mavrelis PG, Carter BJ, Bell RC, Sewell RW, Ihde GM, Dargis D, Hoddinott KM, Shughoury AB, Gill BD, Fox MA, Turgeon DG, Freeman KD, Gunsberger T, Hausmann MG, Leblanc KA, Deljkich E, Trad KS. The effects of transoral incisionless fundoplication on chronic GERD patients: 12-month prospective multicenter experience. *Surg Laparosc Endosc Percutan Tech* 2014; **24**: 36-46 [PMID: 24487156 DOI: 10.1097/SLE.0b013e3182a2b05c]

43 **Testoni PA**, Testoni S, Mazzoleni G, Vailati C, Passaretti S. Long-term efficacy of transoral incisionless fundoplication with Esophyx (Tif 2.0) and factors affecting outcomes in GERD patients followed for up to 6 years: a prospective single-center study. *Surg Endosc* 2015; **29**: 2770-2780 [PMID: 25480624 DOI: 10.1007/s00464-014-4008-6]

44 **Stefanidis G**, Viazis N, Kotsikoros N, Tsoukalas N, Lala E, Theocharis L, Fassaris A, Manolakopoulos S. Long-term benefit of transoral incisionless fundoplication using the esophyx device for the management of gastroesophageal reflux disease responsive to medical therapy. *Dis Esophagus* 2017; **30**: 1-8 [PMID: 27868281 DOI: 10.1111/dote.12525]

45 **Chimukangara M**, Jalilvand AD, Melvin WS, Perry KA. Long-term reported outcomes of transoral incisionless fundoplication: an 8-year cohort study. *Surg Endosc* 2019; **33**: 1304-1309 [PMID: 30167944 DOI: 10.1007/s00464-018-6403-x]

46 **Testoni PA**, Testoni S, Mazzoleni G, Pantaleo G, Cilona MB, Distefano G, Fanti L, Antonelli M, Passaretti S. Transoral incisionless fundoplication with an ultrasonic surgical endostapler for the treatment of gastroesophageal reflux disease: 12-month outcomes. *Endoscopy* 2020; **52**: 469-473 [PMID: 32187630 DOI: 10.1055/a-1124-3187]

47 **Rinsma NF**, Farré R, Bouvy ND, Masclee AA, Conchillo JM. The effect of endoscopic fundoplication and proton pump inhibitors on baseline impedance and heartburn severity in GERD patients. *Neurogastroenterol Motil* 2015; **27**: 220-228 [PMID: 25348594 DOI: 10.1111/nmo.12468]

48 **Witteman BP**, Conchillo JM, Rinsma NF, Betzel B, Peeters A, Koek GH, Stassen LP, Bouvy ND. Randomized controlled trial of transoral incisionless fundoplication vs. proton pump inhibitors for treatment of gastroesophageal reflux disease. *Am J Gastroenterol* 2015; **110**: 531-542 [PMID: 25823768 DOI: 10.1038/ajg.2015.28]

49 **Hunter JG**, Kahrilas PJ, Bell RC, Wilson EB, Trad KS, Dolan JP, Perry KA, Oelschlager BK, Soper NJ, Snyder BE, Burch MA, Melvin WS, Reavis KM, Turgeon DG, Hungness ES, Diggs BS. Efficacy of transoral fundoplication *vs* omeprazole for treatment of regurgitation in a randomized controlled trial. *Gastroenterology* 2015; **148**: 324-333.e5 [PMID: 25448925 DOI: 10.1053/j.gastro.2014.10.009]

50 **Håkansson B**, Montgomery M, Cadiere GB, Rajan A, Bruley des Varannes S, Lerhun M, Coron E, Tack J, Bischops R, Thorell A, Arnelo U, Lundell L. Randomised clinical trial: transoral incisionless fundoplication vs. sham intervention to control chronic GERD. *Aliment Pharmacol Ther* 2015; **42**: 1261-1270 [PMID: 26463242 DOI: 10.1111/apt.13427]

51 **Trad KS**, Barnes WE, Prevou ER, Simoni G, Steffen JA, Shughoury AB, Raza M, Heise JA, Fox MA, Mavrelis PG. The TEMPO Trial at 5 Years: Transoral Fundoplication (TIF 2.0) Is Safe, Durable, and Cost-effective. *Surg Innov* 2018; **25**: 149-157 [PMID: 29405886 DOI: 10.1177/1553350618755214]

52 **Huang X**, Chen S, Zhao H, Zeng X, Lian J, Tseng Y, Chen J. Efficacy of transoral incisionless fundoplication (TIF) for the treatment of GERD: a systematic review with meta-analysis. *Surg Endosc* 2017; **31**: 1032-1044 [PMID: 27495332 DOI: 10.1007/s00464-016-5111-7]

53 **Richter JE**, Kumar A, Lipka S, Miladinovic B, Velanovich V. Efficacy of Laparoscopic Nissen Fundoplication *vs* Transoral Incisionless Fundoplication or Proton Pump Inhibitors in Patients With Gastroesophageal Reflux Disease: A Systematic Review and Network Meta-analysis. *Gastroenterology* 2018; **154**: 1298-1308.e7 [PMID: 29305934 DOI: 10.1053/j.gastro.2017.12.021]

54 **Roy-Shapira A**, Bapaye A, Date S, Pujari R, Dorwat S. Trans-oral anterior fundoplication: 5-year follow-up of pilot study. *Surg Endosc* 2015; **29**: 3717-3721 [PMID: 25783833 DOI: 10.1007/s00464-015-4142-9]

55 **Kim HJ**, Kwon CI, Kessler WR, Selzer DJ, McNulty G, Bapaye A, Bonavina L, Lehman GA. Long-term follow-up results of endoscopic treatment of gastroesophageal reflux disease with the MUSE™ endoscopic stapling device. *Surg Endosc* 2016; **30**: 3402-3408 [PMID: 26537905 DOI: 10.1007/s00464-015-4622-y]

56 **Zacherl J**, Roy-Shapira A, Bonavina L, Bapaye A, Kiesslich R, Schoppmann SF, Kessler WR, Selzer DJ, Broderick RC, Lehman GA, Horgan S. Endoscopic anterior fundoplication with the Medigus Ultrasonic Surgical Endostapler (MUSE™) for gastroesophageal reflux disease: 6-month results from a multi-center prospective trial. *Surg Endosc* 2015; **29**: 220-229 [PMID: 25135443 DOI: 10.1007/s00464-014-3731-3]

57 **Danalioglu A**, Cipe G, Toydemir T, Kocaman O, Ince AT, Muslumanoglu M, Senturk H. Endoscopic stapling in comparison to laparoscopic fundoplication for the treatment of gastroesophageal reflux disease. *Dig Endosc* 2014; **26**: 37-42 [PMID: 23560891 DOI: 10.1111/den.12081]

58 **Sowa P**, Samarasena JB. Nonablative Radiofrequency Treatment for Gastroesophageal Reflux Disease (STRETTA). *Gastrointest Endosc Clin N Am* 2020; **30**: 253-265 [PMID: 32146945 DOI: 10.1016/j.giec.2019.12.006]

59 **Xie P**, Yan J, Ye L, Wang C, Li Y, Chen Y, Li G. Efficacy of different endoscopic treatments in patients with gastroesophageal reflux disease: a systematic review and network meta-analysis. *Surg Endosc* 2021; **35**: 1500-1510 [PMID: 33650003 DOI: 10.1007/s00464-021-08386-1]

60 **Coron E**, Sebille V, Cadiot G, Zerbib F, Ducrotte P, Ducrot F, Pouderoux P, Arts J, Le Rhun M,

Piche T, Bruley des Varannes S, Galmiche JP; Consortium de Recherche Indépendant sur le Traitement et L'exploration du Reflux Gastro-oesophagien et de L'endobrachyoesophage (CRITERE). Clinical trial: Radiofrequency energy delivery in proton pump inhibitor-dependent gastro-oesophageal reflux disease patients. *Aliment Pharmacol Ther* 2008; **28**: 1147-1158 [PMID: 18616516 DOI: 10.1111/j.1365-2036.2008.03790.x]

61 **Corley DA**, Katz P, Wo JM, Stefan A, Patti M, Rothstein R, Edmundowicz S, Kline M, Mason R, Wolfe MM. Improvement of gastroesophageal reflux symptoms after radiofrequency energy: a randomized, sham-controlled trial. *Gastroenterology* 2003; **125**: 668-676 [PMID: 12949712 DOI: 10.1016/s0016-5085(03)01052-7]

62 **Aziz AM**, El-Khayat HR, Sadek A, Mattar SG, McNulty G, Kongkam P, Guda MF, Lehman GA. A prospective randomized trial of sham, single-dose Stretta, and double-dose Stretta for the treatment of gastroesophageal reflux disease. *Surg Endosc* 2010; **24**: 818-825 [PMID: 19730952 DOI: 10.1007/s00464-009-0671-4]

63 **Arts J**, Bisschops R, Blondeau K, Farré R, Vos R, Holvoet L, Caenepeel P, Lerut A, Tack J. A double-blind sham-controlled study of the effect of radiofrequency energy on symptoms and distensibility of the gastro-esophageal junction in GERD. *Am J Gastroenterol* 2012; **107**: 222-230 [PMID: 22108449 DOI: 10.1038/ajg.2011.395]

64 **Lipka S**, Kumar A, Richter JE. No evidence for efficacy of radiofrequency ablation for treatment of gastroesophageal reflux disease: a systematic review and meta-analysis. *Clin Gastroenterol Hepatol* 2015; **13**: 1058-67.e1 [PMID: 25459556 DOI: 10.1016/j.cgh.2014.10.013]

65 **Fass R**, Cahn F, Scotti DJ, Gregory DA. Systematic review and meta-analysis of controlled and prospective cohort efficacy studies of endoscopic radiofrequency for treatment of gastroesophageal reflux disease. *Surg Endosc* 2017; **31**: 4865-4882 [PMID: 28233093 DOI: 10.1007/s00464-017-5431-2]

66 **Vaezi MF**, Shaheen NJ, Muthusamy VR. State of Evidence in Minimally Invasive Management of Gastroesophageal Reflux: Findings of a Scoping Review. *Gastroenterology* 2020; **159**: 1504-1525 [PMID: 32621903 DOI: 10.1053/j.gastro.2020.05.097]

67 **Weitzendorfer M**, Spaun GO, Antoniou SA, Tschoner A, Schredl P, Emmanuel K, Koch OO. Interim Report of a Prospective Trial on the Clinical Efficiency of a New Full-thickness Endoscopic Plication Device for Patients With GERD: Impact of Changed Suture Material. *Surg Laparosc Endosc Percutan Tech* 2017; **27**: 163-169 [PMID: 28383316 DOI: 10.1097/SLE.0000000000000396]

68 **Weitzendorfer M**, Spaun GO, Antoniou SA, Witzel K, Emmanuel K, Koch OO. Clinical feasibility of a new full-thickness endoscopic plication device (GERDx™) for patients with GERD: results of a prospective trial. *Surg Endosc* 2018; **32**: 2541-2549 [PMID: 29602998 DOI: 10.1007/s00464-018-6153-9]

69 **Inoue H**, Ito H, Ikeda H, Sato C, Sato H, Phalanusitthepha C, Hayee B, Eleftheriadis N, Kudo SE. Anti-reflux mucosectomy for gastroesophageal reflux disease in the absence of hiatus hernia: a pilot study. *Ann Gastroenterol* 2014; **27**: 346-351 [PMID: 25330784]

70 **Monino L**, Gonzalez JM, Vitton V, Barthet M. Antireflux mucosectomy band in treatment of refractory gastroesophageal reflux disease: a pilot study for safety, feasibility and symptom control. *Endosc Int Open* 2020; **8**: E147-E154 [PMID: 32010747 DOI: 10.1055/a-1038-4012]

71 **Debourdeau A**, Vitton V, Monino L, Barthet M, Gonzalez JM. Antireflux Mucosectomy Band (ARM-b) in Treatment of Refractory Gastroesophageal Reflux Disease After Bariatric Surgery. *Obes Surg* 2020; **30**: 4654-4658 [PMID: 32676843 DOI: 10.1007/s11695-020-04753-4]

72 **Sumi K**, Inoue H, Kobayashi Y, Iwaya Y, Abad MRA, Fujiyoshi Y, Shimamura Y, Ikeda H, Onimaru M. Endoscopic treatment of proton pump inhibitor-refractory gastroesophageal reflux disease with anti-reflux mucosectomy: Experience of 109 cases. *Dig Endosc* 2021; **33**: 347-354 [PMID: 32415898 DOI: 10.1111/den.13727]

73 **Li X**, Zhang W, Chen M, Wei S, Zhao X, Zhang G. A Prospective Randomized Trial to Assess the Antireflux Effect of Antireflux Mucosectomy in the Porcine Model. *Gastroenterol Res Pract* 2019; **2019**: 3286738 [PMID: 30944560 DOI: 10.1155/2019/3286738]

74 **Yoo IK**, Ko WJ, Kim HS, Kim HK, Kim JH, Kim WH, Hong SP, Yeniova AÖ, Cho JY. Anti-reflux mucosectomy using a cap-assisted endoscopic mucosal resection method for refractory gastroesophageal disease: a prospective feasibility study. *Surg Endosc* 2020; **34**: 1124-1131 [PMID: 31139995 DOI: 10.1007/s00464-019-06859-y]

75 **Inoue H**, Tanabe M, de Santiago ER, Abad MRA, Shimamura Y, Fujiyoshi Y, Ueno A, Sumi K, Tomida H, Iwaya Y, Ikeda H, Onimaru M. Anti-reflux mucosal ablation (ARMA) as a new treatment for gastroesophageal reflux refractory to proton pump inhibitors: a pilot study. *Endosc Int Open* 2020; **8**: E133-E138 [PMID: 32010745 DOI: 10.1055/a-1031-9436]

76 **Hernández Mondragón OV**, Zamarripa Mottú RA, García Contreras LF, Gutiérrez Aguilar RA, Solórzano Pineda OM, Blanco Velasco G, Murcio Perez E. Clinical feasibility of a new antireflux ablation therapy on gastroesophageal reflux disease (with video). *Gastrointest Endosc* 2020; **92**: 1190-1201 [PMID: 32343977 DOI: 10.1016/j.gie.2020.04.046]

77 **Wong HJ**, Su B, Attaar M, Kuchta K, Stearns S, Linn JG, Haggerty SP, Denham W, Ujiki MB. Anti-reflux mucosectomy (ARMS) results in improved recovery and similar reflux quality of life outcomes compared to laparoscopic Nissen fundoplication. *Surg Endosc* 2020 [PMID: 33237465 DOI: 10.1007/s00464-020-08144-9]

78 **Patil G**, Dalal A, Maydeo A. Feasibility and outcomes of anti-reflux mucosectomy for proton pump inhibitor dependent gastroesophageal reflux disease: First Indian study (with video). *Dig Endosc*

2020; **32**: 745-752 [PMID: 31834663 DOI: 10.1111/den.13606]

79 **Bapaye A**, Mahadik M, Pujari R, Bharadwaj T, Vare S, Date S, Dubale N, Bapaye J, Kulkarni A. Anti-reflux mucosectomy (ARMS) for refractory GERD-Initial clinical experience. *J Gastroenterol Hepatol* 2017; **32**: 255

80 **Vasilevskiy DI**, Bagnenko SF, Smirnov A, Lapshin AS, Dvoretskiy SU, Pryadko AS. Antireflux mucosectomy (Arms) in the treatment of patients with gerd and columnar-cell lined (barrett's) esophagus. First experiences. *Surg Endosc* 2017; **31**: S405 [PMID: 28488176 DOI: 10.1007/s00464-017-5565-2]

81 **Shah R**, Maydeo AP, Dhir V. Anti reflux mucosectomy (ARMS) for refractory gastro esophageal reflux disease (GERD)-are we there yet? *United European Gastroenterol J* 2017; **5**: A354-A355 [DOI: 10.1177/2050640617725676]

82 **Ota K**, Takeuchi T, Harada S, Edogawa S, Kojima Y, Inoue T, Higuchi K. A novel endoscopic submucosal dissection technique for proton pump inhibitor-refractory gastroesophageal reflux disease. *Scand J Gastroenterol* 2014; **49**: 1409-1413 [PMID: 25384555 DOI: 10.3109/00365521.2014.978815]

83 **Ortega A**, Rosón P, Fern, ez F, Angeles Romero M, Angeles Perez Aisa M, Cotta J, Lozano M. Antireflux mucosectomy. preliminary results of a prospective study. *Endoscopy* 2019; **51**: S240-S241

84 **Mondragón OVH**, Pintor JC, Aguilar RAG, Garcia-Contreras L, Pineda OS, Mottú RAZ, Blanco-Velasco G, Murcio-Pérez E. Sa1247 Antireflux ablation therapy (ARAT), for reflux disease after poem procedure. Early clinical experience. *Gastrointest Endosc* 2020; **91**: AB130

85 **Schuitenmaker JM**, van Hoeij FB, Schijven MP, Tack J, Conchillo JM, Hazebroek EJ, Smout AJPM, Bredenoord AJ. Pneumatic dilation for persistent dysphagia after antireflux surgery, a multicentre single-blind randomised sham-controlled clinical trial. *Gut* 2021 [PMID: 33452179 DOI: 10.1136/gutjnl-2020-322355]

86 **Seleem WM**, Hanafy AS, Mohamed SI. Endoscopic management of refractory gastroesophageal reflux disease. *Scand J Gastroenterol* 2018; **53**: 390-397 [PMID: 29488430 DOI: 10.1080/00365521.2018.1445775]

87 **Hu HQ**, Li HK, Xiong Y, Zhang XB, Zhi JL, Wang XX, Ling-Hu EQ. Peroral endoscopic cardial constriction in gastroesophageal reflux disease. *Medicine (Baltimore)* 2018; **97**: e0169 [PMID: 29642142 DOI: 10.1097/MD.0000000000010169]

88 **Liu S**, Chai N, Zhai Y, Zou J, Feng X, Li Z, Li L, Zhang X, Wang X, Wang S, Linghu EQ. New treatment method for refractory gastroesophageal reflux disease (GERD): C-BLART (clip band ligation anti-reflux therapy)-a short-term study. *Surg Endosc* 2020; **34**: 4516-4524 [PMID: 31728750 DOI: 10.1007/s00464-019-07238-3]

89 **Benias PC**, D'Souza L, Lan G, Gluckman C, Inamdar S, Trindade AJ, Miller LS, Carr-Locke DL. Initial experience with a novel resection and plication (RAP) method for acid reflux: a pilot study. *Endosc Int Open* 2018; **6**: E443-E449 [PMID: 29607397 DOI: 10.1055/s-0044-101453]

90 **Janu P**, Shughoury AB, Venkat K, Hurwich D, Galouzis T, Siatras J, Streeter D, Korman K, Mavrelis G, Mavrelis P. Laparoscopic Hiatal Hernia Repair Followed by Transoral Incisionless Fundoplication With EsophyX Device (HH + TIF): Efficacy and Safety in Two Community Hospitals. *Surg Innov* 2019; **26**: 675-686 [PMID: 31431138 DOI: 10.1177/1553350619869449]

91 **Fundacion para la Investigacion Biomedica del Hospital Universitario Ramon y Cajal**. Double-blind, Placebo-controlled Clinical Trial on the Efficacy of Antireflux Ablation of the Cardiac Mucosa for the Treatment of Gastroesophageal Reflux Disease. Available from: https://clinicaltrials.gov/ct2/show/NCT04711655

92 **Gyawali CP**, Kahrilas PJ, Savarino E, Zerbib F, Mion F, Smout AJPM, Vaezi M, Sifrim D, Fox MR, Vela MF, Tutuian R, Tack J, Bredenoord AJ, Pandolfino J, Roman S. Modern diagnosis of GERD: the Lyon Consensus. *Gut* 2018; **67**: 1351-1362 [PMID: 29437910 DOI: 10.1136/gutjnl-2017-314722]

93 **Yadlapati R**, Kahrilas PJ, Fox MR, Bredenoord AJ, Prakash Gyawali C, Roman S, Babaei A, Mittal RK, Rommel N, Savarino E, Sifrim D, Smout A, Vaezi MF, Zerbib F, Akiyama J, Bhatia S, Bor S, Carlson DA, Chen JW, Cisternas D, Cock C, Coss-Adame E, de Bortoli N, Defilippi C, Fass R, Ghoshal UC, Gonlachanvit S, Hani A, Hebbard GS, Wook Jung K, Katz P, Katzka DA, Khan A, Kohn GP, Lazarescu A, Lengliner J, Mittal SK, Omari T, Park MI, Penagini R, Pohl D, Richter JE, Serra J, Sweis R, Tack J, Tatum RP, Tutuian R, Vela MF, Wong RK, Wu JC, Xiao Y, Pandolfino JE. Esophageal motility disorders on high-resolution manometry: Chicago classification version 4.0©. *Neurogastroenterol Motil* 2021; **33**: e14058 [PMID: 33373111 DOI: 10.1111/nmo.14058]

94 **Funk LM**, Zhang JY, Drosdeck JM, Melvin WS, Walker JP, Perry KA. Long-term cost-effectiveness of medical, endoscopic and surgical management of gastroesophageal reflux disease. *Surgery* 2015; **157**: 126-136 [PMID: 25262216 DOI: 10.1016/j.surg.2014.05.027]

95 **ASGE Standards of Practice Committee**, Muthusamy VR, Lightdale JR, Acosta RD, Chandrasekhara V, Chathadi KV, Eloubeidi MA, Fanelli RD, Fonkalsrud L, Faulx AL, Khashab MA, Saltzman JR, Shaukat A, Wang A, Cash B, DeWitt JM. The role of endoscopy in the management of GERD. *Gastrointest Endosc* 2015; **81**: 1305-1310 [PMID: 25863867 DOI: 10.1016/j.gie.2015.02.021]

World Journal of Gastroenterology

Submit a Manuscript: https://www.f6publishing.com

World J Gastroenterol 2021 October 21; 27(39): 6615-6630

DOI: 10.3748/wjg.v27.i39.6615

ISSN 1007-9327 (print) ISSN 2219-2840 (online)

ORIGINAL ARTICLE

Basic Study

Cold exposure and capsaicin promote 1,2-dimethylhyrazine-induced colon carcinogenesis in rats correlates with extracellular matrix remodeling

Jing-Chun Qin, Wei-Tao Yu, Hui-Xuan Li, Yu-Qi Liang, Fei-Fei Nong, Bin Wen

ORCID number: Jing-Chun Qin 0000-0001-7680-6076; Wei-Tao Yu 0000-0001-8308-3558; Hui-Xuan Li 0000-0003-0847-2208; Yu-Qi Liang 0000-0002-7481-116X; Fei-Fei Nong 0000-0002-2306-0108; Bin Wen 0000-0001-9096-3115.

Author contributions: Qin JC wrote the manuscript and performed the research; Wen B designed the study; Qin JC, Yu WT, Li HX, and Liang YQ conducted the experiments and analyzed the data; Nong FF reviewed and edited the manuscript; Wen B revised the manuscript.

Supported by National Natural Science Foundation of China, No. 81673944.

Institutional animal care and use committee statement: The study was reviewed and approved by the Institutional Animal Ethics Committee of the Guangzhou University of Chinese Medicine (approval No. 20130001).

Conflict-of-interest statement: We declare that we have no financial and personal relationships with other people or organizations that can inappropriately influence our work, there is no professional or other personal interest of any

Jing-Chun Qin, Yu-Qi Liang, Fei-Fei Nong, Bin Wen, Institute of Science and Technology Innovation Center, Guangzhou University of Chinese Medicine, Guangdong 530001, Guangdong Province, China

Jing-Chun Qin, Liuzhou People's Hospital, Guangxi, 545006, Guangxi Province China

Wei-Tao Yu, Traditional Chinese Medicine Department, The Second People's Hospital of Lianyungang, Lianyungang 222000, Jiangsu Province, China

Hui-Xuan Li, National Center for Respiratory Medicine, Guangzhou Institute of Respiratory Health, The First Affiliated Hospital of Guangzhou Medical University, Guangzhou, State Key Laboratory of Respiratory Disease and National Clinical Research Center for Respiratory Disease, Guangdong 510000, Guangdong Province, China

Corresponding author: Bin Wen, PhD, Academic Research, Full Professor, Institute of Science and Technology Innovation Center, Guangzhou University of Chinese Medicine, No. 12 Airport Road, Guangdong 530001, Guangdong Province, China. wenbin@gzucm.edu.cn

Abstract

BACKGROUND

Extracellular matrix (ECM) remodeling and stiffening, which are correlated with tumor malignancy, drives tumor development. However, the relationship between ECM remodeling and rat experimental model of 1,2-dimethylhyrazine (DMH)-induced colorectal cancer (CRC) imposed by cold and capsaicin exposure remains unclear.

AIM

To explore the effects of cold exposure and capsaicin on ECM remodeling and ECM enzymes in DMH-induced CRC.

METHODS

For histopathological analysis, the sections of colon tissues were stained with hematoxylin and eosin, Masson's trichrome, Picrosirius red, and Weigert's Resorcin-Fuchsin to observe the remodeling of collagen and elastin. Additionally, the protein expression level of type I collagen (COL I), type 3 collagen (COL III0, elastin, matrix metalloproteinase (MMP) 1, MMP2, MMP9, and tissue-specific

nature or kind in any product, service and/or company that could be construed as influencing the position presented in, or the review of, the manuscript entitled "Cold exposure and Capsaicin promote 1,2-dimethylhydrazine-induced colon carcinogenesis in rats correlates with extracellular matrix remodeling".

Data sharing statement: Technical appendix, statistical code, and dataset available from the corresponding author at wenbin@gzucm.edu.cn. Participants gave informed consent for data sharing.

ARRIVE guidelines statement: The authors have read the ARRIVE Guidelines, and the manuscript was prepared and revised according to the ARRIVE Guidelines.

Open-Access: This article is an open-access article that was selected by an in-house editor and fully peer-reviewed by external reviewers. It is distributed in accordance with the Creative Commons Attribution NonCommercial (CC BY-NC 4.0) license, which permits others to distribute, remix, adapt, build upon this work non-commercially, and license their derivative works on different terms, provided the original work is properly cited and the use is non-commercial. See: http://creativecommons.org/Licenses/by-nc/4.0/

Manuscript source: Unsolicited manuscript

Specialty type: Gastroenterology and hepatology

Country/Territory of origin: China

Peer-review report's scientific quality classification

Grade A (Excellent): A
Grade B (Very good): 0
Grade C (Good): 0
Grade D (Fair): 0
Grade E (Poor): 0

Received: March 31, 2021
Peer-review started: April 1, 2021

matrix metalloproteinase 1 (TIMP1) was assessed by immunohistochemistry. The messenger RNA (mRNA) levels of COL I, COL III, elastin, and lysyl oxidase-like-2 (LOXL2) in the colon tissues of rats was measured by reverse-transcriptase quantitative polymerase chain reaction.

RESULTS

Although no differences were observed in the proportion of adenomas, a trend towards the increase of invasive tumors was observed in the cold and capsaicin group. The cold exposure group had a metastasis rate compared with the other groups. Additionally, abnormal accumulation of both collagen and elastin was observed in the cold exposure and capsaicin group. Specifically, collagen quantitative analysis showed increased length, width, angle, and straightness compared with the DMH group. Collagen deposition and straightness were significantly increased in the cold exposure group compared with the capsaicin group. Cold exposure and capsaicin significantly increased the protein levels of COL I, elastin, and LOXL2 along with increases in their mRNA levels in the colon tissues compared with the DMH group, while COL III did not show a significant difference. Furthermore, in immunohistochemical evaluations, MMP1, MMP2, MMP9, and TIMP1 staining increased in the cold exposure and capsaicin group compared with the DMH group.

CONCLUSION

These results suggest that chronic cold and capsaicin exposure further increased the deposition of collagen and elastin in the colonic tissue. Increased COL I and elastin mRNA and protein levels expression may account for the enhanced ECM remodel and stiffness variations of colon tissue. The upregulated expression of the LOXL2 and physiological imbalance between MMP/TIMP activation and deactivation could contribute to the progression of the CRC resulting from cold and capsaicin exposure.

Key Words: Colon cancer; Cold exposure; Capsaicin; Extracellular matrix remodeling; Extracellular matrix enzymes

©The Author(s) 2021. Published by Baishideng Publishing Group Inc. All rights reserved.

Core Tip: In this study, we discovered that remodeling of extracellular matrix (ECM) plays an important role in the progression of colorectal cancer (CRC). These results suggest that increased stiffness of colonic tissue and the remodeling of ECM mediated by ECM enzymes resulting from cold and capsaicin exposure predisposes an environment suitable for CRC development and progression. To target ECM in CRC tumor tissue could represent a novel potential therapeutic strategy.

Citation: Qin JC, Yu WT, Li HX, Liang YQ, Nong FF, Wen B. Cold exposure and capsaicin promote 1,2-dimethylhyrazine-induced colon carcinogenesis in rats correlates with extracellular matrix remodeling. *World J Gastroenterol* 2021; 27(39): 6615-6630
URL: https://www.wjgnet.com/1007-9327/full/v27/i39/6615.htm
DOI: https://dx.doi.org/10.3748/wjg.v27.i39.6615

INTRODUCTION

Colorectal cancer (CRC), a common cause of cancer deaths in the world, is a multifactorial disease driven by genetic predisposition, epigenetic alterations, and environmental factors[1]. Only a minority of CRC is caused by the accumulation of genetic epigenetic alterations, while the majority is linked to environmental factors such as dietary intake, alcohol consumption, and ambient environment[2,3]. Increasing epidemiological data have indicated that cold weather might be associated with an increased occurrence of cancer[4]. Additionally, the consumption of chili-pepper and cancer incidence have a positive correlation[5,6]. However, the mechanisms under-

First decision: June 24, 2021
Revised: July 2, 2021
Accepted: July 30, 2021
Article in press: July 30, 2021
Published online: October 21, 2021

P-Reviewer: Dahiya DS
S-Editor: Gao CC
L-Editor: Filipodia
P-Editor: Yuan YY

lying the effects of cold exposure and capsaicin in 1,2-dimethylhyrazine (DMH)-induced CRC tumorigenesis and progression remain poorly understood. Extracellular matrix (ECM) is a non-cellular structure that is essential for the maintenance of normal tissue and organ function and disease pathophysiology[7]. Collagen is a major component of the ECM. It provides cellular components with physical support and is an important contributor to tumor growth and progression[8]. Tumor progression is accompanied by the dysregulation of collagen structure and deposition. Tumor associated-collagen is usually compacted to thick collagen bundles and the anisotropic arrangement of relatively straight in the matrix of malignancies compared with healthy tissues[9,10]. In clinical samples of breast tumors, collagen deposition increased, and linearization and thickening of collagen occurred; these processes can be linked to poor prognosis and high risk of mortality[11,12].

Elastin is another important fibrous ECM protein that provides elastic recoil to tissue. Importantly, excessive accumulation of ECM, particularly collagen and elastin, gradually leads to progressive organ fibrosis[13]. The fibrosis results in tissue stiffness and can predispose tissue to malignancy. Several human studies indicated that patients with liver fibrosis and stiffness are positively correlated with the risk hepatocellular carcinoma[14]. ECM remodeling is mainly orchestrated by ECM modifying enzymes such as lysyl oxidase-like-2 (LOXL2), matrix metalloproteinases (MMP), and tissue-specific matrix metalloproteinase inhibitors (TIMPs)[15]. LOXL2 is a key factor in ECM remodeling and is a copper-dependent amine oxidase that catalyzes the cross-linking of collagen or elastin in the ECM and thus regulates the tensile strength of tissues. LOXL2 causes disorganization and composition of ECM, resulting in many pathological conditions, including fibrosis and cancer[16]. Active LOXL2 is involved in stiffness-associated cancer progression, whereas inhibition of LOXL2 result in less collagen cross-linking and impeded cancer progression[17]. Moreover, LOXL2 expression is overexpressed in many types of tumors and is associated with poor prognosis[18-20].

MMP has been implicated in cancer development, progression, invasiveness, and dissemination by promoting a protumorigenic microenvironment and modulating the ECM and intercellular junctions[21]. MMPs and TIMPs are the main enzymes involved in the regulation of ECM remodeling and collagen degradation process[22]. Their expression and activity are upregulated in almost all human cancers with disparate changes, and this phenomenon is associated with advanced tumor stage, poor prognosis, and decreased overall survival rate[23,24]. Increased MMP expression/activity or decreased TIMPs could lead to MMP/TIMP imbalance, resulting in various pathological conditions including fibrosis and cancers[25].

Limited information, however, is available about ECM remolding and ECM enzyme activity in the progression of experimental colorectal malignancy. We have previously shown that cold exposure and long-term administration of capsaicin at a low dose further promote the development and progression of CRC[26]. However, the specific mechanisms underlying cold and capsaicin exposure tumor promotion remained unknown. This study aimed to investigate the effects of cold exposure and capsaicin on ECM remodeling and ECM enzymes in DMH-induced CRC. Moreover, we determined whether excessive ECM deposition, particular whether collagen and elastin and dysregulation of ECM enzymes expression and/or secretion in rat treatment with cold exposure, could further stiffen the colon tissues and disrupt the intestinal morphogenesis to exacerbate the experimental colorectal malignancy.

MATERIALS AND METHODS

Experimental design in adult male rats

Wistar rats weighing 200-250 g (6-wk-old) were obtained from Experimental Animal Center in Guangzhou University of Chinese Medicine. Animals were housed in plastic cages under a controlled environment (24 ± 2 °C, 50% ± 5% humidity, 12 h/12 h light-dark cycle) with *ad libitum* food and water access. All the experimental protocols were approved by the Institutional Animal Ethics Committee of the Guangzhou University of Chinese Medicine (No. 20130001). Briefly, after 3 d of acclimation, the animals were randomly assigned into four groups (n = 10). Rats in group A received no treatment and served as control. Five weeks later, rats in groups B-D received subcutaneous injection of DMH (25 mg/kg) once a week for 12 wk. In addition to DMH, Group C rats received cold distilled water (10 mg/kg) until the end of 38 wk. Group D rats were given capsaicin (0.9 mg/mL) every day throughout the experiment. By the end of the week, 10 rats from each group were sacrificed. For macroscopic evaluation of the

incidence of polyps at the end of the experimental period, rats were sacrificed and colons were incised and washed with physiological saline. Then cleaned colons were cut opened longitudinally and the total number of polyps/tumors was carefully counted and later verified with histopathological examination. The counting and histopathological analysis of gross macroscopic neoplastic lesions was carried out by two investigators from this study. If the histopathological types of these two investigators were different, then tumor histology was classified as adenomas and adenocarcinomas by one pathologist under blinded conditions from the Pathology Department in Guangzhou University of Chinese Medicine. Microscope findings were classified as adenomas and adenocarcinomas according to previous criteria described by Jikihara *et al*[27]. Tumor incidence is the percentage of rat bearing the indicated type of tumor.

Histopathological staining

All specimens were fixed in 4% paraformaldehyde solution for 24 h and embedded in paraffin and processed by standard histological processing techniques. Serial issue sections (8-μm thick) were obtained from each sample with the microtome and then were stained with hematoxylin and eosin (HE), picrosirius red, Masson's trichrome (MT), and Weigert's Resorcin-Fuschin (WRF). For Picrosirius red staining, sections were stained in picrosirius red solution 0.1) (Sirius red F3B; Sigma-Aldrich Co., St Louis, MO, United States) in a saturated aqueous solution of picric acid for 1 h at room temperature for collagen bundle staining. Images were subsequently analyzed using ImageJ to calculate the fiber density, which was measured as image % area coverage. MT was performed according to the manufacture's protocol including Weigert's Iron Hematoxylin Solution, Ponceau acid fuchsin, and Aniline Blue as reagents. The collagen volume fraction was measured by ImageJ software and calculated as the proportion of blue positive areas in the total section areas. The process of WRF used reagents and kits from Solarbio (Beijing, China). Sections were then mounted for observation under polarized light microscopy (NIKON Eclipse Ci, Tokyo, Japan) and light microscopy, respectively. Three microphotographs of the reticular dermis were taken with a 400 × magnification with light microscopy and polarized microscopy, respectively. Digitized images of histological sections obtained under final magnification of × 400 were analyzed using the Image-Pro Plus 4.5 software.

Collagen fiber analysis

CT-FIRE, an open-resource software (http://Loci.wisc.edu/software/cifire), was used as previously described to quantify automatically collagen fibers[28]. The quantitative parameters included alignment of collagen fibers as well as individual length, straightness, and width. These features of collagen fibers are widely used to investigate collagen organization in a various of cancer[29]. All the picrosirius red images were converted to 8-bit images and threshold values between 10-255 to eliminate background noise using FIJI ImageJ[30]. These images were uploaded to CT-FIRE; collagen fiber extraction parameters were set to default parameters.

Real-time quantitative reverse-transcriptase polymerase chain reaction

Total RNA extracts of colon tissues were prepared using TRIZOL reagent (TaKaRa, Kusatsu, Japan). RNA (1 μg) was reverse transcribed in a 20 μL reaction mixture using Prime Script RT Master Mix (TaKaRa). The purity of total RNA was evaluated by measuring the concentration and $OD_{260:280}$ values with a Nanodrop 2000 spectrophotometer (Thermo Fisher Scientific, Waltham, MA, United States). The mRNA levels of collagen type 1, alpha1 (COL1A1), collagen type 3, alpha1 (COL3A1), LOXL2, and elastin in colon mucosa were assessed using a Step One Plus real-time polymerase chain reaction system (CFX384TM Real-time System; Thermo Fisher Scientific). The relative levels of gene expression were enumerated using the comparative formula 2-ΔΔCt. The primer sequences used in this polymerase chain reaction amplification were as follows: 5′-AGCCATGTACGTAGCCATCC-3′/3′-ACCCTCATAGATGGGCACAG-5′ for β-actin; 5′-AGGCATAAAGGGTCATCGTGGCTT-3′/3′-AGTCCATCTTTGC-CAGGAGAACCA-5′ for COL1a1; 5′-GGTTTGGAGAATCTATGAATGGTGG-3′/3′-GCTGGAAAGAAGTCTGAGGAAGG-5′ for Col3a1; 5′-AGCCTATAAGCCG-GAGCAAC-3′/3′-GTCCCACTTGTCATCGCAGA-5 'for LOXL2; 5′-CGCCTGTAAT-GCCTCCAATC-3′/3′-AGCAGCTAAAGCAGCGAAGT-5′ for elastin.

Immunohistochemistry

Colonic tissue sections were deparaffinized and rehydrated through a series of xylene and ethanol/water. The sections were placed in a 95 °C antigen retrieval solution (citrate buffer; PH 6.0) for 15 min. After cooling in retrieval solutions for 20 min at

Table 1 Incidence of various tumors induced in different treatment groups

Group	Total number of tumors	Adenoma incidence, %			Adenocarcinoma incidence, %				With lymphytic metastasis (%)
		Mild	Moderate	Severe	Well-differentiated	Moderate-differentiated	Poor-differentiated	Mucinous	Metastasis rate
Control	-	-	-	-	-	-	-	-	-
DMH	23	2/23 (8.7)	2/23 (8.7)	3/23 (13)	12/23 (52.2)	4/23 (17.4)	3/23 (13.0)	-	-
Cold exposure	38	1/38 (2.6)	2/38 (5.3)	3/38 (7.8)	5/38 (15.8)[b]	8/38 (21.1)	15/38 (36.8)[a]	4/38 (10.5)	20.0
Capsaicin	34	2/31 (5.9)	1/34 (2.9)	4/31 (12.9)	7/31(22.6)[a]	12/31 (38.7)	7/31(22.6)	1/31 (3.2)	-

Values are expressed as the proportion of lesions-bearing rats. n = 10 rats/group. Incidence data was analyzed by using chi-square or Fisher's exact test.
[a]$P < 0.05$.
[b]$P < 0.01$.
1,2-dimethylhyrazine compared with cold exposure and capsaicin-treated group. DMH: 1,2-Dimethylhyrazine.

room temperature, the slides were treated with hydrogen peroxide for 10 min to block endogenous peroxidase activity. Primary rabbit anti-histone polyclonal antibodies were applied for 14 h at 4 °C overnight at the following dilutions: Type I collagen (COL I) (1:500; ab34710; Abcam, Cambridge, United Kingdom), type III collagen (COL III) (1:200, ab7778; Abcam), LOXL2 (1:400), elastin (1:600; ab217356; Abcam), MMP1 (1:500; 10371-2-AP; Proteintech, Rosemont, IL, United States), MMP2 (1:200; ab86607; Abcam), MMP9 (1:800; ab38898; Abcam), and TIMP1 (1:600, ab61224; Abcam). The next day, biotin-conjugated secondary antibody and streptavidin-biotin peroxidase were applied each for 20 min. 3,3'-Diaminobenzidine tetrahydrochloride (0.05%) was used as the substrate, and nuclear contrast was performed using hematoxylin counter-staining. Each section was analyzed in three different fields using Image Pro Plus software. The density of yellow reflects the expression levels of target proteins. Integral optical density sum / area SUM was applied to quantify the relative expression of COL I, COL III, LOXL2, elastin, MMP1, MMP2, MMP9, and TIMP1.

Statistical analysis

All the data are summarized as mean ± SD, and data were analyzed using SPSS 23.0 statistical software. We performed the data with a one-way analysis of variance with the post-hoc comparison by the L.S.D. method and Fisher's exact test was employed to compare tumor incidence. Differences with values of $P < 0.05$ were considered statistically significant.

RESULTS

Macroscopic and pathological observation study of colon tumor

No visible colon tumor was found in the normal control. We observed findings such as colonic mucosal thickening, stiffness, and not tiled completely on filter paper in the majority of rats of the cold exposure group (Figure 1C). As shown in Figure 1B, the length of colon in the DMH and normal group was not significantly different. However, the length of the colon in the cold exposure and capsaicin group was shorter than that of DMH group. The pathological classification of colonic tumors in each group is shown in Table 1. No difference was observed in the proportion of adenomas among groups. In the DMH-induced group of animals, most tumors had well-differentiated tubular adenocarcinomas. Invasive tumors increased in the cold and capsaicin group. Histopathological analysis showed in the cold exposure group that an evident malignant transformation occurred in the colon with the features of poor-differentiated mucinous adenocarcinomas, and some of the glands were filled with mucinous material (Figure 2C). In addition, the mesenteric lymph nodes of rats in each group were stained with hematoxylin and eosin, and the lymphatic metastasis was observed under light microscope (Figure 2B). No lymphatic metastasis was observed in the DMH and capsaicin group, while a mesocolic lymph node was totally replaced by

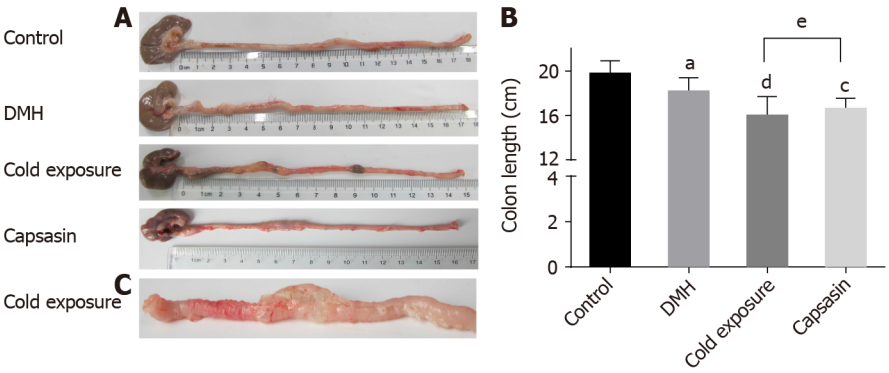


Figure 1 Colonic morphology of rats in different groups. A and B: Changes in colon length and colonic morphology; C: Stiff colonic tissues in cold exposure group. [a]*P* < 0.05, control compared with 1,2-dimethylhyrazine (DMH); [c]*P* < 0.05, [d]*P* < 0.01, DMH compared with cold exposure and capsaicin-treated group; [e]*P* < 0.05, cold exposure compared with capsaicin-treated group.

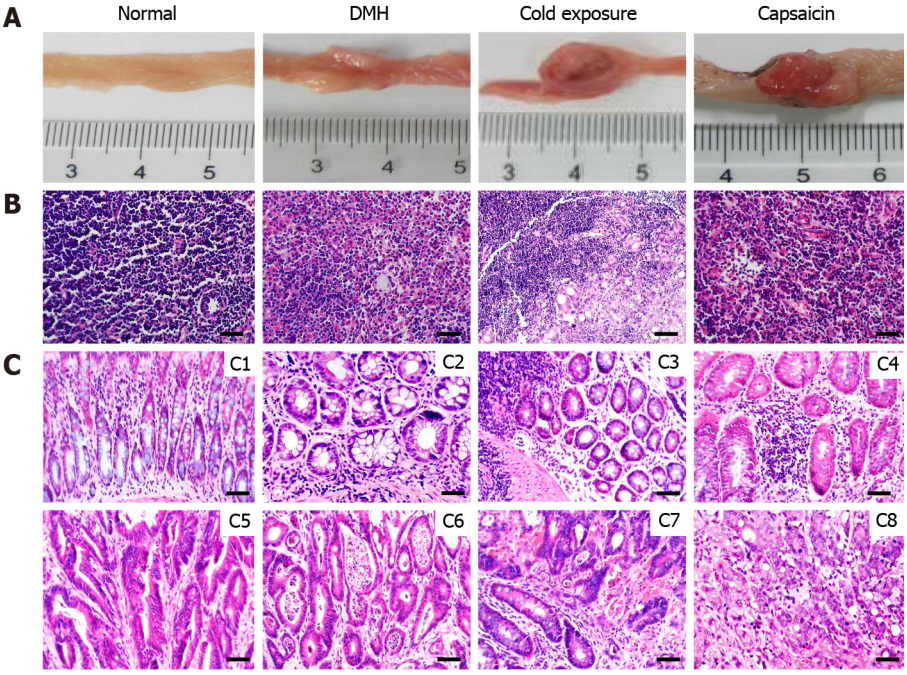


Figure 2 Pathological observation and lymph node metastases of different groups. A: Macroscopic image of the colonic tumors; B: Representative sections stained with hematoxylin and eosin (HE) showing the histopathology of the mesocolic lymph node in the different groups; C: Representative sections stained with HE showing the histopathology of the colonic mucosa in the different groups. Normal architecture of colon was observed in the control groups (C1), adenoma with mild dysplasia with massive infiltration of inflammatory cells (C2). Histology of adenoma with moderate dysplasia in cold exposure groups (C3). Histology of adenoma with severe dysplasia (C4). Histology of well-differentiated tubular adenocarcinomas (C5). Histology of Moderately differentiated adenocarcinomas (C6). Histology of Poorly differentiated adenocarcinomas (C7). Histology of Mucinous adenocarcinoma with signet ring cells (C8) (HE staining, × 400, scalar bar 20 μm). DMH: 1,2-Dimethylhyrazine.

metastatic cancer tissue in the cold exposure group; the lymph node metastasis rate was 20.0% (Table 1, Figures 1 and 2).

Alterations in collagens after cold exposure and capsaicin

Colon tissue sections were stained by MT and picrosirius red to identify the total collagen in the colon mucosa. As shown in Figure 3A, there were few collagen fibers in normal colonic mucosa. After DMH treatment, wave shape collagens stained blue were markedly increased around the glands, and this was increased further in the cold exposure and capsaicin treatment group. The collagen density was quantified using ImageJ, and it was significantly increased in the colonic tissue of cold exposure and capsaicin group. This excessive collagen deposition was further confirmed by picrosirius red staining. As shown in Figure 3B, picrosirius red staining revealed in normal tissue the collagen fibers with sparse deposition composed of thin collagen fibers. The collagen fibers in the DMH group were denser than that in normal collagen

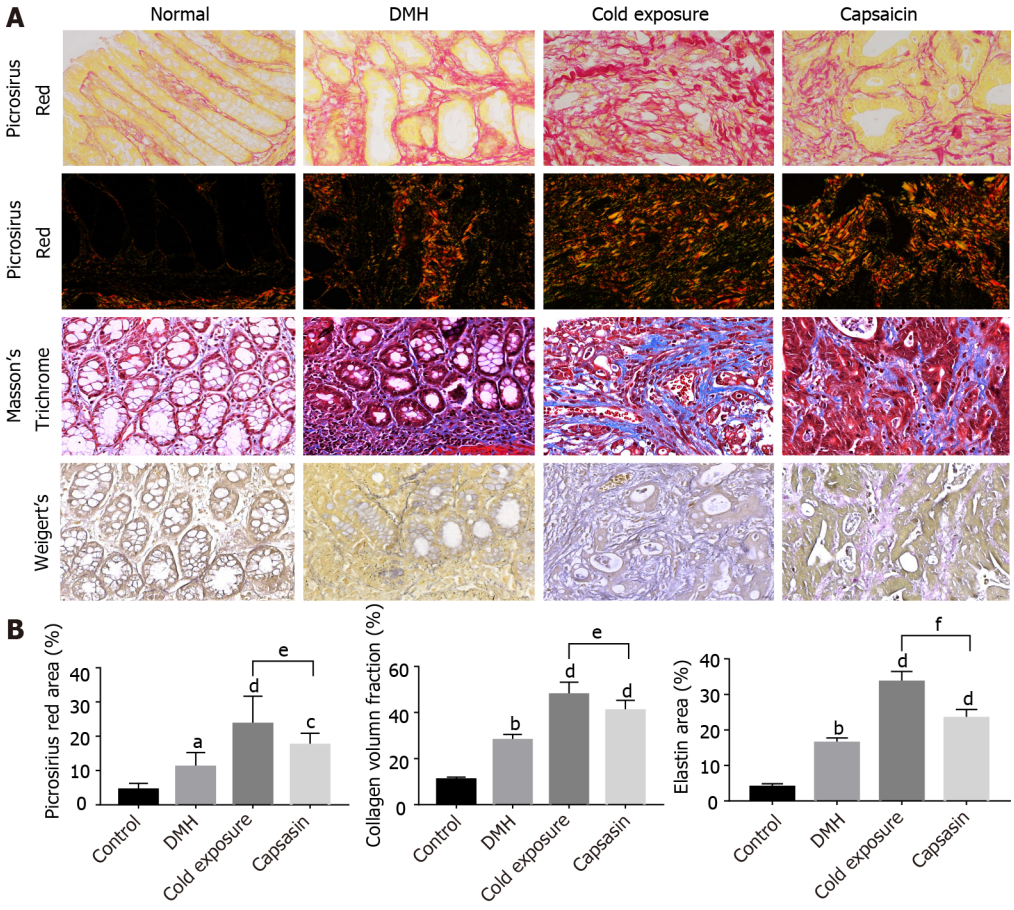


Figure 3 Changes in extracellular matrix components (collagen fibers and elastin) in colonic mucosa of different treatment groups. A: Representative photographs of colonic tissues in rats of normal, 1,2-dimethylhyrazine (DMH), cold exposure and capsaicin groups using Masson's trichrome: collagen (blue), nuclei and cytoplasm (red); picrosirius red in bright-field: collagen (red); polarized light: collagen (yellow-orange to green birefringence) and Weigert's Resorcin-Fuschin: elastin (blue-black), myofibers (yellow). Magnification, × 400, scalar bar 20 μm; B: Quantitative analysis of picrosirius red staining, trichrome and Weigert's staining as a measure of collagen and elastin density.

fibers. In the capsaicin treatment group, collagen fibers showed an evident increase and were crosslinked into bundles. On the other hand, the cold exposure group apparently displayed an increased amount of collagen fibers with heterogeneous thickness and alignment. The collagen in the cold exposure and capsaicin group exhibited a predominant reddish or yellow-orange. The structure and organization of collagen fibers were evaluated in colon tissue sections by quantifying the polarization microscopy images. As shown in Figure 4A, visualized collagen fibers were extracted and analyzed for fiber width, angle, length, and straightness using CT-FIRE software. As shown in Figure 4B, compared with the DMH group, collagen fibers in the cold exposure and capsaicin group showed a significant increase in angle, length, width, and straightness. These results revealed that cold exposure and capsaicin induced a progressive increase in the content and orientation of collagen fibers in CRC as a function of malignancy.

Alterations in elastin after cold exposure and capsaicin

Treatment WRF was used to identify the elastin fibers, which were stained black. As shown in Figure 3A, elastin was hardly expressed in the colonic mucosa of the normal rats. After treatment with DMH, the elastin fibers aligned surrounding the epithelium and stroma. After cold exposure and capsaicin treatment, the amount of elastin fibers increased, and thick elastic fibers was found highly disorganized between the gland compared with their respective control and DMH groups. Alterations in the mRNA levels of COL I, COL III, LOXL2, and elastin. The expression levels of COL I, COL III, LOXL2, and elastin mRNAs in colonic tissue are shown in Figure 5. The COL I, LOXL2, and elastin mRNA levels were higher in the DMH-induced cancer group than in the control group. In comparison with the DMH group, a significant increase was detected both in the cold exposure and capsaicin treatment group, but the mRNA levels of COL III were not significantly different between DMH and capsaicin ex-

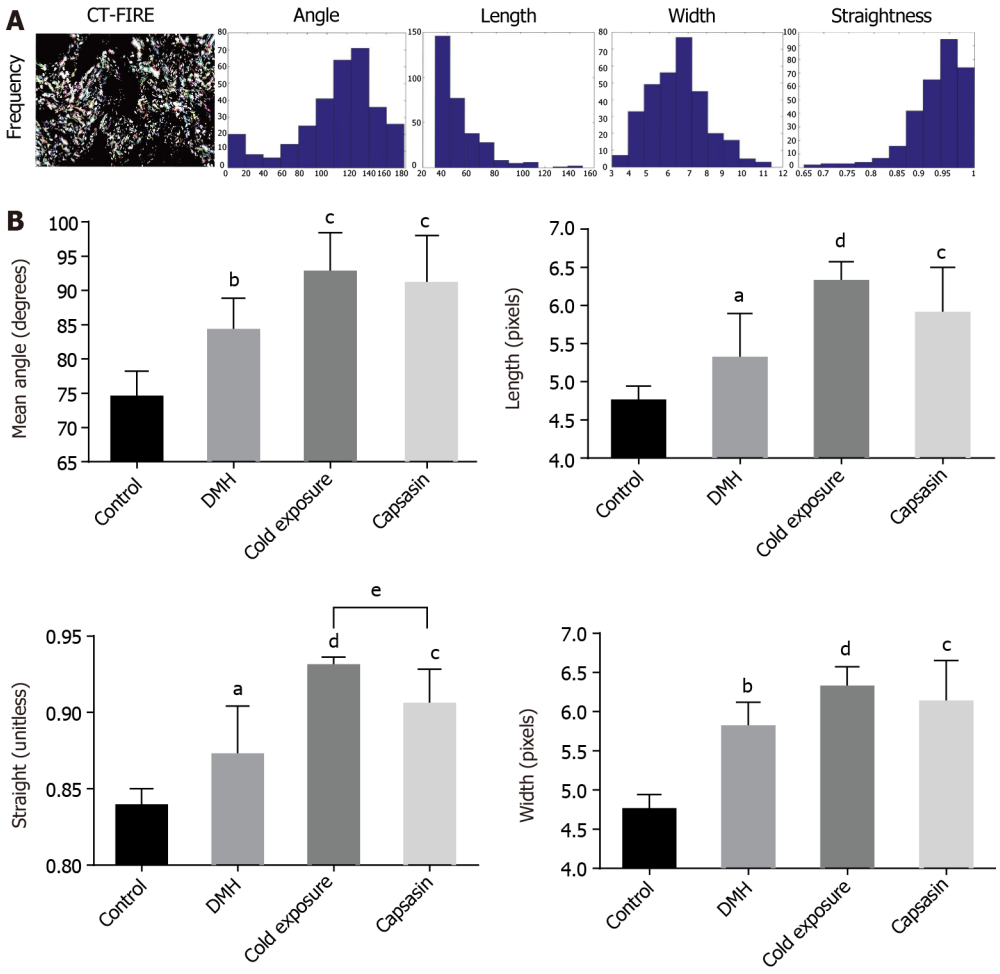


Figure 4 Collagen fibers were automatically extracted for analysis using open-source software CT-FIRE. A: Histograms were generated to show the distribution of various parameters in each polarized light microscopy imaging; B: Quantitative analysis of collagen fibers from polarized light microscopy imaging in the colonic mucosa of different treatment groups. Data are mean ± SE of three images per tissues region. $^{a}P < 0.05$, $^{b}P < 0.01$, control compared with 1,2-dimethylhyrazine (DMH); $^{c}P < 0.05$, $^{d}P < 0.01$, DMH compared with cold exposure and capsaicin-treated group; $^{e}P < 0.05$, Cold exposure compared with capsaicin-treated group.

posure group.

Alterations in the protein levels of COL I, COL III, LOXL2, and elastin

The expression levels of COL I, COL III, LOXL2, and elastin in colonic tissue are shown in Figure 6A and B. The protein expression levels of collagen type I, III, LOXL2, and elastin were significantly elevated in colonic tissue from DMH-treated rats in comparison to the control group. The expression level of proteins in the cold exposure and capsaicin treatment group increased. COL I and LOXL2 levels were significantly higher in the cold exposure group, but no statistical difference was observed in the change of COL III and elastin between cold exposure and capsaicin group.

Alterations in the protein levels of MMP1, MMP2, MMP9, and TIMP1

The expression levels of MMP1, MMP2, MMP9, and TIMP1 in colonic tissue are shown in Figure 7. Significantly elevated MMP1, MMP2, MMP9, and TIMP1 immunoreactivity was observed in DMH-treated rats compared with the control group. The expression levels of proteins in the cold and capsaicin group increased compared with the DMH group. In comparison with the capsaicin group, the expression of MMP2, MMP9, and TIMP1 increased in the cold exposure group.

DISCUSSION

ECM has been increasingly considered as an important regulator at diverse aspects of tumor initiation, promotion, neoplastic transformation, invasion, and metastasis[31].

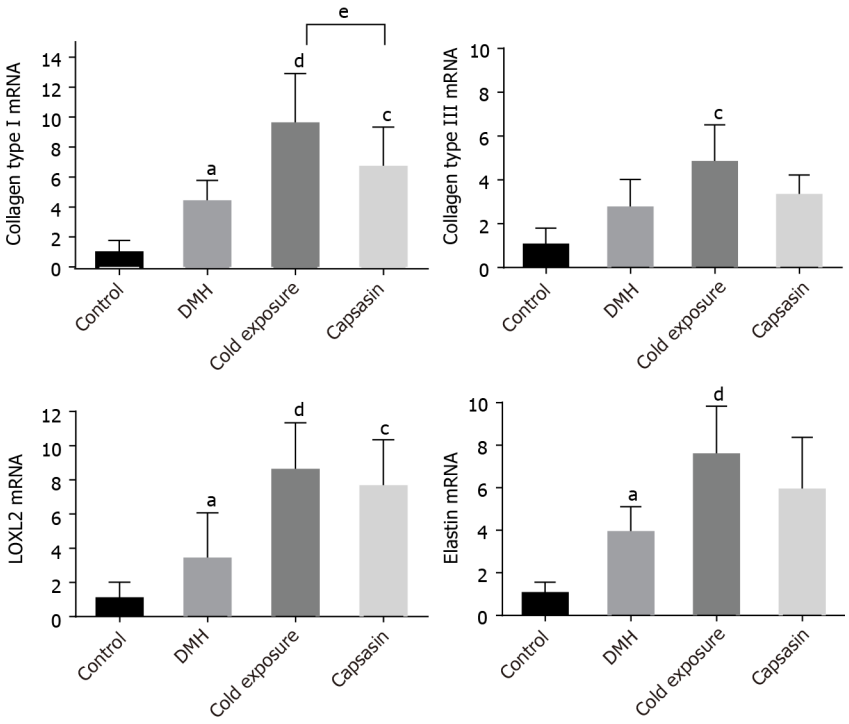


Figure 5 The mRNA expression levels of collagen type I, III, elastin and lysyl oxidase-like-2 in the colon tissues of rats in different groups. Data were presented as the mean ± SD form six independent experiments. [a]*P* < 0.05, control compared with 1,2-dimethylhyrazine (DMH); [c]*P* < 0.05, [d]*P* < 0.01, DMH compared with cold exposure and capsaicin-treated group; [e]*P* < 0.05, cold exposure compared with capsaicin-treated group. LOXL2: Lysyl oxidase-like-2.

Furthermore, ECM remodeling is a consequence of or increases risk for malignant transformation of colonic, hepatic, pulmonary, and pancreatic cells[32,33]. Collagen and elastin are the major components of ECM, and their excessive deposition has been implicated in a number of diseases, particularly fibrosis and cancer. However, the morphology and structure of collagen and elastin fibers in the animal models of CRC remains unclear. In the present study, we analyzed the morphology and structure of collagen and elastin fibers in rat experimental model of DMH-induced CRC imposed by cold and capsaicin exposure. Results showed an association between collagen expression or ECM modifying enzymes and CRC development, thus supporting ECM remodeling is highly relevant to CRC cancer progression. Tumor tissue often exhibits fibrosis, and this fibrotic state is characterized by the excessive deposition of collagen and elastin[34].

Fibrosis can develop in nearly any organ, and it is an important driver of tissue stiffness and increases the risk of malignancy[35]. In fibrotic kidney biopsy specimens or multiple experimental kidney fibrosis rodent models, the accumulation of elastin can be observed in renal tissue[36]. In human fibrosis of the liver, kidney, and pancreas, the ECM on average becomes stiffer than normal. Our previous study indicated in human CRC that the collagen development features numerous changes in composition and organization compared with normal colonic tissues[37]. In the present study, we found that collagen components were quantitatively and qualitatively changed in the rat experimental model of CRC. By using picrosirius red, MT, and WRF staining, we revealed a marked increase in collagen and elastin deposition in rats exposed to cold and capsaicin treatment. Furthermore, they were more orderly organized based on the collagen fibers being more aligned with each other, longer, wider, and slightly straighter.

The structure, orientation, and physical properties of collagen regulate the aggressive behavior of cancer. For example, in glioblastoma, Pointer *et al*[38] showed that patients with more organized glioblastoma multiforme collagen survive longer than patients with less organized glioblastoma multiforme collagen. Zhou *et al*[39] also demonstrated that the increased density, length, or width of collagen negatively affects patients with gastric cancer prognosis. The stromal tissue in CRC has also shown that an increase in the collagen content of the ECM increases mechanical stiffness, which predisposes to aggressive CRC[40]. In human breast cancer, linear organization and relatively straight collagen that facilitates migration of tumor cells indicate poor cancer outcome[41]. Similarly, our data indicated that cold and capsaicin exposure increased

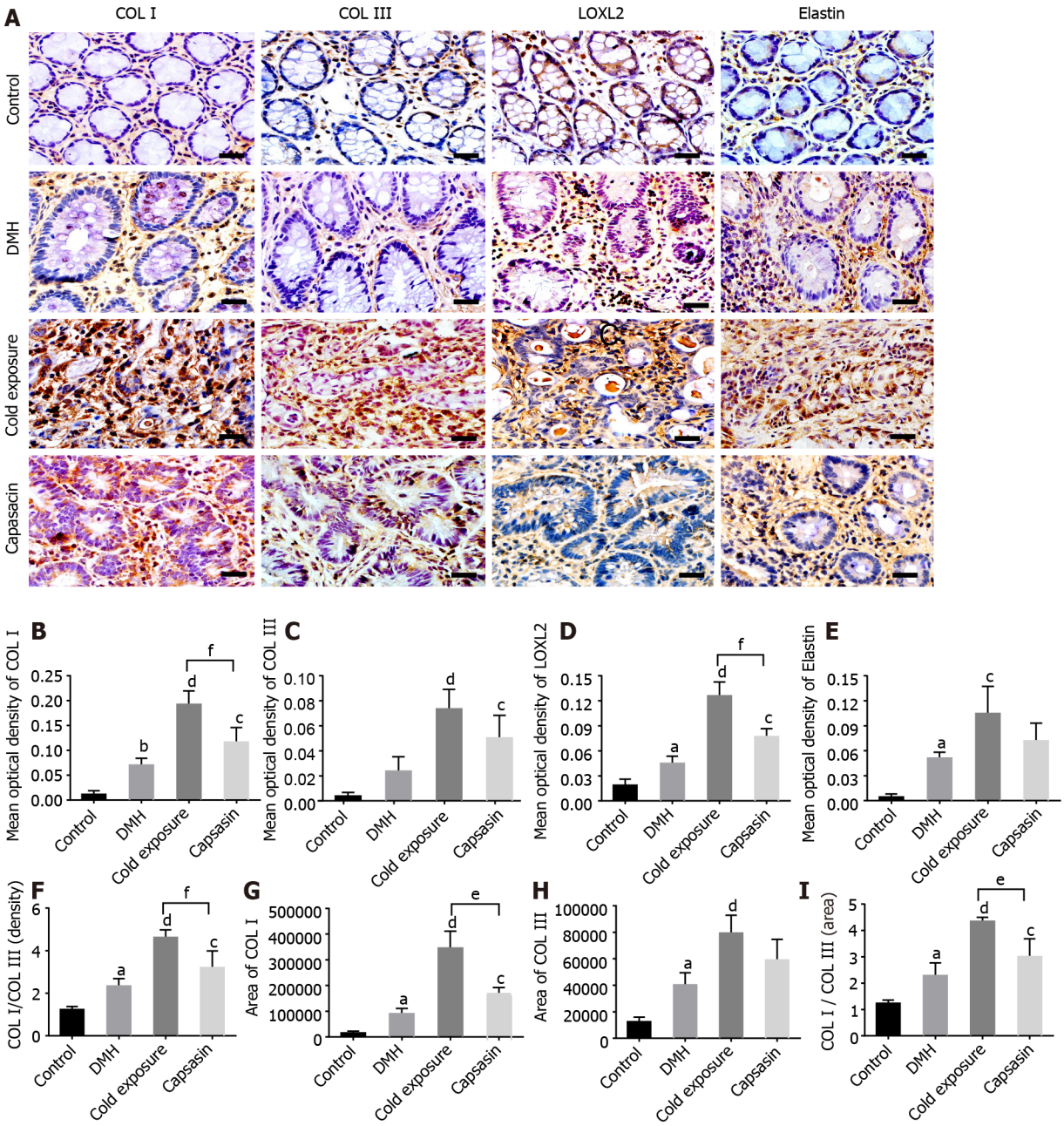


Figure 6 Changes in collagen, elastin and lysyl oxidase-like-2 proteins in the colonic tissues of different treatment groups. A: Protein expressions of type I collagen (COL I), type III collagen (COL III), lysyl oxidase-like-2 (LOXL2), and elastin in the colonic tissues *via* immunohistochemical staining. Magnification, × 400, scalar bar 20 μm; B-I: Densitometric analysis of COL I (B), COL III (C), LOXL2 (D), elastin(E), COL I/COL III (F), COL I area (G), COL III area (H), and COL I area/COL III area (I) during immunohistochemical staining. $^{a}P < 0.05$, $^{b}P < 0.01$, control compared with 1,2-dimethylhyrazine (DMH); $^{c}P < 0.05$, $^{d}P < 0.01$, DMH compared with cold exposure and capsaicin-treated group; $^{e}P < 0.05$, $^{f}P < 0.01$, cold exposure compared with capsaicin-treated group.

collagen and elastin deposition, thus triggering alterations in the ECM architecture and organization in the DMH-induced CRC for further tumor development and progression. Furthermore, all parameters of collagen fibers (*e.g.*, density, angle, length, width, and straightness) significantly increased in the cold exposure group and could accurately explain the cold-induced CRC more seriously.

Recently, the relationship between ECM remodeling and malignant transformation of cancer has attracted much attention[42]. COL I is the most abundant protein present in the body. COL I, a major component of collagen, was significantly up-regulated in CRC tissues and showed enhanced CRC migratory capabilities through the overexpression of WNT/planar cell polarity signaling pathway[43]. Moreover, the elevated expression of type I collagen in CRC tissues is correlated to patients with high metastasis that was due to activation of phosphatidylinositol-3-kinase/AKT signaling [44]. Bode *et al*[45] also showed that the expression of COL was increased in malignant colon tissue compared with COL III. Moreover, the elevated expression of COL I has

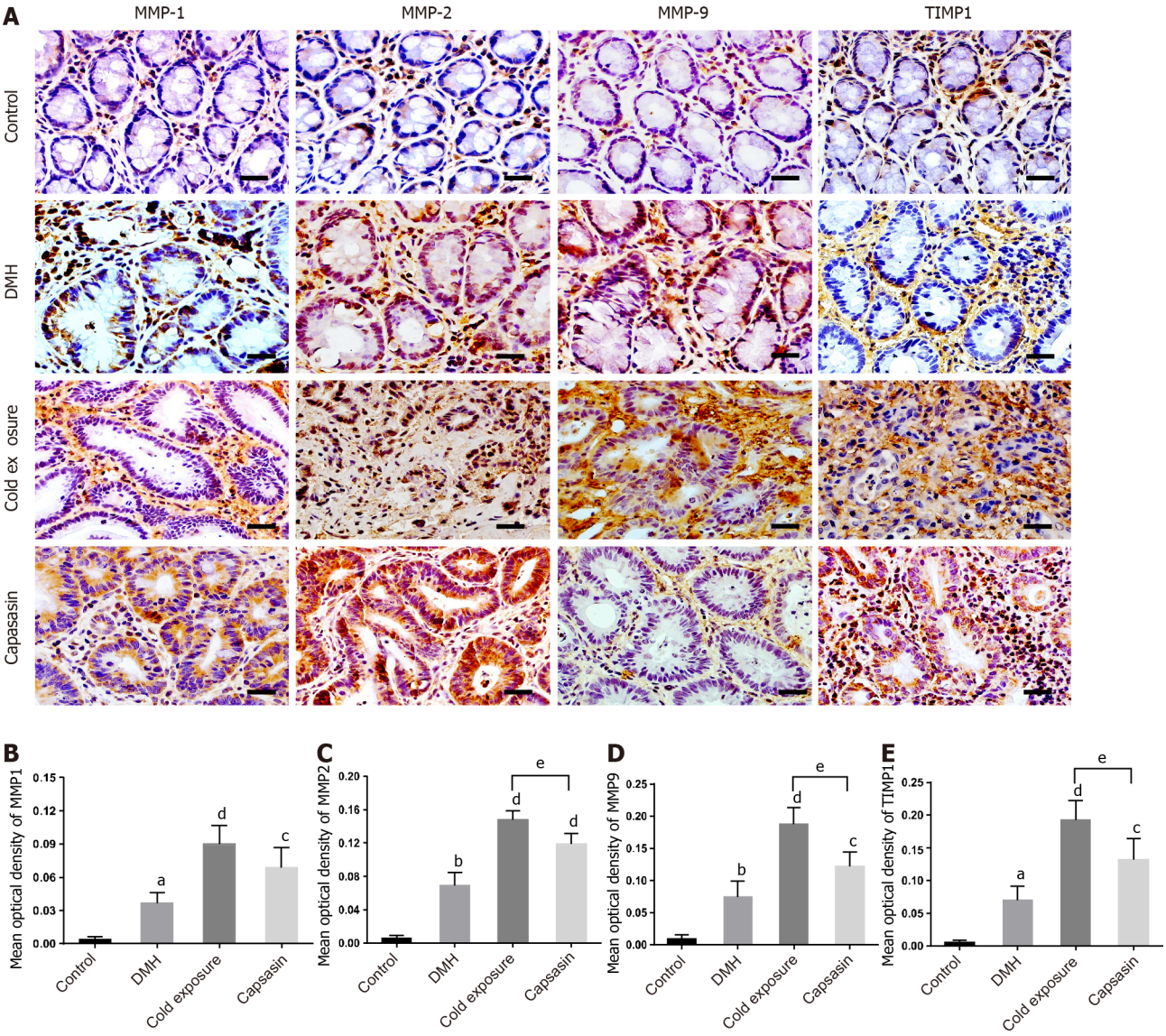


Figure 7 Changes in matrix metalloproteinase 1, matrix metalloproteinase 2, matrix metalloproteinase 9, and tissue-specific matrix metalloproteinase 1 proteins in the colonic tissues of different treatment groups. A: Protein expressions of matrix metalloproteinase (MMP) 1, MMP2, MMP9 and tissue-specific matrix metalloproteinase 1 (TIMP1) in the colonic tissues *via* immunohistochemical staining. Magnification, × 400, scalar bar 20 μm; B-E: Densitometric analysis of MMP1 (B), MMP2 (C), MMP9 (D) and TIMP1 (E) during immunohistochemical staining. $^{a}P < 0.05$, $^{b}P < 0.01$, control compared with 1,2-dimethylhyrazine (DMH); $^{c}P < 0.05$, $^{d}P < 0.01$, DMH compared with cold exposure and capsaicin-treated group; $^{e}P < 0.05$, cold exposure compared with capsaicin-treated group.

been linked to the invasive and aggressive behavior of CRC[46]. In the present study, we also evaluated the expression of COL I in cold exposure and capsaicin treatment CRC colonic tissue. The increase in expression levels of COL I in our study is consistent with other reports in CRC. However, the mRNA level of COL III was not significantly different between the DMH and capsaicin group. In addition, compared with other groups, the COL I/ COL III in cold exposure group was significantly increased. With the increase in collagen expression, distribution area, and collagen ratio, the degree of fibrosis in ECM pathological characteristics was aggravated[47,48]. Therefore, the colonic tissue stiffness was significantly higher than that of the other groups, and the degree of ECM fibrosis in CRC with cold exposure was more serious than that in other groups. ECM remodeling is regulated by ECM enzymes such as LOXL2, MMPs, and TIMPs. ECM-crosslinking enzyme LOXL2 has been implicated in stiffness-associated tumor progression[49]. The LOXL2-mediated collagen cross-linking, both *in vitro* and *in vivo* models of CRC, results in increased tissue stiffness and activation of the focal adhesion kinase/SRC signaling[50].

MMP1, MMP-2, and MMP-9 play a fundamental role in many pathophysiological processes such as cell migration, angiogenesis, and the invasion and metastasis of malignant tumors[51]. TIMPs are the most important physiological inhibitors of MMP,

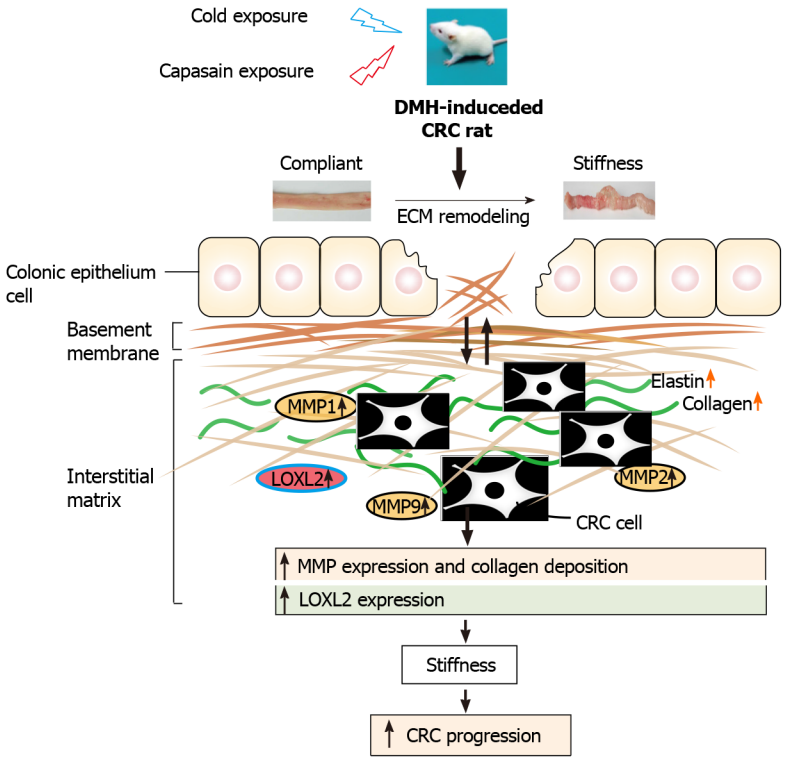


Figure 8 Schematic diagram depicting the role of extracellular matrix and extracellular matrix enzymes in promoting colorectal cancer pathogenesis. Comparison with the normal rats, rats exposed to cold and capsaicin with profound remodeling of extracellular matrix (ECM) in the colonic tissue, which was mediated by ECM enzymes. These results implicate a crucial role of ECM remodeling on cold and capsaicin exposure colorectal cancer development and progression. CRC: Colorectal cancer; DMH: 1,2-Dimethylhyrazine; MMP: Matrix metalloproteinase.

and they are also commonly expressed in tumor sites[52]. The expression of both MMP-2 MMP9 and TIMP-2 is higher in invasive tumors and is strongly associated with angiogenesis in DMH-induced CRC[24]. A previous study indicated that the cross-linking of collagen is known to activate enzymes involved in matrix remodeling, such as LOXL2, MMPs, and TIMPs[53,54]. MMPs are responsible for the degradation of ECM; LOXL2 mediate ECM cross-linking and stiffening[55]. However, recent studies indicated that LOXL2 activity promotes breast cancer metastasis by regulating the expression of MMPs and TIMPs involved in matrix remodeling[56]. LOXL2, TIMP1, and MMP9 are co-expressed during mammary metastasis, suggesting that they function together in glandular remodeling. Our previous study also found that expression levels of LOXL2, MMP1, MMP2, and MMP9 are positively correlated in CRC tissues, and they play synergistic roles in ECM remodeling of human CRC[37].

In the present study, the LOXL2, MMP1, MMP2, MMP9, and TIMP parameters were analyzed, and the results indicated a significant increase in the expression of these proteins in the cold exposure and capsaicin group accompanied by the enhancement of collagen and elastin deposition. Therefore, they may act together in regulating ECM remodeling. Growing insights from experimental studies on the roles of the ECM in CRC suggest that the quantitative and qualitative changes in ECM mediated by specific enzymes promote numerous cellular functions that steer cancer progression and metastasis[57,58]. In the present study, the ECM remodeling in the colonic tissue under cold and capsaicin exposure was more serious, thus increasing the exacerbation severity of CRC. Therefore, environmental factors, such as diet, will affect the internal and external constitutions of organism, causing different manifestations and disease progression in the organism. In the cold exposure and capsaicin treatment group, remodeling of the ECM and stromal stiffness is associated with increased propensity for progression to invasive CRC. Therefore, the levels of ECM remodeling can distinguish different organism characteristics and evaluate the CRC progression successfully, thus providing a novel pathological direction of analysis for clinicians. Furthermore, nanoscale mechanical imaging can be used to observe patients with heterogenous features of ECM, who would benefit most from ECM target therapies.

CONCLUSION

In summary, as shown in Figure 8, the present study revealed profound remodeling of the ECM in cold exposure and long-term administration of capsaicin at a low dose in rats. Collagen signatures including angle, length, width, and straightness have a great impact on CRC progression. Additionally, our results show that higher colonic tissue stiffness might result from ECM enzymes-mediated ECM crosslinking and excessive deposition of collagen and elastin, and such changes are strongly associated with the tumor progression of cold and capsaicin exposure CRC. A better understanding of the role of ECM remodeling and ECM enzymes on the pathogenic mechanisms of colon cancer may help in determining the molecular mechanism of CRC progression and could afford a novel therapeutic intervention in the treatment of this disease.

ARTICLE HIGHLIGHTS

Research background

Colorectal cancer (CRC) is a cancer with high prevalence and mortality in the world. Extracellular matrix (ECM) is a dynamic compartment that regulates tissue development and homeostasis, and its remodeling contributes to neoplastic progression. The cancerous ECM can change cell phenotype and has profound influence on the colonization of metastatic cancer cells. However, the relationship between ECM remodeling and progression and aggression CRC from imposed by cold and capsaicin exposure remains unclear.

Research motivation

To identify the effect of cold exposure and capsaicin on ECM remodeling, ECM enzymes, and the underlying mechanism.

Research objectives

To explore the role of ECM remodeling and ECM enzymes in the 1,2-dimethylhydrazine (DMH)-induced CRC progression and the underlying mechanism.

Research methods

The CRC rat model was conducted by adding DMH and examining the role of ECM remodeling and ECM enzymes on DMH-induced CRC in the model. We investigated the morphology and structure of collagen and elastin using Masson's trichrome, Picrosirius red, and Weigert's Resorcin-Fuchsin stains. Additionally, we evaluated the protein expression level of type I collagen (COL I), type III collagen (COL III), elastin, lysyl oxidase-like 2 (LOXL2), matrix metalloproteinase (MMP) 1, MMP2, MMP9, and tissue-specific matrix metalloproteinase 1 by immunohistochemistry and observed the expression of COL I, COL III, elastin, and LOXL2 in the colon tissues of rats by reverse-transcriptase quantitative polymerase chain reaction.

Research results

We found that although there were no differences in the proportion of adenomas, a trend towards the increase of invasive tumors was observed in the cold and capsaicin group. Cold exposure group had a metastasis rate comparative with the other groups. Additionally, abnormal accumulation of both collagen and elastin was observed in the cold exposure and capsaicin group. Specifically, collagen quantitative analysis showed increased length, width, angle, and straightness compared with the DMH group. Collagen deposition and straightness were significantly increased in the cold exposure group compared with the capsaicin group. Cold exposure and capsaicin significantly increased the protein levels of COL I, elastin, and LOXL2 along with increases in their messenger RNA levels in the colon tissues compared with the DMH group, while COL III did not show a significant difference. Furthermore, in immunohistochemical evaluations, MMP1, MMP2, MMP9, and tissue-specific matrix metalloproteinase 1 staining increased in the cold exposure and capsaicin group compared with the DMH group.

Research conclusions

Increased stiffness of colonic tissue and the remodeling of ECM mediated by ECM enzymes resulted from cold and capsaicin exposure, predisposing an environment suitable for CRC development and progression.

Research perspectives

To target ECM in CRC tumor tissue could represent a novel potential therapeutic strategy.

ACKNOWLEDGEMENTS

The authors would like to acknowledge Xiao XX for skillful technical assistance.

REFERENCES

1 **Okugawa Y**, Grady WM, Goel A. Epigenetic Alterations in Colorectal Cancer: Emerging Biomarkers. *Gastroenterology* 2015; **149**: 1204-1225.e12 [PMID: 26216839 DOI: 10.1053/j.gastro.2015.07.011]

2 **Dionigi G**, Bianchi V, Rovera F, Boni L, Annoni M, Castano P, Villa F, Dionigi R. Genetic alteration in hereditary colorectal cancer. *Surg Oncol* 2007; **16** Suppl 1: S11-S15 [PMID: 18023570 DOI: 10.1016/j.suronc.2007.10.020]

3 **Murphy N**, Moreno V, Hughes DJ, Vodicka L, Vodicka P, Aglago EK, Gunter MJ, Jenab M. Lifestyle and dietary environmental factors in colorectal cancer susceptibility. *Mol Aspects Med* 2019; **69**: 2-9 [PMID: 31233770 DOI: 10.1016/j.mam.2019.06.005]

4 **Lehrer S**, Rosenzweig KE. Cold Climate Is a Risk Factor for Thyroid Cancer. *Clin Thyroidol* 2014; **26**: 273-276 [PMID: 25558467 DOI: 10.1089/ct.2014;26.273-276]

5 **López-Carrillo L**, López-Cervantes M, Robles-Díaz G, Ramírez-Espitia A, Mohar-Betancourt A, Meneses-García A, López-Vidal Y, Blair A. Capsaicin consumption, Helicobacter pylori positivity and gastric cancer in Mexico. *Int J Cancer* 2003; **106**: 277-282 [PMID: 12800206 DOI: 10.1002/ijc.11195]

6 **Serra I**, Yamamoto M, Calvo A, Cavada G, Báez S, Endoh K, Watanabe H, Tajima K. Association of chili pepper consumption, low socioeconomic status and longstanding gallstones with gallbladder cancer in a Chilean population. *Int J Cancer* 2002; **102**: 407-411 [PMID: 12402311 DOI: 10.1002/ijc.10716]

7 **Frantz C**, Stewart KM, Weaver VM. The extracellular matrix at a glance. *J Cell Sci* 2010; **123**: 4195-4200 [PMID: 21123617 DOI: 10.1242/jcs.023820]

8 **Nissen NI**, Karsdal M, Willumsen N. Collagens and Cancer associated fibroblasts in the reactive stroma and its relation to Cancer biology. *J Exp Clin Cancer Res* 2019; **38**: 115 [PMID: 30841909 DOI: 10.1186/s13046-019-1110-6]

9 **Malik R**, Lelkes PI, Cukierman E. Biomechanical and biochemical remodeling of stromal extracellular matrix in cancer. *Trends Biotechnol* 2015; **33**: 230-236 [PMID: 25708906 DOI: 10.1016/j.tibtech.2015.01.004]

10 **Drifka CR**, Tod J, Loeffler AG, Liu Y, Thomas GJ, Eliceiri KW, Kao WJ. Periductal stromal collagen topology of pancreatic ductal adenocarcinoma differs from that of normal and chronic pancreatitis. *Mod Pathol* 2015; **28**: 1470-1480 [PMID: 26336888 DOI: 10.1038/modpathol.2015.97]

11 **Esbona K**, Yi Y, Saha S, Yu M, Van Doorn RR, Conklin MW, Graham DS, Wisinski KB, Ponik SM, Eliceiri KW, Wilke LG, Keely PJ. The Presence of Cyclooxygenase 2, Tumor-Associated Macrophages, and Collagen Alignment as Prognostic Markers for Invasive Breast Carcinoma Patients. *Am J Pathol* 2018; **188**: 559-573 [PMID: 29429545 DOI: 10.1016/j.ajpath.2017.10.025]

12 **Provenzano PP**, Eliceiri KW, Campbell JM, Inman DR, White JG, Keely PJ. Collagen reorganization at the tumor-stromal interface facilitates local invasion. *BMC Med* 2006; **4**: 38 [PMID: 17190588 DOI: 10.1186/1741-7015-4-38]

13 **Herrera J**, Henke CA, Bitterman PB. Extracellular matrix as a driver of progressive fibrosis. *J Clin Invest* 2018; **128**: 45-53 [PMID: 29293088 DOI: 10.1172/JCI93557]

14 **Kendall TJ**, Dolman GE, Duff CM, Paish EC, Zaitoun A, Irving W, Fallowfield JA, Guha IN. Hepatic elastin content is predictive of adverse outcome in advanced fibrotic liver disease. *Histopathology* 2018; **73**: 90-100 [PMID: 29464815 DOI: 10.1111/his.13499]

15 **Schmelzer CEH**, Heinz A, Troilo H, Lockhart-Cairns MP, Jowitt TA, Marchand MF, Bidault L, Bignon M, Hedtke T, Barret A, McConnell JC, Sherratt MJ, Germain S, Hulmes DJS, Baldock C, Muller L. Lysyl oxidase-like 2 (LOXL2)-mediated cross-linking of tropoelastin. *FASEB J* 2019; **33**: 5468-5481 [PMID: 30676771 DOI: 10.1096/fj.201801860RR]

16 **Wang TH**, Hsia SM, Shieh TM. Lysyl Oxidase and the Tumor Microenvironment. *Int J Mol Sci* 2016; **18** [PMID: 28036074 DOI: 10.3390/ijms18010062]

17 **Rachman-Tzemah C**, Zaffryar-Eilot S, Grossman M, Ribero D, Timaner M, Mäki JM, Myllyharju J, Bertolini F, Hershkovitz D, Sagi I, Hasson P, Shaked Y. Blocking Surgically Induced Lysyl Oxidase Activity Reduces the Risk of Lung Metastases. *Cell Rep* 2017; **19**: 774-784 [PMID: 28445728 DOI: 10.1016/j.celrep.2017.04.005]

18 **Cui X**, Wang G, Shen W, Huang Z, He H, Cui L. Lysyl oxidase-like 2 is highly expressed in colorectal cancer cells and promotes the development of colorectal cancer. *Oncol Rep* 2018; **40**: 932-942 [PMID: 29845296 DOI: 10.3892/or.2018.6452]

19 **Zhan P**, Lv XJ, Ji YN, Xie H, Yu LK. Increased lysyl oxidase-like 2 associates with a poor prognosis in non-small cell lung cancer. *Clin Respir J* 2018; **12**: 712-720 [PMID: 27860390 DOI: 10.1111/crj.12584]

20 **Choi J**, Chung T, Rhee H, Kim YJ, Jeon Y, Yoo JE, Noh S, Han DH, Park YN. Increased Expression of the Matrix-Modifying Enzyme Lysyl Oxidase-Like 2 in Aggressive Hepatocellular Carcinoma with Poor Prognosis. *Gut Liver* 2019; **13**: 83-92 [PMID: 29938458 DOI: 10.5009/gnl17569]

21 **Cui N**, Hu M, Khalil RA. Biochemical and Biological Attributes of Matrix Metalloproteinases. *Prog Mol Biol Transl Sci* 2017; **147**: 1-73 [PMID: 28413025 DOI: 10.1016/bs.pmbts.2017.02.005]

22 **Page-McCaw A**, Ewald AJ, Werb Z. Matrix metalloproteinases and the regulation of tissue remodelling. *Nat Rev Mol Cell Biol* 2007; **8**: 221-233 [PMID: 17318226 DOI: 10.1038/nrm2125]

23 **Li BH**, Zhao P, Liu SZ, Yu YM, Han M, Wen JK. Matrix metalloproteinase-2 and tissue inhibitor of metallo-proteinase-2 in colorectal carcinoma invasion and metastasis. *World J Gastroenterol* 2005; **11**: 3046-3050 [PMID: 15918187 DOI: 10.3748/wjg.v11.i20.3046]

24 **Gungor H**, Ilhan N, Eroksuz H. The effectiveness of cyclooxygenase-2 inhibitors and evaluation of angiogenesis in the model of experimental colorectal cancer. *Biomed Pharmacother* 2018; **102**: 221-229 [PMID: 29562216 DOI: 10.1016/j.biopha.2018.03.066]

25 **Xu GF**, Li PT, Wang XY, Jia X, Tian DL, Jiang LD, Yang JX. Dynamic changes in the expression of matrix metalloproteinases and their inhibitors, TIMPs, during hepatic fibrosis induced by alcohol in rats. *World J Gastroenterol* 2004; **10**: 3621-3627 [PMID: 15534918 DOI: 10.3748/wjg.v10.i24.3621]

26 **Li HX**, Tan JQ, Lv ZH, Liang YQ, Wen B. Colorectal Cancer Modeling and Difference Analysis in Cold and Heat Conditions. *Zhongguo Shiyan Fangji Xue Zazhi* 2020; **26**: 109-117 [DOI: 10.13422/j.cnki.syfjx.20201964]

27 **Jikihara H**, Qi G, Nozoe K, Hirokawa M, Sato H, Sugihara Y, Shimamoto F. Aged garlic extract inhibits 1,2-dimethylhydrazine-induced colon tumor development by suppressing cell proliferation. *Oncol Rep* 2015; **33**: 1131-1140 [PMID: 25573280 DOI: 10.3892/or.2014.3705]

28 **Liu Y**, Keikhosravi A, Mehta GS, Drifka CR, Eliceiri KW. Methods for Quantifying Fibrillar Collagen Alignment. *Methods Mol Biol* 2017; **1627**: 429-451 [PMID: 28836218 DOI: 10.1007/978-1-4939-7113-8_28]

29 **Keikhosravi A**, Bredfeldt JS, Sagar AK, Eliceiri KW. Second-harmonic generation imaging of cancer. *Methods Cell Biol* 2014; **123**: 531-546 [PMID: 24974046 DOI: 10.1016/B978-0-12-420138-5.00028-8]

30 **Schindelin J**, Arganda-Carreras I, Frise E, Kaynig V, Longair M, Pietzsch T, Preibisch S, Rueden C, Saalfeld S, Schmid B, Tinevez JY, White DJ, Hartenstein V, Eliceiri K, Tomancak P, Cardona A. Fiji: an open-source platform for biological-image analysis. *Nat Methods* 2012; **9**: 676-682 [PMID: 22743772 DOI: 10.1038/nmeth.2019]

31 **Walker C**, Mojares E, Del Río Hernández A. Role of Extracellular Matrix in Development and Cancer Progression. *Int J Mol Sci* 2018; **19** [PMID: 30287763 DOI: 10.3390/ijms19103028]

32 **Crotti S**, Piccoli M, Rizzolio F, Giordano A, Nitti D, Agostini M. Extracellular Matrix and Colorectal Cancer: How Surrounding Microenvironment Affects Cancer Cell Behavior? *J Cell Physiol* 2017; **232**: 967-975 [PMID: 27775168 DOI: 10.1002/jcp.25658]

33 **Mohan V**, Das A, Sagi I. Emerging roles of ECM remodeling processes in cancer. *Semin Cancer Biol* 2020; **62**: 192-200 [PMID: 31518697 DOI: 10.1016/j.semcancer.2019.09.004]

34 **Pickup MW**, Mouw JK, Weaver VM. The extracellular matrix modulates the hallmarks of cancer. *EMBO Rep* 2014; **15**: 1243-1253 [PMID: 25381661 DOI: 10.15252/embr.201439246]

35 **Cernaro V**, Lacquaniti A, Donato V, Fazio MR, Buemi A, Buemi M. Fibrosis, regeneration and cancer: what is the link? *Nephrol Dial Transplant* 2012; **27**: 21-27 [PMID: 22102616 DOI: 10.1093/ndt/gfr567]

36 **Sun Q**, Baues M, Klinkhammer BM, Ehling J, Djudjaj S, Drude NI, Daniel C, Amann K, Kramann R, Kim H, Saez-Rodriguez J, Weiskirchen R, Onthank DC, Botnar RM, Kiessling F, Floege J, Lammers T, Boor P. Elastin imaging enables noninvasive staging and treatment monitoring of kidney fibrosis. *Sci Transl Med* 2019; **11** [PMID: 30944168 DOI: 10.1126/scitranslmed.aat4865]

37 **Liang Y**, Lv Z, Huang G, Qin J, Li H, Nong F, Wen B. Prognostic significance of abnormal matrix collagen remodeling in colorectal cancer based on histologic and bioinformatics analysis. *Oncol Rep* 2020; **44**: 1671-1685 [PMID: 32945508 DOI: 10.3892/or.2020.7729]

38 **Pointer KB**, Clark PA, Schroeder AB, Salamat MS, Eliceiri KW, Kuo JS. Association of collagen architecture with glioblastoma patient survival. *J Neurosurg* 2017; **126**: 1812-1821 [PMID: 27588592 DOI: 10.3171/2016.6.JNS152797]

39 **Zhou ZH**, Ji CD, Xiao HL, Zhao HB, Cui YH, Bian XW. Reorganized Collagen in the Tumor Microenvironment of Gastric Cancer and Its Association with Prognosis. *J Cancer* 2017; **8**: 1466-1476 [PMID: 28638462 DOI: 10.7150/jca.18466]

40 **Nebuloni M**, Albarello L, Andolfo A, Magagnotti C, Genovese L, Locatelli I, Tonon G, Longhi E, Zerbi P, Allevi R, Podestà A, Puricelli L, Milani P, Soldarini A, Salonia A, Alfano M. Insight On Colorectal Carcinoma Infiltration by Studying Perilesional Extracellular Matrix. *Sci Rep* 2016; **6**: 22522 [PMID: 26940881 DOI: 10.1038/srep22522]

41 **Conklin MW**, Eickhoff JC, Riching KM, Pehlke CA, Eliceiri KW, Provenzano PP, Friedl A, Keely PJ. Aligned collagen is a prognostic signature for survival in human breast carcinoma. *Am J Pathol* 2011; **178**: 1221-1232 [PMID: 21356373 DOI: 10.1016/j.ajpath.2010.11.076]

42 **Lu P**, Weaver VM, Werb Z. The extracellular matrix: a dynamic niche in cancer progression. *J Cell Biol* 2012; **196**: 395-406 [PMID: 22351925 DOI: 10.1083/jcb.201102147]

43 **Zhang Z**, Wang Y, Zhang J, Zhong J, Yang R. COL1A1 promotes metastasis in colorectal cancer by regulating the WNT/PCP pathway. *Mol Med Rep* 2018; **17**: 5037-5042 [PMID: 29393423 DOI: 10.3892/mmr.2018.8533]

44 **Wu X**, Cai J, Zuo Z, Li J. Collagen facilitates the colorectal cancer stemness and metastasis through an integrin/PI3K/AKT/Snail signaling pathway. *Biomed Pharmacother* 2019; **114**: 108708 [PMID: 30913493 DOI: 10.1016/j.biopha.2019.108708]

45 **Bode MK**, Karttunen TJ, Mäkelä J, Risteli L, Risteli J. Type I and III collagens in human colon cancer and diverticulosis. *Scand J Gastroenterol* 2000; **35**: 747-752 [PMID: 10972180 DOI: 10.1080/003655200750023435]

46 **Wei B**, Zhou X, Liang C, Zheng X, Lei P, Fang J, Han X, Wang L, Qi C, Wei H. Human colorectal cancer progression correlates with LOX-induced ECM stiffening. *Int J Biol Sci* 2017; **13**: 1450-1457 [PMID: 29209148 DOI: 10.7150/ijbs.21230]

47 **Beam J**, Botta A, Ye J, Soliman H, Matier BJ, Forrest M, MacLeod KM, Ghosh S. Excess Linoleic Acid Increases Collagen I/III Ratio and "Stiffens" the Heart Muscle Following High Fat Diets. *J Biol Chem* 2015; **290**: 23371-23384 [PMID: 26240151 DOI: 10.1074/jbc.M115.682195]

48 **Gilkes DM**, Semenza GL, Wirtz D. Hypoxia and the extracellular matrix: drivers of tumour metastasis. *Nat Rev Cancer* 2014; **14**: 430-439 [PMID: 24827502 DOI: 10.1038/nrc3726]

49 **Piersma B**, Bank RA. Collagen cross-linking mediated by lysyl hydroxylase 2: an enzymatic battlefield to combat fibrosis. *Essays Biochem* 2019; **63**: 377-387 [PMID: 31324706 DOI: 10.1042/EBC20180051]

50 **Baker AM**, Bird D, Lang G, Cox TR, Erler JT. Lysyl oxidase enzymatic function increases stiffness to drive colorectal cancer progression through FAK. *Oncogene* 2013; **32**: 1863-1868 [PMID: 22641216 DOI: 10.1038/onc.2012.202]

51 **Hojilla CV**, Mohammed FF, Khokha R. Matrix metalloproteinases and their tissue inhibitors direct cell fate during cancer development. *Br J Cancer* 2003; **89**: 1817-1821 [PMID: 14612884 DOI: 10.1038/sj.bjc.6601327]

52 **Deryugina EI**, Quigley JP. Matrix metalloproteinases and tumor metastasis. *Cancer Metastasis Rev* 2006; **25**: 9-34 [PMID: 16680569 DOI: 10.1007/s10555-006-7886-9]

53 **Dittmore A**, Silver J, Sarkar SK, Marmer B, Goldberg GI, Neuman KC. Internal strain drives spontaneous periodic buckling in collagen and regulates remodeling. *Proc Natl Acad Sci USA* 2016; **113**: 8436-8441 [PMID: 27402741 DOI: 10.1073/pnas.1523228113]

54 **Erler JT**, Bennewith KL, Cox TR, Lang G, Bird D, Koong A, Le QT, Giaccia AJ. Hypoxia-induced lysyl oxidase is a critical mediator of bone marrow cell recruitment to form the premetastatic niche. *Cancer Cell* 2009; **15**: 35-44 [PMID: 19111879 DOI: 10.1016/j.ccr.2008.11.012]

55 **Afratis NA**, Klepfish M, Karamanos NK, Sagi I. The apparent competitive action of ECM proteases and cross-linking enzymes during fibrosis: Applications to drug discovery. *Adv Drug Deliv Rev* 2018; **129**: 4-15 [PMID: 29627371 DOI: 10.1016/j.addr.2018.03.004]

56 **Barker HE**, Chang J, Cox TR, Lang G, Bird D, Nicolau M, Evans HR, Gartland A, Erler JT. LOXL2-mediated matrix remodeling in metastasis and mammary gland involution. *Cancer Res* 2011; **71**: 1561-1572 [PMID: 21233336 DOI: 10.1158/0008-5472.CAN-10-2868]

57 **Bonnans C**, Chou J, Werb Z. Remodelling the extracellular matrix in development and disease. *Nat Rev Mol Cell Biol* 2014; **15**: 786-801 [PMID: 25415508 DOI: 10.1038/nrm3904]

58 **Brauchle E**, Kasper J, Daum R, Schierbaum N, Falch C, Kirschniak A, Schäffer TE, Schenke-Layland K. Biomechanical and biomolecular characterization of extracellular matrix structures in human colon carcinomas. *Matrix Biol* 2018; **68-69**: 180-193 [PMID: 29605717 DOI: 10.1016/j.matbio.2018.03.016]

World Journal of Gastroenterology

Submit a Manuscript: https://www.f6publishing.com

World J Gastroenterol 2021 October 21; 27(39): 6631-6646

DOI: 10.3748/wjg.v27.i39.6631

ISSN 1007-9327 (print) ISSN 2219-2840 (online)

ORIGINAL ARTICLE

Basic Study

Detection and analysis of common pathogenic germline mutations in Peutz-Jeghers syndrome

Guo-Li Gu, Zhi Zhang, Yu-Hui Zhang, Peng-Fei Yu, Zhi-Wei Dong, Hai-Rui Yang, Ying Yuan

ORCID number: Guo-Li Gu 0000-0002-9998-047X; Zhi Zhang 0000-0001-5870-1940; Yu-Hui Zhang 0000-0002-3224-9017; Peng-Fei Yu 0000-0002-0528-1839; Zhi-Wei Dong 0000-0102-0548-1859; Hai-Rui Yang 0020-0202-0228-1829; Ying Yuan 0000-0002-3922-9553.

Author contributions: Gu GL and Zhang Z contributed equally to this study; Gu GL and Yuan Y designed the research; Gu GL, Zhang Z, Yang HR, Yu PF, Dong ZW and Zhang YH conducted experiments and analyzed the clinical data; Gu GL and Zhang Z wrote the manuscript; and Yuan Y revised the manuscript.

Supported by Beijing Capital Medical Development Research Fund, No. Shoufa2020-2-5122.

Institutional review board statement: The study was reviewed and approved by the Ethics Committee of the Air Force Medical Center (Approval No. 2020-105-PJ01), and the Second Affiliated Hospital of Zhejiang University School of Medicine (Approval No. 2017-066).

Conflict-of-interest statement: The authors declare that they have no conflicting interests.

Data sharing statement: All

Guo-Li Gu, Zhi Zhang, Yu-Hui Zhang, Peng-Fei Yu, Zhi-Wei Dong, Hai-Rui Yang, Department of General Surgery, Air Force Medical Center, Chinese People's Liberation Army, Beijing 100142, China

Yu-Hui Zhang, Graduate School, Hebei North University, Zhangjiakou 075000, Hebei Province, China

Ying Yuan, Department of Medical Oncology, Cancer Institute, The Second Affiliated Hospital, Zhejiang University School of Medicine, Hangzhou 310009, Zhejiang Province, China

Corresponding author: Ying Yuan, MD, PhD, Chief Doctor, Professor, Department of Medical Oncology, Cancer Institute, The Second Affiliated Hospital, Zhejiang University School of Medicine, No. 88 Jiefang Road, Hangzhou 310009, Zhejiang Province, China.
yuanying1999@zju.edu.cn

Abstract

BACKGROUND

Different types of pathogenic mutations may produce different clinical phenotypes, but a correlation between Peutz-Jeghers syndrome (PJS) genotype and clinical phenotype has not been found. Not all patients with PJS have detectable mutations of the *STK11/LKB1* gene, what is the genetic basis of clinical phenotypic heterogeneity of PJS? Do PJS cases without *STK11/LKB1* mutations have other pathogenic genes? Those are clinical problems that perplex doctors.

AIM

The aim was to investigate the specific gene mutation of PJS, and the correlation between the genotype and clinical phenotype of PJS.

METHODS

A total of 24 patients with PJS admitted to the Air Force Medical Center, PLA (formerly the Air Force General Hospital, PLA) from November 1994 to January 2020 were randomly selected for inclusion in the study. One hundred thirty-nine common hereditary tumor-related genes including *STK11/LKB1* were screened and analyzed for pathogenic germline mutations by high-throughput next-generation sequencing (NGS). The mutation status of the genes and their relationship with clinical phenotypes of PJS were explored.

RESULTS

Twenty of the 24 PJS patients in this group (83.3%) had *STK11/LKB1* gene mutations, 90% of which were pathogenic mutations, and ten had new mutation sites. Pathogenic mutations in exon 7 of *STK11/LKB1* gene were significantly lower than in other exons. Truncation mutations are more common in exons 1 and 4 of *STK11/LKB1*, and their pathogenicity was significantly higher than that of missense mutations. We also found *SLX4* gene mutations in PJS patients.

CONCLUSION

PJS has a relatively complicated genetic background. Changes in the sites responsible for coding functional proteins in exon 1 and exon 4 of *STK11/LKB1* may be one of the main causes of PJS. Mutation of the *SLX4* gene may be a cause of genetic heterogeneity in PJS.

Key Words: Peutz-Jeghers syndrome; Genotype; Phenotype; STK11; Mutation

©The Author(s) 2021. Published by Baishideng Publishing Group Inc. All rights reserved.

Core Tip: It is currently believed that Peutz-Jeghers syndrome (PJS) is an autosomal dominant genetic disease predominantly caused by germline mutations in the *STK11/LKB1* gene. No correlation of the PJS genotype and clinical phenotype has been found so far. The correlation of genotype and clinical phenotype and exploration of the internal molecular mechanism of different clinical phenotypes were studied in 24 treated PJS patients with different clinical phenotypes. Peripheral venous blood or normal tissue adjacent to polyps were collected for high-throughput next-generation sequencing (NGS) of 139 hereditary colorectal tumor-related genes including *STK11/LKB1*. A newly discovered likely pathogenic gene (*SLX4*) provided new data explaining the genetic heterogeneity of PJS.

Citation: Gu GL, Zhang Z, Zhang YH, Yu PF, Dong ZW, Yang HR, Yuan Y. Detection and analysis of common pathogenic germline mutations in Peutz-Jeghers syndrome. *World J Gastroenterol* 2021; 27(39): 6631-6646
URL: https://www.wjgnet.com/1007-9327/full/v27/i39/6631.htm
DOI: https://dx.doi.org/10.3748/wjg.v27.i39.6631

INTRODUCTION

It is currently believed that Peutz-Jeghers syndrome (PJS) is an autosomal dominant genetic disease predominantly caused by germline mutations in the *STK11/LKB1* gene. PJS is characterized by multiple hamartoma polyps in the gastrointestinal tract, pigmentation at specific sites, and hereditary tumors[1-4]. Pathogenic mutations of *STK11/LKB1* lead to inactivation of its expression product and loss of inhibition of mammalian target of rapamycin (mTOR) activity, which leads to abnormal activation of the LKB1/mTOR signal pathway and the occurrence of black spots on the skin and gastrointestinal hamartoma polyps[5]. More than 400 different pathogenic *STK11/LKB1* gene mutations are included in the Human Gene Mutation Database (HGMD), most of which are microminiature. Different types of pathogenic mutations may produce different clinical phenotypes, but no correlations of PJS genotype and clinical phenotype has been found so far[6], Not all patients with PJS have detectable mutations in the *STK11/LKB1* gene. What is the genetic basis of clinical phenotypic heterogeneity in PJS? Do PJS patients without *STK11/LKB1* mutations have other pathogenic genes? These are clinical problems that perplex doctors[7,8]. We enrolled 24 patients treated for PJS. Peripheral venous blood and normal tissue adjacent to polyps were collected for high-throughput next-generation sequencing (NGS) of 139 hereditary colorectal tumor-related genes including *STK11/LKB1* to study the correlation between genotype and clinical phenotype of PJS and explore the internal molecular mechanism of the clinical phenotypes.

patients (legal guardians of minors) understood the process and purpose of this study and signed an informed consent form. In the process of sample collection, follow the principles of informed consent in the Declaration of Helsinki, the Universal Declaration of Human Genome and Human Rights, and the Declaration of the Human Genome Ethics Committee on DNA Sampling, Control, and Acquisition. No additional data are available.

Open-Access: This article is an open-access article that was selected by an in-house editor and fully peer-reviewed by external reviewers. It is distributed in accordance with the Creative Commons Attribution NonCommercial (CC BY-NC 4.0) license, which permits others to distribute, remix, adapt, build upon this work non-commercially, and license their derivative works on different terms, provided the original work is properly cited and the use is non-commercial. See: http://creativecommons.org/licenses/by-nc/4.0/

Manuscript source: Unsolicited manuscript

Specialty type: Gastroenterology and hepatology

Country/Territory of origin: China

Peer-review report's scientific quality classification

Grade A (Excellent): A
Grade B (Very good): B, B
Grade C (Good): 0
Grade D (Fair): 0
Grade E (Poor): 0

Received: April 15, 2021
Peer-review started: April 15, 2021
First decision: May 24, 2021
Revised: May 31, 2021
Accepted: August 11, 2021
Article in press: August 11, 2021
Published online: October 21, 2021

P-Reviewer: Auranen A, Jelsig AM, Winship I
S-Editor: Ma YJ
L-Editor: Filipodia
P-Editor: Xing YX

MATERIALS AND METHODS

Study participants

Patients with PJS, from 18-70 years of age, met the clinical diagnostic criteria of PJs, had complete clinicopathological data, well preserved specimens, were eligible for inclusion. All participants gave their signed informed consent. Patients who could not provide experimental specimens or did not agree to participate in the study were excluded. Twenty-four PJS patients admitted to the Air Force Medical Center (formerly the Air Force General Hospital) from November 1994 to January 2020 met the above criteria and were enrolled. Their clinical information is shown in Table 1. Twenty-three were inpatients, one was an outpatient, 11 had family histories, and 12 had early onset pigment spots that had appeared when they were younger than 3 years of age. All patients met the PJS diagnostic criteria recommended by the National Comprehensive Cancer Network (NCCN)[9]. The experimental samples included 5 mL peripheral venous blood samples collected from 19 patients into tubes containing EDTA-2Na, and paraffin-embedded normal tissue surgically removed from areas adjacent to polyps in five patients. The study was reviewed and approved by the Ethics Committee of the Air Force Medical Center and the Second Affiliated Hospital of Zhejiang University School of Medicine. All patients or the legal guardians of minors, understood the process and purpose of this study and signed an informed consent form. Sample collection followed the ethical principles of the Declaration of Helsinki, the Universal Declaration of Human Genome and Human Rights, and the Declaration of the Human Genome Ethics Committee on DNA Sampling, Control, and Acquisition.

Methods

DNA was extracted from peripheral venous blood samples with TGuide Blood Genomic DNA Kits (CHI-TIANGEN) following the manufacturer's instructions. DNA was extracted from paraffin-embedded tissue specimens with QIAamp DNA FFPE micro sample tissue kits (GER-QIAGEN). Nucleic acids were broken into small, random 150-200 bp fragments by ultrasonic fragmentation (Covaris S220) and separated and evaluated with a Tapestation 2200 electrophoresis working platform (Agilent) to check whether the fragments met the requirements for library construction. A standard gene library was constructed using KAPA HyperPlus Kit (Illumina). A panel of 139 common tumor genetic susceptibility genes including colorectal cancer (Table 2) was selected and provided by Genetron Health Co.(Beijing). The specific gene capture probe was hybridized with the library in the environment of a hybridization buffer, and purified by the magnetic bead method. High-throughput NGS was performed with a Novaseq 6000 sequencer (Illumina, United States). Trimmomatic (version 0.33) was used to crop and filter the original data, which was stored in FastQ format, after sequencing. The reads at the end of each pair were aligned with the human reference sequence GRCh37 (hg19) using the BWA-MEM algorithm (BWA version 0.7.10-r789) and the default parameters. The Picard tool (version 1.103 http://broadinstitute.github.io/picard/) was used to delete duplicate readings, and GATK (version 3.1-0-g72492bb) was used to realign the sequences around the known insertion loss at the single sample level and to recalibrate the base quality. Integrative Genomics Viewer version 2.3.34 (https://software.broadinstitute.org/software/igv/) was used to check the mutations in the coding region.

The Chinese (1000 CN), general population (1000 MAF). and dbSNP (https://www.ncbi.nlm.nih.gov/) at 1000 Genome Project (http://ftp.ncbi.nih.gov/) Snip/), ESP6500 AA/EA (NHLBI GO Exome Sequencing Project https://evs gs.washington.edu/EVS/), ExAC MAF (The Exome Aggregation Consortium) and other population databases were searched for the mutation frequency of this gene. The location of genes with a mutation frequency < 0.01 in the HGMD database (HGMD-PUBLIC version 20152) were used for pathogenicity analysis.

The diseases that the variant gene was related to were searched in the OMIM disease database (https://omim.org/) by ClinVar (https://www.ncbi.nlm.nih.gov/clinvar/). HGMD https://www.hgmd.cf.ac.uk) retrieved the description of the mutation. SIFT[10] (http://sift.jcvi.org), PolyPhen2[11] (http://genetics.bwh.harvard.edu/pph2), and Mutation Assessor (http://mutationassessor.org) make conservative predictions of amino acid sequences. The results were used to evaluate the pathogenicity of the mutations[12,13].

SPSS 24.0 was used for statistical analysis of the acquired data. Qualitative results were reported as numbers and percentages. The chi-square test or Fisher's exact probability method was used for between-group comparisons. $P < 0.05$ was considered

Table 1 Clinical characteristics of 24 enrolled Peutz-Jeghers syndrome patients

No.	Gender	Specimen	Time since onset of pigment spots (yr)	Early or late onset	Family history (members)	Number of hospitalizations	Number of operations	Stomach and enteroscopy times	Age at initial diagnosis of polyps	Age at first treatment	Polyp pathology	Load of Gastric polyps/Max. diameter (mm)	Load of small intestinal polyps/Max. diameter (mm)	Load of colorectal polyps/Max. diameter (mm)
1	Male	Paraffin section	20	Late	No	2	1	6	20	15	1	/	20/30	/
2	Male	Paraffin section	6	Late	Yes (mother and sister)	1	2	3	9	9	1	2/16	20/40	1/8
3	Female	Paraffin section	4	Late	No	2	1	4	9	9	1	/	3/28	/
4	Male	Paraffin section	5	Late	No	1	2	1	21	21	3	20/4	6/50	/
5	Male	Paraffin section	1	Early	Yes (mother)	4	2	1	4	4	1	2/12	2/60	/
6	Female	Blood	5	Late	Yes (father)	1	0	1	29	29	1	/	/	/
7	Female	Blood	1	Early	Yes (father and sister)	4	0	11	7	7	1	1/8	2/30	3/40
8	Male	Blood	0	Early	Yes (father and sister)	1	0	1	10	10	1	/	10/50	/
9	Male	Blood	6	Late	Yes (mother and grandmother)	4	1	7	6	7	1	5/12	2/30	3/35
10	Female	Blood	2	Early	No	1	0	3	7	7	1	2/15	/	1/30
11	Male	Blood	3	Late	No	1	4	0	22	32	1	/	1/30	/
12	Male	Blood	2	Early	No	2	1	10	4	4	1	1/6	2/50	/
13	Male	Blood	2	Early	No	1	2	1	25	24	1	/	10/20	/
14	Female	Blood	3	Late	No	8	2	8	6	6	1	1/10	8/80	1/20
15	Male	Blood	5	Late	No	1	2	3	20	19	2	1/6	1/80	2/30
16	Male	Blood	1	Early	Yes (mother)	3	0	2	10	9	1	/	1/25	/
17	Male	Blood	1	Early	No	3	1	4	6	6	1	8/40	10/30	/
18	Female	Blood	1	Early	No	6	2	9	11	10	1	1/15	3/35	1/50
19	Female	Blood	3	Late	Yes (mother)	2	0	4	15	15	1	1/12	2/12	1/25

20	Female	Blood	3	Late	Yes (father, uncle, and grandmother)	2	2	5	7	7	1	/	18/50	/
21	Female	Blood	1	Early	Yes (mother, uncle, and aunt)	2	0	4	31	31	1	/	10/50	10/40
22	Female	Blood	2	Early	Yes (father and brother)	1	0	1	6	6	1	10/10	8/50	/
23	Male	Blood	5	Late	No	1	0	2	11	11	1	1/30	5/70	1/30
24	Male	Blood	2	Early	No	1	0	4	5	4	1	10/15	/	/

(1) *STK11* mutation, *SLX4* mutation, other gene mutation groups: 0: None 1: Yes; (2) Early onset: Pigment spots appeared at < 3 years of age; Late onset: Pigment spots appeared at ≥ 3 years of age; (3) Polyp pathology: 1 hamartoma, 2 hamartoma with adenoma, 3 hamartoma with cancer; (4) Polyp load is the number of polyps, the largest diameter unit is mm; and (5) 6 was an outpatient, the results of previous endoscopy are unknown.

statistically significant.

RESULTS

STK11/LKB1 gene detection results and pathogenicity analysis

Twenty of the 24 PJS patients (83.3%) in this group had *STK11/LKB1* gene mutations (Table 3). All were heterozygous and ten were newly discovered mutation sites not included in the dbSNP database. There were eight frameshift mutations, five splice-site mutations, four missense mutations and three nonsense mutations. The mutations occurred in eight of the ten exons in the *STK11/LKB1* gene, mutations in exons 1 and 4 and 4 each in exon 7, two in each exons 5 and 8, and one in exons 2, 3, and 6. Frameshift mutations, splice-site mutations, and nonsense mutations were all related to pathogenicity. Frameshift mutations accounted for 62.5% (5/8) that were clearly pathogenic, and 37.5% (3/8) that might cause disease. Splice-site mutations accounted for 40% (2/5) that are clearly pathogenic, and 60% (3/5) that might cause disease. All three nonsense mutations were clearly pathogenic, and the missense mutations were related to and might cause disease. Sites of unclear clinical significance accounted for 50% (2/4); of the 11 truncated mutations, eight cases were clearly pathogenic and three were likely to cause disease. The pathogenicity of STK11 gene mutations in exon 7 was significantly lower than that of other exons (P = 0.000). Truncation mutations were significantly more pathogenic than missense mutations (P = 0.012). The prediction results of bioinformatics tools for missense mutations are shown in Table 4, and the relevant database records and the pathogenicity judgment of all mutations are shown in Table 5.

Table 2 Cancer genetic susceptibility 139 gene panel coverage

AIP	*CYLD*	*FANCL*	*MLH3*	*PRSS1*	*SMARCA4*
ALK	*DDB2*	*FANCM*	*MRE11A*	*PTCH1*	*SMARCB1*
APC	*DICER1*	*FAS*	*MSH2*	*PTCH2*	*SMARCE1*
ATM	*DIS3L2*	*FH*	*MSH6*	*PTEN*	*SOS1*
ATR	*EGFR*	*FLCN*	*MTAP*	*PTPN11*	*STAT3*
AXIN2	*ELANE*	*GALNT12*	*MTUS1*	*RAD50*	*STK11*
BAP1	*EPCAM*	*GATA2*	*MUTYH*	*RAD51B*	*SUFU*
BARD1	*ERCC1*	*GEN1*	*NBN*	*RAD51C*	*TERT*
BLM	*ERCC2*	*GJB2*	*NF1*	*RAD51D*	*TGFBR1*
BMPR1A	*ERCC3*	*GPC3*	*NF2*	*RB1*	*TMEM127*
BRCA1	*ERCC4*	*GREM1*	*NSD1*	*RECQL*	*TP53*
BRCA2	*ERCC5*	*HMBS*	*NTRK1*	*RECQL4*	*TSC1*
BRIP1	*EXT1*	*HNF1A*	*PALB2*	*RET*	*TSC2*
BUB1B	*EXT2*	*HOXB13*	*PALLD*	*RHBDF2*	*UROD*
CBL	*EZH2*	*HRAS*	*PDGFRA*	*RUNX1*	*USHBP1*
CDC73	*FANCA*	*KIT*	*PHOX2B*	*SBDS*	*VEGFA*
CDH1	*FANCB*	*LASP1*	*PMS1*	*SDHA*	*VHL*
CDK4	*FANCC*	*MAX*	*PMS2*	*SDHAF2*	*WRN*
CDKN1B	*FANCD2*	*MC1R*	*POLD1*	*SDHB*	*WT1*
CDKN1C	*FANCE*	*MEN1*	*POLE*	*SDHC*	*XPA*
CDKN2A	*FANCF*	*MET*	*POLH*	*SDHD*	*XPC*
CEBPA	*FANCG*	*MTTF*	*PPM1D*	*SLX4*	*XRCC2*
CHEK1	*FANCI*	*MLH1*	*PRKAR1A*	*SMAD4*	*ZMAT3*
CHEK2					

Considering that the type of specimen may impact on the detection rate of *STK11/LKB1* gene mutations, we analyzed the paraffin-embedded tissue and blood samples separately. The detection rate of *STK11/LKB1* mutations in 60 patients with paraffin samples was 60% (3/5), slightly less than the 89.4% (17/19) of the blood samples from 19 patients. The difference in mutation detection rate of this gene in the two types of sample was not statistically different (P = 0.116).

SLX4 gene detection results and pathogenicity analysis

SLX4 gene mutation (Table 6) was detected in 5 PJS patient samples in this group, with a total detection rate of 20.83% (5/24), all of which were heterozygous mutations. The mutation occurred in 4 of 15 exons of *SLX4* gene. Mutation types include: 3 missense mutations, one splice-site mutation, and one non-frameshift mutation. No truncation mutation was found. The *SLX4* gene is a tumor suppressor gene, and there are three newly discovered mutation sites. The prediction results of three cases of missense mutations by bioinformatics tools (Table 7), the collection of relevant databases and the judgment of the pathogenicity of all mutations (Table 8) are as follows.

Other gene detection results and pathogenicity analysis

A total of 55 mutations of 46 genes other than *STK11/LKB1* and *SLX4* were detected in 21 cases (Table 9), f a detection rate of 87.5% (21/24). Twenty-three of the genes were related to cancer suppression and had 32 different mutation sites. Two mismatch repair *MMR* genes were detected, *MSH2*, *MSH6*. Except for a frameshift mutation (frameshift deletion) in the *BRIP1* gene detected in one patient (No. 18), the rest were missense mutations (Table 10).

Table 3 Characteristics of *STK11/LKB1* gene mutations

No.	Mutation type	dbSNP RS	Mutation site	Amino acid change	Exon	Variant type
2	Frameshift	rs372511774	c.357delC	p.N119Kfs	2|10	SNV
4	Splice-site variant	rs398123406	c.921-1G>A	/	8|10	SNP
5	Frameshift	rs1060499961	c.131dupA	p.L45Afs	1|10	INS
6	Missense	/	c.869T>C	p.L290P	7|10	SNP
7	Nonsense	/	c.658C>T	p.Q220X	5|10	SNP
8	Frameshift	/	c.548del	p.L183Rfs	4|10	DEL
9	Splice-site variant	rs398123406	c.921-1G>C	/	8|10	SNP
10	Frameshift	/	c.471_472del	p.F157Lfs	4|10	DEL
12	Frameshift	/	c.180del	p.Y60X	1|10	DEL
13	Missense	/	c.869T>A	p.L290H	7|10	SNP
14	Splice-site variant	/	c.598-2A>G	/	5|10	SNP
15	Missense	rs121913315	c.580G>A	p.D194N	4|10	SNP
16	Missense	rs730881978	c.890G>A	p.R297K	7|10	SNP
17	Frameshift	/	c.577_578del	p.S193Rfs	4|10	DEL
18	Splice-site variant	/	c.863-2A>G	/	7|10	SNP
19	Splice-site variant	rs1555735080	c.290+1G>T	/	1|10	SNP
20	Nonsense	/	c.179dup	p.Y60X	1|10	INS
21	Frameshift	rs587782584	c.842dup	p.L282Afs	6|10	INS
23	Frameshift	rs786203886	c.228dup	p.V77Rfs	1|10	INS
24	Nonsense	rs730881970	c.409C>T	p.Q137X	3|10	SNP

DEL; Deletion; INS: Insertion; SNP: Single nucleotide polymorphism; SNV: Single nucleotide variation.

Table 4 Prediction of protein function change caused by *STK11/LKB1* mutation

No.	PolyPhen		Mutation Assessor		SIFT	
	Score	Prediction	Score	Prediction	Score	Prediction
6	1	Probably damaging	0.98351; 4.21	High	0	Deleterious
13	1	Probably damaging	0.99415; 4.555	High	0	Deleterious
15	1	Probably damaging	0.98178; 4.165	High	0	Deleterious
16	1	Probably damaging	0.98818; 4.34	High	0.01	Deleterious
23	0.022	Benign	0.56769; 1.78	Low	0.26	Tolerated

STK11/LKB1 genotype-phenotype correlation analysis

Investigation of the relationship between genotype and family history found that the proportion of patients with truncated mutations was slightly higher in those with a family history than in those without a history (60% *vs* 50%). The proportion of splice-site mutations was lower in those with a family history (20% *vs* 30%), and the proportion of nonsense mutations was higher in patients with a family history (20.0% *vs* 11.1%). The proportions of missense mutations were the same (20% *vs* 20%), and the proportion of frameshift mutations were also equal (40% *vs* 10%). There were no significant difference between-group differences in $P_{truncation\ mutation} = 0.653$, $P_{splice\ site\ mutation} = 0.606$, $P_{nonsense\ mutation} = 0.371$, $P_{missense\ mutation} = 1.000$, and $P_{frameshift\ mutation} = 1.000$.

Evaluation of the relationship between genotype and early onset/late onset found that the proportion of truncated mutations in patients with early onset was higher than that in patients with late onset (72.7% *vs* 33.3%). In patients with early onset, the

Table 5 *STK11/LKB1* mutation-related databases and pathogenicity analysis

No.	cDNA/protein	Disease database			Pathogenic judgment
		HGMD	ClinVar	OMIM	
2	p.N119Kfs	/	(1/1) pathogenic	/	Pathogenic
4	c.921-1G>A	√	/	PJS	Pathogenic
5	p.L45Afs	/	/	/	Pathogenic
6	p.L290P	√	(1/1) pathogenic	PJS	Clinical significance unknown
7	p.Q220X	/	(3/3) pathogenic	PJS	Pathogenic
8	p.L183Rfs	/	/	PJS	Pathogenic
9	c.921-1G>C	√	(2/2) pathogenic	PJS	Pathogenic
10	p.F157Lfs	√	/	PJS	Likely pathogenic
12	p.Y60X	√	√	PJS	Pathogenic
13	p.L290H	/	/	PJS	Clinical significance unknown
14	c.598-2A>G	/	(1/1) pathogenic	PJS	Likely pathogenic
15	p.D194N	√	(4/6) likely pathogenic; (2/6) pathogenic	PJS	Likely pathogenic
16	p.R297K	√	(1/2) pathogenic; (1/2) unknown	PJS	Likely pathogenic
17	p.S193Rfs	/	/	PJS	Likely pathogenic
18	c.863-2A>G	/	(1/1) pathogenic	PJS	Likely pathogenic
19	c.290+1G>T	Pathogenic	/	PJS	Likely pathogenic
20	p.Y60X	Pathogenic	(2/2) pathogenic	PJS	Pathogenic
21	p.L282Afs	Pathogenic	(1/1) pathogenic	PJS	Pathogenic
23	p.V77Rfs	/	/	PJS	Likely pathogenic
24	p.Q137X	Pathogenic	(1/1) pathogenic	PJS	Pathogenic

(4/6) likely pathogenic: A total of six institutions have judged this mutation, four of which are judged as probably pathogenic, the same below. PJS: Peutz-Jeghers syndrome.

Table 6 Characteristics of *SLX4* gene mutations

No.	Mutation type	dbSNP RS	Mutation site	Amino acid changes	Exon	Variant type
1	Missense	rs551385115	c.5072A>G	p.N1691S	14|15	SNP
2	Splice-site variant	/	c.1683+1G>A	splice	7|15	SNP
3	Missense	rs774243118	c.2990C>T	p.P997L	12|15	SNP
18	Missense	/	c.2425G>C	p.E809Q	12|15	SNP
22	Non-frameshift	/	c.568_570del	p.P190del	3|15	DEL

DEL: Deletion; SNP: Single nucleotide polymorphism.

percentages of frameshift mutations (54.5% *vs* 22.2%) and sense mutations (18.2% *vs* 11.1%) were higher than those in late onset patients. The percentages of splice-site mutations (9% *vs* 44.4%) and missense mutations were lower (18.2% *vs* 22.2%). There were no significant between-group differences in $P_{truncation\ mutation} = 0.078$, $P_{frameshift\ mutation} = 0.142$, $P_{nonsense\ mutation} = 0.660$, $P_{splice\ site\ mutation} = 0.069$, $P_{missense\ mutation} = 0.822$.

DISCUSSION

The *STK11/LKB1* gene located on chromosome 19p13.3 is considered to be a tumor

Table 7 Prediction of protein function change caused by *SLX4* mutation

No.	PolyPhen		Mutation assessor		SIFT	
	Score	Prediction	Score	Prediction	Score	Prediction
1	0	Benign	0.08118; 0	Neutral	0.16	Tolerated
3	0.004	Benign	0.05510; -0.035	Neutral	1	Tolerated /
18	0.341	Benign	0.59436; 1.845	Low	0.04	Deleterious

Table 8 *SLX4* mutation-related databases and pathogenicity analysis

No.	cDNA/Protein	Disease database			Pathogenic judgment
		HGMD	ClinVar	OMIM	
1	p.N1691S	/	(1/1)Uncertain Significance	BTB/POZ domain containing 12*SLX4* structure-specific	Clinical significance unknown
2	c.1683+1G>A	/	/	BTB/POZ domain containing 12\SLX4 structure-specific	Likely pathogenic
3	p.P997L	/	/	BTB/POZ domain containing 12\SLX4 structure-specific	Clinical significance unknown
18	p.E809Q	√	/	BTB (POZ) domain containing 12\SLX4 structure-specific	Clinical significance unknown
22	p.P190del	/	/	BTB (POZ) domain containing 12\SLX4 structure-specific	Clinical significance unknown

suppressor gene[14] and is widely expressed in human tissues. Pathogenic mutation of *STK11* can inactivate its expressed product, which results in the loss of its inhibitory effect on the activity of mammalian target of rapamycin (mTOR), leading to the occurrence of skin and mucous membrane black spots and gastrointestinal polyps[5]. Methylation of the *STK11/LKB1* gene promoter has an important role in the process of malignant transformation of gastrointestinal polyps[15]. At present, the comprehensive mutation rate of *STK11/LKB1* gene in PJS patients detected by multiple sequencing methods is about 80%-94%[8,15,16]. The detection rate of *STK11/LKB1* gene mutation in PJS patients in this study was 83.3% (20/24), 90% of which are related to pathogenicity. Analysis of the pathogenicity of all the detected mutation sites included in the Mendelian Inheritance in Man (OMIM) database found that about 90% of the *STK11/LKB1* mutations were related to PJS. Except for the *STK11/LKB1* gene and one case of *SLX4* gene mutation, no other gene mutations related to the disease or the possibility of disease were found.

Research on whether there is a correlation between the PJS genotype and clinical phenotype is ongoing. Although the correlation is currently unclear[6,17], some studies have reported positive results. For example, Forcet *et al*[18] reported that patients often present with only black spots and without gastrointestinal polyps when heterozygous mutations occur in exon 8 of the *STK11* gene. Amos *et al*[19] found that PJS patients with missense mutations had a first episode of polypectomy and appearance of other symptoms significantly later than those with truncated mutations or no detectable mutations. In a study including 116 PJS patients in 52 families, Wang *et al*[20] found that nearly 30% of the mutations occurred in exon 7, and some of those mutations affected the protein Kinase domain XI region, which is associated with 90% of cases with gastrointestinal polyp dysplasia. An analysis of the start region of the *STK11/LKB1* coding sequence by Hearle *et al*[21] found that a change in promoter sequence was unlikely to be the cause of PJS. In this study the time that dark spots first appeared, which is a relatively objective indicator, was the basis of clinical classification, and was used to determine whether there was a correlation between the appearance of the spots and any of the genotypes. Spots that appear in early childhood will be noticed. On the other hand, unless there are obvious clinical symptoms, it is extremely difficult to know about gastrointestinal polyps that appear in early childhood. Also, PJS is an autosomal dominant genetic disease and does not completely follow Mendelian inheritance[6]. In clinical practice, it is often found that neither parent has a family history but their child has the disease. This is difficult to fully explain if the disease is caused by a single gene. Therefore, whether the patient has a family history was also included in the basis of clinical classification.

This study did not found that patients with different clinical phenotypes (early onset/late onset and with or without a family history) had statistically significant differences in their *STK11/LKB1* gene mutations and loci. However, we found that the

Table 9 Other gene mutations and inclusion in relevant database

No.	Gene	Type	Mutation site	Amino acid changes	Exon	Disease database		
						HGMD	ClinVar	OMIM
1	*BARD1*	TSG	c.556A>G	p.S186G	4|11	/	(6/6)Uncertain Significance	/
	EGFR	/	c.61G>A	p.A21T	1|28	/	/	Epidermal growth factor receptor
2	*GEN1*	/	c.181T>A	p.S61T	3|14	/	/	Gen endonuclease homolog 1
	BRCA1	TSG	c.2387C>T	p.T796I	10|23	/	(8/8)Uncertain Significance	/
4	*NTRK1*	/	c.1604A>G	p.E535G	13|17	/	/	/
	PDGFRA	/	c.1423G>A	p.E475K	10|23	/	/	/
	TSC2	TSG	c.521C>T	p.S174L	6|42	/	(2/2)Uncertain Significance	/
	MSH6	/	c.1063G>A	p.G355S	4|10		(4/7)Uncertain Significance(3/7)likely benign	/
5	*EGFR*	/	c.3040G>A	p.D1014N	25|28	/	/	Epidermal growth factor receptor
	MTUS1	TSG	c.2282G>A	p.S761N	3|15	/	/	Mitochondrial tumor suppressor 1
	PTCH1	TSG	c.2222C>T	p.A741V	14|24	/	(3/4)benign, (1/4)likely benign	/
6	*SDHA*	TSG	c.715A>G	p.I239V	6|15	√	(2/2)Uncertain significance	/
	MTUS1	TSG	c.1866C>G	p.N622K	2|15	√	√	Mitochondrial tumor suppressor 1
7	*RECQL4*	/	c.1048A>G	p.R350G	5|21	/	(1/1)Uncertain Significance	/
	RECQL4	/	c.236G>A	p.G79E	4|21	/	/	/
8	*ATM*	TSG	c.6503C>T	p.S2168L	45|63	/	(7/7)Uncertain Significance	Ataxia telangiectasia mutated
10	*TSC2*	TSG	c.3475C>T	p.R1159W	30|42	/	(2/4)benign, (2/4)likely benign	/
	FANCG	TSG	c.458C>G	p.A153G	4|14	/	(1/1)Uncertain Significance	/
11	*SBDS*	/	c.98A>G	p.K33R	1|5	/	/	/
12	*VHL*	TSG	c.134C>T	p.P45L	1|3	/	/	Von Hippel-Lindau syndrome
	FANCA	/	c.3031C>T	p.R1011C	31|43	/	(1/1)likely benign	/
	TP53	TSG	c.620A>G	p.D207G	6|11	√	/	/
13	*FANCA*	/	c.2944A>G	p.T982A	30|43	/	(2/2)Uncertain Significance	/
14	*PALLD*	/	c.1011C>A	p.D337E	3|21	/	/	/
	MLH3	TSG	c.1519A>G	p.M507V	2|13	/	(1/1)Uncertain Significance	Mutl (E. Coli) homolog 3
	SMARCA4	TSG	c.3791C>T	p.T1264M	28|36	/	(3/3)Uncertain Significance	/
	NF1	TSG	c.3940T>C	p.W1314R	29|58	/	(1/1)Uncertain Significance	/
15	*PTCH1*	TSG	c.2222C>T	p.A741V	14|24	/	(1/1)likely benign	/
	GALNT12	/	c.148C>A	p.P50T	1|10	/	/	/
16	*ATR*	TSG	c.325C>T	p.R109W	4|47	/	(1/1)Uncertain Significance	Ataxia telangiectasia and Rad3 related
	VEGFA	TSG	c.1039G>A	p.V347I	6|8	/	/	Vascular endothelial growth factor
	DIS3L2	/	c.1642G>A	p.A548T	13|21	/	/	/
17	*TSC1*	TSG	c.2693C>G	p.T898S	21|23	√	(3/5)likely benign, (1/5)benign, (1/5)Uncertain significance	/
18	*PTCH1*	TSG	c.109G>T	p.G37W	1|24	√	(1/1)Uncertain Significance	/

	BRIP1	/	c.3072del	p.S1025Hfs	20|20	√	(1/2)likely pathogenic, (1/2)Uncertain significance	/
	WRN	/	c.3778G>A	p.A1260T	32|35	/	(2/2)Uncertain significance	werner syndrome
	RECQL	/	c.166G>A	p.G56R	4|16	/	/	/
19	*BARD1*	TSG	c.1148T>G	p.M383R	4|11	/	/	/
	USHBP1	/	c.1358C>T	p.P453L	9|13	/	/	/
	APC	TSG	c.2882A>G	p.N961S	16|16	/	(1/1)Uncertain Significance	Adenomatosis polyposis coli
20	*DICER1*	TSG	c.2113A>G	p.I705V	13|27	/	/	Multinodular goiter
	FANCM	/	c.2762G>A	p.C921Y	14|23	/	/	/
	APC	TSG	c.5257G>C	p.A1753P	16|16	/	(3/3)Uncertain Significance	Adenomatosis polyposis coli
	NSD1	/	c.5493T>G	p.D1831E	16|23	/	/	Sotos syndrome
	SDHA	TSG	c.739A>G	p.I247V	6|15	/	(4/4)Uncertain Significance	/
	MTUS1	TSG	c.908A>G	p.N303S	2|15	/	/	Mitochondrial tumor suppressor 1
22	*EXT2*	TSG	c.896G>A	p.R299H	5|14	√	(1/2)likely benign, (1/2)uncategorized	/
	ATM	TSG	c.1555G>A	p.V519I	10|63	√	(3/3)Uncertain Significance	Ataxia telangiectasia mutated
	BRCA2	TSG	c.1568A>G	p.H523R	10|27	√	(1/12)benign, (9/12)likely benign, (2/12)Uncertain Significance	Fanconi anemia
	TP53	TSG	c.214C>G	p.P72A	4|11	√	(5/5)Uncertain Significance	/
23	*FLCN*	TSG	c.1366G>C	p.D456H	12|14	/	/	
	MSH2	TSG	c.1789G>A	p.D597N	12|16	/	(1/1)Uncertain Significance	Colon cancer, nonpolyposis type 1
	KIT	/	c.2263G>A	p.A755T	16|21	/	(1/2)Uncertain Significance,(1/2)uncategorized	Piebald trait
24	*BAP1*	TSG	c.1154G>A	p.R385Q	12|17	/	(2/2)Uncertain Significance	/
	TSC2	TSG	c.1609C>T	p.R537C	16|42	√	(1/5)benign, (2/5)likely benign; (1/5)Uncertain Significance; (1/5)uncategorized	/

HGMD: Human Gene Mutation Database; OMIM: Online Mendelian Inheritance in Man; TSG: Tumor suppressor gene.

most truncation mutations of the *STK11/LKB1* gene mostly occurred in exons 1 and 4, most missense mutations occurred in exon 7, and that truncation mutations were significantly more pathogenic than missense mutations. The results indicate that changes in the sites encoding functional proteins in exon regions 1 and 4 may be among the main causes of PJS. Also, the percentage of *STK11/LKB1* truncation mutations in patients with early onset PJS was higher than that in patients with late onset PJS, and the between-group difference in the percentage of missense mutations was not significant. Because the evidence of a correlation with missense mutations was not strong, it suggests that early onset PJS is more likely to be caused by pathogenic mutations in *STK11/LKB1*, while late onset disease is likely to be clinically heterogeneous. The study results also suggest that analysis of the age of appearance of dark spots in a large sample of PJS patients would yield some interesting findings.

For the first time, we detected more concentrated mutations in the *SLX4* gene in PJS patients. The *SLX4* (*FANCP*) gene is a tumor suppressor gene located on chromosome 16p13.3[21]. It serves as a key scaffold element for the assembly of multiprotein complexes containing enzymes involved in DNA maintenance and repair[22] and has low to moderate expression in all adult and fetal tissues and specific adult brain regions[23]. It has been reported that[24] truncated mutations in the *SLX4* gene were detected in families with Fanconi anemia, and it was determined that *SLX4* mutations are clearly related to one of the subtypes of the disease. Fanconi anemia is a rare autosomal recessive genetic disease[25]. In addition to blood system-related manifestations, the clinical manifestations of FA include multiple congenital malformations, brown pigmentation of the skin, and tumor susceptibility[26]. There are many similarities with PJS, mutations in the *SLX4* gene have been detected in patients with PJS in previous studies, the first of which was found in this group. *SLX4* is considered

Table 10 Prediction of protein function changes caused by other gene mutations

Gene	SIFT		PolyPhen		Mutation Assessor	
	Score	Prediction	Score	Prediction	Score	Prediction
BARD1	0	Deleterious	0.144	Benign	0.66939; 2.045	Medium
EGFR	0.4	Tolerated	0.956	Probably damaging	0.33485; 1.01	Low
GEN1	0	Deleterious	0.999	Probably damaging	0.34521; 1.04	Low
BRCA1	0.02	Deleterious	0.775	Probably damaging	0.78223; 2.4	Medium
NTRK1	0.01	Deleterious	0.639	Probably damaging	0.02685; -0.53	Neutral
PDGFRA	0.1	Tolerated	0.05	Benign	0.38838; 1.175	Low
TSC2	0.15	Tolerated	0.327	Benign	0.57536; 1.79	Low
MSH6	0.45	Tolerated	0.176	Benign	0.08118; 0	Neutral
EGFR	0	Deleterious	0.814	Possibly damaging	0.83953; 2.67	Medium
MTUS1	0.09	Tolerated	0.044	Benign	0.27053; 0.805	Low
PTCH1	0	Deleterious	0.7	Possibly damaging	0.88377; 2.95	Medium
SDHA	0.01	Deleterious low confidence	0.078	Benign	0.49699; 1.58	Low
MTUS1	0.01	Deleterious	0.096	Benign	0.29908; 0.895	Low
RECQL4	/	/	/	/	/	/
RECQL4	/	/	/	/	/	/
ATM	0	Deleterious	0.294	Benign	0.67953; 2.075	Medium
TSC2	0.01	Deleterious	0.226	Benign	0.08118; 0	Neutral
FANCG	0.03	Deleterious	0.018	Benign	0.14661; 0.345	Neutral
SBDS	0.12	Tolerated	0.051	Benign	0.71920; 2.185	Medium
VHL	0.06	Tolerated	0.012	Benign	0.19112; 0.55	Neutral
FANCA	0.24	Tolerated	0	Benign	0.02315; -0.6	Neutral
TP53	0.03	Deleterious	0.386	Benign	0.45228; 1.405	Low
FANCA	0.79	Tolerated	0.007	Benign	0.52573; 1.65	Low
PALLD	0.7	Tolerated	0.159	Benign	0.00602; -1.34	Neutral
MLH3	0.47	Tolerated	0	Benign	0.55103; 1.725	Low
SMARCA4	0.05	Deleterious	0.007	Benign	0.29908; 0.895	Low
NF1	0.62	Tolerated	0.015	Benign	0.08118; 0	Neutral
PTCH1	0	Deleterious	0.626	Possibly damaging	0.88377; 2.95	Medium
GALNT12	0.11	Tolerated	0.007	Benign	0.51422; 1.61	Low
ATR	0	Deleterious	0.998	Probably damaging	0.65975; 2.015	Medium
VEGFA	0.25	Tolerated low confidence	0.695	Probably damaging	0.08118; 0	Neutral
DIS3L2	0.05	Tolerated	0.996	Probably damaging	0.87328; 2.875	Medium
TSC1	/	/		/	0.00621; -1.32	Neutral
PTCH1	0.03	Deleterious low confidence	0.259	Benign	0.36672; 1.1	Low
BRIP1	/	/	/	/	/	/
WRN	0.59	Tolerated	0.164	Benign	0.70595; 2.14	Medium
RECQL	0.5	Tolerated	0.005	Benign	0.41079; 1.255	Low
BARD1	0.4	Tolerated	0	Benign	0.08118; 0	Neutral
USHBP1	0.05	Tolerated	0.521	Possibly damaging	0.56769; 1.78	Low
APC	0.16	Tolerated	0.82	Possibly damaging	0.46157; 1.445	Low

DICER1	0.29	Tolerated	0.664	Possibly damaging	0.34521; 1.04	Low
FANCM	1	Tolerated	0	Benign	0.40543; 1.245	Low
APC	0.57	Tolerated low confidence	0.003	Benign	0.14661; 0.345	Neutral
NSD1	0.03	Deleterious	0.684	Possibly damaging	0.66939; 2.045	Medium
SDHA	0.02	Deleterious low confidence	0.02	Benign	0.20574; 0.59	Neutral
MTUS1	0.87	Tolerated	0	Benign	0.12746; 0.255	Neutral
EXT2	0.03	Deleterious	0.993	Possibly damaging	0.82323; 2.585	Medium
ATM	0.58	Tolerated	0.007	Benign	0.56769; 1.78	Low
BRCA2	0.09	Tolerated	0.003	Benign	0.08118; 0	Neutral
TP53	0.94	Tolerated	0	Benign	0.03608; -0.345	Neutral
FLCN	0.03	Deleterious	0	Benign	0.47716; 1.5	Low
MSH2	0.25	Tolerated	0.023	Benign	0.39692;1.235	Low
KIT	0.15	Tolerated	0.472	Possibly damaging	0.03608; -0.345	Neutral
BAP1	0	Deleterious low confidence	0.968	Possibly damaging	0.59436; 1.845	Low
TSC2	0.02	Deleterious	0.446	Possibly damaging	0.75777; 2.31	Medium

to be an important regulator of DNA repair. Studies have shown that repairing specific types of DNA damage requires *SLX4* and other endonucleases to participate together [22]. At present, it is believed that[27-29] the loss of DNA MMR genes causes the accumulation of mismatches in the process of DNA replication, resulting in the occurrence of microsatellite instability and partial junctions. Colorectal cancer has obvious genetic characteristics. We also detected mutations in some MMR genes (*MSH2* and *MSH6*) in PJS, and the role of *SLX4* gene is highly similar to that. Perhaps the mutation of the *SLX4* gene may explain the genetic heterogeneity of PJS to some extent.

CONCLUSION

In conclusion, we discovered a series of new gene mutation sites, analyzed their pathogenicity, and enriched the mutation spectrum of PJS pathogenic genes. And through the summary of the clinical phenotypes with different *STK11* genotypes, to explore whether they are related, and get some tendentious research results. The detection of *SLX4* gene mutations in patients with PJS was reported for the first time. The relationship between *SLX4* gene mutations and the occurrence of PJS is still unclear, but may help to explain the genetic heterogeneity of PJS.

ARTICLE HIGHLIGHTS

Research background

Different types of pathogenic mutations may produce different clinical phenotypes, but no exact correlation between Peutz-Jeghers syndrome (PJS) genotype and clinical phenotype has been found so far. So it is necessary to study the correlation between genotype and clinical phenotype of PJS, and explore the internal molecular mechanism of different clinical phenotypes.

Research motivation

The authors included 24 cases of treated PJS cases as study participants, collected peripheral venous blood or normal tissue adjacent to polyps for high-throughput next-generation sequencing (NGS) of 139 hereditary colorectal tumor-related genes including *STK11/LKB1* to study the correlation between genotype and clinical phenotype of PJS.

Research objectives

To investigate the correlation between the genotype and clinical phenotype of PJS.

Research methods

Twenty-four patients with PJS were randomly selected for study inclusion. A total of 139 common hereditary tumor-related genes including *STK11/LKB1* were screened and analyzed for pathogenic germline mutations by high-throughput next-generation sequencing (NGS), and the pathogenicity of these mutations was evaluated.

Research results

STK11/LKB1 gene mutations were identified in 20 PJS patients, 90% of which were pathogenic mutations. 10 cases had new mutation sites. Pathogenic mutations were significantly less frequent in exon 7 of the *STK11/LKB1* gene than in other exons. Truncation mutations were more common in exons 1 and 4, and their pathogenicity was significantly higher than that of missense mutations. We also identified *SLX4* gene mutations in PJS patients.

Research conclusions

PJS has a relatively complicated genetic background. Changes in the sites responsible for coding functional proteins in exon 1 and exon 4 of *STK11/LKB1* may be one of the main causes of PJS. Mutation of the *SLX4* gene may help to explain the genetic heterogeneity of PJS.

Research perspectives

Exploration of the relationships of clinical phenotypes with different *STK11* genotypes, may help to interpret some controversial research results. The detection of *SLX4* gene mutations in patients with PJS was reported for the first time.

REFERENCES

1 **van Lier MG**, Wagner A, Mathus-Vliegen EM, Kuipers EJ, Steyerberg EW, van Leerdam ME. High cancer risk in Peutz-Jeghers syndrome: a systematic review and surveillance recommendations. *Am J Gastroenterol* 2010; **105**: 1258-64; author reply 1265 [PMID: 20051941 DOI: 10.1038/ajg.2009.725]

2 **Hearle N**, Schumacher V, Menko FH, Olschwang S, Boardman LA, Gille JJ, Keller JJ, Westerman AM, Scott RJ, Lim W, Trimbath JD, Giardiello FM, Gruber SB, Offerhaus GJ, de Rooij FW, Wilson JH, Hansmann A, Möslein G, Royer-Pokora B, Vogel T, Phillips RK, Spigelman AD, Houlston RS. Frequency and spectrum of cancers in the Peutz-Jeghers syndrome. *Clin Cancer Res* 2006; **12**: 3209-3215 [PMID: 16707622 DOI: 10.1158/1078-0432.CCR-06-0083]

3 **Lim W**, Olschwang S, Keller JJ, Westerman AM, Menko FH, Boardman LA, Scott RJ, Trimbath J, Giardiello FM, Gruber SB, Gille JJ, Offerhaus GJ, de Rooij FW, Wilson JH, Spigelman AD, Phillips RK, Houlston RS. Relative frequency and morphology of cancers in STK11 mutation carriers. *Gastroenterology* 2004; **126**: 1788-1794 [PMID: 15188174 DOI: 10.1053/j.gastro.2004.03.014]

4 **Hemminki A**, Markie D, Tomlinson I, Avizienyte E, Roth S, Loukola A, Bignell G, Warren W, Aminoff M, Höglund P, Järvinen H, Kristo P, Pelin K, Ridanpää M, Salovaara R, Toro T, Bodmer W, Olschwang S, Olsen AS, Stratton MR, de la Chapelle A, Aaltonen LA. A serine/threonine kinase gene defective in Peutz-Jeghers syndrome. *Nature* 1998; **391**: 184-187 [PMID: 9428765 DOI: 10.1038/34432]

5 **Jia Y**, Fu H, Li N, Kang Q, Sheng J. [Diagnosis and treatment for 46 cases of Peutz-Jeghers syndrome]. *Zhong Nan Da Xue Xue Bao Yi Xue Ban* 2018; **43**: 1323-1327 [PMID: 30643048 DOI: 10.11817/j.issn.1672-7347.2018.12.007]

6 **Beggs AD**, Latchford AR, Vasen HF, Moslein G, Alonso A, Aretz S, Bertario L, Blanco I, Bülow S, Burn J, Capella G, Colas C, Friedl W, Møller P, Hes FJ, Järvinen H, Mecklin JP, Nagengast FM, Parc Y, Phillips RK, Hyer W, Ponz de Leon M, Renkonen-Sinisalo L, Sampson JR, Stormorken A, Tejpar S, Thomas HJ, Wijnen JT, Clark SK, Hodgson SV. Peutz-Jeghers syndrome: a systematic review and recommendations for management. *Gut* 2010; **59**: 975-986 [PMID: 20581245 DOI: 10.1136/gut.2009.198499]

7 **Riegert-Johnson DL**, Westra W, Roberts M. High cancer risk and increased mortality in patients with Peutz-Jeghers syndrome. *Gut* 2012; **61**: 322; author reply 322-322; author reply 323 [PMID: 21330574 DOI: 10.1136/gut.2011.238642]

8 **de Leng WW**, Jansen M, Carvalho R, Polak M, Musler AR, Milne AN, Keller JJ, Menko FH, de Rooij FW, Iacobuzio-Donahue CA, Giardiello FM, Weterman MA, Offerhaus GJ. Genetic defects underlying Peutz-Jeghers syndrome (PJS) and exclusion of the polarity-associated MARK/Par1 gene family as potential PJS candidates. *Clin Genet* 2007; **72**: 568-573 [PMID: 17924967 DOI: 10.1111/j.1399-0004.2007.00907.x]

9 **Williams CD**, Grady WM, Zullig LL. Use of NCCN Guidelines, Other Guidelines, and Biomarkers

for Colorectal Cancer Screening. *J Natl Compr Canc Netw* 2016; **14**: 1479-1485 [PMID: 27799515 DOI: 10.6004/jnccn.2016.0154]

10 **Kumar P**, Henikoff S, Ng PC. Predicting the effects of coding non-synonymous variants on protein function using the SIFT algorithm. *Nat Protoc* 2009; **4**: 1073-1081 [PMID: 19561590 DOI: 10.1038/nprot.2009.86]

11 **Adzhubei IA**, Schmidt S, Peshkin L, Ramensky VE, Gerasimova A, Bork P, Kondrashov AS, Sunyaev SR. A method and server for predicting damaging missense mutations. *Nat Methods* 2010; **7**: 248-249 [PMID: 20354512 DOI: 10.1038/nmeth0410-248]

12 **Thompson BA**, Spurdle AB, Plazzer JP, Greenblatt MS, Akagi K, Al-Mulla F, Bapat B, Bernstein I, Capellá G, den Dunnen JT, du Sart D, Fabre A, Farrell MP, Farrington SM, Frayling IM, Frebourg T, Goldgar DE, Heinen CD, Holinski-Feder E, Kohonen-Corish M, Robinson KL, Leung SY, Martins A, Moller P, Morak M, Nystrom M, Peltomaki P, Pineda M, Qi M, Ramesar R, Rasmussen LJ, Royer-Pokora B, Scott RJ, Sijmons R, Tavtigian SV, Tops CM, Weber T, Wijnen J, Woods MO, Macrae F, Genuardi M. Application of a 5-tiered scheme for standardized classification of 2,360 unique mismatch repair gene variants in the InSiGHT locus-specific database. *Nat Genet* 2014; **46**: 107-115 [PMID: 24362816 DOI: 10.1038/ng.2854]

13 **MacArthur DG**, Manolio TA, Dimmock DP, Rehm HL, Shendure J, Abecasis GR, Adams DR, Altman RB, Antonarakis SE, Ashley EA, Barrett JC, Biesecker LG, Conrad DF, Cooper GM, Cox NJ, Daly MJ, Gerstein MB, Goldstein DB, Hirschhorn JN, Leal SM, Pennacchio LA, Stamatoyannopoulos JA, Sunyaev SR, Valle D, Voight BF, Winckler W, Gunter C. Guidelines for investigating causality of sequence variants in human disease. *Nature* 2014; **508**: 469-476 [PMID: 24759409 DOI: 10.1038/nature13127]

14 **Yoo LI**, Chung DC, Yuan J. LKB1--a master tumour suppressor of the small intestine and beyond. *Nat Rev Cancer* 2002; **2**: 529-535 [PMID: 12094239 DOI: 10.1038/nrc843]

15 **Chen C**, Zhang X, Wang D, Wang F, Pan J, Wang Z, Liu C, Wu L, Lu H, Li N, Wei J, Shi H, Wan H, Zhu M, Chen S, Zhou Y, Zhou X, Yang L, Liu J. Genetic Screening and Analysis of LKB1 Gene in Chinese Patients with Peutz-Jeghers Syndrome. *Med Sci Monit* 2016; **22**: 3628-3640 [PMID: 27721366 DOI: 10.12659/msm.897498]

16 **Aretz S**, Stienen D, Uhlhaas S, Loff S, Back W, Pagenstecher C, McLeod DR, Graham GE, Mangold E, Santer R, Propping P, Friedl W. High proportion of large genomic STK11 deletions in Peutz-Jeghers syndrome. *Hum Mutat* 2005; **26**: 513-519 [PMID: 16287113 DOI: 10.1002/humu.20253]

17 **Forcet C**, Etienne-Manneville S, Gaude H, Fournier L, Debilly S, Salmi M, Baas A, Olschwang S, Clevers H, Billaud M. Functional analysis of Peutz-Jeghers mutations reveals that the LKB1 C-terminal region exerts a crucial role in regulating both the AMPK pathway and the cell polarity. *Hum Mol Genet* 2005; **14**: 1283-1292 [PMID: 15800014 DOI: 10.1093/hmg/ddi139]

18 **Amos CI**, Keitheri-Cheteri MB, Sabripour M, Wei C, McGarrity TJ, Seldin MF, Nations L, Lynch PM, Fidder HH, Friedman E, Frazier ML. Genotype-phenotype correlations in Peutz-Jeghers syndrome. *J Med Genet* 2004; **41**: 327-333 [PMID: 15121768 DOI: 10.1136/jmg.2003.010900]

19 **Wang Z**, Wu B, Mosig RA, Chen Y, Ye F, Zhang Y, Gong W, Gong L, Huang F, Wang X, Nie B, Zheng H, Cui M, Wang Y, Wang J, Chen C, Polydorides AD, Zhang DY, Martignetti JA, Jiang B. STK11 domain XI mutations: candidate genetic drivers leading to the development of dysplastic polyps in Peutz-Jeghers syndrome. *Hum Mutat* 2014; **35**: 851-858 [PMID: 24652667 DOI: 10.1002/humu.22549]

20 **Hearle NC**, Tomlinson I, Lim W, Murday V, Swarbrick E, Lim G, Phillips R, Lee P, O'Donohue J, Trembath RC, Morrison PJ, Norman A, Taylor R, Hodgson S, Lucassen A, Houlston RS. Sequence changes in predicted promoter elements of STK11/LKB1 are unlikely to contribute to Peutz-Jeghers syndrome. *BMC Genomics* 2005; **6**: 38 [PMID: 15774015 DOI: 10.1186/1471-2164-6-38]

21 **Fekairi S**, Scaglione S, Chahwan C, Taylor ER, Tissier A, Coulon S, Dong MQ, Ruse C, Yates JR 3rd, Russell P, Fuchs RP, McGowan CH, Gaillard PHL. Human SLX4 is a Holliday junction resolvase subunit that binds multiple DNA repair/recombination endonucleases. *Cell* 2009; **138**: 78-89 [PMID: 19596236 DOI: 10.1016/j.cell.2009.06.029]

22 **Svendsen JM**, Smogorzewska A, Sowa ME, O'Connell BC, Gygi SP, Elledge SJ, Harper JW. Mammalian BTBD12/SLX4 assembles a Holliday junction resolvase and is required for DNA repair. *Cell* 2009; **138**: 63-77 [PMID: 19596235 DOI: 10.1016/j.cell.2009.06.030]

23 **Nagase T**, Kikuno R, Ohara O. Prediction of the coding sequences of unidentified human genes. XXII. The complete sequences of 50 new cDNA clones which code for large proteins. *DNA Res* 2001; **8**: 319-327 [PMID: 11853319 DOI: 10.1093/dnares/8.6.319]

24 **Stoepker C**, Hain K, Schuster B, Hilhorst-Hofstee Y, Rooimans MA, Steltenpool J, Oostra AB, Eirich K, Korthof ET, Nieuwint AW, Jaspers NG, Bettecken T, Joenje H, Schindler D, Rouse J, de Winter JP. SLX4, a coordinator of structure-specific endonucleases, is mutated in a new Fanconi anemia subtype. *Nat Genet* 2011; **43**: 138-141 [PMID: 21240277 DOI: 10.1038/ng.751]

25 **Jacquemont C**, Taniguchi T. The Fanconi anemia pathway and ubiquitin. *BMC Biochem* 2007; **8** Suppl 1: S10 [PMID: 18047734 DOI: 10.1186/1471-2091-8-S1-S10]

26 **Kutler DI**, Singh B, Satagopan J, Batish SD, Berwick M, Giampietro PF, Hanenberg H, Auerbach AD. A 20-year perspective on the International Fanconi Anemia Registry (IFAR). *Blood* 2003; **101**: 1249-1256 [PMID: 12393516 DOI: 10.1182/blood-2002-07-2170]

27 **Picard E**, Verschoor CP, Ma GW, Pawelec G. Relationships Between Immune Landscapes, Genetic Subtypes and Responses to Immunotherapy in Colorectal Cancer. *Front Immunol* 2020; **11**: 369 [PMID: 32210966 DOI: 10.3389/fimmu.2020.00369]

28 **Bourhis A**, De Luca C, Cariou M, Vigliar E, Barel F, Conticelli F, Marcorelles P, Nousbaum JB, Robaszkiewicz M, Samaison L, Badic B, Doucet L, Troncone G, Uguen A. Evaluation of *KRAS*, *NRAS* and *BRAF* mutational status and microsatellite instability in early colorectal carcinomas invading the *submucosa* (pT1): towards an in-house molecular prognostication for pathologists? *J Clin Pathol* 2020; **73**: 741-747 [PMID: 32273401 DOI: 10.1136/jclinpath-2020-206496]

29 **Vageli DP**, Doukas SG, Markou A. Mismatch DNA repair mRNA expression profiles in oral melanin pigmentation lesion and hamartomatous polyp of a child with Peutz-Jeghers syndrome. *Pediatr Blood Cancer* 2013; **60**: E116-E117 [PMID: 23677888 DOI: 10.1002/pbc.24579]

World Journal of Gastroenterology

Submit a Manuscript: https://www.f6publishing.com

World J Gastroenterol 2021 October 21; 27(39): 6647-6658

DOI: 10.3748/wjg.v27.i39.6647

ISSN 1007-9327 (print) ISSN 2219-2840 (online)

ORIGINAL ARTICLE

Clinical and Translational Research

Validation of the Italian translation of the perceived stigma scale and resilience assessment in inflammatory bowel disease patients

Sara Cococcia, Marco Vincenzo Lenti, Caterina Mengoli, Catherine Klersy, Federica Borrelli de Andreis, Matteo Secco, Jihane Ghorayeb, Mariangela Delliponti, Gino Roberto Corazza, Antonio Di Sabatino

ORCID number: Sara Cococcia 0000-0002-1507-6513; Marco Vincenzo Lenti 0000-0002-6654-4911; Caterina Mengoli 0000-0002-2253-7795; Catherine Klersy 0000-0003-0314-8548; Federica Borrelli de Andreis 0000-0003-2933-8825; Matteo Secco 0000-0002-8285-3706; Jihane Ghorayeb 0000-0002-8382-4106; Mariangela Delliponti 0000-0002-3184-0673; Gino Roberto Corazza 0000-0001-9532-0573; Antonio Di Sabatino 0000-0002-0302-8645.

Author contributions: All authors significantly participated in the drafting of the manuscript or critical revision of the manuscript for important intellectual content and provided approval of the final submitted version. Individual contributions are as follows: Lenti MV and Cococcia S designed and coordinated the study, enrolled subjects, interpreted data, and wrote the manuscript; Klersy C designed the study, did statistical analyses, and reviewed the manuscript; Ghorayeb J interpreted data and critically reviewed the manuscript; Di Sabatino A and Corazza GR reviewed the paper and made final critical revision for important intellectual content; All other authors enrolled patients and collected and analyzed data.

Institutional review board

Sara Cococcia, Marco Vincenzo Lenti, Caterina Mengoli, Federica Borrelli de Andreis, Matteo Secco, Mariangela Delliponti, Gino Roberto Corazza, Antonio Di Sabatino, First Department of Internal Medicine, San Matteo Hospital Foundation, University of Pavia, Pavia 27100, Lombardia, Italy

Catherine Klersy, Service of Biometry & Statistics, Foundation IRCCS Policlinico San Matteo, Pavia 27100, Lombardia, Italy

Jihane Ghorayeb, Psychology, Zayed University, Dubai 00000, United Arab Emirates

Corresponding author: Marco Vincenzo Lenti, MD, Academic Research, Doctor, Research Assistant Professor, Research Scientist, First Department of Internal Medicine, San Matteo Hospital Foundation, University of Pavia, Viale Camillo Golgi, 19, Pavia 27100, Lombardia, Italy. marco.lenti@unipv.it

Abstract

BACKGROUND

Stigmatization is the separation of an individual from a group due to aspects that make them different. Resilience may in turn influence the perception of stigma. Patients with inflammatory bowel disease (IBD) are susceptible to stigma, although data are very limited.

AIM

To validate an Italian translation of the IBD perceived stigma scale (PSS) in relation to patients' resilience.

METHODS

Consecutive IBD outpatients were prospectively enrolled (December 2018-September 2019) in an Italian, tertiary referral, IBD center. Clinical and demographic data were collected. Stigma and resilience were evaluated through the IBD-PSS and the 25-item Connor-Davidson Resilience Scale, respectively. The International Quality of Life Assessment Project approach was followed to translate the IBD-PSS into Italian and to establish data quality. Higher scores represent greater perceived stigma and resilience. Multivariable analysis for factors associated with greater stigma was computed.

RESULTS

statement: The study was approved by the local Ethics Committee (Protocol Number 20190003611). The study protocol conforms to the ethical guidelines of the 1975 Declaration of Helsinki as reflected in a priori approval by the institution's human research committee.

Informed consent statement: All participants gave their informed written consent to take part to the study and for the anonymized publication of data.

Conflict-of-interest statement: The authors of this manuscript having no conflicts of interest to disclose.

Data sharing statement: There is no additional data available.

Open-Access: This article is an open-access article that was selected by an in-house editor and fully peer-reviewed by external reviewers. It is distributed in accordance with the Creative Commons Attribution NonCommercial (CC BY-NC 4.0) license, which permits others to distribute, remix, adapt, build upon this work non-commercially, and license their derivative works on different terms, provided the original work is properly cited and the use is non-commercial. See: http://creativecommons.org/Licenses/by-nc/4.0/

Manuscript source: Unsolicited manuscript

Specialty type: Gastroenterology and Hepatology

Country/Territory of origin: Italy

Peer-review report's scientific quality classification

Grade A (Excellent): A
Grade B (Very good): B
Grade C (Good): 0
Grade D (Fair): 0
Grade E (Poor): 0

Received: February 14, 2021
Peer-review started: February 14, 2021
First decision: March 14, 2021
Revised: March 21, 2021
Accepted: October 11, 2021

Overall, 126 IBD patients (mean age 46.1 ± 16.9) were enrolled. The International Quality of Life Assessment criteria for acceptable psychometric properties of the scale were satisfied, with optimal data completeness. There was no ceiling effect, whilst floor effect was present (7.1%). The discriminant validity and the internal consistency reliability were good (Cronbach alpha = 0.87). The overall internal consistency was 95%, and the test-retest reliability was excellent 0.996. The median PSS score was 0.45 (0.20-0.85). Resilience negatively correlated with perceived stigma (Spearman's correlation = -0.18, 95% confidence intervals: -0.42-0.08, P = 0.03).

CONCLUSION
We herein validated the Italian translation of the PSS scale, also demonstrating that resilience negatively impacts perceived stigma.

Key Words: Crohn's disease; Quality of life; Stress; Ulcerative colitis

©The Author(s) 2021. Published by Baishideng Publishing Group Inc. All rights reserved.

Core Tip: We have here validated an Italian version of the Perceived Stigma Scale for patients with inflammatory bowel disease. We have also found that resilience levels negatively correlated with perceived stigma. This is the first study assessing this issue in patients with inflammatory bowel disease.

Citation: Cococcia S, Lenti MV, Mengoli C, Klersy C, Borrelli de Andreis F, Secco M, Ghorayeb J, Delliponti M, Corazza GR, Di Sabatino A. Validation of the Italian translation of the perceived stigma scale and resilience assessment in inflammatory bowel disease patients. *World J Gastroenterol* 2021; 27(39): 6647-6658
URL: https://www.wjgnet.com/1007-9327/full/v27/i39/6647.htm
DOI: https://dx.doi.org/10.3748/wjg.v27.i39.6647

INTRODUCTION

Stigmatization is defined as the societal identification of an individual as abnormal and worthy of separation from the group, leading to discrimination and loss of their social status[1]. It has been reported that inflammatory bowel disease (IBD) is susceptible to stigmatization, not only because of the *taboo* around its symptoms, but also due to the assumption of being a psychosomatic condition affecting people because of their "obsessive behavior"[2] and because it affects sexual life[3]. Stigmatization in IBD patients was reported to be as high as 84%, regardless of disease activity [4].

An important aim of taking care of chronic patients should be the improvement of their quality of life (QoL), taking into account the social context and their needs[5]. Nonetheless, it emerged from a recent review that the burden of stigmatization in IBD, and the ability to positively cope with the disease (*i.e.* resilience), are not adequately addressed by clinicians[6]. In IBD patients, resilience has been found to be influenced by individual characteristics, including age, sex, and employment status and to influence positively the disease prognosis[7-9]. Stigma can be evaluated through the use of different scales, including the IBD perceived stigma scale (PSS)[10], which has been adapted and used in IBD patients[11]. Similarly, resilience can be measured through the Connor-Davidson resilience scale (CD-RISC), a 25-item self-administrated scale exploring different aspects related to the individual ability to cope with adversity and stress[12]. The CD-RISC was initially designed for psychiatric American patients, and it has now been translated into more than 70 languages, being the most widely used resilience scale in a variety of conditions[13].

The first study looking into perceived stigma in IBD showed that functional impairment was mainly due to IBD patients' psychological dimension rather than to their physical one. They also reported that patients with Crohn's disease (CD) had a higher degree of perceived stigma than patients with ulcerative colitis (UC)[14]. While perceived stigma is difficult to address and modify, resilience is responsive to

Article in press: October 11, 2021
Published online: October 21, 2021

P-Reviewer: Sipos F, Truyens M
S-Editor: Chang KL
L-Editor: Filipodia
P-Editor: Chang KL



behavioral intervention and is independently associated with better QoL and lower disease activity in IBD[9].

There are very limited data regarding perceived stigma in IBD, and no validated translation of the PSS into Italian is available. As a consequence, perceived stigma in Italian IBD patients has never been assessed. Therefore, we aimed to validate the Italian version of the PSS in IBD patients in order to obtain a meaningful instrument for assessing stigmatization and compare with international studies. We also assessed resilience and its relation with stigmatization.

MATERIALS AND METHODS

Study population

All IBD patients followed-up at the IBD Clinical & Research Centre of the San Matteo Hospital Foundation were consecutively enrolled between December 2018 and September 2019. IBD diagnosis was established according to internationally agreed criteria[15]. Patients were eligible for inclusion if they had at least a 3-mo history of IBD, were aged ≥ 18, were able to complete a questionnaire, and were willing to give written informed consent. Patients with an inconclusive or uncertain diagnosis of IBD or those diagnosed less than 3 mo before or unwilling to provide informed consent were excluded. Demographic and clinical characteristics were gathered, including IBD type, disease activity and duration, comorbidities, and previous IBD-related surgery. Clinical activity was assessed using the Harvey-Bradshaw index (HBI)[16,17] for CD and the partial Mayo score (pMayo)[18] for UC. For CD patients, HBI < 5 was defined as clinical remission, HBI 5-7 as mild disease, HBI 8-16 as moderate disease, and HBI > 16 as severe disease[16,17]. For UC patients, pMayo < 2 was defined as remission, pMayo 2-4 was defined as mild activity, pMayo 5-7 was defined as moderate activity, and pMayo > 7 was defined as severe activity[18]. The study was approved by the local Ethics Committee (Protocol Number 20190003611), and all participants gave their informed written consent to take part to the study and for the anonymized publication of data. The study protocol conforms to the ethical guidelines of the 1975 Declaration of Helsinki as reflected in a priori approval by the institution's human research committee.

Assessment of the PSS

The PSS was initially designed to assess stigma in irritable bowel syndrome (IBS) patients and was validated in IBD in 2009 in a cohort of patients from the United States [4]. The PSS is a self-administered questionnaire designed to measure perceived stigma through 10 items on a five-point Likert scale (ranging from 0 = never to 4 = always), with a higher score reflecting a greater level of perceived stigma. Each item is assessed on two different domains: Significant others (SO) and healthcare professionals (HP), leading to a total of 20 items. The two-domain PSS version has already been used for different gastrointestinal disease and was found to have an excellent internal consistency and split-half reliability (≥ 0.89)[19].

The score indicating the perceived stigma ranges from 0 to 4 and is obtained by calculating the mean of all the values and the values within each domain.

Translation and cultural validation

We aimed to create a version that was easy to understand and complete by Italian IBD patients, without losing the original English version's equivalence and psychometric validity. The translation and adaptation were made in accordance with the International QoL Assessment (IQOLA) Project approach, which consists of three steps: A forward translation, a backward translation, and a cognitive testing[20,21].

Step 1—Forward translation: Two bilingual physicians (Lenti MV and Cococcia S) blindly translated the questionnaire from English into Italian. The two versions were compared, and discrepancies reconciled. Difficulty and degree of agreement of the translation were rated on a 1 to 100 scale (lowest–highest). For each item, the agreed forward translation was accepted if the scores were ≥ 75, otherwise retranslation was independently performed and scoring repeated.

Step 2—Backward translation: The Italian translation was blindly translated back into British English by two mother-tongue English people with a high educational level (graduated). The same reconciliation process reported for the forward translation was applied. The equivalence of the agreed backward translation to the original version

was rated and expected to be ≥ 75. If that threshold was not reached, the four translators had to agree on a new forward translation.

Step 3—Cognitive testing: Cognitive testing of the agreed Italian version was performed on 10 individuals with different age, sex, and educational background to verify that the translation was clear and understandable by a range of different people. Finally, a panel discussion was held to approve the final version (see Supplementary data).

Resilience assessment

Resilience was assessed through the Italian validated translation of the CD-RISC scale, a self-administered questionnaire assessing resilience through 25 items on a five-point Likert scale (ranging from 0 = totally disagree to 4 = totally agree)[12]. The score is calculated by summing the score of each item (ranging from 0 to 100) with higher scores meaning higher resilience.

Statistical analysis and psychometric evaluation

The sample size was computed based on the primary endpoint. A sample of 100 subjects responding to 20 items would achieve 80% power to detect the difference between the coefficient alpha under the null hypothesis of 0.70 and the coefficient alpha under the alternative hypothesis of 0.81, using a two-sided *F*-test with a significance level of 0.05. Twenty-six extra patients were enrolled to account for possible dropouts.

The PSS scoring was performed according to the scoring manuals, meaning that higher scores represent a higher level of perceived stigma. The psychometric evaluation of the Italian version of the PSS questionnaire included evaluation of data quality, including completeness (Table 1). Results were described as mean and standard deviation, and ceiling and floor effect were evaluated. Reliability was assessed and expressed by means of Cronbach's alpha for internal consistency, alpha = k × r/[1+(k-1) × r]; with k = number of items and r = mean correlation. Item internal consistency (correlation of item and corresponding scale, corrected for overlap), equality of item-scale correlations, and item discriminant validity (correlation of item with the corresponding scale *vs* correlation of item with other scales) were evaluated through the multi-trait/multi-item correlation matrix. Means of Pearson's correlation coefficient and intraclass correlation coefficient were used to evaluate the test-retest correlation for temporal stability (within 1 mo), with 95% confidence intervals (95%CI). External validity was assessed through the comparison of PSS scores in patients with different characteristics by means of the Kruskall Wallis test, the test for trend; the correlation with continuous variables was assessed with the Spearman R. Stata 16 (StataCorp, College Station, TX, United States) was used for all computations. All tests were two-sided, and a P value < 0.05 was considered statistically significant. In the presence of missing data, missing items were replaced by the median of the corresponding scale, unless more than 50% of the items were missing, in which instance the questionnaire was dropped.

RESULTS

Demographic and clinical characteristics

Overall, 146 IBD patients were screened for inclusion in the study. Of these, 20 patients did not participate because denied consent (15 patients) or because were due to be followed up in another hospital. Hence, 126 IBD patients (mean age 46.1 ± 16.9, male 56.4%), 57 with CD and 69 with UC, were consecutively enrolled in the study. The demographic and clinical characteristics of the enrolled patients are reported in Table 2. CD patients were significantly younger than UC patients (42.3 ± 15.7 *vs* 49.3 ± 17.4; P = 0.03). Psychiatric disorders, including anxiety and depression, were the most common concomitant diseases (25.4%), followed by hypertension (22.2%) and cardiomyopathy (11.9%), which was significantly more common among UC patients (17.4% *vs* 5.26%; P = 0.05). Overall, the median disease duration was 8 years [interquartile range (IQR) 3-16]. The majority of the CD patients had a disease with an inflammatory behavior (56.1%), 43.9% had a structuring behavior, and 28.1% had a penetrating disease. Almost half of the CD patients (49.1%) had ileo-colonic involvement, and 33.3% had perianal disease. Among UC patients, half (52.2%) had an extensive disease, 37.7% had a left UC, 10.1% had an ulcerative proctitis, and 4.4% had

Table 1 Thresholds defining acceptable psychometric properties according to the International Quality of Life Assessment project

	Definition	Threshold
Data quality		
Missing items	Unanswered items	< 5%-10%
	Incomplete scales (< 50% of items answered)	< 5%-10%
Floor and ceiling effect	Extreme scores (either on the lower- or higher-end)	< 10%
Scaling assumption		
Internal consistency		
Item	Correlation among items of the same scale (Pearson correlation ≥ 0.4)	> 90%
Reliability	Overall consistency of the scale (Cronbach's alpha coefficient)	> 0.7
Discriminant validity	Items whose Pearson correlation with other scales is higher than with their scale	0%
Test-retest evaluation	Correlation between the results scales filled in twice by the same patients at defined time points (Pearson correlation)	> 0.7

a pouch. The proportion of patients with severe disease activity was higher among UC patients (10.1% *vs* 0%), while two-thirds were in remission in both groups. A quarter of the enrolled patients had an extraintestinal manifestation (28.6%), including anemia, arthritis, uveitis, and dermatological manifestations. When available, calprotectin and C-reactive protein (CRP) were used as inflammatory markers. Overall, 34.1% of the patients had a calprotectin < 50 mg/kg, 16.2% between 51-250 mg/kg, and 12.7% > 250 mg/kg with no difference according to the disease (P = 0.54). Similarly, 61.1% of the patients had a normal CRP, whilst roughly a third had raised levels of CRP (31.0%), with no difference between UC and CD patients (P = 1.00).

Translation and cultural validation

The PSS was translated according to the IQOLA project guidelines[20,21]. For the forward translation, the median difficulty was rated as 10 (range: 10-60) and the agreement was found to be 95 (range: 70-100). Items 1, 5, and 10 were adjusted after discussion. The backward translation equivalence was rated at 95 (range: 80-100). Minor changes were made to item 2 and 4 of the Italian translation to improve the original version's equivalence. A cognitive testing of the agreed Italian version was performed on 10 individuals with different ages (median 48-years-old, range: 29-88), sex (5 female), and educational background (5 graduated), which did not lead to any adjustment of the scale. Supplementary data show the validated Italian version of the PSS-IBD, while the questions of the original English version have already been published elsewhere[4].

Psychometric evaluation

The majority of the IQOLA criteria for acceptable psychometric properties of the scale were satisfied in our cohort as reported in Table 3. We reached an optimal data completeness, and we did not have any ceiling effect, whilst a floor effect was present in 7.1% of the cases (overall domain). The floor effect was greater for the HP domain when compared to the SO domain (42.1% *vs* 8.7%). When looking at scaling assumption, the internal consistency reliability of the Italian version of the PSS was good, with an overall Cronbach alpha coefficient of 0.87 (0.83 for SO and 0.81 for HP). Although an excellent item, internal consistency was found in each domain, with a Pearson correlation ranging from 0.4 to 0.6, and one item (item 8, SO domain) did not reach the predetermined threshold of 0.4, determining an overall item internal consistency of 95% (still indicative of an excellent item internal consistency). The discriminant validity of the scale was good for items 1 to 7 in both domains, whereas items 8 to 10 had exactly the same Pearson correlation with their domain and the other one for both SO and HP.

The test-retest reliability was excellent, being 0.999 (0.997-1.000) overall, 0.99 (0.997-1.000) in the SO domain and 0.994 (0.979-0.998) in the HP domain. The median PSS score was 0.45 (0.20-0.85) with a significantly higher score for the SO domain (0.70 IQR 0.40-1.40 *vs* 0.10 IQR 0.00-0.40, P < 0.001), whilst the median resilience score was 64 (IQR 53-78). The level of perceived stigma did not differ according to sex (P = 0.51), IBD type (P = 0.33), disease activity, age (P = 0.11), or disease duration (P = 0.49) (See

Table 2 Demographic and clinical characteristics of the validating cohort

	Overall (*n* = 126)	CD (*n* = 57)	UC (*n* = 69)	*P* value
Age (mean ± SD)	46.13 (± 16.95)	42.29 (± 15.7)	49.29 (± 17.38)	0.03
Male	71 (56.4%)	33 (57.9%)	38 (55.1%)	0.86
BMI	23.9 (± 4.1)	23.9 (± 4.3)	23.9 (± 3.9)	0.67
Disease duration (median, IQR)	8 (3-16)	10 (3-17)	8 (3.5-13)	0.44
Disease characteristics (CD)				
Location (CD)	-		-	
Terminal ileum (L1)		13 (22.8%)		
Colon (L2)		8 (14.0%)		
Ileo-colon (L3)		28 (49.1%)		
Upper GI (L4)		2 (3.5%)		
Perianal disease (p)		19 (33.3%)		
Behavior (CD)	-	-		
Inflammatory (B1)		32 (56.1%)		
Stricturing (B2)		25 (43.9%)		
Penetrating (B3)		16 (28.1%)		
Disease activity (HBI)	-	-		
< 5		38 (66.7%)		
5-7		14 (24.6%)		
8-16		5 (8.8%)		
> 16	-	0 (0%)		
Disease characteristics (UC)			-	
Location	-	-	7 (10.1%)	
Proctitis (E1)			26 (37.7%)	
Left sided (E2)			36 (52.2%)	
Extensive (E3)				
Disease activity (pMayo)	-			
< 2			45 (65.2%)	
2-4			13 (18.8%)	
5-7			4 (5.8%)	
> 7			7 (10.1%)	
Pouch			3 (4.4%)	
Extraintestinal manifestations	36 (28.6%)	17 (29.8%)	19 (27.5%)	0.84
Previous abdominal surgery	38 (30.2%)	22 (38.6%)	16 (42.1%)	0.07
Calprotectin				0.54
< 50	43(34.1%)	15 (26.3%)	28 (40.6%)	
51-250	33 (16.2%)	17 (29.8%)	16 (23.2.%)	
> 250	16 (12.7%)	7 (12.3%)	9 (13.4%)	
Missing	34 (27.0%)	18 (31.6%)	16 (23.2%)	
CRP				1.00
Normal	77 (61.1)	35 (62.4%)	42 (60.9%)	
Raised	39 (31.0%)	18 (31.6%)	21 (30.4%)	

Missing	10 (7.9%)	4 (7.0%)	6 (8.7%)	
Comorbidities	40 (31.8%)	16 (28.1%)	24 (34.8%)	0.45
Cardiomyopathy	15 (11.9%)	3 (5.26%)	12 (17.4%)	0.05
Hypertension	28 (22.2%)	12 (42.9%)	16 (23.2%)	0.83
Diabetes	11 (8.73%)	4 (7.0%)	7 (10.1%)	0.75
Hepatic failure	1 (0.8%)	1 (1.8%)	0 (0.0%)	0.45
Kidney failure	4 (3.17%)	3 (5.26%)	1 (1.45%)	0.32
Respiratory failure	2 (1.6%)	1 (1.8%)	1 (1.5%)	1.00
Neurologic diseases	5 (4.0%)	1 (1.8%)	4 (5.8%)	0.37
Psychiatric disorder	15 (11.9%)	7 (12.3%)	8 (11.6%)	1.00
Onco-hematological diseases	12 (9.5%)	2 (3.5%)	10 (14.5%)	0.06

BMI: Body mass index; CD: Crohn's disease; CRP: C-reactive protein; GI: Gastrointestinal; HBI: Harvey-Bradshaw Index; IQR: Interquartile range; PMS: Partial Mayo Score; SD: Standard deviation; UC: Ulcerative colitis.

Table 3 Psychometric characteristics of perceived stigma scale and its sub-scales

	Overall	Significant others	Healthcare professionals
Median score	0.45 (0.20-0.85)	0.70 (0.30-1.40)	0.10 (0-0.40)
Data quality			
Missing items	0 (0%)	0 (0%)	0 (0%)
Floor effect	9 (7.1%)	11 (8.7%)	53 (42.1%)
Ceiling effect	0 (0%)	0 (0%)	0 (0%)
Scaling assumption			
Internal consistency			
Item	19/20 (95.0%)	10/10 (100%)	10/10 (100%)
Reliability (Cronbach alpha)	0.87	0.83	0.81
Discriminant validity	-	30.0%	30.0%
Test-retest	0.99 (0.99-1.00)	0.999 (0.99-1.00)	0.99 (0.97-0.99)
Evaluation[a]			

[a]Intraclass correlation coefficient (95% confidence interval).

Table 4). On the contrary, disease activity was found to significantly reduce resilience (Spearman's correlation -0.18, 95%CI: -0.42-0.08, P = 0.03) in CD patients, whilst no significant difference was found in UC patients according to the disease activity (P = 0.23). When exploring the relations between perceived stigma and resilience, a significant negative Spearman's correlation was found (-0.20, 95%CI: -0.36 to -0.02; P = 0.03).

DISCUSSION

Stigmatization is an important, though often unattended, issue in clinical medicine. Whilst for other conditions (*e.g.*, human immunodeficiency virus, mental illness, and lung cancer) stigmatization has been widely studied[22-25], IBD data are scant and fragmentary. This might be partly due to the lack of a validated tool to be used for this purpose. We herein validated an Italian version of the PSS questionnaire that performs well, has good psychometric properties, and is easily understandable. The psychometric evaluation of the Italian PSS version showed an excellent Cronbach alpha coefficient, item internal consistency, and test-retest reliability. Our results are in line

Table 4 Correlation between inflammatory bowel disease perceived stigma scale scores and demographic or clinical characteristics

	PSS	*P*	Spearman's correlation (95%CI)	PSS SO	*P*	Spearman's correlation (95%CI)	PSS HP	*P*	Spearman's correlation (95%CI)
Median score (IQR)	0.45 (0.20 to 0.85)			0.70 (0.30 to 1.40)			0.10 (0.00 to 0.40)		
Age		0.11	-0.14 (-0.31 to 0.03)		0.08	-0.157 (-0.33 to 0.02)		0.20	-0.116 (-0.29 to 0.06)
Sex		0.51			0.26			0.29	
Female	0.45 (0.30 to 0.85)			0.70 (0.50 to 1.40)			0.10 (0.00 to 0.40)		
Male	0.45 (0.15 to 0.90)			0.70 (0.20 to 1.40)			0.10 (0.00 to 0.50)		
Diagnosis		0.33			0.35			0.34	
CD	0.55 (0.25 to 0.95)			0.80 (0.40 to 1.40)			0.10 (0.00 to 0.50)		
UC	0.45 (0.20 to 0.85)			0.70 (0.30 to 1.30)			0.10 (0.00 to 0.40)		
HBI		0.91	0.05 (-0.22 to 0.30)		0.91	0.05 (-0.21 to 0.31)		0.70	0.11 (-0.16 to 0.36)
< 5	0.53 (0.25 to 0.80)			0.75 (0.50 to 1.30)			0.10 (0.00 to 0.50)		
5-7	0.60 (0.10 to 1.15)			0.90 (0.20 to 1.60)			0.30 (0.00 to 0.50)		
8-16	0.40 (0.10 to 1.40)			0.70 (0.20 to 1.80)			0.10 (0.00 to 0.80)		
pMS		0.52	0.06 (-0.18 to 0.29)		0.44	0.03 (-0.21 to 0.26)		0.81	0.11 (-0.13 to 0.34)
< 2	0.40 (0.20 to 0.85)			0.60 (0.40 to 1.30)			0.10 (0.00 to 0.30)		
2-4	0.45 (0.05 to 0.75)			0.60 (0.10 to 1.20)			0.20 (0.00 to 0.40)		
5-7	0.75 (0.48 to 1.22)			1.40 (0.90 to 1.75)			0.15 (0.05 to 0.70)		
> 7	0.35 (0.15 to 1.50)			0.70 (0.00 to 2.70)			0.10 (0.00 to 0.70		
CD-RISC25	-	0.03	-0.20 (-0.36 to -0.02)	-	0.02	-0.20 (-0.36 to -0.03)	-	0.12	-0.14 (-0.31 to 0.04)

CD: Crohn's disease; CD-RISC25: 25-item Connor-Davidson Resilience Scale; CI: Confidence interval; HBI: Harvey-Bradshaw Index; HP: Healthcare professionals; IQR: Interquartile range; pMS: Partial Mayo Score; SO: Significant others; UC: Ulcerative colitis.

with previous literature validating stigma scales in different settings[4,10,26,27], showing that our translation is reliable and offers a tool to assess stigma in Italian IBD patients. In our cohort, the main concern is the high floor effect recorded, especially in the HP domain. However, this result was partially expected since all the included patients were followed-up at a tertiary IBD center. These patients likely experience lower levels of perceived stigma since they are looked after by IBD dedicated HP, whereas a different result might be obtained if the questionnaire would be administered in different settings, such as community centers or private practices. Even considering the setting bias, the level of perceived stigma was found to be lower than expected (median 0.45, IQR 0.20-0.85), when compared to previous literature showing a low-to-moderate level of perceived stigma among IBD patients, using the PSS[4]. This might be explained by the fact that the PSS has been originally designed to address perceived stigma in patients affected by a functional disorder rather than by an organic disease, such as IBD. In the PSS questionnaire, there are no questions addressing some of IBD patients' main concerns, including the fear of relapsing or of incontinence. Therefore, even if this scale offers a useful tool to assess stigma in IBD, it is our opinion that some adjustments are needed.

Additionally, levels of perceived stigma in IBD patients tend to decrease in long-standing disease, in contrast with what happens for IBS[11]. Since IBD is an organic disease not associated with unhealthy or socially unacceptable vices, it is therefore

more likely to be recognized and accepted as a "real" organic disease over time, especially when compared to IBS[11]. Most of the included patients have a longstanding history, which could have led to lower levels of perceived stigma in our sample.

Stigmatization is multifactorial and is influenced by both patient-dependent and environment-dependent factors[28-30]. Among these factors, we have previously speculated that a relation between stigma and resilience may exist[6]. In line with previous literature, we found a moderate level of resilience in our cohort[9]. We have here shown for the first time that, in IBD patients, higher levels of resilience correlate with lower levels of perceived stigma (overall and for SO) and, conceivably, to better QoL. Such correlation was not found for the HP domain, which might be due to the high floor effect reported in this domain. In case of adversity, resilience can modulate catecholamine and cortisol production reducing long-term effects on the body[31] and leading to better outcome also in IBD, which requires continuous adaptation to the unpredictable course of the disease. This hypothesis is supported by a recent study in which higher levels of resilience are associated with lower disease activity, although it is unclear if this result was due to reverse causation[9]. Our findings suggest that downstream public health intervention that focus on patients' resilience may reduce the level of perceived stigma and consequently may improve the patients' QoL. Follow-up data are being gathered to support this hypothesis, since resilience is easily influenced by other events and a single assessment might be misleading. In addition to intervention focused on building individual resilience, upstream public health interventions are needed to reduce stigma around IBD improving the awareness on the disease.

This study has some limitations. Firstly, the sample size was calculated to validate the Italian translation of the PSS and was not adequate to draw firm conclusions about the level of perceived stigma among IBD patients. Larger prospective studies are needed to explore this aspect. Secondly, the majority of the included patients had a low disease activity and that could represent a bias in interpreting the results. Stigma is internalized over time and, since IBD is a chronic disease, the level of perceived stigma is influenced mostly by the social environment rather than by acute events. On the contrary, resilience is strongly influenced by contextual events and can be improved through behavioral intervention, and this is why the ongoing follow-up of these patients will be useful to better assess the relation between stigma and resilience in IBD. Additionally, the level of resilience of the sampled patients ranged from average to good, and this might have played a role in lowering the stigma scores.

CONCLUSION

To conclude, we have herein developed a validated Italian version of the PSS. Also, we have assessed for the first-time stigmatization and its relation with resilience in a cohort of IBD patients. Interventions aimed at building a stronger resilience may reduce perceived stigma. The follow-up data on the variation of stigma and resilience levels over time are being collected.

ARTICLE HIGHLIGHTS

Research background

Patients living with inflammatory bowel disease (IBD) often experience a poor quality of life due to stigmatization that can be assessed through the IBD perceived stigma scale (PSS). Resilience is the ability to cope positively with a specific disease or situation.

Research motivation

Stigmatization in IBD patients, especially in relation to one's own resilience, has been poorly characterized. A validated Italian version of the IBD-PSS is not available.

Research objectives

To validate an Italian version of the PSS in IBD patients and to assess patients' resilience and its relation with stigmatization.

Research methods

We enrolled 126 consecutive IBD patients (mean age 46.1 ± 16.9, male 56.4%), 57 with CD and 69 with UC, in an Italian, tertiary referral, IBD center. Clinical and demographic data were collected, and stigma and resilience were evaluated through the IBD-PSS and the 25-item Connor-Davidson Resilience Scale, respectively. Psychometric validity of the IBD-PSS was assessed, and a multivariable analysis for factors associated with greater stigma was computed.

Research results

We found that the Italian version of the IBD-PSS had an acceptable reliability, having a Cronbach alpha of 0.87, with an excellent test-retest score. The median PSS score was 0.45 (0.20-0.85), and resilience negatively correlated with perceived stigma (Spearman's correlation -0.18, 95%CI: -0.42-0.08, $P = 0.03$).

Research conclusions

We have developed a reliable tool to be used in clinical practice for assessing stigmatization in Italian IBD patients. Also, we found that resilience may have an influence on stigmatization, possibly improving patients' illness perception.

Research perspectives

The Italian IBD-PSS should be used extensively in order to assess this important endpoint in the care of IBD patients. More prospective, long-term studies looking at more detailed factors influencing stigmatization and resilience are urgently needed.

ACKNOWLEDGEMENTS

Dr. Marco Vincenzo Lenti is grateful to the University of Pavia for supporting his research projects. Mr. Tim Brown and Mrs. Joan Brown kindly provided backward translation for free. We also thank Prof. Tiffany Taft for providing the English version of the PSS-IBD. Dr. Marco Vincenzo Lenti has been awarded for presenting the abstract of this research project to the Italian Group for the study of Inflammatory Bowel Disease National Congress (2019; Best Clinical Communication).

REFERENCES

1 **Link BG**, Phelan JC. Conceptualizing stigma. *Annu Rev Sociol* 2001; **27**: 363-385 [DOI: 10.1146/annurev.soc.27.1.363]

2 **Sheffield BF**, Carney MW. Crohn's disease: a psychosomatic illness? *Br J Psychiatry* 1976; **128**: 446-450 [PMID: 1276548 DOI: 10.1192/bjp.128.5.446]

3 **Taft TH**, Keefer L. A systematic review of disease-related stigmatization in patients living with inflammatory bowel disease. *Clin Exp Gastroenterol* 2016; **9**: 49-58 [PMID: 27022294 DOI: 10.2147/CEG.S83533]

4 **Taft TH**, Keefer L, Leonhard C, Nealon-Woods M. Impact of perceived stigma on inflammatory bowel disease patient outcomes. *Inflamm Bowel Dis* 2009; **15**: 1224-1232 [PMID: 19180581 DOI: 10.1002/ibd.20864]

5 **Levenstein S**, Li Z, Almer S, Barbosa A, Marquis P, Moser G, Sperber A, Toner B, Drossman DA. Cross-cultural variation in disease-related concerns among patients with inflammatory bowel disease. *Am J Gastroenterol* 2001; **96**: 1822-1830 [PMID: 11419836 DOI: 10.1111/j.1572-0241.2001.03878.x]

6 **Lenti MV**, Cococcia S, Ghorayeb J, Di Sabatino A, Selinger CP. Stigmatisation and resilience in inflammatory bowel disease. *Intern Emerg Med* 2020; **15**: 211-223 [PMID: 31893346 DOI: 10.1007/s11739-019-02268-0]

7 **Luo D**, Lin Z, Shang XC, Li S. "I can fight it! *Int J Nurs Sci* 2019; **6**: 127-133 [PMID: 31406881 DOI: 10.1016/j.ijnss.2018.12.008]

8 **Acciari AS**, Leal RF, Coy CSR, Dias CC, Ayrizono MLS. Relationship among psychological well-being, resilience and coping with social and clinical features in crohn's disease patients. *Arq Gastroenterol* 2019; **56**: 131-140 [PMID: 31460575 DOI: 10.1590/S0004-2803.201900000-27]

9 **Sehgal P**, Ungaro RC, Foltz C, Iacoviello B, Dubinsky MC, Keefer L. High Levels of Psychological Resilience Associated With Less Disease Activity, Better Quality of Life, and Fewer Surgeries in Inflammatory Bowel Disease. *Inflamm Bowel Dis* 2021; **27**: 791-796 [PMID: 32696966 DOI: 10.1093/ibd/izaa196]

10 **Jones MP**, Keefer L, Bratten J, Taft TH, Crowell MD, Levy R, Palsson O. Development and initial validation of a measure of perceived stigma in irritable bowel syndrome. *Psychol Health Med* 2009;

14: 367-374 [PMID: 19444714 DOI: 10.1080/13548500902865956]
11 **Taft TH**, Keefer L, Artz C, Bratten J, Jones MP. Perceptions of illness stigma in patients with inflammatory bowel disease and irritable bowel syndrome. *Qual Life Res* 2011; **20**: 1391-1399 [PMID: 21424542 DOI: 10.1007/s11136-011-9883-x]
12 **Connor KM**, Davidson JR. Development of a new resilience scale: the Connor-Davidson Resilience Scale (CD-RISC). *Depress Anxiety* 2003; **18**: 76-82 [PMID: 12964174 DOI: 10.1002/da.10113]
13 **Connor KM**, Davidson JR. Translations of the CD-RISC [cited February 14, 2021]. In: Connor-Davidson Resilience Scale. Available from: http://www.connordavidson-resiliencescale.com/translations.php
14 **Drossman DA**, Patrick DL, Mitchell CM, Zagami EA, Appelbaum MI. Health-related quality of life in inflammatory bowel disease. Functional status and patient worries and concerns. *Dig Dis Sci* 1989; **34**: 1379-1386 [PMID: 2766905 DOI: 10.1007/BF01538073]
15 **Maaser C**, Sturm A, Vavricka SR, Kucharzik T, Fiorino G, Annese V, Calabrese E, Baumgart DC, Bettenworth D, Borralho Nunes P, Burisch J, Castiglione F, Eliakim R, Ellul P, González-Lama Y, Gordon H, Halligan S, Katsanos K, Kopylov U, Kotze PG, Krustinš E, Laghi A, Limdi JK, Rieder F, Rimola J, Taylor SA, Tolan D, van Rheenen P, Verstockt B, Stoker J; European Crohn's and Colitis Organisation [ECCO] and the European Society of Gastrointestinal and Abdominal Radiology [ESGAR]. ECCO-ESGAR Guideline for Diagnostic Assessment in IBD Part 1: Initial diagnosis, monitoring of known IBD, detection of complications. *J Crohns Colitis* 2019; **13**: 144-164 [PMID: 30137275 DOI: 10.1093/ecco-jcc/jjy113]
16 **Harvey RF**, Bradshaw JM. A simple index of Crohn's-disease activity. *Lancet* 1980; **1**: 514 [PMID: 6102236 DOI: 10.1016/s0140-6736(80)92767-1]
17 **Sandborn WJ**, Feagan BG, Hanauer SB, Lochs H, Löfberg R, Modigliani R, Present DH, Rutgeerts P, Schölmerich J, Stange EF, Sutherland LR. A review of activity indices and efficacy endpoints for clinical trials of medical therapy in adults with Crohn's disease. *Gastroenterology* 2002; **122**: 512-530 [PMID: 11832465 DOI: 10.1053/gast.2002.31072]
18 **Rutgeerts P**, Sandborn WJ, Feagan BG, Reinisch W, Olson A, Johanns J, Travers S, Rachmilewitz D, Hanauer SB, Lichtenstein GR, de Villiers WJ, Present D, Sands BE, Colombel JF. Infliximab for induction and maintenance therapy for ulcerative colitis. *N Engl J Med* 2005; **353**: 2462-2476 [PMID: 16339095 DOI: 10.1056/NEJMoa050516]
19 **Guadagnoli L**, Taft TH, Keefer L. Stigma perceptions in patients with eosinophilic gastrointestinal disorders. *Dis Esophagus* 2017; **30**: 1-8 [PMID: 28475723 DOI: 10.1093/dote/dox014]
20 **Bullinger M**, Alonso J, Apolone G, Leplège A, Sullivan M, Wood-Dauphinee S, Gandek B, Wagner A, Aaronson N, Bech P, Fukuhara S, Kaasa S, Ware JE Jr. Translating health status questionnaires and evaluating their quality: the IQOLA Project approach. International Quality of Life Assessment. *J Clin Epidemiol* 1998; **51**: 913-923 [PMID: 9817108 DOI: 10.1016/s0895-4356(98)00082-1]
21 **Ware JE Jr**, Gandek B. Methods for testing data quality, scaling assumptions, and reliability: the IQOLA Project approach. International Quality of Life Assessment. *J Clin Epidemiol* 1998; **51**: 945-952 [PMID: 9817111 DOI: 10.1016/s0895-4356(98)00085-7]
22 **Rössler W**. The stigma of mental disorders: A millennia-long history of social exclusion and prejudices. *EMBO Rep* 2016; **17**: 1250-1253 [PMID: 27470237 DOI: 10.15252/embr.201643041]
23 **Henderson C**, Noblett J, Parke H, Clement S, Caffrey A, Gale-Grant O, Schulze B, Druss B, Thornicroft G. Mental health-related stigma in health care and mental health-care settings. *Lancet Psychiatry* 2014; **1**: 467-482 [PMID: 26361202 DOI: 10.1016/S2215-0366(14)00023-6]
24 **Rueda S**, Mitra S, Chen S, Gogolishvili D, Globerman J, Chambers L, Wilson M, Logie CH, Shi Q, Morassaei S, Rourke SB. Examining the associations between HIV-related stigma and health outcomes in people living with HIV/AIDS: a series of meta-analyses. *BMJ Open* 2016; **6**: e011453 [PMID: 27412106 DOI: 10.1136/bmjopen-2016-011453]
25 **Chapple A**, Ziebland S, McPherson A. Stigma, shame, and blame experienced by patients with lung cancer: qualitative study. *BMJ* 2004; **328**: 1470 [PMID: 15194599 DOI: 10.1136/bmj.38111.639734.7C]
26 **Zhu M**, Zhou H, Zhang W, Deng Y, Wang X, Bai X, Li M, Hu R, Hou J, Liu Y. The Stroke Stigma Scale: a reliable and valid stigma measure in patients with stroke. *Clin Rehabil* 2019; **33**: 1800-1809 [PMID: 31307214 DOI: 10.1177/0269215519862329]
27 **Pourmarzi D**, Khoramirad A, Ahmari Tehran H, Abedini Z. Validity and Reliability of Persian Version of HIV/AIDS Related Stigma Scale for People Living With HIV/AIDS in Iran. *J Family Reprod Health* 2015; **9**: 164-171 [PMID: 27047562]
28 **Bifftu BB**, Dachew BA. Perceived Stigma and Associated Factors among People with Schizophrenia at Amanuel Mental Specialized Hospital, Addis Ababa, Ethiopia: A Cross-Sectional Institution Based Study. *Psychiatry J* 2014; **2014**: 694565 [PMID: 24967300 DOI: 10.1155/2014/694565]
29 **Chandra**, A Minkovitz CS. Factors that Influence Mental Health Stigma Among 8th Grade Adolescents. *J Youth Adolescence* 2007; **36**: 763-774 [DOI: 10.1007/s10964-006-9091-0]
30 **Brown RL**. Perceived stigma among people with chronic health conditions: the influence of age, stressor exposure, and psychosocial resources. *Res Aging* 2015; **37**: 335-360 [PMID: 25651574 DOI: 10.1177/0164027514533133]
31 **Bowirrat A**, Chen TJ, Blum K, Madigan M, Bailey JA, Chuan Chen AL, Downs BW, Braverman ER, Radi S, Waite RL, Kerner M, Giordano J, Morse S, Oscar-Berman M, Gold M. Neuro-psychopharmacogenetics and Neurological Antecedents of Posttraumatic Stress Disorder: Unlocking the Mysteries of Resilience and Vulnerability. *Curr Neuropharmacol* 2010; **8**: 335-358 [PMID:

21629442 DOI: 10.2174/157015910793358123]

World Journal of Gastroenterology

Submit a Manuscript: https://www.f6publishing.com

World J Gastroenterol 2021 October 21; 27(39): 6659-6672

DOI: 10.3748/wjg.v27.i39.6659

ISSN 1007-9327 (print) ISSN 2219-2840 (online)

ORIGINAL ARTICLE

Retrospective Cohort Study

Prognostic factors of minimally invasive surgery for gastric cancer: Does robotic gastrectomy bring oncological benefit?

Masaya Nakauchi, Koichi Suda, Susumu Shibasaki, Kenichi Nakamura, Shinichi Kadoya, Kenji Kikuchi, Kazuki Inaba, Ichiro Uyama

ORCID number: Masaya Nakauchi 0000-0002-1338-8556; Koichi Suda 0000-0002-0423-1565; Susumu Shibasaki 0000-0003-2454-5083; Kenichi Nakamura 0000-0002-9665-3940; Shinichi Kadoya 0000-0003-0526-6222; Kenji Kikuchi 0000-0002-6091-9292; Kazuki Inaba 0000-0003-0666-4687; Ichiro Uyama 0000-0003-1044-2948.

Author contributions: Nakauchi M, Suda K, Shibasaki S, and Uyama I provided substantial contributions to the conception and design of the study; Nakauchi M, Shibasaki S, Nakamura K, Kikuchi K, Kadoya S, and Inaba K contributed to the acquisition, analysis, and interpretation of the data; Nakauchi M performed the statistical analysis; Nakauchi M, Suda K, and Uyama I drafted the article and made critical revisions related to important intellectual content of the manuscript; all the authors have read and approved the final version to be published.

Institutional review board statement: This study was approved by the institutional review board of Fujita Health University.

Informed consent statement: Informed consent was obtained from all patients.

Masaya Nakauchi, Koichi Suda, Susumu Shibasaki, Kenichi Nakamura, Kenji Kikuchi, Kazuki Inaba, Ichiro Uyama, Department of Gastroenterological Surgery, Fujita Health University, Toyoake 470-1192, Aichi, Japan

Shinichi Kadoya, Department of Gastroenterological Surgery, Ishikawa Prefectural Central Hospital, Kanazawa 920-8535, Ishikawa, Japan

Corresponding author: Koichi Suda, FACS, MD, PhD, Professor, Department of Gastroenterological Surgery, Fujita Health University, 1-98 Dengakugakubo, Kutsukake, Toyoake 470-1192, Aichi, Japan. ko-suda@nifty.com

Abstract

BACKGROUND

Gastric cancer is the third leading cause of cancer-related death worldwide and surgical resection remains the sole curative treatment for gastric cancer. Minimally invasive gastrectomy including laparoscopic and robotic approaches has been increasingly used in a few decades. Thus far, only a few reports have investigated the oncological outcomes following minimally invasive gastrectomy.

AIM

To determine the 5-year survival following minimally invasive gastrectomy for gastric cancer and identify prognostic predictors.

METHODS

This retrospective cohort study identified 939 patients who underwent gastrectomy for gastric cancer during the study period. After excluding 125 patients with non-curative surgery (n = 77), other synchronous cancer (n = 2), remnant gastric cancer (n = 25), insufficient physical function (n = 13), and open gastrectomy (n = 8), a total of 814 consecutive patients with primary gastric cancer who underwent minimally invasive R0 gastrectomy at our institution between 2009 and 2014 were retrospectively examined. Accordingly, 5-year overall and recurrence-free survival were analyzed using the Kaplan–Meier method with the log-rank test and Cox regression analyses, while factors associated with survival were determined using multivariate analysis.

RESULTS

Our analysis showed that age > 65 years, American Society of Anesthesiologists

Conflict-of-interest statement: All authors have no commercial association or financial involvement that might pose a conflict of interest in connection with the submitted article. I. U. received lecture fees from Intuitive Surgical, Inc. K. S. and K. K. received funding from Medicaroid, Inc. in relation to Collaborative Laboratory for Research and Development in Advanced Surgical Technology. K.S. also received advisory fees from Medicaroid, Inc. outside of the submitted work.

Data sharing statement: No additional data are available.

STROBE statement: The authors have read the STROBE Statement—checklist of items, and the manuscript was prepared and revised according to the STROBE Statement—checklist of items.

Open-Access: This article is an open-access article that was selected by an in-house editor and fully peer-reviewed by external reviewers. It is distributed in accordance with the Creative Commons Attribution NonCommercial (CC BY-NC 4.0) license, which permits others to distribute, remix, adapt, build upon this work non-commercially, and license their derivative works on different terms, provided the original work is properly cited and the use is non-commercial. See: http://creativecommons.org/Licenses/by-nc/4.0/

Manuscript source: Invited manuscript

Specialty type: Gastroenterology and hepatology

Country/Territory of origin: Japan

Peer-review report's scientific quality classification

Grade A (Excellent): A
Grade B (Very good): 0
Grade C (Good): 0
Grade D (Fair): 0
Grade E (Poor): 0

Received: April 26, 2021

(ASA) physical status 3, total or proximal gastrectomy, and pathological T4 and N positive status were independent predictors of both 5-year overall and recurrence-free survival. Accordingly, the included patients had a 5-year overall and recurrence-free survival of 80.3% and 78.2%, respectively. Among the 814 patients, 157 (19.3%) underwent robotic gastrectomy, while 308 (37.2%) were diagnosed with pathological stage II or III disease. Notably, our findings showed that robotic gastrectomy was an independent positive predictor for recurrence-free survival in patients with pathological stage II/III [hazard ratio: 0.56 (0.33-0.96), P = 0.035]. Comparison of recurrence-free survival between the robotic and laparoscopic approach using propensity score matching analysis verified that the robotic group had less morbidity (P = 0.005).

CONCLUSION

Age, ASA status, gastrectomy type, and pathological T and N status were prognostic factors of minimally invasive gastrectomy, with the robot approach possibly improving long-term outcomes of advanced gastric cancer.

Key Words: Laparoscopy; Gastric cancer; Minimally invasive surgery; Prognostic factor; Stomach neoplasms

©The Author(s) 2021. Published by Baishideng Publishing Group Inc. All rights reserved.

Core Tip: This retrospective cohort study on 814 patients undergoing minimally invasive surgery for primary gastric cancer revealed a 5-year overall and recurrence-free survival of 80.3% and 78.2%, respectively. Moreover, our analysis identified age, American Society of Anesthesiologists status, type of gastrectomy, and pathological T and N status as prognostic predictors for overall and recurrence-free survival. The robotic approach was also identified as an independent positive predictor for recurrence-free survival in patients with pathological stage II/III disease, confirmed by the lesser morbidity in the robotic group following propensity score analysis.

Citation: Nakauchi M, Suda K, Shibasaki S, Nakamura K, Kadoya S, Kikuchi K, Inaba K, Uyama I. Prognostic factors of minimally invasive surgery for gastric cancer: Does robotic gastrectomy bring oncological benefit? *World J Gastroenterol* 2021; 27(39): 6659-6672
URL: https://www.wjgnet.com/1007-9327/full/v27/i39/6659.htm
DOI: https://dx.doi.org/10.3748/wjg.v27.i39.6659

INTRODUCTION

Gastric cancer is the fifth most common malignancy and the third leading cause of cancer-related death worldwide[1]. Surgical resection remains the sole curative treatment for gastric cancer, with regional lymphadenectomy being recommended as a component of radical gastrectomy[2]. Laparoscopic gastrectomy has been increasingly used, considering its better short-term effects and comparable long-term outcomes compared to open gastrectomy[2].

The da Vinci surgical system (DVSS; Intuitive Surgical, Sunnyvale, CA, United States) had been developed to overcome several disadvantages identified for standard minimally invasive laparoscopic surgery[2]. Most laparoscopic surgeons expect that utilizing the DVSS for gastric surgery would allow them to overcome the technical difficulties of laparoscopic gastrectomy, thereby improving its safety, reproducibility, teachability, and long-term outcomes. However, only one large, nonrandomized prospective study (NCT01309256) has compared DVSS with laparoscopic gastrectomy. Accordingly, the study results mentioned above demonstrated that DVSS had higher operative time and cost than laparoscopic gastrectomy with no difference in morbidity, suggesting that DVSS might reduce cost-effectiveness[3]. Concurrently, robotic gastrectomy, which has been actively used for operable patients with resectable gastric cancer at the patient's own expense[2], was introduced at our institution in 2009. Analysis of patient outcomes following robotic gastrectomy had demonstrated that its morbidity was approximately one-fifth of that observed with

Peer-review started: April 26, 2021
First decision: June 13, 2021
Revised: June 18, 2021
Accepted: September 23, 2021
Article in press: September 23, 2021
Published online: October 21, 2021

P-Reviewer: Preda SD
S-Editor: Wu YXJ
L-Editor: A
P-Editor: Li JH

laparoscopic gastrectomy, with such a reduction in morbidity, including decreased incidences of postoperative pancreatic fistula, certainly improving the short-term postoperative course[2]. Moreover, our previous study had compared the oncological outcomes, particularly 3-year survival rates, between robotic gastrectomy and laparoscopic gastrectomy[2]. Thus far, only a few reports have investigated the oncological outcomes following robotic gastrectomy, considering that DVSS remains a relatively new technology. Therefore, the current study aimed to determine the prognostic factors of minimally invasive gastrectomy, including laparoscopic and robotic procedures.

MATERIALS AND METHODS

Patients

This single-center retrospective cohort study included patients who underwent curative gastrectomy for gastric cancer at our institution between January 2009 and September 2014. The inclusion criteria were patients with primary gastric adenocarcinoma who underwent curative resection using minimally invasive surgery (MIS). The exclusion criteria were patients with other synchronous cancer and those whose resection was limited due to poor physical functioning. Among the 939 patients who underwent gastrectomy for gastric cancer during the study period, 125 were excluded due to non-curative surgery (n = 77), other synchronous cancer (n = 2), remnant gastric cancer (n = 25), insufficient physical function (n = 13), and open gastrectomy (n = 8). Thus, the 814 patients who satisfied the study criteria were ultimately analyzed. The clinicopathological variables collected included age, sex, body mass index (BMI), American Society of Anesthesiologists (ASA) physical status classification, date of surgery, type of approach, histologic type, lymphovascular invasion status, TNM staging (Japanese Gastric Cancer Association classification, 14th edition), number of harvested lymph nodes, postoperative complications determined by Clavien–Dindo (C-D) classification[4], date of the first recurrence, and date and status of the last follow-up. The extent of gastrectomy and lymphadenectomy was defined based on Japanese gastric cancer treatment guidelines[5]. Overall survival (OS) was calculated from the date of resection to the date of the last follow-up or death of any cause. Recurrence-free survival (RFS) was calculated from the date of resection to the date of first recurrence, last follow-up, or death of any cause, whichever occurred first. Details regarding indications for radical gastrectomy, including the selection of laparoscopic or robotic approach, surgical procedures, perioperative management, adjuvant chemotherapy, and oncologic follow-up, have been previously reported[2]. Neoadjuvant chemotherapy (NAC) (S-1 80 mg/m^2 days 1-21 + CDDP 60 mg/m^2 day 8 or S-1 80 mg/m^2 days 1-28) was offered to patients with clinical T ≥ 2, tumor size ≥ 5 cm, and/or swollen locoregional lymph nodes ≥ 1.5 cm[2]. All patients were uniformly offered robotic surgery without considering their backgrounds, including physical and oncological status. Patients who agreed to the uninsured use of the surgical robot underwent robotic gastrectomy, whereas those who wished for insured treatment underwent laparoscopic gastrectomy[2]. All patients were completely involved in the decision-making process and provided informed consent prior to participation. All surgical procedures were performed or guided by surgeons qualified by the Japanese Society for Endoscopic Surgical Skill Qualification System, initiated in 2004 by the Japanese Society for Endoscopic Surgery to develop a tool for the reliable and reproducible evaluation of trainees' surgical techniques[6]. All procedures were supervised by an expert gastric surgeon (I.U.) who had performed more than 1500 Laparoscopic gastrectomies and 400 robotic gastrectomies. This study was approved by the institutional review board of Fujita Health University.

Statistical analysis

All statistical analyses were conducted using IBM SPSS Statistics 25 (IBM Corporation, Armonk, NY, United States). Long-term outcomes were analyzed using the Kaplan–Meier method with the log-rank test and Cox regression analyses. Considering our relatively small sample size, multivariate analysis was conducted using all variables determined to be significant (P < 0.1) during univariate analysis as independent variables. Data were expressed as median, interquartile range, or hazard ratio (HR) with the 95% confidence interval (CI) unless otherwise stated. A P value of < 0.05 (two-tailed) was considered statistically significant. Propensity score matching analysis was used to reduce selection bias with regard to potential confounding factors when establishing the laparoscopic and robotic groups. Possible confounders were

selected based on their potential association with the outcome of interest according to clinical knowledge. Therefore, clinicopathological characteristics (age, BMI, sex, ASA status, pathological T and N factor, type of surgery, tumor size, and NAC) were used to adjust differences between the laparoscopic and robotic groups through one-to-one pair matching using optimal match without replacement. Propensity scores were matched using a caliper width 1/5 Logit of the standard deviation. The absolute standardized difference was used to measure covariate balance, in which an absolute standardized mean difference above represented a meaningful imbalance[7]. Independent continuous variables were compared using the Mann–Whitney *U* test or Kruskal-Wallis test. Categorical variables were compared using the χ^2 test or Fisher's exact test.

RESULTS

Patient characteristics

Table 1 summarizes the characteristics of all patients included herein. Accordingly, the included patients had a median age of 68 years, among whom 31.4% (n = 256) were diagnosed with clinical stage II or more disease, while 14.6% (n = 119) underwent NAC. Laparoscopic and robotic gastrectomy was performed in 657 (80.7%) and 157 (19.3%) patients, respectively. None of the patients required intraoperative conversion to open procedure from MIS. Pathological stage II and III disease was diagnosed in 160 (19.7%) and 148 (18.2%) patients, respectively. Morbidity of C-D grade ≥ III was observed in 72 patients (8.8%).

Survival outcomes

The median follow-up period was 59.5 mo, while the 5-year OS and RFS were 80.3% and 78.2%, respectively (Figure 1A and B). Patients with pStage I, II, and III had a 5-year OS of 91.9%, 76.3%, and 43.7%, and a 5-year RFS of 91.6%, 74.7%, and 36.0%, respectively.

Factors related to survival

Univariate analysis identified age > 65 years, ASA status 3, total or proximal gastrectomy, D2 lymphadenectomy, tumor size > 30 mm, lymphovascular invasion, C–D grade ≥ III morbidity, NAC administration, adjuvant chemotherapy administration, and higher pT and pN status as factors significantly associated with OS (Table 2). However, multivariate analysis revealed that only age > 65 years [HR: 1.62 (1.09-2.40), P = 0.017], ASA status 3 [HR: 1.91 (1.18-3.10), P = 0.009], total or proximal gastrectomy [HR: 1.45 (1.03-2.05), P = 0.036], pT4 [HR: 4.31 (2.37–7.82), P < 0.001], and pN positive status were significantly and independently associated with OS (Table 2). Similarly, multivariate analysis identified age > 65 years [HR: 1.48 (1.02-2.14), P = 0.038], ASA status 3 [HR: 1.62 (1.02-2.60), P = 0.043], total or proximal gastrectomy [HR: 1.55 (1.12–2.15), P = 0.009], pT4 [HR: 4.20 (2.38–7.41), P < 0.001], and pN positive status as factors significantly and independently associated with RFS (Table 3). Moreover, multivariate analysis showed that robotic approach could likely be a positive predictor for RFS, although no significant association was observed [HR 0.68 (0.44-1.06), P = 0.088] (Table 3).

Survival outcomes following the laparoscopic and robotic approach

The laparoscopic and robotic approach had a 5-year OS of 79.4% and 83.4% (P = 0.243) and a 5-year RFS of 76.9% and 84.2% (P = 0.085), respectively. No significant difference in the 5-year OS and RFS was noted between both groups for patients with pStage I (91.6% *vs* 93.4%, P = 0.471 and 91.4% *vs* 92.7%, P = 0.634) (Figure 2A and B). Notably, among patients with pStage II/III, those in the robotic group had significantly better RFS compared to those in the laparoscopic group (74.1% *vs* 51.7%, P = 0.006) (Figure 2D), although no significant difference in the 5-year OS was observed (P = 0.071) (Figure 2C).

Factors associated with survival in pStage II/III diseases

Our analysis showed that pT4 [HR: 4.02 (1.21-13.42), P = 0.024] and pN positive status were significantly and independently associated with OS. Notably, univariate analysis showed that robotic gastrectomy (P = 0.007), total or proximal gastrectomy (P = 0.004), tumor size > 30 mm (P = 0.014), pT4 (P = 0.007), and pN positive status were significantly associated with RFS. Meanwhile, multivariate analysis found that robotic

Table 1 Clinicopathological characteristics of the entire cohort

Variables	*n* = 814
Age, yr [IQR]	68[61-74]
Sex, *n* (%)	
Male	562 (69.0)
Female	252 (31.0)
BMI, kg/m^2 [IQR]	22.2 [20.0-24.1]
ASA, *n* (%)	
1	314 (38.6)
2	396 (48.6)
3	104 (12.8)
Clinical stage, *n* (%)	
I	558 (68.6)
II	125 (15.3)
III	121 (14.9)
IV	10 (1.2)
Neoadjuvant chemotherapy, *n* (%)	119 (14.6)
Neoadjuvant radiotherapy, *n* (%)	0 (0)
Approach, *n* (%)	
Laparoscopic	657 (80.7)
Robotic	157 (19.3)
Type of gastrectomy, *n* (%)	
Distal	559 (68.7)
Total	238 (29.2)
Proximal	16 (2.0)
Pylorus preserving	1 (0.1)
Lymphadenectomy, *n* (%)	
D1+	378 (46.4)
D2	436 (53.6)
Dissected nodes, *n* [IQR]	38[28-48]
Tumor size, mm [IQR]	30[20-50]
pT, *n* (%)	
1	469 (57.6)
2	87 (10.7)
3	112 (13.8)
4	138 (17.0)
CR	8 (1.0)
pN, *n* (%)	
0	559 (68.7)
1	98 (12.0)
2	79 (9.7)
3	78 (9.6)
pStage, *n* (%)	

I	498 (61.2)
II	160 (19.7)
III	148 (18.2)
TCRNany	8 (1.0)
WHO histologic type, *n* (%)	
Tub/pap	402 (49.4)
Por/sig	352 (43.2)
Mixed/other	60 (7.4)
Lymphovascular invasion, *n* (%)	531 (65.2)
Adjuvant chemotherapy, *n* (%)	242 (29.7)
Adjuvant radiotherapy, *n* (%)	0 (0)
Morbidity (C–D grade ≥ III), *n* (%)	72 (8.8)
Anastomotic leakage	22 (2.7)
Pancreatic fistula	30 (3.7)

Categorical and continuous data are presented as *n* (%) and median [IQR], respectively. IQR: Interquartile range; ASA: American Society of Anesthesiologists; BMI: Body mass index; CR: Complete response at the primary site; C-D: Clavien-Dindo classification.

gastrectomy was independently and positively associated with RFS [HR: 0.56 (0.33–0.96), P = 0.035]. Apart from robotic gastrectomy, only pT4 and pN positive status were identified as factors independently associated with RFS (Table 4).

Comparison between robotic and laparoscopic gastrectomy in pStage II/III diseases

To account for confounding factors between both groups, propensity score matching was performed (Table 5). In the prematched cohort of 308 patients with pStage II/III disease, 67 and 241 patients belonged to the robotic and laparoscopic groups, respectively. After matching, each group comprised 61 patients. The matched cohort had a considerably better balance of covariates, with < 0.245 of the cutoff value of an absolute standardized difference. In the postmatched cohort, no differences in clinicopathological variables were observed between the laparoscopic and robotic groups, although the robotic group had lower morbidity (4.9% *vs* 16.4%, P = 0.04) (Table 5). Furthermore, the robotic group had significantly better 5-year OS (70.4% *vs* 50.2%, P = 0.039) and RFS (74.1% *vs* 44.5%, P = 0.005) than the laparoscopic group in the postmatched cohort (Figure 3A and B).

DISCUSSION

The current study clearly identified factors related to survival in patients with gastric cancer who underwent MIS, subsequently presenting three significant findings.

First, the present study highlighted the feasibility and safety of MIS for gastric cancer as determined by the 5-year outcomes. While the long-term outcomes of laparoscopic surgery have been increasingly reported in recent years, only a few studies have investigated the long-term outcomes of the robotic approach[2,8,9]. Consistent with previous studies, including those from our group, the current study demonstrated no significant difference in OS and RFS between the laparoscopic and robotic approaches [2,8,9]. However, among patients with pStage II/III, those in the robotic group demonstrated significantly better RFS than those in the laparoscopic group (P = 0.006).

Second, our results showed that pT and pN status was independently associated with both OS and RFS. Currently, multidisciplinary treatment for gastric cancer utilizing various chemotherapeutic options has been developed worldwide. In Western countries, neoadjuvant and adjuvant chemotherapy combined with curative resection has been the standard treatment for advanced gastric cancer[10,11], whereas adjuvant chemotherapy following curative resection remains the standard approach in Japan[5]. Regardless of treatment options, however, evidence has shown that the pN factor is consistently strongly associated with survival following gastric cancer treatment[12-14]. The results of the current study are consistent with those presented

Table 2 Factors associated with overall survival for the entire cohort (*n* = 814)

	Univariate			Multivariate		
	HR	95%CI	*P*	HR	95%CI	*P*
Age > 65 yr	1.46	1.04–2.06	0.031	1.62	1.09–2.40	0.017
Female sex	0.75	0.52–1.09	0.129			
BMI > 23 kg/m^2	0.77	0.55–1.07	0.123			
ASA						
1	1			1		
2	0.96	0.68–1.38	0.837	1.06	0.72–1.57	0.753
3	1.97	1.27–3.05	0.003	1.91	1.18–3.10	0.009
Neoadjuvant chemotherapy	1.84	1.27–2.67	0.001	1.34	0.88–2.04	0.166
Robotic approach	0.77	0.50–1.21	0.258			
Type of gastrectomy						
Distal/pylorus-preserving	1			1		
Total/proximal	2.17	1.58–2.99	< 0.001	1.45	1.03–2.05	0.036
D2 lymphadenectomy	1.86	1.32–2.61	< 0.001	0.87	0.57–1.33	0.528
Tumor > 30 mm	3.23	2.20–4.75	< 0.001	1.05	0.66–1.69	0.832
WHO histologic type						
Tub/pap	1			1		
Por/sig/mixed/other	1.54	1.12–2.13	0.009	1.26	0.89–1.78	0.190
Lymphovascular invasion	4.38	2.68–7.17	< 0.001	1.17	0.60–2.26	0.651
pT						
1	1			1		
2	2.82	1.62–4.91	< 0.001	1.72	0.90–3.27	0.099
3	3.03	1.82–5.03	< 0.001	1.54	0.82–2.91	0.184
4	9.78	6.54–14.60	< 0.001	4.31	2.37–7.82	< 0.001
CR	1.67	0.23–12.17	0.613	1.34	0.16–10.97	0.784
pN						
0	1			1		
1	2.76	1.74–4.39	< 0.001	2.02	1.22–3.34	0.007
2	4.05	2.56–6.41	< 0.001	1.97	1.15–3.36	0.013
3	8.08	5.40–12.10	< 0.001	2.92	1.79–4.78	< 0.001
Adjuvant chemotherapy	3.27	2.37–4.50	< 0.001	1.21	0.80–1.82	0.371
Morbidity (C-D grade ≥ III)	1.85	1.18–2.91	0.008	1.27	0.79–2.05	0.325

HR: Hazard ratio; CI: Confidence interval; ASA: American Society of Anesthesiologists; BMI: Body mass index; CR: Complete response at the primary site; C-D: Clavien–Dindo classification.

in previous studies.

Third, the use of the surgical robot was significantly associated with improved RFS among propensity score-matched patients with pStage II/III disease. This could have been attributed to lower morbidity in the robotic gastrectomy group, a causal relationship between morbidity and survival, and higher morbidity in patients undergoing surgery for advanced disease. First, a few studies have shown that robotic gastrectomy was technically safe and feasible but did not have superior morbidity compared to the laparoscopic approach[3]. However, Wang *et al*[15] who compared morbidity between robotic and laparoscopic gastrectomy using propensity score-

Table 3 Factors associated with recurrence-free survival for the entire cohort (*n* = 814)

	Univariate			Multivariate		
	HR	95%CI	*P*	HR	95%CI	*P*
Age > 65 yr	1.33	0.97–1.84	0.076	1.48	1.02–2.14	0.038
Female sex	0.76	0.54–1.06	0.108			
BMI > 23 kg/m^2	0.77	0.56–1.05	0.100			
ASA						
1	1			1		
2	0.95	0.68–1.32	0.761	1.08	0.75–1.55	0.692
3	1.67	1.09–2.55	0.018	1.62	1.02–2.60	0.043
Neoadjuvant chemotherapy	1.91	1.34–2.71	< 0.001	1.39	0.93–2.08	0.104
Robotic approach	0.69	0.45–1.06	0.087	0.68	0.44–1.06	0.088
Type of gastrectomy						
Distal/pylorus-preserving	1			1		
Total/proximal	2.24	1.66–3.02	< 0.001	1.55	1.12–2.15	0.009
D2 lymphadenectomy	2.08	1.50–2.86	< 0.001	0.99	0.66–1.48	0.957
Tumor > 30 mm	3.19	2.23–4.56	< 0.001	0.95	0.61–1.48	0.827
WHO histologic type						
Tub/pap	1			1		
Por/sig/mixed/other	0.54	0.14–2.08	0.005	1.20	0.86–1.66	0.284
Lymphovascular invasion	4.93	3.06–7.94	< 0.001	1.29	0.69–2.43	0.430
pT						
1	1			1		
2	2.87	1.69–4.85	< 0.001	1.57	0.85–2.89	0.148
3	3.42	2.13–5.48	< 0.001	1.60	0.89–2.89	0.120
4	10.62	7.26–15.53	< 0.001	4.20	2.38–7.41	< 0.001
CR	1.41	0.19–10.24	0.737	0.96	0.12–7.77	0.967
pN						
0	1			1		
1	3.08	1.99–4.77	< 0.001	2.23	1.39–3.58	0.001
2	5.01	3.29–7.62	< 0.001	2.24	1.36–3.70	0.002
3	8.92	6.07–13.11	< 0.001	3.32	2.06–5.34	< 0.001
Adjuvant chemotherapy	3.53	2.62–4.77	< 0.001	1.18	0.80–1.73	0.410
Morbidity (C-D grade ≥ III)	1.69	1.09–2.62	0.019	1.04	0.65–1.67	0.868

ASA: American Society of Anesthesiologists; BMI: Body mass index; CR: Complete response at the primary site; C-D: Clavien–Dindo classification; HR: Hazard ratio; CI: Confidence interval.

matched analysis, reported that the robotic group exhibited significantly lower morbidity, particularly with regard to infectious complications (*e.g.*, anastomotic leakage and intra-abdominal abscess)[15]. Furthermore, a multicenter, prospective, single-arm study by our group recently reported that robotic gastrectomy promoted lesser morbidity than laparoscopic gastrectomy among historical controls[2]. Similarly, the present study showed that the robotic group had significantly lesser morbidity compared to the laparoscopic in the postmatched cohort. Second, several studies have demonstrated that morbidity was associated with worse survival in gastric cancer[16-19]. In fact, Jin *et al*[16] reported that patients with and without postoperative complic-

Table 4 Factors associated with recurrence-free survival for patients with pathological stage II/III disease (*n* = 308)

	Univariate			Multivariate		
	HR	95%CI	*P*	HR	95%CI	*P*
Age > 65 yr	1.04	0.73–1.48	0.848			
Female sex	1.08	0.75–1.58	0.673			
BMI > 23 kg/m^2	0.69	0.47–1.00	0.052	0.92	0.62–1.35	0.657
ASA						
1	1					
2	0.82	0.56–1.19	0.297			
3	1.07	0.63–1.80	0.809			
Neoadjuvant chemotherapy	1.37	0.93–2.01	0.114			
Robotic approach	0.50	0.30–0.83	0.007	0.56	0.33–0.96	0.035
Type of gastrectomy						
Distal/pylorus-preserving	1			1		
Total/proximal	1.67	1.18–2.37	0.004	1.32	0.91–1.90	0.145
D2 lymphadenectomy	1.26	0.80–2.00	0.320			
Tumor > 30 mm	2.17	1.17–4.03	0.014	1.34	0.69–2.60	0.303
WHO histologic type						
Tub/pap	1			1		
Por/sig/mixed/other	1.38	0.95–2.00	0.089	1.29	0.88–1.90	0.197
pT						
1	1			1		
2	1.82	0.60–5.53	0.292	1.33	0.42–4.23	0.628
3	1.32	0.47–3.75	0.6	1.45	0.49–4.30	0.505
4	3.96	1.45–10.83	0.007	3.52	1.23–10.07	0.019
pN						
0	1			1		
1	2.07	1.16–3.69	0.014	2.86	1.57–5.24	0.001
2	2.24	1.29–3.90	0.004	2.45	1.38–4.34	0.002
3	3.74	2.21–6.32	< 0.001	3.25	1.88–5.61	< 0.001
Adjuvant chemotherapy	1.37	0.92–2.04	0.119			
Morbidity (C-D grade ≥ III)	1.58	0.97–2.58	0.066	1.22	0.73–2.05	0.453

ASA: American Society of Anesthesiologists; BMI: Body mass index; C–D: Clavien–Dindo classification; HR: Hazard ratio; CI: Confidence interval.

ations had RFS rates of 23% and 40%, respectively ($P < 0.001$). Third, advanced gastric cancer requires complicated procedures, which can cause more complications. Notably, studies have reported that patient with advanced disease had morbidity rates of 8.3%-15.2% following minimally invasive gastrectomy, respectively[20,21]. The aforementioned findings therefore indicate that utilizing surgical robots, which cause less morbidity, might at least partly contribute to the better RFS in patients with advanced gastric cancer, suggesting that surgical robots may be more beneficial for patients with advanced disease. However, although univariate analysis found morbidity to be significantly associated with RFS, multivariate analysis did not identify the same as a significant independent factor associated with RFS in the entire cohort. As such, further investigations are warranted to confirm such findings.

The current study has several limitations worth noting. First, this study was retrospective in nature and involved only a single institution. Moreover, the sample

Table 5 Clinicopathological characteristics of pStage II/III patients in the pre- and postmatched cohort

	Prematched				Postmatched			
	Lap (*n* = 241)	Robotic (*n* = 67)	*P*	ASD	Lap (*n* = 61)	Robotic (*n* = 61)	*P*	ASD
Sex, *n* (%)			0.132	0.204			0.580	0.100
Male	174 (72.2)	42 (62.7)			35 (57.4)	38 (62.3)		
Female	67 (27.8)	25 (37.3)			26 (42.6)	23 (37.7)		
Age, yr [IQR]	69 [61–75]	65 [60–77]	0.134	0.235	68 [61–75]	65 [60–77]	0.824	0.042
BMI, kg/m^2 [IQR]	21.6 [19.2–23.7]	23.1 [20.0–24.8]	0.008	0.329	22.6 [20.4–24.9]	23.0 [20.0–24.9]	0.810	0.007
ASA, *n* (%)			0.074	0.315			0.959	0.052
1	89 (36.9)	35 (52.2)			31 (50.8)	30 (49.2)		
2	118 (49.0)	24 (35.8)			23 (37.7)	23 (37.7)		
3	34 (14.1)	8 (11.9)			7 (11.5)	8 (13.1)		
Neoadjuvant chemotherapy, *n* (%)	61 (25.3)	11 (16.4)	0.128	0.220	10 (16.4)	11 (18.0)	0.810	0.043
Type of gastrectomy, *n* (%)			0.075	0.329			1	< 0.001
Distal	136 (56.4)	48 (71.6)			42 (68.9)	42 (68.9)		
Total	104 (43.2)	19 (28.4)			19 (31.1)	19 (31.1)		
Proximal	1 (0.4)	0 (0)			0 (0)	0 (0)		
Tumor size, mm [IQR]	50[35-70]	40[30-63]	0.026	0.265	50 [35–77]	43 [30–65]	0.192	0.187
pT, *n* (%)			0.042	0.391			0.860	0.158
1	11 (4.6)	8 (11.9)			4 (6.6)	6 (9.8)		
2	35 (14.5)	4 (6.0)			4 (6.6)	4 (6.6)		
3	85 (35.3)	27 (40.3)			21 (34.4)	23 (37.7)		
4	110 (45.6)	28 (41.8)			32 (52.5)	28 (45.9)		
pN, *n* (%)			0.15	0.338			0.617	0.244
0	65 (27.0)	24 (35.8)			16 (26.2)	22 (36.1)		
1	48 (19.9)	15 (22.4)			17 (27.9)	13 (21.3)		
2	68 (28.2)	10 (14.9)			9 (14.8)	10 (16.4)		
3	60 (24.9)	18 (26.9)			19 (31.1)	16 (26.2)		
pStage, *n* (%)			0.246				0.716	
II	121 (50.2)	39 (58.2)			32 (52.5)	34 (55.7)		
III	120 (49.8)	28 (41.8)			29 (47.5)	27 (44.3)		
Dissected nodes, *n* [IQR]	44 [35–53]	43 [35–51]	0.858		45 [35–54]	43 [30-65]	0.556	
WHO histological type, *n* (%)			0.667				0.229	
Tub/pap	88 (36.5)	27 (41.8)			17 (27.9)	26 (42.6)		
Por/sig	129 (53.5)	34 (50.7)			37 (60.7)	30 (49.2)		
Mixed/other	24 (10.0)	5 (7.5)			7 (11.5)	5 (8.2)		
Lymphovascular invasion, *n* (%)	241 (100)	66 (98.5)	0.218		61 (100)	60 (98.4)	0.5	
Adjuvant chemotherapy, *n* (%)	161 (66.8)	47 (70.1)	0.605		38 (62.3)	43 (70.5)	0.338	
Morbidity (C-D grade ≥ III), *n* (%)	31 (12.9)	3 (4.5)	0.053		10 (16.4)	3 (4.9)	0.04	

Categorical and continuous data are presented as *n* (%) and median [IQR], respectively. ASA: American Society of Anesthesiologists; BMI: Body mass

index; CR: Complete response at the primary site; C–D: Clavien–Dindo classification; ASD: Absolute standardized mean difference.

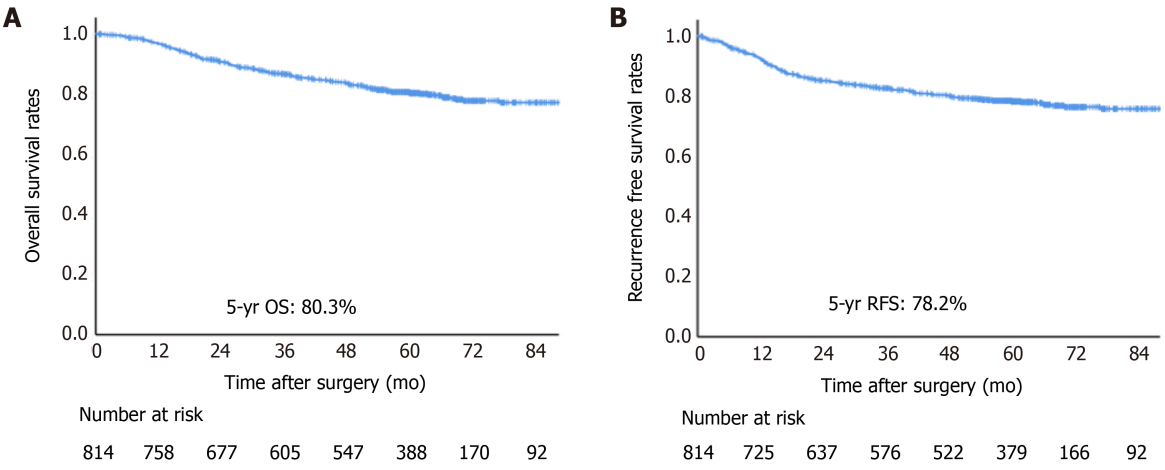


Figure 1 Kaplan-Meier curves. Kaplan-Meier estimates in the entire cohort A: Overall survival probability; B: Recurrence-free survival probability. OS: Overall survival; RFS: Recurrence-free survival.

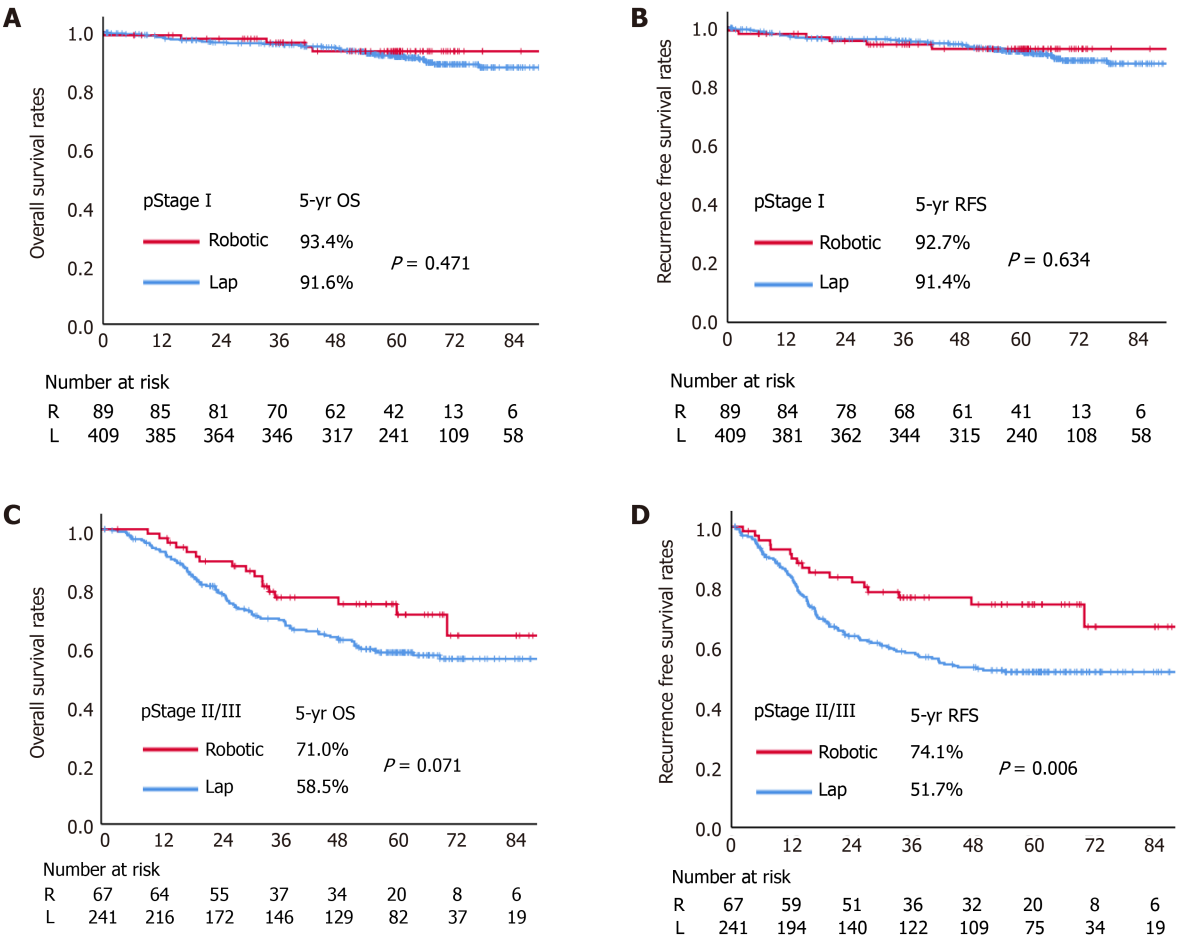


Figure 2 Kaplan-Meier curves. A and C: Kaplan–Meier estimates of overall survival probability for pathological stage I and II/III, B and D: Kaplan–Meier estimates of recurrence-free survival probability for pathological stage I and II/III. OS: Overall survival; RFS: Recurrence-free survival.

size, particularly that of the robotic group, was relatively small. Therefore, given that biases may exist in our data, the overall results should be interpreted with caution. As described in our previous reports[2,6], patients were selected according to whether the they agreed to the uninsured use of robot-assisted surgery, which may have caused

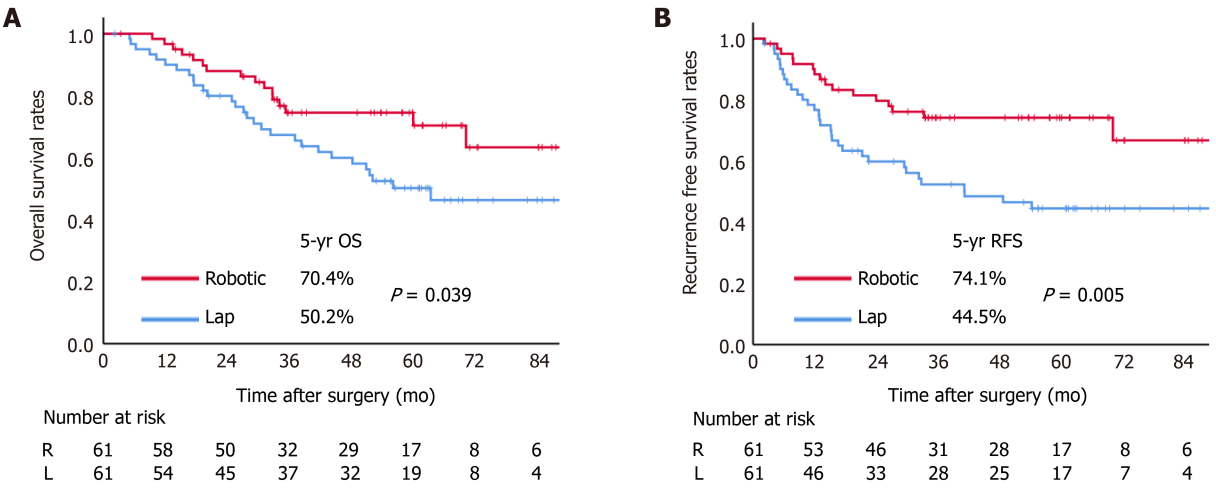


Figure 3 Kaplan-Meier curves. Kaplan-Meier estimates in the postmatched cohort. A: Overall survival probability; B: Recurrence-free survival probability. OS: Overall survival; RFS: Recurrence-free survival.

selection bias due to a possible preference for robotic gastrectomy in patients of higher economic status. However, this was an inherent limitation at the time of study enrollment considering that the DVSS was not covered by the medical insurance in Japan at the time the enrolled patients underwent gastrectomy, whereas conventional laparoscopic gastrectomy was covered. Second, propensity score matching between the laparoscopic and robotic group did not account for adjuvant chemotherapy administration given that, similarly to postoperative complications, adjuvant chemotherapy was determined after robotic or laparoscopic gastrectomy was conducted. Considering that both adjuvant chemotherapy and postoperative complications may affect prognosis[2,6,21], well-designed prospective trials are needed to determine a cause-effect relationship between robotic or laparoscopic gastrectomy and postoperative complications, as well as adjuvant chemotherapy administration.

CONCLUSION

In conclusion, the current study identified age, ASA status, type of gastrectomy, and pathological T and N status are prognostic factors of minimally invasive gastrectomy for gastric cancer. Moreover, the use of robotic assistance was associated with reduced early morbidity, as well as potentially better oncological outcomes in advanced gastric cancer.

ARTICLE HIGHLIGHTS

Research background

Minimally invasive surgery (MIS) including laparoscopic and robotic approaches for gastric cancer has been increasingly used because of its beneficial short-term effects over the open approach. However, oncological outcomes are not established.

Research motivation

There have been few reports on the oncological outcomes of MIS for gastric cancer patients, especially for the robotic approach, because a surgical robot remains a relatively new technology. Therefore, this study aimed to determine the prognostic factors of minimally invasive gastrectomy, including laparoscopic and robotic approaches.

Research objectives

This study aimed to determine the prognostic factors of minimally invasive gastrectomy, including laparoscopic and robotic approaches.

Research methods

This single-institutional retrospective cohort study included 814 consecutive patients with primary gastric cancer who underwent minimally invasive R0 gastrectomy between 2009 and 2014. We retrospectively examined 5-year overall survival and recurrence-free survival and investigated factors related to survival.

Research results

Age > 65 years, American Society of Anesthesiologists (ASA) physical status 3, total or proximal gastrectomy, and pathological T4 and N positive status were independent predictors of overall survival and recurrence-free survival. The five-year overall survival and recurrence-free survival were 80.3% and 78.2%, respectively. Of all 814 patients, 157 patients (19.3%) underwent robotic gastrectomy and 308 (37.2%) were diagnosed with pathological stage II or III disease. Robotic gastrectomy was an independent positive predictor for recurrence-free survival in pathological stage II/III patients (hazard ratio: 0.56 [0.33-0.96], P = 0.035). Comparison of recurrence-free survival between robotic and laparoscopic approach using propensity score matching analysis verified that with less morbidity in the robotic group (P = 0.005).

Research conclusions

Age, ASA status, type of gastrectomy, and pathological T and N status were prognostic factors of minimally invasive gastrectomy for gastric cancer, and the use of a surgical robot may improve its long-term outcomes for advanced gastric cancer.

Research perspectives

Future studies to better prove the efficacy of robotic gastrectomy for advanced gastric cancer patients are warranted.

REFERENCES

1 **Bray F**, Ferlay J, Soerjomataram I, Siegel RL, Torre LA, Jemal A. Global cancer statistics 2018: GLOBOCAN estimates of incidence and mortality worldwide for 36 cancers in 185 countries. *CA Cancer J Clin* 2018; **68**: 394-424 [PMID: 30207593 DOI: 10.3322/caac.21492]

2 **Shibasaki S**, Suda K, Obama K, Yoshida M, Uyama I. Should robotic gastrectomy become a standard surgical treatment option for gastric cancer? *Surg Today* 2020; 50: 955-965 [PMID: 31512060 DOI: 10.1007/s00595-019-01875-w]

3 **Kim HI**, Han SU, Yang HK, Kim YW, Lee HJ, Ryu KW, Park JM, An JY, Kim MC, Park S, Song KY, Oh SJ, Kong SH, Suh BJ, Yang DH, Ha TK, Kim YN, Hyung WJ. Multicenter Prospective Comparative Study of Robotic Versus Laparoscopic Gastrectomy for Gastric Adenocarcinoma. *Ann Surg* 2016; **263**: 103-109 [PMID: 26020107 DOI: 10.1097/SLA.0000000000001249]

4 **Clavien PA**, Barkun J, de Oliveira ML, Vauthey JN, Dindo D, Schulick RD, de Santibañes E, Pekolj J, Slankamenac K, Bassi C, Graf R, Vonlanthen R, Padbury R, Cameron JL, Makuuchi M. The Clavien-Dindo classification of surgical complications: five-year experience. *Ann Surg* 2009; **250**: 187-196 [PMID: 19638912 DOI: 10.1097/SLA.0b013e3181b13ca2]

5 **Japanese Gastric Cancer Association**. Japanese gastric cancer treatment guidelines 2014 (ver. 4). *Gastric Cancer* 2017; **20**: 1-19 [PMID: 27342689 DOI: 10.1007/s10120-016-0622-4]

6 **Mori T**, Kimura T, Kitajima M. Skill accreditation system for laparoscopic gastroenterologic surgeons in Japan. *Minim Invasive Ther Allied Technol* 2010; **19**: 18-23 [PMID: 20095893 DOI: 10.3109/13645700903492969]

7 **Austin PC**. Balance diagnostics for comparing the distribution of baseline covariates between treatment groups in propensity-score matched samples. *Stat Med* 2009; **28**: 3083-3107 [PMID: 19757444 DOI: 10.1002/sim.3697]

8 **Jiang Y**, Zhao Y, Qian F, Shi Y, Hao Y, Chen J, Li P, Yu P. The long-term clinical outcomes of robotic gastrectomy for gastric cancer: a large-scale single institutional retrospective study. *Am J Transl Res* 2018; **10**: 3233-3242 [PMID: 30416664]

9 **Okumura N**, Son T, Kim YM, Kim HI, An JY, Noh SH, Hyung WJ. Robotic gastrectomy for elderly gastric cancer patients: comparisons with robotic gastrectomy in younger patients and laparoscopic gastrectomy in the elderly. *Gastric Cancer* 2016; **19**: 1125-1134 [PMID: 26541766 DOI: 10.1007/s10120-015-0560-6]

10 **Cunningham D**, Allum WH, Stenning SP, Thompson JN, Van de Velde CJ, Nicolson M, Scarffe JH, Lofts FJ, Falk SJ, Iveson TJ, Smith DB, Langley RE, Verma M, Weeden S, Chua YJ, MAGIC Trial Participants. Perioperative chemotherapy *vs* surgery alone for resectable gastroesophageal cancer. *N Engl J Med* 2006; **355**: 11-20 [PMID: 16822992 DOI: 10.1056/NEJMoa055531]

11 **Al-Batran SE**, Homann N, Pauligk C, Goetze TO, Meiler J, Kasper S, Kopp HG, Mayer F, Haag GM, Luley K, Lindig U, Schmiegel W, Pohl M, Stoehlmacher J, Folprecht G, Probst S, Prasnikar N, Fischbach W, Mahlberg R, Trojan J, Koenigsmann M, Martens UM, Thuss-Patience P, Egger M,

Block A, Heinemann V, Illerhaus G, Moehler M, Schenk M, Kullmann F, Behringer DM, Heike M, Pink D, Teschendorf C, Löhr C, Bernhard H, Schuch G, Rethwisch V, von Weikersthal LF, Hartmann JT, Kneba M, Daum S, Schulmann K, Weniger J, Belle S, Gaiser T, Oduncu FS, Güntner M, Hozaeel W, Reichart A, Jäger E, Kraus T, Mönig S, Bechstein WO, Schuler M, Schmalenberg H, Hofheinz RD; FLOT4-AIO Investigators. Perioperative chemotherapy with fluorouracil plus leucovorin, oxaliplatin, and docetaxel *vs* fluorouracil or capecitabine plus cisplatin and epirubicin for locally advanced, resectable gastric or gastro-oesophageal junction adenocarcinoma (FLOT4): a randomised, phase 2/3 trial. *Lancet* 2019; **393**: 1948-1957 [PMID: 30982686 DOI: 10.1016/S0140-6736(18)32557-1]

12 **Kodera Y**, Yamamura Y, Shimizu Y, Torii A, Hirai T, Yasui K, Morimoto T, Kato T, Kito T. Metastatic gastric lymph node rate is a significant prognostic factor for resectable stage IV stomach cancer. *J Am Coll Surg* 1997; **185**: 65-69 [PMID: 9208963 DOI: 10.1016/s1072-7515(97)00006-9]

13 **Zhao BW**, Chen YM, Jiang SS, Chen YB, Zhou ZW, Li YF. Lymph Node Metastasis, a Unique Independent Prognostic Factor in Early Gastric Cancer. *PLoS One* 2015; **10**: e0129531 [PMID: 26154617 DOI: 10.1371/journal.pone.0129531]

14 **Smyth EC**, Fassan M, Cunningham D, Allum WH, Okines AF, Lampis A, Hahne JC, Rugge M, Peckitt C, Nankivell M, Langley R, Ghidini M, Braconi C, Wotherspoon A, Grabsch HI, Valeri N. Effect of Pathologic Tumor Response and Nodal Status on Survival in the Medical Research Council Adjuvant Gastric Infusional Chemotherapy Trial. *J Clin Oncol* 2016; **34**: 2721-2727 [PMID: 27298411 DOI: 10.1200/JCO.2015.65.7692]

15 **Wang WJ**, Li HT, Yu JP, Su L, Guo CA, Chen P, Yan L, Li K, Ma YW, Wang L, Hu W, Li YM, Liu HB. Severity and incidence of complications assessed by the Clavien-Dindo classification following robotic and laparoscopic gastrectomy for advanced gastric cancer: a retrospective and propensity score-matched study. *Surg Endosc* 2019; **33**: 3341-3354 [PMID: 30560498 DOI: 10.1007/s00464-018-06624-7]

16 **Jin LX**, Sanford DE, Squires MH 3rd, Moses LE, Yan Y, Poultsides GA, Votanopoulos KI, Weber SM, Bloomston M, Pawlik TM, Hawkins WG, Linehan DC, Schmidt C, Worhunsky DJ, Acher AW, Cardona K, Cho CS, Kooby DA, Levine EA, Winslow E, Saunders N, Spolverato G, Colditz GA, Maithel SK, Fields RC. Interaction of Postoperative Morbidity and Receipt of Adjuvant Therapy on Long-Term Survival After Resection for Gastric Adenocarcinoma: Results From the U.S. Gastric Cancer Collaborative. *Ann Surg Oncol* 2016; **23**: 2398-2408 [PMID: 27006126 DOI: 10.1245/s10434-016-5121-7]

17 **Tokunaga M**, Tanizawa Y, Bando E, Kawamura T, Terashima M. Poor survival rate in patients with postoperative intra-abdominal infectious complications following curative gastrectomy for gastric cancer. *Ann Surg Oncol* 2013; **20**: 1575-1583 [PMID: 23076557 DOI: 10.1245/s10434-012-2720-9]

18 **Wang S**, Xu L, Wang Q, Li J, Bai B, Li Z, Wu X, Yu P, Li X, Yin J. Postoperative complications and prognosis after radical gastrectomy for gastric cancer: a systematic review and meta-analysis of observational studies. *World J Surg Oncol* 2019; **17**: 52 [PMID: 30885211 DOI: 10.1186/s12957-019-1593-9]

19 **Yuan P**, Wu Z, Li Z, Bu Z, Wu A, Wu X, Zhang L, Shi J, Ji J. Impact of postoperative major complications on long-term survival after radical resection of gastric cancer. *BMC Cancer* 2019; **19**: 833 [PMID: 31443699 DOI: 10.1186/s12885-019-6024-3]

20 **Hu Y**, Huang C, Sun Y, Su X, Cao H, Hu J, Xue Y, Suo J, Tao K, He X, Wei H, Ying M, Hu W, Du X, Chen P, Liu H, Zheng C, Liu F, Yu J, Li Z, Zhao G, Chen X, Wang K, Li P, Xing J, Li G. Morbidity and Mortality of Laparoscopic Versus Open D2 Distal Gastrectomy for Advanced Gastric Cancer: A Randomized Controlled Trial. *J Clin Oncol* 2016; **34**: 1350-1357 [PMID: 26903580 DOI: 10.1200/JCO.2015.63.7215]

21 **Lee JH**, Son SY, Lee CM, Ahn SH, Park DJ, Kim HH. Morbidity and mortality after laparoscopic gastrectomy for advanced gastric cancer: results of a phase II clinical trial. *Surg Endosc* 2013; **27**: 2877-2885 [PMID: 23404155 DOI: 10.1007/s00464-013-2848-0]

World Journal of Gastroenterology

Submit a Manuscript: https://www.f6publishing.com

World J Gastroenterol 2021 October 21; 27(39): 6673-6688

DOI: 10.3748/wjg.v27.i39.6673

ISSN 1007-9327 (print) ISSN 2219-2840 (online)

ORIGINAL ARTICLE

Observational Study

Diagnostic usefulness of selected proteases and acute phase factors in patients with colorectal adenocarcinoma

Tadeusz Sebzda, Jan Gnus, Barbara Dziadkowiec, Miroslaw Latka, Jakub Gburek

ORCID number: Tadeusz Sebzda 0000-0003-3985-5834; Jan Gnus 0000-0002-6220-950X; Barbara Dziadkowiec 0000-0003-0824-626X; Miroslaw Latka 0000-0002-2827-9029; Jakub Gburek 0000-0001-7844-3547.

Author contributions: Sebzda T, Gnus J and Gburek J performed the clinical studies; Sebzda T and Gburek J wrote the initial manuscript; All authors contributed to data analysis and the manuscript revisions.

Institutional review board statement: The study protocol was approved by the Ethics Committee of Wroclaw Medical University (KB 185/2013).

Informed consent statement: All study participants, or their legal guardian, provided informed written consent prior to study enrollment.

Conflict-of-interest statement: The authors declare that the research was conducted in the absence of any commercial or financial relationships that could be construed as a potential conflict of interest.

Data sharing statement: The raw data supporting the conclusions of this article will be made available

Tadeusz Sebzda, Barbara Dziadkowiec, Department of Pathophysiology, Wroclaw Medical University, Wroclaw 50-368, Poland

Jan Gnus, Department of Physiotherapy, Wroclaw Medical University, Wroclaw 50-355, Poland

Miroslaw Latka, Department of Biomedical Engineering, Wroclaw University of Science and Technology, Wroclaw 50-370, Poland

Jakub Gburek, Department of Pharmaceutical Biochemistry, Wroclaw Medical University, Wroclaw 50-556, Poland

Corresponding author: Barbara Dziadkowiec, MD, Doctor, Department of Pathophysiology, Wroclaw Medical University, Marcinkowskiego 1, Wroclaw 50-368, Poland.
dziadkowiecbarbara@gmail.com

Abstract

BACKGROUND

Uncontrolled growth and loss of control over basic metabolic functions, leading to invasive proliferation and metastases, are the salient traits of malignant tumors in general and colorectal cancer in particular. Invasion and metastases hinder effective tumor treatment. While surgical techniques and radiotherapy can be used to remove tumor focus, only chemotherapy can eliminate dispersed neoplastic cells. However, the efficacy of the latter method is limited in the advanced stages of the disease. Therefore, recognition of the mechanisms involved in neoplastic cell spreading is indispensable for developing effective therapies.

AIM

To use a number of biomarkers involved in cancer progression and identify a panel that could be used for effective early diagnosis.

METHODS

We recruited 185 patients with colorectal adenocarcinoma (98 men, 87 women with median age 63). Thirty-five healthy controls were sex and age-matched. Dukes' staging was as follows: A = 22, B = 52, C = 72, D = 39. We analyzed patients' blood serum before surgery. We determined: (1) Cathepsin B (CB) with Barrett's method (fluorogenic substrate); (2) Leukocytic elastase (LE) in a complex

by the authors, without undue reservation, to any qualified researcher.

STROBE statement: The authors have read the STROBE Statement-checklist of items, and the manuscript was prepared and revised according to the STROBE Statement-checklist of items.

Open-Access: This article is an open-access article that was selected by an in-house editor and fully peer-reviewed by external reviewers. It is distributed in accordance with the Creative Commons Attribution NonCommercial (CC BY-NC 4.0) license, which permits others to distribute, remix, adapt, build upon this work non-commercially, and license their derivative works on different terms, provided the original work is properly cited and the use is non-commercial. See: http://creativecommons.org/Licenses/by-nc/4.0/

Manuscript source: Unsolicited manuscript

Specialty type: Gastroenterology and hepatology

Country/Territory of origin: Poland

Peer-review report's scientific quality classification

Grade A (Excellent): A
Grade B (Very good): 0
Grade C (Good): 0
Grade D (Fair): 0
Grade E (Poor): 0

Received: April 7, 2021
Peer-review started: April 7, 2021
First decision: May 27, 2021
Revised: July 7, 2021
Accepted: September 2, 2021
Article in press: September 2, 2021
Published online: October 21, 2021

P-Reviewer: Batyrbekov K
S-Editor: Gao CC
L-Editor: Filipodia
P-Editor: Li JH

with alpha 1 trypsin inhibitor (AAT) using the immunoenzymatic MERCK test; (3) Total sialic acid (TSA) with the colorimetric periodate-resorcinol method; (4) Lipid-bound sialic acid (LASA) with the colorimetric Taut's method; and (5) The antitrypsin activity (ATA) employing the colorimetric test.

RESULTS

In patients, the values of the five biochemical parameters were as follows: CB = 16.1 ± 8.8 mU/L, LE = 875 ± 598 μg/L, TSA = 99 ± 31 mg%, LASA = 0.68 ± 0.33 mg%, and ATA = 3211 ± 1504 U/mL. Except for LASA, they were significantly greater than those of controls: CB = 11.4 ± 6.5 mU/L, LE = 379 ± 187 μg/L, TSA = 71.4 ± 15.1 mg%, LASA = 0.69 ± 0.28 mg%, and ATA = 2016 ± 690 U/mL. For CB and LASA, the differences between the four Dukes' stages and controls were not statistically significant. The inter-stage differences for CB and LASA were also absent. The receiver operating characteristic (ROC) analysis revealed the potential diagnostic value of CB, TSA, and ATA. The area under ROC, sensitivity, and specificity for these three parameters were: 0.85, 72%, 90%; 0.75, 66%, 77%; and 0.77, 63%, 84%, respectively. The sensitivity and specificity for the three-parameter panel CB-TSA-ATA were equal to 88.2% and 100%, respectively.

CONCLUSION

The increased value of CB, TSA, and ATA parameters are associated with tumor biology, invasion, and metastasis of colorectal cancer. The presented evidence suggests the potential value of the CB-TSA-ATA biochemical marker panel in early diagnostics.

Key Words: Colorectal cancer; Cathepsin B; Acute phase reactants; Colorectal adenocarcinoma; Acute phase factor

©The Author(s) 2021. Published by Baishideng Publishing Group Inc. All rights reserved.

Core Tip: We searched for biomarkers applicable to the early detection of colorectal adenocarcinoma. Five parameters were determined in sera of patients and healthy individuals: Cathepsin B activity, total sialic acids concentration, lipid-associated sialic acids concentration, elastase concentration, and alpha 1 antitrypsin activity. We performed receiver operating characteristic analysis for single and multiple parameters. While the sensitivity and specificity were not very high for single parameters, the combined analysis of cathepsin B, alpha 1 antitrypsin, and total sialic acids concentration yielded 88% sensitivity and 100% specificity. We believe that this set of markers can be useful in clinical practice.

Citation: Sebzda T, Gnus J, Dziadkowiec B, Latka M, Gburek J. Diagnostic usefulness of selected proteases and acute phase factors in patients with colorectal adenocarcinoma. *World J Gastroenterol* 2021; 27(39): 6673-6688
URL: https://www.wjgnet.com/1007-9327/full/v27/i39/6673.htm
DOI: https://dx.doi.org/10.3748/wjg.v27.i39.6673

INTRODUCTION

The process of neoplastic invasion consists of two main stages: Penetration of tissues surrounding cancer and creation of metastases in places distant from the original location. During migration, cancer-transformed cells encounter anatomical barriers: The basement membrane and connective tissue. Cathepsins play an important role in the process of overcoming them.

Under normal conditions, cathepsins do not occur extracellularly or appear outside the cell only in small quantities. Their main function is to participate in processes related to the "turn-over" of endogenous proteins and degradation of exogenous proteins absorbed in the process of endocytosis[1-4]. In smaller concentrations, *e.g.*, in extralysosomal spaces, the enzymes can catalyze — by means of limited proteolysis — posttranslational processes of conversion of many peptides and proteins, including

growth factors and hormones such as albumins, insulins, endorphins, and enkephalins [5,6]. The release of cathepsins from cancer cells and their expression in the plasma membrane of cancer cells facilitates the dissolution of the basement membrane and participation in the proteolytic metastatic cascade. In clinical practice, a significant increase in the activity of cathepsin B (CB) is observed in the serum of patients with malignant tumors. This phenomenon occurs regardless of the location of the tumor and is closely related to the severity of ovarian, cervical, breast, laryngeal and colorectal cancer. It was also found that the activation of CB, which takes place with the participation of elastase coming from the neutrophil intumescence and tumor tissue, has an impact on its invasiveness and metastatic capacity. Studies have also confirmed that an increase in cathepsin expression in colorectal tumor tissue homogenates may be a sensitive marker for cancer progression[7-16].

Leukocytic elastase (LE) belongs to the group of serine proteases. It is located mainly in the azurophilic granules of neutrophils, where it is an active component of the phagocytic system along with other hydrolyses and reactive oxygen species. The enzyme is also cytochemically detected in the nuclear membrane, the Golgi complex, endoplasmic reticulum, and mitochondria[17,18]. It also participates in remodeling and tissue repair processes and modulates the activity of cytokines and their receptors (*e.g.*, mitogen-activated protein kinase 3). It can degrade elements of connective tissue by hydrolysis of elastin, various types of collagen, and other extracellular matrix proteins such as fibronectin, laminin, or proteoglycans. The physiological regulation of the activity and prevention of potentially destructive effects of elastase in pathological states is caused by protein inhibitors present in the blood serum. They include alfa 1 trypsin inhibitor (AAT), alpha 2-macroglobulin (alpha-2-MG), a secretory leukocytic protease inhibitor (SLPI), and elaphin[19-21]. In a healthy organism, LE remains in balance with them, and after the secretion from the cells, it is directly bound by inhibitors. The inhibitor molecules are thermally very stable and do not undergo proteolysis. Increased levels of LE in blood plasma, most often determined as LE-AAT complexes, have been found in many associated inflammatory conditions and are therefore considered acute-phase factors. Many authors regard the concentration of the above complexes to be a measure of the activity of the inflammatory process itself and be a marker of stimulation of neutrophils in the inflammatory focus. Lowering the level of AAT, caused by genetic or environmental factors, enables uncontrolled elastase activity and leads to many serious pathological conditions. This is caused by the enzyme-inhibitor imbalance and overexpression of the enzyme or a decrease in inhibitor concentration.

Sialic acid (N-acetyloneuraminic acid, NANA) is an organic compound from the sugar group, a derivative of neuraminic acid. It is a sugar component of glycoproteins and glycolipids. It occupies a terminal position in carbohydrate glycoprotein residues and has an important function in cell physiology as well as in the metabolism and maintenance of the proper concentration of glycoproteins in serum. It is also part of the ligand for the selectin and lectin receptors on leukocytes, T lymphocytes, platelets, and endothelium. It plays a key role in the immune response and hemostasis[22].

In the blood of patients suffering from metabolic disorders (*e.g.*, diabetes mellitus, atherosclerosis), a clear increase in the glycoprotein fraction is observed, while the sialic acid content remains low. In the case of cancer, the level of glycoproteins that contain normal or increased amounts of sialic acid increases in the blood. Increased sialisation is associated with the development of a neoplastic tumor and malignant cell metastasis. An increase in sialic acid concentration is observed in the case of malignant melanoma, lung, larynx, breast, ovary, prostate, liver, or colorectal cancer. It has been shown that the sialyltransferase activity in blood serum taken from people with cancer is increased and reaches its highest concentration at advanced stages of cancer development. The main areas of protein glycosylation include the endoplasmic reticulum and Golgi apparatus[23]. During the transformation of normal cells into cancer cells, there are significant differences in the biosynthesis of the sugar parts of proteins and membrane lipids. These changes are primarily of a qualitative nature. The external part of the plasma membrane of cancer cells has an increased number of sialic acid molecules compared to normal cells. Glycoproteins rich in sialic acids are more frequently found in case of metastatic cancer. The increased level of sialoglycoproteins and sialoglycolipids in neoplasms is mainly due to increased disintegration of cancer cells, increased synthesis and secretion of glycoconjugates (glycoproteins and glycolipids) containing sialic acid[24-32].

Recently, many works have been published on the activity of proteolytic enzymes and their inhibitors in blood serum. However, they do not solve all the problems related to the diagnostic and prognostic usefulness of these parameters in neoplastic diseases.

In this study, a statistically consistent group of colorectal cancer patients was collected: Women and men. The division of colorectal cancer into the colon and rectal cancer, histopathological criteria (adenocarcinoma), a clinical division system based on Dukes' cancer staging were considered.

The study presented below has both basic and diagnostic-clinical nature. The results of the study may be used in the future in the complementary diagnosis of colorectal adenocarcinoma to determine the severity of the disease and in further monitoring of patients under outpatient control and prognosis.

MATERIALS AND METHODS

Patients

One hundred and eighty-five patients were recruited from the Lower Silesian Oncology Center and the Provincial Specialist Hospital in Wroclaw. The study material presented in this paper was blood serum from patients with colorectal adenocarcinoma. The patients' blood serum was examined before surgery.

The examined patients were evaluated in terms of their age, sex, location of neoplastic lesions (colon, sigmoid colon, rectum), histopathological differentiation of neoplastic cells (G), and their clinical stages were based on the Dukes' classification. The characteristics of the examined patients are summarized in Table 1.

Biochemical measurements

The following tests were performed in blood serum according to the methods given below: (1) CB was determined with the use of fluorogenic substrate using the Barrett method[33]; (2) LE in a complex with AAT was determined immunoenzymatically using the MERCK test; (3) Total sialic acid (TSA) was determined colorimetrically using the periodate-resorcinol method, according to Jourdian *et al*[34]; (4) Lipid-bound sialic acid (LASA) was determined colorimetrically using Tautu *et al*[35]; and (5) The antitrypsin activity (ATA) in blood plasma (in the study referred to as antitrypsin capacity — ATA) was determined colorimetrically against trypsin using the method proposed by Warwas *et al*[36] and Dietz *et al*[37].

Statistical analysis

The examined continuous features were characterized by the distribution parameters of these features, *i.e.*, mean value (M), standard deviation (SD), and the number of patients (*n*). For the analysis of the statistical material, the following were used: For continuous features — single-factor analysis of variance (ANOVA), using Tukey's *post hoc* tests and multi-factor analysis of variance (MANOVA). The t-Student's *t*-test was also used for dependent samples. For features deviating from the normal distribution, which were also characterized by a median value, non-parametric tests were used: For independent samples — the Mann-Whitney *U* test, and for dependent samples — the Wilcoxon test. For categorized or dichotomous features, the χ^2 test and the non-parametric Kruskal-Wallis test were used. The relationship between these features was also studied by determining the Spearman correlation coefficient. The receiver operating characteristic (ROC) curve method was used to determine the threshold values of clinical markers (continuous variables) with optimal precision. The significance threshold *P* for all statistical tests was set to 0.05. The statistical analysis was conducted using Statistica v. 10.

RESULTS

Table 2 presents the results of biochemical parameters examined, their M, SD, *n*, including the group of colorectal cancer patients and the control group of healthy individuals.

In the group of patients with colorectal cancer, differences were observed in the values of examined biochemical parameters in blood serum compared to the control group. Despite clear changes in the levels and activity of the studied factors, not in all groups, these differences were statistically significant. Relevance was observed between patient groups suffering from colorectal cancers and the control group for CB, LE, TSA, and ATA.

Table 3 presents statistically significant differences between the examined groups of patients according to Dukes' classification and the control group. There were no

Table 1 Characteristics of patients with colorectal cancer

Number of patients with colorectal cancer	**185**
Age, median (age range)	63 (18-86)
Sex, *n* (%)	
Men	98 (55)
Women	87 (45)
Anatomical location, *n* (%)	
Colon	77 (42)
Sigmoid colon	37 (20)
Rectum	71 (38)
Histological differentiation of cells, *n* (%)	
G1	8 (4)
G2	103 (56)
G3	74 (40)
Division of patients according to Dukes' classification, *n* (%)	
A	22 (12)
B	52 (28)
C	72 (39)
D	39 (21)
Number of patients in the control group	**35**
Age, median (age range)	61 (19-85)
Sex, *n* (%)	
Men	19 (54)
Women	16 (46)

significant differences for CB and LASA ($P > 0.05$), while the differences for other parameters were: LE ($P < 0.001$), TSA ($P < 0.001$), ATA ($P < 0.01$).

Table 4 presents a comparison of statistically significant differences between individual parameters in the patient groups (A, B, C, D, according to Dukes' classification) and control group. There were statistically significant differences for all groups except for group A. Statistically significant differences between patient groups were also being observed. For LE, the most statistically significant difference was observed between groups C and D ($P < 0.002$). For TSA, the difference was most strongly pronounced for A and D ($P < 0.05$). There were no stage differences for ATA.

In Table 5 the correlations between in main parameters are summarized. The values of all the above-mentioned correlation coefficients were positive except for CB and ATA and LASA and ATA. The highest correlations were observed between CB and ATA; LE and TSA; TSA and ATA ($P < 0.001$).

No statistically significant differences in the examined parameters in respect to histopathological differentiation of tumor cells (G1, G2, G3) were observed (data not shown).

The examined biochemical factors in the blood serum were also examined using ROC analysis. The analyses are summarized in Figure 1. The highest diagnostic value was observed for a single value for CB in blood serum, with a threshold value of 11.22 mU/L. The sensitivity of the method was 72%, and its specificity was 90%. Then, respectively: for TSA, with a threshold value of 75.34 mg% — 66% and 77%; for LASA with a threshold value of 0.562mg% — 80% and 41%; for LE with a threshold value of 543 μg/L — 49% and 89% and ATA in blood serum with a threshold value of 2400 U/mL — 63% and 84%.

The analysis of the ROC curves of the two associated parameters has shown that the connection between CB and TSA gives a sensitivity of 73% and a specificity of 100%, with a value under the curve reaching 95%.

Table 2 Characteristics of the tested biochemical parameters in blood serum in all patients and in the control group

No.	Biochemical parameters tested	Groups	ABCD	K	Significance level *P* value
1	CB, mU/L	M	16.1	11.4	< 0.050
		n	185	35	
		SD	8.8	6.5	
2	LE, μg/L	M	875.1	379.1	< 0.001
		n	51	30	
		SD	597.9	187.3	
3	TSA, mg%	M	98.9	71.4	< 0.001
		n	71	31	
		SD	30.8	15.1	
4	LASA, mg%	M	0.68	0.69	NS
		n	68	35	
		SD	0.33	0.28	
5	ATA, U/mL	M	3211.4	2015.9	< 0.001
		n	74	29	
		SD	1504.1	689.6	

ABCD: All patients with colorectal adenocarcinoma; ATA: Antitrypsin activity; CB: Cathepsin B; K: Control group; LASA: Lipid-bound sialic acid; LE: Leukocytic elastase; M: Mean value; NS: Not significant; TSA: Total sialic acid.

Combining three parameters for the ROC curve: CB, TSA, and ATA, in blood serum, gives a sensitivity of 88% and a specificity of 100%, respectively, with a value of area under the curve of 95%.

In conclusion, ROC analysis has a high diagnostic value and can be helpful, especially in the combined analysis (biomarker panel determination).

DISCUSSION

The ability of the tumor to invade and metastasize is associated, among other pathogenic issues, with an increase in the expression of cysteine peptides. The source of these enzymes may be, in addition to the neoplastic tissue, neutrophils infiltrating the tumor. It is believed that CB determination may be helpful in the diagnosis and monitoring of colon and rectal cancer therapy[38-40].

In our study, the average CB activity determined in the blood serum of patients with colorectal cancers using a synthetic Z-Arg-Arg-N-MC substrate was about 1.5 times higher than that of healthy individuals ($P < 0.05$). Statistically significant results were obtained in the group of patients with different degrees of clinical advancement (ABCD: $P < 0.05$) (Table 2 and Figure 1A). On the other hand, CB did not statistically significantly differentiate patients according to Dukes' staging of colorectal cancer (A, B, C, D), although the average values in patients exceeded the average values in the control group (Table 3). Among other parameters, CB correlated only with ATA ($P < 0.001$) (Table 5).

The activity of CB in serums of patients with colon and rectal cancers was also studied by other authors. Dufek *et al*[41] observed a fivefold increase in this parameter. It was found that the CB activity in patients with colon and rectal cancers was significantly higher than in patients with polyps and in healthy individuals. This difference may be due to the use of the other substrate (Z-Ala-Arg-Arg-N-MC), which may also have been hydrolyzed by other proteases. These studies have also shown a high level of alkali-stable form of CB. In people with mild lesions (polyps) and in healthy people, the level of this form did not reach the threshold of determination. After the effective treatment, CB levels decreased significantly and increased again in case of metastases or resistant chemotherapy.

Table 3 Characteristics of biochemical parameters in patients' blood serum in relation to the severity according to the Dukes' classification

No.	Biochemical parameters tested	Groups	A	B	C	D	K	Significance level *P* value
1	CB, mU/L	M	19.9	15.4	16.8	15.5	11.4	NS
		n	22	52	72	39	35	
		SD	19.3	9.4	8.4	7.6	6.5	
2	LE, μg/L	M	386.1	929.9	602.1	1129.5	379.1	< 0.001
		n	5	16	15	15	30	
		SD	190.2	637.5	389.6	651.7	187.3	
3	TSA, mg%	M	67.8	100.8	92.9	107.2	71.4	< 0.001
		n	6	21	24	20	31	
		SD	7.4	39.3	25.1	26.3	15.1	
4	LASA, mg%	M	0.44	0.8	0.6	0.6	0.7	NS
		n	6	21	24	21	37	
		SD	0.12	0.51	0.23	0.20	0.31	
5	ATA, U/mL	M	3100.0	2925.0	3152.1	3576.2	2015.9	< 0.010
		n	2	21	24	21	29	
		SD	424.3	1294.5	1684.7	1548.8	689.6	

Dukes' classification system for colorectal cancer: A, B, C, D: All patients with colorectal adenocarcinoma; ATA: Antitrypsin activity; CB: Cathepsin B; K: Control group; LASA: Lipid-bound sialic acid; LE: Leukocytic elastase; M: Mean value; NS: Not significant; TSA: Total sialic acid.

Kos *et al*[40] also observed the fivefold increase in CB concentration using immune-enzymatic method. The CB level correlated well with stage C and D of Dukes' staging system. As in our research, no correlation between CB and age or gender was observed. However, it should be stressed that the antibodies used in this method detected both the active and non-active precursor form of this enzyme and their complexes with inhibitors, such as cystatins.

Similar studies on the proteolytic activity of blood serum with colon and rectal cancer were performed by Amiguet *et al*[42]. Similar to our research, the proteolytic activities of CB and elastase, were determined. Patients in Dukes' B and D stages were examined. The activities of the examined proteases were increased in relation to the control group of healthy individuals. In Dukes' stage D, the increase in CB levels was directly proportional to the weight of the tumor. In metastatic carcinomas, the increase in CB was accompanied by an increase in AAT concentration.

Padilla *et al*[43] showed, with the use of the immunoreactive method, that CB levels in colorectal cancer patients were different from the control group.

Clinical and pathological evaluation of patients with the use of serum CB and cathepsin D, based on the TNM system before and after the operation, was performed by Skrzydlewska *et al*[44]. The CB activity before the cancer tumor resection was significantly higher. However, in relation to the control group, both before and after the procedure, the CB activity was approximately 8.4 times lower. The authors concluded that the postoperative level of CB was associated with the involvement of the surrounding lymph nodes and higher when not accompanied by lymph node involvement. However, a relatively non-specific Z-Arg-pNA substrate was used to test the CB activity, and thus the observations might have been biased by the activity of other proteases.

Zore *et al*[45] examined CB levels in the complex with cystatin C using the ELISA method. Their observations show that CB in the Dukes' CD stage was significantly lower than in the AB stage (P = 0.02). Our study did not observe any significant differences between these groups (the results are not presented). The inhibitory capacity of cystatin C does not compensate for the increase in CB levels in patients suffering from colorectal cancers. This supports the hypothesis that inhibitory capacity might have been impaired during colorectal cancer progression.

Table 4 Statistical analysis of differences in the activity or concentration of examined parameters in serum of patients with adenocarcinoma and the control group

Patients' Groups					
LE	**A**	**B**	**C**	**D**	**K**
A	NS	NS	NS	NS	NS
B	NS	NS	$P < 0.05$	NS	$P < 0.001$
C	NS	$P < 0.05$	NS	$P < 0.002$	$P < 0.004$
D	NS	NS	$P < 0.002$	NS	$P < 0.001$
K	NS	$P < 0.001$	$P < 0.004$	NS	NS
TSA	**A**	**B**	**C**	**D**	**K**
A	NS	NS	NS	NS	NS
B	NS	NS	NS	NS	$P < 0.001$
C	NS	NS	NS	NS	$P < 0.003$
D	$P < 0.05$	NS	NS	NS	$P < 0.001$
K	NS	$P < 0.001$	$P < 0.003$	$P < 0.001$	NS
ATA	**A**	**B**	**C**	**D**	**K**
A	NS	NS	NS	NS	NS
B	NS	NS	NS	NS	$P < 0.02$
C	NS	NS	NS	NS	$P < 0.002$
D	NS	NS	NS	NS	$P < 0.001$
K	NS	$P < 0.02$	$P < 0.002$	$P < 0.001$	NS

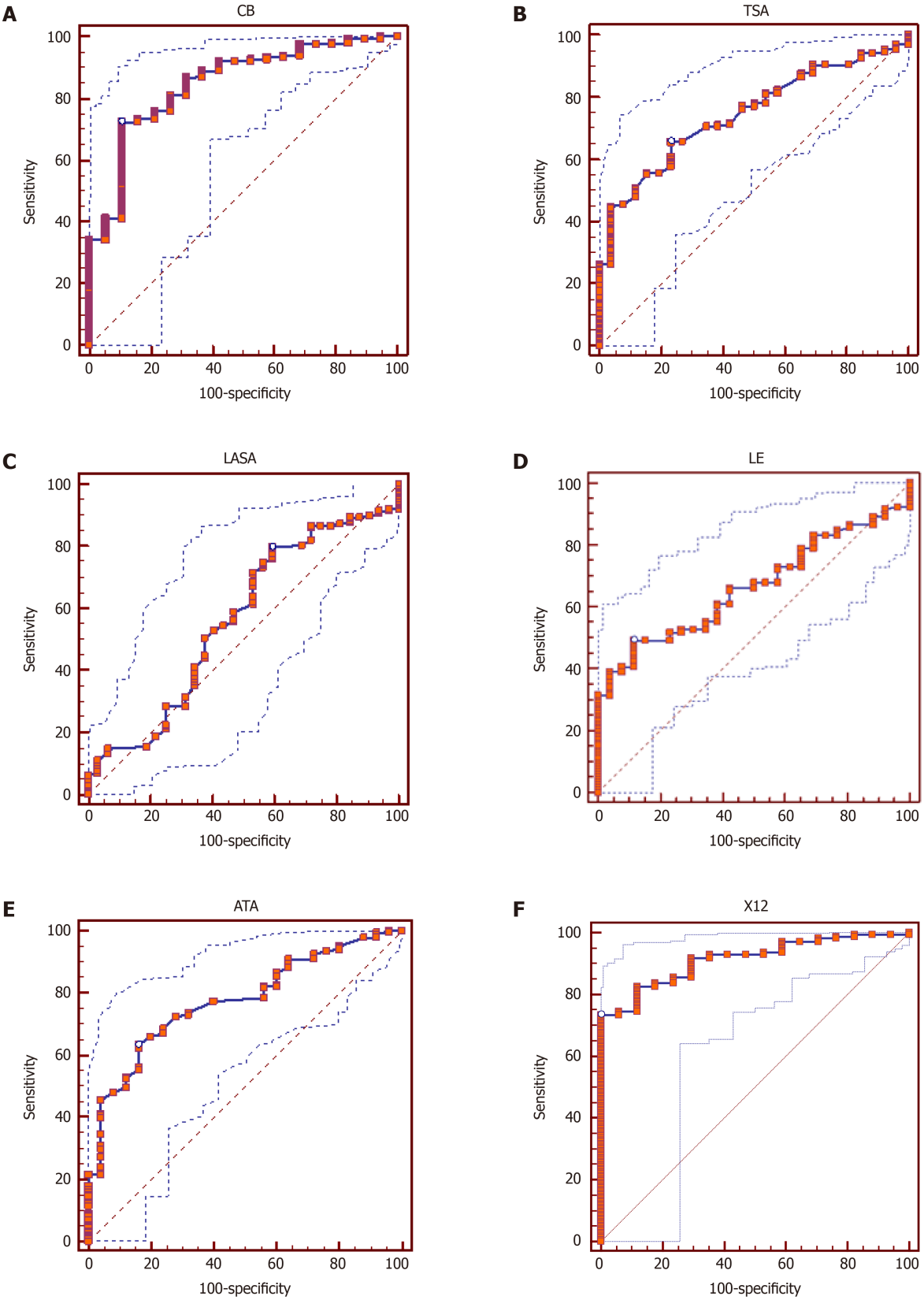
Significance levels of differences in the expected values of the analyzed biochemical parameters in patients divided into colorectal cancer patients (Dukes' stage A, B, C, D) and control group (K). The values of statistical significance — *P* were provided. A, B, C, D: All patients with colorectal adenocarcinoma; ATA: Antitrypsin activity; K: Control group; LE: Leukocytic elastase; NS: Not significant; TSA: Total sialic acid.

Table 5 Statistical analysis of correlations between the biochemical parameters examined in blood serum in all patients

Studied parameters	CB, mU/L	LE, μg/L	TSA, mg%	LASA, mg%	ATA, U/mL
CB, mU/L					-0.24 (187), $P < 0.001$
LE, μg/L			0.37 (140), $P < 0.001$	0.17 (141), $P < 0.05$	
TSA, mg%		0.37 (140), $P < 0.001$		0.19 (212), $P < 0.01$	0.33 (209), $P < 0.001$
LASA, mg%		0.17 (141), $P < 0.05$	0.19 (212), $P < 0.006$		-0.14 (210), $P < 0.05$
ATA, U/mL	-0.24 (187), $P < 0.001$		0.33 (209), $P < 0.001$	-0.14 (210), $P < 0.05$	

Values of linear correlation coefficients between concentrations or activities of the studied biochemical parameters (number of the examined). Description of other parts as in Table 2. ATA: Antitrypsin activity; CB: Cathepsin B; LASA: Lipid-bound sialic acid; LE: Leukocytic elastase; TSA: Total sialic acid.

Cysteine proteases — CB and cathepsin L levels in blood serum in patients with colorectal cancer were studied by Herszényi *et al*[46], who used the ELISA method for this purpose. CB correlated with the progressive Dukes' scale, reaching a 2.3 times higher level in patients compared to the control group. Analysis of the ROC curve confirmed the diagnostic importance of the examined factors, including CB. The sensitivity and specificity in the ROC analysis of CB were similar to the results obtained in our study (72 and 89% respectively *vs* 82 and 88%, and the areas under the ROC curve 0.85 *vs* 0.87), thus confirming the high diagnostic value of the studied parameter. Comparing CB with other biochemical parameters such as TSA and ATA in the ROC analysis results in an even higher level of sensitivity and specificity. Also, other researchers noticed that proteolytic enzymes are excellent indicators for colorectal cancers, often better than the commonly used tumor markers[47].


A
CB
B
TSA
C
LASA
D
LE
E
ATA
F
X12
Sensitivity
100-specificity
0
20
40
60
80
100

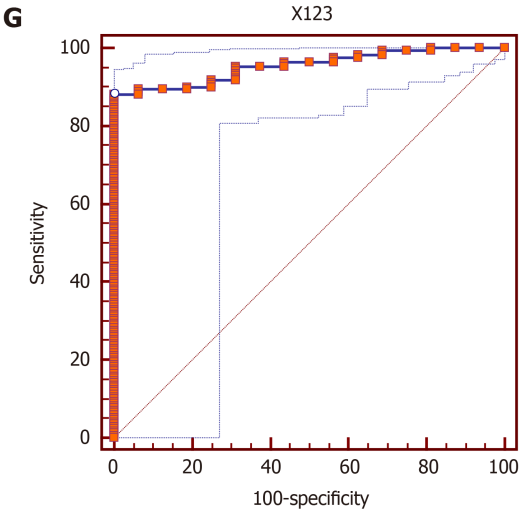


Figure 1 Diagram of receiver operating characteristic curve. A: For cathepsin B (CB). Threshold value of > 11.22 mU/L yielded sensitivity of 72.3% and specificity of 90%. Area under the receiver operating characteristic curve = 0.85; B: For total sialic acid (TSA). Threshold value > 75.34 mg% yielded sensitivity of 65.8% and specificity of 76.9%. Area under the receiver operating characteristic curve = 0.75; C: For lipid-bound sialic acid (LASA). Threshold value > 0.739 mg% yielded sensitivity of 79.7% and specificity of 40.6%. Area under the receiver operating characteristic curve = 0.56; D: For leukocytic elastase (LE). Threshold value > 543 μg/L yielded sensitivity of 49.2% and specificity of 88.5%. Area under the receiver operating characteristic curve = 0.56; E: For antitrypsin activity (ATA). Threshold value > 2400 U/mL yielded sensitivity of 63.2% and specificity of 84.0%. Area under the receiver operating characteristic curve = 0.77; F: For the combined two biochemical parameters. Threshold value > 0.4757 yielded sensitivity of 73.4% and specificity of 100%. Area under the receiver operating characteristic curve = 0.91; G: The three parameters combined (X123): CB, TSA, and ATA. Threshold value > 1.3457 yielded sensitivity of 88.2% and specificity of 100%. Area under the receiver operating characteristic curve = 0.95.

The imbalance of protease/inhibitors ratio is particularly relevant for LE and AAT involvement in the pathogenesis of cancer. The level of AAT, an acute-phase protein, increases in cancer patients in response to the increased levels of proteolytic enzymes released from leukocytes into circulation. In patients, despite an increase in their levels, the functional activity of the inhibitor decreases, thus disturbing the LE/AAT balance. This imbalance is further exacerbated by the fact that membrane forms of proteases, such as CB or elastase are more resistant to these inhibitors. Moreover, LE has itself ability to degrade those inhibitors[48]. A disturbed balance between LE and AAT may be associated with an increased risk of liver, cholecystitis, bladder, lymphoma, or lung cancer[49-55]. Apart from AAT, other protein inhibitors present in the blood serum are also responsible for the physiological regulation of LE: α2MG, SLPI, or elaphin. SLPI, as it is clear from the work by Sugino *et al*[54], performed in various types of cancer, including colorectal cancer, has a dual effect. On the one hand, it suppresses the invasion of neoplastic cells, and on the other hand, it promotes metastasis that transmits through blood circulation.

The inclusion of serum ATA and LE, as indicated by the results of our research, may be a factor informing about the balance of serine proteases.

LE in all listed patient groups according to the Dukes' classification: Combined ABCD stages and A, B, C, D stages separately (Table 2 and Figure 1D), shows a clear statistically significant difference when compared to the control group. Its activity reached the highest values in groups B and D. It is possible that it is associated with subsequent stages of cancer spread and the presence of metastatic foci rich in granulocytic intumescence, increased elastase-induced adhesion of cancer cells to the endothelium of vessels, or through mitogenic activity[56,57].

The different activity of serum elastase, in successive stages of the disease according to the Dukes' classification eliminates the possibility of using this parameter for early diagnosis in colorectal cancers. In addition, serum elastase is characterized by relatively low sensitivity in the ROC analysis (49%) (Figure 1D). On the other hand, some authors have found it as a putative diagnostic biomarker and also a potential therapeutic target[58].

AAT is a blood plasma protein belonging to α_1-globulin fraction, one of the strongest inhibitors of circulating serine proteases (serpins). It is also an acute-phase protein, synthesized mainly in the liver but also by macrophages. AAT has the ability to inactivate many proteolytic enzymes, but its most important effect is the inactivation of LE released by neutrophils as a result of an inflammatory reaction.

In our study, statistically significant ($P < 0.001$) elevated ATA levels were observed in the cumulative group of patients, regardless of the Dukes' classification stage (ABCD) in relation to the control group. In the B, C, and D stages, in relation to the control, these levels were highly statistically significant ($P < 0.001$; $P < 0.004$; $P < 0.001$). Also, ATA differentiated very well patients with Dukes' stages B against C and C against D ($P < 0.05$ and $P < 0.002$, respectively). In our ROC analysis, with the cut-off value > 2400 U/mL, the ATA value reached the sensitivity of 63% and specificity of 84%, respectively. The listed sensitivity and specificity parameters are lower than in the ROC analysis for CB (72% and 90%, respectively).

There is little clinical work on the contribution of AAT to the diagnosis or monitoring of the treatment of colorectal cancer[59-64]. Yüceyar *et al*[65] and Gallardo-Valverde *et al*[66] did not find relationship between the AAT and the severity of colorectal cancer and showed a statistically significant correlation between AAT and other biochemical factors such as acute-phase protein, carcinoembryonic antigen (CEA), or tumor-associated trypsin inhibitor (TATI).

Bernacka *et al*[67] studied plasma levels of AAT in patients with gastrointestinal cancers: Stomach and colorectal cancers of adenocarcinoma type. This marker did not differentiate colorectal cancer patients in terms of local and metastatic lesions. However, it had the highest level in stage C and differentiated patients in terms of the histological degree of tumor stage (G). The author postulates that AAT levels are associated with increased production by liver cells in response to the increased release of lysosomal proteases of tumor cells or from mononuclear inflammatory tumor-infiltrating cells. It seems that tumor cells may be the third source of antiproteases.

Ward *et al*[68], using proteomic profiling, identified AAT as having the potential to classify the colorectal patients with 95% sensitivity and 91% specificity.

Interesting conclusions were drawn from the work of Bujanda *et al*[64], who studied a group of 42 colorectal cancer patients using combined AAT, matrix metalloproteinase 7 (MMP-7), urokinase-type plasmin activator receptor (uPAR), and cyclooxygenase-2 (COX-2). Compared to the control group, AAT levels were about 1.4 times higher at stages B and C, and the AAT level was high and reached its value under the ROC curve (0.88). The above results are similar to those obtained in our study. The level under the ROC curve was 0.77. In patients in stages B and C, ATA levels were 1.5 and 1.6 times higher, respectively, than in the control group. AAT has a promising diagnostic profile and, most importantly, at the early stages of colorectal cancer.

The neoplastic process is associated not only with the activation of the cascade system of proteolytic enzymes, the activation of which mainly takes place with the participation of CB and LE, but also induces the activation of acute-phase proteins.

The interest in the sialic acids (TSA, LASA) as markers useful in diagnosing and monitoring the course of many diseases, including colorectal cancer, is reflected in the publications briefly reviewed in[69-72]. Increased levels of sialic acid expression are associated with changes in biosynthesis and posttranslational processes of acute-phase proteins glycosylation in the liver. This phenomenon is associated with increased expression of sialyltransferases by cancer cells[73]. The mechanism of increased TSA levels in serum takes the following into account: (1) Spontaneous release of the compounds from the surface of cancer cells; (2) Increase in concentration and/or glycosylation of serum glycoproteins; and (3) Secondary inflammatory reaction associated with the increase in acute-phase proteins[32,74]. Increased sialyltransferases activities, observed in cancer cells, results in increased glycoprotein secretion as well as the secretion of cell membrane components into the culture medium. The cancer cell hypoxia may also contribute to the above[75]. Increased sialisation of glycosphingolipids leads to abnormal adhesion and a disturbed premembranous signal exchange [75]. Determination of sialic acids is a laboratory marker of many pathological lesions. A significant increase in serum levels of sialic acids was observed in many malignant diseases[76]. Elevated levels of TSA or LASA were observed in malignant melanoma, lung, breast, ovary, and laryngeal cancers[28,32,77], as well as in colorectal cancer[26,31,70,78-82].

In our study, TSA in blood serum was elevated and statistically significantly different from the control group. The above observation concerns the cumulative group of patients (ABCD: $P < 0.001$) as well as individual groups (B, C, D in relation to the control: $P < 0.001$; $P < 0.003$; $P < 0.001$ respectively). The lowest level among patients was found in group A, and the highest in group D. The above clearly shows differences between particular patient groups. TSA was only less effective than ATA. The TSA level moderately but statistically significantly correlates with LE and ATA. The results of the ROC analysis are interesting. With a cut-off value for TSA > 75.34 mg%, the sensitivity of the method was 66%, and its specificity was 77%. In ROC analysis TSA clearly benefits when combined CB with the same cut-off values)

sensitivity 74% and specificity 100%were obtained. The sensitivity further increases if we also take the ATA into account, which is also studied by the authors and reflects the AAT level. In the TSA test, the main component determined is the sialic acid associated with proteins. The level of sialic acids increases in the sera of cancer patients as a result of increased concentration of acute-phase proteins rather than gangliosides from decaying cancer cells[65,74,75,83].

CONCLUSION

We have found a statistically significant increase in the CB activity in the blood serum of the examined individuals suffering from colorectal cancers. The highest CB level was observed in Dukes' stage A patients, and in stages B, C and D, it was lower and comparable to each other.

Concordantly, the following increased concentrations in blood serum of investigated markers were observed: LE, TSA, and ATA. According to Dukes' classification, these values were statistically significantly increased with respect to the control group, gradually rising from the A to D stage.

The ROC analysis showed the high diagnostic value of CB, TSA, ATA determinations in blood serum, both in the single and combined analysis (biomarker panels) with two biochemical parameters: CB and TSA, and with three parameters: CB, TSA, and ATA. The above results suggest high diagnostic usefulness in determining these 2 or 3 combined parameters in relation to single determinations, obtaining sensitivity and specificity of 88.2% and 100% for three parameters.

ARTICLE HIGHLIGHTS

Research background

Recognition of the mechanisms involved in neoplastic cell spreading is indispensable for the early diagnosis and detection of colorectal cancer.

Research motivation

Colorectal cancer is the third most common type of cancer, making up about 10% of all cases. In 2018, there were 1.09 million new cases and 551000 deaths from the disease. Consequently, early diagnosis of colorectal cancer remains a significant medical and economic problem.

Research objectives

Using several biomarkers involved in cancer progression, we have tried to identify a panel that could be used for effective early diagnosis.

Research methods

Before surgery, we analyzed the blood serum of 185 patients with colorectal cancer and determined: Cathepsin B (CB), leukocytic elastase (LE), total sialic acid (TSA), lipid-bound sialic acid (LASA), and antitrypsin activity (ATA).

Research results

The receiver operating characteristic analysis revealed the potential diagnostic value of CB, TSA, and ATA. The sensitivity and specificity for the three-parameter panel CB-TSA-ATA were equal to 88.2% and 100%, respectively.

Research conclusions

The increased value of CB, TSA, and ATA parameters are associated with tumor biology, invasion, and metastasis of colorectal cancer.

Research perspectives

The presented evidence suggests the potential diagnostic and prognostic value of the CB-TSA-ATA biochemical marker panel.

ACKNOWLEDGEMENTS

We thank Dr. Filipowski H, PhD, for help with the statistical analysis.

REFERENCES

1 **Guinec N**, Dalet-Fumeron V, Pagano M. "In vitro" study of basement membrane degradation by the cysteine proteinases, cathepsins B, B-like and L. Digestion of collagen IV, laminin, fibronectin, and release of gelatinase activities from basement membrane fibronectin. *Biol Chem Hoppe Seyler* 1993; **374**: 1135-1146 [PMID: 8129860 DOI: 10.1515/bchm3.1993.374.7-12.1135]

2 **Korzus G**, Turyna B. [Cysteine proteinases and their endogenous inhibitors]. *Postepy Biochem* 1988; **34**: 23-46 [PMID: 3064060]

3 **Calkins CC**, Sameni M, Koblinski J, Sloane BF, Moin K. Differential localization of cysteine protease inhibitors and a target cysteine protease, cathepsin B, by immuno-confocal microscopy. *J Histochem Cytochem* 1998; **46**: 745-751 [PMID: 9603786 DOI: 10.1177/002215549804600607]

4 **Olszewska D**, Drewa T, Makarewicz R, Drewa J, Woźniak A, Maciak R. [Significance of cathepsin B and D in physiologic and pathologic processes]. *Pol Merkur Lekarski* 2001; **10**: 65-70 [PMID: 11320558]

5 **Qian F**, Chan SJ, Gong QM, Bajkowski AS, Steiner DF, Frankfater A. The expression of cathepsin B and other lysosomal proteinases in normal tissues and in tumors. *Biomed Biochim Acta* 1991; **50**: 531-540 [PMID: 1801719]

6 **Howie AJ**, Burnett D, Crocker J. The distribution of cathepsin B in human tissues. *J Pathol* 1985; **145**: 307-314 [PMID: 3889245 DOI: 10.1002/path.1711450404]

7 **Nomura T**, Katunuma N. Involvement of cathepsins in the invasion, metastasis and proliferation of cancer cells. *J Med Invest* 2005; **52**: 1-9 [PMID: 15751268 DOI: 10.2152/jmi.52.1]

8 **Talieri M**, Papadopoulou S, Scorilas A, Xynopoulos D, Arnogianaki N, Plataniotis G, Yotis J, Agnanti N. Cathepsin B and cathepsin D expression in the progression of colorectal adenoma to carcinoma. *Cancer Lett* 2004; **205**: 97-106 [PMID: 15036666 DOI: 10.1016/j.canlet.2003.09.033]

9 **Sheahan K**, Shuja S, Murnane MJ. Cysteine protease activities and tumor development in human colorectal carcinoma. *Cancer Res* 1989; **49**: 3809-3814 [PMID: 2544258]

10 **Troy AM**, Sheahan K, Mulcahy HE, Duffy MJ, Hyland JM, O'Donoghue DP. Expression of Cathepsin B and L antigen and activity is associated with early colorectal cancer progression. *Eur J Cancer* 2004; **40**: 1610-1616 [PMID: 15196548 DOI: 10.1016/j.ejca.2004.03.011]

11 **Shuja S**, Sheahan K, Murnane MJ. Cysteine endopeptidase activity levels in normal human tissues, colorectal adenomas and carcinomas. *Int J Cancer* 1991; **49**: 341-346 [PMID: 1917131 DOI: 10.1002/ijc.2910490305]

12 **Kruszewski WJ**, Rzepko R, Wojtacki J, Skokowski J, Kopacz A, Jaśkiewicz K, Drucis K. Overexpression of cathepsin B correlates with angiogenesis in colon adenocarcinoma. *Neoplasma* 2004; **51**: 38-43 [PMID: 15004658]

13 **Campo E**, Muñoz J, Miquel R, Palacín A, Cardesa A, Sloane BF, Emmert-Buck MR. Cathepsin B expression in colorectal carcinomas correlates with tumor progression and shortened patient survival. *Am J Pathol* 1994; **145**: 301-309 [PMID: 7519824]

14 **Berquin IM**, Sloane BF. Cathepsin B expression in human tumors. *Adv Exp Med Biol* 1996; **389**: 281-294 [PMID: 8861022 DOI: 10.1007/978-1-4613-0335-0_35]

15 **Hirai K**, Yokoyama M, Asano G, Tanaka S. Expression of cathepsin B and cystatin C in human colorectal cancer. *Hum Pathol* 1999; **30**: 680-686 [PMID: 10374777 DOI: 10.1016/s0046-8177(99)90094-1]

16 **Adenis A**, Huet G, Zerimech F, Hecquet B, Balduyck M, Peyrat JP. Cathepsin B, L, and D activities in colorectal carcinomas: relationship with clinico-pathological parameters. *Cancer Lett* 1995; **96**: 267-275 [PMID: 7585467 DOI: 10.1016/0304-3835(95)03930-u]

17 **Travis J**, Dubin A, Potempa J, Watorek W, Kurdowska A. Neutrophil proteinases. Caution signs in designing inhibitors against enzymes with possible multiple functions. *Ann N Y Acad Sci* 1991; **624**: 81-86 [PMID: 1905897 DOI: 10.1111/j.1749-6632.1991.tb17008.x]

18 **Watorek W**, Farley D, Salvesen G, Travis J. Neutrophil elastase and cathepsin G: structure, function, and biological control. *Adv Exp Med Biol* 1988; **240**: 23-31 [PMID: 3266707 DOI: 10.1007/978-1-4613-1057-0_3]

19 **Imamura T**, Maeda H. [Alpha1-proteinase inhibitor: structure and functions]. *Nihon Rinsho* 2005; **63** Suppl 4: 81-87 [PMID: 15861638]

20 **Okada Y**, Watanabe S, Nakanishi I, Kishi J, Hayakawa T, Watorek W, Travis J, Nagase H. Inactivation of tissue inhibitor of metalloproteinases by neutrophil elastase and other serine proteinases. *FEBS Lett* 1988; **229**: 157-160 [PMID: 3162216 DOI: 10.1016/0014-5793(88)80817-2]

21 **Potempa J**, Dubin A, Watorek W, Travis J. An elastase inhibitor from equine leukocyte cytosol belongs to the serpin superfamily. Further characterization and amino acid sequence of the reactive center. *J Biol Chem* 1988; **263**: 7364-7369 [PMID: 3366785]

22 **Varki NM**, Varki A. Diversity in cell surface sialic acid presentations: implications for biology and disease. *Lab Invest* 2007; **87**: 851-857 [PMID: 17632542 DOI: 10.1038/Labinvest.3700656]

23 **Sillanaukee P**, Pönniö M, Jääskeläinen IP. Occurrence of sialic acids in healthy humans and different

disorders. *Eur J Clin Invest* 1999; **29**: 413-425 [PMID: 10354198 DOI: 10.1046/j.1365-2362.1999.00485.x]

24 **Akcay F**, Taysi S, Uslu C, Doğru Y, Gümüştekin K. Levels of soluble intercellular adhesion molecule-1 and total sialic acid in serum of patients with laryngeal cancer. *Jpn J Clin Oncol* 2001; **31**: 584-588 [PMID: 11902488 DOI: 10.1093/jjco/hye128]

25 **de Albuquerque Garcia Redondo P**, Nakamura CV, de Souza W, Morgado-Díaz JA. Differential expression of sialic acid and N-acetylgalactosamine residues on the cell surface of intestinal epithelial cells according to normal or metastatic potential. *J Histochem Cytochem* 2004; **52**: 629-640 [PMID: 15100240 DOI: 10.1177/002215540405200507]

26 **Feijoo-Carnero C**, Rodríguez-Berrocal FJ, Páez de la Cadena M, Ayude D, de Carlos A, Martínez-Zorzano VS. Clinical significance of preoperative serum sialic acid levels in colorectal cancer: utility in the detection of patients at high risk of tumor recurrence. *Int J Biol Markers* 2004; **19**: 38-45 [PMID: 15077925 DOI: 10.5301/jbm.2008.576]

27 **Katopodis N**, Hirshaut Y, Geller NL, Stock CC. Lipid-associated sialic acid test for the detection of human cancer. *Cancer Res* 1982; **42**: 5270-5275 [PMID: 7139630]

28 **López Sáez JJ**, Senra-Varela A. Evaluation of lipid-bound sialic acid (LSA) as a tumor marker. *Int J Biol Markers* 1995; **10**: 174-179 [PMID: 8551061]

29 **Miyazaki K**, Ohmori K, Izawa M, Koike T, Kumamoto K, Furukawa K, Ando T, Kiso M, Yamaji T, Hashimoto Y, Suzuki A, Yoshida A, Takeuchi M, Kannagi R. Loss of disialyl Lewis(a), the ligand for lymphocyte inhibitory receptor sialic acid-binding immunoglobulin-like lectin-7 (Siglec-7) associated with increased sialyl Lewis(a) expression on human colon cancers. *Cancer Res* 2004; **64**: 4498-4505 [PMID: 15231659 DOI: 10.1158/0008-5472.CAN-03-3614]

30 **Shen Y**, Tiralongo J, Kohla G, Schauer R. Regulation of sialic acid O-acetylation in human colon mucosa. *Biol Chem* 2004; **385**: 145-152 [PMID: 15101557 DOI: 10.1515/BC.2004.033]

31 **Shen Y**, Kohla G, Lrhorfi AL, Sipos B, Kalthoff H, Gerwig GJ, Kamerling JP, Schauer R, Tiralongo J. O-acetylation and de-O-acetylation of sialic acids in human colorectal carcinoma. *Eur J Biochem* 2004; **271**: 281-290 [PMID: 14717696 DOI: 10.1046/j.1432-1033.2003.03927.x]

32 **Uslu C**, Taysi S, Akcay F, Sutbeyaz MY, Bakan N. Serum free and bound sialic acid and alpha-1-acid glycoprotein in patients with laryngeal cancer. *Ann Clin Lab Sci* 2003; **33**: 156-159 [PMID: 12817619]

33 **Barrett AJ**. Fluorimetric assays for cathepsin B and cathepsin H with methylcoumarylamide substrates. *Biochem J* 1980; **187**: 909-912 [PMID: 6897924 DOI: 10.1042/bj1870909]

34 **Jourdian GW**, Dean L, Roseman S. The sialic acids. XI. A periodate-resorcinol method for the quantitative estimation of free sialic acids and their glycosides. *J Biol Chem* 1971; **246**: 430-435 [PMID: 5542012]

35 **Tautu C**, Verazin G, Prorok JJ, Alhadeff JA. Improved procedure for determination of serum lipid-associated sialic acid: application for early diagnosis of colorectal cancer. *J Natl Cancer Inst* 1988; **80**: 1333-1337 [PMID: 3172258 DOI: 10.1093/jnci/80.16.1333]

36 **Warwas M**, Knapik-Kordecka M, Kowal-Gierczak B. Stężenie i aktywność alfa1-inhibitora proteaz oraz alfa-2 makroglobuliny w osoczu krwi chorych na cukrzycę typu II. *Diagn Lab* 1991; **44**: 552-556

37 **Dietz AA**, Rubinstein HM, Hodges LK. Use of alpha-N-benzoyl-L-arginine-p-nitroanilide as trypsin substrate in estimation of alpha 1-antitrypsin. *Clin Chem* 1976; **22**: 1754-1755 [PMID: 10097]

38 **Herszényi L**, Farinati F, Plebani M, Carraro P, Roveroni G, De Paoli M, Cardin R, Naccarato R, Tulassay Z. [Prognostic role of cisteine and serin proteases in gastriC cancer]. *Orv Hetil* 1996; **137**: 1637-1641 [PMID: 9019701]

39 **Herszényi L**, Farinati F, Plebani M, István G, Sápi Z, Carraro P, De Paoli M, Naccarato R, Tulassay Z. [The role of cathepsins and the plasminogen activator/inhibitor system in colorectal cancer]. *Orv Hetil* 1999; **140**: 1833-1836 [PMID: 10489782]

40 **Kos J**, Nielsen HJ, Krasovec M, Christensen IJ, Cimerman N, Stephens RW, Brünner N. Prognostic values of cathepsin B and carcinoembryonic antigen in sera of patients with colorectal cancer. *Clin Cancer Res* 1998; **4**: 1511-1516 [PMID: 9626470]

41 **Dufek V**, Jirásek V, Král V, Matous B, Drazná E. Changes in serum cathepsin B-like activity in patients with colorectal cancer. *Neoplasma* 1985; **32**: 51-54 [PMID: 3982561]

42 **Amiguet JA**, Jiménez J, Monreal JI, Hernández MJ, López-Vivanco G, Vidán JR, Conchillo F, Liso P. Serum proteolytic activities and antiproteases in human colorectal carcinoma. *J Physiol Biochem* 1998; **54**: 9-13 [PMID: 9732103]

43 **Padilla D**, Cubo T, Molina JM, García M, De la Osa G, Palomino T, Pardo R, Martín J, Arévalo E, Hernández Calvo J. [Prognostic significance and clinic utility of serum and immunohistochemical cathepsin B levels in colorectal cancer]. *An Med Interna* 2003; **20**: 521-525 [PMID: 14585038]

44 **Skrzydlewska E**, Sulkowska M, Wincewicz A, Koda M, Sulkowski S. Evaluation of serum cathepsin B and D in relation to clinicopathological staging of colorectal cancer. *World J Gastroenterol* 2005; **11**: 4225-4229 [PMID: 16015694 DOI: 10.3748/wjg.v11.i27.4225]

45 **Zore I**, Krasovec M, Cimerman N, Kuhelj R, Werle B, Nielsen HJ, Brünner N, Kos J. Cathepsin B/cystatin C complex levels in sera from patients with lung and colorectal cancer. *Biol Chem* 2001; **382**: 805-810 [PMID: 11517934 DOI: 10.1515/BC.2001.097]

46 **Herszényi L**, Plebani M, Carraro P, De Paoli M, Roveroni G, Cardin R, Foschia F, Tulassay Z, Naccarato R, Farinati F. Proteases in gastrointestinal neoplastic diseases. *Clin Chim Acta* 2000; **291**:

171-187 [PMID: 10675722 DOI: 10.1016/s0009-8981(99)00227-2]
47 **Herszényi L**, Farinati F, Cardin R, István G, Molnár LD, Hritz I, De Paoli M, Plebani M, Tulassay Z. Tumor marker utility and prognostic relevance of cathepsin B, cathepsin L, urokinase-type plasminogen activator, plasminogen activator inhibitor type-1, CEA and CA 19-9 in colorectal cancer. *BMC Cancer* 2008; **8**: 194 [PMID: 18616803 DOI: 10.1186/1471-2407-8-194]
48 **Geraghty P**, Rogan MP, Greene CM, Boxio RM, Poiriert T, O'Mahony M, Belaaouaj A, O'Neill SJ, Taggart CC, McElvaney NG. Neutrophil elastase up-regulates cathepsin B and matrix metalloprotease-2 expression. *J Immunol* 2007; **178**: 5871-5878 [PMID: 17442971 DOI: 10.4049/jimmunol.178.9.5871]
49 **Sun Z**, Yang P. Role of imbalance between neutrophil elastase and alpha 1-antitrypsin in cancer development and progression. *Lancet Oncol* 2004; **5**: 182-190 [PMID: 15003202 DOI: 10.1016/S1470-2045(04)01414-7]
50 **Xu Y**, Zhang J, Han J, Pan X, Cao Y, Guo H, Pan Y, An Y, Li X. Curcumin inhibits tumor proliferation induced by neutrophil elastase through the upregulation of α1-antitrypsin in lung cancer. *Mol Oncol* 2012; **6**: 405-417 [PMID: 22507634 DOI: 10.1016/j.molonc.2012.03.005]
51 **Sato T**, Takahashi S, Mizumoto T, Harao M, Akizuki M, Takasugi M, Fukutomi T, Yamashita J. Neutrophil elastase and cancer. *Surg Oncol* 2006; **15**: 217-222 [PMID: 17320378 DOI: 10.1016/j.suronc.2007.01.003]
52 **Kataoka H**, Nabeshima K, Komada N, Koono M. New human colorectal carcinoma cell lines that secrete proteinase inhibitors in vitro. *Virchows Arch B Cell Pathol Incl Mol Pathol* 1989; **57**: 157-165 [PMID: 2570482 DOI: 10.1007/BF02899077]
53 **Keppler D**, Markert M, Carnal B, Berdoz J, Bamat J, Sordat B. Human colon carcinoma cells synthesize and secrete alpha 1-proteinase inhibitor. *Biol Chem Hoppe Seyler* 1996; **377**: 301-311 [PMID: 8828821 DOI: 10.1515/bchm3.1996.377.5.301]
54 **Sugino T**, Yamaguchi T, Ogura G, Kusakabe T, Goodison S, Homma Y, Suzuki T. The secretory leukocyte protease inhibitor (SLPI) suppresses cancer cell invasion but promotes blood-borne metastasis *via* an invasion-independent pathway. *J Pathol* 2007; **212**: 152-160 [PMID: 17455170 DOI: 10.1002/path.2156]
55 **Korkmaz B**, Attucci S, Jourdan ML, Juliano L, Gauthier F. Inhibition of neutrophil elastase by alpha1-protease inhibitor at the surface of human polymorphonuclear neutrophils. *J Immunol* 2005; **175**: 3329-3338 [PMID: 16116225 DOI: 10.4049/jimmunol.175.5.3329]
56 **Meyer-Hoffert U**, Wiedow O. Neutrophil serine proteases: mediators of innate immune responses. *Curr Opin Hematol* 2011; **18**: 19-24 [PMID: 21042214 DOI: 10.1097/MOH.0b013e32834115d1]
57 **Nozawa F**, Hirota M, Okabe A, Shibata M, Iwamura T, Haga Y, Ogawa M. Elastase activity enhances the adhesion of neutrophil and cancer cells to vascular endothelial cells. *J Surg Res* 2000; **94**: 153-158 [PMID: 11104655 DOI: 10.1006/jsre.2000.6002]
58 **Ho AS**, Chen CH, Cheng CC, Wang CC, Lin HC, Luo TY, Lien GS, Chang J. Neutrophil elastase as a diagnostic marker and therapeutic target in colorectal cancers. *Oncotarget* 2014; **5**: 473-480 [PMID: 24457622 DOI: 10.18632/oncotarget.1631]
59 **Kovcić V**, Jelić S, Filipović I, Tomasević Z. [Serum haptoglobin and alpha-1 antitrysin levels as biological evolution markers in patients with gastric and colorectal cancer]. *Srp Arh Celok Lek* 1994; **122**: 311-313 [PMID: 17974404]
60 **Millán Núñez-Cortés J**. [Biological and clinical aspects of alpha 1-antitrypsin with special reference to malignant tumor processes]. *Rev Esp Oncol* 1981; **28**: 591-641 contd [PMID: 6764960]
61 **Simpson WG**, Heys SD, Whiting PH, Eremin O, Broom J. Acute phase proteins and recombinant IL-2 therapy: prediction of response and survival in patients with colorectal cancer. *Clin Exp Immunol* 1995; **99**: 143-147 [PMID: 7531626 DOI: 10.1111/j.1365-2249.1995.tb05524.x]
62 **Stamatiadis AP**, St Toumanidou M, Vyssoulis GP, Manouras AJ, Apostolidis NS. Value of serum acute-phase reactant proteins and carcinoembryonic antigen in the preoperative staging of colorectal cancer. A multivariate analysis. *Cancer* 1990; **65**: 2055-2057 [PMID: 1695546 DOI: 10.1002/1097-0142(19900501)65:9<2055::aid-cncr2820650927>3.0.co;2-6]
63 **Jaberie H**, Hosseini SV, Naghibalhossaini F. Evaluation of Alpha 1-Antitrypsin for the Early Diagnosis of Colorectal Cancer. *Pathol Oncol Res* 2020; **26**: 1165-1173 [PMID: 31183614 DOI: 10.1007/s12253-019-00679-0]
64 **Bujanda L**, Sarasqueta C, Cosme A, Hijona E, Enríquez-Navascués JM, Placer C, Villarreal E, Herreros-Villanueva M, Giraldez MD, Gironella M, Balaguer F, Castells A. Evaluation of alpha 1-antitrypsin and the levels of mRNA expression of matrix metalloproteinase 7, urokinase type plasminogen activator receptor and COX-2 for the diagnosis of colorectal cancer. *PLoS One* 2013; **8**: e51810 [PMID: 23300952 DOI: 10.1371/journal.pone.0051810]
65 **Yüceyar S**, Ertürk S, Dirican A, Cengiz A, Saner H. The role of acute-phase reactant proteins, carcinoembryonic antigen and CA 19-9 as a marker in the preoperative staging of colorectal cancer: a prospective clinical study. *Int Surg* 1996; **81**: 136-139 [PMID: 8912078]
66 **Gallardo-Valverde JM**, Calañas-Continente A, Baena-Delgado E, Zurera-Tendero L, Vázquez-Martínez C, Membrives-Obrero A, Muntané J, Arévalo-Jiménez E. Obstruction in patients with colorectal cancer increases morbidity and mortality in association with altered nutritional status. *Nutr Cancer* 2005; **53**: 169-176 [PMID: 16573378 DOI: 10.1207/s15327914nc5302_6]
67 **Bernacka K**, Kuryliszyn-Moskal A, Sierakowski S. The levels of alpha 1-antitrypsin and alpha 1-antichymotrypsin in the sera of patients with gastrointestinal cancers during diagnosis. *Cancer* 1988; **62**: 1188-1193 [PMID: 3261623 DOI:

10.1002/1097-0142(19880915)62:6<1188::aid-cncr2820620624>3.0.co;2-e]

68 **Ward DG**, Suggett N, Cheng Y, Wei W, Johnson H, Billingham LJ, Ismail T, Wakelam MJ, Johnson PJ, Martin A. Identification of serum biomarkers for colon cancer by proteomic analysis. *Br J Cancer* 2006; **94**: 1898-1905 [PMID: 16755300 DOI: 10.1038/sj.bjc.6603188]

69 **Kątnik-Prastowska I**. Struktura i biologia kwasów sjalowych. *Adv Clin Exp Med* 2003; **5**: 653-663

70 **Painbeni T**, Gamelin E, Cailleux A, Le Bouil A, Boisdron-Celle M, Daver A, Larra F, Allain P. Plasma sialic acid as a marker of the effect of the treatment on metastatic colorectal cancer. *Eur J Cancer* 1997; **33**: 2216-2220 [PMID: 9470809 DOI: 10.1016/s0959-8049(97)00318-3]

71 **Romppanen J**, Eskelinen M, Tikanoja S, Mononen I. Total and lipid-bound serum sialic acid in benign and malignant breast disease. *Anticancer Res* 1997; **17**: 1249-1253 [PMID: 9137482]

72 **Varki A**. Sialic acids in human health and disease. *Trends Mol Med* 2008; **14**: 351-360 [PMID: 18606570 DOI: 10.1016/j.molmed.2008.06.002]

73 **Brockhausen I**, Yang JM, Burchell J, Whitehouse C, Taylor-Papadimitriou J. Mechanisms underlying aberrant glycosylation of MUC1 mucin in breast cancer cells. *Eur J Biochem* 1995; **233**: 607-617 [PMID: 7588808 DOI: 10.1111/j.1432-1033.1995.607_2.x]

74 **Inagaki Y**, Tang W, Guo Q, Kokudo N, Sugawara Y, Karako H, Konishi T, Nakata M, Nagawa H, Makuuchi M. Sialoglycoconjugate expression in primary colorectal cancer and metastatic lymph node tissues. *Hepatogastroenterology* 2007; **54**: 53-57 [PMID: 17419230]

75 **Miyagi T**, Wada T, Yamaguchi K. Roles of plasma membrane-associated sialidase NEU3 in human cancers. *Biochim Biophys Acta* 2008; **1780**: 532-537 [PMID: 18023981 DOI: 10.1016/j.bbagen.2007.09.016]

76 **Schutter EM**, Visser JJ, van Kamp GJ, Mensdorff-Pouilly S, van Dijk W, Hilgers J, Kenemans P. The utility of lipid-associated sialic acid (LASA or LSA) as a serum marker for malignancy. A review of the literature. *Tumour Biol* 1992; **13**: 121-132 [PMID: 1626178 DOI: 10.1159/000217755]

77 **Cylwik B**, Chrostek L, Szmitkowski M. [Diagnostic value of total and lipid-bound sialic acid in malignancies]. *Pol Merkur Lekarski* 2005; **19**: 237-241 [PMID: 16245443]

78 **Feijoo C**, Páez de la Cadena M, Rodríguez-Berrocal FJ, Martínez-Zorzano VS. Sialic acid levels in serum and tissue from colorectal cancer patients. *Cancer Lett* 1997; **112**: 155-160 [PMID: 9066722 DOI: 10.1016/s0304-3835(96)04564-8]

79 **Sebzda T**, Saleh Y, Gburek J, Warwas M, Andrzejak R, Siewinski M, Rudnicki J. Total and lipid-bound plasma sialic acid as diagnostic markers in colorectal cancer patients: correlation with cathepsin B expression in progression to Dukes stage. *J Exp Ther Oncol* 2006; **5**: 223-229 [PMID: 16528972]

80 **İliklerden ÜH**, Peksen C, Kalayci T, Kemik O. Evaluation of preoperative and postoperative total serum sialic acid levels in patients with colon cancer. *Ann Ital Chir* 2020; **91**: 649-647 [PMID: 33554943]

81 **Zhang Z**, Wuhrer M, Holst S. Serum sialylation changes in cancer. *Glycoconj J* 2018; **35**: 139-160 [PMID: 29680984 DOI: 10.1007/s10719-018-9820-0]

82 **Herszényi L**, Barabás L, Hritz I, István G, Tulassay Z. Impact of proteolytic enzymes in colorectal cancer development and progression. *World J Gastroenterol* 2014; **20**: 13246-13257 [PMID: 25309062 DOI: 10.3748/wjg.v20.i37.13246]

83 **Yin J**, Hashimoto A, Izawa M, Miyazaki K, Chen GY, Takematsu H, Kozutsumi Y, Suzuki A, Furuhata K, Cheng FL, Lin CH, Sato C, Kitajima K, Kannagi R. Hypoxic culture induces expression of sialin, a sialic acid transporter, and cancer-associated gangliosides containing non-human sialic acid on human cancer cells. *Cancer Res* 2006; **66**: 2937-2945 [PMID: 16540641 DOI: 10.1158/0008-5472.CAN-05-2615]

World Journal of Gastroenterology

Submit a Manuscript: https://www.f6publishing.com

World J Gastroenterol 2021 October 21; 27(39): 6689-6700

DOI: 10.3748/wjg.v27.i39.6689

ISSN 1007-9327 (print) ISSN 2219-2840 (online)

ORIGINAL ARTICLE

Observational Study

Impact of a colorectal cancer screening program implantation on delays and prognosis of non-screening detected colorectal cancer

Joaquin Cubiella, María Lorenzo, Franco Baiocchi, Coral Tejido, Alejandro Conde, María Sande-Meijide, Margarita Castro

ORCID number: Joaquin Cubiella 0000-0002-9994-4831; María Lorenzo 0000-0003-4898-3889; Franco Baiocchi 0000-0002-6518-8169; Coral Tejido 0000-0003-1068-7224; Alejandro Conde 0000-0002-0183-1119; María Sande-Meijide 0000-0002-5697-9292; Margarita Castro 0000-0001-9605-9709.

Author contributions: Cubiella J, Sande-Meijide M and Castro M contributed to the conception and design of the article; Cubiella J, Sande-Meijide M, Castro M and Lorenzo M contributed to obtaining funding; Lorenzo M, Baiocchi F, Tejido C and Conde A contributed to acquisition of data; Cubiella J contributed to analysis, interpretation of data and drafting the article; all authors made critical revisions related to the manuscript's important intellectual content and gave final approval of the version of the article to be published.

Supported by the Spain's Carlos III Health Care Institute by means of project PI17/00837 (Co-funded by European Regional Development Fund/European Social Fund "A way to make Europe"/"Investing in your future").

Institutional review board statement: The study was

Joaquin Cubiella, Coral Tejido, Department of Gastroenterology, Complexo Hospitalario Universitario de Ourense, Ourense 32005, Orense, Spain

María Lorenzo, Alejandro Conde, María Sande-Meijide, Department of Preventive Medicine, Complexo Hospitalario Universitario de Ourense, Ourense 32003, Orense, Spain

Franco Baiocchi, Department of Gastroenterology, Hospital del Bierzo, Ponferrada 24404, Leon, Spain

Margarita Castro, Dirección Xeral de Saúde Pública, Conselleria de Sanidade, Santiago de Compostela 15703, Spain

Corresponding author: Joaquin Cubiella, MD, PhD, Doctor, Staff Physician, Statistician, Department of Gastroenterology, Complexo Hospitalario Universitario de Ourense, Rúa Ramón Puga 52-54, Ourense 32005, Orense, Spain. joaquin.cubiella.fernandez@sergas.es

Abstract

BACKGROUND

The implementation of a colorectal cancer (CRC) screening programme may increase the awareness of Primary Care Physicians, reduce the diagnostic delay in CRC detected outside the scope of the screening programme and thus improve prognosis.

AIM

To determine the effect of implementation of a CRC screening programme on diagnostic delays and prognosis of CRC detected outside the scope of a screening programme.

METHODS

We performed a retrospective intervention study with a pre-post design. We identified 322 patients with incident and confirmed CRC in the pre-implantation cohort (June 2014 – May 2015) and 285 in the post-implantation cohort (June 2017 - May 2018) in the Cancer Registry detected outside the scope of a CRC screening programme. In each patient we calculated the different healthcare diagnostics delays: global, primary and secondary healthcare, referral and colonoscopy-related delays. In addition, we collected the initial healthcare that evaluated the patient, the home location (urban/rural), and the CRC stage at diagnosis. We

determined the two-year survival and we performed a multivariate proportional hazard regression analysis to determine the variables associated with survival.

RESULTS

We did not detect any differences in the patient or CRC baseline-related variables. A total of 20.1% of patients was detected with metastatic disease. There was a significant increase in direct referral to colonoscopy from primary healthcare (25.5%, 35.8%; P = 0.04) in the post-implantation cohort. Diagnostic delay was reduced by 24 d (106.64 ± 148.84 days, 82.84 ± 109.31 d; P = 0.02) due to the reduction in secondary healthcare delay (46.01 ± 111.65 d; 29.20 ± 60.83 d; P = 0.02). However, we did not find any differences in CRC stage at diagnosis or in two-year survival (70.3%; P = 0.9). Variables independently associated with two-year risk of death were age (Hazard Ratio-HR: 1.06, 95%CI: 1.04-1.07), CRC stage (II HR: 2.17, 95%CI: 1.07-4.40; III HR: 3.07, 95%CI: 1.56-6.08; IV HR: 19.22, 95%CI: 9.86-37.44; unknown HR: 9.24, 95%CI: 4.27-19.99), initial healthcare consultation (secondary HR: 2.93, 95%CI: 1.01-8.55; emergency department HR: 2.06, 95%CI: 0.67-6.34), hospitalization during the diagnostic process (HR: 1.67, 95%CI: 1.17-2.38) and urban residence (HR: 1.44, 95%CI: 1.06-1.98).

CONCLUSION

Although implementation of a CRC screening programme can reduce diagnostic delays for CRC detected in symptomatic patients, this has no effect on CRC stage or survival.

Key Words: Colorectal cancer; Population based screening; Primary healthcare; Diagnostic delay; Prognosis

©The Author(s) 2021. Published by Baishideng Publishing Group Inc. All rights reserved.

Core Tip: We have designed a retrospective intervention study with a pre-post design to confirm the hypothesis that the implementation of a colorectal cancer (CRC) screening program may increase the awareness of primary care physicians and, thus, reduce the diagnostic delays in CRC detected outside the screening program and improve prognosis. Our results confirm that the implementation of the CRC screening program reduced the diagnostic delays due to an increase in the direct referrals to colonoscopy from primary healthcare. However, this reduction in the delays had no effect on the stage at diagnosis or in the two year survival. These later results were confirmed in a multivariable Cox regression analysis.

Citation: Cubiella J, Lorenzo M, Baiocchi F, Tejido C, Conde A, Sande-Meijide M, Castro M. Impact of a colorectal cancer screening program implantation on delays and prognosis of non-screening detected colorectal cancer. *World J Gastroenterol* 2021; 27(39): 6689-6700
URL: https://www.wjgnet.com/1007-9327/full/v27/i39/6689.htm
DOI: https://dx.doi.org/10.3748/wjg.v27.i39.6689

INTRODUCTION

Colorectal cancer (CRC) is one of the most important health problems in the Western world. In 2018, almost half a million new cases were diagnosed in Europe and 250,000 patients died due to CRC[1]. In order to reduce the disease burden, population-based CRC screening programmes have been established in the Western world. This strategy has demonstrated its efficacy to reduce CRC mortality and incidence in randomized controlled trials. Furthermore, we have real data showing that implementation of CRC screening programmes has achieved its expected efficiency in reducing both CRC mortality and incidence[2,3].

In spite of the implementation of CRC screening programmes, most CRC are detected among symptomatic patients outside the scope of CRC screening mainly due to the limited participation and the detection in age cohorts that are not candidates for CRC screening[4,5]. However, as in breast cancer screening, the implementation of

conducted in accordance with the Declaration of Helsinki, and the protocol was approved by the Ethics Committee of Galicia, Spain (code 2016/274). As long as the study was based on database use, no informed consent was required. The information was accessed according to prevailing European and Spanish legislation.

Informed consent statement: All study participants, or their legal guardian, provided informed written consent prior to study enrollment.

Conflict-of-interest statement: There are no conflicts of interest to report.

Data sharing statement: We will share the data base on demand and according to European legislation.

STROBE statement: The authors have read the STROBE Statement—checklist of items, and the manuscript was prepared and revised according to the STROBE Statement—checklist of items.

Open-Access: This article is an open-access article that was selected by an in-house editor and fully peer-reviewed by external reviewers. It is distributed in accordance with the Creative Commons Attribution NonCommercial (CC BY-NC 4.0) license, which permits others to distribute, remix, adapt, build upon this work non-commercially, and license their derivative works on different terms, provided the original work is properly cited and the use is non-commercial. See: http://creativecommons.org/Licenses/by-nc/4.0/

Manuscript source: Invited manuscript

Specialty type: Oncology

Country/Territory of origin: Spain

Peer-review report's scientific quality classification

Grade A (Excellent): 0
Grade B (Very good): B
Grade C (Good): C
Grade D (Fair): D

Grade E (Poor): 0

Received: April 14, 2021
Peer-review started: April 14, 2021
First decision: July 14, 2021
Revised: July 15, 2021
Accepted: September 8, 2021
Article in press: September 8, 2021
Published online: October 21, 2021

P-Reviewer: Bordonaro M, Ji J, Rompianesi G
S-Editor: Wang LL
L-Editor: A
P-Editor: Xing YX

CRC screening may have an additional positive effect on these patients due to increased awareness and creation of multidisciplinary teams[6]. In this sense, CRC screening may increase the CRC awareness of patients and primary care physicians (PCPs) and promote use of faecal immunochemical test (FIT) as a triage test to refer patients to colonoscopy[7].

The delay to diagnosis in cancer is due to factors related to the patient and health system. The period from initial symptoms until final diagnosis is made can be highly variable. Although the common belief is that a longer delay can lead to an advanced stage at diagnosis and worse prognosis, evidence on CRC is controversial[8]. Patients seeking assistance with more severe symptoms are diagnosed in a shorter period and have more advanced disease[9]. In contrast, there is no evidence that a health system delay lower than six months worsens prognosis in the context of an outpatient diagnosis[10].

Based on the hypothesis that implementation of a mass CRC screening programme could raise awareness of patients and PCPs, we decided to design a retrospective intervention study to determine whether implementation of a CRC screening programme could reduce health system delays and, secondarily, improve CRC staging at diagnosis and long term survival.

MATERIALS AND METHODS

Study design

We designed a retrospective intervention study with a pre-post design without a control group.

Description of the intervention

The intervention was the first round of the Galician CRC screening programme that took place between 1 July 2015 and 30 June 2017 in Ourense, Spain. Galician CRC mass screening is based on biennial FIT with a 20 μg haemoglobin/g of faeces threshold. FIT is offered to subjects aged 50 to 69 years. It is coordinated by the Public Health Department of the Galician Regional Health Department. They are in charge of the identification of subjects, invitation to participate, reception of FIT results, citation of patients with a positive result to perform a colonoscopy and final evaluation of the endoscopic and histological results. Primary healthcare clinics are in charge of promoting participation in the screening programme, collecting FIT kits and evaluation of subjects with a positive FIT prior to colonoscopy. The hospitals in each health area are responsible for FIT analysis, colonoscopies, histological analysis and evaluation and treatment of patients with a CRC. Finally, personnel at the Coordination Unit key in data into the screening programme's information system regarding CRC stage according to the AJCC classification,[11]. the final classification of patients with a positive result[12]. as well as several quality endoscopist indicators according to the Spanish guideline on quality in screening colonoscopy[13]. During the implantation of the CRC screening program no change was performed in the diagnostic pathways for CRC diagnosis in symptomatic patients.

Inclusion criteria and definition of the cohorts

Pre cohort: We included all invasive incident CRC histologically confirmed detected in the natural year before implementation of the CRC screening programme (1 July 2014 – 30 June 2015) in Ourense.

Post cohort: We included all invasive incident CRC histologically confirmed and detected outside the scope of the CRC screening programme in the natural year after the first round: (1 July 2017- 30 June 2018).

Identification of the incident CRC

We identified the incident using the case identification structure developed and validated by the project for implementation of the Galician Tumour Registry (Project REGAT). REGAT uses the topographic codes ICD-O-3.1 C18-C19-C20 to identify the CRC[14]. Codes C18.1 (appendix), C21 (anus and anal canal) were excluded. REGAT data were crosslinked with the Galician CRC screening information system to exclude those patients with a CRC diagnosed within the screening programme.

Variables analyzed

We collected information regarding: (1) Demographics (age and sex); and (2) Tumour

location in relation to the splenic flexure: proximal (caecum, ascending colon, hepatic flexure and transverse colon) and distal (rectum, sigma, descending colon and splenic flexure).

Cancer stage at diagnosis according to the TNM classification (AJCC 7th edition) [11]. We used the following data to determine the stage at diagnosis: clinical or anatomo-pathological stage for metastatic disease, imaging tests for the local rectal cancer stage (T and N), anatomo-pathological evaluation for the remaining situations (colon cancer T and N).

We searched in IANUS, the unified clinical record database of the Galician Health Department, for information regarding the contacts and referrals in the healthcare system. IANUS includes all information regarding attendance in primary and secondary healthcare as well as emergency departments and hospitalization. We determined the first contact in the health system (primary, secondary, emergency), whether the patient required hospitalization during the diagnostic process and the diagnostic delays. We defined five diagnostic delays (Figure 1): (1) Global diagnostic delay: Overall delay from the first consultation to definitive diagnosis; (2) Primary healthcare delay: Delay from the initial evaluation in primary healthcare until the decision to refer to secondary healthcare. In the event of colonoscopy being directly requested from primary healthcare, this date was considered as the referral date; (3) Referral delay: Delay from the primary healthcare referral to the first attendance in secondary healthcare (either clinical consultation or performing of colonoscopy); (4) Secondary healthcare delay: Delay from the first attendance in secondary healthcare to final diagnosis; and (5) Colonoscopy delay: Delay from the colonoscopy request to the performing of colonoscopy.

Statistical analysis

First, we performed a descriptive analysis of the variables included: number and frequencies in the qualitative variables and mean and standard deviation in the quantitative variables. We determined whether there were differences between both cohorts in the diagnostic pathways (hospitalization, direct referral to colonoscopy from primary healthcare) using the Chi-square test. In order to detect whether there were differences in the referral delays between both cohorts we used the Student *t* test. We analyzed whether there were differences in two-year survival between both cohorts in the Kaplan-Meier analysis using the log-rank test. Finally, to control confounding variables we performed a Cox multivariate regression analysis and we determined which variables were independently associated with survival after diagnosis. The study was statistically reviewed by a biomedical statistician.

Ethics aspects

The study was conducted in accordance with the Declaration of Helsinki, and the protocol was approved by the Ethics Committee of Galicia, Spain (code 2016/274). As long as the study was based on database use, no informed consent was required. The information was accessed according to prevailing European and Spanish legislation.

RESULTS

Description of the sample

We identified records from 757 patients in the two periods analyzed in the cancer registry. We excluded 92 patients that did not meet the inclusion criteria and 58 patients with CRC detected within the CRC screening programme in the post-implantation cohort. Finally, the pre-implantation and post-implantation cohort consisted of 322 and 285 patients, respectively (Figure 2).

As we show in Table 1, we did not detect baseline differences between both cohorts. CRC was detected more commonly in males (59.6%) with a mean age of 74.5 ± 11.5 years and more than two thirds were distal to the splenic flexure. There were no differences with respect to the place of residence either. Most patients were initially evaluated in primary healthcare but up to 41.0% required hospitalization before reaching final diagnosis. Diagnosis was made through colonoscopy in 89.8% of detected CRC. In this sense, we detected a significant increase in the colonoscopy directly requested from primary healthcare in the post-implantation cohort (P = 0.04). When we limited the analysis to those patients initially seen in primary healthcare (522), the results were similar. In this sense, we only found differences in the rate of colonoscopy directly referred from primary healthcare (29.2%, 42.3%; P = 0.005).

Table 1 Characteristics of the patients included

	Pre-implantation cohort (*n* = 322)	Post-implantation cohort (*n* = 285)	*P* value[1]
Sex			0.1
Male	184 (57.1%)	178 (62.5%)	
Female	138 (42.9%)	107 (37.5%)	
Age (yr)	74.1 ± 11.8	74.8 ± 11.1	0.4
Colorectal location			0.8
Distal to splenic	221 (68.6%)	197 (69.1%)	
Proximal to splenic	101 (31.4%)	88 (30.9%)	
TNM			
I	45 (14.0%)	47 (16.5%)	
II	93 (26.9%)	71 (24.9%)	
III	101 (31.4%)	99 (34.7%)	0.5
IV	65 (20.2%)	57 (20.0%)	
Unknown	18 (5.6%)	11 (3.9%)	
Rural/Urban			
Rural	218 (67.9%)	195 (68.4%)	0.8
Urban	103 (32.1%)	90 (31.6%)	
Initial consultation			
Primary healthcare	281 (87.3%)	241 (84.6%)	
Secondar y healthcare	33 (10.2%)	37 (13.0%)	0.5
Emergency department	8 (2.5%)	7 (2.5%)	
Hospitalization			
Yes	135 (41.9%)	114 (40.0%)	0.6
No	187 (52.2%)	171 (60.0%)	
Colonoscopy request			
Primary healthcare	82 (25.5%)	102 (35.8%)	
Secondary healthcare			0.04
After referral	160 (49.7%)	116 (40.7%)	
Direct request	45 (14.0%)	40 (14.0%)	
No colonoscopy	35 (10.9%)	27 (9.5%)	

[1]Statistical significance in the univariate analysis using the Chi-square test for qualitative variables and the Student *t* test for quantitative variables.

Delay to diagnosis

The delay to diagnosis was reduced in 24 d after implantation of the CRC screening programme (P = 0.02). We did not detect any differences in the primary healthcare, referral or colonoscopy delay. The reduction was due to a secondary healthcare delay in relation to an increased rate of direct referral to colonoscopy from primary healthcare, as we show in Table 2 and Figure 3.

The global delay was also reduced by 27 d in patients evaluated initially in primary healthcare (117.66 ± 154.08 days, 90.06 ± 111.31 days; P = 0.02) also due to a reduction in secondary healthcare delay (48.17 ± 116.42 d, 26.89 ± 54.50 d; P = 0.02). There were no differences in primary healthcare, referral or colonoscopy delay.

Factors associated with survival

The incidence of metastatic CRC remained stable (20.1%) in both cohorts and overall survival after one and two years was 71.3% and 70.3% without differences in the log-

Table 2 Delay to colorectal cancer diagnosis in the pre and post-implantation cohorts

	Pre-implantation cohort (*n* = 322)	Post-implantation cohort (*n* = 285)	*P* value[1]
Global diagnostic delay (d)	106.64 ± 148.84	82.84 ± 109.31	0.02
Primary healthcare delay (d)	35.88 ± 84.47	39.28 ± 98.03	0.7
Referral delay (d)	13.18 ± 25.77	16.02 ± 41.63	0.4
Secondary healthcare delay (d)	46.01 ± 111.65	29.20 ± 60.83	0.02
Colonoscopy delay (d)	43.71 ± 78.22	37.75 ± 53.37	0.3

[1]Statistical significance in the univariate analysis using the Student *t* test.

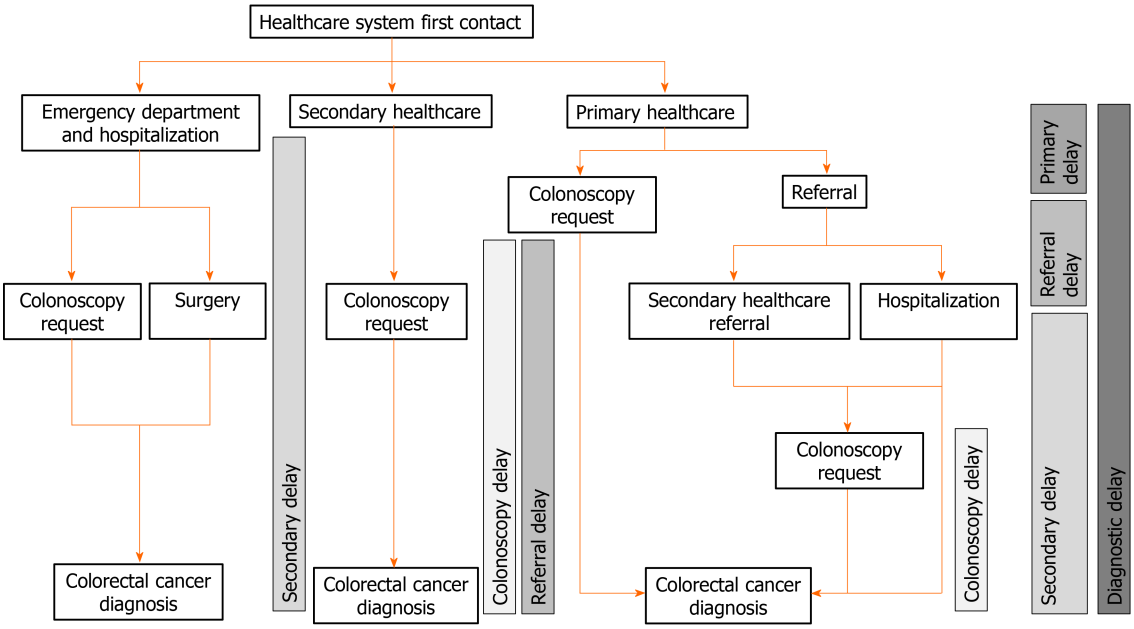


Figure 1 Flowchart of the referral and diagnostic pathways.

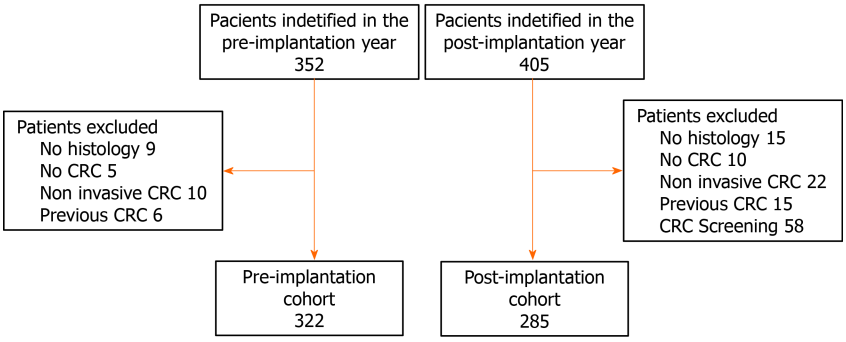


Figure 2 Flowchart of the patients included in the analysis.

rank test (P = 0.9) as we show in Figure 4. These results were confirmed in the Cox multivariate regression analysis and there were no differences in the survival between both cohorts (post-implantation cohort HR: 1.12, 95%CI: 0.83-1.51). As we show in Table 3, only age, CRC staging according to TNM classification, initial healthcare consultation, hospitalization during the diagnostic process and residence were independently associated with death after CRC diagnosis.

Table 3 Factors associated with survival

	Hazard ratio[1] (95%CI)
Sex	
Male	1
Female	1.18 (0.89-1.58)
Age (yr)	1.06 (1.04-1.07)
Colorectal location	
Distal to splenic	1
Proximal to splenic	0.84 (0.62-1.13)
Cohort	
Pre-implantation	1
Post-implantation	1.12 (0.83-1.51)
TNM	
I	1
II	2.17 (1.07-4.40)
III	3.07 (1.56-6.08)
IV	19.22 (9.86-37.44)
Unknown	9.24 (4.27-19.99)
Initial consultation	
Primary healthcare	1
Secondary healthcare	2.93 (1.01-8.55)
Emergency department	2.06 (0.67-6.34)
Hospitalization	
Yes	1.67 (1.17-2.38)
No	1
Colonoscopy request	
Primary healthcare	1.79 (0.96-3.35)
Secondary healthcare	1.54 (0.92-2.58)
After referral from Primary Healthcare	0.74 (0.25-2.21)
Direct request	1
No colonoscopy	
Rural/Urban	
Rural	1
Urban	1.44 (1.06-1.98)
Diagnostic delay (d)	1.001 (1.00-1.002)

[1]Hazard Ratio and its 95% confidence interval calculated using a multivariate proportional hazard regression analysis.

DISCUSSION

Our study shows that implementation of the CRC screening programme reduced healthcare referral delays due to the direct request of colonoscopy from primary healthcare. Unfortunately, this reduction in referral delay had no effect on CRC staging at diagnosis nor on the two-year survival. Finally, although we detected several variables associated with overall survival, multivariate logistic analysis confirms that neither implantation of the CRC screening nor diagnostic delay were related to the prognosis of CRC detected outside the scope of CRC screening.

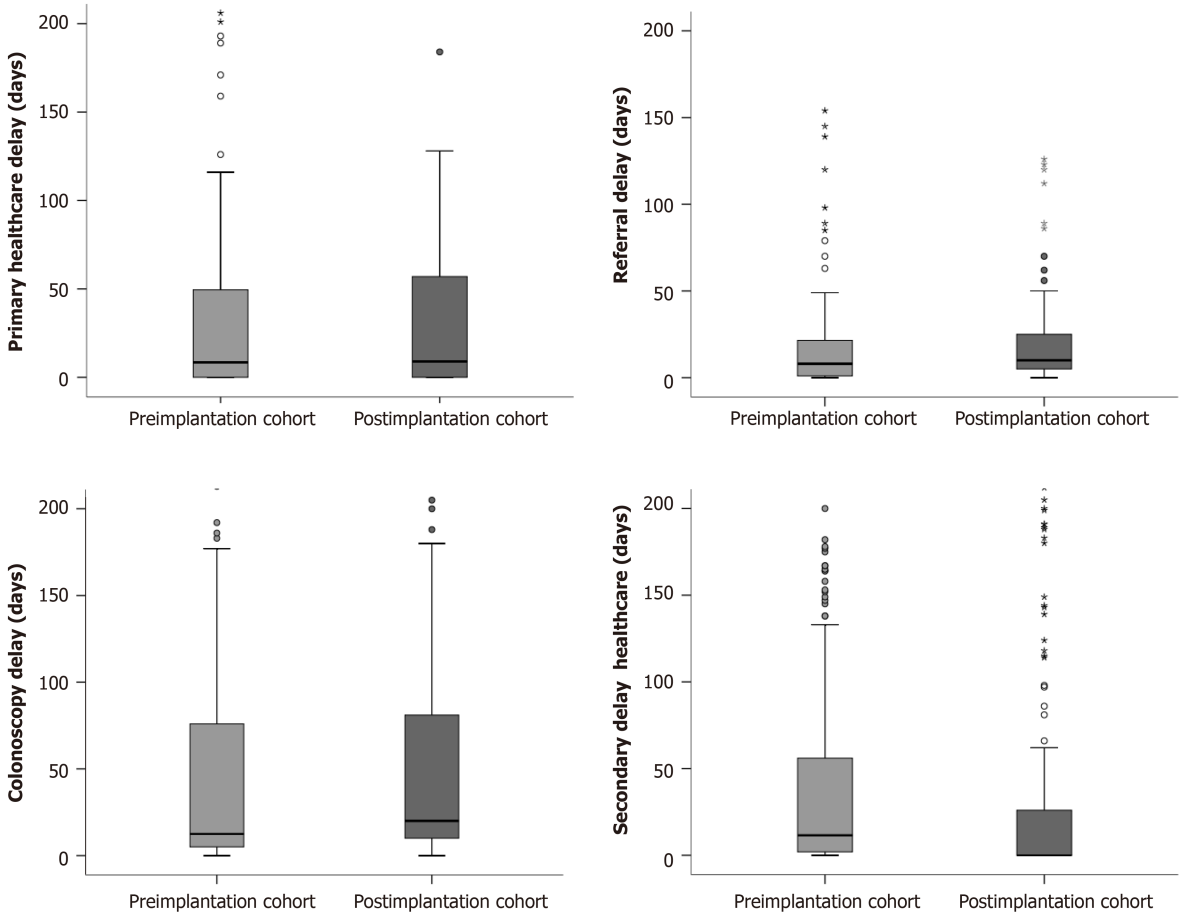


Figure 3 Healthcare diagnostic delays. We show the distribution of the primary and secondary healthcare, referral and colonoscopy delays expressed in days.

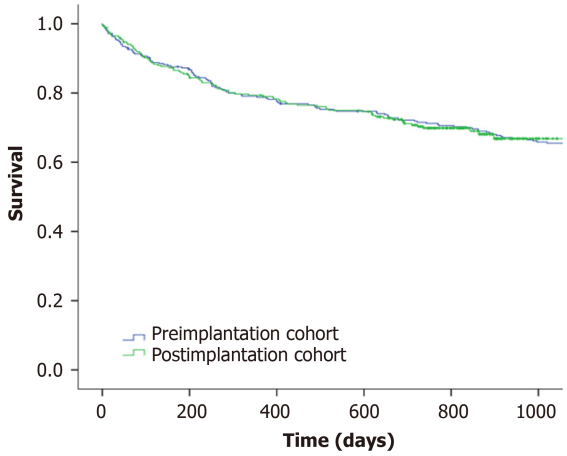


Figure 4 Survival curves of the pre and post-implantation cohorts. Survival curves were calculated using the Kaplan-Meier method.

PCPs play an important role in CRC care, from encouraging screening and accurate diagnosis to providing care during and after treatment for cancer and any comorbid complications. The implication of PCPs on CRC screening is variable according to the screening programme. Participation rates are increased when PCPs are involved in the invitation process. However, in the European population-based programmes in Europe PCPs play a rather supportive, informative or facilitating role[15]. In our case, PCPs receive full information on the screening programme organization and they are in charge of promoting participation as well as resolving any doubts. Within the training, PCPs are reminded which symptoms may lead to suspicion of CRC as well as the established referral pathways, including direct referral criteria for colonoscopy evaluation from primary healthcare[8,16].

We designed this analysis under the hypothesis that increased awareness on CRC and training in the diagnosis of CRC and the established protocols could reduce delays attributed to the health system. In this sense, our results confirm that implementation of the screening programme enabled a reduction in the diagnostic delay due to an increase in direct referrals to colonoscopy from primary healthcare. PCPs, as demonstrated in our study, are the main gateway and responsible for a significant part of the delay[17-19]. The role of PCPs in CRC diagnosis is complex since gastrointestinal symptoms that may suggest CRC are very common, the CRC prevalence low and the diagnostic performance of available symptom-based tools is very limited[20]. Recently, implementation of the faecal immunochemical test to triage patients with gastrointestinal symptoms in primary healthcare has improved diagnostic referral pathways[20,21]. In the health area of Ourense, faecal immunochemical test was implemented as a triage test seven years ago, so we cannot attribute the decreases in delay to this modification[16].

However, it is relevant that, despite the reduction in delay, we have not detected any changes in the stage at diagnosis or in the prognosis of CRC. These data are in accordance with results previously published by our group[8]. and with the data in the available meta-analysis on the effect of diagnostic delays in CRC prognosis[9]. In this sense, the prognosis of patients with shorter diagnostic delay is worse due to presentation with urgent symptoms that require hospitalization or more serious systemic symptoms[19]. In fact, in our study, hospitalization during admission was associated with a higher risk of mortality after diagnosis. In our research, although initial urgent presentation was rare, up to 40% of patients required hospitalization during the diagnostic process, similar to the information available on literature[22-24]. This lack of relationship between delay and prognosis may be related to different forms of presentation. In this sense, a prospective study on patients that met the National Institute for Health and Care Excellence referral criteria demonstrated that a delay of more than six months was associated with a worse prognosis compared to patients with the same symptoms diagnosed in an interval of less than one month[10].

Our study has two main strengths. We had the opportunity to evaluate the effect of the CRC screening programme on the diagnostic delays of CRC detected in symptomatic patients. This is the first study that evaluates additional impacts of the implementation of CRC screening on CRC diagnosis. No study has evaluated whether a CRC screening programme can increase the awareness of patients and PCPs, reduce delays and improve prognosis. However, we could identify all the CRC through the Galician cancer registry, confirm the diagnosis in IANUS, the centralized clinical record and determine when the patient was evaluated in the health system and thus calculate all the referral delays[25].

There are several limitations. Due to the design of the study, we could not evaluate the effect of CRC screening on the patient delays to seek assistance. Patient delay accounts for a relevant proportion of the delay between the onset of symptoms and the final diagnosis[26]. Moreover, we did not collect the initial symptoms as long as they were not collected uniformly in the clinical records.

CONCLUSION

To conclude, the implementation of a CRC screening programme enabled reduction of health system diagnostic delay by means of increased patients referred directly by PCPs to colonoscopy. However, this reduction in referral delay did not modify either CRC stage at diagnosis or two-year survival.

ARTICLE HIGHLIGHTS

Research background

In spite of the implementation of colorectal cancer (CRC) screening programmes, most CRC are detected among symptomatic patients outside the scope of CRC screening. However, they may increase the CRC awareness of patients and primary care physicians (PCP).

Research motivation

The implementation of a mass CRC screening programme could raise awareness of patients and PCPs, we decided to design a retrospective intervention study to

determine whether implementation of a CRC screening programme could reduce health system delays and, secondarily, improve CRC staging at diagnosis and long term survival.

Research objectives

To determine the effect of implementation of a CRC screening programme on diagnostic delays and prognosis of CRC detected outside the scope of a screening programme.

Research methods

We designed a retrospective intervention study with a pre-post design without a control group. We compared diagnostic delays, CRC stage and two year survival of a yearly CRC diagnosed before the implementation of a CRC screening programa with a CRC cohort diagnosed the year after the first round.

Research results

There was a significant increase in direct referral to colonoscopy from primary healthcare (25.5%, 35.8%; $P = 0.04$) in the post-implantation cohort. Diagnostic delay was reduced by 24 d (106.64 ± 148.84 d, 82.84 ± 109.31 d; $P = 0.02$) due to the reduction in secondary healthcare delay (46.01 ± 111.65 d; 29.20 ± 60.83 d; $P = 0.02$). However, we did not find any differences in CRC stage at diagnosis or in two-year survival (70.3%; $P = 0.9$).

Research conclusions

Although implementation of a CRC screening programme can reduce diagnostic delays for CRC detected in symptomatic patients, this has no effect on CRC stage or survival.

Research perspectives

We need more research on the motivations and perspectives of patients seeking help in primary healthcare.

REFERENCES

1 **World Health Organization**. Cancer Today. International Agency for Research on Cancer [Internet]. [cited 23 May 2020]. Available from: https://gco.iarc.fr/today/home

2 **Zorzi M**, Fedeli U, Schievano E, Bovo E, Guzzinati S, Baracco S, Fedato C, Saugo M, Dei Tos AP. Impact on colorectal cancer mortality of screening programmes based on the faecal immunochemical test. *Gut* 2015; **64**: 784-790 [PMID: 25179811 DOI: 10.1136/gutjnl-2014-307508]

3 **Levin TR**, Corley DA, Jensen CD, Schottinger JE, Quinn VP, Zauber AG, Lee JK, Zhao WK, Udaltsova N, Ghai NR, Lee AT, Quesenberry CP, Fireman BH, Doubeni CA. Effects of Organized Colorectal Cancer Screening on Cancer Incidence and Mortality in a Large Community-Based Population. *Gastroenterology* 2018; **155**: 1383-1391.e5 [PMID: 30031768 DOI: 10.1053/j.gastro.2018.07.017]

4 **Mansouri D**, McMillan DC, Crearie C, Morrison DS, Crighton EM, Horgan PG. Temporal trends in mode, site and stage of presentation with the introduction of colorectal cancer screening: a decade of experience from the West of Scotland. *Br J Cancer* 2015; **113**: 556-561 [PMID: 26158422 DOI: 10.1038/bjc.2015.230]

5 **Gutierrez-Stampa MA**, Aguilar V, Sarasqueta C, Cubiella J, Portillo I, Bujanda L. Impact of the faecal immunochemical test on colorectal cancer survival. *BMC Cancer* 2020; **20**: 616 [PMID: 32611328 DOI: 10.1186/s12885-020-07074-y]

6 **Kalager M**, Zelen M, Langmark F, Adami HO. Effect of screening mammography on breast-cancer mortality in Norway. *N Engl J Med* 2010; **363**: 1203-1210 [PMID: 20860502 DOI: 10.1056/NEJMoa1000727]

7 **Gutierrez-Stampa MA**, Aguilar V, Sarasqueta C, Cubiella J, Portillo I, Bujanda L. Colorectal Cancer Survival in 50- to 69-Year-Olds after Introducing the Faecal Immunochemical Test. *Cancers (Basel)* 2020; **12** [PMID: 32854370 DOI: 10.3390/cancers12092412]

8 **Fernández-de Castro JD**, Baiocchi Ureta F, Fernández González R, Pin Vieito N, Cubiella Fernández J. The effect of diagnostic delay attributable to the healthcare system on the prognosis of colorectal cancer. *Gastroenterol Hepatol* 2019; **42**: 527-533 [PMID: 31421857 DOI: 10.1016/j.gastrohep.2019.03.012]

9 **Tørring ML**, Murchie P, Hamilton W, Vedsted P, Esteva M, Lautrup M, Winget M, Rubin G. Evidence of advanced stage colorectal cancer with longer diagnostic intervals: a pooled analysis of seven primary care cohorts comprising 11 720 patients in five countries. *Br J Cancer* 2017; **117**: 888-897 [PMID: 28787432 DOI: 10.1038/bjc.2017.236]

10 **Alonso-Abreu I**, Alarcón-Fernández O, Gimeno-García AZ, Romero-García R, Carrillo-Palau M, Nicolás-Pérez D, Jiménez A, Quintero E. Early Colonoscopy Improves the Outcome of Patients With Symptomatic Colorectal Cancer. *Dis Colon Rectum* 2017; **60**: 837-844 [PMID: 28682969 DOI: 10.1097/DCR.0000000000000863]

11 **Edge SB**, Byrd DR, Compton CC, Fritz AG, Greene FL. In: Trotti A, editor. AJCC Cancer Staging Manual [Internet]. 7th edition. Springer, 2010. [cited 23 May 2020]. Available from: http://www.springer.com/medicine/surgery/book/978-0-387-88440-0

12 **European Colorectal Cancer Screening Guidelines Working Group**, von Karsa L, Patnick J, Segnan N, Atkin W, Halloran S, Lansdorp-Vogelaar I, Malila N, Minozzi S, Moss S, Quirke P, Steele RJ, Vieth M, Aabakken L, Altenhofen L, Ancelle-Park R, Antoljak N, Anttila A, Armaroli P, Arrossi S, Austoker J, Banzi R, Bellisario C, Blom J, Brenner H, Bretthauer M, Camargo Cancela M, Costamagna G, Cuzick J, Dai M, Daniel J, Dekker E, Delicata N, Ducarroz S, Erfkamp H, Espinàs JA, Faivre J, Faulds Wood L, Flugelman A, Frkovic-Grazio S, Geller B, Giordano L, Grazzini G, Green J, Hamashima C, Herrmann C, Hewitson P, Hoff G, Holten I, Jover R, Kaminski MF, Kuipers EJ, Kurtinaitis J, Lambert R, Launoy G, Lee W, Leicester R, Leja M, Lieberman D, Lignini T, Lucas E, Lynge E, Mádai S, Marinho J, Maučec Zakotnik J, Minoli G, Monk C, Morais A, Muwonge R, Nadel M, Neamtiu L, Peris Tuser M, Pignone M, Pox C, Primic-Zakelj M, Psaila J, Rabeneck L, Ransohoff D, Rasmussen M, Regula J, Ren J, Rennert G, Rey J, Riddell RH, Risio M, Rodrigues V, Saito H, Sauvaget C, Scharpantgen A, Schmiegel W, Senore C, Siddiqi M, Sighoko D, Smith R, Smith S, Suchanek S, Suonio E, Tong W, Törnberg S, Van Cutsem E, Vignatelli L, Villain P, Voti L, Watanabe H, Watson J, Winawer S, Young G, Zaksas V, Zappa M, Valori R. European guidelines for quality assurance in colorectal cancer screening and diagnosis: overview and introduction to the full supplement publication. *Endoscopy* 2013; **45**: 51-59 [PMID: 23212726 DOI: 10.1055/s-0032-1325997]

13 **Jover R**, Herráiz M, Alarcón O, Brullet E, Bujanda L, Bustamante M, Campo R, Carreño R, Castells A, Cubiella J, García-Iglesias P, Hervás AJ, Menchén P, Ono A, Panadés A, Parra-Blanco A, Pellisé M, Ponce M, Quintero E, Reñé JM, Sánchez del Río A, Seoane A, Serradesanferm A, Soriano Izquierdo A, Vázquez Sequeiros E; Spanish Society of Gastroenterology; Spanish Society of Gastrointestinal Endoscopy Working Group. Clinical practice guidelines: quality of colonoscopy in colorectal cancer screening. *Endoscopy* 2012; **44**: 444-451 [PMID: 22438159 DOI: 10.1055/s-0032-1306690]

14 **World Health Organization**. The International Classification of Diseases for Oncology (ICD-O) - 3 rd edition, 1st revision [Internet]. 2013. [cited 31 January 2021]. Available from: https://apps.who.int/iris/handle/10665/96612

15 **Triantafillidis JK**, Vagianos C, Gikas A, Korontzi M, Papalois A. Screening for colorectal cancer: the role of the primary care physician. *Eur J Gastroenterol Hepatol* 2017; **29**: e1-e7 [PMID: 27676092 DOI: 10.1097/MEG.0000000000000759]

16 **Vega-Villaamil P**, Salve-Bouzo M, Cubiella J, Valentín-Gómez F, Sánchez-Hernández E, Gómez-Fernández I, Fernández-Seara J. Evaluation of the implementation of Galician Health Service indications and priority levels for colonoscopy in symptomatic patients: prospective, cross-sectional study. *Rev Esp Enferm Dig* 2013; **105**: 600-608 [PMID: 24641457 DOI: 10.4321/s1130-01082013001000005]

17 **van Erp NF**, Helsper CW, Olyhoek SM, Janssen RRT, Winsveen A, Peeters PHM, de Wit NJ. Potential for Reducing Time to Referral for Colorectal Cancer Patients in Primary Care. *Ann Fam Med* 2019; **17**: 419-427 [PMID: 31501203 DOI: 10.1370/afm.2446]

18 **Brandenbarg D**, Groenhof F, Siewers IM, van der Voort A, Walter FM, Berendsen AJ. Possible missed opportunities for diagnosing colorectal cancer in Dutch primary care: a multimethods approach. *Br J Gen Pract* 2018; **68**: e54-e62 [PMID: 29203683 DOI: 10.3399/bjgp17X693905]

19 **Esteva M**, Leiva A, Ramos M, Pita-Fernández S, González-Luján L, Casamitjana M, Sánchez MA, Pértega-Díaz S, Ruiz A, Gonzalez-Santamaría P, Martín-Rabadán M, Costa-Alcaraz AM, Espí A, Macià F, Segura JM, Lafita S, Arnal-Monreal F, Amengual I, Boscá-Watts MM, Hospital A, Manzano H, Magallón R; DECCIRE GROUP. Factors related with symptom duration until diagnosis and treatment of symptomatic colorectal cancer. *BMC Cancer* 2013; **13**: 87 [PMID: 23432789 DOI: 10.1186/1471-2407-13-87]

20 **Cubiella J**, Marzo-Castillejo M, Mascort-Roca JJ, Amador-Romero FJ, Bellas-Beceiro B, Clofent-Vilaplana J, Carballal S, Ferrándiz-Santos J, Gimeno-García AZ, Jover R, Mangas-Sanjuán C, Moreira L, Pellisè M, Quintero E, Rodríguez-Camacho E, Vega-Villaamil P; Sociedad Española de Medicina de Familia y Comunitaria y Asociación Española de Gastroenterología. Clinical practice guideline. Diagnosis and prevention of colorectal cancer. 2018 Update. *Gastroenterol Hepatol* 2018; **41**: 585-596 [PMID: 30245076 DOI: 10.1016/j.gastrohep.2018.07.012]

21 **Pin Vieito N**, Zarraquiños S, Cubiella J. High-risk symptoms and quantitative faecal immunochemical test accuracy: Systematic review and meta-analysis. *World J Gastroenterol* 2019; **25**: 2383-2401 [PMID: 31148909 DOI: 10.3748/wjg.v25.i19.2383]

22 **Renzi C**, Lyratzopoulos G, Card T, Chu TP, Macleod U, Rachet B. Do colorectal cancer patients diagnosed as an emergency differ from non-emergency patients in their consultation patterns and symptoms? *Br J Cancer* 2016; **115**: 866-875 [PMID: 27537389 DOI: 10.1038/bjc.2016.250]

23 **Esteva M**, Ruidíaz M, Sánchez MA, Pértega S, Pita-Fernández S, Macià F, Posso M, González-Luján L, Boscá-Wats MM, Leiva A, Ripoll J; DECCIRE GROUP. Emergency presentation of colorectal patients in Spain. *PLoS One* 2018; **13**: e0203556 [PMID: 30273339 DOI:

10.1371/journal.pone.0203556]

24 **Borowski DW**, Cawkwell S, Zaidi SM, Toward M, Maguire N, Gill TS. Primary care referral practice, variability and socio-economic deprivation in colorectal cancer. *Colorectal Dis* 2016; **18**: 1072-1079 [PMID: 27110954 DOI: 10.1111/codi.13360]

25 **Leiva A**, Esteva M, Llobera J, Macià F, Pita-Fernández S, González-Luján L, Sánchez-Calavera MA, Ramos M. Time to diagnosis and stage of symptomatic colorectal cancer determined by three different sources of information: A population based retrospective study. *Cancer Epidemiol* 2017; **47**: 48-55 [PMID: 28126583 DOI: 10.1016/j.canep.2016.10.021]

26 **Weller D**, Menon U, Zalounina Falborg A, Jensen H, Barisic A, Knudsen AK, Bergin RJ, Brewster DH, Cairnduff V, Gavin AT, Grunfeld E, Harland E, Lambe M, Law RJ, Lin Y, Malmberg M, Turner D, Neal RD, White V, Harrison S, Reguilon I; ICBP Module 4 Working Group, Vedsted P. Diagnostic routes and time intervals for patients with colorectal cancer in 10 international jurisdictions; findings from a cross-sectional study from the International Cancer Benchmarking Partnership (ICBP). *BMJ Open* 2018; **8**: e023870 [PMID: 30482749 DOI: 10.1136/bmjopen-2018-023870]

World Journal of Gastroenterology

Submit a Manuscript: https://www.f6publishing.com

World J Gastroenterol 2021 October 21; 27(39): 6701-6714

DOI: 10.3748/wjg.v27.i39.6701

ISSN 1007-9327 (print) ISSN 2219-2840 (online)

ORIGINAL ARTICLE

Prospective Study

Standard liver weight model in adult deceased donors with fatty liver: A prospective cohort study

Bo Li, Pan-Yu Chen, Yi-Fei Tan, He Huang, Min Jiang, Zhen-Ru Wu, Chen-Hao Jiang, Dao-Feng Zheng, Diao He, Yu-Jun Shi, Yan Luo, Jia-Yin Yang

ORCID number: Bo Li 0000-0003-2458-754X; Pan-Yu Chen 0000-0001-7416-8904; Yi-Fei Tan 0000-0001-8168-3971; He Huang 0000-0002-9439-9512; Min Jiang 0000-0002-0932-4904; Zhen-Ru Wu 0000-0001-5974-8265; Chen-Hao Jiang 0000-0001-5465-7743; Dao-Feng Zheng 0000-0002-2124-8377; Diao He 0000-0001-7379-4284; Yu-Jun Shi 0000-0003-0494-6023; Yan Luo 0000-0003-2985-1768; Jia-Yin Yang 0000-0001-9134-1959.

Author contributions: Li B and Chen PY contributed equally to this work; Li B collected all the clinical data, analyzed the data, drafted the manuscript and prepared the revised materials; Chen PY collected the data of donor liver weight in the operating room and assisted with data analysis; Tan YF analyzed the data, drafted the manuscript and prepared the revised materials; Huang H and Luo Y assisted with ultrasound examination and data processing; Wu ZR and Shi YJ helped with tissue staining and histological assessment; Zheng DF, He D and Jiang CH assisted with donor liver weight measurement and tissue Sampling; Jiang M participated in design of the study, data processing and data analysis; Yang JY participated in design and oversight of the study and was

Bo Li, Yi-Fei Tan, Chen-Hao Jiang, Dao-Feng Zheng, Diao He, Jia-Yin Yang, Department of Liver Surgery, Liver Transplantation Centre, West China Hospital of Sichuan University, Chengdu 610041, Sichuan Province, China

Bo Li, Yi-Fei Tan, Chen-Hao Jiang, Dao-Feng Zheng, Diao He, Jia-Yin Yang, Laboratory of Liver Transplantation, Frontiers Science Center for Disease-related Molecular Network, West China Hospital of Sichuan University, Chengdu 610041, Sichuan Province, China

Pan-Yu Chen, Operating Room, West China Hospital, Sichuan University/West China School of Nursing, Sichuan University, Chengdu 610041, Sichuan Province, China

He Huang, Yan Luo, Department of Medical Ultrasound, West China Hospital of Sichuan University, Chengdu 610041, Sichuan Province, China

Min Jiang, Department of Epidemiology and Health Statistics, West China School of Public Health and West China Fourth Hospital, Sichuan University, Chengdu 610041, Sichuan Province, China

Zhen-Ru Wu, Yu-Jun Shi, Laboratory of Pathology, Key Laboratory of Transplant Immunology and Engineering, National Health Commission, West China Hospital of Sichuan University, Chengdu 610041, Sichuan Province, China

Corresponding author: Jia-Yin Yang, MD, PhD, Chief Doctor, Director, Professor, Surgeon, Department of Liver Surgery, Liver Transplantation Centre, West China Hospital of Sichuan University, No. 37 Guo Xue Xiang, Chengdu 610041, Sichuan Province, China.
doctoryjy@scu.edu.cn

Abstract

BACKGROUND

Standard liver weight (SLW) is frequently used in deceased donor liver transplantation to avoid size mismatches with the recipient. However, some deceased donors (DDs) have fatty liver (FL). A few studies have reported that FL could impact liver size. To the best of our knowledge, there are no relevant SLW models for predicting liver size.

AIM

To demonstrate the relationship between FL and total liver weight (TLW) in detail

involved with drafting of the manuscript; all authors have read and approve the final manuscript.

Supported by New Clinical Technology Project, West China Hospital, Sichuan University, No. 20HXJS012; and National Natural Science Foundation of China, No. 81770653 and No. 82070674.

Institutional review board statement: This study was reviewed and approved by the West China Hospital of Sichuan University Institutional Review Board.

Clinical trial registration statement: This study was registered at http://www.chictr.org.cn. The registration identification number is ChiCTR2000041406.

Informed consent statement: All study participants, or their legal guardians, provided informed written consent prior to study enrollment.

Conflict-of-interest statement: The authors of this manuscript have no conflicts of interest to disclose.

Data sharing statement: No additional data are available.

CONSORT 2010 statement: The authors have read the CONSORT 2010 Statement, and the manuscript was prepared and revised according to the CONSORT 2010 Statement.

Open-Access: This article is an open-access article that was selected by an in-house editor and fully peer-reviewed by external reviewers. It is distributed in accordance with the Creative Commons Attribution NonCommercial (CC BY-NC 4.0) license, which permits others to distribute, remix, adapt, build upon this work non-commercially, and license their derivative works on different terms, provided the original work is properly cited and the use is non-commercial. See: http://creativecommons.org/Licenses/by-nc/4.0/

Manuscript source: Unsolicited

and present a related SLW formula.

METHODS

We prospectively enrolled 212 adult DDs from West China Hospital of Sichuan University from June 2019 to February 2021, recorded their basic information, such as sex, age, body height (BH) and body weight (BW), and performed abdominal ultrasound (US) and pathological biopsy (PB). The chi-square test and kappa consistency score were used to assess the consistency in terms of FL diagnosed by US relative to PB. Simple linear regression analysis was used to explore the variables related to TLW. Multiple linear regression analysis was used to formulate SLW models, and the root mean standard error and interclass correlation coefficient were used to test the fitting efficiency and accuracy of the model, respectively. Furthermore, the optimal formula was compared with previous formulas.

RESULTS

Approximately 28.8% of DDs had FL. US had a high diagnostic ability (sensitivity and specificity were 86.2% and 92.9%, respectively; kappa value was 0.70, $P < 0.001$) for livers with more than a 5% fatty change. Simple linear regression analysis showed that sex (R^2, 0.226; $P < 0.001$), BH (R^2, 0.241; $P < 0.001$), BW (R^2, 0.441; $P < 0.001$), BMI (R^2, 0.224; $P < 0.001$), BSA (R^2, 0.454; $P < 0.001$) and FL (R^2, 0.130; $P < 0.001$) significantly impacted TLW. In addition, multiple linear regression analysis showed that there was no significant difference in liver weight between the DDs with no steatosis and those with steatosis within 5%. Furthermore, in the context of hepatic steatosis, TLW increased positively (non-linear); compared with the TLW of the non-FL group, the TLW of the groups with hepatic steatosis within 5%, between 5% and 20% and more than 20% increased by 0 g, 90 g, and 340 g, respectively. A novel formula, namely, -348.6 + (110.7 x Sex [0 = Female, 1 = Male]) + 958.0 x BSA + (179.8 x FL_{US} [0 = No, 1 = Yes]), where FL was diagnosed by US, was more convenient and accurate than any other formula for predicting SLW.

CONCLUSION

FL is positively correlated with TLW. The novel formula deduced using sex, BSA and FL_{US} is the optimal formula for predicting SLW in adult DDs.

Key Words: Standard liver weight; Body surface area; Fatty liver; Sex; Deceased donors

©The Author(s) 2021. Published by Baishideng Publishing Group Inc. All rights reserved.

Core Tip: This study was the first to explore the relationship between fatty liver (FL) and total liver weight (TLW) in detail using pathological biopsy based on adult deceased donors (DDs) and developed a new standard liver weight (SLW) formula. Moreover, to conveniently apply the SLW formula to the clinic, we introduced ultrasound (US). Notably, we found that FL was positively correlated with TLW and that US had a high diagnostic ability for mild to severe FL, which could increase liver weight significantly. The formula deduced using sex, BSA and FL_{US} is the optimal formula for predicting SLW in adult DDs.

Citation: Li B, Chen PY, Tan YF, Huang H, Jiang M, Wu ZR, Jiang CH, Zheng DF, He D, Shi YJ, Luo Y, Yang JY. Standard liver weight model in adult deceased donors with fatty liver: A prospective cohort study. *World J Gastroenterol* 2021; 27(39): 6701-6714
URL: https://www.wjgnet.com/1007-9327/full/v27/i39/6701.htm
DOI: https://dx.doi.org/10.3748/wjg.v27.i39.6701

INTRODUCTION

Standard liver weight (SLW) is a key parameter in liver surgery. Its accurate evaluation is the basis for patient safety in both hepatectomy and liver transplantation

manuscript

Specialty type: Transplantation

Country/Territory of origin: China

Peer-review report's scientific quality classification

Grade A (Excellent): 0
Grade B (Very good): B
Grade C (Good): 0
Grade D (Fair): 0
Grade E (Poor): 0

Received: June 20, 2021
Peer-review started: June 20, 2021
First decision: August 8, 2021
Revised: August 22, 2021
Accepted: September 16, 2021
Article in press: September 16, 2021
Published online: October 21, 2021

P-Reviewer: Yang M
S-Editor: Ma YJ
L-Editor: A
P-Editor: Liu JH

(LT). In hepatectomy, the underestimation of SLW may lead to residual liver failure[1,2], and in living donor liver transplantation (LDLT)/split liver transplantation (SLT), the underestimation of SLW can lead to small-for-size syndrome (SFSS)[3-5]. Since the establishment of Urata's standard liver volume (SLV) model[6], approximately 14 SLV models have been published worldwide, most of which are based on healthy people, living donors and autopsy donors from various medical centres. Deceased donor liver transplantation (DDLT) is a crucial donor liver source for alleviating the shortage of donor livers. Subsequently, SLT was established and further expanded the donor liver pool. Previous studies[7-10] have reported that SLT is not inferior to whole liver transplantation in terms of patient prognosis, which has encouraged the extensive use of SLT and necessitated an urgent demand for an SLW formula for DDLT to avoid severe mismatches, large-for-size syndrome[11,12] or SFSS. Moreover, deceased donors (DDs) and living donors (LDs) are from the general population and may have hepatic steatosis, which has a reported global incidence of 15%-30%[13,14]. To our knowledge, fatty liver (FL) may be associated with marginal grafts, as severe steatosis is a risk factor related to graft survival[15] and may affect liver size[16,17]. However, these associations have not been quantified conclusively. To the best of our knowledge, only one model[18] has been published for DDs, and it was based on a Western population and did not address FL. Therefore, this study prospectively collected adult DDs' clinical data combined with FL parameters to develop an SLW model.

MATERIALS AND METHODS

The present study prospectively enrolled consecutive deceased liver donors from West China Hospital of Sichuan University from June 2019 to February 2021 and recorded basic patient information, such as sex, age, body height (BH) and body weight (BW). This study was reviewed and approved by the West China Hospital of Sichuan University Institutional Review Board and registered at http://www.chictr.org.cn. The registration identification number is ChiCTR2000041406. All the study participants, or their legal guardians, provided informed written consent prior to study enrollment, and the study protocol conformed to the ethical guidelines of the 1975 Declaration of Helsinki as reflected in a priori approval by the ethics committee. No executed prisoners were included in the study. A total of 212 DDs were enrolled, and brain death was confirmed in all of them before organ procurement. Advanced life support was maintained in an intensive care unit (ICU); moreover, abdominal ultrasound (US) examinations, liver function tests and kidney function tests were completed for each donor. Pathological biopsy (PB) was performed for all enrolled donor livers after they were obtained.

US examination

A US examination was carried out for all DDs before organ procurement. Scanning and diagnosis were conducted by 2 experienced (> 5 years) US doctors who were blinded to the final PB diagnosis. The examinations were performed by using a MultiWave ultrasound system (Aixplorer, France) equipped with an SC6–1 (1–6 MHz) transducer. FL was identified as a diffuse increase in fine echoes in the liver parenchyma. Representative images[19] are presented in Figure 1.

Donor liver weight measurement, tissue sampling and histological assessment

Donor livers were procured and trimmed in the operating room and were then weighed with a precision electronic balance (unit: kg, accurate to 0.001 kg, Figure 2) on a back table.

A single tissue wedge of approximately 1.0 cm × 1.0 cm × 1.0 cm was excised from the left lateral lobe surface of the donor liver, fixed in formalin and embedded in paraffin. Each donor liver was stained with haematoxylin and eosin (HE) and Masson's trichrome. The histological degree of liver pathology, including hepatic steatosis, ballooning of hepatocytes, lobular inflammation, necrosis, and fibrosis, was evaluated by two expert liver pathologists blinded to any other clinical information and laboratory data. The extent of hepatic steatosis was assessed by the percentage of hepatocytes containing large- and medium-sized intracytoplasmic lipid droplets (but not foamy microvesicles). The definition of ballooning of hepatocytes and lobular inflammation was as described by Kleiner *et al*[20] and Bedossa *et al*[21]. The definition of necrosis is described in Table 1. Fibrosis was scored according to the standard grading (inflammation) and staging (fibrosis) method based on the modified Scheuer

Table 1 Characteristics of the deceased donors

Characteristic	Total, *n* = 212
Sex, male, *n* (%)	167 (78.8)
Age, median (range), yr	49 (18–68)
BH, median (range), cm	168 (150–185)
BW, median (range), kg	65 (45–90)
BMI, median (range), kg/m^2	23.35 (15.57–30.48)
BSA, median (range), m^2	1.73 (1.37–2.10)
TLW, median (range), g	1400 (830–2100)
Cause of death, *n* (%)	
Trauma	106 (50.0)
Cerebrovascular	97 (45.8)
Other	9 (4.2)
Degree of fatty change, median (range)	0 (0–40%)
0, *n* (%)	151 (71.2)
> 0, < 5%, *n* (%)	32 (15.1)
5%–33%, *n* (%)	22 (10.4)
> 33%, *n* (%)	7 (3.3)
Ballooning of hepatocytes	
None	24 (11.1)
Ballooned hepatocyte with normal size	116 (54.9)
Enlarged ballooned hepatocyte	72 (34.0)
Lobular inflammation	
None	66 (30.9)
< 2 foci per lobule	131 (61.7)
> 2 foci per lobule	15 (7.4)
Necrosis	
None	200 (94.4)
Focal or unicellular necrosis	8 (3.7)
More extensive necrosis and above	4 (1.9)
Stage of fibrosis[1]	
0	72 (33.8)
1	88 (41.6)
2	47 (22.1)
3	4 (1.9)
4	1 (0.6)

[1]According to the modified Scheuer system[22]. BH: Body height; BW: Body weight; BMI: Body mass index; BSA: Body surface area; TLW: Total liver weight.

system[22].

Estimating SLW using previous formulas

According to previous studies at our centre[23] and other centres[24-26], the density of the liver was determined to be 1 g/cm^3; that is, the weight and volume of the donor liver were equal. For comparison, we calculated the estimated SLW according to

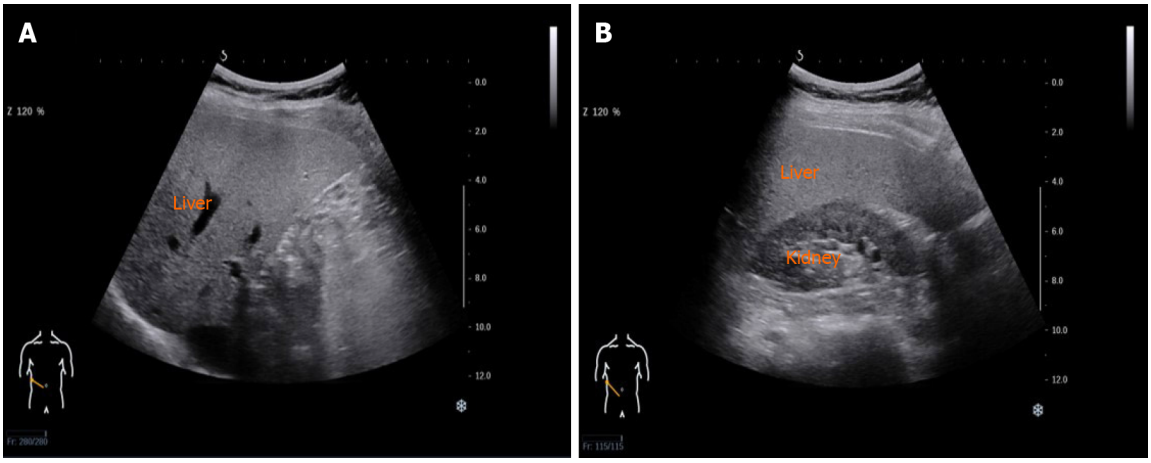


Figure 1 Diagram of fatty liver diagnosed by ultrasound from the view of the liver and kidney. A: Diffuse increase in fine echoes in liver parenchyma with normal visualization of intrahepatic vessel borders; B: Diffuse increase in fine echoes in liver parenchyma. There was an increase in echogenicity of the liver compared with the echogenicity of the renal cortex.

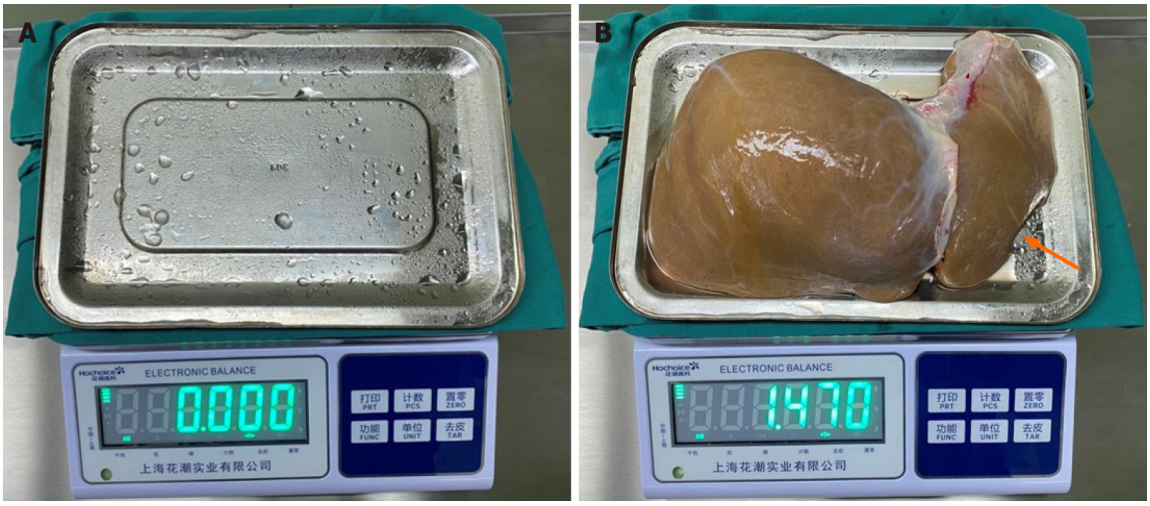


Figure 2 Actual liver weight measurement by electronic balance. A: Zero correction of electronic balance; B: Donor liver weighing. The arrow indicates that a single tissue wedge of approximately 1.0 cm × 1.0 cm × 1.0 cm was excised from the left lateral lobe surface of the donor liver.

previous formulas for adults[6-19]. Body mass index (BMI) = BW/BH^2 and body surface area (BSA) = $BW^{0.425}$ x $BH^{0.725}$ x 0.007184 using the Dubois formula[27] were also calculated.

Statistical analysis

In this study, simple linear regression analysis was used to explore the variables related to TLW. Multiple linear regression analysis was used to formulate the SLW. As BH, BW, BMI and BSA are collinear variables, each was applied in a different prediction model. The root mean standard error (RMSE) and interclass correlation coefficient (ICC) were used to test the fitting efficiency and accuracy of the model, respectively. The chi-square test and kappa consistency score were used to assess the consistency in terms of FL diagnosed by US relative to PB. Continuous variables were analysed by a paired-samples *t* test. Two-tailed statistical analysis was used, and *P* values less than 0.05 were considered to be statistically significant. SPSS, version 25.0 (IBM, Armonk, NY, United States) was used for all statistical analyses. GraphPad Prism 7.0 (GraphPad Software, Inc.) was used for drawing.

RESULTS

Baseline data

This study included 167 males (78.8%). The median age was 49 years, ranging from 18 to 68 years. The median BH, BW, BMI, BSA and TLW were 1.68 m, 65 kg, 23.35 kg/m^2, 1.73 m^2 and 1400 g, respectively. The main causes of death of the DDs were trauma (50%), cerebrovasculature (45.8%), and other (4.2%), which included brain tumours and hypoxic-ischaemic encephalopathy. There were 151 DDs (71.2%) with no steatosis, 32 (15.1%) with steatosis within 5%, 22 (10.4%) with steatosis between 5% and 33%, and 7 (3.3%) with steatosis greater than 33%. Moreover, hepatocyte ballooning was observed in 88.9% of DDs. Lobular inflammation was observed in approximately 69.1% of DDs. Necrosis (focal or unicellular necrosis, in 3.7% of DDs samples, and more extensive necrosis, in 1.9% of DDs samples) was observed in only a few DDs liver tissue samples. Stage 0–2 Liver fibrosis was observed in approximately 97.5% of DDs (Table 1).

Impact factors related to the TLW of deceased donors

Simple linear regression analysis showed that sex, BH, BW, BMI, BSA and FL significantly impacted TLW ($P < 0.001$) (Table 2). BSA was the most influential factor related to liver size [R^2, 0.454; 95% confidence interval (CI): 1024.56–1383.79]. Multiple linear regression analysis showed that there was no significant difference in TLW between no steatosis and steatosis within 5% ($P = 0.147$, Figure 3A). Furthermore, in the context of hepatic steatosis, TLW increased positively (non-linear); compared with the TLW of the non-FL group, the TLW of the groups with hepatic steatosis within 5%, between 5% and 20% and more than 20% increased by 0 g, 90 g, and 340 g, respectively (Figure 3B).

Consistency test for FL diagnosis between US and PB

This study investigated 61 hepatic steatosis cases, which accounted for 28.8% of all cases, and moderate and severe steatosis cases, which accounted for 3.3%. The cases of hepatic steatosis and non-hepatic steatosis diagnosed by US were 38 and 174, respectively. The sensitivity and specificity of US were 55.7% and 97.4%, respectively, and the kappa value was 0.598 ($P < 0.001$). That is, its diagnostic consistency was good (Supplementary Table 1). Furthermore, when setting 5% as the cut-off value for diagnosing FL by PB, there were 174 cases within a 5% fatty change and 38 cases with more than a 5% fatty change diagnosed by US, with a sensitivity and specificity of 86.2% and 92.9%, respectively, and a kappa value of 0.70 ($P < 0.001$). Therefore, the diagnostic consistency between US and PB was high (Table 3).

Current formulas for estimating SLW

The SLW models were separately formulated based on four collinear variables, namely, BH, BW, BMI and BSA. Subsequently, three prediction model groups were established, two of which were used to assess the presence of FL based on US or PB; the third group did not include FL as an indicator. The present study showed that the SLW models based on BSA, FL and sex had the best fitness, and the adjusted R^2 and RMSE for PB and US were 0.546 and 169.985 and 0.546 and 169.913, respectively. The fitting efficiency of these two models was almost equal and better than that of the traditional method (adjusted R^2, 0.485; RMSE, 181.095) (Table 4).

Comparison between the current formula and previous formulas

Previously reported formulas were used to assess our DDs cohort, and the results showed that the fitting efficiency and accuracy of the SLW model introducing FL diagnosed by US were 168.3 (RMSE) and 0.71 (ICC), with a non-significant difference ($P = 1.00$) between the SLW and TLW of 1.5 g. The RMSE and ICC of Yu *et al*[25]'s and Lin *et al*[28]'s models were 187.5 and 0.61 and 188.0 and 0.63, respectively. There were no significant differences between the SLW and actual TLW for these two formulas, but those of the remaining formulas were significantly different (Table 5)[6,18,25-37].

DISCUSSION

The shortage of donor livers is a problem worldwide and has become a major obstacle hindering the development of LT. To date, experts in the LT field have explored expanding the donor liver pool, including *via* SLT, marginal donor LT, domino LT and

Table 2 Factors related to the total liver weight of the deceased donors

Factor	R^2	*P* value	95%CI
Sex	0.226	< 0.001	220.89–369.68
BH	0.241	< 0.001	13.92–22.78
BW	0.441	< 0.001	15.25–20.77
BSA	0.454	< 0.001	1024.56–1383.79
BMI	0.224	< 0.001	32.28–54.18
Degree of fatty change (< 5%, 5%–20%, > 20%)	0.130	< 0.001	116.89–244.17
Hepatic steatosis[1]	0.125	< 0.001	149.67–318.33

[1]Diagnosed by ultrasound. BH: Body height; BW: Body weight; BSA: Body surface area; BMI: Body mass index.

Table 3 Results for livers with more than 5% fatty change diagnosed by ultrasound and pathological biopsy in the deceased donors

Ultrasound	Pathological biopsy		Total
	+	-	
+	25	13	38
-	4	170	174
Total	29	183	212

According to the table above, livers with a fatty change of more than 5% were diagnosed by ultrasound, and the sensitivity and specificity were 86.2% and 92.9%, respectively. The chi-square test showed that the kappa value was 0.70, $P < 0.001$.

so on. These schemes have successfully and significantly expanded the donor liver pool, and SLT has become one of the most valuable means of promotion. Graft weight (GW) plays a key role in recipients, especially in DDLT and LDLT. Therefore, it is necessary to evaluate the donor liver size in LT.

DDs are patients with brain death caused by non-liver diseases. This study illustrated that 95.8% of DDs died from trauma or cardiovascular and cerebrovascular accidents. Biopsies showed that many donor livers had hepatocyte oedema and lobular inflammation, which can be explained by the cause of death. Trauma and cardiovascular and cerebrovascular accidents can cause instability of the circulatory system, leading to long-term ICU stays and the requirement for resuscitative therapy, which may cause unstable organ perfusion (hypoperfusion or hyperperfusion) and reperfusion injury. In addition, the use of a large number of vasoactive drugs may aggravate organ microcirculation disorder. Thus, the graft may have acute injury, such as lobular inflammation, hepatocyte oedema and even necrosis. The present study found that 28.8% of DDs had hepatic steatosis and that 2.5% had stage 3–4 Liver fibrosis. Unlike DDs, LDs screened from healthy populations rarely have FL or other acute liver injuries. In addition, it was unclear whether there was a difference in the SLW between DDs and LDs. To the best of our knowledge, there have been few relevant reports. Therefore, we explored the SLW model based on DDs data derived from West China Hospital.

Simple linear regression analysis showed that liver size was correlated with sex. The liver size of males was larger than that of females, which was in line with previous studies[30,33]. We speculated that this might be related to the fact that the body size of men is generally larger than that of women and that men have a larger skeletal muscle system and higher daily consumption and metabolic requirements. Therefore, a larger liver mass is needed to meet physiological needs[38,39]. In addition, the present study found that BH, BW, BMI and BSA were closely related to liver size, which was similar to previous studies[6,25,31,40]. Indeed, multiple linear regression analysis revealed that the above four variables were collinear. From the perspective of morphology, liver size and physical indicators are supposed to be positively correlated. Moreover, in terms of energy requirements, to meet metabolic needs, a larger body size needs more organ support. Furthermore, the current study found that BSA was the most influential factor impacting TLW, which was consistent with previous studies[6,29,

Table 4 Results of multiple linear regression analysis performed to predict the total liver weight using each of the body anthropometric measures divided into groups of the traditional method and two new methods, which introduce the parameter of fatty liver diagnosed by ultrasound and pathological biopsy

Groups	Formulas	Adjusted R^2	RMSE
Traditional method			
BH	- 809.4 + 167.3 x Sex + 12.6 x BH	0.29	212.0
BW	322.1 + 147.0 x Sex + 15.2 x BW	0.49	181.1
BSA	- 466.9 + 99.0 x Sex + 1051.0 x BSA	0.48	182.8
BMI	329.2 + 264.5 x Sex + 37.8 x BMI	0.39	196.5
Ultrasound method			
BH	- 1011.9 + 149.7 x Sex + 13.6 x BH + 240.7 x FL_{US}	0.43	191.1
BW	392.7 + 158.3 x Sex + 13.5 x BW + 158.6 x FL_{US}	0.54	171.4
BSA	- 348.6 + 110.7 x Sex + 958.0 x BSA + 179.8 x FL_{US}	0.55	169.9
BMI	453.7 + 264.5 x Sex + 31.2 x BMI + 162.9 x FL_{US}	0.45	187.5
Pathological biopsy method (< 5%, 5%–20%, > 20%)			
BH	- 803.7 + 178.5 x sex + 12.3 x BH + FL_{PB} (0 = 0, 1 = 163.5, 2 = 393.0)	0.43	190.0
BW	414.5 + 172.6 x sex + 13.1 x BW + FL_{PB} (0 = 0, 1 = 79.8, 2 = 280.7)	0.54	170.8
BSA	- 288.8 + 129.5 x sex + 919.6 x BSA + FL_{PB} (0 = 0, 1 = 93.9, 2 = 304.5)	0.55	170.0
BMI	478.1 + 276.5 x Sex + 30.0 x BMI + FL_{PB} (0 = 0, 1 = 105.3, 2 = 299.1)	0.46	185.4

Sex and FL_{US} are binary variables; FL_{PB} is a dummy variable. Sex: 0 = Female, 1 = Male; FL_{US}: 0 = No, 1 = Yes; FL_{PB}: 0 < 5%, 1 = 5%–20%, 2 > 20%. BH: Body height; BW: Body weight; BSA: Body surface area; BMI: Body mass index; FL_{US}: Fatty liver diagnosed by ultrasound; FL_{PB}: Fatty liver diagnosed by pathological biopsy; RMSE: Root mean standard error.

31]. BSA is a widely used parameter in physiology and clinical medicine for normalizing biological function with respect to variations in body size and conformation. Thus, we believe that the liver size required to meet the metabolic demands of the individual may correlate more closely with BSA than with any other parameter. Additionally, previous studies[30,34] reported that age was associated with TLW; however, similar to Poovathumkadavil's study[35], we failed to identify an association between age and TLW. Several previous studies[31,40] reported that the partial regression coefficient of age was very small, and the authors considered the effect of this variable in adults to be negligible. Therefore, our negative result may be explained by the age distribution of patients in our study and the sample size, and further studies with larger sample sizes are needed to confirm the relation between age and TLW.

Interestingly, this study found that more than a quarter of DDs from the general population had hepatic steatosis, which was similar to Zhou *et al*[41]'s report (29.2%). To our knowledge, an increasing number of individuals, especially those who are obese, suffer from FL worldwide[42,43]. Furthermore, the present study also found that 10.4% and 3.3% of livers had mild and moderate steatosis, respectively, while no liver was detected to have severe steatosis. Several studies have confirmed that mild steatosis grafts (< 33%) can be used safely in LT. However, the eligibility of livers with moderate steatosis is controversial, while livers with severe steatosis are generally discarded because of the increased probability of primary non-function[15,44,45]. Importantly, in the current study, simple linear regression analysis demonstrated that FL was correlated with TLW. Moreover, multivariate analysis showed that steatosis significantly affected TLW, and the degree of steatosis was positively correlated with liver size, which was consistent with previous studies[16,46,47]. Multiple linear regression analysis showed that compared with non-FLs, the presence of hepatic steatosis within 5%, 5%–20% and over 20% resulted in an increase in liver weight by 0 g, 93.9 g, and 304.5 g, respectively. In LT, we generally evaluate the feasibility of SLT

Table 5 Differences between the estimated and actual liver weights calculated using previous formulas in our deceased donor cohort.

Ref.	Formula	Difference[1] (g)	RMSE	ICC	*P* value[2]
Autopsy					
DeLand *et al*[29]	1020 × BSA - 220	135.5 (-366–632)	221.2	0.52	< 0.01
Heinemann *et al*[26]	1072.8 × BSA - 345.7	95 (-421–556)	202.5	0.56	< 0.01
Yu *et al*[25]	$21.585 \times BW^{0.732} \times BH^{0.225}$	34.5 (-490–576)	187.5	0.61	0.102
Choukèr *et al*[30]	[16–50 yr] 452 + 16.34 x BW + 11.85 × age - 166 × sex (1 = female, 0 = male) 51–70 yr] 1390 + 15.94 × BW - 12.86 × age	435 (-301–1000)	484.0	0.24	< 0.01
General population/living donor					
Urata[6]	706.2 × BSA + 2.4	-185 (-713–337)	278.1	0.32	< 0.01
Lin *et al*[28]	13 × BH + 12 × BW - 1530	11.5 (-546–445)	188.0	0.63	0.472
Vauthey *et al*[31][3]	1267.28 × BSA - 794.41	-15 (-544–421)	188.1	0.64	< 0.01
Hashimoto *et al*[32]	961.3 × BSA - 404.8	-161 (-668–317)	253.4	0.42	< 0.01
Chan *et al*[33]	218 + BW × 12.3 + sex × 51 (0 = female, 1 = male)	-356.5 (-859–175)	411.1	0.21	< 0.01
Yuan *et al*[34]	949.7 × BSA - 247.4–48.3 x age factor (1, < 40; 2, 41–60; 3, > 60)	-106 (-646–359)	228.0	0.48	< 0.01
Fu-Gui *et al*[23]	11.508 × BW + 334.024	-319 (-845–241)	393.6	0.19	< 0.01
Poovathumkadavil *et al*[35]	12.26 × BW + 555.65	-57 (-572–510)	207.5	0.47	< 0.01
Um *et al*[36]	893.485 x BSA − 439.169	-312.5 (-816–173)	372.8	0.24	< 0.01
Cadaveric population					
Yoshizumi *et al*[18][3]	772 × BSA	-79 (-602–416)	214.6	0.45	< 0.01
Current	- 348.6 + 110.7 x Sex (0 = Female, 1 = Male) + 958.0 x BSA + 179.8 x FL_{US} (0 = No, 1 = Yes)	1.5 (-477.0–450.0)	168.3	0.71	1

[1]Difference between estimated and actual liver weight using previous formulas.
[2]Paired-samples *t* test.
[3]Mosteller's formula[37] was adopted for BSA, and the remaining formulas used the Dubois formula[27].
BH: Body height; BW: Body weight; BSA: Body surface area; BMI: Body mass index; FL_{US}: Fatty liver diagnosed by ultrasound; ICC: Interclass correlation coefficient; RMSE: Root mean standard error.

based on the criteria of GW/SLW (30%–40%) or GW/BW (0.8%)[11]. Thus, for FL, the GW required for recipients would be underestimated if calculated according to the traditional SLV method, leading to an increased risk of SFSS. Therefore, the current study introduced the FL variable for the first time to develop an SLW model. To diagnose FL before organ procurement, US was performed for all DDs. Notably, for a diagnosis of mild steatosis and greater (≥ 5%), the sensitivity and specificity of US were 86.2% and 92.9%, respectively, and the ICC was 0.70 ($P < 0.001$). That is, US had a higher diagnostic consistency with PB. In addition, this study revealed that the size of livers with a fatty change less than 5% was not different from that of livers without fatty change but was different from that of livers with a fatty change of 5% or greater. The gap of liver size between these two hepatic steatosis categories was significant (180 g, $P < 0.001$), which laid a solid theoretical foundation to apply US in the diagnosis of FL and develop the SLW model, highlighting its clinical practical value.

In this study, the deduced best fit formula based on US had equivalence with that based on PB and was better than the best fit traditional model. Furthermore, the present study showed that the formulas of Deland *et al*[29], Heinemann *et al*[26], and Choukèr *et al*[30] overestimated liver size, while the formulas of Urata *et al*[6], Vauthey *et al*[31], Yoshizumi *et al*[18], Hashimoto *et al*[32], Chan *et al*[33], Yuan *et al*[34], Fu Gui *et al*[23], Poovathumkadavil *et al*[35], and Um *et al*[36] underestimated liver size. On the other hand, there was no significant difference between the actual liver weight and the predicted liver weight calculated by Yu *et al*[25]'s and Lin *et al*[28]'s formulas. This was speculated to be related to the characteristics of the study samples. Deland *et al*[29]'s, Heinemann *et al*[26]'s and Choukèr *et al*[30]'s cohorts were autopsy samples. To

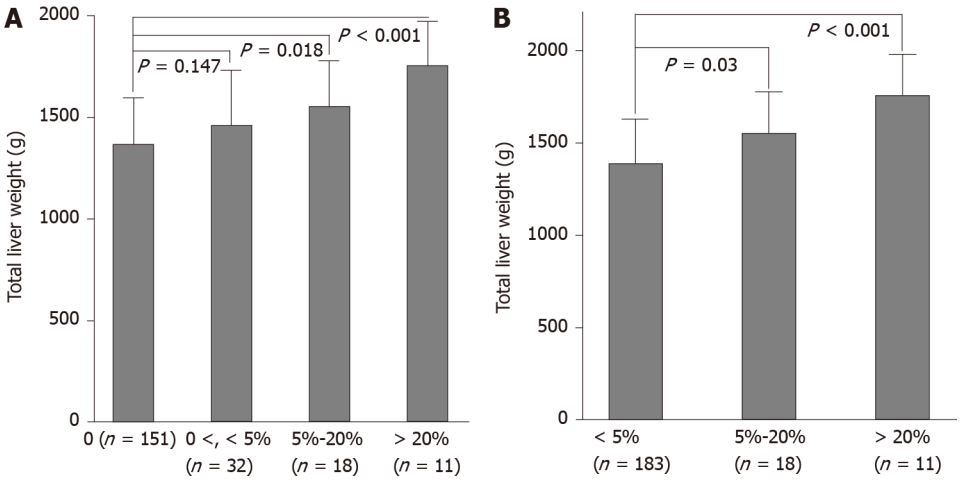


Figure 3 Total liver weight comparison of different groups according to the degree of fatty change of donor livers. A: Groups according to the degree of fatty change of 0, (0 <, < 5%), (5%–20%) and > 20%; B: Groups according to the degree of fatty change of < 5%, (5%–20%) and > 20%. Multiple linear regression analysis including parameters of sex, BSA, and FL_{PB}, which were dummy variables divided into groups according to the degree of fatty change in donor livers, was used. FL_{PB}, fatty liver diagnosed by pathological biopsy.

our knowledge, data from autopsy studies[29] includes the weight of the gallbladder, the attached ligaments, and the hepatic vena cava. In addition, various causes of death, *i.e.*, cardiac failure and traffic accidents, might increase liver weight through mechanisms associated with shock-related hepatic congestion. On the other hand, due to long-term immersion in the fixed solution, the weight of the specimen may exceed the actual size *in vivo*. However, the autopsy study of Yu *et al*[25] was not consistent with the other three autopsy studies but was similar to our study, which may be explained by racial differences. Additionally, the cohorts of Vauthey *et al*[31], Hashimoto *et al*[32], Chan *et al*[33], Yuan *et al*[34], Fu Gui *et al*[23], Poovathumkadavil *et al*[35], and Um *et al*[36] were based on healthy populations without liver disease. However, Lin *et al*[28]'s study cohort comprised 44 (57.1%) patients with chronic liver disease (alcoholic hepatitis, 9; hepatitis B, 24; and hepatitis C, 11), which may explain the difference from other studies based on the general population. Notably, the difference was significant between actual liver weight and estimated liver weight using the formula of Yoshizumi *et al*[18], which was the only previous study based on a cadaveric population. Their study included DDs of several races, most of which were Western, and subjects under 18 years were enrolled. These confounding factors may explain the difference. Therefore, for different study populations, the model for predicting liver size is supposed to be different, which highlights the need for this study for adult DDs. In addition, this study shows the practicability and rationality of the current SLW model in DDLT. Theoretically, it suggests that the current formula is the most suitable for recipients assigned with FL in SLT, and use of this formula is anticipated to reduce the risk of SFSS.

However, the sample size of this study was relatively small, especially in regard to cases of moderate to severe hepatic steatosis. Therefore, studies with larger sample sizes are warranted to optimize the SLW model. Additionally, the extrapolation and clinical practicability of the current SLW model need to be further verified.

CONCLUSION

In conclusion, this study was the first to demonstrate the positive correlation between the degree of hepatic steatosis and liver size based on pathological findings. Furthermore, this study creatively proposed and verified the equivalent value of FL diagnosed by US instead of that diagnosed by PB in terms of the FL variable in the SLW model as follows: SLW (g)= -348.6 + [110.7 x Sex (0 = Female, 1 = Male)] + 958.0 x BSA + [179.8 x FL_{US} (0 = No, 1 = Yes)]. This formula can be used to estimate the liver weight before liver procurement. Additionally, our formula lays a theoretical and practical basis for the further application of donor livers with fatty changes in SLT.

ARTICLE HIGHLIGHTS

Research background

Standard liver weight (SLW) is frequently used in liver transplantation, especially for living donor liver transplantation/split liver transplantation (SLT). However, some deceased donors (DDs) have fatty liver (FL). There have been a few studies to report that FL could impact liver size. This study was to develop a new formula including FL to predict liver size.

Research motivation

To explore SLW model in adult DDs with FL and help transplant doctors make allocation decisions, especially for recipients assigned with FL in SLT to reduce the risk of small-for-size syndrome.

Research objectives

To explore the liver pathology of DDs, such as hepatic steatosis, and diagnostic ability of ultrasound for FL, as well as the relationship between FL and total liver weight. Furthermore, to develop an SLW formula, combined with FL parameter, used to predict graft weight required for recipients in SLT.

Research methods

This study prospectively enrolled consecutive DDs from West China Hospital of Sichuan University from June 2019 to February 2021 and recorded basic patient information, and abdominal ultrasound (US) examination and pathological biopsy (PB) were performed for them. Furthermore, the chi-square test and kappa consistency score were used to assess the consistency in terms of FL diagnosed by US relative to PB. Simple linear regression analysis was used to explore the variables related to TLW. Multiple linear regression analysis was used to formulate SLW models.

Research results

More than a quarter of DDs had hepatic steatosis, and US had a high diagnostic ability for mild to severe FL. Furthermore, this study found that FL was positively correlated with liver size and deduced an optimal SLW formula in adult DDs with FL. However, the extrapolation and clinical practicability of the current SLW model need to be further verified in the future.

Research conclusions

FL is positively correlated with liver size. Our novel formula deduced using sex, BSA and FL_{US} is the optimal formula for predicting SLW in adult DDs with FL.

Research perspectives

To verify the extrapolation of the current SLW model using multicentre data and its clinical practicability in SLT.

ACKNOWLEDGEMENTS

We gratefully acknowledge Dr. Qi-Qi Zhou (Institute of Clinical Pathology, West China Hospital of Sichuan University, Chengdu 610041, Sichuan Province, China) for helping us scan pathological sections and process data. We gratefully acknowledge Dr. Min Jiang (Department of Epidemiology and Health Statistics, West China School of Public Health and West China Fourth Hospital, Sichuan University, Chengdu 610041, Sichuan Province, China) for reviewing the statistical methods of this study.

REFERENCES

1 **Ribero D**, Amisano M, Bertuzzo F, Langella S, Lo Tesoriere R, Ferrero A, Regge D, Capussotti L. Measured versus estimated total liver volume to preoperatively assess the adequacy of the future liver remnant: which method should we use? *Ann Surg* 2013; **258**: 801-806; discussion 806 [PMID: 24045451 DOI: 10.1097/SLA.0000000000000213]

2 **Mullen JT**, Ribero D, Reddy SK, Donadon M, Zorzi D, Gautam S, Abdalla EK, Curley SA, Capussotti L, Clary BM, Vauthey JN. Hepatic insufficiency and mortality in 1,059 noncirrhotic

patients undergoing major hepatectomy. *J Am Coll Surg* 2007; **204**: 854-862; discussion 862 [PMID: 17481498 DOI: 10.1016/j.jamcollsurg.2006.12.032]

3 **Dahm F**, Georgiev P, Clavien PA. Small-for-size syndrome after partial liver transplantation: definition, mechanisms of disease and clinical implications. *Am J Transplant* 2005; **5**: 2605-2610 [PMID: 16212618 DOI: 10.1111/j.1600-6143.2005.01081.x]

4 **Soejima Y**, Taketomi A, Yoshizumi T, Uchiyama H, Harada N, Ijichi H, Yonemura Y, Shimada M, Maehara Y. Feasibility of left lobe living donor liver transplantation between adults: an 8-year, single-center experience of 107 cases. *Am J Transplant* 2006; **6**: 1004-1011 [PMID: 16611337 DOI: 10.1111/j.1600-6143.2006.01284.x]

5 **Emond JC**, Renz JF, Ferrell LD, Rosenthal P, Lim RC, Roberts JP, Lake JR, Ascher NL. Functional analysis of grafts from living donors. Implications for the treatment of older recipients. *Ann Surg* 1996; **224**: 544-552; discussion 552 [PMID: 8857858 DOI: 10.1097/00000658-199610000-00012]

6 **Urata K**, Kawasaki S, Matsunami H, Hashikura Y, Ikegami T, Ishizone S, Momose Y, Komiyama A, Makuuchi M. Calculation of child and adult standard liver volume for liver transplantation. *Hepatology* 1995; **21**: 1317-1321 [PMID: 7737637]

7 **Park GC**, Hwang S, Song GW, Jung DH, Ha TY, Ahn CS, Moon DB, Kim KH, Yoon YI, Kang WH, Cho HD, Choi JU, Kim M, Na BG, Kim SH, Lee SG. Prognosis of Split Liver Transplantation Compared with Whole Liver Transplantation in Adult Patients: Single-center Results under the Korean MELD Score-based Allocation Policy. *J Korean Med Sci* 2020; **35**: e304 [PMID: 32959541 DOI: 10.3346/jkms.2020.35.e304]

8 **Cherukuru R**, Reddy MS, Shanmugam NP, Rajalingam R, Kota V, Gunasekaran V, Narasimhan G, Kaliamoorthy I, Rela M. Feasibility and Safety of Split-Liver Transplantation in a Nascent Framework of Deceased Donation. *Liver Transpl* 2019; **25**: 450-458 [PMID: 30586233 DOI: 10.1002/lt.25405]

9 **Valentino PL**, Emre S, Geliang G, Li L, Deng Y, Mulligan D, Rodriguez-Davalos MI. Frequency of whole-organ in lieu of split-liver transplantation over the last decade: Children experienced increased wait time and death. *Am J Transplant* 2019; **19**: 3114-3123 [PMID: 31152483 DOI: 10.1111/ajt.15481]

10 **Chul Yoon K**, Song S, Jwa EK, Lee S, Man Kim J, Kim OK, Kyun Hong S, Yi NJ, Lee KW, Soo Kim M, Hwang S, Suh KS, Lee SK. Survival Outcomes in Split Compared With Whole Liver Transplantation. *Liver Transpl* 2018; **24**: 1411-1424 [PMID: 29747216 DOI: 10.1002/lt.25196]

11 **Kiuchi T**, Kasahara M, Uryuhara K, Inomata Y, Uemoto S, Asonuma K, Egawa H, Fujita S, Hayashi M, Tanaka K. Impact of graft size mismatching on graft prognosis in liver transplantation from living donors. *Transplantation* 1999; **67**: 321-327 [PMID: 10075602 DOI: 10.1097/00007890-199901270-00024]

12 **Tanaka A**, Tanaka K, Tokuka A, Kitai T, Shinohara H, Hatano E, Sato S, Inomoto T, Takada Y, Higashiyama H, Nakamura Y, Yamamoto Y, Egawa H, Uemoto S, Ikai I, Ozaki N, Inomata Y, Yamaoka Y. Graft size-matching in living related partial liver transplantation in relation to tissue oxygenation and metabolic capacity. *Transpl Int* 1996; **9**: 15-22 [PMID: 8748406 DOI: 10.1007/BF00336807]

13 **Younossi ZM**, Koenig AB, Abdelatif D, Fazel Y, Henry L, Wymer M. Global epidemiology of nonalcoholic fatty liver disease-Meta-analytic assessment of prevalence, incidence, and outcomes. *Hepatology* 2016; **64**: 73-84 [PMID: 26707365 DOI: 10.1002/hep.28431]

14 **Gao X**, Fan JG; Study Group of Liver and Metabolism, Chinese Society of Endocrinology. Diagnosis and management of non-alcoholic fatty liver disease and related metabolic disorders: consensus statement from the Study Group of Liver and Metabolism, Chinese Society of Endocrinology. *J Diabetes* 2013; **5**: 406-415 [PMID: 23560695 DOI: 10.1111/1753-0407.12056]

15 **Spitzer AL**, Lao OB, Dick AA, Bakthavatsalam R, Halldorson JB, Yeh MM, Upton MP, Reyes JD, Perkins JD. The biopsied donor liver: incorporating macrosteatosis into high-risk donor assessment. *Liver Transpl* 2010; **16**: 874-884 [PMID: 20583086 DOI: 10.1002/lt.22085]

16 **Kromrey ML**, Ittermann T, vWahsen C, Plodeck V, Seppelt D, Hoffmann RT, Heiss P, Kühn JP. Reference values of liver volume in Caucasian population and factors influencing liver size. *Eur J Radiol* 2018; **106**: 32-37 [PMID: 30150048 DOI: 10.1016/j.ejrad.2018.07.005]

17 **Bian H**, Hakkarainen A, Zhou Y, Lundbom N, Olkkonen VM, Yki-Järvinen H. Impact of non-alcoholic fatty liver disease on liver volume in humans. *Hepatol Res* 2015; **45**: 210-219 [PMID: 24698021 DOI: 10.1111/hepr.12338]

18 **Yoshizumi T**, Gondolesi GE, Bodian CA, Jeon H, Schwartz ME, Fishbein TM, Miller CM, Emre S. A simple new formula to assess liver weight. *Transplant Proc* 2003; **35**: 1415-1420 [PMID: 12826175 DOI: 10.1016/s0041-1345(03)00482-2]

19 **Saadeh S**, Younossi ZM, Remer EM, Gramlich T, Ong JP, Hurley M, Mullen KD, Cooper JN, Sheridan MJ. The utility of radiological imaging in nonalcoholic fatty liver disease. *Gastroenterology* 2002; **123**: 745-750 [PMID: 12198701 DOI: 10.1053/gast.2002.35354]

20 **Kleiner DE**, Brunt EM, Van Natta M, Behling C, Contos MJ, Cummings OW, Ferrell LD, Liu YC, Torbenson MS, Unalp-Arida A, Yeh M, McCullough AJ, Sanyal AJ; Nonalcoholic Steatohepatitis Clinical Research Network. Design and validation of a histological scoring system for nonalcoholic fatty liver disease. *Hepatology* 2005; **41**: 1313-1321 [PMID: 15915461 DOI: 10.1002/hep.20701]

21 **Bedossa P**; FLIP Pathology Consortium. Utility and appropriateness of the fatty liver inhibition of progression (FLIP) algorithm and steatosis, activity, and fibrosis (SAF) score in the evaluation of biopsies of nonalcoholic fatty liver disease. *Hepatology* 2014; **60**: 565-575 [PMID: 24753132 DOI:

10.1002/hep.27173]
22 **Batts KP**, Ludwig J. Chronic hepatitis. An update on terminology and reporting. *Am J Surg Pathol* 1995; **19**: 1409-1417 [PMID: 7503362 DOI: 10.1097/00000478-199512000-00007]
23 **Fu-Gui L**, Lu-Nan Y, Bo L, Yong Z, Tian-Fu W, Ming-Qing X, Wen-Tao W, Zhe-Yu C. Estimation of standard liver volume in Chinese adult living donors. *Transplant Proc* 2009; **41**: 4052-4056 [PMID: 20005340 DOI: 10.1016/j.transproceed.2009.08.079]
24 **Van Thiel DH**, Hagler NG, Schade RR, Skolnick ML, Heyl AP, Rosenblum E, Gavaler JS, Penkrot RJ. In vivo hepatic volume determination using sonography and computed tomography. Validation and a comparison of the two techniques. *Gastroenterology* 1985; **88**: 1812-1817 [PMID: 3888769 DOI: 10.1016/0016-5085(85)90005-8]
25 **Yu HC**, You H, Lee H, Jin ZW, Moon JI, Cho BH. Estimation of standard liver volume for liver transplantation in the Korean population. *Liver Transpl* 2004; **10**: 779-783 [PMID: 15162473 DOI: 10.1002/Lt.20188]
26 **Heinemann A**, Wischhusen F, Püschel K, Rogiers X. Standard liver volume in the Caucasian population. *Liver Transpl Surg* 1999; **5**: 366-368 [PMID: 10477836 DOI: 10.1002/Lt.500050516]
27 **Du Bois D**, Du Bois EF. A formula to estimate the approximate surface area if height and weight be known. 1916. *Nutrition* 1989; **5**: 303-311; discussion 312 [PMID: 2520314]
28 **Lin XZ**, Sun YN, Liu YH, Sheu BS, Cheng BN, Chen CY, Tsai HM, Shen CL. Liver volume in patients with or without chronic liver diseases. *Hepatogastroenterology* 1998; **45**: 1069-1074 [PMID: 9756008]
29 **DeLand FH**, North WA. Relationship between liver size and body size. *Radiology* 1968; **91**: 1195-1198 [PMID: 5699624 DOI: 10.1148/91.6.1195]
30 **Choukèr A**, Martignoni A, Dugas M, Eisenmenger W, Schauer R, Kaufmann I, Schelling G, Löhe F, Jauch KW, Peter K, Thiel M. Estimation of liver size for liver transplantation: the impact of age and gender. *Liver Transpl* 2004; **10**: 678-685 [PMID: 15108261 DOI: 10.1002/Lt.20113]
31 **Vauthey JN**, Abdalla EK, Doherty DA, Gertsch P, Fenstermacher MJ, Loyer EM, Lerut J, Materne R, Wang X, Encarnacion A, Herron D, Mathey C, Ferrari G, Charnsangavej C, Do KA, Denys A. Body surface area and body weight predict total liver volume in Western adults. *Liver Transpl* 2002; **8**: 233-240 [PMID: 11910568 DOI: 10.1053/jlts.2002.31654]
32 **Hashimoto T**, Sugawara Y, Tamura S, Hasegawa K, Kishi Y, Kokudo N, Makuuchi M. Estimation of standard liver volume in Japanese living liver donors. *J Gastroenterol Hepatol* 2006; **21**: 1710-1713 [PMID: 16984594 DOI: 10.1111/j.1440-1746.2006.04433.x]
33 **Chan SC**, Liu CL, Lo CM, Lam BK, Lee EW, Wong Y, Fan ST. Estimating liver weight of adults by body weight and gender. *World J Gastroenterol* 2006; **12**: 2217-2222 [PMID: 16610024 DOI: 10.3748/wjg.v12.i4.2217]
34 **Yuan D**, Lu T, Wei YG, Li B, Yan LN, Zeng Y, Wen TF, Zhao JC. Estimation of standard liver volume for liver transplantation in the Chinese population. *Transplant Proc* 2008; **40**: 3536-3540 [PMID: 19100432 DOI: 10.1016/j.transproceed.2008.07.135]
35 **Poovathumkadavil A**, Leung KF, Al Ghamdi HM, Othman Iel H, Meshikhes AW. Standard formula for liver volume in Middle Eastern Arabic adults. *Transplant Proc* 2010; **42**: 3600-3605 [PMID: 21094823 DOI: 10.1016/j.transproceed.2010.07.098]
36 **Um EH**, Hwang S, Song GW, Jung DH, Ahn CS, Kim KH, Moon DB, Park GC, Lee SG. Calculation of standard liver volume in Korean adults with analysis of confounding variables. *Korean J Hepatobiliary Pancreat Surg* 2015; **19**: 133-138 [PMID: 26693231 DOI: 10.14701/kjhbps.2015.19.4.133]
37 **Mosteller RD**. Simplified calculation of body-surface area. *N Engl J Med* 1987; **317**: 1098 [PMID: 3657876 DOI: 10.1056/NEJM198710223171717]
38 **Midorikawa T**, Kondo M, Beekley MD, Koizumi K, Abe T. High REE in Sumo wrestlers attributed to large organ-tissue mass. *Med Sci Sports Exerc* 2007; **39**: 688-693 [PMID: 17414807 DOI: 10.1249/mss.0b013e31802f58f6]
39 **Abe T**, Kearns CF, Fukunaga T. Sex differences in whole body skeletal muscle mass measured by magnetic resonance imaging and its distribution in young Japanese adults. *Br J Sports Med* 2003; **37**: 436-440 [PMID: 14514537 DOI: 10.1136/bjsm.37.5.436]
40 **Feng LM**, Wang PQ, Yu H, Chen RT, Wang J, Sheng X, Yuan ZL, Shi PM, Xie WF, Zeng X. New formula for predicting standard liver volume in Chinese adults. *World J Gastroenterol* 2017; **23**: 4968-4977 [PMID: 28785151 DOI: 10.3748/wjg.v23.i27.4968]
41 **Zhou F**, Zhou J, Wang W, Zhang XJ, Ji YX, Zhang P, She ZG, Zhu L, Cai J, Li H. Unexpected Rapid Increase in the Burden of NAFLD in China From 2008 to 2018: A Systematic Review and Meta-Analysis. *Hepatology* 2019; **70**: 1119-1133 [PMID: 31070259 DOI: 10.1002/hep.30702]
42 **Loomba R**, Sanyal AJ. The global NAFLD epidemic. *Nat Rev Gastroenterol Hepatol* 2013; **10**: 686-690 [PMID: 24042449 DOI: 10.1038/nrgastro.2013.171]
43 **Li J**, Zou B, Yeo YH, Feng Y, Xie X, Lee DH, Fujii H, Wu Y, Kam LY, Ji F, Li X, Chien N, Wei M, Ogawa E, Zhao C, Wu X, Stave CD, Henry L, Barnett S, Takahashi H, Furusyo N, Eguchi Y, Hsu YC, Lee TY, Ren W, Qin C, Jun DW, Toyoda H, Wong VW, Cheung R, Zhu Q, Nguyen MH. Prevalence, incidence, and outcome of non-alcoholic fatty liver disease in Asia, 1999-2019: a systematic review and meta-analysis. *Lancet Gastroenterol Hepatol* 2019; **4**: 389-398 [PMID: 30902670 DOI: 10.1016/S2468-1253(19)30039-1]
44 **McCormack L**, Dutkowski P, El-Badry AM, Clavien PA. Liver transplantation using fatty livers: always feasible? *J Hepatol* 2011; **54**: 1055-1062 [PMID: 21145846 DOI: 10.1016/j.jhep.2010.11.004]

45 **Wong TC**, Fung JY, Chok KS, Cheung TT, Chan AC, Sharr WW, Dai WC, Chan SC, Lo CM. Excellent outcomes of liver transplantation using severely steatotic grafts from brain-dead donors. *Liver Transpl* 2016; **22**: 226-236 [PMID: 26359934 DOI: 10.1002/lt.24335]

46 **Chen TY**, Chen CL, Tsang LL, Huang TL, Wang CC, Concejero AM, Lu CH, Cheng YF. Correlation between hepatic steatosis, hepatic volume, and spleen volume in live liver donors. *Transplant Proc* 2008; **40**: 2481-2483 [PMID: 18929772 DOI: 10.1016/j.transproceed.2008.08.045]

47 **Busetto L**, Tregnaghi A, De Marchi F, Segato G, Foletto M, Sergi G, Favretti F, Lise M, Enzi G. Liver volume and visceral obesity in women with hepatic steatosis undergoing gastric banding. *Obes Res* 2002; **10**: 408-411 [PMID: 12006641 DOI: 10.1038/oby.2002.56]

World Journal of Gastroenterology

Submit a Manuscript: https://www.f6publishing.com

World J Gastroenterol 2021 October 21; 27(39): 6715-6732

DOI: 10.3748/wjg.v27.i39.6715

ISSN 1007-9327 (print) ISSN 2219-2840 (online)

SYSTEMATIC REVIEWS

Microbiota shaping — the effects of probiotics, prebiotics, and fecal microbiota transplant on cognitive functions: A systematic review

Simone Baldi, Tiziana Mundula, Giulia Nannini, Amedeo Amedei

ORCID number: Simone Baldi 0000-0002-5151-2618; Tiziana Mundula 0000-0002-3021-454X; Giulia Nannini 0000-0002-6481-6864; Amedeo Amedei 0000-0002-6797-9343.

Author contributions: Baldi S and Mundula T contributed equally to writing the manuscript; Baldi S, Mundula T, Nannini G, and Amedei A contributed to the conceptualization and design of the study; Baldi S, Mundula T, Nannini G, and Amedei A critically revised the paper; Amedei A contributed to the supervision of the study; Baldi S, Mundula T, Nannini G, and Amedei A approved the final version of the paper.

Supported by Università degli Studi di Firenze, No. EX60%2020.

Conflict-of-interest statement: The authors declare no competing interests.

PRISMA 2009 Checklist statement: The authors have read the PRISMA 2009 Checklist, and the manuscript was prepared and revised according to the PRISMA 2009 Checklist.

Open-Access: This article is an open-access article that was selected by an in-house editor and fully peer-reviewed by external reviewers. It is distributed in

Simone Baldi, Tiziana Mundula, Giulia Nannini, Amedeo Amedei, Department of Experimental and Clinical Medicine, University of Florence, Florence 50134, Italy

Amedeo Amedei, SOD of Interdisciplinary Internal Medicine, Azienda Ospedaliera Universitaria Careggi, Florence 50134, Italy

Corresponding author: Amedeo Amedei, BSc, Reader (Associate Professor), Department of Experimental and Clinical Medicine, University of Florence, Largo Brambilla 3, Florence 50134, Italy. aamedei@unifi.it

Abstract

BACKGROUND

Dementia is a chronic progressive neurological disease affecting millions of people worldwide, and represents a relevant economic burden for healthcare systems. Although its pathogenesis is still unknown, recent findings have reported that a dysregulated gut-brain axis communication, a fundamental relationship mediated by several host and microbial molecules, is associated with cognitive disorders. In addition, gut microbiota manipulation reduces neuroinflammation, improving cognitive function by restoring the functional gut-brain axis.

AIM

To better define the effects of probiotics, prebiotics, synbiotics, and fecal microbiota transplant (FMT) on cognitive function.

METHODS

We performed a literature search of human randomized clinical trials to examine the effects of the administration of probiotics, prebiotics, synbiotics, or FMT on cognition outcomes in healthy or sick people of every age, sex, and nationality. We systematically searched Embase, Medline/PubMed, Cochrane Library, central and clinicaltrials.gov databases with a combination of comprehensive terms related to cognition and gut microbiota manipulation. Then we carefully reviewed and synthesized the data by type of study design and setting, characteristics of the studied population, kind of intervention (strain type or mixture type, dosage, and frequency of administration), control treatment, inclusion and exclusion criteria, follow-up duration, and cognitive or memory outcomes.

RESULTS

After examining the titles and abstracts, the initial literature screening identified

accordance with the Creative Commons Attribution NonCommercial (CC BY-NC 4.0) license, which permits others to distribute, remix, adapt, build upon this work non-commercially, and license their derivative works on different terms, provided the original work is properly cited and the use is non-commercial. See: http://creativecommons.org/Licenses/by-nc/4.0/

Manuscript source: Invited manuscript

Specialty type: Gastroenterology and hepatology

Country/Territory of origin: Italy

Peer-review report's scientific quality classification

Grade A (Excellent): 0
Grade B (Very good): B, B
Grade C (Good): C, C
Grade D (Fair): 0
Grade E (Poor): 0

Received: February 25, 2021
Peer-review started: February 25, 2021
First decision: April 18, 2021
Revised: May 12, 2021
Accepted: September 2, 2021
Article in press: September 2, 2021
Published online: October 21, 2021

P-Reviewer: García-Mena J, Qi R, Sales-Campos H
S-Editor: Gao CC
L-Editor: Filipodia
P-Editor: Liu JH

995 articles, but we added 23 papers in our systematic review. The analyses of these selected studies highlighted that both probiotic supplementation and FMT improved cognitive function regardless of the type and posology of administration and the adopted cognitive tests and questionnaires. We found that most of the studies conducted in healthy people showed a significant positive effect of the intervention on at least one of the performed cognitive tests. Regarding unhealthy subjects, while FMT and especially probiotic administration had multiple beneficial effects on different cognitive functions, supplementation with prebiotics did not provide any cognitive improvement.

CONCLUSION
Probiotic supplementation and FMT may represent a promising strategy to restore gut eubiosis and enhance the cognitive functions of healthy people and patients with neurological disorders.

Key Words: Dementia; Cognitive disorders; Gut microbiota; Probiotics; Prebiotics; Fecal microbiota transplant

©The Author(s) 2021. Published by Baishideng Publishing Group Inc. All rights reserved.

Core Tip: Dementia and cognitive impairment are age-related conditions that are on the rise worldwide. Recent studies have demonstrated the existence of a gut-brain axis and that the manipulation of gut microbiota composition can exert positive effects on cognition. The administration of probiotics, prebiotics, and fecal microbiota transplant may represent a good strategy to counteract gut dysbiosis and ameliorate cognitive dysfunction by reducing neuroinflammation and brain damage.

Citation: Baldi S, Mundula T, Nannini G, Amedei A. Microbiota shaping — the effects of probiotics, prebiotics, and fecal microbiota transplant on cognitive functions: A systematic review. *World J Gastroenterol* 2021; 27(39): 6715-6732
URL: https://www.wjgnet.com/1007-9327/full/v27/i39/6715.htm
DOI: https://dx.doi.org/10.3748/wjg.v27.i39.6715

INTRODUCTION

Global population ageing, defined as the increasing proportion of older people around the globe, represents a deep shift in society and a considerable challenge for the sustainability of healthcare systems due to the rise of geriatric illnesses[1,2]. Currently, the prevalence of cognition impairment, particularly dementia, is estimated worldwide in 50 million people with an economic burden of 818 billion dollars in 2016 and a forecast of about 115 million people by 2050[3,4].

Dementia is an acquired, gradual, and progressive disorder involving multiple adverse neurocognitive changes that can affect learning processes, memory, executive function, language, complex attention, mood, perceptual-motor function or social cognition. Moreover, although its detailed pathological mechanism is still not well understood, dementia often occurs in association with advanced age or the presence of contributing causes, usually Alzheimer's disease (AD), Parkinson's disease (PD), or cerebrovascular pathology[5-7]. Unfortunately, current therapies are only symptomatic, and notably, no treatment stops the disease progression[8].

Recent studies have shown that that the gut microbiota, with more than 100 trillion microorganisms carrying three times of human genes, plays a pivotal role in human health; manipulation of the intestinal microbiota can modify the release of neuroactive metabolites, which affect brain health[9,10]. This role can be further explained by the documented existence of the gut-brain axis, a complex bidirectional system in which communication occurs through three parallel and interplaying pathways that involve nervous, endocrine, and immune signals[11]. Therefore, different preclinical and observational studies have demonstrated that the gut dysbiosis is responsible for increased intestinal permeability, which correlates with both neuroinflammation and a decline of cognitive abilities[12-15].

Dietary interventions (in nutritional supplements or specific diets) have often been applied in clinical practice to restore intestinal eubiosis and prevent and treat cognitive disorders. For example, a Mediterranean diet and/or a healthy diet based on fruits, vegetables, and fish seems to stabilize or slow cognitive decline[16].

Nevertheless, the most promising strategy to counteract gut dysbiosis and to maintain cognitive function seems represented by the administration of probiotics, prebiotics, and fecal microbiota transplant (FMT).

Interestingly, administration in animal models of an adequate posology of multistrain probiotics reduces both Firmicutes/Bacteroidetes ratio and intestinal permeability, slowing cognitive decline and reducing neuroinflammation[17,18]. Moreover, using specific prebiotics seems to ameliorate cognitive performance with a direct effect on gut microbiota[19].

Moreover, even FMT has demonstrated remarkable efficacy in healthy subjects and people affected by various diseases caused by gut microbiota perturbation, particularly *Clostridium difficile* infection. It could represent a promising therapy for cognitive impairment improvement because of its capability to re-establish a healthy gut microbial community[20,21].

Therefore, since the evidence derived from human randomized clinical trials (RCTs) is currently limited, this systematic review identified the available RCTs and better defined the effects of probiotics, prebiotics, synbiotics, and FMT on cognitive functions.

MATERIALS AND METHODS

Literature search

Our study followed the PRISMA statement guidelines. A computerized search of the articles published until 24 October 2019 was conducted in Embase, Medline/PubMed, Cochrane Library, central and clinicaltrials.gov databases and other individual journal sources, using the following search string: (memory OR cognition OR dementia) AND (lactobacillus OR bifidobacteria OR streptococcus OR enterococcus OR probiotic OR prebiotic OR symbiotic OR fecal, transplantation). In the PubMed database, we activated the filter "Humans"; in Embase, we selected the filter "Research articles"; in Cochrane Library, we activated the filter "Trials"; and in clinicaltrials.gov, we selected the filter "recruitment: terminated or completed." The search did not apply filters for language, country, duration of follow-up, and participants' characteristics (age and sex).

Study selection

Two authors independently reviewed the titles and abstracts of the collected articles, applying predefined inclusion/exclusion criteria. The inclusion criteria were as follows: RCTs; availability of full text; patients regardless of age, nationality, sex, and health status; comparison between oral intake of probiotics, prebiotics, or symbiotic and control treatment or placebo; and outcome as cognitive or memory evaluation. The adopted exclusion criteria were as follows: Studies with fewer than 10 participants; reviews, articles, and case reports; or studies with incomplete outcomes.

Data extraction

The same two authors performed analyses of the full text and data extraction with the intervention of a third author in case of poor agreement or discrepancies. Each reviewer independently recorded the data in a predefined data extraction form. The following data, if reported, were obtained from each selected trial: First author name, year of publication, study design, setting (institution, city, and country), characteristics of the studied population (mainly age and health status), number of total participants and their gender, number of subjects in both treatment and control groups, characteristics of the intervention (strain type or mixture type, dosage and frequency of administration), control treatment, inclusion and exclusion criteria, follow-up duration, cognitive or memory outcomes and compliance data.

Outcome assessment

For each selected study, cognitive functions were assessed through specific tests which evaluated the eight main cognitive skills: sustained attention, speed of information processing, cognitive flexibility and control, multiple simultaneous attention, working memory (short-term memory), category formation, pattern recognition, and response

inhibition[22]. A detailed description of all cognitive tests performed in the selected papers for this systematic review is annexed in Supplementary material.

RESULTS

Study selection

The initial literature screening identified 995 papers. Eight studies were excluded for duplication and another 964 papers were removed after the title and abstract screening because they did not respect inclusion criteria. The selection process, in accordance with the PRISMA statement 2009, is illustrated in Figure 1.

Characteristics of the included studies

An overview of the 23 studies included in this systematic review is reported in Table 1. All 23 included papers were RCTs published from 2007 to 2019[23-45]. The total number of participants was 1285 (491 males and 650 females); unfortunately, both articles published by Tamtaji *et al*[44,45] did not report the gender of the participants. Regarding the age of the enrolled subjects, one study was conducted in healthy scholars (7-9 years)[31], four studies enrolled young adults (19-30 years)[25,36,40,43], and most of the studies involved adults or older people (48-95 years)[23,24,26-30,32-35,37-39,40,42,44,45]. Most studies (four) were performed in Iran[22,24,44,45]; three in the United States[26-28] and Japan[34,37,39]; two in the United Kingdom[29,31], South Korea[33,35], and Spain[30,41]; and one in Austria[25], Italy[32], Ireland[36], Malaysia [38], Poland[42], Wales[43] and the Netherlands[40].

Concerning the patients' health state, most studies enrolled healthy people[25,29,31,33-36,40,43], whereas three studies involved patients with AD[23,24,44] or cirrhotic subjects with recurrent encephalopathy[26-28]. The other studies were focused on stressed adults[38], patients with PD[45], human immunodeficiency virus (HIV)-1-infected individuals[32], subjects affected by fibromyalgia syndrome[41], people with major depression[42], elderly with frailty syndrome[30], and adults with forgetfulness [39] and mild cognitive impairment[37].

In the trials, subjects were administered probiotics[22-25,26,29,32-42,44,45], prebiotics[30,31,43], or FMT[27,28] and its duration lasted a maximum of 24 wk[32] and a minimum of 4 h[43]; however, the trials continued for 12 wk for most of the studies[23,24,31,33-35,37,38,44,45]. No studies have reported the administration of synbiotics. In the studies examining the effects of probiotics, a total of 21 different bacterial species were administered (alone or in combination) in a dosage ranging from 1×10^9 CFU/mL to 2.5×10^{10} CFU/mL; the most represented species were *Lactobacillus plantarum*, *L. acidophilus*, and *Bifidobacterium bifidum*. On the other side, the administered prebiotics was composed of inulin or galacto-oligosaccharides (GOS), in a dosage that ranged from 5 g/d to 7.5 g/d. In FMT studies, subjects were administered a capsule containing 550 μL stool and buffer solution or enema infusion of 90 mL FMT solution. Lastly, only five studies reported their compliance[31,33-35,44,45], and it was generally considered high because it ranged from 82.69% to 100%.

Effects of probiotics and prebiotics on the cognitive functions of healthy people

Regarding the healthy subjects, three studies showed no significant difference between probiotic and placebo groups[29,31,36]. In comparison, five studies showed a significant positive effect of the intervention on at least one of the performed cognitive tests[25,33,35,40,43].

In Benton *et al*[29], the healthy enrolled subjects ingested fermented milk containing *L. casei* Shirota daily for 3 wk. However, no significant differences between the probiotic and placebo groups were reported regarding episodic and long-term memory, assessed with the Wechsler Memory Scale test and the ability to remember the capitals of 30 countries. Moreover, the healthy people treated with *L. rhamnosus* supplement in Kelly *et al*[36] did not report any cognitive improvement, as assessed with the Paired Associates Learning, Attention Switching Task, Rapid Visual Information-Processing task (RVIP), Emotion Recognition Task and electroencephalography tests.

Considering the five studies reporting a significant cognitive improvement, Bagga *et al*[25] found that 4 wk administration of a multistrain probiotic increased Positive and Negative Affect Schedule (PANAS) score (paired with the response accuracy to unpleasant stimuli test) and showed the activation of the cingulum, pre-cuneum and cerebellum areas, involved in decision making and memory process.

Table 1 Summarizing of all selected studies

Ref.	Study design	Setting	Characteristics of the studied population	Number of participants (M/F)	Intervention	Comparison	Duration of intervention	Outcomes	Compliance
Agahi *et al*[23], 2018	RCT	Cities: Emam Ali, Golabchi, Miad, Barekat; Country: Iran	Patients with Alzheimer disease; Age: 65-90 yr; Control group: 80.57 ± 1.79 yr; Intervention group: 79.70 ± 1.72 yr	Total: 48; Control group = 23 (10/13); Intervention group = 25 (7/18)	1 capsule with *L. fermentum, L. plantarum, B. lactis* and 1 capsule with *L. acidophilus, B. bifidum, and B. longum* (3×10^9 CFU)	Placebo	12 wk	TYM	-
Akbari *et al* [24], 2016	RCT	Cities: Golabchi, Sadeghyeh; Country: Iran	Patients with Alzheimer disease; Age: 60-95 yr; Control group: 82.00 ± 1.69 yr; Intervention group: 77.67 ± 2.62 yr	Total: 60; Control group = 30 (24/6); Intervention group = 30 (24/6)	200 mL/d probiotic milk containing *L. acidophilus*, *L. casei*, *B. bifidum*, and *L. fermentum* (2×10^9 CFU each)	Placebo	12 wk	MMSE	-
Bagga *et al*[25], 2018	RCT	City: Graz Country: Austria	Healthy volunteers; Age: 20-40 yr; Control group (placebo): 27.25 ± 5.78 yr; No intervention group: 23.87 ± 4.97 yr; Intervention group: 28.27 ± 4.2 yr	Total: 45; Control group = 15 (9/6); No intervention group = 15 (7/8); Intervention group = 15 (7/8)	1 sachet/d with 3 g freeze-dried powder containing *L. casei* W56, *L. acidophilus* W22, *L. paracasei* W20, *B. lactis* W51, *L. salivarius* W24, *L. lactis* W19, *B. lactis* W52, *L. plantarum* W62 and *B. bifidum* W23(7.5×10^6 CFU/g)	Placebo or no intervention	4 wk	PANAS, SCL-90, ADS, LEIDS, RM task, ED task	-
Bajaj *et al*[26], 2014	RCT	City: Richmond, Virginia Country: United States	Patients with hepatic encephalopathy; Age: 18-65 yr; Control group: 58.5 ± 4.5 yr; Intervention group: 58.4 ± 3.8 yr	Total: 30; Control group = 16 (12/4); Intervention group = 14 (10/4)	*L. rhamnosus* GG (ATCC 53103)(> 50 billion CFU/gm)	Placebo	8 wk	NCT-A, NCT-B, DS, BDT	-
Bajaj *et al*[27], 2017	RCT	City: Richmond, Virginia Country: United States	Patients with hepatic encephalopathy; Mean age: 62 yr; Control group: 62.9 ± 9.8 yr; Intervention group: 64.5 ± 5.1 yr	Total: 20; Control group = 10 (10/0); Intervention group = 10 (10/0)	FMT units (90 mL total) instilled by enema and retained for 30 min	Standard of care	20 wk	EncephalApp-Stroop, PHES	-
Bajaj *et al*[28], 2019	RCT	City: Richmond, Virginia Country: United States	Patients with hepatic encephalopathy; Control group: 64.2 ± 6.2 yr; Intervention group: 63.3 ± 4.2 yr	Total: 20; Control group = 10 (8/2); Intervention group = 10 (8/2)	FMT capsules (550 µL of stool and buffer solution)	Placebo	20 wk	EncephalApp-Stroop, PHES	-
Benton *et al* [29], 2007	RCT	City: Swansea Country: Wales	Healthy volunteers; Age: 48-79 yr; Average age 61.8 ±7.3 yr	Total: 126 (51/75)	65 mL of milk drink containing *L. casei* Shirota (10^8/mL)	Placebo	3 wk	POMS, WMS, VFT, NART, Ability to recall the capital cities of countries	-
Buigues *et al* [30], 2016	RCT	City: Valencia Country: Spain	People with frailty syndrome; Age: 66-90 yr; Control group: 73.4 ± 1.8 yr; Intervention group: 74.2 ± 1.6 yr	Total: 50; Control group = 22 (6 /16); Intervention group = 28 (9/19)	7.5 g/d of Darmocare Pre® (Inulin 3375 mg, FOS 3488)	Placebo	13 wk	MMSE	-

Capitão *et al* [31], 2020	RCT	Cities: Swindon, Milton Keynes, London Country: United Kingdom	Healthy scholars; Age: 7-9 yr; Control group: 9.12 ± 1.02 yr; Intervention group: 8.54 ± 0.79 yr	Total: 35; Control group = 18 (12/6); Intervention group = 17 (12/5)	5.5 g/d of Bimuno (B-GOS, Lactose, Glucose, Galactose)	Placebo	12 wk	BAS-III, CogTrackTM battery, STAIC, MFQ	High (> 80%)
Ceccarelli *et al* [32], 2017	RCT	City: Rome Country: Italy	HIV-1 infected individuals; Median age: 48 (IQR: 38-54) yr; Intervention group: 45 (35-52.5) yr; Control group: 43 (38.2-53) yr	Total: 35; Control group = 26 (24/2); Intervention group = 9 (9/0)	Sachet containing *L. plantarum* DSM 24730 *S. thermophilus* DSM 24731, *B. breve* DSM 24732, *L. paracasei* DSM 24733, *L. delbrueckii subsp. bulgaricus* DSM 24734, *L. acidophilus* DSM 24735 *B. longum* DSM 24736, and *B. infantis* DSM 24737(450×10^9 bacteria)	Control group	24 wk	ROCF, RAVLT, STEP, VST, PVF, SVF, SPM, DS, CBTT, AAT, TMT A, TMT B	-
Chung *et al* [33], 2014	RCT	City: Jeonju Country: Korea	Healthy volunteers; Age: 60-75 yr; Control group: 64.50 ± 4.84 yr; Intervention group (500 mg): 64.50 ± 2.17 yr; Intervention group (1000 mg): 64.43 ± 4.47 yr; Intervention group (2000 mg): 66.56 ± 4.98 yr	Total: 36; Control group = 10 (4/6); Intervention group (500 mg) = 10 (9/1); Intervention group (1000 mg) = 7 (2/5); Intervention group (2000 mg) = 9 (5/4)	Daily doses of 500, 1000, or 2000 mg. of tablet containing *L. helveticus* IDCC3801	Placebo	12 wk	DS, SRT, VLT, RVIP, SCWT	> 70%
Inoue *et al*[34], 2018	RCT	City; Hyogo prefecture, Country: Japan	Healthy volunteers; Average age: 70.3 ± 3.1 yr; Control group: 70.9 ± 3.2 yr; Intervention group: 69.9 ± 3.0 yr	Total: 38; Control group = 18 (7/11); Intervention group = 20 (7/13)	Sachet containing lyophilised powder of *B. longum* BB536, *B. infantis* M-63, *B. breve* M-16V and *B.breve* B-3 (1.25×10^{10} CFU each)	Placebo	12 wk	MoCA, Modified flanker task, PHQ-9, GAD-7	> 99%
Hwang *et al* [35], 2019	RCT	City: Jeonju Country: South Korea	People with mild cognitive impairment; Age: 55-85 yr; Control group: 69.2 ± 7.00 yr; Intervention group: 68.0 ± 5.12 yr	Total: 100; Control group = 50 (14/36); Intervention group = 50 (20/30)	Mixture of fermented soybean powder and *L. plantarum* C29 (1.25×10^{10} CFU/g)	Placebo	12 wk	VLT, DS, ACPT	> 90%
Kelly *et al*[36], 2017	RCT	City: Cork Country: Ireland	Healthy volunteers; Age: 20-33 yr; Placebo/Probiotic group: 23.6 ± 0.97 yr; Probiotic/Placebo group: 25.64 ± 1.14 yr	Total: 29; Placebo/Probiotic group = 15 (15/0); Probiotic/Placebo group = 14 (14/0)	Active capsules contained corn starch, magnesium stearate, silicon dioxide and *L. Rhamnosus*(1×10^9 CFU)	Placebo	8 wk	MOT, PAL, AST, RVIP, ERT, Emotional Stroop	-
Kobayashi *et al* [37], 2019	RCT	City: Tokyo Country: Japan	People with memory complaints; Age: 50-80 yr; Control group: 61.6 ± 6.37 yr; Intervention group: 61.5 ± 6.83 yr	Total: 117; Control group = 58 (29/29); Intervention group = 59 (29/30)	1 capsule per day with *B. breve* A1 ($> 2 \times 10^{10}$ CFU)	Placebo	12 wk	RBANS, MMSE	-
Lew *et al*[38], 2019	RCT	Cities: Penang, Kubang Kerian Country: Malaysia	Stressed adults; Age: 18-60 yr; Control group: 32.1 ± 11.4 yr; Intervention group: 31.3 ± 10.8 yr	Total: 103; Control group = 51 (12/39); Probiotic group = 52 (12/40)	*L. plantarum* P8 (10^{10} CFU/sachet per day)	Placebo	12 wk	PSS-10, DASS-42, CBB	-
Ohsawa *et al* [39], 2018	RCT	Country: Japan	People with forgetfulness; 50-70 yr; Control group: 57.8	Total: 60; Control group = 29 (13/16); Intervention	One bottle per day (190 g per bottle) of a *L. helveticus*-fermented	Placebo	8 wk	RBANS, POMS	-

			± 5.9 yr; Intervention group: 58.5 ± 6.5 yr	group = 31 (13/18)	milk contained 2.4 mg of lactononadecapeptide				
Papalini *et al* [40], 2019	RCT	City: Nijmegen Country: The Netherlands	Healthy volunteers; Age:18-40 yr; Control group: 22 yr (SE = 0.5); Intervention group: 21 yr (SE = 0.4)	Total: 58; Control group = 29 (0/29); Intervention group = 29 (0/29)	2 g/d of powder diluted in water or milk containing *B. bifidum* W23, *B. lactis* W51, *B. lactis* W52, *L. acidophilus* W37, *L. brevis* W63, *L. casei* W56, *L. salivarius* W24, *L. lactis* W19 *L. lactis* W58(5×10^9 CFU)	Placebo	4 wk	BDI, LEIDS-r, Emotional face-word Stroop task, Emotional face-matching paradigm, SCWT, DS, SECPT	-
Roman *et al* [41], 2018	RCT	City: Almeria Country: Spain	Fibromyalgia patients; Control group: 50.27 ± 2.03 yr; Intervention group: 55.00 ± 2.09 yr	Total: 31; Control group = 15 (2/13); Intervention group = 16 (1/15)	4 pills/d containing *L. Rhamnosus* GG®, *L. casei*, *L. acidophilus*, and *B. Bifidus* (6×10^6 bacteria per capsule)	Placebo	8 wk	MMSE, BDI, IGT, Two-choice Task	-
Rudzki *et al* [42], 2019	RCT	City: Bialystok Country: Poland	People with major depression; Control group: 38.90 (12) yr (SD); Intervention group: 39.13 (9.96) yr	Total: 60; Control group = 30 (10/20); Intervention group = 30 (7/23)	2 capsules/d containing *L. plantarum* 299v (10×10^9 CFU per capsule)	Placebo	8 wk	HAM-D 17, SCL-90, PSS-10, APT, RFFT, TMT A, TMT B, CVLT Stroop Test parts A and B	-
Smith *et al*[43], 2015	RCT	City: Cardiff Country: Galles	Healthy volunteers; Age: 19-30 yr; Mean age 23.0 yr	Total: 47 (19/28)	One sachet of Inulin per day (5 mg)	Placebo	4 h	Mood, Performance Tasks, Memory Tasks, Psychomotor Tasks, Selective Attention Tasks, Sustained Attention Task	-
Tamtaji *et al* [44], 2019	RCT	City: Kashan, Shahrekord Country: Iran	Patients with Alzheimer disease; Age: 55-100 yr; Control group: 78.5 ± 8.0 yr; Intervention group (Selenium): 78.8 ± 10.2 yr; Intervention group (Selenium + probiotic): 76.2 ± 8.1 yr	Total: 79; Control group = 26; Intervention group (Selenium) = 26; Intervention group (Selenium + probiotic) = 27	Selenium (200 μg/d) and probiotic containing *L. acidophilus*, *B. bifidum*, and *B. longum* (2×10^9 CFU/d each)	Placebo or only selenium (200 μg/d)	12 wk	MMSE	100%
Tamtaji *et al* [45], 2019	RCT	City: Kashan Country: Iran	Patients with Parkinson disease; Age: 50-90 yr; Control group: 67.7 ± 10.2 yr; Intervention group: 68.2 ± 7.8 yr	Total: 60; Control group = 30; Intervention group = 30	Probiotic containing *L. acidophilus*, *B. bifidum*, *L. reuteri*, and *L. fermentum* (each 2×10^9 CFU/g)	Placebo	12 wk	MDS-UPDRS	90%

AAT: Aachener Aphasia Test; ACPT: Auditory Continuous Performance Test; ADS: Allgemeine Depressionsskala; APT: Attention and Perceptivity Test; AST: Attention Switching Task; BAS-III: British Ability Scales III; BDI: Beck Depression Inventory; BDT: Block Design Test; CBB: Cogstate Brief Battery; CBTT: Corsi Block Tapping Test; CFU: Colony-forming unit; CVLT: California Verbal Learning Test; DASS-42: Depression Anxiety and Stress Scale questionnaire; DS: Digit Symbol Test; ED: Emotional Decision Making; ERT: Emotion Recognition Task; F: Female; GAD-7: Generalised Anxiety Disorder Questionnaire-7; HAM-D 17: Hamilton Depression Rating-17; IGT: Iowa Gambling Task; LEIDS: Leiden Index of Depression Severity; M: Male; MDS-UPDRS: Movement Disorders Society-Unified Parkinson's Disease Rating Scale; MMSE: Mini Mental State Evaluation; MoCA: Montreal Cognitive Assessment instrument; MOT: Motor Screening Test; NART: National Adult Reading Test; NCT-A: Number Connection Test A; NCT-B: Number Connection Test B; PAL: Paired Associates Learning; PANAS: Positive and Negative Affect Schedule; PHES: Psychometric Hepatic Encephalopathy Score; PHQ-9: Patient Health Questionnaire-9; POMS: Profile of Mood States; PSS-10: Perceived Stress Scale-10; PVFT: Phonological Verbal Fluency (PVF) test; RAVLT: Rey Auditory Verbal Learning Test; RBANS: Repeatable Battery for the Assessment of Neuropsychological Status; RCT: Randomized controlled trial; RFFT: Ruff Figural Fluency Test; RM: Emotional Recognition Memory; ROCF: Rey-Osterrieth Complex Figure Test; RVIP: Rapid

Visual Information-Processing task; SCL-90: Symptom Checklist 90; SCWT: Stroop Color and Word Test; SECPT: Socially Evaluated Cold Pressor Test; SPM: Raven's Standard Progressive Matrices; SRT: Story Recall Test; STAIC: State-Trait Anxiety Inventory for Children; STEP: Test of Time and Weights Estimation; SVF: Semantic Verbal Fluency test; TMT-A: Trail Making Test A; TMT-B: Trail Making Test B; TYM: Test your memory; VFT: Verbal Fluency test; WMS: Wechsler Memory Scale MFQ: Children Mood and Feelings Questionnaire; VLT: Verbal Learning Test; VST: Visual Search Test.

Papalini *et al*[40] tested a probiotic multistrain mixture in women who underwent a stressful condition for 4 wk. The results showed that the trial reduced the unfavorable stress effect on working memory performance measured by the DS backward test. In addition, Chung *et al*[33] demonstrated a significant improvement in Verbal Learning Test, Story Recall Test, RVIP and Stroop Color and Word Test after 12 wk administration of *L. helveticus* in healthy subjects compared to placebo. Finally, Inoue *et al*[34] demonstrated that intervention with *Bifidobacterium spp.* for 12 wk, added to resistance training, significantly improved response accuracy and reaction time tests in healthy elderly subjects. Regarding the cognitive effects of prebiotic administration, the study conducted in healthy children by Capitão *et al*[31] reported that 12 wk GOS supplement only improved memory retrieval speed assessed with the CogTrackTM test battery. By contrast, Smith *et al*[43] investigated the acute effects of inulin intake on healthy volunteers and reported improving memory tasks, especially immediate free and delayed recall. No FMT intervention has been carried out in healthy subjects. Hence, although three of eight studies conducted in healthy subjects showed no significant difference between intervention and placebo groups, probiotics resulted were more effective in improving cognitive function than prebiotics.

Patients with different pathologies and the impact of probiotics/prebiotics/FMT on cognitive functions

The effects of probiotics, prebiotics, and FMT on cognitive functions were also assessed in different diseases, of which the most represented were hepatic encephalopathy (HE) and AD. Bajaj *et al*[26] conducted three studies on HE. In particular, the authors first investigated the effect of *Lactobacillus GG* administration on HE but did not report changes in cognition. However, they also treated HE patients with FMT *via* enema and reported a significant improvement in PHES and EncephalApp Stroop tests[27]. Moreover, Bajaj *et al*[28] evaluated the treatment with FMT capsules effects on HE patients, and they reported only a significant improvement in the EncephalApp Stroop test.

Regarding AD, Agahi *et al*[23] administered two different multistrain probiotic capsules to patients affected by severe disease for 12 wk, but no effect on TYM cognitive tests were reported. By contrast, Akbari *et al*[24] found that daily administration of probiotic milk enriched with *Lactobacillus spp.* led to a decline in Mini Mental State Evaluation (MMSE) score in AD patients compared to placebo. Moreover, Tamtaji *et al*[44] found that a probiotic and selenium co-supplement in AD patients was responsible for a significant increase in MMSE score. In addition, Hwang *et al*[35] found that people with mild cognitive impairment showed an improvement in a

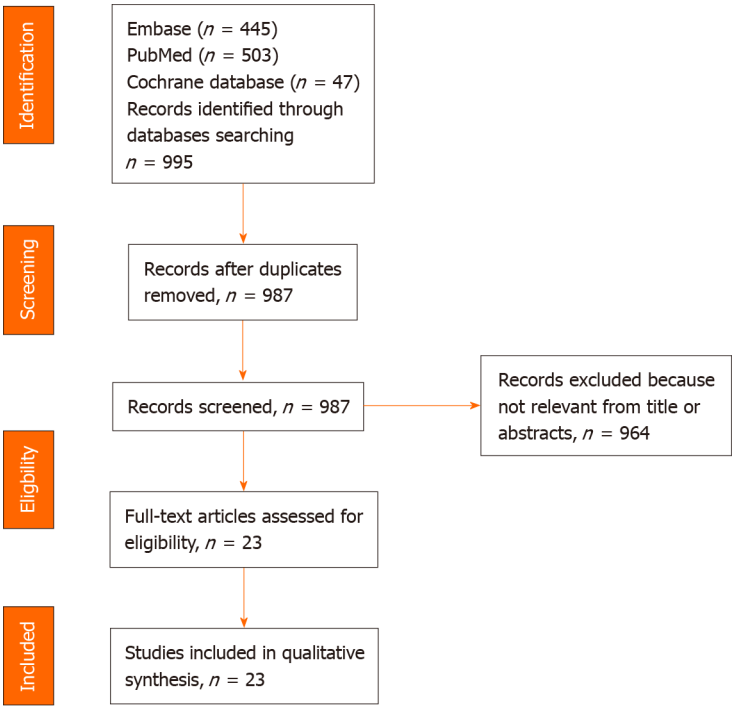


Figure 1 PRISMA flow diagram.

battery of tests related to verbal memory and attention domains after ingesting a mixture of *L. plantarum* C29 and fermented soybean powder. Finally, Lew *et al*[38] reported that daily administration of *L. plantarum* P8 for 12 wk in stressed adults led to a reduction of stress score and enhanced cognition and verbal learning memory, assessed through the CBB. Another study, conducted by Roman *et al*[41], explored the effect of a multispecies probiotic on fibromyalgia patients and found a significantly reduced number of impulsive choices. Moreover, Kobayashi *et al*[37] carried out a 12-wk treatment with *Bifidobacterium breve* A1 in elderly subjects with memory complaints, documenting a significant decline of total scores of both Repeatable Battery for the Assessment of Neuropsychological Status (RBANS) and MMSE tests. Regarding patients affected by PD, Tamtaji *et al*[45] highlighted a favorable reduction of the Movement Disorders Society-Unified PD Rating Scale (MDS-UPDRS) after ingesting a probiotic mixture for 12 wk. In addition, Ohsawa *et al*[39] reported improved attention, coding, and delayed memory scores (assessed with RBANS) in people with forgetfulness after 8 wk intake of a *L. helveticus* fermented milk drink. Also, Rudzki *et al*[42] reported a significant improvement in CVLT and APT in people with major depression treated with *L. plantarum 299v*. Moreover, Ceccarelli *et al*[32] demonstrated a significant improvement in several cognitive functions in HIV-1 infected patients ingesting a multistrain probiotic for 24 wk (primarily in the following neurocognitive tests: Rey-Osterrieth Complex Figure, Rey Auditory Verbal Learning Test, Test of Time and Weights Estimation, Phonological Verbal Fluency Test, Corsi Block Tapping Test and Trail Making Test A). Finally, the only study which assessed the effectiveness of a prebiotic intake (inulin and fructooligosaccharides), conducted by Buigues *et al*[30] on elderly affected by frailty syndrome, the MMSE did not report significant cognitive improvement. As a result, while the FMT and especially probiotics played multiple beneficial effects on different cognitive functions of unhealthy subjects, the prebiotics' supplementation did not provide any cognitive improvement, maybe because of their short-term administration.

DISCUSSION

Dementia is a chronic, gradual, and progressive neurological disease that affects millions of people in both industrialized and rural countries. Cognitive decline and daily activities impairment limits patients' self-care and causes a severe burden to parents, friends, caregivers, and especially to the healthcare systems[46,47]. Increasing evidence suggests that the prevalence of dementia rises with age and is strongly

associated with other comorbidities, including AD and cardiovascular risk factors such as hypertension and hypercholesterolaemia[48].

Although the specific dementia pathogenesis is not yet understood and current therapies only attempt to counterbalance the disturbance, several studies recently highlighted the central role of the gut microbiota in brain health and the onset and persistence of neurodegenerative diseases[49,50]. Nevertheless, our systematic review of human RCTs reported contradictory results due to the diverse type, posology, and duration of interventions and the different responses of healthy or diseased people to the treatment.

In general, supplementation with probiotics and prebiotics determined the positive effects on healthy subjects. Five (63%) out[25,33,34,40,43] of the eight studies conducted in volunteers reported beneficial effects on the cognitive functions, while the other three[29,31,36] studies did not find any difference between the intervention and control groups.

Regarding the different evaluated patients, only 3 (20%)[23,26,30] of the 15 studies did not report an amelioration of cognitive functions for other possible reasons. For example, the probiotics' administration performed by Bajaj *et al*[26] probably did not last for a sufficient time to obtain cognitive improvement in patients with HE. In contrast, with 13 wk of prebiotics' supplementation, Buigues *et al*[30] did not observe effects on cognitive behaviour because MMSE does not represent a sensitive tool to detect the small changes in cognition that may occur after inulin and FOS supplementation. In addition, in the study conducted by Agahi *et al*[23], the 12 wk probiotic administration did not lead to cognitive amelioration in patients with AD; a probable explanation could be the enrollment of only patients with advanced disease.

Probiotic supplementation improves cognitive functions in many different diseases such as HIV[32], PD[45], fibromyalgia, major depression[42], AD[24,44], and other mild cognitive deficits[35,37-39]. Furthermore, studies evaluating the effects of FMT on patients with HE highlighted a significant amelioration in cognitive functionality[27,28]. It is well established that a balanced gut microbiota composition (eubiosis condition) plays a crucial role in our health; a dysbiotic status (meaning a reduced gut microbiota diversity) is related to many human gastrointestinal, immunological, and neurodegenerative diseases[51]. Concerning neurological impairments, recent findings elucidated the importance of the gut microbiota in the bidirectional communication between the central and enteric nervous systems, called the gut-brain axis[52]. Hence, the main factors responsible for intestinal dysbiosis such as stress, unbalanced diet, and drug abuse also determine an alteration of the gut-brain axis by causing a loss of epithelial integrity. The loss of this barrier functionality allows microbial-derived molecules to enter the systemic circulation, promoting endotoxemia, oxidative stress and low-grade inflammation responsible for the blood-brain barrier disruption[53,54] (Figure 2); these factors represent a signature for neurodegenerative disorders, especially AD. Consequently, given the importance of the intestinal barrier integrity for the prevention of neuroinflammation and brain damage, gut microbiota modulation by psychobiotics, namely beneficial bacteria (probiotics) or support for such bacteria (prebiotics) and FMT, represent an excellent strategy to restore the intestinal permeability and prevent the consequences of a leaky gut[55-57].

However, although several studies have highlighted the local beneficial effects of probiotics, prebiotics and FMT (*e.g.*, modification of the gut microbiota composition, strengthening of the gut epithelial barrier and modulation of the local (mucosal) immune system), they also exerted systemic effects, in particular on the central nervous system[58,60]. More specifically, recent studies have reported that the intestinal microbiota affects neurodevelopment and diverse brain functions by regulating the gut-brain axis, for example, by acting on the electrophysiological thresholds of the enteric nervous system neurons, which interact *via* neurotransmitters (adrenaline, noradrenaline, and acetylcholine) with the central nervous system[61].

Another important neuronal pathway in gut-brain communication involves the vagus nerve, and many effects of probiotics strains influence its activity[62]. Furthermore, since the gut houses the most extensive collection of lymphoid tissues in the human body and various intestinal immune cells can cross the blood-brain barrier, gut microbiota manipulation represents a key indirect route for communication between the gut microbiota and the central nervous system[63]. Intriguingly, specific probiotic formulations have also been shown an ability to stimulate the production of neurotransmitters (*e.g.*, GABA, serotonin, and dopamine) or are even microbially neuroactive. These microbial metabolites can trigger epigenetic signals on human brain genes involved in various complex networks or act as a ligand for specific human receptors[64].

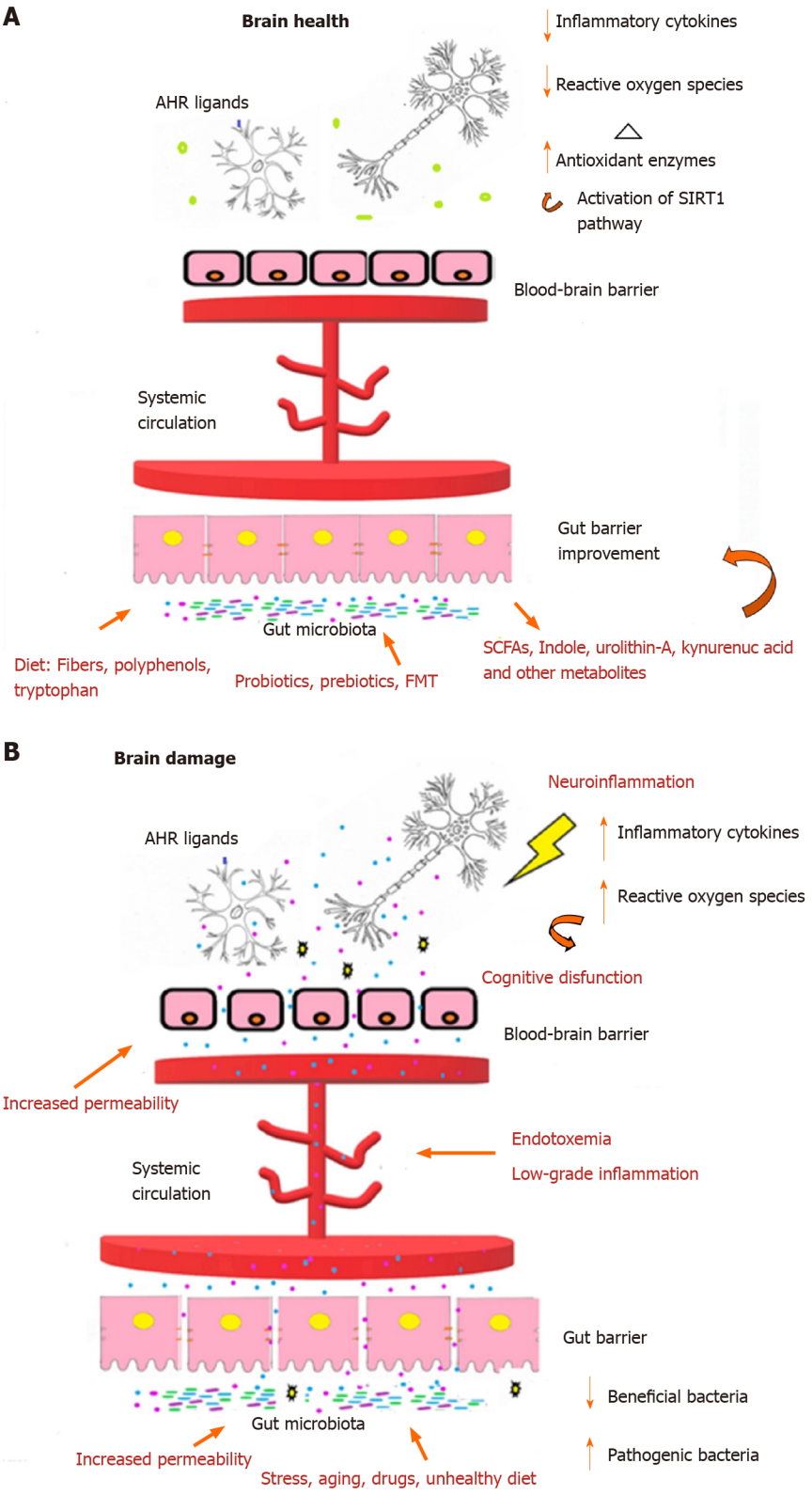


Figure 2 Gut-brain axis in eubiosis and dysbiosis condition. A: Eubiosis; B: Dysbiosis condition. AHR: Aryl hydrocarbon receptor; FMT: Fecal microbiota transplant; SCFA: Short-chain fatty acid; SIRT1: Sirtuin 1.

For instance, the probiotic activated Sirtuin 1 pathway, which regulates the brain antioxidant enzymes such as superoxide dismutase and glutathione peroxidase, could favor cognitive improvements by preventing oxidative stress and deposition of beta-amyloid in the brain[65]. Even the modulation of kynurenine metabolism, the primary route for tryptophan catabolism, which is closely related to the structural and functional dynamics of the gut microbiota, could positively affect brain health[66]. Indeed, *in vivo L. plantarum* administration demonstrated a beneficial reduction of

kynurenines as most act as neurotoxic compounds[42,67,68]. Notably, although *L. plantarum* was administered to healthy or ill people in most of our selected RCTs, its positive effects have been probably underestimated because of the unknown impact of the other components of the probiotic formula that include it.

By contrast, indole-3-lactic acid (ILA) is an interesting neuroprotective tryptophan metabolite mainly produced by *Bifidobacterium spp*. acting as an aryl hydrocarbon receptor (AhR) agonist, expressed by intestinal and neuronal cells[69,70]. In detail, microbial agonists produced by *L. bulgaricus* and *L. reuteri* could activate microglia and astrocytes AhRs, suppressing pro-inflammatory signals and preventing neuronal damage[71-73]. Furthermore, the administration of some probiotics (especially *L. helveticus*, *L. casei* and *L. rhamnosus*) and prebiotics could also improve cognitive functions by stimulating the production of short-chain fatty acids as they enhance the transcription of the brain-derived neurotrophic factor that stimulates neuronal plasticity, protecting against neuroinflammation and neuronal apoptosis[74-78]. Moreover, the FMT represents a very promising strategy to re-establish gut eubiosis and improve cognitive functions. For instance, in transgenic mice, FMT significantly improved cognitive deficits, beta-amyloid accumulation, and neuroinflammation while reducing UPDRS score and tremor in people with Parkinson disease[79].

Finally, our recent study demonstrated that age-associated shifts of the microbiota have a detrimental impact on the central nervous system's protein expression and critical functions. Still, FMT represents an excellent strategy to restore a young-like microbiota and improve cognitive functions[80]. Therefore, although the modulation of intestinal microbiota represents a new precious therapeutic opportunity, it also shows some restrictions and risks. In particular, even if probiotics are generally considered safe and have many advantages such as a tolerated mode of administration (orally) and the possibility to integrate them with other pharmacological/non-pharmacological approaches, they displayed some limitations mainly due to potential side effects, especially in some patients (including immunocompromised people), or to their long-term safety[81]. Besides, even if probiotics can promote the production of several compounds such as lactic acid, bioamines, bile salts and other molecules that could play detrimental effects on the host, most of them are sold as dietetic supplements, and the regulatory agencies do not require safety studies in humans before their commercialization[82,83].

Although reported to be fairly safe in most clinical trials, FMT can be responsible for acute or prolonged adverse effects such as diarrhea, abdominal pain, nausea, headaches, and fatigue[84]. In particular, immunological concerns have been raised regarding safety assessments for both probiotics and the FMT because either indigenous or transient microorganisms could impact the immune system's functionality. Hence, the FMT application or the administration of probiotics to specific vulnerable populations and stressed or aged people, immunocompromised patients, newborns or pregnant women must be well evaluated to prevent microbial translocation and sepsis[85-87]. Moreover, the current literature lacks information about the long-term administration of probiotics; therefore, the possible horizontal transfer of antibiotic resistance genes favored by their supplementation cannot be excluded. Likewise, because stool contains thousands of microorganisms and a vast number of metabolites, FMT represents a constant risk of pathogens or commensals transfer to donors that may harmfully affect them[88].

CONCLUSION

As a final note, the different defects found in the evaluated studies highlighted some methodical limitations such as small sample sizes, the limited sampling time and the wide range of other cognitive tests. Supplementation of probiotics and FMT could represent a non-invasive successful strategy to restore gut eubiosis and enhance cognitive functions in healthy people and patients with different neurological/neurodegenerative diseases. Of course, further specific and clinical studies with numerous patients are needed to confirm this encouraging hypothesis.

ARTICLE HIGHLIGHTS

Research background

Due to the global population aging, cognitive impairments will affect approximately

115 million people by 2050. Since current therapies only attempt to counterbalance cognitive disorders, many recent studies recently highlighted the central role of the gut microbiota in brain health.

Research motivation

The pathogenesis of several cognitive disorders is still not fully understood; however, it has been recently established that a dysregulated gut-brain axis communication is associated with the onset and persistence of neurodegenerative diseases. Thus, gut microbiota manipulation could restore a functional gut-brain axis improving cognitive functions.

Research objectives

Since the evidence derived from human randomized clinical trials (RCTs) is currently limited, the main purpose of this systematic review was to detect the currently available RCTs, to define better the effects of probiotics, prebiotics, and fecal microbiota transplant (FMT) on cognitive functions.

Research methods

We systematically searched Embase, Medline/PubMed, Cochrane Library, central and clinicaltrials.gov databases with a combination of comprehensive terms related to cognition and gut microbiota manipulation. Then, we carefully reviewed and synthesized the data by types of study design and setting, characteristics of the studied population, kind of the intervention (strain type or mixture type, dosage and frequency of administration), control treatment, inclusion and exclusion criteria, follow-up duration, and cognitive or memory outcomes.

Research results

The analysis of the 23 included in our systematic review highlighted that, although the different type and posology of administration and the various cognitive tests and questionnaires adopted, both probiotics supplementation and FMT improved the cognitive functions in most of healthy people and patients affected by different neurological pathologies.

Research conclusions

The gut microbiota manipulation could represent a good strategy to counteract gut dysbiosis and so ameliorate cognitive dysfunction.

Research perspectives

The supplementation of probiotics and FMT could represent a non-invasive successful strategy to restore gut eubiosis and enhance cognitive functions in healthy people and patients with different neurological/neurodegenerative diseases.

ACKNOWLEDGEMENTS

We thank Dr. Stroobant M for the language editing of the manuscript.

REFERENCES

1 **Land KC**, Lamb VL. Demography of Aging. In: Heggenhougen K, Stella Q. International Encyclopedia of Public Health. San Diego: Academic Press, 2008: 89-95
2 **Brayne C**, Miller B. Dementia and aging populations-A global priority for contextualized research and health policy. *PLoS Med* 2017; **14**: e1002275 [PMID: 28350794 DOI: 10.1371/journal.pmed.1002275]
3 **Tomaskova H**, Kuhnova J, Cimler R, Dolezal O, Kuca K. Prediction of population with Alzheimer's disease in the European Union using a system dynamics model. *Neuropsychiatr Dis Treat* 2016; **12**: 1589-1598 [PMID: 27418826 DOI: 10.2147/NDT.S107969]
4 **Prince MJ**, Wu F, Guo Y, Gutierrez Robledo LM, O'Donnell M, Sullivan R, Yusuf S. The burden of disease in older people and implications for health policy and practice. *Lancet* 2015; **385**: 549-562 [PMID: 25468153 DOI: 10.1016/S0140-6736(14)61347-7]
5 **Sacuiu SF**. Dementias. *Handb Clin Neurol* 2016; **138**: 123-151 [PMID: 27637956 DOI: 10.1016/B978-0-12-802973-2.00008-2]
6 **Snyder HM**, Corriveau RA, Craft S, Faber JE, Greenberg SM, Knopman D, Lamb BT, Montine TJ,

Nedergaard M, Schaffer CB, Schneider JA, Wellington C, Wilcock DM, Zipfel GJ, Zlokovic B, Bain LJ, Bosetti F, Galis ZS, Koroshetz W, Carrillo MC. Vascular contributions to cognitive impairment and dementia including Alzheimer's disease. *Alzheimers Dement* 2015; **11**: 710-717 [PMID: 25510382 DOI: 10.1016/j.jalz.2014.10.008]

7 **Raz L**, Knoefel J, Bhaskar K. The neuropathology and cerebrovascular mechanisms of dementia. *J Cereb Blood Flow Metab* 2016; **36**: 172-186 [PMID: 26174330 DOI: 10.1038/jcbfm.2015.164]

8 **Yiannopoulou KG**, Papageorgiou SG. Current and future treatments for Alzheimer's disease. *Ther Adv Neurol Disord* 2013; **6**: 19-33 [PMID: 23277790 DOI: 10.1177/1756285612461679]

9 **Boem F**, Amedei A. Healthy axis: Towards an integrated view of the gut-brain health. *World J Gastroenterol* 2019; **25**: 3838-3841 [PMID: 31413521 DOI: 10.3748/wjg.v25.i29.3838]

10 **Cussotto S**, Sandhu KV, Dinan TG, Cryan JF. The Neuroendocrinology of the Microbiota-Gut-Brain Axis: A Behavioural Perspective. *Front Neuroendocrinol* 2018; **51**: 80-101 [PMID: 29753796 DOI: 10.1016/j.yfrne.2018.04.002]

11 **Cryan JF**, Dinan TG. Mind-altering microorganisms: the impact of the gut microbiota on brain and behaviour. *Nat Rev Neurosci* 2012; **13**: 701-712 [PMID: 22968153 DOI: 10.1038/nrn3346]

12 **Mangiola F**, Ianiro G, Franceschi F, Fagiuoli S, Gasbarrini G, Gasbarrini A. Gut microbiota in autism and mood disorders. *World J Gastroenterol* 2016; **22**: 361-368 [PMID: 26755882 DOI: 10.3748/wjg.v22.i1.361]

13 **Noble EE**, Hsu TM, Kanoski SE. Gut to Brain Dysbiosis: Mechanisms Linking Western Diet Consumption, the Microbiome, and Cognitive Impairment. *Front Behav Neurosci* 2017; **11**: 9 [PMID: 28194099 DOI: 10.3389/fnbeh.2017.00009]

14 **Ticinesi A**, Tana C, Nouvenne A, Prati B, Lauretani F, Meschi T. Gut microbiota, cognitive frailty and dementia in older individuals: a systematic review. *Clin Interv Aging* 2018; **13**: 1497-1511 [PMID: 30214170 DOI: 10.2147/CIA.S139163]

15 **Bonfili L**, Cecarini V, Berardi S, Scarpona S, Suchodolski JS, Nasuti C, Fiorini D, Boarelli MC, Rossi G, Eleuteri AM. Microbiota modulation counteracts Alzheimer's disease progression influencing neuronal proteolysis and gut hormones plasma levels. *Sci Rep* 2017; **7**: 2426 [PMID: 28546539 DOI: 10.1038/s41598-017-02587-2]

16 Risk Reduction of Cognitive Decline and Dementia: WHO Guidelines. Geneva: World Health Organization; 2019 [PMID: 31219687]

17 **Chen D**, Yang X, Yang J, Lai G, Yong T, Tang X, Shuai O, Zhou G, Xie Y, Wu Q. Prebiotic Effect of Fructooligosaccharides from *Morinda officinalis* on Alzheimer's Disease in Rodent Models by Targeting the Microbiota-Gut-Brain Axis. *Front Aging Neurosci* 2017; **9**: 403 [PMID: 29276488 DOI: 10.3389/fnagi.2017.00403]

18 **Larsen N**, Vogensen FK, Gøbel RJ, Michaelsen KF, Forssten SD, Lahtinen SJ, Jakobsen M. Effect of Lactobacillus salivarius Ls-33 on fecal microbiota in obese adolescents. *Clin Nutr* 2013; **32**: 935-940 [PMID: 23510724 DOI: 10.1016/j.clnu.2013.02.007]

19 **Cammarota G**, Ianiro G, Tilg H, Rajilić-Stojanović M, Kump P, Satokari R, Sokol H, Arkkila P, Pintus C, Hart A, Segal J, Aloi M, Masucci L, Molinaro A, Scaldaferri F, Gasbarrini G, Lopez-Sanroman A, Link A, de Groot P, de Vos WM, Högenauer C, Malfertheiner P, Mattila E, Milosavljević T, Nieuwdorp M, Sanguinetti M, Simren M, Gasbarrini A; European FMT Working Group. European consensus conference on faecal microbiota transplantation in clinical practice. *Gut* 2017; **66**: 569-580 [PMID: 28087657 DOI: 10.1136/gutjnl-2016-313017]

20 **Sun J**, Xu J, Ling Y, Wang F, Gong T, Yang C, Ye S, Ye K, Wei D, Song Z, Chen D, Liu J. Fecal microbiota transplantation alleviated Alzheimer's disease-like pathogenesis in APP/PS1 transgenic mice. *Transl Psychiatry* 2019; **9**: 189 [PMID: 31383855 DOI: 10.1038/s41398-019-0525-3]

21 **Goloshchapov OV**, Olekhnovich EI, Sidorenko SV, Moiseev IS, Kucher MA, Fedorov DE, Pavlenko AV, Manolov AI, Gostev VV, Veselovsky VA, Klimina KM, Kostryukova ES, Bakin EA, Shvetcov AN, Gumbatova ED, Klementeva RV, Shcherbakov AA, Gorchakova MV, Egozcue JJ, Pawlowsky-Glahn V, Suvorova MA, Chukhlovin AB, Govorun VM, Ilina EN, Afanasyev BV. Long-term impact of fecal transplantation in healthy volunteers. *BMC Microbiol* 2019; **19**: 312 [PMID: 31888470 DOI: 10.1186/s12866-019-1689-y]

22 **Neisser U**. Cognitive psychology. Englewood Cliffs: Prentice-Hall ll, Inc., 1967

23 **Agahi A**, Hamidi GA, Daneshvar R, Hamdieh M, Soheili M, Alinaghipour A, Esmaeili Taba SM, Salami M. Does Severity of Alzheimer's Disease Contribute to Its Responsiveness to Modifying Gut Microbiota? *Front Neurol* 2018; **9**: 662 [PMID: 30158897 DOI: 10.3389/fneur.2018.00662]

24 **Akbari E**, Asemi Z, Daneshvar Kakhaki R, Bahmani F, Kouchaki E, Tamtaji OR, Hamidi GA, Salami M. Effect of Probiotic Supplementation on Cognitive Function and Metabolic Status in Alzheimer's Disease: A Randomized, Double-Blind and Controlled Trial. *Front Aging Neurosci* 2016; **8**: 256 [PMID: 27891089 DOI: 10.3389/fnagi.2016.00256]

25 **Bagga D**, Reichert JL, Koschutnig K, Aigner CS, Holzer P, Koskinen K, Moissl-Eichinger C, Schöpf V. Probiotics drive gut microbiome triggering emotional brain signatures. *Gut Microbes* 2018; **9**: 486-496 [PMID: 29723105 DOI: 10.1080/19490976.2018.1460015]

26 **Bajaj JS**, Heuman DM, Hylemon PB, Sanyal AJ, Puri P, Sterling RK, Luketic V, Stravitz RT, Siddiqui MS, Fuchs M, Thacker LR, Wade JB, Daita K, Sistrun S, White MB, Noble NA, Thorpe C, Kakiyama G, Pandak WM, Sikaroodi M, Gillevet PM. Randomised clinical trial: Lactobacillus GG modulates gut microbiome, metabolome and endotoxemia in patients with cirrhosis. *Aliment Pharmacol Ther* 2014; **39**: 1113-1125 [PMID: 24628464 DOI: 10.1111/apt.12695]

27 **Bajaj JS**, Kassam Z, Fagan A, Gavis EA, Liu E, Cox IJ, Kheradman R, Heuman D, Wang J, Gurry T,

Williams R, Sikaroodi M, Fuchs M, Alm E, John B, Thacker LR, Riva A, Smith M, Taylor-Robinson SD, Gillevet PM. Fecal microbiota transplant from a rational stool donor improves hepatic encephalopathy: A randomized clinical trial. *Hepatology* 2017; **66**: 1727-1738 [PMID: 28586116 DOI: 10.1002/hep.29306]

28 **Bajaj JS**, Salzman NH, Acharya C, Sterling RK, White MB, Gavis EA, Fagan A, Hayward M, Holtz ML, Matherly S, Lee H, Osman M, Siddiqui MS, Fuchs M, Puri P, Sikaroodi M, Gillevet PM. Fecal Microbial Transplant Capsules Are Safe in Hepatic Encephalopathy: A Phase 1, Randomized, Placebo-Controlled Trial. *Hepatology* 2019; **70**: 1690-1703 [PMID: 31038755 DOI: 10.1002/hep.30690]

29 **Benton D**, Williams C, Brown A. Impact of consuming a milk drink containing a probiotic on mood and cognition. *Eur J Clin Nutr* 2007; **61**: 355-361 [PMID: 17151594 DOI: 10.1038/sj.ejcn.1602546]

30 **Buigues C**, Fernández-Garrido J, Pruimboom L, Hoogland AJ, Navarro-Martínez R, Martínez-Martínez M, Verdejo Y, Mascarós MC, Peris C, Cauli O. Effect of a Prebiotic Formulation on Frailty Syndrome: A Randomized, Double-Blind Clinical Trial. *Int J Mol Sci* 2016; **17** [PMID: 27314331 DOI: 10.3390/ijms17060932]

31 **Capitão LP**, Baião R, Baek HK, Kappelmann N, Sharman R, Harvey CJ, Montgomery P, Burnet PW. Prebiotic supplementation does not affect reading and cognitive performance in children: A randomised placebo-controlled study. *J Psychopharmacol* 2020; **34**: 148-152 [PMID: 31342840 DOI: 10.1177/0269881119862534]

32 **Ceccarelli G**, Brenchley JM, Cavallari EN, Scheri GC, Fratino M, Pinacchio C, Schietroma I, Fard SN, Scagnolari C, Mezzaroma I, Vullo V, d'Ettorre G. Impact of High-Dose Multi-Strain Probiotic Supplementation on Neurocognitive Performance and Central Nervous System Immune Activation of HIV-1 Infected Individuals. *Nutrients* 2017; **9** [PMID: 29160817 DOI: 10.3390/nu9111269]

33 **Chung YC**, Jin HM, Cui Y, Kim DS, Jung JM, Park JI, Jung ES, Choi EK, Chae SW. Fermented milk of Lactobacillus helveticus IDCC3801 improves cognitive functioning during cognitive fatigue tests in healthy older adults. *J Funct Foods* 2014; **10**: 465-474 [DOI: 10.1016/j.jff.2014.07.007]

34 **Inoue T**, Kobayashi Y, Mori N, Sakagawa M, Xiao JZ, Moritani T, Sakane N, Nagai N. Effect of combined bifidobacteria supplementation and resistance training on cognitive function, body composition and bowel habits of healthy elderly subjects. *Benef Microbes* 2018; **9**: 843-853 [PMID: 30198326 DOI: 10.3920/BM2017.0193]

35 **Hwang YH**, Park S, Paik JW, Chae SW, Kim DH, Jeong DG, Ha E, Kim M, Hong G, Park SH, Jung SJ, Lee SM, Na KH, Kim J, Chung YC. Efficacy and Safety of *Lactobacillus Plantarum* C29-Fermented Soybean (DW2009) in Individuals with Mild Cognitive Impairment: A 12-Week, Multi-Center, Randomized, Double-Blind, Placebo-Controlled Clinical Trial. *Nutrients* 2019; **11** [PMID: 30717153 DOI: 10.3390/nu11020305]

36 **Kelly JR**, Allen AP, Temko A, Hutch W, Kennedy PJ, Farid N, Murphy E, Boylan G, Bienenstock J, Cryan JF, Clarke G, Dinan TG. Lost in translation? *Brain Behav Immun* 2017; **61**: 50-59 [PMID: 27865949 DOI: 10.1016/j.bbi.2016.11.018]

37 **Kobayashi Y**, Kuhara T, Oki M, Xiao JZ. Effects of *Bifidobacterium breve* A1 on the cognitive function of older adults with memory complaints: a randomised, double-blind, placebo-controlled trial. *Benef Microbes* 2019; **10**: 511-520 [PMID: 31090457 DOI: 10.3920/BM2018.0170]

38 **Lew LC**, Hor YY, Yusoff NAA, Choi SB, Yusoff MSB, Roslan NS, Ahmad A, Mohammad JAM, Abdullah MFIL, Zakaria N, Wahid N, Sun Z, Kwok LY, Zhang H, Liong MT. Probiotic Lactobacillus plantarum P8 alleviated stress and anxiety while enhancing memory and cognition in stressed adults: A randomised, double-blind, placebo-controlled study. *Clin Nutr* 2019; **38**: 2053-2064 [PMID: 30266270 DOI: 10.1016/j.clnu.2018.09.010]

39 **Ohsawa K**, Nakamura F, Uchida N, Mizuno S, Yokogoshi H. Lactobacillus helveticus-fermented milk containing lactononadecapeptide (NIPPLTQTPVVVPPFLQPE) improves cognitive function in healthy middle-aged adults: a randomised, double-blind, placebo-controlled trial. *Int J Food Sci Nutr* 2018; **69**: 369-376 [PMID: 28819993 DOI: 10.1080/09637486.2017.1365824]

40 **Papalini S**, Michels F, Kohn N, Wegman J, van Hemert S, Roelofs K, Arias-Vasquez A, Aarts E. Stress matters: Randomized controlled trial on the effect of probiotics on neurocognition. *Neurobiol Stress* 2019; **10**: 100141 [PMID: 30937347 DOI: 10.1016/j.ynstr.2018.100141]

41 **Roman P**, Estévez AF, Miras A, Sánchez-Labraca N, Cañadas F, Vivas AB, Cardona D. A Pilot Randomized Controlled Trial to Explore Cognitive and Emotional Effects of Probiotics in Fibromyalgia. *Sci Rep* 2018; **8**: 10965 [PMID: 30026567 DOI: 10.1038/s41598-018-29388-5]

42 **Rudzki L**, Ostrowska L, Pawlak D, Małus A, Pawlak K, Waszkiewicz N, Szulc A. Probiotic Lactobacillus Plantarum 299v decreases kynurenine concentration and improves cognitive functions in patients with major depression: A double-blind, randomized, placebo controlled study. *Psychoneuroendocrinology* 2019; **100**: 213-222 [PMID: 30388595 DOI: 10.1016/j.psyneuen.2018.10.010]

43 **Smith AP**, Sutherland D, Hewlett P. An Investigation of the Acute Effects of Oligofructose-Enriched Inulin on Subjective Wellbeing, Mood and Cognitive Performance. *Nutrients* 2015; **7**: 8887-8896 [PMID: 26516908 DOI: 10.3390/nu7115441]

44 **Tamtaji OR**, Heidari-Soureshjani R, Mirhosseini N, Kouchaki E, Bahmani F, Aghadavod E, Tajabadi-Ebrahimi M, Asemi Z. Probiotic and selenium co-supplementation, and the effects on clinical, metabolic and genetic status in Alzheimer's disease: A randomized, double-blind, controlled trial. *Clin Nutr* 2019; **38**: 2569-2575 [PMID: 30642737 DOI: 10.1016/j.clnu.2018.11.034]

45 **Tamtaji OR**, Taghizadeh M, Daneshvar Kakhaki R, Kouchaki E, Bahmani F, Borzabadi S, Oryan S,

Mafi A, Asemi Z. Clinical and metabolic response to probiotic administration in people with Parkinson's disease: A randomized, double-blind, placebo-controlled trial. *Clin Nutr* 2019; **38**: 1031-1035 [PMID: 29891223 DOI: 10.1016/j.clnu.2018.05.018]

46 **Lee MT**, Jang Y, Chang WY. How do impairments in cognitive functions affect activities of daily living functions in older adults? *PLoS One* 2019; **14**: e0218112 [PMID: 31173607 DOI: 10.1371/journal.pone.0218112]

47 **Bunn F**, Burn AM, Goodman C, Rait G, Norton S, Robinson L, Schoeman J, Brayne C. Comorbidity and dementia: a scoping review of the literature. *BMC Med* 2014; **12**: 192 [PMID: 25358236 DOI: 10.1186/s12916-014-0192-4]

48 **Qiu C**, Kivipelto M, von Strauss E. Epidemiology of Alzheimer's disease: occurrence, determinants, and strategies toward intervention. *Dialogues Clin Neurosci* 2009; **11**: 111-128 [PMID: 19585947 DOI: 10.31887/DCNS.2009.11.2/cqiu]

49 **Vuotto C**, Battistini L, Caltagirone C, Borsellino G. Gut Microbiota and Disorders of the Central Nervous System. *Neuroscientist* 2020; **26**: 487-502 [PMID: 32441219 DOI: 10.1177/1073858420918826]

50 **Sarkar A**, Lehto SM, Harty S, Dinan TG, Cryan JF, Burnet PWJ. Psychobiotics and the Manipulation of Bacteria-Gut-Brain Signals. *Trends Neurosci* 2016; **39**: 763-781 [PMID: 27793434 DOI: 10.1016/j.tins.2016.09.002]

51 **Cryan JF**, O'Riordan KJ, Cowan CSM, Sandhu KV, Bastiaanssen TFS, Boehme M, Codagnone MG, Cussotto S, Fulling C, Golubeva AV, Guzzetta KE, Jaggar M, Long-Smith CM, Lyte JM, Martin JA, Molinero-Perez A, Moloney G, Morelli E, Morillas E, O'Connor R, Cruz-Pereira JS, Peterson VL, Rea K, Ritz NL, Sherwin E, Spichak S, Teichman EM, van de Wouw M, Ventura-Silva AP, Wallace-Fitzsimons SE, Hyland N, Clarke G, Dinan TG. The Microbiota-Gut-Brain Axis. *Physiol Rev* 2019; **99**: 1877-2013 [PMID: 31460832 DOI: 10.1152/physrev.00018.2018]

52 **Martin CR**, Osadchiy V, Kalani A, Mayer EA. The Brain-Gut-Microbiome Axis. *Cell Mol Gastroenterol Hepatol* 2018; **6**: 133-148 [PMID: 30023410 DOI: 10.1016/j.jcmgh.2018.04.003]

53 **Liu S**, Gao J, Zhu M, Liu K, Zhang HL. Gut Microbiota and Dysbiosis in Alzheimer's Disease: Implications for Pathogenesis and Treatment. *Mol Neurobiol* 2020; **57**: 5026-5043 [PMID: 32829453 DOI: 10.1007/s12035-020-02073-3]

54 **Cerovic M**, Forloni G, Balducci C. Neuroinflammation and the Gut Microbiota: Possible Alternative Therapeutic Targets to Counteract Alzheimer's Disease? *Front Aging Neurosci* 2019; **11**: 284 [PMID: 31680937 DOI: 10.3389/fnagi.2019.00284]

55 **Rao RK**, Samak G. Protection and Restitution of Gut Barrier by Probiotics: Nutritional and Clinical Implications. *Curr Nutr Food Sci* 2013; **9**: 99-107 [PMID: 24353483 DOI: 10.2174/1573401311309020004]

56 **Cheng S**, Ma X, Geng S, Jiang X, Li Y, Hu L, Li J, Wang Y, Han X. Fecal Microbiota Transplantation Beneficially Regulates Intestinal Mucosal Autophagy and Alleviates Gut Barrier Injury. *mSystems* 2018; **3** [PMID: 30320222 DOI: 10.1128/mSystems.00137-18]

57 **Li LL**, Wang YT, Zhu LM, Liu ZY, Ye CQ, Qin S. Inulin with different degrees of polymerization protects against diet-induced endotoxemia and inflammation in association with gut microbiota regulation in mice. *Sci Rep* 2020; **10**: 978 [PMID: 31969646 DOI: 10.1038/s41598-020-58048-w]

58 **Bermudez-Brito M**, Plaza-Díaz J, Muñoz-Quezada S, Gómez-Llorente C, Gil A. Probiotic mechanisms of action. *Ann Nutr Metab* 2012; **61**: 160-174 [PMID: 23037511 DOI: 10.1159/000342079]

59 **Plaza-Diaz J**, Ruiz-Ojeda FJ, Gil-Campos M, Gil A. Mechanisms of Action of Probiotics. *Adv Nutr* 2019; **10**: S49-S66 [PMID: 30721959 DOI: 10.1093/advances/nmy063]

60 **Ma Q**, Xing C, Long W, Wang HY, Liu Q, Wang RF. Impact of microbiota on central nervous system and neurological diseases: the gut-brain axis. *J Neuroinflammation* 2019; **16**: 53 [PMID: 30823925 DOI: 10.1186/s12974-019-1434-3]

61 **Wang Y**, Kasper LH. The role of microbiome in central nervous system disorders. *Brain Behav Immun* 2014; **38**: 1-12 [PMID: 24370461 DOI: 10.1016/j.bbi.2013.12.015]

62 **Bonaz B**, Bazin T, Pellissier S. The Vagus Nerve at the Interface of the Microbiota-Gut-Brain Axis. *Front Neurosci* 2018; **12**: 49 [PMID: 29467611 DOI: 10.3389/fnins.2018.00049]

63 **Kim N**, Yun M, Oh YJ, Choi HJ. Mind-altering with the gut: Modulation of the gut-brain axis with probiotics. *J Microbiol* 2018; **56**: 172-182 [PMID: 29492874 DOI: 10.1007/s12275-018-8032-4]

64 **Qin Y**, Wade PA. Crosstalk between the microbiome and epigenome: messages from bugs. *J Biochem* 2018; **163**: 105-112 [PMID: 29161429 DOI: 10.1093/jb/mvx080]

65 **Bonfili L**, Cecarini V, Cuccioloni M, Angeletti M, Berardi S, Scarpona S, Rossi G, Eleuteri AM. SLAB51 Probiotic Formulation Activates SIRT1 Pathway Promoting Antioxidant and Neuroprotective Effects in an AD Mouse Model. *Mol Neurobiol* 2018; **55**: 7987-8000 [PMID: 29492848 DOI: 10.1007/s12035-018-0973-4]

66 **Agus A**, Planchais J, Sokol H. Gut Microbiota Regulation of Tryptophan Metabolism in Health and Disease. *Cell Host Microbe* 2018; **23**: 716-724 [PMID: 29902437 DOI: 10.1016/j.chom.2018.05.003]

67 **Birner A**, Platzer M, Bengesser SA, Dalkner N, Fellendorf FT, Queissner R, Pilz R, Rauch P, Maget A, Hamm C, Herzog-Eberhard S, Mangge H, Fuchs D, Moll N, Zelzer S, Schütze G, Schwarz M, Reininghaus B, Kapfhammer HP, Reininghaus EZ. Increased breakdown of kynurenine towards its neurotoxic branch in bipolar disorder. *PLoS One* 2017; **12**: e0172699 [PMID: 28241062 DOI: 10.1371/journal.pone.0172699]

68 **Bansal Y**, Singh R, Parhar I, Kuhad A, Soga T. Quinolinic Acid and Nuclear Factor Erythroid 2-

Related Factor 2 in Depression: Role in Neuroprogression. *Front Pharmacol* 2019; **10**: 452 [PMID: 31164818 DOI: 10.3389/fphar.2019.00452]

69 **Wong CB**, Tanaka A, Kuhara T, Xiao JZ. Potential Effects of Indole-3-Lactic Acid, a Metabolite of Human Bifidobacteria, on NGF-induced Neurite Outgrowth in PC12 Cells. *Microorganisms* 2020; **8** [PMID: 32178456 DOI: 10.3390/microorganisms8030398]

70 **Cuartero MI**, Ballesteros I, de la Parra J, Harkin AL, Abautret-Daly A, Sherwin E, Fernández-Salguero P, Corbí AL, Lizasoain I, Moro MA. L-kynurenine/aryl hydrocarbon receptor pathway mediates brain damage after experimental stroke. *Circulation* 2014; **130**: 2040-2051 [PMID: 25359166 DOI: 10.1161/CIRCULATIONAHA.114.011394]

71 **Rothhammer V**, Quintana FJ. The aryl hydrocarbon receptor: an environmental sensor integrating immune responses in health and disease. *Nat Rev Immunol* 2019; **19**: 184-197 [PMID: 30718831 DOI: 10.1038/s41577-019-0125-8]

72 **Takamura T**, Harama D, Fukumoto S, Nakamura Y, Shimokawa N, Ishimaru K, Ikegami S, Makino S, Kitamura M, Nakao A. Lactobacillus bulgaricus OLL1181 activates the aryl hydrocarbon receptor pathway and inhibits colitis. *Immunol Cell Biol* 2011; **89**: 817-822 [PMID: 21321579 DOI: 10.1038/icb.2010.165]

73 **Lamas B**, Hernandez-Galan L, Galipeau HJ, Constante M, Clarizio A, Jury J, Breyner NM, Caminero A, Rueda G, Hayes CL, McCarville JL, Bermudez Brito M, Planchais J, Rolhion N, Murray JA, Langella P, Loonen LMP, Wells JM, Bercik P, Sokol H, Verdu EF. Aryl hydrocarbon receptor ligand production by the gut microbiota is decreased in celiac disease leading to intestinal inflammation. *Sci Transl Med* 2020; **12** [PMID: 33087499 DOI: 10.1126/scitranslmed.aba0624]

74 **Liang S**, Wang T, Hu X, Luo J, Li W, Wu X, Duan Y, Jin F. Administration of Lactobacillus helveticus NS8 improves behavioral, cognitive, and biochemical aberrations caused by chronic restraint stress. *Neuroscience* 2015; **310**: 561-577 [PMID: 26408987 DOI: 10.1016/j.neuroscience.2015.09.033]

75 **Gu F**, Wu Y, Liu Y, Dou M, Jiang Y, Liang H. Lactobacillus casei improves depression-like behavior in chronic unpredictable mild stress-induced rats by the BDNF-TrkB signal pathway and the intestinal microbiota. *Food Funct* 2020; **11**: 6148-6157 [PMID: 32578646 DOI: 10.1039/d0fo00373e]

76 **Orlando A**, Chimienti G, Lezza AMS, Pesce V, Gigante I, D'Attoma B, Russo F. *Lactobacillus Rhamnosus* GG Affects the BDNF System in Brain Samples of Wistar Rats with Pepsin-Trypsin-Digested Gliadin (PTG)-Induced Enteropathy. *Nutrients* 2020; **12** [PMID: 32120967 DOI: 10.3390/nu12030629]

77 **McLoughlin RF**, Berthon BS, Jensen ME, Baines KJ, Wood LG. Short-chain fatty acids, prebiotics, synbiotics, and systemic inflammation: a systematic review and meta-analysis. *Am J Clin Nutr* 2017; **106**: 930-945 [PMID: 28793992 DOI: 10.3945/ajcn.117.156265]

78 **Silva YP**, Bernardi A, Frozza RL. The Role of Short-Chain Fatty Acids From Gut Microbiota in Gut-Brain Communication. *Front Endocrinol (Lausanne)* 2020; **11**: 25 [PMID: 32082260 DOI: 10.3389/fendo.2020.00025]

79 **Vendrik KEW**, Ooijevaar RE, de Jong PRC, Laman JD, van Oosten BW, van Hilten JJ, Ducarmon QR, Keller JJ, Kuijper EJ, Contarino MF. Fecal Microbiota Transplantation in Neurological Disorders. *Front Cell Infect Microbiol* 2020; **10**: 98 [PMID: 32266160 DOI: 10.3389/fcimb.2020.00098]

80 **D'Amato A**, Di Cesare Mannelli L, Lucarini E, Man AL, Le Gall G, Branca JJV, Ghelardini C, Amedei A, Bertelli E, Regoli M, Pacini A, Luciani G, Gallina P, Altera A, Narbad A, Gulisano M, Hoyles L, Vauzour D, Nicoletti C. Faecal microbiota transplant from aged donor mice affects spatial learning and memory *via* modulating hippocampal synaptic plasticity- and neurotransmission-related proteins in young recipients. *Microbiome* 2020; **8**: 140 [PMID: 33004079 DOI: 10.1186/s40168-020-00914-w]

81 **Sanders ME**, Akkermans LM, Haller D, Hammerman C, Heimbach J, Hörmannsperger G, Huys G, Levy DD, Lutgendorff F, Mack D, Phothirath P, Solano-Aguilar G, Vaughan E. Safety assessment of probiotics for human use. *Gut Microbes* 2010; **1**: 164-185 [PMID: 21327023 DOI: 10.4161/gmic.1.3.12127]

82 **Lerner A**, Shoenfeld Y, Matthias T. Probiotics: If It Does Not Help It Does Not Do Any Harm. Really? *Microorganisms* 2019; **7** [PMID: 30979072 DOI: 10.3390/microorganisms7040104]

83 **Zawistowska-Rojek A**, Tyski S. Are Probiotic Really Safe for Humans? *Pol J Microbiol* 2018; **67**: 251-258 [PMID: 30451441 DOI: 10.21307/pjm-2018-044]

84 **Sbahi H**, Di Palma JA. Faecal microbiota transplantation: applications and limitations in treating gastrointestinal disorders. *BMJ Open Gastroenterol* 2016; **3**: e000087 [PMID: 27239328 DOI: 10.1136/bmjgast-2016-000087]

85 **Gill HS**, Rutherfurd KJ, Cross ML. Dietary probiotic supplementation enhances natural killer cell activity in the elderly: an investigation of age-related immunological changes. *J Clin Immunol* 2001; **21**: 264-271 [PMID: 11506196 DOI: 10.1023/a:1010979225018]

86 **Snydman DR**. The safety of probiotics. *Clin Infect Dis* 2008; **46** Suppl 2: S104-11; discussion S144 [PMID: 18181712 DOI: 10.1086/523331]

87 **Wardill HR**, Secombe KR, Bryant RV, Hazenberg MD, Costello SP. Adjunctive fecal microbiota transplantation in supportive oncology: Emerging indications and considerations in immunocompromised patients. *EBioMedicine* 2019; **44**: 730-740 [PMID: 30940601 DOI: 10.1016/j.ebiom.2019.03.070]

88 **Merrick B**, Allen L, Masirah M Zain N, Forbes B, Shawcross DL, Goldenberg SD. Regulation, risk

and safety of Faecal Microbiota Transplant. *Infect Prev Pract* 2020; **2**: 100069 [PMID: 34316559 DOI: 10.1016/j.infpip.2020.100069]

World Journal of Gastroenterology

Submit a Manuscript: https://www.f6publishing.com

World J Gastroenterol 2021 October 21; 27(39): 6733-6736

DOI: 10.3748/wjg.v27.i39.6733

ISSN 1007-9327 (print) ISSN 2219-2840 (online)

LETTER TO THE EDITOR

Impact of COVID-19 pandemic on the neuropsychiatric status of Wilson's disease

Giuseppe Lanza, Massimiliano Godani, Raffaele Ferri, Alberto Raggi

ORCID number: Giuseppe Lanza 0000-0002-5659-662X; Massimiliano Godani 0000-0002-3268-0229; Raffaele Ferri 0000-0001-6937-3065; Alberto Raggi 0000-0001-9414-1995.

Author contributions: Lanza G designed the study; Godani M and Raggi A performed research; Ferri R analyzed the data; Lanza G and Godani M wrote the letter; Ferri R and Raggi A revised the letter.

Conflict-of-interest statement: Dr. Ferri R declared a personal Participation on a Data Safety Monitoring Board or Advisory Board for Jazz in the past 36 mo. Drs. Lanza G, Godani M, and Raggi A declared no conflict of interest.

Open-Access: This article is an open-access article that was selected by an in-house editor and fully peer-reviewed by external reviewers. It is distributed in accordance with the Creative Commons Attribution NonCommercial (CC BY-NC 4.0) license, which permits others to distribute, remix, adapt, build upon this work non-commercially, and license their derivative works on different terms, provided the original work is properly cited and the use is non-commercial. See: http://creativecommons.org/Licenses/by-nc/4.0/

Giuseppe Lanza, Department of Surgery and Medical-Surgical Specialties, University of Catania, Catania 95123, Italy

Giuseppe Lanza, Clinical Neurophysiology Research Unit, Oasi Research Institute-IRCCS, Troina 94018, Italy

Massimiliano Godani, Neurology Unit, Sant'Andrea Civic Hospital, La Spezia 19121, Italy

Raffaele Ferri, Department of Neurology IC, Sleep Research Center, Oasi Research Institute-IRCCS, Troina 94018, Italy

Alberto Raggi, Unit of Neurology, G.B. Morgagni - L. Pierantoni Hospital, Forlì 47121, Italy

Corresponding author: Giuseppe Lanza, MD, PhD, MSc, Senior Academic Research, Assistant Professor, Consultant Neurologist, Department of Surgery and Medical-Surgical Specialties, University of Catania, Via Santa Sofia 78, Catania 95123, Italy. Clinical Neurophysiology Research Unit, Oasi Research Institute-IRCCS, Via Conte Ruggero 73, Troina 94018, Italy glanza@oasi.en.it

Abstract

We have read with interest the Letter to the Editor by Drs. Zhuang and Zhong, who presented the clinical data of 68 patients with Wilson's disease (WD) who were admitted to the hospital before and during the coronavirus disease 2019 (COVID-19) pandemic, and appreciated their findings on hepatic and some extrahepatic manifestations. Nevertheless, given the strong impact of the pandemic on patients with neurological and psychiatric disorders, we would have expected a worsening of the psychiatric and/or neurological impairments in these patients. In contrast, according to the authors, these manifestations remained, somewhat unexpectedly, unchanged. This finding is in contrast with most of the current literature that highlights not only an increased incidence of mental health disorders in the general population but also an exacerbation of neurological and psychiatric symptoms in patients with chronic diseases, especially in those with pre-existing neuropsychiatric disorders, such as WD. Although the study was mainly focused on the hepatic features of WD patients taking anti-copper treatment, a generic and cumulative definition of neurological and psychiatric manifestations, as in this study, does not allow for further considerations. Future studies during and after the pandemic are necessary to clarify the real impact, either direct or indirect, of the COVID-19 pandemic on the neurological and psychiatric symptoms of WD patients.

Manuscript source: Unsolicited manuscript

Specialty type: Gastroenterology and hepatology

Country/Territory of origin: Italy

Peer-review report's scientific quality classification
Grade A (Excellent): 0
Grade B (Very good): 0
Grade C (Good): C
Grade D (Fair): 0
Grade E (Poor): E

Received: July 17, 2021
Peer-review started: July 17, 2021
First decision: August 9, 2021
Revised: August 11, 2021
Accepted: September 22, 2021
Article in press: September 22, 2021
Published online: October 21, 2021

P-Reviewer: Kumar A, Rodríguez CV
S-Editor: Gao CC
L-Editor: Filipodia
P-Editor: Li JH



Key Words: Wilson's disease; Extra-hepatic manifestations; Neuropsychiatric symptoms; COVID-19; Therapy; Resilience

©The Author(s) 2021. Published by Baishideng Publishing Group Inc. All rights reserved.

Core Tip: In the interesting letter by Drs. Zhuang and Zhong, the psychiatric and neurological manifestations of 68 patients with Wilson's disease who were treated with anti-copper therapy unexpectedly remained unchanged after the pandemic. Given the impact of the pandemic on patients with neurological and psychiatric disorders, a worsening in the severity or frequency of these manifestations could have been expected. The possible reasons underlying this finding, including the relatively small sample size, the effect of therapy, and the patients' resilience, are discussed.

Citation: Lanza G, Godani M, Ferri R, Raggi A. Impact of COVID-19 pandemic on the neuropsychiatric status of Wilson's disease. *World J Gastroenterol* 2021; 27(39): 6733-6736
URL: https://www.wjgnet.com/1007-9327/full/v27/i39/6733.htm
DOI: https://dx.doi.org/10.3748/wjg.v27.i39.6733

TO THE EDITOR

We have read with interest the Letter to the Editor by Zhuang and Zhong[1], who presented the clinical data of 68 patients with Wilson's disease (WD) who were admitted to the hospital before and during the coronavirus disease 2019 (COVID-19) pandemic in Guangzhou (China). Of note, none of the patients had COVID-19. As WD is a rare chronic systemic disease, the impact of the pandemic on the multiorgan clinical status of these patients is still unclear and, therefore, certainly worth investigating. Indeed, we have appreciated the findings that showed a marked shortage of medical resources for the clinical management of patients with WD during the pandemic, as well as the findings that patients who consistently took anti-copper medications showed no significant difference in hepatic and some extrahepatic features, although the incidence of their complications (especially those related to infections) significantly increased. For these reasons, we fully support the authors' recommendations to strictly adhere to the anti-copper therapy and closely monitor these patients to prevent complications[1].

However, given the strong psychological and socio-behavioral impacts of the pandemic on the clinical symptoms of different neuropsychiatric disorders[2,3], a worsening, or at least an increase in the frequency or severity, of psychiatric and/or neurological manifestations in WD patients could have been expected. Conversely, according to the authors, before the COVID-19 pandemic, 50 out of the 68 patients had neurological involvement, and three had psychiatric manifestations, which remained, somewhat unexpectedly, unchanged after the pandemic (49 and 4 out of the 68 patients, respectively)[1]. Although this study was mainly focused on the hepatic features of WD, only a generic and cumulative definition of neurological and psychiatric manifestations was adopted without additional specifications (*e.g.*, type, onset, severity, and duration), which did not allow for any further considerations; indeed, these apparently negative results were not discussed. Moreover, it was not specified how neurological and psychiatric manifestations were evaluated (*e.g.*, were specific scales used?), both at the study entry and at the end of the study. A more detailed stratification, for instance, by type of manifestation (such as cognitive or motor deficits, among the neurological aspects, and anxiety or mood disorders, among the psychiatric conditions), would have likely disclosed additional findings.

In this context, COVID-19, being the major infectious outbreak in the 21st century, has led to an unprecedented global hazard to mental health. A recent systematic review[4] on the impact of the pandemic on mental health in the general population found significantly higher rates of symptoms of anxiety (6.3%-50.9%), depression (14.6%-48.3%), post-traumatic stress disorder (7.0%-53.8%), psychological distress (34.4%-38.0%), and stress in general (8.1%-81.9%) in several countries worldwide, including China. Although a certain degree of heterogeneity was noted across the studies, the risk factors associated with these manifestations included, among others, a

younger age (≤ 40 years) and comorbid chronic or neuropsychiatric illnesses[4], such as WD.

On the other hand, the negative effect of the COVID-19 outbreak on mental health and health care services has been and will likely continue to be significant because of the unpredictability and uncertainty of the pandemic, the associated lockdowns, physical distancing, and other containment strategies, and the resulting economic breakdown[5]. Reasonably, as also observed in the Letter discussed here[1], the impact of the COVID-19 pandemic on the utilization of health care services, in terms of outpatient visits, hospital admissions, diagnostic exams, and therapeutic interventions, decreased by approximately one-third during the pandemic, with considerable variations and greater reductions among people with less severe illness[6]. Throughout the pandemic and even still, there has also been evidence of increased levels of relapse, in people with pre-existing mental health conditions and even in people with no previous history of a mental health disorder[7]. In particular, patients with pre-existing anxiety, depression, panic, delirium, psychosis, and suicidality appear to be extremely vulnerable[8].

Nevertheless, the matter is still debated, since it has also been observed that some individuals with severe mental illnesses, such as schizophrenia and affective disorders, may not report a worsening of symptoms, thus appearing to be resilient to the negative effects of the pandemic[9]. However, frequent assessments and periodic follow-up are needed to determine whether this resilience will persist as the pandemic progresses or after its end. In this context, in addition to the relatively small sample size, the potential effect of anti-copper therapy in this cohort, and the fact that none of the patients were affected by COVID-19, the patients' resilience might also represent a possible reason that supports the findings reported by Zhuang and Zhong[1]. However, their patients did not seem to be affected by severe psychopathologies, thus making this possibility less likely to justify the authors' conclusions. Moreover, although WD is a rare pathology, it is worth mentioning some methodological issues in the study[1] that may be appropriate and relevant for discussion. In particular, the relatively small sample size, the fact that not all patients were admitted to the hospital during the pandemic, and the possibility of the patients' resilience raise crucial questions that need to be addressed in the near future. Further multicenter prospective cohort studies, retrospective studies, and case-control studies on inpatients and outpatients with WD, both before and after anti-copper treatment, should be performed.

Less is known about the effects of the COVID-19 pandemic on neurological disorders, although a recent systematic review concluded that patients with pre-existing conditions (including those characterized by cognitive impairments or parkinsonism, which may be part of the clinical spectrum of WD) can develop exacerbation of their neurological symptoms, thus encouraging clinicians to be aware of this risk and to focus on its prevention and early management[10]. In this context, it is known that concomitant infections, especially infections of the respiratory and urinary tracts (such as those reported in the letter[1]), frequently worsen the symptoms and the course of several neurological diseases, including parkinsonism and dementia[11,12]. Therefore, the fact that the increased infection incidence detected in the study[1] did not induce an even transient worsening of the patients' clinical status remains to be explained or at least briefly commented on.

In conclusion, the study by Zhuang and Zhong[1] provides a valid clinical basis for the proper management of WD patients during the pandemic, thus representing an advance in this field of clinical and research interest. However, further independent multicenter studies during and after the pandemic are necessary to clarify the real impact, either direct (*i.e.*, infected patients) or indirect (*i.e.*, psychological and sociobehavioral consequences), of the COVID-19 pandemic on the neurological and psychiatric symptoms of WD.

REFERENCES

1 **Zhuang YP**, Zhong HJ. Impact of COVID-19 on the clinical status of patients with Wilson disease. *World J Gastroenterol* 2021; **27**: 4248-4251 [PMID: 34326624 DOI: 10.3748/wjg.v27.i26.4248]

2 **Fisicaro F**, Di Napoli M, Liberto A, Fanella M, Di Stasio F, Pennisi M, Bella R, Lanza G, Mansueto G. Neurological Sequelae in Patients with COVID-19: A Histopathological Perspective. *Int J Environ Res Public Health* 2021; **18** [PMID: 33546463 DOI: 10.3390/ijerph18041415]

3 **Pennisi M**, Lanza G, Cantone M, Ricceri R, Ferri R, D'Agate CC, Pennisi G, Di Lazzaro V, Bella R. Cortical involvement in celiac disease before and after long-term gluten-free diet: A Transcranial Magnetic Stimulation study. *PLoS One* 2017; **12**: e0177560 [PMID: 28489931 DOI:

10.1371/journal.pone.0177560]
4 **Xiong J**, Lipsitz O, Nasri F, Lui LMW, Gill H, Phan L, Chen-Li D, Iacobucci M, Ho R, Majeed A, McIntyre RS. Impact of COVID-19 pandemic on mental health in the general population: A systematic review. *J Affect Disord* 2020; **277**: 55-64 [PMID: 32799105 DOI: 10.1016/j.jad.2020.08.001]
5 **Moreno C**, Wykes T, Galderisi S, Nordentoft M, Crossley N, Jones N, Cannon M, Correll CU, Byrne L, Carr S, Chen EYH, Gorwood P, Johnson S, Kärkkäinen H, Krystal JH, Lee J, Lieberman J, López-Jaramillo C, Männikkö M, Phillips MR, Uchida H, Vieta E, Vita A, Arango C. How mental health care should change as a consequence of the COVID-19 pandemic. *Lancet Psychiatry* 2020; **7**: 813-824 [PMID: 32682460 DOI: 10.1016/S2215-0366(20)30307-2]
6 **Moynihan R**, Sanders S, Michaleff ZA, Scott AM, Clark J, To EJ, Jones M, Kitchener E, Fox M, Johansson M, Lang E, Duggan A, Scott I, Albarqouni L. Impact of COVID-19 pandemic on utilisation of healthcare services: a systematic review. *BMJ Open* 2021; **11**: e045343 [PMID: 33727273 DOI: 10.1136/bmjopen-2020-045343]
7 **Gavin B**, Lyne J, McNicholas F. Mental health and the COVID-19 pandemic: looking back and moving forward. *Ir J Psychol Med* 2020; **37**: 247-249 [PMID: 33323135 DOI: 10.1017/ipm.2020.128]
8 **Tsamakis K**, Tsiptsios D, Ouranidis A, Mueller C, Schizas D, Terniotis C, Nikolakakis N, Tyros G, Kympouropoulos S, Lazaris A, Spandidos DA, Smyrnis N, Rizos E. COVID-19 and its consequences on mental health (Review). *Exp Ther Med* 2021; **21**: 244 [PMID: 33603852 DOI: 10.3892/etm.2021.9675]
9 **Pinkham AE**, Ackerman RA, Depp CA, Harvey PD, Moore RC. A Longitudinal Investigation of the Effects of the COVID-19 Pandemic on the Mental Health of Individuals with Pre-existing Severe Mental Illnesses. *Psychiatry Res* 2020; **294**: 113493 [PMID: 33038789 DOI: 10.1016/j.psychres.2020.113493]
10 **Kubota T**, Kuroda N. Exacerbation of neurological symptoms and COVID-19 severity in patients with preexisting neurological disorders and COVID-19: A systematic review. *Clin Neurol Neurosurg* 2021; **200**: 106349 [PMID: 33172719 DOI: 10.1016/j.clineuro.2020.106349]
11 **Lanza G**, Ferri R. The neurophysiology of hyperarousal in restless legs syndrome: Hints for a role of glutamate/GABA. *Adv Pharmacol* 2019; **84**: 101-119 [PMID: 31229167 DOI: 10.1016/bs.apha.2018.12.002]
12 **Deleidi M**, Isacson O. Viral and inflammatory triggers of neurodegenerative diseases. *Sci Transl Med* 2012; **4**: 121ps3 [PMID: 22344685 DOI: 10.1126/scitranslmed.3003492]

Published by **Baishideng Publishing Group Inc**
7041 Koll Center Parkway, Suite 160, Pleasanton, CA 94566, USA
Telephone: +1-925-3991568
E-mail: bpgoffice@wjgnet.com
Help Desk: https://www.f6publishing.com/helpdesk
https://www.wjgnet.com

© 2021 Baishideng Publishing Group Inc. All rights reserved.

ISSN 1007-9327 (print)
ISSN 2219-2840 (online)

World Journal of *Gastroenterology*

World J Gastroenterol 2021 October 28; 27(40): 6737-7004



Published by Baishideng Publishing Group Inc

World Journal of Gastroenterology

Contents

Weekly Volume 27 Number 40 October 28, 2021

FRONTIER

6737 Hepatocellular carcinoma risk after viral response in hepatitis C virus-advanced fibrosis: Who to screen and for how long?

Ahumada A, Rayón L, Usón C, Bañares R, Alonso Lopez S

OPINION REVIEW

6750 Higher doses of ascorbic acid may have the potential to promote nutrient delivery *via* intestinal paracellular absorption

Sequeira IR

EVIDENCE REVIEW

6757 Venous and arterial thromboembolism in patients with inflammatory bowel diseases

Stadnicki A, Stadnicka I

REVIEW

6775 Understanding the immune response and the current landscape of immunotherapy in pancreatic cancer

Ostios-Garcia L, Villamayor J, Garcia-Lorenzo E, Vinal D, Feliu J

6794 Artificial intelligence in gastroenterology: A state-of-the-art review

Kröner PT, Engels MM, Glicksberg BS, Johnson KW, Mzaik O, van Hooft JE, Wallace MB, El-Serag HB, Krittanawong C

MINIREVIEWS

6825 Emerging artificial intelligence applications in liver magnetic resonance imaging

Hill CE, Biasiolli L, Robson MD, Grau V, Pavlides M

6844 Role of human nucleoside transporters in pancreatic cancer and chemoresistance

Carter CJ, Mekkawy AH, Morris DL

6861 Management of hepatitis B and C in special population

Kulkarni AV, Duvvuru NR

6874 Endoscopic ultrasound-guided vascular interventions: Current insights and emerging techniques

Mann R, Goyal H, Perisetti A, Chandan S, Inamdar S, Tharian B

World Journal of Gastroenterology

Weekly Volume 27 Number 40 October 28, 2021

Contents

ORIGINAL ARTICLE

Basic Study

6888 Metabolomics of *Fuzi-Gancao* in CCl_4 induced acute liver injury and its regulatory effect on bile acid profile in rats

Wang MF, Zhao SS, Thapa DM, Song YL, Xiang Z

6908 Transforming growth factor beta-1 upregulates glucose transporter 1 and glycolysis through canonical and noncanonical pathways in hepatic stellate cells

Zhou MY, Cheng ML, Huang T, Hu RH, Zou GL, Li H, Zhang BF, Zhu JJ, Liu YM, Liu Y, Zhao XK

Retrospective Cohort Study

6927 Serum hepatitis B core-related antigen as a surrogate marker of hepatitis B e antigen seroconversion in chronic hepatitis B

Chi XM, Wang XM, Wang ZF, Wu RH, Gao XZ, Xu HQ, Ding YH, Niu JQ

6939 Long-term follow-up of liver alveolar echinococcosis using echinococcosis multilocularis ultrasound classification

Schuhbaur J, Schweizer M, Philipp J, Schmidberger J, Schlingeloff P, Kratzer W

Observational Study

6951 Hepatic and gastrointestinal disturbances in Egyptian patients infected with coronavirus disease 2019: A multicentre cohort study

Shousha HI, Afify S, Maher R, Asem N, Fouad E, Mostafa EF, Medhat MA, Abdalazeem A, Elmorsy H, Aziz MM, Mohammed RS, Ibrahem M, Elgarem H, Omran D, Hassany M, Elsayed B, Abdelaziz AY, El Kassas M

6967 Factors affecting anxiety, depression, and self-care ability in patients who have undergone liver transplantation

Akbulut S, Ozer A, Saritas H, Yilmaz S

META-ANALYSIS

6985 Prophylactic transcatheter arterial embolization reduces rebleeding in non-variceal upper gastrointestinal bleeding: A meta-analysis

Boros E, Sipos Z, Hegyi P, Teutsch B, Frim L, Váncsa S, Kiss S, Dembrovszky F, Oštarijaš E, Shawyer A, Erőss B

LETTER TO THE EDITOR

7000 Gastrointestinal and hepatic involvement during COVID-19 pandemic: A focus on pediatric population and possible future implications

Sica R, Pennoni S, Penta L, Riccioni S, Di Cara G, Verrotti A

World Journal of Gastroenterology

Weekly Volume 27 Number 40 October 28, 2021

Contents

ABOUT COVER

Editorial Board Member of *World Journal of Gastroenterology*, Pietro Fusaroli, MD, Associate Professor, Chief, Gastrointestinal Unit, University of Bologna at the Hospital of Imola, Via Montericco 4, Imola 40026, Italy. pietro.fusaroli@unibo.it

AIMS AND SCOPE

The primary aim of *World Journal of Gastroenterology* (*WJG*, *World J Gastroenterol*) is to provide scholars and readers from various fields of gastroenterology and hepatology with a platform to publish high-quality basic and clinical research articles and communicate their research findings online. *WJG* mainly publishes articles reporting research results and findings obtained in the field of gastroenterology and hepatology and covering a wide range of topics including gastroenterology, hepatology, gastrointestinal endoscopy, gastrointestinal surgery, gastrointestinal oncology, and pediatric gastroenterology.

INDEXING/ABSTRACTING

The *WJG* is now indexed in Current Contents®/Clinical Medicine, Science Citation Index Expanded (also known as SciSearch®), Journal Citation Reports®, Index Medicus, MEDLINE, PubMed, PubMed Central, and Scopus. The 2021 edition of Journal Citation Report® cites the 2020 impact factor (IF) for *WJG* as 5.742; Journal Citation Indicator: 0.79; IF without journal self cites: 5.590; 5-year IF: 5.044; Ranking: 28 among 92 journals in gastroenterology and hepatology; and Quartile category: Q2. The *WJG*'s CiteScore for 2020 is 6.9 and Scopus CiteScore rank 2020: Gastroenterology is 19/136.

RESPONSIBLE EDITORS FOR THIS ISSUE

Production Editor: *Jia-Hui Li*; **Production Department Director:** *Yu-Jie Ma*; **Editorial Office Director:** *Ze-Mao Gong*.

NAME OF JOURNAL
World Journal of Gastroenterology

ISSN
ISSN 1007-9327 (print) ISSN 2219-2840 (online)

LAUNCH DATE
October 1, 1995

FREQUENCY
Weekly

EDITORS-IN-CHIEF
Andrzej S Tarnawski, Subrata Ghosh

EDITORIAL BOARD MEMBERS
http://www.wjgnet.com/1007-9327/editorialboard.htm

PUBLICATION DATE
October 28, 2021

COPYRIGHT
© 2021 Baishideng Publishing Group Inc

INSTRUCTIONS TO AUTHORS
https://www.wjgnet.com/bpg/gerinfo/204

GUIDELINES FOR ETHICS DOCUMENTS
https://www.wjgnet.com/bpg/GerInfo/287

GUIDELINES FOR NON-NATIVE SPEAKERS OF ENGLISH
https://www.wjgnet.com/bpg/gerinfo/240

PUBLICATION ETHICS
https://www.wjgnet.com/bpg/GerInfo/288

PUBLICATION MISCONDUCT
https://www.wjgnet.com/bpg/gerinfo/208

ARTICLE PROCESSING CHARGE
https://www.wjgnet.com/bpg/gerinfo/242

STEPS FOR SUBMITTING MANUSCRIPTS
https://www.wjgnet.com/bpg/GerInfo/239

ONLINE SUBMISSION
https://www.f6publishing.com

© 2021 Baishideng Publishing Group Inc. All rights reserved. 7041 Koll Center Parkway, Suite 160, Pleasanton, CA 94566, USA
E-mail: bpgoffice@wjgnet.com https://www.wjgnet.com

World Journal of Gastroenterology

Submit a Manuscript: https://www.f6publishing.com

World J Gastroenterol 2021 October 28; 27(40): 6737-6749

DOI: 10.3748/wjg.v27.i40.6737

ISSN 1007-9327 (print) ISSN 2219-2840 (online)

FRONTIER

Hepatocellular carcinoma risk after viral response in hepatitis C virus-advanced fibrosis: Who to screen and for how long?

Adriana Ahumada, Laura Rayón, Clara Usón, Rafael Bañares, Sonia Alonso Lopez

ORCID number: Adriana Ahumada 0000000329653016; Laura Rayón 0000-0002-0240-1858; Clara Usón 0000-0002-7896-4278; Rafael Bañares 0000-0002-0412-8437; Sonia Alonso Lopez 0000000276270846.

Author contributions: Ahumada A, Bañares R and Alonso López S have been involved in conception and drafting the article; Bañares R and Alonso López S have made critical revisions related to important intellectual content of the manuscript; Rayón L and Usón C have been involved in acquisition of data and drafting the article; Ahumada A, Rayón L, Usón C, Bañares R and Alonso López S have read and approved the final manuscript.

Conflict-of-interest statement: Adriana Ahumada has received fees for serving as a speaker and a grant from Abbvie and personal fees for serving as a speaker and for Gilead. Laura Rayón, Clara Usó n and Rafael Bañares have nothing to disclose. Sonia Alonso has received fees for serving as a speaker and consultant from Abbvie and Gilead.

Open-Access: This article is an open-access article that was selected by an in-house editor and fully peer-reviewed by external reviewers. It is distributed in accordance with the Creative

Adriana Ahumada, Laura Rayón, Clara Usón, Rafael Bañares, Sonia Alonso Lopez, Liver Unit, Hospital General Universitario Gregorio Marañón, Madrid 28007, Spain

Adriana Ahumada, Rafael Bañares, Sonia Alonso Lopez, Liver Unit, Instituto de Investigación Sanitaria Gregorio Marañón (IiSGM), Madrid 28007, Spain

Rafael Bañares, Medicine, Universidad Complutense de Madrid, Madrid 28006, Spain

Rafael Bañares, Sonia Alonso Lopez, Centro de Investigación Biomédica En Red de Enfermedades Hepáticas y Digestivas (CIBERehd), Instituto de Salud Carlos III, Madrid 28029, Spain

Corresponding author: Sonia Alonso Lopez, MD, PhD, Attending Doctor, Consultant Physician-Scientist, Doctor, Senior Researcher, Liver Unit, Hospital General Universitario Gregorio Marañón, Doctor Esquerdo 46, Madrid 28007, Spain. salonsol@telefonica.net

Abstract

Hepatitis C virus (HCV) chronic infection is associated with fibrosis progression, end-stage liver complications and HCC. Not surprisingly, HCV infection is a leading cause of liver-related morbidity and mortality worldwide. After sustained virological response (SVR), the risk of developing hepatocellular carcinoma is not completely eliminated in patients with established cirrhosis or with advanced fibrosis. Therefore, lifelong surveillance is currently recommended. This strategy is likely not universally cost-effective and harmless, considering that not all patients with advanced fibrosis have the same risk of developing HCC. Factors related to the severity of liver disease and its potential to improve after SVR, the molecular and epigenetic changes that occur during infection and other associated comorbidities might account for different risk levels and are likely essential for identifying patients who would benefit from screening programs after SVR. Efforts to develop predictive models and risk calculators, biomarkers and genetic panels and even deep learning models to estimate the individual risk of HCC have been made in the direct-acting antiviral agents era, when thousands of patients with advanced fibrosis and cirrhosis have reached SVR. These tools could help to identify patients with very low HCC risk in whom surveillance might not be justified. In this review, factors affecting the probability of HCC development after SVR, the benefits and risks of surveillance, suggested strategies to estimate individualized HCC risk and the current evidence to recommend lifelong surveillance are discussed.

Commons Attribution NonCommercial (CC BY-NC 4.0) license, which permits others to distribute, remix, adapt, build upon this work non-commercially, and license their derivative works on different terms, provided the original work is properly cited and the use is non-commercial. See: http://creativecommons.org/Licenses/by-nc/4.0/

Manuscript source: Invited manuscript

Specialty type: Gastroenterology and hepatology

Country/Territory of origin: Spain

Peer-review report's scientific quality classification
Grade A (Excellent): 0
Grade B (Very good): B
Grade C (Good): 0
Grade D (Fair): 0
Grade E (Poor): 0

Received: April 11, 2021
Peer-review started: April 11, 2021
First decision: June 13, 2021
Revised: June 24, 2021
Accepted: September 19, 2021
Article in press: September 19, 2021
Published online: October 28, 2021

P-Reviewer: Djuric O
S-Editor: Wang LL
L-Editor: A
P-Editor: Yu HG



Key Words: Hepatitis C virus; Hepatocellular carcinoma; Liver fibrosis; Surveillance; Sustained virologic response; Epigenetic changes; Predictive models; Cost-effectiveness

©The Author(s) 2021. Published by Baishideng Publishing Group Inc. All rights reserved.

Core Tip: Hepatocellular carcinoma (HCC) risk is reduced after sustained viral response, but a substantial threat persists over time. Understanding the natural history of hepatitis C virus infection and the variable influence of viral eradication in the molecular and epigenetic changes that occur during infection are essential to explain the different risk of developing HCC in patients with advanced fibrosis. The definition of the appropriate tools to estimate the individual risk of HCC after antiviral treatment providing reliable recommendations about HCC surveillance is probably the most important challenge to be clarified in this field.

Citation: Ahumada A, Rayón L, Usón C, Bañares R, Alonso Lopez S. Hepatocellular carcinoma risk after viral response in hepatitis C virus-advanced fibrosis: Who to screen and for how long? *World J Gastroenterol* 2021; 27(40): 6737-6749
URL: https://www.wjgnet.com/1007-9327/full/v27/i40/6737.htm
DOI: https://dx.doi.org/10.3748/wjg.v27.i40.6737

INTRODUCTION

Hepatitis C virus (HCV) chronic infection is a major cause of liver-related morbidity and mortality worldwide. Direct-acting antiviral agents (DAAs) have definitely changed the natural history of the disease by reducing liver-related complications in patients with advanced liver fibrosis (including those with cirrhosis) and improving the survival rate. Nonetheless, the risk of developing hepatocellular carcinoma is not completely eliminated with viral clearance. Not surprisingly, clinical guidelines still recommend life-long ultrasound surveillance in all patients with advanced fibrosis (F3) and cirrhosis (F4)[1,2].

However, the risk of HCC occurrence is not homogenous within the spectrum of compensated advanced chronic liver disease (c-ACLD). Therefore, surveillance strategies might not be cost-effective or harmless in all patients. Thus, the identification of patients who truly benefit from screening programs and for how long is a matter of debate.

HCC risk factors are associated with the severity of liver disease and the degree of improvement after sustained virological response but also with the presence of other comorbidities and preneoplastic changes induced by HCV. All of them are discussed in this review, as well as their predictive capacity to estimate individualized HCC risk. We also discuss the current evidence to recommend surveillance.

FACTORS AFFECTING HCC OCCURRENCE IN HCV PATIENTS

A combination of different factors, occurring either before or after SVR, is involved in the risk of HCC associated with HCV chronic infection (Figure 1).

Development of fibrosis during HCV infection

Chronic HCV infection typically causes damage and inflammation in the liver parenchyma, which can be followed by fibrosis deposition of different severities. Fibrogenesis is a dynamic process characterized by the synthesis of extracellular matrix (ECM), composed of a mixed complex of glycoproteins (collagen, elastin, fibronectin, laminin) and proteoglycans organized in a three-dimensional network[3]. Therefore, fibrosis is a physiological mechanism that can become pathological when viral infection and chronic hepatocellular injury persist[4].

In chronic hepatitis, including hepatitis C, active fibrosis begins around the portal areas (periportal or zone 1 fibrosis) and gradually extends out into the lobules toward the central veins (zone 3), with septum formation and then bridging fibrosis[5]. The

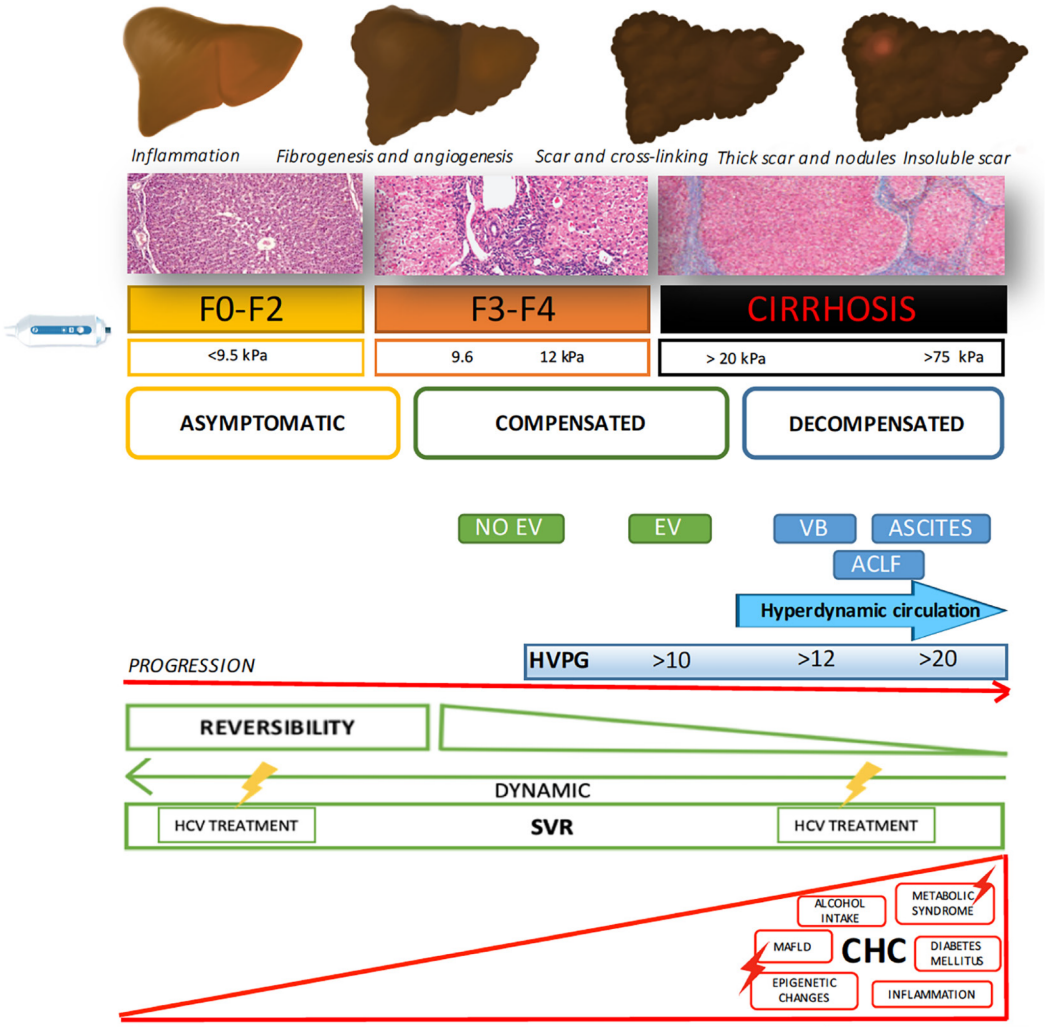


Figure 1 Factors involved in increasing or decreasing hepatocellular carcinoma risk, either before or after sustained virologic response. EV: Esophageal varices; VB: Variceal bleeding; ACLF: Acute on chronic liver failure; PH: Portal hypertension; SVR: Sustained virologic response; HCC: Hepatocellular carcinoma; MAFLD: Metabolic associated fatty liver disease.

final stage of this process constitutes cirrhosis, in which extensive fibrosis linking portal and central areas and nodular regeneration of the liver parenchyma appear. Collagen and matrix proteins are largely produced by activated hepatic stellate cells (HSCs). In contrast, activated liver sinusoidal endothelial cells (LSECs) contribute to ECM production, including the synthesis of basement membrane components, leading to perisinusoidal fibrosis. They also produce cytokines that activate HSCs and secrete factors that contribute to intrahepatic vasoconstriction and to portal hypertension in cirrhosis[6]. It has been widely demonstrated that the severity of liver fibrosis and the development of cirrhosis are the most important risk factors for HCC[7-9]. Therefore, the earlier that this process is discontinued by means of SVR, the lower that the likelihood is of HCC occurrence.

Epigenetic changes involved in hepatitis C infection

Cirrhosis of all causes can be complicated by the appearance of liver tumors, but the risk is higher in patients with chronic liver disease of a viral etiology[7]. In 2018, a large cohort study aimed to compare HCC risk according to the etiology of liver disease and showed that patients with HCV-related cirrhosis had a 3-fold increased HCC risk compared to ALD or NAFLD-related cirrhosis, suggesting that hepatitis C virus itself might have a direct carcinogenic effect[10].

HCV is an RNA virus with limited potential for integration into the host genome and therefore requires continuous replication to maintain chronic infection. HCV directly contributes to hepatocarcinogenesis, interrupting the signal transduction pathways that affect cell survival, proliferation, and transformation *via* HCV protein or RNA and indirectly by inducing chronic inflammation[8,11].

Epigenetic regulation is an indispensable process for the normal development and preservation of tissue-specific gene expression profiles. Thus, any perturbation of the epigenetic landscape can lead to shifted gene function and malignant cellular transformation. The changed epigenome of HCC is characterized by gene-specific hypermethylation or hypomethylation, global genomic hypomethylation, abnormal expression of DNA methyltransferases and histone modifying enzymes, altered histone modification patterns, and aberrant expression of microRNAs, which can affect the expression of oncogenes, tumor suppressor genes and other tumor-related genes altering the cancer development pathways over time[12]. In fact, a recent study showed a clear, positive correlation between epigenetic changes and fibrosis stages in HCV chronic infection[13], which persist after SVR.

Reversibility of liver fibrosis

Effective antiviral treatment has proved to change the natural history of HCV-related liver disease, reducing the risk of liver events and HCC, even in patients with advanced liver disease and cirrhosis. A recent meta-analysis[14] showed a significant absolute risk reduction in HCC after SVR, which was even greater in patients with cirrhosis (22%; 95%CI: 13-31) than in patients with any stage of fibrosis (6.7%; 95%CI: 5-8). It has been suggested that regression of fibrosis is one of the key mechanisms. In contrast to what was previously believed, there is currently substantial evidence indicating that the removal of fibrosis, hepatocyte repopulation and microvasculature remodeling occur after SVR following several cellular processes[15,16]. Mechanisms of the resolution of liver fibrosis involve senescence and apoptosis of activated HSCs/myofibroblasts caused by deprivation of fibrogenic cytokines. Reversal of these cells to an inactive phenotype during liver fibrosis regression[6,15] has also been described. However, regression of liver disease depends on the severity of fibrosis before antiviral therapy, with total regression being more likely in patients with mild/moderate fibrosis than in those with established cirrhosis due to the presence of a stronger cross-linking matrix, which is more difficult to remove by methaloproteases. Furthermore, the presence of architectural distortion with vascular shunts also contributes to the persistence of architectural changes[17-21]. However, the "point of no return" is controversial. A Canadian study[16] examined explants of patients with cirrhosis or precirrhosis who underwent transplantation, in which the causative agent of the liver disease was controlled or had been removed. The authors found that regression involves two main processes: removal of fibrosis and repopulation of scarred regions with hepatocytes, concluding that reversibility is possible in all stages of fibrosis, including precirrhotic stages and even macronodular cirrhosis. Interestingly, "sinusoidal capillarization" was considered the "point of no return". Moreover, advanced stages of cirrhosis with thicker septa and smaller micronodules are associated with the presence of clinically significant portal hypertension and therefore with a lower likelihood of reversibility[20].

An Italian study including patients with cirrhosis with paired biopsies after achieving SVR with PEGINF/RBV showed that, in more than half of the patients, regression of cirrhosis was observed during follow-up. Patients who did not change their METAVIR scores after SVR also presented a decrease in the amount of collagen fibers, coinciding with the transformation of micronodular cirrhosis into a macronodular form or incomplete septal cirrhosis[21]. Finally, a Spanish study published in 2018 evaluated the regression of fibrosis using paired biopsies in 112 patients with posttransplant recurrence of HCV infection after treatment with DAAs [22]. Fibrosis regression occurred in 72-85% of the patients without liver cirrhosis (F1-F3) and in 43% of the patients with cirrhosis. Interestingly, in this study, more than 50% of the cirrhotic patients had a history of decompensation, suggesting that patients with liver cirrhosis without clinically significant portal hypertension are more likely to have improved liver injury, likely decreasing the risk of developing HCC after SVR.

Therefore, among patients with advanced fibrosis and cirrhosis, the risk of HCC seems to be lower in patients with less severe disease, who are in fact those who benefit the most after SVR.

One important issue is how to assess fibrosis regression since liver biopsy is an invasive procedure, does not distinguish early from advanced stages of cirrhosis and cannot be performed repeatedly after SVR. Not surprisingly, noninvasive elastographic and direct or indirect serological markers have been widely used to assess fibrosis regression[23]. However, in regressed cirrhosis, macronodules and aberrant vasculature with capillarization of the sinusoids can persist despite a decrease in liver stiffness assessed by TE. The study from D' Ambrosio *et al*[24] revealed that, after 61 mo of follow-up, 38% of patients with biopsy-proven F4 had liver stiffness < 12 kPa, resulting in low predictive power of TE to diagnose cirrhosis after viral

eradication. Thus, a combination of TE and serological noninvasive markers might improve the capacity to assess fibrosis regression.

Inflammation and liver cancer

Another factor specifically affecting HCC risk during HCV chronic infection is the presence of inflammation. Various types of cancer arise in the setting of chronic inflammation, indicating a strong link between inflammation and cancer. It has been estimated that approximately 15% of all human cancers are associated with inflammation and chronic infections[25]. During chronic viral hepatitis, host immune responses to HBV or HCV are often not sufficiently strong to completely eradicate the infection, inducing persistent stimulation of antigen-specific immune responses. Host immune cells are known to destroy virus-infected liver cells, resulting in the production of different cytokines and growth factors, consequently inducing compensatory regeneration of hepatocytes. The persistent cycle of hepatocyte necroinflammation and regeneration has a synergistic effect with the severity of liver fibrosis and cirrhosis, promoting architectural distortion and portal hypertension with reduced sinusoidal perfusion favoring hypoxia, which is the substrate for the formation of hypervascular tumors. These factors increase the risk of genetic changes in hepatocytes, promoting the survival and expansion of the initiated cells and leading to dysregulated hepatocyte proliferation, which contributes to the development and progression of liver cancer. Furthermore, oxidative stress accelerates hepatocarcinogenesis through several mechanisms, including transcription and activation of cytokines and growth factors, oxidative DNA damage, DNA methylation, and hepatocyte injury[26-30]. Therefore, HCC risk is expected to decrease after eradicating infection and the subsequent decrease in inflammation mechanisms.

HCC RISK CAN PERSIST AFTER SUSTAINED VIROLOGICAL RESPONSE

Although SVR is associated with a reduction in some of the HCC pathogenetic factors mentioned above, there are many other contributors to HCC occurrence that can persist after viral eradication, related either to the stage of liver disease (*e.g.*, Child B, portal hypertension, low platelet count) or to the presence of comorbidities, such as diabetes, alcohol consumption, smoking and older age[31-34].

A recent publication suggested that regression of liver damage after SVR can last for years, with HCC risk persisting during this period; in other patients, liver injury is not reversed due to advanced cirrhosis stage, or it progresses because of the coexistence of other factors, such as obesity, diabetes, and alcohol intake[35]. In addition, older age contributes, even years after SVR, to the progression of liver fibrosis and to an increased risk of HCC.

Epigenetic memory is another of the possible mechanisms involved in HCC risk persistence after SVR. As mentioned above, HCV infection induces epigenetic alterations. DAA treatment eliminates the virus inside cells, but it is not able to restore the concomitant epigenetic signatures already produced and associated with the risk of HCC. Available data suggest that, when infection has already induced epigenetic changes, gene expression is conserved in cells; therefore, the presence of the virus is no longer necessary to exert oncogenic effects on host cells, producing what is known as epigenetic memory or persistent epigenetic changes[13,36].

HCC SURVEILLANCE AFTER SVR: CURRENT RECOMMENDATIONS

Current guidelines from EASL[1] and AASLD[37] agree regarding the recommendation of hepatocellular carcinoma surveillance after SVR in all patients with cirrhosis. However, EASL recommends indefinite HCC screening in patients with advanced fibrosis (F3) by ultrasound every six months, whereas AASLD does not. These differences are likely related to controversy regarding the risk of developing HCC in F3 patients due to the heterogeneity of this population, which could include misclassified patients (over- or underestimating the severity of fibrosis).

ACCURACY IN THE DIAGNOSIS OF ADVANCED FIBROSIS AND CIRRHOSIS

Considering that advanced fibrosis and especially cirrhosis are the main factors contributing to HCC risk, an accurate diagnosis prior to antiviral therapy is mandatory to predict individual risk after SVR. Liver biopsy remains the gold standard for the assessment of hepatic fibrosis, although noninvasive methods for estimating liver fibrosis are increasingly used. However, the accuracy of fibrosis staging in the noninvasive assessment era is imperfect -- even more so after sustained virological response. This fact is especially important in patients with advanced fibrosis but without cirrhosis, in which liver stiffness measurements (LSMs) can occasionally overestimate fibrosis, especially when marked inflammation is present[38]. Another problem is the definition of F3 stage by LSM, with cutoffs varying from 9.5 kPa to 14.5 kPa according to Castera's[39] study or up to 12.5 kPa as Ziol *et al*[40] suggested. Therefore, a substantial proportion of patients might be misclassified, overestimating or underestimating fibrosis and leading to an indefinite link to medical care or, alternatively, mistaken discharge. Thus, other clinical or serological markers should be available to accurately define the severity of compensated advanced liver disease and the remaining HCC risk after SVR.

COST-EFFECTIVENESS, BENEFITS AND RISKS OF HCC SURVEILLANCE

HCC surveillance aims to prolong patient survival and quality of life by improving early diagnosis and curative therapy. Based on estimated tumor doubling times, current guidelines recommend ultrasound every six months, and they establish an incidence of at least 1.5% per year to justify HCC surveillance. Although this threshold is likely too high due to the clinical benefits induced by DAA after SVR and the improvement in HCC therapies, it is not clear whether HCC surveillance remains cost effective in all patients with advanced fibrosis after SVR. Regarding this point, a study suggested that HCC surveillance is unlikely to be cost effective in patients with F3 fibrosis, whereas both annual and biannual modalities are likely to be cost effective for patients with cirrhosis compared with no surveillance[41]. The study suggested that an annual HCC incidence greater than 0.5% might be currently cost-effective, and it proved that both an APRI greater than 2 or an FIB-4 greater than 3.25 allow for the identification of patients for whom HCC surveillance becomes cost effective, suggesting that patients with values less than these thresholds should be discharged from follow-up evaluation. Another study evaluated the cost-effectiveness of risk-stratified HCC screening in cirrhosis based on a combination of biomarkers and clinical variables, including epidermal growth factor single-nucleotide polymorphism, age, sex, smoking status, alkaline phosphatase level, and platelet count. The study showed that HCC surveillance strategies targeting high- and intermediate-risk patients with cirrhosis are cost-effective. Finally, the authors suggested that omitting screening in the lowest-risk subjects was cost-effective compared with biannual screening, without sacrificing net survival benefit[42].

Moreover, in a recent opinion article, Jepsen *et al*[43] argued that randomized trials of HCC surveillance *vs* no surveillance are necessary to make formal recommendations involving thousands of patients. The authors made their arguments indicating that universal surveillance could negatively impact patients' quality of life by generating anxiety about the possibility of a cancer diagnosis. Furthermore, the problems associated with false positives in screening procedures and the need to be connected for life to hospital care in patients with negligible HCC risk are also matters of concern. Therefore, accurate models including predictive factors to identify different risk levels are likely the key to adequate follow-up of patients after SVR.

PREDICTIVE FACTORS OF HCC RISK

Multiple models including clinical, serological, molecular and elastographic variables have attempted to stratify HCC risk in patients with advanced fibrosis. Importantly, there are controversies about the markers that should be used and when they should be measured, considering the dynamic changes that occur after SVR. Table 1 summarizes some studies that have assessed the risk of HCC according to both baseline and dynamic risk factors.

Table 1 Studies assessing the risk of hepatocellular carcinoma according to baseline and dynamic risk factors

Ref.	Country	*n*	Population at risk	Diagnosis of cirrhosis	Treatment regimens	Baseline risk factors	Dynamic risk factors
Lleo *et al*[33], 2019	Italy	1766	All cirrhosis 11.4% Child B/C	1 or more of the following: Stage 4 fibrosis by METAVIR score, esophageal and/or gastric varices at endoscopy, LSM > 12.5 kPa	All were treated with DAA	Age > 50 years old and presence of esophageal varices, platelets < 110000/L and LSM > 25 kPa	Lack of SVR
Ioannou *et al* [44], 2018	United States	45810	23% cirrhosis	Clinical, based on ICD-9 or 10 codes for cirrhosis or its complications	Either IFN or DAA	Cirrhosis, SVR, ALT, AST, platelets, albumin, age	
Ioannou *et al* [45], 2019	United States	48135	9784 with pretreatment cirrhosis	Clinical, based on ICD-9 or 10 codes for cirrhosis or its complications	Either IFN or DAA	Cirrhosis and FIB-4 ≥ 3.25 before treatment	FIB-4 ≥ 3.25 post-SVR
Ravaioli *et al* [47], 2018	Italy	139	All cirrhosis; Included previous HCC 11.5% Child B		All were treated with DAA	History of previous HCC	Child B and LSM reduction after DAA treatment < 30%
Pons *et al*[48], 2019	Spain	572	All LSM ≥ 10 kPa; All compensated	cACLD defined by LSM ≥ 10 kPa	All were treated with DAA	High risk: baseline albumin < 4 g/dL; Low risk: Baseline albumin ≥ 4 g/dL	High risk: LSM ≥ 20 kPa or LSM 10-20 kPa and albumin < 4.4 g/dL; Low risk: LSM < 10 kPa or LSM 10-20 kPa and albumin ≥ 4.4 g/dL
Fan *et al*[50], 2020	China	3566	75.3% cirrhosis compensated and decompensated	Histological and/or radiological	Either IFN or DAA	aMAP score; Low risk: 0-50; Intermediate risk: 50-60; High risk: 60-100	
Alonso *et al* [49], 2020	Spain	993	Advanced fibrosis or compensated cirrhosis	Clinical or histological; advanced fibrosis defined by a LSM by TE > 9.5 Kpa	All were treated with DAA	Albumin < 4.2 g/dL; LSM > 17,3 kPaFIB-4 > 3.7	Delta LSM < 25.5%; FIB-4 > 3.3; GGT > 42 IU
Ioannou *et al* [62], 2020	United States	48151	All cirrhosis compensated and decompensated	Clinical, based on ICD-9 or 10 codes for cirrhosis or its complications	Either IFN or DAA	Deep learning RNN model Cirrhosis diagnosis, sex, race and HCV genotype 3	Development of cirrhosis, SVR, BMI, AST, ALT, bilirubin, FIB-4, APRI, platelets

LSM: Liver stiffness measurement; TE: Transient elastography; INF: Interferon, DAA: Direct-acting antiviral agent; HCV: Hepatitis C virus; SVR: Sustained virologic response; FIB-4: Fibrosis 4; HCC: Hepatocellular carcinoma; c-ACLD: Compensated advanced chronic liver disease; CP: Child-Pugh; FU: Follow-up; amap: age, male, ALBI and platelets; GGT: Gamma-glutamyltransferase; RNN: Recurrent neural networks; APRI: AST to platelet ratio index; ALT: Alanine aminotransferase; AST: Aspartate aminotransferase; BMI: Body mass index.

The study by Ioannou *et al*[44] introduced the need for risk modeling, suggesting that screening strategies based on HCC risk models were superior to "screen-all" or "screen-none" strategies. The proposed HCC risk model, which included the presence of cirrhosis, SVR, baseline ALT, AST, platelets, albumin and age, allowed us to calculate the individual risk of HCC. However, the definition of cirrhosis was made based on the presence of portal hypertension signs and/or clinical complications, suggesting that perhaps patients with advanced fibrosis or with early stages of cirrhosis could be misclassified as not having cirrhosis.

In a further study, the authors used a different evaluation of liver disease severity, introducing not only baseline data but also changes in FIB-4 over time, to assess

different HCC risk levels. In this second study, the authors showed that patients in whom FIB-4 was less than 3.25 before treatment and after SVR had a lower risk of HCC[45].

Other predictive models have included different combinations of laboratory and elastographic parameters. A study from Italy[33] aimed to evaluate the risk of HCC occurrence and recurrence in cirrhotic patients after DAA therapy. The authors identified a subgroup of patients with SVR and the "Extended Baveno Criteria"[46] (> 110000 platelets and LSM < 25 kPa), with an HCC incidence of 0.5%/per year, suggesting that the Baveno Criteria could be an appropriate tool for stratification, advising less frequent follow-up in this population.

Models that include dynamic changes after SVR could be especially relevant since they can identify patients with less severe disease more likely to regress or improve after SVR. The dynamic change in LSM as an HCC risk factor was previously described in a study showing that a reduction in liver stiffness > 30% at the end of treatment was associated with a significantly lower risk of HCC at one year after EOT [47]. In this study, TE was likely performed too early to detect regression or improvement, although it could identify those patients with overestimated fibrosis at baseline, in whom the resolution of inflammatory activity accounts for the rapid decrease in liver stiffness.

A Spanish study developed a model to estimate HCC risk in patients with c-ACLD after SVR. This study revealed that the combination of follow-up LSM and serum albumin levels at one year after SVR was able to identify different HCC risk groups. The authors observed that patients with LSM < 10 kPa or with LSM between 10-20 kPa and high albumin levels at follow-up had an incidence rate of HCC of less than 1/100 patients per year; thus, the authors considered them a low-risk group[48].

Furthermore, a recent large, multicenter cohort study performed in our unit[49] confirmed the impact of both baseline and dynamic changes in noninvasive markers on the risk of HCC development. We constructed two simple models: the first one included baseline albumin (g/dL) and LSM (Kpa) and the percentage of LSM variation one year after EOT. Patients with baseline albumin > 4.2 g/dL, baseline LSM ≤ 17.3 kPa, and 1-year DeltaLSM > 25.5% had the lowest HCC risk (cumulative incidence of HCC at 3 years of 0%). Considering that LSM might not be universally available, we also built a second model that exclusively included noninvasive serological markers. Similarly, the FIB-4-based model identified patients with baseline albumin > 4.2 g/dL, baseline FIB-4 ≤ 3.7, 1-year FIB-4 score ≤ 3.3, and 1-year GGT ≤ 42 IU/mL as the group with the lowest HCC risk (cumulative incidence of 0.4% at 3 years). Notably, our results suggested that baseline and dynamic LSM (or FIB-4, when TE is not available) could identify patients with a lower incidence of HCC after SVR that does not justify continuous HCC screening. Approximately 20% of the patients were considered to have low or very low HCC risk, and according to our findings, they could be safely discharged from surveillance.

Another recently validated predictive model is the aMAP score[50], which includes laboratory and clinical parameters such as the albumin-bilirubin score (ALBI score) platelets, age and sex. The score identifies two different risk groups, suggesting that only patients belonging to the high-risk group (aMAP score > 60) should undergo intensive surveillance to detect early HCC. This prognostic tool was externally validated in patients with different cirrhosis etiologies from 11 global prospective studies; interestingly, the score properly discriminated 5-year HCC irrespective of etiology of liver disease and ethnicity.

Thus, predictive models and risk scores, preferably based on baseline data and dynamic changes, are likely the best approach for determining the individual risk of HCC after SVR.

LONG-TERM RISK OF HCC: DOES IT DECREASE OVER TIME?

Different long-term studies in HCV patients treated with IFN-based regimens have documented a reduction in the incidence of HCC by 75% in patients with SVR[51-53]. Currently, there is growing evidence that the same occurs after DAA therapy. Several data have shown that SVR after DAAs does not have a significant impact on the development of HCC in the short or medium term since many of the patients were treated with a more advanced disease, it but reduces the risk of HCC in the medium and long term, like what occurs in patients treated with IFN-based regimens[9].

Conversely, it has been suggested that HCC risk persists for up to 10 years after HCV eradication in patients with baseline cirrhosis or high FIB-4 scores[45]. In this

study, HCC incidence remained > 2% per year even 10 years after antiviral treatment in patients with a high baseline FIB-4 ≥ 3.25, especially if it remained ≥ 3.25 after SVR. Conversely, patients with baseline FIB-4 < 3.25 had an HCC incidence < 1%.

Moreover, aging and comorbidities that can occur or progress over time could have an additive effect on HCC risk. Consequently, there is no strong evidence to support a dynamic assessment of HCC risk over time, and the best strategy is likely to continue screening patients with intermediate and high HCC risk until they reach an age when it is no longer cost effective.

HCC SCREENING: WHO DOES BENEFIT AND FOR HOW LONG?

It seems clear that the current recommendations regarding HCC screening after SVR in HCV patients with advanced fibrosis at baseline should be modified in the future. While changes become formal, we provide below a proposal based on the current data (Figure 2).

Cirrhotic patients with baseline decompensated or compensated advanced liver disease with significant portal hypertension. HCC risk in this population remains greater than the accepted threshold for surveillance; therefore, biannual US screening is recommended.

Patients with findings of advanced chronic liver disease without clear evidence of baseline portal hypertension. In our opinion, these patients should be screened for HCC at least 1 year after EOT to evaluate early dynamic changes and make more accurate estimations of the individual HCC risk.

FUTURE STRATEGIES IN SURVEILLANCE

As previously stated, several questions remain concerning surveillance strategies. Most likely, the most important concern is that we do not have accurate information about whether HCC risk persists constantly over the long term and therefore for how long patients with medium or high risk should continue HCC surveillance.

It is possible that, in the near future, patients will benefit from a more specific biomarker panel, genetic and molecular profiles and even deep learning models to predict the risk of developing HCC.

Circulating biomarkers are promising tools for better stratification of patients[54-56]. Biomarker panels, such as the GALAD score, are excellent tools for the detection of early-stage HCC, including tumors with negative AFP (AUC of 0.96 for detection of early-stage HCC)[57,58]. As previously exposed, HCV induces epigenetic alterations persisting after DAA cure[13], so the opportunity to detect epigenetic changes of histones bound to circulating DNA in plasma represents a new opportunity to uncover biomarkers of HCC risk. These approaches could represent personalized, noninvasive and cost-effective alternatives based on clinical and biological findings for HCC screening.

The use of deep learning models, which have also been successfully applied in other settings to predict clinical events[59], could also be relevant. Various types of model architectures, such as recurrent neural networks, have been used to capture temporal dynamics and long-term information over time[60]. Recently, it was suggested that some machine-learning algorithms accurately stratify the risk of HCC in patients with cirrhosis, identifying those at high risk for developing HCC[61]. Additionally, it has been shown that, in terms of cost-effectiveness, deep learning and recurrent neural network models were able to improve HCC surveillance strategies in HCV patients, thereby identifying high-risk cases[62].

CONCLUSION

In conclusion, HCC surveillance in HCV patients should likely be based on an evaluation of individualized risk rather than exclusively based on baseline fibrosis stage. Currently available risk scores should be improved and validated, likely by including novel approaches, such as personalized biomarkers and deep learning methods.

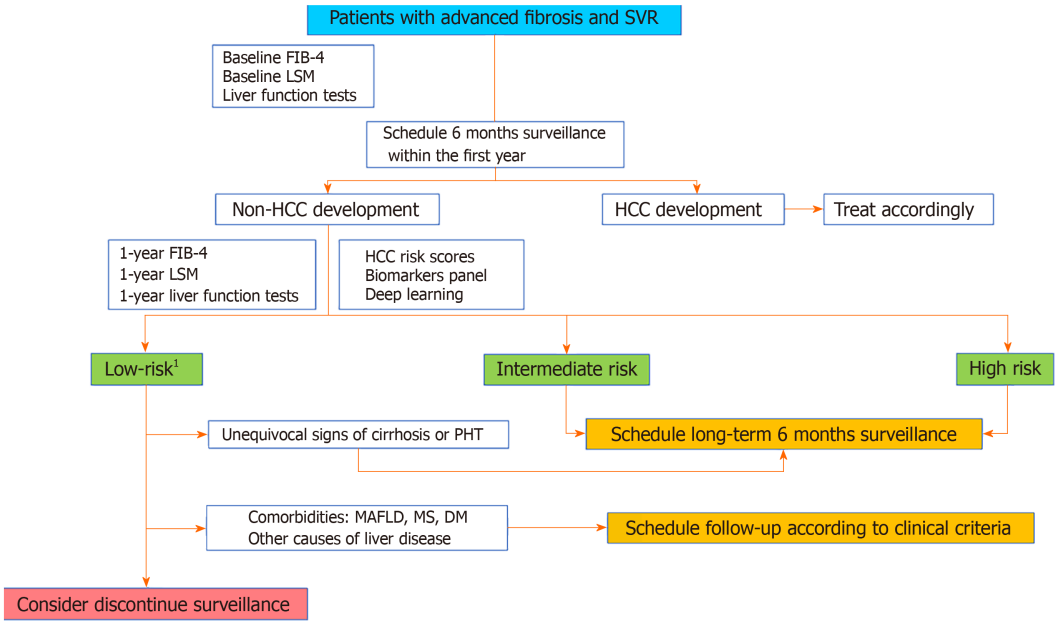


Figure 2 Surveillance hepatocellular carcinoma algorithm proposed. [1]Most likely, annual incidence < 0.5% per year. FIB-4: Fibrosis 4; LSM: Liver stiffness measurement; TE: Transient elastography; PHT: Portal hypertension; DM: Diabetes mellitus; MS: Metabolic syndrome; MAFLD: Metabolic associated fatty liver disease.

REFERENCES

1 **European Association for the Study of the Liver**. EASL Recommendations on Treatment of Hepatitis C 2018. *J Hepatol* 2018; **69**: 461-511 [PMID: 29650333 DOI: 10.1016/j.jhep.2018.03.026]

2 **Singal AG**, Lim JK, Kanwal F. AGA Clinical Practice Update on Interaction Between Oral Direct-Acting Antivirals for Chronic Hepatitis C Infection and Hepatocellular Carcinoma: Expert Review. *Gastroenterology* 2019; **156**: 2149-2157 [PMID: 30878469 DOI: 10.1053/j.gastro.2019.02.046]

3 **Schuppan D**, Ruehl M, Somasundaram R, Hahn EG. Matrix as a modulator of hepatic fibrogenesis. *Semin Liver Dis* 2001; **21**: 351-372 [PMID: 11586465 DOI: 10.1055/s-2001-17556]

4 **Marcellin P**, Asselah T, Boyer N. Fibrosis and disease progression in hepatitis C. *Hepatology* 2002; **36**: S47-S56 [PMID: 12407576 DOI: 10.1053/jhep.2002.36993]

5 **Goodman ZD**, Ishak KG. Histopathology of hepatitis C virus infection. *Semin Liver Dis* 1995; **15**: 70-81 [PMID: 7597446 DOI: 10.1055/s-2007-1007264]

6 **Jung YK**, Yim HJ. Reversal of liver cirrhosis: current evidence and expectations. *Korean J Intern Med* 2017; **32**: 213-228 [PMID: 28171717 DOI: 10.3904/kjim.2016.268]

7 **European Association for the Study of the Liver**. EASL Clinical Practice Guidelines: Management of hepatocellular carcinoma. *J Hepatol* 2018; **69**: 182-236 [PMID: 29628281 DOI: 10.1016/j.jhep.2018.03.019]

8 **Bandiera S**, Billie Bian C, Hoshida Y, Baumert TF, Zeisel MB. Chronic hepatitis C virus infection and pathogenesis of hepatocellular carcinoma. *Curr Opin Virol* 2016; **20**: 99-105 [PMID: 27741441 DOI: 10.1016/j.coviro.2016.09.010]

9 **Rinaldi L**, Nevola R, Franci G, Perrella A, Corvino G, Marrone A, Berretta M, Morone MV, Galdiero M, Giordano M, Adinolfi LE, Sasso FC. Risk of Hepatocellular Carcinoma after HCV Clearance by Direct-Acting Antivirals Treatment Predictive Factors and Role of Epigenetics. *Cancers (Basel)* 2020; **12** [PMID: 32466400 DOI: 10.3390/cancers12061351]

10 **Ioannou GN**, Green P, Lowy E, Mun EJ, Berry K. Differences in hepatocellular carcinoma risk, predictors and trends over time according to etiology of cirrhosis. *PLoS One* 2018; **13**: e0204412 [PMID: 30260995 DOI: 10.1371/journal.pone.0204412]

11 **Hoshida Y**, Villanueva A, Sangiovanni A, Sole M, Hur C, Andersson KL, Chung RT, Gould J, Kojima K, Gupta S, Taylor B, Crenshaw A, Gabriel S, Minguez B, Iavarone M, Friedman SL, Colombo M, Llovet JM, Golub TR. Prognostic gene expression signature for patients with hepatitis C-related early-stage cirrhosis. *Gastroenterology* 2013; **144**: 1024-1030 [PMID: 23333348 DOI: 10.1053/j.gastro.2013.01.021]

12 **Zhang Y**. Detection of epigenetic aberrations in the development of hepatocellular carcinoma. *Methods Mol Biol* 2015; **1238**: 709-731 [PMID: 25421688 DOI: 10.1007/978-1-4939-1804-1_37]

13 **Hamdane N**, Jühling F, Crouchet E, El Saghire H, Thumann C, Oudot MA, Bandiera S, Saviano A, Ponsolles C, Roca Suarez AA, Li S, Fujiwara N, Ono A, Davidson I, Bardeesy N, Schmidl C, Bock C, Schuster C, Lupberger J, Habersetzer F, Doffoël M, Piardi T, Sommacale D, Imamura M, Uchida T, Ohdan H, Aikata H, Chayama K, Boldanova T, Pessaux P, Fuchs BC, Hoshida Y, Zeisel MB, Duong FHT, Baumert TF. HCV-Induced Epigenetic Changes Associated With Liver Cancer Risk Persist

After Sustained Virologic Response. *Gastroenterology* 2019; **156**: 2313-2329.e7 [PMID: 30836093 DOI: 10.1053/j.gastro.2019.02.038]

14 **Messori A**, Badiani B, Trippoli S. Achieving Sustained Virological Response in Hepatitis C Reduces the Long-Term Risk of Hepatocellular Carcinoma: An Updated Meta-Analysis Employing Relative and Absolute Outcome Measures. *Clin Drug Investig* 2015; **35**: 843-850 [PMID: 26446006 DOI: 10.1007/s40261-015-0338-y]

15 **Sun M**, Kisseleva T. Reversibility of liver fibrosis. *Clin Res Hepatol Gastroenterol* 2015; **39** Suppl 1: S60-S63 [PMID: 26206574 DOI: 10.1016/j.clinre.2015.06.015]

16 **Wanless IR**, Nakashima E, Sherman M. Regression of human cirrhosis. Morphologic features and the genesis of incomplete septal cirrhosis. *Arch Pathol Lab Med* 2000; **124**: 1599-1607 [PMID: 11079009 DOI: 10.1043/0003-9985(2000)124<1599:ROHC>2.0.CO;2]

17 **Shiratori Y**, Imazeki F, Moriyama M, Yano M, Arakawa Y, Yokosuka O, Kuroki T, Nishiguchi S, Sata M, Yamada G, Fujiyama S, Yoshida H, Omata M. Histologic improvement of fibrosis in patients with hepatitis C who have sustained response to interferon therapy. *Ann Intern Med* 2000; **132**: 517-524 [PMID: 10744587 DOI: 10.7326/0003-4819-132-7-200004040-00002]

18 **Poynard T**, McHutchison J, Manns M, Trepo C, Lindsay K, Goodman Z, Ling MH, Albrecht J. Impact of pegylated interferon alfa-2b and ribavirin on liver fibrosis in patients with chronic hepatitis C. *Gastroenterology* 2002; **122**: 1303-1313 [PMID: 11984517 DOI: 10.1053/gast.2002.33023]

19 **Romero-Gómez M**, Del Mar Viloria M, Andrade RJ, Salmerón J, Diago M, Fernández-Rodríguez CM, Corpas R, Cruz M, Grande L, Vázquez L, Muñoz-De-Rueda P, López-Serrano P, Gila A, Gutiérrez ML, Pérez C, Ruiz-Extremera A, Suárez E, Castillo J. Insulin resistance impairs sustained response rate to peginterferon plus ribavirin in chronic hepatitis C patients. *Gastroenterology* 2005; **128**: 636-641 [PMID: 15765399 DOI: 10.1053/j.gastro.2004.12.049]

20 **Nagula S**, Jain D, Groszmann RJ, Garcia-Tsao G. Histological-hemodynamic correlation in cirrhosis-a histological classification of the severity of cirrhosis. *J Hepatol* 2006; **44**: 111-117 [PMID: 16274836 DOI: 10.1016/j.jhep.2005.07.036]

21 **D'Ambrosio R**, Aghemo A, Rumi MG, Ronchi G, Donato MF, Paradis V, Colombo M, Bedossa P. A morphometric and immunohistochemical study to assess the benefit of a sustained virological response in hepatitis C virus patients with cirrhosis. *Hepatology* 2012; **56**: 532-543 [PMID: 22271347 DOI: 10.1002/hep.25606]

22 **Mauro E**, Crespo G, Montironi C, Londoño MC, Hernández-Gea V, Ruiz P, Sastre L, Lombardo J, Mariño Z, Díaz A, Colmenero J, Rimola A, Garcia-Pagán JC, Brunet M, Forns X, Navasa M. Portal pressure and liver stiffness measurements in the prediction of fibrosis regression after sustained virological response in recurrent hepatitis C. *Hepatology* 2018; **67**: 1683-1694 [PMID: 28960366 DOI: 10.1002/hep.29557]

23 **Poynard T**, Moussalli J, Munteanu M, Thabut D, Lebray P, Rudler M, Ngo Y, Thibault V, Mkada H, Charlotte F, Bismut FI, Deckmyn O, Benhamou Y, Valantin MA, Ratziu V, Katlama C; FibroFrance-GHPS group. Slow regression of liver fibrosis presumed by repeated biomarkers after virological cure in patients with chronic hepatitis C. *J Hepatol* 2013; **59**: 675-683 [PMID: 23712051 DOI: 10.1016/j.jhep.2013.05.015]

24 **D'Ambrosio R**, Aghemo A, Fraquelli M, Rumi MG, Donato MF, Paradis V, Bedossa P, Colombo M. The diagnostic accuracy of Fibroscan for cirrhosis is influenced by liver morphometry in HCV patients with a sustained virological response. *J Hepatol* 2013; **59**: 251-256 [PMID: 23528378 DOI: 10.1016/j.jhep.2013.03.013]

25 **Coussens LM**, Werb Z. Inflammation and cancer. *Nature* 2002; **420**: 860-867 [PMID: 12490959 DOI: 10.1038/nature01322]

26 **Wang YH**, Huang JH, Tian ZF, Zhou YF, Yang J. The role of CXC cytokines as biomarkers and potential targets in hepatocellular carcinoma. *Math Biosci Eng* 2019; **17**: 1381-1395 [PMID: 32233584 DOI: 10.3934/mbe.2020070]

27 **Nakagawa H**, Maeda S. Inflammation- and stress-related signaling pathways in hepatocarcinogenesis. *World J Gastroenterol* 2012; **18**: 4071-4081 [PMID: 22919237 DOI: 10.3748/wjg.v18.i31.4071]

28 **Marra M**, Sordelli IM, Lombardi A, Lamberti M, Tarantino L, Giudice A, Stiuso P, Abbruzzese A, Sperlongano R, Accardo M, Agresti M, Caraglia M, Sperlongano P. Molecular targets and oxidative stress biomarkers in hepatocellular carcinoma: an overview. *J Transl Med* 2011; **9**: 171 [PMID: 21985599 DOI: 10.1186/1479-5876-9-171]

29 **Bishayee A**. The role of inflammation and liver cancer. *Adv Exp Med Biol* 2014; **816**: 401-435 [PMID: 24818732 DOI: 10.1007/978-3-0348-0837-8_16]

30 **Morse MA**, Sun W, Kim R, He AR, Abada PB, Mynderse M, Finn RS. The Role of Angiogenesis in Hepatocellular Carcinoma. *Clin Cancer Res* 2019; **25**: 912-920 [PMID: 30274981 DOI: 10.1158/1078-0432.CCR-18-1254]

31 **Poynard T**, Bedossa P, Opolon P. Natural history of liver fibrosis progression in patients with chronic hepatitis C. The OBSVIRC, METAVIR, CLINIVIR, and DOSVIRC groups. *Lancet* 1997; **349**: 825-832 [PMID: 9121257 DOI: 10.1016/S0140-6736(96)07642-8]

32 **Finkelmeier F**, Dultz G, Peiffer KH, Kronenberger B, Krauss F, Zeuzem S, Sarrazin C, Vermehren J, Waidmann O. Risk of de novo Hepatocellular Carcinoma after HCV Treatment with Direct-Acting Antivirals. *Liver Cancer* 2018; **7**: 190-204 [PMID: 29888208 DOI: 10.1159/000486812]

33 **Lleo A**, Aglitti A, Aghemo A, Maisonneuve P, Bruno S, Persico M; collaborators. Predictors of hepatocellular carcinoma in HCV cirrhotic patients treated with direct acting antivirals. *Dig Liver Dis*

2019; **51**: 310-317 [PMID: 30473220 DOI: 10.1016/j.dld.2018.10.014]

34 **van der Meer AJ**, Feld JJ, Hofer H, Almasio PL, Calvaruso V, Fernández-Rodríguez CM, Aleman S, Ganne-Carrié N, D'Ambrosio R, Pol S, Trapero-Marugan M, Maan R, Moreno-Otero R, Mallet V, Hultcrantz R, Weiland O, Rutter K, Di Marco V, Alonso S, Bruno S, Colombo M, de Knegt RJ, Veldt BJ, Hansen BE, Janssen HLA. Risk of cirrhosis-related complications in patients with advanced fibrosis following hepatitis C virus eradication. *J Hepatol* 2017; **66**: 485-493 [PMID: 27780714 DOI: 10.1016/j.jhep.2016.10.017]

35 **Ioannou GN**. HCC surveillance after SVR in patients with F3/F4 fibrosis. *J Hepatol* 2021; **74**: 458-465 [PMID: 33303216 DOI: 10.1016/j.jhep.2020.10.016]

36 **Perez S**, Kaspi A, Domovitz T, Davidovich A, Lavi-Itzkovitz A, Meirson T, Alison Holmes J, Dai CY, Huang CF, Chung RT, Nimer A, El-Osta A, Yaari G, Stemmer SM, Yu ML, Haviv I, Gal-Tanamy M. Hepatitis C virus leaves an epigenetic signature post cure of infection by direct-acting antivirals. *PLoS Genet* 2019; **15**: e1008181 [PMID: 31216276 DOI: 10.1371/journal.pgen.1008181]

37 **Ghany MG**, Morgan TR; AASLD-IDSA Hepatitis C Guidance Panel. Hepatitis C Guidance 2019 Update: American Association for the Study of Liver Diseases-Infectious Diseases Society of America Recommendations for Testing, Managing, and Treating Hepatitis C Virus Infection. *Hepatology* 2020; **71**: 686-721 [PMID: 31816111 DOI: 10.1002/hep.31060]

38 **Coco B**, Oliveri F, Maina AM, Ciccorossi P, Sacco R, Colombatto P, Bonino F, Brunetto MR. Transient elastography: a new surrogate marker of liver fibrosis influenced by major changes of transaminases. *J Viral Hepat* 2007; **14**: 360-369 [PMID: 17439526 DOI: 10.1111/j.1365-2893.2006.00811.x]

39 **Castéra L**, Vergniol J, Foucher J, Le Bail B, Chanteloup E, Haaser M, Darriet M, Couzigou P, De Lédinghen V. Prospective comparison of transient elastography, Fibrotest, APRI, and liver biopsy for the assessment of fibrosis in chronic hepatitis C. *Gastroenterology* 2005; **128**: 343-350 [PMID: 15685546 DOI: 10.1053/j.gastro.2004.11.018]

40 **Ziol M**, Handra-Luca A, Kettaneh A, Christidis C, Mal F, Kazemi F, de Lédinghen V, Marcellin P, Dhumeaux D, Trinchet JC, Beaugrand M. Noninvasive assessment of liver fibrosis by measurement of stiffness in patients with chronic hepatitis C. *Hepatology* 2005; **41**: 48-54 [PMID: 15690481 DOI: 10.1002/hep.20506]

41 **Farhang Zangneh H**, Wong WWL, Sander B, Bell CM, Mumtaz K, Kowgier M, van der Meer AJ, Cleary SP, Janssen HLA, Chan KKW, Feld JJ. Cost Effectiveness of Hepatocellular Carcinoma Surveillance After a Sustained Virologic Response to Therapy in Patients With Hepatitis C Virus Infection and Advanced Fibrosis. *Clin Gastroenterol Hepatol* 2019; **17**: 1840-1849.e16 [PMID: 30580095 DOI: 10.1016/j.cgh.2018.12.018]

42 **Goossens N**, Singal AG, King LY, Andersson KL, Fuchs BC, Besa C, Taouli B, Chung RT, Hoshida Y. Cost-Effectiveness of Risk Score-Stratified Hepatocellular Carcinoma Screening in Patients with Cirrhosis. *Clin Transl Gastroenterol* 2017; **8**: e101 [PMID: 28640287 DOI: 10.1038/ctg.2017.26]

43 **Jepsen P**, West J. We need stronger evidence for (or against) hepatocellular carcinoma surveillance. *J Hepatol* 2021; **74**: 1234-1239 [PMID: 33465402 DOI: 10.1016/j.jhep.2020.12.029]

44 **Ioannou GN**, Green PK, Beste LA, Mun EJ, Kerr KF, Berry K. Development of models estimating the risk of hepatocellular carcinoma after antiviral treatment for hepatitis C. *J Hepatol* 2018; **69**: 1088-1098 [PMID: 30138686 DOI: 10.1016/j.jhep.2018.07.024]

45 **Ioannou GN**, Beste LA, Green PK, Singal AG, Tapper EB, Waljee AK, Sterling RK, Feld JJ, Kaplan DE, Taddei TH, Berry K. Increased Risk for Hepatocellular Carcinoma Persists Up to 10 Years After HCV Eradication in Patients With Baseline Cirrhosis or High FIB-4 Scores. *Gastroenterology* 2019; **157**: 1264-1278.e4 [PMID: 31356807 DOI: 10.1053/j.gastro.2019.07.033]

46 **Augustin S**, Pons M, Maurice JB, Bureau C, Stefanescu H, Ney M, Blasco H, Procopet B, Tsochatzis E, Westbrook RH, Bosch J, Berzigotti A, Abraldes JG, Genescà J. Expanding the Baveno VI criteria for the screening of varices in patients with compensated advanced chronic liver disease. *Hepatology* 2017; **66**: 1980-1988 [PMID: 28696510 DOI: 10.1002/hep.29363]

47 **Ravaioli F**, Conti F, Brillanti S, Andreone P, Mazzella G, Buonfiglioli F, Serio I, Verrucchi G, Bacchi Reggiani ML, Colli A, Marasco G, Colecchia A, Festi D. Hepatocellular carcinoma risk assessment by the measurement of liver stiffness variations in HCV cirrhotics treated with direct acting antivirals. *Dig Liver Dis* 2018; **50**: 573-579 [PMID: 29567413 DOI: 10.1016/j.dld.2018.02.010]

48 **Pons M**, Rodríguez-Tajes S, Esteban JI, Mariño Z, Vargas V, Lens S, Buti M, Augustin S, Forns X, Mínguez B, Genescà J. Non-invasive prediction of liver-related events in patients with HCV-associated compensated advanced chronic liver disease after oral antivirals. *J Hepatol* 2020; **72**: 472-480 [PMID: 31629779 DOI: 10.1016/j.jhep.2019.10.005]

49 **Alonso López S**, Manzano ML, Gea F, Gutiérrez ML, Ahumada AM, Devesa MJ, Olveira A, Polo BA, Márquez L, Fernández I, Cobo JCR, Rayón L, Riado D, Izquierdo S, Usón C, Real Y, Rincón D, Fernández-Rodríguez CM, Bañares R. A Model Based on Noninvasive Markers Predicts Very Low Hepatocellular Carcinoma Risk After Viral Response in Hepatitis C Virus-Advanced Fibrosis. *Hepatology* 2020; **72**: 1924-1934 [PMID: 33022803 DOI: 10.1002/hep.31588]

50 **Fan R**, Papatheodoridis G, Sun J, Innes H, Toyoda H, Xie Q, Mo S, Sypsa V, Guha IN, Kumada T, Niu J, Dalekos G, Yasuda S, Barnes E, Lian J, Suri V, Idilman R, Barclay ST, Dou X, Berg T, Hayes PC, Flaherty JF, Zhou Y, Zhang Z, Buti M, Hutchinson SJ, Guo Y, Calleja JL, Lin L, Zhao L, Chen Y, Janssen HLA, Zhu C, Shi L, Tang X, Gaggar A, Wei L, Jia J, Irving WL, Johnson PJ, Lampertico P, Hou J. aMAP risk score predicts hepatocellular carcinoma development in patients with chronic

hepatitis. *J Hepatol* 2020; **73**: 1368-1378 [PMID: 32707225 DOI: 10.1016/j.jhep.2020.07.025]

51 **D'Ambrosio R**, Della Corte C, Colombo M. Hepatocellular Carcinoma in Patients with a Sustained Response to Anti-Hepatitis C Therapy. *Int J Mol Sci* 2015; **16**: 19698-19712 [PMID: 26295392 DOI: 10.3390/ijms160819698]

52 **Morgan RL**, Baack B, Smith BD, Yartel A, Pitasi M, Falck-Ytter Y. Eradication of hepatitis C virus infection and the development of hepatocellular carcinoma: a meta-analysis of observational studies. *Ann Intern Med* 2013; **158**: 329-337 [PMID: 23460056 DOI: 10.7326/0003-4819-158-5-201303050-00005]

53 **Nahon P**, Bourcier V, Layese R, Audureau E, Cagnot C, Marcellin P, Guyader D, Fontaine H, Larrey D, De Lédinghen V, Ouzan D, Zoulim F, Roulot D, Tran A, Bronowicki JP, Zarski JP, Leroy V, Riachi G, Calès P, Péron JM, Alric L, Bourlière M, Mathurin P, Dharancy S, Blanc JF, Abergel A, Serfaty L, Mallat A, Grangé JD, Attali P, Bacq Y, Wartelle C, Dao T, Benhamou Y, Pilette C, Silvain C, Christidis C, Capron D, Bernard-Chabert B, Zucman D, Di Martino V, Thibaut V, Salmon D, Ziol M, Sutton A, Pol S, Roudot-Thoraval F; ANRS CO12 CirVir Group. Eradication of Hepatitis C Virus Infection in Patients With Cirrhosis Reduces Risk of Liver and Non-Liver Complications. *Gastroenterology* 2017; **152**: 142-156.e2 [PMID: 27641509 DOI: 10.1053/j.gastro.2016.09.009]

54 **Qiu L**, Xu H, Ji M, Shang D, Lu Z, Wu Y, Tu Z, Liu H. Circular RNAs in hepatocellular carcinoma: Biomarkers, functions and mechanisms. *Life Sci* 2019; **231**: 116660 [PMID: 31319086 DOI: 10.1016/j.lfs.2019.116660]

55 **Mücke VT**, Thomas D, Mücke MM, Waidmann O, Zeuzem S, Sarrazin C, Pfeilschifter J, Vermehren J, Finkelmeier F, Grammatikos G. Serum sphingolipids predict de novo hepatocellular carcinoma in hepatitis C cirrhotic patients with sustained virologic response. *Liver Int* 2019; **39**: 2174-2183 [PMID: 31207039 DOI: 10.1111/Liv.14178]

56 **Pascut D**, Cavalletto L, Pratama MY, Bresolin S, Trentin L, Basso G, Bedogni G, Tiribelli C, Chemello L. Serum miRNA Are Promising Biomarkers for the Detection of Early Hepatocellular Carcinoma after Treatment with Direct-Acting Antivirals. *Cancers (Basel)* 2019; **11** [PMID: 31717959 DOI: 10.3390/cancers11111773]

57 **Johnson PJ**, Pirrie SJ, Cox TF, Berhane S, Teng M, Palmer D, Morse J, Hull D, Patman G, Kagebayashi C, Hussain S, Graham J, Reeves H, Satomura S. The detection of hepatocellular carcinoma using a prospectively developed and validated model based on serological biomarkers. *Cancer Epidemiol Biomarkers Prev* 2014; **23**: 144-153 [PMID: 24220911 DOI: 10.1158/1055-9965.EPI-13-0870]

58 **Yang JD**, Addissie BD, Mara KC, Harmsen WS, Dai J, Zhang N, Wongjarupong N, Ali HM, Ali HA, Hassan FA, Lavu S, Cvinar JL, Giama NH, Moser CD, Miyabe K, Allotey LK, Algeciras-Schimnich A, Theobald JP, Ward MM, Nguyen MH, Befeler AS, Reddy KR, Schwartz M, Harnois DM, Yamada H, Srivastava S, Rinaudo JA, Gores GJ, Feng Z, Marrero JA, Roberts LR. GALAD Score for Hepatocellular Carcinoma Detection in Comparison with Liver Ultrasound and Proposal of GALADUS Score. *Cancer Epidemiol Biomarkers Prev* 2019; **28**: 531-538 [PMID: 30464023 DOI: 10.1158/1055-9965.EPI-18-0281]

59 **Shickel B**, Tighe PJ, Bihorac A, Rashidi P. Deep EHR: A Survey of Recent Advances in Deep Learning Techniques for Electronic Health Record (EHR) Analysis. *IEEE J Biomed Health Inform* 2018; **22**: 1589-1604 [PMID: 29989977 DOI: 10.1109/JBHI.2017.2767063]

60 **Xiao C**, Choi E, Sun J. Opportunities and challenges in developing deep learning models using electronic health records data: a systematic review. *J Am Med Inform Assoc* 2018; **25**: 1419-1428 [PMID: 29893864 DOI: 10.1093/jamia/ocy068]

61 **Singal AG**, Mukherjee A, Elmunzer BJ, Higgins PD, Lok AS, Zhu J, Marrero JA, Waljee AK. Machine learning algorithms outperform conventional regression models in predicting development of hepatocellular carcinoma. *Am J Gastroenterol* 2013; **108**: 1723-1730 [PMID: 24169273 DOI: 10.1038/ajg.2013.332]

62 **Ioannou GN**, Tang W, Beste LA, Tincopa MA, Su GL, Van T, Tapper EB, Singal AG, Zhu J, Waljee AK. Assessment of a Deep Learning Model to Predict Hepatocellular Carcinoma in Patients With Hepatitis C Cirrhosis. *JAMA Netw Open* 2020; **3**: e2015626 [PMID: 32870314 DOI: 10.1001/jamanetworkopen.2020.15626]

World Journal of Gastroenterology

Submit a Manuscript: https://www.f6publishing.com

World J Gastroenterol 2021 October 28; 27(40): 6750-6756

DOI: 10.3748/wjg.v27.i40.6750

ISSN 1007-9327 (print) ISSN 2219-2840 (online)

OPINION REVIEW

Higher doses of ascorbic acid may have the potential to promote nutrient delivery *via* intestinal paracellular absorption

Ivana Roosevelt Sequeira

ORCID number: Ivana Roosevelt Sequeira 0000-0001-5414-9925.

Author contributions: Sequeira IR conceptualized, drafted and wrote the manuscript.

Conflict-of-interest statement: The author declares no conflict of interest.

Open-Access: This article is an open-access article that was selected by an in-house editor and fully peer-reviewed by external reviewers. It is distributed in accordance with the Creative Commons Attribution NonCommercial (CC BY-NC 4.0) license, which permits others to distribute, remix, adapt, build upon this work non-commercially, and license their derivative works on different terms, provided the original work is properly cited and the use is non-commercial. See: http://creativecommons.org/Licenses/by-nc/4.0/

Manuscript source: Unsolicited manuscript

Specialty type: Gastroenterology and hepatology

Country/Territory of origin: New Zealand

Peer-review report's scientific quality classification

Ivana Roosevelt Sequeira, Human Nutrition Unit, School of Biological Science, University of Auckland, Auckland 1024, New Zealand

Corresponding author: Ivana Roosevelt Sequeira, PhD, Research Fellow, Human Nutrition Unit, School of Biological Science, University of Auckland, 18 Carrick Place, Mount Eden, Auckland 1024, New Zealand. i.sequeira@auckland.ac.nz

Abstract

The significance of plasma ascorbic acid (AA) is underscored by its enzymatic and antioxidant properties as well as involvement in many aspects of health including the synthesis of biomolecules during acute illness, trauma and chronic health conditions. Dietary intake supports maintenance of optimal levels with supplementation at higher doses more likely pursued. Transient increased intestinal paracellular permeability following high dose AA may be utilised to enhance delivery of other micronutrients across the intestinal lumen. The potential mechanism following dietary intake however needs further study but may provide an avenue to increase small intestinal nutrient co transport and absorption, including in acute and chronic illness.

Key Words: Aspirin; Ascorbic acid; Paracellular permeability; Antioxidant; Lactulose mannitol test

©The Author(s) 2021. Published by Baishideng Publishing Group Inc. All rights reserved.

Core Tip: The significance of plasma ascorbic acid (AA) is underscored by its enzymatic and antioxidant properties as well as involvement in many aspects of health including the synthesis of biomolecules during acute illness, trauma and chronic health conditions. Dietary intake supports maintenance of optimal levels with supplementation at higher doses more likely pursued. Transient increased intestinal paracellular permeability following high dose AA may be utilised to enhance delivery of other micronutrients across the intestinal lumen. The potential mechanism following dietary intake however needs further study but may provide an avenue to increase small intestinal nutrient co transport and absorption, including in acute and chronic illness.

Grade A (Excellent): 0
Grade B (Very good): B
Grade C (Good): 0
Grade D (Fair): 0
Grade E (Poor): 0

Received: July 1, 2021
Peer-review started: July 1, 2021
First decision: July 13, 2021
Revised: July 16, 2021
Accepted: September 19, 2021
Article in press: September 19, 2021
Published online: October 28, 2021

P-Reviewer: Subramanian VS
S-Editor: Wang JJ
L-Editor: A
P-Editor: Li JH



Citation: Sequeira IR. Higher doses of ascorbic acid may have the potential to promote nutrient delivery *via* intestinal paracellular absorption. *World J Gastroenterol* 2021; 27(40): 6750-6756
URL: https://www.wjgnet.com/1007-9327/full/v27/i40/6750.htm
DOI: https://dx.doi.org/10.3748/wjg.v27.i40.6750

INTRODUCTION

Ascorbic acid (AA) or Vitamin C is an essential micronutrient in the human diet, due to the non-functional gene encoding L-glucono lactone oxidase that is involved in the catalysis of the last biosynthetic step in the pathway. The physiology and pathophysiology of AA has been extensively studied and the estimated plasma half-life reported to be between 7-14 d on the basis of depletion-repletion studies, conducted in healthy male subjects. Ergo, providing an approximation of the plasma half-life in those individuals that may have acute illness, trauma or chronic health conditions. The importance of maintaining optimal AA levels is underscored by both its antioxidant and non-antioxidant, *i.e.*, enzymatic roles and involvement in many aspects of health which include being an essential factor in the synthesis of collagen, carnitine and norepinephrine. Reduced dietary consumption, due to lower intake of fresh fruit and vegetables, or increased utilization *via* intracellular uptake are important aspects in the maintenance of plasma AA levels. Increased cellular distribution of AA has been shown to be associated with high leukocyte turnover and oxidative stress, whereby the redox potential of AA mitigates the production of reactive oxygen species (ROS). Dehydroascorbic acid (DHA), formed by the loss of electron by the ascorbic radical, has the same biological activity as the reduced form. The subsequent hydrolysis of DHA, if not reduced back to AA, to 2,3-diketogulonic acid is an irreversible step that results in the loss of antioxidant properties and its degradation.

Exogenous AA uptake is provided by, but not limited to, dietary intake. Due to AAs proposed antioxidant as well as enzymatic health benefits it is a widely sought-after dietary supplement that is available for consumption alone or as a multivitamin. Notably, AA has been co-formulated not only with other vitamins but also with anti-inflammatory pharmacological agents[1-3], in particular with aspirin. Monotherapy with aspirin has been shown to decrease the concentration of AA not only within the intestinal enterocytes[4] but also in gastric juice[5] potentiating negative impacts by reducing the ability of intestinal mucosal cells to manage oxidative stress[4]. Therefore, the co-formulation of AA with aspirin is considered to mitigate and ameliorate ROS induced gastrointestinal damage that has been implicated with the etiology of aspirin monotherapy[6].

Of interest is, a body of work conducted by our group that demonstrated that a single dose of aspirin has the potential to cause transient increases in small intestinal permeability over a 6 h period in healthy individuals. More importantly that rather than mitigating the aspirin induced increase in intestinal permeability[7], assessed by the lactulose mannitol test[8], the administration of 500 mg AA augmented absorption of lactulose either when given alone or in combination with the single 500 mg dose of aspirin (Table 1).

Therefore, it appears that while simultaneous dosage of AA with aspirin may potentially have longer term beneficial effects, related to the antioxidant properties of AA, in the short term however it may not mitigate the aspirin-induced increase in intestinal permeability. It is notable that, in the investigation, participants received an aspirin drink thirty minutes prior to the AA drink[7] in contrast to other studies where AA and aspirin were administered together as a single solution or in the form of a tablet[1-3,5,9]. Hence, it may be considered that the extent of ionization of each of these weak organic acids could have differed in the intestinal lumen consequentially affecting their ability to access transporters in the gut wall. The proportion of unionized AA increases to 99% and 15% in the stomach (pH 1) and small intestine (pH 5) respectively, and under these conditions passive diffusion is thought to play a significant role in AA uptake[10]. Indeed, it has been previously shown that co-administration of aspirin with AA decreased the rate at which AA was absorbed *in vivo*[11] and could have resulted from interference with sodium dependent secondary active transport *via* sodium-dependent vitamin C transporters (SVCT1 and SVCT2)[12]. These transporters are differentially expressed along the length of the gastrointestinal tract, with the pattern of expression mediated in part by transcriptional and epigenetic mechanisms[13].

Table 1 Variation in the cumulative excretion of lactulose in bulked urine samples collected over two time periods (first three hours and the second three hours) during a six hours collection period in 28 healthy female participants

Treatment	Lactulose excretion (% recovery of ingested dose)	
	First 3 h	Second 3 h
Aspirin	0.37 ± 0.05[a,b]	0.46 ± 0.05[d]
Ascorbic acid	0.47 ± 0.05[a,c]	0.53 ± 0.04
Combined dosage	0.68 ± 0.09[b,c]	0.77 ± 0.14[d]

[a]Statistically significant ($P < 0.05$) differences between treatments during the first 3 h, results expressed as mean ± SEM.
[b]Statistically significant ($P < 0.05$) differences between treatments during the first 3 h, results expressed as mean ± SEM.
[c]Statistically significant ($P < 0.05$) differences between treatments during the first 3 h, results expressed as mean ± SEM.
[d]Statistically significant ($P < 0.05$) differences between treatments during the second 3 h during the lactulose mannitol test, results expressed as mean ± SEM.

Pertinent however is that increased small intestinal mucosal permeability, even if transient, following dosage with AA raises questions as to whether similar changes may occur following dietary ingestion of foods that are rich in AA. It is noteworthy that the dose of 500 mg AA administered in our study[7] is higher than the recommended daily allowance (RDA 60-120 mg)[14], guidelines for which are variable. An increase in the RDA to 200 mg has been proposed[15] to maximize the attributed health benefits, with evidence suggesting that regular supplement users consume more than 1 g AA per day[16]. Whether the increase in intestinal permeability detected in our study was dose dependent is not known and a comparison with other publications is not possible as the effect of AA on intestinal permeability has not been previously studied. We hypothesize that the dose of AA induced increase in intestinal permeability could be due to its action on apical transporters. Glucose has been shown to modulate vitamin C transport at the small intestinal brush border membrane with similar rates of uptake of DHA and AA reported in the absence of glucose[17]. The reduced form, AA, is absorbed *via* SVCT1 and SVCT2[18]. Given that the stoichiometry of the SVCTs are similar to those of the sodium dependent glucose transporter (SGLT1)[19,20] it is possible that absorption of AA may bring about intracellular changes that modulate, *i.e.*, relax, tight junctions in a manner similar to that of glucose transport *via* SGLT1[21]. Additionally, the oxidised form DHA has been shown to compete with glucose for transport *via* glucose transporters[22] in particular GLUT2 and GLUT8[23], which have been suggested along with SGLT1 to cause cytoskeletal contraction[24]. The modulation of the tight junctions in this manner has been shown to increase mucosal permeability[25], allowing greater quantities of larger molecules to be absorbed *via* the paracellular pathway[26].

Relating and extending the results of our study to AA levels from dietary intake maybe difficult and may necessitate human intervention studies using whole foods or extracts at comparable doses. However, an extrapolation of the effect of foods/extract would require careful study design as the amount of available AA in different foods may vary widely[27]. Particularly in fruits and vegetables where the quantity of AA is determined by a variety of factors which include cultivars, environmental conditions including regional and seasonal conditions as well as maturation[28]. Additionally, depending on the levels of hydration it is very likely that there may be inherent variability in the proportion of reduced and oxidized AA within fruits and vegetables, much like AA in solutions which have a greater susceptibility to oxidation. At pH < 4 [29] the concentration of AA deteriorates, with greater losses shown to occur in frozen products that are processed/canned [mean: 26 % (0% - 78 %)] than from frozen fresh products [mean: 18 % (0% - 50 %)][30]. Furthermore, supplementation of products with synthetic AA has been shown to facilitate oxidation within products[31].

The degradation of AA not only occurs during processing and storage of the food/extract but also once it is consumed and introduced into the gastrointestinal lumen. Being an antioxidant, AA gets oxidized in the gastrointestinal tract to maintain the reduced state of other nutrients, *e.g.*, iron or form metal-oxygen-ascorbate complexes[32]. However, the acidic conditions of the gastrointestinal tract protect AA against chemical and enzymatic oxidation[32] with 93% of AA from bioactive broccoli inflorescence[33] and 71% from pomegranate juice[34] shown to be stable following *in vitro* gastric digestion. Conversely, in the small intestinal environment greater amounts

of AA was oxidized, with 39% of AA recovered[35] in this segment of the gut following *in vitro* small intestinal digestion of blended fruit juice. While this information is pertinent to our understanding, the bioavailability of luminal AA also requires consideration of the interaction with other contained dietary constituents *e.g.*, fiber and other bioflavanoids. Micronutrients within fruit juice have been shown to inhibit the absorption of AA[36] at doses between 50-500 mg. One mechanism for the inhibition is thought to occur *via* competition with transporters which has been particularly attributed to flavanoids such as quercetin and myricetin that are shown to decrease ascorbate as well as DHA absorption in *in vitro* models[37,38]. Vinson *et al*[39] further demonstrated in guinea pigs that dosage with a citrus fruit extract, containing 18% bioflavonoids, 15% proteins and 30% carbohydrates, resulted in a significantly slower rise in plasma ascorbate concentrations in comparison to a simple ascorbate solution. In alignment with these findings, a similar effect was also reported in human participants following the intake of citrus fruit extract[40].

Contrary to these findings it has also been shown that flavonoids, following consumption of half a golden kiwi fruit a day (50 g) over six weeks, did not alter the bioavailability of contained AA when compared to 50 g of synthetic AA[41]. This inferred effect appeared consistent as the administration of AA with blackcurrant juice [42] or orange juice[43] containing flavonoids did not impede absorption. Therefore, it seems likely that these differences in the manner in which AA is absorbed when co-administered could have arisen due to the differential gastric transit times[44]. Gastric emptying of liquid meals or beverages is dependent on the pressure gradient across the gastroduodenal junction and in part by the composition of the duodenal content, and hence it is conceivable that the nutrient content and composition of these different solutions or fruit slowed down gastric emptying[44]. Alternatively, these incongruent results may in part have been due to the different forms and dosages at which AA was administered, *i.e.*, as solutions or gels. Ergo resulting in potentially variable gastrointestinal residence and emptying times to influence absorption and the subsequent appearance of AA in sampled biological fluids *i.e.*, plasma, urine *etc.*

Given these inconsistencies in evidence regarding the bioavailability when co-administered with other substances, it remains unclear as to whether the effects of AA on intestinal permeability can be extended to situations when it is delivered in foods. This in particular considering the dose and quantity of the foods/extract that would have to be consumed to show comparable effects. All the same, the ability of a pharmaceutical dose of 500 mg AA to augment absorption of larger inert sugars such as lactulose does raise the possibility that AA could be a putative agent that could be co-administered with poorly absorbed drugs, nutrients or food substances of similar or larger molecular weight to enhance their absorption[45,46].

Increased paracellular permeability, *via* the modulation of tight junctions, has been reported after consumption of a meal especially in the presence of glucose[47] and alanine[48]. Using Caco 2 models, food components such as plant extracts[49-51] and isolated food components[52-54] have been shown to increase paracellular permeability with a the resultant flux in macromolecules, such as mannitol[51,55,56]. These authors, including Kosińska *et al*[57], postulated that food components could be safe alternatives to reversibly 'open' tight junctions in order to enhance the absorption of molecules of interest. Conversely, glutamine, polyunsaturated fatty acids and polyphenols have been shown to 'tighten' tight junctions through increased expression of tight junction associated proteins[58].

CONCLUSION

Whilst the molecular mechanism by which AA increases paracellular permeability remains to be elucidated, a dose of 500 mg, which is higher than the current RDA, has been shown to increase small intestinal permeability in healthy individuals. Whether this effect is dose dependent requires further exploration however together with its antioxidant properties, the alteration of intestinal permeability by AA can be potentially explored as a safe and novel application for the delivery of molecules *via* the paracellular pathway. Indeed it is also conceivable the co-administration of AA, as a supplement or through consumption of a rich food source, with aspirin may potentiate its serum levels and analgesic effects.

ACKNOWLEDGEMENTS

The studies were conducted at the Human Nutrition Unit at Massey University, Palmerston North under the supervision of Prof Roger G Lentle, Prof Marlena C Kruger and Dr Roger D Hurst.

REFERENCES

1 **Konturek PC**, Kania J, Hahn EG, Konturek JW. Ascorbic acid attenuates aspirin-induced gastric damage: role of inducible nitric oxide synthase. *J Physiol Pharmacol* 2006; **57** Suppl 5: 125-136 [PMID: 17218764]
2 **Dammann HG**, Saleki M, Torz M, Schulz HU, Krupp S, Schürer M, Timm J, Gessner U. Effects of buffered and plain acetylsalicylic acid formulations with and without ascorbic acid on gastric mucosa in healthy subjects. *Aliment Pharmacol Ther* 2004; **19**: 367-374 [PMID: 14984384 DOI: 10.1111/j.1365-2036.2004.01742.x]
3 **McAlindon ME**, Muller AF, Filipowicz B, Hawkey CJ. Effect of allopurinol, sulphasalazine, and vitamin C on aspirin induced gastroduodenal injury in human volunteers. *Gut* 1996; **38**: 518-524 [PMID: 8707080 DOI: 10.1136/gut.38.4.518]
4 **Buffinton GD**, Doe WF. Altered ascorbic acid status in the mucosa from inflammatory bowel disease patients. *Free Radic Res* 1995; **22**: 131-143 [PMID: 7704184 DOI: 10.3109/10715769509147535]
5 **Pohle T**, Brzozowski T, Becker JC, Van der Voort IR, Markmann A, Konturek SJ, Moniczewski A, Domschke W, Konturek JW. Role of reactive oxygen metabolites in aspirin-induced gastric damage in humans: gastroprotection by vitamin C. *Aliment Pharmacol Ther* 2001; **15**: 677-687 [PMID: 11328262 DOI: 10.1046/j.1365-2036.2001.00975.x]
6 **Patel V**, Fisher M, Voelker M, Gessner U. Gastrointestinal effects of the addition of ascorbic acid to aspirin. *Pain Pract* 2012; **12**: 476-484 [PMID: 22151399 DOI: 10.1111/j.1533-2500.2011.00517.x]
7 **Sequeira IR**, Kruger MC, Hurst RD, Lentle RG. Ascorbic Acid may Exacerbate Aspirin-Induced Increase in Intestinal Permeability. *Basic Clin Pharmacol Toxicol* 2015; **117**: 195-203 [PMID: 25641731 DOI: 10.1111/bcpt.12388]
8 **Sequeira IR**, Lentle RG, Kruger MC, Hurst RD. Standardising the lactulose mannitol test of gut permeability to minimise error and promote comparability. *PLoS One* 2014; **9**: e99256 [PMID: 24901524 DOI: 10.1371/journal.pone.0099256]
9 **Hanan S**. Ahmed S. Zolfakar. Effect of aspirin versus aspirin and vitamin C on gastric mucosa [fundus] of adult male albino rats: histological and morphometric study. *Egypt J of Histol* 2010; **33**: 313-326
10 **Lykkesfeldt J**, Tveden-Nyborg P. The Pharmacokinetics of Vitamin C. *Nutrients* 2019; **11** [PMID: 31601028 DOI: 10.3390/nu11102412]
11 **Ioannides C**, Stone AN, Breacker PJ, Basu TK. Impairment of absorption of ascorbic acid following ingestion of aspirin in guinea pigs. *Biochem Pharmacol* 1982; **31**: 4035-4038 [PMID: 6818974 DOI: 10.1016/0006-2952(82)90652-9]
12 **Tsukaguchi H**, Tokui T, Mackenzie B, Berger UV, Chen XZ, Wang Y, Brubaker RF, Hediger MA. A family of mammalian Na+-dependent L-ascorbic acid transporters. *Nature* 1999; **399**: 70-75 [PMID: 10331392 DOI: 10.1038/19986]
13 **Subramanian VS**, Srinivasan P, Wildman AJ, Marchant JS, Said HM. Molecular mechanism(s) involved in differential expression of vitamin C transporters along the intestinal tract. *Am J Physiol Gastrointest Liver Physiol* 2017; **312**: G340-G347 [PMID: 27932501 DOI: 10.1152/ajpgi.00369.2016]
14 **Carr AC**, Lykkesfeldt J. Discrepancies in global vitamin C recommendations: a review of RDA criteria and underlying health perspectives. *Crit Rev Food Sci Nutr* 2021; **61**: 742-755 [PMID: 32223303 DOI: 10.1080/10408398.2020.1744513]
15 **Frei B**, Birlouez-Aragon I, Lykkesfeldt J. Authors' perspective: What is the optimum intake of vitamin C in humans? *Crit Rev Food Sci Nutr* 2012; **52**: 815-829 [PMID: 22698272 DOI: 10.1080/10408398.2011.649149]
16 **Johnston CS**. Biomarkers for establishing a tolerable upper intake level for vitamin C. *Nutr Rev* 1999; **57**: 71-77 [PMID: 10101920 DOI: 10.1111/j.1753-4887.1999.tb06926.x]
17 **Malo C**, Wilson JX. Glucose modulates vitamin C transport in adult human small intestinal brush border membrane vesicles. *J Nutr* 2000; **130**: 63-69 [PMID: 10613768 DOI: 10.1093/jn/130.1.63]
18 **Wilson JX**. Regulation of vitamin C transport. *Annu Rev Nutr* 2005; **25**: 105-125 [PMID: 16011461 DOI: 10.1146/annurev.nutr.25.050304.092647]
19 **Lindblad M**, Tveden-Nyborg P, Lykkesfeldt J. Regulation of vitamin C homeostasis during deficiency. *Nutrients* 2013; **5**: 2860-2879 [PMID: 23892714 DOI: 10.3390/nu5082860]
20 **Goldenberg H**, Schweinzer E. Transport of vitamin C in animal and human cells. *J Bioenerg Biomembr* 1994; **26**: 359-367 [PMID: 7844110 DOI: 10.1007/BF00762776]
21 **Turner JR**. Show me the pathway! *Adv Drug Deliv Rev* 2000; **41**: 265-281 [PMID: 10854686 DOI: 10.1016/s0169-409x(00)00046-6]
22 **Vera JC**, Rivas CI, Fischbarg J, Golde DW. Mammalian facilitative hexose transporters mediate the transport of dehydroascorbic acid. *Nature* 1993; **364**: 79-82 [PMID: 8316303 DOI:

10.1038/364079a0]
23 **Corpe CP**, Eck P, Wang J, Al-Hasani H, Levine M. Intestinal dehydroascorbic acid (DHA) transport mediated by the facilitative sugar transporters, GLUT2 and GLUT8. *J Biol Chem* 2013; **288**: 9092-9101 [PMID: 23396969 DOI: 10.1074/jbc.M112.436790]
24 **Schmitt CC**, Aranias T, Viel T, Chateau D, Le Gall M, Waligora-Dupriet AJ, Melchior C, Rouxel O, Kapel N, Gourcerol G, Tavitian B, Lehuen A, Brot-Laroche E, Leturque A, Serradas P, Grosfeld A. Intestinal invalidation of the glucose transporter GLUT2 delays tissue distribution of glucose and reveals an unexpected role in gut homeostasis. *Mol Metab* 2017; **6**: 61-72 [PMID: 28123938 DOI: 10.1016/j.molmet.2016.10.008]
25 **Pappenheimer JR**. Intestinal absorption of hexoses and amino acids: from apical cytosol to villus capillaries. *J Membr Biol* 2001; **184**: 233-239 [PMID: 11891547 DOI: 10.1007/s00232-001-0094-1]
26 **Groschwitz KR**, Hogan SP. Intestinal barrier function: molecular regulation and disease pathogenesis. *J Allergy Clin Immunol* 2009; **124**: 3-20; quiz 21 [PMID: 19560575 DOI: 10.1016/j.jaci.2009.05.038]
27 **Gregory JF**, III. Ascorbic acid bioavailability in foods and supplements. *Nutr Rev* 1993; **51**: 301-303 [DOI: 10.1111/j.1753-4887.1993.tb03059.x]
28 **Erdman JW**, Klein BP. Harvesting, processing, and cooking influences on vitamin C in foods. In: Seib PA, Tolbert BM, eds. Ascorbic Acid: Chemistry, Metabolism, and Uses. 1982: 499-532
29 **Jeney-Nagymate E**, Fodor P. The stability of vitamin C in different beverages. *Brit Food J* 2008; **110**: 296-309 [DOI: 10.1108/00070700810858709]
30 **Belitz H-D**, Grosch W, Schieberle P. Vitamins. Food Chemistry. Germany: Springer, 2009: 403-420
31 **May J**, Asard H. Ascorbate recycling. In: Asard H, May J, Smirnoff N. Vitamin C: its functions and biochemistry in animals and plants. Taylor & Francis, 2003; 153-175
32 **Ball GFM**. Intestinal absorption and bioavailability of vitamins. In: Vitamins in foods: analysis, bioavailability, and stability. Boca Raton: CRC Press, 2005; 23-3
33 **Vallejo F**, Gil-Izquierdo A, Pérez-Vicente A, García-Viguera C. In vitro gastrointestinal digestion study of broccoli inflorescence phenolic compounds, glucosinolates, and vitamin C. *J Agric Food Chem* 2004; **52**: 135-138 [PMID: 14709026 DOI: 10.1021/jf0305128]
34 **Pérez-Vicente A**, Gil-Izquierdo A, García-Viguera C. In vitro gastrointestinal digestion study of pomegranate juice phenolic compounds, anthocyanins, and vitamin C. *J Agric Food Chem* 2002; **50**: 2308-2312 [PMID: 11929289 DOI: 10.1021/jf0113833]
35 **Rodríguez-Roque MJ**, Rojas-Graü MA, Elez-Martínez P, Martín-Belloso O. Changes in vitamin C, phenolic, and carotenoid profiles throughout in vitro gastrointestinal digestion of a blended fruit juice. *J Agric Food Chem* 2013; **61**: 1859-1867 [PMID: 23374081 DOI: 10.1021/jf3044204]
36 **Uchida E**, Kondo Y, Amano A, Aizawa S, Hanamura T, Aoki H, Nagamine K, Koizumi T, Maruyama N, Ishigami A. Absorption and excretion of ascorbic acid alone and in acerola (Malpighia emarginata) juice: comparison in healthy Japanese subjects. *Biol Pharm Bull* 2011; **34**: 1744-1747 [PMID: 22040889 DOI: 10.1248/bpb.34.1744]
37 **Song J**, Kwon O, Chen S, Daruwala R, Eck P, Park JB, Levine M. Flavonoid inhibition of sodium-dependent vitamin C transporter 1 (SVCT1) and glucose transporter isoform 2 (GLUT2), intestinal transporters for vitamin C and Glucose. *J Biol Chem* 2002; **277**: 15252-15260 [PMID: 11834736 DOI: 10.1074/jbc.M110496200]
38 **Park JB**, Levine M. Intracellular accumulation of ascorbic acid is inhibited by flavonoids *via* blocking of dehydroascorbic acid and ascorbic acid uptakes in HL-60, U937 and Jurkat cells. *J Nutr* 2000; **130**: 1297-1302 [PMID: 10801933 DOI: 10.1093/jn/130.5.1297]
39 **Vinson J BP**. Comparative bioavailability of synthetic and natural vitamin C in guinea pigs. *Nutr Rep Int* 1983; **27**: 875-879
40 **Vinson JA**, Bose P. Comparative bioavailability to humans of ascorbic acid alone or in a citrus extract. *Am J Clin Nutr* 1988; **48**: 601-604 [PMID: 3414575 DOI: 10.1093/ajcn/48.3.601]
41 **Carr AC**, Bozonet SM, Pullar JM, Simcock JW, Vissers MC. A randomized steady-state bioavailability study of synthetic versus natural (kiwifruit-derived) vitamin C. *Nutrients* 2013; **5**: 3684-3695 [PMID: 24067392 DOI: 10.3390/nu5093684]
42 **E J**, RE H. The influence of bioflavonoids on the absorption of vitamin C. *IRCS Med Sci* 1984; **12**: 320
43 **Pelletier O**, Keith MO. Bioavailability of synthetic and natural ascorbic acid. *J Am Diet Assoc* 1974; **64**: 271-275 [PMID: 4813067]
44 **Collins PJ**, Horowitz M, Cook DJ, Harding PE, Shearman DJ. Gastric emptying in normal subjects--a reproducible technique using a single scintillation camera and computer system. *Gut* 1983; **24**: 1117-1125 [PMID: 6642275 DOI: 10.1136/gut.24.12.1117]
45 **Deli MA**. Potential use of tight junction modulators to reversibly open membranous barriers and improve drug delivery. *Biochim Biophys Acta* 2009; **1788**: 892-910 [PMID: 18983815 DOI: 10.1016/j.bbamem.2008.09.016]
46 **Salama NN**, Eddington ND, Fasano A. Tight junction modulation and its relationship to drug delivery. *Adv Drug Deliv Rev* 2006; **58** (1): 15-28 [PMID: 16517003 DOI: 10.1016/j.addr.2006.01.003]
47 **Pappenheimer JR**, Reiss KZ. Contribution of solvent drag through intercellular junctions to absorption of nutrients by the small intestine of the rat. *J Membr Biol* 1987; **100**: 123-136 [PMID: 3430569 DOI: 10.1007/BF02209145]
48 **Sadowski DC**, Meddings JB. Luminal nutrients alter tight-junction permeability in the rat jejunum: an

in vivo perfusion model. *Can J Physiol Pharmacol* 1993; **71**: 835-839 [PMID: 7511482 DOI: 10.1139/y93-125]

49 **Hashimoto K**, Matsunaga N, Shimizu M. Effect of vegetable extracts on the transepithelial permeability of the human intestinal Caco-2 cell monolayer. *Biosci, Biotech, and Bioch* 1994; **58**: 1345-1346 [DOI: 10.1271/bbb.58.1345]

50 **Konishi Y**. Modulations of food-derived substances on intestinal permeability in Caco-2 cell monolayers. *Biosci Biotechnol Biochem* 2003; **67**: 2297-2299 [PMID: 14586128 DOI: 10.1271/bbb.67.2297]

51 **Epriliati I**, D'Arcy B, Gidley M. Nutriomic analysis of fresh and processed fruit products. 2. During in vitro simultaneous molecular passages using Caco-2 cell monolayers. *J Agric Food Chem* 2009; **57**: 3377-3388 [PMID: 19290640 DOI: 10.1021/jf802226n]

52 **Ohno Y**, Naganuma T, Ogawa T, Muramoto K. Effect of lectins on the transport of food factors in caco-2 cell monolayers. *J Agric Food Chem* 2006; **54**: 548-553 [PMID: 16417319 DOI: 10.1021/jf052040y]

53 **Isoda H**, Han J, Tominaga M, Maekawa T. Effects of capsaicin on human intestinal cell line Caco-2. *Cytotechnology* 2001; **36**: 155-161 [PMID: 19003326 DOI: 10.1023/A:1014053306343]

54 **Rapin JR**, Wiernsperger N. Possible links between intestinal permeability and food processing: A potential therapeutic niche for glutamine. *Clinics (Sao Paulo)* 2010; **65**: 635-643 [PMID: 20613941 DOI: 10.1590/S1807-59322010000600012]

55 **Laitinen LA**, Tammela PS, Galkin A, Vuorela HJ, Marvola ML, Vuorela PM. Effects of extracts of commonly consumed food supplements and food fractions on the permeability of drugs across Caco-2 cell monolayers. *Pharm Res* 2004; **21**: 1904-1916 [PMID: 15553239 DOI: 10.1023/b:pham.0000045246.94064.ab]

56 **Vaidyanathan JB**, Walle T. Cellular uptake and efflux of the tea flavonoid (-) epicatechin-3-gallate in the human intestinal cell line Caco-2. *J Pharmacol Exp Ther* 2003; **307**: 745-752 [PMID: 12970388 DOI: 10.1124/jpet.103.054296]

57 **Kosińska A**, Andlauer W. Modulation of tight junction integrity by food components. *Food Res Int* 2013; **54**: 951-960 [DOI: 10.1016/j.foodres.2012.12.038]

58 **Amasheh M**, Andres S, Amasheh S, Fromm M, Schulzke JD. Barrier effects of nutritional factors. *Ann N Y Acad Sci* 2009; **1165**: 267-273 [PMID: 19538315 DOI: 10.1111/j.1749-6632.2009.04063.x]

World Journal of Gastroenterology

Submit a Manuscript: https://www.f6publishing.com

World J Gastroenterol 2021 October 28; 27(40): 6757-6774

DOI: 10.3748/wjg.v27.i40.6757

ISSN 1007-9327 (print) ISSN 2219-2840 (online)

EVIDENCE REVIEW

Venous and arterial thromboembolism in patients with inflammatory bowel diseases

Antoni Stadnicki, Izabela Stadnicka

ORCID number: Antoni Stadnicki 0000-0003-2675-3732; Izabela Stadnicka 0000-0003-3522-4058.

Author contributions: Both authors designated the overall study, collected information, drafted the manuscript, revised the manuscript critically, and approved the final version of manuscript.

Conflict-of-interest statement: Authors declare no conflict of interests and no financial support for this article.

Open-Access: This article is an open-access article that was selected by an in-house editor and fully peer-reviewed by external reviewers. It is distributed in accordance with the Creative Commons Attribution NonCommercial (CC BY-NC 4.0) license, which permits others to distribute, remix, adapt, build upon this work non-commercially, and license their derivative works on different terms, provided the original work is properly cited and the use is non-commercial. See: http://creativecommons.org/Licenses/by-nc/4.0/

Manuscript source: Invited manuscript

Specialty type: Gastroenterology and hepatology

Antoni Stadnicki, Department of Physiology, Faculty of Medicine, University of Technology, Katowice 41-209, Poland

Izabela Stadnicka, Department of Molecular Medicine, Medical University of Silesia, Faculty of Pharmacy, Sosnowiec 41-200, Poland

Corresponding author: Antoni Stadnicki, DSc, MD, PhD, Professor, Department of Physiology, Faculty of Medicine, University of Technology, Ul. Rolna, Katowice 41-209, Poland. astadnic@wp.pl

Abstract

The risk of thromboembolism (TE) is increased in patients with inflammatory bowel disease (IBD), mainly due to an increased risk of venous TE (VTE). The risk of arterial TE (ATE) is less pronounced, but an increased risk of cardiovascular diseases needs to be addressed in IBD patients. IBD predisposes to arterial and venous thrombosis through similar prothrombotic mechanisms, including triggering activation of coagulation, in part mediated by impairment of the intestinal barrier and released bacterial components. VTE in IBD has clinical specificities, *i.e.*, an earlier first episode in life, high rates during both active and remission stages, higher recurrence rates, and poor prognosis. The increased likelihood of VTE in IBD patients may be related to surgery, the use of medications such as corticosteroids or tofacitinib, whereas infliximab is antithrombotic. Long-term complications of VTE can include post-thrombotic syndrome and high recurrence rate during post-hospital discharge. A global clot lysis assay may be useful in identifying patients with IBD who are at risk for TE. Many VTEs occur in IBD outpatients; therefore, outpatient prophylaxis in high-risk patients is recommended. It is crucial to continue focusing on prevention and adequate treatment of VTE in patients with IBD.

Key Words: Inflammatory bowel disease; Thrombosis; Coagulation; Bacterial components; Prophylaxis; Post-thrombotic syndrome

©The Author(s) 2021. Published by Baishideng Publishing Group Inc. All rights reserved.

Core Tip: Patients with inflammatory bowel disease (IBD) are at significantly higher

Country/Territory of origin: Poland

Peer-review report's scientific quality classification
Grade A (Excellent): 0
Grade B (Very good): B
Grade C (Good): 0
Grade D (Fair): 0
Grade E (Poor): E

Received: March 29, 2021
Peer-review started: March 29, 2021
First decision: June 14, 2021
Revised: June 22, 2021
Accepted: August 19, 2021
Article in press: August 19, 2021
Published online: October 28, 2021

P-Reviewer: Kitamura K, Pop TL
S-Editor: Wang LL
L-Editor: Kerr C
P-Editor: Liu JH

risk for venous thromboembolism (VTE) than patients with other inflammatory and immune-mediated diseases. The prevalence of arterial vascular disease is also higher in IBD. Inflammatory and molecular aspects of coagulation cascades are strictly linked and share several common mediators, including bacterial components as a possible link between intestinal microbiota and coagulation. We explored risk factors of thrombosis in IBD including clinical specificity, fibrin clot phenotype, *Clostridium difficile* infection, medication and surgery. We also present long-lasting thromboembolic complications and consider the advantage of post-discharge VTE prophylaxis.

Citation: Stadnicki A, Stadnicka I. Venous and arterial thromboembolism in patients with inflammatory bowel diseases. *World J Gastroenterol* 2021; 27(40): 6757-6774
URL: https://www.wjgnet.com/1007-9327/full/v27/i40/6757.htm
DOI: https://dx.doi.org/10.3748/wjg.v27.i40.6757

INTRODUCTION

Inflammatory bowel disease (IBD) includes ulcerative colitis (UC) that primarily involves the large intestine, and Crohn's disease (CD) that may affect any part of the gastrointestinal tract, from the oral cavity to the rectum. However, about 20%–30% of IBD cases are associated with manifestations in other organs[1]. Venous thromboembolism (VTE) is a common extraintestinal complication in CD and UC, which is related to significant morbidity and mortality[2,3].

The number of hospitalizations of adults with VTE in the USA was estimated at more than 500 000 individuals each year, and 100 000 deaths are attributed to VTE annually, as indicated by data from the National Hospital Discharge Survey[4]. VTE is the third most common cause of vascular death after myocardial infarction and stroke. In recent years, there have been a growing number of reports on the VTE mechanism, risk factors, including medication and surgery, and the management of IBD patients. In light of the recent evidence, this review is focused on prothrombotic factors of VTE and arterial thromboembolism (ATE) and clinical complications of thrombotic events in patients with IBD, and summarizes the approach to the prevention during hospitalization and in the post-discharge period, and treatment of VTE in IBD.

EPIDEMIOLOGY AND LOCATION OF VTE

Population–based cohort studies have shown that patients with IBD seem to have an approximately threefold increased risk for developing VTE compared to the general population, and this relative risk is significantly higher during active IBD[2,3,5-7]. In their cohort study, Bernstein *et al*[5] found that the incidence rate of deep venous thrombosis (DVT) was 31.4/10000 person-years and the incidence rate of pulmonary embolism (PE) was 10.3/10000 person-years in CD, while the incidence rates were 30.0/10000 person-years for DVT and 19.8/10000 person-years for PE in UC. In an Austrian multicenter study, the incidence rate of all VTE was 6.3 per 1000 person-years, which was similar to the rate reported in the earlier study[7]. The incidence of VTE increases with age. However, no significant sex-related differences have been found[7,8]. The mortality associated with IBD-related VTE ranges from 8% to 22%[9,10]. Nguyen and Sam showed a significant, 2.5-fold-increased odds [odds ratio (OR): 1.83–3.43] of mortality associated with VTE-related hospitalization in patients with IBD compared to patients without VTE[2] .

In terms of VTE location, DVT of the lower extremity and PE are the most common VTE complications in IBD. However, VTE may occur in the abdominal (portal, mesenteric and splenic) veins[11]. VTE is also reported in the arm vein, and unusual sites such as the retinal vein, and cerebral sinus veins[7,12]. In an Austrian multicenter study among patients with IBD with a history of VTE, 90.4% of patients presented with DVT and/or PE, whereas 9.6% had portal, mesenteric, cerebral or internal jugular vein thrombosis[7]. The most commonly applied procedures for diagnosis of DVT include ultrasound and venography[13,14].Ventilation-perfusion scan and multidetector helical computer axial tomography are tools for the diagnosis of PE[14].

ATE COMPLICATIONS

ATE occur less frequently than VTE in IBD, including the limb arteries, and even central vessels including the aorta[15-17]. In the past few years, studies have suggested that patients with IBD might also be at an increased risk of coronary heart disease and stroke[16,18]. In a recent meta-analysis, IBD was associated with a modest increase in the risk of cerebrovascular disease incidence [hazard ratio (HR: 1.29)], in both CD (HR: 1.32) and UC (HR: 1.18)[18]. In another meta-analysis, patients with IBD were associated with a modest increase in the risk of coronary artery disease (OR: 1.19) in patients with CD and UC[19]. After adjusting for potential confounders, the meta-analysis of five studies revealed an 18% higher risk of cerebrovascular events in both CD and UC, with no significant differences between the two forms, but a higher risk for women compared to men [OR: 1.28 adjusted, 95% confidence interval (CI): 1.17–1.41]. No increased risk of ATE was found in a French study, including 33 studies with a large cohort of hospitalized IBD patients and controls. However, an increased risk of coronary heart disease and mesenteric ischemia was found[20]. An increased risk for potentially life-threatening arterial vascular diseases in patients with IBD also requires assessment of conventional risk factors such as hypertension, obesity, diabetes and dyslipidemia. However, typical cardiovascular risk factors other than hypertension have not been confirmed in IBD[21].

ETIOPATHOGENESIS OF VTE AND ATE IN IBD

Impairment of hemostasis in patients with IBD

Unregulated activation of the coagulation system may cause thrombosis or embolism. Local hemostasis is initiated when chronic inflammation, surgery or trauma disrupts the vascular endothelial lining, and blood is exposed to subendothelial connective tissue. In primary hemostasis, a platelet plug is formed, and then plasma coagulation proteins are activated to initiate secondary hemostasis. The complex of tissue factor (TF) and active factor VII is the most important initiator of coagulation. Activation of coagulation results in thrombin generation, and in turn may generate fibrin formation as well as platelet activation *via* the cleavage of and binding to thrombin receptors (Figure 1)[22]. Several authors have indicated systemic evidence for impairment of fibrinolysis and intravascular thrombin generation in patients with IBD to measure prothrombin fragments (formed during the conversion of prothrombin to thrombin, F1+2) and thrombin–antithrombin complexes[23,24]. The plasma level of protein C, a natural coagulation inhibitor, has been shown to be unchanged or decreased in IBD[25,26], while its decreased cofactor, the protein S plasma level, was demonstrated in most studies[27]. Importantly, in some studies, thrombin-activatable fibrinolysis inhibitor (TAFI) which provides a link between coagulation and fibrinolysis, has been found to be increased in patients with IBD[28,29]. Activated by thrombin, TAFI removes lysine residues from fibrin, which is essential for plasmin formation in the fibrin network, and in turn inhibits fibrinolysis, which contributes to the prothrombotic state. Elevated D-dimer levels were found mainly in active IBD patients, which provides evidence of fibrin formation and reactive fibrinolysis (Figure 1)[24,25].

The increased platelet count correlates with IBD activity, and higher platelet count is even proposed to distinguish IBD from infectious diarrhea. Abnormal platelet aggregation *in vitro*, and activation *in vivo* are found in both active and inactive IBD[24,25,30]. Thus, platelet activation is a feature of IBD, and along with thrombocytosis, it may have a role in the development of thrombosis. Systemic endothelial cell dysfunction has been reported in UC and CD. Serum concentration of von Willebrand factor and thrombomodulin level, which are the markers of vascular injury, are also increased in the serum of IBD patients in relation to the disease activity[31,32]. In their large epidemiological study, Thompson *et al*[33] indicated an opposite approach showing that IBD occurred less frequently as expected in large cohort patients with the main inherited coagulation deficiency disorders, including hemophilia or von Willebrand disease.

Mutual activation of coagulation and inflammation in IBD

Activation of coagulation is a significant constituent of the inflammatory response and probably is involved in the pathogenesis of IBD[34,35]. Proinflammatory cytokines, such as tumor necrosis factor-α (TNF-α) and interleukin-1 (IL-1), which are elevated in circulation and intestinal lesions in IBD, may initiate coagulation by induction of the TFs in monocytes/macrophages, endothelial cells and platelets. IL-1 and TNF–α are

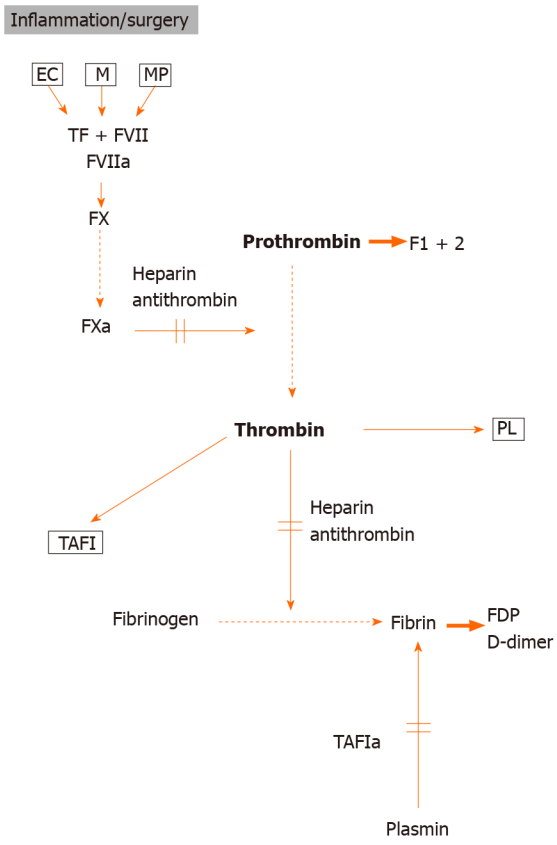


Figure 1 Diagram of the main pathways of the hemostatic process. Solid arrows designate activation, dashed arrows conversion, open arrow indicates release, and interrupted lines indicate inhibition. EC: Endothelial cell; M: Monocyte; MP: Microparticle; PL: Platelet; TF: Tissue factor; TAFI: Thrombin activatable fibrinolysis inhibitor; FDP: Fibrin degradation product.

capable of inducing procoagulant activity and suppressing the anticoagulant activity of thrombomodulin, in part due to a downregulation of endothelial protein C receptor, which is expressed normally by endothelial cells[36]. In addition, the cell components, known as microparticles, are found in plasma of adult and pediatric IBD patients[37-39]. There are vesicles of cell membranes mainly from activated platelets with the expression of TFs on their surface, suggesting their role in the activation of coagulation. Importantly, platelets may mediate leukocyte recruitment to the inflamed colon *via* surface CD40 ligand (CD40L). Danese *et al*[40] found an increased platelet expression of CD40L, and an increased plasma level of platelet soluble CD40L in both UC and CD compared to normal controls. Taken together, it seems that platelets are involved in hemostasis and thrombosis. They also act as inflammatory cells in IBD.

Evidence suggests that thrombin may, in turn, mediate and amplify inflammatory cascades in IBD *via* activating protease activated receptors (PARs), which have been identified as mediators of cellular responses, especially in the context of a link between coagulation and inflammation. Thrombin is an essential mediator of PAR activation as this enzyme can activate PAR1, 3 and 4, and in turn mediate detrimental cellular effects, especially barrier disruption in endothelial cells[41]. In addition, recent studies have shown that the protein C pathway is expressed not only in endothelial cells of the mucosal microvasculature, but also in intestinal epithelial cells and plays a unique role in controlling the integrity of tight junctions[42]. Expression of epithelial protein C pathway is altered in patients with CD and UC, which may enhance intestinal permeability[43].

Due to the overlapping risk factors, patients with VTE are at increased risk for arterial thrombotic events, including coronary heart disease and stroke. Endotheliopathy and abnormalities in the coagulation cascade and their cellular components play a role for the development of VTE and ATE. A growing number of studies have indicated that patients with IBD are at an increased risk of developing cardiovascular disease (CVD). Both diseases are chronic inflammatory conditions and share certain pathophysiological mechanisms that may influence each other. High levels of cytokines, C-reactive protein, and homocysteine in IBD patients may lead to endothelial dysfunction, which is an early sign of atherosclerosis. Platelet–leukocyte

interaction and an increased CD40/CD40L system may be important links in the generation of atherosclerosis and IBD[40]. Higher levels of coagulation factors and an increased number of activated circulating platelets frequently occur in IBD, which may predispose to ATE events[32].

Bacterial components and gut microbiota

Endotoxins (lipopolysaccharide; LPS) are glycolipids found on the outer membrane of Gram-negative bacteria, which originate from the intestine and may activate receptors in monocytes, endothelial cells and platelets directly or *via* augmentation of cytokines, promoting a procoagulant state. The epithelium of the intestine creates a barrier to potentially immunogenic and noxious factors, including microorganisms and dietary components within the intestinal lumen. Luminal proteases include the host's digestive enzymes and the proteases released by the microbiota. PAR1 and PAR2 are expressed throughout the gastrointestinal (GI) tract[41]. Although PARs are traditionally known to affect several vascular responses, recent studies have indicated the functional role of PAR signaling in the GI tract. Proteases A, either from the gut lumen or from the mucosa, are capable of activating PARs, thus influencing gut permeability regulation[44].

Both endothelial cells and platelets possess innate immunity receptors, such as Toll-like receptors (TLRs). After being activated by bacterial components, TLR2 and TLR4 promote cell activation and the subsequent release of different procoagulant molecules [45,46]. The role of the impairment of the intestinal barrier has been recently indicated by Pastorelli *et al*[47] who showed that LPS level increased in systemic circulation of IBD patients and correlated with TLR4 concentrations in both active and remission phases of IBD. Simultaneously, serum LPS level correlated with both D-dimer and F1+2 levels, which supports the role of the impairment of the intestinal barrier in triggering the activation of the coagulation cascade in IBD. In fact, LPS might act as the link between the microbiome and hypercoagulability.

Gut microbiome and TE

Recent reports have suggested that alterations in gut microbiome due to a decrease in commensal anaerobic bacteria and an increase in the abundance of the Gram-negative Enterobacteriaceae family may increase the risk of TE[48]. It was found that dietary nutrients, such as choline, carnitine and butyrobetaine, common in a western diet, can be used by gut microbes to produce trimethylamine (TMA), which is converted into TMA N-oxide (TMAO)[49]. Clinical studies have revealed that TMAO level is associated with thrombotic risk of CVD[49-51]. The mechanisms in which TMAO may enhance CVD risk include endothelial cell activation and vascular inflammation, as well as alterations in tissue sterol metabolism[50]. A recent study has revealed that gut microbes directly contribute to platelet hyper-reactivity through generation of TMAO and increased plasma TMAO levels independently predicted the event of thrombosis [51]. Patients with IBD show microbial imbalance, and a less diverse gut microbiome compared to healthy individuals[52]. Currently, there are no data showing metabolic pathways by specific gut microbiota in IBD that might cause the risk of thrombosis.

RISK FACTORS OF THROMBOEMBOLIC COMPLICATIONS IN IBD

Disease activity and hospitalization

Several IBD-specific risk factors are responsible for the increased risk of VTE, especially in hospitalized IBD patients, which in part may reflect periods of increased inflammation[2,3,53]. The disease phenotype, *e.g.*, pancolitis in patients with UC, extensive colonic involvement and active fistulizing CD are significantly associated with VTE in IBD patients[2,3,10]. Similar data reported by a recent large cohort Swiss study and a recent cohort multinational study in East Asia demonstrated that VTEs were prevalent in CD patients with ileocolonic involvement, and in UC patients with pancolitis[54,55]. During hospitalization, VTE events are also related to immobility, the use of a venous catheter for parenteral nutrition, and fluid depletion due to diarrhea.

Clinical and biochemical specificities

VTEs in IBD patients are characterized by unusual clinical and biochemical specificities (an earlier first episode in life, high rates of remission, and high recurrence rates). The incidence of VTE increases with age. However, it occurs more frequently in younger patients with IBD than in those without this condition[2,3,53,56]. A large

population-based study from Denmark showed that the risk of VTE was particularly high (sixfold higher HR) in young patients with IBD as compared to age and sex-matched patients without IBD[53]. VTE events are more frequent in active IBD. However, in one-third of the patients with IBD, VTE was observed during clinical remission[7,56,57]. Although the epidemiological data demonstrate a relative prevalence of VTE in some immune-mediated disorders[58], especially among many inflammatory and/or immune-mediated conditions, IBD is related to a significantly more prominent risk of VTE[56]. Therefore, IBD is itself prothrombotic.

Polish studies have shown that plasma fibrin clot permeability is reduced and fibrin network is mostly resistant to lysis in patients with IBD, which may represent a mechanism for increasing the thrombotic risk in IBD[59]. Recently, the investigators at the University of Leuven, Belgium indicated that clot lysis parameters (area under the curve, 50% clot lysis time, and amplitude) were significantly higher in IBD compared to controls and in IBD with thrombotic events and a history of thrombosis compared to IBD without thrombosis[60]. Taken together, fibrin clot phenotype in IBD may be considered a potential novel risk factor for TE.

Recurrence of VTE

IBD represents an independent risk factor for the recurrence of VTE. Novacek *et al*[61] showed that patients with IBD who experienced their first episode of unprovoked VTE had 33% likelihood of the second episode of VTE within 5 years compared to 21% in non-IBD patients (HR: 2.5). Recently, Bollen *et al*[62] presented a monocentric cohort of IBD patients with a history of VTE and ATE and focused on the recurrence rate. These authors confirmed the high recurrence rate of thrombotic events in patients with IBD. They found that 30% of patients were identified to have recurrent TE events. In this group, 83% developed VTE, with DVT as the major manifestation (40%), followed by PE (23%). However, a relatively high number of thrombotic events (*i.e.* 17%) became recurrent in arterial circulation. De Fonseka *et al*[63] found that a history of TE was the most significant predictor of VTE in IBD. Similarly, Faye *et al*[64] showed that in patients with IBD, prior VTE was associated with readmission for VTE within 2 mo.

Post-thrombotic syndrome

Post-thrombotic syndrome (PTS) may increase the likelihood of VTE recurrence among IBD patients. It is the most frequent complication of VTE located in the lower limbs, which develops in 20%–50% of cases after proximal DVT and is severe in 5%–10% of cases[65]. Reported risk factors of PTS include extensive proximal character of DVT, involving the popliteal vein or above. Other reported risk factors include pre-existing chronic venous insufficiency (especially with mild or severe contralateral leg venous ectasia), older age and high body mass index[65]. The risk of PTS is substantial but significantly lower after an isolated distal infrapopliteal DVT. Since signs and symptoms of DVT and PTS may be similar, diagnosis of PTS should be delayed for 3–6 mo after DVT diagnosis. Compression ultrasonography, which is based on leg vein compression using the ultrasound probe, should be performed to evaluate the degree of obstruction by clots, the location of these clots, and the detection of venous insufficiency[13].

Clostridium difficile infection

IBD has been shown to be a specific risk factor for the development of *C. difficile* infection, which may lead to higher morbidity and mortality[66]. A large cohort retrospective study assessing the Nationwide Inpatient Sample in the USA found that the rate of VTE was twofold higher in hospitalized patients with IBD and *C. difficile* infection than in those without *C. difficile* infection (adjusted OR: 1.7)[67]. In their most recent study, Faye *et al*[64] found that *C. difficile* infection was an independent risk factor of readmission for VTE in patients with IBD during a 2-month time period. Therefore, clinicians need to be vigilant to assess *C. difficile* infections in patients with IBD with a flare of diarrhea to counteract *C. difficile* and minimize the risk of VTE.

Nonspecific risk factors

IBD-associated comorbidity is prothrombotic in itself and is an independent predictor of VTE; *e.g.*, congestive heart failure, chronic obstructive pulmonary disease, obesity, Behcet's disease, myeloproliferative diseases (polycythemia vera, paroxysmal nocturnal hemoglobinuria, paraproteinemia), liver cirrhosis, or diabetes mellitus[68].

Low serum albumin is a well-recognized risk factor for VTE in nephrotic syndrome [69]. In patients with IBD, low albumin levels may reflect excess loss of intestinal protein, and particularly circulating antithrombotic proteins, especially antithrombin.

Serum level of antithrombin may be a marker of underlying inflammation as a negative acute phase reactant.

An increased level of lipoprotein(a), an independent risk factor for TE, has been shown to account for a tendency toward TE in some CD patients[70]. Autoimmune abnormalities and increased production of various antibodies are often associated with IBD. Serum cardiolipin autoantibodies involved in higher risk of arterial and venous thrombosis are increased in patients with IBD. However, their elevated titer is not associated with higher VTE rates[71]. Similarly, in a recent IBD cohort study, a higher prevalence of various types of antiphospholipid antibodies was documented in patients with CD. However, this status was not associated with more TE events[72].

Provoked VTE and ATE may occur in hyperhomocysteinemia due to deficiency of vitamins B12, B6 or folate, or hereditary genetic abnormalities such as gene mutation of methylenetetrahydrofolate reductase (MTHFR)[73]. In a meta-analysis, the mean plasma homocysteine level was significantly higher in IBD patients compared to controls. However, in this study the risk of hyperhomocysteinemia was not higher among IBD patients who presented with TE complications[74].

In CD patients, oral contraceptive drugs are well-known risk factors for TE[75]. In spite of this, Cotton *et al*[76] in a large internet-based cohort of patients with IBD found that use of hormonal contraceptives in women with multiple risk factors for TE was similar to that in women without risk factors. Thus, patients with IBD should be asked about risk factors for thromboembolic disease to have an opportunity for alternative contraception. Patients with CD are more likely to be smokers, which increases the risk of vascular disease in this condition. However, UC is generally a disease of non-smokers and exsmokers[77].

Extended traveling with prolonged sitting is known as a risk factor for VTE, although it is currently recognized that reduced movement on long distance flights is more significant than immobilization. As summarized by Byard, long-distance flights of ≥ 8 h are associated with a 2–4-fold increased risk of VTE, but only in those individuals who have underlying risk factors. Importantly, the potential impact of lethal pulmonary VTE exists with increasing numbers of flights of > 16-h duration[78].

IBD medications

Some drugs used in IBD treatment can be considered potential thrombotic factors. Glucocorticosteroids used to maintain remission in IBD by multifactorial anti-inflammatory effects are also known to induce hypercoagulability, increasing plasma fibrinogen level, and decreasing tissue plasminogen activator activity and prostacyclin synthesis[79]. The use of corticosteroids prior to hospitalization is an independent risk for VTE[68]. Nguyen *et al*[80] in their large retrospective cohort study compared the risk of postoperative complications between preoperative steroid users and nonusers. They found that preoperative steroid use was associated with an increased risk of VTE in CD (OR: 1.66) and UC (OR: 2.66).

The role of TNF-α that occupies a central position to generate the inflammatory and coagulation cascade has been well defined in CD and UC. Compounds that contain anti-TNF-α antibody are currently the most recommended for biological treatment of moderate and active CD and UC[81]. Hommes *et al*[82] demonstrated that treatment with infliximab decreased thrombin generation, indicating that coagulation activation is mediated by TNF-α or a subsequent cascade of cytokines. In addition, treatment with infliximab reduces the level of circulating and prothrombotic serum-soluble CD40L in patients with CD[83]. Anti-TNF-α therapy with infliximab also downregulates isoprostane generation and thromboxane synthesis, which may reduce thromboxane-dependent platelet activation in IBD patients[84]. Bollen *et al*[85] in a prospective study investigated the effect of infliximab therapy on the hemostatic profile. They documented normalization of the clot lysis profile in responders to infliximab treatment, suggesting that infliximab is especially advisable for patients with IBD with an activated hemostatic profile. Swiss investigators in their single-center retrospective study found that in patients with IBD, TNF-α inhibitor therapy was associated with a reduced risk of TE (OR: 0.20), whereas corticosteroid use increased (OR: 4.62) TE[63]. A recent meta-analysis conducted by Hungarian investigators showed that systemic corticosteroids were associated with a significantly higher rate of VTE complications in IBD patients as compared to IBD patients without steroid medication (OR: 2.202). In contrast, treatment with anti-TNF-α agents resulted in a fivefold decreased risk of VTE compared to steroid medication (OR: 0.267)[86].

Tofacitinib, a small-molecule Janus kinase inhibitor, has been used for the treatment of moderate and severe UC. Recently, safety data for tofacitinib in rheumatology studies showed that tofacitinib 10 mg twice daily increased the frequency of VTE, although the study comprised patients aged ≥ 50 years who presented with other

cardiovascular risk factors[87]. The US Food and Drug Administration has indicated that tofacitinib 10 mg twice daily may increase the risk of VTE[88]. The most recent preliminary analysis of UC patients treated with tofacitinib 10 mg twice daily demonstrated that five presented with VTE (four PE, and one DVT), as compared to two patients receiving placebo[89]. The analysis was limited by the small group of patients, and hence further studies are warranted. At present, since uncertainty exists, the lower dose of tofacitinib (5 mg twice daily) is indicated.

Surgery

Colorectal surgery is a strong predictor of developing VTE[90]. A combination of pathophysiology of IBD and surgical risk factors increases the risk of postoperative VTE in IBD patients. A recently conducted Canadian meta-analysis showed that IBD patients undergoing colorectal surgery were at a higher risk for postoperative VTE as compared to patients undergoing surgery for colorectal cancer[91]. Patients with UC may be at higher risk for postoperative VTE as compared to those with CD. Wilson *et al*[92] found that during admission and within 30 d of hospital discharge, the incidence of VTE was higher in UC patients (2.74%) than in patients with colorectal cancer (1.74%). However, the lowest incidence was seen in patients with CD (1.2%). Similarly, McCurdy *et al*[93] reported that the cumulative incidence of VTE at 1 mo after discharge was higher in surgical patients with UC (HR: 1.68; 95%CI: 1.16–2.45) but not in surgical patients with CD. In UC patients, the risk of VTE is mostly higher in patients after colectomy[94,95]. McKenna *et al*[95] using the American College of Surgeons-National Surgical Quality Improvement Project database found that surgically urgent UC cases showed a higher rate of VTE than non-IBD patients undergoing colorectal resections (6.9% *vs* 3.1%).

PROPHYLAXIS OF VTE IN IBD

Of note, controlling the disease activity as the primary aim of IBD treatment may partly prevent VTE events and also reduce the risk of recurrent VTE episodes. Correction of vitamin deficiencies (particularly B6, B12 and folic acid) can reduce homocysteine levels[74]. In addition, therapy with sulfasalazine or methotrexate may induce folate deficiency, thus supplementation of folic acid is advocated.

Pharmacological prophylaxis

It has been confirmed that that IBD patients have an elevated risk of VTE compared to the general population. Consequently, GI societies from North America and Europe have advocated the use of pharmacological prophylaxis among hospitalized IBD patients[15,96,97]. Low molecular-weight heparin (LMWH) and unfractionated heparin are recommended for thromboprophylaxis in IBD patients. Primary prophylaxis is advocated for all hospitalized IBD patients, because the higher risk of VTE in hospitalized IBD patients also includes those hospitalized for non-IBD related reasons[96-98]. In the period of active bleeding, mechanical prophylaxis is temporarily advisable. If bleeding is not severe, anticoagulant thromboprophylaxis should be substituted for mechanical thromboprophylaxis. Anticoagulant thromboprophylaxis during hospitalization is recommended for IBD patients who underwent major abdominal-pelvic or general surgery. Similarly, anticoagulant thromboprophylaxis during hospitalization is indicated for pregnant women with IBD who underwent cesarean section. Another recommendation for pharmacological prophylaxis is advocated (related to secondary prophylaxis) during moderate-severe IBD flares in outpatients with a history of VTE. The unresolved question is whether thromboprophylaxis should be extended to all outpatients with the disease flare. Thus, the absolute risk of VTE should be assessed for each ambulatory patient with active IBD, including co-morbidity, previous VTE events, the use of oral contraceptives, smoking, and the presence of venous catheters[68,98]. Moreover, disease features could be useful in assessing the individual prothrombotic risk. Another question arises whether thromboprophylaxis should be extended after hospitalization to IBD patients with a higher risk for VTE. In a recent population-based study, McCurdy *et al*[93] found that surgical IBD patients with UC and non-surgical IBD patients were 1.7-fold more likely to develop post-discharge VTE than non-IBD matched controls. These authors showed that the risk score of post-discharge VTE for IBD patients included age over 45 years and the length of admission (more than 7 d), which would indicate prolonged post-hospitalization VTE prophylaxis. In another recent study evaluating predictors of post-hospitalization VTE in patients with IBD, Faye *et al*[64] showed that risk factors such as

older age, discharge to a nursing facility, and a previous C. *difficile* infection at the time of admission increased this risk. In addition, they found that over 90% of VTE readmissions occurred within 60 d post-discharge, with the majority in the first 20 d. These findings should increase alertness and consideration of thromboprophylaxis in this population.

Finally, it is well known that surgery represents a major risk factor for VTE, particularly in patients with IBD, and thromboprophylaxis is universally performed from the day of surgery to discharge. However, as reported before, in the IBD patient population, colorectal surgery is related to an additional VTE risk, including post-discharge period[93,95]. Recent meta-analyses in the United States indicated that IBD patients undergoing colorectal surgery were at a higher in-hospital and post-discharge risk for postoperative VTE compared to non-IBD patients undergoing surgery for colorectal cancer[91,99]. Current prophylaxis may not be sufficient to prevent VTE, especially for UC patients undergoing emergency colorectal procedures who might benefit from extended TE prophylaxis[92,94]. Kaplan *et al*[94] presented a population-based surveillance of UC hospitalized patients during a flare and compared VTE events between UC patients who responded to medical management and patients who underwent colectomy. These authors showed that VTE was significantly higher among patients who underwent colectomy, and mostly higher in patients after emergency colectomy, although more than 90% of surgical patients were given heparin prophylaxis. Despite a large amount of evidence demonstrating the high VTE risk in IBD, no randomized controlled trials specifically assessed the efficacy of anticoagulation in reducing the rate of VTE in IBD patients or in applying extended-duration prophylaxis after surgery to this population.

Implementation of prophylaxis in IBD

Although the increased risk of VTE among IBD patients has been documented, thromboprophylaxis rates in hospitalized patients with IBD seem to be low[98]. Recent and prior studies showed that patients with IBD admitted to surgical service received anticoagulation prophylaxis more often than those admitted to medical centers. In a multicenter retrospective study from Canada, patients with IBD admitted to the surgical setting were more likely to receive VTE prophylaxis than those admitted to medical service (84% *vs* 74%)[100]. Implementation of an electronic alert system seems to be an effective tool for increasing VTE prophylaxis rates in hospitalized patients with IBD. The introduction of this system was associated with a significant improvement in prophylaxis rates in both medical (26.3% *vs* 62.8%) and surgical (83.7% *vs* 95.5%) services[101]. All providers should be educated on the increased risk of VTE as well as the safety of pharmacologic prophylaxis. Inadequate implementation of VTE prophylaxis in patients with IBD is still mainly due to the concern about the safety of anticoagulation. Although prior data of Ra *et al*[102] indicated that the rate of major and minor bleeding was not significantly higher in the group who received pharmacological VTE prophylaxis compared to those who did not receive it, Faye *et al*[103] showed that IBD patients with minor hematochezia (OR: 0.27) were significantly less likely to receive VTE prophylaxis. In addition, these investigators concluded that VTE prophylaxis was not associated with increased blood transfusion rates or a clinically significant decline in hemoglobin level during hospitalization[]. It should be underlined that most patients with hematochezia will have a disease flare, and they are at a significantly increased risk for VTE during this time.

Mechanical prophylaxis

Mechanical thromboprophylaxis, graduated compression stockings, and/or intermittent pneumatic compression devices are indicated for IBD patients hospitalized with major GI bleeding[96]. Early mobilization in hospitalized surgical and non-surgical IBD patients should be always considered. These methods address the venous stasis portion of the Virchow triad by increasing venous blood flow. There are several proposed mechanism for the efficacy of induced venous stasis, including increased level of tissue factor inhibitor, the resultant factor Xa–related coagulation inhibition, and promotion of fibrinolysis by increased release of t-PA from the endothelium[104]. However, in cases of severe limb ischemia, the use of mechanical prophylaxis could worsen the ischemia and should not be used in these patients.

TEST SCREENING FOR THROMBOSIS RISK

Thrombophilia is related to acquired or inherited susceptibility to thrombosis.

However, thrombophilia testing in IBD patients is not routinely recommended. In general, no interaction between IBD and inherited factors of thrombophilia was found. Study results showed that the prevalence of factor V Leiden (which makes factor V resistant to inactivation by activated protein C) in IBD is not different compared to the general population. Studies failed to demonstrate the prevalence of the genetic variant prothrombin G20210A, and MTHFR, or gene mutation related to hyperhomocysteinemia in IBD patients[105,106]. However, hereditary genetic screening should be performed in IBD when a familial history of thrombosis, myocardial infarction, or stroke before the age of 50 is confirmed in first-degree relatives[107]. In addition, myeloproliferative neoplasms should be considered in patients with splanchnic vein thrombosis, particularly in the absence of an additional provoking factor. In these cases, testing for the JAK2V617F mutation, which is present in most patients with a myeloproliferative neoplasm is useful for identifying this disorder[100].

D-dimer, a fibrin degradation product, is effective for VTE screening, and adequately demonstrates the occurrence of VTE in the general population, although this test is characterized by low specificity[108]. However, high prevalence of elevated D-dimer in active patients with IBD usually rules out its utility in IBD[24,25,109].

Search for a biomarker which could select patients with and increased risk for thrombosis among IBD subjects is a challenging dilemma for clinicians. The endogenous thrombin potential (ETP) test may be considered a new tool for prospective studies on IBD patients to assess the risk of TE[110]. As opposed to coagulation intermediates or fragments which are markers of thrombin already generated, the ETP quantifies thrombin activity that can be generated in plasma. The increased ETP has been demonstrated in adult patients with IBD, and in active and quiescent stages in pediatric IBD patients, which indicates that procoagulant potential is a feature of the disease[38,110]. Probably the prospective studies are needed to evaluate clinical value of ETP, which stratifies the VTE risk, especially in pediatric IBD patients, in whom anticoagulation prophylaxis is not routinely recommended. Recently, investigators at the University of Leuven have determined the clot lysis profiles in patients with IBD before and after developing thrombosis and showed that clot lysis parameters differed significantly between IBD patients with and without a history of TE[62]. Therefore, a functional clot lysis assay could be included in the assessment of TE risk[60]. Nevertheless, it should be noted that both ETP test and clot lysis assay have sophisticated methodology, and hence are not routinely used.

TREATMENT OF VTE IN PATIENTS WITH IBD

The general approach to treatment of VTE in patients with IBD is similar to patients without IBD. If there is no hemodynamically significant bleeding, LMWH is the most appropriate treatment. LMWH is usually switched to an oral vitamin K antagonist (*e.g.* warfarin). In terms of VTE treatment, strong recommendations are made for a period of minimum 3 mo of anticoagulant therapy for adult and pediatric IBD patients with a symptomatic VTE, including symptomatic splanchnic vein thrombosis. In patients with active IBD, in the first event of VTE, anticoagulation therapy should be continued until IBD has been in remission for at least 3 mo. For IBD patients with unprovoked VTE presenting during clinical remission, indefinite anticoagulant therapy is recommended with a periodic analysis of the decision. In similar cases, if there is a reversible risk factor, anticoagulation therapy is recommended for at least three months until a risk factor has resolved. In addition, in those cases it is recommended that therapy should be prolonged for at least 1 mo until the risk factor has resolved. The risk-benefit ratio of long-term therapy should be evaluated on an individual basis. Anticoagulant treatment should aim not only at preventing thrombus extension but also at preventing early and late recurrences[111].

Treatment of PTS

The presence of residual vein thrombosis (partial recanalization) at 3 to 6 mo post-DVT is associated with symptomatic PTS and an increased risk of VTE recurrence in about one third in the post-DVT patients after regular discontinuation of anticoagulant treatment. Patients with PTS with delayed recanalization, and venous reflux confirmed by compression ultrasonography should receive extended anticoagulation treatment [112]. In addition, in patients hospitalized at risk of PTS, recurrence prevention includes immediate mobilization and compression stockings[65]. Vitamin K antagonists (mainly warfarin) are effective in treating VTE, but they require frequent monitoring. Poor quality of anticoagulation control (*e.g.*, too low doses during

treatment) may explain why at least some patients develop PTS[65].

OTHER TREATMENT MODALITIES

New oral anticoagulants

Anticoagulation treatment options have undergone a significant change within the last 10 years due to the development of direct oral anticoagulants (DOACs). Direct factor Xa inhibitors (rivaroxaban, apixaban, and edoxaban), and thrombin inhibitor (dabigatran) are currently available. In patients on DOACs, it is not necessary to monitor the INR ratio or heparin bridging. DOACs may allow stable patients with VTE to be treated at home earlier than in the case of warfarin. In fact, DOACs might be superior to vitamin K antagonists in treatment of VTE and prevention of PTS[113]. VTE is a dynamic process resulting from clot propagation exceeding clot lysis over time[114]. Anticoagulant therapy attenuates thrombin generation and promotes clot lysis by preventing thrombin activation of TAFI, and in turn inhibition of clot lysis. A failure to adequately suppress thrombin generation and/or activity will permit continued feedback activation of thrombin generation, fibrin formation, and inhibition of fibrinolysis by activation of TAFI. Some reports indicated that treatment with DOACs of acute symptomatic VTE was associated with a significantly lower risk of bleeding complications as compared with the vitamin K antagonist[115]. However, in case of overdose, there is no reversing agent for these drugs. In relation to IBD, currently there are no data related to the use of these promising drugs. DOACs, and perhaps low-dose DOACs, could have a particularly important role in the management of outpatients with IBD in remission and in outpatients with IBD-associated PTS. In such cases, controlled trials are warranted.

Acetylsalicylic acid

Acetylsalicylic acid (ASA) is commonly used for preventing arterial thrombosis. Some studies showed that aspirin reduced the relative risk of recurrent VTE by 30% in the high risk population compared to placebo[116]. However, the use of ASA in prevention of VTE is currently not routinely recommended. It should be underlined that if patients are scheduled for anticoagulation therapy, and have been on ASA for another indication, the risk of bleeding might be increased. A new generation of antiplatelet compounds which selectively inhibit platelet activation rather than platelet aggregation merits future studies.

Local thrombolysis

Catheter-directed thrombolysis (CDT) is increasingly used to treat acute TE. Currently used thrombolytic agents include t-PA, urokinase or streptokinase. It is accepted that systemic thrombolytic therapy should be considered in patients with massive PE, defined by hemodynamic compromise[117]. The cases of severe thrombosis causing limb ischemia may also require CDT. The role for thrombolysis, particularly CDT in other patients with DVT is less well established. CDT would be favorable in otherwise healthy patients with significant iliofemoral DVT. The rationale here is that CDT may decrease the incidence and severity of PTS. In IBD, a systematic review of outcomes with anticoagulation *vs* CDT was compared. It was found that CDT was more effective to achieve complete or partial symptomatic and radiologic resolution of thrombus in patients with IBD. Although hemorrhagic complication tended to occur more frequently in patients treated with CDT, no statistically significant differences were found in terms of complications between the two groups[118].

CONCLUSION

VTE events in IBD may increase as the incidence of IBD and life expectancy also increase. The risk of arterial TE is significantly lower than VTE, but an increased risk of cardiovascular diseases need to be monitored in IBD patients. Patients with IBD have a higher baseline risk of VTE, which further increases with surgery and corticosteroid therapy. Long-term complications of VTE can include post-thrombotic syndrome or chronic thromboembolic pulmonary hypertension. Thus focus on prevention and consideration of the utility of post-discharge prophylaxis and effort of implementation of VTE prophylaxis should be continued. The pathogenesis of TE in IBD is multifactorial and incompletely understood. The activation of coagulation is

recognized as an important component of the inflammatory response in IBD, and is also significant in the progression and possible pathogenesis. Whereas intestinal bacterial components may trigger the coagulation cascade in IBD, the gut microbiome could be an innovative approach for decreasing the risk of thrombosis in IBD.

REFERENCES

1 **Vegh Z**, Kurti Z, Gonczi L, Golovics PA, Lovasz BD, Szita I, Balogh M, Pandur T, Vavricka SR, Rogler G, Lakatos L, Lakatos PL. Association of extraintestinal manifestations and anaemia with disease outcomes in patients with inflammatory bowel disease. *Scand J Gastroenterol* 2016; **51**: 848-854 [PMID: 26880133 DOI: 10.3109/00365521.2016.1140807]

2 **Nguyen GC**, Sam J. Rising prevalence of venous thromboembolism and its impact on mortality among hospitalized inflammatory bowel disease patients. *Am J Gastroenterol* 2008; **103**: 2272-2280 [PMID: 18684186 DOI: 10.1111/j.1572-0241.2008.02052.x]

3 **Grainge MJ**, West J, Card TR. Venous thromboembolism during active disease and remission in inflammatory bowel disease: a cohort study. *Lancet* 2010; **375**: 657-663 [PMID: 20149425 DOI: 10.1016/S0140-6736(09)61963-2]

4 **Centers for Disease Control and Prevention (CDC)**. Venous thromboembolism in adult hospitalizations - United States, 2007-2009. *MMWR Morb Mortal Wkly Rep* 2012; **61**: 401-404 [PMID: 22672974]

5 **Bernstein CN**, Blanchard JF, Houston DS, Wajda A. The incidence of deep venous thrombosis and pulmonary embolism among patients with inflammatory bowel disease: a population-based cohort study. *Thromb Haemost* 2001; **85**: 430-434 [PMID: 11307809]

6 **Murthy SK**, Nguyen GC. Venous thromboembolism in inflammatory bowel disease: an epidemiological review. *Am J Gastroenterol* 2011; **106**: 713-718 [PMID: 21407182 DOI: 10.1038/ajg.2011.53]

7 **Papay P**, Miehsler W, Tilg H, Petritsch W, Reinisch W, Mayer A, Haas T, Kaser A, Feichtenschlager T, Fuchssteiner H, Knoflach P, Vogelsang H, Platzer R, Tillinger W, Jaritz B, Schmid A, Blaha B, Dejaco C, Sobala A, Weltermann A, Eichinger S, Novacek G. Clinical presentation of venous thromboembolism in inflammatory bowel disease. *J Crohns Colitis* 2013; **7**: 723-729 [PMID: 23127785 DOI: 10.1016/j.crohns.2012.10.008]

8 **Nylund CM**, Goudie A, Garza JM, Crouch G, Denson LA. Venous thrombotic events in hospitalized children and adolescents with inflammatory bowel disease. *J Pediatr Gastroenterol Nutr* 2013; **56**: 485-491 [PMID: 23232326 DOI: 10.1097/MPG.0b013e3182801e43]

9 **Quera R**, Shanahan F. Thromboembolism--an important manifestation of inflammatory bowel disease. *Am J Gastroenterol* 2004; **99**: 1971-1973 [PMID: 15447758 DOI: 10.1111/j.1572-0241.2004.40923.x]

10 **Solem CA**, Loftus EV, Tremaine WJ, Sandborn WJ. Venous thromboembolism in inflammatory bowel disease. *Am J Gastroenterol* 2004; **99**: 97-101 [PMID: 14687149 DOI: 10.1046/j.1572-0241.2003.04026.x]

11 **Landman C**, Nahon S, Cosnes J, Bouhnik Y, Brixi-Benmansour H, Bouguen G, Colombel JF, Savoye G, Coffin B, Abitbol V, Filippi J, Laharie D, Moreau J, Veyrac M, Allez M, Marteau P; Groupe d'Etude Thérapeutique des Affections Inflammatoires du Tube Digestif. Portomesenteric vein thrombosis in patients with inflammatory bowel disease. *Inflamm Bowel Dis* 2013; **19**: 582-589 [PMID: 23385240 DOI: 10.1097/MIB.0b013e31827eea5f]

12 **DeFilippis EM**, Barfield E, Leifer D, Steinlauf A, Bosworth BP, Scherl EJ, Sockolow R. Cerebral venous thrombosis in inflammatory bowel disease. *J Dig Dis* 2015; **16**: 104-108 [PMID: 25395041 DOI: 10.1111/1751-2980.12212]

13 **Michiels JJ**, Michiels JM, Moossdorff W, Lao M, Maasland H, Palareti G. Diagnosis of deep vein thrombosis, and prevention of deep vein thrombosis recurrence and the post-thrombotic syndrome in the primary care medicine setting anno 2014. *World J Crit Care Med* 2015; **4**: 29-39 [PMID: 25685720 DOI: 10.5492/wjccm.v4.i1.29]

14 **Van Assche G**, Dignass A, Reinisch W, van der Woude CJ, Sturm A, De Vos M, Guslandi M, Oldenburg B, Dotan I, Marteau P, Ardizzone A, Baumgart DC, D'Haens G, Gionchetti P, Portela F, Vucelic B, Söderholm J, Escher J, Koletzko S, Kolho KL, Lukas M, Mottet C, Tilg H, Vermeire S, Carbonnel F, Cole A, Novacek G, Reinshagen M, Tsianos E, Herrlinger K, Bouhnik Y, Kiesslich R, Stange E, Travis S, Lindsay J; European Crohn's and Colitis Organisation (ECCO). The second European evidence-based Consensus on the diagnosis and management of Crohn's disease: Special situations. *J Crohns Colitis* 2010; **4**: 63-101 [PMID: 21122490 DOI: 10.1016/j.crohns.2009.09.009]

15 **Vrij AA**, Rijken J, van Wersch JW, Stockbrügger RW. Coagulation and fibrinolysis in inflammatory bowel disease and in giant cell arteritis. *Pathophysiol Haemost Thromb* 2003; **33**: 75-83 [PMID: 14624048 DOI: 10.1159/000073850]

16 **Bernstein CN**, Wajda A, Blanchard JF. The incidence of arterial thromboembolic diseases in inflammatory bowel disease: a population-based study. *Clin Gastroenterol Hepatol* 2008; **6**: 41-45 [PMID: 18063423 DOI: 10.1016/j.cgh.2007.09.016]

17 **Lin TY**, Chen YG, Lin CL, Huang WS, Kao CH. Inflammatory Bowel Disease Increases the Risk of Peripheral Arterial Disease: A Nationwide Cohort Study. *Medicine (Baltimore)* 2015; **94**: e2381

[PMID: 26717386 DOI: 10.1097/MD.0000000000002381]
18 **Xiao Z**, Pei Z, Yuan M, Li X, Chen S, Xu L. Risk of Stroke in Patients with Inflammatory Bowel Disease: A Systematic Review and Meta-analysis. *J Stroke Cerebrovasc Dis* 2015; **24**: 2774-2780 [PMID: 26360973 DOI: 10.1016/j.jstrokecerebrovasdis.2015.08.008]
19 **Singh S**, Singh H, Loftus EV Jr, Pardi DS. Risk of cerebrovascular accidents and ischemic heart disease in patients with inflammatory bowel disease: a systematic review and meta-analysis. *Clin Gastroenterol Hepatol* 2014; **12**: 382-393.e1 quiz e22 [PMID: 23978350 DOI: 10.1016/j.cgh.2013.08.023]
20 **Fumery M**, Xiaocang C, Dauchet L, Gower-Rousseau C, Peyrin-Biroulet L, Colombel JF. Thromboembolic events and cardiovascular mortality in inflammatory bowel diseases: a meta-analysis of observational studies. *J Crohns Colitis* 2014; **8**: 469-479 [PMID: 24183231 DOI: 10.1016/j.crohns.2013.09.021]
21 **Gandhi S**, Narula N, Marshall JK, Farkouh M. Are patients with inflammatory bowel disease at increased risk of coronary artery disease? *Am J Med* 2012; **125**: 956-962 [PMID: 22840916 DOI: 10.1016/j.amjmed.2012.03.015]
22 **Colman RW**. Are hemostasis and thrombosis two sides of the same coin? *J Exp Med* 2006; **203**: 493-495 [PMID: 16533890 DOI: 10.1084/jem.20060217]
23 **Hudson M**, Hutton RA, Wakefield AJ, Sawyerr AM, Pounder RE. Evidence for activation of coagulation in Crohn's disease. *Blood Coagul Fibrinolysis* 1992; **3**: 773-778 [PMID: 1489898 DOI: 10.1097/00001721-199212000-00011]
24 **Stadnicki A**, Gonciarz M, Niewiarowski TJ, Hartleb J, Rudnicki M, Merrell NB, Dela Cadena RA, Colman RW. Activation of plasma contact and coagulation systems and neutrophils in the active phase of ulcerative colitis. *Dig Dis Sci* 1997; **42**: 2356-2366 [PMID: 9398817 DOI: 10.1023/a:1018891323205]
25 **Souto JC**, Martínez E, Roca M, Mateo J, Pujol J, González D, Fontcuberta J. Prothrombotic state and signs of endothelial lesion in plasma of patients with inflammatory bowel disease. *Dig Dis Sci* 1995; **40**: 1883-1889 [PMID: 7555437 DOI: 10.1007/BF02208650]
26 **Larsen TB**, Nielsen JN, Fredholm L, Lund ED, Brandslund I, Munkholm P, Hey H. Platelets and anticoagulant capacity in patients with inflammatory bowel disease. *Pathophysiol Haemost Thromb* 2002; **32**: 92-96 [PMID: 12214155 DOI: 10.1159/000065082]
27 **Saibeni S**, Vecchi M, Valsecchi C, Faioni EM, Razzari C, de Franchis R. Reduced free protein S levels in patients with inflammatory bowel disease: prevalence, clinical relevance, and role of anti-protein S antibodies. *Dig Dis Sci* 2001; **46**: 637-643 [PMID: 11318545 DOI: 10.1023/a:1005675921664]
28 **Saibeni S**, Bottasso B, Spina L, Bajetta M, Danese S, Gasbarrini A, de Franchis R, Vecchi M. Assessment of thrombin-activatable fibrinolysis inhibitor (TAFI) plasma levels in inflammatory bowel diseases. *Am J Gastroenterol* 2004; **99**: 1966-1970 [PMID: 15447757 DOI: 10.1111/j.1572-0241.2004.30203.x]
29 **Owczarek D**, Undas A, Foley JH, Nesheim ME, Jabłonski K, Mach T. Activated thrombin activatable fibrinolysis inhibitor (TAFIa) is associated with inflammatory markers in inflammatory bowel diseases TAFIa level in patients with IBD. *J Crohns Colitis* 2012; **6**: 13-20 [PMID: 22261523 DOI: 10.1016/j.crohns.2011.06.005]
30 **Collins CE**, Cahill MR, Newland AC, Rampton DS. Platelets circulate in an activated state in inflammatory bowel disease. *Gastroenterology* 1994; **106**: 840-845 [PMID: 8143990 DOI: 10.1016/0016-5085(94)90741-2]
31 **Meucci G**, Pareti F, Vecchi M, Saibeni S, Bressi C, de Franchis R. Serum von Willebrand factor levels in patients with inflammatory bowel disease are related to systemic inflammation. *Scand J Gastroenterol* 1999; **34**: 287-290 [PMID: 10232874 DOI: 10.1080/00365529950173708]
32 **Boehme MW**, Autschbach F, Zuna I, Scherbaum WA, Stange E, Raeth U, Sieg A, Stremmel W. Elevated serum levels and reduced immunohistochemical expression of thrombomodulin in active ulcerative colitis. *Gastroenterology* 1997; **113**: 107-117 [PMID: 9207268 DOI: 10.1016/s0016-5085(97)70086-6]
33 **Thompson NP**, Wakefield AJ, Pounder RE. Inherited disorders of coagulation appear to protect against inflammatory bowel disease. *Gastroenterology* 1995; **108**: 1011-1015 [PMID: 7698567 DOI: 10.1016/0016-5085(95)90197-3]
34 **Yoshida H**, Granger DN. Inflammatory bowel disease: a paradigm for the link between coagulation and inflammation. *Inflamm Bowel Dis* 2009; **15**: 1245-1255 [PMID: 19253306 DOI: 10.1002/ibd.20896]
35 **Stadnicki A**. Involvement of coagulation and hemostasis in inflammatory bowel diseases. *Curr Vasc Pharmacol* 2012; **10**: 659-669 [PMID: 22272910 DOI: 10.2174/157016112801784495]
36 **Van de Wouwer M**, Collen D, Conway EM. Thrombomodulin-protein C-EPCR system: integrated to regulate coagulation and inflammation. *Arterioscler Thromb Vasc Biol* 2004; **24**: 1374-1383 [PMID: 15178554 DOI: 10.1161/01.ATV.0000134298.25489.92]
37 **Andoh A**, Tsujikawa T, Hata K, Araki Y, Kitoh K, Sasaki M, Yoshida T, Fujiyama Y. Elevated circulating platelet-derived microparticles in patients with active inflammatory bowel disease. *Am J Gastroenterol* 2005; **100**: 2042-2048 [PMID: 16128950 DOI: 10.1111/j.1572-0241.2005.50381.x]
38 **Deutschmann A**, Schlagenhauf A, Leschnik B, Hoffmann KM, Hauer A, Muntean W. Increased procoagulant function of microparticles in pediatric inflammatory bowel disease: role in increased thrombin generation. *J Pediatr Gastroenterol Nutr* 2013; **56**: 401-407 [PMID: 23164759 DOI: 10.1097/MPG.0b013e31827daf72]

39 **Stadnicki A**. Thrombin generation and microparticles in inflammatory bowel diseases. *J Pediatr Gastroenterol Nutr* 2013; **56**: 343 [PMID: 23531480 DOI: 10.1097/MPG.0b013e31827daf94]

40 **Danese S**, Katz JA, Saibeni S, Papa A, Gasbarrini A, Vecchi M, Fiocchi C. Activated platelets are the source of elevated levels of soluble CD40 ligand in the circulation of inflammatory bowel disease patients. *Gut* 2003; **52**: 1435-1441 [PMID: 12970136 DOI: 10.1136/gut.52.10.1435]

41 **Steinhoff M**, Buddenkotte J, Shpacovitch V, Rattenholl A, Moormann C, Vergnolle N, Luger TA, Hollenberg MD. Proteinase-activated receptors: transducers of proteinase-mediated signaling in inflammation and immune response. *Endocr Rev* 2005; **26**: 1-43 [PMID: 15689571 DOI: 10.1210/er.2003-0025]

42 **Vetrano S**, Ploplis VA, Sala E, Sandoval-Cooper M, Donahue DL, Correale C, Arena V, Spinelli A, Repici A, Malesci A, Castellino FJ, Danese S. Unexpected role of anticoagulant protein C in controlling epithelial barrier integrity and intestinal inflammation. *Proc Natl Acad Sci U S A* 2011; **108**: 19830-19835 [PMID: 22109555 DOI: 10.1073/pnas.1107140108]

43 **Faioni EM**, Ferrero S, Fontana G, Gianelli U, Ciulla MM, Vecchi M, Saibeni S, Biguzzi E, Cordani N, Franchi F, Bosari S, Cattaneo M. Expression of endothelial protein C receptor and thrombomodulin in the intestinal tissue of patients with inflammatory bowel disease. *Crit Care Med* 2004; **32**: S266-S270 [PMID: 15118529 DOI: 10.1097/01.ccm.0000128032.85396.83]

44 **Pontarollo G**, Mann A, Brandão I, Malinarich F, Schöpf M, Reinhardt C. Protease-activated receptor signaling in intestinal permeability regulation. *FEBS J* 2020; **287**: 645-658 [PMID: 31495063 DOI: 10.1111/febs.15055]

45 **Cognasse F**, Hamzeh H, Chavarin P, Acquart S, Genin C, Garraud O. Evidence of Toll-like receptor molecules on human platelets. *Immunol Cell Biol* 2005; **83**: 196-198 [PMID: 15748217 DOI: 10.1111/j.1440-1711.2005.01314.x]

46 **Faure E**, Equils O, Sieling PA, Thomas L, Zhang FX, Kirschning CJ, Polentarutti N, Muzio M, Arditi M. Bacterial lipopolysaccharide activates NF-kappaB through toll-like receptor 4 (TLR-4) in cultured human dermal endothelial cells. Differential expression of TLR-4 and TLR-2 in endothelial cells. *J Biol Chem* 2000; **275**: 11058-11063 [PMID: 10753909 DOI: 10.1074/jbc.275.15.11058]

47 **Pastorelli L**, Dozio E, Pisani LF, Boscolo-Anzoletti M, Vianello E, Munizio N, Spina L, Tontini GE, Peyvandi F, Corsi Romanelli MM, Vecchi M. Procoagulatory state in inflammatory bowel diseases is promoted by impaired intestinal barrier function. *Gastroenterol Res Pract* 2015; **2015**: 189341 [PMID: 25767508 DOI: 10.1155/2015/189341]

48 **Hasan RA**, Koh AY, Zia A. The gut microbiome and thromboembolism. *Thromb Res* 2020; **189**: 77-87 [PMID: 32192995 DOI: 10.1016/j.thromres.2020.03.003]

49 **Warrier M**, Shih DM, Burrows AC, Ferguson D, Gromovsky AD, Brown AL, Marshall S, McDaniel A, Schugar RC, Wang Z, Sacks J, Rong X, Vallim TA, Chou J, Ivanova PT, Myers DS, Brown HA, Lee RG, Crooke RM, Graham MJ, Liu X, Parini P, Tontonoz P, Lusis AJ, Hazen SL, Temel RE, Brown JM. The TMAO-Generating Enzyme Flavin Monooxygenase 3 Is a Central Regulator of Cholesterol Balance. *Cell Rep* 2015; **10**: 326-338 [PMID: 25600868 DOI: 10.1016/j.celrep.2014.12.036]

50 **Wang Z**, Klipfell E, Bennett BJ, Koeth R, Levison BS, Dugar B, Feldstein AE, Britt EB, Fu X, Chung YM, Wu Y, Schauer P, Smith JD, Allayee H, Tang WH, DiDonato JA, Lusis AJ, Hazen SL. Gut flora metabolism of phosphatidylcholine promotes cardiovascular disease. *Nature* 2011; **472**: 57-63 [PMID: 21475195 DOI: 10.1038/nature09922]

51 **Zhu W**, Gregory JC, Org E, Buffa JA, Gupta N, Wang Z, Li L, Fu X, Wu Y, Mehrabian M, Sartor RB, McIntyre TM, Silverstein RL, Tang WHW, DiDonato JA, Brown JM, Lusis AJ, Hazen SL. Gut Microbial Metabolite TMAO Enhances Platelet Hyperreactivity and Thrombosis Risk. *Cell* 2016; **165**: 111-124 [PMID: 26972052 DOI: 10.1016/j.cell.2016.02.011]

52 **Alam MT**, Amos GCA, Murphy ARJ, Murch S, Wellington EMH, Arasaradnam RP. Microbial imbalance in inflammatory bowel disease patients at different taxonomic levels. *Gut Pathog* 2020; **12**: 1 [PMID: 31911822 DOI: 10.1186/s13099-019-0341-6]

53 **Kappelman MD**, Horvath-Puho E, Sandler RS, Rubin DT, Ullman TA, Pedersen L, Baron JA, Sørensen HT. Thromboembolic risk among Danish children and adults with inflammatory bowel diseases: a population-based nationwide study. *Gut* 2011; **60**: 937-943 [PMID: 21339206 DOI: 10.1136/gut.2010.228585]

54 **Alatri A**, Schoepfer A, Fournier N, Engelberger RP, Safroneeva E, Vavricka S, Biedermann L, Calanca L, Mazzolai L; Swiss IBD Cohort Study Group. Prevalence and risk factors for venous thromboembolic complications in the Swiss Inflammatory Bowel Disease Cohort. *Scand J Gastroenterol* 2016; **51**: 1200-1205 [PMID: 27211077 DOI: 10.1080/00365521.2016.1185464]

55 **Weng MT**, Park SH, Matsuoka K, Tung CC, Lee JY, Chang CH, Yang SK, Watanabe M, Wong JM, Wei SC. Incidence and Risk Factor Analysis of Thromboembolic Events in East Asian Patients With Inflammatory Bowel Disease, a Multinational Collaborative Study. *Inflamm Bowel Dis* 2018; **24**: 1791-1800 [PMID: 29726897 DOI: 10.1093/ibd/izy058]

56 **Miehsler W**, Reinisch W, Valic E, Osterode W, Tillinger W, Feichtenschlager T, Grisar J, Machold K, Scholz S, Vogelsang H, Novacek G. Is inflammatory bowel disease an independent and disease specific risk factor for thromboembolism? *Gut* 2004; **53**: 542-548 [PMID: 15016749 DOI: 10.1136/gut.2003.025411]

57 **van Bodegraven AA**, Schoorl M, Linskens RK, Bartels PC, Tuynman HA. Persistent activation of coagulation and fibrinolysis after treatment of active ulcerative colitis. *Eur J Gastroenterol Hepatol* 2002; **14**: 413-418 [PMID: 11943956 DOI: 10.1097/00042737-200204000-00014]

58 **Zöller B**, Li X, Sundquist J, Sundquist K. Autoimmune diseases and venous thromboembolism: a review of the literature. *Am J Cardiovasc Dis* 2012; **2**: 171-183 [PMID: 22937487]

59 **Owczarek D**, Cibor D, Sałapa K, Głowacki MK, Mach T, Undas A. Reduced plasma fibrin clot permeability and susceptibility to lysis in patients with inflammatory bowel disease: a novel prothrombotic mechanism. *Inflamm Bowel Dis* 2013; **19**: 2616-2624 [PMID: 24108112 DOI: 10.1097/01.MIB.0000437041.59208.44]

60 **Bollen L**, Vande Casteele N, Peeters M, Van Assche G, Ferrante M, Van Moerkercke W, Declerck P, Vermeire S, Gils A. The Occurrence of Thrombosis in Inflammatory Bowel Disease Is Reflected in the Clot Lysis Profile. *Inflamm Bowel Dis* 2015; **21**: 2540-2548 [PMID: 26313696 DOI: 10.1097/MIB.0000000000000531]

61 **Novacek G**, Weltermann A, Sobala A, Tilg H, Petritsch W, Reinisch W, Mayer A, Haas T, Kaser A, Feichtenschlager T, Fuchssteiner H, Knoflach P, Vogelsang H, Miehsler W, Platzer R, Tillinger W, Jaritz B, Schmid A, Blaha B, Dejaco C, Eichinger S. Inflammatory bowel disease is a risk factor for recurrent venous thromboembolism. *Gastroenterology* 2010; **139**: 779-787, 787.e1 [PMID: 20546736 DOI: 10.1053/j.gastro.2010.05.026]

62 **Bollen L**, Vande Casteele N, Ballet V, van Assche G, Ferrante M, Vermeire S, Gils A. Thromboembolism as an important complication of inflammatory bowel disease. *Eur J Gastroenterol Hepatol* 2016; **28**: 1-7 [PMID: 26513610 DOI: 10.1097/MEG.0000000000000495]

63 **deFonseka AM**, Tuskey A, Conaway MR, Behm BW. Antitumor Necrosis Factor-α Therapy Is Associated With Reduced Risk of Thromboembolic Events in Hospitalized Patients With Inflammatory Bowel Disease. *J Clin Gastroenterol* 2016; **50**: 578-583 [PMID: 26368297 DOI: 10.1097/MCG.0000000000000408]

64 **Faye AS**, Wen T, Ananthakrishnan AN, Lichtiger S, Kaplan GG, Friedman AM, Lawlor G, Wright JD, Attenello FJ, Mack WJ, Lebwohl B. Acute Venous Thromboembolism Risk Highest Within 60 D After Discharge From the Hospital in Patients With Inflammatory Bowel Diseases. *Clin Gastroenterol Hepatol* 2020; **18**: 1133-1141.e3 [PMID: 31336196 DOI: 10.1016/j.cgh.2019.07.028]

65 **Galanaud JP**, Holcroft CA, Rodger MA, Kovacs MJ, Betancourt MT, Wells PS, Anderson DR, Chagnon I, Le Gal G, Solymoss S, Crowther MA, Perrier A, White RH, Vickars LM, Ramsay T, Kahn SR. Predictors of post-thrombotic syndrome in a population with a first deep vein thrombosis and no primary venous insufficiency. *J Thromb Haemost* 2013; **11**: 474-480 [PMID: 23279046 DOI: 10.1111/jth.12106]

66 **Anderson A**, Click B, Ramos-Rivers C, Cheng D, Babichenko D, Koutroubakis IE, Hashash JG, Schwartz M, Swoger J, Barrie AM 3rd, Dunn MA, Regueiro M, Binion DG. Lasting Impact of Clostridium difficile Infection in Inflammatory Bowel Disease: A Propensity Score Matched Analysis. *Inflamm Bowel Dis* 2017; **23**: 2180-2188 [PMID: 29084081 DOI: 10.1097/MIB.0000000000001251]

67 **Bhandari S**, Mohammed Abdul MK, Dhakal B, Kreuziger LB, Saeian K, Stein D. Increased Rate of Venous Thromboembolism in Hospitalized Inflammatory Bowel Disease Patients with Clostridium Difficile Infection. *Inflamm Bowel Dis* 2017; **23**: 1847-1852 [PMID: 28837518 DOI: 10.1097/MIB.0000000000001218]

68 **Ananthakrishnan AN**, Cagan A, Gainer VS, Cheng SC, Cai T, Scoville E, Konijeti GG, Szolovits P, Shaw SY, Churchill S, Karlson EW, Murphy SN, Kohane I, Liao KP. Thromboprophylaxis is associated with reduced post-hospitalization venous thromboembolic events in patients with inflammatory bowel diseases. *Clin Gastroenterol Hepatol* 2014; **12**: 1905-1910 [PMID: 24632349 DOI: 10.1016/j.cgh.2014.02.034]

69 **Ismail G**, Mircescu G, Ditoiu AV, Tacu BD, Jurubita R, Harza M. Risk factors for predicting venous thromboembolism in patients with nephrotic syndrome: focus on haemostasis-related parameters. *Int Urol Nephrol* 2014; **46**: 787-792 [PMID: 24078010 DOI: 10.1007/s11255-013-0574-0]

70 **van Bodegraven AA**, Meuwissen SG. Lipoprotein (a), thrombophilia and inflammatory bowel disease. *Eur J Gastroenterol Hepatol* 2001; **13**: 1407-1409 [PMID: 11742187 DOI: 10.1097/00042737-200112000-00002]

71 **Koutroubakis IE**, Petinaki E, Anagnostopoulou E, Kritikos H, Mouzas IA, Kouroumalis EA, Manousos ON. Anti-cardiolipin and anti-beta2-glycoprotein I antibodies in patients with inflammatory bowel disease. *Dig Dis Sci* 1998; **43**: 2507-2512 [PMID: 9824143 DOI: 10.1023/a:1026602803622]

72 **Sipeki N**, Davida L, Palyu E, Altorjay I, Harsfalvi J, Szalmas PA, Szabo Z, Veres G, Shums Z, Norman GL, Lakatos PL, Papp M. Prevalence, significance and predictive value of antiphospholipid antibodies in Crohn's disease. *World J Gastroenterol* 2015; **21**: 6952-6964 [PMID: 26078573 DOI: 10.3748/wjg.v21.i22.6952]

73 **Bjerregaard LT**, Nederby NJ, Fredholm L, Brandslund I, Munkholm P, Hey H. Hyperhomocysteinaemia, coagulation pathway activation and thrombophilia in patients with inflammatory bowel disease. *Scand J Gastroenterol* 2002; **37**: 62-67 [PMID: 11843038 DOI: 10.1080/003655202753387374]

74 **Oussalah A**, Guéant JL, Peyrin-Biroulet L. Meta-analysis: hyperhomocysteinaemia in inflammatory bowel diseases. *Aliment Pharmacol Ther* 2011; **34**: 1173-1184 [PMID: 21967576 DOI: 10.1111/j.1365-2036.2011.04864.x]

75 **Danese S**, Sans M, Fiocchi C. Inflammatory bowel disease: the role of environmental factors. *Autoimmun Rev* 2004; **3**: 394-400 [PMID: 15288007 DOI: 10.1016/j.autrev.2004.03.002]

76 **Cotton CC**, Baird D, Sandler RS, Long MD. Hormonal Contraception Use is Common Among

Patients with Inflammatory Bowel Diseases and an Elevated Risk of Deep Vein Thrombosis. *Inflamm Bowel Dis* 2016; **22**: 1631-1638 [PMID: 27306071 DOI: 10.1097/MIB.0000000000000800]

77 **Stadnicki A**, Bojko B, Myczkowska K, Witalińska-Łabuzek J. [Selected risk factors of thrombotic complications in patients with ulcerative colitis]. *Wiad Lek* 2003; **56**: 341-347 [PMID: 14969162]

78 **Byard RW**. Deep venous thrombosis, pulmonary embolism and long-distance flights. *Forensic Sci Med Pathol* 2019; **15**: 122-124 [PMID: 29948593 DOI: 10.1007/s12024-018-9991-9]

79 **Maxwell SR**, Moots RJ, Kendall MJ. Corticosteroids: do they damage the cardiovascular system? *Postgrad Med J* 1994; **70**: 863-870 [PMID: 7870631 DOI: 10.1136/pgmj.70.830.863]

80 **Nguyen GC**, Elnahas A, Jackson TD. The impact of preoperative steroid use on short-term outcomes following surgery for inflammatory bowel disease. *J Crohns Colitis* 2014; **8**: 1661-1667 [PMID: 25107847 DOI: 10.1016/j.crohns.2014.07.007]

81 **Błoński W**, Stadnicki A, Lichtenstein G, Burke A. Infliximab use in ulcerative colitis. In: Ulcerative Colitis. The complete quid to medical management. Ed: GR Lichtenstein, EJ Scherl. New York, Slack Inc, 2011: 237-254

82 **Hommes DW**, van Dullemen HM, Levi M, van der Ende A, Woody J, Tytgat GN, van Deventer SJ. Beneficial effect of treatment with a monoclonal anti-tumor necrosis factor-alpha antibody on markers of coagulation and fibrinolysis in patients with active Crohn's disease. *Haemostasis* 1997; **27**: 269-277 [PMID: 9731107 DOI: 10.1159/000217467]

83 **Danese S**, Sans M, Scaldaferri F, Sgambato A, Rutella S, Cittadini A, Piqué JM, Panes J, Katz JA, Gasbarrini A, Fiocchi C. TNF-alpha blockade down-regulates the CD40/CD40L pathway in the mucosal microcirculation: a novel anti-inflammatory mechanism of infliximab in Crohn's disease. *J Immunol* 2006; **176**: 2617-2624 [PMID: 16456024 DOI: 10.4049/jimmunol.176.4.2617]

84 **Di Sabatino A**, Santilli F, Guerci M, Simeone P, Ardizzone S, Massari A, Giuffrida P, Tripaldi R, Malara A, Liani R, Gurini E, Aronico N, Balduini A, Corazza GR, Davě G. Oxidative stress and thromboxane-dependent platelet activation in inflammatory bowel disease: effects of anti-TNF-α treatment. *Thromb Haemost* 2016; **116**: 486-495 [PMID: 27305860 DOI: 10.1160/TH16-02-0167]

85 **Bollen L**, Vande Casteele N, Peeters M, Bessonov K, Van Steen K, Rutgeerts P, Ferrante M, Hoylaerts MF, Vermeire S, Gils A. Short-term effect of infliximab is reflected in the clot lysis profile of patients with inflammatory bowel disease: a prospective study. *Inflamm Bowel Dis* 2015; **21**: 570-578 [PMID: 25659086 DOI: 10.1097/MIB.0000000000000301]

86 **Szemes K**, Soós A, Hegyi P, Farkas N, Erős A, Erőss B, Mezősi E, Szakács Z, Márta K, Sarlós P. Comparable Long-Term Outcomes of Cyclosporine and Infliximab in Patients With Steroid-Refractory Acute Severe Ulcerative Colitis: A Meta-Analysis. *Front Med (Lausanne)* 2019; **6**: 338 [PMID: 32039218 DOI: 10.3389/fmed.2019.00338]

87 **Desai RJ**, Pawar A, Weinblatt ME, Kim SC. Comparative Risk of Venous Thromboembolism in Rheumatoid Arthritis Patients Receiving Tofacitinib Versus Those Receiving Tumor Necrosis Factor Inhibitors: An Observational Cohort Study. *Arthritis Rheumatol* 2019; **71**: 892-900 [PMID: 30552833 DOI: 10.1002/art.40798]

88 Communication, FDS FDA approves Boxed Warning about increased risk of blood clots and death with higher dose of arthritis and ulcerative colitis medicine tofacitinib (Xeljanz, Xeljanz XR); FDA Drug Safety Communication 2019. [cited 20 February 2021]. Available from: https://www.fda.gov/drugs/drug-safety-and-availability/

89 **Sandborn WJ**, Panés J, Sands BE, Reinisch W, Su C, Lawendy N, Koram N, Fan H, Jones TV, Modesto I, Quirk D, Danese S. Venous thromboembolic events in the tofacitinib ulcerative colitis clinical development programme. *Aliment Pharmacol Ther* 2019; **50**: 1068-1076 [PMID: 31599001 DOI: 10.1111/apt.15514]

90 **Fleming F**, Gaertner W, Ternent CA, Finlayson E, Herzig D, Paquette IM, Feingold DL, Steele SR. The American Society of Colon and Rectal Surgeons Clinical Practice Guideline for the Prevention of Venous Thromboembolic Disease in Colorectal Surgery. *Dis Colon Rectum* 2018; **61**: 14-20 [PMID: 29219916 DOI: 10.1097/DCR.0000000000000982]

91 **McKechnie T**, Wang J, Springer JE, Gross PL, Forbes S, Eskicioglu C. Extended thromboprophylaxis following colorectal surgery in patients with inflammatory bowel disease: a comprehensive systematic clinical review. *Colorectal Dis* 2020; **22**: 663-678 [PMID: 31490000 DOI: 10.1111/codi.14853]

92 **Wilson MZ**, Connelly TM, Tinsley A, Hollenbeak CS, Koltun WA, Messaris E. Ulcerative Colitis Is Associated With an Increased Risk of Venous Thromboembolism in the Postoperative Period: The Results of a Matched Cohort Analysis. *Ann Surg* 2015; **261**: 1160-1166 [PMID: 24983992 DOI: 10.1097/SLA.0000000000000788]

93 **McCurdy JD**, Kuenzig ME, Smith G, Spruin S, Murthy SK, Carrier M, Nguyen GC, Benchimol EI. Risk of Venous Thromboembolism After Hospital Discharge in Patients With Inflammatory Bowel Disease: A Population-based Study. *Inflamm Bowel Dis* 2020; **26**: 1761-1768 [PMID: 31995204 DOI: 10.1093/ibd/izaa002]

94 **Kaplan GG**, Lim A, Seow CH, Moran GW, Ghosh S, Leung Y, Debruyn J, Nguyen GC, Hubbard J, Panaccione R. Colectomy is a risk factor for venous thromboembolism in ulcerative colitis. *World J Gastroenterol* 2015; **21**: 1251-1260 [PMID: 25632199 DOI: 10.3748/wjg.v21.i4.1251]

95 **McKenna NP**, Behm KT, Ubl DS, Glasgow AE, Mathis KL, Pemberton JH, Habermann EB, Cima RR. Analysis of Postoperative Venous Thromboembolism in Patients With Chronic Ulcerative Colitis: Is It the Disease or the Operation? *Dis Colon Rectum* 2017; **60**: 714-722 [PMID: 28594721

DOI: 10.1097/DCR.0000000000000846]

96 **Nguyen GC**, Bernstein CN, Bitton A, Chan AK, Griffiths AM, Leontiadis GI, Geerts W, Bressler B, Butzner JD, Carrier M, Chande N, Marshall JK, Williams C, Kearon C. Consensus statements on the risk, prevention, and treatment of venous thromboembolism in inflammatory bowel disease: Canadian Association of Gastroenterology. *Gastroenterology* 2014; **146**: 835-848.e6 [PMID: 24462530 DOI: 10.1053/j.gastro.2014.01.042]

97 **Mowat C**, Cole A, Windsor A, Ahmad T, Arnott I, Driscoll R, Mitton S, Orchard T, Rutter M, Younge L, Lees C, Ho GT, Satsangi J, Bloom S. IBD Section of the British Society of Gastroenterology. Guidelines for the management of inflammatory bowel disease in adults. Gut 2011; 60: 571-607 [PMID: 21464096 DOI: 10.1136/gut.2010.224154]

98 **Scoville EA**, Konijeti GG, Nguyen DD, Sauk J, Yajnik V, Ananthakrishnan AN. Venous thromboembolism in patients with inflammatory bowel diseases: a case-control study of risk factors. *Inflamm Bowel Dis* 2014; **20**: 631-636 [PMID: 24552828 DOI: 10.1097/MIB.0000000000000007]

99 **Alhassan N**, Trepanier M, Sabapathy C, Chaudhury P, Liberman AS, Charlebois P, Stein BL, Lee L. Risk factors for post-discharge venous thromboembolism in patients undergoing colorectal resection: a NSQIP analysis. *Tech Coloproctol* 2018; **22**: 955-964 [PMID: 30569263 DOI: 10.1007/s10151-018-1909-8]

100 **Nguyen GC**, Murthy SK, Bressler B, Lam MCW, Alali A, Toumi A, Reinglas J, Rampersad A, Weizman AV, Afif W; CINERGI group. Quality of Care and Outcomes Among Hospitalized Inflammatory Bowel Disease Patients: A Multicenter Retrospective Study. *Inflamm Bowel Dis* 2017; **23**: 695-701 [PMID: 28426451 DOI: 10.1097/MIB.0000000000001068]

101 **Mathers B**, Williams E, Bedi G, Messaris E, Tinsley A. An Electronic Alert System Is Associated With a Significant Increase in Pharmacologic Venous Thromboembolism Prophylaxis Rates Among Hospitalized Inflammatory Bowel Disease Patients. *J Healthc Qual* 2017; **39**: 307-314 [PMID: 27153049 DOI: 10.1097/JHQ.0000000000000021]

102 **Ra G**, Thanabalan R, Ratneswaran S, Nguyen GC. Predictors and safety of venous thromboembolism prophylaxis among hospitalized inflammatory bowel disease patients. *J Crohns Colitis* 2013; **7**: e479-e485 [PMID: 23537817 DOI: 10.1016/j.crohns.2013.03.002]

103 **Faye AS**, Hung KW, Cheng K, Blackett JW, Mckenney AS, Pont AR, Li J, Lawlor G, Lebwohl B, Freedberg DE. Minor Hematochezia Decreases Use of Venous Thromboembolism Prophylaxis in Patients with Inflammatory Bowel Disease. *Inflamm Bowel Dis* 2020; **26**: 1394-1400 [PMID: 31689354 DOI: 10.1093/ibd/izz269]

104 **Laryea J**, Champagne B. Venous thromboembolism prophylaxis. *Clin Colon Rectal Surg* 2013; **26**: 153-159 [PMID: 24436666 DOI: 10.1055/S-0033-135113]

105 **Papa A**, De Stefano V, Gasbarrini A, Chiusolo P, Cianci R, Casorelli I, Paciaroni K, Cammarota G, Leone G, Gasbarrini G. Prevalence of factor V Leiden and the G20210A prothrombin-gene mutation in inflammatory bowel disease. *Blood Coagul Fibrinolysis* 2000; **11**: 499-503 [PMID: 10937811 DOI: 10.1097/00001721-200007000-00013]

106 **Guédon C**, Le Cam-Duchez V, Lalaude O, Ménard JF, Lerebours E, Borg JY. Prothrombotic inherited abnormalities other than factor V Leiden mutation do not play a role in venous thrombosis in inflammatory bowel disease. *Am J Gastroenterol* 2001; **96**: 1448-1454 [PMID: 11374681 DOI: 10.1111/j.1572-0241.2001.03797.x]

107 **Tsiolakidou G**, Koutroubakis IE. Thrombosis and inflammatory bowel disease-the role of genetic risk factors. *World J Gastroenterol* 2008; **14**: 4440-4444 [PMID: 18680221 DOI: 10.3748/wjg.14.4440]

108 **Jacobs B**, Obi A, Wakefield T. Diagnostic biomarkers in venous thromboembolic disease. *J Vasc Surg Venous Lymphat Disord* 2016; **4**: 508-517 [PMID: 27639008 DOI: 10.1016/j.jvsv.2016.02.005]

109 **Nguyen GC**, Wu H, Gulamhusein A, Rosenberg M, Thanabalan R, Yeo EL, Bernstein CN, Steinhart AH, Margolis M. The utility of screening for asymptomatic lower extremity deep venous thrombosis during inflammatory bowel disease flares: a pilot study. *Inflamm Bowel Dis* 2013; **19**: 1053-1058 [PMID: 23429463 DOI: 10.1097/MIB.0b013e3182802a65]

110 **Saibeni S**, Saladino V, Chantarangkul V, Villa F, Bruno S, Vecchi M, de Franchis R, Sei C, Tripodi A. Increased thrombin generation in inflammatory bowel diseases. *Thromb Res* 2010; **125**: 278-282 [PMID: 19914688 DOI: 10.1016/j.thromres.2009.10.012]

111 **Kearon C**, Akl EA, Ornelas J, Blaivas A, Jimenez D, Bounameaux H, Huisman M, King CS, Morris TA, Sood N, Stevens SM, Vintch JRE, Wells P, Woller SC, Moores L. Antithrombotic Therapy for VTE Disease: CHEST Guideline and Expert Panel Report. *Chest* 2016; **149**: 315-352 [PMID: 26867832 DOI: 10.1016/j.chest.2015.11.026]

112 **Prandoni P**, Prins MH, Lensing AW, Ghirarduzzi A, Ageno W, Imberti D, Scannapieco G, Ambrosio GB, Pesavento R, Cuppini S, Quintavalla R, Agnelli G; AESOPUS Investigators. Residual thrombosis on ultrasonography to guide the duration of anticoagulation in patients with deep venous thrombosis: a randomized trial. *Ann Intern Med* 2009; **150**: 577-585 [PMID: 19414836 DOI: 10.7326/0003-4819-150-9-200905050-00003]

113 **Rennenberg RJ**. Oral anticoagulants, effect on thrombus resolution and post-thrombotic syndrome. *Phlebology* 2016; **31**: 24-27 [PMID: 26916765 DOI: 10.1177/0268355516632101]

114 **Sweetland S**, Green J, Liu B, Berrington de González A, Canonico M, Reeves G, Beral V; Million Women Study collaborators. Duration and magnitude of the postoperative risk of venous thromboembolism in middle aged women: prospective cohort study. *BMJ* 2009; **339**: b4583 [PMID: 19959589 DOI: 10.1136/bmj.b4583]

115 **van der Hulle T**, Kooiman J, den Exter PL, Dekkers OM, Klok FA, Huisman MV. Effectiveness and safety of novel oral anticoagulants as compared with vitamin K antagonists in the treatment of acute symptomatic venous thromboembolism: a systematic review and meta-analysis. *J Thromb Haemost* 2014; **12**: 320-328 [PMID: 24330006 DOI: 10.1111/jth.12485]

116 **Brighton TA**, Eikelboom JW, Mann K, Mister R, Gallus A, Ockelford P, Gibbs H, Hague W, Xavier D, Diaz R, Kirby A, Simes J; ASPIRE Investigators. Low-dose aspirin for preventing recurrent venous thromboembolism. *N Engl J Med* 2012; **367**: 1979-1987 [PMID: 23121403 DOI: 10.1056/NEJMoa1210384]

117 **Comerota AJ**. Pharmacologic and Pharmacomechanical Thrombolysis for Acute Deep Vein Thrombosis: Focus on ATTRACT[CME]. *Methodist Debakey Cardiovasc J* 2018; **14**: 219-227 [PMID: 30410653 DOI: 10.14797/mdcj-14-3-219]

118 **Tabibian JH**, Streiff MB. Inflammatory bowel disease-associated thromboembolism: a systematic review of outcomes with anticoagulation *vs* catheter-directed thrombolysis. *Inflamm Bowel Dis* 2012; **18**: 161-171 [PMID: 21805543 DOI: 10.1002/ibd.21307]

World Journal of Gastroenterology

Submit a Manuscript: https://www.f6publishing.com

World J Gastroenterol 2021 October 28; 27(40): 6775-6793

DOI: 10.3748/wjg.v27.i40.6775

ISSN 1007-9327 (print) ISSN 2219-2840 (online)

REVIEW

Understanding the immune response and the current landscape of immunotherapy in pancreatic cancer

Lorena Ostios-Garcia, Julia Villamayor, Esther Garcia-Lorenzo, David Vinal, Jaime Feliu

ORCID number: Lorena Ostios-Garcia 0000-0001-9052-5609; Julia Villamayor 0000-0002-9980-9971; Esther Garcia-Lorenzo 0000-0001-5574-9180; David Vinal 0000-0002-9905-3270; Jaime Feliu 0000-0003-4867-1420.

Author contributions: Ostios-Garcia L performed the review, wrote the manuscript and reviewed the data; Villamayor J and Garcia-Lorenzo E helped write the manuscript; Vinal D and Feliu J reviewed the data.

Supported by the Instituto de Salud Carlos III, Ministerio de Economia, Industria y Competitividad, No. PI18/01604.

Conflict-of-interest statement: Authors declare no conflict of interest for this manuscript.

Open-Access: This article is an open-access article that was selected by an in-house editor and fully peer-reviewed by external reviewers. It is distributed in accordance with the Creative Commons Attribution NonCommercial (CC BY-NC 4.0) license, which permits others to distribute, remix, adapt, build upon this work non-commercially, and license their derivative works on different terms, provided the original work is properly cited and the use is non-commercial. See: htt

Lorena Ostios-Garcia, Julia Villamayor, Esther Garcia-Lorenzo, David Vinal, Jaime Feliu, Department of Oncology, La Paz University Hospital, IDIPAZ, CIBERONC, Cátedra UAM-AMGEN, Madrid 28046, Spain

Corresponding author: Jaime Feliu, MD, PhD, Associate Professor, Chief Physician, Department of Oncology, La Paz University Hospital, IDIPAZ, CIBERONC, Cátedra UAM-AMGEN, Paseo de la Castellana, 261, Madrid 28046, Spain. jaimefeliu@hotmail.com

Abstract

Pancreatic ductal adenocarcinoma (PDAC) is an aggressive tumor with high lethality. Even with surgery, radiotherapy, chemotherapy, and other locoregional or systemic therapies, the survival rates for PDAC are low and have not significantly changed in the past decades. The special characteristics of the PDAC's microenvironment and its complex immune escape mechanism need to be considered when designing novel therapeutic approaches in this disease. PDAC is characterized by chronic inflammation with a high rate of tumor-associated macrophages and myeloid-derived suppressor cells and a low rate of natural killer and effector T cells. The pancreatic microenvironment is a fibrotic, microvascularized stroma that isolates the tumor from systemic vascularization. Immunotherapy, a novel approach that has demonstrated effectiveness in certain solid tumors, has failed to show any practice-changing results in pancreatic cancer, with the exception of PDACs with mismatch repair deficiency and high tumor mutational burden, which show prolonged survival rates with immunotherapy. Currently, numerous clinical trials are attempting to assess the efficacy of immunotherapeutic strategies in PDAC, including immune checkpoint inhibitors, cancer vaccines, and adoptive cell transfer, alone or in combination with other immunotherapeutic agents, chemoradiotherapy, and other targeted therapies. A deep understanding of the immune response will help in the development of new therapeutic strategies leading to improved clinical outcomes for patients with PDAC.

Key Words: Pancreatic cancer; Immunity; Immune evasion; Tumor microenvironment; Immunotherapy; Cancer vaccines

©The Author(s) 2021. Published by Baishideng Publishing Group Inc. All rights reserved.

p://creativecommons.org/Licenses/by-nc/4.0/

Manuscript source: Invited manuscript

Specialty type: Gastroenterology and hepatology

Country/Territory of origin: Spain

Peer-review report's scientific quality classification

Grade A (Excellent): 0
Grade B (Very good): B
Grade C (Good): 0
Grade D (Fair): 0
Grade E (Poor): 0

Received: February 23, 2021
Peer-review started: February 23, 2021
First decision: June 14, 2021
Revised: June 28, 2021
Accepted: September 19, 2021
Article in press: September 19, 2021
Published online: October 28, 2021

P-Reviewer: Chawla S
S-Editor: Wang LL
L-Editor: A
P-Editor: Yu HG



Core Tip: Immunotherapy has demonstrated effectiveness in treating several solid tumors and has become a major revolution in oncology. In pancreatic ductal adenocarcinoma, however, the outcomes continue to be poor due to its special immune response and microenvironmental characteristics. In this review, we summarize the most important concepts of the immune system and the current landscape of immunotherapy in pancreatic cancer.

Citation: Ostios-Garcia L, Villamayor J, Garcia-Lorenzo E, Vinal D, Feliu J. Understanding the immune response and the current landscape of immunotherapy in pancreatic cancer. *World J Gastroenterol* 2021; 27(40): 6775-6793
URL: https://www.wjgnet.com/1007-9327/full/v27/i40/6775.htm
DOI: https://dx.doi.org/10.3748/wjg.v27.i40.6775

INTRODUCTION

Pancreatic ductal adenocarcinoma cancer (PDAC) derives from pancreatic glandular tissue and is considered the fourth most lethal malignant tumor worldwide, with high mortality and poor prognosis[1]. The aggressive nature of PDAC is the result of a multifactorial condition related to its desmoplastic stroma and characteristic tumor microenvironment (TME), the ability to evade the immune response, the low tumor mutational burden (TMB) and the lack of effective treatments[2].

Despite the use of various approaches and therapies such as surgical resection, radiotherapy, systemic chemotherapy and the combination of these therapies[3], 80% of such patients will die within a year of the diagnosis[4]. Even for patients with resectable disease who undergo R0 pancreatic surgery, the 5-year survival rate is less than 20%[5,6], and the 5-year overall survival (OS) is lower than 7% for those with metastatic PDAC[7]. Novel therapeutic strategies such as adjuvant modified FOLFIRINOX (folinic acid, 5-fluorouracil, irinotecan, and oxaliplatin) have improved postoperative survival rates[8]. For advanced and metastatic PDAC, chemotherapy is the only treatment option. Despite the new chemotherapy regimens developed over the past few years (FOLFIRINOX and gemcitabine plus nab-paclitaxel), however, the median OS is still under 12 mo[1,8]. Most of the driver mutations identified in PDAC lack targeted therapies. Nevertheless, patients might benefit from platinum-based chemotherapy and poly (ADP-ribose) polymerase (PARP) inhibitors in the case of BRCA1/2 mutation[9], immune checkpoint inhibitors in microsatellite instability[10] and tyrosine-kinase inhibitors for patients harboring neurotrophic-tropomyosin receptor kinase (NTRK) gene fusions[11], although the improvement in survival is not as successful as in other tumors. Even with all these advances, the OS for PDAC has hardly improved in recent decades.

Immunotherapy is a classic treatment approach and has been recognized since 2017 as the fourth pillar of treatment for many solid tumors[12]. A high number of preclinical and clinical studies are evaluating the efficacy of immunotherapeutic strategies in PDAC, including immune checkpoint inhibitors, cancer vaccines, and adoptive cell transfer, combined with other immunotherapeutic agents, chemoradiotherapy or other molecularly targeted agents. However, this new strategy still fails to meet the clinical needs of patients with PDAC, a consequence of the complex immune escape mechanisms, which need to be understood to improve the efficacy of new therapies.

In this review, we summarize the immune response mechanisms, the current landscape and the limitations of immunotherapy in PDAC.

IMMUNE RESPONSE IN PANCREATIC CANCER

The immune system and inflammatory state involve numerous interactions with premalignant and malignant lesions. While chronic inflammation induced by the immune system is associated with tumor growth[13], tumors cause tissue destruction and trigger inflammatory signals leading to the recruitment of cells of the innate immune system such as natural killer (NK), T cells, macrophages, and dendritic cells

(DCs)[13]. Inflammation is characterized by supporting hallmarks capabilities that contribute to tumor progression by providing cytokines, chemokines, proteases, and growth and proangiogenic factors; encouraging angiogenesis and tissue remodeling, assisting in the invasion and metastasis and ultimately driving local and systemic immune suppression[13].

In an effort to understand the dynamics of the immune response from preinvasive pancreatic intraepithelial neoplasia (PanIN) to invasive and metastatic PDAC, a study with genetically engineered *KRAS* and p53 mutant mice showed that immune system cells with suppressive properties are involved from the earliest stages of tumorigenesis. The *RAS* oncogene induces inflammation and immune suppression in the microenvironment, and both carry immune privilege in the tumor[14]. The predominant cells in the tumor stroma are immunosuppressive leukocytes that weakens the antitumor functions of lymphocytes infiltrating the pancreas and promote disease progression[15]. In contrast, many other solid tumors harbor a larger infiltration of effector T cells, which has been associated with enhanced clinical outcomes [14].

Immune system cells in pancreatic ductal adenocarcinoma

The most common immune cells in the tumor microenvironment (from PanIN to PDAC) include tumor-associated macrophages (TAM), myeloid-derived suppressor cells (MDSC), neutrophils, regulatory T cells (Treg), a smaller number of effector T cells and, rarely, NK cells[13-15].

TAMs and MDSCs are innate immune cells that play a dual role in PDAC and are involved in cancer cell recognition and antitumor response but also lead to chronic inflammation[16,17]. Macrophages are predominant in the initial stages of the disease, but the ratio of TAMs and MDSCs becomes similar as the disease progresses[15]. There are very few lymphocytes in the tumor; CD4+ T cells, along with a high portion of Tregs, are the most frequent. NK and CD8+ T cells are extremely rare at any stage [15].

Tumor-associated macrophages

Two types of TAMs have been identified: M1 and M2 macrophages. M1 macrophages secrete proinflammatory cytokines with antineoplastic effects, while M2 macrophages release cytokines that lead to tumor progression[18,19]. Macrophages are the most common immune cells in the tumor microenvironment at the early stage. Several reports have shown an inverse correlation between the prognosis and M2 TAM infiltration in vairous tumors, including PDAC[20,21].

TAMs produce cytokines, proteases and metabolites, such as indoleamine dioxygenase and reactive oxygen species, which inhibit T-cell activity against tumor and attract Tregs to the tumor site[22]. Moreover, TAMs facilitate tumor angiogenesis by releasing pro-angiogenic factors such as vascular endothelial growth factor (VEGF) and participate in matrix remodeling to facilitate invasion and metastasis[23].

Myeloid derived suppressor cells

MDSCs are a heterogeneous group of immature cells divided into polymorphonuclear (PMN-MDSC) and monocytic (M-MDSC), resembling neutrophils and monocytes, respectively[24,25]. Myeloid cells are more frequent in the advanced stages of PDAC, when the number of these cells is comparable to TAMs'. MDSCs inhibit the innate antitumor immunity[26].

MDSCs have a variety of mechanisms to attenuate immune response. They inhibit the antigen-specific response of CD4+ and CD8+ T cells. Some of these mechanisms occur through direct cell-to-cell contact between MDSCs and lymphocytes with the participation of programmed death-ligand 1 (PD-L1) and programmed death-1 (PD-1). MDSCS therefore induce the suppression of T-cell activation and self-tolerance[26]. In addition, MDSCs suppress the proliferation, cytokine production, and cytotoxic function of T cells[27]; decrease T-cell receptor signaling[28]; and induce apoptosis of intratumor T cells[28]. Furthermore, MDSCs induce Treg expansion through interleukin (IL)-10[29], resulting in additional suppression of T-cell function. As with TAMs, an increase in MDSCs in patients with cancer is related to high levels of VEGF [30].

Natural Killer cells

NK cells are an important immune component in controlling the antitumor immune response. These immune cells can interact with DCs, macrophages, T cells and endothelial cells through cell-to-cell contact and secreting cytokines[31]. A number of studies have found that natural killer (NK) cells are positively correlated with survival

in patients with PDAC[32]. However, PDAC is characterized by a very low count of NK cells in the tumor site (< 0.5%)[33]. Furthermore, the antitumor effect of NK cells decreases by the action of pancreatic stellate cells[34] and the expression of IL-10, transforming growth factor beta (TGF-b), indoleamine 2,3-dioxygenase (IDO), and matrix metalloproteinases (MMPs)[35].

Tumor associated Neutrophils

Tumor associated neutrophils (TANs) are typically localized at the periphery of the tumor site in early stages of the disease and infiltrate the center of the tumor in advanced stages. The neutrophil-to-lymphocyte ratio (NLR) has been studied as a predictor, and high TAN counts are correlated with poor prognoses[36-38]. However, the value of the NLR with regard to prognosis and survival prediction requires further validation.

There are two types of TANs: N1 and N2 which have different functions[39]. N1 TANs are proinflammatory and releases IL-12, tumor necrosis factor (TNF)-a and other immunostimulatory cytokines involved in the migration and activation of CD8+ T cells[40]. N2 TANs are immunosuppressive and promote angiogenesis, invasion and metastases. These tumor-promoting activities are mediated by hepatocyte growth factor (HGF), oncostatin M, reactive oxygen species (ROS), reactive nitrogen species (RNS), matrix metalloproteinase (MMPS), and neutrophil elastase (NE)[39].

T cells

PDAC presents a variable number of T cells, encompassing several T-cell subpopulations. The immunosuppressive microenvironment, compounded by fibroblast and desmoplastic stroma, prevents T-cell infiltration and influences their spatial distribution in the tumor site[41]. CD4+ and CD8+ T cells have specific regulation, produce several cytokines, and have different functions in immunity[42]. Consequently, the effects of T cells in PDAC depend on the subpopulation type, their spatial distribution, and macrophage infiltration. A high infiltration of CD4+ and CD8+ T cells, low infiltration of Treg cells, and high ratio of M1/M2 macrophages are therefore associated with greater survival in PDAC[43,44].

CD4+ lymphocytes are differentiated into T helper (Th) 1, Th2, Th17 and Treg subpopulations. Th1 produces interferon gamma (IFN-γ) and cytotoxic molecules that support cellular type I immunity (priming, activation and recruitment of cytotoxic T lymphocytes, M1 macrophages and NK cells) that attack intracellular pathogens and tumors immunity[45]. Th2 produces IL-4, IL-5 and IL-3, participates in humoral type II immunity (inducing M2 macrophages) and contributes to allergy and asthma[45]. Th2 is predominant in PDAC and is associated with disease progression[46] and shorter OS[47]. Th17 produces IL-17, IL-21 and IL-22 and protects against extracellular bacterial and fungal infections[48]. Oncogenic *KRAS*, expressed in pancreatic cells, induces the recruitment of Th17 cells into the TME[49]. Th17 and IL-17 are involved in PDAC progression[49]. A high proportion of Th17 cells in tumor site is correlated with shorter OS and distant disease.

Regulatory T cells or suppressor T cells are a subpopulation of CD4+ lymphocytes that infiltrate the tumor. The main function of Treg in healthy patients is to maintain tolerance to self-antigen and prevent autoimmune disease[50]. Treg counts increases from PanIN to advanced PDAC[15]. In case of PDAC, Tregs have differing roles depending on the tumor stage. Tregs promote tumorigenesis by suppressing the cytotoxic function of T cells, IFN- γ and IL-2, induced by tumor antigens[15]. In contrast, Tregs can delay tumor progression by assessing the suppressive myeloid cells [51]. Tregs are associated with worse prognosis and decreased survival[52].

CD8+ T cells, also Known as cytotoxic T lymphocytes and effector T lymphocytes, produce IFN-γ, TNF and cytotoxic molecules against tumor cells and protect from cancer recurrence[53]. CD8+ T cells are scarce in PDAC.

T cell evasion

The most well-known mechanism of immune tolerance in cancer is the exhaustion of effector T cells (CD8+ T lymphocytes), produced by the binding of cytotoxic T lymphocyte antigen 4 (CTLA-4) to CD80 and of PD-L1 (CD86) to PD-1. However, effector T lymphocytes are scarce in pancreatic cancer, and the inflammatory immune reaction develops early, suppressing the development of an adaptative immune response.

T cell evasion in PDAC has been describe as a 4-step process[14,15]: 1) Induction: mutations in oncogenes (*i.e.*, *KRAS*) and tumor suppressor genes initiate the process of tumorigenesis from normal pancreatic cells to PDAC. 2) Inflammation: PanIN, a

preinvasive lesion, produces soluble factors inducing local inflammation and recruitment of immune cells in the tumor site. 3) Immunosuppression: chronic inflammatory reaction and enrollment of TAMs, MDSCs and Treg cells produce immunosuppressive cytokines and suppressive response with cell-to-cell contact. Macrophages and suppressive T cells prevent effector T cells from entering the TME[54], while cytokines such as IL-10 and TGF inactivate the few effector T cells present in TME[55]. This condition prevents an efficient adaptive response against the tumor. 4) Immune Privilege: in the advanced stage of the disease, immune evasion persists, and the TME becomes a site of immune privilege for pancreatic tumor cells.

Tumor microenvironment: A barrier for immunotherapy

The PDAC microenvironment is a classical barrier involved in tumor progression[56], and low microvascular density hinders the diffusion of therapeutic agents[57,58]. This fibroinflammatory structure is a mixture of immune cells, malignant cells, and a dense desmoplastic stroma, which includes fibroblasts, blood vessels, and pancreatic stellate cells[59,60]. The stroma is a traditional characteristic of PDAC that participates in tumor growth, vascularization, drug diffusion, resistance to treatment, and metastasis [61]. Tumor cells and stromal cells undergo into a continuous change throughout the transformation process from a healthy pancreatic tissue to an invasive malignance[13]. TME plays a key role in this immunosuppression and presents similar characteristics in both primary and metastatic lesions[62].

Based on the biological, prognostic, and predictive characteristics, it is possible to differentiate two molecular subtypes (classical and basal-like)[63-65] and two stromal subtypes of PDAC (normal and activated)[66]. The basal-like subtype is associated with an activated stroma and poor prognosis[64,65]. Patients with the activated stromal PDAC subtype have a poorer prognosis compared with the normal stromal subtype, presenting a median OS of 15 *vs* 24 mo, respectively[66]. Activated stroma is associated with a greater presence of macrophages and activated fibroblasts, both responsible for poor clinical outcomes[66]. Modulating the TME would possibly redirect the immune system to eliminate the tumor, achieving greater efficiency in antitumor therapies.

Tumor mutational burden and mismatch repair deficiency: Assistance for immunotherapy

TMB is defined as the total number of nonsynonymous mutations per coding area of a tumor gene[67]. A high number of somatic mutations produces and releases neoantigens in the TME which lead to increase in inflammatory cytokines and effector T cells[2,10,68]. A high TMB therefore stimulates the efficacy of immunotherapy[67, 69]. PDAC is characterized by low immunogenicity and low TMB (1 mutation/megabase) compared with other tumors such as melanoma (10 mutations/megabase) [67] and lung or bladder cancer (just under 10 mutations/megabase)[70].

There is a known association between mismatch repair deficiency (dMMR) and high TMB, and PDAC is not an exception[71]. dMMR represents a loss of function of the mismatch repair (MMR) pathway, a DNA repair pathway that plays a key role in maintaining genomic stability. Random mutations occurring in small repetitive elements define microsatellite instability (MSI)[72]. dMMR is defined as the loss of expression of one or more of the MLH1, MSH2, MSH6, and PMS2 proteins. Characteristically, dMMR is correlated with high TMB[72] and increased effector T cells in tumor site[63]. A high MSI status, an emerging predictor of immunotherapy response in PDAC, has a prevalence of 0.3-1.3% in this tumor type[73]. Patients with this condition present prolonged survival rates[71,74]. Neoantigens must be presented by antigen-presenting cells (APCs) to achieve a T-cell response and, in the case of PDAC, DCs (the major APCs), are usually immature or scarce, causing weakened T-cell activation[75].

LANDSCAPE OF IMMUNOTHERAPY IN PANCREATIC DUCTAL ADENOCARCINOMA

Our understanding of the immune response in cancer is still incomplete and continues to be investigated, with the reported relationships between the various cell populations and microenvironment composition[59,60] the basis for the development of immune-based therapies in PDAC. The combination of several immune strategies, such as checkpoints inhibitors, immune checkpoints inhibitors or vaccines plus

chemotherapy, and the use of adoptive cellular therapy are some of these new approaches[76].

Immune checkpoints agents

Whereas immune checkpoint inhibitors have proven their efficacy in many tumors, they have falied to do so in PDAC due to its low immunogenicity and low TMB[67]. These inhibitors help to interrupt the intratumoral T-cell dysfunction and provide the block of the overexpressed receptors involved in its exhaustion such as PD-1 and CTLA-4[77]. The union between PD-L1 or PD-L2 and PD-1 induces the cessation of T-cell effector functions causing a suppression in T-cell motility[78], an antagonization of T cell receptor (TCR) signaling[79] and a suppression in gene transcription[80]. PD-L1 expression is therefore inversely correlated with survival. Thus, anti-PD-L1 and anti-PD-1 therapies have been shown to reduce tumor volume in mice that were subcutaneously injected with a murine PDAC cell line[81].

Antibody anticytotoxic T lymphocyte antigen-4

Several phase II clinical trials in PDAC have been developed using antibodies against CTLA-4, such as Ipilimumab[82] and Tremelimumab[83] as single agents; however, these studies have not achieved an impact in OS[82,83]. Ipilimumab in a phase II trial (NCT00112580) of pretreated patients with locally advanced and metastatic pancreatic cancer showed a median OS of 4.5 mo, with no responders except for one patient who had a delayed objective response. A phase II trial of Tremelimumab (NCT02527434) in metastatic pancreatic cancer had a median OS of 4 mo (95%CI 2.83-5.42), with 18 out 20 patients with progressive disease.

Antibody anti-programmed death-1

The efficacy of pembrolizumab in MSI-H PDAC has been reported in the phase II NTC02628067 study. The OS and progression-free survival (PFS) were 4 mo and 2.1 mo, respectively[76], highly disappointing results compared with those obtained in other tumors such as colorectal cancer in which a PFS of 16.5 mo was reported in the KEYNOTE-177 trial[84]. We do not have results for nivolumab or pembrolizumab as single agents in microsatellite stable tumors.

Antibody anti-programmed death-ligand 1

A phase I/II clinical trial (NCT03829501) assessing the efficacy of atezolizumab in advanced PDAC and other tumors refractory to first-line treatment is currently ongoing.

Combination of immune checkpoints agents

The combination of anti–PD-1/anti–PD-L1 and anti–CTLA-4 might have additive or synergistic activity[85]. In fact, the combination has shown enhanced activity in certain tumor types such as melanoma and non-small cell-lung cancer[85]. Several clinical trials have therefore sought to assess the efficacy of this combination.

Durvalumab alone or in combination with tremelimumab for patients with previously treated metastatic PDAC (NCT 02558894) did not achieved any improvement in OS. The combination achieved a median of 3.1 mo, while durvalumab alone achieved 3.6 mo[85]. However, the evaluation of the combination of other immunotherapy agents such as nivolumab and ipilimumab (NCT01928394) is still ongoing, with no results posted yet[86]. Table 1 Lists other immunotherapy agents that have been employed in treating PDAC.

Combination of immune checkpoints and chemotherapy

It has been suggested that the efficacy of immune checkpoint inhibitors could improve when combined with chemotherapy, the latter acting by activating the intratumoral immune response when inducing immunogenic cell death. This type of cell death is characterized by a necrolytic release of danger signals that can modify the stroma, change cytokine rates, reduce the presence of suppressive cells such as MDSCs and Tregs, promote the expression of molecules of the major histocompatibility complex (MHC) in cancerous cells and stimulate DC maturation[87]. In animal models, a synergetic effect has been observed between the combination of gemcitabine and anti-PDL1[88].

Several clinical trials have investigated the combination of immune checkpoint inhibitors and chemotherapy in PDAC. Table 2 Lists the main clinical trials in this field.

Table 1 Clinical trials on pancreatic ductal adenocarcinoma using immunotherapy

National clinical trial number	Sample	Phase	Settings	Drug	Results
NCT00112580	82	II	Advanced; Metastatic; Any line	Ipilimumab	No improvement in survival rate
NCT02527434	64	II	Advanced; Metastatic; ≥ Second line	Tremelimumab	OS 4 m (95%CI: 2.83-5.42)
NCT02558894	65	II	Metastatic; ≥ Second line	Tremelimumab + Durvalumab *vs* Durvalumab alone	OS 3.1 m (95%CI: 2.2-6.1) Combination therapy; OS 3.6 m (95%CI: 2.7-6.1) Durvalumab alone
NCT00112580	27	II	Advanced; Metastatic; ≥ Second line	Ipilimumab	No improvement in survival rate
NCT03379259	14	I	Advanced (PDAC and other tumors); ≥ Second line	Anti-PD-L1 (BMS-936559)	No improvement in survival rate
NCT01928394	1131	I/II	Advanced (PDAC and other tumors) Any line	Nivolumab ± Ipilimumab	Ongoing
NCT03829501	412	I/II	Advanced (PDAC and other tumors); ≥ Second line	Atezolizumab	Ongoing
NCT03080974	10	I	Advanced (stage III) Any line	Nivolumab +Irreversible electroporation	PFS 6.3 m (95%CI: 3.5-10.0); OS 18 m (95%CI: 9.2-26.8)

OS: Overall survival; PDAC: Pancreatic ductal adenocarcinoma; PFS: Progression-free survival.

A phase I/II clinical trial (NCT02331251) of metastatic PDAC naïve chemotherapy, tested the combination of pembrolizumab (anti-PDL1), nab-pacliatxel and gemcitabine [89], achieving a median PFS and OS of 9,1 and 15.0 mo, respectively[89].

Other combinations such as ipilimumab plus gemcitabine (NCT01473940)[90] or CD40 agonist plus gemcitabine[91] in a phase I clinical trial in first-line treatment have also improved OS in the experimental arm , with an OS of 8.5 mo and 8.4 mo, respectively. CD40 is a member of the tumor necrosis factor receptor superfamily. The binding of CD40 by its ligand or by an agonistic monoclonal antibody activates the receptor and results in APC activation, including DCs, B cells and monocytes. In mouse pancreatic cancer models, the combination of agonistic CD40 monoclonal antibody with gemcitabine plus nab-paclitaxel triggers T-cell-dependent tumor regressions and improves survival benefit, which are further augmented by the addition of an anti-PD-1 monoclonal antibody. The preliminary results from the combination of a CD40 monoclonal antibody agonist combined with gemcitabine plus nab-paclitaxel and PD1 inhibitor have been published, showing a 58% response rate from 24 evaluable patients[92].

The COMBAT/Keynote-2020 clinical trial deserves special mention. This trial is based on CXC chemokine receptor 4 (CXCR4) blockades, that promotes T-cell tumor infiltration and is synergistic with anti-PD-1 therapy in PDAC mouse models. One cohort included 22 patients and combined the CXCR4 antagonist BL-8040 (motixafortide) with pembrolizumab-nanoliposomal irinotecan-fluorouracil-folinic acid in PDAC second-line treatment. The preliminary results showed an objective response rate, disease control rate and median duration of response of 32%, 77% and 7.8 mo, respectively, suggesting that it is indeed a promising strategy in treating PDAC[93].

According to trial results, patients, who received only immunotherapy, experienced 9%-11% of grade ≥ 3 immune related adverse events[76], while patients receiving immunotherapy in combination with chemotherapy presented grade ≥ 3 adverse effects in up to 53%. In these cases the most common toxicities were hematologic[2].

Vaccines treatment as a single agent or in combination

Several types of vaccines have been tested as single agents (Table 3) or in combination with chemotherapy (Table 4) or immunotherapy (Table 5), including whole-cell vaccines, DCs, DNA and peptide vaccines that entail the presentation of immunogenic cancer antigens to the immune system, resulting in the activation of cancer antigen-specific cytotoxic T lymphocytes *in vivo* and the subsequent anticancer immune response[94].

Table 2 Clinical trials on pancreatic ductal adenocarcinoma combining immunotherapy and chemotherapy

National clinical trial number	Sample	Phase	Settings	Drug	Results
NCT01473940	21	I	Advanced; Metastatic; Any line	Ipilimumab; Gemcitabine	OS 8,5 m (95%CI: 2.2-10.3)
NCT00556023	34	I	Metastatic Chemotherapy naïve	Tremelimumab Gemcitabine	OS 7.4 m (95%CI: 5.8-9.4)
NCT02331251	81	I/II	Metastatic (PDAC and other tumors) Chemotherapy naïve	Pembrolizumab; Nab-Paclitaxel Gemcitabine	OS 15 m (95%CI: 6.8-22.6)
Beatty *et al*, *Clin Cancer Res* 2013; **19**: 6286–6295	22	I	Advanced; First line	CD40 agonist (CP-870893); Gemcitabine	PFS 5.2 m (95%CI: 1.9-7.4); OS 8.4 m (95%CI: 5.3-11.8); 1-y OS 28.6%
NCT01413022	47	I	Borderline; Locally advanced Chemotherapy naïve	CCR2 inhibitor (PF-04136309); FOLFIRINOX	Combination arm: 49% OR Chemotherapy arm: 0% OR
NCT02268825	39	I	Advanced; Metastatic (gastrointestinal malignancies) ; Any line	Pembrolizumab mFOLFOX	No results posted
NCT02309177	138	I	Advanced; Metastatic (PDAC and other tumors); Any treatment naive	Nivolumab; Nab-Paclitaxel Gemcitabine	No results posted
NCT02077881	98	I/II	Metastatic; First line	IDO inhibitor (indoximod); Nab-Paclitaxel; Gemcitabine	No results posted
NCT04045730	17	I/II	Metastatic First line	Gemcitabine; Nab-Pacliatxel; Pembrolizumab	PFS 9.1 m (95%CI: 4.9-13.3); OS 15 m (95%CI: 6.8-23)
NCT03214250	30	I	Metastatic; First line	Gemcitabine; Nab-Paclitaxel; Nivolumab; CD40 (agonistic monoclonal antibody) APX005M (sotigalimab)	Ongoing
NCT02826486	80	II	Metastatic; Any line	BL-8040; Pembrolizumab; Pegylated liposomal Irinotecan + 5FU	Disease Control Rate 34.5%; OS: 3.3 m Patients receiving study drugs as second-line therapy: 7.5 m

OS: Overall survival; PDAC: Pancreatic ductal adenocarcinoma; PFS: Progression-free survival; OR: Objective response.

GVAX

The mechanism of actions of GVAX vaccines is the stimulation of APC antigen uptake and T-cell priming through PDAC cell modification to express granulocyte-macrophage colony-stimulating factor (GM-CSF)[95].

A number of phase I and II clinical trials have been conducted on localized PDAC. A phase II clinical trial (NCT00084383) with 60 randomized patients evaluated the effectiveness of the GVAX vaccine administrated in two times: 1) after surgery and before 5-fluoracil based chemotherapy and 2) after chemotherapy had finished. The median PFS was 17.3 mo, and the median OS of 24.8 mo[96].

The GVAX vaccine has also been tested in metastatic PDAC. A phase II clinical trial (NCT01417000) in which 93 patients were randomized to the combination of GVAX plus cyclophosphamide with or without CRS-207 reported an OS of 6.1 mo in the experimental arm *vs* 3.9 mo in the control arm[97]. However, a phase IIb clinical trial (NCT02004262) showed no benefit in its primary endpoint of OS[98].

Algenpantucel

Algenpantucel is a whole cell vaccine that works by harnessing a natural robust immune response against pancreatic cancer[99]. The vaccine has been tested in combination with gemcitabine plus 5-Fluoracil chemoraditherapy in patients with resected PDAC, achieving a 12 mo PFS of 65% and a 12 mo OS of 83% (*vs* 45% and 63% in the control arm, respectively)[99]. This trial is still on-going for patients with borderline and locally advanced PDAC[99].

KIF20A-66 and survivin-2B 80-88 peptides

KIF20A and survivin are two up-regulated HLA-A24-restricted peptides that have been employed as epitopes in vaccines development[100,101]. KIF20A-66 was tested in a phase I/II clinical trial for patients with metastatic HLA-2402-positive PDAC who

Table 3 Clinical trials on pancreatic ductal adenocarcinoma using vaccines

National clinical trial number	Sample	Phase	Settings	Drug	Results
UMIN000004919	31	I/II	Metastatic ≥ Second line	KIF20A-66	KIF20A-66 vaccine: OS 4.7 m ± 0.8; Best supportive care: OS 2.7 m ± 1.1
UMIN000000905	6	I	Advanced (gastrointestinal and endocrine malignancies) ; Any line	SVN-2B; IFA; INFa	> 50% of the patients had positive clinical and immunological responses
NCT00569387	73	II	Adjuvant treatment	Algenpantucel-L	12-m OS: 86%
Kaufman *et al, J Transl Med* 2007; **5**: 60	10	I	Advanced; Metastatic; Any line	MUC1; HLA-A2; ICAM-1; LFA-3; CM-CSF	antiCEA/MUC-1 positive: OS 15.1 m; antiCEA/MUC-1 negative: OS 3.9 m
Lepisto *et al*, *Cancer Ther* 2008; **6**: 955–964	12	I/II	Adjuvant treatment	MUC1 peptide-loaded DC vaccine	Four of twelve patients are still alive without disease recurrence
NCT01410968	12	I	Advanced; Metastatic; Any line	w/Poly-ICLC peptide-pulsed DC-CIK	OS 7.7 m
Gjertsen *et al, Int J Cancer* 2001; **92**: 441–50	48	I/II	Surgically resected; Advanced; Any line	K-Ras vaccine GM-CSF	Resected: OS 25.6 m (95%CI: 10-39); Unresectable: OS 10.2 m (95%CI: 3-28)
Abou-Alfa *et al, Am J Clin Oncol* 2011; **34**: 321–5	24	I	Adjuvant (KRAS mutant)	Ras-peptide GM-CSF	OS 20.3 (95%CI: 11.6-45.3)
Bernhardt *et al, Br J Cancer* 2006; **95**: 1474–1482	48	I/II	Advanced Treatment naive	GV1001; GM-CSF	Responders: OS 7.2 m (95%CI: 4.8-10.7); Non-responders: OS 2.9 m (95%CI: 1.7-6.30)
Shima *et al*, *Cancer Sci* 2019; **110**: 2378-2385	83	II	Unresectable ≥ Second line	Survivin 2B peptide (SVN-2B); Interferon-β	SVN-2B + IFNβ: OS 312 d (95%CI: 43-460); IFNβ: OS 39 d (95%CI: 13-153)

CIK: cytokine-induced killer ; DC: dendritic cells; GM-CSF: granulocyte-macrophage colony-stimulating factor; IFN: interferon; m: months; OS: overall survival; PDAC: pancreatic ductal adenocarcinoma; PFS: progression-free survival.

had progressed to first-line gemcitabine chemotherapy (UMIN000004919). The OS was 4.7 mo in the treated arm *vs* 2.7 mo in the best supportive care arm. The PFS was 1.8 mo in the vaccine arm[100].

Survivine-2B (SVN-2B) is an HLA-A24 restricted peptide that has been investigated since 2003 with inconspicuous results. A clinical trial (UMIN000000905) with 6 HLA-A2402-positive patients was conducted, resulting in a clinical y immunogenic response in 50% of patients[101].

Other vaccines targeting KRAS and MUC-1

These vaccines target distinct tumor antigens based on the identification of mutated oncogenes, such as *KRAS*, altered tumor suppressor genes, such as *TP53*, *CDKN2A*, *DPC4*, *BRCA2*, and *ERBB2*, as well as the overexpression of tumor-associated antigens, such as *CEA* and *MUC-1*, in pancreatic carcinoma cells[102]. A phase I clinical trial was conducted using MUC-1 vaccines in advanced PDAC, the results of which confirmed that a specific T-cell immune response was obtained, achieving a significant improvement in OS (15.3 mo *vs* 3.9 mo)[103].

A phase I/II clinical trial was conducted in the adjuvant setting, the results of which revealed that 4 out of 12 patients survived without disease recurrence[104].

Clinical trials using *KRAS* against vaccines have also been developed. There is a phase I/II study that combines mutant RAS peptides and GM-CSF in patients with resected or locally advanced PDAC, with an OS of 25.6 mo and 10.2 mo, respectively [105].

GV1001 is another tested vaccine. A phase I/II trial combining this vaccine with GM-CSF for unresectable PDAC[106], and observed an immune response in 63% of patients, with an OS of 7.2 mo *vs* 2.9 mo in no-immune responders. After these encouraging results, a phase III study for locally advanced PDAC was conducted [107]. However, the combination of GV1001 plus gemcitabine plus capecitabine did not improve OS compared with chemotherapy alone (6.9 mo *vs* 7.9 mo).

Combination of vaccines treatment with immune checkpoints

Preclinical reports have supported the concept of synergy between cancer vaccines and immune checkpoint blockade in non-immunogenic tumors. Based on these results, several clinical trials have been conducted to assess the efficacy of this combination in

Table 4 Clinical trials on pancreatic ductal adenocarcinoma combining vaccines and chemotherapy

National clinical trial number	Sample	Phase	Settings	Drug	Results
Jaffee *et al, J Clin Oncol* 2001; **19**: 145–56	14	I	Adjuvant (stage I/II/III)	CVAX, Chemorradiation	Effective anti-tumor immunty
NCT00084383	60	II	Adjuvant (stage I/II)	GVAX; 5FU; Chemorradiation	Combination: OS 24.8 m (95%CI: 21.2-31.6); 5FU/Chemorradiation: OS 20.3 m (95%CI: 18-23.9)
NCT01417000	93	IIa	Metastatic ≥ Second line	GVAX/Cy CRS-207	Combination: OS 6.28 m (95%CI: 4.47-9.40); GVAX/Cy: OS 4.07 m (95%CI: 3.32-5.42)
NCT02004262	303	IIb	Metastatic ≥ Second line	GVAX/Cy CRS-207 Chemotherapy	Combination: OS 3.7 m (95%CI: 2.9-5.3); CRS-207 alone: OS 5.4 m (95%CI: 4.2-6.4); Chemotherapy: OS 4.6 m (95%CI: 4.2-5.7)
UMIN000008082	60	II	Advanced First line	KIF20A; VEGFR1/2; Gemcitabine	OS 9 m HLA matched; OS 10 m HLA unmatched
NCT01072981	722	III	Adjuvant treatment	Algenpantucel-L; Gemcitabine-5FU	1-y DFS 86% algenpantucel-L *vs* 63% Gemcitabine-5FU; 1-y OS 65% algenpantucel-L *vs* 45% Gencitabine-5FU
NCT01836432	302	III	Borderline resectable; Locally advanced usresectable; First line	Algenpantucel-L; FOLFIRINOX; Gemcitabine; Nab-Paclitaxel; Capecitabine; 5FU	No results posted
NCT01781520	47	I/II	Unresectable locally advancedMetastatic Chemotherapy naïve	DC-CIK Chemotherapy S-1	DC-CIK+Chemotherapy S-1: OS 7 m; DC-CIK alone: OS 4.2 m; Chemotherapy S-1 alone: OS 4.7 m; Supportive care only: OS 1.73 m
Muscarella *et al, J Clin Oncol* 2012; **30**: e14501-e.	176	II	Resected (KRAS mutant) adjuvant	GI-4000 Gemcitabine	GI-4000+Gemcitabine OS 19.8 m; Placebo-gemcitabine: OS 14.8 m
Middleton *et al, Lancet Oncol* 2014; **15**: 829–840	1062	III	AdvancedMetastatic Chemotherapy naïve	GV1001 Gemcitabine Capecitabine	Treated group: OS 6.9 m (95%CI: 6.4-7.6); Chemotherapy alone: OS 7.9 m (95% 7.1-8.8)
Yanagisawa *et al*, *Anticancer Res* 2018; **38**: 2217-2225	8	I	Adjuvant (I, II, III)	WT1-DC VaccineS-1 Chemotherapy Gemcitabine	No results posted
Suzuki *et al, Cancer Sci* 2017; **108**: 73-80	66	II	Advanced First line	Antiangiogenic cancer vaccines targeting VEGFR1 and VEGFR2 in addition to the KIF20A peptide; Gemcitabine	PFS HLA matched: 4.7 m; PFS HLA unmatched: 5.2 m

OS: overall survival; PDAC: pancreatic ductal adenocarcinoma: PFS: progression-free survival; Cy: Cyclophosphamide; VEGFR: vascular endothelial growth factor receptor.

PDAC therapy[108].

In clinical trial NCT00836407, 30 patients with previously treated metastatic PDAC were randomized to a high dose of Ipilimumab (10mg/kg) as the single agent or in combination with the GVAX vaccine. Five patients showed stable disease, and an OS of 5.7 mo was achieved in the experimental arm compared with 3.6 mo in the control arm[108].

Other studies that included patients with metastatic PDAC combined with nivolumab and ipilimumab, with or without GVAX and CRS-207, showed enhanced T-cell responses. Studies are currently evaluating the role of immune checkpoint inhibitors in combination with cyclophosphamide/GVAX and CRS-207 vaccines (NCT02243371, NCT02451982), and the results have yet to be published[99].

Pembrolizumab combined with the modified p53-expressing Ankara virus (p53MVA) vaccine has been studied in patients with several malignancies included PDAC, with clinical responses observed in 3 of 11 patients and disease stabilization for 30, 32 and 49 wk[109].

Vaccines were well tolerated. Most common toxicities were grade 1-2 induration/erythema or pain/soreness at the vaccine sites, pyrexia, chills, fatigue and nausea, with < 5% of patients reporting serious adverse events[96,98-99,106]. There were not reported clinical signs of auto-immune disease, abnormal biochemical or

Table 5 Clinical trials on pancreatic ductal adenocarcinoma combining vaccines and immunotherapy

National clinical trial number	Sample	Phase	Settings	Drug	Results
NCT00836407	30	I	Metastatic ≥ Second line	Ipilimumab GVAX	Combination: OS 5.7 m (95%CI: 4.3-14.7); Ipilimumab: OS 3.6 m (95%CI: 2.5-9.2)
NCT02243371	93	II	Metastatic ≥ Second line	Nivolumab Cy; GVAX; CRS-207	No results posted
NCT02451982	62	I/II	Neoadjuvant Adjuvant	Nivolumab Cy GVAX Urelumab	No results posted
NCT04627246	3	I/II	Adjuvant	DC vaccine loaded with personalized peptides (PEP-DC); Nivolumab SOC	No results posted
NCT02432963	11	I	Advanced (solid malignancies) ≥ Second line	Pembrolizumab p53MVA	Clinical responses in three out of eleven patients

OS: overall survival; Cy: Cyclophosphamide; SOC: Standard of Care Chemotherapy; p53MVA: Modified Vaccinia Virus Ankara Vaccine Expressing p53.

haematological parameters related with the vaccinations[105]. A grade 5 fatal myocarditis was reported with Pembrolizumab combined with the p53MVA vaccine [109].

Adoptive cell transfer

The most clinically important form of adoptive cell transfer therapy is chimeric antigen receptor (CAR) T-cell therapy (Table 6). CAR-T cells can target any extracellular molecular structure recognizable by an antibody, thereby avoiding the MHC restriction. CAR consists of an extracellular domain of a single-chain variable fragment (scFv) of an antibody that recognizes a specific tumor antigen and an intracellular domain that contains the T cell receptor signal transduction sequence[39]. To generate the appropriate cell therapy product for adaptive transfer, T cells are collected from patients *via* leukapheresis, manipulated to target the specific antigen, expanded, and then reinfused[110].

The ideal target antigen is one that is selectively expressed in tumor cells; however, most targets of CAR-T cells are also expressed in normal tissues such as the mesothelin, CD24, carcinoembryonic antigen (CEA) and human epidermal growth factor receptor 2 (HER2), and have been considered as targets in PDAC[110].

Several clinical trials have followed this approach; however, the use of CAR-T cell therapy in PDAC is scarce, and the clinical results are moderate. For example, a phase I study of Her2-specific CAR-T cells (NCT01935843) showed that 5 out of the 11 treated patients achieved stable disease, while 2 patients achieved partial response with a median PFS of 4.8 mo[111].

However, CAR-T cell therapy might trigger a cytokine release syndrome, a severe complication that consists of the release of cytokines that cause several symptoms including fever and hypotension[110].

The most characteristic toxicity associated with CAR-T therapy is the cytokine release syndrome. If the antigen selected for CAR-T cell therapy is expressed on normal tissues, toxicity and autoimmunity might appear[2].

CONCLUSION

The immune response in cancer is a complex process that involves the balance between tumor-promoting innate immune responses and tumor-suppressing adaptive immune responses. In PDAC, immune evasion is an early event during tumorigenesis and is associated with proinflammatory signals, infiltration of immunosuppressive cells (Tregs and MDSCs), and a sophisticated TME where numerous interactions occur between stromal signals, the immune system and tumor cells. As a consequence, PDAC is characterized by low immunogenicity and antigenicity, a critical concept when developing novel immunotherapeutic approaches for treating PDAC.

The emergence of immunotherapy as a new treatment approach for solid tumors has become a revolution in modern oncology. Immune checkpoint inhibitors improve survival in several tumors, such as melanoma, lung cancer, head and neck, and genitourinary. These tumors, known as “hot tumors”, present numerous mutations

Table 6 Clinical trials on pancreatic ductal adenocarcinoma using adoptive cell transfer

National clinical trial number	Sample	Phase	Settings	Drug	Results
NCT00570713	155	II	Unresectable First-line	MORb-009 Gemcitabine	Combination: OS 6.5 m (95%CI: 4.5-8.10); Placebo plus Gemcitabine: OS 6.9 m (95%CI: 5.4-8.8)
NCT01935843	10	I/II	Advanced (PDAC and other tumors Her2-positive) ≥ Second line	Her2-specific CAR-T cells	OS 4.8 m (95%CI: 1.5-8.3)
NCT01781520	47	I/II	Advanced; Any line	DC-CIK Chemoterapy S-1	DC-CIK + Chemotherapy S-1: OS 7 m DC-CIK alone: OS 4.2 m; Chemotherapy S-1 alone: OS 4.7 m; Supportive care only: OS 1.73 m
Aoki *et al*, *Cytotherapy* 2017; **19**: 473-485	48	I	Adjuvant	Gemcitabine; Autologous γδ; T-cell transfer	PFS 26 m (no statistical diference); OS No statistical difference
NCT01959672	11	I/II	Neoadjuvant	Gemcitabine; Leucovorin-Fluorouracil; Oregovomab; Nelfinavir + SBRT	Prematurely closed; PFS 8.6 m; OS 13 m (95%CI: 7-22)
NCT00720785	40	I	Metastatic (PDAC and other tumors) ≥ Second line	Irreversible electroporation (IRE); Allogeneic natural killer cell therapy	No results posted
NCT04212026	67	I	Metastatic ≥ Second line	Irreversible electroporation; Allogeneic natural killer cell therapy	Stage III PFS 9,1 m (IRE-NK) *vs* 7.9 m (IRE); Stage III OS 13.6 m (IRE-NK) *vs* 12.2 m (IRE); Stage IV OS 10.2 m (IRE-NK) *vs* 9.1 m (IRE)
NCT01583686	6	I	Metastatic ≥ Second line	Mesothelin-CART	2 patients stabilized diseasePFS patient 1: 3.8 mPFS patient 2: 5.4 m

CAR: chimeric antigen receptor; DC-CIK: dendritic cell-activated cytokine-induced killer cell; IRE: irreversible electroporation; OS: overall survival; NK: natural killer; PFS: progression-free survival; SBRT: stereotactic body radiation therapy.

that create a high number of neoantigens recognized by effector T cells that are released to fight the cancerous cells. However, in the case of PDAC, these results have not been as spectacular as other tumors' due to the intrinsic characteristics of PDAC, which enable it to self-isolate through a complex stroma, thereby evading the immune system.

Immune checkpoint inhibitors as single agents do not provide a benefit in PDAC. However, their combination with chemotherapy may transform PDAC into a "hot tumor" that is more susceptible to immunotherapy. The outcomes in phase I/II clinical trials using this approach are encouraging, with a benefit in OS in several combinations. Cancer vaccines employed as single-agent treatments or combined with classical chemotherapy, chemoradiotherapy or immunotherapy have promising results in the early phases of clinical trials. However, these outcomes have not been confirmed in more advanced studies. Lastly, adoptive cell transfer, specifically the CART-T cell approach, is still in very early phase of development.

Despite advances in treating PDAC, this tumor continues to be associated with extremely poor outcomes and high mortality. Systemic therapies and new strategies therefore need to be developed to improve patient prognoses, which will depend on an ever-increasing understanding of basic immunity and its role in PDAC. They keys to achieving significant changes in the treatment of PDAC include research into safe novel inhibitors (such as immunosuppressive factor, TAMs, MDSCs, and Tregs), increasing the prophylactic efforts in the early stages of carcinogenesis, deepening the understanding of molecular subtyping in PDAC and conducting appropriate patient selection.

REFERENCES

1 **Von Hoff DD**, Ervin T, Arena FP, Chiorean EG, Infante J, Moore M, Seay T, Tjulandin SA, Ma WW, Saleh MN, Harris M, Reni M, Dowden S, Laheru D, Bahary N, Ramanathan RK, Tabernero J, Hidalgo M, Goldstein D, Van Cutsem E, Wei X, Iglesias J, Renschler MF. Increased survival in pancreatic cancer with nab-paclitaxel plus gemcitabine. *N Engl J Med* 2013; **369**: 1691-1703 [PMID: 24131140 DOI: 10.1056/NEJMoa1304369]

2 **Young K**, Hughes DJ, Cunningham D, Starling N. Immunotherapy and pancreatic cancer: unique challenges and potential opportunities. *Ther Adv Med Oncol* 2018; **10**: 1758835918816281 [PMID: 30574212 DOI: 10.1177/1758835918816281]

3 **Ilic M**, Ilic I. Epidemiology of pancreatic cancer. *World J Gastroenterol* 2016; **22**: 9694-9705 [PMID: 27956793 DOI: 10.3748/wjg.v22.i44.9694]

4 **Seufferlein T**, Bachet JB, Van Cutsem E, Rougier P; ESMO Guidelines Working Group. Pancreatic adenocarcinoma: ESMO-ESDO Clinical Practice Guidelines for diagnosis, treatment and follow-up. *Ann Oncol* 2012; **23** Suppl 7: vii33-vii40 [PMID: 22997452 DOI: 10.1093/annonc/mds224]

5 **Mayo SC**, Nathan H, Cameron JL, Olino K, Edil BH, Herman JM, Hirose K, Schulick RD, Choti MA, Wolfgang CL, Pawlik TM. Conditional survival in patients with pancreatic ductal adenocarcinoma resected with curative intent. *Cancer* 2012; **118**: 2674-2681 [PMID: 21935914 DOI: 10.1002/cncr.26553]

6 **Hidalgo M**. Pancreatic cancer. *N Engl J Med* 2010; **362**: 1605-1617 [PMID: 20427809 DOI: 10.1056/NEJMra0901557]

7 **Kamisawa T**, Wood LD, Itoi T, Takaori K. Pancreatic cancer. *Lancet* 2016; **388**: 73-85 [PMID: 26830752 DOI: 10.1016/S0140-6736(16)00141-0]

8 **Conroy T**, Hammel P, Hebbar M, Ben Abdelghani M, Wei AC, Raoul JL, Choné L, Francois E, Artru P, Biagi JJ, Lecomte T, Assenat E, Faroux R, Ychou M, Volet J, Sauvanet A, Breysacher G, Di Fiore F, Cripps C, Kavan P, Texereau P, Bouhier-Leporrier K, Khemissa-Akouz F, Legoux JL, Juzyna B, Gourgou S, O'Callaghan CJ, Jouffroy-Zeller C, Rat P, Malka D, Castan F, Bachet JB; Canadian Cancer Trials Group and the Unicancer-GI–PRODIGE Group. FOLFIRINOX or Gemcitabine as Adjuvant Therapy for Pancreatic Cancer. *N Engl J Med* 2018; **379**: 2395-2406 [PMID: 30575490 DOI: 10.1056/NEJMoa1809775]

9 **Golan T**, Hammel P, Reni M, Van Cutsem E, Macarulla T, Hall MJ, Park JO, Hochhauser D, Arnold D, Oh DY, Reinacher-Schick A, Tortora G, Algül H, O'Reilly EM, McGuinness D, Cui KY, Schlienger K, Locker GY, Kindler HL. Maintenance Olaparib for Germline *BRCA*-Mutated Metastatic Pancreatic Cancer. *N Engl J Med* 2019; **381**: 317-327 [PMID: 31157963 DOI: 10.1056/NEJMoa1903387]

10 **Le DT**, Durham JN, Smith KN, Wang H, Bartlett BR, Aulakh LK, Lu S, Kemberling H, Wilt C, Luber BS, Wong F, Azad NS, Rucki AA, Laheru D, Donehower R, Zaheer A, Fisher GA, Crocenzi TS, Lee JJ, Greten TF, Duffy AG, Ciombor KK, Eyring AD, Lam BH, Joe A, Kang SP, Holdhoff M, Danilova L, Cope L, Meyer C, Zhou S, Goldberg RM, Armstrong DK, Bever KM, Fader AN, Taube J, Housseau F, Spetzler D, Xiao N, Pardoll DM, Papadopoulos N, Kinzler KW, Eshleman JR, Vogelstein B, Anders RA, Diaz LA Jr. Mismatch repair deficiency predicts response of solid tumors to PD-1 blockade. *Science* 2017; **357**: 409-413 [PMID: 28596308 DOI: 10.1126/science.aan6733]

11 **O'Reilly EM**, Hechtman JF. Tumour response to TRK inhibition in a patient with pancreatic adenocarcinoma harbouring an NTRK gene fusion. *Ann Oncol* 2019; **30**: viii36-viii40 [PMID: 31605106 DOI: 10.1093/annonc/mdz385]

12 **Emens LA**, Ascierto PA, Darcy PK, Demaria S, Eggermont AMM, Redmond WL, Seliger B, Marincola FM. Cancer immunotherapy: Opportunities and challenges in the rapidly evolving clinical landscape. *Eur J Cancer* 2017; **81**: 116-129 [PMID: 28623775 DOI: 10.1016/j.ejca.2017.01.035]

13 **Hanahan D**, Weinberg RA. Hallmarks of cancer: the next generation. *Cell* 2011; **144**: 646-674 [PMID: 21376230 DOI: 10.1016/j.cell.2011.02.013]

14 **Vonderheide RH**, Bayne LJ. Inflammatory networks and immune surveillance of pancreatic carcinoma. *Curr Opin Immunol* 2013; **25**: 200-205 [PMID: 23422836 DOI: 10.1016/j.coi.2013.01.006]

15 **Clark CE**, Beatty GL, Vonderheide RH. Immunosurveillance of pancreatic adenocarcinoma: insights from genetically engineered mouse models of cancer. *Cancer Lett* 2009; **279**: 1-7 [PMID: 19013709 DOI: 10.1016/j.canlet.2008.09.037]

16 **de Visser KE**, Eichten A, Coussens LM. Paradoxical roles of the immune system during cancer development. *Nat Rev Cancer* 2006; **6**: 24-37 [PMID: 16397525 DOI: 10.1038/nrc1782]

17 **Hinshaw DC**, Shevde LA. The Tumor Microenvironment Innately Modulates Cancer Progression. *Cancer Res* 2019; **79**: 4557-4566 [PMID: 31350295 DOI: 10.1158/0008-5472.CAN-18-3962]

18 **Mosser DM**, Edwards JP. Exploring the full spectrum of macrophage activation. *Nat Rev Immunol* 2008; **8**: 958-969 [PMID: 19029990 DOI: 10.1038/nri2448]

19 **Biswas SK**, Mantovani A. Macrophage plasticity and interaction with lymphocyte subsets: cancer as a paradigm. *Nat Immunol* 2010; **11**: 889-896 [PMID: 20856220 DOI: 10.1038/ni.1937]

20 **Zhang R**, Liu Q, Peng J, Wang M, Li T, Liu J, Cui M, Zhang X, Gao X, Liao Q, Zhao Y. CXCL5 overexpression predicts a poor prognosis in pancreatic ductal adenocarcinoma and is correlated with immune cell infiltration. *J Cancer* 2020; **11**: 2371-2381 [PMID: 32201508 DOI: 10.7150/jca.40517]

21 **Hu H**, Hang JJ, Han T, Zhuo M, Jiao F, Wang LW. The M2 phenotype of tumor-associated macrophages in the stroma confers a poor prognosis in pancreatic cancer. *Tumour Biol* 2016; **37**: 8657-8664 [PMID: 26738860 DOI: 10.1007/s13277-015-4741-z]

22 **Pollard JW**. Tumour-educated macrophages promote tumour progression and metastasis. *Nat Rev Cancer* 2004; **4**: 71-78 [PMID: 14708027 DOI: 10.1038/nrc1256]

23 **Wyckoff J**, Wang W, Lin EY, Wang Y, Pixley F, Stanley ER, Graf T, Pollard JW, Segall J, Condeelis J. A paracrine loop between tumor cells and macrophages is required for tumor cell migration in mammary tumors. *Cancer Res* 2004; **64**: 7022-7029 [PMID: 15466195 DOI: 10.1158/0008-5472.CAN-04-1449]

24 **Thyagarajan A**, Alshehri MSA, Miller KLR, Sherwin CM, Travers JB, Sahu RP. Myeloid-Derived Suppressor Cells and Pancreatic Cancer: Implications in Novel Therapeutic Approaches. *Cancers (Basel)* 2019; **11** [PMID: 31652904 DOI: 10.3390/cancers11111627]

25 **Trovato R**, Fiore A, Sartori S, Canè S, Giugno R, Cascione L, Paiella S, Salvia R, De Sanctis F, Poffe O, Anselmi C, Hofer F, Sartoris S, Piro G, Carbone C, Corbo V, Lawlor R, Solito S, Pinton L, Mandruzzato S, Bassi C, Scarpa A, Bronte V, Ugel S. Immunosuppression by monocytic myeloid-derived suppressor cells in patients with pancreatic ductal carcinoma is orchestrated by STAT3. *J Immunother Cancer* 2019; **7**: 255 [PMID: 31533831 DOI: 10.1186/s40425-019-0734-6]

26 **Pinton L**, Solito S, Damuzzo V, Francescato S, Pozzuoli A, Berizzi A, Mocellin S, Rossi CR, Bronte V, Mandruzzato S. Activated T cells sustain myeloid-derived suppressor cell-mediated immune suppression. *Oncotarget* 2016; **7**: 1168-1184 [PMID: 26700461 DOI: 10.18632/oncotarget.6662]

27 **Gabrilovich DI**, Velders MP, Sotomayor EM, Kast WM. Mechanism of immune dysfunction in cancer mediated by immature Gr-1+ myeloid cells. *J Immunol* 2001; **166**: 5398-5406 [PMID: 11313376 DOI: 10.4049/jimmunol.166.9.5398]

28 **Otsuji M**, Kimura Y, Aoe T, Okamoto Y, Saito T. Oxidative stress by tumor-derived macrophages suppresses the expression of CD3 zeta chain of T-cell receptor complex and antigen-specific T-cell responses. *Proc Natl Acad Sci U S A* 1996; **93**: 13119-13124 [PMID: 8917554 DOI: 10.1073/pnas.93.23.13119]

29 **Huang B**, Pan PY, Li Q, Sato AI, Levy DE, Bromberg J, Divino CM, Chen SH. Gr-1+CD115+ immature myeloid suppressor cells mediate the development of tumor-induced T regulatory cells and T-cell anergy in tumor-bearing host. *Cancer Res* 2006; **66**: 1123-1131 [PMID: 16424049 DOI: 10.1158/0008-5472.CAN-05-1299]

30 **Melani C**, Chiodoni C, Forni G, Colombo MP. Myeloid cell expansion elicited by the progression of spontaneous mammary carcinomas in c-erbB-2 transgenic BALB/c mice suppresses immune reactivity. *Blood* 2003; **102**: 2138-2145 [PMID: 12750171 DOI: 10.1182/blood-2003-01-0190]

31 **Chiossone L**, Dumas PY, Vienne M, Vivier E. Natural killer cells and other innate lymphoid cells in cancer. *Nat Rev Immunol* 2018; **18**: 671-688 [PMID: 30209347 DOI: 10.1038/s41577-018-0061-z]

32 **Davis M**, Conlon K, Bohac GC, Barcenas J, Leslie W, Watkins L, Lamzabi I, Deng Y, Li Y, Plate JM. Effect of pemetrexed on innate immune killer cells and adaptive immune T cells in subjects with adenocarcinoma of the pancreas. *J Immunother* 2012; **35**: 629-640 [PMID: 22996369 DOI: 10.1097/CJI.0b013e31826c8a4f]

33 **Lim SA**, Kim J, Jeon S, Shin MH, Kwon J, Kim TJ, Im K, Han Y, Kwon W, Kim SW, Yee C, Kim SJ, Jang JY, Lee KM. Defective Localization With Impaired Tumor Cytotoxicity Contributes to the Immune Escape of NK Cells in Pancreatic Cancer Patients. *Front Immunol* 2019; **10**: 496 [PMID: 31024520 DOI: 10.3389/fimmu.2019.00496]

34 **Huang Q**, Huang M, Meng F, Sun R. Activated pancreatic stellate cells inhibit NK cell function in the human pancreatic cancer microenvironment. *Cell Mol Immunol* 2019; **16**: 87-89 [PMID: 29628497 DOI: 10.1038/s41423-018-0014-2]

35 **Peng YP**, Zhang JJ, Liang WB, Tu M, Lu ZP, Wei JS, Jiang KR, Gao WT, Wu JL, Xu ZK, Miao Y, Zhu Y. Elevation of MMP-9 and IDO induced by pancreatic cancer cells mediates natural killer cell dysfunction. *BMC Cancer* 2014; **14**: 738 [PMID: 25274283 DOI: 10.1186/1471-2407-14-738]

36 **Arima K**, Okabe H, Hashimoto D, Chikamoto A, Tsuji A, Yamamura K, Kitano Y, Inoue R, Kaida T, Higashi T, Taki K, Imai K, Komohara Y, Beppu T, Takeya M, Baba H. The diagnostic role of the neutrophil-to-lymphocyte ratio in predicting pancreatic ductal adenocarcinoma in patients with pancreatic diseases. *Int J Clin Oncol* 2016; **21**: 940-945 [PMID: 27023215 DOI: 10.1007/s10147-016-0975-z]

37 **Tao L**, Zhang L, Peng Y, Tao M, Li G, Xiu D, Yuan C, Ma C, Jiang B. Preoperative neutrophil-to-lymphocyte ratio and tumor-related factors to predict lymph node metastasis in patients with pancreatic ductal adenocarcinoma (PDAC). *Oncotarget* 2016; **7**: 74314-74324 [PMID: 27494847 DOI: 10.18632/oncotarget.11031]

38 **Pu N**, Yin H, Zhao G, Nuerxiati A, Wang D, Xu X, Kuang T, Jin D, Lou W, Wu W. Independent effect of postoperative neutrophil-to-lymphocyte ratio on the survival of pancreatic ductal adenocarcinoma with open distal pancreatosplenectomy and its nomogram-based prediction. *J Cancer* 2019; **10**: 5935-5943 [PMID: 31762803 DOI: 10.7150/jca.35856]

39 **Huber M**, Brehm CU, Gress TM, Buchholz M, Alashkar Alhamwe B, von Strandmann EP, Slater EP, Bartsch JW, Bauer C, Lauth M. The Immune Microenvironment in Pancreatic Cancer. *Int J Mol Sci* 2020; **21** [PMID: 33022971 DOI: 10.3390/ijms21197307]

40 **Mollinedo F**. Neutrophil Degranulation, Plasticity, and Cancer Metastasis. *Trends Immunol* 2019; **40**: 228-242 [PMID: 30777721 DOI: 10.1016/j.it.2019.01.006]

41 **Balli D**, Rech AJ, Stanger BZ, Vonderheide RH. Immune Cytolytic Activity Stratifies Molecular Subsets of Human Pancreatic Cancer. *Clin Cancer Res* 2017; **23**: 3129-3138 [PMID: 28007776 DOI: 10.1158/1078-0432.CCR-16-2128]

42 **Ino Y**, Yamazaki-Itoh R, Shimada K, Iwasaki M, Kosuge T, Kanai Y, Hiraoka N. Immune cell infiltration as an indicator of the immune microenvironment of pancreatic cancer. *Br J Cancer* 2013; **108**: 914-923 [PMID: 23385730 DOI: 10.1038/bjc.2013.32]

43 **Feig C**, Jones JO, Kraman M, Wells RJ, Deonarine A, Chan DS, Connell CM, Roberts EW, Zhao Q, Caballero OL, Teichmann SA, Janowitz T, Jodrell DI, Tuveson DA, Fearon DT. Targeting CXCL12 from FAP-expressing carcinoma-associated fibroblasts synergizes with anti-PD-L1 immunotherapy

in pancreatic cancer. *Proc Natl Acad Sci U S A* 2013; **110**: 20212-20217 [PMID: 24277834 DOI: 10.1073/pnas.1320318110]

44 **Hiraoka N**, Onozato K, Kosuge T, Hirohashi S. Prevalence of FOXP3+ regulatory T cells increases during the progression of pancreatic ductal adenocarcinoma and its premalignant lesions. *Clin Cancer Res* 2006; **12**: 5423-5434 [PMID: 17000676 DOI: 10.1158/1078-0432.CCR-06-0369]

45 **Huber M**, Lohoff M. IRF4 at the crossroads of effector T-cell fate decision. *Eur J Immunol* 2014; **44**: 1886-1895 [PMID: 24782159 DOI: 10.1002/eji.201344279]

46 **De Monte L**, Reni M, Tassi E, Clavenna D, Papa I, Recalde H, Braga M, Di Carlo V, Doglioni C, Protti MP. Intratumor T helper type 2 cell infiltrate correlates with cancer-associated fibroblast thymic stromal lymphopoietin production and reduced survival in pancreatic cancer. *J Exp Med* 2011; **208**: 469-478 [PMID: 21339327 DOI: 10.1084/jem.20101876]

47 **Galon J**, Bruni D. Tumor Immunology and Tumor Evolution: Intertwined Histories. *Immunity* 2020; **52**: 55-81 [PMID: 31940273 DOI: 10.1016/j.immuni.2019.12.018]

48 **Dobrzanski MJ**. Expanding roles for CD4 T cells and their subpopulations in tumor immunity and therapy. *Front Oncol* 2013; **3**: 63 [PMID: 23533029 DOI: 10.3389/fonc.2013.00063]

49 **Vizio B**, Novarino A, Giacobino A, Cristiano C, Prati A, Ciuffreda L, Montrucchio G, Bellone G. Potential plasticity of T regulatory cells in pancreatic carcinoma in relation to disease progression and outcome. *Exp Ther Med* 2012; **4**: 70-78 [PMID: 23060925 DOI: 10.3892/etm.2012.553]

50 **Wing K**, Fehérvári Z, Sakaguchi S. Emerging possibilities in the development and function of regulatory T cells. *Int Immunol* 2006; **18**: 991-1000 [PMID: 16720616 DOI: 10.1093/intimm/dxl044]

51 **Chellappa S**, Hugenschmidt H, Hagness M, Line PD, Labori KJ, Wiedswang G, Taskén K, Aandahl EM. Regulatory T cells that co-express RORγt and FOXP3 are pro-inflammatory and immunosuppressive and expand in human pancreatic cancer. *Oncoimmunology* 2016; **5**: e1102828 [PMID: 27141387 DOI: 10.1080/2162402X.2015.1102828]

52 **Curiel TJ**, Coukos G, Zou L, Alvarez X, Cheng P, Mottram P, Evdemon-Hogan M, Conejo-Garcia JR, Zhang L, Burow M, Zhu Y, Wei S, Kryczek I, Daniel B, Gordon A, Myers L, Lackner A, Disis ML, Knutson KL, Chen L, Zou W. Specific recruitment of regulatory T cells in ovarian carcinoma fosters immune privilege and predicts reduced survival. *Nat Med* 2004; **10**: 942-949 [PMID: 15322536 DOI: 10.1038/nm1093]

53 **Tassi E**, Gavazzi F, Albarello L, Senyukov V, Longhi R, Dellabona P, Doglioni C, Braga M, Di Carlo V, Protti MP. Carcinoembryonic antigen-specific but not antiviral CD4+ T cell immunity is impaired in pancreatic carcinoma patients. *J Immunol* 2008; **181**: 6595-6603 [PMID: 18941250 DOI: 10.4049/jimmunol.181.9.6595]

54 **Blazquez JL**, Benyamine A, Pasero C, Olive D. New Insights Into the Regulation of γδ T Cells by BTN3A and Other BTN/BTNL in Tumor Immunity. *Front Immunol* 2018; **9**: 1601 [PMID: 30050536 DOI: 10.3389/fimmu.2018.01601]

55 **von Bernstorff W**, Voss M, Freichel S, Schmid A, Vogel I, Jöhnk C, Henne-Bruns D, Kremer B, Kalthoff H. Systemic and local immunosuppression in pancreatic cancer patients. *Clin Cancer Res* 2001; **7**: 925s-932s [PMID: 11300493]

56 **Torphy RJ**, Zhu Y, Schulick RD. Immunotherapy for pancreatic cancer: Barriers and breakthroughs. *Ann Gastroenterol Surg* 2018; **2**: 274-281 [PMID: 30003190 DOI: 10.1002/ags3.12176]

57 **Heinemann V**, Reni M, Ychou M, Richel DJ, Macarulla T, Ducreux M. Tumour-stroma interactions in pancreatic ductal adenocarcinoma: rationale and current evidence for new therapeutic strategies. *Cancer Treat Rev* 2014; **40**: 118-128 [PMID: 23849556 DOI: 10.1016/j.ctrv.2013.04.004]

58 **Feig C**, Gopinathan A, Neesse A, Chan DS, Cook N, Tuveson DA. The pancreas cancer microenvironment. *Clin Cancer Res* 2012; **18**: 4266-4276 [PMID: 22896693 DOI: 10.1158/1078-0432.CCR-11-3114]

59 **Watt J**, Kocher HM. The desmoplastic stroma of pancreatic cancer is a barrier to immune cell infiltration. *Oncoimmunology* 2013; **2**: e26788 [PMID: 24498555 DOI: 10.4161/onci.26788]

60 **Neesse A**, Algül H, Tuveson DA, Gress TM. Stromal biology and therapy in pancreatic cancer: a changing paradigm. *Gut* 2015; **64**: 1476-1484 [PMID: 25994217 DOI: 10.1136/gutjnl-2015-309304]

61 **Kleeff J**, Beckhove P, Esposito I, Herzig S, Huber PE, Löhr JM, Friess H. Pancreatic cancer microenvironment. *Int J Cancer* 2007; **121**: 699-705 [PMID: 17534898 DOI: 10.1002/ijc.22871]

62 **Whatcott CJ**, Diep CH, Jiang P, Watanabe A, LoBello J, Sima C, Hostetter G, Shepard HM, Von Hoff DD, Han H. Desmoplasia in Primary Tumors and Metastatic Lesions of Pancreatic Cancer. *Clin Cancer Res* 2015; **21**: 3561-3568 [PMID: 25695692 DOI: 10.1158/1078-0432.CCR-14-1051]

63 **Bailey P**, Chang DK, Nones K, Johns AL, Patch AM, Gingras MC, Miller DK, Christ AN, Bruxner TJ, Quinn MC, Nourse C, Murtaugh LC, Harliwong I, Idrisoglu S, Manning S, Nourbakhsh E, Wani S, Fink L, Holmes O, Chin V, Anderson MJ, Kazakoff S, Leonard C, Newell F, Waddell N, Wood S, Xu Q, Wilson PJ, Cloonan N, Kassahn KS, Taylor D, Quek K, Robertson A, Pantano L, Mincarelli L, Sanchez LN, Evers L, Wu J, Pinese M, Cowley MJ, Jones MD, Colvin EK, Nagrial AM, Humphrey ES, Chantrill LA, Mawson A, Humphris J, Chou A, Pajic M, Scarlett CJ, Pinho AV, Giry-Laterriere M, Rooman I, Samra JS, Kench JG, Lovell JA, Merrett ND, Toon CW, Epari K, Nguyen NQ, Barbour A, Zeps N, Moran-Jones K, Jamieson NB, Graham JS, Duthie F, Oien K, Hair J, Grützmann R, Maitra A, Iacobuzio-Donahue CA, Wolfgang CL, Morgan RA, Lawlor RT, Corbo V, Bassi C, Rusev B, Capelli P, Salvia R, Tortora G, Mukhopadhyay D, Petersen GM; Australian

Pancreatic Cancer Genome Initiative, Munzy DM, Fisher WE, Karim SA, Eshleman JR, Hruban RH, Pilarsky C, Morton JP, Sansom OJ, Scarpa A, Musgrove EA, Bailey UM, Hofmann O, Sutherland RL, Wheeler DA, Gill AJ, Gibbs RA, Pearson JV, Waddell N, Biankin AV, Grimmond SM. Genomic analyses identify molecular subtypes of pancreatic cancer. *Nature* 2016; **531**: 47-52 [PMID: 26909576 DOI: 10.1038/nature16965]

64 **Aguirre AJ**, Nowak JA, Camarda ND, Moffitt RA, Ghazani AA, Hazar-Rethinam M, Raghavan S, Kim J, Brais LK, Ragon D, Welch MW, Reilly E, McCabe D, Marini L, Anderka K, Helvie K, Oliver N, Babic A, Da Silva A, Nadres B, Van Seventer EE, Shahzade HA, St Pierre JP, Burke KP, Clancy T, Cleary JM, Doyle LA, Jajoo K, McCleary NJ, Meyerhardt JA, Murphy JE, Ng K, Patel AK, Perez K, Rosenthal MH, Rubinson DA, Ryou M, Shapiro GI, Sicinska E, Silverman SG, Nagy RJ, Lanman RB, Knoerzer D, Welsch DJ, Yurgelun MB, Fuchs CS, Garraway LA, Getz G, Hornick JL, Johnson BE, Kulke MH, Mayer RJ, Miller JW, Shyn PB, Tuveson DA, Wagle N, Yeh JJ, Hahn WC, Corcoran RB, Carter SL, Wolpin BM. Real-time Genomic Characterization of Advanced Pancreatic Cancer to Enable Precision Medicine. *Cancer Discov* 2018; **8**: 1096-1111 [PMID: 29903880 DOI: 10.1158/2159-8290.CD-18-0275]

65 **Aung KL**, Fischer SE, Denroche RE, Jang GH, Dodd A, Creighton S, Southwood B, Liang SB, Chadwick D, Zhang A, O'Kane GM, Albaba H, Moura S, Grant RC, Miller JK, Mbabaali F, Pasternack D, Lungu IM, Bartlett JMS, Ghai S, Lemire M, Holter S, Connor AA, Moffitt RA, Yeh JJ, Timms L, Krzyzanowski PM, Dhani N, Hedley D, Notta F, Wilson JM, Moore MJ, Gallinger S, Knox JJ. Genomics-Driven Precision Medicine for Advanced Pancreatic Cancer: Early Results from the COMPASS Trial. *Clin Cancer Res* 2018; **24**: 1344-1354 [PMID: 29288237 DOI: 10.1158/1078-0432.CCR-17-2994]

66 **Moffitt RA**, Marayati R, Flate EL, Volmar KE, Loeza SG, Hoadley KA, Rashid NU, Williams LA, Eaton SC, Chung AH, Smyla JK, Anderson JM, Kim HJ, Bentrem DJ, Talamonti MS, Iacobuzio-Donahue CA, Hollingsworth MA, Yeh JJ. Virtual microdissection identifies distinct tumor- and stroma-specific subtypes of pancreatic ductal adenocarcinoma. *Nat Genet* 2015; **47**: 1168-1178 [PMID: 26343385 DOI: 10.1038/ng.3398]

67 **Champiat S**, Ferté C, Lebel-Binay S, Eggermont A, Soria JC. Exomics and immunogenics: Bridging mutational load and immune checkpoints efficacy. *Oncoimmunology* 2014; **3**: e27817 [PMID: 24605269 DOI: 10.4161/onci.27817]

68 **Upadhrasta S**, Zheng L. Strategies in Developing Immunotherapy for Pancreatic Cancer: Recognizing and Correcting Multiple Immune "Defects" in the Tumor Microenvironment. *J Clin Med* 2019; **8** [PMID: 31527414 DOI: 10.3390/jcm8091472]

69 **Kleeff J**, Korc M, Apte M, La Vecchia C, Johnson CD, Biankin AV, Neale RE, Tempero M, Tuveson DA, Hruban RH, Neoptolemos JP. Pancreatic cancer. *Nat Rev Dis Primers* 2016; **2**: 16022 [PMID: 27158978 DOI: 10.1038/nrdp.2016.22]

70 **Alexandrov LB**, Nik-Zainal S, Wedge DC, Aparicio SA, Behjati S, Biankin AV, Bignell GR, Bolli N, Borg A, Børresen-Dale AL, Boyault S, Burkhardt B, Butler AP, Caldas C, Davies HR, Desmedt C, Eils R, Eyfjörd JE, Foekens JA, Greaves M, Hosoda F, Hutter B, Ilicic T, Imbeaud S, Imielinski M, Jäger N, Jones DT, Jones D, Knappskog S, Kool M, Lakhani SR, López-Otín C, Martin S, Munshi NC, Nakamura H, Northcott PA, Pajic M, Papaemmanuil E, Paradiso A, Pearson JV, Puente XS, Raine K, Ramakrishna M, Richardson AL, Richter J, Rosenstiel P, Schlesner M, Schumacher TN, Span PN, Teague JW, Totoki Y, Tutt AN, Valdés-Mas R, van Buuren MM, van 't Veer L, Vincent-Salomon A, Waddell N, Yates LR; Australian Pancreatic Cancer Genome Initiative; ICGC Breast Cancer Consortium; ICGC MMML-Seq Consortium; ICGC PedBrain, Zucman-Rossi J, Futreal PA, McDermott U, Lichter P, Meyerson M, Grimmond SM, Siebert R, Campo E, Shibata T, Pfister SM, Campbell PJ, Stratton MR. Signatures of mutational processes in human cancer. *Nature* 2013; **500**: 415-421 [PMID: 23945592 DOI: 10.1038/nature12477]

71 **Nakata B**, Wang YQ, Yashiro M, Nishioka N, Tanaka H, Ohira M, Ishikawa T, Nishino H, Hirakawa K. Prognostic value of microsatellite instability in resectable pancreatic cancer. *Clin Cancer Res* 2002; **8**: 2536-2540 [PMID: 12171881]

72 **Salem ME**, Puccini A, Grothey A, Raghavan D, Goldberg RM, Xiu J, Korn WM, Weinberg BA, Hwang JJ, Shields AF, Marshall JL, Philip PA, Lenz HJ. Landscape of Tumor Mutation Load, Mismatch Repair Deficiency, and PD-L1 Expression in a Large Patient Cohort of Gastrointestinal Cancers. *Mol Cancer Res* 2018; **16**: 805-812 [PMID: 29523759 DOI: 10.1158/1541-7786.MCR-17-0735]

73 **Hu ZI**, Shia J, Stadler ZK, Varghese AM, Capanu M, Salo-Mullen E, Lowery MA, Diaz LA Jr, Mandelker D, Yu KH, Zervoudakis A, Kelsen DP, Iacobuzio-Donahue CA, Klimstra DS, Saltz LB, Sahin IH, O'Reilly EM. Evaluating Mismatch Repair Deficiency in Pancreatic Adenocarcinoma: Challenges and Recommendations. *Clin Cancer Res* 2018; **24**: 1326-1336 [PMID: 29367431 DOI: 10.1158/1078-0432.CCR-17-3099]

74 **Fraune C**, Burandt E, Simon R, Hube-Magg C, Makrypidi-Fraune G, Kluth M, Büscheck F, Höflmayer D, Blessin NC, Mandelkow T, Li W, Perez D, Izbicki JR, Wilczak W, Sauter G, Schrader J, Neipp M, Mofid H, Daniels T, Isbert C, Clauditz TS, Steurer S. MMR Deficiency is Homogeneous in Pancreatic Carcinoma and Associated with High Density of Cd8-Positive Lymphocytes. *Ann Surg Oncol* 2020; **27**: 3997-4006 [PMID: 32108923 DOI: 10.1245/s10434-020-08209-y]

75 **Fukunaga A**, Miyamoto M, Cho Y, Murakami S, Kawarada Y, Oshikiri T, Kato K, Kurokawa T, Suzuoki M, Nakakubo Y, Hiraoka K, Itoh T, Morikawa T, Okushiba S, Kondo S, Katoh H. CD8+

tumor-infiltrating lymphocytes together with CD4+ tumor-infiltrating lymphocytes and dendritic cells improve the prognosis of patients with pancreatic adenocarcinoma. *Pancreas* 2004; **28**: e26-e31 [PMID: 14707745 DOI: 10.1097/00006676-200401000-00023]

76 **Schizas D**, Charalampakis N, Kole C, Economopoulou P, Koustas E, Gkotsis E, Ziogas D, Psyrri A, Karamouzis MV. Immunotherapy for pancreatic cancer: A 2020 update. *Cancer Treat Rev* 2020; **86**: 102016 [PMID: 32247999 DOI: 10.1016/j.ctrv.2020.102016]

77 **Hodi FS**, O'Day SJ, McDermott DF, Weber RW, Sosman JA, Haanen JB, Gonzalez R, Robert C, Schadendorf D, Hassel JC, Akerley W, van den Eertwegh AJ, Lutzky J, Lorigan P, Vaubel JM, Linette GP, Hogg D, Ottensmeier CH, Lebbé C, Peschel C, Quirt I, Clark JI, Wolchok JD, Weber JS, Tian J, Yellin MJ, Nichol GM, Hoos A, Urba WJ. Improved survival with ipilimumab in patients with metastatic melanoma. *N Engl J Med* 2010; **363**: 711-723 [PMID: 20525992 DOI: 10.1056/NEJMoa1003466]

78 **Freeman GJ**, Long AJ, Iwai Y, Bourque K, Chernova T, Nishimura H, Fitz LJ, Malenkovich N, Okazaki T, Byrne MC, Horton HF, Fouser L, Carter L, Ling V, Bowman MR, Carreno BM, Collins M, Wood CR, Honjo T. Engagement of the PD-1 immunoinhibitory receptor by a novel B7 family member leads to negative regulation of lymphocyte activation. *J Exp Med* 2000; **192**: 1027-1034 [PMID: 11015443 DOI: 10.1084/jem.192.7.1027]

79 **Zinselmeyer BH**, Heydari S, Sacristán C, Nayak D, Cammer M, Herz J, Cheng X, Davis SJ, Dustin ML, McGavern DB. PD-1 promotes immune exhaustion by inducing antiviral T cell motility paralysis. *J Exp Med* 2013; **210**: 757-774 [PMID: 23530125 DOI: 10.1084/jem.20121416]

80 **Patsoukis N**, Brown J, Petkova V, Liu F, Li L, Boussiotis VA. Selective effects of PD-1 on Akt and Ras pathways regulate molecular components of the cell cycle and inhibit T cell proliferation. *Sci Signal* 2012; **5**: ra46 [PMID: 22740686 DOI: 10.1126/scisignal.2002796]

81 **Pauken KE**, Sammons MA, Odorizzi PM, Manne S, Godec J, Khan O, Drake AM, Chen Z, Sen DR, Kurachi M, Barnitz RA, Bartman C, Bengsch B, Huang AC, Schenkel JM, Vahedi G, Haining WN, Berger SL, Wherry EJ. Epigenetic stability of exhausted T cells limits durability of reinvigoration by PD-1 blockade. *Science* 2016; **354**: 1160-1165 [PMID: 27789795 DOI: 10.1126/science.aaf2807]

82 **Royal RE**, Levy C, Turner K, Mathur A, Hughes M, Kammula US, Sherry RM, Topalian SL, Yang JC, Lowy I, Rosenberg SA. Phase 2 trial of single agent Ipilimumab (anti-CTLA-4) for locally advanced or metastatic pancreatic adenocarcinoma. *J Immunother* 2010; **33**: 828-833 [PMID: 20842054 DOI: 10.1097/CJI.0b013e3181eec14c]

83 Study of Tremelimumab in Patients With Advanced Solid Tumors - Study Results - ClinicalTrials.gov. [cited 20 January 2021]. Available from: https://clinicaltrials.gov/ct2/show/results/NCT02527434

84 Pembrolizumab in Microsatellite-Instability–High Advanced Colorectal Cancer | NEJM. [cited 20 January 2021]. Available from: https://www.nejm.org/doi/full/10.1056/NEJMoa2017699

85 **O'Reilly EM**, Oh D-Y, Dhani N, Renouf DJ, Lee MA, Sun W, Fisher G, Hezel A, Chang S-C, Vlahovic G, Takahashi O, Yang Y, Fitts D, Philip PA. Durvalumab With or Without Tremelimumab for Patients With Metastatic Pancreatic Ductal Adenocarcinoma: A Phase 2 Randomized Clinical Trial. *JAMA Oncol* (e-pub ahead of print 18 July 2019 [DOI: 10.1001/jamaoncol.2019.1588]

86 **Bristol-Myers Squibb**. A Phase 1/2, Open-label Study of Nivolumab Monotherapy or Nivolumab Combined With Ipilimumab in Subjects With Advanced or Metastatic Solid Tumors. ClinicalTrials.gov. [cited 20 January 2021]. Available from: https://clinicaltrials.gov/ct2/show/NCT01928394

87 **Beatty GL**, Gladney WL. Immune escape mechanisms as a guide for cancer immunotherapy. *Clin Cancer Res* 2015; **21**: 687-692 [PMID: 25501578 DOI: 10.1158/1078-0432.CCR-14-1860]

88 **Ho TTB**, Nasti A, Seki A, Komura T, Inui H, Kozaka T, Kitamura Y, Shiba K, Yamashita T, Mizukoshi E, Kawaguchi K, Wada T, Honda M, Kaneko S, Sakai Y. Combination of gemcitabine and anti-PD-1 antibody enhances the anticancer effect of M1 macrophages and the Th1 response in a murine model of pancreatic cancer liver metastasis. *J Immunother Cancer* 2020; **8** [PMID: 33188035 DOI: 10.1136/jitc-2020-001367]

89 **Weiss GJ**, Blaydorn L, Beck J, Bornemann-Kolatzki K, Urnovitz H, Schütz E, Khemka V. Phase Ib/II study of gemcitabine, nab-paclitaxel, and pembrolizumab in metastatic pancreatic adenocarcinoma. *Invest New Drugs* 2018; **36**: 96-102 [PMID: 29119276 DOI: 10.1007/s10637-017-0525-1]

90 **Mohindra NA**, Kircher SM, Nimeiri HS, Benson AB, Rademaker A, Alonso E, Blatner N, Khazaie K, Mulcahy MF. Results of the phase Ib study of ipilimumab and gemcitabine for advanced pancreas cancer. *J Clin Oncol* 2015; **33**: e15281-e15281 [DOI: 10.1200/jco.2015.33.15_suppl.e15281]

91 **Aglietta M**, Barone C, Sawyer MB, Moore MJ, Miller WH Jr, Bagalà C, Colombi F, Cagnazzo C, Gioeni L, Wang E, Huang B, Fly KD, Leone F. A phase I dose escalation trial of tremelimumab (CP-675,206) in combination with gemcitabine in chemotherapy-naive patients with metastatic pancreatic cancer. *Ann Oncol* 2014; **25**: 1750-1755 [PMID: 24907635 DOI: 10.1093/annonc/mdu205]

92 **O'Hara MH**, O'Reilly EM, Varadhachary G, Wolff RA, Wainberg ZA, Ko AH, Fisher G, Rahma O, Lyman JP, Cabanski CR, Mick R, Gherardini PF, Kitch LJ, Xu J, Samuel T, Karakunnel J, Fairchild J, Bucktrout S, LaVallee TM, Selinsky C, Till JE, Carpenter EL, Alanio C, Byrne KT, Chen RO, Trifan OC, Dugan U, Horak C, Hubbard-Lucey VM, Wherry EJ, Ibrahim R, Vonderheide RH. CD40 agonistic monoclonal antibody APX005M (sotigalimab) and chemotherapy, with or without

nivolumab, for the treatment of metastatic pancreatic adenocarcinoma: an open-label, multicentre, phase 1b study. *Lancet Oncol* 2021; **22**: 118-131 [PMID: 33387490 DOI: 10.1016/S1470-2045(20)30532-5]

93 **Bockorny B**, Semenisty V, Macarulla T, Borazanci E, Wolpin BM, Stemmer SM, Golan T, Geva R, Borad MJ, Pedersen KS, Park JO, Ramirez RA, Abad DG, Feliu J, Muñoz A, Ponz-Sarvise M, Peled A, Lustig TM, Bohana-Kashtan O, Shaw SM, Sorani E, Chaney M, Kadosh S, Vainstein Haras A, Von Hoff DD, Hidalgo M. BL-8040, a CXCR4 antagonist, in combination with pembrolizumab and chemotherapy for pancreatic cancer: the COMBAT trial. *Nat Med* 2020; **26**: 878-885 [PMID: 32451495 DOI: 10.1038/s41591-020-0880-x]

94 **Janikashvili N**, Larmonier N, Katsanis E. Personalized dendritic cell-based tumor immunotherapy. *Immunotherapy* 2010; **2**: 57-68 [PMID: 20161666 DOI: 10.2217/imt.09.78]

95 **Le DT**, Pardoll DM, Jaffee EM. Cellular vaccine approaches. *Cancer J* 2010; **16**: 304-310 [PMID: 20693840 DOI: 10.1097/PPO.0b013e3181eb33d7]

96 **Lutz E**, Yeo CJ, Lillemoe KD, Biedrzycki B, Kobrin B, Herman J, Sugar E, Piantadosi S, Cameron JL, Solt S, Onners B, Tartakovsky I, Choi M, Sharma R, Illei PB, Hruban RH, Abrams RA, Le D, Jaffee E, Laheru D. A lethally irradiated allogeneic granulocyte-macrophage colony stimulating factor-secreting tumor vaccine for pancreatic adenocarcinoma. A Phase II trial of safety, efficacy, and immune activation. *Ann Surg* 2011; **253**: 328-335 [PMID: 21217520 DOI: 10.1097/SLA.0b013e3181fd271c]

97 **Whiting C**, Lutz E, Nair N, Chang S, Lemmens E, Chen S-Y, Solt S, Ferber S, Maecker H, Murphy A, Brockstedt DG, Jaffee EM, Le DT. Phase II, randomized study of GVAX pancreas and CRS-207 immunotherapy in patients with metastatic pancreatic cancer: Clinical update on long term survival and biomarker correlates to overall survival. *J Clin Oncol* 2015; **33**: 261-261 [DOI: 10.1200/jco.2015.33.3_suppl.261]

98 **Le DT**, Picozzi VJ, Ko AH, Wainberg ZA, Kindler H, Wang-Gillam A, Oberstein P, Morse MA, Zeh HJ 3rd, Weekes C, Reid T, Borazanci E, Crocenzi T, LoConte NK, Musher B, Laheru D, Murphy A, Whiting C, Nair N, Enstrom A, Ferber S, Brockstedt DG, Jaffee EM. Results from a Phase IIb, Randomized, Multicenter Study of GVAX Pancreas and CRS-207 Compared with Chemotherapy in Adults with Previously Treated Metastatic Pancreatic Adenocarcinoma (ECLIPSE Study). *Clin Cancer Res* 2019; **25**: 5493-5502 [PMID: 31126960 DOI: 10.1158/1078-0432.CCR-18-2992]

99 **McCormick KA**, Coveler AL, Rossi GR, Vahanian NN, Link C, Chiorean EG. Pancreatic cancer: Update on immunotherapies and algenpantucel-L. *Hum Vaccin Immunother* 2016; **12**: 563-575 [PMID: 26619245 DOI: 10.1080/21645515.2015.1093264]

100 **Asahara S**, Takeda K, Yamao K, Maguchi H, Yamaue H. Phase I/II clinical trial using HLA-A24-restricted peptide vaccine derived from KIF20A for patients with advanced pancreatic cancer. *J Transl Med* 2013; **11**: 291 [PMID: 24237633 DOI: 10.1186/1479-5876-11-291]

101 **Kameshima H**, Tsuruma T, Kutomi G, Shima H, Iwayama Y, Kimura Y, Imamura M, Torigoe T, Takahashi A, Hirohashi Y, Tamura Y, Tsukahara T, Kanaseki T, Sato N, Hirata K. Immunotherapeutic benefit of α-interferon (IFNα) in survivin2B-derived peptide vaccination for advanced pancreatic cancer patients. *Cancer Sci* 2013; **104**: 124-129 [PMID: 23078230 DOI: 10.1111/cas.12046]

102 **Laheru D**, Jaffee EM. Immunotherapy for pancreatic cancer-science driving clinical progress. *Nat Rev Cancer* 2005; **5**: 459-467 [PMID: 15905855 DOI: 10.1038/nrc1630]

103 **Kaufman HL**, Kim-Schulze S, Manson K, DeRaffele G, Mitcham J, Seo KS, Kim DW, Marshall J. Poxvirus-based vaccine therapy for patients with advanced pancreatic cancer. *J Transl Med* 2007; **5**: 60 [PMID: 18039393 DOI: 10.1186/1479-5876-5-60]

104 **Lepisto AJ**, Moser AJ, Zeh H, Lee K, Bartlett D, McKolanis JR, Geller BA, Schmotzer A, Potter DP, Whiteside T, Finn OJ, Ramanathan RK. A phase I/II study of a MUC1 peptide pulsed autologous dendritic cell vaccine as adjuvant therapy in patients with resected pancreatic and biliary tumors. *Cancer Ther* 2008; **6**: 955-964 [PMID: 19129927]

105 **Gjertsen MK**, Buanes T, Rosseland AR, Bakka A, Gladhaug I, Søreide O, Eriksen JA, Møller M, Baksaas I, Lothe RA, Saeterdal I, Gaudernack G. Intradermal ras peptide vaccination with granulocyte-macrophage colony-stimulating factor as adjuvant: Clinical and immunological responses in patients with pancreatic adenocarcinoma. *Int J Cancer* 2001; **92**: 441-450 [PMID: 11291084 DOI: 10.1002/ijc.1205]

106 **Bernhardt SL**, Gjertsen MK, Trachsel S, Møller M, Eriksen JA, Meo M, Buanes T, Gaudernack G. Telomerase peptide vaccination of patients with non-resectable pancreatic cancer: A dose escalating phase I/II study. *Br J Cancer* 2006; **95**: 1474-1482 [PMID: 17060934 DOI: 10.1038/sj.bjc.6603437]

107 **Middleton G**, Silcocks P, Cox T, Valle J, Wadsley J, Propper D, Coxon F, Ross P, Madhusudan S, Roques T, Cunningham D, Falk S, Wadd N, Harrison M, Corrie P, Iveson T, Robinson A, McAdam K, Eatock M, Evans J, Archer C, Hickish T, Garcia-Alonso A, Nicolson M, Steward W, Anthoney A, Greenhalf W, Shaw V, Costello E, Naisbitt D, Rawcliffe C, Nanson G, Neoptolemos J. Gemcitabine and capecitabine with or without telomerase peptide vaccine GV1001 in patients with locally advanced or metastatic pancreatic cancer (TeloVac): an open-label, randomised, phase 3 trial. *Lancet Oncol* 2014; **15**: 829-840 [PMID: 24954781 DOI: 10.1016/S1470-2045(14)70236-0]

108 **Le DT**, Lutz E, Uram JN, Sugar EA, Onners B, Solt S, Zheng L, Diaz LA Jr, Donehower RC, Jaffee EM, Laheru DA. Evaluation of ipilimumab in combination with allogeneic pancreatic tumor cells transfected with a GM-CSF gene in previously treated pancreatic cancer. *J Immunother* 2013; **36**:

382-389 [PMID: 23924790 DOI: 10.1097/CJI.0b013e31829fb7a2]

109 **Chung V**, Kos FJ, Hardwick N, Yuan Y, Chao J, Li D, Waisman J, Li M, Zurcher K, Frankel P, Diamond DJ. Evaluation of safety and efficacy of p53MVA vaccine combined with pembrolizumab in patients with advanced solid cancers. *Clin Transl Oncol* 2019; **21**: 363-372 [PMID: 30094792 DOI: 10.1007/s12094-018-1932-2]

110 **Sunami Y**, Kleeff J. Immunotherapy of pancreatic cancer. In: Progress in Molecular Biology and Translational Science. Elsevier, 2019: 189–216

111 **Feng K**, Liu Y, Guo Y, Qiu J, Wu Z, Dai H, Yang Q, Wang Y, Han W. Phase I study of chimeric antigen receptor modified T cells in treating HER2-positive advanced biliary tract cancers and pancreatic cancers. *Protein Cell* 2018; **9**: 838-847 [PMID: 28710747 DOI: 10.1007/s13238-017-0440-4]

World Journal of Gastroenterology

Submit a Manuscript: https://www.f6publishing.com

World J Gastroenterol 2021 October 28; 27(40): 6794-6824

DOI: 10.3748/wjg.v27.i40.6794

ISSN 1007-9327 (print) ISSN 2219-2840 (online)

REVIEW

Artificial intelligence in gastroenterology: A state-of-the-art review

Paul T Kröner, Megan ML Engels, Benjamin S Glicksberg, Kipp W Johnson, Obaie Mzaik, Jeanin E van Hooft, Michael B Wallace, Hashem B El-Serag, Chayakrit Krittanawong

ORCID number: Paul T Kröner 0000-0002-7361-7883; Megan ML Engels 0000-0002-4708-3750; Benjamin S Glicksberg 0000-0003-4515-8090; Kipp W Johnson 0000-0002-5102-741X; Obaie Mzaik 0000-0001-7315-2548; Jeanin E van Hooft 0000-0002-4424-0079; Michael B Wallace 0000-0002-6446-5785; Hashem B El-Serag 0000-0001-5964-7579; Chayakrit Krittanawong 0000-0001-7953-335X.

Author contributions: Kröner PT contributed complete manuscript drafting, review of literature and data adquisition, critical manuscript revision; Engels MM contributed review of the literature, data adquisition, figure construction, table construction, manuscript review; Mzaik O contributed literature review, table construction; van Hooft JE and El-Serag HB contributed critical manuscript review; Wallace MB contributed manuscript structure, critical manuscript review; Krittanawong C contributed literature review, editing, critical manuscript review.

Conflict-of-interest statement: Dr. Krittanawong C discloses the following relationships – Member of the American College of Cardiology Solution Set Oversight Committee, the American Heart Association Committee of the Council on Genomic and Precision Medicine, and the American College of Cardiology/American

Paul T Kröner, Megan ML Engels, Obaie Mzaik, Michael B Wallace, Division of Gastroenterology and Hepatology, Mayo Clinic, Jacksonville, FL 32224, United States

Megan ML Engels, Cancer Center Amsterdam, Department of Gastroenterology and Hepatology, Amsterdam UMC, Location AMC, Amsterdam 1105, The Netherlands

Benjamin S Glicksberg, Kipp W Johnson, The Hasso Plattner Institute for Digital Health, Icahn School of Medicine at Mount Sinai, New York, NY 10029, United States

Jeanin E van Hooft, Department of Gastroenterology and Hepatology, Leiden University Medical Center, Amsterdam 2300, The Netherlands

Michael B Wallace, Division of Gastroenterology and Hepatology, Sheikh Shakhbout Medical City, Abu Dhabi 11001, United Arab Emirates

Hashem B El-Serag, Section of Gastroenterology and Hepatology, Michael E. DeBakey VA Medical Center and Baylor College of Medicine, Houston, TX 77030, United States

Hashem B El-Serag, Chayakrit Krittanawong, Section of Health Services Research, Michael E. DeBakey VA Medical Center and Baylor College of Medicine, Houston, TX 77030, United States

Chayakrit Krittanawong, Section of Cardiology, Michael E. DeBakey VA Medical Center, Houston, TX 77030, United States

Corresponding author: Chayakrit Krittanawong, MD, Doctor, Section of Health Services Research, Michael E. DeBakey VA Medical Center and Baylor College of Medicine, 1 Baylor Plaza, Houston, TX 77030, United States. chayakrit.krittanawong@bcm.edu

Abstract

The development of artificial intelligence (AI) has increased dramatically in the last 20 years, with clinical applications progressively being explored for most of the medical specialties. The field of gastroenterology and hepatology, substantially reliant on vast amounts of imaging studies, is not an exception. The clinical applications of AI systems in this field include the identification of premalignant or malignant lesions (*e.g.*, identification of dysplasia or esophageal adenocarcinoma in Barrett's esophagus, pancreatic malignancies), detection of lesions (*e.g.*, polyp identification and classification, small-bowel bleeding lesion on capsule endoscopy, pancreatic cystic lesions), development of objective scoring systems for risk stratification, predicting disease prognosis or treatment response [*e.g.*,

Heart Association (ACC/AHA) Task Force on Performance Measures, The Lancet Digital Health (Advisory Board), European Heart Journal Digital Health (Editorial board), Journal of the American Heart Association (Editorial board), JACC: Asia (Section Editor), The Journal of Scientific Innovation in Medicine (Associate Editor), and Frontiers in Cardiovascular Medicine (Associate Editor).

Open-Access: This article is an open-access article that was selected by an in-house editor and fully peer-reviewed by external reviewers. It is distributed in accordance with the Creative Commons Attribution NonCommercial (CC BY-NC 4.0) license, which permits others to distribute, remix, adapt, build upon this work non-commercially, and license their derivative works on different terms, provided the original work is properly cited and the use is non-commercial. See: http://creativecommons.org/licenses/by-nc/4.0/

Manuscript source: Invited manuscript

Specialty type: Gastroenterology and hepatology

Country/Territory of origin: United States

Peer-review report's scientific quality classification

Grade A (Excellent): 0
Grade B (Very good): B
Grade C (Good): 0
Grade D (Fair): 0
Grade E (Poor): 0

Received: May 11, 2021
Peer-review started: May 11, 2021
First decision: June 12, 2021
Revised: June 15, 2021
Accepted: September 15, 2021
Article in press: September 15, 2021
Published online: October 28, 2021

P-Reviewer: Shafqat S
S-Editor: Gao CC
L-Editor: A
P-Editor: Yuan YY

determining survival in patients post-resection of hepatocellular carcinoma), determining which patients with inflammatory bowel disease (IBD) will benefit from biologic therapy], or evaluation of metrics such as bowel preparation score or quality of endoscopic examination. The objective of this comprehensive review is to analyze the available AI-related studies pertaining to the entirety of the gastrointestinal tract, including the upper, middle and lower tracts; IBD; the hepatobiliary system; and the pancreas, discussing the findings and clinical applications, as well as outlining the current limitations and future directions in this field.

Key Words: Artificial intelligence; Machine learning; Deep learning; Clinical applications; Gastroenterology

©The Author(s) 2021. Published by Baishideng Publishing Group Inc. All rights reserved.

Core Tip: Artificial intelligence (AI) clinical applications in gastroenterology and hepatology, which heavily relies on imaging, have dramatically expanded in the last 20 years. These applications include the detection of lesions, identification of pre-malignant or malignant lesions, development of objective scoring systems for risk stratification, predicting disease prognosis or treatment response, or evaluation of metrics such as bowel preparation score or quality of endoscopic examination. The objective of this review is to pool the available AI-related studies pertaining to the entire gastrointestinal tract, discussing findings and clinical applications, as well as outlining the current limitations and future directions in this field.

Citation: Kröner PT, Engels MM, Glicksberg BS, Johnson KW, Mzaik O, van Hooft JE, Wallace MB, El-Serag HB, Krittanawong C. Artificial intelligence in gastroenterology: A state-of-the-art review. *World J Gastroenterol* 2021; 27(40): 6794-6824
URL: https://www.wjgnet.com/1007-9327/full/v27/i40/6794.htm
DOI: https://dx.doi.org/10.3748/wjg.v27.i40.6794

INTRODUCTION

As artificial intelligence (AI) continues to rapidly evolve in medicine, the clinical applications of this technology are becoming increasingly evident[1]. Relying heavily on endoscopic and radiologic imaging, gastroenterology has become an attractive field in which to apply AI. Special interest has already been devoted to several areas, including the detection of gastrointestinal neoplastic lesions to assist with rapid diagnosis, reduction of misdiagnosis, improvement in quality of imaging, reduction of interobserver variability in visual classifications, and radiologic and histopathologic interpretation[2-4].

AI is a broad term that encompasses disciplines such as machine learning (ML) and subdisciplines or specific techniques such as deep learning (DL) (Figure 1). The central motivation of ML to use large datasets to recognize patterns of interactions between variables, often ultimately in a way that allows the learned function to be applied to new data[5]. ML is composed of both "supervised" and "unsupervised" learning methods. The goal of supervised learning is to predict a labelled output focusing primarily on classifying data input into specific subgroups, or alternately for prediction of quantitative outcomes[6]. An example of supervised learning is training a system to assist in identifying gastric intestinal metaplasia (GIM) using a large database of lesions that have previously been identified by an operator as corresponding to GIM. In comparison, unsupervised learning does not have an output to predict. It relies on attempting to identify naturally occurring patterns from within the input, often to then group them accordingly (*e.g.*, tissue sample clustering based on similar gene expression values)[6]. DL is a subset of ML, based on artificial neural networks (ANN), which are loosely inspired by the neuronal interplay in the human brain. DL autonomously utilizes the data input to learn, identify, and leverage predictive factors of an outcome, which can use multi-layered systems [*i.e.*, convolutional neural networks (CNN)] to process complex information[3,7]. The realization of

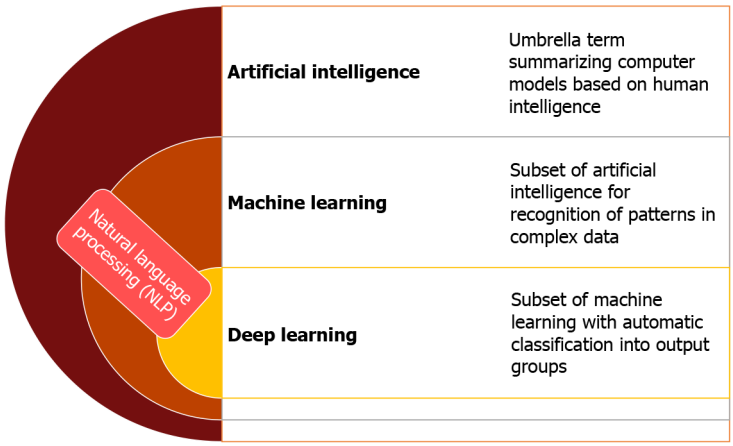


Figure 1 Primary concepts of artificial intelligence.

the concept of DL has recently become possible with rapid advancements in specialized computer hardware, such as increased graphics processing unit power, and accompanying software and algorithmic achievements.

With increased recognition of the importance of AI in gastroenterology, the first global AI in gastroenterology and endoscopy summit was held in Washington D.C. in late 2019, which included multiple experts in the domains of academia, industry and regulatory institutions. The consortium anticipated that in the next 10 years the clinical applications of AI in gastroenterology will positively influence patient care and clinical workflow. The consortium recognized the importance of a close multidisciplinary collaboration between gastroenterologists, industry, and regulatory institutions in the development and application of new technologies in the clinical setting[8]. Therefore, the main objective of this review is to introduce the topic of AI and its clinical applications, outline current limitations and knowledge gaps, and trace the future directions in each field by summarizing the global rapidly expanding pool of ever-changing literature to date (Figures 2 and 3).

UPPER GASTROINTESTINAL TRACT

Detection of premalignant and malignant lesions

The upper gastrointestinal tract has several areas of interest for detection of premalignant and malignant lesions, such as identification of dysplasia and early neoplasia in Barrett's esophagus (BE), esophageal squamous cell carcinoma (SCC), and gastric cancer (GC)[9] (Supplementary Table 1).

Despite the fact that histopathologic analysis is the gold standard to establish the diagnosis of BE and determine the presence of dysplasia, it is of paramount importance for endoscopists to obtain targeted biopsies from specific locations that harbor the actual lesion. By identifying areas that may harbor BE with or without dysplasia, AI can orient the clinician in performing directed biopsies instead of relying on random sampling. Importantly, detection of early esophageal neoplasia with conventional white light imaging (WLI) and digital chromoendoscopy [*i.e.*, narrow band imaging (NBI)] represents a challenge, an issue for which AI has been proposed as a possible solution[10,11].

In total, we included 8 studies that examined BE, all of which addressed the detection of dysplasia or early esophageal adenocarcinoma (EAC) based on endoscopic imaging or laser endomicroscopy[10-17]. The most popular analytic models were CNNs and support vector machines (SVMs), while cross-validation techniques were the primary basis of validation methods. In general, the models were able to discern between normal and dysplastic/neoplastic images with an accuracy of at least 89.9%, performing better than nonexpert endoscopists. De Groof *et al*[12] developed a DL algorithm based on a hybrid ResNet-UNet model using 4-fold per-patient cross-validation to detect early neoplasia in BE. The model was trained in a stepwise fashion, using a database with over 490000 endoscopic still images of the gastrointestinal tract for training, out of which 1247 corresponded to early BE neoplasia. This model achieved higher level of accuracy than non-expert endoscopists and could also detect the optimal biopsy site in up to 97% of patients. Ebigbo *et al*[14] developed a

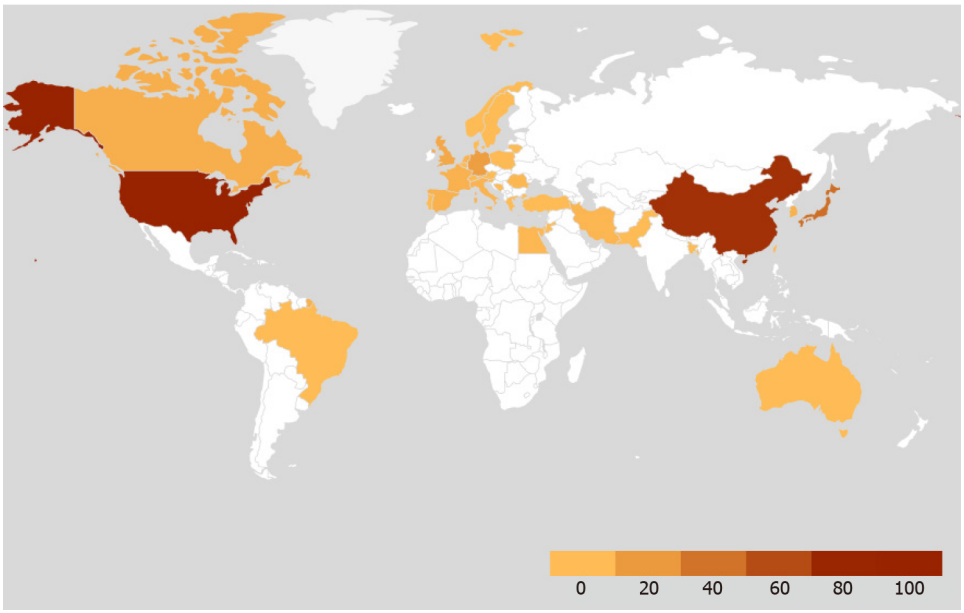


Figure 2 Geographic distribution of country from which the included studies originated.

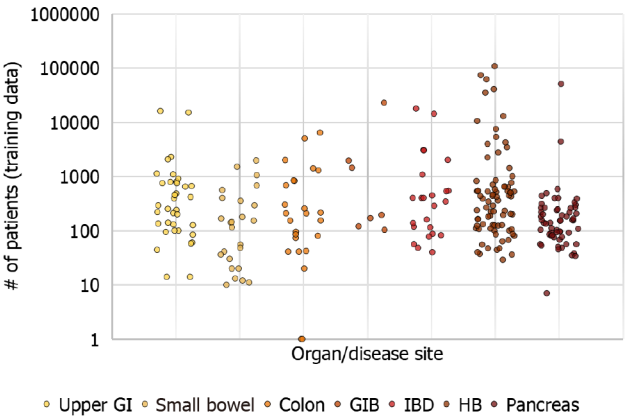


Figure 3 Scatterplot depicting distribution of studies across the organ systems in gastroenterology and hepatology. GI: Gastrointestinal; GIB: Gastrointestinal bleeding; IBD: Inflammatory bowel disease; HB: Hepatobiliary.

computer-aided diagnosis model based on ResNet that differentiated between normal BE and early EAC, with 89.9% accuracy, 83.7 sensitivity and 100% specificity.

Similarly, identification of SCC poses a similar clinical challenge, as traditional diagnostic techniques (*e.g.*, chromoendoscopy with lugol or NBI) have relatively low specificity[18]. As complex novel methods that rely heavily on endoscopic imaging such as endocytoscopy or volumetric laser endomicroscopy have been progressively implemented in clinical practice, the interpretation of large volumes of images has been noted to be a challenging and time-consuming issue[19]. Therefore, AI-assisted image interpretation has also found a use in identifying abnormalities in the image inputs[17].

Thirteen studies examining esophageal cancer were examined, of which 11 specifically studied SCC. Nine of the studies targeted to develop DL models for malignancy detection, while two studies aimed to develop models that predict malignancy depth of invasion with DL models. Most studies (8) were based on CNN models, while others used joint diagonalization principal component analysis (JDPCA), VGG16 Net, or GoogLeNet as classifiers. Although the values of accuracy, sensitivity and specificity in esophageal SCC detection varied between the studies, all models performed at least as good as endoscopists in lesion detection and characterization or substantially improved the endoscopists' lesion detection[20-30]. Fukuda *et al*[21] developed a DL model aimed at detecting suspicious lesions and characterize SCC using more than 28000 NBI-enhanced images in the construction of the model. The model achieved a higher sensitivity for SCC detection and higher accuracy for

SCC characterization from normal tissue than endoscopic experts. Two studies by Nakagawa *et al*[31] and Shimamoto *et al*[32] aimed at developing models that predicted esophageal malignancy depth utilizing a DL model based on a CNN with a belief-propagation decoder using independent validation datasets. These models achieved an accuracy of 89.2% and 91% in predicting invasion depth, with sensitivities of 70.8% and 90.1%, and specificities of 94.4% and 95.8%, respectively.

GC is the fourth most common cause of cancer-related death in the world. Identification of premalignant lesions or early gastric neoplasia is of paramount importance. Unfortunately, as with esophageal diseases, several studies have shown that conventional endoscopic imaging (*e.g.*, WLI or NBI) or other advanced endoscopic modalities (*e.g.*, magnifying endoscopy, blue laser imaging) have relatively low sensitivity and specificity in identifying premalignant or early neoplastic gastric lesions[33-36].

Twenty-four studies examined gastric malignancy or premalignant conditions. Eleven (46%) studies directly addressed early GC (EGC) detection, of which eight models used DL, two used SVM and one used JDPCA. The sample size in the training and validation datasets varied from less than 100 million to 1.03 million. The accuracy in EGC detection of all models ranged from 86.5%-98.7%, with sensitivity of 80.0%-96.7% and specificity of 89.2%-100%[30-37-51]. Specifically, Wu *et al*[52] developed a CNN-based model using over 9000 images to train the algorithm, which not only detected EGC lesions with a 92.5% accuracy, 94.0% sensitivity and 91.0% specificity but also performed significantly better than expert endoscopists at this task. Two studies, one based on faster region-based CNNs and another one based on quantum neural networks, used biomarkers, histology and computed tomography (CT) images to predict metastasis to the liver or lymph nodes. These models predicted metastasis to liver and lymph nodes with sensitivity of 66.7%, specificity 97.1% and an area under the curve (AUC) of 0.95[53,54]. Four studies developed models predicting survival in GC or stratification of risk of developing GC[55,56]. While 1 model based on SVM achieved higher accuracy than the tumor, nodes, metastasis cancer staging (TNM) system to predict overall survival and disease-free survival[57], another model based on a preoperative ANN was not superior in predicting survival compared to TNM [58]. Zhu *et al*[59] developed a ResNet50-based computer-aided detection and diagnosis (CAD) model to predict GC invasion depth, based on endoscopic images. The model achieved an accuracy of 89.16% in identifying GC invasion depth, compared to 71.49% in endoscopists.

Non-malignant conditions

Currently, diagnosis of *Helicobacter pylori (H. pylori)* infection (a known risk factor for the development of peptic ulcer disease and GC) relies on stool or breath testing and histopathology (invasive and expensive). Endoscopic identification of *H. pylori* has been a target for AI-assisted systems[60,61]. For *H. pylori* detection and classification, 4 of 4 studies used a CNN model[62-65]. A study by Martin *et al*[62] using gastric biopsy histopathology images as an input with small number of samples (n = 210 in training dataset and 90-106 in 2 test datasets) had diagnostic accuracy of 98.9%-99.1% for detecting current *H. pylori* infection. This result was higher than the accuracy achieved in 2 studies using esophagogastroduodenoscopy images as an input with higher number of samples (98.9%-99.1% *vs* 77.5%-87.7%). The mean accuracy of endoscopists for detecting currently infected *H. pylori* in 2 studies was around 79.0%-79.4%[62]. A study by Shichijo *et al*[64] found that the average *H. pylori* diagnostic time for the AI model was 194 s, while it was 230 ± 65 min for endoscopists. The AI model also had a significantly higher accuracy than the endoscopists by 5.3%, demonstrating that AI algorithms had significantly better accuracy and faster diagnostic time for *H. pylori* than the endoscopists. More recently, Nakashima *et al*[63] developed a CAD system based on linked color imaging combined with DL, which achieved 82.5% accuracy, demonstrating comparable diagnostic accuracy of *H. pylori* to that of experienced endoscopists.

In the area of gastrointestinal bleeding (GIB), risk stratification is of paramount importance not only to identify high-risk patients and guide clinical decision-making but to also identify areas where relatively scarce resources require allocation. In general, risk-stratification tools examine risk factors that are associated with a condition to predict one or several outcomes (*e.g.*, survival, length of hospitalization, rebleeding rates, need for endoscopic therapy, response to treatment)[66-68]. Regarding upper GIB, studies focused on developing prognostic models that predict rebleeding or the need for endoscopic/surgical therapy[69].

Seven studies examining outcome measures in GIB were included, all of which were developed by reviewing medical record parameters to construct ML algorithms, which were primarily based on ANN[67-73]. Half of the studies had both internal and

external validation cohorts, and patient sample sizes varied from 147 to over 22800. Shung *et al*[69] developed a gradient-boosting ML model that identified patients with upper GIB who met a composite endpoint with superior AUC, sensitivity and specificity to that of the Glasgow-Blatchford (GBS), Rockall and AIMS-65 scores. Seo *et al*[68] developed 4 different ML algorithms in patients with nonvariceal upper GIB that achieved superior AUC for mortality, rebleeding and hypotension than that of the GBS, particularly with the use of the random forest (RF) analytic model. However, for rebleeding prediction, a gradient-boosting model developed by Ayaru *et al*[73] showed a higher accuracy than the VC model in the aforementioned study (88% *vs* 78.5%). Das *et al*[70] developed a predictive ML model in lower GIB and compared it in internal and external validation cohorts to the validated BLEED score. Both internal and external validation cohorts reached accuracies, sensitivities, and specificities that were superior to the BLEED score.

LOWER GASTROINTESTINAL TRACT

Direct endoscopic visualization of the colon continues to be the gold standard for detection and resection of colonic premalignant lesions. In addition, patient- and polyp-specific characteristics have also been identified as predictors of missed colorectal cancer (CRC)[74]. Therefore, quality measures such as cecal intubation time, withdrawal time, bowel preparation quality and adenoma detection rates (ADR) have been instituted to attempt and standardize practice and mitigate the rates of missed CRC[74,75]. Since colonoscopy is an operator-dependent procedure, this may lead to variability in polyp detection rates, polyp characterization and estimation of depth of invasion of malignant lesions between endoscopists. CAD has been studied to address these current shortcomings, as well as to improve ADR and reduce CRC risk and colon cancer-related deaths[76] (Supplementary Table 2).

Detection of premalignant and malignant lesions

Polyp detection during colonoscopy is the cornerstone of CRC prevention. It is estimated that CRC develops in 2%-6% of cases after colonoscopy but before the next scheduled surveillance and, therefore, could represent missed or new postcolonoscopy CRC[74,77]. A large number of research studies have been devoted to identifying factors that play a role in the detection of premalignant lesions during colonoscopy, as well as factors that are associated with missed CRC[77]. An observation that has gained considerable attention is that the presence of experienced endoscopy nurses, fellows or any trained second observer during the procedure itself improves ADR[78,79]. Therefore, and answering the call for improved polyp detection measures during colonoscopy, AI has become a promising technology serving the role of a more standardized "second observer," appropriately termed "computer-aided detection" (CADe).

Eighteen studies that evaluated polyp detection were included in this review, thirteen of which employed DL models, while five used other ML models. Nearly all the studies were limited to having internal validation only. The training datasets in these studies utilized still images from colonoscopy videos ranging from 176 to more than 8600 images. Seven studies calculated the ADR of the developed model and compared it to that of endoscopists, most of which found that the AI had significantly higher ADR than endoscopists, with a decreased reaction time, while the remaining studies showed equivalent ADR[80-87]. Repici *et al*[82] conducted a multicenter study showing that the ADR was 40.4% in the study's participating endoscopists alone, while it was 54.8% in the group using the CADe-based GI-Genius (®Medtronic, Minneapolis, MN) module. Similarly, Wang *et al*[85] conducted a study that evaluated over 520 colonoscopies, also examining the use of a CADe model, and found that the ADR increased from 20.34% in endoscopists alone to 29.12% in the CADe-assisted group. Other studies explored the accuracy, sensitivity and specificity of polyp-detection AI models, displaying accuracies of up to 96.4%, sensitivity of up to 99.7% and specificity of up to 93.7%[88-98]. Kominami *et al*[93] designed an SVM-based model using real-time images with NBI and magnification enhancement to detect colon polyps, achieving an accuracy, sensitivity, and specificity of 93.2%, 93.0%, and 93.3%, respectively. Three studies addressed subjects in the realm of CRC, specifically detecting malignancy on colonoscopy with chromoendoscopy and NBI enhancement, hematoxylin-eosin histopathology slides, or estimating invasion depth on regular WLI colonoscopy images[99-101]. Ito *et al*[100] developed a DL model based on CNN to detect deeply invasive CRC based on WLI colonoscopy, which utilized over 9900

images from 41 patients to train the model. Furthermore, over 5000 images were used in the testing cohort, achieving an accuracy, sensitivity and specificity in differentiating invasion depth of 81.2%, 67.5%, and 89.0%, respectively. Kudo *et al*[101] developed a model based on EndoBRAIN (®Cybernet Systems Co., Tokyo, Japan) using colonoscopy with chromoendoscopy and NBI enhancement to detect malignant lesions in the colon. The training sample used over 69000 images and achieved accuracies of 98.0% and 96.0% for chromoendoscopy and NBI enhancement, respectively. These diagnostic parameters were higher than those of expert and nonexpert endoscopists.

In an attempt to morphologically classify polyps according to their malignant potential, numerous classification systems have been developed. As an example, the Paris classification classifies polyps according to whether they are pedunculated, sessile, slightly raised, or excavated[102]. These visual characteristics are then used to predict whether the polyp has invasive potential or lymph node involvement and potentially contribute to clinical decision-making, such as determining whether the polyp is resectable endoscopically[103]. Unfortunately, research has shown that interobserver variability with this classification is moderately high, suggesting that this visual classification should not be routinely used in research or practice[104]. In addition, considering that most resected polyps during colonoscopy are diminutive and that histopathologic analysis of resected polyps is costly, optical diagnosis has been proposed in this subset of polyps and termed "optical biopsy"[105]. The concept of optical biopsy has been proposed to support cost-effective strategies in CRC screening such as resecting-and-discarding, as well as diagnosing-and-leaving this subset of polyps[106]. However, the concept of optical biopsy has the same limitations as endoscopic polyp characterization does: relatively high interobserver variability. Hence, computer-aided diagnosis has been proposed as a potential solution to standardization of interpretation of endoscopic images.

Nine studies pertaining to colonic polyp classification or differentiation were included in this review[107-115]. While some studies did not report on validation methods, others had cross-validation, internal, and external methods. Most studies relied on ML-based algorithms to assess colonoscopy with enhancement measures (*e.g.*, magnification, NBI, endocytoscopy), while deep CNN models were used in studies evaluating real-time polyp differentiation. Sánchez-Montes *et al*[114] developed an SVM-based model to predict polyp histologic classification using high-definition WLI from 225 colonoscopies, achieving accuracy, sensitivity, and specificity of 91.1%, 92.3%, and 89.2%, respectively. Additionally, Misawa *et al*[111] evaluated the performance of EndoBRAIN (®Cybernet Systems Co., Tokyo) analyzing endocytoscopic images obtained during colonoscopy to characterize polyps as neoplastic *vs* non-neoplastic with an accuracy, sensitivity, and specificity of 96.9%, 97.6%, and 95.8%, respectively. These findings hold promise in determining screening and surveillance schedules, and in instituting cost-effective strategies such as "resect-and-leave".

Knowledge on the depth of invasion of early CRC is critical for determining resection modality. Intramucosal and submucosal cancerous lesions can be resected with endoscopic techniques such as endoscopic mucosal resection or endoscopic submucosal dissection[116]. However, lesions that invade the deeper layers have a higher association with lymph node metastasis and, hence, may require a combined surgical and oncologic approach[116,117]. Several features on direct endoscopic visualization have been associated with deep invasion of a lesion, including lesion depression, fold convergence, and significantly irregular, and heterogeneous surface capillary pattern[118]. As with any image-based field, a significant degree of interobserver variability exists in characterizing lesions and determining their depth or invasion, for which CAD represents an attractive option to standardize the approach of estimating lesion invasion depth.

Finally, 6 studies assessed other subjects within the realm of the lower gastrointestinal tract, including developing models that predict outcomes in patients with CRC, models examining quality of colonoscopy performance, and studies estimating cost reductions of the use of AI[119-122]. Of 4 studies examining prediction of outcomes, 2 were based on DL (*i.e.*, CNN-based) models, using a wide numerical range of histopathologic images: from 300 million to 12 million. Skrede *et al*[123] developed a DL model using over 12 million histopathological images to develop a biomarker for automatic prediction of cancer-specific survival, which outperformed existing markers. The authors conclude this strategy can potentially be utilized in the treatment selection process by identifying high-risk groups. Thakkar *et al*[120] recently developed a DL model aimed at automatically quantifying quality metrics during colonoscopy, providing intra-procedural feedback to the performing endoscopist.

Non-malignant conditions

Video capsule endoscopy: Owing to its ease of use and noninvasiveness, video capsule endoscopy (VCE) is the current diagnostic method of choice to assess the small bowel for conditions such as occult GIB and Crohn's disease (CD). However, since it lacks self-locomotion, it relies on the motility of the bowel to advance within the gastrointestinal tract. Therefore, it requires a very large number of images (up to 60000 per examination) to be automatically obtained, rendering the process of interpretation lengthy and tedious[124]. VCE has been an area of focus for AI since its early stages, seeing the initial AI classifying methods such as SVM and multilayer perceptron network[125-127]. With faster processors, increased computational power by improved graphics processing units and evolving CNNs, DL algorithms have become the modality of choice for image analysis in VCE[128,129]. As in the lower gastrointestinal tract, the same principles of CADe and computer-aided diagnosis could be applied to deep balloon-assisted or motorized enteroscopy systems (Supplementary Table 3).

A total of 31 studies pertaining to VCE were identified. Fifteen studies (48%) developed models to assist in detection of active GIB or angioectasia. Four studies used CNN, five used SVM, and the remaining ones used ML-based analytic models. Five studies reported cross-validation methods. All studies reported accuracy ranging from 94% to 98% in identifying GIB and angioectasias, with sensitivity of 92.0%-100% and specificity of 82.9%-99.9%[130-142]. Specifically, Tsuboi *et al*[140] developed a DL model based on CNN for angioectasia detection, which achieved an AUC of 0.998, with a sensitivity and specificity of 98.8% and 98.4%, respectively.

Six studies assessed for the presence of small-intestinal ulcers, of which five used DL models based on CNN and one used SVM[128,134,143-146]. Aoki *et al*[128,143] conducted 2 studies in testing DL models to detect ulcerations, yielding a sensitivity of 88.2%, a specificity of 90.9%, and an AUC of 0.958, respectively. Two more studies evaluated the detection of small-bowel CD by identifying ulcers on VCE[147,148]. Klang *et al*[147] developed a DL model based on CNN that used over 17000 VCE images to identify CD ulcers, achieving an AUC of 0.99. Two studies examined small intestinal polyp detection using NN-based models, both achieving an accuracy of at least 98%, with sensitivity and specificity of up to 95.5% and 98.5%, respectively[149,150].

Regarding celiac disease (CeD) detection, 4 studies were evaluated, 3 of which used CNN and 1 that used a clinical decision support system[151]. A study by Zhou *et al*[152] reported 100% sensitivity and specificity in detecting CeD using GoogLeNet as classifier. A study by Wimmer *et al*[153] using AlexNet, VGGf net, and VGG-16 net as classifiers obtained an optimal accuracy of 92.5% using VGG-16, although the report did not include sample size. More recently, Wang *et al*[154] developed a DL model using the CNN-based InceptionV3 as well as the SVM-based ResNet50 that was 95.94% accurate, 97.20% sensitive and 95.63% specific in identifying CeD in VCE images.

Hookworm infection represents a significant healthcare issue in the developing world, with an estimated 600 million people harboring this infection[155]. As this helminth typically dwells in the small bowel, it may occasionally be a finding in VCE. Three studies evaluated hookworm detection, of which two used CNN and one used SVM with all using cross-validation[156-158]. Specifically, He *et al*[157] developed a DL model based on deep CNN, which was trained on a large VCE dataset consisting of more than 440000 images. The model outperformed other handcrafted, feature-based methods, reaching an accuracy of 88.5% and a sensitivity of 84.6% in detecting hookworm in the small bowel.

To assess for quality of bowel preparation during VCE Leenhardt *et al*[159] and Noorda *et al*[160] developed a DL models based on CNN. Both models achieved accuracy of over 95%, with sensitivity and specificity of 94.7%-96.18% and 94.0%-94.33%, respectively. Overall, Ding *et al*[131] developed a DL model based on CNN to identify and categorize all small-bowel ulcers, polyps, bleeding, lymphangiectasia, follicular hyperplasia, protruding lesions, diverticula or inflammation using over 100 million VCE images. The model achieved an impressive 99.90% overall sensitivity and 99.88% specificity, whereas gastroenterologists identified lesions with a 74.57% sensitivity in the per-patient analysis and 76.89% sensitivity in the per-lesion analysis. Furthermore, the reading time per patient was 5.9 min by the CNN model, compared to 96.6 min by conventional reading.

Inflammatory bowel disease: The complex interplay of pathophysiological factors in inflammatory bowel disease (IBD) has led to the realization that differences in patients' biology may confer differences in disease activity and response to therapy- an example of "precision medicine"[161]. Integration of AI algorithms into the IBD realm

brings promise not only in diagnosis or reducing interobserver variability in severity grading but also opens up the possibility of analyzing large databases to identify complex or occult patterns of disease[162-167].

A total of 25 studies pertaining to IBD were included in this review, of which 9 dealt with CD, 6 studied ulcerative colitis (UC,) and 10 investigated both. Five studies aimed to detect CD, UC, or IBD in general from VCE images, endoscopic images, histology, magnetic resonance imaging (MRI) images, and genetics. Most of the studies used cross-validated ML methods, of which SVM was the method of choice; while another study used DL-based CNN. These studies displayed high levels of accuracy in detecting IBD, from 83.3%-90.8%[143,168-171]. Aoki *et al*[143] developed a DL model based on CNN that used more than 10000 VCE images in the validation dataset to detect CD ulcers in the small bowel, achieving an accuracy, sensitivity and specificity of 90.8%, 88.2% and 90.9%, respectively.

Nine studies that addressed predicting disease severity were primarily based on endoscopic imaging; although other studies also used laboratory studies, demographics, histopathology and CT enterography[172-179]. Five studies utilized ML-based analytic models, while the remaining four utilized DL-based models, of which CNNs were the preferred ones. Five studies reported internal validation, and two studies had external validation cohorts; while two studies did not report validation. The size of patient cohorts varied greatly, from 87 to over 3000, with studies reporting up to 40000 images in the validation datasets. Yao *et al*[179] designed a DL model based on CNN to grade the severity of UC using colonoscopy images, which was constructed with over 16000 images from 3000 patients. The reported accuracy, sensitivity, and specificity was 87.6%, 90.2%, and 87.0%, respectively. The authors concluded that these results support the use of AI in UC severity grading , which approximates the scoring of experienced human reviewers. Maeda *et al*[172] designed a ML model with CAD to detect histologic inflammation based on colonoscopy images enhanced with endocytoscopy. The model achieved an accuracy, sensitivity and specificity of 90.0%, 74.0%, and 91.0%, respectively, using over 9900 images from 100 patients in the validation cohort.

To predict therapeutic response in patients with IBD treated with thiopurines or biologics seven studies constructed internally validated ML algorithms, based on RF analytic models. All models achieved an accuracy of 80.0%-89.8% or an AUC of 0.73-0.846 in identifying patients who will respond at 6-8 wk to therapeutic regimens[180-186]. Waljee *et al*[186] designed a model using only demographic and laboratory data from 401 patients to predict response at 8 wk in patients receiving ustekinumab with an AUC of 0.78, potentially laying the foundation to avoid costly therapeutic drug monitoring. Waljee *et al*[184] also constructed a model based on laboratory values and demographics with a validation dataset of over 6100 patients to predict IBD-related hospitalization and outpatient steroid use, achieving an AUC of 0.87, suggesting such AI models could be used to identify patients at risk of an IBD flare and enable precision medicine-based therapeutic approaches (Supplementary Table 4).

A further 2 internally validated ML models using SVM and RF were developed to predict the risk of IBD based on a genomic datasets[187,188]. Isakov *et al*[187] developed a gene prioritization model using 4 combined analytic models (RF, SVM GB, and an elastic net regularized generalized linear model) to identify genes related to IBD, achieving an accuracy of 80.8%. An internally validated natural language processing (NLP) model by Hou *et al*[189] used histopathology reports to identify surveillance *vs* nonsurveillance colonoscopy in patients with IBD, with an accuracy of 80.0%. Lastly, Firouzi *et al*[190] developed an internally validated model based on Waikato Environment for Knowledge Analysis that identified, with an accuracy of up to 89.8%, patients with IBD who required a bone mineral density scan, using electronic health record data.

HEPATOBILIARY SYSTEM

Liver diseases are broad and complex, ranging from asymptomatic liver chemistry elevation to life-threatening conditions such as acute liver failure or orthotopic liver transplantation (OLT). Hepatology is can be a fertile ground for applying AI in survival models (*e.g.*, model for end-stage liver disease), disease detection models [*e.g.*, early detection of non-alcoholic fatty liver disease (NAFLD)], disease severity models (*e.g.*, alcoholic hepatitis discriminant function), or disease estimation models (*e.g.*, aspartate aminotransferase-to-platelet ratio index), but also for pattern recognition in radiological images, histopathology and even selection of LT candidates[191,192]. A

total of eighty-five studies pertaining to hepatology were examined, out of which twenty assessed prediction of outcome measures, forty-one examined prediction or detection of steatosis, fibrosis or cirrhosis, nine studies examined differentiation of malignant liver neoplasms, six studies explored predictive models for portal hypertension, and eight studies investigated AI models for other purposes.

Nine studies developed models that assisted with detection or classification of hepatobiliary neoplastic lesion, six of which involved DL-based CNN[193-202]. Schmauch *et al*[197] constructed an internally validated CNN-based DL model using ultrasonographic images of the liver to detect and classify focal liver lesions, achieving an overall AUC of 0.891. Six studies constructed models assisting in predicting the presence of portal hypertension complications in patients with all-cause cirrhosis, based on clinical data or radiological images obtained from modalities such as CT scans[203-208]. Dong *et al*[204] constructed an ML-based model on an RF analytic model that used clinical data and predicted the presence of esophageal varices in patients with cirrhosis with an AUC of 0.82, potentially being useful in performing a better triage of patients who actually require an upper endoscopy for variceal screening. Liu *et al*[206] developed an ML model that had a higher diagnostic performance than conventional noninvasive tools (either conventional image-based or serum-based tools) in identifying clinically significant portal hypertension from contrast-enhanced CT or MRI, with an accuracy of 91.1% and 88.9%, respectively.

Forty-two studies developed models addressing detection of steatosis, fibrosis, or cirrhosis based on clinical data, shear-wave elastography, CT or MRI scans, histopathology, or genetics. Of these, 27 studies developed models to detect, quantify, or predict steatosis, fibrosis, or cirrhosis[202,209-234]. Forlano *et al*[215] developed a ML-based model for quantification of steatosis, inflammation, ballooning, and fibrosis using biopsies from patients with NAFLD. The model identified characteristics of NAFLD with intra- and inter-observer agreement from 0.95-0.99, and has a potential use in objective assessment of treatment response in patients with NAFLD. Yasaka *et al*[202] constructed a DCCN model based on over 144000 MRI images from 534 patients to stage hepatic fibrosis, achieving AUCs of 0.84, 0.84, and 0.85 for F4, F3, and F2 fibrosis, respectively. In assessing fibrosis in patients with hepatitis B virus, Wang *et al*[232] created a DL-based CNN model that used ultrasonographic and elastography data from 132 patients to predict fibrosis, with AUCs of 0.97, 0.98 and 0.82 for F4, F3 and F2 fibrosis, respectively. Eight studies developed AI models to establish the diagnosis of fatty liver disease or distinguish between the causes of liver disease[235-242]. In distinguishing NAFLD from non-alcoholic steatohepatitis (NASH), Fialoke *et al*[237] constructed an ML model testing decision tree, linear regression,, RF, and extreme gradient boosting (XGB) analytic models, of which the XGB achieved the highest accuracy, AUC, sensitivity, and specificity at 79.7%. 0.876, 77.4%, and 80.8%, respectively. Taylor-Weiner *et al*[239] constructed an ML model that enabled quantitative measurement of liver histology and disease monitoring in NASH, characterizing disease severity, heterogeneity and treatment response in NASH.

Of 20 studies examining outcome predictors, 8 evaluated predictor models in OLT involving donor-recipient matching, recipient survival at determined time frame, graft survival at different time frames, survival predictors, and morbidity predictors[243-250]. Bertsimas *et al*[245] constructed an internally-validated decision tree-based ML model using clinical data that predicted 3-mo waitlist mortality or removal with an AUC of 0.895. Five studies designed models for outcome prediction in patients with hepatocellular carcinoma (HCC), including response to trans-arterial chemoembolization (TACE), recurrence or survival after resection, most of which were based on CNN[251-255]. Saillard *et al*[254] designed an externally-validated model based on a pre-trained CNN based on histology slides from 328 patients that independently predicted survival after HCC resection with a c-index of 0.75. Other studies evaluated outcomes in patients with acetaminophen-related ALF, primary sclerosing cholangitis, predicted the presence of choledocholithiasis, predicted hepatotoxicity of stereotactic body radiation, or mortality in patients with cirrhosis[256-263]. Eaton *et al*[256] constructed a ML model with XGB that accurately predicted hepatic decompensation in patients with primary sclerosing cholangitis with a C-statistic of 0.90.

Other studies focused on developing models for miscellaneous topics such as estimating liver stiffness from MRI, assessing pretransplant cognitive impairment, detecting spectral differences between normal and hepatitis B virus serum samples, classifying seroconversion to HBeAg, predicting hepatotoxicity in early stages of drug development, predicting fibrosis in hepatitis C virus, or AI-assisted liver tumor segmentation[264-272]. Williams *et al*[271] developed a ML model based on a Bayesian network using hepatic safety assays to predict drug-induced liver injury in compounds during drug development, achieving an accuracy, sensitivity, and specificity

of 86.0%, 87.0%, and 85.0%, respectively. An externally-validated ML model based on SVM and radiomics by He *et al*[267] used MRI and clinical data to estimate liver stiffness, achieving an AUC of 0.80, with an accuracy, sensitivity, and specificity of 75.0%, 63.6%, and 82.4%, respectively. Lastly, models addressing prediction of NAFLD or NASH based on clinical or genetic data, as well as models analyzing donor liver texture for steatosis, have also been developed[272-278] (Supplementary Table 5).

PANCREATIC DISEASES

Pancreatic diseases contain areas where AI can be effectively applied. Of primary interest is the use of AI in improving existing disease severity scoring systems or prognostic models in complicated acute pancreatitis (AP) or chronic pancreatitis (CP), based on clinical and radiological data, detection and differentiation of pancreas cystic neoplasms (PCN) with prediction of malignant potential, radiologic early detection of pancreatic ductal adenocarcinoma (PDAC), radiologic differentiation between PDAC and benign pancreatic conditions [*e.g.*, autoimmune pancreatitis (AIP)], and histopathologic interpretation of tissue samples[279-282]. A total of 59 studies pertaining to the pancreas were reviewed. Of these, 20 (34%) addressed prediction of outcomes in patients with pancreatic diseases ranging from AP to neoplasia.

Eleven of these studies examined outcome prediction in AP. All of the studies' ANN models outperformed logistic regression models, Glasgow, and APACHE-II scoring systems in predicting AP severity; while requiring less number of parameters[283-293]. Qiu *et al*[292] compared the performance of SVM, logistic regression analysis, and ANN models to predict multiorgan failure in AP. All 3 models predicted multiorgan failure, with AUC of 0.840, 0.832, and 0.834, respectively, with ANN requiring a lesser number of parameters.

Seven (12%) studies used AI algorithms to construct clinical registries, segment the pancreas based on imaging, or differentiate between certain pancreatic diseases based on cross-sectional imaging or endoscopic ultrasound (EUS)[294-300]. Zhang *et al*[298] constructed a DL station classification model and a segmentation model to reduce the difficulty in EUS interpretation for trainees. The trainee station recognition accuracy improved from 67.2% to 78.4% in the crossover study. Interobserver agreement between endoscopists and deep CNN with Cohen's kappa coefficient was substantial, ranging from 0.826-0.879. The authors conclude that this technology may play a key role in shortening the learning curve of EUS among trainees.

Fifteen studies (25%) addressed prediction of malignancy based on imaging findings, or differentiation of benign from malignant pancreatic conditions[280,301-315]. Marya *et al*[280] developed an EUS-based CNN model that distinguished AIP from normal pancreas with 99% sensitivity and 98% specificity, AIP from CP with 94% sensitivity and 71% specificity, and AIP from PDAC with 90% sensitivity and 93% specificity. Chu *et al*[301] conducted a study utilizing CT radiomics features to differentiate PDAC from normal pancreas tissue. The accuracy of the RF binary classification was 99.2%, with an AUC of 99.9%. All cases of PDAC were correctly identified, with a sensitivity of 100% and specificity of 98.5%.

Eleven studies (19%) evaluated differentiation of PCNs by classifying them into their respective subtypes based on their characteristics on imaging[316-326]. Springer *et al*[324] developed a multimodality ML model that integrated clinical, radiological and genetic/biochemical markers data to determine whether patients with pancreas cyst should undergo surgery, monitoring, or no further surveillance. The model correctly identified serous cystic neoplasms in 65% of the cases with 99% specificity, clearly outperforming the current standard of care of clinical identification in only 18% of cases. The authors conclude that these systems may serve an adjunct role in clinical practice, enabling the clinician to take better-informed clinical decisions[324].

Eight studies addressed PDAC, from developing risk scores for development of PDAC based on urinary biomarkers, predicting clinical performance and response to celiac plexus neurolysis, to prediction of survival time. AI models performed at least as well as the logistic regression models in predicting the selected outcome[327-334].

Six studies directly examined early pancreatic cancer detection in PDAC or PCN by examining the imaging characteristics or identifying high-risk patients on electronic health records based on factors such as family history of pancreatic cancer[335-340]. Roch *et al*[339] developed NLP-based algorithms based on common terminology used by physicians in describing pancreatic cysts and applied them to automatically conduct searches in electronic health records. The algorithm tracked patients with cysts with a 99.9% sensitivity and 98.8% specificity, demonstrating its utility in

capturing patients swiftly and with more ease than manual review. Ozkan *et al*[338] developed a CAD image-processing system using EUS images to diagnose PDAC, taking patient age into consideration. The accuracy of the model was 87.5, with sensitivity and specificity of 83.3% and 93.3%, respectively (Supplementary Table 6).

CURRENT LIMITATIONS AND KNOWLEDGE GAPS

Despite the numerous positive advances in AI, there remain several limitations to current studies and obstacles to overcome for future studies. Most current models are based on labeled data and, hence, interpretation is only as good as the observer who labeled the "gold-standard" data. Current algorithms are specifically fitted for a determined dataset. A sizeable proportion of the AI models applied to the clinical setting are only internally validated. Ideally, models should be externally validated on diverse cohorts to ensure that overfitting does not become an issue. Therefore, this issue could be potentially addressed by the creation of a universal, well-annotated, high-quality dataset, and by creating algorithms with more plasticity. However, creating "universal datasets" creates additional challenges, particularly related to data integrity and privacy. A potential solution to this is the decentralized "federated datasets", which involves combining multiple datasets stored on their respective servers, addressing these challenges[341]. Specific protocols are required for choosing an analytic model and selecting or developing validation techniques (*e.g.*, external-, internal-, cross-validation) for data fine-tuning or augmentation. Algorithms that yield the best accuracy should be promoted. Calibration has translated into improvements in probability prediction, for which they should be instituted in all models. Most current studies were cohort studies, whereas well-designed randomized controlled trials would be needed to better support conclusions. Some studies utilized custom-built models, which are not explained in detail. Therefore, custom-built algorithms should have their background and processes thoroughly declared. The studies presented numerous different newly developed models, which would require validation to determine whether these can be applied to other datasets. Several studies examine different techniques during an equivalent endoscopic procedure (*e.g.*, endoscopic image processing in NBI, WLI, or chromoendoscopy), which renders comparisons between techniques cumbersome or not possible. Data matrixes should be completely reported[342]. Significant efforts have been devoted to developing guidelines, such as the CONSORT-AI extension, to standardize reporting in trials evaluating performance of the AI. Adherence to current guidelines and flexibility to revise them as technology continues to advance is of paramount importance. The majority of studies use still images and high-definition images, which is not in line with the "real-world experience" of real-time settings, imaging affected by motion artifact or poor image processing from outdated technical equipment.

APPLICATION IN CLINICAL CARE (ARTICLE HIGHLIGHTS)

ML and DL could assist clinicians in the diagnosis of gastrointestinal and liver neoplasms, bleeding, infection, and inflammatory process, and also predict outcome measures in these conditions.

The initial use of ML or DL models might be used in backing up clinicians in establishing diagnoses or determining a treatment plan.

Given its high predictive value, if AI suggestions match the clinician's reasoning, clinicians could make a decision more confidently. If the answers are discrepant, careful investigation should be undertaken.

In the future, if ML or DL models find a place to be integrated in standard clinical care, to guide in establishing diagnoses, selecting treatment interventions, predicting outcomes, and influencing clinical decision-making. However, future studies are also necessary to explore avenues of how these measures can be better instituted in clinical practice as a whole.

FUTURE DIRECTIONS

As demonstrated by this review, AI applications in clinical gastroenterology and hepatology continue to rapidly expand and evolve at many different levels. For

general clinical care, the recent proliferation in AI applications is likely to enable "precision medicine" on a broader scale. Clinically, it is predicted that invasive diagnostic interventions will generally fall out of favor for some conditions, as better noninvasive ML-based algorithms pave the way for improved clinical prediction models. Some diagnostic interventions, such as VCE interpretation, may see a considerable decrease in human interpretation, minimizing the human role to that of supervision and attestation of findings of the model. AI-assisted technology will prove important in real-time clinical settings (*e.g.*, polyp detection during colonoscopy). Integration of monitoring devices (*e.g.*, smartphones, smart watches) with ML in the management of selected diseases is also predicted to significantly receive more attention the coming years. The creation of a universal, large, high-quality, well-labelled dataset is a necessity, from which algorithms could be developed to better define the epidemiology and risk factors of diseases. Well-harnessed AI assistance should decrease physician workload or at least maximize their productivity by allowing them to shift from menial tasks to faster, more accurate clinical decision-making. ML algorithms based on these datasets can also be used for other quality measures, such as improvement of process efficiency or identifying cost-effective interventions. In terms of data analysis, traditional analytic models (*e.g.*, logistic regression and clinical scoring systems) may be substituted or augmented by ML algorithms to achieve greater capability and accuracy. Developing and maintaining multidisciplinary teams of data scientists, physicians, content subject experts and industry is of paramount importance in the advancement of AI in gastroenterology and hepatology. Finally, educating clinicians and patients in the future paths of AI applications is critical to increase understanding of future value and decrease reluctance in engagement.

CONCLUSION

The latest advances in AI in gastroenterology and hepatology are promising for aspect many fields of clinical care, from detection of neoplastic lesions on endoscopic assessment and improving current survival models to predicting treatment response. The application of AI to large and complex datasets may assist in the identification of new associations between variables, potentially leading to changes in clinical practice. Furthermore, the use of AI-assisted technologies has the potential to dramatically improve the quality of care. Finally, the time for assisted precision medicine is at hand, with the AI being able to tailor a treatment regimen or potentially predict the response to treatment in a specific patient based on extensive amounts of clinical data from large patient datasets. It is important to realize that, while AI currently does not substitute human clinical reasoning, it has a bright future in the betterment of patient care.

ACKNOWLEDGEMENTS

The authors are grateful to for Wang Z, PhD, Zhang HJ, PhD, Sun T, MD, PhD, Hassan Virk H, MD, and Aiumtrakul N, MD assistance with the additional literature search.

REFERENCES

1 **Noorbakhsh-Sabet N**, Zand R, Zhang Y, Abedi V. Artificial Intelligence Transforms the Future of Health Care. *Am J Med* 2019; **132**: 795-801 [PMID: 30710543 DOI: 10.1016/j.amjmed.2019.01.017]

2 **Calderaro J**, Kather JN. Artificial intelligence-based pathology for gastrointestinal and hepatobiliary cancers. *Gut* 2021; **70**: 1183-1193 [PMID: 33214163 DOI: 10.1136/gutjnl-2020-322880]

3 **Le Berre C**, Sandborn WJ, Aridhi S, Devignes MD, Fournier L, Smaïl-Tabbone M, Danese S, Peyrin-Biroulet L. Application of Artificial Intelligence to Gastroenterology and Hepatology. *Gastroenterology* 2020; **158**: 76-94.e2 [PMID: 31593701 DOI: 10.1053/j.gastro.2019.08.058]

4 **Kather JN**, Calderaro J. Development of AI-based pathology biomarkers in gastrointestinal and liver cancer. *Nat Rev Gastroenterol Hepatol* 2020; **17**: 591-592 [PMID: 32620817 DOI: 10.1038/s41575-020-0343-3]

5 **Hoogenboom SA**, Bagci U, Wallace MB. Artificial intelligence in gastroenterology. The current state of play and the potential. How will it affect our practice and when? *Tech Gastrointest Endosc* 2019; **22**: 42-47 [DOI: 10.1016/j.tgie.2019.150634]

6 **Deo RC**. Machine Learning in Medicine. *Circulation* 2015; **132**: 1920-1930 [PMID: 26572668 DOI: 10.1161/CIRCULATIONAHA.115.001593]

7 **Wu J**, Chen J, Cai J. Application of Artificial Intelligence in Gastrointestinal Endoscopy. *J Clin Gastroenterol* 2021; **55**: 110-120 [PMID: 32925304 DOI: 10.1097/MCG.0000000000001423]

8 **Parasa S**, Wallace M, Bagci U, Antonino M, Berzin T, Byrne M, Celik H, Farahani K, Golding M, Gross S, Jamali V, Mendonca P, Mori Y, Ninh A, Repici A, Rex D, Skrinak K, Thakkar SJ, van Hooft JE, Vargo J, Yu H, Xu Z, Sharma P. Proceedings from the First Global Artificial Intelligence in Gastroenterology and Endoscopy Summit. *Gastrointest Endosc* 2020; **92**: 938-945.e1 [PMID: 32343978 DOI: 10.1016/j.gie.2020.04.044]

9 **Mori Y**, Kudo SE, Mohmed HEN, Misawa M, Ogata N, Itoh H, Oda M, Mori K. Artificial intelligence and upper gastrointestinal endoscopy: Current status and future perspective. *Dig Endosc* 2019; **31**: 378-388 [PMID: 30549317 DOI: 10.1111/den.13317]

10 **Hashimoto R**, Requa J, Dao T, Ninh A, Tran E, Mai D, Lugo M, El-Hage Chehade N, Chang KJ, Karnes WE, Samarasena JB. Artificial intelligence using convolutional neural networks for real-time detection of early esophageal neoplasia in Barrett's esophagus (with video). *Gastrointest Endosc* 2020; **91**: 1264-1271.e1 [PMID: 31930967 DOI: 10.1016/j.gie.2019.12.049]

11 **van der Sommen F**, Zinger S, Curvers WL, Bisschops R, Pech O, Weusten BL, Bergman JJ, de With PH, Schoon EJ. Computer-aided detection of early neoplastic lesions in Barrett's esophagus. *Endoscopy* 2016; **48**: 617-624 [PMID: 27100718 DOI: 10.1055/s-0042-105284]

12 **de Groof AJ**, Struyvenberg MR, van der Putten J, van der Sommen F, Fockens KN, Curvers WL, Zinger S, Pouw RE, Coron E, Baldaque-Silva F, Pech O, Weusten B, Meining A, Neuhaus H, Bisschops R, Dent J, Schoon EJ, de With PH, Bergman JJ. Deep-Learning System Detects Neoplasia in Patients With Barrett's Esophagus With Higher Accuracy Than Endoscopists in a Multistep Training and Validation Study With Benchmarking. *Gastroenterology* 2020; **158**: 915-929.e4 [PMID: 31759929 DOI: 10.1053/j.gastro.2019.11.030]

13 **de Groof J**, van der Sommen F, van der Putten J, Struyvenberg MR, Zinger S, Curvers WL, Pech O, Meining A, Neuhaus H, Bisschops R, Schoon EJ, de With PH, Bergman JJ. The Argos project: The development of a computer-aided detection system to improve detection of Barrett's neoplasia on white light endoscopy. *United European Gastroenterol J* 2019; **7**: 538-547 [PMID: 31065371 DOI: 10.1177/2050640619837443]

14 **Ebigbo A**, Mendel R, Probst A, Manzeneder J, Prinz F, de Souza LA Jr, Papa J, Palm C, Messmann H. Real-time use of artificial intelligence in the evaluation of cancer in Barrett's oesophagus. *Gut* 2020; **69**: 615-616 [PMID: 31541004 DOI: 10.1136/gutjnl-2019-319460]

15 **Riaz F**, Ribeiro MD, Pimentel-Nunes P, Coimbra MT. Integral scale histogram local binary patterns for classification of narrow-band gastroenterology images. *Annu Int Conf IEEE Eng Med Biol Soc* 2013; **2013**: 3714-3717 [PMID: 24110537 DOI: 10.1109/EMBC.2013.6610350]

16 **Swager AF**, van der Sommen F, Klomp SR, Zinger S, Meijer SL, Schoon EJ, Bergman JJGHM, de With PH, Curvers WL. Computer-aided detection of early Barrett's neoplasia using volumetric laser endomicroscopy. *Gastrointest Endosc* 2017; **86**: 839-846 [PMID: 28322771 DOI: 10.1016/j.gie.2017.03.011]

17 **Trindade AJ**, McKinley MJ, Fan C, Leggett CL, Kahn A, Pleskow DK. Endoscopic Surveillance of Barrett's Esophagus Using Volumetric Laser Endomicroscopy With Artificial Intelligence Image Enhancement. *Gastroenterology* 2019; **157**: 303-305 [PMID: 31078625 DOI: 10.1053/j.gastro.2019.04.048]

18 **Morita FH**, Bernardo WM, Ide E, Rocha RS, Aquino JC, Minata MK, Yamazaki K, Marques SB, Sakai P, de Moura EG. Narrow band imaging *vs* lugol chromoendoscopy to diagnose squamous cell carcinoma of the esophagus: a systematic review and meta-analysis. *BMC Cancer* 2017; **17**: 54 [PMID: 28086818 DOI: 10.1186/s12885-016-3011-9]

19 **Pannala R**, Krishnan K, Melson J, Parsi MA, Schulman AR, Sullivan S, Trikudanathan G, Trindade AJ, Watson RR, Maple JT, Lichtenstein DR. Artificial intelligence in gastrointestinal endoscopy. *VideoGIE* 2020; **5**: 598-613 [PMID: 33319126 DOI: 10.1016/j.vgie.2020.08.013]

20 **Cai SL**, Li B, Tan WM, Niu XJ, Yu HH, Yao LQ, Zhou PH, Yan B, Zhong YS. Using a deep learning system in endoscopy for screening of early esophageal squamous cell carcinoma (with video). *Gastrointest Endosc* 2019; **90**: 745-753.e2 [PMID: 31302091 DOI: 10.1016/j.gie.2019.06.044]

21 **Fukuda H**, Ishihara R, Kato Y, Matsunaga T, Nishida T, Yamada T, Ogiyama H, Horie M, Kinoshita K, Tada T. Comparison of performances of artificial intelligence *vs* expert endoscopists for real-time assisted diagnosis of esophageal squamous cell carcinoma (with video). *Gastrointest Endosc* 2020; **92**: 848-855 [PMID: 32505685 DOI: 10.1016/j.gie.2020.05.043]

22 **Guo L**, Xiao X, Wu C, Zeng X, Zhang Y, Du J, Bai S, Xie J, Zhang Z, Li Y, Wang X, Cheung O, Sharma M, Liu J, Hu B. Real-time automated diagnosis of precancerous lesions and early esophageal squamous cell carcinoma using a deep learning model (with videos). *Gastrointest Endosc* 2020; **91**: 41-51 [PMID: 31445040 DOI: 10.1016/j.gie.2019.08.018]

23 **Horie Y**, Yoshio T, Aoyama K, Yoshimizu S, Horiuchi Y, Ishiyama A, Hirasawa T, Tsuchida T, Ozawa T, Ishihara S, Kumagai Y, Fujishiro M, Maetani I, Fujisaki J, Tada T. Diagnostic outcomes of esophageal cancer by artificial intelligence using convolutional neural networks. *Gastrointest Endosc* 2019; **89**: 25-32 [PMID: 30120958 DOI: 10.1016/j.gie.2018.07.037]

24 **Kumagai Y**, Takubo K, Kawada K, Aoyama K, Endo Y, Ozawa T, Hirasawa T, Yoshio T, Ishihara S, Fujishiro M, Tamaru JI, Mochiki E, Ishida H, Tada T. Diagnosis using deep-learning artificial

intelligence based on the endocytoscopic observation of the esophagus. *Esophagus* 2019; **16**: 180-187 [PMID: 30547352 DOI: 10.1007/s10388-018-0651-7]

25 **Li B**, Cai SL, Tan WM, Li JC, Yalikong A, Feng XS, Yu HH, Lu PX, Feng Z, Yao LQ, Zhou PH, Yan B, Zhong YS. Comparative study on artificial intelligence systems for detecting early esophageal squamous cell carcinoma between narrow-band and white-light imaging. *World J Gastroenterol* 2021; **27**: 281-293 [PMID: 33519142 DOI: 10.3748/wjg.v27.i3.281]

26 **Ohmori M**, Ishihara R, Aoyama K, Nakagawa K, Iwagami H, Matsuura N, Shichijo S, Yamamoto K, Nagaike K, Nakahara M, Inoue T, Aoi K, Okada H, Tada T. Endoscopic detection and differentiation of esophageal lesions using a deep neural network. *Gastrointest Endosc* 2020; **91**: 301-309.e1 [PMID: 31585124 DOI: 10.1016/j.gie.2019.09.034]

27 **Tan MC**, Bhushan S, Quang T, Schwarz R, Patel KH, Yu X, Li Z, Wang G, Zhang F, Wang X, Xu H, Richards-Kortum RR, Anandasabapathy S. Automated software-assisted diagnosis of esophageal squamous cell neoplasia using high-resolution microendoscopy. *Gastrointest Endosc* 2021; **93**: 831-838.e2 [PMID: 32682812 DOI: 10.1016/j.gie.2020.07.007]

28 **Zhao YY**, Xue DX, Wang YL, Zhang R, Sun B, Cai YP, Feng H, Cai Y, Xu JM. Computer-assisted diagnosis of early esophageal squamous cell carcinoma using narrow-band imaging magnifying endoscopy. *Endoscopy* 2019; **51**: 333-341 [PMID: 30469155 DOI: 10.1055/a-0756-8754]

29 **Liu G**, Hua J, Wu Z, Meng T, Sun M, Huang P, He X, Sun W, Li X, Chen Y. Automatic classification of esophageal lesions in endoscopic images using a convolutional neural network. *Ann Transl Med* 2020; **8**: 486 [PMID: 32395530 DOI: 10.21037/atm.2020.03.24]

30 **Liu DY**, Gan T, Rao NN, Xing YW, Zheng J, Li S, Luo CS, Zhou ZJ, Wan YL. Identification of lesion images from gastrointestinal endoscope based on feature extraction of combinational methods with and without learning process. *Med Image Anal* 2016; **32**: 281-294 [PMID: 27236223 DOI: 10.1016/j.media.2016.04.007]

31 **Nakagawa K**, Ishihara R, Aoyama K, Ohmori M, Nakahira H, Matsuura N, Shichijo S, Nishida T, Yamada T, Yamaguchi S, Ogiyama H, Egawa S, Kishida O, Tada T. Classification for invasion depth of esophageal squamous cell carcinoma using a deep neural network compared with experienced endoscopists. *Gastrointest Endosc* 2019; **90**: 407-414 [PMID: 31077698 DOI: 10.1016/j.gie.2019.04.245]

32 **Shimamoto Y**, Ishihara R, Kato Y, Shoji A, Inoue T, Matsueda K, Miyake M, Waki K, Kono M, Fukuda H, Matsuura N, Nagaike K, Aoi K, Yamamoto K, Nakahara M, Nishihara A, Tada T. Real-time assessment of video images for esophageal squamous cell carcinoma invasion depth using artificial intelligence. *J Gastroenterol* 2020; **55**: 1037-1045 [PMID: 32778959 DOI: 10.1007/s00535-020-01716-5]

33 **Pimentel-Nunes P**, Libânio D, Lage J, Abrantes D, Coimbra M, Esposito G, Hormozdi D, Pepper M, Drasovean S, White JR, Dobru D, Buxbaum J, Ragunath K, Annibale B, Dinis-Ribeiro M. A multicenter prospective study of the real-time use of narrow-band imaging in the diagnosis of premalignant gastric conditions and lesions. *Endoscopy* 2016; **48**: 723-730 [PMID: 27280384 DOI: 10.1055/s-0042-108435]

34 **White JR**, Sami SS, Reddiar D, Mannath J, Ortiz-Fernández-Sordo J, Beg S, Scott R, Thiagarajan P, Ahmad S, Parra-Blanco A, Kasi M, Telakis E, Sultan AA, Davis J, Figgins A, Kaye P, Robinson K, Atherton JC, Ragunath K. Narrow band imaging and serology in the assessment of premalignant gastric pathology. *Scand J Gastroenterol* 2018; **53**: 1611-1618 [PMID: 30600732 DOI: 10.1080/00365521.2018.1542455]

35 **Kimura-Tsuchiya R**, Dohi O, Fujita Y, Yagi N, Majima A, Horii Y, Kitaichi T, Onozawa Y, Suzuki K, Tomie A, Okayama T, Yoshida N, Kamada K, Katada K, Uchiyama K, Ishikawa T, Takagi T, Handa O, Konishi H, Kishimoto M, Naito Y, Yanagisawa A, Itoh Y. Magnifying Endoscopy with Blue Laser Imaging Improves the Microstructure Visualization in Early Gastric Cancer: Comparison of Magnifying Endoscopy with Narrow-Band Imaging. *Gastroenterol Res Pract* 2017; **2017**: 8303046 [PMID: 28947900 DOI: 10.1155/2017/8303046]

36 **Mouri R**, Yoshida S, Tanaka S, Oka S, Yoshihara M, Chayama K. Evaluation and validation of computed virtual chromoendoscopy in early gastric cancer. *Gastrointest Endosc* 2009; **69**: 1052-1058 [PMID: 19152892 DOI: 10.1016/j.gie.2008.08.032]

37 **Guimarães P**, Keller A, Fehlmann T, Lammert F, Casper M. Deep-learning based detection of gastric precancerous conditions. *Gut* 2020; **69**: 4-6 [PMID: 31375599 DOI: 10.1136/gutjnl-2019-319347]

38 **Hirasawa T**, Aoyama K, Tanimoto T, Ishihara S, Shichijo S, Ozawa T, Ohnishi T, Fujishiro M, Matsuo K, Fujisaki J, Tada T. Application of artificial intelligence using a convolutional neural network for detecting gastric cancer in endoscopic images. *Gastric Cancer* 2018; **21**: 653-660 [PMID: 29335825 DOI: 10.1007/s10120-018-0793-2]

39 **Ishioka M**, Hirasawa T, Tada T. Detecting gastric cancer from video images using convolutional neural networks. *Dig Endosc* 2019; **31**: e34-e35 [PMID: 30449050 DOI: 10.1111/den.13306]

40 **Korhani Kangi A**, Bahrampour A. Predicting the Survival of Gastric Cancer Patients Using Artificial and Bayesian Neural Networks. *Asian Pac J Cancer Prev* 2018; **19**: 487-490 [PMID: 29480983 DOI: 10.22034/APJCP.2018.19.2.487]

41 **Li L**, Chen Y, Shen Z, Zhang X, Sang J, Ding Y, Yang X, Li J, Chen M, Jin C, Chen C, Yu C. Convolutional neural network for the diagnosis of early gastric cancer based on magnifying narrow band imaging. *Gastric Cancer* 2020; **23**: 126-132 [PMID: 31332619 DOI: 10.1007/s10120-019-00992-2]

42 **Miyaki R**, Yoshida S, Tanaka S, Kominami Y, Sanomura Y, Matsuo T, Oka S, Raytchev B, Tamaki T, Koide T, Kaneda K, Yoshihara M, Chayama K. A computer system to be used with laser-based endoscopy for quantitative diagnosis of early gastric cancer. *J Clin Gastroenterol* 2015; **49**: 108-115 [PMID: 24583752 DOI: 10.1097/MCG.0000000000000104]

43 **Togo R**, Yamamichi N, Mabe K, Takahashi Y, Takeuchi C, Kato M, Sakamoto N, Ishihara K, Ogawa T, Haseyama M. Detection of gastritis by a deep convolutional neural network from double-contrast upper gastrointestinal barium X-ray radiography. *J Gastroenterol* 2019; **54**: 321-329 [PMID: 30284046 DOI: 10.1007/s00535-018-1514-7]

44 **Wang S**, Zhu Y, Yu L, Chen H, Lin H, Wan X, Fan X, Heng PA. RMDL: Recalibrated multi-instance deep learning for whole slide gastric image classification. *Med Image Anal* 2019; **58**: 101549 [PMID: 31499320 DOI: 10.1016/j.media.2019.101549]

45 **Luo H**, Xu G, Li C, He L, Luo L, Wang Z, Jing B, Deng Y, Jin Y, Li Y, Li B, Tan W, He C, Seeruttun SR, Wu Q, Huang J, Huang DW, Chen B, Lin SB, Chen QM, Yuan CM, Chen HX, Pu HY, Zhou F, He Y, Xu RH. Real-time artificial intelligence for detection of upper gastrointestinal cancer by endoscopy: a multicentre, case-control, diagnostic study. *Lancet Oncol* 2019; **20**: 1645-1654 [PMID: 31591062 DOI: 10.1016/S1470-2045(19)30637-0]

46 **Namikawa K**, Hirasawa T, Nakano K, Ikenoyama Y, Ishioka M, Shiroma S, Tokai Y, Yoshimizu S, Horiuchi Y, Ishiyama A, Yoshio T, Tsuchida T, Fujisaki J, Tada T. Artificial intelligence-based diagnostic system classifying gastric cancers and ulcers: comparison between the original and newly developed systems. *Endoscopy* 2020; **52**: 1077-1083 [PMID: 32503056 DOI: 10.1055/a-1194-8771]

47 **Ueyama H**, Kato Y, Akazawa Y, Yatagai N, Komori H, Takeda T, Matsumoto K, Ueda K, Hojo M, Yao T, Nagahara A, Tada T. Application of artificial intelligence using a convolutional neural network for diagnosis of early gastric cancer based on magnifying endoscopy with narrow-band imaging. *J Gastroenterol Hepatol* 2021; **36**: 482-489 [PMID: 32681536 DOI: 10.1111/jgh.15190]

48 **Zhou C**, Hu J, Wang Y, Ji MH, Tong J, Yang JJ, Xia H. A machine learning-based predictor for the identification of the recurrence of patients with gastric cancer after operation. *Sci Rep* 2021; **11**: 1571 [PMID: 33452440 DOI: 10.1038/s41598-021-81188-6]

49 **Zhang Y**, Li F, Yuan F, Zhang K, Huo L, Dong Z, Lang Y, Zhang Y, Wang M, Gao Z, Qin Z, Shen L. Diagnosing chronic atrophic gastritis by gastroscopy using artificial intelligence. *Dig Liver Dis* 2020; **52**: 566-572 [PMID: 32061504 DOI: 10.1016/j.dld.2019.12.146]

50 **Kanesaka T**, Lee TC, Uedo N, Lin KP, Chen HZ, Lee JY, Wang HP, Chang HT. Computer-aided diagnosis for identifying and delineating early gastric cancers in magnifying narrow-band imaging. *Gastrointest Endosc* 2018; **87**: 1339-1344 [PMID: 29225083 DOI: 10.1016/j.gie.2017.11.029]

51 **Sakai Y**, Takemoto S, Hori K, Nishimura M, Ikematsu H, Yano T, Yokota H. Automatic detection of early gastric cancer in endoscopic images using a transferring convolutional neural network. *Annu Int Conf IEEE Eng Med Biol Soc* 2018; **2018**: 4138-4141 [PMID: 30441266 DOI: 10.1109/EMBC.2018.8513274]

52 **Wu L**, Zhou W, Wan X, Zhang J, Shen L, Hu S, Ding Q, Mu G, Yin A, Huang X, Liu J, Jiang X, Wang Z, Deng Y, Liu M, Lin R, Ling T, Li P, Wu Q, Jin P, Chen J, Yu H. A deep neural network improves endoscopic detection of early gastric cancer without blind spots. *Endoscopy* 2019; **51**: 522-531 [PMID: 30861533 DOI: 10.1055/a-0855-3532]

53 **Gao Y**, Zhang ZD, Li S, Guo YT, Wu QY, Liu SH, Yang SJ, Ding L, Zhao BC, Lu Y. Deep neural network-assisted computed tomography diagnosis of metastatic lymph nodes from gastric cancer. *Chin Med J (Engl)* 2019; **132**: 2804-2811 [PMID: 31856051 DOI: 10.1097/CM9.0000000000000532]

54 **Jagric T**, Potrc S, Jagric T. Prediction of liver metastases after gastric cancer resection with the use of learning vector quantization neural networks. *Dig Dis Sci* 2010; **55**: 3252-3261 [PMID: 20186483 DOI: 10.1007/s10620-010-1155-z]

55 **Chen T**, Zhang C, Liu Y, Zhao Y, Lin D, Hu Y, Yu J, Li G. A gastric cancer LncRNAs model for MSI and survival prediction based on support vector machine. *BMC Genomics* 2019; **20**: 846 [PMID: 31722674 DOI: 10.1186/s12864-019-6135-x]

56 **Nakahira H**, Ishihara R, Aoyama K, Kono M, Fukuda H, Shimamoto Y, Nakagawa K, Ohmori M, Iwatsubo T, Iwagami H, Matsuno K, Inoue S, Matsuura N, Shichijo S, Maekawa A, Kanesaka T, Yamamoto S, Takeuchi Y, Higashino K, Uedo N, Matsunaga T, Tada T. Stratification of gastric cancer risk using a deep neural network. *JGH Open* 2020; **4**: 466-471 [PMID: 32514455 DOI: 10.1002/jgh3.12281]

57 **Jiang Y**, Xie J, Han Z, Liu W, Xi S, Huang L, Huang W, Lin T, Zhao L, Hu Y, Yu J, Zhang Q, Li T, Cai S, Li G. Immunomarker Support Vector Machine Classifier for Prediction of Gastric Cancer Survival and Adjuvant Chemotherapeutic Benefit. *Clin Cancer Res* 2018; **24**: 5574-5584 [PMID: 30042208 DOI: 10.1158/1078-0432.CCR-18-0848]

58 **Que SJ**, Chen QY, Qing-Zhong, Liu ZY, Wang JB, Lin JX, Lu J, Cao LL, Lin M, Tu RH, Huang ZN, Lin JL, Zheng HL, Li P, Zheng CH, Huang CM, Xie JW. Application of preoperative artificial neural network based on blood biomarkers and clinicopathological parameters for predicting long-term survival of patients with gastric cancer. *World J Gastroenterol* 2019; **25**: 6451-6464 [PMID: 31798281 DOI: 10.3748/wjg.v25.i43.6451]

59 **Zhu Y**, Wang QC, Xu MD, Zhang Z, Cheng J, Zhong YS, Zhang YQ, Chen WF, Yao LQ, Zhou PH, Li QL. Application of convolutional neural network in the diagnosis of the invasion depth of gastric cancer based on conventional endoscopy. *Gastrointest Endosc* 2019; **89**: 806-815.e1 [PMID: 30452913 DOI: 10.1016/j.gie.2018.11.011]

60 **Nakashima H**, Kawahira H, Kawachi H, Sakaki N. Artificial intelligence diagnosis of *Helicobacter pylori* infection using blue laser imaging-bright and linked color imaging: a single-center prospective study. *Ann Gastroenterol* 2018; **31**: 462-468 [PMID: 29991891 DOI: 10.20524/aog.2018.0269]

61 **Shichijo S**, Endo Y, Aoyama K, Takeuchi Y, Ozawa T, Takiyama H, Matsuo K, Fujishiro M, Ishihara S, Ishihara R, Tada T. Application of convolutional neural networks for evaluating Helicobacter pylori infection status on the basis of endoscopic images. *Scand J Gastroenterol* 2019; **54**: 158-163 [PMID: 30879352 DOI: 10.1080/00365521.2019.1577486]

62 **Martin DR**, Hanson JA, Gullapalli RR, Schultz FA, Sethi A, Clark DP. A Deep Learning Convolutional Neural Network Can Recognize Common Patterns of Injury in Gastric Pathology. *Arch Pathol Lab Med* 2020; **144**: 370-378 [PMID: 31246112 DOI: 10.5858/arpa.2019-0004-OA]

63 **Nakashima H**, Kawahira H, Kawachi H, Sakaki N. Endoscopic three-categorical diagnosis of Helicobacter pylori infection using linked color imaging and deep learning: a single-center prospective study (with video). *Gastric Cancer* 2020; **23**: 1033-1040 [PMID: 32382973 DOI: 10.1007/s10120-020-01077-1]

64 **Shichijo S**, Nomura S, Aoyama K, Nishikawa Y, Miura M, Shinagawa T, Takiyama H, Tanimoto T, Ishihara S, Matsuo K, Tada T. Application of Convolutional Neural Networks in the Diagnosis of Helicobacter pylori Infection Based on Endoscopic Images. *EBioMedicine* 2017; **25**: 106-111 [PMID: 29056541 DOI: 10.1016/j.ebiom.2017.10.014]

65 **Zheng W**, Zhang X, Kim JJ, Zhu X, Ye G, Ye B, Wang J, Luo S, Li J, Yu T, Liu J, Hu W, Si J. High Accuracy of Convolutional Neural Network for Evaluation of Helicobacter pylori Infection Based on Endoscopic Images: Preliminary Experience. *Clin Transl Gastroenterol* 2019; **10**: e00109 [PMID: 31833862 DOI: 10.14309/ctg.0000000000000109]

66 **Yang YJ**, Bang CS. Application of artificial intelligence in gastroenterology. *World J Gastroenterol* 2019; **25**: 1666-1683 [PMID: 31011253 DOI: 10.3748/wjg.v25.i14.1666]

67 **Wong GL**, Ma AJ, Deng H, Ching JY, Wong VW, Tse YK, Yip TC, Lau LH, Liu HH, Leung CM, Tsang SW, Chan CW, Lau JY, Yuen PC, Chan FK. Machine learning model to predict recurrent ulcer bleeding in patients with history of idiopathic gastroduodenal ulcer bleeding. *Aliment Pharmacol Ther* 2019; **49**: 912-918 [PMID: 30761584 DOI: 10.1111/apt.15145]

68 **Seo DW**, Yi H, Park B, Kim YJ, Jung DH, Woo I, Sohn CH, Ko BS, Kim N, Kim WY. Prediction of Adverse Events in Stable Non-Variceal Gastrointestinal Bleeding Using Machine Learning. *J Clin Med* 2020; **9** [PMID: 32796647 DOI: 10.3390/jcm9082603]

69 **Shung DL**, Au B, Taylor RA, Tay JK, Laursen SB, Stanley AJ, Dalton HR, Ngu J, Schultz M, Laine L. Validation of a Machine Learning Model That Outperforms Clinical Risk Scoring Systems for Upper Gastrointestinal Bleeding. *Gastroenterology* 2020; **158**: 160-167 [PMID: 31562847 DOI: 10.1053/j.gastro.2019.09.009]

70 **Das A**, Ben-Menachem T, Cooper GS, Chak A, Sivak MV Jr, Gonet JA, Wong RC. Prediction of outcome in acute lower-gastrointestinal haemorrhage based on an artificial neural network: internal and external validation of a predictive model. *Lancet* 2003; **362**: 1261-1266 [PMID: 14575969 DOI: 10.1016/S0140-6736(03)14568-0]

71 **Das A**, Ben-Menachem T, Farooq FT, Cooper GS, Chak A, Sivak MV Jr, Wong RC. Artificial neural network as a predictive instrument in patients with acute nonvariceal upper gastrointestinal hemorrhage. *Gastroenterology* 2008; **134**: 65-74 [PMID: 18061180 DOI: 10.1053/j.gastro.2007.10.037]

72 **Loftus TJ**, Brakenridge SC, Croft CA, Smith RS, Efron PA, Moore FA, Mohr AM, Jordan JR. Neural network prediction of severe lower intestinal bleeding and the need for surgical intervention. *J Surg Res* 2017; **212**: 42-47 [PMID: 28550920 DOI: 10.1016/j.jss.2016.12.032]

73 **Ayaru L**, Ypsilantis PP, Nanapragasam A, Choi RC, Thillanathan A, Min-Ho L, Montana G. Prediction of Outcome in Acute Lower Gastrointestinal Bleeding Using Gradient Boosting. *PLoS One* 2015; **10**: e0132485 [PMID: 26172121 DOI: 10.1371/journal.pone.0132485]

74 **Bressler B**, Paszat LF, Chen Z, Rothwell DM, Vinden C, Rabeneck L. Rates of new or missed colorectal cancers after colonoscopy and their risk factors: a population-based analysis. *Gastroenterology* 2007; **132**: 96-102 [PMID: 17241863 DOI: 10.1053/j.gastro.2006.10.027]

75 **Jover R**, Zapater P, Polanía E, Bujanda L, Lanas A, Hermo JA, Cubiella J, Ono A, González-Méndez Y, Peris A, Pellisé M, Seoane A, Herreros-de-Tejada A, Ponce M, Marín-Gabriel JC, Chaparro M, Cacho G, Fernández-Díez S, Arenas J, Sopeña F, de-Castro L, Vega-Villaamil P, Rodríguez-Soler M, Carballo F, Salas D, Morillas JD, Andreu M, Quintero E, Castells A; COLONPREV study investigators. Modifiable endoscopic factors that influence the adenoma detection rate in colorectal cancer screening colonoscopies. *Gastrointest Endosc* 2013; **77**: 381-389.e1 [PMID: 23218945 DOI: 10.1016/j.gie.2012.09.027]

76 **Hassan C**, Spadaccini M, Iannone A, Maselli R, Jovani M, Chandrasekar VT, Antonelli G, Yu H, Areia M, Dinis-Ribeiro M, Bhandari P, Sharma P, Rex DK, Rösch T, Wallace M, Repici A. Performance of artificial intelligence in colonoscopy for adenoma and polyp detection: a systematic review and meta-analysis. *Gastrointest Endosc* 2021; **93**: 77-85.e6 [PMID: 32598963 DOI: 10.1016/j.gie.2020.06.059]

77 **Samadder NJ**, Curtin K, Tuohy TM, Pappas L, Boucher K, Provenzale D, Rowe KG, Mineau GP, Smith K, Pimentel R, Kirchhoff AC, Burt RW. Characteristics of missed or interval colorectal cancer and patient survival: a population-based study. *Gastroenterology* 2014; **146**: 950-960 [PMID: 24417818 DOI: 10.1053/j.gastro.2014.01.013]

78 **Lee CK**, Park DI, Lee SH, Hwangbo Y, Eun CS, Han DS, Cha JM, Lee BI, Shin JE. Participation by

experienced endoscopy nurses increases the detection rate of colon polyps during a screening colonoscopy: a multicenter, prospective, randomized study. *Gastrointest Endosc* 2011; **74**: 1094-1102 [PMID: 21889137 DOI: 10.1016/j.gie.2011.06.033]

79 **Aslanian HR**, Shieh FK, Chan FW, Ciarleglio MM, Deng Y, Rogart JN, Jamidar PA, Siddiqui UD. Nurse observation during colonoscopy increases polyp detection: a randomized prospective study. *Am J Gastroenterol* 2013; **108**: 166-172 [PMID: 23381064 DOI: 10.1038/ajg.2012.237]

80 **Gong D**, Wu L, Zhang J, Mu G, Shen L, Liu J, Wang Z, Zhou W, An P, Huang X, Jiang X, Li Y, Wan X, Hu S, Chen Y, Hu X, Xu Y, Zhu X, Li S, Yao L, He X, Chen D, Huang L, Wei X, Wang X, Yu H. Detection of colorectal adenomas with a real-time computer-aided system (ENDOANGEL): a randomised controlled study. *Lancet Gastroenterol Hepatol* 2020; **5**: 352-361 [PMID: 31981518 DOI: 10.1016/S2468-1253(19)30413-3]

81 **Klare P**, Sander C, Prinzen M, Haller B, Nowack S, Abdelhafez M, Poszler A, Brown H, Wilhelm D, Schmid RM, von Delius S, Wittenberg T. Automated polyp detection in the colorectum: a prospective study (with videos). *Gastrointest Endosc* 2019; **89**: 576-582.e1 [PMID: 30342029 DOI: 10.1016/j.gie.2018.09.042]

82 **Repici A**, Badalamenti M, Maselli R, Correale L, Radaelli F, Rondonotti E, Ferrara E, Spadaccini M, Alkandari A, Fugazza A, Anderloni A, Galtieri PA, Pellegatta G, Carrara S, Di Leo M, Craviotto V, Lamonaca L, Lorenzetti R, Andrealli A, Antonelli G, Wallace M, Sharma P, Rosch T, Hassan C. Efficacy of Real-Time Computer-Aided Detection of Colorectal Neoplasia in a Randomized Trial. *Gastroenterology* 2020; **159**: 512-520.e7 [PMID: 32371116 DOI: 10.1053/j.gastro.2020.04.062]

83 **Su JR**, Li Z, Shao XJ, Ji CR, Ji R, Zhou RC, Li GC, Liu GQ, He YS, Zuo XL, Li YQ. Impact of a real-time automatic quality control system on colorectal polyp and adenoma detection: a prospective randomized controlled study (with videos). *Gastrointest Endosc* 2020; **91**: 415-424.e4 [PMID: 31454493 DOI: 10.1016/j.gie.2019.08.026]

84 **Urban G**, Tripathi P, Alkayali T, Mittal M, Jalali F, Karnes W, Baldi P. Deep Learning Localizes and Identifies Polyps in Real Time With 96% Accuracy in Screening Colonoscopy. *Gastroenterology* 2018; **155**: 1069-1078.e8 [PMID: 29928897 DOI: 10.1053/j.gastro.2018.06.037]

85 **Wang P**, Berzin TM, Glissen Brown JR, Bharadwaj S, Becq A, Xiao X, Liu P, Li L, Song Y, Zhang D, Li Y, Xu G, Tu M, Liu X. Real-time automatic detection system increases colonoscopic polyp and adenoma detection rates: a prospective randomised controlled study. *Gut* 2019; **68**: 1813-1819 [PMID: 30814121 DOI: 10.1136/gutjnl-2018-317500]

86 **Wang P**, Liu X, Berzin TM, Glissen Brown JR, Liu P, Zhou C, Lei L, Li L, Guo Z, Lei S, Xiong F, Wang H, Song Y, Pan Y, Zhou G. Effect of a deep-learning computer-aided detection system on adenoma detection during colonoscopy (CADe-DB trial): a double-blind randomised study. *Lancet Gastroenterol Hepatol* 2020; **5**: 343-351 [PMID: 31981517 DOI: 10.1016/S2468-1253(19)30411-X]

87 **Liu WN**, Zhang YY, Bian XQ, Wang LJ, Yang Q, Zhang XD, Huang J. Study on detection rate of polyps and adenomas in artificial-intelligence-aided colonoscopy. *Saudi J Gastroenterol* 2020; **26**: 13-19 [PMID: 31898644 DOI: 10.4103/sjg.SJG_377_19]

88 **Bernal J**, Tajkbaksh N, Sanchez FJ, Matuszewski BJ, Hao Chen, Lequan Yu, Angermann Q, Romain O, Rustad B, Balasingham I, Pogorelov K, Sungbin Choi, Debard Q, Maier-Hein L, Speidel S, Stoyanov D, Brandao P, Cordova H, Sanchez-Montes C, Gurudu SR, Fernandez-Esparrach G, Dray X, Jianming Liang, Histace A. Comparative Validation of Polyp Detection Methods in Video Colonoscopy: Results From the MICCAI 2015 Endoscopic Vision Challenge. *IEEE Trans Med Imaging* 2017; **36**: 1231-1249 [PMID: 28182555 DOI: 10.1109/TMI.2017.2664042]

89 **Blanes-Vidal V**, Baatrup G, Nadimi ES. Addressing priority challenges in the detection and assessment of colorectal polyps from capsule endoscopy and colonoscopy in colorectal cancer screening using machine learning. *Acta Oncol* 2019; **58**: S29-S36 [PMID: 30836800 DOI: 10.1080/0284186X.2019.1584404]

90 **Fernández-Esparrach G**, Bernal J, López-Cerón M, Córdova H, Sánchez-Montes C, Rodríguez de Miguel C, Sánchez FJ. Exploring the clinical potential of an automatic colonic polyp detection method based on the creation of energy maps. *Endoscopy* 2016; **48**: 837-842 [PMID: 27285900 DOI: 10.1055/s-0042-108434]

91 **Figueiredo PN**, Figueiredo IN, Pinto L, Kumar S, Tsai YR, Mamonov AV. Polyp detection with computer-aided diagnosis in white light colonoscopy: comparison of three different methods. *Endosc Int Open* 2019; **7**: E209-E215 [PMID: 30705955 DOI: 10.1055/a-0808-4456]

92 **Hassan C**, Wallace MB, Sharma P, Maselli R, Craviotto V, Spadaccini M, Repici A. New artificial intelligence system: first validation study *vs* experienced endoscopists for colorectal polyp detection. *Gut* 2020; **69**: 799-800 [PMID: 31615835 DOI: 10.1136/gutjnl-2019-319914]

93 **Kominami Y**, Yoshida S, Tanaka S, Sanomura Y, Hirakawa T, Raytchev B, Tamaki T, Koide T, Kaneda K, Chayama K. Computer-aided diagnosis of colorectal polyp histology by using a real-time image recognition system and narrow-band imaging magnifying colonoscopy. *Gastrointest Endosc* 2016; **83**: 643-649 [PMID: 26264431 DOI: 10.1016/j.gie.2015.08.004]

94 **Lequan Yu**, Hao Chen, Qi Dou, Jing Qin, Pheng Ann Heng. Integrating Online and Offline Three-Dimensional Deep Learning for Automated Polyp Detection in Colonoscopy Videos. *IEEE J Biomed Health Inform* 2017; **21**: 65-75 [PMID: 28114049 DOI: 10.1109/JBHI.2016.2637004]

95 **Misawa M**, Kudo SE, Mori Y, Cho T, Kataoka S, Yamauchi A, Ogawa Y, Maeda Y, Takeda K, Ichimasa K, Nakamura H, Yagawa Y, Toyoshima N, Ogata N, Kudo T, Hisayuki T, Hayashi T, Wakamura K, Baba T, Ishida F, Itoh H, Roth H, Oda M, Mori K. Artificial Intelligence-Assisted Polyp Detection for Colonoscopy: Initial Experience. *Gastroenterology* 2018; **154**: 2027-2029.e3

[PMID: 29653147 DOI: 10.1053/j.gastro.2018.04.003]

96 **Misawa M**, Kudo SE, Mori Y, Hotta K, Ohtsuka K, Matsuda T, Saito S, Kudo T, Baba T, Ishida F, Itoh H, Oda M, Mori K. Development of a computer-aided detection system for colonoscopy and a publicly accessible large colonoscopy video database (with video). *Gastrointest Endosc* 2021; **93**: 960-967.e3 [PMID: 32745531 DOI: 10.1016/j.gie.2020.07.060]

97 **Mori Y**, Kudo SE, Misawa M, Saito Y, Ikematsu H, Hotta K, Ohtsuka K, Urushibara F, Kataoka S, Ogawa Y, Maeda Y, Takeda K, Nakamura H, Ichimasa K, Kudo T, Hayashi T, Wakamura K, Ishida F, Inoue H, Itoh H, Oda M, Mori K. Real-Time Use of Artificial Intelligence in Identification of Diminutive Polyps During Colonoscopy: A Prospective Study. *Ann Intern Med* 2018; **169**: 357-366 [PMID: 30105375 DOI: 10.7326/M18-0249]

98 **Wang P**, Xiao X, Glissen Brown JR, Berzin TM, Tu M, Xiong F, Hu X, Liu P, Song Y, Zhang D, Yang X, Li L, He J, Yi X, Liu J, Liu X. Development and validation of a deep-learning algorithm for the detection of polyps during colonoscopy. *Nat Biomed Eng* 2018; **2**: 741-748 [PMID: 31015647 DOI: 10.1038/s41551-018-0301-3]

99 **Echle A**, Grabsch HI, Quirke P, van den Brandt PA, West NP, Hutchins GGA, Heij LR, Tan X, Richman SD, Krause J, Alwers E, Jenniskens J, Offermans K, Gray R, Brenner H, Chang-Claude J, Trautwein C, Pearson AT, Boor P, Luedde T, Gaisa NT, Hoffmeister M, Kather JN. Clinical-Grade Detection of Microsatellite Instability in Colorectal Tumors by Deep Learning. *Gastroenterology* 2020; **159**: 1406-1416.e11 [PMID: 32562722 DOI: 10.1053/j.gastro.2020.06.021]

100 **Ito N**, Kawahira H, Nakashima H, Uesato M, Miyauchi H, Matsubara H. Endoscopic Diagnostic Support System for cT1b Colorectal Cancer Using Deep Learning. *Oncology* 2019; **96**: 44-50 [PMID: 30130758 DOI: 10.1159/000491636]

101 **Kudo SE**, Misawa M, Mori Y, Hotta K, Ohtsuka K, Ikematsu H, Saito Y, Takeda K, Nakamura H, Ichimasa K, Ishigaki T, Toyoshima N, Kudo T, Hayashi T, Wakamura K, Baba T, Ishida F, Inoue H, Itoh H, Oda M, Mori K. Artificial Intelligence-assisted System Improves Endoscopic Identification of Colorectal Neoplasms. *Clin Gastroenterol Hepatol* 2020; **18**: 1874-1881.e2 [PMID: 31525512 DOI: 10.1016/j.cgh.2019.09.009]

102 . The Paris endoscopic classification of superficial neoplastic lesions: esophagus, stomach, and colon: November 30 to December 1, 2002. *Gastrointest Endosc* 2003; **58**: S3-43 [PMID: 14652541 DOI: 10.1016/s0016-5107(03)02159-x]

103 **Endoscopic Classification Review Group**. Update on the paris classification of superficial neoplastic lesions in the digestive tract. *Endoscopy* 2005; **37**: 570-578 [PMID: 15933932 DOI: 10.1055/s-2005-861352]

104 **van Doorn SC**, Hazewinkel Y, East JE, van Leerdam ME, Rastogi A, Pellisé M, Sanduleanu-Dascalescu S, Bastiaansen BA, Fockens P, Dekker E. Polyp morphology: an interobserver evaluation for the Paris classification among international experts. *Am J Gastroenterol* 2015; **110**: 180-187 [PMID: 25331346 DOI: 10.1038/ajg.2014.326]

105 **Wang TD**, Van Dam J. Optical biopsy: a new frontier in endoscopic detection and diagnosis. *Clin Gastroenterol Hepatol* 2004; **2**: 744-753 [PMID: 15354274 DOI: 10.1016/S1542-3565(04)00345-3]

106 **Hassan C**, Pickhardt PJ, Rex DK. A resect and discard strategy would improve cost-effectiveness of colorectal cancer screening. *Clin Gastroenterol Hepatol* 2010; **8**: 865-869, 869.e1 [PMID: 20621680 DOI: 10.1016/j.cgh.2010.05.018]

107 **Byrne MF**, Chapados N, Soudan F, Oertel C, Linares Pérez M, Kelly R, Iqbal N, Chandelier F, Rex DK. Real-time differentiation of adenomatous and hyperplastic diminutive colorectal polyps during analysis of unaltered videos of standard colonoscopy using a deep learning model. *Gut* 2019; **68**: 94-100 [PMID: 29066576 DOI: 10.1136/gutjnl-2017-314547]

108 **Chen PJ**, Lin MC, Lai MJ, Lin JC, Lu HH, Tseng VS. Accurate Classification of Diminutive Colorectal Polyps Using Computer-Aided Analysis. *Gastroenterology* 2018; **154**: 568-575 [PMID: 29042219 DOI: 10.1053/j.gastro.2017.10.010]

109 **Gross S**, Trautwein C, Behrens A, Winograd R, Palm S, Lutz HH, Schirin-Sokhan R, Hecker H, Aach T, Tischendorf JJ. Computer-based classification of small colorectal polyps by using narrow-band imaging with optical magnification. *Gastrointest Endosc* 2011; **74**: 1354-1359 [PMID: 22000791 DOI: 10.1016/j.gie.2011.08.001]

110 **Horiuchi H**, Tamai N, Kamba S, Inomata H, Ohya TR, Sumiyama K. Real-time computer-aided diagnosis of diminutive rectosigmoid polyps using an auto-fluorescence imaging system and novel color intensity analysis software. *Scand J Gastroenterol* 2019; **54**: 800-805 [PMID: 31195905 DOI: 10.1080/00365521.2019.1627407]

111 **Misawa M**, Kudo SE, Mori Y, Nakamura H, Kataoka S, Maeda Y, Kudo T, Hayashi T, Wakamura K, Miyachi H, Katagiri A, Baba T, Ishida F, Inoue H, Nimura Y, Mori K. Characterization of Colorectal Lesions Using a Computer-Aided Diagnostic System for Narrow-Band Imaging Endocytoscopy. *Gastroenterology* 2016; **150**: 1531-1532.e3 [PMID: 27072671 DOI: 10.1053/j.gastro.2016.04.004]

112 **Mori Y**, Kudo SE, Chiu PW, Singh R, Misawa M, Wakamura K, Kudo T, Hayashi T, Katagiri A, Miyachi H, Ishida F, Maeda Y, Inoue H, Nimura Y, Oda M, Mori K. Impact of an automated system for endocytoscopic diagnosis of small colorectal lesions: an international web-based study. *Endoscopy* 2016; **48**: 1110-1118 [PMID: 27494455 DOI: 10.1055/s-0042-113609]

113 **Mori Y**, Kudo SE, Wakamura K, Misawa M, Ogawa Y, Kutsukawa M, Kudo T, Hayashi T, Miyachi H, Ishida F, Inoue H. Novel computer-aided diagnostic system for colorectal lesions by using endocytoscopy (with videos). *Gastrointest Endosc* 2015; **81**: 621-629 [PMID: 25440671 DOI:

10.1016/j.gie.2014.09.008]
114 **Sánchez-Montes C**, Sánchez FJ, Bernal J, Córdova H, López-Cerón M, Cuatrecasas M, Rodríguez de Miguel C, García-Rodríguez A, Garcés-Durán R, Pellisé M, Llach J, Fernández-Esparrach G. Computer-aided prediction of polyp histology on white light colonoscopy using surface pattern analysis. *Endoscopy* 2019; **51**: 261-265 [PMID: 30360010 DOI: 10.1055/a-0732-5250]
115 **Tischendorf JJ**, Gross S, Winograd R, Hecker H, Auer R, Behrens A, Trautwein C, Aach T, Stehle T. Computer-aided classification of colorectal polyps based on vascular patterns: a pilot study. *Endoscopy* 2010; **42**: 203-207 [PMID: 20101564 DOI: 10.1055/s-0029-1243861]
116 **Ikehara H**, Saito Y, Matsuda T, Uraoka T, Murakami Y. Diagnosis of depth of invasion for early colorectal cancer using magnifying colonoscopy. *J Gastroenterol Hepatol* 2010; **25**: 905-912 [PMID: 20546444 DOI: 10.1111/j.1440-1746.2010.06275.x]
117 **Kitajima K**, Fujimori T, Fujii S, Takeda J, Ohkura Y, Kawamata H, Kumamoto T, Ishiguro S, Kato Y, Shimoda T, Iwashita A, Ajioka Y, Watanabe H, Watanabe T, Muto T, Nagasako K. Correlations between lymph node metastasis and depth of submucosal invasion in submucosal invasive colorectal carcinoma: a Japanese collaborative study. *J Gastroenterol* 2004; **39**: 534-543 [PMID: 15235870 DOI: 10.1007/s00535-004-1339-4]
118 **Matsuda T**, Saito Y, Nakajima T, Sakamoto T, Ikematsu H, Sano Y, Fu KI, Fujii T. Macroscopic estimation of submucosal invasion in the colon. *Tech Gastrointest Endosc* 2011; **13**: 24-32 [DOI: 10.1016/j.tgie.2011.01.004]
119 **Mori Y**, Kudo SE, East JE, Rastogi A, Bretthauer M, Misawa M, Sekiguchi M, Matsuda T, Saito Y, Ikematsu H, Hotta K, Ohtsuka K, Kudo T, Mori K. Cost savings in colonoscopy with artificial intelligence-aided polyp diagnosis: an add-on analysis of a clinical trial (with video). *Gastrointest Endosc* 2020; **92**: 905-911.e1 [PMID: 32240683 DOI: 10.1016/j.gie.2020.03.3759]
120 **Thakkar S**, Carleton NM, Rao B, Syed A. Use of Artificial Intelligence-Based Analytics From Live Colonoscopies to Optimize the Quality of the Colonoscopy Examination in Real Time: Proof of Concept. *Gastroenterology* 2020; **158**: 1219-1221.e2 [PMID: 31945357 DOI: 10.1053/j.gastro.2019.12.035]
121 **Reichling C**, Taieb J, Derangere V, Klopfenstein Q, Le Malicot K, Gornet JM, Becheur H, Fein F, Cojocarasu O, Kaminsky MC, Lagasse JP, Luet D, Nguyen S, Etienne PL, Gasmi M, Vanoli A, Perrier H, Puig PL, Emile JF, Lepage C, Ghiringhelli F. Artificial intelligence-guided tissue analysis combined with immune infiltrate assessment predicts stage III colon cancer outcomes in PETACC08 study. *Gut* 2020; **69**: 681-690 [PMID: 31780575 DOI: 10.1136/gutjnl-2019-319292]
122 **Kather JN**, Krisam J, Charoentong P, Luedde T, Herpel E, Weis CA, Gaiser T, Marx A, Valous NA, Ferber D, Jansen L, Reyes-Aldasoro CC, Zörnig I, Jäger D, Brenner H, Chang-Claude J, Hoffmeister M, Halama N. Predicting survival from colorectal cancer histology slides using deep learning: A retrospective multicenter study. *PLoS Med* 2019; **16**: e1002730 [PMID: 30677016 DOI: 10.1371/journal.pmed.1002730]
123 **Skrede OJ**, De Raedt S, Kleppe A, Hveem TS, Liestøl K, Maddison J, Askautrud HA, Pradhan M, Nesheim JA, Albregtsen F, Farstad IN, Domingo E, Church DN, Nesbakken A, Shepherd NA, Tomlinson I, Kerr R, Novelli M, Kerr DJ, Danielsen HE. Deep learning for prediction of colorectal cancer outcome: a discovery and validation study. *Lancet* 2020; **395**: 350-360 [PMID: 32007170 DOI: 10.1016/S0140-6736(19)32998-8]
124 **Yang YJ**. The Future of Capsule Endoscopy: The Role of Artificial Intelligence and Other Technical Advancements. *Clin Endosc* 2020; **53**: 387-394 [PMID: 32668529 DOI: 10.5946/ce.2020.133]
125 **Liu G**, Yan G, Kuang S, Wang Y. Detection of small bowel tumor based on multi-scale curvelet analysis and fractal technology in capsule endoscopy. *Comput Biol Med* 2016; **70**: 131-138 [PMID: 26829705 DOI: 10.1016/j.compbiomed.2016.01.021]
126 **Li B**, Meng MQ. Tumor recognition in wireless capsule endoscopy images using textural features and SVM-based feature selection. *IEEE Trans Inf Technol Biomed* 2012; **16**: 323-329 [PMID: 22287246 DOI: 10.1109/TITB.2012.2185807]
127 **Li B**, Meng MQ. Computer-based detection of bleeding and ulcer in wireless capsule endoscopy images by chromaticity moments. *Comput Biol Med* 2009; **39**: 141-147 [PMID: 19147126 DOI: 10.1016/j.compbiomed.2008.11.007]
128 **Aoki T**, Yamada A, Aoyama K, Saito H, Fujisawa G, Odawara N, Kondo R, Tsuboi A, Ishibashi R, Nakada A, Niikura R, Fujishiro M, Oka S, Ishihara S, Matsuda T, Nakahori M, Tanaka S, Koike K, Tada T. Clinical usefulness of a deep learning-based system as the first screening on small-bowel capsule endoscopy reading. *Dig Endosc* 2020; **32**: 585-591 [PMID: 31441972 DOI: 10.1111/den.13517]
129 **Soffer S**, Klang E, Shimon O, Nachmias N, Eliakim R, Ben-Horin S, Kopylov U, Barash Y. Deep learning for wireless capsule endoscopy: a systematic review and meta-analysis. *Gastrointest Endosc* 2020; **92**: 831-839.e8 [PMID: 32334015 DOI: 10.1016/j.gie.2020.04.039]
130 **Aoki T**, Yamada A, Kato Y, Saito H, Tsuboi A, Nakada A, Niikura R, Fujishiro M, Oka S, Ishihara S, Matsuda T, Nakahori M, Tanaka S, Koike K, Tada T. Automatic detection of blood content in capsule endoscopy images based on a deep convolutional neural network. *J Gastroenterol Hepatol* 2020; **35**: 1196-1200 [PMID: 31758717 DOI: 10.1111/jgh.14941]
131 **Ding Z**, Shi H, Zhang H, Meng L, Fan M, Han C, Zhang K, Ming F, Xie X, Liu H, Liu J, Lin R, Hou X. Gastroenterologist-Level Identification of Small-Bowel Diseases and Normal Variants by Capsule Endoscopy Using a Deep-Learning Model. *Gastroenterology* 2019; **157**: 1044-1054.e5 [PMID: 31251929 DOI: 10.1053/j.gastro.2019.06.025]

132 **Fu Y**, Zhang W, Mandal M, Meng MQ. Computer-aided bleeding detection in WCE video. *IEEE J Biomed Health Inform* 2014; **18**: 636-642 [PMID: 24608063 DOI: 10.1109/JBHI.2013.2257819]

133 **Hassan AR**, Haque MA. Computer-aided gastrointestinal hemorrhage detection in wireless capsule endoscopy videos. *Comput Methods Programs Biomed* 2015; **122**: 341-353 [PMID: 26390947 DOI: 10.1016/j.cmpb.2015.09.005]

134 **Iakovidis DK**, Koulaouzidis A. Automatic lesion detection in capsule endoscopy based on color saliency: closer to an essential adjunct for reviewing software. *Gastrointest Endosc* 2014; **80**: 877-883 [PMID: 25088924 DOI: 10.1016/j.gie.2014.06.026]

135 **Leenhardt R**, Vasseur P, Li C, Saurin JC, Rahmi G, Cholet F, Becq A, Marteau P, Histace A, Dray X; CAD-CAP Database Working Group. A neural network algorithm for detection of GI angiectasia during small-bowel capsule endoscopy. *Gastrointest Endosc* 2019; **89**: 189-194 [PMID: 30017868 DOI: 10.1016/j.gie.2018.06.036]

136 **Lv G**, Yan G, Wang Z. Bleeding detection in wireless capsule endoscopy images based on color invariants and spatial pyramids using support vector machines. *Annu Int Conf IEEE Eng Med Biol Soc* 2011; **2011**: 6643-6646 [PMID: 22255862 DOI: 10.1109/IEMBS.2011.6091638]

137 **Noya F**, Alvarez-Gonzalez MA, Benitez R. Automated angiodysplasia detection from wireless capsule endoscopy. *Annu Int Conf IEEE Eng Med Biol Soc* 2017; **2017**: 3158-3161 [PMID: 29060568 DOI: 10.1109/EMBC.2017.8037527]

138 **Pan G**, Yan G, Song X, Qiu X. BP neural network classification for bleeding detection in wireless capsule endoscopy. *J Med Eng Technol* 2009; **33**: 575-581 [PMID: 19639509 DOI: 10.1080/03091900903111974]

139 **Sainju S**, Bui FM, Wahid KA. Automated bleeding detection in capsule endoscopy videos using statistical features and region growing. *J Med Syst* 2014; **38**: 25 [PMID: 24696394 DOI: 10.1007/s10916-014-0025-1]

140 **Tsuboi A**, Oka S, Aoyama K, Saito H, Aoki T, Yamada A, Matsuda T, Fujishiro M, Ishihara S, Nakahori M, Koike K, Tanaka S, Tada T. Artificial intelligence using a convolutional neural network for automatic detection of small-bowel angioectasia in capsule endoscopy images. *Dig Endosc* 2020; **32**: 382-390 [PMID: 31392767 DOI: 10.1111/den.13507]

141 **Xing X**, Jia X, Meng MQ. Bleeding Detection in Wireless Capsule Endoscopy Image Video Using Superpixel-Color Histogram and a Subspace KNN Classifier. *Annu Int Conf IEEE Eng Med Biol Soc* 2018; **2018**: 1-4 [PMID: 30440286 DOI: 10.1109/EMBC.2018.8513012]

142 **Yuan Y**, Li B, Meng MQ. Bleeding Frame and Region Detection in the Wireless Capsule Endoscopy Video. *IEEE J Biomed Health Inform* 2016; **20**: 624-630 [PMID: 25675468 DOI: 10.1109/JBHI.2015.2399502]

143 **Aoki T**, Yamada A, Aoyama K, Saito H, Tsuboi A, Nakada A, Niikura R, Fujishiro M, Oka S, Ishihara S, Matsuda T, Tanaka S, Koike K, Tada T. Automatic detection of erosions and ulcerations in wireless capsule endoscopy images based on a deep convolutional neural network. *Gastrointest Endosc* 2019; **89**: 357-363.e2 [PMID: 30670179 DOI: 10.1016/j.gie.2018.10.027]

144 **Otani K**, Nakada A, Kurose Y, Niikura R, Yamada A, Aoki T, Nakanishi H, Doyama H, Hasatani K, Sumiyoshi T, Kitsuregawa M, Harada T, Koike K. Automatic detection of different types of small-bowel lesions on capsule endoscopy images using a newly developed deep convolutional neural network. *Endoscopy* 2020; **52**: 786-791 [PMID: 32557474 DOI: 10.1055/a-1167-8157]

145 **Fan S**, Xu L, Fan Y, Wei K, Li L. Computer-aided detection of small intestinal ulcer and erosion in wireless capsule endoscopy images. *Phys Med Biol* 2018; **63**: 165001 [PMID: 30033931 DOI: 10.1088/1361-6560/aad51c]

146 **Wang S**, Xing Y, Zhang L, Gao H, Zhang H. A systematic evaluation and optimization of automatic detection of ulcers in wireless capsule endoscopy on a large dataset using deep convolutional neural networks. *Phys Med Biol* 2019; **64**: 235014 [PMID: 31645019 DOI: 10.1088/1361-6560/ab5086]

147 **Klang E**, Barash Y, Margalit RY, Soffer S, Shimon O, Albshesh A, Ben-Horin S, Amitai MM, Eliakim R, Kopylov U. Deep learning algorithms for automated detection of Crohn's disease ulcers by video capsule endoscopy. *Gastrointest Endosc* 2020; **91**: 606-613.e2 [PMID: 31743689 DOI: 10.1016/j.gie.2019.11.012]

148 **Charisis VS**, Hadjileontiadis LJ. Potential of hybrid adaptive filtering in inflammatory lesion detection from capsule endoscopy images. *World J Gastroenterol* 2016; **22**: 8641-8657 [PMID: 27818583 DOI: 10.3748/wjg.v22.i39.8641]

149 **Saito H**, Aoki T, Aoyama K, Kato Y, Tsuboi A, Yamada A, Fujishiro M, Oka S, Ishihara S, Matsuda T, Nakahori M, Tanaka S, Koike K, Tada T. Automatic detection and classification of protruding lesions in wireless capsule endoscopy images based on a deep convolutional neural network. *Gastrointest Endosc* 2020; **92**: 144-151.e1 [PMID: 32084410 DOI: 10.1016/j.gie.2020.01.054]

150 **Yuan Y**, Meng MQ. Deep learning for polyp recognition in wireless capsule endoscopy images. *Med Phys* 2017; **44**: 1379-1389 [PMID: 28160514 DOI: 10.1002/mp.12147]

151 **Tenório JM**, Hummel AD, Cohrs FM, Sdepanian VL, Pisa IT, de Fátima Marin H. Artificial intelligence techniques applied to the development of a decision-support system for diagnosing celiac disease. *Int J Med Inform* 2011; **80**: 793-802 [PMID: 21917512 DOI: 10.1016/j.ijmedinf.2011.08.001]

152 **Zhou T**, Han G, Li BN, Lin Z, Ciaccio EJ, Green PH, Qin J. Quantitative analysis of patients with celiac disease by video capsule endoscopy: A deep learning method. *Comput Biol Med* 2017; **85**: 1-6 [PMID: 28412572 DOI: 10.1016/j.compbiomed.2017.03.031]

153 **Wimmer G**, Vécsei A, Uhl A. CNN transfer learning for the automated diagnosis of celiac disease. *IEEE* 2016; 1-6 [DOI: 10.1109/IPTA.2016.7821020]

154 **Wang X**, Qian H, Ciaccio EJ, Lewis SK, Bhagat G, Green PH, Xu S, Huang L, Gao R, Liu Y. Celiac disease diagnosis from videocapsule endoscopy images with residual learning and deep feature extraction. *Comput Methods Programs Biomed* 2020; **187**: 105236 [PMID: 31786452 DOI: 10.1016/j.cmpb.2019.105236]

155 **Fenwick A**. The global burden of neglected tropical diseases. *Public Health* 2012; **126**: 233-236 [PMID: 22325616 DOI: 10.1016/j.puhe.2011.11.015]

156 **Chen H**, Chen J, Peng Q, Sun G, Gan T. Automatic hookworm image detection for wireless capsule endoscopy using hybrid color gradient and contourlet transform. *Int Conf Biomed Eng Inf* 2013; 116-120 [DOI: 10.1109/BMEI.2013.6746918]

157 **He JY**, Wu X, Jiang YG, Peng Q, Jain R. Hookworm Detection in Wireless Capsule Endoscopy Images With Deep Learning. *IEEE Trans Image Process* 2018; **27**: 2379-2392 [PMID: 29470172 DOI: 10.1109/TIP.2018.2801119]

158 **Wu X**, Chen H, Gan T, Chen J, Ngo CW, Peng Q. Automatic Hookworm Detection in Wireless Capsule Endoscopy Images. *IEEE Trans Med Imaging* 2016; **35**: 1741-1752 [PMID: 26886971 DOI: 10.1109/TMI.2016.2527736]

159 **Leenhardt R**, Souchaud M, Houist G, Le Mouel JP, Saurin JC, Cholet F, Rahmi G, Leandri C, Histace A, Dray X. A neural network-based algorithm for assessing the cleanliness of small bowel during capsule endoscopy. *Endoscopy* 2021; **53**: 932-936 [PMID: 33137834 DOI: 10.1055/a-1301-3841]

160 **Noorda R**, Nevárez A, Colomer A, Pons Beltrán V, Naranjo V. Automatic evaluation of degree of cleanliness in capsule endoscopy based on a novel CNN architecture. *Sci Rep* 2020; **10**: 17706 [PMID: 33077755 DOI: 10.1038/s41598-020-74668-8]

161 **Borg-Bartolo SP**, Boyapati RK, Satsangi J, Kalla R. Precision medicine in inflammatory bowel disease: concept, progress and challenges. *F1000Res* 2020; **9** [PMID: 32047622 DOI: 10.12688/f1000research.20928.1]

162 **Seyed Tabib NS**, Madgwick M, Sudhakar P, Verstockt B, Korcsmaros T, Vermeire S. Big data in IBD: big progress for clinical practice. *Gut* 2020; **69**: 1520-1532 [PMID: 32111636 DOI: 10.1136/gutjnl-2019-320065]

163 **Olivera P**, Danese S, Jay N, Natoli G, Peyrin-Biroulet L. Big data in IBD: a look into the future. *Nat Rev Gastroenterol Hepatol* 2019; **16**: 312-321 [PMID: 30659247 DOI: 10.1038/s41575-019-0102-5]

164 **Bossuyt P**, Vermeire S, Bisschops R. Scoring endoscopic disease activity in IBD: artificial intelligence sees more and better than we do. *Gut* 2020; **69**: 788-789 [PMID: 30954951 DOI: 10.1136/gutjnl-2019-318235]

165 **Iacucci M**, Furfaro F, Matsumoto T, Uraoka T, Smith S, Ghosh S, Kiesslich R. Advanced endoscopic techniques in the assessment of inflammatory bowel disease: new technology, new era. *Gut* 2019; **68**: 562-572 [PMID: 30580249 DOI: 10.1136/gutjnl-2017-315235]

166 **Ozawa T**, Ishihara S, Fujishiro M, Saito H, Kumagai Y, Shichijo S, Aoyama K, Tada T. Novel computer-assisted diagnosis system for endoscopic disease activity in patients with ulcerative colitis. *Gastrointest Endosc* 2019; **89**: 416-421.e1 [PMID: 30367878 DOI: 10.1016/j.gie.2018.10.020]

167 **Zezos P**, Borowski K, Bajaj G, Boland K, Sheasgreen C, Tessolini JM, Silverberg MS. 439 - Toward Computer-Based Automated Mayo Score Classification in Ulcerative Colitis through Classical and Deep Machine Learning. *Gastroenterology* 2018; **154**: S-99 [DOI: 10.1016/S0016-5085(18)30773-X]

168 **Khorasani HM**, Usefi H, Peña-Castillo L. Detecting ulcerative colitis from colon samples using efficient feature selection and machine learning. *Sci Rep* 2020; **10**: 13744 [PMID: 32792678 DOI: 10.1038/s41598-020-70583-0]

169 **Kumar R**, Zhao Q, Seshamani S, Mullin G, Hager G, Dassopoulos T. Assessment of Crohn's disease lesions in wireless capsule endoscopy images. *IEEE Trans Biomed Eng* 2012; **59**: 355-362 [PMID: 22020661 DOI: 10.1109/TBME.2011.2172438]

170 **Mahapatra D**, Vos FM, Buhmann JM. Active learning based segmentation of Crohns disease from abdominal MRI. *Comput Methods Programs Biomed* 2016; **128**: 75-85 [PMID: 27040833 DOI: 10.1016/j.cmpb.2016.01.014]

171 **Mossotto E**, Ashton JJ, Coelho T, Beattie RM, MacArthur BD, Ennis S. Classification of Paediatric Inflammatory Bowel Disease using Machine Learning. *Sci Rep* 2017; **7**: 2427 [PMID: 28546534 DOI: 10.1038/s41598-017-02606-2]

172 **Maeda Y**, Kudo SE, Mori Y, Misawa M, Ogata N, Sasanuma S, Wakamura K, Oda M, Mori K, Ohtsuka K. Fully automated diagnostic system with artificial intelligence using endocytoscopy to identify the presence of histologic inflammation associated with ulcerative colitis (with video). *Gastrointest Endosc* 2019; **89**: 408-415 [PMID: 30268542 DOI: 10.1016/j.gie.2018.09.024]

173 **Matalka II**, Al-Omari FA, Salama RM, Mohtaseb AH. A novel approach for quantitative assessment of mucosal damage in inflammatory bowel disease. *Diagn Pathol* 2013; **8**: 156 [PMID: 24053788 DOI: 10.1186/1746-1596-8-156]

174 **Niehaus KE**, Uhlig HH, Clifton DA. Phenotypic characterisation of Crohn's disease severity. *Annu Int Conf IEEE Eng Med Biol Soc* 2015; **2015**: 7023-7026 [PMID: 26737909 DOI: 10.1109/EMBC.2015.7320009]

175 **Reddy BK**, Delen D, Agrawal RK. Predicting and explaining inflammation in Crohn's disease patients using predictive analytics methods and electronic medical record data. *Health Informatics J*

2019; **25**: 1201-1218 [PMID: 29320910 DOI: 10.1177/1460458217751015]
176 **Stidham RW**, Enchakalody B, Waljee AK, Higgins PDR, Wang SC, Su GL, Wasnik AP, Al-Hawary M. Assessing Small Bowel Stricturing and Morphology in Crohn's Disease Using Semi-automated Image Analysis. *Inflamm Bowel Dis* 2020; **26**: 734-742 [PMID: 31504540 DOI: 10.1093/ibd/izz196]
177 **Stidham RW**, Liu W, Bishu S, Rice MD, Higgins PDR, Zhu J, Nallamothu BK, Waljee AK. Performance of a Deep Learning Model *vs* Human Reviewers in Grading Endoscopic Disease Severity of Patients With Ulcerative Colitis. *JAMA Netw Open* 2019; **2**: e193963 [PMID: 31099869 DOI: 10.1001/jamanetworkopen.2019.3963]
178 **Takenaka K**, Ohtsuka K, Fujii T, Negi M, Suzuki K, Shimizu H, Oshima S, Akiyama S, Motobayashi M, Nagahori M, Saito E, Matsuoka K, Watanabe M. Development and Validation of a Deep Neural Network for Accurate Evaluation of Endoscopic Images From Patients With Ulcerative Colitis. *Gastroenterology* 2020; **158**: 2150-2157 [PMID: 32060000 DOI: 10.1053/j.gastro.2020.02.012]
179 **Yao H**, Najarian K, Gryak J, Bishu S, Rice MD, Waljee AK, Wilkins HJ, Stidham RW. Fully automated endoscopic disease activity assessment in ulcerative colitis. *Gastrointest Endosc* 2021; **93**: 728-736.e1 [PMID: 32810479 DOI: 10.1016/j.gie.2020.08.011]
180 **Doherty MK**, Ding T, Koumpouras C, Telesco SE, Monast C, Das A, Brodmerkel C, Schloss PD. Fecal Microbiota Signatures Are Associated with Response to Ustekinumab Therapy among Crohn's Disease Patients. *mBio* 2018; **9** [PMID: 29535202 DOI: 10.1128/mBio.02120-17]
181 **Douglas GM**, Hansen R, Jones CMA, Dunn KA, Comeau AM, Bielawski JP, Tayler R, El-Omar EM, Russell RK, Hold GL, Langille MGI, Van Limbergen J. Multi-omics differentially classify disease state and treatment outcome in pediatric Crohn's disease. *Microbiome* 2018; **6**: 13 [PMID: 29335008 DOI: 10.1186/s40168-018-0398-3]
182 **Waljee AK**, Joyce JC, Wang S, Saxena A, Hart M, Zhu J, Higgins PD. Algorithms outperform metabolite tests in predicting response of patients with inflammatory bowel disease to thiopurines. *Clin Gastroenterol Hepatol* 2010; **8**: 143-150 [PMID: 19835986 DOI: 10.1016/j.cgh.2009.09.031]
183 **Waljee AK**, Lipson R, Wiitala WL, Zhang Y, Liu B, Zhu J, Wallace B, Govani SM, Stidham RW, Hayward R, Higgins PDR. Predicting Hospitalization and Outpatient Corticosteroid Use in Inflammatory Bowel Disease Patients Using Machine Learning. *Inflamm Bowel Dis* 2017; **24**: 45-53 [PMID: 29272474 DOI: 10.1093/ibd/izx007]
184 **Waljee AK**, Liu B, Sauder K, Zhu J, Govani SM, Stidham RW, Higgins PDR. Predicting corticosteroid-free endoscopic remission with vedolizumab in ulcerative colitis. *Aliment Pharmacol Ther* 2018; **47**: 763-772 [PMID: 29359519 DOI: 10.1111/apt.14510]
185 **Waljee AK**, Sauder K, Patel A, Segar S, Liu B, Zhang Y, Zhu J, Stidham RW, Balis U, Higgins PDR. Machine Learning Algorithms for Objective Remission and Clinical Outcomes with Thiopurines. *J Crohns Colitis* 2017; **11**: 801-810 [PMID: 28333183 DOI: 10.1093/ecco-jcc/jjx014]
186 **Waljee AK**, Wallace BI, Cohen-Mekelburg S, Liu Y, Liu B, Sauder K, Stidham RW, Zhu J, Higgins PDR. Development and Validation of Machine Learning Models in Prediction of Remission in Patients With Moderate to Severe Crohn Disease. *JAMA Netw Open* 2019; **2**: e193721 [PMID: 31074823 DOI: 10.1001/jamanetworkopen.2019.3721]
187 **Isakov O**, Dotan I, Ben-Shachar S. Machine Learning-Based Gene Prioritization Identifies Novel Candidate Risk Genes for Inflammatory Bowel Disease. *Inflamm Bowel Dis* 2017; **23**: 1516-1523 [PMID: 28795970 DOI: 10.1097/MIB.0000000000001222]
188 **Wei Z**, Wang W, Bradfield J, Li J, Cardinale C, Frackelton E, Kim C, Mentch F, Van Steen K, Visscher PM, Baldassano RN, Hakonarson H; International IBD Genetics Consortium. Large sample size, wide variant spectrum, and advanced machine-learning technique boost risk prediction for inflammatory bowel disease. *Am J Hum Genet* 2013; **92**: 1008-1012 [PMID: 23731541 DOI: 10.1016/j.ajhg.2013.05.002]
189 **Hou JK**, Chang M, Nguyen T, Kramer JR, Richardson P, Sansgiry S, D'Avolio LW, El-Serag HB. Automated identification of surveillance colonoscopy in inflammatory bowel disease using natural language processing. *Dig Dis Sci* 2013; **58**: 936-941 [PMID: 23086115 DOI: 10.1007/s10620-012-2433-8]
190 **Firouzi F**, Rashidi M, Hashemi S, Kangavari M, Bahari A, Daryani NE, Emam MM, Naderi N, Shalmani HM, Farnood A, Zali M. A decision tree-based approach for determining low bone mineral density in inflammatory bowel disease using WEKA software. *Eur J Gastroenterol Hepatol* 2007; **19**: 1075-1081 [PMID: 17998832 DOI: 10.1097/MEG.0b013e3282202bb8]
191 **Ahn JC**, Connell A, Simonetto DA, Hughes C, Shah VH. Application of Artificial Intelligence for the Diagnosis and Treatment of Liver Diseases. *Hepatology* 2021; **73**: 2546-2563 [PMID: 33098140 DOI: 10.1002/hep.31603]
192 **Spann A**, Yasodhara A, Kang J, Watt K, Wang B, Goldenberg A, Bhat M. Applying Machine Learning in Liver Disease and Transplantation: A Comprehensive Review. *Hepatology* 2020; **71**: 1093-1105 [PMID: 31907954 DOI: 10.1002/hep.31103]
193 **Chen T**, Tu S, Wang H, Liu X, Li F, Jin W, Liang X, Zhang X, Wang J. Computer-aided diagnosis of gallbladder polyps based on high resolution ultrasonography. *Comput Methods Programs Biomed* 2020; **185**: 105118 [PMID: 31671340 DOI: 10.1016/j.cmpb.2019.105118]
194 **Hamm CA**, Wang CJ, Savic LJ, Ferrante M, Schobert I, Schlachter T, Lin M, Duncan JS, Weinreb JC, Chapiro J, Letzen B. Deep learning for liver tumor diagnosis part I: development of a convolutional neural network classifier for multi-phasic MRI. *Eur Radiol* 2019; **29**: 3338-3347

[PMID: 31016442 DOI: 10.1007/s00330-019-06205-9]

195 **Kim DW**, Lee G, Kim SY, Ahn G, Lee JG, Lee SS, Kim KW, Park SH, Lee YJ, Kim N. Deep learning-based algorithm to detect primary hepatic malignancy in multiphase CT of patients at high risk for HCC. *Eur Radiol* 2021; **31**: 7047-7057 [PMID: 33738600 DOI: 10.1007/s00330-021-07803-2]

196 **Kim JW**, Ye Q, Forgues M, Chen Y, Budhu A, Sime J, Hofseth LJ, Kaul R, Wang XW. Cancer-associated molecular signature in the tissue samples of patients with cirrhosis. *Hepatology* 2004; **39**: 518-527 [PMID: 14768006 DOI: 10.1002/hep.20053]

197 **Schmauch B**, Herent P, Jehanno P, Dehaene O, Saillard C, Aubé C, Luciani A, Lassau N, Jégou S. Diagnosis of focal liver lesions from ultrasound using deep learning. *Diagn Interv Imaging* 2019; **100**: 227-233 [PMID: 30926443 DOI: 10.1016/j.diii.2019.02.009]

198 **Singal AG**, Mukherjee A, Elmunzer BJ, Higgins PD, Lok AS, Zhu J, Marrero JA, Waljee AK. Machine learning algorithms outperform conventional regression models in predicting development of hepatocellular carcinoma. *Am J Gastroenterol* 2013; **108**: 1723-1730 [PMID: 24169273 DOI: 10.1038/ajg.2013.332]

199 **Sun C**, Xu A, Liu D, Xiong Z, Zhao F, Ding W. Deep Learning-Based Classification of Liver Cancer Histopathology Images Using Only Global Labels. *IEEE J Biomed Health Inform* 2020; **24**: 1643-1651 [PMID: 31670686 DOI: 10.1109/JBHI.2019.2949837]

200 **Wang CJ**, Hamm CA, Savic LJ, Ferrante M, Schobert I, Schlachter T, Lin M, Weinreb JC, Duncan JS, Chapiro J, Letzen B. Deep learning for liver tumor diagnosis part II: convolutional neural network interpretation using radiologic imaging features. *Eur Radiol* 2019; **29**: 3348-3357 [PMID: 31093705 DOI: 10.1007/s00330-019-06214-8]

201 **Yasaka K**, Akai H, Abe O, Kiryu S. Deep Learning with Convolutional Neural Network for Differentiation of Liver Masses at Dynamic Contrast-enhanced CT: A Preliminary Study. *Radiology* 2018; **286**: 887-896 [PMID: 29059036 DOI: 10.1148/radiol.2017170706]

202 **Yasaka K**, Akai H, Kunimatsu A, Abe O, Kiryu S. Liver Fibrosis: Deep Convolutional Neural Network for Staging by Using Gadoxetic Acid-enhanced Hepatobiliary Phase MR Images. *Radiology* 2018; **287**: 146-155 [PMID: 29239710 DOI: 10.1148/radiol.2017171928]

203 **Abd El-Salam SM**, Ezz MM, Hashem S, Elakel W, Salama R, ElMakhzangy H, ElHefnawi M. Performance of machine learning approaches on prediction of esophageal varices for Egyptian chronic hepatitis C patients. *Inform Med Unlocked* 2019; **17**: 100267 [DOI: 10.1016/j.imu.2019.100267]

204 **Dong TS**, Kalani A, Aby ES, Le L, Luu K, Hauer M, Kamath R, Lindor KD, Tabibian JH. Machine Learning-based Development and Validation of a Scoring System for Screening High-Risk Esophageal Varices. *Clin Gastroenterol Hepatol* 2019; **17**: 1894-1901.e1 [PMID: 30708109 DOI: 10.1016/j.cgh.2019.01.025]

205 **Hong WD**, Ji YF, Wang D, Chen TZ, Zhu QH. Use of artificial neural network to predict esophageal varices in patients with HBV related cirrhosis. *Hepat Mon* 2011; **11**: 544-547 [PMID: 22087192]

206 **Liu Y**, Ning Z, Örmeci N, An W, Yu Q, Han K, Huang Y, Liu D, Liu F, Li Z, Ding H, Luo H, Zuo C, Liu C, Wang J, Zhang C, Ji J, Wang W, Wang Z, Yuan M, Li L, Zhao Z, Wang G, Li M, Liu Q, Lei J, Tang T, Akçalar S, Çelebioğlu E, Üstüner E, Bilgiç S, Ellik Z, Asiller ÖÖ, Liu Z, Teng G, Chen Y, Hou J, Li X, He X, Dong J, Tian J, Liang P, Ju S, Zhang Y, Qi X. Deep Convolutional Neural Network-Aided Detection of Portal Hypertension in Patients With Cirrhosis. *Clin Gastroenterol Hepatol* 2020; **18**: 2998-3007.e5 [PMID: 32205218 DOI: 10.1016/j.cgh.2020.03.034]

207 **Marozas M**, Zykus R, Sakalauskas A, Kupčinskas L, Lukoševičius A. Noninvasive Evaluation of Portal Hypertension Using a Supervised Learning Technique. *J Healthc Eng* 2017; **2017**: 6183714 [PMID: 29158886 DOI: 10.1155/2017/6183714]

208 **Qi X**, An W, Liu F, Qi R, Wang L, Liu Y, Liu C, Xiang Y, Hui J, Liu Z, Qi X, Peng B, Ding H, Yang Y, He X, Hou J, Tian J, Li Z. Virtual Hepatic Venous Pressure Gradient with CT Angiography (CHESS 1601): A Prospective Multicenter Study for the Noninvasive Diagnosis of Portal Hypertension. *Radiology* 2019; **290**: 370-377 [PMID: 30457484 DOI: 10.1148/radiol.2018180425]

209 **Ahmed Y**, Hussein RS, Basha TA, Khalifa AM, Ibrahim AS, Abdelmoaty AS, Abdella HM, Fahmy AS. Detecting liver fibrosis using a machine learning-based approach to the quantification of the heart-induced deformation in tagged MR images. *NMR Biomed* 2020; **33**: e4215 [PMID: 31730265 DOI: 10.1002/nbm.4215]

210 **Byra M**, Styczynski G, Szmigielski C, Kalinowski P, Michałowski Ł, Paluszkiewicz R, Ziarkiewicz-Wróblewska B, Zieniewicz K, Sobieraj P, Nowicki A. Transfer learning with deep convolutional neural network for liver steatosis assessment in ultrasound images. *Int J Comput Assist Radiol Surg* 2018; **13**: 1895-1903 [PMID: 30094778 DOI: 10.1007/s11548-018-1843-2]

211 **Chang EK**, Yu CY, Clarke R, Hackbarth A, Sanders T, Esrailian E, Hommes DW, Runyon BA. Defining a Patient Population With Cirrhosis: An Automated Algorithm With Natural Language Processing. *J Clin Gastroenterol* 2016; **50**: 889-894 [PMID: 27348317 DOI: 10.1097/MCG.0000000000000583]

212 **Chen Y**, Luo Y, Huang W, Hu D, Zheng RQ, Cong SZ, Meng FK, Yang H, Lin HJ, Sun Y, Wang XY, Wu T, Ren J, Pei SF, Zheng Y, He Y, Hu Y, Yang N, Yan H. Machine-learning-based classification of real-time tissue elastography for hepatic fibrosis in patients with chronic hepatitis B. *Comput Biol Med* 2017; **89**: 18-23 [PMID: 28779596 DOI: 10.1016/j.compbiomed.2017.07.012]

213 **Choi KJ**, Jang JK, Lee SS, Sung YS, Shim WH, Kim HS, Yun J, Choi JY, Lee Y, Kang BK, Kim

JH, Kim SY, Yu ES. Development and Validation of a Deep Learning System for Staging Liver Fibrosis by Using Contrast Agent-enhanced CT Images in the Liver. *Radiology* 2018; **289**: 688-697 [PMID: 30179104 DOI: 10.1148/radiol.2018180763]

214 **Cui E**, Long W, Wu J, Li Q, Ma C, Lei Y, Lin F. Predicting the stages of liver fibrosis with multiphase CT radiomics based on volumetric features. *Abdom Radiol (NY)* 2021; **46**: 3866-3876 [PMID: 33751193 DOI: 10.1007/s00261-021-03051-6]

215 **Forlano R**, Mullish BH, Giannakeas N, Maurice JB, Angkathunyakul N, Lloyd J, Tzallas AT, Tsipouras M, Yee M, Thursz MR, Goldin RD, Manousou P. High-Throughput, Machine Learning-Based Quantification of Steatosis, Inflammation, Ballooning, and Fibrosis in Biopsies From Patients With Nonalcoholic Fatty Liver Disease. *Clin Gastroenterol Hepatol* 2020; **18**: 2081-2090.e9 [PMID: 31887451 DOI: 10.1016/j.cgh.2019.12.025]

216 **Gatos I**, Tsantis S, Spiliopoulos S, Karnabatidis D, Theotokas I, Zoumpoulis P, Loupas T, Hazle JD, Kagadis GC. A new computer aided diagnosis system for evaluation of chronic liver disease with ultrasound shear wave elastography imaging. *Med Phys* 2016; **43**: 1428-1436 [PMID: 26936727 DOI: 10.1118/1.4942383]

217 **Gatos I**, Tsantis S, Spiliopoulos S, Karnabatidis D, Theotokas I, Zoumpoulis P, Loupas T, Hazle JD, Kagadis GC. A Machine-Learning Algorithm Toward Color Analysis for Chronic Liver Disease Classification, Employing Ultrasound Shear Wave Elastography. *Ultrasound Med Biol* 2017; **43**: 1797-1810 [PMID: 28634041 DOI: 10.1016/j.ultrasmedbio.2017.05.002]

218 **Gatos I**, Tsantis S, Spiliopoulos S, Karnabatidis D, Theotokas I, Zoumpoulis P, Loupas T, Hazle JD, Kagadis GC. Temporal stability assessment in shear wave elasticity images validated by deep learning neural network for chronic liver disease fibrosis stage assessment. *Med Phys* 2019; **46**: 2298-2309 [PMID: 30929260 DOI: 10.1002/mp.13521]

219 **Heinemann F**, Birk G, Stierstorfer B. Deep learning enables pathologist-like scoring of NASH models. *Sci Rep* 2019; **9**: 18454 [PMID: 31804575 DOI: 10.1038/s41598-019-54904-6]

220 **Huang H**, Shiffman ML, Friedman S, Venkatesh R, Bzowej N, Abar OT, Rowland CM, Catanese JJ, Leong DU, Sninsky JJ, Layden TJ, Wright TL, White T, Cheung RC. A 7 gene signature identifies the risk of developing cirrhosis in patients with chronic hepatitis C. *Hepatology* 2007; **46**: 297-306 [PMID: 17461418 DOI: 10.1002/hep.21695]

221 **Konerman MA**, Beste LA, Van T, Liu B, Zhang X, Zhu J, Saini SD, Su GL, Nallamothu BK, Ioannou GN, Waljee AK. Machine learning models to predict disease progression among veterans with hepatitis C virus. *PLoS One* 2019; **14**: e0208141 [PMID: 30608929 DOI: 10.1371/journal.pone.0208141]

222 **Konerman MA**, Zhang Y, Zhu J, Higgins PD, Lok AS, Waljee AK. Improvement of predictive models of risk of disease progression in chronic hepatitis C by incorporating longitudinal data. *Hepatology* 2015; **61**: 1832-1841 [PMID: 25684666 DOI: 10.1002/hep.27750]

223 **Kuppili V**, Biswas M, Sreekumar A, Suri HS, Saba L, Edla DR, Marinho RT, Sanches JM, Suri JS. Extreme Learning Machine Framework for Risk Stratification of Fatty Liver Disease Using Ultrasound Tissue Characterization. *J Med Syst* 2017; **41**: 152 [PMID: 28836045 DOI: 10.1007/s10916-017-0797-1]

224 **Lara J**, López-Labrador F, González-Candelas F, Berenguer M, Khudyakov YE. Computational models of liver fibrosis progression for hepatitis C virus chronic infection. *BMC Bioinformatics* 2014; **15** Suppl 8: S5 [PMID: 25081062 DOI: 10.1186/1471-2105-15-S8-S5]

225 **Li W**, Huang Y, Zhuang BW, Liu GJ, Hu HT, Li X, Liang JY, Wang Z, Huang XW, Zhang CQ, Ruan SM, Xie XY, Kuang M, Lu MD, Chen LD, Wang W. Multiparametric ultrasomics of significant liver fibrosis: A machine learning-based analysis. *Eur Radiol* 2019; **29**: 1496-1506 [PMID: 30178143 DOI: 10.1007/s00330-018-5680-z]

226 **Meffert PJ**, Baumeister SE, Lerch MM, Mayerle J, Kratzer W, Völzke H. Development, external validation, and comparative assessment of a new diagnostic score for hepatic steatosis. *Am J Gastroenterol* 2014; **109**: 1404-1414 [PMID: 24957156 DOI: 10.1038/ajg.2014.155]

227 **Perakakis N**, Polyzos SA, Yazdani A, Sala-Vila A, Kountouras J, Anastasilakis AD, Mantzoros CS. Non-invasive diagnosis of non-alcoholic steatohepatitis and fibrosis with the use of omics and supervised learning: A proof of concept study. *Metabolism* 2019; **101**: 154005 [PMID: 31711876 DOI: 10.1016/j.metabol.2019.154005]

228 **Piscaglia F**, Cucchetti A, Benlloch S, Vivarelli M, Berenguer J, Bolondi L, Pinna AD, Berenguer M. Prediction of significant fibrosis in hepatitis C virus infected liver transplant recipients by artificial neural network analysis of clinical factors. *Eur J Gastroenterol Hepatol* 2006; **18**: 1255-1261 [PMID: 17099373 DOI: 10.1097/01.meg.0000243885.55562.7e]

229 **Raoufy MR**, Vahdani P, Alavian SM, Fekri S, Eftekhari P, Gharibzadeh S. A novel method for diagnosing cirrhosis in patients with chronic hepatitis B: artificial neural network approach. *J Med Syst* 2011; **35**: 121-126 [PMID: 20703578 DOI: 10.1007/s10916-009-9348-8]

230 **Redman JS**, Natarajan Y, Hou JK, Wang J, Hanif M, Feng H, Kramer JR, Desiderio R, Xu H, El-Serag HB, Kanwal F. Accurate Identification of Fatty Liver Disease in Data Warehouse Utilizing Natural Language Processing. *Dig Dis Sci* 2017; **62**: 2713-2718 [PMID: 28861720 DOI: 10.1007/s10620-017-4721-9]

231 **Sowa JP**, Heider D, Bechmann LP, Gerken G, Hoffmann D, Canbay A. Novel algorithm for non-invasive assessment of fibrosis in NAFLD. *PLoS One* 2013; **8**: e62439 [PMID: 23638085 DOI: 10.1371/journal.pone.0062439]

232 **Wang K**, Lu X, Zhou H, Gao Y, Zheng J, Tong M, Wu C, Liu C, Huang L, Jiang T, Meng F, Lu Y,

Ai H, Xie XY, Yin LP, Liang P, Tian J, Zheng R. Deep learning Radiomics of shear wave elastography significantly improved diagnostic performance for assessing liver fibrosis in chronic hepatitis B: a prospective multicentre study. *Gut* 2019; **68**: 729-741 [PMID: 29730602 DOI: 10.1136/gutjnl-2018-316204]

233 **Wei R**, Wang J, Wang X, Xie G, Wang Y, Zhang H, Peng CY, Rajani C, Kwee S, Liu P, Jia W. Clinical prediction of HBV and HCV related hepatic fibrosis using machine learning. *EBioMedicine* 2018; **35**: 124-132 [PMID: 30100397 DOI: 10.1016/j.ebiom.2018.07.041]

234 **Lee JH**, Joo I, Kang TW, Paik YH, Sinn DH, Ha SY, Kim K, Choi C, Lee G, Yi J, Bang WC. Deep learning with ultrasonography: automated classification of liver fibrosis using a deep convolutional neural network. *Eur Radiol* 2020; **30**: 1264-1273 [PMID: 31478087 DOI: 10.1007/s00330-019-06407-1]

235 **Canbay A**, Kälsch J, Neumann U, Rau M, Hohenester S, Baba HA, Rust C, Geier A, Heider D, Sowa JP. Non-invasive assessment of NAFLD as systemic disease-A machine learning perspective. *PLoS One* 2019; **14**: e0214436 [PMID: 30913263 DOI: 10.1371/journal.pone.0214436]

236 **Docherty M**, Regnier SA, Capkun G, Balp MM, Ye Q, Janssens N, Tietz A, Löffler J, Cai J, Pedrosa MC, Schattenberg JM. Development of a novel machine learning model to predict presence of nonalcoholic steatohepatitis. *J Am Med Inform Assoc* 2021; **28**: 1235-1241 [PMID: 33684933 DOI: 10.1093/jamia/ocab003]

237 **Fialoke S**, Malarstig A, Miller MR, Dumitriu A. Application of Machine Learning Methods to Predict Non-Alcoholic Steatohepatitis (NASH) in Non-Alcoholic Fatty Liver (NAFL) Patients. *AMIA Annu Symp Proc* 2018; **2018**: 430-439 [PMID: 30815083]

238 **Sowa JP**, Atmaca Ö, Kahraman A, Schlattjan M, Lindner M, Sydor S, Scherbaum N, Lackner K, Gerken G, Heider D, Arteel GE, Erim Y, Canbay A. Non-invasive separation of alcoholic and non-alcoholic liver disease with predictive modeling. *PLoS One* 2014; **9**: e101444 [PMID: 24988316 DOI: 10.1371/journal.pone.0101444]

239 **Taylor-Weiner A**, Pokkalla H, Han L, Jia C, Huss R, Chung C, Elliott H, Glass B, Pethia K, Carrasco-Zevallos O, Shukla C, Khettry U, Najarian R, Taliano R, Subramanian GM, Myers RP, Wapinski I, Khosla A, Resnick M, Montalto MC, Anstee QM, Wong VW, Trauner M, Lawitz EJ, Harrison SA, Okanoue T, Romero-Gomez M, Goodman Z, Loomba R, Beck AH, Younossi ZM. A Machine Learning Approach Enables Quantitative Measurement of Liver Histology and Disease Monitoring in NASH. *Hepatology* 2021; **74**: 133-147 [PMID: 33570776 DOI: 10.1002/hep.31750]

240 **Van Vleck TT**, Chan L, Coca SG, Craven CK, Do R, Ellis SB, Kannry JL, Loos RJF, Bonis PA, Cho J, Nadkarni GN. Augmented intelligence with natural language processing applied to electronic health records for identifying patients with non-alcoholic fatty liver disease at risk for disease progression. *Int J Med Inform* 2019; **129**: 334-341 [PMID: 31445275 DOI: 10.1016/j.ijmedinf.2019.06.028]

241 **Vanderbeck S**, Bockhorst J, Kleiner D, Komorowski R, Chalasani N, Gawrieh S. Automatic quantification of lobular inflammation and hepatocyte ballooning in nonalcoholic fatty liver disease liver biopsies. *Hum Pathol* 2015; **46**: 767-775 [PMID: 25776030 DOI: 10.1016/j.humpath.2015.01.019]

242 **Vanderbeck S**, Bockhorst J, Komorowski R, Kleiner DE, Gawrieh S. Automatic classification of white regions in liver biopsies by supervised machine learning. *Hum Pathol* 2014; **45**: 785-792 [PMID: 24565203 DOI: 10.1016/j.humpath.2013.11.011]

243 **Andres A**, Montano-Loza A, Greiner R, Uhlich M, Jin P, Hoehn B, Bigam D, Shapiro JAM, Kneteman NM. A novel learning algorithm to predict individual survival after liver transplantation for primary sclerosing cholangitis. *PLoS One* 2018; **13**: e0193523 [PMID: 29543895 DOI: 10.1371/journal.pone.0193523]

244 **Ayllón MD**, Ciria R, Cruz-Ramírez M, Pérez-Ortiz M, Gómez I, Valente R, O'Grady J, de la Mata M, Hervás-Martínez C, Heaton ND, Briceño J. Validation of artificial neural networks as a methodology for donor-recipient matching for liver transplantation. *Liver Transpl* 2018; **24**: 192-203 [PMID: 28921876 DOI: 10.1002/lt.24870]

245 **Bertsimas D**, Kung J, Trichakis N, Wang Y, Hirose R, Vagefi PA. Development and validation of an optimized prediction of mortality for candidates awaiting liver transplantation. *Am J Transplant* 2019; **19**: 1109-1118 [PMID: 30411495 DOI: 10.1111/ajt.15172]

246 **Bhat V**, Tazari M, Watt KD, Bhat M. New-Onset Diabetes and Preexisting Diabetes Are Associated With Comparable Reduction in Long-Term Survival After Liver Transplant: A Machine Learning Approach. *Mayo Clin Proc* 2018; **93**: 1794-1802 [PMID: 30522594 DOI: 10.1016/j.mayocp.2018.06.020]

247 **Briceño J**, Cruz-Ramírez M, Prieto M, Navasa M, Ortiz de Urbina J, Orti R, Gómez-Bravo MÁ, Otero A, Varo E, Tomé S, Clemente G, Bañares R, Bárcena R, Cuervas-Mons V, Solórzano G, Vinaixa C, Rubín A, Colmenero J, Valdivieso A, Ciria R, Hervás-Martínez C, de la Mata M. Use of artificial intelligence as an innovative donor-recipient matching model for liver transplantation: results from a multicenter Spanish study. *J Hepatol* 2014; **61**: 1020-1028 [PMID: 24905493 DOI: 10.1016/j.jhep.2014.05.039]

248 **Kazemi A**, Kazemi K, Sami A, Sharifian R. Identifying Factors That Affect Patient Survival After Orthotopic Liver Transplant Using Machine-Learning Techniques. *Exp Clin Transplant* 2019; **17**: 775-783 [PMID: 30968757 DOI: 10.6002/ect.2018.0170]

249 **Lau L**, Kankanige Y, Rubinstein B, Jones R, Christophi C, Muralidharan V, Bailey J. Machine-Learning Algorithms Predict Graft Failure After Liver Transplantation. *Transplantation* 2017; **101**:

e125-e132 [PMID: 27941428 DOI: 10.1097/TP.0000000000001600]

250 **Lee HC**, Yoon SB, Yang SM, Kim WH, Ryu HG, Jung CW, Suh KS, Lee KH. Prediction of Acute Kidney Injury after Liver Transplantation: Machine Learning Approaches vs. Logistic Regression Model. *J Clin Med* 2018; **7** [PMID: 30413107 DOI: 10.3390/jcm7110428]

251 **Abajian A**, Murali N, Savic LJ, Laage-Gaupp FM, Nezami N, Duncan JS, Schlachter T, Lin M, Geschwind JF, Chapiro J. Predicting Treatment Response to Intra-arterial Therapies for Hepatocellular Carcinoma with the Use of Supervised Machine Learning-An Artificial Intelligence Concept. *J Vasc Interv Radiol* 2018; **29**: 850-857.e1 [PMID: 29548875 DOI: 10.1016/j.jvir.2018.01.769]

252 **Chaudhary K**, Poirion OB, Lu L, Garmire LX. Deep Learning-Based Multi-Omics Integration Robustly Predicts Survival in Liver Cancer. *Clin Cancer Res* 2018; **24**: 1248-1259 [PMID: 28982688 DOI: 10.1158/1078-0432.CCR-17-0853]

253 **Morshid A**, Elsayes KM, Khalaf AM, Elmohr MM, Yu J, Kaseb AO, Hassan M, Mahvash A, Wang Z, Hazle JD, Fuentes D. A machine learning model to predict hepatocellular carcinoma response to transcatheter arterial chemoembolization. *Radiol Artif Intell* 2019; **1** [PMID: 31858078 DOI: 10.1148/ryai.2019180021]

254 **Saillard C**, Schmauch B, Laifa O, Moarii M, Toldo S, Zaslavskiy M, Pronier E, Laurent A, Amaddeo G, Regnault H, Sommacale D, Ziol M, Pawlotsky JM, Mulé S, Luciani A, Wainrib G, Clozel T, Courtiol P, Calderaro J. Predicting Survival After Hepatocellular Carcinoma Resection Using Deep Learning on Histological Slides. *Hepatology* 2020; **72**: 2000-2013 [PMID: 32108950 DOI: 10.1002/hep.31207]

255 **Shan QY**, Hu HT, Feng ST, Peng ZP, Chen SL, Zhou Q, Li X, Xie XY, Lu MD, Wang W, Kuang M. CT-based peritumoral radiomics signatures to predict early recurrence in hepatocellular carcinoma after curative tumor resection or ablation. *Cancer Imaging* 2019; **19**: 11 [PMID: 30813956 DOI: 10.1186/s40644-019-0197-5]

256 **Eaton JE**, Vesterhus M, McCauley BM, Atkinson EJ, Schlicht EM, Juran BD, Gossard AA, LaRusso NF, Gores GJ, Karlsen TH, Lazaridis KN. Primary Sclerosing Cholangitis Risk Estimate Tool (PREsTo) Predicts Outcomes of the Disease: A Derivation and Validation Study Using Machine Learning. *Hepatology* 2020; **71**: 214-224 [PMID: 29742811 DOI: 10.1002/hep.30085]

257 **Garcia MS**, Agarwal B, Mookerjee RP, Jalan R, Doyle G, Ranco G, Arroyo V, Pavesi M, Garcia E, Saliba F, Banares R, Fernandez J. An Accurate Data Preparation Approach for the Prediction of Mortality in ACLF Patients using the CANONIC Dataset. *Annu Int Conf IEEE Eng Med Biol Soc* 2019; **2019**: 1371-1377 [PMID: 31946148 DOI: 10.1109/EMBC.2019.8857239]

258 **Ibragimov B**, Toesca D, Chang D, Yuan Y, Koong A, Xing L. Development of deep neural network for individualized hepatobiliary toxicity prediction after liver SBRT. *Med Phys* 2018; **45**: 4763-4774 [PMID: 30098025 DOI: 10.1002/mp.13122]

259 **Jovanovic P**, Salkic NN, Zerem E. Artificial neural network predicts the need for therapeutic ERCP in patients with suspected choledocholithiasis. *Gastrointest Endosc* 2014; **80**: 260-268 [PMID: 24593947 DOI: 10.1016/j.gie.2014.01.023]

260 **Kanwal F**, Taylor TJ, Kramer JR, Cao Y, Smith D, Gifford AL, El-Serag HB, Naik AD, Asch SM. Development, Validation, and Evaluation of a Simple Machine Learning Model to Predict Cirrhosis Mortality. *JAMA Netw Open* 2020; **3**: e2023780 [PMID: 33141161 DOI: 10.1001/jamanetworkopen.2020.23780]

261 **Speiser JL**, Karvellas CJ, Wolf BJ, Chung D, Koch DG, Durkalski VL. Predicting daily outcomes in acetaminophen-induced acute liver failure patients with machine learning techniques. *Comput Methods Programs Biomed* 2019; **175**: 111-120 [PMID: 31104700 DOI: 10.1016/j.cmpb.2019.04.012]

262 **Speiser JL**, Lee WM, Karvellas CJ; US Acute Liver Failure Study Group. Predicting outcome on admission and post-admission for acetaminophen-induced acute liver failure using classification and regression tree models. *PLoS One* 2015; **10**: e0122929 [PMID: 25885260 DOI: 10.1371/journal.pone.0122929]

263 **Konerman MA**, Lu D, Zhang Y, Thomson M, Zhu J, Verma A, Liu B, Talaat N, Balis U, Higgins PDR, Lok ASF, Waljee AK. Assessing risk of fibrosis progression and liver-related clinical outcomes among patients with both early stage and advanced chronic hepatitis C. *PLoS One* 2017; **12**: e0187344 [PMID: 29108017 DOI: 10.1371/journal.pone.0187344]

264 **Ai H**, Chen W, Zhang L, Huang L, Yin Z, Hu H, Zhao Q, Zhao J, Liu H. Predicting Drug-Induced Liver Injury Using Ensemble Learning Methods and Molecular Fingerprints. *Toxicol Sci* 2018; **165**: 100-107 [PMID: 29788510 DOI: 10.1093/toxsci/kfy121]

265 **Banerjee I**, Choi HH, Desser T, Rubin DL. A Scalable Machine Learning Approach for Inferring Probabilistic US-LI-RADS Categorization. *AMIA Annu Symp Proc* 2018; **2018**: 215-224 [PMID: 30815059]

266 **Dickerson LK**, Rouhizadeh M, Korotkaya Y, Bowring MG, Massie AB, McAdams-Demarco MA, Segev DL, Cannon A, Guerrerio AL, Chen PH, Philosophe BN, Mogul DB. Language impairment in adults with end-stage liver disease: application of natural language processing towards patient-generated health records. *NPJ Digit Med* 2019; **2**: 106 [PMID: 31701020 DOI: 10.1038/s41746-019-0179-9]

267 **He L**, Li H, Dudley JA, Maloney TC, Brady SL, Somasundaram E, Trout AT, Dillman JR. Machine Learning Prediction of Liver Stiffness Using Clinical and T2-Weighted MRI Radiomic Data. *AJR Am J Roentgenol* 2019; **213**: 592-601 [PMID: 31120779 DOI: 10.2214/AJR.19.21082]

268 **Khan S**, Ullah R, Khan A, Ashraf R, Ali H, Bilal M, Saleem M. Analysis of hepatitis B virus infection in blood sera using Raman spectroscopy and machine learning. *Photodiagnosis Photodyn Ther* 2018; **23**: 89-93 [PMID: 29787817 DOI: 10.1016/j.pdpdt.2018.05.010]

269 **Li X**, Chen H, Qi X, Dou Q, Fu CW, Heng PA. H-DenseUNet: Hybrid Densely Connected UNet for Liver and Tumor Segmentation From CT Volumes. *IEEE Trans Med Imaging* 2018; **37**: 2663-2674 [PMID: 29994201 DOI: 10.1109/TMI.2018.2845918]

270 **Mueller-Breckenridge AJ**, Garcia-Alcalde F, Wildum S, Smits SL, de Man RA, van Campenhout MJH, Brouwer WP, Niu J, Young JAT, Najera I, Zhu L, Wu D, Racek T, Hundie GB, Lin Y, Boucher CA, van de Vijver D, Haagmans BL. Machine-learning based patient classification using Hepatitis B virus full-length genome quasispecies from Asian and European cohorts. *Sci Rep* 2019; **9**: 18892 [PMID: 31827222 DOI: 10.1038/s41598-019-55445-8]

271 **Williams DP**, Lazic SE, Foster AJ, Semenova E, Morgan P. Predicting Drug-Induced Liver Injury with Bayesian Machine Learning. *Chem Res Toxicol* 2020; **33**: 239-248 [PMID: 31535850 DOI: 10.1021/acs.chemrestox.9b00264]

272 **Shousha HI**, Awad AH, Omran DA, Elnegouly MM, Mabrouk M. Data Mining and Machine Learning Algorithms Using IL28B Genotype and Biochemical Markers Best Predicted Advanced Liver Fibrosis in Chronic Hepatitis C. *Jpn J Infect Dis* 2018; **71**: 51-57 [PMID: 29279441 DOI: 10.7883/yoken.JJID.2017.089]

273 **Garcia-Carretero R**, Vigil-Medina L, Barquero-Perez O, Ramos-Lopez J. Relevant Features in Nonalcoholic Steatohepatitis Determined Using Machine Learning for Feature Selection. *Metab Syndr Relat Disord* 2019; **17**: 444-451 [PMID: 31675274 DOI: 10.1089/met.2019.0052]

274 **Ma H**, Xu CF, Shen Z, Yu CH, Li YM. Application of Machine Learning Techniques for Clinical Predictive Modeling: A Cross-Sectional Study on Nonalcoholic Fatty Liver Disease in China. *Biomed Res Int* 2018; **2018**: 4304376 [PMID: 30402478 DOI: 10.1155/2018/4304376]

275 **Moccia S**, Mattos LS, Patrini I, Ruperti M, Poté N, Dondero F, Cauchy F, Sepulveda A, Soubrane O, De Momi E, Diaspro A, Cesaretti M. Computer-assisted liver graft steatosis assessment *via* learning-based texture analysis. *Int J Comput Assist Radiol Surg* 2018; **13**: 1357-1367 [PMID: 29796834 DOI: 10.1007/s11548-018-1787-6]

276 **Perveen S**, Shahbaz M, Keshavjee K, Guergachi A. A Systematic Machine Learning Based Approach for the Diagnosis of Non-Alcoholic Fatty Liver Disease Risk and Progression. *Sci Rep* 2018; **8**: 2112 [PMID: 29391513 DOI: 10.1038/s41598-018-20166-x]

277 **Wu CC**, Yeh WC, Hsu WD, Islam MM, Nguyen PAA, Poly TN, Wang YC, Yang HC, Jack Li YC. Prediction of fatty liver disease using machine learning algorithms. *Comput Methods Programs Biomed* 2019; **170**: 23-29 [PMID: 30712601 DOI: 10.1016/j.cmpb.2018.12.032]

278 **Yip TC**, Ma AJ, Wong VW, Tse YK, Chan HL, Yuen PC, Wong GL. Laboratory parameter-based machine learning model for excluding non-alcoholic fatty liver disease (NAFLD) in the general population. *Aliment Pharmacol Ther* 2017; **46**: 447-456 [PMID: 28585725 DOI: 10.1111/apt.14172]

279 **Gorris M**, Hoogenboom SA, Wallace MB, van Hooft JE. Artificial intelligence for the management of pancreatic diseases. *Dig Endosc* 2021; **33**: 231-241 [PMID: 33065754 DOI: 10.1111/den.13875]

280 **Marya NB**, Powers PD, Chari ST, Gleeson FC, Leggett CL, Abu Dayyeh BK, Chandrasekhara V, Iyer PG, Majumder S, Pearson RK, Petersen BT, Rajan E, Sawas T, Storm AC, Vege SS, Chen S, Long Z, Hough DM, Mara K, Levy MJ. Utilisation of artificial intelligence for the development of an EUS-convolutional neural network model trained to enhance the diagnosis of autoimmune pancreatitis. *Gut* 2021; **70**: 1335-1344 [PMID: 33028668 DOI: 10.1136/gutjnl-2020-322821]

281 **Tonozuka R**, Mukai S, Itoi T. The Role of Artificial Intelligence in Endoscopic Ultrasound for Pancreatic Disorders. *Diagnostics (Basel)* 2020; **11** [PMID: 33374181 DOI: 10.3390/diagnostics11010018]

282 **van den Heever M**, Mittal A, Haydock M, Windsor J. The use of intelligent database systems in acute pancreatitis--a systematic review. *Pancreatology* 2014; **14**: 9-16 [PMID: 24555973 DOI: 10.1016/j.pan.2013.11.010]

283 **Andersson B**, Andersson R, Ohlsson M, Nilsson J. Prediction of severe acute pancreatitis at admission to hospital using artificial neural networks. *Pancreatology* 2011; **11**: 328-335 [PMID: 21757970 DOI: 10.1159/000327903]

284 **Fei Y**, Gao K, Li WQ. Artificial neural network algorithm model as powerful tool to predict acute lung injury following to severe acute pancreatitis. *Pancreatology* 2018; **18**: 892-899 [PMID: 30268673 DOI: 10.1016/j.pan.2018.09.007]

285 **Fei Y**, Gao K, Li WQ. Prediction and evaluation of the severity of acute respiratory distress syndrome following severe acute pancreatitis using an artificial neural network algorithm model. *HPB (Oxford)* 2019; **21**: 891-897 [PMID: 30591306 DOI: 10.1016/j.hpb.2018.11.009]

286 **Fei Y**, Hu J, Li WQ, Wang W, Zong GQ. Artificial neural networks predict the incidence of portosplenomesenteric venous thrombosis in patients with acute pancreatitis. *J Thromb Haemost* 2017; **15**: 439-445 [PMID: 27960048 DOI: 10.1111/jth.13588]

287 **Hong WD**, Chen XR, Jin SQ, Huang QK, Zhu QH, Pan JY. Use of an artificial neural network to predict persistent organ failure in patients with acute pancreatitis. *Clinics (Sao Paulo)* 2013; **68**: 27-31 [PMID: 23420153 DOI: 10.6061/clinics/2013(01)rc01]

288 **Keogan MT**, Lo JY, Freed KS, Raptopoulos V, Blake S, Kamel IR, Weisinger K, Rosen MP, Nelson RC. Outcome analysis of patients with acute pancreatitis by using an artificial neural network. *Acad Radiol* 2002; **9**: 410-419 [PMID: 11942655 DOI: 10.1016/s1076-6332(03)80186-1]

289 **Mofidi R**, Duff MD, Madhavan KK, Garden OJ, Parks RW. Identification of severe acute

pancreatitis using an artificial neural network. *Surgery* 2007; **141**: 59-66 [PMID: 17188168 DOI: 10.1016/j.surg.2006.07.022]

290 **Pearce CB**, Gunn SR, Ahmed A, Johnson CD. Machine learning can improve prediction of severity in acute pancreatitis using admission values of APACHE II score and C-reactive protein. *Pancreatology* 2006; **6**: 123-131 [PMID: 16327290 DOI: 10.1159/000090032]

291 **Pofahl WE**, Walczak SM, Rhone E, Izenberg SD. Use of an artificial neural network to predict length of stay in acute pancreatitis. *Am Surg* 1998; **64**: 868-872 [PMID: 9731816 DOI: 10.1016/S0016-5085(98)81989-6]

292 **Qiu Q**, Nian YJ, Guo Y, Tang L, Lu N, Wen LZ, Wang B, Chen DF, Liu KJ. Development and validation of three machine-learning models for predicting multiple organ failure in moderately severe and severe acute pancreatitis. *BMC Gastroenterol* 2019; **19**: 118 [PMID: 31272385 DOI: 10.1186/s12876-019-1016-y]

293 **Qiu Q**, Nian YJ, Tang L, Guo Y, Wen LZ, Wang B, Chen DF, Liu KJ. Artificial neural networks accurately predict intra-abdominal infection in moderately severe and severe acute pancreatitis. *J Dig Dis* 2019; **20**: 486-494 [PMID: 31328389 DOI: 10.1111/1751-2980.12796]

294 **Al-Haddad MA**, Friedlin J, Kesterson J, Waters JA, Aguilar-Saavedra JR, Schmidt CM. Natural language processing for the development of a clinical registry: a validation study in intraductal papillary mucinous neoplasms. *HPB (Oxford)* 2010; **12**: 688-695 [PMID: 21083794 DOI: 10.1111/j.1477-2574.2010.00235.x]

295 **Gao X**, Wang X. Performance of deep learning for differentiating pancreatic diseases on contrast-enhanced magnetic resonance imaging: A preliminary study. *Diagn Interv Imaging* 2020; **101**: 91-100 [PMID: 31375430 DOI: 10.1016/j.diii.2019.07.002]

296 **Mashayekhi R**, Parekh VS, Faghih M, Singh VK, Jacobs MA, Zaheer A. Radiomic features of the pancreas on CT imaging accurately differentiate functional abdominal pain, recurrent acute pancreatitis, and chronic pancreatitis. *Eur J Radiol* 2020; **123**: 108778 [PMID: 31846864 DOI: 10.1016/j.ejrad.2019.108778]

297 **Roth HR**, Lu L, Lay N, Harrison AP, Farag A, Sohn A, Summers RM. Spatial aggregation of holistically-nested convolutional neural networks for automated pancreas localization and segmentation. *Med Image Anal* 2018; **45**: 94-107 [PMID: 29427897 DOI: 10.1016/j.media.2018.01.006]

298 **Zhang J**, Zhu L, Yao L, Ding X, Chen D, Wu H, Lu Z, Zhou W, Zhang L, An P, Xu B, Tan W, Hu S, Cheng F, Yu H. Deep learning-based pancreas segmentation and station recognition system in EUS: development and validation of a useful training tool (with video). *Gastrointest Endosc* 2020; **92**: 874-885.e3 [PMID: 32387499 DOI: 10.1016/j.gie.2020.04.071]

299 **Zheng H**, Chen Y, Yue X, Ma C, Liu X, Yang P, Lu J. Deep pancreas segmentation with uncertain regions of shadowed sets. *Magn Reson Imaging* 2020; **68**: 45-52 [PMID: 31987903 DOI: 10.1016/j.mri.2020.01.008]

300 **Zhu J**, Wang L, Chu Y, Hou X, Xing L, Kong F, Zhou Y, Wang Y, Jin Z, Li Z. A new descriptor for computer-aided diagnosis of EUS imaging to distinguish autoimmune pancreatitis from chronic pancreatitis. *Gastrointest Endosc* 2015; **82**: 831-836.e1 [PMID: 25952089 DOI: 10.1016/j.gie.2015.02.043]

301 **Chu LC**, Park S, Kawamoto S, Fouladi DF, Shayesteh S, Zinreich ES, Graves JS, Horton KM, Hruban RH, Yuille AL, Kinzler KW, Vogelstein B, Fishman EK. Utility of CT Radiomics Features in Differentiation of Pancreatic Ductal Adenocarcinoma From Normal Pancreatic Tissue. *AJR Am J Roentgenol* 2019; **213**: 349-357 [PMID: 31012758 DOI: 10.2214/AJR.18.20901]

302 **Das A**, Nguyen CC, Li F, Li B. Digital image analysis of EUS images accurately differentiates pancreatic cancer from chronic pancreatitis and normal tissue. *Gastrointest Endosc* 2008; **67**: 861-867 [PMID: 18179797 DOI: 10.1016/j.gie.2007.08.036]

303 **Gao X**, Wang X. Deep learning for World Health Organization grades of pancreatic neuroendocrine tumors on contrast-enhanced magnetic resonance images: a preliminary study. *Int J Comput Assist Radiol Surg* 2019; **14**: 1981-1991 [PMID: 31555998 DOI: 10.1007/s11548-019-02070-5]

304 **Kaissis G**, Ziegelmayer S, Lohöfer F, Steiger K, Algül H, Muckenhuber A, Yen HY, Rummeny E, Friess H, Schmid R, Weichert W, Siveke JT, Braren R. A machine learning algorithm predicts molecular subtypes in pancreatic ductal adenocarcinoma with differential response to gemcitabine-based *vs* FOLFIRINOX chemotherapy. *PLoS One* 2019; **14**: e0218642 [PMID: 31577805 DOI: 10.1371/journal.pone.0218642]

305 **Kaissis GA**, Ziegelmayer S, Lohöfer FK, Harder FN, Jungmann F, Sasse D, Muckenhuber A, Yen HY, Steiger K, Siveke J, Friess H, Schmid R, Weichert W, Makowski MR, Braren RF. Image-Based Molecular Phenotyping of Pancreatic Ductal Adenocarcinoma. *J Clin Med* 2020; **9** [PMID: 32155990 DOI: 10.3390/jcm9030724]

306 **E L**, Xu Y, Wu Z, Li L, Zhang N, Yang H, Schwartz LH, Lu L, Zhao B. Differentiation of Focal-Type Autoimmune Pancreatitis From Pancreatic Ductal Adenocarcinoma Using Radiomics Based on Multiphasic Computed Tomography. *J Comput Assist Tomogr* 2020; **44**: 511-518 [PMID: 32697521 DOI: 10.1097/RCT.0000000000001049]

307 **Momeni-Boroujeni A**, Yousefi E, Somma J. Computer-assisted cytologic diagnosis in pancreatic FNA: An application of neural networks to image analysis. *Cancer Cytopathol* 2017; **125**: 926-933 [PMID: 28885766 DOI: 10.1002/cncy.21915]

308 **Norton ID**, Zheng Y, Wiersema MS, Greenleaf J, Clain JE, Dimagno EP. Neural network analysis of EUS images to differentiate between pancreatic malignancy and pancreatitis. *Gastrointest Endosc*

2001; **54**: 625-629 [PMID: 11677484 DOI: 10.1067/mge.2001.118644]
309 **Qiu W**, Duan N, Chen X, Ren S, Zhang Y, Wang Z, Chen R. Pancreatic Ductal Adenocarcinoma: Machine Learning-Based Quantitative Computed Tomography Texture Analysis For Prediction Of Histopathological Grade. *Cancer Manag Res* 2019; **11**: 9253-9264 [PMID: 31802945 DOI: 10.2147/CMAR.S218414]
310 **Săftoiu A**, Vilmann P, Dietrich CF, Iglesias-Garcia J, Hocke M, Seicean A, Ignee A, Hassan H, Streba CT, Ioncică AM, Gheonea DI, Ciurea T. Quantitative contrast-enhanced harmonic EUS in differential diagnosis of focal pancreatic masses (with videos). *Gastrointest Endosc* 2015; **82**: 59-69 [PMID: 25792386 DOI: 10.1016/j.gie.2014.11.040]
311 **Săftoiu A**, Vilmann P, Gorunescu F, Gheonea DI, Gorunescu M, Ciurea T, Popescu GL, Iordache A, Hassan H, Iordache S. Neural network analysis of dynamic sequences of EUS elastography used for the differential diagnosis of chronic pancreatitis and pancreatic cancer. *Gastrointest Endosc* 2008; **68**: 1086-1094 [PMID: 18656186 DOI: 10.1016/j.gie.2008.04.031]
312 **Săftoiu A**, Vilmann P, Gorunescu F, Janssen J, Hocke M, Larsen M, Iglesias-Garcia J, Arcidiacono P, Will U, Giovannini M, Dietrich CF, Havre R, Gheorghe C, McKay C, Gheonea DI, Ciurea T; European EUS Elastography Multicentric Study Group. Efficacy of an artificial neural network-based approach to endoscopic ultrasound elastography in diagnosis of focal pancreatic masses. *Clin Gastroenterol Hepatol* 2012; **10**: 84-90.e1 [PMID: 21963957 DOI: 10.1016/j.cgh.2011.09.014]
313 **Yeaton P**, Sears RJ, Ledent T, Salmon I, Kiss R, Decaestecker C. Discrimination between chronic pancreatitis and pancreatic adenocarcinoma using artificial intelligence-related algorithms based on image cytometry-generated variables. *Cytometry* 1998; **32**: 309-316 [PMID: 9701400 DOI: 10.1002/(sici)1097-0320(19980801)32:4<309::aid-cyto8>3.0.co;2-c]
314 **Zhu M**, Xu C, Yu J, Wu Y, Li C, Zhang M, Jin Z, Li Z. Differentiation of pancreatic cancer and chronic pancreatitis using computer-aided diagnosis of endoscopic ultrasound (EUS) images: a diagnostic test. *PLoS One* 2013; **8**: e63820 [PMID: 23704940 DOI: 10.1371/journal.pone.0063820]
315 **Luo Y**, Chen X, Chen J, Song C, Shen J, Xiao H, Chen M, Li ZP, Huang B, Feng ST. Preoperative Prediction of Pancreatic Neuroendocrine Neoplasms Grading Based on Enhanced Computed Tomography Imaging: Validation of Deep Learning with a Convolutional Neural Network. *Neuroendocrinology* 2020; **110**: 338-350 [PMID: 31525737 DOI: 10.1159/000503291]
316 **Chakraborty J**, Midya A, Gazit L, Attiyeh M, Langdon-Embry L, Allen PJ, Do RKG, Simpson AL. CT radiomics to predict high-risk intraductal papillary mucinous neoplasms of the pancreas. *Med Phys* 2018; **45**: 5019-5029 [PMID: 30176047 DOI: 10.1002/mp.13159]
317 **Corral JE**, Hussein S, Kandel P, Bolan CW, Bagci U, Wallace MB. Deep Learning to Classify Intraductal Papillary Mucinous Neoplasms Using Magnetic Resonance Imaging. *Pancreas* 2019; **48**: 805-810 [PMID: 31210661 DOI: 10.1097/MPA.0000000000001327]
318 **Dmitriev K**, Kaufman AE, Javed AA, Hruban RH, Fishman EK, Lennon AM, Saltz JH. Classification of Pancreatic Cysts in Computed Tomography Images Using a Random Forest and Convolutional Neural Network Ensemble. *Med Image Comput Comput Assist Interv* 2017; **10435**: 150-158 [PMID: 29881827 DOI: 10.1007/978-3-319-66179-7_18]
319 **Kurita Y**, Kuwahara T, Hara K, Mizuno N, Okuno N, Matsumoto S, Obata M, Koda H, Tajika M, Shimizu Y, Nakajima A, Kubota K, Niwa Y. Diagnostic ability of artificial intelligence using deep learning analysis of cyst fluid in differentiating malignant from benign pancreatic cystic lesions. *Sci Rep* 2019; **9**: 6893 [PMID: 31053726 DOI: 10.1038/s41598-019-43314-3]
320 **Kuwahara T**, Hara K, Mizuno N, Okuno N, Matsumoto S, Obata M, Kurita Y, Koda H, Toriyama K, Onishi S, Ishihara M, Tanaka T, Tajika M, Niwa Y. Usefulness of Deep Learning Analysis for the Diagnosis of Malignancy in Intraductal Papillary Mucinous Neoplasms of the Pancreas. *Clin Transl Gastroenterol* 2019; **10**: 1-8 [PMID: 31117111 DOI: 10.14309/ctg.0000000000000045]
321 **Li H**, Shi K, Reichert M, Lin K, Tselousov N, Braren R, Fu D, Schmid R, Li J, Menze B. Differential Diagnosis for Pancreatic Cysts in CT Scans Using Densely-Connected Convolutional Networks. *Annu Int Conf IEEE Eng Med Biol Soc* 2019; **2019**: 2095-2098 [PMID: 31946314 DOI: 10.1109/EMBC.2019.8856745]
322 **Okoń K**, Tomaszewska R, Nowak K, Stachura J. Application of neural networks to the classification of pancreatic intraductal proliferative lesions. *Anal Cell Pathol* 2001; **23**: 129-136 [PMID: 12082293 DOI: 10.1155/2001/657268]
323 **Song JW**, Lee JH, Choi JH, Chun SJ. Automatic differential diagnosis of pancreatic serous and mucinous cystadenomas based on morphological features. *Comput Biol Med* 2013; **43**: 1-15 [PMID: 23200461 DOI: 10.1016/j.compbiomed.2012.10.009]
324 **Springer S**, Masica DL, Dal Molin M, Douville C, Thoburn CJ, Afsari B, Li L, Cohen JD, Thompson E, Allen PJ, Klimstra DS, Schattner MA, Schmidt CM, Yip-Schneider M, Simpson RE, Fernandez-Del Castillo C, Mino-Kenudson M, Brugge W, Brand RE, Singhi AD, Scarpa A, Lawlor R, Salvia R, Zamboni G, Hong SM, Hwang DW, Jang JY, Kwon W, Swan N, Geoghegan J, Falconi M, Crippa S, Doglioni C, Paulino J, Schulick RD, Edil BH, Park W, Yachida S, Hijioka S, van Hooft J, He J, Weiss MJ, Burkhart R, Makary M, Canto MI, Goggins MG, Ptak J, Dobbyn L, Schaefer J, Sillman N, Popoli M, Klein AP, Tomasetti C, Karchin R, Papadopoulos N, Kinzler KW, Vogelstein B, Wolfgang CL, Hruban RH, Lennon AM. A multimodality test to guide the management of patients with a pancreatic cyst. *Sci Transl Med* 2019; **11** [PMID: 31316009 DOI: 10.1126/scitranslmed.aav4772]
325 **Wei R**, Lin K, Yan W, Guo Y, Wang Y, Li J, Zhu J. Computer-Aided Diagnosis of Pancreas Serous Cystic Neoplasms: A Radiomics Method on Preoperative MDCT Images. *Technol Cancer Res Treat*

2019; **18**: 1533033818824339 [PMID: 30803366 DOI: 10.1177/1533033818824339]

326 **Yang J**, Guo X, Ou X, Zhang W, Ma X. Discrimination of Pancreatic Serous Cystadenomas From Mucinous Cystadenomas With CT Textural Features: Based on Machine Learning. *Front Oncol* 2019; **9**: 494 [PMID: 31245294 DOI: 10.3389/fonc.2019.00494]

327 **Blyuss O**, Zaikin A, Cherepanova V, Munblit D, Kiseleva EM, Prytomanova OM, Duffy SW, Crnogorac-Jurcevic T. Development of PancRISK, a urine biomarker-based risk score for stratified screening of pancreatic cancer patients. *Br J Cancer* 2020; **122**: 692-696 [PMID: 31857725 DOI: 10.1038/s41416-019-0694-0]

328 **Facciorusso A**, Del Prete V, Antonino M, Buccino VR, Muscatiello N. Response to repeat echoendoscopic celiac plexus neurolysis in pancreatic cancer patients: A machine learning approach. *Pancreatology* 2019; **19**: 866-872 [PMID: 31375433 DOI: 10.1016/j.pan.2019.07.038]

329 **Hayward J**, Alvarez SA, Ruiz C, Sullivan M, Tseng J, Whalen G. Machine learning of clinical performance in a pancreatic cancer database. *Artif Intell Med* 2010; **49**: 187-195 [PMID: 20483571 DOI: 10.1016/j.artmed.2010.04.009]

330 **Kaissis G**, Ziegelmayer S, Lohöfer F, Algül H, Eiber M, Weichert W, Schmid R, Friess H, Rummeny E, Ankerst D, Siveke J, Braren R. A machine learning model for the prediction of survival and tumor subtype in pancreatic ductal adenocarcinoma from preoperative diffusion-weighted imaging. *Eur Radiol Exp* 2019; **3**: 41 [PMID: 31624935 DOI: 10.1186/s41747-019-0119-0]

331 **Li K**, Xiao J, Yang J, Li M, Xiong X, Nian Y, Qiao L, Wang H, Eresen A, Zhang Z, Hu X, Wang J, Chen W. Association of radiomic imaging features and gene expression profile as prognostic factors in pancreatic ductal adenocarcinoma. *Am J Transl Res* 2019; **11**: 4491-4499 [PMID: 31396352]

332 **Walczak S**, Velanovich V. An Evaluation of Artificial Neural Networks in Predicting Pancreatic Cancer Survival. *J Gastrointest Surg* 2017; **21**: 1606-1612 [PMID: 28776157 DOI: 10.1007/s11605-017-3518-7]

333 **Xu W**, Liu Y, Lu Z, Jin ZD, Hu YH, Yu JG, Li ZS. A new endoscopic ultrasonography image processing method to evaluate the prognosis for pancreatic cancer treated with interstitial brachytherapy. *World J Gastroenterol* 2013; **19**: 6479-6484 [PMID: 24151368 DOI: 10.3748/wjg.v19.i38.6479]

334 **Zhang Y**, Lobo-Mueller EM, Karanicolas P, Gallinger S, Haider MA, Khalvati F. CNN-based survival model for pancreatic ductal adenocarcinoma in medical imaging. *BMC Med Imaging* 2020; **20**: 11 [PMID: 32013871 DOI: 10.1186/s12880-020-0418-1]

335 **Li S**, Jiang H, Wang Z, Zhang G, Yao YD. An effective computer aided diagnosis model for pancreas cancer on PET/CT images. *Comput Methods Programs Biomed* 2018; **165**: 205-214 [PMID: 30337075 DOI: 10.1016/j.cmpb.2018.09.001]

336 **Liu SL**, Li S, Guo YT, Zhou YP, Zhang ZD, Lu Y. Establishment and application of an artificial intelligence diagnosis system for pancreatic cancer with a faster region-based convolutional neural network. *Chin Med J (Engl)* 2019; **132**: 2795-2803 [PMID: 31856050 DOI: 10.1097/CM9.0000000000000544]

337 **Mehrabi S**, Krishnan A, Roch AM, Schmidt H, Li D, Kesterson J, Beesley C, Dexter P, Schmidt M, Palakal M, Liu H. Identification of Patients with Family History of Pancreatic Cancer--Investigation of an NLP System Portability. *Stud Health Technol Inform* 2015; **216**: 604-608 [PMID: 26262122]

338 **Ozkan M**, Cakiroglu M, Kocaman O, Kurt M, Yilmaz B, Can G, Korkmaz U, Dandil E, Eksi Z. Age-based computer-aided diagnosis approach for pancreatic cancer on endoscopic ultrasound images. *Endosc Ultrasound* 2016; **5**: 101-107 [PMID: 27080608 DOI: 10.4103/2303-9027.180473]

339 **Roch AM**, Mehrabi S, Krishnan A, Schmidt HE, Kesterson J, Beesley C, Dexter PR, Palakal M, Schmidt CM. Automated pancreatic cyst screening using natural language processing: a new tool in the early detection of pancreatic cancer. *HPB (Oxford)* 2015; **17**: 447-453 [PMID: 25537257 DOI: 10.1111/hpb.12375]

340 **Zhang MM**, Yang H, Jin ZD, Yu JG, Cai ZY, Li ZS. Differential diagnosis of pancreatic cancer from normal tissue with digital imaging processing and pattern recognition based on a support vector machine of EUS images. *Gastrointest Endosc* 2010; **72**: 978-985 [PMID: 20855062 DOI: 10.1016/j.gie.2010.06.042]

341 **Liu X**, Rivera SC, Moher D, Calvert MJ, Denniston AK; SPIRIT-AI and CONSORT-AI Working Group. Reporting guidelines for clinical trial reports for interventions involving artificial intelligence: the CONSORT-AI Extension. *BMJ* 2020; **370**: m3164 [PMID: 32909959 DOI: 10.1136/bmj.m3164]

342 **Krittanawong C**, Johnson KW, Rosenson RS, Wang Z, Aydar M, Baber U, Min JK, Tang WHW, Halperin JL, Narayan SM. Deep learning for cardiovascular medicine: a practical primer. *Eur Heart J* 2019; **40**: 2058-2073 [PMID: 30815669 DOI: 10.1093/eurheartj/ehz056]

World Journal of Gastroenterology

Submit a Manuscript: https://www.f6publishing.com

World J Gastroenterol 2021 October 28; 27(40): 6825-6843

DOI: 10.3748/wjg.v27.i40.6825

ISSN 1007-9327 (print) ISSN 2219-2840 (online)

MINIREVIEWS

Emerging artificial intelligence applications in liver magnetic resonance imaging

Charles E Hill, Luca Biasiolli, Matthew D Robson, Vicente Grau, Michael Pavlides

ORCID number: Charles E Hill 0000-0001-5825-030X; Luca Biasiolli 0000-0002-0452-8756; Matthew D Robson 0000-0002-5902-1012; Vicente Grau 0000-0001-8139-3480; Michael Pavlides 0000-0001-9882-8874.

Author contributions: Hill CE did the literature search and drafted the manuscript; all other authors revised the manuscript for important intellectual content.

Supported by the Engineering and Physical Sciences Research Council and Medical Research Council, No. EP/L016052/1.

Conflict-of-interest statement: Pavlides M is a shareholder for the company Perspectum Ltd. and has applied for a patent for medical imaging; All other authors declare no conflicts of interest; Robson M is an employee and shareholder for the company Perspectum Ltd.; Hill CE is partially funded by the company Perspectum Ltd.

Open-Access: This article is an open-access article that was selected by an in-house editor and fully peer-reviewed by external reviewers. It is distributed in accordance with the Creative Commons Attribution NonCommercial (CC BY-NC 4.0) license, which permits others to distribute, remix, adapt, build upon this work non-commercially,

Charles E Hill, Department of Engineering Science, University of Oxford, Oxford OX3 7DQ, United Kingdom

Luca Biasiolli, Radcliffe Department of Medicine, University of Oxford, Oxford OX3 9DU, United Kingdom

Matthew D Robson, MR Physics, Perspectum Ltd, Oxford OX4 2LL, United Kingdom

Vicente Grau, Department of Engineering, University of Oxford, Oxford OX3 7DQ, United Kingdom

Michael Pavlides, Oxford Centre for Clinical Magnetic Resonance Research, Division of Cardiovascular Medicine, Radcliffe Department of Medicine, University of Oxford, Oxford OX3 9DU, United Kingdom

Michael Pavlides, Translational Gastroenterology Unit, University of Oxford, Oxford OX3 9DU, United Kingdom

Michael Pavlides, Oxford NIHR Biomedical Research Centre, University of Oxford, Oxford OX3 9DU, United Kingdom

Corresponding author: Michael Pavlides, BSc, DPhil, MBBS, MRCP, Consultant Physician-Scientist, Doctor, Oxford Centre for Clinical Magnetic Resonance Research, Division of Cardiovascular Medicine, Radcliffe Department of Medicine, University of Oxford, Level 0, John Radcliffe Hospital, Headley Way, Headington, Oxford OX3 9DU, United Kingdom. michael.pavlides@cardiov.ox.ac.uk

Abstract

Chronic liver diseases (CLDs) are becoming increasingly more prevalent in modern society. The use of imaging techniques for early detection, such as magnetic resonance imaging (MRI), is crucial in reducing the impact of these diseases on healthcare systems. Artificial intelligence (AI) algorithms have been shown over the past decade to excel at image-based analysis tasks such as detection and segmentation. When applied to liver MRI, they have the potential to improve clinical decision making, and increase throughput by automating analyses. With Liver diseases becoming more prevalent in society, the need to implement these techniques to utilize liver MRI to its full potential, is paramount. In this review, we report on the current methods and applications of AI methods in liver MRI, with a focus on machine learning and deep learning methods. We

and license their derivative works on different terms, provided the original work is properly cited and the use is non-commercial. See: http://creativecommons.org/licenses/by-nc/4.0/

Manuscript source: Invited manuscript

Specialty type: Gastroenterology and hepatology

Country/Territory of origin: United Kingdom

Peer-review report's scientific quality classification

Grade A (Excellent): A
Grade B (Very good): B
Grade C (Good): 0
Grade D (Fair): 0
Grade E (Poor): 0

Received: February 6, 2021
Peer-review started: February 6, 2021
First decision: March 29, 2021
Revised: April 16, 2021
Accepted: September 26, 2021
Article in press: September 30, 2021
Published online: October 28, 2021

P-Reviewer: Karavaş E, Wang CY
S-Editor: Gong ZM
L-Editor: A
P-Editor: Gong ZM

assess four main themes of segmentation, classification, image synthesis and artefact detection, and their respective potential in liver MRI and the wider clinic. We provide a brief explanation of some of the algorithms used and explore the current challenges affecting the field. Though there are many hurdles to overcome in implementing AI methods in the clinic, we conclude that AI methods have the potential to positively aid healthcare professionals for years to come.

Key Words: Liver diseases; Magnetic resonance imaging; Machine learning; Deep learning; Artificial intelligence; Computer vision

©The Author(s) 2021. Published by Baishideng Publishing Group Inc. All rights reserved.

Core Tip: Artificial Intelligence (AI) algorithms are becoming increasingly prevalent in magnetic resonance imaging (MRI) after their proven success in computer vision tasks. With regards to liver MRI, these methods have been shown to be successful in tasks from hepatocellular carcinoma detection, to motion reduction to improve undiagnostic scans. They have also been shown in some cases to outperform radiographer level performance. The widespread use of these techniques could positively aid clinicians for years to come, if implemented properly into clinical workflows.

Citation: Hill CE, Biasiolli L, Robson MD, Grau V, Pavlides M. Emerging artificial intelligence applications in liver magnetic resonance imaging. *World J Gastroenterol* 2021; 27(40): 6825-6843
URL: https://www.wjgnet.com/1007-9327/full/v27/i40/6825.htm
DOI: https://dx.doi.org/10.3748/wjg.v27.i40.6825

INTRODUCTION

Since the advent of magnetic resonance imaging (MRI) in the 1970s, its use has grown exponentially worldwide, due to its ability to give high resolution images in the body, allowing the early diagnosis and accurate prognosis of many diseases[1,2]. In contrast to computed tomography (CT), MRI uses no ionising radiation, has superior soft tissue contrast and allows the probing of metabolic processes due to the ubiquitous nature of water in our bodies. With regards to the liver, it has become an essential tool for anatomical assessment. In addition, current cutting edge methods allow for quantification of liver fat, liver iron and staging of fibrosis levels within the liver[3-5]. These methods have the possibility to provide early detection and staging of many chronic liver diseases (CLDs), and are becoming more in demand with the rising prevalence in liver disease in western society. With 1/3 of adults believed to have non-alcoholic fatty liver disease (NAFLD) and 12% the more severe non-alcoholic steatohepatitis (NASH), NAFLD has been defined as a silent pandemic and the most prevalent liver disease in human history[6-9]. As there is currently no medical treatment for NAFLD beyond lifestyle interventions, the need for early detection is paramount, so that the disease progression can be halted and reversed, and MRI can play an important role in this [10].

The need for early detection is not only limited to CLDs but is also important in detection of liver cell cancer (hepatocellular cancer; HCC). With mortality rates from HCC predicted to rise to become the third highest leading cause of cancer-related deaths in the US by 2030, the need for early diagnosis is needed so that treatment can be effective[11]. Currently this requires expert radiologists studying liver MRI scans trying to find a tumour. Though many tumours are identified, some tumours can also be missed, with one study finding that 16% of lesions were missed in multiparametric MR imaging of the prostate, highlighting the need for a method for identifying these missed cases[12].

Early detection can be addressed in many liver diseases using liver MRI. The current gold standard for staging is liver biopsy, however, it is invasive, is localized (sampling error) and has risk of complications[13]. Liver MRI is overtaking this standard, due to being non-invasive and allowing global metrics to be calculated across the whole liver. When diagnosing liver fibrosis stage, an important biomarker

in staging NAFLD, many different sequences have predictive potential, such as MRE, T1 and T2* mapping, diffusion weighted imaging (DWI) and hepatocellular function imaging using contrast agents[14]. When identifying HCC within the liver, hepatocellular function imaging is commonly used, however DWI also has good predictive power[15,16]. These methods all require a level of expert analysis to interpret the images, similarly to biopsies, which means they are prime candidates for automation using AI methods.

Artificial intelligence (AI) techniques, have been shown to perform well when applied to computer vision problems, from classification of objects in a photograph to fast object segmentation of video frames for self-driving cars[17,18]. These techniques have also been applied successfully to many areas of MRI in the body, such as segmentation of brain tissue, ejection fraction prediction and diagnosis of heart conditions[19-21]. An AI approach to report mammograms for the presence of breast cancer has been shown to outperform radiologist reporting[22]. AI techniques in Liver MRI are relatively underdeveloped compared to brain and cardiac MRI, but nevertheless, they provide opportunities to alleviate workload in many settings.

In this review, we assess the current gold standard of AI in liver imaging. Specifically, we review the recent application of AI techniques for segmentation (Table 1), classification (Table 2) and image synthesis for different CLDs and MR imaging techniques. We briefly provide an overview of AI techniques in the field, describe the implementation of AI to achieve these applications and explain how they are quantitatively and qualitatively assessed. We explore the publications that have sought to solve these problems and assess the challenges that still face the field.

AI ALGORITHMS

We broadly focus on two subsets of AI algorithms: traditional machine learning (ML) algorithms and deep learning (DL) algorithms. Traditional machine learning algorithms often rely on the input of handcrafted features, an additional piece of data which has been derived from acquired data. In the case of MR images, these handcrafted features are often statistical measurements such as the mean intensity of the image or a sub region of the image, and are called radiomic features as they are derived from medical images. These radiomic features are then passed to a statistical model, such as a support vector machine (SVM), kMeans Clustering, random forests or a naïve bayes algorithm among many others[23,24]. These models can either be supervised, where you have a desired target outcome, or unsupervised, where no target outcome is enforced. When you have selected the appropriate model for your task, the model is then trained. In the case of supervised models, the model updates its parameters to minimise the error between your desired output and the model output, as new data is sequentially passed to it. An example would be inputting radiomic features extracted from tumours and the model getting better at classifying the tumours into their classes, such as hepatocellular carcinoma (HCC) or intrahepatic cholangiocarcinoma (ICC), as it updates its parameters to minimise the error between its output prediction and the ground truth. In the case of unsupervised models, the model updates its parameters to be able to separate input data into a predefined number of classes, without knowledge of what those classes may be. In the above example, you would input the radiomic features from different tumours and ask the model to output two distinct classes for HCC and ICC, without explicitly giving the model information about which tumour corresponds to which class. During training you monitor the success at a desired task and stop training once the model performance meets some predefined criteria, such as the model no longer improving even when new data is added. If the model is accurate, *i.e.*, it rivals human performance, it can then be used in a research or clinical setting.

LeCun *et al*[25] defines DL methods as ML methods with multiple levels of features, obtained by composing simple but non-linear modules that each transform the feature at one level (starting with the raw input) into a feature at a higher, slightly more abstract level. In essence, this means that DL algorithms calculate successive features based on the features or data that you provide it. The most common way of doing this in MR images is to employ convolutional layers. A convolution, in terms of images, is a filter of a defined size, which when applied to a portion of an MR image of the liver equal to the size of the filter, outputs a singular value, as shown in Figure 1. When applied sequentially to a whole scan, it outputs an image containing these values, known as a feature map. Additional convolutional layers are applied to these feature maps, to produce feature maps with deeper information. When these layers are

Table 1 Applications of artificial intelligence segmentation methods to liver magnetic resonance imaging

Ref.	Task	Method	MR image	DICE
Mole *et al*[37], 2020	Segment liver from T1 mapping technique to aid surgical planning	3D U-Net	T1 map	0.97
Winther *et al*[27], 2020	Segment liver from Gd-EOB-DTPA-enhanced MRI for volume calculations	3D U-Net	Gadoxetic acid-enhanced MRI	0.96 ± 1.9
Liu *et al*[30], 2020	Segment liver for automated liver iron quantification	2D U-Net	T2* map	0.86 ± 0.01
Wang *et al*[43], 2019	Segment Liver across multiple imaging modalities and techniques	2D U-Net	T1- and T2*- weighted	T1-w: 0.95 ± 0.03 T2-w: 0.92 ± 0.05
Cunha *et al*[46], 2020	Segment liver to classify if adequate contrast uptake has occurred in contrast enhanced scans	2D U-Net	Pre- and post-contrast T1-weighted, and T2- weighted	Not reported
Chen *et al*[31], 2020	Segment multiple organs in abdominal scans, to aid radiotherapy planning	2D Dense U-Net	T1-weighted	Liver: 0.96 ± 0.009
Bousabarah *et al*[36], 2020	Segment and delineate HCCs	2D U-Net	Gadoxetic acid-enhanced MRI	Liver: 0.91 ± 0.01 Tumour: 0.68 ± 0.03
Ivashchenko *et al*[41], 2019	Segment liver, vasculature and biliary tree	4D k-mean clustering	Gadoxetic acid-enhanced MRI	Liver: 0.95 ± 0.01
Irving *et al*[44], 2017	Segment liver with vessel exclusion to assist in liver assessment	2D U-Net	T1 map	0.95
Yang *et al*[45], 2019	Segment liver across multiple domains *via* domain transfer	Cycle GAN and 2D U-Net	Gadoxetic acid-enhanced MRI	0.891 ± 0.040
Christ *et al*[39], 2017	Segment liver and tumours within, in CT and MRI	Two sequential 2D U-Nets	Diffusion-weighted	Liver: 0.87 Tumour: 0.697
Fu *et al*[35], 2018	Segment multiple organs in abdominal scans, to aid radiotherapy planning	Three Dense CNNs	T2/T1-weighted	Liver: 0.953 ± 0.007
Valindria *et al*[33], 2018	Segment multiple organs in multi-modal (MR,CT) scans	ResNet Encoder Decoder	T2-weighted	Liver: 0.914
Masoumi *et al*[42], 2012	Segment the liver	Watershed (non-AI) + ANN	Abdominal MRI	0.94 (IoU not DICE)
Jansen *et al*[40], 2019	Segment liver and metastases	CNN	DCE-MR and diffusion-weighted	Liver: 0.95

MRI: Magnetic resonance imaging; CT: Computed tomography; DCE-MR: Dynamic contrast enhanced magnetic resonance; HCC: Hepatocellular carcinoma; GAN: Generative adversarial network; CNN: Convolutional neural network; ANN: Artificial neural network; IoU: Intersect over union.

stacked together, a convolutional neural network (CNN) is generated. The final convolutional layer generates the desired size of your output, anything from a single value to classify the disease state, or a new image which could be a segmentation map of the liver. Like traditional machine learning, the accuracy of the output compared to a gold standard measurement, is maximised during training.

SEGMENTATION

Segmentation describes the process by which anatomical structures can be selected from a radiological image. Anatomical structures can be organs like the liver, tissues like subcutaneous and visceral fat or malignant deposits. Metrics resulting from the segmentation process and segmentation maps can help with estimation of volumes (*e.g.*, liver volume), important metabolic ratios (ratio of visceral to subcutaneous fat) and provide important anatomical information that can help in the radiotherapy and surgical planning for the treatment of malignant tumours[26,27]. Segmentation can therefore play an important role in many aspects of clinical decision making. Segmentation maps are also often used in quantitative techniques, such as T1 mapping and MRE, to give accurate measurements across the whole liver and not just in a region of interest[26,28].

Table 2 Applications of artificial intelligence classification methods using liver magnetic resonance imaging

Ref.	Task	Method	MR image	Accuracy	Sensitivity	Specificity	AUROC
Hectors *et al* [60], 2020	Stage liver fibrosis	VGG16 CNN	Gadoxetic acid-enhanced MRI	F1-4: 0.69 F2-4: 0.85 F3-4: 0.85 F4: 0.78	F1-4: 0.64 F2-4: 0.82 F3-4: 0.87 F4: 0.73	F1-4: 0.90 F2-4: 0.93 F3-4: 0.83 F4: 0.81	F1-4: 0.77 F2-4: 0.91 F3-4: 0.90 F4: 0.85
Liu *et al*[55], 2021	Classify cHCC-CC *vs* non-cHCC-CC and HCC *vs* non-HCC	Radiomics + SVM	Gadoxetic acid-enhanced MRI	cHCC-CC *vs* non-cHCC-CC: 0.77 HCC *vs* non-HCC: -	cHCC-CC *vs* non-cHCC-CC: 0.65 HCC *vs* non-HCC: 0.68	cHCC-CC *vs* non-cHCC-CC: 0.81 HCC *vs* non-HCC: 0.88	cHCC-CC *vs* non-cHCC-CC: 0.77 HCC *vs* non-HCC: 0.79
Wu *et al*[48], 2020	Classify tumours according to their LI-RADS grade	AlexNet CNN	Gadoxetic acid-enhanced MRI	0.9	1	0.835	0.95
Messaoudi *et al*[50], 2020	Classify tumours into HCC or non-HCC	Patch based CNN	Multiphase 3D fast spoiled gradient echo T1	0.9	?	?	?
Hamm *et al* [51], 2019	Classify tumours into type and LI-RADS derived classes	CNN	Multiphase contrast-enhanced T1-weighted MRI	Lesion class: 0.919 LI-RADS: 0.943	Lesion class: 0.90 LI-RADS: 0.92	Lesion class: 0.98 LI-RADS: 0.97	LI-RADS (HCC): 0.922
Trivizakis *et al*[54], 2018	Classify tumours into primary or metastatic	3D CNN + SVM	Diffusion weighted MRI	0.83	0.93	0.67	0.8
He *et al*[65], 2019	Correctly predict liver stiffness using clinical and radiomic data	Radiomics + SVM	T2-weighted MRI	0.818	0.722	0.87	0.84
Schawkat *et al*[61], 2020	Stage liver fibrosis into low-stage (F0-2) and high-stage (F3-4)	Radiomics + SVM	T1-weighted MRI, T2-weighted MRI	T1-w: 0.857 T2-w: 0.619	?	?	T1-w: 0.82 T2-w: 0.57
Lewis *et al* [56], 2019	Distinguish HCC from other primary cancers	Radiomics + Binary logistic regression	Diffusion weighted MRI	Observer 1: 0.815 Observer 2: 0.80	Observer 1: 0.793 Observer 2: 0.862	Observer 1: 0.889 Observer 2: 0.778	Observer 1: 0.90 Observer 2: 0.89
Wu *et al*[57], 2019	Classify tumours into HCC and HH	Radiomics + logistic regression	T2-weighted MRI, Diffusion weighted MRI, T1-weighted GRE in phase and out of phase MRI	?	0.822	0.714	0.89
Oyama *et al* [58], 2019	Classification of hepatic tumours into HCC, HH and MT	Radiomics + logistic regression/XGBoost	T1-weighted MRI	HCC *vs* MT: 0.92 HCC *vs* HH: 0.9 MT *vs* HH: 0.73	HCC *vs* MT: 1.0 HCC *vs* HH: 0.96 MT *vs* HH: 0.72	HCC *vs* MT: 0.84 HCC *vs* HH: 0.84 MT *vs* HH: 0.74	HCC *vs* MT: 0.95 HCC *vs* HH: 0.95 MT *vs* HH: 0.75
Wu *et al*[59], 2019	Predict pre-operative HCC grade	Combined clinical data and Radiomics + logistic regression	T2/T1-weighted	0.761	0.85	0.65	0.8
Chen *et al* [69], 2019	Predict pre-treatment immunscore in HCC	Combined clinical data and radiomics + multi-vote decision trees	Gadoxetic acid-enhanced MRI	0.842	0.846	0.841	0.934
Park *et al* [63], 2019	Stage liver fibrosis	Radiomics + logistic regression	Gadoxetic acid-enhanced MRI	F2-4: 0.803 F3-4: 0.803 F4: 0.813	F2-4: 0.814 F3-4: 0.789 F4: 0.921	F2-4: 0.784 F3-4: 0.820 F4: 0.754	F2-4: 0.91 F3-4: 0.88 F4: 0.87
Zhao *et al* [67], 2019	Predict early reoccurrence of IMCC	Combined clinical data and radiomics + logistic regression	T2-weighted MRI, gadoxetic acid-enhanced MRI	0.872	0.938	0.839	0.949

Reimer *et al* [68], 2018	Predict therapy response to transarterial radioembolization	Radiomics + logistic regression	Gadoxetic acid-enhanced MRI	?	Arterial phase: 0.83 Venous phase: 0.71	Arterial phase: 0.62 Venous phase: 0.85	Arterial phase: 0.73 Venous phase: 0.76
Zhen *et al* [53], 2020	Classify liver tumours into benign , HCC, metastatic or other primary malignancy	CNN with clinical input	T2, diffusion, Pre-contrast T1, late arterial, portal venous, and equilibrium phase	0.919	HCC: 0.957 Metastatic: 0.946 Other primary: 0.733	HCC: 0.904 Metastatic: 1.0 Other primary: 0.964	HCC: 0.951 Metastatic: 0.985 Other primary: 0.989
Yasaka *et al* [62], 2017	Stage liver fibrosis	CNN	Gadoxetic acid-enhanced MRI	F4 *vs* F3-0: 0.75 F4-3 *vs* F2-0: 0.77 F4-2 *vs* F1-0: 0.80	F4 *vs* F3-0: 0.76 F4-3 *vs* F2-0: 0.78 F4-2 *vs* F1-0: 0.84	F4 *vs* F3-0: 0.76 F4-3 *vs* F2-0: 0.74 F4-2 *vs* F1-0: 0.65	F4 *vs* F3-0: 0.84 F4-3 *vs* F2-0: 0.84 F4-2 *vs* F1-0: 0.84
Kim *et al* [70], 2019	Predict postoperative early and late recurrence of single HCC	Radiomics + random forests	Gadoxetic acid-enhanced MRI	Harrel C-statistic: 0.716 in combined radiomic and clinicopathologic model, no significant difference to clinicopathologic model (0.696)			
Kim *et al* [52], 2020	Detect HCC	CNN	Gadoxetic acid-enhanced MRI	0.937	0.94	0.99	0.97
Liu *et al*[71], 2020	Identify clinically significant portal hypertension	CNN + logistic regression	?	?	0.929	0.846	0.94

MRI: Magnetic resonance imaging; GRE: Gradient recalled echo; LI-RADS: Liver Imaging Reporting and Data System; HCC: Hepatocellular carcinoma; HH: Hepatic hemangioma; MT: Metastatic tumour; CC: Cholangiocarcinoma; cHCC-CC: Combined hepatocellular cholangiocarcinoma; IMCC: Intrahepatic mass-forming cholangiocarcinoma; CNN: Convolutional neural network; SVM: Support vector machine; AUROC: Area under the receiver operating characteristic curve.

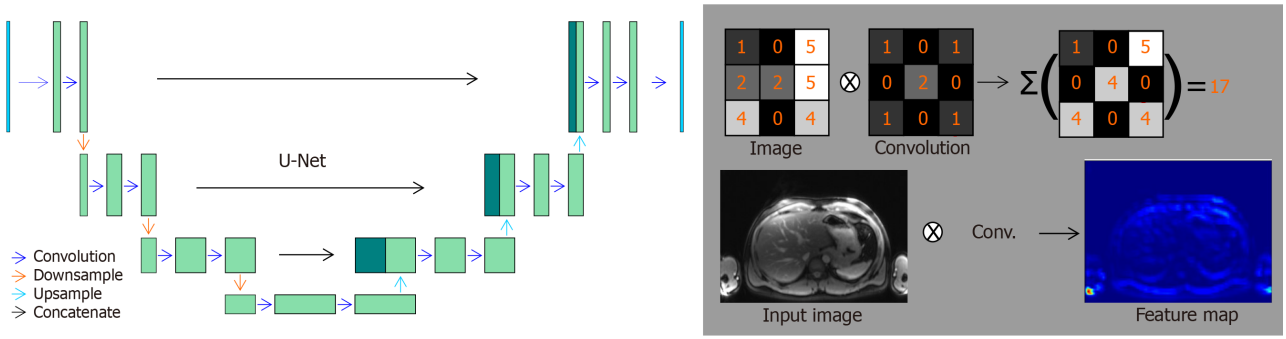


Figure 1 A deep convolutional network. An example deep learning segmentation network, the U-Net. A series of convolutions, combined with downsampling and upsampling to learn feature maps at different scales, are used to output a segmentation map. An example of a convolution, and feature map are shown on the right.

The segmentation processes are usually carried out manually using software tools for this purpose. However, these manual processes can be time consuming and inaccurate, and the introduction of automated AI methods can reliably supersede these methods, improving output and reliability by performing close to the level of expert radiologists in a much shorter time[28]. For example, automatic segmentation to measure liver fat, adipose tissue depots and muscle volume and fat content led to an improved risk stratification for the presence of type 2 diabetes and cardiovascular disease compared to discrete categorisations of body composition in a large population study (n = 10000)[29]. Such a study would not be possible without automatic segmentation to measure the parameters of interest.

When applying AI algorithms to segmentation tasks, the aim is to highlight every voxel in an MR image that applies to a certain class. For example, this could be that the voxel contains the liver, a tumour, or neither. Though different algorithms have different approaches to achieving this goal, they are all evaluated by their ability to

correctly identify which voxel of the MR image corresponds to which class. One common metric for evaluating this is the DICE score, which is defined as follows (Formula 1):

$$DICE = \frac{2TP}{2TP + FP + FN}$$

Where TP is the number of true positives, where the voxel has been correctly classified, FP the false positives, where the voxel has been incorrectly given a class instead of no class, and FN the false negatives, where a voxel which belongs to a desired class has been labelled as belonging to no class. If the DICE score is high, then the segmentation map is accurate. Additional metrics of performance do exist, such as intersect over union (IoU), where the closer to 1 the result is, the better the segmentation.

Though non-deep learning AI segmentation methods do exist, the majority of papers presented here are based on deep learning methods due to the successful application of these methods in natural image space, an example being the U-Net, as shown in Figure 1[30]. Though other methods are used, the U-Net is the most common due to its proven performance in segmentation maps, in part down to its ability to learn features at different scales due to the downsampling, and inclusion of previous feature maps in the concatenation steps.

Segmentation for surgical and radiotherapy planning

Segmentation maps are crucial in surgical planning, especially in giving the clinician information of the size and location of tumours, to allow for safe and successful surgery. They are also useful in radiotherapy planning, allowing the therapy to be performed such that there is minimal risk to organs and maximal damage to tumours.

Chen *et al*[31] and Huang *et al*[32] implemented a 2D U-Net, with densely connected blocks, to segment up to 10 organs at risk in radiotherapy. They achieved a DICE coefficient of 0.963 ± 0.0010 in the liver with high metrics in most of all the other organs studied. Likewise, Valindria *et al*[33] and He *et al*[34] trained a 2D residual network to segment out multiple organs in CT or MR scans which can similarly be used for radiotherapy planning. The use of both modalities increased performance in both their segmentation maps, achieving a DICE score of 0.914 in the liver, when compared to training with just one modality. This is still less than that achieved by Chen *et al*[31], even with the additional information from the CT scans used in the Valindria study. This may be due to the use of T2-weighted MR images being used by Valindria *et al*[33] as opposed to T1 -weighted. Fu *et al*[35] used a trio of CNNs to segment multiple organs in images acquired on a dual radiotherapy MR machine, in order to expediate the MRI guided adaptive radiotherapy. They achieved a DICE score of 0.953 ± 0.007 in the liver. The segmentations took approximately 5 s to produce and as such could not be used yet in a real-time radiotherapy setting, however, the method does still alleviate radiologist workflow, where they only quality control the output which takes a quarter of the time of a full manual segmentation. Bousabarah *et al*[36] automate the segmentation of the liver and classification of tumours within into the Liver Imaging Reporting and Data System (LI-RADS) classes. They used a 2D U-Net to segment contrast enhanced MR images into two segmentation maps, one of the liver and one of any tumours within. The proposed tumour segmentation then undergoes post-processing by using a random forest classifier using radiomic features extracted from the proposed region. The combined model detected 75% of lesions in the test data, when there was a DICE score of 0.2 or greater between the detected and actual tumour. The output could not only be used in surgery and radiotherapy planning, but also be used in conjunction with a radiologist's assessment to improve detection accuracy. They achieved a similar performance as Valindria *et al*[33], but with the harder task of segmenting out bodies within the liver itself, which will likely decrease performance in liver segmentation. Mole *et al*[37] and Owler *et al*[38] used a 3D U-Net to segment out the liver in a pipeline for surgical planning. They segmented the liver in a T1-mapping acquisition with a DICE score of 0.970. The metrics calculated using this segmentation map were used to predict post-operative liver function with a high degree of accuracy. This shows that the method could be used in determining whether a patient should go for surgery or whether other treatments should be considered. Christ *et al*[39] implemented two 2D U-Nets to segment out the liver and metastases within the liver, in both CT and MRI images, which could be used both for radiotherapy planning and measuring response to therapy. The first U-Net segments out the liver region, which is used to process the input MR image. The second U-Net segments out any tumours within this identified region. They achieved a DICE score of 0.87 when applied to diffusion weighted MRI images. Jansen *et al*[40] utilised

information from both dynamic contrast enhanced MRI (DCE-MRI) and DW-MRI to segment out the liver and metastases within, achieving a DICE score of 0.95 in the liver, and an accuracy of 96% in detecting the liver metastases.

Non-CNN based methods have also been used to segment out the liver in multi-phase contrast enhanced MRI[41]. Ivashchenko *et al*[41] used a K-means clustering algorithm on multiple phases of the contrast enhancement to generate 8 initial compartments. They then select a best candidate and apply multiple post-processing non-AI methods to generate a full segmentation of the liver, achieving a DICE score of 0.949 ± 1.2. This method could also be used to segment out the vessels and biliary tree, allowing safer execution of complicated liver resections. Masoumi *et al*[42] also used a non -CNN based method using both traditional non-AI methods, the watershed algorithm, and an artificial neural network (ANN) to automate the traditional algorithm. Six ANNs were trained to estimate 6 chosen features from the image, such as the ratio of the maximum and minimum diameter of the liver. These also extracted from the watershed algorithm and the error between the two feature sets calculated. This error is then iteratively used to update the watershed algorithm parameters until there is no longer a reduction in the error between the two feature sets. They achieved a mean Intersect over Union (IoU) of 0.94.

Segmentation of the liver when applied to surgical planning is, in most studies covered, exceeding a DICE score of 0.9. Variations in this value for the liver will likely be down to imaging protocol used (T1-weighted, T2-weighted, *etc.*), the patient group of interest, and the target outcome, in this case whether you are optimising to segment out the liver or whether it is a subtask among others, *e.g.*, segmenting out metastases or multiple over organs.

Segmentation for liver function assessment

Another application area for AI segmentation methods is liver function assessment. A full liver segmentation provides a more comprehensive estimation of liver function compared to region of interest placement. To get an overview of whole liver quantitative measures, radiologists must take the time to create these segmentations, that can easily be automated. Winther *et al*[27] showed that it is possible to segment out Gd-EOB-DTPA-enhanced liver MR images to calculate liver volumetry to assess hepatic functional reserve. They trained a 3D U-Net using the liver images of 100 patients, achieving a DICE score of 0.967 ± 0.019, when compared to two experts who had a corresponding DICE score of 0.952 ± 0.028. The segmentation time using a 3D U-Net took on average 60 s to generate a 3D segmentation map, compared to 10 min for an expert. Another study seeks to automate quantification of liver iron using a liver segmentation[30]. Liu *et al*[30] used a 2D U-Net to output a segmentation map for a T2* quantitative map, generated using 16 slices from the T2* relaxometry method used to calculate it. They achieved a DICE score of 0.86 ± 0.01 with the manual segmentations and subsequently a strong correlation of the liver iron in mg/g calculated using the automated and manual methods. This lower DICE score in T2*-weighted images correlates with the lower DICE score seen in the Valindria *et al*[33] study above, suggesting that it is harder for these networks to segment the liver in T2* weighted images, or that it is harder for humans to segment out the liver accurately in T2*-weighted images leading to a larger variation in your training dataset. Wang *et al*[43] implemented a 2D U-Net to segment the liver from abdominal MRI and CT scans. They achieved a DICE score of 0.95 in 100 T1-weighted MRI scans, and 0.92 in T2*-weighted MRI scans. They used the segmentations to automate the calculation of liver volumetry and hepatic PDFF, both of which had good agreement with manual segmentation derived values. Liver function assessment can also be performed during scanning. Irving *et al*[44], used a 2D U-Net to segment out the liver with exclusion of internal vasculature, so that quantitative liver T1 scores could be calculated. They achieved a DICE score of 0.95. The above four studies, all showed to have liver function assessment measurements that correlate with the current methods. Though, most of the measurements derived from the automated segmentations are usually derived from manual segmentations and so if the segmentation is accurate, then it should be expected that the output measurement would correlate highly. Yang *et al*[45] also used a 2D U-Net to generate segmentation maps of the liver, however by using a process known as disentangled representation, they were able to transform MR and CT images into a shared image space which contains only shared content. On these images, they achieved a DICE score or 0.891 ± 0.040. This segmentation network could be applied to multiple imaging modalities, which could be useful in clinical uptake as the end user won't have to carefully choose which model they apply. However, if accuracy of segmentation is the most important outcome, then many of the papers

covered here have shown better performance when seeking to maximise the segmentation accuracy in a single use case. Cunha *et al*[46] used AI methods to determine the optimal point for hepatobiliary phase acquisition in contrast enhanced MRI, thus avoiding overwaiting. They used a 2D U-Net to segment out a liver mask, which is applied to the original image. This masked liver is then passed to a classification CNN, which outputs a contrast uptake quality ranging from 0, minimal uptake, to 1, adequate uptake. They achieve an area under the receiver operating characteristic (AUROC) curve of 0.952 in the test set, indicating good classification accuracy. By applying their model in situ, they could reduce examination time in 48% of patients, by detecting when optimal uptake of contrast has occurred.

CLASSIFICATION

Classification or stratification is an important step in any disease treatment in healthcare. Without a proper classification of the disease causing symptoms, it is not possible to implement the correct medical response. Unfortunately, some diseases are hard to differentiate, even by experienced healthcare professionals. Providing additional support in this task could help ensure that patients are stratified correctly and swiftly. AI algorithms have been shown to deal well with image-to-class-based tasks, as demonstrated in applications to the ImageNet dataset[47].

AI classification algorithms are almost identical in their approach as segmentation networks. Whereas segmentation networks classify each voxel in an image, a classification seeks to classify all voxel in an image into a single class. They are evaluated against their ability to do this, by use of metrics such as accuracy, the percentage true positives and true negatives, sensitivity, the rate of true positives, specificity, the true negative rate, and by using receiver operating characteristic (ROC) curves, the true positive rate *vs* the false positive rate (1 – true negative rate/specificity), as shown in Figure 2.

Tumour detection and classification

Tumour classification is a useful tool in staging the severity of the cancer. The ability to differentiate between the various types of liver tumours would give the ability to medical professionals to implement an optimised treatment plan. Wu *et al*[48] used the AlexNet network architecture to classify cropped HCC tumours into either LR-3 (intermediate probability for HCC) or the combined class LR-4/LR-5 (likely/definite HCC respectively)[48,49]. They achieved a 90% accuracy in classification and an AUROC 0.95 with reference to an expert radiologist. Messaoudi *et al*[50] achieved similar accuracy when applying a CNN to classify HCC tumours from liver dynamic contrast enhanced (DCE) MRI sequences with an accuracy of 90% when classifying between HCC and non-HCC. Hamm *et al*[51] also implemented a CNN for the classification of tumours into both the LI-RADS grading system and the lesion class. Their input to the network was the three phases, arterial, venous and equilibrium phases, of the contrast enhanced scans. They achieved an accuracy of 91.9% when classifying into the distinct lesion classes, and an accuracy of 94.3% when classifying into the LI-RADS score. This was both more accurate and faster (1.0ms runtime of the model) than two radiologists on the same dataset. When comparing to the study by Wu *et al*[48], though they both sought to differentiate cases using the LI-RADS system, Hamm *et al*[51] differentiated into more classes (LR-1,LR-4,LR-M) instead of just between LR-3 and LR-4/5. Hamm *et al*[51] outperformed the performance of Wu *et al*[48], however it is likely that it is harder to differentiate between LR-3 and 4/5, so they are not directly comparable. Ideally a neural network would be able to differentiate between all LI-RADS classes. Kim *et al*[52] used a CNN to detect presence of HCC in liver MRI scans. By simplifying the problem into detection without segmentation, they get a high accuracy of 93.7% in detecting liver HCC lesions. This was comparable to the performance of a junior radiologist with an AUROC of 0.9 compared to 0.893, though was outperformed by an expert radiologist who had an AUROC of 0.957. Zhen *et al*[53] used a CNN to classify tumours into multiple classes of benign, primary malignant and metastatic tumours using a combination of MR, clinical data and laboratory results. When using all the data together they achieved their best model performance with AUROCs of 0.951, 0.985 and 0.989 when classifying HCC, metastatic malignancy and primary malignancy (excluding HCC) respectively. Trivizakis *et al*[54] trained both a 2D and 3D CNN to classify liver tumours into primary and metastatic classes. The 2D network took the axial slices as input, whereas the 3D network took the abdominal volume. Unlike the papers above, they then used the features learnt

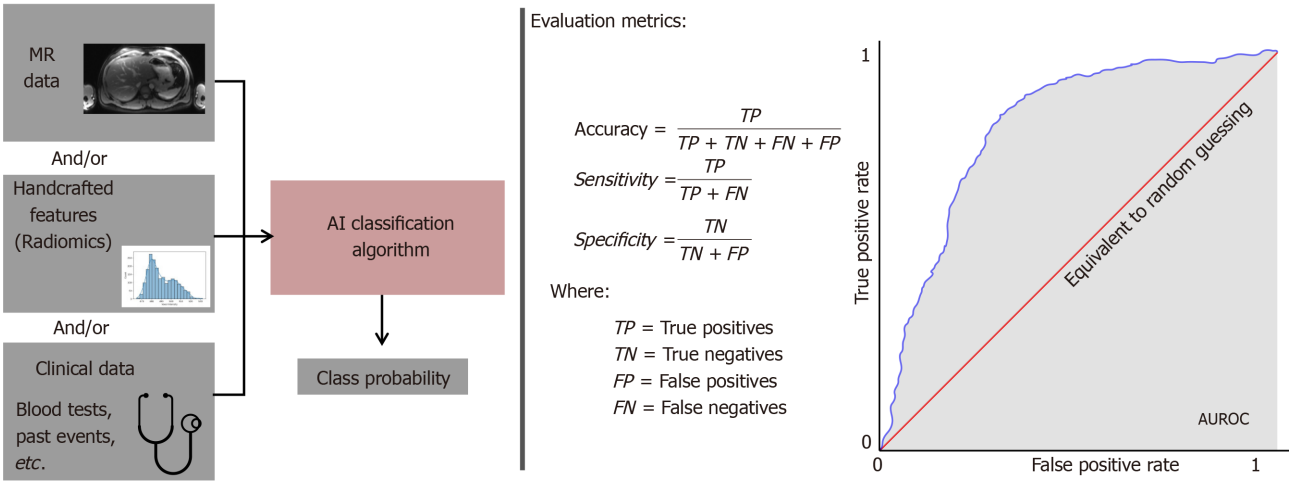


Figure 2 Classification algorithms and their performance metrics. Artificial intelligence classification algorithms use the combination of data provided to them and output a class probability. They are often evaluated according to the metrics on the right. MR: Magnetic resonance; AUROC: Area under the receiver operating characteristic curve.

during the training of these networks to train a support vector machine (SVM), a non-CNN based AI approach. They achieved an accuracy of 83% in the SVM trained on the features from the 3D network, and 67.4% in the SVM trained on the features from the 2D network. When not using the SVM as an additional step, they achieved an accuracy of 85.5% in the 3D network, with unreported accuracy in the 2D network though they conclude that the 3D model outperforms this. It shows that the inclusion of additional data, in this case more slices as a volume, often leads to an increased performance in the network performance. Though that does not always hold true, as in the study by Hamm *et al*[51] where the inclusion of all phases of a gadoxetic acid-enhanced MRI scan produced worse results that selected phases. It is important that the addition of data is performed with care, such that you are not adding more noise to the data.

Radiomic-based approaches have also been shown to be successful in classifying detected tumours into potential classes. Liu *et al*[55] extract radiomic features from tumours manually segmented from Gd-EOB-DTPA-enhanced liver MR images. These features are input into two support vector machines (SVM), with the first classifying into combined hepatocellular cholangiocarcinoma (cHCC-CC) or non-cHCC-CC, and the second classifying into HCC and non-HCC. They achieved a mean AUROC of 0.77 ± 0.19 and 0.81 ± 0.13 for the first and second methods respectively. Conversely, radiologists misdiagnosed cHCC-CC as HCC or CC in 69% of cases. With the model accuracy higher than that of the radiologists, having the model available as an additional tool for radiologists would help improve the diagnostic accuracy. Lewis *et al*[56] used extracted radiomic features from diffusion weighted imaging (DWI) MR, combined with LI-RADS category, to classify whether a tumour is HCC or another primary liver cancer such as intrahepatic cholangiocarcinoma (ICC) and combined HCC-ICC. Using binary logistic regression, they achieved an AUROC of 0.9 and 0.89 when compared to two observers. This is comparable in performance to similar LI-RADS based studies above, but without the expertise an training time needed for a large neural network. Another radiomic based study, by Wu *et al*[57], similarly extracted radiomic features from lesions detected in T2-weighted and DWI images. They achieved a similar AUROC score of 0.89, when compared to Lewis *et al*[56], by also using logistic regression on their extracted features. They additionally showed that their model outperformed a junior radiologist with 2 years' experience and rivalled a senior radiographer with 10 years' experience. Other radiomic based studies have shown similar performance, when applied to tumour classification, when using a variety of MR sequences and often the addition of additional non-MR features such as BMI and medical records[58,59].

Liver disease staging and response

Liver fibrosis staging is used clinically in predicting the prognosis of liver diseases and helps in determining the appropriate action to take in treatment[60]. Several approaches of AI applications on liver MR have been described for the assessment of liver fibrosis. Hectors *et al*[60], used a VGG16 network to predict the fibrosis stage from F1-4 using Gd-EOB-DTPA-enhanced liver MR images. The network, which was

pretrained on image net with only the last few layers being trainable, predicted a class from F1-F4, F2-F4, F3-F4 and F4, achieving an AUROC of 0.77, 0.91, 0.91 and 0.85 respectively, showing good diagnostic ability. This was comparable to the use of MRE with no significant difference between MRE and the use of deep learning methods for fibrosis prediction. The diagnostic performance of combined MRE and AI classification of contrast enhanced MRI was better overall at 0.87, 0.93, 0.95 and 0.87 for F1-F4, F2-F4, F3-F4, and F4 respectively, but was not significantly better than MRE alone. Schawkat *et al*[61] also sought to quantify the liver fibrosis from T1- or T2-weighted MR images. To do this, they did an initial texture analysis, to extract handmade features from the data. These handmade features underwent some pre-processing, then were input into an SVM which was trained to output whether the patient had a high fibrosis score, 3-4 on a standardized scale using multiple different scoring approaches, or low fibrosis score, 0-2. They achieved an AUROC of 0.82 for T1 and an AUROC of 0.57 for T2. However, when applied to MRE they achieved an AUROC of 0.92. This shows that machine learning methods are only as good as the data that is input. In the above two cases, MRE contains the information needed to output an accurate classification. However, MRE is often expensive and limited to highly funded MRI centres, therefore it is still important that techniques that don't use MRE are explored and developed while uptake of MRE is limited. The two studies above have shown in this case that deep learning methods are outperforming more traditional methods, however the use of two different scanning sequences doesn't allow for a direct comparison, as any difference in performance could be down to the data provided. Yasaka *et al*[62] also used a CNN with contrast enhanced MR images and clinical information as input, to stage liver fibrosis. They achieved AUROCs of 0.84, 0.84 and 0.85 for classifying into cirrhosis, advanced fibrosis and substantial fibrosis respectively. They were unable to differentiate fibrosis scores as well as Hectors *et al*[60] with similar methods, likely due to the Hectors study pre-training on Image Net data and so compensating for the small datasets that these study have to train on. Radiomics combined with a logistic regression model has also been used to classify into liver fibrosis scores. Park *et al*[63] extracted radiomic features from Gd-EOB-DTPA-enhanced liver MR images, and used these to classify into F0 to F4 fibrosis stages, achieving an accuracy of 80.3% in classifying F2-F4, 80.3% in F3-F4 and 81.3% in F4. Gallego-Duran *et al*[64] used radiomics approaches, combined with a logistic regression classifier, on non-contrast enhanced MRI scans to define the NASH-MRI and fibro-MRI score that could diagnose non-alcoholic steatohepatitis and advanced fibrosis with an AUROC of 0.83 and 0.85 respectively. He *et al*[65] utilised an SVM to classify patient groups into MR elastography liver stiffness measurement of ≤ 3 kPa and ≥ 3 kPa as surrogates of low and high fibrosis burden respectively, They combine radiomic features derived from T2-weighted images, with clinical data such as blood scores, BMI and their medical history. The SVM achieves an accuracy of 81.8% with an AUROC of 0.84.

Portal hypertension is one of the complications of liver fibrosis and develops in late stage disease. Portal hypertension is usually assessed by the hepatic vein pressure gradient with a gradient of ≥ 10 mmHg signifying "clinically significant portal hypertension (CSPH)" which is associated with a higher risk of adverse outcomes. AI techniques to identify CSPH have been applied to CT and MR images with some promising results. Liu *et al*[66], used a CNN to predict the presence of CSPH in both the liver and the spleen, which were then input into a logistic regression model to output an overall prediction. They achieved an AUROC of 0.940 in their test set when classifying between CSPH and non-CSPH.

Zhao *et al*[67] extracted radiomics from four MRI acquisitions (fat suppressed T2-weighted images, arterial phase, portal venous phase and delayed phase of contrast enhanced imaging) to predict early recurrence of intrahepatic mass-forming cholangiocarcinoma (IMCC). This was combined with biomarkers from histology studies, and input into a logistic regression model, to achieve an AUROC of 0.949 in predicting early recurrence of IMCC. This would assist in personalising a treatment plan for each patient. Reimer *et al*[68] utilised a radiomics approach combined with logistic regression, to predict the response to therapy in patients with liver metastases. They classified patients into two classes of stable disease and progressive disease based on features extracted from dynamic contrast enhanced MR images taken at a mean of 2.2 d after transarterial radioembolization. They achieved an AUROC of 0.73 and 0.76 in the radiomics extracted from the arterial and venous phase respectively. Chen *et al*[69] used a combination of clinical data and radiomics with decision trees to predict the immunoscore of HCC pre-treatment and therefore its response to therapy. Their best model, when using all the clinical and radiomics data, achieved and AUROC of 0.926 when classifying into high (≥ 3) and low (≤ 2) immunoscores. Finally Kim *et al*[70] utilise random forests with radiomics to predict the postoperative reoccurrence time of

single HCC. Additionally, they combine their radiomics model with a clinicopathologic model. When evaluating their model using Harrell c-index, a measure where higher than 0.5 has predictive value, their combined model was 0.716. This was better than the current clinicopathologic model (0.696), however the difference was not significant. As Kim *et al*[70] and Zhao *et al*[67] use different performance metrics, it is hard to compare their ability in tumour reoccurrence, regardless of each study focusing on different tumour types. It is important that these studies, where possible, quote similar metrics so that future researchers can determine which one is best for their task.

IMAGE SYNTHESIS

It is often the case that, when training an AI model, we are limited by the data that we have available. This is also true in healthcare settings when making clinical decisions. The simplest way to rectify this lack of data is to find more, however, this is not always possible due to many reasons both medical and logistical. The field of image synthesis or domain transfer seeks to address this. These algorithms can generate synthetic MR data based on information they are provided with, allowing this data to be either used in a setting where you might not have access to a particular technique, *e.g.*, hospitals without an MR scanner, or used to improve AI algorithms by giving it more data to train on. A common group of networks for image synthesis are conditional generative adversarial networks (cGAN). A cGAN combines a generator network, *e.g.*, a U-Net for generating the new MR image, and a discriminator network, a classification network to distinguish between real ground truth MR image and fake generated image. These networks compete against each other. The generator seeks to create an output that the discriminator believes is anatomically plausible, and the discriminator seeks to detect the output of the generator. This adversarial training often leads to improved results in segmentation or domain transfer tasks.

Liu *et al*[71] developed a cGAN to generate CT images from T1-weighted MR images, also to aid clinicians in radiotherapy treatment planning. They achieved a low mean absolute error of 72.87 HU in their generated CT scans. Jiang *et al*[72] used a cGAN to perform the opposite transformation of synthesising MR images from CT images in order to improve segmentation maps of organs at risk in MR for radiotherapy planning. They achieve a DICE score of 0.91, 0.92 in the liver when applied to real non-synthesised T2-weighted images and T1-weighted images respectively.

GANs were also implemented in Zhao *et al*[73] study to synthesise contrast enhanced MR images from non-contrast enhanced images, in order to improve tumour detection. They combined this with an additional tumour detection CNN which was applied to synthetic images in order to help improve the quality of the synthesised image, and the detection of tumours. The combined synthesis and detection networks achieved a classification accuracy of 91.3% when classifying between healthy and hemangioma present, 88.4% when classifying between healthy and HCC present and 89.2% when classifying between hemangioma and HCC. This combination of networks not only allows for accurate detection of tumours, but also supersedes the need for a contrast enhanced scan, while still giving the radiographer a proposed contrast scan to aid in their diagnosis.

ARTEFACT DETECTION

Motion detection and removal

Artefacts can occur in many forms in MRI scans, from patient induced breathing artefacts to scanner related field susceptibility artefacts. AI based methods, as shown with classification and image synthesis, have the potential to detect these artefacts and generate artefact free images which can then be used in a clinical setting. Motion is the dominating artefact present in many MR techniques. Breath holding is necessary in most scanning protocols to reduce movement artefacts. New scanning sequences are specifically designed to be shorter (*i.e.*, shorter breath-holds) and produce the same output in order to reduce these problems[74,75]. However, motion still occurs even when these steps are implemented. AI offers us the opportunity to detect, so that re-acquisition of the scans can occur; remove, so that a motion degraded scan can be used clinically; and predict, so that free-breathing methods can be used with optimal

acquisition.

Romaguera *et al*[76] have developed a spatial transformer network that takes an image sequence and predicts the next image in the sequence with an error in vessel localisation of 0.45 ± 0.55 mm when 320 ms has passed. This rises to 0.77 ± 1.36 mm at 1.6 s, but still allows the accurate prediction of frames in the future based on what has been acquired so far. This would be useful in predicting when to acquire a scan so that any data is motion free, and can also be useful in the MR-Linac systems so that radiotherapy is only applied to any tumours within the liver, reducing damage to the organs. Esses *et al*[77] used a CNN, similar to those presented in the classification section, to classify artefact degraded images into a quality score of diagnostic to non-diagnostic. They achieve a concordance rate with two trained radiographers of 79% and 73%. Tamada *et al*[78] utilise a CNN to reduce motion artefacts caused by respiratory motion in DCE-MRI. They generated simulated motion data from the ground truth data and then trained a network to predict the residual between that and collected ground truth data. They then tested on non-simulated motion degraded data, with radiographers rating on a scale of no artefact (0) to non-diagnostic (5). The output of the network was better by a mean score of 0.37 and 0.35 when rated by two radiologists. Kromrey *et al*[79] utilised the same CNN to reduce motion artifacts in arterial phase contrast enhanced MRI by 0.56 on average, on a scale of no artifact (0) to severe artifact (4). Küstner *et al*[80] try both a GAN and a variational autoencoder to remove motion artefacts from both brain and abdominal liver scans. The GAN was able to reduce the presence of motion artefacts by 67% and 65% when evaluated by two experienced radiologists. The same group had also previously used a patch based CNN to predict the amount of motion in a specific region of an image, achieving an accuracy of 72% ± 5% in classifying the images into motion from no motion to strong motion[81]. As many of the above techniques rely on radiologist qualitative assessment, they can be heavily biased by the skill of those doing the check, and as such can't be compared well as the improvement is highly subjective. More importantly though all studies showed an improvement when comparing before and after, and all the radiologists were suitably blinded. Oh *et al*[82] used an unsupervised GAN to correct for motion in Gd-EOB-DTPA-enhanced MR images. They did this by down sampling k space in each input image and regenerating the fully sampled image. This would train the network to reconstruct the missing data from what it is given, and so generate data without artefacts if clean data is given. They then apply it to artefact degraded images, achieving an improvement from 3.20 ± 1.28 to 1.95 ± 0.94 on a scale of 1 (no artefacts) to 5 (non-diagnostic) when applied to artefact degraded images. Wang *et al*[83] used a two-step approach by segmenting the liver from MR scans using a U-Net, then using this to extract patches from the liver which are classified into diagnostic and non-diagnostic. They achieved a DICE of 0.90 ± 0.05 in their liver segmentation, and an AUROC of 0.911 [95% confidence interval (CI): 0.882-0.939, $P < 0.05$] when classifying. The predictive performance when using patches extracted from the liver was better than trying to directly classify from the whole image (AUROC of 0.802, 95%CI: 0.759-0.846, $P < 0.05$). Though this final method shows a greater performance when using patches, we believe it is unlikely that each individual patch was classified for whether it was diagnostic or non-diagnostic, therefore this process would fail if applied to artefacts which only have affect a sub region of an image.

IMAGE REGISTRATION

Registration of two MR images into a shared cartesian space is an important step in allowing comparisons to be made. This could be longitudinal comparisons in a single participant in order to stage disease progression and treatment response, or it could be latitudinal comparisons within a patient cohort for research studies. Additionally, the registration of two different modalities is important when differing but complimentary clinical information is in different scan types such as CT and MR. In all cases, the manual task of registering images can be time consuming and is often composed of rigid body transformations and as such it is hard to compare between two participants of differing dimensions. AI methods can help solve these issues by introducing fast, reliable non-rigid deformation techniques for image registration.

Kuznetsova *et al*[84] looked into the use of a commercial AI based registration software for the registration of CT and MRI. They assessed the performance of their registration for three different seed points, using the liver contour, using an internal liver structures such as the inferior vena cava (IVC) or portal region (PR), and using

internal liver structures along with the liver contour. They achieved the highest performance when using just the liver contour, with a DICE score of 0.89 in the liver segmentation and 0.76 in the IVC segmentation when compared between MR and CT segmentations. As they used commercial software, we are not able to comment on the model used, however it does show that these methods have already been developed for those who need them. Fu *et al*[85] similarly assessed the performance of their bespoke MRI and CT registration CNN by assessing the DICE score between the two segmentations. They achieved a score of 0.93 ± 0.02 in the whole liver segmentation, outperforming the previous study.

CONCLUSION

Current challenges and future directions

Though the benefits of AI algorithms in Liver MRI have been displayed above, there are also many obstacles in the way of application in the clinic where they can have an impact. The first and foremost is that of open data, *i.e.*, the access to large publicly-available clinical databanks. Many of the studies above have used internal datasets which are specific to a certain hospital or patient group. Though performing well in their specific setting, they are limited in scope and generalizability due to un-modelled variations across different hospitals. Additionally, these datasets are rather small for the purpose of training ML algorithms which perform better when trained on more data, and will thus benefit from a larger suitable dataset. However, of the large datasets available, such as UKBiobank, most are focused on healthy volunteers and not clinically relevant patient cohorts. This means any AI algorithm trained on these datasets must be applied with care and knowledge of their limitations. By pooling datasets of clinical patients, the AI algorithms will both perform better, due to the increased data to learn from, and be universally applicable, due to the increased variation.

The second challenge will be overcoming scepticism towards AI algorithms. Deep learning algorithms are often termed "black boxes", due to their lack of interpretability. This is problematic when the model fails, as it is impossible to reason why. Therefore, care must be taken to apply models in their correct setting, *i.e.*, on data that fits within the distribution of that which the model was trained and tested. If interpretability is desired and a-priori knowledge and physical/biological assumptions are to be incorporated in the model, then traditional ML methods should be used, as they allow to select features and focus on ROIs more easily than with DL. Radiomics is an example of this, as you are able to determine how the model you use weighs the importance of each input feature. From this you can start to reason why the model might fail. As with deep learning methods though, when used in conjunction with radiologists, it can be a vital tool in getting the cases which are traditionally missed.

Finally, the third challenge is translating these networks into clinical workflows. The above papers have shown an ability to either speed up or achieve a radiologist level accuracy in many tasks they perform. However, until recently, there was no standard protocol into getting these networks approved for mainstream use. In April 2019, the US Food and Drug Administration published a paper on the proposed regulatory framework for AI/ML based software as a medical device and have since developed new rules and processes for approval of AI assisted software[86]. Since these new rules have been implemented, multiple AI methods have been given approval, but their wide spread use is still limited. Therefore, developing a framework for widespread distribution should be implemented.

If the above challenges can be addressed, the techniques shown in this review and those yet to be invented can positively transform many aspects of medical imaging in years to come.

REFERENCES

1 **Tenner S**, Baillie J, DeWitt J, Vege SS; American College of Gastroenterology. American College of Gastroenterology guideline: management of acute pancreatitis. *Am J Gastroenterol* 2013; **108**: 1400-15; 1416 [PMID: 23896955 DOI: 10.1038/ajg.2013.218]

2 **Kasivisvanathan V**, Rannikko AS, Borghi M, Panebianco V, Mynderse LA, Vaarala MH, Briganti A, Budäus L, Hellawell G, Hindley RG, Roobol MJ, Eggener S, Ghei M, Villers A, Bladou F, Villeirs GM, Virdi J, Boxler S, Robert G, Singh PB, Venderink W, Hadaschik BA, Ruffion A, Hu JC,

Margolis D, Crouzet S, Klotz L, Taneja SS, Pinto P, Gill I, Allen C, Giganti F, Freeman A, Morris S, Punwani S, Williams NR, Brew-Graves C, Deeks J, Takwoingi Y, Emberton M, Moore CM; PRECISION Study Group Collaborators. MRI-Targeted or Standard Biopsy for Prostate-Cancer Diagnosis. *N Engl J Med* 2018; **378**: 1767-1777 [PMID: 29552975 DOI: 10.1056/nejmoa1801993]

3 **Pavlides M**, Banerjee R, Tunnicliffe EM, Kelly C, Collier J, Wang LM, Fleming KA, Cobbold JF, Robson MD, Neubauer S, Barnes E. Multiparametric magnetic resonance imaging for the assessment of non-alcoholic fatty liver disease severity. *Liver Int* 2017; **37**: 1065-1073 [PMID: 27778429 DOI: 10.1111/Liv.13284]

4 **Loomba R**, Cui J, Wolfson T, Haufe W, Hooker J, Szeverenyi N, Ang B, Bhatt A, Wang K, Aryafar H, Behling C, Valasek MA, Lin GY, Gamst A, Brenner DA, Yin M, Glaser KJ, Ehman RL, Sirlin CB. Novel 3D Magnetic Resonance Elastography for the Noninvasive Diagnosis of Advanced Fibrosis in NAFLD: A Prospective Study. *Am J Gastroenterol* 2016; **111**: 986-994 [PMID: 27002798 DOI: 10.1038/ajg.2016.65]

5 **St Pierre TG**, El-Beshlawy A, Elalfy M, Al Jefri A, Al Zir K, Daar S, Habr D, Kriemler-Krahn U, Taher A. Multicenter validation of spin-density projection-assisted R2-MRI for the noninvasive measurement of liver iron concentration. *Magn Reson Med* 2014; **71**: 2215-2223 [PMID: 23821350 DOI: 10.1002/mrm.24854]

6 **Wong VW**, Chu WC, Wong GL, Chan RS, Chim AM, Ong A, Yeung DK, Yiu KK, Chu SH, Woo J, Chan FK, Chan HL. Prevalence of non-alcoholic fatty liver disease and advanced fibrosis in Hong Kong Chinese: a population study using proton-magnetic resonance spectroscopy and transient elastography. *Gut* 2012; **61**: 409-415 [PMID: 21846782 DOI: 10.1136/gutjnl-2011-300342]

7 **Williams CD**, Stengel J, Asike MI, Torres DM, Shaw J, Contreras M, Landt CL, Harrison SA. Prevalence of nonalcoholic fatty liver disease and nonalcoholic steatohepatitis among a largely middle-aged population utilizing ultrasound and liver biopsy: a prospective study. *Gastroenterology* 2011; **140**: 124-131 [PMID: 20858492 DOI: 10.1053/j.gastro.2010.09.038]

8 **Lazarus JV**, Colombo M, Cortez-Pinto H, Huang TT, Miller V, Ninburg M, Schattenberg JM, Seim L, Wong VWS, Zelber-Sagi S. NAFLD - sounding the alarm on a silent epidemic. *Nat Rev Gastroenterol Hepatol* 2020; **17**: 377-379 [PMID: 32514153 DOI: 10.1038/s41575-020-0315-7]

9 **Younossi ZM**, Koenig AB, Abdelatif D, Fazel Y, Henry L, Wymer M. Global epidemiology of nonalcoholic fatty liver disease-Meta-analytic assessment of prevalence, incidence, and outcomes. *Hepatology* 2016; **64**: 73-84 [PMID: 26707365 DOI: 10.1002/hep.28431]

10 **Romero-Gómez M**, Zelber-Sagi S, Trenell M. Treatment of NAFLD with diet, physical activity and exercise. *J Hepatol* 2017; **67**: 829-846 [PMID: 28545937 DOI: 10.1016/j.jhep.2017.05.016]

11 **Rahib L**, Smith BD, Aizenberg R, Rosenzweig AB, Fleshman JM, Matrisian LM. Projecting cancer incidence and deaths to 2030: the unexpected burden of thyroid, liver, and pancreas cancers in the United States. *Cancer Res* 2014; **74**: 2913-2921 [PMID: 24840647 DOI: 10.1158/0008-5472.CAN-14-0155]

12 **Hajdinjak T**, Pelzer AE. Re: What Are We Missing? *Eur Urol* 2018; **73**: 637 [PMID: 29273407 DOI: 10.1016/j.eururo.2017.12.006]

13 **Sumida Y**, Nakajima A, Itoh Y. Limitations of liver biopsy and non-invasive diagnostic tests for the diagnosis of nonalcoholic fatty liver disease/nonalcoholic steatohepatitis. *World J Gastroenterol* 2014; **20**: 475-485 [PMID: 24574716 DOI: 10.3748/wjg.v20.i2.475]

14 **Petitclerc L**, Sebastiani G, Gilbert G, Cloutier G, Tang A. Liver fibrosis: Review of current imaging and MRI quantification techniques. *J Magn Reson Imaging* 2017; **45**: 1276-1295 [PMID: 27981751 DOI: 10.1002/jmri.25550]

15 **Roberts LR**, Sirlin CB, Zaiem F, Almasri J, Prokop LJ, Heimbach JK, Murad MH, Mohammed K. Imaging for the diagnosis of hepatocellular carcinoma: A systematic review and meta-analysis. *Hepatology* 2018; **67**: 401-421 [PMID: 28859233 DOI: 10.1002/hep.29487]

16 **Sutherland T**, Watts J, Ryan M, Galvin A, Temple F, Vuong J, Little AF. Diffusion-weighted MRI for hepatocellular carcinoma screening in chronic liver disease: Direct comparison with ultrasound screening. *J Med Imaging Radiat Oncol* 2017; **61**: 34-39 [PMID: 27558976 DOI: 10.1111/1754-9485.12513]

17 **Redmon J**, Divvala S, Girshick R, Farhadi A. You only look once: Unified, real-time object detection. *Proc IEEE Comput Soc Conf Comput Vis Pattern Recognit* 2016; 779-788 [DOI: 10.1109/CVPR.2016.91]

18 **Tao A**, Sapra K, Catanzaro B. Hierarchical Multi-Scale Attention for Semantic Segmentation. *arXiv* 2020; 1-11

19 **Dolz J**, Desrosiers C, Ben Ayed I. 3D fully convolutional networks for subcortical segmentation in MRI: A large-scale study. *Neuroimage* 2018; **170**: 456-470 [PMID: 28450139 DOI: 10.1016/j.neuroimage.2017.04.039]

20 **Oktay O**, Ferrante E, Kamnitsas K, Heinrich M, Bai W, Caballero J, Cook SA, de Marvao A, Dawes T, O'Regan DP, Kainz B, Glocker B, Rueckert D. Anatomically Constrained Neural Networks (ACNNs): Application to Cardiac Image Enhancement and Segmentation. *IEEE Trans Med Imaging* 2018; **37**: 384-395 [PMID: 28961105 DOI: 10.1109/TMI.2017.2743464]

21 **Ko WY**, Siontis KC, Attia ZI, Carter RE, Kapa S, Ommen SR, Demuth SJ, Ackerman MJ, Gersh BJ, Arruda-Olson AM, Geske JB, Asirvatham SJ, Lopez-Jimenez F, Nishimura RA, Friedman PA, Noseworthy PA. Detection of Hypertrophic Cardiomyopathy Using a Convolutional Neural Network-Enabled Electrocardiogram. *J Am Coll Cardiol* 2020; **75**: 722-733 [PMID: 32081280 DOI: 10.1016/j.jacc.2019.12.030]

22 **McKinney SM**, Sieniek M, Godbole V, Godwin J, Antropova N, Ashrafian H, Back T, Chesus M, Corrado GS, Darzi A, Etemadi M, Garcia-Vicente F, Gilbert FJ, Halling-Brown M, Hassabis D, Jansen S, Karthikesalingam A, Kelly CJ, King D, Ledsam JR, Melnick D, Mostofi H, Peng L, Reicher JJ, Romera-Paredes B, Sidebottom R, Suleyman M, Tse D, Young KC, De Fauw J, Shetty S. International evaluation of an AI system for breast cancer screening. *Nature* 2020; **577**: 89-94 [PMID: 31894144 DOI: 10.1038/s41586-019-1799-6]

23 **Cortes C**, Vapnik V. Support-vector networks. *Mach Learn* 1995; **20**: 273-297 [DOI: 10.1007/BF00994018]

24 **Ho TK**. Random decision forests. *Proc Int Conf Doc Anal Recognition* 1995; **1**: 278-282 [DOI: 10.1109/ICDAR.1995.598994]

25 **LeCun Y**, Bengio Y, Hinton G. Deep learning. *Nature* 2015; **521**: 436-444 [PMID: 26017442 DOI: 10.1038/nature14539]

26 **Dzyubak B**, Glaser K, Yin M, Talwalkar J, Chen J, Manduca A, Ehman RL. Automated liver stiffness measurements with magnetic resonance elastography. *J Magn Reson Imaging* 2013; **38**: 371-379 [PMID: 23281171 DOI: 10.1002/jmri.23980]

27 **Winther H**, Hundt C, Ringe KI, Wacker FK, Schmidt B, Jürgens J, Haimerl M, Beyer LP, Stroszczynski C, Wiggermann P, Verloh N. A 3D Deep Neural Network for Liver Volumetry in 3T Contrast-Enhanced MRI. *Rofo* 2021; **193**: 305-314 [PMID: 32882724 DOI: 10.1055/a-1238-2887]

28 **Mio M**, Fujiwara Y, Tani K, Toyofuku T, Maeda T, Inoue T. Quantitative evaluation of focal liver lesions with T1 mapping using a phase-sensitive inversion recovery sequence on gadoxetic acid-enhanced MRI. *Eur J Radiol Open* 2021; **8**: 100312 [PMID: 33392362 DOI: 10.1016/j.ejro.2020.100312]

29 **Linge J**, Whitcher B, Borga M, Dahlqvist Leinhard O. Sub-phenotyping Metabolic Disorders Using Body Composition: An Individualized, Nonparametric Approach Utilizing Large Data Sets. *Obesity (Silver Spring)* 2019; **27**: 1190-1199 [PMID: 31094076 DOI: 10.1002/oby.22510]

30 **Liu M**, Vanguri R, Mutasa S, Ha R, Liu YC, Button T, Jambawalikar S. Channel width optimized neural networks for liver and vessel segmentation in liver iron quantification. *Comput Biol Med* 2020; **122**: 103798 [PMID: 32658724 DOI: 10.1016/j.compbiomed.2020.103798]

31 **Chen Y**, Ruan D, Xiao J, Wang L, Sun B, Saouaf R, Yang W, Li D, Fan Z. Fully automated multiorgan segmentation in abdominal magnetic resonance imaging with deep neural networks. *Med Phys* 2020; **47**: 4971-4982 [PMID: 32748401 DOI: 10.1002/mp.14429]

32 **Huang G**, Liu Z, Van Der Maaten L, Weinberger KQ. Densely connected convolutional networks. *2017 IEEE Conference on Computer Vision and Pattern Recognition (CVPR)* 2017; 2261-2269 [DOI: 10.1109/CVPR.2017.243]

33 **Valindria VV**, Pawlowski N, Rajchl M, Lavdas I, Aboagye EO, Rockall AG, Rueckert D. Multi-modal Learning from Unpaired Images: Application to Multi-organ Segmentation in CT and MRI. *2018 IEEE Winter Conference on Applications of Computer Vision (WACV)* 2018; 547-556 [DOI: 10.1109/WACV.2018.00066]

34 **He K**, Zhang X, Ren S, Sun J. Deep residual learning for image recognition. *2016 IEEE Conference on Computer Vision and Pattern Recognition (CVPR)* 2016; 770-778 [DOI: 10.1109/CVPR.2016.90]

35 **Fu Y**, Mazur TR, Wu X, Liu S, Chang X, Lu Y, Li HH, Kim H, Roach MC, Henke L, Yang D. A novel MRI segmentation method using CNN-based correction network for MRI-guided adaptive radiotherapy. *Med Phys* 2018; **45**: 5129-5137 [PMID: 30269345 DOI: 10.1002/mp.13221]

36 **Bousabarah K**, Letzen B, Tefera J, Savic L, Schobert I, Schlachter T, Staib LH, Kocher M, Chapiro J, Lin M. Automated detection and delineation of hepatocellular carcinoma on multiphasic contrast-enhanced MRI using deep learning. *Abdom Radiol (NY)* 2021; **46**: 216-225 [PMID: 32500237 DOI: 10.1007/s00261-020-02604-5]

37 **Mole DJ**, Fallowfield JA, Sherif AE, Kendall T, Semple S, Kelly M, Ridgway G, Connell JJ, McGonigle J, Banerjee R, Brady JM, Zheng X, Hughes M, Neyton L, McClintock J, Tucker G, Nailon H, Patel D, Wackett A, Steven M, Welsh F, Rees M; HepaT1ca Study Group. Quantitative magnetic resonance imaging predicts individual future liver performance after liver resection for cancer. *PLoS One* 2020; **15**: e0238568 [PMID: 33264327 DOI: 10.1371/journal.pone.0238568]

38 **Owler J**, Irving B, Ridgway G, Wojciechowska M, McGonigle J, Brady M. Comparison of Multi-atlas Segmentation and U-Net Approaches for Automated 3D Liver Delineation in MRI. In: Zheng Y, Williams BM, Chen K, eds. Medical Image Understanding and Analysis. Springer International Publishing, 2020 [DOI: 10.1007/978-3-030-39343-4_41]

39 **Christ PF**, Ettlinger F, Grün F, Elshaera MEA, Lipkova J, Schlecht S, Freba A, Tatavarty S, Bickel M, Bilic P, Rempfler M, Hofmann F, Anastasi MD, Ahmadi SA, Kaissis G, Holch J, Sommer W, Braren R, Heinemann V, Menze B. Automatic liver and tumor segmentation of CT and MRI volumes using cascaded fully convolutional neural networks. *arXiv* 2017; 1-20

40 **Jansen MJA**, Kuijf HJ, Niekel M, Veldhuis WB, Wessels FJ, Viergever MA, Pluim JPW. Liver segmentation and metastases detection in MR images using convolutional neural networks. *J Med Imaging (Bellingham)* 2019; **6**: 044003 [PMID: 31620549 DOI: 10.1117/1.JMI.6.4.044003]

41 **Ivashchenko OV**, Rijkhorst EJ, Ter Beek LC, Hoetjes NJ, Pouw B, Nijkamp J, Kuhlmann KFD, Ruers TJM. A workflow for automated segmentation of the liver surface, hepatic vasculature and biliary tree anatomy from multiphase MR images. *Magn Reson Imaging* 2020; **68**: 53-65 [PMID: 31935445 DOI: 10.1016/j.mri.2019.12.008]

42 **Masoumi H**, Behrad A, Pourmina MA, Roosta A. Automatic liver segmentation in MRI images using an iterative watershed algorithm and artificial neural network. *Biomed Signal Process Control* 2012;

7: 429-437 [DOI: 10.1016/j.bspc.2012.01.002]
43 **Wang K**, Mamidipalli A, Retson T, Bahrami N, Hasenstab K, Blansit K, Bass E, Delgado T, Cunha G, Middleton MS, Loomba R, Neuschwander-Tetri BA, Sirlin CB, Hsiao A; members of the NASH Clinical Research Network. Automated CT and MRI Liver Segmentation and Biometry Using a Generalized Convolutional Neural Network. *Radiol Artif Intell* 2019; **1** [PMID: 32582883 DOI: 10.1148/ryai.2019180022]
44 **Irving B**. Deep Quantitative Liver Segmentation and Vessel Exclusion to Assist in Liver Assessment. In: Valdés Hernández M, González-Castro V. eds. Medical Image Understanding and Analysis. Springer International Publishing, 2017: 663-673
45 **Yang J**, Dvornek NC, Zhang F, Chapiro J, Lin M, Duncan JS. Unsupervised Domain Adaptation *via* Disentangled Representations: Application to Cross-Modality Liver Segmentation. *Med Image Comput Comput Assist Interv* 2019; **11765**: 255-263 [PMID: 32377643 DOI: 10.1007/978-3-030-32245-8_29]
46 **Cunha GM**, Hasenstab KA, Higaki A, Wang K, Delgado T, Brunsing RL, Schlein A, Schwartzman A, Hsiao A, Sirlin CB, Fowler KJ. Convolutional neural network-automated hepatobiliary phase adequacy evaluation may optimize examination time. *Eur J Radiol* 2020; **124**: 108837 [PMID: 31958630 DOI: 10.1016/j.ejrad.2020.108837]
47 **Russakovsky O**, Deng J, Su H, Krause J, Satheesh S, Ma S, Huang Z, Karpathy A, Khosla A, Bernstein M, Berg AC, Li FF. ImageNet Large Scale Visual Recognition Challenge. *Int J Comput Vis* 2015; **115**: 211-252 [DOI: 10.1007/s11263-015-0816-y]
48 **Wu Y**, White GM, Cornelius T, Gowdar I, Ansari MH, Supanich MP, Deng J. Deep learning LI-RADS grading system based on contrast enhanced multiphase MRI for differentiation between LR-3 and LR-4/LR-5 Liver tumors. *Ann Transl Med* 2020; **8**: 701 [PMID: 32617321 DOI: 10.21037/atm.2019.12.151]
49 **Krizhevsky A**, Sutskever I, Hinton GE. ImageNet classification with deep convolutional neural networks. Commun. *ACM* 2017; **60**: 84-90 [DOI: 10.1145/3065386]
50 **Messaoudi R**, Jaziri F, Vacavant A, Mtibaa A, Gargouri F. A Novel Deep Learning Approach for Liver MRI Classification and HCC Detection. In: Lu Y. eds. Pattern Recognition and Artificial Intelligence. Springer International Publishing, 2020: 635-645
51 **Hamm CA**, Wang CJ, Savic LJ, Ferrante M, Schobert I, Schlachter T, Lin M, Duncan JS, Weinreb JC, Chapiro J, Letzen B. Deep learning for liver tumor diagnosis part I: development of a convolutional neural network classifier for multi-phasic MRI. *Eur Radiol* 2019; **29**: 3338-3347 [PMID: 31016442 DOI: 10.1007/s00330-019-06205-9]
52 **Kim J**, Min JH, Kim SK, Shin SY, Lee MW. Detection of Hepatocellular Carcinoma in Contrast-Enhanced Magnetic Resonance Imaging Using Deep Learning Classifier: A Multi-Center Retrospective Study. *Sci Rep* 2020; **10**: 9458 [PMID: 32527998 DOI: 10.1038/s41598-020-65875-4]
53 **Zhen SH**, Cheng M, Tao YB, Wang YF, Juengpanich S, Jiang ZY, Jiang YK, Yan YY, Lu W, Lue JM, Qian JH, Wu ZY, Sun JH, Lin H, Cai XJ. Deep Learning for Accurate Diagnosis of Liver Tumor Based on Magnetic Resonance Imaging and Clinical Data. *Front Oncol* 2020; **10**: 680 [PMID: 32547939 DOI: 10.3389/fonc.2020.00680]
54 **Trivizakis E**, Manikis GC, Nikiforaki K, Drevelegas K, Constantinides M, Drevelegas A, Marias K. Extending 2-D Convolutional Neural Networks to 3-D for Advancing Deep Learning Cancer Classification With Application to MRI Liver Tumor Differentiation. *IEEE J Biomed Health Inform* 2019; **23**: 923-930 [PMID: 30561355 DOI: 10.1109/JBHI.2018.2886276]
55 **Liu X**, Khalvati F, Namdar K, Fischer S, Lewis S, Taouli B, Haider MA, Jhaveri KS. Can machine learning radiomics provide pre-operative differentiation of combined hepatocellular cholangiocarcinoma from hepatocellular carcinoma and cholangiocarcinoma to inform optimal treatment planning? *Eur Radiol* 2021; **31**: 244-255 [PMID: 32749585 DOI: 10.1007/s00330-020-07119-7]
56 **Lewis S**, Peti S, Hectors SJ, King M, Rosen A, Kamath A, Putra J, Thung S, Taouli B. Volumetric quantitative histogram analysis using diffusion-weighted magnetic resonance imaging to differentiate HCC from other primary liver cancers. *Abdom Radiol (NY)* 2019; **44**: 912-922 [PMID: 30712136 DOI: 10.1007/s00261-019-01906-7]
57 **Wu J**, Liu A, Cui J, Chen A, Song Q, Xie L. Radiomics-based classification of hepatocellular carcinoma and hepatic haemangioma on precontrast magnetic resonance images. *BMC Med Imaging* 2019; **19**: 23 [PMID: 30866850 DOI: 10.1186/s12880-019-0321-9]
58 **Oyama A**, Hiraoka Y, Obayashi I, Saikawa Y, Furui S, Shiraishi K, Kumagai S, Hayashi T, Kotoku J. Hepatic tumor classification using texture and topology analysis of non-contrast-enhanced three-dimensional T1-weighted MR images with a radiomics approach. *Sci Rep* 2019; **9**: 8764 [PMID: 31217445 DOI: 10.1038/s41598-019-45283-z]
59 **Wu M**, Tan H, Gao F, Hai J, Ning P, Chen J, Zhu S, Wang M, Dou S, Shi D. Predicting the grade of hepatocellular carcinoma based on non-contrast-enhanced MRI radiomics signature. *Eur Radiol* 2019; **29**: 2802-2811 [PMID: 30406313 DOI: 10.1007/s00330-018-5787-2]
60 **Hectors SJ**, Kennedy P, Huang KH, Stocker D, Carbonell G, Greenspan H, Friedman S, Taouli B. Fully automated prediction of liver fibrosis using deep learning analysis of gadoxetic acid-enhanced MRI. *Eur Radiol* 2020 [PMID: 33201285 DOI: 10.1007/s00330-020-07475-4]
61 **Schawkat K**, Ciritsis A, von Ulmenstein S, Honcharova-Biletska H, Jüngst C, Weber A, Gubler C, Mertens J, Reiner CS. Diagnostic accuracy of texture analysis and machine learning for quantification of liver fibrosis in MRI: correlation with MR elastography and histopathology. *Eur Radiol* 2020; **30**:

4675-4685 [PMID: 32270315 DOI: 10.1007/s00330-020-06831-8]
62 **Yasaka K**, Akai H, Kunimatsu A, Abe O, Kiryu S. Liver Fibrosis: Deep Convolutional Neural Network for Staging by Using Gadoxetic Acid-enhanced Hepatobiliary Phase MR Images. *Radiology* 2018; **287**: 146-155 [PMID: 29239710 DOI: 10.1148/radiol.2017171928]
63 **Park HJ**, Lee SS, Park B, Yun J, Sung YS, Shim WH, Shin YM, Kim SY, Lee SJ, Lee MG. Radiomics Analysis of Gadoxetic Acid-enhanced MRI for Staging Liver Fibrosis. *Radiology* 2019; **290**: 380-387 [PMID: 30615554 DOI: 10.1148/radiol.2018181197]
64 **Gallego-Durán R**, Cerro-Salido P, Gomez-Gonzalez E, Pareja MJ, Ampuero J, Rico MC, Aznar R, Vilar-Gomez E, Bugianesi E, Crespo J, González-Sánchez FJ, Aparcero R, Moreno I, Soto S, Arias-Loste MT, Abad J, Ranchal I, Andrade RJ, Calleja JL, Pastrana M, Iacono OL, Romero-Gómez M. Imaging biomarkers for steatohepatitis and fibrosis detection in non-alcoholic fatty liver disease. *Sci Rep* 2016; **6**: 31421 [PMID: 27514671 DOI: 10.1038/srep31421]
65 **He L**, Li H, Dudley JA, Maloney TC, Brady SL, Somasundaram E, Trout AT, Dillman JR. Machine Learning Prediction of Liver Stiffness Using Clinical and T2-Weighted MRI Radiomic Data. *AJR Am J Roentgenol* 2019; **213**: 592-601 [PMID: 31120779 DOI: 10.2214/AJR.19.21082]
66 **Liu Y**, Ning Z, Örmeci N, An W, Yu Q, Han K, Huang Y, Liu D, Liu F, Li Z, Ding H, Luo H, Zuo C, Liu C, Wang J, Zhang C, Ji J, Wang W, Wang Z, Yuan M, Li L, Zhao Z, Wang G, Li M, Liu Q, Lei J, Tang T, Akçalar S, Çelebioğlu E, Üstüner E, Bilgiç S, Ellik Z, Asiller ÖÖ, Liu Z, Teng G, Chen Y, Hou J, Li X, He X, Dong J, Tian J, Liang P, Ju S, Zhang Y, Qi X. Deep Convolutional Neural Network-Aided Detection of Portal Hypertension in Patients With Cirrhosis. *Clin Gastroenterol Hepatol* 2020; **18**: 2998-3007.e5 [PMID: 32205218 DOI: 10.1016/j.cgh.2020.03.034]
67 **Zhao L**, Ma X, Liang M, Li D, Ma P, Wang S, Wu Z, Zhao X. Prediction for early recurrence of intrahepatic mass-forming cholangiocarcinoma: quantitative magnetic resonance imaging combined with prognostic immunohistochemical markers. *Cancer Imaging* 2019; **19**: 49 [PMID: 31307551 DOI: 10.1186/s40644-019-0234-4]
68 **Reimer RP**, Reimer P, Mahnken AH. Assessment of Therapy Response to Transarterial Radioembolization for Liver Metastases by Means of Post-treatment MRI-Based Texture Analysis. *Cardiovasc Intervent Radiol* 2018; **41**: 1545-1556 [PMID: 29881933 DOI: 10.1007/s00270-018-2004-2]
69 **Chen S**, Feng S, Wei J, Liu F, Li B, Li X, Hou Y, Gu D, Tang M, Xiao H, Jia Y, Peng S, Tian J, Kuang M. Pretreatment prediction of immunoscore in hepatocellular cancer: a radiomics-based clinical model based on Gd-EOB-DTPA-enhanced MRI imaging. *Eur Radiol* 2019; **29**: 4177-4187 [PMID: 30666445 DOI: 10.1007/s00330-018-5986-x]
70 **Kim S**, Shin J, Kim DY, Choi GH, Kim MJ, Choi JY. Radiomics on gadoxetic acid-enhanced magnetic resonance imaging for prediction of postoperative early and late recurrence of single hepatocellular carcinoma. *Clin Cancer Res* 2019; **25**: 3847-3855 [PMID: 30808773 DOI: 10.1158/1078-0432.CCR-18-2861]
71 **Liu Y**, Lei Y, Wang T, Kayode O, Tian S, Liu T, Patel P, Curran WJ, Ren L, Yang X. MRI-based treatment planning for liver stereotactic body radiotherapy: validation of a deep learning-based synthetic CT generation method. *Br J Radiol* 2019; **92**: 20190067 [PMID: 31192695 DOI: 10.1259/bjr.20190067]
72 **Jiang J**, Hu YC, Tyagi N, Rimner A, Lee N, Deasy JO, Berry S, Veeraraghavan H. PSIGAN: Joint Probabilistic Segmentation and Image Distribution Matching for Unpaired Cross-Modality Adaptation-Based MRI Segmentation. *IEEE Trans Med Imaging* 2020; **39**: 4071-4084 [PMID: 32746148 DOI: 10.1109/TMI.2020.3011626]
73 **Zhao J**, Li D, Kassam Z, Howey J, Chong J, Chen B, Li S. Tripartite-GAN: Synthesizing liver contrast-enhanced MRI to improve tumor detection. *Med Image Anal* 2020; **63**: 101667 [PMID: 32375101 DOI: 10.1016/j.media.2020.101667]
74 **Messroghli DR**, Radjenovic A, Kozerke S, Higgins DM, Sivananthan MU, Ridgway JP. Modified Look-Locker inversion recovery (MOLLI) for high-resolution T1 mapping of the heart. *Magn Reson Med* 2004; **52**: 141-146 [PMID: 15236377 DOI: 10.1002/mrm.20110]
75 **Piechnik SK**, Ferreira VM, Dall'Armellina E, Cochlin LE, Greiser A, Neubauer S, Robson MD. Shortened Modified Look-Locker Inversion recovery (ShMOLLI) for clinical myocardial T1-mapping at 1.5 and 3 T within a 9 heartbeat breathhold. *J Cardiovasc Magn Reson* 2010; **12**: 69 [PMID: 21092095 DOI: 10.1186/1532-429X-12-69]
76 **Romaguera LV**, Plantefève R, Romero FP, Hébert F, Carrier JF, Kadoury S. Prediction of in-plane organ deformation during free-breathing radiotherapy *via* discriminative spatial transformer networks. *Med Image Anal* 2020; **64**: 101754 [PMID: 32580056 DOI: 10.1016/j.media.2020.101754]
77 **Esses SJ**, Lu X, Zhao T, Shanbhogue K, Dane B, Bruno M, Chandarana H. Automated image quality evaluation of T_2 -weighted liver MRI utilizing deep learning architecture. *J Magn Reson Imaging* 2018; **47**: 723-728 [PMID: 28577329 DOI: 10.1002/jmri.25779]
78 **Tamada D**, Kromrey ML, Ichikawa S, Onishi H, Motosugi U. Motion Artifact Reduction Using a Convolutional Neural Network for Dynamic Contrast Enhanced MR Imaging of the Liver. *Magn Reson Med Sci* 2020; **19**: 64-76 [PMID: 31061259 DOI: 10.2463/mrms.mp.2018-0156]
79 **Kromrey ML**, Tamada D, Johno H, Funayama S, Nagata N, Ichikawa S, Kühn JP, Onishi H, Motosugi U. Reduction of respiratory motion artifacts in gadoxetate-enhanced MR with a deep learning-based filter using convolutional neural network. *Eur Radiol* 2020; **30**: 5923-5932 [PMID: 32556463 DOI: 10.1007/s00330-020-07006-1]
80 **Küstner T**, Armanious K, Yang J, Yang B, Schick F, Gatidis S. Retrospective correction of motion-

affected MR images using deep learning frameworks. *Magn Reson Med* 2019; **82**: 1527-1540 [PMID: 31081955 DOI: 10.1002/mrm.27783]

81 **Küstner T**, Liebgott A, Mauch L, Martirosian P, Bamberg F, Nikolaou K, Yang B, Schick F, Gatidis S. Automated reference-free detection of motion artifacts in magnetic resonance images. *MAGMA* 2018; **31**: 243-256 [PMID: 28932991 DOI: 10.1007/s10334-017-0650-z]

82 **Oh G**, Lee JE, Ye JC. Unsupervised MR Motion Artifact Deep Learning using Outlier-Rejecting Bootstrap Aggregation. 2020: 1-10

83 **Wang Y**, Song Y, Wang F, Sun J, Gao X, Han Z, Shi L, Shao G, Fan M, Yang G. A two-step automated quality assessment for liver MR images based on convolutional neural network. *Eur J Radiol* 2020; **124**: 108822 [PMID: 31951895 DOI: 10.1016/j.ejrad.2020.108822]

84 **Kuznetsova S**, Grendarova P, Ploquin N, Thind K. Multimodality Image Fusion of the Liver Using Structure-Guided Deformable Image Registration in Velocity AI---What Is the Preferred Approach? In: Lhotska L, Sukupova L, Lacković I, Ibbott G (eds). World Congress on Medical Physics and Biomedical Engineering 2018. IFMBE Proceedings, Singapore, 2019: 273-277 [DOI: 10.1007/978-981-10-9035-6_49]

85 **Fu Y**, Lei Y, Wang T, Zhou J, Curran WJ, Patel P, Liu T, Yang X. Deformable MRI-CT liver image registration using convolutional neural network with modality independent neighborhood descriptors. In: Mazurowski MA, Drukker K (eds). Medical Imaging 2021: Computer-Aided Diagnosis 2021; 11597: 102-107 [DOI: 10.1117/12.2581082]

86 **FDA**. Proposed Regulatory Framework for Modifications to Artificial Intelligence/Machine Learning (AI/ML)-Based Software as a Medical Device (SaMD)-Discussion Paper and Request for Feedback. 2019: 1-20

World Journal of Gastroenterology

Submit a Manuscript: https://www.f6publishing.com

World J Gastroenterol 2021 October 28; 27(40): 6844-6860

DOI: 10.3748/wjg.v27.i40.6844

ISSN 1007-9327 (print) ISSN 2219-2840 (online)

MINIREVIEWS

Role of human nucleoside transporters in pancreatic cancer and chemoresistance

Carly Jade Carter, Ahmed H Mekkawy, David L Morris

ORCID number: Carly Jade Carter 0000-0003-3219-4076; Ahmed H Mekkawy 0000-0001-7162-8936; David L Morris 0000-0001-9377-8521.

Author contributions: Carter CJ wrote the manuscript and designed the figures with the support of Mekkawy AH; Mekkawy AH and Morris DL revised and supervised the manuscript; all authors have read and approved the final manuscript.

Conflict-of-interest statement: Morris DL is one of the inventors of BromAc and owns stocks in Mucpharm. Carter CJ and Mekkawy AH are employees of Mucpharm Pty Ltd.

Open-Access: This article is an open-access article that was selected by an in-house editor and fully peer-reviewed by external reviewers. It is distributed in accordance with the Creative Commons Attribution NonCommercial (CC BY-NC 4.0) license, which permits others to distribute, remix, adapt, build upon this work non-commercially, and license their derivative works on different terms, provided the original work is properly cited and the use is non-commercial. See: http://creativecommons.org/Licenses/by-nc/4.0/

Carly Jade Carter, Ahmed H Mekkawy, David L Morris, Hepatobiliary and Surgical Oncology Unit, Department of Surgery, St George Hospital, University of New South Wales, Sydney 2217, New South Wales, Australia

Carly Jade Carter, Ahmed H Mekkawy, David L Morris, Mucpharm Pty Ltd, Australia

Corresponding author: David L Morris, FRCS, FRCS (Ed), MBChB, MD, PhD, Professor, Hepatobiliary and Surgical Oncology Unit, Department of Surgery, St George Hospital, University of New South Wales, Kogarah, Sydney 2217, New South Wales, Australia. david.morris@unsw.edu.au

Abstract

The prognosis of pancreatic cancer is poor with the overall 5-year survival rate of less than 5% changing minimally over the past decades and future projections predicting it developing into the second leading cause of cancer related mortality within the next decade. Investigations into the mechanisms of pancreatic cancer development, progression and acquired chemoresistance have been constant for the past few decades, thus resulting in the identification of human nucleoside transporters and factors affecting cytotoxic uptake *via* said transporters. This review summaries the aberrant expression and role of human nucleoside transports in pancreatic cancer, more specifically human equilibrative nucleoside transporter 1/2 (hENT1, hENT2), and human concentrative nucleoside transporter 1/3 (hCNT1, hCNT3), while briefly discussing the connection and importance between these nucleoside transporters and mucins that have also been identified as being aberrantly expressed in pancreatic cancer. The review also discusses the incidence, current diagnostic techniques as well as the current therapeutic treatments for pancreatic cancer. Furthermore, we address the importance of chemoresistance in nucleoside analogue drugs, in particular, gemcitabine and we discuss prospective therapeutic treatments and strategies for overcoming acquired chemoresistance in pancreatic cancer by the enhancement of human nucleoside transporters as well as the potential targeting of mucins using a combination of mucolytic compounds with cytotoxic agents.

Key Words: Pancreatic cancer; Gemcitabine; Human nucleoside transporters; Human equilibrative nucleoside transporters; Human concentrative nucleotide transporters; Mucins

Manuscript source: Unsolicited manuscript

Specialty type: Gastroenterology and hepatology

Country/Territory of origin: Australia

Peer-review report's scientific quality classification

Grade A (Excellent): 0
Grade B (Very good): B, B
Grade C (Good): 0
Grade D (Fair): 0
Grade E (Poor): 0

Received: February 17, 2021
Peer-review started: February 17, 2021
First decision: April 5, 2021
Revised: April 19, 2021
Accepted: September 14, 2021
Article in press: September 14, 2021
Published online: October 28, 2021

P-Reviewer: Fernández-Placencia RM, Jin Y
S-Editor: Gong ZM
L-Editor: A
P-Editor: Ma YJ

©The Author(s) 2021. Published by Baishideng Publishing Group Inc. All rights reserved.

Core Tip: Pancreatic cancer continues to be one of the leading causes of cancer-related mortality worldwide, with prevalence expected to increase drastically within the next decade primarily due to difficulties in diagnosis and acquired resistance to chemotherapeutic drugs. Due to this, in-depth work is extremely important for the future diagnosis and treatment of the disease. Human Nucleoside Transporters have been identified as a key target in not only diagnosis but also overcoming chemoresistance. Here, we summarize the information currently available on Pancreatic Cancer and the role of Nucleoside Transporters in chemoresistance.

Citation: Carter CJ, Mekkawy AH, Morris DL. Role of human nucleoside transporters in pancreatic cancer and chemoresistance. *World J Gastroenterol* 2021; 27(40): 6844-6860
URL: https://www.wjgnet.com/1007-9327/full/v27/i40/6844.htm
DOI: https://dx.doi.org/10.3748/wjg.v27.i40.6844

INTRODUCTION

Pancreatic cancer is the seventh leading cause of cancer-related mortality[1], and is ranked as the 14th most common cancer worldwide[2]. The prognosis of pancreatic cancer is often poor with an average five-year survival rate of less than 5%[3]. This poor prognosis has been attributed, in part, to the difficulties in early-stage detection, advancement of disease at the time of diagnosis, frequent recurrence and lack of effective treatment therapies specifically targeting tumour cells[4,5].

Pancreatic ductal adenocarcinoma (PDAC), which accounts for > 90% of all pancreatic cancer cases is characterized by dense desmoplastic stromal development proximal to cancerous tissue, as well as the aberrant expression of mucins and nucleoside transporters[6,7]. Three different preneoplastic lesions of the pancreatic duct have been identified as precursors of PDAC those being, pancreatic intraepithelial neoplasia (PanIN), mucinous cystic neoplasm (MCN) and intraductal papillary mucinous neoplasm (IPMN)[3].

PanIN accounts for 85% of PDAC cases and is categorised into PanIN1A, PanIN1B, PanIN2 and PanIN3[8]. Prior to PanIN progression, normal pancreatic ductal cells express mucin proteins MUC1/5AB/6/17 which have been identified in assisting cancer cell in evading immune systems[3]. PanIN1A/1B is described as hyperplasia without dysplasia, followed by PanIN2 with dysplasia at variable rates and a loss of polarity and finally PanIN3, representative of an in-situ carcinoma. For all PanIN, increased expression can be seen for MUC1/6/16 and neoexpression is observed for MUC3/4/5AC (Figure 1)[4,9].

MCN and IPMN account for the remainder 15% of PDAC cases, with MCN characterized as cyst forming pancreatic epithelial neoplasms that produce mucin, have a distinct stroma type, and have a broad spectrum of dysplasia. Importantly, MCN's are also representative of early Kras mutations as well as late oncogene SMAD4 and proto-oncogene TP53 inactivation and lastly, increased MUC1 expression and neoexpression of MUC2/5AC [2-4].

IPMN which originates from the main pancreatic duct is characterized by the increased secretion of select mucins (MUC1/6), neoexpression of MUC2/4/5AC, and a large dilation of the ducts or cysts formation. Much like MCN, IPMN presents with a Kras mutation and the inactivation of TP53 and P16/CDKN2A. MCN and IPMN may further progress into adenocarcinoma where an increased expression of MUC1/6 and neoexpression of MUC3/4/5AC/5AB/7/13/16/17 is observed (Figure 1)[3,4].

The aim of this review is to outline the role of nucleoside transporters in pancreatic cancer progression and their contribution to chemotherapeutic drug resistance. This review will also examine the current treatments and therapies to overcome cancer progression and acquired resistance to nucleoside analogue drugs, specifically, gemcitabine.

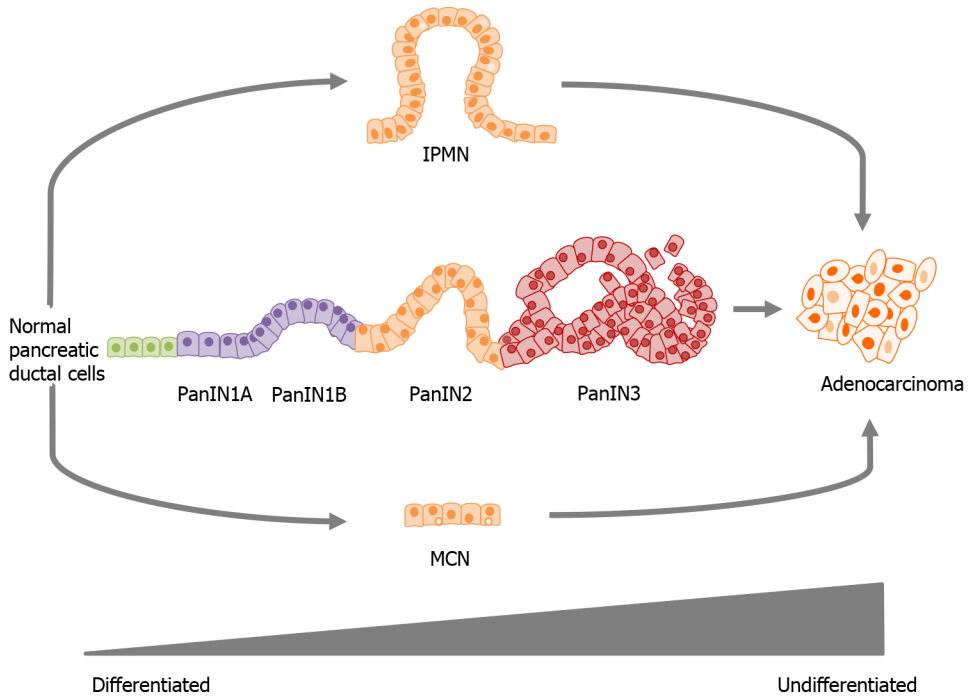


Figure 1 Pancreatic cancer progression beginning with normal pancreatic ductal cells which express MUC1, MUC5AB, MUC6, MUC17, and MUC20. Pancreatic ductal cells progress to hyperplasia (PanIN21A/1B) with columnar cells, followed by dysplasia (PanIN2) with a loss of polarity, papillary and finally In-situ carcinoma (PanIN3) with a loss in cell polarity, papillary, budding off and mitosis. An increased expression of MUC1, MUC6, MUC16 and neoexpression of MUC3, MUC4, and MUC5AC can be seen in pancreatic intraepithelial neoplasia's. Pancreatic ductal cells also progress into MCN which has an increased expression of MUC1 and the neoexpression of MUC2 and MUC5AC. Early Kras mutation as well as late SMAD4 and TP53 inactivation is seen in both PanIN and MCN. Finally pancreatic ductal cells can progress into IPMN which are mucin producing neoplasms that present with an increased expression of MUC1 and MUC6 as well as neoexpression of MUC2, MUC4 and MUC5AC. IPMN also presents with a Kras mutation and the inactivation of TP53 and P16/CDKN2A. IPMN and MCN further progress to adenocarcinoma where MUC1, and MUC6 expression is increased and MUC3, MUC4, MUC5AC, MUC5AB, MUC7, MUC13, MUC16 and MUC17 are neoexpressed[2-4,68]. IPMN: Intraductal papillary mucinous neoplasm; PanIN: Pancreatic intraepithelial neoplasia; MCN: Mucinous cystic neoplasm.

INCIDENCE

The incidence rates of pancreatic cancer have significant variation between countries; however, the higher rates can be seen in developed countries (North America and Europe) compared to developing countries (South Central Asia and Africa). World-wide incidence and mortality rates correlate with ageing and a higher prevalence is observed in men compared to woman. In western societies, the incidence of pancreatic cancer has been steadily increasing with predictions that by 2030 it will be the 2nd greatest cause of death related to cancer in the United States[1,2]

Despite the cause of pancreatic cancer being multifactorial and complex, several factors whether modifiable or non-modifiable have been identified as having a direct association. Non-modifiable factors include age, sex, ethnicity, blood group, family history, genetic susceptibility, gut microbiota, and diabetes. The modifiable risk factors that have been identified are smoking, alcohol consumption, obesity, chronic pancreatitis, dietary factors, and helicobacter pylori infections[1,2,10].

DIAGNOSIS

There are significant challenges with the diagnosis of pancreatic cancer with most patients presenting with late-stage tumour development at the time of diagnosis. The reasons of late-stage progression diagnosis are multi-factorial and therefore, several factors must be assessed[1,10]. Firstly, the initial stage of pancreatic cancer is, for the most part, clinically silent. This results in patients not presenting with symptoms until being in advanced stages of disease. Presenting symptoms are non-specific and can include jaundice, dark urine, abdominal pain, acholic stools and pruritus. Due to the broad range of non-specific symptoms, there are several diseases that require differentiation, including but not limited to: pancreatitis, gastritis, abdominal aortic aneurysm, and pancreas. As a result, diagnosis can be missed or delayed which results in

pancreatic cancer being the most commonly detected tumour during autopsy studies [2,10,11].

Currently, several diagnostic tools are available for the diagnosis of pancreatic cancer, such as magnetic resonance imaging (MRI), abdominal ultrasonography, endoscopic ultrasound-guided fine-needle aspiration and the standard for staging and diagnosis tri-phase pancreatic protocol CT. Additionally, the cancer biomarker serum cancer antigen 19-9 (CA 19-9) is the only approved marker for pancreatic cancer and is used to assist in diagnosis and to predict patient prognosis and recurrence post resection. Unfortunately, the CA19-9 biomarker is not tumour-specific and therefore is not capable for use as a screening tool for the patients that are asymptomatic[1,2,10].

Recently, biomarkers for early diagnosis have been investigated, including plasma-based metabolite panels, increased concentrations of volatile organic compounds in exhaled air, DNA mutations such as p53 in pancreatic juice, and tumour markers such as CA125, CA242, CEA, NSE[2,12]. Despite continued investigation into diagnostic biomarkers, the lack of a specific and validated biomarker as well as sensitive screening programs remains a major issue.

TREATMENT

The treatment strategy for pancreatic cancer is dependent on the primary tumour resectability, which is defined by the absence of distance metastasis as well as the locoregional anatomical contacts allowing for a R0 resection. For patients eligible, the primary treatment that presents a possible cure for pancreatic cancer is surgical resection in addition to chemotherapy[2,13].

The surgical options for achieving surgical resection are open Pacnreatico-duodenectomy and total or distal pancreatectomy, either open or laparoscopic. The surgical method employed is dependent on the tumour or tumour's anatomical location. It is important to mention that the survival rates following surgical resection alone are low with approximately 10% after 5 years. Despite observed benefits when adjuvant therapies are utilised, the recurrence rates remain high, with a 2-year relapse of approximately 70%[2,13,14].

Unfortunately, as previously mentioned, at the time of diagnosis approximately 90% of patients present with tumours that are locally advanced or metastatic, making them ineligible for surgical resection. The only options for these patients are the management of jaundice, system control, palliative radiotherapy, and chemotherapy. A variety of chemotherapeutic drugs are used to treat pancreatic cancer including Oxaliplatin, Paclitaxel, Leucovorin, Irinotecan, Doxorubicin, and 5-fluorouracil (5-FU) (Table 1)[15,16]. Currently, the standard of care for patient's ineligible for surgical resection remains FOLFIRINOX (Fluorouracil, Oxaliplatin, Leucovorin and Irinotecan) or Gemcitabine (2′,2′-diflurodeoxyxytidine) either in combination with Paclitaxel or as a single agent[3,4,14,17,18].

The most effective treatment regimen is guided by patient fitness, FOLFIRNOX is administered to fit patients with tumours in the tail, body, and head of the pancreas, with treatment resulting in significant longer cancer-specific, metastasis-free, disease-free, and overall survival (11.1 mo) when compared to Gemcitabine (6.8 mo). However, a significantly increased risk of adverse effects and complications is seen in patients that receive FOLFIRNOX when compared to Gemcitabine. Gemcitabine +/- Capecitabine is relative safe compared to other chemotherapy options and is therefore the standard treatment for patients that are ineligible for FOLFIRNOX treatment regimens. It has been found to provide improved system control, a higher response rate and a greater overall survival rate compared to 5-FU (4.41 mo)[2,14,19]. Despite the poor survival outcomes, 5-FU is used for periampullary tumours primarily due to insufficient evidence for other chemotherapeutic agents specifically targeting said tumour types[2]. Due to the clinical benefits of Gemcitabine compared to other treatment regimes, it has become the standard reference agent in the first line treatment choice of pancreatic cancer[20,21]. This shows that the patient benefit to current treatments is minimal, hence identifying better targets and more efficient treatments is required.

GEMCITABINE

Gemcitabine is a cytotoxic pyrimidine nucleoside analogue that has been utilized as a chemotherapeutic agent for not only pancreatic cancer but for a variety of solid

Table 1 The current chemotherapeutic and chemoprotectant agents used to treat pancreatic cancer, their classification, action, and chemical structure

Drug	Classification	Action
Gemcitabine (Gemzar)	Antimetabolite	Pyrimidine antagonist
Doxorubicin (Rubex)	Anthracycline Antibiotic	Cell-cycle specific antagonist
Fluorouracil (5-FU)	Antimetabolite	Pyrimidine antagonist
Paclitaxel (Abraxane)	Plant alkaloid, Taxane, Antimircotubule	Inhibition of cell microtubule structures
Oxaliplatin (Eloxatin)	Alkylating agent	Cell-cycle non-specific antagonist
Leucovorin (Folinic acid)	Chemoprotectant	Enhancement anti-cancer effects
Irinotecan (Camptosar)	Plant alkaloid, Topoisomerase I inhibitor	Camptothecan analogs
Erlotinib (Tarceva)	Tyrosine kinase inhibitor	Ant-EGFR
Cetuximab (Erbitux)	Biologic	Anti-EGFR
Bevacizumab (Avastin)	Biologic	Anti-VEGF

Citation: National Center for Biotechnology Information, 2021 [cited 12 April 2021]. Database: PubChem Compound Summary [Internet]. Available from: https://pubchem.ncbi.nlm.nih.gov/compound/Gemcitabine[70,71].

tumours and more recently in certain lymphomas[22]. Due to the hydrophilic nature of gemcitabine, passive diffusion is slow through cellular membranes and therefore requires transportation into cells by specialized integral membrane proteins known as human nucleotide transporters (NTs)[16,23,24].

To exert clinical action, gemcitabine needs to be metabolized and requires multiple kinases to initiate serial phosphorylation. Once transported intracellularly, gemcitabine (dFdC) is catalyzed by deoxycytidine kinase (dCK) resulting in gemcitabine monophosphate (dFdCMP) and is then phosphorylated to gemcitabine diphosphate (dFdCDP) by nucleotide monophosphate kinase (NMPK) and finally gemcitabine triphosphate (dFdCTP) by nucleoside-diphosphate kinase (NDPK). The successful uptake and metabolism of gemcitabine to results in the inhibition of DNA repair and replication (Figure 2). Finally, Gemcitabine or its phosphorylated metabolites are exported into the extracellular space by multidrug resistance protein 5 (MRP5). An additional mechanism that gemcitabine exerts actions is self-potentiation by the inhibition of enzymes associated with deoxynucleotide metabolism[22,25-27].

Although gemcitabine and other chemotherapeutic drugs have been proven effective among patients with various stages of pancreatic cancer, the effectiveness of gemcitabine is severely limited due to the development of chemoresistance[19]. Chemoresistance is simply the ability of cancer cells to survive or evade therapeutics and can be intrinsic or acquired during treatment[28]. Chemotherapeutic drug resistance is widely common in pancreatic cancer with less than 30% of patients showing improvement post treatment and previous studies have identifying a heightened resistance to gemcitabine in comparison to other chemotherapeutic drugs in pancreatic cancer cells[19,29,30].

To date, several mechanisms have been identified as contributors to acquired gemcitabine resistance in pancreatic cancer due to the drugs rapid metabolism and hydrophilic nature including increased levels of ribonucleotide reductase subunit II and II (RRM1/2), mucins, deoxycytidine kinase (dCK), as well as concentrative and equilibrative nucleoside transporters (hCNT/hENT). Regrettably, many of these mechanisms are complex and the identification of their specific roles and consequences in chemoresistance remains unclear[19,31,32]. As nucleoside transporters are required for gemcitabine uptake into pancreatic cancer cells, they have been identified as key contributing factors to chemoresistance which will be discussed in the following sections.

NUCLEOSIDE TRANSPORTERS

Nucleoside transporters (NTs) are a group of membrane proteins that transport the analogs of both natural and synthetic nucleosides that act as anticancer agents across

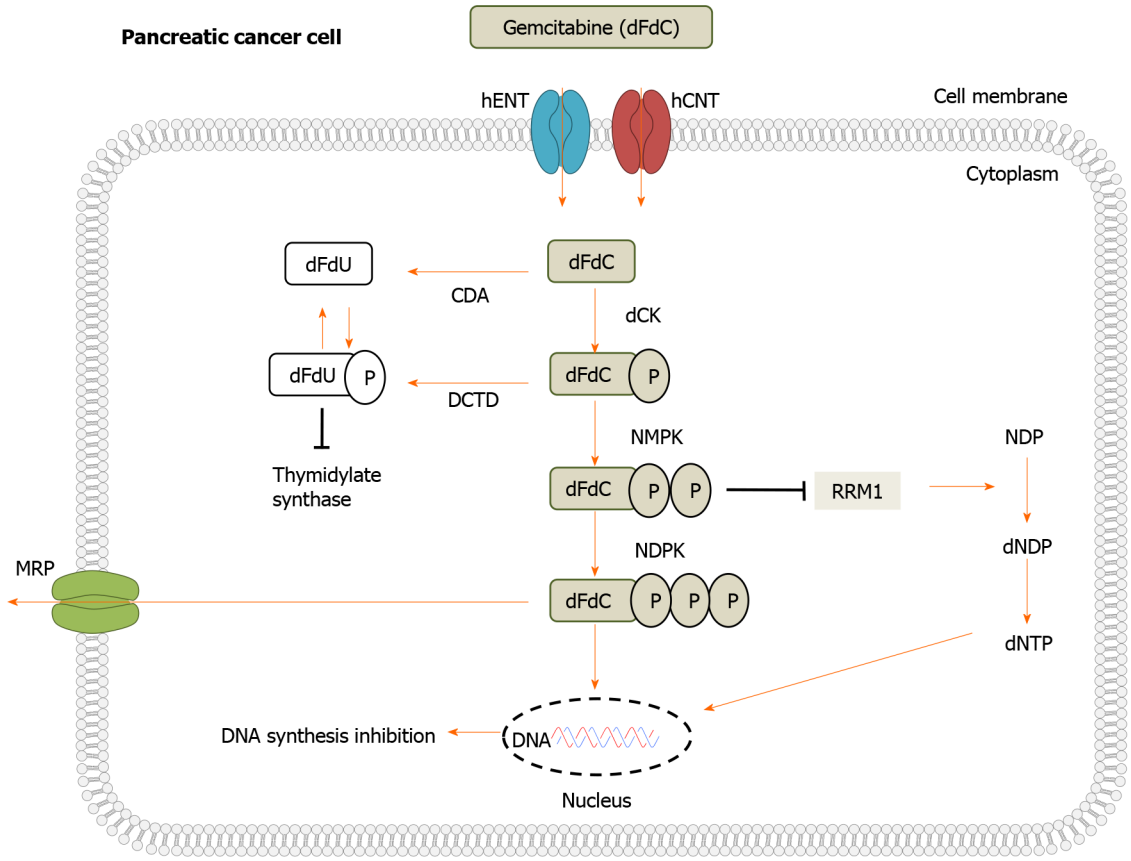


Figure 2 Schematic representation of Gemcitabine transport, metabolism, intracellular activation, and deactivation. Gemcitabine (dFdC) is transported into the cell by nucleoside transporters: human equilibrative nucleoside transporter (hENT) human concentrative nucleoside transporter (hCNT) and is then catalysed by deoxycytidine kinase (dCK), which results in gemcitabine monophosphate (dFdCMP). It is then phosphorylated by nucleotide monophosphate kinase (NMPK) to gemcitabine diphosphate (dFdCDP). Finally, it is phosphorylated into gemcitabine triphosphate (dFdCTP) by nucleoside-diphosphate kinase (NDPK). Once metabolism is completed, gemcitabine enters the DNA resulting in the inhibition of DNA repair and replication. Gemcitabine or its phosphorylated metabolites are finally exported into the extracellular matrix by multidrug resistance protein 5 (MRP5)[22,26,27,41,69]. RRM1: Ribonucleotide reductase; CDA: Cytidine deaminase; DCTD: Deoxycytidylate deaminase; NDP: Nucleotide diphosphate.

the membranes of vesicles and cells. There are two classes of transporter proteins that are encoded by two different solute carrier families (SLC), SLC28 known as human concentrative nucleoside transports and SLC29 also known as human equilibrative nucleoside transporters[33].

There are three members of the human concentrative nucleoside transporter family including, hCNT1, hCNT2 and hCNT3. These transporters mediate the unidirectional co-transport of Na+ and/or H+ and nucleosides into cells at a 1:1 coupling ratio for hCNT1 and hCNT2 and a 2:1 ratio for hCNT3. Initially, hCNTs were believed to be expressed only in polarized epithelia, however, recent studies have identified the expression to be considerably broader. These proteins favour nucleoside transepithelial flux as they present at an ideal localization on the apical side of polarized epithelial tissue[33].

Human equilibrative nucleoside transporters include four members, hENT1, hENT2, hENT3 and hENT4. These proteins are bio-directional and mediate the facilitative transport of nucleosides and select hENTs also facilitate the transportation of nucleobases dependent on their concentration gradient. Except for hENT4, hENT proteins can transport both pyrimidines and purines, they have a broad permeant selectivity, and are widely distributed in a variety of cell types. Despite their similarities, hENT1, 2 and 3 differ in in nucleoside specificity, however, they all present with a lower substrate affinity then the members of the hCNT family[16,23,33].

NUCLEOSIDE TRANSPORTERS AND PANCR-EATIC CANCER

Due to the importance of gemcitabine in pancreatic cancer treatment and the requirement of transporters for drug uptake, extensive research has been undertaken

on transports and their role in tumorigenesis. Alterations in the expression of transporters have been identified in the progression of normal pancreatic cells to malignant pancreatic cancer cells. Despite significant efforts of researchers to identify the roles transporters undertake in substrate translocation and their functions in cell physiology, more research evaluating the clinical application of transporters as potential biomarkers or therapeutical targets is required. The primary transporter that efficiently mediates the cellular uptake of gemcitabine is hENT1 (SLC29A1), however, evidence suggests minor cellular uptake of gemcitabine *via* hENT2 (SLC29A2), hCNT1 (SLC28A1) and hCNT3 (SLC28A3)[15,16,23,26]. Each transporter undertakes specific functions (Table 2), and each will be discussed as follows:

HUMAN EQUILIBRATIVE NUCLEOSIDE TRANSPORTERS IN PANCREATIC CANCER

hENT1

The hENT1 protein is a transmembrane glycoprotein that is localized to plasma membranes and is widely expressed with a broad selectivity for pyrimidines and purines[16]. In a healthy pancreas, hENT1 has medium expression in exocrine glandular cells and low expression in islets of Langerhans. In comparison, pancreatic tumours present with a decrease in hENT1 expression[34].

Previous clinical studies on pancreatic cancer patients and various cell lines have identified that that low levels of hENT1 expression on pancreatic tumour cells correlates with a significant reduction in progression free survival (PFS) and disease-free survival (DFS) when compared to patients with medium to high levels of hENT1 expression[7,35]. If gemcitabine is incapable of cellular uptake due to a lack of transportation into the cell, it is unable to inhibit cell growth and therefore the abundance of hENT1 may contribute to gemcitabine resistance as a result of reduced intracellular build-up. In fact, previous studies reported the inhibition of hENT1 in cancer cell lines with NBMPR (nucleoside analogue nitrobenzylmercaptopurine ribonucleoside - a potent inhibitor of hENT1) resulted in cell chemoresistance to gemcitabine[34,36,37]. Thus, further supporting the importance of hENT1 in gemcitabine sensitivity.

This research indicates that hENT1 Levels are correlated with gemcitabine response as the upregulation of hENT1 proteins results in the enhancement of gemcitabine's cytotoxic effects, while the loss of hENT1 protein expression results in the development of gemcitabine resistance. Due to this, hENT1 is an attractive potential prognostic biomarker in pancreatic cancer patients for gemcitabine treated patients[7,19].

It is important to note that the hENT1 gene itself is not reduced in the development of chemoresistance to gemcitabine, nor does it correlate with gemcitabine's IC_{50} values for several pancreatic cancer cell lines. This suggests that hENT1 expression is not solely alone in patients acquired and inherent chemoresistance to gemcitabine[34].

hENT2

The hENT2 protein is encoded by the gene SLC29A2 and transports a range purine and pyrimidine nucleosides as well as select nucleobases across cells membranes with broad affinity. The protein is present in a wide range of cell types though its gene expression is greatest in the skeletal muscle. The hENT2 protein is highly expressed in the pancreatic cells of healthy individuals but is shown to be reduced in pancreatic cancer patients and pancreatic cancer cell lines[38,39].

hENT2 has recently been identified as being a key element in the regulation of nucleotide and nucleoside pool for effective cell cycle progression and synthesis of DNA. This evidence indicates that hENT2 is partly responsible for transporting, into the nucleus, the supply of nucleotides required for DNA replication. Therefore, the dysregulation of this transporter protein may have adverse effects on cell homeostasis and possibly contribute to tumour progression[33].

hENT2 has also been the subject of several investigations due to its ability to transport gemcitabine into cells. It is however proven to transport the chemotherapeutic drug with a much lower affinity when compared to hENT1[38]. Unlike the extensive research undertaken on hENT1 which has proven a link between the protein and chemoresistance, there are few studies investigating the importance of hENT2 [22]. hENT2 protein expression has been identified in various pancreatic cancer cell lines, although less than the expression of hENT1 transporters[25].

Table 2 The mechanisms, efficacy, toxicity, affinity, and disadvantages of human nucleoside transporters

Transporter	Mechanisms of action	Efficacy, toxicity, and affinity	Known disadvantages	Ref.
hENT1 (SLC29A1)	Nucleoside-derived anticancer drug update. Antiviral drug uptake. Cellular uptake of nucleosides for RNA or DNA synthesis. Adenosine signalling	Clear correlation between the efficacy of nucleoside analog chemotherapeutic treatment and expression of hENT1. Increase in chemotherapeutic drug efficacy with an increase in transporter expression. Highly sensitive to NBMPR, draflazine, dilazep, and dipyridamole.Increase in cell toxicity with an increase in transporter expression. Highest affinity for gemcitabine uptake	Mutations in the SLC29A1 gene associated with Faisalabad histiocytosis, pigmented hypertrichosis including insulin dependent diabetes, and H syndrome. Select variants of the gene highly immunogenic, may result in haemolytic disease of newborns and foetus as well as acute haemolytic transfusion reaction	[72-77]
hENT2 (SLC29A2)	Nucleoside-derived anticancer drug update. Antiviral drug uptake Mediates the influx and efflux of pyrimidine and purine nucleosides as well as the purine base hypoxanthine. Transport's bile salts, metal ions, organic acids, amine compounds, glucose and other sugars	Although identified to transport gemcitabine into cells, it is less effective than hENT1 at cytotoxic drug uptake. Minimally sensitive to inhibition *via* NBMPR, draflazine, dilazep, and dipyridamole. Higher affinity for nucleobases when compared to hENT1	Mutations in the SLC29A2 gene associated with familial and Histiocytosis-Lymphadenopathy Plus Syndrome and hepatic Adenomas. Dysregulation may result in have adverse effects on cell homeostasis and possibly contribute to tumour progression	[33, 37, 38, 40, 78]
hCNT1 (SLC28A1)	Transport's bile salts, metal ions, organic acids, amine compounds, glucose and other sugars. Transport's nucleosides, related molecules, and vitamins. Nucleoside binding. Nucleoside sodium symporter activity. Nucleoside-derived anticancer drug update. Antiviral pyrimidine nucleoside analog drug uptake	Minimally effective at cytotoxic drug uptake. Expression is negatively regulated by MUC4 in gemcitabine resistant pancreatic cancer cells. Has a selective inhibition for thymidine, adenosine, uridine, inosine, guanosine, and cytidine	Mutations in the SLC28A1 gene are associated with Uridine-Cytidineuria disease. Overexpression of protein may result in translocation of pyrimidine alone, resulting in modifications of cell physiology	[16, 45, 51, 79]
hCNT3 (SLC28A3)	Regulates cellular processes, such as vascular tone, neurotransmission, surface receptors, the concentration of adenosine in the vicinity of cell as well as transport, and finally the metabolism of nucleoside drugs. hCNT3 has a broad specificity for pyrimidine and purine nucleosides	Clear correlation between hCNT3 downregulation and gemcitabine toxicity	Mutations in the *SLC28A3* gene results in the altered sensitivity to the compound BMS-536924	[80-82]

hENT1/2: Human equilibrative nucleoside transporter 1/2; hCNT1/3: Human concentrative nucleoside transporter 1/3.

Previous studies aimed at investigating hENT2 Levels in chemoresistance pancreatic cancer cell lines identified the expressed protein had a lower expression after gemcitabine treatment[37,40]. In cohesion with the reduction in protein expression, hENT2 mRNA levels are also reduced following gemcitabine treatment. Furthering these studies, the inactivation of hENT2 *via* exposure to dilazep (a hENT2 inhibitor), in conjunction with the inhibition of hENT1 *via* NBMPR, results in a reduction of gemcitabine uptake and sensitivity. However, the decrease in hENT2 expression may not provide an explanation for the limited uptake of gemcitabine into cells and therefore chemoresistance, as the expression of other gemcitabine transporters are not affected by hENT2 downregulation[37,40].

These results provide evidence that hENT2 when aberrantly expressed may contribute to gemcitabine resistance, however, more extensive research is required to understand the exact impact hENT2 expression has on other mechanisms of chemoresistance in addition to pancreatic cancer cells.

HUMAN CONCENTRATIVE NUCLEOTIDE TRANSPORTERS IN PANCREATIC CANCER

hCNT1

The hCNT1 protein, encoded by the SLAC28A1 gene, is a sodium dependant transporter with a high affinity for pyrimidines[25]. It is broadly detected in epithelia with a moderate to high expression in healthy pancreatic tissue. The expression of hCNT1 is decreased to an almost negligible in undifferentiated states such as fetal hepatocytes, intestinal crypt cells and human tumours, namely pancreatic and breast tumours[41].

The exact role hCNT1 undertakes in the regulation of gemcitabine resistance and cytotoxicity in pancreatic cancer cells is yet to be described, however, data obtained from multiple studies have indicated that the hCNT1 expression is frequently reduced in pancreatic cancer cell lines and tumours when compared to unaffected pancreatic cells[42-44]. In chemoresistant pancreatic cancer cells, hCNT1 expression is limited and can be correlated with limited influx of gemcitabine into target cells. However, investigations into the pharmacological inhibition of the degradation of hCNT1 results in a moderate increase of the cellular transport of gemcitabine thus suggesting the transporter as a possible target mechanism for increasing chemosensitivity and drug transport[42].

Due to the correlation between decreased hCNT1 expression levels and the increased chemoresistance of pancreatic cancer cells, recent research has investigated the mechanisms that decrease transporter expression. As a result, it has been identified that the transmembrane mucin MUC4 utilises the NF-KB pathway to inhibit hCNT1 [45]. The increase of MUC4 expression is commonly observed in pancreatic cancer cells, which results in a higher rate of inhibition of hCNT1 transporters and therefore an increase in chemoresistance. Importantly, studies have shown that the inhibition of MUC4 oncogenic receptor Erb2 resulted in the increase of hCNT1 expression and an increased uptake and sensitivity to gemcitabine[42]. Although more extensive work is needed to determine the processes affecting hCNT1 expression, mucins are an interesting contributing factor.

hCNT3

The hCNT3 transporter belongs to the SLC28 family and is characterized by the broadest tissue specificity and tissue distribution. It is a symporter that couples the transportation of a nucleoside to the symport of one proton or two Na^+ ions. In healthy individuals the transporter is expressed at high levels in the pancreas, mammary glands and in bone marrow. HCNT3 is also expressed in low levels in the prostate, liver, testis, lungs, and intestines[46].

The importance of hCNT3 in pancreatic cancer is of clinical and pharmacological significance due to its ability to transport a large variety of nucleoside-derived drugs such as valacyclovir for viral infections and more importantly gemcitabine for solid tumors. Due to this, it is identified as a crucial mediator of drug response and the development of resistance to anti-cancer drugs[46].

The aberrant expression of hCNT3 has been observed in various pancreatic tumors and pancreatic cancer cell lines. More specifically, a decrease in expression is observed which has been correlated with increased gemcitabine cytotoxicity[45]. Furthermore, uncharacterized polymorphisms of hCHT3 such as the nonsynonymous A25G mutation, have been associate with tumor response to drug toxicity and therapy in pancreatic cancer patients[24]. It has also been shown that hCNT3 expression in pancreatic tumors correlates with overall patient survival, with an increased expression of the transporter associated with a longer overall patient survival[45]. Recent studies investigating the mechanisms that regulate hCNT3 expression in tumor cells suggest that ErbB2 expression and epithelial to mesenchymal transition (EMT) have a negative impact on the regulation of transporter expression[47].

hCNT3 has been observed to have multiple advantages over other NTs capable of gemcitabine uptake, primarily as a potential therapeutic target for reducing resistance of toxic nucleoside analog treatments. Despite extensive research aimed at hENT1 as a therapeutic target for overcoming gemcitabine resistance in pancreatic cancer patients, Paproski *et al*[23] identified an 8-fold uptake of gemcitabine in hCNT3 transfected cells with functional hENTs and 142-434-fold uptake in cells without hENT activity. The evidence suggesting that functional hENTs present in cells result in a decrease in gemcitabine uptake. However, another study undertaken by Maréchal *et al*[26] identified pancreatic cancer patients that presented with both high hENT1 and high hCNT3 expression had a 5-fold longer overall survival than those with one favorable prognostic factor and a 7-fold overall survival length than individuals with no favorable prognostic factors.

POSSIBLE STRATEGIES TO OVERCOME CHEMORESISTANCE

To date, several strategies aim at effectively treating pancreatic cancer and overcoming chemoresistance commonly seen in patients undertaking chemotherapeutic treatments. A variety of techniques and agents are currently or have previously been investigated for their effectiveness against not only pancreatic cancer, but also

gastrointestinal, peritoneal, and respiratory mucous tumours[3,48].

Numerous target treatments have been investigated and evaluated either alone or in combination with chemotherapeutic agents for pancreatic cancer. Currently, the only targeted therapeutic agent to have statistically significant benefit for patient survival is the tyrosine kinase inhibitor (TKI) erlotinib in combination with gemcitabine with a 2-week mean survival benefit over gemcitabine as a single agent. Though promising, erlotinib is clinically marginal and further investigations are required[48,49].

Other investigated drugs include multikinase inhibitors exhibiting antiangiogenic activity like axitinib, sunitinib and sorafenib and antiangiogenic drugs including vascular endothelial growth factor (VEGF) inhibitors aflibercept and bevacizumab. Recently, compounds targeting signalling cascades such as the multikinase inhibitor masitinib67, phosphoinositide 3-kinase inhibitor rigosertib, and anti-insulin-like growth factor 1 receptor antibodies cixutumumab65,66 and ganitumab have been investigated in combination with gemcitabine. Regrettably, these agents have shown no improvement in patient survival, they have however, provided insight into the cause of futility, with the dense stroma surrounding pancreatic cancer cells speculated to be a key contributor[48,50].

The microenvironment of pancreatic tumours is composed of fibrotic stroma including inflammatory cells, fibroblasts, nerve cells, blood vessels, hyaluronan, fibronectin, and collagen. The theory of targeting the stroma of pancreatic tumours to enhance the effectiveness of chemotherapeutic drugs is of great interest. It is hypothesised that due to the poor vascularization and deposition of extracellular matrix component causes increased hydrostatic pressure and stiffness resulting in a barrier of drug uptake. Currently investigated treatments included calcipotriol for the inactivation of pancreatic stellate cells (PSCs), smoothened homologue inhibitor IPI-926 for the inhibition of collagen deposition and myofibroblast growth and finally evofosfamide which inhibits DNA replication. As seen with other therapeutic treatments, agents attacking the stroma are still in the early stages of investigation and more work is required[48,50].

POSSIBLE STRATEGIES TO ENHANCE NUCLEOSIDE TRANSPORTERS

To date, no viable agents specifically targeting nucleoside transporters in relation to chemoresistance has been developed. Though *in vivo* investigations into the upregulation of hCNT1 expression have shown promising results, the clinical application of these techniques is not yet applicable[51,52]. Although, it has been hypothesised that the overexpression of selected mucins in pancreatic cancer is a contributing factor to nucleoside transporter efficacy and therefore chemoresistance[53]. This mucin overexpression results in the production of a thick, mucinous physical barrier between cancer cells and the extracellular matrix, thus inhibiting the ability of intracellular drug uptake *via* nucleoside transporters and affecting the drugs cytotoxicity. Due to this, several agents have been investigated for their mucolytic properties[42,53].

Much of this research has focused on agents that involve the immune system, such as adoptive immunotherapy, oncolytic viral therapy, peptide vaccines to enhance the cytotoxic T cell or T helper cell response, or specific antibodies. These techniques have shown promising results for patients with metastasised disease, when implemented in pre-clinical as well as early-stage clinical trials. However, many of these approaches are limited in their targeting abilities and have only been examined in small patient cohorts[2,3].

Another avenue readily investigated is gene editing technology specifically targeting the mechanisms that have been identified as contributors of disease progression. These methods can include transfection of cells, silencing, and upregulating genes *via* gene promotors, and at the transcriptional level, targeting epigenetic regulation. It is important to note, despite the promising results obtained *in vitro* and in early clinical stages for these treatments, there are issues surrounding the effectiveness of treatment delivery *in vivo*. Due to this, further research is required on the feasibilities of implementing these treatments to patients[2,3,54].

A variety of micro RNAs (miRs), pharmacological and natural agents have also been investigated for their ability to limit pancreatic cancer progression by specifically targeting and downregulating well known mucins such as MUC1 and MUC4[54,55].

miRs are small noncoding RNAs that occur naturally, functioning in gene regulation and have been identified as possible regulators of mucin expression in pancreatic cancer. Four key miRs have been investigated and provided positive results, those being, miR-Let-7b, miR-150, miR-219-1-3p, and miR-200c. All mentioned miRs have

been found to downregulate MUC4 expression, miR-150 directly targets MUC4 resulting in inhibition and is therefore a MUC4-regulating miR. Despite the promising effect of miRs in regulating mucins, there are minimal studies aimed at assessing their viability against established pancreatic tumors *in vivo* and further studies are required prior to clinical application[36,56-58].

Regarding pharmacological agents, the modulation of mucins, specifically MUC4, is achieved through anti-inflammatory drugs, corticosteroids. Key investigated corticosteroids include dexamethasone, as well as afatinib and canertinib, two pan-EGFR family inhibitors. These agents had various levels of effectiveness with dexamethasone providing variable modulation results, while afatinib and canertinib resulted in the downregulation of MUC4 expression. Interestingly, canertinib, unlike afatinib, is an irreversible inhibitor and treatment resulted in not only downregulation of MUC4, but also reduction in tumor growth. Though promising, the variable effects due to corticosteroids not only on mucins, but other mechanisms of disease have limited the possibility of clinical application[54,59,60].

Natural agents are of great significance in the treatment of pancreatic cancer due to their ability to target inflammation signaling pathways and regulate the expression of mucins. Several of these agents have been identified as possible pancreatic cancer treatments, including, Thymoquinone, Guggulsterone, Graviola extract, Bromelain and N-acetylcysteine.

Guggulsterone is a phytosteroid derived from the resin of Commiphora Mukul plants. Historically, it has been utilized for the treatment of atherosclerosis, hyperlipidemia, diabetes, hypertension, and obesity. More recently, it has been investigated for its anti-proliferative activity, ability to induce apoptosis and inhibit cell invasion and motility in various tumor types whether *in vitro* or *vivo*. Furthermore, Guggulsterone has shown a synergistic effect with gemcitabine against pancreatic cancer, as well as the reversal of multidrug resistance in breast cancer cell lines. In addition to its anti-tumor properties, Guggulsterone has been identified to decrease the activation of STAT/JAK pathways, downregulating MUC4 as a result. Accounting for all the possible benefits of Guggulsterone it is an attractive agent for clinical application in combination with Gemcitabine against pancreatic cancer[54,61].

Thymoquinone is a bioactive constitute derived from black seed oil (Nigella sativa). It has previously been identified as having several promising pharmacological properties against diseases due to its anti-inflammatory, antioxidant, and anticancer activities. More recently, it has been shown to exhibit antineoplastic properties against pancreatic cancer cell lines FG/ COLO357 and CD18/HPAF. Treatment with Thymoquinone against these cell lines resulted in the downregulation of MUC4 resulting in the increased apoptosis and decrease of migration of tumor cells. The downregulation of MUC4 results in the activation of c-Jun-(NH2)-terminal kinase and p38 MAP kinase, thereby implicating MUC4 as a key target of Thymoquinone. As seen with other natural agents, synergistic effects have been observed both *in vitro* and vivo with Thymoquinone and chemotherapeutic agents, specifically, Gemcitabine and Oxaliplatin[54,62,63].

Annona muricata (Graviola) evergreen trees are the source of medicinal treatment for inflammatory conditions such as insomnia, hypertension, rheumatism, diabetes, and neuralgia. Within the last decade, investigations into the effect of extracted graviola on pancreatic cancer cell lines have been undertaken *in vitro* and vivo. It has been identified that graviola downregulated genes associated with glycolysis and hypoxia, and more importantly, downregulated MUC4, while exhibiting antimetastatic and antiproliferative effects[54,64]. Interestingly, graviola has been shown effective in destroying chemoresistant breast cancer cells[65]. This study indicating graviola to be an attractive agent of investigation for chemoresistant cancer cells.

Bromelain is a cysteine proteolytic enzyme extracted from the stem of immature pineapple plants (Ananas comosus). The enzyme is well known for its anti-inflammatory and mucolytic properties as well as its uses for relief of indigestion, thrombosis, fevers, wound debridement, and edema. Bromelain was originally utilised for its anti-cancer properties in ovarian and breast cancer, with clinical trials of administration resulting in a decrease of metastasis and the resolution of tumour masses. When administered in combination treatments with chemotherapeutic agents such as 5-FU greater patient outcomes and further tumour regression has been observed[66]. Interestingly, bromelain has been recently investigated for its proteolytic properties, specifically its ability to target and disrupt glycosidic linkages in mucins resulting in the disruption of the protective mucolytic layer. The disruption of mucolytic layers produced by mucins on cancerous cells enables the effective uptake of cytotoxic drugs into cells resulting in better patient survival[3,53,66].

N-acetyl cystine (NAC) is a sulphur containing amino acid that is commonly used for the treatment of acetaminophen toxicity and to liquify the thick mucus formed in respiratory diseases such as chronic obstructive pulmonary disorder (COPD) and cystic fibrosis[66]. Due to its chemical composition, NAC holds the ability to reduce disulphide bonds (S-S) to sulphydryl (S-H) bonds in glycoproteins and therefore convert purulent and viscous mucin into an aqueous state resulting in ciliary elimination in the respiratory system[66].

A further strategy for overcoming chemoresistance and increasing patient survival is combination therapy with chemotherapeutic and mucolytic agent. Two natural agents have been identified as effective against mucous cancers when combined, those being bromelain and NAC[67].

Recently, studies into the efficiency of these agents as single agents, in combination with each other and in combination with gemcitabine and 5-FU against pancreatic cancer cell lines has been investigate with promising results[53]. This can present beneficial outcomes for clinical application due to the ease of application as well as a reduction in required chemotherapeutic doses therefore reduced toxicity when compared to currently utilised chemotherapeutic drugs[3,53].

The combination of bromelain and NAC has been shown to have a synergistic cytotoxic effect against several tumour types. It is known that late-stage pancreatic tumours express high amounts of MUC1, MUC4, MUC16 which have been associated with invasiveness, cellular proliferation, metastasis and chemoresistance. Previous studies have shown that a bromelain and NAC combination treatment resulted in the reduction of mucin expression both *in vitro* and *vivo*[53,68]. Recent *in vivo* investigations into combination therapy of bromelain and NAC with the addition of cytotoxic agents such as gemcitabine resulted in observed synergism and introduce the possibility of reducing the clinical cytotoxic dosage required for treatment and therefore reducing side effects that commonly present with high dose treatments[53]. It is thought that the combination of bromelain and NAC will disrupt the glycosylic linkages and disulphate bonds within mucins allowing for gemcitabine to effectively enter the cells *via* nucleoside transporters resulting in its ability to incite its cytotoxic effect[53].

CONCLUSION

Pancreatic cancer is a deadly disease with a high mortality rate attributed to late tumour detection, disease aggressiveness and chemoresistance. Although predicted to be the second leading cause of cancer associated mortality within the next 10 years, steady progress has been achieved in determining the mechanisms that contributes to the poor progression of the disease, which, in turn contributes to the development of diagnostic and therapeutic targets.

One of these mechanisms has been identified as human nucleoside transporters, namely for their importance in the transportation of chemotherapeutic drugs into diseased cells along with their contribution to acquired chemoresistance. Primarily, investigations have been undertaken on the nucleoside transporters hENT1, hENT2, hCNT1, and hCNT3, namely due to their ability to transport the nucleoside analogue gemcitabine, however, more research is needed to evaluate their use not only as diagnostic markers but as therapeutic targets.

The expression of nucleoside transporter proteins has been shown to be adverse in pancreatic cancer cells, with decreased protein expression correlating with not only reductions in progression and disease-free patient survival but also an increase in acquired chemoresistance. The lack or inability of nucleoside transporter proteins to facilitate the uptake of chemotherapeutic drugs has been identified as a contributor of gemcitabine chemoresistance and although the majority of research has been focused on hENT1, all examine nucleoside transporters have exhibited this correlation.

There have been several suggestions on overcoming the factors contributing to nucleoside transport related chemoresistance, with treatment options such as mucins being of great interest. Specific mucins have been shown to be overexpressed in pancreatic cancer cells and new combination treatment therapies, such as bromelain + NAC + gemcitabine, targeting the linkages seen in mucins expose the encased nucleoside transporters, allowing for the uptake of cytotoxic drugs which is advantageous for several reasons. The two main benefits being increased drug uptake, and reduction of required cytotoxic dose although further research of this strategy for not only the treatment of pancreatic cancer but also overcoming chemoresistance is required.

ACKNOWLEDGEMENTS

We would like to thank the team at the Department of Surgery at St George Hospital, UNSW for all of their support.

REFERENCES

1 **Rawla P**, Sunkara T, Gaduputi V. Epidemiology of Pancreatic Cancer: Global Trends, Etiology and Risk Factors. *World J Oncol* 2019; **10**: 10-27 [PMID: 30834048 DOI: 10.14740/wjon1166]
2 **McGuigan A**, Kelly P, Turkington RC, Jones C, Coleman HG, McCain RS. Pancreatic cancer: A review of clinical diagnosis, epidemiology, treatment and outcomes. *World J Gastroenterol* 2018; **24**: 4846-4861 [PMID: 30487695 DOI: 10.3748/wjg.v24.i43.4846]
3 **Suh H**, Pillai K, Morris DL. Mucins in pancreatic cancer: biological role, implications in carcinogenesis and applications in diagnosis and therapy. *Am J Cancer Res* 2017; **7**: 1372-1383 [PMID: 28670497]
4 **Jonckheere N**, Skrypek N, Van Seuningen I. Mucins and pancreatic cancer. *Cancers (Basel)* 2010; **2**: 1794-1812 [PMID: 24281201 DOI: 10.3390/cancers2041794]
5 **Kaur S**, Kumar S, Momi N, Sasson AR, Batra SK. Mucins in pancreatic cancer and its microenvironment. *Nat Rev Gastroenterol Hepatol* 2013; **10**: 607-620 [PMID: 23856888 DOI: 10.1038/nrgastro.2013.120]
6 **Murthy D**, Attri KS, Singh PK. Phosphoinositide 3-Kinase Signaling Pathway in Pancreatic Ductal Adenocarcinoma Progression, Pathogenesis, and Therapeutics. *Front Physiol* 2018; **9**: 335 [PMID: 29670543 DOI: 10.3389/fphys.2018.00335]
7 **Attia F**, Fathy S, Anani M, Hassan A, Attia F, Ibrahim G, Elazab M. Human equilibrative nucleoside transporter-1 and deoxycytidine kinase can predict gemcitabine effectiveness in Egyptian patients with Hepatocellular carcinoma. *J Clin Lab Anal* 2020; **34**: e23457 [PMID: 32671914 DOI: 10.1002/jcla.23457]
8 **Ringel J**, Löhr M. The MUC gene family: their role in diagnosis and early detection of pancreatic cancer. *Mol Cancer* 2003; **2**: 9 [PMID: 12556240]
9 **Moniaux N**, Andrianifahanana M, Brand RE, Batra SK. Multiple roles of mucins in pancreatic cancer, a lethal and challenging malignancy. *Br J Cancer* 2004; **91**: 1633-1638 [PMID: 15494719 DOI: 10.1038/sj.bjc.6602163]
10 **Zhang L**, Sanagapalli S, Stoita A. Challenges in diagnosis of pancreatic cancer. *World J Gastroenterol* 2018; **24**: 2047-2060 [PMID: 29785074 DOI: 10.3748/wjg.v24.i19.2047]
11 **Mohammed S**, Van Buren G 2nd, Fisher WE. Pancreatic cancer: advances in treatment. *World J Gastroenterol* 2014; **20**: 9354-9360 [PMID: 25071330 DOI: 10.3748/wjg.v20.i28.9354]
12 **Liu F**, Du F, Chen X. Multiple tumor marker protein chip detection system in diagnosis of pancreatic cancer. *World J Surg Oncol* 2014; **12**: 333 [PMID: 25381564 DOI: 10.1186/1477-7819-12-333]
13 **Yamamoto T**, Uchida Y, Terajima H. Clinical impact of margin status on survival and recurrence pattern after curative-intent surgery for pancreatic cancer. *Asian J Surg* 2019; **42**: 93-99 [PMID: 29249392 DOI: 10.1016/j.asjsur.2017.09.003]
14 **Conroy T**, Hammel P, Hebbar M, Ben Abdelghani M, Wei AC, Raoul JL, Choné L, Francois E, Artru P, Biagi JJ, Lecomte T, Assenat E, Faroux R, Ychou M, Volet J, Sauvanet A, Breysacher G, Di Fiore F, Cripps C, Kavan P, Texereau P, Bouhier-Leporrier K, Khemissa-Akouz F, Legoux JL, Juzyna B, Gourgou S, O'Callaghan CJ, Jouffroy-Zeller C, Rat P, Malka D, Castan F, Bachet JB; Canadian Cancer Trials Group and the Unicancer-GI–PRODIGE Group. FOLFIRINOX or Gemcitabine as Adjuvant Therapy for Pancreatic Cancer. *N Engl J Med* 2018; **379**: 2395-2406 [PMID: 30575490 DOI: 10.1056/NEJMoa1809775]
15 **Tsujie M**, Nakamori S, Nakahira S, Takahashi Y, Hayashi N, Okami J, Nagano H, Dono K, Umeshita K, Sakon M, Monden M. Human equilibrative nucleoside transporter 1, as a predictor of 5-fluorouracil resistance in human pancreatic cancer. *Anticancer Res* 2007; **27**: 2241-2249 [PMID: 17695509]
16 **Spratlin JL**, Mackey JR. Human Equilibrative Nucleoside Transporter 1 (hENT1) in Pancreatic Adenocarcinoma: Towards Individualized Treatment Decisions. *Cancers (Basel)* 2010; **2**: 2044-2054 [PMID: 24281217 DOI: 10.3390/cancers2042044]
17 **Conroy T**, Desseigne F, Ychou M, Bouché O, Guimbaud R, Bécouarn Y, Adenis A, Raoul JL, Gourgou-Bourgade S, de la Fouchardière C, Bennouna J, Bachet JB, Khemissa-Akouz F, Péré-Vergé D, Delbaldo C, Assenat E, Chauffert B, Michel P, Montoto-Grillot C, Ducreux M; Groupe Tumeurs Digestives of Unicancer; PRODIGE Intergroup. FOLFIRINOX versus gemcitabine for metastatic pancreatic cancer. *N Engl J Med* 2011; **364**: 1817-1825 [PMID: 21561347 DOI: 10.1056/NEJMoa1011923]
18 **Jonckheere N**, Skrypek N, Van Seuningen I. Mucins and tumor resistance to chemotherapeutic drugs. *Biochim Biophys Acta* 2014; **1846**: 142-151 [PMID: 24785432 DOI: 10.1016/j.bbcan.2014.04.008]
19 **Zeng S**, Pöttler M, Lan B, Grützmann R, Pilarsky C, Yang H. Chemoresistance in Pancreatic Cancer. *Int J Mol Sci* 2019; **20** [PMID: 31514451 DOI: 10.3390/ijms20184504]
20 **Manji GA**, Olive KP, Saenger YM, Oberstein P. Current and Emerging Therapies in Metastatic Pancreatic Cancer. *Clin Cancer Res* 2017; **23**: 1670-1678 [PMID: 28373365 DOI:

10.1158/1078-0432.Ccr-16-2319]
21 **Conroy T**, Bachet JB, Ayav A, Huguet F, Lambert A, Caramella C, Maréchal R, Van Laethem JL, Ducreux M. Current standards and new innovative approaches for treatment of pancreatic cancer. *Eur J Cancer* 2016; **57**: 10-22 [PMID: 26851397 DOI: 10.1016/j.ejca.2015.12.026]
22 **Alvarellos ML**, Lamba J, Sangkuhl K, Thorn CF, Wang L, Klein DJ, Altman RB, Klein TE. PharmGKB summary: gemcitabine pathway. *Pharmacogenet Genomics* 2014; **24**: 564-574 [PMID: 25162786 DOI: 10.1097/fpc.0000000000000086]
23 **Paproski RJ**, Yao SY, Favis N, Evans D, Young JD, Cass CE, Zemp RJ. Human concentrative nucleoside transporter 3 transfection with ultrasound and microbubbles in nucleoside transport deficient HEK293 cells greatly increases gemcitabine uptake. *PLoS One* 2013; **8**: e56423 [PMID: 23441192 DOI: 10.1371/journal.pone.0056423]
24 **Maréchal R**, Bachet JB, Mackey JR, Dalban C, Demetter P, Graham K, Couvelard A, Svrcek M, Bardier-Dupas A, Hammel P, Sauvanet A, Louvet C, Paye F, Rougier P, Penna C, André T, Dumontet C, Cass CE, Jordheim LP, Matera EL, Closset J, Salmon I, Devière J, Emile JF, Van Laethem JL. Levels of gemcitabine transport and metabolism proteins predict survival times of patients treated with gemcitabine for pancreatic adenocarcinoma. *Gastroenterology* 2012; **143**: 664-674.e6 [PMID: 22705007 DOI: 10.1053/j.gastro.2012.06.006]
25 **García-Manteiga J**, Molina-Arcas M, Casado FJ, Mazo A, Pastor-Anglada M. Nucleoside transporter profiles in human pancreatic cancer cells: role of hCNT1 in 2',2'-difluorodeoxycytidine-induced cytotoxicity. *Clin Cancer Res* 2003; **9**: 5000-5008 [PMID: 14581375]
26 **Maréchal R**, Mackey JR, Lai R, Demetter P, Peeters M, Polus M, Cass CE, Young J, Salmon I, Devière J, Van Laethem JL. Human equilibrative nucleoside transporter 1 and human concentrative nucleoside transporter 3 predict survival after adjuvant gemcitabine therapy in resected pancreatic adenocarcinoma. *Clin Cancer Res* 2009; **15**: 2913-2919 [PMID: 19318496 DOI: 10.1158/1078-0432.Ccr-08-2080]
27 **Hagmann W**, Jesnowski R, Löhr JM. Interdependence of gemcitabine treatment, transporter expression, and resistance in human pancreatic carcinoma cells. *Neoplasia* 2010; **12**: 740-747 [PMID: 20824050 DOI: 10.1593/neo.10576]
28 **Yeldag G**, Rice A, Del Río Hernández A. Chemoresistance and the Self-Maintaining Tumor Microenvironment. *Cancers (Basel)* 2018; **10** [PMID: 30487436 DOI: 10.3390/cancers10120471]
29 **Shukla SK**, Purohit V, Mehla K, Gunda V, Chaika NV, Vernucci E, King RJ, Abrego J, Goode GD, Dasgupta A, Illies AL, Gebregiworgis T, Dai B, Augustine JJ, Murthy D, Attri KS, Mashadova O, Grandgenett PM, Powers R, Ly QP, Lazenby AJ, Grem JL, Yu F, Matés JM, Asara JM, Kim JW, Hankins JH, Weekes C, Hollingsworth MA, Serkova NJ, Sasson AR, Fleming JB, Oliveto JM, Lyssiotis CA, Cantley LC, Berim L, Singh PK. MUC1 and HIF-1alpha Signaling Crosstalk Induces Anabolic Glucose Metabolism to Impart Gemcitabine Resistance to Pancreatic Cancer. *Cancer Cell* 2017; **32**: 71-87.e7 [PMID: 28697344 DOI: 10.1016/j.ccell.2017.06.004]
30 **Dauer P**, Nomura A, Saluja A, Banerjee S. Microenvironment in determining chemo-resistance in pancreatic cancer: Neighborhood matters. *Pancreatology* 2017; **17**: 7-12 [PMID: 28034553 DOI: 10.1016/j.pan.2016.12.010]
31 **de Sousa Cavalcante L**, Monteiro G. Gemcitabine: metabolism and molecular mechanisms of action, sensitivity and chemoresistance in pancreatic cancer. *Eur J Pharmacol* 2014; **741**: 8-16 [PMID: 25084222 DOI: 10.1016/j.ejphar.2014.07.041]
32 **Mittal A**, Chitkara D, Behrman SW, Mahato RI. Efficacy of gemcitabine conjugated and miRNA-205 complexed micelles for treatment of advanced pancreatic cancer. *Biomaterials* 2014; **35**: 7077-7087 [PMID: 24836307 DOI: 10.1016/j.biomaterials.2014.04.053]
33 **Pastor-Anglada M**, Pérez-Torras S. Emerging Roles of Nucleoside Transporters. *Front Pharmacol* 2018; **9**: 606 [PMID: 29928232 DOI: 10.3389/fphar.2018.00606]
34 **Nakano Y**, Tanno S, Koizumi K, Nishikawa T, Nakamura K, Minoguchi M, Izawa T, Mizukami Y, Okumura T, Kohgo Y. Gemcitabine chemoresistance and molecular markers associated with gemcitabine transport and metabolism in human pancreatic cancer cells. *Br J Cancer* 2007; **96**: 457-463 [PMID: 17224927 DOI: 10.1038/sj.bjc.6603559]
35 **Farrell JJ**, Elsaleh H, Garcia M, Lai R, Ammar A, Regine WF, Abrams R, Benson AB, Macdonald J, Cass CE, Dicker AP, Mackey JR. Human equilibrative nucleoside transporter 1 levels predict response to gemcitabine in patients with pancreatic cancer. *Gastroenterology* 2009; **136**: 187-195 [PMID: 18992248 DOI: 10.1053/j.gastro.2008.09.067]
36 **Wang C**, Lin W, Playa H, Sun S, Cameron K, Buolamwini JK. Dipyridamole analogs as pharmacological inhibitors of equilibrative nucleoside transporters. Identification of novel potent and selective inhibitors of the adenosine transporter function of human equilibrative nucleoside transporter 4 (hENT4). *Biochem Pharmacol* 2013; **86**: 1531-1540 [PMID: 24021350 DOI: 10.1016/j.bcp.2013.08.063]
37 **Paproski RJ**, Young JD, Cass CE. Predicting gemcitabine transport and toxicity in human pancreatic cancer cell lines with the positron emission tomography tracer 3'-deoxy-3'-fluorothymidine. *Biochem Pharmacol* 2010; **79**: 587-595 [PMID: 19788890 DOI: 10.1016/j.bcp.2009.09.025]
38 **Liu Y**, Zuo T, Zhu X, Ahuja N, Fu T. Differential expression of hENT1 and hENT2 in colon cancer cell lines. *Genet Mol Res* 2017; **16** [PMID: 28218790 DOI: 10.4238/gmr16019549]
39 **Griffiths M**, Yao SY, Abidi F, Phillips SE, Cass CE, Young JD, Baldwin SA. Molecular cloning and characterization of a nitrobenzylthioinosine-insensitive (ei) equilibrative nucleoside transporter from human placenta. *Biochem J* 1997; **328** (Pt 3): 739-743 [PMID: 9396714 DOI: 10.1042/bj3280739]

40 **Zhang S**, Furugawa T, Takahashi H, Che X, Zhao H, Akiyama S, Li Y. Analysis of gene expression in gemcitabine resistant cells derived from human pancreatic cancer cell. Proceedings of the Proceedings 2011 International Conference on Human Health and Biomedical Engineering. 2011: 182-185

41 **Amrutkar M**, Gladhaug IP. Pancreatic Cancer Chemoresistance to Gemcitabine. *Cancers (Basel)* 2017; **9** [PMID: 29144412 DOI: 10.3390/cancers9110157]

42 **Spratlin J**, Sangha R, Glubrecht D, Dabbagh L, Young JD, Dumontet C, Cass C, Lai R, Mackey JR. The absence of human equilibrative nucleoside transporter 1 is associated with reduced survival in patients with gemcitabine-treated pancreas adenocarcinoma. *Clin Cancer Res* 2004; **10**: 6956-6961 [PMID: 15501974 DOI: 10.1158/1078-0432.Ccr-04-0224]

43 **Bhutia YD**, Hung SW, Patel B, Lovin D, Govindarajan R. CNT1 expression influences proliferation and chemosensitivity in drug-resistant pancreatic cancer cells. *Cancer Res* 2011; **71**: 1825-1835 [PMID: 21343396 DOI: 10.1158/0008-5472.Can-10-2736]

44 **Skrypek N**, Duchêne B, Hebbar M, Leteurtre E, van Seuningen I, Jonckheere N. The MUC4 mucin mediates gemcitabine resistance of human pancreatic cancer cells *via* the Concentrative Nucleoside Transporter family. *Oncogene* 2013; **32**: 1714-1723 [PMID: 22580602 DOI: 10.1038/onc.2012.179]

45 **Stecula A**, Schlessinger A, Giacomini KM, Sali A. Human Concentrative Nucleoside Transporter 3 (hCNT3, SLC28A3) Forms a Cyclic Homotrimer. *Biochemistry* 2017; **56**: 3475-3483 [PMID: 28661652 DOI: 10.1021/acs.biochem.7b00339]

46 **Hesler RA**, Huang JJ, Starr MD, Treboschi VM, Bernanke AG, Nixon AB, McCall SJ, White RR, Blobe GC. TGF-β-induced stromal CYR61 promotes resistance to gemcitabine in pancreatic ductal adenocarcinoma through downregulation of the nucleoside transporters hENT1 and hCNT3. *Carcinogenesis* 2016; **37**: 1041-1051 [PMID: 27604902 DOI: 10.1093/carcin/bgw093]

47 **Neoptolemos JP**, Kleeff J, Michl P, Costello E, Greenhalf W, Palmer DH. Therapeutic developments in pancreatic cancer: current and future perspectives. *Nat Rev Gastroenterol Hepatol* 2018; **15**: 333-348 [PMID: 29717230 DOI: 10.1038/s41575-018-0005-x]

48 **Moore MJ**, Goldstein D, Hamm J, Figer A, Hecht JR, Gallinger S, Au HJ, Murawa P, Walde D, Wolff RA, Campos D, Lim R, Ding K, Clark G, Voskoglou-Nomikos T, Ptasynski M, Parulekar W; National Cancer Institute of Canada Clinical Trials Group. Erlotinib plus gemcitabine compared with gemcitabine alone in patients with advanced pancreatic cancer: a phase III trial of the National Cancer Institute of Canada Clinical Trials Group. *J Clin Oncol* 2007; **25**: 1960-1966 [PMID: 17452677 DOI: 10.1200/jco.2006.07.9525]

49 **Michl P**, Gress TM. Current concepts and novel targets in advanced pancreatic cancer. *Gut* 2013; **62**: 317-326 [PMID: 23112132 DOI: 10.1136/gutjnl-2012-303588]

50 **Pérez-Torras S**, Vidal-Pla A, Cano-Soldado P, Huber-Ruano I, Mazo A, Pastor-Anglada M. Concentrative nucleoside transporter 1 (hCNT1) promotes phenotypic changes relevant to tumor biology in a translocation-independent manner. *Cell Death Dis* 2013; **4**: e648 [PMID: 23722537 DOI: 10.1038/cddis.2013.173]

51 **Pastor-Anglada M**, Pérez-Torras S. Nucleoside transporter proteins as biomarkers of drug responsiveness and drug targets. *Front Pharmacol* 2015; **6**: 13 [PMID: 25713533 DOI: 10.3389/fphar.2015.00013]

52 **Pillai K**, Mekkawy AH, Akhter J, Badar S, Dong L, Liu AI, Morris DL. Enhancing the potency of chemotherapeutic agents by combination with bromelain and N-acetylcysteine - an in vitro study with pancreatic and hepatic cancer cells. *Am J Transl Res* 2020; **12**: 7404-7419 [PMID: 33312377]

53 **Gautam SK**, Kumar S, Cannon A, Hall B, Bhatia R, Nasser MW, Mahapatra S, Batra SK, Jain M. MUC4 mucin- a therapeutic target for pancreatic ductal adenocarcinoma. *Expert Opin Ther Targets* 2017; **21**: 657-669 [PMID: 28460571 DOI: 10.1080/14728222.2017.1323880]

54 **Torres MP**, Chakraborty S, Souchek J, Batra SK. Mucin-based targeted pancreatic cancer therapy. *Curr Pharm Des* 2012; **18**: 2472-2481 [PMID: 22372499 DOI: 10.2174/13816128112092472]

55 **Srivastava SK**, Bhardwaj A, Singh S, Arora S, Wang B, Grizzle WE, Singh AP. MicroRNA-150 directly targets MUC4 and suppresses growth and malignant behavior of pancreatic cancer cells. *Carcinogenesis* 2011; **32**: 1832-1839 [PMID: 21983127 DOI: 10.1093/carcin/bgr223]

56 **Arora S**, Swaminathan SK, Kirtane A, Srivastava SK, Bhardwaj A, Singh S, Panyam J, Singh AP. Synthesis, characterization, and evaluation of poly (D,L-lactide-co-glycolide)-based nanoformulation of miRNA-150: potential implications for pancreatic cancer therapy. *Int J Nanomedicine* 2014; **9**: 2933-2942 [PMID: 24971005 DOI: 10.2147/ijn.S61949]

57 **Lahdaoui F**, Delpu Y, Vincent A, Renaud F, Messager M, Duchêne B, Leteurtre E, Mariette C, Torrisani J, Jonckheere N, Van Seuningen I. miR-219-1-3p is a negative regulator of the mucin MUC4 expression and is a tumor suppressor in pancreatic cancer. *Oncogene* 2015; **34**: 780-788 [PMID: 24608432 DOI: 10.1038/onc.2014.11]

58 **Seshacharyulu P**, Ponnusamy MP, Rachagani S, Lakshmanan I, Haridas D, Yan Y, Ganti AK, Batra SK. Targeting EGF-receptor(s) - STAT1 axis attenuates tumor growth and metastasis through downregulation of MUC4 mucin in human pancreatic cancer. *Oncotarget* 2015; **6**: 5164-5181 [PMID: 25686822 DOI: 10.18632/oncotarget.3286]

59 **Gollub EG**, Waksman H, Goswami S, Marom Z. Mucin genes are regulated by estrogen and dexamethasone. *Biochem Biophys Res Commun* 1995; **217**: 1006-1014 [PMID: 8554551 DOI: 10.1006/bbrc.1995.2870]

60 **Macha MA**, Rachagani S, Gupta S, Pai P, Ponnusamy MP, Batra SK, Jain M. Guggulsterone decreases proliferation and metastatic behavior of pancreatic cancer cells by modulating JAK/STAT

and Src/FAK signaling. *Cancer Lett* 2013; **341**: 166-177 [PMID: 23920124 DOI: 10.1016/j.canlet.2013.07.037]

61 **Torres MP**, Ponnusamy MP, Chakraborty S, Smith LM, Das S, Arafat HA, Batra SK. Effects of thymoquinone in the expression of mucin 4 in pancreatic cancer cells: implications for the development of novel cancer therapies. *Mol Cancer Ther* 2010; **9**: 1419-1431 [PMID: 20423995 DOI: 10.1158/1535-7163.Mct-10-0075]

62 **Woo CC**, Kumar AP, Sethi G, Tan KH. Thymoquinone: potential cure for inflammatory disorders and cancer. *Biochem Pharmacol* 2012; **83**: 443-451 [PMID: 22005518 DOI: 10.1016/j.bcp.2011.09.029]

63 **Torres MP**, Rachagani S, Purohit V, Pandey P, Joshi S, Moore ED, Johansson SL, Singh PK, Ganti AK, Batra SK. Graviola: a novel promising natural-derived drug that inhibits tumorigenicity and metastasis of pancreatic cancer cells in vitro and in vivo through altering cell metabolism. *Cancer Lett* 2012; **323**: 29-40 [PMID: 22475682 DOI: 10.1016/j.canlet.2012.03.031]

64 **Syed Najmuddin SU**, Romli MF, Hamid M, Alitheen NB, Nik Abd Rahman NM. Anti-cancer effect of Annona Muricata Linn Leaves Crude Extract (AMCE) on breast cancer cell line. *BMC Complement Altern Med* 2016; **16**: 311 [PMID: 27558166 DOI: 10.1186/s12906-016-1290-y]

65 **Pillai K**. Anti-Tumour and Chemosensitising Effect of a Combination of Bromelain + N-Acetyl Cysteine with Cisplatin or 5-Fu on Malignant Peritoneal Mesothelioma Cells. *J Glycobiol* 2013; s1 [DOI: 10.4172/2168-958X.S1-005]

66 **Amini A**, Masoumi-Moghaddam S, Ehteda A, Liauw W, Morris DL. Potentiation of chemotherapeutics by bromelain and N-acetylcysteine: sequential and combination therapy of gastrointestinal cancer cells. *Am J Cancer Res* 2016; **6**: 350-369 [PMID: 27186409]

67 **Zheng HC**. The molecular mechanisms of chemoresistance in cancers. *Oncotarget* 2017; **8**: 59950-59964 [PMID: 28938696 DOI: 10.18632/oncotarget.19048]

68 **Goral V**. Pancreatic Cancer: Pathogenesis and Diagnosis. *Asian Pac J Cancer Prev* 2015; **16**: 5619-5624 [PMID: 26320426 DOI: 10.7314/apjcp.2015.16.14.5619]

69 **Maher DM**, Gupta BK, Nagata S, Jaggi M, Chauhan SC. Mucin 13: structure, function, and potential roles in cancer pathogenesis. *Mol Cancer Res* 2011; **9**: 531-537 [PMID: 21450906 DOI: 10.1158/1541-7786.Mcr-10-0443]

70 **Chemocare**. Chemotherapy Drugs and Drugs Often Used During Chemotherapy. 2020 [cited 12 April 2021] Available from: https://pubchem.ncbi.nlm.nih.gov/compound/Gemcitabine

71 **National Center for Biotechnology Information**. PubChem Compound Summary for CID 60750, Gemcitabine. 2020 [cited 12 April 2021] Available from: https://pubchem.ncbi.nlm.nih.gov/compound/Gemcitabine

72 **Wright NJ**, Lee SY. Structures of human ENT1 in complex with adenosine reuptake inhibitors. *Nat Struct Mol Biol* 2019; **26**: 599-606 [PMID: 31235912 DOI: 10.1038/s41594-019-0245-7]

73 **Rehan S**, Paavilainen VO, Jaakola VP. Functional reconstitution of human equilibrative nucleoside transporter-1 into styrene maleic acid co-polymer lipid particles. *Biochim Biophys Acta Biomembr* 2017; **1859**: 1059-1065 [PMID: 28254415 DOI: 10.1016/j.bbamem.2017.02.017]

74 **Vincenzi B**, Stacchiotti S, Collini P, Pantano F, Rabitti C, Perrone G, Iuliani M, Baldi A, Badalamenti G, Sanfilippo R, Santini D, Muda AO, Gronchi A, Casali P, Dei Tos AP, Tonini G. Human equilibrative nucleoside transporter 1 gene expression is associated with gemcitabine efficacy in advanced leiomyosarcoma and angiosarcoma. *Br J Cancer* 2017; **117**: 340-346 [PMID: 28641307 DOI: 10.1038/bjc.2017.187]

75 **Kim J**, Kim H, Lee JC, Kim JW, Paik WH, Lee SH, Hwang JH, Ryu JK, Kim YT. Human equilibrative nucleoside transporter 1 (hENT1) expression as a predictive biomarker for gemcitabine chemotherapy in biliary tract cancer. *PLoS One* 2018; **13**: e0209104 [PMID: 30557411 DOI: 10.1371/journal.pone.0209104]

76 **Bolze A**, Abhyankar A, Grant AV, Patel B, Yadav R, Byun M, Caillez D, Emile JF, Pastor-Anglada M, Abel L, Puel A, Govindarajan R, de Pontual L, Casanova JL. A mild form of SLC29A3 disorder: a frameshift deletion leads to the paradoxical translation of an otherwise noncoding mRNA splice variant. *PLoS One* 2012; **7**: e29708 [PMID: 22238637 DOI: 10.1371/journal.pone.0029708]

77 **Daniels G**. An update on the Augustine blood group system. *Immunohematology* 2019; **35**: 1-2 [PMID: 30908068]

78 **Owen RP**, Lagpacan LL, Taylor TR, De La Cruz M, Huang CC, Kawamoto M, Johns SJ, Stryke D, Ferrin TE, Giacomini KM. Functional characterization and haplotype analysis of polymorphisms in the human equilibrative nucleoside transporter, ENT2. *Drug Metab Dispos* 2006; **34**: 12-15 [PMID: 16214850 DOI: 10.1124/dmd.105.006270]

79 **Cano-Soldado P**, Gorraitz E, Errasti-Murugarren E, Casado FJ, Lostao MP, Pastor-Anglada M. Functional analysis of the human concentrative nucleoside transporter-1 variant hCNT1S546P provides insight into the sodium-binding pocket. *Am J Physiol Cell Physiol* 2012; **302**: C257-C266 [PMID: 21998139 DOI: 10.1152/ajpcell.00198.2011]

80 **Koczor CA**, Torres RA, Lewis W. The role of transporters in the toxicity of nucleoside and nucleotide analogs. *Expert Opin Drug Metab Toxicol* 2012; **8**: 665-676 [PMID: 22509856 DOI: 10.1517/17425255.2012.680885]

81 **Yao SYM**, Young JD. Inward- and outward-facing homology modeling of human concentrative nucleoside transporter 3 (hCNT3) predicts an elevator-type transport mechanism. *Channels (Austin)* 2018; **12**: 291-298 [PMID: 30096006 DOI: 10.1080/19336950.2018.1506665]

82 **Ritzel MW**, Ng AM, Yao SY, Graham K, Loewen SK, Smith KM, Ritzel RG, Mowles DA,

Carpenter P, Chen XZ, Karpinski E, Hyde RJ, Baldwin SA, Cass CE, Young JD. Molecular identification and characterization of novel human and mouse concentrative Na+-nucleoside cotransporter proteins (hCNT3 and mCNT3) broadly selective for purine and pyrimidine nucleosides (system cib). *J Biol Chem* 2001; **276**: 2914-2927 [PMID: 11032837 DOI: 10.1074/jbc.M007746200]

World Journal of Gastroenterology

Submit a Manuscript: https://www.f6publishing.com

World J Gastroenterol 2021 October 28; 27(40): 6861-6873

DOI: 10.3748/wjg.v27.i40.6861

ISSN 1007-9327 (print) ISSN 2219-2840 (online)

MINIREVIEWS

Management of hepatitis B and C in special population

Anand V Kulkarni, Nageshwar Reddy Duvvuru

ORCID number: Anand V Kulkarni 0000-0002-1240-1675; Nageshwar Reddy Duvvuru 0000-0001-7540-0496.

Author contributions: Kulkarni AV and Duvvuru NR made the study concept; Kulkarni AV did the initial drafting and DNR critically assessed and edited the manuscript; all authors approved the final manuscript.

Conflict-of-interest statement: The authors declare no conflicts of interest.

Open-Access: This article is an open-access article that was selected by an in-house editor and fully peer-reviewed by external reviewers. It is distributed in accordance with the Creative Commons Attribution NonCommercial (CC BY-NC 4.0) license, which permits others to distribute, remix, adapt, build upon this work non-commercially, and license their derivative works on different terms, provided the original work is properly cited and the use is non-commercial. See: http://creativecommons.org/Licenses/by-nc/4.0/

Manuscript source: Invited manuscript

Specialty type: Gastroenterology and hepatology

Country/Territory of origin: India

Anand V Kulkarni, Department of Hepatology, Asian Institute of Gastroenterology, Hyderabad 500032, Telangana, India

Nageshwar Reddy Duvvuru, Department of Gastroenterology, Asian Institute of Gastroenterology, Hyderabad 500032, Telanagana, India

Corresponding author: Anand V Kulkarni, MD, Consultant Physician-Scientist, Department of Hepatology, Asian Institute of Gastroenterology, 6-3-661, Somajiguda, Hyderabad 500032, Telangana, India. anandvk90@gmail.com

Abstract

Chronic viral hepatitis is one of the leading causes of cirrhosis worldwide. Chronic hepatitis B is more common in the Asia-Pacific region due to the larger population and lower screening availability. Hepatitis C predominates in the west due to injection drug abuse. The discovery of (oral) direct-acting antiviral agents (DAAs) has changed the landscape of chronic hepatitis C (CHC) management. Nucleos(t)ide analogs (NUCs) have also changed the approach to the treatment of chronic hepatitis B (CHB). Oral NUCs and DAAs have excellent efficacy and patient acceptance as well as a lower risk of resistance. However, certain populations have no robust data and safety and efficacy of such oral drugs is still evolving. In this review, we provide an overview of the management of CHB and CHC in special populations, such as those with chronic kidney disease, pregnant women, healthcare workers, and those undergoing chemo- or immunosuppressive therapy.

Key Words: Chronic kidney disease; Pregnancy; Hepatitis B; Hepatitis C; Health care professionals; Tenofovir

©The Author(s) 2021. Published by Baishideng Publishing Group Inc. All rights reserved.

Core Tip: Hepatitis B and hepatitis C are leading causes of liver disease and pose significant burdens on healthcare and the economy, especially in developing countries. The management of chronic hepatitis B and C in special populations is less known. In this review, we discuss the indications, timing of treatment, and safety of drugs in special populations infected with hepatitis B or C. The special populations discussed herein are those with chronic kidney disease, pregnant women, coinfected patients, healthcare workers, and patients undergoing chemotherapy.

Peer-review report's scientific quality classification
Grade A (Excellent): 0
Grade B (Very good): B
Grade C (Good): 0
Grade D (Fair): 0
Grade E (Poor): 0

Received: February 22, 2021
Peer-review started: February 22, 2021
First decision: May 13, 2021
Revised: May 30, 2021
Accepted: September 14, 2021
Article in press: September 14, 2021
Published online: October 28, 2021

P-Reviewer: Ikegami T
S-Editor: Wu YXJ
L-Editor: A
P-Editor: Wu RR

Citation: Kulkarni AV, Duvvuru NR. Management of hepatitis B and C in special population. *World J Gastroenterol* 2021; 27(40): 6861-6873
URL: https://www.wjgnet.com/1007-9327/full/v27/i40/6861.htm
DOI: https://dx.doi.org/10.3748/wjg.v27.i40.6861

INTRODUCTION

Hepatitis B and C together constitute a major etiology of cirrhosis of the liver, especially in the Asia-Pacific region[1-3]. Nucleos(t)ide analogs and direct-acting antivirals (DAAs) are breakthrough treatments for chronic hepatitis B (CHB) and chronic hepatitis C (CHC), respectively. The management of Hepatitis B and C in an adult population without comorbidities is well known. Special population groups are those who are less often studied, and the drugs cannot be tested in such populations due to ethical reasons. The data on management strategies are still evolving for special populations. Such populations include patients with chronic kidney disease (CKD), patients on hemodialysis (HD), pregnant women, coinfected patients, healthcare workers, and patients undergoing chemotherapy[4]. In this review, we discuss the indications and safety of antiviral agents in special populations.

CHRONIC KIDNEY DISEASE AND HEMODIALYSIS

Hepatitis B and CKD

Hepatitis B is associated with proteinuria and a higher risk of CKD[5,6]. Hepatitis B virus (HBV)-infected treatment naïve patients have a higher incidence of hematuria, glycosuria, and leukocyturia[7]. Nearly 28%-40% of CHB patients have a glomerular filtration rate (GFR) < 90 mL/min/1.73 m^2[7,8]. The prevalence of CKD in CHB patients is 3%-8%, with increasing prevalence with age[9]. This translates into an enormous burden of CKD due to the higher prevalence of CHB in the Asia-Pacific region. The presence of hypertension, diabetes mellitus, and cirrhosis further increases the risk of CKD in CHB[9]. Smoking and physical inactivity can also increase the risk of CKD[10]. The presence of CKD can also increase the risk of HBV infection due to immuno-suppression (rising the risk of viral infections), frequent requirements of blood transfusions (for anemia of chronic disease), and HD. The ideal endpoints of CHB treat-ment are HBsAg loss and anti-HBs seroconversion, which are challenging to attain. Long-term DNA suppression, normalization of alanine transaminase (ALT), and HBeAg loss (in those who are HBe-positive with or without anti-HBe seroconversion) remain the primary achievable endpoints in the treatment of CHB[4]. The data on the management of CHB in CKD are limited. Since ALT levels are suppressed in CKD (and those on HD), initiating treatment in individuals with HBV DNA > 2000 IU/mL (irrespective of ALT levels) is recommended, especially if > F1 fibrosis is documented either by biopsy or noninvasively[11]. Vaccination remains the best preventive strategy for CKD and HD patients. One milliliter each (containing 20 mcg) should be given intramuscularly (in deltoid muscle) four times at 0, 1 mo, 2 mo and 6 mo. The initial anti-HBs titer should be done two months after the first schedule and then annually thereafter. A booster dose is recommended if the anti-HBs is < 10 IU/mL in CKD patients[12]. Tenofovir disoproxil fumarate (TDF), tenofovir alafenamide fumarate (TAF), and entecavir (ETV) have a low risk of resistance and high efficacy in CKD patients[11,13]. Lamivudine, telbivudine, and adefovir are less effective, nephrotoxic, and are associated with risk of resistance. Interferon-α therapy is less tolerated and is not preferred over NUCs, although the advantage of IFN-α of limited duration therapy cannot be ignored. IFN-α can be used in young patients without cirrhosis, psychosis, or autoimmune disease and GFR > 30 mL/min/1.73 $m^2$13 (Table 1).

Hepatitis C and CKD

Extrahepatic manifestations are more common in hepatitis C virus (HCV) than HBV [14]. CHC patients may have renal failure even in the absence of liver disease[15]. HCV-infected individuals have a 23% higher risk of developing CKD than non-HCV-infected individuals[16]. Hepatitis C is a leading cause of liver disease among patients with CKD, particularly those on dialysis. The seroprevalence of HCV in the Asian population in patients on dialysis ranges between 1%-18%, with higher a prevalence in

Table 1 Hepatitis B in chronic kidney disease

	HBV and CKD
Prevalence of CKD in HBV patients	8%
Pathogenesis	Direct cytopathic effect of the HBV on cells of the kidney; Glomerular deposition of immune complexes; Virus-induced specific immunological effector mechanisms (specific T lymphocyte or antibody); CHB induced cytokine toxicity on renal tissue
Risk factors	Smoking, diabetes mellitus, hypertension, cirrhosis.
Common type of renal injury	Membranous GN; Membranoproliferative GN; Polyarteritis nodosa; IgA nephropathy
Treatment indication	HBV DNA 2000 IU/mL with or without elevated ALT; Liver biopsy-chronic hepatitis with > F1 fibrosis; If planned for renal transplant, initiate NUCs 2 wk before transplant even if DNA ≤ 2000 IU/mL
Safe drugs	TAF (no dose adjustment till eGFR < 15 mL); ETV and TDF (If GFR > 50: ETV 0.5 mg/d or TDF 300 mg/d; GFR 30-49: ETV 0.5 mg alternate day or TDF 300 mg alternate day; GFR 10-29: ETV 0.5 mg once in 3 d and TDF 300 mg once in 3 d; on HD-ETV 0.5 mg or TDF 300 mg after every dialysis or every 7 d)
Prevention	Regular screening; Vaccination (double dose); Serology should be performed every year, and a booster dose should be given if antibody titers are below 10 mIU/mL.

HBV: Hepatitis B virus; CKD: Chronic kidney disease; CHB: Chronic hepatitis B; NUC: Nucleos(t)ide analogues; TDF: Tenofovir disoproxil fumarate; TAF: Tenofovir alafenamide fumarate; ETV: Entecavir; GFR: Glomerular filtration rate; GN: Glomerulonephritis; ALT: Alanine transaminase.

those on HD than in those on peritoneal dialysis, *i.e.*, 8 ± 5.5%[17]. Due to a higher number of adverse effects, the use of pegylated IFN plus ribavirin is not recommended [18]. Glecaprevir and pibrentasvir are NS3/4A protease and NS5A inhibitors, respectively, which have pangenotypic activity. Glecapravir 300 mg and pibrentasvir 120 mg in a fixed-dose combination are the treatments of choice for patients with chronic hepatitis C and stage 4 or 5 CKD (including those on HD)[19,20]. In patients with stage 1-3 CKD, similar dosing of DAA without dose adjustments is recommended. However, glecaprevir and pibrentasvir are not available in all countries. Another option for genotype 1b CHC is grazoprevir, 100 mg and elbasvir, 50 mg for 12 wk, which is still unavailable in many countries[21]. Sofosbuvir-based regimens are also safe in patients with renal impairment and cirrhosis (both decompensated and compensated)[22]. Sofosbuvir 400 mg and velpatasvir 100 mg fixed-dose combination is safe and effective for renal impairment patients (even HD patients) with CHC[23]. In patients with CHC and compensated cirrhosis, the recommended duration is 12 wk, while it is 24 wk for decompensated cirrhosis[20]. Sofosbuvir (400 mg) + ledipasvir (90 mg) also has proven efficacy for Genotype 1b with renal impairment but not on HD [24]. Ribavirin may be added for decompensated cirrhosis patients in combination with sofosbuvir-ledipasvir or in persons with HCV genotype 1a who are receiving treatment with elbasvir-grazoprevir and who have baseline NS5A resistance-associated variants for elbasvir. The dose of ribavirin is 200 mg/d for patients with creatinine clearance < 30 mL/min and 200/400 mg alternate day for patients with creatinine clearance between 30 mL/min and 50 mL/min. American Association for the study of Liver Disease (AASLD)/Infectious Disease Society of America (IDSA) has approved the use of sofosbuvir-velpatasvir; however, in some countries, it is still used as an off-label indication in patients with renal impairment[25]. Strict adherence to infection control protocols during dialysis is the only way to prevent HCV spread[26]. To date, no vaccines have succeeded in preventing chronic HCV infection[27]. Anti-HCV antibodies should be tested before initiation of dialysis and then biannually[28]. Monthly ALT estimation is also recommended for those on dialysis (Table 2).

Pregnancy

Pregnancy is an opportunity to diagnose chronic viral hepatitis. Screening for hepatitis B and C is recommended for all individuals to prevent mother-to-child transmission (MTCT) and prevent transmission to health care professionals[29].

HBV and pregnancy: Nearly 10% of childbearing women in the Asia-Pacific region are infected with HBV[30]. There can be four situations in pregnancy: (1) First time incidentally diagnosed CVH during pregnancy; (2) Individuals are infected and are already on treatment with antiviral therapy; (3) Individuals are under surveillance for CVH and are contemplating pregnancy; and (4) Cirrhosis due to viral hepatitis.

Table 2 Hepatitis C in chronic kidney disease

	HCV and CKD
Prevalence of HCV in CKD patients	10%-14%
Pathogenesis	Pronounced leucocyte infiltration of glomerular capillaries and the precipitation of immunoglobulins, immune complexes/cryoglobulins; Glomerular deposition of HCV protein
Risk factors	Age, male gender, lack of HCV treatment, concomitant HAV/HBV infection; Diabetes mellitus
Common types of renal injury	Membranous GN; Membranoproliferative GN; Essential mixed cryoglobulinemia (type II); IgA nephropathy; Polyarteritis nodosa
Treatment indication	Viremia
Safe drugs	Glecapravir + Pibrentasvir; Sofofbuvir + Velpatasvir; Sofosbuvir + Ledipasvir; Grazoprevir + Elbasvir
Prevention	Regular screening and strict infection control procedures; Effective dialysis machine decontamination

HCV: Hepatitis C virus; CKD: Chronic kidney disease; HAV: Hepatitis A virus; GN: Glomerulonephritis.

The risk of transmission to the newborn is as high as 90% if the mother is HBeAg (e antigen)-positive and 10%-12% if the mother is HBeAg-negative and HBeAb (e antibody)-positive[31]. The risk of transmission is also directly proportional to viral load. The risk of progression to chronicity is nearly 90% if the newborn becomes infected[30]. Hence, preventing MTCT is of utmost importance. Screening for HBsAg is mandatory for all pregnant individuals in the first trimester. It is prudent to test HBeAg, HBeAb, and DNA levels by the end of the second trimester. Treatment is indicated if HBV DNA > 200000 IU/mL or HBsAg levels > 4 Log10 IU/mL. TDF can be started at 24-32 wk of gestation and must be continued for up to 12 wk after delivery[4]. Currently, TAF has no data to support its use during pregnancy. However, an initial review of data on TAF in pregnancy is encouraging[32]. If a woman is infected and is already on treatment with antivirals, the treatment must be continued. TDF is the recommended drug of choice during pregnancy, and if the individual is on ETV or any other antivirals, she should be switched to TDF[29]. If the individual is infected and is contemplating pregnancy, it is advised to postpone the treatment until childbirth unless the woman fulfills CHB treatment criteria (presence of advanced fibrosis or high viral load)[29]. Cirrhosis patients who wish to becomes pregnant should be counseled about the risk of decompensations during pregnancy. Pregnancy-induced volume disturbances are similar to cirrhosis, *i.e.*, reduction in systemic vascular resistance and rise in blood volume and splanchnic vasodilation, which may exacerbate pre-existing portal hypertension[29]. Newborns of HBV-positive mothers should receive active and passive immunization. The newborn should be tested for HBsAb 3 mo after complete immunization (*i.e.*, > 9 mo of age)[33]. Chronic HBV infection may not influence pregnancy outcomes; however, postpregnancy, there may be a flare of HBV due to immune restoration[29,30]. Breastfeeding is not contraindicated, and cesarean section is not indicated for HBV-infected mothers.

HCV and pregnancy: The prevalence of HCV infection is high in Western countries due to injection drug abuse; however, the Asia-Pacific region has a lower prevalence than the west. Due to the large population, the incidence of HCV is considered high in the Asia-Pacific region. The prevalence of HCV in the Asia-Pacific region is 0.1%-5% [34]. The lack of sensitive universal testing in developing countries is a major hindrance to diagnose HCV infection. Further transient elastography is not recommended in pregnant individuals to stage fibrosis.

HCV can affect pregnancy outcomes. HCV, a cytopathic virus, has been linked to intrahepatic cholestasis of pregnancy[35]. HCV can also downregulate multidrug resistance protein 2 (MRP2), which would induce a failure to transport toxic substances and subsequent defects in bile transport; high estrogen and progesterone levels would further compound this effect on MRP2 during pregnancy[35,36]. HCV-infected women also have a higher risk of preterm birth[37]. In contrast, pregnancy being immunosuppressed does not affect HCV. However, in the postpartum period, women may clear the virus spontaneously due to immune reconstitution and HCV-specific T-cell response development[36]. The pooled incidence of MTCT is 6%[38]. Concomitant human immunodeficiency virus (HIV) infection, high HCV viral load, and injection drug abusers (due to acute hepatitis) are at higher risk of transmitting the infection to the newborn[38,39]. MTCT occurs most often in late stages, either during

intrauterine or intrapartum transmission[29]. There is no added benefit of cesarean section and hence is not indicated for patients with HCV infection to prevent transmission. Breastfeeding is not contraindicated[40]. Prolonged rupture of membranes (> 6 h) and invasive tests such as internal fetal monitoring, amniocentesis, and chorionic villous sampling have the potential risk of transmission[41]. Episiotomy should also be avoided, if possible, in HCV-infected pregnant individuals[41]. None of the DAAs have been approved to be used in pregnancy yet. DAAs are category B drugs in pregnancy. Sofosbuvir with ledipasvir has been shown to be effective and safe in pregnancy[42]. The drug was initiated in the 2nd or early third trimester. There are two trials underway assessing DAAs in pregnancy. The first trial evaluating sofosbuvir plus ledipasvir initiated at 24 wk of gestation (ClinicalTrials.gov Identifier: NCT02683005). Another trial assessing sofosbuvir plus velpatasvir commenced six months postpartum (ClinicalTrials.gov Identifier: NCT03570112). The results of these trials are expected soon. Differences in HBV and HCV management are shown in Table 3.

HEALTHCARE WORKERS

Healthcare workers (HCWs) are attending clinicians, surgeons, employees, students, contractors, public-safety workers, or volunteers whose activities involve contact with patients or with blood or other body fluids from patients in healthcare, laboratory, or public-safety settings[43]. HCWs are at risk of becoming infected and can also be a potential source of transmission to patients. The risk of transmission is, although rare from providers to patients, it is recommended to treat HCWs even with a low viral load (HBV DNA < 1000 IU/mL)[44]. Prior to universal vaccination, the risk of transmission was 5%-13% from HBeAg-positive HCWs to patients and 0.8%-3.5% from HBeAg-negative HCWs to patients[45]. The prevalence of HBV among HCWs ranges between 5%-7% in developing countries[46,47]. The presence of HBV infection does not preclude the HCWs from practicing medicine (dentistry or surgery, or any allied health care work) as per the Centers for Disease control and Prevention (CDC) [44]. The European Association for the Study of the Liver recommends treating HCWs if DNA levels are more than 200 IU/mL[4]. The CDC recommends treating HCWs if DNA >1000 IU/mL and prohibits HCWs from performing exposure-prone procedures if DNA >1000 IU/mL[44]. In contrast, transmission of HCV from HCWs to patients is rare. HCWs are at higher risk of becoming infected by patients. A meta-analysis reported higher odds of infection among HCWs than controls[48]. HCWs with viremia should be treated.

COINFECTION

HBV with HIV: The prevalence of HBV HIV coinfection ranges between 5%-20%, with a higher prevalence among injection drug abusers[49]. The risk of liver-related mortality is twice as high in patients with coinfection as in those with HIV monoinfection[50]. HBV also increases overall mortality and hepatocellular carcinoma in HIV-infected patients[51,52]. Coinfected patients have higher levels of HBV viremia and lower rates of HBeAg clearance[53]. HIV-infected patients are prone to drug-induced liver injuries (especially from nevirapine-based regimens) and hepatitis flares[54]. HBV is reported to increase the risk of acquired immunodeficiency syndrome development, but this report was contraindicated in later studies[55]. All coinfected patients should be treated with ART (antiretroviral therapy) irrespective of the CD4 count[4,56]. ART should contain tenofovir as a part of the regimen. Lamivudine + emtricitabine and tenofovir (TDF or TAF) should be used for treating coinfected patients. TDF + lamivudine+ efavirenz or nevirapine combination has a lower attrition rate and is associated with lower mortality in HIV/HBV infected patients[57]. A fixed drug combination of elvitegravir, cobicistat, emtricitabine, and TAF has excellent efficacy in HIV/HBV coinfected patients[58]. Dolutegravir, emtricitabine and TDF/TAF fixed dose combinations may also be considered for patients with HIV/HBV coinfection[59]. All HBsAg patients should be screened for HIV infection prior to initiating tenofovir-based therapy (to prevent resistance), and HIV-infected patients should be screened for HBsAg prior to initiation of ART[56]. If negative, it is recommended to vaccinate the individual to achieve an anti-HBs of ≥ 10 mIU/mL.

Table 3 Hepatitis B and Hepatitis C in pregnancy

	HBV	HCV
MTCT	90% if HBeAg+; 10% if HBeAg-; Directly proportional to viral load	6%; Higher risk with concomitant HIV infection, higher viral load, IV drug abuse; Higher risk with PROM and CVS
Treatment	TDF is safe; Can be initiated in third trimester	DAAs are not approved; Treat prior to pregnancy or 6 mo postpartum
Effect on pregnancy outcome	None	Preterm birth, ICP
Effect of pregnancy on virus	None	None
Effect of postpartum (immune restoration) on virus	Risk of HBV flares	Higher chance of viral clearance
Timing of transmission	Intrapartum > intrauterine	Intrapartum > intrauterine
C-section for all	Not indicated	Not indicated
Breastfeeding	Not contraindicated	Not contraindicated
Prevention	Active and passive immunization to child prevents 90% of transmission; Failure is nearly 15% if the viral load in mother is > log6	None
Confirming the perinatal transmission	Persistence of HBsAg in newborn for > 6 mo	Anti-HCV positive at 18 mo of age HCV RNA positive after 2 mo on 2 different samples
Confirming the protection	Anti-HBs titers at 9 mo	Negative Anti-HCV at 18 mo

HBV: Hepatitis B virus; HCV: Hepatitis C virus; HIV: Human immunodeficiency virus; IV: Intravenous; MTCT: Mother-to-child transmission; PROM: Prolonged rupture of membranes; CVS: Chorionic villous sampling; Ag: Antigen; ICP: Intrahepatic cholestasis of pregnancy; C-section: Cesarean section.

HCV and HIV coinfection is common in injection drug abusers. HCV does not alter the natural history of HIV; however, HIV infection significantly alters the natural history of HCV. HIV leads to a rapid worsening of liver disease, shortens survival, and increases the risk of decompensations in HCV-related cirrhosis patients[60]. HIV also hastens fibrosis progression in CHC patients. Spontaneous clearance of HCV is noted in 5%-10% of patients with HIV infection, whereas nearly 15%-30% of HIV noninfected patients clear HCV spontaneously[61]. The indication for treating HCV and HIV is similar to those infected with either alone. However, it is recommended to avoid HCV treatment until the CD4 count > 200/μL in coinfected patients[62]. Sofosbuvir (400 mg) plus velpatasvir (100 mg) is the recommended drug of choice for HCV for 12 wk in cirrhosis and noncirrhosis[63]. Glecapravir and pibrentasvir are other options for HIV and HCV coinfected patients for 8 wk (no cirrhosis) or 12 wk (cirrhosis)[20] (Figure 1).

HBV with HCV coinfection: The prevalence of HBV/HCV coinfection varies across the globe. The prevalence of HBV coinfection in HCV-positive individuals ranges from 0.7%-5.8%, and the prevalence of HCV coinfection in HBsAg-positive individuals is between 3.4%-23.0%[64,65]. The presence of HCV coinfection leads to rapid progression of liver disease, fibrosis and accelerates the development of hepatocellular carcinoma (HCC)[65]. Patients with HCV viremia should be treated with DAAs, and those satisfying criteria for treatment for HBV should be treated with NUCs. However, if the patient is HBsAg-positive (not satisfying the treatment criteria for HBV) but requires DAA therapy for HCV, NUCs should be initiated[4]. NUCs should be continued for 12 wk post DAA to prevent reactivation of HBV[4]. HCV core protein strongly inhibits HBV replication, and post DAA lack of HCV core poses a risk for HBV reactivation. The incidence of HBV reactivation is around 12%-14% after HCV treatment[66].

CHEMOTHERAPY AND HEMATOLOGICAL MALIGNANCIES

Patients planned for chemotherapy or immunosuppression should be evaluated for HBV and HCV infection[4]. HBV and HCV are strongly associated with non-Hodgkin's lymphoma[67-69]. Approximately 7%-23% of NHL patients have HBV infection, and 3%-10% harbor HCV infection[69-71]. The risk of HBV reactivation in HBsAg-positive patients undergoing chemotherapy ranges from 26%-53%[72]. HCV

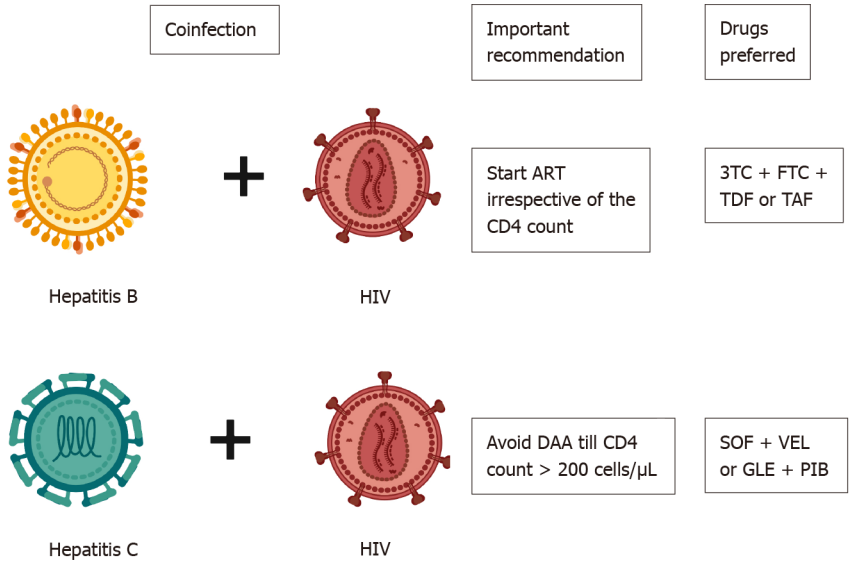


Figure 1 Management of coinfection. Created with biorender.com. HIV: Human immunodeficiency virus; ART: Antiretroviral therapy; 3TC: Lamivudine; FTC: Emtricitabine; TDF: Tenofovir disoproxil fumarate; TAF: Tenofovir alafenamide fumarate; DAA: Directly acting antiviral agents; SOF: Sofosbuvir; VEL: Velpatasvir; GLE: Glecaprevir; PIB: Pibrentasvir.

reactivation is noted in 11% of patients undergoing chemotherapy[73]. If the surface antigen is positive (irrespective of viremia), it is recommended to start NUCs (TDF, TAF, or ETV)[4,72]. Therapy should be continued for 12 mo (18 mo for those on rituximab) after the cessation of immunosuppressive therapy. The stopping rules for those satisfying the standard treatment criteria are the same as those not on immunosuppression.

Patients with HCV viremia should be treated with DAA therapy; however, the timing of therapy is still controversial. If malignancy treatment is deemed urgent, then DAA can be initiated six months after malignancy remission. However, the patient should be monitored for flares. If the malignancy is suspected to be related to the virus itself, then DAAs should be initiated, and viral suppression should be documented prior to chemotherapy initiation[74].

CHILDREN

HBV and children

Chronicity in children is common and depends on the age of acquisition of infection. Perinatally infected patients have a 90% chance of progression to chronicity, while patients infected before 5 years of age have a 25%-50% chance of progression to chronicity. Data on the treatment of the pediatric population are limited. The global prevalence of HBsAg positivity of among children < 5 years of age is 1.3%[75]. The indication for treatment is slightly different from that in the adult population. The presence of cirrhosis (regardless of decompensation status) requires treatment[56]. However, it is recommended to assess the inflammation and stage of fibrosis *via* liver biopsy in all patients prior to therapy. Children with persistently elevated ALT levels (> 1.5 times the upper limit) for ≥ 6 mo who are HBeAg-positive (or ≥ 1 year for HBeAg-negative) with a DNA > 2000 IU/mL and biopsy evidence of moderate to severe necroinflammation or fibrosis require treatment[76]. For patients with a family history of HCC treatment should be initiated even if necroinflammation/fibrosis is mild or absent provided that DNA is > 2000 IU/mL and the ALT levels are elevated [56,76]. TAF (25 mg/d) and ETV (0.015 mg/kg; maximum of 0.5 mg/d) are drugs with high genetic barriers to resistance that are approved for patients aged ≥ 12 years and ≥ 2 years, respectively[75,77]. Last, interferon α-2b (6 million IU/m^2 thrice weekly) is also approved for children aged ≥ 1 year[75]. For HBeAg-positive children, the drug can be stopped 1 year after HBeAg seroconversion[77]. However, the duration of therapy for HBeAg-negative patients is unknown.

HCV and Children: Nearly 0.15% of the global population aged < 18 years has HCV viremia, which corresponds to 3.26 million (2.07-3.9) children. The seropositivity ranges between 0.2% and 0.4% of the population aged < 18 years[78,79]. Interestingly,

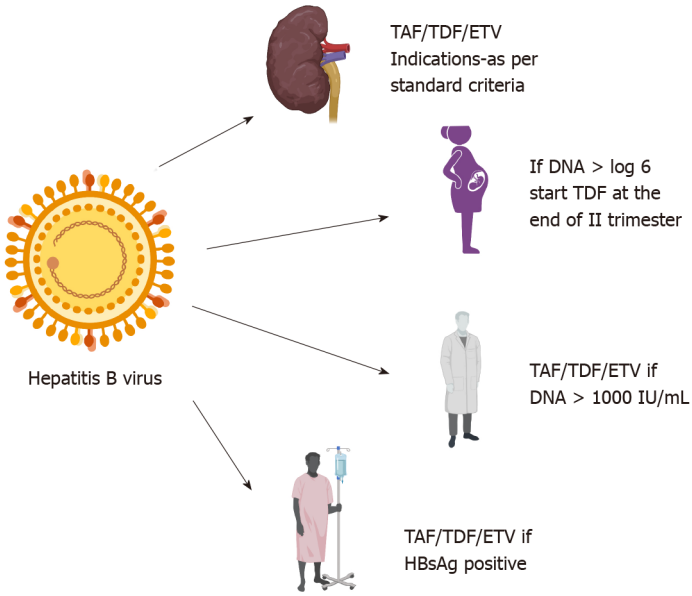


Figure 2 Indications and safety of drugs in special circumstances for hepatitis B. Created with biorender.com. TAF: Tenofovir alafenamide fumarate; TDF: Tenofovir disoproxil fumarate; ETV: Entecavir.

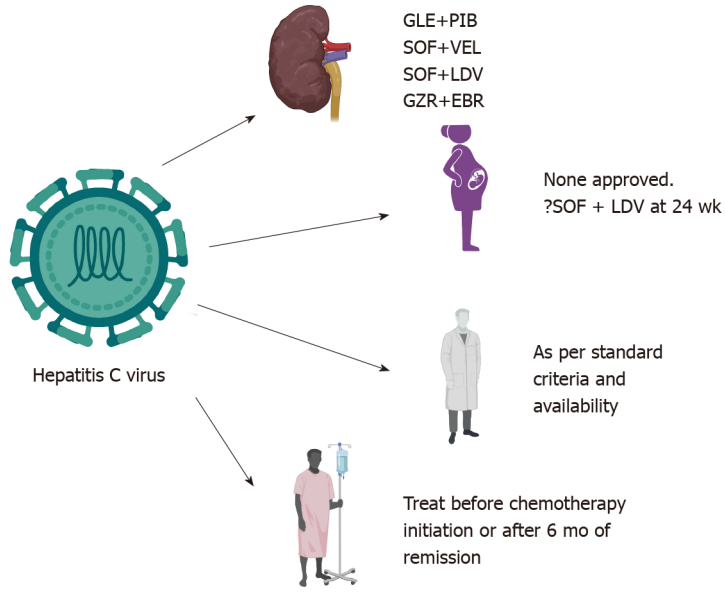


Figure 3 Indications and safety of drugs in special circumstances for hepatitis C. Created with biorender.com. GLE: Glecaprevir; PIB: Pibrentasvir; SOF: Sofosbuvir; VEL: Velpatasvir; LDV: Ledipasvir; GZR: Grazoprevir; EBR: Elbasvir.

25%-40% of children with perinatal transmission spontaneously achieve viral clearance, usually by age 2, and an additional 6%-12% of those with chronic hepatitis C infection may clear the virus before adulthood[80]. Hence, children born to HCV-positive mothers should undergo antibody testing after 18 mo of age[36]. If they are antibody-positive, then their HCV RNA should be assessed after the age of 3 years to confirm the chronicity of infection. The AASLD/IDSA approved drugs widely available are sofosbuvir/Ledipasvir for children aged ≥ 3 years and sofosbuvir/velpatasvir for children aged ≥ 6 years. The doses of these drugs are weight based (sofosbuvir/ledipasvir: < 17 kg: 150 mg/33.75 mg; 17-35 kg: 200 mg/45 mg; ≥ 35 kg: 400 mg/90 mg and sofosbuvir/velpatasvir: 17-30 kg: 200 mg/50 mg; ≥ 30 kg: 400 mg/100 mg) (https://www.hcvguidelines.org/node/2376/summary).

CONCLUSION

Although there are recommendations for each of the above conditions described, further research is required in many areas. The role of TAF in pregnancy is unknown. Since newborns have a higher risk of progression to chronicity if infected, is it prudent to treat all the pregnant mothers' pre-emptively needs to be assessed. Furthermore, in countries in which vertical transmission is the most common mode of infection and testing resources (or ability to provide passive immunization to newborns) are limited, is it beneficial to treat all pregnant women infected with HBV needs to be evaluated. There are some data on the safety of concomitant DAA therapy in patients undergoing chemotherapy without any adverse drug-drug interactions[81]. However, prospective trials are still lacking. The most important aspects of managing HBV and HCV in CKD, pregnant patients, HCWs, and immunosuppressed patients are depicted in Figure 2 and 3.

REFERENCES

1 **Sarin SK**, Kumar M, Eslam M, George J, Al Mahtab M, Akbar SMF, Jia J, Tian Q, Aggarwal R, Muljono DH, Omata M, Ooka Y, Han KH, Lee HW, Jafri W, Butt AS, Chong CH, Lim SG, Pwu RF, Chen DS. Liver diseases in the Asia-Pacific region: a Lancet Gastroenterology & Hepatology Commission. *Lancet Gastroenterol Hepatol* 2020; **5**: 167-228 [PMID: 31852635 DOI: 10.1016/S2468-1253(19)30342-5]

2 **Razavi H**. Global Epidemiology of Viral Hepatitis. *Gastroenterol Clin North Am* 2020; **49**: 179-189 [PMID: 32389357 DOI: 10.1016/j.gtc.2020.01.001]

3 **Jefferies M**, Rauff B, Rashid H, Lam T, Rafiq S. Update on global epidemiology of viral hepatitis and preventive strategies. *World J Clin Cases* 2018; **6**: 589-599 [PMID: 30430114 DOI: 10.12998/wjcc.v6.i13.589]

4 **European Association for the Study of the Liver**. EASL 2017 Clinical Practice Guidelines on the management of hepatitis B virus infection. *J Hepatol* 2017; **67**: 370-398 [PMID: 28427875 DOI: 10.1016/j.jhep.2017.03.021]

5 **Hong YS**, Ryu S, Chang Y, Caínzos-Achirica M, Kwon MJ, Zhao D, Shafi T, Lazo M, Pastor-Barriuso R, Shin H, Cho J, Guallar E. Hepatitis B virus infection and development of chronic kidney disease: a cohort study. *BMC Nephrol* 2018; **19**: 353 [PMID: 30537940 DOI: 10.1186/s12882-018-1154-4]

6 **Du Y**, Zhang S, Hu M, Wang Q, Liu N, Shen H, Zhang Y, Yan D, Zhang M. Association between hepatitis B virus infection and chronic kidney disease: A cross-sectional study from 3 million population aged 20 to 49 years in rural China. *Medicine (Baltimore)* 2019; **98**: e14262 [PMID: 30702585 DOI: 10.1097/MD.0000000000014262]

7 **Amet S**, Bronowicki JP, Thabut D, Zoulim F, Bourliere M, Mathurin P, de Ledinghen V, Benhamou Y, Larrey DG, Janus N, Deray G, Launay-Vacher V, Pol S. Prevalence of renal abnormalities in chronic HBV infection: the HARPE study. *Liver Int* 2015; **35**: 148-155 [PMID: 24502506 DOI: 10.1111/liv.12480]

8 **Ha NB**, Ha NB, Garcia RT, Trinh HN, Vu AA, Nguyen HA, Nguyen KK, Levitt BS, Nguyen MH. Renal dysfunction in chronic hepatitis B patients treated with adefovir dipivoxil. *Hepatology* 2009; **50**: 727-734 [PMID: 19517525 DOI: 10.1002/hep.23044]

9 **Ning L**, Lin W, Hu X, Fan R, Liang X, Wu Y, Shen S, Yu R, Sun J, Hou J. Prevalence of chronic kidney disease in patients with chronic hepatitis B: A cross-sectional survey. *J Viral Hepat* 2017; **24**: 1043-1051 [PMID: 28581186 DOI: 10.1111/jvh.12733]

10 **Si J**, Yu C, Guo Y, Bian Z, Qin C, Yang L, Chen Y, Yin L, Li H, Lan J, Chen J, Chen Z, Lv J, Li L; China Kadoorie Biobank Collaborative Group. Chronic hepatitis B virus infection and risk of chronic kidney disease: a population-based prospective cohort study of 0.5 million Chinese adults. *BMC Med* 2018; **16**: 93 [PMID: 29909773 DOI: 10.1186/s12916-018-1084-9]

11 **Pipili C**, Cholongitas E, Papatheodoridis G. Review article: nucleos(t)ide analogues in patients with chronic hepatitis B virus infection and chronic kidney disease. *Aliment Pharmacol Ther* 2014; **39**: 35-46 [PMID: 24299322 DOI: 10.1111/apt.12538]

12 Guidelines for vaccination in patients with chronic kidney disease. *Indian J Nephrol* 2016; **26**: S15-18

13 **Cholongitas E**, Tziomalos K, Pipili C. Management of patients with hepatitis B in special populations. *World J Gastroenterol* 2015; **21**: 1738-1748 [PMID: 25684938 DOI: 10.3748/wjg.v21.i6.1738]

14 **Chacko EC**, Surrun SK, Mubarack Sani TP, Pappachan JM. Chronic viral hepatitis and chronic kidney disease. *Postgrad Med J* 2010; **86**: 486-492 [PMID: 20709771 DOI: 10.1136/pgmj.2009.092775]

15 **Radhakrishnan J**, Uppot RN, Colvin RB. Case records of the Massachusetts General Hospital. Case 5-2010. A 51-year-old man with HIV infection, proteinuria, and edema. *N Engl J Med* 2010; **362**: 636-646 [PMID: 20164488 DOI: 10.1056/NEJMcpc0910091]

16 **Park H**, Adeyemi A, Henry L, Stepanova M, Younossi Z. A meta-analytic assessment of the risk of

chronic kidney disease in patients with chronic hepatitis C virus infection. *J Viral Hepat* 2015; **22**: 897-905 [PMID: 25904153 DOI: 10.1111/jvh.12413]

17 **Johnson DW**, Dent H, Yao Q, Tranaeus A, Huang CC, Han DS, Jha V, Wang T, Kawaguchi Y, Qian J. Frequencies of hepatitis B and C infections among haemodialysis and peritoneal dialysis patients in Asia-Pacific countries: analysis of registry data. *Nephrol Dial Transplant* 2009; **24**: 1598-1603 [PMID: 19096083 DOI: 10.1093/ndt/gfn684]

18 **Gordon CE**, Berenguer MC, Doss W, Fabrizi F, Izopet J, Jha V, Kamar N, Kasiske BL, Lai CL, Morales JM, Patel PR, Pol S, Silva MO, Balk EM, Earley A, Di M, Cheung M, Jadoul M, Martin P. Prevention, Diagnosis, Evaluation, and Treatment of Hepatitis C Virus Infection in Chronic Kidney Disease: Synopsis of the Kidney Disease: Improving Global Outcomes 2018 Clinical Practice Guideline. *Ann Intern Med* 2019; **171**: 496-504 [PMID: 31546256 DOI: 10.7326/M19-1539]

19 **Gane E**, Lawitz E, Pugatch D, Papatheodoridis G, Bräu N, Brown A, Pol S, Leroy V, Persico M, Moreno C, Colombo M, Yoshida EM, Nelson DR, Collins C, Lei Y, Kosloski M, Mensa FJ. Glecaprevir and Pibrentasvir in Patients with HCV and Severe Renal Impairment. *N Engl J Med* 2017; **377**: 1448-1455 [PMID: 29020583 DOI: 10.1056/NEJMoa1704053]

20 **European Association for the Study of the Liver**. Clinical Practice Guidelines Panel: Chair; EASL Governing Board representative; Panel members:. EASL recommendations on treatment of hepatitis C: Final update of the series. *J Hepatol* 2020; **73**: 1170-1218 [PMID: 32956768 DOI: 10.1016/j.jhep.2020.08.018]

21 **Roth D**, Nelson DR, Bruchfeld A, Liapakis A, Silva M, Monsour H Jr, Martin P, Pol S, Londoño MC, Hassanein T, Zamor PJ, Zuckerman E, Wan S, Jackson B, Nguyen BY, Robertson M, Barr E, Wahl J, Greaves W. Grazoprevir plus elbasvir in treatment-naive and treatment-experienced patients with hepatitis C virus genotype 1 infection and stage 4-5 chronic kidney disease (the C-SURFER study): a combination phase 3 study. *Lancet* 2015; **386**: 1537-1545 [PMID: 26456905 DOI: 10.1016/S0140-6736(15)00349-9]

22 **Cox-North P**, Hawkins KL, Rossiter ST, Hawley MN, Bhattacharya R, Landis CS. Sofosbuvir-based regimens for the treatment of chronic hepatitis C in severe renal dysfunction. *Hepatol Commun* 2017; **1**: 248-255 [PMID: 29404457 DOI: 10.1002/hep4.1035]

23 **Borgia SM**, Dearden J, Yoshida EM, Shafran SD, Brown A, Ben-Ari Z, Cramp ME, Cooper C, Foxton M, Rodriguez CF, Esteban R, Hyland R, Lu S, Kirby BJ, Meng A, Markova S, Dvory-Sobol H, Osinusi AO, Bruck R, Ampuero J, Ryder SD, Agarwal K, Fox R, Shaw D, Haider S, Willems B, Lurie Y, Calleja JL, Gane EJ. Sofosbuvir/velpatasvir for 12 weeks in hepatitis C virus-infected patients with end-stage renal disease undergoing dialysis. *J Hepatol* 2019; **71**: 660-665 [PMID: 31195062 DOI: 10.1016/j.jhep.2019.05.028]

24 **Lawitz E**, Landis CS, Flamm SL, Bonacini M, Ortiz-Lasanta G, Huang J, Zhang J, Kirby BJ, De-Oertel S, Hyland RH, Osinusi AO, Brainard DM, Robson R, Maliakkal BJ, Gordon SC, Gane EJ. Sofosbuvir plus ribavirin and sofosbuvir plus ledipasvir in patients with genotype 1 or 3 hepatitis C virus and severe renal impairment: a multicentre, phase 2b, non-randomised, open-label study. *Lancet Gastroenterol Hepatol* 2020; **5**: 918-926 [PMID: 32531259 DOI: 10.1016/S2468-1253(19)30417-0]

25 **AASLD/IDSA HCV Guidance Panel**. Hepatitis C guidance: AASLD-IDSA recommendations for testing, managing, and treating adults infected with hepatitis C virus. *Hepatology* 2015; **62**: 932-954 [PMID: 26111063 DOI: 10.1002/hep.27950]

26 **Nguyen DB**, Bixler D, Patel PR. Transmission of hepatitis C virus in the dialysis setting and strategies for its prevention. *Semin Dial* 2019; **32**: 127-134 [PMID: 30569604 DOI: 10.1111/sdi.12761]

27 **Page K**, Melia MT, Veenhuis RT, Winter M, Rousseau KE, Massaccesi G, Osburn WO, Forman M, Thomas E, Thornton K, Wagner K, Vassilev V, Lin L, Lum PJ, Giudice LC, Stein E, Asher A, Chang S, Gorman R, Ghany MG, Liang TJ, Wierzbicki MR, Scarselli E, Nicosia A, Folgori A, Capone S, Cox AL. Randomized Trial of a Vaccine Regimen to Prevent Chronic HCV Infection. *N Engl J Med* 2021; **384**: 541-549 [PMID: 33567193 DOI: 10.1056/NEJMoa2023345]

28 **Roth D**, Bloom RD, Molnar MZ, Reese PP, Sawinski D, Sise ME, Terrault NA. KDOQI US Commentary on the 2018 KDIGO Clinical Practice Guideline for the Prevention, Diagnosis, Evaluation, and Treatment of Hepatitis C. *Am J Kidney Dis* 2020; **75**: 665-683 [PMID: 32279907 DOI: 10.1053/j.ajkd.2019.12.016]

29 **Sarkar M**, Brady CW, Fleckenstein J, Forde KA, Khungar V, Molleston JP, Afshar Y, Terrault NA. Reproductive Health and Liver Disease: Practice Guidance by the American Association for the Study of Liver Diseases. *Hepatology* 2021; **73**: 318-365 [PMID: 32946672 DOI: 10.1002/hep.31559]

30 **Trehanpati N**, Hissar S, Shrivastav S, Sarin SK. Immunological mechanisms of hepatitis B virus persistence in newborns. *Indian J Med Res* 2013; **138**: 700-710 [PMID: 24434322]

31 **Borgia G**, Carleo MA, Gaeta GB, Gentile I. Hepatitis B in pregnancy. *World J Gastroenterol* 2012; **18**: 4677-4683 [PMID: 23002336 DOI: 10.3748/wjg.v18.i34.4677]

32 **Eke AC**, Brooks KM, Gebreyohannes RD, Sheffield JS, Dooley KE, Mirochnick M. Tenofovir alafenamide use in pregnant and lactating women living with HIV. *Expert Opin Drug Metab Toxicol* 2020; **16**: 333-342 [PMID: 32125906 DOI: 10.1080/17425255.2020.1738384]

33 **Nelson NP**, Jamieson DJ, Murphy TV. Prevention of Perinatal Hepatitis B Virus Transmission. *J Pediatric Infect Dis Soc* 2014; **3** Suppl 1: S7-S12 [PMID: 25232477 DOI: 10.1093/jpids/piu064]

34 **Lim SG**, Aghemo A, Chen PJ, Dan YY, Gane E, Gani R, Gish RG, Guan R, Jia JD, Lim K, Piratvisuth T, Shah S, Shiffman ML, Tacke F, Tan SS, Tanwandee T, Win KM, Yurdaydin C. Management of hepatitis C virus infection in the Asia-Pacific region: an update. *Lancet Gastroenterol*

Hepatol 2017; **2**: 52-62 [PMID: 28404015 DOI: 10.1016/S2468-1253(16)30080-2]

35 **Wijarnpreecha K**, Thongprayoon C, Sanguankeo A, Upala S, Ungprasert P, Cheungpasitporn W. Hepatitis C infection and intrahepatic cholestasis of pregnancy: A systematic review and meta-analysis. *Clin Res Hepatol Gastroenterol* 2017; **41**: 39-45 [PMID: 27542514 DOI: 10.1016/j.clinre.2016.07.004]

36 **Kushner T**, Terrault NA. Hepatitis C in Pregnancy: A Unique Opportunity to Improve the Hepatitis C Cascade of Care. *Hepatol Commun* 2019; **3**: 20-28 [PMID: 30619991 DOI: 10.1002/hep4.1282]

37 **Huang QT**, Huang Q, Zhong M, Wei SS, Luo W, Li F, Yu YH. Chronic hepatitis C virus infection is associated with increased risk of preterm birth: a meta-analysis of observational studies. *J Viral Hepat* 2015; **22**: 1033-1042 [PMID: 26081198 DOI: 10.1111/jvh.12430]

38 **Benova L**, Mohamoud YA, Calvert C, Abu-Raddad LJ. Vertical transmission of hepatitis C virus: systematic review and meta-analysis. *Clin Infect Dis* 2014; **59**: 765-773 [PMID: 24928290 DOI: 10.1093/cid/ciu447]

39 **Syriopoulou V**, Nikolopoulou G, Daikos GL, Theodoridou M, Pavlopoulou I, Nicolaidou P, Manolaki N. Mother to child transmission of hepatitis C virus: rate of infection and risk factors. *Scand J Infect Dis* 2005; **37**: 350-353 [PMID: 16051571 DOI: 10.1080/00365540510032105]

40 **Cottrell EB**, Chou R, Wasson N, Rahman B, Guise JM. Reducing risk for mother-to-infant transmission of hepatitis C virus: a systematic review for the U.S. Preventive Services Task Force. *Ann Intern Med* 2013; **158**: 109-113 [PMID: 23437438 DOI: 10.7326/0003-4819-158-2-201301150-00575]

41 **Society for Maternal-Fetal Medicine (SMFM)**, Hughes BL, Pag CM, Kuller JA. Hepatitis C in pregnancy: screening, treatment, and management. *Am J Obstet Gynecol* 2017; **217**: B2-B12 [PMID: 28782502 DOI: 10.1016/j.ajog.2017.07.039]

42 **Yattoo N**. Treatment of chronic hepatitis C with ledipasvir/sofosbuvir combination during pregnancy. *Hepatol Int* 2018; **12**: S292-S293

43 **Singhal V**, Bora D, Singh S. Hepatitis B in health care workers: Indian scenario. *J Lab Physicians* 2009; **1**: 41-48 [PMID: 21938248 DOI: 10.4103/0974-2727.59697]

44 **Centers for Disease Control and Prevention (CDC)**. Updated CDC recommendations for the management of hepatitis B virus-infected health-care providers and students. *MMWR Recomm Rep* 2012; **61**: 1-12 [PMID: 22763928]

45 **Gerlich WH**. Reduction of infectivity in chronic hepatitis B virus carriers among healthcare providers and pregnant women by antiviral therapy. *Intervirology* 2014; **57**: 202-211 [PMID: 25034489 DOI: 10.1159/000360949]

46 **Ganju SA**, Goel A. Prevalence of HBV and HCV infection among health care workers (HCWs). *J Commun Dis* 2000; **32**: 228-230 [PMID: 11407011]

47 **Mueller A**, Stoetter L, Kalluvya S, Stich A, Majinge C, Weissbrich B, Kasang C. Prevalence of hepatitis B virus infection among health care workers in a tertiary hospital in Tanzania. *BMC Infect Dis* 2015; **15**: 386 [PMID: 26399765 DOI: 10.1186/s12879-015-1129-z]

48 **Westermann C**, Peters C, Lisiak B, Lamberti M, Nienhaus A. The prevalence of hepatitis C among healthcare workers: a systematic review and meta-analysis. *Occup Environ Med* 2015; **72**: 880-888 [PMID: 26438666 DOI: 10.1136/oemed-2015-102879]

49 **Singh KP**, Crane M, Audsley J, Avihingsanon A, Sasadeusz J, Lewin SR. HIV-hepatitis B virus coinfection: epidemiology, pathogenesis, and treatment. *AIDS* 2017; **31**: 2035-2052 [PMID: 28692539 DOI: 10.1097/QAD.0000000000001574]

50 **van Griensven J**, Phirum L, Choun K, Thai S, De Weggheleire A, Lynen L. Hepatitis B and C co-infection among HIV-infected adults while on antiretroviral treatment: long-term survival, CD4 cell count recovery and antiretroviral toxicity in Cambodia. *PLoS One* 2014; **9**: e88552 [PMID: 24533106 DOI: 10.1371/journal.pone.0088552]

51 **Shiels MS**, Engels EA. Evolving epidemiology of HIV-associated malignancies. *Curr Opin HIV AIDS* 2017; **12**: 6-11 [PMID: 27749369 DOI: 10.1097/coh.0000000000000327]

52 **Pinchoff J**, Tran OC, Chen L, Bornschlegel K, Drobnik A, Kersanske L, Fuld J. Impact of hepatitis B on mortality and specific causes of death in adults with and without HIV co-infection in NYC, 2000-2011. *Epidemiol Infect* 2016; **144**: 3354-3364 [PMID: 27510414 DOI: 10.1017/S0950268816001801]

53 **Thio CL**. Hepatitis B in the human immunodeficiency virus-infected patient: epidemiology, natural history, and treatment. *Semin Liver Dis* 2003; **23**: 125-136 [PMID: 12800066 DOI: 10.1055/s-2003-39951]

54 **Yang R**, Gui X, Xiong Y, Gao SC, Yan Y. Impact of hepatitis B virus infection on HIV response to antiretroviral therapy in a Chinese antiretroviral therapy center. *Int J Infect Dis* 2014; **28**: 29-34 [PMID: 25236390 DOI: 10.1016/j.ijid.2014.07.018]

55 **Rockstroh JK**. Influence of viral hepatitis on HIV infection. *J Hepatol* 2006; **44**: S25-S27 [PMID: 16338020 DOI: 10.1016/j.jhep.2005.11.007]

56 **Sarin SK**, Kumar M, Lau GK, Abbas Z, Chan HL, Chen CJ, Chen DS, Chen HL, Chen PJ, Chien RN, Dokmeci AK, Gane E, Hou JL, Jafri W, Jia J, Kim JH, Lai CL, Lee HC, Lim SG, Liu CJ, Locarnini S, Al Mahtab M, Mohamed R, Omata M, Park J, Piratvisuth T, Sharma BC, Sollano J, Wang FS, Wei L, Yuen MF, Zheng SS, Kao JH. Asian-Pacific clinical practice guidelines on the management of hepatitis B: a 2015 update. *Hepatol Int* 2016; **10**: 1-98 [PMID: 26563120 DOI: 10.1007/s12072-015-9675-4]

57 **Zhu J**, Yang W, Feng Y, Lo C, Chen H, Zhu Q, Shen Z, Lan G, Chen Y, Tang Z, Xing H, Shao Y, Ruan Y, Li L. Treatment effects of the differential first-line antiretroviral regimens among HIV/HBV

coinfected patients in southwest China: an observational study. *Sci Rep* 2019; **9**: 1006 [PMID: 30700732 DOI: 10.1038/s41598-018-37148-8]

58 **Gallant J**, Brunetta J, Crofoot G, Benson P, Mills A, Brinson C, Oka S, Cheng A, Garner W, Fordyce M, Das M, McCallister S; GS-US-292-1249 Study Investigators. Brief Report: Efficacy and Safety of Switching to a Single-Tablet Regimen of Elvitegravir/Cobicistat/Emtricitabine/Tenofovir Alafenamide in HIV-1/Hepatitis B-Coinfected Adults. *J Acquir Immune Defic Syndr* 2016; **73**: 294-298 [PMID: 27171740 DOI: 10.1097/qai.0000000000001069]

59 **Venter WDF**, Moorhouse M, Sokhela S, Fairlie L, Mashabane N, Masenya M, Serenata C, Akpomiemie G, Qavi A, Chandiwana N, Norris S, Chersich M, Clayden P, Abrams E, Arulappan N, Vos A, McCann K, Simmons B, Hill A. Dolutegravir plus Two Different Prodrugs of Tenofovir to Treat HIV. *N Engl J Med* 2019; **381**: 803-815 [PMID: 31339677 DOI: 10.1056/NEJMoa1902824]

60 **Pineda JA**, Romero-Gómez M, Díaz-García F, Girón-González JA, Montero JL, Torre-Cisneros J, Andrade RJ, González-Serrano M, Aguilar J, Aguilar-Guisado M, Navarro JM, Salmerón J, Caballero-Granado FJ, García-García JA; Grupo Andaluz para el Estudio de las Enfermedades Infecciosas; Grupo Andaluz para el Estudio del Hígado. HIV coinfection shortens the survival of patients with hepatitis C virus-related decompensated cirrhosis. *Hepatology* 2005; **41**: 779-789 [PMID: 15800956 DOI: 10.1002/hep.20626]

61 **Thomas DL**. Hepatitis C and human immunodeficiency virus infection. *Hepatology* 2002; **36**: S201-S209 [PMID: 12407595 DOI: 10.1053/jhep.2002.36380]

62 **Omata M**, Kanda T, Wei L, Yu ML, Chuang WL, Ibrahim A, Lesmana CR, Sollano J, Kumar M, Jindal A, Sharma BC, Hamid SS, Dokmeci AK, Mamun-Al-Mahtab, McCaughan GW, Wasim J, Crawford DH, Kao JH, Yokosuka O, Lau GK, Sarin SK. APASL consensus statements and recommendation on treatment of hepatitis C. *Hepatol Int* 2016; **10**: 702-726 [PMID: 27130427 DOI: 10.1007/s12072-016-9717-6]

63 **Wyles D**, Bräu N, Kottilil S, Daar ES, Ruane P, Workowski K, Luetkemeyer A, Adeyemi O, Kim AY, Doehle B, Huang KC, Mogalian E, Osinusi A, McNally J, Brainard DM, McHutchison JG, Naggie S, Sulkowski M; ASTRAL-5 Investigators. Sofosbuvir and Velpatasvir for the Treatment of Hepatitis C Virus in Patients Coinfected With Human Immunodeficiency Virus Type 1: An Open-Label, Phase 3 Study. *Clin Infect Dis* 2017; **65**: 6-12 [PMID: 28369210 DOI: 10.1093/cid/cix260]

64 **Holmes JA**, Yu ML, Chung RT. Hepatitis B reactivation during or after direct acting antiviral therapy - implication for susceptible individuals. *Expert Opin Drug Saf* 2017; **16**: 651-672 [PMID: 28471314 DOI: 10.1080/14740338.2017.1325869]

65 **Caccamo G**, Saffioti F, Raimondo G. Hepatitis B virus and hepatitis C virus dual infection. *World J Gastroenterol* 2014; **20**: 14559-14567 [PMID: 25356020 DOI: 10.3748/wjg.v20.i40.14559]

66 **Chen G**, Wang C, Chen J, Ji D, Wang Y, Wu V, Karlberg J, Lau G. Hepatitis B reactivation in hepatitis B and C coinfected patients treated with antiviral agents: A systematic review and meta-analysis. *Hepatology* 2017; **66**: 13-26 [PMID: 28195337 DOI: 10.1002/hep.29109]

67 **Li M**, Gan Y, Fan C, Yuan H, Zhang X, Shen Y, Wang Q, Meng Z, Xu D, Tu H. Hepatitis B virus and risk of non-Hodgkin lymphoma: An updated meta-analysis of 58 studies. *J Viral Hepat* 2018; **25**: 894-903 [PMID: 29532605 DOI: 10.1111/jvh.12892]

68 **Rattotti S**, Ferretti VV, Rusconi C, Rossi A, Fogazzi S, Baldini L, Pioltelli P, Balzarotti M, Farina L, Ferreri AJM, Laszlo D, Speziale V, Varettoni M, Sciarra R, Morello L, Tedeschi A, Frigeni M, Defrancesco I, Zerbi C, Flospergher E, Nizzoli ME, Morra E, Arcaini L; "Rete Ematologica Lombarda" (REL - Hematology Clinical Network of Lombardy - Lymphoma Workgroup). Lymphomas associated with chronic hepatitis C virus infection: A prospective multicenter cohort study from the Rete Ematologica Lombarda (REL) clinical network. *Hematol Oncol* 2019; **37**: 160-167 [PMID: 30726562 DOI: 10.1002/hon.2575]

69 **Kang J**, Cho JH, Suh CW, Lee DH, Oh HB, Sohn YH, Chi HS, Park CJ, Jang SS, Lee KH, Lee JH, Lee SW, Chung YH, Kim TH, Shin HR, Huh J. High prevalence of hepatitis B and hepatitis C virus infections in Korean patients with hematopoietic malignancies. *Ann Hematol* 2011; **90**: 159-164 [PMID: 20821327 DOI: 10.1007/s00277-010-1055-5]

70 **Takai S**, Tsurumi H, Ando K, Kasahara S, Sawada M, Yamada T, Hara T, Fukuno K, Takahashi T, Oyama M, Onishi H, Tomita E, Takami T, Imawari M, Moriwaki H. Prevalence of hepatitis B and C virus infection in haematological malignancies and liver injury following chemotherapy. *Eur J Haematol* 2005; **74**: 158-165 [PMID: 15654908 DOI: 10.1111/j.1600-0609.2004.00376.x]

71 **Chen MH**, Hsiao LT, Chiou TJ, Liu JH, Gau JP, Teng HW, Wang WS, Chao TC, Yen CC, Chen PM. High prevalence of occult hepatitis B virus infection in patients with B cell non-Hodgkin's lymphoma. *Ann Hematol* 2008; **87**: 475-480 [PMID: 18327583 DOI: 10.1007/s00277-008-0469-9]

72 **Huang H**, Li X, Zhu J, Ye S, Zhang H, Wang W, Wu X, Peng J, Xu B, Lin Y, Cao Y, Li H, Lin S, Liu Q, Lin T. Entecavir *vs* lamivudine for prevention of hepatitis B virus reactivation among patients with untreated diffuse large B-cell lymphoma receiving R-CHOP chemotherapy: a randomized clinical trial. *JAMA* 2014; **312**: 2521-2530 [PMID: 25514302 DOI: 10.1001/jama.2014.15704]

73 **Mahale P**, Kontoyiannis DP, Chemaly RF, Jiang Y, Hwang JP, Davila M, Torres HA. Acute exacerbation and reactivation of chronic hepatitis C virus infection in cancer patients. *J Hepatol* 2012; **57**: 1177-1185 [PMID: 22871500 DOI: 10.1016/j.jhep.2012.07.031]

74 **Torres HA**, McDonald GB. How I treat hepatitis C virus infection in patients with hematologic malignancies. *Blood* 2016; **128**: 1449-1457 [PMID: 27443290 DOI: 10.1182/blood-2016-05-718643]

75 **Indolfi G**, Easterbrook P, Dusheiko G, Siberry G, Chang MH, Thorne C, Bulterys M, Chan PL, El-Sayed MH, Giaquinto C, Jonas MM, Meyers T, Walsh N, Wirth S, Penazzato M. Hepatitis B virus

infection in children and adolescents. *Lancet Gastroenterol Hepatol* 2019; **4**: 466-476 [PMID: 30982722 DOI: 10.1016/S2468-1253(19)30042-1]

76 **Sokal EM**, Paganelli M, Wirth S, Socha P, Vajro P, Lacaille F, Kelly D, Mieli-Vergani G; European Society of Pediatric Gastroenterology, Hepatology and Nutrition. Management of chronic hepatitis B in childhood: ESPGHAN clinical practice guidelines: consensus of an expert panel on behalf of the European Society of Pediatric Gastroenterology, Hepatology and Nutrition. *J Hepatol* 2013; **59**: 814-829 [PMID: 23707367 DOI: 10.1016/j.jhep.2013.05.016]

77 **Lai MW**, Chang MH. Updates in the management of hepatitis B in children. *Expert Rev Gastroenterol Hepatol* 2019; **13**: 1065-1076 [PMID: 31663387 DOI: 10.1080/17474124.2019.1686975]

78 **Schmelzer J**, Dugan E, Blach S, Coleman S, Cai Z, DePaola M, Estes C, Gamkrelidze I, Jerabek K, Ma S, Montoya S, Razavi-Shearer D, Razavi-Shearer K, Robbins-Scott S, Razavi H, El Sayed MH. Global prevalence of hepatitis C virus in children in 2018: a modelling study. *Lancet Gastroenterol Hepatol* 2020; **5**: 374-392 [PMID: 31954439 DOI: 10.1016/S2468-1253(19)30385-1]

79 **Pawlowska M**, Sobolewska-Pilarczyk M, Domagalski K. Hepatitis C virus infection in children in the era of direct-acting antiviral. *World J Gastroenterol* 2018; **24**: 2555-2566 [PMID: 29962813 DOI: 10.3748/wjg.v24.i24.2555]

80 **Squires JE**, Balistreri WF. Hepatitis C virus infection in children and adolescents. *Hepatol Commun* 2017; **1**: 87-98 [PMID: 29404447 DOI: 10.1002/hep4.1028]

81 **Economides MP**, Mahale P, Kyvernitakis A, Turturro F, Kantarjian H, Naing A, Hosry J, Shigle TL, Kaseb A, Torres HA. Concomitant use of direct-acting antivirals and chemotherapy in hepatitis C virus-infected patients with cancer. *Aliment Pharmacol Ther* 2016; **44**: 1235-1241 [PMID: 27730654 DOI: 10.1111/apt.13825]

World Journal of Gastroenterology

Submit a Manuscript: https://www.f6publishing.com

World J Gastroenterol 2021 October 28; 27(40): 6874-6887

DOI: 10.3748/wjg.v27.i40.6874

ISSN 1007-9327 (print) ISSN 2219-2840 (online)

MINIREVIEWS

Endoscopic ultrasound-guided vascular interventions: Current insights and emerging techniques

Rupinder Mann, Hemant Goyal, Abhilash Perisetti, Saurabh Chandan, Sumant Inamdar, Benjamin Tharian

ORCID number: Rupinder Mann 0000-0001-9139-7411; Hemant Goyal 0000-0002-9433-9042; Abhilash Perisetti 0000-0003-4074-6395; Saurabh Chandan 0000-0002-2661-6693; Sumant Inamdar 0000-0002-1002-2823; Benjamin Tharian 0000-0002-7797-3738.

Author contributions: Perisetti A, Goyal H and Mann R concepted and designed the article, did a literature search; Mann R finished the first draft; all authors critically revised and edited manuscript.

Conflict-of-interest statement: Rupinder Mann, Hemant Goyal, Abhilash Perisetti, Saurabh Chandan, Sumant Inamdar has nothing to disclose; Benjamin Tharian acts as a consultant to Boston Scientific and Medtronic which are not relevant for this manuscript.

Open-Access: This article is an open-access article that was selected by an in-house editor and fully peer-reviewed by external reviewers. It is distributed in accordance with the Creative Commons Attribution NonCommercial (CC BY-NC 4.0) license, which permits others to distribute, remix, adapt, build upon this work non-commercially, and license their derivative works on different terms, provided the original work is properly cited and

Rupinder Mann, Department of Internal Medicine, Saint Agnes Medical Center, Fresno, CA 93730, United States

Hemant Goyal, Department of Internal Medicine, The Wright Center for Graduate Medical Education, Scranton, PA 18503, United States

Abhilash Perisetti, Department of Gastroenterology and Hepatology, The University of Arkansas for Medical Sciences, Little Rock, AR 72205, United States

Saurabh Chandan, Department of Gastroenterology and Hepatology, CHI Creighton University Medical Center, Omaha, NE 68107, United States

Sumant Inamdar, Benjamin Tharian, Department of Internal Medicine, Gastroenterology and Hepatology Division, University of Arkansas for Medical Sciences, Little Rock, AR 72205, United States

Corresponding author: Abhilash Perisetti, FACP, MBBS, MD, Academic Fellow, Department of Gastroenterology and Hepatology, The University of Arkansas for Medical Sciences, 4301 W Markham St, Little Rock, AR 72205, United States. abhilash.perisetti@gmail.com

Abstract

Endoscopic ultrasound (EUS) is one of the significant breakthroughs in the field of advanced endoscopy. In the last two decades, EUS has evolved from a diagnostic tool to a real-time therapeutic modality. The luminal gastrointestinal (GI) tract provides a unique opportunity to access multiple vascular structures, especially in the mediastinum and abdomen, thus permitting a variety of EUS-guided vascular interventions. The addition of the doppler and contrast-enhanced capability to EUS has further helped provide real-time visualization of blood flow in vessels through the GI tract. EUS-guided vascular interventions rely on standard endoscopic accessories and interventional tools such as fine-needle aspiration needles and fine-needle biopsy. EUS allows the visualization of various structures in real-time by differentiating tissue densities and vascularity, thus, avoiding radiation exposure. EUS-guided techniques also allow real-time microscopic examination after target biopsy. Furthermore, many necessary interventions can be done during the same procedure after diagnosis. This article provides an overview of EUS-guided vascular interventions such as variceal, non-variceal bleeding interventions, EUSguided portal vein (PV) access with the formation of an intrahepatic portosystemic shunt, and techniques related to diagnosis of GI malignancies. Furthermore, we discuss current insights and future outlook of

the use is non-commercial. See: http://creativecommons.org/Licenses/by-nc/4.0/

Manuscript source: Invited manuscript

Specialty type: Gastroenterology and hepatology

Country/Territory of origin: United States

Peer-review report's scientific quality classification

Grade A (Excellent): A
Grade B (Very good): B
Grade C (Good): 0
Grade D (Fair): 0
Grade E (Poor): 0

Received: March 16, 2021
Peer-review started: March 16, 2021
First decision: May 1, 2021
Revised: May 3, 2021
Accepted: September 14, 2021
Article in press: September 14, 2021
Published online: October 28, 2021

P-Reviewer: Harada R, Mitri RD
S-Editor: Fan JR
L-Editor: A
P-Editor: Liu JH

therapeutic modalities like PV embolization, PV sampling, angiography, drug administration, and portal pressure measurement.

Key Words: Endoscopic ultrasound; Vascular intervention; Esophageal varices; Gastric varices; Portal vein; Therapeutic endoscopy

©The Author(s) 2021. Published by Baishideng Publishing Group Inc. All rights reserved.

Core Tip: Endoscopic ultrasound (EUS) technology has evolved rapidly in clinical practice, first as merely a diagnostic tool and now a therapeutic modality. EUS-guided interventions involve combining real-time imaging capability with invasive therapeutic interventions. The gastrointestinal (GI) tract has proximity to various vascular structures in the abdomen and mediastinum and thus provides a unique window to access these structures with EUS to render EUS-guided vascular interventions. Herein, this article provides an overview of EUS-guided vascular interventions for GI bleeding, portal vein access, and therapeutic implications, tumor diagnosis, and access to non-GI structures.

Citation: Mann R, Goyal H, Perisetti A, Chandan S, Inamdar S, Tharian B. Endoscopic ultrasound-guided vascular interventions: Current insights and emerging techniques. *World J Gastroenterol* 2021; 27(40): 6874-6887
URL: https://www.wjgnet.com/1007-9327/full/v27/i40/6874.htm
DOI: https://dx.doi.org/10.3748/wjg.v27.i40.6874

INTRODUCTION

Endoscopic ultrasound (EUS) is a minimally invasive specialized procedure that blends endoscopy with ultrasound. The endoscope allows visualizing the gastrointestinal (GI) tract lining, and ultrasound allows visualization of the GI tract walls, surrounding organs, and blood vessels with high-frequency waves. Three different types of echoendoscopes are available: Linear, radial, and mini-probes. Linear echoendoscopes are preferred for pancreaticobiliary interventions such as acquiring tissue, drainage of collections, and injections. Radial echoendoscopes are preferred for the staging of esophageal and gastric cancers[1,2]. Mini probes are more useful in diagnosing mucosal malignancy, pancreaticobiliary diseases (such as malignancy or stricture) because of their high frequency[1]. EUS can visualize both solid and fluid structures in the GI lumen and extraluminal. Various structures accessible with EUS include the luminal wall of the GI tract (esophagus, stomach, duodenum, and rectum), liver, pancreas, gallbladder, biliary tree, mediastinum, and lymph nodes. In addition, EUS can identify various arterial and venous vascular structures in proximity to the GI tract are accessible. Feeding vessels from small branches of vessels and aberrant vascular shunts can also be visualized by EUS[2,3].

Since the introduction of EUS in 1980 for diagnostic purposes, significant evolution has occurred (Figures 1 and 2). Its application on humans dates back to 1982[4]. This evolved in 1991 when EUS-guided fine-needle aspiration (FNA) was first introduced, and it allowed to do therapeutic interventions outside the lumen of the GI tract[5]. In 1996, EUS-guided cholangiography and EUS-guided biliary drainage were introduced [6]. Furthermore, the role of EUS expanded rapidly over the last 20 years from the diagnostic to the therapeutic tool as it provides direct visualization, access to structures within and outside the GI tract. Several new advancements in EUS-guided vascular procedures have emerged due to the proximity of many blood vessels to the GI tract and the ability to deliver precise real-time interventions. It has been further expanded to target gastric variceal bleeding by cyanoacrylate (CYA) injection[7]. In 2008, EUS-guided glue injection and micro coil embolization were used to treat a patient with refractory gastric variceal bleeding. Additionally, EUS can obtain real-time portal pressures in patients suspected of portal hypertension (PH) and obtain liver core biopsies to evaluate for fibrosis in one setting. Given its ability to access the portal vein (PV), interventions such as PV thrombectomy have been possible. Given these advances, we aim to discuss updates and emerging trends in EUS related

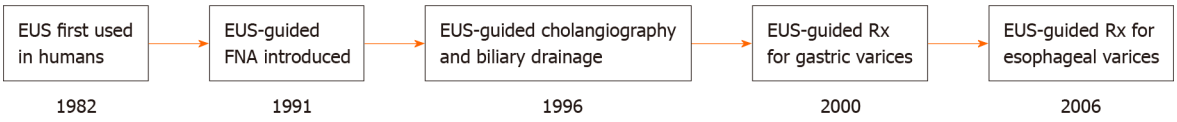


Figure 1 Endoscopic ultrasound history. EUS: Endoscopic ultrasound; FNA: Fine-needle aspiration; Rx: Treatment.

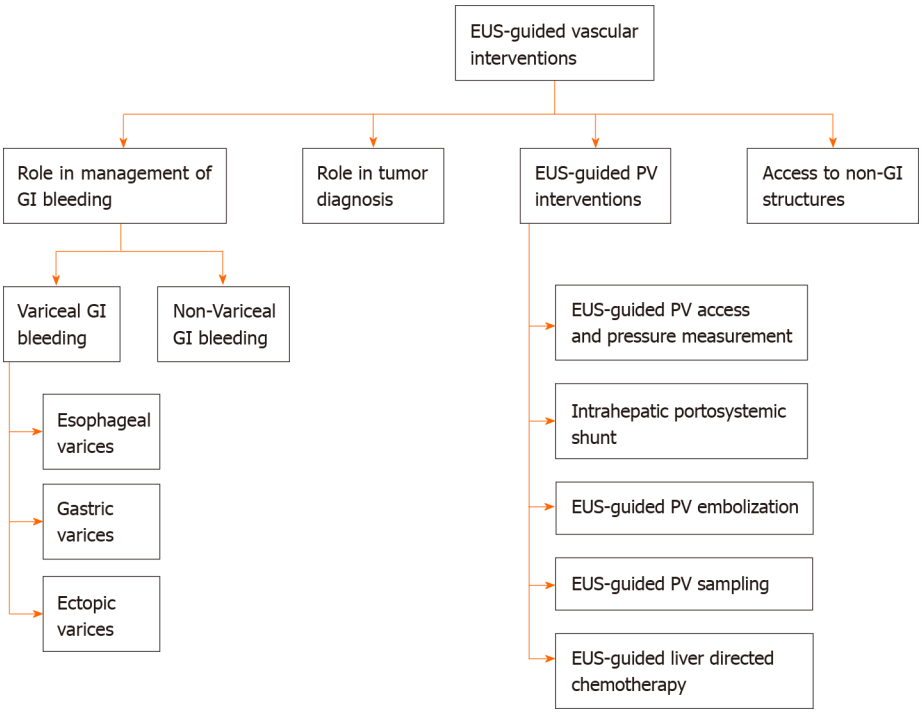


Figure 2 Different types of endoscopic ultrasound guided vascular interventions. PV: Portal vein; EUS: Endoscopic ultrasound; GI: Gastrointestinal.

vascular interventions.

ROLE OF EUS IN THE MANAGEMENT OF GI BLEEDING

Variceal bleeding

Esophageal varices: Endoscopic band ligation (EBL) is the preferred treatment for bleeding and non-bleeding esophageal varices. However, endoscopic sclerotherapy is an additional treatment that is still used, especially when EBL is not feasible[8]. Although these therapies are successful, the rate of recurrent bleeding can range up to 15%-65%[9]. The higher recurrence is most likely due to failure to treat perforating and collateral vessels. Echoendoscope provides benefits over endoscope due to its ability to visualize and target these high-risk vessels under direct visualization[10,11]. EUS-guided sclerotherapy for esophageal varices was first described in 2000 by Lahoti *et al* [12] in a study of 5 patients. A sclerosing agent such as sodium morrhuate was injected into target perforating vessels under EUS guidance until complete blood flow cessation was confirmed with the doppler. A mean of 2.2 sessions (range 2-3 sessions) were required to achieve the complete eradication of varices. No recurrence of bleeding or death was reported during 15 mo follow-up. Only one patient developed esophageal stricture, which was managed with balloon dilation[12].

The above study showed comparable results of EUS-guided sclerotherapy for esophageal varices. Therefore, EBL is still a preferred treatment for esophageal varices. Large, randomized trials are needed to show the clinical benefits of EUS-guided sclerotherapy compared to EBL to consider it as one of the first-line treatments.

Gastric varices: Although gastric varices (GV) are less common than esophageal varices, it affects around 20% of patients with PH[13,14]. GV can occasionally cause bleeding, leading to iron deficiency anemia, and the risk of rebleeding (34%-89%) is much higher than compared to esophageal varices (15%-65%)[13]. There are no well-

established treatment guidelines for the management of GV compared to esophageal varices[15]. EBL is not recommended for managing GV as they are larger in size, with thick overlying gastric mucosa making it difficult to band. EBL of GV can lead to life-threatening bleeding due to post-band ulcerations, developed due to a failure to capture the contralateral wall of varices during the procedure[16]. In a study of 22 patients with bleeding GV treated with EBL, 18.2% developed early rebleeding even after complete hemostasis was achieved in all cases on EBL[17]. Endoscopic sclerosing therapy should also be avoided in bleeding GV as it provides only temporary control of bleed and a higher incidence of adverse events like gastric ulcerations, perforations, and rebleeding in 37%–53% of cases[18].

Glue therapy with CYA is the primary treatment of choice for GV. It was first described in 1986 as it has higher rates (> 90%) of achieving hemostasis and a lower rate of rebleeding (0%-40%) compared to other therapies (EBL and sclerotherapy)[19, 20]. However, there are reports of significant adverse effects associated with CYA injections like systemic embolization (cardiac embolism, pulmonary embolism, splenic vein thrombosis, splenic artery embolism, renal vein thrombosis, and cerebral infarct), which is thought to be related to the volume of CYA injection[21]. EUS assists in both the diagnosis and treatment of GV. It helps in diagnosis and allows a precise evaluation of pathological vessels, improving therapeutic targeting. Color doppler also permits to differentiation of GV from other structures and can help confirm eradication of varices. EUS has provided us a new array of treatment options, including coil embolization with or without glue therapy and thrombin injection *etc.*, in the treatment of GV[13,20].

Glue therapy. Endoscopic-CYA injection has been shown to control bleeding, but there is a high recurrence of bleeding, probably due to incomplete obliteration of varices. EUS-guided CYA glue injection can minimize recurrent bleeding and decrease CYA volume by directly visualizing the perforating vessels, thus more precise obliteration of varices. Theoretically, the risk of embolization also decreases as it allows precise CYA injection into the target vessel[7].

A total of six patients with GV, including four for secondary prophylaxis, were treated with EUS-guided coil embolization followed by CYA glue injection in a single-center retrospective study. Complete eradication of GV was achieved in 3 patients. One patient had pulmonary embolism as a complication of CYA glue injection[22]. In a large single-center study, 40 patients underwent EUS-guided n-butyl-2-CYA for GV. Out of 40 patients, 13 patients were treated during active bleeding and another 23 within 24 h of bleeding. Thus, bleeding was acutely controlled in 100% of cases after treatment with EUS-guided n-butyl-2-CYA therapy. Only six patients required additional intervention for long-term management (Table 1)[23].

In a single-center study, 40 patients with actively/recently bleeding or high-risk GV treated with direct endoscopic injection of CYA were compared with 64 patients treated prospectively with EUS-guided fine needle injection CYA. Gastroesophageal varices type 2 was the most common type of varices seen in both groups. During the procedure, a greater number of varices were obliterated in EUS-guided fine needle injection of the CYA group (1.6 ± 0.7) than the direct endoscopic injection of the CYA group (1.1 ± 0.4, $P < 0.001$). Whereas the mean volume of CYA was injected more in the direct endoscopic injection-CYA group (3.3 ± 1.3 mL) compared to EUS-guided fine needle injection of the CYA group (2.0 ± 0.8 mL, $P < 0.001$). Overall post-procedure GV rebleeding (23.7% *vs* 8.8%, $P = 0.045$) and non-GV-related GI bleeding (GIB) (27.5% *vs* 10.9%, $P = 0.030$) were found to be higher in the direct endoscopic injection of CYA group compared to EUS-guided fine needle injection of CYA group. No significant difference was found in the overall rate of adverse events in the direct endoscopic injection of CYA group (17.5%) and EUS-guided fine needle injection of CYA (20.3%, $P = 0.361$)[24]. EUS-guided glue injection appears to be safe and effective in decreasing the risk of rebleeding in patients with active or recent bleeding GV when compared to the endoscopic injection of CYA.

Coil embolization. EUS-guided coil application is another treatment modality for GV. Coils are commonly used for various interventional radiology procedures (Table 1). These micro coils can obliterate GV and avoids adverse effects associated with CYA use, such as embolization coils are made up of light metal alloy and are covered with synthetic fibers to induce clot formation and subsequent hemostasis. Furthermore, fibers can act as a scaffold for CYA if injected during the same procedure. Varices are identified and punctured through standard FNA size needles like 19G (0.035-inch coil) or a 22G (0.018-inch coil). These coils are then advanced from the needle into varix using the stylet as a pusher. The coil sizes are selected based on the size of varix[25,26].

Table 1 Endoscopic ultrasound-guided gastric varices treatment

Type of Intervention	Year	Ref.	Number of patients, *n* (%)	Follow up (mo)	Obliteration of varices/Clinical success %	Recurrent bleeding rate %	Adverse events %
CYA glue	2019	Lôbo *et al*[13]	16	9.9	75%	-	50%
CYA glue	2014	Gubler and Bauerfeind[23]	40	-	100%	15%	5%
CYA glue	2019	Bick *et al*[24]	64	6.6	96.9%	8.8%	17.5%
CYA glue	2013	Romero-Castro *et al*[26]	19	6	94.7%	0%	57.9%
CYA glue	2018	Krill *et al*[62]	10	4	100%	-	0%
Coil	2013	Romero-Castro *et al*[26]	11	6	90.9%	0%	9.1%
Coil	2018	Krill *et al*[62]	6	4	100%	-	0%
Coil	2010	Romero-Castro *et al*[63]	4	5 (1-3)	75%	0%	0%
Coil and CYA Glue	2019	Lôbo *et al*[13]	16	9.9	73.3%	-	25%
Coil and CYA Glue	2019	Kozieł *et al*[14]	16	10.9	100%	-	37.5%
Coil and CYA Glue	2018	Krill *et al*[62]	12	4	100%	-	8%

CYA: Cyanoacrylate.

A retrospective multicenter study compared EUS-guided CYA injection (n = 19) to EUS-guided coil embolization (n = 11) patients with GV. There was no statistically significant difference in obliteration rate, the mean number of sessions required, and recurrence noted during follow-up. However, adverse events were reported to be higher in the CYA group in [11/19 (57%)] when compared to EUS-guided coil embolization [1/11 (9.1%), P < 0.01]. A post-procedure computed tomography (CT) scan was performed in all patients, and nine patients in the CYA group were found to have asymptomatic glue embolism on imaging[26] (Table 1). This was the first study to compare coil embolization and CYA directly. Both procedures showed comparable results in terms of GV obliteration, but fewer adverse events were noted with coil embolization.

In another study, ten patients with GV underwent EUS-guided coil embolization and then reinforcement by gelatin sponges. Nine patients had either active bleeding or recently bled GV. A 100% obliteration of GV was achieved. Patients were followed for six mo, and only 1/10 patients developed severe abdominal pain as a complication. Further large prospective studies are needed describing its direct comparison with other treatment modalities like CYA or CYA and coil embolization combined[27].

Combined coiling and glue therapy. Although endoscopic CYA injection is considered primary therapy for GV, it is associated with systemic glue embolization. Synthetic fibers in the covering of coils function as a scaffold to keep CYA in varices; thus, a decrease of CYA reagent is needed to eradicate gastric fundal varices (GFV) and also may reduce the risk of glue embolization. In another study by Kozieł *et al*[14], four patients were treated with coils, and 12 patients were treated with EUS-guided coil and CYA injection. These patients were followed for an average of 327 d. The technical success rate was 94%, and the mean number of CYA volume and coils needed *per* procedure was 2 mL and 1.7, respectively. No serious complications like embolization or death were noted (Table 1).

A randomized pilot trial was conducted comparing the safety and efficacy of EUS-guided coil and CYA (n = 16) to EUS-guided CYA in GV patients, and these patients were followed for an average of 9.9 mo. EUS doppler was done in all cases to determine flow within varix after the procedure, and thoracic and abdomen CT was done in all cases 1 wk after the procedure. Repeat CT scans were done in symptomatic cases only afterward. In the EUS-guided coil and CYA *vs* EUS-guided CYA group, the total reduction inflow in the treated vessel was 37.5% *vs* 50% (P = 0.476) and 73% *vs* 80% (P = 1) immediately and at 30 d after the procedure, respectively. In addition,

asymptomatic pulmonary embolism was found to be in 25%, and 50% cases (P = 0.144) in EUS-guided combined coil and CYA and EUS-guided CYA, respectively[13] (Table 1).

A metanalysis and systematic review was conducted comparing EUS-guided CYA injection, EUS-guided coil embolization and CYA injection combined, and EUS-guided coil injection alone. Combined EUS-guided CYA and coiling were found to have better technical and clinical success rate compared coil embolization alone (99% *vs* 97%; P < 0.001 and 96% *vs* 90%; P < 0.001) and CYA alone (100% *vs* 97%; P < 0.001 and 98% *vs* 96%; P < 0.001). Similarly, lower adverse events were found to be with EUS-guided CYA and coil combined compared to coil embolization (10% *vs* 3%; P = 0.057) and CYA alone (10% *vs* 21%; P < 0.001)[15]. Given the above results from various studies, EUS-guided coil embolization and CYA injection combined therapy could be preferred compared to EUS-guided monotherapy with either coil or CYA injection alone.

Thrombin injection. Recently, a study of eight patients (three with active bleeding and five as elective prevention) with GFV treated with EUS-guided thrombin injection was published. About 2/3 of patients with active bleeding had successful hemostasis and obliteration of varices. All five patients who underwent the procedure for prevention of future bleeding had complete obliteration of varices. No direct procedure-related complications were observed. Although this series showed positive results, further large prospective studies are needed[19].

Ectopic varices: Ectopic varices can develop at any site, including duodenal, small bowel, colon, rectum, common bile duct, and peristomal, with duodenum ectopic varices are being the most frequent to bleed[25,28]. Many case reports have described the use of EUS for variceal bleeding at ectopic sites. Cases of duodenal variceal bleed treated with EUS-guided coil and CYA have been described without any complications[29].

Rectal varies are reported in 44%-89% of cirrhosis patients because of PH[30]. It can also be seen in patients with vascular anomalies, mesenteric vein obstruction, adhesions, and heart failure. However, rectal varices are a lower bleeding risk than esophageal and GV[11]. EUS can help detect and treat the presence of rectal varices better than the endoscopy (Table 2). Although most of the data for EUS-guided intervention for bleeding ectopic varices is based on case reports/series, it is emerging as a viable option.

Non-variceal GIB

GIB can be due to variceal or non-variceal causes[31]. Standard endoscopic treatments for non-variceal bleeding include injection (epinephrine), thermal (argon plasma coagulation, electrosurgical coagulation), and mechanical therapy (such as clipping). Despite these interventions, rebleeding or refractory bleeding is reported as high as 10%-24% in these patients[31]. EUS-guided therapies are advantageous over endoscopic therapy due to the ability to directly visualize target vessels buried in the walls of the organ along with real-time doppler. A literature review of 35 patients who underwent EUS-guided treatment of non-variceal GIB (NVGIB) showed a favorable clinical outcome in 32/35 (91.4%) patients, with recurrent bleeding in only three patients. Moreover, bleeding eventually stopped in all cases. The median follow-up time was 11 mo, and no complications or adverse events were reported during or after the procedure[32]. EUS-guided treatment can also be used as an adjunct treatment in refractory and recurrent disease.

Dieulafoy's lesions

The first use of EUS-guided therapy for Dieulafoy's lesion was described in 1996 when EUS was used to detect and treat eight patients referred for suspicion of Dieulafoy's lesion. A large vessel was identified in the stomach wall in all eight patients, which was treated with adrenaline/polidocanol injection using a sclerotherapy needle. Two patients had rebleeding during follow-up, one with recurrent bleeding from Dieulafoy's lesion and the other from duodenal ulcer. EUS-guided angiotherapy was described by Levy *et al*[33] in a case series of five patients with refractory bleeding due to hemosuccus pancreaticus, Dieulafoy lesion, duodenal ulcer, GI stromal tumor (GIST), and occult GIB. These patients had failed at least two conventional treatment options and received an average of 18 units of packed red blood cell transfusions. Patients were treated by injecting CYA (3-5 mL) or 99% alcohol into a feeding vessel using a 22G FNA needle under EUS-guidance. Doppler was used to ensuring the absence of blood flow after treatment. These patients were followed up for a mean 12-mo period (range 0.4-23 mo), no rebleeding or complication was reported[33].

Table 2 Case report studies on endoscopic ultrasound-guided rectal varices treatment

Ref.	Presenting symptom	Number of patients, age, sex	Rectal varices size	Therapy	Results	Follow up	Results on follow up
Philips and Augustine[64], 2017	Rectal bleeding	1, 48 yr, M	Large rectal varix	EUS-guided embolization coil and glue	No further bleeding	1 mo	No rebleeding
Bazarbashi *et al* [65], 2020	Rectal bleeding	1, 71 yr, M	Large rectal varices (4 mm in diameter)	EUS-guided coil embolization	No further bleeding	6 mo	No bleeding
Mukkada *et al* [66], 2017	Rectal bleeding	1, 65 yr, M	Large rectal varices	First EUS-guided sclerotherapy, but unable to achieve hemostasis, EUS guided glue	No further bleeding	1 wk	Rebleeding and then required EUS-guided coil embolization

F: Female; M: Male; EUS: Endoscopic ultrasound; N/A: Not applicable.

Law *et al*[34] performed EUS-guided hemostatic interventions between June 2003 to May 2014 for 17 patients with refractory NVGIB. Causes of GIB were GIST, colorectal, vascular malformations, Dieulafoy lesions, duodenal ulcers, masses or polyps, rectally invasive prostate cancer, pancreatic pseudoaneurysms, ulcerated esophageal cancer, and ulceration after Roux-en-Y gastric bypass. These patients were treated with epinephrine, 99% ethanol, coil embolization, band ligation, hyaluronate, and CYA using a therapeutic curvilinear echoendoscope with a 22G standard FNA needle. On median follow-up of 12 mo (range 3 wk-120 mo), 15/17 (88%) patients didn't have any recurrence. However, one patient required repeat EUS-guided band ligation for gastric Dieulafoy lesion, and another patient with rectally invasive prostate cancer experienced ongoing bleeding despite a decrease in vessel flow after treatment with 99% ethanol injection.

Pseudoaneurysms

Pseudoaneurysms are a known complication of pancreatitis with a risk of rupture and life-threatening bleeding. The risk of rupture is as high as 50%, with 15%-40% of mortality after rupture. Gamanagatti *et al*[35] described a case series of three patients with pancreatitis-related pseudoaneurysm, which were technically challenging to treat by the endovascular route. These cases were managed with EUS-guided thrombin injection, which resulted in complete thrombosis of the pseudoaneurysms. There were no immediate or late complications on follow-up. In a prospective study, eight patients with symptomatic visceral artery pseudoaneurysm who were unable to undergo angioembolization underwent EUS-guided thrombin injection for pseudoaneurysm. Out of eight patients, 5 had pseudoaneurysm of the splenic artery, 2 had pseudoaneurysm of the hepatic artery, and one patient had pseudoaneurysm of the gastroduodenal artery. Five patients with splenic artery and gastroduodenal artery aneurysms had chronic pancreatitis due to alcohol abuse. The pseudoaneurysm's median size was 2.9 cm × 2.6 cm (range 1.8 cm × 1.9-4 cm × 5 cm), and the median dose of thrombin injected was 400 IU (200-500 IU). Thrombin was injected under EUS guidance with 100% technical success. Repeat EUS after 72 h and 4 wk showed obliteration of pseudoaneurysm in all patients. Whereas on median six mo (1-9 mo) follow up, EUS showed obliterated pseudoaneurysm in 7 patients, and one patient had recurrence requiring recanalization after 6 wk[36]. There are few case reports describing the use of EUS-guided intervention for pseudoaneurysms (Table 3).

GIST

EUS is traditionally used to evaluate GI luminal tumors and obtain a tissue diagnosis. Bleeding GISTs are traditionally managed by either surgical resection, radiologic embolization, or rarely with endoscopic therapies like hemoclips and endoloop® ligation. In an elderly patient with a bleeding ulcer due to GIST who was not a candidate for surgery due to comorbidities, EUS-guided angiotherapy was done. A deep vessel was identified to bleeding GIST ulcer *via* echoendoscope, and the target vessel was treated with CYA, which stopped bleeding. Doppler confirmed the absence of vascularity, and the patient had no further bleeding at 6 mo follow-up[37]. In a study, 32 consecutive patients with submucosal tumors of the upper GI tracts underwent EUS examination with either radial or linear echoendoscope with color and

Table 3 Case report studies on endoscopic ultrasound-guided treated for pseudoaneurysm

Ref.	Presenting symptom	Number of patients, age and sex	Pseudoaneurysm artery	Therapy	Results	Follow up	Results on follow up
Gamanagatti *et al*[35], 2015	Pancreatitis with upper GI bleed in all three cases	3; 56, 45 and 30 yr; M	Gastroduodenal artery-1, splenic artery for 2 patients	EUS-guided thrombin injection	Bleeding stopped, Obliteration of pseudoaneurysm	1 mo	No bleeding
Robb *et al*[67], 2012	Infected pseudoaneurysm	1, 54 yr, M	Superior mesenteric artery branch	EUS-guided embolization	Obliteration of pseudoaneurysm	5 mo	Asymptomatic
Somani *et al* [68], 2017	Melena	1, 50 yr, M	Gastroduodenal artery	EUS-guided coil embolization and thrombin injection	Obliteration of pseudoaneurysm	2 wk	No further bleeding
Jhajharia *et al* [69], 2018	Chronic pancreatitis, GI bleed	3; 43, 25 and 55 yr; M	Gastroduodenal artery, hepatic artery, splenic artery	EUS-guided thrombin injection	Obliteration of pseudoaneurysm	14 d	No rebleeding

F: Female; M: Male; EUS: Endoscopic ultrasound; GI: Gastrointestinal; N/A: Not applicable.

Doppler capabilities: 51.4% had a discrepancy between suspected endoscopic and EUS diagnosis, 83.3% of malignant GISTs had significant intratumoral vessels seen on doppler or color EUS compared to 28% in benign GIST. Three patients were found to have vascular lesions, hemangioma on color Doppler EUS. In two patients, these lesions were treated with EUS-directed therapy consisted of ligation, coagulation, injection of sclerosing agents, or histoacryl resulting in complete eradication of lesions. One patient required surgery due to the severity of the bleeding. The patients remained asymptomatic on a mean follow-up of 48 mo[38].

Although the results of EUS-guided therapies in non-variceal bleeding are encouraging, most of the data is based on case reports and case series. No studies have compared EUS treatment with other management therapies such as endoscopic, surgical, and interventional radiology. Further large-scale studies comparing the standard treatment are needed. At present, EUS-guided therapies are available only at high-level care centers when other treatment options fail.

EUS-GUIDED PV INTERVENTIONS

PV access and pressure measurement

PV access can help to manage patients with the hepatobiliary diseases and PH. PV is not easy to access with traditional routes. Nevertheless, PV can easily be seen from the stomach and duodenum with EUS and accessed using a standard FNA needle. EUS, along with doppler, is used for needle puncture and withdrawal without hemorrhage [39]. Initial studies of EUS-guided PV access were performed in animals.

The measurement of PH can help to stage cirrhosis and thus prognosis. Portal pressure gradient (PPG) reflects the degree of PH. PPG ≥ 10 mmHg is associated with esophageal varices, and ≥ 12 mmHg is associated with variceal bleeding[40]. Currently, PH is evaluated by indirect measurement of the hepatic venous pressure gradient (HVPG), which poorly correlates with directly measured portal pressure in presinusoidal PH. Presinusoidal PH can be seen in the case of PV thrombosis, schistosomiases, and non-cirrhotic portal fibrosis[41-43].

The first human pilot study conducted to measure EUS-guided PPG measurement included 28 patients with a history of liver disease or suspected cirrhosis. The PV and hepatic vein (or inferior vena cava) were punctured with a 25G FNA needle under EUS guidance either through a transgastric or transduodenal approach. A 100% technical success with no complications was reported. PPG measurement showed a correlation with clinical and endoscopic parameters of PH, including the presence of varices (P = 0.0002), portal hypertensive gastropathy (P = 0.007), and thrombocytopenia (P = 0.036). PPG was shown to increase in patients with high clinical evidence of cirrhosis (P = 0.005)[40]. This study showed that the EUS-guided PPG measurement is safe in humans and further large clinical trials to evaluate safety and efficacy, especially compared to standard HVPG measurement methods, as intrahepatic portosystemic shunt (IPSS).

Transjugular IPSS (TIPS) is performed by interventional radiologists to reduce the PPG. TIPS decompresses the portal system and reduces complications due to PH, such as recurrent variceal bleeding and refractory ascites. It is usually performed in patients with refractory variceal bleed. TIPS involves catheter advancement and guidewire through the right heart and then inferior venacava (IVC) *via* transjugular route. It can expose patients to unintentional carotid or tracheal puncture, cardiac arrhythmias, and pneumothorax. Also, the transjugular approach for TIPS can be technically challenging in patients with IVC and hepatic vein obstruction, including Budd-Chiari syndrome. EUS-guided IPSS offer benefit as it does not involve heart catheterization, avoiding the related complications[44-48].

A study was conducted to create IPSS using lumen opposing metal stent (LAMS) in a porcine model. PV was accessed by puncturing through the stomach wall and IVC with a 19G needle under EUS guidance. A distal flange of the stent was deployed in the PV and the proximal flange in IVC. Gross necropsy of all five animals showed the correct placement of a stent and no tissue injury or hematoma[49]. Although IPSS has shown promising results in animal models, more studies are needed to evaluate the efficacy and safety of this technique.

PV embolization

Preoperative PV embolization induces the atrophy of the embolized liver lobe to be resected and compensatory hypertrophy of non-embolized remnant liver to increase future liver volume to prevent postoperative liver dysfunction. It is performed in patients with hepatocellular carcinoma (HCC), intrahepatic or hilar cholangiocarcinoma receiving extensive liver resection[25,50]. Liver resection should be performed 2 to 6 wk after PV embolization as compensatory hypertrophy of non-embolized remnant liver occurs in 6 wk with a maximum in the first 2 wk after the procedure. Proceduralists should have meticulous knowledge of liver and portal venous system anatomy before performing this procedure[51]. Presently it is performed through a percutaneous transhepatic approach by vascular interventional radiologist[50]. In a live porcine model to study EUS-guided selective intrahepatic PV embolization, PV was punctured with a 19G FNA needle under EUS guidance, the first coil, and then CYA was injected through the same FNA needle. Doppler was used to evaluating the blood flow. Coil and CYA delivery had a success rate of 88.9% and 87.5%, respectively. In one case, the embolized coil migrated to hepatic parenchyma, and CYA injection failed one case due to the early clogging of CYA in the FNA needle. One wk later, postoperative necropsy showed total occlusion of selected PV with embolus and no evidence of damage to any other organ[50]. Further studies are needed comparing the EUS-guided PV embolization to the percutaneous approach and evaluate the long-term effects.

Portal venous blood sampling

Pancreaticobiliary cancers (PBCs) are usually at advance to late stages at the time of diagnosis. Circulating tumor cells (CTCs) circulate from the primary tumor to distant sites through vascular supply, and their number is usually low in peripheral blood. In the case of PBCs, CTCs can be detected in the portal circulation before the peripheral blood and can be used to detect metastasis[25,52,53].

In a single-center cohort study, 18 patients with suspected PBCs had blood aspirated from PV *via* a 19G FNA needle through a EUS-guided transhepatic approach. Paired peripheral blood samples were also collected. Epithelial-derived CTCs were isolated. CTCs were detected from PV samples in all 18 patients (100%), whereas only in peripheral blood samples of four patients (22.2%). These CTCs isolated from PV can also provide sufficient cells to do genomic and proteomic tumor profiling[52].

In another study performed on patients undergoing pancreaticoduodenectomy for presumed periampullary or pancreatic adenocarcinoma without metastatic disease, PV and peripheral venous samples were collected simultaneously at the time of surgery. Sixty patients were monitored postoperatively every three months for one year with imaging for liver metastasis. CTCs were detected in 58% of cases in PV blood compared to 40% in a peripheral blood sample ($P = 0.0098$). CTCs count was also high PV sample than peripheral blood sample (mean, 230.1 *vs* 71.7, $P = 0.0002$). Liver metastasis was detected in 11 of 13 patients with high portal CTCs count (> 112 CMx Platform estimated CTCs in 2 mL blood) compared to 6 of 47 patients with low portal CTCs count ($P < 0.0001$) at 6-mo follow-up after surgery. The results of this study concluded that the CTCs can be used as a predictor for liver metastases within six months after surgery in patients undergoing pancreaticoduodenectomy for presumed periampullary or pancreatic adenocarcinoma[53]. Unfortunately, PV blood sampling with an evaluation of CTCs is only available in the limited number of specialized

tertiary care centers. Further larger studies are needed to ensure the efficacy and safety of the procedure before making it standard of care to predict hepatic metastasis in patients with pancreatic adenocarcinoma.

FNA of PV thrombus

PV thrombosis due to tumor invasion by direct venous extension or metastasis is seen in up to 70% of cases of HCC[54]. Patients with HCC can also have nontumor (bland) thrombosis of PV. It could be challenging to differentiate PV tumor thrombosis (PVTT) from bland PV thrombosis based on routine radiographic imaging. It is essential to diagnose PVTT as it is a poor prognostic sign, and curative resection or liver transplantation is contraindicated if the patient has PVTT. Transabdominal ultrasound-guided FNA has limited utility due to the difficulty of sample thrombus in the central main PV without contaminating with normal hepatocytes or liver mass, which can affect results. Furthermore, this procedure can have several complications, including vascular injury, pseudoaneurysm formation, and bile duct injury. EUS-guided FNA can directly access the extrahepatic PV without passing the needle through liver tissue[54,55]. Several case reports of EUS-guided FNA of PV thrombosis for diagnosis and staging of HCC even in patients when imaging did not show any liver mass[54-56].

Liver-directed PV injection chemotherapy

The liver is a common site of metastasis from other primary tumors. Patients with diffuse liver metastasis usually resort to palliative systemic chemotherapy given limited options available. It is hypothesized that the direct injection of chemotherapy into PV may increase the drug level in hepatic tissue while decreasing systemic side effects[25,57]. In a study, EUS-guided portal injection chemotherapy (EPIC) was performed by injecting irinotecan (100 mg) loaded microbeads by using a 22G FNA needle, and the control group had saline injected to PV and irinotecan (100 mg) injected into the jugular vein. EPIC resulted in twice a level of irinotecan in hepatic tissue after 1 h. and half the irinotecan level in plasma after 15 min[57]. These animal studies showed that EPIC could be an option for patients with diffuse liver metastasis; however, no human studies are available currently.

ROLE IN TUMOR DIAGNOSIS

Invasion of the vascular structures by tumor impacts staging and therapeutic options, including tumor resectability. Vascular invasion can often be diagnosed based on radiographic imaging like CT, magnetic resonance imaging (MRI), or positron emission tomography scans. However, sometimes it is difficult to judge based on the imaging as in pancreatic ductal adenocarcinoma. Similarly, tumor thrombi can be challenging to differentiate from bland thrombi based on imaging. EUS-guided FNA and elastography can be helpful in these cases.

In a retrospective study, forty-four patients with pancreatic ductal adenocarcinoma underwent dynamic CT and EUS, EUS-B mode imaging was taken, and also EUS elastography was done in all cases. Sensitivity, specificity and accuracy (95%CI) for vascular invasion were 0.733, 0.697 and 0.708 on dynamic CT; 0.733, 0.606 and 0.646 in EUS B-mode; and 0.917, 0.900 and 0.906 in EUS elastography. EUS-B mode and EUS elastography should be considered in patients with pancreatic ductal adenocarcinoma, where dynamic cannot detect vascular invasion[58].

ACCESS TO NON-GI STRUCTURES

The heart and pulmonary vascular systems can be easily accessed *via* EUS because of their proximity to the esophagus. Transesophageal echocardiography is routinely done in cardiac patients for various conditions[59]. Fritscher-Ravens *et al*[60] conducted a study where they performed EUS-guided puncture of the heart in a porcine model using a linear array echoendoscope followed by three clinical cases. In the porcine study, 22- and 19-gauge EUS needles were used to access the left atrium, left ventricle, coronary arteries, and aortic valve. In the porcine group, procedures performed included needle biopsy of cardiac muscle; contrast injection into the left atrium, ventricle, coronary arteries; radiofrequency ablation of aortic and mitral valves; and passage of a guidewire. No arrhythmias were reported during the procedures. During

necropsy, penetration sites were identified, but they were unremarkable in appearance; no bleeding or hematoma was noticed. Subsequently, EUS-guided cardiac access was performed in three patients. In two patients, pericardial fluid was aspirated for diagnostic purposes using a 22-gauge EUS needle, and the third patient had the FNA of atrial mass. No adverse events were observed after procedures in these patients.

Somani *et al*[61] described EUS-guided thrombolysis of pulmonary artery thrombus in a 57-year-old patient who presented with shortness of breath, shock, and acute abdominal pain. The patient had a superior mesenteric vein and right pulmonary artery thrombus. Given the shock state and history of recent hemorrhagic stroke, EUS-guided thrombolysis of pulmonary artery thrombus was done with Tenecteplase using 25G needle. Repeat EUS after 48 h and one before 15 d showed a reduction in the volume of thrombus.

Gaps in knowledge

The GI tract provides access to several vascular structures in the mediastinum, abdominal, and pelvis. Currently, most vascular interventions are done by an interventional radiologist through a percutaneous route. EUS provides access to most of the vasculature through the GI tract and the ability to do real-time interventions. Various studies have shown promising results for the safety, clinical and technical success of EUS-guided vascular intervention concluding that it should be considered either as first-line therapy or when conventional treatment fails. Although results are promising, it is based on case reports and series except in GV management, for which relatively more extensive studies are available.

Given that most data is available from case studies and series, it increases the risk of selection bias. Furthermore, these studies are available from tertiary care centers due to the limited availability of EUS and specialist trained in echoendoscope. EUS will eventually offer a less invasive and safer approach to various vascular interventions as this field expands further.

CONCLUSION

The GI tract provides a unique window to vascular structures in the mediastinum and abdomen, which can be accessed through FNA needle. Various studies have shown promising results for the safety, clinical and technical success of EUS-guided vascular intervention concluding that it should be considered either as first-line therapy or when conventional treatment fails. Although results are promising, it is based on case reports and series except in GV management for which relatively more extensive studies are available. Given that most data is available from case studies and series, it increases the risk of selection bias. Furthermore, these studies are available from tertiary care centers due to the limited availability of EUS and specialist trained in echoendoscope. As this field advances, EUS will offer a less invasive and safer approach to various vascular interventions.

REFERENCES

1 **Deprez PH**. Choice of endosonographic equipment and normal endosonographic anatomy. *Best Pract Res Clin Gastroenterol* 2009; **23**: 623-637 [PMID: 19744628 DOI: 10.1016/j.bpg.2009.07.001]

2 **Burmester E**, Tiede U. Longitudinal Endoscopic Ultrasound–Anatomical Guiding Structures in the Upper Abdomen (Cranial–Right). *J Enc GI End* 2013; **1**: 501-504 [DOI: 10.1016/s2212-0971(13)70220-6]

3 **Snady H**. Identification of major retroperitoneal vascular anatomy with endoscopic ultrasonography. *Acta Endosc* 1995; **25**: 491-498 [DOI: 10.1007/bf02966485]

4 **DiMagno EP**, DiMagno MJ. Endoscopic Ultrasonography: From the Origins to Routine EUS. *Dig Dis Sci* 2016; **61**: 342-353 [PMID: 26694170 DOI: 10.1007/s10620-015-3999-8]

5 **Friedberg SR**, Lachter J. Endoscopic ultrasound: Current roles and future directions. *World J Gastrointest Endosc* 2017; **9**: 499-505 [PMID: 29085560 DOI: 10.4253/wjge.v9.i10.499]

6 **Prachayakul V**, Aswakul P. Endoscopic ultrasound-guided interventions in special situations. *World J Gastrointest Endosc* 2016; **8**: 104-112 [PMID: 26839650 DOI: 10.4253/wjge.v8.i2.104]

7 **Oleas R**, Robles-Medranda C. Insights into the role of endoscopic ultrasound-guided vascular therapy. *Ther Adv Gastrointest Endosc* 2019; **12**: 2631774519878282 [PMID: 31633107 DOI: 10.1177/2631774519878282]

8 **Krige JE**, Bornman PC, Goldberg PA, Terblanche J. Variceal rebleeding and recurrence after

endoscopic injection sclerotherapy: a prospective evaluation in 204 patients. *Arch Surg* 2000; **135**: 1315-1322 [PMID: 11074888 DOI: 10.1001/archsurg.135.11.1315]

9 **Hou MC**, Lin HC, Lee FY, Chang FY, Lee SD. Recurrence of esophageal varices following endoscopic treatment and its impact on rebleeding: comparison of sclerotherapy and ligation. *J Hepatol* 2000; **32**: 202-208 [PMID: 10707859 DOI: 10.1016/s0168-8278(00)80064-1]

10 **Bokun T**, Grgurevic I, Kujundzic M, Banic M. EUS-Guided Vascular Procedures: A Literature Review. *Gastroenterol Res Pract* 2013; **2013**: 865945 [PMID: 23737766 DOI: 10.1155/2013/865945]

11 **Artifon ELA**, Marson FP, Khan MA. Endoscopic Ultrasonography-Guided Hemostasis Techniques. *Gastrointest Endosc Clin N Am* 2017; **27**: 741-747 [PMID: 28918809 DOI: 10.1016/j.giec.2017.06.011]

12 **Lahoti S**, Catalano MF, Alcocer E, Hogan WJ, Geenen JE. Obliteration of esophageal varices using EUS-guided sclerotherapy with color Doppler. *Gastrointest Endosc* 2000; **51**: 331-333 [PMID: 10699783 DOI: 10.1016/s0016-5107(00)70363-4]

13 **Lôbo MRA**, Chaves DM, DE Moura DTH, Ribeiro IB, Ikari E, DE Moura EGH. Safety and efficacy of EUS-guided coil plus cyanoacrylate versus conventional cyanoacrylate technique in the treatment of gastric varices: A randomized controlled trial. *Arq Gastroenterol* 2019; **56**: 99-105 [PMID: 31141079 DOI: 10.1590/S0004-2803.201900000-08]

14 **Koziel S**, Pawlak K, Błaszczyk Ł, Jagielski M, Wiechowska-Kozłowska A. Endoscopic Ultrasound-Guided Treatment of Gastric Varices Using Coils and Cyanoacrylate Glue Injections: Results after 1 Year of Experience. *J Clin Med* 2019; **8** [PMID: 31731504 DOI: 10.3390/jcm8111786]

15 **McCarty TR**, Bazarbashi AN, Hathorn KE, Thompson CC, Ryou M. Combination therapy *versus* monotherapy for EUS-guided management of gastric varices: A systematic review and meta-analysis. *Endosc Ultrasound* 2020; **9**: 6-15 [PMID: 31417066 DOI: 10.4103/eus.eus_37_19]

16 **Ríos Castellanos E**, Seron P, Gisbert JP, Bonfill Cosp X. Endoscopic injection of cyanoacrylate glue versus other endoscopic procedures for acute bleeding gastric varices in people with portal hypertension. *Cochrane Database Syst Rev* 2015; CD010180 [PMID: 25966446 DOI: 10.1002/14651858.CD010180.pub2]

17 **Lee TH**, Shih LN. Clinical experience of endoscopic banding ligation for bleeding gastric varices. *Hepatogastroenterology* 2008; **55**: 766-769 [PMID: 18613450]

18 **Sarin SK**, Lahoti D, Saxena SP, Murthy NS, Makwana UK. Prevalence, classification and natural history of gastric varices: a long-term follow-up study in 568 portal hypertension patients. *Hepatology* 1992; **16**: 1343-1349 [PMID: 1446890 DOI: 10.1002/hep.1840160607]

19 **Frost JW**, Hebbar S. EUS-guided thrombin injection for management of gastric fundal varices. *Endosc Int Open* 2018; **6**: E664-E668 [PMID: 29868631 DOI: 10.1055/a-0599-0440]

20 **Wang X**, Yu S, Chen X, Duan L. Endoscopic ultrasound-guided injection of coils and cyanoacrylate glue for the treatment of gastric fundal varices with abnormal shunts: a series of case reports. *J Int Med Res* 2019; **47**: 1802-1809 [PMID: 30819006 DOI: 10.1177/0300060519830207]

21 **Hwang SS**, Kim HH, Park SH, Kim SE, Jung JI, Ahn BY, Kim SH, Chung SK, Park YH, Choi KH. N-butyl-2-cyanoacrylate pulmonary embolism after endoscopic injection sclerotherapy for gastric variceal bleeding. *J Comput Assist Tomogr* 2001; **25**: 16-22 [PMID: 11176287 DOI: 10.1097/00004728-200101000-00003]

22 **George N**, Perisetti A, Banerjee D, Raghavapuram S, Garcia-Saenz-de-Sicilia M, Tharian B. EUS-Guided Treatment of Gastric Varices: A Single Center Experience: 783. *Am J Gastroenterol* 2017; 112 [DOI: 10.14309/00000434-201710001-00784]

23 **Gubler C**, Bauerfeind P. Safe and successful endoscopic initial treatment and long-term eradication of gastric varices by endoscopic ultrasound-guided Histoacryl (N-butyl-2-cyanoacrylate) injection. *Scand J Gastroenterol* 2014; **49**: 1136-1142 [PMID: 24947448 DOI: 10.3109/00365521.2014.929171]

24 **Bick BL**, Al-Haddad M, Liangpunsakul S, Ghabril MS, DeWitt JM. EUS-guided fine needle injection is superior to direct endoscopic injection of 2-octyl cyanoacrylate for the treatment of gastric variceal bleeding. *Surg Endosc* 2019; **33**: 1837-1845 [PMID: 30259158 DOI: 10.1007/s00464-018-6462-z]

25 **Anastasiou J**, Berzin TM. Endoscopic Ultrasound-Guided Vascular Interventions: From Diagnosis to Treatment. *Saudi J Med Med Sci* 2018; **6**: 61-67 [PMID: 30787823 DOI: 10.4103/sjmms.sjmms_131_17]

26 **Romero-Castro R**, Ellrichmann M, Ortiz-Moyano C, Subtil-Inigo JC, Junquera-Florez F, Gornals JB, Repiso-Ortega A, Vila-Costas J, Marcos-Sanchez F, Muñoz-Navas M, Romero-Gomez M, Brullet-Benedi E, Romero-Vazquez J, Caunedo-Alvarez A, Pellicer-Bautista F, Herrerias-Gutierrez JM, Fritscher-Ravens A. EUS-guided coil versus cyanoacrylate therapy for the treatment of gastric varices: a multicenter study (with videos). *Gastrointest Endosc* 2013; **78**: 711-721 [PMID: 23891417 DOI: 10.1016/j.gie.2013.05.009]

27 **Bazarbashi AN**, Wang TJ, Thompson CC, Ryou M. Endoscopic ultrasound-guided treatment of gastric varices with coil embolization and absorbable hemostatic gelatin sponge: a novel alternative to cyanoacrylate. *Endosc Int Open* 2020; **8**: E221-E227 [PMID: 32010757 DOI: 10.1055/a-1027-6708]

28 **Grgurevic I**, Kujundzic M, Banic M, Kusec R, Bokun T, Vukelic-Markovic M, Bogdanovic Z, Lukic A, Tsochatzis E, Brkljacic B. Subtypes and clinical significance of common bile duct varices in portal vein thrombosis: diagnosis and follow-up by Doppler US and EUS. *Abdom Radiol (NY)* 2016; **41**: 476-484 [PMID: 27039318 DOI: 10.1007/s00261-015-0596-4]

29 **Kinzel J**, Pichetshote N, Dredar S, Aslanian H, Nagar A. Bleeding from a duodenal varix: a unique case of variceal hemostasis achieved using EUS-guided placement of an embolization coil and

cyanoacrylate. *J Clin Gastroenterol* 2014; **48**: 362-364 [PMID: 24518801 DOI: 10.1097/MCG.0000000000000004]

30 **Sharma M**, Rai P, Bansal R. EUS-Assisted Evaluation of Rectal Varices before Banding. *Gastroenterol Res Pract* 2013; **2013**: 619187 [PMID: 23781241 DOI: 10.1155/2013/619187]

31 **Maggio D**, Barkun AN, Martel M, Elouali S, Gralnek IM; Reason Investigators. Predictors of early rebleeding after endoscopic therapy in patients with nonvariceal upper gastrointestinal bleeding secondary to high-risk lesions. *Can J Gastroenterol* 2013; **27**: 454-458 [PMID: 23936874 DOI: 10.1155/2013/128760]

32 **De Angelis CG**, Cortegoso Valdivia P, Rizza S, Venezia L, Rizzi F, Gesualdo M, Saracco GM, Pellicano R. Endoscopic Ultrasound-Guided Treatments for Non-Variceal Upper GI Bleeding: A Review of the Literature. *J Clin Med* 2020; **9** [PMID: 32245209 DOI: 10.3390/jcm9030866]

33 **Levy MJ**, Wong Kee Song LM, Farnell MB, Misra S, Sarr MG, Gostout CJ. Endoscopic ultrasound (EUS)-guided angiotherapy of refractory gastrointestinal bleeding. *Am J Gastroenterol* 2008; **103**: 352-359 [PMID: 17986314 DOI: 10.1111/j.1572-0241.2007.01616.x]

34 **Law R**, Fujii-Lau L, Wong Kee Song LM, Gostout CJ, Kamath PS, Abu Dayyeh BK, Gleeson FC, Rajan E, Topazian MD, Levy MJ. Efficacy of endoscopic ultrasound-guided hemostatic interventions for resistant nonvariceal bleeding. *Clin Gastroenterol Hepatol* 2015; **13**: 808-12.e1 [PMID: 25245627 DOI: 10.1016/j.cgh.2014.09.030]

35 **Gamanagatti S**, Thingujam U, Garg P, Nongthombam S, Dash NR. Endoscopic ultrasound guided thrombin injection of angiographically occult pancreatitis associated visceral artery pseudoaneurysms: Case series. *World J Gastrointest Endosc* 2015; **7**: 1107-1113 [PMID: 26421108 DOI: 10.4253/wjge.v7.i13.1107]

36 **Maharshi S**, Sharma SS, Sharma D, Sapra B, Nijhawan S. Endoscopic ultrasound-guided thrombin injection, a management approach for visceral artery pseudoaneurysms. *Endosc Int Open* 2020; **8**: E407-E412 [PMID: 32118114 DOI: 10.1055/a-1070-9168]

37 **Kumbhari V**, Gondal B, Okolo Iii PI, Lennon AM, Law JK, Singh VK, Saxena P, Shin EJ, Canto MI, Kalloo AN, Khashab MA. Endoscopic ultrasound-guided angiotherapy of a large bleeding gastrointestinal stromal tumor. *Endoscopy* 2013; **45** Suppl 2 UCTN: E326-E327 [PMID: 24101603 DOI: 10.1055/s-0033-1344875]

38 **Săftoiu A**, Vilmann P, Hassan H, Krag Jacobsen G. Utility of colour Doppler endoscopic ultrasound evaluation and guided therapy of submucosal tumours of the upper gastrointestinal tract. *Ultraschall Med* 2005; **26**: 487-495 [PMID: 16453220 DOI: 10.1055/s-2005-858905]

39 **Crowe DR**, Eloubeidi MA, Chhieng DC, Jhala NC, Jhala D, Eltoum IA. Fine-needle aspiration biopsy of hepatic lesions: computerized tomographic-guided versus endoscopic ultrasound-guided FNA. *Cancer* 2006; **108**: 180-185 [PMID: 16634071 DOI: 10.1002/cncr.21912]

40 **Huang JY**, Samarasena JB, Tsujino T, Lee J, Hu KQ, McLaren CE, Chen WP, Chang KJ. EUS-guided portal pressure gradient measurement with a simple novel device: a human pilot study. *Gastrointest Endosc* 2017; **85**: 996-1001 [PMID: 27693644 DOI: 10.1016/j.gie.2016.09.026]

41 **Sarin SK**, Khanna R. Non-cirrhotic portal hypertension. *Clin Liver Dis* 2014; **18**: 451-476 [PMID: 24679506 DOI: 10.1016/j.cld.2014.01.009]

42 **Suk KT**. Hepatic venous pressure gradient: clinical use in chronic liver disease. *Clin Mol Hepatol* 2014; **20**: 6-14 [PMID: 24757653 DOI: 10.3350/cmh.2014.20.1.6]

43 **Pomier-Layrargues G**, Kusielewicz D, Willems B, Villeneuve JP, Marleau D, Côté J, Huet PM. Presinusoidal portal hypertension in non-alcoholic cirrhosis. *Hepatology* 1985; **5**: 415-418 [PMID: 3997071 DOI: 10.1002/hep.1840050312]

44 **Colombato L**. The role of transjugular intrahepatic portosystemic shunt (TIPS) in the management of portal hypertension. *J Clin Gastroenterol* 2007; **41** Suppl 3: S344-S351 [PMID: 17975487 DOI: 10.1097/MCG.0b013e318157e500]

45 **Wong F**. The use of TIPS in chronic liver disease. *Ann Hepatol* 2006; **5**: 5-15 [PMID: 16531959]

46 **Quateen A**, Pech M, Berg T, Bergk A, Podrabsky P, Felix R, Ricke J. Percutaneous transjugular direct porto-caval shunt in patients with Budd-Chiari syndrome. *Cardiovasc Intervent Radiol* 2006; **29**: 565-570 [PMID: 16729230 DOI: 10.1007/s00270-005-0103-3]

47 **Perry BC**, Kwan SW. Portosystemic Shunts: Stable Utilization and Improved Outcomes, Two Decades After the Transjugular Intrahepatic Portosystemic Shunt. *J Am Coll Radiol* 2015; **12**: 1427-1433 [PMID: 26410348 DOI: 10.1016/j.jacr.2015.06.037]

48 **Silva RF**, Arroyo PC Jr, Duca WJ, Silva AA, Reis LF, Cabral CM, Sgnolf A, Domingues RB, Barao GT, Coelho DJ, Deberaldini M, Felício HC, Silva RC. Complications following transjugular intrahepatic portosystemic shunt: a retrospective analysis. *Transplant Proc* 2004; **36**: 926-928 [PMID: 15194319 DOI: 10.1016/j.transproceed.2004.03.117]

49 **Kenneth F**. Janak NS. Sa1428 EUS-Guided Transgastric Intrahepatic Portosystemic Shunt Using the Axios Stent. *Gastro Endos* 2011; 73 [DOI: 10.1016/j.gie.2011.03.162]

50 **Park TY**, Seo DW, Kang HJ, Song TJ, Park DH, Lee SS, Lee SK, Kim MH. Feasibility and safety of EUS-guided selective portal vein embolization with a coil and cyanoacrylate in a live porcine model. *Endosc Ultrasound* 2018; **7**: 389-394 [PMID: 30246708 DOI: 10.4103/eus.eus_18_18]

51 **Loffroy R**, Favelier S, Chevallier O, Estivalet L, Genson PY, Pottecher P, Gehin S, Krausé D, Cercueil JP. Preoperative portal vein embolization in liver cancer: indications, techniques and outcomes. *Quant Imaging Med Surg* 2015; **5**: 730-739 [PMID: 26682142 DOI: 10.3978/j.issn.2223-4292.2015.10.04]

52 **Catenacci DV**, Chapman CG, Xu P, Koons A, Konda VJ, Siddiqui UD, Waxman I. Acquisition of

Portal Venous Circulating Tumor Cells From Patients With Pancreaticobiliary Cancers by Endoscopic Ultrasound. *Gastroenterology* 2015; **149**: 1794-1803.e4 [PMID: 26341722 DOI: 10.1053/j.gastro.2015.08.050]

53 **Tien YW**, Kuo HC, Ho BI, Chang MC, Chang YT, Cheng MF, Chen HL, Liang TY, Wang CF, Huang CY, Shew JY, Chang YC, Lee EY, Lee WH. A High Circulating Tumor Cell Count in Portal Vein Predicts Liver Metastasis From Periampullary or Pancreatic Cancer: A High Portal Venous CTC Count Predicts Liver Metastases. *Medicine (Baltimore)* 2016; **95**: e3407 [PMID: 27100430 DOI: 10.1097/MD.0000000000003407]

54 **Kayar Y**, Turkdogan KA, Baysal B, Unver N, Danalioglu A, Senturk H. EUS-guided FNA of a portal vein thrombus in hepatocellular carcinoma. *Pan Afr Med J* 2015; **21**: 86 [PMID: 26491529 DOI: 10.11604/pamj.2015.21.86.6991]

55 **Michael H**, Lenza C, Gupta M, Katz DS. Endoscopic Ultrasound -guided Fine-Needle Aspiration of a Portal Vein Thrombus to Aid in the Diagnosis and Staging of Hepatocellular Carcinoma. *Gastroenterol Hepatol (N Y)* 2011; **7**: 124-129 [PMID: 21475421]

56 **Storch I**, Gomez C, Contreras F, Schiff E, Ribeiro A. Hepatocellular carcinoma (HCC) with portal vein invasion, masquerading as pancreatic mass, diagnosed by endoscopic ultrasound-guided fine needle aspiration (EUS-FNA). *Dig Dis Sci* 2007; **52**: 789-791 [PMID: 17268833 DOI: 10.1007/s10620-006-9325-8]

57 **Faigel D**, Lake D, Landreth T, Kelman C, Marler R. Endoscopic ultrasonography-guided portal injection chemotherapy for hepatic metastases. *Endosc Ultrasound* 2014; **3**: S1 [PMID: 26425503]

58 **Yamada K**, Kawashima H, Ohno E, Ishikawa T, Tanaka H, Nakamura M, Miyahara R, Ishigami M, Hirooka Y, Fujishiro M. Diagnosis of vascular invasion in pancreatic ductal adenocarcinoma using endoscopic ultrasound elastography. *BMC Gastroenterol* 2020; **20**: 81 [PMID: 32228472 DOI: 10.1186/s12876-020-01228-9]

59 **Kühl HP**, Hanrath P. The impact of transesophageal echocardiography on daily clinical practice. *Eur J Echocardiogr* 2004; **5**: 455-468 [PMID: 15556822 DOI: 10.1016/j.euje.2004.04.007]

60 **Fritscher-Ravens A**, Ganbari A, Mosse CA, Swain P, Koehler P, Patel K. Transesophageal endoscopic ultrasound-guided access to the heart. *Endoscopy* 2007; **39**: 385-389 [PMID: 17516342 DOI: 10.1055/s-2007-966440]

61 **Somani P**, Talele R, Sharma M. Endoscopic Ultrasound-Guided Thrombolysis of Pulmonary Artery Thrombus and Mesenteric Vein Thrombus. *Am J Gastroenterol* 2019; **114**: 379 [PMID: 30840604 DOI: 10.14309/ajg.0000000000000139]

62 **Krill JT**, Othman MO, Munot K, Jalal PK, Patel K. Su1411 EUS-Guided coil application with glue injection for gastric variceal obliteration is associated with less endoscopic reintervention compared to glue injection alone. *Gastro Endos* 2018; **87**: AB345 [DOI: 10.1016/j.gie.2018.04.1741]

63 **Romero-Castro R**, Pellicer-Bautista F, Giovannini M, Marcos-Sánchez F, Caparros-Escudero C, Jiménez-Sáenz M, Gomez-Parra M, Arenzana-Seisdedos A, Leria-Yebenes V, Herrerias-Gutiérrez JM. Endoscopic ultrasound (EUS)-guided coil embolization therapy in gastric varices. *Endoscopy* 2010; **42** Suppl 2: E35-E36 [PMID: 20073010 DOI: 10.1055/s-0029-1215261]

64 **Philips CA**, Augustine P. Endoscopic Ultrasound-Guided Management of Bleeding Rectal Varices. *ACG Case Rep J* 2017; **4**: e101 [PMID: 28879206 DOI: 10.14309/crj.2017.101]

65 **Bazarbashi AN**, Thompson CC, Ryou M. Targeting the perforator vein: EUS-guided coil embolization for the treatment of bleeding rectal varices. *VideoGIE* 2020; **5**: 434-436 [PMID: 32954109 DOI: 10.1016/j.vgie.2020.05.008]

66 **Mukkada RJ**, Mathew PG, Francis Jose V, Paul Chettupuzha A, Antony R, Koshy A. EUS-guided coiling of rectal varices. *VideoGIE* 2017; **2**: 208-210 [PMID: 30175307 DOI: 10.1016/j.vgie.2017.05.005]

67 **Robb PM**, Yeaton P, Bishop T, Wessinger J. Endoscopic Ultrasound Guided Embolization of a Pancreatic Pseudoaneurysm. *Gastroenterology Res* 2012; **5**: 239-241 [PMID: 27785215 DOI: 10.4021/gr500w]

68 **Somani P**, Sharma M, Jindal S. EUS-Guided Coil Embolization and Thrombin Injection of Bleeding Gastroduodenal Artery Pseudoaneurysm: 1611. *Am College Gastroenterol* 2017; **112**: S876 [DOI: 10.14309/00000434-201710001-01612]

69 **Jhajharia A**, Wanjari S, Ashdhir P, Sharma D, Pokharna R, Nijhawan S. Endoscopic ultrasound-guided thrombin injection for management of visceral artery pseudoaneurysm: A novel approach. *Indian J Gastroenterol* 2018; **37**: 271-275 [PMID: 29971689 DOI: 10.1007/s12664-018-0865-6]

World Journal of Gastroenterology

Submit a Manuscript: https://www.f6publishing.com

World J Gastroenterol 2021 October 28; 27(40): 6888-6907

DOI: 10.3748/wjg.v27.i40.6888

ISSN 1007-9327 (print) ISSN 2219-2840 (online)

ORIGINAL ARTICLE

Basic Study

Metabolomics of *Fuzi-Gancao* in CCl_4 induced acute liver injury and its regulatory effect on bile acid profile in rats

Mo-Fei Wang, Song-Song Zhao, Dil Momin Thapa, Yu-Ling Song, Zheng Xiang

ORCID number: Mo-Fei Wang 0000-0002-3221-608X; Song-Song Zhao 0000-0003-2401-8769; Dil Momin Thapa 0000-0003-2856-6324; Yu-Ling Song 0000-0002-6330-957X; Zheng Xiang 0000-0003-4983-1019.

Author contributions: Xiang Z and Wang MF designed and coordinated the study; Wang MF, Thapa DM, and Song YL performed the experiments and acquired and analyzed the data; Wang MF and Zhao SS wrote the manuscript; all authors approved the final version of the article.

Supported by Scientific Research Projects for Higher Education in Inner Mongolia Autonomous Region, No. NJZZ21027; Support Plan for the Innovation and Entrepreneurship Initiation Plan for Overseas Students in Inner Mongolia Autonomous Region, No. MOHRSS2020122; Doctoral Start-up Fund of the Affiliated Hospital of Inner Mongolia University for the Nationalities, No. MDFY2020001.

Institutional animal care and use committee statement: All animal experiments conformed to the internationally accepted principles for the care and use of laboratory animals. The study was reviewed and approved by the Liaoning

Mo-Fei Wang, Dil Momin Thapa, Yu-Ling Song, The Second Department of General Surgery, The Affiliated Hospital of Inner Mongolia University for the Nationalities, Tongliao 028000, Inner Mongolia Autonomous Region, China

Song-Song Zhao, Department of Educational Administration, The First Affiliated Hospital of Liaoning Medical University, Jinzhou 121000, Liaoning Province, China

Zheng Xiang, School of Pharmaceutical Science, Liaoning University, Shenyang 110032, Liaoning Province, China

Corresponding author: Mo-Fei Wang, PhD, Professor, The Second Department of General Surgery, The Affiliated Hospital of Inner Mongolia University for the Nationalities, No. 1742 East Section of Huolinhe Street, Tongliao 028000, Inner Mongolia Autonomous Region, China. wangm1228@sina.com

Abstract

BACKGROUND

Fuzi (*Radix aconiti* lateralis)-*Gancao* (*Radix glycyrrhizae*) is one of the most classical drug pairs of traditional Chinese medicine. In clinical practice, decoctions containing *Fuzi-Gancao* (F-G) are often used in the treatment of liver diseases such as hepatitis and liver failure.

AIM

To investigate the metabolomics of F-G in CCl_4 induced acute liver injury in rats and its regulatory effect on the bile acid profile.

METHODS

The pharmacodynamic effect of F-G on CCl_4 induced acute liver injury in rats was evaluated, and an ultra performance liquid chromatography-tandem mass spectrometry (UPLC-MS/MS) method for the simultaneous determination of 92 metabolites from multiple pathways was established to explore the protective metabolic mechanism of F-G in serum on the liver.

RESULTS

Twenty-four differential metabolites were identified in serum samples. The primary bile acid biosynthetic metabolic pathway was the major common pathway in the model group and F-G group. Subsequently, a UPLC-MS/MS method for simultaneous determination of 11 bile acids, including cholic acid,

University Research Ethics Committee.

Conflict-of-interest statement: There are no conflicts of interest to disclose.

Data sharing statement: No additional data are available.

ARRIVE guidelines statement: The authors have read the ARRIVE guidelines, and the manuscript was prepared and revised according to the ARRIVE guidelines.

Open-Access: This article is an open-access article that was selected by an in-house editor and fully peer-reviewed by external reviewers. It is distributed in accordance with the Creative Commons Attribution NonCommercial (CC BY-NC 4.0) license, which permits others to distribute, remix, adapt, build upon this work non-commercially, and license their derivative works on different terms, provided the original work is properly cited and the use is non-commercial. See: http://creativecommons.org/Licenses/by-nc/4.0/

Manuscript source: Unsolicited manuscript

Specialty type: Gastroenterology and hepatology

Country/Territory of origin: China

Peer-review report's scientific quality classification

Grade A (Excellent): 0
Grade B (Very good): B
Grade C (Good): 0
Grade D (Fair): 0
Grade E (Poor): 0

Received: April 17, 2021
Peer-review started: April 17, 2021
First decision: June 23, 2021
Revised: June 28, 2021
Accepted: August 25, 2021
Article in press: August 25, 2021
Published online: October 28, 2021

P-Reviewer: Saraiva MM
S-Editor: Wu YXJ
L-Editor: Wang TQ

ursodeoxycholic acid, glycochenodeoxycholic acid, glycochenodeoxycholic acid, taurocholic acid, glycocholic acid, chenodeoxycholic acid, deoxycholic acid, taurochenodeoxycholic acid, taurocholic acid, and glycinic acid, was established to analyze the regulatory mechanism of F-G in serum. F-G decreased the contents of these 11 bile acids in serum in a dose-dependent manner compared with those in the model control group.

CONCLUSION

F-G could protect hepatocytes by promoting the binding of free bile acids to glycine and taurine, and reducing the accumulation of free bile acids in the liver. F-G could also regulate the compensatory degree of taurine, decreasing the content of taurine-conjugated bile acids to protect hepatocytes.

Key Words: *Radix aconiti* lateralis; *Radix glycyrrhizae*; Liver injury; Metabolites; Bile acid; *Fuzi-Gancao*

©The Author(s) 2021. Published by Baishideng Publishing Group Inc. All rights reserved.

Core Tip: *Fuzi-Gancao* (F-G) could protect hepatocytes by promoting the binding of free bile acids to glycine and taurine, and reducing the accumulation of free bile acids in the liver. F-G could also regulate the compensatory degree of taurine, decreasing the content of taurine-conjugated bile acids to protect hepatocytes.

Citation: Wang MF, Zhao SS, Thapa DM, Song YL, Xiang Z. Metabolomics of *Fuzi-Gancao* in CCl_4 induced acute liver injury and its regulatory effect on bile acid profile in rats. *World J Gastroenterol* 2021; 27(40): 6888-6907
URL: https://www.wjgnet.com/1007-9327/full/v27/i40/6888.htm
DOI: https://dx.doi.org/10.3748/wjg.v27.i40.6888

INTRODUCTION

The liver is an important metabolic organ of the human body that has the physiological functions of detoxification, phagocytosis, and defense[1]. With the development of modern industry, liver injury caused by environmental pollution is gradually increasing. Liver injury is an important pathophysiological process in the development of hepatitis, liver fibrosis, liver cirrhosis, and liver cancer. Therefore, the treatment of liver injury is important for the prevention, treatment, and recovery of a variety of liver diseases[2,3].

Bile acids are one of the most sensitive indicators for the clinical diagnosis of liver diseases[4,5]. When the liver system is diseased, it can cause a disturbance in the metabolism of bile acids in the body, thus causing a significant change in the amount of bile acids in the blood. Therefore, biomarkers of the bile acid metabolism pathway are very important diagnostic and therapeutic indicators for liver disease[4-6]. Liver diseases such as liver injury, hepatitis, cirrhosis, and hepatocellular carcinoma have significantly increased serum total bile acid levels, and changes in total bile acid levels are usually analyzed in clinical tests but are not highly specific[6,7]. Therefore, the changes in the bile acid profile based on the metabolic pathway of bile acids have important significance for the prevention and treatment of liver diseases. Bile acids can be divided into primary and secondary bile acids[8,9]. Primary bile acids are bile acids synthesized directly from cholesterol by hepatocytes and mainly include cholic acid (CA) and chenodeoxycholic acid (CDCA). Secondary bile acids are free bile acids produced by the primary bile acids deoxycholic acid (DCA) and lithocholic acid (LCA) after 7α-hydroxy deoxygenation of the intestinal flora. These free bile acids bind with glycine and taurine to form conjugated secondary bile acids such as glycocholic acid (GCA), glycochenodeoxycholic acid (GCDCA), glycochenodeoxycholic acid (GDCA), taurocholic acid (TCA), taurochenodeoxycholic acid (TCDCA), ursodeoxycholic acid (UDCA), glycinic acid (GLCA), and taurocholic acid (TUDCA).

Chinese herbal compounds have been used clinically for thousands of years in the treatment of liver system diseases, among which *Fuzi* (*Radix aconiti* Lateralis)-*Gancao* (

P-Editor: Li JH

Radix glycyrrhizae) is one of the most common drug pairs in Chinese herbal compounds, and Chinese herbal compounds containing *Fuzi-Gancao* (F-G), such as *Yinchen Sifu* decoction, *Sini* decoction, and *Fuzi Lizhong* decoction, are often used in the treatment of liver diseases such as hepatitis and liver failure[10-13]. Modern pharmacological studies have shown that herbal compounds containing *Fuzi* and *Gancao* can reduce the biochemical indexes of liver injury model animals by inhibiting inflammatory stress, lipid peroxidation, and apoptosis and have significant pharmacological activity to prevent liver injury[14-16].

Fuzi and *Gancao* are important medicinal materials in classic prescriptions, such as *Sini* decoction and *Fuzi Lizhong* decoction. Aconite alkaloids in *Fuzi* and flavonoids in *Gancao* are the main active ingredients in F-G drug pairs. Alkaloids are the main active ingredients in aconite, and thus far, nearly 200 alkaloids have been isolated and identified. These alkaloids are mainly classified into nonester alkaloids, monoester diterpene alkaloids (MDAs), diester diterpene alkaloids (DDAs), and lipoalkaloids according to their structural properties[17]. MDAs and DDAs have very well-defined pharmacological activities, such as cardiotonic[18-20], anti-inflammatory and analgesic [21], antitumor[22], antioxidation[23], and hepatoprotective[24,25] activities. Flavonoids are the main active ingredients of *Gancao* and have well-defined pharmacological anti-inflammatory[26-28], antibacterial[29], antioxidant[30], hepatoprotective, and antitumor[31] activities. The Chinese Pharmacopoeia (2015 edition) prescribes the compatibility ratio of *Fuzi* and *Gancao* as 1:1, which could decrease the toxins caused by aconite alkaloids and enhance the treatment effect compared with other ratios[32-34].

In a previous study, a rapid, convenient, and stable method for the simultaneous quantitative determination of six alkaloids and three flavonoids in *Radix aconiti* lateralis and *Radix glycyrrhizae* by ultra performance liquid chromatography-tandem mass spectrometry (UPLC-MS/MS) was established[17]. In this study, the effects of the F-G water extract on the prevention of liver injury induced by tetrachloride (CCl_4) were evaluated. Then, the metabolic mechanism was studied by UPLC-MS/MS. Finally, a method of simultaneous quantitative detection of 11 bile acids was established, and the mechanism of F-G in the regulation of the serum bile acid profile was analyzed by UPLC-MS/MS.

MATERIALS AND METHODS

Plant materials

Radix aconiti lateralis (*Fuzi*) pieces were purchased from Huang Gang Jingui Traditional Chinese Medicine Industry Development Co., Ltd. (Sichuan, China), and *Radix glycyrrhizae* (*Gancao*) was purchased from Bozhou Jinshaotang Herbal Decoction Co., Ltd. (Anhui, China). The medicinal materials were identified by Professor Fu Xiao at the First Affiliated Hospital of Jinzhou Medical University.

Chemicals and Reagents

The aspartate aminotransferase (AST) and alanine aminotransferase (ALT) assay kits were purchased from Nanjing Jiancheng Bioengineering Co., Ltd.; silybin was purchased from Solarbio Biotech Co., Ltd.; L-leucine, L-tryptophan, L-kynurenine, 5-Hydroxytryptamine (5-HT), 5-hydroxytryptophan (5-HTP), cholic acid, N-phenylacetylglycine, glutathione (GSH), glutathione oxidized (GSSG), N-ethylmaleimide, and formic acid were purchased from Sigma-Aldrich (United States); L-phenylalanine (Ring-D5) was purchased from Cambridge isotope laboratories; UDCA, GDCA, GCDCA-Na, TCA-Na, and GCA were purchased from Meryer Co., Ltd.; CDCA, DCA, TCDCA, TUDCA, and GLCA were obtained from Shanghai Macklin Biochemical Co., Ltd; d4-GCDCA was purchased from Shanghai Zhenzun Biochemical Co., Ltd; MS-grade methanol and acetonitrile were purchased from Merck; water for MS analysis was prepared using a Milli-Q water purification system; phosphate buffered solution (PBS) was purchased from HyClone Co., Ltd; CCl4 was purchased from Yongsheng Chemical Co., Ltd; alcohol was purchased from Kermel Chemical Co.; pentobarbital sodium was purchased from Shanghai Experimental Chemical Reagent Co., Ltd.; and normal saline was purchased from Qingdao Huaren Pharmaceutical Co., Ltd.

Animals

Male Sprague-Dawley rats (200 g ± 20 g) were purchased from the Laboratory Animal Center of Chinese Medical University (animal license No.: SCXK (Liao) 2008-0005). The rats were housed under SPF laboratory conditions at a temperature of 25 ± 2 °C, a

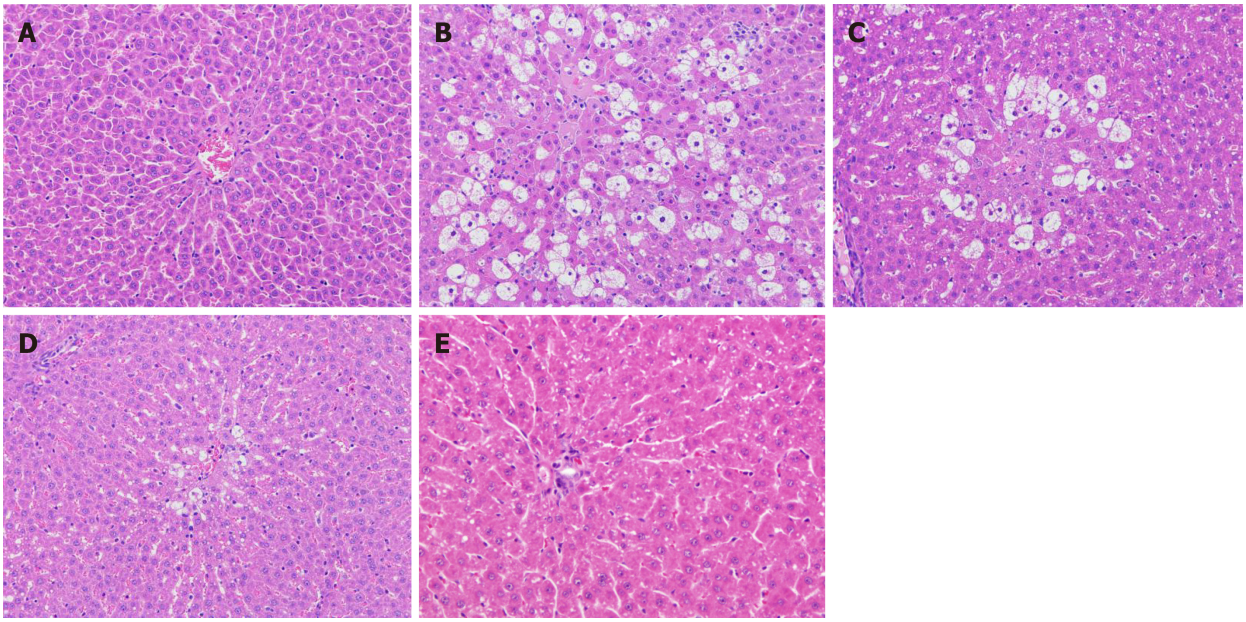


Figure 1 Histological changes in various groups of rats. HE staining, magnification: 400 ×. A: Normal control group; B: Model control group; C: *Fuzi-Gancao* (F-G) group (15 g/kg); D: F-G group (30 g/kg); E: Positive control group (silybin).

relative humidity of 40 ± 5%, and a 12-h circadian cycle for 1 wk. All procedures were performed according to the National Institute of Health guidelines regarding the principles of animal care.

Preparation of the F-G extract

Fuzi (1.3 kg) and *Gancao* (1.3 kg) were mixed and soaked in water (26 L) for 0.5 h, and then the mixture was refluxed for 2 h. The supernatant was then concentrated under vacuum to obtain the F-G extract. The extract was diluted with water to a final concentration of 1.5 g/mL (crude drug), and all the extracts were stored at 4 °C before use.

Protective effect of F-G on acute liver injury induced by CCl_4

Forty male rats were randomly divided into five groups (n = 8): Normal control group, model control group, positive control group, F-G group with 15 g/kg crude drug, and F-G group with 30 g/kg crude drug. The positive control group was orally administered with silybin at 50 mg/kg daily, and the normal control group and model control group were given the same volume of normal saline daily by gavage once a day for 8 d.

On the 7th day, 40% CCl_4 (v/v, olive oil) was intraperitoneally injected in the positive control group, model control group, and F-G groups at a dose of 2 mL/kg. The rats were anesthetized using sodium pentobarbital 2 h after administration on the 8th day. Blood samples were collected from the abdominal aorta and centrifuged at 3500 rpm for 10 min (4 °C) to obtain serum samples for transaminase (ALT and AST) and metabolic analysis. Liver tissue samples were taken for pathological analysis.

Metabolic analysis

To elucidate the mechanism of F-G in the treatment of liver injury, three groups of serum samples, including that from the normal control group, model control group, and F-G group (30 g/kg), were used for metabolic analysis by UPLC-MS according to a method published by the authors with minor modifications[35].

Preparation of "stripped" serum: One hundred milliliters of rat serum including activated charcoal powder (6 g) was incubated at room temperature for 2 h. After centrifugation at 13000 rpm for 20 min (4 °C), the supernatant was filtered successively through microporous membranes with pore sizes of 5 μm, 1.2 μm, and 0.45 μm to obtain "stripped" serum.

Samples for metabolic analysis: Two hundred microliters of the serum sample was pipetted into a 1.5 mL centrifuge tube, followed by adding 200 μL of PBS solution containing NEM (10 mmol/L) and 1000 μL of methanol solution with L-phenylalanine (Ring-D5; 10 ng/mL, internal standard) in sequence, vortexing for 30 s, and incubating

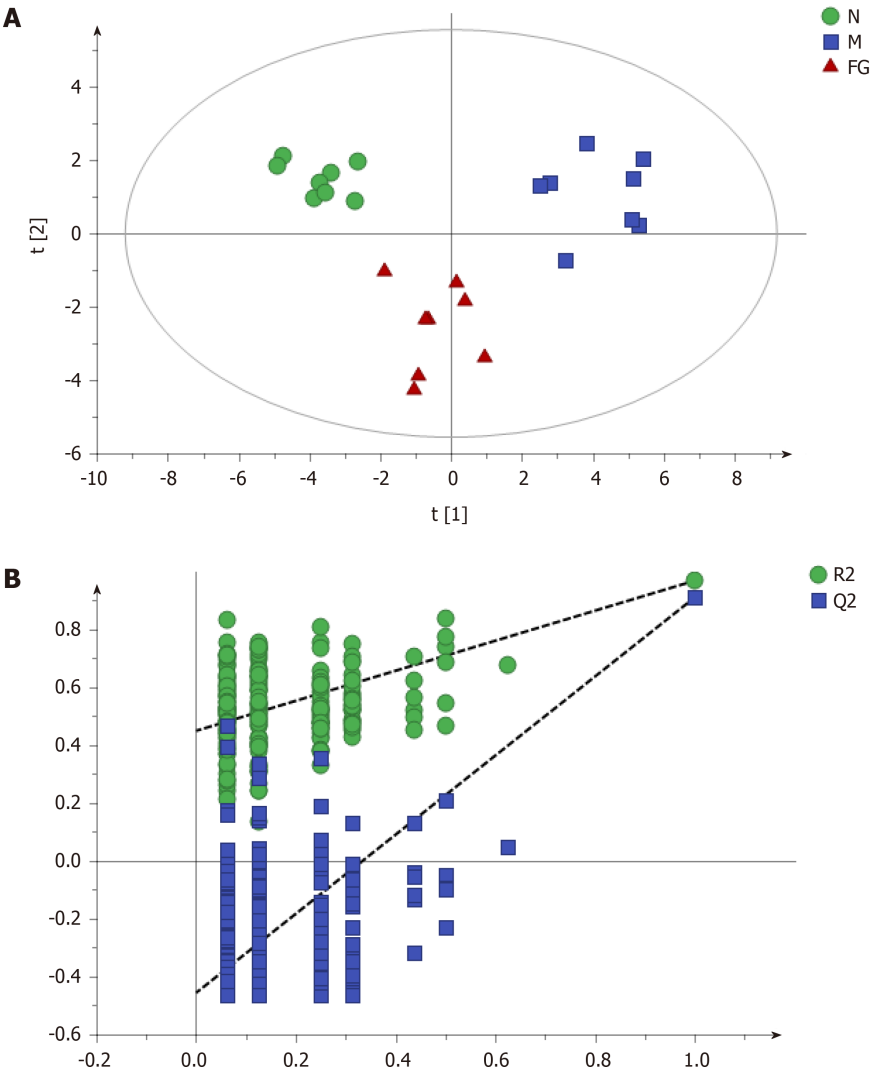


Figure 2 Serum metabolites in rats. A: Partial Least-Squares Discriminant Analysis; B: P-test analysis. M: Model control group; N: Negative control group; F-G: *Fuzi-Gancao* group.

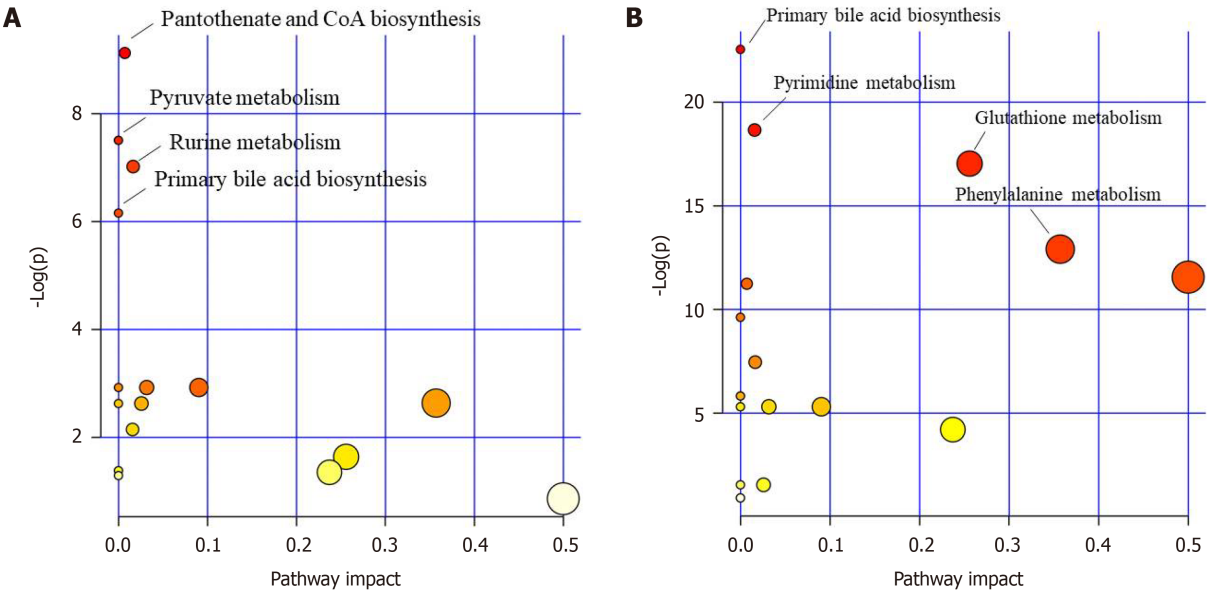


Figure 3 Metabolic pathway analysis of serum in rats. A: Negative control group *vs* model control group; B: *Fuzi-Gancao* group *vs* model control group.

the sample at -20 °C for 15 min after mixing. After incubation, 1000 μL of supernatant

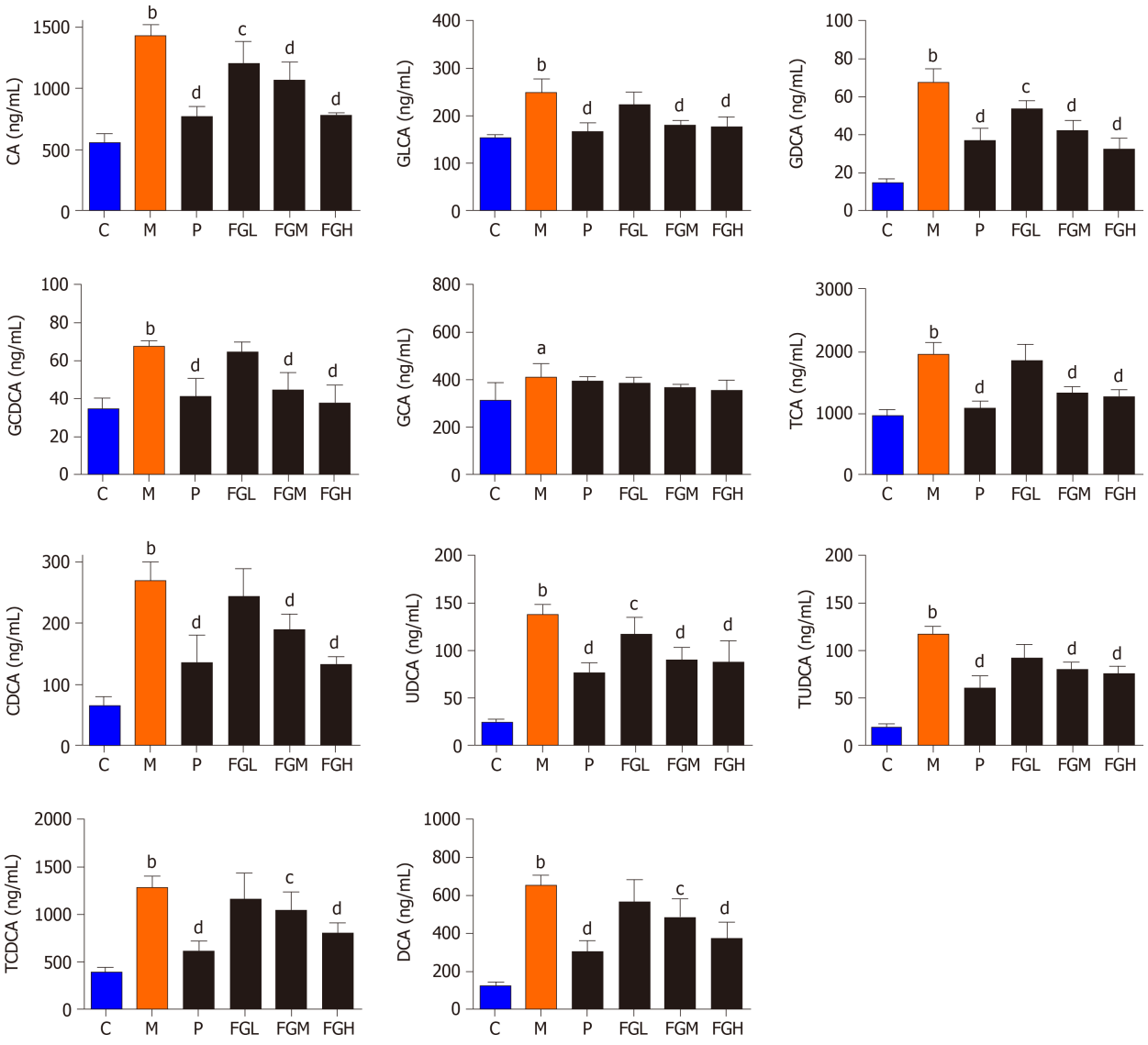


Figure 4 Bile acids in rats (*n* = 6, mean ± SD). $^{a}P < 0.05$, $^{b}P < 0.01$ for each treatment group and model control group, respectively; $^{c}P < 0.05$, $^{d}P < 0.01$ for the model control group and normal control group, respectively.

Preparation of standard solution: L-Leucine, 5-HT, N-phenylacetylglycine, L-tryptophan, L-kynurenine, 5-HTP, cholic acid, and GSSG were accurately weighed and dissolved in methanol to make stock solutions at a concentration of 1 mg/mL. GSH was accurately weighed and dissolved in methanol containing NEM (10 mmol/L) to make a solution at a concentration of 0.5 mg/mL. Each standard solution was mixed proportionally and serially diluted with 50% methanol-water to obtain a series of mixed standard solutions.

Method validation: Calibrators of the nine metabolites (L-Leu, 5-HT, N-Phe, L-Try, L-Kyn, 5-HTP, CA, GSH, and GSSG) were generated from the mixed standard working solutions in "stripped" serum. The linear regression standard curve was calculated with 1/x weighting and plotted with the concentrations and the peak area ratio of each analyte to the internal standard.

Pooled standard solutions were added to "stripped" serum to prepare QC samples of three different concentrations, which were then processed as described in "Samples for metabolic analysis". Intraday precision was calculated according to the content of nine metabolites from the QC sample in six consecutive analyses. The interday precision was obtained after continuous analysis of the QC sample for 3 d. Precision is expressed as the relative standard deviation (RSD, %).

Three concentrations of the mixed standard solutions were added to the samples of a definite content and processed for analysis six times to obtain recovery. Recovery was calculated according to the formula:

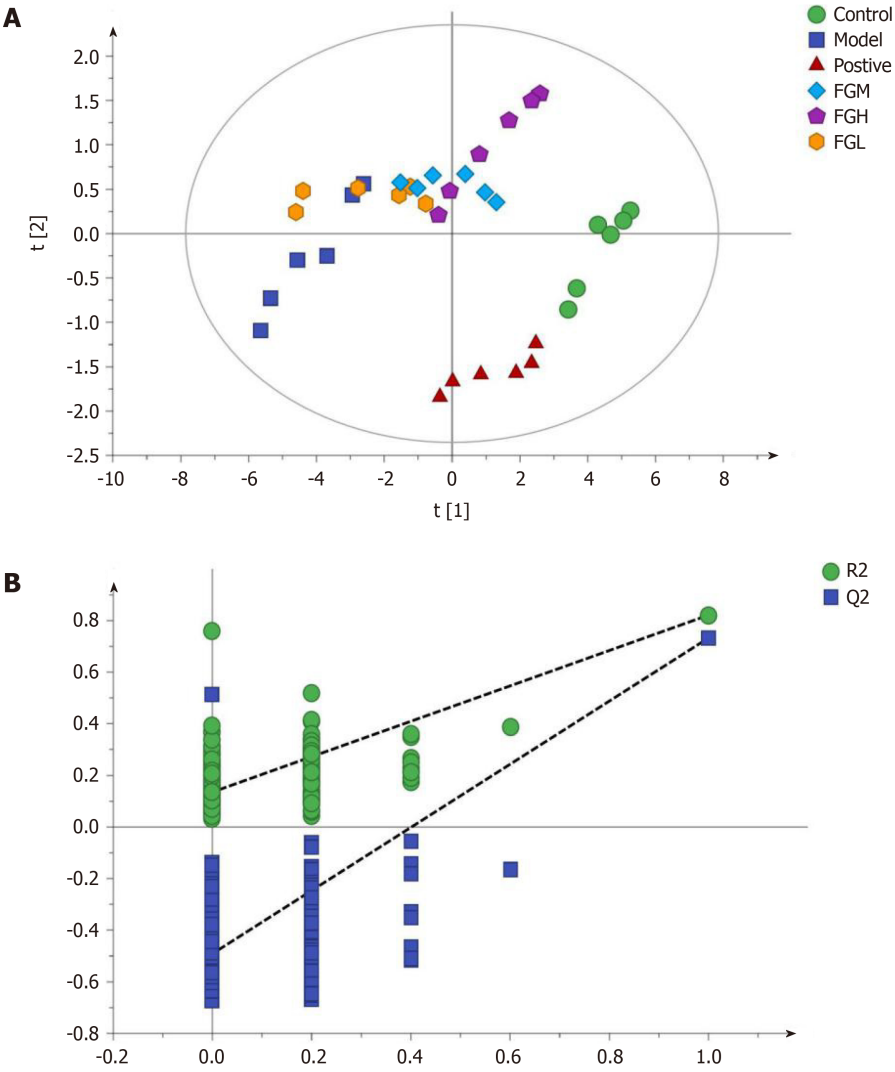


Figure 5 Bile acids in rats. A: Partial Least-Squares Discriminant Analysis; B: P-test analysis.

Recovery (%) = (C-A)/B × 100% (A is the measured content of the test sample, B is the amount of standard content, and C is the measured content).

UPLC-MS/MS analysis: Samples were separated using a Waters ACQUITY ultra-performance liquid chromatographer with a Waters BEH column (1.7 μm, 2.1 × 50 mm, C-18) and a mobile phase consisting of 0.1% formic acid in water (A) and acetonitrile (B) using a gradient system with the following elution procedures: 0-2.0 min, 5% B; 2.0-5.0 min, 5-50% B; 5.0-6.0 min, 50% B; 6.0-17.0 min, 50-95% B; 18.0-22.0 min, 95-5% B; and 22.0-25.0 min, 5% B. The flow rate was 0.3 mL/min, and the column temperature was set at 25 °C. Mass spectral analysis was achieved using an AB 4000 Q-TRAP system with ESI in positive and negative ionization modes and multiple reaction monitoring (MRM) mode. The MS parameters were as follows: Ion spray voltage, ± 4500 V; curtain gas, 20 psi; temperature, 450 °C; and ion source gas, 40 psi. All the metabolites were analyzed using precursor ions (Q1), product ions (Q3), declustering energy, entrance pressure, collision energy, and collision cell exit potential as detection parameters.

Bile acid analysis

Thirty-six male SD rats were randomly divided into six groups (n = 6): Normal control group, model control group, positive control group, and F-G groups including FGL (10 g/kg), FGM (20 g/kg), and FGH (30 g/kg). The positive control group was given 50 mg/kg silybin, the normal group and model group were given the same volume of normal saline, and all the groups were administered for 8 d.

On the 7th day, 40% CCl_4 (v/v, olive oil) solution was injected intraperitoneally (2 mL/kg), and the same dose of olive oil was injected intraperitoneally in the control group. The rats were anesthetized 2 h after administration on the 8th day. Blood

Table 1 Alanine aminotransferase and aspartate aminotransferase in serum of rats (*n* = 8)

Group	ALT (U/L)	AST (U/L)
Normal control	43.6 ± 8.7	131.6 ± 25.1
Model control	187.3 ± 29.6[a]	285.1 ± 31.5[a]
Positive control	86.7 ± 13.7[c]	184.2 ± 37.8[c]
F-G (15 g/kg)	151.2 ± 24.3	246.2 ± 39.8
F-G (30 g/kg)	119.4 ± 19.5[c]	224.0 ± 34.1[b]

[a]$P < 0.01$ for the model control group and normal control group.
[b]$P < 0.05$.
[c]$P < 0.01$ for each treatment group and model control group, respectively. F-G: *Fuzi-Gancao*; ALT: Alanine aminotransferase; AST: Aspartate aminotransferase.

Table 2 Calibration curve, R^2, and concentration range of nine metabolites

Compound	Standard curve	R^2	Range (ng/mL)
L-Leu	Y = 0.0627X - 4.9797	0.9952	100-10000
5-HT	Y = 0.0385X - 0.0269	0.9939	0.8-80
N-phe	Y = 0.0229X - 4.9120	0.9958	250-25000
L-Try	Y = 0.0048X - 2.4673	0.9926	600-60000
L-Kyn	Y = 0.0331X + 0.0123	0.9960	5-500
5-HTP	Y = 0.0492X - 0.0001	0.9983	0.2-20
CA	Y = 0.00004X - 0.0010	0.9959	40-4000
GSH	Y = 0.0032X - 0.2362	0.9975	150-20000
GSSG	Y = 0.0001X + 0.0010	0.9949	50-10000

L-Leu: L-leucine; 5-HT: 5-Hydroxytryptamine; N-phe: N-phenylacetylglycine; L-Try: L-tryptophan; L-Kyn: L-kynurenine; 5-HTP: 5-hydroxytryptophan; CA: Cholic acid; GSH: Glutathione; GSSG: Glutathione oxidized.

samples were collected from the abdominal aorta and centrifuged at 4000 rpm for 10 min (4 °C) to obtain serum samples for the analysis of bile acids.

Preparation of standard solutions: CDCA, DCA, UDCA, GLCA, GCDCA, GDCA, GCA, TCDCA, TCDCA, TUDCA, and TCA were accurately weighed and dissolved in methanol to prepare stock solutions at a concentration of 1 mg/mL and stored at -80 °C. Solutions were serially diluted with 50% methanol-water prior to testing. d_4-GCDCA was accurately weighed and dissolved in methanol to make an internal standard solution. All the solutions were stored at -80 °C prior to use.

Sample preparation: Two hundred microliters of serum was added to 1000 μL of methanol containing internal standard (d4-GCDCA, 20 ng/mL). The samples were centrifuged at 12000 rpm for 15 min (4 °C) after mixing, and then 1000 μL of the supernatant was dried with nitrogen and stored at -80 °C. The dried residue was reconstituted with 50 μL of 80% methanol-water solution prior to analysis, vortexed for 1 min, and centrifuged at 12000 rpm for 15 min (4 °C). Then, 30 μL of supernatant was aspirated accurately into an injection vial, and 10 μL of each sample was injected into the UPLC-MS/MS system for bile acid quantification.

UPLC-MS analysis: Samples were separated using a Waters Acquity Uplc instrument and an Agilent ZORBAX SB-C18 column (3.5 μm, 2.1 mm × 100 mm) and a mobile phase consisting of 0.1% formic acid in water (A) and methanol (B) using a gradient system with the following elution procedure: 0-2.0 min, 10% B; 2.0-9.0 min, 10%-80% B; 9.0-11.0 min, 80% B; 11.0-20.0 min, 80%-90% B; and 20.0-25.0 min, 90%-10% B. Ten microliters of the sample was injected at a flow rate of 0.4 mL/min and column temperature of 25 °C. Mass spectral analysis was achieved using a Thermo Scientific

Table 3 Accuracy and precision of the developed ultra performance liquid chromatography-tandem mass spectrometry method (n = 6)

Ingredient	Concentration (ng/mL)	Accuracy %	Precision %	Repeatability %	Stability %
L-Leu	750	100.35 ± 3.20	3.19	3.69	0.41
	1000	105.20 ± 6.45	6.13	6.91	1.69
	5000	95.53 ± 4.55	4.76	4.98	1.85
5-HT	6	99.78 ± 8.61	8.63	8.10	2.78
	8	101.78 ± 4.32	4.24	2.87	3.80
	40	101.76 ± 4.50	4.42	4.24	2.14
N-phe	1800	100.29 ± 4.32	4.31	4.72	3.07
	2500	98.97 ± 4.13	4.17	3.71	3.18
	12500	92.24 ± 5.12	5.55	5.95	1.09
L-Try	4500	97.33 ± 3.25	3.34	3.75	0.71
	6000	95.45 ± 4.12	4.32	4.22	3.35
	30000	94.89 ± 4.77	5.03	4.22	4.00
L-Kyn	37	99.61 ± 4.66	4.68	5.00	2.98
	50	102.43 ± 4.15	4.05	4.41	1.73
	250	99.76 ± 4.11	4.12	4.15	2.09
5-HTP	300	102.45 ± 4.51	4.40	3.98	3.65
	400	95.20 ± 8.80	9.24	7.50	6.16
	2000	101.77 ± 8.11	7.97	7.89	7.36
CA	1.5	99.88 ± 3.70	3.70	3.83	1.47
	2	97.00 ± 3.19	3.29	2.97	2.47
	10	96.76 ± 5.30	5.48	4.17	5.22
GSH	1500	101.91 ± 4.65	4.56	5.19	1.45
	2000	96.05 ± 3.98	4.14	4.63	0.89
	10000	97.51 ± 5.88	6.03	4.45	2.45
GSSG	750	99.64 ± 3.97	3.98	4.43	1.56
	1000	100.8 ± 6.45	6.40	7.23	4.89
	5000	98.39 ± 4.54	4.61	3.90	3.80

L-Leu: L-leucine; 5-HT: 5-Hydroxytryptamine; N-phe: N-phenylacetylglycine; L-Try: L-tryptophan; L-Kyn: L-kynurenine; 5-HTP: 5-hydroxytryptophan; CA: Cholic acid; GSH: Glutathione; GSSG: Glutathione oxidized.

TSQ Quantum with ESI in negative ionization mode and MRM mode. The ion spray voltage was -3200 v and the temperature was 380 °C.

Method validation: Eleven bile acids (CDCA, DCA, UDCA, CA, GLCA, GCDCA, GDCA, GCA, TCDCA, TCDCA, TUDCA, and TCA) were diluted with 50% methanol solution to prepare a series of solutions and mixed with "stripped" serum to generate calibrators for validation of the UPLC-MS/MS method. The linear regression standard curve was calculated with 1/x weighting and plotted with the concentrations and the peak area ratio of each analyte to the internal standard.

Pooled standard solutions were added to "stripped" serum to prepare QC samples of three different concentrations for analysis. Intraday precision was calculated according to the contents of 11 bile acids from QC samples for six consecutive analyses. The interday precision was obtained after continuous analysis of QC samples for 3 d. Interday precision and intraday precision are expressed as the relative standard deviation (RSD, %). Three concentrations of mixed standard solutions were added to the samples of a definite content and processed as described above for bile

Table 4 Recovery of the developed ultra performance liquid chromatography-tandem mass spectrometry method (*n* = 6)

Ingredient	Baseline (ng/mL)	Spiked (ng/mL)	Recovery %
L-Leu	1000	250	92.53 ± 7.13
		500	93.42 ± 11.52
		750	87.53 ± 9.59
5-HT	8	2	85.37 ± 9.79
		4	90.52 ± 13.47
		6	93.05 ± 10.16
N-phe	2500	625	94.54 ± 12.15
		1250	89.46 ± 6.54
		1875	86.72 ± 8.19
L-Try	6000	1500	93.04 ± 13.23
		3000	85.42 ± 7.12
		4500	91.16 ± 12.25
L-Kyn	50	12.5	90.48 ± 6.18
		25	85.30 ± 10.42
		37.5	86.20 ± 6.13
5-HTP	2	0.5	91.49 ± 5.36
		1	94.64 ± 7.46
		1.5	93.58 ± 5.15
CA	400	100	91.83 ± 12.12
		200	93.29 ± 8.62
		300	90.22 ± 7.28
GSH	1000	250	88.17 ± 6.33
		500	91.16 ± 6.15
		750	90.85 ± 9.81
GSSG	2000	500	91.15 ± 10.08
		1000	93.92 ± 12.15
		1500	89.27 ± 10.92

L-Leu: L-leucine; 5-HT: 5-Hydroxytryptamine; N-phe: N-phenylacetylglycine; L-Try: L-tryptophan; L-Kyn: L-kynurenine; 5-HTP: 5-hydroxytryptophan; CA: Cholic acid; GSH: Glutathione; GSSG: Glutathione oxidized.

acid analysis six times to obtain recovery.

Three concentrations of 11 mixed bile acid standard solutions were used to investigate the stability of QC samples under different storage conditions and processing procedures. Short-term stability was assessed by analyzing the QC samples that were kept at room temperature for 12 h. Long-term stability was assessed by storing the QC samples at -20 °C for 20 d. Freeze-thaw stability was assessed after the QC samples were frozen at -80 °C and thawed at 4 °C in 1 d for 3 consecutive days. Postpreparation stability was assessed by analyzing the QC samples that were kept at 4 °C for 12 h.

Data analysis

Metabolic analysis was calibrated and integrated using AB Analyst (version 1.6.2, AB Applied Biosystems). Quantitative analyses of bile acids were performed using Thermo Scientific TSQ Quantum Workstation analysis software. Pathway analyses were achieved using SIMCA-P, Metaboanalyst, and KEGG software. The experimental data are expressed as the mean ± SD. The data were analyzed with SPSS 19.0 statistical software ($P < 0.05$ and $P < 0.01$).

Table 5 Serum metabolites in CCl_4-induced acute liver injury in rats (n = 8)

Metabolite	Model group	Control group	FG group
L-leucine	431.1 ± 54.32	331.4 ± 48.78[d]	393.5 ± 53.83
N-phenylacetylglycine	5.350 ± 0.938	1.417 ± 0.351[d]	2.915 ± 0.496[b,d]
L-tryptophan	17.96 ± 3.014	14.63 ± 2.724[c]	17.05 ± 2.679[a]
L-kynurenine	6.270 ± 0.729	3.948 ± 0.450[d]	6.646 ± 1.214[b]
Cholic acid	1.342 ± 0.230	0.047 ± 0.004[d]	1.001 ± 0.124[b,d]
GSH	2.562 ± 0.433	0.991 ± 0.285[d]	2.317 ± 0.632[b]
GSSG	0.108 ± 0.016	0.021 ± 0.002[d]	0.051 ± 0.009[b,d]
lactate	257.8 ± 32.57	230.8 ± 37.30	185.3 ± 31.52[b,d]
Choline	3.548 ± 0.539	2.639 ± 0.451	2.802 ± 0.413
(E)-butenedioic acid	163.6 ± 18.57	79.48 ± 8.625[d]	87.82 ± 10.55[d]
Hypoxanthine	0.052 ± 0.003	0.021 ± 0.002[d]	0.022 ± 0.003[d]
Carnitine	23.55 ± 5.024	13.52 ± 1.370[d]	20.05 ± 1.323[b]
Phenylalanine	289.5 ± 37.51	165.6 ± 23.76[d]	261.4 ± 32.33[b]
Uric acid	4.523 ± 0.863	2.769 ± 0.474[d]	2.927 ± 0.488[d]
Hippuric acid	95.58 ± 16.47	65.78 ± 13.92[d]	76.53 ± 16.92[d]
Citric acid	11.86 ± 1.531	15.62 ± 2.437[d]	13.51 ± 2.002
Pantothenic acid	7.852 ± 0.953	4.602 ± 0.560[d]	4.831 ± 0.693[d]
Uridine	19.37 ± 2.772	6.816 ± 0.829[d]	17.53 ± 2.503[b]
Glucosamine-1-phosphate	0.025 ± 0.005	0.017 ± 0.004[c]	0.020 ± 0.004
8-OH-dG	0.008 ± 0.001	0.007 ± 0.001[c]	0.007 ± 0.001[c]
C16:1 Lyso PC	3.215 ± 0.491	4.813 ± 0.503[d]	6.293 ± 1.337[b,d]
C16:0 Lyso PC	13.37 ± 2.434	16.62 ± 3.027	18.39 ± 3.316[c]
C18:1 Lyso PC	16.837 ± 2.392	23.699 ± 4.427[d]	26.647 ± 4.339[a,d]
C18:0 LysoPC	11.42 ± 1.130	18.332 ± 1.833[d]	16.66 ± 2.603[a,d]

[a]$P < 0.05$.
[b]$P < 0.01$ compared with the negative control group.
[c]$P < 0.05$.
[d]$P < 0.01$ compared with the model control group. GSH: Glutathione; GSSG: Glutathione oxidized.

RESULTS

Effects of F-G on acute liver injury

Histological analysis: The liver tissue of rats in each group was macroscopically observed. The livers of the normal control group rats had a normal morphology, a red color, no adhesion between the lobules, a smooth surface, and no bleeding spots. In the model group, the surface of the liver was milky white, and there was obvious adhesion between the lobules of the liver and the mucous membranes. In the F-G group, the adhesion degree between the lobules and mucous membrane was significantly decreased, and the color was rosier than that of the model rats. The morphological results showed that F-G extract could significantly relieve liver injury induced by CCl_4 (Figure 1).

Histological analysis indicated that the structure of liver tissue in the normal control group was normal, the liver cells were neatly arranged, and there were no pathological changes, such as hepatocyte swelling, inflammatory cell infiltration, blood stasis, or steatosis of hepatocytes. Compared with the normal control group, the model control group showed a significant increase in the number of hepatocytes with extensive hydrodegeneration, steatosis, hepatocyte necrosis, and inflammatory cell infiltration. Compared with the model control group, F-G groups (15 g/kg and 30 g/kg) indicated

Table 6 Variable importance in the projection values of serum metabolites and effects of CCl_4 on their changes (model group *vs* negative group)

Var ID (primary)	M1-VIP	Variation trend
GSSG	1.19631	↑↑
Cholic acid	1.18964	↑↑
Uridine	1.18609	↑↑
N-phenylacetylglycine	1.16986	↑↑
Hypoxanthine	1.13469	↑↑
(E)-butenedioic acid	1.1299	↑↑
GSH	1.12862	↑↑
C18:0LPC	1.12325	↓↓
Pantothenic acid	1.08663	↑↑
Carnitine	1.08264	↑↑
Phenylalanine	1.07794	↑↑
Hippuric acid	1.06083	↑↑
C16:1LPC	1.05866	↓↓
Uric acid	1.01621	↑↑
C18:1LPC	0.943612	↓↓
L-kynurenine	0.919692	↑
L-leucine	0.90164	↑↑
Glucosamine-1-phosphate	0.893372	↑
Citric acid	0.866932	↓↓
L-tryptophan	0.842517	↑
8-OH-dG	0.711595	↑
Lactate	0.704198	NS
Choline	0.639509	NS
C16:0LPC	0.514772	NS

↑ represents a P value ≤ 0.05 for the increase in mean content; ↑↑ represents a P value ≤ 0.01 for the increase in mean content; ↓ represents a P value ≤ 0.05 for the mean content decrease; ↓↓ represents a P value ≤ 0.01 for the mean content decrease; NS: The mean concentrations of metabolites in the model group were not statistically significant; GSSG: Glutathione oxidized; GSH: Glutathione; VIP: Variable importance in the projection.

a decrease in the amount of water-like degeneration in the liver, steatotic cells, and swelling hepatocytes with a significant dose-effect relationship.

Assay of ALT and AST: ALT and AST in the serum of rats were detected by ELISA. The results indicated that the contents of ALT and AST in the model control group were significantly higher than those in the normal control group ($P < 0.01$). Both transaminase levels were significantly reduced in the F-G groups compared to those in the model control group, but the magnitude of the reduction was still different from that of the positive control group (Table 1).

Metabolic analysis

Linearity: The calibration curve of each standard was plotted with the concentrations of nine biomarkers and the ratio of the peak area of each component to that of the internal standard with weighted (1/x) least-square linear regression. The calibration curves of the nine analytes exhibited a good linearity with coefficient of correlation (R^2) values better than 0.9926. The lowest concentration of the linear regression for each sample was determined to be the limit of quantification (Table 2).

Accuracy, precision, and recovery: The accuracy and precision of analytes in the QC samples were less than 9.24% and 8.10%, respectively (Table 3), and the recovery of

Table 7 Variable importance in the projection values of serum metabolites and effects of *Fuzi-Gancao* on their changes (*Fuzi-Gancao* group *vs* model group)

Var ID (primary)	M1-VIP	Variation trend
Hypoxanthine	1.37706	↓↓
GSSG	1.36516	↓↓
Pantothenic acid	1.28548	↓↓
C18:1LPC	1.27880	↑↑
C16:1LPC	1.25881	↑↑
N-phenylacetylglycine	1.22022	↓↓
Lactate	1.21835	↓↓
Hippuric acid	1.21598	↓↓
Uric acid	1.21291	↓↓
(E)-butenedioic acid	1.21107	↓↓
Cholic acid	1.17091	↓↓
C18:0LPC	1.15078	↑↑
C16:0LPC	1.00088	↑
Choline	0.906949	NS
L-kynurenine	0.893225	↑↑
Uridine	0.810356	NS
8-OH-dG	0.777736	NS
Citric acid	0.633654	NS
GSH	0.512313	NS
L-leucine	0.497685	NS
Carnitine	0.447434	NS
Phenylalanine	0.427897	NS
Glucosamine-1-phosphate	0.312245	NS
L-tryptophan	0.0800812	NS

↑ represents a P value ≤ 0.05 for the increase in mean content; ↑↑ represents a P value ≤ 0.01 for the increase in mean content; ↓ represents a P value ≤ 0.05 for the mean content decrease; ↓↓ represents a P value ≤ 0.01 for the mean content decrease; NS: No statistically significant change in the mean concentration of metabolites in the *Fuzi-Gancao* group; GSSG: Glutathione oxidized; GSH: Glutathione; VIP: Variable importance in the projection.

analytes is shown in Table 4. All the analytical values of the nine analytes had satisfactory results within the acceptable criteria according to the bioanalytical method validation guidance of the United States FDA.

Metabolic analysis: Analysis of 92 metabolites was achieved by UPLC-QTRAP-LC-MS/MS. NEM was used to improve the stability of GSH. Twenty-four differential metabolites in the serum (normal control group *vs* model control group and F-G groups *vs* model control group) were confirmed according to statistical analysis (Table 5).

Partial Least-Squares Discriminant Analysis (PLS-DA) (Figure 2) was performed on the data matrix of the variation in individual metabolites in Table 4. The results showed that the samples of the negative control group, model control group, and F-G groups were distributed in different areas and could be separated completely, but samples of the same group had the tendency to aggregate (Figure 2A). The results showed that the difference in all metabolites between the negative control group and the model control group was significant, indicating that the contents of these 24 metabolites were significantly changed in acute liver injury induced by CCl_4. The difference in all metabolites between the F-G groups and the model control group was also significant, indicating that the administration of the F-G extract could cause a

Table 8 Standard curve, R^2, and concentration range of 11 bile acids in serum

Compound	Standard curve	R^2	Range (ng/mL)
CDCA	Y = 0.0235X - 0.0056	0.9981	2.5-1000
UDCA	Y = 0.0013X + 0.2156	0.9972	1.25-500
GCA	Y = 0.0164X + 1.1577	0.9956	1.25-500
GDCA	Y = 0.0025X + 0.833	0.9982	1.25-500
TCA	Y = 0.0198X - 0.0113	0.9953	1.25-500
TUDCA	Y = 0.0332X + 0.0023	0.9985	2.5-1000
TCDCA	Y = 0.0306X + 0.00422	0.9923	2.5-1000
GCDCA	Y = 0.0133X - 0.00324	0.9915	2.5-1000
GLCA	Y = 0.0018X + 0.00242	0.9931	2.5-1000
DCA	Y = 0.0076X + 0.00614	0.9956	2.5-1000
CA	Y = 0.0916X - 0.00465	0.9987	2.5-1000

CDCA: Chenodeoxycholic acid; UDCA: Ursodeoxycholic acid; GCA: Glycocholic acid; GDCA: Glycochenodeoxycholic acid; TCA: Taurocholic acid; TUDCA: Taurocholic acid; GCDCA: Glycochenodeoxycholic acid; GLCA: Glycinic acid; DCA: Deoxycholic acid; CA: Cholic acid.

significant reduction in the metabolite contents in the serum of rats with acute liver injury induced by CCl_4, which could cause a significant change in the metabolic network. In the PLS-DA plot, samples of the F-G groups were closer to those of the negative control group than those of the model control group, indicating a significant difference in the metabolite contents in rats with liver injury compared to those in the negative control group after treatment with F-G. P-test analysis (Figure 2B) showed that there was no overfitting of the separation model between groups.

Combined with the variable importance in the projection (VIP) value based on PLS-DA, it was shown that the metabolites with a VIP value greater than 1.0 contributed greatly to the difference before and after treatment with the F-G extract and were the key metabolites. There were 14 key metabolites in the model control group *vs* the negative control group (Table 6) and 13 key metabolites in the F-G groups *vs* the model control group (Table 7). Ten common metabolites, namely, GSSG, cholic acid, N-phenylacetylglycine, hippuric acid, uric acid, hypoxanthine, (E)-butenedioic acid, pantothenic acid, C16:1 LPC, and C18:0 LPC, were observed.

Pathway analysis: Metaboanalyst software was used to analyze the metabolic mechanism. Metabolic pathway differences between the negative control group and model control group and between the model control group and F-G group were analyzed by topological and enrichment analyses to confirm the important metabolic pathway effects of F-G in acute liver injury induced by CCl_4.

The results indicated that the primary bile acid biosynthesis pathway was the most important metabolic pathway affected in the model control group *vs* the negative control group (Figure 3A). Other pathways, such as pyrimidine metabolism, glutathione metabolism, glutamate metabolism, and phenylalanine metabolism, are also affected by CCl_4. The pantothenate and CoA biosynthesis, primary bile acid biosynthesis, and pyruvate metabolism pathways were significantly affected by the administration of the F-G extract (Figure 3B).

Bile acids analysis

Method validation: The calibration curve of each standard was plotted on the concentrations of 11 bile acids and the ratio of the peak area of each component to that of the internal standard with weighted (1/x) least square linear regression. The calibration curves of the 11 analytes exhibited a good linearity (Table 8).

The intraday precision of QC samples with three concentrations of bile acids ranged from 1.20% to 6.57%, the interday precision ranged from 2.10% to 6.35%, and the recovery of each analyte was greater than 80% (Table 9). Eleven bile acid analytes exhibited good stability (short-term stability, long-term stability, freeze-thaw stability, and postpreparation stability) (Table 10). All the analytical values of the 11 analytes had satisfactory results within the acceptable criteria.

Table 9 Precision, accuracy, and recovery of bile acids in serum samples (n = 6, mean ± SD)

Compound	Concentration (ng/mL)	Recovery (%)	Intraday		Interday	
			Accuracy (%)	Precision (%)	Accuracy (%)	Precision (%)
CA	2.5	90.12 ± 2.16	96.44 ± 2.05	4.26	91.83 ± 3.32	5.03
	500	88.21 ± 5.34	91.65 ± 4.14	3.60	94.42 ± 4.55	4.36
	2000	85.60 ± 7.22	92.11 ± 4.11	5.42	94.54 ± 8.35	6.00
GLCA	1.25	91.52 ± 5.51	92.13 ± 2.97	5.71	98.48 ± 2.22	3.75
	250	86.74 ± 7.12	87.31 ± 1.92	4.23	93.42 ± 3.67	5.40
	1000	90.48 ± 3.31	91.55 ± 5.31	6.13	89.24 ± 4.63	4.57
GDCA	1.25	88.54 ± 2.93	90.67 ± 6.87	6.22	88.55 ± 3.87	3.28
	250	98.43 ± 1.26	97.24 ± 7.86	6.38	101.53 ± 2.54	2.76
	1000	95.56 ± 4.01	89.34 ± 2.65	2.81	89.23 ± 6.25	6.16
GCDCA	1.25	96.02 ± 3.11	93.24 ± 3.78	6.30	89.32 ± 4.32	3.19
	250	90.13 ± 3.42	97.43 ± 2.82	5.03	88.54 ± 4.75	2.10
	1000	89.32 ± 3.13	86.53 ± 4.27	2.96	89.52 ± 3.63	3.28
GCA	1.25	80.87 ± 3.83	99.31 ± 5.19	4.18	89.42 ± 1.71	2.32
	250	91.43 ± 6.38	101.33 ± 2.23	2.59	112.53 ± 5.76	2.29
	1000	92.43 ± 2.14	88.76 ± 1.46	1.20	89.16 ± 3.46	3.09
TCA	2.5	84.77 ± 2.38	103.55 ± 1.27	1.50	98.24 ± 2.14	5.51
	500	86.92 ± 4.96	89.04 ± 6.42	5.53	95.33 ± 2.86	3.82
	2000	81.34 ± 1.84	88.57 ± 4.85	4.77	97.81 ± 3.08	4.50
CDCA	1.25	80.33 ± 3.23	94.33 ± 4.62	4.39	90.49 ± 4.83	5.18
	250	86.34 ± 2.45	92.33 ± 4.93	3.70	91.49 ± 7.39	4.49
	1000	84.62 ± 3.21	92.33 ± 6.03	5.58	92.77 ± 4.83	6.18
DCA	1.25	95.54 ± 2.17	94.67 ± 4.93	5.88	104.21 ± 7.22	3.87
	250	82.56 ± 4.32	106.33 ± 7.37	4.36	99.31 ± 5.66	5.57
	1000	94.45 ± 5.34	101.33 ± 5.77	6.31	89.83 ± 4.53	4.71
UDCA	1.25	83.32 ± 1.43	91.67 ± 4.62	6.41	93.43 ± 4.63	3.38
	250	88.13 ± 5.94	95.33 ± 4.73	6.57	92.12 ± 4.49	2.84
	1000	85.26 ± 3.01	94 ± 4.58	2.90	91.79 ± 5.74	6.35
TCDCA	1.25	86.04 ± 3.36	93.67 ± 5.86	6.49	92.77 ± 4.83	3.28
	250	87.98 ± 3.11	94.67 ± 4.93	5.18	89.83 ± 4.53	2.17
	1000	83.72 ± 2.19	91.67 ± 4.62	3.05	92.77 ± 7.36	3.38
TUDCA	1.25	87.17 ± 4.61	94.67 ± 7.51	4.31	96.69 ± 9.82	2.39
	250	87.41 ± 4.09	98.67 ± 10.02	2.66	98.33 ± 8.33	2.36
	1000	99.06 ± 3.56	100.33 ± 8.5	1.23	92.45 ± 4.53	3.18

CDCA: Chenodeoxycholic acid; UDCA: Ursodeoxycholic acid; GCA: Glycocholic acid; GDCA: Glycochenodeoxycholic acid; TCA: Taurocholic acid; TUDCA: Taurocholic acid; GCDCA: Glycochenodeoxycholic acid; GLCA: Glycinic acid; DCA: Deoxycholic acid; CA: Cholic acid.

Bile acids analysis: Liver injury induced by CCl_4 in rats could reduce bile secretion and rapidly alter the distribution of bile acid stores, resulting in a significant increase in serum bile acid concentrations. The results indicated that the contents of 11 analytes (CDCA, DCA, UDCA, GLCA, GLCA, GCDCA, GDCA, GCA, TCDCA, TUDCA, and TCA) in the serum of the model control group, compared with the negative control group, were significantly increased (P < 0.01), and the contents of the 11 bile acids in

Table 10 Stability of bile acid standards in serum samples (n = 6, mean ± SD)

Compound	Concentration (ng/mL)	Concentration (mean ± SD)				
		Initial	Freeze-thaw	Short-term	Long-term	Post-preparation
CA	2.5	2.35 ± 0.17	2.3 ± 0.16	2.56 ± 0.18	2.33 ± 0.17	2.52 ± 0.08
	500	495.43 ± 12.15	485.52 ± 11.91	538.93 ± 13.22	511.98 ± 12.56	505.09 ± 5.54
	2000	2080.38 ± 101	2038.77 ± 98.98	2263.03 ± 109.87	2149.88 ± 104.38	2194.52 ± 99.16
GLCA	1.25	1.24 ± 0.14	1.22 ± 0.13	1.17 ± 0.15	1.21 ± 0.14	1.25 ± 0.14
	250	247.1 ± 10.76	242.15 ± 10.55	258.79 ± 11.71	255.35 ± 11.12	250.24 ± 10.9
	1000	979.04 ± 40.32	959.46 ± 39.51	985 ± 43.86	1011.75 ± 41.66	991.52 ± 40.83
GDCA	1.25	1.27 ± 0.05	1.24 ± 0.05	1.24 ± 0.06	1.19 ± 0.06	1.26 ± 0.08
	250	240.43 ± 3.98	235.62 ± 3.9	261.54 ± 4.33	248.46 ± 4.12	249.32 ± 5.42
	1000	975.71 ± 45.93	956.19 ± 45.01	1061.38 ± 49.96	1008.31 ± 47.46	1035.03 ± 14.83
GCDCA	1.25	1.27 ± 0.06	1.23 ± 0.08	1.36 ± 0.08	1.21 ± 0.09	1.21 ± 0.08
	250	243.49 ± 4.03	242.1 ± 19.01	237.25 ± 18.63	263.35 ± 20.68	250.18 ± 19.64
	1000	988.14 ± 46.51	1047.04 ± 49.29	1026.1 ± 48.31	1108.97 ± 53.62	1082.02 ± 50.94
GCA	1.25	1.19 ± 0.03	1.27 ± 0.03	1.27 ± 0.03	1.22 ± 0.03	1.21 ± 0.04
	250	237.1 ± 1.93	232.35 ± 1.9	257.91 ± 2.1	245.02 ± 2	244.16 ± 1.88
	1000	982.38 ± 30.18	962.73 ± 29.58	1068.63 ± 32.83	1015.2 ± 31.19	1014.36 ± 44.06
TCA	2.5	2.25 ± 0.17	2.21 ± 0.16	2.45 ± 0.18	2.33 ± 0.17	2.42 ± 0.08
	500	492.1 ± 28.22	482.25 ± 27.65	535.3 ± 30.69	508.54 ± 29.16	494.76 ± 23.69
	2000	2013.71 ± 105.21	1973.43 ± 103.1	2190.51 ± 114.44	2080.99 ± 108.72	2142.85 ± 26.09
CDCA	1.25	1.19 ± 0.1	1.28 ± 0.1	1.23 ± 0.11	1.24 ± 0.1	1.22 ± 0.08
	250	232.1 ± 6.9	227.45 ± 6.77	252.47 ± 7.51	239.85 ± 7.14	236.41 ± 5.54
	1000	1010.38 ± 39.44	990.17 ± 38.65	1099.09 ± 42.91	1044.13 ± 40.76	1057.77 ± 46.98
DCA	1.25	1.13 ± 0.03	1.15 ± 0.06	1.18 ± 0.13	1.23 ± 0.13	1.24 ± 0.14
	250	236.33 ± 13.65	229.67 ± 21.36	233 ± 10.15	244.65 ± 10.66	247.1 ± 10.76
	1000	967.67 ± 15.82	947.67 ± 106.82	1031 ± 115.66	982.55 ± 53.41	979.04 ± 40.32
UDCA	1.25	1.22 ± 0.06	1.19 ± 0.06	1.23 ± 0.07	1.26 ± 0.07	1.28 ± 0.07
	250	252.1 ± 6.9	247.05 ± 6.77	244.23 ± 7.51	250.52 ± 7.14	257.07 ± 5.54
	1000	931.71 ± 85.92	971.43 ± 120.15	958.15 ± 108.46	940.89 ± 109.04	1061.11 ± 99.16
TCDCA	1.25	1.22 ± 0.06	1.25 ± 0.06	1.28 ± 0.07	1.22 ± 0.06	1.19 ± 0.06
	250	251.76 ± 3.11	246.73 ± 3.05	273.87 ± 3.39	260.17 ± 3.22	261.73 ± 2.5
	1000	1013.71 ± 69.97	993.43 ± 68.57	1102.71 ± 76.11	1047.58 ± 72.31	1057.77 ± 99.16
TUDCA	1.25	1.22 ± 0.02	1.2 ± 0.02	1.23 ± 0.03	1.26 ± 0.02	1.27 ± 0.03
	250	249.1 ± 6.47	244.11 ± 6.34	270.97 ± 7.04	257.42 ± 6.68	259.14 ± 8.46
	1000	977.04 ± 18.84	957.5 ± 18.46	1062.83 ± 20.49	1009.69 ± 19.47	1006.1 ± 26.09

CDCA: Chenodeoxycholic acid; UDCA: Ursodeoxycholic acid; GCA: Glycocholic acid; GDCA: Glycochenodeoxycholic acid; TCA: Taurocholic acid; TUDCA: Taurocholic acid; GCDCA: Glycochenodeoxycholic acid; GLCA: Glycinic acid; DCA: Deoxycholic acid; CA: Cholic acid.

the serum of the F-G groups were decreased in a dose-dependent manner (Figure 4).

PLS-DA analysis was performed using a data matrix on the effect of F-G on serum bile acid levels in rats with CCl_4 induced acute liver injury. As seen from the PLS-DA analysis (Figure 5A), the samples of the negative control group and model control group are distributed in different areas and far away from each other and can be completely separated from each other. The content differences of bile acids between

the negative control group and model control group were significant. At the same time, the samples of the F-G group (10 g/kg) were partially overlapping those of the model control group, but with increasing dose, the samples of the mid-dose and high-dose F-G groups (20 g/kg and 30 g/kg) were clearly separated from those of the model control group, indicating that the dose-dependent relationship between the bile acid level and the dose of F-G extract was apparent in the overall analysis. P-test analysis showed that there was no overfitting of the between-group separation model (Figure 5B).

DISCUSSION

Analysis of 24 differential metabolites by UPLC-QTRAP-LC-MS/MS showed that CCl_4 could affect a variety of metabolic pathways, such as primary bile acid biosynthesis, glutathione metabolism, pyrimidine metabolism, and phenylalanine metabolism. The F-G extract could affect the metabolic pathways of pantothenic acid and CoA biosynthesis, primary bile acid biosynthesis, and pyruvate biosynthesis. The primary bile acid synthesis pathway was the most important common pathway affected by CCl_4 and the F-G extract. Subsequently, a UPLC-QQQ-LC-MS/MS method was established for the simultaneous quantitative detection of 11 bile acids, and the regulatory mechanism of the F-G extract on bile acids in the prevention of acute liver injury induced by CCl_4 was obtained.

Since the content of different bile acids varied greatly in the serum, we first used the relative variation in each bile acid for analysis. This analysis evaluated the relative changes in bile acids for each group based on their primary contents (1.0) in the negative control group (Table 11). Free and conjugated bile acids are the two bile acid types in the liver and blood. CA, CDCA, and DCA are the main free bile acids, and bile acids conjugated with glycine or taurine compose the combined bile acids. In this study, a relatively higher increase in taurine-conjugated bile acids, except TCA, was observed in the model control group than in the negative control group (TUDCA, 6.00; TCDCA, 3.24), whereas the increase in glycine conjugated bile acids, except GDCA, was relatively low (GLCA, 1.61; GCDCA, 1.74; GCA, 1.30). Taurine possessed protective effects on hepatocellular injury and apoptosis. When hepatocellular injury occurs, the body can regulate the compensatory increase in taurine and further increase the content of taurine-conjugated bile acids[36]. The content of taurine conjugated bile acids was significantly decreased after treatment with the F-G extract in a dose-dependent manner.

Bile acids exhibit different hydrophilic and hydrophobic properties according to their chemical structure. Hydrophobic bile acids can lyse cell membrane lipids, exhibiting "decontamination", resulting in hepatocellular necrosis. Therefore, the accumulation of hydrophobic bile acids in the liver is a major and important cause of liver injury. UDCA is a nontoxic hydrophilic bile acid. Taurine conjugated bile acids (TCA, TCDCA, and TDCA) and glycine conjugated bile acids (GLCA, GDCA, GCDCA, and GCA) exhibit low toxicity due to some hydrophobicity, while CA, CDCA, and DCA are free and hydrophobic bile acids that show strong hepatotoxicity. DCA is one of the most toxic bile acids. The accumulation of DCA in the liver or blood leads to mitochondrial destruction, cell membrane rupture, and the production of reactive oxygen species in hepatocytes, leading to apoptosis and necrosis[36,37]. In this study, three hydrophobic components, CA, CDCA, and DCA, were significantly increased in the model control group, showing a positive correlation with the toxic effects reported[38]. The F-G extract can promote the binding of CA, CDCA, and DCA to taurine and glycine to reduce the accumulation of free CA, CDCA, and DCA *in vivo*, thus preventing acute liver injury induced by CCl_4.

When acute liver injury was caused by CCl_4 in rats, the hepatocytes were damaged, and the activities of cholesterol 7α-hydroxylase and cholesterol 12α-hydroxylase in hepatocytes were decreased, resulting in decreased CA and CDCA produced by cholesterol synthesis. However, due to impaired hepatic uptake of bile acids, the uptake of these two bile acids in the enterohepatic circulation is greatly reduced, resulting in a significant increase in the concentrations of bile acids in the serum. In this study, CA and CDCA were significantly increased in the model control group, showing liver damage and leading to bile acid malabsorption in the hepatoenteric circulation. The F-G extract decreased the contents of CA and CDCA in serum in a dose-dependent manner, indicating that the F-G extract could repair liver injury, improve enterohepatic circulation, and promote the absorption of CA and CDCA, exhibiting almost the same pharmacological effect as silybin.

Table 11 Ratio of bile acids in each experimental group to corresponding composition of negative control group

Bile acid	Negative	Model	Positive	FGL	FGM	FGH
CA	1.00	2.57	1.38	2.16	1.92	1.40
GLCA	1.00	1.61	1.08	1.45	1.17	1.15
GDCA	1.00	4.45	2.43	3.53	2.78	2.14
GCDCA	1.00	1.74	1.18	1.85	1.28	1.09
GCA	1.00	1.30	1.25	1.22	1.16	1.12
TCA	1.00	1.99	1.11	1.90	1.37	1.31
CDCA	1.00	4.12	2.08	3.76	2.90	2.03
UDCA	1.00	5.68	3.17	4.87	3.72	3.62
TUDCA	1.00	6.00	3.08	4.73	4.13	3.87
TCDCA	1.00	3.24	1.57	2.92	2.63	2.03
DCA	1.00	5.16	2.40	4.48	3.84	2.95

CDCA: Chenodeoxycholic acid; UDCA: Ursodeoxycholic acid; GCA: Glycocholic acid; GDCA: Glycochenodeoxycholic acid; TCA: Taurocholic acid; TUDCA: Taurocholic acid; GCDCA: Glycochenodeoxycholic acid; GLCA: Glycinic acid; DCA: Deoxycholic acid; CA: Cholic acid.

CONCLUSION

In this study, the effects of F-G extract in preventing acute liver injury induced by CCl_4 have been assayed. The F-G extract decreases the adhesion between the lobules and the mucosa, reduces the bleeding point on the surface of the liver, effectively decreases ALT and AST in a rat model of acute liver injury in a dose-dependent manner, and reduces hepatocellular swelling, inflammatory cell infiltration, blood stasis, hepatic steatosis, and other pathological changes in rats.

ARTICLE HIGHLIGHTS

Research background

Fuzi (*Radix aconiti* lateralis)-*Gancao* (*Radix glycyrrhizae*) (F-G) is often used in the treatment of liver diseases such as hepatitis and liver failure.

Research motivation

This study can clarify the bile acid mechanism of F-G in the treatment of liver injury, and establish a complete bile acid spectrum research method, so as to provide reference for future research.

Research objectives

To study the molecular mechanism and action mechanism of F-G in the treatment of liver injury, and to provide a theoretical basis for the clinical research of F-G.

Research methods

An ultra performance liquid chromatography tandem mass spectrometry (UPLC-MS/MS) method for the simultaneous determination of 92 metabolites from multiple pathways was established to explore the protective metabolic mechanism of F-G in serum on the liver.

Research results

A UPLC-MS/MS method for simultaneous determination of 11 bile acids was established to analyze the regulatory mechanism of F-G in serum. F-G decreased the contents of 11 bile acids in the serum in a dose-dependent manner.

Research conclusions

F-G could promote the conjugation of free bile acids to glycine and taurine, reduce the

accumulation of free bile acids in the liver, regulate the compensatory degree of taurine, and decrease the content of taurine conjugated bile acids.

Research perspectives

The research group will continue to study the effect of bile acid metabolism regulation on molecular regulation in the body.

REFERENCES

1 **Wu H**, Zhang G, Huang L, Pang H, Zhang N, Chen Y, Wang G. Hepatoprotective Effect of Polyphenol-Enriched Fraction from *Folium Microcos* on Oxidative Stress and Apoptosis in Acetaminophen-Induced Liver Injury in Mice. *Oxid Med Cell Longev* 2017; **2017**: 3631565 [PMID: 28626497 DOI: 10.1155/2017/3631565]

2 **Yang Y**, He Q, Wang H, Hu X, Luo Y, Liang G, Kuang S, Mai S, Ma J, Tian X, Chen Q, Yang J. The protection of meloxicam against chronic aluminium overload-induced liver injury in rats. *Oncotarget* 2017; **8**: 23448-23458 [PMID: 28423583 DOI: 10.18632/oncotarget.15588]

3 **Navarro VJ**, Khan I, Björnsson E, Seeff LB, Serrano J, Hoofnagle JH. Liver injury from herbal and dietary supplements. *Hepatology* 2017; **65**: 363-373 [PMID: 27677775 DOI: 10.1002/hep.28813]

4 **Russell DW**, Setchell KD. Bile acid biosynthesis. *Biochemistry* 1992; **31**: 4737-4749 [PMID: 1591235 DOI: 10.1021/bi00135a001]

5 **Chiang JY**. Bile acids: regulation of synthesis. *J Lipid Res* 2009; **50**: 1955-1966 [PMID: 19346330 DOI: 10.1194/jlr.R900010-JLR200]

6 **Li T**, Chiang JY. Bile acid signaling in metabolic disease and drug therapy. *Pharmacol Rev* 2014; **66**: 948-983 [PMID: 25073467 DOI: 10.1124/pr.113.008201]

7 **Trauner M**, Boyer JL. Bile salt transporters: molecular characterization, function, and regulation. *Physiol Rev* 2003; **83**: 633-671 [PMID: 12663868 DOI: 10.1152/physrev.00027.2002]

8 **Maillette de Buy Wenniger L**, Beuers U. Bile salts and cholestasis. *Dig Liver Dis* 2010; **42**: 409-418 [PMID: 20434968 DOI: 10.1016/j.dld.2010.03.015]

9 **Russell DW**. The enzymes, regulation, and genetics of bile acid synthesis. *Annu Rev Biochem* 2003; **72**: 137-174 [PMID: 12543708 DOI: 10.1146/annurev.biochem.72.121801.161712]

10 **Zhou W**. Clinical observation on treatment of acute-on-chronic liver failure with Traditional Chinese Medicine. *Zhongguo Xiandai Yaowu Yingyong Zazhi* 2016; **10**: 263-264 [DOI: 10.14164/j.cnki.cn11-5581/r.2016.17.172]

11 **Liu QL**, Sun YW. Clinical observation of Fuzi Lizhong decoction combined with western medicine in the treatment of chemotherapy-induced liver injury. *Zhongguo Laonian Baojian Yixue***13**: 73-74 [DOI: 10.3969/j.issn.1672-4860.2015.02.027]

12 **Luo JX**, Zhang Y, Hu XY, Yu C. The Effect of Modified Sini Decoction on Survival Rates of Patients with Hepatitis B Virus Related Acute-on-Chronic Liver Failure. *Evid Based Complement Alternat Med* 2019; **2019**: 2501847 [PMID: 30915144 DOI: 10.1155/2019/2501847]

13 **Li RX**, Chen ZY, Liu X, Yang CS. Effect of modified Sini decoction combined with magnesium isoglycyrrhizinate on acute drug-induced liver injury and its influence on oxidative stress and humoral immune function. *Xiandai Zhongxiyi Jiehe Zazhi* 2018; **27**: 25-29 [DOI: 10.3969/j.issn.1008-8849.2018.36.005]

14 **Chen L**, Yang H, Zhang FX, Liu N, Li XY, Zhao F. Protective effects of modified Sini decoction on hepatocyte apopto-sis induced by Con A. *Yunnan Daxue Zhongyiyao Zazhi* 2014; **37**: 5-7

15 **Yang JH**, Shi SH, Ma W, Tao DQ, Liu S, Chen L, Zhou XL. Effect of Fuzi Lizhong decoction in reducing fiver injury of rats with non-alcoholic fatty liver *via* activating AMPK and suppressing NF-κBp65 pathway. *Zhongguo Zhongyao Zazhi* 2018; **43**: 3176-3183

16 **Luo J**, Zhang Y, Hu X, Zhong S, Chen G, Wang Y, Lin W, Yi C, Zhu H. The effects of modified sini decoction on liver injury and regeneration in acute liver failure induced by D-galactosamine in rats. *J Ethnopharmacol* 2015; **161**: 53-59 [PMID: 25499312 DOI: 10.1016/j.jep.2014.12.003]

17 **Fu X**, Lu R, Zhao S. Simultaneous quantitation of six aconitum alkaloids and three flavonoids in the herb couple of radix aconiti lateralis-radix glycyrrhizae (Fuzi-Gancao) by UHPLC-ESI-MS/MS. *Pharmacogn Mag* 2017; **13**: 425-429 [PMID: 28839367 DOI: 10.4103/pm.pm_141_16]

18 **Liu XX**, Jian XX, Cai XF, Chao RB, Chen QH, Chen DL, Wang XL, Wang FP. Cardioactive C_{19}-diterpenoid alkaloids from the lateral roots of Aconitum carmichaeli "Fu Zi". *Chem Pharm Bull (Tokyo)* 2012; **60**: 144-149 [PMID: 22223386 DOI: 10.1248/cpb.60.144]

19 **Wang L**, Ding JY, Liu XX, Tang MH, Chao RB, Wang FP. [Identification of aminoalcohol-diterpenoid alkaloids in Aconiti Lateralis Radix Praeparata and study of their cardiac effects]. *Yao Xue Xue Bao* 2014; **49**: 1699-1704 [PMID: 25920200]

20 **Lu ZQ**, Zhang YJ, Zhuang PW, Zhang JB, Zhou HF, Chen Z, Sun M, Xu LM. Effect of Aconiti Lateralis Radix Preparata on hemodynamics of rats with acute heart failure and its mechanism. *Zhong Cao Yao* 2015; **46**: 3223-3234

21 **Shao F**, Li SL, Liu RH, Huang HL, Ren G, Yao YX, Hao XC. Analgesic and Anti-inflammatory Effects of Different Processed Products of Aconiti lateralis radix praeparata. *Shizhen Guoyi Guoyao* 2011; **22**: 2329-2330 [DOI: 10.3969/j.issn.1008-0805.2011.10.006]

22 **Gao F**, Li YY, Wang D, Huang X, Liu Q. Diterpenoid alkaloids from the Chinese traditional herbal "Fuzi" and their cytotoxic activity. *Molecules* 2012; **17**: 5187-5194 [PMID: 22628040 DOI: 10.3390/molecules17055187]

23 **Zhang T**, Wang GJ, Bai SG. Effect of Aconiti Lateralis Radix Preparata on antioxidant system in aged rats. *Zhongguo Laonianxue Zazhi* 2001; **21**: 135-136 [DOI: 10.3969/j.issn.1005-9202.2001.02.031]

24 **Luo JX**, Zhang Y, Hu XY, Chen G, Liu XY, Nie HM, Liu JL, Wen DC. Aqueous extract from Aconitum carmichaelii Debeaux reduces liver injury in rats *via* regulation of HMGB1/TLR4/NF-KB/caspase-3 and PCNA signaling pathways. *J Ethnopharmacol* 2016; **183**: 187-192 [PMID: 26806574 DOI: 10.1016/j.jep.2016.01.020]

25 **Konda VGR**, Eerike M, Prabhu L. Evaluation of hepatoprotective activity of ethanolic extract of aconitum heterophyllum root in paracetamol induced liver toxicity. *Int J Pharma Bio Sci* 2013; **4**: 714-721

26 **Yang XX**, Liu D, Bian K, Zhang DD. Study on *in vitro* anti-inflammatory activity of total flavonoids from Glycyrrhizae Radix et Rhizoma and its ingredients. *Zhongguo Zhongyao Zazhi* 2013; **38**: 99-104 [DOI: 10.4268/cjcmm20130120]

27 **Furusawa J**, Funakoshi-Tago M, Tago K, Mashino T, Inoue H, Sonoda Y, Kasahara T. Licochalcone A significantly suppresses LPS signaling pathway through the inhibition of NF-kappaB p65 phosphorylation at serine 276. *Cell Signal* 2009; **21**: 778-785 [PMID: 19168128 DOI: 10.1016/j.cellsig.2009.01.021]

28 **Fu Y**, Chen J, Li YJ, Zheng YF, Li P. Antioxidant and anti-inflammatory activities of six flavonoids separated from licorice. *Food Chem* 2013; **141**: 1063-1071 [PMID: 23790887 DOI: 10.1016/j.foodchem.2013.03.089]

29 **Ahn SJ**, Cho EJ, Kim HJ, Park SN, Lim YK, Kook JK. The antimicrobial effects of deglycyrrhizinated licorice root extract on Streptococcus mutans UA159 in both planktonic and biofilm cultures. *Anaerobe* 2012; **18**: 590-596 [PMID: 23123832 DOI: 10.1016/j.anaerobe.2012.10.005]

30 **Dong Y**, Zhao M, Zhao T, Feng M, Chen H, Zhuang M, Lin L. Bioactive profiles, antioxidant activities, nitrite scavenging capacities and protective effects on H2O2-injured PC12 cells of Glycyrrhiza glabra L. leaf and root extracts. *Molecules* 2014; **19**: 9101-9113 [PMID: 24983860 DOI: 10.3390/molecules19079101]

31 **Kim YW**, Park SM, Seo HL, Jang MH, Jung JY, Lee JH, Jang EJ, Cho IJ, Byun SH, Kim SC. Licorice and its flavonoids inhibit oxidative damage in the liver. *Integr Med Res* 2015; **4**: 77 [DOI: 10.1016/j.imr.2015.04.109]

32 **Zhang GP**, Xie SH, Zhu XG, Zhang SY, Zhai JY, Meng H, Ye ZG. Experimental Study on Effects of Radix Glycyr-rhizae on Toxicity and Efficacy of Radix Aconiti Carmichaeli in Compatibility. *Zhongguo Zhongyiyao Xinxi Zazhi* 2012; **19**: 31-34 [DOI: 10.3969/j.issn.1005-5304.2012.06.012]

33 **Ma LN**, Ye ZG, Zhang GP. Detoxification mechanism of Aconiti lateralis radix praeparata with Glycyrrhizae Radix et Rhizoma compatibility based on the change of components in vitro-metabolism in vivo-antagonism of biological effects. *Zhongguo Zhongyao Zazhi* 2019; **44**: 99-104 [DOI: 10.19540/j.cnki.cjcmm.20190701.404]

34 **Li H**, Zhang GP, Ma M, Su P, Yang YF, Chen TF, Ye ZG. Attenuation Mechanism of Aconti Lateralis Radix Praeparata Combined with Glycyrrhizae Radix et Rhizoma Based on Heart CYP450 Isozymes. *Zhongguo Shiyan Fangjixue Zazhi* 2020; **26**: 59-64 [DOI: 10.13422/j.cnki.syfjx.20192026]

35 **Song H**, Li W, Liu B, Sun X, Ding J, Chen N, Ji Y, Xiang Z. Study of the estrogenic-like mechanism of glycosides of cistanche using metabolomics. *RSC Adv* 2017; **7**: 39403-39410 [DOI: 10.1039/C7RA06930H]

36 **Xu Y**, Chen CC, Yang L, Wang JM, Ji LL, Wang ZT, Hu ZB. Evaluation on hepatotoxicity caused by Dioscorea bulbifera based on analysis of bile acids. *Acta Pharm Sin* 2011; **46**: 39-44 [DOI: 10.1007/s11606-010-1517-4]

37 **He XL**, Guan H, Li PF. Research progress of taurochodeoxycholic acid. *Anim Husb Feed Sci* 2008; **29**: 57-60

38 **Zheng JC**, Wang WF, Pei XT. Effects of bile acids metabolism on hepatocytes function. *Ganzhang* 2007; **12**: 308-310 [DOI: 10.3969/j.issn.1008-1704.2007.04.032]

World Journal of Gastroenterology

Submit a Manuscript: https://www.f6publishing.com

World J Gastroenterol 2021 October 28; 27(40): 6908-6926

DOI: 10.3748/wjg.v27.i40.6908

ISSN 1007-9327 (print) ISSN 2219-2840 (online)

ORIGINAL ARTICLE

Basic Study

Transforming growth factor beta-1 upregulates glucose transporter 1 and glycolysis through canonical and noncanonical pathways in hepatic stellate cells

Ming-Yu Zhou, Ming-Liang Cheng, Tao Huang, Rui-Han Hu, Gao-Liang Zou, Hong Li, Bao-Fang Zhang, Juan-Juan Zhu, Yong-Mei Liu, Yang Liu, Xue-Ke Zhao

ORCID number: Ming-Yu Zhou 0000-0002-5130-5950; Ming-Liang Cheng 0000-0001-6962-4012; Tao Huang 0000-0001-6849-5378; Rui-Han Hu 0000-0003-0668-2025; Gao-Liang Zou 0000-0002-9460-0802; Hong Li 0000-0003-0601-3198; Bao-Fang Zhang 0000-0002-5396-540X; Juan-Juan Zhu 0000-0003-0692-9200; Yong-Mei Liu 0000-0003-4334-4340; Yang Liu 0000-0002-1140-2588; Xue-Ke Zhao 0000-0002-3032-4933.

Author contributions: Zhao XK and Cheng ML designed the study; Zhou MY, Huang T and Hu RH performed most of the experiments and wrote the article; all authors contributed to the design and interpretation of the study; Zhou MY, Huang T and Hu RH contributed equally to this work; all authors approved the final version of the article.

Supported by National Natural Science Foundation of China, No. 82060116, No. 81860115 and No. 81960118; and Guizhou Science and Technology Support Project Fund, No. [2021] 058.

Institutional review board statement: This study was approved by the Institutional Review Board of the Affiliated

Ming-Yu Zhou, Ming-Liang Cheng, Tao Huang, Rui-Han Hu, Xue-Ke Zhao, Department of Internal Medicine, Guizhou Medical University, Guiyang 550001, Guizhou Province, China

Ming-Yu Zhou, Ming-Liang Cheng, Gao-Liang Zou, Hong Li, Bao-Fang Zhang, Juan-Juan Zhu, Yang Liu, Xue-Ke Zhao, Department of Infectious Diseases, Affiliated Hospital of Guizhou Medical University, Guiyang 550004, Guizhou Province, China

Yong-Mei Liu, Clinical Laboratory Center, Affiliated Hospital of Guizhou Medical University, Guiyang 550004, Guizhou Province, China

Corresponding author: Xue-Ke Zhao, MD, PhD, Chief Physician, Professor, Department of Infectious Diseases, Affiliated Hospital of Guizhou Medical University, No. 28 Guiyi Road, Guiyang 550004, Guizhou Province, China. zhaoxueke1@163.com

Abstract

BACKGROUND

Hepatic stellate cells (HSCs) are the key effector cells mediating the occurrence and development of liver fibrosis, while aerobic glycolysis is an important metabolic characteristic of HSC activation. Transforming growth factor-β1 (TGF-β1) induces aerobic glycolysis and is a driving factor for metabolic reprogramming. The occurrence of glycolysis depends on a high glucose uptake level. Glucose transporter 1 (GLUT1) is the most widely distributed glucose transporter in the body and mainly participates in the regulation of carbohydrate metabolism, thus affecting cell proliferation and growth. However, little is known about the relationship between TGF-β1 and GLUT1 in the process of liver fibrosis and the molecular mechanism underlying the promotion of aerobic glycolysis in HSCs.

AIM

To investigate the mechanisms of action of GLUT1, TGF-β1 and aerobic glycolysis in the process of HSC activation during liver fibrosis.

METHODS

Immunohistochemical staining and immunofluorescence assays were used to examine GLUT1 expression in fibrotic liver tissue. A Seahorse extracellular flux (XF) analyzer was used to examine changes in aerobic glycolytic flux, lactate

Hospital of Guizhou Medical University.

Institutional animal care and use committee statement: All animal experiments conformed to the internationally accepted principles for the care and use of laboratory animals (license No. 2000719). All animal interventions were approved by the Institutional Animal Care and Use Committee (IACUC) of Guizhou Medical University.

Conflict-of-interest statement: The authors declare no conflicts of interest related to this study.

Data sharing statement: No additional data are available.

ARRIVE guidelines statement: The authors have read the ARRIVE Guidelines, and the manuscript was prepared and revised according to the ARRIVE Guidelines.

Open-Access: This article is an open-access article that was selected by an in-house editor and fully peer-reviewed by external reviewers. It is distributed in accordance with the Creative Commons Attribution NonCommercial (CC BY-NC 4.0) license, which permits others to distribute, remix, adapt, build upon this work non-commercially, and license their derivative works on different terms, provided the original work is properly cited and the use is non-commercial. See: http://creativecommons.org/Licenses/by-nc/4.0/

Manuscript source: Unsolicited manuscript

Specialty type: Gastroenterology and hepatology

Country/Territory of origin: China

Peer-review report's scientific quality classification

Grade A (Excellent): 0
Grade B (Very good): B, B, B
Grade C (Good): 0
Grade D (Fair): 0
Grade E (Poor): 0

production levels and glucose consumption levels in HSCs upon TGF-β1 stimulation. The mechanism by which TGF-β1 induces GLUT1 protein expression in HSCs was further explored by inhibiting/promoting the TGF-β1/mothers-against-decapentaplegic-homolog 2/3 (Smad2/3) signaling pathway and inhibiting the p38 and phosphoinositide 3-kinase (PI3K)/AKT signaling pathways. In addition, GLUT1 expression was silenced to observe changes in the growth and proliferation of HSCs. Finally, a GLUT1 inhibitor was used to verify the *in vivo* effects of GLUT1 on a mouse model of liver fibrosis.

RESULTS

GLUT1 protein expression was increased in both mouse and human fibrotic liver tissues. In addition, immunofluorescence staining revealed colocalization of GLUT1 and alpha-smooth muscle actin proteins, indicating that GLUT1 expression was related to the development of liver fibrosis. TGF-β1 caused an increase in aerobic glycolysis in HSCs and induced GLUT1 expression in HSCs by activating the Smad, p38 MAPK and P13K/AKT signaling pathways. The p38 MAPK and Smad pathways synergistically affected the induction of GLUT1 expression. GLUT1 inhibition eliminated the effect of TGF-β1 on HSC proliferation and migration. A GLUT1 inhibitor was administered in a mouse model of liver fibrosis, and GLUT1 inhibition reduced the degree of liver inflammation and liver fibrosis.

CONCLUSION

TGF-β1 induces GLUT1 expression in HSCs, a process related to liver fibrosis progression. *In vitro* experiments revealed that TGF-β1-induced GLUT1 expression might be one of the mechanisms mediating the metabolic reprogramming of HSCs. In addition, *in vivo* experiments also indicated that the GLUT1 protein promotes the occurrence and development of liver fibrosis.

Key Words: Gene regulation; Glycolysis; Liver fibrosis; Glucose transporter 1; Transforming growth factor-β1

©The Author(s) 2021. Published by Baishideng Publishing Group Inc. All rights reserved.

Core Tip: Liver fibrosis is a repair response of the liver to various chronic injuries. However, fibrosis may eventually evolve into liver cirrhosis or even liver cancer if it progresses. Hepatic stellate cell activation is the initiating factor for liver fibrosis. Transforming growth factor-β1 (TGF-β1) is a pleiotropic cytokine that induces aerobic glycolysis. Glucose transporter 1 (GLUT1) regulates glucose metabolism. This study examined the effects of TGF-β1-mediated pathways on GLUT1 expression *in vivo* and *in vitro*, explored the relationship between GLUT1 and TGF-β1 and further investigated the potential underlying mechanisms.

Citation: Zhou MY, Cheng ML, Huang T, Hu RH, Zou GL, Li H, Zhang BF, Zhu JJ, Liu YM, Liu Y, Zhao XK. Transforming growth factor beta-1 upregulates glucose transporter 1 and glycolysis through canonical and noncanonical pathways in hepatic stellate cells. *World J Gastroenterol* 2021; 27(40): 6908-6926
URL: https://www.wjgnet.com/1007-9327/full/v27/i40/6908.htm
DOI: https://dx.doi.org/10.3748/wjg.v27.i40.6908

INTRODUCTION

Liver fibrosis is the inevitable result of chronic liver inflammation caused by various etiologies. With progressive destruction of liver parenchymal cells, liver fibrosis eventually develops into liver cirrhosis and even liver cancer[1,2]. Although liver cirrhosis and liver cancer are irreversible, liver fibrosis can be reversed. Therefore, the mechanism of and clinical studies on liver fibrosis have always been the focus of liver disease research. The main pathological feature of liver fibrosis is the excessive

Received: April 30, 2021
Peer-review started: April 30, 2021
First decision: July 2, 2021
Revised: July 19, 2021
Accepted: September 8, 2021
Article in press: September 8, 2021
Published online: October 28, 2021

P-Reviewer: Rojas A, Vela D, Wang Z
S-Editor: Gao CC
L-Editor: A
P-Editor: Xing YX



deposition of extracellular matrix (ECM), while the key initiating factors are activation of quiescent hepatic stellate cells (HSCs) and transformation of their phenotypes and functions[3]. The transforming growth factor-β1 (TGF-β1) pathway is the key fibrogenic pathway that drives HSC activation and induces ECM production. HSC activation requires metabolic reprogramming and a continuous energy supply[4,5]. Aerobic glycolysis is an important metabolic characteristic of the transdifferentiation of quiescent stellate cells, a process similar to the Warburg effect in tumor cells, and the core metabolic changes include a transition from oxidative phosphorylation to aerobic glycolysis[6]. Dysregulated glycolysis has been implicated in experimental models of lung and liver fibrosis, and inhibition of glycolysis reduces ECM accumulation[7]. In view of the mechanisms involved, targeting and inhibiting the metabolic reprogramming of activated HSCs during liver fibrosis may be a promising anti-liver fibrosis strategy.

TGF-β1 is a multifunctional cytokine and a major profibrotic cytokine that regulates cell differentiation, cell proliferation and ECM production and directly regulates multiple cellular signal transduction networks[8]. In the canonical TGF-β1/mothers-against-decapentaplegic-homolog 2/3 (Smad2/3) pathway, ligands induce the assembly of the TGF-β1 receptor I (TβRI)/TGF-β1 receptor II (TβRII) heterocomplex, which targets Smad4 *via* Smad2 and Smad3 proteins to form the Smad complex, leading to phosphorylation and nuclear translocation of Smad2/3; this R-Smad/Co-Smad4 complex translocates to the nucleus where it binds to DNA either directly or in association with other DNA-binding proteins[9-11]. Phosphorylated Smad2/3 binds to specific Smad binding elements (SBEs) in gene promoter regions to activate/suppress the expression of target genes[12,13]. In addition to Smads, TGF-β1 also triggers other protein-mediated signaling pathways, *e.g.*, p38, mitogen-activated protein kinases (MAPKs) and phosphoinositide 3-kinase (PI3K). Some functions of TGF-β1 have been studied in depth, such as the mediation of cell differentiation and proliferation. However, TGF-β1 has recently been reported to induce aerobic glycolysis and is considered a driving factor in metabolic reprogramming[14]. TGF-β is also a strong activator of glycolysis in mesenchymal cells[15]. Extracellular accumulation of lactic acid induces epithelial-mesenchymal transition (EMT) by directly reconstituting the ECM and releasing activated TGF-β1. EMT induced by TGF-β in hepatocellular carcinoma cells reprograms lipid metabolism to sustain the elevated energy requirements associated with this process[16]. Research on the mechanism of idiopathic pulmonary fibrosis has shown that TGF-β1-induced aerobic glycolysis causes lactic acid accumulation and changes the cellular microenvironment, thereby activating latent TGF-β1 in the ECM and eventually forming a positive feedback loop to promote the effects of TGF-β1[17].

Glucose transporter 1 (GLUT1) is a member of the GLUT transporter family, the most conserved and most widely distributed glucose transporter in mammals and the main transporter regulating glucose uptake[18]. An increasing number of studies have found that GLUT1 plays an important role in accelerated metabolism. Research on the mechanism of neurodegenerative diseases has revealed that GLUT1 controls the activation of microglia by promoting aerobic glycolysis[19]. GLUT1 enhances the stimulating effect of TGF-β1 on mesangial cells, breast cancer cells and pancreatic cancer cells. As glucose uptake increases during TGF-β1-induced EMT of breast cancer cells, GLUT1 expression also increases and is correlated with EMT markers (including E-cadherin and vimentin). GLUT1 is the key mediator of the aerobic glycolysis phenotype in ovarian cancer and is required to maintain a high level of basic aerobic glycolysis. In models of bleomycin-induced pulmonary fibrosis, GLUT1-dependent aerobic glycolysis has been reported to be essential for pulmonary parenchymal fibrosis[20-23]. Certain signaling molecules (such as cAMP, p53, PI3K and AKT) reduce alpha-smooth muscle actin (α-SMA) protein expression in primary mouse fibroblasts by inhibiting GLUT1 expression. Exosomes secreted by activated HSCs affect the metabolic switch of liver nonparenchymal cells through delivery of the glycolysis-related proteins GLUT1 and PKM2; GLUT1 is involved in metabolic reprogramming of HSCs[24]. TGF-β1 and GLUT1 play important regulatory roles in metabolic reprogramming. To date, however, researchers have not explored whether the increases in TGF-β1 and GLUT1 Levels during HSC activation are related. Therefore, this study investigated the effect of the TGF-β1 signaling pathway on the regulation of GLUT1 and aerobic glycolysis. We hypothesized that TGF-β1 drives HSC activation and aerobic glycolysis by inducing GLUT1 expression, thereby promoting liver fibrosis progression. As shown in the present study, GLUT1 expression was significantly increased in mouse and human fibrotic liver tissue samples. Further *in vitro* experiments showed that the aerobic glycolysis capacity of HSCs was enhanced and GLUT1 expression increased with increasing TGF-β1 Levels. Inhibition/

promotion of the Smad2/3 signaling pathway and inhibition of the p38 and PI3K/AKT signaling pathways confirmed that TGF-β1 induced GLUT1 expression by targeting the pSmad2/3, p38 and PI3K/AKT pathways, thus promoting HSC activation. Finally, administration of a specific GLUT1 inhibitor in a mouse model of liver fibrosis resulted in a significant reduction in liver fibrosis. Based on these findings, the TGF-β1 signaling pathway enhances aerobic glycolysis by promoting GLUT1 expression, thereby promoting the development of liver fibrosis.

MATERIALS AND METHODS

Reagents and antibodies

The TGF-β1 antibody was purchased from R&D Systems (Minneapolis, MN, United States); antibodies against GLUT1, p-Smad2/3, Smad2/3, p-P38, p-AKT and desmin were purchased from Abcam (Cambridge, MA, United States), and the tubulin antibody was purchased from Research Diagnostics (Flanders, NJ, United States). The anti-α-SMA antibody, carbon tetrachloride (CCl_4), corn oil, OptiPrep and other chemicals and reagents were purchased from Sigma-Aldrich (St. Louis, MO, United States) and Fisher Scientific (Waltham, MA, United States). A TβRI/II inhibitor (APExBIO Technology, United States) was used at 2 μmol/L. Inhibitors of p38 MAPK and PI3K, namely, SB203580 and LY294002, respectively, were purchased from Abcam (Cambridge, MA, United States). The Smad3 inhibitors SIS3 and phloretin were purchased from Abcam (Cambridge, MA, United States).

Generation of a mouse model of liver fibrosis

The animal protocol was designed to minimize pain or discomfort to the animals. The animals were acclimated to laboratory conditions (22 °C, 12-h/12-h light/dark cycle, 50% humidity, *ad libitum* access to food and water) for 1 wk prior to experimentation. The methods and experimental procedures were carried out in accordance with the relevant guidelines and regulations. Mice (C57BL6, eight to ten weeks old) were housed in standard conditions, and sex-matched mice were treated with 2.0 μL/g body weight CCl_4 [diluted 1:10 (v/v) with corn oil] or corn oil as a control by intraperitoneal (i.p.) injections three times per week for 4 wk[25]. Mice were challenged with CCl_4 or corn oil (control), followed by an i.p. injection of phloretin (10 mg/kg, three times per week for 2 wk) or 0.9% saline (vehicle). Mice were sacrificed at 48 h after the experiment ended, and tissues were harvested.

Patient liver samples

Normal and liver fibrosis tissue samples were obtained from patients treated at the Department of Hepatobiliary Surgery of the Affiliated Hospital of Guizhou Medical University (Guiyang, China). Written informed consent was obtained from the patients.

Western blot analysis

Immunoblotting was performed using whole-liver tissue lysates or whole-cell lysates prepared in buffer containing 1% NP-40 as described previously[26]. Total proteins were extracted and quantified using Bradford protein quantification kits. Protein samples (40 μg each) were resolved by sodium dodecyl sulfate-polyacrylamide gel electrophoresis (SDS-PAGE). The proteins were transferred onto polyvinylidene fluoride (PVDF) membranes and incubated with primary antibodies overnight at 4 °C. On the next day, signals were developed with an electrochemiluminescence detection kit after incubation with the appropriate secondary antibodies.

Cells and cell culture

Primary mouse HSCs were isolated and cultured as described previously[26]. Briefly, cells were isolated from livers through in situ liver perfusion with pronase, Liberase and collagenase followed by density gradient centrifugation. The dispersed cell suspension was filtered and gradiently centrifuged for 2 min to remove hepatocytes. The remaining cell fraction was washed and resuspended in 11.5% OptiPrep and then gently transferred to a tube containing 15% OptiPrep at the bottom, followed by PBS addition as the top layer. The cell fraction was then centrifuged at 1400 rpm/min for 20 min. The HSC fraction layer was obtained at the interface between the top and intermediate layers. The purity of the HSC fraction was estimated based on autofluorescence 1 d after isolation and was always greater than 97%. Flow cytometry was used

to identify the purity of primary cells. In brief, the cells were digested with trypsin, centrifuged at 1000 rpm/min for 10 min, washed twice with PBS, resuspended in EP tubes (100 μL/tube) and centrifuged at 2000 rpm/min for 6 min. Then, the supernatant was discarded, 100 μL of PBS was added, and the cells were resuspended and dispersed. A mouse monoclonal antibody against desmin (desmin is a typical molecular marker of HSCs) was added, and the cells were incubated at 1:100 for 1.5 h and centrifuged at 2000 rpm/min for 6 min. Centrifugation was repeated twice. The cells were resuspended and dispersed by adding 100 μL of PBS. Fluorescence-labeled anti-mouse secondary antibody (1:1000) was added, followed by incubation at 4 °C for 30 min in the dark. Next, 1 mL of PBS was added to each tube, followed by centrifugation at 2000 rpm/min for 6 min, which was repeated twice. Finally, 0.5 mL of PBS was added to resuspend the cells, and then the cells were subjected to flow cytometry measurements. HSCs were also confirmed to lack E-cadherin expression. Cell viability was also examined, and HSCs were maintained in Dulbecco's modified Eagle's medium (DMEM) supplemented with 10% fetal bovine serum and antibiotics as described previously[26]. Cells were starved or treated on day 2 after isolation, and the duration of starvation or treatment is described in each figure legend. The duration of the whole experiment was 5-7 d after HSC isolation, and cells at passages 1-2 were used (as cells were passaged from regular culture flasks to experimental cell culture wells for some experiments).

Histological and immunohistochemical studies

Liver samples were fixed with formalin, embedded in paraffin, sectioned and processed routinely for Masson's trichrome and Sirius red staining. Antibodies used for immunohistochemical (IHC) staining of GLUT1 and α-SMA were purchased from Abcam Technology, United States.

RNA interference

Cells were transfected with small interfering RNAs (siRNAs) using Lipofectamine 3000 (Invitrogen, Carlsbad, CA, United States) according to the manufacturer's recommendations. The siRNAs used were an siRNA mix targeting sequences in Smad2 and Smad3 purchased from Santa Cruz Biotechnology (siRNA Smad2/3) and siRNAs targeting four different sequences of Smad4 purchased from Santa Cruz Biotechnology. GLUT1 siRNA was purchased from Cell Signaling Technology. The sequences of the siRNAs used are shown in Table 1.

Glycolytic function assay and lactate measurements

Primary mouse HSCs were plated on XF96 cell culture microplates. The extracellular acidification rate (ECAR), a glycolytic flux parameter, was measured with a Seahorse XF96 bioanalyzer using the XF Glycolysis Stress Test kit according to the manufacturer's instructions (102194-100, Seahorse Bioscience). Lactate levels were measured spectrophotometrically in 700 μL of supernatants from cells receiving the corresponding treatment using standard enzymatic methods.

Cell counting kit-8 assay

Primary mouse HSCs were seeded in a 96-well plate at a density of 3000 cells per well. CCK-8 reagent was added to each well every 24 h, and the plates were incubated for an additional 1 h at 37 °C and measured by recording the absorbance at 450 nm with an Elx800™ spectrophotometer (BioTek, Winooski, VT, United States).

Biochemical function analysis

Alanine aminotransferase (ALT) and aspartate transaminase (AST) levels in mouse serum samples and the supernatant of cell culture medium were detected using an automatic biochemical analyzer (Siemens Advia 1650; Siemens, Bensheim, Germany).

RNA extraction and real-time polymerase chain reaction

GLUT1, hexokinase 2 (HK-2), pyruvate kinase 2 (PKM-2) and α-SMA mRNA levels were determined using real-time polymerase chain reaction (RT-PCR) with a SYBR Green Master Mix Kit (Roche, Indianapolis, IN, United States). The primer sequences used are shown in Table 2.

Transwell migration assay

The migratory properties of HSCs were assessed using a Transwell assay. Cells were seeded at a density of 4×10^5 cells/well in the upper compartment of Transwell chambers with serum-free medium, and the lower compartment contained 700 μL of

Table 1 Small interfering RNA sequences

	Forward	Reverse
siGlut1-1	5′-CACCGGGAGTGACAAAGACTTTGTTCAAGCA-3′	5′-GATCCAAAAAAGGGAGTGACAAAGACTTCTC-3′
Negative control	5′-ATCCGACTTCATAAGGCGCATGCT-3′	5′-AGTATTCCGCGTACGAAGTTCTGC-3′
	siRNA Smad4 targeting four different sequences1	
	GCAAUUGAAAGUUUGGUAA, CCCACAACCUUUAGACUGA, GAAUCCAUAUCACUACGAA and GUACAGAGUUACUACUUAG	
	Sense	**Antisense**
siRNA Smad2/3[1]		
sc-37239A	CUUGCUGGAUUGAACUUCAtt	UGAAGUUCAAUCCAGCAAGtt
sc-37239B	CCGUCGUAGUAUUCAUGUAtt	UACAUGAAUACUACGACGGtt
sc-37239C	CUGACUCCUUGUUUAAUGAtt	UCAUUAAACAAGGAGUCAGtt
sc-37239D	GGAAGCUGAGAGUUAUAGAtt	UCUAUAACUCUCAGCUUCCtt

[1]Purchased from Santa Cruz Biotechnology. sc-37239: Smad2/3 siRNA (m) is a pool of four different siRNA duplexes.

Table 2 Primer sequences for real-time polymerase chain reaction

Gene	Forward sequence	Reverse sequence
HK2	5′-GGGTAGCCACGGAGTACAAA-3′	5′-TGGATTGAAAGCCAACTTCC-3′
GLUT1	5′-GCTTCTCCAACTGGACCTC-3′	5′-AAGAAGAGCACGAGGAGCAC-3′
PKM2	5′-TGGGATGGAAACTGTGAAGAG-3′	5′-CGGAGTTCCTCGAATAGCTG-3′
α-SMA	5′-AAGAGCATCCGACACTGCTGAC-3′	5′-AGCACAGCCTGAATAGCCACATAC-3′

5% glucose-containing medium per well. Migration was subsequently observed and measured.

Tissue immunofluorescence staining

Tissue sections were placed at room temperature for 10 min and deparaffinized in water for further antigen retrieval. After the sections were dried slightly, a histochemical pen was used to draw circles around the tissue, and 3%-5% BSA was added dropwise inside the circle for blocking, followed by incubation for 30 min. The primary antibody was added dropwise at the recommended ratio to the sections, and the sections were placed in a refrigerator (4 °C) and incubated overnight. After 3 washes, the sections were incubated with a FITC (CK-18)-labeled secondary antibody at room temperature for 45 min, and nuclei were stained with DAPI (300 nmol/L) for 1-5 min. After 3 washes, an antifluorescence quencher was added, and the sections were sealed with resin. Photographs of random fields were taken under an upright fluorescence microscope (ZEISS Axiovert).

Statistical analysis

Data were analyzed using Student's t test (SigmaPlot, SPSS 17.0, United States) to determine differences between two groups and are presented as the mean ± SE. For comparisons between multiple groups, three-way analysis of variance was performed, followed by t tests with Bonferroni correction using SAS 9.3 software (SAS Institute Inc., Cary, NC, United States). In addition, a log-rank test was used for survival analysis. All experiments were repeated at least three times. Differences were considered statistically significant at $P < 0.05$ ($^{a}P < 0.05$, $^{b}P < 0.01$).

RESULTS

GLUT1 expression is correlated with liver fibrosis progression

The classic mouse model of CCl_4-induced liver fibrosis was used to first clarify whether GLUT1 is related to liver fibrosis. Successful establishment of the liver fibrosis model was confirmed by Sirius red staining and α-SMA IHC staining (Figure 1A-C). Notably, a significant increase in GLUT1 expression was detected in the liver tissue specimens from the model group (Figure 1A and D). Subsequently, tissue immunofluorescence staining was performed, and the results showed significantly increased GLUT1 expression in liver tissue samples from the CCl_4 liver fibrosis model. More importantly, GLUT1 colocalized with α-SMA, indicating a correlation between GLUT1 and liver fibrosis (Figure 1E). IHC staining for GLUT1 and α-SMA was performed using human liver fibrosis specimens and liver specimens from a healthy control group; as expected, GLUT1 expression was significantly higher in the human liver fibrosis specimens (Figure 1F). Finally, whole-liver lysates were prepared from human liver tissue specimens and specimens from the mouse liver fibrosis model, and GLUT1 protein expression was analyzed. The results were consistent with the IHC data (Figure 1G-H). In summary, these results indicate that GLUT1 expression is related to liver fibrosis progression.

TGF-β1 stimulates HSC activation by inducing GLUT1 expression and promoting aerobic glycolysis

We found that GLUT1 colocalized with α-SMA, indicating that GLUT1 expression was increased mainly in activated HSCs because α-SMA is a major marker of HSC transdifferentiation. TGF-β1 is a very important profibrotic factor and regulates metabolic reprogramming in pulmonary fibrosis[27], as reported in some studies. Therefore, we questioned whether the increase in GLUT1 expression in liver fibrosis and TGF-β1 are related. This study first determined the effect of TGF-β1 on glycolysis in HSCs. To assess the dose responses to TGF-β1, we incubated HSCs with different TGF-β1 concentrations ranging from 3 ng/mL to 5 ng/mL, and the results showed similar effects on GLUT1 protein levels (Supplementary Figure 1). Therefore, a TGF-β1 concentration of 3 ng/mL was used for subsequent experiments. Mouse primary HSCs were isolated and cultured, and the cells were stimulated with TGF-β1 for 24 h prior to the experiments. TGF-β1 stimulation led to an early and continuous increase in the ECAR (an indicator of extracellular acid production) in HSCs, indicating that glycolysis was enhanced in these cells (Figure 2A and B). In addition, the intracellular and extracellular levels (in the medium) of lactic acid were examined to further confirm the glycolytic changes in HSCs. Both intracellular and extracellular lactic acid levels were significantly increased. Consistent with the increase in glycolysis, the level of glucose consumption also increased in these cells (Figure 2C and D). Therefore, TGF-β1 induces glycolysis during the process of HSC transdifferentiation. The expression levels of key glycolytic enzymes in these cells were evaluated; the expression levels of HK-2, PKM-2 and GLUT1 were upregulated, and the increase in GLUT1 expression was particularly significant (Figure 2F-H). Based on these findings, the increase in glycolysis during HSC transdifferentiation is related to the upregulation of key glycolysis enzymes. Similarly, the expression of α-SMA, a marker of transdifferentiation, also increased during the TGF-β1-mediated activation of HSCs (Figure 2I). GLUT1 protein expression was examined at various time points after stimulating HSCs with TGF-β1 (3 ng/mL) to determine whether TGF-β1 stimulates GLUT1 expression in a time-dependent manner, and the results showed that GLUT1 expression increased 2 h after stimulation with TGF-β1 and peaked at 8 h. These results indicate a time-dependent relationship between the increase in GLUT1 expression and TGF-β1 stimulation, which is consistent with the early increase in aerobic glycolysis in HSCs (Figure 2J). Finally, the addition of an inhibitor of the type 1 TGF-β1 receptor inhibited TGF-β1-induced GLUT1 expression in HSCs, suggesting that GLUT1 induction was mediated by TGF-β1 (Figure 2K). Based on these data, TGF-β1 is involved in glycolysis during HSC transdifferentiation and mediates GLUT1 expression, thereby promoting HSC transdifferentiation.

TGF-β1 induces GLUT1 expression through the Smad pathway

After finding that TGF-β1 stimulation induces GLUT1 expression, the specific mechanism by which TGF-β1 induces GLUT1 expression was further explored. Changes in the expression levels of Smad proteins in the canonical pathway activated by TGF-β1 stimulation were first examined. Western blot analysis revealed a time-dependent relationship between Smad2/Smad3 phosphorylation and TGF-β1

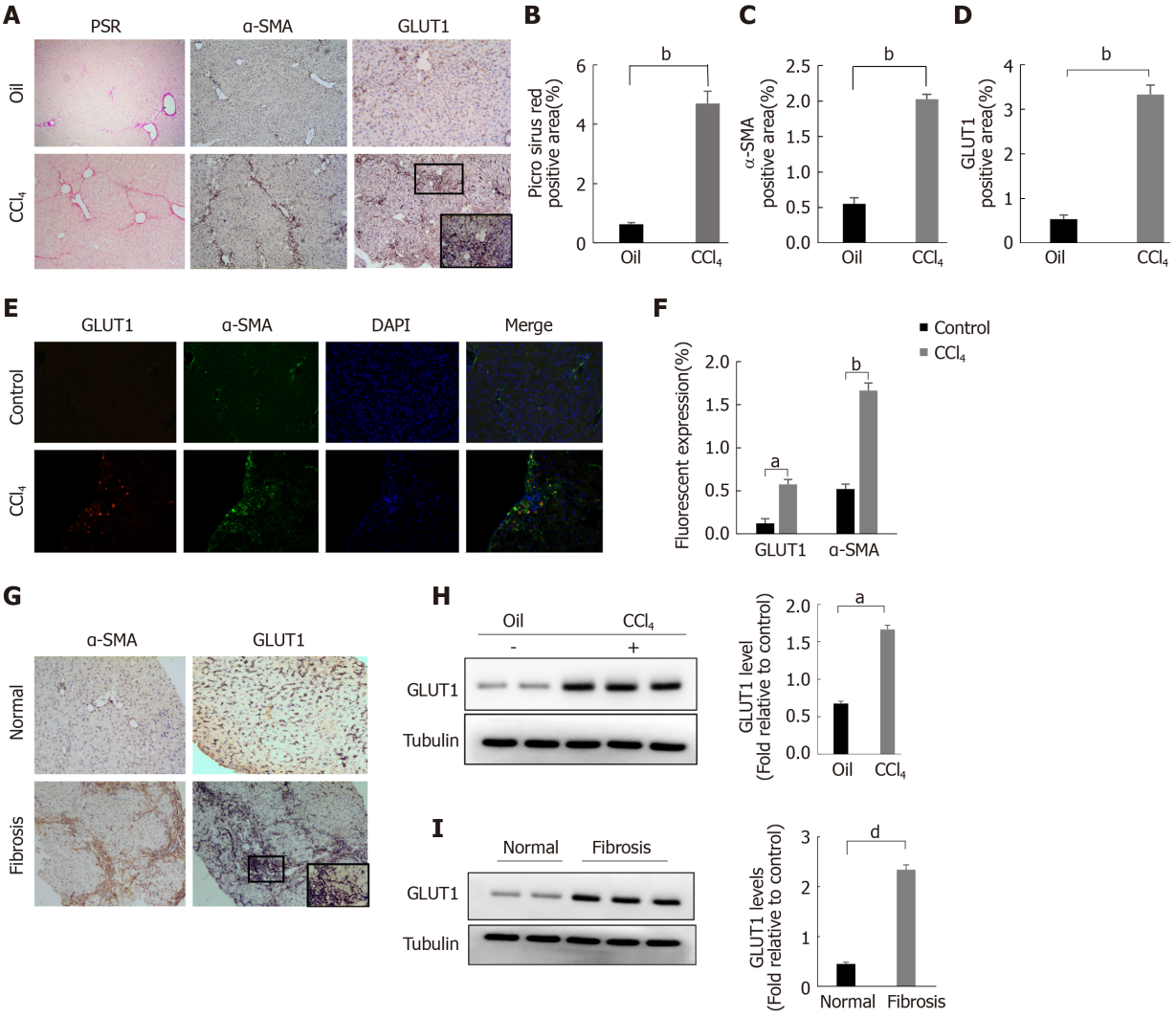


Figure 1 Glucose transporter 1 expression is correlated with liver fibrosis progression. A-D: The classic mouse model of CCl_4-induced liver fibrosis was used to first clarify whether glucose transporter 1 (GLUT1) is related to liver fibrosis. Sirius red staining and alpha-smooth muscle actin (α-SMA) immunohistochemical (IHC) staining were used to confirm that the liver fibrosis model was successfully established, and then the mice were randomly divided into the CCl_4 group and the control oil group (n = 6-10 mice/group) (A); Evaluation of liver fibrosis using Sirius red staining (B); Determination of the area ratio of positive IHC staining for α-SMA in the mouse CCl_4-induced liver fibrosis model (C); GLUT1 expression was more abundant in the liver tissue samples from the model group (D); E and F: Immunofluorescence staining for GLUT1 (red) and α-SMA (green) in the CCl_4 model. Cell nuclei were counterstained with DAPI. Scale bar for immunofluorescence staining, 200 μm; scale bars for IHC staining and Sirius red staining, 200 μm; G: IHC staining for α-SMA and GLUT1 in the healthy control and liver fibrosis groups (scale bar, 100 μm); H: Western blot analysis of changes in GLUT1 protein levels in the oil group and the CCl_4 model group; I: Western blot analysis of GLUT1 protein expression in human liver tissues from the healthy control group and the liver fibrosis group. Data in B-D, G and H are presented as the mean ± SE. Statistically significant differences were detected (compared with the oil group, $^aP < 0.05$ and $^bP < 0.01$; compared with the healthy control group, $^dP < 0.05$). GLUT1: Glucose transporter 1; α-SMA: Alpha-smooth muscle actin.

stimulation (Figure 3A and B), and phosphorylation occurred at time points close to when GLUT1 expression increased. Next, the direct role of Smads in GLUT1 induction was explored. Smad3 or Smad4 overexpression plasmids were first transiently transfected into HSCs, and then certain groups of HSCs were induced with TGF-β1 for 4 h. Smad3 or Smad4 overexpression promoted GLUT1 expression, and TGF-β1 addition amplified these effects, resulting in a further increase in GLUT1 expression (Figure 3C and D). Smad2/3 and/or Smad4 siRNAs were used to silence their expression levels and to better understand the roles of Smads in the relationship between TGF-β1 and GLUT1 expression, and the analysis performed at 48 h after the transfection of Smad2/3 and/or Smad4 siRNAs showed that TGF-β1-mediated GLUT1 expression was significantly reduced. This change was more significant and the decrease in GLUT1 expression was more substantial when the cells were transfected simultaneously with both siRNAs (Figure 3G and H). Finally, HSCs were sequentially treated with the Smad inhibitor SIS3 for 2 h and then with TGF-β1 for 4 h, resulting in

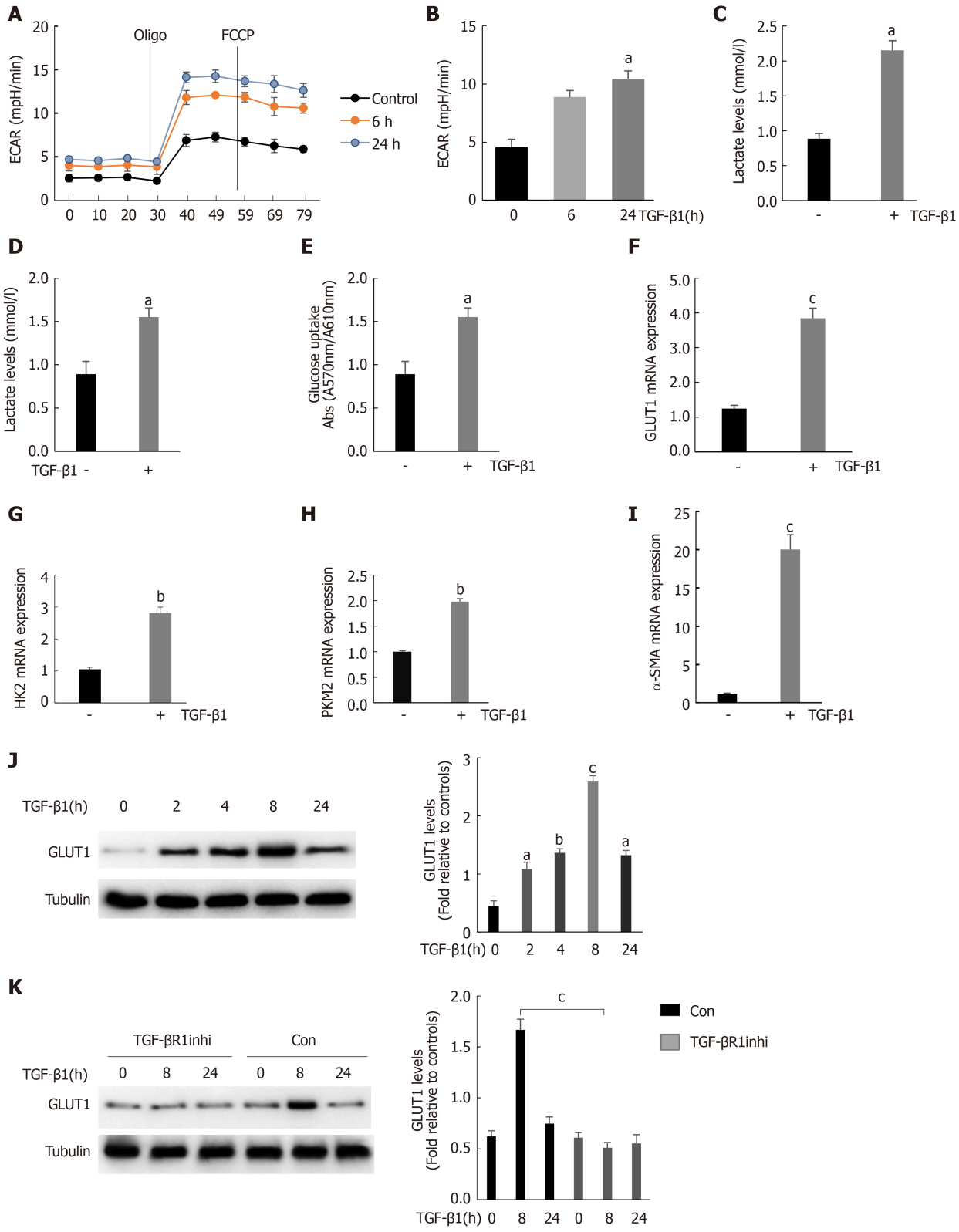


Figure 2 Stimulation of hepatic stellate cells with transforming growth factor-β1 induces glucose transporter 1 expression and promotes glycolysis. A: Serum-starved (for 20 h) primary mouse hepatic stellate cells (HSCs) were seeded into Seahorse XF-24 cell culture microplates (5×10^4 cells/well). The cells were first treated with transforming growth factor-β1 (TGF-β1) (3 ng/mL) for 0, 6 or 24 h, followed by sequential treatment with oligomycin (Oligo) and carbonyl cyanide 4-(trifluoromethoxy)phenylhydrazone (FCCP). The extracellular acidification rate (ECAR) was recorded in real time; B: The basic ECAR. $n = 6$; the mean ± SE; $^aP < 0.05$ compared to the level before TGF-β1 treatment (0 h); unpaired *t* test; C and D: Mouse HSCs were treated with or without TGF-β1 (3 ng/mL) for 24 h. The cells were then lysed, and the lactic acid contents in the cell lysate (C) and the culture medium (D) were examined; E: Determination of glucose consumption in the culture medium; F-I: Mouse HSCs were treated with or without TGF-β1 (3 ng/mL) for 24 h. RNA was purified, and RT-PCR was performed to examine the expression levels of glucose transporter 1 (GLUT1) (F), HK-2 (G), PKM-2 (H) and α-SMA (I), $n = 5$, the mean ± SE; $^aP < 0.05$, $^bP < 0.01$ and $^cP < 0.001$ compared with those at 0 h or those in the TGF-β1-untreated group; one-way analysis of variance (ANOVA); J: Western blot analysis of the expression levels of

GLUT1 and tubulin at various time points after HSCs were treated with TGF-β1 (3 ng/mL); K: Examination of the changes in GLUT1 and tubulin levels after sequential treatment with a type 1 TGF-β receptor inhibitor (LY2109761, 2 μm) for 1 h and then with TGF-β1 (3 ng/mL) for 0, 8 or 24 h. All experiments shown in A-E and F-I were performed 2-3 times. Inhi: Inhibitor; Con: Control; FCCP: Carbonyl cyanide 4-(trifluoromethoxy)phenylhydrazone; ECAR: Extracellular acidification rate; GLUT1: Glucose transporter 1; TGF-β1: Transforming growth factor-β1.

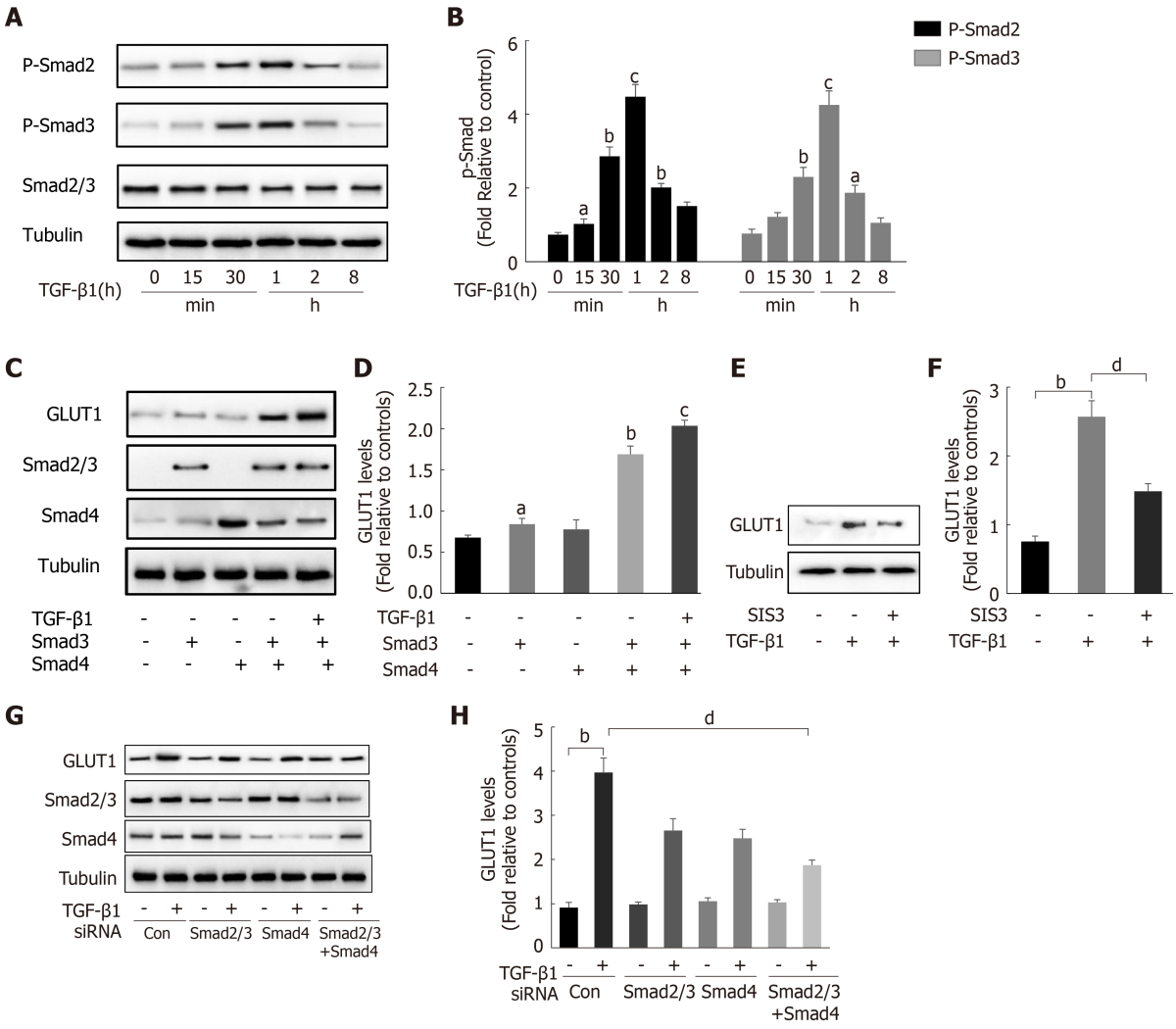


Figure 3 Transforming growth factor-β1 induces glucose transporter 1 expression through the Smad pathway. A and B: Serum-starved (for 20 h) primary mouse hepatic stellate cells (HSCs) were treated with transforming growth factor-β1 (TGF-β1) (3 ng/mL) and examined at various time points. Western blot analysis using specific antibodies (A). Quantitative analysis of the levels of the p-Smad2 and p-Smad3 proteins in five independent experiments (B); C and D: After transiently transfecting HSCs with 2 μg of Smad3 and/or Smad4 expression plasmids, the cells were cultured in serum-free medium for 48 h and then treated with TGF-β1 (3 ng/mL) for 4 h. Green fluorescent protein (GFP) was used as a transfection control. Western blot analysis using specific antibodies (C). Quantitative analysis of glucose transporter 1 (GLUT1) protein expression in five independent experiments (D); E and F: HSCs were first pretreated with a Smad3 inhibitor (SIS3, 20 μm) for 1 h and then treated with TGF-β1 (3 ng/mL) for 4 h. Western blot analysis using specific antibodies (E). Quantitative analysis of the GLUT1 protein level in five independent experiments (F); G and H: Mouse primary HSCs were transfected with 20 μmol/L control small interfering RNAs (siRNAs) or siRNAs targeting Smad2/3 and Smad4. After transfection in serum-free medium for 48 h, the cells were treated with TGF-β1 (3 ng/mL) for 4 h. Western blot analysis using specific antibodies (G). Quantitative analysis of the GLUT1 protein level in five independent experiments (H) (the mean ± SE; $^{a}P < 0.05$, $^{b}P < 0.01$ and $^{c}P < 0.001$ compared with that in the group of cells without TGF-β1; $^{d}P < 0.05$ for the comparison of the groups treated with TGF-β1 and the groups treated with TGF-β1 and different additional reagents; Student's *t* test). GLUT1: Glucose transporter 1; TGF-β1: Transforming growth factor-β1; Con: Control; siRNAs: Small interfering RNAs.

a significant decrease in GLUT1 protein expression (Figure 3E and F). These results preliminarily indicate the important regulatory role of Smad proteins in TGF-β1-mediated GLUT1 expression and suggest that Smad proteins directly participate in the regulation of GLUT1 by TGF-β1.

The noncanonical p38 MAPK and PI3K/AKT signaling pathways are also involved in TGF-β1-mediated GLUT1 induction

During fibrosis development, TGF-β1 activates not only the canonical Smad pathway

but also noncanonical pathways (such as the PI3K/AKT and p38 MAPK signaling pathways). In addition, the Smad pathway and non-Smad pathways are mutually dependent[28]. Therefore, we questioned whether a non-Smad pathway is involved in the TGF-β1-mediated induction of GLUT1. Changes in the phosphorylation levels of p38 and AKT in HSCs after TGF-β1 stimulation were examined to answer this question. Western blot analyses showed increased levels of phosphorylated p38 and AKT in HSCs after TGF-β1 treatment (Figure 4A-C). HSCs were pretreated with the specific p38 MAPK inhibitor SB203580 and the PI3K inhibitor LY294002 for 1 h and then induced with TGF-β1 to understand the bridging role of p38 MAPK and AKT in TGF-β1-mediated GLUT1 expression. Western blot analyses showed that p-AKT activity was significantly inhibited and that GLUT1 protein expression was significantly reduced (Figure 4D). S6 ribosomal protein and heat shock protein 25 (Hsp25) are downstream proteins in the PI3K/AKT and p38 MAPK pathways, and their phosphorylation was also inhibited. Addition of the p38 inhibitor reduced the phosphorylation of the S6 protein, and the phosphorylation level of Smad2 was also affected; however, Smad3 was not significantly affected (Figure 4D and E). The above results indicate that (1) GLUT1 expression in HSCs did not rely solely on the TGF-β1-mediated Smad pathway, *i.e.*, the p38 MAPK and PI3K/AKT signaling pathways were also involved in TGF-β1-mediated GLUT1 expression, and (2) TGF-β1-mediated pathways did not act independently, as mutual restrictions and interactions between the pathways were observed. Based on the results described above, the effects of inhibiting the Smad3, p38 MAPK and PI3K/AKT pathways on GLUT1 expression were analyzed, and the simultaneous addition of inhibitors of the Smad3, p38 MAPK and PI3K/AKT pathways significantly reduced TGF-β1-mediated GLUT1 expression (Figure 4F and G). In summary, TGF-β1 requires the participation of non-Smad pathways to induce GLUT1 expression during HSC activation.

The effect of GLUT1 on HSC migration and proliferation

Cells were first treated with phloretin (a specific inhibitor of GLUT1) for 30 min or transfected with an siRNA targeting GLUT1, followed by treatment with TGF-β1 for 4 h. The targeted inhibition of GLUT1 by phloretin and the siRNA suppressed the effect of TGF-β1 on the migration and proliferation of HSCs (Figure 5A, B and E). Western blot analyses also showed that siRNA transfection effectively inhibited TGF-β1-induced GLUT1 expression (Figure 5C and D). Therefore, inhibition of GLUT1 expression reverses the effect of TGF-β1 on the migration and proliferation of HSCs and delays the process of HSC transdifferentiation into myofibroblasts. No noticeable effect of the control siRNA on proliferation was identified between TGF-β1-treated cells and TGF-β1/siRNA-control-treated cells or between control/saline-treated cells and saline/siRNA-control-treated cells (Figure 5E). In addition, no obvious effect of siRNA interference on cell viability (Supplementary Figure 2) or the expression of TGF-β receptors was found (Supplementary Figure 3).

GLUT1 inhibition delays the development of liver fibrosis in a mouse model of liver fibrosis

In vitro experiments confirmed the importance of GLUT1 in liver fibrosis. Next, we examined whether inhibition of GLUT1 expression suppressed liver fibrosis *in vivo*. Phloretin, a specific inhibitor of GLUT1, was used, and its effect on CCl_4-induced liver fibrosis was examined. After successful establishment of the CCl_4-induced model, an i.p. injection of phloretin was administered three times a week; the intervention was discontinued after 2 wk. A simple technical roadmap is shown in Figure 6A. Compared with those in the model group, the areas of collagen fiber deposition were significantly reduced in the liver tissues from mice in the drug intervention group; these findings were confirmed by Masson's trichrome and Sirius red staining (Figure 6B-D). The degree of liver inflammation was determined by performing serological assessments of changes in ALT and AST levels, and the results indicated that the degree of inflammation was significantly reduced in the drug intervention group (Figure 6E and F). Therefore, the *in vivo* results revealed that GLUT1 inhibition reduces CCl_4-induced liver fibrosis.

DISCUSSION

In normal liver tissues, quiescent HSCs express TGF-β1 at low levels, while TGF-β1 is immediately upregulated after acute or chronic liver injury and interacts with multiple signaling pathways to induce HSC activation and proliferation and extensive ECM

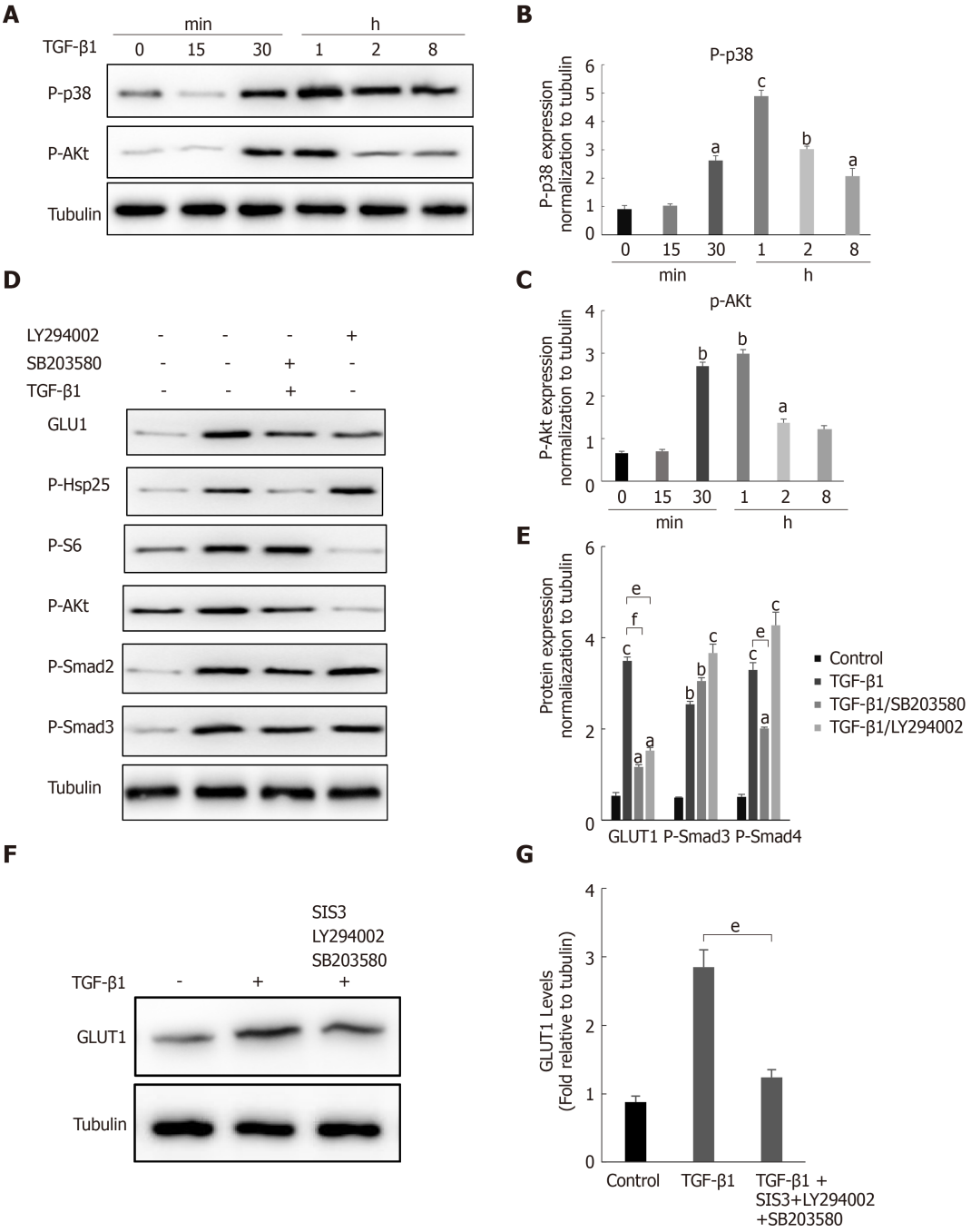


Figure 4 The noncanonical p38 MAPK and PI3K/AKT signaling pathways are also involved in transforming growth factor-β1-mediated glucose transporter 1 expression. A-C: Serum-starved (for 20 h) primary mouse hepatic stellate cells (HSCs) were treated with transforming growth factor-β1 (TGF-β1) (3 ng/mL) and examined at different time points. Western blot analysis using specific antibodies (A). Five independent experiments were performed to quantitatively analyze the levels of phosphorylated p38 (B) MAPK and AKT (C); D and E: HSCs cultured in serum-free medium were pretreated with the p38 MAPK inhibitor SB203580 (10 μm) or the PI3K inhibitor LY294002 (10 μm) for 1 h and then treated with TGF-β1 (3 ng/mL) for 4 h. Western blot analysis using specific antibodies (D). Quantitative analysis of the levels of glucose transporter 1 (GLUT1) and phosphorylated Smad2 and Smad3 proteins (E); F and G: HSCs cultured in serum-free medium were pretreated with the p38 MAPK inhibitor SB203580 (10 μm), the PI3K inhibitor LY294002 (10 μm) and the Smad inhibitor SIS3 (20 μm) for 1 h and then treated with TGF-β1 (3 ng/mL) for 4 h. Western blot analysis using specific antibodies (F). Quantitative analysis of the GLUT1 protein level (G) (the mean ± SE; $^{a}P < 0.05$, $^{b}P < 0.01$ and $^{c}P < 0.001$ compared with the TGF-β1-treated group or the TGF-β1-untreated group, $^{d}P < 0.05$, $^{e}P < 0.01$ and $^{f}P < 0.001$ for the comparison of the group treated with TGF-β1 and the groups treated with TGF-β1 and the corresponding inhibitors; Student's *t* test). GLUT1: Glucose transporter 1; TGF-β1: Transforming growth factor-β1.

production[29,30]. TGF-β1 enhances aerobic glycolysis, amino acid uptake and lactic acid production in Ras- and Myc-transformed cells. TGF-β1 contributes to the metabolic reprogramming of cancer cells and tumor-associated stromal cells[31]. When used to replace a peritoneal dialysis solution, TGF-β1 stimulates glycolysis and inhibits mitochondrial respiration of mesothelial cells, thus promoting the development of peritoneal fibrosis[32]. Preliminary yet strong evidence supporting the importance of

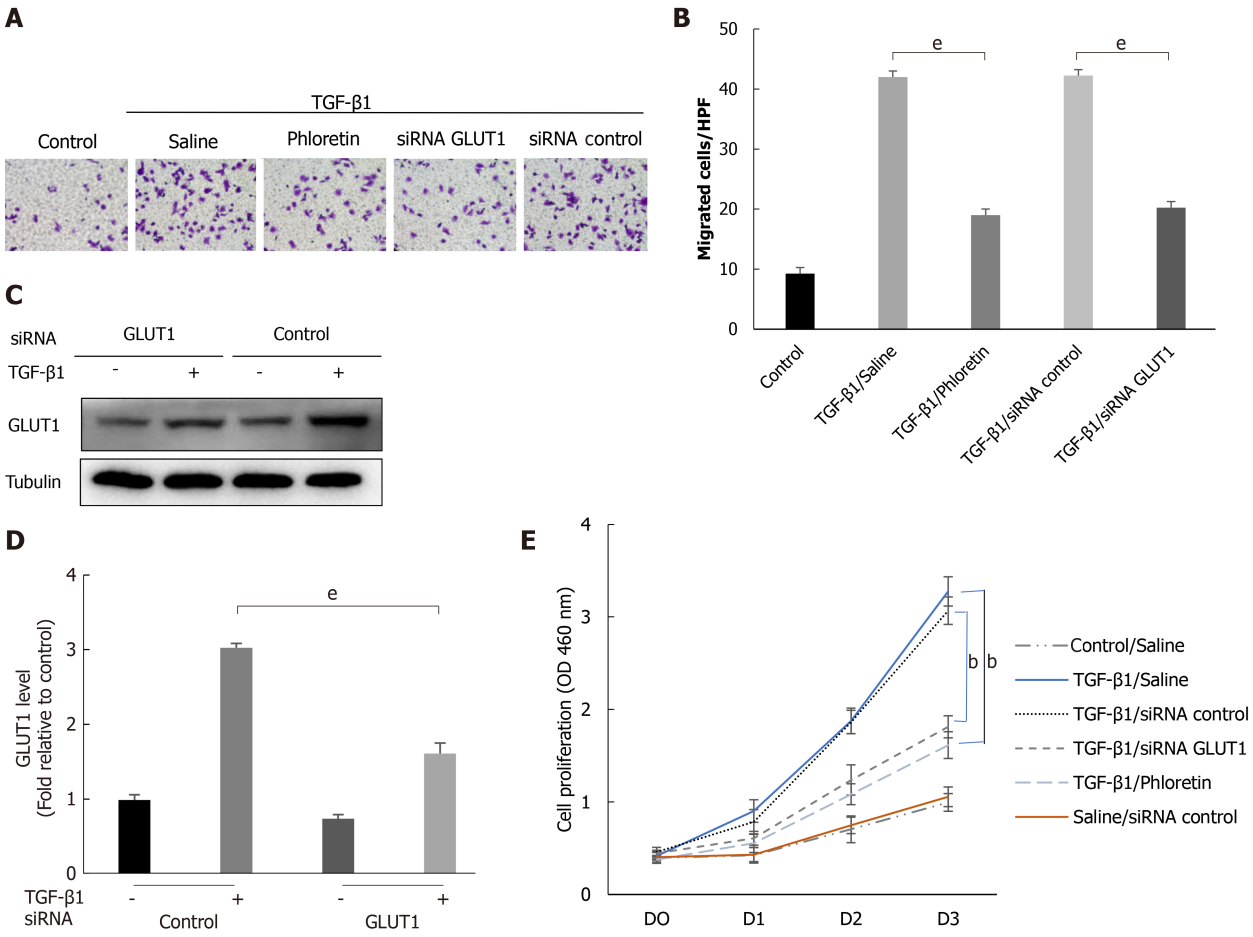


Figure 5 The effect of glucose transporter 1 on the growth and proliferation of hepatic stellate cell. Mouse primary hepatic stellate cells (HSCs) were 1) pretreated with the glucose transporter 1 (GLUT1) inhibitor phloretin (50 μm) for 30 min and then treated with transforming growth factor-β1 (TGF-β1) (3 ng/mL) for 4 h or 2) transiently transfected with small interfering RNAs that inhibited GLUT1 expression, cultured in serum-free medium for 24 h and then treated with TGF-β1 (3 ng/mL) for 4 h. A: Cells were seeded in serum-free medium (4 × 10^5 cells/well) in the upper chambers of a Transwell system. The lower chambers were filled with 5% glucose medium (700 μL per well). Changes in cell migration were observed. Representative images of crystal violet staining are shown; B: Quantitative data showing the number of migrating cells in each group; C: Western blot analysis using specific antibodies; D: Quantitative analysis of GLUT1 protein expression in three independent experiments; E: The effect of GLUT1 inhibition on the growth/proliferation of HSCs (mean ± SE; $^bP < 0.01$ and $^cP < 0.001$ compared with the group without TGF-β1; $^eP < 0.01$ for the comparison of the TGF-β1-treated group with the groups subjected to TGF-β1 treatment and different interventions; Student's *t* test). GLUT1: Glucose transporter 1; TGF-β1: Transforming growth factor-β1; siRNAs: Small interfering RNAs.

metabolic reprogramming in the activation of fibroblasts is steadily accumulating. Research on the mechanism of organ fibrosis also shows that TGF-β1 is related to the occurrence of aerobic glycolysis and mitochondrial dysfunction. The transdifferentiation of resting HSCs into hepatic fibroblasts has been confirmed to be related to mutual transformation between glycolytic enzymes and gluconeogenic enzymes triggered by Hedgehog signaling[33]. Glycolysis is an important pathway of glucose metabolism, and GLUT1 is the most widely expressed glucose transporter in mammals; its expression is regulated by changes in metabolic status and oxidative stress. GLUT1 is also an important marker of liver carcinogenesis and metabolic liver diseases[34]. GLUT1-dependent glycolysis exacerbates lung fibrogenesis during *Streptococcus pneumoniae* infection *via* AIM2 inflammasome activation[35]. In the pathogenesis of diabetic glomerulosclerosis, TGF-β1 triggers GLUT1 activation by stretching glomerular mesangial cells. In breast cancer cells, long-term exposure to TGF-β1 restores GLUT1 expression and results in stable EMT and unlimited cell proliferation[36,37]. Therefore, we questioned whether TGF-β1 and GLUT1 are related to liver fibrosis.

This study showed a significant increase in GLUT1 expression in human and mouse fibrotic liver tissues, which is consistent with the research results of Wan *et al*[24]. With the increase in TGF-β1 Levels, the gene expression levels of key enzymes, including GLUT1, in the glycolytic pathway are elevated, glucose consumption and intracellular lactate production are also increased, and glycolytic flux by HSCs is enhanced. As expected, the results of this study are consistent with those of previous studies

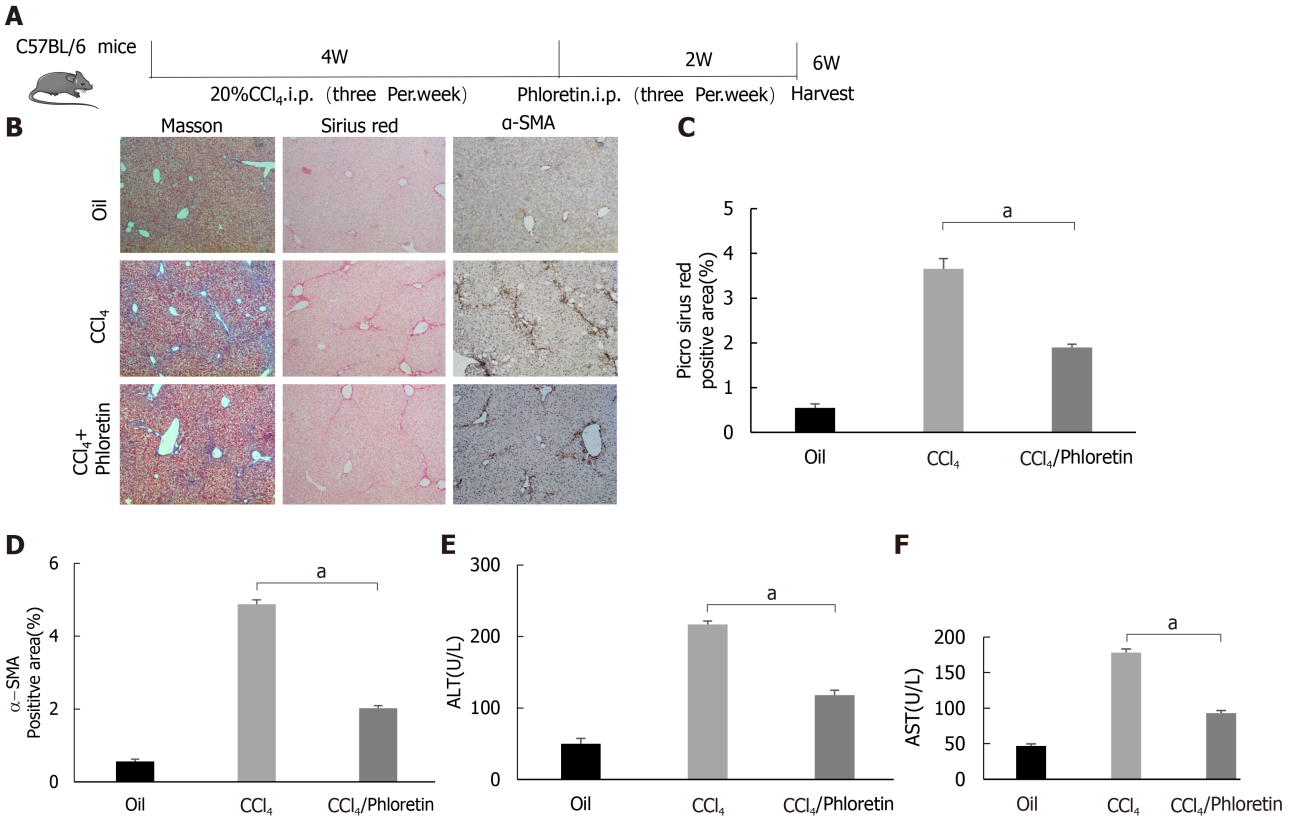


Figure 6 Glucose transporter 1 inhibition delays the development of liver fibrosis in a mouse model of liver fibrosis. A: Schematic diagram of the experiment. C57BL/6 mice were injected intraperitoneally with CCl_4 to induce liver fibrosis. The model was successfully established after 4 wk. Among the treatment groups, the CCl_4 + phloretin group was intraperitoneally injected with phloretin (10 mg/kg) three times a week, and the CCl_4 group was injected with normal saline as a control. The treatments were discontinued after 2 wk; B: Mouse livers were collected, and liver tissue sections were prepared. The sections were subjected to Masson's trichrome staining, Sirius red staining and alpha-smooth muscle actin (α-SMA) immunohistochemical (IHC) staining (original magnification, × 10); C: The positive area ratio detected using Sirius red staining; D: The positive area ratio for α-SMA IHC staining; E and F: Serological analysis of ALT (E) and AST (F) levels (n = 5-7; the mean ± SE; scale bar, 100 μm; $^aP < 0.05$ for the comparison between the CCl_4 group and the CCl_4 + phloretin group; Student's t test). α-SMA: Alpha-smooth muscle actin.

assessing the mechanism of metabolic reprogramming of pulmonary fibrotic fibroblasts[38], indicating that TGF-β1 induces aerobic glycolysis and drives the occurrence of metabolic reprogramming during the process of stromal cell transdifferentiation. Increased GLUT1 expression also contributes to an elevated glycolytic rate, increased lactic acid production and enhanced glucose-dependent metabolic pathways in cells. In contrast, GLUT1 expression decreased significantly after the addition of a TGF-β1 receptor inhibitor, indicating that GLUT1 expression is related to TGF-β1 signaling. Experiments involving Smad overexpression, siRNA-mediated knockout and Smad inhibitors showed that the response of GLUT1 to TGF-β1 was at least partially dependent on the Smad pathway. Studies have identified a cascade of related pathways activated by TGF-β1. Therefore, this study attempted to verify whether non-Smad pathways were also involved in the induction of GLUT1 expression in HSCs. The noncanonical PI3K/AKT and p38 MAPK pathways activated by TGF-β1 were examined. In colorectal cancer (CRC) cells, silencing GLUT1 expression inactivates the TGF-β1/PI3K/AKT signaling pathway, inhibits the proliferation of CRC cells and promotes apoptosis. MAPK activation by TGF-β1 may trigger GLUT1 synthesis[39, 40]. Based on the results of the present study, the simultaneous addition of specific inhibitors of the PI3K/AKT and p38 pathways, *i.e.*, SB203580 and LY294002, respectively, reduced TGF-β1-induced GLUT1 protein expression. The addition of the p38 pathway inhibitor resulted in a decrease in Smad2 protein phosphorylation, changes in the phosphorylated AKT level and changes in the phosphorylation level of a protein downstream of PI3K/AKT signaling (namely, S6); therefore, we speculated that the p38 MAPK pathway acted as a bridge between the TGF-β1-mediated Smad and AKT pathways in HSCs and that reduced activation of the p38 MAPK pathway would inhibit the latter two pathways. In addition, the p38 MAPK pathway might limit Smad pathway-mediated GLUT1 expression to a certain extent. These results are consistent with the previously reported crosstalk between Smad and p38 MAPK in

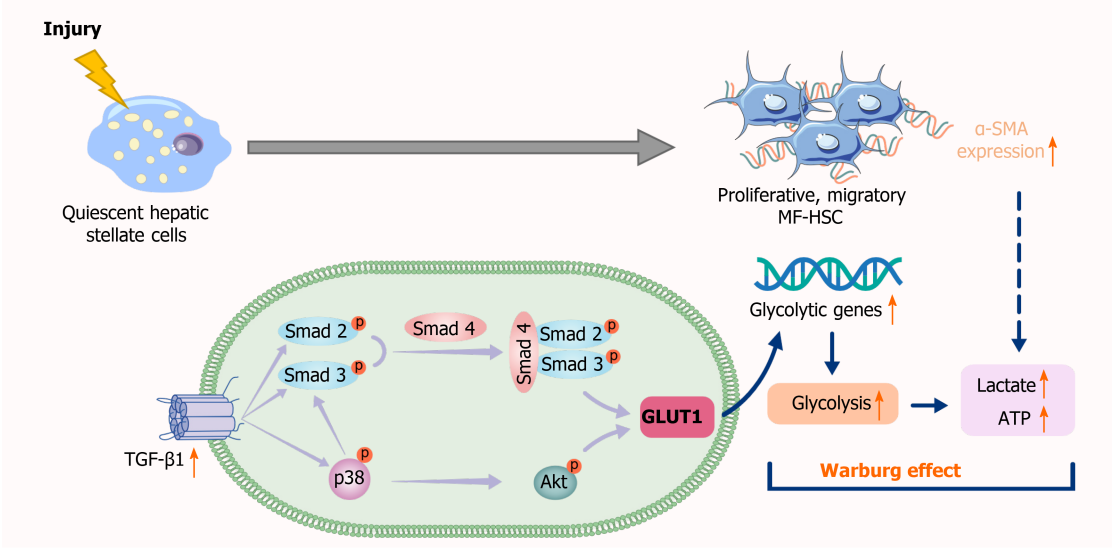


Figure 7 Schematic representation of the mechanisms implicated in canonical and noncanonical transforming growth factor-β pathways regulating glucose transporter 1 expression. TGF-β1: Transforming growth factor-β1; GLUT1: Glucose transporter 1; MF-HSC: Myofibroblasts-hepatic stellate cells; α-SMA: Alpha-smooth muscle actin.

TGF-β1 signal transduction in human glioblastoma cells[41]. However, the specific mechanism underlying the interaction among TGF-β1 pathways in the induction of aerobic glycolysis in stellate cells requires further study. The significant reduction in GLUT1 protein expression was related to the simultaneous inhibition of the Smad3, p38 MAPK and PI3K signaling pathways, indicating that GLUT1 protein expression during stellate cell activation requires the activation and signaling of these three pathways. Moreover, activation of the p38 MAPK pathway might result in a certain synergistic effect with the Smad2/3 pathway (Figure 7).

TGF-β1 is a pleiotropic cytokine with an important role in the occurrence of liver fibrosis. According to previous studies, TGF-β1 signaling clearly promotes cell migration, matrix synthesis and HSC differentiation toward myofibroblasts. Moreover, the effect of TGF-β1 on fibroblast migration and proliferation depends on changes in the microenvironment[42]. As shown in the present study, TGF-β1 promoted the proliferative and migratory capabilities of HSCs, functions that are hallmarks of cell transformation. The addition of a pharmacological inhibitor of GLUT1 activity (phloretin, an effective GLUT1 inhibitor capable of inhibiting bleomycin-induced pulmonary fibrosis *in vivo*[43]) and silencing of the GLUT1 gene eliminated TGF-β1-induced proliferation, growth and migration. Finally, a GLUT1 inhibitor was used in *in vivo* experiments, and the degree of mouse liver fibrosis improved, collagen fiber deposition decreased, and the degree of inflammation decreased. Given the importance of GLUT1, the experimental results revealed that GLUT1 is involved in aerobic glycolysis during HSC activation and that aerobic glycolysis is a response to TGF-β1 signaling mediated by the Smad, PI3K/AKT and p38 MAPK pathways.

CONCLUSION

In summary, TGF-β1-induced GLUT1 expression may be one of the mechanisms involved in the reprogramming of HSCs, providing an expanded basis and new insights for the mechanism of action of TGF-β1 in metabolic reprogramming during liver fibrosis. GLUT1 plays an important role in aerobic glycolysis in HSCs and in promoting cell proliferation and transformation. GLUT1 inhibition may be an alternative therapy to the current traditional treatments for liver fibrosis. However, the extent to which GLUT1 inhibition contributes to elimination of the profibrotic effect of TGF-β1 and the specific molecular mechanisms of the interaction between the two may require verification using approaches combining proteomics and single-cell sequencing, which may be an attractive research direction in the future.

ARTICLE HIGHLIGHTS

Research background

Liver fibrosis is a refractory disease that develops progressively and eventually evolves into liver cirrhosis or even liver cancer. Hepatic stellate cell (HSC) activation is the initiating factor for liver fibrosis, while aerobic glycolysis is one of the main metabolic characteristics. Transforming growth factor-β1 (TGF-β1) is the most important profibrotic factor in HSCs, and TGF-β1 drives metabolic reprogramming. Glucose transporter 1 (GLUT1) is the most widely distributed glucose transporter in mammals and is related to glycolytic metabolism. However, the role of GLUT1 in liver fibrosis and the relationship between GLUT1 and TGF-β1 remain unclear and require further investigation.

Research motivation

The results of this study might provide a basis for the application of GLUT1 in the treatment of liver fibrosis and provide an expanded basis for understanding the mechanism of action of TGF-β1 in metabolic reprogramming during liver fibrosis.

Research objectives

This study examined changes in GLUT1 expression in human and mouse fibrotic liver tissues and differences in extracellular acid production and in the expression levels of key glycolytic enzymes and GLUT1 during HSC activation induced by TGF-β1-related pathways. In addition, this study further explored the relationship between TGF-β1 pathways and GLUT1 expression and the potential underlying molecular mechanisms.

Research methods

IHC was employed to examine changes in GLUT1 expression in human and mouse fibrotic liver tissues. Immunofluorescence staining was performed to examine changes in GLUT1 and alpha-smooth muscle actin (α-SMA) expression in mouse fibrotic liver tissue. Primary mouse stellate cells were isolated. After activation of the cells by TGF-β 1 stimulation, changes in extracellular acid production, key glycolytic enzymes and glucose consumption were examined. In addition, changes in GLUT1 expression were explored by activating/inhibiting the Smad2/3 pathway and inhibiting the expression of proteins related to the p38 and PI3K/AKT pathways. Finally, in mice with liver fibrosis, the effect of a GLUT1 inhibitor on liver fibrosis was investigated by performing Masson's trichrome staining and Sirius red staining and analyzing serological inflammatory markers.

Research results

The expression of the GLUT1 protein was increased in both mouse and human fibrotic liver tissue.immunofluorescence staining revealed the colocalization of GLUT1 and α-SMA proteins, indicating that GLUT1 expression was related to the development of liver fibrosis. TGF-β1 induced an increase in aerobic glycolysis in HSCs and induced GLUT1 expression in HSCs by activating the canonical and noncanonical signaling pathways. The p38 MAPK pathway and the Smad pathway synergistically affected the induction of GLUT1 expression. GLUT1 inhibition eliminated the effect of TGF-β1 on the proliferation and migration of HSCs. A GLUT1 inhibitor was administered to a mouse model of liver fibrosis, and GLUT1 inhibition reduced the degree of liver inflammation.

Research conclusions

GLUT1 expression was upregulated in liver fibrosis, and the underlying mechanism was related to activation of the Smad2/3, p38 and PI3K/AKT pathways by TGF-β1, which directly induced GLUT1 expression and promoted glycolysis. GLUT1 inhibition eliminated TGF-β1-induced HSC activation, proliferation and migration, and GLUT1 inhibition exerted an antifibrotic effect.

Research perspectives

The results of this study reveal that the TGF-β1 pathway directly induces GLUT1 expression and aerobic glycolysis, thus promoting liver fibrosis. This study preliminarily clarified the mechanism underlying the interaction between TGF-β1 and GLUT1 in liver fibrosis, thus providing a deeper understanding of the mechanism of liver fibrosis and providing guidance for the selection of targets to treat liver fibrosis. The results from this study indicate that GLUT1 inhibitors may have certain

prospective applications as therapeutic drugs for liver fibrosis.

ACKNOWLEDGEMENTS

The authors thank Dr. Ding Q for expert technical assistance.

REFERENCES

1 **Ni Y**, Li JM, Liu MK, Zhang TT, Wang DP, Zhou WH, Hu LZ, Lv WL. Pathological process of liver sinusoidal endothelial cells in liver diseases. *World J Gastroenterol* 2017; **23**: 7666-7677 [PMID: 29209108 DOI: 10.3748/wjg.v23.i43.7666]

2 **Hernandez-Gea V**, Friedman SL. Pathogenesis of liver fibrosis. *Annu Rev Pathol* 2011; **6**: 425-456 [PMID: 21073339 DOI: 10.1146/annurev-pathol-011110-130246]

3 **Higashi T**, Friedman SL, Hoshida Y. Hepatic stellate cells as key target in liver fibrosis. *Adv Drug Deliv Rev* 2017; **121**: 27-42 [PMID: 28506744 DOI: 10.1016/j.addr.2017.05.007]

4 **Vallée A**, Lecarpentier Y, Vallée JN. Thermodynamic Aspects and Reprogramming Cellular Energy Metabolism during the Fibrosis Process. *Int J Mol Sci* 2017; **18** [PMID: 29186898 DOI: 10.3390/ijms18122537]

5 **Vander Heiden MG**, Cantley LC, Thompson CB. Understanding the Warburg effect: the metabolic requirements of cell proliferation. *Science* 2009; **324**: 1029-1033 [PMID: 19460998 DOI: 10.1126/science.1160809]

6 **Chen Y**, Choi SS, Michelotti GA, Chan IS, Swiderska-Syn M, Karaca GF, Xie G, Moylan CA, Garibaldi F, Premont R, Suliman HB, Piantadosi CA, Diehl AM. Hedgehog controls hepatic stellate cell fate by regulating metabolism. *Gastroenterology* 2012; **143**: 1319-1329.e11 [PMID: 22885334 DOI: 10.1053/j.gastro.2012.07.115]

7 **Henderson NC**, Rieder F, Wynn TA. Fibrosis: from mechanisms to medicines. *Nature* 2020; **587**: 555-566 [PMID: 33239795 DOI: 10.1038/s41586-020-2938-9]

8 **Syed V**. TGF-β Signaling in Cancer. *J Cell Biochem* 2016; **117**: 1279-1287 [PMID: 26774024 DOI: 10.1002/jcb.25496]

9 **Zhang YE**. Non-Smad Signaling Pathways of the TGF-β Family. *Cold Spring Harb Perspect Biol* 2017; **9** [PMID: 27864313 DOI: 10.1101/cshperspect.a022129]

10 **Derynck R**, Budi EH. Specificity, versatility, and control of TGF-β family signaling. *Sci Signal* 2019; **12** [PMID: 30808818 DOI: 10.1126/scisignal.aav5183]

11 **Heldin CH**, Moustakas A. Signaling Receptors for TGF-β Family Members. *Cold Spring Harb Perspect Biol* 2016; **8** [PMID: 27481709 DOI: 10.1101/cshperspect.a022053]

12 **Wrana JL**, Attisano L, Wieser R, Ventura F, Massagué J. Mechanism of activation of the TGF-beta receptor. *Nature* 1994; **370**: 341-347 [PMID: 8047140 DOI: 10.1038/370341a0]

13 **Dennler S**, Itoh S, Vivien D, ten Dijke P, Huet S, Gauthier JM. Direct binding of Smad3 and Smad4 to critical TGF beta-inducible elements in the promoter of human plasminogen activator inhibitor-type 1 gene. *EMBO J* 1998; **17**: 3091-3100 [PMID: 9606191 DOI: 10.1093/emboj/17.11.3091]

14 **Dewidar B**, Meyer C, Dooley S, Meindl-Beinker AN. TGF-β in Hepatic Stellate Cell Activation and Liver Fibrogenesis-Updated 2019. *Cells* 2019; **8** [PMID: 31718044 DOI: 10.3390/cells8111419]

15 **Zhao X**, Kwan JYY, Yip K, Liu PP, Liu FF. Targeting metabolic dysregulation for fibrosis therapy. *Nat Rev Drug Discov* 2020; **19**: 57-75 [PMID: 31548636 DOI: 10.1038/s41573-019-0040-5]

16 **Soukupova J**, Malfettone A, Bertran E, Hernández-Alvarez MI, Peñuelas-Haro I, Dituri F, Giannelli G, Zorzano A, Fabregat I. Epithelial-Mesenchymal Transition (EMT) Induced by TGF-β in Hepatocellular Carcinoma Cells Reprograms Lipid Metabolism. *Int J Mol Sci* 2021; **22** [PMID: 34073989 DOI: 10.3390/ijms22115543]

17 **Kottmann RM**, Kulkarni AA, Smolnycki KA, Lyda E, Dahanayake T, Salibi R, Honnons S, Jones C, Isern NG, Hu JZ, Nathan SD, Grant G, Phipps RP, Sime PJ. Lactic acid is elevated in idiopathic pulmonary fibrosis and induces myofibroblast differentiation *via* pH-dependent activation of transforming growth factor-β. *Am J Respir Crit Care Med* 2012; **186**: 740-751 [PMID: 22923663 DOI: 10.1164/rccm.201201-0084OC]

18 **Chen LQ**, Cheung LS, Feng L, Tanner W, Frommer WB. Transport of sugars. *Annu Rev Biochem* 2015; **84**: 865-894 [PMID: 25747398 DOI: 10.1146/annurev-biochem-060614-033904]

19 **Wang L**, Pavlou S, Du X, Bhuckory M, Xu H, Chen M. Glucose transporter 1 critically controls microglial activation through facilitating glycolysis. *Mol Neurodegener* 2019; **14**: 2 [PMID: 30634998 DOI: 10.1186/s13024-019-0305-9]

20 **Hua W**, Ten Dijke P, Kostidis S, Giera M, Hornsveld M. TGFβ-induced metabolic reprogramming during epithelial-to-mesenchymal transition in cancer. *Cell Mol Life Sci* 2020; **77**: 2103-2123 [PMID: 31822964 DOI: 10.1007/s00018-019-03398-6]

21 **Liu M**, Quek LE, Sultani G, Turner N. Epithelial-mesenchymal transition induction is associated with augmented glucose uptake and lactate production in pancreatic ductal adenocarcinoma. *Cancer Metab* 2016; **4**: 19 [PMID: 27777765 DOI: 10.1186/s40170-016-0160-x]

22 **Li W**, Wei Z, Liu Y, Li H, Ren R, Tang Y. Increased 18F-FDG uptake and expression of Glut1 in the

EMT transformed breast cancer cells induced by TGF-beta. *Neoplasma* 2010; **57**: 234-240 [PMID: 20353274 DOI: 10.4149/neo_2010_03_234]

23 **Inoki K**, Haneda M, Maeda S, Koya D, Kikkawa R. TGF-beta 1 stimulates glucose uptake by enhancing GLUT1 expression in mesangial cells. *Kidney Int* 1999; **55**: 1704-1712 [PMID: 10231432 DOI: 10]

24 **Wan L**, Xia T, Du Y, Liu J, Xie Y, Zhang Y, Guan F, Wu J, Wang X, Shi C. Exosomes from activated hepatic stellate cells contain GLUT1 and PKM2: a role for exosomes in metabolic switch of liver nonparenchymal cells. *FASEB J* 2019; **33**: 8530-8542 [PMID: 30970216 DOI: 10.1096/fj.201802675R]

25 **Zhao XK**, Yu L, Cheng ML, Che P, Lu YY, Zhang Q, Mu M, Li H, Zhu LL, Zhu JJ, Hu M, Li P, Liang YD, Luo XH, Cheng YJ, Xu ZX, Ding Q. Focal Adhesion Kinase Regulates Hepatic Stellate Cell Activation and Liver Fibrosis. *Sci Rep* 2017; **7**: 4032 [PMID: 28642549 DOI: 10.1038/s41598-017-04317-0]

26 **Zou GL**, Zuo S, Lu S, Hu RH, Lu YY, Yang J, Deng KS, Wu YT, Mu M, Zhu JJ, Zeng JZ, Zhang BF, Wu X, Zhao XK, Li HY. Bone morphogenetic protein-7 represses hepatic stellate cell activation and liver fibrosis *via* regulation of TGF-β/Smad signaling pathway. *World J Gastroenterol* 2019; **25**: 4222-4234 [PMID: 31435175 DOI: 10.3748/wjg.v25.i30.4222]

27 **Morikawa M**, Derynck R, Miyazono K. TGF-β and the TGF-β Family: Context-Dependent Roles in Cell and Tissue Physiology. *Cold Spring Harb Perspect Biol* 2016; **8** [PMID: 27141051 DOI: 10.1101/cshperspect.a021873]

28 **Xu F**, Liu C, Zhou D, Zhang L. TGF-β/SMAD Pathway and Its Regulation in Hepatic Fibrosis. *J Histochem Cytochem* 2016; **64**: 157-167 [PMID: 26747705 DOI: 10.1369/0022155415627681]

29 **Simeone DM**, Zhang L, Graziano K, Nicke B, Pham T, Schaefer C, Logsdon CD. Smad4 mediates activation of mitogen-activated protein kinases by TGF-beta in pancreatic acinar cells. *Am J Physiol Cell Physiol* 2001; **281**: C311-C319 [PMID: 11401854 DOI: 10.1152/ajpcell.2001.281.1.C311]

30 **Fan W**, Liu T, Chen W, Hammad S, Longerich T, Hausser I, Fu Y, Li N, He Y, Liu C, Zhang Y, Lian Q, Zhao X, Yan C, Li L, Yi C, Ling Z, Ma L, Xu H, Wang P, Cong M, You H, Liu Z, Wang Y, Chen J, Li D, Hui L, Dooley S, Hou J, Jia J, Sun B. ECM1 Prevents Activation of Transforming Growth Factor β, Hepatic Stellate Cells, and Fibrogenesis in Mice. *Gastroenterology* 2019; **157**: 1352-1367.e13 [PMID: 31362006 DOI: 10.1053/j.gastro.2019.07.036]

31 **Olsson N**, Piek E, Sundström M, ten Dijke P, Nilsson G. Transforming growth factor-beta-mediated mast cell migration depends on mitogen-activated protein kinase activity. *Cell Signal* 2001; **13**: 483-490 [PMID: 11516623 DOI: 10.1016/s0898-6568(01)00176-0]

32 **Si M**, Wang Q, Li Y, Lin H, Luo D, Zhao W, Dou X, Liu J, Zhang H, Huang Y, Lou T, Hu Z, Peng H. Inhibition of hyperglycolysis in mesothelial cells prevents peritoneal fibrosis. *Sci Transl Med* 2019; **11** [PMID: 31167927 DOI: 10.1126/scitranslmed.aav5341]

33 **Nigdelioglu R**, Hamanaka RB, Meliton AY, O'Leary E, Witt LJ, Cho T, Sun K, Bonham C, Wu D, Woods PS, Husain AN, Wolfgeher D, Dulin NO, Chandel NS, Mutlu GM. Transforming Growth Factor (TGF)-β Promotes de Novo Serine Synthesis for Collagen Production. *J Biol Chem* 2016; **291**: 27239-27251 [PMID: 27836973 DOI: 10.1074/jbc.M116.756247]

34 **Cho SJ**, Moon JS, Nikahira K, Yun HS, Harris R, Hong KS, Huang H, Choi AMK, Stout-Delgado H. GLUT1-dependent glycolysis regulates exacerbation of fibrosis *via* AIM2 inflammasome activation. *Thorax* 2020; **75**: 227-236 [PMID: 31822523 DOI: 10.1136/thoraxjnl-2019-213571]

35 **Chadt A**, Al-Hasani H. Glucose transporters in adipose tissue, liver, and skeletal muscle in metabolic health and disease. *Pflugers Arch* 2020; **472**: 1273-1298 [PMID: 32591906 DOI: 10.1007/s00424-020-02417-x]

36 **Jiang L**, Deberardinis R, Boothman DA. The cancer cell 'energy grid': TGF-β1 signaling coordinates metabolism for migration. *Mol Cell Oncol* 2015; **2**: e981994 [PMID: 27308459 DOI: 10.4161/23723556.2014.981994]

37 **Nilchian A**, Giotopoulou N, Sun W, Fuxe J. Different Regulation of Glut1 Expression and Glucose Uptake during the Induction and Chronic Stages of TGFβ1-Induced EMT in Breast Cancer Cells. *Biomolecules* 2020; **10** [PMID: 33271824 DOI: 10.3390/biom10121621]

38 **Xie N**, Tan Z, Banerjee S, Cui H, Ge J, Liu RM, Bernard K, Thannickal VJ, Liu G. Glycolytic Reprogramming in Myofibroblast Differentiation and Lung Fibrosis. *Am J Respir Crit Care Med* 2015; **192**: 1462-1474 [PMID: 26284610 DOI: 10.1164/rccm.201504-0780OC]

39 **Fujishiro M**, Gotoh Y, Katagiri H, Sakoda H, Ogihara T, Anai M, Onishi Y, Ono H, Funaki M, Inukai K, Fukushima Y, Kikuchi M, Oka Y, Asano T. MKK6/3 and p38 MAPK pathway activation is not necessary for insulin-induced glucose uptake but regulates glucose transporter expression. *J Biol Chem* 2001; **276**: 19800-19806 [PMID: 11279172 DOI: 10.1074/jbc.M101087200]

40 **Yamamoto Y**, Yoshimasa Y, Koh M, Suga J, Masuzaki H, Ogawa Y, Hosoda K, Nishimura H, Watanabe Y, Inoue G, Nakao K. Constitutively active mitogen-activated protein kinase kinase increases GLUT1 expression and recruits both GLUT1 and GLUT4 at the cell surface in 3T3-L1 adipocytes. *Diabetes* 2000; **49**: 332-339 [PMID: 10868953 DOI: 10.2337/diabetes.49.3.332]

41 **Dziembowska M**, Danilkiewicz M, Wesolowska A, Zupanska A, Chouaib S, Kaminska B. Cross-talk between Smad and p38 MAPK signalling in transforming growth factor beta signal transduction in human glioblastoma cells. *Biochem Biophys Res Commun* 2007; **354**: 1101-1106 [PMID: 17276399 DOI: 10.1016/j.bbrc.2007.01.113]

42 **Lu Y**, Jiang F, Zheng X, Katakowski M, Buller B, To SS, Chopp M. TGF-β1 promotes motility and invasiveness of glioma cells through activation of ADAM17. *Oncol Rep* 2011; **25**: 1329-1335 [PMID:

21359495 DOI: 10.3892/or.2011.1195]

43 **Cho SJ**, Moon JS, Lee CM, Choi AM, Stout-Delgado HW. Glucose Transporter 1-Dependent Glycolysis Is Increased during Aging-Related Lung Fibrosis, and Phloretin Inhibits Lung Fibrosis. *Am J Respir Cell Mol Biol* 2017; **56**: 521-531 [PMID: 27997810 DOI: 10.1165/rcmb.2016-0225OC]

World Journal of Gastroenterology

Submit a Manuscript: https://www.f6publishing.com

World J Gastroenterol 2021 October 28; 27(40): 6927-6938

DOI: 10.3748/wjg.v27.i40.6927

ISSN 1007-9327 (print) ISSN 2219-2840 (online)

ORIGINAL ARTICLE

Retrospective Cohort Study

Serum hepatitis B core-related antigen as a surrogate marker of hepatitis B e antigen seroconversion in chronic hepatitis B

Xiu-Mei Chi, Xiao-Mei Wang, Zhong-Feng Wang, Rui-Hong Wu, Xiu-Zhu Gao, Hong-Qin Xu, Yan-Hua Ding, Jun-Qi Niu

ORCID number: Xiu-Mei Chi 0000-0002-6291-8496; Xiao-Mei Wang 0000-0003-2606-4013; Zhong-Feng Wang 0000-0001-9588-4985; Rui-Hong Wu 0000-0001-7585-0059; Xiu-Zhu Gao 0000-0001-6310-1456; Hong-Qin Xu 0000-0002-5841-2230; Yan-Hua Ding 0000-0003-2320-4404; Jun-Qi Niu 0000-0001-5415-2024.

Author contributions: Chi XM contributed to design and data analysis and drafted the manuscript; Wang XM contributed to data analysis and critically revised the manuscript; Wang ZF, Wu RH, Gao XZ and Xu HQ contributed to data acquisition and analysis; Ding YH critically revised the manuscript; Niu JQ contributed to the conception and critically revised the manuscript; All authors read and approved the final manuscript.

Supported by National Science and Technology Major Project, No. 2017ZX10302201, No. 2017ZX09304004 and No. 2014ZX10002002; and National Program on Key Basic Research Project (973 Program), No. 2015CB554304.

Institutional review board statement: This study was approved by the ethics committee of the First Hospital of Jilin

Xiu-Mei Chi, Xiao-Mei Wang, Zhong-Feng Wang, Rui-Hong Wu, Xiu-Zhu Gao, Hong-Qin Xu, Jun-Qi Niu, Department of Hepatology, Key Laboratory of Zoonosis Research, Ministry Education, The First Hospital of Jilin University, Changchun 130021, Jilin Province, China

Xiu-Mei Chi, Yan-Hua Ding, Phase I Clinical Trials Unit, The First Hospital of Jilin University, Changchun 130021, Jilin Province, China

Corresponding author: Jun-Qi Niu, MD, PhD, Academic Research, Dean, Director, Doctor, Professor, Research Scientist, Department of Hepatology, Key Laboratory of Zoonosis Research, Ministry Education, The First Hospital of Jilin University, No. 71 Xinmin Street, Changchun 130021, Jilin Province, China. junqiniu@jlu.edu.cn

Abstract

BACKGROUND

Quantitative hepatitis B core-related antigen (qHBcrAg) has a better correlation with intrahepatic hepatitis B virus (HBV) covalently closed circular DNA (cccDNA) than HBV DNA or hepatitis B e antigen (HBeAg), but data are still lacking for its clinical application.

AIM

The aim was to investigate serum qHBcrAg levels in patients with chronic hepatitis B and assess the correlation of serum qHBcrAg with pregenomic RNA (pgRNA), cccDNA, and HBeAg seroconversion.

METHODS

This study was a secondary analysis of patients who underwent percutaneous liver biopsy between July 2014 and June 2019 in two multicenter randomized controlled clinical trials of peginterferon *vs* nucleos(t)ide analog (NUC)-based therapy (NCT03509688 and NCT03546530). Serum qHBcrAg, pgRNA, HBV DNA, hepatitis B core antigen, HBeAg, liver cccDNA, and HBV DNA were measured. The correlations of serum qHBcrAg with other biomarkers were analyzed.

RESULTS

A total of 139 patients were included. The mean qHBcrAg levels were 5.32 ± 1.18 $\log_{10}$ U/mL at baseline and decreased during treatment (all $P < 0.0001$). Serum qHBcrAg levels were positively correlated with pgRNA ($r = 0.597$, $P < 0.0001$) and cccDNA ($r = 0.527$, $P < 0.0001$) levels. The correlation of serum qHBcrAg level and

University.

Informed consent statement: Informed consent was obtained from each patient for the original trials, with clauses for possibly secondary analyses. The original studies were registered (ClinicalTrials.gov NCT03509688 and NCT03546530).

Conflict-of-interest statement: The authors declare that they have no conflicting interests.

Data sharing statement: The datasets used and/or analyzed during the current study are available from the corresponding author on reasonable request.

STROBE statement: The authors have read the STROBE Statement-checklist of items, and the manuscript was prepared and revised according to the STROBE Statement-checklist of items.

Open-Access: This article is an open-access article that was selected by an in-house editor and fully peer-reviewed by external reviewers. It is distributed in accordance with the Creative Commons Attribution NonCommercial (CC BY-NC 4.0) license, which permits others to distribute, remix, adapt, build upon this work non-commercially, and license their derivative works on different terms, provided the original work is properly cited and the use is non-commercial. See: http://creativecommons.org/Licenses/by-nc/4.0/

Manuscript source: Unsolicited manuscript

Specialty type: Gastroenterology and hepatology

Country/Territory of origin: China

Peer-review report's scientific quality classification

Grade A (Excellent): 0
Grade B (Very good): 0
Grade C (Good): C, C
Grade D (Fair): 0
Grade E (Poor): 0

Received: March 11, 2021

intrahepatic HBV DNA levels at baseline was weak but significant (r = 0.399, P < 0.0001). HBcrAg predicted HBeAg seroconversion, with areas under the receiver operating characteristics curve of 0.788 at 24 wk and 0.825 at 48 wk. Log HBcrAg at wk 24 and 48 was independently associated with HBeAg seroconversion [odds ratio (OR) = 2.402, 95% confidence interval (CI): 1.314-4.391, P = 0.004; OR = 3.587, 95%CI: 1.315-9.784, P = 0.013].

CONCLUSION

Serum HBcrAg levels were correlated with HBV virological markers and could be used to predict HBeAg seroconversion.

Key Words: Hepatitis B virus; Hepatitis B core antigen; Hepatitis B virus DNA; Detection; Liver biopsy; Pregenomic RNA; Quantitative hepatitis B core-related antigen; Receiver operating characteristic; Seroconversion; Correlation

©The Author(s) 2021. Published by Baishideng Publishing Group Inc. All rights reserved.

Core Tip: The mean quantitative hepatitis B core-related antigen (qHBcrAg) levels were decreased post treatment. Serum qHBcrAg levels were positively associated with pregenomic RNA and covalently closed circular DNA levels. qHBcrAg predicted hepatitis B e antigen (HBeAg) seroconversion with an area under the receiver operating characteristics curve of 0.788 at 24 wk and 0.825 at 48 wk. Log qHBcrAg at wk 24 and wk 48 was independently associated with HBeAg seroconversion (odds ratio = 2.402, 95% confidence interval: 1.314-4.391, P = 0.004; odds ratio = 3.587, 95% confidence interval: 1.315-9.784, P = 0.013, respectively).

Citation: Chi XM, Wang XM, Wang ZF, Wu RH, Gao XZ, Xu HQ, Ding YH, Niu JQ. Serum hepatitis B core-related antigen as a surrogate marker of hepatitis B e antigen seroconversion in chronic hepatitis B. *World J Gastroenterol* 2021; 27(40): 6927-6938
URL: https://www.wjgnet.com/1007-9327/full/v27/i40/6927.htm
DOI: https://dx.doi.org/10.3748/wjg.v27.i40.6927

INTRODUCTION

Chronic hepatitis B (CHB) is a liver disease caused by a chronic infection with the hepatitis B virus (HBV) and is potentially life-threatening. CHB is a global health problem that affects about 250 million people worldwide, with a prevalence of < 2% in the United States and other Western countries and > 5% in East Asia, Southeast Asia, and sub-Saharan Africa[1-3]. The disease is particularly endemic in China, where there are about 84 million individuals infected with HBV[4], with a prevalence as high as 6.3% in some rural areas[5]. All-cause mortality associated with HBV infection is about 6%-8%, and 15%-40% of untreated patients with CHB develop serious conditions such as cirrhosis and hepatocellular carcinoma[3,6].

The HBV genome exists in the nuclei of infected hepatocytes as a 3.2-kb double-stranded episomal DNA called covalently closed circular DNA (cccDNA). cccDNA is a key component in the HBV life cycle since it is the template for all viral genomic and subgenomic transcripts, including pregenomic RNA (pgRNA), and its level is correlated with the proliferative potential of HBV[7]. cccDNA serves as the template for pgRNA production, which is the main step in HBV replication[7]. The control of intrahepatic levels of HBV cccDNA and/or controlling the transcriptional activity of cccDNA are critical to prevent the occurrence of decompensated cirrhosis and hepatocellular carcinoma, which is the ultimate goal of anti-HBV therapies[8,9]. Hence, changes in the intrahepatic level of cccDNA can be used to monitor the efficacy of antiviral therapies and evaluate the possibility of viral rebound after stopping treatment[10-12]. The direct method to measure liver cccDNA levels is liver biopsy, but it is an invasive procedure not easily accepted by the patients[13]. Therefore, searching for surrogate indicators of intrahepatic HBV cccDNA is important to optimize patient management and quality of life.

Peer-review started: March 11, 2021
First decision: April 5, 2021
Revised: May 6, 2021
Accepted: September 1, 2021
Article in press: September 1, 2021
Published online: October 28, 2021

P-Reviewer: El-Nakeep S, Simsek H
S-Editor: Gao CC
L-Editor: Filipodia
P-Editor: Yuan YY

Although sustained serum HBV DNA suppression and hepatitis B e antigen (HBeAg) seroconversion are associated with disease remission[8], their performance in reflecting the changes in intrahepatic cccDNA is poor[14,15]. Hepatitis B core-related antigen (HBcrAg) is an emerging marker of HBV DNA suppression[16,17]. HBcrAg consists of hepatitis B core antigen (HBcAg), HBeAg, and p22cr. HBcAg and HBeAg share the first 149 amino acids (aa) encoded by the core gene, overlapping the -10 to 183 aa region[18]. A study showed that quantitative HBcrAg (qHBcrAg) better reflects intrahepatic cccDNA levels than HBV DNA or HBeAg[15]. In addition, intrahepatic cccDNA can be determined with an enzyme immunoassay for HBcrAg[19,20]. Nevertheless, HBcrAg is still not widely used by clinicians worldwide because not enough data are currently available.

Therefore, this study aimed to investigate the serum qHBcrAg levels of patients with CHB and assess the correlation of serum qHBcrAg with pgRNA, cccDNA, and HBeAg seroconversion. The results will add to the sparse literature about qHBcrAg and could eventually lead to its wider use in the clinical setting.

MATERIALS AND METHODS

Study design and patients

This study was a secondary analysis of a cohort of patients who underwent percutaneous liver biopsy at baseline and after 48 wk of therapy between July 2014 and June 2019 during their participation in two multicenter randomized controlled clinical trials of peginterferon (Peg-IFN) or nucleos(t)ide analog (NUC)-based therapy. The study was approved by the ethics committee of the First Hospital of Jilin University. Informed consent was obtained from each patient for the original trials, with clauses for possible secondary analyses. The original studies were registered (ClinicalTrials.gov NCT03509688 and NCT03546530).

All patients were diagnosed with CHB according to the criteria of detectable HBV DNA ≥ 10^5 IU/mL, alanine aminotransferase (ALT) 1.5-10 times the upper limit of normal, and HBeAg positivity[3,6]. The inclusion criteria were: (1) Diagnosis of CHB; (2) Treatment with Peg-IFN or NUC-based therapy for at least 48 wk; and (3) Available serum samples and liver specimens at baseline and 48 wk. The exclusion criteria were: (1) A history of hepatitis C virus or hepatitis D virus infection; (2) Human immunodeficiency virus; (3) Inflammatory diseases such as rheumatoid arthritis, diabetes, autoimmune hepatitis, hypertension, or kidney disease; or (4) Recent infectious disease.

Treatment

The treatment regimens followed the clinical practice guidelines OF the Asian-Pacific Association for the Study of the Liver on the management of hepatitis B[21]. In one of the original trials, the patients received entecavir (ETV) (Cosunter Pharmaceutical, China) 0.5 mg once daily po for 144 wk with/without resveratrol 1000 mg once daily for 48 wk or thymosin α1 twice-weekly sc for 24 wk. In the other trial, the patients received interferon (IFN, Kawin Technology, China) 1.5 μg/kg per week sc for 48 wk with/without resveratrol 1000 mg once daily for 48 wk. The patients who underwent liver biopsy before and after 48 wk of treatment were included in the present study. In the two trials, 139 patients completed 48 wk treatment with both biopsies (Figure 1). In each original trial[22-24], the patients were randomly assigned to the trial drugs.

Quantitative serum HBcrAg assay

The quantification of HBcrAg was performed using a fully automated Lumipulse chemiluminescence enzyme immunoassay analyzer (Fujirebio Inc., Tokyo, Japan) according to the manufacturer's instructions. Serum was pretreated with sodium dodecyl sulfate and incubated with monoclonal antibodies against denatured HBcAg and HBeAg. After washing and incubation with secondary antibodies, the concentrations of HBcrAg were determined by relative chemiluminescence intensity and compared with a standard curve. Because the general analytic measurement range of the assay was between 1000 U/mL (3 $\log_{10}$ U/mL) and 10000000 U/mL (7 $\log_{10}$ U/mL), serial dilutions of the serum sample were needed when the serum qHBcrAg level was above the detection limit of the assay.

Biochemistry and other indicators

Fasting venous blood was centrifuged at 4000 rpm for 10 min to obtain serum. All laboratory assessments were performed at baseline and weeks 4, 12, 24, 48, and 96.

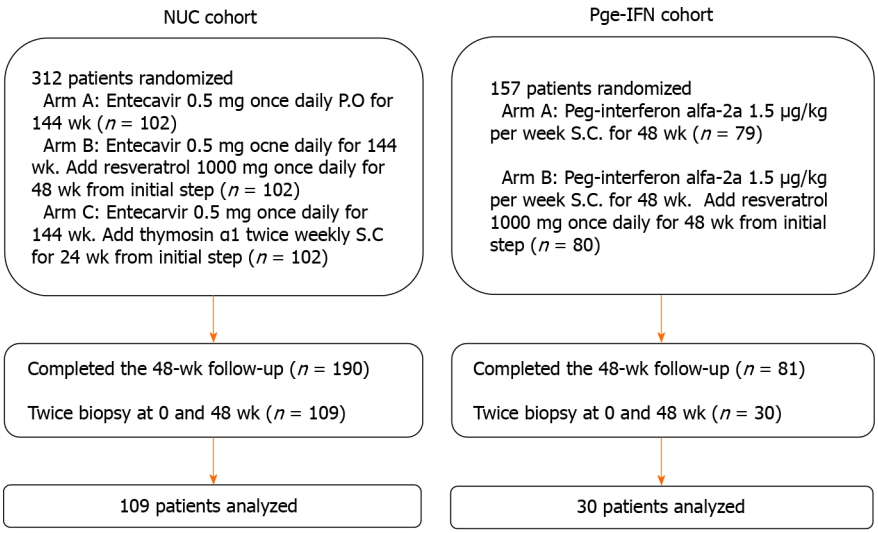


Figure 1 Patient flowchart. NUC: Nucleos(t)ide analog; Peg-IFN: Peginterferon.

HBV DNA was detected by quantitative polymerase chain reaction (PCR) using the Roche COBAS AmpliPrep/COBAS TaqMan system (Roche Diagnostics, Basel, Switzerland). The lowest detection limit was 20 IU/mL. Hepatitis B surface antigen (HBsAg), anti-HBs, HBeAg, anti-HBe, and anti-HBc were detected by chemiluminescence microparticle immunoassays using the Architect i2000SR platform and Abbott Architect reagents (Abbott Laboratories, Abbott Park, IL, United States). Serum HBsAg levels were measured with a dynamic range of 0-250 IU/mL. If qHBsAg levels were > 250 IU/mL, the samples were retested with a stepwise dilution of 1:10,000. ALT and aspartate aminotransferase were measured at each participating medical site. ALT, HBsAg, HBeAg, and HBV DNA were directly detected immediately at each time point. The HBV genotype was determined at screening. HBV pgRNA was measured at Peking University Health Science Center (Beijing, China), as previously described[25]. HBV genotypes were determined by real-time PCR with Taqman probe technology (Shanghai ZJ Bio-Tech, Shanghai, China). A FibroScan system was used to measure liver stiffness (Echosens, Paris, France).

Intrahepatic indicators

All patients in this study underwent liver biopsy before treatment and after 48 wk of treatment. The remaining liver tissue was stored in liquid nitrogen. Quantitative intrahepatic cccDNA was detected by PCR-fluorescent probing (SUPBIO Biotechnology, Beijing, China) following the manufacturer's instructions. Intrahepatic HBV DNA was detected by quantitative PCR using the Roche COBAS AmpliPrep/COBAS TaqMan system (Roche Diagnostics, Basel, Switzerland).

Statistical analyses

Continuous data were expressed as means ± SD and analyzed using Student's *t*-test or Mann-Whitney *U*-test, as appropriate based on the results of the Kolmogorov-Smirnov test. Intragroup analyses were performed using the paired ˆ-test or repeated-measure analysis of variance. Categorical variables were reported as numbers and percentages (%) and analyzed using Fisher's exact test. The correlation between two continuous variables was analyzed using Spearman's bivariate correlation, with a two-tailed significance level of $P < 0.01$. Receiver operating characteristic (ROC) curves were generated to compare the relative sensitivity and specificity of HBcrAg as a predictor of HBeAg seroconversion. A multivariable logistic regression model was used to determine whether the level of HBcrAg was a risk factor of HBeAg seroconversion. Otherwise, two-tailed *P* values of < 0.05 were considered statistically significant in all analyses. The statistical analysis were performed with SPSS 18.0 (IBM, Armonk, NY, United States).

RESULTS

Patient Characteristics

From the two original trials, 139 patients were eligible (Table 1). Among them, 69.1% were men, and 30.9% were women. There were more patients with HBV genotype C (79.9%) than B (20.1%). At baseline, the mean levels of intrahepatic HBV cccDNA were 26.65 ± 11.03 copies/cell. The mean levels of serum HBV DNA and HBsAg were 7.59 ± 1.05 $\log_{10}$ IU/mL and 3.81 ± 0.69 $\log_{10}$ IU/mL, respectively. The detailed baseline characteristics of the patients in the ETV and Peg-IFN cohorts are shown in Supplementary Table 1. The patients in the Peg-IFN cohort were younger than those in the ETV cohort (P = 0.045); there were no significant differences in the other characteristics.

Serum HBcrAg distribution

The serum qHBcrAg levels were different among the 139 patients with different phases of HBV infection and treatment. Indeed, the levels of qHBcrAg were 2.30-7.80 $\log_{10}$ U/mL. The mean levels were 5.24 ± 1.07 $\log_{10}$ U/mL in the ETV group (Figure 2A) and 5.38 ± 1.22 in the Peg-IFN group (Figure 2B) at baseline. The mean levels of qHBcrAg were 5.32 ± 1.18 $\log_{10}$ U/mL at baseline and 3.50 ± 1.31 $\log_{10}$ U/mL at week 48, showing decreases at each time point after treatment initiation (all P < 0.0001. Figure 2A-C), and there were no differences between the two groups (P = 0.6291, Figure 2D).

Comparison of the changes in qHBcrAg with other markers during treatment

Among the 139 patients, the serum qHBcrAg levels were positively correlated with cccDNA (r = 0.527, P < 0.0001; r = 0.323, P = 0.0001) and pgRNA (r = 0.597, P < 0.0001; r = 0.592, P = 0.0001) levels before and after treatment (Figure 3A and B). The correlation of serum qHBcrAg levels and intrahepatic HBV DNA levels was statistically significant at week 0 (r = 0.399, P < 0.0001, Figure 3A) and at week 48 (r = 0.213, P = 0.001) (Figure 3B). The serum qHBcrAg levels and FibroScan score weakly correlated (r = −0.278, P = 0.0099) (Supplementary Figure 1). Correlations were also observed between serum HBsAg (r = 0.514, P < 0.0001) and HBeAg (r = 0.744, P < 0.0001), but there was no significant correlation with HBcAb (r = −0.151, P = 0.0758) (Supplementary Figure 1).

Correlation between serum HBsAg and cccDNA

Serum HBsAg was weakly correlated with cccDNA levels at baseline (r = 0.265, P < 0.001) and week 48 (r = 0.141, P = 0.092; Figure 4A and B). The correlation between HBsAg and cccDNA levels at week 48 was weak in both treatment cohorts (Figure 4C and D).

Performance of HBcrAg levels for HBeAg negative conversion prediction

The levels of serum HBcrAg were significantly lower in patients with HBeAg conversion compared with those without (Figure 5A). The area under the ROC curve of HBcrAg levels for the prediction of HBeAg seroconversion was 0.643 [95% confidence interval (CI): 0.484-0.802, P = 0.072], 0.750 (95%CI: 0.629-0.872, P = 0.002), 0.794 (95%CI: 0.679-0.908, P < 0.001), and 0.825 (95%CI: 0.738-0.913, P < 0.001) at baseline, 12, 24, and 48 wk, respectively (Figure 5B). At baseline, the best cutoff of HBcrAg was 5.29 $\log_{10}$ U/mL, with 73.3% sensitivity and 66.5% specificity for predicting HBeAg seroconversion. At 12 wk, the cutoff of HBcrAg was 3.22 $\log_{10}$ U/mL, with 66.7% sensitivity and 78.2% specificity. At 24 wk, the cutoff of HBcrAg was 3.00 $\log_{10}$ U/mL, with 86.7% sensitivity and 74.8% specificity. At 48 wk, the cutoff of HBcrAg was 2.68 $\log_{10}$ U/mL, with 80.0% sensitivity and 78.6% specificity. In the multivariable model of HBeAg seroconversion, Log_{10}HBcrAg at weeks 24 and 48 was independently associated with HBeAg [odds ratio (OR) = 2.402, 95%CI: 1.314-4.391, P = 0.004; OR = 3.587, 95%CI: 1.315-9.784, P = 0.013].

DISCUSSION

qHBcrAg better represents intrahepatic levels of HBV cccDNA than HBV DNA or HBeAg[19,20,26], but data are still lacking in support of its wide clinical application. Therefore, this study aimed to investigate serum qHBcrAg levels in patients with CHB and assess the correlation of serum qHBcrAg with pgRNA and cccDNA. As expected,

Table 1 Baseline characteristics of the patients

Characteristic	*n* = 139
Age, yr, median (range)	30.4 (19-62)
Sex (male/female, %)	96/43 (69.1/30.9)
HBV genotype, *n* (%)	
B	28 (20.1)
C	111 (79.9)
ALT, U/mL, mean ± SD	174.07 ± 119.82
Serum HBV DNA, $\log_{10}$ IU/mL, mean ± SD	7.59 ± 1.05
Serum pgRNA, $\log_{10}$ copies/mL, mean ± SD	7.82 ± 1.17
ihHBV cccDNA, copies/cell	26.65 ± 11.03
ihHBV DNA, copies/cell	385.13 ± 86.09
Serum HBsAg, $\log_{10}$ IU/mL, mean ± SD	3.81 ± 0.69
Serum HBeAg, $\log_{10}$ S/CO, mean ± SD	2.49 ± 0.82
HBcrAg, $\log_{10}$ U/mL, mean ± SD	5.32 ± 1.18

ALT: Alanine transaminase; cccDNA: Covalently closed circular DNA; HBcrAg: Hepatitis B core-related antigen. HBeAg: Hepatitis B e antigen; HBsAg: Hepatitis B surface antigen; HBV: Hepatitis B virus; ihHBV: Intrahepatic hepatitis B virus.

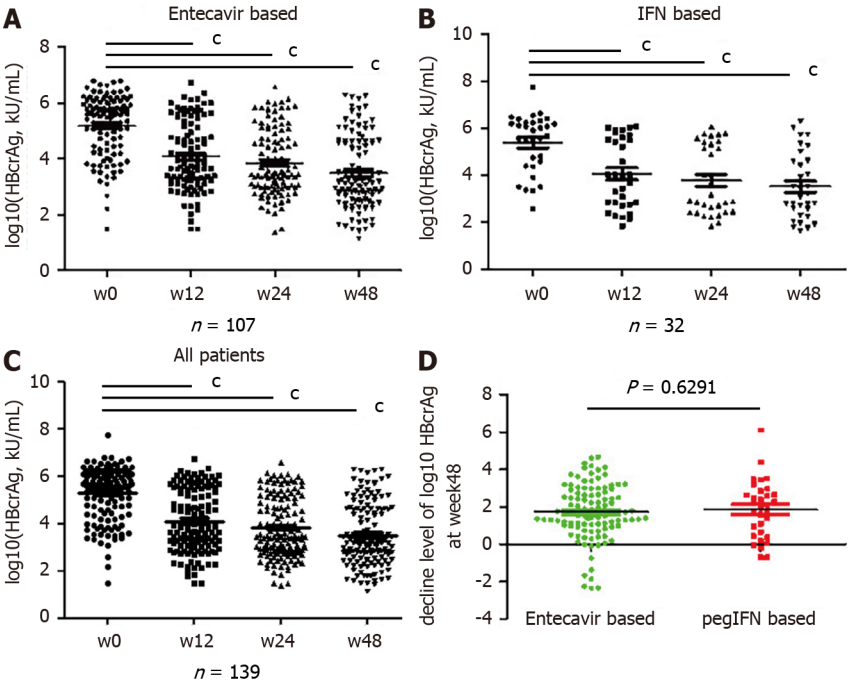


Figure 2 Time-dependent distribution of serum quantitative hepatitis B core-related antigen in patients with chronic hepatitis B and treated with different regimens. A: Changes in hepatitis B core-related antigen (HBcrAg) levels during treatment in the entecavir group; B: Changes in HBcrAg levels during treatment in the peginterferon group; C: Changes in HBcrAg levels during treatment in all patients; D: Comparison of the decrease in HBcrAg levels from baseline to week 48 between the entecavir and peginterferon groups. °P < 0.0001. HBcrAg: Hepatitis B core-related antigen; IFN: Interferon.

serum qHBcrAg was significantly and positively associated with the intrahepatic levels of cccDNA in CHB, and the association was stronger than the correlation between serum qHBsAg and intrahepatic cccDNA. Furthermore, antiviral therapy reduced the serum levels of HBcrAg and HBV DNA and the intrahepatic levels of cccDNA. The results suggest that serum HBcrAg levels correlate with HBV virological markers and could be used to predict CHB treatment outcomes, especially HBeAg seroconversion.

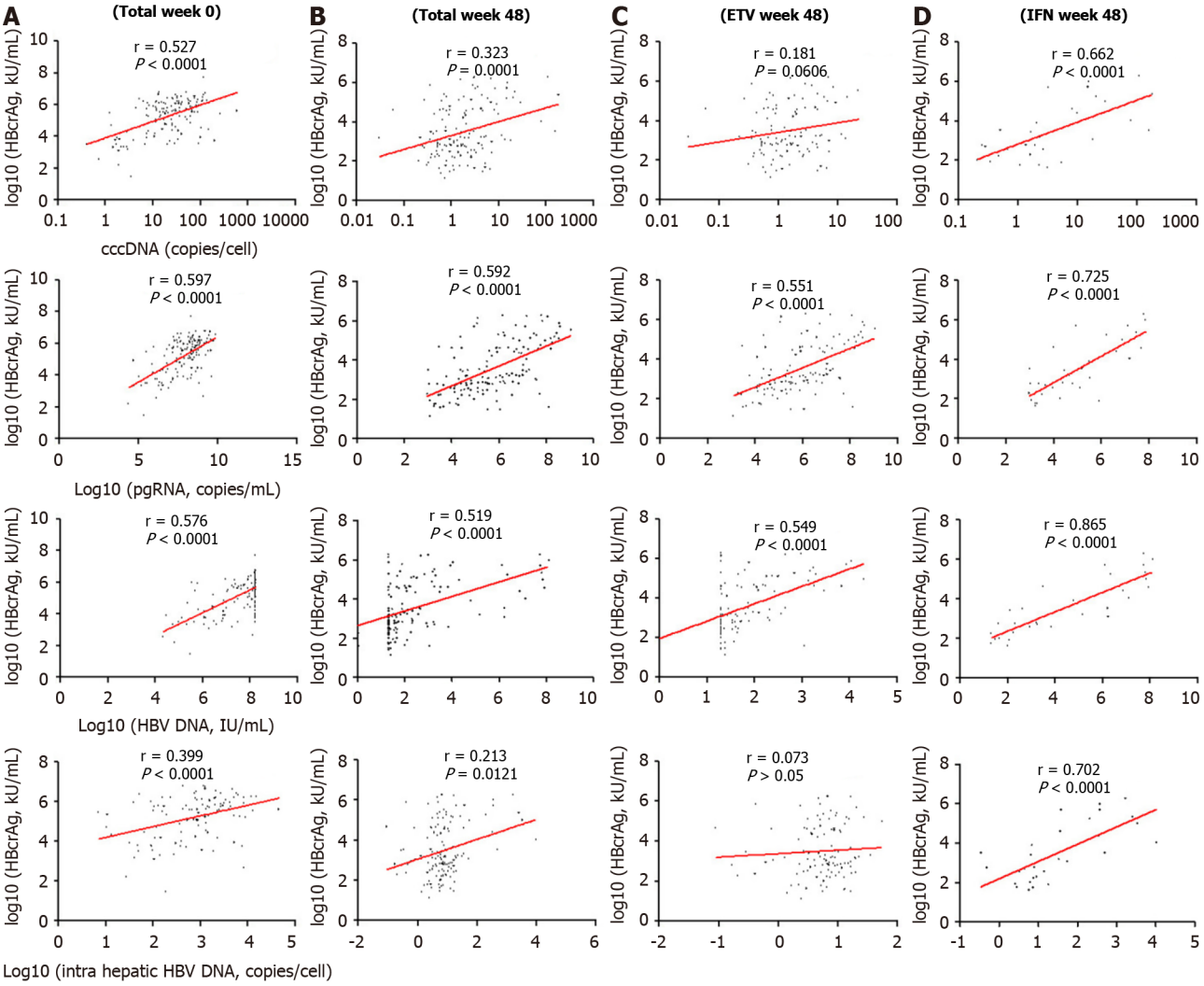


Figure 3 Correlation of serum quantitative hepatitis B core-related antigen with covalently closed circular DNA, pregenomic RNA, serum, and intrahepatic hepatitis B virus DNA level. A: In all patients at baseline; B: In all patients at week 48; C: Entecavir at week 48; D: Peginterferon at week 48. cccDNA: Covalently closed circular DNA; ETV: Entecavir; HBV: Hepatitis B virus; IFN: Interferon. pgRNA: Pregenomic RNA.

Serum levels of HBV DNA have been considered for many decades as a marker of the intrahepatic levels of cccDNA in untreated patients with CHB, but not when they are under treatment with NUCs. Indeed, under treatment, the decrease of the intrahepatic levels of cccDNA was not proportional to the steep decrease of the serum levels of HBV DNA[19,20]. Therefore, more reliable biomarkers were sought, and HBcrAg was found to be a potential additional biomarker of HBV infection, with a good correlation with intrahepatic levels of cccDNA[19,25,26]. HBcrAg was also suggested to be a reliable surrogate of cccDNA in two previous studies, as qHBcrAg was strongly correlated with intrahepatic cccDNA (r = 0.929 and 0.70, respectively), which is superior to that of qHBsAg and HBV DNA[27,28]. Hence, this study first aimed to investigate the correlation between the serum levels of qHBcrAg and the intrahepatic levels of cccDNA during CHB in Chinese patients. It showed that qHBcrAg was correlated with cccDNA before and after 48 wk of treatment, and the findings are supported by two previous studies[14,29]. HBcrAg more effectively represents cccDNA levels because HBcrAg includes three proteins: HBeAg, p22cr, and HBsAg. HBeAg is secreted by hepatocytes, p22cr represents empty virions, and HBsAg represents both empty virions and viable Dane particles[30]. Therefore, HBcrAg comprehensively encompasses the whole process of viral replication from cccDNA.

Of importance, decreases of the serum HBcrAg level were positively associated with decreases of the intrahepatic levels of cccDNA, even under therapy. Hence, the serum levels of HBcrAg could be a biomarker for the intrahepatic levels of cccDNA. In addition, because the changes in HBcrAg parallel those of intrahepatic cccDNA during treatment, it might be a better long-term prognostic indicator of CHB outcomes than

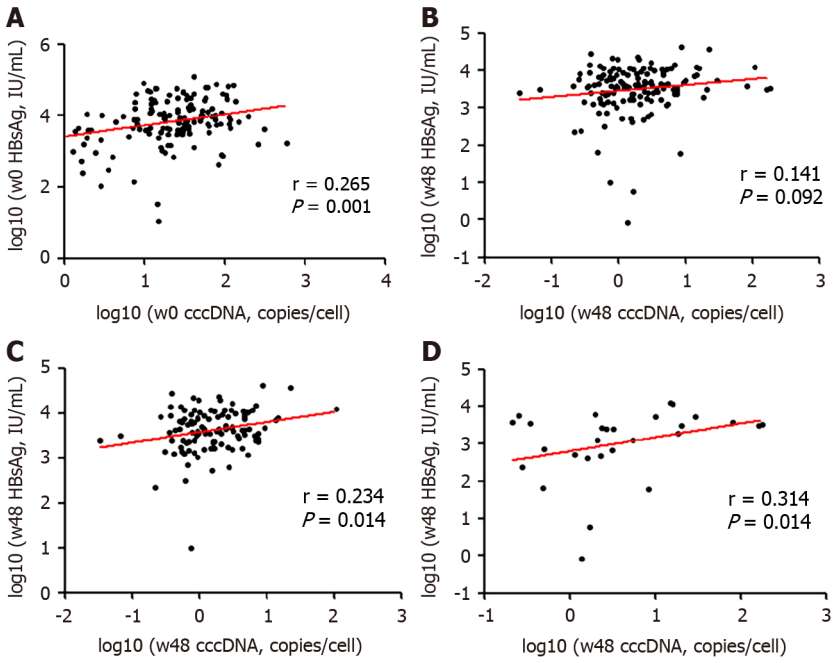
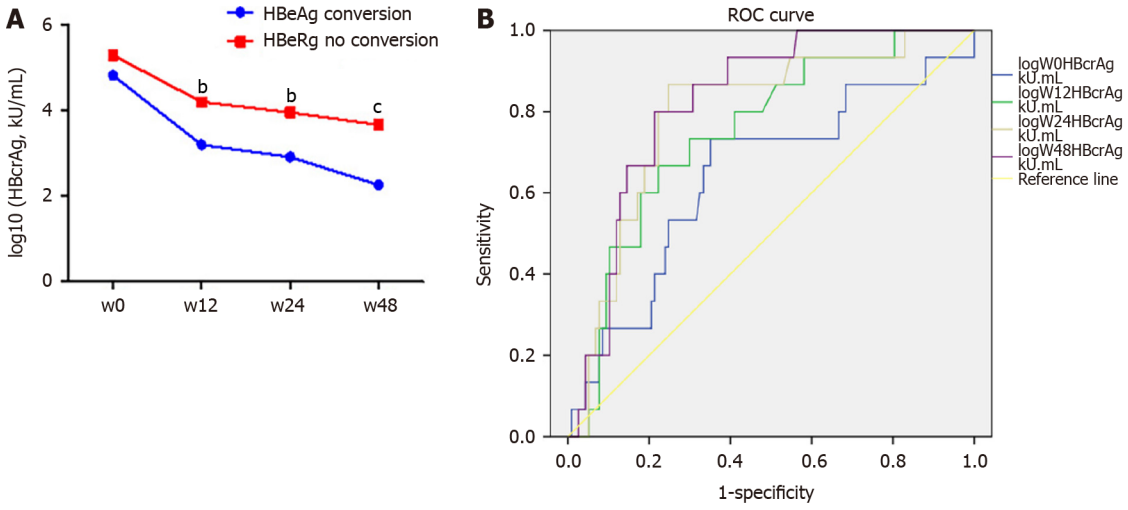


Figure 4 Correlation of serum hepatitis B surface antigen with covalently closed circular DNA. A: Correlation between serum hepatitis B surface antigen (HBsAg) and intrahepatic covalently closed circular DNA (cccDNA) at baseline; B: Correlation between serum HBsAg and intrahepatic cccDNA and at week 48; C: Correlation between cccDNA and HBsAg levels at weeks 48 in the entecavir cohort; D: Correlation between cccDNA and HBsAg levels at weeks 48 in the interferon cohort. HBsAg: Hepatitis B surface antigen; cccDNA: Covalently closed circular DNA.



			95% confidence interval	
	Area	*P* value	Lower bound	Upper bound
LogW0 HBcrAg	0.643	0.072	0.484	0.802
LogW12 HBcrAg	0.750	0.002	0.629	0.872
LogW24 HBcrAg	0.794	0.000	0.679	0.908
LogW48 HBcrAg	0.825	0.000	0.738	0.913

Figure 5 Hepatitis B core-related antigen prediction of hepatitis B e antigen seroconversion at 48 wk. A: Concentration of hepatitis B core-related antigen (HBcrAg) at different times in the two groups of hepatitis B e antigen (HBeAg) seroconversion; B: Receiver operating characteristic curve analysis of HBcrAg to predict HBeAg seroconversion. HBcrAg: Hepatitis B core-related antigen; HBeAg: Hepatitis B e antigen; ROC: Receiver operating characteristic; W: Week.

other biomarkers (*i.e.* serum HBV DNA and HBeAg). HBcrAg levels are determined by the transcription level of cccDNA. Therefore, decline of the HBcrAg levels with NUCs is slower than the decline of the serum levels of HBV DNA in patients. The slower decline might also explain why the serum levels of HBcrAg were positively correlated with the intrahepatic levels of cccDNA, either before or after ETV treatment.

In addition, the levels of serum qHBcrAg were higher in this study than in a previous study[31], which might have been the result of the high proportion of HBeAg-positive patients in this study. Considering that viral replication and host immune responses can be influenced by the HBV genotype, the distribution of the serum levels of HBcrAg was examined between patients carrying the HBV genotypes B and C, but the difference was not statistically significant. HBcrAg is a pre-core protein encoded by the pre-core/core regions of the HBV genome. Hence, the production of HBcrAg is not affected by the promoters found in the S region[18], possibly explaining the similar distribution of HBcrAg between the genotypes.

The serum levels of qHBsAg reflect the intrahepatic levels of cccDNA[19,20]. Still, in this study, the correlation between qHBsAg and intrahepatic cccDNA was weaker than the correlation between serum qHBcrAg and intrahepatic cccDNA, both without and under treatment. Most patients with HBsAg loss or seroconversion still had detectable levels of intrahepatic cccDNA and HBV DNA. Thus, according to the currently available evidence, serum levels of qHBcrAg could be more appropriate than HBsAg as a biomarker of the intrahepatic levels of cccDNA, but that needs to be confirmed in larger studies. The predictive value of qHBcrAg for HBeAg seroconversion was the best at 24 and 48 wk. That could be because baseline qHBcrAg is not predictive of the response to treatment, and that 12 wk is too early to observe a proper response. Additional studies are necessary to determine the best timing of qHBcrAg measurement for the prognosis of CHB. Nevertheless, qHBcrAg levels at the other time points were still associated with HBeAg seroconversion, as observed in previous studies[32-35]. HBsAg and HBeAg each represent only a part of the process of HBV production and assembly, and that could explain why they have a lower prognostic value, especially HBsAg at 48 wk[30].

The study has limitations. It was a secondary analysis of patients from two different trials with two different antiviral treatments and different regimens. Not all patients underwent two biopsies, leading to a selection bias and a small sample size. Importantly, a biopsy was performed at 48 wk in both studies. Still, the patients were followed for up to 144 wk in the ETV group and 96 wk in the Peg-IFN group, but the patients were only treated with Peg-IFN for 48 wk, and the long-term changes in HBcrAg are unknown. HBV genotype D is very rare in China and was not included in the two trials. Therefore, future studies should address those points.

CONCLUSION

Serum qHBcrAg levels were correlated with the intrahepatic levels of cccDNA in patients with CHB and might be an acceptable surrogate marker for cccDNA. HBcrAg levels correlated with HBV virological markers and could be used to predict CHB treatment outcomes, especially HBeAg seroconversion. Hence, serum qHBcrAg might be used in the clinical setting for monitoring intrahepatic HBV status and determining the long-term prognosis of patients with CHB.

ACKNOWLEDGMENTS

We are very grateful to the following professors for their selfless help in the process of collecting and treating clinical cases: Yu L, Chen YP, Shang J, Liu LG, Zhang SQ, Jiang YF, Zhang MX, Tong QX, Zhang LL, Tan YW, Ma AL, Dang SS, Xu B, Jin ZJ, Li J and Li XB.

ARTICLE HIGHLIGHTS

Research background

Quantitative hepatitis B core-related antigen (qHBcrAg) had a better correlation with intrahepatic hepatitis B virus (HBV) covalently closed circular DNA (cccDNA) than either HBV DNA or hepatitis B e antigen (HBeAg).

Research motivation

Data are still lacking for the widespread clinical application of qHBcrAg.

Research objectives

This study aimed to investigate the serum qHBcrAg levels in patients with chronic hepatitis B (CHB) and to assess the correlation of serum qHBcrAg with pregenomic RNA (pgRNA), cccDNA, and HBeAg seroconversion.

Research methods

This was a secondary analysis of patients who underwent percutaneous liver biopsy in two multicenter, randomized, controlled clinical trials. Serum qHBcrAg, pgRNA, HBV DNA, hepatitis B core antigen, and HBeAg and liver cccDNA, and HBV DNA were measured. The correlations of serum qHBcrAg with other biomarkers were tested.

Research results

Serum qHBcrAg levels were positively associated with pgRNA ($r = 0.597$, $P < 0.0001$) and cccDNA ($r = 0.527$, $P < 0.0001$) levels. HBcrAg predicted HBeAg seroconversion, with an area under the receiver operating characteristics curve of 0.788 at 24 wk and 0.825 at 48 wk.

Research conclusions

Serum HBcrAg levels correlated with HBV virological markers and could be used to predict HBeAg seroconversion.

Research perspectives

Serum qHBcrAg might be used in the clinical setting to monitor intrahepatic HBV status and determine the long-term prognosis of patients with CHB.

REFERENCES

1 **Schweitzer A**, Horn J, Mikolajczyk RT, Krause G, Ott JJ. Estimations of worldwide prevalence of chronic hepatitis B virus infection: a systematic review of data published between 1965 and 2013. *Lancet* 2015; **386**: 1546-1555 [PMID: 26231459 DOI: 10.1016/S0140-6736(15)61412-X]

2 **Terrault NA**, Lok ASF, McMahon BJ, Chang KM, Hwang JP, Jonas MM, Brown RS Jr, Bzowej NH, Wong JB. Update on prevention, diagnosis, and treatment of chronic hepatitis B: AASLD 2018 hepatitis B guidance. *Hepatology* 2018; **67**: 1560-1599 [PMID: 29405329 DOI: 10.1002/hep.29800]

3 **Trépo C**, Chan HL, Lok A. Hepatitis B virus infection. *Lancet* 2014; **384**: 2053-2063 [PMID: 24954675 DOI: 10.1016/S0140-6736(14)60220-8]

4 **Wang H**, Men P, Xiao Y, Gao P, Lv M, Yuan Q, Chen W, Bai S, Wu J. Hepatitis B infection in the general population of China: a systematic review and meta-analysis. *BMC Infect Dis* 2019; **19**: 811 [PMID: 31533643 DOI: 10.1186/s12879-019-4428-y]

5 **Liu J**, Zhang S, Wang Q, Shen H, Zhang M, Zhang Y, Yan D, Liu M. Seroepidemiology of hepatitis B virus infection in 2 million men aged 21-49 years in rural China: a population-based, cross-sectional study. *Lancet Infect Dis* 2016; **16**: 80-86 [PMID: 26268687 DOI: 10.1016/S1473-3099(15)00218-2]

6 **Lok AS**, McMahon BJ. Chronic hepatitis B: update 2009. *Hepatology* 2009; **50**: 661-662 [PMID: 19714720 DOI: 10.1002/hep.23190]

7 **Tang H**, Banks KE, Anderson AL, McLachlan A. Hepatitis B virus transcription and replication. *Drug News Perspect* 2001; **14**: 325-334 [PMID: 12813595]

8 **Tang CM**, Yau TO, Yu J. Management of chronic hepatitis B infection: current treatment guidelines, challenges, and new developments. *World J Gastroenterol* 2014; **20**: 6262-6278 [PMID: 24876747 DOI: 10.3748/wjg.v20.i20.6262]

9 **Nassal M**. HBV cccDNA: viral persistence reservoir and key obstacle for a cure of chronic hepatitis B. *Gut* 2015; **64**: 1972-1984 [PMID: 26048673 DOI: 10.1136/gutjnl-2015-309809]

10 **Yang HC**, Kao JH. Persistence of hepatitis B virus covalently closed circular DNA in hepatocytes: molecular mechanisms and clinical significance. *Emerg Microbes Infect* 2014; **3**: e64 [PMID: 26038757 DOI: 10.1038/emi.2014.64]

11 **Shi M**, Sun WL, Hua YY, Han B, Shi L. Effects of entecavir on hepatitis B virus covalently closed circular DNA in hepatitis B e antigen-positive patients with hepatitis B. *PLoS One* 2015; **10**: e0117741 [PMID: 25647607 DOI: 10.1371/journal.pone.0117741]

12 **Zheng Q**, Zhu YY, Chen J, Liu YR, You J, Dong J, Zeng DW, Gao LY, Chen LH, Jiang JJ. Decline in intrahepatic cccDNA and increase in immune cell reactivity after 12 weeks of antiviral treatment were associated with HBeAg loss. *J Viral Hepat* 2014; **21**: 909-916 [PMID: 24888640 DOI: 10.1111/jvh.12261]

13 **Thampanitchawong P**, Piratvisuth T. Liver biopsy:complications and risk factors. *World J Gastroenterol* 1999; **5**: 301-304 [PMID: 11819452 DOI: 10.3748/wjg.v5.i4.301]

14 **Tanaka E**, Matsumoto A, Yoshizawa K, Maki N. Hepatitis B core-related antigen assay is useful for monitoring the antiviral effects of nucleoside analogue therapy. *Intervirology* 2008; **51** Suppl 1: 3-6

[PMID: 18544941 DOI: 10.1159/000122592]
15 **Liu YY**, Liang XS. Progression and status of antiviral monitoring in patients with chronic hepatitis B: From HBsAg to HBV RNA. *World J Hepatol* 2018; **10**: 603-611 [PMID: 30310538 DOI: 10.4254/wjh.v10.i9.603]
16 **Mak LY**, Wong DK, Cheung KS, Seto WK, Lai CL, Yuen MF. Review article: hepatitis B core-related antigen (HBcrAg): an emerging marker for chronic hepatitis B virus infection. *Aliment Pharmacol Ther* 2018; **47**: 43-54 [PMID: 29035003 DOI: 10.1111/apt.14376]
17 **Shimakawa Y**, Ndow G, Njie R, Njai HF, Takahashi K, Akbar SMF, Cohen D, Nayagam S, Jeng A, Ceesay A, Sanneh B, Baldeh I, Imaizumi M, Moriyama K, Aoyagi K, D'Alessandro U, Mishiro S, Chemin I, Mendy M, Thursz MR, Lemoine M. Hepatitis B Core-related Antigen: An Alternative to Hepatitis B Virus DNA to Assess Treatment Eligibility in Africa. *Clin Infect Dis* 2020; **70**: 1442-1452 [PMID: 31102406 DOI: 10.1093/cid/ciz412]
18 **Kimura T**, Rokuhara A, Sakamoto Y, Yagi S, Tanaka E, Kiyosawa K, Maki N. Sensitive enzyme immunoassay for hepatitis B virus core-related antigens and their correlation to virus load. *J Clin Microbiol* 2002; **40**: 439-445 [PMID: 11825954 DOI: 10.1128/jcm.40.2.439-445.2002]
19 **Suzuki F**, Miyakoshi H, Kobayashi M, Kumada H. Correlation between serum hepatitis B virus core-related antigen and intrahepatic covalently closed circular DNA in chronic hepatitis B patients. *J Med Virol* 2009; **81**: 27-33 [PMID: 19031469 DOI: 10.1002/jmv.21339]
20 **Matsuzaki T**, Tatsuki I, Otani M, Akiyama M, Ozawa E, Miuma S, Miyaaki H, Taura N, Hayashi T, Okudaira S, Takatsuki M, Isomoto H, Takeshima F, Eguchi S, Nakao K. Significance of hepatitis B virus core-related antigen and covalently closed circular DNA levels as markers of hepatitis B virus re-infection after liver transplantation. *J Gastroenterol Hepatol* 2013; **28**: 1217-1222 [PMID: 23432697 DOI: 10.1111/jgh.12182]
21 **Sarin SK**, Kumar M, Lau GK, Abbas Z, Chan HL, Chen CJ, Chen DS, Chen HL, Chen PJ, Chien RN, Dokmeci AK, Gane E, Hou JL, Jafri W, Jia J, Kim JH, Lai CL, Lee HC, Lim SG, Liu CJ, Locarnini S, Al Mahtab M, Mohamed R, Omata M, Park J, Piratvisuth T, Sharma BC, Sollano J, Wang FS, Wei L, Yuen MF, Zheng SS, Kao JH. Asian-Pacific clinical practice guidelines on the management of hepatitis B: a 2015 update. *Hepatol Int* 2016; **10**: 1-98 [PMID: 26563120 DOI: 10.1007/s12072-015-9675-4]
22 **Sonneveld MJ**, van Oord GW, van Campenhout MJ, De Man RA, Janssen HLA, de Knegt RJ, Boonstra A, van der Eijk AA. Relationship between hepatitis B core-related antigen levels and sustained HBeAg seroconversion in patients treated with nucleo(s)tide analogues. *J Viral Hepat* 2019; **26**: 828-834 [PMID: 30896057 DOI: 10.1111/jvh.13097]
23 **Song G**, Rao H, Feng B, Wei L. Prediction of spontaneous HBeAg seroconversion in HBeAg-positive chronic hepatitis B patients during the immune clearance phase. *J Med Virol* 2014; **86**: 1838-1844 [PMID: 25088043 DOI: 10.1002/jmv.24032]
24 **Song G**, Yang R, Rao H, Feng B, Ma H, Jin Q, Wei L. Serum HBV core-related antigen is a good predictor for spontaneous HBeAg seroconversion in chronic hepatitis B patients. *J Med Virol* 2017; **89**: 463-468 [PMID: 27505145 DOI: 10.1002/jmv.24657]
25 **Maasoumy B**, Wiegand SB, Jaroszewicz J, Bremer B, Lehmann P, Deterding K, Taranta A, Manns MP, Wedemeyer H, Glebe D, Cornberg M. Hepatitis B core-related antigen (HBcrAg) levels in the natural history of hepatitis B virus infection in a large European cohort predominantly infected with genotypes A and D. *Clin Microbiol Infect* 2015; **21**: 606.e1-606.10 [PMID: 25700889 DOI: 10.1016/j.cmi.2015.02.010]
26 **Wang L**, Cao X, Wang Z, Gao Y, Deng J, Liu X, Zhuang H. Correlation of HBcrAg with Intrahepatic Hepatitis B Virus Total DNA and Covalently Closed Circular DNA in HBeAg-Positive Chronic Hepatitis B Patients. *J Clin Microbiol* 2019; **57** [PMID: 30355757 DOI: 10.1128/JCM.01303-18]
27 **Wong DK**, Seto WK, Cheung KS, Chong CK, Huang FY, Fung J, Lai CL, Yuen MF. Hepatitis B virus core-related antigen as a surrogate marker for covalently closed circular DNA. *Liver Int* 2017; **37**: 995-1001 [PMID: 27992681 DOI: 10.1111/liv.13346]
28 **Chen EQ**, Feng S, Wang ML, Liang LB, Zhou LY, Du LY, Yan LB, Tao CM, Tang H. Serum hepatitis B core-related antigen is a satisfactory surrogate marker of intrahepatic covalently closed circular DNA in chronic hepatitis B. *Sci Rep* 2017; **7**: 173 [PMID: 28282964 DOI: 10.1038/s41598-017-00111-0]
29 **van Campenhout MJ**, Brouwer WP, van Oord GW, Xie Q, Zhang Q, Zhang N, Guo S, Tabak F, Streinu-Cercel A, Wang J, Pas SD, Sonneveld MJ, de Knegt RJ, Boonstra A, Hansen BE, Janssen HL. Hepatitis B core-related antigen levels are associated with response to entecavir and peginterferon add-on therapy in hepatitis B e antigen-positive chronic hepatitis B patients. *Clin Microbiol Infect* 2016; **22**: 571.e5-571.e9 [PMID: 26898481 DOI: 10.1016/j.cmi.2016.02.002]
30 **Inoue T**, Tanaka Y. The Role of Hepatitis B Core-Related Antigen. *Genes (Basel)* 2019; **10** [PMID: 31075974 DOI: 10.3390/genes10050357]
31 **Wong DK**, Tanaka Y, Lai CL, Mizokami M, Fung J, Yuen MF. Hepatitis B virus core-related antigens as markers for monitoring chronic hepatitis B infection. *J Clin Microbiol* 2007; **45**: 3942-3947 [PMID: 17942661 DOI: 10.1128/JCM.00366-07]
32 **Ma H**, Yang RF, Li XH, Jin Q, Wei L. HBcrAg Identifies Patients Failing to Achieve HBeAg Seroconversion Treated with Pegylated Interferon Alfa-2b. *Chin Med J (Engl)* 2016; **129**: 2212-2219 [PMID: 27625094 DOI: 10.4103/0366-6999.189904]
33 **Chuaypen N**, Posuwan N, Payungporn S, Tanaka Y, Shinkai N, Poovorawan Y, Tangkijvanich P. Serum hepatitis B core-related antigen as a treatment predictor of pegylated interferon in patients with

HBeAg-positive chronic hepatitis B. *Liver Int* 2016; **36**: 827-836 [PMID: 26678018 DOI: 10.1111/liv.13046]

34 **Matsumoto A**, Yatsuhashi H, Nagaoka S, Suzuki Y, Hosaka T, Tsuge M, Chayama K, Kanda T, Yokosuka O, Nishiguchi S, Saito M, Miyase S, Kang JH, Shinkai N, Tanaka Y, Umemura T, Tanaka E. Factors associated with the effect of interferon-α sequential therapy in order to discontinue nucleoside/nucleotide analog treatment in patients with chronic hepatitis B. *Hepatol Res* 2015; **45**: 1195-1202 [PMID: 25594111 DOI: 10.1111/hepr.12488]

35 **Martinot-Peignoux M**, Lapalus M, Maylin S, Boyer N, Castelnau C, Giuily N, Pouteau M, Moucari R, Asselah T, Marcellin P. Baseline HBsAg and HBcrAg titres allow peginterferon-based 'precision medicine' in HBeAg-negative chronic hepatitis B patients. *J Viral Hepat* 2016; **23**: 905-911 [PMID: 27375231 DOI: 10.1111/jvh.12565]

World Journal of Gastroenterology

Submit a Manuscript: https://www.f6publishing.com

World J Gastroenterol 2021 October 28; 27(40): 6939-6950

DOI: 10.3748/wjg.v27.i40.6939

ISSN 1007-9327 (print) ISSN 2219-2840 (online)

ORIGINAL ARTICLE

Retrospective Cohort Study

Long-term follow-up of liver alveolar echinococcosis using echinococcosis multilocularis ultrasound classification

Jasmin Schuhbaur, Melissa Schweizer, Jana Philipp, Julian Schmidberger, Patrycja Schlingeloff, Wolfgang Kratzer

ORCID number: Jasmin Schuhbaur 0000-0003-2284-9948; Melissa Schweizer 0000-0002-5826-942X; Jana Philipp 0000-0001-8091-1864; Julian Schmidberger 0000-0002-9960-9574; Patrycja Schlingeloff 0000-0003-3514-7347; Wolfgang Kratzer 0000-0002-9727-3843.

Author contributions: Kratzer W and Schuhbaur J planned and designed the study; The data were evaluated by Kratzer W and Schuhbaur J; all authors were involved in the interpretation of the results; Kratzer W, Schuhbaur J, Schmidberger J, Schlingeloff P, Schweizer M and Philipp J prepared the first draft; the statistical analysis was performed by Schmidberger J and Schlingeloff P; all authors read, amended, and approved the final version of the manuscript.

Institutional review board statement: The study was approved by the local ethics committee and conducted in accordance with the Declaration of Helsinki (ref. No. 166/13). Because of its retrospective design and pseudonymised evaluation of imaging, no ethics approval was necessary. All data were analysed anonymously.

Jasmin Schuhbaur, Melissa Schweizer, Jana Philipp, Julian Schmidberger, Patrycja Schlingeloff, Wolfgang Kratzer, Department of Internal Medicine I, University Hospital Ulm, Ulm 89081, Germany

Corresponding author: Wolfgang Kratzer, MD, Professor, Department of Internal Medicine I, University Hospital Ulm, Albert-Einstein-Allee 23, Ulm 89081, Germany.
wolfgang.kratzer@uniklinik-ulm.de

Abstract

BACKGROUND

When *Echinococcus multilocularis* infects humans as a false intermediate host, alveolar echinococcosis (AE) usually manifests primarily intrahepatically and is initially asymptomatic. If the disease remains undiagnosed and untreated, progressive growth occurs, reminiscent of malignant tumours. The only curative therapy is complete resection, which is limited to localised stages, and palliative drug therapy is used otherwise. Consequently, early diagnosis and reliable detection of AE lesions are important. For this reason, abdominal ultrasonography, as the most common primary imaging for AE, relies on classification systems.

AIM

To investigate how hepatic AE lesion sonomorphology changes over time in the Echinococcosis Multilocularis Ulm Classification (EMUC)-ultrasound (US) classification.

METHODS

Based on data from Germany's national echinococcosis database, we evaluated clinical and US imaging data for 59 patients according to the AE case definition in our preliminary retrospective longitudinal study. There had to be at least two liver sonographies ≥ 6 mo apart, ≥ 1 hepatic AE lesion, and complete documentation in all US examinations. The minimum interval between two separately evaluated US examinations was 4 wk. The AE reference lesion was the largest hepatic AE lesion at the time of the first US examination. To classify the sonomorphologic pattern, we used EMUC-US. In addition to classifying the findings of the original US examiner, all reference lesions at each examination time point were assigned EMUC-US patterns in a blinded fashion by two investigators experienced in US diagnosis. Statistical analysis was performed using SAS version

Informed consent statement: Because of retrospective and anonymous character of this study, the need for informed consent was waived by the institutional review board.

Conflict-of-interest statement: The authors declare that they have no competing interests.

Data sharing statement: The datasets used and analyzed during the current study are available from the corresponding author on reasonable request (wolfgang.kratzer@uniklinik-ulm.de).

STROBE statement: The authors have read the STROBE Statement-checklist of items, and the manuscript was prepared and revised according to the STROBE Statement-checklist of items.

Open-Access: This article is an open-access article that was selected by an in-house editor and fully peer-reviewed by external reviewers. It is distributed in accordance with the Creative Commons Attribution NonCommercial (CC BY-NC 4.0) license, which permits others to distribute, remix, adapt, build upon this work non-commercially, and license their derivative works on different terms, provided the original work is properly cited and the use is non-commercial. See: http://creativecommons.org/Licenses/by-nc/4.0/

Manuscript source: Unsolicited manuscript

Specialty type: Gastroenterology and hepatology

Country/Territory of origin: Germany

Peer-review report's scientific quality classification

Grade A (Excellent): 0
Grade B (Very good): B
Grade C (Good): 0
Grade D (Fair): 0
Grade E (Poor): 0

Received: July 20, 2021
Peer-review started: July 20, 2021

9.4 (SAS Institute Inc., Cary, NC, United Stated). *P* values < 0.05 were considered statistically significant.

RESULTS

The preliminary study included 59 patients, 38 (64.5%) women and 21 (35.6%) men. The mean age at initial diagnosis was 59.9 ± 16.9 years. At the time of initial ultrasonography, a hailstorm pattern was present in 42.4% (25/59) of cases, a hemangioma-like pattern in 16.9% (10/59), a pseudocystic pattern in 15.3% (9/59), and a metastasis-like pattern in 25.4% (15/59). For the hailstorm pattern, the average lesion size was 67.4 ± 26.3 mm. The average lesion size was 113.7 ± 40.8 mm with the pseudocystic pattern and 83.5 ± 27.3 mm with the hemangioma-like pattern. An average lesion size of 21.7 ± 11.0 mm was determined for the metastasis-like pattern. Although the sonomorphologic pattern remained unchanged in 84.7% (50/59) of AE reference lesions, 15.3% (9/59) showed a change over time. A change in pattern was seen exclusively for AE lesions initially classified as hemangioma-like or pseudocystic. A total of 70% (7/10) of AE lesions initially classified as hemangioma-like showed a relevant change in pattern over time, and 85.7% (6/7) of these were secondarily classified as having a hailstorm pattern, with the remainder (1/7; 14.3%) classified as having a pseudocystic pattern. A total of 22.2% (2/9) of AE lesions initially classified as pseudocystic showed a relevant change in pattern over time and were classified as having a hailstorm pattern. For AE lesions initially classified as having a hailstorm or metastatic pattern, no pattern change was evident. All patients with pattern change were on continuous drug therapy with albendazole.

CONCLUSION

The sonomorphology of hepatic AE lesions may change over time. The hemangioma-like and pseudocystic patterns are affected.

Key Words: Alveolar echinococcosis; *Echinococcus multilocularis*; Ultrasonography; Sonomorphology; Pattern change

©The Author(s) 2021. Published by Baishideng Publishing Group Inc. All rights reserved.

Core Tip: Alveolar echinococcosis is potentially fatal. In approximately 98% of cases, it manifests in the liver, similar to a primary malignant or metastatic tumour. The sonomorphological appearance of the disease is varied and easily confused with other differential diagnoses. Sonography is the most important tool in diagnostics, but how the known patterns change over time is unclear. The evidence that certain sonographic patterns in particular change over time shows a possible evolutionary approach to the disease and may, in the long term, make lifelong drug therapy unnecessary in non-operable patients when non-active stages can be clearly identified.

Citation: Schuhbaur J, Schweizer M, Philipp J, Schmidberger J, Schlingeloff P, Kratzer W. Long-term follow-up of liver alveolar echinococcosis using echinococcosis multilocularis ultrasound classification. *World J Gastroenterol* 2021; 27(40): 6939-6950
URL: https://www.wjgnet.com/1007-9327/full/v27/i40/6939.htm
DOI: https://dx.doi.org/10.3748/wjg.v27.i40.6939

INTRODUCTION

Fox tapeworm disease (alveolar echinococcosis, AE) is a zoonotic disease caused by the larval stage of the cestode *Echinococcus multilocularis*, in which humans act as the major false intermediate host[1,2]. After a host accidentally ingests infectious worm eggs, the eggs penetrate the wall of the small intestine and usually first reach the liver, the most common primary site of AE in humans, Via the enterohepatic circulation[1,3,4].

First decision: August 19, 2021
Revised: September 1, 2021
Accepted: September 22, 2021
Article in press: September 22, 2021
Published online: October 28, 2021

P-Reviewer: Okasha HH
S-Editor: Gao CC
L-Editor: A
P-Editor: Yu HG

AE is primarily asymptomatic and progressive in the therapy-naive state[5]. Only as the disease progresses do patients develop nonspecific symptoms, including abdominal tenderness or pain, jaundice, unwanted weight loss, and diffuse deterioration of general condition[6,7]. In Europe, the diagnosis of AE is usually made as an incidental finding in asymptomatic stages, and in China, diagnosis frequently is made in the setting of locally advanced growth with a complicated clinical course. Radical surgical resection of an AE lesion is considered the only potentially curative therapeutic option, followed by anthelmintic therapy for 2 years[8]. In case of an unresectable finding at diagnosis, long-term and often lifelong conservative medical therapy with benzimidazoles is required.

The high rate of advanced AE foci and inoperable disease at diagnosis underscore the need for early, definitive diagnosis. In clinical practice, B-scan ultrasonography is the most common primary imaging modality for evaluating nonspecific abdominal complaints and for the differential diagnostic assessment of hepatic incidentalomas[9].

The sonomorphology of hepatic AE foci is heterogeneous. The Echinococcosis Multilocularis Ulm Classification (EMUC)-ultrasound (US) classification, published in 2015, describes five sonomorphologic appearances of hepatic AE lesions and provides important guidance for their recognition and follow-up[10]. Five patterns are distinguished: hailstorm, hemangioma-like, pseudocystic, metastasis-like, and ossification. Conventional cross-sectional imaging [computed tomography (CT), magnetic resonance imaging (MRI)], with the appropriate classification schemes, is particularly useful for assessing spatial spread, potential infiltration of adjacent organs, and extrahepatic manifestations[11]. The gold standard for estimating parasitic activity is ^{18}FDG positron emission tomography (PET)[12,13]. Contrast-enhanced sonography of the liver also plays an increasing role in the evaluation of hepatic AE[14-16]. Available studies and analyses on the sonomorphology of AE have largely been cross-sectional, and we are not aware of any longitudinal studies assessing sonomorphology and a classification scheme for individual AE lesions.

The aim of our preliminary study is to investigate whether a change in pattern and size over time can be identified in patients with hepatic AE during follow-up, using the EMUC-US classification.

MATERIALS AND METHODS

Ethics statement

The study was approved by the local ethics committee and conducted in accordance with the Declaration of Helsinki (ref. No. 166/13). Because of its retrospective design and pseudonymised evaluation of imaging, no ethics approval was necessary. All data were analysed anonymously.

Study collective

For our preliminary retrospective evaluation, we used the clinical and imaging data of the national Echinococcosis Database in Germany. A main prerequisite for inclusion was confirmed or probable AE disease according to the AE case definition "confirmed" or "probable"[5]. Other inclusion criteria were at least two liver sonographies performed over a period of at least 6 mo, the presence of at least one hepatic AE lesion at the time of US 1, and complete documentation of the AE lesion defined as the reference lesion at all further observation time points. In total, 59 patients with data included in the Echinococcosis Database Germany were included (Figure 1 and Table 1).

Parameter

Initially, a hepatic AE reference lesion was defined per patient; this was measured by the largest diameter (in mm) at the time of the first US examination (US 1). At each time point, the number of all hepatic AE lesions in each patient was documented. The reference lesion was evaluated according to its maximum diameter and its EMUC-US pattern classification[10]. In addition to the AE case definition ("confirmed", "probable", "possible"), the clinical data included the therapy (surgical, conservative). A surgical procedure resulted in study exclusion. All study patients received oral anthelmintic therapy, and the preparation, time of initiation of therapy, and daily medication dose were documented.

Table 1 Overview of patient characteristics as well as sonomorphological aspects of the total collective

	n (%)	mean ± SD
Number of patients	59 (100.0)	
Number of sonographies	244 (100.0)	
Sex		
Female	38 (64.5)	
Male	21 (35.6)	
AE case definition		
Confirmed	26 (44.1)	
Probable	33 (55.9)	
Age at first diagnosis (yr)		59.9 ± 16.9
Age at initial ultrasound (yr)		60.4 ± 16.8
Localisation of the reference lesion		
Right hepatic	34 (57.6)	
Left hepatic	19 (32.3)	
Bihepatic	6 (10.2)	
Number of AE lesions on US 1		
1	29 (49.2)	
2-5	28 (47.5)	
6-10	1 (1.7)	
> 10	1 (1.7)	
Lesion size according to EMUC-US pattern (mm)		65.6 ± 39.7
Hailstorm pattern		67.4 ± 26.3
Pseudohemangioma-like pattern		83.5 ± 27.3
Pseudocystic pattern		113.7 ± 40.8
Metastasis-like pattern		21.7 ± 11.0
Drug therapy		
Initial albendazole	58 (98.3)	
Initial mebendazole	0 (0)	
Therapy change to mebendazole	2 (3.4)	
Continuous therapy	50 (86.2)	
Discontinuous therapy	8 (13.8)	
No therapy (rejection by patients)	1 (1.7)	

AE: Alveolar echinococcosis; US: Ultrasound.

US examinations and EMUC-US

All US examinations were performed using convex probes (C5-1 MHz, C9-1 MHz) with state-of-the-art US equipment (Aplio 500 Toshiba, Siemens S3000, Philips Epiqu 7, Philips IU22). The sonomorphology of the hepatic AE reference lesion was assigned to a pattern according to EMUC-US in each examination[10]. At each examination time point, three different examiners performed a pattern assignment of the reference lesion. The pattern assignment of examiner 1 was taken from the written documentation as the initial examiner. Investigators 2 and 3 performed follow-up of all US images relevant to the study in all included patients. The physicians who performed the follow-up were blinded to the initial examination and independently performed an EMUC-US assessment (Figure 2).

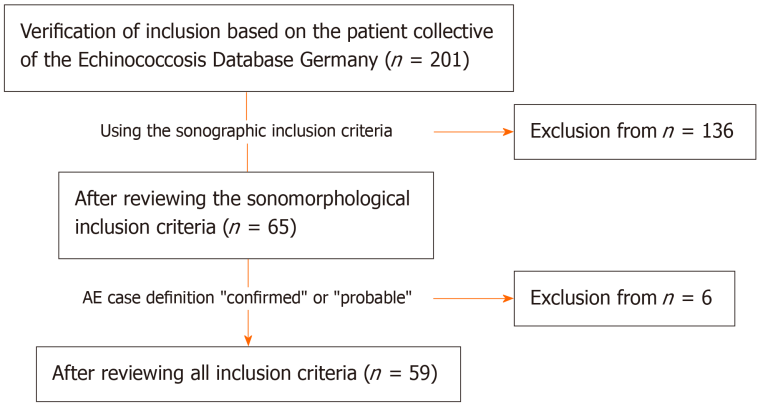


Figure 1 Flowchart illustrating case selection, including inclusion and exclusion criteria starting from the patient collective of the alveolar echinococcosis database in Germany. AE: Alveolar echinococcosis.

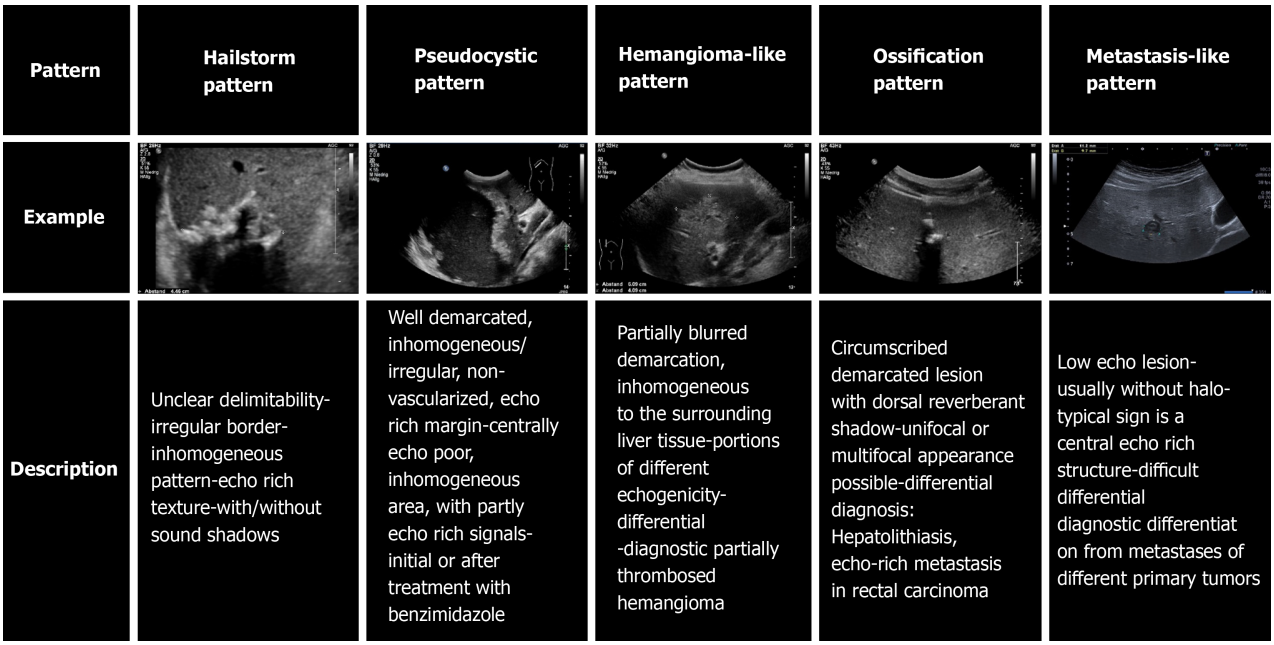


Figure 2 Echinococcosis Multilocularis Ulm Classification-ultrasound.

Statistical analysis

We performed statistical analyses using SAS Version 9.4 (SAS Institute Inc., Cary, NC, United Stated). Descriptive analysis of the data was performed to obtain absolute and relative frequencies, as well as measures of central tendency and dispersion. Pearson's χ^2 and exact fisher tests were used to determine possible relationships and differences in the frequency distribution between dichotomous variables. Wilcoxon rank sum test was performed to determine differences between variables without a normal distribution. All tests were performed two-sided. The level of significance was set at $\alpha = 0.05$, and a $P < 0.05$ was considered to be statistically significant with a 5% probability of error.

Biostatistics

The statistical methods of this study were reviewed by Dr. Schmidberger J, MPH, Ph.D., from the Department of Internal Medicine I, University Hospital Ulm, Albert-Einstein-Allee 23, 89081 Ulm, Germany.

RESULTS

Patient collective

The study included 59 patients, including 38 (64.5%) women and 21 (35.6%) men. The mean age at initial diagnosis was 59.9 ± 16.9 years, with a mean age at first sonographic examination of 60.4 ± 16.8 years. A World Health Organization case definition of "confirmed" was present in 26 (44.1%) patients, and a case definition of "probable" was present in 33 (55.9%). The 59 included patients underwent a total of 244 US examinations for a mean of 4.1 sonographic examinations per patient (2-15 ± 2.1 US examinations). A total of 58/59 (98.3%) received initial benzimidazole therapy using albendazole (Tables 1 and 2).

Lesion sizes, localisation, and distribution of EMUC-US patterns

At the time of initial US, 42.4% (25/59) corresponded to the hailstorm pattern, 16.9% (10/59) to the hemangioma-like pattern, 15.3% (9/59) to the pseudocystic pattern, and 25.4% (15/59) to the metastasis-like pattern. None of the reference lesions were initially assigned to the ossification pattern. For those with the hailstorm pattern, the mean lesion size was 67.4 ± 26.3 mm. The average lesion size with the pseudocystic pattern was 113.7 ± 40.8 mm, and that of the hemangioma-like pattern was 83.5 ± 27.3 mm. An average lesion size of 21.7 ± 11.0 mm was determined for the metastasis-like pattern (Figure 3).

In 34/59 (57.6%) of patients, the reference echinococcosis-associated lesion was right hepatic, and in 19/59 (32.3%), it was left hepatic. Bihepatic involvement was identified in 6/59 (10.2%).

Change in EMUC-US patterns

Over the whole observation period, the predominant pattern of hepatic AE reference lesions according to EMUC-US remained unchanged in 50/59 (84.7%). In 9/59 (15.3%) of the findings, however, a change in sonomorphology was observed. Of the 10 reference lesions initially classified as hemangioma-like, 7/10 (70.0%) showed a relevant change in sonomorphologic criteria. Of these, 6/7 (85.7%) were assigned to the hailstorm pattern in subsequent US examinations, and 1/7 (14.3%) showed a change toward the pseudocystic pattern. Lesions initially classified as having a pseudocystic pattern showed a change to a hailstorm pattern over time in 2/9 (22.2%) of cases. In all cases of a change in the pattern of AE reference lesions over time, the patients had taken albendazole continuously through the observation period (Figures 4 and 5). For the metastatic pattern, there were no pattern changes over time, but an increase in the size of the central echo-rich laminar body was observed (Figure 6). The mean time from initial diagnosis of AE to a pattern change was 24.2 ± 35.6 mo.

Number of lesions and lesion size according to EMUC-US

The study further revealed statistically significant differences in the number of hepatic AE lesions among EMUC-US types ($P < 0.05$) (Table 2). There were further statistically significant differences in lesion size between the metastatic pattern compared to the hailstorm pattern (21.7 ± 11.0 *vs* 67.4 ± 26.3; $P < 0.0001$), the pseudocystic pattern (21.7 ± 11.0 *vs* 113.7 ± 40.8; $P < 0.0001$), and the hemangioma-like pattern (21.7 ± 11.0 *vs* 83.5 ± 27.3; $P < 0.0001$) (Table 3). In the 9/59 (15.3%) cases with morphologic change in the EMUC-US pattern, there was a nonsignificant size regrowth from the initial examination (88.8 ± 30.6 *vs* 71.9 ± 29.6; $P = 0.1641$). For the 7/9 (77.8%) cases initially classified as having a hemangioma-like pattern, the mean average lesion size was 81.4 ± 29.4 mm initially *vs* 72.4 ± 21.4 mm after the pattern change. For the 2/9 (22.2%) cases initially classified as having a pseudocystic pattern, the mean lesion size at initial examination was 114.5 ± 24.8 mm *vs* 70.0 ± 65.1 mm after the pattern change.

DISCUSSION

Our work is the first preliminary longitudinal study tracking changes in sonomorphology during the follow-up of hepatic AE lesions using a sonomorphologic classification scheme. We found that the sonographic characteristics of individual subtypes of hepatic AE lesions change over time under anthelmintic therapy and exhibit size regrowth, resulting in a pattern classification that diverges from that assigned at the initial examination. A change in sonomorphology leading to pattern reclassification

Table 2 Number of hepatic alveolar echinococcosis reference lesions at the time of ultrasound 1, subdivided by Echinococcosis Multilocularis Ulm Classification-ultrasound classification

Number of AE lesions US 1	*n* (%)	*P* value		
Hailstorm pattern (*n* = 25)				
1	15 (60)	Reference	1.0000	0.4385
> 1	10 (40)			
2-5	9 (36)	-		
6-10	1 (4)			
> 10	0 (0)			
Pseudohemangioma-like pattern (*n* = 10)				
1	6 (60)	1.0000	Reference	0.6284
> 1	4 (40)			
2-5	4 (40)	-		
6-10	0 (0)			
> 10	0 (0)			
Pseudocystic pattern (*n* = 9)				
1	7 (77.8)	0.4385	0.6284	Reference
> 1	2 (22.2)			
2-5	2 (22.2)	-		
6-10	0 (0)			
> 10	0 (0)			
Metastasis-like pattern (*n* = 15)				
1	1 (6.7)	0.0009	0.0068	0.0007
> 1	14 (93.4)			
2-5	13 (86.7)	-		
6-10	0 (0)			
> 10	1 (6.7)			

AE: Alveolar echinococcosis; US: Ultrasound.

was seen for the hemangioma-like and pseudocystic patterns. A total of 70% of the reference lesions initially classified as hemangioma-like shifted to a different pattern classification. Of these, 85% were assigned to the hailstorm pattern and 15% to the pseudocystic pattern. A total of 22.2% (2/9) of the hepatic AE lesions initially described as pseudocystic were assigned to the hailstorm pattern during follow-up (Figures 5 and 7).

In agreement with our results, a Polish working group using the EMUC-US classification confirmed the hailstorm pattern as the most frequent[14]. However, a correlation between the sonographic EMUC-US patterns and the PNM (P = parasitic mass in the liver, N = involvement of neighbouring organs, and M = metastasis) scheme could not be demonstrated in this retrospective work[16]. In addition to the EMUC-US scheme, classification schemes are currently available for CT and MRI[11]. In a recent 39.8-mo follow-up study of our working group 72 patients on albendazole therapy with hepatic AE using the EMUC-CT classification, only one case had a pattern change reassignment from type IIIa (primarily cystoid) to type V (calcified). This result clearly contrasts with our current findings. To compare the different patterns of hepatic AE between the different imaging modalities, appropriate prospective comparative studies are necessary and as yet are unavailable. However, in a further retrospective study we compared EMUC-US and EMUC-CT, no clear assignment could be found for the sonographic hemangioma-like pattern in the EMUC-CT classification. In that study, the sonographic pseudocystic pattern could be

Table 3 Diameter of hepatic alveolar echinococcosis reference lesions at the time of ultrasound 1, subdivided by Echinococcosis Multilocularis Ulm Classification-ultrasound classification

	mean ± SD, min-max		*P* value
	EMUC-US	**Hailstorm pattern (*n* = 25)**	
Pseudohemangioma-like pattern (*n* = 10)	83.5 ± 27.3, 44-121	67.4 ± 26.3, 12-124	0.1491
Pseudocystic pattern (*n* = 9)	113.7 ± 40.8, 54-198	67.4 ± 26.3, 12-124	0.0017
Metastasis-like pattern (*n* = 15)	21.7 ± 11.0, 7-44	67.4 ± 26.3, 12-124	< 0.0001
	EMUC-US	**Pseudohemangioma-like pattern (*n* = 10)**	
Pseudocystic pattern (*n* = 9)	113.7 ± 40.8, 54-198	83.5 ± 27.3, 44-121	0.1304
Metastasis-like pattern (*n* = 15)	21.7 ± 11.0, 7-44	83.5 ± 27.3, 44-121	< 0.0001
	EMUC-US	**Pseudocystic pattern (*n* = 9)**	
Metastasis-like pattern (*n* = 15)	21.7 ± 11.0, 7-44	113.7 ± 40.8, 54-198	< 0.0001

EMUC-US: Echinococcosis Multilocularis Ulm Classification-ultrasound.

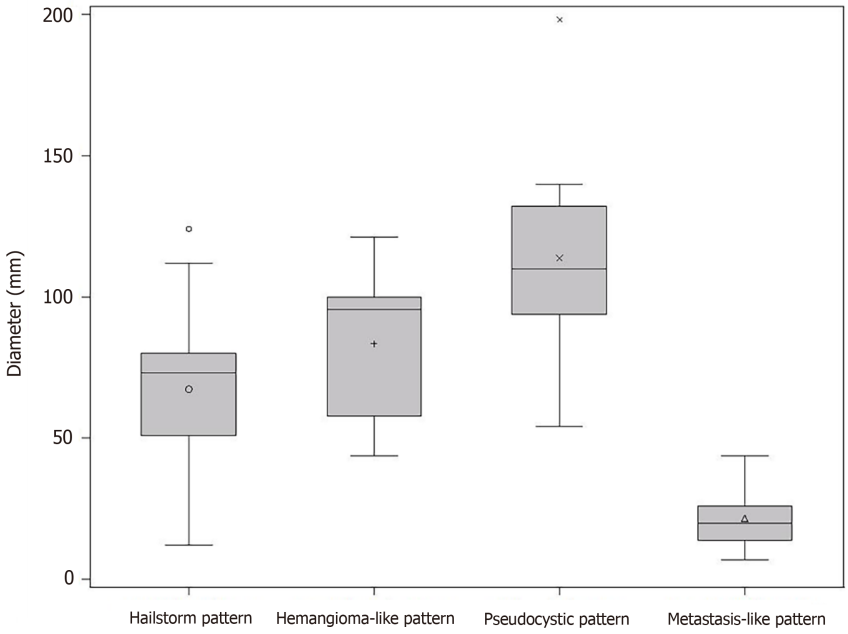


Figure 3 Diameter of hepatic alveolar echinococcosis reference lesion sorted by sonomorphological pattern analogous to Echinococcosis Multilocularis Ulm Classification-ultrasound classification.

predominantly classified as type I (diffuse-infiltrating) of the EMUC-CT classification. A study comparing MRI and PET-CT demonstrated an association between positron emission activity of hepatic AE lesions and microcysts[17]. A correlation between increased PET activity and calcifications could not be shown in this work[17]. This result contrasts with those of others results of our group who reported increased PET activity depending in particular on microcalcifications. The hailstorm pattern has significantly more calcifications than the hemangioma-like pattern, so these findings offer support for our hypothesis that a shift from hemangioma-like to hailstorm may indicate disease progression. In a recent retrospective study using the EMUC-CT classification in comparison to histology, a possible disease progression could be postulated for EMUC-CT patterns I-III[18]. In further confirmation of our hypothesis that the hemangioma-like pattern may represent an earlier disease stage, Zeng *et al* [19], using contrast-enhanced sonography with a four-type classification, visualised echo-rich masses corresponding to the EMUC-US hemangioma-like pattern.

The development of different manifestation patterns does not seem to be exclusively an expression of the temporal course of the disease, however, and appears to be

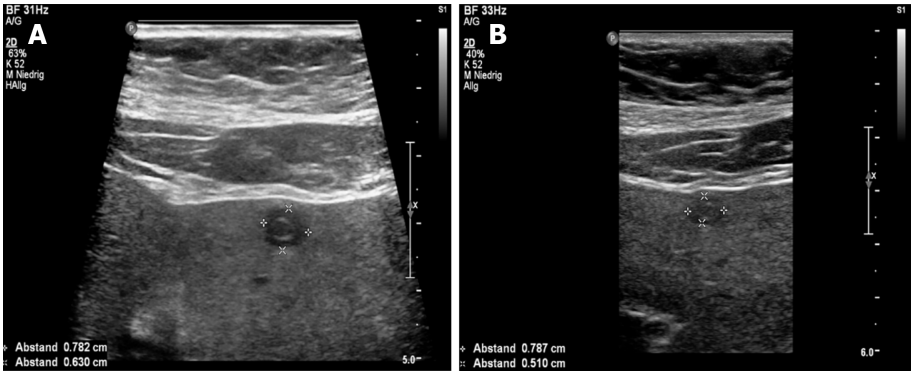


Figure 4 Hepatic alveolar echinococcosis reference lesion in segment II with pseudocystic pattern. A: Initially sharply delineated with individual centrally echo-rich portions; B: Through the disease course, more blurred delineation and increase of centrally echo-rich portions. The ultrasound images shown are from the current patient collective.

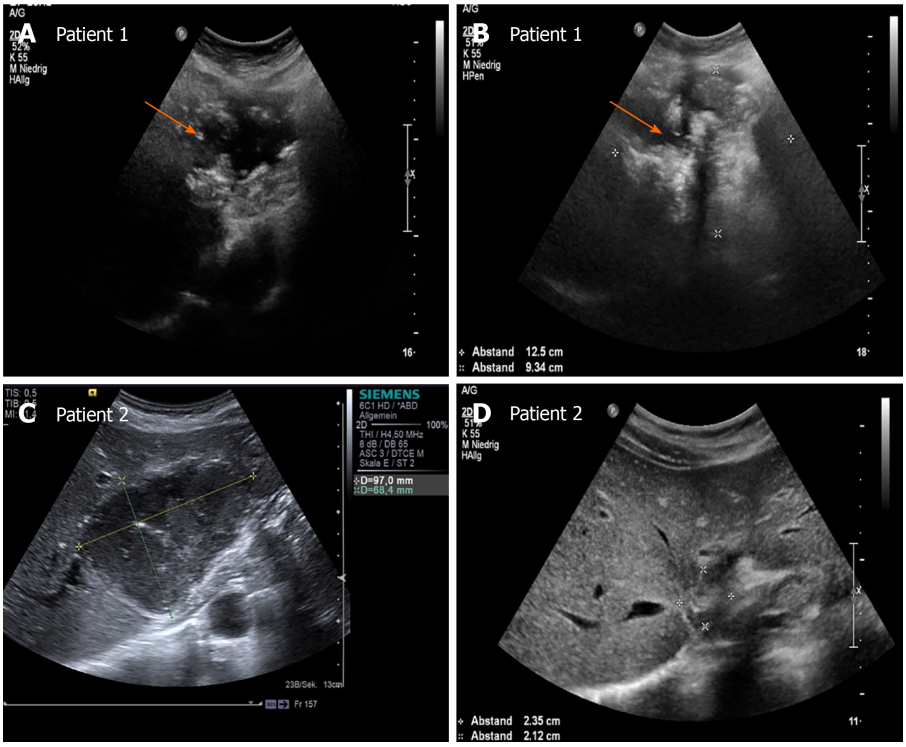


Figure 5 Hepatic alveolar echinococcosis reference lesions (arrow) in segment II/IVa/VIII (patient 1) and segment II/III (patient 2), respectively. A and C: initially classified as pseudocystic pattern (patient 1: A, patient 2: C); B and D: In the course of each case loss of the centrally echo-poor, liquid-impressive zone and increasing calcification structures, indicating a change in sonomorphology with a transition to a hailstorm pattern (patient 1: B; patient 2: D). The ultrasound images shown are from the current patient collective.

significantly related to the immunological and constitutional state of the host/misintermediate host (patient)[20]. In addition to the intraindividual immune response of the patient, one of the major difficulties in performing longitudinal imaging morphological studies is the apparent slow growth of the parasite with corresponding morphological changes in the liver. The use of international prospective database analysis studies could address this problem in the long term.

Limits of the study

The retrospective design of the preliminary cohort study must be seen as a limitation. It must also be taken into account that the number of cases in the individual EMUC-US patterns is very small, so that small effects may not be validly detected. Due to the sample size and study design, no calculation of interobserver variability between examiner 1 and examiner 2 and 3 was performed. Further prospective studies with larger numbers of cases, especially multicentre and international studies, are necessary

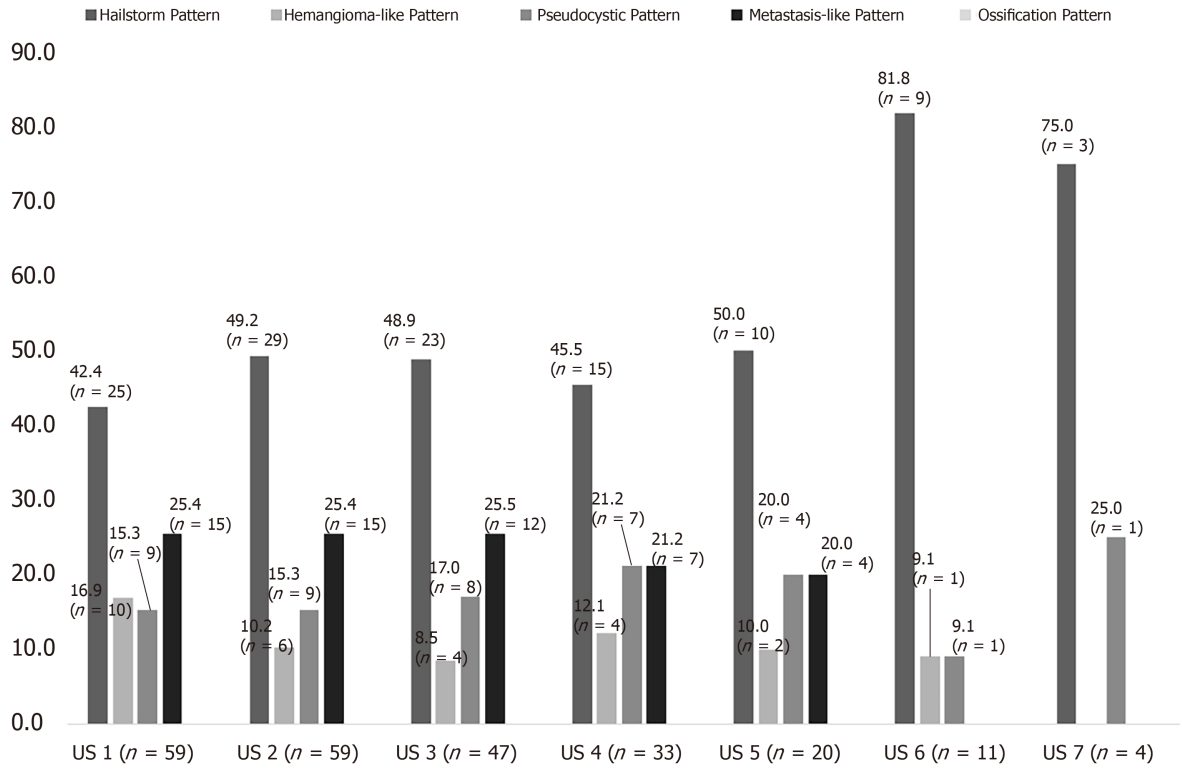


Figure 6 Predominant sonomorphological pattern of alveolar echinococcosis reference lesion subdivided according to Echinococcosis Multilocularis Ulm Classification-ultrasound classification, ultrasound 1 to ultrasound 7. US: Ultrasound.

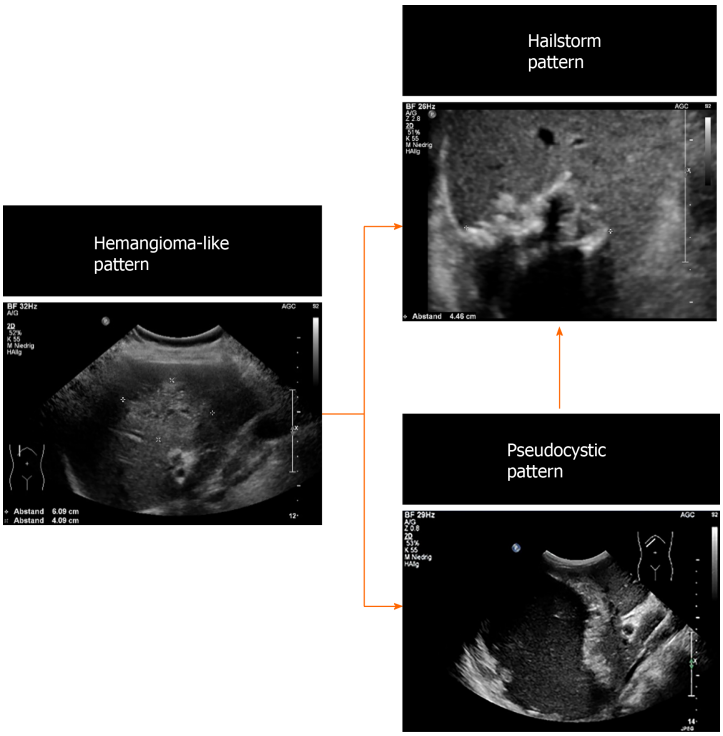


Figure 7 Potential pattern change over time.

to confirm the preliminary study results.

CONCLUSION

Our preliminary study demonstrates not only great heterogeneity in the sonomorphology of hepatic AE lesions at the initial diagnosis but also that sonomorphologic classification can change during disease progression.

ARTICLE HIGHLIGHTS

Research background

Alveolar echinococcosis (AE) is a human parasitosis caused by *Echinococcus multilocularis*.

Research motivation

Early diagnosis of AE is important to initiate prompt therapy and improve patient prognosis. Abdominal ultrasonography is the most common primary imaging modality and allows for classification of hepatic lesion morphology.

Research objectives

We address the question of whether (and how) the sonomorphology of individual AE lesions can change over time.

Research methods

In our preliminary retrospective longitudinal study, based on data from the national echinococcosis database in Germany, we evaluated clinical and ultrasound (US) imaging data for 59 patients according to AE case definition of confirmed (n = 26) or probable (n = 33) AE. The AE reference lesion was the largest hepatic AE lesion at the time of the first US examination. We used the Echinococcosis Multilocularis Ulm Classification (EMUC)-US to classify the sonomorphologic pattern.

Research results

The study included 59 patients, 38 (64.5%) women and 21 (35.6%) men. The mean median age at initial diagnosis was 59.9 ± 16.9 years. At the time of initial US, 42.4% (25/59) had a hailstorm pattern, 16.9% (10/59) had a pseudohemangioma-like pattern, 15.3% (9/59) had a pseudocystic pattern, and 25.4% (15/59) had a metastasis-like pattern. Although the sonomorphologic pattern remained unchanged in 84.7% (50/59) of the AE reference lesions, 15.3% (9/59) showed a pattern change over time. A change in pattern was seen exclusively for AE lesions initially classified as hemangioma-like or pseudocystic.

Research conclusions

The sonomorphology of hepatic AE lesions may change over time, particularly hemangioma-like and pseudocystic patterns.

Research perspectives

Further research should clarify whether the patterns evolve and change according to a sonomorphological evolution.

ACKNOWLEDGEMENTS

Members of the Echinococcosis Working Group Ulm: Barth TFE, Baumann S, Fischer I, Graeter T, Henne-Bruns D, Hillenbrand A, Kratzer W, Schlingeloff P, Schmidberger J, and Shi R.

REFERENCES

1 **Pawlowski ZS**, Vuitton DA, Ammann RW, Kern P, Craig P; World Health Organization. WHO/OIE Manual on echinococcosis in humans and animals: a public health problem of global concern. Paris, France: World Organization for Animal Health, 2001

2 **Eckert J**, Deplazes P. Biological, epidemiological, and clinical aspects of echinococcosis, a zoonosis

of increasing concern. *Clin Microbiol Rev* 2004; **17**: 107-135 [PMID: 14726458 DOI: 10.1128/CMR.17.1.107-135.2004]

3 **Kantarci M**, Bayraktutan U, Karabulut N, Aydinli B, Ogul H, Yuce I, Calik M, Eren S, Atamanalp SS, Oto A. Alveolar echinococcosis: spectrum of findings at cross-sectional imaging. *Radiographics* 2012; **32**: 2053-2070 [PMID: 23150858 DOI: 10.1148/rg.327125708]

4 **Polat P**, Kantarci M, Alper F, Suma S, Koruyucu MB, Okur A. Hydatid disease from head to toe. *Radiographics* 2003; **23**: 475-94; quiz 536 [PMID: 12640161 DOI: 10.1148/rg.232025704]

5 **Brunetti E**, Kern P, Vuitton DA; Writing Panel for the WHO-IWGE. Expert consensus for the diagnosis and treatment of cystic and alveolar echinococcosis in humans. *Acta Trop* 2010; **114**: 1-16 [PMID: 19931502 DOI: 10.1016/j.actatropica.2009.11.001]

6 **Vuitton DA**, Azizi A, Richou C, Vuitton L, Blagosklonov O, Delabrousse E, Mantion GA, Bresson-Hadni S. Current interventional strategy for the treatment of hepatic alveolar echinococcosis. *Expert Rev Anti Infect Ther* 2016; **14**: 1179-1194 [PMID: 27686694 DOI: 10.1080/14787210.2016.1240030]

7 **Wen H**, Vuitton L, Tuxun T, Li J, Vuitton DA, Zhang W, McManus DP. Echinococcosis: Advances in the 21st Century. *Clin Microbiol Rev* 2019; **32** [PMID: 30760475 DOI: 10.1128/CMR.00075-18]

8 **Yang C**, He J, Yang X, Wang W. Surgical approaches for definitive treatment of hepatic alveolar echinococcosis: results of a survey in 178 patients. *Parasitology* 2019; **146**: 1414-1420 [PMID: 31267889 DOI: 10.1017/S0031182019000891]

9 **Liu W**, Delabrousse É, Blagosklonov O, Wang J, Zeng H, Jiang Y, Qin Y, Vuitton DA, Wen H. Innovation in hepatic alveolar echinococcosis imaging: best use of old tools, and necessary evaluation of new ones. *Parasite* 2014; **21**: 74 [PMID: 25531446 DOI: 10.1051/parasite/2014072]

10 **Kratzer W**, Gruener B, Kaltenbach TE, Ansari-Bitzenberger S, Kern P, Fuchs M, Mason RA, Barth TF, Haenle MM, Hillenbrand A, Oeztuerk S, Graeter T. Proposal of an ultrasonographic classification for hepatic alveolar echinococcosis: Echinococcosis multilocularis Ulm classification-ultrasound. *World J Gastroenterol* 2015; **21**: 12392-12402 [PMID: 26604646 DOI: 10.3748/wjg.v21.i43.12392]

11 **Kodama Y**, Fujita N, Shimizu T, Endo H, Nambu T, Sato N, Todo S, Miyasaka K. Alveolar echinococcosis: MR findings in the liver. *Radiology* 2003; **228**: 172-177 [PMID: 12750459 DOI: 10.1148/radiol.2281020323]

12 **Brumpt E**, Blagosklonov O, Calame P, Bresson-Hadni S, Vuitton DA, Delabrousse E. AE hepatic lesions: correlation between calcifications at CT and FDG-PET/CT metabolic activity. *Infection* 2019; **47**: 955-960 [PMID: 31165442 DOI: 10.1007/s15010-019-01328-z]

13 **Yangdan CR**, Wang C, Zhang LQ, Ren B, Fan HN, Lu MD. Recent advances in ultrasound in the diagnosis and evaluation of the activity of hepatic alveolar echinococcosis. *Parasitol Res* 2021; **120**: 3077-3082 [PMID: 34370071 DOI: 10.1007/s00436-021-07262-0]

14 **Cai D**, Li Y, Jiang Y, Wang H, Wang X, Song B. The role of contrast-enhanced ultrasound in the diagnosis of hepatic alveolar echinococcosis. *Medicine (Baltimore)* 2019; **98**: e14325 [PMID: 30702614 DOI: 10.1097/MD.0000000000014325]

15 **Wa ZC**, Du T, Li XF, Xu HQ, Suo-Ang QC, Chen LD, Hu HT, Wang W, Lu MD. Differential diagnosis between hepatic alveolar echinococcosis and intrahepatic cholangiocarcinoma with conventional ultrasound and contrast-enhanced ultrasound. *BMC Med Imaging* 2020; **20**: 101 [PMID: 32854653 DOI: 10.1186/s12880-020-00499-8]

16 **Sulima M**, Nahorski W, Gorycki T, Wołyniec W, Wąż P, Felczak-Korzybska I, Szostakowska B, Sikorska K. Ultrasound images in hepatic alveolar echinococcosis and clinical stage of the disease. *Adv Med Sci* 2019; **64**: 324-330 [PMID: 31003201 DOI: 10.1016/j.advms.2019.04.002]

17 **Azizi A**, Blagosklonov O, Lounis A, Berthet L, Vuitton DA, Bresson-Hadni S, Delabrousse E. Alveolar echinococcosis: correlation between hepatic MRI findings and FDG-PET/CT metabolic activity. *Abdom Imaging* 2015; **40**: 56-63 [PMID: 24970734 DOI: 10.1007/s00261-014-0183-0]

18 **Grimm J**, Beck A, Nell J, Schmidberger J, Hillenbrand A, Beer AJ, Dezsényi B, Shi R, Beer M, Kern P, Henne-Bruns D, Kratzer W, Moller P, Barth TF, Gruener B, Graeter T. Combining Computed Tomography and Histology Leads to an Evolutionary Concept of Hepatic Alveolar Echinococcosis. *Pathogens* 2020; **9** [PMID: 32759781 DOI: 10.3390/pathogens9080634]

19 **Zeng H**, Wang J, Xie W, Liu W, Wen H. Assessment of early hepatic echinococcus multilocularis infection in rats with real-time contrast-enhanced ultrasonography. *Ultrasound Med Biol* 2012; **38**: 1982-1988 [PMID: 22929653 DOI: 10.1016/j.ultrasmedbio.2012.07.007]

20 **Deplazes P**, Grimm F, Sydler T, Tanner I, Kapel CM. Experimental alveolar echinococcosis in pigs, lesion development and serological follow up. *Vet Parasitol* 2005; **130**: 213-222 [PMID: 15869842 DOI: 10.1016/j.vetpar.2005.03.034]

World Journal of Gastroenterology

Submit a Manuscript: https://www.f6publishing.com

World J Gastroenterol 2021 October 28; 27(40): 6951-6966

DOI: 10.3748/wjg.v27.i40.6951

ISSN 1007-9327 (print) ISSN 2219-2840 (online)

ORIGINAL ARTICLE

Observational Study

Hepatic and gastrointestinal disturbances in Egyptian patients infected with coronavirus disease 2019: A multicentre cohort study

Hend Ibrahim Shousha, Shimaa Afify, Rabab Maher, Noha Asem, Eman Fouad, Ehab F Mostafa, Mohammed A Medhat, Amr Abdalazeem, Hazem Elmorsy, Miriam M Aziz, Rateba S Mohammed, Mohamed Ibrahem, Hassan Elgarem, Dalia Omran, Mohamed Hassany, Bassem Elsayed, Ahmed Y Abdelaziz, Mohamed El Kassas

ORCID number: Hend Ibrahim Shousha 0000-0002-0928-4738; Shimaa Afify 0000-0001-5937-4240; Rabab Maher 0000-0002-8728-2156; Noha Asem 0000-0003-3400-0159; Eman Fouad 0000-0002-2802-3082; Ehab F Mostafa 0000-0002-9805-3850; Mohammed A Medhat 0000-0002-3866-2283; Amr Abdalazeem 0000-0001-7205-0697; Hazem Elmorsy 0000-0001-7639-7567; Miriam M Aziz 0000-0003-0777-8555; Rateba S Mohammed 0000-0001-7697-0001; Mohamed Ibrahem 0000-0002-4570-2917; Hassan Elgarem 0000-0003-4521-5876; Dalia Omran 0000-0002-5513-6955; Mohamed Hassany 0000-0002-6001-8793; Bassem Elsayed 0000-0003-4806-0443; Ahmed Y Abdelaziz 0000-0002-9389-9371; Mohamed El Kassas 0000-0002-3396-6894.

Author contributions: Shousha HI was the guarantor and designed the study; Afify S, Maher R, Mostafa EF, Medhat MA, Abdelazeem A, Elmorsy H, Mohammed RS, Ibrahem M, Hassany M, Elsayed B, and El Kassas M participated in the acquisition of the data; Asem N and Fouad E participated in the analysis and interpretation of the data; Shousha HI and El Kassas M drafted the initial manuscript; Afify S, Aziz MM, Maher R,

Hend Ibrahim Shousha, Endemic Medicine, Faculty of Medicine, Cairo University, Cairo 11562, Egypt

Shimaa Afify, Mohamed Hassany, Bassem Elsayed, Gastroenterology Department, National Hepatology & Tropical Medicine Research Institute, Cairo 11563, Egypt

Rabab Maher, Hepatology Department, Students Hospital, Cairo University, Giza 12566, Egypt

Noha Asem, Eman Fouad, The Public Health Department, Faculty of Medicine, Cairo University, Cairo 11562, Egypt

Noha Asem, Mohamed Hassany, Egyptian, Ministry of Health and Population, Cairo 11567, Egypt

Ehab F Mostafa, Mohammed A Medhat, Department of Tropical Medicine and Gastroenterology, Faculty of Medicine, Assiut University, Assiut 15655, Egypt

Amr Abdalazeem, Mohamed El Kassas, Endemic Medicine Department, Faculty of Medicine, Helwan University, Cairo 13544, Egypt

Hazem Elmorsy, Internal Medicine, 15 Mayo Smart Hospital, Ministry of Health and Population, Cairo 13488, Egypt

Miriam M Aziz, Pediatrics Department, Faculty of Medicine, Cairo University, Cairo 11562, Egypt

Rateba S Mohammed, Occupational and Environmental Medicine Department, Faculty of Medicine, Cairo University, Cairo 11562, Egypt

Mohamed Ibrahem, Clinical Biochemistry Department, Faculty of medicine, Cairo University, Cairo 11562, Egypt

Hassan Elgarem, Dalia Omran, Endemic Medicine Department, Faculty of Medicine, Cairo University, Cairo 11562, Egypt

Ahmed Y Abdelaziz, Urology Department, Cairo University, Cairo 11562, Egypt

Corresponding author: Hend Ibrahim Shousha, MD, MSc, Associate Professor, Endemic

Mostafa EF, Medhat MA, Elgarem H, Omran D, Hassan M, Abdelaziz AY, and Elsayed B critically revised the article for important intellectual content.

Institutional review board statement: This study was approved by the research ethics committee of the Faculty of Medicine at Cairo University (No. N-37-2020, May 14, 2020) and the research ethics committee of the Egyptian Ministry of Health and Population (No. 17-2020/8, June 21, 2020).

Informed consent statement: All study subjects gave written informed consent before study inclusion.

Conflict-of-interest statement: There are no conflicts of interest to report.

Data sharing statement: No additional data are available.

STROBE statement: The authors have read the STROBE Statement checklist of items, and the manuscript was prepared and revised according to the STROBE Statement—checklist of items.

Open-Access: This article is an open-access article that was selected by an in-house editor and fully peer-reviewed by external reviewers. It is distributed in accordance with the Creative Commons Attribution NonCommercial (CC BY-NC 4.0) license, which permits others to distribute, remix, adapt, build upon this work non-commercially, and license their derivative works on different terms, provided the original work is properly cited and the use is non-commercial. See: http://creativecommons.org/Licenses/by-nc/4.0/

Manuscript source: Invited manuscript

Specialty type: Gastroenterology and hepatology

Country/Territory of origin: Egypt

Peer-review report's scientific quality classification

Medicine, Faculty of Medicine, Cairo University, Kasr Alainy Street, Cairo 11562, Egypt. hendshousha@kasralainy.edu.eg

Abstract

BACKGROUND

Various liver and gastrointestinal involvements occur in patients with coronavirus disease 2019 (COVID-19) at variable prevalence. Most studies report mild liver function disturbances correlated with COVID-19 severity, though liver failure is unusual.

AIM

To study liver and gastrointestinal dysfunctions in Egyptian patients with COVID-19 and their relation to disease outcomes

METHODS

This multicentre cohort study was conducted on 547 Egyptian patients from April 15, 2020 to July 29, 2020. Consecutive polymerase chain reaction-confirmed COVID-19 cases were included from four quarantine hospitals affiliated to the Egyptian ministry of health. Demographic information, laboratory characteristics, treatments, fibrosis-4 (FIB-4) index, COVID-19 severity, and outcomes were recorded and compared according to the degree of liver enzyme elevation and the presence of gastrointestinal symptoms. Follow-ups were conducted until discharge or death. Regression analyses were performed to determine the independent factors affecting mortality.

RESULTS

This study included 547 patients, of whom 53 (9.68%) died during hospitalization and 1 was discharged upon his request. Patients' mean age was 45.04 ± 17.61 years, and 21.98% had severe or critical COVID-19. Alanine aminotransferase (ALT) and aspartate aminotransferase (AST) were available for 430 and 428 patients, respectively. In total, 26% and 32% of patients had elevated ALT and AST, respectively. Significant liver injury with ALT or AST elevation exceeding 3-fold was recorded in 21 (4.91%) and 16 (3.73%) patients, respectively. Male gender, smoking, hypertension, chronic hepatitis C, and lung involvement were associated with elevated AST or ALT. AST was elevated in 50% of patients over 60-years-old. FIB-4 was significantly higher in patients admitted to the intensive care unit (ICU), those with more severe COVID-19, and non-survivors. The independent variables affecting outcome were supplementary vitamin C intake (1 g daily capsules) [odds ratio (OR): 0.05, 95% confidence interval (CI): 0.008–0.337]; lung consolidation (OR: 4.540, 95%CI: 1.155–17.840); ICU admission (OR: 25.032, 95%CI: 7.110–88.128); and FIB-4 score > 3.25 (OR: 10.393, 95%CI: 2.459-43.925). Among 60 (13.98%) patients with gastrointestinal symptoms, 52 (86.67%) had diarrhoea. Patients with gastrointestinal symptoms were predominantly females with higher body mass index, and 50 (83.40%) patients had non-severe COVID-19.

CONCLUSION

Few Egyptian patients with COVID-19 developed a significant liver injury. The independent variables affecting mortality were supplementary vitamin C intake, lung consolidation, ICU admission, and FIB-4 score.

Key Words: COVID-19; Egypt; Liver injury; Gastrointestinal symptoms; Fibrosis-4; Liver enzymes

©The Author(s) 2021. Published by Baishideng Publishing Group Inc. All rights reserved.

Core Tip: The prevalence and severity of liver and gastrointestinal dysfunction in patients with coronavirus disease 2019 (COVID-19) vary among populations with different underlying characteristics and disease outcomes. This is the first report from Egypt specifically exploring hepatic and gastrointestinal involvement in Egyptian

Grade A (Excellent): 0
Grade B (Very good): 0
Grade C (Good): C, C
Grade D (Fair): 0
Grade E (Poor): 0

Received: February 4, 2021
Peer-review started: February 4, 2021
First decision: March 6, 2021
Revised: March 17, 2021
Accepted: August 25, 2021
Article in press: August 25, 2021
Published online: October 28, 2021

P-Reviewer: Salvatore S
S-Editor: Liu M
L-Editor: Filipodia
P-Editor: Li JH



patients with COVID-19. In this study, we analyzed multicentre data of patients with polymerase chain reaction-confirmed COVID-19 from April 15, 2020 to July 29, 2020. Based on these data, we assessed the degree of liver injury and presence of gastrointestinal symptoms concerning COVID-19 disease severity, intensive care unit admission, and outcome.

Citation: Shousha HI, Afify S, Maher R, Asem N, Fouad E, Mostafa EF, Medhat MA, Abdalazeem A, Elmorsy H, Aziz MM, Mohammed RS, Ibrahem M, Elgarem H, Omran D, Hassany M, Elsayed B, Abdelaziz AY, El Kassas M. Hepatic and gastrointestinal disturbances in Egyptian patients infected with coronavirus disease 2019: A multicentre cohort study. *World J Gastroenterol* 2021; 27(40): 6951-6966
URL: https://www.wjgnet.com/1007-9327/full/v27/i40/6951.htm
DOI: https://dx.doi.org/10.3748/wjg.v27.i40.6951

INTRODUCTION

Hepatic and gastrointestinal (GI) involvement occurs in 16% to 78% of patients infected with the novel coronavirus, severe acute respiratory syndrome coronavirus 2 (SARS-CoV-2)[1-3]. In some of these populations, liver enzyme elevation exceeds five times the upper limit of normal (ULN)[4]. Most studies report mild liver function disturbances correlated with coronavirus disease 2019 (COVID-19) severity, though liver failure is unusual[5]. Hepatic and GI involvement can occur with and without pulmonary manifestations of COVID-19[1]. Different underlying mechanisms may contribute to liver injury related to COVID-19, including a direct viral effect, as the virus enters through the angiotensin-converting enzyme-2 receptor on cholangiocytes. Other indirect pathways include sepsis, drug-related hepatic injury, uncontrolled immune reactions, and cytokine storm[6].

Diarrhoea is the most frequently recorded GI symptom reported with COVID-19, ranging from 3% to 30%, followed by anorexia, nausea, vomiting, and abdominal pain [7]. SARS-CoV-2 RNA has been detected in stool specimens from patients with polymerase chain reaction-confirmed COVID-19 in respiratory samples. Those patients showed extended viral shedding in stool up to 11.2 d after viral eradication from respiratory specimens, suggesting faecal-oral transmission and warranting subsequent precautions[8]. The possible underlying mechanisms for GI involvement are the direct viral invasion of cells in the GI tract *via* the angiotensin-converting enzyme-2 receptor on gastric and duodenal glandular cells and proximal and distal enterocytes[8]. This viral invasion disrupts absorption and intestinal secretions, which activates the enteric nervous system and causes diarrhoea[9]. Other indirect mechanisms include antibiotic-associated diarrhoea, indirect inflammatory damage, and the ''gut-lung axis'' theory of immune-mediated effects on the respiratory tract by disturbed digestive tract flora[1,10]. This study aimed to determine the prevalence and extent of liver and GI derangements in Egyptian patients with COVID-19 infection and their relation to COVID-19 disease outcomes.

MATERIALS AND METHODS

Study population and data collection

This multicentre, prospective cohort study recruited 547 consecutive patients from April 15, 2020 to July 29, 2020 who were hospitalized in four quarantine centres affiliated to the Egyptian Ministry of Health and Population in three Egyptian governorates: 15 Mayo Smart Hospital in Cairo governorate, National Hepatology and Tropical Medicine Research Institute in Cairo governorate, Students Hospital in Giza governorate, and Alraghy Hospital in Assuit Governorate. This study included patients with a confirmed diagnosis of SARS-CoV-2, defined as a positive real-time reverse-transcriptase polymerase chain reaction assay of nasal and pharyngeal swab specimens. Patients were followed until discharge or death.

Table 1 Patients characteristics according to the degree of aspartate transaminase elevation, *n* (%)

Variable		AST level					*P* value
		Normal291 (67.99)	1-2 UNL97 (22.66)	2-3 UNL19 (4.44)	> 3UNL21 (4.91)	Total	
Age	< 18	7 (87.5)	1 (12.5)	0 (0.0)	0 (0.0)	8 (100.0)	< 0.001
	18:60	237 (72.7)	65 (19.9)	9 (2.8)	15 (4.6)	326 (100.0)	
	> 60	47 (50.0)	32 (34.0)	9 (9.6)	6 (6.4)	94 (100.0)	
Gender	Male	142 (61.2)	66 (28.4)	10 (4.3)	14 (6.0)	232 (100)	0.009
	Female	149 (76.0)	32 (16.3)	8 (4.1)	7 (3.6)	196 (100)	
Cigarette smoking		10 (47.6)	10 (47.6)	0 (0.0)	1 (4.8)	21 (100)	0.04
Diabetes mellitus		68 (61.8)	32 (29.1)	6 (5.5)	4 (3.6)	110 (100)	0.23
Hypertension		60 (55.6)	34 (31.5)	10 (9.3)	4 (3.7)	108 (100)	0.001
Chronic hepatitis C		3 (21.4)	7 (50.0)	0 (0.0)	4 (28.6)	14 (100)	< 0.001
CT chest	Normal	105 (78.9)	21 (15.8)	5 (3.8)	2 (1.5)	133 (100)	0.008
	Abnormal	181 (63.1)	76 (26.5)	13 (4.5)	17 (5.9)	287 (100)	
Lung consolidation		37 (56.1)	20 (30.3)	6 (9.1)	3 (4.5)	66 (100)	0.05

AST: Aspartate transaminase; CT: computed tomography; UNL: Upper limit of normal.

Ethics statement

The authors assert that all procedures contributing to this work complied with the ethical standards of the relevant national and institutional committees on human experimentation and with the Helsinki Declaration of 1975, as revised in 2008. All procedures involving human subjects or patients were approved by the research ethics committee of the Faculty of Medicine at Cairo University (number N-37-2020, May 14, 2020) and the research ethics committee of the Ministry of Health and Population (number 17-2020/8, June 21, 2020). Written informed consent was obtained from all patients before they participated in the study.

Methods

Collected baseline data included demographic information (age, gender, cigarette smoking, comorbidities), presenting symptoms (general, respiratory, GI), and laboratory features [complete blood count, liver and renal function, coagulation test, D-dimer, ferritin, C-reactive protein (CRP)]. Liver injury was defined as transaminase elevation exceeding three times the ULN[5]. The fibrosis-4 index (FIB-4) was calculated on admission using Sterling's formula: Age (years) × aspartate aminotransferase (AST) (IU/L) / platelet count (10^9/L) × [alanine aminotransferase (ALT) (IU/L) × 1/2][11]. Patients were classified according to the respective FIB-4 cut-off values (≤ 1.45 and ≥ 3.25) for predicting advanced liver fibrosis. Other baseline data included chest computed tomography (CT) findings, treatments administered, and COVID-19 disease classification and outcome. Laboratory results before discharge were collected.

COVID-19 severity was categorized as mild, moderate, or severe according to the management protocol of the Egyptian Ministry of Health and Population. Mild cases included asymptomatic and symptomatic cases with lymphopenia (defined as an absolute lymphocyte count < 1.0 × 10^3/L)[12] or leukopenia[12] (defined as a total leucocyte count < 4.0 × 10^3/L) and no radiological evidence of pneumonia. Moderate cases included symptomatic patients with radiological features of pneumonia with or without leukopenia and lymphopenia. Severe and critical cases were defined by the presence of any of the following: Respiratory rate > 30 per min, SaO_2 < 92 without oxygen therapy; PaO_2/FiO_2 ratio < 300 without oxygen or < 200 with oxygen, chest radiology showing more than 50% lung involvement, or progressive lung involvement within 24 h to 48 h. Severe and critical cases were indicated for intensive care unit (ICU) admission. Treatments were applied according to the protocol[13].

Statistical analysis

Analysis of data was performed using SPSS 25 for Windows (Armonk, NY, United States). Numerical variables are presented as mean, standard deviation, median, and

Table 2 Laboratory characteristics according to the degree of aspartate transaminase elevation, *n* (%)

Variable	AST level					*P* value
	Normal291 (67.99)	1-2 UNL97 (22.66)	2-3 UNL19 (4.44)	> 3UNL21 (4.91)	Total	
Hemoglobin (gm/L) median (IQR)	12.80 (11.80:14.00)	13.00 (12.00:14.23)	12.85 (11.23:14.05)	13.00 (10.75:15.00)	12.60 (12.00:13.90)	0.49
white blood cell count ($\times 10^9$)	5.00 (3.80:7.00)	6.20 (4.88:10.68)	6.30 (4.73:9.48)	7.40 (4.35:9.85)	5.00 (4.40:7.60)	< 0.001
Neutrophils absolute count	2.58 (1.58:4.40)	3.90 (2.20:7.87)	4.60 (3.01:8.13)	6.00 (2.74:8.33)	2.95 (1.70:5.60)	< 0.001
Neutrophils percentage	53.00 (42.00:69.00)	61.50 (43.13:80.85)	55.50 (42.75:68.25)	73.00 (55.00:89.88)	56.50 (42.63:70.75)	0.25
Lymphocytes absolute count	1.63 (1.30:2.30)	1.40 (1.01:2.35)	1.50 (0.89:1.92)	1.07 (0.80:1.48)	1.58 (1.10:2.20)	< 0.001
Lymphocytes percentages	38.00 (26.00:45.90)	23.30 (14.50:37.60)	23.40 (16.85:28.90)	14.00 (8.00:28.00)	32.70 (20.15:45.00)	< 0.001
Neutrophils/lymphocytes ratio	2.16 (1.30:3.73)	6.11 (2.12:11.26)	3.66 (3.26)	5.31 (3.83:6.84)	3.11 (1.56:6.16)	0.002
Platelet Count	225.00 (173.00:283.00)	221.00 (174.50:286.50)	251.00 (180.75:319.75)	210.00 (146.50:293.50)	208.00 (184.00:272.00)	0.62
AST	22.00 (17.00:28.00)	46.00 (41.00:55.50)	85.00 (72.75:95.25)	156.00 (117.00:252.00)	28.00 (19.00:43.00)	< 0.001
ALT	22.00 (16.00:30.00)	48.00 (36.00:68.00)	68.00 (44.00:92.75)	142.00 (93.50:217.50)	27.00 (18.00:46.00)	< 0.001
Alkaline phosphatase	89.00 (68.50:112.00)	82.50 (76.50:88.50)	155.00 (125.25:349.00)	111.00 (84.00:144.00)	89.00 (71.00:114.50)	0.01
GGT	31.00 (20.00:34.00)	39.50 (31.25:62.25)	67.50 (65.00)	90.00 (65.00)	34.00 (22.00:50.00)	0.005
Total bilirubin	0.80 (0.50:1.10)	0.90 (0.70:1.13)	1.15 (0.88:1.65)	1.80 (0.75:2.15)	0.80 (0.60 :1.13)	0.09
Serum albumin	4.20 (3.80:4.50)	4.10 (3.90:4.45)	3.80 (3.80)	3.80 (2.90:4.10)	4.20 (3.80:4.50)	0.13
D-dimer	0.54 (0.35:1.02)	0.57 (0.40:1.21)	1.08 (0.55:1.50)	0.90 (0.40:2.24)	0.58 (0.40:1.10)	0.005
Ferritin	230.00 (110.00:486.00)	406.85 (200.00:773.25)	804.00 (317.50:960.50)	540.00 (231.45:1219.10)	300.00 (132.80:590.00)	< 0.001
C-reactive protein	32.00 (5.00:64.00)	43.22 (14.40:64.00)	64.00 (31.50:109.85)	39.23 (32.00:64.00)	45.00 (8.25:64.00)	0.002
Recovery	273 (93.8)	78 (81.3)	11 (61.1)	17 (81.0)	379 (89.0)	< 0.001
Death	18 (6.2)	18 (18.8)	7 (38.9)	4 (19.0)	47 (11.0)	

Data are presented as median and interquartile range (IQR). AST: Aspartate transaminase; ALT: Alanine aminotransferase; GGT: Gamma-glutamyl transferase; IQR: Interquartile range.

25th and 75th percentiles. Categorical variables are presented as numbers (*n*) and percentages (%). According to the distribution of numerical data, suitable tests for inferential statistics were used. The Kruskal-Wallis and Wilcoxon or the Mann–Whitney U test was used for comparing two groups of independent variables [14]. Comparisons between categorical variables were carried out by Chi-square test (χ^2)[15]. Fisher's exact test was used instead of the Chi-square test when one expected cell or more was ≤ 5[15]. Results are expressed as *P*-values. Both univariate and multivariate logistic regression analyses were performed to identify the factors associated with outcome (death/recovery)[16].

RESULTS

This study included 547 COVID-19 patients hospitalized in four quarantine hospitals affiliated to the Egyptian Ministry of Health and Population (see Supplementary Tables 1 and 2 for baseline clinical, laboratory, imaging, treatment, and outcome features of the studied cohort). Of the 547 patients, 53 (9.68%) died during hospitalization, 493 (90.46%) recovered and were discharged, and 1 was discharged upon his request. The most common symptoms were fever (54.66%), cough (52.47%), dyspnoea (32.54%), and fatigue (30.71%), and 118 (21.57%) patients were asymptomatic. The mean age of the studied patients was 45.04 ± 17.61 years (the median age interquartile range) was 45.00 (30.00:60.00) years and 300 (54.84%) were male. Diabetes was the

Table 3 Patients characteristics according to the degree of alanine transaminase elevation, *n* (%)

Variable		ALT levels					*P* value
		Normal318 (74.0)	1-2 UNL73 (17.0)	2-3 UNL23 (5.3)	> 3UNL16 (3.7)	Total	
Age	< 18	9 (100.0)	0 (0.0)	0 (0.0)	0 (0.0)	9 (100.0)	0.53
	18:60	246 (75.0)	53 (16.2)	18 (5.5)	11 (3.4)	328 (100.0)	
	> 60	63 (67.7)	20 (21.5)	5 (5.4)	5 (5.4)	93 (100.0)	
Gender	Male	157 (67.4)	50 (21.5)	16 (6.9)	10 (4.3)	233 (100.0)	0.02
	Female	160 (81.6)	23 (11.7)	7 (3.6)	6 (3.1)	196 (100.0)	
Cigarette smoking		10 (47.6)	5 (23.8)	4 (19.0)	2 (9.5)	21 (100.0)	0.02
Diabetes mellitus		79 (71.2)	27 (24.3)	3 (2.7)	2 (1.8)	111 (100.0)	0.04
Hypertension		79 (73.1)	25 (23.1)	2 (1.9)	2 (1.9)	108 (100.0)	0.05
Chronic hepatitis C		5 (35.7)	6 (42.9)	1 (7.1)	2 (14.3)	14 (100.0)	0.005
CT chest	Normal	110 (82.1)	16 (11.9)	7 (5.2)	1 (.7)	134 (100.0)	0.04
	Abnormal	203 (70.5)	56 (19.4)	16 (5.6)	13 (4.5)	288 (100.0)	
Consolidation		43 (65.2)	17 (25.8)	3 (4.5)	3 (4.5)	66 (100.0)	0.06

AST: Aspartate transaminase; CT: Computed tomography.

most common comorbidity (24.86%), followed by hypertension (23.77%) and coronary artery disease (4.20%). Chronic liver disease was reported in 18 (3.29%) patients: 14 had chronic hepatitis C (of whom 7 had liver cirrhosis), 2 had chronic hepatitis B, and 2 had fatty liver disease. We confirmed their liver condition using their most recent abdominal ultrasound study before hospitalization for COVID-19. Regarding COVID-19, 427 (78.02%) had mild and moderate disease, 120 (21.98%) had severe or critical disease, and 122 (22.34%) were admitted to the ICU during their hospitalization. Flow chart of the study cohort is illustrated in Figure 1.

In our study, ALT and AST were available for 430 and 428 patients, respectively, and their other liver function tests and inflammatory markers were also available. Most patients had normal AST (291; 67.99%) and normal ALT levels (318; 74%). We divided patients as follows: Those with liver enzyme levels within the normal range, 1–2 fold over the ULN, 2–3 fold over the ULN, or >3 fold over the ULN (Tables 1-4). Among patients who required ICU admission, 48.50% had elevated AST and 35.60% had elevated ALT. On admission, FIB-4 was significantly higher in patients admitted to the ICU, those with more severe COVID-19 disease, and non-survivors (Supplementary Table 3).

We found that male gender, cigarette smoking, systemic hypertension, chronic hepatitis C, and abnormal chest CT findings were associated with significant elevation of baseline AST and ALT. Also, AST levels were elevated in patients older than 60 years, and diabetes mellitus was associated with elevation of baseline ALT. Elevated AST was also associated with elevated white blood cell count, absolute neutrophils count, neutrophils/lymphocytes ratio, ALT, gamma-glutamyl transferase (GGT), D-dimer, ferritin, and CRP and negatively correlated with absolute lymphocyte count and serum albumin. Elevated ALT was associated with elevated white blood cell count, Absolute Neutrophils count, neutrophils/lymphocytes ratio, AST, alkaline phosphatase (ALP), GGT, D-dimer, ferritin, and CRP and negatively correlated with absolute lymphocyte count and serum albumin (Tables 1-4).

No patient under 18-years-old showed elevated ALT levels, and only 1 had less than a 2-fold elevation of AST. All patients under 18 recovered and were discharged. Elevated AST levels were observed in 32 (18.4%) patients with mild disease and 23 (44.20%) with the critical disease, whereas elevated ALT levels were observed in 33 (19%) patients with mild disease and 32 (61.5%) with the critical disease (Supplementary Table 3).

Univariate analysis revealed several factors associated with survival (age < 60 years; no fever; no dyspnoea; normal findings on chest CT) and several associated with increased mortality (age > 60 years; leucocytosis; increased neutrophil/lymphocyte ratio; elevated AST, CRP, D-dimer or ferritin; baseline renal function impairment with elevations 1–2 above ULN) (Table 5).

Table 4 Laboratory characteristics according to the degree of alanine transaminase elevation, *n* (%)

Variable	ALT levels					*P* value
	Normal318 (74.0)	1-2 UNL73 (17.0)	2-3 UNL23 (5.3)	> 3UNL16 (3.7)	Total	
Hemoglobin (gm/L) median (IQR)	12.75 (11.78:14.00)	13.00 (12.10:14.45)	13.30 (12.30:14.80)	13.35 (10.63:14.98)	12.60 (12.00:13.90)	0.09
white blood cell count (× 10^9)	5.00 (4.00:7.40)	6.30 (4.70:10.55)	6.30 (4.20:9.80)	7.55 (3.88:9.33)	5.00 (4.40:7.60)	0.003
Neutrophils absolute count	2.70 (1.60:4.69)	4.00 (2.40:7.73)	2.70 (1.80:7.10)	5.00 (2.60:6.97)	2.95 (1.70:5.60)	0.02
Neutrophils percentage	53.00 (41.50:66.50)	57.00 (46.00:77.50)	82.60 (44.93:92.08)	66.50 (53.25:74.50)	56.50 (42.63:70.75)	0.17
Lymphocytes absolute count	1.60 (1.20:2.30)	1.60 (1.02:2.00)	1.26 (1.06:1.80)	1.07 (0.83:1.50)	1.58 (1.10:2.20)	0.04
Lymphocytes percentages	36.00 (24.23:45.00)	22.00 (15.70:43.40)	25.55 (15.05:42.38)	22.60 (13.75:33.75)	32.70 (20.15:45.00)	0.01
Neutrophils/lymphocytes ratio	2.19 (1.40:4.19)	6.07 (2.96:9.15)	6.24 (2.83:7.96)	4.14 (2.70:15.85)	3.11 (1.56:6.16)	0.002
Platelet count	220.00 (168.00:273.25)	238.00 (168.00:309.00)	219.00 (202.00:297.00)	271.00 (160.00:343.75)	208.00 (184.00:272.00)	0.11
AST	23.00 (17.00:31.00)	46.00 (34.00:60.00)	61.00 (52.00:84.00)	154.50 (109.25:236.00)	28.00 (19.00:43.00)	< 0.001
ALT	22.00 (16.00:29.25)	56.00 (48.00:63.60)	96.00 (91.00:110.00)	183.50 (144.50:228.50)	27.00 (18.00:46.00)	< 0.001
Alkaline phosphatase	88.00 (65.50:108.50)	88.00 (77.50:134.00)	86.00 (86.00:86.00)	120.00 (90.00:151.00)	89.00 (71.00:114.50)	0.19
GGT	23.00 (20.00:34.00)	39.50 (34.00:67.75)	34.00 (22.00:50.00)	77.50 (65.00:101.25)	34.00 (22.00:50.00)	0.001
Total bilirubin	0.80 (0.50:0.90)	1.10 (0.75:1.40)	0.80 (0.35: 0.88)	1.80 (1.25:2.15)	0.80 (0.60 :1.13)	0.01
Serum albumin	4.20 (3.70:4.50)	4.00 (3.83:4.45)	3.10 (2.60)	3.80 (3.50:4.10)	4.20 (3.80:4.50)	0.29
D-dimer	0.55 (0.36:1.02)	0.58 (0.40:1.27)	0.63 (0.36:1.50)	0.58 (0.40:1.48)	0.58 (0.40:1.10)	0.23
Ferritin	245.20M (122.93:540.00)	427.80 (200.00:847.00)	438.00 (86.50:922.00)	430.50 (215.73:1076.00)	300.00 (132.80:590.00)	0.009
C-reactive protein	32.00 (5.00:64.00)	32.00 (20.00:64.00)	32.00 (9.40:64.00)	55.44 (32.00:78.23)	45.00 (8.25:64.00)	0.09
Recovery	286 (90.2)	60 (83.3)	22 (95.7)	13 (81.3)	381 (89.0)	0.18
Death	31 (9.8)	12 (16.7)	1 (4.3)	3 (18.8)	47 (11.0)	

AST: Aspartate transaminase; ALT: Alanine aminotransferase; GGT: Gamma-glutamyl transferase; IQR: Interquartile range; UNL: Upper limit normal.

Patients were followed up till discharge or death. On discharge, patients showed significant improvement in haemoglobin, gamma-glutamyl transferase, serum albumin, ferritin, CRP, and lactate dehydrogenase levels with mild elevations in ALT and AST levels (Supplementary Table 4).

Multiple stepwise logistic regression analyses were conducted to identify significant predictors for outcomes of death and recovery. Independent variables included age, asymptomatic status, fever, dry cough, dyspnoea, sore throat, steroid use, supplementary vitamin C intake, azithromycin intake, subcutaneous heparin, chest CT findings, ICU admission, FIB-4 score, creatinine level, and urea level. The model was significant [χ^2 (144)], and the *P*-value was < 0.001, meaning the independent variable could explain the change in the dependent variable by up to 90.8%. Significant predictors in our model included treatment with supplementary vitamin C (1 g daily capsules according to the Egyptian Ministry of Health protocol[13]) [odds ratio (OR): 0.05, 95% confidence interval (CI): 0.008–0.337]; lung consolidation (OR: 4.540, 95%CI: 1.155–17.840); ICU admission (OR: 25.032, 95%CI: 7.110–88.128), and FIB-4 score > 3.25 (OR: 10.393, 95%CI: 2.459-43.925). The most significant predictor was ICU admission (Table 6).

Within our cohort, 60 (13.98%) patients presented with GI symptoms in addition to respiratory symptoms. They were predominantly females with significantly higher body mass index. Diarrhoea was the most common symptom, affecting 52 (86.67%) patients. Headache and sore throat were more frequent in patients with GI symptoms compared to those without GI symptoms; 83.4% of patients with GI symptoms had non-severe COVID-19 presentations with fewer ICU admissions. There was no difference in FIB-4 scores among patients with and without GI symptoms (Table 7).

Table 5 Univariate analysis for factors affecting the outcome, *n* (%)

Variable		Outcome			*P* value
		Death	Recovery	Total	
Age	< 18 yr	0 (0.0)	20 (100.0)	20 (100.0)	< 0.001
	18-60 yr	25 (6.1)	384 (93.9)	409 (100.0)	
	> 60 yr	27 (23.5)	88 (76.5)	115 (100.0)	
Gender	Male	29 (9.7)	270 (90.3)	299 (100.0)	0.94
	Female	23 (9.4)	221 (90.6)	244 (100.0)	
BMI (mean ± SD)		24.90 ± 2.08	28.11 ± 4.9		0.36
Cigarette smoking		2 (9.5)	19 (90.5)	21 (100.0)	0.64
Diabetes mellitus		17 (12.6)	118 (87.4)	135 (100.0)	0.17
Hypertension		17 (13.2)	112 (86.8)	129 (100.0)	0.11
Pulmonary diseases		2 (40.0)	3 (60.0)	5 (100.0)	0.07
Symptoms	Asymptomatic	1 (0.9)	116 (99.1)	117 (100.0)	< 0.001
	Respiratory	47 (12.8)	320 (87.2)	367 (100.0)	0.17
	GIT	4 (6.7)	56 (93.3)	60 (100.0)	
	Fever	43 (14.5)	254 (85.5)	297 (100.0)	< 0.001
	Headache	16 (10.3)	140 (89.7)	156 (100.0)	0.73
	Dry cough	40 (14.0)	245 (86.0)	285 (100.0)	< 0.001
	Dyspnea	38 (21.5)	139 (78.5)	177 (100.0)	< 0.001
	Sore throat	2 (2.3)	86 (97.7)	88 (100.0)	0.01
	Diarrhoea	2 (3.8)	50 (96.2)	52 (100.0)	0.21
Steroids		18 (14.2)	109 (85.8)	127 (100.0)	0.04
Lactoferrin		1 (2.2)	45 (97.8)	46 (100.0)	0.11
Hydroxy-chloroquine		12 (8.8)	124 (91.2)	136 (100.0)	0.74
Chloroquine sulphate		26 (8.3)	287 (91.7)	313 (100.0)	0.25
Vitamin C		22 (6.5)	318 (93.5)	340 (100.0)	0.002
Azithromycin		5 (4.1)	117 (95.9)	122 (100.0)	0.02
Other antibiotic		21 (10.9)	171 (89.1)	192 (100.0)	0.42
Subcutaneous heparin		43 (19.4)	179 (80.6)	222 (100.0)	< 0.001
Oral anticoagulants		0 (0.0)	33 (100.0)	33 (100.0)	0.06
COVID-19 disease classification	Mild	1 (0.4)	247 (99.6)	248 (100.0)	< 0.001
	Moderate	7 (4.0)	169 (96.0)	176 (100.0)	
	Severe	10 (17.2)	48 (82.8)	58 (100.0)	
	Critical	34 (55.7)	27 (44.3)	61 (100.0)	
CT chest	Normal	4 (2.0)	194 (98.0)	198 (100.0)	< 0.001
	Abnormal	48 (14.2)	290 (85.8)	338 (100.0)	
Lug consolidation		29 (42.6)	39 (57.4)	68 (100.0)	< 0.001
ICU admission		45 (37.2)	76 (62.8)	121 (100.0)	< 0.001
Fibrosis 4-score	< 1.45	17 (6.1)	263 (93.9)	280 (100.0)	< 0.001
	1.45:3.25	16 (15.1)	90 (84.9)	106 (100.0)	
	> 3.25	14 (38.9)	22 (61.1)	36 (100.0)	
Creatinine	Normal	35 (7.3)	445 (92.7)	480 (100.0)	< 0.001

	1-2 UNL	14 (25.9)	40 (74.1)	54 (100.0)	
	2-3 UNL	1 (50.0)	1 (50.0)	2 (100.0)	
	> 3UNL	2 (28.6)	5 (71.4)	7 (100.0)	
Urea	Normal	24 (7.5)	295 (92.5)	319 (100.0)	< 0.001
	1-2 UNL	18 (26.5)	50 (73.5)	68 (100.0)	
	2-3 UNL	3 (37.5)	5 (62.5)	8 (100.0)	
	> 3UNL	4 (44.4)	5 (55.6)	9 (100.0)	
Estimated-glomerular filtration rate	< 15	2 (28.6)	5 (71.4)	7 (100.0)	< 0.001
	15:29	4 (50.0)	4 (50.0)	8 (100.0)	
	30:44	4 (22.2)	14 (77.8)	18 (100.0)	
	45:59	10 (18.2)	45 (81.8)	55 (100.0)	
	60:89	17 (8.6)	181 (91.4)	198 (100.0)	
	≥ 90	15 (5.8)	243 (94.2)	258 (100.0)	
Hemoglobin (gm/L)[1]		12.35 (11.28:13.70)	12.60 (12.00: 13.90)	12.60 (12.00:13.90)	0.23
white blood cell count ($\times 10^9$)[1]		8.95 (5.08:13.68)	5.00 (4.30:6.90)	5.00 (4.40:7.60)	< 0.001
Neutrophils/lymphocytes ratio		9.85 (5.14:14.85)	2.71 (1.56:5.14)	3.11 (1.56:6.16)	0.003
Platelet count[1]		201.50 (182.25:278.50)	210.00 (187.00:271.50)	208.00 (184.00:272.00)	0.84
AST[1]		43.00 (28.00:67.00)	26.00 (18.00:40.00)	28.00 (19.00:43.00)	< 0.001
ALT[1]		31.00 (18.00:51.00)	26.70 (18.00:45.00)	27.00 (18.00:46.00)	0.35
Alkaline phosphatase[1]		152.00 (49.00)	89.00 (71.50:114.00)	89.00 (71.00:114.50)	0.37
Total bilirubin[1]		0.75 (0.70:0.80)	0.90 (0.60:1.20)	0.80 (0.60 :1.13)	0.38
Serum albumin[1]		4.00 (2.60)	4.20 (3.80:4.50)	4.20 (3.80:4.50)	0.36
D-dimer[1]		0.89 (0.40:1.96)	0.56 (0.40:1.05)	0.58 (0.40:1.10)	0.01
Ferritin[1]		429.40 (200.00:957.00)	269.00 (125.80:550.00)	300.00 (132.80:590.00)	0.001
C-reactive protein[1]		60.60 (32.00:64.00)	44.90 (7.00:64.00)	45.00 (8.25:64.00)	0.02

[1]Data are presented as median (interquartile range). COVID-19: Coronavirus disease 2019; AST: Aspartate transaminase; ALT: Alanine aminotransferase; IQR: Interquartile range; CT: Computed tomography; ICU: Intensive care unit; BMI: Body mass index; GIT: Gastrointestinal tract.

DISCUSSION

This is the first report from Egypt specifically exploring hepatic and GI disturbances in patients with COVID-19. Within our cohort, AST was more frequently elevated (32.10% of cases), compared with ALT (26% of cases). Only 21 (4.91%) and 16 (3.70%) patients, respectively, had a significant liver injury with AST or ALT elevation > 3-fold. The cholestatic pattern of elevated bilirubin > 1.1 mg/dL, elevated ALP >147 U/L, and GGT > 48 U/L was observed in only 8 (1.86%) patients. Our study findings align with those of other studies showing a direct relationship between elevated liver enzymes and COVID-19 disease activity.

Similar to our study, most other studies reveal a predominant pattern of disturbances in liver enzymes in COVID-19 patients, specifically higher AST elevation than ALT elevation[17-19]. A meta-analysis by Wu *et al*[20] found that low serum albumin and high GGT were the most frequent abnormalities on admission and that ALT elevation occurred most frequently during hospitalization, which they speculate may be due to the inclusion of patients with pre-existing liver disease. In our study, we observed no difference between survivors and non-survivors in serum albumin level. Wu *et al*[20] and Liu *et al*[21] found that serum albumin was significantly lower in non-survivors.

Chronic liver disease was reported in 3.29% of our patients. Phipps *et al*[4] reported that the severity and type of underlying chronic liver disease (*e.g.*, non-alcoholic fatty liver disease and chronic hepatitis B or C) were not significantly associated with hepatic disturbances related to COVID-19, which could be due to the small numbers of

Table 6 Multivariate analysis for factors associated with mortality

Variable	B	*P* value	adjusted OR	95% confidence interval for OR	
				Lower	Upper
Vitamin C intake	-2.960	0.002	0.05	0.008	0.337
Lung consolidation	1.513	0.030	4.540	1.155	17.840
ICU admission	3.220	< 0.001	25.032	7.110	88.128
FIB-4 score levels		0.001			
FIB-4 index levels (1.45:3.25)	0.054	0.921	1.055	0.368	3.025
Fib-4 index levels (above 3.25)	2.341	0.001	10.393	2.459	43.925
Constant	-4.821		0.008		

ICU: Intensive care unit; FIB-4: Fibrosis-4; OR: Odds ratio.

those cases with chronic liver diseases in their study.

In our study, AST was significantly higher in non-survivors, but no significant difference was observed in ALT levels between survivors and non-survivors, which is similar to previous meta-analyses[17,18]. Patients with severe COVID-19 and patients admitted to the ICU had higher transaminase levels, as confirmed by previous meta-analyses[17-19,21,22]. Ponziani *et al*[23] reported that alterations in transaminase levels in patients with COVID-19 were mild to moderate, whereas significant liver injury with transaminases > 3 times the ULN and pure cholestatic injuries occurred in a minority of patients[23]. Phipps *et al*[4] showed that 6.4% of their patients had a severe liver injury with ALT > 5 times above the ULN. They also found that peak ALT, older age, diabetes mellitus, and intubation were independent predictors of mortality. A meta-analysis by Kulkarni *et al*[22] found that severe liver injury occurred in 10.7% of 3440 patients with COVID-19: 24.9% among 358 patients with the non-severe disease and 41.5% among 317 patients with severe disease.

Other causes of liver injury in patients with COVID-19 include medication, such as acetaminophen at doses exceeding 7.5–10 g and combined use of antivirals and antibiotics. Systemic effects of SARS-CoV-2 infection can be hepatotoxic. For example, hypoxia due to lung injury and, in severe cases, sepsis, acute respiratory distress syndrome, and multi-organ failure precipitate hypoxia and ischemia of the liver, causing elevated serum ALT, AST, and total bilirubin levels[17].

In this study, baseline FIB-4 was an independent factor affecting mortality, and it was significantly higher in patients admitted to the ICU, those with more severe COVID-19 disease, and non-survivors. FIB-4, which predicts significant hepatic fibrosis in patients with liver disease, comprises four variables: Age, AST, ALT, and platelet count[11]. These factors are deranged in COVID-19 disease due to systemic inflammation, bone marrow suppression, injury of the skeletal muscles, elevated pressure in the right heart system with subsequent liver congestion, and elevated liver stiffness that occurs in the disease[24,25]. Sterling *et al*[23] showed that gender, diabetes mellitus, and FIB-4 ≥ 2.67 were associated with increased mortality. Another recent study by Li *et al*[25] found that FIB-4 correlated with mortality and severe COVID-19, noting that FIB-4 normalized in the survivors only. They also found that baseline FIB-4 correlated with SARS-CoV-2 viral load and their studied monocyte/interferon-I-related cytokines (interleukin-6 and interferon-gamma–induced protein 10)[25]. Rentsch *et al*[26] and Price-Haywood *et al*[27] found that FIB-4 scores > 3.25 and ≥ 2.67, respectively, were associated with hospitalization and with ICU admission and mechanical support.

Within our cohort, 60 patients (13.98%) presented with GI symptoms in addition to respiratory symptoms. The prevalence of diarrhoea, nausea, vomiting, and abdominal pain was 9.51%, 2.01%, 3.11%, and 3.84%, respectively. Diarrhoea was the most common GI symptom in our cohort, similar to findings from Wang *et al*[28].

The prevalence of diarrhoea, nausea/vomiting, and abdominal pain in their systematic review and meta-analysis was 9.1%, 5.2%, and 3.5%, respectively. The predominant GI symptoms differ among countries[28-30]. In China, for example, Luo *et al*[29] reported anorexia, nausea, and vomiting as the frequent symptoms in two-thirds of their patients, while diarrhoea and abdominal pain presented in 37%and 25% of their patients, respectively. A meta-analysis by Wan *et al*[30] (included 55 studies

Table 7 Features of patients with and without gastrointestinal manifestations, *n* (%)

Variable		Respiratory, *n* = 369 (86.02)	Respiratory and GIT, *n* = 60 (13.98)	Total	*P* value
Age	< 18	2 (0.5)	0 (0.0)	2 (0.5)	0.12
	18:60	271 (73.4)	51 (85.0)	322 (75.1)	
	> 60	96 (26.0)	9 (15.0)	105 (24.5)	
Gender	Male	210 (56.9)	22 (36.7)	232 (54.1)	0.004
	Female	159 (43.1)	38 (63.3)	197 (45.9)	
BMI median (IQR)		25.96 (23.34:31.25)	29.02 (26.91:33.36)	27.76 (23.74:32.01)	0.04
Cigarette smoking		15 (18.3)	6 (18.2)	21 (18.3)	1.00
Diabetes mellitus		103 (27.9)	18 (30.0)	121 (28.2)	0.74
Hypertension		101 (27.4)	21 (35.0)	122 (28.4)	0.22
Pulmonary diseases		5 (1.4)	0 (0.0)	5 (1.2)	0.36
Symptoms	Fever	255 (69.1)	44 (73.3)	299 (69.7)	0.51
	Headache	124 (33.6)	34 (56.7)	158 (36.8)	0.001
	Dry cough	252 (68.3)	35 (58.3)	287 (66.9)	0.13
	Dyspnea	154 (41.7)	24 (40.0)	178 (41.5)	0.80
	Sore throat	68 (18.4)	20 (33.3)	88 (20.5)	0.008
Steroids		101 (27.4)	24 (40.0)	125 (29.1)	0.05
Lactoferrin		28 (7.6)	18 (30.0)	46 (10.7)	<0.001
Hydroxy-chloroquine		101 (27.4)	31 (51.7)	132 (30.8)	<0.001
Chloroquine sulfate		200 (54.2)	24 (40.0)	224 (52.2)	0.04
Vitamin C		201 (54.5)	50 (83.3)	251 (58.5)	<0.001
Azithromycin		80 (21.7)	33 (55.0)	113 (26.3)	<0.001
Other parenteral antibiotics		149 (40.4)	36 (60.0)	185 (43.1)	0.004
Subcutaneous heparin		186 (50.4)	22 (36.7)	208 (48.5)	0.05
Oral anticoagulants		20 (5.4)	13 (21.7)	33 (7.7)	<0.001
COVID-19 disease Classification	Mild	122 (33.2)	16 (26.7)	138 (32.2)	0.03
	Moderate	137 (37.2)	34 (56.7)	171 (40.0)	
	Severe	53 (14.4)	6 (10.0)	59 (13.8)	
	Critical	56 (15.2)	4 (6.7)	60 (14.0)	
Outcome	Recovery	320 (87.2)	56 (93.3)	376 (88.1)	0.17
	Death	47(12.8)	4 (6.7)	51(11.9)	
CT chest	Normal	91 (25.0)	11 (19.3)	102 (24.2)	0.35
	Abnormal	273 (75.0)	46 (80.7)	319 (75.8)	
Lug consolidation		61 (17.0)	4 (7.1)	65 (15.7)	0.06
ICU admission		111 (30.2)	10 (16.7)	121 (28.3)	0.03
Fibrosis 4-score	< 1.45	202 (64.7)	34 (64.2)	236 (64.7)	0.99
	1.45:3.25	81 (26.0)	14 (26.4)	95 (26.0)	
	> 3.25	29 (9.3)	5 (9.4)	34 (9.3)	
Creatinine	Normal	319 (86.4)	53 (88.3)	372 (86.7)	0.89
	1-2 UNL	41 (11.1)	7 (11.7)	48 (11.2)	
	2-3 UNL	2 (0.5)	0 (0.0)	2 (0.5)	

	> 3UNL	7 (1.9)	0 (0.0)	7 (1.6)	
Urea	Normal	226 (75.8)	46 (85.2)	272 (77.3)	0.49
	1-2 UNL	57 (19.1)	7 (13.0)	64 (18.2)	
	2-3 UNL	7 (2.3)	1 (1.9)	8 (2.3)	
	> 3UNL	8 (2.7)	0 (0.0)	8 (2.3)	
Estimated-GFR	< 15	7 (1.9)	0 (0.0)	7 (1.6)	0.84
	15:29	5 (1.4)	1 (1.7)	6 (1.4)	
	30:44	17 (4.6)	1 (1.7)	18 (4.2)	
	45:59	42 (11.4)	8 (13.3)	50 (11.7)	
	60:89	135 (36.6)	21 (35.0)	156 (36.4)	
	≥ 90	163 (44.2)	29 (48.3)	192 (44.8)	
Hemoglobin (gm/L)		12.80 (12.00:14.00)	12.05 (11.00:13.35)	12.60 (12.00:13.90)	0.02
White blood cell count ($\times 10^9$)		5.30 (4.35:8.40)	5.00 (3.63:7.08)	5.00 (4.40:7.60)	0.12
Neutrophils/lymphocytes ratio		3.71 (1.91:6.81)	4.20 (2.13:6.83)	3.11 (1.56:6.16)	0.85
Platelet count		213.00 (175.50:282.50)	225.50 (187.00:278.25)	208.00 (184.00:272.00)	0.87
AST		29.00 (20.00:44.00)	26.00 (17.00:45.63)	28.00 (19.00:43.00)	0.63
ALT		28.00 (19.00:46.00)	27.00 (18.00:55.50)	27.00 (18.00:46.00)	0.96
Alkaline phosphatase		86.50 (70.00:112.25)	99.00 (78.00:117.00)	89.00 (71.00:114.50)	0.18
Total bilirubin		0.80 (0.55:0.90)	0.90 (0.65:1.20)	0.80 (0.60:1.13)	0.06
Serum albumin		4.20 (3.80:4.50)	4.20 (3.70:4.40)	4.20 (3.80:4.50)	0.75
D-dimer		0.58 (0.40:1.10)	0.60 (0.40:1.22)	0.58 (0.40:1.10)	0.08
Ferritin		317.80 (156.10:615.90)	350.00 (112.50:723.98)	300.00 (132.80:590.00)	0.93
C-reactive protein		47.34 (13.81:64.00)	40.00 (7.00:64.00)	45.00 (8.25:64.00)	0.48

AST: Aspartate transaminase; ALT: Alanine aminotransferase; CT: computed tomography; COVID-19: Coronavirus disease 2019; BMI: Body mass index; QR: Interquartile range; GIT: Gastrointestinal tract.

from China, 1 from Austria, 1 from the United States, 1 from Spain, and 2 from Singapore) reported the prevalence of GI symptoms as diarrhoea (53 studies, 8604 patients: 11.2%), nausea and vomiting (33 studies, 6165 patients: 10.0%), loss of appetite (15 studies, 2540 patients: 21.3%), and abdominal pain 14 studies, 2203 patients: (4.6%). Another meta-analysis by Parasa *et al*[31] reported that diarrhoea occurred in 4.3%–12.2%, and nausea, or vomiting occurred in 2.6%–8.0% of their included 4805 patients[31]. A study from the United States showed that GI symptoms were present in 61.3% of their patients (the most common was loss of appetite (34.8%) followed by diarrhoea (33.7%) and nausea (26.4%))[32].

In our study, 83.4% of patients with GI symptoms had non-severe COVID-19. The presence of diarrhoea or other GI symptoms did not impact COVID-19 mortality. Wang *et al*[28] also found no difference in the prevalence of diarrhoea among severe and non-severe cases, and the presence of GI symptoms did not affect mortality. Nobel *et al*[33] found that COVID-19 patients with GI symptoms had lower mortality and no difference in ICU admission rates, compared with patients without GI symptoms[33]. In contrast, Zhong *et al*[8] and Wan *et al*[30] reported a correlation between diarrhoea and severity of COVID-19, showing that patients with diarrhoea needed more ICU care and ventilator support.

In our cohort, there was no significant difference in transaminases level among patients with and without GI symptoms, which contrasts with a meta-analysis by Wijarnpreecha *et al*[17] showing higher transaminases in patients with GI symptoms. The results of our study are similar to Zhou *et al*[34], who found that GI symptoms were more common in females, sore throat was also more common in their patients with GI symptoms, and haemoglobin level was significantly lower in their patients with GI symptoms. In contrast to our study, ALT was higher in their non-medical group of patients with GI symptoms but not in the medical group, and CRP was

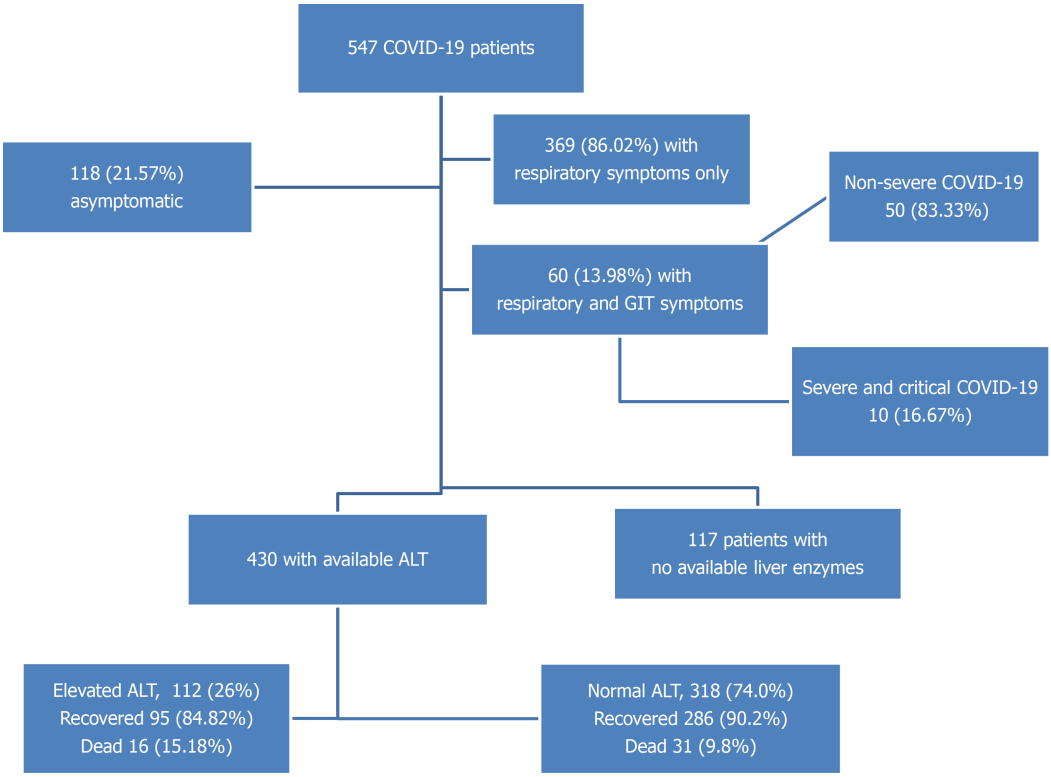


Figure 1 Flow chart of the study cohort. COVID-19: Coronavirus disease 2019; ALT: Alanine aminotransferase.

higher in their patients with GI symptoms. Limitations of our study include inconclusive reports about medications received before hospitalization and the possibility of underlying undiagnosed liver disease, such as non-alcoholic fatty liver disease and unavailability of creatine phosphokinase enzyme results, as it was not tested at the time of the study in the quarantine hospitals affiliated with the Egyptian Ministry of Health.

CONCLUSION

In conclusion, within our cohort of Egyptian patients with COVID-19, elevated AST, ALT, total bilirubin ,and GGT were present in 32.1%, 26%, 5.8%, and 1.86% of our patients, respectively. Significant liver injury (AST and ALT three times higher than the ULN) affected 4.91% and 3.70% of patients, respectively. Male gender, smoking, hypertension, chronic hepatitis C, and lung involvement were significantly associated with elevated AST and ALT. FIB-4 scores were significantly higher in patients admitted to the ICU, those with more severe COVID-19, and non-survivors. The independent variables affecting outcome were supplementary vitamin C intake, lung consolidation, ICU admission, and FIB-4 score. GI symptoms were significantly more frequent in women, patients with higher body mass index, and those with non-severe COVID-19.

ARTICLE HIGHLIGHTS

Research background

Hepatic and gastrointestinal (GI) disturbances have been reported in patients with coronavirus disease 2019 (COVID-19) with variable prevalence according to disease severity and population characteristics. This could be due to direct severe acute respiratory syndrome coronavirus 2 invasion through the angiotensin-converting enzyme 2 receptors or indirect effects such as an uncontrolled immune response, drug-induced injury, or sepsis.

Research motivation

Comprehensive researches on hepatic and GI derangements in patients with COVID-19 are still lacking, and they are needed for better understanding of the underlying factors, clinical presentations, and disease outcome

Research objectives

We aimed to study the prevalence and severity of liver and GI derangements in Egyptian patients with COVID-19 infection and their relation to disease outcomes.

Research methods

This multicentre cohort study was conducted on 547 COVID-19 cases from four quarantine hospitals during the period from April 15, 2020 to July 29, 2020. Clinical, laboratory features, fibrosis-4 (FIB-4) index, COVID-19 severity, and outcomes were recorded. Follow-ups were conducted until discharge or death.

Research results

Alanine aminotransferase (ALT) and aspartate aminotransferase (AST) were elevated in 26% and 32% of patients while elevations above 3 fold were recorded in 4.91% and 3.73% patients, respectively. Male gender, smoking, hypertension, chronic hepatitis C, and lung involvement were associated with elevated AST or ALT. FIB-4 was significantly higher in patients admitted to the intensive care unit (ICU), those with more severe COVID-19, and non-survivors. The independent variables affecting outcome were supplementary vitamin C intake, lung consolidation, ICU admission, and FIB-4 score > 3.25. GI symptoms were present in 60 (13.98%) patients. They were predominantly females with higher body mass index, and 50 (83.40%) patients had non-severe COVID-19.

Research conclusions

Significant liver injury was uncommon among Egyptian patients with COVID-19. The independent variables affecting mortality were supplementary vitamin C intake, lung consolidation, ICU admission, and FIB-4 score.

Research perspectives

Variables independently affecting mortality were supplementary vitamin C intake, FIB-4 score > 3.25, lung consolidation, and ICU admission. GI symptoms occurred in patients with non-severe COVID-19.

REFERENCES

1 **Musa S**. Hepatic and gastrointestinal involvement in coronavirus disease 2019 (COVID-19): What do we know till now? *Arab J Gastroenterol* 2020; **21**: 3-8 [PMID: 32253172 DOI: 10.1016/j.ajg.2020.03.002]

2 **Youssef M**, H Hussein M, Attia AS, M Elshazli R, Omar M, Zora G, S Farhoud A, Elnahla A, Shihabi A, Toraih EA, S Fawzy M, Kandil E. COVID-19 and liver dysfunction: A systematic review and meta-analysis of retrospective studies. *J Med Virol* 2020; **92**: 1825-1833 [PMID: 32445489 DOI: 10.1002/jmv.26055]

3 **Feng G**, Zheng KI, Yan QQ, Rios RS, Targher G, Byrne CD, Poucke SV, Liu WY, Zheng MH. COVID-19 and Liver Dysfunction: Current Insights and Emergent Therapeutic Strategies. *J Clin Transl Hepatol* 2020; **8**: 18-24 [PMID: 32274342 DOI: 10.14218/JCTH.2020.00018]

4 **Phipps MM**, Barraza LH, LaSota ED, Sobieszczyk ME, Pereira MR, Zheng EX, Fox AN, Zucker J, Verna EC. Acute Liver Injury in COVID-19: Prevalence and Association with Clinical Outcomes in a Large U.S. Cohort. *Hepatology* 2020; **72**: 807-817 [PMID: 32473607 DOI: 10.1002/hep.31404]

5 **Ghoda A**, Ghoda M. Liver Injury in COVID-19 Infection: A Systematic Review. *Cureus* 2020; **12**: e9487 [PMID: 32879813 DOI: 10.7759/cureus.9487]

6 **Jothimani D**, Venugopal R, Abedin MF, Kaliamoorthy I, Rela M. COVID-19 and the liver. *J Hepatol* 2020; **73**: 1231-1240 [PMID: 32553666 DOI: 10.1016/j.jhep.2020.06.006]

7 **Suresh Kumar VC**, Harne PS, Mukherjee S, Gupta K, Masood U, Sharma AV, Lamichhane J, Dhamoon AS, Sapkota B. Transaminitis is an indicator of mortality in patients with COVID-19: A retrospective cohort study. *World J Hepatol* 2020; **12**: 619-627 [PMID: 33033568 DOI: 10.4254/wjh.v12.i9.619]

8 **Zhong P**, Xu J, Yang D, Shen Y, Wang L, Feng Y, Du C, Song Y, Wu C, Hu X, Sun Y. COVID-19-associated gastrointestinal and liver injury: clinical features and potential mechanisms. *Signal Transduct Target Ther* 2020; **5**: 256 [PMID: 33139693 DOI: 10.1038/s41392-020-00373-7]

9 **Zhang H**, Kang Z, Gong H, Xu D, Wang J, Li Z, Cui X, Xiao J, Zhan J, Meng T, Zhou W, Liu J, Xu

H. Digestive system is a potential route of COVID-19: an analysis of single-cell coexpression pattern of key proteins in viral entry process. *Gut* 2020; **69**: 1010-1018 [DOI: 10.1136/gutjnl-2020-320953]

10 **Villapol S**. Gastrointestinal symptoms associated with COVID-19: impact on the gut microbiome. *Transl Res* 2020; **226**: 57-69 [PMID: 32827705 DOI: 10.1016/j.trsl.2020.08.004]

11 **Sterling RK**, Lissen E, Clumeck N, Sola R, Correa MC, Montaner J, S Sulkowski M, Torriani FJ, Dieterich DT, Thomas DL, Messinger D, Nelson M; APRICOT Clinical Investigators. Development of a simple noninvasive index to predict significant fibrosis in patients with HIV/HCV coinfection. *Hepatology* 2006; **43**: 1317-1325 [PMID: 16729309 DOI: 10.1002/hep.21178]

12 **Frater JL**, Zini G, d'Onofrio G, Rogers HJ. COVID-19 and the clinical hematology laboratory. *Int J Lab Hematol* 2020; **42** Suppl 1: 11-18 [PMID: 32311826 DOI: 10.1111/ijlh.13229]

13 **Ministry of Health and Population**, Egypt Management protocol for COVID-19 Patients. [cited 30 May 2020]. Available from: https://www.elwatannews.com/data/iframe/pdf/17175200761591035127.pdf

14 **Chan YH**. Biostatistics 102: quantitative data--parametric & non-parametric tests. *Singapore Med J* 2003; **44**: 391-396 [PMID: 14700417]

15 **Chan YH**. Biostatistics 103: qualitative data - tests of independence. *Singapore Med J* 2003; **44**: 498-503 [PMID: 15024452]

16 **Chan YH**. Biostatistics 202: logistic regression analysis. *Singapore Med J* 2004; **45**: 149-153 [PMID: 15094982]

17 **Wijarnpreecha K**, Ungprasert P, Panjawatanan P, Harnois DM, Zaver HB, Ahmed A, Kim D. COVID-19 and liver injury: a meta-analysis. *Eur J Gastroenterol Hepatol* 2021; **33**: 990-995 [PMID: 32639420 DOI: 10.1097/MEG.0000000000001817]

18 **Wu ZH**, Yang DL. A meta-analysis of the impact of COVID-19 on liver dysfunction. *Eur J Med Res* 2020; **25**: 54 [PMID: 33148326 DOI: 10.1186/s40001-020-00454-x]

19 **Xing QQ**, Dong X, Ren YD, Chen WM, Zeng DY, Cai YY, Hong MZ, Pan JS. Liver Chemistries in Patients with COVID-19 Who Discharged alive or Died: A Meta-analysis. *Hepatol Commun* 2020; **5**: 12-23 [PMID: 32838104 DOI: 10.1002/hep4.1585]

20 **Wu Y**, Li H, Guo X, Yoshida EM, Mendez-Sanchez N, Levi Sandri GB, Teschke R, Romeiro FG, Shukla A, Qi X. Incidence, risk factors, and prognosis of abnormal liver biochemical tests in COVID-19 patients: a systematic review and meta-analysis. *Hepatol Int* 2020; **14**: 621-637 [PMID: 32710250 DOI: 10.1007/s12072-020-10074-6]

21 **Liu C**, Yang J, Wang W, Zheng P, Tang Y. Liver injury could be associated with severe disease in COVID-19 patients: a meta-analysis. *Eur J Gastroenterol Hepatol* 2020 [PMID: 33031191 DOI: 10.1097/MEG.0000000000001953]

22 **Kulkarni AV**, Kumar P, Tevethia HV, Premkumar M, Arab JP, Candia R, Talukdar R, Sharma M, Qi X, Rao PN, Reddy DN. Systematic review with meta-analysis: liver manifestations and outcomes in COVID-19. *Aliment Pharmacol Ther* 2020; **52**: 584-599 [PMID: 32638436 DOI: 10.1111/apt.15916]

23 **Ponziani FR**, Del Zompo F, Nesci A, Santopaolo F, Ianiro G, Pompili M, Gasbarrini A; "Gemelli against COVID-19" group. Liver involvement is not associated with mortality: results from a large cohort of SARS-CoV-2-positive patients. *Aliment Pharmacol Ther* 2020; **52**: 1060-1068 [PMID: 32628793 DOI: 10.1111/apt.15996]

24 **Sterling RK**, Oakes T, Gal TS, Stevens MP, deWit M, Sanyal AJ. The Fibrosis-4 Index Is Associated With Need for Mechanical Ventilation and 30-Day Mortality in Patients Admitted With Coronavirus Disease 2019. *J Infect Dis* 2020; **222**: 1794-1797 [PMID: 32856702 DOI: 10.1093/infdis/jiaa550]

25 **Li Y**, Regan J, Fajnzylber J, Coxen K, Corry H, Wong C, Rosenthal A, Atyeo C, Fischinger S, Gillespie E, Chishti R, Baden L, Yu XG, Alter G, Kim A, Li JZ. Liver Fibrosis Index FIB-4 Is Associated With Mortality in COVID-19. *Hepatol Commun* 2020; **5**: 434-445 [PMID: 33363264 DOI: 10.1002/hep4.1650]

26 **Rentsch CT**, Kidwai-Khan F, Tate JP, Park LS, King JT, Skanderson M, Hauser RG, Schultze A, Jarvis CI, Holodniy M, Lo Re V, Akgun KM, Crothers K, Taddei TH, Freiberg MS, Justice AC. Covid-19 Testing, Hospital Admission, and Intensive Care Among 2,026,227 United States Veterans Aged 54-75 Years. 2020 Preprint. Available from: medRxiv [PMID: 32511595 DOI: 10.1101/2020.04.09.20059964]

27 **Price-Haywood EG**, Burton J, Fort D, Seoane L. Hospitalization and Mortality among Black Patients and White Patients with Covid-19. *N Engl J Med* 2020; **382**: 2534-2543 [PMID: 32459916 DOI: 10.1056/NEJMsa2011686]

28 **Wang H**, Qiu P, Liu J, Wang F, Zhao Q. The liver injury and gastrointestinal symptoms in patients with Coronavirus Disease 19: A systematic review and meta-analysis. *Clin Res Hepatol Gastroenterol* 2020; **44**: 653-661 [PMID: 32418852 DOI: 10.1016/j.clinre.2020.04.012]

29 **Luo S**, Zhang X, Xu H. Don't Overlook Digestive Symptoms in Patients With 2019 Novel Coronavirus Disease (COVID-19). *Clin Gastroenterol Hepatol* 2020; **18**: 1636-1637 [PMID: 32205220 DOI: 10.1016/j.cgh.2020.03.043]

30 **Wan J**, Wang X, Su S, Zhang Y, Jin Y, Shi Y, Wu K, Liang J. Digestive symptoms and liver injury in patients with coronavirus disease 2019 (COVID-19): A systematic review with meta-analysis. *JGH Open* 2020; **4**: 1047-1058 [PMID: 33319036 DOI: 10.1002/jgh3.12428]

31 **Parasa S**, Desai M, Thoguluva Chandrasekar V, Patel HK, Kennedy KF, Roesch T, Spadaccini M, Colombo M, Gabbiadini R, Artifon ELA, Repici A, Sharma P. Prevalence of Gastrointestinal Symptoms and Fecal Viral Shedding in Patients With Coronavirus Disease 2019: A Systematic Review and Meta-analysis. *JAMA Netw Open* 2020; **3**: e2011335 [PMID: 32525549 DOI:

10.1001/jamanetworkopen.2020.11335]

32 **Redd WD**, Zhou JC, Hathorn KE, McCarty TR, Bazarbashi AN, Thompson CC, Shen L, Chan WW. Prevalence and Characteristics of Gastrointestinal Symptoms in Patients With Severe Acute Respiratory Syndrome Coronavirus 2 Infection in the United States: A Multicenter Cohort Study. *Gastroenterology* 2020; **159**: 765-767. e2 [PMID: 32333911 DOI: 10.1053/j.gastro.2020.04.045]

33 **Nobel YR**, Phipps M, Zucker J, Lebwohl B, Wang TC, Sobieszczyk ME, Freedberg DE. Gastrointestinal Symptoms and Coronavirus Disease 2019: A Case-Control Study From the United States. *Gastroenterology* 2020; **159**: 373-375. e2 [PMID: 32294477 DOI: 10.1053/j.gastro.2020.04.017]

34 **Zhou Z**, Zhao N, Shu Y, Han S, Chen B, Shu X. Effect of Gastrointestinal Symptoms in Patients With COVID-19. *Gastroenterology* 2020; **158**: 2294-2297 [PMID: 32199880 DOI: 10.1053/j.gastro.2020.03.020]

World Journal of Gastroenterology

Submit a Manuscript: https://www.f6publishing.com

World J Gastroenterol 2021 October 28; 27(40): 6967-6984

DOI: 10.3748/wjg.v27.i40.6967

ISSN 1007-9327 (print) ISSN 2219-2840 (online)

ORIGINAL ARTICLE

Observational Study

Factors affecting anxiety, depression, and self-care ability in patients who have undergone liver transplantation

Sami Akbulut, Ali Ozer, Hasan Saritas, Sezai Yilmaz

ORCID number: Sami Akbulut 0000-0002-6864-7711; Ali Ozer 0000-0002-7144-4915; Hasan Saritas 0000-0001-7558-8812; Sezai Yilmaz 0000-0002-8044-0297.

Author contributions: Akbulut S and Saritas H collected the data; Akbulut S and Ozer A performed the statistical analysis; Akbulut S and Ozer A wrote the manuscript; Akbulut S, Ozer A and Yilmaz S reviewed the final version of the manuscript.

Institutional review board statement: This study was reviewed and approved by the Inonu University institutional review board for non-interventional studies (2019/3-27).

Informed consent statement: Verbal and written consents were obtained from all living liver donor candidates.

Conflict-of-interest statement: The authors declare no conflicts of interest regarding this manuscript.

Data sharing statement: There are no additional data available for this study.

STROBE statement: The authors have read the STROBE Statement-checklist of items, and the manuscript was prepared and

Sami Akbulut, Sezai Yilmaz, Liver Transplant Institute, Inonu University Faculty of Medicine, Malatya 44280, Turkey

Sami Akbulut, Ali Ozer, Department of Public Health, Inonu University Faculty of Medicine, Malatya 44280, Turkey

Hasan Saritas, Department of Surgical Nursing, Siirt University Faculty of Nursing, Siirt 56100, Turkey

Corresponding author: Sami Akbulut, MD, PhD, Professor, Liver Transplant Institute, Inonu University Faculty of Medicine, Elazig Yolu 10.Km, Malatya 44280, Turkey.
akbulutsami@gmail.com

Abstract

BACKGROUND

Depression, anxiety, and altered self-care ability are among the most important factors affecting the quality of life of liver transplant recipients. Depending on the severity of the underlying liver disease, signs and symptoms of anxiety and depression may become more pronounced.

AIM

To evaluate the factors affecting depression, anxiety and self-care abilities of liver transplant recipients.

METHODS

Recipients who are ≥ 18 years and who underwent liver transplantation at Inonu University Liver Transplantation Institute were included in this descriptive and cross-sectional study. Sample size analysis showed that the minimum number of recipients should be 301 (confidence level = 95%, confidence interval = 2.5, population = 1382). Three hundred and twenty recipients were interviewed and 316 recipients that have answered the questionnaires accurately were analyzed. The dependent variables were the Beck Depression Scale, State-Trait Anxiety Scale (Form I and II), and Self-Care Agency Scale. The independent variables of the study were sociodemographic characteristics, biliary complications, hepato-cellular carcinoma, recommending liver transplantation to other patients, and the interval of out-patient clinic visits.

RESULTS

Self-care ability scores were lower (P = 0.002) and anxiety scores were higher (P = 0.004) in recipients with biliary complications. On the other hand, in recipients with hepatocellular carcinoma, self-care scores were lower (P = 0.006) while depression (P = 0.003) and anxiety scores (P = 0.009) were higher. Liver transplantation recipients with a monthly income < 3000 Turkish liras had higher depression (P < 0.001) and anxiety (P = 0.003) scores. The recipients who stated that they would not recommend liver transplantation to others had lower self-care scores (P = 0.002), higher depression (P < 0.001), higher state anxiety (P = 0.02), and trait anxiety (P < 0.001) scores.

CONCLUSION

Presence of biliary complications and hepatocellular carcinoma, low income level, and an obligation for monthly visits to the outpatient clinic are factors that are found to affect self-care capability, depression, and anxiety.

Key Words: Liver transplantation; Biliary complications; Hepatocellular carcinoma; Socioeconomic status; Depression; Anxiety; Self-care capabilities

©The Author(s) 2021. Published by Baishideng Publishing Group Inc. All rights reserved.

Core Tip: Depression, anxiety, and deficiency in self-care ability are among the most important factors affecting the quality of life of liver transplant recipients. This descriptive, cross-sectional questionnaire-based study shows that presence of biliary complications and hepatocellular carcinoma, low monthly income level, and monthly visits to the outpatient clinic are factors that affect self-care capability, depression, and anxiety.

Citation: Akbulut S, Ozer A, Saritas H, Yilmaz S. Factors affecting anxiety, depression, and self-care ability in patients who have undergone liver transplantation. *World J Gastroenterol* 2021; 27(40): 6967-6984
URL: https://www.wjgnet.com/1007-9327/full/v27/i40/6967.htm
DOI: https://dx.doi.org/10.3748/wjg.v27.i40.6967

INTRODUCTION

Since the first successful liver transplantation (LT) performed by Starzl *et al*[1] in 1967, LT has become the gold standard treatment modality for end stage liver failure and acute liver failure. In recent years, advancements in immunosuppressive medication, management of postoperative complications, and surgical technique have resulted in extended survival periods for transplant recipients[2,3]. The expectations in quality of life (QOL) of the LT recipients became more prominent with the increased survival rates of the recipients.

The parameters, signs, and symptoms related to QOL, such as the preoperative depression, anxiety, or need for support of a relative, can be exacerbated or can initially be seen in the postoperative period depending on the severity of preoperative psychosocial problems, operative trauma of a major operation, such as LT, long duration of hospitalization in either intensive care unit or in patient-wards, adverse effects of immunosuppressive agents (diabetes mellitus, osteoporosis, infection risk, hypertension, renal failure *etc*.), development of postoperative biliary complications that require interventions, the fear of recurrence of the underlying disease, such as hepatocellular carcinoma (HCC), the fear of the risk of acute or chronic organ rejection, loss of occupation that result in economic losses, and the need for regular postoperative follow-up[4-13]. The major factors affecting the QOL related with health are presence of preoperative co-morbidities (diabetes, hypertension, pulmonary disease), advanced age, female gender, occupation, low socioeconomic status, and financial burden[14-16]. Therefore, all these data suggest that strict surveillance of the transplant recipients in the preoperative and postoperative period in terms of psychosocial status and treatment of any psychosocial problems with psychotherapy and medication may increase the physical and mental QOL and may have a positive

revised according to the STROBE Statement-checklist of items.

Open-Access: This article is an open-access article that was selected by an in-house editor and fully peer-reviewed by external reviewers. It is distributed in accordance with the Creative Commons Attribution NonCommercial (CC BY-NC 4.0) license, which permits others to distribute, remix, adapt, build upon this work non-commercially, and license their derivative works on different terms, provided the original work is properly cited and the use is non-commercial. See: http://creativecommons.org/Licenses/by-nc/4.0/

Manuscript source: Invited manuscript

Specialty type: Gastroenterology and hepatology

Country/Territory of origin: Turkey

Peer-review report's scientific quality classification
Grade A (Excellent): 0
Grade B (Very good): B, B, B
Grade C (Good): 0
Grade D (Fair): 0
Grade E (Poor): 0

Received: July 6, 2021
Peer-review started: July 6, 2021
First decision: August 7, 2021
Revised: August 15, 2021
Accepted: October 11, 2021
Article in press: September 30, 2021
Published online: October 28, 2021

P-Reviewer: Goktepe HM, Kowalewski G, Li HL
S-Editor: Gao CC
L-Editor: Filipodia
P-Editor: Gao CC

impact on the life expectancy of the individuals[7,8].

Depression, anxiety, and the ability of self-care seem to be the most important parameters in the recipients in the postoperative period. Furthermore, some recipients may develop anxiety and depression depending on the risk factors mentioned above that may have an impact on the postoperative mental and physical QOL of the individual. In the present study on patients who received a LT, the anxiety was evaluated by State-Trait Anxiety Scale (STAI; Form I and II), depression was evaluated using the Beck Depression Scale (BDS), and the self-care was evaluated using the Self-Care Agency Scale (SCAS). All these scoring systems and scales were individually used in previous studies involving solid organ transplantation[17-19]. However, we have not encountered any study involving all three scales used together to evaluate a population of recipients. The aim of the present study is to analyze the relationship between sociodemographic characteristics, presence of biliary complications, presence of HCC, preference of recommendation of LT to others, and frequency of out-patient clinic control and some post-transplant QOL indicators (depression, anxiety, self-care ability).

MATERIALS AND METHODS

Type, duration, and location of the study

The preset study is descriptive, cross-sectional questionnaire-based study on patients transplanted between March 2002 and December 2018 at Inonu University Liver Transplant Institute. The recipients that are compliant with regular out-patient follow-up were selected for evaluation in the study, and face-to-face interview technique was applied to all these recipients. This study was reviewed and approved by the Inonu University institutional review board for non-interventional studies (3/27/2019).

Study population and sample size

The study population included 1382 recipients who met the above-mentioned criteria. The sample size was calculated (from the website https://www.surveysystem.com/sscalc.htm) using the confidence level of 95% and patient population (n = 1382) and the calculation showed that minimum of 301 individuals were required for evaluation in the present study. We interviewed 320 recipients in the present study considering the proportion of the recipients with missing data. Of those, the 316 recipients who answered the questionnaire forms accurately were included in the present study.

Inclusion and exclusion criteria

LT recipients who were discharged that were equal to or greater than 18 years old, who can communicate verbally, and understand and answer the questions were included in the present study. At the time of this study, LT was not performed for patients with intellectual disability in our liver transplant institute. Foreigners who lacked sufficient Turkish to answer the questions and recipients younger than 18 years were excluded from the study.

Parameters and scales used in the study

Demographic and clinical characteristics form: Age, gender, marital status, blood type, residency (city center, town, or village), monthly income [≤ 1000 Turkish liras (TL), 1000-3000 TL, ≥ 3000 TL], underlying liver disease (hepatitis B, hepatitis C, HCC *etc.*), type of LT (living donor LT, deceased donor LT), smoking status, alcohol consumption, type of immunosuppressive agent that is being used (tacrolimus, everolimus, cyclosporin, mycophenolate mofetil, corticosteroids, *etc.*), presence of postoperative biliary complications, co-morbidities (cardiac, pulmonary, metabolic *etc.*), and the frequency of the out-patient visits [monthly or once in every 3 mo (quarterly)] were all evaluated for the present study.

BDS: BDS is designed to evaluate how the individual feels about one-self that was defined by Beck *et al*[20] for the first time in 1961. Hisli[21] evaluated the validity and reliability of the Turkish version in 1989 (Cronbach's alpha = 0.80). BDS includes 21 articles that are scored between 0 and 3 points. The scores obtained from BDS range between 0 and 63 points and it evaluates the presence and the severity of depression in individuals. The severity of depression according to the scores of the individuals are minimal depression (0-9 points), mild depression (10-16 points), moderate depression (17-29 points), and severe depression (30-63 points)[22].

STAI: STAI was first defined by Spielberger *et al*[23] in 1970 to define the reaction of individuals with newly-developed or pre-existent anxiety. The validity and reliability of the scale was performed by Oner and LeCompte in 1983[24]. The Cronbach's alpha reliability coefficient for instantaneous and continuous anxiety scores calculated were 0.96 and 0.83, respectively[24]. The scale includes STAI Form-I (State) and STAI Form-II (Trait) parts. The first part of the form evaluates the recent anxiety status of the individual and the later part of the form evaluates the general anxiety status of the patient. The answers to the first part of the form are as follows: not at all (= 1), somewhat (= 2), moderately so (= 3), and very much so (= 4). The answers to the second part of the form are as follows: almost never (= 1), sometime (= 2), often (= 3), and almost always (= 4). In the STAI-I scale questions 1, 2, 5, 8, 10, 11, 15, 16, 19, and 20 are graded inversely (1 = 4 points, 2 = 3 points, 3 = 2 points, and 4 = 1 points). The other questions are graded directly (1 = 1 points, 2 = 2 points, 3 = 3 points, 4 = 4 points). In a similar fashion, in the STAI-II scale, 21, 26, 27, 30, 36, and 39th questions are graded inversely as explained before. At the end of evaluation, the anxiety is classified as high if the points are high; and is considered as low if the points are low. The total points from the instantaneous and the continuous parts is also helpful for the diagnosis of anxiety. If the total points are ≥ 35 points, this indicates the presence of anxiety and if the total points are < 35, this suggests that there is no anxiety in the patients[24,25].

SCAS: SCAS was first developed in 1979 by Kearney and Fleischer[26] to evaluate the self-care ability of individuals. The validation of the Turkish version in healthy subjects was performed by Nahcivan[27] in 1993 (Cronbach's alpha = 0.89). All 35 questions in the questionnaire are designed in a five-point Likert scale: It does not define me at all (= 0), it does not define me entirely (= 1), I have no idea (= 2), it defines me a little (= 3), and it defines me completely (= 4). In the questionnaire, the question 6, 9, 13, 19, 22, 26, and 31 are graded inversely (0 = 4 points, 1 = 3 points, 2 = 2 points, 3 = 1 points, 4 = 1 points). The other questions are graded directly (0 = 1 points, 1 = 1 points, 2 = 2 points, 3 = 3 points, 4 = 4 points). Maximum points obtained from the scale can be 140, and higher scores indicate higher self-care ability.

Statistical analysis

All statistical analyses are performed by Statistical Software Package for Social Sciences (SPSS v. 25). The Kolmogorov-Smirnov test was used to evaluate the normality of distribution of the variables. Some of the variables did not distribute normally and, therefore, all the continuous variables were expressed as median and interquartile range (IQR = Q3-Q1). Qualitative variables were expressed as the number of affected individuals (*n*) and percentage (%). Two-independent groups were compared using the Mann-Whitney *U* test, Pearson Chi-Square test, and Chi-Square test with Yates correction. For three-independent group comparisons, the Chi-Square test was used for qualitative variables and the Kruskal-Wallis test was used for continuous variables. For parameters that showed significant differences in the Kruskal-Wallis test, these parameters were further evaluated with Kruskal-Wallis One-way ANOVA (k sample) to determine the source of difference among the multiple groups. The correlation between the discrete variables was evaluated using Spearman's Rho correlation analysis. The correlation between the qualitative and quantitative variables were evaluated using the Point Double-Series Correlation Coefficient. Partial correlation analysis was performed to evaluate the individual contribution of variables to the correlation. The Correlation coefficient (r) was classified according to the power of the correlation; as defined before: very weak (*r* = 0.00-0.25), weak (*r* = 0.00-0.25), moderate (*r* = 0.50-0.69), high (*r* = 0.70-0.89), and very high (*r* = 0.90-1.00). Any *P* value less than 0.05 was considered as being statistically significant.

RESULTS

A total 316 patient with an age ranging from 18 to 76 years (median = 50, IQR = 58-36) were included in the present study. There were 189 (59.8%) male and 127 (40.2%) female patients included in the study. The demographic and sociocultural characteristics, clinical characteristics related with LT, and data regarding self-care ability, depression and anxiety status of the recipients are summarized in Tables 1-3.

Table 1 Sociodemographic characteristics of the study group

Parameters	*n*	%
Gender		
Female	127	40.2
Male	189	59.8
Age (yr)		
Median	50	
IQR	58-36	
BMI (kg/m^2)		
Median	25	
IQR	28-22	
Marital status		
Married	245	77.5
Unmarried	58	18.4
Divorced	13	4.1
Residency		
City Center	175	55.4
Town	106	33.5
Village	35	11.1
Levels of education		
Unschooled	48	15.2
Primary school	156	49.4
Secondary school	23	7.3
High school	61	19.3
Bachelor's degree or more	28	8.9
Career		
Housewife	90	28.5
Employed	27	8.6
Retired	78	24.7
Tradesman	40	12.7
Unemployed	81	25.6
Monthly income (Turkish liras)		
≤ 1000	18	5.7
1000-3000	260	82.3
≥ 3000	38	12.0
Chronic disease (except liver disease)		
Yes	113	35.8
No	203	64.2
Smoking (pre-LT)		
Yes	127	40.2
No	189	59.8
Smoking (post-LT)		
Yes	12	3.8

No	304	96.2
Alcohol use (pre-LT)		
Yes	37	11.7
No	279	88.3
Alcohol use (post-LT)		
Yes	7	2.2
No	309	97.8

BMI: Body mass index; IQR (Q3-Q1): Inter-quartile range.

Evaluation of the patients according to the presence of biliary complications

The recipients were classified into two groups according to presence (n = 200) and absence (n = 116) of biliary complications. Body mass index (P = 0.038), type of liver graft (P < 0.001), SCAS (P = 0.002), and STAI-I (P = 0.004) were significantly different among the groups. In recipients with biliary complications SCAS scores were found to be low and STAI-I scores were high. The median BDS scores did not significantly change. However, when the BDS scores were classified, there was a significant difference among the recipients with and without biliary complications (P = 0.04). The moderate to severe depression rate was higher in recipients with biliary complications. Total STAI scores were classified according to the anxiety of the recipients and the severity of anxiety was higher in recipients with biliary complications (57.5%, P = 0.009). There was no statistically significant difference in other variables according to the presence of biliary complications (Table 4).

Evaluation of the patients according to the presence of HCC

The recipients were classified according to presence (n = 32) or absence (n = 284) of HCC (Table 5). SCAS (P = 0.006), BDS (P = 0.003), and STAI-II scores (P = 0.009) were significantly different among recipients with and without HCC. While mild and moderate depressive symptoms were more pronounced in recipients with HCC, minimal depressive symptoms were higher in recipients without HCC. Other variables showed no difference according to presence or absence of HCC (Table 5).

Evaluation of the patients according to monthly income

The recipients were grouped in to three groups according to their monthly income (TL): ≤ 1000 (n = 18), 1000-3000 (n = 260), and ≥ 3000 (n = 38) (Table 6). There were significant differences in gender (P < 0.001), place or residence (P = 0.002), BDS scores (P < 0.001), and STAI-II scores (P = 0.003) among groups. In recipients with monthly income ≥ 3000 TL, the depressive symptoms were minimal; while, in recipients with low income, higher rates of mild and moderate depressive symptoms were observed. Other parameters did not show difference according to income of the recipients (Table 6).

Evaluation of the patients according to their inclination towards recommendation of LT to others

The recipients were grouped according to their preference of recommending (n = 285) or not recommending (n = 31) LT to others. The groups showed statistically significant difference in terms of SCAS (P = 0.002), BDS scores (P < 0.001), STAI-I (P = 0.02), and STAI-II scores (P < 0.001). In the group of recipients that do not recommend LT to others, about half of the individuals had moderate to severe depressive symptoms which was significantly higher than the recipients in the group that do recommend LT (48.5% *vs* 11.6%; P < 0.001). All STAI scores were stratified according to the anxiety of the recipients and the rate of anxiety was significantly higher in recipients in the group that do not recommend LT (100% *vs* 85.6%; P = 0.021). There was no significant difference in other variables according to inclination towards recommending or not recommending LT to others (Table 7).

Evaluation of the patients according to frequency of out-patient clinic visits

The data of the 264 LT recipients that come to out-patient clinic monthly were compared to 52 recipients who come to out-patient visits quarterly. Age (P = 0.047) and BDS scores (P = 0.028) showed significant difference among the groups. The

Table 2 Clinical characteristics of the study group associated with liver transplantation

Parameters	*n*	%
Underlying liver disease		
HBV	157	49.7
Cryptogenic	25	7.9
HCC	32	10.1
Wilson	15	4.7
HCV	19	6.0
Autoimmune	22	6.9
Others	46	14.5
Type of LT		
LDLT	291	92.1
DDLT	25	7.9
Biliary complications		
Presence	200	63.3
Absence	116	36.7
Antiviral agents use (HBV/HCV)		
Yes	196	62.0
No	120	38.0
Ursodeoxycholic use		
Yes	229	72.5
No	87	27.5
Tacrolimus use		
Yes	286	90.5
No	30	9.5
Everolimus use		
Yes	108	34.2
No	208	65.8
Corticosteroid use		
Yes	96	30.4
No	220	69.6
Mycophenolate mofetil use		
Yes	212	67.1
No	104	32.9
PPI Inhibitors use		
Yes	314	99.4
No	2	0.6
Inclination towards recommendation of LT to others		
I recommend	285	90.2
I do not recommend	31	9.8
Frequency of out-patient visits		
Monthly	264	83.5
Quarterly	52	16.5

DDLT: Deceased donor liver transplantation; HBV: Hepatitis B virus; HCC: Hepatocellular carcinoma; HCV: Hepatitis C virus; LDLT: Living donor liver transplantation; LT: Liver transplantation.

Table 3 Evaluation of the Study group according to the scores obtained Self-Care Agency Scale, Beck Depression Scale and State-Trait Anxiety Scale

Parameters	Results
SCAS scores	
Median	95
IQR	108-86
BDS scores	
Median	9
IQR	14-5
STAI-I (state) scores	
Median	35
IQR	41-28
STAI-II (trait) scores	
Median	42
IQR	50-36
STAI-I (state) (categorized form)	
Presence anxiety (≥ 35 point)	164 (51.9)
Absence anxiety (< 35 point)	152 (48.1)
STAI-II (trait) (categorized form)	
Presence anxiety (≥ 35 point)	275 (87.0)
Absence anxiety (< 35 point)	41 (13.0)
BDS (categorized form)	
Minimal depression (0-9 point)	183 (57.9)
Mild depression (10-16 point)	85 (26.9)
Moderate depression (17-29 point)	45 (14.2)
Severe depression (30-63 point)	3 (0.9)

BDS: Beck Depression Scale; IQR (Q3-Q1): Inter-quartile range; SCAS: Self-Care Agency Scale; STAI: State-Trait Anxiety Scale.

moderate depression rate of the recipients that come to monthly controls were significantly higher (16.7% *vs* 1.9%; $P = 0.004$). Other variables did not show significant difference according to the frequency of out-patient clinical visits (Table 8).

The results of correlation statistics between the scales

SCAS and BDS showed a significant but weak and negative correlation ($P < 0.001$; $r = -0.340$). There was also a significant but weak and negative correlation between SCAS and STAI-I scales ($P < 0.001$; $r = -0.473$) and SCAS and STAI-II scales ($P < 0.001$; $r = -0.391$). There was a significant but weak positive correlation between BDS and STAI-I scores ($P < 0.001$; $r = +0.498$) and between BDS and STAI-II scores ($P < 0.001$; $r = +0.455$). There was a significant, moderate, and positive correlation between STAI-I and STAI-II scores ($P < 0.001$; $r = +0.539$). The impact of presence of biliary complications, HCC, and the frequency of out-patient clinic visits on correlations observed between STAI-I, STAI-II, BDS, and SCAS scores were further analyzed using partial correlation analyses techniques which showed that the correlation between different scales were independent from the factors that were investigated.

Table 4 Comparison of various characteristics of the study group according to presence of postoperative biliary complications

Parameters	Biliary complications (+) (*n* = 200)	Biliary complications (-) (*n* = 116)	*P* value
Age (yr)			0.126
Median	48	53	
IQR	56-36	60-40	
Gender (%)			0.533
Female	83 (41.5)	44 (37.9)	
Male	117 (58.5)	72 (62.1)	
BMI (kg/m^2)			0.038
Median	26	25	
IQR	28-22	27-22	
Type of LT			**< 0.001**
LDLT	194 (97)	97 (83.6)	
DDLT	6 (3)	19 (16.4)	
SCAS scores			**0.002**
Median	94	98	
IQR	108-82	107-89	
BDS scores			0.375
Median	9	9	
IQR	15-5	12-7	
STAI-I (state) scores			**0.004**
Median	37	32	
IQR	43-29	41-27	
STAI-II (trait) scores			0.454
Median	42	42	
IQR	50-36	54-37	
BDS (categorized form)			**0.040**
Minimal depression	114 (57)	69 (59.5)	
Mild depression	52 (26)	33 (28.4)	
Moderate depression	34 (17)	11 (9.5)	
Severe depression	0(0)	3 (2.6)	
STAI-I (state)			**0.009**
Presence anxiety	115(57.5)	49(42.2)	
Absence anxiety	85(42.5)	67(57.8)	
STAI-II (trait)			1.000
Presence anxiety	174 (87.0)	101 (87.1)	
Absence anxiety	26 (13.0)	15 (12.9)	

BDS: Beck Depression Scale; BMI: Body mass index; IQR (Q3-Q1): Inter-quartile range; SCAS: Self-Care Agency Scale; STAI: State-Trait Anxiety Scale.

DISCUSSION

With the advances in surgical techniques, perioperative patient management, the treatment of postoperative complications with minimally invasive methods, and the development of targeted immunosuppressive treatment protocols with fewer side effects, significant reductions in mortality and morbidity rates have been achieved in

Table 5 Comparison of various characteristics of the study group according to presence of hepatocellular carcinoma

Parameters	HCC (+) (*n* = 32)	HCC (-) (*n* = 284)	*P* value
Age (yr)			0.195
Median	52	50	
IQR	59-44	58-36	
BMI (kg/m^2)			0.063
Median	26	25	
IQR	29-23	28-22	
Gender (%)			1.000
Female	13 (40.6)	114 (40.1)	
Male	19 (59.4)	170 (59.9)	
Biliary complications			0.147
Presence	16 (50)	184 (64.8)	
Absence	16 (50)	100 (35.2)	
SCAS scores			**0.006**
Median	92	96	
IQR	95-68	108-86	
BDS scores			**0.003**
Median	13	9	
IQR	17-8	13-5	
STAI-I (state) scores			0.856
Median	34	35	
IQR	50-26	41-28	
STAI-II (trait) scores			**0.009**
Median	45	42	
IQR	56-39	50-36	
BDS (categorized form)			**0.004**
Minimal depression	10 (31.3)	173 (60.9)	
Mild depression	12 (37.5)	73 (25.7)	
Moderate depression	10 (31.3)	35 (12.3)	
Severe depression	0 (0)	3 (0.9)	
STAI-I (state) (categorized form)			0.968
Presence anxiety	16 (50)	148 (52.1)	
Absence anxiety	16 (50)	136 (47.9)	
STAI-II (trait) (categorized form)			0.402
Presence anxiety	30 (93.8)	245 (86.3)	
Absence anxiety	2 (6.2)	39 (13.7)	

BDS: Beck Depression Scale; BMI: Body mass index; IQR (Q3-Q1): Inter-quartile range; SCAS: Self-Care Agency Scale; STAI: State-Trait Anxiety Scale.

patients who received LT during the last quarter century[8]. The 1- and 5-years survival rates of the patients following LT were 85%-86% and 68%-74%, respectively [28]. On the other hand, together with the long-term survival rates obtained, the QOL of the recipients started to become one of the major concerns for both the physicians and the relatives of the recipients[8].

Table 6 Comparison of various characteristics of the study group according to monthly income

Parameters	≤ 1000 TL (*n* = 18)	1000-3000 TL (*n* = 260)	≥ 3000 TL (*n* = 38)	*P* value
Age (yr)				0.921
Median	44	51	50	
IQR	60-30	58-36	57-43	
Gender (%)				**< 0.001**
Female	13 (72.2)	107 (41.2)	7 (18.4)	
Male	5 (27.8)	153 (58.8)	31 (81.6)	
Residency (%)				*0.002*
City center	12 (66.7)	131 (50.4)	32(84.2)	
Town	4 (22.2)	96 (36.9)	6 (15.8)	
Village	2 (11.1)	33 (12.7)	0 (0)	
SCAS scores				0.119
Median	94	94	97	
IQR	109-86	105-86	112-87	
BDS scores				**< 0.001**
Median	9	9	6	
IQR	16-5	15-6	9-3	
STAI-I (state) scores				0.106
Median	35	35	33	
IQR	46-26	42-28	41-25	
STAI-II (trait) scores				**0.003**
Median	48	42	39	
IQR	52-43	50-36	45-36	
BDS (categorized form)				**0.004**
Minimal depression	10 (55.6)	139 (53.5)	34 (89.5)	
Mild depression	4 (22.2)	78 (30)	3 (7.9)	
Moderate depression	4 (22.2)	40 (15.4)	1 (2.6)	
Severe depression	0 (0)	3 (1.2)	0 (0)	

BDS: Beck Depression Scale; IQR (Q3-Q1): Inter-quartile range; SCAS: Self-Care Agency Scale; STAI: State-Trait Anxiety Scale; TL: Turkish liras.

According to the World Health Organization (WHO), healthy individual is not only free of disease or disability but also defined as a state of psychological and physical well-being[8-10]. From this WHO's perspective, technical and medical success following LT does not necessarily indicate health of the individual; the recipients should also be in the acceptable range of well-being in psychosocial terms as well. For this reason, physicians should also aim to mediate the factors that affect the psychosocial QOL of the individuals following the LT procedures. In the last two decades the studies regarding the QOL of the living donors and recipients after LT have increased tremendously[8,29-33].

Biliary complications are frequently encountered following LT and especially after living donor LT[34,35]. The treatment involves a combination of surgical therapy and endoscopic or interventional radiology assisted percutaneous stenting or catheter placement[36-39]. These complications result in prolonged hospitalization, repeated interventions, and frequent outpatient clinic visits. Therefore, the QOL of the recipients with biliary complications are expected to be lower than recipients without biliary complications[6,40-42]. We have seen that there are no studies analyzing the relationship between biliary complications and the QOL of the recipients. The majority of the published studies state that the biliary complications that develop can adversely

Table 7 Evaluation of the study group according to their inclination towards recommendation of liver transplantation to other patients

Parameters	I recommend (*n* = 285)	I do not recommend (*n* = 31)	*P* value
Age (yr)			0.519
Median	51	50	
IQR	58-36	62-40	
Gender (%)			1.000
Female	115 (40.4)	12 (38.7)	
Male	170 (59.6)	19 (61.3)	
Residency (%)			0.551
City center	155 (54.4)	20 (64.5)	
Town	98 (34.4)	8 (25.8)	
Village	32 (11.2)	3 (9.7)	
Biliary complications			0.660
Presence	182 (63.9)	18 (58.1)	
Absence	103 (36.1)	13 (41.9)	
SCAS scores			**0.002**
Median	95	74	
IQR	108-87	101-69	
BDS scores			**< 0.001**
Median	9	15	
IQR	13-5	29-9	
STAI-I (state) scores			**0.020**
Median	35	42	
IQR	41-28	51-27	
STAI-II (trait) scores			**< 0.001**
Median	42	49	
IQR	50-36	53-43	
BDS (categorized form)			**< 0.001**
Minimal depression	173 (60.7)	10 (32.3)	
Mild depression	79 (27.7)	6 (19.4)	
Moderate depression	33 (11.6)	12 (38.7)	
Severe depression	0 (0)	3 (9.8)	
STAI-I (state) (categorized form)			0.095
Presence anxiety	143 (50.2)	21 (67.7)	
Absence anxiety	142 (49.8)	10 (32.3)	
STAI-II (trait) (categorized form)			**0.021**
Presence anxiety	244 (85.6)	31 (100)	
Absence anxiety	41 (14.4)	0 (0.0)	

BDS: Beck Depression Scale; IQR (Q3-Q1): Inter-quartile range; SCAS: Self-Care Agency Scale; STAI: State-Trait Anxiety Scale.

affect the QOL of the recipients[6,8,40]. In the present study, the self-care ability of the recipients with biliary complications was found to be low (P = 0.002) and the instantaneous anxiety index was found to be increased (P = 0.004). Furthermore, in recipients with biliary complications, 17% showed moderate depression and 57.5% showed signs

Table 8 Comparison of various characteristics of the study group according to frequency of out-patient clinic visits

Parameters	Monthly control (*n* = 264)	Quarterly control (*n* = 52)	*P* value
Age (yr)			**0.047**
Median	52	44	
IQR	58-38	56-29	
Gender (%)			1.000
Female	106 (40.2)	21 (40.4)	
Male	158 (59.8)	31 (56.9)	
Residency (%)			0.077
City center	150 (56.8)	25 (48.1)	
Town	82 (31.1)	24 (46.2)	
Village	32 (12.1)	3 (5.8)	
SCAS scores			0.664
Median	95	94	
IQR	108-86	108-87	
BDS scores			**0.028**
Median	9	9	
IQR	15-6	10-3	
STAI-I (state) scores			0.728
Median	35	38	
IQR	41-28	44-29	
STAI-II (trait) scores			0.519
Median	42	40	
IQR	50-36	50-36	
BDS (categorized form)			**0.004**
Minimal depression	147 (55.7)	36 (69.2)	
Mild depression	72 (27.3)	13 (25)	
Moderate depression	44 (16.7)	1 (1.9)	
Severe depression	1 (0.4)	2 (3.8)	
STAI-I (state) (categorized form)			0.360
Presence anxiety	134 (50.8)	30 (57.7)	
Absence anxiety	130 (49.2)	22 (42.3)	
STAI-II (trait) (categorized form)			0.506
Presence anxiety	228 (86.4)	47 (90.4)	
Absence anxiety	36 (13.6)	5 (9.6)	

BDS: Beck Depression Scale; IQR (Q3-Q1): Inter-quartile range; SCAS: Self-Care Agency Scale; STAI: State-Trait Anxiety Scale.

of instantaneous anxiety. In our opinion, this observation can be explained by prolonged hospitalization, pain and discomfort that is caused by percutaneous catheter placement, the fear of losing the transplanted organ, and the necessity of frequent outpatient clinic visits.

Another factor that has a major impact on the QOL is the presence of HCC diagnosis before the LT. Mabrouk *et al*[43] have stated that the QOL parameters in recipients transplanted for HCC were significantly worse than that of the recipients transplanted for other etiologies; the reason for this was correlated with anxiety related with the probability of a recurrence of the HCC in the post-LT period. On the

other hand, Castaldo *et al*[44] suggested that the diagnosis of HCC had a positive impact on the physical and mental components of QOL for the recipients. On the other hand, Heits *et al*[45] have found no relation between HCC and QOL parameters. In Europe and the United States, recipients with HCC receive additional points during the waiting list and recipients are transplanted in early disease stages, which results in a favorable prognosis compared to recipients without HCC. In the present study, in patients with HCC, the self-care ability was low (P = 0.006) while depression (P = 0.003) and continuous anxiety indices (P = 0.009) were higher than recipients without HCC. Furthermore, 31.3% of the patients with HCC had signs and symptoms of moderate depression. We agree with the Mabrouk *et al*[43] regarding this issue; however, we believe that the negative effect on the QOL parameters should be further investigated regarding the impact of HCC diagnosis and the cumulative effect of the various other factors on this outcome. The cadaveric organ donations in Turkey are significantly lower than that of the developed western countries, and, for this reason, the recipients with HCC have almost no chance for deceased donor LT and the majority need a living liver donation from a family member or a relative[46]. Therefore, the patients have to live with HCC for a period of time before the LT, with some patients requiring bridging procedures, such as chemoembolization, radioembolization, microwave or radiofrequency ablation, and surgical resection. This prolonged and hard waiting period may be the cause of the adverse effects observed on the QOL parameters in the post-LT period.

Other important factors that have an impact on the QOL of the recipients following LT is the income and the frequency of the required out-patient clinic visits of the recipients. The studies have shown that the recipients taking long journeys to come for an out-patient control visit had detrimental economical consequences and reduction in QOL of the recipients[47]. Furthermore, the prolonged hospitalization and frequent hospital visits delay the time to return to work, which reduce the household income. This will inevitably result in psychosocial problems in the recipients. Previous studies from our institute have shown that families of pediatric recipients with a low incomes experienced severe social and economic problems following the transplant procedure [48]. In the present study, we have shown that as the monthly income increased, the parameters related with depression (P < 0.001) and continuous anxiety indices (P = 0.003) decreased significantly. The symptoms related with moderate depression was observed in 22.2% of the patients with a monthly income lower than 1000 TL; on the other hand, patients with 1000-3000 TL and ≥ 3000 TL had moderate depression rate of 15.4% and 2.6%, respectively (P = 0.004). Similarly, the depression level of the recipients who were required to attend frequent visits to the out-patient clinic were significantly higher than recipients who only had to attend quarterly (P = 0.028). In other words, 22.2% of the patients that had to come to out-patient clinic monthly showed signs and symptoms of moderate depression (P = 0.004).

Immunosuppressive drugs that are being used to prevent organ rejection also have a significant impact on the QOL of the recipients. Zaydfudim *et al*[49] have stated that high dose steroid use in recipients have reduced the physical and mental health of the recipients and caused majority of the anxiety related symptoms of the individuals. Lerut[50] stated that reduction or even discontinuation of steroids and other immunosuppressives would eliminate their adverse effects and would increase the QOL of the recipients. In the preset study, we found no difference between the Beck's depression score, instantaneous or continuous anxiety indices, and self-care ability of the patients who did or did not use steroids. Braun *et al*[51] have suggested that recipients that are treated with cyclosporin had better QOL when compared to patients treated with tacrolimus. However, there are contradicting studies that show better QOL with tacrolimus treatment when compared to patients that are on cyclosporin treatment[52,53]. In the present study, the type of immunosuppressive (tacrolimus *vs* cyclosporin) did not have significant impact on the BDS, STAI-I, STAI-II, and SCAS scores of the recipients. Similarly, we found no difference in terms of the BDS, STAI-I, STAI-II, and SCAS among the patients who did or did not receive cyclosporin treatment. However, we found that the BDS scores of the recipients that are on tacrolimus therapy were significantly higher (P = 0.018) and the SCAS scores (P = 0.001) were significantly lower than the recipients that are not receiving tacrolimus therapy. In general, our results suggest that there is no impact of either cyclosporin or tacrolimus on the QOL parameters of the recipients. However, our results regarding the impact of tacrolimus on the self-care abilities of the recipients are original and need to be validated by prospective studies.

The decision to recommend LT to others and its relationship with the QOL parameters requires further analysis. Our review of current literature showed that there are no studies addressing this problem. In the present study, we have found that

the SCAS scores were lower (P = 0.002) and BDS (P < 0.001), STAI-I (P = 0.020), and STAI-II (P < 0.001) scores were higher in patients who stated that they would not to recommend LT to others. Furthermore, moderate depression rate and signs of prominent anxiety was present in 38.7% and 100% of the recipients who did not recommend LT to others, respectively. The recipients that did or did not recommend LT did not differ in terms of incidence of biliary complications (P = 0.660), presence of HCC (P = 1.000), and use of tacrolimus (P = 0.056) as immunosuppressive treatment. However, 36.1% of the recipients that did recommend LT and 16.1% of the recipients that did not recommend LT were using everolimus (P = 0.042). Patients that do or do not use everolimus did not significantly differ in terms of depression, anxiety, and self-care ability. Therefore, our results need validation and further analyses by studies that will be conducted in future.

CONCLUSION

Biliary complications cause depression, reduced self-care ability, and cause anxiety in patients after LT. This has a major impact on the QOL of the recipients. HCC reduces the QOL by increasing depression and anxiety and reducing self-care ability of the recipients. These recipients have HCC that exceed the acceptable limits in the preoperative period, and they receive multiple procedures to down-stage the tumors. This results in frustration and concerns of recurrence of the tumor in the postoperative period. The monthly income and frequent out-patient clinic visits have a significant impact on the QOL of the recipients. The recipients and their relatives cannot return to work until they recover fully after the LT procedure. Furthermore, frequent visits to the out-patient clinic further compromise return to work for the recipients which has a major impact on the income of the recipients. All recipients should be examined by psychiatry in the preoperative period and should receive medico-social therapy in necessary situations. Routine postoperative follow-up of the recipients with a psychologist and physiotherapists are very important for physical and mental QOL of the recipients. Transplant centers should also employ physiotherapists and psychologists that will work with specifically with recipients.

ARTICLE HIGHLIGHTS

Research background

Depression, anxiety, and status of self-care ability are among the most important factors affecting the quality of life of patients who have undergone liver transplantation. Depending on the severity of the underlying liver disease, signs and symptoms of anxiety and depression may become more pronounced.

Research motivation

Depression, anxiety, and deficiency in self-care ability are among the most important factors affecting the quality of life of liver transplant recipients. This descriptive, cross-sectional questionnaire-based study shows that presence of biliary complications and hepatocellular carcinoma, low monthly income level, and monthly visits to the outpatient clinic are factors that are found to affect self-care capability, depression, and anxiety.

Research objectives

The main objective of this study is to analyze the relationship between sociodemographic characteristics, presence of biliary complications, presence of hepatocellular carcinoma, preference of recommendation of liver transplantation to others, and frequency of out-patient clinic control, and some post-transplant quality of life indicators (depression, anxiety, self-care ability).

Research methods

This study is descriptive, cross-sectional questionnaire-based study on patients transplanted between 2002 and 2018 at our Liver Transplant Institute. The recipients who were discharged that were equal to or greater than 18-years-old and who can communicate verbally and understand and answer the questions were included in the present study. We interviewed 320 liver transplant recipients in the present study

considering the proportion of the recipients with missing data. Of those, 316 recipients who answered the questionnaire forms accurately were included in the present study. The dependent variables were Beck Depression Scale, State-Trait Anxiety Scale (Form I and II) and Self-Care Agency Scale. The independent variables of the study were sociodemographic characteristics, biliary complications, hepatocellular carcinoma, recommending liver transplantation to other patients, and the interval of out-patient clinic visits.

Research results

Self-care ability scores were lower and anxiety scores were higher in recipients with biliary complications. On the other hand, in recipients with hepatocellular carcinoma, self-care scores were lower and depression and anxiety scores were higher. In liver transplantation recipients with a monthly income < 3000 Turkish liras had higher depression and anxiety scores. The recipients who stated that they would not recommend liver transplantation to others had lower self-care scores and higher depression, state anxiety, and trait anxiety scores.

Research conclusions

Presence of biliary complications and hepatocellular carcinoma, low income level, and an obligation monthly visits to the outpatient clinic are factors that are found to affect self-care capability, depression and anxiety.

Research perspectives

To our knowledge, this study is one of the most comprehensive studies examining the relationships between post liver transplant quality of life indicators and various clinical parameters.

REFERENCES

1 **Akbulut S**, Yilmaz S. Liver transplantation in Turkey: historical review and future perspectives. *Transplant Rev (Orlando)* 2015; **29**: 161-167 [PMID: 25535023 DOI: 10.1016/j.trre.2014.12.002]

2 **Akbulut S**, Sahin TT, Yilmaz S. Comment on pediatric living donor liver transplantation decade progress in Shanghai: Characteristics and risks factors of mortality. *World J Gastroenterol* 2020; **26**: 4564-4566 [PMID: 32874065 DOI: 10.3748/wjg.v26.i30.4564]

3 **Pillai AA**, Levitsky J. Overview of immunosuppression in liver transplantation. *World J Gastroenterol* 2009; **15**: 4225-4233 [PMID: 19750565 DOI: 10.3748/wjg.15.4225]

4 **Åberg F**. Quality of life after liver transplantation. *Best Pract Res Clin Gastroenterol* 2020; **46-47**: 101684 [PMID: 33158471 DOI: 10.1016/j.bpg.2020.101684]

5 **Medved V**, Medved S, Skočić Hanžek M. Transplantation Psychiatry: an Overview. *Psychiatr Danub* 2019; **31**: 18-25 [PMID: 30948685 DOI: 10.24869/psyd.2019.18]

6 **Coelho JCU**, Leite LO, Molena A, Freitas ACT, Matias JEF. Biliary complications after liver transplantation. *Arq Bras Cir Dig* 2017; **30**: 127-131 [PMID: 29257849 DOI: 10.1590/0102-6720201700020011]

7 **Benson AA**, Rowe M, Eid A, Bluth K, Merhav H, Khalaileh A, Safadi R. Pre-liver transplant psychosocial evaluation predicts post-transplantation outcomes. *Psychol Health Med* 2018; **23**: 788-796 [PMID: 29278010 DOI: 10.1080/13548506.2017.1417610]

8 **Onghena L**, Develtere W, Poppe C, Geerts A, Troisi R, Vanlander A, Berrevoet F, Rogiers X, Van Vlierberghe H, Verhelst X. Quality of life after liver transplantation: State of the art. *World J Hepatol* 2016; **8**: 749-756 [PMID: 27366301 DOI: 10.4254/wjh.v8.i18.749]

9 **Bownik H**, Saab S. Health-related quality of life after liver transplantation for adult recipients. *Liver Transpl* 2009; **15** Suppl 2: S42-S49 [PMID: 19876941 DOI: 10.1002/lt.21911]

10 **Jay CL**, Butt Z, Ladner DP, Skaro AI, Abecassis MM. A review of quality of life instruments used in liver transplantation. *J Hepatol* 2009; **51**: 949-959 [PMID: 19775771 DOI: 10.1016/j.jhep.2009.07.010]

11 **Golfieri L**, Gitto S, Vukotic R, Andreone P, Marra F, Morelli MC, Cescon M, Grandi S. Impact of psychosocial status on liver transplant process. *Ann Hepatol* 2019; **18**: 804-809 [PMID: 31471202 DOI: 10.1016/j.aohep.2019.06.011]

12 **Duffy JP**, Kao K, Ko CY, Farmer DG, McDiarmid SV, Hong JC, Venick RS, Feist S, Goldstein L, Saab S, Hiatt JR, Busuttil RW. Long-term patient outcome and quality of life after liver transplantation: analysis of 20-year survivors. *Ann Surg* 2010; **252**: 652-661 [PMID: 20881772 DOI: 10.1097/SLA.0b013e3181f5f23a]

13 **Miller LR**, Paulson D, Eshelman A, Bugenski M, Brown KA, Moonka D, Abouljoud M. Mental health affects the quality of life and recovery after liver transplantation. *Liver Transpl* 2013; **19**: 1272-1278 [PMID: 23959592 DOI: 10.1002/lt.23728]

14 **Polis S**, Fernandez R. Impact of physical and psychological factors on health-related quality of life in

adult patients with liver cirrhosis: a systematic review protocol. *JBI Database System Rev Implement Rep* 2015; **13**: 39-51 [PMID: 26447006 DOI: 10.11124/jbisrir-2015-1987]
15 **Šumskienė J**, Kupčinskas L, Šumskas L. Health-related quality of life measurement in chronic liver disease patients. *Medicina (Kaunas)* 2015; **51**: 201-208 [PMID: 26424183 DOI: 10.1016/j.medici.2015.06.006]
16 **Sobhonslidsuk A**, Silpakit C, Kongsakon R, Satitpornkul P, Sripetch C, Khanthavit A. Factors influencing health-related quality of life in chronic liver disease. *World J Gastroenterol* 2006; **12**: 7786-7791 [PMID: 17203521 DOI: 10.3748/wjg.v12.i48.7786]
17 **Mendes KD**, Lopes AR, Martins TA, Lopes GF, Ziviani LC, Rossin FM, Castro-e-Silva O, Galvão CM. Relevance of anxiety and stress levels on sleep quality after liver transplantation. *Transplant Proc* 2014; **46**: 1822-1826 [PMID: 25131046 DOI: 10.1016/j.transproceed.2014.05.051]
18 **Mohamed S**, Sabki ZA, Zainal NZ. Depression and psychosocial correlates of liver transplant candidates: a systematic review. *Asia Pac Psychiatry* 2014; **6**: 447-453 [PMID: 25132651 DOI: 10.1111/appy.12145]
19 **Celikturk N**, Edeer AD. Self-Care Agency and Associated Factors in Heart Transplant Patients. *Turkiye Klinikleri J Cardiovasc Sci* 2019; **31**: 148-154 [DOI: 10.5336/cardiosci.2019-70586]
20 **Beck AT**, Ward CH, Mendelson M, Mock J, Erbaugh J. An inventory for measuring depression. *Arch Gen Psychiatry* 1961; **4**: 561-571 [PMID: 13688369 DOI: 10.1001/archpsyc.1961.01710120031004]
21 **Hisli N**. Beck depresyon ölçeğinin üniversite öğrencileri için geçerliği, güvenirliği. *Psikoloji Dergisi* 1989; **7**: 3-13
22 **Ardic A**. The Relationship Between Depression, Anxiety and Stress Levels of Overweight and Obese Adolescents: The Sample of Istanbul. *TJFMPC* 2020; **14**: 384-390
23 **Spielberger CD**, Gorsuch RL, Lushene RE. Manual for the State-Trait Anxiety Scale (Self Evaluation Questionnaire). Palo Alto, CA: Consulting Psychologists Press, 1970
24 **Oner N**, LeCompte A. Durumluk Surekli Kaygi Ölçeği El Kitabi. Istanbul: Bogazici Universitesi Yayinlari, 1983: 1-26
25 **Kacmaz N**, Balas GU. The Psychosocial Status of Liver Transplant Patients and Their Relatives Regarding the Procedure's Effects on Their Quality of Life. *J Psychiat Nursg* 2014; **5**: 1-8
26 **Kearney BY**, Fleischer BJ. Development of an instrument to measure exercise of self-care agency. *Res Nurs Health* 1979; **2**: 25-34 [PMID: 254279 DOI: 10.1002/nur.4770020105]
27 **Nahcivan NO**. A Turkish language equivalence of the Exercise of Self-Care Agency Scale. *West J Nurs Res* 2004; **26**: 813-824 [PMID: 15466617 DOI: 10.1177/0193945904267599]
28 **Becchetti C**, Dirchwolf M, Banz V, Dufour JF. Medical management of metabolic and cardiovascular complications after liver transplantation. *World J Gastroenterol* 2020; **26**: 2138-2154 [PMID: 32476781 DOI: 10.3748/wjg.v26.i18.2138]
29 **Tome S**, Wells JT, Said A, Lucey MR. Quality of life after liver transplantation. A systematic review. *J Hepatol* 2008; **48**: 567-577 [PMID: 18279999 DOI: 10.1016/j.jhep.2007.12.013]
30 **Yang LS**, Shan LL, Saxena A, Morris DL. Liver transplantation: a systematic review of long-term quality of life. *Liver Int* 2014; **34**: 1298-1313 [PMID: 24703371 DOI: 10.1111/liv.12553]
31 **Janik MK**, Księżopolska A, Kostrzewa K, Kobryń K, Moskwa M, Raszeja-Wyszomirska J, Kornasiewicz O, Patkowski W, Milkiewicz P, Krawczyk M, Zieniewicz K. Long-Term Health-Related Quality of Life in Living Liver Donors. *Ann Transplant* 2019; **24**: 45-51 [PMID: 30666044 DOI: 10.12659/AOT.911109]
32 **Ladner DP**, Dew MA, Forney S, Gillespie BW, Brown RS Jr, Merion RM, Freise CE, Hayashi PH, Hong JC, Ashworth A, Berg CL, Burton JR Jr, Shaked A, Butt Z. Long-term quality of life after liver donation in the adult to adult living donor liver transplantation cohort study (A2ALL). *J Hepatol* 2015; **62**: 346-353 [PMID: 25195558 DOI: 10.1016/j.jhep.2014.08.043]
33 **Chandran B**, Bharathan VK, Shaji Mathew J, Amma BSPT, Gopalakrishnan U, Balakrishnan D, Menon RN, Dhar P, Vayoth SO, Surendran S. Quality of life of liver donors following donor hepatectomy. *Indian J Gastroenterol* 2017; **36**: 92-98 [PMID: 28393329 DOI: 10.1007/s12664-017-0743-7]
34 **Daniel K**, Said A. Early Biliary complications after liver transplantation. *Clin Liver Dis (Hoboken)* 2017; **10**: 63-67 [PMID: 30992762 DOI: 10.1002/cld.654]
35 **Simoes P**, Kesar V, Ahmad J. Spectrum of biliary complications following live donor liver transplantation. *World J Hepatol* 2015; **7**: 1856-1865 [PMID: 26207167 DOI: 10.4254/wjh.v7.i14.1856]
36 **Moy BT**, Birk JW. A Review on the Management of Biliary Complications after Orthotopic Liver Transplantation. *J Clin Transl Hepatol* 2019; **7**: 61-71 [PMID: 30944822 DOI: 10.14218/JCTH.2018.00028]
37 **Crismale JF**, Ahmad J. Endoscopic Management of Biliary Issues in the Liver Transplant Patient. *Gastrointest Endosc Clin N Am* 2019; **29**: 237-256 [PMID: 30846151 DOI: 10.1016/j.giec.2018.11.003]
38 **Koksal AS**, Eminler AT, Parlak E, Gurakar A. Management of biliary anastomotic strictures after liver transplantation. *Transplant Rev (Orlando)* 2017; **31**: 207-217 [PMID: 28427741 DOI: 10.1016/j.trre.2017.03.002]
39 **Czubkowski P**, Markiewicz-Kijewska M, Janiszewski K, Rurarz M, Kaliciński P, Jarzębicka D, Pertkiewicz J, Kamińska D, Jankowska I, Teisseyre M, Szymczak M, Pawłowska J. Percutaneous Treatment of Biliary Strictures After Pediatric Liver Transplantation. *Ann Transplant* 2018; **23**: 845-851 [PMID: 30531688 DOI: 10.12659/AOT.910528]

40 **Silva ACDS**, Andrade AMDF, Lisboa QC, Lima CXD, Araujo JP, Gambogi TR, Borges VO, Filho IJZ. Epidemiologic Study on the Incidence of Biliary Complications after Liver Transplantation. *J Liver* 2018; **7**: 229 [DOI: 10.4172/2167-0889.1000229]

41 **Fang C**, Yan S, Zheng S. Bile Leakage after Liver Transplantation. *Open Med (Wars)* 2017; **12**: 424-429 [PMID: 29318188 DOI: 10.1515/med-2017-0062]

42 **Palanisamy AP**, Taber DJ, Sutter AG, Nadig SN, Dowden JE, McGillicuddy JW, Baliga PK, Chavin KD. Clinical outcomes and costs associated with in-hospital biliary complications after liver transplantation: a cross-sectional analysis. *J Gastrointest Surg* 2015; **19**: 282-289 [PMID: 25319035 DOI: 10.1007/s11605-014-2675-1]

43 **Mabrouk M**, Esmat G, Yosry A, El-Serafy M, Doss W, Zayed N, El-Sahhar M, Awny S, Omar A. Health-related quality of life in Egyptian patients after liver transplantation. *Ann Hepatol* 2012; **11**: 882-890 [PMID: 23109452 DOI: 10.1016/S1665-2681(19)31414-0]

44 **Castaldo ET**, Feurer ID, Russell RT, Pinson CW. Correlation of health-related quality of life after liver transplant with the Model for End-Stage Liver Disease score. *Arch Surg* 2009; **144**: 167-172 [PMID: 19221329 DOI: 10.1001/archsurg.2008.563]

45 **Heits N**, Meer G, Bernsmeier A, Guenther R, Malchow B, Kuechler T, Becker T, Braun F. Mode of allocation and social demographic factors correlate with impaired quality of life after liver transplantation. *Health Qual Life Outcomes* 2015; **13**: 162 [PMID: 26420554 DOI: 10.1186/s12955-015-0360-z]

46 **Kutluturk K**, Akbulut S, Baskiran A, Gonultas F, Dirican A, Isık B, Yilmaz S. Aborted donor hepatectomy in living donor liver transplantation: lessons learned. *S Afr J Surg* 2020; **58**: 91-100 [PMID: 32644313]

47 **O'Connell Francischetto E**, Damery S, Ferguson J, Combes G; myVideoClinic randomised evaluation steering group. Video clinics *vs* standard face-to-face appointments for liver transplant patients in routine hospital outpatient care: study protocol for a pragmatic randomised evaluation of myVideoClinic. *Trials* 2018; **19**: 574 [PMID: 30340637 DOI: 10.1186/s13063-018-2953-4]

48 **Akbulut S**, Gunes G, Saritas H, Aslan B, Karipkiz Y, Demyati K, Gungor S, Yilmaz S. Differences in parents of pediatric liver transplantation and chronic liver disease patients. *World J Clin Cases* 2020; **8**: 2162-2172 [PMID: 32548146 DOI: 10.12998/wjcc.v8.i11.2162]

49 **Zaydfudim V**, Feurer ID, Landman MP, Moore DE, Wright JK, Pinson CW. Reduction in corticosteroids is associated with better health-related quality of life after liver transplantation. *J Am Coll Surg* 2012; **214**: 164-173 [PMID: 22137824 DOI: 10.1016/j.jamcollsurg.2011.10.006]

50 **Lerut J**. Minimalization of immunosuppression in liver transplantation: steps from 'how' to 'now'. Interview by Emily Reeve. *Expert Rev Clin Immunol* 2012; **8**: 605-607 [PMID: 23078057 DOI: 10.1586/eci.12.53]

51 **Braun F**, Teren K, Wilms P, Günther R, Allmann J, Broering DC, Küchler T. Quality of life after liver transplantation. *Transplant Proc* 2009; **41**: 2564-2566 [PMID: 19715975 DOI: 10.1016/j.transproceed.2009.06.030]

52 **Felser I**, Wagner S, Depee J, Johnson N, Staschak S, Jain A, Fung JJ, Starzl TE. Changes in quality of life following conversion from CyA to FK 506 in orthotopic liver transplant patients. *Transplant Proc* 1991; **23**: 3032-3034 [PMID: 1721350]

53 **Scholler G**, Rose M, Neuhaus R, Neuhaus P, Klapp BF. Comparison of cyclosporine A and FK506 with regard to complaints and psychosocial characteristics before and after liver transplantation. *Transplant Proc* 1997; **29**: 2491-2493 [PMID: 9270822 DOI: 10.1016/s0041-1345(97)00461-2]

World Journal of Gastroenterology

Submit a Manuscript: https://www.f6publishing.com

World J Gastroenterol 2021 October 28; 27(40): 6985-6999

DOI: 10.3748/wjg.v27.i40.6985

ISSN 1007-9327 (print) ISSN 2219-2840 (online)

META-ANALYSIS

Prophylactic transcatheter arterial embolization reduces rebleeding in non-variceal upper gastrointestinal bleeding: A meta-analysis

Eszter Boros, Zoltán Sipos, Péter Hegyi, Brigitta Teutsch, Levente Frim, Szilárd Váncsa, Szabolcs Kiss, Fanni Dembrovszky, Eduard Oštarijaš, Andrew Shawyer, Bálint Erőss

ORCID number: Eszter Boros 0000-0002-7831-163X; Zoltán Sipos 0000-0001-7845-8116; Péter Hegyi 0000-0003-0399-7259; Brigitta Teutsch 0000-0002-9530-7886; Levente Frim 0000-0003-0097-6663; Szilárd Váncsa 0000-0002-9347-8163; Szabolcs Kiss 0000-0001-5032-866X; Fanni Dembrovszky 0000-0001-6953-3591; Eduard Oštarijaš 0000-0001-9999-9886; Andrew Shawyer 0000-0003-1700-3307; Bálint Erőss 0000-0003-3658-8427.

Author contributions: Boros E, Sipos Z, Hegyi P, Teutsch B, Frim L, Váncsa S, Kiss S, Dembrovszky F, Oštarijaš E, Shawyer A, and Erőss B provided the conceptualization; Boros E is the project administration; Boros E and Sipos Z formally analyze the original draft; Boros E and Teutsch B did the systematic search and selection, and wrote the original draft; Sipos Z made the visualisation, and wrote the original draft; Hegyi P contributed to the funding acquisition; Hegyi P, Frim L, Váncsa S, Kiss S, Dembrovszky F, Oštarijaš E, and Shawyer A wrote, reviewed and edited the manuscript; Frim L contributed to the data curation, quality and risk assessment; Vá ncsa S and Kiss S provided the methodology, and made the data curation; Dembrovszky F provided the methodology, and made the

Eszter Boros, Zoltán Sipos, Péter Hegyi, Brigitta Teutsch, Levente Frim, Szilárd Váncsa, Szabolcs Kiss, Fanni Dembrovszky, Eduard Oštarijaš, Bálint Erőss, Institute for Translational Medicine, University of Pecs, Medical School, Pécs 7624, Hungary

Eszter Boros, First Department of Internal Medicine, St. George University Teaching Hospital of County Fejér, Székesfehérvár 8000, Hungary

Péter Hegyi, Szentágothai Research Center, University of Pecs, Pécs 7624, Hungary

Szabolcs Kiss, Doctoral School of Clinical Medicine, University of Szeged, Szeged 6720, Hungary

Andrew Shawyer, Department of Interventional Radiology, University Hospitals Dorset NHS Foundation Trust, Bournemouth BH7 7DW, United Kingdom

Corresponding author: Bálint Erőss, MD, PhD, Assistant Professor, Doctor, Institute for Translational Medicine, University of Pecs, Medical School, 12 Szigeti Street, Pécs 7624, Hungary. eross.balint@pte.hu

Abstract

BACKGROUND

Despite the improvement in the endoscopic hemostasis of non-variceal upper gastrointestinal bleeding (NVUGIB), rebleeding remains a major concern.

AIM

To assess the role of prophylactic transcatheter arterial embolization (PTAE) added to successful hemostatic treatment among NVUGIB patients.

METHODS

We searched three databases from inception through October 19th, 2020. Randomized controlled trials (RCTs) and observational cohort studies were eligible. Studies compared patients with NVUGIB receiving PTAE to those who did not get PTAE. Investigated outcomes were rebleeding, mortality, reintervention, need for surgery and transfusion, length of hospital (LOH), and intensive care unit (ICU) stay. In the quantitative synthesis, odds ratios (ORs) and weighted mean differences (WMDs) were calculated with the random-effects model and interpreted with 95% confidence intervals (CIs).

quality and risk assessment; Oš tarijaš E did the visualisation; Erőss B did the conceptualization, supervision, and wrote the original draft; All authors certify that they have participated sufficiently in the work to take public responsibility for the content, including participation in the concept, design, analysis, writing, or revision of the manuscript.

Supported by Economic Development and Innovation Operative Programme Grant, No. GINOP 2.3.2-15-2016-00048 and No. GINOP-2.3.4-15-2020-00010; and Human Resources Development Operational Programme Grant, No. EFOP-3.6.2-16-2017-00006 and No. EFOP-3.6.1.-16-2016-00004.

Conflict-of-interest statement: No conflict of interest to declare.

PRISMA 2009 Checklist statement: The authors have read the PRISMA 2020 Checklist, and was prepared and revised according to the PRISMA 2020 Checklist.

Open-Access: This article is an open-access article that was selected by an in-house editor and fully peer-reviewed by external reviewers. It is distributed in accordance with the Creative Commons Attribution NonCommercial (CC BY-NC 4.0) license, which permits others to distribute, remix, adapt, build upon this work non-commercially, and license their derivative works on different terms, provided the original work is properly cited and the use is non-commercial. See: http://creativecommons.org/Licenses/by-nc/4.0/

Manuscript source: Unsolicited manuscript

Specialty type: Gastroenterology and hepatology

Country/Territory of origin: Hungary

Peer-review report's scientific quality classification

Grade A (Excellent): A
Grade B (Very good): B, B, B

RESULTS

We included a total of 3 RCTs and 9 observational studies with a total of 1329 patients, with 486 in the intervention group. PTAE was associated with lower odds of rebleeding (OR = 0.48, 95%CI: 0.29–0.78). There was no difference in the 30-d mortality rates (OR = 0.82, 95%CI: 0.39–1.72) between the PTAE and control groups. Patients who underwent PTAE treatment had a lower chance for reintervention (OR = 0.48, 95%CI: 0.31–0.76) or rescue surgery (OR = 0.35, 95%CI: 0.14–0.92). The LOH and ICU stay was shorter in the PTAE group, but the difference was non-significant [WMD = -3.77, 95%CI: (-8.00)–0.45; WMD = -1.33, 95%CI: (-2.84)–0.18, respectively].

CONCLUSION

PTAE is associated with lower odds of rebleeding and any reintervention in NVUGIB. However, further RCTs are needed to have a higher level of evidence.

Key Words: Prophylactic transcatheter arterial embolization; Non-variceal upper gastrointestinal bleeding; Rebleeding; Reintervention; Meta-analysis; Review

©The Author(s) 2021. Published by Baishideng Publishing Group Inc. All rights reserved.

Core Tip: Rebleeding remains a significant concern in patients with non-variceal upper gastrointestinal bleeding (NVUGIB), despite the improvements in endoscopic and pharmacologic treatments. Our systematic review and meta-analysis indicate that prophylactic transcatheter arterial embolization (PTAE) compared to standard of care is accompanied by lower odds of rebleeding, need for rescue surgery, and reinterventions NVUGIB. However, we could not justify a beneficial effect of PTAE on mortality rates compared with the standard of care. In line with our results, we suggest using PTAE in selected cases, where risk stratification predicts high rebleeding risk or the anatomical situation makes the secure and permanent endoscopic hemostasis impossible.

Citation: Boros E, Sipos Z, Hegyi P, Teutsch B, Frim L, Váncsa S, Kiss S, Dembrovszky F, Oštarijaš E, Shawyer A, Erőss B. Prophylactic transcatheter arterial embolization reduces rebleeding in non-variceal upper gastrointestinal bleeding: A meta-analysis. *World J Gastroenterol* 2021; 27(40): 6985-6999
URL: https://www.wjgnet.com/1007-9327/full/v27/i40/6985.htm
DOI: https://dx.doi.org/10.3748/wjg.v27.i40.6985

INTRODUCTION

Acute upper gastrointestinal bleeding (UGIB) remains a common medical emergency with an incidence of 47-90/100000[1-3]. The age-standardized incidence of ulcer bleeding decreased by 41.6% between 1983 and 2004 in a prospective observational study; notable the decrease occurred only in people younger than 70 years of age[1]. Mortality in UGIB ranges between 1.1%–11%[4], although it has significantly decreased due to improvements and innovation in both endoscopic and pharmacologic treatments[1,4]. The UGIB population characteristics have changed considerably, the mean age of the patients has increased, the prevalence of co-morbidities is higher than before, and the use of nonsteroidal anti-inflammatory, antiplatelet and anticoagulant drugs is more widespread[1,5,6].

Rebleeding is a significant concern in patients with UGIB, occurring in 7%–16% of cases despite endoscopic therapy[6]. As published in a study from the United Kingdom in 2007, rebleeding is associated with a higher mortality rate, potentially induces more extended hospital stay and need for reintervention[5]. Thus, preventing rebleeding is a critical factor from the patients' and a healthcare economic view. The management of non-variceal UGIB (NVUGIB) is well established in guidelines based on a high level of evidence. In the post-endoscopy care of NVUGIB, a strong recommendation is to use high-dose proton pump inhibitors and eradicate *Helicobacter pylori (H. pylori)* if presence is established[7]. On the other hand, if rebleeding happens,

Grade C (Good): 0
Grade D (Fair): 0
Grade E (Poor): 0

Received: June 16, 2021
Peer-review started: June 16, 2021
First decision: July 14, 2021
Revised: July 25, 2021
Accepted: September 16, 2021
Article in press: September 16, 2021
Published online: October 28, 2021

P-Reviewer: Liu XM, Papadopoulos VP, Xiong A, Ziogas IA
S-Editor: Ma YJ
L-Editor: A
P-Editor: Ma YJ

the patient should receive a repeat upper gastrointestinal endoscopy[7]. In the case of failure of this second attempt with endoscopic hemostasis, either transcatheter angiographic embolization (TAE) or rescue surgery are indicated, as they provide the same level of efficacy[8,9].

In contrast, there are only a few studies about the potential role of prophylactic transcatheter arterial embolization (PTAE) in the management of NVUGIB. A recent randomized controlled trial suggested that PTAE may reduce the incidence of recurrent bleeding (10.2% *vs* 11.4%, $P = 0.745$), but they could not show a clear benefit in adding angiographic embolization to endoscopic hemostasis in NVUGIB patients [10]. Investigating a subset of patients with ulcers 15mm or more in size, PTAE significantly reduced the risk of rebleeding (23.1% *vs* 4.5%, $P = 0.027$)[10]. A similar improvement in the rebleeding rate after PTAE was observed in some cohort studies [11-13].

Our study aimed to assess the role of PTAE among NVUGIB patients. We hypothesized that PTAE could reduce the risk of rebleeding and even the mortality rate among NVUGIB patients and improve other outcomes.

MATERIALS AND METHODS

We are reporting our systematic review and meta-analysis in line with the Preferred Reporting Items for Systematic Reviews and Meta-Analyses (PRISMA) 2020 Statement [14] (Supplementary Table 1) and also in line with the Meta-analysis Of Observational Studies in Epidemiology (MOOSE) guidelines[15] because we included both RCTs and observational cohort studies. Methods of the analysis and inclusion criteria were established in advance, and the protocol was documented on the International Prospective Register of Systematic Reviews (PROSPERO, registration number CRD42021223726).

Systematic search

Three databases, MEDLINE (via PubMed), EMBASE, and Cochrane Central Register of Controlled Trials (CENTRAL), were searched from inception through October 19th, 2020. We applied the following search key: (embolization OR embolisation) AND (peptic OR ulcer OR "gastrointestinal bleeding" OR nonvariceal OR non-variceal OR "gastrointestinal hemorrhage" OR "gastrointestinal haemorrhage"). We did not use any restrictions or filters during the search. We provide the complete search strategy in Supplementary Appendix 1.

Selection and eligibility

After the automatic and manual removal of duplicates with a reference manager software (EndNote X9, Clarivate Analytics, Philadelphia, PA, United States), screening and selection for the title, abstract, and full text were undertaken independently by two review authors. Cohen's kappa coefficient (κ) was calculated after each step to measure inter-reviewer reliability[16]. Disagreements were resolved through discussion with a third author. The references of the selected studies were examined to identify any additional relevant studies.

To identify eligible studies, we used the population-intervention-control-outcome (PICO) framework. Our investigated population (P) consisted of adult patients (age > 18 years) with endoscopy, digital subtraction angiography, or computed tomography angiography proved NVUGIB source, who either underwent successful endoscopic hemostasis or during angiography, there was no detectable contrast extravasation described. Studies compared the outcomes of patients who received PTAE (I) to patients who did not receive PTAE (C). The primary outcomes (O) were rebleeding and 30-d mortality rate, and the secondary outcomes were in-hospital or overall mortality rate, reintervention, need for salvage surgery, need of transfusion, length of hospital (LOH), and intensive care unit (ICU) stay. We pooled studies with different measurement time points regarding rebleeding (such as in-hospital, 28- and 30-d). If articles did not provide a precise measurement time point for mortality, we referred to that as "overall mortality". We defined reintervention as any repeated invasive treatment of rebleeding such as embolization, endoscopy, or surgery. Randomized controlled trials, prospective and retrospective observational cohort studies were eligible. Case reports, case series with less than ten patients, and review articles that did not report original research were excluded. In the case of publications using data with overlapping study populations, we used the one with the bigger sample size.

Data collection

Two independent review authors extracted data from eligible studies into a predesigned data collection form. The following data were collected from each study: first author, year of publication, study design, study period, study site (country), demographic features of the study population, the number of participants with PTAE, the number of patients without PTAE, bleeding etiology, type of embolic agents, data on outcomes (rebleeding, surgery, mortality, reintervention, LOH stay, ICU stay, and blood transfusion) in the intervention and control groups. In the case of the RCTs, intention-to-treat and per-protocol data were collected separately.

Data synthesis and statistical analysis

A biomedical statistician performed the statistical analysis of the study. Calculations were made by Stata 16 data analysis and statistical software (Stata Corp LLC, College Station, TX, United States). In the case of dichotomous categorical outcomes (mortality, rebleeding rate, *etc.*), we determined odds ratios (ORs) with 95% confidence intervals (95%CIs) from two-by-two tables (intervention *vs* control, outcome present and absent). For continuous variables, weighted mean difference (WMD) with 95%CIs were calculated. A P value less than 0.05 was considered a statistically significant difference. The random-effects model, according to the method of DerSimonian-Laird [17], was used to calculate the pooled estimates. We used forest plots to present the results of the meta-analyses.

I^2 and χ^2 tests were performed to assess heterogeneity. I^2 values were described as "minimal" (0%–40%), "moderate" (30%–60%), "substantial" (50%–90%), and "considerable" (75%–100%) heterogeneity, with a P value < 0.1 considered significant, as suggested by the Cochrane Handbook[18]. For the outcome of rebleeding, publication bias was assessed by visual inspection of a funnel plot and Egger's test. As for the other outcomes, we were unable to determine the presence of publication bias because of the low number of studies included in each analysis.

Sensitivity analysis was carried out by removing each trial analysis in turn in the case of rebleeding, reintervention, surgery, and need of transfusion outcome (the leave-one-out-method).

We performed a subgroup analysis for rebleeding and compared randomized controlled studies (RCTs) with non-randomized studies. For RCTs, we analyzed the intention-to-treat and per-protocol analysis results separately. Trial Sequential Analysis (TSA 0.9.5.10.) was performed for the RCTs regarding rebleeding to control random errors and estimate the optimal information size.

Risk of bias assessment and certainty of the evidence

Two independent review authors carried out the risk of bias assessment. Discrepancies were resolved by third-party arbitration. We followed the recommendations of the Cochrane Prognosis Methods group, and we used the revised Risk of Bias (RoB) 2 tool for randomized and the Risk of Bias In Non-randomized Studies - of Interventions (ROBINS-I) tool for non-randomized studies[19,20]. We used the Risk-of-bias VISualization (robvis) web-based tool[21].

Two independent review authors assessed the overall quality of evidence following the recommendation of the "Grades of Recommendation, Assessment, Development, and Evaluation (GRADE)" workgroup[22]. A third author resolved disagreements. Summary of Findings table and the additional tables were prepared with the GRADE profiler (GRADEpro) tool [GRADEpro Guideline Development Tool (Software)]. McMaster University, 2020 (developed by Evidence Prime, Inc.).

RESULTS

Search and selection

We identified 10591 records in three databases for evaluation. After removing duplicates and careful selection by title and abstract, 46 articles were eligible for full-text assessment. Altogether, 14 papers were retrieved for qualitative and 12 for quantitative synthesis. Two studies[23,24] were excluded from the quantitative synthesis due to major differences in intervention or outcome compared to other included articles. In the study of Ying *et al*[23], the intervention group got not only PTAE but also superior mesenteric arterial hypophysin infusion, which was too much alteration from our PICO and inclusion criteria. In the publication of Yonemoto *et al* [24], different outcomes (statistical analysis for laboratory data, number of endoscopic

treatments) were presented than we were assessing in our meta-analysis. The selection process is detailed in Figure 1.

Characteristics of the studies included

The 14 included studies are summarized in Table 1. We included in the quantitative synthesis three randomized controlled trials[10,25,26], two prospective[11,12], and seven retrospective cohort studies[13,27-32]. The source of bleeding was peptic ulcer lesions in eight studies[10-13,25,29,30,32], while in four studies[26-28,31], NVUGIB lesion was used as a generic term for various bleeding sources (*e.g.*, angiodysplasia, solid tumors, peptic ulcers). Each study had a relatively small sample size, with similar characteristics between intervention groups. The eligibility criteria of the studies included are presented in Supplementary Table 2. Most of the studies did not report any adverse events during or after PTAE. Information about the reported endoscopic treatments, technical success rate of PTAE, adverse events, and standard of care are summarized in Supplementary Table 3.

Prophylactic transcatheter arterial embolization is associated with lower odds of rebleeding

In our meta-analysis, we included a total of twelve studies with 1329 patients evaluating the clinical effect of PTAE on various outcomes. In the intervention group, 486 patients received PTAE in addition to standard of care. There was a total of 843 patients in the control group.

PTAE is connected with significantly lower chance for rebleeding compared to the control group (OR = 0.48, 95%CI: 0.29–0.78, P = 0.003; in a mildly heterogenous dataset, I^2 = 33.0%, P = 0.126) (Figure 2).

For this comparison, publication bias assessment by visual inspection of a funnel-plot and Egger's test was carried out, suggesting a likelihood for publication bias. (Supplementary Figure 1). Leave-one-out analysis showed no significant change in the overall odds for rebleeding (Supplementary Figure 2).

According to the RCT subgroup analysis with intention-to-treat data, there was no significant difference between the PTAE and control group in the rate of rebleeding (OR = 0.58, 95%CI: 0.27–1.25, P = 0.165; in a mildly heterogeneous dataset, I^2 = 12.6%, P = 0.319) (Figure 2). However, with available per-protocol analysis results, the odds of rebleeding were significantly lower in the PTAE group, compared to the control group even according to the RCT subgroup analysis (OR = 0.42, 95%CI: 0.19–0.93, P = 0.033; [I^2 = 0.0%, P = 0.712]) (Supplementary Figure 3). The performed TSA showed that the required information size was reached neither in the intention-to-treat nor in the per-protocol calculation (Supplementary Figure 4A and 4B).

Prophylactic transcatheter arterial embolization is not associated with mortality in non-variceal upper gastrointestinal bleeding

There was no significant difference neither in 30-day mortality [OR = 0.82, 95%CI: 0.39–1.72, P = 0.594; (I^2 = 19.6%, P = 0.290)], nor in in-hospital mortality rates [OR = 0.46, 95%CI: 0.19–1.14, P = 0.092; (I^2 = 0.0%, P = 0.713), respectively] between the PTAE and control group (Figure 3A).

Prophylactic transcatheter arterial embolization seems to improve secondary outcomes in non-variceal upper gastrointestinal bleeding

Patients who underwent PTAE treatment were less likely to need any kind of reintervention caused by rebleeding, compared to those without PTAE (OR = 0.48, 95%CI: 0.31–0.76, P = 0.002; in a homogenous dataset, I^2 = 0.0%, P = 0.636) (Figure 3B). We found that PTAE group has significantly lower odds of rescue surgery in contrast with the control group [OR = 0.35, 95%CI: 0.14–0.92, P = 0.033; (I^2 = 44.1%, P = 0.128)] (Supplementary Figure 5). Leave-one-out analysis showed no major change in the overall odds of reintervention or rescue surgery (Supplementary Figure 6 and 7).

The length of hospital stay was reported in four studies[10-12,25]. Our meta-analysis established no statistically significant difference between the intervention and the control group in the length of hospital stay [WMD = -3.77 days, 95%CI: (-8.00)–0.45, P = 0.08; considerable heterogenous dataset, I^2 = 90.7%, P < 0.001] (Figure 3C). In parallel, three publications[10-12] reported the length of ICU stay, however the difference between the PTAE and control group was non-significant [WMD = -1.33 days, 95%CI: (-2.84)–0.18, P = 0.084; I^2 = 84.8%, P = 0.001] (Supplementary Figure 8).

Table 1 Basic characteristics of included studies in the systematic review and meta-analysis

Ref.	Country	Study design	Study period	Number of patients/ intervention group	Female %	Age,[1] (yr)	Bleeding etiology	Outcome(s)	Embolic agents
Arrayeah *et al*[27]	United States, Israel	Retrospective cohort	1997–2009	73/56	40	61.1	NVUGIB	Rebleeding, 30-d mortality, reintervention, surgery	Microcoils, gelatin sponge, polyvinyl alcohol particles
Dixon *et al* [28]	United Kingdom	Retrospective cohort	05.2008–11.2010	27/20	18.5	66	NVUGIB of duodenal origin	Rebleeding, 30-d mortality, reintervention	Microcoils alone or combined with gelatin/gelfoam sponge, polyvinyl alcohol particles
Kaminskis *et al*[11]	Latvia	Prospective cohort	2014–2018	399/58	44.4	67	High-risk peptic ulcer	Rebleeding, in-hospital mortality, surgery, hospital stay, ICU stay, transfused blood units	ND
Kaminskis *et al*[12]	Latvia	Prospective cohort	2010–2013	75/25	66.6	64	High-risk peptic ulcer	Rebleeding, in-hospital mortality, surgery, hospital stay, ICU stay, transfused blood units	Coil or sandwich technique
Lau *et al* [10]	China	Randomized controlled trial	2010–2014	241/118	24.9	66	High-risk peptic ulcer	Rebleeding, 30-d mortality, reintervention, surgery, hospital stay, ICU stay, transfused blood units	Sandwich technique: Coils and gel foam particles
Laursen *et al*[25]	Denmark	Randomized controlled trial	11.2009–05.2012	105/49	44	73	High-risk peptic ulcer	Rebleeding, in-hospital and 30-d mortality, hospital stay, readmission	Coils
Lebedev *et al*[29]	Russia	Retrospective cohort	1991–2016	90/30	ND	ND	Peptic ulcer	Rebleeding, mortality	Microcoils, polyvinyl alcohol
Mille *et al* [30]	Germany	Retrospective cohort	2008–2012	102/55	31.4	70.7	Duodenal ulcer	Rebleeding, 30-d mortality, surgery, transfused blood units	Coils, cyanoacrylate glue or both
Sildiroglu *et al*[31]	United States	Retrospective cohort	10.2001–11.2011	43/18	ND	60.1	NVUGIB	Rebleeding, mortality	Coils, gelfoam, polyvinyl alcohol
Tong *et al* [13]	China	Retrospective cohort	2014–2016	74/16	23	57.2	High-risk peptic ulcer	Rebleeding	ND
Wu *et al* [32]	Australia	Retrospective cohort	01.2008–12.2012	34/8	ND	70.1	Peptic ulcer	Rebleeding	ND
Ying *et al* [26]	China	Randomized controlled trial	05.2012–06.2013	66/33	25	51.5	Upper GIB	Rebleeding	Gelatin sponge particles
Ying *et al* [23]	China	Randomized controlled trial	06.2010–06.2014	78/39	46.2	46.5	Upper GIB	Short term haemostasis, long term haemostasis, hospital stay, transfusion	Coils, gelatin sponge
Yonemoto *et al*[24]	Japan	Retrospective cohort	04.2005–12.2017	141/11	22.7	62.8	Duodenal ulcer	Laboratory data at initial diagnosis, the amount of blood transfusion, 30-d mortality	ND

[1]Age is given in mean or median. GIB: Gastrointestinal bleeding, ICU: Intensive care unit, ND: No data, NVUGIB: Non-variceal upper GIB.

Lastly, the PTAE group needed significantly more units of blood transfusion, than

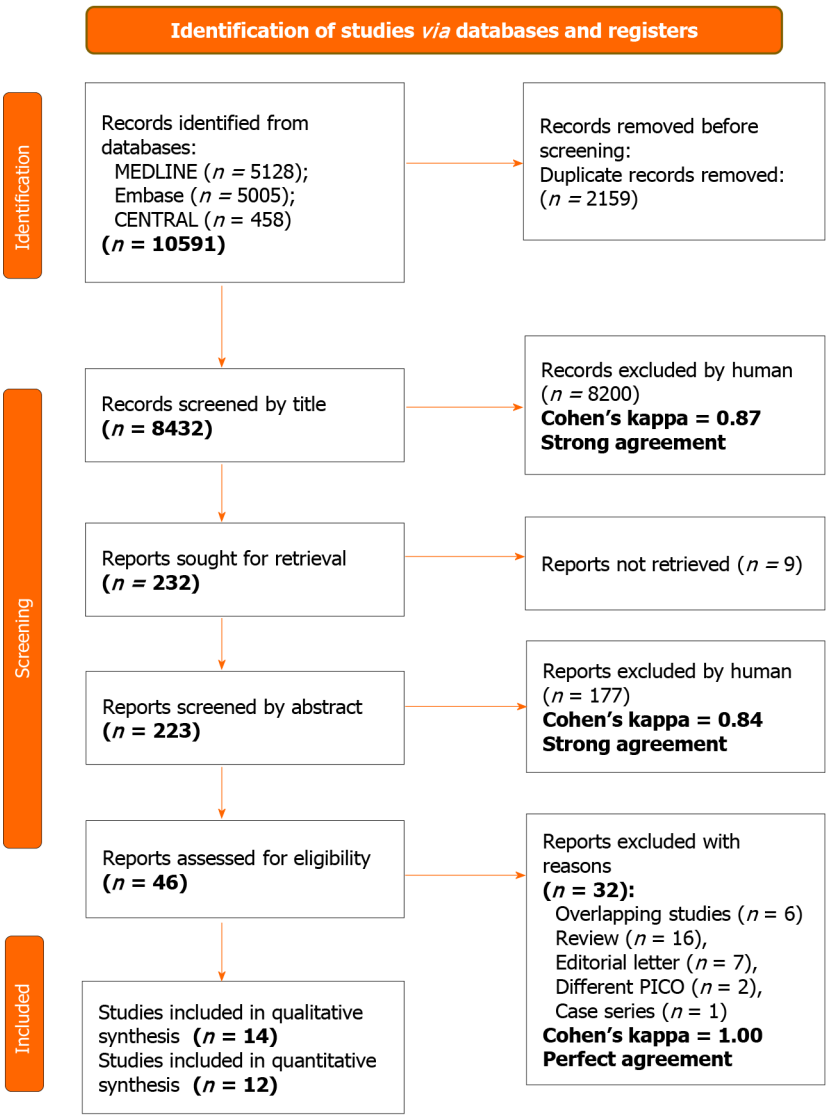


Figure 1 Preferred reporting in systematic reviews and meta-analyses flowchart showing the selection process.

Risk of bias assessment and quality of evidence

Among the included studies, four[10-12,25] were of low overall risk of bias, two[29,30] were of high overall risk of bias, all the other studies were rated to carry moderate overall risk of bias. The summary of the risk of bias assessment is shown in Supplementary Figure 11-18.

We included all outcomes in the "Summary of findings table" (Supplementary Table 4). The certainty of the evidence is very low for every outcome because our meta-analysis mainly contained observational studies. We calculated the quality of evidence among the RCT subgroup in rebleeding, and we found a moderate certainty of the evidence for PTAE, lowering the chance of rebleeding.

DISCUSSION

In this study, we assessed the effect of PTAE in addition to the successful endoscopic treatment of NVGUIB or PTAE as the first treatment option in case of not actively bleeding patients with NVUGIB lesions. Based on our findings, PTAE is associated with lower odds of rebleeding, need for additional reintervention, and rescue surgery compared to standard of care. We found a roughly 50% lower rate of the outcomes mentioned above, which is a considerable proportion, especially considering the prevalence of NVUGIB.

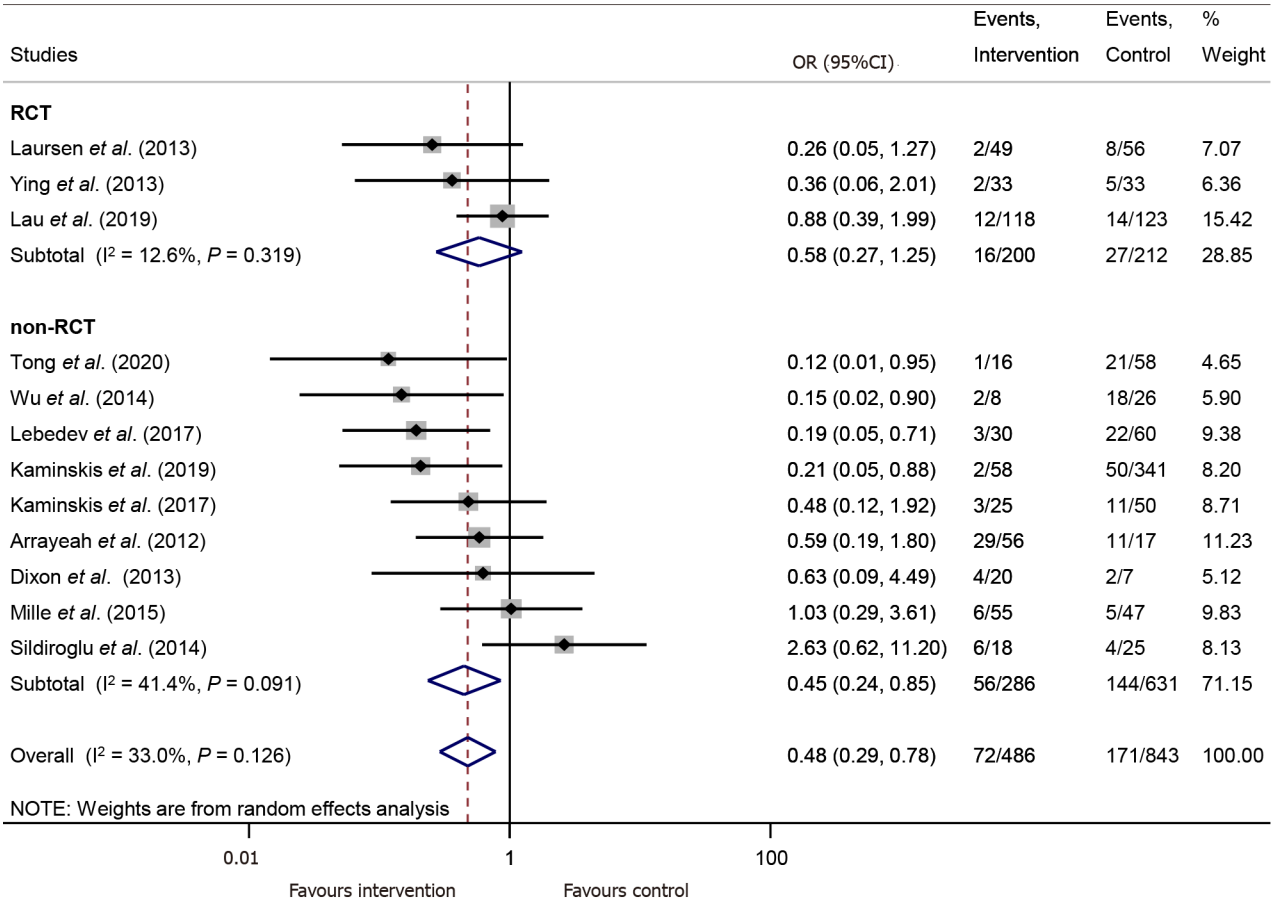


Figure 2 Forest plot of studies divided into subgroups representing that the overall odds of rebleeding were significantly lower in the prophylactic transcatheter arterial embolization group. However, among the RCT studies, the difference was not statistically significant. RCT: Randomized controlled trial; OR: Odds ratio; 95%CI: Confidence interval.

A recent meta-analysis of Chang *et al*[33] attempted to evaluate the role of PTAE in the management of patients with high-risk peptic ulcer bleeding. They included only 2 RCTs and 3 observational studies in their meta-analysis while narrowing their search to patients with a high risk of rebleeding. We designed our systematic search for NVUGIB without restriction to high-risk peptic ulcer bleeding because of the various NVUGIB bleeding etiologies that could be treated with TAE[9].

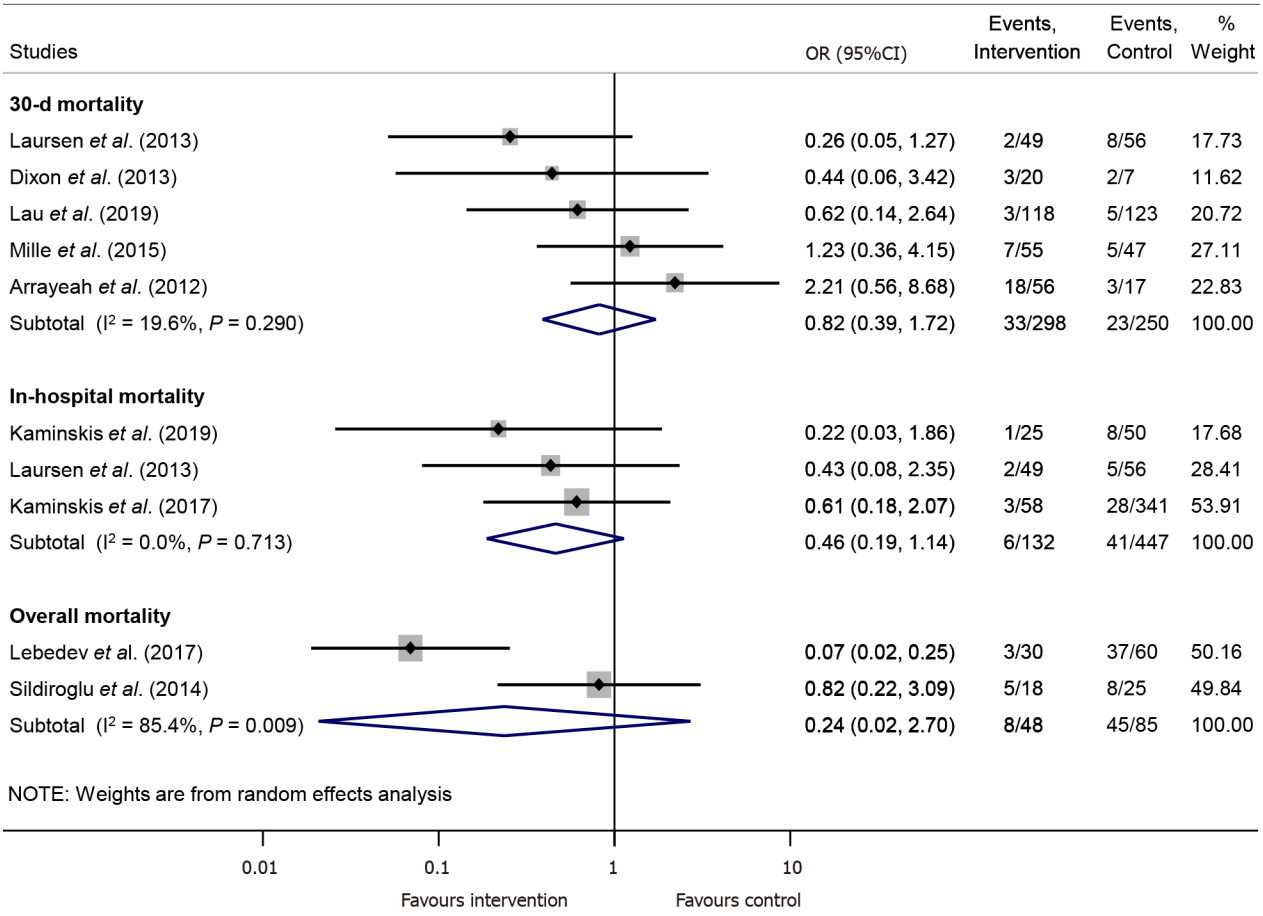
Rebleeding in the randomized controlled trials

We found three eligible RCTs[10,25,26], which provide the core of our meta-analysis and the highest level of evidence. When we performed a subgroup analysis of the RCTs for the rebleeding outcome, we found no significant difference between PTAE and the control group. We think that the main reason why with intention-to-treat data, we could not demonstrate the clear beneficial effect of PTAE is that in Lau *et al*[10]'s study, 22 patients out of 118 (18.6%), and Laursen *et al*[25], 18 out of 49 (36.7%) did not receive embolization at all despite being in the embolization arm of the studies. When we used per-protocol data, also in the RCT subgroup, there was a significantly lower risk for rebleeding in the PTAE group. However, the TSA calculation showed that the required information size was not reached, and our results are inconclusive.

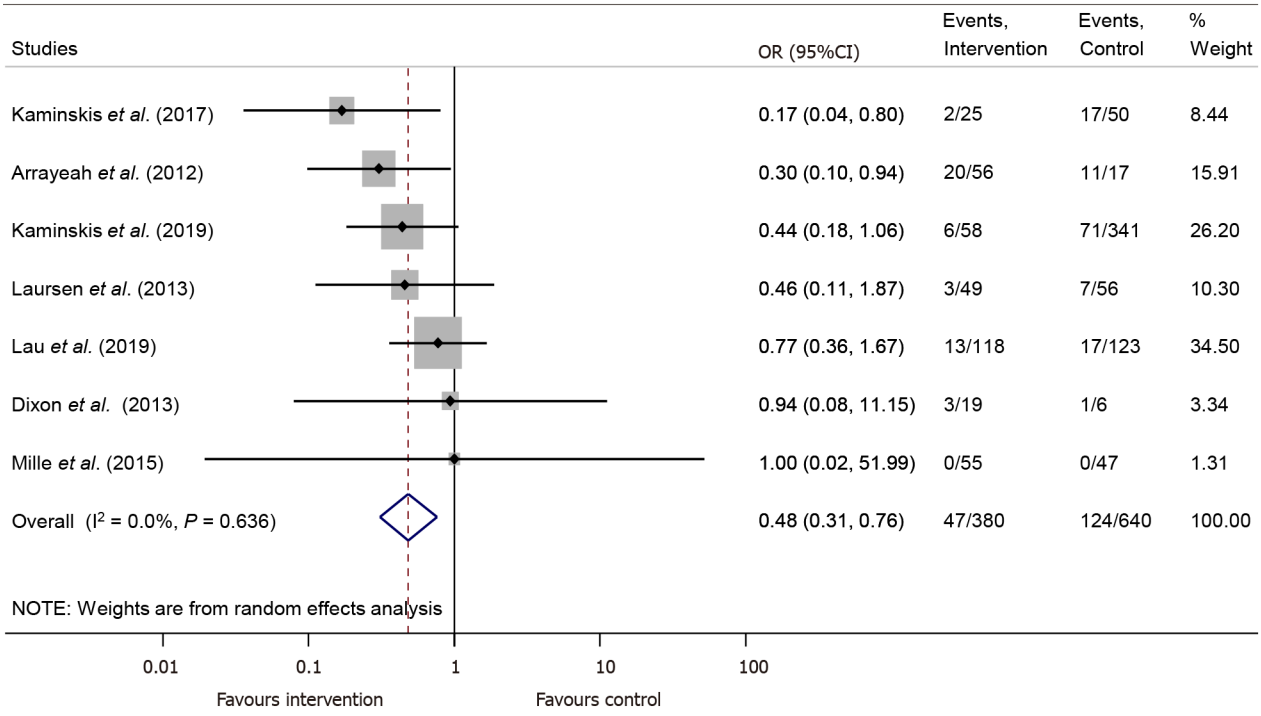
It is important to note that in Laursen *et al*[25]'s study, 9% of the potentially eligible patients were excluded because they were admitted to the hospital on weekends. These patients could not receive the allocated intervention due to the lack of staff in interventional radiology. This highlights that PTAE could be the most beneficial treatment option in centers with well-established interventional radiology units.

According to Lau *et al*[10], the chance of recurrent bleeding was significantly reduced in ulcers 15 mm in size or greater. Unfortunately, there was not enough data on the size of the culprit lesions in the other included studies to perform a meta-analysis. Nevertheless, risk stratification is essential before choosing between multiple possible treatment modalities in the case of NVUGIB. Several studies[10-13,25] used the Forrest classification, Rockall score, or the American Society of Anesthesiologists

A


Studies
OR (95%CI)
Events, Intervention
Events, Control
% Weight
30-d mortality
Laursen et al. (2013) 0.26 (0.05, 1.27) 2/49 8/56 17.73
Dixon et al. (2013) 0.44 (0.06, 3.42) 3/20 2/7 11.62
Lau et al. (2019) 0.62 (0.14, 2.64) 3/118 5/123 20.72
Mille et al. (2015) 1.23 (0.36, 4.15) 7/55 5/47 27.11
Arrayeah et al. (2012) 2.21 (0.56, 8.68) 18/56 3/17 22.83
Subtotal (I² = 19.6%, P = 0.290) 0.82 (0.39, 1.72) 33/298 23/250 100.00
In-hospital mortality
Kaminskis et al. (2019) 0.22 (0.03, 1.86) 1/25 8/50 17.68
Laursen et al. (2013) 0.43 (0.08, 2.35) 2/49 5/56 28.41
Kaminskis et al. (2017) 0.61 (0.18, 2.07) 3/58 28/341 53.91
Subtotal (I² = 0.0%, P = 0.713) 0.46 (0.19, 1.14) 6/132 41/447 100.00
Overall mortality
Lebedev et al. (2017) 0.07 (0.02, 0.25) 3/30 37/60 50.16
Sildiroglu et al. (2014) 0.82 (0.22, 3.09) 5/18 8/25 49.84
Subtotal (I² = 85.4%, P = 0.009) 0.24 (0.02, 2.70) 8/48 45/85 100.00
NOTE: Weights are from random effects analysis
0.01
0.1
1
10
Favours intervention
Favours control

B


Studies
OR (95%CI)
Events, Intervention
Events, Control
% Weight
Kaminskis et al. (2017) 0.17 (0.04, 0.80) 2/25 17/50 8.44
Arrayeah et al. (2012) 0.30 (0.10, 0.94) 20/56 11/17 15.91
Kaminskis et al. (2019) 0.44 (0.18, 1.06) 6/58 71/341 26.20
Laursen et al. (2013) 0.46 (0.11, 1.87) 3/49 7/56 10.30
Lau et al. (2019) 0.77 (0.36, 1.67) 13/118 17/123 34.50
Dixon et al. (2013) 0.94 (0.08, 11.15) 3/19 1/6 3.34
Mille et al. (2015) 1.00 (0.02, 51.99) 0/55 0/47 1.31
Overall (I² = 0.0%, P = 0.636) 0.48 (0.31, 0.76) 47/380 124/640 100.00
NOTE: Weights are from random effects analysis
0.01
0.1
1
10
100
Favours intervention
Favours control

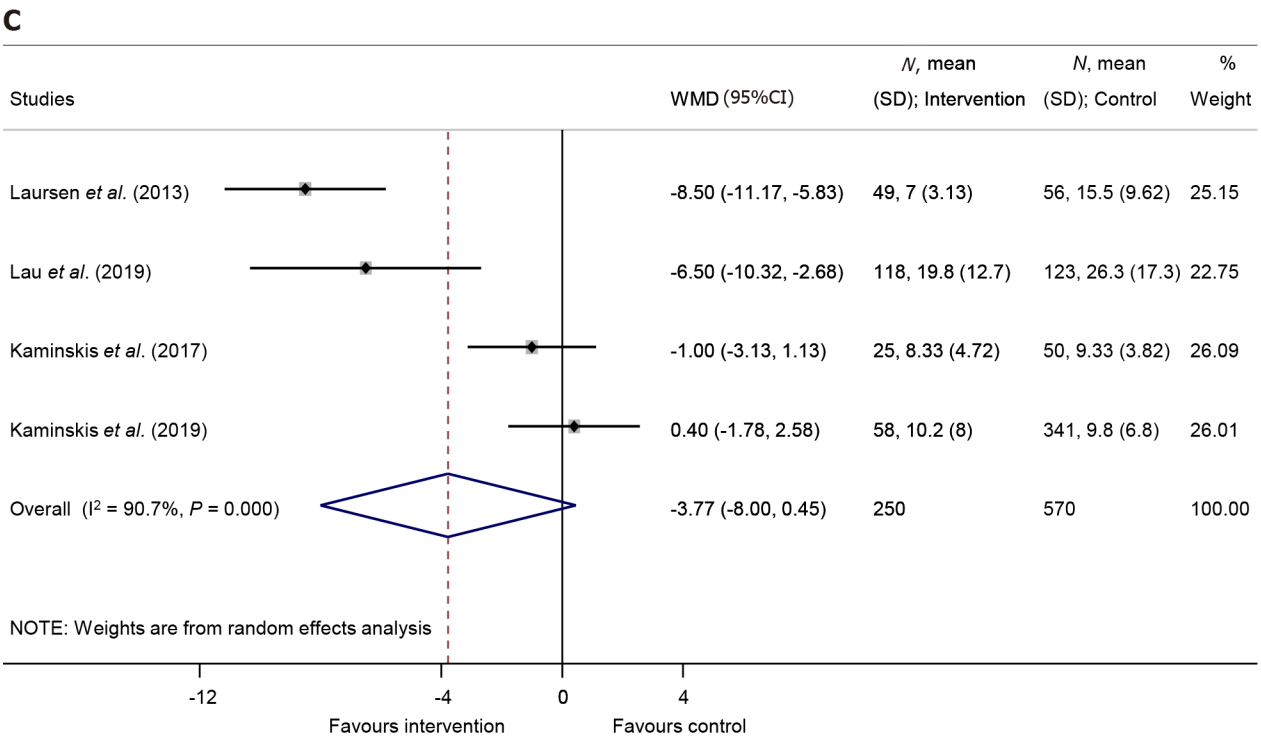


Figure 3 Forest plot of studies. A: Representing no significant difference in mortality rates between the prophylactic transcatheter arterial embolization and the control group; B: Representing significantly lower odds of reintervention in the prophylactic transcatheter arterial embolization than the control group; C: representing no significant difference in length of hospital stay in days between the prophylactic transcatheter arterial embolization and the control group. OR: Odds ratio; 95%CI: Confidence interval; WMD: Weighted mean difference; SD: Standard deviation.

score to assess the baseline risk of rebleeding or mortality among the patients, and it was approximately the same between the PTAE and the control group.

Rebleeding in cohort studies

The publication of Mille *et al*[30] described that only high rebleeding risk patients got PTAE, and in the control group were only low-risk patients. We consider this a selection bias, causing confounding of the measured outcomes, which could explain why they did not manage to find any difference in the rebleeding, reintervention, or rescue surgery rate between the intervention and the control group. Applying the leave-one-out method in the case of the study of Mille *et al*[30], there was no major change in the overall odds for rebleeding, reintervention, and rescue surgery.

The study of Sildiroglu *et al*[31] was the only one where the PTAE group had a worse rebleeding rate than the control group. There was no data on the baseline characteristics of the two treatment groups, so we cannot explain this contradicting result.

We included in our analyses four studies[26-28,31], with a definition of NVUGIB including various sources such as peptic ulcers, tumors, Dieulafoy lesion, Mallory-Weiss tear. Arrayeh *et al*[27] carried out a retrospective analysis that compared three therapeutic options: angiography without embolization, PTAE, and TAE with an abnormal angiogram. They published the interesting observation that patients with duodenal bleeding due to a mass (various types of malignant) lesion had a greater primary hemostasis rate 30 d after angiography compared with patients with nonmass (different types of benign) sources of duodenal bleeding (100% *vs* 54%; $P = 0.008$). This difference was not detectable between mass and nonmass lesions in the case of gastric bleeding. We did not find data in other studies about the investigated outcomes separated by the type of the bleeding lesion.

The rebleeding rate could also depend on whether NVUGIB has a gastric or duodenal source. According to Arrayeh *et al*[27], PTAE may be advantageous in patients with a duodenal source of bleeding but not in patients with gastric hemorrhage. We did not identify enough evidence to support this inference because none of the other included studies reported gastric and duodenal bleeding separately.

Evidence about secondary outcomes

Our results indicated that PTAE does not improve the mortality rates of NVUGIB significantly. We could not draw a clear conclusion about this outcome because of the different time-frames for mortality assessment used between the different studies: 30-d mortality was used in five studies[10,25,27,28,30], in-hospital mortality in three[11,12,25] and two studies[29,31] did not report any time-frame for mortality. Mortality is strongly associated with pre-endoscopy and complete Rockall score, according to Hearnshaw *et al*[5] We can only speculate that numerous major confounding factors affect the mortality of NVUGIB patients, and only one of them is the chosen treatment modality.

We had predicted a shorter hospital stay and ICU stay in the PTAE group, but our findings could not prove a significant difference between the two groups. Interestingly, if we analyzed only the data coming from RCTs, there was an apparent reduction in the length of hospital and ICU stay in the PTAE group compared with the control group. This result highlights the possible bias of the observational cohort studies.

The PTAE group needed slightly more red blood cell transfusion than the control group, although the heterogeneity between the studies suggests a careful interpretation of this finding. Since we assume a major confounding factor in the publication of Mille *et al*[30], the difference was no longer statistically significant between the PTAE and the control group after applying the leave-one-out method.

Methods reducing rebleeding risk in non-variceal upper gastrointestinal bleeding

There are a few therapies, which are already proved to reduce rebleeding from NVUGIB. Proton pump inhibitors (PPI) significantly decrease the recurrence of bleeding compared to control (placebo or histamine type 2 receptor antagonists); pooled rates were 10.6% with PPI *vs* 17.3% with control treatment (OR = 0.49; 95%CI: 0.37-0.65) in a Cochrane review comprising 24 RCTs[34]. Our recent meta-analysis showed that PPIs given either orally or intravenously are equally efficacious in preventing rebleeding[35].

After peptic ulcer bleeding, investigation for the presence of *H. pylori* should be mandatory. Our network meta-analysis[36] demonstrated that none of the individual tests or the strategy of combined tests is superior in detecting *H. pylori*. Gisbert *et al*[37] reported that rebleeding did not occur in patients with complicated ulcers after *H. pylori* eradication; moreover, maintenance of anti-ulcer therapy is unnecessary if eradication was achieved.

Endoscopic Doppler probe guided hemostasis significantly reduced the 30-d rates of rebleeding compared with standard visually guided hemostasis in an RCT (11.1% *vs* 26.3%), and the use of the endoscopic Doppler probe was suggested for risk stratification in the management of NVUGIB[38].

Another promising endoscopic technique to reduce the rebleeding rate of peptic ulcers is over-the-scope clipping (OTSC), which is superior to standard therapy with through-the-scope clips in preventing further bleeding according to the prospective RCT of Schmidt *et al*[39].

A recent meta-analysis[40] showed that the routine second-look endoscopy was not superior to a single endoscopy with complete endoscopic hemostasis in reducing the risk of recurrent bleeding, mortality, or need for surgery in patients with acute UGIB due to peptic ulcer disease. In contrast, according to our results, PTAE added to the standard of care could decrease the probability of rebleeding. Moreover, PTAE might reduce the need for surgery and any reintervention.

Strengths and limitations

Our work is assessing the potential effects of PTAE compared to the standard of care in the treatment of NVUGIB. We used a rigorous methodology and followed a transparent protocol, combined with a comprehensive statistical analysis as possible. We collected a total of 486 patients who received PTAE, which is an infrequent therapeutic choice so far.

The main limitation of our meta-analysis is that we collected our data mostly from observational cohort studies, and we found only three RCTs comparing PTAE to the standard of care. Thus, the quality of evidence for every outcome in our meta-analysis is very low based on the GRADE framework. When we assessed the quality of evidence regarding rebleeding in the RCT subgroup, we found moderate evidence for the risk reduction with PTAE. The diversity of the NVUGIB population in some studies could also limit our results and explain the statistical heterogeneity in some cases. Significant differences are present in the embolic agents utilized for PTAE

among publications. There was very restricted data on the endoscopic treatment before PTAE, which could also influence the outcomes. The included studies contain only limited information on secondary outcomes, so our conclusions about these are less certain.

Implications for practice

In selected cases, where the previous risk stratification suggests high rebleeding risk or the anatomical situation makes the secure and permanent endoscopic hemostasis impossible, we can consider the routine use of PTAE. Considering the demographic trends of NVUGIB, we predict that elderly, high-risk patients with co-morbidities could benefit the most from PTAE as a therapeutic approach.

Implications for research

Further RCTs are warranted to achieve a higher level of evidence about the potentially beneficial effects of PTAE. Developing an accurate risk stratification system would be crucial to select the ideal candidates for PTAE. Clinical trials investigating the use of existing risk scores or creating a new risk stratification tool of NVUGIB could help clinicians choose between the emerging number of treatment options.

CONCLUSION

PTAE is accompanied by lower odds of rebleeding, need for surgery, and reinterventions in NVUGIB. However, our meta-analysis could not justify a beneficial effect of *PTAE* on mortality rates compared with the standard of care in *NVUGIB*.

ARTICLE HIGHLIGHTS

Research background

The prevention of rebleeding is one of the main goals in managing non-variceal upper gastrointestinal bleeding (NVUGIB). Prophylactic transcatheter arterial embolization (PTAE) can be used in NVUGIB as second-line therapy.

Research motivation

The results of the individual studies about the beneficial effects of PTAE among NVUGIB patients were contradictory.

Research objectives

The authors aimed to carry out a comprehensive systematic review and meta-analysis. The authors compared the PTAE to no embolization as a second line, prophylactic treatment among NVUGIB patients.

Research methods

The authors conducted a systematic search in three databases (MEDLINE, EMBASE, CENTRAL). The eligible studies compared patients with NVUGIB receiving PTAE to those who did not get PTAE. The authors calculated odds ratios (ORs) with 95% confidence intervals (CI) for rebleeding, mortality, reintervention, need for surgery, and weighted mean differences (WMDs) of need for transfusion, length of hospital (LOH), and intensive care unit (ICU) stay.

Research results

PTAE was associated with significantly lower odds of rebleeding, reintervention and rescue surgery (OR = 0.48, 95%CI: 0.29–0.78; OR = 0.48, 95%CI: 0.31–0.76; OR = 0.35, 95%CI: 0.14–0.92; respectively). There was no significant difference in the mortality rates, LOH, and ICU stays between the PTAE and control groups. The quality of evidence for every outcome in our meta-analysis is very low based on the GRADE framework.

Research conclusions

The results suggest that PTAE is a reasonable therapeutic choice to prevent rebleeding or reintervention in NVUGIB, although it did not improve the mortality rates of NVUGIB.

Research perspectives

Further randomized controlled trials are needed about the use of PTAE. We also propose a clinical trial that could recommend a new risk stratification tool of NVUGIB, helping clinicians choose between treatment options.

REFERENCES

1 **Loperfido S**, Baldo V, Piovesana E, Bellina L, Rossi K, Groppo M, Caroli A, Dal Bò N, Monica F, Fabris L, Salvat HH, Bassi N, Okolicsanyi L. Changing trends in acute upper-GI bleeding: a population-based study. *Gastrointest Endosc* 2009; **70**: 212-224 [PMID: 19409558 DOI: 10.1016/j.gie.2008.10.051]

2 **Oakland K**. Changing epidemiology and etiology of upper and lower gastrointestinal bleeding. *Best Pract Res Clin Gastroenterol* 2019; **42-43**: 101610 [PMID: 31785737 DOI: 10.1016/j.bpg.2019.04.003]

3 **Wuerth BA**, Rockey DC. Changing Epidemiology of Upper Gastrointestinal Hemorrhage in the Last Decade: A Nationwide Analysis. *Dig Dis Sci* 2018; **63**: 1286-1293 [PMID: 29282637 DOI: 10.1007/s10620-017-4882-6]

4 **Jairath V**, Martel M, Logan RF, Barkun AN. Why do mortality rates for nonvariceal upper gastrointestinal bleeding differ around the world? *Can J Gastroenterol* 2012; **26**: 537-543 [PMID: 22891179 DOI: 10.1155/2012/862905]

5 **Hearnshaw SA**, Logan RF, Lowe D, Travis SP, Murphy MF, Palmer KR. Acute upper gastrointestinal bleeding in the UK: patient characteristics, diagnoses and outcomes in the 2007 UK audit. *Gut* 2011; **60**: 1327-1335 [PMID: 21490373 DOI: 10.1136/gut.2010.228437]

6 **van Leerdam ME**. Epidemiology of acute upper gastrointestinal bleeding. *Best Pract Res Clin Gastroenterol* 2008; **22**: 209-224 [PMID: 18346679 DOI: 10.1016/j.bpg.2007.10.011]

7 **Gralnek IM**, Stanley AJ, Morris AJ, Camus M, Lau J, Lanas A, Laursen SB, Radaelli F, Papanikolaou IS, Cúrdia Gonçalves T, Dinis-Ribeiro M, Awadie H, Braun G, de Groot N, Udd M, Sanchez-Yague A, Neeman Z, van Hooft JE. Endoscopic diagnosis and management of nonvariceal upper gastrointestinal hemorrhage (NVUGIH): European Society of Gastrointestinal Endoscopy (ESGE) Guideline - Update 2021. *Endoscopy* 2021; **53**: 300-332 [PMID: 33567467 DOI: 10.1055/a-1369-5274]

8 **Nykänen T**, Peltola E, Kylänpää L, Udd M. Bleeding gastric and duodenal ulcers: case-control study comparing angioembolization and surgery. *Scand J Gastroenterol* 2017; **52**: 523-530 [PMID: 28270041 DOI: 10.1080/00365521.2017.1288756]

9 **Tarasconi A**, Baiocchi GL, Pattonieri V, Perrone G, Abongwa HK, Molfino S, Portolani N, Sartelli M, Di Saverio S, Heyer A, Ansaloni L, Coccolini F, Catena F. Transcatheter arterial embolization versus surgery for refractory non-variceal upper gastrointestinal bleeding: a meta-analysis. *World J Emerg Surg* 2019; **14**: 3 [PMID: 30733822 DOI: 10.1186/s13017-019-0223-8]

10 **Lau JYW**, Pittayanon R, Wong KT, Pinjaroen N, Chiu PWY, Rerknimitr R, Holster IL, Kuipers EJ, Wu KC, Au KWL, Chan FKL, Sung JJY. Prophylactic angiographic embolisation after endoscopic control of bleeding to high-risk peptic ulcers: a randomised controlled trial. *Gut* 2019; **68**: 796-803 [PMID: 29802172 DOI: 10.1136/gutjnl-2018-316074]

11 **Kaminskis A**, Ivanova P, Kratovska A, Ponomarjova S, Ptašņuka M, Demičevs J, Demičeva R, Boka V, Pupelis G. Endoscopic hemostasis followed by preventive transarterial embolization in high-risk patients with bleeding peptic ulcer: 5-year experience. *World J Emerg Surg* 2019; **14**: 45 [PMID: 31516544 DOI: 10.1186/s13017-019-0264-z]

12 **Kaminskis A**, Kratovska A, Ponomarjova S, Tolstova A, Mukans M, Stabiņa S, Gailums R, Bernšteins A, Ivanova P, Boka V, Pupelis G. Preventive transarterial embolization in upper nonvariceal gastrointestinal bleeding. *World J Emerg Surg* 2017; **12**: 3 [PMID: 28101125 DOI: 10.1186/s13017-016-0114-1]

13 **Tong H**, Lan T, Tang CW. Prophylactic angiographic embolisation after endoscopic treatment of bleeding for high-risk peptic ulcers: what are the more appropriate indications? *Gut* 2020; **69**: 1897-1898 [PMID: 31776229 DOI: 10.1136/gutjnl-2019-319818]

14 **Page MJ**, McKenzie JE, Bossuyt PM, Boutron I, Hoffmann TC, Mulrow CD, Shamseer L, Tetzlaff JM, Akl EA, Brennan SE, Chou R, Glanville J, Grimshaw JM, Hróbjartsson A, Lalu MM, Li T, Loder EW, Mayo-Wilson E, McDonald S, McGuinness LA, Stewart LA, Thomas J, Tricco AC, Welch VA, Whiting P, Moher D. The PRISMA 2020 statement: an updated guideline for reporting systematic reviews. *BMJ* 2021; **372**: n71 [PMID: 33782057 DOI: 10.1136/bmj.n71]

15 **Stroup DF**, Berlin JA, Morton SC, Olkin I, Williamson GD, Rennie D, Moher D, Becker BJ, Sipe TA, Thacker SB. Meta-analysis of observational studies in epidemiology: a proposal for reporting. Meta-analysis Of Observational Studies in Epidemiology (MOOSE) group. *JAMA* 2000; **283**: 2008-2012 [PMID: 10789670 DOI: 10.1001/jama.283.15.2008]

16 **McHugh ML**. Interrater reliability: the kappa statistic. *Biochem Med (Zagreb)* 2012; **22**: 276-282 [PMID: 23092060]

17 **DerSimonian R**, Laird N. Meta-analysis in clinical trials. *Control Clin Trials* 1986; **7**: 177-188 [PMID: 3802833 DOI: 10.1016/0197-2456(86)90046-2]

18 **Higgins JPT**, Thomas J, Chandler J, Cumpston M, Li T, Page MJ, Welch VA (editors). Cochrane

Handbook for Systematic Reviews of Interventions version 6.2 (updated February 2021). Cochrane, 2021. Available from: https://training.cochrane.org/handbook

19 **Sterne JA**, Hernán MA, Reeves BC, Savović J, Berkman ND, Viswanathan M, Henry D, Altman DG, Ansari MT, Boutron I, Carpenter JR, Chan AW, Churchill R, Deeks JJ, Hróbjartsson A, Kirkham J, Jüni P, Loke YK, Pigott TD, Ramsay CR, Regidor D, Rothstein HR, Sandhu L, Santaguida PL, Schünemann HJ, Shea B, Shrier I, Tugwell P, Turner L, Valentine JC, Waddington H, Waters E, Wells GA, Whiting PF, Higgins JP. ROBINS-I: a tool for assessing risk of bias in non-randomised studies of interventions. *BMJ* 2016; **355**: i4919 [PMID: 27733354 DOI: 10.1136/bmj.i4919]

20 **Sterne JAC**, Savović J, Page MJ, Elbers RG, Blencowe NS, Boutron I, Cates CJ, Cheng HY, Corbett MS, Eldridge SM, Emberson JR, Hernán MA, Hopewell S, Hróbjartsson A, Junqueira DR, Jüni P, Kirkham JJ, Lasserson T, Li T, McAleenan A, Reeves BC, Shepperd S, Shrier I, Stewart LA, Tilling K, White IR, Whiting PF, Higgins JPT. RoB 2: a revised tool for assessing risk of bias in randomised trials. *BMJ* 2019; **366**: l4898 [PMID: 31462531 DOI: 10.1136/bmj.l4898]

21 **McGuinness LA**, Higgins JPT. Risk-of-bias VISualization (robvis): An R package and Shiny web app for visualizing risk-of-bias assessments. *Res Synth Methods* 2021; **12**: 55-61 [PMID: 32336025 DOI: 10.1002/jrsm.1411]

22 **Iorio A**, Spencer FA, Falavigna M, Alba C, Lang E, Burnand B, McGinn T, Hayden J, Williams K, Shea B, Wolff R, Kujpers T, Perel P, Vandvik PO, Glasziou P, Schunemann H, Guyatt G. Use of GRADE for assessment of evidence about prognosis: rating confidence in estimates of event rates in broad categories of patients. *BMJ* 2015; **350**: h870 [PMID: 25775931 DOI: 10.1136/bmj.h870]

23 **Ying Y**, Luo JF, He X, Zeng FL, Xie YL. Clinical effects of preventive interventional therapy in gastrointestinal bleeding patients with negative digital subtraction angiography findings. *Shijie Huaren Xiaohua Zazhi* 2014; **22**: 5556-5560 [DOI: 10.11569/wcjd.v22.i35.5556]

24 **Yonemoto Y**, Fukami Y, Hara H, Mochida T, Machida T, Sugiyama Y, Watanabe A, Kaneshiro M, Ikemiyagi H, Yoshino K, Sakita S. The statistical comparison of endoscopic procedure and transarterial embolization for hemorrhage caused by duodenal ulcer. *United European Gastroenterol J* 2018; **6**: A496-A497 [DOI: 10.1177/2050640618792819]

25 **Laursen SB**, Hansen JM, Andersen PE, Schaffalitzky de Muckadell OB. Supplementary arteriel embolization an option in high-risk ulcer bleeding--a randomized study. *Scand J Gastroenterol* 2014; **49**: 75-83 [PMID: 24256098 DOI: 10.3109/00365521.2013.854829]

26 **Ying Y**, Luo JF, Zhang WH, Wang XN, He X. Effects of vasopressin infusion aided prophylactic gastroduodenal artery embolization in DSA-negative gastrointestinal bleeding patients. *Shijie Huaren Xiaohua Zazhi* 2013; **21**: 4180-4184 [DOI: 10.11569/wcjd.v21.i36.4180]

27 **Arrayeh E**, Fidelman N, Gordon RL, LaBerge JM, Kerlan RK Jr, Klimov A, Bloom AI. Transcatheter arterial embolization for upper gastrointestinal nonvariceal hemorrhage: is empiric embolization warranted? *Cardiovasc Intervent Radiol* 2012; **35**: 1346-1354 [PMID: 22302348 DOI: 10.1007/s00270-012-0351-y]

28 **Dixon S**, Chan V, Shrivastava V, Anthony S, Uberoi R, Bratby M. Is there a role for empiric gastroduodenal artery embolization in the management of patients with active upper GI hemorrhage? *Cardiovasc Intervent Radiol* 2013; **36**: 970-977 [PMID: 23152041 DOI: 10.1007/s00270-012-0511-0]

29 **Lebedev NV**, Belozerov GE, Klimov AE, Sokolova PY, Spasskiy AA, Barkhudarov AA. [Transcatheter embolization in prevention of recurrent bleeding from stomach ulcers]. *Khirurgiia (Mosk)* 2017; 31-35 [PMID: 28514380 DOI: 10.17116/hirurgia2017531-35]

30 **Mille M**, Huber J, Wlasak R, Engelhardt T, Hillner Y, Kriechling H, Aschenbach R, Ende K, Scharf JG, Puls R, Stier A. Prophylactic Transcatheter Arterial Embolization After Successful Endoscopic Hemostasis in the Management of Bleeding Duodenal Ulcer. *J Clin Gastroenterol* 2015; **49**: 738-745 [PMID: 25319738 DOI: 10.1097/MCG.0000000000000259]

31 **Sildiroglu O**, Muasher J, Arslan B, Sabri SS, Saad WE, Angle JF, Matsumoto AH, Turba UC. Outcomes of patients with acute upper gastrointestinal nonvariceal hemorrhage referred to interventional radiology for potential embolotherapy. *J Clin Gastroenterol* 2014; **48**: 687-692 [PMID: 25014238 DOI: 10.1097/MCG.0000000000000181]

32 **Wu P**, Szczesniak MM, Craig PI, Choo L. A novel predictor of rebleeding in high risk peptic ulcer disease selects patients who would benefit most from prophylactic arterial embolisation. *Gastroenterology* 2014; **146**: S-183 [DOI: 10.1016/S0016-5085(14)60650-8]

33 **Chang JHE**, Lye TJY, Zhu HZ, Syn NL, Tang SS, Gogna A, Chan WH, Ong HS, Tan JTH, Lim CH. Systematic Review and Meta-Analysis of Prophylactic Transarterial Embolization for High-Risk Bleeding Peptic Ulcer Disease. *J Vasc Interv Radiol* 2021; **32**: 576-584.e5 [PMID: 33526343 DOI: 10.1016/j.jvir.2020.12.005]

34 **Leontiadis GI**, Sharma VK, Howden CW. Proton pump inhibitor treatment for acute peptic ulcer bleeding. *Cochrane Database Syst Rev* 2006; CD002094 [PMID: 16437441 DOI: 10.1002/14651858.CD002094.pub3]

35 **Csiki E**, Szabó H, Hanák L, Szakács Z, Kiss S, Vörhendi N, Pécsi D, Hegyi E, Hegyi P, Erőss B. Oral Proton Pump Inhibitors May Be as Effective as Intravenous in Peptic Ulcer Bleeding: A Systematic Review and Meta-analysis. *Clin Transl Gastroenterol* 2021; **12**: e00341 [PMID: 33988530 DOI: 10.14309/ctg.0000000000000341]

36 **Vörhendi N**, Soós A, Anne Engh M, Tinusz B, Szakács Z, Pécsi D, Mikó A, Sarlós P, Hegyi P, Erőss B. Accuracy of the *Helicobacter pylori* diagnostic tests in patients with peptic ulcer bleeding: a systematic review and network meta-analysis. *Therap Adv Gastroenterol* 2020; **13**: 1756284820965324 [PMID: 33403002 DOI: 10.1177/1756284820965324]

37 **Gisbert JP**, Calvet X, Cosme A, Almela P, Feu F, Bory F, Santolaria S, Aznárez R, Castro M, Fernández N, García-Grávalos R, Benages A, Cañete N, Montoro M, Borda F, Pérez-Aisa A, Piqué JM; H. pylori Study Group of the Asociación Española de Gastroenterología (Spanish Gastroenterology Association). Long-term follow-up of 1,000 patients cured of Helicobacter pylori infection following an episode of peptic ulcer bleeding. *Am J Gastroenterol* 2012; **107**: 1197-1204 [PMID: 22613904 DOI: 10.1038/ajg.2012.132]

38 **Jensen DM**, Kovacs TOG, Ohning GV, Ghassemi K, Machicado GA, Dulai GS, Sedarat A, Jutabha R, Gornbein J. Doppler Endoscopic Probe Monitoring of Blood Flow Improves Risk Stratification and Outcomes of Patients With Severe Nonvariceal Upper Gastrointestinal Hemorrhage. *Gastroenterology* 2017; **152**: 1310-1318.e1 [PMID: 28167214 DOI: 10.1053/j.gastro.2017.01.042]

39 **Schmidt A**, Gölder S, Goetz M, Meining A, Lau J, von Delius S, Escher M, Hoffmann A, Wiest R, Messmann H, Kratt T, Walter B, Bettinger D, Caca K. Over-the-Scope Clips Are More Effective Than Standard Endoscopic Therapy for Patients With Recurrent Bleeding of Peptic Ulcers. *Gastroenterology* 2018; **155**: 674-686.e6 [PMID: 29803838 DOI: 10.1053/j.gastro.2018.05.037]

40 **Kamal F**, Khan MA, Lee-Smith W, Sharma S, Imam Z, Henry C, Jowhar D, Khan Z, Petryna E, Iqbal U, Tombazzi C, Ismail MK, Howden CW. Role of routine second-look endoscopy in patients with acute peptic ulcer bleeding: meta-analysis of randomized controlled trials. *Gastrointest Endosc* 2021; **93**: 1228-1237.e5 [PMID: 33417896 DOI: 10.1016/j.gie.2020.12.039]

World Journal of Gastroenterology

Submit a Manuscript: https://www.f6publishing.com

World J Gastroenterol 2021 October 28; 27(40): 7000-7004

DOI: 10.3748/wjg.v27.i40.7000

ISSN 1007-9327 (print) ISSN 2219-2840 (online)

LETTER TO THE EDITOR

Gastrointestinal and hepatic involvement during COVID-19 pandemic: A focus on pediatric population and possible future implications

Rossella Sica, Serena Pennoni, Laura Penta, Sara Riccioni, Giuseppe Di Cara, Alberto Verrotti

ORCID number: Rossella Sica 0000-0002-3990-4117; Serena Pennoni 0000-0002-4238-436X; Laura Penta 0000-0003-0945-2997; Sara Riccioni 0000-0003-1989-9549; Giuseppe Di Cara 0000-0002-7632-6774; Alberto Verrotti 0000-0001-6323-4187.

Author contributions: Sica R drafted the manuscript; Sica R, Pennoni S, Penta L, Riccioni S, Di Cara G and Verrotti A edited and revised the manuscript; Verrotti A supervised and approved the final version of the manuscript; all authors have read and agreed to the published version of the manuscript.

Conflict-of-interest statement: The authors declare no conflict of interest.

Open-Access: This article is an open-access article that was selected by an in-house editor and fully peer-reviewed by external reviewers. It is distributed in accordance with the Creative Commons Attribution NonCommercial (CC BY-NC 4.0) license, which permits others to distribute, remix, adapt, build upon this work non-commercially, and license their derivative works on different terms, provided the original work is properly cited and the use is non-commercial. See: htt

Rossella Sica, Serena Pennoni, Laura Penta, Sara Riccioni, Giuseppe Di Cara, Alberto Verrotti, Department of Pediatrics, University of Perugia, Perugia 06132, PG, Italy

Corresponding author: Alberto Verrotti, MD, PhD, Chief Doctor, Professor, Department of Pediatrics, University of Perugia, Piazza L Severi 1, Perugia 06132, PG, Italy. alberto.verrottidipianella@unipg.it

Abstract

Since the coronavirus disease 2019 (COVID-19) pandemic caused by severe acute respiratory syndrome coronavirus 2 (SARS-CoV-2) has rapidly spread worldwide, there is still limited knowledge about this condition and its natural history. Children have been relatively spared during COVID-19 pandemic but a novel syndrome known as multisystem inflammatory syndrome (MIS-C) has emerged, following a SARS-CoV-2 infection in children and adolescents. This syndrome can lead to shock and multiple organ failure requiring intensive care. Although COVID-19 clinical research focuses on respiratory symptoms, extrapulmonary involvement such as gastrointestinal (GI) and hepatic manifestations should also be considered. In fact, GI and hepatic involvement play an important role among the most common presenting symptoms of both pediatric and adult COVID-19 and MIS-C. This involvement can not only be one of the most common presenting clinical features but also one of the sequelae of these syndromes. Abdominal ultrasonography monitoring could be very useful to identify a potential involvement of the GI tract and liver. Moreover, long-term follow-up is needed and would be essential to define the long-term outcomes of these patients.

Key Words: SARS-CoV-2; COVID-19; Multisystem inflammatory syndrome; Gastrointestinal tract; Liver; Ultrasonography

©The Author(s) 2021. Published by Baishideng Publishing Group Inc. All rights reserved.

Core Tip: Gastrointestinal and hepatic symptoms are a common clinical feature of the coronavirus disease 2019 (COVID-19). Moreover, a novel syndrome known as multisystem inflammatory syndrome (MIS-C) associated with COVID-19 in children

p://creativecommons.org/Licenses/by-nc/4.0/

Manuscript source: Unsolicited manuscript

Specialty type: Medicine, research and experimental

Country/Territory of origin: Italy

Peer-review report's scientific quality classification

Grade A (Excellent): 0
Grade B (Very good): 0
Grade C (Good): C, C
Grade D (Fair): 0
Grade E (Poor): 0

Received: August 5, 2021
Peer-review started: August 5, 2021
First decision: August 19, 2021
Revised: August 30, 2021
Accepted: September 15, 2021
Article in press: September 15, 2021
Published online: October 28, 2021

P-Reviewer: Freij BJ, Nabil A
S-Editor: Gao CC
L-Editor: A
P-Editor: Li JH

and adolescents has emerged. Among the most common presenting symptoms of MIS-C, we found gastrointestinal and hepatic involvement. As gastrointestinal and hepatic involvement might play a major role in the clinical spectrum and possible sequelae of this novel condition, physicians should not underestimate these clinical manifestations. Therefore, abdominal ultrasonography monitoring and long-term follow-up could be useful to evaluate this potential damage and the possible outcome of these patients.

Citation: Sica R, Pennoni S, Penta L, Riccioni S, Di Cara G, Verrotti A. Gastrointestinal and hepatic involvement during COVID-19 pandemic: A focus on pediatric population and possible future implications. *World J Gastroenterol* 2021; 27(40): 7000-7004
URL: https://www.wjgnet.com/1007-9327/full/v27/i40/7000.htm
DOI: https://dx.doi.org/10.3748/wjg.v27.i40.7000

TO THE EDITOR

We read with great interest the review by Mohamed *et al*[1] about manifestations, mechanisms and management of the gastrointestinal (GI) and hepatic diseases during the coronavirus disease 2019 (COVID-19) pandemic. Although the large majority of concern about COVID-19 and its outcomes is centered on pulmonary manifestations and sequelae, we must be aware that GI and hepatic involvement could play a major role in the clinical spectrum of this novel disease as well as in virus transmission *via* the fecal-oral route. Hence, we agree with the authors' purpose that physicians should not underestimate digestive symptoms during COVID-19. In fact, GI manifestations in COVID-19 patients, including diarrhea, nausea, vomiting, anorexia and abdominal pain are common features of the disease with diarrhea being the most common among these symptoms[2,3].

The pathophysiologic mechanism of GI and hepatic injury during COVID-19 is still debated. Mohamed *et al*[1] reported that GI damage might be due to direct infection of GI cells. We appreciate the great relevance the authors gave to angiotensin-converting enzyme 2 (ACE2) receptors' expression over the small intestine cells, cholangiocytes and hepatocytes and the role it plays in severe acute respiratory syndrome coronavirus 2 (SARS-CoV-2) infection and in the pathophysiology of both GI and hepatic injury. Also, SARS-CoV-2 can induce cells expressing ACE2 to release inflammatory cytokines leading to a cytokine storm and multiple organ failure[4]. As Mohamed *et al*[1] well reported, SARS-CoV-2 binding to ACE2 receptor can lower the critical receptor level, reducing the absorption of tryptophan on the lumen surface of intestinal epithelial cells. It is known that tryptophan is absorbed on the lumen surface of intestinal epithelial cells *via* the B0AT1/ACE2 transport route inducing the mammalian target of rapamycin which controls the appearance of antimicrobial peptides influencing the components of gut flora. Therefore, the reduced absorption of tryptophan caused by SARS-CoV-2 can ultimately unbalance the gut flora resulting in diarrhea. The changings in the GI flora also stimulate the polarization of T helper 17 cells, and eventually, interleukin 17A induces the recruitment of neutrophils[1]. Moreover, changes in intestinal flora might affect the respiratory tract and *vice versa via* the gut-lung axis, subsequently enhancing the inflammatory and immune-mediated damage in the small intestine.

A study by Pirola and Sookoian[5] demonstrates that gene expression levels for ACE2 are highest in cholangiocytes compared to alveolar type 2 cells, followed in turn by sinusoidal endothelial cells and hepatocytes, thus supporting the possibility that SARS-CoV-2 may cause direct liver injury through a viral cytopathic effect. Nevertheless, GI mucosal damage and unbalance in the gut flora may lead to liver dysfunction through the gut-liver axis.

However, we should not forget that GI tract symptoms and liver injury may also be due to cytokine storm, hypoxic-shock conditions due to acute respiratory distress syndrome and drug-induced injury[6,7].

It is generally accepted that the existence of comorbidities in COVID-19 patients can dramatically increase the risk of poor outcome. Besides, the impact of the COVID-19 pandemic on preexisting GI, liver and pancreatic diseases is still under investigation. We appreciate the importance the authors gave to patients affected by inflammatory bowel diseases (IBD). Actually, these patients are more at risk for infectious diseases

due to the immunosuppressive therapy they undergo. Thus, IBD patients may potentially be more at risk for SARS-CoV-2 infection and severe COVID-19. The prognostic value of the elevation of liver enzymes and indices of cholestasis reflecting hepatic injury and cholangiocellular damage respectively, is still debated. Conversely, pre-existing chronic liver diseases seem to be independent risk factors for poor outcome in COVID-19, and cirrhosis grade has been defined as a predictor of mortality in SARS-CoV-2 infected patients[6].

We are thankful to the authors for their contribution to current literature and we would like to implement the authors' excellent work by reporting our experience with SARS-CoV-2 infection in the Pediatric population.

We would like to emphasize that COVID-19 in children and adolescents may often be asymptomatic or cause only mild symptoms. The most prevalent symptom of COVID-19 in children and adolescents is fever, followed by cough, upper respiratory tract symptoms, diarrhea and nausea/vomiting. In a multinational, multicenter cohort study, 22% of patients had GI symptoms and 7% of those had no respiratory symptoms[8]. Also, neurological manifestations must be considered as they might be a direct result of central nervous system viral invasion or post-infection immuno-mediated disease[9]. Interestingly, in the latter half of April 2020 a previously unknown SARS-CoV-2-related clinical syndrome emerged. Initially this novel entity was named pediatric inflammatory multisystem syndrome temporally associated with SARS-CoV-2 (PIMS-TS) by the European Centre for Disease Prevention and Control and then multisystem inflammatory syndrome in children (MIS-C) by the Centers for Disease Control and Prevention (CDC) in the United States and by the World Health Organization. This syndrome can lead to shock and multiple organ failure requiring a Pediatric Intensive Care Unit. Its features resemble those of known entities such as Kawasaki Disease, toxic shock syndrome, and macrophage activation syndrome. The CDC issued a case definition of MIS-C specifying that the patient should be < 21-year-old, have fever, laboratory evidence of inflammation, and evidence of a clinically severe illness requiring hospitalization, with multisystem (> 2) organ involvement (cardiac, renal, respiratory, hematological, GI, dermatological, or neurological), in the absence of an alternative plausible diagnosis, and evidence of SARS-CoV-2 infection or exposure[10]. It was initially thought that this syndrome was specific of children, but recent reports have shown that it can also occur in adults. In a case series comparing children and adolescents with MIS-C *vs* those with severe COVID-19, MIS-C was distinguished by having a more severe cardiovascular and mucocutaneous involvement and a worse inflammation with a higher neutrophil/Leukocyte ratio, higher c-reactive protein level and lower thrombocytopenia compared to patients with COVID-19[11].

The pathophysiology of this syndrome is under intense investigation but so far it remains unclear. It is believed that this syndrome results from an abnormal immune response to the virus. Interestingly, among the most common presenting symptoms of MIS-C from reports worldwide we found GI involvement, including vomiting, abdominal pain, and/or diarrhea. Moreover, there are reports in literature reporting cases of MIS-C presenting with acute abdomen and pseudo appendicular syndrome with shock, clinical symptoms suggestive of appendicitis, functional intestinal obstruction and ischemic bowel lesions[12,13]. Furthermore, abdominal imaging findings such as hepatomegaly, nephromegaly, gallbladder wall edema, ascites, intestinal inflammation and mesenteric lymphadenopathy are very common[14]. The role of SARS-CoV-2 in some of these clinical presentations seems more likely to be temporal rather than causative but it causes diagnostic and management dilemmas for treating physicians.

Regarding the experience of our Department of Pediatrics, we recently reported the case of a 14-year-old non-obese boy with MIS-C who presented with jaundiced skin, a diffusely painful abdomen and palpable hepatosplenomegaly. He was in a condition of multiorgan failure with a compromised hemodynamic status with reduction of left ventricular ejection fraction and elevated values of alanine aminotransferase, aspartate aminotransferase and indices of cholestasis. Notably, our patient fully recovered from MIS-C, with an excellent cardiac and renal outcome but during the follow-up visit program he was diagnosed with a new onset hepatic steatosis. Therefore, we suggest that hepatic steatosis might be one of the sequelae following SARS-CoV-2 infection, MIS-C or its treatment, mainly due to prolonged use of corticosteroids, probably through an inhibition of mitochondrial fatty acid oxidation[15].

We fully agree with the authors' suggestion that liver function should be monitored during COVID-19, particularly in more severe cases. Furthermore, we think that hepatic involvement after COVID-19 and MIS-C could be underdiagnosed as few patients undergo abdominal ultrasonography monitoring. Diagnosis of hepatic

steatosis is easily accessible through an abdominal ultrasound, which is a low-cost, non-invasive examination. To date, abdominal ultrasound monitoring for these patients is not supported by evidence but we suggest that it could be very useful to identify this potential damage early and evaluate the possible outcome of these patients.

In conclusion, GI and hepatic involvement in COVID-19 and MIS-C should not be underestimated because potential damage could be underdiagnosed. Further studies and long-term follow ups are needed to completely understand the pathophysiology and possible implications that GI and hepatic involvement might have in COVID-19 and MIS-C.

REFERENCES

1 **Mohamed DZ**, Ghoneim ME, Abu-Risha SE, Abdelsalam RA, Farag MA. Gastrointestinal and hepatic diseases during the COVID-19 pandemic: Manifestations, mechanism and management. *World J Gastroenterol* 2021; **27**: 4504-4535 [PMID: 34366621 DOI: 10.3748/wjg.v27.i28.4504]

2 **Wang D**, Hu B, Hu C, Zhu F, Liu X, Zhang J, Wang B, Xiang H, Cheng Z, Xiong Y, Zhao Y, Li Y, Wang X, Peng Z. Clinical Characteristics of 138 Hospitalized Patients With 2019 Novel Coronavirus-Infected Pneumonia in Wuhan, China. *JAMA* 2020; **323**: 1061-1069 [PMID: 32031570 DOI: 10.1001/jama.2020.1585]

3 **Huang C**, Wang Y, Li X, Ren L, Zhao J, Hu Y, Zhang L, Fan G, Xu J, Gu X, Cheng Z, Yu T, Xia J, Wei Y, Wu W, Xie X, Yin W, Li H, Liu M, Xiao Y, Gao H, Guo L, Xie J, Wang G, Jiang R, Gao Z, Jin Q, Wang J, Cao B. Clinical features of patients infected with 2019 novel coronavirus in Wuhan, China. *Lancet* 2020; **395**: 497-506 [PMID: 31986264 DOI: 10.1016/S0140-6736(20)30183-5]

4 **Gu J**, Korteweg C. Pathology and pathogenesis of severe acute respiratory syndrome. *Am J Pathol* 2007; **170**: 1136-1147 [PMID: 17392154 DOI: 10.2353/ajpath.2007.061088]

5 **Pirola CJ**, Sookoian S. SARS-CoV-2 virus and liver expression of host receptors: Putative mechanisms of liver involvement in COVID-19. *Liver Int* 2020; **40**: 2038-2040 [PMID: 32352224 DOI: 10.1111/liv.14500]

6 **Nardo AD**, Schneeweiss-Gleixner M, Bakail M, Dixon ED, Lax SF, Trauner M. Pathophysiological mechanisms of liver injury in COVID-19. *Liver Int* 2021; **41**: 20-32 [PMID: 33190346 DOI: 10.1111/liv.14730]

7 **McDermott CV**, Cox EJ, Scanlan JM, Alicic RZ. COVID-19 and Gastrointestinal Tract Symptoms: Recognition, Containment, and Learning From the Past. *Mayo Clin Proc* 2020; **95**: 2320-2324 [PMID: 33153620 DOI: 10.1016/j.mayocp.2020.08.023]

8 **Götzinger F**, Santiago-García B, Noguera-Julián A, Lanaspa M, Lancella L, Calò Carducci FI, Gabrovska N, Velizarova S, Prunk P, Osterman V, Krivec U, Lo Vecchio A, Shingadia D, Soriano-Arandes A, Melendo S, Lanari M, Pierantoni L, Wagner N, L'Huillier AG, Heininger U, Ritz N, Bandi S, Krajcar N, Roglić S, Santos M, Christiaens C, Creuven M, Buonsenso D, Welch SB, Bogyi M, Brinkmann F, Tebruegge M; ptbnet COVID-19 Study Group. COVID-19 in children and adolescents in Europe: a multinational, multicentre cohort study. *Lancet Child Adolesc Health* 2020; **4**: 653-661 [PMID: 32593339 DOI: 10.1016/S2352-4642(20)30177-2]

9 **Verrotti A**, Mazzocchetti C, Iannetti P. Definitive pathognomonic signs and symptoms of paediatric neurological COVID-19 are still emerging. *Acta Paediatr* 2021; **110**: 1774-1777 [PMID: 33641209 DOI: 10.1111/apa.15827]

10 **CDC Health Alert Network**. Multisystem Inflammatory Syndrome in Children (MIS-C) Associated with Coronavirus Disease 2019 (COVID-19). [cited 14 May 2020]. In: CDC Health Alert Network [Internet]. Available from: https://emergency.cdc.gov/han/2020/han00432.asp

11 **Feldstein LR**, Tenforde MW, Friedman KG, Newhams M, Rose EB, Dapul H, Soma VL, Maddux AB, Mourani PM, Bowens C, Maamari M, Hall MW, Riggs BJ, Giuliano JS Jr, Singh AR, Li S, Kong M, Schuster JE, McLaughlin GE, Schwartz SP, Walker TC, Loftis LL, Hobbs CV, Halasa NB, Doymaz S, Babbitt CJ, Hume JR, Gertz SJ, Irby K, Clouser KN, Cvijanovich NZ, Bradford TT, Smith LS, Heidemann SM, Zackai SP, Wellnitz K, Nofziger RA, Horwitz SM, Carroll RW, Rowan CM, Tarquinio KM, Mack EH, Fitzgerald JC, Coates BM, Jackson AM, Young CC, Son MBF, Patel MM, Newburger JW, Randolph AG; Overcoming COVID-19 Investigators. Characteristics and Outcomes of US Children and Adolescents With Multisystem Inflammatory Syndrome in Children (MIS-C) Compared With Severe Acute COVID-19. *JAMA* 2021; **325**: 1074-1087 [PMID: 33625505 DOI: 10.1001/jama.2021.2091]

12 **Khesrani LS**, Chana K, Sadar FZ, Dahdouh A, Ladjadj Y, Bouguermouh D. Intestinal ischemia secondary to Covid-19. *J Pediatr Surg Case Rep* 2020; **61**: 101604 [PMID: 32839689 DOI: 10.1016/j.epsc.2020.101604]

13 **Hwang M**, Wilson K, Wendt L, Pohlman J, Densmore E, Kaeppler C, Van Arendonk K, Yale S. The Great Gut Mimicker: A case report of MIS-C and appendicitis clinical presentation overlap in a teenage patient. *BMC Pediatr* 2021; **21**: 258 [PMID: 34074244 DOI: 10.1186/s12887-021-02724-x]

14 **Morparia K**, Park MJ, Kalyanaraman M, McQueen D, Bergel M, Phatak T. Abdominal Imaging Findings in Critically Ill Children With Multisystem Inflammatory Syndrome Associated With COVID-19. *Pediatr Infect Dis J* 2021; **40**: e82-e83 [PMID: 33298763 DOI:

10.1097/INF.0000000000002967]

15 **Sica R**, Pennoni S, Penta L, Di Cara G, Verrotti A. New Onset of Hepatic Steatosis Post-Severe Multisystem Inflammatory Syndrome in Children (MIS-C): A Case Report. *Int J Environ Res Public Health* 2021; **18** [PMID: 34209719 DOI: 10.3390/ijerph18136961]

Published by **Baishideng Publishing Group Inc**
7041 Koll Center Parkway, Suite 160, Pleasanton, CA 94566, USA
Telephone: +1-925-3991568
E-mail: bpgoffice@wjgnet.com
Help Desk: https://www.f6publishing.com/helpdesk
https://www.wjgnet.com

© 2021 Baishideng Publishing Group Inc. All rights reserved.